JANUARY 1978
VOLUME 67 NUMBER 1

JOURNAL OF PHARMACEUTICAL SCIENCES

MARY H. FERGUSON
Editor

SHELLY ELLIOTT
Production Editor

JANET D. SHOFF
Copy Editor

EDWARD G. FELDMANN
Contributing Editor

SAMUEL W. GOLDSTEIN
Contributing Editor

BELLE R. BECK
Editorial Secretary

DAVID BOHARDT
Director of Publications

L. LUAN CORRIGAN
Assistant Director of Publications

EDITORIAL ADVISORY BOARD

JOHN AUTIAN
NORMAN R. FARNSWORTH
WILLIAM O. FOYE
WILLIAM J. JUSKO
HERBERT A. LIEBERMAN
DAVID E. MANN, JR.
GERALD J. PAPARIELLO
EDWARD G. RIPPIE

The *Journal of Pharmaceutical Sciences* is published monthly by the American Pharmaceutical Association at 2215 Constitution Ave., N.W., Washington, DC 20037. Second-class postage paid at Washington, D.C., and at additional mailing office.

All expressions of opinion and statements of supposed fact appearing in articles or editorials carried in this journal are published on the authority of the writer over whose name they appear and are not to be regarded as necessarily expressing the policies or views of the American Pharmaceutical Association.

Offices—Editorial, Advertising, and Subscription Offices: 2215 Constitution Ave., N.W., Washington, DC 20037. Printing Offices: 20th & Northampton Streets, Easton, PA 18042.

Annual Subscriptions—United States and foreign, industrial and government institutions $50, educational institutions $50, individuals *for personal use only* $30; single copies $5. All foreign subscriptions add $5 for postage. Subscription rates are subject to change without notice. Members of the American Pharmaceutical Association may elect to receive the *Journal of Pharmaceutical Sciences* as a part of their annual $70 (foreign $75) APhA membership dues.

Claims—Missing numbers will not be supplied if dues or subscriptions are in arrears for more than 60 days or if claims are received more than 60 days after the date of the issue, or if loss was due to failure to give notice of change of address. The Association cannot accept responsibility for foreign delivery when its records indicate shipment has been made.

Change of Address—Members and subscribers should notify at once both the Post Office and the American Pharmaceutical Association, 2215 Constitution Ave., N.W., Washington, DC 20037, of any change of address.

Microfilm—Microfilm volumes are available from University Microfilms International, 300 N. Zeeb Road, Ann Arbor, MI 48106.

© Copyright 1978, American Pharmaceutical Association, 2215 Constitution Ave., N.W., Washington, DC 20037; all rights reserved.

MOMENT OF TRUTH FOR OTA

When the federal government was first established, the number of employees in the executive branch was a mere handful. Indeed, there may have been more congressional delegates from the thirteen original states than the total work force in the executive branch.

Over the intervening years, there has been a tremendous expansion in the federal work force. Although appropriations have been made for sizable support staffs for individual members of Congress and for congressional committees, the growth in the legislative branch has been extremely modest by comparison with the explosive expansion of personnel within the executive branch.

As a result, within the past decade, Congress found itself—collectively and individually—coming more and more to rely on the technical expertise within executive agencies because it lacked any such resource itself. Moreover, as this situation developed, the issues coming before Congress—whether they dealt with space exploration, sophisticated military hardware, supersonic aircraft, energy resources, environmental concerns, and so on—increasingly required accurate and reliable technical facts as well as good, sound interpretations of those data.

Having to rely exclusively on the executive agencies for such information or assessments left Congress understandably uneasy. For example, a Defense Department official would be expected to support the need for a new bomber and to describe the virtues of that airplane with a favorable bias when testifying before a congressional committee or otherwise being consulted by Congress.

The obvious answer seemed to be for Congress to establish its own scientific and technical advisory office staffed with appropriately qualified people. And that was just the step that Congress took about five years ago.

The resultant agency was named the Office of Technology Assessment (OTA), and former Congressman Emilio Q. Daddario was named its first director. He was a very logical choice, having served with distinction as chairman of the science subcommittee within the House, as well as being generally credited as the originator of OTA.

However, OTA never seemed to live up to its potential or to the expectations of its followers. With the single exception of the drug bioequivalence study, which was conducted by a panel of outside people and staffed by OTA, the agency maintained a very low profile and seemed to side-step controversial issues. At least it managed to avoid taking any definitive stand on those issues that might have controversial overtones. Although this is a good formula for survival in the political jungle, it doesn't lead to any noteworthy track record with respect to achievement.

Within the past six months, it appears that Congress has decided to do some assessment of its own—specifically, to conduct a series of oversight hearings under the chairmanship of Rep. Ray Thornton (D-Ala.) of the House Subcommittee on Science, Research, and Technology. The hearings were announced shortly after a strange scenario in which there were mass resignations by Senate and House members of the joint Congressional Board which is charged with overseeing the OTA, and then an announcement by Daddario that he, too, was resigning as the agency's full-time director.

Although there were recurring mumbles of dissatisfaction, some of which were elaborated upon in press interviews, the real basis of congressional unhappiness remains somewhat fuzzy and obscure. This is attributed, in part, to a reluctance by resigning Board members to criticize publicly and openly the alleged interference in OTA's operation practiced by one of their Senate colleagues.

Whatever the reasons, it was expected that Daddario—having already submitted his resignation as director—would "let it all hang out" when he appeared as a witness before Thornton's Subcommittee. But the prevailing characteristic of Daddario's operation of OTA was to avoid controversy and the hard issues, and his appearance before the Subcommittee was true to form. In short, he ducked again, even when leading questions afforded him the opportunity to be candid.

Well, the search is now on for a new OTA director. At this writing, the leading candidate is Russell W. Peterson who certainly has the credentials: research chemist and then senior executive at Du Pont, governor of Delaware, chairman of the Council on Environmental Quality, and currently chief executive officer of New Directions, a respected citizens' organization. In fact, he is so "leading" that one recent press report said his appointment to the post has gone "from speculation to expectation."

In sharp contrast to Daddario, Peterson has a reputation as a decisive manager with very strong-willed ideas. Clearly, if appointed, he would not be content to let OTA meander along as a subservient puppet. The question now being asked is whether Congress is quite ready to accept such a dramatic change. We hope they are, and that they will bite the bullet in proceeding with the appointment of a strong administrator such as Peterson. For OTA, the gestation period is over; if it does not begin to produce, it does not deserve to survive.

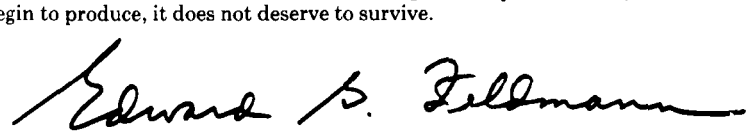

JANUARY 1978
VOLUME 67 NUMBER 1

JOURNAL OF PHARMACEUTICAL SCIENCES

MARY H. FERGUSON
Editor

SHELLY ELLIOTT
Production Editor

JANET D. SHOFF
Copy Editor

EDWARD G. FELDMANN
Contributing Editor

SAMUEL W. GOLDSTEIN
Contributing Editor

BELLE R. BECK
Editorial Secretary

DAVID BOHARDT
Director of Publications

L. LUAN CORRIGAN
Assistant Director of Publications

EDITORIAL ADVISORY BOARD

JOHN AUTIAN
NORMAN R. FARNSWORTH
WILLIAM O. FOYE
WILLIAM J. JUSKO
HERBERT A. LIEBERMAN
DAVID E. MANN, JR.
GERALD J. PAPARIELLO
EDWARD G. RIPPIE

The *Journal of Pharmaceutical Sciences* is published monthly by the American Pharmaceutical Association at 2215 Constitution Ave., N.W., Washington, DC 20037. Second-class postage paid at Washington, D.C., and at additional mailing office.

All expressions of opinion and statements of supposed fact appearing in articles or editorials carried in this journal are published on the authority of the writer over whose name they appear and are not to be regarded as necessarily expressing the policies or views of the American Pharmaceutical Association.

Offices—Editorial, Advertising, and Subscription Offices: 2215 Constitution Ave., N.W., Washington, DC 20037. Printing Offices: 20th & Northampton Streets, Easton, PA 18042.

Annual Subscriptions—United States and foreign, industrial and government institutions $50, educational institutions $50, individuals *for personal use only* $30; single copies $5. All foreign subscriptions add $5 for postage. Subscription rates are subject to change without notice. Members of the American Pharmaceutical Association may elect to receive the *Journal of Pharmaceutical Sciences* as a part of their annual $70 (foreign $75) APhA membership dues.

Claims—Missing numbers will not be supplied if dues or subscriptions are in arrears for more than 60 days or if claims are received more than 60 days after the date of the issue, or if loss was due to failure to give notice of change of address. The Association cannot accept responsibility for foreign delivery when its records indicate shipment has been made.

Change of Address—Members and subscribers should notify at once both the Post Office and the American Pharmaceutical Association, 2215 Constitution Ave., N.W., Washington, DC 20037, of any change of address.

Microfilm—Microfilm volumes are available from University Microfilms International, 300 N. Zeeb Road, Ann Arbor, MI 48106.

© Copyright 1978, American Pharmaceutical Association, 2215 Constitution Ave., N.W., Washington, DC 20037; all rights reserved.

MOMENT OF TRUTH FOR OTA

When the federal government was first established, the number of employees in the executive branch was a mere handful. Indeed, there may have been more congressional delegates from the thirteen original states than the total work force in the executive branch.

Over the intervening years, there has been a tremendous expansion in the federal work force. Although appropriations have been made for sizable support staffs for individual members of Congress and for congressional committees, the growth in the legislative branch has been extremely modest by comparison with the explosive expansion of personnel within the executive branch.

As a result, within the past decade, Congress found itself—collectively and individually—coming more and more to rely on the technical expertise within executive agencies because it lacked any such resource itself. Moreover, as this situation developed, the issues coming before Congress—whether they dealt with space exploration, sophisticated military hardware, supersonic aircraft, energy resources, environmental concerns, and so on—increasingly required accurate and reliable technical facts as well as good, sound interpretations of those data.

Having to rely exclusively on the executive agencies for such information or assessments left Congress understandably uneasy. For example, a Defense Department official would be expected to support the need for a new bomber and to describe the virtues of that airplane with a favorable bias when testifying before a congressional committee or otherwise being consulted by Congress.

The obvious answer seemed to be for Congress to establish its own scientific and technical advisory office staffed with appropriately qualified people. And that was just the step that Congress took about five years ago.

The resultant agency was named the Office of Technology Assessment (OTA), and former Congressman Emilio Q. Daddario was named its first director. He was a very logical choice, having served with distinction as chairman of the science subcommittee within the House, as well as being generally credited as the originator of OTA.

However, OTA never seemed to live up to its potential or to the expectations of its followers. With the single exception of the drug bioequivalence study, which was conducted by a panel of outside people and staffed by OTA, the agency maintained a very low profile and seemed to side-step controversial issues. At least it managed to avoid taking any definitive stand on those issues that might have controversial overtones. Although this is a good formula for survival in the political jungle, it doesn't lead to any noteworthy track record with respect to achievement.

Within the past six months, it appears that Congress has decided to do some assessment of its own—specifically, to conduct a series of oversight hearings under the chairmanship of Rep. Ray Thornton (D-Ala.) of the House Subcommittee on Science, Research, and Technology. The hearings were announced shortly after a strange scenario in which there were mass resignations by Senate and House members of the joint Congressional Board which is charged with overseeing the OTA, and then an announcement by Daddario that he, too, was resigning as the agency's full-time director.

Although there were recurring mumbles of dissatisfaction, some of which were elaborated upon in press interviews, the real basis of congressional unhappiness remains somewhat fuzzy and obscure. This is attributed, in part, to a reluctance by resigning Board members to criticize publicly and openly the alleged interference in OTA's operation practiced by one of their Senate colleagues.

Whatever the reasons, it was expected that Daddario—having already submitted his resignation as director—would "let it all hang out" when he appeared as a witness before Thornton's Subcommittee. But the prevailing characteristic of Daddario's operation of OTA was to avoid controversy and the hard issues, and his appearance before the Subcommittee was true to form. In short, he ducked again, even when leading questions afforded him the opportunity to be candid.

Well, the search is now on for a new OTA director. At this writing, the leading candidate is Russell W. Peterson who certainly has the credentials: research chemist and then senior executive at Du Pont, governor of Delaware, chairman of the Council on Environmental Quality, and currently chief executive officer of New Directions, a respected citizens' organization. In fact, he is so "leading" that one recent press report said his appointment to the post has gone "from speculation to expectation."

In sharp contrast to Daddario, Peterson has a reputation as a decisive manager with very strong-willed ideas. Clearly, if appointed, he would not be content to let OTA meander along as a subservient puppet. The question now being asked is whether Congress is quite ready to accept such a dramatic change. We hope they are, and that they will bite the bullet in proceeding with the appointment of a strong administrator such as Peterson. For OTA, the gestation period is over; if it does not begin to produce, it does not deserve to survive.

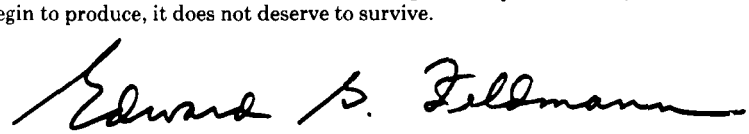

Biological Foreign Particle Film Encapsulation

All foreign, biologically "inert" particles that are at least initially insoluble in biological fluids are enveloped by films composed of endogenous macromolecular and/or tissue surfactants. Marck *et al.*[1] reported that, under the conditions of their investigation, particles of different degrees of hydrophilicity showed different degrees of tissue interaction. They felt that their findings were relevant for bioadhesives, suture materials, and controlled drug release carriers[1]. It is our belief that the process of film formation has broad significance for the total field of the health sciences.

Ecanow[2,3] theorized that the presence of foreign particles, regardless of whether they are introduced as drug carriers, environmental pollutants, or whatever, can initiate pathological processes. Foreign particles are not "inert" in a physical–chemical sense[4]. The data developed in our studies of the relationship between pathology and particulate matter have resulted in a classification of inert particles similar to that of Marck *et al.*[1]

Class A particles are very hydrophobic and are wetted with great difficulty by tissue fluids. Such particulate matter is generally phagocytosed or walled off or floats on the tissue fluids as in the respiratory tract.

Class B particles sorb strongly onto cellular surfaces; these particles produce abnormal membrane-structuring effects. These effects, in turn, may initiate the process of uncontrolled cellular growth[3–5].

Class C particles are dissolved by the biological fluids after varying periods of time.

Particulate matter of Class A is the least biologically toxic. Particles of Class B are potentially the most pathogenic. Class C particulates are toxic only if they result in, among other responses, chemical or free radical reactions that may have a protein-denaturing effect.

Drugs and other therapeutic agents must be tested for their toxic potential. We wish to suggest that toxicity studies be expanded to include investigation of the possibility of encapsulation or partial film formation to determine the long-term biological effects. Aside from the pharmaceutical implications, films may contain significant etiological inferences. Thus, foreign inert particles, most of which are of Class A or C, are almost continuously present in the GI tract. Therefore, it is critical that no agent, *e.g.*, a surfactant, be introduced that will convert these particles to the Class B type.

If the matter of film formation is placed in the context of a lesion, its importance can be made explicit. In many respects, the lesion surface is similar to that of a foreign particle surface. In an ulcer, the crater edge contains fragments of denatured protein. If surfactants are introduced that can combine with these denatured particles and, in time, form a film matrix, then interference with normal healing of the ulcer may take place or a neoplasm might begin[3].

It is our belief that before any given substance is introduced into the body, there must be evidence that it does not initiate or promote adverse tissue reaction of the type discussed. Thus, products containing agents that conceivably bind inert particles to tissue membranes (*e.g.*, antacids that contain surfactants) should be studied to determine whether the surface-active components do initiate tissue changes and whether the surfactant involved adsorbs onto the surface of any lesion and, in the case of an ulcer, prevents normal healing. Failure to satisfy these requirements may cause patients an unacceptable risk.

Bernard Ecanow
Bernard H. Gold
Byong H. Moon
University of Illinois at the Medical Center
Chicago, IL 60680
and the
Rush-Presbyterian-St. Luke's Medical Center
Chicago, IL 60612

R. Saul Levinson
University of Oklahoma
Oklahoma City, OK 73118

Received October 3, 1977.

[1] K. W. Marck, C. Wildevuur, W. L. Sederel, A. Bantjes, and J. Feijen, *J. Biomed. Mater. Res.*, 11, 405 (1977).
[2] B. Ecanow, U.S. Copyright A 895 763 (Ecanow, Skokie, Ill.) (1966).
[3] B. Ecanow and H. Klawans, in "Models of Human Neurological Disease," H. Klawans, Ed., Excerpta Medica, Amsterdam, The Netherlands, 1974, chap. 9.
[4] B. Ecanow, B. H. Gold, and M. Sadove, *Br. J. Cancer*, in press.
[5] B. Ecanow, B. Gold, and W. McCreery, *Clin. Oncol.*, in press.

JOURNAL OF PHARMACEUTICAL SCIENCES

JANUARY 1978
VOLUME 67 NUMBER 1

REVIEW ARTICLE

Contamination of Pharmaceutical Products

IRA FLAUM

Received from the *Food and Drug Administration, Department of Health, Education, and Welfare, Brooklyn, NY 11232.*

Keyphrases □ Contamination—in pharmaceutical formulations, various origins, prevention methods, and detection procedures, review □ Pharmaceutical formulations—presence of contaminants, various origins, prevention methods, and detection procedures, review

CONTENTS

Nature of Contaminants 1
Mechanical Contamination 1
Chemical Contamination 2
Microbiological Contamination 3
Prevention of Contamination 3
Premises 3
Personnel 4
Raw Materials 4
Working Processes 4
Formulation 5
Control 5
Equipment 5
Packaging 5
Detection of Contamination 5
Chemical Contaminants 6
Microbiological Contaminants 7
Mechanical Contaminants 7
Suggested Approaches to the Contamination Problem 8

The ubiquitous problem of contamination of pharmaceutical products is well known to anyone involved in drug manufacture, control, or distribution. In fact, the types of contaminants, their relative hazard to human health, the sources of contamination, and the methods for prevention and detection of such contamination are so varied and numerous as almost to defy compilation. This paper attempts to condense some of the more pertinent literature as well as to put forth possible paths of action with the hope of reducing the future incidence of contaminated drugs.

An indication of the importance of this problem is the fact that the Federal Food, Drug, and Cosmetic Act of the United States (1) appears to place even more emphasis on what should not be included in a drug or its packaging than on what should. In making this point, Wright (2) mentioned five specific conditions listed in the Act as constituting adulteration and not related to the potency of the active ingredients. Although the Act does require drugs to meet standards of potency, quality, and purity of active ingredients, these standards are more measures of ingredients that do not belong in a drug than of those that do.

The point is reinforced when one examines the fact that official compendial standards (3, 4) invariably provide for only one assay method but usually several other tests for the identity of specific expected impurities as well as the presence of materials not included in the formula.

NATURE OF CONTAMINANTS

Mechanical Contamination—Mechanical contaminants are foreign extraneous materials that get into drugs (5, 6). They may be easily seen and explained, such as an iron screw in a drug substance for ingestion or chips and fragments broken from processing equipment, and can be incorporated into products during manufacturing. They may be environmental such as metal fragments, wood slivers, rust, rubber particles, plant fibers, lint, hair, glass, ashes, starch, talc, or asbestos. They may come from the packaging containers such as pieces of glass, plastic, or metal.

A persistent contamination problem continues to be that of metal particles in ophthalmic ointments which result from the stamping and thread cutting operation (7). The potential hazard to sight is obvious. Recognizing this problem, the USP set limits for the number and size of discrete metal particles allowable in ophthalmic ointments (8).

A problem creating much current concern is that of particulate matter (9–29), especially asbestos (30, 31) in parenterals. The inhalation of fibers of the chrysotile form

of asbestos has been associated with serious health hazards, including pulmonary fibrosis and cancer. It is now known that much less exposure than that received by asbestos workers, as little as that received by a person living in a household with an asbestos worker, is associated with neoplastic disease.

To remove foreign material, asbestos filters have been used extensively at many stages of the pharmaceutical manufacturing process, including the final filtration of parenterals. Because of its rapid filtering properties, minimizing bacterial growth, the chrysotile variety is most often chosen. When used in this way, chrysotile fibrils tend to flake off into solutions, with the possibility of finding their way into the human bloodstream and settling at points in the body.

The suspicion that these particles may be foci for disease is supported by experiments with animals and indications of increased GI cancer among asbestos workers. In view of this hazard, the Food and Drug Administration (FDA) ruled that by September 14, 1976, parenteral manufacturers must eliminate asbestos or other fiber-releasing filters from their manufacturing process unless it is impossible to produce a particular drug otherwise. In that case, subsequent filtration with a nonfiber-releasing filter is required (32, 33).

Coincidentally, talc, widely used in the pharmaceutical industry as a tablet excipient, often contains asbestos minerals. There are no current regulations concerning the purity of talc used in this manner. Blejer and Arlon (34) suggested, based on findings relative to talc-coated rice, that analyses for asbestos contamination be performed on talc that can be expected to be significantly exposed to humans. Ominously, they also suggested that studies be made to determine the carcinogenicity of pure talc itself.

Starch, plant fibers, glass particles (35), lint, and undissolved crystalline material from the formulation are other common particles found as contaminants (36–39). Cellulose fibers or particles of powdered plastics, injected intravenously, can cause granulomas and microthrombi in the lungs of rabbits and dogs (6). Autopsies on patients who had received large amounts of intravenous fluids indicated similar lesions (40–42). The particle sizes involved in these observations are about 50 μm, the limit of unmagnified visibility. Medical disagreement surrounds the question of what size particle is hazardous. It is clear, however, that the risk with particulate matter is real and that parenteral drugs should contain as few extraneous particles of any kind as possible.

Chemical Contamination—Chemical contamination occurs in many ways (43). Material obtained from natural sources may contain important contaminants, even after purification. Natural pituitary hormone preparations, corticotropin (adrenocorticotropic hormone), and human growth hormone (HGH) have been found to contain the vasopressor antidiuretic hormone (ADH). This finding explains the occurrence of water retention among some patients receiving 48-hr intravenous infusions of corticotropin or human growth hormone (44).

Incorrect ingredients are sometimes added to the product by mistake, such as the use of an excipient not called for in the formula (2). The addition of an incorrect physiologically active ingredient is, of course, more serious. In deliberate ingredient substitution, there is a different kind of contamination, one commonly known as "sophistication." This substitution would ordinarily be done for economic reasons, such as the substitution of a cheaper synthetic for a "natural" ingredient (synthetic B vitamins for yeast extract), or for reasons of convenience based on the greater availability of one excipient over another.

Because of limitations in purification steps, precursors, reactants, and intermediates from the synthesis of the drug may occur in the final product beyond limits defined by safety and regulations. Soluble equipment components and interaction and degradation products also may be found (45). To control these impurities, tests are instituted, either as called for by the official compendia or as deemed necessary by the manufacturer. These may be tests for specific anions, specific cations, nonspecific impurities, or drug congeners. For example, the USP monograph for chlorpromazine requires a test for an objectionable congener, 4-chlorpromazine, a structural isomer.

Similarly, limit tests are often devised for contaminants expected in very small amounts in the final product, originating from some vessels, catalysts, pipes, stirrers, filters, or other utensils used to process or handle the drugs. These are usually tests for specific metals or for general classes of compounds such as heavy metals (46) or halides.

If nonmetallic processing equipment is used, tests for oxidizable or foreign organic substances may be required.

Drug breakdown and interaction (47, 48) may necessitate tests such as those for salicylic acid in an aspirin product (2). Peculiar and original formulations may often lead to unforeseen contamination problems. Wright (2) cited the reaction between the active ingredient in isoproterenol injection and an added antioxidant, sodium bisulfite, in which the isoproterenol side-chain hydroxyl group is replaced by a sulfo ($HOSO_2$—) group, creating a therapeutically inactive compound. Wright (2) also described the effect of warm humid storage conditions on tetracycline hydrochloride capsules containing citric acid. Not only is tetracycline degraded, but the situation is aggravated by the fact that one degradation product, epianhydrotetracycline, is quite toxic.

Breakdown and contamination after packaging may occur from reactions between liquid drugs and rubber closures (49) or plastic containers (50, 51). Sulfides, added to rubbers as vulcanizers, react with mercury preservatives to form mercuric sulfide. Plastics may release salts into solutions or absorb active ingredients.

Crude drugs (52), although rarely dispensed in this country, have been contaminated with organochlorine pesticides. Noguchi *et al.* (53) found cyclodiene insecticides and benzene hexachloride isomers, including chlorophenothane (DDT), in many Far Eastern commercial crude drugs and in their processed products.

Herlihy (54) described an isolated incident of the contamination of a medical oxygen cylinder. Although the source of the problem was not found, the experimental combustion of polytef yielded products whose IR spectra were identical to the contaminants.

During the last decade, there has been increased awareness of another problem, that of cross-contamination. This problem may be described as the unintended,

unexpected presence of one drug in another, generally resulting from the spread of dust particles arising from the manufacture of other drugs in the area or from equipment not completely cleaned after use in the manufacture of other products (55).

Historically, the increased attention paid to this problem began with attempts to control penicillin cross-contamination (56). The unusual concern shown penicillin is a result of its allergenicity. An individual receiving very small doses of penicillin as a contaminant in another drug may become sensitized, setting up an allergic response or even a severe anaphylactic shock when a full dose (or less) is adminstered (57). Thus, as a result of an ad hoc Advisory Committee on Penicillin Contamination convened by the FDA Commissioner in 1965 (58, 59), penicillin limits were fixed at 0.5 IU (0.3 μg) for oral drugs and at 0.05 IU (0.03 μg) for parenteral drugs for the highest single recommended dose. Proposed new regulations would reduce the tolerance to zero (60). Ironically, penicillin's allergic properties may be traceable to penicillin itself being contaminated. It has been suggested that macromolecular proteinaceous and nonproteinaceous substances, as well as polymers of penicillin, present in trace amounts are important in precipitating allergic reactions (61).

Penicillin is usually used as a very fine, dry powder, easily becoming airborne and migratory (62). It is particularly difficult to clean a penicillin production facility because the drug clings electrostatically to processing equipment (63). Also, the weight of a penicillin tablet is typically about 70% active ingredient, giving a very high yield of penicillin in the dust produced by the tableting operation (55).

Some investigators agree that, because of its high potency and ease of dissemination, if penicillin could be prevented from contaminating other products in a plant, cross-contamination in general within that plant would be under control (56, 64). In this regard, penicillin may be considered as a test substance, since it is possible to detect and quantitate it at very low levels by the simple and specific agar plate-zone inhibition technique (65).

Microbiological Contamination—Regarding microbiological contamination, injections, intravenous infusion fluids, and drugs intended for ophthalmic use are required to be sterile; the presence of even one live microorganism, of any type, is not tolerated (66–68). The literature is replete with unfortunate violations of this requirement (69–74).

The great danger in contaminated intravenous infusion fluid was painfully learned during the "Devonport Incident" in England (75–80). At least four, and possibly six, people collapsed and died as a direct result of receiving 5% dextrose infusions following surgery. A committee of inquiry deduced that an autoclave that left air in the chamber during the pressure cycle was at fault. The dextrose bottles were stacked in three layers, and the effect was that the bottles in the lowest layer were not sterilized. Bacteriological control samples were taken only from the uppermost layer, preventing the detection of the problem. More than 1 year passed before the solutions were administered, allowing heavy bacterial growth and accumulation of endotoxin. The cloudy solutions that resulted were not recognized by the hospital staff. Eventually, *Klebsiella aerogenes*, other Enterobacteriaceae, *Erwinia herbiocola*, *Pseudomonas thomasii*, and coryneform organisms were identified in the bottles.

The microbiological condition of drugs not intended to be sterile represents a different problem (81–91). About 200 cases of salmonellosis in Sweden in 1966, traced to thyroid tablets contaminated with defatted thyroid powder containing over 30 million bacteria/g, proved to be one stimulus to study in this area (92). Yet a random sampling of 660 production batches of various drugs marketed in Sweden revealed remarkably high levels of bacteria and fungi not apparently associated with disease. Counts of up to millions per gram were common. Of 160 tablet batches, 38 contained coliform bacteria, an indication of poor sanitation somewhere in the manufacturing procedure.

Just why one set of conditions represents a hazard to health and another does not is defined by certain parameters, namely, the intended use of the drug, the pathogenicity and virulence of the organisms in relation to the immunological state of the patients, and the total numbers of organisms present in the preparation. Other parameters to be considered include the possibility of changes in pharmacological activity, side effects, and shelflife resulting from the presence of microorganisms.

Ignorance of some of these parameters resulted in reduced sight and the loss of an eye from the use of an ophthalmic ointment containing two broad spectrum antibiotics and a steroid (92). The manufacturer failed to use a preservative, wrongly thinking that the low water content and two antibiotics would prevent bacterial growth. What resulted were tubes heavily contaminated with *Pseudomonas aeruginosa* in pure culture. Since 1965, the USP has required sterility in solutions and ointments for ophthalmic use (66–68).

PREVENTION OF CONTAMINATION

The prevention of contamination, particularly cross-contamination, is a problem whose solution is best summed up by Elias' (93) three I's: "The integrity and identity of the product are assured by isolation." However, this simple statement should not obscure the fact that the problem is multifaceted (63).

With particular reference to the prevention of microbiological contamination, Moller (94) listed the following key areas: premises, personnel, raw materials, working processes, formulation, and control. Molin (64) added equipment and packaging. The proper control of these factors will serve equally well to prevent chemical and mechanical contamination.

Premises—"Premises" refers to the layout and general construction of the plant (94–101). Production areas and adjacent formulation, storage, and cleaning facilities, as well as product transportation routes, should be separated from each other as much as possible (64). They also should be isolated from similar areas used in making other products. In fact, the current dominant guiding principle in plant design calls for the subdivision of production areas into cellular units where it is possible for personnel to pass physically through production departments without going through the actual working areas. Also, admission to various areas is possible only through lock arrangements, with concurrent facilities for the changing of clothes.

The importance of this cellular isolation varies with the

particular procedure involved. For the production of some drugs, separate rooms are required. For others, such as the redoubtable penicillin, separate rooms and, additionally, equipment not used for any other product are necessary. The isolated rooms are kept at negative air pressure relative to the surrounding areas to prevent the escape of particles to other parts of the plant.

An additional important feature in a modern, well-designed plant is a suction system with inlets to remove dust at crucial points in the manufacturing process such as tableting and coating.

Also important are the materials used for the interior surfaces of the production buildings. Smooth-surfaced, easily cleaned, and seamless polyurethane is a popular and serviceable material.

The judicious use of underpressure and filtered, recirculated air throughout the plant helps prevent cross-contamination and bacterial spread (102), as does the HEPA filter, which is usually used where sterile air is a requirement (103–105).

The last decade has seen a great increase in clean room design utilizing the principle of laminar air flow in the pharmaceutical industry (106–115). HEPA-filtered air is blown uniformly through a work area or entire room and exhausted on the opposite side. This system can be done horizontally or vertically. The resultant sweeping effect leads to a considerable improvement in air cleanliness over that achieved by conventional HEPA filtration. However, despite its proven utility, the laminar flow technique must be examined carefully for effectiveness in a particular situation; it should not be thought of as a panacea (116).

The general subject of "clean room" technology was discussed previously (117–125). Kinsky (126) described the conversion of ordinary office space into a sterile filling and sealing facility. Three rooms were constructed: a gown room, a sterile storage room, and a main production room. The original sheetrock walls and ceiling were replaced by plaster, sealed, and finished with epoxy paint and sheet metal. The original vinyl tile floor was replaced by sheet vinyl curved upward at the walls to form a cove molding. Horizontal laminar air flow was provided in the main production area. The storage and gown rooms, thought not to require full recirculated laminar flow, were utilized for the removal of air and the introduction of makeup air. A smoke generator and photometer[1] were then used to evaluate the efficiency of the system and to check for leaks. Finally, plate counts of sampled air and control production samples confirmed the suitability of the complex for the beginning of routine sterile production.

Federal Standard No. 209B (127), whose provisions must be met by U.S. Government contractors manufacturing under conditions requiring clean rooms, is an often-quoted document which has become widely accepted as a guide to clean room requirements and standards.

Personnel—Personnel immediately involved in the production process, their very presence and what they do, are crucial to the quality of the product (128). People who move into, out of, and about production areas are inevitably carriers of potential contamination (129). Walking, talking, and breathing can spread bacteria and chemical dust. People who work in production areas should be free from communicable disease and be subject to essentially the same health requirements as are food workers. Pharmaceutical workers should have the proper facilities and follow prescribed routines for the changing of clothes, shoes, and gloves.

Just as important, they should have the proper knowledge and education. A program of continuing education, such as that introduced by the Swedish Drug Industry Association, is useful (94). Austin (130) described various approaches effective in the training of clean room personnel. Lecture techniques, slide shows, and on-site demonstrations are recommended. However, knowledge and education count for nothing if the proper motivation is not present. Neglect and indifference can overwhelm the most sophisticated system. Failure to check a weight and careless cleaning and inspection of a mixer are examples of behavior that are greatly influenced by the employer–employee relationship. A strong sense of responsibility must be instilled in people who work with pharmaceuticals.

Raw Materials—Perhaps the most essential single factor that can guarantee the quality of a drug product is high quality raw materials (64). All materials used in formulations should be obtained from reliable sources, quarantined after receipt at the plant, and tested prior to use (56). They should be kept in sealed containers, in isolated quarters, and not opened except in formulation or weighing rooms.

For sterile production, the most important single raw material is undoubtedly water. Tap water is well recognized as a carrier and incubator of microorganisms. This fact, plus its mineral content, makes it unsuitable for all pharmaceutical production (131). Distilled water, if not properly collected and stored, may also harbor bacteria. Rubber and plastic connections in a still may be sources of infection, necessitating either frequent sterilization of the system or the introduction of all-glass equipment. For nonsterile preparations, demineralization, followed by filtration[2] and continuous holding at 80°, was described (94). This system resulted in sterile and pyrogen-free water.

Working Processes—The systematic study of new working processes and procedures is necessary to discover potential trouble spots (132, 133). Weak points might be an inadequate drying time or temperature for granulations, water condensation on the surfaces of ointments or solutions, and taps containing residual water after cleaning (94).

An interesting method for discovering potential trouble is to substitute a broth or buffer solution for the product and to pass it through the process (64). Sampling at different stages is performed to locate sources of contamination.

A key area of concern that could be considered a processing problem is the production schedule itself (56). Drugs that are in any way incompatible should not be scheduled in succession on the same equipment. For example, barbiturates stimulate the metabolic breakdown of anticoagulants in the body, reducing their efficiency. Therefore, it would be prudent not to schedule anticoagulant manufacture immediately after the production of

[1] Royco.

[2] Millipore.

a barbiturate. If cross-contamination has to occur, it should be kept as harmless as possible.

Tablet production is inevitably dusty. Some steps that should be taken to control it (55, 134) include: (*a*) limiting the weighing area to the ingredient that is actually being weighed, (*b*) maintaining negative pressure in the vicinity of tablet machines, (*c*) avoiding hand-scooping of granulations by elevating the drums and using continuous flow into the hoppers, (*d*) cleaning containers that accumulate dust before removing them from the area, (*e*) thoroughly cleaning each piece of equipment between runs of different products, and (*f*) providing facilities for the disposal of operators' clothes that have accumulated dust.

Otto (135) described the large-volume parenteral manufacturing procedure with emphasis on minimizing particulate matter. The solution itself, ambient air, the interior glass surface, and the closure affect the residue of particles in the final product. Recommended steps are: the proper filtration of the solution, efficient cap and bottle wash and rinse procedures, a short time lapse between washing and final production steps, inspections and quality control checks (136) during filling (137), and the use of enclosures to limit fallout from the air. It is currently anticipated that the Code of Federal Regulations will soon require stringent procedures to be followed in the manufacture of large-volume parenterals.

In the production of sterile solids for injection, the filtration prior to recovery of the solid is the last step to reduce particulate matter. Hammer (138) discussed factors in subsequent steps that influence the final particulate content: spray or drum drying (139) usually results in fewer particles than the recrystallization procedure, simpler machinery with fewer moving and grinding parts generates less particulate matter, large room-size laminar flow units throughout the manufacturing procedure reduce particulate fallout from the air, and shrink-wrapped vials (140) contain fewer particles than those shipped in corrugated boxes and result in less contamination after washing.

The difficulty of the problem can be seen in the fact that, even with proper knowledge and consideration of these factors, particulate contamination was reduced by only about half in the Hammer (138) study—and at great expense.

Formulation—The protection of a nonsterile formulation against microbial growth both during and after its preparation is affected by the control of certain factors (94). For granulations, these factors may be the lowering of pH, the change or elimination of the granulating liquid, and the introduction of preservatives. For liquid preparations, a pH change, the use of preservatives, or a change in osmotic pressure may be necessary.

Basically, what a good master formula must do is carefully spell out every step in the procedure with respect to the equipment used, the order of addition of ingredients, the duration of mixing, safety precautions, *etc.* The batch master formula is the key to a contamination-free operation.

Control—Once a satisfactory system is achieved, it is a permanent function of the quality control system to maintain it (94).

To guard against error in labeling or processing, assay, identity, and limit tests should be scrupulously performed on all finished products. Although acceptance of protocol for raw materials received from suppliers is permissible according to good manufacturing practices (141, 142), additional identity tests should be instituted (142). For sterile productions, every raw material and finished product, as well as some intermediates and the production environment, should be checked for all microorganisms (143, 144) according to a fixed schedule. Tap water, demineralized water, and distilled water especially should be checked regularly.

The method, described earlier (64), of broth substitution for the product is a useful periodic check on the microbiological cleanliness of a procedure. However, as a routine in-process test, it is not generally acceptable because of its cost, incompatibility with normal production runs in terms of the duration of the run, and the danger of accidentally leaving a bacteriological medium where it may become a substrate for microbial growth.

Hess *et al.* (145) published a generalized scheme and routine procedures for determining low level microbiological contamination in topical preparations used on open skin wounds or mucous membranes. These preparations are unique in that, while they must be initially sterilized and contain preservatives that will maintain their freedom from pathogens, they are not required to remain sterile. However, they must not support the growth of high numbers of microorganisms of any kind (146).

Another indispensable part of the control system is the use of trained, on-site inspectors, who visually check every part of the production, packaging, and labeling procedure.

Equipment—Equipment should be constructed so as to facilitate cleaning and sterilization, especially between changes in product, to prevent the seeding of new batches with the residue from the old (64).

Machines such as mills and granulators with bushings and packing glands are usually difficult to clean. For this reason, they should be dismantled to an extent sufficient to permit proper cleaning.

Packaging—The packaging step in the production procedure is particularly important. Miller and Korczynski (147) outlined various aspects of drug and cosmetic packing from the point of view of a contract packing firm not involved in the prior manufacturing steps. The great variety of products handled requires that the firm carefully analyze the sterility requirements and problems of each product. Products are classified into groups and subgroups according to dosage form, label claim, intended use, and stability. For instance, a sterile parenteral is quarantined until tested whereas ointments, creams, liquids and powders for external use are merely screened (based on results from the first few lots) for an increase in microorganisms and the absence of undesirable microorganisms following handling and packaging.

DETECTION OF CONTAMINATION

The detection of drug contaminants is a broad problem, often requiring great ingenuity and imagination. Much depends on the amount of detailed information available to the analyst. Alexander (148) summarized his own experience at FDA in analyzing drugs for impurities. As an example, he cited a customer complaint of a manufacturer producing drugs and pesticides in the same apparatus

without proper cleaning of the equipment between product runs. Knowledge of what contaminant to expect simplified the chemist's task in detecting insecticide contamination of the drugs.

Once an analyst knows what to look for, the procedures used depend on the nature and level of the contamination, the nature of the drug, the equipment and instrumentation available, and the amount of time available.

Perception of the contamination problem has been influenced greatly by the development of modern sophisticated techniques and instrumentation (149). Contamination at the parts-per-million and parts-per-billion level can be detected with TLC (150–153), GLC (154–156) with its sensitive detectors, mass spectrometry (157–159), neutron activation analysis (160, 161), and microcrystalline tests (162–164).

Although it is impossible to describe here all of the methods that might be used to detect trace materials, the information relating to specific approaches to the problem will be reviewed.

Chemical Contaminants—An FDA procedure describes the general method for detecting and measuring penicillin contamination in drugs (65). The procedure is divided into three sections. In Section A, several microbiological assays are described using the method of bacterial growth inhibition on agar plates. Section B describes several methods of preparing samples for assay. Section C lists, in tabular form, the appropriate combination of assay and sample preparation for specific drugs. These methods comprise the basic approach to the detection and quantitation of penicillin as a cross-contaminant.

After the development of these methods, many semisynthetic penicillin and cephalosporin antibiotics were introduced. A study was made to determine if the existing methods were satisfactory for their detection (165). It was discovered that new methods were needed to detect ampicillin in other drugs and antibiotics.

Using high-speed liquid chromatography (HSLC), Bracey (166) determined trace ampicillin in nitrofurantoin capsules. The powder from 10 capsules is suspended in water, filtered through glass wool, and extracted with chloroform. A portion is injected into a liquid–liquid chromatograph with a UV detector. A strong anion-exchange column and a mobile phase of pH 6.5 phosphate buffer are used. With this procedure, the sensitivity limit is 0.1 mg or more/dose, which is too low to be of much use. It is suggested that the method, with proper sample preparation, could be applied to the determination of ampicillin in other drugs.

Although penicillin levels of 1 μg/g can be detected conveniently with microbiological methods, a rapid chemical method is advantageous where other antibiotics are present or the growth of the test microorganism is affected by the drug substance itself. A TLC method was developed (57). Two grams of sample is shaken with 10 ml of water, and the pH is adjusted to 6.5–7.0. After centrifugation, the supernate is washed with chloroform and acidified with phosphoric acid (pH about 2). Free penicillinic acids are extracted with methylene chloride, which is then dried by being passing through anhydrous sodium sulfate.

The combined extracts are evaporated to dryness, and the residue is extracted with isopropyl acetate. After evaporation to about 0.05 ml (a 90% yield is expected), 5 μl is spotted on TLC plates; penicillin G spotted in amounts from 0.5 to 5 μg is used as a standard. Any of four separate solvent systems are used, yielding different R_f values. The penicillin compounds may be visualized or monitored in different ways. No specific penicillin spray reagents are indicated, but several alternative sprays are listed.

An alternative to spraying is the bioautographic process of Stahl (167). The material in the penicillin-suspected spots is brought into contact with an agar gel inoculated with a microorganism, and the observed biological activity represents proof of the presence of penicillin. If it is assumed that the weakest standard spot represents the lower level of method sensitivity, 2.5 μg/g is the least amount that can be detected.

Specialized methodology for the determination of antibiotic dust dissemination has been published (168, 169). The general procedure involves passing a known volume of air through a 0.22-μm pore size filter[2]. Any residue is dissolved in a buffer, and portions are incubated on agar plates containing a suspension of test organism. Zones of growth inhibition as diameters in millimeters are measured and compared with those obtained from known concentrations of the same antibiotic, *i.e.*, a standard curve. The sensitivity of the procedure is 0.001 unit for penicillin and 0.004 μg for chlortetracycline.

An adaptation of this method was made by Garth *et al.* (170) for the purpose of making an environmental survey of a six-story building that housed the laboratories of the National Center for Antibiotics and Insulin Analysis. Qualitative and quantitative tests for penicillin and tetracycline were performed on air samples from various parts of the building. Initial tests were made using agar plates, and the results were used as a guide for the vacuum sampling of air at points in the building thought to be the most easily contaminated.

The results (170) of the tests indicated that the incidence of contamination by antibiotic dust was negligible other than in the actual laboratory rooms where testing was performed. The exception to this finding was a cleanup area where soap powders, antiseptics, and antibiotic-contaminated glassware were processed. The investigators concluded that persons in the building not testing antibiotics were not exposed to them by the atmosphere whereas antibiotic analysts were exposed minimally. While, strictly speaking, this paper did not concern pharmaceutical contamination, the general approach can certainly be applied analogously to a drug plant.

A comprehensive approach to the detection of foreign active drug ingredients in pharmaceutical preparations was made by Cieri (171). General procedures were discussed where the suspected contaminant was extracted with a suitable solvent and separated from the other extracted ingredients, usually by column chromatography. TLC was used to detect the contaminants, with a spiked sample being simultaneously run through the identical procedure for comparison. Specific methods were detailed for the detection of the following drugs: barbiturates, diethylstilbestrol, reserpine, cardiac glycosides, quinine or tropane alkaloids, pyrilamine or chlorpheniramine, phenylethylamines, steroids, methapyrilene or its salts, acetaminophen, and meprobamate. The author suggested the pos-

sibility of scraping the spots from the TLC plates and, after suitable extraction, using UV absorption as an identity confirmation.

Senov *et al.* (172) and Edmond (173) also described the use of TLC for the quantitative evaluation and determination of drug purity.

Adapting the Cieri TLC procedures, an FDA regulatory analyst detected drug residue in cotton balls that had been used to swab various parts of a drug plant. Positive results were obtained from acetaminophen, saccharin, and quinidine sulfate. Additionally, acetaminophen was confirmed on the basis of its UV absorption maximum.

Expanding on the problem of pharmaceutical factory dust, Page (174) published a general scheme for its analysis, concentrating mainly on ingredients found in relatively high dose level dosage forms. Direct IR spectra of the dust is occasionally useful, as is X-ray diffraction or X-ray fluorescence of the residue, following ignition at 600°. More often, purification is required. A subsample of the dust is mixed with aluminum oxide, and the mixture is then added to an aluminum oxide chromatographic column. Elution of the drugs is accomplished with chloroform, followed by methanol and, finally, water. Water deactivates the column. The separated eluates are then resolved by TLC using one or two of the solvent systems described. The TLC spots can be identified either with fluorescence quenchers or with spray reagents, with the probable detection limit for fluorescence quenchers being about 100 ng. Several confirmation tests are suggested, using IR, UV, GLC, or HSLC.

Another approach to the factory dust problem, using combined GLC–mass spectrometry, will be discussed later.

The manufacture of counterfeit drugs and illegal distribution of legitimate drugs are major societal and enforcement problems. Reynolds *et al.* (175) described the use of neutron activation analysis to identify the source of a drug product. The approach is based on the fact that natural trace elements may be present in a drug, giving it a characteristic "fingerprint" and establishing its origin. Manufacturers may also deliberately add trace elements to a drug to achieve the same effect. Neutron activation analysis, effective for about two-thirds of the chemical elements, is used to determine the patterns of trace elements. A nuclear reactor activates the sample, creating radioactive nuclides. After radiochemical separation, the radioactivity is measured directly or by direct γ-ray spectrometry with a scintillation detector and multichannel analyzer. The latter was used in this case. Five samples of dextroamphetamine tablets or capsules, along with several common tablet and capsule excipients, were analyzed for contaminants. Seventeen elements were detected in amounts ranging from less than 1 ppb to more than 0.1%. The results indicated that the tablet and capsule samples were readily distinguishable.

Microbiological Contaminants—The USP (176) describes detailed tests, where called for in compendial monographs, for the presence of viable bacteria, fungi, and yeasts. Procedures are given for opening containers, sampling, preparation of media, and incubation. The technique of membrane filtration (177) is also described. Other methods are acceptable, but the results of the official procedure take precedence in the event of contradictory findings. No sampling and testing format can guarantee that untested units of a given batch are sterile. This fact recalls one aspect of an expression often used in the pharmaceutical industry: "You can't test in quality."

Holdowsky (178) solved the problem of the determination of viable sensitive bacteria in antibacterial drugs. USP sterility tests could rarely recover bacteria from antibiotics that inhibited their growth unless a deactivator was available (*e.g.*, penicillinase for penicillin). The membrane filter was used to separate the bacteria from the antibiotics. Of 15 dihydrostreptomycin samples contaminated by the method, only one could be confirmed by the official USP test.

Wargo (89) performed sterility tests on topical ointments, utilizing a technique developed by Tsuji and Robinson (179). The ointment is dissolved in a mixture of isopropyl myristate, carbon disulfide, and xylene and then passed through a sterile membrane filter. The filter is divided in two, and retained bacterial contaminants are incubated on agar and in a fluid medium. Although only 11% of 180 previously unopened tubes were contaminated in this study, 93% of 80 tubes used in a patient care area were nonsterile. Isopropyl myristate is less toxic to microorganisms than the Tsuji and Robinson mixture of solvents. Therefore, the USP adopted a method using isopropyl myristate alone as the extracting solvent.

Mechanical Contaminants—The quantitation and identification of particulate matter in parenterals are relatively new fields and the subject of much recent study (180–186). The USP XIX (187) established an official procedure and particle-count limits for large-volume injections for single-dose infusions. Standards are met if the product contains "not more than 50 particles per ml that are equal to or larger than 10.0 μm and not more than 5 particles per ml that are equal to or larger than 25.0 μm."

The USP method is essentially a membrane filtration, followed by microscopic examination of the filter for particulate count and size. Other methods are allowed providing they are of equivalent reliability. Several instrumental methods have been developed, but their limitations must be considered. For instance, microscopic air bubbles, electrical disturbances, physical vibrations, or the formation of particle agglomerates may give rise to erroneous results (188–193).

A conductometric particle counter[3] was described (194, 195). An electrolyte solution containing the particles to be counted is sucked through a capillary across which resistance is continuously measured. When a particle passes through the capillary, a resistance change occurs and an impulse proportional to the particle size is generated and recorded. The use of "discriminators" that eliminate impulses below a threshold level permits the simultaneous counting of particles above given sizes (196).

An automated counter[4] was used to count particles of the 2–12-μm diameter range in intravenous infusions (19). Eighteen samples contained from 217 ± 49 to 6110 ± 343 particles/ml above 2.7 μm in diameter. Tests after autoclaving several times showed that, when new silanized rubber stoppers were used, it could not be concluded that

[3] Celloscope 202.
[4] Coulter.

repeated autoclaving increased the particle count. In fact, the count seemed to decrease, perhaps because of fragmentation into particles smaller than 2.7 μm. Other tests led to the conclusion that patients would receive fewer particles if the first 50–100 ml of intravenous solutions was used to flush out particulate matter present in intravenous administration sets.

A new instrument, the prototron, utilizes a laser light-scattering principle. It was used to count and size particulate matter in normal saline and 5% dextrose solutions (198). From three to five times as many particles were found greater than 1 μm than were found greater than 5 μm. This result is fairly typical of the skew in size distribution that other researchers have reported. Fortunately, it is felt that emboli are more likely to form with particles greater than 5 μm, the diameter of an erythrocyte being about 4.5 μm.

The determination of the silting index was proposed as an alternative to particle counting (199). The silting index is dependent on the flow rate decrease resulting from the tendency of particles to clog a filter. This decrease is, in turn, proportional to the number of particles as well as, to a certain extent, the size distribution of the particles. Values derived from three runs per sample were within 15% of the true value with 90% confidence.

The identification of particles requires the skilled use of a microscope (200). Oblique reflected light is used for opaque materials (metals and gelatinous debris) (201). Most common particulates of higher birefringence (fibers, starch crystals, plant tissue, and mold) are accessible to transmitted light microscopy techniques, which include polarized light, phase contrast, and differential interference contrast.

SUGGESTED APPROACHES TO THE CONTAMINATION PROBLEM

At this point, we might ask ourselves: "What is a rational basis for sampling to detect drug contamination?" The deciding criterion seems to be a logical, systematic approach that would yield the maximum, meaningful, practical amount of information for remedial action after subsequent analysis.

Many factors govern this criterion. Several questions need to be answered. Does the investigation have a clinical background or is it a general inquiry to determine the extent of suspected problems? If there has been a precipitating incident, is the source of the problem at the plant or a result of contaminated and/or mislabeled raw material? Might there be a repacking or storage-related problem? Are there initial laboratory findings to serve as a basis for further investigations? What is the potential health hazard? Are there specific, sensitive analytical procedures available for practical analyses?

In answering these and other questions, comprehensive scientific knowledge, experience, and sleuth-like qualities are required of the investigator. A routine, fixed approach does not exist, but certain recurrent themes will govern the approach to be taken.

For a plant survey, without clinical or laboratory findings as a starting point, a complete picture of the physical layout, production processes, manufacturing scheduling, flow of materials, in-process controls, and cleaning routines should be obtained. Personal observations should be made to see if the prescribed routines are being followed. Deficiencies can then be identified and potential problem areas can be investigated in depth.

Observers should be as unobtrusive as possible and not disturb the normal routine. It is important that the plant personnel not be so aware of being watched that they alter their normal procedures. What is remarkable, however, is the extent to which people, out of ignorance or habit, will continue to do things the way they have in the past, even though they know they are being observed[5].

Environmental analyses may provide indicators of trouble spots. For sterile production, testing for airborne bacteria by the use of agar plates left in fixed positions for various times has become an accepted, useful procedure.

However, the use of routine procedures for estimating airborne, particulate contamination risks during production and for determining the effectiveness of prophylactic measures (202) has been essentially neglected, as indicated by the paucity of literature. A start was made by Buogo and Eboli (203), who adapted an electrostatic bacterial air sampler to collect micronized drug particles. With a highly susceptible strain of *Sarcina lutea* seeded on Mueller–Hinton medium, penicillin, tetracycline, paromomycin, and sulfapyrazine were identified and quantitated. Penicillin G was detected at a level of 0.3 $\mu g/m^3$ of air. When 20–40 min had elapsed after the drugs were sprayed into the air, small quantities of penicillin were still detectable.

Ernerot and Molin (204) used an air sampling method[6] and two sedimentation methods (particle-fallout photometer and the analysis of penicillin fallout on petri dishes). Penicillin powder was artificially dispersed at regular intervals and under different conditions of ventilation in a "clean room," and the fallout pattern was observed at various locations in the room. Similarly, a penicillin vial filling room, penicillin tableting area, general tableting department, and granulation room were surveyed for particle fallout. The results from the different methods used correlated well and provided useful information about the dispersion pattern of chemical dust in the room.

A point to be kept in mind is the advantage of sampling product material at the earliest production stage after the suspected occurrence of contamination, *i.e.*, at that point where contamination will be the most concentrated. This is important for the analytical chemist as well as for pinpointing the trouble area. Those who have attempted to detect parts-per-million levels of estrogen in a multivitamin tablet, for instance, will attest to the great difficulty that may be encountered in recovering trace drugs from complex mixtures.

Nevertheless, the demonstration of a contaminant in the dosage form to be administered provides the most information about the extent of the health hazard as well as the

[5] The following incident involving an FDA investigator may serve as an extreme example. One of two weighers, who were supposedly checking each other's work, left the weighing area to obtain dextroamphetamine sulfate. He returned with a handscoop filled with white powder. After weighing the prescribed amount, he took the excess powder back to where he had obtained it, accompanied by the investigator. The material was returned to one of two adjacent, open drums, both containing white powder. There was no check of the drum from which the powder came or was returned to, and a potent drug was carried open, some distance through material storage areas, with the possibility of airborne cross-contamination. The chief weigher remained at the weighing scale throughout, apparently unaware of the multiple dangers in the procedure.

[6] Royco particle counter.

strongest legal evidence[7].

As an example of the solution of a sequential cross-contamination problem, Banes (205) cited the classic case of diethylstilbestrol contamination of isoniazid tablets. Initially, suspicions were aroused by the appearance of premature sexual maturation among young girls being treated for tuberculosis with isoniazid tablets. After ruling out environmental factors as a cause, isoniazid therapy was discontinued and the symptoms disappeared. Animals were fed the tablets and showed a positive estrogen response. Chemical analysis of the tablet batch then yielded an extract whose IR and UV spectra and chromatographic properties were identical to those of diethylstilbestrol. Production records revealed that isoniazid had been compressed immediately after a high potency diethylstilbestrol batch. This evidence and the observation of lax cleaning procedures and, eventually, the discovery of other batches sequentially contaminated with diethylstilbestrol represented an irrefutable chain of evidence.

A final philosophical point should be made. Surely, many of the cited examples of contaminated pharmaceuticals are real and severe dangers to the public. However, what of an innocuous condition represented by a trace of ascorbic acid in an aspirin tablet? It might be argued that the expense of eliminating the possibility of this occurring is not worth the doubtful benefit. It must be decided what kind of general attitude should be fostered in pharmaceutical manufacturers, whether they are small private label houses with limited funds or large multinational corporations. Aside from the fact that the consumer of an item so important as a drug is entitled to receive no more and no less than what he or she is paying for and not a mixture of traces of everything present in a plant, an attitude of scrupulous attention to detail, anticipation of problems, and even seeking out of problems is well worth whatever it costs if one "Devonport Incident" is avoided.

[7] The solution of a sampling and detection problem that arose at this agency is presented, not as an exact model to be followed but as a particular solution to a special situation. Hopefully, it will provide some insight into similar and related problems facing drug manufacturers and regulatory agencies.

During an inspection of a large ethical drug manufacturing plant, an FDA inspector observed substantial concentrations of dust throughout various parts of a general tablet compression room. There was dust on the walls of the room, on vacuum air returns atop the room partitions, and at the fresh air return. In instances where hand loading of granulations into the hoppers was observed, considerable dusting occurred despite the operator's care and the use of vacuum equipment. Nine tablet compression machines were separated only by 1.7-m high partitions.

The inspector felt that, to reduce the chance of cross-contamination under the prevailing manufacturing conditions, ceiling-high partitions between the compression machines should be installed. Although the amount of dust was small, it was felt that if this dust could be shown to contain drug material that had migrated from tableting cubicles some distance away, the potential of cross-contamination would be demonstrated. In addition, records were obtained of the firm's tablet compression schedules for the 2-week period prior to sampling. The New York FDA laboratory was then given the assignment of determining the drug content of cotton swabs used for the sampling of the various dust deposits. To complete the picture, a comprehensive listing of the firm's tableted drugs was obtained.

The method of analysis adopted was combined GLC–mass spectrometry. The procedures used in general by this author were as follows. The contents of a swab plus any loose powder were extracted into alcohol, filtered through Whatman No. 41 paper, and brought to volume. A portion of the alcohol solution was cleaned up (as found necessary) using acid and basic washes and reextractions. Eventually, a very small volume of chloroform extract was obtained, and a portion was injected into a system consisting of a Barber-Coleman 5000 gas chromatograph interfaced to an A.E.I. M.S.-12 mass spectrometer through a Markey glass frit separator.

The column liquid phase was 10% DC 200 on a support of 80–100-mesh Gas Chrom W (HP) with the column effluent split between a flame-ionization detector and the mass spectrometer source. As a peak appeared on the GLC recorder, the total ion current monitor of the mass spectrometer indicated a peak and the mass spectrum was scanned. GLC retention times and mass spectra were compared with standards, and identifications were made. The areas under the GLC peaks could be used for approximate quantitation.

Seven swabs were analyzed. All seven contained phenobarbital, and four contained caffeine. These positive results were obtained from widely disparate parts of the room. While the origin of the phenobarbital and caffeine as to date of manufacture and compression machine used could not be proven, a serious dust problem was demonstrated. Upon being presented with the findings, the firm acceded to the agency's recommendations.

REFERENCES

(1) M. N. Lehnhard, "A Brief Legislative History of the Food, Drug, and Cosmetic Act," Committee Print No. 14, 93rd Congress, 2nd Session, 26-062, U.S. Government Printing Office, Washington, D.C., 1974, p. 24.

(2) W. W. Wright, *FDA By-Lines*, **5**, 37 (1974).

(3) "The United States Pharmacopeia," 19th rev., Mack Publishing Co., Easton, Pa., 1975.

(4) "The National Formulary," 14th ed., Mack Publishing Co., Easton, Pa., 1975.

(5) L. Lachman and R. J. Lantz, Jr., *J. Mond. Pharm.*, **14**, 90 (1971).

(6) H. Hellberg, in "Contamination in the Manufacture of Pharmaceutical Products," Secretariat of the European Free Trade Association, Geneva, Switzerland, 1973, pp. 7–15.

(7) A. Brunzell and G. Nilsson, *Acta Pharm. Suec.*, **10**, 247 (1973).

(8) "The United States Pharmacopeia," 19th rev., Mack Publishing Co., Easton, Pa., 1975, p. 652.

(9) M. L. Yakowitz, in "FDA Symposium on Safety of Large Volume Parenteral Solutions Proceedings," July 1966, pp. 3–5.

(10) *Med. Lett. Drugs Ther.*, **10**, 42 (1968).

(11) S. M. Edirimanasinghe, A. P. Lemberger, and J. H. Perrin, *Acta Pharm. Suec.*, **5**, 501 (1968).

(12) L. Ernerot and G. Millstrom, *ibid.*, **6**, 283 (1969).

(13) M. J. Groves, *Analyst (London)*, **94**, 992 (1969).

(14) N. S. Jaffe, *Bull. Parenter. Drug Assoc.*, **24**, 218 (1970).

(15) N. N. Davis, S. Turco, and E. Sivelly, *ibid.*, **24**, 257 (1970).

(16) N. M. Davis, S. Turco, and E. Sivelly, *Am. J. Hosp. Pharm.*, **27**, 822 (1970).

(17) T. C. Lyon, Jr., D. E. Cutright, and J. W. Nunley, *Pharmacol. Ther. Dent.*, **1**, 216 (1971).

(18) J. M. Garvan and B. W. Gunner, *Br. J. Clin. Pract.*, **25**, 119 (1971).

(19) S. J. Turco and N. M. Davis, *Am. J. Hosp. Pharm.*, **30**, 611 (1973).

(20) *Ibid.*, **30**, 770 (1973).

(21) S. J. Turco, N. M. Davis, and R. Bhatia, *Am. J. Hosp. Pharm.*, **31**, 222 (1974).

(22) *Ibid.*, **31**, 825 (1974).

(23) L. P. Jeffrey and T. F. Pinkus, *Am. J. Hosp. Pharm.*, **31**, 334 (1974).

(24) D. E. Bailey, *ibid.*, **31**, 30 (1974).

(25) L. Ernerot and E. Sandell, *Acta Pharm. Suec.*, **4**, 293 (1967).

(26) L. Ernerot, *ibid.*, **5**, 101 (1968).

(27) E. Sandell and L. Ernerot, *ibid.*, **5**, 111 (1968).

(28) L. Ernerot and L. Dahlinder, *ibid.*, **6**, 401 (1969).

(29) W. H. Thomas and Y. K. Lee, *N. Z. Med. J.*, **80**, 170 (1974).

(30) W. J. Nicholson, C. J. Maggiore, and I. J. Selikoff, *Science*, **177**, 171 (1972).

(31) T. J. Haley, *J. Pharm. Sci.*, **64**, 1435 (1975).

(32) *Fed. Regist.*, **38** (188), 27,076 (Sept. 28, 1973).

(33) *Ibid.*, **40** (51), 11,865–11,869 (Mar. 14, 1975).

(34) H. P. Blejer and R. Arlon, *J. Occup. Med.*, **15**, 92 (1973).

(35) H. Hoar, S. Turco, Y. S. Kim, and N. M. Davis, *Am. J. Hosp. Pharm.*, **29**, 470 (1972).

(36) *Br. Med. J.*, **1**, 307 (1973).

(37) H. Katz, H. Borden, and D. Hirscher, *J. Am. Med. Assoc.*, **229**, 1169 (1974).

(38) "The United States Pharmacopeia," 19th rev., Mack Publishing Co., Easton, Pa., 1975, p. 584.

(39) S. Turco and N. M. Davis, *Hosp. Pharm.*, **8**, 137 (1973).

(40) A. M. Jonas, in "FDA Symposium on Safety of Large Volume Parenteral Solutions Proceedings," July 1966, pp. 23–27.

(41) J. D. Lockhart, in *ibid.*, pp. 28–30.

(42) A. Gross and C. J. Carter, in *ibid.*, pp. 31–37.

(43) M. Hoeke, *Pharm. Weekbl.*, **106**, 709 (1971).

(44) G. Baumann, E. J. Rayfield, L. I. Rose, G. H. Williams, and J. F. Dingman, *J. Clin. Endocrinol. Metab.*, **34**, 801 (1972).

(45) J. H. Perrin, in "FDA Symposium on Safety of Large Volume Parenteral Solutions Proceedings," July 1966, pp. 73–78.

(46) G. Reinhardt, F. Scholz, and J. Wettengel, *Pharmazie*, **29**, 482 (1974).
(47) "The Stability and Stability Testing of Pharmaceuticals, 1939–1963," Pharmaceutical Manufacturers Association, Washington, D.C., 1964.
(48) "The Stability and Stability Testing of Pharmaceuticals, 1964–1970," Pharmaceutical Manufacturers Association, Washington, D.C., 1972.
(49) L. Lachman, in "FDA Symposium on Safety of Large Volume Parenteral Solutions Proceedings," July 1966, pp. 51–55.
(50) J. Autian, in *ibid.*, pp. 38–47.
(51) H. J. Senf, H. Wellman, and K. Kottke, *Pharmazie*, **28**, 440 (1973).
(52) B. L. Chia, C. K. Leng, F. P. Hsii, M. H. L. Yap, and Y. K. Lee, *Br. Med. J.*, **1**, 534 (1973).
(53) M. Noguchi, Y. Kaneda, K. Mochida, and K. Yoshimura, *Shoyakugaku Zasshi*, **25**, 33 (1971).
(54) W. J. Herlihy, *Anaesth. Intensive Care*, **1**, 240 (1973).
(55) J. Bergman, in "Contamination in the Manufacture of Pharmaceutical Products," Secretariat of the European Free Trade Association, Geneva, Switzerland, 1973, pp. 43–49.
(56) L. Greenberg, *Bull. Parenter. Drug Assoc.*, **24**, 157 (1970).
(57) P. J. O'Neil, *Proc. Soc. Anal. Chem.*, **11**, 30 (1974).
(58) *Fed. Regist.*, **30** (19), 932, 933 (Jan. 29, 1965).
(59) "Code of Federal Regulations," Part 211,58j, Title 21, 1975.
(60) C. M. Mitchell, *Bull. Parenter. Drug Assoc.*, **28**, 146 (1974).
(61) W. E. Walsh, H. Markowitz, J. D. Jones, and G. J. Gleich, *J. Allergy*, **47**, 159 (1971).
(62) P. P. Lamy, E. W. Parsons, Jr., and M. W. Kitler, *Am. J. Hosp. Pharm.*, **26**, 294 (1969).
(63) J. H. Guill, Jr., *Bull. Parenter. Drug Assoc.*, **20**, 151 (1966).
(64) O. Molin, in "Contamination in the Manufacture of Pharmaceutical Products," Secretariat of the European Free Trade Association, Geneva, Switzerland, 1973, pp. 33–41.
(65) "Procedure for Detecting and Measuring Penicillin Contamination in Drugs," DHEW, FDA, Bureau of Scientific Standards and Evaluation, Division of Antibiotics and Insulin Certification, Washington, D.C., Oct. 1965, and Addendum, 1967.
(66) "The United States Pharmacopeia," 19th rev., Mack Publishing Co., Easton, Pa., 1975, p. 701.
(67) *Ibid.*, p. 702.
(68) F. W. Bowman and S. Holdowsky, *J. Am. Pharm. Assoc., Sci. Ed.*, **48**, 95 (1959).
(69) F. W. Bowman, *J. Pharm. Sci.*, **58**, 277 (1969).
(70) S. Wahlgren, *Dan. Tidsskr. Farm.*, **44**, 1 (1970).
(71) F. W. Bowman, E. W. Knoll, M. White, and P. Mislivec, *J. Pharm. Sci.*, **61**, 532 (1972).
(72) W. Wozniak, B. Werakso, and E. Zembrzuska, *Acta Pol. Pharm.*, **29**, 518 (1972).
(73) J. B. Guynn, Jr., D. M. Poretz, and R. J. Duma, *Am. J. Hosp. Pharm.*, **30**, 321 (1973).
(74) L. Ernerot, S. Thoren, and E. Sandell, *Acta Pharm. Suec.*, **10**, 141 (1973).
(75) *Br. Med. J.*, **1**, 707 (1972).
(76) I. Phillips and S. Eykyn, *ibid.*, **1**, 746 (1972).
(77) P. G. T. Ford, *ibid.*, **2**, 111 (1972).
(78) A. C. Maddocks and G. Raine, *ibid.*, **2**, 231 (1972).
(79) P. D. Meers, M. W. Calder, M. M. Mazhar, and G. M. Lawrie, *Lancet*, **2**, 1189 (1973).
(80) J. H. Tenney, R. E. Dixon, and J. V. Bennett, *ibid.*, **1**, 679 (1974).
(81) B. Fuglsang-Smidt and K. Ulrich, *Dan. Tiddskr. Farm.*, **43**, 257 (1968).
(82) J. Cragg and A. V. Andrews, *Br. Med. J.*, **3**, 57 (1969).
(83) N. A. Simmons and D. A. Gardner, *ibid.*, **2**, 668 (1969).
(84) F. W. Bowman, M. White, and R. L. Lyles, *J. Pharm. Sci.*, **60**, 1099 (1971).
(85) E. P. Robinson, *ibid.*, **60**, 604 (1971).
(86) K. Ulrich, B. Fuglsang-Smidt, B. Hastrup, H. Hansen, and A. Fischer, *Dan. Tiddskr. Pharm.*, **45**, 39 (1971).
(87) R. F. Waterman, E. D. Sumner, J. N. Baldwin, and F. W. Warren, *J. Pharm. Sci.*, **62**, 1317 (1973).
(88) J. S. Hansen and C. Hepler, *Am. J. Hosp. Pharm.*, **30**, 326 (1973).
(89) E. J. Wargo, *ibid.*, **30**, 332 (1973).
(90) W. Wozniak, B. Werakso, and E. Zembrzuska, *Acta Pol. Pharm.*, **30**, 339 (1973).
(91) D. Kruger, *Drugs Made Ger.*, **16**, 111 (1973).
(92) L. O. Kallings, in "Contamination in the Manufacture of Pharmaceutical Products," Secretariat of the European Free Trade Association, Geneva, Switzerland, 1973, pp. 17–24.
(93) W. F. Elias, *Bull. Parenter. Drug Assoc.*, **28**, 263 (1966).
(94) M. Moller, in "Contamination in the Manufacture of Pharmaceutical Products," Secretariat of the European Free Trade Association, Geneva, Switzerland, 1973, pp. 25–31.
(95) *Contam. Control*, **10** (3–4), 10 (1971).
(96) D. E. Bishop, *ibid.*, **10** (5–6), 20 (1971).
(97) *Ibid.*, **10** (7–8), 17 (1971).
(98) H. A. Frediani, *Bull. Parenter. Drug Assoc.*, **20**, 189 (1966).
(99) V. A. DiBenedetto, *Drug Cosmet. Ind.*, **113**, 39 (1973).
(100) R. H. Avery and J. Luciano, *Bull. Parenter. Drug Assoc.*, **19**, 176 (1965).
(101) J. A. Kotaski, *Contam. Control*, **9**, 10 (1970).
(102) T. F. Aronson and P. Friedman, "Non-Contaminant Production of Liquid and Powder Drugs, AD 68–534," American Society of Tool and Manufacturing Engineers, Dearborn, Mich., 1968, p. 8.
(103) P. R. Austin, *Contam. Control*, **8** (1), 26 (1969).
(104) C. A. Burchsted, *ibid.*, **8** (5), 16 (1969).
(105) A. R. Walters and J. C. Hurgeton, *Contam. Control/Biomed. Environ.*, **11** (5–6), 20 (1972).
(106) R. C. Marsh, W. J. Whitfield, W. E. Neitzel, J. C. Mashburn, and L. C. Trujillo, "Standard Tests for Laminar Flow Devices, SC-TM-64-637," Sandia Corp., Albuquerque, N.M., June 1964.
(107) "The Laminar Flow Clean Room Handbook," Agnew-Higgins, Garden Grove, Calif., 1968.
(108) J. E. Woods, *Contam. Control*, **8** (4), 13 (1969).
(109) H. Loughhead and A. Vellutato, *Bull. Parenter. Drug Assoc.*, **23**, 17 (1969).
(110) K. Goddard, *ibid.*, **23**, 69 (1969).
(111) H. O. Loughhead and J. A. Moffett, *ibid.*, **26**, 102 (1972).
(112) D. Leach, *ibid.*, **26**, 104 (1972).
(113) J. Kotaski, *ibid.*, **26**, 108 (1972).
(114) H. P. Hurtig, *ibid.*, **27**, 38 (1973).
(115) R. I. Gross, *ibid.*, **30**, 143 (1976).
(116) A. L. Hanson and R. M. Shelley, *Am. J. Hosp. Pharm.*, **31**, 733 (1974).
(117) P. R. Austin and S. W. Timmerman, "Design and Operation of Clean Rooms," Business News Publishing Co., Detroit, Mich., 1970.
(118) "Contamination Control Principles," NASA SP-5045, National Aeronautics and Space Administration (Code DHA-11), Washington, D.C., 1967.
(119) P. R. Austin, "Clean Rooms of the World," Ann Arbor Science Publishers, Ann Arbor, Mich., 1967.
(120) "Clean Rooms and Work Stations for Microbially Controlled Environment," NASA Standard NHB53402, National Aeronautics and Space Administration (Code DHA-11), Washington, D.C., Aug. 1967.
(121) D. M. Carlberg, *Contam. Control*, **7** (8), 10 (1968).
(122) D. J. Raper, *ibid.*, **8** (6), 20 (1969).
(123) C. R. Havighorst, *Food Eng.*, **42**, 91 (1970).
(124) W. R. Howarth, *Bull. Parenter. Drug Assoc.*, **26**, 147 (1972).
(125) P. A. Kiritsy and R. Engvall, *ibid.*, **27**, 279 (1973).
(126) R. A. Kinsky, *Contam. Control*, **7** (2), 24 (1968).
(127) "Clean Room and Work Station Requirements, Controlled Environment," Federal Standard No. 209B, General Services Administration, Washington, D.C., Apr. 1973.
(128) J. A. Kotaski, *Bull. Parenter. Drug Assoc.*, **25**, 203 (1971).
(129) H. Heuring, *Contam. Control*, **9**, 18 (1970).
(130) P. R. Austin, *ibid.*, **8** (2), 28 (1969).
(131) G. Sykes, *J. Mond. Pharm.*, **14**, 8 (1971).
(132) R. F. Schmitt, J. J. Brennan, and R. Berube, *Bull. Parenter. Drug Assoc.*, **27**, 15 (1973).
(133) C. J. Endicott, R. Giles, and R. Pecina, in "FDA Symposium on Safety of Large Volume Parenteral Solutions Proceedings," July 1966, pp. 62–70.
(134) N. J. Leonard, *East Afr. Pharm. J.*, **39**, 53 (1972).
(135) R. H. Otto, in "FDA Symposium on Safety of Large Volume Parenteral Solutions Proceedings," July 1966, pp. 56–58.
(136) S. Levine, in *ibid.*, pp. 71, 72.
(137) W. A. Lennox, in *ibid.*, pp. 59–61.
(138) H. F. Hammer, *Bull. Parenter. Drug Assoc.*, **28**, 205 (1974).
(139) J. Y. Masuda and J. B. Beckerman, *Am. J. Hosp. Pharm.*, **30**, 297 (1973).
(140) A. B. McGinn, *Bull. Parenter. Drug Assoc.*, **26**, 26 (1972).
(141) "Code of Federal Regulations," Parts 210 and 211, Title 21,

1975.
(142) S. H. Willig, M. M. Tuckerman, and W. S. Hitchings, IV, "Good Manufacturing Practices for Pharmaceuticals," Dekker, New York, N.Y., 1975.
(143) A. N. Parisi and P. M. Borick, *Contam. Control*, **8** (1), 31 (1969).
(144) R. Ravin, J. Bahr, F. Luscomb, J. Gooch, S. Mutta, and S. D. Spittell, *Am. J. Hosp. Pharm.*, **31**, 340 (1974).
(145) H. Hess, F. Knusel, and K. Muller, *Pharm. Acta Helv.*, **44**, 174 (1969).
(146) "The United States Pharmacopeia," 19th rev., Mack Publishing Co., Easton, Pa., 1975, p. 588.
(147) W. S. Miller and M. S. Korczynski, *Drug Cosmet. Ind.*, **110**, 38 (1972).
(148) T. G. Alexander, *Bureau By-Lines*, **4**, 81 (1963).
(149) W. Alternschmidt and T. Liske, *Drugs Made Ger.*, **15**, 11 (1972).
(150) I. Sunshine, "Handbook of Analytical Toxicology," CRC Press, Cleveland, Ohio, 1969, pp. 772–808.
(151) E. G. C. Clarke and J. Berle, "Isolation and Identification of Drugs," Pharmaceutical Press, London, England, 1969, pp. 43–58, 637–655.
(152) E. Stahl, "Thin-Layer Chromatography—A Laboratory Handbook," 2nd ed., Springer-Verlag, New York, N.Y., 1969.
(153) G. Zweig and J. Sherma, "Handbook of Chromatography," vol. I and II, CRC Press, Cleveland, Ohio, 1972, pp. 89–189, 310–317, 437–467.
(154) H. S. Kroman and S. R. Bender, "Theory and Application of Gas Chromatography in Industry and Medicine," Grune and Stratton, New York, N.Y., 1968.
(155) B. Gudzinowicz, "Gas Chromatographic Analysis of Drugs and Pesticides," Dekker, New York, N.Y., 1967.
(156) E. G. C. Clarke and J. Berle, "Isolation and Identification of Drugs," Pharmaceutical Press, London, England, 1969, pp. 59–83.
(157) B. J. Millard, *Adv. Drug Res.*, **6**, 157 (1971).
(158) G. R. Waller, "Biochemical Applications of Mass Spectrometry," Wiley–Interscience, New York, N.Y., 1972.
(159) W. H. McFadden, III, "Techniques of Combined Gas Chromatography/Mass Spectrometry: Applications in Organic Analysis," Wiley–Interscience, New York, N.Y., 1973.
(160) H. T. Hopkins, *Bureau By-Lines*, **4**, 7 (1963).
(161) D. Taylor, "Neutron Activation and Activation Analysis," Van Nostrand-Reinhold, New York, N.Y., 1964.
(162) C. C. Fulton, "Modern Microcrystal Tests for Drugs," Wiley–Interscience, New York, N.Y., 1969.
(163) E. G. C. Clarke and J. Berle, "Isolation and Identification of Drugs," Pharmaceutical Press, London, England, 1969, pp. 123–141.
(164) "Official Methods of Analysis of the Association of Official Analytical Chemists," 12th ed., Association of Official Analytical Chemists, Washington, D.C., 1975, pp. 670–680.
(165) D. V. Herbst and H. H. Bryant, "F.D.A. Laboratory Information Bulletin," No. 1585, May 1973.
(166) A. Bracey, *J. Pharm. Sci.*, **62**, 1695 (1973).
(167) E. Stahl, "Thin-Layer Chromatography—A Laboratory Workbook," 2nd ed., Springer-Verlag, New York, N.Y., 1969, p. 568.
(168) "Millipore Application Procedure," A.P. 201, Millipore Corp., Bedford, Mass., 1973.
(169) *Millipore Pharm. Rev.*, **4**, 6 (1973).
(170) M. A. Garth, H. Bryant, J. Kramer, and A. Kirshbaum, *J. Pharm. Sci.*, **60**, 63 (1971).
(171) U. R. Cieri, *ibid.*, **58**, 1532 (1969).
(172) P. L. Senov, V. E. Chichiro, and Z. P. Kosmennikova, *Farmatsiya (Moscow)*, **22**, 72 (1973).
(173) J. D. Edmond, *Proc. Anal. Div. Chem. Soc.*, **13** (1), 28 (1976).
(174) J. H. Page, *Proc. Soc. Anal. Chem.*, **10**, 294 (1973).
(175) L. M. Reynolds, W. V. Kessler, J. E. Christian, and L. Ziemer, *J. Pharm. Sci.*, **56**, 437 (1967).
(176) "The United States Pharmacopeia," 19th rev., Mack Publishing Co., Easton, Pa., 1975, p. 592.
(177) N. Stojtschew, *Pharm. Ind.*, **32**, 968 (1970).
(178) S. Holdowsky, *Antibiot. Chemother.*, **7**, 49 (1957).
(179) K. Tsuji and J. H. Robinson, *Appl. Microbiol.*, **20**, 802 (1970).
(180) G. F. Archambault and A. W. Dodds, in "FDA Symposium on Safety of Large Volume Parenteral Solutions Proceedings," July 1966, pp. 15–17.
(181) M. J. Groves, *J. Pharm. Pharmacol., Suppl.*, **23**, 238S (1971).
(182) R. C. Louer, Jr., J. A. Russoman, and P. R. Rasanen, *Bull. Parenter. Drug Assoc.*, **25**, 54 (1971).
(183) J. V. Tatke, *Hind. Antibiot. Bull.*, **11**, 115 (1968).
(184) J. Tatke, *ibid.*, **11**, 262 (1969).
(185) E. Kirnbauer, *Bull. Parenter. Drug Assoc.*, **24**, 53 (1970).
(186) "Detection and Analysis of Particulate Contamination," Millipore Publication ADM 30, Millipore Corp., Bedford, Mass., 1966.
(187) "1st Supplement to the United States Pharmacopeia, 19th rev., and the National Formulary, 14th ed.," United States Pharmacopeial Convention, Rockville, Md., 1975, p. 56.
(188) E. Sandell and L. Ernerot, *Acta Pharm. Suec.*, **3**, 229 (1966).
(189) L. Ernerot, I. Helmstein, and E. Sandell, *ibid.*, **7**, 50 (1970).
(190) B. A. Taliaferro, T. G. Alexander, M. R. Howlett, and P. J. Weiss, *FDA By-Lines*, **4**, 55 (1973).
(191) L. Ernerot, *Acta Pharm. Suec.*, **11**, 1 (1974).
(192) G. H. Hopkins and R. W. Young, *Bull. Parenter. Drug Assoc.*, **28**, 15 (1974).
(193) L. Ernerot, *Sven. Farm. Tidskr.*, **78**, 129 (1974).
(194) E. Trieber, *ibid.*, **69**, 699 (1965).
(195) L. Ernerot, *Farm. Revy*, **64**, 721 (1965).
(196) L. Ernerot and E. Sandell, *Acta Pharm. Suec.*, **2**, 411 (1965).
(197) R. G. Draftz and J. Graf, *Bull. Parenter. Drug Assoc.*, **28**, 174 (1974).
(198) S. M. Blaug and R. E. Sarabia, *ibid.*, **29**, 74 (1975).
(199) L. Ernerot, *Acta Pharm. Suec.*, **11**, 15 (1974).
(200) *Duke Stand. Chron.*, **2**, 1 (1973).
(201) "Microchemical and Industrial Analysis," Millipore Publication ADM 70, Millipore Corp., Bedford, Mass., 1963, pp. 9, 10.
(202) "Filters and Associated Products," Millipore Publication MF-67, Millipore Corp., Bedford, Mass., 1966, p. 38.
(203) A. Buogo and V. Eboli, *Appl. Microbiol.*, **23**, 1149 (1972).
(204) L. Ernerot and O. Molin, *Acta Pharm. Suec.*, **10**, 75 (1973).
(205) D. Banes, "Principles of Regulatory Drug Analysis," Association of Official Analytical Chemists, Washington, D.C., 1966, pp. 4, 5.

ACKNOWLEDGMENTS

The author thanks Thomas Medwick, Food and Drug Administration, New York District, and College of Pharmacy, Rutgers—The State University, New Brunswick, N.J., and William M. Plank, Food and Drug Administration, New York District, for their invaluable assistance in the preparation of this paper. He also thanks the following personnel of the Food and Drug Administration, New York District and Washington, D.C., for their helpful suggestions: Cyril Osbrack, Keith S. Ehrlich, Leonora Auerbach, Martin Finkelson, Samuel Eskenazi, Henry A. Sinsabaugh, Evelyn Sarnoff, Ted M. Hopes, Helen L. Reynolds, and Laura A. Kovach.

General Method for Determining Macrodissociation Constants of Polyprotic, Amphoteric Compounds from Solubility Measurements

CARL C. PECK ˣ and LESLIE Z. BENET *

Received April 30, 1976, from the *Letterman Army Institute of Research, Blood Research Division, Department of Surgery, Presidio of San Francisco, CA 94129.* Accepted for publication March 21, 1977. * Present address: Department of Pharmacy, School of Pharmacy, University of California, San Francisco, CA 94143.

Abstract □ Equilibrium solubility and pH measurements can be used to determine macrodissociation constants of weak acids and bases of some highly insoluble substances. Equations are derived extending solubility, pH, and pKa (macroscopic) relationships to polyprotic, amphoteric substances. A general method for estimating pKa values, given a set of solubility and pH measurements, is presented. Included in the estimation procedure is a subroutine for approximating thermodynamic pKa values. The method was tested on two data sets (tyrosine and 2,8-dihydroxyadenine) and rendered pKa (thermodynamic) estimates in close agreement with those using other methods.

Keyphrases □ Dissociation constants—polyprotic, amphoteric compounds, determined using solubility and pH measurements □ pKa values—polyprotic, amphoteric compounds, determined using solubility and pH measurements □ Solubility measurements—used to determine dissociation constants for polyprotic, amphoteric compounds □ pH measurements—used to determine dissociation constants for polyprotic, amphoteric compounds

Dissociation behavior of weak acids and bases is unambiguously characterized by determination of the thermodynamic microdissociation constant pertaining to each dissociation reaction. The microdissociation constant of a monoprotic species (or that of an amphoteric compound with widely separated acidity constants) can often be determined directly from potentiometric measurements. Dissociation constants of polyprotic species estimated by this method (macrodissociation constants) generally represent apparent dissociation reactions which do not precisely relate to actual ionic forms present at equilibrium. Nevertheless, macrodissociation constants provide useful estimates of apparent dissociation behavior which can be utilized for characterizing buffer systems, acid strength, and solubility–pH relationships. Thermodynamic macrodissociation constants are preferred over apparent macrodissociation constants since thermodynamic constants are applicable to any aqueous solution in which the activities of participating ions can be estimated.

Several methods exist for determining aqueous macrodissociation constants of weak acids and bases. While potentiometric titrations and conductimetry generally suffice for readily soluble substances, estimating pKa values of poorly soluble compounds is sometimes impossible by these methods (1, 2). UV and fluorescent spectrophotometry can be applied in such cases, provided there is sufficient shift in the spectra with a changing hydrogen-ion concentration (1, 3). Where molecular and ionic spectra are too similar or totally lacking, the solubility method may be uniquely suited (1). This technique takes advantage of the fact that sparingly soluble weak acids become predictably soluble in basic media while poorly soluble weak bases become soluble in acid media. This phenomenon can be modeled mathematically in a form that relates solubility to pH and pKa.

No general treatment extending the solubility method of pKa determination to polyprotic species has been published. Moreover, all previously published pKa determinations by the solubility method have resulted in estimation of apparent pKa values (pKa′). Determination of the thermodynamic pKa by the solubility method has apparently been considered indeterminate (1, 4).

A general method is presented for obtaining estimates of macro pKa values (thermodynamic) of polyprotic, amphoteric compounds of limited solubility from pH and solubility measurements. The method is applied experimentally to two data sets: (*a*) tyrosine solubilities published previously and (*b*) 2,3-dihydroxyadenine solubilities measured in this laboratory. The equivalence of the solubility method is then investigated by comparing resulting pKa estimates to pKa values determined by other methods.

THEORETICAL

Let H_nS be a weak, polyvalent, sparingly soluble amphoteric compound that may acquire m additional hydrogens in its most acidic state $(H_{n+m}S)^{+m}$ and lose n hydrogens in its most basic state $(S)^{-n}$. At any given pH, its *apparent* equilibrium reaction may be as shown in Scheme I, with the net charge of each species indicated above it.

For clarity, the molecular and ionic species of the solute are abbreviated only as $S^{+m} \ldots S^{+1}$ and $S^{-1} \ldots S^{-n}$. The thermodynamic dissociation constant, K_a, for the dissociation of the amphoteric or molecular species, *i.e.*, the $m + 1$th hydrogen dissociation, is given by:

$$K_{a_{m+1}} = \{H\}[S^{-1}]f_{S^{-1}}/[S_0]f_{S_0} \qquad \text{(Eq. 1}a\text{)}$$

where $\{H\}$ is the hydrogen-ion activity; $[S^{-1}]$ is the concentration of S^{-1}; $[S_0]$ is the concentration of S_0, the solubility of the uncharged (or net charge equal to zero) species; and f_{S_0} and $f_{S^{-1}}$ are activity coefficients for S_0 and S^{-1} species, respectively. Solving Eq. 1*a* for $[S^{-1}]$ yields:

$$(H_{n+m}S)^{+m} \cdots \underset{}{\overset{K_{a_1}}{\rightleftharpoons}} (H_{n+2}S)^{+2} \overset{K_{a_{n-1}}}{\rightleftharpoons} (H_{n+1}S)^{+1} \overset{K_{a_m}}{\rightleftharpoons} (H_nS)^{0} \overset{K_{a_{m+1}}}{\rightleftharpoons} (H_{n-1}S)^{-1} \overset{K_{a_{m+2}}}{\rightleftharpoons} (H_{n-2}S)^{-2} \overset{K_{a_{m+n}}}{\rightleftharpoons} \cdots (S)^{-n}$$

$$\longleftarrow \downarrow \text{pH} \uparrow \longrightarrow$$

Scheme I

$$[S^{-1}] = K_{a_{m+1}}[S_0]f_{S_0}/\{H\}f_{S^{-1}} \quad \text{(Eq. 1}b\text{)}$$

The second hydrogen dissociation from the molecular or amphoteric species is given by:

$$K_{a_{m+2}} = \{H\}[S^{-2}]f_{S^{-2}}/[S^{-1}]f_{S^{-1}} \quad \text{(Eq. 2)}$$

Substituting Eq. 1*b* into Eq. 2 and canceling appropriate terms yield:

$$K_{a_{m+2}} = \{H\}^2[S^{-2}]f_{S^{-2}}/K_{a_{m+1}}[S_0]f_{S_0} \quad \text{(Eq. 3}a\text{)}$$

$$[S^{-2}] = K_{a_{m+1}}K_{a_{m+2}}[S_0]f_{S_0}/\{H\}^2f_{S^{-2}} \quad \text{(Eq. 3}b\text{)}$$

In general:

$$K_{a_{m+r}} = \{H\}^r[S^{-r}]f_{S^{-r}}/[S_0]f_{S_0}\prod_{i=m+1}^{m+r-1}(K_{a_i}) \quad \text{(Eq. 4}a\text{)}$$

$$[S^{-r}] = [S_0]f_{S_0}\prod_{i=m+1}^{m+r}(K_{a_i})/\{H\}^rf_{S^{-r}} \quad \text{(Eq. 4}b\text{)}$$

where r is the rth hydrogen dissociation, and numbering begins from the molecular or amphoteric form and increases toward the right in the dissociation scheme.

To convert Eq. 4*b* to contain the frequently used terms pH (= −log {H}) and pKa (= −log K_a), the $\log_{10}$ of each side of Eq. 4*b* is taken and pKa and pH are substituted:

$$\log_{10}[S^{-r}] = \log_{10}(S_0) + r\text{pH} - \sum_{i=m+1}^{m+r}(\text{pKa}_i) + \log_{10}(f_{S_0}/f_{S^{-r}}) \quad \text{(Eq. 4}c\text{)}$$

The antilog$_{10}$ of Eq. 4*c* yields:

$$[S^{-r}] = 10^{[\log_{10}(S_0)+r\text{pH}-\sum_{i=m+1}^{m+r}(\text{pKa}_i)+\log_{10}(f_{S_0}/f_{S^{-r}})]} \quad \text{(Eq. 5)}$$

Making the usual assignment of unity to f_{S_0} and bringing $\log_{10}$ (S_0) down out of the exponent result in:

$$[S^{-r}] = S_0 10^{[r\text{pH}-\sum_{i=m+1}^{m+r}(\text{pKa}_i)-\log_{10}f_{S^{-r}}]} \quad \text{(Eq. 6)}$$

Identical treatment of the dissociation constants for addition of m hydrogens yields:

$$[S^{+\upsilon}] = S_0 10^{[\sum_{i=m-\upsilon+1}^{m}(\text{pKa}_i)-\upsilon\text{pH}-\log_{10}f_{S^{+\upsilon}}]} \quad \text{(Eq. 7)}$$

where υ is the υth dissociation, numbering from the amphoteric form, S_0, to the left in Scheme I.

Now, at any given pH, the total concentration of the compound in solution, S, is given by:

$$S = [S_0] + \sum_{r=1}^{n}[S^{-r}] + \sum_{\upsilon=1}^{m}[S^{+\upsilon}] \quad \text{(Eq. 8)}$$

Inserting Eqs. 6 and 7 into 8, the generalized equation becomes (the brackets about all S species have been removed but *concentration* is understood):

$$S = S_0\left[1 + \sum_{r=1}^{n}10^{(r\text{pH}-\sum_{i=m+1}^{m+r}\text{pKa}_i-\log_{10}f_{S^{-r}})} + \sum_{\upsilon=1}^{m}10^{(\sum_{i=m-\upsilon+1}^{m}\text{pKa}_i-\upsilon\text{pH}-\log_{10}f_{S^{+\upsilon}})}\right] \quad \text{(Eq. 9)}$$

Equation 9 represents the generalized relationship for thermodynamic pKa values. The equivalent equation for apparent pKa′ values in which the activity terms have been set equal to unity is:

$$S = S_0'\left[1 + \sum_{r=1}^{n}10^{(r\text{pH}-\sum_{i=m+1}^{m+r}\text{pKa}_i')} + \sum_{\upsilon=1}^{m}10^{(\sum_{i=m-\upsilon+1}^{m}\text{pKa}_i'-\upsilon\text{pH})}\right] \quad \text{(Eq. 10)}$$

where S_0' is an estimate of the basal solubility when all activity terms are set equal to one.

Faced with Eqs. 9 and 10 and a set of solubilities at given pH values, it may not be intuitively clear which values of n and m specify the proper equations for fitting to get estimates of S_0', S_0, and the various apparent and thermodynamic pKa values. Moreover, it is desirable to use the simplest equation giving the best fit.

An easy solution to the problem involves making a preliminary plot of $\log_{10}$ ($S/S_0'' - 1$) *versus* pH:

$$\log_{10}(S/S_0'' - 1) = \log_{10}\left[\sum_{r=1}^{n}10^{(r\text{pH}-\sum_{i=m+1}^{m+r}\text{pKa}_i')} + \sum_{\upsilon=1}^{m}10^{(\sum_{i=m-\upsilon+1}^{m}\text{pKa}_i'-\upsilon\text{pH})}\right] \quad \text{(Eq. 11)}$$

where S_0'' is the minimum solubility experimentally.

Examination of the plot generally reveals one or several connecting straight lines. The slopes of individual and final segments reveal information relevant to the functional form to be used in the estimation procedures. This approach is equivalent to taking the first derivative of Eq. 11 and evaluating it within given pH intervals. The function (Eq. 11) is such that generally one or, at most, two terms of the equation make the major contribution to the value of $\log_{10}$ ($S/S_0'' - 1$) in any given pH region. Likewise, the straight-line portions result from only the predominant term. The derivatives thus obtained are integer functions of the number of associations or dissociations occurring, and their signs reflect the anionic or cationic nature of the reaction. Depending upon the proximity of pKa′ values, intermediate linear portions of the plot may exhibit slopes that change in serial integer fashion.

Furthermore, a more detailed study of this plot can yield preliminary estimates for apparent pKa values. Solving the terms of Eq. 11 representing each linear portion of the curve for its x-intercept yields expressions for pKa$_i$ values, i = 1 to m:

$$x_{\text{intercept}_j} = \sum_{i=j}^{m}\text{pKa}_i'/(m + 1 - j) \quad \text{(Eq. 12)}$$

and for pKa$_i$ values, $i = m + 1$ to $m + n$:

$$x_{\text{intercept}_j} = \sum_{i=m+1}^{j}\text{pKa}_i'/(j - m) \quad \text{(Eq. 13)}$$

where the x-intercept is the intercept on the pH axis of the projection of a given linear portion, numbering left to right from j = 1 to $j = n + m$.

Preliminary pKa$_i$ values are then found by solving the equations serially in order from the simpler to the more complex. Even though the accuracy of this procedure depends upon the pKa values being separated sufficiently to reveal definitive slopes, the general region of the pKa values should be evident even where they lie close together.

GENERAL METHOD AND APPLICATION

A flow diagram outlining the general method is shown in Scheme II. Given a suitable set of pH and solubility measurements, the basic approach is to estimate the preliminary basal solubility, S_0', and apparent pKa′ values from a nonlinear least-squares fit of the data to Eq. 10. The preliminary estimates contribute to the calculation of ionic strengths of the various solutions, which then allow computation of sample-specific

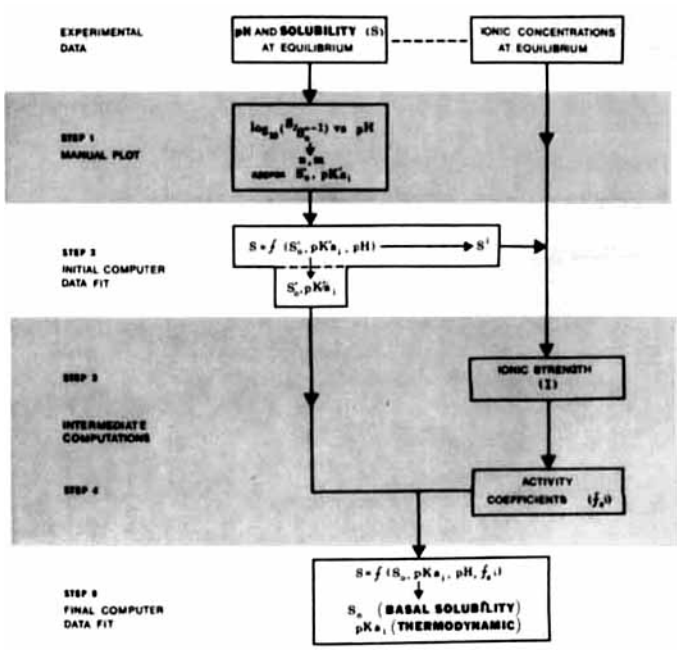

Scheme II

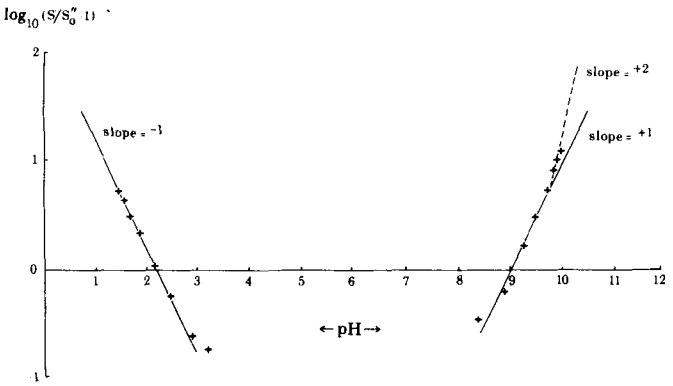

Figure 1—*Plot of* $\log_{10}(S/S_0'' - 1)$ versus *pH [Hitchcock's tyrosine data (5)]. The terminal slopes specify* m *and* n.

activity coefficients for the substance under study. Finally, the activities enter into a final fit of the data to Eq. 9, rendering estimates of the thermodynamic macrodissociation constants.

A step-by-step approach is given here, detailing the general method and applying this method to the tyrosine solubility measurements reported by Hitchcock (5). Briefly, Hitchcock added excess tyrosine to hydrochloric acid or sodium hydroxide solutions of varying starting concentrations, and saturated solutions were obtained by rotation at 25° for 1 or 2 days. After filtration, the concentration of tyrosine was obtained by Kjeldahl determination of nitrogen. The pH was measured with Clark electrodes at 25°. The data appear in Table I.

1. The first step is to specify the values of n and m, the highest valences of anions and cations existent at the upper and lower pH limits, respectively. Since this information may not be reasonably known *a priori*, n and m may be extracted from a visual analysis of the data by plotting $\log_{10}(S/S_0'' - 1)$ *versus* pH, S_0'' being the minimum solubility obtained by inspection of the data. This plot yields a curve from which n and m can be determined by inspection of terminal slopes. The terminal slope in the upper pH region determines n; expected slopes are multiples of 1. If a slope lies between two integers, the higher integer should be chosen. The value of m is determined in an identical fashion. Once n and m are substituted in Eqs. 9 and 10, the functional forms for the data-fitting process are specified.

When this procedure is applied to the tyrosine data, S_0'' is noted to be around 2.62 m*M* (Table I). A plot of $\log_{10}(S/S_0'' - 1)$ *versus* pH is shown in Fig. 1. The terminal slope in the lower pH region is −1, thereby establishing $m = 1$. The terminal slope at higher pH lies between +1 and +2, so $n = 2$.

From the same plot, preliminary estimates of the pKa values can be obtained to provide the nonlinear data-fitting procedure with starting points and limits. Figure 2 illustrates the procedure for gaining preliminary estimates of the apparent pKa′ values.

2. The next step is to estimate S_0' and the apparent pKa′ values. These values result from a nonlinear least-squares fit of the solubility and pH measurements to Eq. 10.

Table I—Tyrosine Data of Hitchcock (5)

$[HCl]_{initial}$, m*M*	$[Tyrosine]_{equilibrium}$, m*M*	$pH_{equilibrium}$
50.00	16.50	1.450
40.00	13.80	1.560
30.00	10.80	1.675
20.00	8.43	1.861
9.99	5.39	2.160
4.99	4.10	2.457
2.00	3.25	2.857
1.00	3.09	3.190
H_2O	2.62	5.300
$[NaOH]_{initial}$, m*M*		
0.98	3.54	8.342
1.95	4.30	8.865
4.88	7.06	9.249
9.76	10.70	9.484
19.50	17.50	9.726
29.90	24.70	9.841
39.80	30.40	9.881
49.80	35.80	9.953

Table II—Results of Solubility Method pKa Estimates for Tyrosine and Values Reported by Other Workers

Methods and Conditions	Apparent pK′ Values	Thermodynamic pK Values (Adjusted to 25° $I \simeq 0.00$)	Reference
Solubility, 25°, $I \leq 0.07$	$pKa_1' = 2.13$ $pKa_2' = 9.21$ $pKa_3' = 9.91$ $S_0' = 2.86\ \mu M$	$pKa_1 = 2.06$ $pKa_2 = 9.18$ $pKa_3 = 10.40$ $S_0 = 2.89\ \mu M$	This work
Potentiometry, 20°, I = 0.005	$pKa_1' = 2.20$ $pKa_2' = 9.19$ $pKa_3' = 10.43$	$pKa_1 = 2.11$ $pKa_2 = 9.12$ $pKa_3 = 10.43$	14
Spectrophotometry, 25°, I = 0.04	$pKa_2' = 9.12$ $pKa_3' = 10.28$	$pKa_2 = 9.19$ $pKa_3 = 10.47$	10
Spectrophotometry, 25°, I = 0.1	$pKa_2' = 8.95$ $pKa_3' = 10.08$	$pKa_2 = 9.04$ $pKa_3 = 10.34$	15

Substituting m and n for tyrosine into Eq. 10 yields:

$$S = S_0' [1 + 10^{(pH - pKa_2')} + 10^{(2pH - pKa_2' - pKa_3')} + 10^{(pKa_1' - pH)}] \quad \text{(Eq. 14)}$$

A nonlinear least-squares fit[1] of the data in Table I to Eq. 14 results in estimates for the preliminary basal solubility, S_0', and apparent pKa′ values shown in the upper part of Table II.

3. The ionic strength at each pH is next computed by summing the ionic concentrations of all ions present as follows (7):

$$I = 0.5 \left[\sum_{|i|=1}^{|p|} a_{|i|} Z_i^2 + \sum_{i=1}^{m} S^{+i} Z_i^2 + \sum_{i=1}^{n} S^{-i} Z_i^2 \right] \quad \text{(Eq. 15)}$$

where I is the ionic strength; $a_{|i|}$ is the ionic concentration of all non-S-ions at equilibrium; $|p|$ is the absolute value of the highest charged species present; $S^{\pm i}$ is the ionic concentration of all S-ions at each pH; m and n are the absolute values of highest cationic and anionic charges, respectively; and Z_i is the net charge.

Computation of ionic strength requires the ionic concentration of all ions present at equilibrium. These ions include the various tyrosine ions, which are computed from Eqs. 6 and 7 by using the S_0' and pKa′ values estimated and setting activity coefficients equal to unity; $[Na^+]$ and $[Cl^-]$ obtained from Table I; and, finally, $[H^+]$ and $[OH^-]$ computed from a mass balance estimation of hydrogen and hydroxide ions, taking into account those lost in forming the various tyrosine ions.

4. The ionic strength computations, I, allow for approximation of the activity coefficient, f_{S^i}, for ionic strengths below 0.1 according to the Debye–Hückel equation (25°) (8):

$$-\log_{10}(f_{S^i}) = \frac{0.5\, Z_i^2 \sqrt{I}}{1 + 0.329\, \mathring{A}_{S^i} \sqrt{I}} \quad \text{(Eq. 16)}$$

where f_{S^i} is the activity coefficient of the S-ion with charge i, $\mathring{A}_{S^i}$ is the

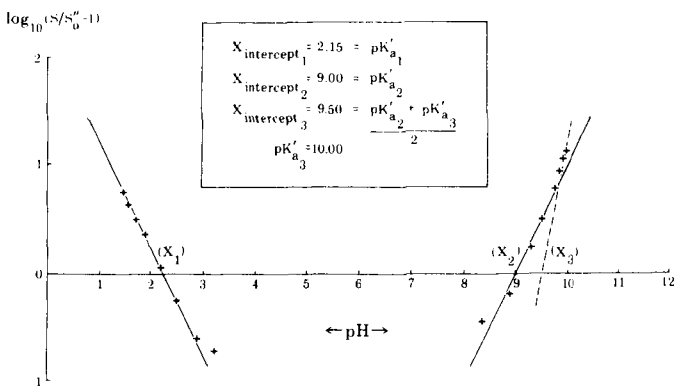

Figure 2—*Plot of* $\log_{10}(S/S_0'' - 1)$ versus *pH [tyrosine data of Hitchcock (5)]. The intercepts allow for preliminary estimates of pKa′ values.*

[1] Nonlinear Regression Program (6), modified by C. C. Peck and B. B. Barrett, Letterman Army Institute of Research, San Francisco, Calif., and implemented on a Hewlett-Packard 9830-A desktop calculator.

Table III—Comparison of Thermodynamic pKa Values for Tyrosine at 25° (Mean ± 1 *SD*)

Source	pKa_1	pKa_2	pKa_3
Published values[a]	2.11 (n = 1)	9.11 ± 0.08 (n = 3)	10.41 ± 0.07 (n = 3)
Solubility method (this paper)	2.06 ± 0.05	9.18 ± 0.06	10.40 ± 0.09

[a] Reported (12, 14, 15) as $-\log_{10}(\overline{X}_{K_{a_i}})$, where $\overline{X}_{K_{a_i}}$ = mean of published dissociation constants (K_{a_i}).

effective ionic radius in angstroms, and all other terms are as defined previously.

Approximate values for $Å_{Si}$ may be obtained from the data of Kielland (9) by choosing an ionic radius corresponding to an ion in his list whose dimensions are similar to those of the compound under study.

The effective ionic radius used in the activity calculations for tyrosine was 7.5 Å. This value is identical to that used by Martin *et al.* (10), who based their choice on Kielland's data (9). The validity of this choice is supported by the study of Edsall *et al.* (11). These investigators estimated the distance between the amino nitrogen and the hydroxyl hydrogen of tyrosine to be 6.95 Å using the Kirkwood–Westheimer equation and experimentally determined microdissociation constants. (Using Å = 6.95 leaves the final estimate for pK_1 and pK_2 unchanged and changes pK_3 to 10.42.)

5. Thermodynamic pKa values can now be estimated by substituting the activity coefficients obtained in Step 4 into Eq. 9 and performing a final nonlinear least-squares fit of the solubility data and pH measurements to Eq. 9.

In practice, Steps 1 and 2 are done as separate procedures; then Steps 3–5 can be performed in a single computer run. Thus, having obtained S_0' and the apparent pKa′ values, a repeat nonlinear least-squares fit of pH, solubility measurements, and activity estimates to Eq. 9 was carried out, resulting in the thermodynamic constants given in Table II.

A consideration of the type of measurement error may be important in the data-fitting process. Since the nonlinear model assumes an additive error in S, one should be confident that the type of measurement error in S emerges as an additive term. Such analytical work, where pipetting errors are carried through, for example, frequently results in a multiplicative type of measurement error. Such an error component can be rendered additive by taking the $\log_{10}$ of each solubility measurement. This approach was shown to be appropriate for a similar exercise by Krüger-Thiemer *et al.* (12). The $\log_{10}$ of both sides of Eqs. 9 and 10 must be taken in Steps 2 and 5 if such a procedure is followed. Alternatively, if the variance of the measurements is known, a weighted analysis can be performed (13). For example, a weight of the reciprocal of the square of the measured solubility is appropriate for a multiplicative error component.

In addition, Table II presents published pKa values for tyrosine that fulfill the criterion of an accurately reported ionic strength of the test solutions in which the total ionic strength was less than 0.1 (10, 14, 15). To exemplify exclusions, close examination of two papers (16, 17) indicated that the ionic strength values were underestimated by virtue of improper assignment of a charge of −1 to tyrosine in the pH region >9.0. Likewise, some pK_1 estimates (10, 17) were made in solutions of $I > 0.15$, rendering the Debye–Hückel approximation for activity in doubt.

Since the published values in Table II were apparent pKa′ values, some at 20°, adjustments were made to obtain thermodynamic pKa values at 25°. The temperature adjustment used was that suggested by Albert and Serjeant (1) based on the work of Hall and Sprinkle (18). Conversion to thermodynamic pKa from apparent pKa′ was made by correcting to zero ionic strength by means of activities computed from Eq. 16 (ionic radius = 7.5 Å), using the ionic strength reported in each paper.

Table III compares the pKa values estimated by the solubility method described here with the means of acceptable published values. The standard deviations about the values calculated by this method are those reported in the computer program. Caution should be exercised in interpreting confidence limits about the parameters (S_0 and pKa values) estimated in Step 5 by the nonlinear fitting procedure. Since the same solubility and pH measurements are used twice in arriving at final estimates of the thermodynamic pKa values, confidence regions would be expected to be broadened by a suitable reduction in the degrees of freedom that contribute to this computation. Apparently, however, no sound theoretical statistical basis currently exists to solve this problem. However, dispersion about the estimated parameters can be established by one or more complete duplications of the experiment.

Table IV—2,8-Dihydroxyadenine Solubility at Various pH Values (37°)

[2,8-Dihydroxyadenine], mg/liter	$pH_{equilibrium}$
603.58	0.018
581.42	0.022
131.60	0.533
137.91	0.535
138.10	0.536
134.09	0.562
129.31	0.573
125.29	0.579
79.55	1.164
80.60	1.175
10.51	2.280
10.40	2.250
1.47	5.08
1.55	5.08
1.43	5.08
1.51	7.06
1.49	7.06
40.49	9.468
46.61	9.615
50.99	9.672
65.80	9.737
68.86	9.748
62.46	9.777
79.55	9.811
76.12	9.825
93.78	9.901
86.33	9.902
117.18	9.971
168.09	10.011
139.43	10.073
140.39	10.087
347.92	10.196
467.29	10.378
3883.34	11.048
4187.80	11.211

EXPERIMENTAL

As a second test of the solubility method, three thermodynamic macrodissociation constants of 2,8-dihydroxyadenine were estimated by the solubility method and by UV spectrophotometry. All measurements relevant to the solubility method were made at 37°. UV absorption was measured at 25 or 37°. The pH was measured with a digital pH meter, and all pH values are reported as the final equilibrium pH. Buffers were made at ionic strengths of 0.1 and were adjusted with hydrochloric acid or sodium hydroxide and citrate and phosphate buffers.

Anhydrous 2,8-dihydroxyadenine was certified[2] to be 98.52% pure. 2,8-Dihydroxyadenine was assayed in aqueous buffer as follows. The final equilibrium sample was filtered through a 0.22-μm filter and diluted as necessary with a solution of the same buffer of similar pH. This prefinal solution was then diluted 1:1 with 6 *N* HCl, and the UV absorbance at 305 nm was read against an identical blank. The 2,8-dihydroxyadenine concentration was computed using the experimentally determined molar absorptivity of 17,130 for 2,8-dihydroxyadenine in 3 *N* HCl at 25°. The quantitative lower limit of sensitivity of this procedure is 0.1 mg/liter, and precision is ±3% for concentrations above 1 mg/liter.

The experimental procedure consisted of massively exceeding the 2,8-dihydroxyadenine solubility in test solutions by heating to 100° for 30 min followed by agitation at 37°. Agitation was continued for no less than 65 hr and for as long as 504 hr. The criterion for attainment of stable solubility for a given sample was a solubility change of less than 3% in three successive 24-hr checks.

RESULTS AND DISCUSSION

The pH and solubility data for 2,8-dihydroxyadenine appear in Table IV. The data analysis procedure for estimating thermodynamic macrodissociation constants by the solubility method was identical to that used for tyrosine, except that the nonlinear regressions were weighted by the reciprocal of the square of the 2,8-dihydroxyadenine concentration because of multiplicative errors due to dilution procedures as discussed previously. The results are presented in Table V.

The solubility method for determining aqueous pKa values was used with some frequency 30–50 years ago (5, 19–24) but only sporadically in

[2] Aldrich Chemical Co., Milwaukee, WI 53233.

Table V—Thermodynamic pKa Values for 2,8-Dihydroxyadenine (37°) (Mean ± 1 *SD*)

Method	pKa_1	pKa_2	pKa_3
Solubility	2.45 ± 0.06	8.12 ± 0.05	11.38 ± 0.16
Spectral	2.49[a]	8.09[a]	11.52[b]

[a] UV absorbance was measured at 25°; resulting pKa values were adjusted to 37° (1, 18). [b] All measurements were performed at 37°.

recent years (4, 12, 25, 26). In part, this change may be accounted for by the relative simplicity and ease of potentiometric and spectrophotometric methods. In addition to the awkward and complicated graphic solutions recommended by early protagonists of the solubility method, it may have been underutilized because it has never been generalized to estimation of thermodynamic pKa values for polyprotic species. Recently, one investigator asserted that a dibasic acid pKa could not be determined by the solubility method (4). Examination of his report, however, suggests no reason why it could not be accomplished using the method described here.

Krebs and Speakman (22) first provided a derivation of the fundamental solubility–dissociation equation in a form relating solubility to pH and pKa′, linearly and separately for monoprotic acids and bases. They correctly predicted the upward change in the terminal slope of the $\log_{10}(S/S_0' - 1)$ *versus* pH plot when a dibasic dissociation becomes operative. However, no generalized derivation was provided, nor was there serious suggestion of extension to dibasic species. They mentioned the problem of correcting the apparent pKa′ to zero ionic strength to obtain the thermodynamic pKa but made no comment on the proper correction for polyprotic species. The Krebs and Speakman approach, however, was useful for studying aqueous pKa′ values of a number of substances (4, 22, 25–27).

Krüger-Thiemer *et al.* (12) published a nonlinear solubility equation for amphoteric substances and suggested the use of a least-squares data fitting procedure for estimating S_0' and pKa′. They applied this approach to a number of monoprotic sulfonamides and found that it yielded pKa′ estimates in close agreement with values obtained by conventional methods. The advantage of this technique over a simple plotting routine is its provision of an automated estimation procedure. It is uniquely suited to cases of amphoteric and/or polyprotic compounds that cannot be fitted by a linear regression.

Krüger-Thiemer *et al.* (12) also reported the $\log_{10}$ form of Eq. 10 to eliminate inaccuracies in the estimation procedures produced by multiplicative errors. Since the tyrosine data of Hitchcock (5) were reported as means of two or more analyses, it was impossible to examine the data for the measurement error type. Therefore, the values from Table I were fit in both the transformed ($\log_{10}$) and untransformed manner. Final estimates by the transformed manner are as follows: S_0 = 2.81 m*M*, pKa_1 = 2.08, pKa_2 = 9.14, and pKa_3 = 10.47. The estimates thus obtained are approximately as close as the untransformed estimates are to the means for the published dissociation values (Table III). However, in this case, there is no compelling argument in favor of the $\log_{10}$ transform approach. Therefore, the values estimated by the untransformed equation remain the best estimates.

An extensive search of the world literature failed to reveal a general treatment of the solubility–dissociation relationships as described here. However, two reports that used solubility–pKa considerations should be mentioned. An equation that can be made equivalent to Eqs. 6 and 7 was included (without derivation) as part of a general discussion of solubility (28); it was not used to provide a basis for the determination of thermodynamic pKa values of polyprotic species. Levy and Rowland (29) proposed a pKa determination method that allows use of potentiometry in pH regions where precipitation of a sparingly soluble substance has occurred.

The validity of the solubility method for determining thermodynamic pKa values described here was tested on tyrosine solubility measurements published by Hitchcock (5) and on 2,8-dihydroxyadenine solubilities measured in this laboratory. Tables III and V indicate substantial agreement between solubility-determined thermodynamic pKa values and those determined by independent methods. All solubility-estimated pKa values fall within ±1 *SD* of the means of acceptable published values for tyrosine and are acceptably close to spectral pKa values in the dihydroxyadenine case.

The maximum number of pKa values of a given compound that can be determined by this method remains unexplored. There appears to be no limitation on the estimation of apparent pKa′ values beyond the requirement of chemical stability at the pH extremes. However, the ionic strength for such apparent pKa′ values would be impossible to summarize in a single number unless a swamping electrolyte was utilized. Accurate estimation of multiple thermodynamic pKa values would be limited by the inaccuracy of the Debye–Hückel activity approximation at ionic strengths greater than 0.1. Although activity approximations exist for ionic strengths greater than 0.1 (30), estimation of thermodynamic pKa values in this circumstance would be tenuous at best. Thus, where the initial pH is ≤1 or ≥13, the contribution of acid or base alone to ionic strength represents a limitation to this method. Moreover, the ionic strength contribution of other ions, especially those of the compound under study, shrinks these limits further.

In summary, a derivation of solubility, pH, and pKa (macroscopic) relationships is presented and is generalized to polyprotic, amphoteric species in aqueous solutions. A general method is provided for determining apparent and thermodynamic macrodissociation constants from a set of solubility and pH measurements using a data-fitting procedure. Finally, this approach is validated by estimating thermodynamic pKa values on two data sets. Solubility-estimated pKa values for tyrosine and 2,8-dihydroxyadenine compare favorably with those using independent methods.

REFERENCES

(1) A. Albert and E. D. Serjeant, "Ionization Constants of Acids and Bases," Wiley, New York, N.Y., 1962.

(2) L. Z. Benet and J. E. Goyan, *J. Pharm. Sci.*, **56**, 655 (1967).

(3) D. C. Ward and E. Reich, *J. Biol. Chem.*, **244**, 1228 (1969).

(4) J. A. W. Dalziel and A. K. Slawinski, *Talanta*, **19**, 1240 (1972).

(5) D. I. Hitchcock, *J. Gen. Physiol.*, **6**, 747 (1924).

(6) D. L. Horowitz and L. D. Hoover, Naval Medical Research Institute Report No. 25, Project No. MR005.20-0287, 1970.

(7) S. Glasstone and D. Lewis, "Elements of Physical Chemistry," Van Nostrand, Princeton, N.J., 1960, p. 510.

(8) H. S. Harned and B. B. Owen, "The Physical Chemistry of Electrolyte Solutions," 3rd ed., Reinhold, New York, N.Y., 1958, p. 488.

(9) J. Kielland, *J. Am. Chem. Soc.*, **59**, 1675 (1937).

(10) R. B. Martin, J. T. Edsall, D. B. Wetlaufer, and B. R. Hollingworth, *J. Biol. Chem.*, **233**, 1429 (1958).

(11) J. T. Edsall, R. B. Martin, and B. R. Hollingworth, *Proc. Natl. Acad. Sci. USA*, **44**, 505 (1958).

(12) E. Krüger-Thiemer, B. Schlender, and J. Seydel, *Arzneim.-Forsch.*, **13**, 894 (1963).

(13) K. A. Brownlee, "Statistical Theory and Methodology in Science and Engineering," Wiley, New York, N.Y., 1960.

(14) A. Albert, *Biochem. J.*, **50**, 690 (1952).

(15) P. J. Niebergall, R. L. Schnaare, and E. T. Sugita, *J. Pharm. Sci.*, **61**, 232 (1972).

(16) J. L. Grammer and A. Neuberger, *Biochem. J.*, **37**, 302 (1943).

(17) C. Tanford and G. L. Roberts, *J. Am. Chem. Soc.*, **74**, 2509 (1952).

(18) N. F. Hall and M. R. Sprinkle, *ibid.*, **54**, 3469 (1932).

(19) K. Sano, *Biochem. Z.*, **168**, 14 (1925).

(20) H. L. Johnston and H. L. LeLand, *J. Am. Chem. Soc.*, **60**, 1439 (1938).

(21) L. A. McDowell and H. L. Johnston, *ibid.*, **58**, 2009 (1936).

(22) H. A. Krebs and J. C. Speakman, *J. Chem. Soc.*, **1945**, 593.

(23) S. Glasstone, *Chem. Soc. J.*, **119**, 1689 (1921).

(24) D. L. Davidson, *J. Chem. Educ.*, **19**, 221 (1942).

(25) R. Alric and R. Peuch, *J. Pharmacol.*, **2**, 141 (1971).

(26) B. D. Berezin, O. I. Koifman, and V. A. Andrianov, *J. Phys. Chem.*, **47**, 823 (1973).

(27) H. A. Krebs and J. C. Speakman, *Br. Med. J.*, **1**, 47 (1946).

(28) F. J. C. Rossotti and H. Rossotti, "The Determination of Stability Constants in Solution," McGraw-Hill, New York, N.Y., 1961, p. 194.

(29) R. H. Levy and M. Rowland, *J. Pharm. Sci.*, **60**, 1155 (1971).

(30) R. A. Robinson and R. H. Stokes, "Electrolyte Solutions," Butterworths Scientific Publications, London, England, 1959, p. 231.

ACKNOWLEDGMENTS

The authors gratefully acknowledge the technical assistance of Mr. Fred J. Bailey as well as the advice given by Ms. Margaret Wrensch, Dr. G. L. Moore, Dr. L. B. Sheiner, and Dr. T. N. Tozer.

The opinions or assertions contained herein are those of the authors and are not to be construed as reflecting the views of the Department of the Army.

Analysis of Tricyclic Antidepressants in Human Plasma by GLC–Chemical-Ionization Mass Spectrometry with Selected Ion Monitoring

RAND G. JENKINS and ROBERT O. FRIEDEL *x

Received April 26, 1976, from the *Department of Psychiatry and Behavioral Sciences, University of Washington, Seattle, WA 98195.* Accepted for publication December 3, 1976. * Present address: Department of Psychiatry, Medical College of Virginia, MCV Station, Richmond, VA 23298.

Abstract □ A method is described for the analysis of amitriptyline, doxepin, imipramine, nortriptyline, desmethyldoxepin, desipramine, and protriptyline in human plasma utilizing GLC–chemical-ionization mass spectrometry with selected ion monitoring. The assay is highly specific and is quantitative to at least 1 ng/ml with a standard error typically less than 5%. Representative concentrations of the parent compounds and their monodemethylated metabolites, as measured in plasma samples from patients under treatment with tertiary amine tricyclic antidepressants, are given.

Keyphrases □ Antidepressants, various tricyclic—GLC–chemical-ionization mass spectrometric analyses, human plasma □ GLC–chemical-ionization mass spectrometry—analysis, various tricyclic antidepressants in human plasma □ Mass spectrometry, chemical ionization—analysis, various tricyclic antidepressants in human plasma

Tricyclic antidepressants are the most commonly used medications for the treatment of depression. Approximately 60–70% of patients treated with these substances respond favorably. The lack of response in the remaining 30–40% may be attributed, in part, to interpatient differences in drug absorption, distribution, metabolism, and elimination, resulting in nontherapeutic blood levels of the drugs and their active metabolites (1–6).

To evaluate the importance of these pharmacokinetic processes on the response of depression to tricyclic antidepressant treatment, selective and sensitive assay methods for these compounds and their metabolites must be utilized. Previous approaches include TLC (7–10), photometry (11–16), radioisotopic derivatization (17, 18), GLC (9, 13, 19–28), and GLC–mass spectrometry with selected ion monitoring (4, 29–39), which is the most accurate and among the most sensitive. To date, assays with this method have utilized electron-impact ionization techniques.

The purpose of the present study was to develop GLC–mass spectrometric assays with selected ion monitoring for the most commonly used tricyclic antidepressants utilizing the more recently developed chemical-ionization method.

EXPERIMENTAL

Blood samples, 5–10 ml, were drawn in heparinized tubes[1] from patients under treatment for depression. The plasma was separated by centrifugation at 2000 rpm for 10 min, transferred to tubes with polytef-lined screw caps, and stored frozen at −20° until analysis. The following were used as reference compounds: amitriptyline[2], protriptyline[2], nortriptyline[3], doxepin[4], desmethyldoxepin[4], imipramine[5], and desipramine[6].

All solvents were either high purity[7] or glass distilled[8]. Trifluoroacetic, heptafluorobutyric[9], and pentafluoropropionic[10] anhydrides were reagent grade; perfluorotributylamine[10] was mass spectrometric grade. All other reagents were ACS reagent grade. Glassware was acid washed, and silanization of glassware with dimethylchlorosilane or the inclusion of an alcohol such as isobutyl in the extraction solvent was essential to prevent serious drug adsorption on the extraction glassware. Addition of isobutyl alcohol was preferred as a matter of convenience.

A gas chromatograph–mass spectrometer system[11] interfaced with a data system[12] was equipped with a differentially pumped chemical-ionization source that received the total effluent from the gas chromatograph.

A series of standards was prepared daily and analyzed along with each set of unknowns. Standards were prepared by spiking 2-ml aliquots of drug-free human plasma with known concentrations of the drugs of interest along with the appropriate internal standards as aqueous solutions of their hydrochloride salts. (These solutions were stable for several weeks when prepared in 0.01 *N* HCl and stored at 4°.) Tertiary and secondary amine analogs from the tricyclic class were chosen as internal standards. A range of 5–150 ng/ml in the spiked standards generally coincided with the range of actual blood levels measured in most patients. Internal standards were added at a concentration falling approximately in the center of the standard range. The standards were extracted simultaneously and identically with the unknowns.

The unknown plasmas were thawed, and 2.0-ml aliquots of each were pipetted into 8-ml screw-capped tubes with polytef-lined caps[13]. The same quantities of the internal standards were added to these as were added to the known standards, again as aqueous solutions of their hydrochloride salts. The pH of the samples was adjusted to 10.5–11.5 by dropwise addition of 1 *N* NaOH. Control of the pH with bicarbonate or other buffers was unnecessary, and dilution of the plasma with these buffers generally resulted in excessive emulsion formation with shaking.

Samples were extracted twice with 3 ml of 1.5% (v/v) isobutyl alcohol–heptane by shaking vigorously for 2 min and then centrifuging at 1500 rpm for 10 min to effect complete phase separation. The aqueous phases were discarded, and the combined organic phases were back-extracted into 1 ml of 0.1 *N* H_2SO_4, again with 2 min of shaking followed by centrifugation. The heptane phases were discarded, and the acidic aqueous phases were washed once with 4 ml of fresh extraction solvent; again the organic phases were discarded after centrifugation.

It was necessary to include this back-extraction step to eliminate interfering substances that gave mass fragments at identical *m/e* values to those being selectively monitored as well as late eluting contaminants that excessively prolonged the chromatography time. Three common contaminants, other than neutral lipids, substantially removed by this step were identified from their mass spectra as tributoxyethyl phosphate,

[1] Vacutainer, Becton-Dickenson, Rutherford, N.J.
[2] Merck Sharp and Dohme, West Point, Pa.
[3] Eli Lilly and Co., Indianapolis, Ind.
[4] Pfizer Research Laboratories, Groton, Conn.
[5] Ciba-Geigy Corp., Summit, N.J.
[6] Lakeside Laboratories, Milwaukee, Wis.
[7] Nanograde, Mallinckrodt, St. Louis, Mo.
[8] Burdick & Jackson Laboratories, Rockford, Mich.
[9] Pierce Chemical Co., Rockford, Ill.
[10] PCR, Gainesville, Fla.
[11] Model 3200E, Finnigan Corp., Sunnyvale, Calif.
[12] Model 6100, Finnigan Corp., Sunnyvale, Calif.
[13] Corning Glass Works, Corning, N.Y.

dibutyl phthalate, and dioctyl phthalate. The vacuum blood collection tubes[1] or their stoppers contain these compounds (40).

The samples were then readjusted to pH 10.5–11.5 by dropwise addition of 1 *N* NaOH and extracted twice with 2 ml of extraction solvent, followed by shaking and centrifuging as before. The upper organic phases were then transferred to clean, dry, screw-capped tubes and evaporated under a stream of dry gaseous nitrogen at 40°. Imipramine samples had to be analyzed at this point due to degradation of this tertiary amine by the derivatization reaction conditions of the next step. Samples were then derivatized to convert the secondary amine metabolites to products more easily analyzed by GLC.

To the dried residues in each tube were added 25 μl of ethyl acetate and 50 μl of heptafluorobutyric anhydride. The tubes were tightly capped and heated at 60° in a block-type heater. The maximal reaction yield was achieved in 30–60 min. The samples were dried again under gaseous nitrogen at 40°, with a few drops of toluene added near the end of drying to facilitate complete removal of unreacted heptafluorobutyric anhydride and residual heptafluorobutyric acid. The residues were taken up in 20–50 μl of ethyl acetate just prior to analysis.

Samples were stable for several days when stored either dry or in ethyl acetate at 4°. Samples, 1–5 μl, were then analyzed by GLC–chemical-ionization mass spectrometry with selected ion monitoring.

Reference Spectra—Aliquots of 100–200 ng of each pure reference compound (or the heptafluorobutyramide derivative of the secondary amines) were injected into the gas chromatograph–mass spectrometer–computer system and chromatographed using the following conditions. The silanized glass column, 6 mm o.d., 2 mm i.d. × 1.5 m, was packed with 3% SP-2250DB on 100–120-mesh Supelcoport[14]. The column oven was maintained at 205° isothermal, and the injector temperature was 235° isothermal. The carrier gas was methane, and the flow rate was adjusted to give a source pressure of 1000 μm (equivalent to a flow rate of 20 ml-atm/min).

The mass spectrometer conditions were: interface temperature, 170°; ion source temperature, at equilibrium (130–135°); emission current, 500 μamp; electron multiplier, 2100 v; electron energy, 105 ev; and preamplifier range, 10^{-9} amp/v.

The computerized data system produced an internal mass calibration table by scanning a spectrum of perfluorotributylamine for its known mass peaks. To the two or four masses selected, 0.1 or 0.2 amu was added for mass defect compensation. The integration time was automatically selected by the data system to optimize the signal-to-noise ratio, and the scan time was 1 sec. The mass spectrometer was operated under computer control in the scan mode (over the appropriate mass range).

Scans were taken at 2–3-sec intervals using an integration time of 8 msec/amu and stored on the computer disk memory. A reconstructed gas chromatogram was generated by the data system in real time from these scans as they were acquired. Each reference spectrum represents the scan corresponding to the chromatogram peak apex minus a background scan taken prior to the peak elution. The spectra were normalized on the base peak and plotted on a digital plotter[15].

GLC–Chemical-Ionization Mass Spectrometry—The selected ions monitored were chosen from the reference spectra (Table I). Up to four ions were monitored simultaneously by the data system. Although the ions as listed in Table I are of integer mass, they were actually monitored with +0.1 or +0.2 amu offset to compensate for mass defect. The quadrupole mass set voltages corresponding to these ions were automatically set by the computer referenced to a mass calibration table, with perfluorotributylamine[16] as the calibration compound. Integration times were determined by a computer algorithm to maximize the signal-to-noise ratio.

The standard curves were computer constructed from a multiple linear regression analysis of the mass chromatogram area ratios (standard drug–internal standard) *versus* the corresponding concentration ratios (nanograms per milliliter).

The final drug concentrations of the samples were determined mathematically from the ratios of the mass chromatogram peak areas (unknown drug–internal standard) using the slope and intercept of the standard curve.

RESULTS

Reference Mass Spectra—Methane chemical-ionization mass spectra of pure reference compounds, or their heptafluorobutyramide derivatives where appropriate, are shown in Figs. 1–7. The structures indicated are not those of the molecular ion(s) because the adduct protons or alkyl chains are not shown. The left ordinates represent the relative intensity normalized on the base peak (100%) of the mass range indicated. The right ordinates represent the percent of the sum of the total ions over the indicated mass range.

Table I—Selected Ions Monitored for Analysis of Tricyclic Antidepressants[a]

Compound	Base Peak (*m/e*)	Reference Peaks (*m/e*)
Amitriptyline	278 (MH^+)	233, 276
Nortriptyline heptafluorobutyramide	233	460 (MH^+)
Doxepin	280 (MH^+)	235, 278
Desmethyldoxepin heptafluorobutyramide	235	462 (MH^+)
Imipramine	281 (MH^+)	208, 279, 280
Desipramine bis(heptafluorobutyryl) derivative	228	430, 657 (MH^+)
Protriptyline heptafluorobutyramide	191	233, 460 (MH^+)

[a] Mass spectra were prepared from solutions of pure reference compounds (Figs. 1–7). The base peak in each spectrum was chosen for quantitation, and one or more other major peaks were selected as reference peaks for qualitative verification.

The spectra (Figs. 1–7) include the significant ions above *m/e* 100, extending approximately from the mass of the intact tricyclic ring system to the $(M + 41)^+$ ion. The most abundant ions found below this range and, therefore, not included were those at *m/e* 58 of the tertiary amines. The relative abundances of *m/e* 58 were 100, 95, and 30% for amitriptyline, doxepin, and imipramine, respectively, and represented 75, 30, and 8%, respectively, of the sum of the total ions between 50 and 350 amu for these compounds.

Amitriptyline, mol. wt. 277, gave a relatively simple spectrum (Fig. 1), with the base peak at *m/e* 278 from the protonated molecular ion MH^+. Also present were the molecular adduct ions at *m/e* 306 $(M + 29)^+$ and 318 $(M + 41)^+$ from the addition of $C_2H_5^+$ and $C_3H_5^+$, respectively. The $(M - 1)^+$ ion at *m/e* 276 was derived from hydride abstraction.

The spectrum of doxepin, mol. wt. 279, was analogous to that of amitriptyline, with the base peak at *m/e* 280 from the MH^+ ion and associated adduct ions at *m/e* 308 and 320 (Fig. 2). The $(M - 1)^+$ ion at *m/e* 278 was much less prominent relative to the MH^+ ion in this spectrum than were the corresponding ions in the spectrum of amitriptyline, probably due to the oxygen in the ethylene bridge of the doxepin ring system.

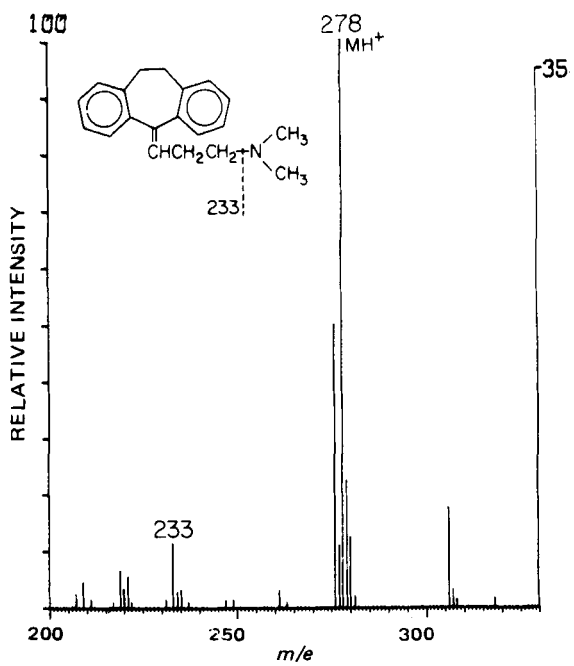

Figure 1—*Chemical-ionization mass spectrum and structure of amitriptyline.*

[14] Supelco, Inc., Bellefonte, Pa.
[15] Zeta Research Inc., Lafayette, Calif.
[16] FC-43.

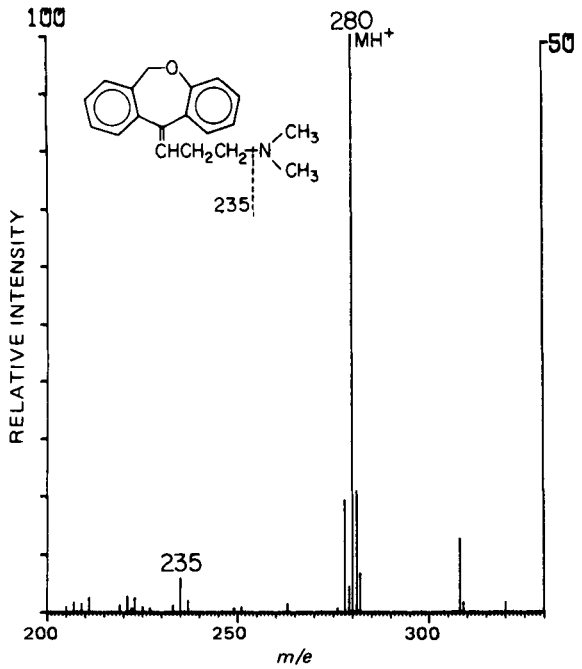

Figure 2—*Chemical-ionization mass spectrum and structure of doxepin.*

Imipramine, mol. wt. 280, yielded a spectrum analogous to spectra of amitriptyline and doxepin, with the MH^+ ion at *m/e* 281 as the base peak and the expected adduct ions at *m/e* 309 and 321 (Fig. 3). A relatively large M^+ ion at *m/e* 280 derived from charge exchange ionization and a relatively small $(M - 1)^+$ ion from hydride abstraction are the reverse of the relative intensities seen for amitriptyline and doxepin.

Nortriptyline heptafluorobutyramide, mol. wt. 459, gave a more complex spectrum than that of amitriptyline, with a fragment ion at *m/e* 233 as the base peak (Fig. 4). This ion (identical to *m/e* 233 of amitriptyline) was derived from inductive cleavage of the MH^+ ion with neutral loss of $C_3F_7CONHCH_3$. The MH^+ ion at *m/e* 460 and the associated ions at *m/e* 488 and 500 were much less stable than the analogous ions in the spectrum of amitriptyline and were, therefore, comparatively low in relative abundance (note that the intensities of all ions above 400

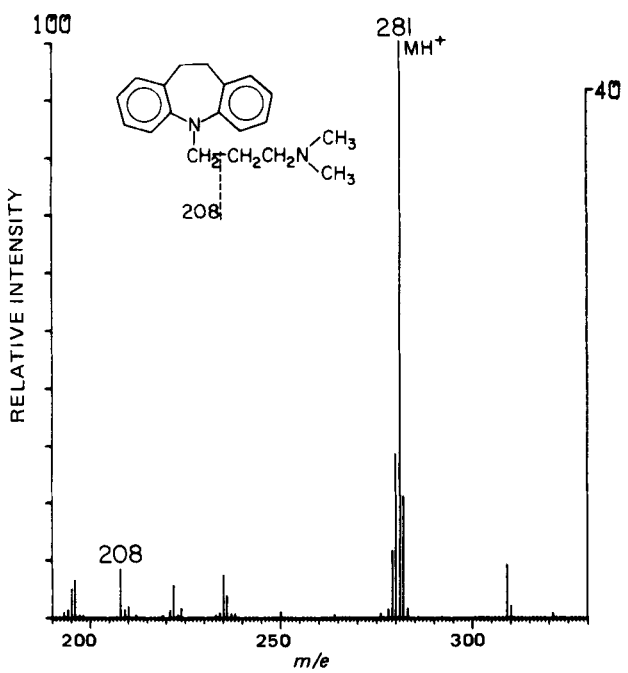

Figure 3—*Chemical-ionization mass spectrum and structure of imipramine.*

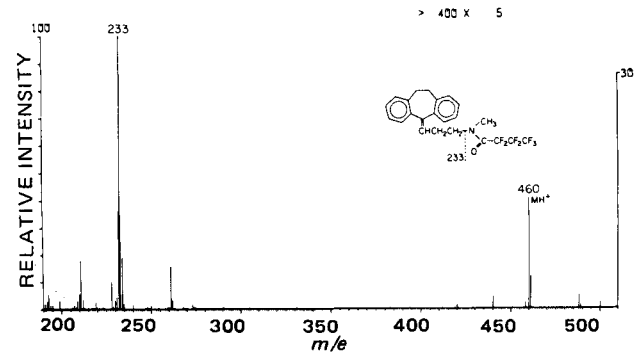

Figure 4—*Chemical-ionization mass spectrum and structure of nortriptyline heptafluorobutyramide.*

were magnified five times). Ions at *m/e* 440 and 420 were from single and double loss of HF, respectively. Fragments at *m/e* 261 and 273 were probably derived from *m/e* 388 $(M + 29)^+$ and 500 $(M + 41)^+$ by the same cleavage that produced *m/e* 233 from *m/e* 460.

Desmethyldoxepin heptafluorobutyramide, mol. wt. 461, gave a spectrum (Fig. 5) analogous to that of nortriptyline heptafluorobutyramide, with the base peak at *m/e* 235 formed from the MH^+ ion as described for the base peak of nortriptyline heptafluorobutyramide. The MH^+ ion was present at *m/e* 462 along with the accompanying adduct ions at *m/e* 490 and 502, all of low relative abundance. Ions at *m/e* 263 and 275 were probably from cleavage of *m/e* 490 $(M + 29)^+$ and 502 $(M + 41)^+$, as described for the analogous ions of nortriptyline heptafluorobutyramide.

Desipramine was converted by reaction with heptafluorobutyric anhydride to a diacyl derivative, mol. wt. 656, of uncertain structure. The spectrum of desipramine bis(heptafluorobutyramide) (Fig. 6) gave an MH^+ ion at *m/e* 657. The base peak at *m/e* 228 was structurally identified as $C_3F_7CON^+H_2CH_3$. Another prominent ion at *m/e* 430 $(MH - 227)^+$ was derived from loss of $C_3F_7CONHCH_3$ from the MH^+ ion. Reaction of desipramine with trifluoroacetic anhydride or pentafluoropropionic anhydride produced diacyl derivatives analogous to desipramine diheptafluorobutyramide. The yields of these reactions were essentially quantitative.

Protriptyline heptafluorobutyramide, mol. wt. 459, gave a spectrum significantly different from that of nortriptyline heptafluorobutyramide, mol. wt. 459 (Fig. 7). The base peak of protriptyline heptafluorobutyramide was at *m/e* 191, derived from loss of the side chain from the tricyclic ring system. A significant ion at *m/e* 268 probably represented charge retention by the cleaved side chain. The MH^+ ion at *m/e* 460 and accompanying ions at *m/e* 488 and 500 were of much greater relative abundance than the analogous ions in the spectra of the other secondary amine tricyclic heptafluorobutyramide derivatives (spectrum is shown with no vertical expansion). Prominent ions at *m/e* 233, 261, and 273 were probably from cleavage of MH^+, $(M + 29)^+$, and $(M + 41)^+$ ions as described for nortriptyline heptafluorobutyramide.

Relative Retention Times—Relative GLC retention times of the tricyclic antidepressants are listed in Table II. The values were normalized relative to amitriptyline (first column) and nortriptyline heptafluorobutyramide (second column), since these compounds were used as

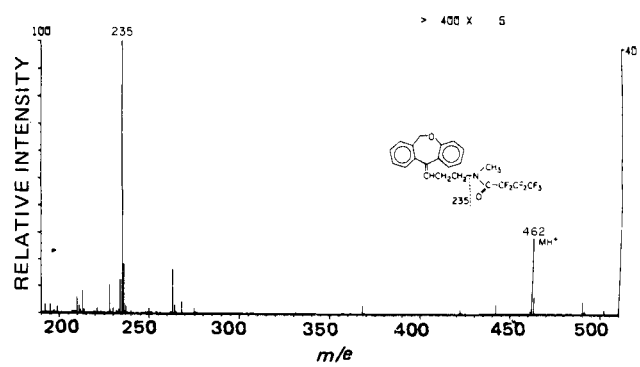

Figure 5—*Chemical-ionization mass spectrum and structure of desmethyldoxepin heptafluorobutyramide.*

Table II—Relative GLC Retention Times of Tricyclic Antidepressants[a]

Compound	Relative Retention Time
Amitriptyline	1.00
Doxepin (*cis-trans*)	1.70
Imipramine	1.40
Nortriptyline heptafluorobutyramide	3.25, 1.00
Desmethyldoxepin heptafluorobutyramide	
cis	3.90, 1.20
trans	4.52, 1.39
Desipramine bis(heptafluorobutyryl) derivative	1.23, 0.38
Protriptyline heptafluorobutyramide	4.33, 1.30

[a] The GLC effluent containing the solvent front was vacuum diverted ahead of the mass spectrometer ion source for 3.0 min from the point of injection until the start of data acquisition. The values were normalized relative to amitriptyline in the first column and nortriptyline heptafluorobutyramide in the second column.

the internal standards for the analysis of the other tricyclics. Doxepin and desmethyldoxepin were used as internal standards for the analysis of amitriptyline and nortriptyline. Doxepin and imipramine eluted later than, and were completely resolved from, amitriptyline under the conditions described. The *cis*- and *trans*-isomers of doxepin were not separable on this stationary phase.

Nortriptyline heptafluorobutyramide and desmethyldoxepin heptafluorobutyramide were separated, eluting much later than their tertiary amine counterparts, amitriptyline and doxepin. The *cis*- and *trans*-isomers of desmethyldoxepin heptafluorobutyramide were well resolved, in contrast to those of doxepin, eluting in that order after nortriptyline heptafluorobutyramide. Desipramine diheptafluorobutyramide eluted well ahead of nortriptyline heptafluorobutyramide, having the shortest retention time of any of the secondary amine acyl derivatives. Protriptyline heptafluorobutyramide was completely separated from nortriptyline heptafluorobutyramide.

GLC–Chemical-Ionization Mass Spectrometry—Typical mass chromatograms of four different ions (*m/e* values) monitored during a doxepin and desmethyldoxepin analysis are shown in Figs. 8 and 9. A slight separation of the *cis–trans*-isomers of doxepin was observed in Fig. 8. The *cis*-isomer appeared as a small shoulder on the leading edge of the much larger *trans*-isomer peak (the isomer ratio of the reference compound as supplied was 15:85 *cis–trans*). This was apparent in both peak 1 from the MH^+ ion (*m/e* 280) and the smaller peak from the $(M - 1)^+$ ion (*m/e* 278).

The *cis–trans*-isomers of desmethyldoxepin heptafluorobutyramide are separated in Fig. 9 (peaks 5 and 3). No *cis*-isomer is seen in Fig. 8 because the pure reference sample of desmethyldoxepin contained only the *trans*-isomer (verified by melting-point analysis). That peak 5 in Fig. 9 truly represents *cis*-desmethyldoxepin heptafluorobutyramide was confirmed by analyzing plasma from a doxepin overdosed patient. Identical mass spectra were obtained from both isomer peaks. The unnumbered fragmentogram peaks present at the same scan number (retention time) as a numbered peak were all generated from the single drug component eluting at that retention time. These smaller peaks represent ions with different *m/e* values and lower relative abundances than the base peak ion (producing the numbered peak) in the mass spectrum of the particular drug component.

Efficiency of Extraction—The extraction efficiency was measured by comparing samples containing internal standards with those containing external standards. Typical recoveries were greater than 95%.

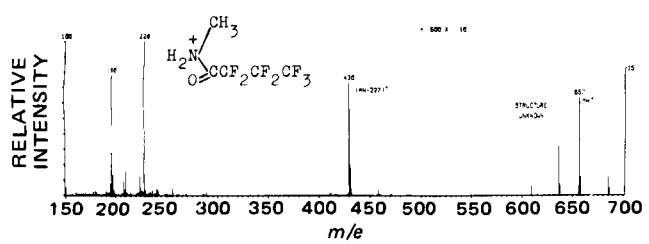

Figure 6—*Chemical-ionization mass spectrum and structure of desipramine bis(heptafluorobutyramide).*

Table III—Assay Precision[a]

Plasma Standard	Plasma Doxepin[a], ng/ml	*x* Area[b] Ratios	*n*	*SE*	*SE*, %
A	10	0.26	5	0.012	4.6
B	25	0.76	5	0.026	3.5
C	50	1.61	5	0.077	4.8
D	100	3.56	5	0.119	3.4
E	150	5.88	4	0.145	2.5
Plasma Standard	**Plasma Desmethyl-doxepin, ng/ml**	***x* Area[c,d] Ratios**	***n***	***SE***	***SE*, %**
A	10	0.29	5	0.014	4.8
B	25	0.81	5	0.030	3.7
C	50	1.59	5	0.124	7.8
D	100	3.55	5	0.148	4.2
E	150	5.04	3	0.254	5.0

[a] Forty nanograms per milliliter each of amitriptyline and nortriptyline were used as internal standards with doxepin and desmethyldoxepin, respectively. [b] Mass chromatogram peak area ratio = doxepin (*m/e* 280)/amitriptyline (*m/e* 278). [c] Mass chromatogram peak area ratio = desmethyldoxepin (*m/e* 235)/nortriptyline (*m/e* 233). [d] Combined area of *cis*- and *trans*-peaks.

Assay Precision—The precision of the described method is illustrated by the data in Table III from an analysis of doxepin and desmethyldoxepin. The standard error was generally less than 5% and is typical of results obtained for the other tricyclic compounds assayable by this method.

Standard Curve Linearity—Statistical analysis of 16 standard curves from the analyses of the three tertiary amine tricyclics gave a mean regression coefficient of 0.996 ± 0.003 ($\bar{r} \pm SD$). Similar analysis of 16 curves from the analyses of the four secondary amine tricyclic heptafluorobutyramide derivatives yielded a slightly better mean coefficient of 0.998 ± 0.002.

Patient Plasma Samples—The data in Table IV are representative of the plasma concentrations of the parent compounds and their monodemethylated metabolites as measured in samples from patients under treatment with the tertiary amine tricyclics. The dosages represent the total daily amount regardless of administration schedule. Indicated dosages were maintained for at least 4–5 days prior to sampling.

DISCUSSION

The measurement of blood tricyclic antidepressant levels is useful in the evaluation of the treatment of patients with these agents (1–5, 29). However, the routine clinical measurement of these compounds has only recently become feasible because of the sensitivity and specificity required.

Many techniques have been applied to the analyses of these substances. Qualitative and some semiquantitative analyses were reported using conventional TLC (7, 9). Quantitative application of TLC with 5–10-ng/ml sensitivity (4–5 ml of plasma required) was demonstrated using both UV and fluorometric direct densitometry (8, 10). Interference by other concurrently administered drugs is possible because qualitative accuracy is based upon R_f values and spot color tests.

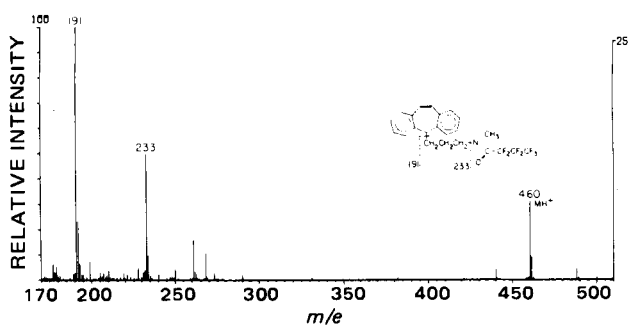

Figure 7—*Chemical-ionization mass spectrum and structure of protriptyline heptafluorobutyramide.*

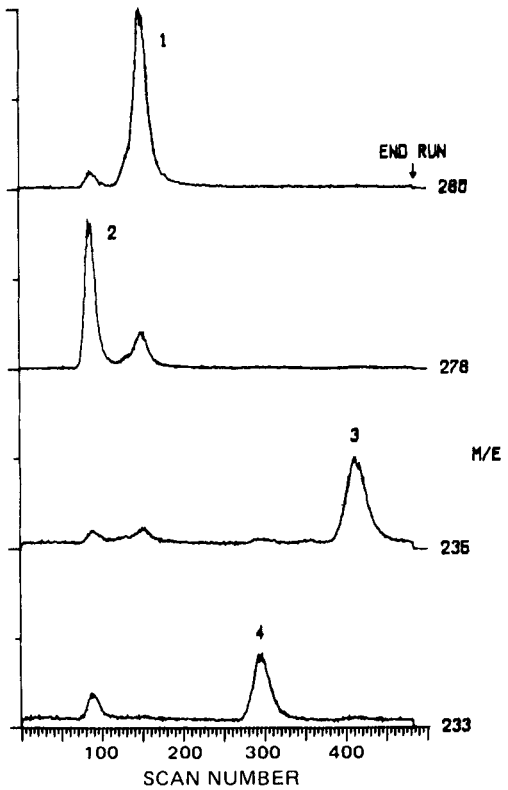

Figure 8—*Representative mass fragmentograms from doxepin and desmethyldoxepin analysis of a spiked plasma standard. Amitriptyline (2) and nortriptyline (4) were used as internal standards (40 ng/ml) for* cis-trans-*doxepin (1) and* trans-*desmethyldoxepin (3), respectively.*

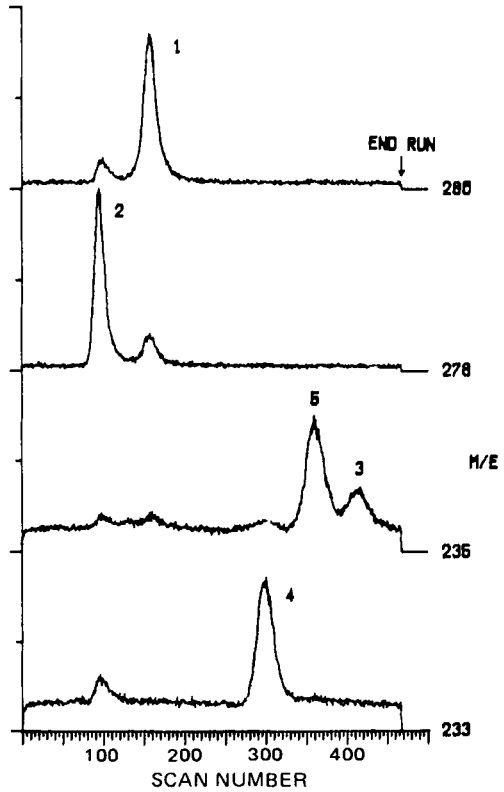

Figure 9—*Representative mass fragmentograms from doxepin and desmethyldoxepin analysis of plasma from a patient receiving doxepin. Amitriptyline (2) and nortriptyline (4) were used as internal standards (40 ng/ml) for* cis-trans-*doxepin (1) and* cis-*desmethyldoxepin (5), respectively.*

Photometric methods, including visible and UV spectrophotometry and fluorometry, were developed (11–16). Reported sensitivities ranged from 2 ng/ml to 2 μg/ml. Photometric methods lacking chromatographic separations generally showed poor selectively because of interferences by many compounds including metabolites and other drugs.

Radioisotopic derivatization methods were described (4, 17) for some primary and secondary amine tricyclics by acylation with ^{3}H-acetic anhydride. A method using ^{14}C-methyl iodide to convert imipramine to a radiolabeled quaternary amine has been the only application of isotopic techniques to the tertiary amine compounds (26). The reported sensitivities varied from 5 to 20 ng/ml. These methods are difficult to reproduce and are subject to interference by any compounds with derivatizable functional groups (including many concurrently administered drugs). These methods are unable to differentiate between the primary and secondary amine tricyclics, and only the method using ^{14}C-methyl iodide is applicable to the tertiary amine parent compounds.

Many GLC methods were described, differing primarily in the type of detector used. The flame-ionization detector yielded reported sensitivities ranging from 2 to 50 ng/ml (9, 20, 21, 28, 35). Qualitative accuracy necessarily was based upon relative retention times because of the nonspecificity of the flame-ionization detector. Cochromatography of contaminants with compounds of interest and prolonged chromatography times due to late eluting contaminants were common difficulties. Correction factors are required to compensate for variable flame-ionization detector responses to different compounds.

The electron-capture detector achieved sensitivities of 5–10 ng/ml for derivatives of some tricyclics (13, 19, 22, 26), but conversion of the tricyclics to products capable of capturing electrons was mandatory for detectability. Two approaches were used: acylation to polyfluorinated amides and oxidation to polyaromatic carbonyl derivatives. The first method was applied to desipramine (22), protriptyline (25), and nortriptyline (27) and its metabolites (19) but was not applicable to the tertiary amine tricyclics. Amitriptyline and nortriptyline were analyzed by the second method as anthraquinone, the product of their oxidation with ceric sulfate–sulfuric acid (13, 26). The oxidation of amitriptyline and nortriptyline yielded the same product, so only combined values were obtained. Protriptyline and cyproheptadine are also converted to anthraquinone and are potential sources of interference.

Difficulties associated with the electron-capture detector in general are: lack of sensitivity to nonelectrophilic compounds (*e.g.*, unaltered tricyclics), limited dynamic range, nonlinearity of response, foil contamination, and susceptibility to interference from electron-capturing contaminants. A nitrogen-specific detector was applied (24) to assays of amitriptyline and nortriptyline, with reported sensitivities of 5 and 10–15 ng/ml, respectively. Of several benzodiazepines and metabolites tested, only 3-hydroxydiazepam interfered. However, many other nitrogen-containing compounds and drugs cannot be ruled out as potential sources of interference.

Table IV—Typical Plasma Tricyclic Antidepressant Levels

Patient	Dose, mg/day	Plasma Concentration[a], ng/ml		
	Imipramine	Imipramine	Desipramine	Total
1	150	18	8	26
2	150	12	28	40
3	200	54	100	154
4	200	15	66	81
5	300	66	97	163
	Amitriptyline	Amitriptyline	Nortriptyline	Total
6	100	24	69	93
7	150	52	37	89
8	200	46	61	107
9	225	97	87	184
10	300	198	125	323
	Doxepin	Doxepin	Desmethyldoxepin	Total
11	75	22	24	46
12	100	17	27	44
13	150	26	40	66
14	225	103	118	221
15	300	122	115	237

[a] Blood was drawn 8–10 hr after the preceding dose of drug.

The application of the mass spectrometer as a gas chromatograph detector (41) made possible the direct identification of compounds as they eluted from the gas chromatograph. Initially, the sensitivity of the gas chromatograph–mass spectrometer was much less than some of the previously mentioned techniques due to the conventional mode of mass spectrometer operation by repetitive scanning over wide mass ranges. Selected ion monitoring (36, 42–44) increased the sensitivity of GLC–mass spectrometry up to 10,000-fold relative to the conventional scanning techniques.

Selective monitoring of single mass ions allowed detection of as low as 10^{-12} g of many compounds in some GLC–mass spectrometer systems (45). Single mass monitoring does not yield the qualitative information obtained by scanning complete mass spectra. However, partial mass spectra may still be obtained by simultaneous selective monitoring of several ions characteristic of the compound(s) of interest (chosen from complete spectra).

GLC–mass spectrometry with and without selected ion monitoring was applied to the analysis of nortriptyline and its metabolites (4, 29, 31, 35–38) and imipramine and desipramine (32–34, 39). Recently, a method was reported for the analysis of all commonly prescribed tricyclic antidepressants by GLC–electron-impact mass spectrometry with selected ion monitoring (30) with reported sensitivities of generally 10 ng/ml or less. An important feature common to all of these studies was the use of electron-impact ionization mass spectrometer systems.

Some additional problems are common to GLC as well as GLC–mass spectrometric analyses of the tricyclics. Column adsorption due to the chemical characteristics and small quantities of these compounds frequently occurs. Biggs *et al.* (30) reported the necessity of "priming" the chromatographic column with eight to 10 100-ng injections of drug prior to actual sample analyses. The present results support this finding, especially with new or infrequently used columns. Injection of 10–20 μl of the silylation reagent[17] also is beneficial. Adsorption is most serious for the free secondary amine tricyclics. However, their acyl derivatives (acetyl, trifluoroacetamide, pentafluoropropionamide, and heptafluorobutyramide) are chromatographed with comparative ease, showing little adsorption.

Imipramine and desipramine react differently to the acid anhydrides in the presence of ethyl acetate than any of the other tricyclics. Imipramine is degraded, and desipramine is converted to a diacyl derivative of uncertain structure. This problem was observed by several investigators (30, 46, 47), and a tentative structure for the diacyl derivative was proposed (47). Molecular weight, spectroscopic, and other data indicate that the compound is an enamine (1,2- or 2,3-). In the absence of ethyl acetate, using pure anhydride, only a monoacyl derivative is obtained, as with the other secondary amine tricyclics (47).

In the present report, a two-part analysis for imipramine and its desmethyl metabolite and utilization of the enamine derivative of the latter for quantitation are proposed. Under the reported reaction conditions, quantitative yields of the diacyl enamine product were obtained; with nortriptyline as an internal standard, the analytical accuracy and precision were equal to those achieved for the other secondary amine tricyclics forming monoacyl derivatives. Although it may be possible to eliminate the two-step analysis of imipramine and desipramine by use of a different solvent system or straight anhydride, a single consistent procedure applicable to the entire tricyclic class was desired, and some of these alternatives were not evaluated thoroughly. The use of *N*-perfluoroacylimidazoles was evaluated using nortriptyline and desmethyldoxepin and was unacceptable. The reaction by-products such as imidazole caused severe chromatographic tailing and interference at some of the masses monitored. A new reagent, *N*-methylbis(trifluoroacetamide), has not been tried. The acid anhydrides are preferred due to the ease of removal of the unreacted excess anhydride and free acid by evaporation prior to GLC analysis, thereby presenting no interferences.

The chromatography time required for separation of sample components sometimes is quite long and can be a problem when the number of samples is large. The method described generally requires 8–12 min/injection, depending on column length and compounds analyzed. This requirement can be complicated by late eluting contaminants such as plastisizers and cholesterol. Dioctyl phthalate and cholesterol are not completely removed during extraction, and it has been necessary to wait between injections for their elution (retention times of both are slightly longer than all of the compounds in Table II under the described conditions). Cholesterol specifically interferes at *m/e* 233 and 235, and dioctyl phthalate interferes at *m/e* 280.

[17] Silyl-8, Pierce Chemical, Rockford, Ill.

The methane chemical-ionization mass spectra of the tricyclics reported here differ significantly from those obtained by electron-impact ionization methods (30–32, 34, 36). A brief comparison of the characteristics of chemical ionization and electron-impact ionization of importance to their applicability to the assay of tricyclics should be noted. More comprehensive treatment is given elsewhere (40, 45, 48–51).

In chemical ionization, the energy transfer during ionization is much lower than in electron-impact ionization; consequently, less fragmentation occurs, resulting in simpler spectra with a predominance of intense high mass ions. The most characteristic ions of a compound are those of a high mass, including parent ion(s), since low mass fragment ions may originate from many compounds. For example, in the quantitative analysis of amitriptyline by chemical ionization, the intense parent ion at *m/e* 278 MH^+ is monitored; in electron-impact analysis, the base peak ion at *m/e* 58 is monitored (30).

No molecular ion (*m/e* 277) is observed in the electron-impact mass spectrum at the nanogram level. It is readily apparent that *m/e* 278 is much more diagnostic of the tertiary amine tricyclic amitriptyline than is *m/e* 58, an ion common to many amines. Also, background from column bleed and other sources is significant at low masses but is generally low or absent at high masses (*i.e.*, molecular ion region). A greater measure of selectivity is possible with chemical ionization by the monitoring of its characteristically abundant high mass ions while achieving sensitivity equivalent with electron-impact ionization.

The described method was applicable to the quantitative analysis of all commonly prescribed tricyclic antidepressants to a level of 1 ng/ml, with only a single minor modification necessary for imipramine and desipramine. The use of the members of this class of drugs as internal standards for each other eliminated the necessity of obtaining stable isotopically labeled compounds for this purpose.

With these selective and sensitive GLC–mass spectrometric assays for tricyclic antidepressants now available, it seems reasonable to expect that the other less expensive and more available assay methods for these substances be validated against these norms. Even when this is done, however, the lack of selectivity of these other techniques, as already noted, must be considered a serious limitation. It is hoped that the problem will be resolved by the development of inexpensive, selective, and sensitive radioimmunoassay methods. The major difficulty with the radioimmunoassay approach will be in developing a degree of selectivity sufficient to distinguish between the tricyclics as well as their metabolites. To date, no assay meeting these criteria has been reported.

REFERENCES

(1) R. A. Braithwaite, R. Goulding, G. Theano, J. Bailey, and A. Coppen, *Lancet*, **1**, 1297 (1972).

(2) R. O. Friedel and M. A. Raskind, "Sinequan: A Monograph of Recent Clinical Studies," Excerpta Medica, Princeton, N.J., 1975, pp. 51, 53.

(3) A. H. Glassman, M. Shostak, S. J. Kantor, and J. M. Perel, *Psychopharmacol. Bull.*, **14**, 27 (1975).

(4) P. Kragh-Sørenson, M. Asberg, and C. E. Hansen, *Lancet*, **1**, 113 (1973).

(5) P. Kragh-Sørenson, C. E. Hansen, N. E. Larsen, J. Nasestoft, and E. F. Hvidberg, *Psychol. Med.*, **4**, 174 (1974).

(6) E. S. Vesell, *Clin. Pharmacol. Ther.*, **16**, 135 (1974).

(7) E. Eschenhof and J. Rieder, *Arzneim.-Forsch.*, **19**, 957 (1969).

(8) D. G. Faber, C. Mulder, and W. A. 'T Veld, *J. Chromatogr.*, **100**, 55 (1974).

(9) D. C. Hobbs, *Biochem. Pharmacol.*, **18**, 1941 (1969).

(10) A. Nagy and L. Treiber, *J. Pharm. Pharmacol.*, **25**, 599 (1973).

(11) A. Devriendt, I. Weemaes, and F. H. Jansen, *Arzneim.-Forsch.*, **23**, 863 (1973).

(12) J. V. Dingell, F. Sulser, and J. R. Gillette, *J. Pharmacol. Exp. Ther.*, **143**, 14 (1964).

(13) H. E. Hamilton, J. E. Wallace, and K. Blum, *Anal. Chem.*, **47**, 1139 (1975).

(14) J. P. Moody, A. C. Tait, and A. Todrick, *Br. J. Psychol.*, **113**, 183 (1967).

(15) J. P. Moody, S. F. Whtyte, and G. J. Naylor, *Clin. Chim. Acta*, **43**, 355 (1973).

(16) J. E. Wallace and E. V. Dahl, *J. Forensic Sci.*, **12**, 484 (1967).

(17) W. M. Hammer and B. B. Brodie, *J. Pharmacol. Exp. Ther.*, **157**, 503 (1967).

(18) F. Sjöqvist, W. Hammer, O. Borgå, and D. L. Azarnoff, "Collequim International Neuro-Psychopharmacologicum. Proceedings of the International Congress. 6th," 1968, pp. 123, 136.

(19) O. Borgå and M. Garle, *J. Chromatogr.*, **68**, 77 (1972).
(20) R. A. Braithwaite and J. A. Whatley, *ibid.*, **49**, 303 (1970).
(21) R. A. Braithwaite and B. Widdop, *Clin. Chim. Acta*, **35**, 461 (1971).
(22) M. Ervik, T. Walle, and H. Ehrsson, *Acta Pharm. Suec.*, **7**, 625 (1970).
(23) H. B. Hucker and S. C. Stauffer, *J. Pharm. Sci.*, **63**, 296 (1974).
(24) A. Jørgensen, *Acta Pharmacol. Toxicol.*, **36**, 79 (1975).
(25) S. F. Sisenwine, J. A. Knowles, and H. W. Rulius, *Anal. Lett.*, **2**, 315 (1969).
(26) J. E. Wallace, H. E. Hamilton, L. K. Goggin, and K. Blum, *Anal. Chem.*, **47**, 1516 (1975).
(27) T. Walle and H. Ehrsson, *Acta Pharm. Suec.*, **8**, 27 (1971).
(28) H. J. Weder and M. H. Bickel, *J. Chromatogr.*, **37**, 181 (1968).
(29) M. Åsberg, B. Cronholm, F. Sjöqvist, and D. Tuck, *Br. Med. J.*, **3**, 331 (1971).
(30) J. T. Biggs, W. R. Holland, S. S. Chang, P. P. Hipps, and W. R. Sherman, *J. Pharm. Sci.*, **65**, 261 (1976).
(31) O. Borgå, L. Palmer, A. Linnarsson, and B. Holmstedt, *Anal. Lett.*, **4**, 837 (1971).
(32) A. Frigerio, *Finnigan Spectra*, **5** (1975).
(33) A. Frigerio, K. M. Baker, and P. L. Mosselli, "Mass Spectrometry in Biochemistry and Medicine," Raven, New York, N.Y., 1974, pp. 65, 82.
(34) A. Frigerio, G. Belvedere, F. DeNadai, R. Fanelli, C. Pantarotto, E. Riva, and P. L. Mosselli, *J. Chromatogr.*, **74**, 201 (1972).
(35) T. E. Gaffney, C.-G. Hammar, B. Holmstedt, and R. E. McMahon, *Anal. Chem.*, **43**, 307 (1971).
(36) C.-G. Hammar, B. Alexanderson, B. Holmstedt, and F. Sjöqvist, *Clin. Pharmacol. Ther.*, **12**, 496 (1971).
(37) D. R. Knapp, T. E. Gaffney, and R. E. McMahon, *Biochem. Pharmacol.*, **21**, 425 (1972).
(38) D. R. Knapp, T. E. Gaffney, R. E. McMahon, and G. Kiplinger, *J. Pharmacol. Exp. Ther.*, **180**, 784 (1972).
(39) P. A. Taylor and L. P. Egan, *Finnigan Spectra*, **4** (1974).
(40) R. L. Foltz, P. A. Clark, D. A. Knowlton, and J. R. Hoyland, Center for Studies of Narcotic and Drug Abuse, National Institute of Drug Abuse, Columbus, Ohio, 1974.
(41) R. Ryhage, *Anal. Chem.*, **36**, 759 (1964).
(42) C.-G. Hammar, B. Holmstedt, and R. Ryhage, *Anal. Biochem.*, **25**, 532 (1968).
(43) L. Palmer and B. Holmstedt, *Sci. Tools*, **2**, 25 (1975).
(44) C. C. Sweeley, W. H. Elliott, I. Fries, and R. Ryhage, *Anal. Chem.*, **38**, 1549 (1966).
(45) E. C. Horning, M. G. Horning, D. I. Carroll, I. Dzidic, and R. N. Stilwell, *ibid.*, **45**, 936 (1973).
(46) M. Claeys, G. Muscettola, and S. Markey, *Biomed. Mass Spectrom.*, **3**, 110 (1976).
(47) T. Walle, H. Ehrsson, C. Bogentoft, and J. Dolby, *Acta Pharm. Suec.*, **9**, 509 (1972).
(48) M. S. B. Munson and F. H. Field, *J. Am. Chem. Soc.*, **88**, 2621 (1966).
(49) F. H. Field, *Acc. Chem. Res.*, **1**, 42 (1968).
(50) B. Munson, *Anal. Chem.*, **43**, 28A (1971).
(51) G. P. Arsenault, "Biochemical Applications of Mass Spectrometry," Wiley–Interscience, New York, N.Y., 1972, pp. 817, 832.

ACKNOWLEDGMENTS

Supported in part by General Research Support Grant S01 RR05432 from the National Institutes of Health.

The authors thank Mrs. Patti Peterson for the preparation of the manuscript and Merck Sharp and Dohme, Eli Lilly, Pfizer, and Ciba for providing the pure samples of tricyclic antidepressants.

In Vitro Studies on Drug–Antibiotic Interactions I: Analgesics, Antipyretics, Antimalarials, and Tranquilizers

MOHAMED A. TOAMA *x, HAMED M. EL FATATRY *, and BAHGAT EL FALAHA

Received August 11, 1976, from the *Faculty of Pharmacy, Cairo University, Cairo, Egypt.* Accepted for publication January 25, 1977. * Present address: Faculty of Pharmacy, Riyadh University, Riyadh, Saudi Arabia.

Abstract □ The antimicrobial effects of some analgesics, antipyretics, antimalarials, and tranquilizers were determined. The phenothiazines were the most active group. The effect of the chosen drugs when combined with a selected number of antibiotics was studied on *Staphylococcus aureus* and *Escherichia coli* to determine the type of interaction. Most analgesics, antipyretics, and antimalarials showed either no effect or a synergistic action. However, some exhibited antagonistic effects. All tested tranquilizers were synergistic. Preliminary studies, using electronic absorption spectrometry, indicated that the antagonistic action may be attributed to a physical interaction.

Keyphrases □ Antimicrobial activity—evaluated in various analgesics, antipyretics, antimalarials, and tranquilizers, effect of combination with various antibiotics □ Drug–antibiotic interactions—various analgesics, antipyretics, antimalarials, and tranquilizers, effect of combination with various antibiotics □ Antibiotics, various—effect of combination with various analgesics, antipyretics, antimalarials, and tranquilizers □ Analgesics, various—antimicrobial activity, effect of combination with various antibiotics □ Antipyretics, various—antimicrobial activity, effect of combination with various antibiotics □ Antimalarials, various—antimicrobial activity, effect of combination with various antibiotics □ Tranquilizers, various—antimicrobial activity, effect of combination with various antibiotics

The bioavailability of drugs at their sites of action can be enhanced or reduced by interaction with other drugs. Several studies concerned the biochemical and pharmacological effects of antimicrobial agents when given with other drugs (1, 2). The type of interactions reported involved competition for renal tubular excretion, displacement from carrier sites, increased metabolism by stimulation of hepatic enzymes, decreased protein synthesis, and increased tissue toxicity (3, 4).

Analgesics, antipyretics, antimalarials, and tranquilizers generally are prescribed along with antibiotics for the treatment of infectious diseases. The pharmacological and

(19) O. Borgå and M. Garle, *J. Chromatogr.*, **68**, 77 (1972).
(20) R. A. Braithwaite and J. A. Whatley, *ibid.*, **49**, 303 (1970).
(21) R. A. Braithwaite and B. Widdop, *Clin. Chim. Acta*, **35**, 461 (1971).
(22) M. Ervik, T. Walle, and H. Ehrsson, *Acta Pharm. Suec.*, **7**, 625 (1970).
(23) H. B. Hucker and S. C. Stauffer, *J. Pharm. Sci.*, **63**, 296 (1974).
(24) A. Jørgensen, *Acta Pharmacol. Toxicol.*, **36**, 79 (1975).
(25) S. F. Sisenwine, J. A. Knowles, and H. W. Rulius, *Anal. Lett.*, **2**, 315 (1969).
(26) J. E. Wallace, H. E. Hamilton, L. K. Goggin, and K. Blum, *Anal. Chem.*, **47**, 1516 (1975).
(27) T. Walle and H. Ehrsson, *Acta Pharm. Suec.*, **8**, 27 (1971).
(28) H. J. Weder and M. H. Bickel, *J. Chromatogr.*, **37**, 181 (1968).
(29) M. Åsberg, B. Cronholm, F. Sjöqvist, and D. Tuck, *Br. Med. J.*, **3**, 331 (1971).
(30) J. T. Biggs, W. R. Holland, S. S. Chang, P. P. Hipps, and W. R. Sherman, *J. Pharm. Sci.*, **65**, 261 (1976).
(31) O. Borgå, L. Palmer, A. Linnarsson, and B. Holmstedt, *Anal. Lett.*, **4**, 837 (1971).
(32) A. Frigerio, *Finnigan Spectra*, **5** (1975).
(33) A. Frigerio, K. M. Baker, and P. L. Mosselli, "Mass Spectrometry in Biochemistry and Medicine," Raven, New York, N.Y., 1974, pp. 65, 82.
(34) A. Frigerio, G. Belvedere, F. DeNadai, R. Fanelli, C. Pantarotto, E. Riva, and P. L. Mosselli, *J. Chromatogr.*, **74**, 201 (1972).
(35) T. E. Gaffney, C.-G. Hammar, B. Holmstedt, and R. E. McMahon, *Anal. Chem.*, **43**, 307 (1971).
(36) C.-G. Hammar, B. Alexanderson, B. Holmstedt, and F. Sjöqvist, *Clin. Pharmacol. Ther.*, **12**, 496 (1971).
(37) D. R. Knapp, T. E. Gaffney, and R. E. McMahon, *Biochem. Pharmacol.*, **21**, 425 (1972).
(38) D. R. Knapp, T. E. Gaffney, R. E. McMahon, and G. Kiplinger, *J. Pharmacol. Exp. Ther.*, **180**, 784 (1972).
(39) P. A. Taylor and L. P. Egan, *Finnigan Spectra*, **4** (1974).
(40) R. L. Foltz, P. A. Clark, D. A. Knowlton, and J. R. Hoyland, Center for Studies of Narcotic and Drug Abuse, National Institute of Drug Abuse, Columbus, Ohio, 1974.
(41) R. Ryhage, *Anal. Chem.*, **36**, 759 (1964).
(42) C.-G. Hammar, B. Holmstedt, and R. Ryhage, *Anal. Biochem.*, **25**, 532 (1968).
(43) L. Palmer and B. Holmstedt, *Sci. Tools*, **2**, 25 (1975).
(44) C. C. Sweeley, W. H. Elliott, I. Fries, and R. Ryhage, *Anal. Chem.*, **38**, 1549 (1966).
(45) E. C. Horning, M. G. Horning, D. I. Carroll, I. Dzidic, and R. N. Stilwell, *ibid.*, **45**, 936 (1973).
(46) M. Claeys, G. Muscettola, and S. Markey, *Biomed. Mass Spectrom.*, **3**, 110 (1976).
(47) T. Walle, H. Ehrsson, C. Bogentoft, and J. Dolby, *Acta Pharm. Suec.*, **9**, 509 (1972).
(48) M. S. B. Munson and F. H. Field, *J. Am. Chem. Soc.*, **88**, 2621 (1966).
(49) F. H. Field, *Acc. Chem. Res.*, **1**, 42 (1968).
(50) B. Munson, *Anal. Chem.*, **43**, 28A (1971).
(51) G. P. Arsenault, "Biochemical Applications of Mass Spectrometry," Wiley–Interscience, New York, N.Y., 1972, pp. 817, 832.

ACKNOWLEDGMENTS

Supported in part by General Research Support Grant S01 RR05432 from the National Institutes of Health.

The authors thank Mrs. Patti Peterson for the preparation of the manuscript and Merck Sharp and Dohme, Eli Lilly, Pfizer, and Ciba for providing the pure samples of tricyclic antidepressants.

In Vitro Studies on Drug–Antibiotic Interactions I: Analgesics, Antipyretics, Antimalarials, and Tranquilizers

MOHAMED A. TOAMA *x, HAMED M. EL FATATRY *, and BAHGAT EL FALAHA

Received August 11, 1976, from the *Faculty of Pharmacy, Cairo University, Cairo, Egypt.* Accepted for publication January 25, 1977. * Present address: Faculty of Pharmacy, Riyadh University, Riyadh, Saudi Arabia.

Abstract □ The antimicrobial effects of some analgesics, antipyretics, antimalarials, and tranquilizers were determined. The phenothiazines were the most active group. The effect of the chosen drugs when combined with a selected number of antibiotics was studied on *Staphylococcus aureus* and *Escherichia coli* to determine the type of interaction. Most analgesics, antipyretics, and antimalarials showed either no effect or a synergistic action. However, some exhibited antagonistic effects. All tested tranquilizers were synergistic. Preliminary studies, using electronic absorption spectrometry, indicated that the antagonistic action may be attributed to a physical interaction.

Keyphrases □ Antimicrobial activity—evaluated in various analgesics, antipyretics, antimalarials, and tranquilizers, effect of combination with various antibiotics □ Drug–antibiotic interactions—various analgesics, antipyretics, antimalarials, and tranquilizers, effect of combination with various antibiotics □ Antibiotics, various—effect of combination with various analgesics, antipyretics, antimalarials, and tranquilizers □ Analgesics, various—antimicrobial activity, effect of combination with various antibiotics □ Antipyretics, various—antimicrobial activity, effect of combination with various antibiotics □ Antimalarials, various—antimicrobial activity, effect of combination with various antibiotics □ Tranquilizers, various—antimicrobial activity, effect of combination with various antibiotics

The bioavailability of drugs at their sites of action can be enhanced or reduced by interaction with other drugs. Several studies concerned the biochemical and pharmacological effects of antimicrobial agents when given with other drugs (1, 2). The type of interactions reported involved competition for renal tubular excretion, displacement from carrier sites, increased metabolism by stimulation of hepatic enzymes, decreased protein synthesis, and increased tissue toxicity (3, 4).

Analgesics, antipyretics, antimalarials, and tranquilizers generally are prescribed along with antibiotics for the treatment of infectious diseases. The pharmacological and

Table I—Concentrations of Drugs and Antibiotics in the Different Tubes

Drug	Antibiotic		
	One-Fourth MIC	One-Half MIC	MIC
One-fourth MIC	1	2	3
One-half MIC	4	5	6
MIC	7	8	9

biochemical actions of these drugs as well as their interactions in humans have been studied thoroughly (1–4).

However, few *in vitro* studies on the effects of these drugs and their interaction with antibiotics on microorganisms have been reported. The antimicrobial effect of chlorpromazine, quinine, and quinacrine was the subject of several studies, and these drugs proved to be synergistic with antibiotics by preventing the emergence of resistant microorganisms (5–9). Their mechanisms of action include complexation of the cationic groups of such drugs with the phosphate groups of nucleic acids, alteration or lysis of the cell wall, alteration of cell permeability, inhibition of spore germination, blockade of RNA synthesis, interference with the cytochrome system, and inhibition of oxygen consumption (10–14).

In this investigation, it was of interest to determine the antimicrobial activity of certain drugs, generally prescribed with antibiotics in the treatment of infectious diseases, when tested alone and in combination with antibiotics. The types of interaction are reported.

EXPERIMENTAL

Stock Cultures and Test Organisms[1]—Cultures of *Escherichia coli, Proteus vulgaris, Salmonella typhi, Pseudomonas aeruginosa, Staphylococcus aureus, Streptococcus pyogenes, Bacillus subtilis,* and *Candida albicans* were maintained on slants of dextrose nutrient agar or blood agar and stored at 4°. Subculturing was carried out every 2 weeks.

Determination of Minimum Inhibitory Concentration (MIC) of Drugs and Antibiotics—A stock solution was prepared to contain 4 mg/ml of the drug or 1 mg/ml of antibiotic. Compounds that are insoluble in water were first dissolved in small quantities of either 95% alcohol or 50% dimethyl sulfoxide, and then the solutions were diluted to volume with sterile distilled water or 1% phosphate buffer, pH 6–8 (15).

Twofold serial dilution of the stock solutions were carried out in nutrient broth, except with *Str. pyogenes* where dilution was carried out in brain heart infusion; the diluted solutions were distributed in 5-ml quantities in test tubes. Each tube was inoculated with 0.1 ml of the suspension of the test organism ($1–2 \times 10^6$ cells/ml). The inoculated media were incubated at 37° for 18–24 hr, and the MIC was then recorded. Each experiment was performed in triplicate.

Procedure for Interaction Study—Nine test tubes, each containing 3 ml of dextrose nutrient broth (1.66×), were diluted to 5 ml by adding 1 ml each of the antibiotic and the drug solution. The final concentrations of the drug and the antibiotic in the tubes in terms of the MIC are shown in Table I. For drugs that did not show antimicrobial activity, 100 μg/ml was used instead of the MIC. Each tube was then inoculated with 0.1 ml of the suspension of the test organism and incubated for 18–24 hr. Each experiment was performed in triplicate.

A positive control for growth and a negative control for the MIC of both the drug and the antibiotic were carried out concurrently with each experiment.

The interactions between the drug and the antibiotic were recorded as synergistic (S) when the bacteriostatic action was manifested in tubes 1, 2, and 4 (Table I) and antagonistic (A) when growth was produced in tubes 3 and 5–9.

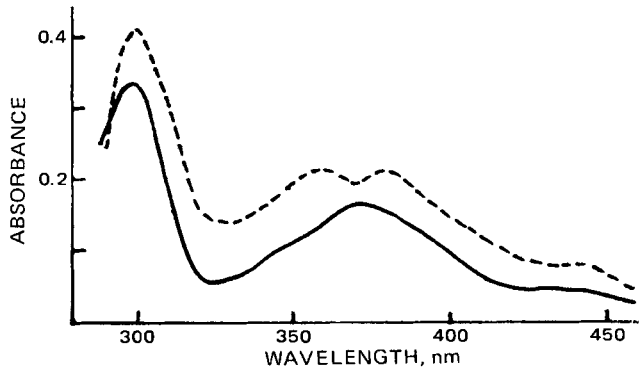

Figure 1—*Electronic absorption spectra of acetanilide–tetracycline hydrochloride aqueous solutions (0.125×10^{-4} M each). Key: ——, experimentally obtained spectrum; and - - -, calculated spectrum.*

Electronic Absorption Spectrometric Studies—For combinations showing an antagonistic effect, preliminary studies were carried out on selected systems using electronic absorption spectrometry. Accordingly, the electronic absorption spectra of the following aqueous solutions at pH 6.8 were determined in the range of 300–600 nm[2]: 1, 0.250×10^{-4} *M* quinine dihydrochloride; 2, 0.250×10^{-4} *M* streptomycin sulfate; 3, 0.125×10^{-4} *M* of both quinine dihydrochloride and streptomycin sulfate; 4, 0.5×10^{-4} *M* chloroquine diphosphate; 5, 0.500×10^{-4} *M* penicillin G sodium; 6, 0.250×10^{-4} *M* of both chloroquine diphosphate and penicillin G sodium; 7, 0.250×10^{-4} *M* acetanilide; 8, 0.250×10^{-4} *M* tetracycline; and 9, 0.125×10^{-4} *M* of both tetracycline hydrochloride and acetanilide.

The data obtained from the spectra of Solutions 1 and 2 were used to calculate the spectrum of Solution 3. The calculated spectrum was compared to the experimentally obtained one. Similarly, the calculated spectra of Solutions 6 and 9 were computed from the data obtained from the spectra of Solutions 4 and 5 and 7 and 8, respectively.

RESULTS AND DISCUSSION

The activities of the tested drugs on the different microorganisms are shown in Table II. The phenothiazines were the most active group; for example, the MIC of trifluoperazine hydrochloride against *Str. pyogenes* was 4.0 μg/ml. The salicylates had low antimicrobial activity (250–1000 μg/ml), and the other analgesics and antimalarials investigated had moderate antimicrobial activity.

The tested Gram-positive microorganisms were generally more responsive than the Gram-negative ones. *Ps. aeruginosa* was the most resistant.

Interaction between Drugs and Antibiotics—Synergism and antagonism between different antimicrobial agents have been studied using various methods (16–18). To study the interactions of the drugs with antibiotics, it was necessary to determine the MIC of the antibiotics against the two strains of *Staph. aureus* and *E. coli.* The types of interactions between the different drugs and antibiotics are shown in Tables III–V.

Aspirin and antipyrine salicylate were synergistic with the antibiotics in Table III except neomycin. With *Staph. aureus,* acetanilide, antipyrine, and dipyrone were antagonistic with tetracycline hydrochloride, nafcillin, and oxacillin, respectively, but no interactions occurred with the other antibiotics.

Quinine dihydrochloride was antagonistic with streptomycins, oxacillin, and nafcillin, while chloroquine diphosphate was antagonistic with penicillin G and penicillin V. However, both showed a synergistic effect with chlortetracycline hydrochloride and demeclocycline hydrochloride. On the other hand, the other antimalarials quinacrine and primaquine were synergistic with most of the tested antibiotics (Table IV).

Most tranquilizers were synergistic with all tested antibiotics (Table V).

[1] Culture collection of the Microbiology Department, Faculty of Pharmacy, Cairo University, Cairo, Egypt.

[2] Pye Unicam SP 8000 recording spectrophotometer and two matched 1-cm fused silica cells.

Table II—MIC of the Analgesics, Antipyretics, Antimalarials, and Tranquilizers against Different Microorganisms

Drug	*E. coli*	*P. vulgaris*	*S. typhi*	*Ps. aeruginosa*	*Staph. aureus*	*Str. pyogenes*	*B. subtilis*	*C. albicans*
Analgesics and antipyretics								
Salicylamide	N[a]	N	N	N	N	N	N	N
Sodium salicylate	N	500	250	N	N	N	1000	N
Aspirin	1000	500	500	1000	500	N	500	N
Sodium gentisate	N	N	N	N	N	N	N	N
Antipyrine salicylate	1000	1000	500	N	500	N	500	N
Acetanilide	N	N	N	N	N	N	N	N
Acetaminophen	N	N	N	N	N	N	N	N
Phenacetin	N	N	N	N	N	N	N	N
Dipyrone	N	N	N	N	N	N	N	N
Antipyrine	N	N	N	N	N	N	N	N
Indomethacin	N	N	N	N	N	N	1000	N
Antimalarials								
Quinine dihydrochloride	N	500	500	1000	N	125	1000	N
Chloroquine diphosphate	N	N	1000	N	N	500	N	N
Primaquine diphosphate	1000	N	25	N	1000	63	1000	1000
Quinacrine	500	N	125	N	1000	16	N	1000
Tranquilizers								
Chlorpromazine hydrochloride	31	16	8	125	125	8	31	31
Promethazine hydrochloride	125	250	125	500	500	31	250	125
Acetophenazine maleate	250	N	250	1000	N	63	250	250
Trifluoperazine dihydrochloride	31	250	125	500	31	4	31	31
Thioridazine hydrochloride	31	63	31	250	63	16	16	31
Triethylperazine dimaleate	63	63	63	250	31	16	31	31
Hydroxyzine hydrochloride	250	500	250	N	500	63	500	1000

[a] N = no effect at 1000 μg of drug/ml.

Table III—Interaction between Aspirin and Antipyrine Salicylate with Antibiotics as Shown by Their Effect on *Staph. aureus* and *E. coli*[a]

Antibiotic	Aspirin		Antipyrine Salicylate	
	Staph. aureus	*E. coli*	*Staph. aureus*	*E. coli*
Kanamycin sulfate	S	S	S	—
Neomycin sulfate	A	A	A	A
Chloramphenicol	—	—	S	—
Oleandomycin phosphate	—	S	—	—
Penicillin G sodium	—	S	S	S
Ampicillin sodium	S	S	—	S
Oxacillin sodium	S	—	S	—
Nafcillin sodium	S	S	—	—
Polymyxin B sulfate	—	S	—	—
Chlortetracycline hydrochloride	S	—	—	—
Novobiocin sodium	—	S	—	S

[a] A = antagonistic; S = synergistic. The dash (—) indicates that the results were found as expected; either *no growth occurred* (the total concentration was equal to MIC or more) or *growth occurred* (the total concentration was less than the MIC).

All synergistic effects (Tables III–V) occurred at one-fourth of the MIC of both the drugs and the antibiotics.

Electronic Absorption Spectrometric Studies—Preliminary studies using electronic absorption spectrometry were done on some combinations that showed antagonistic action, namely quinine–streptomycin, chloroquine–penicillin G sodium, and acetanilide–tetracycline.

With the quinine dihydrochloride–streptomycin sulfate and chloroquine diphosphate–penicillin G sodium combinations, the calculated spectra of their solutions, containing equimolar concentrations, were more or less identical with the experimentally obtained spectra. On the other hand, Fig. 1 shows that the experimentally obtained spectrum of the solution containing 0.250×10^{-4} *M* of both acetanilide and tetracycline hydrochloride was different from the calculated spectrum. This result suggests that, under these experimental conditions, no physical interaction occurs in the first two systems (19). On the contrary, there is some sort of physical interaction between acetanilide and tetracycline.

Further studies on the mechanism of action of drugs showing synergistic and antagonistic effects are in progress. In conclusion, it seems that the indiscriminate administration of drug–antibiotic combinations is questionable and may not be advisable because such *in vitro* interactions may occur *in vivo*.

Table IV—Interaction between Antimalarials with Antibiotics as Shown by Their Effect on *Staph. aureus* and *E. coli*[a]

Antibiotic	Quinine Dihydrochloride		Chloroquine Diphosphate		Primaquine Diphosphate		Quinacrine	
	Staph. aureus	*E. coli*	*Staph. aureus*	*E. coli*	*Staph. aureus*	*E. coli*	*Staph. aureus*	*E. coli*
Dihydrostreptomycin sulfate	A	A	—	—	S	S	S	S
Streptomycin sulfate	A	A	—	—	S	S	S	S
Kanamycin sulfate	—	—	—	—	—	S	—	S
Neomycin sulfate	—	—	—	—	S	S	S	S
Chloramphenicol	—	—	—	—	S	S	S	S
Erythromycin	—	—	—	—	S	S	S	S
Oleandomycin phosphate	—	S	—	S	S	S	S	S
Penicillin G sodium	—	—	A	—	S	S	S	S
Penicillin V potassium	—	—	A	—	S	S	S	S
Ampicillin sodium	—	—	—	—	S	S	S	S
Oxacillin sodium	A	—	—	—	S	S	S	S
Nafcillin sodium	A	—	—	—	S	S	S	S
Gramicidin	—	—	—	—	S	S	S	S
Polymyxin B sulfate	—	—	—	—	S	S	S	S
Tetracycline hydrochloride	—	—	—	—	S	—	S	S
Oxytetracycline hydrochloride	—	—	—	—	S	S	S	S
Chlortetracycline hydrochloride	S	S	S	S	S	S	S	S
Demeclocycline hydrochloride	S	S	S	S	S	S	S	S
Methacycline hydrochloride	—	—	—	S	S	S	S	S
Novobiocin sodium	—	—	—	—	S	S	S	S
Vancomycin hydrochloride	—	—	—	—	S	S	S	S

[a] See Table III.

Table V—Interaction between Tranquilizers with Antibiotics as Shown by Their Effect on *Staph. aureus* and *E. coli*[a]

Antibiotic	Chlorpromazine Hydrochloride		Promethazine Hydrochloride		Acetophenazine Maleate		Trifluoperazine Dihydrochloride		Thioridazine Hydrochloride		Triethylperazine Dimaleate		Hydroxyzine Hydrochloride	
	Staph. aureus	*E. coli*	*Staph. aureus*	*E. coli*	*Staph. aureus*	*E. coli*	*Staph. aureus*	*E. coli*	*Staph. aureus*	*E. coli*	*Staph. aureus*	*E. coli*	*Staph. aureus*	*E. coli*
Dihydrostreptomycin sulfate	S	—	—	—	—	—	S	—	—	—	—	—	—	—
Streptomycin sulfate	S	—	S	—	—	—	S	—	—	—	—	—	—	—
Kanamycin sulfate	S	S	S	—	—	—	—	S	S	—	S	S	—	—
Neomycin sulfate	S	S	S	S	—	—	S	—	S	—	S	—	S	—
Chloramphenicol	S	S	S	—	—	—	S	—	S	—	S	S	S	—
Erythromycin	S	S	S	S	S	—	S	S	S	—	S	S	—	—
Oleandomycin phosphate	S	S	S	S	S	S	S	—	S	—	S	S	S	—
Penicillin G sodium	S	S	S	S	—	S	—	—	S	—	S	—	S	—
Penicillin V potassium	S	S	S	S	—	S	S	—	S	S	S	—	S	S
Ampicillin sodium	S	S	S	S	—	S	S	—	—	S	S	S	—	S
Oxacillin sodium	S	S	S	S	—	S	S	—	S	S	S	—	—	S
Nafcillin sodium	—	S	—	S	—	S	—	S	—	S	—	S	—	—
Gramicidin	S	S	S	S	—	S	S	S	S	S	S	—	—	—
Polymyxin B sulfate	—	S	—	S	—	S	—	S	—	S	—	S	—	S
Tetracycline hydrochloride	S	S	S	—	—	S	—	S	S	S	—	S	—	S
Oxytetracycline hydrochloride	S	—	S	S	—	—	—	—	S	—	—	—	S	—
Chlortetracycline hydrochloride	S	S	S	S	—	—	—	S	S	—	—	S	—	S
Demeclocycline hydrochloride	S	S	S	S	—	S	—	S	S	S	—	S	—	S
Methacycline hydrochloride	S	S	S	—	—	S	—	S	S	—	—	S	S	S
Novobiocin sodium	S	S	S	S	—	S	—	S	S	S	—	S	—	S
Vancomycin hydrochloride	S	—	S	S	—	S	S	—	S	—	S	—	S	S

[a] See Table III.

REFERENCES

(1) S. A. Kabins, *J. Am. Med. Assoc.*, **219**, 206 (1972).
(2) L. F. Prescott, *Lancet*, **2**, 1239 (1969).
(3) I. H. Stockley, *Pharm. J.*, **206**, 377 (1971).
(4) *Ibid.*, **210**, 36 (1973).
(5) J. L. Bourdon, *Ann. Inst. Pasteur*, **101**, 878 (1961).
(6) S. F. DeCourcy and M. G. Sevag, *Nature*, **209**, 373 (1966).
(7) C. S. Heller and M. G. Sevag, *Appl. Microbiol.*, **14**, 879 (1966).
(8) A. J. Richard and E. R. Garrett, *J. Pharm. Sci.*, **63**, 894 (1974).
(9) M. G. Sevag, *Arch. Biochem. Biophys.*, **108**, 85 (1964).
(10) M. J. Allen, *Electrochim. Acta*, **11**, 1 (1966).
(11) P. Hele, *Biochim. Biophys. Acta*, **76**, 647 (1963).
(12) P. Klubes, P. J. Fay, and I. Cerna, *Biochem. Pharmacol.*, **20**, 265 (1971).
(13) L. Lilov, D. Zahn, and G. Ignatov, *Acta Biol. Med.*, **15**, 365 (1965).
(14) H. A. Nathan, *Nature*, **192**, 471 (1961).
(15) F. Kavanagh, "Analytical Microbiology," Academic, New York, N.Y., 1963.
(16) P. J. Hymas, M. S. Simberkoff, and J. J. Rahal, *Antimicrob. Agents Chemother.*, **5**, 571 (1974).
(17) R. M. E. Richards and R. J. McBride, *J. Pharm. Sci.*, **63**, 54 (1974).
(18) M. Sonne and E. Jawetz, *Appl. Microbiol.*, **17**, 893 (1969).
(19) F. J. G. Rossotti and H. Rossotti, "The Determination of Stability Constants," McGraw-Hill, New York, N.Y., 1961.

ACKNOWLEDGMENTS

The drugs used in this study were supplied by El-Nasr Pharmaceutical Co., Egypt; Swiss-Pharma, Egypt; B.D.H., England; May and Baker, England; Bristol Laboratories, England; Merck Sharp and Dohme; Schering Corp.; Lederle; Pfizer Inc.; Upjohn Co.; and Eli Lilly & Co.

The authors thank Dr. Hassan Y. Aboul-Enein, Faculty of Pharmacy, Riyadh University, for proofreading the manuscript.

Stability of Tetrahydrocannabinols II

EDWARD R. GARRETT ˣ, ALAIN J. GOUYETTE, and HENDRIK ROSEBOOM *

Received September 27, 1976, from *The Beehive, College of Pharmacy, University of Florida, Gainesville, FL 32610.* Accepted for publication March 29, 1977. * Present address: School of Pharmacy, University of Utrecht, Utrecht, The Netherlands.

Abstract □ The biphasic degradation of Δ^9-tetrahydrocannabinol (I), as monitored by flame-ionization GLC, produced Δ^8-tetrahydrocannabinol (II), cannabidiol (X), 9-hydroxyhexahydrocannabinol (IV), 9,10-dihydro-9-hydroxyisocannabidiol (VI), and 6,12-dihydro-6-hydroxycannabidiol (VIII) in acidic solutions. Further identification was made by GLC, mass spectrometry, and comparison with authentic samples. Only II and IV were produced above pH 4 in the neutral region by first-order kinetics. The acidic degradation of cannabidiol (X) gave I and the products of the acidic degradation of I. The initial phase of acidic I degradation was assigned to the development of solvolytic equilibria among I, VIII, X, and, possibly, isocannabidiol (IX), with the concomitant production of II and IV. Compounds VIII, IX, and X did not appear in the neutral region since ether cleavage occurred only in strong mineral acids. Hydration of the Δ^9-double bond resulted only in acid-catalyzed equilibria of cleaved ethers with the Δ^8-configurations and characterized the second phase of acid degradation of I. Cannabinol and hexahydrocannabinol were found together in several cases due to the disproportionation of I as catalyzed by silicic acid, silica gel, and chloroform.

Keyphrases □ Δ^9-Tetrahydrocannabinol—kinetics of biphasic degradation in acidic solution □ Degradation—Δ^9-tetrahydrocannabinol in acidic solution, kinetics □ Cannabinoids—Δ^9-tetrahydrocannabinol, kinetics of biphasic degradation in acidic solution

Previous studies (1) on the stability of Δ^9-tetrahydrocannabinol (I) in acidic media below pH 4, monitored by GLC, demonstrated an apparent biphasic semilogarithmic plot of undegraded I against time. Two alternative rationalizations were possible. Either an intermediate was formed that had the same retention time as I and gave rise to the observed products, or there was a relatively rapid equilibration of I with other compound(s) and slower, further, irreversible degradation of one or all of these compounds. Both explanations were consistent with transformations (Scheme I) of I, by hydrogen-ion-catalyzed double bond migration to Δ^8-tetrahydrocannabinol (II) and by hydrogen-ion-catalyzed hydrolysis of the ether linkage, with possible dehydration and acid-catalyzed hydration of the isolated Δ^9-double bond.

The products observed on GLC and identified (1) were

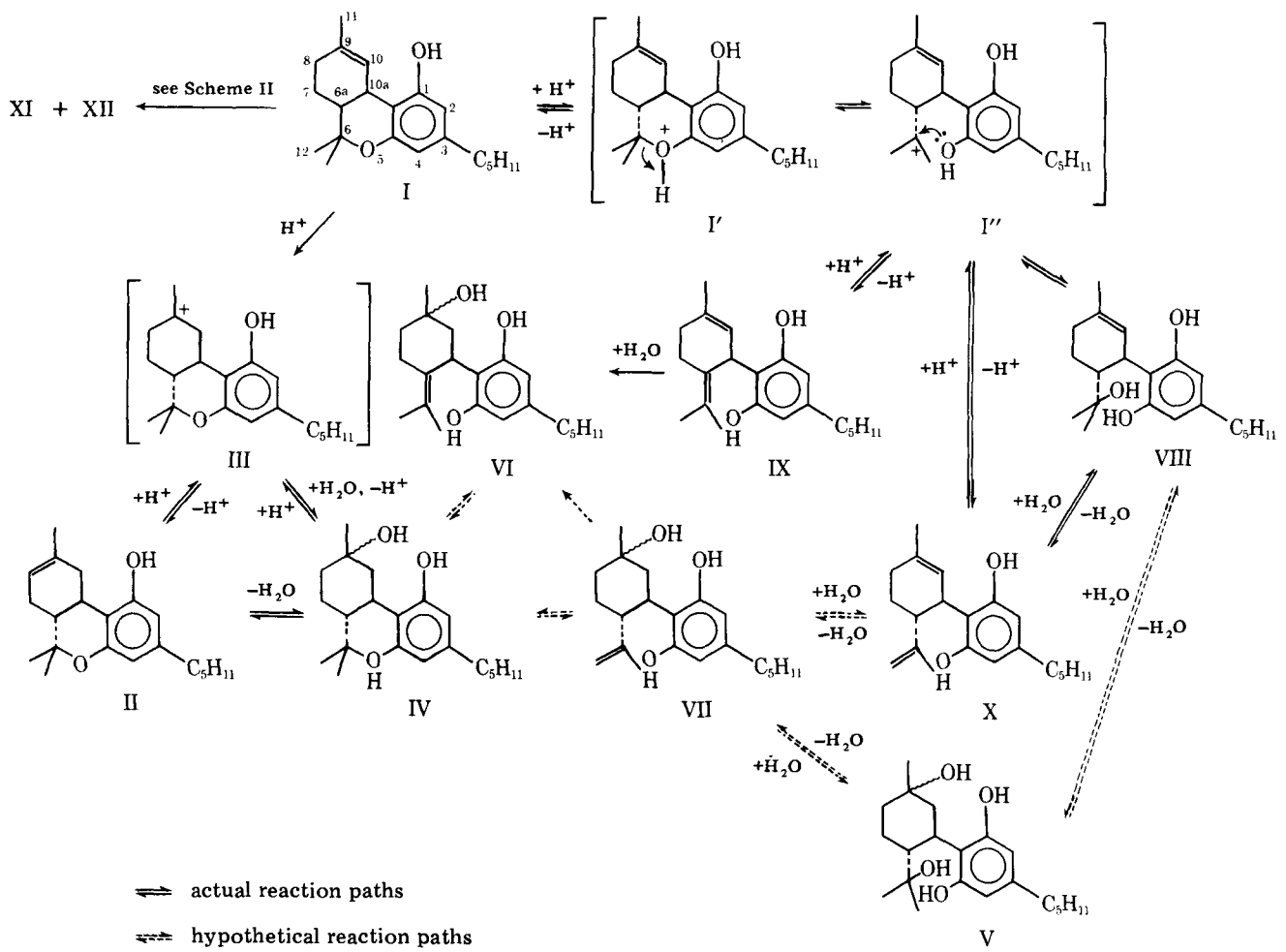

Scheme I

II, 9,10-dihydro-9-hydroxyisocannabidiol (VI), 9-hydroxyhexahydrocannabinol (IV), and cannabinol (XII). Compounds I, II, IV, and VI, on acid degradation, gave final similar ratios of II:IV:VI under the same acidic conditions to indicate the final equilibria among them. The fact that XII resulted from I under anaerobic conditions was anomalous and difficult to explain.

These studies were conducted to rationalize the apparent biphasic nature of I degradation in acid and the anomalous appearance of XII. The purpose was also to identify other products in the acidic and nonacidic degradations. New high-pressure liquid chromatographic (HPLC) techniques for cannabinoid separation and purification were developed, GLC methods were modified, and additional kinetic studies were conducted.

EXPERIMENTAL

Materials—*trans*-Δ^9-Tetrahydrocannabinol[1] (I), *trans*-cannabidiol[2] (X), and cannabinol[3] (XII) were used only after TLC[4] or HPLC[5] purification. The various degradation products were isolated and purified (TLC or HPLC). The internal standards for the GLC studies were tetraphenylethylene[6] and 4-androsten-3,17-dione[7]. The solvents werechromatographic grade *n*-heptane fraction[8] (bp 95–99°), ether[8], and chloroform[8] or UV grade *n*-hexane[8] and tetrahydrofuran[8]; all were distilled in glass.

Isoamyl alcohol was analytical reagent grade[9], as were the other chemicals (mono- and dibasic sodium phosphates[10]). Hydrochloric acid was made from concentrates in plastic ampuls[11] and extracted with chloroform prior to use to remove the plasticizers (phthalate diesters revealed by mass spectrometry) or was taken from a glass bottle[10]. Pure absolute ethanol[12] was used. The double-distilled water was stored in glass containers or purified by means of HPLC[13]. All degradations were conducted in a dark hood.

HPLC Methods for Purification of I and X and Separation of Products on Acid Degradation—HPLC techniques were developed that improved on the previously described (1, 2) TLC purification techniques for cannabinoids. A flow rate of 0.5 ml/min of tetrahydrofuran–*n*-hexane (5:95) quantitatively separated I and II, with respective retention volumes on a 4-mm i.d. × 30-cm column[14] of 6.62 and 6.37 ml. In the same system, cannabidiol had a retention volume of 6.06 ml. The same column with a 3:7 ratio of solvents separated XII, I, and II at 4.5 ml from the products of acid degradation, VI and IV, with respective retention volumes of 8.5 and 11 ml. The collection fraction of the tetrahydrocannabinol could then be evaporated under nitrogen at 60° and separated and purified on HPLC with the 5:95 solvent ratio.

The stock solution of X originally analyzed by GLC[15] (column length of 1.8 m, 3% OV-17 on 100–120-mesh Gas Chrom Q, 240°) showed the following composition by percent areas[16] under a specific peak to the total area (compound, retention time in minutes, and percent area): unknown, 2.25, and 0.39%; unknown, 2.96, and 0.13%; unknown, 3.12, and 0.14%; X with traces of hexahydrocannabinol (XI), 3.85, and 86.4%; I, 5.28, and 12.28%; and XII, 6.70, and 0.65%. Two milliliters of this stock solution was evaporated to dryness and reconstituted in 0.5 ml of the HPLC solvent, 5% tetrahydrofuran in *n*-hexane, which was used to purify X on two columns[14] in series. The retention volumes in this system were 13.3, 14.0, and 14.6 ml for X, II, and I, respectively. GLC analysis of the X fractions showed greater than 99.5% purity with less than 0.3% contamination by I and negligible other peaks.

Table I—Comparison of Retention Times of a Mixture of HPLC-Purified Cannabinoids and Products of Acid Degradation on Different Columns

Compound	OV-225 Retention Time, min	OV-225 Retention Time Relative to IV	OV-17 Retention Time, min	OV-17 Retention Time Relative to IV
II	4.93	0.38	4.65	0.58
I	5.53	0.41	5.19	0.64
XII	8.45	0.64	6.43	0.80
VI	10.62	0.81	7.35	0.91
IV	13.14	1.00	8.07	1.00

GLC Procedures—Cannabinoid separation on GLC has been largely performed on a 3% OV-17 column (2, 3), although 3% OV-225 on 100–120-mesh Gas Chrom Q also was used (1, 4). The efficiencies of separation of the two columns were compared for a mixture of the HPLC-purified products of the acid degradation of I by flame-ionization detection under the following conditions: column length, 1.8 m; column temperature, 235°; detector and injector temperature, 260°; hydrogen flow, 30 ml/min; air flow, 300 ml/min; and helium flow, 35 ml/min. The retention times for both columns are given in Table I and clearly show the superiority of OV-225 in peak separation of these particular compounds. However, OV-17 columns do have the greater thermal stability, and their use is favored for repetitive studies at 235°.

Determination when Products of Acid Degradation Had Same Retention Time as I on GLC—An aqueous solution of I (1 mg/liter of 0.1 *N* HCl) was purged with nitrogen, reacted at 60° for 1 hr, and adjusted to pH 6 with 0.5 *M* phosphate buffer. Three 500-ml chloroform extracts were combined, evaporated to dryness at 50° under nitrogen, and reconstituted in 1 ml of chloroform. Half (500 μl) was streaked on TLC sheets and developed with cyclohexane–acetone (10:1) for 15 cm. The dried sheet was cut into 15 × 1-cm strips, and each was eluted with absolute ethanol. The dried eluates from each zone were reconstituted in chloroform and gas chromatographed (OV-17). Aliquots of the other half of the reconstituted chloroform extracts were taken to dryness and treated as discussed under HPLC methods. All fractions, including those that gave no UV signals, were gas chromatographed.

The TLC and HPLC fractions of the acid degradations corresponding to those from pure I were silylated (5) with bis(trimethylsilyl)trifluoroacetamide with 1% trimethylchlorosilane in pyridine[17] and gas chromatographed (3% OV-17).

Similar studies were conducted with the other HPLC- and TLC-separated products. The known degradation products, their retention times at 235°, and the retention times of their silylated derivatives at 220° in minutes were, respectively: II, 4.21 and 3.56; I, 4.64 and 3.93; XII, 5.90 and 4.82; VI, 6.49 and 5.54; and IV, 7.3 and 5.9. The peak areas of the nonsilylated compounds and the relative peak area ratios of nonsilylated compound to the silylated derivative were, respectively: II, 72,330 and 0.77; I, 171,456 and 0.79; XII, 10,448 and 0.42; VI, 115,228 and 0.57; and IV, 102,833 and 0.59.

Investigation of Degradation Intermediates in Equilibrium with I in Acid Degradation—Similar studies were conducted with ^{14}C-I. The material was degraded at 60° in 0.1 *N* HCl. The reaction was inhibited at timed intervals by adding 5 ml of a 0.5 *M* Na_2HPO_4–NaH_2PO_4 (1:1) buffer to 20-ml aliquots, which were then extracted with chloroform. The extracts were dried under nitrogen at 60°, and the reconstituted residues in 100 μl of chloroform were thin layered on sheets (previously activated at 100° for 2 hr) with cyclohexane–acetone (9:1).

The sheets were dried and then scanned with a radiochromatogram scanner[18], and the area of each peak was recorded as a percentage of the total for the aliquots taken at different times. The total radioactivity in an aliquot of the extract was also counted[19] and was the same for each sample taken with time; this finding implies equal extraction efficiency for the degradation products as for the parent compound. No detectable activity was observed in the aqueous sample after chloroform extraction. The extraction efficiency of radiolabeled material with the chloroform was determined to be 98%. Three pronounced peaks were found on the TLC sheets at R_f 0.07, 0.40, and 0.67. Elution of the first peak (R_f 0.07) with ethanol gave counts that increased with time over 240 min and contained IV and VI by GLC. The second peak (R_f 0.40) gave counts that

[1] Lot SSC 79124, National Institute of Mental Health, Bethesda, MD 20014.
[2] Lot NMH-IV-65C.
[3] Lot SSC 61565, National Institute of Mental Health, Bethesda, MD 20014.
[4] Eastman Chromatogram Sheet 6060, Eastman Kodak Co., Rochester, NY 14650.
[5] Model 440 liquid chromatograph (absorbance UV detector at 254 nm), Waters Associates, Milford, MA 01757.
[6] Aldrich Chemical Co., Milwaukee, WI 53233.
[7] Batch 10751, Applied Science Laboratories, State College, PA 16801.
[8] Burdick and Jackson Laboratories, Muskegon, MI 49442.
[9] Reagent ACS, Matheson, Coleman and Bell, Norwood, OH 45212.
[10] Fisher Scientific Co., Fair Lawn, NJ 07410.
[11] Dilut-it, J. T. Baker Chemical Co., Phillipsburg, NJ 08865.
[12] U.S. Industrial Chemicals Co., New York, NY 10016.
[13] Bondapak C_{18} column.
[14] μPorasil.
[15] Varian Aerograph 2400, Walnut Creek, CA 94598.
[16] HP 3380 A integrator, Hewlett-Packard, Palo Alto, CA 94303.
[17] Pierce Chemical Co., Rockford, IL 61105.
[18] Model 7201 C, Packard Instrument Co., Downers Grove, IL 60515.
[19] Beckman liquid scintillation, Beckman Instruments, Fullerton, CA 92634.

decreased with time over 240 min and contained XII, I, and II. The R_f 0.67 peak was not detectable under UV light on the plate and gave no significant GLC peaks on elution. Its radioactive content was reasonably constant over the studied time interval. The original solution showed material at the same R_f value, so this R_f may be assigned to a nondegradable impurity.

Studies to Seek Other Degradation Products of I—One liter of 20% ethanolic 0.1 *N* HCl, preextracted with chloroform, was purged with nitrogen and preequilibrated at 61°; 15 mg of purified I in 1.5 ml of ethanol was added. After 30 min at 60°, the solution was extracted with 3 × 500 ml of ether, and the ether extract was washed with 3 × 250 ml of water to remove any acid. The extract was taken to dryness at room temperature under nitrogen and reconstituted in 0.5 ml of ethanol. Aliquots were injected into the gas chromatograph. Room temperature instead of 50° was preferred since less cannabinol was formed.

Studies to Determine If X Solutions Gave Rise to I—HPLC purified X (20 μg) (chromatographic purity greater than 99.5%) was reacted in 20 ml of 0.1 *N* HCl and in 0.05 *M* phosphate buffers at pH 5.72, 7.03, and 9.12 for 3.3 hr at 60°. The solution was then adjusted to pH 5.5. A 20-ml ether extract, washed with 20 ml of distilled water, was taken to dryness under nitrogen at room temperature and reconstituted in 0.5 ml of ethanol. Aliquots were analyzed by GLC.

Production of XII in Acid Degradation of I—Purified (HPLC or TLC) I (50 μg) was degraded in 50 ml of nitrogen-purged 0.1 *N* HCl, preequilibrated at 60.0°, and then maintained for 30 min. The reaction was halted by adjustment to pH 5.5 with phosphate buffer, and the mixture was extracted with 3 × 10 ml of chloroform. The internal standard (4-androsten-3,17-dione solution) was added to the extract, which was evaporated to dryness and reconstituted in 20–50 μl of chloroform. Then 1 μl was injected on the gas chromatograph equipped with the OV-17 column, and the areas were determined under all peaks.

The reactions were made under different conditions and with differently treated reactants including: (*a*) distilled water cleaned on HPLC[13], (*b*) distilled water preextracted with chloroform, (*c*) concentrated hydrochloric acid[10], (*d*) hydrochloric acid concentrate[11], (*e*) TLC purified I, (*f*) HPLC-purified I, (*g*) unsilylated glassware, (*h*) glassware coated with a water-soluble silicone concentration[20], and (*i*) glassware presilylated with a trimethylsilyl compound[21]. Blank solutions without material were studied in the same manner.

Kinetic Studies on Degradation of I—Aliquots of HPLC-purified I in aqueous hydrochloric acid (1.00 mg/liter) at pH 0.70 and 1.40, preequilibrated and reacted at 60°, were taken with time. Each 20-ml aliquot was neutralized with 5 ml of phosphate buffer and extracted with 3 × 10 ml of dichloromethane[8], which was evaporated to dryness under nitrogen at 50°. The internal standard, 200 μl of a tetraphenylethylene[6] solution (300 μg/ml), was added to the residue, which was reconstituted in 200 μl of chloroform at 0°. Then 1.0 μl was injected.

Studies in the neutral pH region at 5.28, 7.36, and 9.22 were performed by adding 1 mg/liter of HPLC-purified I to the appropriate nitrogen-purged, 60°-preequilibrated, 0.05 *M* phosphate buffer. Aliquots of 20 ml, taken with time, were extracted with 24 ml of *n*-heptane containing 1.5% isoamyl alcohol. The extraction efficiency was the same as chloroform. The organic layer was dried under nitrogen after the addition of the internal standard: 100 μl of a solution of 140 μg of 4-androsten-3,17-dione/ml of chloroform. This internal standard was preferred because there was a greater potential for XI formation and the retention times of the alternative internal standard, tetraphenylethylene (1), were too close to those of XI. The residue was reconstituted in 100 μl of absolute ethanol, and 1.0 μl was injected for GLC analysis (OV-17). At the higher pH values, adequate volumes of 1.0 *N* HCl were added to adjust the pH to 5.5 before extraction.

Kinetic Studies on Degradation of X at pH 1.12—A solution containing 100 ml of 1.0 *N* HCl, 200 ml of absolute ethanol, and 700 ml of distilled water (apparent pH 1.12) was purged with nitrogen and then preequilibrated at 60°. HPLC-purified X (6.35 mg in 1 ml of absolute ethanol) was added. Aliquots (24 ml) were taken with time and delivered in a 50-ml conical centrifuge tube containing 250 μl of the internal standard solution (140 μg of steroid/ml of chloroform) and 6.0 ml of 0.5 *M* Na_2HPO_4–NaH_2PO_4 (1:1) buffer. The cannabinoids were then extracted with 2 × 10 ml of ether[8].

The pH after extraction was in the 5.71–5.74 range. The ether extracts were dried under nitrogen, and the residues were reconstituted in 100 μl of absolute ethanol. Aliquots (1.0 μl) were analyzed by GLC (OV-17) under the following conditions: column temperature, 240°; helium flow rate, 40 ml/min; air flow, 300 ml/min; hydrogen flow, 30 ml/min; injector, 290°; and detector, 300°.

[20] Siliclad, Clay-Adams, Parsippany, NJ 07054.
[21] Regisil, Regis Chemical Co., Morton Grove, IL 60053.

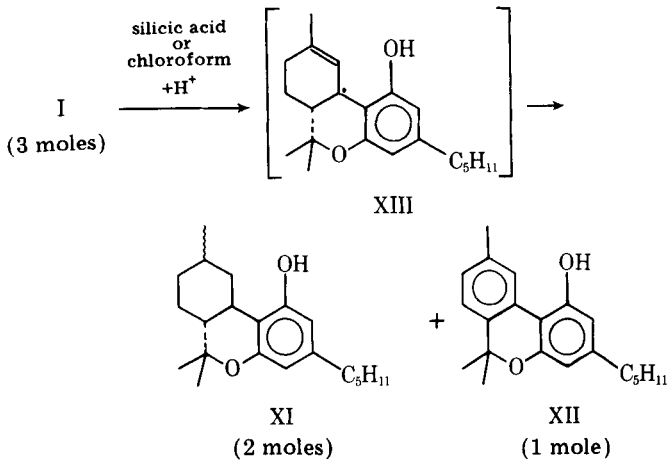

Scheme II

RESULTS AND DISCUSSION

Production of XII in Acid Degradation of I—The formation of XII in nitrogen-purged acidic solutions is difficult to explain in the absence of oxidizing agents. The probable route is a disproportionation of I to XI and XII. GLC analyses of the contents of aqueous solutions (0.1 *N* HCl) of I, reacted at 60° for 30 min under various conditions, not only demonstrated the peaks assignable to I, II, IV, and VI but also significant areas under the peaks assignable to XI (relative retention time with respect to the steroid of 0.36) and XII (relative retention time of 0.63). Both peaks

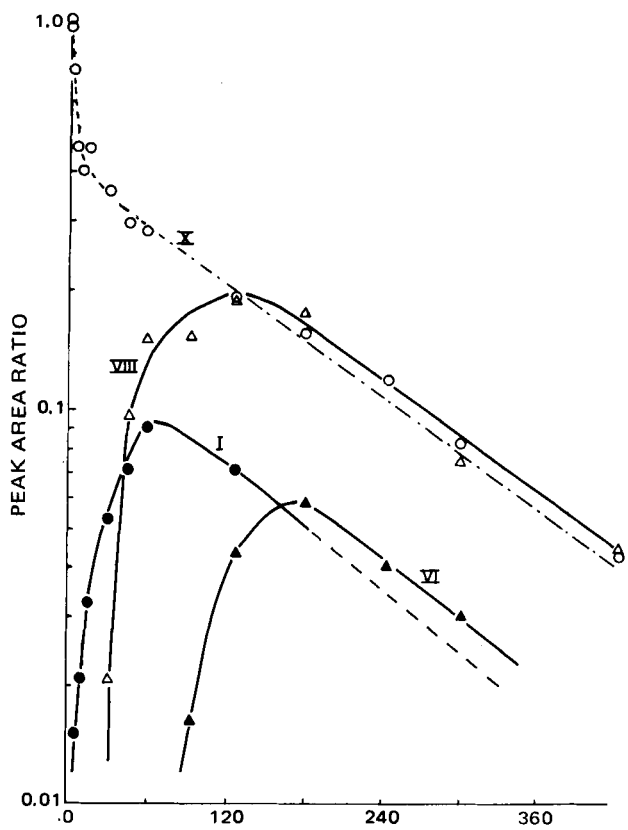

Figure 1—*Semilogarithmic plots against time of the ratios of the area of the GLC peaks for cannabinoids to the peak area of the internal standard 4-androsten-3,17-dione for the degradation of a 20% ethanolic solution (0.1 N HCl) of HPLC-purified X at 60°. The dashed curve for X was based on a nonlinear digital computer fitting.*

Table II—GLC[a] Characterization of Acid Degradation[b] of HPLC-Purified I in 20% Ethanol in 0.1 *N* HCl

Retention Time, min	Percent of Total Area[c]	Compound
4.00	0.66	X
4.90	1.49	II
5.44	81.53	I
6.66	9.62	XII
7.43	2.57	VI
8.34	1.55	IV
9.18	2.16	VIII

[a] Conditions: OV-17 column, 240°; injector, 290°; detector, 300°; helium, 35 ml/min; air, 300 ml/min; and hydrogen, 30 ml/min. [b] In 100 ml of 1.0 *N* HCl, 200 ml of ethanol, and 700 ml of water at 60° for 30 min. [c] The total is not 100% since there are some minor unidentified peaks.

were always present together. Both were absent when degradations occurred in HPLC-purified water with both sources of hydrochloric acid when the glassware was previously silylated. The use of TLC-purified, but not HPLC-purified, I showed both products. Also, when the water used was preextracted with chloroform for both untreated glassware or aqueous silicone-coated glassware, both of these products were present in high evidence.

Thus, it can be concluded that traces of chloroform in the reaction mixture and traces of silicic acid from TLC catalyze the formation of free radicals of I and lead to its disproportionation to XI and XII (Scheme II). Untreated and aqueous silicone-coated glassware also catalyze this reaction. It was shown previously that the latter greatly adsorbed I (3). The radical XIII can be stabilized by the benzene ring and the allylic activation of the C-10 benzylic hydrogen.

The peak for XI was not observed previously (1) since its small amount was obliterated by that of the internal standard (tetraphenylethylene) which, unfortunately, occurred at the same retention time [0.74 of that for I (1)] in the system used.

Determination If Products of Acid Degradation Had Same Retention Time as I—One possible explanation of the biphasic kinetics in acid solution, monitored by the loss of the peak assigned to I, on GLC was that an intermediate degradation product was formed with the same retention time that degraded more slowly. The maximum amount of this intermediate should occur at 60° in 0.1 *N* HCl at about 1 hr (Fig. 1). TLC analysis of the chloroform extracts showed that only the eluted material from TLC with the I R_f value gave a GLC peak at the retention time of I. The eluates of the zones with R_f values corresponding to the known degradation products gave only their respective GLC peaks. The eluates of other zones gave no significant peaks on GLC.

HPLC analysis of the chloroform extract showed no other peaks than those assigned to the known degradation products. The collected fractions, other than those encompassing the retention volume of I, did not show the GLC retention time of this compound. Silylation of fractions eluted from TLC and collected on HPLC from the chloroform extract gave silylated products that only showed one peak on GLC. Specifically, the HPLC collections and the TLC elutions at the retention volume and

Table III—GLC[a] Characterization of Degradation Products from Cannabidiol at Different pH Values[b]

Compound	Retention Time, min	Retention Time Relative to Steroid	Percent of Total Area[c] pH 0.3	pH 1.10	pH 5.72	pH 7.03	pH 9.12
X	3.19	0.36	72.33	81.71	94.71	99.30	97.11
XI	3.23	0.37	—	—	—	—	—
II	3.97	0.45	5.65	—	—	—	—
I	4.34	0.50	10.61	8.87	3.88	0.57	2.71
XII	5.48	0.63	—	1.48	1.19	—	—
VI	6.10	0.70	8.13	1.54	—	—	—
IV	6.95	0.80	0.25	—	—	—	—
Unknown (VII?)	7.27	0.83	0.30	—	—	—	—
VIII	7.68	0.88	2.02	5.16	—	—	—
4-Androsten-3,17-dione	8.73	1.00					

[a] Conditions: OV-17 column, 240°; injector, 290°; detector, 295°; helium, 40 ml/min; hydrogen, 30 ml/min; and air, 300 ml/min. [b] In aqueous hydrochloric acid (pH 0.3 for 20 hr; pH 1.1 for 3 hr) or in 0.05 *M* phosphate buffer for 200 min. [c] The total is not 100% since there are some minor unidentified peaks.

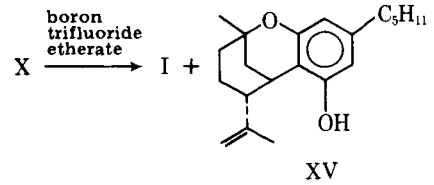

XV

Scheme III

R_f values, respectively, of I gave silylated products that had only the one peak given by silylated pure compound.

Thus, it can be concluded that the hypothesized degradation product could exist only if it had the same retention time on GLC, had the same R_f value on TLC, had the same retention volume on HPLC, and had a silyl ether with the same GLC retention time of the trimethylsilylated I. This is highly improbable.

Existence of Degradation Intermediates in Equilibrium with I on Acid Degradation—The alternative hypothesis to explain the biphasic kinetics in acid media is that I undergoes an initial relatively rapid loss due to its equilibration with other compounds and that the subsequent slower loss of assayed aliquots at its GLC retention time is due to further irreversible transformations. Attempts were made with 1 mg of radiolabeled substance/liter to discover additional spots by radiochromatogram scanning of TLC plates other than those assignable to previously reported compounds (*e.g.*, I, II, IV, VI, and XII). None was observed.

Other Degradation Products of I—Since a possible reason was that the specific activity or the concentration was too low, additional studies of 30 min of degradation in 0.1 *N* HCl with 20% ethanol at 10 mg of I/liter were conducted. The entire reaction mixture was extracted, taken to dryness, and reconstituted in 0.5 ml of ethanol. It was then analyzed on GLC (3% OV-17), and the results are given in Table II. These retention times were the same as for purified authentic materials.

The identification of X [*m/e* (%) 314 (M^+) (21.3), 299 ($M - CH_3\cdot$) (5.6), 271 ($M - C_3H_7\cdot$) (5.4), 258 ($M - C_4H_8\cdot$) (4.6), 246 (19.7), 231 (100), and 193 (7.7)] at a retention time of 4.00 min and of 6,12-dihydro-6-hydroxycannabidiol (VIII) [*m/e* (%) 332 (M^+) (18.5), 314 ($M - H_2O$) (31.5), 299, (14.0), 273 ($M - 59$) (6.5), 271 (16.5), 258 (13.5), 231 (100), 193 (16.0), and 59 ($CH_3C^+(OH)CH_3$) (2.5)] as the trihydroxy derivative of I at 9.18 min was effected by GLC–mass spectrometry[22]. The presence of these two compounds had been predicted (1) as shown in Scheme I.

Thus, the postulated equilibria among I, X, VIII, and possibly isocannabidiol (IX) were confirmed.

Determination If X Solutions Gave Rise to I—These postulated equilibria were challenged by subjecting HPLC-purified X (with a I content less than 0.3%) to degradation and assaying the resultant products by GLC (Table III). The appearance of I and VIII and the appearance of the product VI of I degradation were confirmatory.

The acid-catalyzed cyclization of X to I was first reported by Adams *et al.* (6, 7) and, in the presence of boron trifluoride etherate (8), gave I in 60% yield and isotetrahydrocannabinol (XV) in 13% yield (Scheme III). Compound XV, at the GLC retention time of an authentic sample[23], was not found in the present acidic degradations. This result is consistent with the fact that boiling X with *p*-toluenesulfonic acid in benzene gave II in practically quantitative yield (9, 10). In *trans*-I, the olefinic C-10 hydrogen is very close to the free hydroxyl group (11) and the double bond migration would tend to relieve this nonbonded interaction.

The formation of I from X in the alkaline region can also be expected

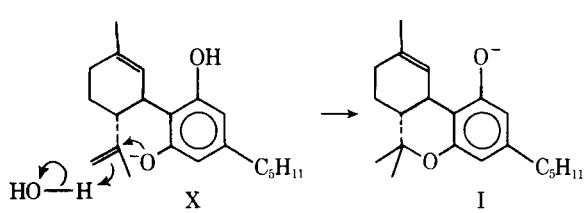

X I

Scheme IV

[22] Varian 2700 gas chromatograph equipped with an OV-17 column (20 psi of helium); column temperature from 55 to 300° (10°/min); and du Pont 21-490F mass spectrometer, E. I. du Pont de Nemours and Co., Instrument Products Division, Monrovia, CA 91016, electron impact mode (70 ev).

[23] Gift of R. Mechoulam, Laboratory of Natural Products, School of Pharmacy, Hebrew University, Jerusalem, Israel.

Table IV—GLC[a] Characterization of Degradation Products from I at Different pH Values[b]

Compound	Retention Time, min	Retention Time Relative to Steroid	Percent of Total Area								
			pH 5.28			pH 7.36			pH 9.22		
			30 sec	6 hr	100 hr	30 sec	6 hr	192 hr	30 sec	6 hr	192 hr
XI	3.24	0.37	0.14	—	—	0.42	0.05	Traces	0.06	0.31	0.25
II	3.95	0.45	0.93	0.95	Traces	0.79	0.89	8.42	0.79	3.73	11.46
I	4.38	0.50	62.48	61.78	43.00	64.18	63.65	13.20	63.56	59.06	5.32
XII	5.52	0.63	Traces	Traces	4.23	3.44	2.36	3.55	1.66	1.86	1.38
VI	6.15	0.70	Traces	Traces	Traces	—	—	—	—	—	—
IV	7.02	0.80	0.56	0.55	—	0.79	0.50	0.02	0.61	0.65	1.15
4-Androsten-3,17-dione	8.77	1.00	35.65	36.62	52.76	30.36	32.53	74.80	33.26	34.36	80.42
Total area of cannabinoids/area of steroid			1.80	1.73	0.89	2.29	2.07	0.34	2.00	1.91	0.24

[a] Conditions: OV-17 column, 240°; injector, 290°; detector, 300°; helium, 40 ml/min; hydrogen, 30 ml/min; and air, 300 ml/min. [b] In 0.05 *M* phosphate buffers for the reported reaction times at 60°.

(Scheme IV), but it would be anticipated that the ether linkage would be affected only by concentrated acids and high temperatures. Negligible products of ether solvolysis (*e.g.*, VI) were observed on neutral degradation of I (Ref. 1 and Table IV) or of X (Table III), which gives rise to I, to confirm this hypothesis.

Degradation of X at pH 1.12—A kinetic study of X degradation in 0.1 *N* HCl with 20% ethanol, using 4-androsten-3,17-dione as an internal standard, showed a biphasic decline on semilogarithmic plotting against time (Fig. 1). Concomitant with the initial decline was the appearance of I, undoubtedly due to acid-catalyzed cyclization. The almost simultaneous appearance of the trihydroxy compound (VIII) could be due to the reversible acid-catalyzed hydration of the exocyclic double bond of X or the acidic cleavage of the ether linkage of I in the equilibrium (Scheme I). The retarded appearance of VI indicates that acid-catalyzed hydration of the endocyclic double bond may preferentially be effected only when the intact ether of I exists. The final equilibria must favor VI, IV, and II, where dehydration of IV favors the Δ^8-configuration (11).

Degradation of I—The kinetics of I degradation in an acidic medium, using an OV-17 column with 4-androsten-3,17-dione as the internal standard and peak area ratios, confirmed the prior studies (1) using peak height ratios.

Previously (1), it had been argued that the peak height ratios of each degradation product would be proportional to the number of molecules observed if each compound had the same retention time as II. On this basis, the final molar ratios of products II, IV, and VI were shown to be invariant under the same acidic conditions for peak height ratios corrected to the same retention time and were independent of which product was studied.

The premise for the peak height correction was that the ratio of the peak heights for equal amounts of I or II at their normal retention time, R_{t_n}, to their peak heights at another retention time, R_{t_i} (obtained by chromatography at other temperatures), gave factors that could be used for correction of product peak heights at their respective R_{t_i} retention times. Multiplication of the peak height of a product by the pertinent factor should give a corrected peak height for that compound that would be proportional to its amount in the gas chromatographed mixture. This premise would be valid if the detector response for each compound were the same, even though a compound of longer retention time but of the same quantity would demonstrate a lower peak height ratio without correction since the peak areas would be the same.

This method to correct peak heights is theoretically correct and reasonably accurate in practice. The relation between peak width, w, and its retention time, R_t, is (12):

$$w = 4R_t/\sqrt{N} \qquad \text{(Eq. 1)}$$

where N is the number of theoretical plates of a column and w is the length of a baseline cut by the two tangents drawn on either side of the peak at the inflection points. The area of the peak is directly related to the amount of the related compound and can be estimated with reasonable accuracy by multiplying this width by half of the height, h, of the peak:

$$\text{area} = \alpha(\text{amount of drug}) = hw/2 = 2hR_t/\sqrt{N} \qquad \text{(Eq. 2)}$$

Thus, the height of the peak against its retention time for the same amount of drug (as measured at different column temperatures) should give the curved line observed previously (Fig. 11 in Ref. 1).

The validity of the method can be checked by plotting the ratio of the area to the peak height for the same substance against the retention time in minutes in accordance with a rearrangement of Eq. 2:

$$\text{area}/h = 2R_t/\sqrt{N} \qquad \text{(Eq. 3)}$$

The linearity of such plots (Fig. 2) with an intercept of zero and the same slope of $2/\sqrt{N}$ for each of the tetrahydrocannabinol degradation products chromatographed at different temperatures confirms this premise and the reliability of the yield estimates given previously (1).

The log k–pH profile at 60° (Fig. 3) shows the results of both previous and present kinetic studies. The first phase of the biphasic acid degradation, characterized by k_1, can now be assigned (Scheme I) in its greater part to the equilibration of I with VIII, X, and, possibly, IX with slower production of IV and II. It appears that subsequent dehydration of IV favors the II configuration because of the previously mentioned steric hindrance between the Δ^9-double bond and the phenolic hydroxyl. The second phase, characterized by k_2 and encountered only in acidic regions, can now be largely assigned to products of ether solvolysis: VIII–X. This reverses the assignments of the hydrolysis in the neutral region given previously (1), which was taken as related to the k_2 phase rather than the k_1 phase in the acidic region.

The degradations of I in the more neutral regions were studied for as long as 192 hr (Table IV). The GLC-observed products had terminal areas (relative to the internal standard) that, in total, did not account for more than 49% (pH 5.28 for 100 hr), 15% (pH 7.36 for 192 hr), and 12% (pH 9.22 for 192 hr) of the original area of I (Table IV).

These results were confirmed with ^{14}C-radiolabeled I. The chloroform extract of I, degraded under the same conditions for the same time, was

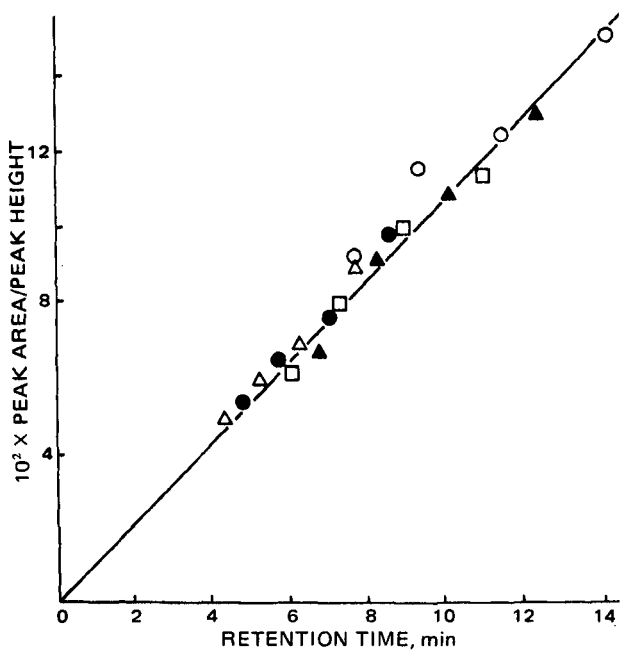

Figure 2—*Plots of the ratios of the peak area to the peak height for different cannabinoids against their respective retention times. The retention times were obtained by varying the column temperatures. Key:* ●, *I;* △, *II;* ○, *IV;* ▲, *VI; and* □, *XII.*

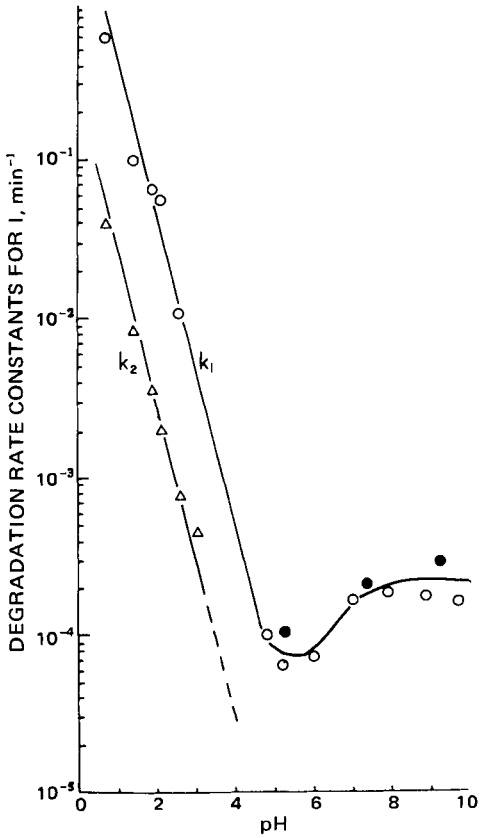

Figure 3—*Log* k–*pH profile for the degradation of I at 60.8°, where the concentration could be expressed as* $C = C_1e^{-k_1t} + C_2e^{-k_2t}$ *as a function of time, t, in minutes. The open symbols are previous data (1) and the closed symbols are additional data. The rate constants for monophasic degradation above pH 4 are taken as related to* k_1 *(see text) in contrast to the previous assignment (1).*

evaporated to dryness and reconstituted in 200 μl of chloroform. The solution was streaked on TLC sheets, developed for 15 cm in cyclohexane–acetone (9:1), and the sheets were analyzed by radiochromatogram scanner. No additional R_f values were observed other than those for GLC-identified products and a large amount of radioactivity at the origin. This result implies polar or polymeric degradation products that gave no pertinent signals under the GLC conditions, even after treatment of the methanolic extract of the origin with bis(trimethylsilyl)trifluoroacetamide containing 1% trimethylchlorosilane[21].

REFERENCES

(1) E. R. Garrett and J. Tsau, *J. Pharm. Sci.*, **63,** 1563 (1974).
(2) C. E. Turner and K. W. Hadley, *ibid.*, **62,** 251 (1973).
(3) C. E. Turner, K. W. Hadley, J. Henry, and M. L. Mole, *ibid.*, **63,** 1872 (1974).
(4) E. R. Garrett and C. A. Hunt, *ibid.*, **62,** 1211 (1973).
(5) C. E. Turner and K. W. Hadley, *ibid.*, **62,** 1083 (1973).
(6) R. Adams, D. C. Pease, C. K. Cain, B. R. Baker, J. H. Clark, H. Wolff, and R. B. Wearn, *J. Am. Chem. Soc.*, **62,** 2245 (1940).
(7) R. Adams, D. C. Pease, C. K. Cain, and J. H. Clark, *ibid.*, **62,** 2402 (1940).
(8) Y. Gaoni and R. Mechoulam, *ibid.*, **93,** 217 (1971).
(9) R. Adams, C. K. Cain, W. D. McPhee, and R. B. Wearn, *ibid.*, **63,** 2209 (1941).
(10) Y. Gaoni and R. Mechoulam, *Tetrahedron*, **22,** 1481 (1966).
(11) R. Mechoulam, "Marijuana," Academic, New York, N.Y., 1973, chap. I, p. 61.
(12) H. M. McNair and E. J. Bonelli, "Basic Gas Chromatography," Consolidated Printers, Berkeley, Calif., 1969, p. 23.

ACKNOWLEDGMENTS

Supported in part by Grant DA-00743-03 from the National Institute of Mental Health, Bethesda, MD 20014, and in part by the NATO Grant in support of A. J. Gouyette.

The authors are grateful to Dr. Brian D. Andresen (Analytical Toxicology Laboratory) for the GLC–mass spectral studies and to Professor R. Mechoulam (Hebrew University of Jerusalem) for authentic samples of isotetrahydrocannabinols. The technical assistance of Mr. George L. Perry is appreciated.

Direct Spectrophotometric Determination of Thebaine in Arya II Population Capsules of *Papaver bracteatum* Lindl

ROSTAM H. MAGHSSOUDI ˣ and AHMAD B. FAWZI

Received February 9, 1976, from the *Department of Pharmaceutical Chemistry, College of Pharmacy, Tehran University, Tehran, Iran.*
Accepted for publication March 18, 1977.

Abstract □ A simple spectrophotometric determination of thebaine based on the complexation reaction with bromcresol green was developed. The yellow complex was extracted with chloroform over the pH 1.5–4.5 range. The solution of the complex in chloroform showed the maximum absorption at 415 nm and obeyed Beer's law over the concentration range of 4.0–14.0 μg/ml. The molar absorptivity of the complex was 1.9460×10^4. The ratio of thebaine to bromcresol green in the complex was 1:1. The method was applied successfully to the direct determination of thebaine in the Arya II population capsules of *Papaver bracteatum* Lindl. The thebaine content of the dried capsules was 3.14%.

Keyphrases □ Thebaine—spectrophotometric analysis in Arya II population capsules of *Papaver bracteatum* □ *Papaver bracteatum*—Arya II population capsules, spectrophotometric analysis of thebaine □ Spectrophotometry—analysis, thebaine in Arya II population capsules of *Papaver bracteatum* □ Narcotics—thebaine, spectrophotometric analysis in Arya II population capsules of *Papaver bracteatum*

Most methods for the quantitative determination of thebaine (I) were based on chromatographic techniques (1–9). Other procedures include ion-exchange separation (10, 11), IR spectrophotometric determination (12, 13), and nonaqueous titration (14).

Several spectrophotometric methods have been reported (15–23). The UV spectrophotometric method (18) determines thebaine, when present alone, in completely pure solutions. Sulfuric acid methods (19–22) are specific but complicated and with low extinction values. A selective but

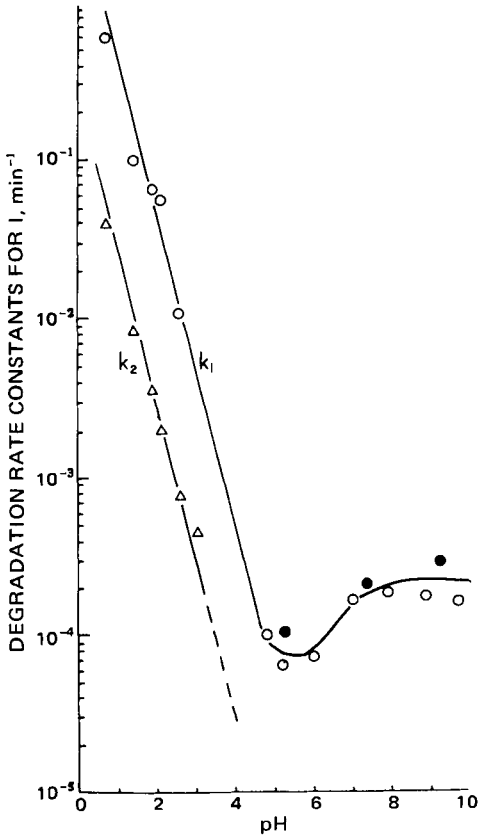

Figure 3—*Log* k–*pH profile for the degradation of I at 60.8°, where the concentration could be expressed as* $C = C_1e^{-k_1t} + C_2e^{-k_2t}$ *as a function of time, t, in minutes. The open symbols are previous data (1) and the closed symbols are additional data. The rate constants for monophasic degradation above pH 4 are taken as related to* k_1 *(see text) in contrast to the previous assignment (1).*

evaporated to dryness and reconstituted in 200 μl of chloroform. The solution was streaked on TLC sheets, developed for 15 cm in cyclohexane–acetone (9:1), and the sheets were analyzed by radiochromatogram scanner. No additional R_f values were observed other than those for GLC-identified products and a large amount of radioactivity at the origin. This result implies polar or polymeric degradation products that gave no pertinent signals under the GLC conditions, even after treatment of the methanolic extract of the origin with bis(trimethylsilyl)trifluoroacetamide containing 1% trimethylchlorosilane[21].

REFERENCES

(1) E. R. Garrett and J. Tsau, *J. Pharm. Sci.*, **63,** 1563 (1974).
(2) C. E. Turner and K. W. Hadley, *ibid.*, **62,** 251 (1973).
(3) C. E. Turner, K. W. Hadley, J. Henry, and M. L. Mole, *ibid.*, **63,** 1872 (1974).
(4) E. R. Garrett and C. A. Hunt, *ibid.*, **62,** 1211 (1973).
(5) C. E. Turner and K. W. Hadley, *ibid.*, **62,** 1083 (1973).
(6) R. Adams, D. C. Pease, C. K. Cain, B. R. Baker, J. H. Clark, H. Wolff, and R. B. Wearn, *J. Am. Chem. Soc.*, **62,** 2245 (1940).
(7) R. Adams, D. C. Pease, C. K. Cain, and J. H. Clark, *ibid.*, **62,** 2402 (1940).
(8) Y. Gaoni and R. Mechoulam, *ibid.*, **93,** 217 (1971).
(9) R. Adams, C. K. Cain, W. D. McPhee, and R. B. Wearn, *ibid.*, **63,** 2209 (1941).
(10) Y. Gaoni and R. Mechoulam, *Tetrahedron*, **22,** 1481 (1966).
(11) R. Mechoulam, "Marijuana," Academic, New York, N.Y., 1973, chap. I, p. 61.
(12) H. M. McNair and E. J. Bonelli, "Basic Gas Chromatography," Consolidated Printers, Berkeley, Calif., 1969, p. 23.

ACKNOWLEDGMENTS

Supported in part by Grant DA-00743-03 from the National Institute of Mental Health, Bethesda, MD 20014, and in part by the NATO Grant in support of A. J. Gouyette.

The authors are grateful to Dr. Brian D. Andresen (Analytical Toxicology Laboratory) for the GLC–mass spectral studies and to Professor R. Mechoulam (Hebrew University of Jerusalem) for authentic samples of isotetrahydrocannabinols. The technical assistance of Mr. George L. Perry is appreciated.

Direct Spectrophotometric Determination of Thebaine in Arya II Population Capsules of *Papaver bracteatum* Lindl

ROSTAM H. MAGHSSOUDI ˣ and AHMAD B. FAWZI

Received February 9, 1976, from the *Department of Pharmaceutical Chemistry, College of Pharmacy, Tehran University, Tehran, Iran.*
Accepted for publication March 18, 1977.

Abstract □ A simple spectrophotometric determination of thebaine based on the complexation reaction with bromcresol green was developed. The yellow complex was extracted with chloroform over the pH 1.5–4.5 range. The solution of the complex in chloroform showed the maximum absorption at 415 nm and obeyed Beer's law over the concentration range of 4.0–14.0 μg/ml. The molar absorptivity of the complex was 1.9460×10^4. The ratio of thebaine to bromcresol green in the complex was 1:1. The method was applied successfully to the direct determination of thebaine in the Arya II population capsules of *Papaver bracteatum* Lindl. The thebaine content of the dried capsules was 3.14%.

Keyphrases □ Thebaine—spectrophotometric analysis in Arya II population capsules of *Papaver bracteatum* □ *Papaver bracteatum*—Arya II population capsules, spectrophotometric analysis of thebaine □ Spectrophotometry—analysis, thebaine in Arya II population capsules of *Papaver bracteatum* □ Narcotics—thebaine, spectrophotometric analysis in Arya II population capsules of *Papaver bracteatum*

Most methods for the quantitative determination of thebaine (I) were based on chromatographic techniques (1–9). Other procedures include ion-exchange separation (10, 11), IR spectrophotometric determination (12, 13), and nonaqueous titration (14).

Several spectrophotometric methods have been reported (15–23). The UV spectrophotometric method (18) determines thebaine, when present alone, in completely pure solutions. Sulfuric acid methods (19–22) are specific but complicated and with low extinction values. A selective but

complicated method for the spectrophotometric determination of I also was reported (23).

In western Iran, a new population, Arya II, of *Papaver bracteatum* Lindl produced a high yield of I (24). The importance of I for the preparation of codeine and other medicinally important alkaloids prompted the use of this population as a natural source for I. Thus, a simple, rapid, and precise quantitative determination of I was needed to evaluate the plant samples.

This paper describes a new sensitive spectrophotometric method for I based on the complexation reaction between I and bromcresol green (II) followed by extraction with chloroform. Previously, II was investigated for the absorptiometric determination of small amounts of long-chain alkylamines and quaternary ammonium salts (25) in aqueous solution in a solvent extraction procedure that has the disadvantage of a blank depending on both the pH and concentration of excess reagent.

Prior separation of the alkaloid fraction, by chromatography or solvent extraction, is necessary for the determination by the reported methods. The present II method determines substances with a tertiary amine group, including thebaine, in aqueous acidic solutions without prior separation.

EXPERIMENTAL[1]

Reagents and Chemicals—All solutions were prepared from reagent grade[2] chemicals. Freshly prepared 10^{-4} *M* I, 10^{-4} *M* II aqueous solution, and pH 3 (BP standard) phthalate buffer were used.

Arya II Capsule Powder—The capsule powder[3] was sifted through a No. 42 sieve, and the remaining woody coarse particles were subjected to a current of air to free the fine powder.

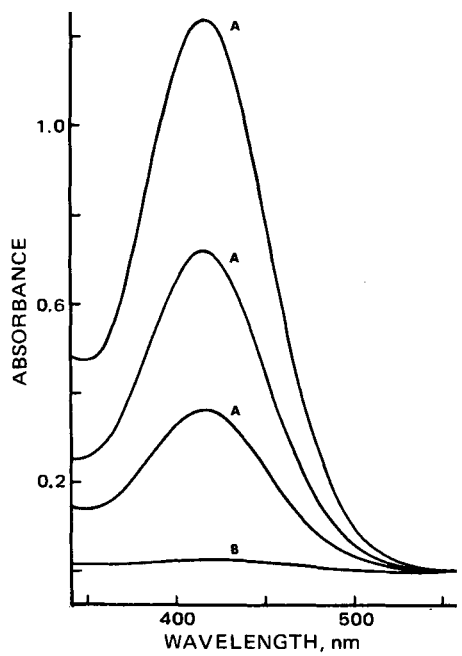

Figure 1—*Absorption spectra of chloroform solutions of various concentrations of I–II complex against the reagent blank (A) and of the reagent blank against chloroform (B).*

[1] A Beckman DB-GT spectrophotometer with 1.00-cm glass or quartz cells and a Beckman H3 type pH meter were used.

[2] Analar.

[3] Obtained from the Laboratory of Organic Chemistry, College of Pharmacy, Tehran University.

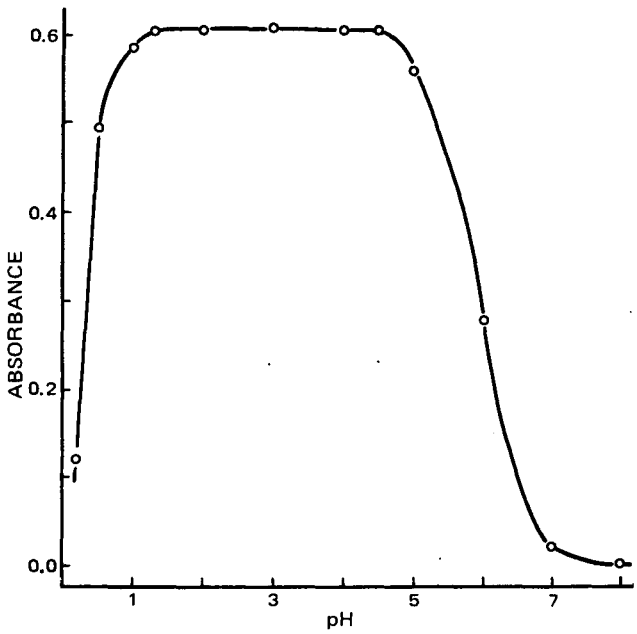

Figure 2—*Effect of pH on the complex formation and extraction. The concentration of I was 3 × 10⁻⁴ M.*

General Procedure—Pipet a sufficient quantity of I solution containing 40–140 μg of I into a 100-ml separator. Add 15 ml of 10^{-4} *M* II followed by a few drops of 0.1 *N* HCl or NaOH to obtain a yellow color. Then add 10 ml of pH 3 buffer and extract the yellow complex by vigorous shaking with 5, 3, and 2 ml of chloroform successively. Combine the extracts into a 10-ml volumetric flask, adjust the volume with chloroform, and measure the absorbance of the solution against a similarly prepared reagent blank at 415 nm.

The total operation requires about 10 min.

Direct Determination of Thebaine in Capsules—Digest accurately about 1.00 g of the Arya II capsule powder (fine powder, unsieved powder, and coarse particles) in 50 ml of 0.1 *N* HCl with intermittent shaking for 20 min. Filter the solution directly into a 250-ml volumetric flask. Repeat the digestion four times with 50 ml of 0.1 *N* HCl and filter immediately. Adjust the volume of the solution with distilled water to 250 ml and determine the I content as described in the general procedure.

Wash the clean glass apparatus with 0.1 *N* HCl followed by distilled water.

The following methods were employed to evaluate the proposed method.

Benzene Extraction Method (24)—The alkaloid was isolated by extraction with benzene and evaporation of the extract to dryness. The residue was dissolved in 0.1 *N* HCl, and the extinction at 285 nm (maximum) was measured using an $E_{1\%}$ (1 cm) value of 250.

In the present investigation, the proposed II method was employed, instead of extinction measurements at 285 nm, for the determination of thebaine content.

Sulfuric Acid Method (22)—The alkaloid was isolated by chloroform extraction and evaporation of the extract to dryness. The thebaine content of the residue was determined by using the color reaction with 29 *N* H_2SO_4.

RESULTS AND DISCUSSION

The yellow I–II complex solution in chloroform gave maximum absorption at 415 nm (Fig. 1). Complex formation and extraction were complete and quantitative between pH 1.5 and 4.5 (Fig. 2). The absorbance of the complex in chloroform was measured at selected times up to 1 week and was constant.

Composition of Complex—The composition of the complex was ascertained by the following methods.

Continuous Variation Method (26, 27)—The method was applied for the total constant concentration of the mixtures, [I + II], first at 10×10^{-4} *M* and then at 6×10^{-4} *M*; the complex was determined as described in the general procedure. Figure 3 shows that a maximum occurs at a 0.5 mole fraction of I, indicating thereby the formation of a 1:1 complex.

Mole Ratio Method—The method of Yoe and Jones (28) was applied

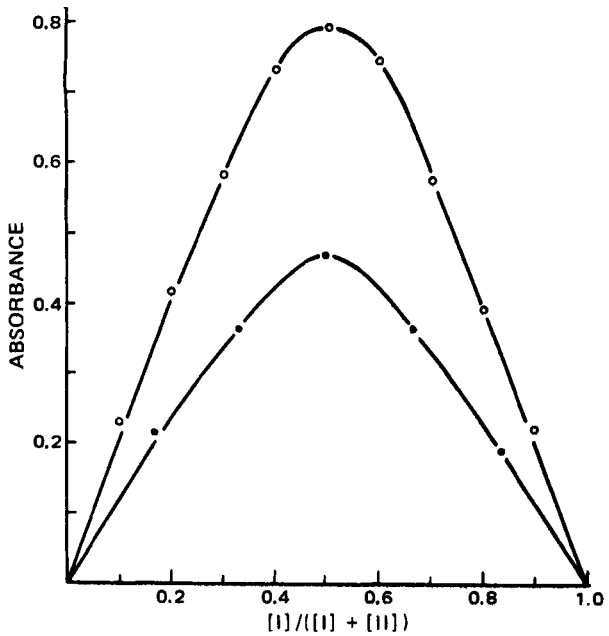

Figure 3—*Job's plot for the I–II system. Key (total concentration of I and II):* ○, *10 × 10⁻⁴ M; and* ●, *6 × 10⁻⁴ M.*

for a standard I solution at a fixed concentration of 4×10^{-4} *M* and different amounts of standard II solution of 10^{-4} *M*. The complex was determined as described. As shown in Fig. 4, the ratio of I to II in the complex was 1:1, but the required ratio for complete complexation and extraction was 1:3.

Beer's Law, Range, and Precision—The optimum concentration range for the measurements, which conforms to Beer's law, at 415 nm and a 1.00-cm optical path was about 4.0–14.0 μg/ml; the molar absorptivity of the complex solution in chloroform was 1.9460×10^4. The relative standard deviation of the calculated absorptivities in the optimum concentration range was 0.9%; at concentrations below 5.0 μg/ml, it was 2.2%.

Compound II Reactions—Acid dyes react with amines or quaternary ammonium salts to form colored compounds (29, 30). Compound II was used for the determination of small amounts of long-chain tertiary alkylamines and quaternary ammonium salts (25).

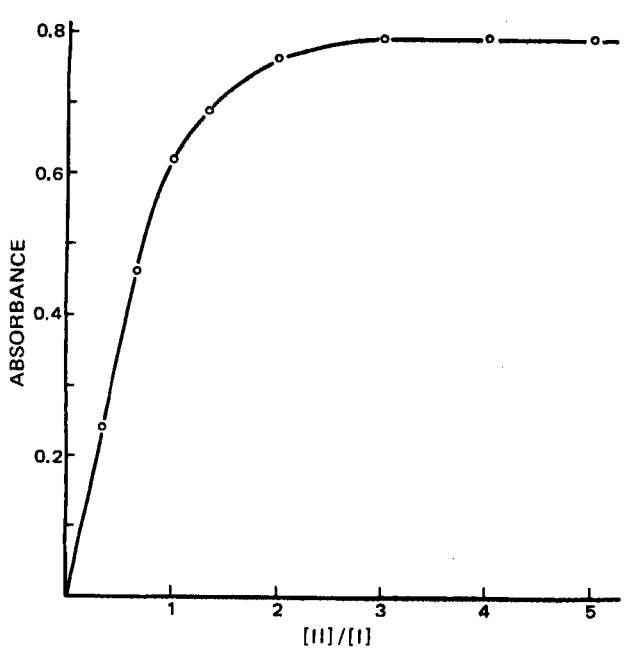

Figure 4—*Mole ratio plot. The final concentration of I was* 4×10^{-4} M.

Table I—Thebaine Content of the Arya II Population Capsules of *P. bracteatum* Lindl

Powder Portion[b]	Direct Determination[a] % Thebaine, Mean $\bar{X}$	Direct Determination[a] *RSD*, %	Indirect Determination[a] % Thebaine, Mean $\bar{X}$	Indirect Determination[a] *RSD*, %
Fine powder	4.17	1.13	3.70	1.43
Unsieved powder	3.14	1.10	2.71	1.29
Coarse particles	1.75	1.14	1.57	1.38

[a] Each determination was repeated six times on each portion. [b] The sample was collected during June 1974.

In an acidic medium, most organic compounds with a tertiary amine group react with II, forming yellow complexes extractable with chloroform. Antihistaminic agents and most alkaloids show selective positive reactions, and the proposed method was found to be suitable for their spectrophotometric determination. Further investigations on the validity of II for the determination of medicinally active substances in pharmaceutical preparations are currently being undertaken and will be the subject of future reports.

Determination of Thebaine Content of Arya II Population Capsules—Since thebaine is the only alkaloidal constituent of the Arya II population of *P. bracteatum* (24), it can be measured directly as described. The I content of different portions of the powdered capsules was determined directly after digestion with 0.1 *N* HCl and indirectly after benzene extraction (24), both with the II method (Table I). Moreover, the I content of each sample was determined by the sulfuric acid method (22), and identical results to the II method were obtained in each case.

In contrast to the sulfuric acid method (22), this method shows no interference from the other contents of the capsules. The indirect determination of the alkaloid based on benzene extraction gives a lower recovery (86–89%) of the alkaloid (Table I). This method, compared with the previously reported methods, was easier and more precise.

The presence of a high percentage of thebaine (1.75%) in the coarse particles, which are commonly discarded, necessitate their use as a source for thebaine production.

REFERENCES

(1) K. Macek, J. Hacaperkova, and B. Kakac, *Pharmazie*, **11**, 533 (1956).

(2) K. Genest and C. G. Farmilo, *J. Am. Pharm. Assoc., Sci. Ed.*, **48**, 286 (1959).

(3) A. Kaess and C. Mathis, *Ann. Pharm. Fr.*, **23**, 739 (1965).

(4) M. S. Shipalov and S. D. Mekhtikhanov, *Prikl. Biokhim. Mikrobiol.*, **4**, 444 (1968).

(5) V. E. Chichiro, Z. P. Kostennikova, and S. D. Mekhtikhanov, *Farmatsiya*, **20**, 37 (1971).

(6) J. Buchi and R. Huber, *Pharm. Acta Helv.*, **36**, 571 (1961).

(7) E. Brochmann-Hanssen and T. Furuya, *J. Pharm. Sci.*, **53**, 1549 (1964).

(8) E. Brochmann-Hanssen and A. B. Svendsen, *ibid.*, **51**, 1095 (1962).

(9) D. W. Smith, T. H. Beasley, Sr., R. L. Charles, and H. W. Ziegler, *ibid.*, **62**, 1691 (1973).

(10) J. Buechi and R. von Moos, *Pharm. Acta Helv.*, **41**, 142 (1966).

(11) W. Kamp, *Pharm. Weekbl.*, **92**, 1 (1957).

(12) V. J. Bakre, Z. Karaata, J. C. Bartlet, and C. G. Farmilo, *J. Pharm. Pharmacol.*, **11**, 234 (1959).

(13) V. M. Merlis, E. I. Kryukova, A. A. Chemerisskaya, E. M. Peresleni, and A. A. Ivanov, *Bull. Narc.*, **20**, 5 (1968).

(14) H. Sakurai and E. Awada, *J. Pharm. Soc. Jpn.*, **76**, 1026 (1956).

(15) K.-T. Lee, *J. Pharm. Pharmacol.*, **12**, 666 (1960).

(16) E. G. Clair, *Analyst*, **87**, 499 (1962).

(17) H. Fukamauchi, R. Ideno, and N. Sanbongi, *Yakugaku Zasshi*, **90**, 1039 (1970).

(18) F. Y. Kagan, G. A. Vaisman, F. A. Mitchenko, and L. O. Kirichenko, *Farm. Zh.*, **19**, 24 (1964).

(19) E. Wegner, *Pharmazie*, **5**, 33 (1950).

(20) S. Pfeifer and F. Weiss, *ibid.*, **15**, 349 (1960).

(21) J. Castel and M. F. Viallefont, *Trav. Soc. Pharm. Montpellier*, **26**, 127 (1966).

(22) I. Reifer and K. Toczko, *Acta Biochim. Polon.*, **3**, 381 (1956).

(23) H. Sakurai and M. Umeda, *Yakugaku Zasshi*, **83**, 1000 (1963).

(24) I. Lalezari, P. Nasseri, and R. Asgharian, *J. Pharm. Sci.*, **63**, 1331 (1974).
(25) H. M. N. H. Irving and J. J. Markham, *Anal. Chim. Acta*, **39**, 7 (1967).
(26) P. Job, *Ann. Chim.*, **9**, 113 (1928).
(27) *Ibid.*, **16**, 97 (1936).
(28) J. H. Yoe and A. L. Jones, *Ind. Eng. Chem., Anal. Ed.*, **16**, 111 (1944).
(29) M. E. Auerbach, *ibid.*, **15**, 492 (1943).
(30) P. B. Marshall and E. W. Rogers, *Biochem. J.*, **39**, 258 (1945).

ACKNOWLEDGMENTS

The authors are grateful to Ali Shafiee for providing research facilities.

Inhibition by Paromomycin of R-Factor Transfer of Tetracycline Resistance between *Escherichia coli* and *Salmonella pullorum*

ALDO BUOGO ˣ and PIERANGELO CATTANEO

Received October 12, 1976, from the *Farmitalia Research Laboratories, 20014 Nerviano, Milan, Italy.* Accepted for publication February 2, 1977.

Abstract □ *In vitro* assays showed that low concentrations (5–10 and 20 μg/ml) of the antimicrobial paromomycin sulfate are able to block or diminish significantly the transfer of the tetracycline resistance R-factor between *Escherichia coli* and *Salmonella pullorum*. This observation is important because it offers the possibility of preventing the formation of tetracycline-resistant pathogens, a limiting factor of tetracycline use in both human and veterinary medicine.

Keyphrases □ Paromomycin—effect on R-factor transfer of tetracycline resistance from *Escherichia coli* to *Salmonella pullorum* □ Tetracycline resistance—R-factor transfer from *Escherichia coli* to *Salmonella pullorum*, effect of paromomycin □ Bacterial resistance—to tetracycline, R-factor transfer from *Escherichia coli* to *Salmonella pullorum*, effect of paromomycin □ Antibacterials—effect of paromomycin on R-factor transfer of tetracycline resistance from *Escherichia coli* to *Salmonella pullorum* □ Antimicrobials—effect of paromomycin on R-factor transfer of tetracycline resistance from *Escherichia coli* to *Salmonella pullorum*

Previously (1), it was demonstrated that *in vitro* pretreatment of *Escherichia coli* with low doses of tetracycline inhibits the production of mutants resistant to paromomycin sulfate (I), an oligosaccharide antimicrobial with a broad antibacterial spectrum including Gram-positive, Gram-negative, and acid-fast bacteria (2–4). Compound I also inhibits some protozoa (5, 6).

The effect of I on the development of tetracycline-resistant strains was studied by evaluating its action on the R-factor transfer capacity between a strain of *E. coli* (donor) and a strain of *Salmonella pullorum* (recipient) (7).

Salmonellosis is an increasing health hazard (8–11). The spread of drug-resistant pathogenic *Salmonella* has encouraged investigation of methods to reduce this phenomenon, which affects both human and animal bacterial flora.

EXPERIMENTAL

Bacterial Strains—*E. coli* (FI 3632), tetracycline resistant and rifamide sensitive, and *S. pullorum* (FI 741), tetracycline sensitive and rifamide resistant, were used. The *Salmonella* strain was used because only mutants with acquired resistance to tetracycline develop in subcultures on a solid medium containing 30 μg of tetracycline/ml plus 40 μg of rifamide/ml.

In these transfer assays, the two strains can be immediately distinguished on a solid medium containing lactose and a pH indicator by the formation of acidifying (*E. coli*) or nonacidifying (*S. pullorum*) colonies. The usual cultural, biochemical, and serological tests were employed to identify the parent and revertant strains.

Assay Media—Medium 1 was liquid tryptose broth[1]. Medium 2 (solid) contained tryptose agar[1], 1% lactose, and 0.01% bromthymol blue (Wurtz medium) with and without tetracycline[2] (30 μg/ml), rifamide[3] (40 μg/ml), paromomycin[4] (30 μg/ml), or tetracycline (30 μg/ml) plus rifamide (40 μg/ml). Medium 3 was TSI medium[1], and Medium 4 was SIM medium[1].

Medium 1 was used for the conjugation assays and the determination of the minimum inhibitory concentrations (MIC) of the three antimicrobials. Medium 2 served as a control for the conjugation experiments and for the sensitivity tests following the Kirby–Bauer method. The medicated media were employed for checking the drug resistance of the parent and revertant strains. Media 3 and 4 were employed for an initial differentiation between *E. coli* and *S. pullorum* colonies.

Reagents—Sensitivity disks were prepared according to the "Code of Federal Regulations" (12) and contained 30 μg of tetracycline, 40 μg of rifamide, or 30 μg of I. The somatic serodiagnostic antiserum of *E. coli* was obtained by rabbit immunization as described by Kauffmann (13), and the somatic serodiagnostic antiserum of *S. pullorum* was purchased[1].

Antibiotic Sensitivity Test—This test was performed in tryptose broth by determining the MIC values, in solid Medium 2 according to the Kirby–Bauer method, and by evaluating the bacterial growth in Medium 2 containing 30 μg of the single antimicrobial/ml.

Conjugation Assays in Presence of I—*Single Strains with I and 2–4 hr of Contact Time*—Compound I (final concentrations of 5, 10, and 20 μg/ml) was added to tryptose broth cultures of the single strains after 2 hr of incubation at 37°. After further incubation (2 and 4 hr), the cultures were washed (three times by centrifugation) to remove I and the pellets were resuspended and brought to volume with sterile tryptose broth.

Under these conditions, the drug concentration remaining in the cultures was lower than the minimum assayable microbiologically (0.05 μg/ml) by the agar plate method (12). Broth cultures of the two test strains grown in the absence of I were treated identically. The final bacterial suspensions thus obtained were mixed in a chessboard scheme according to the different concentrations of I with which the bacteria had previously been in contact.

[1] Difco Laboratories, Detroit, Mich.
[2] Lot 241/5, Farmitalia Research Laboratories, Milan, Italy.
[3] Lot 011, Gruppo Lepetit, spa, Milan, Italy.
[4] Aminosidine, lot 501.2, Farmitalia Research Laboratories, Milan, Italy.

(24) I. Lalezari, P. Nasseri, and R. Asgharian, *J. Pharm. Sci.*, **63**, 1331 (1974).
(25) H. M. N. H. Irving and J. J. Markham, *Anal. Chim. Acta*, **39**, 7 (1967).
(26) P. Job, *Ann. Chim.*, **9**, 113 (1928).
(27) *Ibid.*, **16**, 97 (1936).
(28) J. H. Yoe and A. L. Jones, *Ind. Eng. Chem., Anal. Ed.*, **16**, 111 (1944).
(29) M. E. Auerbach, *ibid.*, **15**, 492 (1943).
(30) P. B. Marshall and E. W. Rogers, *Biochem. J.*, **39**, 258 (1945).

ACKNOWLEDGMENTS

The authors are grateful to Ali Shafiee for providing research facilities.

Inhibition by Paromomycin of R-Factor Transfer of Tetracycline Resistance between *Escherichia coli* and *Salmonella pullorum*

ALDO BUOGO ˣ and PIERANGELO CATTANEO

Received October 12, 1976, from the *Farmitalia Research Laboratories, 20014 Nerviano, Milan, Italy.* Accepted for publication February 2, 1977.

Abstract □ *In vitro* assays showed that low concentrations (5–10 and 20 μg/ml) of the antimicrobial paromomycin sulfate are able to block or diminish significantly the transfer of the tetracycline resistance R-factor between *Escherichia coli* and *Salmonella pullorum*. This observation is important because it offers the possibility of preventing the formation of tetracycline-resistant pathogens, a limiting factor of tetracycline use in both human and veterinary medicine.

Keyphrases □ Paromomycin—effect on R-factor transfer of tetracycline resistance from *Escherichia coli* to *Salmonella pullorum* □ Tetracycline resistance—R-factor transfer from *Escherichia coli* to *Salmonella pullorum*, effect of paromomycin □ Bacterial resistance—to tetracycline, R-factor transfer from *Escherichia coli* to *Salmonella pullorum*, effect of paromomycin □ Antibacterials—effect of paromomycin on R-factor transfer of tetracycline resistance from *Escherichia coli* to *Salmonella pullorum* □ Antimicrobials—effect of paromomycin on R-factor transfer of tetracycline resistance from *Escherichia coli* to *Salmonella pullorum*

Previously (1), it was demonstrated that *in vitro* pretreatment of *Escherichia coli* with low doses of tetracycline inhibits the production of mutants resistant to paromomycin sulfate (I), an oligosaccharide antimicrobial with a broad antibacterial spectrum including Gram-positive, Gram-negative, and acid-fast bacteria (2–4). Compound I also inhibits some protozoa (5, 6).

The effect of I on the development of tetracycline-resistant strains was studied by evaluating its action on the R-factor transfer capacity between a strain of *E. coli* (donor) and a strain of *Salmonella pullorum* (recipient) (7).

Salmonellosis is an increasing health hazard (8–11). The spread of drug-resistant pathogenic *Salmonella* has encouraged investigation of methods to reduce this phenomenon, which affects both human and animal bacterial flora.

EXPERIMENTAL

Bacterial Strains—*E. coli* (FI 3632), tetracycline resistant and rifamide sensitive, and *S. pullorum* (FI 741), tetracycline sensitive and rifamide resistant, were used. The *Salmonella* strain was used because only mutants with acquired resistance to tetracycline develop in subcultures on a solid medium containing 30 μg of tetracycline/ml plus 40 μg of rifamide/ml.

In these transfer assays, the two strains can be immediately distinguished on a solid medium containing lactose and a pH indicator by the formation of acidifying (*E. coli*) or nonacidifying (*S. pullorum*) colonies. The usual cultural, biochemical, and serological tests were employed to identify the parent and revertant strains.

Assay Media—Medium 1 was liquid tryptose broth[1]. Medium 2 (solid) contained tryptose agar[1], 1% lactose, and 0.01% bromthymol blue (Wurtz medium) with and without tetracycline[2] (30 μg/ml), rifamide[3] (40 μg/ml), paromomycin[4] (30 μg/ml), or tetracycline (30 μg/ml) plus rifamide (40 μg/ml). Medium 3 was TSI medium[1], and Medium 4 was SIM medium[1].

Medium 1 was used for the conjugation assays and the determination of the minimum inhibitory concentrations (MIC) of the three antimicrobials. Medium 2 served as a control for the conjugation experiments and for the sensitivity tests following the Kirby–Bauer method. The medicated media were employed for checking the drug resistance of the parent and revertant strains. Media 3 and 4 were employed for an initial differentiation between *E. coli* and *S. pullorum* colonies.

Reagents—Sensitivity disks were prepared according to the "Code of Federal Regulations" (12) and contained 30 μg of tetracycline, 40 μg of rifamide, or 30 μg of I. The somatic serodiagnostic antiserum of *E. coli* was obtained by rabbit immunization as described by Kauffmann (13), and the somatic serodiagnostic antiserum of *S. pullorum* was purchased[1].

Antibiotic Sensitivity Test—This test was performed in tryptose broth by determining the MIC values, in solid Medium 2 according to the Kirby–Bauer method, and by evaluating the bacterial growth in Medium 2 containing 30 μg of the single antimicrobial/ml.

Conjugation Assays in Presence of I—*Single Strains with I and 2–4 hr of Contact Time*—Compound I (final concentrations of 5, 10, and 20 μg/ml) was added to tryptose broth cultures of the single strains after 2 hr of incubation at 37°. After further incubation (2 and 4 hr), the cultures were washed (three times by centrifugation) to remove I and the pellets were resuspended and brought to volume with sterile tryptose broth.

Under these conditions, the drug concentration remaining in the cultures was lower than the minimum assayable microbiologically (0.05 μg/ml) by the agar plate method (12). Broth cultures of the two test strains grown in the absence of I were treated identically. The final bacterial suspensions thus obtained were mixed in a chessboard scheme according to the different concentrations of I with which the bacteria had previously been in contact.

[1] Difco Laboratories, Detroit, Mich.
[2] Lot 241/5, Farmitalia Research Laboratories, Milan, Italy.
[3] Lot 011, Gruppo Lepetit, spa, Milan, Italy.
[4] Aminosidine, lot 501.2, Farmitalia Research Laboratories, Milan, Italy.

Table I—Antibiotic Sensitivity of the Test Strains[a]

Strain	Tetracycline MIC, μg/ml	Tetracycline ST, mm	Tetracycline NC, %	Rifamide MIC, μg/ml	Rifamide ST, mm	Rifamide NC, %	I MIC, μg/ml	I ST, mm	I NC, %
E. coli	200	0	100	12.5	16.7	0	33	12.1	0
S. pullorum	1.5	26.2	0	150	0	100	25	13.5	0

[a] MIC = minimum inhibitory concentration in tryptose broth after 24 hr of incubation; ST = inhibition zone diameter in millimeters (average of four zones); and NC = number of colonies developed in medium containing 30–40 μg/ml of the antimicrobials, reported as percentage of the control tests (number of colonies grown in medium without antibiotic).

After static incubation at 37° for 3, 20, and 40 hr, known quantities of the microbial suspensions were seeded on plates of Medium 2 containing rifamide plus tetracycline. Following incubation at 37° for 18–24 hr, the acidifying and nonacidifying colonies were counted. Two to 10 colonies per plate were checked for identification purposes in Medium 3 and 4 tubes and by slide agglutination.

Mixed Strains with I and 3–20 hr of Contact Time—A few tests were carried out by placing the two strains in contact with I for the whole conjugation time. The subcultures were carried out after 3, 20, and 40 hr.

Tests for Bacteriophages—Experiments were carried out on *E. coli* to exclude bacteriophage carriers and the transduction phenomena. The experiments were performed both by seeding the filtrates of *E. coli* broth cultures on plain Medium 2 inoculated with the recipient strain and by the method of phage liberation after UV irradiation (14).

RESULTS

S. pullorum is resistant to rifamide and sensitive to tetracycline and I; *E. coli* is only resistant to tetracycline (Table I).

Table II—Mean Number (Three Replicates), Reported in Factorial Design, of *S. pullorum* Colonies that Developed on Wurtz Medicated Medium (30 μg of Tetracycline/ml and 40 μg of Rifamide/ml) after Conjugation

Conjugation Time = 20 hr[a]

	E. coli I, μg/ml	0 (A)	10 (B)	20 (C)	Assay
S. pullorum	20 (X)	3,203	2,940	787	a
		4,056	2,201	832	b
		10,446	0	5	c
		5,503	3,616	0	d
	10 (Y)	3,221	2,850	2743	a
		3,922	3,353	2790	b
		12,375	5,019	0	c
		6,070	2,955	2	d
	0 (Z)	3,287	3,102	1807	a
		8,960	5,438	4064	b
		17,220	14,392	1	c
		12,523	12,680	7869	d

Conjugation Time = 40 hr[b]

	E. coli I, μg/ml	0 (A)	10 (B)	20 (C)	Assay
S. pullorum	20 (X)	7,529	8,420	671	a
		94,667	9,366	337	b
		44,098	0	0	c
		21,647	23,298	0	d
	10 (Y)	11,764	7,702	1,522	a
		415,664	56,331	1,450	b
		11,836	28,130	0	c
		30,478	16,504	370	d
	0 (Z)	22,365	8,142	7,431	a
		318,665	115,668	54,667	b
		35,900	2,864	0	c
		44,235	43,574	18,073	d

[a] Out of 72 possible combinations of the data of the same assay, only 14 were statistically nonsignificant ($p > 0.5$): BYa *versus* CYa, AZa *versus* BZa, AZc *versus* BZc, AZd *versus* BZd, CYc *versus* CZc, BXa *versus* BYa, BXd *versus* BYd, BXa *versus* BZa, AXa *versus* AYa, AXb *versus* AYb, AXc *versus* AYc, AXd *versus* AYd, AXa *versus* AZa, and AYa *versus* AZa. [b] Out of 72 possible combinations of the data of the same assay, only eight were statistically nonsignificant ($p > 0.5$): BXc *versus* CXc, AXd *versus* BXd, AZd *versus* BZd, CXc *versus* CYc, CXc *versus* CZc, CYc *versus* CZc, BYa *versus* BZa, and AXc *versus* AZc.

Table II gives the data obtained from four conjugation tests (a, b, c, and d), and Table III gives the results of two tests (a and b). These tables report the average results (three replicates for each determination) of the *S. pullorum* colonies that had become tetracycline resistant after 2 hr of precontact with various concentrations of I and successive conjugation with the donor strain for 20 and 40 hr at 37°. The statistical significance (p) of all possible combinations between *E. coli* and *S. pullorum* treated with I was calculated, and the few nonsignificant confrontations are reported in the tables. On the average, 87% of the combinations showed statistically significant differences, that is, positive R-factor transfer with p values ranging from <0.001 to <0.05 (analysis of variance).

The data from the conjugation tests calculated as percentages of revertants and the range limits reported in Figs. 1 and 2 allow an immediate evaluation of the transfer decrease associated with the I treatment.

The lowest value was reached when both strains were exposed to the highest concentration of I (20 μg/ml). When only the donor strain (*E. coli*) and, to a lesser extent, when only the recipient strain were treated with I, a significant reduction in transfer also was noted. In both cases, the lowest value was again associated with the pretreatment with the highest concentration of I. Conjugation periods of 3 hr or less did not modify the transfer, in agreement with Anderson (15).

Separate analogous tests demonstrated that the presence of 3 μg/ml or less of I did not interfere with the acquisition of tetracycline resistance.

The experiments performed to show the presence of bacteriophages in the donor strain were negative.

DISCUSSION

These assays show that contact with subinhibitory concentrations of I impedes the acquisition and donation of tetracycline resistance in *S.*

Table III—Mean Number (Three Replicates), Reported in Factorial Design, of *S. pullorum* Colonies that Developed on Wurtz Medicated Medium (30 μg of Tetracycline/ml and 40 μg of Rifamide/ml) after Conjugation

Conjugation Time = 20 hr[a]

	E. coli I, μg/ml	0 (A)	5 (B)	10 (C)	Assay
S. pullorum	10 (X)	24,668	31,132	37,332	a
		25,768	35,465	28,536	b
	5 (Y)	28,534	27,466	31,170	a
		43,499	35,600	29,531	b
	0 (Z)	140,334	35,302	27,266	a
		285,666	32,466	31,102	b

Conjugation Time = 40 hr[b]

	E. coli I, μg/ml	0 (A)	5 (B)	10 (C)	Assay
S. pullorum	10 (X)	185,334	302,152	85,766	a
		125,332	95,666	37,800	b
	5 (Y)	165,667	62,168	95,667	a
		105,332	44,798	5,366	b
	0 (Z)	314,666	275,334	163,666	a
		310,332	40,766	121,000	b

[a] Out of 36 possible combinations of the data of the same assay, only five were statistically nonsignificant ($p > 0.5$): AYa *versus* BYa, BZb *versus* CZb, CXb *versus* CYb, BXb *versus* BYb, and CXb *versus* CYb. [b] Out of 36 possible combinations of the data of the same assay, none was statistically nonsignificant.

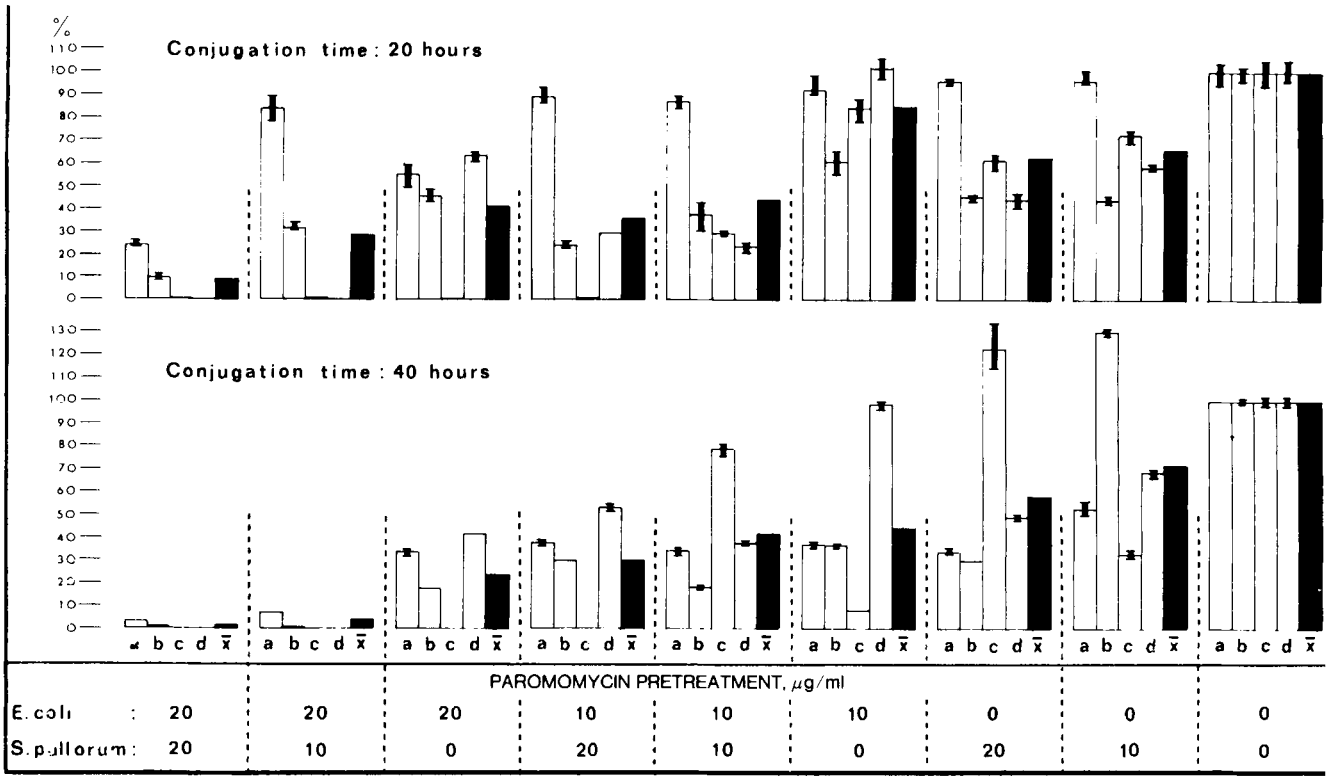

Figure 1—*Percent of* S. pullorum *colonies (with respect to the controls) that became tetracycline resistant after pretreatment of* E. coli *and/or* S. pullorum *with 20 and 10 μg of I/ml during 2 hr at 37°. Data are from four assays (a, b, c, and d) and their averages (x̄). The* I *represents the range limits for three determinations.*

pullorum and *E. coli*. Analogous effects were described for the acridine derivatives, mitomycin and sodium lauryl sulfate (16).

The effects of I may be attributed either to the induced synthesis of anomalous proteins, according to the mechanism of action common to the oligosaccharide antibiotics, or to a I-induced change of the superficial electrical charge of the bacterial cells, in a way analogous to that which occurs in *E. coli* in the presence of streptomycin, another oligosaccharide antibacterial (17).

The experimental evidence suggests that the emergence of tetracycline-resistant bacteria through conjugation resistance transfer may be prevented by the presence of I in low concentrations.

This acquisition seemed to be relevant even *in vivo*, because orally administered I is not absorbed through the GI tract and can reach intestinal concentrations high enough to inhibit the transfer of resistance factors between the ubiquitous, usually harmless, *E. coli* and the pathogenic *Salmonella*.

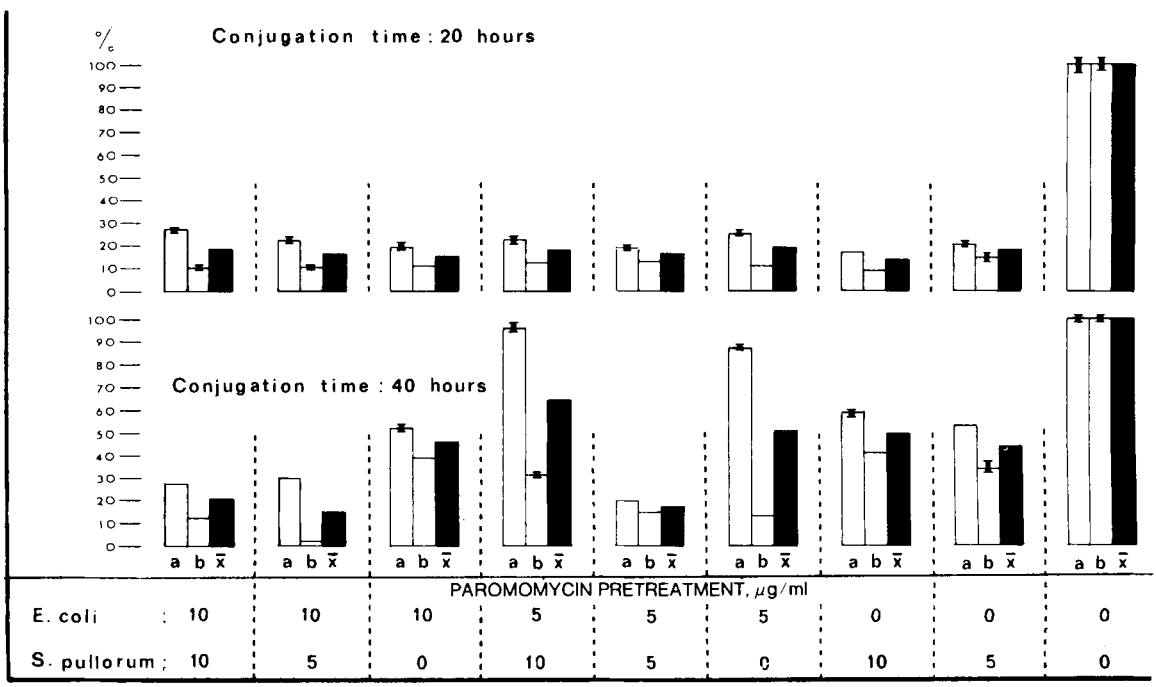

Figure 2—*Percent of* S. pullorum *colonies (with respect to the controls) that became tetracycline resistant after pretreatment of* E. coli *and/or* S. pullorum *with 10 and 5 μg of I/ml during 2 hr at 37°. Data are from two assays (a and b) and their averages (x̄). The* I *represents the range limits for three determinations.*

REFERENCES

(1) E. R. Garrett and J. K. Lewis, *J. Pharm. Sci.*, **64**, 1936 (1975).
(2) M. Ghione, A. Buogo, and A. Sanfilippo, *G. Microbiol.*, **8**, 9 (1960).
(3) F. Arcamone, C. Bertazzoli, A. Buogo, G. Cassinelli, and A. Vigevani, *Panminerva Med.*, **16**, 9 (1974).
(4) A. Buogo and P. Cattaneo, *Gazz. Med. Ital.*, **133**, 1 (1974).
(5) W. Almeida, *Hospital*, **59**, 947 (1961).
(6) G. K. Daikos, P. Kontomichalou, E. Petassis, and D. Bilasis, *Antimicrob. Agents Chemother.*, **4**, 765 (1963).
(7) A. Buogo and P. Cattaneo, *Arch. Vet. Ital.*, **26**, 111 (1975).
(8) P. J. Christopher, P. D. Claxton, D. C. Dorman, B. F. O'Connor, R. W. Proudford, and R. G. A. Sutton, *Med. J. Aust.*, **1**, 337 (1974).
(9) N. Datta, *J. Hyg. (London)*, **60**, 301 (1962).
(10) D. W. Pocurull, S. A. Gaines, and H. D. Mercer, *Appl. Microbiol.*, **21**, 258 (1971).
(11) M. Finland, C. Garner, C. Wilcox, and L. D. Sabath, *J. Am. Med. Assoc.*, **229**, 1309 (1974).
(12) Code of Federal Regulations, 21 Food and Drugs, Parts 300 to 199, Apr. 1, 1975.
(13) F. Kauffmann, "The Bacteriology of Enterobacteriaceae," Munksgaard, Copenhagen, Denmark, 1966, pp. 90, 91.
(14) P. Frédéricq and A. Gratia, *C. R. Soc. Biol.*, **143**, 560 (1949).
(15) E. S. Anderson, *Ann. Rev. Microbiol.*, **22**, 131 (1968).
(16) Y. Masanosuke and M. G. Sevag, *J. Bacteriol.*, **93**, 245 (1967).
(17) A. Buogo, *G. Microbiol.*, **6**, 57 (1958).

Pharmacokinetic Model for Salicylate in Cerebrospinal Fluid, Blood, Organs, and Tissues

C. N. CHEN, D. L. COLEMAN, J. D. ANDRADE ˣ, and A. R. TEMPLE

Received May 10, 1976, from the *College of Engineering and College of Pharmacy, University of Utah, Salt Lake City, UT 84112.*
Accepted for publication April 6, 1977.

Abstract □ The developed pharmacokinetic model, an extension of the Bischoff–Dedrick model, simultaneously predicts the kinetic behavior of salicylate in cerebrospinal fluid, blood, organs, and tissues. The model, which is entirely different from conventional compartment models, is derived from basic considerations of drug distribution with biochemical and physiological meaning. The dog was studied at three different dosages of salicylate: therapeutic, moderate intoxication, and severe intoxication. The predicted kinetics of salicylate in cerebrospinal fluid, blood, plasma, liver, muscle, and adipose tissue by the model agreed well with the experimental data. The effectiveness of hemoperfusion treatment for the severely intoxicated dog by albumin-coated activated carbon and its effect on the kinetic behavior of salicylate in cerebrospinal fluid, blood, organs, and tissues were studied. The model was also applied to predict the kinetic changes of salicylate in the body during and after the extracorporeal treatment. The predicted results also agreed with the experimental data.

Keyphrases □ Models, pharmacokinetic—developed to predict behavior of salicylate in cerebrospinal fluid, blood, organs, and tissues, compared to experimental data with dogs □ Pharmacokinetic models—developed to predict behavior of salicylate in cerebrospinal fluid, blood, organs, and tissues, compared to experimental data with dogs □ Salicylate—pharmacokinetic model developed to predict behavior in cerebrospinal fluid, blood, organs, and tissues, compared to experimental data with dogs

Blood or plasma drug levels have been used as an index of dose scheduling for therapeutics under the assumption that the drug level in blood or plasma corresponds to the pharmacological effect of the drug. Conventional pharmacokinetic models have been widely applied to simulate the kinetic behavior of drug levels in blood or plasma. However, the knowledge of drug levels in blood or plasma with time may not provide sufficient information for adequate therapy. The kinetic information of drug levels in brain, cerebrospinal fluid, blood, organs, and tissues of pharmacological interest may be necessary for the development of more appropriate dosage regimens.

The model developed and used in this study is an extension of the Bischoff–Dedrick model (1, 2). This model is derived from basic considerations of drug distribution with biochemical and physiological meaning. The model has been applied successfully to predict the pharmacokinetics of thiopental (2, 3), methotrexate (1, 4, 5), and cytarabine (6).

Previously, an extended version of the Bischoff–Dedrick model was used to predict thiopental kinetics in the dog (2). In this paper, the model previously presented (2) is modified and applied to salicylate in the dog. The model also is modified to consider the effects of activated carbon hemoperfusion on the pharmacokinetics of salicylate in the dog. Since drug–protein binding plays an important role in pharmacological effect and pharmacokinetics, the model also is applied to predict the pharmacokinetics of free (unbound) salicylate levels in plasma water, which is more related to the pharmacological effect of the drug.

THEORETICAL

A diagram of blood circulation through various body regions is shown in Scheme I. The blood pool is the blood volume excluding the blood contained in the capillary beds of organs and tissues in the body.

The transient mass balance for any organ or body region can be expressed as (2):

$$\begin{bmatrix}\text{drug accumulation rate}\\ \text{in both capillary bed and}\\ \text{tissue portion}\end{bmatrix} = \begin{bmatrix}\text{drug inflow rate from}\\ \text{blood pool and/or}\\ \text{other body regions}\end{bmatrix} + [\text{drug ingestion rate, if any}] - \begin{bmatrix}\text{drug outflow rate}\\ \text{from body region}\end{bmatrix} - \begin{bmatrix}\text{drug metabolism rate and/or}\\ \text{excretion rate, if any}\end{bmatrix} \quad \text{(Eq. 1)}$$

The mathematical equation of the transient mass balance for any body region (Yz) is:

$$\frac{d(V_{YzB}C_{T,YzB})}{dt} + \frac{d(V_{YzT}C_{T,YzT})}{dt} = Q_{Yz}(C_{T,B} - C_{T,YzB}) \quad \text{(Eq. 2)}$$

where the subscripts mean the following: B, blood; T, total or tissue; and Yz, a body region such as Ad (adipose), Br (brain), GI (gastrointestinal), Li (liver), Mu (muscle), and Vi (viscera); and where $C_{T,B}$ is the total

REFERENCES

(1) E. R. Garrett and J. K. Lewis, *J. Pharm. Sci.*, **64**, 1936 (1975).
(2) M. Ghione, A. Buogo, and A. Sanfilippo, *G. Microbiol.*, **8**, 9 (1960).
(3) F. Arcamone, C. Bertazzoli, A. Buogo, G. Cassinelli, and A. Vigevani, *Panminerva Med.*, **16**, 9 (1974).
(4) A. Buogo and P. Cattaneo, *Gazz. Med. Ital.*, **133**, 1 (1974).
(5) W. Almeida, *Hospital*, **59**, 947 (1961).
(6) G. K. Daikos, P. Kontomichalou, E. Petassis, and D. Bilasis, *Antimicrob. Agents Chemother.*, **4**, 765 (1963).
(7) A. Buogo and P. Cattaneo, *Arch. Vet. Ital.*, **26**, 111 (1975).
(8) P. J. Christopher, P. D. Claxton, D. C. Dorman, B. F. O'Connor, R. W. Proudford, and R. G. A. Sutton, *Med. J. Aust.*, **1**, 337 (1974).
(9) N. Datta, *J. Hyg. (London)*, **60**, 301 (1962).
(10) D. W. Pocurull, S. A. Gaines, and H. D. Mercer, *Appl. Microbiol.*, **21**, 258 (1971).
(11) M. Finland, C. Garner, C. Wilcox, and L. D. Sabath, *J. Am. Med. Assoc.*, **229**, 1309 (1974).
(12) Code of Federal Regulations, 21 Food and Drugs, Parts 300 to 199, Apr. 1, 1975.
(13) F. Kauffmann, "The Bacteriology of Enterobacteriaceae," Munksgaard, Copenhagen, Denmark, 1966, pp. 90, 91.
(14) P. Frédéricq and A. Gratia, *C. R. Soc. Biol.*, **143**, 560 (1949).
(15) E. S. Anderson, *Ann. Rev. Microbiol.*, **22**, 131 (1968).
(16) Y. Masanosuke and M. G. Sevag, *J. Bacteriol.*, **93**, 245 (1967).
(17) A. Buogo, *G. Microbiol.*, **6**, 57 (1958).

Pharmacokinetic Model for Salicylate in Cerebrospinal Fluid, Blood, Organs, and Tissues

C. N. CHEN, D. L. COLEMAN, J. D. ANDRADE ˣ, and A. R. TEMPLE

Received May 10, 1976, from the *College of Engineering and College of Pharmacy, University of Utah, Salt Lake City, UT 84112.*
Accepted for publication April 6, 1977.

Abstract □ The developed pharmacokinetic model, an extension of the Bischoff–Dedrick model, simultaneously predicts the kinetic behavior of salicylate in cerebrospinal fluid, blood, organs, and tissues. The model, which is entirely different from conventional compartment models, is derived from basic considerations of drug distribution with biochemical and physiological meaning. The dog was studied at three different dosages of salicylate: therapeutic, moderate intoxication, and severe intoxication. The predicted kinetics of salicylate in cerebrospinal fluid, blood, plasma, liver, muscle, and adipose tissue by the model agreed well with the experimental data. The effectiveness of hemoperfusion treatment for the severely intoxicated dog by albumin-coated activated carbon and its effect on the kinetic behavior of salicylate in cerebrospinal fluid, blood, organs, and tissues were studied. The model was also applied to predict the kinetic changes of salicylate in the body during and after the extracorporeal treatment. The predicted results also agreed with the experimental data.

Keyphrases □ Models, pharmacokinetic—developed to predict behavior of salicylate in cerebrospinal fluid, blood, organs, and tissues, compared to experimental data with dogs □ Pharmacokinetic models—developed to predict behavior of salicylate in cerebrospinal fluid, blood, organs, and tissues, compared to experimental data with dogs □ Salicylate—pharmacokinetic model developed to predict behavior in cerebrospinal fluid, blood, organs, and tissues, compared to experimental data with dogs

Blood or plasma drug levels have been used as an index of dose scheduling for therapeutics under the assumption that the drug level in blood or plasma corresponds to the pharmacological effect of the drug. Conventional pharmacokinetic models have been widely applied to simulate the kinetic behavior of drug levels in blood or plasma. However, the knowledge of drug levels in blood or plasma with time may not provide sufficient information for adequate therapy. The kinetic information of drug levels in brain, cerebrospinal fluid, blood, organs, and tissues of pharmacological interest may be necessary for the development of more appropriate dosage regimens.

The model developed and used in this study is an extension of the Bischoff–Dedrick model (1, 2). This model is derived from basic considerations of drug distribution with biochemical and physiological meaning. The model has been applied successfully to predict the pharmacokinetics of thiopental (2, 3), methotrexate (1, 4, 5), and cytarabine (6).

Previously, an extended version of the Bischoff–Dedrick model was used to predict thiopental kinetics in the dog (2). In this paper, the model previously presented (2) is modified and applied to salicylate in the dog. The model also is modified to consider the effects of activated carbon hemoperfusion on the pharmacokinetics of salicylate in the dog. Since drug–protein binding plays an important role in pharmacological effect and pharmacokinetics, the model also is applied to predict the pharmacokinetics of free (unbound) salicylate levels in plasma water, which is more related to the pharmacological effect of the drug.

THEORETICAL

A diagram of blood circulation through various body regions is shown in Scheme I. The blood pool is the blood volume excluding the blood contained in the capillary beds of organs and tissues in the body.

The transient mass balance for any organ or body region can be expressed as (2):

$$\begin{bmatrix}\text{drug accumulation rate}\\ \text{in both capillary bed and}\\ \text{tissue portion}\end{bmatrix} = \begin{bmatrix}\text{drug inflow rate from}\\ \text{blood pool and/or}\\ \text{other body regions}\end{bmatrix} + [\text{drug ingestion rate, if any}] - \begin{bmatrix}\text{drug outflow rate}\\ \text{from body region}\end{bmatrix} - \begin{bmatrix}\text{drug metabolism rate and/or}\\ \text{excretion rate, if any}\end{bmatrix} \quad \text{(Eq. 1)}$$

The mathematical equation of the transient mass balance for any body region (Yz) is:

$$\frac{d(V_{YzB}C_{T,YzB})}{dt} + \frac{d(V_{YzT}C_{T,YzT})}{dt} = Q_{Yz}(C_{T,B} - C_{T,YzB}) \quad \text{(Eq. 2)}$$

where the subscripts mean the following: B, blood; T, total or tissue; and Yz, a body region such as Ad (adipose), Br (brain), GI (gastrointestinal), Li (liver), Mu (muscle), and Vi (viscera); and where $C_{T,B}$ is the total

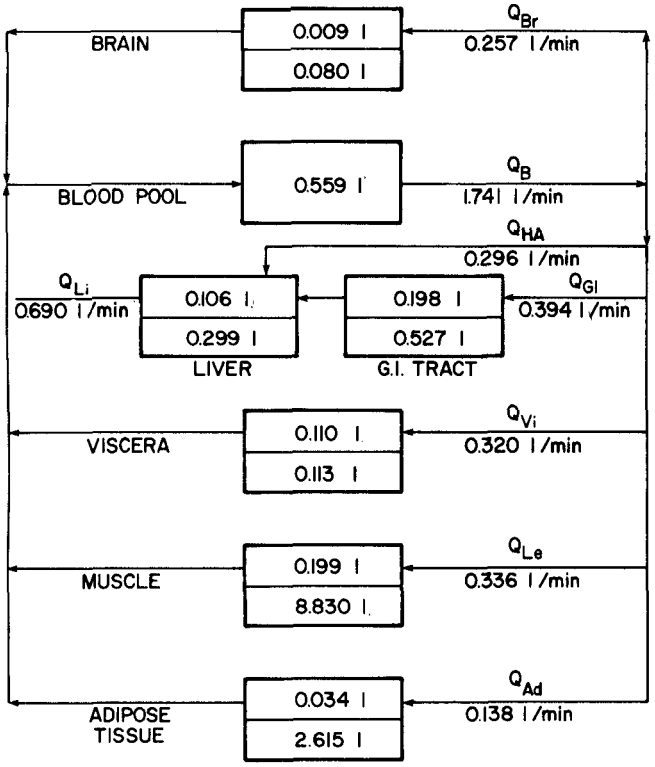

Scheme I—Body regions and blood flows for a 15-kg (average) dog. Key: l = liters.

(bound and unbound) drug concentration in blood from the blood pool, $C_{T,YzB}$ is the total drug concentration in the capillary bed (blood portion) of the body region (Yz), $C_{T,YzT}$ is the total drug concentration in the tissue portion of the body region (Yz), Q_{Yz} is the blood flow rate from the body region (Yz), t is time, V_{YzB} is the blood volume in the capillary bed of the body region (Yz), and V_{YzT} is the tissue volume in the tissue portion of the body region (Yz).

Most drugs can be bound to plasma proteins, especially to albumin, and to various tissue components (7). The free (unbound) drug level in the target organ(s) is more related to the pharmacological effect of the drug. The model considers this factor by correlating the total drug concentration with the free drug concentration in blood, organs, and tissues. The relationship between the total drug concentration, $C_{T,B}$, and the free drug concentration, $C_{F,B}$, in blood can be determined *in vitro*. Thus:

$$C_{T,B} = f_B(C_{F,B}) \qquad \text{(Eq. 3)}$$

where $f_B(C_{F,B})$ is a mathematical expression of the total drug concentration in terms of the free drug concentration in blood.

The mathematical relation between the total drug concentration, $C_{T,YzB}$, and the free drug concentration, $C_{F,YzB}$, in the blood of any organ capillary bed, YzB, is the same as that in Eq. 3:

$$C_{T,YzB} = f_B(C_{F,YzB}) \qquad \text{(Eq. 4)}$$

Similarly, the total drug concentration, $C_{T,YzT}$, in the tissue portion of the body region, Yz, can be expressed in terms of the corresponding free drug concentration, $C_{F,YzT}$, by another function, $f_{YzT}(C_{F,YzT})$:

$$C_{T,YzT} = f_{YzT}(C_{F,YzT}) \qquad \text{(Eq. 5)}$$

After Eqs. 3–5 are substituted into Eq. 2, Eq. 2 becomes:

$$\frac{d[V_{YzB}f_B(C_{F,YzB})]}{dt} + \frac{d[V_{YzT}f_{YzT}(C_{F,YzT})]}{dt} = Q_{Yz}[f_B(C_{F,B}) - f_B(C_{F,YzB})] \qquad \text{(Eq. 6)}$$

Equation 6 can be developed to the following equation:

$$V_{YzB}f_B'(C_{F,YzB})\frac{dC_{F,YzB}}{dt} + f_B(C_{F,YzB})\frac{dV_{YzB}}{dt} + V_{YzT}f'_{YzT}(C_{F,YzT})\frac{dC_{F,YzT}}{dt} + f_{YzT}(C_{F,YzT})\frac{dV_{YzT}}{dt} = Q_{Yz}[f_B(C_{F,B}) - f_B(C_{F,YzB})] \qquad \text{(Eq. 7)}$$

where $f_B'(C_{F,YzB}) = df_B(C_{F,YzB})/dC_{F,YzB}$ and $f'_{YzT}(C_{F,YzT}) = df_{YzT}(C_{F,YzT})/dC_{F,YzT}$.

Capillaries in organs and tissues differ widely in their permeability characteristics. There are two types of mass transfer between the capillaries and the surrounding tissue. One type is the nearly instantaneous establishment of an equilibrium free drug concentration between the capillaries and the tissue. The capillaries of the liver permit the passage of substances quite readily (8). The equilibrium free drug concentration between the liver capillaries and the surrounding tissue can be established rapidly. In this case, the free drug concentration, $C_{F,YzT}$, in the tissue effectively equals the free drug concentration, $C_{F,YzB}$, in the capillaries. That is:

$$C_{F,YzT} = C_{F,YzB} \qquad \text{(Eq. 8)}$$

Substitution of Eq. 8 into Eq. 5 gives:

$$C_{T,YzT} = f_{YzT}(C_{F,YzB}) \qquad \text{(Eq. 9)}$$

Equations 8 and 9 are substituted into Eq. 7, rearranged, and simplified to:

$$[V_{YzB}f_B'(C_{F,YzB}) + V_{YzT}f'_{YzT}(C_{F,YzB})]\frac{dC_{F,YzB}}{dt} + f_B(C_{F,YzB})\frac{dV_{YzB}}{dt} + f_{YzT}(C_{F,YzB})\frac{dV_{YzT}}{dt} = Q_{Yz}[f_B(C_{F,B}) - f_B(C_{F,YzB})] \qquad \text{(Eq. 10)}$$

The second type of mass transport through the capillary wall is the restricted passage between the capillaries and the tissue. For instance, the capillary wall in muscle is composed of an interlocking mosaic of endothelial cells with slits (junctions) between them that could function as the postulated pores and could account for the restricted passage of water-soluble compounds (9). The restricted transport of salicylate through the muscle capillary wall does not allow the instantaneous establishment of the equilibrium free salicylate concentration between the capillaries and the muscle tissue.

The restricted transport of drugs between the capillaries and the tissue may be described in terms of Fick's law. The changing rate of the free drug concentration, $C_{F,YzT}$, in the tissue is proportional to the free concentration difference between the capillaries and the tissue, which gives:

$$\frac{dC_{F,YzT}}{dt} = P_{Yz}(C_{F,YzB} - C_{F,YzT}) \qquad \text{(Eq. 11)}$$

where P_{Yz} is a proportionality constant called the permeability constant and $C_{F,YzB}$ and $C_{F,YzT}$ are the free drug concentrations in the capillaries and the tissue of the body region, Yz.

Substituting Eq. 11 into Eq. 7 gives:

$$V_{YzB}f_B'(C_{F,YzB})\frac{dC_{F,YzB}}{dt} + f_B(C_{F,YzB})\frac{dV_{YzB}}{dt} + V_{YzT}f'_{YzT}(C_{F,YzT})P_{Yz} \times (C_{F,YzB} - C_{F,YzT}) + f_{YzT}(C_{F,YzT})\frac{dV_{YzT}}{dt} = Q_{Yz}[f_B(C_{F,B}) - f_B(C_{F,YzB})] \qquad \text{(Eq. 12)}$$

MODEL

This study attempted to apply the model to predict the kinetic behavior of salicylate in cerebrospinal fluid, blood, liver, muscle, and adipose tissue because experimental kinetic data of salicylate in these body regions are available (10). At least five body regions may be defined: brain, liver, muscle, adipose tissue, and the blood pool (the blood volume excluding those blood volumes in the capillary beds of body regions). In mammals, blood from the GI area perfuses the liver. Thus, GI tissues are added as another body region. Since there is little interest in the kinetics of salicylate in the kidneys or heart, these two organs may be included in the body region called viscera.

A diagram of blood circulation in the seven body regions with physiological data of blood volumes, tissue volumes, and blood flows for a 15-kg (average) dog is shown in Scheme I. Some physiological data are revised and different from those given previously (2). These revised data represent the actually measured statistical data (11–18).

The transient mass balance for the blood pool can be expressed as:

$$\frac{d(V_{B,t}C_{T,B})}{dt} = (Q_{Br}C_{T,BrB} + Q_{Li}C_{T,LiB} + Q_{Vi}C_{T,ViB} + Q_{Mu}C_{T,MuB} + Q_{Ad}C_{T,AdB}) + Mg(t) - Q_BC_{T,B} \qquad \text{(Eq. 13a)}$$

Table I—Parameters and Constants for the Model[a]

	Blood Pool	Brain	Liver	Viscera	GI Area	Muscle	Adipose Tissue
$F_{V,YzB}$[b]	0.460	0.007	0.087	0.091	0.163	0.164	0.028
$F_{W,YzT}$[c]	—	0.7936	0.7326	0.7824	0.7410	0.7757	0.1922

[a] A (mg/liter) = 72.6645, M = 1.1571, B (mg/liter) = 175.1879, N = 1.2441, P_{CSF} (21, 22) (min^{-1}) = 0.0040, P_{Mu} (8, 23) (min^{-1}) = 4.5550, Q_{BL} (liter/min) = 0.001, Q_{ET} (liter/min) = 0.065, Q_{SE} (liter/min) = 0.00167, Q_{CSF} (8, 23) (ml/min) = 0.08, and V_{CSF} (ml) (8, 23) = 32 for a 15-kg (average) dog. [b] Fraction of the blood volume in organ capillaries to the total blood volume in the body. [c] Taken from Table 1 of Ref. 2.

or:

$$\begin{bmatrix}\text{drug accumulation}\\ \text{rate in blood pool}\end{bmatrix} = \begin{bmatrix}\text{summation of drug inflow rates}\\ \text{from five body regions}\end{bmatrix}$$

$$+ [\text{ingestion rate}] - [\text{drug outflow rate from blood pool}] \quad \text{(Eq. 13}b\text{)}$$

Plasma protein binding of salicylate was studied by the equilibrium dialysis technique (19). A linear relation was found between the total salicylate concentration, $C_{T,P}$, and the free concentration, $C_{F,P}$, in plasma in the range of salicylate levels investigated (10):

$$C_{T,P} = f_P(C_{F,P}) = B + NC_{F,P} \quad \text{(Eq. 14)}$$

where B and N are constants (10) given in Table I.

The relationship between the total salicylate concentration and the free concentration in whole blood may be determined indirectly. Since the free (unbound) drug in plasma water is in equilibrium with the bound drug in both plasma and blood, simultaneous determination of both total salicylate concentrations in blood and plasma from the same samples makes it possible to find the free concentration corresponding to both total concentrations in plasma and blood from Eq. 14. The relation thus constructed between the total salicylate concentration, $C_{T,B0}$, in original (nondiluted) blood and the free concentration, $C_{F,B}$, in blood water is also linear (10):

$$C_{T,B0} = f_B(C_{F,B}) = A + MC_{F,B} \quad \text{(Eq. 15)}$$

The values for A and M are also listed in Table I.

The experimental salicylate distribution data were obtained during a 6-hr experiment (10) in which blood loss occurred due to the surgical trauma from taking tissue samples. Normal saline was given continuously to maintain adequate blood pressure and blood volume. Therefore, the blood in the body was gradually diluted during the experiment. The fraction of whole (nondiluted) blood at time t in the continuously diluted blood, $F_B(t)$, can be calculated from the solution to a differential equation of the mass balance for the whole (nondiluted) blood. The rate of change of the total whole (nondiluted) blood volume in the body is equal to the loss rate of the whole blood, $Q_{BL}F_B(t)$, due to bleeding. It gives:

$$\frac{d[V_{TB,t}F_B(t)]}{dt} = -Q_{BL}F_B(t) \quad \text{(Eq. 16)}$$

where:

$$V_{TB,t} = V_{TB,0} + (Q_{SE} - Q_{BL})t \quad \text{(Eq. 17)}$$

and $F_B(t)$ is the fraction of whole (nondiluted) blood in the continuously diluted blood at time t, Q_{BL} is the blood loss rate due to bleeding from tissues, Q_{SE} is the saline-entering rate to the vein, $V_{TB,0}$ is the total blood volume in the body at time zero, and $V_{TB,t}$ is the total blood volume (diluted blood) in the body at time t.

In this study, the normal saline infusion rate was kept constant while the bleeding rate of blood loss from tissues was assumed to be constant (Table I). After Eq. 17 is substituted into Eq. 16, the solution to Eq. 16, under the conditions of both Q_{SE} and Q_{BL} being constants, gives:

$$F_B(t) = F_B(0)\left[1 + \frac{(Q_{SE} - Q_{BL})t}{V_{TB,0}}\right]^{-[Q_{SE}/(Q_{SE}-Q_{BL})]} \quad \text{(Eq. 18)}$$

Since time zero is the time just prior to blood dilution from saline infusion (10), the fraction of whole (nondiluted) blood at time zero, $F_B(0)$, is one.

The amount of salicylate in the diluted blood equals the amount of salicylate in the whole blood fraction plus that of salicylate in the water fraction of the diluted blood. Thus, it gives:

$$V_{TB,t}C_{T,B} = [V_{TB,t}F_B(t)]C_{T,B0} + \{V_{TB,t}[1 - F_B(t)]\}C_{F,B} \quad \text{(Eq. 19)}$$

Equation 19 may be simplified to:

$$C_{T,B} = F_B(t)C_{T,B0} + [1 - F_B(t)]C_{F,B} \quad \text{(Eq. 20)}$$

Substituting Eq. 15 into Eq. 20 and rearranging give:

$$C_{T,B} = F_B(t)A + H_m(t)C_{F,B} \quad \text{(Eq. 21)}$$

where $H_m(t) = 1 + (M - 1)F_B(t)$, A and M are constants in Eq. 15 and their values are shown in Table I, $C_{F,B}$ is the free salicylate concentration in blood water, $C_{T,B0}$ is the total salicylate concentration in whole (undiluted) blood, and $C_{T,B}$ is the total salicylate concentration in the diluted blood at time t.

Similarly, the total salicylate concentration in the blood of the capillary bed of any body region, Yz, can be expressed as:

$$C_{T,YzB} = F_B(t)A + H_m(t)C_{F,YzB} \quad \text{(Eq. 22)}$$

where $C_{F,YzB}$ is the free salicylate concentration in the capillary blood of any body region, Yz, and $C_{T,YzB}$ is the total salicylate concentration in the capillary blood of any body region, Yz. The blood volume of the blood pool, $V_{B,t}$, at time t can be calculated by:

$$V_{B,t} = V_{B,0} + (Q_{SE} - Q_{BL})tF_{V,B} \quad \text{(Eq. 23)}$$

where $F_{V,B}$ is the fraction of the blood volume of the blood pool in the total blood volume, $V_{B,0}$ is the blood volume of the blood pool at time zero, and $V_{B,t}$ is the blood volume of the blood pool at time t. Substituting Eqs. 21–23 into Eq. 13 and rearranging result in:

$$\frac{dC_{F,B}}{dt} = (Q_{Br}C_{F,BrB} + Q_{Li}C_{F,LiB} + Q_{Vi}C_{F,ViB} + Q_{Mu}C_{F,MuB} + Q_{Ad}C_{F,AdB})/V_{B,t} + Mg(t)/[V_{B,t}H_m(t)] - J_B(t)C_{F,B} - G_B(t) \quad \text{(Eq. 24)}$$

where:

$$G_B(t) = A\{F_B'(t)/H_m(t) + (Q_{SE} - Q_{BL})F_{V,B}F_B(t)/[V_{B,t}H_m(t)]\} \quad \text{(Eq. 25}a\text{)}$$

and:

$$J_B(t) = [H_m'(t)/H_m(t) + (Q_{SE} - Q_{BL})F_{V,B}/V_{B,t} + Q_B/V_B] \quad \text{(Eq. 25}b\text{)}$$

where $F_B'(t) = dF_B(t)/dt$; $H_m'(t) = dH_m(t)/dt$; $C_{F,B}$ is the free salicylate concentration in the blood pool; $C_{F,YzB}$ is the free salicylate concentration in the capillary bed of any body region, Yz; Q_{Yz} is the blood flow rate from the body region, Yz; and $V_{B,t}$ is the blood volume of the blood pool at time t.

An infusion pump was used to infuse the drug solution at a constant rate over 5 min (10). Thus, the ingestion term, $Mg(t)$, in Eq. 24 is equal to the dose divided by 5.

Liver—The transient mass balance for the liver (Li) is:

$$\frac{d(V_{LiB,t}C_{T,LiB})}{dt} + \frac{d(V_{LiT}C_{T,LiT})}{dt} = (Q_{HA}C_{T,B} + Q_{GI}C_{T,GIB}) - Q_{Li}C_{T,LiB} - R_m \quad \text{(Eq. 26}a\text{)}$$

or:

$$\begin{bmatrix}\text{drug accumulation rate}\\ \text{in capillary bed and}\\ \text{tissue portion of liver}\end{bmatrix} = \begin{bmatrix}\text{drug inflow rates from}\\ \text{blood pool (hepatic artery) and}\\ \text{GI tissue (portal vein)}\end{bmatrix} - \begin{bmatrix}\text{drug outflow}\\ \text{rate from liver}\end{bmatrix} - [\text{metabolism rate}] \quad \text{(Eq. 26}b\text{)}$$

Salicylate did not bind with the tissue components of the liver (10), which suggests that the amount of salicylate in the liver tissue equals the free salicylate concentration, $C_{F,LiT}$, multiplied by the volume of liver tissue water, $V_{LiT}F_{w,LiT}$:

$$V_{LiT}C_{T,LiT} = (V_{LiT}F_{w,LiT})C_{F,LiT} \quad \text{(Eq. 27)}$$

where $C_{F,LiT}$ and $C_{T,LiT}$ are the free and total salicylate concentrations

in the tissue portion of the liver, respectively; $F_{w,LiT}$ is the volume fraction of water in the tissue portion of the liver; and V_{LiT} is the volume of the tissue portion of the liver. Since the liver capillaries are highly permeable to salicylate, the equilibrium salicylate concentration (unbound concentration) between the capillaries and the liver tissue may be established nearly instantaneously:

$$C_{F,LiT} = C_{F,LiB} \quad \text{(Eq. 28)}$$

Substitution of Eq. 28 into Eq. 27 yields:

$$V_{LiT}C_{T,LiT} = (V_{LiT}F_{w,LiT})C_{F,LiB} \quad \text{(Eq. 29)}$$

The total salicylate concentration, $C_{T,LiB}$, and the blood volume, $V_{LiB,t}$, in the liver capillaries at time t have similar formulas as those in Eqs. 22 and 23:

$$C_{T,LiB} = F_B(t)A + H_m(t)C_{F,LiB} \quad \text{(Eq. 30)}$$

and:

$$V_{LiB,t} = V_{LiB,0} + (Q_{SE} - Q_{BL})tF_{V,LiB} \quad \text{(Eq. 31)}$$

where $F_{V,LiB}$ is the fraction of the blood volume of the liver capillary bed in the total blood volume, and $V_{LiB,0}$ and $V_{LiB,t}$ are the blood volumes of the liver capillary bed at time zero and t, respectively.

Substituting Eqs. 29–31 into Eq. 26*a* and rearranging yield:

$$\frac{dC_{F,LiB}}{dt} = (Q_{HA}C_{F,B} + Q_{GI}C_{F,GIB})H_m(t)/L_{Li}(t) - J_{Li}(t)C_{F,LiB} - R_m/L_{Li}(t) - G_{Li}(t) \quad \text{(Eq. 32)}$$

where:

$$L_{Li}(t) = V_{LiB,t}H_m(t) + V_{LiT}F_{w,LiT}$$

$$G_{Li}(t) = A[V_{LiB,t}F_B'(t) + (Q_{SE} - Q_{BL})F_{V,LiB}F_B(t)]/L_{Li}(t)$$

$$J_{Li}(t) = [V_{LiB,t}H_m'(t) + (Q_{SE} - Q_{BL})F_{V,LiB}H_m(t) + Q_{Li}H_m(t)]/L_{Li}(t)$$

Q_{HA} = blood flow rate of the hepatic artery

Q_{GI} = blood flow rate from the GI body region

The metabolism rate, R_m, can generally be described in terms of the simple Michaelis–Menten form:

$$R_m = \frac{K_{Li}C_{F,LiT}}{K_{M,Li} + C_{F,LiT}} \quad \text{(Eq. 33)}$$

There are two special cases: (*a*) if $C_{F,LiT} \gg K_{M,Li}$, then $R_m = K_{Li}$ (zero order), and (*b*) if $C_{F,LiT} \ll K_{M,Li}$, then $R_m = (K_{Li}/K_{M,Li})C_{F,LiT}$ (first order).

Since the metabolism mainly occurs in the liver, it was assumed that all salicylate metabolism occurs in the liver. In general, similar terms could be added to the other body regions if necessary. It was found previously (10) that the total excretion rate of unchanged salicylate and its metabolites (salicylurate, salicylglucuronide, and gentisate) was zero order and was 1.70 mg/min for the three dosages studied. Davis and Westfall (20) found that the amount of unchanged salicylate excreted in dog urine was 38% while that of its metabolites was 62% of the total amount excreted. The salicylate metabolism rate, which was assumed to be 62% of the total excretion rate, was 1.05 mg/min for the three dosages investigated.

Viscera—The transient mass balance for the viscera body region (Vi) is:

$$\frac{d(V_{ViB,t}C_{T,ViB})}{dt} + \frac{d(V_{ViT}C_{T,ViT})}{dt} = Q_{Vi}(C_{T,B} - C_{T,ViB}) - R_r \quad \text{(Eq. 34)}$$

The renal excretion rate, R_r, of unchanged salicylate was 0.65 mg/min for the three dosages studied (10). The total salicylate concentration, $C_{T,ViB}$, and blood volume, $V_{ViB,t}$, in the viscera capillaries at time t may be written in a form similar to that for the liver capillaries. The permeability of the visceral (kidneys and heart) capillaries is assumed to be similar to that of the liver capillaries. Salicylate does not bind with the tissue components of the viscera either. Thus:

$$V_{ViT}C_{T,ViT} = (F_{w,ViT}V_{ViT})C_{F,ViT} = (F_{w,ViT}V_{ViT})C_{F,ViB} \quad \text{(Eq. 35)}$$

$$C_{T,ViB} = F_B(t)A + H_m(t)C_{F,ViB} \quad \text{(Eq. 36)}$$

and:

$$V_{ViB,t} = V_{ViB,0} + (Q_{SE} - Q_{BL})tF_{V,ViB} \quad \text{(Eq. 37)}$$

Substituting Eqs. 35–37 into Eq. 34 and rearranging yield:

$$\frac{dC_{F,ViB}}{dt} = [Q_{Vi}H_m(t)/L_{Vi}(t)]C_{F,B} - J_{Vi}(t)C_{F,ViB} - G_{Vi}(t) - R_r/L_{Vi}(t) \quad \text{(Eq. 38)}$$

where:

$$L_{Vi}(t) = V_{ViB,t}H_m(t) + V_{ViT}F_{w,ViT}$$

$$G_{Vi}(t) = A[V_{ViB,t}F_B'(t) + (Q_{SE} - Q_{BL})F_{V,ViB}F_B(t)]/L_{Vi}(t)$$

$$J_{Vi}(t) = [V_{ViB,t}H_m'(t) + (Q_{SE} - Q_{BL})F_{V,ViB}H_m(t) + Q_{Vi}H_m(t)]/L_{Vi}(t)$$

R_r = renal excretion rate of unchanged salicylate

GI Region—The transit mass balance for the GI region (GI) is:

$$\frac{d(V_{GIB,t}C_{T,GIB})}{dt} + \frac{d(V_{GIT}C_{T,GIT})}{dt} = Q_{GI}(C_{T,B} - C_{T,GIB}) \quad \text{(Eq. 39)}$$

where:

$$V_{GIT}C_{T,GIT} = (V_{GIT}F_{w,GIT})C_{F,GIT} = (V_{GIT}F_{w,GIT})C_{F,GIB} \quad \text{(Eq. 40)}$$

$$C_{T,GIB} = F_B(t)A + H_m(t)C_{F,GIB} \quad \text{(Eq. 41)}$$

and:

$$V_{GIB,t} = V_{GIB,0} + (Q_{SE} - Q_{BL})tF_{V,GIB} \quad \text{(Eq. 42)}$$

The following equation results from the substitution of Eqs. 40–42 into Eq. 39:

$$\frac{dC_{F,GIB}}{dt} = [Q_{GI}H_m(t)/L_{GI}(t)]C_{F,B} - J_{GI}(t)C_{F,GIB} - G_{GI}(t) \quad \text{(Eq. 43)}$$

where:

$$L_{GI}(t) = V_{GIB,t}H_m(t) + V_{GIT}F_{w,GIT}$$

$$G_{GI}(t) = A[V_{GIB,t}F_B'(t) + (Q_{SE} - Q_{BL})F_{V,GIB}F_B(t)]/L_{GI}(t)$$

$$J_{GI}(t) = [V_{GIB,t}H_m'(t) + (Q_{SE} - Q_{BL})F_{V,GIB}H_m(t) + Q_{GI}H_m(t)]/L_{GI}(t)$$

Adipose Tissue—The transit mass balance for the adipose tissue region (Ad) is:

$$\frac{d(V_{AdB,t}C_{T,AdB})}{dt} + \frac{d(V_{AdT}C_{T,AdT})}{dt} = Q_{Ad}(C_{T,B} - C_{T,AdB}) \quad \text{(Eq. 44)}$$

The tissue "binding" in adipose tissue is primarily due to the lipid solubility of the drug. Salicylate that is ionized at physiological pH is not lipid soluble. Salicylate in the small portion (about 19%) of water in adipose tissue accounts for the total amount of salicylate in the tissue portion, giving:

$$V_{AdT}C_{T,AdT} = (V_{AdT}F_{w,AdT})C_{F,AdT} = (V_{AdT}F_{w,AdT})C_{F,AdB} \quad \text{(Eq. 45)}$$

Also:

$$C_{T,AdB} = F_B(t)A + H_m(t)C_{F,AdB} \quad \text{(Eq. 46)}$$

and:

$$V_{AdB,t} = V_{AdB,0} + (Q_{SE} - Q_{BL})tF_{V,AdB} \quad \text{(Eq. 47)}$$

Substituting Eqs. 45–47 into Eq. 44 and rearranging yield:

$$\frac{dC_{F,AdB}}{dt} = [Q_{Ad}H_m(t)/L_{Ad}(t)]C_{F,B} - J_{Ad}(t)C_{F,AdB} - G_{Ad}(t) \quad \text{(Eq. 48)}$$

where:

$$L_{Ad}(t) = V_{AdB,t}H_m(t) + V_{AdT}F_{w,AdT}$$

$$G_{Ad}(t) = A[V_{AdB,t}F_B'(t) + (Q_{SE} - Q_{BL})F_{V,AdB}F_B(t)]/L_{Ad}(t)$$

$$J_{Ad}(t) = [V_{AdB,t}H_m'(t) + (Q_{SE} - Q_{BL})F_{V,AdB}H_m(t) + Q_{Ad}H_m(t)]/L_{Ad}(t)$$

Muscle—The transit mass balance for the muscle body region (Mu) is:

$$\frac{d(V_{MuB,t}C_{T,MuB})}{dt} + \frac{d(V_{MuT}C_{T,MuT})}{dt} = Q_{Mu}(C_{T,B} - C_{T,MuB}) \quad \text{(Eq. 49)}$$

Salicylate does not bind with the tissue components of muscle. Hence:

$$V_{MuT}C_{T,MuT} = (V_{MuT}F_{w,MuT})C_{F,MuT} \quad \text{(Eq. 50)}$$

$$C_{T,MuB} = F_B(t)A + H_m(t)C_{F,MuB} \quad \text{(Eq. 51)}$$

and:

$$V_{MuB,t} = V_{MuB,0} + (Q_{SE} - Q_{BL})tF_{V,MuB} \quad \text{(Eq. 52)}$$

It has been stated that the passage of water-soluble compounds such as salicylate through the muscle capillaries is restricted. The restricted drug transport can be described by:

$$\frac{dC_{F,MuT}}{dt} = P_{Mu}(C_{F,MuB} - C_{F,MuT}) \quad \text{(Eq. 53)}$$

Substituting Eqs. 50–53 into Eq. 49 and rearranging give:

$$\frac{dC_{F,MuB}}{dt} = (Q_{Mu}/V_{MuB,t})C_{F,B} - I_{Mu}(t)C_{F,MuB} + \{P_{Mu}V_{MuT}F_{w,MuT}/[V_{MuB,t}H_m(t)]\}C_{F,MuT} - S_{Mu}(t) \quad \text{(Eq. 54)}$$

where:

$$I_{Mu}(t) = [V_{MuB,t}H_m'(t) + (Q_{SE} - Q_{BL})F_{V,MuB}H_m(t) + P_{Mu}V_{MuT}F_{w,MuT} + Q_{Mu}H_m(t)]/[V_{MuB,t}H_m(t)]$$

$$S_{Mu}(t) = A\{F_B'(t)/H_m(t) + (Q_{SE} - Q_{BL})F_{V,MuB}F_B(t)/[V_{MuB,t}H_m(t)]\}$$

Brain—The transit mass balance for the brain region (Br) is

$$\frac{d(V_{BrB,t}C_{T,BrB})}{dt} + \frac{d(V_{BrT}C_{T,BrT})}{dt} = Q_{Br}(C_{T,B} - C_{T,BrB}) \quad \text{(Eq. 55)}$$

No binding between salicylate and the brain tissue was found (10). Hence:

$$V_{BrT}C_{T,BrT} = (V_{BrT}F_{w,BrT})C_{F,BrT} \quad \text{(Eq. 56)}$$

$$C_{T,BrB} = F_B(t)A + H_m(t)C_{F,BrB} \quad \text{(Eq. 57)}$$

and:

$$V_{BrB,t} = V_{BrB,0} + (Q_{SE} - Q_{BL})tF_{V,BrB} \quad \text{(Eq. 58)}$$

In the brain, the capillaries are much less permeable to water-soluble substances, perhaps because the endothelium of brain capillaries appears to be a continuous sheet of the glial connective tissue cells without visible pores (8). The cellular sheath of the brain capillaries highly impedes the passage of water-soluble compounds and accounts for the blood–brain barrier. The kinetics of salicylate penetration into cerebrospinal fluid and brain were studied previously (21, 22). The permeability constant, P_{CSF}, for salicylate penetration into cerebrospinal fluid (21, 22) is in the 0.0026–0.006-min^{-1} range. Materials diffuse relatively freely in either direction between the cerebrospinal fluid and extracellular fluid deep into brain tissue (23). Therefore, the value of the permeability constant for the blood–cerebrospinal fluid barrier may be adopted as that for the passage of the drug between the brain capillaries and the brain tissue, *i.e.*, $P_{Br} = P_{CSF}$.

The highly restricted transport of the drug in the brain can be written in terms of the free concentration difference between the capillaries and the brain tissue:

$$\frac{dC_{F,BrT}}{dt} = P_{Br}(C_{F,BrB} - C_{F,BrT}) \quad \text{(Eq. 59)}$$

Substituting Eqs. 56–59 into Eq. 55 and rearranging give:

$$\frac{dC_{F,BrB}}{dt} = (Q_{Br}/V_{BrB,t})C_{F,B} - I_{Br}(t)C_{F,BrB} + \{P_{Br}V_{BrT}F_{w,BrT}/[V_{BrB,t}H_m(t)]\}C_{F,BrT} - S_{Br}(t) \quad \text{(Eq. 60)}$$

where:

$$I_{Br}(t) = [V_{BrB,t}H_m'(t) + (Q_{SE} - Q_{BL})F_{V,BrB}H_m(t) + P_{Br}V_{BrT}F_{w,BrT} + Q_{Br}H_m(t)]/[V_{BrB,t}H_m(t)]$$

$$S_{Br}(t) = A\{F_B'(t)/H_m(t) + (Q_{SE} - Q_{BL})F_{V,BrB}F_B(t)/[V_{BrB,t}H_m(t)]\}$$

Kinetics of Salicylate Penetration into Cerebrospinal Fluid—In humans, the production rate of cerebrospinal fluid is in the 0.3–0.5-ml/min range with a total volume of about 120–200 ml (8, 23). The cerebrospinal fluid moves by bulk flow out of the ventricular system into the subarachnoid space and eventually returns to the bloodstream. The drug in the cerebrospinal fluid is removed as it returns to the general circulation.

The drug accumulation rate in the cerebrospinal fluid equals the drug penetration rate from the brain capillaries to the cerebrospinal fluid minus the drug removal rate due to the cerebrospinal fluid returning to the bloodstream. Thus:

$$\frac{d(V_{CSF}C_{CSF})}{dt} = V_{CSF}P_{CSF}(C_{F,BrB} - C_{CSF}) - Q_{CSF}C_{CSF} \quad \text{(Eq. 61)}$$

Equation 61 may be simplified to:

$$\frac{dC_{CSF}}{dt} = P_{CSF}(C_{F,BrB} - C_{CSF}) - (Q_{CSF}/V_{CSF})C_{CSF} \quad \text{(Eq. 62)}$$

where $C_{F,BrB}$ and C_{CSF} are the free concentrations in the brain capillaries and in the cerebrospinal fluid, respectively; P_{CSF} is the permeability constant for drug passage into the cerebrospinal fluid; Q_{CSF} is the production or removal rate of the cerebrospinal fluid; and V_{CSF} is the total cerebrospinal fluid volume.

There are 10 unknown variables (seven free concentrations in the blood pool and in the capillaries of the other six body regions plus three free concentrations in the cerebrospinal fluid and in the tissue portions of brain and muscle) in a system of 10 simultaneous equations (Eqs. 24, 32, 38, 43, 48, 53, 54, 59, 60, and 62). Ten equations can serve to solve 10 variables. Therefore, a system of the 10 simultaneous first-order ordinary differential equations can be solved numerically. In this study, the Runge-Kutta fourth-order method (10, 24) for solution of ordinary differential equations was employed to solve the 10 simultaneous equations. The solution gives simultaneously the kinetics of the 10 variables (free salicylate concentrations in this case).

Since the total salicylate concentration, $C_{T,B}$, in the blood pool and both the total salicylate concentration, $C_{T,YzB}$, in the capillary blood and the total salicylate concentration, $C_{T,YzT}$, in the tissue portion of any body region, Yz, can be correlated with their corresponding free salicylate concentrations by Eqs. 21, 22, 29, 35, 40, 45, 50, and 56, all kinetics of total salicylate concentrations in the blood pool and in both the capillary blood and tissue portions of various body regions can also be determined by the model. Model feasibility can be demonstrated by comparing the experimental kinetic data with the model-predicted results. Since the experimentally determined salicylate concentration in any organ, Yz, represents the total salicylate concentration, $C_{T,Yz}$, in that organ, which can be calculated in terms of the total salicylate concentration, $C_{T,YzB}$, in the capillary blood and the total salicylate concentration $C_{T,YzT}$, in the tissue portion of the body region by the following equation:

$$C_{T,Yz}(V_{YzB} + V_{YzT}) = C_{T,YzB}V_{YzB} + C_{T,YzT}V_{YzT} \quad \text{(Eq. 63)}$$

the pharmacokinetics of total salicylate levels in various organs and tissues can be predicted by the model.

During the 6-hr experiment, blood loss occurred due to the bleeding from taking various tissue samples to obtain experimental kinetic data. Normal saline was continuously supplied to maintain adequate blood pressure and blood volume. The factors accounting for the blood dilution and the drug loss accompanying blood loss were considered in constructing the pharmacokinetic model. However, the kinetic behavior of salicylate distribution in the body of an intact dog in which tissue samples are not taken is expected to be a little different from that in the dog from which various tissue samples are taken. When tissue samples are not taken, neither blood loss nor blood dilution occurs. The fraction of whole (nondiluted) blood, $F_B(t)$, is always one, and the rates of saline supply and blood loss are zero. The solution to a system of the 10 simultaneous differential equations will give slightly higher salicylate levels in the body because there is no drug loss accompanying blood loss.

Effect of Hemoperfusion on Salicylate Kinetics—The effectiveness of hemoperfusion using albumin-coated activated carbon for acute, severely intoxicated cases was evaluated in terms of its effect on the salicylate body distribution (10). It was also attempted to apply the model to predict the salicylate pharmacokinetics in the body due to the extracorporeal treatment. A blood pump was used to shunt part of the femoral arterial blood through the extracorporeal device, and the "clean" blood out of the device was conducted into the femoral vein during the treatment. Thus:

$$Q_{Mu,ET} = Q_{Mu} - Q_{ET} \quad \text{(Eq. 64)}$$

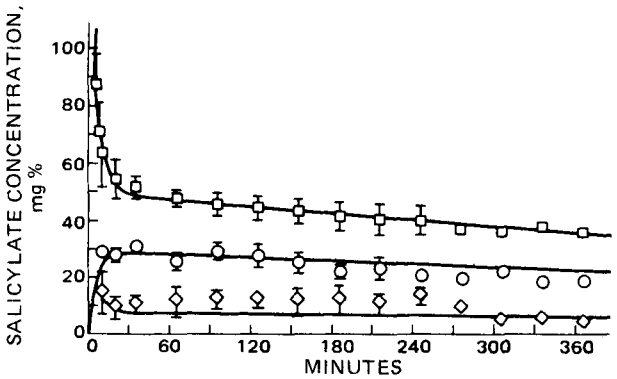

Figure 1—*Predicted (solid lines) and experimental salicylate concentrations in blood (□), muscle (○), and adipose tissue (◇) at a dose of 285 mg/kg (sodium salicylate).*

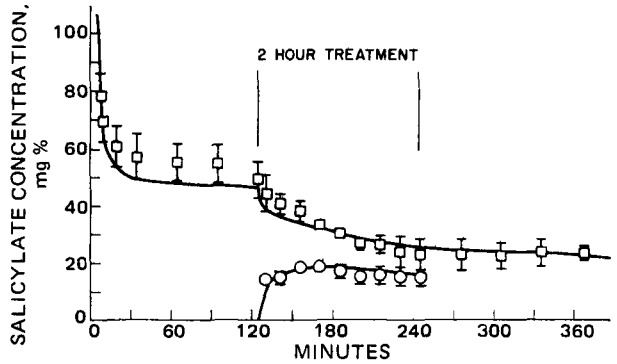

Figure 3—*Predicted (solid lines) and experimental salicylate concentrations in blood under the influence of 2-hr hemoperfusion treatment at a dose of 285 mg/kg. Key: □, inflow blood; and ○, outflow blood.*

where $Q_{Mu,ET}$ is the blood flow rate through the muscle during the extracorporeal treatment, Q_{ET} is the blood perfusion rate shunted through the extracorporeal device, and Q_{Mu} is the blood flow rate through the muscle without shunting blood through the device.

The salicylate removal rate by the extracorporeal treatment, R_{ET}, can be calculated by:

$$R_{ET} = Q_{ET}(C_{T,B} - C_{T,B,\text{out}}) \quad \text{(Eq. 65)}$$

where $C_{T,B}$ is the total drug concentration from the blood pool entering the extracorporeal device and $C_{T,B,\text{out}}$ is the total drug concentration in the outflow blood from the device.

During extracorporeal treatment, Eqs. 13 and 49 of transient mass balance for the blood pool and for the muscle region should be modified to:

$$\frac{d(V_{B,t}C_{T,B})}{dt} = (Q_{Br}C_{T,BrB} + Q_{Li}C_{T,LiB} + Q_{Vi}C_{T,ViB} + Q_{Mu,ET}C_{T,MuB} + Q_{ET}C_{T,B,\text{out}} + Q_{Ad}C_{T,AdB}) + Mg(t) - Q_BC_{T,B} \quad \text{(Eq. 66)}$$

and:

$$\frac{d(V_{MuB,t}C_{T,MuB})}{dt} + \frac{d(V_{MuT}C_{T,MuT})}{dt} = Q_{Mu,ET}(C_{T,B} - C_{T,MuB}) \quad \text{(Eq. 67)}$$

The right-hand side of Eq. 66 can also be written in terms of the salicylate removal rate by the extracorporeal treatment, R_{ET}, from Eq. 65 and becomes:

$$\frac{d(V_{B,t}C_{T,B})}{dt} = (Q_{Br}C_{T,BrB} + Q_{Li}C_{T,LiB} + Q_{Vi}C_{T,ViB} + Q_{Mu,ET}C_{T,MuB} + Q_{Ad}C_{T,AdB}) + Mg(t) - (Q_B - Q_{ET})C_{T,B} - R_{ET} \quad \text{(Eq. 68)}$$

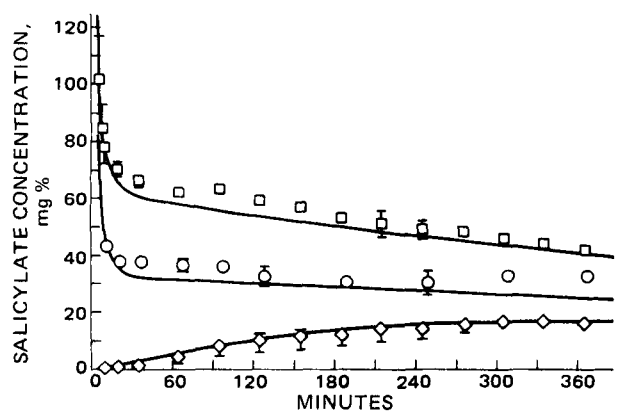

Figure 2—*Predicted (solid lines) and experimental salicylate concentrations in plasma (□), liver (○), and cerebrospinal fluid (◇) at a dose of 285 mg/kg (sodium salicylate).*

Therefore, the pharmacokinetic behavior of salicylate in the body during the extracorporeal treatment also can be predicted by solving a system of 10 simultaneous equations.

RESULTS AND DISCUSSION

The values of parameters and constants necessary for solving the system of 10 simultaneous differential equations are shown in Table I and Scheme I.

Three different dosages of sodium salicylate were used: 135 mg/kg (therapeutic), 210 mg/kg (moderate intoxication), and 285 mg/kg (severe intoxication). Only the 285-mg/kg data are given here; data for the other dosages are available, however (10). Three or four mongrel dogs (15–25 kg) were evaluated with each dosage. An infusion pump was employed to infuse each dose at a constant rate over 5 min. A detailed description of the experimental method for quantitative studies on salicylate kinetics in cerebrospinal fluid, blood, plasma, liver, muscle, and adipose tissue is available (10).

The mean values ($\pm SD$) of the experimentally determined salicylate concentrations with time and the predicted pharmacokinetics (solid lines) by the model are shown in Figs. 1 and 2 for the 285-mg/kg dose. If a calculated standard deviation is within the size of a symbol representing a mean value, then the standard deviation is not shown in the figures. Time zero in the figures is the time just prior to infusing a dose. The good agreement between predicted kinetics and experimental data demonstrates model feasibility.

In an experiment with hemoperfusion treatment, a severely intoxicating dose (285 mg/kg) of sodium salicylate was administered intravenously to dogs (19–26 kg, average 23 kg) at a constant rate for 5 min. Two hours later, the poisoned dog was treated by an extracorporeal device containing 250 g (wet weight) of albumin-coated activated carbon[1] for 2 hr (10). The arterial blood from the femoral artery was shunted through the extracorporeal cartridge; salicylate in the blood was adsorbed by the carbon, and the outflow "clean" blood returned to the femoral vein.

The salicylate removal rate by hemoperfusion was calculated, as stated previously, in terms of the blood perfusion rate and the concentration difference between inflow and outflow blood samples (Fig. 3). The blood perfusion rate shunted from the femoral artery of a 23-kg (average) dog in the experiment (10) was kept at 100 ml/min by a blood pump. However, the physiological parameters employed in the pharmacokinetic modeling are based on a 15-kg (average) dog. Hence, the blood perfusion rate used in this model was adjusted to that for a 15-kg dog and gave 65 ml/min as the result of multiplying a ratio of the two body weights.

Figures 4–6 show the experimental kinetic data of salicylate levels (mean value ± SD) in blood, plasma, muscle, adipose tissue, and cerebrospinal fluid and the predicted kinetics (solid lines) by the model under the effect of the 2-hr treatment. The kinetic changes of salicylate levels in the body during and after the hemoperfusion are also well predicted by the model with certain modifications in blood flows and in equations as expressed in the previous section.

The pharmacological effect of a drug is generally reflected better by the free (unbound) drug levels in blood or target organ(s). The relationships between free and total drug concentrations in blood and various

[1] Witco 517, Witco Chemical Co.

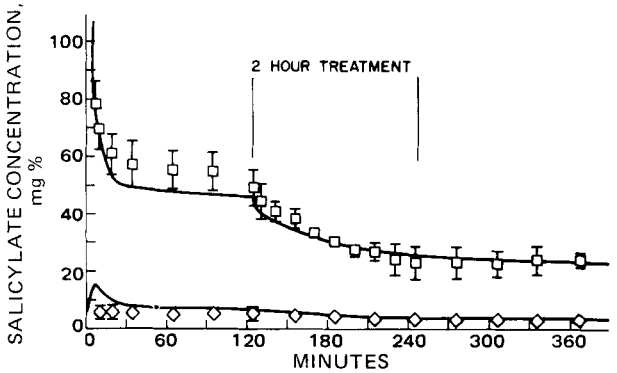

Figure 4—*Predicted (solid lines) and experimental salicylate concentrations in blood (□) and adipose tissue (◇) under the influence of 2-hr hemoperfusion treatment at a dose of 285 mg/kg.*

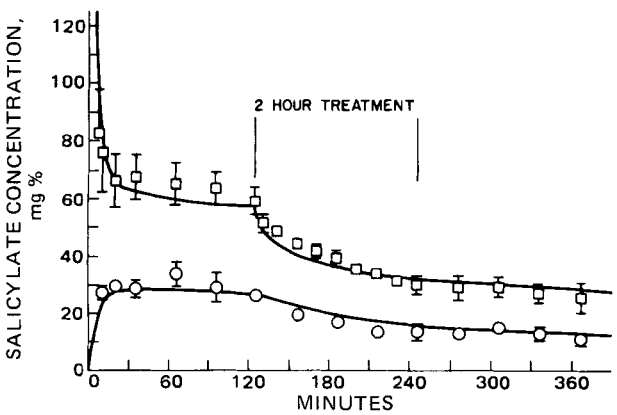

Figure 5—*Predicted (solid lines) and experimental salicylate concentrations in plasma (□) and muscle (○) under the influence of 2-hr hemoperfusion treatment at a dose of 285 mg/kg.*

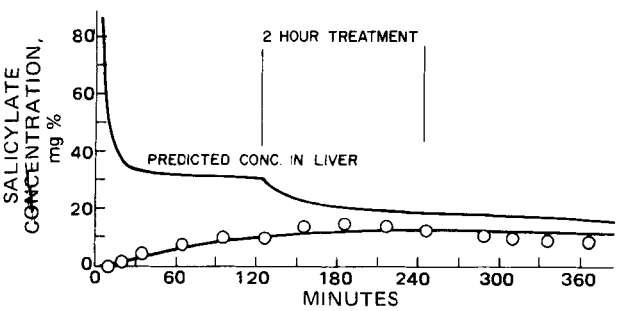

Figure 6—*Predicted (solid lines) and experimental salicylate concentrations in cerebrospinal fluid (○) and liver under the influence of 2-hr hemoperfusion treatment at a dose of 285 mg/kg. No experimental data were obtained for liver as a result of heparin therapy being applied to the dog with the hemoperfusion treatment (10).*

tissues were considered in constructing the equations for the model. Figures 7 and 8 show experimental (mean value ± *SD*) and predicted (solid lines) kinetics of free and total salicylate levels in plasma with and without the hemoperfusion treatment. The results predicted by the model agree with the experimental data.

Curves and data comparable to those reported in Figs. 1–8 are also available for the 135- and 210-mg/kg doses (10).

CONCLUSIONS

Since knowledge of the kinetic behavior of a drug in blood or plasma may not provide sufficient information for appropriate therapy, kinetic information of drug levels in brain, cerebrospinal fluid, blood, organs, and tissues of pharmacological interest may be necessary for the development of improved dosage regimens. The pharmacokinetic model

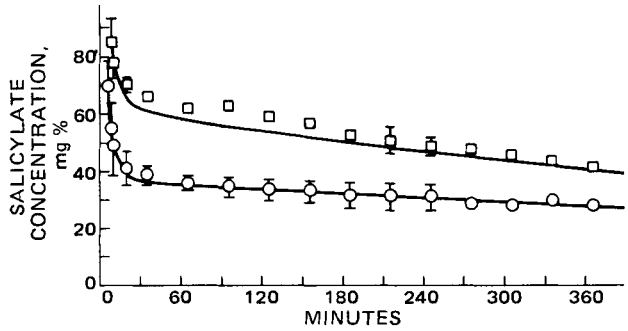

Figure 7—*Predicted (solid lines) and experimental free salicylate concentration (○) and total salicylate concentration (□) in plasma at a dose of 285 mg/kg (sodium salicylate).*

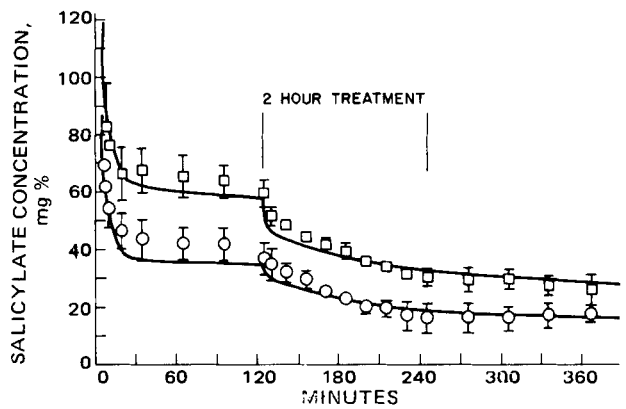

Figure 8—*Predicted (solid lines) and experimental free salicylate concentration (○) and total salicylate concentration (□) in plasma under the influence of 2-hr hemoperfusion treatment at a dose of 285 mg/kg.*

presented in this study can predict salicylate levels not only in blood or plasma but also in cerebrospinal fluid, liver, and other tissues. Conventional compartment models are unable to do so.

Free drug concentrations (variables to be solved) in all body regions (Scheme I) are involved in Eq. 24 while the free drug concentration in the blood pool appears in the equation for each body region. Thus, each equation in a system of simultaneous differential equations is not independent but interrelated to the others. This feature of the model has an important application in clinical pharmacokinetics. If the model for a given drug can be verified in a species pharmacokinetically similar to humans, then it can be applied to predict pharmacokinetics of the drug in human blood, organs, and tissues of pharmacological importance by using the physiological and biochemical parameters of humans.

The experimentally observed kinetics of drug levels in blood or plasma may be used to compare with the corresponding kinetics predicted by the model. If they agree well, the model-predicted kinetics of drug distribution in the other body regions that are difficult to sample may be expected to represent closely the actual kinetic courses because of the interrelated characteristics of the equations. Therefore, the model can furnish more complete and valuable information for optimal therapeutic regimens. The model has been successfully applied to predict the pharmacokinetics of salicylate in the dog with and without extracorporeal activated carbon treatment.

REFERENCES

(1) R. J. Lutz, R. L. Dedrick, J. A. Straw, M. M. Hart, P. Klubes, and D. S. Zaharko, *J. Pharmacokinet. Biopharm.*, **3**, 77 (1975).

(2) C. N. Chen and J. D. Andrade, *J. Pharm. Sci.*, **65**, 717 (1976).

(3) K. B. Bischoff and R. L. Dedrick, *ibid.*, **57**, 1346 (1968).

(4) D. S. Zaharko, R. L. Dedrick, K. B. Bischoff, J. A. Longstreth, and V. T. Oliverio, *J. Natl. Cancer Inst.*, **46**, 775 (1971).

(5) R. L. Dedrick, S. C. Zaharko, and R. J. Lutz, *J. Pharm. Sci.*, **62**, 882 (1973).

(6) R. L. Dedrick, D. D. Forrester, J. N. Cannon, S. M. El Dareer, and L. B. Mellett, *Biochem. Pharmacol.*, **22**, 2405 (1973).

(7) R. L. Dedrick, D. D. Forrester, and D. H. W. Ho, *ibid.*, **21**, 1 (1972).
(8) A. Goldstein, L. Aronow, and S. W. Kalman, "Principles of Drug Action," 2nd ed., Wiley, New York, N.Y., 1974, p. 167.
(9) J. G. Luft, in "The Inflammatory Process," B. W. Zweifach, L. Grant, and R. T. McCluskey, Eds., Academic, New York, N.Y., 1965, p. 121.
(10) C. N. Chen, Ph.D. dissertation, University of Utah, Salt Lake City, Utah, 1976.
(11) S. A. Duwe, G. L. DeNardo, M. A. Helikson, K. S. Watanabe, and L. G. Crowley, *Surg. Forum*, **21**, 376 (1970).
(12) J. G. Gibson, A. M. Seligman, W. C. Peacock, J. C. Aub, J. Fine, and R. D. Evans, *J. Clin. Invest.*, **25**, 848 (1946).
(13) V. A. Levin and D. D. Gilboe, *Stroke*, **1**, 270 (1970).
(14) M. T. Velasquez, A. V. Notargioacomo, and J. N. Cohn, *Am. J. Physiol.*, **224**, 322 (1973).
(15) E. G. Ohlsson, R. B. Rutherford, M. M. P. Haalebos, H. N. Wagner, and G. D. Zuidema, *J. Surg. Res.*, **10**, 201 (1970).
(16) W. J. Kane and E. Grim, *J. Bone Joint Surg.*, **51**, 309 (1969).
(17) P. A. Nielsen and N. J. Secher, *Life Sci.*, **9**, 75 (1970).
(18) U. Finsterer, P. Pruchsunand, and H. Brechtelsbauer, *Pfluegers Arch. Eur. J. Physiol.*, **341**, 63 (1973).
(19) C. Davison and P. K. Smith, *J. Pharmacol. Exp. Ther.*, **133**, 161 (1961).
(20) L. E. Davis and B. A. Westfall, *Am. J. Vet. Res.*, **33**, 1253 (1972).
(21) S. Mayer, R. P. Maickel, and B. B. Brodie, *J. Pharmacol. Exp. Ther.*, **127**, 205 (1959).
(22) B. B. Brodie, H. Kurz, and L. S. Schanker, *ibid.*, **130**, 20 (1960).
(23) D. P. Rall, in "Fundamentals of Drug Metabolism and Drug Disposition," B. N. LaDu, H. G. Mandel, and E. L. Way, Eds., Williams & Wilkins, Baltimore, Md., 1971, p. 76.
(24) B. Carnahan, H. A. Luther, and J. O. Wilkes, "Applied Numerical Methods," Wiley, New York, N.Y., 1969, p. 361.

ACKNOWLEDGMENTS

Supported by National Institutes of Health Grant FD 00480-03 and National Science Foundation Grant GH 38996X.

The assistance of Dr. S. M. Fang, C. M. Chen, and A. Atwood is gratefully acknowledged.

Frequency Distribution of Bilirubin Intrinsic Clearance in Adult Male Sprague–Dawley Rats

SVEIN ØIE and GERHARD LEVY ˣ

Received September 7, 1976, from the *Department of Pharmaceutics, School of Pharmacy, State University of New York at Buffalo, Amherst, NY 14260.* Accepted for publication March 22, 1977.

Abstract □ The intrinsic body clearance of bilirubin was determined in 48 adult male Sprague–Dawley rats that received an intravenous infusion of bilirubin. The intrinsic body clearance was calculated from the infusion rate, the steady-state plasma concentration of total (free and protein-bound) bilirubin, and the free fraction of bilirubin in plasma. The intrinsic body clearance of bilirubin ranged from 5.05 to 13.20 liters/kg/min and was bimodally distributed, with half of the animals in each group. The plasma free fraction of bilirubin ranged from 0.00025 to 0.00077 (mean 0.00053) in the 24 intrinsically rapid metabolizers of bilirubin and from 0.00048 to 0.00103 (mean 0.00075) in the intrinsically slow metabolizers of the pigment. Thus, interindividual differences in the *total* clearance of bilirubin in the rats are due to differences in both intrinsic body clearance and plasma protein binding.

Keyphrases □ Bilirubin—intrinsic body clearance, frequency distribution, rats □ Clearance, intrinsic body—bilirubin, frequency distribution, rats □ Pigments—bilirubin, intrinsic body clearance, frequency distribution, rats

The heme pigment bilirubin is eliminated in humans and animals almost entirely by conjugative pathways (1). The concentration of bilirubin in plasma is a frequently used diagnostic index because it reflects changes in the formation and elimination rates of the pigment that may be caused by hemolysis, liver disease, and other pathologic conditions.

Preliminary studies on a small group of rats revealed pronounced interindividual differences in the total body clearance of bilirubin which could be ascribed largely to corresponding differences in the plasma protein binding of the pigment (2). This study has been extended to a total of 48 animals to determine the magnitude of interindividual differences in total body clearance, intrinsic clearance, and plasma free fraction of bilirubin.

EXPERIMENTAL

Forty-eight male Sprague–Dawley rats[1], 300–400 g, were maintained on a standard diet[2] and received an infusion of bilirubin into the right jugular vein. Forty animals received bilirubin at a rate of 0.8 mg/kg/min for 15 min and then 0.32 mg/kg/min for up to 4 hr; the other eight rats were infused at a rate of 0.8 mg/kg/min for the entire period (except for three of these animals that received 2 mg/kg/min for the first 15 min). Blood samples were obtained periodically, and plasma was assayed for free (3) and total (4) unconjugated bilirubin.

Steady-state conditions were ascertained as previously described (2). The total body clearance of bilirubin was calculated by dividing the maintenance infusion rate by the steady-state concentration of total bilirubin in plasma. The intrinsic body clearance was determined (5) by dividing the total body clearance by the free fraction of bilirubin in plasma (free fraction = free ÷ total concentration of bilirubin). These experiments were carried out over 2 years, 1–4 weeks after receipt of the animals.

Histograms to describe the frequency distribution of intrinsic clearance and log intrinsic clearance values were constructed by iteratively changing the class interval to maximize the number of bars in the respective graph while minimizing the number of regional reversals (modes and antimodes), as suggested by Martin *et al.* (6). For the bimodal characterization, the mean value, standard deviation, and fraction of the total population in each Gaussian component were estimated (7) by dividing the appropriate histogram at the antimode and considering each segment of the population as a separate Gaussian or log-normally distributed component.

[1] Blue Spruce Farms, Altamont, N.Y.
[2] Charles River Formula 4RF.

(7) R. L. Dedrick, D. D. Forrester, and D. H. W. Ho, *ibid.*, **21**, 1 (1972).
(8) A. Goldstein, L. Aronow, and S. W. Kalman, "Principles of Drug Action," 2nd ed., Wiley, New York, N.Y., 1974, p. 167.
(9) J. G. Luft, in "The Inflammatory Process," B. W. Zweifach, L. Grant, and R. T. McCluskey, Eds., Academic, New York, N.Y., 1965, p. 121.
(10) C. N. Chen, Ph.D. dissertation, University of Utah, Salt Lake City, Utah, 1976.
(11) S. A. Duwe, G. L. DeNardo, M. A. Helikson, K. S. Watanabe, and L. G. Crowley, *Surg. Forum*, **21**, 376 (1970).
(12) J. G. Gibson, A. M. Seligman, W. C. Peacock, J. C. Aub, J. Fine, and R. D. Evans, *J. Clin. Invest.*, **25**, 848 (1946).
(13) V. A. Levin and D. D. Gilboe, *Stroke*, **1**, 270 (1970).
(14) M. T. Velasquez, A. V. Notargioacomo, and J. N. Cohn, *Am. J. Physiol.*, **224**, 322 (1973).
(15) E. G. Ohlsson, R. B. Rutherford, M. M. P. Haalebos, H. N. Wagner, and G. D. Zuidema, *J. Surg. Res.*, **10**, 201 (1970).
(16) W. J. Kane and E. Grim, *J. Bone Joint Surg.*, **51**, 309 (1969).
(17) P. A. Nielsen and N. J. Secher, *Life Sci.*, **9**, 75 (1970).
(18) U. Finsterer, P. Pruchsunand, and H. Brechtelsbauer, *Pfluegers Arch. Eur. J. Physiol.*, **341**, 63 (1973).
(19) C. Davison and P. K. Smith, *J. Pharmacol. Exp. Ther.*, **133**, 161 (1961).
(20) L. E. Davis and B. A. Westfall, *Am. J. Vet. Res.*, **33**, 1253 (1972).
(21) S. Mayer, R. P. Maickel, and B. B. Brodie, *J. Pharmacol. Exp. Ther.*, **127**, 205 (1959).
(22) B. B. Brodie, H. Kurz, and L. S. Schanker, *ibid.*, **130**, 20 (1960).
(23) D. P. Rall, in "Fundamentals of Drug Metabolism and Drug Disposition," B. N. LaDu, H. G. Mandel, and E. L. Way, Eds., Williams & Wilkins, Baltimore, Md., 1971, p. 76.
(24) B. Carnahan, H. A. Luther, and J. O. Wilkes, "Applied Numerical Methods," Wiley, New York, N.Y., 1969, p. 361.

ACKNOWLEDGMENTS

Supported by National Institutes of Health Grant FD 00480-03 and National Science Foundation Grant GH 38996X.

The assistance of Dr. S. M. Fang, C. M. Chen, and A. Atwood is gratefully acknowledged.

Frequency Distribution of Bilirubin Intrinsic Clearance in Adult Male Sprague–Dawley Rats

SVEIN ØIE and GERHARD LEVY ˣ

Received September 7, 1976, from the *Department of Pharmaceutics, School of Pharmacy, State University of New York at Buffalo, Amherst, NY 14260.* Accepted for publication March 22, 1977.

Abstract □ The intrinsic body clearance of bilirubin was determined in 48 adult male Sprague–Dawley rats that received an intravenous infusion of bilirubin. The intrinsic body clearance was calculated from the infusion rate, the steady-state plasma concentration of total (free and protein-bound) bilirubin, and the free fraction of bilirubin in plasma. The intrinsic body clearance of bilirubin ranged from 5.05 to 13.20 liters/kg/min and was bimodally distributed, with half of the animals in each group. The plasma free fraction of bilirubin ranged from 0.00025 to 0.00077 (mean 0.00053) in the 24 intrinsically rapid metabolizers of bilirubin and from 0.00048 to 0.00103 (mean 0.00075) in the intrinsically slow metabolizers of the pigment. Thus, interindividual differences in the *total* clearance of bilirubin in the rats are due to differences in both intrinsic body clearance and plasma protein binding.

Keyphrases □ Bilirubin—intrinsic body clearance, frequency distribution, rats □ Clearance, intrinsic body—bilirubin, frequency distribution, rats □ Pigments—bilirubin, intrinsic body clearance, frequency distribution, rats

The heme pigment bilirubin is eliminated in humans and animals almost entirely by conjugative pathways (1). The concentration of bilirubin in plasma is a frequently used diagnostic index because it reflects changes in the formation and elimination rates of the pigment that may be caused by hemolysis, liver disease, and other pathologic conditions.

Preliminary studies on a small group of rats revealed pronounced interindividual differences in the total body clearance of bilirubin which could be ascribed largely to corresponding differences in the plasma protein binding of the pigment (2). This study has been extended to a total of 48 animals to determine the magnitude of interindividual differences in total body clearance, intrinsic clearance, and plasma free fraction of bilirubin.

EXPERIMENTAL

Forty-eight male Sprague–Dawley rats[1], 300–400 g, were maintained on a standard diet[2] and received an infusion of bilirubin into the right jugular vein. Forty animals received bilirubin at a rate of 0.8 mg/kg/min for 15 min and then 0.32 mg/kg/min for up to 4 hr; the other eight rats were infused at a rate of 0.8 mg/kg/min for the entire period (except for three of these animals that received 2 mg/kg/min for the first 15 min). Blood samples were obtained periodically, and plasma was assayed for free (3) and total (4) unconjugated bilirubin.

Steady-state conditions were ascertained as previously described (2). The total body clearance of bilirubin was calculated by dividing the maintenance infusion rate by the steady-state concentration of total bilirubin in plasma. The intrinsic body clearance was determined (5) by dividing the total body clearance by the free fraction of bilirubin in plasma (free fraction = free ÷ total concentration of bilirubin). These experiments were carried out over 2 years, 1–4 weeks after receipt of the animals.

Histograms to describe the frequency distribution of intrinsic clearance and log intrinsic clearance values were constructed by iteratively changing the class interval to maximize the number of bars in the respective graph while minimizing the number of regional reversals (modes and antimodes), as suggested by Martin *et al.* (6). For the bimodal characterization, the mean value, standard deviation, and fraction of the total population in each Gaussian component were estimated (7) by dividing the appropriate histogram at the antimode and considering each segment of the population as a separate Gaussian or log-normally distributed component.

[1] Blue Spruce Farms, Altamont, N.Y.
[2] Charles River Formula 4RF.

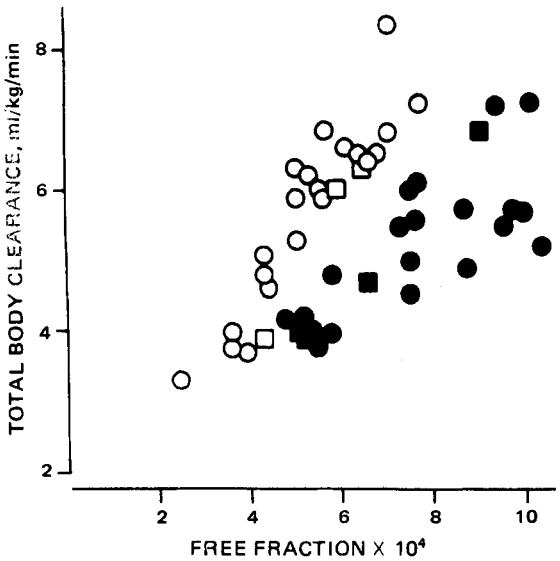

Figure 1—*Relationship between total body clearance of bilirubin and the free fraction of bilirubin in the plasma of individual rats. The 48 animals yielded data indicative of two separate populations, designated by open and closed symbols. Key: ○, ●, animals that received a bilirubin "loading" infusion of 0.8 mg/kg/min for 15 min and a maintenance infusion of 0.32 mg/kg/min thereafter; and □, ■, animals that received a maintenance infusion of 0.8 mg/kg/min (three animals first received a "loading" infusion of 2 mg/kg/min for 15 min). Correlation coefficients are 0.91 (p < 0.001) for data represented by open symbols and 0.79 (p < 0.001) for data represented by closed symbols.*

The various frequency distribution curves were fitted to the respective frequency–clearance value or frequency–log clearance value histograms by a standard method (8). The expected frequencies for overlapping components were summed prior to evaluating the agreement of the distribution model with the histogram by a χ-square test. For this test, classes were pooled when the expected frequency was three or less.

RESULTS

The average bilirubin concentration in the plasma of the rats before infusion of exogenous bilirubin was 0.06 mg/100 ml, which is less than 2% of the steady-state concentration during the infusion of the pigment. Thus, no correction had to be made for endogenous bilirubin.

The total body clearance of bilirubin in the 48 rats ranged from 3.3 to 8.3 ml/kg/min, and the plasma free fraction of bilirubin ranged from 0.00025 to 0.00103, indicating 99.897–99.975% protein binding. There is a statistically significant correlation ($r = 0.53$, $p < 0.001$) between total body clearance and free fraction values. This correlation becomes stronger if the data are treated as being representative of two different populations (Fig. 1). The existence of two different populations becomes even more apparent in the histogram of the intrinsic body clearance values (Fig. 2).

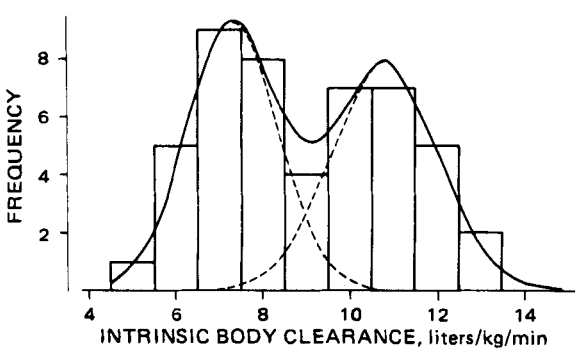

Figure 2—*Histogram showing the frequency distribution of bilirubin intrinsic body clearance by 48 male Sprague-Dawley rats. Also shown is the bimodal theoretical distribution curve, with the dotted line indicating the overlapping portions of the individual Gaussian components.*

Table I—Evaluation of Different Types of Frequency Distribution Curves for Bilirubin Intrinsic Clearance by Sprague–Dawley Rats

Type of Distribution	Mean(s), liters/kg/min	*SD*	χ^2	Degrees of Freedom	*p*
Normal	8.91	2.12	5.23	4	>0.26
Log-normal	8.65	+2.42, −1.89	4.59	3	>0.20
Bimodal	7.30	1.00	0.50	2	>0.77
	10.80	1.20			
Log-bimodal	7.24	+1.08, −0.93	2.18	1	>0.13
	10.72	+1.52, −1.39			

The data are best described by a bimodal frequency distribution curve, with one-half the animals in each Gaussian component (Table I). The intrinsic clearance data were examined for a possible seasonal or time-related effect (9), and none of the runs above or below the median for any one of the populations or for the combined group of 48 animals exceeded the length predictable entirely by chance ($0.10 < p < 0.50$).

There is a statistically significant negative correlation between the intrinsic body clearance and the plasma free fraction of bilirubin for the entire 48 animals ($r = -0.711$, $p < 0.001$) and for the intrinsically rapid and slow metabolizers of bilirubin considered separately (Fig. 3). Taken as a whole, the 48 plasma free fraction values are log-normally distributed.

DISCUSSION

The total body clearance of bilirubin in male Sprague–Dawley rats, as determined in this investigation, is significantly lower than their liver perfusion rate (about 93 ml of blood/kg/min) (10). Therefore, an approximately linear relationship between total body clearance and plasma free fraction may be expected on theoretical grounds if the intrinsic body clearance is relatively constant (5). Such a linear relationship is apparent in Fig. 1, but the data in this figure suggest that there may be two populations, one consisting of intrinsically rapid metabolizers of bilirubin (high intrinsic body clearance) and the other consisting of intrinsically slow metabolizers (low intrinsic body clearance).

The existence of such bimodality was verified by statistical analysis of the frequency distribution of the intrinsic body clearance values for bilirubin in the 48 animals (Fig. 2). However, there is also an unanticipated, although relatively weak, negative correlation between the intrinsic body clearance and the plasma free fraction of bilirubin (Fig. 3).

A change in plasma free fraction has a relatively modest effect on the intrinsic body clearance when the rapid and slow metabolizers are considered separately. This result suggested the possibility that the negative correlation apparent in Fig. 3 may be a consequence of a small influence of the hepatic perfusion rate on the body clearance of bilirubin. Such an

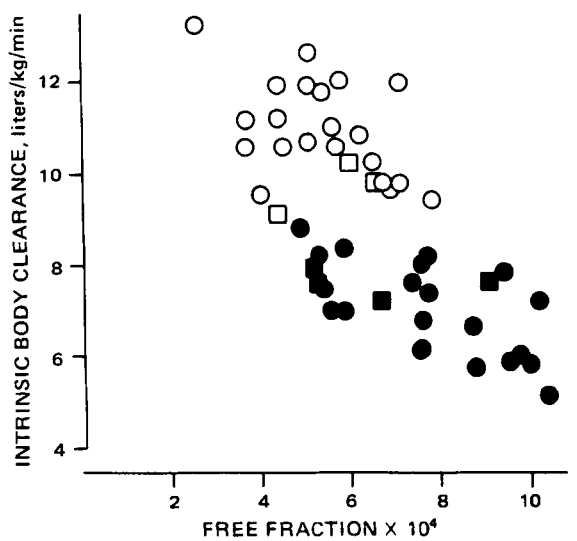

Figure 3—*Relationship between intrinsic body clearance of bilirubin and free fraction of bilirubin in the plasma of individual rats. Key: same as Fig. 1. Correlation coefficients are −0.426 (p < 0.05) for data represented by open symbols and −0.651 (p < 0.001) for data represented by closed symbols.*

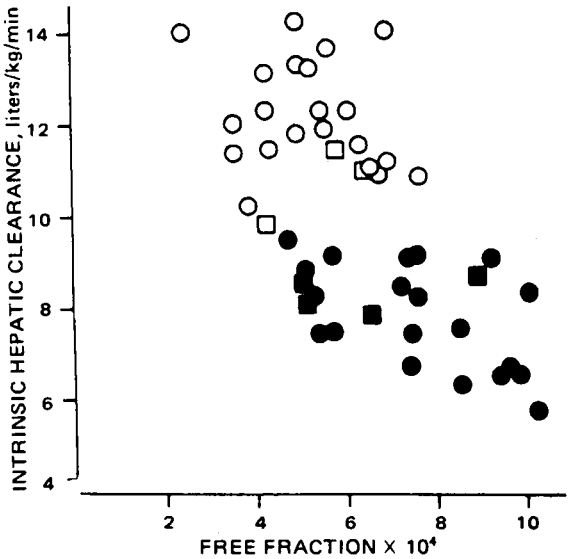

Figure 4—*Relationship between intrinsic hepatic plasma clearance of bilirubin and the free fraction of bilirubin in plasma of individual rats. Key: same as Fig. 1. Correlation coefficients are −0.194 (p > 0.30) for open symbols and −0.527 (p < 0.01) for closed symbols.*

influence, although small in magnitude, cannot be neglected in the interpretation of the data. The total body clearance values were, therefore, converted to total *hepatic* plasma clearances on the basis of the relationship (11):

$$\text{total body clearance} = \frac{\text{THPC} \times \text{PPR}}{\text{THPC} + \text{PPR}} \qquad \text{(Eq. 1)}$$

where THPC is the total hepatic plasma clearance and PPR is the plasma perfusion rate of the liver, which was assumed to be 55.8 ml/kg/min (60% of blood flow). Determination of plasma rather than blood clearance presents no interpretative difficulty since less than 10% of the bilirubin in rat blood is in or on erythrocytes. The total hepatic plasma clearance was divided by the plasma free fraction value to obtain the intrinsic hepatic plasma clearance (IHPC).

The relationship between the intrinsic hepatic plasma clearance and the plasma free fraction of bilirubin is shown in Fig. 4. The correlation between these variables is statistically not significant ($r = -0.194$, $p > 0.30$) for the intrinsically rapid metabolizers but significant ($r = -0.527$, $p < 0.01$) for the slow metabolizers. Even if the plasma perfusion rate is decreased by one-third to 37.2 ml/kg/min, the negative correlation between the intrinsic hepatic plasma clearance and the free fraction is marginally significant ($r = -0.448$, $p < 0.05$).

The reason for this negative correlation is not readily apparent. One possibility, entirely speculative, is that certain endogenous inhibitor(s) of bilirubin binding to plasma proteins may be eliminated by the same conjugative pathways as bilirubin itself. Rapid intrinsic metabolizers of bilirubin may then also be rapid eliminators of the endogenous inhibitor(s), resulting in lower inhibitor concentrations and more extensive plasma protein binding of bilirubin.

The results of this investigation show that there are appreciable interindividual differences in the total body clearance of bilirubin by adult male Sprague–Dawley rats and that these differences are due to interindividual differences in both determinants of the total body clearance, plasma protein binding and intrinsic clearance. The intrinsic body clearance values were bimodally distributed. No similar study has been carried out in human subjects, but it has been established that there are significant interindividual differences in plasma protein binding of bilirubin in normal adult volunteers and in newborn infants (12).

Indirect evidence, namely an inverse correlation between the conjugation of salicylamide with glucuronic acid and the plasma concentration of bilirubin in newborn infants together with pronounced interindividual differences in the formation of salicylamide glucuronide (13), suggests that the intrinsic metabolic clearance of bilirubin differs appreciably among human neonates. Similar differences are likely in adults, particularly in relation to changes in liver function. For example, Pirotte (14) found that the total body clearance of exogenous bilirubin ranged from 22.7 to 66.8 ml/min in normal adult humans and from 2.25 to 78.6 ml/min in patients with cirrhosis of the liver. Therefore, the results of this study probably apply in principle also to humans.

REFERENCES

(1) B. H. Billing and F. H. Jansen, *Gastroenterology*, **61**, 258 (1971).

(2) S. Øie and G. Levy, *J. Pharm. Sci.*, **64**, 1433 (1975).

(3) J. Jacobsen and O. Fedders, *Scand. J. Clin. Lab. Invest.*, **26**, 237 (1970).

(4) R. Broderson and I. Vind, *ibid.*, **15**, 107 (1963).

(5) G. Levy and A. Yacobi, *J. Pharm. Sci.*, **63**, 805 (1974).

(6) H. F. Martin, B. J. Gudzinowicz, and H. Fanger, "Normal Values in Clinical Chemistry; A Guide to Statistical Analysis of Laboratory Data," Dekker, New York, N.Y., 1975, pp. 142–154.

(7) C. G. Bhattacharya, *Biometrics*, **23**, 115 (1967).

(8) I. M. Chakravarti, R. G. Laha, and J. Roy, "Handbook of Methods of Applied Statistics: Techniques of Computation, Descriptive Methods and Statistical Inference," vol. I, Wiley, New York, N.Y., 1967, p. 152.

(9) "Scientific Tables," K. Diem and C. Lentner, Eds., 7th ed., J. R. Geigy, Basle, Switzerland, 1970, p. 130.

(10) E. E. Ohnhaus and J. T. Locher, *Eur. J. Pharmacol.*, **31**, 161 (1975).

(11) M. Gibaldi and D. Perrier, "Pharmacokinetics," Dekker, New York, N.Y., 1975, p. 246.

(12) S. Øie and G. Levy, *Clin. Pharmacol. Ther.*, **21**, 627 (1977).

(13) L. Stern, N. N. Khanna, G. Levy, and S. J. Yaffe, *Am. J. Dis. Child.*, **120**, 26 (1970).

(14) J. Pirotte, *Biol. Gastroenterol. (Paris)*, **6**, 183 (1973).

ACKNOWLEDGMENTS

Supported in part by Grant GM 19568 from the National Institute of General Medical Sciences, National Institutes of Health, Bethesda, MD 20014.

USP Dissolution Test II: Sigmoid Dissolution Profiles from Directly Compressed Tablets

J. T. CARSTENSEN ˣ, JAMES L. WRIGHT, KENNETH W. BLESSEL *, and JANE SHERIDAN *

Received December 16, 1976, from the *School of Pharmacy, University of Wisconsin, Madison, WI 53706.* Accepted for publication March 25, 1977. *Present address: Hoffmann-La Roche Inc., Nutley, NJ 07110.

Abstract □ The basic steps involved in the dissolution of a directly compressed tablet in a USP basket dissolution apparatus were examined *via* data generation. The proposed model explains why a dissolution curve can be sigmoid shaped and why the portion past the lag time has a log-linear undissolved mass *versus* time correlation.

Keyphrases □ Dissolution—directly compressed tablet in USP basket apparatus, sigmoid-shaped curve explained □ Apparatus, dissolution—USP basket, directly compressed tablet, sigmoid-shaped curve explained

Dissolution curves of dosage forms in the USP dissolution apparatus often are S-shaped. Only a few attempts to explain the basic phenomena leading to an S-shaped curve have been reported (1, 2). An explanation is given here for the dissolution of a drug substance in a directly compressed tablet, where the drug substance is monodisperse with diameter d_0.

THEORETICAL

The situation considered is one where a tablet disintegrates into prime drug particles. Without a loss of generality, it can be considered that the tablet consists of drug particles only and that it is made up of a total of T_0 drug particles of diameter d_0 initially, *i.e.*, that it has a weight of $w = T_0\pi d_0^3\rho/6$. The tablet weight in the basket, after the onset of the dissolution test, decreases exponentially (3); *i.e.*:

$$T = T_0e^{-q\theta} \qquad \text{(Eq. 1)}$$

where θ is the experimentally observed time and q is denoted as an erosion constant.

The dissolution process can be examined in three portions. The first phase (Fig. 1*a*) is where the drug particles dislodged from the tablet have not yet decreased sufficiently in size to pass through the basket, which has an opening of d_1 cm. In the USP apparatus, this opening is $d_1 = 0.042$ cm (40 mesh). The dislodged particles will decrease in size according to the cube root law provided that they are isometric and that sink conditions prevail (4):

$$d = d_0 - F_0t \qquad \text{(Eq. 2)}$$

where:

$$F_0 = 2k_0S/\rho \qquad \text{(Eq. 3)}$$

and k_0 is the intrinsic dissolution rate constant (centimeters per second) in the basket and S is the drug solubility. At a certain time, θ_1, the particles that dislodged first will have decreased in size sufficiently to pass through the basket. Time θ_1 is given by:

$$d_1 = d_0 - F_0\theta_1 \qquad \text{(Eq. 4)}$$

The second phase is at time points beyond θ_1 but prior to the time, θ_2, where the particles that dislodged first will have completely dissolved (Fig. 1*b*). This point in time is arrived at in the following fashion. If k_1 is considered the intrinsic dissolution rate constant in the *vessel*, it will obviously differ from k_0 because of the different hydrodynamic conditions in the vessel. In general (5):

$$k_0 = 1.5k_1 \qquad \text{(Eq. 5)}$$

so that:

$$F_0 = 1.5F_1 \qquad \text{(Eq. 6)}$$

Time θ_2 is then given by:

$$0 = d_1 - F_1(\theta_2 - \theta_1) \qquad \text{(Eq. 7)}$$

and the three phases can be characterized as depicted in Fig. 1. The three phases according to time are given by: first phase, $\theta < \theta_1$; second phase, $\theta_1 < \theta < \theta_2$; and third phase, $\theta_2 < \theta$.

To arrive at an expression for the mass undissolved at time θ, one can consider the first phase. The number of particles formed (eroded off) t sec after the experiment is started, *i.e.*, in a time element $(t|t + dt)$, is given by:

$$-dT = qT_0e^{-qt}\,dt \qquad \text{(Eq. 8)}$$

After θ sec, these particles, which were created at time t, have been exposed to dissolution for a period of time equaling $\tau = (\theta - t)$. Therefore, their diameter (Eq. 2) is given by $d = d_0 - F_0(\theta - t)$, and the undissolved mass (m) of the particles dislodged at time t will at time θ be:

$$m = qT_0e^{-qt}(\rho\pi/6)[d_0 - F_0(\theta - t)]^3\,dt \qquad \text{(Eq. 9)}$$

Integrating this equation from $t = 0$ to $t = \theta$ then gives the total mass of the *particles* that are not dissolved at time θ; the mass of the *tablet* that is not dissolved at time θ is $T_0e^{-q\theta}\rho d_0^3\pi/6$. Therefore, the expression for the mass undissolved at time θ is:

$$m = T_0e^{-q\theta}\rho d_0^3\pi/6 + T_0(\pi\rho/6)\int_0^\theta qe^{-qt}[d_0 - F_0(\theta - t)]^3\,dt \qquad \text{(Eq. 10)}$$

The integral can be evaluated through integration by parts and has the value:

$$-\left[e^{-qt}\left\{(d_0 - F_0(\theta - t))^3 + 3\left(\frac{F_0}{q}\right)(d_0 - F_0(\theta - t))^2 + 6\left(\frac{F_0}{q}\right)^2(d_0 - F_0(\theta - t)) + 6\left(\frac{F_0}{q}\right)^3\right\}\right]\Bigg|_0^\theta$$

$$= \left[\{d_0 - F_0\theta\}^3 + 3\left(\frac{F_0}{q}\right)\{d_0 - F_0\theta\}^2 + 6\left(\frac{F_0}{q}\right)^2\{d_0 - F_0\theta\} + 6\left\{\frac{F_0}{q}\right\}^3\right] - e^{-q\theta}\left[d_0^3 + 3\left(\frac{F_0}{q}\right)d_0^2 + 6\left(\frac{F_0}{q}\right)^2 d_0 + 6\left(\frac{F_0}{q}\right)^3\right] \qquad \text{(Eq. 11)}$$

In general, if τ is the time elapsed from the time a particle has size d_i, then the integral may be written:

$$\int_{\zeta_1}^{\zeta_2} qe^{-qt}(d_i - F_i\tau)^3\,dt = I(i, \tau, \{\zeta_1\ \zeta_2\}) \qquad \text{(Eq. 12)}$$

This nomenclature facilitates the writing of the expressions for the mass undissolved as a function of time in the three phases.

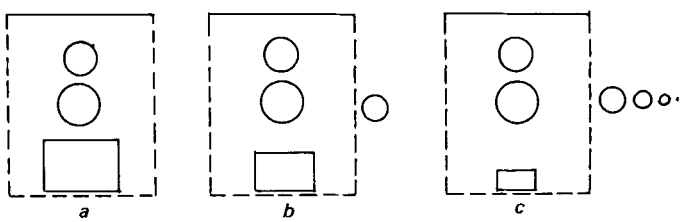

Figure 1—*Schematic of a tablet in a basket dissolution apparatus at various stages. Key:* a, *some disintegration, but dislodged particles have not decreased in size sufficiently to pass through basket mesh;* b, *more disintegration than* a *and the particles first formed have decreased in size sufficiently to pass through the basket but no particles have completely dissolved; and* c, *more disintegration than* b *and the particles formed first have completely dissolved.*

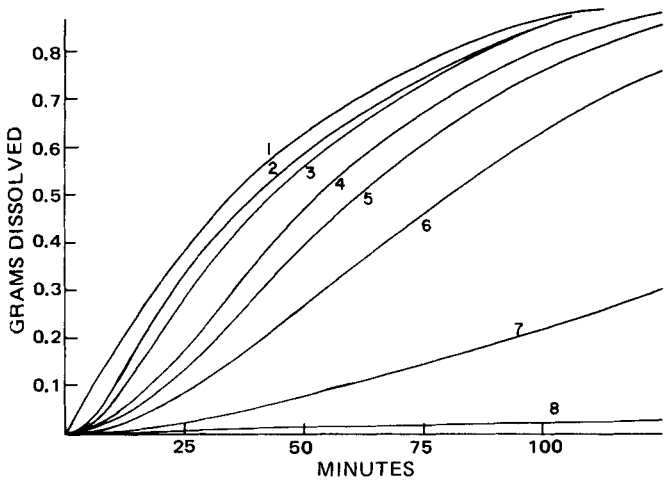

Figure 2—*Dissolution rate curves generated from 1 g of drug in a tablet, with* q = *0.02 min*$^{-1}$. *The* F *values (in centimeters per minute) are: 0.15 (1), 0.045 (2), 0.003 (3), 0.0015 (4), 0.00105 (5), 0.0006 (6), 0.00015 (7), and 0.000015 (8).*

In the first phase:

$$m = T_0 e^{-q\theta} \rho \pi d_0^3/6 + I(0, (\theta - t), \{0, \theta\}) \qquad \text{(Eq. 13)}$$

In the second phase:

$$m = T_0 e^{-q\theta} \rho \pi d_0^3/6 + I(0, (\theta - t), \{\theta - \theta_1, \theta\}) + I(1, (\theta - \theta_1 - t), \{0, \theta - \theta_1\}) \qquad \text{(Eq. 14}a\text{)}$$

In the third phase:

$$m = T_0 e^{-q\theta} \rho \pi d_0^3/6 + I(0, (\theta - t), \{\theta - \theta_1, \theta\}) + I(1, (\theta - \theta_1 - t), \{\theta - \theta_2, \theta - \theta_1\}) \qquad \text{(Eq. 14}b\text{)}$$

The actual expressions for Eqs. 14*a* and 14*b* are given in Eqs. 15*a* and 15*b*, respectively.

The expansion of Eq. 13 is shown in Eq. 11.

In the second phase:

$$m = T_0 e^{-q\theta} \rho \pi d_0^3/6 + T_0 \frac{\rho\pi}{6} \left\{ (d_1 - F_1(\theta - \theta_1))^3 + 3\left(\frac{F_1}{q}\right)(d_1 - F_1(\theta - \theta_1))^2 + 6\left(\frac{F_1}{q}\right)^2 (d_1 - F_1(\theta - \theta_1)) + 6\left(\frac{F_1}{q}\right)^3 - e^{-\theta q}\left[d_0^3 + 3\left(\frac{F_0}{q}\right) d_0^2 + 6\left(\frac{F_0}{q}\right)^2 d_0 + 6\left(\frac{F_0}{q}\right)^3 \right] + e^{-(\theta-\theta_1)q}\left[3\left\{\left(\frac{F_0}{q}\right) - \left(\frac{F_1}{q}\right)\right\} d_1^2 + 6\left\{\left(\frac{F_0}{q}\right)^2 - \left(\frac{F_1}{q}\right)^2\right\} d_1 + 6\left\{\left(\frac{F_0}{q}\right)^3 - \left(\frac{F_1}{q}\right)^3\right\}\right]\right\} \qquad \text{(Eq. 15}a\text{)}$$

In the third phase:

$$m = T_0 e^{-q\theta} \rho \pi d_0^3/6 + T_0 \frac{\rho\pi}{6} \left\{ e^{-(\theta-\theta_2)q}\, 6\left(\frac{F_1}{q}\right)^3 + e^{-(\theta-\theta_1)q}\left\{ 3\left[\left(\frac{F_0}{q}\right) - \left(\frac{F_1}{q}\right)\right] d_1^2 + 6\left[\left(\frac{F_0}{q}\right)^2 - \left(\frac{F_1}{q}\right)^2\right] d_1 + 6\left[\left(\frac{F_0}{q}\right)^3 - \left(\frac{F_1}{q}\right)^3\right]\right\} - e^{-q\theta}\left\{ d_0^3 + 3\left(\frac{F_0}{q}\right) d_0^2 + 6\left(\frac{F_0}{q}\right)^2 d_0 + 6\left(\frac{F_0}{q}\right)^3 \right\}\right\} \qquad \text{(Eq. 15}b\text{)}$$

If q is small and if $F/q \ll 1$, then the leading term at long times predominates, *i.e.*:

$$m \sim (\pi/6) \rho T_0 e^{-q\theta} d_0^3 \qquad \text{(Eq. 16)}$$

or:

$$\ln m = -q\theta + \ln m_0 \qquad \text{(Eq. 17)}$$

If q is large, then the term with the lowest exponent predominates and, at long times:

$$m \sim (\pi/6)\, \rho T_0 6 (F_1/q)^3 e^{-(\theta-\theta_2)q} \qquad \text{(Eq. 18)}$$

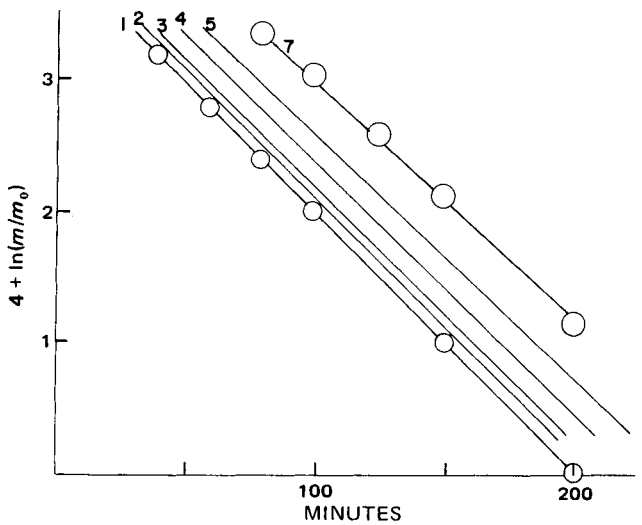

Figure 3—*Data in Fig. 2 treated according to Eq. 19. The curves are not experimental curves; the points in curves 1 and 7 are calculated points included (in these two cases) to demonstrate the goodness of fit.*

or:

$$\ln m = -q\theta + q\theta_2 + \ln m_0 6 (F/q)^3 \qquad \text{(Eq. 19)}$$

In the latter case, the intercept of a plot of the logarithm of the undissolved amount *versus* time will not intercept at ln m_0, although it will be linear at high time values.

Because of the initial lag, the curves will all have skewed S-shapes and adhere to either Weibull or log-normal distributions when the percent dissolved is plotted *versus* time.

DISCUSSION

Several generated curves are shown in Fig. 2. In each case, d_0 = 0.1 cm (1000 μm), d_1 = 0.042 cm (420 μm, 40 mesh), and ρ is $(6/\pi)$. The value of T_0 is 1000 so that the initial weight of drug is $1000(\pi/6)(6/\pi)0.1^3$ = 1.0 g. The factor in front of each integral is then 1000.

It is seen from Fig. 3 that the generated curves adhere to Eq. 19. Seven time points (40, 60, 80, 100, 125, 150, and 200 min) were selected for the generated curves in Fig. 2 to arrive at the curves in Fig. 3; the least-squares fit parameters based on these seven time values are listed in Table I. For q = 0.02 min^{-1}, F values of 0.006–0.15 cm/min give slopes close to the value of q. The length of time for a particle to dissolve completely, θ_2, is related to F by $\theta_2 = 0.081/F$ or:

$$\ln \theta_2 = -\ln F + \ln 0.081 = -\ln F - 2.52 \qquad \text{(Eq. 20)}$$

The intercept to slope ratio (θ') of the lines in Table I are the "lag times" obtained by log-linear plotting (and, hence, is biased by the fact that approximations are made). The values of the lag times are plotted *versus* the values of F on a log–log plot in Fig. 4. The least-squares fit of this plot is:

$$\ln \theta' = -1.02F - 3.809 \qquad \text{(Eq. 21)}$$

As predicted in Eq. 20, the slope is −1, but the intercepts are different. Equation 21 holds for $F > 0.006$ when $q = 0.02$, *i.e.*, for F/q ratios above 0.3. The intercepts do not coincide, which means that the lag time from

Table I—Least-Squares Fit Parameters of Lines in Fig. 3

Curve	F, cm/min	Slope, min^{-1}	Correlation Coefficient ($-R$)	Intercept
1	0.15	−0.0200	1.000	0.0029
2	0.0045	−0.0200	1.000	0.1165
3	0.0030	−0.0200	1.000	0.1769
4	0.0015	−0.0199	1.000	0.3658
5	0.00105	−0.0195	0.9996	0.4923
6	0.0006	−0.0167	0.9952	0.5969
7	0.00015[a]	−0.0158	0.9988	1.2888

[a] All fits are based on the time points indicated in the text above 40 min, except curve 7 for which points above 100 min only were used.

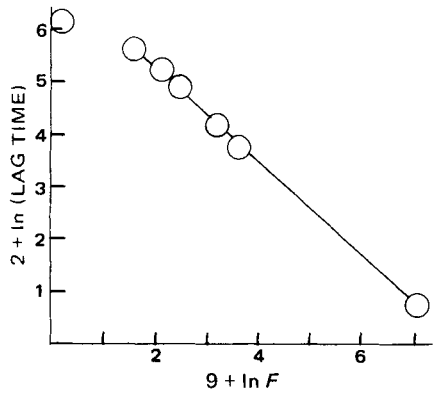

Figure 4—*Logarithm of the lag times of the lines in Fig. 3 (Table I) plotted* versus *the logarithm of the corresponding* F *values.*

log-time plots (θ') are proportional to the appropriate θ_2 values since ln (θ_2/θ') = 1.29, *i.e.*:

$$\theta_2 = 3.63\theta' \qquad \text{(Eq. 22)}$$

Although time is shown in minutes, it could be in any time unit; the important parameter is the F/q ratio. Therefore, the same curves would be generated if all time units are multiplied by ($^1/_{60}$) (to give the data in seconds) or by 15 to give the data in quarter hours, and so on.

In summary, directly compressed tablets can have sigmoid-shaped USP dissolution rate curves in which the tail is log-linear in time if sink conditions are applicable.

REFERENCES

(1) J. H. Wood, presented at the Industrial Pharmaceutics Section, APhA Academy of Pharmaceutical Sciences, Dallas meeting, Apr. 1966.

(2) J. T. Carstensen, in "Dissolution Technology," L. Leeson and J. T. Carstensen, Eds., Industrial Pharmaceutical Technology Section, Academy of Pharmaceutical Sciences, American Pharmaceutical Association, Washington, D.C., 1974, p. 192.

(3) J. T. Carstensen, J. Wright, K. Blessel, and J. Sheridan, *J. Pharm. Sci.*, in press.

(4) J. T. Carstensen, "Pharmaceutics of Solids and Solid Dosage Forms," Wiley, New York, N.Y., 1977, p. 77.

(5) J. T. Carstensen, T. Lai, and V. K. Prasad, *J. Pharm. Sci.*, **66**, 607 (1977).

ACKNOWLEDGMENTS

Presented at the APhA Academy of Pharmaceutical Sciences, Orlando meeting, November 1976 ["Abstracts," vol. 6, p. 114, paper 79].

Evaluation of Acceptance Criteria for Particulate Limits for Small-Volume Parenteral Products

KIYOSHI TSUJI ˣ **and A. R. LEWIS**

Received December 17, 1976, from *Control Analytical Research and Development and Mathematical Services, The Upjohn Company, Kalamazoo, MI 49001.* Accepted for publication March 31, 1977.

Abstract □ The precision of and correlation between the USP membrane filtration–microscopic method and the instrumental method for sizing and quantifying particulate matter in small-volume parenteral products were determined using simulated products. The total variance for the instrumental counts was lower than the USP method for all products in the 10–25-μm particle range and for most products in the ≥25–50-μm range. A linear relationship between the instrumental counts and the USP counts was demonstrated for the 10–25-μm particle range. However, the instrumental reading was higher than the USP method for counts of 10 or more particles/ml. The instrumental and the USP methods failed to correlate on particulate sizes greater than 25 μm. The content of particulate matter in over 100 small-volume parenteral products was sized and quantified by the USP and the instrumental methods. From the instrumental data, a statistical treatment for the analysis of particulate data is presented as an objective method of evaluating acceptance criteria on particulate matter in small-volume parenteral products.

Keyphrases □ *Particle* content determinations—small-volume parenterals, USP membrane filtration–microscopic and instrumental methods compared □ Parenterals, small volume—particle content determinations, USP membrane filtration–microscopic and instrumental methods compared □ Dosage forms—various small-volume parenterals, particle content determinations, USP membrane filtration–microscopic and instrumental methods compared

Interest in particulate matter in parenteral products was dramatically heightened by Garvan and Gunner (1, 2), who became concerned over the large number of visible particles in intravenous solutions manufactured in Australia. They presented evidence of the harmful effects of such contaminants by infusing intravenous solutions into rabbits; granulomas were produced in the lung, each containing fragments of cellulose particles. They identified the source of most particles as originating from locally produced rubber closures; other particulates were identified as cellulose fibers. They also examined numerous brands of intravenous solutions manufactured in Australia, England, Europe, the Philippines, and the United States and found particles in most products.

In 1966, Vessey and Kendall (3) published a method of determining particulate matter in large-volume parenteral solutions using an automated counter. They proposed an arbitrary limit for particulate matter in these solutions. This proposal was modified and adopted by the British Pharmacopoeia in 1973 (4); the limits are less than 1000 particles/ml equal to or larger than 2 μm and less than 100 particles/ml equal to or larger than 5 μm. Recently, Bikhazi *et al.* (5) extrapolated the BP regulation and proposed that the average counts per 1 ml of parenteral preparation should contain not more than 700 particles equal to or greater than 1 μm, 200 equal to or greater than 2 μm, 100 equal to or greater than 3 μm, and 40 equal to or greater than 5 μm.

"The First Supplement to the USP XIX and NF XIV" (6) established the limit for particulate matter in large-volume parenteral products as not more than 50 parti-

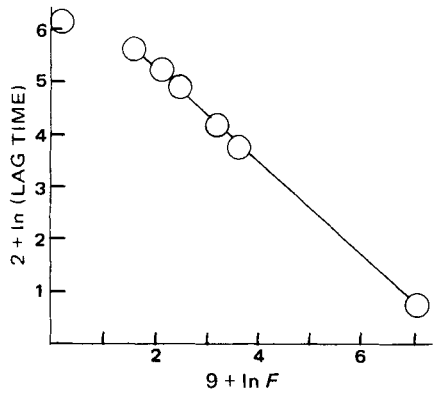

Figure 4—*Logarithm of the lag times of the lines in Fig. 3 (Table I) plotted* versus *the logarithm of the corresponding* F *values.*

log-time plots (θ') are proportional to the appropriate θ_2 values since ln (θ_2/θ') = 1.29, *i.e.*:

$$\theta_2 = 3.63\theta' \qquad \text{(Eq. 22)}$$

Although time is shown in minutes, it could be in any time unit; the important parameter is the F/q ratio. Therefore, the same curves would be generated if all time units are multiplied by ($^1/_{60}$) (to give the data in seconds) or by 15 to give the data in quarter hours, and so on.

In summary, directly compressed tablets can have sigmoid-shaped USP dissolution rate curves in which the tail is log-linear in time if sink conditions are applicable.

REFERENCES

(1) J. H. Wood, presented at the Industrial Pharmaceutics Section, APhA Academy of Pharmaceutical Sciences, Dallas meeting, Apr. 1966.

(2) J. T. Carstensen, in "Dissolution Technology," L. Leeson and J. T. Carstensen, Eds., Industrial Pharmaceutical Technology Section, Academy of Pharmaceutical Sciences, American Pharmaceutical Association, Washington, D.C., 1974, p. 192.

(3) J. T. Carstensen, J. Wright, K. Blessel, and J. Sheridan, *J. Pharm. Sci.*, in press.

(4) J. T. Carstensen, "Pharmaceutics of Solids and Solid Dosage Forms," Wiley, New York, N.Y., 1977, p. 77.

(5) J. T. Carstensen, T. Lai, and V. K. Prasad, *J. Pharm. Sci.*, **66**, 607 (1977).

ACKNOWLEDGMENTS

Presented at the APhA Academy of Pharmaceutical Sciences, Orlando meeting, November 1976 ["Abstracts," vol. 6, p. 114, paper 79].

Evaluation of Acceptance Criteria for Particulate Limits for Small-Volume Parenteral Products

KIYOSHI TSUJI ˣ **and A. R. LEWIS**

Received December 17, 1976, from *Control Analytical Research and Development and Mathematical Services, The Upjohn Company, Kalamazoo, MI 49001.* Accepted for publication March 31, 1977.

Abstract □ The precision of and correlation between the USP membrane filtration–microscopic method and the instrumental method for sizing and quantifying particulate matter in small-volume parenteral products were determined using simulated products. The total variance for the instrumental counts was lower than the USP method for all products in the 10–25-μm particle range and for most products in the ≥25–50-μm range. A linear relationship between the instrumental counts and the USP counts was demonstrated for the 10–25-μm particle range. However, the instrumental reading was higher than the USP method for counts of 10 or more particles/ml. The instrumental and the USP methods failed to correlate on particulate sizes greater than 25 μm. The content of particulate matter in over 100 small-volume parenteral products was sized and quantified by the USP and the instrumental methods. From the instrumental data, a statistical treatment for the analysis of particulate data is presented as an objective method of evaluating acceptance criteria on particulate matter in small-volume parenteral products.

Keyphrases □ *Particle* content determinations—small-volume parenterals, USP membrane filtration–microscopic and instrumental methods compared □ Parenterals, small volume—particle content determinations, USP membrane filtration–microscopic and instrumental methods compared □ Dosage forms—various small-volume parenterals, particle content determinations, USP membrane filtration–microscopic and instrumental methods compared

Interest in particulate matter in parenteral products was dramatically heightened by Garvan and Gunner (1, 2), who became concerned over the large number of visible particles in intravenous solutions manufactured in Australia. They presented evidence of the harmful effects of such contaminants by infusing intravenous solutions into rabbits; granulomas were produced in the lung, each containing fragments of cellulose particles. They identified the source of most particles as originating from locally produced rubber closures; other particulates were identified as cellulose fibers. They also examined numerous brands of intravenous solutions manufactured in Australia, England, Europe, the Philippines, and the United States and found particles in most products.

In 1966, Vessey and Kendall (3) published a method of determining particulate matter in large-volume parenteral solutions using an automated counter. They proposed an arbitrary limit for particulate matter in these solutions. This proposal was modified and adopted by the British Pharmacopoeia in 1973 (4); the limits are less than 1000 particles/ml equal to or larger than 2 μm and less than 100 particles/ml equal to or larger than 5 μm. Recently, Bikhazi *et al.* (5) extrapolated the BP regulation and proposed that the average counts per 1 ml of parenteral preparation should contain not more than 700 particles equal to or greater than 1 μm, 200 equal to or greater than 2 μm, 100 equal to or greater than 3 μm, and 40 equal to or greater than 5 μm.

"The First Supplement to the USP XIX and NF XIV" (6) established the limit for particulate matter in large-volume parenteral products as not more than 50 parti-

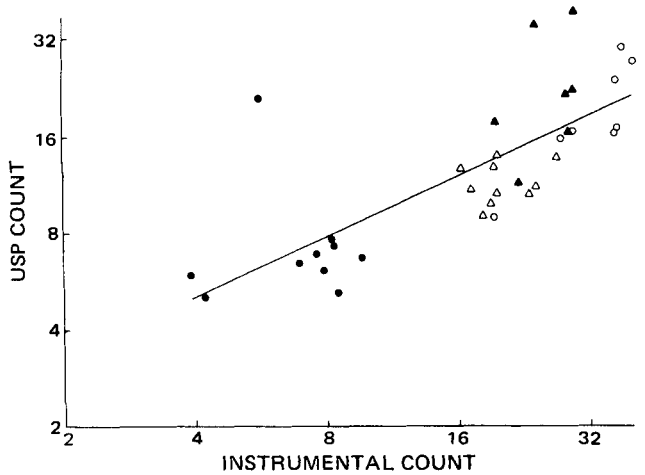

Figure 1—*Correlation between the USP method and the instrumental counts by day for particles of the 10–25-μm range in simulated products. Key: ○, Product I; △, Product II; ●, Product III; and ▲, Product IV.*

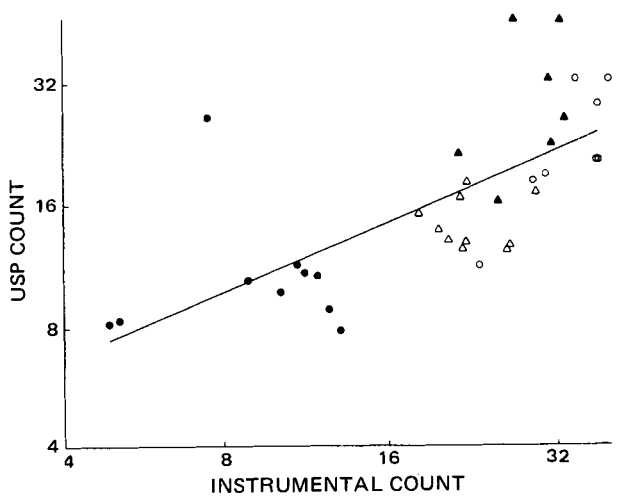

Figure 2—*Correlation between the USP method and the instrumental counts by day for particles of the ≥10-μm range in simulated products. Key: same as Fig. 1.*

cles/ml equal to or larger than 10 μm and not more than 5 particles/ml equal to or larger than 25 μm. The USP also recognized the membrane filtration–microscopic method as the official method for particulate determination. These methods and limits became effective July 1, 1975.

This report provides data on the precision of and correlation between the USP and the instrumental methods. It also presents data on particulate matter in over 100 small-volume parenteral products and suggests an approach for evaluating acceptance criteria on particulate matter in small-volume parenteral products.

EXPERIMENTAL

The membrane filtration–microscopic method used to size and quantitate particulate matter was described in "The Second Supplement to the USP XIX and NF XIV" (7). The sample preparation procedure includes opening of ampuls by the melt-open technique. This technique involves placing the upper widest part, above the breakline, of an ampul into the oxygen–gas torch flame. As the glass softens, the internal pressure forces the glass to pop out, forming a hole. As soon as the hole appears, a glass rod is used to melt away and remove the upper portion of the ampul. Thus, the particulate matter in an ampul can be counted without interference by the broken glass formed during an ampul-opening operation. The superiority of the melt-open technique over the break-open technique was amply demonstrated (8).

The particle-size analyzer[1] used was equipped with a small-volume sampler and a six-channel line printer. This instrument, which operates by the principle of light blockage, was used at a flow rate of 20 ml/min with 1-ml sample size. The small-volume sampler worked well at 20 ml/min but not at 60 ml/min.

The six channels were set to operate in the delta mode to record the following particle-size ranges: 5–10, 10–25, 50–100, 100–125, and over 125 μm. Due to extreme difficulty in obtaining reproducible results on particulate counts in the 5–10-μm range, this size range was not used in the statistical evaluation. Any proposal limiting particulate matter in this or a smaller size range (4.5) would be beyond the capability of the current particulate monitoring technology.

To minimize container-to-container variations, four simulated bulk product solutions (I–IV) were prepared. These solutions were aseptically dispensed into particle-free 50-ml vials and capped with clean butyl rubber stoppers. The vials, after machine washing, were manually cleaned by rinsing several times with particulate-free distilled water through a 0.22-μm membrane filter. Vials were then dry heat sterilized at 280° for 1 hr.

To establish the precision of the particle-size analyzer readings, a calibration solution[2] containing latex spheres of various sizes was used. The solution was aseptically dispensed into particle-free 50-ml vials. These bulk solutions were examined by the USP and the instrumental methods for up to 10 consecutive days. Instrumental drift was checked each day by examining the calibration solution three times a day.

The following test scheme and order were used each day.

1. The calibration solution was analyzed by the instrumental method (10 1-ml readings).
2. Product I was analyzed in the following order: USP method (one 5-ml sample), instrumental method (10 1-ml readings), USP method, instrumental method, USP method, and instrumental method.
3. Product II was analyzed in the same order as Product I.
4. The calibration solution was analyzed by the instrumental method.
5. Product III was analyzed in the same order as Product I.
6. Product IV was analyzed in the same order as Product I.
7. The calibration solution was analyzed by the instrumental method.

Thus, each product solution was examined consecutively by both the USP and the instrumental methods, repeating the sequence three times. The actual sequence of the product examination was randomized after the 1st day.

RESULTS AND DISCUSSION

The first experiment was designed to determine the correlation and precision of the USP and the instrumental methods. The experiment was then followed by the application of these two methods to obtain particulate levels in over 100 small-volume parenteral products.

Correlation Study—Each of the four bulk product samples yielded three USP counts and 30 instrumental counts per day. Preliminary analysis indicated that there was no short time trend in either the USP or the instrumental method. Since these within-day variations appeared to be random, daily averages were used in the correlation study. Additionally, the distribution of the counts appeared to be log-normal. Thus, the statistical evaluation of the data was performed using the number formed by the natural log of the sum of the observed count plus 0.5.

The transformed data of the USP and the instrumental counts were plotted against each other (Figs. 1–4), and the linear regression analyses were run. Since regression analysis assumes that the independent variable (the instrumental count) is known without error, the regression lines in Figs. 1–4 should be regarded as approximate. The results of these regression analyses for 35 daily average USP counts against 35 daily average instrumental counts fell into two groups (Groups 1 and 2, Table I) depending on the particle size. Thus, there appears to be a rough linear relationship between the USP and the instrumental counts for the 10–25-μm particle range. The effect of one outlier point (Product III) in Figs. 1 and 2 on the correlation coefficient is minimal.

In the 10–25-μm particle range, the instrumental method gave higher counts than the USP method for counts of 10 or more. This discrepancy may result from the use of the membrane filter required in the USP method; *i.e.*, silicone stopcock grease is used to hold the membrane filter on a plastic petri slide for microscopic counting, and any particles soluble

[1] HIAC model PC-320 with an E5-150 sensor, Pacific Scientific Co., Montclair, Calif.

[2] Lot 292, Pacific Scientific Co.

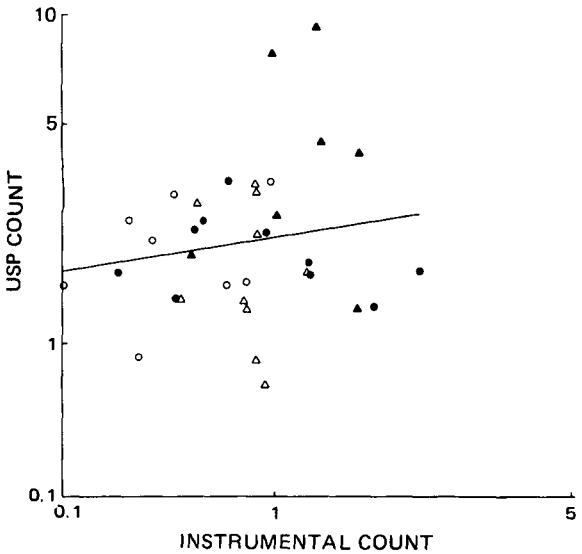

Figure 3—*Comparison of the USP method and the instrumental counts by day for particles of the 25–50-μm range in simulated products. Key: same as Fig. 1.*

in the grease may not be counted. Also, as the count becomes larger, the chance of clumping increases, thus giving falsely lower counts in the subvisual range (<20 μm).

It was not totally unexpected that the USP and the instrumental methods failed to correlate on particle sizes greater than 25 μm (9). This difficulty was most likely due to one or both of the following physical properties of the four simulated bulk products. The first property was the similarity of the particle densities (counts per milliliter) in the ≥ 25-μm size range. This similarity of densities, relative to the variation in densities within each product, would mask any correlation between the methods. The correlations reported above the 10–25- and ≥10-μm ranges were observable because there were distinct differences between the particle densities of the bulk products. The within-product correlation was largely masked by measurement error.

The second property was the shape of the ≥25-μm particles in relation to the difference in the mode of sizing used by the USP and instrumental methods. The particle-size analyzer is operated on the concept of light blockage or geometric shadowing. A beam of light is focused through the window of a flowcell onto a photocell. As particles, in a fluid flow, individually pass the window, a fraction of the light beam is interrupted, thus generating a series of pulses. These pulses are fed into six counting channels to record the particle size as a sphere corresponding to its equivalent geometric mean diameter.

The USP method, on the other hand, measures the longest axis or effective linear dimension (6, 7). Therefore, differences in the numerical results of the two methods become greater when the particle shape deviates further from the spherical shape. For example, a fiber 50 μm long, 2 μm wide, and 2 μm thick will be sized as a 50-μm particle by the USP method. The particle-size analyzer will recognize the fiber as a spherical particle having a geometric mean diameter of 11.3 μm.

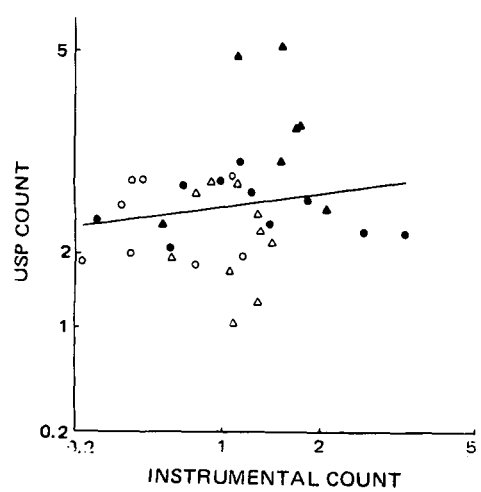

Figure 4—*Comparison of the USP method and the instrumental counts by day for particles of the ≥25-μm range in simulated products. Key: same as Fig. 1.*

Table I—Correlation Results for Bulk Product Samples

Group 1, 10–25- and ≥10-μm Particle-Size Range	Group 2, 25–50- and ≥25-μm Particle-Size Range
1. Data form a distinct cluster for each product. Center of cluster is near regression line[a].	1. A large amount of scatter is in the data; product clusters overlap.
2. Instrumental counts greater than 10 generally exceed corresponding USP count (Figs. 1 and 2).	2. Instrumental counts are usually lower than USP counts (Figs. 3 and 4).
3. Linear regression is statistically significant. Correlation coefficients were 0.75 and 0.68 for 10–25- and ≥10-μm ranges, respectively.	3. Linear regression is not significant. Correlation coefficients were less than 0.20.

[a] Linear regression equations were $\ln(USP + \frac{1}{2}) = 0.80 + 0.63 \ln(\text{instrumental} + \frac{1}{2})$ for the 10–25-μm range and $\ln(USP + \frac{1}{2}) = 1.13 + 0.57 \ln(\text{instrumental} + \frac{1}{2})$ for the ≥10-μm range.

Need for a Particulate Standard—The instrumental counter can be calibrated to compensate for the difference in shape of particles once the shape is defined. The National Fluid Power Association recognized the problems and established an acceptance criterion (AC) fine test dust standard for particles normally encountered in hydraulic fluids. The instrument calibrated with this standard correlates extremely well with the data gathered by the microscopic method (10).

It is unlikely that the particulate matter in pharmaceutical preparations is in spherical form; therefore, establishment of a standard with well-characterized and defined particles normally encountered in parenterals is highly desirable. The pharmaceutical industry may not have recognized this need. Pollen (spherical) was used in two of four collaborative studies conducted by the Pharmaceutical Manufacturers Association to simulate particulate matter in injectables.

An interim report on physical attributes of parenteral preparations by two Australian committees (11) stated that a quantitative method for particle-size determination should be based on the counter[1] used in this study. They considered that a method based on membrane filtration, such as the USP method, would be inappropriate in view of the difficulty in visualizing particles of less than 20 μm in diameter. Therefore, it would be appropriate to use the instrument and to supplement the data with the USP method to investigate particulate matter in injectable products.

Among the various instrumental particle-size analyzers, many investigators have chosen the instrument based on the light blockage principle since it operates independent of the presence of electrolyte and the color, shape, or composition of particles have a minimum effect on size measurement. Light-scattering and electrolyte instruments would be influenced greatly by these factors.

Precision of Instrumental and USP Methods—The data on the four simulated bulk product samples were used to estimate the within- and between-day variances for both methods. The within-day variance of the instrumental method has been divided by 5 to correct for the larger sample volume used in the USP method (the USP method used 5 ml; the instrumental used 1 ml of sample). The resultant variance is equivalent to averaging five 1-ml sample counts from the instrument.

Day-to-day differences (Table II) were statistically significant for Products I, III, and IV; however, these differences appeared to be random. The day-to-day differences were small and sometimes nonexistent for Product II.

The total variance (sum of between and within variances) for the instrument was lower than for the USP method for all four products in the 10–25- and ≥10-μm ranges and for three of the four products in the 25–50- and ≥25-μm ranges. Thus, overall the instrument was more precise than the USP method.

The latex sphere calibration suspensions run consecutively with the four product samples were used to determine the absolute precision of the instrument. The variance estimates (Table III) indicate that most variation is between samples in one container within days. The overall variation (expressed as a relative standard deviation, *RSD*) varied from 3.1 to 7.8%, depending upon the particle-size range. The average for the 50–100-μm size quoted by the manufacturer on the latex sphere calibration suspension (860/ml) differed slightly from the average count

Table II—Estimated Variance Components for the Instrumental and the USP Methods

Range of Particulate Matter, μm	Product		Variance, ln[(counts/ml + 0.5)²] Instrumental	USP
≥10	I	Between day	0.031	0.098
		Within day	0.038	0.048
		Total	0.068	0.146
	II	Between day	0.002	0.000
		Within day	0.019	0.128
		Total	0.021	0.128
	III	Between day	0.100	0.056
		Within day	0.037	0.173
		Total	0.137	0.229
	IV	Between day	0.019	0.103
		Within day	0.013	0.094
		Total	0.032	0.197
≥25	I	Between day	0.056	0.045
		Within day	0.127	0.109
		Total	0.183	0.154
	II	Between day	0.000	0.088
		Within day	0.102	0.096
		Total	0.102	0.185
	III	Between day	0.106	0.000
		Within day	0.147	0.146
		Total	0.253	0.146
	IV	Between day	0.050	0.188
		Within day	0.116	0.122
		Total	0.166	0.310
10–25	I	Between day	0.044	0.108
		Within day	0.050	0.059
		Total	0.094	0.167
	II	Between day	0.004	0.000
		Within day	0.019	0.171
		Total	0.023	0.171
	III	Between day	0.075	0.075
		Within day	0.043	0.203
		Total	0.117	0.283
	IV	Between day	0.016	0.114
		Within day	0.014	0.118
		Total	0.031	0.232
25–50	I	Between day	0.059	0.069
		Within day	0.119	0.135
		Total	0.178	0.204
	II	Between day	0.000	0.131
		Within day	0.106	0.116
		Total	0.106	0.247
	III	Between day	0.073	0.006
		Within day	0.134	0.138
		Total	0.208	0.144
	IV	Between day	0.044	0.305
		Within day	0.127	0.164
		Total	0.171	0.469

obtained (744/ml).

Small-Volume Parenteral Products—Samples from over 100 small-volume parenteral products on the market were examined by both the USP and the instrumental methods. For the USP method, four containers/lot were tested and the total content of each container was filtered through a membrane filter. The results were expressed per milliliter of solution tested. For the instrumental method, 10 containers/lot were examined. The vials were sampled by taking as many 1-ml samples as possible up to a maximum of 10/vial, and the results were expressed on a per milliliter basis.

In general, the variation in particle count between the containers within a given lot was extremely large. The results of the USP and instrumental counts indicated a similar trend. The variation in these products was from

Table III—Variance Components of the Instrumental Method by Latex Sphere Samples

Particle-Size Range, μm	Arithmetic Average Count	Estimated Variance, ln[(counts/ml)²] Between Days	Within Days	Total	*RSD*, %
10–25	698	0.0	0.044	0.044	3.2
25–50	44.9	0.008	0.079	0.086	7.8
50–100	1.20	0	0.574	0.574	294
≥10	744	0	0.042	0.042	3.1
≥25	46.2	0.007	0.077	0.084	7.6

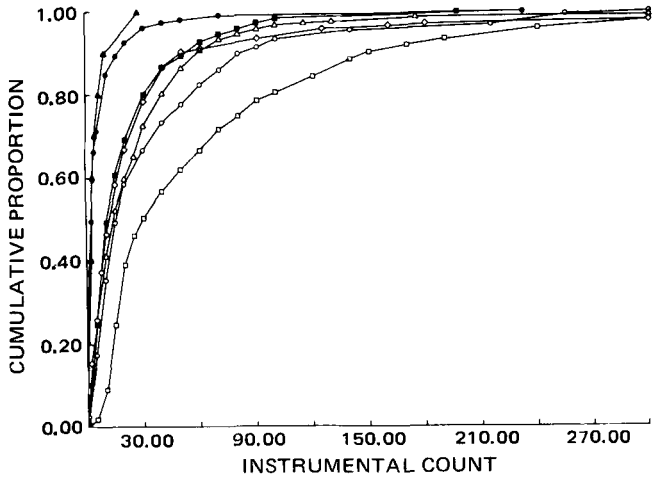

Figure 5—*Cumulative relative frequency distribution plots of the instrumental counts by product type for the ≥10-μm particle range. Key: △, aqueous solution, vials; ●, aqueous solution, ampuls; ▲, aqueous solution, syringes; ○, aqueous solutions; □, freeze-dried products; ■, oil solutions; and ◇, sterile powders.*

two to 10 times larger than the variation found in the four simulated bulk product samples tested earlier. This large variation would make a correlation study between the instrumental and the USP methods based on actual product samples extremely difficult.

The balance of the statistical analysis was conducted using the instrumental data, since the USP test requires the entire contents of each container, resulting in the complete confounding of measurement as well as container-to-container variations and in a high frequency of "too numerous to count" results that made statistical treatment of these data impossible.

Summarization of the instrumental data by product type, *i.e.*, aqueous solutions, oil, *etc.*, is given in Table IV. For the same raw data, cumulative particle frequency distribution curves (by product type) were constructed (Figs. 5 and 6). The difference between the arithmetic mean and the median (50th percentile) demonstrates the skewness in these raw count distributions.

Effects of Varying Acceptance Criteria—The effects of various acceptance criteria were demonstrated by computing lot rejection rates for the product samples for various acceptance criteria. The accept/reject decisions were based on the following statistical decision rule: accept a lot whose estimated proportion of container average particle counts exceeding the maximum allowable particulate count (MAPC) was greater than the unacceptable quality level (UQL). Since the distribution of counts was approximately log-normal, the calculations required to apply this rule were performed on the number formed by the natural log of the sum of the observed count plus 0.5.

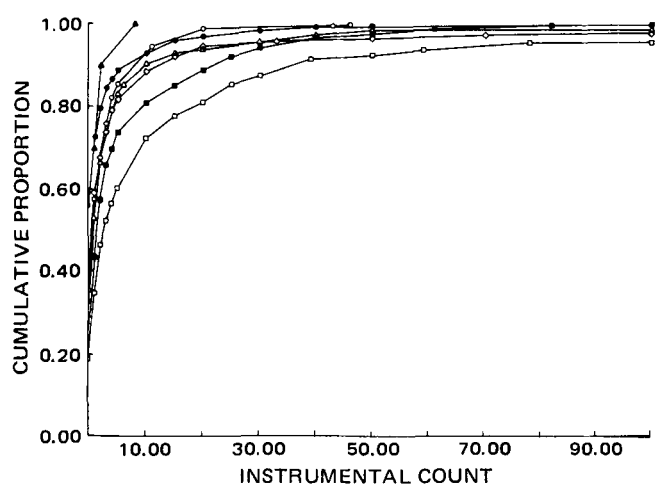

Figure 6—*Cumulative relative frequency distribution plots of the instrumental counts by product type for the ≥25-μm particle range. Key: same as Fig. 5.*

Table IV—Particle Counts in Small-Volume Parenterals by Instrumental Method

Product Type	Level	Particle-Size Range, μm					
		10–25	25–50	50–100	≥100	≥10	≥25
Aqueous solution: vial (n = 990)	Minimum	0	0	0	0	0	0
	Maximum	161	430	241	17	796	635
	Average	19.9	5.0	2.9	0.3	28.1	8.2
	50th percentile	11	1	0	0	15	1
	90th percentile	52	6	4	0	59	10
	95th percentile	66	13	9	1	84	26
	99th percentile	99	70	71	6	223	174
Aqueous solution: ampul (n = 610)	Minimum	0	0	0	0	0	0
	Maximum	144	110	55	13	232	168
	Average	4.2	1.5	1.1	0.3	7.0	2.8
	50th percentile	2	0	0	0	3	0
	90th percentile	10	3	3	1	16	7
	95th percentile	15	6	5	2	26	14
	99th percentile	40	20	18	6	68	40
Aqueous solution: syringe (n = 10)	Minimum	0	0	0	0	0	0
	Maximum	19	6	2	0	27	8
	Average	4.3	0.9	0.6	0	5.8	1.5
	50th percentile	2	0	0	0	3	1
	90th percentile	9	1	2	0	9	2
	95th percentile	19	6	2	0	27	8
	99th percentile	19	6	2	0	27	8
Oil solution (n = 630)	Minimum	0	0	0	0	0	0
	Maximum	176	36	69	28	197	105
	Average	13.3	1.9	3.6	1.5	20.3	7.0
	50th percentile	6	1	0	0	11	2
	90th percentile	30	4	12	5	51	22
	95th percentile	55	7	19	8	72	34
	99th percentile	110	18	38	22	130	63
Sterile powder (n = 719)	Minimum	0	0	0	0	0	0
	Maximum	1067	403	362	12	1306	727
	Average	28.8	6.6	3.8	0.2	39.4	10.6
	50th percentile	9	1	0	0	12	1
	90th percentile	41	9	4	0	49	13
	95th percentile	86	18	8	1	112	23
	99th percentile	403	140	99	6	1002	233
Sterile freeze-dried product (n = 350)	Minimum	2	0	0	0	2	0
	Maximum	362	177	148	13	589	299
	Average	46.9	10.2	5.9	0.3	63.3	16.4
	50th percentile	23	2	1	0	30	3
	90th percentile	107	25	10	1	149	37
	95th percentile	139	51	29	2	226	78
	99th percentile	288	129	108	5	415	227

The proportion of a given lot exceeding the limit was estimated in the following way:

1. The within- and between-container variances (σ_w^2 and σ_b^2, respectively) are estimated by analysis of variance.
2. The variance of the container average ($\sigma_{\bar{x}}^2$) is given by:

$$\sigma_{\bar{x}}^2 = \sigma_b^2 + \frac{\sigma_w^2}{NS} \qquad \text{(Eq. 1)}$$

where NS is the number of samples per container examined. The value of NS must be greater than 1 or separate estimates of σ_w^2 and σ_b^2 are not obtainable.

3. The proportion of the lot above the MAPC is the area under the standard normal curve to the right of z, where:

$$z = \frac{\text{MAPC} - \bar{\bar{x}}}{\sigma_{\bar{\bar{x}}}} \qquad \text{(Eq. 2)}$$

and $\bar{\bar{x}}$ is the average particulate count over all containers and samples in the lot.

This accept/reject procedure was applied to the product sample data for nine acceptance criteria consisting of all combinations of three UQL's and three MAPC's. The UQL's were arbitrarily set at 5, 10, and 25%. The first MAPC was set equal to the USP limit for large-volume parenterals, and the remaining two were equated to the 95th and 99th percentiles of the cumulative relative particle count frequency distribution for freeze-dried products (Table IV and Figs. 5 and 6). The cumulative relative frequency plotted in Figs. 5 and 6 is the proportion of the counts in a product group less than or equal to a given count. For example, 0.5 (or 50%) of the particle counts in the ≥10-μm range (Fig. 5) for sterile powder are less than or equal to 30.

The number of lots rejected by each criterion was tabulated and converted to percentages. These percentages are given in Tables V and VI

Table V—Percent of Lots Tested that Fail Acceptance Criteria for ≥10-μm Particle Range

Product Type	UQL, %	Maximum Allowable Particle Count[a]		
		LVP	A_1	A_2
Aqueous solution	5	39	8	4
	10	29	4	4
	25	17	2	2
Freeze-dried product	5	55	23	13
	10	48	10	10
	25	32	7	3
Oil solution	5	47	7	7
	10	33	0	0
	25	27	0	0
Average	5	45	12	13
	10	36	5	5
	25	24	3	2

[a] LVP = NMT 50 ≥10-μm particles, A_1 = NMT 200 ≥10-μm particles, and A_2 = NMT 420 ≥10-μm particles.

Table VI—Percent of Lots Tested that Fail Acceptance Criteria for ≥25-μm Particle Range

Product Type	UQL, %	Maximum Allowable Particle Count[a]		
		LVP	B_1	B_2
Aqueous solution	5	46	6	2
	10	44	6	2
	25	31	4	0
Freeze-dried product	5	65	19	3
	10	52	19	3
	25	36	7	3
Oil solution	5	100	7	0
	10	87	0	0
	25	53	0	0
Average	5	60	10	2
	10	53	9	2
	25	36	4	1

[a] LVP = NMT 5 ≥25-μm particles, B_1 = NMT 50 ≥25-μm particles, and B_2 = NMT 230 ≥25-μm particles.

Table VII—Percent of Lots Tested that Fail Acceptance Criteria for ≥10- and ≥25-μm Particle Ranges Simultaneously

Product Type	UQL, %	Maximum Allowable Particle Count[a] LVP	C_1	C_2
Aqueous solution	5	62	8	4
	10	58	6	4
	25	37	4	2
Freeze-dried product	5	71	29	13
	10	61	23	10
	25	42	6	3
Oil solution	5	100	13	7
	10	93	0	0
	25	67	0	0
Average	5	70	15	7
	10	64	10	7
	25	43	4	2

[a] LVP = NMT 50 ≥10-μm and NMT 5 ≥25-μm particles, C_1 = NMR 200 ≥10-μm and NMT 50 ≥25-μm particles, and C_2 = NMT 420 ≥10-μm and NMT 230 ≥25-μm particles.

for the ≥10- and ≥25-μm ranges, respectively. Table VII presents the overall rejection rate when both particulate ranges are considered simultaneously. The overall reject rates for product samples at or beyond their expiration date are not significantly different from those reported in Table VII. Thus, the direct application of the USP large-volume parenteral limits to the present data resulted in an overall rejection rate of 43–70%, depending upon the UQL. If the present data are indeed representative of the current industrial technology, adoption of the large-volume parenteral limits for small-volume parenterals would cause extreme difficulty.

Guidelines in Establishing Small-Volume Parenterals—The medical consequences of subvisual-size particulate matter in parenteral formulations are believed to be dependent on the total number and nature of particles that a patient receives from injectables. The standard criteria for particulate matter in a small-volume parenteral could be established based on the concept of the maximum injectable dose.

The USP requirement for particulate matter in large-volume parenterals allows up to 50 and 5 particles for the ≥10- and ≥25-μm size ranges, respectively. Therefore, a patient could receive up to 5000 particles ≥10 μm and 500 particles ≥25 μm from a dose of a 100-ml large-volume parenteral (the minimum size for large-volume parenterals). Infusion from 1 liter of parenteral solution could subject a patient with as many as 50,000 and 5000 particles in the respective size ranges. Therefore, any proposal limiting the particulate matter in small-volume parenteral products could be established based on the concept of the maximum injectable dose and on the statistical acceptance criteria.

This paper represents only the beginning of an evaluation of the quantitative aspects of particulate level methodology. More quantitative data together with the investigation of large numbers of lots and wide varieties of products are needed prior to the establishment of particulate limits in small-volume parenterals. In view of the inevitability that particles of various sizes will be generated by manipulations necessary prior to injection, *e.g.*, breaking a glass ampul and piercing a rubber septum, an in-line final filter is recommended as an efficient means of eliminating particulate introduction into a patient.

REFERENCES

(1) J. M. Garvan and B. W. Gunner, *Med. J. Aust.*, **2**, 140 (1963).

(2) *Ibid.*, **1**, 1 (1964).

(3) I. Vessey and C. E. Kendall, *Analyst*, **91**, 273 (1966).

(4) "British Pharmacopoeia 1973," Her Majesty's Stationery Office, London, England, 1973, p. A123.

(5) A. B. Bikhazi, J. A. Shiatis, and A. F. Haddad, *J. Pharm. Sci.*, **66**, 181 (1977).

(6) "First Supplement to the USP XIX and NF XIV," United States Pharmacopeial Convention, Rockville, Md., July 1, 1975.

(7) "Second Supplement to the USP XIX and NF XIV," United States Pharmacopeial Convention, Rockville, Md., Jan. 30, 1976.

(8) W. E. Hamlin, presented at the 16th Annual National Industrial Pharmaceutical Research Conference, Land O'Lakes, Wis., June 10–14, 1974.

(9) G. H. Hopkins and R. W. Young, *Bull. Parenteral Drug Assoc.*, **28**, 15 (1974).

(10) J. O. Robinson and J. B. Bayle, *J. Am. Assoc. Contamination Control*, Jan. 1964.

(11) "Australian Therapeutic Goods Standards Committee and Therapeutic Goods Advisory Committee Report. Interim Report on Uniformity and Physical Attributes of Parenteral Preparations," Feb. 18, 1975.

ACKNOWLEDGMENTS

The authors thank Rena R. Butler and E. B. Ferrer for technical assistance.

Chemical Constituents of Gentianaceae XXIII: Tetraoxygenated and Pentaoxygenated Xanthones and Xanthone *O*-Glucosides of *Swertia angustifolia* Buch.-Ham.

S. GHOSAL ˣ, P. V. SHARMA, and D. K. JAISWAL

Received November 11, 1976, from the *Pharmaceutical Chemistry Research Laboratory, Department of Pharmaceutics, Banaras Hindu University, Varanasi-5, India.* Accepted for publication April 1, 1977.

Abstract □ The whole plant extract of *Swertia angustifolia* Buch.-Ham., collected at different stages of growth, contained 14 tetraoxygenated and five pentaoxygenated xanthones and xanthone 1-*O*-glucosides. Of the eight xanthone 1-*O*-glucosides isolated, five were previously unreported in nature. The xanthones are broadly based on 1,3,5,8- and 1,3,7,8-oxygenated systems, with an added oxygen function at C-4 in some compounds, and represent a number of methoxylated patterns. The content and relative abundance of the free xanthones and their 1-*O*-glucosides changed with plant growth. These results are the first demonstration of the variation in chemical characters in the different parts of a *Swertia* species during its ontogeny. The biological significance of these results is appraised.

Keyphrases □ Xanthones and *O*-glucosides—isolated and identified in *Swertia angustifolia*, whole plant extract, various growth stages compared □ *Swertia angustifolia*—whole plant extract, various xanthones and *O*-glucosides isolated and identified, various growth stages compared

Swertia angustifolia (var. *angustifolia*) Buch.-Ham., native to the subtropical Himalayas from the Chenub to Bhutan, 304.8–1828.8 m (1000–6000 ft), is a small flowering species. It is used as a substitute for the Indian pharmacopeial drug *S. chirata* Buch.-Ham. Extracts of this plant are used as a bitter tonic, as a febrifuge, in epilepsy, and

Table VII—Percent of Lots Tested that Fail Acceptance Criteria for ≥10- and ≥25-μm Particle Ranges Simultaneously

Product Type	UQL, %	Maximum Allowable Particle Count[a] LVP	C_1	C_2
Aqueous solution	5	62	8	4
	10	58	6	4
	25	37	4	2
Freeze-dried product	5	71	29	13
	10	61	23	10
	25	42	6	3
Oil solution	5	100	13	7
	10	93	0	0
	25	67	0	0
Average	5	70	15	7
	10	64	10	7
	25	43	4	2

[a] LVP = NMT 50 ≥10-μm and NMT 5 ≥25-μm particles, C_1 = NMR 200 ≥10-μm and NMT 50 ≥25-μm particles, and C_2 = NMT 420 ≥10-μm and NMT 230 ≥25-μm particles.

for the ≥10- and ≥25-μm ranges, respectively. Table VII presents the overall rejection rate when both particulate ranges are considered simultaneously. The overall reject rates for product samples at or beyond their expiration date are not significantly different from those reported in Table VII. Thus, the direct application of the USP large-volume parenteral limits to the present data resulted in an overall rejection rate of 43–70%, depending upon the UQL. If the present data are indeed representative of the current industrial technology, adoption of the large-volume parenteral limits for small-volume parenterals would cause extreme difficulty.

Guidelines in Establishing Small-Volume Parenterals—The medical consequences of subvisual-size particulate matter in parenteral formulations are believed to be dependent on the total number and nature of particles that a patient receives from injectables. The standard criteria for particulate matter in a small-volume parenteral could be established based on the concept of the maximum injectable dose.

The USP requirement for particulate matter in large-volume parenterals allows up to 50 and 5 particles for the ≥10- and ≥25-μm size ranges, respectively. Therefore, a patient could receive up to 5000 particles ≥10 μm and 500 particles ≥25 μm from a dose of a 100-ml large-volume parenteral (the minimum size for large-volume parenterals). Infusion from 1 liter of parenteral solution could subject a patient with as many as 50,000 and 5000 particles in the respective size ranges. Therefore, any proposal limiting the particulate matter in small-volume parenteral products could be established based on the concept of the maximum injectable dose and on the statistical acceptance criteria.

This paper represents only the beginning of an evaluation of the quantitative aspects of particulate level methodology. More quantitative data together with the investigation of large numbers of lots and wide varieties of products are needed prior to the establishment of particulate limits in small-volume parenterals. In view of the inevitability that particles of various sizes will be generated by manipulations necessary prior to injection, *e.g.*, breaking a glass ampul and piercing a rubber septum, an in-line final filter is recommended as an efficient means of eliminating particulate introduction into a patient.

REFERENCES

(1) J. M. Garvan and B. W. Gunner, *Med. J. Aust.*, **2**, 140 (1963).

(2) *Ibid.*, **1**, 1 (1964).

(3) I. Vessey and C. E. Kendall, *Analyst*, **91**, 273 (1966).

(4) "British Pharmacopoeia 1973," Her Majesty's Stationery Office, London, England, 1973, p. A123.

(5) A. B. Bikhazi, J. A. Shiatis, and A. F. Haddad, *J. Pharm. Sci.*, **66**, 181 (1977).

(6) "First Supplement to the USP XIX and NF XIV," United States Pharmacopeial Convention, Rockville, Md., July 1, 1975.

(7) "Second Supplement to the USP XIX and NF XIV," United States Pharmacopeial Convention, Rockville, Md., Jan. 30, 1976.

(8) W. E. Hamlin, presented at the 16th Annual National Industrial Pharmaceutical Research Conference, Land O'Lakes, Wis., June 10–14, 1974.

(9) G. H. Hopkins and R. W. Young, *Bull. Parenteral Drug Assoc.*, **28**, 15 (1974).

(10) J. O. Robinson and J. B. Bayle, *J. Am. Assoc. Contamination Control*, Jan. 1964.

(11) "Australian Therapeutic Goods Standards Committee and Therapeutic Goods Advisory Committee Report. Interim Report on Uniformity and Physical Attributes of Parenteral Preparations," Feb. 18, 1975.

ACKNOWLEDGMENTS

The authors thank Rena R. Butler and E. B. Ferrer for technical assistance.

Chemical Constituents of Gentianaceae XXIII: Tetraoxygenated and Pentaoxygenated Xanthones and Xanthone *O*-Glucosides of *Swertia angustifolia* Buch.-Ham.

S. GHOSAL ˣ, P. V. SHARMA, and D. K. JAISWAL

Received November 11, 1976, from the *Pharmaceutical Chemistry Research Laboratory, Department of Pharmaceutics, Banaras Hindu University, Varanasi-5, India.* Accepted for publication April 1, 1977.

Abstract □ The whole plant extract of *Swertia angustifolia* Buch.-Ham., collected at different stages of growth, contained 14 tetraoxygenated and five pentaoxygenated xanthones and xanthone 1-*O*-glucosides. Of the eight xanthone 1-*O*-glucosides isolated, five were previously unreported in nature. The xanthones are broadly based on 1,3,5,8- and 1,3,7,8-oxygenated systems, with an added oxygen function at C-4 in some compounds, and represent a number of methoxylated patterns. The content and relative abundance of the free xanthones and their 1-*O*-glucosides changed with plant growth. These results are the first demonstration of the variation in chemical characters in the different parts of a *Swertia* species during its ontogeny. The biological significance of these results is appraised.

Keyphrases □ Xanthones and *O*-glucosides—isolated and identified in *Swertia angustifolia*, whole plant extract, various growth stages compared □ *Swertia angustifolia*—whole plant extract, various xanthones and *O*-glucosides isolated and identified, various growth stages compared

Swertia angustifolia (var. *angustifolia*) Buch.-Ham., native to the subtropical Himalayas from the Chenub to Bhutan, 304.8–1828.8 m (1000–6000 ft), is a small flowering species. It is used as a substitute for the Indian pharmacopeial drug *S. chirata* Buch.-Ham. Extracts of this plant are used as a bitter tonic, as a febrifuge, in epilepsy, and

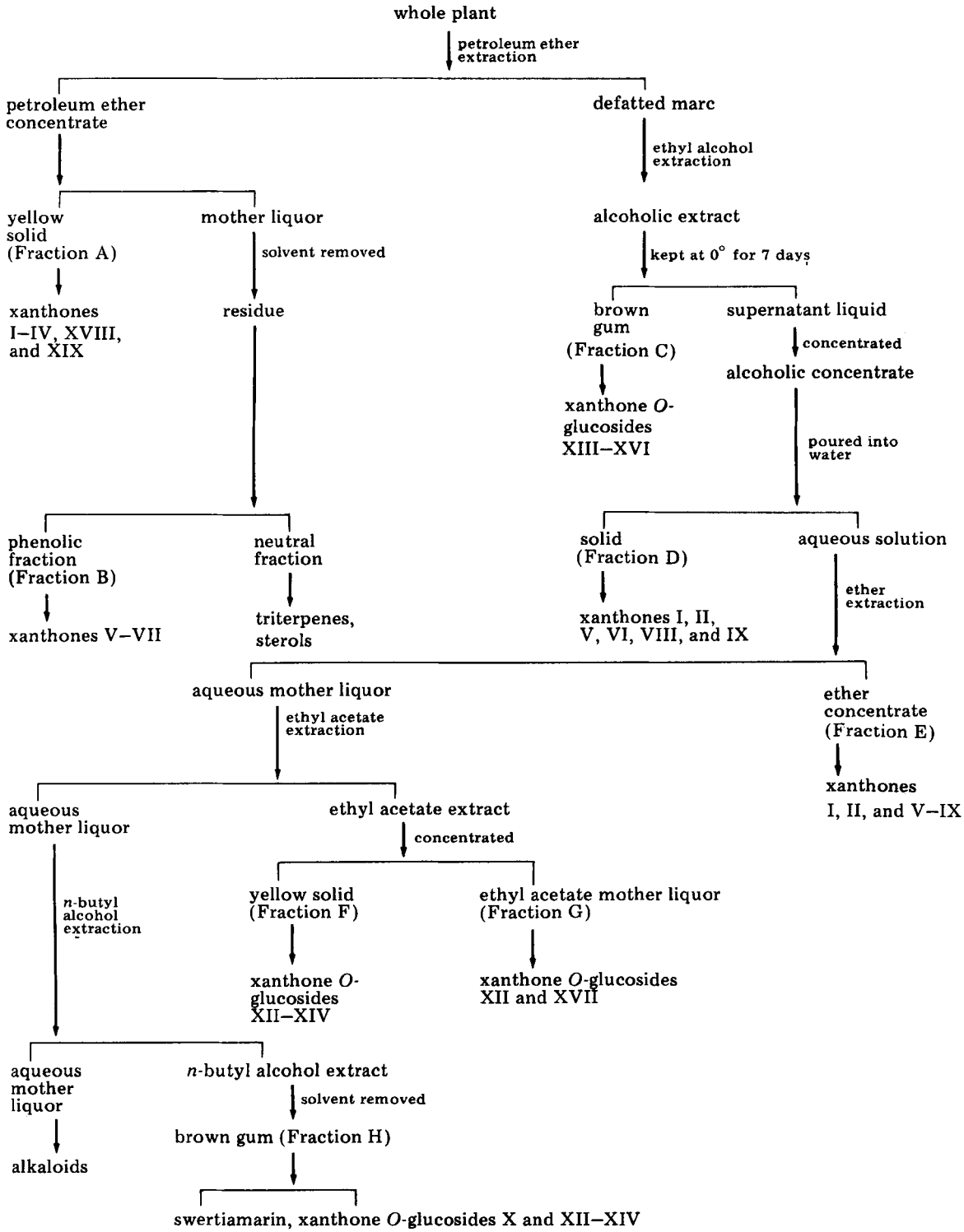

Scheme I

in certain mental disorders (1).

Work in this laboratory previously demonstrated the chemotaxonomic significance of the xanthonic constituents of members of the genus *Swertia* and of related genera (2–4). The present investigation, with previously unexplored *S. angustifolia*, complements the earlier studies. Additionally, it provides information concerning the content and relative abundance of the free xanthones and xanthone *O*-glucosides in the different parts of this species during its vegetation.

EXPERIMENTAL[1]

Extraction of *S. angustifolia*[2]—The isolation of xanthones and xanthone *O*-glucosides from the whole plant, harvested at three different stages of growth (1–2 weeks, 4–6 weeks, and with fruits), was accomplished following the general procedure shown in Scheme I. The changes

[1] The general directions were reported previously (5).

[2] The plant materials were collected by Mr. V. K. Lal, Central Council of Research in Indian Medicine and Homeopathy, Ranikhet, Almora, India. Voucher specimens are available at the Pharmaceutical Chemistry Research Laboratory, Department of Pharmaceutics, Banaras Hindu University, Varanasi-5, India.

in the content and patterns of the xanthones are recorded in Table I.

In a typical experiment, dried and milled aerial parts with fruits (about 200 g) were batch extracted, at ordinary temperature, in a percolator with petroleum ether (bp 60–80°) and then with ethyl alcohol (4 weeks each). The two extracts were separately processed.

Isolation of Xanthones from Petroleum Extract—The petroleum ether extract was concentrated (about 100 ml), and the concentrate was kept at room temperature (24 ± 8°) overnight. A yellow solid (1.5 g, Fraction A) separated. The solid was collected by filtration, and the mother liquor was evaporated to dryness (2.2 g). A portion (0.2 g) of this residue was dissolved in ether, and the phenolic and nonphenolic constitutents were separated by extraction with an aqueous solution of sodium hydroxide (2%, 3 × 30 ml). The alkaline solution after the usual workup afforded a brown solid (24 mg, Fraction B).

The neutral fraction was column chromatographed according to a previously described procedure (6). TLC and mass spectrometry of the eluted fractions suggested the presence of *n*-alkanes (C_{27}–C_{31}), alkanols (C_{26}–C_{32}), phytosterols (a typical mixture of sitosterol, stigmasterol, and campesterol), and two triterpenes (friedelin and β-amyrin).

Separation of Xanthones from Fraction A—A portion of the solid (0.15 g) was mixed with silica gel[3] (about 1 g) and placed in a 25 × 1.8-cm silica gel column. Elution was carried out with petroleum ether (1 liter), benzene (2 liters), chloroform (1 liter), and chloroform–methanol (90:10, 1 liter). Fractions (500 ml) were collected. The presence of xanthonic constituents in the eluates was monitored by analytical TLC, using silica gel G[4] as the adsorbent.

The petroleum ether eluates gave only a small quantity of an intractable gum, and the gum was not processed further.

Xanthone I (1,5,8-Trihydroxy-3-methoxyxanthone)—The first benzene fraction was concentrated, and the concentrate was subjected to preparative TLC on silica gel G[4] plates (2-mm thickness), developed with benzene–acetic acid (100:2). The upper pale-yellow zone, R_f 0.35, was eluted with chloroform–methanol (10:1). The solution was evaporated to give a dull-yellow solid (3 mg), mp 270–271°. Its melting point, mixed melting point, R_f value, and UV and IR absorption spectra were identical with those of 1,5,8-trihydroxy-3-methoxyxanthone (2).

Xanthone II (1,7,8-Trihydroxy-3-methoxyxanthone)—The third and fourth benzene eluates were combined and concentrated to give a yellow solid (47 mg). This solid crystallized from ethyl alcohol as yellowish-orange needles, mp 218°. Its melting point, mixed melting point, R_f value, and UV and PMR spectra were identical with those of 1,7,8-trihydroxy-3-methoxyxanthone (3). The 7,8-dimethyl ether of the xanthone, prepared with ethereal diazomethane, crystallized from ethyl alcohol as yellow needles; the melting point and mixed melting point with decussatin (2) were 149–150°.

The chloroform eluates also were combined and concentrated. The concentrate showed two major and one minor ferric positive spots on analytic TLC. The components, however, could not be separated by preparative TLC. Therefore, the mixture was methylated with dimethyl sulfate and potassium carbonate in anhydrous acetone under reflux (45 hr). The permethyl ethers were separated by preparative TLC.

Xanthone XVIII (1,3,4,5,8-Pentamethoxyxanthone)—The upper pale-yellow zone, R_f 0.5 (chloroform–acetic acid, 100:1), which also showed a strong fluorescence under shortwave UV light, was eluted with chloroform. The residue (1.8 mg) from the chloroform solution showed an R_f value and UV absorption spectrum that indicated it was 1,3,4,5,8-pentamethoxyxanthone (7). The mass spectrum of the compound, *m/e* 346 (M^+, relative intensity 100%), 331 (30), 329 (7), 317 (18), 316 (18), 303 (42), 275 (12), and 260 (5), was also consistent with this conclusion.

Xanthone XIX (1,3,4,7,8-Pentamethoxyxanthone)—The lower yellow zone, R_f 0.32, was eluted with chloroform. The residue (2.5 mg) from the chloroform solution showed an R_f value, UV absorption spectrum, and mass spectrum (M^+, 346) identical with those of 1,3,4,7,8-pentamethoxyxanthone (7).

When the chloroform–methanol (90:10) eluates were combined and concentrated, a triterpene (22 mg), mp 300–302°, was obtained. The melting point, mixed melting point, and IR and PMR spectra of the compound established its identity as oleanolic acid. The mother liquor showed the presence of two strongly polar xanthones on analytical TLC. The R_f values of the two compounds corresponded with 1,3,5,8- and 1,3,7,8-tetrahydroxyxanthones (2).

The mixture of xanthones was acetylated with acetic anhydride and pyridine. Workup in the usual fashion afforded the corresponding tetraacetate derivatives, which were separated by column chromatography over silica gel. Petroleum ether, benzene, and benzene–chloroform (1:1), 1 liter each, were used as the eluents. Fractions (100 ml) were collected, and each fraction was monitored by analytical TLC.

Xanthone III (1,3,5,8-Tetrahydroxyxanthone)—The early benzene

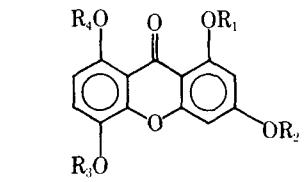

I: $R_1 = R_3 = R_4 = H$, $R_2 = CH_3$
III: $R_1 = R_2 = R_3 = R_4 = H$
VI: $R_1 = R_4 = H$, $R_2 = R_3 = CH_3$
X: R_1 = β-D-glucopyranosyl, $R_2 = CH_3$, $R_3 = R_4 = H$
XI: R_1 = β-D-glucopyranosyl, $R_2 = R_3 = CH_3$, $R_4 = H$
XIII: R_1 = β-D-glucopyranosyl, $R_2 = R_3 = R_4 = H$

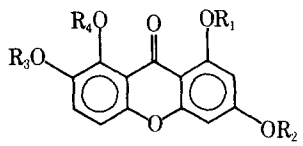

II: $R_1 = R_3 = R_4 = H$, $R_2 = CH_3$
IV: $R_1 = R_2 = R_3 = R_4 = H$
VII: $R_1 = R_4 = H$, $R_2 = R_3 = CH_3$
VIII: $R_1 = H$, $R_2 = R_3 = R_4 = CH_3$
IX: $R_1 = R_2 = R_4 = H$, $R_3 = CH_3$
XIV: R_1 = β-D-glucopyranosyl, $R_2 = R_3 = R_4 = H$
XVII: R_1 = β-D-glucopyranosyl, $R_2 = CH_3$, $R_3 = R_4 = H$

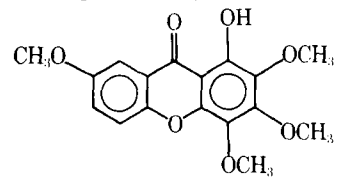

V

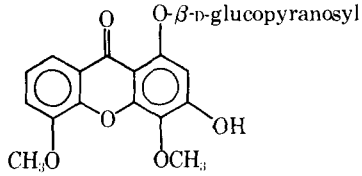

XII

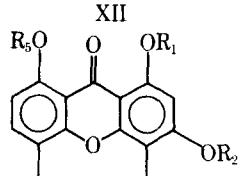

XV: R_1 = β-D-glucopyranosyl, $R_2 = R_3 = R_4 = R_5 = H$
XVIII: $R_1 = R_2 = R_3 = R_4 = R_5 = CH_3$

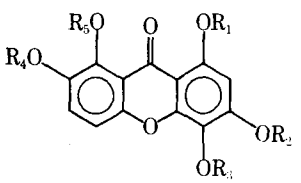

XVI: R_1 = β-D-glucopyranosyl, $R_2 = R_3 = R_4 = R_5 = H$
XIX: $R_1 = R_2 = R_3 = R_4 = R_5 = CH_3$

[3] British Drug Houses (60–120 mesh).
[4] E. Merck AG, Darmstadt, Germany.

Table I—Xanthonic Patterns (Relative Percent Yield) of *S. angustifolia* during Growth[a,b]

Xanthones	4–6-Week-Old Plant		Plant with Fruits	
	Roots	Aerial Parts	Roots	Aerial Parts
Tetraoxygenated free xanthones	60	48	22	10
Pentaoxygenated free xanthones	12	17	2	6
Tetraoxygenated xanthone *O*-glucosides	2	10	50	64
Pentaoxygenated xanthone *O*-glucosides	—	3	5	6
Unidentified phenolic constituents	26	22	21	14
Yield, %	0.038	0.22	1.8	5.5

[a] The mean of three experiments is recorded. [b] One- to two-week-old seedlings, grown on a potting soil, gave only traces of 1,3,5,8- and 1,3,7,8-tetraoxygenated xanthones but relatively larger amounts of polyphenols which could not be identified.

eluates afforded 1,3,5,8-tetraacetoxyxanthone (5.5 mg). This compound, on hydrolysis with methanolic potassium hydroxide (5%) and the usual workup of the hydrolyzed product, gave 1,3,5,8-tetrahydroxyxanthone as a brown solid; the melting point and mixed melting point were 295–300° (2).

Xanthone IV (1,3,7,8-Tetrahydroxyxanthone)—The later benzene and benzene–chloroform eluates, in a similar way, furnished 1,3,7,8-tetrahydroxyxanthone (11 mg); the melting point and mixed melting point were 330–333° (3).

Separation of Xanthones from Fraction B—The total phenolic constituents from this fraction showed five iodine-positive spots on analytical TLC. Preparative TLC, using benzene–acetic acid (100:2) as the developer, afforded three xanthones as pure entities.

Xanthone V (1-Hydroxy-2,3,4,7-tetramethoxyxanthone)—The upper bright-yellow zone, R_f 0.75, was eluted with chloroform. The solution was evaporated to give a yellow solid (3 mg), mp 114–115°. Its melting point, mixed melting point, R_f value, and UV and mass spectra (M^+, 332) were identical with those of 1-hydroxy-2,3,4,7-tetramethoxyxanthone (4).

Xanthone VI (1,8-Dihydroxy-3,5-dimethoxyxanthone)—The middle yellow zone, R_f 0.62, was eluted with chloroform, and the chloroform concentrate showed an elongated spot on analytical TLC. It was subjected again to preparative TLC and, after the usual workup, the residue (about 1 mg) was obtained as a yellow microcrystalline solid, mp 184–186°. Its melting point, mixed melting point, R_f values, and UV absorption spectrum suggested its identity as 1,8-dihydroxy-3,5-dimethoxyxanthone. The diacetate derivative, prepared by treating it with acetic anhydride and pyridine on a steam bath (4 hr), was found to be identical to 1,8-diacetoxy-3,5-dimethoxyxanthone by co-TLC.

Xanthone VII (1,8-Dihydroxy-3,7-dimethoxyxanthone)—After the usual workup, the lowest yellow zone, R_f 0.45, gave yellow crystals (7 mg), mp 177–178°. The melting point, mixed melting point, R_f value, and UV and PMR spectra of the compound were identical with those of 1,8-dihydroxy-3,7-dimethoxyxanthone (2).

Isolation of Xanthones from Alcoholic Extract—The alcoholic extract was concentrated (to about 200 ml) and kept at 0° for 7 days, and a brown gum (5.8 g, Fraction C) separated. The alcoholic supernate was further concentrated to a syrupy liquid. It was poured into water (100 ml), and the mixture was kept at ambient temperature overnight. The precipitated yellow solid (0.72 g, Fraction D) was collected by filtration. The aqueous mother liquor was successively extracted with ether, ethyl acetate, and *n*-butyl alcohol (5 × 100 ml each).

The solvent was evaporated from the combined ether extracts, and a yellow solid (0.18 g, Fraction E) was obtained. The combined ethyl acetate extracts, on concentration, gave a yellow solid (0.42 g, Fraction F). On evaporation, the ethyl acetate mother liquor gave a second yellow solid (0.08 g, Fraction G). Likewise, the *n*-butyl alcohol extract gave a brown gum (2.1 g, Fraction H).

Separation of Xanthone *O*-Glucosides from Fraction C—Analytical TLC (*n*-butyl alcohol–acetic acid–water, 4:1:2) and paper chromatography[5] (aqueous acetic acid, 15%) indicated the presence of four xanthone *O*-glucosides in this fraction. A small portion (40 mg) of this mixture was hydrolyzed with emulsin according to a previously described procedure (4). In the aqueous hydrolysate, the presence of glucose as the only glucone moiety was detected by cochromatography (4). The aglucone moieties were identified as I, II, 1,3,4,5,8-pentahydroxyxanthone, and 1,3,4,7,8-pentahydroxyxanthone by their melting points, mixed melting points, co-TLC with reference samples, and comparison of UV absorption spectra of the individual compounds and their methyl ethers with those of authentic markers (4, 7).

A larger portion (0.5 g) of this fraction was permethylated with methyl iodide and sodium hydride in tetrahydrofuran at ordinary temperature (4). The product was dissolved in chloroform and chromatographed over a 40 × 1.8-cm silica gel column. The elution was carried out with chloroform (500 ml) and chloroform–ethyl acetate (2:1 and 1:1, 500 ml each). Fractions (50 ml) were collected and monitored by TLC.

Permethyl Ether of Xanthone *O*-Glucoside XIII (2′,3′,4′,6′-Tetra-*O*-methyl-1-*O*-β-D-glucopyranosyl -3,5,8-trimethoxyxanthone)—Fractions 3–6, on evaporation, yielded a straw-colored amorphous powder (22 mg). The 60-MHz PMR spectrum of the compound in deuterochloroform was characteristic of the heptamethyl ether of 3,5,8-trioxygenated xanthone 1-*O*-glucoside. Thus, the glucosyl six protons and 21 methoxyl protons appeared in the 3.2–4.0-ppm region; the glucosyl anomeric proton showed a broad one-proton signal around 5 ppm; and the aromatic protons appeared at 6.40 (1H, d, J = 2 Hz), 6.64 (1H, d, J = 2 Hz), 6.76 (1H, d, J = 9 Hz), and 7.34 (1H, d, J = 9 Hz) ppm. It did not give any molecular ion peak in its mass spectrum, but characteristic fragment ion peaks appeared at *m/e* 302 and 219 due to 1-hydroxy-3,5,8-trimethoxyxanthone and 2,3,4,6-tetra-*O*-methylglucosyl moieties, respectively.

The glucoside methyl ether was hydrolyzed with 2 *N* HCl, and the aglucone was extracted with chloroform. The residue from the chloroform solution crystallized from ethyl alcohol as pale-yellow needles, mp 204–205°. The melting point, mixed melting point, R_f value, and UV absorption spectrum of the compound established its identity as 1-hydroxy-3,5,8-trimethoxyxanthone (2). The glucone fraction from the aqueous hydrolysate was obtained as a syrup, $[\alpha]_D^{30}$ +74° (c 0.52, water), *m/e* 236 (M^+). The R_f value and spectral (PMR and mass) and optical properties of the compound were indistinguishable from those of 2,3,4,6-tetra-*O*-methylglucose.

Permethyl Ether of Xanthone *O*-Glucoside XIV (2′,3′,4′,6′-Tetra-*O*-methyl-1-*O*-β-D-glucopyranosyl -3,7,8-trimethoxyxanthone)—Fractions 8–10, on evaporation, gave a yellow solid (172 mg); *m/e* 302 and 219.

Anal.—Calc. for $C_{26}H_{32}O_{11}$: C, 60.00; H, 6.15. Found: C, 59.61; H, 6.42.

Hydrolysis of the glucoside with 2 *N* HCl and the usual workup of the aglucone afforded a yellow solid, mp 148–149°. The compound was identical with decussatin in all respects (melting point, mixed melting point, co-TLC, and UV absorption spectrum) (2). The glucone part was identified as 2,3,4,6-tetra-*O*-methylglucose as shown previously.

The chloroform–ethyl acetate (1:1) eluates, on evaporation, gave an ivory-colored solid (14 mg); it showed two major spots, R_f 0.38 and 0.28, on analytical TLC. These compounds were separated by preparative TLC using chloroform–acetic acid (100:2).

Permethyl Ether of Xanthone *O*-Glucoside XV (2′,3′,4′,6′-Tetra-*O*-methyl-1-*O*-β-D-glucopyranosyl -3,4,5,8-tetramethoxyxanthone)—The less polar component, R_f 0.38, from preparative TLC was obtained as a glassy solid (8 mg); *m/e* 332 and 219.

Anal.—Calc. for $C_{27}H_{36}O_{12}$: C, 61.13; H, 6.79. Found: C, 60.62; H, 6.88.

Hydrolysis of the glucoside with 2 *N* HCl and workup of the product in the usual manner furnished 1-hydroxy-3,4,5,8-tetramethoxyxanthone (melting point, mixed melting point, co-TLC, and UV absorption spectrum) (7) and 2,3,4,6-tetra-*O*-methylglucose (co-TLC and PMR spectrum).

Permethyl Ether of Xanthone *O*-Glucoside XVI (2′,3′,4′,6′-Tetra-*O*-methyl-1-*O*-β-D-glucopyranosyl -3,4,7,8-tetramethoxyxanthone)—The more polar component, R_f 0.28, from the preparative TLC was obtained as a pale-yellow gum (17 mg); *m/e* 332 and 219.

Anal.—Calc. for $C_{27}H_{36}O_{12}$: C, 61.13; H, 6.79. Found: C, 60.82; H, 6.94.

The compound, on hydrolysis with 2 *N* HCl, gave 1-hydroxy-3,4,7,8-tetramethoxyxanthone (melting point, mixed melting point, co-TLC, and PMR spectrum) (7) and 2,3,4,6-tetra-*O*-methylglucose (co-TLC and PMR spectrum).

Separation of Xanthones from Fraction D—The yellow solid showed two major and four minor spots on analytical TLC. Co-TLC behavior of the minor components suggested that these compounds were xanthones I, II, V, and VI (2, 7). The two major components were sepa-

[5] Whatman No. 1.

rated by repeated preparative TLC using benzene–acetic acid (100:2).

Xanthone VIII (1-Hydroxy-3,7,8-trimethoxyxanthone)—The upper zone, R_f 0.35, was eluted with chloroform, and the solvent was evaporated. The residue crystallized from ethyl alcohol as bright-yellow needles (18 mg), mp 149–150°. The melting point, mixed melting point, R_f value, and UV absorption spectrum of the compound were in excellent agreement with those of decussatin (2).

Xanthone IX (1,3,8-Trihydroxy-7-methoxyxanthone)—The lower zone, R_f 0.18, was eluted with chloroform. The residue from chloroform crystallized from acetone as yellow needles (5 mg), mp 295–298°; λ_{max} (ethyl alcohol) (log ϵ): 238 (4.44), 262 (4.54), and 336 (4.29) nm; *m/e* 274 (M^+, relative intensity, 100%), 259 (18), 245 (22), 231 (24), 203 (5), and 202 (4). The melting point and UV absorption spectrum of the compound were indistinguishable from those reported for 1,3,8-trihydroxy-7-methoxyxanthone (8). The compound, on methylation with ethereal diazomethane, gave decussatin (2).

Separation of Xanthones from Fraction E—Analytical TLC indicated the presence of seven xanthones, I, II, and V–IX, which were separated as described previously.

Separation of Xanthone *O*-Glucosides from Fraction F—This fraction showed one major and two minor spots on analytical TLC, R_f 0.52, 0.48, and 0.33 (chlorofrom–methanol, 2:1).

Xanthone *O*-Glucoside XII (3-Hydroxy-1-*O*-β-D-glucopyranosyl-4,5-dimethoxyxanthone)—The major component, R_f 0.52, crystallized from ethyl alcohol as pale-yellow crystals (24 mg), mp 268–270°: $[\alpha]_D^{30}$ −112.8° (c 0.32, methyl alcohol).

Anal.—Calc. for $C_{21}H_{22}O_{11}\cdot H_2O$: C, 53.84; H, 5.12. Found: C, 54.27; H, 5.06.

Hydrolysis of the compound with emulsin gave 1,3-dihydroxy-4,5-dimethoxyxanthone (4) and glucose. Permethylation of the glucoside followed by acid hydrolysis yielded 1-hydroxy-3,4,5-trimethoxyxanthone (melting point, mixed melting point, co-TLC, and PMR spectrum) (4) and 2,3,4,6-tetra-*O*-methylglucose (co-TLC and PMR spectrum). These properties were identical with those reported for 3-hydroxy-1-*O*-β-D-glucopyranosyl-4,5-dimethoxyxanthone (9).

From the alcoholic mother liquor, after the separation of the glucoside (XII), further quantities of xanthone *O*-glucosides XIII (7 mg) and XIV (12 mg) were obtained as their permethyl ethers following the procedure described for Fraction C.

Separation of Xanthone *O*-Glucosides from Fraction G—This fraction showed one major and one minor spot, R_f 0.46 and 0.37, respectively, on analytical TLC (chloroform–methanol, 2:1).

Xanthone *O*-Glucoside XVII (3-Methoxy-1-*O*-β-D-glucopyranosyl-7,8-dihydroxyxanthone)—The major component crystallized from ethyl alcohol as straw-colored crystals (26 mg), mp 198–203°; $[\alpha]_D^{30}$ −103° (c 0.28, methyl alcohol).

Anal.—Calc. for $C_{20}H_{20}O_{11}\cdot H_2O$: C, 52.86; H, 4.84. Found: C, 52.51; H, 4.98.

Hydrolysis of the glucoside with emulsin gave 1,7,8-trihydroxy-3-methoxyxanthone and glucose. Permethylation followed by acid hydrolysis gave decussatin and 2,3,4,6-tetra-*O*-methylglucose.

Separation of Xanthone *O*-Glucosides from Fraction H—This fraction, when processed for the isolation of heterosides (7), gave swertiamarin (melting point, mixed melting point, and PMR spectrum of the tetraacetate) (1.8 g) (10) as the major constituent plus small quantities of xanthone *O*-glucosides X and XII–XIV. The xanthone *O*-glucosides were identified as before.

RESULTS AND DISCUSSION

Preliminary examination of the petroleum ether and alcoholic extracts of the roots of *S. angustifolia* by analytical TLC suggested the presence of over a dozen xanthones of varying polarity. The TLC patterns of these constituents and those obtained from the aerial portions (stems, leaves, and flowers) did not show any significant qualitative difference. Therefore, the whole plant was used for batch extractions with larger samples. The individual parts were also extracted in small batches to determine the quantities of free xanthones and xanthone *O*-glucosides during plant growth. The results are recorded in Table I.

From the whole plant of *S. angustifolia*, 14 tetraoxygenated and five pentaoxygenated xanthonic constituents were isolated. Chemical transformation, spectroscopic analyses (UV, IR, PMR, and mass spectra), and comparison with reference samples (2–7) established their structures. Xanthones XVIII and XIX were isolated from a permethylated sample of the natural mixture of xanthones. The xanthone *O*-glucosides XI and XIV–XVII were previously unreported in nature.

The occurrence of V and XII in this species is taxonomically significant. Xanthones containing these two oxygenation patterns were encountered only once before in *Swertia*—*viz.*, *S. bimaculata* (4). These two types of xanthones, however, constitute major characters in a number of *Frasera* species (11). Until recently, the genus *Frasera* was considered chemotaxonomically different from *Swertia* on the basis of differences in the oxygenation patterns of their contained xanthones. Work in this laboratory has shown (4) for the first time that xanthones of *S. bimaculata* bear oxygenation patterns characteristic of both *Swertia* and *Frasera* species. The isolation of xanthone V and xanthone *O*-glucoside XII from *S. angustifolia* provides additional support in favor of the proposed phylogentic similarity of the two genera.

Another aspect of this investigation that has taxonomic significance was the relative abundance of the differently oxygenated xanthones occurring in *S. angustifolia*. The relative abundance of the complementary pair of 1,3,5,8- and 1,3,7,8-tetraoxygenated xanthones was inversely proportional in all members of the genera *Swertia* and *Gentiana* investigated so far (3). In *S. angustifolia* also, 1,3,7,8-tetraoxygenated xanthones constituted the major oxygenation pattern. The glucosylation in the xanthone *O*-glucosides of this species was exclusively at the 1-position.

The formation of xanthone *O*-glucosides in *S. angustifolia* was discernible only from the onset of maturity (4–6-week-old plant). This phenomenon is rather surprising in view of the fact that glycosides are less toxic to plants than their phenolic aglucones (12); therefore, glycosidation of xanthones is expected at an early stage of growing but was not observed in *S. angustifolia*.

Phenolic substances are known to be responsible for the general resistance showed by higher plants toward parasitic bacteria and fungi (13). The question of whether an unaltered phenol or the corresponding *O*-glycoside is a true protective agent of a higher plant was answered recently (14) for the case of the wilting disease of safflower (*Carthamus tinctorius* L.) caused by *Fusarium oxysporum* f. sp. *carthami*. Carthamidin (4′,5,7,8-tetrahydroxyflavanone), a constituent of healthy safflower, was strongly effective as a protective agent against the fusarial wilt while the corresponding 5-*O*-glucoside was practically inactive. Further work is clearly necessary to establish whether or not the observed difference between the free phenolic compound and the corresponding *O*-glucoside as a protective agent is a general phenomenon.

The content of the xanthone *O*-glucosides was greater in the aerial portions than in the roots (Table I). This result is particularly germane to the use of the plant extract for therapeutic purposes (1). Recent investigations in this laboratory have shown that free xanthones and their *O*-glucosides have different biological properties (2, 7, 15–18).

REFERENCES

(1) R. N. Chopra, S. L. Nayar, and I. C. Chopra, "Glossary of Indian Medicinal Plants," C.S.I.R., New Delhi, India, 1956, p. 237.

(2) S. Ghosal, P. V. Sharma, R. K. Chaudhuri, and S. K. Bhattacharya, *J. Pharm. Sci.*, **62,** 926 (1973).

(3) S. Ghosal, P. V. Sharma, and R. K. Chaudhuri, *Phytochemistry*, **14,** 1393 (1975).

(4) *Ibid.*, **14,** 2671 (1975).

(5) S. Ghosal, P. V. Sharma, and R. K. Chaudhuri, *J. Pharm. Sci.*, **63,** 1286 (1974).

(6) R. K. Chaudhuri and S. Ghosal, *Phytochemistry*, **9,** 1895 (1970).

(7) S. Ghosal, P. V. Sharma, R. K. Chaudhuri, and S. K. Bhattacharya, *J. Pharm. Sci.*, **64,** 80 (1975).

(8) K. R. Markham, *Tetrahedron*, **21,** 3687 (1965).

(9) H. Inouye, S. Ueda, M. Inada, and M. Tsujii, *Yakugaku Zasshi*, **91,** 1022 (1971).

(10) S. K. Bhattacharya, P. K. S. P. Reddy, S. Ghosal, A. K. Singh, and P. V. Sharma, *J. Pharm. Sci.*, **65,** 1547 (1976).

(11) G. H. Stout, E. N. Christensen, W. J. Balkenhol, and K. L. Stevens, *Tetrahedron*, **25,** 1961 (1969).

(12) L. P. Miller, in "Phytochemistry," vol. I, L. P. Miller, Ed., Van Nostrand, New York, N.Y., 1973, p. 297.

(13) R. K. S. Wood, in "Physiological Plant Pathology," Blackwell, Oxford, England, 1967, p. 413.

(14) S. Ghosal, K. Biswas, D. K. Chakrabarti, and K. C. Basu Chaudhary, *Phytopathology*, **67,** 548 (1977).

(15) S. K. Bhattacharya, S. Ghosal, R. K. Chaudhuri, and A. K. Sanyal, *J. Pharm. Sci.*, **61,** 1838 (1972).

(16) S. K. Bhattacharya, A. K. Sanyal, and S. Ghosal, in "Drugs and Central Synaptic Transmission," P. B. Bradley and B. N. Dhawan, Eds., Macmillan, London, England, 1976, p. 333.
(17) S. Ghosal and R. K. Chaudhuri, *J. Pharm. Sci.*, **64**, 888 (1975).
(18) S. Ghosal, S. K. Bhattacharya, and R. K. Chaudhuri, "Abstracts of the 35th International Pharmaceutical Congress (FIP)," Dublin, Ireland, 1975, p. 82.

ACKNOWLEDGMENTS

Supported in part by a grant from the University Grants Commission, New Delhi, India.

The authors are grateful to Professor T. R. Govindachari, Ciba-Geigy Research Centre, Bombay, India, and to Dr. R. K. Chaudhuri, Pharmazeutisches Institut der Universität, Bonn, Germany, for some spectral data.

Quantitative Determination of Amitriptyline in Blood

PUSHKAR N. KAUL ˣ, LLOYD R. WHITFIELD, and MERVIN L. CLARK

Received February 25, 1977, from the *University of Oklahoma Health Sciences Center and Central State Griffin Memorial Hospital, Norman, OK 73070.* Accepted for publication March 29, 1977.

Abstract □ An assay was developed and standardized for amitriptyline and its hydroxylated tertiary amine metabolites in blood and other biological tissues. This method is capable of determining 5–15 ng of these compounds/ml and is based on reacting the drug as base with 9-bromomethylacridine to form a quaternary product which, on photolysis, yields fluorescence in a stoichiometric fashion. The precision of the method is usually around ±5%.

Keyphrases □ Amitriptyline—fluorometric analysis, blood and tissues □ Fluorometry—analysis, amitriptyline, blood and tissues □ Antidepressants—amitriptyline, fluorometric analysis, blood and tissues

Blood amitriptyline levels in humans following a single oral dose are generally 20 ng/ml or less (1). These low levels were difficult to determine until recently, primarily because of a lack of appropriate methods with adequate sensitivity and precision.

Several methods were reported (1–6), but only three were capable of assaying blood levels of less than 20 ng/ml. A GLC method (3) has not yet been used to study amitriptyline pharmacokinetics. A method based on UV reflectance photometry was used for various psychoactive drugs including amitriptyline (5), but its ability to determine blood levels of this tricyclic compound following a single oral dose has not been demonstrated. One GLC method (6) was reported to exhibit reasonably good sensitivity and precision.

A method based on a fluorometric approach (7–9) could determine the absorption and elimination profiles of amitriptyline in humans following a single oral dose of 1 mg/kg (4). In this method, amitriptyline extracted from blood is reacted with 9-bromomethylacridine to form a quaternary ammonium product which, on photolysis, yields fluorescence. Both quaternization and photolysis are stoichiometric with a high degree of precision.

This paper describes the development of a fluorometric assay capable of determining levels as low as 5 ng of amitriptyline/ml in biological fluids. The method has been applied to assaying patient blood samples and is being used to generate basic pharmacokinetic data on amitriptyline in animals and humans.

EXPERIMENTAL

Materials and Equipment—The acridine reagent was synthesized as described earlier (8). Various chemicals and solvents, the laboratory equipment, and other instrumentation were essentially the same as described previously (9). Amitriptyline[1] was used as a hydrochloride salt.

Table I—Percent Maximum Extraction of Amitriptyline from Blood (n = 4)

Solvent	Relative Fluorescence	Blood Blank	Maximum Extraction, %
Hexane	2762 ± 345[a,b]	100 ± 21[a,c]	100
Hexane–1.5% isoamyl alcohol	2707 ± 242	86 ± 5	98
Toluene–1.5% isoamyl alcohol	2020 ± 106	180 ± 0	73
Benzene–1.5% isoamyl alcohol	2435 ± 78	202 ± 53	88
Toluene	2030 ± 259	138 ± 30	73
Benzene	2148 ± 43	108 ± 11	78

[a] Mean ± *SD*. [b] Formed emulsions. [c] n = 2.

General Procedure—*Amitriptyline, as the base, was reacted with* excess 9-bromomethylacridine in 200 μl of acetonitrile in the presence of glass beads as the catalyst. The reaction mixture was incubated at 50° for 18 hr, evaporated to dryness, and finally reconstituted in 100 μl of acetonitrile. An aliquot was subjected to TLC to separate the quaternary salt. The separated quaternary salt was photolyzed under UV light, and the fluorescent material was eluted with methanolic sulfuric acid for fluorometric determination[2].

Standardization of Assay—Various steps, starting from the isolation of amitriptyline from blood, its reaction with the acridine reagent, and finally fluorometric determination, were standardized to derive the optimum conditions. Since the assay primarily would be applied to blood, all standardization steps were carried out in the presence of a blank blood extract, *i.e.*, amitriptyline was added either to the blank whole blood and extracted out or to the evaporated extract of 3-ml blank blood, prior to reaction with the acridine reagent.

Extraction from Blood—Of the organic solvents examined, n-hexane containing 1.5% isoamyl alcohol was optimum for single extraction (Table I). Other optimum conditions included a blood-to-solvent ratio of 3:20, an extraction pH of 13 ± 0.5, and a shake time of 30 min at 150 cpm (Table II).

Quaternization Reaction—A range of 9-bromomethylacridine concentrations was reacted with amitriptyline and assayed. The optimum acridine concentration for the quaternization of 0.1–1 μg of amitriptyline was 0.47×10^{-3} M and higher (Table III).

TLC and Photolysis—A 20-μl aliquot of the reconstituted mixture was spotted on the synthetic-backed 100-μm silica gel plate. The plate was dried and developed in many trial solvents, including ethyl acetate–methanol–water–acetic acid–cyclohexane (100:20:12:5:5). This solvent system caused a good separation of the amitriptyline quaternary product (R_f 0.42) from the quaternary products of 10-hydroxy and

[1] Supplied by Merck Sharp & Dohme Research Laboratories, West Point, Pa.
[2] Aminco-Bowman spectrophotofluorometer.

(16) S. K. Bhattacharya, A. K. Sanyal, and S. Ghosal, in "Drugs and Central Synaptic Transmission," P. B. Bradley and B. N. Dhawan, Eds., Macmillan, London, England, 1976, p. 333.
(17) S. Ghosal and R. K. Chaudhuri, *J. Pharm. Sci.*, **64**, 888 (1975).
(18) S. Ghosal, S. K. Bhattacharya, and R. K. Chaudhuri, "Abstracts of the 35th International Pharmaceutical Congress (FIP)," Dublin, Ireland, 1975, p. 82.

ACKNOWLEDGMENTS

Supported in part by a grant from the University Grants Commission, New Delhi, India.

The authors are grateful to Professor T. R. Govindachari, Ciba-Geigy Research Centre, Bombay, India, and to Dr. R. K. Chaudhuri, Pharmazeutisches Institut der Universität, Bonn, Germany, for some spectral data.

Quantitative Determination of Amitriptyline in Blood

PUSHKAR N. KAUL ˣ, LLOYD R. WHITFIELD, and MERVIN L. CLARK

Received February 25, 1977, from the *University of Oklahoma Health Sciences Center and Central State Griffin Memorial Hospital, Norman, OK 73070.* Accepted for publication March 29, 1977.

Abstract □ An assay was developed and standardized for amitriptyline and its hydroxylated tertiary amine metabolites in blood and other biological tissues. This method is capable of determining 5–15 ng of these compounds/ml and is based on reacting the drug as base with 9-bromomethylacridine to form a quaternary product which, on photolysis, yields fluorescence in a stoichiometric fashion. The precision of the method is usually around ±5%.

Keyphrases □ Amitriptyline—fluorometric analysis, blood and tissues □ Fluorometry—analysis, amitriptyline, blood and tissues □ Antidepressants—amitriptyline, fluorometric analysis, blood and tissues

Blood amitriptyline levels in humans following a single oral dose are generally 20 ng/ml or less (1). These low levels were difficult to determine until recently, primarily because of a lack of appropriate methods with adequate sensitivity and precision.

Several methods were reported (1–6), but only three were capable of assaying blood levels of less than 20 ng/ml. A GLC method (3) has not yet been used to study amitriptyline pharmacokinetics. A method based on UV reflectance photometry was used for various psychoactive drugs including amitriptyline (5), but its ability to determine blood levels of this tricyclic compound following a single oral dose has not been demonstrated. One GLC method (6) was reported to exhibit reasonably good sensitivity and precision.

A method based on a fluorometric approach (7–9) could determine the absorption and elimination profiles of amitriptyline in humans following a single oral dose of 1 mg/kg (4). In this method, amitriptyline extracted from blood is reacted with 9-bromomethylacridine to form a quaternary ammonium product which, on photolysis, yields fluorescence. Both quaternization and photolysis are stoichiometric with a high degree of precision.

This paper describes the development of a fluorometric assay capable of determining levels as low as 5 ng of amitriptyline/ml in biological fluids. The method has been applied to assaying patient blood samples and is being used to generate basic pharmacokinetic data on amitriptyline in animals and humans.

EXPERIMENTAL

Materials and Equipment—The acridine reagent was synthesized as described earlier (8). Various chemicals and solvents, the laboratory equipment, and other instrumentation were essentially the same as described previously (9). Amitriptyline[1] was used as a hydrochloride salt.

Table I—Percent Maximum Extraction of Amitriptyline from Blood (n = 4)

Solvent	Relative Fluorescence	Blood Blank	Maximum Extraction, %
Hexane	2762 ± 345[a,b]	100 ± 21[a,c]	100
Hexane–1.5% isoamyl alcohol	2707 ± 242	86 ± 5	98
Toluene–1.5% isoamyl alcohol	2020 ± 106	180 ± 0	73
Benzene–1.5% isoamyl alcohol	2435 ± 78	202 ± 53	88
Toluene	2030 ± 259	138 ± 30	73
Benzene	2148 ± 43	108 ± 11	78

[a] Mean ± *SD*. [b] Formed emulsions. [c] n = 2.

General Procedure—*Amitriptyline, as the base, was reacted with* excess 9-bromomethylacridine in 200 μl of acetonitrile in the presence of glass beads as the catalyst. The reaction mixture was incubated at 50° for 18 hr, evaporated to dryness, and finally reconstituted in 100 μl of acetonitrile. An aliquot was subjected to TLC to separate the quaternary salt. The separated quaternary salt was photolyzed under UV light, and the fluorescent material was eluted with methanolic sulfuric acid for fluorometric determination[2].

Standardization of Assay—Various steps, starting from the isolation of amitriptyline from blood, its reaction with the acridine reagent, and finally fluorometric determination, were standardized to derive the optimum conditions. Since the assay primarily would be applied to blood, all standardization steps were carried out in the presence of a blank blood extract, *i.e.*, amitriptyline was added either to the blank whole blood and extracted out or to the evaporated extract of 3-ml blank blood, prior to reaction with the acridine reagent.

Extraction from Blood—Of the organic solvents examined, n-hexane containing 1.5% isoamyl alcohol was optimum for single extraction (Table I). Other optimum conditions included a blood-to-solvent ratio of 3:20, an extraction pH of 13 ± 0.5, and a shake time of 30 min at 150 cpm (Table II).

Quaternization Reaction—A range of 9-bromomethylacridine concentrations was reacted with amitriptyline and assayed. The optimum acridine concentration for the quaternization of 0.1–1 μg of amitriptyline was 0.47×10^{-3} M and higher (Table III).

TLC and Photolysis—A 20-μl aliquot of the reconstituted mixture was spotted on the synthetic-backed 100-μm silica gel plate. The plate was dried and developed in many trial solvents, including ethyl acetate–methanol–water–acetic acid–cyclohexane (100:20:12:5:5). This solvent system caused a good separation of the amitriptyline quaternary product (R_f 0.42) from the quaternary products of 10-hydroxy and

[1] Supplied by Merck Sharp & Dohme Research Laboratories, West Point, Pa.
[2] Aminco-Bowman spectrophotofluorometer.

Table II—Effect of Varying the Blood-to-Solvent Volume Ratio and Shake Time on the Extraction Efficiency Based on 3-ml Blood Samples Containing 100 ng of Amitriptyline/ml

Solvent Volume[a], ml	Maximum Extraction at Shake Time (n = 3), %		
	15 min	30 min	60 min
10	83 ± 7.4	83 ± 7.3	90 ± 8.0
15	86[b]	88 ± 5.0	97 ± 9.1
20	92 ± 10.8	97 ± 4.7	100 ± 1.6

[a] Extraction solvent was hexane containing 1.5% isoamyl alcohol. [b] n = 1.

10,11-dihydroxy metabolites of amitriptyline. Both hydroxy compounds moved to the same spot (R_f 0.26).

The optimum exposure time for photolysis appeared to be approximately 3 min (Table IV). The photolysis products were reconfirmed to be the same as previously reported (4). Both quaternization and photolysis were stoichiometric over a wide concentration range with a high degree of precision (coefficient of variation ≤5).

Stability of Amitriptyline—Since, in actual practice, the blood samples are generally stored until assayed and since the described assay involves rendering the blood to pH 13, amitriptyline stability was studied in aqueous solution as well as in whole blood at pH 7.4 and 13. These solutions were maintained at 5 and 22° for up to 72 hr. Additional quantitative chromatographic procedures were developed for this work to separate and detect possible decomposition products.

Optimum Assay Procedure—A 3-ml sample of blood was sonicated, adjusted to pH 13 ± 0.05 in a 35-ml screw-capped centrifuge tube by adding 2 ml of 2 N NaOH, and treated with 20 ml of n-hexane containing 1.5% isoamyl alcohol. Then the tube was capped and shaken horizontally at 150 cpm for 30 min. Following centrifugation at 2250 rpm for 10 min, an aliquot (19 ml) was transferred to an evaporation tube. The extract was evaporated at room temperature under nitrogen to 0.5 ml and quantitatively transferred into a 1.5-ml tapered polypropylene tube. The contents were then evaporated to dryness under nitrogen.

Fifty milligrams of 200-μm glass beads and 0.2 ml of the acridine reagent (0.94×10^{-3} M 9-bromomethylacridine in acetonitrile) were added to the reaction tube. The tube was capped, vortexed for 20 sec, and placed in an oven at 50° for 18 hr. Following centrifugation, the contents were evaporated to dryness under nitrogen at room temperature and reconstituted in 100 μl of acetonitrile. A 20-μl aliquot was spotted on a scribed, plastic-backed, 100-μm silica gel TLC plate without fluorescent indicator and developed in ethyl acetate–methanol–water–acetic acid–cyclohexane (100:20:12:5:5) in a saturation chamber.

The plate was dried at 85° for 15 min and placed under a UV lamp (λ_{max} 254 nm) at 12–14 cm for 3 min to generate fluorescence. Then the fluorescent spot was cut out and eluted by vortexing for 20 sec into 10 ml of 0.01 N H_2SO_4 containing 20% methanol in a test tube. The fluorescence was then quantitated on a spectrofluorometer set at an excitation wavelength of 350 nm and an emission wavelength of 474 nm.

Standard curves were obtained by adding known amounts of amitriptyline and/or 10-hydroxyamitriptyline to whole blood and assaying the samples in replicate sets as described. The blanks were run similarly, except that no amitriptyline was added to the blood sample.

RESULTS AND DISCUSSION

The data scatter in the stability experiments was well within the range of experimental error. Thus, no significant loss of amitriptyline in aqueous and blood solutions at basic pH values was observed for up to 72 hr.

Table III—Optimum Concentration of 9-Bromomethylacridine (I) Required for Quaternization of Amitriptyline

I Concentration $\times 10^{-3}$ M	Relative Fluorescence ± SD (n = 3)		Maximum Yield, %
	Blood Blank	Drug[a]	
0.16	90 ± 14	4670 ± 177	64 ± 3.8
0.31	103 ± 11	6731 ± 116	92 ± 1.7
0.47	160 ± 64	7440 ± 173	100 ± 2.3
0.63	130 ± 0	7187 ± 301	98 ± 4.2
0.78	230 ± 85	7103 ± 450	97 ± 6.3
0.94	205 ± 14	7311 ± 368	100 ± 5.0
1.25	203 ± 4	7313 ± 202	100 ± 2.8

[a] Amitriptyline, 1 μg, reacted in the presence of blood extract.

Table IV—Effect of Varying the Duration of Photolysis of the Amitriptyline Quaternary Product in the Presence and Absence of Blank Blood Extract

Minutes	Photolytic Yield (Direct Reaction)		Photolytic Yield (Extracted from Blood)	
	Relative Fluorescence	% Maximum	Relative Fluorescence	% Maximum
0.5	1373 ± 32[a]	78	1023 ± 15[a]	76
1.5	1733 ± 6	98	1320 ± 36	98
2.5	1750 ± 10	99	1337 ± 6	99
3.5	1763 ± 21	100	1353 ± 12	100
4.0	1763 ± 6	100	1340 ± 26	99
5.5	1710 ± 10	97	1327 ± 35	98
6.0	1730 ± 0	98	1297 ± 29	96
8.0	1677 ± 6	95	1260 ± 20	93
10.0	1633 ± 21	93	1143 ± 55	84

[a] n = 3–5.

The previously used solvent system, acetonitrile–water (9:1), separated the quaternary products of chlorpromazine (9) and amitriptyline from the reactants rather well. However, it did not separate the amitriptyline product from the quaternary products of the 10-hydroxy and 10,11-dihydroxy metabolites of amitriptyline, which may be present *in vivo*. Of the various solvent systems tried, ethyl acetate–methanol–water–acetic acid–cyclohexane (100:20:12:5:5) proved effective in solving the separation problem. Thus, in the developed method, the hydroxy tertiary amine metabolites do not interfere. As with chlorpromazine (9), the desmethyl metabolites of amitriptyline also do not interfere.

Blanks, Sensitivity, and Precision—Based on a 3-ml sample, the relative fluorescence values from blank blood and plasma were approximately numerically equivalent to those of the reagent blank. The fluorescence values obtained from analyses of blank organ homogenates were generally greater than those for plasma or blood. However, due to the good precision of the method, it is possible to quantitate accurately low nanogram amitriptyline concentrations in organ homogenates. Since a larger blood or plasma sample did not yield higher blank values, quantities of amitriptyline in the range of 5–15 ng/ml could be assayed by utilizing 6–9-ml samples. The precision within an experiment on the blood and plasma samples was usually within ±5% but occasionally was as high as 10%. Abnormal values (> ±10%) generally warrant repeat analyses.

Addition and Recovery—When known concentrations of amitriptyline, ranging from 20 to 200 ng/ml, were assayed, recoveries of 75–89% were obtained based on the described single-extraction procedure. However, nearly 100% recoveries were attained on triple extraction.

The plasma yielded 76–86% recoveries for a 25–100-ng/ml concentration range. For concentrations of 10 ng/ml or less, better precision and sensitivity could be achieved when larger plasma samples were used for assay, *i.e.*, 6–9 ml instead of 3 ml.

The addition and recovery data from various organs are summarized in Table V.

The addition–recovery experiments were also carried out in whole mouse homogenates (Table VI) to derive the amitriptyline metabolism rate profile in the whole organism.

Hydroxylated Metabolites—Since a solvent system capable of separating from each other the quaternary products of amitriptyline and its two hydroxylated metabolites has not yet been found, it is not possible to quantitate individually 10-hydroxyamitriptyline and 10,11-dihydroxyamitriptyline simultaneously. However, one solvent system did separate the free base of each of the three substances. The free bases can be eluted, evaporated, and then reacted with the acridine reagent to accomplish quantitation.

This approach was used to quantitate the tertiary amine hydroxylated

Table V—Percent Recovery of Amitriptyline from Various Organ Homogenates of Dog [a]

Concentration, ng/ml	Percent Recovery from (Mean ± SD, n = 3)				
	Heart	Liver	Lung	Muscle	Brain
25	77 ± 12	115 ± 17	90 ± 6	80 ± 8	82 ± 11
50	70 ± 11	91 ± 13	81 ± 2	88 ± 4	86 ± 1
100	65 ± 3	88 ± 2	80 ± 4	86 ± 5	76 ± 6

[a] The tissues were homogenized in 20 ml of 0.1 N NaOH/g of tissue.

Table VI—Percent Recovery of Amitriptyline from Whole Mouse Homogenate [a]

Concentration, ng/ml	25	50	100	200	400	600	1000
Percent recovery ± *SD*	74 ± 14[b]	89 ± 7	92 ± 2	89 ± 1	89 ± 1	91 ± 1	92 ± 5

[a] The mice were homogenized in 20 ml of 0.1 *N* NaOH/g of body weight. [b] n = 3.

Table VII—Blood Amitriptyline and 10-Hydroxyamitriptyline Levels in Subjects Receiving 100 mg of Amitriptyline at Bedtime

Subject	Time since Last Dose, hr	Amitriptyline, ng/ml	10-Hydroxyamitriptyline, ng/ml
G.M.	19	42 ± 1	6 ± 1
K.F.	11	34 ± 3	10 ± 1
S.B.	17	165 ± 6	6[a]
M.F.	10	33 ± 2	6 ± 0

[a] Single spot only. All other values are mean ± *SD* of values from duplicate spots derived from a single blood sample per subject.

metabolites added to blood[3]. In the blood samples from both humans and dogs, 10,11-dihydroxyamitriptyline could not be detected. Therefore, the hydroxylated metabolite data may be assumed to represent 10-hydroxyamitriptyline only.

Application to Biological Specimens—*Dog Studies*—Blood levels of amitriptyline were determined in a 9.1-kg dog following a rapid dose of 1 mg/kg iv. Blood specimens were drawn at suitable intervals up to 6 hr. Figure 1 shows the blood level–time profile of amitriptyline and one metabolite, 10-hydroxyamitriptyline. The blood amitriptyline levels declined very rapidly and had an apparent elimination half-life of about 3 hr.

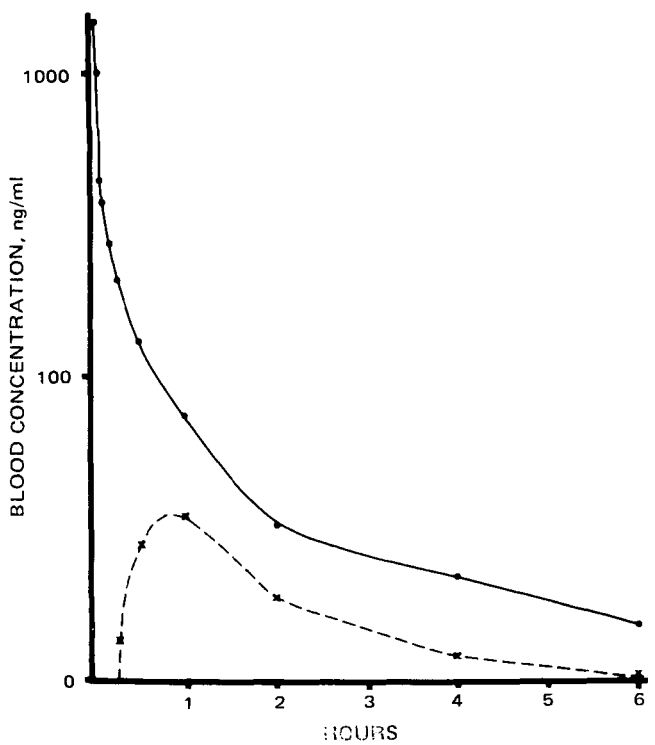

Figure 1—*Blood levels of amitriptyline (●) and 10-hydroxyamitriptyline (×) after 1 mg/kg iv.*

[3] Unpublished results.

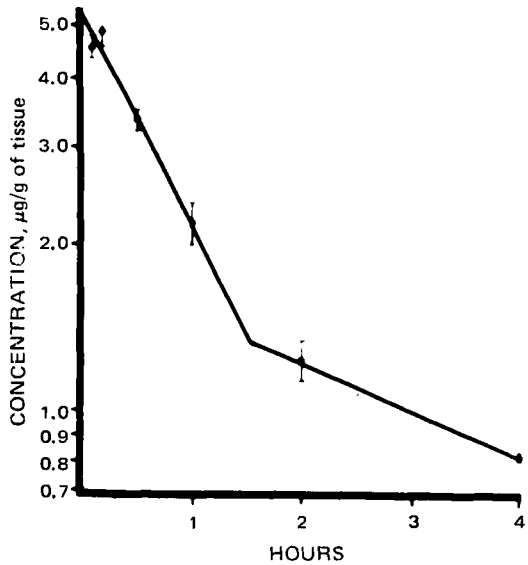

Figure 2—*Disappearance with time of amitriptyline in whole mouse given 5 mg/kg iv. Each point is the mean of two mice with a triplicate analysis on each mouse.*

The 10-hydroxyamitriptyline data indicate a rapid appearance in blood, with a measurable level seen within 3 min. The observed peak blood level was 36 ng/ml and occurred at 1 hr. The metabolite had an apparent elimination half-life of approximately 8 hr. A detailed pharmacokinetic analysis of these data will be published.

Mouse Studies—The method is also amenable to the analysis of biological materials other than blood and plasma. Figure 2 shows the results of applying the method to the determination of amitriptyline from whole mouse homogenates. The mice received a 5-mg/kg iv dose and were subsequently sacrificed at intervals up to 4 hr. Duplicate mice were assayed for each time period. The data show a biphasic decline of the amitriptyline levels. The first phase had a half-life of approximately 0.5 hr, and the second phase had a half-life of approximately 3.5 hr.

Human Studies—Table VII shows the blood levels of amitriptyline and 10-hydroxyamitriptyline in subjects described as suffering from depressive neurosis. Each subject received 100 mg po of amitriptyline at bedtime. Each subject had been receiving treatment for at least 1 week.

REFERENCES

(1) R. A. Braithwaite and B. Widdop, *Clin. Chim. Acta*, **35**, 461 (1971).

(2) H. B. Hucker and S. C. Stauffer, *J. Pharm. Sci.*, **63**, 296 (1974).

(3) A. Jørgensen, *Acta Pharmacol. Toxicol.*, **36**, 79 (1975).

(4) P. N. Kaul and L. R. Whitfield, *West. Pharmacol. Soc.*, **18**, 251 (1975).

(5) U. Breyer and K. Villumsen, *Eur. J. Clin. Pharmacol.*, **4**, 457 (1976).

(6) T. B. Cooper, D. Allen, and G. M. Simpson, *Psychopharm. Commun.*, **2**, 105 (1976).

(7) P. N. Kaul *et al.*, *Int. Res. Commun. Syst.*, **2**, 1343 (1974).

(8) R. E. Lehr and P. N. Kaul, *J. Pharm. Sci.*, **64**, 950 (1975).

(9) P. N. Kaul, L. R. Whitfield, and M. L. Clark, *ibid.*, **65**, 689 (1976).

ACKNOWLEDGMENTS

Supported by National Institutes of Health Grant NS-12004-01.

The authors are grateful to Teresa Paxton for technical assistance and to Dr. John Rush for providing the patient blood samples.

Potential of Liquid Membranes for Drug Overdose Treatment: *In Vitro* Studies

CHIA-WHEI CHIANG *, GEORGE C. FULLER ‡, JOHN W. FRANKENFELD §, and C. T. RHODES *x

Received July 21, 1976, from the **Department of Pharmacy and the* ‡*Department of Pharmacology and Toxicology, College of Pharmacy, University of Rhode Island, Kingston, RI 02881,* and §*Exxon Corporate Research, Linden, NJ 07036.* Accepted for publication March 29, 1977.

Abstract □ The *in vitro* removal of six barbiturates from pH 2 donor solutions by liquid membranes with pH control was evaluated. More than 90% of amobarbital, phenobarbital, and secobarbital were removed within 10 min by the liquid membranes. Drug transport obeyed first-order kinetics initially, and Fick's law was obeyed. The transport rate of phenobarbital by a liquid membrane was temperature dependent. An Arrhenius plot revealed that the activation energy was 10 kcal/mole. The liquid membranes showed some instability in the presence of bile salts.

Keyphrases □ Liquid membranes—*in vitro* removal of various barbiturates from pH 2 donor solutions, effect of temperature, phase ratio, and bile salts □ Membranes, liquid—*in vitro* removal of various barbiturates from pH 2 donor solutions, effect of temperature, phase ratio, and bile salts □ Barbiturates, various—*in vitro* removal by liquid membranes from pH 2 donor solutions, effect of temperature, phase ratio, and bile salts

Human poisoning involving drug ingestion is common in the United States (1). Barbiturate poisoning accounts for 75% of suicides by drugs or 50% of all suicides by chemicals (2). Traditionally, acute poisoning treatment involves attempts to reduce drug absorption from the GI tract. Activated charcoal has been used for this purpose. Also, emetics and peritoneal dialysis have been recommended, although these methods have limitations.

Recently, liquid membranes (stable water-in-oil-in-water emulsions) were patented (3). They have many potential applications, *e.g.*, separation of hydrocarbon types (4), purification of waste water (5), and removal of uremia toxins (6). They also may have potential as an emergency treatment of a drug overdose (7). Preliminary *in vitro* studies indicated that liquid membranes were capable of rapid uptake of phenobarbital and aspirin from either pH 2 or 7 buffered donor solutions (7).

To understand the properties of liquid membranes in drug overdose treatment, *in vitro* studies were conducted under different temperatures and phase ratios of liquid membranes to the donor solutions. Since barbiturates are a common cause of drug overdoses, several barbiturates were employed as model drugs. The stability of liquid membranes in the presence of bile salts also was investigated.

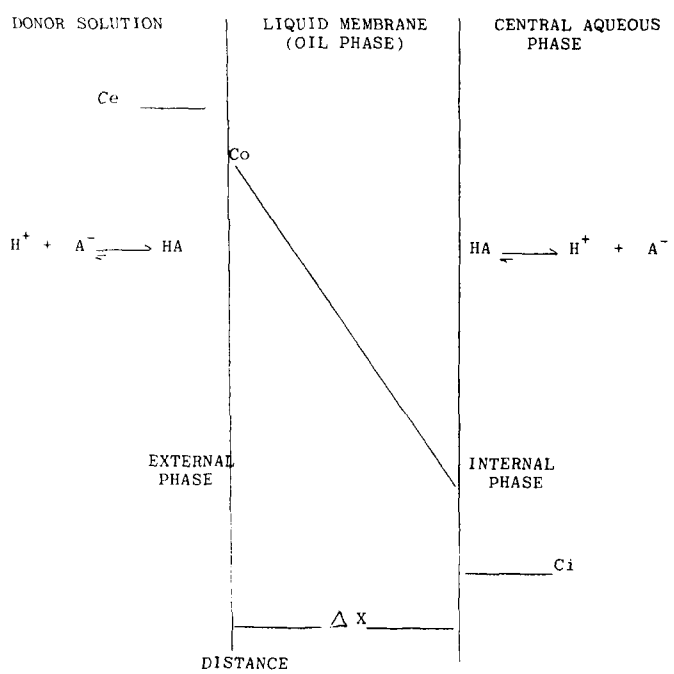

Figure 1—*Simplified scheme of drug transport through liquid membranes.*

THEORETICAL

The central aqueous phase of liquid membranes can be formulated to form a high capacity sink for the drug in the donor phase by (*a*) pH control, (*b*) plasma proteins to bind the drug, (*c*) activated charcoal, or (*d*) specific drug antibodies. The liquid membranes with pH control will be used as a model.

A simplified schematic diagram of the removal of acidic drug from the donor phase (pH 2) by the liquid membrane with pH control is shown in Fig. 1. Drug transfer from the donor solution to the central aqueous phase is accomplished by solution of the drug in the membrane and diffusion in the direction of the concentration gradient. Since a membrane made from a hydrocarbon is virtually impenetrable to ions, only the uncharged species in the donor phase can be dissolved in the membrane and transported through it to the central aqueous phase where an appropriate trapping agent is present. In this study, a pH 12 buffer solution was used as this trapping agent. According to pH partition theory, the acidic unionized species transported from the donor solution will be ionized at this high pH in the central aqueous phase and be unable to diffuse out of the membrane.

The uptake rate of the drug from the donor solution by a liquid membrane is discussed using the following symbols:

C_e = concentration of drug in the donor phase
C_e^o = concentration of drug in the external, *i.e.*, oil, phase of the membrane
C_i = concentration of drug in the internal, *i.e.*, aqueous, phase of the membrane
P = apparent partition coefficient of unionized drug (HA) between oil and aqueous phases
D = diffusion coefficient of drug in the membrane
ΔX = membrane thickness
A = area of contact between the donor solution and liquid membrane (this is a function of the volume of the liquid membrane used when the stirring speed is kept constant)

According to Fick's law, the transport of unionized drug across the membrane is:

$$\frac{dC_o}{dt} = -DA\frac{\Delta C}{\Delta X} = \frac{-DA}{\Delta X}(C_o - C_i) \qquad \text{(Eq. 1)}$$

Since $C_e = C_o/P$, then:

$$\frac{dC_e}{dt} = \frac{1}{P}\frac{dC_o}{dt} = \frac{-DA}{\Delta X}\frac{1}{P}(PC_e - C_i) \qquad \text{(Eq. 2)}$$

When a trapping agent, pH 12 buffer, is used in the central aqueous phase, the unionized species transported is ionized at this pH and C_i is negligible.

Equation 2 can be written as:

$$\frac{dC_e}{dt} = \frac{DA}{\Delta X} C_e = kC_e \quad \frac{dC_e}{dt} = \frac{-DA}{\Delta X} C_e = -kC_e \qquad \text{(Eq. 3)}$$

By integration:

$$C_e = C_e{}^o e^{-kt} \qquad \text{(Eq. 3a)}$$

According to Eq. 3, first-order kinetics are followed if the transport is governed by simple Fickian diffusion; the rate constant k is a function of the diffusion coefficient of drug used, the area of contact between the donor phase and liquid membrane, and the membrane thickness.

The dependence of the first-order rate constants with temperature could be expressed by the Arrhenius equation:

$$k = Ae^{-E_a/RT} \qquad \text{(Eq. 4)}$$

where k is the transport rate constant, E_a is the activation energy, R is the universal gas constant, and T is the absolute temperature.

EXPERIMENTAL

Materials and Methods—Three different liquid membranes, A, B, and C, were made with a 1:1 ratio of oil to aqueous phase. Liquid Membrane A was made from an isoparaffinic oil phase[1] with 0.1 *N* NaOH as the central aqueous phase. Membranes B and C were both made from 83% of the isoparaffinic oil and 15% of a normal paraffinic oil of lower viscosity[2], but pH 12 buffer was used as the central aqueous phase for B and pH 2 buffer was used as the central aqueous phase for C.

The barbiturates were barbital[3], amobarbital[4], phenobarbital sodium[5], pentobarbital sodium[6], secobarbital sodium[7], butabarbital[8], and ring ^{14}C-labeled pentobarbital[9] (0.1 mCi/ml). Standard pH 2 and 6 donor solutions were made from potassium chloride–hydrochloric acid and monobasic potassium phosphate–sodium hydroxide buffers, respectively.

The drugs were dissolved in either pH 2 or 6 buffer. Appropriate amounts of the liquid membrane were mixed with the drug solution in a beaker and stirred at a constant speed with a magnetic stirrer. The whole system was maintained at required temperatures (±1°) using a water bath.

At appropriate intervals, the mixture of liquid membrane and donor solution was sampled and filtered through a filter paper[10]. An appropriate volume of the filtrate was made alkaline with 1 *N* NaOH, and the absorbance was determined[11] at 255 nm. A standard curve of the absorbance as a function of drug concentration was prepared for each experiment. A blank also was run each time by using the same buffer solution without drug. The radioactivity assay for carbon-14 was accomplished by using the internal standard method to correct the color quench of sodium glycocholate[12].

The first-order rate constants for drug removal were calculated by using a log–linear least-squares fitting program. The regression coefficients for all studies were >0.95.

Partition Coefficient Studies—Accurately weighed (W_{LM}) liquid Membrane C was stirred with 100 ml of a barbiturate (six were tested) in pH 2 buffer solution at 37°. Samples were withdrawn and assayed. When an equilibrium was reached, the concentration of barbiturate in the donor solution was equal to that of the central aqueous phase of the liquid membrane. Therefore, the barbiturate concentration in the oil phase could be calculated as:

$$C_{oil} = \left[(C_e)(V_e - C_e)\left(V_e + \frac{W_{LM}}{2}\right) \right] / (W_{LM}/2) \qquad \text{(Eq. 5)}$$

The barbiturate uptake rates in pH 2 buffer by Membrane B, whose central aqueous phase, a pH 12 buffer, served as a sink for the barbiturates, also were determined at 37°.

Phase Ratio Studies—Pentobarbital sodium in pH 2 buffer and Membrane A were utilized. The ratios of the weight of Membrane A to the volume of pentobarbital solution (pH 2, 500 mg/liter) ranged from 0.1 to 1.0. The uptake rates of pentobarbital sodium with different phase ratios were investigated at 37°.

Temperature Effect—The uptake rates of a 500-mg/liter phenobarbital solution (pH 2, 100 ml) by 50 g of Membrane B were studied at 22, 30, 37, 45, and 50°.

Effects of Bile Salt—The pentobarbital sodium uptake in pH 6 buffer at 37° by Membrane B in the absence of bile salt and in the presence of 0.5 and 2% sodium glycocholate was studied; 0.1 ml of ^{14}C-labeled pentobarbital was added to a 500-mg/liter pentobarbital solution in pH 6 buffer with 0.5 or 2% sodium glycocholate. The radioactive assay was used for systems containing sodium glycocholate.

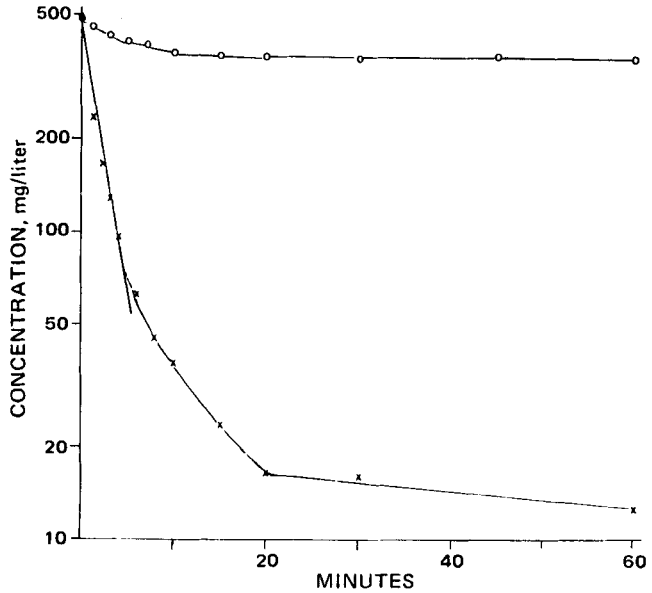

Figure 2—*Pentobarbital transport by liquid Membranes B and C from donor solution. Key: ×, Membrane B (pH 12 buffer); and ○, Membrane C (pH 2 buffer).*

RESULTS AND DISCUSSION

Partition Coefficient Studies—The semilogarithmic plot of pentobarbital concentration in pH 2 buffer after treatment with liquid Membrane B is shown in Fig. 2. It indicates that first-order kinetics were followed from time zero to 4 min. Because the pentobarbital concentration in the central aqueous phase was negligible in comparison with that in the donor phase during that time, Eq. 3 was obeyed. However, the drug concentration in the donor phase decreased with increasing drug concentration in the central aqueous phase. Therefore, C_i was no longer negligible relative to C_o, and Eq. 2 should be used.

Figure 2 also shows pentobarbital transport from pH 2 donor solution by Membrane C, with pH 2 buffer as the central aqueous phase. Liquid Membrane B could effectively remove 90% of pentobarbital in the donor solution in 7 min, while Membrane C only removed 20% of the drug. At equilibrium, only 27% of pentobarbital was transported into Membrane C.

Table I—Comparison of the Fractions of Drugs Remaining in the Donor Phase after Treatment with Liquid Membranes B and C

Barbiturate	B				C,
	10 min	30 min	60 min	155 min	$C_e/C_e{}^o$
Barbital	0.68	0.46	0.35	0.19	0.82
Butabarbital	0.14	0.05	0.05	—	0.79
Phenobarbital	0.35	0.18	0.10	—	0.77
Amobarbital	0.04	0.03	0.02	—	0.75
Pentobarbital	0.07	0.03	0.03	—	0.73
Secobarbital	0.03	0.02	0.02	—	0.69

[1] Exxon S100N.
[2] Exxon Norpar 13.
[3] Gane's Chemical Works.
[4] Eli Lilly, Indianapolis, Ind.
[5] Mallinckrodt Chemical Works.
[6] Abbott, Chicago, Ill.
[7] Ruger Chemical Co.
[8] McNeil Laboratories, Fort Washington, Pa.
[9] New England Nuclear.
[10] Whatman No. 42.
[11] Perkin-Elmer spectrophotometer.
[12] Amend Chemical Co.

Table II—Apparent Partition Coefficients, Dissociation Constants, and Transport Constants for Six Barbiturates

Barbiturate	Dissociation Constant, pKa[a]	Apparent Partition Coefficient	Transport Rate Constant, min^{-1}
Barbital	7.86	0.00	0.037
Butabarbital	8.01	0.07	0.188
Phenobarbital	7.37	0.21	0.116
Amobarbital	7.87	0.36	0.662
Pentobarbital	8.03	0.50	0.401
Secobarbital	7.90	0.83	0.727

[a] From Ref. 8.

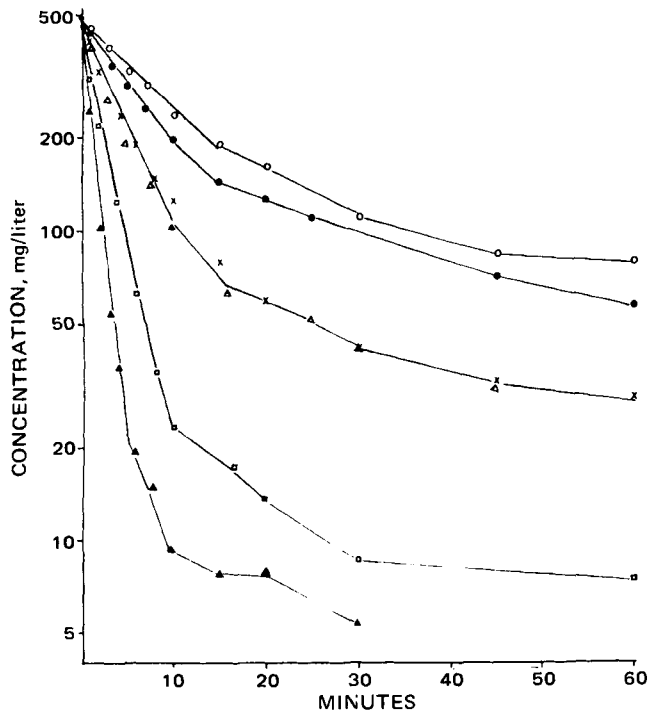

Figure 3—*Pentobarbital uptake by liquid Membrane A. Different phase ratios of the amount of liquid membrane to the volume of donor phase are presented. Key (phase volume ratio): ○, 0.1; ●, 0.14; × and △, 0.20; □, 0.50; and ▲, 1.00.*

The percentages of six different barbiturates remaining in the donor solution at 10, 30, 60, and 155 min after they were treated with Membrane B, as well as the final fraction (at equilibrium) of the same drug treated with Membrane C under the same experimental conditions, are listed in Table I. Ninety-five percent of the barbiturate except barbital and phenobarbital was removed from the donor phase in 30 min by B, while only 18–31% of the drug was trapped inside C.

Table II shows the partition coefficients, P, calculated from Eq. 6, the first-order transport rate constants, k, and the dissociation constants, pKa (8). There is no obvious linear relationship.

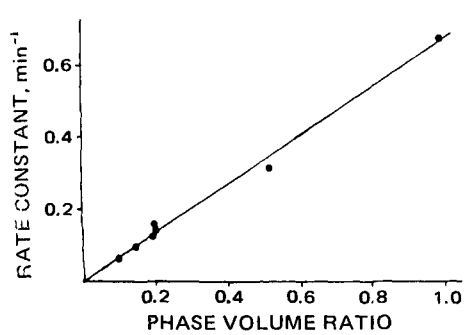

Figure 4—*Transport rate constants as a function of the relative amount of liquid membrane present.*

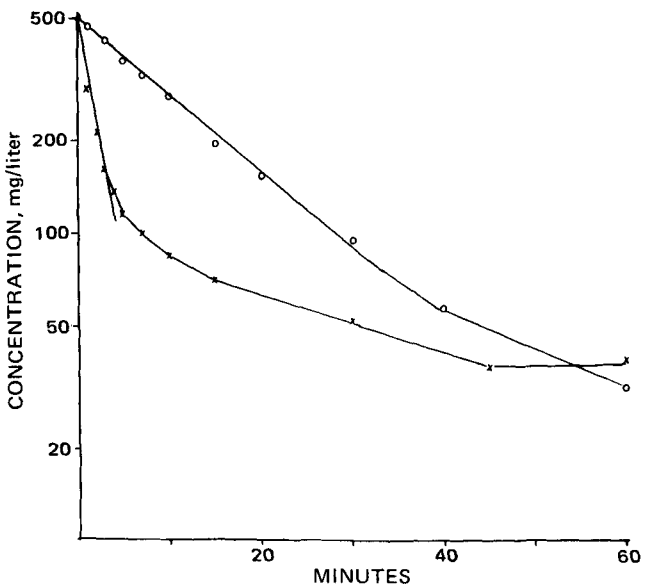

Figure 5—*Pentobarbital transport by liquid Membrane B at 50° (×) and 22° (○).*

Phase Ratio—Figure 3 shows the semilogarithmic plots of the pentobarbital concentrations in the donor phase after treatment with different amounts of Membrane A. Initially, all plots followed monoexponential decay kinetics with different rate constants. After equilibrium, the pentobarbital concentration in the donor phase also was a function of the amount of liquid membrane used. A plot of the first-order transport rate constants of pentobarbital as a function of the phase ratios of liquid membrane used to the volume of the donor phase gave a straight line with a regression coefficient of 0.99 (Fig. 4). Therefore, the transport rate of pentobarbital from the donor phase was directly dependent on the phase ratio.

Temperature—The semilogarithmic plots of the phenobarbital concentrations in a donor phase of pH 2 treated with Membrane B at 22 and 50° are shown in Fig. 5. The same studies were also carried out at 30, 37, and 45°. The results indicated that the higher the temperature, the faster the phenobarbital transport rate, but the final equilibrium concentrations of phenobarbital were very similar in all studies.

The plot of the logarithm of the first-order transport constants of phenobarbital as a function of reciprocal temperatures is presented in Fig. 6. A straight line with a regression coefficient of 0.97 was obtained.

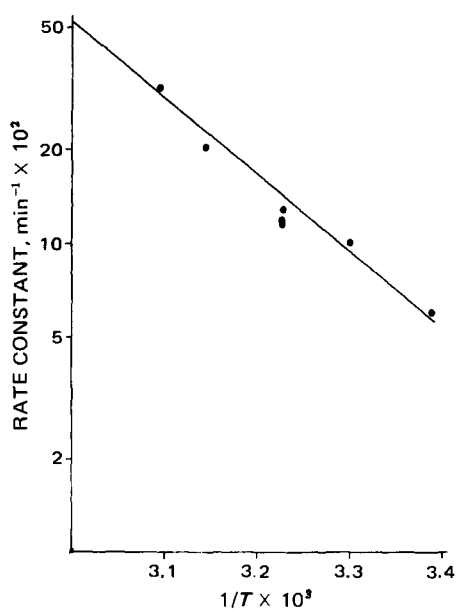

Figure 6—*Semilogarithmic plot of transport constant as a function of the reciprocal of absolute temperature.*

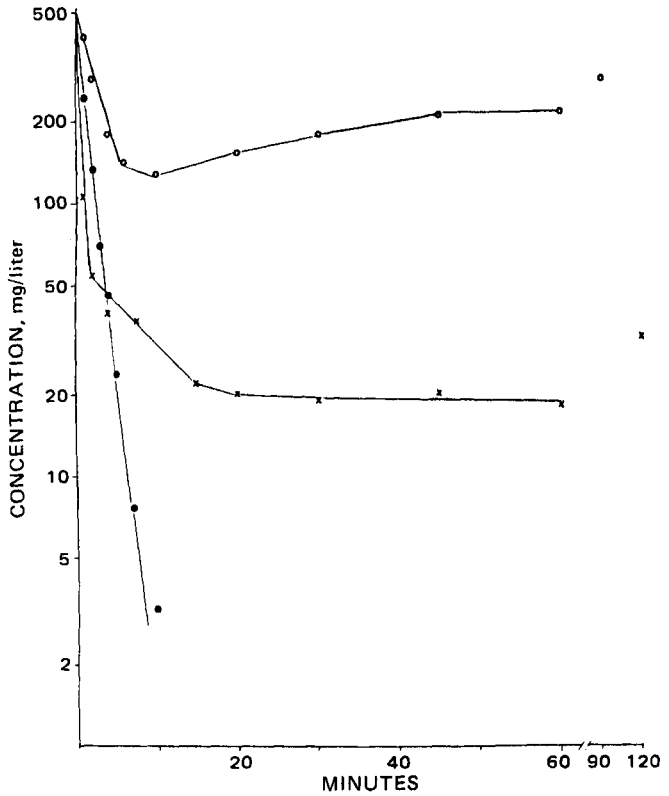

Figure 7—*Pentobarbital transport from pH 6 buffer solution by liquid Membrane B. Key:* ●, *no bile salt present;* ×, *0.5% bile salt present; and* ○, *2% bile salt present.*

From the Arrhenius equation, the activation energy of the system was calculated to be 10.8 kcal/mole (45 kjoules/mole).

Effect of Bile Salt—Figure 7 shows pentobarbital uptake in pH 6 buffered donor solution in the presence of 0.5 and 2% sodium glycocholate. Pentobarbital uptake by Membrane B in the presence of 0.5% sodium glycocholate (which corresponds to the approximate concentration of the total conjugated bile salts in the upper jejunum of fasting humans) was initially faster than in the system without bile salt. This faster pentobarbital transport may perhaps result from the bile salt changing the permeability of the liquid membrane to the drug. It has been observed that bile salt alters the permeability of intestine to drugs (10). However, after 4 min, the transport rate of pentobarbital tended to decrease.

When 2% sodium glycocholate [the approximate total concentration of conjugated bile salts commonly found in the jejunum after fat digestion (11)] was added to the liquid membrane system, pentobarbital transport was much slower and reached a maximum in 10 min. Thereafter, the pentobarbital concentration in the donor phase tended to increase. Even though these *in vitro* studies showed that bile salt may adversely affect the liquid membrane in the intestine, *in vivo* studies may give different results. Because there is food present in the intestine, which interacts with bile salts, the free bile salt concentration may well be less than in these *in vitro* studies.

Further studies will be conducted in animals to evaluate the effectiveness and applicabilities of these liquid membranes.

REFERENCES

(1) "FDA Poison Control Statistics for 1971," National Clearinghouse for Poison Control Centers, Washington, D.C., 1972.

(2) US-DHEW, National Center for Health Statistics, 1968.

(3) N. N. Li, U.S. pat. 3,410,794 (Nov. 12, 1968).

(4) N. N. Li, *Ind. Eng. Chem. Process Des. Dev.*, **10,** 215 (1971).

(5) N. N. Li and A. L. Shrier, "Recent Developments in Separation Sciences," vol. 1, CRC Press, Cleveland, Ohio, 1972, chap. 9.

(6) W. J. Asher, K. C. Bovee, J. W. Frankenfeld, R. W. Hamilton, L. W. Henderson, P. G. Holtzapple, and N. N. Li, *Kidney Int.*, **7,** s-409 (1975).

(7) J. W. Frankenfeld, G. C. Fuller, and C. T. Rhodes, *Drug Dev. Commun.*, **2,** 405 (1976).

(8) D. A. Doornbos and R. A. deZeeuw, *Pharm. Weekbl.*, **104,** 233 (1969).

(9) S. Tebaqchali, J. Hatzioannon, and C. C. Booth, *Lancet*, **2,** 12 (1968).

(10) M. Gibaldi and S. Feldman, *J. Pharm. Sci.*, **59,** 579 (1970).

(11) J. Sjovall, *Acta Physiol. Scand.*, **46,** 229 (1959).

Three-Dimensional Molecular Illustrations I: Isoelectron Density Contours and Isoelectrostatic Energy Contours

THOMAS L. BREON *, HAROLD PETERSEN, Jr. ‡, and ANTHONY N. PARUTA *x

Received May 21, 1976, from the *College of Pharmacy and the ‡Department of Chemistry, University of Rhode Island, Kingston, RI 02881. Accepted for publication April 1, 1977.

Abstract □ A method of depicting dimensional illustrations of molecules *in vacuo* that are sensitive to small electronic perturbations was attempted. This method would be useful in determining the effects of either perturbing groups from other molecules or changes produced by the addition or modification of an existing atom or chemical group on the same molecule. Isoelectron density contours for small molecules such as benzene, ammonia, and formaldehyde were first considered using the CNDO/2 molecular approximation method and then extended to the use of deorthogonalized CNDO/2 eigenvectors. These methods were similar in molecular projections but insensitive to electronic alterations. Therefore, the electrostatic potential energy was considered in developing contour surfaces of several of the molecules studied. In this case, acute and visually discernible changes were evidenced by electron exchange in the three-dimensional illustration of formaldehyde. The effect on the two-dimensional contour map of ammonia was strikingly altered by the addition of a proton, further substantiating the sensitivity of electrostatic contours to perturbing influences. These methods are considered and amplified in this report.

Keyphrases □ Molecular structure—method of depicting three-dimensional illustrations sensitive to small electronic perturbations developed, electrostatic potential energy contours considered □ Electrostatic potential energy contours—considered in depicting three-dimensional illustrations of molecular structure sensitive to small electronic perturbations

The concept that a three-dimensional picture of a molecule can be drawn and visualized is attractive. Additional importance can be attached to this configurational viewing of molecules when one attempts to relate the physical shape with the pharmacological response of the therapeutic agent. On occasion, molecules possessing unrelated configurations produce similar pharmacological responses. In many instances, these dissimilar molecules may be spatially manipulated to assume similar configurations.

The utility of three-dimensional molecular illustrations becomes apparent from the vast number of investigations and publications dealing with stereochemistry and structure–activity relationships of medicinal agents (1–8).

BACKGROUND

Many series of biologically active compounds have been investigated with respect to the effects caused by the addition, deletion, or alteration of a functional group on a parent moiety. Generally, these investigations have dealt with the chemical group as a whole rather than the more detailed electronic configuration of the individual atoms. In some advanced studies, a more comprehensive analysis of the compounds has been used, taking into consideration more detailed parameters such as the charge distribution and the position of lone-pair electrons.

Atoms and functional groups do not exist as single entities that can be considered independently of each other but rather as a complex arrangement of electrons surrounding the nuclei. Therefore, the spatial configuration of a molecule should not be considered simply as a collection of atoms but rather as a summation of the complex interactions among all of the nuclei and electrons of the entire molecule.

Therefore, this work involved the development of illustrating simple molecules, initially in terms of their isoelectron density contour surfaces. This technique, however, was insensitive to electronic changes in these molecules and led to the consideration of isoelectrostatic energy contours. Both the isoelectron density and the isoelectrostatic energy contours will be discussed.

Schnaare and Martin (9) reviewed the application of quantum theory to the study of drug systems. Theoretical calculations on the π-electron systems of several drugs were correlated with physical–chemical parameters. The orientation of the molecules involved in the benzocaine–caffeine complex was proposed. Also, the preferred site of hydroxylation on indole derivatives and the pKa values of a series of sulfonamides were correlated with electronic charge.

A detailed examination of this subject explained the many types of molecular interactions involved when a drug is introduced into a biological system (10). Various methods used to calculate molecular orbital indexes were discussed, as well as the shortcomings of each. Extensive consideration was given to the application of quantum mechanical calculations to drug systems. Many types of physical–chemical interactions and pharmacological classes of drugs were examined by this approach.

Graphical illustrations were produced showing how the value of the wavefunction varies with increasing distance on a radius from the nucleus (11–13). Bordass and Linnett (14), using isometric projections, illustrated how the magnitude of the wavefunction varies concurrently with two spatial coordinates. A computer line printer was utilized to produce a two-dimensional matrix of data representing the electron density probability on a plane through the atom (15). Isodensity contour lines may then be drawn through equal values of electron density probability. Other isodensity contours of atomic orbitals also were reported (12, 13).

Pictorial descriptions of molecular orbitals produced by methods similar to those for atomic orbitals include the line printer (15–17) and isometric projections (18, 19). A series of three-membered ring molecules was investigated with respect to the shape of two-dimensional isodensity contours (20, 21). In one attempt to examine the three-dimensional character of these contours, a series of charge density contour maps, each on a successive plane through the gallium arsenide crystal, were combined into a movie (22). Furthermore, the electrostatic potential was investigated with respect to its ability to predict the most stable conformation in a bimolecular system (23).

COMPUTATION

Electron Density Calculations—The proposed methods of illustrating molecules required a large number of repetitious numerical evaluations of algebraic functions, which were performed by a computer[1] using Fortran IV language. The molecular illustrations were produced on an incremental plotter[2], which was operated off-line from the computer.

The method developed to produce three-dimensional electron density illustrations of molecules involves the following sequence: determining the atomic coordinates, calculating the orthogonalized and deorthogonalized orbital populations, producing a matrix of data representing the electron density probability at numerous points surrounding the molecule, determining the points in this matrix that represent the boundary corresponding to the desired level of probability, and plotting these points by a method that produces a three-dimensional illustration.

The atomic coordinates of the system being investigated may be obtained from various sources. For purely qualitative interpretation of the resulting illustrations, the atomic positions may be derived from tables of standard bond lengths and bond angles (24). More accurate data concerning specific compounds may be derived from X-ray crystallographic techniques.

The orbital electron populations were determined by the CNDO/2

[1] IBM 370/155.
[2] Broomall Industries M-2000 drum-type.

molecular orbital approximation (25)[3] using computer program CNINDO (26). This method considers only the outer shell or valence orbitals. Since the electrons contained in the inner or nonvalence shells participate only to a very limited extent in any type of sharing or transfer with other atoms, these orbitals were assumed to contain 2.0 electrons each unless otherwise noted.

In theory, a box representing a three-dimensional array is placed over the molecule. With formaldehyde as a model, it was found that when the boundaries were restricted to a distance no less than 0.9 Å from the nearest hydrogen atom and 1.5 Å from the nearest second row atom, approximately 99.5% of all electrons were included. These restrictions were adhered to for all electron cloud illustrations.

The illustrations produced from these data are contour plots where points of equal density probability are connected with a line.

The nuclear coordinates, Slater atomic orbitals, ϕ, and the corresponding orbital population coefficients, $P_{\mu\mu}$, are utilized to calculate the electron density probability, D, at all points, r, according to:

$$D(r) = \sum_{\mu} P_{\mu\mu}\phi(r)^2 \qquad \text{(Eq. 1)}$$

Simultaneously, a total is accumulated representing the total density probability in the matrix.

Deorthogonalized CNDO/2 Eigenvectors—The orbital populations, $P_{\mu\mu}$, obtained by the CNDO/2 method are considered to be compatible with the Slater-type orbitals in spite of the zero differential overlap approximation of the method. However, the CNDO/2 eigenvectors may be considered as orthogonalized orbitals derived from Slater orbitals by the Lowdin transformation (27). Since the Slater orbitals are nonorthogonal, a more exact interpretation of the electron density probability will be provided if the eigenvectors are deorthogonalized by the matrix product:

$$C^x = S^{-1/2}C^\lambda \qquad \text{(Eq. 2)}$$

where S is the overlap matrix and C^λ and C^x are the CNDO/2 and deorthogonalized eigenvectors, respectively. This procedure was used previously (28, 29) in conjunction with Slater-type orbitals.

With the deorthogonalized CNDO/2 eigenvectors, C, the density probability at point r may be determined by the double summation:

$$D(r) = 2\sum_{i}\left[\sum_{\mu} c_{\mu i}\phi_\mu(r)\right]^2 \qquad \text{(Eq. 3)}$$

The summation over i includes only the occupied molecular orbitals. The summation over μ represents the combination of atomic orbitals, ϕ_μ, composing the ith molecular orbital.

To produce a three-dimensional isodensity contour illustration, it is necessary to choose the appropriate level of density probability. An arbitrary value of $D(r)$ is chosen, and the data are scanned for all values equal to or greater than this cutoff value. Several more values are chosen, and the procedure is repeated. A plot of these percentages *versus* the cutoff values allows selection of an appropriate limiting value of $D(r)$ corresponding to the desired probability.

The data needed to produce the actual electron density illustration (*i.e.*, for the plotting program) include only the three cartesian coordinates for each grid point located on the contour surface.

To plot these data, a program was developed to generate instructions subsequently used to drive the plotting instrument. The resulting illustration is a three-dimensional plot consisting of a series of contour lines in either the xy or yz plane. Each contour represents the data found in one slice or plane of the coordinate matrix. Plotting begins with the plane closest to the viewer, and subsequent planes are plotted until the back of the object is reached.

A total of 36 possible views is provided by this program. The data matrix, or object, may be viewed from any one of the four sides. Thus, the molecule may be rotated about the y axis 360° in 90° increments. For each side of the object, there are nine possible viewing angles.

An integral part of this routine is its ability to eliminate lines that are hidden from the viewer. The plotting surface is divided into many columns. The area plotted in each column is stored, and these data are referred to each time subsequent lines are to be drawn.

The resulting illustrations are only pseudo three dimensional because no consideration is given to perspective. The scale is identical in the front and rear portions of the illustration, allowing measurement of actual molecular distances on any plane parallel to the page. Because perspective is neglected, the hidden-line problem is simplified and the computer processing time is minimized.

The program also has the additional ability to plot several colors on one illustration. This feature is not necessary for the electron density models where only one variable is plotted (*e.g.*, isodensity contours) but enhances illustrations where several variables are plotted simultaneously (*e.g.*, electrostatic potential energy contours).

[3] The program was altered to allow input of a maximum of 50 atoms or 120 basis functions.

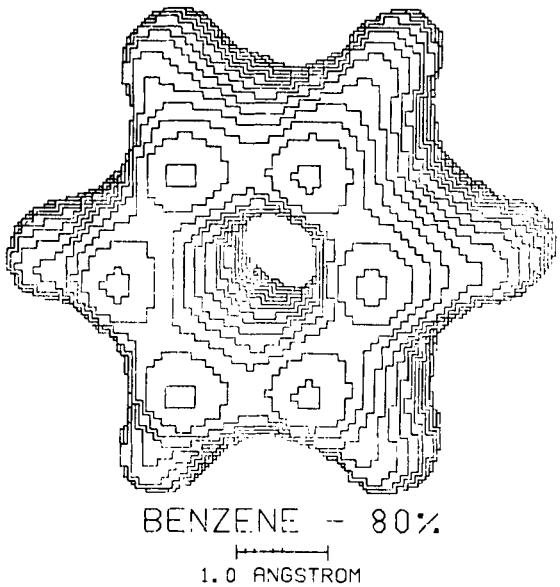

Figure 1—*Electron density probability contour surface of benzene using a minimal basis set and CNDO/2 orbital population coefficients.*

RESULTS

Electron Density for Small Molecules—Three fairly simple molecules, benzene, ammonia, and formaldehyde, were chosen to test the programs that produce three-dimensional electron density illustrations. In each case, standard bond lengths and bond angles (24) were used to determine the nuclear coordinates.

Figure 1 represents the electron cloud of the benzene molecule at an isodensity value of 80%. If the 100% isodensity contour were chosen, the contours would simply be slightly larger; the 80% contours retained all features required for these illustrations. The data for this figure were generated from a minimal basis set (*i.e.*, all atomic orbitals up to and including the valence shell of each atom). As might be expected, this il-

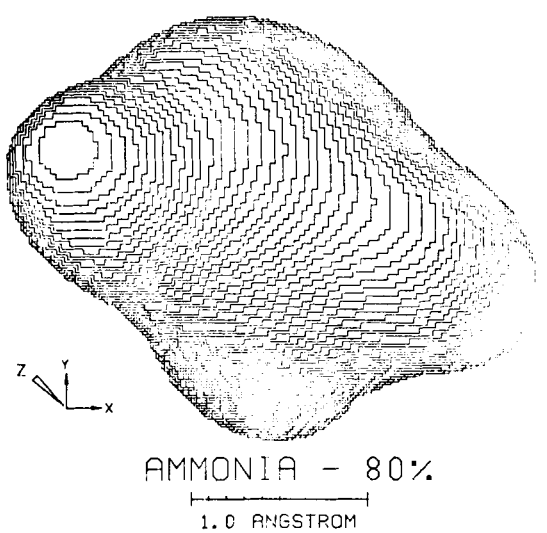

Figure 2—*Electron density probability contour surface of ammonia using a minimal basis set and CNDO/2 orbital population coefficients.*

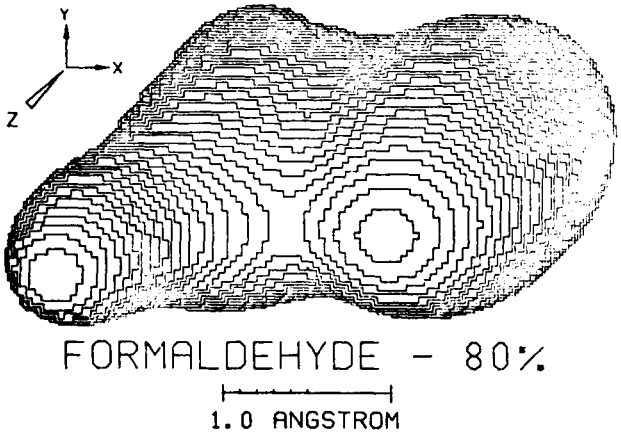

Figure 3—*Electron density contour surface of formaldehyde at 80% probability using a minimal basis set and CNDO/2 orbital population coefficients.*

lustration clearly shows the hole through this aromatic system. Another distinctive feature is the relative size of the carbon and hydrogen atoms. The density is more pronounced in the region between bonded atoms, but the areas separating nonbonded atoms are deficient in this respect.

The mechanism of the plotting routine may be better understood from this figure. Close examination reveals the contours for each of the many slices through the molecule. These individual contours, each on a plane parallel to the page, are superimposed upon each other to form the three-dimensional structure. The viewing angle is controlled by displacing each plane in the vertical and/or horizontal direction. The contours are drawn in stepwise fashion; each step represents one of the many points at which the electron density probability functions were evaluated. Although the curves are not smooth, the illustration possesses visual clarity.

From orbital populations, an illustration of ammonia at an isodensity value of 80% is given in Fig. 2. The atoms of the molecule are located at the corners of a tetrahedron, with the nitrogen atom positioned at its center. Again, the drawing shows the relative sizes of the atoms and allows the heteroatom to be distinguished from the hydrogen atoms. The lone pair of electrons associated with the nitrogen atom extends the contour surface in the vertical direction, parallel to the y axis.

A similar illustration of formaldehyde, obtained from a minimal basis set and the atomic orbital populations, is given in Fig. 3. An oxygen atom would be expected to be slightly smaller in size than a carbon atom. In this case, the slightly greater electronegativity of the oxygen atom withdraws electrons from the carbon atom, thus increasing the electron population of the atomic orbitals associated with the oxygen atom. As a consequence of these excess electrons, the oxygen atom is enlarged in comparison to the carbon atom. Most of these electrons are in the $2px$ and $2pz$ orbitals; the oxygen atom is elongated in the xz plane, which is perpendicular to the page.

Figure 4 illustrates the 60% probability contour surface of formaldehyde. A discontinuity of electron density appears between the carbon and

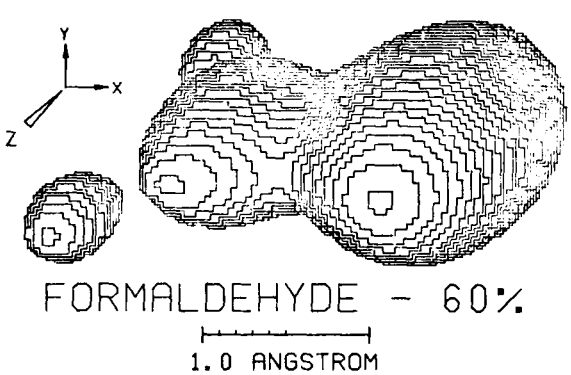

Figure 4—*Electron density contour surface of formaldehyde at 60% probability using a minimal basis set and CNDO/2 orbital population coefficients.*

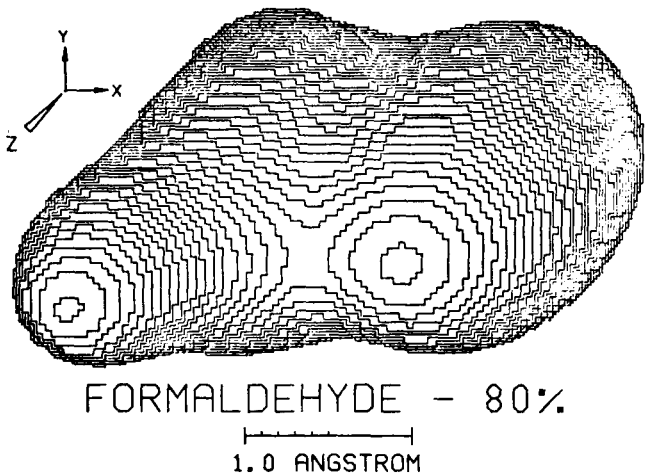

Figure 5—*Electron density probability contour surface of formaldehyde using only a valence basis set and CNDO/2 orbital population coefficients.*

hydrogen atoms but not between the nonhydrogen atoms. This phenomenon is fully expected when the relative number of electrons participating in the various bonds is considered. Further reductions of the probability will, in sequence, produce a gap in the carbon–oxygen bond, eliminate the hydrogens, and, finally, eliminate the carbon atom. Such a series of illustrations, produced by successively reducing the probability, allows one to distinguish the most densely populated area in the molecule.

By eliminating the calculations involving the $1s$ orbitals of all second-row atoms, such as carbon and oxygen, isodensity contours may be produced in terms of the valence orbitals only. The resulting illustration of formaldehyde, at 80% probability, is shown in Fig. 5. A comparison may be made with Fig. 6, where all atomic orbitals were utilized. It can be visually discerned from Fig. 6 that the molecule is slightly enlarged. These larger contours are a result of the nuclear cores of the nonhydrogen atoms being very sparsely populated. To enclose the same percentage of electrons, the contour surface has to extend outward. A similar comparison of the ammonia molecule, with and without the nonvalence orbitals, also shows this enlarging effect. In that case, the effect is less pronounced because of the smaller number of nonvalence electrons.

In the method that conforms strictly to the CNDO/2 approximation, the eigenvectors must first be deorthogonalized. The illustrations are then produced by summing the molecular orbital contributions to the density probability, as opposed to those of the atomic orbitals. Figure 6 is a result of these computations performed on formaldehyde.

A comparison between Figs. 5, where atomic orbital approximation was used, and 6 reveals only very slight differences in the overall shape

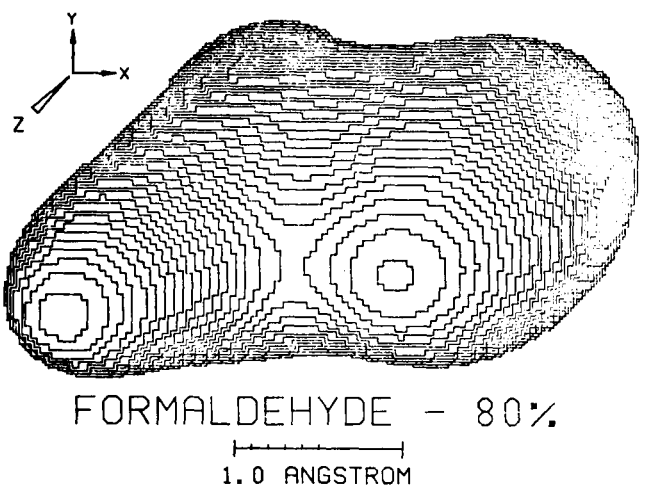

Figure 6—*Electron density probability contour surface of formaldehyde using only a valence basis set and deorthogonalized CNDO/2 eigenvectors.*

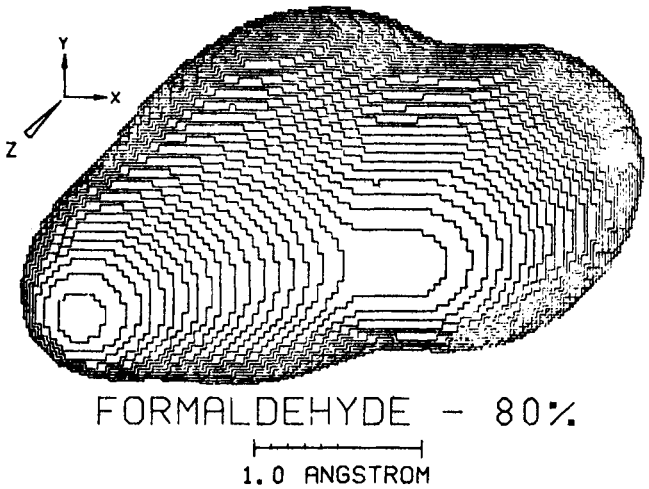

Figure 7—*Electron density probability contour surface of formaldehyde using only a valence basis set and CNDO/2 orbital population coefficients. The coefficients for the carbon and oxygen atoms are reversed.*

and size of the portrayed molecule. A similar comparison using ammonia also reveals only very slight differences in size and shape.

It may be inferred from these comparisons that the approximation utilizing the CNDO/2 atomic orbital populations is probably a valid and accurate method that can lead to electron density illustrations of molecules. The importance of this approximation is the substantial reduction in the total number of calculations necessary and the corresponding reduction in the computer processing time compared with the method utilizing the deorthogonalized CNDO/2 eigenvector matrix. It is more efficient to utilize this method for illustrations of larger molecules such as drug entities.

To test the sensitivity of the electron density illustrations, another set of data was generated for formaldehyde using only the valence orbitals. The orbital populations corresponding to the oxygen and carbon atoms were reversed. In the resulting illustration (Fig. 7), the shift of electrons caused a corresponding change in the relative sizes of the constituent atoms. When this surface contour is compared with Fig. 5, it is seen that the carbon atom is now slightly larger than the oxygen atom. However, the differences between these two illustrations are not as pronounced as might be expected. As a result of the exchange, the total valence population of carbon has increased by 63% and that of oxygen has decreased by 39% compared to those populations used to generate Fig. 5. The magnitude of even this gross and unrealistic shift of electrons does not radically change the appearance of the molecule. The exponential portion of the Slater orbitals has such a large influence that, although the number of electrons associated with the atoms is significantly altered, they are still confined to approximately the same volume in space.

The ability of the electron density illustrations to show much smaller and more realistic electron shifts would, therefore, leave much to be desired. Comparisons among a series of similar compounds would illustrate little, if any, differences in the electron clouds of the common portions of the molecules. As a result of this insensitivity, the electrostatic potential energy was investigated for its capacity to portray visually small changes in the electron distribution of a molecule.

The isoelectron density contours that had been computed and the illustrations derived from these molecular elements were insensitive to electronic perturbations of significant magnitude.

The major intent of this work was to develop a method that would produce a molecular projection with sensitivity to small electronic differences of similar molecules. This molecular parameter would have to discern visually the changes caused by these shifts or various chemical groupings. It would be desirable to illustrate various molecules in a three-dimensional fashion when only relatively minor chemical changes were made. For this purpose, the electrostatic potential was chosen as the molecular parameter.

In a molecular system, the nuclear charges are fixed quantities at relatively stationary positions. However, the electrons are distributed in molecular orbitals. As a result, the charge distribution varies throughout the molecular environment. Electrostatic potential energy is derived from the magnitudes of the electronic and nuclear charges and their relative positions. A great deal of information about a molecule may be obtained from this parameter.

Electrostatic Potential Energy: Calculations—Three-dimensional illustrations of molecules represented by isoelectrostatic potential energy contour surfaces are generated by the following sequence: determining the atomic coordinates, calculating the atomic populations, producing a matrix of potential energy data at points in the molecular environment, determining which points are isoenergy values, and plotting these points. The procedures followed in this method are similar to those required for the electron density illustrations.

The electrostatic potential energy, V, at a point, r, is determined by summing the electrostatic interactions of the protons and electrons in a molecule with a unit positive charge placed at point r (5):

$$V(r) = \sum_a \frac{Za}{R} - \sum_{\mu\nu} P_{\mu\nu} \int \frac{X_\mu X_\nu}{R} d\tau \qquad \text{(Eq. 4)}$$

where Za is the nuclear charge of atom a and R is the distance between atom a and point r. The second summation represents the nuclear attraction integrals of the distribution $X_\mu X_\nu$ with the proton. The molecular charge distribution is considered unperturbed by the proton.

The orbital populations, $P_{\mu\nu}$, obtained from CNINDO must be deorthogonalized to be strictly compatible with Slater-type orbitals. This step results in the evaluation of a large number of integrals. The computer time necessary to perform these calculations prohibits the consideration of even moderate size molecules.

An approximation to the true electrostatic potential is given by (28):

$$V(r) = \sum_a \left(\frac{Za}{r} - Pa\,Vah\right) \qquad \text{(Eq. 5)}$$

where Pa is the total electron population of atom a and Za is its effective nuclear charge. This quantity is made equal to the number of valence electrons of a neutral atom, in keeping with the all-valence orbital CNDO/2 method. The term Vah is the nuclear attraction integral of atom a with the point charge at r. This integral extends over s atomic orbitals to retain spherical symmetry. As a result of this approximation, only one calculation per atom per point is necessary. Algebraic evaluation of this integral was published previously (30).

The program performs a function in that a three-dimensional grid of data is calculated. In this instance, the electrostatic potential energy function replaces the atomic orbital basis functions. The size of the matrix and the required computer processing time to fill the matrix with data are greatly reduced in comparison to the electron density calculations.

Several reasons account for this increased efficiency. The size of the box enclosing the molecule is usually much smaller. The restriction of enclosing essentially 100% of the electrons does not apply. Consequently, the boundaries need not extend as far from the molecule. In the electrostatic potential illustrations, the curvature of the contours is much more gradual than that produced by the isodensity contours. As a result, less points per unit area are needed to describe the contours.

Another feature is that the calculations are performed on the atoms as a whole rather than on the individual atomic orbitals, resulting in an overall reduction in the number of calculations necessary for each grid point.

The large matrix containing the potential energy data is searched for the desired isoenergy value(s). The y coordinate of each point is calculated and placed in a second smaller matrix. With this type of molecular illustration, it is often desirable to draw contours at several specific values of electrostatic potential. The resulting triply subscripted array contains the y coordinates, and the x and z coordinates are generated from two of the array subscripts.

The third subscript not only identifies the point as being located on an upper or lower surface but also identifies to which isoenergy contour it corresponds. This information is necessary if the illustration contains more than one isoenergy contour surface and is plotted in two or more colors.

The type of plot produced by this program is similar to the electron density plot. However, it can distinguish between the various levels of the coordinate matrix and associates the desired colors with these levels. Thus, a multicolored plot may be drawn, each color representing a particular isoenergy contour surface.

Positioning the molecule in the box in preparation for running the program is sometimes difficult. Unless the user has some idea as to the position and magnitude of the negative energy lobes, these may be omitted or truncated by improper positioning. The program used produces a two-dimensional illustration of the isoenergy contours on a plane representing a slice through the molecule.

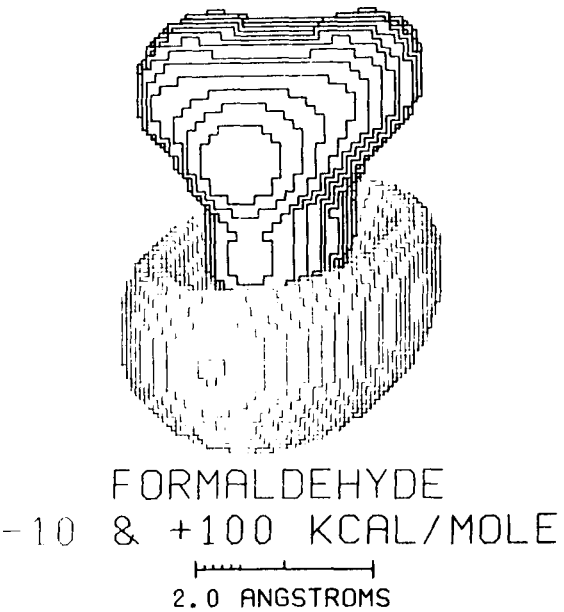

Figure 8—*Electrostatic potential energy contour surface of formaldehyde.*

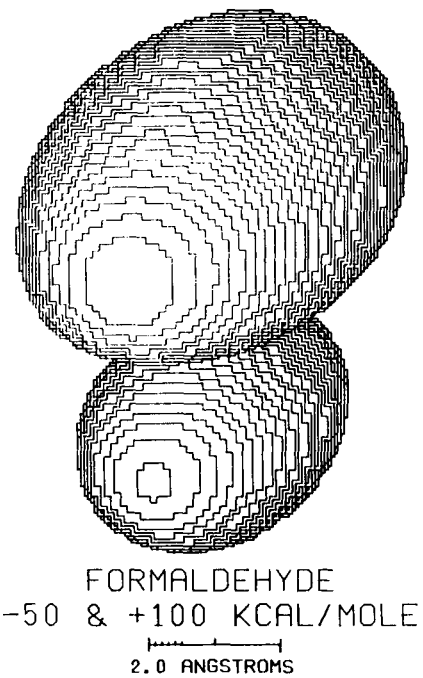

Figure 9—*Electrostatic potential energy contour surfaces of formaldehyde. The population coefficients for the carbon and oxygen atoms are reversed.*

This program is a modified version of that used previously[4]. The resulting illustrations are produced by the computer line printer. This type of illustration is produced with much less computer time than is necessary for three-dimensional illustrations. It is advantageous to use this program to obtain a preliminary view of the various electrostatic potential energy contours of a molecule and to position the molecule properly for the full three-dimensional illustration. Also, for many symmetrical molecules, a two-dimensional view provides the same information as a three-dimensional view.

The electrostatic potential at any point in space is derived from a nuclear repulsion term and an integral representing the affinity of a proton for the various electrons of the atoms in a molecule. This integral determines how much of the nuclear charge is screened by the electrons associated with a particular atom. The repulsion term varies inversely with the distance from the nucleus while the attraction integral decreases exponentially. The numerical difference between these two terms is the net electrostatic potential energy.

A positive potential is always present near the nucleus of an atom because of the greater influence of the repulsion term. As one proceeds on a vector away from the atomic center, this term diminishes at a much larger rate than the attraction integral. Thus, the individual atoms of a molecule will always be identifiable by a region of positive potential about the nucleus.

An atom with excess electrons effectively screens the nucleus and possesses an affinity for a proton. This condition is demonstrated by a net negative potential in the immediate vicinity of the atom. Conversely, a deficiency in the electron population produces a larger than normal positive potential about the atom, resulting in an atmosphere repulsive to the proton.

Figure 8 is a composition illustration of the −10- and +100-kcal/mole electrostatic potential energy contour surfaces pertaining to formaldehyde. The molecule is oriented such that the molecular plane is parallel to the page, with the hydrogen atoms positioned at the top.

The area surrounding the carbon and hydrogen atoms is repulsive for an attacking proton. Although the hydrogens possess a slight excess of electrons, no center of negative potential is found in this region of the molecule. The carbon atom is deficient in electrons, creating a large positive potential, and the influence of this atom mitigates any negative potential generated by the hydrogen atoms.

The oxygen atom radiates a negative potential due to its excess electrons. As this contour surface of negative potential is penetrated, the potential progressively decreases until a minimum is reached. In this case, a minimum of −21 kcal/mole is found.

Because of the spherical symmetry of the *s* orbitals used in the attraction integral, only one minimum is found; it is located on the molecular axis below the oxygen atom. The characteristics of this illustration are in agreement with those previously found (28) from two-dimensional contours.

The sensitivity of this method of producing molecular illustrations was evaluated by a means identical to that used for the electron cloud drawings. In the resulting illustration (Fig. 9), the molecule is positioned in the same manner as in Fig. 8. A large and significant change in the overall contour surface can be noted. Exchanging the atomic valence populations on the carbon and oxygen atoms results in a large net positive charge associated with the oxygen atom. This result is demonstrated by the enlarged contour surface representing +100 kcal/mole.

The negative potentials generated by the excess electrons on the carbon and hydrogen atoms combine to form a large negative lobe. In this figure, the negative contour represents −50 kcal/mole. Again, the minimum is found on the molecular axis, but it is positioned at the opposite end of the molecule. At this point, an electrostratic potential of −274 kcal/mole is found. At points in close proximity to the hydrogen atoms, the potential is positive as a result of the greater influence of the nuclear repulsion term. As the distance from these atoms increases, the energy rapidly decreases because of the overpowering effect of the large electron population in this region. Thus, the hydrogen atoms are embedded in the negative lobe in a lock-and-key fashion.

A comparative analysis of Figs. 8 and 9 reveals the acute sensitivity of this method of producing molecular illustrations. The potential energy calculations not only consider the probability of finding an electron at a particular point in space but also take into account the interaction of these electrons with the nuclei. The net result is the electrostatic force that an approaching molecule would encounter.

Further investigations were carried out on other small symmetrical

Table I—CNDO/2 Net Atomic Charges for Ammonia, Ammonium Ion, and Nitrogen Trifluoride

Ammonia		Ammonium Ion		Nitrogen Trifluoride	
Atom	Net Atomic Charge	Atom	Net Atomic Charge	Atom	Net Atomic Charge
N	−0.2458	N	−0.0750	N	0.3464
H-1	0.0819	H-1	0.2688	F-1	−0.1155
H-2	0.0819	H-2	0.2688	F-2	−0.1155
H-3	0.0819	H-3	0.2688	F-3	−0.1155
		H-4	0.2686		

[4] Upon request, Program VSS was supplied; it performs the calculations corresponding to Approximation II of Ref. 28.

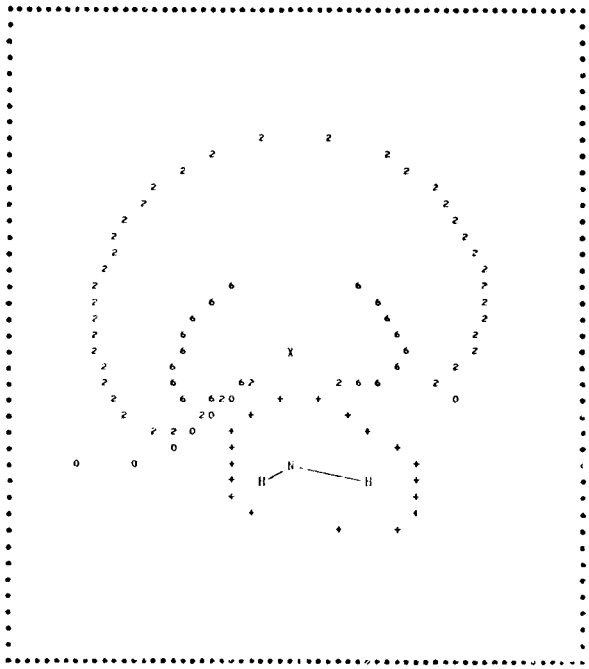

Figure 10—*Electrostatic potential energy contours of ammonia. Key: +, 100 kcal/mole; 0, 0.0 kcal/mole; 2, −2 kcal/mole; 6, −6 kcal/mole; and X, minimum energy of −13.4 kcal/mole.*

molecules (ammonia and nitrogen trifluoride) to assess the accuracy, specificity, and sensitivity of this method. Nuclear coordinates were derived from tables of standard bond lengths and angles. Due to the symmetry of these molecules, two-dimensional contour maps were drawn in the interest of expediency and efficiency of computer utilization (Figs. 10 and 11). The net atomic charges assigned to the atoms of each molecule are listed in Table I. Each map represents a molecular symmetry plane containing the nitrogen atom and the hydrogen or fluorine atom on the right. The atomic symbol shown at the left represents two atoms, one above and one below this plane.

In Fig. 10, a large negative lobe is found in proximity to the nitrogen atom. The single lone pair of electrons associated with this atom is responsible for this energy well. A minimum value of −13 kcal/mole is located at its center.

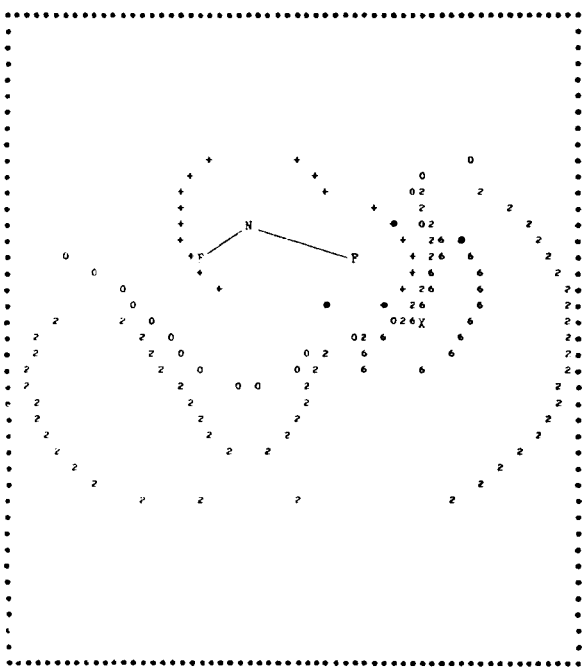

Figure 11—*Electrostatic potential energy contours of nitrogen trifluoride. Key: +, 100 kcal/mole; 0, 0.0 kcal/mole; 2, −2 kcal/mole; 6, −6 kcal/mole; and X, minimum energy of −9.0 kcal/mole.*

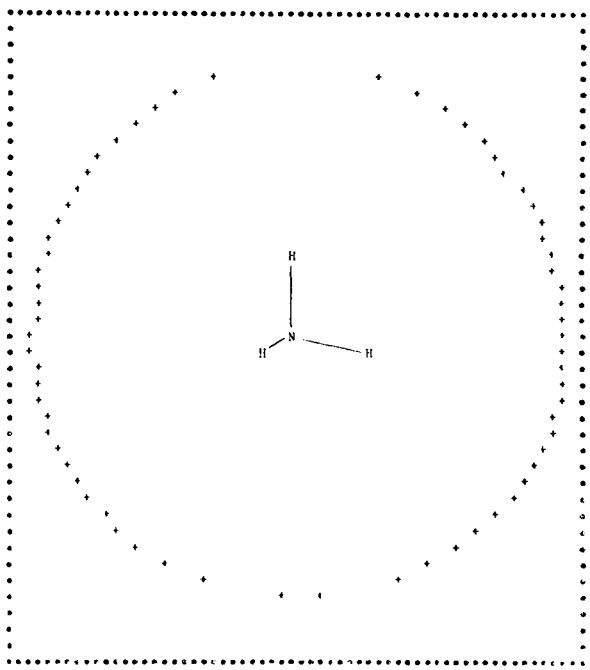

Figure 12—*Electrostatic potential energy contour of the ammonium ion. Key: +, 100 kcal/mole.*

The contours associated with nitrogen trifluoride show a marked difference from those corresponding to ammonia. In the latter compound, the peripheral atoms are more electronegative than the nitrogen, resulting in a net reduction in the electron population of the central atom. The negative energy contours in Fig. 11 are in the neighborhood of the halogen atoms. Each of these negative lobes possesses a minimum electrostatic potential energy of −9 kcal/mole.

A unique situation is observed in that the negative lobe of each fluorine atom merges at a point below the molecule on the symmetry axis. This region of low potential makes the entire lower portion of the molecule vulnerable to electrophilic attack.

The third illustration in the series (Fig. 12) represents the electrophilic potential energy contours of the ammonium ion. The net atomic charges for these atoms are also listed in Table I. To produce this figure, a proton was added to the ammonia structure on the symmetry axis.

The resulting contour diagram illustrates only a positive potential: no negative values are found in the environment of this ion. The effect of adding a single positive charge to ammonia results in a profound change in the magnitude of the potential energy. A comparison of Figs. 10 and 12 reveals the radius of the +100-kcal/mole contour to be increased approximately threefold, indicating the widespread influence of the positive charge. This cation is effectively shielded from electrophilic agents as a result of this positive field created by its charge, consistent with known chemical facts.

It can be seen that the electrostatic potential energy can be utilized as a sensitive molecular probe where changes or pertubations occur such as electronic shifts or protonation causes large, visually portrayable effects in these three-dimensional illustrations.

It was felt to be judicious to apply these considerations to large molecules such as morphine, meperidine, and alphaprodine; the results are reported in a subsequent paper.

CONCLUSIONS

Nonperspective, three-dimensional, computer-derived and drawn illustrations of small molecules were presented by a consideration of various molecular parameters.

Initially, the commonly used isoelectron density contours were considered and produced clear illustrations compatible with chemical, configurational, and molecular reasoning. However, the illustrations drawn from the computer-generated elements were rather insensitive to electronic changes. A somewhat more accurate and more sophisticated method of molecular parameter calculations was attempted with the deorthogonalized CNDO/2 eigenvectors. This method also produced clear

illustrations very similar to the isoelectron density contours without any increase in sensitivity to electronic alterations.

The electrostatic potential energy was then investigated for its utility to produce either two- or three-dimensional aspects of molecules. These isoelectrostatic energy contours produced pictorially clear illustrations with the additional characteristic of sensitivity to electron shifts and an attacking proton in these molecular projections.

REFERENCES

(1) J. E. Falk, *Aust. J. Sci.*, **7**, 48 (1944).

(2) T. Sabaltschka and H. Tietz, *Pharm. Acta Helv.*, **5**, 286 (1930).

(3) G. Barger and H. H. Dale, *J. Physiol.*, **41**, 19 (1910).

(4) "The Pharmacological Basis of Therapeutics," 4th ed., L. S. Goodman and A. Gilman, Eds., Macmillan, New York, N.Y., 1970, p. 1604.

(5) A. L. Tatum, *Physiol. Rev.*, **19**, 472 (1939).

(6) R. F. Doerge, in "Textbook of Organic Medicinal and Pharmaceutical Chemistry," 4th ed., C. O. Wilson and O. Gisvold, Eds., Lippincott, Philadelphia, Pa., 1962, p. 534.

(7) P. N. Patil, J. B. LaPidus, and A. Tye, *J. Pharm, Sci.*, **59**, 1205 (1970).

(8) N. B. Eddy, *Chem. Ind.*, **1959**, 1462.

(9) R. S. Schnaare and A. N. Martin, *J. Pharm. Sci.*, **54**, 1707 (1965).

(10) L. B. Kier, "Molecular Orbital Theory in Drug Research," Academic, New York, N.Y., 1971.

(11) I. Cohen, *J. Chem. Educ.*, **38**, 20 (1961).

(12) E. A. Ogryzlo and G. B. Porter, *ibid.*, **40**, 256 (1963).

(13) F. Daniels and R. Alberty, "Physical Chemistry," 3rd ed., Wiley, New York, N.Y., 1966, p. 451.

(14) W. T. Bordass and J. W. Linnett, *J. Chem. Educ.*, **47**, 672 (1970).

(15) N. C. Craig, D. D. Sherertz, T. S. Carlton, and M. N. Ackermann, *ibid.*, **48**, 310 (1970).

(16) R. C. Reiter and J. E. House, Jr., *ibid.*, **45**, 465 (1968).

(17) D. L. Peterson and M. E. Fuller, *ibid.*, **48**, 314 (1971).

(18) R. J. Olcott, *ibid.*, **49**, 614 (1972).

(19) M. S. Dewar and J. Kelemen, *ibid.*, **48**, 494 (1971).

(20) R. Bonaccorsi, C. Petrongolo, E. Scrocco, and J. Tomasi, in "The Jerusalem Symposia on Quantum Chemistry and Biochemistry," vol. II, 1970, p. 181.

(21) R. Bonaccorsi, E. Scrocco, and J. Tomasi, *J. Chem. Phys.*, **52**, 5270 (1970).

(22) N. W. Dalton and D. E. Schreiber, *Solid State Phys.*, **27**, 183 (1972).

(23) R. Bonaccorsi, C. Petrongolo, E. Scrocco, and J. Tomasi, *ibid.*, **20**, 331 (1971).

(24) J. A. Pople and D. L. Beveridge, "Approximate Molecular Orbital Theory," McGraw-Hill, New York, N.Y., 1970, p. 111.

(25) *Ibid.*, p. 62.

(26) Program 141, Quantum Chemistry Program Exchange, Department of Chemistry, Indiana University, Bloomington, Ind.

(27) P. Lowdin, *J. Chem. Phys.*, **18**, 365 (1950).

(28) C. Giessner-Prettre and A. Pullman, *Theor. Chim. Acta (Berl.)*, **25**, 83 (1972).

(29) J. W. McIver, Jr., P. Coppens, and D. Nowak, *Chem. Phys. Lett.*, **11**, 82 (1971).

(30) J. A. Pople and D. L. Beveridge, "Approximate Molecular Orbital Theory," McGraw-Hill, New York, N.Y., 1970, p. 202.

ACKNOWLEDGMENTS

Abstracted in part from a dissertation submitted by T. L. Breon to the Graduate School, University of Rhode Island, in partial fulfillment of the Doctor of Philosophy degree requirements.

Three-Dimensional Molecular Illustrations II: Isoelectrostatic Energy Contour Spheres of Influence Applied to Narcotic Molecules

THOMAS L. BREON *, HAROLD PETERSEN, Jr. ‡, and ANTHONY N. PARUTA *x

Received May 21, 1976, from the **College of Pharmacy and the* ‡*Department of Chemistry, University of Rhode Island, Kingston, RI 02881.* Accepted for publication April 1, 1977.

Abstract □ A computer-generated method using quantum mechanics was applied to the calculation and subsequent plotting of nonperspective three-dimensional illustrations of molecules *in vacuo*. The purpose was to generate isoelectrostatic energy contour spheres for larger molecules and current drugs. The molecules chosen, morphine, meperidine, and alphaprodine, possess similar pharmacological properties. Minor configurational manipulation of the meperidine and alphaprodine molecules was made to approximate the spatial configuration of the rigid morphine molecule so that direct comparisons were possible. Common areas of reactivity, potential energy minima, net atomic charges, spatial regions, and near neighbor influences are considered.

Keyphrases □ Molecular structure—three-dimensional illustrations of narcotic molecules calculated and plotted with computer-generated method using electrostatic energy contours □ Narcotic molecules—three-dimensional illustrations of molecular structure calculated and plotted with computer-generated method using electrostatic energy contours □ Electrostatic potential energy—considered in depicting three-dimensional illustrations of molecular structure of narcotic molecules

In this study, molecular projections utilizing electrostatic potential energy contours were prepared for morphine, meperidine, and alphaprodine. These narcotic agents were chosen because their large molecular sizes show that the methods developed are adaptable to large molecular systems characteristic of most medicinal agents. Moreover, although the spatial configurations of the molecules are dissimilar, they possess common pharmacological properties. The molecular illustrations derived from the electrostatic potential energy function show that these molecules possess common regions of reactivity in their molecular environments.

BACKGROUND

The stereochemical configuration of compounds possessing narcotic activity was presented (1–5) and reviewed (6). Another study (7) dealt

illustrations very similar to the isoelectron density contours without any increase in sensitivity to electronic alterations.

The electrostatic potential energy was then investigated for its utility to produce either two- or three-dimensional aspects of molecules. These isoelectrostatic energy contours produced pictorially clear illustrations with the additional characteristic of sensitivity to electron shifts and an attacking proton in these molecular projections.

REFERENCES

(1) J. E. Falk, *Aust. J. Sci.*, **7**, 48 (1944).

(2) T. Sabaltschka and H. Tietz, *Pharm. Acta Helv.*, **5**, 286 (1930).

(3) G. Barger and H. H. Dale, *J. Physiol.*, **41**, 19 (1910).

(4) "The Pharmacological Basis of Therapeutics," 4th ed., L. S. Goodman and A. Gilman, Eds., Macmillan, New York, N.Y., 1970, p. 1604.

(5) A. L. Tatum, *Physiol. Rev.*, **19**, 472 (1939).

(6) R. F. Doerge, in "Textbook of Organic Medicinal and Pharmaceutical Chemistry," 4th ed., C. O. Wilson and O. Gisvold, Eds., Lippincott, Philadelphia, Pa., 1962, p. 534.

(7) P. N. Patil, J. B. LaPidus, and A. Tye, *J. Pharm, Sci.*, **59**, 1205 (1970).

(8) N. B. Eddy, *Chem. Ind.*, **1959**, 1462.

(9) R. S. Schnaare and A. N. Martin, *J. Pharm. Sci.*, **54**, 1707 (1965).

(10) L. B. Kier, "Molecular Orbital Theory in Drug Research," Academic, New York, N.Y., 1971.

(11) I. Cohen, *J. Chem. Educ.*, **38**, 20 (1961).

(12) E. A. Ogryzlo and G. B. Porter, *ibid.*, **40**, 256 (1963).

(13) F. Daniels and R. Alberty, "Physical Chemistry," 3rd ed., Wiley, New York, N.Y., 1966, p. 451.

(14) W. T. Bordass and J. W. Linnett, *J. Chem. Educ.*, **47**, 672 (1970).

(15) N. C. Craig, D. D. Sherertz, T. S. Carlton, and M. N. Ackermann, *ibid.*, **48**, 310 (1970).

(16) R. C. Reiter and J. E. House, Jr., *ibid.*, **45**, 465 (1968).

(17) D. L. Peterson and M. E. Fuller, *ibid.*, **48**, 314 (1971).

(18) R. J. Olcott, *ibid.*, **49**, 614 (1972).

(19) M. S. Dewar and J. Kelemen, *ibid.*, **48**, 494 (1971).

(20) R. Bonaccorsi, C. Petrongolo, E. Scrocco, and J. Tomasi, in "The Jerusalem Symposia on Quantum Chemistry and Biochemistry," vol. II, 1970, p. 181.

(21) R. Bonaccorsi, E. Scrocco, and J. Tomasi, *J. Chem. Phys.*, **52**, 5270 (1970).

(22) N. W. Dalton and D. E. Schreiber, *Solid State Phys.*, **27**, 183 (1972).

(23) R. Bonaccorsi, C. Petrongolo, E. Scrocco, and J. Tomasi, *ibid.*, **20**, 331 (1971).

(24) J. A. Pople and D. L. Beveridge, "Approximate Molecular Orbital Theory," McGraw-Hill, New York, N.Y., 1970, p. 111.

(25) *Ibid.*, p. 62.

(26) Program 141, Quantum Chemistry Program Exchange, Department of Chemistry, Indiana University, Bloomington, Ind.

(27) P. Lowdin, *J. Chem. Phys.*, **18**, 365 (1950).

(28) C. Giessner-Prettre and A. Pullman, *Theor. Chim. Acta (Berl.)*, **25**, 83 (1972).

(29) J. W. McIver, Jr., P. Coppens, and D. Nowak, *Chem. Phys. Lett.*, **11**, 82 (1971).

(30) J. A. Pople and D. L. Beveridge, "Approximate Molecular Orbital Theory," McGraw-Hill, New York, N.Y., 1970, p. 202.

ACKNOWLEDGMENTS

Abstracted in part from a dissertation submitted by T. L. Breon to the Graduate School, University of Rhode Island, in partial fulfillment of the Doctor of Philosophy degree requirements.

Three-Dimensional Molecular Illustrations II: Isoelectrostatic Energy Contour Spheres of Influence Applied to Narcotic Molecules

THOMAS L. BREON *, HAROLD PETERSEN, Jr. ‡, and ANTHONY N. PARUTA *x

Received May 21, 1976, from the **College of Pharmacy and the* ‡*Department of Chemistry, University of Rhode Island, Kingston, RI 02881.* Accepted for publication April 1, 1977.

Abstract □ A computer-generated method using quantum mechanics was applied to the calculation and subsequent plotting of nonperspective three-dimensional illustrations of molecules *in vacuo*. The purpose was to generate isoelectrostatic energy contour spheres for larger molecules and current drugs. The molecules chosen, morphine, meperidine, and alphaprodine, possess similar pharmacological properties. Minor configurational manipulation of the meperidine and alphaprodine molecules was made to approximate the spatial configuration of the rigid morphine molecule so that direct comparisons were possible. Common areas of reactivity, potential energy minima, net atomic charges, spatial regions, and near neighbor influences are considered.

Keyphrases □ Molecular structure—three-dimensional illustrations of narcotic molecules calculated and plotted with computer-generated method using electrostatic energy contours □ Narcotic molecules—three-dimensional illustrations of molecular structure calculated and plotted with computer-generated method using electrostatic energy contours □ Electrostatic potential energy—considered in depicting three-dimensional illustrations of molecular structure of narcotic molecules

In this study, molecular projections utilizing electrostatic potential energy contours were prepared for morphine, meperidine, and alphaprodine. These narcotic agents were chosen because their large molecular sizes show that the methods developed are adaptable to large molecular systems characteristic of most medicinal agents. Moreover, although the spatial configurations of the molecules are dissimilar, they possess common pharmacological properties. The molecular illustrations derived from the electrostatic potential energy function show that these molecules possess common regions of reactivity in their molecular environments.

BACKGROUND

The stereochemical configuration of compounds possessing narcotic activity was presented (1–5) and reviewed (6). Another study (7) dealt

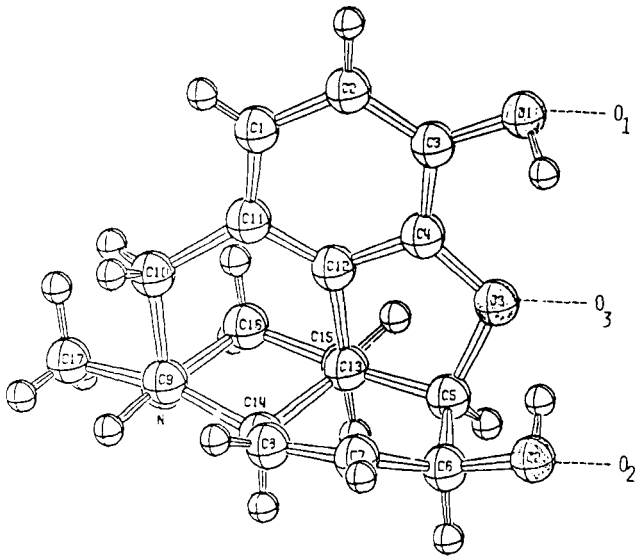

Figure 1—*Skeletal illustration of morphine depicting the spatial relationships of the atoms obtained from the ORTEP program.*

with the topography of the narcotic receptor. Binding modes by the use of free energy relationships were presented (8), and receptor perturbation by interacting molecules was suggested (9). The possibility of unrelated chemical species assuming a conformation similar to active compounds also was discussed (10). The chemical configuration of opium alkaloids (11, 12) and the total synthesis of codeine and morphine (13) confirmed earlier studies.

The structure of the phenanthrene fragment and its relative configuration were reported (14). Independent studies (15–18) confirmed this work. Stereochemical configurations from X-ray crystallographic studies of this type of compound were derived (19, 20), and the absolute configurations were determined by chemical means (21). Subsequent three-dimensional analysis of crystallographic data confirmed the absolute stereochemistry of morphine (22) and codeine (23). Through similar methods, the stereochemistry of several synthetic narcotics was determined (24–26).

PROCEDURES

Computations—The calculation of electrostatic potential energy was accomplished with a computer[1] utilizing Fortran IV language. These procedures were described in Part I. The molecular projections or illustrations were effected by the use of an available program[2] and an incremental plotter[3] slaved to the computer output.

Electrostatic Potential Energy Projections—*Morphine*—All molecules discussed in Part I had relatively small structures. To demonstrate the applicability of this method to large molecular systems of more practical interest, the electrostatic potential energy computations were performed on several narcotic agents. Morphine was chosen because of its potent pharmacological properties, widespread interest, and well-defined conformation.

A skeletal illustration of this molecule, utilizing the ORTEP method (27), is found in Fig. 1. The characteristic features of this molecule include a piperidine and phenyl ring joined by a common asymmetric carbon atom, C-13. Two more six-membered rings and a five-membered ring containing an ether linkage, O-3, complete the main structure. Peripheral groups necessary for pharmacological activity include a methyl, C-17, an alcoholic hydroxyl, O-2, and a phenolic hydroxyl, O-1. The basic structure consists of five ring systems bonded to each other at multiple points. This structure is rigid and may preclude any significant conformational changes caused by biological systems. The skeletal configuration and numbering system for this molecule were taken from the crystallographic data of Gylbert (22), as corrected[4].

[1] IBM 370/155.
[2] ORTEP.
[3] Broomall Industries M-2000 drum-type.
[4] The correct x positional coordinate, in Table I of Ref. 22, for C-3 is 1806 (5) (Dr. Leif Gylbert, Department of Medical Physica, Karolinska Institutet, S-104-01 Stockholm 60, Sweden, personal communication, Sept. 1974).

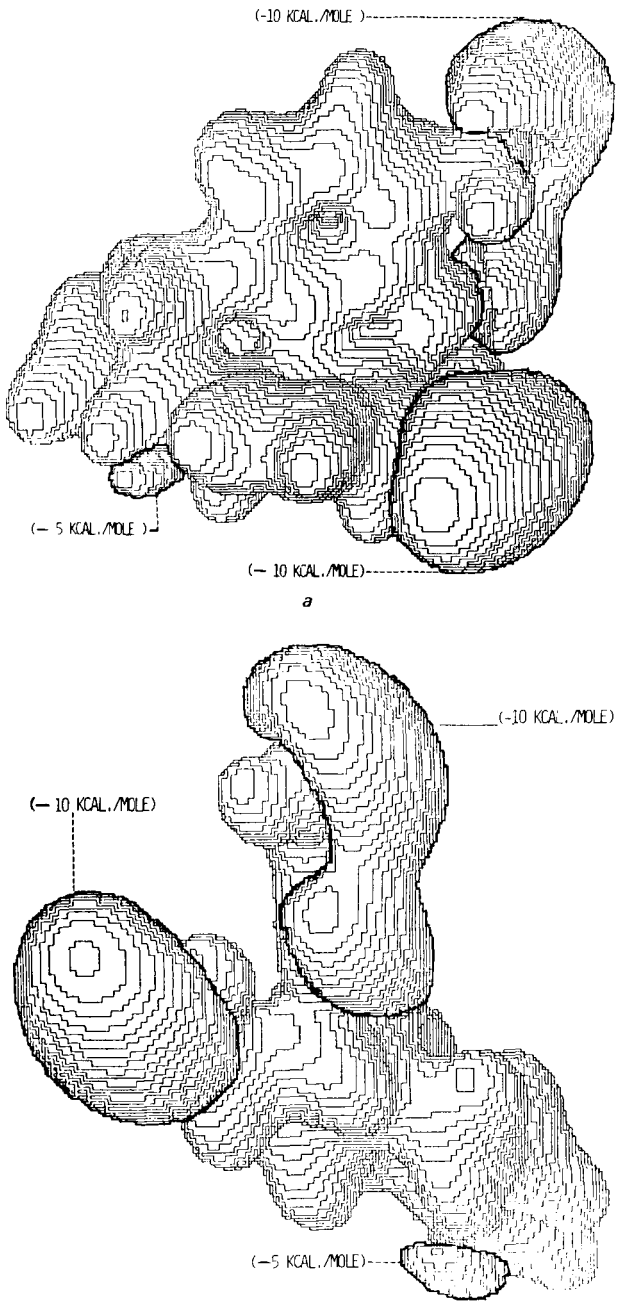

Figure 2—(a) *Illustration of the electrostatic potential energy contours of morphine (ORTEP facing). The negative lobes are at −10 kcal/mole for O-1, O-2, and O-3 and at −5 kcal/mole for N; all other lobes are at +100 kcal/mole.* (b) *Illustration of the electrostatic potential energy contours of morphine from Fig. 2a, where the molecule is rotated 90° about a vertical axis toward the viewer.*

The electrostatic potential energy contours pertaining to morphine are presented in Fig. 2. Figure 2*a* represents a frontal view in which the molecule is positioned identically to Fig. 1. Figure 2*b* is a view after the molecule was rotated 90° about a vertical axis. For comparison, the net atomic charges of the molecular constituents are listed in Table I. These data were calculated from the CNDO/2 valence orbital populations. These populations compare favorably with those published previously (28).

Virtually the entire molecule is surrounded by a field of positive potential. As expected, the potential diminishes near the center of the various ring systems. In Fig. 2*a*, "holes" may be seen in the two six-membered rings parallel to the plane of the page as well as in the ring containing the ether bridge. The *N*-methyl group is readily distinguishable at the far left. The phenolic hydroxyl group is at the upper right,

Table I—CNDO/2 Net Atomic Charges for Morphine

Atom	Net Atomic Charge	Atom	Net Atomic Charge
O-1	−0.2445	C-17	0.0430
O-2	−0.3067	H–O-1	0.1433
O-3	−0.2382	H-1	0.0156
N	−0.1744	H-2	0.0103
C-1	−0.0298	H-5	−0.0001
C-2	−0.0364	H-6	−0.0035
C-3	0.1285	H-7	0.0253
C-4	0.1116	H-8	0.0239
C-5	0.1082	H-9	−0.0253
C-6	0.1397	H-10a	0.0251
C-7	−0.0442	H-10b	0.0022
C-8	−0.0280	H-14	0.0007
C-9	0.0968	H-15a	0.0051
C-10	−0.0282	H-15b	0.0022
C-11	0.0221	H-16a	−0.0117
C-12	−0.0178	H-16b	−0.0009
C-13	0.0288	H-17a	−0.0065
C-14	0.0101	H-17b	0.0169
C-15	−0.0070	H-17c	−0.0094
C-16	0.0752	H–O-2	0.1781

adjacent to the aromatic ring; the alcoholic hydroxyl is positioned at the lower right but is hidden from view.

Four regions of negative potential, each associated with a heteroatom, can be noted.

The minima, expressed in kilocalories per mole, found at the center of each of these energy wells are ranked as follows: −32.2 (O-2, alcoholic hydroxyl) > −24.4 (O-1, phenolic hydroxyl) > −20.7 (O-3, ether) > −7.1 (N). These regions represent prime areas for electrophilic interaction or attack and are of particular interest when considering drug–receptor mechanisms. Each lobe is on the periphery of the molecule, thus providing a relatively large number of possible conformations in its approach to, or interaction with, a biophase.

Because of the close physical proximity of the lobes associated with the phenolic and ether oxygen atoms, the −10-kcal/mole contours merge to form one large, odd-shaped negative site. Within this dumbell-shaped lobe, two wells exist, having minimum energies of −24.4 and −20.7 kcal/mole.

The negative potential corresponding to the ether oxygen atom is nonuniformly distributed about the nucleus. In a molecule where there is no steric hindrance, the negative lobe of an ether linkage would possess a quarter-moon shape and lay on a plane perpendicular to the ether linkage, corresponding to the approximate position of the two lone pairs of electrons. In the present case, the −10-kcal/mole contour associated with the ether oxygen atom is concentrated only on one side of it. The additive effect of the phenolic hydroxyl may partially account for this uneven distribution.

Of greater significance is the alcoholic hydroxyl group at C-6. The O–H bond of this group is directed toward the ether bridge. The O-2–H···O-3 interatomic distance is 2.72 Å, and the angle is 146°. As suggested previously (22), the geometric configurations of these atoms present conditions that may be favorable to intramolecular hydrogen bonding, and the potential for forming a five-membered ring exists.

The partial positive charge on the hydrogen atom, H–O-2, generates a large sphere of positive potential, and a region of negative potential is generated by the excess electrons of the ether. In this case, these atoms are close enough together that the potential energies generated by each blend together, resulting in a net positive electrostatic potential in this entire region.

The illustrated isoelectrostatic energy values were chosen because these values provide a contiguous picture of the entire molecule. Greater or smaller values would cause the illustration to "balloon out" or "become nodules" in space; the values chosen give the best pictorial guide compatible with chemical reasoning.

Table II—CNDO/2 Conformational Energies for Various Configurations of Meperidine

Configuration	Total Energy, kcal/mole
Crystal, from Ref. 24	−107,453
Piperidine ring inverted	−107,455
Phenyl ring rotated about C-3–C-1′ onto a plane perpendicular to N–C-3	−107,452
Ester linkage rotated about C-3–C-7	−107,448

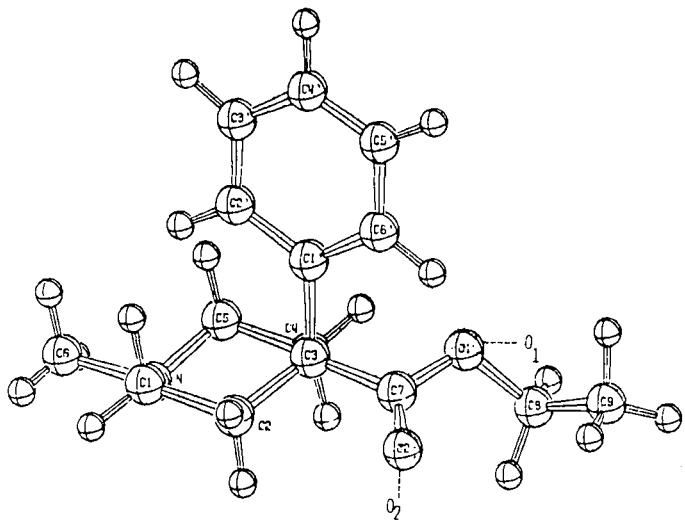

Figure 3—*Skeletal illustration of meperidine depicting the spatial relationships of the atoms obtained from the ORTEP program.*

Meperidine—Meperidine, a synthetic narcotic, has several structural features similar to morphine. This molecule is composed of a piperidine ring, containing an *N*-methyl group, with a phenyl ring and an ester linkage positioned on an asymmetric carbon atom. The crystal structure of this compound (24) indicates the aromatic ring to be equatorial and the ester linkage to be axial to the piperidine ring.

In this investigation, the conformation of meperidine was altered to reposition the negative lobes that might be generated by the heteroatoms. Manipulation of the atomic coordinates allows these lobes to be placed in positions similar to those occupied by the negative lobes of morphine.

When altering the configuration of a molecule, one must also be concerned with the change in conformational energy that may occur. Table II lists the steps used in manipulating the meperidine molecule and the total energy of each resulting conformer.

By inverting the piperidine ring, the phenyl ring now becomes axial and the ester becomes equatorial (Fig. 3). In this position, this molecule is in a configuration similar to the structure of morphine. Conformational energies indicate a small change in total energy between the crystal and inverted configurations.

The next step involves the rotation of the aromatic ring about the C-3–C-1′ axis onto a plane perpendicular to the nitrogen and asymmetric carbon atoms of the piperidine ring. Again, a very small change in the conformational energy is noted. Finally, rotation of the ester fragment about the C-3–C-7 bond allows the two ester oxygen atoms to be positioned in the same relative positions as the ether and alcohol oxygen

Table III—CNDO/2 Net Atomic Charges for Meperidine

Atom	Net Atomic Charge	Atom	Net Atomic Charge
O-1	−0.2735	H-2a	0.0013
O-2	−0.3291	H-2b	0.0039
N	−0.1565	H-4a	−0.0057
C-1	0.0811	H-4b	−0.0042
C-2	0.0086	H-5a	−0.0075
C-3	−0.0184	H-5b	−0.0090
C-4	0.0179	H-6a	−0.0029
C-5	0.0786	H-6b	0.0224
C-6	0.0273	H-6c	0.0003
C-7	0.3985	H-8a	−0.0011
C-8	0.1541	H-8b	−0.0099
C-9	−0.0377	H-9a	0.0117
C-1′	0.0416	H-9b	0.0261
C-2′	−0.0222	H-9c	0.0160
C-3′	0.0110	H-2′	0.0103
C-4′	0.0065	H-3′	−0.0038
C-5′	0.0050	H-4′	−0.0093
C-6′	−0.0273	H-5′	0.0027
H-1a	−0.0166	H-6′	0.0217
H-1b	−0.0117		

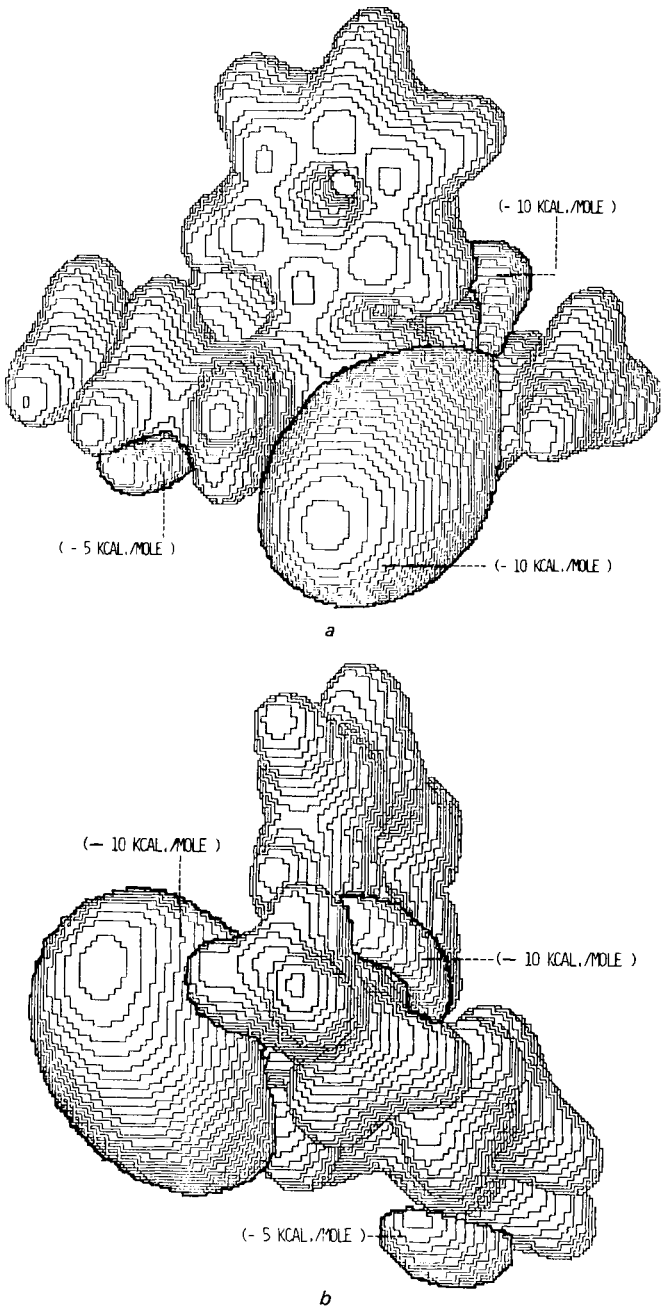

Figure 4—(a) *Illustration of the electrostatic potential energy contours of meperidine (ORTEP facing). The negative lobes are at −10 kcal/mole for O-1 and O-2 and at −5 kcal/mole for N; all other lobes are at +100 kcal/mole.* (b) *Illustration of the electrostatic potential energy contours of meperidine from Fig. 4a, where the molecule is rotated 90° about a vertical axis toward the viewer.*

atoms of morphine. A small loss in the conformational energy of 4 kcal/mole occurs as a result of this step. The net change in conformational energy between the first and the last step is a loss of 5 kcal/mole (Table II).

The skeletal structure of meperidine resulting from these manipulations is found in Fig. 3. This structure is used in all subsequent illustrations. The numbering system is identical to that previously published (24). In Ref. 24, only the positions of the nonhydrogen atoms were reported. In the present investigation, standard bond lengths and bond angles were used to add the hydrogen atoms. Table III lists the net atomic charges calculated from the CNDO/2 orbital populations.

The potential energy contour surfaces corresponding to meperidine are shown in Fig. 4. The energy values represented by the various contours and the orientation of the molecule are identical to the morphine illustrations.

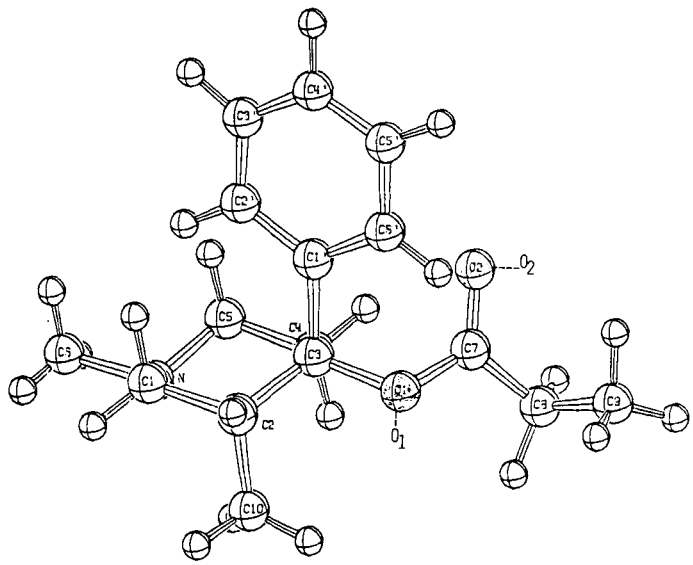

Figure 5—*Skeletal illustration of alphaprodine depicting the spatial relationships of atoms obtained from the ORTEP program.*

Three lobes of negative electrostatic potential energy are found, and each of these energy wells is associated with an atom possessing lone-pair orbitals and a rather large negative net atomic charge. The energy minima, in kilocalories per mole, associated with each lobe are ranked as follows: −41.7 (O-2, carbonyl) > −18.7 (O-1, ether) > −7.8 (N).

The −10-kcal/mole contours generated by the ester oxygens merge in an area approximately midway between the two minima. This phenomenon may not be explicitly evident from these illustrations but was visually confirmed using other viewing angles. The remainder of the molecule is surrounded by a field of positive electrostatic potential.

Alphaprodine—The molecular structure of alphaprodine, another synthetic narcotic agent, is similar to meperidine in that it is composed of a phenyl ring, an ester linkage, and a piperidine ring containing an *N*-methyl group. In alphaprodine, however, the ester linkage is reversed from that in meperidine. The only other feature unique to this compound is a second methyl group substituted on the piperidine ring.

The spatial relationships among the two ring systems and the ester group are identical to the crystal configuration of meperidine (25). The additional methyl group is equatorial to the heterocyclic ring.

Because of the similar stereochemical relationships of meperidine and alphaprodine, it was presupposed that the latter molecule could be subjected to conformational alterations with virtually no change in conformational energy. The resulting configuration is similar to that found in Fig. 5. As seen in the previous illustrations, the ester group may be rotated, within limits, to orient the expected regions of negative potential into positions mimicking meperidine and morphine. As a result of the type of ester found in alphaprodine, only one oxygen atom may be displaced by a rotation about the C-3–O-1 bond. The other oxygen atom, which lies on the axis, cannot be displaced by rotation, but the anticipated lobe of negative potential associated with the ether oxygen atom may be reoriented into a more favorable position.

In the previous illustrations of meperidine, the carbonyl produced the largest region of negative potential. Because of the close stereochemical similarities, the carbonyl of alphaprodine would, in all probability, generate the largest region of low electrostatic potential energy. This portion of the molecule was manipulated independently so that the position of this lobe would reside in the same general area as the lobe generated by the ether group of morphine.

A conformational change of this nature affords the opportunity to assess the difference in the potential energy contour surfaces resulting from interchanging the two types of oxygen atoms. In meperidine, an ether oxygen is located in the same relative spatial position as the ether oxygen of morphine; in alphaprodine, this region is occupied by the carbonyl oxygen.

The nuclear coordinates of the atomic constituents of alphaprodine were taken from the corresponding atoms of the meperidine molecule. The C-10 methyl group was added and the ester linkage was reversed, utilizing standard bond lengths and angles. The ester group was then rotated about the C-3–O-1 bond as described. The resulting configuration (Fig. 5) was utilized in the CNDO/2 computations to determine the

Table IV—CNDO/2 Net Atomic Charges for Alphaprodine

Atom	Net Atomic Charge	Atom	Net Atomic Charge
O-1	−0.2943	H-2	−0.0014
O-2	−0.3376	H-4a	0.0042
N	−0.1588	H-4b	0.0019
C-1	0.0873	H-5a	−0.0027
C-2	0.0127	H-5b	−0.0064
C-3	0.1668	H-6a	−0.0017
C-4	−0.0169	H-6b	0.0229
C-5	0.0843	H-6c	0.0022
C-6	0.0283	H-8a	0.0331
C-7	0.4082	H-8b	0.0145
C-8	−0.0529	H-9a	0.0039
C-9	0.0049	H-9b	0.0147
C-10	−0.0084	H-9c	0.0090
C-1′	−0.0061	H-10a	−0.0097
C-2′	−0.0133	H-10b	0.0105
C-3′	−0.0070	H-10c	0.0082
C-4′	0.0155	H-2′	0.0
C-5′	−0.0194	H-3′	−0.0083
C-6′	0.0242	H-4′	−0.0142
H-1a	−0.0177	H-5′	−0.0006
H-1b	−0.0082	H-6′	0.0282

atomic electron populations, from which the net atomic charges (Table IV) were derived.

Two views of the electrostatic potential energy contour surfaces representing alphaprodine are shown in Fig. 6. The viewing angle in each is the same as the corresponding illustrations of morphine and meperidine. The negative isoenergy contour associated with the nitrogen atom is not drawn at the same energy level as in the previous illustrations. In the present case, this contour represents a value of −2 kcal/mole.

This molecule is unique, among the three narcotics presented, in that the minimum energy in the nitrogen atom region does not attain a value of −5 kcal/mole, the level at which this contour was drawn for the previous molecules. This positive shift in the potential energy may be due to the close proximity of the C-10 methyl group. The positive potential generated by this group partially neutralizes the negative potential radiated by the nitrogen atom, resulting in a net increase in the minimum energy of this lobe.

The energy minima, in kilocalories per mole, associated with each lobe are: −40.5 (O-2, carbonyl) > −22.7 (O-1, ether) > −4.8 (N). As expected, the largest region of negative potential, as well as the lowest minimum, was found in the vicinity of the carbonyl oxygen atom.

DISCUSSION

The atomic coordinates and the spatial orientation of these narcotic compounds have been manipulated so that comparisons may be readily made among them. The illustration pertaining to morphine (Fig. 2*a*) indicates three lobes of negative potential on the right side of the molecule. If the quantity of energy representing these contours is made less negative, it would become apparent that this entire region is attractive to an electrophilic group in a biophase. The region on the opposite side of the molecule is positive and repulsive to a reactant of this type.

Meperidine and alphaprodine each possess a similar large region of positive potential surrounding the phenyl ring and the top of the piperidine ring. They differ from morphine in the shape of their regions of negative potential. In these compounds, the ethane substituent attached to the ester linkage radiates a dense field of positive energy that pierces or attenuates this otherwise large field of negative potential. As a result, an approaching electrophilic agent must be more selective in its direction of attack.

Each of these molecules demonstrates a decreased propensity toward electrostatic interactions in an area directly beneath the nitrogen atoms. The energy minima in these regions are significantly less negative than those generated by the other electronegative atoms. The affinity of these areas for an electrophilic agent is greatly reduced. Of importance also is the greater amount of shielding produced by the surrounding region of positive potential. Unlike the other energy wells, the lobes associated with each nitrogen atom are tucked in close to the underside of the molecule. This shielding effect is more pronounced for alphaprodine, which has a methyl group axial to the piperidine ring. In these regions, the direction from which an electrophilic agent might approach the molecule is more restrictive than when the lobes are associated with the oxygen atoms.

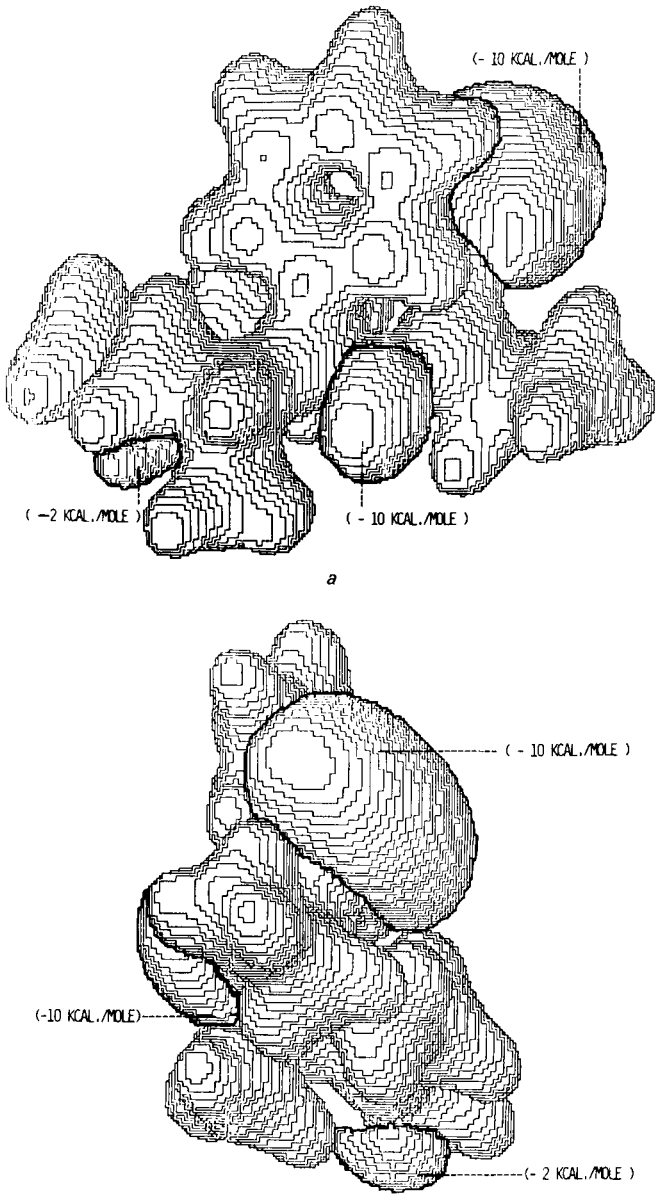

Figure 6—(a) *Illustration of the electrostatic potential energy contours of alphaprodine (ORTEP facing). The negative lobes are at −10 kcal/mole for O-1 and O-2 and at −2 kcal/mole for N; all other lobes are at +100 kcal/mole.* (b) *Illustration of the electrostatic energy contours of alphaprodine from Fig. 6a, where the molecule is rotated 90° about a vertical axis toward the viewer.*

The type of atom involved in these electrostatic potential energy calculations should dictate the magnitude of the energy minimum. An oxygen atom, having a greater ability to attract electrons than a nitrogen atom, is expected to generate an energy minimum somewhat more negative than that produced by a nitrogen atom. This fact is substantiated by the data presented in Table V. Each nitrogen atom generates an energy minimum significantly less negative than any oxygen atom.

The oxygen atoms can be further segregated by the type of group in which they reside. In general, the net atomic charges become more negative as one descends this list of chemical groups. An alcoholic oxygen atom is expected to possess a larger number of excess electrons than an ether oxygen because of the greater ease of extracting an electron from a hydrogen atom. In an ether group, the oxygen atom incurs more competition from the two adjacent carbon atoms, and its net atomic charge is less negative.

A phenolic hydroxyl group is much the same as an alcoholic hydroxyl group, but the resonating aromatic ring competes with the oxygen from the electrons to a greater extent than a single carbon atom. As a result,

Table V—Summary of the Potential Energy Minimums [a] and the Net Atomic Charge [b] Associated with the Noted Atom or Functional Group for the Narcotic Molecules Utilized in This Study

Group	Morphine	Meperidine	Alphaprodine
N	−7.1 [−0.1744]	−7.8 [−0.1565]	−4.8 [−0.1588]
Ether	−20.7 [−0.2382]	−18.6 [−0.2735]	−22.7 [−0.2943]
Phenolic hydroxyl	−24.4 [−0.2554]	—	—
Alcoholic hydroxyl	−32.2 [−0.3067]	—	—
Carbonyl	—	−41.7 [−0.3291]	−40.5 [−0.3376]

[a] Expressed in kilocalories per mole. [b] Values appear in brackets.

Table VII—Summary of the Distances between the Points of Minimum Energy Found in Each Common Region [a] and the Triangular Area Enclosed by These Points for the Narcotic Molecules Utilized in This Study [b]

Molecule	Vector, Å			Area, Å²
	1–2	1–3	2–3	
Morphine	6.8 [5.22]	7.7 [6.50]	4.2 [2.72]	14.3 [6.8]
Meperidine	6.3 [5.10]	5.8 [4.98]	4.2 [2.27]	12.0 [5.6]
Alphaprodine	6.8 [5.39]	5.3 [4.33]	4.2 [2.44]	11.0 [4.7]

[a] See the text for a description of the heteroatoms associated with each region. [b] Values denoted in brackets were derived in a similar manner from the nuclear coordinates of the heteroatoms associated with each region.

the net atomic charge on the oxygen atom is similar to that of an ether oxygen. Finally, a carbonyl oxygen atom has the largest electron-withdrawing capability because of the reduced number of protons, on the single carbon atom, competing with the oxygen atom. To summarize, as the list is descended, the total number of protons on the atoms adjacent to the oxygen atom gain excess electrons. As a result of this ordering of net atomic charges, the energy minima also vary in the same general pattern (Table V).

Another factor also must be considered when discussing the ordering of the energy minima associated with the oxygen atoms. As the list is descended, the number and size of the atoms bonded to the oxygen atom diminish. The number and magnitude of the spheres of influence generated by these nearest neighbors also diminish, resulting in less attenuation of the negative energy lobe.

Of particular interest is the smaller variation of the energy minima among the nitrogen atoms themselves (Table V). In each of the three molecules listed, the net atomic charge of the nitrogen atoms is nearly identical. This fact in itself would lead one to expect identical energy minima. However, the value for alphaprodine is nearly half that of the other molecules. This aberrant behavior pointedly demonstrates the steric effect created by the C-10 methyl group of alphaprodine. The spatial location of this substituent is close enough to the nitrogen atom that its sphere of positive influence mitigates the negative potential generated by the nitrogen atom, thus rendering the minimum less negative. With nearly identical net atomic charges, electron density illustrations would not show any discernible differences in this region of the molecules.

Several other irregularities also demonstrate the significant influence of neighboring atoms on the energy minima (Table V). One would expect the energy minimum to become more negative as the number of electrons in a given atom increases. Comparing the ether groups of morphine and meperidine, one finds the minimum energies to be proportional to the net atomic charges. An analogous situation exists with the meperidine and alphaprodine carbonyl groups.

These trends illustrate the specificity and sensitivity of this method to depict small changes in the electronic character of a molecule and to depict uniquely the steric effects caused by interactions of molecular constituents.

In any discussion of drug–receptor mechanisms, electrostatic interactions between the pharmacophore and receptor must be considered. In a given series of similar pharmacological agents, such as the narcotics presently being discussed, a comparison of their electrostatic potential energy characteristics is essential. Each of these molecules possesses at least three energy wells in similar geometrical or spatial regions. The minimum energies in each region in the molecular environment are listed in Table VI.

Region 1 includes the energy wells generated by the nitrogen atoms, and Region 2 is comprised of the ether oxygens of morphine and meperidine and the carbonyl oxygen of alphaprodine. The alcoholic hydroxyl of morphine, the carbonyl oxygen of meperidine, and the ether oxygen of alphaprodine are located in Region 3. Morphine has a fourth energy well generated by the phenolic hydroxyl group. Meperidine and alphaprodine do not possess a corresponding region of low potential energy.

Table VI—Summary of the Potential Energy Minimums [a] Associated with the Common Spatial Regions for the Narcotic Molecules Utilized in This Study

Molecule	Region [b]			
	1	2	3	4
Morphine	−7.1	−20.7	−32.2	−24.4
Meperidine	−7.8	−18.6	−41.7	—
Alphaprodine	−4.8	−40.5	−22.7	—

[a] Expressed in kilocalories per mole. [b] See the text for a description of the heteroatoms associated with each region.

The energy minima for morphine and meperidine are ranked in the same order but differ slightly in magnitude. In each molecule, the lobes occupying Regions 1 and 2 are generated by a nitrogen atom and an ether oxygen atom, respectively. On this basis, one might expect similar minimum energies, barring any steric influence from neighboring atoms. The lowest potential energy in Region 2 of meperidine is somewhat less negative than the corresponding value for morphine. The sphere of negative potential energy in this region of the morphine molecule possesses spatial contours larger in volume because of the additive effect of the phenolic hydroxyl in Region 4. This condition undoubtedly accounts for the slightly more negative minimum in Region 2 of morphine.

A somewhat larger deviation is found when comparing the minimum energies in Region 3 of morphine and meperidine. These energy wells are generated by an alcoholic hydroxyl and a carbonyl oxygen atom, respectively. Previously, it was noted that the alcoholic oxygen atom possessed a less negative net atomic charge, thus accounting for part of this deviation. A large sphere of positive potential is generated by the alcoholic hydrogen atom, which tends to produce a less negative minimum energy in Region 2 of morphine.

The smaller minimum energy found in Region 1 of alphaprodine has already been discussed in regard to the sphere of influence generated by the extra methyl group in this molecule. The relative strengths of the minima in Regions 2 and 3 of alphaprodine are reversed from those in morphine and meperidine (Table VI), partially as a result of the ester group being approximately 180° out of phase with the same chemical group of meperidine.

The ester groups of these two molecules have about the same geometrical configuration and spatial coordinates. It would be expected that the relative order and magnitudes of the alphaprodine minimums could be made to conform to those of morphine and meperidine by rotation of the ester linkage. In such a configuration, a close correlation would be noted among the energy minima found in nearly identical regions of each of these narcotic molecules.

The electrostatic potential energy surface contours are unique in that they can be utilized to combine elements from both the stereochemical and quantum mechanical approaches to the elucidation of drug–receptor conformations. The magnitude of the electrostatic interactions is an indicator of the intermolecular affinity between two or more species. As noted from the illustrations, these forces are not evenly distributed about the molecule but are localized in specific regions; each region radiates a sphere of influence from its nucleus or point of minimum energy. Therefore, critical distances should not be calculated from the nuclear coordinates of the reactive atoms but from the centers of the minimum energy wells. Since these energy minima are not symmetrically distributed about an atom because of the influence of its neighbors, a more accurate description of the location of the "reactive sites" is obtained from the point of minimum energy.

Table VII lists the distances calculated between these points in similar regions of low electrostatic potential. The regions are numbered by the same convention used in the previous table. For comparison purposes, the distances between the nuclei of the atoms generating these minimum energies are included in brackets. The distance between each pair of minima occupying similar regions are nearly identical among the three molecules. The major exception is the Region 1–3 interval in morphine. This deviation is a consequence of the alcoholic hydroxyl group of Region

3 being approximately one carbon–carbon bond length further removed from the nitrogen atom.

The positions of the energy minima associated with the three negative lobes common to each molecule may be thought of as representing the vertices of a triangle. The similarities of the geometrical configuration of the electrostatic potential energy field surrounding each compound is demonstrated by a comparison of the areas of these triangles (Table VII). The values corresponding to meperidine and alphaprodine are nearly identical. As a result of the increased distance between Regions 1 and 3, the area corresponding to morphine is slightly larger.

The data in Table VII derived from the nuclear coordinates show approximately the same rank correlation as those derived from the positions of minimum energy. The significant feature is the larger magnitude of the distances calculated by the latter method. This result indicates the much larger total sphere of influence a molecule presents to a receptor than might be implied by using measurements taken from the nuclear coordinates.

At the beginning of this investigation, it was noted that the molecular structures of meperidine and alphaprodine were systematically manipulated so that the anticipated positions of the energy wells would occupy approximately the same spatial regions in each molecule. Examination of the illustrations and the data of Table VII shows the manipulations to be effective in achieving this end.

If the original coordinates, derived from the crystallographic data, were used to generate the electrostatic potential energy contour surfaces, the distances between Regions 1 and 2 and 1 and 3 would be reduced for both meperidine and alphaprodine. The vector from Region 2 to Region 3 would not be altered due to the rigidness of the ester group. In these molecules, the inversion of the piperidine ring reorients the ester group from an axial to an equatorial position, resulting in electrostatic potential energy contours that closely mimic those of morphine with a minimum expenditure of conformational energy.

Much smaller variations in the distances between the energy wells may be achieved by rotation of the individual functional groups about their adjacent bonds. With the exception of the carbonyl group, the points of minimum energy are remote from the bond axis. Rotation about a bond would reorient the negative energy lobe.

Rotation about the C–O bonds of the hydroxyl groups of morphine would alter only slightly the positions of the energy minima associated with the oxygen atoms. In meperidine, the ester linkage may be rotated about the C-3–C-7 bond, within the limits dictated by the conformational energy. A similar rotation could be applied to the C-3–O-1 bond of alphaprodine. In each case, the positions of the energy wells would be offset by a small distance. In any case, the effect created by the extra carbon–carbon length between the nitrogen atom and alcoholic hydroxyl of morphine could not be compensated for by these manipulations.

A more important point is the effect of any molecular configurational modification on the magnitudes of the various energy wells. Each negative energy lobe is oriented on a vector away from all other neighboring atoms. Small rotations about the bonds specified would tend to bring these lobes into closer proximity to the neighboring atoms. The steric relationships of these atoms would have a profound effect on the electrostatic energy minima, resulting in less negative values and changes in the shapes of the isopotential surfaces.

If it is assumed that the electrostatic forces play an important role in drug–receptor interactions, these spheres of influence would determine the proper and maximal alignment of a pharmacophore with a receptor. An affinity for the receptor could result if proper alignment could occur. The minimum energies, as well as the spatial location of the negative energy lobes, would be of utmost importance. Under these conditions, the members of a homologous series of pharmacophores would not have to possess identical energy minima at exactly the same spatial locations. Any small deviation from the optimum position for an energy well could be compensated for by a more negative energy minimum associated with that well. In such a situation, the net attractive force between a molecule and a receptor would remain constant.

A comparison of morphine and meperidine can be used to illustrate this principle. If one assumes that the negative energy lobes associated with the nitrogen atom and the oxygen atom of the alcoholic hydroxyl group of morphine are in "perfect" alignment with complementary receptor sites, the meperidine molecule would not physically match these sites identically. In the latter compound, the carbonyl oxygen atom and its corresponding point of minimum energy would be far removed from the receptor site. However, the energy minimum (Table VI, Region 3) in this region is significantly more negative, producing a sphere of influence much larger in volume than that in the corresponding position of morphine. Because of this magnified effect, it is conceivable that this region of low electrostatic potential extends away from the molecule far enough to engage the same receptor site. If the ester group of alphaprodine is rotated, as mentioned previously, this same reasoning would apply to that compound.

The possibility of the receptor itself modifying the conformation of the pharmacophore also must be considered. Just as the drug molecule is considered as a field of electrostatic forces, the receptor must be thought of likewise. The fields of electrostatic attraction and/or repulsion generated by the receptor molecule could perturb the pharmacophore to a small degree. This effect, in turn, could aid in the proper alignment of these species and increase the efficiency of the drug–receptor interaction. This ability of drugs to undergo molecular reorganization upon interacting with a receptor also was recognized by Portoghese (29).

It is also possible to alter the magnitude and position of the minimum energy at a point in the molecular environment by altering neighboring substituent groups. The C-10 methyl group of alphaprodine significantly changed the magnitude of the minimum energy associated with the nitrogen atom to a less negative value. The opposite effect might also be designed into a drug molecule. For example, the addition of an electronegative group on a position in close proximity to one already present in a molecule would enhance the minimum energy, producing a more negative value. This result, in turn, would increase the volume of its sphere of influence. The position of the energy minimum may also be altered by such an additional chemical group.

CONCLUSIONS

The purpose of this study was to devise a method by which three-dimensional illustrations could be produced to allow visualization of the electronic characteristics of a molecule. To devise a viable research tool to accomplish this task, it was necessary to introduce some assumptions and approximations to reduce the computational efforts involved.

The electrostatic potential energy contour surface illustrations were prepared from molecules that admittedly exist *in vacuo*. In reality, a molecule cannot exist as a single entity but always coexists with other molecules of its own or of a differing kind. Such a close relationship of molecular entities tends to influence the electronic structure of each. In an analogous manner, the association of a drug with a receptor could cause mutual perturbations in both the pharmacophore and molecular constituents of the biophase. However, the amount of computational effort necessary to consider the perturbations is beyond the realm of reality at this time. The method presented fulfilled the objectives initially set forth. It allows one to view the physical configuration of a molecule in terms of the electrostatic forces generated by the constituent atoms and to discern how these contours are perturbed by molecular modifications.

The superiority of the electrostatic potential contour surface illustrations may also be substantiated by some features found in the narcotic illustrations. The unsymmetrical shape of the region of negative potential associated with the ether group of morphine provided evidence of possible intramolecular hydrogen bonding.

In comparing the molecules of the narcotic series, the attenuating effect of the fields of electrostatic potential energy about a molecule was noted from the significant influence of the C-10 methyl group of alphaprodine in rendering less negative the minimum energy associated with the nitrogen atom. The electron population assigned to this nitrogen atom is nearly identical to that in meperidine and morphine.

The electrostatic potential energy contour surface illustrations allow one to discern readily the regions in the molecular environment that are attractive or repulsive to an approaching electrophilic group.

A sensitive probe has been developed which makes clearly perceptible one force within a molecule that is important in any discussion of drug interactions in the biophase.

REFERENCES

(1) A. H. Beckett and A. F. Casey, *J. Pharm. Pharmacol.*, **6**, 986 (1954).

(2) A. H. Beckett and J. Walker, *ibid.*, **7**, 1039 (1955).

(3) A. H. Beckett, *ibid.*, **8**, 848 (1956).

(4) A. H. Beckett, A. F. Casey, N. J. Harper, and P. M. Phillips, *ibid.*, **8**, 860 (1956).

(5) A. H. Beckett, A. F. Casey, and N. J. Harper, *ibid.*, **8**, 874 (1956).

(6) A. H. Beckett, in "Progress in Drug Research," vol. 1, E. Jucker, Ed., Birkhauser A. G., Basel, Switzerland, 1959, p. 519.

(7) P. Portoghese, *J. Med. Chem.*, **8**, 609 (1965).

(8) H. H. Jaffe, *Chem. Rev.*, **53**, 191 (1953).
(9) B. Belleau, *J. Med. Chem.*, **7**, 776 (1964).
(10) A. Korolkovas, "Essentials of Molecular Pharmacology," Wiley-Interscience, New York, N.Y., 1970, p. 191.
(11) J. M. Gulland and R. Robinson, *Nature*, **115**, 625 (1925).
(12) L. F. Small, "Chemistry of the Opium Alkaloids," U. S. Government Printing Office, Washington, D.C., 1932.
(13) M. Gates and G. Tschudi, *J. Am. Chem. Soc.*, **74**, 1109 (1952).
(14) G. Stork, *ibid.*, **74**, 768 (1952).
(15) H. Rapoport and J. B. Lavigne, *ibid.*, **75**, 5329 (1953).
(16) H. Rapoport and G. B. Payne, *J. Org. Chem.*, **15**, 1093 (1950).
(17) H. Rapoport and G. B. Payne, *J. Am. Chem. Soc.*, **74**, 2630 (1952).
(18) A. K. Bose, *Chem. Ind.*, **1954**, 130.
(19) J. M. Lindsey and W. H. Barnes, *Acta Crystallogr.*, **8**, 227 (1955).
(20) M. Mackay and D. C. Hodgkin, *J. Chem. Soc.*, **1955**, 3261.
(21) J. Kalvoda, P. Buchschacher, and O. Jeger, *Helv. Chim. Acta*, **38**, 1847 (1955).
(22) L. Gylbert, *Acta Crystallogr.*, **B29**, 1630 (1973).
(23) G. Kartha, F. R. Ahmed, and W. H. Barnes, *ibid.*, **15**, 326 (1962).
(24) H. VanKoningsveld, *Rec. Trav. Chim. Pays-Bas*, **89**, 375 (1970).
(25) G. Kartha, F. R. Ahmed, and W. H. Barnes, *Acta Crystallogr.*, **13**, 525 (1960).
(26) F. R. Ahmed, W. H. Barnes, and L. Masironi, *ibid.*, **16**, 237 (1963).
(27) C. K. Johnson, ORTEP, Report ORNL-3794, Oak Ridge National Laboratories, Oak Ridge, Tenn., 1965.
(28) J. J. Kaufman, E. Kerman, and W. S. Koski, *Int. J. Quantum Chem., Quantum Biol. Symp.*, **1**, 289 (1974).
(29) P. S. Portoghese, *Ann. Rev. Pharmacol.*, **10**, 51 (1970).

ACKNOWLEDGMENTS

Abstracted in part from a dissertation submitted by T. L. Breon to the Graduate School, University of Rhode Island, in partial fulfillment of the Doctor of Philosophy degree requirements.

Potential Hypocholesteremic Derivatives of Styrylacetic Acid II: *cis*- and *trans*-3-Methyl-4-phenyl-3-butenoic Acid Analogs

E. S. STRATFORD *[x], L. M. SMITH [1], and G. W. TOMECKO [1]

Received December 20, 1976, from the *Section of Medicinal Chemistry and Pharmacognosy, School of Pharmacy, University of Connecticut, Storrs, CT 06268.* Accepted for publication April 7, 1977. *Present address: School of Pharmacy, West Virginia University Medical Center, Morgantown, WV 26505.

Abstract □ The synthesis and preliminary biological testing for *in vitro* cholesterol biosynthesis inhibitory activity of 2-indeneacetic acid, 2-methyl-1,2-dihydro-2-naphthoic acid, and their 5- and 7-chloro derivatives, respectively, are described. These compounds were prepared as *trans*- and *cis*-analogs of the known antilipemic agent 3-methyl-4-phenyl-3-butenoic acid. Although both series of compounds showed cholesterol biosynthesis inhibitory properties, chloro substitution enchanced potency only in the *cis*-system. These findings are discussed in terms of a possible relationship between the *cis*-compounds and clofibrate-type antilipemic agents.

Keyphrases □ *cis*- and *trans*-3-Methyl-4-phenyl-3-butenoic acid analogs—synthesized, evaluated for effect on cholesterol biosynthesis in rat liver homogenates □ 2-Indeneacetic acid and 5-chloro derivative—synthesized, evaluated for effect on cholesterol biosynthesis in rat liver homogenates □ 2-Naphthoic acids, substituted—synthesized, evaluated for effect on cholesterol biosynthesis in rat liver homogenates □ Cholesterol biosynthesis—effect of 2-indeneacetic acid and substituted 2-naphthoic acids and chloro derivatives, rat liver homogenates □ Structure–activity relationships—effects of 2-indeneacetic acid and substituted 2-naphthoic acids and chloro derivatives on cholesterol biosynthesis in rat liver homogenates

In continuing investigations (1) of the structure–activity relationships for cholesterol biosynthesis inhibition by compounds related to 3-methyl-4-phenyl-3-butenoic acid (benzalbutyric acid) (I), the influence of the double bond stereochemistry on biological activity was examined. Compound I exists in the (*E*)-configuration (2), but it has not been established that this configuration represents the optimal geometry for biological action.

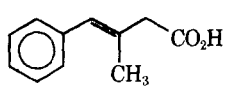

I

In an initial attempt to obtain information relating to this question, the synthesis of indeneacetic acids (II*a* and II*b*) and dihydronaphthoic acids (III*a* and III*b*) as *trans*- and *cis*-congeners of the parent system was undertaken. Although these compounds also differ with respect to the α-carbon substitution pattern, they were believed to be useful as initial probes. This report describes their synthesis and preliminary *in vitro* testing.

DISCUSSION

The synthesis of II*a* and II*b* is outlined in Scheme I (also see *Experimental*). Although the mixture of hydroxy acid X and lactone XI could be converted entirely into the lactone by prolonged stirring in dilute sulfuric acid, for preparative runs it was more convenient to use the mixture directly for the subsequent reaction.

Synthesis of the *cis*-analogs was accomplished according to the sequence outlined in Scheme II.

Interestingly, if the methanolysis of XVIII or the mixture of XVII and XVIII was terminated after refluxing for only 4 hr and the product was saponified, methoxy acid XX could be obtained from the reaction product mixture. This finding is in agreement with the suggestion advanced previously (3) that methanolyses of similar tricyclic lactones, including XI, proceed *via* an intermediate benzyl carbonium ion. This conclusion was based largely on the fact that methanolysis of γ-phenylbutyrolactone afforded methyl 4-methoxy-4-phenylbutanoate instead of the anticipated

[1] Undergraduate research participant.

(8) H. H. Jaffe, *Chem. Rev.*, **53**, 191 (1953).
(9) B. Belleau, *J. Med. Chem.*, **7**, 776 (1964).
(10) A. Korolkovas, "Essentials of Molecular Pharmacology," Wiley-Interscience, New York, N.Y., 1970, p. 191.
(11) J. M. Gulland and R. Robinson, *Nature*, **115**, 625 (1925).
(12) L. F. Small, "Chemistry of the Opium Alkaloids," U. S. Government Printing Office, Washington, D.C., 1932.
(13) M. Gates and G. Tschudi, *J. Am. Chem. Soc.*, **74**, 1109 (1952).
(14) G. Stork, *ibid.*, **74**, 768 (1952).
(15) H. Rapoport and J. B. Lavigne, *ibid.*, **75**, 5329 (1953).
(16) H. Rapoport and G. B. Payne, *J. Org. Chem.*, **15**, 1093 (1950).
(17) H. Rapoport and G. B. Payne, *J. Am. Chem. Soc.*, **74**, 2630 (1952).
(18) A. K. Bose, *Chem. Ind.*, **1954**, 130.
(19) J. M. Lindsey and W. H. Barnes, *Acta Crystallogr.*, **8**, 227 (1955).
(20) M. Mackay and D. C. Hodgkin, *J. Chem. Soc.*, **1955**, 3261.
(21) J. Kalvoda, P. Buchschacher, and O. Jeger, *Helv. Chim. Acta*, **38**, 1847 (1955).
(22) L. Gylbert, *Acta Crystallogr.*, **B29**, 1630 (1973).
(23) G. Kartha, F. R. Ahmed, and W. H. Barnes, *ibid.*, **15**, 326 (1962).
(24) H. VanKoningsveld, *Rec. Trav. Chim. Pays-Bas*, **89**, 375 (1970).
(25) G. Kartha, F. R. Ahmed, and W. H. Barnes, *Acta Crystallogr.*, **13**, 525 (1960).
(26) F. R. Ahmed, W. H. Barnes, and L. Masironi, *ibid.*, **16**, 237 (1963).
(27) C. K. Johnson, ORTEP, Report ORNL-3794, Oak Ridge National Laboratories, Oak Ridge, Tenn., 1965.
(28) J. J. Kaufman, E. Kerman, and W. S. Koski, *Int. J. Quantum Chem., Quantum Biol. Symp.*, **1**, 289 (1974).
(29) P. S. Portoghese, *Ann. Rev. Pharmacol.*, **10**, 51 (1970).

ACKNOWLEDGMENTS

Abstracted in part from a dissertation submitted by T. L. Breon to the Graduate School, University of Rhode Island, in partial fulfillment of the Doctor of Philosophy degree requirements.

Potential Hypocholesteremic Derivatives of Styrylacetic Acid II: *cis*- and *trans*-3-Methyl-4-phenyl-3-butenoic Acid Analogs

E. S. STRATFORD *[x], L. M. SMITH [1], and G. W. TOMECKO [1]

Received December 20, 1976, from the *Section of Medicinal Chemistry and Pharmacognosy, School of Pharmacy, University of Connecticut, Storrs, CT 06268.* Accepted for publication April 7, 1977. *Present address: School of Pharmacy, West Virginia University Medical Center, Morgantown, WV 26505.

Abstract □ The synthesis and preliminary biological testing for *in vitro* cholesterol biosynthesis inhibitory activity of 2-indeneacetic acid, 2-methyl-1,2-dihydro-2-naphthoic acid, and their 5- and 7-chloro derivatives, respectively, are described. These compounds were prepared as *trans*- and *cis*-analogs of the known antilipemic agent 3-methyl-4-phenyl-3-butenoic acid. Although both series of compounds showed cholesterol biosynthesis inhibitory properties, chloro substitution enchanced potency only in the *cis*-system. These findings are discussed in terms of a possible relationship between the *cis*-compounds and clofibrate-type antilipemic agents.

Keyphrases □ *cis*- and *trans*-3-Methyl-4-phenyl-3-butenoic acid analogs—synthesized, evaluated for effect on cholesterol biosynthesis in rat liver homogenates □ 2-Indeneacetic acid and 5-chloro derivative—synthesized, evaluated for effect on cholesterol biosynthesis in rat liver homogenates □ 2-Naphthoic acids, substituted—synthesized, evaluated for effect on cholesterol biosynthesis in rat liver homogenates □ Cholesterol biosynthesis—effect of 2-indeneacetic acid and substituted 2-naphthoic acids and chloro derivatives, rat liver homogenates □ Structure–activity relationships—effects of 2-indeneacetic acid and substituted 2-naphthoic acids and chloro derivatives on cholesterol biosynthesis in rat liver homogenates

In continuing investigations (1) of the structure–activity relationships for cholesterol biosynthesis inhibition by compounds related to 3-methyl-4-phenyl-3-butenoic acid (benzalbutyric acid) (I), the influence of the double bond stereochemistry on biological activity was examined. Compound I exists in the (*E*)-configuration (2), but it has not been established that this configuration represents the optimal geometry for biological action.

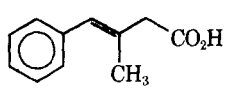

I

In an initial attempt to obtain information relating to this question, the synthesis of indeneacetic acids (II*a* and II*b*) and dihydronaphthoic acids (III*a* and III*b*) as *trans*- and *cis*-congeners of the parent system was undertaken. Although these compounds also differ with respect to the α-carbon substitution pattern, they were believed to be useful as initial probes. This report describes their synthesis and preliminary *in vitro* testing.

DISCUSSION

The synthesis of II*a* and II*b* is outlined in Scheme I (also see *Experimental*). Although the mixture of hydroxy acid X and lactone XI could be converted entirely into the lactone by prolonged stirring in dilute sulfuric acid, for preparative runs it was more convenient to use the mixture directly for the subsequent reaction.

Synthesis of the *cis*-analogs was accomplished according to the sequence outlined in Scheme II.

Interestingly, if the methanolysis of XVIII or the mixture of XVII and XVIII was terminated after refluxing for only 4 hr and the product was saponified, methoxy acid XX could be obtained from the reaction product mixture. This finding is in agreement with the suggestion advanced previously (3) that methanolyses of similar tricyclic lactones, including XI, proceed *via* an intermediate benzyl carbonium ion. This conclusion was based largely on the fact that methanolysis of γ-phenylbutyrolactone afforded methyl 4-methoxy-4-phenylbutanoate instead of the anticipated

[1] Undergraduate research participant.

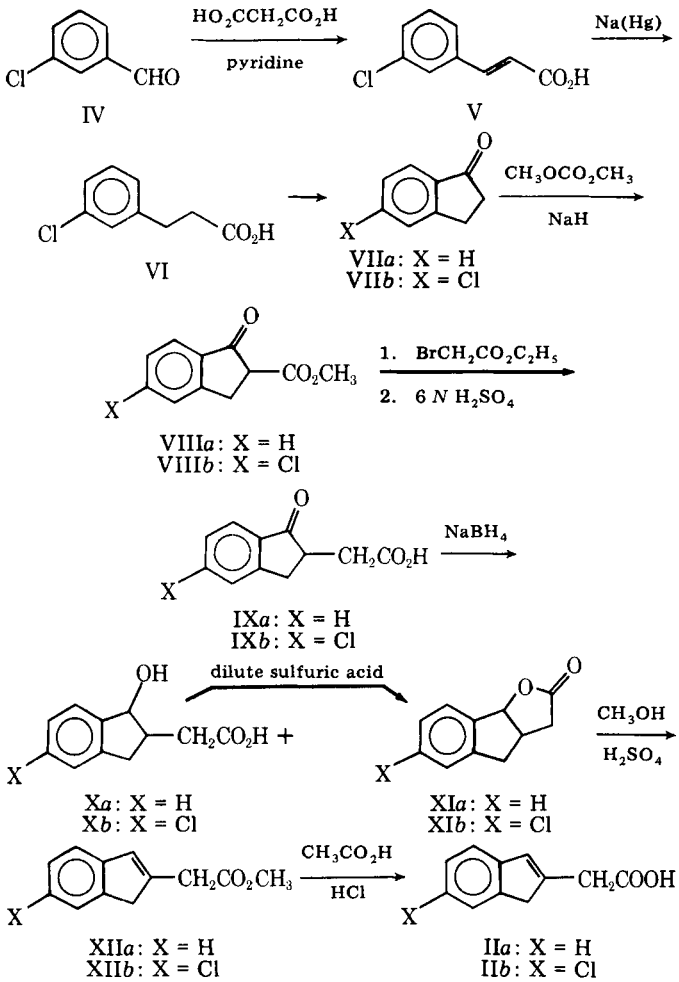

Scheme I

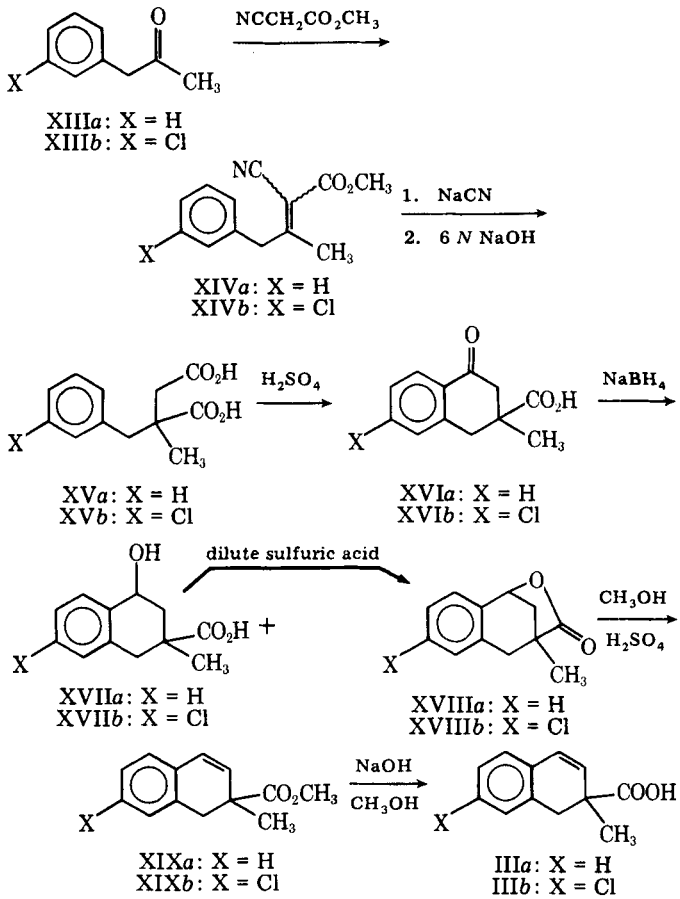

Scheme II

β,γ-unsaturated ester. This report (3) suggested that the methoxy compound was produced because substitution by methoxide occurred in preference to elimination, as in the tricyclic lactones. The results obtained in the present case, however, imply that the γ-methoxy esters either are intermediates in the formation of the β,γ-unsaturated esters or, more likely, are in equilibrium with the benzyl carbonium ion since none of the methoxy acid was detected when the methanolysis was allowed to continue for 24 hr.

EXPERIMENTAL[2]

2-Indeneacetic Acid (IIa)—Compound II*a* was prepared as described previously (3), affording slightly yellow flakes from 20% aqueous acetic acid, mp 122–123° [lit. (3) mp 124–125°].

Anal.—Calc. for $C_{11}H_{10}O_2$: C, 75.84; H, 5.79. Found: C, 75.79; H, 5.70.

5-Chloro-1-indanone (VII*b*)—Compound VII*b* was prepared as described previously (4) from *m*-chlorobenzaldehyde (5) and sublimed at 80°, affording white crystals, mp 72–88°, apparently as a mixture of keto and enol forms since the material appeared chromatographically (TLC) and spectroscopically pure. Crystallization from ethyl acetate afforded colorless crystals, mp 93–95° [lit. (4) mp 100°].

Anal.—Calc. for C_9H_7ClO: C, 64.88; H, 4.23; Cl, 21.28. Found: C, 64.66; H, 4.32; Cl, 21.56.

5-Chloro-2-methoxycarbonyl-1-indanone (VIII*b*)—According to the method of House and Hudson (6), a solution of 8.0 g (48 mmoles) of VII*b* in 65 ml of sodium-dried benzene was added dropwise over 2 hr to a mixture of 34 ml of dimethyl carbonate and 3 equivalents of sodium hydride (6.91 g of a 50% dispersion in mineral oil) in 85 ml of benzene at 85°. Heating was continued for 2 hr after the complete addition. The mixture was then cooled at 15° and acidified with 15 ml of acetic acid.

The resulting mixture was poured onto ice–hydrochloric acid, and the organic phase was washed successively with saturated sodium bicarbonate and brine and then dried. The solvent was removed *in vacuo*, affording a dark-green oil. The oil was distilled with the aid of a heat lamp to prevent crystallization in the distilling head. The distillate was recrystallized from hot hexane after treatment with charcoal, affording 5.2 g (48%) of VIII*b* as white crystals, mp 83–84°.

Anal.—Calc. for $C_{11}H_9ClO_3$: C, 58.81; H, 4.04; Cl, 15.78. Found: C, 58.37; H, 4.09; Cl, 15.41.

5-Chloro-1-indanone-2-acetic Acid (IX*b*)—A mixture of 6.0 g (26.7 mmoles) of VIII*b*, 5.5 g (33 mmoles) of ethyl bromoacetate, and 3.8 g (37.6 mmoles) of triethylamine in 300 ml of sodium-dried ether was heated at reflux for 24 hr. The solvent was removed *in vacuo*, and 375 ml of 6 *N* H_2SO_4 was added. The resulting mixture was heated at reflux overnight. The reaction mixture was allowed to cool and was then extracted with ether.

The ether solution was extracted several times with saturated sodium bicarbonate solution, and the combined bicarbonate extracts were acidified with dilute sulfuric acid. The precipitate was isolated and dried in a heated vacuum desiccator, affording 4.6 g (77%) of crude IX*b* as a

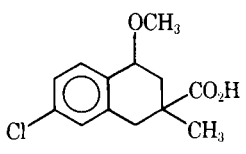

XX

[2] Melting points were determined with a Thomas-Hoover apparatus and are uncorrected. Elemental analyses were performed by Galbraith Laboratories, Knoxville, Tenn., or by Baron Consulting Co., Orange, Conn. IR spectra were recorded on a Beckman Acculab 3 spectrophotometer. NMR spectra were obtained with a Hitachi Perkin-Elmer model R-24 spectrometer, using tetramethylsilane as the internal standard. In all cases, the spectra obtained were consistent with proposed structures.

For biological evaluations, ^{14}C-counting was performed with a Packard Tri-Carb liquid scintillation spectrometer, model 3375. Where unspecified, organic solutions were dried prior to evaporation of the solvent with either anhydrous sodium sulfate or anhydrous magnesium sulfate. Brine refers to a saturated solution of sodium chloride.

colorless solid, mp 158–161°. Recrystallization from ethyl acetate afforded an analytical sample, mp 162–163°.

Anal.—Calc. for $C_{11}H_9ClO_3$: C, 58.81; H, 4.04; Cl, 15.78. Found: C, 58.40; H, 4.22; Cl, 15.94.

5-Chloro-1-hydroxy-2-indaneacetic Acid Lactone (XI*b*)—To a solution of IX*b* (2.5 g, 11.1 mmoles) in 90 ml of 2 *N* NaOH was added 0.41 g (11.1 mmoles) of sodium borohydride. The solution was allowed to stir at room temperature for 24 hr and was then acidified with 4 *N* H_2SO_4.

The resulting mixture was extracted with ether, the organic phase was dried, and the solvent was removed *in vacuo*, affording 2.19 g of white solid as a mixture of X*b* and XI*b*. The mixture was then stirred in 200 ml of 4 *N* H_2SO_4 for 3 days, and the solid was filtered and dried *in vacuo*, affording 2.04 g (89%) of XI*b*, mp 111–114°. Recrystallization from heptane–ethyl acetate afforded an analytical sample, mp 119.5–121°.

Anal.—Calc. for $C_{11}H_9ClO_2$: C, 63.32; H, 4.35; Cl, 16.99. Found: C, 63.06; H, 4.45; Cl, 17.00.

5-Chloro-2-indeneacetic Acid (II*b*)—A solution of XI*b* (1.62 g, 7.77 mmoles) in 50 ml of methanol containing 1 ml of concentrated sulfuric acid was heated at reflux for 18 hr. The cooled solution was diluted with 100 ml of ether and washed with 100 ml of distilled water. The aqueous layer was extracted with 100 ml of ether, and the combined organic layers were washed successively with 100 ml of saturated sodium bicarbonate and brine.

The resulting solution was dried, and the solvent was removed *in vacuo*, affording a yellow-orange oil. The oil was dissolved in 100 ml of acetic acid–concentrated hydrochloric acid (4:1) and heated on a steam bath for 2 hr. The cooled reaction mixture was poured onto 300 g of ice. The precipitate was isolated and dried, affording 1.16 g (72%) of crude product, mp 129–132°. Recrystallization from heptane–ethyl acetate afforded pure II*b*, mp 134.5–136°.

Anal.—Calc. for $C_{11}H_9ClO_2$: C, 63.32; H, 4.35; Cl, 16.99. Found: C, 63.47; H, 4.28; Cl, 16.85.

2-Benzyl-2-methylsuccinic Acid (XV*a*)—Compound XV*a* was prepared as described by Foucaud (7), affording a white powder, mp 140–142° [lit. (7) mp 144°].

Anal.—Calc. for $C_{12}H_{14}O_4$: C, 64.85; H, 6.35. Found: C, 65.24; H, 6.43.

2-Methyl-4-oxo-1,2,3,4-tetrahydro-2-naphthoic Acid (XVI*a*)—A mixture of 5.8 g (26.1 mmoles) of diacid XV*a* and 50 ml of concentrated sulfuric acid was stirred at 45–50° for 4 hr. The cooled mixture was poured onto ice (300 g) and extracted with ether (3 × 100 ml). The combined ether extracts were washed with brine and dried, and the solvent was evaporated. Recrystallization of the solid residue from ethyl acetate afforded 4.1 g (78%) of XVI*a* as white crystals, mp 163–166°. A further recrystallization afforded an analytical sample, mp 172.5–174.5°.

Anal.—Calc. for $C_{12}H_{12}O_3$: C, 70.57; H, 5.92. Found: C, 70.56; H, 6.08.

2-Methyl-1,2-dihydro-2-naphthoic Acid (III*a*)—To a solution of XVI*a* (20.4 g, 0.1 mole) in 300 ml of 2 *N* NaOH was added 3.8 g (0.1 mole) of sodium borohydride, and the solution was allowed to stir at room temperature. After 24 hr, the solution was acidified by dropwise addition of 4 *N* H_2SO_4 and was then extracted with ether. The ether extract was washed with brine and dried, and the solvent was removed *in vacuo*, affording 19.5 g of a mixture of XVII*a* and XVIII*a* in an undetermined ratio. Without further purification, the mixture was dissolved in 500 ml of methanol, and 5 ml of concentrated sulfuric acid was added.

The resulting solution was heated at reflux for 30 hr, cooled to room temperature, and concentrated *in vacuo* to about 60% of the original volume. The concentrate was then partitioned between 250 ml each of ether and distilled water. The aqueous phase was removed and extracted with 3 × 150 ml of ether, and the combined organic layers were washed with brine and dried. Evaporation of the solvent afforded 20 g of crude XIX*a* as a yellow-orange liquid. Although the procedure was not performed routinely, the hydroxy acid XVII*a* could be isolated from the crude mixture by crystallization from ethyl acetate as colorless crystals, mp 181–183°.

Anal.—Calc. for $C_{12}H_{14}O_3$: C, 69.88; H, 6.84. Found: C, 69.75; H, 6.86.

Lactone XVIII*a* was obtained by evaporating the filtrate, redissolving in ether, and washing with saturated sodium bicarbonate solution. The remaining ether solution was dried, and the solvent was evaporated. Recrystallization of the residue from hexane afforded pure XVIII*a*, mp 86.5–87.5°.

Anal.—Calc. for $C_{12}H_{12}O_2$: C, 76.57; H, 6.43. Found: C, 76.37; H, 6.35.

Crude XIX*a* was dissolved in 450 ml of methanol, and 16.5 g (0.25 mole) of 85% potassium hydroxide was added. The solution was refluxed for 12 hr, cooled, concentrated *in vacuo* to about 100 ml, and diluted with 200 ml of distilled water. The resulting aqueous solution was washed with 3 × 100 ml of ether and acidified with 4 *N* H_2SO_4. The resulting mixture was extracted with 3 × 100 ml of ether, and the combined ether extracts were washed with brine and dried. The solvent was then removed *in vacuo*, affording 16.8 g (89% overall from XVI*a*) of crude III*a* as a slightly yellow solid, mp 89–92°. Recrystallization from hexane afforded pure III*a*, mp 93–94.5°.

Anal.—Calc. for $C_{12}H_{12}O_2$: C, 76.57; H, 6.43. Found: C, 76.72; H, 6.51.

4-Methoxy-2-methyl-1,2,3,4-tetrahydro-2-naphthoic Acid (XX)—A solution of 5.0 g of XVIII*a* in 50 ml of methanol was refluxed for 4 hr and worked up as described above to give 5.1 g of a cloudy liquid. Distillation (105–115°/0.6 mm) afforded 4.7 g of an impure oil. A 3.0-g portion of this material was refluxed for 2.5 hr in a mixture of 15 ml of methanol and 15 ml of 2 *N* NaOH. Workup gave 2.7 g of a viscous oil, which was dissolved in hot hexane. The solution was allowed to stand at room temperature overnight, and 0.5 g of a white solid, mp 142–145°, was isolated. A further recrystallization from hexane afforded pure XX, mp 145–147°.

Anal.—Calc. for $C_{13}H_{16}O_3$: C, 70.89; H, 7.32. Found: C, 70.71; H, 7.48.

Methyl 2-Cyano-4-(3′-chlorophenyl)-3-methyl-2-butenoate (XIV*b*)—A mixture of 26.0 g (0.154 mole) of *m*-chlorophenylacetone (8), 19.1 g (0.193 mole, 1.25 equivalents) of methyl cyanoacetate, 0.5 ml of piperidine, and 0.5 ml of acetic acid in 100 ml of sodium-dried benzene was refluxed for 18 hr; water was collected in a Dean–Stark trap. The reaction mixture was allowed to cool to room temperature; it was then diluted with 200 ml of ether and washed successively with 100-ml portions of distilled water, saturated sodium bicarbonate, brine, 3 *N* HCl, and brine.

The resulting solution was dried, and the solvent was removed *in vacuo*. Distillation of the residue afforded 32.6 g (85%) of XIV*b* as a slightly yellow liquid, bp 138–148°/0.3 mm. This liquid was shown to be approximately a 1:1 mixture of (*E*)- and (*Z*)-isomers by NMR analysis, with the methyl groups appearing as sharp singlets at δ 2.14 and 2.25 ppm, the methoxyl protons appearing at δ 3.80 and 3.83 ppm, the methylene protons appearing at δ 3.83 (shoulder on methoxyl resonance) and 4.13 ppm, and the aromatic protons appearing as a multiplet centered at δ 7.18 ppm. No attempts were made to purify the material further or to separate the isomers.

2-(3′-Chlorobenzyl)-2-methylsuccinic Acid (XV*b*)—A solution of 5.0 g (0.020 mole) of XIV*b* in 50 ml of absolute ethanol was warmed to about 60° and 3.4 ml of 50% aqueous potassium cyanide was added. The mixture was heated at reflux for 18 hr, and 50 ml of 6 *N* NaOH was added. The ethanol was removed by distillation, and the resulting mixture was refluxed an additional 12 hr. The cooled reaction mixture was poured into ice–sulfuric acid (300 g, 30 ml) and extracted with ether.

The organic solution was then washed with brine and dried. The solvent was then removed *in vacuo*, leaving a viscous oil which crystallized from benzene–heptane, affording 4.6 g (89%) of crude XV*b*, mp 138–143°. Recrystallization from benzene afforded white crystals, mp 144–146°.

Anal.—Calc. for $C_{12}H_{13}ClO_4$: C, 56.15; H, 5.10; Cl, 13.81. Found: C, 55.80; H, 4.90; Cl, 14.14.

7-Chloro-2-methyl-4-oxo-1,2,3,4-tetrahydro-2-naphthoic Acid (XVI*b*)—A solution of 5.80 g (22.6 mmoles) of XV*b* in 60 ml of concentrated sulfuric acid was stirred at 50° for 3 hr. The resulting solution was poured onto ice (300 g); the precipitate was filtered and dried, affording 4.6 g (85%) of crude product, mp 158–162°. Recrystallization from ethyl acetate afforded pure XVI*b* as colorless crystals, mp 163–165°.

Anal.—Calc. for $C_{12}H_{11}ClO_3$: C, 60.39; H, 4.65; Cl, 14.86. Found: C, 60.29; H, 4.58; Cl, 15.04.

7-Chloro-4-hydroxy-2-methyl-1,2,3,4-tetrahydro-2-naphthoic Acid Lactone (XVIII*b*)—To a solution of 1.07 g (4.5 mmoles) of XVI*b* in 50 ml of 2 *N* NaOH was added 0.17 g (4.5 mmoles) of sodium borohydride. After 24 hr, the solution was acidified and extracted with ether (3 × 50 ml). The combined organic layers were washed with brine and dried, and the solvent was removed *in vacuo*. The resulting solid was stirred for 4 days in 4 *N* H_2SO_4 at room temperature, filtered, and dried, affording 0.93 g (93%) of the crude lactone, mp 102–105°. Recrystallization from ethyl acetate afforded pure XVI*b*, mp 105–106°.

Anal.—Calc. for $C_{12}H_{11}ClO_2$: C, 64.73; H, 4.98. Found: C, 64.43; H, 4.63.

7-Chloro-2-methyl-1,2-dihydro-2-naphthoic Acid (III*b*)—A solution of 2.0 g (9.0 mmoles) of XVIII*b* in 50 ml of methanol containing 1 ml of concentrated sulfuric acid was heated at reflux for 18 hr. The cooled solution was diluted with 100 ml of ether and washed with 100 ml

Table I—Effect of Compounds on Incorporation of 2-^{14}C-Acetate into Neutral Sterols by Rat Liver Homogenate Preparations

Compound	Concentration, m*M*	Percent Incorporation[a]
I	10	6.7 ± 0.51[c]
	1	40.9 ± 0.95
	0.5	54.4 ± 2.00
	0.1	72.7 ± 9.90
II*a*	10	8.1 ± 1.85
	5	18.9 ± 1.65
	1	64.1 ± 2.03
	0.5	75.0 ± 2.08
II*b*	10	1.8 ± 0.57
	5	7.8 ± 4.06
	1	60.3 ± 1.01
	0.5	85.9 ± 1.34
III*a*	10	20.8 ± 2.62
	5	54.3 ± 2.11
	1	95.9 ± 6.72
	0.5	106.9 ± 3.72
III*b*	10	0.7 ± 0.17
	5	6.2 ± 3.35
	1	57.7 ± 6.91
	0.5	66.8 ± 2.91

[a] Relative to incorporation in controls being defined as 100%. [b] Data taken from Ref. 1. [c] Standard error of mean of three experiments.

of distilled water. The aqueous layer was extracted with 100 ml of ether, and the combined organic layers were washed with 100-ml portions of saturated sodium bicarbonate and brine and dried. The solvent was evaporated *in vacuo*.

The resulting oil was dissolved in 50 ml of methanol and 1.2 g of potassium hydroxide. The solution was allowed to reflux overnight and acidified with 100 ml of 2 *N* H_2SO_4. The mixture was then extracted with 2 × 100 ml of ether. The combined extracts were washed with brine and dried. The solvent was then removed *in vacuo*, affording 1.74 g (87%) of crude product, mp 132–135°. Recrystallization from heptane gave pure III*b*, mp 138–140°.

Anal.—Calc. for $C_{12}H_{11}ClO_2$: C, 64.73; H, 4.98; Cl, 15.92. Found: C, 64.52; H, 5.30; Cl, 16.20.

RESULTS

Compounds II*a*, II*b*, III*a*, and III*b* were examined for their ability to inhibit the incorporation of 2-^{14}C-acetate into nonsaponifiable sterols by rat liver homogenates using the method described previously (1) (Table I).

In the unsubstituted compounds, the *trans*-analog II*a* is considerably more potent than the *cis*-III*a*, as was anticipated. However, the effect of *para*-substitution in the two systems is quite different. Incorporation of the chloro group in the *trans*-system, on the other hand, produced a marked increase in potency.

The variable response observed for the two systems cannot be accounted for on the basis of available information since several alternative explanations are possible. From among those possible, however, certain rationalizations readily lend themselves to further examination by extension of the series of compounds employed in this study.

On the basis of earlier studies with acyclic analogs of I (1), it was anticipated that chloro substitution *para* to the point of attachment of the double bond would enhance potency, especially in the *trans*-system, which is structurally more closely related to the acyclic analogs. However, this effect was demonstrated only for compounds in which the carbon alpha to the carboxyl group is tetrasubstituted. Previously, it was suggested that the apparent reduction in potency resulting from *p*-chloro substitution in I (9) might be due to contamination of material with the less active β,γ-unsaturated isomer. In view of the results reported herein, such an explanation is less attractive. These observations would, however, be consistent with the suggestion that the mode of action depends on the substitution pattern at the α-carbon atom. The synthesis of additional analogs that should help clarify the situation is currently in progress.

The difference in the effect of substitution in the two systems also allows an interesting interpretation on the basis of geometrical properties. One original goal of this research program was to obtain information that could be used in relation to the speculation that I and 2-(4′-chlorophenoxy)-2-methylpropanoic acid (XXI), the active metabolite of clofibrate, might be affecting cholesterol biosynthesis by similar mechanisms. Examination of Dreiding models of II*a*, II*b*, III*a*, III*b*, and XXI reveals that only the *cis*-compounds can adopt conformations in which the distance between the center of the aromatic ring and the carboxyl group is similar to that possible for XXI. The interatomic distances between the centroid of the aromatic ring and the carboxyl carbon as measured using Dreiding models fall in the possible ranges of 3.5–4.9 Å for XXI, 4.2–5.3 Å for III*a* and III*b*, and 5.8 Å for II*a* and II*b*. Furthermore, it is known that removal of the chloro substituent in XXI and its analogs lowers their potency as inhibitors of cholesterol biosynthesis (10, 11). It seems possible, therefore, that III*a* and III*b* may be interacting with the same receptor site(s) as XXI. The additional analogs currently being prepared should provide additional information for assessing these and other possible explanations.

REFERENCES

(1) E. S. Stratford, *J. Med. Chem.*, **18**, 242 (1975).

(2) S. G. Boots, M. R. Boots, and K. E. Guyer, *J. Pharm. Sci.*, **60**, 614 (1971).

(3) S. K. Dasgupta, S. R. Ghosh, and A. S. Sarma, *Tetrahedron Lett.*, **1969**, 2331.

(4) L. Novak and M. Protiva, *Coll. Czech. Chem. Commun.*, **27**, 2413 (1962).

(5) K. C. Pandya and R. B. Pandya, *Proc. Indian Acad. Sci.*, **14A**, 112 (1941).

(6) H. O. House and C. B. Hudson, *J. Org. Chem.*, **35**, 647 (1970).

(7) A. Foucaud, *Bull. Soc. Chim. Fr.*, 873 (1963).

(8) K. L. Nelson, J. C. Robertson, and J. J. Duvall, *J. Am. Chem. Soc.*, **86**, 684 (1964).

(9) U. Valcavi and L. Gaudenzi, *Farmaco, Ed. Sci.*, **16**, 571 (1961).

(10) D. T. Witiak, T. C.-L. Ho, R. E. Hackney, and W. E. Connor, *J. Med. Chem.*, **11**, 1086 (1968).

(11) D. T. Witiak, E. S. Stratford, R. Nazareth, G. Wagner, and D. R. Feller, *ibid.*, **14**, 758 (1971).

ACKNOWLEDGMENTS

Supported by Grant HL 14950 from the National Institutes of Health.

GLC Determination of Warfarin in Human Plasma

S. HANNA ˣ, M. ROSEN, P. EISENBERGER, L. RASERO, and L. LACHMAN

Received April 19, 1976, from the *Quality Control Department, Endo Laboratories, Inc., Garden City, NY 11530 (Subsidiary of E. I. du Pont de Nemours & Co., Inc.).* Accepted for publication April 8, 1977.

Abstract □ A specific and quantitative GLC method for warfarin in human plasma is described. The procedure uses papaverine as the internal standard and involves a dichloroethane extraction of the acidified specimen. The organic extract is evaporated, and the evaporated extract is dissolved in 50 μl of chloroform. Aliquots of 2–3 μl are injected into a gas chromatograph equipped with a flame-ionization detector. The sensitivity of the method is such that 0.3 μg of intact warfarin can be detected in 1 ml of plasma. Statistical analyses indicate a recovery of 97.26 ± 1.89% *SD*. The procedure was successfully applied to plasma drug level studies in humans.

Keyphrases □ Warfarin—GLC analysis in human plasma □ GLC—analysis, warfarin in human plasma □ Anticoagulants—warfarin, GLC analysis in human plasma

It has been more than 30 years since the oral anticoagulant warfarin was first used medically (1). Because of the numerous disease states in which warfarin is potentially useful, drug interactions appear to occur more frequently with it than with any other pharmacological class of drugs (2).

Warfarin measurement in human blood facilitated many pharmacokinetic and bioavailability studies. Analysis of warfarin in human plasma by spectrophotometric (3–10), fluorometric (11, 12), and TLC combined with spectrophotometric or fluorometric (13–19) techniques were described. Recently, GLC methods using warfarin methyl or trimethylsilyl ester, acetate, trichloroacetate, trifluoroacetate, and pentafluorobenzyl derivatives were reported (20–23). A high-pressure liquid chromatographic procedure also was used for the quantitative estimation of warfarin in human plasma (24). These methods are complex and lengthy or require large amounts of plasma samples.

This paper describes a relatively simple, easily reproducible, sensitive, and specific GLC method that eliminates the need for derivatization or special instrumentation.

EXPERIMENTAL

Reagents and Materials—Warfarin[1] and papaverine[2] were used as supplied. Spectral grade chloroform[3], analytical reagent grade sulfuric acid[4] (1 *N*), dichloroethane[4], and vinyl methyl silicone[5] on 80–100-mesh Gas Chrom WHP[6] were employed.

Instrumentation—A gas chromatograph[7] equipped with a flame-ionization detector was used. The column was a spiral glass tube (1.8 m × 0.25 cm i.d.) packed with 3.8% (w/w) vinyl methyl silicone on 80–100-mesh Gas Chrom WHP. The column was conditioned by being maintained at 275° for 12 hr with helium gas at a flow rate of 15 ml/min.

The injection port, detector, and oven temperatures were maintained isothermally at 300, 300, and 270°, respectively; helium as a carrier gas was maintained at a flow rate of 60 ml/min. Hydrogen and compressed air flow rates were adjusted to give maximum response. Chromatograms were recorded on a 1-mv recorder[8].

Table I—Recovery of Warfarin after *In Vitro* Addition to 5 ml of Human Plasma

Warfarin Added, μg	Warfarin Added per Milliliter of Blank Plasma, μg	Warfarin Recovered per Milliliter of Blank Plasma, μg	Average Recovery[a]	*SD*, %
1.50	0.300	0.2907	96.90	±0.678
3.0	0.600	0.5844	97.40	±0.919
5.0	1.00	0.9953	99.53	±0.674
10.0	2.00	1.9443	97.21	±0.680
		Mean	97.26	±1.89

[a] Mean of five samples.

Determination of Warfarin in Human Plasma—Throughout the procedure, scrupulously clean glassware was used; the glassware had been washed successively with hydrochloric acid, water, and ethanol, carefully dried, rinsed with dichloroethane, and then dried.

A 2-ml plasma sample (spiked or from dosed volunteers) was acidified with a few drops of 1 *N* H_2SO_4 to pH 1. The sample was then extracted with 3 × 5 ml of dichloroethane. The combined dichloroethane extracts were filtered through a dichloroethane-wetted glass wool pledget into a centrifuge tube containing 5.0 ml of a 5-μg/ml solution of papaverine in dichloroethane as the internal standard. The organic solvent was evaporated to dryness under a gentle stream of dry nitrogen over a steam bath.

The walls of the centrifuge tube were washed down with 1 ml of dichloroethane and evaporated to dryness with nitrogen over a steam bath. The tube was allowed to cool to room temperature, and the residue was dissolved in 50 μl of chloroform by mixing for 30 sec. A 2–3-μl aliquot was injected into the gas chromatograph.

Plasma Level Studies—All subjects[9] were between the ages of 21 and 50 years and ranged in body weight from 65 to 90 kg and in height from

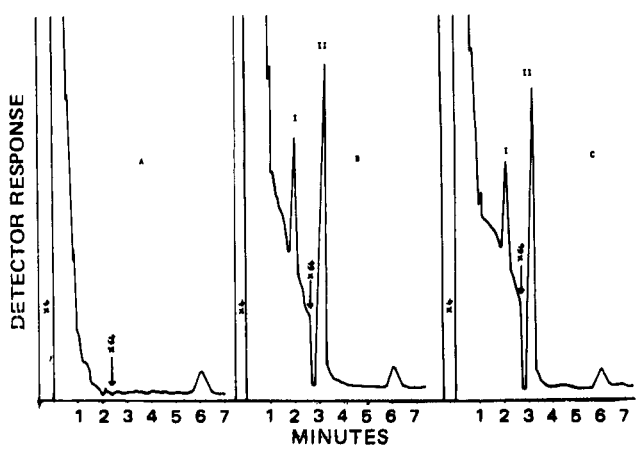

Figure 1—*Chromatograms of human plasma extracts. Key: A, control plasma; B, plasma containing 3 μg of warfarin/ml and 30 μg of papaverine/ml; and C, plasma from a human volunteer who had been given 15 mg of warfarin sodium, 2nd-hr plasma sample. Peaks I and II are peaks of warfarin and papaverine, respectively.*

[1] USP reference standard.
[2] Endo Laboratories, Garden City, N.Y.
[3] Burdick & Jackson Laboratories, Muskegon, Mich.
[4] J. T. Baker Chemical Co., Phillipsburg, N.J.
[5] UCW-98, Applied Science Laboratories, State College, Pa.
[6] Applied Science Laboratories, State College, Pa.
[7] Model 3920, Perkin-Elmer, Norwalk, Conn.
[8] Model 690, Perkin-Elmer, Norwalk, Conn.
[9] Informed written consent was obtained from each of the normal, healthy, male Caucasian volunteers prior to participation.

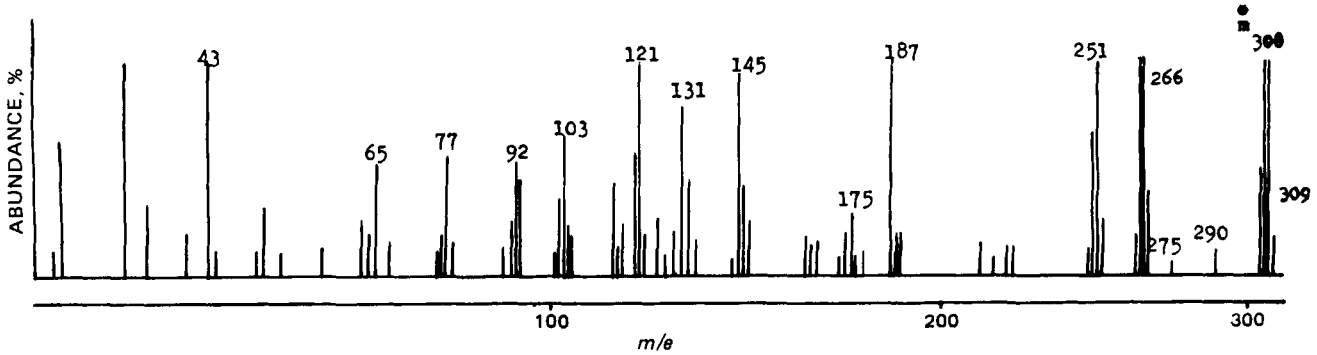

Figure 2—*GLC–mass spectrum of warfarin (normalized).*

1.5 to 1.9 m. Each subject had a drug history taken, and a physical examination was given which included measurement of blood pressure, pulse, and respiration rates. Before and after the study, adequate clinical pathological screening including hematology, blood chemistry, and urinalysis was performed. Seven subjects were selected who had all parameters in the normal range.

All subjects received no medication for 7 days preceding initiation of the studies and only the prescribed medication during the study. Subjects were fasted overnight with water *ad libitum* (at least 12 hr predosing) and for 4 hr after drug administration. Then a standard light meal was eaten. Each subject swallowed three whole 5-mg crystalline warfarin sodium[10] tablets with 200–500 ml of water.

Blood samples of 30 ml were withdrawn from a forearm vein into heparinized evacuated tubes[11] at zero time and at 1, 2, 4, 6, 8, 12, 48, 72, and 96 hr after dosing. The blood samples were centrifuged[12] at 2000 rpm for 10 min, and the plasma was transferred to another tube before being stored at −20°.

Calculations—Peak height ratios were calculated by dividing the height of the peak due to warfarin by that due to papaverine. Calibration curves were constructed from the results of spiked control plasma samples by plotting the peak height ratios against the warfarin concentration, expressed as micrograms of warfarin per milliliter of plasma. Values of unknown concentrations of warfarin in plasma specimens, obtained in the same manner, were then read directly from the graph or calculated from the slope of a two-point standard curve.

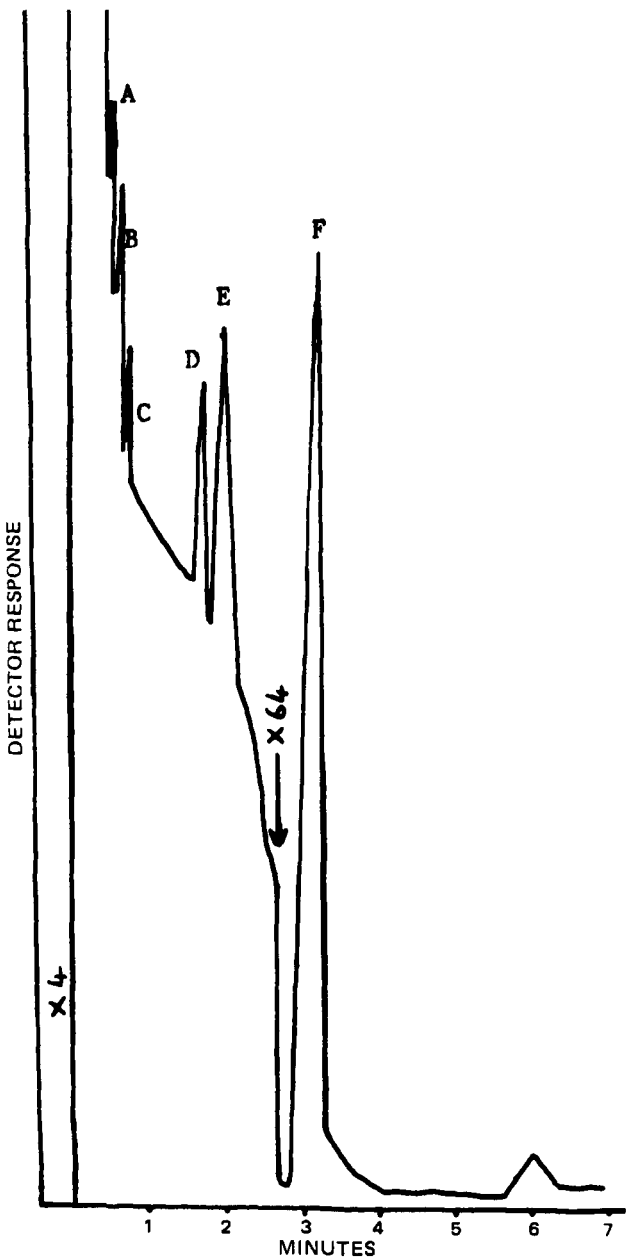

Figure 3—*Chromatogram of warfarin and its degradation and metabolic products. Key: A, 5-hydroxywarfarin; B, 7-hydroxywarfarin; C, 8-hydroxywarfarin; D, 3-(o-hydroxyphenyl)-5-phenyl-2-cyclohexen-1-one; E, warfarin; and F, papaverine.*

RESULTS AND DISCUSSION

Under the assay conditions described, a linear relationship between detector response and concentration was obtained for warfarin over the range of 0.3–2 μg/ml of plasma with a correlation coefficient of 0.9944. Regression analysis showed that the regression equation was $y = 0.338x - 0.081$ with a standard error of the estimate of y on x of 0.021 and standard errors of the estimate of the intercept and slope of 0.107 and 0.675, respectively. The retention times of warfarin and papaverine were 2 and 3.1 min, respectively (Fig. 1).

Several plasma samples taken at the predetermined intervals were pooled, extracted, and chromatographed using the described method. The material obtained within the warfarin peak (retention time of 2 min) was trapped and analyzed by mass spectrometry[13]. The mass spectrum of the collected warfarin peak was identical with that obtained from a USP reference standard (Fig. 2). The mass spectrum showed a molecular ion at *m/e* 308 and abundant ions at *m/e* 43, 65, 77, 92, 103, 121, 131, 145, 175, 187, 249, 251, 265, 266, 275, and 290.

The accuracy and precision of the GLC assay procedure are demonstrated in Table I. The quantitative lower limit of detection sensitivity for warfarin in human plasma was 0.3 μg/ml. The average recovery of warfarin from spiked plasma was 97.26 ± 1.89%. The resolution factor between warfarin and internal standard peaks was 4.6 (25). The degradation product, 3-(*o*-hydroxyphenyl)-5-phenyl-2-cyclohexen-1-one[2], and three metabolic products of warfarin (16, 23, 24), 5-hydroxywarfarin[14], 7-hydroxywarfarin[14], and 8-hydroxywarfarin[14], do not interfere with the assay since they gave retention times of 1.65, 0.6, 0.7, and 0.75 min, respectively, under the assay conditions described (Fig. 3).

The GLC procedure was compared with a UV spectrophotometric assay (14). Results from measurements of plasma warfarin levels in seven normal human subjects after single-dose oral administration of crystalline warfarin sodium, 15 mg, are shown in Fig. 4. A peak mean level of warfarin (1.80 μg/ml) was observed at 1.0 hr after oral drug administration, fol-

[10] Coumadin, Endo Laboratories, Garden City, N.Y.
[11] Becton, Dickinson and Co., Rutherford, N.J.
[12] Model IEC-HN-S, Damon IEC Division, Needham Heights, Mass.
[13] Model 1015, Finnigan Corp., Sunnyvale, Calif.
[14] Dr. C. Schroder, WARF Institute, Madison, Wis.

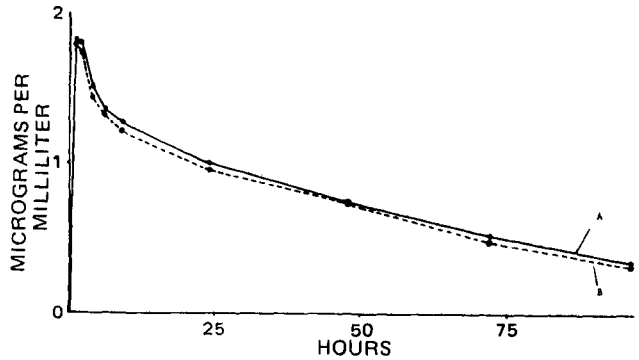

Figure 4—*Mean plasma warfarin concentrations in seven volunteers following a single oral dose of 15 mg of crystalline warfarin sodium. Key: A, UV method; and B, GLC method.*

lowed by a smooth, gradual decline from 24 to 96 hr, indicating slow drug disappearance from peripheral circulation. The estimated areas under the plasma concentration–time curves from 0 to 96 hr were 73.58 and 75.86 μg/ml × hr while the elimination half-lives were 50.9 and 51.4 hr as determined by the GLC and UV methods, respectively.

REFERENCES

(1) I. Wright, *Geriatrics*, **24**, 96 (1969).
(2) D. Deykin, *N. Engl. J. Med.*, **283**, 691, 801 (1970).
(3) R. A. O'Reilly, P. M. Aggeler, M. S. Hoag, and L. Leong, *Thromb. Diath. Haemorrh.*, **8**, 82 (1962).
(4) R. A. O'Reilly, P. M. Aggeler, and L. S. Leong, *J. Clin. Invest.*, **42**, 1542 (1963).
(5) J. G. Pool, R. A. O'Reilly, L. J. Schneiderman, and M. Alexander, *Am. J. Physiol.*, **215**, 627 (1968).
(6) R. A. O'Reilly and P. M. Aggeler, *Circulation*, **38**, 169 (1968).
(7) M. G. McDonald, D. S. Robinson, D. Slywester, and J. J. Jaffe, *Clin. Pharmacol. Ther.*, **10**, 80 (1969).
(8) J. G. Wagner, P. G. Welling, K. P. Lee, and J. E. Walker, *J. Pharm. Sci.*, **60**, 666 (1971).
(9) R. A. O'Reilly, *Fed. Proc.*, **32**, 289 Abstr. (1973).
(10) G. Levy, R. A. O'Reilly, and L. B. Wingard, Jr., *Res. Commun. Chem. Pathol. Pharmacol.*, **7**, 359 (1974).
(11) M. Corn and R. Berberich, *Clin. Chem.*, **13**, 126 (1967).
(12) R. Nagashima and G. Levy, *J. Pharm. Sci.*, **58**, 845 (1969).
(13) R. J. Lewis and L. P. Ilnicki, *Clin. Res.*, **17**, 332 (1969).
(14) P. G. Welling, K. P. Lee, V. Khanna, and J. G. Wagner, *J. Pharm. Sci.*, **59**, 1621 (1970).
(15) R. J. Lewis, L. P. Ilnicki, and M. Carlstrim, *Biochem. Med.*, **4**, 376 (1970).
(16) R. J. Lewis and W. F. Trager, *Ann. N.Y. Acad. Sci.*, **179**, 205 (1971).
(17) R. J. Lewis, *J. Pharm. Sci.*, **60**, 1271 (1971).
(18) J. G. Wagner, *ibid.*, **60**, 1272 (1971).
(19) D. S. Hewick and J. McEwen, *J. Pharm. Pharmacol.*, **25**, 458 (1973).
(20) F. W. Deckert, *J. Chromatogr.*, **64**, 201 (1972).
(21) *Ibid.*, **64**, 355 (1972).
(22) D. G. Kaiser and R. S. Martin, *J. Pharm. Sci.*, **63**, 1579 (1974).
(23) K. K. Midha, I. J. McGilveray, and J. K. Cooper, *ibid.*, **63**, 1725 (1974).
(24) E. S. Vesell and C. A. Shivley, *Science*, **184**, 466 (1974).
(25) "The National Formulary," 14th ed., Mack Publishing Co., Easton, Pa., 1975, p. 868.

ACKNOWLEDGMENTS

The authors gratefully acknowledge the assistance of E. Newkom, Endo Laboratories, and T. Foster, College of Pharmacy, University of Kentucky, in the clinical study.
This report is Contribution 108 from Endo Laboratories.

Determination of Time Course of Tablet Disintegration II: Method Using Continuous Functions

K. G. NELSON ˣ and L. Y. WANG

Received March 15, 1977, from the *College of Pharmacy, University of Minnesota, Minneapolis, MN 55455.* Accepted for publication April 14, 1977.

Abstract □ An analysis of the disintegration–dissolution sequence of drug release from a tablet leads to a mathematical expression relating disintegration to the dissolution profile of the tablet and the dissolution rate of the primary drug particles in the tablet. The equation describing the disintegration of an acetaminophen tablet is determined to demonstrate the application of the theory.

Keyphrases □ Disintegration, tablet—related to dissolution profile of tablet and dissolution rate of primary drug particles □ Dissolution—profile of tablet and rate of primary drug particles related to tablet disintegration

A method involving numerical analysis was described recently (1) that accounts for both the disintegration and dissolution aspects of drug release from a tablet. If the dissolution characteristics of the primary drug particles in the tablet are known, it is possible to determine the time course of the disintegration process from tablet dissolution data. This disintegration–dissolution analysis requires a numerical data analysis over many small time intervals. The purpose of the present paper is to extend this method to provide a model based on continuum mathematics.

THEORETICAL

The principle of the disintegration–dissolution analysis described previously (1) is to consider the processes of disintegration and dissolution to be discrete events over many small, equal time intervals. At any arbitrary interval, the fraction of drug in the tablet that has dissolved is considered to be the sum of the amounts dissolved from all disintegrated fractions, calculated using the cube-root equation for the time periods between the disintegration intervals and the arbitrary interval. The mathematical expression given that describes this phenomenon is:

$$M_n = \sum_{i=0}^{n} w_i\{1 - [1 - K(t_n - t_i)]^3\} \qquad \text{(Eq. 1)}$$

where M_n is the fraction of drug in the tablet dissolved after n time intervals and corresponds to time t_n. The fraction disintegrated at the ith interval is w_i, and K is the cube-root law dissolution constant. The term

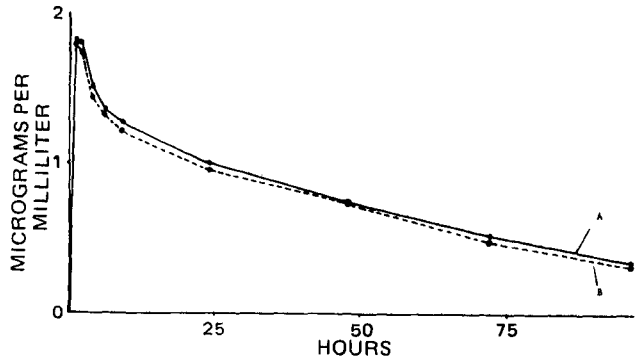

Figure 4—*Mean plasma warfarin concentrations in seven volunteers following a single oral dose of 15 mg of crystalline warfarin sodium. Key: A, UV method; and B, GLC method.*

lowed by a smooth, gradual decline from 24 to 96 hr, indicating slow drug disappearance from peripheral circulation. The estimated areas under the plasma concentration–time curves from 0 to 96 hr were 73.58 and 75.86 μg/ml × hr while the elimination half-lives were 50.9 and 51.4 hr as determined by the GLC and UV methods, respectively.

REFERENCES

(1) I. Wright, *Geriatrics*, **24**, 96 (1969).
(2) D. Deykin, *N. Engl. J. Med.*, **283**, 691, 801 (1970).
(3) R. A. O'Reilly, P. M. Aggeler, M. S. Hoag, and L. Leong, *Thromb. Diath. Haemorrh.*, **8**, 82 (1962).
(4) R. A. O'Reilly, P. M. Aggeler, and L. S. Leong, *J. Clin. Invest.*, **42**, 1542 (1963).
(5) J. G. Pool, R. A. O'Reilly, L. J. Schneiderman, and M. Alexander, *Am. J. Physiol.*, **215**, 627 (1968).
(6) R. A. O'Reilly and P. M. Aggeler, *Circulation*, **38**, 169 (1968).
(7) M. G. McDonald, D. S. Robinson, D. Slywester, and J. J. Jaffe, *Clin. Pharmacol. Ther.*, **10**, 80 (1969).
(8) J. G. Wagner, P. G. Welling, K. P. Lee, and J. E. Walker, *J. Pharm. Sci.*, **60**, 666 (1971).
(9) R. A. O'Reilly, *Fed. Proc.*, **32**, 289 Abstr. (1973).
(10) G. Levy, R. A. O'Reilly, and L. B. Wingard, Jr., *Res. Commun. Chem. Pathol. Pharmacol.*, **7**, 359 (1974).
(11) M. Corn and R. Berberich, *Clin. Chem.*, **13**, 126 (1967).
(12) R. Nagashima and G. Levy, *J. Pharm. Sci.*, **58**, 845 (1969).
(13) R. J. Lewis and L. P. Ilnicki, *Clin. Res.*, **17**, 332 (1969).
(14) P. G. Welling, K. P. Lee, V. Khanna, and J. G. Wagner, *J. Pharm. Sci.*, **59**, 1621 (1970).
(15) R. J. Lewis, L. P. Ilnicki, and M. Carlstrim, *Biochem. Med.*, **4**, 376 (1970).
(16) R. J. Lewis and W. F. Trager, *Ann. N.Y. Acad. Sci.*, **179**, 205 (1971).
(17) R. J. Lewis, *J. Pharm. Sci.*, **60**, 1271 (1971).
(18) J. G. Wagner, *ibid.*, **60**, 1272 (1971).
(19) D. S. Hewick and J. McEwen, *J. Pharm. Pharmacol.*, **25**, 458 (1973).
(20) F. W. Deckert, *J. Chromatogr.*, **64**, 201 (1972).
(21) *Ibid.*, **64**, 355 (1972).
(22) D. G. Kaiser and R. S. Martin, *J. Pharm. Sci.*, **63**, 1579 (1974).
(23) K. K. Midha, I. J. McGilveray, and J. K. Cooper, *ibid.*, **63**, 1725 (1974).
(24) E. S. Vesell and C. A. Shivley, *Science*, **184**, 466 (1974).
(25) "The National Formulary," 14th ed., Mack Publishing Co., Easton, Pa., 1975, p. 868.

ACKNOWLEDGMENTS

The authors gratefully acknowledge the assistance of E. Newkom, Endo Laboratories, and T. Foster, College of Pharmacy, University of Kentucky, in the clinical study.
This report is Contribution 108 from Endo Laboratories.

Determination of Time Course of Tablet Disintegration II: Method Using Continuous Functions

K. G. NELSON ˣ and L. Y. WANG

Received March 15, 1977, from the *College of Pharmacy, University of Minnesota, Minneapolis, MN 55455.* Accepted for publication April 14, 1977.

Abstract □ An analysis of the disintegration–dissolution sequence of drug release from a tablet leads to a mathematical expression relating disintegration to the dissolution profile of the tablet and the dissolution rate of the primary drug particles in the tablet. The equation describing the disintegration of an acetaminophen tablet is determined to demonstrate the application of the theory.

Keyphrases □ Disintegration, tablet—related to dissolution profile of tablet and dissolution rate of primary drug particles □ Dissolution—profile of tablet and rate of primary drug particles related to tablet disintegration

A method involving numerical analysis was described recently (1) that accounts for both the disintegration and dissolution aspects of drug release from a tablet. If the dissolution characteristics of the primary drug particles in the tablet are known, it is possible to determine the time course of the disintegration process from tablet dissolution data. This disintegration–dissolution analysis requires a numerical data analysis over many small time intervals. The purpose of the present paper is to extend this method to provide a model based on continuum mathematics.

THEORETICAL

The principle of the disintegration–dissolution analysis described previously (1) is to consider the processes of disintegration and dissolution to be discrete events over many small, equal time intervals. At any arbitrary interval, the fraction of drug in the tablet that has dissolved is considered to be the sum of the amounts dissolved from all disintegrated fractions, calculated using the cube-root equation for the time periods between the disintegration intervals and the arbitrary interval. The mathematical expression given that describes this phenomenon is:

$$M_n = \sum_{i=0}^{n} w_i\{1 - [1 - K(t_n - t_i)]^3\} \qquad \text{(Eq. 1)}$$

where M_n is the fraction of drug in the tablet dissolved after n time intervals and corresponds to time t_n. The fraction disintegrated at the ith interval is w_i, and K is the cube-root law dissolution constant. The term

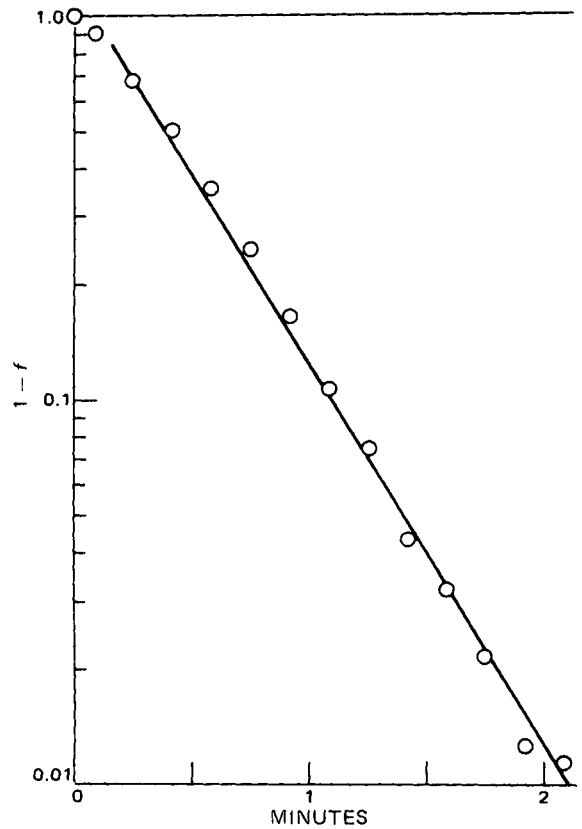

Figure 1—*Linearized plot of dissolution data for acetaminophen powder.*

in braces should be defined equal to one once it attains that value. The w_i can be obtained by applying Eq. 1 at each interval for the dissolution curve of the tablet. The cumulative fraction of drug disintegrated from the tablet, W_n, up to time t_n is given by:

$$W_n = \sum_{i=0}^{n} w_i \qquad \text{(Eq. 2)}$$

The disintegration profile for the tablet can be constructed by application of Eq. 2 at each time interval.

To make the transition from the numerical analysis type of expressions of Eqs. 1 and 2 to equations involving analytical functions, Eq. 1 should first be generalized as:

$$M_n = \sum_{i=0}^{n} w(t_i) f(t_n - t_i)\,\Delta t \qquad \text{(Eq. 3)}$$

where w is the differential disintegration function and Δt is the length of the time interval. The function f describes the dissolution of the primary drug particles. The term in braces in Eq. 1 is $f(t_n - t_i)$ for the Hixson–Crowell cube-root model for particle dissolution.

In the limit as $\Delta t \to 0$ and $n \to \infty$, Eq. 3 becomes the convolution integral:

$$M(t) = \int_0^t w(\theta) f(t - \theta)\, d\theta = w(t) * f(t) \qquad \text{(Eq. 4)}$$

where M now becomes a continuous function of time t, θ is an integration variable, and $*$ represents convolution. The convolution integral is well characterized and is dealt with on the basis of operational calculus (2). Because $w(t)$ is the differential disintegration function, the cumulative fraction of the tablet disintegrated as a function of time, $W(t)$, is given as:

$$W(t) = \int_0^t w(t)\, dt \qquad \text{(Eq. 5)}$$

If Laplace transforms are taken for the convolution equation $M(t) = w(t) * f(t)$, then the relationship for the transforms is:

$$\overline{M}(s) = \overline{w}(s)\overline{f}(s) \qquad \text{(Eq. 6)}$$

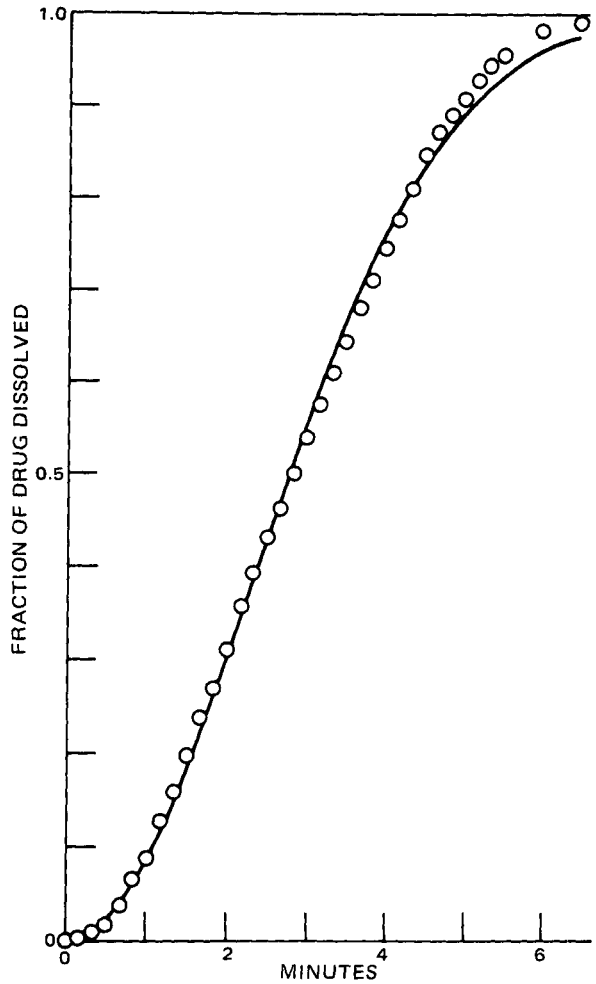

Figure 2—*Dissolution of the acetaminophen tablet (points). The curve is the Weibull function with* a = *11.15 and* b = *1.996.*

The bar over the function and the s represent the Laplace transform for the function. A rearrangement of Eq. 6 yields:

$$\overline{w}(s) = \frac{\overline{M}(s)}{\overline{f}(s)} \qquad \text{(Eq. 7)}$$

Equation 7 indicates that the function w can be obtained from the inverse transform of the ratio of the Laplace transforms of M and f.

The function M is a continuous function that describes the fraction of drug in a tablet dissolved with time. To obtain this function on a practical basis, an empirical equation can be fit to experimental tablet dissolution data. An equation found to be useful is the Weibull function (3):

$$M(t) = 1 - e^{-(t^b/a)} \qquad \text{(Eq. 8)}$$

The adjustable parameters are a and b, the scale factor and the shape factor, respectively. The Weibull function normally contains a lag time, but this term has been omitted because it is usually zero for tablet dissolution experiments.

The function f describes the dissolution of the primary drug particles in the tablet; it is initially zero and approaches unity as the particles completely dissolve. This function can be developed from a model that describes dissolution of powders, *e.g.*, the term in braces in Eq. 1 is $f(t_n - t_i)$ developed from the cube-root law, or it may be an empirical function fit to powder dissolution data. The latter approach is taken for the present work because a smooth function that facilitates the solution of Eq. 4 may be chosen. Functions f that arise from the powder dissolution models usually have a discontinuity in the first derivative at the time of complete dissolution, making the mathematics more complex. For the present, an exponential function is assumed to describe the particle dissolution:

$$f(t) = 1 - e^{-kt} \qquad \text{(Eq. 9)}$$

where k is an adjustable parameter.

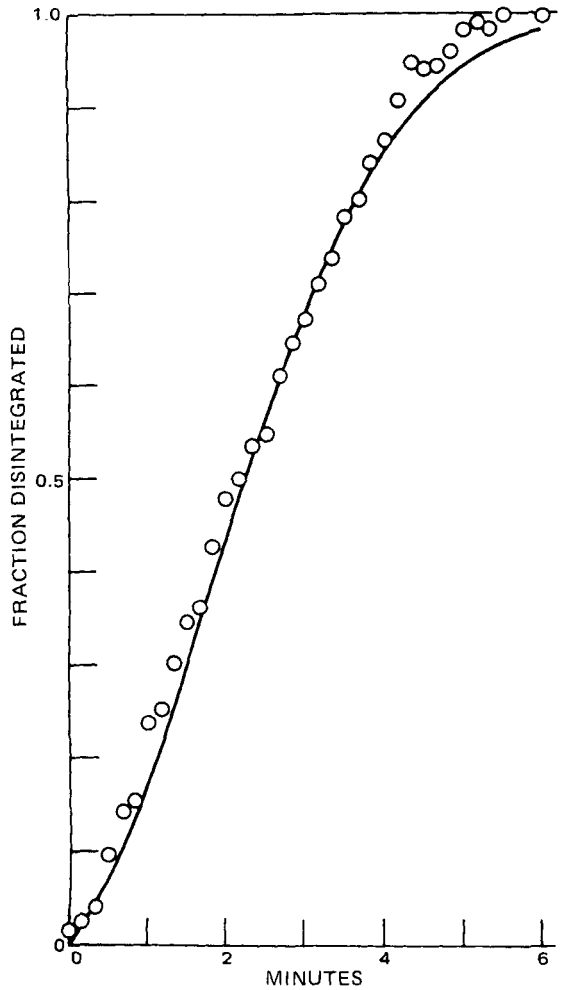

Figure 3—*Disintegration profile (curve) determined with Eq. 14. The points are the results of the numerical method using Eq. 9.*

If the Laplace transform of Eq. 9 is substituted into Eq. 7 and rearranged:

$$\overline{w}(s) = \frac{1}{k} s^2 \overline{M}(s) + s\overline{M}(s) \qquad \text{(Eq. 10)}$$

Thus:

$$w(t) = \frac{1}{k} L^{-1}[s^2\overline{M}(s)] + L^{-1}[s\overline{M}(s)] \qquad \text{(Eq. 11)}$$

where L^{-1} represents the inverse transform. Because of the fundamental relationship between the derivative of a function (denoted by a prime) and the transform, if $M'(0) = 0$ and $M(0) = 0$, Eq. 11 becomes:

$$w(t) = \frac{1}{k} M''(t) + M'(t) \qquad \text{(Eq. 12)}$$

Integration of Eq. 12 yields:

$$W(t) = \frac{1}{k} M'(t) + M(t) \qquad \text{(Eq. 13)}$$

If M from Eq. 8 is substituted into Eq. 13:

$$W(t) = 1 - \left(1 - \frac{bt^{b-1}}{ka}\right) e^{-(t^b/a)} \qquad \text{(Eq. 14)}$$

Equation 14 thus represents the disintegration profile for a tablet whose dissolution curve is represented by the Weibull function with parameters a and b and whose particles dissolve according to Eq. 9 with parameter k.

RESULTS AND DISCUSSION

In the report where the disintegration profile was determined by a numerical technique (1), the method was applied to an acetaminophen tablet prepared with a direct compaction formulation which included a monodisperse sample of the drug. The same data are used for the present analysis. The dissolution behavior of the acetaminophen powder sample is shown in Fig. 1, plotted as the linearized form of Eq. 9. The straight line is the least-squares fit and yields a good correlation coefficient ($r^2 = 0.995$). A nonlinear regression of Eq. 9 with the data gives $k = 1.824$.

Figure 2 shows the data points for the dissolution profile of the acetaminophen tablet. The continuous line is the Weibull function for $a = 11.15$ and $b = 1.996$. These parameters were determined by a nonlinear regression of the Weibull function to the data. The fit is quite good, although the function is below the data at large times.

The disintegration profile constructed from Eq. 14 with the above-mentioned values for a, b, and k is given in Table I and as the continuous curve in Fig. 3. The shape is sigmoidal. The profile determined before had slight curvature but was sufficiently linear that a straight line was fitted to it and utilized for simulation purposes. Data for the profile determined previously are included in Table I for comparison. Because W in Fig. 3 appears to have more curvature than the profile determined previously, it is of interest to evaluate the possible reasons for this change. Two functions used in the present report that differ from the earlier work are the exponential function (Eq. 9) instead of the cube-root law and the Weibull function (Eq. 8) instead of the actual data.

To evaluate whether the use of the exponential function contributed to the discrepancy, Eq. 9 was used in Eq. 3 and the numerical analysis technique was applied using the actual data to generate the disintegration profile (Table I). These results closely follow those of the previous work using the cube-root law. The results of this calculation are also shown in Fig. 3. It is apparent from Figs. 2 and 3 that the problem resides in the Weibull function at higher times where it does not fit the experimental dissolution data with a high degree of accuracy. With this in mind, the agreement between the discrete and continuous mathematical treatments is quite satisfactory.

Equation 13 arises primarily from the application of Eqs. 7 and 5 to the exponential description of the dissolution of primary particles (Eq.

Table I—Fraction Dissolved and Fraction Disintegrated from an Acetaminophen Tablet

		W		
Minutes	M	Discrete Case, Cube Root (1)	Discrete Case, Exponential	Continuous Function (Eq. 14)
0.00	0.000	0.018	0.015	0.000
0.17	0.004	0.028	0.025	0.019
0.33	0.009	0.043	0.039	0.042
0.50	0.017	0.109	0.096	0.070
0.67	0.038	0.156	0.142	0.103
0.83	0.065	0.158	0.154	0.137
1.00	0.088	0.251	0.237	0.176
1.17	0.128	0.255	0.253	0.217
1.33	0.159	0.306	0.303	0.258
1.50	0.198	0.347	0.346	0.303
1.67	0.237	0.356	0.362	0.348
1.83	0.269	0.428	0.427	0.392
2.00	0.311	0.480	0.479	0.438
2.17	0.356	0.497	0.501	0.483
2.33	0.393	0.531	0.536	0.525
2.50	0.431	0.540	0.549	0.568
2.67	0.462	0.614	0.613	0.609
2.83	0.501	0.648	0.649	0.646
3.00	0.540	0.669	0.674	0.684
3.17	0.576	0.708	0.711	0.719
3.33	0.610	0.734	0.738	0.749
3.50	0.644	0.781	0.783	0.779
3.67	0.681	0.795	0.801	0.807
3.83	0.711	0.837	0.840	0.831
4.00	0.746	0.860	0.864	0.854
4.17	0.777	0.906	0.907	0.874
4.33	0.810	0.949	0.949	0.891
4.50	0.847	0.931	0.941	0.908
4.67	0.872	0.933	0.945	0.922
4.83	0.891	0.950	0.960	0.934
5.00	0.909	0.978	0.983	0.945
5.17	0.929	0.986	0.991	0.954
5.33	0.945	0.976	0.984	0.962
5.50	0.955	0.995	0.999	0.969
6.00	0.982	0.994	0.997	0.983
6.50	0.991			0.991

9) along with the restrictions on M of $M(0) = 0$ and $M'(0) = 0$. Within these limitations, Eq. 13 is a rather general relationship between the disintegration and dissolution of a tablet. Any function M that fits the tablet dissolution data and meets these restrictions may be substituted into Eq. 13 to give an explicit expression for the disintegration.

Another ramification of Eq. 13 is that it would be possible to determine the disintegration profile in real time if k is known by using the output signal from the spectrophotometer or potentiometer that is monitoring the tablet dissolution as input for an analog computer programmed for Eq. 13. The dissolution and disintegration profiles could thereby be determined simultaneously.

REFERENCES

(1) K. G. Nelson and L. Y. Wang, *J. Pharm. Sci.*, **66**, 1758 (1977).

(2) R. V. Churchill, "Operational Mathematics," 3rd ed., McGraw-Hill, New York, N.Y., 1972.

(3) F. Langenbucher, *J. Pharm. Pharmacol.*, **24**, 979 (1972).

ACKNOWLEDGMENTS

The authors thank Mr. David C. Lin for assisting in the mathematical development. They also gratefully acknowledge support for this study from a grant from the Pharmacy Research Unit, The Upjohn Co., Kalamazoo, Mich.

Binding of 3-Aminoacridinium and 7-Aminoquinolinium Monocations to Double-Stranded DNA: Evidence for Nonlinear Binding Isotherm in Intercalative Region

ANTHONY C. CAPOMACCHIA * and STEPHEN G. SCHULMAN ˣ

Received October 14, 1976, from the *College of Pharmacy, University of Florida, Gainesville, FL 32610.* Accepted for publication April 8, 1977.

* Present address: College of Pharmacy, University of Georgia, Athens, GA 30602.

Abstract □ The complexations of the singly charged cations of 3-aminoacridine and 7-aminoquinoline by double-stranded, calf thymus DNA were studied by electronic absorption spectrophotometry. At high ratios of total DNA phosphate concentration to total probe concentration (the region associated with intercalative binding), four DNA phosphate units are associated with each bound monocation. However, a binding isotherm based on four DNA phosphate groups in a single binding site does not yield a reproducible equilibrium constant for the binding process. Rather, the sequestration of the monocations by two binding sites, each containing two DNA phosphate units, yields a satisfactory equilibrium expression. This result suggests that the intercalative mode of binding by DNA is not a simple one-step process, which is in agreement with previous kinetic studies. In the region of low DNA phosphate concentration to monocation concentration (the external binding region), the binding is described adequately by a linear isotherm.

Keyphrases □ 3-Aminoacridinium monocations—binding to double-stranded DNA, equilibrium expressions developed □ 7-Aminoquinolinium monocations—binding to double-stranded DNA, equilibrium expressions developed □ Binding—3-aminoacridinium and 7-aminoquinolinium monocations to double-stranded DNA, equilibrium expressions developed □ DNA, double stranded—binding to 3-aminoacridinium and 7-aminoquinolinium monocations, equilibrium expressions developed

Numerous investigators have examined the binding of aminoacridines and aminoquinolines to double-stranded and denatured deoxyribonucleic acid (DNA) (1–8). The aminoacridines have received particular attention because of their well-known antibacterial activity, which has been attributed to their binding by bacterial DNA (9–11). The ability of aminoacridinium compounds to induce frameshift mutations by causing a deletion or insertion of a single nucleotide in the complementary chain of a replicating chromosome is believed to be due to the strong or intercalative binding of these compounds to nucleic acid (12–14).

Aminoquinolines, particularly the 4-amino and 8-amino analogs, have been employed extensively as antimalarial agents (15). Their antimalarial activity has been said to be due to their interaction with the DNA of infectious plasmodia found in malaria-infested mammals (16).

BACKGROUND

The various interactions of aminoacridines and aminoquinolines with nucleic acids can be classified into two groups: intercalation and external binding (6, 11). Intercalation or strong binding of the aminoacridine or aminoquinoline involves insertion of these compounds, to varying degrees, into the DNA molecule and results in some disruption of the latter (1–3). The intercalative binding of drugs or probes to double-stranded DNA is strongest with compounds possessing three fused aromatic rings, linearly annulated, as in the aminoacridines (6–17). A decrease in the size of the aromatic portion of the intercalating probe results in weaker intercalative binding, as demonstrated by DNA–aminoquinoline complexes (18).

Previous studies (19–23) utilizing temperature-jump relaxation kinetics indicated that the intercalation of the singly charged cations of proflavine and acridine orange may occur in two kinetically discrete steps at high DNA phosphorus to probe ratios. However, this behavior has not been established for all aminoacridine cations. External binding to the double-stranded DNA polyanion occurs after all intercalative binding sites are saturated. The interaction apparently occurs mainly between the cationic probe molecule and the negatively charged DNA phosphate groups and, as such, is primarily an electrostatic interaction (6).

Albert (9) demonstrated that it is the cation of aminoacridine that is necessary for bacteriostasis. The inference is that the cationic form is a necessary condition for intercalation of aminoacridines and aminoquinolines. Therefore, electrostatic forces are believed to provide the initial driving force behind the formation of the DNA–probe complex, prior to intercalation of the probe into the DNA molecule, as well as a substantial portion of the forces that maintain the integrity of the complex (6, 9, 18). However, electrostatic forces are said to be less important in intercalative binding than in the binding of cationic drugs or probes to the exterior of the DNA molecule (5, 6).

Data obtained from investigations of the complexation of small cations to DNA are usually treated according to a model developed by Scatchard (24) to describe the binding of small molecules to proteins. This model was later modified and adapted by other investigators to describe binding to nucleic acids (5, 6, 11, 25).

As a consequence of the pharmacological and physicochemical significance of the complexation of aminoquinolines and aminoacridines to double-stranded and denatured DNA, as well as of an interest in im-

9) along with the restrictions on M of $M(0) = 0$ and $M'(0) = 0$. Within these limitations, Eq. 13 is a rather general relationship between the disintegration and dissolution of a tablet. Any function M that fits the tablet dissolution data and meets these restrictions may be substituted into Eq. 13 to give an explicit expression for the disintegration.

Another ramification of Eq. 13 is that it would be possible to determine the disintegration profile in real time if k is known by using the output signal from the spectrophotometer or potentiometer that is monitoring the tablet dissolution as input for an analog computer programmed for Eq. 13. The dissolution and disintegration profiles could thereby be determined simultaneously.

REFERENCES

(1) K. G. Nelson and L. Y. Wang, *J. Pharm. Sci.*, **66**, 1758 (1977).

(2) R. V. Churchill, "Operational Mathematics," 3rd ed., McGraw-Hill, New York, N.Y., 1972.

(3) F. Langenbucher, *J. Pharm. Pharmacol.*, **24**, 979 (1972).

ACKNOWLEDGMENTS

The authors thank Mr. David C. Lin for assisting in the mathematical development. They also gratefully acknowledge support for this study from a grant from the Pharmacy Research Unit, The Upjohn Co., Kalamazoo, Mich.

Binding of 3-Aminoacridinium and 7-Aminoquinolinium Monocations to Double-Stranded DNA: Evidence for Nonlinear Binding Isotherm in Intercalative Region

ANTHONY C. CAPOMACCHIA * and STEPHEN G. SCHULMAN ˣ

Received October 14, 1976, from the *College of Pharmacy, University of Florida, Gainesville, FL 32610.* Accepted for publication April 8, 1977.

* Present address: College of Pharmacy, University of Georgia, Athens, GA 30602.

Abstract □ The complexations of the singly charged cations of 3-aminoacridine and 7-aminoquinoline by double-stranded, calf thymus DNA were studied by electronic absorption spectrophotometry. At high ratios of total DNA phosphate concentration to total probe concentration (the region associated with intercalative binding), four DNA phosphate units are associated with each bound monocation. However, a binding isotherm based on four DNA phosphate groups in a single binding site does not yield a reproducible equilibrium constant for the binding process. Rather, the sequestration of the monocations by two binding sites, each containing two DNA phosphate units, yields a satisfactory equilibrium expression. This result suggests that the intercalative mode of binding by DNA is not a simple one-step process, which is in agreement with previous kinetic studies. In the region of low DNA phosphate concentration to monocation concentration (the external binding region), the binding is described adequately by a linear isotherm.

Keyphrases □ 3-Aminoacridinium monocations—binding to double-stranded DNA, equilibrium expressions developed □ 7-Aminoquinolinium monocations—binding to double-stranded DNA, equilibrium expressions developed □ Binding—3-aminoacridinium and 7-aminoquinolinium monocations to double-stranded DNA, equilibrium expressions developed □ DNA, double stranded—binding to 3-aminoacridinium and 7-aminoquinolinium monocations, equilibrium expressions developed

Numerous investigators have examined the binding of aminoacridines and aminoquinolines to double-stranded and denatured deoxyribonucleic acid (DNA) (1–8). The aminoacridines have received particular attention because of their well-known antibacterial activity, which has been attributed to their binding by bacterial DNA (9–11). The ability of aminoacridinium compounds to induce frameshift mutations by causing a deletion or insertion of a single nucleotide in the complementary chain of a replicating chromosome is believed to be due to the strong or intercalative binding of these compounds to nucleic acid (12–14).

Aminoquinolines, particularly the 4-amino and 8-amino analogs, have been employed extensively as antimalarial agents (15). Their antimalarial activity has been said to be due to their interaction with the DNA of infectious plasmodia found in malaria-infested mammals (16).

BACKGROUND

The various interactions of aminoacridines and aminoquinolines with nucleic acids can be classified into two groups: intercalation and external binding (6, 11). Intercalation or strong binding of the aminoacridine or aminoquinoline involves insertion of these compounds, to varying degrees, into the DNA molecule and results in some disruption of the latter (1–3). The intercalative binding of drugs or probes to double-stranded DNA is strongest with compounds possessing three fused aromatic rings, linearly annulated, as in the aminoacridines (6–17). A decrease in the size of the aromatic portion of the intercalating probe results in weaker intercalative binding, as demonstrated by DNA–aminoquinoline complexes (18).

Previous studies (19–23) utilizing temperature-jump relaxation kinetics indicated that the intercalation of the singly charged cations of proflavine and acridine orange may occur in two kinetically discrete steps at high DNA phosphorus to probe ratios. However, this behavior has not been established for all aminoacridine cations. External binding to the double-stranded DNA polyanion occurs after all intercalative binding sites are saturated. The interaction apparently occurs mainly between the cationic probe molecule and the negatively charged DNA phosphate groups and, as such, is primarily an electrostatic interaction (6).

Albert (9) demonstrated that it is the cation of aminoacridine that is necessary for bacteriostasis. The inference is that the cationic form is a necessary condition for intercalation of aminoacridines and aminoquinolines. Therefore, electrostatic forces are believed to provide the initial driving force behind the formation of the DNA–probe complex, prior to intercalation of the probe into the DNA molecule, as well as a substantial portion of the forces that maintain the integrity of the complex (6, 9, 18). However, electrostatic forces are said to be less important in intercalative binding than in the binding of cationic drugs or probes to the exterior of the DNA molecule (5, 6).

Data obtained from investigations of the complexation of small cations to DNA are usually treated according to a model developed by Scatchard (24) to describe the binding of small molecules to proteins. This model was later modified and adapted by other investigators to describe binding to nucleic acids (5, 6, 11, 25).

As a consequence of the pharmacological and physicochemical significance of the complexation of aminoquinolines and aminoacridines to double-stranded and denatured DNA, as well as of an interest in im-

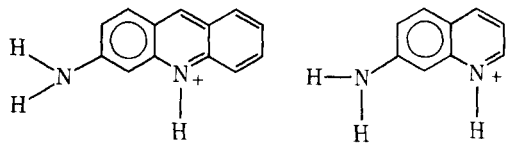

I II

proving the methods employed in developing experimental data obtained from these complexation studies, it seemed desirable to investigate the comparative binding affinities of these compounds. The 3-aminoacridinium (I) and 7-aminoquinolinium (II) monocations were chosen as model compounds since they are not only benzologs of each other but are directly related to the much studied compounds proflavine and acridine orange but are less susceptible to problems associated with molecular aggregation (6, 11, 25–28).

EXPERIMENTAL

Instrumentation—Electronic absorption spectra were taken in 1-cm silica cells on a spectrophotometer[1]. The pH measurements were made on a pH meter[2] with a combination silver–silver chloride glass electrode[1]. Calculations were made on a programmable calculator[3] utilizing an extensive cassette program library. Solutions were mixed on a rotating mixer[4] and an ultrasonic mixer[5]. Solutions of DNA or probe were delivered with micropipets[6].

Materials and Solutions—Aqueous buffered solutions at a specified pH were prepared from analytical grade monobasic and dibasic potassium phosphates[7] in which the ionic strength was maintained at 0.005 *M*. Calf thymus DNA[8] as the A grade sodium salt, containing 8.04% phosphorus and 12.21% nitrogen, was used without further purification. A sufficient amount of the DNA sodium salt was added to 10 ml of buffer solution in a volumetric flask to make a stock DNA solution (1.10×10^{-2} mole of DNA phosphorus/liter).

Solutions of DNA were prepared at the desired pH for each titration and were mixed for 6 hr on a rotating mixer at room temperature. After mixing, the flask containing the stock solution was placed in an ultrasonic mixer for 10 min. These solutions were then divided into 0.5-ml aliquots and stored at 0° for not more than 2 weeks prior to use.

3-Aminoacridine, prepared by a literature method (29), and 7-aminoquinoline[9] were determined to be at least 98% pure according to literature melting-point and molar absorptivity values (29–32).

Methods—Ethanolic solutions ($\sim 1.00 \times 10^{-3}$ *M*) of the compounds to be studied were delivered from a 20-μl micropipet into a 1-cm silica cell containing 2.00 ml of the aqueous buffer solution at the desired pH. This 2 ml of solution was titrated, in the cell, with small increments of the DNA solution at the desired pH. Several micropipets that delivered 5–100 μl reproducibly were employed during each titration. The inherent viscosity of the DNA solution did not appear to be a factor in its reproducible delivery.

The total concentration of DNA phosphorus at each point in the titration was calculated from the dilution of the added DNA stock solution by the 2 ml of test solution. The total concentration of I or II at each point in the titration was calculated from the initial value, taking account of dilution by the volume of added DNA solution. All experiments were conducted at ambient temperature.

Calculations—The concentrations of free base, [B], free monocation, [BH^+], and bound monocation, [BHS_q], in solution were calculated from the simultaneous solution of the equations representing the protolytic equilibrium:

$$K_a = \frac{[H^+][B]}{[BH^+]} \qquad \text{(Eq. 1)}$$

the conservation of mass for the probe I or II:

$$C_t = [B] + [BH^+] + [BHS_q] \qquad \text{(Eq. 2)}$$

and the photometric absorbance at any point in the titration of I or II with DNA:

$$A = \epsilon_B[B]l + \epsilon_{BH^+}[BH^+]l + \epsilon_{BHS_q}[BHS_q]l \qquad \text{(Eq. 3)}$$

Explicitly:

$$[BHS_q] = \frac{\left(\epsilon_B \frac{K_a}{[H^+]} + \epsilon_{BH^+}\right)C_t l - A(1 + K_a/[H^+])}{\left\{\epsilon_B \frac{K_a}{[H^+]} + \epsilon_{BH^+} - \epsilon_{BHS_q}(1 + K_a/[H^+])\right\}l} \qquad \text{(Eq. 4)}$$

$$[BH^+] = \frac{A - \epsilon_{BHS_q}C_t l}{\left\{\epsilon_B \frac{K_a}{[H^+]} + \epsilon_{BH^+} - \epsilon_{BHS_q}(1 + K_a/[H^+])\right\}l} \qquad \text{(Eq. 5)}$$

$$[B] = \frac{(A - \epsilon_{BHS_q}C_t l)K_a/[H^+]}{\left\{\epsilon_B \frac{K_a}{[H^+]} + \epsilon_{BH^+} - \epsilon_{BHS_q}\left(1 + \frac{K_a}{[H^+]}\right)\right\}l} \qquad \text{(Eq. 6)}$$

It was also useful to calculate the ratio directly:

$$\frac{[BHS_q]}{[BH^+]} = \frac{\left(\epsilon_B \frac{K_a}{[H^+]} + \epsilon_{BH^+}\right)C_t l - A(1 + K_a/[H^+])}{A - \epsilon_{BHS_q}C_t l} \qquad \text{(Eq. 7)}$$

K_a = dissociation constant for the drug or probe
$[H^+]$ = hydronium-ion concentration
ϵ_{BHS_q} = molar absorptivity of the bound monocation at the specified analytical wavelength
ϵ_{BH^+} = molar absorptivity of the free monocation at the specified analytical wavelength
ϵ_B = molar absorptivity of the free base at the specified analytical wavelength
l = absorption cell path (1 cm)
A = absorbance at any point during the titration at the specified analytical wavelength
C_t = total concentration of drug or probe

The molar absorptivities of I and II were calculated at each absorption maximum as well as at each distinct vibrational band and agreed with published values (31, 32). The molar absorptivities of the bound monocations of I and II were calculated from the absorbances of solutions of the probes in which pH = pKa − 2 and to which a sufficient excess of DNA was added so that further addition of DNA produced no perceptible changes in the absorption. Since C_t is equal to [BHS_q] when I or II is completely sequestered by the DNA, ϵ_{BHS_q} for I and II may be readily calculated as $A/C_t l$.

The analytical wavelengths at which all calculations were made were 363 and 453 nm for I and 393 nm for II.

The pKa values of 8.04 and 6.65 of I and II, respectively, were taken from the literature (9, 31).

RESULTS AND DISCUSSION

Figures 1 and 2 are representative of the absorption spectra obtained when aqueous solutions of I and II were titrated with double-stranded DNA. Titrations were conducted at five different pH values from 5.90 to 7.90 for I and at three different pH values from 4.90 to 6.40 for II. Figures 1 and 2 contain the electronic absorption spectra of the free drug or probe, three intermediate spectra, and a final spectrum of the DNA–probe complex in which the probe has been sequestered completely by the DNA. Each titration consisted of 13–18 spectral measurements. However, some intermediate spectra were omitted from these figures for clarity.

Calculation of the solution concentrations of the free base, [B], the free monocation, [BH^+], and the bound monocation, [BHS_q], derived from I and II represents an attempt to account for all spectroscopically distinct species derived from the probes throughout the titration with DNA. The advantage of this approach is that the pH of a solution titrated with DNA need not be maintained such that the drug or probe is fully protonated. The ability to vary the pH of the test solution offers the alternative of measuring either BHS_q or B in cases where the spectra of BHS_q and BH^+ overlap to a great extent or when the affinity of BH^+ for DNA is so great that little free BH^+ is in solution.

Moreover, the reproducibility of binding constants at different values of solution pH is a good test of the absence of processes competing with the binding equilibria of interest over a given pH range. Therefore, a wider

[1] Beckman Instruments, Fullerton, Calif.
[2] Orion Research, Cambridge, Mass.
[3] Wang Laboratories, Tewksburg, Mass.
[4] Scientific Industries, Springfield, Mass.
[5] Precision Cells, Hicksville, N.Y.
[6] Unimetrics Universal Corp., Anaheim, Calif.
[7] Mallinckrodt Chemical Corp., Anaheim, Calif.
[8] Calbiochem, LaJolla, Calif.
[9] Courtesy of Dr. D. Jackman, Texas Tech University, Lubbock, Tex.

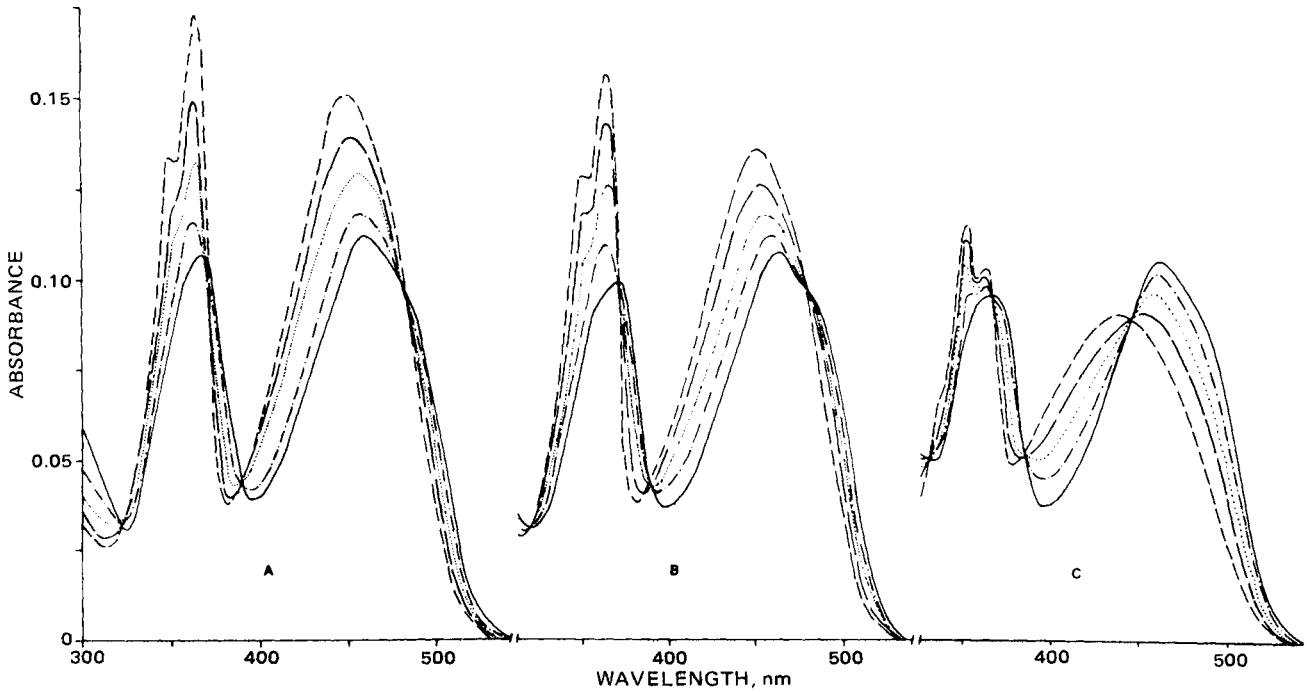

Figure 1—*Variation of the electronic absorption spectra accompanying the titrations of 1.00 × 10^{-5} M I with double-stranded DNA at pH 5.90 (A), 6.90 (B), and 7.90 (C). The* P_t *is the total DNA phosphate concentration at any point during the titration. Key:* $P_t = 0$, –; $P_t = 1.38 \times 10^{-5}$ *mole* P/l, —; $P_t = 4.13 \times 10^{-5}$ *mole* P/l, . . . ; $P_t = 8.19 \times 10^{-5}$ *mole* P/l, –·–; *and* $P_t = 14.9 \times 10^{-5}$ *mole* P/l, *solid line.*

variety of compounds may be utilized to study the complexation behavior of DNA. In studies with double-stranded DNA, this approach is limited to the pH range in which the integrity of the double helix is maintained [*i.e.*, double-stranded DNA becomes denatured at pH values below 4.00 and greater than 11.00 (33)]. Furthermore, at a high pH (pH > pKa), the competition of alkali metal ions with BH^+ for the DNA binding sites may complicate the interpretation of the titration curves.

Stoichiometry of Binding—The number of DNA phosphate groups associated with each bound monocation was estimated by the mole ratio method (34). Plots of absorbance against P_t/C_t (total DNA phosphate concentration/total probe concentration) for I with double-stranded DNA were obtained in acidic solution (pH 5.90). The stoichiometry of binding is apparently four or five phosphates for each bound BH^+. The stoichiometry is in agreement with that obtained by other investigators for different amino-substituted acridines such as proflavine, acridine orange, 9-aminoacridine, and ethidium bromide (5, 6, 35, 36).

The high degree of curvature of the mole ratio plots for II with double-stranded DNA prevented estimation of the binding stoichiometry and suggested that II is more weakly bound by double-stranded DNA than is I. This observation is supported by the weaker association constants calculated for II relative to those calculated for I (Table I).

Methods for Determining Binding Constants—Most available information concerning the binding of the aminoacridines and aminoquinolines to DNA has been gathered using the method first proposed by Scatchard (24) and then modified by Peacocke and Skerrett (5, 6) to explain spectrophotometric data acquired directly or subsequent to separation of the free and bound probes by equilibrium dialysis. In this approach, the average number of moles of probe bound per mole of DNA phosphate, $[BHS_q]/P_t$, is divided by the free protonated probe concentration, $[BH^+]$, and plotted against $[BH^+]$. This plot yields a hyperbolic curve resolvable into two linear components, one of steep slope at high values of $[BHS_q]/P_t[BH^+]$ (low values of $[BH^+]$) and one of shallow slope at low values of $[BHS_q]/P_t[BH^+]$ (high values of $[BH^+]$). The line of steep slope is associated with the intercalative (strong) binding, and the line of shallow slope is associated with external (weak) binding of the probe.

The slope of each line segment is taken to be the negative of the equilibrium constant and the intercept on the vertical axis, the product of the equilibrium constant, and the number of DNA phosphates associated with each mode of binding. It is implicit in this treatment that the number of DNA phosphate groups associated with each mode of binding is equivalent to a single binding site (*i.e.*, regardless of the number of phosphates in each type of binding site, $q = 1$ in BHS_q). Upon careful examination of the data obtained for the strong binding of I and II using this treatment, definite curvature was exhibited in the plots of $[BHS_q]/P_t[BH^+]$ against $[BH^+]$ at low values of $[BH^+]$. This result suggested that the linearity in binding site concentration, implicit in the method of Peacocke and Skerrett (5), might not adequately describe the chemistry of binding in the intercalative region. Therefore, the binding of I and II by DNA was examined by employing an empirical mass action approach.

For the systems under study, the binding equilibria may be expressed as:

$$BH^+ + qS \rightleftarrows BHS_q$$

Scheme I

where BH^+ is the free I or II monocation, q is the number of DNA binding sites that complex one BH^+, and S is the free DNA binding site, which may contain $1, 2, 3, \ldots, m$ DNA phosphates. The binding sites are defined in terms of DNA phosphate since the formal concentration of the DNA and the stoichiometry are expressed in these terms. Although binding sites on the exterior of the DNA may differ physically and chemically from intercalative (internal) binding sites, each is defined, for the present, in terms of the number of DNA phosphates engaged in binding since DNA phosphate is their common component.

The association constant, K, may be determined from:

$$K = \frac{[BHS_q]}{[BH^+][S]^q} \qquad \text{(Eq. 8)}$$

Table I—Binding Constants for the Association of I and II at Different pH Values with Double-Stranded DNA[a]

I			II	
pH	$K_1 \times 10^{-9}$	$K_2 \times 10^{-5}$	pH	$K_1 \times 10^{-6}$
5.90	6.8 ± 0.5	0.97 ± 0.04	4.90	4.2 ± 0.1
6.40	8.0 ± 0.5	1.3 ± 0.3	5.40	6.5 ± 0.7
6.90	8.3 ± 0.6	1.0 ± 0.06	6.40	6.2 ± 0.6
7.40	8.9 ± 0.7	1.0 ± 0.1		
7.90	7.0 ± 0.7	—		

[a] The constants in the intercalative (strong-binding) region of the titration of the probe with DNA (K_1) were calculated from the expression:

$$K_1 = \frac{[BHS_q]}{[BH^+](P_t/2 - [BHS_q])^2}$$

The constants in the external (weak-binding) region of the titration were calculated from the expression:

$$K_2 = \frac{[BHS_q]}{[BH^+](P_t/3 - [BHS_q])}$$

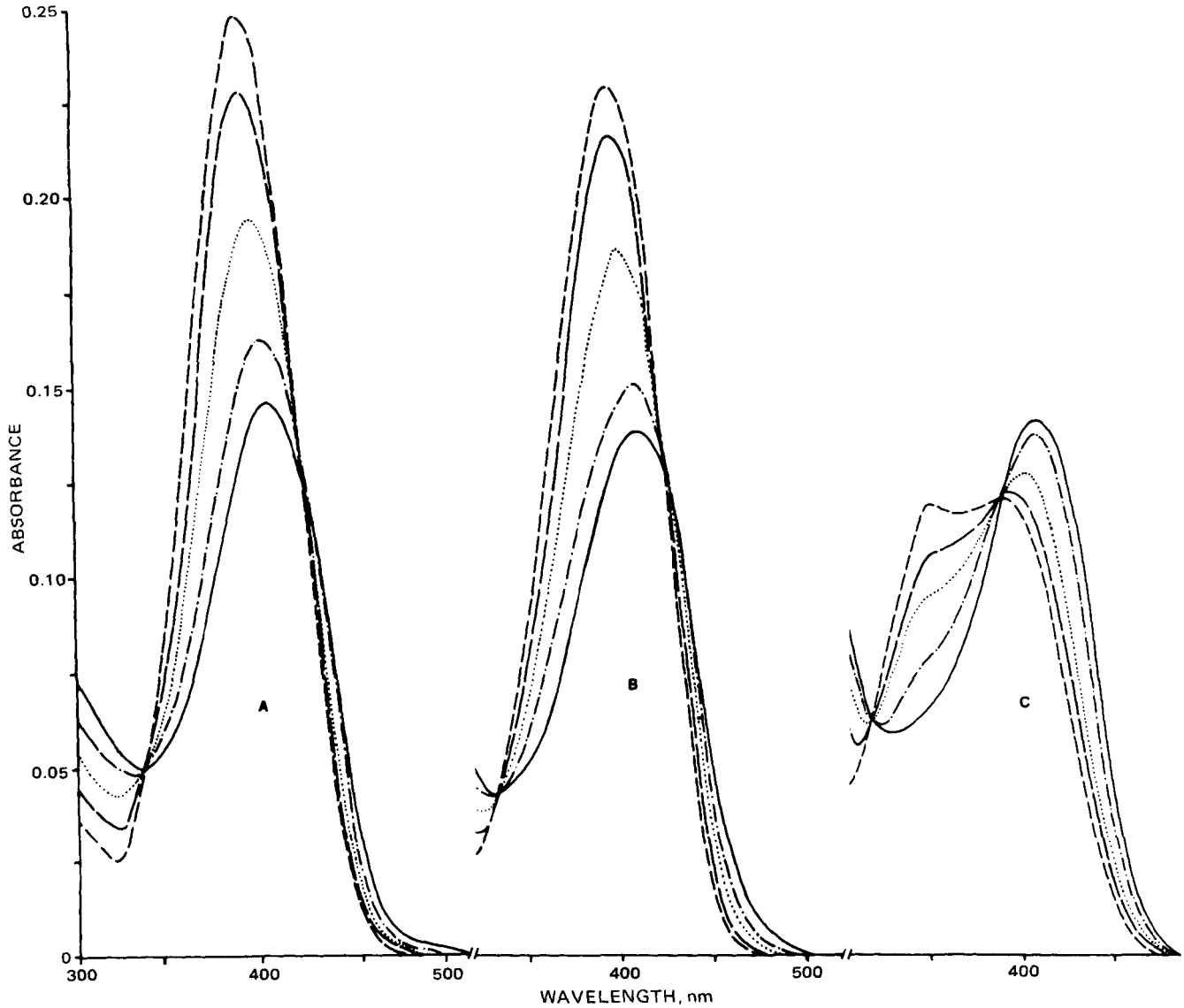

Figure 2—*Variation of the electronic absorption spectra accompanying the titrations of 1.00 × 10^{-5} M II with double-stranded DNA at pH 4.90 (A), 5.90 (B), and 6.90 (C). The* P_t *is the total DNA phosphate concentration at any point during the titration. Key:* P_t *= 0, –; P_t = 52.4 × 10^{-5} mole* P/l, —; P_t = *100 × 10^{-5} mole* P/l, . . . ; P_t = *183 × 10^{-5} mole* P/l, – –; *and* P_t = *285 × 10^{-5} mole* P/l, *solid line.*

The equilibrium concentration of free binding sites, in a given class [S], is evaluated by:

$$S_t = [S] + S_c \qquad \text{(Eq. 9)}$$

where S_t is the total concentration of DNA binding sites in moles per liter and S_c is the equilibrium concentration of complexed DNA binding sites in moles per liter. If q is the number of occupied sites, S_c, in each complex of a given class, then:

$$S_c/q = [\mathrm{BHS}_q] \qquad \text{(Eq. 10)}$$

and since P_t is the total concentration of DNA phosphate in moles per liter:

$$S_t = P_t/m \qquad \text{(Eq. 11)}$$

where m is the number of DNA phosphates in a binding site. Then [S] becomes:

$$[S] = (P_t/m - q[\mathrm{BHS}_q]) \qquad \text{(Eq. 12)}$$

Substituting Eq. 12 into Eq. 8 yields:

$$K = \frac{[\mathrm{BHS}_q]}{[\mathrm{BH}^+](P_t/m - q[\mathrm{BHS}_q])^q} \qquad \text{(Eq. 13)}$$

which, upon rearrangement, becomes:

$$[\mathrm{BHS}_q]/[\mathrm{BH}^+] = K(P_t/m - q[\mathrm{BHS}_q])^q \qquad \text{(Eq. 14)}$$

Values for [BH^+] and [BHS_q] were calculated at each point in the titration using methods described under *Experimental.*

The appropriate values for m and q were empirically determined by solving for K in Eq. 13 using probable combinations of the two constants based on the approximate stoichiometry obtained from the mole-ratio plots (the stoichiometric number of DNA phosphates bound must equal $m \times q$). Combinations of q = 1 and m = 1–6, q = 2 and m = 1–4, q = 3 and m = 1–3, and q = 4 and m = 1, 2 were attempted to fit the data of the titrations to Eq. 13. The combination of q = 2 and m = 2 gave the best fit of K to the data points in the intercalative region. In the region generally associated with external binding, the combination of q = 1 and m = 3 gave the most reproducible value of K. The results of these calculations are shown in Table I.

Equation 14 can be expressed in logarithmic form such that:

$$\log [\mathrm{BHS}_q]/[\mathrm{BH}^+] = \log K + q \log (P_t/m - q[\mathrm{BHS}_q]) \qquad \text{(Eq. 15)}$$

This equation allows a rapid graphical estimate of the suitability of estimated values of m and q over an extended titration range. Log [BHP]/[BH^+] against log ($P_t/m - q[\mathrm{BHS}_q]$) was plotted for I and II, with double-stranded DNA, using the empirically chosen value of 2 for both

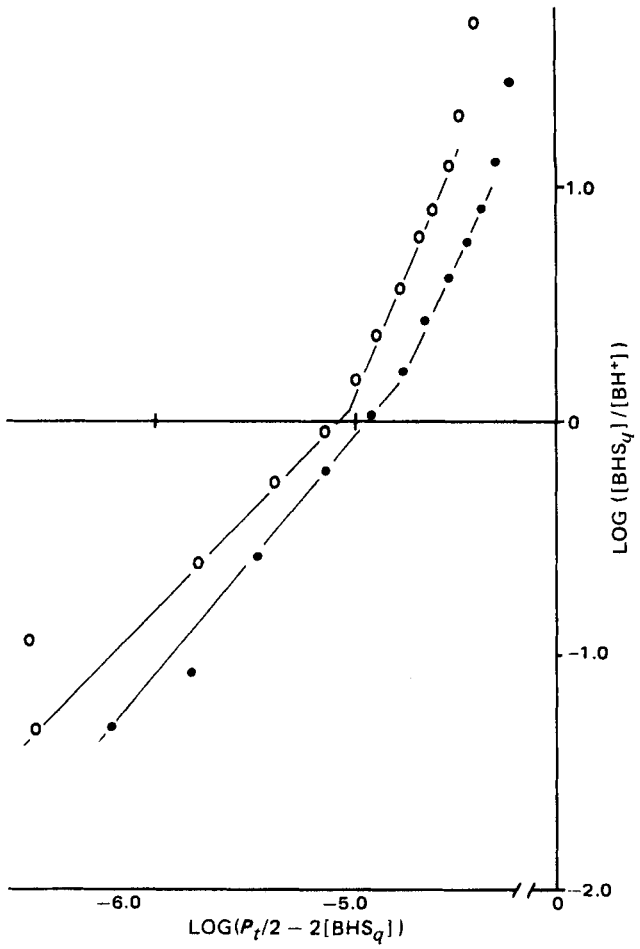

Figure 3—*Logarithmic plots of the ratio of bound monocation [BHS$_q$] to free monocation [BH$^+$] against (P_t/2 − 2[BHS$_q$]) for I titrated with double-stranded DNA at pH 6.40 (○) and 7.40 (●).*

m in the P_t/m term and q in the q[BHS$_q$] term. The slope of the plot should be 2 and the intercept should be log K where $m = q = 2$ correctly represents the binding isotherm.

Representative results for I with double-stranded DNA are found in Fig. 3. This figure exhibits two distinct regions of linearity. The linear region of least slope corresponds to the external binding region of each titration, although this line segment has no rigorous physical significance when m and q are chosen as 2. The linear region of greatest slope corresponds to the intercalative region of each titration. The presence of two regions of linearity strongly suggests that there are at least two separate modes of binding. One occurs at the beginning of the titration at concentrations of I such that only external binding sites on the DNA molecule are available. The other occurs near the latter part of the titration at total concentrations of I such that intercalative binding could predominate (*i.e.*, $P_t/([BH^+] + [BHS_q]) > 10$).

The slopes of these two linear regions, $q = 2.0 \pm 0.3$ and $q = 1.00 \pm 0.04$, indicate that the nature of the binding site differs in each mode of binding. The poor precision in the former slope may indicate overlap of the two modes of binding when the free binding site concentration is high. If $q = 2$ is substituted in Scheme I:

$$BH^+ + 2S \rightleftarrows BHS_2$$

Scheme II

However, the binding stoichiometry of I to double-stranded DNA was determined to be four or five DNA phosphates per BH$^+$. This result can be accounted for by considering that one BH$^+$ may be complexed by two binding sites, each containing two phosphate groups, in separate steps. Scheme II will then be equivalent to:

$$BH^+ + 2[PO_4]_2 \rightleftarrows BH([PO_4]_2)_2$$

Scheme III

where $[PO_4]_2$ is conceived as representing one binding site. Kinetic studies demonstrated that the binding of proflavine and acridine orange to

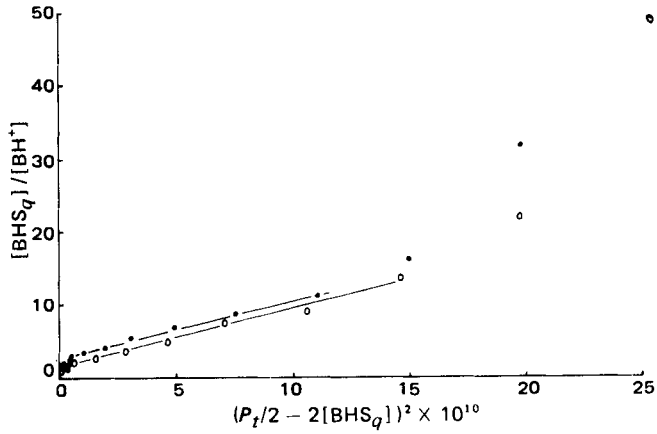

Figure 4—*Linear plots of the ratio of bound monocation [BHS$_q$] to free monocation [BH$^+$] against (P_t/2 − 2[BHP])^2 for I titrated with double-stranded DNA at pH 6.40 (○) and 7.40 (●).*

double-stranded DNA occurs in two discrete steps at concentrations of probe and DNA such that only intercalative binding can occur (19–23).

The mathematical model of the binding equilibrium in the intercalative region, represented in Scheme III, does not establish a detailed mechanism for the interaction. Moreover, the physical significance of the occurrence of two DNA phosphates in each intercalative binding site is not clear from the present study. The diphosphate units are not independently diffusing entities and, on the DNA polyanion, may actually represent two singly charged phosphate groups, two adjacent bases on one DNA strand, or one DNA base pair on complimentary strands.

Furthermore, it is even possible that the two diphosphate units represented in Scheme III may not represent identical physical entities but may actually be a combination of two different binding sites of the types just mentioned. For example, the intercalative process could entail a diffusion-controlled encounter of a monocation with the phosphate backbone of DNA, with a strong electrostatic interaction occurring between the cation and two neighboring phosphate groups. As suggested by the experiments of Li and Crothers (19), the externally bound cation could then move, in a second discrete step, into the interior of the double helix. This would require that two more DNA phosphates (and their associated bases) would be removed from the pool of "free" phosphate groups and thereby account for the four phosphates associated with each intercalated monocation. However, at equilibrium, the interaction with the DNA base pairs may actually be more important than the interaction with the phosphate groups.

The complexation of II by double-stranded DNA was comparable to that observed for I. Empirically determined values for m and q were the same as those for I under the same conditions ($m = q = 2$). However, values for the slopes of the logarithmic plots were not as consistent as those calculated for I. The correlation coefficients, although still indicating that the slopes drawn correlate to the equation for a straight line, were not quite as good, nor were the errors as small, as those obtained for I. Moreover, it was not possible to observe a well-defined region of weaker external binding for II. Possibly this is because external binding is so weak that it does not occur to a significant degree with the concentrations of reagents and buffer species employed in the present experiments.

The adherence of the binding reaction to an isotherm linear in the concentration of the binding site appears to be valid in the beginning of the titration of the monocations with DNA where saturation of the intercalative binding sites of double-stranded DNA by the monocations exists. The available DNA binding sites in this region of the titration contain three DNA phosphates.

General Power Curve, $y = Kx^b$—A nonlinear regression analysis was conducted at each pH to test the two regions of linearity observed in the logarithmic plots obtained from titrations of I and II with double-stranded DNA. The data points constituting the region of greatest slope in these plots followed the equation of the power curve and:

$$[BHS_q]/[BH^+] = K(P_t/2 - 2[BHS_q])^b \qquad \text{(Eq. 16)}$$

The power $b \simeq q \cong 2.0 \pm 0.2$ while the average correlation coefficient was 0.996 ± 0.003. This result supports the conclusion that the power, q, cannot be neglected when writing equilibrium expressions to describe the strong complexation (intercalation) of I and II and perhaps other aminoacridines and aminoquinolines to double-stranded DNA. The data

points comprising the region of least slope in these logarithmic plots also followed Eq. 16, with $b \cong a \cong 1 \pm 0.1$. The average correlation coefficient was 0.997 ± 0.002.

Linear Plots—To confirm the significance of the exponent q in the equilibrium expression describing the intercalative binding region, elements of Eq. 14 were plotted against each other. Linear plots of $[BHS_q]/[BH^+]$ against $(P_t/2 - 2[BHS_q])$ were drawn in which the power, q, was set equal to 2 for each pH at which the titrations were conducted. Figure 4, which is representative, shows that the linear plots exhibit a definite region of linearity, corresponding to the intercalative region of the titration.

A linear regression analysis of the linear portions in these plots revealed an average correlation coefficient of 0.997 ± 0.002 for I titrated with double-stranded DNA; the value for a similar titration of II was 0.991 ± 0.006. The results indicate that Eq. 14 fits well the experimental data obtained from the titrations of I with double-stranded DNA, when q is set equal to 2. The experimental fit of the data obtained from similar titrations with II, however, is more approximate.

CONCLUSIONS

The complexation of I and II by double-stranded DNA at high P_t/C_t (total DNA phosphate concentration/total probe concentration) values may be described by a nonlinear binding isotherm in which one monocation is sequestered in at least two successive steps by two separate entities on the DNA polymer, each containing two phosphate groups. This process may be described by Scheme III.

However, the complexation of the same compounds by double-stranded DNA, having only external binding sites vacant, evidently follows a linear binding isotherm in which one monocation is complexed by one binding site containing three phosphate groups. The latter binding process may be described by:

$$BH^+ + [PO_4]_3 \rightleftarrows BH([PO_4]_3)$$

Scheme IV

REFERENCES

(1) L. S. Lerman, *J. Mol. Biol.*, **3,** 18 (1961).

(2) L. S. Lerman, *Proc. Natl. Acad. Sci. USA,* **49,** 94 (1963).

(3) L. S. Lerman, *J. Cell. Comp. Physiol., Suppl. 1,* **64** (1964).

(4) N. J. Pritchard, A. Blake, and A. R. Peacocke, *Nature,* **212,** 1360 (1966).

(5) A. R. Peacocke and J. N. H. Skerrett, *Trans. Faraday Soc.,* **52,** 261 (1956).

(6) A. R. Peacocke, in "Acridines," 2nd ed., R. M. Acheson, Ed., Interscience, New York, N.Y., 1973, chap. 14.

(7) W. Kersten, H. Kersten, and W. Szybalski, *Biochemistry,* **5,** 236 (1966).

(8) W. Muller, D. M. Crothers, and M. S. Waring, *Eur. J. Biochem.,* **39,** 223 (1973).

(9) A. Albert, "The Acridines," 2nd ed., Arnold, London, England, 1966, chap. II.

(10) C. N. Hinshelwood, "The Kinetics of Bacterial Change," Clarendon Press, Oxford, England, 1946.

(11) A. Blake and A. R. Peacocke, *Biopolymers,* **6,** 1225 (1968).

(12) S. Brenner, L. Barnett, F. H. C. Crick, and A. Orgel, *J. Mol. Biol.,* **3,** 121 (1961).

(13) F. H. C. Crick, L. Barnett, S. Brenner, and R. J. Watts-Tobin, *Nature,* **192,** 1227 (1961).

(14) J. Hurwitz, J. J. Furth, M. Malamy, and M. Alexander, *Proc. Natl. Acad. Sci. USA,* **48,** 1222 (1962).

(15) B. H. Nicholson and A. R. Peacocke, *Biochem. J.,* **100,** 50 (1966).

(16) "The Pharmacological Basis of Therapeutics," 4th ed., L. S. Goodman and A. Gilman, Eds., Macmillan, New York, N.Y., 1970, chap. XIII.

(17) A. Albert, "Selective Toxicity," 4th ed., Methuen & Co., London, England, 1968, chap. 3.

(18) *Ibid.*, chap. 8.

(19) J. H. Li and D. M. Crothers, *J. Mol. Biol.,* **39,** 461 (1969).

(20) W. Muller and D. M. Crothers, *ibid.*, **35,** 251 (1968).

(21) K. Akasaka, M. Sakoda, and K. Hiromi, *Biochem. Biophys. Res. Commun.,* **40,** 1239 (1970).

(22) M. Sakoda, K. Hiromi, and K. Akasaka, *Biopolymers,* **10,** 1003 (1971).

(23) M. Sakoda, K. Hiromi, and K. Akasaka, *J. Biochem.,* **71,** 891 (1972).

(24) G. Scatchard, *Ann. N.Y. Acad. Sci.,* **51,** 660 (1949).

(25) R. W. Armstrong, T. Kurucsev, and U. P. Strauss, *J. Am. Chem. Soc.,* **92,** 3174 (1970).

(26) C. Gatli, C. Houssier, and E. Fredericq, *Biochim. Biophys. Acta,* **407,** 308 (1975).

(27) T. Meites and L. Meites, *Talanta,* **19,** 1130 (1972).

(28) S. G. Schulman, K. Abate, P. J. Kovi, A. C. Capomacchia, and D. Jackman, *Anal. Chim. Acta,* **65,** 59 (1973).

(29) R. F. Martin and J. H. Y. Tong, *Aust. J. Chem.,* **22,** 487 (1969).

(30) K. Matsumara, *J. Am. Chem. Soc.,* **61,** 2247 (1939).

(31) E. V. Brown and A. Plasz, *J. Heterocycl. Chem.,* **7,** 335 (1970).

(32) A. Albert, *J. Chem. Soc.,* **1965,** 4653.

(33) A. L. Lehninger, "Biochemistry," Worth, New York, N.Y., 1970, p. 645.

(34) J. H. Yoe and A. L. Jones, *Ind. Eng. Chem., Anal. Ed.,* **16,** 111 (1944).

(35) J. B. Lepecq and C. Paoletti, *J. Mol. Biol.,* **27,** 87 (1967).

(36) G. Löber, *Stud. Biophys.,* **8,** 99 (1968).

ACKNOWLEDGMENTS

Adapted in part from a dissertation submitted by A. C. Capomacchia to the University of Florida in partial fulfillment of the Doctor of Philosophy degree requirements.

The authors are grateful to Ms. Rebecca McKinley for typing the manuscript and to P. F. Eisenhardt for helpful suggestions.

Estimation of Dissolution Rate of Salicylamide in Complexing Media Using a Theoretical Diffusion Model

M. DONBROW ˣ **and E. TOUITOU**

Received June 24, 1976, from the *Department of Pharmacy, School of Pharmacy, Hebrew University of Jerusalem, Jerusalem, Israel.* Accepted for publication April 15, 1977.

Abstract □ Dissolution rates of salicylamide in water and caffeine solutions under perfect sink conditions were predicted by theoretical diffusion equations applicable to dissolution in complexing media. Experimental dissolution rates were measured using a compartmentalized rotating-basket apparatus under two sets of conditions. Agreement was found between experimental and predicted rates. Use of the theoretical equation for estimating dissolution rates involves simple calculations of diffusion coefficients and diffusion layer thickness under the operative dissolution conditions. The increase in dissolution rate caused by addition of the complexant can be calculated for diffusion-controlled dissolution directly if the stability constant and the drug solubility in water are known or measured.

Keyphrases □ Dissolution rates—salicylamide in water and caffeine solutions, estimated using theoretical diffusion model, compared to experimental results □ Salicylamide—dissolution rates in water and caffeine solutions, estimated using theoretical diffusion model, compared to experimental results □ Diffusion model, theoretical—used to estimate dissolution rates of salicylamide in water and caffeine solutions, compared to experimental results □ Complexes—salicylamide and caffeine, dissolution rates estimated using theoretical diffusion model, compared to experimental results

Dissolution rates of solid drug products in media containing substances capable of reaction with the drug have aroused much interest in view of their possible influence on bioavailability. Three main classes of interactions affecting dissolution have been recognized. The first, involving pH equilibria and their effects on the degree of drug ionization, has been investigated extensively, and theoretical treatments have been developed and tested (1–3). The second is the interaction between drugs and macromolecules, such as colloids or surfactant micelles, generally added as formulating agents; this area also has received considerable study (4–8).

Much less attention has been paid, however, to the third type, complex formation, which may occur between the drug and formulating agents, other drugs, food ingredients, enzymes, and toxins. Interaction of solid phase components was treated theoretically as one case of dissolution from polyphase mixtures, and the equations developed agreed with the dissolution behavior of caffeine–benzocaine disks (9). The initial dissolution rates of solid complexes of caffeine and gentisic acid were compared with those of caffeine using a simplified mathematical treatment (10). With regard to the interacting medium, the dissolution rate of 2-naphthol was studied in several complexing media. Experimental results were not reproducible, nor did they obey the Noyes–Whitney equation; a "concentration jump" extrapolation technique was developed to compare dissolution rates during individual experiments (11).

The purpose of the present studies was to determine whether a general diffusional mathematical treatment was applicable to prediction of dissolution rates over a range of complexant concentrations under experimental conditions used for *in vitro* testing. Such a treatment would permit theoretical estimation of dissolution rates in various complexing media since stability constants of many complexes are available or are easily measured; the necessary hydrodynamic parameters of the dissolution apparatus may be estimated for standard conditions.

THEORETICAL

The treatment used is based on the general theory previously developed (1) for the influence of bases on the dissolution of acidic solids undergoing diffusion-controlled transport through a liquid film. The complexation equilibrium replaces the ionization equilibrium, and the formation constant of the complex is the factor determining the activities of the free and complexed drug in the film and bulk medium. Complexation is considered to occur throughout a single liquid film at the solid interface through which there is a continuous concentration gradient rather than at a plane surface of contact somewhere within the film. Concentration gradients in the film need not be linear, but the chemical equilibrium must be rapid compared to transport. Diffusion coefficients are considered to be concentration independent. The treatment is based on the "unstirred" diffusion layer model.

In the test apparatus used in the present work (see *Experimental*), in which solvent flow occurs through a tube cut into a cylindrical block, the velocity gradient for streamline flow may be considered to be zero at the sides of the tube. In effect, the tube is bisected by the large flat compressed disk inserted in the center, which gives two hemispherical streamlined flows, with the velocity gradient approximated to zero over the disk surface. Equations for dealing with convective flow components were proposed previously (12–14) but are applicable to idealized model systems and are not valid for the apparatus used here. For the defined test apparatus, the film thickness is considered to be dependent on the stirring rate but independent of all other factors except viscosity.

For dissolution of a solid unionized substrate, S, in the presence of an unionized complexant molecule, C, with which it forms complexes in solution by the Scheme I reactions:

$$S + C \rightleftarrows SC$$

$$S + 2C \rightleftarrows SC_2, \textit{ etc.}$$

Scheme I

the thermodynamic stability constants $K_{a(1:1)}$, $K_{a(1:2)}$, *etc.*, are given by:

$$K_{a(1:1)} = (SC)/(S)(C) \qquad \text{(Eq. 1}a\text{)}$$

$$K_{a(1:1)} = K_{c(1:1)}\,\gamma_{SC}/\gamma_S\gamma_C \qquad \text{(Eq. 1}b\text{)}$$

$$K_{a(1:2)} = (SC_2)/(S)(C)^2 \qquad \text{(Eq. 1}c\text{)}$$

$$K_{a(1:2)} = K_{c(1:2)}\,\gamma_{SC_2}/\gamma_S\gamma_C{}^2 \qquad \text{(Eq. 1}d\text{)}$$

where parentheses represent activities and γ activity coefficients of the various species and K_c is the concentration equilibrium constant. Concentrations and concentration stability constants are applicable to dilute aqueous solutions of nonelectrolytes, for which $\gamma \rightarrow 1$, and are used here.

With Olander's treatment (15), the solution rate of S is given by the fluxes of all species containing S—*viz.*, S, SC_2, . . . , SC_n. The concentration of each species SC_n formed can be evaluated, in principle, if the individual $K_{1:n}$ constants are known and used in conjunction with the appropriate diffusion coefficient of the species to write a flux equation. For weak complexes formed at low concentrations in water, measured K values are generally overall values or represent the dominant complex.

By designating steady-state concentrations at the solid–liquid interface with the subscript 0 and in the bulk solution with the subscript h, the

Table I—Estimated Diffusion Coefficients of Salicylamide, Caffeine, and Their 1:1 Complexes at 25 and 37°

Species	Partial Molal Volume, v, cm³/mole[a]	Diffusion Coefficient, D, cm²/sec × 10⁵[b] 25°	37°
Salicylamide	100	1.06	1.42
Caffeine	127	0.978	1.31
1:1 Complex	228	0.806	1.08

[a] The v values were calculated using data from Ref. 22. [b] The D values were calculated by means of Eq. 11.

concentrations of the components on the two sides of a film of thickness h (considered as one dimensional) are given by: $[S]_0$, $[C]_0$, and $[SC]_0$ and $[S]_h$, $[C]_h$, and $[SC]_h$, respectively. Application of Fick's second law (16) and Higuchi's treatment (1) to the steady-state condition leads to:

$$V_D = \frac{D_S([S]_0 - [S]_h)}{h} + \frac{D_C D_{SC} K([S]_0 - [S]_h)(D_{SC}[SC]_h + D_C[C]_h)}{h(D_{SC}[S]_0 K + D_C)(D_{SC}[S]_h K + D_C)} \quad \text{(Eq. 2)}$$

where V_D is the dissolution rate per unit area of substrate in the complexant solution in which a 1:1 complex of stability constant K is formed; D_S, D_C, and D_{SC} are the diffusion coefficients of the respective species. This equation is parallel to that developed for a nonionic acid–base equilibrium (1). Equation 2 may be simplified by using Eq. 1 to eliminate $[SC]_h$, giving:

$$V_D = \frac{D_S([S]_0 - [S]_h)}{h} + \frac{D_C D_{SC} K[C]_h([S]_0 - [S]_h)}{h(D_{SC}K[S]_0 + D_C)} \quad \text{(Eq. 3)}$$

When K is very small, Eq. 3 reduces to the usual Noyes–Whitney equation for dissolution of the pure solid:

$$V_D = \frac{D_S}{h}([S]_0 - [S]_h) \quad \text{(Eq. 4)}$$

When K is very large, Eq. 3 takes the form:

$$V_D = \frac{D_S}{h}([S]_0 - [S]_h) + \frac{D_C}{h}[C]_h \quad \text{(Eq. 5)}$$

Further simplifications of the general equation may be made under zero sink conditions when $(S)_h = (SC)_h = 0$. Equation 3 then reduces to:

$$V_D = \frac{[S]_0}{h}\left(D_S + \frac{D_C D_{SC} K[C]_h}{D_{SC}K[S]_0 + D_C}\right) \quad \text{(Eq. 6)}$$

or:

$$V_D = L_1 + L_2[C]_h \quad \text{(Eq. 7)}$$

where $L_1 = ([S]_0 D_S)/h$ and $L_2 = ([S]_0 D_C D_{SC} K)/h(D_{SC}K[S]_0 + D_C)$. Equation 7 predicts a linear increase of the dissolution rate with the complexant concentration, $[C]_h$.

When the diffusion coefficients have similar values, as with interactants differing in molecular weight by a factor of less than three (10), Eqs. 3–7 may be further simplified. Equation 6, for example, gives:

$$V_D = \frac{[S]_0 D}{h}\left(1 + \frac{K[C]_h}{K[S]_0 + 1}\right) \quad \text{(Eq. 8a)}$$

$$V_D = \frac{[S]_0 D}{h}\left(1 + \frac{[C]_h}{[S]_0 + 1/K}\right) \quad \text{(Eq. 8b)}$$

By rearrangement and substitution of $(K[S]_0[C]_h)/(K[S]_0 + 1)$ by $[SC]_0$[1], Eq. 8a approximates:

$$V_D = \frac{D}{h}([S]_0 + [SC]_0) = \frac{D}{h}c_S \quad \text{(Eq. 9)}$$

where c_S is the apparent salicylamide solubility; *i.e.*, $c_S = [S]_0 + [SC]_0$.

By using this relation, the ratio, R, of the dissolution rates in the caffeine solutions to those in water (Eq. 4 with $[S]_h = 0$) are given, under these limitations, by:

$$R = c_S/[S]_0 \quad \text{(Eq. 10)}$$

Table II—Diffusion Layer Thickness (h) at 25° and 48 rpm and at 37° and 90 rpm

Caffeine Concentration, $M \times 10^2$	Salicylamide Solubility, $M \times 10^2$	f_S/f_{SC}	D_m, cm²/sec × 10⁵[a]	h, cm × 10²[b]
		37° and 90 rpm		
1.00	—	—	—	—
2.90	4.50	2.11/1	1.31	0.87
3.00	—	—	—	—
5.00	—	—	—	—
5.75	6.07	1.07/1	1.25	0.97
8.12	7.38	1/1.32	1.22	1.03
		25° and 48 rpm		
2.25	—	—	—	—
2.90	2.85	1.02/1	0.93	1.35
3.50	—	—	—	—
4.00	3.36	1/1.25	0.92	1.36
8.12	5.27	1/2.74	0.87	1.34

[a] Calculated by means of Eq. 13. [b] Calculated by means of Eq. 12. The values of h for this apparatus estimated from benzoic acid dissolution rates were 0.82×10^{-2} at 37° and 90 rpm and 1.73×10^{-2} cm at 25° and 48 rpm.

EXPERIMENTAL

Materials—Salicylamide[2] and caffeine[3] were NF grade.

Viscosity and Density—The viscosity of filtered solutions containing mixtures of salicylamide and salicylamide–caffeine complex, prepared by saturation with salicylamide at the various caffeine concentrations, was measured at 25 and 37° using a capillary viscometer[4]. The densities of these solutions were measured at 25 and 37° pycnometrically.

Solubility of Salicylamide—The solubilities of salicylamide in water at 25 and 37° and the stability constants of its complex with caffeine were obtained by the solubility method. Experimental conditions and phase diagrams were reported elsewhere (18).

Dissolution Rate Determinations—Salicylamide was compressed into cylindrical tablets (diameter, 13.1 mm; thickness, 2.9 mm; and weight, 493 mg ± 1.5%) in a vacuum potassium bromide die with a laboratory press at high pressure[5]. Release of the drug was measured using a rotating-disk dissolution apparatus (19) in 1 liter of dissolution medium containing increasing concentrations of caffeine. Experiments were run at 48 rpm and 25° and at 90 rpm and 37° over 3 hr. Samples were assayed for total salicylamide content spectrophotometrically at λ_{max} 525 nm using a modified Trinder's reagent (18).

Corrections were applied for cumulative dilution caused by replacement of samples by equal volumes of the original medium. Two tablets were used per test; experiments were run in duplicate and the results were averaged. Reproducibility was within ±3%. The data were treated by means of the Hixson–Crowell equation (20), and dissolution rates ($3K'$) were obtained from the slopes ($K'a$) of $(W_0^{1/3} - W^{1/3})$ against time[6], which were linear throughout each experiment. The tablets maintained a constant shape throughout the measurements.

RESULTS AND DISCUSSION

Dissolution rates were predicted by Eq. 6, with perfect sink conditions prevailing throughout the measurements. The values used for $[S]_0$, the solubility of salicylamide in water, were 1.50×10^{-2} M at 25° and 2.90×10^{-2} M at 37°; the stability constants, K, at these temperatures were 57.9 and 44.1 M^{-1}, respectively (18). The diffusion coefficients (Table I) of the species S, C, and SC were calculated by the Stokes–Einstein equation (Eq. 11) (22):

$$D = \frac{RT}{4\pi\eta N}\left(\frac{4\pi N}{3v}\right)^{1/3} \quad \text{(Eq. 11)}$$

where R is the molar gas constant, T is the absolute temperature, η is the viscosity of the solvent, N is Avogadro's number, and v is the partial molal volume.

For the apparatus used in the present work, calculation of the apparent diffusion layer thickness, h, involved hydrodynamic properties, which are not readily definable. Therefore, this parameter was estimated experimentally by using compressed disks of a model solute, benzoic acid, reported to give diffusion-controlled dissolution (23).

[1] Here, $[SC] = Sl[C]_h$ and $Sl = K[S]_0/(1 + K[S]_0)$, where Sl is the slope of substrate solubility *versus* ligand concentration in the phase diagram (17).
[2] Sigma Chemical Co., St. Louis, Mo.
[3] Merck, Darmstadt, West Germany.
[4] Ostwald type U tube, A. Gallenkamp & Co., London, England.
[5] Research and Industrial Instruments Co., London, England.
[6] The notation used is that of Parrott *et al.* (21), except that K' replaces K.

Table III—Dissolution Rate, Experimental and Estimated Data

Caffeine Concentration, $M \times 10^2$	Salicylamide Concentration, c_S, $M \times 10^2$	Dissolution Rate, moles $cm^{-2}/sec \times 10^8$ [a]		Dissolution Rate Ratio[b]			
		Experimental	Estimated	R_1	R_2	R_3	R_4
		25° and 48 rpm					
0	1.50	0.98	1.09	—	—	—	—
0.26	1.62	1.09	1.12	1.11	1.14	1.02	1.08
0.47	1.72	1.22	1.23	1.24	1.26	1.12	1.14
0.94	1.92	1.34	1.36	1.37	1.39	1.24	1.28
2.00	2.43	1.66	1.66	1.70	1.70	1.31	1.62
2.90	2.85	1.96	1.92	2.00	1.96	1.75	1.90
4.70	3.68	2.39	2.43	2.44	2.48	2.21	2.45
8.12	5.27	3.43	3.40	3.50	3.47	3.09	3.47
		37° and 90 rpm					
0	2.90	4.25	4.11	—	—	—	—
1.99	4.00	6.38	5.44	1.50	1.28	1.32	1.37
3.26	4.70	6.86	6.30	1.61	1.48	1.53	1.62
4.08	5.15	7.23	6.86	1.69	1.61	1.66	1.76
5.57	5.97	7.75	7.85	1.82	1.84	1.90	2.06
7.42	6.99	8.50	8.63	2.00	2.00	2.10	2.41

[a] Slope of dissolution rate against caffeine concentration. At 25° and 48 rpm: experimental = 2.95×10^{-4} ($r = 0.998$), and predicted = 2.89×10^{-4} ($r = 0.999$). At 37° and 90 rpm, experimental = 5.36×10^{-4} ($r = 0.962$), and predicted = 6.21×10^{-4} ($r = 0.999$). Slope units are centimeters per second. [b] Ratio of dissolution rate in caffeine solution to that in water: R_1, both from experimental data; R_2, predicted values from Eq. 6 for caffeine solutions and experimental data for water; R_3, both predicted from Eq. 6; and R_4, predicted from Eq. 10.

The apparent h value was obtained from the experimental dissolution rates and solubilities measured in 0.01 N HCl and substituted in Eq. 12 based on the Nernst theory (24):

$$h = \frac{Dc_S}{3K'} \qquad \text{(Eq. 12)}$$

The h values (Table II) were close to those calculated from the experimental parameters of the salicylamide–caffeine system, obtained using the same equation.

In calculating the thickness from dissolution rates corresponding to different forms of the diffusing substrate, D_m is the weighted mean diffusion coefficient—*viz.*:

$$D_m = f_S D_S + f_{SC} D_{SC} = \sum f_i D_i \qquad \text{(Eq. 13)}$$

where f_S and f_{SC} are the fractions of free and complexed salicylamide, respectively. These values were calculated from the complexation data (18) using the relations $f_S = 1/(K[C]_h + 1)$ and $f_{SC} = K[C]_h/(K[C]_h + 1)$, in which $[C]_h$ is the total caffeine concentration (Table II).

Estimated and experimental dissolution rates are given in Table III for caffeine concentrations used in the dissolution medium. At 25° and 48 rpm, the predicted and measured rates are virtually identical over the full concentration range.

There is reasonable agreement also at 37° and 90 rpm; the deviation of the first two points is the cause of the lower correlation coefficient, 0.962, of the experimental regression line; its source is apparently interfacial control of the dissolution process when the transport is largely of free salicylamide (25). There is evidence of a similar deviation of the initial point at 25 and 48 rpm, but it is small.

Participation of the interfacial control in the process is supported by point-to-point comparison of experimental and estimated ratios of the dissolution rates. Ratios of the dissolution rates in the caffeine solutions to those in water are included in Table III. When calculated with respect to the experimental dissolution rate in water at the respective temperature and agitation rate, the experimental ratios, R_1, and theoretical ratios, R_2, are in good agreement. However, when estimated with respect to the predicted dissolution rate of salicylamide in water, the predicted ratios, R_3, agree much less well with the experimental values.

Evidently, R_3 values based on rate equations that assume diffusion control for salicylamide dissolution in both caffeine solutions and water are incorrect for comparison with the experimental systems, so agreement is rather poor. However, the predicted ratios calculated with respect to the experimental rates in water, R_2, do take into account the initial interfacial control. Therefore, they become virtually identical with the experimental R_1 values as soon as the caffeine concentration is sufficient for the process to become diffusion controlled. The addition of the caffeine shifts the process from interfacial to diffusion control because of the increase of salicylamide concentration in the diffusion layer in the form of the complexed species.

Deviation from the linear diffusion model used in the present study might also be expected in three other cases: (*a*) where insoluble complexes are formed that coat the surface of the solid substrate, (*b*) where the complex contains more than one molecule of the ligand, and (*c*) where there is multiple complexation. In the first case, the dissolution rate–ligand concentration plot would exhibit a break; in the other cases, it would be curved since powers of $[C]_h$ would be involved. Ratios calculated in accordance with Eq. 10 (Table III, R_4) are also of the same order as the experimental ratios, R_1, the deviations presumably arising from the D approximation made. Thus, this simple equation yields a rapid estimate of the dissolution rate change obtained on complexation in these systems.

CONCLUSIONS

Complexation between the two drugs doubled the salicylamide dissolution rate at 37° and increased it fourfold at 25° over the range used. The experimental conditions selected covered substantial differences in K values, solubilities, and agitation rates. Therefore, since Eq. 6 and the estimated parameters correctly predicted the diffusion behavior during dissolution, they might afford a general procedure for estimating dissolution rates for a range of ligands without point-by-point experimental studies[7].

On the other hand, the dissolution rate of the substrate in water should always be measured since, should it differ appreciably from the predicted value, one would suspect interfacial control of dissolution rate to be present[8]. It would then be necessary to extend the experimental studies over a ligand concentration range sufficient to clarify the onset of diffusion control.

REFERENCES

(1) W. I. Higuchi, E. L. Parrott, D. E. Wurster, and T. Higuchi, *J. Am. Pharm. Assoc., Sci. Ed.*, **47**, 376 (1958).

(2) W. E. Hamlin and W. I. Higuchi, *J. Pharm. Sci.*, **55**, 205 (1966).

(3) J. H. Collett, J. A. Rees, and N. A. Dickinson, *J. Pharm. Pharmacol.*, **24**, 724 (1972).

(4) P. W. Taylor, Jr., and D. E. Wurster, *J. Pharm. Sci.*, **54**, 1654 (1965).

(5) E. L. Parrott and V. K. Sharma, *ibid.*, **56**, 1341 (1967).

(6) S. Feldman, M. Gibaldi, and M. Reinhard, *ibid.*, **60**, 1105 (1971).

(7) J. A. Rees and J. H. Collett, *J. Pharm. Pharmacol.*, **26**, 956 (1974).

(8) M. Z. Biber and C. T. Rhodes, *Acta Pharm. Suec.*, **11**, 275 (1974).

(9) W. I. Higuchi, N. A. Mir, and S. J. Desai, *J. Pharm. Sci.*, **54**, 1405 (1965).

[7] The procedure has not yet been tested with other types of dissolution apparatus, but further studies are underway.

[8] The water experiment would also permit detection of surface area deviations (12). If the ligand possessed surface activity, it might influence the dissolution rate even before an appreciable amount of complex was formed. There is no evidence of such an effect with caffeine.

(10) T. Higuchi and I. H. Pitman, *ibid.*, **62**, 55 (1973).
(11) T. Higuchi, S. Dayal, and I. H. Pitman, *ibid.*, **61**, 659 (1972).
(12) L. L. Bircumshaw and A. C. Riddiford, *Q. Rev.*, **6**, 157 (1952).
(13) K. G. Nelson and A. C. Shah, *J. Pharm. Sci.*, **64**, 610 (1975).
(14) A. C. Shah and K. G. Nelson, *ibid.*, **64**, 1519 (1975).
(15) D. R. Olander, *Am. J. Ch. E.*, **6**, 233 (1960).
(16) W. Jost, "Diffusion," Academic, New York, N.Y., 1960.
(17) M. Donbrow and Z. A. Jan, *J. Pharm. Pharmacol., Suppl.*, **17**, 129S (1965).
(18) M. Donbrow, E. Touitou, and H. Ben-Shalom, *ibid.*, **28**, 766 (1976).
(19) D. L. Simmons, M. Frechette, R. J. Ranz, W. S. Chen, and N. K. Patel, *Can. J. Pharm. Sci.*, **7**, 62 (1972).
(20) A. W. Hixson and J. H. Crowell, *Ind. Eng. Chem.*, **23**, 923 (1931).
(21) E. L. Parrott, D. E. Wurster, and T. Higuchi, *J. Am. Pharm. Assoc., Sci. Ed.*, **44**, 269 (1955).
(22) G. L. Flynn, S. H. Yalkowsky, and T. J. Roseman, *J. Pharm. Sci.*, **63**, 479 (1974).
(23) R. J. Braun and E. L. Parrott, *ibid.*, **61**, 592 (1972).
(24) W. Nernst and E. Brunner, *Z. Phys. Chem.*, **47**, 52 (1904).
(25) M. Donbrow and E. Touitou, *J. Pharm. Pharmacol.*, **29**, 524 (1977).

ACKNOWLEDGMENTS

The authors thank Miss Ruth Moshe for technical assistance.

Dihydroergotoxine: Separation and Determination of Four Components by High-Performance Liquid Chromatography

V. HARTMANN, M. RÖDIGER, W. ABLEIDINGER, and H. BETHKE ˣ

Received December 16, 1976, from *Analytical Research and Development, Pharmaceutical Department, Sandoz Ltd., CH 4002 Basle, Switzerland.* Accepted for publication April 18, 1977.

Abstract □ The evaluation of a new high-performance liquid chromatographic method is described. It permits the separation and determination of the four components of dihydroergotoxine (dihydroergocristine, dihydroergocornine, dihydro-α-ergocryptine, and dihydro-β-ergocryptine) in a single step. On reversed-phase microparticles, complete baseline separation is possible with different mobile phases containing about 10^{-2} *M* base. The analysis of dihydroergotoxine mesylate drug substance or its dosage forms can be carried out in about 15 min. No reference substance is required for the determination of the proportions of the components. This method is simple and exhibits high accuracy, reproducibility, and selectivity. It permits the analytical control of dosage forms containing dihydroergotoxine mesylate to ensure that they comply with the specifications for the drug substance used in clinical and pharmacological studies.

Keyphrases □ Dihydroergotoxine—high-performance liquid chromatographic analyses of four components in bulk drug and pharmaceutical formulations □ High-performance liquid chromatography—analyses, four components of dihydroergotoxine in bulk drug and pharmaceutical formulations □ Antiadrenergic agents—dihydroergotoxine, high-performance liquid chromatographic analyses of four components in bulk drug and pharmaceutical formulations

Ergotoxine is the name given to a particular group of ergot alkaloids derived from lysergic acid; they contain peptide moieties with similar chemical structures and have almost the same chemical and physical properties. These alkaloids are produced together by many strains of *Claviceps purpurea.*

Ergotoxine was believed to consist of three components: ergocristine (I), ergocornine (II), and ergocryptine (1, 2). In 1967, however, ergocryptine was shown to be composed of two isomers (3, 4), designated α-ergocryptine (III) and β-ergocryptine (IV) (5), differing only in one isomeric amino acid.

BACKGROUND

Ergotoxine, the actual product from *Claviceps,* is not used as such but in the form of the 9,10-dihydro derivative, generally called dihydroergotoxine (V–VIII). In the mesylate form, it is now widely used for the treatment of symptoms of impairment of mental function in the elderly.

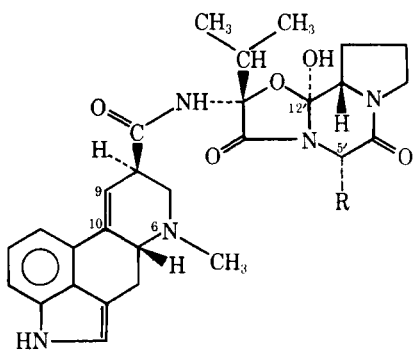

I: R = $CH_2C_6H_5$
II: R = $CH(CH_3)_2$
III: R = $CH_2CH(CH_3)_2$
IV: R = $CH(CH_3)CH_2CH_3$
V: R = $CH_2C_6H_5$; 9,10-dihydro
VI: R = $CH(CH_3)_2$; 9,10-dihydro
VII: R = $CH_2CH(CH_3)_2$; 9,10-dihydro
VIII: R = $CH(CH_3)CH_2CH_3$; 9,10-dihydro

Proof of safety and efficacy was obtained with material[1] containing the four constituents in specified proportions, representing the amounts found in natural ergotoxine isolated from selected, cultivated strains of *C. purpurea.* This defined dihydroergotoxine mesylate[2] consists of equal amounts of the mesylates of dihydroergocristine (V), dihydroergocornine (VI) and dihydroergocryptine (both isomers taken together), the ratio of dihydro-α-ergocryptine (VII) to dihydro-β-ergocryptine (VIII) being 2:1.

An analytical method is required to check the compliance of active ingredient and dosage forms with these specifications[3]. No simultaneous

[1] Hydergine, Sandoz Ltd.
[2] Dergocrine, generic name proposed to WHO.
[3] The tolerance ranges are 30.3–36.3% for V and VI as well as for the sum of VII and VIII and 1.5:1–2.5:1 for the ratio of VII to VIII.

(10) T. Higuchi and I. H. Pitman, *ibid.*, **62**, 55 (1973).
(11) T. Higuchi, S. Dayal, and I. H. Pitman, *ibid.*, **61**, 659 (1972).
(12) L. L. Bircumshaw and A. C. Riddiford, *Q. Rev.*, **6**, 157 (1952).
(13) K. G. Nelson and A. C. Shah, *J. Pharm. Sci.*, **64**, 610 (1975).
(14) A. C. Shah and K. G. Nelson, *ibid.*, **64**, 1519 (1975).
(15) D. R. Olander, *Am. J. Ch. E.*, **6**, 233 (1960).
(16) W. Jost, "Diffusion," Academic, New York, N.Y., 1960.
(17) M. Donbrow and Z. A. Jan, *J. Pharm. Pharmacol., Suppl.*, **17**, 129S (1965).
(18) M. Donbrow, E. Touitou, and H. Ben-Shalom, *ibid.*, **28**, 766 (1976).
(19) D. L. Simmons, M. Frechette, R. J. Ranz, W. S. Chen, and N. K. Patel, *Can. J. Pharm. Sci.*, **7**, 62 (1972).
(20) A. W. Hixson and J. H. Crowell, *Ind. Eng. Chem.*, **23**, 923 (1931).
(21) E. L. Parrott, D. E. Wurster, and T. Higuchi, *J. Am. Pharm. Assoc., Sci. Ed.*, **44**, 269 (1955).
(22) G. L. Flynn, S. H. Yalkowsky, and T. J. Roseman, *J. Pharm. Sci.*, **63**, 479 (1974).
(23) R. J. Braun and E. L. Parrott, *ibid.*, **61**, 592 (1972).
(24) W. Nernst and E. Brunner, *Z. Phys. Chem.*, **47**, 52 (1904).
(25) M. Donbrow and E. Touitou, *J. Pharm. Pharmacol.*, **29**, 524 (1977).

ACKNOWLEDGMENTS

The authors thank Miss Ruth Moshe for technical assistance.

Dihydroergotoxine: Separation and Determination of Four Components by High-Performance Liquid Chromatography

V. HARTMANN, M. RÖDIGER, W. ABLEIDINGER, and H. BETHKE ˣ

Received December 16, 1976, from *Analytical Research and Development, Pharmaceutical Department, Sandoz Ltd., CH 4002 Basle, Switzerland.* Accepted for publication April 18, 1977.

Abstract □ The evaluation of a new high-performance liquid chromatographic method is described. It permits the separation and determination of the four components of dihydroergotoxine (dihydroergocristine, dihydroergocornine, dihydro-α-ergocryptine, and dihydro-β-ergocryptine) in a single step. On reversed-phase microparticles, complete baseline separation is possible with different mobile phases containing about 10^{-2} *M* base. The analysis of dihydroergotoxine mesylate drug substance or its dosage forms can be carried out in about 15 min. No reference substance is required for the determination of the proportions of the components. This method is simple and exhibits high accuracy, reproducibility, and selectivity. It permits the analytical control of dosage forms containing dihydroergotoxine mesylate to ensure that they comply with the specifications for the drug substance used in clinical and pharmacological studies.

Keyphrases □ Dihydroergotoxine—high-performance liquid chromatographic analyses of four components in bulk drug and pharmaceutical formulations □ High-performance liquid chromatography—analyses, four components of dihydroergotoxine in bulk drug and pharmaceutical formulations □ Antiadrenergic agents—dihydroergotoxine, high-performance liquid chromatographic analyses of four components in bulk drug and pharmaceutical formulations

Ergotoxine is the name given to a particular group of ergot alkaloids derived from lysergic acid; they contain peptide moieties with similar chemical structures and have almost the same chemical and physical properties. These alkaloids are produced together by many strains of *Claviceps purpurea.*

Ergotoxine was believed to consist of three components: ergocristine (I), ergocornine (II), and ergocryptine (1, 2). In 1967, however, ergocryptine was shown to be composed of two isomers (3, 4), designated α-ergocryptine (III) and β-ergocryptine (IV) (5), differing only in one isomeric amino acid.

BACKGROUND

Ergotoxine, the actual product from *Claviceps,* is not used as such but in the form of the 9,10-dihydro derivative, generally called dihydroergotoxine (V–VIII). In the mesylate form, it is now widely used for the treatment of symptoms of impairment of mental function in the elderly.

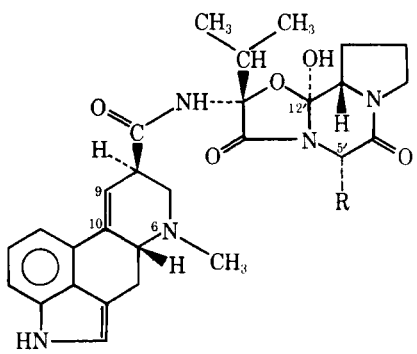

I: R = $CH_2C_6H_5$
II: R = $CH(CH_3)_2$
III: R = $CH_2CH(CH_3)_2$
IV: R = $CH(CH_3)CH_2CH_3$
V: R = $CH_2C_6H_5$; 9,10-dihydro
VI: R = $CH(CH_3)_2$; 9,10-dihydro
VII: R = $CH_2CH(CH_3)_2$; 9,10-dihydro
VIII: R = $CH(CH_3)CH_2CH_3$; 9,10-dihydro

Proof of safety and efficacy was obtained with material[1] containing the four constituents in specified proportions, representing the amounts found in natural ergotoxine isolated from selected, cultivated strains of *C. purpurea.* This defined dihydroergotoxine mesylate[2] consists of equal amounts of the mesylates of dihydroergocristine (V), dihydroergocornine (VI) and dihydroergocryptine (both isomers taken together), the ratio of dihydro-α-ergocryptine (VII) to dihydro-β-ergocryptine (VIII) being 2:1.

An analytical method is required to check the compliance of active ingredient and dosage forms with these specifications[3]. No simultaneous

[1] Hydergine, Sandoz Ltd.
[2] Dergocrine, generic name proposed to WHO.
[3] The tolerance ranges are 30.3–36.3% for V and VI as well as for the sum of VII and VIII and 1.5:1–2.5:1 for the ratio of VII to VIII.

chromatographic separation of the four components has been reported previously.

Incomplete separation without distinguishing between the isomers VII and VIII by paper chromatography (6–11), TLC (12, 13), high-performance liquid chromatography (HPLC) (14, 15), and countercurrent distribution (16) was described. A TLC separation of VII and VIII, derived from a system previously proposed (17), was reported[4]. However, the simultaneous separation into all four components failed because VIII and VI showed the same R_f value.

Amino acid analysis, according to Moore and Stein (18), has been the only technique available for the identification and determination of the four components in the drug substance. The peptide moieties of the alkaloids were hydrolyzed, and the resulting amino acids were determined by ion-exchange chromatography and subsequent reaction with ninhydrin. This indirect determination, however, is usually inadequate for the analysis of pharmaceutical dosage forms.

This paper describes a method, based on HPLC separation, suitable for the analysis of the drug substance and the various liquid and solid dosage forms. Because of its accuracy, reproducibility, and simplicity, this method is suggested for quality control, *e.g.*, to verify compliance with the established specifications.

EXPERIMENTAL

Apparatus—Two solvent delivery systems were used[5]. Sample injections were made with three systems[6] using 20–50 μl. The detectors[7] were set at 280 nm. Peak integrations were performed with a laboratory data system[8]. A pH meter[9] and an NMR spectrometer[10] were used.

Reagents and Solvents—Water was double distilled in a quartz apparatus. The solvents and reagents were analytical grade and were used without further purification; they were triethylamine[11], acetonitrile for pesticide residue analysis[12], methanol[12], absolute ethanol[12], tartaric acid[12], ammonium carbonate[12], and ammonium acetate[12].

The pH 2–13 range was studied using commercial buffer solutions[13]. Phosphate buffers, 5×10^{-2} *M* or 1×10^{-1} *M*, were used for the pH 9–13 range after adjustment to the appropriate pH with sodium hydroxide.

Packings and Columns—Several types (A[14], B[15], and C[16]) of chemically bonded reversed-phase materials were used to pack columns (25 cm long, 3–4 mm i.d., for 10-μm materials or 10–15 cm long, 3–4 mm i.d., for 5-μm materials) according to the procedures described for microparticles, *e.g.*, the balanced density technique (19–21), the dynamic slurry packing technique (22), and the viscosity technique (23–25). Some columns were glass coated[17]. In addition, prepacked columns were used with Phases B[18], C[19], and D[20].

Samples—Sample solutions, 1 mg/ml, were prepared by dissolving the drug substance[21] in methanol or the mobile phase.

Twenty tablets[1] of 1 or 1.5 mg were stirred without grinding in 20 ml of tartaric acid–water–ethanol (0.03:2:1 w/v/v) for about 15 min. The suspensions were centrifuged, and the solutions were injected directly into the column. Liquid dosage forms[1] required no preparation.

Assay—The sample injection size was 50 μl, corresponding to the following amounts of dihydroergotoxine mesylate: 50 μg for 1-mg tablets, 75 μg for 1.5-mg tablets, 15 μg for the injection, and 50 μg for the oral solution.

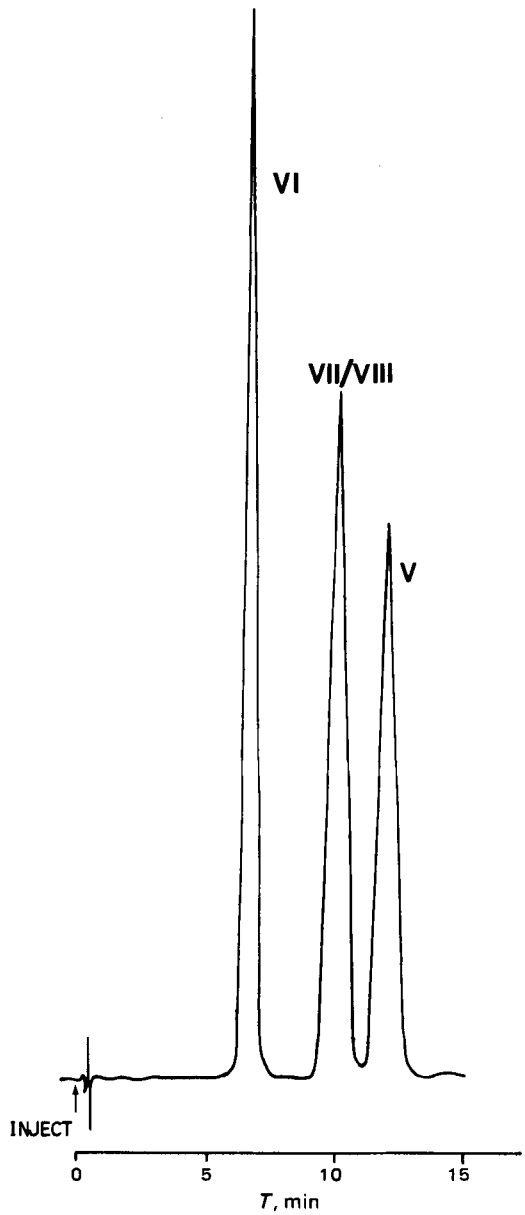

Figure 1—*Dihydroergotoxine mesylate in an oral solution; separation of components V, VI, and VII/VIII. The conditions were: column, 30 cm × 4.6 mm i.d.; stationary phase, C, 10 μm; mobile phase, acetonitrile–10^{-2} M ammonium carbonate in water (0.82:1 v/v); flow, 7 ml/min; pressure, 5000 psi; detection, 280 nm and 0.4 absorbance unit; and injection, 50 μl of oral solution = 50 μg of dihydroergotoxine mesylate.*

Chromatographic conditions for different stationary phases were: Phase C, 5 μm in a 15-cm column, 3 mm i.d., water–acetonitrile–triethylamine (32:8:1 v/v/v) with a 1.0-ml/min flow, corresponding to a linear velocity of 0.3 cm/sec and a pressure of 4000 psi; Phase B, water–acetonitrile–triethylamine (75:40:1 v/v/v) with a 0.8-ml/min flow, corresponding to a linear velocity of 0.3 cm/sec and a pressure of 2000 psi; and Phase D, water–acetonitrile–triethylamine (22.8:11.4:1 v/v/v) with a 2.0-ml/min flow, corresponding to a linear velocity of 0.4 cm/sec and a pressure of 5000 psi.

The general procedure for evaluating the proportions of the components is demonstrated with the following example of 1-mg tablets[1]. Peak areas found were 16.960 (V), 17.079 (VI), 10.602 (VII), and 6.011 (VIII). Molecular weights of the mesylates are 707.8 (V), 659.8 (VI), and 673.8 (VII and VIII). The corrected peak areas are obtained by multiplication of the found areas with the corresponding molecular weights: 11,969 (V), 11,269 (VI), 7144 (VII), and 4050 (VIII). The sum of these corrected peak areas, 34,432, corresponds to 100%. Consequently, the relative amounts of the components are: 34.8% (V), 32.7% (VI), and 32.5% (VII/VIII), and the ratio of VII to VIII is 1.8:1.

[4] R. Brunner, Chemical Production Department, Sandoz Ltd., personal communication.
[5] Model 6000 A, Waters Associates, Milford, Mass.; and model FLM 50/2, Lewa, Leonberg, Germany.
[6] Model 70-10 loop injector, Rheodyne, Berkeley, Calif.; model U6K, Waters Associates, Milford, Mass.; and autosampler system, Varian.
[7] Model 1030 B, Hewlett-Packard; and model LC 55, Perkin-Elmer.
[8] Model 3352 B, Hewlett-Packard.
[9] Model E 500, Metrohm, Herisau, Switzerland.
[10] Model HX-90E, 22.63 MHz, Bruker Physik, Karlsruhe, Germany.
[11] Puriss., Fluka, Buchs, Switzerland.
[12] Merck, Darmstadt, Germany.
[13] Titrisol, Merck, Darmstadt, Germany.
[14] Nucleosil C_{18}, 10 μm, Macherey and Nagel, Düren, Germany.
[15] LiChrosorb RP 8, 5 and 10 μm, Merck, Darmstadt, Germany.
[16] LiChrosorb RP 18, 5 and 10 μm, Merck, Darmstadt, Germany.
[17] Scientific Glass Engineering, Melbourne, Australia.
[18] LiChrosorb RP 8, 7 μm, 25 cm long, 3 mm i.d., Merck, Darmstadt, Germany.
[19] LiChrosorb RP 18, 5 μm, 25 cm long, 3 mm i.d., Merck, Darmstadt, Germany.
[20] μ-Bondapak C_{18}, 10 μm, 30 cm long, 4 mm i.d., Waters Associates, Milford, Mass.
[21] Sandoz Ltd., Basle, Switzerland.

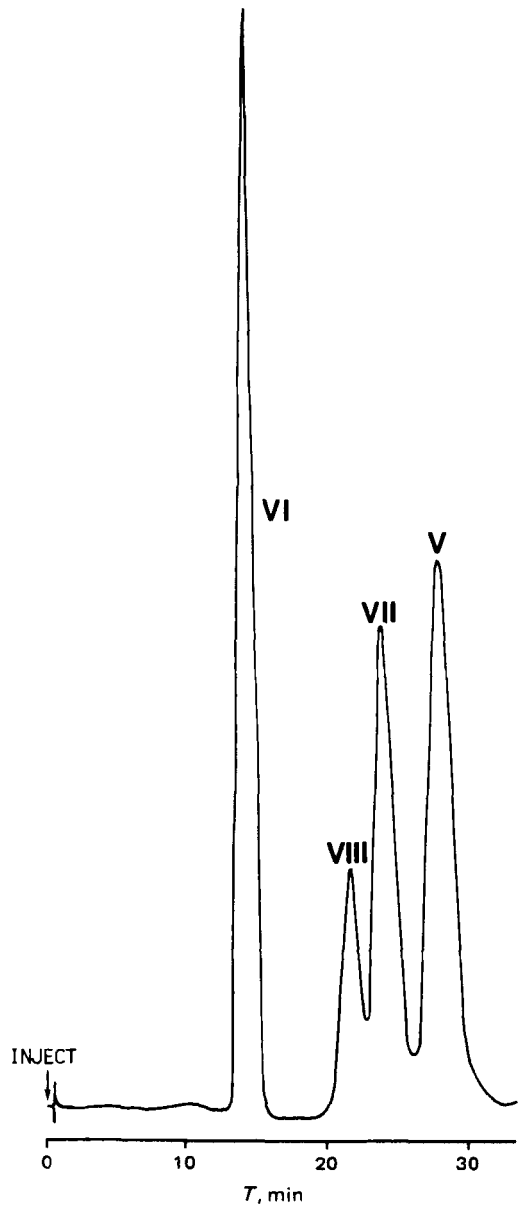

Figure 2—*Sparation of dihydroergotoxine mesylate drug substance into its constituents using a neutral mobile phase. The conditions were: column, 30 cm × 4 mm i.d.; stationary phase, D; mobile phase, methanol–10^{-1} M ammonium acetate in water (1.1:1 v/v); flow, 3.3 ml/min; pressure, 5500 psi; detection, 280 nm and 0.02 absorbance unit; and injection, 30 µl of methanolic solution = 30 µg of drug substance.*

RESULTS AND DISCUSSION

The problem of separating all four components (V–VIII) of dihydroergotoxine mesylate has been tackled in various ways by HPLC. With normal phase partition chromatography, a complete separation into three components, V, VI, and VII/VIII, was achieved, but isomers VII and VIII were only partly separated[22]. The selectivity factor α for this critical pair of compounds was reported to be 1.06.

A separation of components V, VI, and VII/VIII on reversed-phase porous layer beads[23] was described (14) and improved (15) by using the corresponding microparticles[20]. At the same time, determination of the components of dihydroergotoxine mesylate in various dosage forms with reversed-phase microparticles was begun in this laboratory. A representative chromatogram for an oral solution[1] is given in Fig. 1. The chromatographic system is useful for quality control and stability testing.

[22] R. Stampfli and R. Krattiger, Chemical Production Department, Sandoz Ltd., personal communication.

[23] Corasil C_{18}, Waters Associates, Milford, Mass.

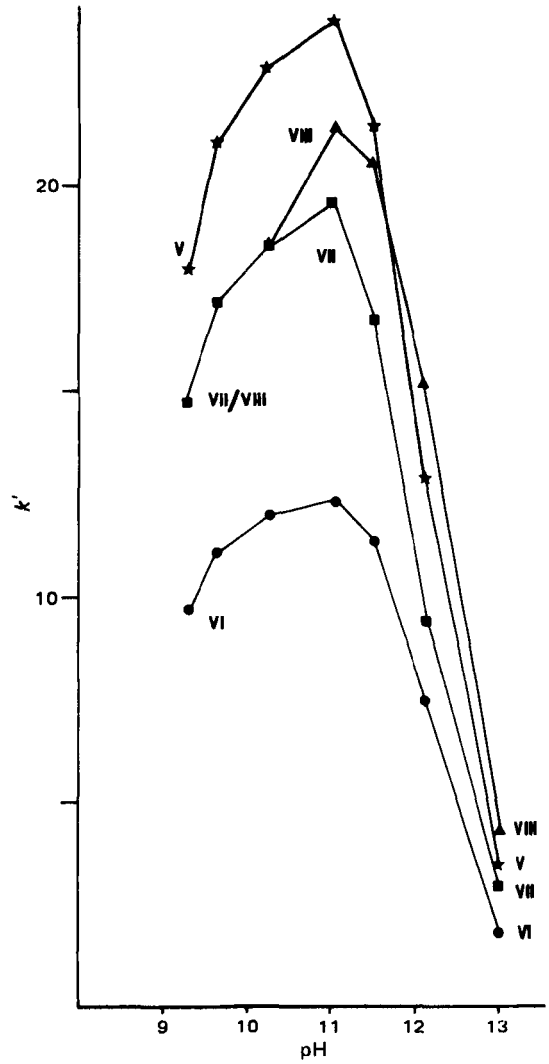

Figure 3—*Capacity factors k′ of V–VIII as a function of the pH of the mobile phase (aqueous part of phosphate buffers and sodium hydroxide mixed with acetonitrile, 1.67:1). Stationary Phase A was used.*

Proper selectivity of the mobile phase is achieved by using a salt concentration of at least 10^{-3} *M* and a pH value adjusted to $7 \leq \text{pH} \leq 9$, *e.g.*, with a mobile phase of acetonitrile–10^{-2} *M* ammonium carbonate in water (0.54:1 v/v).

Insufficient stability was observed for some columns of any reversed-phase material because of the alkaline conditions of a mobile phase with acetonitrile and ammonium carbonate. New experiments showed that the ammonium carbonate solution can be replaced by systems buffered to pH ~ 7.5, prepared either with 0.33 *M* phosphate buffer or with 0.1% (v/v) triethylamine in water and adjusted to the required pH with 1 *N* acetic acid. The ratio of acetonitrile to the aqueous solution is the same as when ammonium carbonate solution is used.

A partial separation of VII and VIII was observed only on columns with extremely high performance ($n > 3000$, determined at the peak of VI). It was, therefore, necessary to improve the selectivity of the phases. Replacement of acetonitrile by methanol led to a slight change in the capacity factors (k') of VII and VIII. To improve the selectivity of this methanolic phase, the effect of certain salts and acids added to the mobile phase was investigated.

A mobile phase of methanol–10^{-1} *M* ammonium acetate in water (1:1–1.2:1) gave reproducible separations of all four components (V–VIII) on Phase D in a column with at least 1000 theoretical plates (determined in the system at the peak for VI). The capacity factors (k') were: 21 (VI), 33 (VIII), 36 (VII), and 42 (V), thus leading to a selectivity factor α for the critical pair of isomers, VII and VIII, of about 1.1 and to a resolution R_S of about 0.9 (Fig. 2).

The advantage of this chromatographic system is that the pH of the mobile phase (pH ~7) causes no difficulties with the stability of the

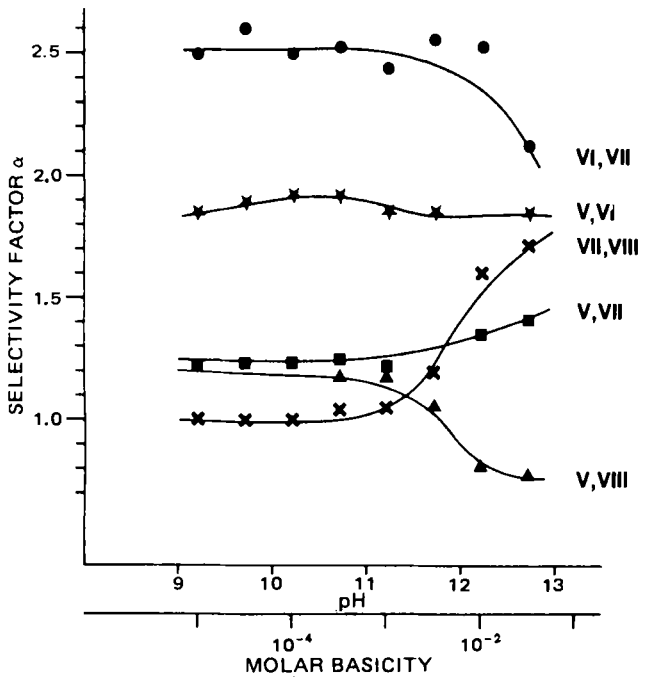

Figure 4—*Selectivity, α, of the different pairs of compounds as a function of the basicity of the mobile phase, corresponding to the pH of the aqueous part (mixed with acetonitrile, 1.67:1). Stationary Phase C was used.*

stationary phase used. Disadvantages result from the high capacity factors (k'), particularly for electronic peak integration.

An improvement of selectivity in drug analysis by pH variation of the mobile phase was reported. Twitchett and Moffat (26) described the correlation between the pKa values of various drugs and their retention time in reversed-phase HPLC. As a result, the optimum pH can be predicted from the pKa value. Hartmann and Rödiger (27) reported that improved selectivity in separation of penicillins and cephalosporins could be obtained by modifying the pH.

For dihydroergotoxine mesylate, a pH variation of the aqueous part of the mobile phase between 2 and 13 influenced the selectivity of the chromatographic system.

Mobile phases with pH < 9 (buffer–acetonitrile) did not improve selectivity. On the other hand, Fig. 3 demonstrates specific influences on the selectivity at pH ≥ 10 by showing the k' values as a function of pH. With increasing basicity, the retention time of VIII becomes longer in comparison with that of the other components, thereby improving the separation between VII and VIII. But at the same time, the separation between V and VIII becomes worse in an intermediate region at pH ~ 11. If the pH is increased still further, the k' value of VIII becomes higher than that of V, and a further improvement of resolution is achieved.

The results for the critical components VI–VIII appear to indicate that the separation of VII and VIII requires a pH above 10.5 using a phosphate buffer system. In the pH 10.5–11.5 range, the peak of VIII emerges between the peaks of VII and V; finally, at pH > 12, VIII is eluted as the last peak.

Figure 4 shows that the selectivities of the pairs VI and VII, V and VI, and V and VII are more or less independent of pH changes. The dramatic variation of the pairs VII and VIII and V and VIII is solely due to the effect of pH on the retardation of VIII. The reasons for this particular effect cannot be found in the ionization constants of the nitrogen in position 6 of the molecules[24].

All explanations of this successful separation remain purely hypothetical. Factors that may influence the retention behavior of VIII are: (*a*) changes in solvation or conformation, (*b*) specific ionization of the amide groups, and (*c*) specific ionization of the 12′-hydroxyl group. Preliminary ^{13}C-NMR investigations were carried out to study the influence of basicity on the carbon skeleton of the molecules.

Table I—Results Deduced from the Calibration for the Proportions of the Four Components, Including the Relative Standard Deviation Found by Repeating the Analyses in the Most Relevant Range under Constant Conditions (100% = 1 mg of Dihydroergotoxine Mesylate/ml)

Component	Proportion		*RSD*, %
	Calculated, %	Found, %	
V	4.8	4.5	
	9.6	9.3	
	19.2	19.1	
	24.0	24.1	
	28.8	28.9	
	30.2	30.7	1.0 (n = 3)
	33.2	33.4	0.7 (n = 9)
	37.2	37.5	0.3 (n = 3)
	38.4	38.7	
VI	4.7	4.7	
	9.5	9.5	
	18.9	18.7	
	23.6	23.6	
	28.4	28.7	
	30.4	30.0	0.6 (n = 4)
	33.4	32.9	0.2 (n = 6)
	37.5	36.8	1.0 (n = 3)
	37.8	37.8	
VII	4.8	4.7	
	9.5	9.8	
	19.1	19.0	
	20.8	20.5	0.3 (n = 3)
	21.8	21.3	0.5 (n = 3)
	22.8	22.5	0.4 (n = 4)
	23.8	23.7	0.4 (n = 2)
	23.9	24.2	
	28.6	29.0	
	38.2	38.3	
VIII	4.8	4.6	
	9.0	9.2	0.9 (n = 8)
	9.7	9.6	
	11.0	11.2	1.5 (n = 3)
	14.0	14.1	0.9 (n = 4)
	19.2	18.5	
	24.0	23.9	
	28.7	28.5	
	38.3	38.0	

Solutions of VII and VIII in dimethyl sulfoxide[25] yielded signals that did not vary as a function of basicity. Nevertheless, there is some evidence for variations in the chemical shifts of isomers VII and VIII in the critical range of pH > 10 when the solvent is as similar as possible to the mobile phase used in HPLC[26].

The conclusion to be drawn from the results of variation in pH is that sufficient selectivity can be achieved only when the concentration of the base is at least 10^{-2} M. This value is far outside the range recommended for chromatographic support materials based on silica gel (pH < 8–9) (24). In fact, the columns cannot resist such an alkaline mobile phase and usually fail after about 2–4 days.

Methylating the remaining silanol groups of the stationary phase produced some improvement in the stability, but it was not sufficient. Therefore, the replacement of the inorganic bases and buffer systems by organic amines was studied[27]. The influence of methanol and acetonitrile was investigated at the same time.

Successful separation of the four components (V–VIII) of dihydroergotoxine was obtained with triethylamine in the specified concentration (10^{-2} M) together with either methanol or acetonitrile to produce the optimum selectivity. Typical conditions for Phase C are water–methanol–triethylamine (25:3.6:1 v/v/v) or water–acetonitrile–triethylamine (32:8:1 v/v/v). The acetonitrile system has the following advantages over the methanol system: (*a*) better selectivity, particularly for the pair V and VII; (*b*) lower pressure and, consequently, fewer technical problems with pumps, injectors, *etc.*; and (*c*) a longer lasting stationary phase since silica gel is not dissolved.

In accordance with the results from pH variation, the important modifier of the selectivity is the amount of the amine. At least 0.5–1% triethylamine (equivalent to 3.5–7 × 10^{-2} M in the mobile phase) is

[24] Maulding and Zoglio (28) reported the pKa values in aqueous solution of V, VI, and VII/VIII to be practically equal (pKa ~ 6.74). A. Wehrli, Chemical Research Department, Sandoz Ltd., determined the following pK_{MCS} values according to the method described by Simon (29): 5.83 (V), 5.78 (VI), 5.81 (VII), and 5.84 (VIII).

[25] F. Erni and H. Loosli, Sandoz Ltd., showed that ^{13}C-NMR spectra can be used to determine the proportions of the four components in dihydroergotoxine mesylate drug substance dissolved in dimethyl sulfoxide.

[26] H. Bethke and H. Loosli, to be published.

[27] H. P. Keller, R. Stampfli, and A. Wehrli, to be published.

Table II—Determination of the Proportions of the Four Components in Dihydroergotoxine Mesylate and Its Preparations, Including the Relative Standard Deviation Found by Repeating the Analyses under Constant Conditions

Sample	Proportion of V Mesylate	Proportion of VI Mesylate	Proportion of Sum of VII Mesylate and VIII Mesylate	Ratio of VII Mesylate to VIII Mesylate
Dihydroergotoxine mesylate (10 determinations)	33.9 ± 0.9%	35.0 ± 0.8%	31.2 ± 0.5%	1.9 ± 1.7%
Oral solution[a] (eight determinations)	33.6 ± 0.7%	32.2 ± 0.8%	34.2 ± 0.4%	2.2 ± 1.8%
Injection solution[a] (10 determinations)	33.7 ± 0.7%	34.2 ± 0.9%	32.1 ± 0.3%	2.1 ± 1.7%
Tablets[a], 1 mg (seven determinations)	34.9 ± 0.6%	32.7 ± 0.9%	32.4 ± 0.5%	1.8 ± 1.2%
Tablets[a], 1.5 mg (eight determinations)	34.5 ± 0.4%	33.8 ± 0.4%	31.7 ± 0.4%	2.0 ± 1.4%

[a] Hydergine, Sandoz Ltd.

necessary for sufficient separation. With larger amounts, the retention times of all components are reduced and the separation between VI and VII is practically unchanged whereas the selectivity for the pair V and VIII is improved. A similar decrease in selectivity is observed for the pair V and VII. Therefore, about 2–3% triethylamine should be optimum, producing sufficient resolution while permitting the analysis to be completed within a reasonable time.

On the other hand, in the range of 20–30%, the amount of acetonitrile has little influence on system selectivity. It only affects the retention times, which decrease with increasing acetonitrile concentration. These results and further experience led to typical chromatographic conditions (Fig. 5) for different reversed stationary phases (see *Experimental*). Under these conditions, baseline separations are achieved for all adjoining peaks. The capacity factors vary between $k' \sim 6$ for VI and $k' \sim 35$ for VIII. By slight modifications of the mobile phase, the system can be adjusted to yield optimum separation and minimum chromatographic time, generally about 15 min.

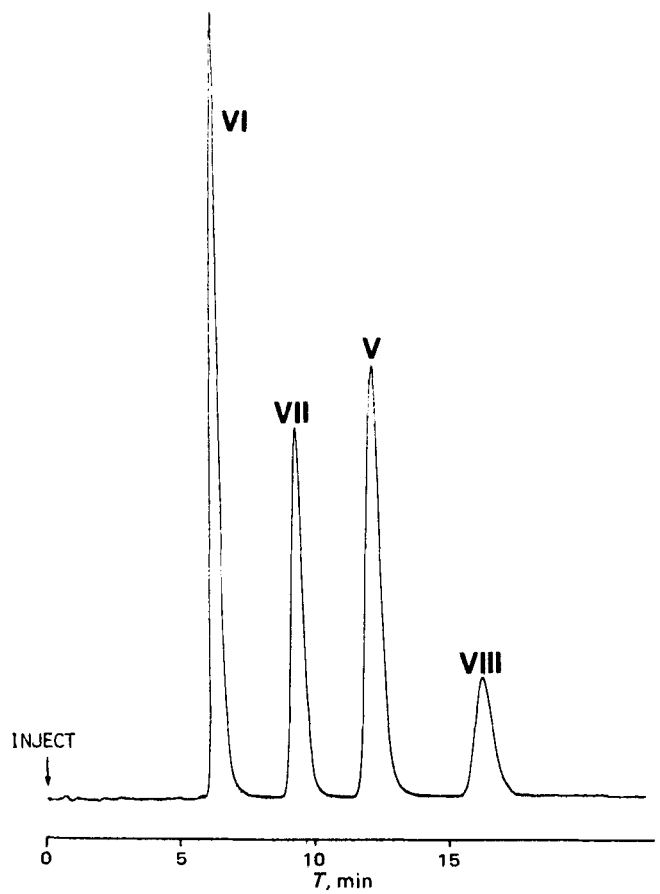

Figure 5—*Separation of dihydroergotoxine mesylate oral solution into its constituents using the optimum mobile phase of pH ~ 12. The conditions were: column, 15 cm × 3 mm i.d. glass-coated steel; stationary phase, C, 5 μm; mobile phase, water–acetonitrile–triethylamine (32:8:1 v/v/v); flow, 1.0 ml/min; pressure, 5500 psi; detection, 280 nm and 0.2 absorbance unit; and injection, 20 μg of dihydroergotoxine mesylate in 20 μl of water–acetonitrile (4:1 v/v).*

Several columns have been in use, some for more than 2 months for hundreds of routine analyses of dihydroergotoxine mesylate drug substance and its dosage forms. The columns are at least as stable as under conditions of low alkalinity (pH 8 with inorganic salts), although the measured pH is about 12.

The top of the column must be inspected routinely and a small amount of the stationary phase must be added, if necessary. Washing the column with water, acetonitrile, or alcohols should be avoided because it adversely affects stability.

Since all peaks show baseline separation, electronic integrators can be used for the quantitative determination. Since the indole group of the lysergic acid constitutes the chromophore of all four components, the molar ratios can be calculated directly from the peak areas obtained at 280 nm. This fact has been verified by calibration experiments, in which the proportions of the single components ranged from 5 to 50% calculated on the total amount of dihydroergotoxine mesylate. At the 95% confidence level, the measured values did not differ significantly from the expected values (Table I).

The precise setting of the detection wavelength is not critical, as was demonstrated by varying it from 275 to 285 nm with 2-nm bandwidth. Calibration with an external standard is not necessary for the determination of the proportion of each component. Consequently, a high level of accuracy is required for integration of the peaks, especially the smallest peak (VIII). Proper column performance, an injected amount of about 20–50 μg of dihydroergotoxine mesylate, and an optimum setting of the peak detection system of the integrator are essential.

For the drug substance dihydroergotoxine mesylate, the proportions are labeled as weight ratios rather than as molar ratios. Therefore, the area of each peak in the chromatogram must be multiplied by the molecular weight of the relevant mesylate. These corrected values give the amount of each component by weight; the proportions can be calculated by using the 100% method (example given in the *Experimental* section).

The proportions of the components were determined for dihydroergotoxine mesylate and for different dosage forms. The results and the standard deviations of the analyses are summarized in Table II. There is a good agreement with the specifications given in the introduction as well as good reproducibility, which demonstrates the suitability of the method for routine analysis.

The preparation of the samples is simple. The drug substance must be dissolved in the mixture of water and acetonitrile used in the mobile phase; liquid dosage forms require no preparation; and an extract of tablets is prepared in a single step (*cf., Experimental*).

Further investigations showed that the HPLC system is not only suitable for the determination of the relative amounts of each component but also for the determination of dihydroergotoxine mesylate as the sum of all components[28].

REFERENCES

(1) A. Stoll and A. Hofmann, *Helv. Chim. Acta*, **26**, 1570 (1943).

(2) A. Stoll, A. Hofmann, and T. Petrzilka, *ibid.*, **34**, 1544 (1951).

(3) W. Schlientz, R. Brunner, A. Rüegger, B. Berde, E. Stürmer, and A. Hofmann, *Experientia*, **23**, 991 (1967).

(4) W. Schlientz, R. Brunner, A. Rüegger, B. Berde, E. Stürmer, and A. Hofmann, *Pharm. Acta Helv.*, **43**, 497 (1968).

(5) P. A. Stadler, S. Guttmann, H. Hauth, R. L. Huguenin, E. Sandrin, G. Wersin, H. Willems, and A. Hofmann, *Helv. Chim. Acta*, **52**, 1549 (1969).

[28] Details will be published later.

(6) A. Stoll and A. Rüegger, *ibid.*, **37**, 1725 (1954).
(7) M. Prošek, E. Kučan, M. Katič, and M. Bano, *Chromatographia*, **9**, 273 (1976).
(8) F. Adamanis, E. Pawelczyk, and Z. Plotkowiakowa, *Bull. Soc. Amis. Sci. Lett. Poznan*, C **10**, 95 (1960); through *Chem. Abstr.*, **55**, 23930h (1961).
(9) W. Schlientz, R. Brunner, A. Hofmann, B. Berde, and E. Stürmer, *Pharm. Acta Helv.*, **36**, 472 (1961).
(10) A. Hofmann, *Pharm. Weekbl.*, **100**, 1261 (1965).
(11) Z. Margasinski, R. Danielak, H. Rafalowska, and Z. Nowakowska, *Acta Pol. Pharm.*, **24**, 301 (1967); through *Chem. Abstr.*, **68**, 62729g (1968).
(12) T. Hohmann and R. Rochelmeyer, *Arch. Pharm.*, **297**, 186 (1964).
(13) M. Prošek, E. Kučan, M. Katič, and M. Bano, *Chromatographia*, **9**, 325 (1976).
(14) I. Jane and B. B. Wheals, *J. Chromatogr.*, **84**, 181 (1973).
(15) R. V. Vivilecchia, R. L. Cotter, R. J. Limpert, N. Z. Thimot, and J. N. Little, *ibid.*, **99**, 407 (1974).
(16) C. Galeffi and E. M. Delle Monache, *ibid.*, **88**, 413 (1974).
(17) M. S. Gibson, *ibid.*, **44**, 631 (1969).
(18) S. Moore and W. H. Stein, *J. Biol. Chem.*, **211**, 893 (1954).
(19) R. E. Majors, *Anal. Chem.*, **44**, 1722 (1972).
(20) J. J. Kirkland, *J. Chromatogr. Sci.*, **10**, 593 (1972).
(21) R. M. Cassidy, D. S. Le Gay, and R. W. Frei, *Anal. Chem.*, **46**, 340 (1974).
(22) H. R. Linder, H. P. Keller, and R. W. Frei, *J. Chromatogr. Sci.*, **14**, 234 (1976).
(23) J. Asshauer and I. Halász, *ibid.*, **12**, 139 (1974).
(24) I. Halász, *Z. Anal. Chem.*, **277**, 257 (1975).
(25) I. Sebestian, Hausmitteilung HPLC/d4/07, Macherey-Nagel, Düren, Germany, 1976.
(26) P. J. Twitchett and A. C. Moffat, *J. Chromatogr.*, **111**, 149 (1975).
(27) V. Hartmann and M. Rödiger, *Chromatographia*, **9**, 266 (1976).
(28) H. V. Maulding and M. A. Zoglio, *J. Pharm. Sci.*, **59**, 700 (1970).
(29) W. Simon, *Helv. Chim. Acta*, **41**, 1835 (1958).

ACKNOWLEDGMENTS

This work was carried out in part at the Analytical Laboratories of Sandoz AG, D 8500 Nuremberg, Germany.

The authors are indebted to many colleagues at Sandoz Ltd. for their help, particularly H. P. Keller, K. Krummen, R. Stampfli, and A. Wehrli. They also thank H. Bosshard, M. Cholet, B. Delz, B. Dobler, B. Hauenstein, C. Karsenty, H. Loosli, and A. Moser for helpful technical assistance.

This report is the 84th paper on ergot alkaloids. For the previous report in this series, see E. Schreier, *Helv. Chim. Acta*, **59**, 585 (1976).

Biosynthesis of Morphine Alkaloids in *Papaver bracteatum* Lindl.

E. BROCHMANN-HANSSEN ˣ and S. W. WUNDERLY

Received January 18, 1977, from the *Department of Pharmaceutical Chemistry, School of Pharmacy, University of California, San Francisco, CA 94143.* Accepted for publication April 18, 1977.

Abstract □ Administration of 1-^{3}H-*N*-methyl-^{14}C-(±)-reticuline to *Papaver bracteatum* gave good incorporation of carbon-14 into thebaine and a decrease in the tritium to carbon-14 ratio indicative of racemization. The incorporation of carbon-14 and the extent of tritium loss were the same whether reticuline was administered to the intact plant or to isolated leaves. Carrier dilution with cold codeine, codeinone, and morphine showed only insignificant incorporation of radioactivity into codeine and none at all into codeinone and morphine. When codeinone was administered to the living plant, it was converted to codeine rapidly and efficiently, but no *O*-demethylation to morphine could be detected. The experimental data indicate that the biosynthesis of thebaine in *P. bracteatum* proceeds by the same pathway as in the opium poppy. The limiting step in the sequence is the demethylation of the enol ether group of thebaine to neopinone.

Keyphrases □ Morphine alkaloids—biosynthesis in *Papaver bracteatum*, radiochemical study □ Alkaloids, morphine—biosynthesis in *Papaver bracteatum*, radiochemical study □ Biosynthesis—morphine alkaloids in *Papaver bracteatum*, radiochemical study □ *Papaver bracteatum*—biosynthesis of morphine alkaloids, radiochemical study □ Radiochemistry—study of biosynthesis of morphine alkaloids in *Papaver bracteatum*

In 1963, Neubauer and Mothes (1) reported on a strain of *Papaver bracteatum* Lindl. that produced thebaine in high yield but apparently contained neither codeine nor morphine. *P. bracteatum* is closely related to *P. orientale* and *P. pseudo-orientale*, which do not synthesize significant amounts of thebaine. They can be differentiated from *P. bracteatum* by cytological examination (2) and chemotaxonomic tests (3). In contrast to the opium poppy (*P. somniferum*), which produces a large number of alkaloids, several in appreciable concentrations, *P. bracteatum* contains mainly thebaine, which may account for 98% of the alkaloid content[1] (1, 4). Isolation and purification of thebaine from *P. bracteatum* are, therefore, relatively simple.

In recent years, considerable interest has developed in this plant as a source of thebaine; in the laboratory, thebaine can be converted to codeine and other narcotic analgesics and antitussives (6–8). Thebaine is also the raw material for naloxone and related narcotic antagonists and for the interesting *endo*-ethenotetrahydrothebaines (9). In 1972, a collaborative research project on *P. bracteatum* was initiated by the United Nations Narcotics Laboratory, which has been coordinating investigations carried out in many countries (10).

The purposes of the present investigation were to study the biosynthetic pathways of hydrophenanthrene alkaloids in *P. bracteatum* and to explore possible sites of biosynthesis.

BACKGROUND

The biosynthesis of morphine alkaloids in the opium poppy has been

[1] Several varieties, or chemical races, of *P. bracteatum* have been found, differing somewhat in alkaloid composition. The Arya II variety from western Iran has a particularly high content of thebaine (5).

(6) A. Stoll and A. Rüegger, *ibid.*, **37**, 1725 (1954).
(7) M. Prošek, E. Kučan, M. Katič, and M. Bano, *Chromatographia*, **9**, 273 (1976).
(8) F. Adamanis, E. Pawelczyk, and Z. Plotkowiakowa, *Bull. Soc. Amis. Sci. Lett. Poznan*, C **10**, 95 (1960); through *Chem. Abstr.*, **55**, 23930h (1961).
(9) W. Schlientz, R. Brunner, A. Hofmann, B. Berde, and E. Stürmer, *Pharm. Acta Helv.*, **36**, 472 (1961).
(10) A. Hofmann, *Pharm. Weekbl.*, **100**, 1261 (1965).
(11) Z. Margasinski, R. Danielak, H. Rafalowska, and Z. Nowakowska, *Acta Pol. Pharm.*, **24**, 301 (1967); through *Chem. Abstr.*, **68**, 62729g (1968).
(12) T. Hohmann and R. Rochelmeyer, *Arch. Pharm.*, **297**, 186 (1964).
(13) M. Prošek, E. Kučan, M. Katič, and M. Bano, *Chromatographia*, **9**, 325 (1976).
(14) I. Jane and B. B. Wheals, *J. Chromatogr.*, **84**, 181 (1973).
(15) R. V. Vivilecchia, R. L. Cotter, R. J. Limpert, N. Z. Thimot, and J. N. Little, *ibid.*, **99**, 407 (1974).
(16) C. Galeffi and E. M. Delle Monache, *ibid.*, **88**, 413 (1974).
(17) M. S. Gibson, *ibid.*, **44**, 631 (1969).
(18) S. Moore and W. H. Stein, *J. Biol. Chem.*, **211**, 893 (1954).
(19) R. E. Majors, *Anal. Chem.*, **44**, 1722 (1972).
(20) J. J. Kirkland, *J. Chromatogr. Sci.*, **10**, 593 (1972).
(21) R. M. Cassidy, D. S. Le Gay, and R. W. Frei, *Anal. Chem.*, **46**, 340 (1974).
(22) H. R. Linder, H. P. Keller, and R. W. Frei, *J. Chromatogr. Sci.*, **14**, 234 (1976).
(23) J. Asshauer and I. Halász, *ibid.*, **12**, 139 (1974).
(24) I. Halász, *Z. Anal. Chem.*, **277**, 257 (1975).
(25) I. Sebestian, Hausmitteilung HPLC/d4/07, Macherey-Nagel, Düren, Germany, 1976.
(26) P. J. Twitchett and A. C. Moffat, *J. Chromatogr.*, **111**, 149 (1975).
(27) V. Hartmann and M. Rödiger, *Chromatographia*, **9**, 266 (1976).
(28) H. V. Maulding and M. A. Zoglio, *J. Pharm. Sci.*, **59**, 700 (1970).
(29) W. Simon, *Helv. Chim. Acta*, **41**, 1835 (1958).

ACKNOWLEDGMENTS

This work was carried out in part at the Analytical Laboratories of Sandoz AG, D 8500 Nuremberg, Germany.

The authors are indebted to many colleagues at Sandoz Ltd. for their help, particularly H. P. Keller, K. Krummen, R. Stampfli, and A. Wehrli. They also thank H. Bosshard, M. Cholet, B. Delz, B. Dobler, B. Hauenstein, C. Karsenty, H. Loosli, and A. Moser for helpful technical assistance.

This report is the 84th paper on ergot alkaloids. For the previous report in this series, see E. Schreier, *Helv. Chim. Acta*, **59**, 585 (1976).

Biosynthesis of Morphine Alkaloids in *Papaver bracteatum* Lindl.

E. BROCHMANN-HANSSEN ˣ and S. W. WUNDERLY

Received January 18, 1977, from the *Department of Pharmaceutical Chemistry, School of Pharmacy, University of California, San Francisco, CA 94143.* Accepted for publication April 18, 1977.

Abstract □ Administration of 1-^{3}H-*N*-methyl-^{14}C-(±)-reticuline to *Papaver bracteatum* gave good incorporation of carbon-14 into thebaine and a decrease in the tritium to carbon-14 ratio indicative of racemization. The incorporation of carbon-14 and the extent of tritium loss were the same whether reticuline was administered to the intact plant or to isolated leaves. Carrier dilution with cold codeine, codeinone, and morphine showed only insignificant incorporation of radioactivity into codeine and none at all into codeinone and morphine. When codeinone was administered to the living plant, it was converted to codeine rapidly and efficiently, but no *O*-demethylation to morphine could be detected. The experimental data indicate that the biosynthesis of thebaine in *P. bracteatum* proceeds by the same pathway as in the opium poppy. The limiting step in the sequence is the demethylation of the enol ether group of thebaine to neopinone.

Keyphrases □ Morphine alkaloids—biosynthesis in *Papaver bracteatum*, radiochemical study □ Alkaloids, morphine—biosynthesis in *Papaver bracteatum*, radiochemical study □ Biosynthesis—morphine alkaloids in *Papaver bracteatum*, radiochemical study □ *Papaver bracteatum*—biosynthesis of morphine alkaloids, radiochemical study □ Radiochemistry—study of biosynthesis of morphine alkaloids in *Papaver bracteatum*

In 1963, Neubauer and Mothes (1) reported on a strain of *Papaver bracteatum* Lindl. that produced thebaine in high yield but apparently contained neither codeine nor morphine. *P. bracteatum* is closely related to *P. orientale* and *P. pseudo-orientale*, which do not synthesize significant amounts of thebaine. They can be differentiated from *P. bracteatum* by cytological examination (2) and chemotaxonomic tests (3). In contrast to the opium poppy (*P. somniferum*), which produces a large number of alkaloids, several in appreciable concentrations, *P. bracteatum* contains mainly thebaine, which may account for 98% of the alkaloid content[1] (1, 4). Isolation and purification of thebaine from *P. bracteatum* are, therefore, relatively simple.

In recent years, considerable interest has developed in this plant as a source of thebaine; in the laboratory, thebaine can be converted to codeine and other narcotic analgesics and antitussives (6–8). Thebaine is also the raw material for naloxone and related narcotic antagonists and for the interesting *endo*-ethenotetrahydrothebaines (9). In 1972, a collaborative research project on *P. bracteatum* was initiated by the United Nations Narcotics Laboratory, which has been coordinating investigations carried out in many countries (10).

The purposes of the present investigation were to study the biosynthetic pathways of hydrophenanthrene alkaloids in *P. bracteatum* and to explore possible sites of biosynthesis.

BACKGROUND

The biosynthesis of morphine alkaloids in the opium poppy has been

[1] Several varieties, or chemical races, of *P. bracteatum* have been found, differing somewhat in alkaloid composition. The Arya II variety from western Iran has a particularly high content of thebaine (5).

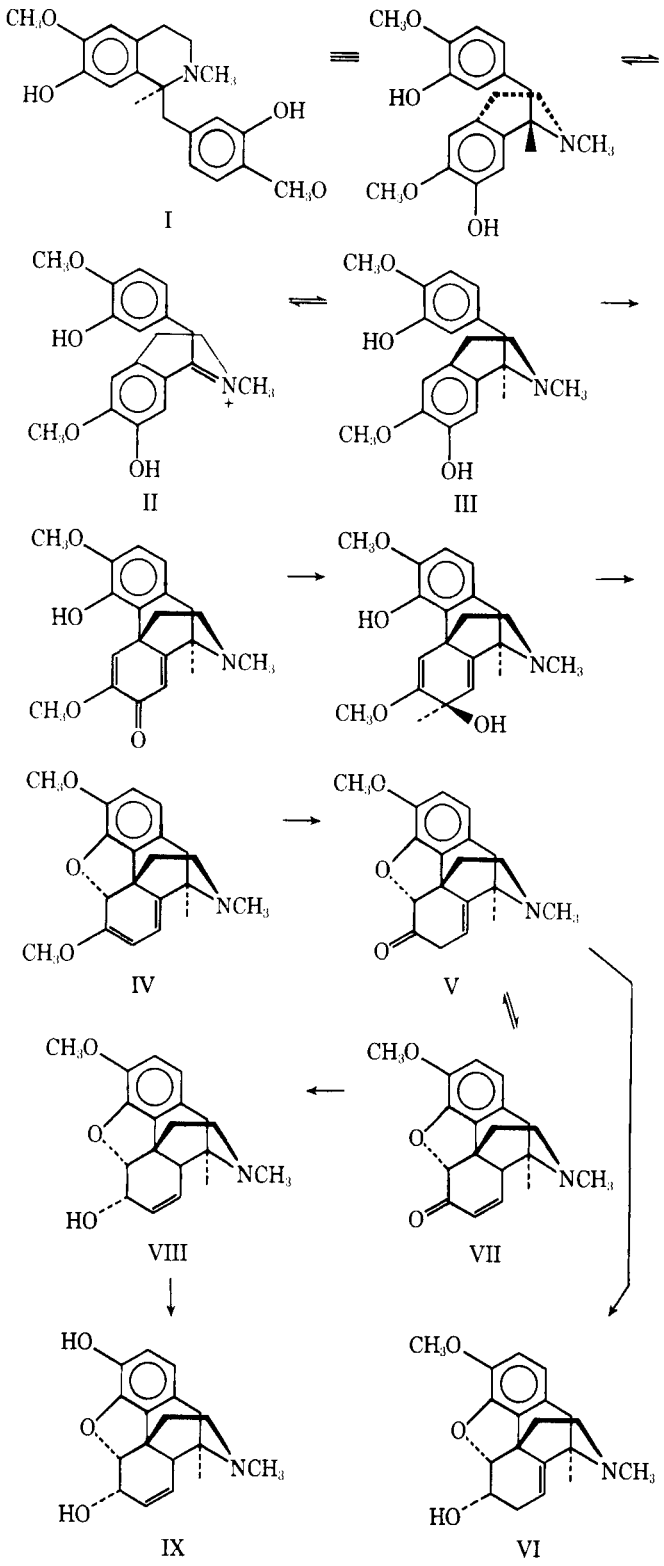

Scheme I

described in detail (11–17). The last few steps of the pathway in *P. somniferum* are illustrated in Scheme I. Reticuline produced from L-tyrosine has the (*S*)-configuration and is dextrorotatory (I). Battersby *et al.* (13) demonstrated that reticuline undergoes racemization in the plant, a reaction essential for the formation of the morphine alkaloids derived from (−)-(*R*)-reticuline (III). This racemization is enzymatic and substrate specific (18) and proceeds by a reversible oxidation–reduction mechanism *via* the 1,2-dehydro derivative (II) (13). While *O*-demethylation of the enol ether group of thebaine (IV) is an enzymatic reaction, the rearrangement of neopinone (V) to codeinone (VII) does not require an enzyme. In aqueous solution, an equilibrium that favors codeinone is established (19).

Table I—Tracer Experiments on *P. bracteatum* with 1-^{3}H-*N*-Methyl-^{14}C-(±)-reticuline

Administration	Incorporation of ^{14}C, %, into Thebaine	Codeine[a]	Codeinone[a]	Morphine[a]
Intact plant by wick	12.03[b]	0.002	0.000	0.000
Isolated shoots	12.08[c]	0.000	—	0.000
Root of whole plant:				
Root	0.30[d]	—	—	—
Shoot	0.06[e]	—	—	—
Root slices	1.60[f]	—	—	—

[a] Isolated by dilution with cold carrier. [b] 4696 dpm/mg (^{14}C); 53.6% ^{3}H-loss. [c] 41,888 dpm/mg (^{14}C); 54.2% ^{3}H-loss. [d] 1071 dpm/mg (^{14}C); 55.3% ^{3}H-loss. [e] 267 dpm/mg (^{14}C); 58.9% ^{3}H-loss. [f] 2762 dpm/mg (^{14}C); 58.0% ^{3}H-loss.

Very few biosynthetic studies have been performed with *P. bracteatum*. Neubauer (20) showed that short-term (6 hr) exposure of leaves to 2-^{14}C-DL-tyrosine gave incorporation of radioactivity into thebaine with a proper labeling pattern. Nordal *et al.* (21) obtained radioactive thebaine from uniformly labeled phenylalanine, tyrosine, glycine, and urea when the radioactive substances were applied to the surface of leaves and stems in a surfactant solution.

To obtain more detailed information about the biosynthetic pathway, reticuline was chosen as the precursor because—unlike the amino acids—it is not a primary metabolite and its racemization plays a crucial part in the biosynthesis of morphine in the opium poppy. Racemization was studied by means of double-labeled (±)-reticuline containing a ^{14}C-*N*-methyl, a ^{3}H-label at the asymmetric center, and a known ratio of specific activities. Previously (12, 13), it was demonstrated that no significant *N*-demethylation takes place in the biosynthesis of thebaine from reticuline in the opium poppy.

If the isotope ratio of the biosynthetic product remains unchanged, no racemization has taken place and only the *levo*-enantiomer has been utilized in the reaction. A ^{3}H-loss of 50% or less means that racemization has occurred, but it may only have affected the dextrorotatory isomer. If the ^{3}H-loss is greater than 50%, even the levorotatory isomer of required stereochemistry must have been subjected to some racemization and, consequently, the reaction is reversible. The labeling pattern of isolated thebaine was established by rearrangement to thebenine (11), followed by exhaustive methylation and Hoffman degradation. Trimethylamine carrying the ^{14}C-label was isolated as benzyltrimethylammonium bromide.

To determine the limiting step in the biosynthesis of hydrophenanthrene alkaloids in *P. bracteatum*, feeding experiments also were performed with codeinone. This alkaloid was administered as the nonradioactive substance. The alkaloids produced by the plant were isolated and identified by GLC and IR spectroscopy.

In young plants of *P. bracteatum*, the thebaine content increases most rapidly in the roots and tends to stabilize there after a few weeks, whereupon the thebaine concentration increases in the shoots (22). It was suggested, therefore, that thebaine is biosynthesized in the root and translocated to the shoots. As the plant reaches maturity during its 2nd year of growth, the highest concentration of thebaine is found in the capsule, reaching a peak 4–6 weeks after flowering (8, 23). If the plant is disbudded and thereby prevented from flowering and forming capsules, most thebaine remains in the roots, which increase in size and weight (7).

RESULTS AND DISCUSSION

The results of the feeding experiments indicate that the biosynthesis of thebaine in *P. bracteatum* occurs by the same route as in the opium poppy. Double-labeled (±)-reticuline showed good incorporation into thebaine by several methods of administration (Table I). The plant is capable of racemization of reticuline, and the reaction is reversible as indicated by a ^{3}H-loss greater than 50%. Chemical degradation of thebaine showed that all ^{14}C-activity was located in the *N*-methyl group (Table II). Rearrangement to thebenine took place without loss of tritium. Immature plants fed (±)-reticuline through their leaves gave thebaine with the highest specific ^{14}C-activity (~42,000 dpm/mg), but the percent incorporation was the same as that obtained by wick feeding because of the much larger amount of thebaine present in the whole plants.

The negligible incorporation of radioactivity into codeine (VIII), codeinone (VII), and morphine (IX), isolated by dilution with cold carriers, indicates that these alkaloids are not present in the plant. However,

Table II—Controlled Degradation of Radioactive Thebaine

Fragment	Relative ^{14}C-Activity in Isolated Fragment, %	^{3}H-Loss
Methebenine methosulfate	99.6	0.00
Benzyltrimethylammonium bromide	99.5	100.0

Küppers *et al.* (24) recently reported the isolation of trace amounts (0.003–0.004%) of neopine (VI) and codeine from the Arya I variety of *P. bracteatum*. Unequivocal detection of such small amounts by the isotope dilution method requires a precursor of much greater specific activity than was used in these experiments. Nevertheless, the small incorporation of reticuline into codeine is consistent with the results of Küppers *et al.* (24).

When codeinone was administered to the intact plant and to isolated leaves, rapid and efficient reduction to codeine took place, as demonstrated by actual isolation of codeine (Table III). Little or no codeinone could be recovered unchanged. The difference between the amount of codeinone administered and the amount of codeine isolated was due primarily to losses during the extensive purification of codeine. No morphine could be detected. Therefore, the limiting step in the biosynthetic sequence apparently is the *O*-6-demethylation of thebaine to neopinone. In view of the large amount of thebaine present in *P. bracteatum* and the facile reduction of the ketones, as demonstrated for codeinone, the minute amounts of codeine and neopine reported by Küppers *et al.* (24) perhaps may be best explained by nonenzymatic hydrolysis of the enol ether group of thebaine because of the acidic conditions prevailing in the plant. Neopinone and codeinone produced in this way would be rapidly reduced to the corresponding alcohols in the living plant.

The feeding experiments with young, isolated leaves prior to stem formation make it clear that alkaloid biosynthesis occurs at a fast rate in the aerial parts (Table I). When labeled reticuline was fed through the roots of young plants placed in vermiculite and the roots and shoots were analyzed separately, significant incorporation of radioactivity into thebaine could be observed in the roots. A much smaller incorporation was found in the aerial parts, perhaps because the time of the experiment was too short (2 days) for an appreciable translocation from the roots.

High incorporation of radioactivity into thebaine was achieved when the roots were cut into small sections and allowed to remain in contact with radioactive reticuline solution. This result was undoubtedly due to the larger surface area and the direct contact of the precursor with the enzymes exposed by the cross-sections of the roots. Therefore, alkaloid biosynthesis in *P. bracteatum* is not limited to any one part of the plant. As in the opium poppy, alkaloid biosynthesis probably takes place in the laticiferous vessels that form an anastomotic network throughout the plant (25, 26). This finding is consistent with the fact that the latex that accumulates in the capsule after petal drop is the single richest source of thebaine, containing as much as 20% on a dry weight basis (27).

EXPERIMENTAL[2]

Synthesis of Precursors—*1-^{3}H-N-Methyl-^{14}C-(±)-reticuline*—*N*-Methyl-^{14}C-(±)-*O,O*-dibenzylreticuline was prepared as described previously (28); the specific activity was 1.65 mCi/mmole.

1-(3-Benzyloxy-4-methoxybenzyl)-7-benzyloxy-6-methoxy-3,4-dihydroisoquinoline methiodide (200 mg) (28) was dissolved in 25 ml of anhydrous dimethyl sulfoxide and reduced with 8 mCi (1.6 mg) of sodium ^{3}H-borohydride overnight. Cold sodium borohydride was added to complete the reduction, and the product was isolated and purified by crystallization to give 166 mg of pure 1-^{3}H-(±)-*O,O*-dibenzylreticuline, specific activity 14.00 mCi/mmole.

N-Methyl-^{14}C-(±)-*O,O*-dibenzylreticuline (667 mg) and 1-^{3}H-(±)-*O,O*-dibenzylreticuline (150 mg) were dissolved in 50 ml of hydrochloric acid (38%) in a 250-ml round-bottom flask. Then 50 ml of benzene was added, and the mixture was stirred vigorously under nitrogen for about 14 hr at room temperature (29). The acid layer was separated, cooled in ice water, and made alkaline to pH 13 with 6 *N* NaOH. After extraction with ether, the aqueous phase was adjusted to pH 9 with ammonium chloride and extracted several times with ether. The ether extracts obtained at pH 9 were dried over anhydrous sodium sulfate and evaporated to dryness. The residue (428 mg) was purified by repeated precipitation from ether–petroleum ether until pure by TLC on silica gel and GLC[3] of the base and its bis(trimethylsilyl) derivative on OV-1 (3%); specific activities were: ^{14}C, 1.35 mCi/mmole; ^{3}H, 2.57 mCi/mmole; and ^{3}H to ^{14}C ratio, 1.90.

Table III—Biosynthetic Conversion of Codeinone to Codeine in *P. bracteatum*

Administration	Codeinone, mg Administered	Codeinone, mg Recovered	Codeine Isolated, mg
Intact plant by wick	6	0	2
Isolated shoots	30	Trace	21

Codeinone—This compound was prepared by oxidation of codeine with manganese dioxide as described by Highet and Wildman (30). It was purified by chromatography on alumina[4] with benzene containing 20% chloroform and by crystallization from benzene–hexane until free of codeine as demonstrated by GLC on OV-1 (3%), mp 185°.

Cultivation of Plants and Administration of Labeled Reticuline—Seeds[5] of *P. bracteatum*, Arya II variety, were sown on free land in December 1974 and in flowerpots in a greenhouse in January 1976. The precursor solutions were prepared by dissolving the compound in an equivalent amount of 0.1 *N* H_2SO_4 and diluting with water to a concentration of 1 mg/ml.

Wick Feeding—A cotton thread was inserted through the main stem near its base of 12 plants, 16–18 months old, as they were just beginning to blossom. Both ends of the thread were twisted together and placed in a vial containing the precursor solution. The amount of precursor per plant ranged from 1 to 3 mg, depending on plant size. The plants were harvested after 10 days and placed in a freezer until they could be extracted.

Feeding of Isolated Shoots—Sixty leaves from 30 immature plants, about 15 months old, were cut off near the roots and immediately placed in a beaker of water. About 1 cm of the end of the leaf stem was cut off under water and the leaf was transferred, with a drop of water clinging to the end, to a small test tube, 15 mm i.d. × 10 cm long. The test tube contained 0.25 mg of labeled reticuline in 1 ml of water. Two leaves were placed in each test tube. Water was added as needed during the experiment, and the leaves were harvested when they showed signs of wilting (36–48 hr).

Root Feeding of Whole Plants—Four immature plants, about 15 months old, were carefully removed from the soil, rinsed with water, and placed in moist vermiculite in test tubes. A solution of the precursor containing 3 mg of labeled reticuline was added to each test tube around the root system. The plants were harvested after 2 days when they began to wilt. About 1 cm of the intersection between the root and the shoot was removed, and the roots and the leaves were extracted separately.

Tracer Experiments with Root Slices—Six immature plants, about 15 months old, were removed carefully from the soil and rinsed with water. The shoots were removed, including about 1 cm of the uppermost part of the root. The rest of the root was cut into 1-cm slices, which were placed in a dark-brown glass bottle and moistened with a solution containing 10 mg of labeled reticuline. The bottle was rotated several times a day for 4 days to allow the root pieces to contact the radioactive precursor solution.

Extraction, Separation, and Purification of Alkaloids—The fresh or frozen plants were extracted with methanol in a high-speed blender[6], and the cold alkaloid carriers were added. The suspension was poured into a glass percolator and extracted with methanol until the extract gave negative tests for alkaloids. The extract was concentrated in a rotary vacuum evaporator to remove the methanol, transferred to a separator, and shaken with several small portions of ethyl acetate. The combined ethyl acetate extracts were washed three times with 0.5 *N* HCl, and the acid washings were combined with the original aqueous solution (total alkaloids).

The total alkaloid solution was cooled in ice water, 6 *N* NaOH was added to pH 13, and the solution was extracted several times with chloroform. Chloroform evaporation gave the nonphenolic alkaloids. The aqueous solution containing the phenolic alkaloids was adjusted to pH 9 with ammonium chloride and extracted with 50, 30, and 20 ml of chlo-

[2] All melting points are uncorrected.

[3] Varian Aerograph model 2100 gas chromatograph with glass column, 1.82 m (6 ft) long, 2 mm i.d.

[4] Neutral aluminum oxide, Woelm, activity III.

[5] Obtained from the United Nations Narcotic Laboratory, courtesy of Dr. O. J. Braenden.

[6] Waring Products Co.

roform–isopropyl alcohol (3:1). The organic extract was shaken, first with 10 ml and then with 5 ml of 0.1 *N* NaOH.

The combined alkaline extracts were placed in a 50-ml glass-stoppered flask and 20 ml of ether, 500 mg of ammonium chloride, and 1 ml of pH 9.0 ammonium chloride–ammonium hydroxide buffer were added. The flask was stoppered, shaken vigorously for about 2 min, and placed in a refrigerator for crystallization of morphine. The crystals were collected and purified by crystallization from methanol to constant radioactivity (31).

The fraction containing the nonphenolic alkaloids was separated by chromatography on alumina[4] with benzene containing 10% chloroform. The elution was monitored by micro-TLC. After thebaine had been collected, the concentration of chloroform in the eluting solvent was increased gradually to 35% for elution of codeinone and codeine. Thebaine was purified by fractional crystallization from benzene–hexane to constant radioactivity. Codeinone and codeine were first purified by preparative TLC on alumina with 8% ethanol in benzene. Codeinone was then crystallized from benzene–hexane to constant radioactivity. Codeine was converted to 6-acetylcodeine by means of acetic anhydride and pyridine and crystallized from hexane to constant radioactivity.

Feeding Experiments with Codeinone—In one experiment, 6 mg of codeinone was administered as the sulfate to a mature flowering plant by cotton wick. The plant was harvested after 7 days and extracted as described. GC of the total alkaloid extract (116 mg) revealed thebaine as the major component with smaller amounts of several other alkaloids. One minor alkaloid had the same retention time as codeine. The gas chromatogram showed no detectable amount of codeinone.

The major portion of thebaine was removed by crystallization from ether, and the minor alkaloids were separated by preparative TLC on silica gel with chloroform–methanol (9:1) into three fractions, one of which contained codeine as its major component. This fraction was further purified by TLC on silica gel with benzene–ethanol (8:2) (double development) to afford pure codeine (2 mg), identified by GLC of the base and of its trimethylsilyl derivative on two stationary phases of different polarity (OV-1 and OV-17). There was no evidence of morphine.

In another experiment, 30 mg of codeinone was administered to 66 large leaves cut from 35 5-month-old plants as described for reticuline. The alkaloids were extracted and separated into phenolic and nonphenolic fractions. The nonphenolic fraction (172 mg), consisting mainly of thebaine, displayed a distinct peak on the gas chromatogram corresponding to codeine but showed only a trace of codeinone. It was separated by preparative TLC on alumina with benzene–ethanol (92:8) into six fractions, one of which was almost pure codeine (21 mg), identified by GLC and IR spectroscopy. The phenolic fraction (91 mg) was purified by preparative TLC on silica gel with chloroform–methanol (9:1). No morphine could be detected by GLC of the fractions obtained.

The same extraction and separation procedures were applied to 45 leaves of *P. bracteatum* that had not received codeinone. No codeine could be detected by GLC of the total nonphenolic fraction or of the fractions obtained by preparative TLC on silica gel with chloroform–methanol (9:1).

Degradation of Thebaine—Thebaine (200 mg) was dissolved in a mixture of 2 ml of 15% hydrochloric acid and 0.4 ml of methanol and refluxed under nitrogen for 2 min. The solution was cooled, and the liquid was decanted from the gummy precipitate of thebenine. Thebenine was methylated at room temperature in a nitrogen stream with dimethyl sulfate. Sodium hydroxide solution (11 *N*) was added dropwise to maintain the pH of about 10. The reaction mixture was cooled in the refrigerator overnight to produce green crystals of methebenine methosulfate (97 mg), mp 270–273° [lit. (11) mp 273–275°]. It was recrystallized from methanol–ether to constant radioactivity.

Methebenine methosulfate (88 mg) was placed in a two-necked flask fitted with a reflux condenser and a nitrogen inlet tube. The top of the condenser was connected to a flask containing 1 ml of benzyl bromide in 10 ml of methylene chloride. A slow nitrogen stream was passed into the reaction flask, bubbling through the solution of benzyl bromide. Five milliliters of 6 *N* NaOH was added to the reaction flask, and the solution was refluxed overnight. The methylene chloride solution was concentrated, and benzyltrimethylammonium bromide was precipitated with ether. The precipitate (26 mg) was recrystallized from ether–chloroform to constant radioactivity, mp 232–234° [lit. (32) mp 235°].

REFERENCES

(1) D. Neubauer and K. Mothes, *Planta Med.*, **11**, 387 (1963).

(2) P. Goldblatt, United Nations Secretariat, Document ST/SOA/Ser.J/19, 1975.

(3) P. G. Vincent, C. E. Bare, and W. A. Gentner, *ibid.*, No. 21, 1975.

(4) A. Shafiee, I. Lalezari, P. Nasseri-Nouri, and R. Asgharian, *J. Pharm. Sci.*, **64**, 1570 (1975).

(5) I. Lalezari, P. Nasseri, and R. Asgharian, *ibid.*, **63**, 1331 (1974).

(6) *Science*, **190**, 1274 (1975).

(7) H. Böhm, *Planta Med.*, **15**, 215 (1967). *Ibid.*, **19**, 93 (1970).

(8) J. W. Fairbairn and F. Hakim, *J. Pharm. Pharmacol.*, **25**, 353 (1973).

(9) K. W. Bentley and D. G. Hardy, *J. Am. Chem. Soc.*, **89**, 3267, 3273, 3281 (1967).

(10) United Nations Secretariat, Documents ST/SOA/SER.J/1,2 (1973), 15 (1974), 23 (1976).

(11) A. R. Battersby, R. Binks, R. J. Francis, D. J. McCaldin, and H. Ramuz, *J. Chem. Soc.*, **1964**, 3600.

(12) D. H. R. Barton, G. W. Kirby, W. Steglich, G. M. Thomas, A. R. Battersby, T. A. Dobson, and H. Ramuz, *ibid.*, **1975**, 2423.

(13) A. R. Battersby, D. M. Foulkes, and R. Binks, *ibid.*, **1965**, 3323.

(14) A. R. Battersby, J. A. Martin, and E. Brochmann-Hanssen, *ibid.*, **1967**, 1785.

(15) G. Blaschke, H. J. Parker, and H. Rapoport, *J. Am. Chem. Soc.*, **89**, 1540 (1967).

(16) D. H. R. Barton, D. S. Bhakuni, R. James, and G. W. Kirby, *J. Chem. Soc. C*, **1967**, 128.

(17) A. R. Battersby, D. M. Foulkes, M. Hirst, G. V. Parry, and J. Staunton, *ibid.*, **1968**, 210.

(18) E. Brochmann-Hanssen, C.-H. Chen, C. R. Chen, H.-C. Chiang, A. Y. Leung, and K. McMurtrey, *ibid.*, **1975**, 1531.

(19) R. B. Barber and H. Rapoport, *J. Med. Chem.*, **19**, 1175 (1976).

(20) D. Neubauer, *Arch. Pharm.*, **298**, 737 (1965).

(21) A. Nordal, B. S. Paulsen, and J. K. Wold, United Nations Secretariat, Document ST/SOA/Ser.J/22, 1976.

(22) C. B. Coffman, C. E. Bare, and W. A. Gentner, *Bull. Narcotics*, **27** (3), 41 (1975).

(23) Y. Aynehchi and S. Jaffarian, *Lloydia*, **36**, 427 (1973).

(24) F. J. M. Küppers, C. A. Salemink, M. Bastart, and M. Paris, *Phytochemistry*, **15**, 444 (1976).

(25) J. W. Fairbairn and L. D. Kapoor, *Planta Med.*, **8**, 49 (1960).

(26) J. W. Fairbairn, F. Hakim, and P. B. Dickenson, *J. Pharm. Pharmacol., Suppl.*, **25**, 113P (1973).

(27) N. Sharghi and I. Lalezari, *Nature*, **213**, 1244 (1967).

(28) E. Brochmann-Hanssen, C.-C. Fu, and G. Zanati, *J. Pharm. Sci.*, **60**, 873 (1971).

(29) W. Wan-Chiu and P. Maitland, *J. Chem. Soc. C*, **1966**, 753.

(30) R. J. Highet and W. C. Wildman, *J. Am. Chem. Soc.*, **77**, 4399 (1955).

(31) E. Brochmann-Hanssen, *J. Pharm. Sci.*, **61**, 1118 (1972).

(32) "Handbook of Chemistry and Physics," 52nd ed., Chemical Rubber Co., Cleveland, Ohio, 1971–1972, p. C-104.

ACKNOWLEDGMENTS

Supported by Grant DA-00014-17 from the National Institute on Drug Abuse.

The authors are indebted to Dr. C.-T. Peng for assistance in making the vacuum transfers of ^{14}C-iodomethane.

Direct and Indirect Determination of Binding Constants of Drug–Protein Complexes with Microparticles

ANITA KOBER, BO EKMAN, and INGVAR SJÖHOLM ˣ

Received February 8, 1977, from the *Department of Pharmaceutical Biochemistry, Biomedical Center, University of Uppsala, S-751 23 Uppsala, Sweden.* Accepted for publication April 15, 1977.

Abstract □ Albumin can be immobilized in microparticles of polyacrylamide in such a way that its ligand-binding properties are retained. With radiolabeled salicylic acid, warfarin, and tryptophan, the same characteristics are obtained for binding to albumin in the microparticles as in free solution. The particles can be used conveniently to determine association constants and the number of binding sites directly. The association constant of a competitive displacer can be determined indirectly as well, as shown with diazepam–salicylic acid and tryptophan–salicylic acid.

Keyphrases □ Binding, protein—salicylic acid, warfarin, and tryptophan to albumin in free solution and in microparticles, direct and indirect determination of constants □ Protein binding—salicylic acid, warfarin, and tryptophan to albumin in free solution and in microparticles, direct and indirect determination of constants □ Microparticles, polyacrylamide—containing albumin, binding of salicylic acid, warfarin, and tryptophan compared to binding in free solution, direct and indirect determination of constants

Considerable efforts have been devoted to the quantitative characterization of ligand–macromolecule complexes, especially between drugs and serum albumin. In the absence of better methods, the time-consuming and laborious equilibrium dialysis technique is still most commonly used and is considered to give correct data when properly applied. Some modifications (1, 2) were tried to speed up equilibrium. Ultrafiltration is a rapid technique, but it generally gives too high a degree of binding because of the increased local concentration of protein just over the membrane (3).

Gel filtration also has been used in ligand binding studies (4), but unspecific interactions with the gels, together with difficulties in correctly calculating the binding constants thermodynamically, have precluded its general application. Circular dichroism measurements (5) can, in some cases, be used to determine binding constants accurately in homogeneous solutions without any interfering membranes or matrixes. However, the limited availability of spectropolarimeters and the costs involved limit the applicability.

It recently was reported (6–8) that immunoglobulins, albumin, and enzymes retain their biological properties when immobilized in microparticles of highly cross-linked polyacrylamide. The proteins are partly entrapped in the network of the polymer and partly fixed in the thick threads forming the network. The relatively large pores of the polyacrylamide allow the equilibrium between the interior of the particles and the environment to be attained rapidly.

The present paper demonstrates that the quantitative relationships for the binding of some drugs to albumin in microparticles and in true solution (as in equilibrium dialysis) are the same. Moreover, it is shown how albumin in microparticles can be used conveniently for both direct and indirect determinations of binding constants.

EXPERIMENTAL

Materials—The purity of the human serum albumin[1] was more than 98% according to the manufacturer's specifications.

^{14}C-Salicylic acid (52 mCi/mmole), ^{14}C-warfarin (23.5 mCi/mmole), and ^{14}C-tryptophan (52 mCi/mmole) were used[2]. The radiochemical purity was checked by TLC and was >98%. The unlabeled drugs were used as received. Other chemicals were analytical grade.

Radioactivity was measured by liquid scintillation counting.

Microparticles of polyacrylamide containing human serum albumin, and with a diameter primarily between 1 and 3 μm, were prepared as described by Ekman and Sjöholm (7). An appropriate amount of human serum albumin was dissolved in a solution of acrylamide (6% w/v) and *N,N'*-methylenebisacrylamide (2% w/v) in 0.1 *M* KCl and 0.005 *M* phosphate buffer, pH 7.4. In general, a concentration of 150 mg of albumin/ml was used.

After the addition of the catalyst system consisting of *N,N,N',N'*-tetramethylethylenediamine and ammonium peroxydisulfate, the water phase (5 ml) was immediately homogenized in 200 ml of an organic phase[3] [toluene–chloroform (4:1)]. The polymerization started immediately and was completed in 5 min. The microparticles were isolated by centrifugation and washed several times with buffer. The amount of human serum albumin incorporated in the particles was determined by amino acid analysis after hydrolysis in 6 *M* HCl at 105° for 20 hr.

Drug–Protein Binding with Microparticles—The experiments were carried out at room temperature (23°). Microparticles containing albumin were suspended in a 0.03 *M* phosphate buffer and 0.1 *M* NaCl, pH 7.4. The concentration of albumin in the suspension was 0.8 mg/ml (1.2×10^{-5} *M*). Aliquots of 1 ml were pipetted into plastic centrifuge tubes. Different amounts of the drug studied, also containing the ^{14}C-labeled compound, were dissolved in the same buffer and added (in 100 μl) to the tubes containing the microparticle suspension. Earlier studies (7) showed that equilibrium is obtained rapidly; the samples were generally centrifuged within 5–15 min for 20 min at 3000×*g*.

After centrifugation, the concentration of the free drug, [*D*], in the system was determined by measuring the radioactivity in 0.1-ml aliquots taken in duplicate from the supernate. The concentration of the bound drug, [*DP*], was calculated by subtracting the free drug from the total concentration of drug added.

Unspecific binding to the polyacrylamide gel of the respective ligands was tested in the same way with microparticles not containing proteins.

In the interaction studies, the displacing drug, which was not radioactively labeled, was added to the microparticle suspension so that a constant molar ratio between displacer and albumin was obtained in all samples in a series. After mixing and centrifuging, the radioactivity was determined as previously described.

Equilibrium Dialysis—The protein binding also was determined by equilibrium dialysis at 23° as described earlier (9). The albumin concentration was determined from the absorption at 278 nm ($A^{1\%}_{1\,cm}$ = 5.80).

Evaluation of Data—The binding data obtained with the different ligands were analyzed according to Scatchard (10). The following equation:

$$\frac{r}{[D]} = n \cdot K_a - r \cdot K_a \qquad \text{(Eq. 1)}$$

was used, where r is the moles of bound drug per mole of albumin, n is the number of binding sites, K_a is the association constant for the

[1] Batch 30299, KABI AB, Stockholm, Sweden.
[2] Radiochemical Centre, Amersham, England.
[3] An Ultraturrax TP 18-10 was used as the homogenizer, and the detergent was Pluronic F68, Wyandotte Chemicals Corp., Wyandotte, Mich.

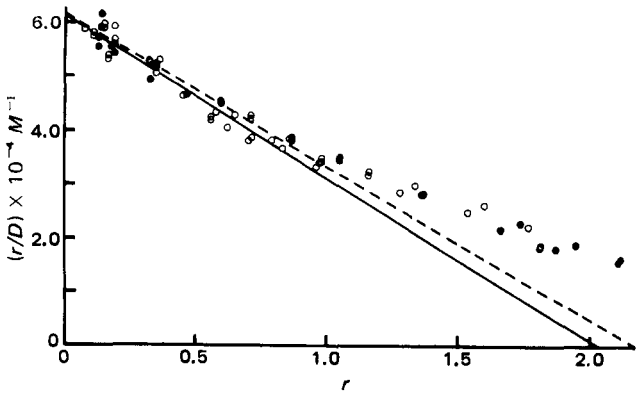

Figure 1—*Scatchard plot showing salicylic acid binding to human serum albumin in free solution determined by equilibrium dialysis (●) and to albumin in microparticles (○). The lines (--- and —, respectively) are the regression lines calculated from the experimental points with r < 1.0. Albumin (1.2 × 10⁻⁵ M) was dissolved or, when present in microparticles, suspended in 1.0 M NaCl with 0.03 M phosphate, pH 7.4; the temperature was 23°.*

drug–albumin complex, and [D] is the concentration of free drug. The data also were evaluated by the double-reciprocal plot:

$$\frac{1}{r} = \frac{1}{nK_a} \cdot \frac{1}{[D]} + \frac{1}{n} \qquad \text{(Eq. 2)}$$

When the binding of a ligand to a particular site on the macromolecule is inhibited by a competitive inhibitor, the following relation exists (11) between the association constant, K_{app}, determined in the presence of the inhibitor, I, and the true association constant, K_a, obtained in the absence of inhibitor:

$$K_{app} = \frac{K_a}{1 + [I]K_i} \qquad \text{(Eq. 3)}$$

where $[I]$ is the concentration of the free displacing drug and K_i is the association constant for the protein–displacer complex. From this equation, the association constant for the displacing drug, K_i, can be calculated if K_a and $[I]$ are known.

In the plots, the data points were fitted to straight lines by linear regression analyses using the values on the x-axis as the independent variable and the values on the y-axis as the dependent variable.

RESULTS

Protein Binding—The unspecific binding to the polyacrylamide gel is generally low, and no such binding was detected for salicylic acid, warfarin, and tryptophan. The characteristics for the binding to human serum albumin in microparticles, as displayed in the Scatchard plots, are shown for salicylic acid, warfarin, and tryptophan in Figs. 1–3, respectively. The binding of the drugs to albumin incorporated in the microparticles is the same, within the experimental errors, as the binding to albumin in free solution as determined by equilibrium dialysis. The straight lines were calculated by linear regression and gave the values of nK_a (intercept on the y-axis), n (intercept on the x-axis), and K_a (Table I).

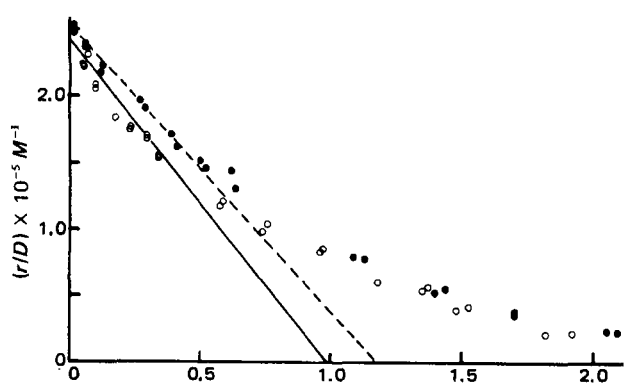

Figure 2—*Scatchard plot showing warfarin binding to human serum albumin in free solution determined by equilibrium dialysis (●) and to albumin in microparticles (○). The lines (--- and —, respectively) are the regression lines calculated from the experimental points with r < 0.6. The experimental conditions were the same as in Fig. 1.*

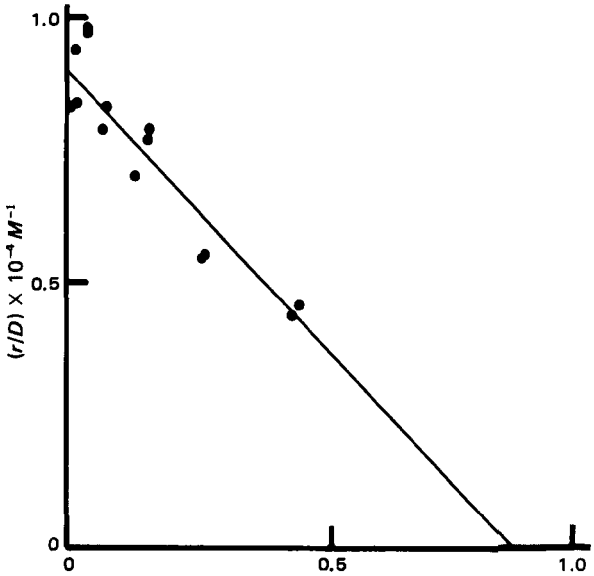

Figure 3—*Scatchard plot showing L-tryptophan binding to human serum albumin in microparticles (●). The line drawn is the regression line. The experimental conditions were the same as in Fig. 1.*

Inhibition of Binding—The changes in the binding of salicylic acid to albumin in microparticles brought about by adding competing ligands are shown in Figs. 4 and 5. These double-reciprocal plots show that both diazepam and tryptophan inhibit ^{14}C-salicylic acid binding.

Diazepam is known to bind to one primary site on human serum albumin (12, 13); this site is evidently one of the two sites to which salicylic acid binds. The two lines have the same intercept, giving $n = 2$; *i.e.*, the binding of salicylic acid is competitively inhibited. From the slopes of the two lines, K_a and K_{app} can be calculated; K_i, the association constant characterizing diazepam binding to albumin, may subsequently be calculated from Eq. 3. Thereby, in Eq. 3, the total concentration of the inhibitor may, as an approximation, be substituted for the value of the free inhibitor concentration, $[I]$. The value of K_i is given in Table I and approaches the value $1.8 \times 10^5\ M^{-1}$ obtained with circular dichroism (13). The albumin used in this investigation was not treated with charcoal, which is usually done to eliminate the strongly bound fatty acids.

Figure 5 shows that salicylic acid binding successively decreased with increasing tryptophan concentration. Tryptophan is probably bound to more than one site on human serum albumin, even if the Scatchard plot in Fig. 3 indicates only one site. Therefore, the approximation that $[I] = [I]_{total}$ is more uncertain, which introduces a larger error in the calculation of K_i.

DISCUSSION

Immobilization of biologically active macromolecules, *e.g.*, proteins, by covalent binding to solid matrixes generally decreases or changes the activity. However, in the microparticles of highly cross-linked polyacrylamide (in this work, T – C = 8–25%)[4], the proteins are only physically entrapped in the network as well as in the threads, and the activity of the immobilized proteins is retained (6, 7).

In the present case, the binding affinity between albumin and several ligands was the same in the microparticles as in free solution. The obvious consequence of this observation is that microparticles with immobilized albumin (or other proteins) might be used to characterize the quantitative relationship between protein and ligand.

The present work showed that the association constant for drug

[4] The gels prepared are characterized according to the nomenclature suggested by Hjertén (15). The first numeral, T, denotes the total amount of monomer (g/100 ml of solvent), and the second numeral, C, denotes the amount of *N,N*-methylenebisacrylamide expressed as the percentage (weight/weight) of the total amount of monomers.

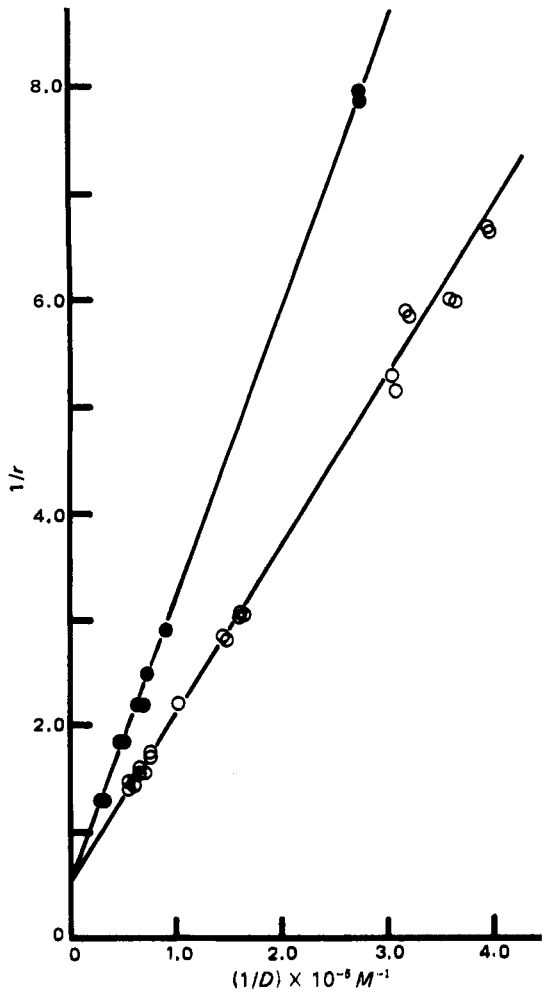

Figure 4—*Double-reciprocal plot showing salicylic acid binding to human serum albumin in microparticles in the absence (○) and presence (●) of 1.5 × 10⁻⁵ M diazepam. The experimental conditions were the same as in Fig. 1.*

binding can conveniently be performed directly. The constants can be determined by the Scatchard plot, especially when the number of binding sites involved, n, is of interest. In addition, the double-reciprocal plot can be used to study the effects of inhibitors. The association constant for the binding of the inhibitor to the specific site can be estimated from the changed slopes of the lines obtained with increasing inhibitor concentration. Certainly, the inhibitor may bind to other sites as well, so some uncertainty will exist as to the approximation that the free inhibitor concentration approaches the total. In this case, information may be obtained from determinations at varying inhibitor concentrations. Consistent values of K_i indicate that the approximation is correct.

The use of microparticles with immobilized protein simplifies the determination of association constants considerably. The procedure is rapid and simple, and the values will be precise when radiolabeled ligands are used or when sensitive methods are available for the determination of the free ligand in the supernate obtained after centrifugation. In these

Table I—Binding Constants for the Binding to Human Serum Albumin

Compound	Microparticles K_a, $M^{-1} \times 10^{-4}$	n	Microparticles K_i, $M^{-1} \times 10^{-4}$	Other Methods K_a, $M^{-1} \times 10^{-4}$	Other Methods n
Salicylic acid	3.0	2.0	—	2.8	2.2[a]
Warfarin	24.0	1.0	—	21.0	1.2[a]
Tryptophan	1.1	0.8	0.9	1.1	0.9[b]
Diazepam	—	—	11.0	18.0	1.0[c]

[a] Equilibrium dialysis (this work). [b] Gel filtration (14). [c] Circular dichroism (13).

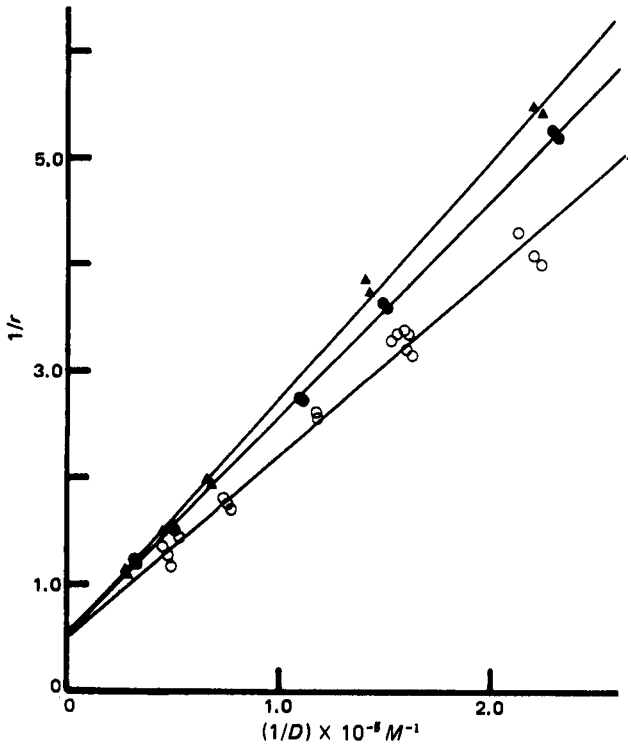

Figure 5—*Double-reciprocal plot of salicylic acid binding to human serum albumin in microparticles, alone (○), in the presence of 5.8 × 10⁻⁵ M tryptophan (●), and in the presence of 9.6 × 10⁻⁵ M tryptophan (▲). The experimental conditions were the same as in Fig. 1.*

cases, low concentrations of protein and ligand can be used, which means that the degree of binding will be low. Such conditions are favorable for the determination of the primary binding constant, which most often represents the physiologically significant binding.

REFERENCES

(1) M. C. Meyer and D. E. Guttman, *J. Pharm. Sci.*, **59**, 33 (1970).
(2) V. P. Shah, S. M. Wallace, and S. Riegelman, *ibid.*, **63**, 1364 (1974).
(3) W. E. Lindrup, *Biochem. Soc. Trans.*, **3** (5), 635 (1975).
(4) J. P. Hummel and W. J. Dreyer, *Biochim. Biophys. Acta*, **63**, 530 (1962).
(5) N. Roosdorp and I. Sjöholm, *Biochem. Pharmacol.*, **25**, 2141 (1976).
(6) B. Ekman and I. Sjöholm, *Nature*, **257**, 825 (1975).
(7) B. Ekman and I. Sjöholm, *Biochemistry*, **15**, 5115 (1976).
(8) S. E. Brolin, A. Ågren, B. Ekman, and I. Sjöholm, *Anal. Biochem.*, **78**, 577 (1977).
(9) I. Sjöholm, A. Kober, I. Odar-Cederlöf, and O. Borgå, *Biochem. Pharmacol.*, **25**, 1205 (1976).
(10) G. Scatchard, *Ann. N.Y. Acad. Sci.*, **51**, 660 (1949).
(11) J. T. Edsall and J. Wyman, *Biophys. Chem.*, 1, 652 (1958).
(12) W. Müller and U. Wollert, *Naunyn-Schmiedeberg's Arch. Pharmacol.*, **280**, 229 (1973).
(13) T. Sjödin, N. Roosdorp, and I. Sjöholm, *Biochem. Pharmacol.*, **25**, 2131 (1976).
(14) W. E. Müller and U. Wollert, *Naunyn-Schmiedeberg's Arch. Pharmacol.*, **288**, 17 (1975).
(15) S. Hjerén, *Arch. Biochem. Biophys., Suppl.*, 1, 147 (1962).

ACKNOWLEDGMENTS

Supported by the Swedish Medical Research Council (Project 13X-3162), the Swedish Board for Technical Development (Project 75-4415), the I.F. Foundation for Pharmaceutical Research, Stockholm, and Apotekarsociteten, Stockholm.

The authors thank Mr. Börje Berg for the preparation of the microparticles.

Polymer-Bound Carbonic Anhydrides in *N*-Acylation of 7-Aminocephalosporanic Acid

GARY E. MARTIN *, MANVENDRA B. SHAMBHU, and GEORGE A. DIGENIS ˣ

Received November 24, 1976, from the *Division of Medicinal Chemistry and Pharmacognosy, College of Pharmacy, University of Kentucky, Lexington, KY 40506.* Accepted for publication February 17, 1977. *Present address: College of Pharmacy, University of Houston, Houston, TX 77004.

Abstract □ 7-Aminocephalosporanic acid *tert*-butyl ester was reacted with polystyrene-bound mixed carbonic–carboxylic anhydrides to give the corresponding *N*-acylated derivatives. Cleavage of the *tert*-butyl protecting group with trifluoroacetic acid gave the corresponding cephalosporanic acid.

Keyphrases □ Cefaloram—synthesized by *N*-acylation of *tert*-butyl 7-aminocephalosporanate using polystyrene-bound anhydrides □ Polymer-bound anhydrides—used in synthesis of cefaloram by *N*-acylation of *tert*-butyl 7-aminocephalosporanate □ Cephalosporins—cefaloram synthesized by *N*-acylation of *tert*-butyl 7-aminocephalosporanate using polystyrene-bound anhydrides □ Solid phase syntheses—cefaloram, *N*-acylation of *tert*-butyl 7-aminocephalosporanate using polystyrene-bound anhydrides □ Antibiotics—cefaloram, synthesized by *N*-acylation of *tert*-butyl 7-aminocephalosporanate using polystyrene-bound anhydrides

The advantages of using insoluble polymer supports in the syntheses of polypeptides (1) and polynucleotides (2) have been well documented. The success of this solid phase technique prompted various syntheses with polymer-bound reagents (3, 4). One dominant reason for using the insoluble support is that the excess reagent and the products arising from it can be removed by simple filtration. Thus, excess reagent can be added to ensure complete conversion of the substrate and the product can be isolated by filtration and solvent evaporation. The ease of this workup procedure is especially important in preparing sensitive molecules such as antibiotics. This report presents initial studies on the use of insoluble reagents in the *N*-acylation of 7-aminocephalosporanic acid.

Mixed carbonic–carboxylic anhydrides have been utilized in the *N*-acylation of both 7-aminocephalosporanic and 6-aminopenicillanic acids (5). Due to their instability, these reagents are prepared *in situ*. These highly reactive anhydride functions can be created on insoluble polystyrene (6), resulting in a polymer capable of benzoylation of simple aliphatic amines. Since *N*-acylation of 7-aminocephalosporanic acid by phenylacetic acid is required to produce an active antibiotic (cefaloram), a study of the formation and utilization of polystyrene with carbonic–phenylacetic anhydride functions was undertaken.

RESULTS AND DISCUSSION

The preparation of polymeric mixed anhydrides is illustrated in Scheme I. "Popcorn polystyrene" (I) was chloromethylated according to the general procedure of Merrifield (1), resulting in the production of resins bearing approximately 1.8 mEq/g of chloromethyl residues. Subsequent reaction of the chloromethyl polystyrene (II) with sodium benzoate and triethylamine gave the benzoate ester (III), which, on alkaline hydrolysis, gave quantitative conversion to the benzyl alcohol-bearing resin (IV).

Treatment of IV with a 12.5% solution of phosgene in benzene converted the alcohol to the corresponding chloroformate (V). The conversion of V to the carbonic–benzoic anhydride (VI*a*) was achieved using triethylamine as the catalyst at 0° in 30 min (6). Attempts to prepare the corresponding phenylacetic anhydride (VI*b*) under the same conditions resulted in poor yields, because of the rapid decomposition of the anhydride functions caused by the presence of triethylamine. Stability studies on such mixed anhydrides in solution have shown that some tertiary amines catalyze their conversion to the corresponding esters, accompanied by the loss of carbon dioxide (7). The use of another tertiary amine, quinoline, as the catalyst at 25° gave the desired resin (VI*b*) in fair yield (0.8 mEq/g of acid).

Prior to the reaction with the resin anhydrides, 7-aminocephalosporanic acid was converted to its *tert*-butyl ester (VII) by the use of 2-methylpropene and sulfuric acid (8) for two reasons. One was the necessity of carrying out the reactions of polystyrene-based reagents in solvents, such as benzene, that swell the resin bead. The solubility of

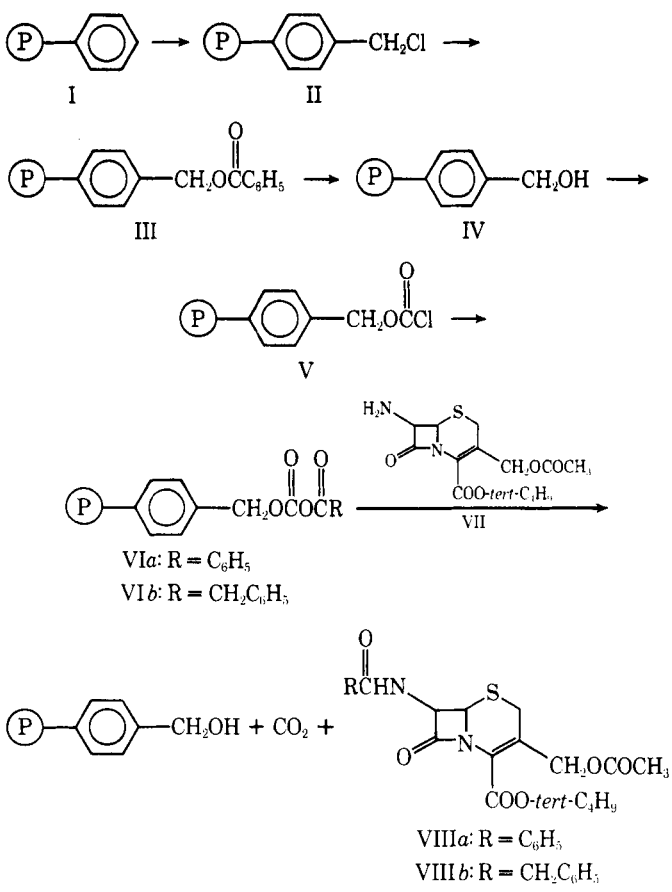

Scheme I

7-aminocephalosporanic acid in benzene is negligible. The second was the blocking of the carboxylic acid function, which left only the amine function to react with the resin-bound reagents (6).

Acylation was carried out by addition of the ester to the benzene suspensions of resins VI*a* and VI*b*. The corresponding *N*-acyl derivatives were obtained after the evaporation of the filtrates in 75 and 50% yields, respectively. Cleavage of the *tert*-butyl ester from *tert*-butyl 7-(*N*-phenylacetamido)cephalosporanate (VIII*b*) resulted in the production of 7-(*N*-phenylacetamido)cephalosporanic acid (cefaloram), a biologically active cephalosporin (5, 8). Subsequent biological activity testing of cefaloram, produced by *N*-acylation with the polymeric mixed anhydride method, by the paper disk method of Bauer *et al.* (9) gave antibiotic activity parallel with that obtained following conventional synthetic preparation (5, 9). Against *Staphylococcus aureus* (3074), a minimum inhibitory concentration of 2.5 μg/ml was obtained.

The reason for the relatively low yields in the acylation reactions was the incomplete conversion of the chloroformate functions of V to the mixed anhydrides. Thus, the polymers VI*a* and VI*b* possessed some chloroformate functions. A portion of the substrate amine was lost because of the reaction with the chloroformate moieties, resulting in binding to the resin as the carbamates. This conclusion was supported by the presence of sulfur in VI*a* and VI*b* after reaction with VII. Attempts are being made to reduce the number of the unreacted chloroformate functions on VI*b*.

Although yields obtained in the *N*-acylation of the cephalosporin nucleus at this time are only comparable to other synthetic procedures, the solid phase method is of potential interest in the preparation of semisynthetic cephalosporins because of its simplicity.

EXPERIMENTAL[1]

Compound I—The resin was prepared according to the procedure described by Letsinger *et al.* (10) and was reduced to 40–100 mesh using a blender[2].

Compound II—To 70 g of I in 500 ml of chloroform at 0° was added, over 30 min, 135 ml of a solution containing 100 ml of chloromethyl methyl ether and 35 ml of anhydrous stannic chloride. The mixture was stirred for 1 additional hr at 0° and then for 2 hr at 25°. The resin was then washed with 500-ml aliquots of each of the following: dioxane, dioxane–water (1:1), 10% HCl (hot), water, dioxane, benzene, and anhydrous ether. The pale-yellow resin was dried *in vacuo* to yield 80.5 g.

Polystyrene Benzyl Alcohol (IV)—To 12.0 g of II in 100 ml of 2-methoxyethanol were added 5 g of potassium benzoate and 2 ml of triethylamine, and the mixture was refluxed for 4 hr. The polymer was washed by decantation with 200 ml of 2-methoxyethanol while still hot. Then the resin was transferred to a second flask containing 4.0 g of potassium hydroxide in 100 ml of 2-methoxyethanol, and the mixture was refluxed for an additional 4 hr. The resin was washed as previously described and dried *in vacuo* to give 11.2 g of IV; IR (4% KBr pellet): 3300 cm^{-1}.

Polystyrene Benzylchloroformate (V)—To a flask containing 75 ml of a 12.5% solution of phosgene in benzene was added 10.0 g of IV. The mixture was shaken at 25° for 5 hr. Then the resin was filtered, washed with benzene (2 × 100 ml) and anhydrous ether (2 × 100 ml), and dried *in vacuo* to give 12.9 g of V; IR (4% KBr pellet): 1765 cm^{-1} (no absorption at 3300 cm^{-1}).

Polystyrene Mixed Carbonic–Carboxylic Anhydrides (VI*a* and VI*b*)—To 8.0 g of V in 50 ml of dry benzene was added 30 m*M* of the desired carboxylic acid and 30 m*M* of the necessary tertiary amine. For benzoic acid, triethylamine was added and the reaction was allowed to proceed at 0° for 30 min; for phenylacetic acid, quinoline was added and the reaction was conducted at 25° for 2 hr. The resin was washed with dioxane–water (1:1) (2 × 100 ml), dioxane (2 × 100 ml), benzene (2 × 100 ml), and anhydrous ether (2 × 100 ml) and dried *in vacuo;* IR (4% KBr pellet): 1740 and 1795 cm^{-1}.

Compound VIII*b*—To 3.0 g of VI*b* in 50 ml of dry benzene at 50° was added 0.85 g of *tert*-butylaminocephalosporanate (VII). The mixture was allowed to react for 2 hr, and then the resin was removed by filtration. After evaporation of the solvent, the residue was recrystallized from methylene chloride–ether to give 0.65 g (50%) of VIII*b*, mp 159–160° [lit. (11) mp 148–150°].

Cefaloram—Cleavage of the *tert*-butyl ester-protecting group was conducted by dissolving 1.0 g of VIII*b* in 10 ml of anhydrous ice-cold trifluoroacetic acid and allowing it to stand at 25° for 30 min (8). Then the solution was concentrated under reduced pressure to give a gummy residue, which was dissolved in a minimum of methylene chloride. The product precipitated with ether to give 0.54 g (62%) of cefaloram (5), mp 168–171° dec.; IR (chloroform): 1780, 1720, 1670, and 1640 cm^{-1}; NMR (acetone-d_6): δ 2.02 (s, 3H, $COCH_3$), 3.45–3.55 (d, 2H, C-2 CH_2), 3.6 (s, 2H, $C_6H_5CH_2$), 4.6–5.2 (m, 3H, C-6 H and CH_2O), 5.75 (quartet, 1H, C-7 H), 7.25 (s, 5H, C_6H_5), and 7.85–8.0 (broad doublet, 1H, NH) ppm.

[1] IR spectra were recorded on a Perkin-Elmer 564 or 700 instrument. NMR spectra were taken on a Varian EM-360 or A-60-A instrument. Mass spectra were obtained on a Perkin-Elmer RMU-67 instrument at 70 ev. Melting points were taken with a Thomas-Hoover capillary melting-point apparatus and are uncorrected. Elemental analyses were performed by Microanalysis Inc., Wilmington, Del., and were within 0.4% of theory.

[2] Waring.

REFERENCES

(1) R. B. Merrifield, *J. Am. Chem. Soc.*, **85**, 2149 (1963).

(2) R. L. Letsinger and V. Mahadevan, *ibid.*, **88**, 5319 (1966).

(3) C. C. Leznoff, *Chem. Soc. Rev.*, **3**, 65 (1974).

(4) J. I. Crowley and H. Rapoport, *Acc. Chem. Res.*, **9**, 135 (1976).

(5) R. R. Chauvette, E. H. Flynn, B. G. Jackson, E. R. Lavagino, R. B. Morin, R. A. Mueller, R. R. Pioch, A. W. Roeske, C. W. Ryan, J. L. Spencer, and E. van Heyningen, *J. Am. Chem. Soc.*, **84**, 3401 (1962).

(6) M. B. Shambhu and G. A. Digenis, *J. Chem. Soc., Chem. Commun.*, **1974**, 619.

(7) D. S. Tarbell and N. E. Leister, *J. Org. Chem.*, **23**, 1149 (1958).

(8) R. J. Stedman, *J. Med. Chem.*, **9**, 444 (1966).

(9) A. W. Bauer, W. M. M. Kirby, J. C. Sherris, and M. Turck, *Am. J. Clin. Pathol.*, **45**, 493 (1966).

(10) R. L. Letsinger, M. J. Kornet, V. Mahadevan, and M. J. Jerina, *J. Am. Chem. Soc.*, **86**, 5163 (1964).

(11) J. Altman, E. Kavoly, and N. Maoz, *J. Med. Chem.*, **18**, 627 (1975).

High-Performance Liquid Chromatographic Assay of Isoquinoline Alkaloid Formation from Reaction of Biogenic Amines and Aldehydes

THOMAS M. KENYHERCZ and PETER T. KISSINGER ˣ

Received January 13, 1977, from the *Department of Chemistry, Purdue University, West Lafayette, IN 47907.* Accepted for publication March 16, 1977.

Abstract □ To understand the role that tetrahydroisoquinoline formation may play in alcoholism and drug toxicology, high-performance liquid chromatography with electrochemical detection was used to monitor the overall rate of reaction, in pH 7.4 buffer, between the catecholamines (dopamine, α-methyldopamine, dihydroxyphenylpropanolamine, deoxyepinephrine, levodopa, α-methyldopa, epinephrine, levarterenol, and isoproterenol) and acetaldehyde. The observed overall rate of reaction varied from 0.38 to 0.0013 liter/mole sec. In addition, the reaction rate of the neurotransmitter dopamine was measured for various aldehydes (formaldehyde, acetaldehyde, glyoxylic acid, paraldehyde, malonaldehyde, glyceraldehyde, and chloral hydrate). The observed overall rate of reaction varied from 5.3 to 0.0011 liters/mole sec. Penicillamine prevented formation of the tetrahydroisoquinoline alkaloids when initially present in concentrations equal to or greater than the aldehyde concentration.

Keyphrases □ Catecholamines, various—reaction with acetaldehyde, formation rate of isoquinoline alkaloids □ Aldehydes, various—reaction with dopamine, formation rate of isoquinoline alkaloids □ Isoquinoline alkaloids—formation rate by reaction of various catecholamines and aldehydes □ Alkaloids, isoquinoline—formation rate by reaction of various catecholamines and aldehydes

An understanding of the mechanism and kinetics of the Pictet–Spengler condensation is significant. The reaction, involving the formation of tetrahydroisoquinoline alkaloids from biogenic amines and aldehydes, may be important in alcoholism and the toxicology of several pharmaceuticals adventitiously coadministered with alcohol (1–9). While some effort has been expended to evaluate the role of these alkaloids *in vivo*, few supporting chemical studies have been reported (10).

Recently, this laboratory developed a new approach to the assay of phenolic alkaloids involving high-performance liquid chromatography (HPLC) with electrochemical detection (11). The new method is sufficiently sensitive to be useful for monitoring isoquinoline alkaloids in biological material, and data have been obtained for the banana (12), cocoa (13), and human urine[1]. The present brief report describes the use of HPLC to determine the overall formation rate of tetrahydroisoquinoline alkaloids from the Pictet–Spengler reaction at physiological pH. The inhibition of alkaloid formation by competitive reaction of penicillamine with acetaldehyde also was examined. This investigation was undertaken as part of a long-term study on the role of *in vivo* isoquinoline formation in drug toxicology.

EXPERIMENTAL

A modular HPLC system[2] was used with an amperometric detector operated at +0.8 v *versus* the saturated calomel electrode. A 50-cm × 2-mm glass column was dry packed with a pellicular cation-exchange resin[3]. The aqueous mobile phase consisted of 0.018 *M* H_2SO_4 and either 0.1 or 0.2 *M* Na_2SO_4, depending upon the relative capacity factors of the alkaloids and parent amines.

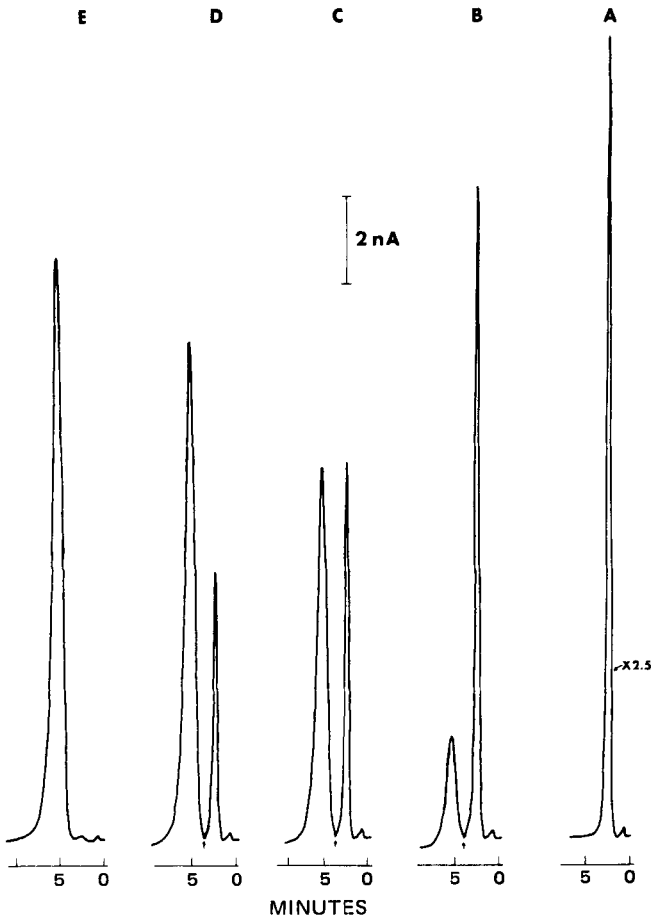

Figure 1—*Representative chromatograms illustrating conversion of dopamine to salsolinol at pH 7.4 monitored by HPLC with electrochemical detection. The initial concentration of dopamine was 1 m*M*, and that of acetaldehyde was 20 m*M*. Key: A, 0 sec; B, 25 sec; C, 101 sec; D, 149 sec; and E, 300 sec.*

Reactions were carried out at 37° in 0.1 *M* phosphate buffer, pH 7.4. The amines tested included dopamine, α-methyldopamine, 3,4-dihydroxyphenylpropanolamine, deoxyepinephrine, levodopa, α-methyldopa, epinephrine, levarterenol, isoproterenol, and serotonin. The compounds (as salts), except α-methyldopa and α-methyldopamine[4], were obtained from commercial suppliers[5].

Acetaldehyde, formaldehyde, malonaldehyde, glyceraldehyde, glyoxylic acid, paraldehyde, or chloral hydrate was added to a 1 m*M* amine solution so that the final analytical concentration of the aldehyde was 20 m*M*. Serial aliquots (25 μl) of the reaction mixture were transferred to test tubes containing 10 ml of the acidic mobile phase at 0°, thereby quenching the reaction both thermally and by dilution. Each tube was

[1] R. M. Riggin and P. T. Kissinger, unpublished results.
[2] Model LC-40, Bioanalytical Systems.
[3] Zipax SCX, du Pont.
[4] Donated by the Merck Institute, West Point, Pa.
[5] Sigma Chemical Co., Aldrich Chemical Co., and Regis Chemical Co.

Table I—Reaction of Catecholamines with Acetaldehyde at pH 7.4

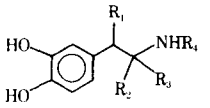

Compound	R_1	R_2	R_3	R_4	k_{obs}, liter/mole sec[a]
Dopamine	H	H	H	H	0.38
α-Methyldopamine	H	CH_3	H	H	0.36
3,4-Dihydroxyphenyl-propanolamine	OH	CH_3	H	H	0.32
Deoxyepinephrine	H	H	H	CH_3	0.30
Levodopa	H	COOH	H	H	0.16
α-Methyldopa	H	COOH	CH_3	H	0.14
Epinephrine	OH	H	H	CH_3	0.10
Levarterenol	OH	H	H	H	0.075
Isoproterenol	OH	H	H	$CH(CH_3)_2$	0.0013

[a] Observed second-order rate constants for the disappearance of catecholamines in the presence of acetaldehyde at pH 7.4 and 37° determined under pseudo-first-order conditions *via* HPLC.

immediately capped, vortexed, and kept on ice prior to chromatographic analysis. A similar sequence was used during competitive inhibition studies, except that penicillamine was mixed with the deoxygenated amine solutions prior to aldehyde addition. All chromatographic data were analyzed by manual peak height measurement and fit, using a simple linear regression analysis assuming pseudo-first-order behavior.

RESULTS AND DISCUSSION

Neuroamines condense *in vivo* with aldehydes to form isoquinoline alkaloids of potential pharmacological importance. Since the reaction is apparently nonenzymatic, the chemistry in homogeneous solution probably has a direct bearing on the *in vivo* process. A thorough study of this chemistry (14) is complicated by the large number of reactions (protonations and hydrations) coupled to the major steps indicated in Scheme I, using dopamine as an example.

While all of the details are not well understood, a useful first step is to assess the influence of amine and aldehyde structure on the overall rate of alkaloid formation. HPLC is well suited to this objective since, in most cases, the irreversible reaction is sufficiently slow to permit discrete analysis of the reaction mixture quenched by acidification, dilution, and temperature. For example, the time course of the reaction between dopamine and acetaldehyde can be examined by HPLC as illustrated in Fig. 1. All alkaloids of interest are phenolic and can be readily oxidized at a graphite electrode following separation by HPLC. The current resulting from this electrochemical reaction is an excellent measure of the quantity eluted from the column.

Rate constants obtained for the condensation of acetaldehyde with several catecholamines are presented in Table I. Where the biogenic amine is β-hydroxylated (*e.g.*, levarterenol), the reaction is complicated by the stereochemistry of the final product(s). Serotonin (5-hydroxytryptamine), which is known to react with acetaldehyde (15, 16), has a k_{obs} of 0.0034 liter/mole sec for the formation of 1-methyl-6-hydroxytryptoline under the conditions described in Table I. Observed rate constants for the condensation of endogenous or exogenous aldehydes with dopamine are reported in Table II. The hypnotic compounds, chloral hydrate and paraldehyde, react, but slowly, as do aldehydes that result from lipid peroxidation (17).

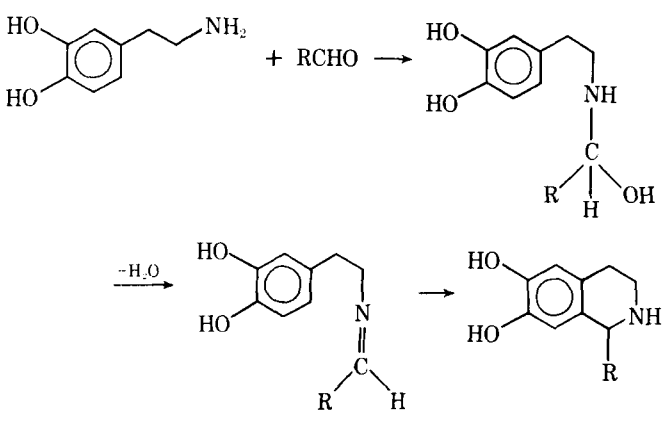

Scheme I

Table II—Reaction of Dopamine with Various Aldehydes at pH 7.4

Compound	k_{obs}, liters/mole sec[a]
Formaldehyde	5.3
Acetaldehyde	0.38
Glyoxylic acid	0.33
Paraldehyde	0.069
Malonaldehyde	0.048
Glyceraldehyde	0.021
Chloral hydrate	0.0011

[a] Observed second-order rate constants for the disappearance of dopamine at pH 7.4, 37°, determined under pseudo-first-order conditions *via* HPLC.

An attempt was made to examine the role of sulfhydryl-containing compounds (*i.e.*, penicillamine and cysteine) in preventing tetrahydroisoquinoline alkaloid formation. With variable amounts of the sulfhydryl compounds present in the initial catecholamine reaction mixture, acetaldehyde combined with the sulfhydryl compound in a 1:1 ratio. With stoichiometric amounts of penicillamine and acetaldehyde, no measurable alkaloid was produced even at catecholamine concentrations 10-fold in excess. Penicillamine and cysteine protect animals from the detrimental effects of acetaldehyde by the formation of the corresponding thiazolidine compounds (18–20). This observation may eventually prove useful in alcohol detoxification therapy.

This HPLC approach is applicable to a number of related problems in alkaloid chemistry because of its excellent selectivity and sensitivity (detection limits below 100 pg are routine). Whether the Pictet–Spengler reaction is important in the pharmacology of amine or aldehyde drugs remains to be determined. *In vivo* experiments bearing on this question are planned. The methodology for brain tissue assay has already been developed (21).

REFERENCES

(1) V. E. Davis and M. J. Walsh, *Science*, **167**, 1005 (1970).
(2) G. Cohen and M. Collins, *ibid.*, **167**, 1749 (1970).
(3) V. E. Davis, M. J. Walsh, and Y. Yamanaka, *J. Pharmacol. Exp. Ther.*, **174**, 401 (1970).
(4) M. Collins and G. Cohen, *Fed. Proc.*, **29**, 608 (1970).
(5) G. Cohen and R. E. Barrett, *ibid.*, **28**, 288 (1969).
(6) G. Cohen, *Biochem. Pharmacol.*, **20**, 1757 (1971).
(7) A. C. Collins, J. L. Cashaw, and V. E. Davis, *ibid.*, **22**, 2337 (1973).
(8) M. A. Collins and M. G. Bigdeli, *Life Sci.*, **16**, 585 (1975).
(9) M. G. Bigdeli and M. A. Collins, *Biochem. Med.*, **12**, 55 (1975).
(10) J. H. Robbins, *Clin. Res.*, **16**, 554 (1968).
(11) P. T. Kissinger, *Anal. Chem.*, **49**, 447A (1977).
(12) R. M. Riggin, M. J. McCarthy, and P. T. Kissinger, *J. Agr. Food Chem.*, **24**, 189 (1976).
(13) R. M. Riggin and P. T. Kissinger, *ibid.*, **24**, 900 (1976).
(14) W. P. Jencks, "Catalysis in Chemistry and Enzymology," McGraw-Hill, New York, N.Y., 1969.
(15) I. Geller, R. Purdy, and J. H. Merritt, *Ann. N.Y. Acad. Sci.*, **215**, 54 (1973).
(16) R. D. Myers and G. E. Martin, *ibid.*, **215**, 135 (1973).
(17) K. S. Chio and A. L. Tappel, *Biochemistry*, **8**, 2821 (1969).
(18) H. T. Nagasawa, D. J. W. Goon, N. U. Constantino, and C. S. Alexander, *Life Sci.*, **17**, 707 (1975).
(19) H. Sprince, C. M. Parker, G. G. Smith, and L. J. Conzales, *Agents Actions*, **4**, 125 (1974).
(20) *Ibid.*, **5**, 164 (1975).
(21) R. M. Riggin and P. T. Kissinger, *Anal. Chem.*, **49**, 530 (1977).

ACKNOWLEDGMENTS

The authors thank Dr. Herb Nagasawa, Mr. Ronald Shoup, and Dr. Ralph Riggin for helpful discussions and gratefully acknowledge financial assistance from the National Institute of General Medical Sciences and the National Science Foundation.

Solid Dispersions of Nitrofurantoin, Ethotoin, and Coumarin with Polyethylene Glycol 6000 and Their Coprecipitates with Povidone 25,000

A. SH. GENEIDI *, A. A. ALI ˣ, and R. B. SALAMA

Received April 30, 1976, from the *Faculty of Pharmacy, University of Khartoum, Khartoum, Egypt.* Accepted for publication November 30, 1976. *Present address: Department of Pharmaceutics, Faculty of Pharmacy, Cairo University, Cairo, Egypt.

Abstract □ The influence of two linear polymers, polyethylene glycol 6000 and povidone 25,000, on the dissolution rate of three poorly soluble drugs, nitrofurantoin, ethotoin, and coumarin, was studied. Povidone 25,000 produced better drug solubilization than polyethylene glycol 6000 with the drug–polymer ratios studied, and an increase in the weight fraction of either polymer gave more rapid dissolution. TLC and IR studies ruled out any interaction between the drugs and polyethylene glycol 6000. IR spectrophotometry provided evidence that there was complex formation between nitrofurantoin and povidone 25,000, probably *via* hydrogen bonding.

Keyphrases □ Nitrofurantoin—solid dispersions with polyethylene glycol 6000, coprecipitates with povidone, effect on dissolution rate □ Ethotoin—solid dispersions with polyethylene glycol 6000, coprecipitates with povidone, effect on dissolution rate □ Coumarin—solid dispersions with polyethylene glycol 6000, coprecipitates with povidone, effect on dissolution rate □ Solid dispersions—nitrofurantoin, ethotoin, and coumarin with polyethylene glycol 6000, effect on dissolution rate □ Coprecipitates—nitrofurantoin, ethotoin, and coumarin with povidone, effect on dissolution rate □ Dissolution rates—nitrofurantoin, ethotoin, and coumarin, solid dispersions with polyethylene glycol 6000 and coprecipitates with povidone □ Polyethylene glycol 6000—solid dispersions with nitrofurantoin, ethotoin, and coumarin, effect on dissolution rates □ Povidone—coprecipitates with nitrofurantoin, ethotoin, and coumarin, effect on dissolution rates

The formation of solid dispersions or coprecipitates of relatively water-insoluble drugs with various pharmacologically inert carriers increases *in vitro* dissolution rates significantly (1–22). However, the use of linear polymeric materials, especially povidone, as carriers in coprecipitate systems has received limited attention (7, 13). In theory, an enhancement in the dissolution rate of a drug should facilitate its GI absorption rate if the absorption process is dissolution rate limited. The mechanism and advantages of increased dissolution rates of drugs coprecipitated in povidone were described (13, 16).

The mechanism underlying the influence of polyethylene glycols in enhancing the dissolution rate of drugs was the subject of intensive study by IR spectral analysis (16), X-ray diffraction (23), differential thermal analysis (24), microscopic examination (24), and TLC (16, 25). Each of these approaches for increasing the dissolution rate requires a unique type of drug molecule (26). The coprecipitation of reserpine with povidone markedly enhanced the absorption characteristics of this hydrophobic drug, and these *in vivo* increases were correlated quantitatively with *in vitro* dissolution rates (14, 17).

Recently, several reports (27, 28) confirmed the existence of a close correlation between *in vitro* dissolution and plasma digoxin levels. Therefore, dissolution experiments were carried out to reflect bioavailability. This study reports the influence of solid dispersions of polyethylene glycol 6000 (I) coprecipitates and physical mixtures of povidone 25,000 (II) on the dissolution rates of three poorly water-soluble drugs: nitrofurantoin, ethotoin, and coumarin.

EXPERIMENTAL

Materials—Nitrofurantoin[1], ethotoin[2], and coumarin[3] were pharmaceutical grade. Compounds I[4] and II[5] had average molecular weights of 6000 and 25,000, respectively. Chloroform, hydrochloric acid, and acetone were analytical reagent grade.

Test Preparation—Solid dispersions of nitrofurantoin, ethotoin, and coumarin in I were prepared by the fusion method. A weighed quantity of the drug was dissolved in a melted quantity of I over a thermostatically heated water bath and then spread in a thin layer on a glass slab. The resultant mixtures were cooled and solidified gradually at room temperature. The formed crust was scraped off, homogeneously mixed, and incubated at 45–50° for 6 hr. It was then pulverized in a mortar, and the 125–180-μm particles were collected.

The 1:2, 1:4, and 1:8 (w/w) drug–II coprecipitates were prepared by dissolving both components in chloroform and subsequently evaporating the organic solvent *in vacuo*. The residue was then dried to constant weight *in vacuo* and screened, and the drug–II weight ratio was confirmed analytically.

The 1:4 (w/w) nitrofurantoin, ethotoin, and coumarin physical mixtures with II were prepared by gently triturating appropriate quantities of each drug and II in a glass mortar. Pure drug possessing the same particle-size range served as a control.

Dissolution Rate Studies—The dissolution apparatus was similar to that employed by Levy and Hayes (29). A 400-ml beaker contained 200 ml of 0.1 *N* HCl as the dissolution medium. The dissolution medium was maintained at 37 ± 0.5° and agitated at 100 rpm with a polytef stirrer blade connected to a constant-speed stirring moter[6].

The test preparations were filled into capsules, each containing a quantity equivalent to 100 mg of drug. At frequent time intervals after the test preparation was added to the dissolution medium, a 2.0-ml sample was withdrawn, filtered, and replaced with 2.0 ml of fresh dissolution medium. The amount of the drug in solution at each time interval, appropriately corrected for this dilution effect (30), was determined spectrophotometrically[7] at 367, 257, and 276 nm for nitrofurantoin, ethotoin, and coumarin, respectively. Compounds I and II in the concentration present in the assay samples did not interfere with the determination of these drugs.

IR Spectral Analysis—A mineral oil mull of each sample was smeared as a thin film between two sodium chloride plates, and the IR spectrum[8] was recorded at the slow scanning speed.

TLC—TLC plates of 0.25-mm thickness were prepared using a slurry of silica gel G[9] (25 g) with 60 ml of water. The solvent systems were chloroform–diethylamine (90:10), benzene–acetone (90:10), and chloroform–acetone (90:10) for nitrofurantoin, coumarin, and ethotoin and their test preparations, respectively. Aliquots (10 μl) of 0.1% alcoholic solutions of each drug and its preparations were spotted on the TLC plates and developed. Nitrofurantoin, coumarin, and their preparations were detected by UV light, but the visualization of ethotoin and its preparations was by UV light after spraying with 2′,7′-dichlorofluorescein alcoholic solution.

[1] Eaton Laboratories, Norwich Pharmacal Co., Norwich, N.Y.
[2] Abbott.
[3] British Drug House Chemicals Ltd., Poole, England.
[4] Hoechst, West Germany.
[5] BASF, Ludwigshafen, West Germany.
[6] Citenco Ltd., England.
[7] Model DU-2, Beckman Instruments.
[8] IR-10, Beckman Instruments.
[9] E. Merck, Darmstadt, West Germany.

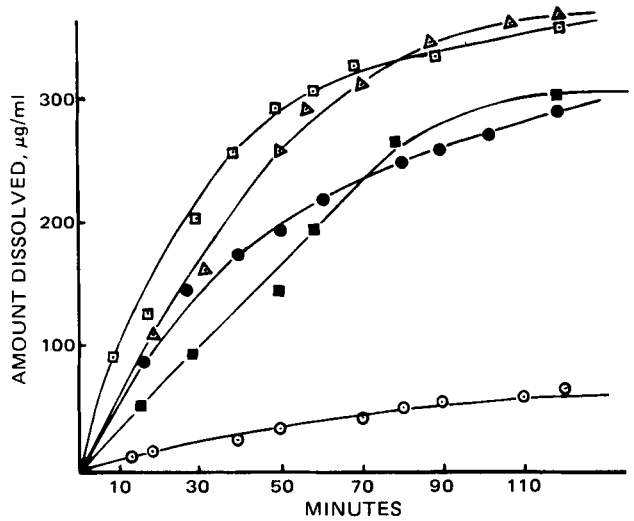

Figure 1—*Dissolution rates of coumarin from test preparations at 37°. Key: ○, pure coumarin; ●, 1:4 (w/w) solid dispersion; □, 1:10 (w/w) solid dispersion; ■, 1:4 (w/w) physical mixture; and △, 1:4 (w/w) coprecipitate.*

RESULTS AND DISCUSSION

Dissolution followed first-order kinetics. Semilogarithmic plots of the percent drug undissolved *versus* time were linear, the correlation coefficient being 0.98–0.99 in all cases. Figures 1–3 show that the dissolution rate of the solid dispersions of coumarin, ethotoin, and nitrofurantoin increased considerably. For capsules containing coumarin only, the release rate was slow and steady (Fig. 1). However, there was almost a sevenfold increase in the dissolution rate of coumarin when present in a 1:10 I solid dispersion system. Figures 2 and 3 show that there were fivefold and sevenfold increases in the dissolution rates of ethotoin and nitrofurantoin, respectively, in the 1:10 and 1:8 drug–I solid dispersion systems.

In addition, there was a progressive increase in the percentage release of the medicament corresponding to the increased weight fraction of I. The maximal release attained depends upon the weight fraction of the polymer (Figs. 1–3). Thus, maximum drug release was achieved after 45 and 60 min from the dispersion system of coumarin–I in ratios of 1:10 and 1:4, respectively. The plain capsules gave only 10% release after 120 min. Similar results were obtained for both ethotoin–I and nitrofurantoin–I dispersion systems. The demonstrated fairly fast *in vitro* release of the selected three compounds from dispersion systems suggests their high potential application for the formulation of most water-insoluble drugs. The bioavailability of such dosage forms as compared to the conventional forms, however, will be the subject of further study.

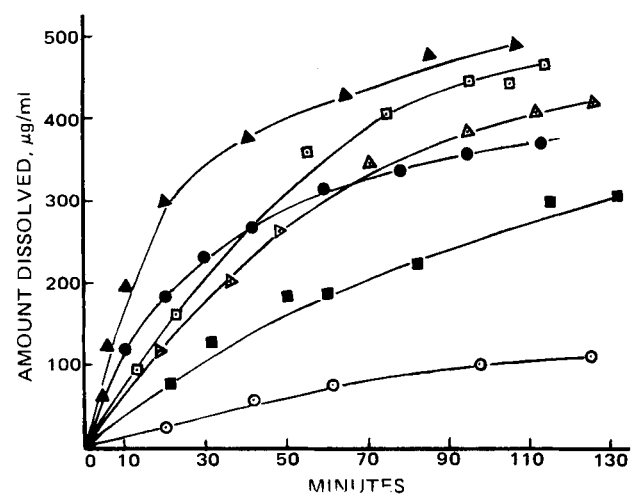

Figure 2—*Dissolution rates of ethotoin from test preparations at 37°. Key: ○, pure ethotoin; ●, 1:4 (w/w) solid dispersion; □, 1:10 (w/w) solid dispersion; ■, 1:4 (w/w) physical mixture; △, 1:4 (w/w) coprecipitate; and ▲, 1:8 (w/w) coprecipitate.*

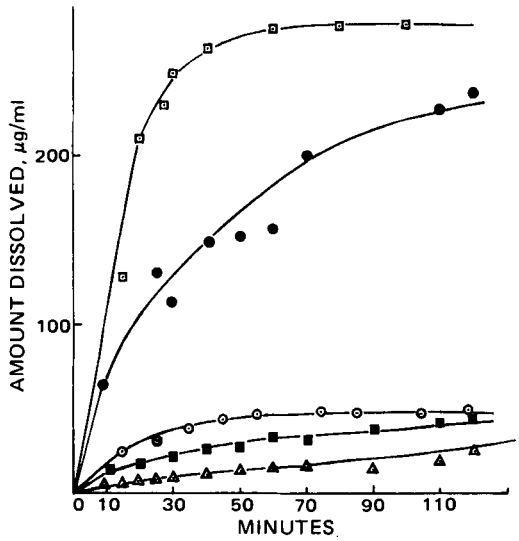

Figure 3—*Dissolution rates of nitrofurantoin from test preparations at 37°. Key: ○, pure nitrofurantoin; ●, 1:4 (w/w) solid dispersion; □, 1:8 (w/w) solid dispersion; ■, 1:4 (w/w) physical mixture; and △, 1:4 (w/w) coprecipitate.*

The dissolution rate profiles for 1:4 (w/w) physical mixtures and 1:4 (w/w) coprecipitates of coumarin, ethotoin, and nitrofurantoin are also shown in Figs. 1–3. At each time interval, marked differences existed between the amount of drug in solution from the coprecipitate and the other two preparations (Figs. 1 and 2). Surprisingly, the capsules prepared from nitrofurantoin–II as a 1:4 physical mixture and a 1:4 coprecipitate achieved dissolution rates essentially lower than pure nitrofurantoin alone (Fig. 3). From these data, it can be concluded that bulk effects due to the presence of II in solution are responsible for the decrease in the dissolution rate observed, since there was a significant difference between nitrofurantoin alone and when present in a 1:4 physical mixture and a 1:4 coprecipitate with II. Therefore, factors such as insoluble complex formation, chemisorption, micelle formation, and other surface phenomena are probably responsible for the decreased nitrofurantoin dissolution rate.

An increase in the weight fraction of II resulted in a corresponding increase in the ethotoin dissolution rate (Fig. 2). However, II induced better solubilization of ethotoin and coumarin than I with the drug–polymer ratios tested. If it is assumed that the dissolution rate from the powder surface is rate limited by the dissolution of the controlling I external layer, analogous to the controlling II layer in the high II weight fractions (13), then the dissolution rate of the drug from the same drug–I dispersion surface will be proportional to the drug–I ratio of the solid dispersion. In other words, the dissolution rate of the drug from a 1:4 solid dispersion will be almost twice as fast as from a 1:2 solid dispersion if the dissolution surface is the same. Other factors, such as the possible complexation between the drug and I or II and the conversion of the molecular dispersion to particulate aggregates of pure compounds, may also affect the dissolution.

Chromatographic Behavior—TLC showed that the drug–I solid dispersion was resolved into two separate spots of R_f (× 100) values of 52, 73, 3, and 78 for I, ethotoin, nitrofurantoin, and coumarin, respectively, which were identical to the pure components. The nitrofurantoin–II coprecipitate was not resolved into two separate spots as were coumarin–II and ethotoin–II coprecipitates. Therefore, TLC indicated the existence of complexation between nitrofurantoin and II, but there was no evidence of complexation between coumarin or ethotoin and II.

IR Spectra—The bands characteristic for each drug were unaffected in the drug–I systems, and the IR spectrum of the drug–I system was simply the summation of the spectra of the two components. There was no evidence of complexation between nitrofurantoin, ethotoin, or coumarin and I. On the other hand, the sharp band at 3300 cm^{-1}, due to the NH stretching vibration of nitrofurantoin, completely disappeared in the nitrofurantoin–II system. Other sharp bands at 680, 820, 975, 1100, and 1239 cm^{-1}, characteristic of nitrofurantoin, disappeared in the nitrofurantoin–II system.

In contrast, the band at 3300 cm^{-1}, due to the NH stretching vibration of ethotoin, was unaffected in the ethotoin–II system, and the IR spec-

trum of the ethotoin–II system was the summation of the spectra of the two components. Again there was no evidence of complexation between the two compounds. The formation of an insoluble complex between nitrofurantoin and II may explain the decrease in the dissolution rates from both the nitrofurantoin–II physical mixture and the coprecipitate.

REFERENCES

(1) K. Sekiguchi and N. Obi, *Chem. Pharm. Bull.*, **9**, 866 (1961).

(2) K. Sekiguchi, N. Obi, and Y. Ueda, *ibid.*, **12**, 134 (1964).

(3) A. H. Goldberg, M. Gibaldi, and J. L. Kanig, *J. Pharm. Sci.*, **54**, 1145 (1965).

(4) *Ibid.*, **55**, 581 (1966).

(5) *Ibid.*, **55**, 487 (1966).

(6) A. H. Goldberg, M. Gibaldi, J. L. Kanig, and M. Mayersohn, *J. Pharm. Sci.*, **55**, 581 (1966).

(7) M. Mayersohn and M. Gibaldi, *ibid.*, **55**, 1323 (1966).

(8) R. G. Stoll, T. R. Bates, K. A. Nieforth, and J. Swarbrick, *ibid.*, **58**, 1457 (1969).

(9) M. Gibaldi, S. Feldman, and T. R. Bates, *ibid.*, **57**, 708 (1968).

(10) W. L. Chiou and S. Riegelman, *ibid.*, **58**, 1505 (1969).

(11) *Ibid.*, **59**, 937 (1970).

(12) *Ibid.*, **60**, 1376, 1569 (1971).

(13) A. P. Simonelli, S. C. Mehta, and W. I. Higuchi, *J. Pharm. Sci.*, **58**, 538 (1969).

(14) T. R. Bates, *J. Pharm. Pharmacol.*, **21**, 710 (1969).

(15) G. H. Svoboda, M. J. Sweeney, and W. D. Walkling, *J. Pharm. Sci.*, **60**, 333 (1971).

(16) S. A. Said, H. M. El Fatatry, and A. S. Geneidi, *Aust. J. Pharm. Sci.*, **3**(2), 42 (1974).

(17) E. I. Stupak and T. R. Bates, *J. Pharm. Sci.*, **61**, 400 (1972).

(18) A. A. Kassen, S. A. Said, and M. El-Samaligy, *Aust. J. Pharm. Sci.*, **4**, 123 (1974).

(19) W. I. Higuchi, N. A. Mir, and S. J. Desai, *J. Pharm. Sci.*, **54**, 1405 (1965).

(20) M. H. Malone, H. I. Hochman, and K. A. Nieforth, *ibid.*, **55**, 972 (1966).

(21) D. J. Allen and K. C. Kwan, *ibid.*, **58**, 1190 (1969).

(22) T. Tachibana and A. Nakamura, *Kolloid-Polym.*, **203**, 130 (1965).

(23) T. Tsuji, K. Foukik, and T. Takaibo, *Bull. Chem. Soc. Jpn.*, **42**, 2193 (1969).

(24) R. Rastogi and P. Bassi, *J. Phys. Chem.*, **68**, 2398 (1964).

(25) S. Said, H. El Fatatry, and M. El Samaligy, *Aust. J. Pharm. Sci.*, **3** (2), (1974).

(26) D. C. Monkhouse and J. L. Lach, *J. Pharm. Sci.*, **61**, 1430 (1972).

(27) T. R. D. Shaw, K. Raymond, M. R. Howard, and J. Hammer, *Br. Med. J.*, **4**, 763 (1973).

(28) J. Linenbaum, V. P. Butler, J. E. Murphy, and R. M. Crosswell, *Lancet*, **1**, 1215 (1973).

(29) G. Levy and B. A. Hayes, *N. Engl. J. Med.*, **262**, 1053 (1960).

(30) T. R. Bates, M. Gibaldi, and J. L. Kanig, *Nature*, **210**, 1331 (1966).

ACKNOWLEDGMENTS

The authors acknowledge the technical help of Mr. M. H. Ibrahim.

GLC Determination of Meperidinic and Normeperidinic Acids in Urine

I. W. WAINER ˣ and J. E. STAMBAUGH

Received December 9, 1976, from the *Department of Pharmacology, Section of Clinical Pharmacology, Thomas Jefferson University, Philadelphia, PA 19107.* Accepted for publication February 10, 1977.

Abstract □ A GLC procedure for the determination of meperidinic and normeperidinic acids in human urine is described. After the extraction of any interfering meperidine or normeperidine, the urine samples are dried and the acids are reesterified using ethanol–sulfuric acid. The resulting meperidine and normeperidine are then extracted and quantified. With this method, the urinary excretion of these metabolites was followed in five subjects who received a single meperidine dose of 36 mg/m^2 im. This method represents an improvement over the previously described methods for meperidinic and normeperidinic acids and can be applied to clinical situations.

Keyphrases □ Meperidine metabolites—meperidinic and normeperidinic acids, GLC analyses, human urine □ GLC—analyses, meperidinic and normeperidinic acids in human urine □ Analgesics, narcotic—meperidine metabolites, GLC analyses in human urine

The pharmacokinetics of meperidine (I) were described previously (1), and its metabolites were identified (2). Unchanged meperidine was identified in the urine along with the *N*-demethylated metabolite normeperidine (II), meperidinic acid (III), normeperidinic acid (IV), and conjugated esters of these acids (Scheme I) (2). These initial studies were limited to high drug doses due to the limitations of the analytical colorimetric method.

The recent development of more sensitive GLC assays for meperidine in serum (3) and for meperidine and normeperidine in urine (4) permitted the study of the pharmacokinetics and metabolism of meperidine in humans using usual clinical doses (5). A sensitive method for the determination of urinary levels of meperidinic and normeperidinic acids has not been reported previously. This report describes a GLC technique for the analysis of these metabolites using small aliquots of urine samples.

EXPERIMENTAL

Ten milliliters of urine, 1 ml of 5 *N* NaOH, and 5 ml of chloroform were shaken for 10 min in a 50-ml glass-stoppered centrifuge tube. Then the tube was centrifuged, and 9 ml of the aqueous phase was transferred to a 50-ml round-bottom flask and evaporated to dryness by freeze drying. Absolute ethanol, 9 ml, and 1 ml of sulfuric acid were added to the residue, and the resulting mixture was refluxed for 3 hr.

After cooling, 1 ml of the reaction mixture was added to a 15-ml screw-capped centrifuge tube containing 2 ml of 2.5 *N* NaOH. Chloroform, 100 μl, containing an internal standard (lidocaine, 20 μg/ml), was added to the solution, and the resulting mixture was vortexed for 30 sec and centrifuged for 5 min. A 5-μl aliquot of the chloroform layer was then injected into the chromatograph[1].

The analysis was carried out using a hydrogen flame-ionization detector

[1] Perkin-Elmer model 3920.

trum of the ethotoin–II system was the summation of the spectra of the two components. Again there was no evidence of complexation between the two compounds. The formation of an insoluble complex between nitrofurantoin and II may explain the decrease in the dissolution rates from both the nitrofurantoin–II physical mixture and the coprecipitate.

REFERENCES

(1) K. Sekiguchi and N. Obi, *Chem. Pharm. Bull.*, **9**, 866 (1961).

(2) K. Sekiguchi, N. Obi, and Y. Ueda, *ibid.*, **12**, 134 (1964).

(3) A. H. Goldberg, M. Gibaldi, and J. L. Kanig, *J. Pharm. Sci.*, **54**, 1145 (1965).

(4) *Ibid.*, **55**, 581 (1966).

(5) *Ibid.*, **55**, 487 (1966).

(6) A. H. Goldberg, M. Gibaldi, J. L. Kanig, and M. Mayersohn, *J. Pharm. Sci.*, **55**, 581 (1966).

(7) M. Mayersohn and M. Gibaldi, *ibid.*, **55**, 1323 (1966).

(8) R. G. Stoll, T. R. Bates, K. A. Nieforth, and J. Swarbrick, *ibid.*, **58**, 1457 (1969).

(9) M. Gibaldi, S. Feldman, and T. R. Bates, *ibid.*, **57**, 708 (1968).

(10) W. L. Chiou and S. Riegelman, *ibid.*, **58**, 1505 (1969).

(11) *Ibid.*, **59**, 937 (1970).

(12) *Ibid.*, **60**, 1376, 1569 (1971).

(13) A. P. Simonelli, S. C. Mehta, and W. I. Higuchi, *J. Pharm. Sci.*, **58**, 538 (1969).

(14) T. R. Bates, *J. Pharm. Pharmacol.*, **21**, 710 (1969).

(15) G. H. Svoboda, M. J. Sweeney, and W. D. Walkling, *J. Pharm. Sci.*, **60**, 333 (1971).

(16) S. A. Said, H. M. El Fatatry, and A. S. Geneidi, *Aust. J. Pharm. Sci.*, **3**(2), 42 (1974).

(17) E. I. Stupak and T. R. Bates, *J. Pharm. Sci.*, **61**, 400 (1972).

(18) A. A. Kassen, S. A. Said, and M. El-Samaligy, *Aust. J. Pharm. Sci.*, **4**, 123 (1974).

(19) W. I. Higuchi, N. A. Mir, and S. J. Desai, *J. Pharm. Sci.*, **54**, 1405 (1965).

(20) M. H. Malone, H. I. Hochman, and K. A. Nieforth, *ibid.*, **55**, 972 (1966).

(21) D. J. Allen and K. C. Kwan, *ibid.*, **58**, 1190 (1969).

(22) T. Tachibana and A. Nakamura, *Kolloid-Polym.*, **203**, 130 (1965).

(23) T. Tsuji, K. Foukik, and T. Takaibo, *Bull. Chem. Soc. Jpn.*, **42**, 2193 (1969).

(24) R. Rastogi and P. Bassi, *J. Phys. Chem.*, **68**, 2398 (1964).

(25) S. Said, H. El Fatatry, and M. El Samaligy, *Aust. J. Pharm. Sci.*, **3** (2), (1974).

(26) D. C. Monkhouse and J. L. Lach, *J. Pharm. Sci.*, **61**, 1430 (1972).

(27) T. R. D. Shaw, K. Raymond, M. R. Howard, and J. Hammer, *Br. Med. J.*, **4**, 763 (1973).

(28) J. Linenbaum, V. P. Butler, J. E. Murphy, and R. M. Crosswell, *Lancet*, **1**, 1215 (1973).

(29) G. Levy and B. A. Hayes, *N. Engl. J. Med.*, **262**, 1053 (1960).

(30) T. R. Bates, M. Gibaldi, and J. L. Kanig, *Nature*, **210**, 1331 (1966).

ACKNOWLEDGMENTS

The authors acknowledge the technical help of Mr. M. H. Ibrahim.

GLC Determination of Meperidinic and Normeperidinic Acids in Urine

I. W. WAINER ˣ and J. E. STAMBAUGH

Received December 9, 1976, from the *Department of Pharmacology, Section of Clinical Pharmacology, Thomas Jefferson University, Philadelphia, PA 19107.* Accepted for publication February 10, 1977.

Abstract □ A GLC procedure for the determination of meperidinic and normeperidinic acids in human urine is described. After the extraction of any interfering meperidine or normeperidine, the urine samples are dried and the acids are reesterified using ethanol–sulfuric acid. The resulting meperidine and normeperidine are then extracted and quantified. With this method, the urinary excretion of these metabolites was followed in five subjects who received a single meperidine dose of 36 mg/m^2 im. This method represents an improvement over the previously described methods for meperidinic and normeperidinic acids and can be applied to clinical situations.

Keyphrases □ Meperidine metabolites—meperidinic and normeperidinic acids, GLC analyses, human urine □ GLC—analyses, meperidinic and normeperidinic acids in human urine □ Analgesics, narcotic—meperidine metabolites, GLC analyses in human urine

The pharmacokinetics of meperidine (I) were described previously (1), and its metabolites were identified (2). Unchanged meperidine was identified in the urine along with the *N*-demethylated metabolite normeperidine (II), meperidinic acid (III), normeperidinic acid (IV), and conjugated esters of these acids (Scheme I) (2). These initial studies were limited to high drug doses due to the limitations of the analytical colorimetric method.

The recent development of more sensitive GLC assays for meperidine in serum (3) and for meperidine and normeperidine in urine (4) permitted the study of the pharmacokinetics and metabolism of meperidine in humans using usual clinical doses (5). A sensitive method for the determination of urinary levels of meperidinic and normeperidinic acids has not been reported previously. This report describes a GLC technique for the analysis of these metabolites using small aliquots of urine samples.

EXPERIMENTAL

Ten milliliters of urine, 1 ml of 5 *N* NaOH, and 5 ml of chloroform were shaken for 10 min in a 50-ml glass-stoppered centrifuge tube. Then the tube was centrifuged, and 9 ml of the aqueous phase was transferred to a 50-ml round-bottom flask and evaporated to dryness by freeze drying. Absolute ethanol, 9 ml, and 1 ml of sulfuric acid were added to the residue, and the resulting mixture was refluxed for 3 hr.

After cooling, 1 ml of the reaction mixture was added to a 15-ml screw-capped centrifuge tube containing 2 ml of 2.5 *N* NaOH. Chloroform, 100 μl, containing an internal standard (lidocaine, 20 μg/ml), was added to the solution, and the resulting mixture was vortexed for 30 sec and centrifuged for 5 min. A 5-μl aliquot of the chloroform layer was then injected into the chromatograph[1].

The analysis was carried out using a hydrogen flame-ionization detector

[1] Perkin-Elmer model 3920.

Table I—Recovery of Meperidine following the Esterification of Urine Samples Containing Meperidinic Acid[a]

Meperidinic Acid Added, μg/ml	Meperidine Recovered, μg/ml	Conversion and Recovery, %
10	7.73 ± 0.15	77.3 ± 1.3
7	5.46 ± 0.15	78.1 ± 2.2
5	3.76 ± 0.32	75.3 ± 6.4
2	1.48 ± 0.08	74.2 ± 4.3

[a] Figures represent the mean ± *SD* for three analyses.

and a 2-mm i.d. × 1.8-m coiled glass column packed with 3% OV-17 on 100–120-mesh Gas Chrom Q[2]. A column temperature of 175° and an injector and detector temperature of 250° were used. The gas flows were: hydrogen, 60 ml/min; air, 500 ml/min; and nitrogen carrier gas, 55 ml/min. Under these conditions, the retention times of meperidine, normeperidine, and lidocaine were approximately 4.4, 5.2, and 6.8 min, respectively (Fig. 1).

Following chromatography, a baseline was drawn and the peak heights of meperidine, normeperidine, and lidocaine were measured. The ratios of meperidine and lidocaine peak heights and normeperidine and lidocaine peak heights were calculated, and the concentrations were obtained from the standard curves.

Standard curves for meperidinic and normeperidinic acids were constructed by the analysis of urine samples to which known amounts of the meperidinic and normeperidinic acids[3] had been added. The concentrations ranged from 20 to 1 μg/ml. The standard curves were described by the equations $y = 19.6x + 0.9$ with a correlation coefficient (r) = 0.99 for normeperidinic acid and $y = 3.9x - 0.4$ (r = 0.99) for meperidinic acid. The percent conversion and the percent recovery were calculated by

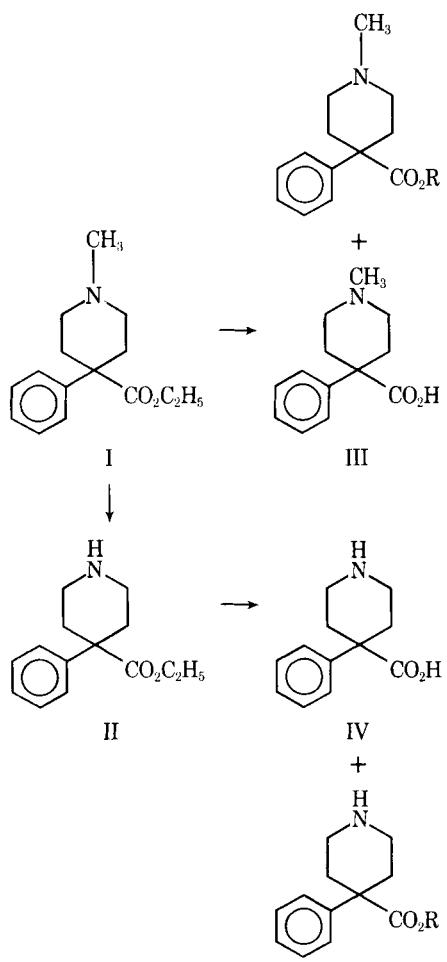

Scheme I

[2] Applied Science Laboratories, State College, Pa.

[3] Standards supplied by Sterling-Winthrop Research Institute, Renssalaer, N.Y.

Table II—Recovery of Normeperidine following the Esterification of Urine Samples Containing Normeperidinic Acid[a]

Normeperidinic Acid Added, μg/ml	Normeperidine Recovered, μg/ml	Conversion and Recovery, %
10	7.85 ± 0.25	78.5 ± 2.5
7	5.30 ± 0.18	75.8 ± 2.6
5	3.72 ± 0.15	74.5 ± 3.1
2	1.45 ± 0.03	72.5 ± 1.5

[a] Figures represent the mean ± *SD* for three analyses.

comparing the final meperidine and normeperidine concentrations with known standards.

For the *in vivo* study, five healthy volunteers were given a single 36-mg/m[2] im injection of meperidine hydrochloride[4]. Venous blood samples were collected at 0.5, 1, 2, 4, 6, 8, 12, and 24 hr and were analyzed for meperidine by previously described methods (5). The cumulative urinary output in each subject was collected 1, 2, 4, 6, 8, 12, and 24 hr after dosing. The volume and pH of these samples were measured, and then the samples were frozen for analysis at a later date. The 24-hr cumulative excretion of meperidinic and normeperidinic acids was determined using 10% aliquots of each sample and analyzing the pooled samples.

RESULTS AND DISCUSSION

The percent conversion of meperidinic and normeperidinic acids to the corresponding ester and the recovery of meperidine and normeperidine are presented in Tables I and II. The mean percent recovery of meperidine from urine samples with initial meperidinic acid concentrations of 2–10 μg/ml was 76.0%. The mean percent recovery of normeperidine from urine samples with initial normeperidinic acid concentrations of 2–10 mg/ml was 74.8%. The low recoveries were probably due to incomplete esterification and degradation of the molecule during the esterification process. Due to the difference in retention time and the similarity of the molecules, meperidinic and normeperidinic acids can be assayed at the same time without interference. The limit of detection was approximately 10 ng/ml of urine.

All subjects displayed normal serum meperidine concentration-time curves, with a maximum at 1 hr and with biological half-lives of 2.8–3.4 hr. The amount of meperidinic acid excreted varied considerably from

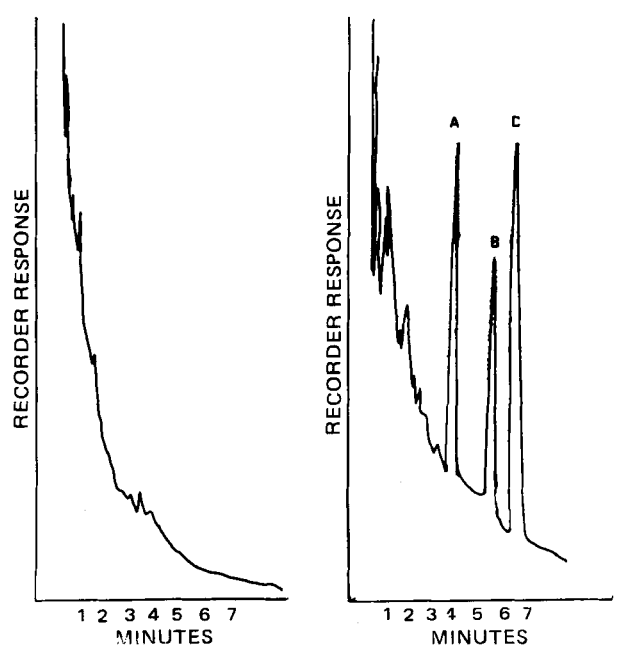

Figure 1—*Gas chromatogram of an extract after the esterification of 10 ml of control human urine containing no drugs (left) and 10 ml of human urine containing 10 μg of meperidinic acid/ml and 10 μg of normeperidinic acid/ml (right). Key: A, normeperidine; B, meperidine; and C, internal standard.*

[4] Elkins-Sinn, Inc., Cherry Hill, N.J.

Table III—Cumulative 24-hr Excretion of Meperidinic and Normeperidinic Acids

Subject	Meperidinic Acid, mg	Percent Dose	Normeperidinic Acid, mg	Percent Dose
1	8.89	17.8	3.56	7.1
2	6.49	12.8	4.73	9.5
3	13.91	27.8	4.17	8.3
4	4.49	9.0	2.22	4.4
5	12.98	26.0	6.51	13.0

subject to subject (Table III), and the 24-hr cumulative excretion of meperidinic acid accounted for between 9.0 and 27.8% of the administered dose. These results are consistent with the previously reported findings for these metabolites of 10.3–40.9% of the administered dose when 200–1180 mg (over 20 hr) (2) and 100 mg (6) of meperidine were administered.

The 24-hr cumulative excretion of normeperidinic acid ranged between 4.4 and 13.0% of the administered dose (Table III); these results are also consistent with previous studies of normeperidinic acid, which accounted for 2.7–28.3% of the administered dose (2, 6). No other attempt was made to quantitate the conjugate esters of meperidinic and normeperidinic acids, which accounted for 0–16.1 and 3.8–22.3% of the administered dose, respectively.

The hourly excretion of meperidine, normeperidine, and meperidinic and normeperidinic acids was followed in one subject (Table IV). The meperidine excretion rate reached a maximum of 3.50 μg/ml hr at 2 hr. Meperidinic acid also reached its maximum at 2 hr with a rate of 10.24 μg/ml hr. The maxima for normeperidine and normeperidinic acid were reached at 6 hr with rates of 0.60 and 2.64 μg/ml hr, respectively.

The described GLC procedure is reliable and easily performed, and it can be applied to the study of the pharmacokinetic and metabolic parameters of meperidine in humans using average clinical doses.

Table IV—Hourly Excretion of Meperidine, Normeperidine, and Meperidinic and Normeperidinic Acids by Subject 3

Hour	Meperidine, mg	Normeperidine, mg	Meperidinic Acid, mg	Normeperidinic Acid, mg
1	0.01	0.00	0.61	0.00
2	0.44	0.08	1.28	0.36
4	0.46	0.06	1.12	0.34
6	0.56	0.28	3.37	0.81
8	0.08	0.08	1.49	0.58
12	0.04	0.24	2.68	0.89
24	0.19	1.07	3.36	1.19
Total	1.71	1.81	13.91	4.17

REFERENCES

(1) J. J. Burns, B. L. Berger, P. A. Lief, A. Walack, E. M. Papper, and B. B. Brodie, *J. Pharmacol. Exp. Ther.*, **114**, 289 (1955).

(2) N. P. Plotnikoff, E. L. Way, and H. W. Elliot, *ibid.*, **117**, 414 (1956).

(3) J. E. Stambaugh and I. W. Wainer, *J. Clin. Pharmacol.*, **14**, 552 (1974).

(4) *Ibid.*, **15**, 269 (1975).

(5) J. E. Stambaugh, I. W. Wainer, J. K. Sanstead, and D. M. Hemphill, *J. Clin. Pharmacol.*, **16**, 245 (1976).

(6) A. M. Asatoor, D. R. London, M. D. Milne, and M. L. Simenhoff, *Br. J. Pharmacol.*, **20**, 285 (1963).

Simultaneous GLC Determination of Phenylpropanolamine and Chlorpheniramine in Urine Using a Nitrogen Selective Detector

H. KINSUN *, M. A. MOULIN *x, and E. C. SAVINI ‡

Received February 8, 1977, from the **Laboratory of Functional Explorations B and Pharmacology, Centre Hospitalier Regional et Universitaire de Caen, 14033 Caen, France,* and the ‡*Laboratory of Toxicology and Pharmacology, Nice Medical School, 06000 Nice, France.* Accepted for publication March 29, 1977.

Abstract □ A simple, rapid, and sensitive simultaneous quantitative determination of phenylpropanolamine and chlorpheniramine in human urine by GLC, using a nitrogen specific detector, is described. After alkaline extraction from urine, phenylpropanolamine and chlorpheniramine are analyzed directly by GLC, without a derivatization step. Promethazine was used as the internal standard. The total assay time is less than 30 min. The method is useful in studies of pharmacokinetic and pharmacological interactions of drug combinations.

Keyphrases □ Phenylpropanolamine—GLC analysis in presence of chlorpheniramine, human urine □ Chlorpheniramine—GLC analysis in presence of phenylpropanolamine, human urine □ GLC—analyses, phenylpropanolamine and chlorpheniramine simultaneously, human urine □ Adrenergic agents—phenylpropanolamine, GLC analysis in presence of chlorpheniramine, human urine □ Antihistaminics—chlorpheniramine, GLC analysis in presence of phenylpropanolamine, human urine

Phenylpropanolamine has been identified and quantitated by a spectrophotometric method after periodate oxidation (1) according to the original method of Shinn and Nicolet (2). This method was time consuming in comparison to GLC for phenylpropanolamine and chlorpheniramine analysis (3–7).

GLC, using a nitrogen selective detector, is sensitive and allows specific detection (8–11).

The purpose of this work was to develop a simultaneous quantitative method for the determination of phenylpropanolamine and chlorpheniramine in human urine by GLC with a nitrogen specific detector.

EXPERIMENTAL

Instrumentation—The gas chromatograph[1] was equipped with flame-ionization and nitrogen detectors[2] connected to a recorder[3] with a scale range of 1 mv. The stainless steel column (2.17 mm × 2 m) was packed with 3% OV-1[4] on 100–120-mesh Gas Chrom Q[5] and conditioned at 260° for 34 hr with 35 ml of nitrogen (U quality)/min.

The chromatographic conditions were as follows: injected quantity of sample, 1–2 μl; injector temperature, 240°; detector temperature, 280°; column temperature, 230° in isotherm; carrier gas (nitrogen U) flow rate, 35 ml/min; hydrogen (U) flow rate, 30 ml/min; air (medical quality) flow

[1] Girdel model 3000 1 ERPT, Paris, France.
[2] Girdel model 15 489, Paris, France.
[3] Servotrace PU Sefram, Paris, France.
[4] Pierce Chemical, Rockford, IL 61105.
[5] Applied Sciences, Inglewood, CA 90304.

Table III—Cumulative 24-hr Excretion of Meperidinic and Normeperidinic Acids

Subject	Meperidinic Acid, mg	Percent Dose	Normeperidinic Acid, mg	Percent Dose
1	8.89	17.8	3.56	7.1
2	6.49	12.8	4.73	9.5
3	13.91	27.8	4.17	8.3
4	4.49	9.0	2.22	4.4
5	12.98	26.0	6.51	13.0

subject to subject (Table III), and the 24-hr cumulative excretion of meperidinic acid accounted for between 9.0 and 27.8% of the administered dose. These results are consistent with the previously reported findings for these metabolites of 10.3–40.9% of the administered dose when 200–1180 mg (over 20 hr) (2) and 100 mg (6) of meperidine were administered.

The 24-hr cumulative excretion of normeperidinic acid ranged between 4.4 and 13.0% of the administered dose (Table III); these results are also consistent with previous studies of normeperidinic acid, which accounted for 2.7–28.3% of the administered dose (2, 6). No other attempt was made to quantitate the conjugate esters of meperidinic and normeperidinic acids, which accounted for 0–16.1 and 3.8–22.3% of the administered dose, respectively.

The hourly excretion of meperidine, normeperidine, and meperidinic and normeperidinic acids was followed in one subject (Table IV). The meperidine excretion rate reached a maximum of 3.50 μg/ml hr at 2 hr. Meperidinic acid also reached its maximum at 2 hr with a rate of 10.24 μg/ml hr. The maxima for normeperidine and normeperidinic acid were reached at 6 hr with rates of 0.60 and 2.64 μg/ml hr, respectively.

The described GLC procedure is reliable and easily performed, and it can be applied to the study of the pharmacokinetic and metabolic parameters of meperidine in humans using average clinical doses.

Table IV—Hourly Excretion of Meperidine, Normeperidine, and Meperidinic and Normeperidinic Acids by Subject 3

Hour	Meperidine, mg	Normeperidine, mg	Meperidinic Acid, mg	Normeperidinic Acid, mg
1	0.01	0.00	0.61	0.00
2	0.44	0.08	1.28	0.36
4	0.46	0.06	1.12	0.34
6	0.56	0.28	3.37	0.81
8	0.08	0.08	1.49	0.58
12	0.04	0.24	2.68	0.89
24	0.19	1.07	3.36	1.19
Total	1.71	1.81	13.91	4.17

REFERENCES

(1) J. J. Burns, B. L. Berger, P. A. Lief, A. Walack, E. M. Papper, and B. B. Brodie, *J. Pharmacol. Exp. Ther.*, **114**, 289 (1955).

(2) N. P. Plotnikoff, E. L. Way, and H. W. Elliot, *ibid.*, **117**, 414 (1956).

(3) J. E. Stambaugh and I. W. Wainer, *J. Clin. Pharmacol.*, **14**, 552 (1974).

(4) *Ibid.*, **15**, 269 (1975).

(5) J. E. Stambaugh, I. W. Wainer, J. K. Sanstead, and D. M. Hemphill, *J. Clin. Pharmacol.*, **16**, 245 (1976).

(6) A. M. Asatoor, D. R. London, M. D. Milne, and M. L. Simenhoff, *Br. J. Pharmacol.*, **20**, 285 (1963).

Simultaneous GLC Determination of Phenylpropanolamine and Chlorpheniramine in Urine Using a Nitrogen Selective Detector

H. KINSUN *, M. A. MOULIN *x, and E. C. SAVINI ‡

Received February 8, 1977, from the **Laboratory of Functional Explorations B and Pharmacology, Centre Hospitalier Regional et Universitaire de Caen, 14033 Caen, France,* and the ‡*Laboratory of Toxicology and Pharmacology, Nice Medical School, 06000 Nice, France.* Accepted for publication March 29, 1977.

Abstract □ A simple, rapid, and sensitive simultaneous quantitative determination of phenylpropanolamine and chlorpheniramine in human urine by GLC, using a nitrogen specific detector, is described. After alkaline extraction from urine, phenylpropanolamine and chlorpheniramine are analyzed directly by GLC, without a derivatization step. Promethazine was used as the internal standard. The total assay time is less than 30 min. The method is useful in studies of pharmacokinetic and pharmacological interactions of drug combinations.

Keyphrases □ Phenylpropanolamine—GLC analysis in presence of chlorpheniramine, human urine □ Chlorpheniramine—GLC analysis in presence of phenylpropanolamine, human urine □ GLC—analyses, phenylpropanolamine and chlorpheniramine simultaneously, human urine □ Adrenergic agents—phenylpropanolamine, GLC analysis in presence of chlorpheniramine, human urine □ Antihistaminics—chlorpheniramine, GLC analysis in presence of phenylpropanolamine, human urine

Phenylpropanolamine has been identified and quantitated by a spectrophotometric method after periodate oxidation (1) according to the original method of Shinn and Nicolet (2). This method was time consuming in comparison to GLC for phenylpropanolamine and chlorpheniramine analysis (3–7).

GLC, using a nitrogen selective detector, is sensitive and allows specific detection (8–11).

The purpose of this work was to develop a simultaneous quantitative method for the determination of phenylpropanolamine and chlorpheniramine in human urine by GLC with a nitrogen specific detector.

EXPERIMENTAL

Instrumentation—The gas chromatograph[1] was equipped with flame-ionization and nitrogen detectors[2] connected to a recorder[3] with a scale range of 1 mv. The stainless steel column (2.17 mm × 2 m) was packed with 3% OV-1[4] on 100–120-mesh Gas Chrom Q[5] and conditioned at 260° for 34 hr with 35 ml of nitrogen (U quality)/min.

The chromatographic conditions were as follows: injected quantity of sample, 1–2 μl; injector temperature, 240°; detector temperature, 280°; column temperature, 230° in isotherm; carrier gas (nitrogen U) flow rate, 35 ml/min; hydrogen (U) flow rate, 30 ml/min; air (medical quality) flow

[1] Girdel model 3000 1 ERPT, Paris, France.
[2] Girdel model 15 489, Paris, France.
[3] Servotrace PU Sefram, Paris, France.
[4] Pierce Chemical, Rockford, IL 61105.
[5] Applied Sciences, Inglewood, CA 90304.

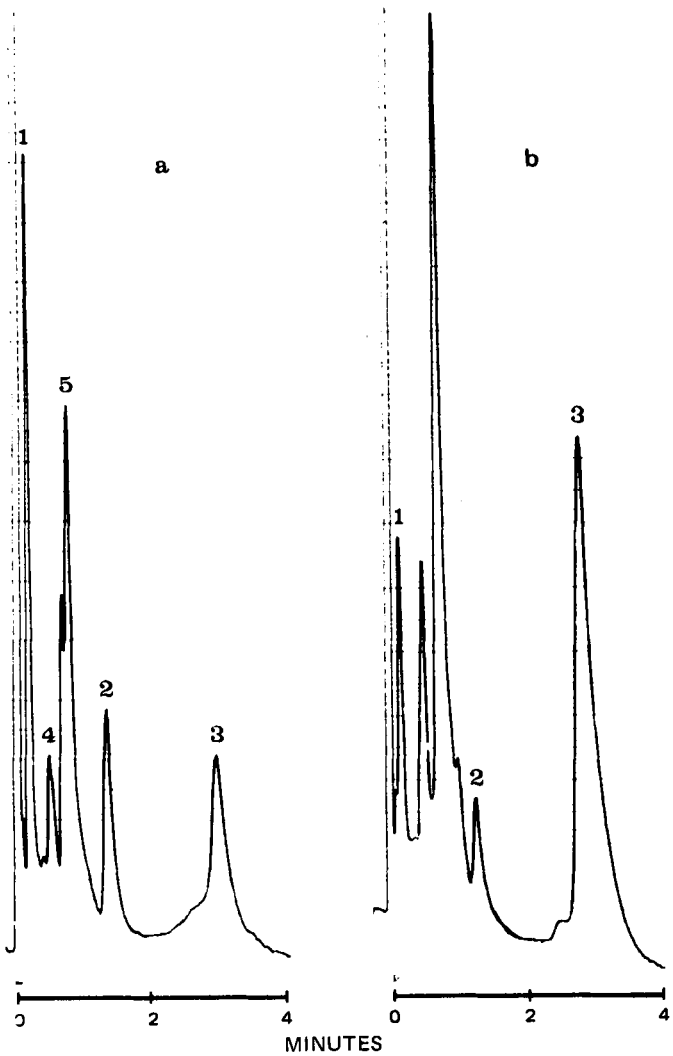

Figure 1—(a) *Gas chromatogram obtained during the peak height ratio standardization in the standard curve, Phenylpropanolamine (1), chlorpheniramine (2), promethazine (3), a constituent of the solvent (4), and a urinary constituent (5) were present.* (b) *Representative chromatogram from a patient receiving an oral dose of 8-mg of chlorpheniramine and 50 mg of phenylpropanolamine in a combination dosage form.*

rate, 350 ml/min; sensitivity and attenuation, 1 × 64; and chart speed, 10 mm/min.

Standard Solutions—The stock standard solutions (1 mg/ml) of promethazine chlorhydrate[6], phenylpropanolamine chlorhydrate[7], and chlorpheniramine maleate[7] were prepared by directly dissolving them in methanol. After some decomposition in the first 48 hr, the promethazine chlorhydrate standard solution was stable for several months (12). The standard solutions were stored at 4° in a cold chamber.

Extraction Procedure—To 1 ml of normal human urine in a glass test tube[8] (polytef-lined screw cap) were added successively 15 μl of promethazine (15 μg), 50–150 μl of phenylpropanolamine (50–150 μg), 2.5–10 μl of chlorpheniramine (2.5–10 μg) from stock standard solutions, and 0.5 ml of 1 *N* NaOH. The mixture was shaken and extracted with 2 × 3 ml of ether with vigorous stirring. The organic fractions were mixed and dried on anhydrous sodium sulfate and then evaporated under an air flow in a water bath at 30°.

The residue was dissolved in methanol (30 μl) by ultrasonic shaking for 30 sec. Then 1–2 μl of the mixture was injected into the gas chromatograph.

[6] Specia, Paris, France.
[7] Smith Kline and French, Paris, France.
[8] Sovirel, Paris, France.

RESULTS AND DISCUSSION

Figure 1*a* represents the gas chromatogram obtained during the peak height ratio standardization of phenylpropanolamine on promethazine and of chlorpheniramine on promethazine in a standard curve. In spite of the nitrogen specific detection, five peaks were observed. Two came from the impurity of the solvent and a urinary constituent. The relative retention times (to the solvent) were 0.3 min for phenylpropanolamine, 1.55 min for chlorpheniramine, and 3.35 min for the internal standard. The total analysis time was 30 min or less, suitable for several analyses.

The chromatographic yield of phenylpropanolamine ($C_{19}H_{13}NO$) with one nitrogen atom was less than that of chlorpheniramine ($C_{16}H_{19}ClN_2$), but phenylpropanolamine had better permeability through the 3% OV-1 packed column.

The selectivity and sensitivity of the nitrogen selective detector (8–10) contribute to the suitable separation of the tailing peak of methanol (solvent) from that of phenylpropanolamine on the weak polar phase OV-1. This separation was not possible with flame-ionization detection because of the short retention time of phenylpropanolamine and the unfavorable ratio of the amount of phenylpropanolamine to the solvent.

Figure 1*b* shows the representative chromatogram of a biological specimen from a patient receiving an oral dose of phenylpropanolamine chlorhydrate (50 mg) and chlorpheniramine maleate (8 mg) in a combination dosage form. One hundred samples were assayed in this laboratory.

The standard curves were prepared from normal human urine samples spiked with 0–150 μg of phenylpropanolamine, 0–10 μg of chlorpheniramine, and a constant quantity of the internal standard. The curves of the peak height ratio *versus* the added amount of phenylpropanolamine and chlorpheniramine were linear over these ranges.

The concentration in urine was within the range of the concentrations found following daily doses of 8–16 mg of chlorpheniramine and 50–100 mg of phenylpropanolamine.

The errors on the peak height ratio in standard curves for any of the three points were 7.5% for phenylpropanolamine (50, 100, and 150 μg) and 6% for chlorpheniramine (2.5, 5, and 10 μg). The recovery for both products was 98.5 ± 3.5%, and the coefficients of variation within and between assays were 2.5 and 7.5%, respectively.

The limit of sensitivity was not reached and might be improved.

After alkaline extraction, phenylpropanolamine, chlorpheniramine, and promethazine were in a relatively volatile basic form. Evaporation at room temperature under nitrogen may be desirable.

REFERENCES

(1) K. R. Heimlich, D. R. Mac Donnell, T. L. Flanagan, and P. D. O'Brien, *J. Pharm. Sci.*, **50**, 232 (1961).

(2) L. A. Shinn and B. H. Nicolet, *J. Biol. Chem.*, **138**, 91 (1941).

(3) C. Hishta and R. G. Lauback, *J. Pharm. Sci.*, **58**, 745 (1969).

(4) P. Cancalon and J. D. Klingman, *J. Chromatogr. Sci.*, **10**, 253 (1972).

(5) N. C. Jain and P. L. Kirk, *Mikrochem. J.*, **12**, 242 (1967).

(6) T. J. Reiss, *J. Assoc. Offic. Anal. Chem.*, **53**, 609 (1970).

(7) R. E. Madsen and D. F. Magin, *J. Pharm. Sci.*, **65**, 924 (1976).

(8) A. Brachet-Liermain and L. Ferrus, *Ann. Falsif. Expert. Chim.*, **67**, 351 (1974).

(9) J. H. Goudie and D. Burnett, *Clin. Chim. Acta*, **43**, 423 (1973).

(10) A. Brachet-Liermain, A. M. Trezeguet, C. Versille, and M. Dubois, *Ann. Biol. Clin.*, **32**, 135 (1974).

(11) M. A. Moulin and H. Kinsun, *Clin. Chem. Acta*, **75**, 491 (1977).

(12) R. Mestre and J. L. Berges, *Trav. Soc. Pharm., Montpellier*, **30**, 69 (1970).

ACKNOWLEDGMENTS

The authors thank M. Herrou for technical assistance and M.-C. Bigot for help in preparing the manuscript.

Convenient Synthesis of (*RS*)-4-Amino-3-hydroxybutyric Acid

MARIO PINZA and GIORGIO PIFFERI ˣ

Received December 17, 1976, from *ISF-Italseber Research Laboratories, Trezzano s/N, Milan 20090, Italy.* Accepted for publication March 14, 1977.

Abstract □ A new three-step synthesis of 4-amino-3-hydroxybutyric acid from an inexpensive starting material and under mild reaction conditions is described. Crotonic acid was brominated by the Wohl–Ziegler reaction to 4-bromocrotonic acid, which, in turn, was converted with ammonium hydroxide into 4-aminocrotonic acid. This compound, refluxed in water in the presence of a strong acid resin, afforded 4-amino-3-hydroxybutyric acid in good yields.

Keyphrases □ 4-Amino-3-hydroxybutyric acid—three-step synthesis from crotonic acid □ Anticonvulsants—4-amino-3-hydroxybutyric acid, three-step synthesis under mild reaction conditions

4-Amino-3-hydroxybutyric acid (III) was first synthesized by Tomita (1) in 1923 and was detected in the rat brain by Hayashi (2) in 1959. The remarkable importance of III stems from its biological function as a neuromodulator in the mammalian central nervous system (3, 4). Moreover, the metabolic correlation of III with 4-aminobutyric acid (5) and thus with glutamic acid and glutamine (6) justifies interest concerning its use in the treatment of epilepsy (7, 8).

In the elaboration of a research program on new 4-hydroxypyrrolidinones (9, 10), it was of interest to develop a versatile synthesis capable of giving fair amounts of III that could eventually be adapted to the preparation of some related compounds (*e.g.*, carnitine).

DISCUSSION

At present, essentially three methods exist for the synthesis of III: starting from material that contains two carbon atoms (*e.g.*, glycine), starting from compounds having three carbon atoms (*e.g.*, epichlorohydrin), and starting from compounds that possess the four-carbon framework (*e.g.*, ethyl acetoacetate).

The difficulties involved in the preparation of the key intermediate, 4-phthalimidocrotonic acid (11, 12), from phthalimidoacetic acid render the first method of limited synthetic utility. Another approach (1) consists of the reaction of phthalimide with epichlorohydrin to form 1-chloro-2-hydroxy-3-phthalimidopropane, exchange with alkaline cyanides, and final hydrolysis to III. In spite of its industrial application (13–15), this method suffers from serious ecological limitations due to the toxicity of epichlorohydrin and cyanides.

The four-step method involves bromination of the ethyl acetoacetate, reduction of the keto group, displacement of the halogen with ammonium hydroxide, and final hydrolysis of the ester (16). This method appears attractive because the material employed is inexpensive and the workup is safe. Unfortunately, the procedure is considerably limited by the low reactivity of ethyl 4-bromo-3-hydroxybutyrate to nucleophilic displacement, which causes a drastic fall in the overall yield.

To circumvent this problem, 4-bromocrotonic acid (I*b*) (17) was used. It possesses the 4-amino-3-hydroxybutyric acid framework and has an allylic bromine, which is highly reactive toward the nucleophiles.

Crotonic acid (I*a*, Scheme I) was brominated by the Wohl–Ziegler reaction with *N*-bromosuccinimide in boiling benzene in the presence of 2,2′-azobisisobutyronitrile as a radical initiator. An effort was made to find the best conditions for optimizing the transformation of I*a* into I*b*, thus avoiding the need of crystallization with severe loss of product (17). The replacement of the bromine by an amino group to yield 4-aminocrotonic acid (II) was performed with ammonium hydroxide in the presence of excess ammonium chloride to minimize the formation of secondary and tertiary amino derivatives (18).

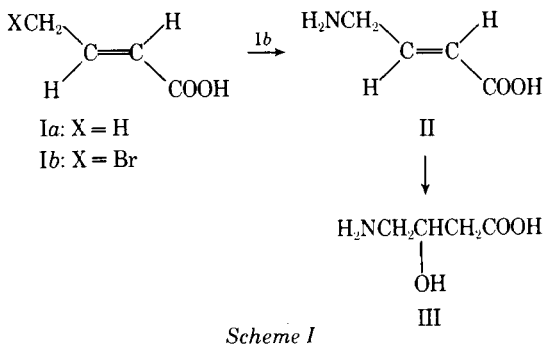

Scheme I

The exchange, carried out in liquid ammonia, contrary to that reported (19), provided only very low yields of II, as could be expected from the poor reactivity of the anhydrous reagent at −33° (20). Addition of water to the double bond of II was catalyzed in boiling water by a strongly acidic resin[1]. This reaction can be regarded as the reverse of the known dehydration of III in warm sulfuric acid to form II (21).

This three-step synthesis of III (Scheme I) provided the final compound in 26% overall yield. Moreover, mild reaction conditions are employed in this preliminary method, which is still open to improvement.

EXPERIMENTAL[2]

4-Bromocrotonic Acid (I*b*)—To a solution of 20 g (0.23 mole) of I*a* in 200 ml of dry benzene, 45.6 g (0.25 mole) of *N*-bromosuccinimide was added under nitrogen. The solution was brought to a gentle reflux while stirring and was treated with 0.5 g (3.7 mmoles) of 2,2′-azobisisobutyronitrile. Refluxing was continued for 2 hr, and the solution was cooled to 10°. The resulting white precipitate was filtered off, and the filtrate was evaporated *in vacuo*.

The residue was taken up with 200 ml of carbon tetrachloride, and the mixture was cooled to 0° and filtered. The filtrate was evaporated *in vacuo* to give 38 g of a mixture of I*a* and I*b* as a brown solid. Examination of the ^{1}H-NMR signals of CH_3 at δ 1.95 ppm for I*a* and of CH_2Br at δ 4.05 ppm for I*b* indicated that about 85% (molar percentage) was the bromo derivative I*b*. An analytical sample of I*b* could be obtained upon several recrystallizations from light petroleum, mp 73–74° [lit. (17) mp 73.5–74.5°].

4-Aminocrotonic Acid (II)—To an ice-cold and stirred solution of 130 g (2.43 moles) of ammonium chloride in 1.3 liters of ammonium hydroxide (density = 0.89 g/ml), 38 g of the crude I*b* dissolved in 50 ml of methanol was added dropwise. The flask was sealed, and stirring was continued at room temperature for 16 hr. The resulting solution was concentrated *in vacuo* at 60° to remove excess ammonia and was then passed through a column (1.3 liters) of acidic resin[1].

The column was washed with water and developed with 5.8 liters of 5% ammonium hydroxide. The eluate was concentrated *in vacuo* to 80 ml and added dropwise to 1.5 liters of ethanol stirred at 0°. The resulting precipitate was collected and dried to yield 10.7 g (50%) of II, mp 157–160° dec. A further precipitation afforded an analytical sample, mp 174–176° dec. [lit. (11) mp 164° dec. and (21) mp 180° dec.].

(*RS*)-4-Amino-3-hydroxybutyric Acid (III)—To a solution of 10.7 g (0.106 mole) of II in 600 ml of water, 260 ml of acidic resin was added; the mixture was then refluxed with stirring for 16 hr. After cooling, the

[1] Amberlite IR 120

[2] Melting points were determined with a Büchi capillary melting-point apparatus and are uncorrected. ^{1}H-NMR spectra were determined on a Perkin-Elmer R-12B spectrometer in carbon tetrachloride, using tetramethylsilane as the internal reference.

resin was transferred to a column, washed with water, and developed with 1.3 liters of 5% ammonium hydroxide. The eluate was concentrated *in vacuo* to 25 ml, treated with active charcoal (5 g), and added dropwise to 1 liter of ethanol stirred at 0°. The precipitation was repeated, yielding 7.18 g (57%) of III, mp 204–206° dec. Recrystallization from water–ethanol afforded an analytical sample, mp 214–215° dec. [lit. (1) mp 214°].

REFERENCES

(1) M. Tomita, *Z. Physiol. Chem.*, **124**, 253 (1923).

(2) T. Hayashi, *J. Physiol.*, **145**, 570 (1959).

(3) M. Otsuka, K. Obata, Y. Miyata, and Y. Tanaka, *J. Neurochem.*, **18**, 287 (1971).

(4) M. Otsuka and Y. Miyata, "Advances in Biochemical Psychopharmacology," vol. 6, Raven, New York, N.Y., 1972, p. 61.

(5) J. J. Pisano, J. D. Wilson, and S. Udenfriend, "Inhibition in the Nervous System and Gamma Aminobutyric Acid," Pergamon, New York, N.Y., 1960, p. 226.

(6) E. Roberts and C. F. Baxter, "Proceedings of the 4th International Congress on Biochemistry, Vienna 1958," Pergamon, London, England, 1959, p. 268.

(7) *Unlisted Drugs*, **16**, 6k (1964).

(8) *Ibid.*, **25**, 1411 (1973).

(9) G. Pifferi, M. Pinza, S. Banfi, and E. Teza, "Abstracts of the Vth International Symposium on Medicinal Chemistry," Paris, France, July 1976, p. 53.

(10) G. Pifferi and M. Pinza, *Farmaco, Ed. Sci.*, **32**, 602 (1977).

(11) K. Balenovic, I. Jambresic, and B. Urbas, *J. Org. Chem.*, **19**, 1589 (1954).

(12) Italseber, Fr. M. 4329 (1966); through *Chem. Abstr.*, **67**, P 100415r (1967).

(13) M. Hayashi, M. Tomita, and K. Nagai, Japanese pat. 772 (1958); through *Chem. Abstr.*, **53**, P 1172d (1959).

(14) A. Gallardo, Spanish pat. 278,780 (1963); through *Chem. Abstr.*, **60**, P 2779a (1964).

(15) T. Hayashi, French pat. 1,348,105 (1964); through *Chem. Abstr.*, **60**, P 11955h (1964).

(16) F. D'Alò and A. Masserini, *Farmaco, Ed. Sci.*, **19**, 30 (1964).

(17) L. Heslinga, H. J. J. Pabon, and D. A. Van Dorp, *Rec. Trav. Chim. Pays-Bas*, **92**, 287 (1973), and references cited therein.

(18) N. D. Cheronis and K. M. Spitzmueller, *J. Org. Chem.*, **6**, 349 (1941).

(19) D. Todd and S. Teich, *J. Am. Chem. Soc.*, **75**, 1895 (1953).

(20) G. Spielberger, "Methoden der Organischen Chemie (Houben-Weyl)," G. Thieme, Stuttgart, Germany, vol. XI-1, 1957, pp. 27–30.

(21) A. Musashi, *Hoppe-Seyler's Z. Physiol. Chem.*, **297**, 71 (1954).

ACKNOWLEDGMENTS

The authors thank Dr. P. Ventura for the NMR spectral data.

Vasodilator Activity of Adenosine Analogs

ALEEM GANGJEE *§, **HARRY P. C. HOGENKAMP** *¶, and **JAN M. KITZEN** ‡x

Received June 17, 1976, from the *Department of Biochemistry and the ‡Department of Pharmacology, College of Medicine, University of Iowa, Iowa City, IA 52242. Accepted for publication March 21, 1977.

§Present address: Department of Medicinal Chemistry, School of Pharmacy, State University of New York at Buffalo, Amherst, NY 14260. ¶Present address: Department of Biochemistry, Medical School, University of Minnesota, Minneapolis, MN 55455.

Abstract □ Various adenosine analogs were evaluated as smooth muscle vasodilators. The compounds were screened initially using a dog hindlimb preparation. Most analogs were less potent than adenosine. The three most potent compounds were tested for coronary vasodilator effects and duration of action on the isolated rabbit heart. 5′-Deoxy-5′-chloroadenosine and 5′-deoxy-5′-bromoadenosine were equipotent with adenosine but possessed a longer duration of action. 2′,3′,5′-Trideoxy-3′,5′-dichloroadenosine, an analog lacking both the 2′- and 3′-hydroxyl groups, had significant vasodilator activity.

Keyphrases □ Adenosine analogs, various—evaluated as smooth muscle vasodilators, dog hindlimb preparation □ Vasodilator activity—various adenosine analogs evaluated, dog hindlimb preparation □ Structure–activity relationships—various adenosine analogs evaluated as smooth muscle vasodilators, dog hindlimb preparation

The coronary vasodilator effects of adenosine (*Ia*) and its analogs have been recognized since 1929 (1). It has also been reported that these compounds cause the dilation of peripheral vessels (2, 3). It was suggested that adenosine is a physiological mediator of vasodilation (4). In all cases, the observed effects of adenosine are of short duration due to the rapid metabolism of the nucleoside to inosine (5) or phosphorylation to the corresponding nucleotide. Recently, Stein and coworkers (6, 7) reported that a series of esters and amides of adenosine-5′-carboxylic acid were potent cardiovascular agents that caused a marked increase in coronary sinus oxygen tension and prolonged

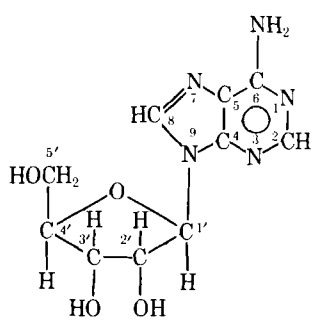

Ia

hypotension. These investigators postulated that these compounds act directly at an "adenosine receptor."

In an attempt to investigate the vasodilator activities of adenosine analogs further, a diverse series of adenosine analogs was synthesized and studied for peripheral activity in the hindlimb vasculature of the dog. Three of the most potent compounds were further studied on the Langendorff heart. The structural modifications included mono- and dihalo substituents in the sugar moiety, the extension of the 5′-position by one and two carbon atoms, an unsaturation in the carbon chain attached to the 5′-position, alterations in the sugar moiety, and a modification in the imidazole ring system. The vasodilatory effects of these compounds were compared to those of adenosine.

resin was transferred to a column, washed with water, and developed with 1.3 liters of 5% ammonium hydroxide. The eluate was concentrated *in vacuo* to 25 ml, treated with active charcoal (5 g), and added dropwise to 1 liter of ethanol stirred at 0°. The precipitation was repeated, yielding 7.18 g (57%) of III, mp 204–206° dec. Recrystallization from water–ethanol afforded an analytical sample, mp 214–215° dec. [lit. (1) mp 214°].

REFERENCES

(1) M. Tomita, *Z. Physiol. Chem.*, **124**, 253 (1923).

(2) T. Hayashi, *J. Physiol.*, **145**, 570 (1959).

(3) M. Otsuka, K. Obata, Y. Miyata, and Y. Tanaka, *J. Neurochem.*, **18**, 287 (1971).

(4) M. Otsuka and Y. Miyata, "Advances in Biochemical Psychopharmacology," vol. 6, Raven, New York, N.Y., 1972, p. 61.

(5) J. J. Pisano, J. D. Wilson, and S. Udenfriend, "Inhibition in the Nervous System and Gamma Aminobutyric Acid," Pergamon, New York, N.Y., 1960, p. 226.

(6) E. Roberts and C. F. Baxter, "Proceedings of the 4th International Congress on Biochemistry, Vienna 1958," Pergamon, London, England, 1959, p. 268.

(7) *Unlisted Drugs*, **16**, 6k (1964).

(8) *Ibid.*, **25**, 1411 (1973).

(9) G. Pifferi, M. Pinza, S. Banfi, and E. Teza, "Abstracts of the Vth International Symposium on Medicinal Chemistry," Paris, France, July 1976, p. 53.

(10) G. Pifferi and M. Pinza, *Farmaco, Ed. Sci.*, **32**, 602 (1977).

(11) K. Balenovic, I. Jambresic, and B. Urbas, *J. Org. Chem.*, **19**, 1589 (1954).

(12) Italseber, Fr. M. 4329 (1966); through *Chem. Abstr.*, **67**, P 100415r (1967).

(13) M. Hayashi, M. Tomita, and K. Nagai, Japanese pat. 772 (1958); through *Chem. Abstr.*, **53**, P 1172d (1959).

(14) A. Gallardo, Spanish pat. 278,780 (1963); through *Chem. Abstr.*, **60**, P 2779a (1964).

(15) T. Hayashi, French pat. 1,348,105 (1964); through *Chem. Abstr.*, **60**, P 11955h (1964).

(16) F. D'Alò and A. Masserini, *Farmaco, Ed. Sci.*, **19**, 30 (1964).

(17) L. Heslinga, H. J. J. Pabon, and D. A. Van Dorp, *Rec. Trav. Chim. Pays-Bas*, **92**, 287 (1973), and references cited therein.

(18) N. D. Cheronis and K. M. Spitzmueller, *J. Org. Chem.*, **6**, 349 (1941).

(19) D. Todd and S. Teich, *J. Am. Chem. Soc.*, **75**, 1895 (1953).

(20) G. Spielberger, "Methoden der Organischen Chemie (Houben-Weyl)," G. Thieme, Stuttgart, Germany, vol. XI-1, 1957, pp. 27–30.

(21) A. Musashi, *Hoppe-Seyler's Z. Physiol. Chem.*, **297**, 71 (1954).

ACKNOWLEDGMENTS

The authors thank Dr. P. Ventura for the NMR spectral data.

Vasodilator Activity of Adenosine Analogs

ALEEM GANGJEE *§, **HARRY P. C. HOGENKAMP** *¶, and **JAN M. KITZEN** ‡x

Received June 17, 1976, from the *Department of Biochemistry and the ‡Department of Pharmacology, College of Medicine, University of Iowa, Iowa City, IA 52242. Accepted for publication March 21, 1977.

§Present address: Department of Medicinal Chemistry, School of Pharmacy, State University of New York at Buffalo, Amherst, NY 14260. ¶Present address: Department of Biochemistry, Medical School, University of Minnesota, Minneapolis, MN 55455.

Abstract □ Various adenosine analogs were evaluated as smooth muscle vasodilators. The compounds were screened initially using a dog hindlimb preparation. Most analogs were less potent than adenosine. The three most potent compounds were tested for coronary vasodilator effects and duration of action on the isolated rabbit heart. 5′-Deoxy-5′-chloroadenosine and 5′-deoxy-5′-bromoadenosine were equipotent with adenosine but possessed a longer duration of action. 2′,3′,5′-Trideoxy-3′,5′-dichloroadenosine, an analog lacking both the 2′- and 3′-hydroxyl groups, had significant vasodilator activity.

Keyphrases □ Adenosine analogs, various—evaluated as smooth muscle vasodilators, dog hindlimb preparation □ Vasodilator activity—various adenosine analogs evaluated, dog hindlimb preparation □ Structure–activity relationships—various adenosine analogs evaluated as smooth muscle vasodilators, dog hindlimb preparation

The coronary vasodilator effects of adenosine (*Ia*) and its analogs have been recognized since 1929 (1). It has also been reported that these compounds cause the dilation of peripheral vessels (2, 3). It was suggested that adenosine is a physiological mediator of vasodilation (4). In all cases, the observed effects of adenosine are of short duration due to the rapid metabolism of the nucleoside to inosine (5) or phosphorylation to the corresponding nucleotide. Recently, Stein and coworkers (6, 7) reported that a series of esters and amides of adenosine-5′-carboxylic acid were potent cardiovascular agents that caused a marked increase in coronary sinus oxygen tension and prolonged

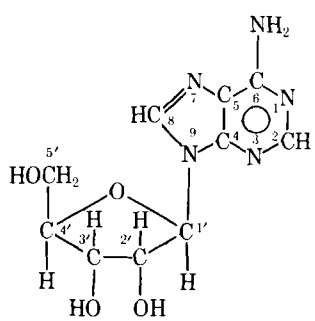

Ia

hypotension. These investigators postulated that these compounds act directly at an "adenosine receptor."

In an attempt to investigate the vasodilator activities of adenosine analogs further, a diverse series of adenosine analogs was synthesized and studied for peripheral activity in the hindlimb vasculature of the dog. Three of the most potent compounds were further studied on the Langendorff heart. The structural modifications included mono- and dihalo substituents in the sugar moiety, the extension of the 5′-position by one and two carbon atoms, an unsaturation in the carbon chain attached to the 5′-position, alterations in the sugar moiety, and a modification in the imidazole ring system. The vasodilatory effects of these compounds were compared to those of adenosine.

Table I—Potency Ratios of Adenosine Analogs on Perfused Hindlimb Preparation

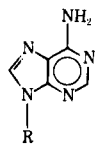

Compound	R	Potency[a]	Synthesis Literature Reference
Ib	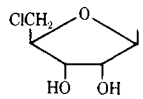	0.810	8
II	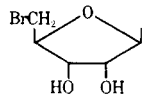	0.360	8
III	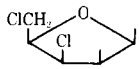	0.160	9
IV	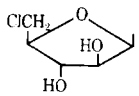	0.008	9
V	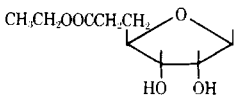	0.011	10
VI	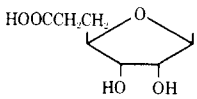	0.009	10
VII	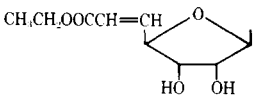	0.008	10
VIII	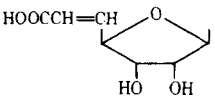	0.003	10
IX	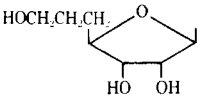	0.012	10
X	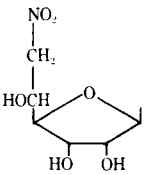	0.006	10
XI	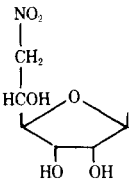	0.027	10
XII	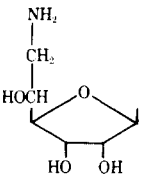	0.025	10
XIII	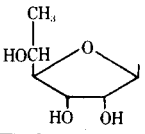	0.038	10

Table I—*Continued*

Compound	R	Potency[a]	Synthesis Literature Reference
XIV	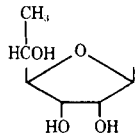	0.009	10
XV	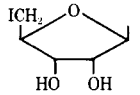	0.049	—
XVI	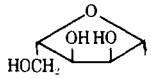	0.011	11, 12
XVII	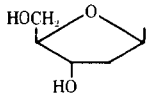	0.004	—
XVIII	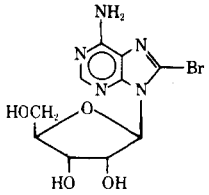	0.0005	—

[a] Vasodilator potency relative to adenosine; n = 3 except for XVIII where n = 2.

EXPERIMENTAL

Chemistry—Compounds Ib, II–XIV, and XVI were prepared by literature methods (Table I). Compounds Ia[1], XVII[2], and XVIII[2] were obtained commercially. Compound XV was prepared by the acid hydrolysis of *N*-formyl-*O*-(2′,3′-isopropylidene)-5′-deoxy-5′-iodoadenosine[3].

Pharmacology—*Perfused Hindlimb Preparation*—All compounds were screened for vasodilator activity in the perfused hindlimbs of mongrel dogs. Briefly, the preparation utilizes the left hindquarter isolated from the circulation by cannulation of the distal iliac artery with polyethylene tubing. The limb is perfused at a constant flow rate, with blood withdrawn from a carotid artery and pumped with a constant flow pump. Adequacy of isolation is determined by turning off the pump and noting a residual pressure of 25–30 mm Hg and the lack of pulsatile flow. Under these conditions, a change in perfusion pressure is proportional to changes in vascular resistance.

Drugs were dissolved in 10 ml of 0.9% saline solution with 1.0 mg of tartaric acid for solubilization and injected directly into the perfusion tubing proximal to the cannula. All test compounds were compared to adenosine as the standard, and relative potencies were determined according to Finney (13). Since this procedure was utilized for screening, any compounds that were less than 0.100 as active as adenosine were not studied in the isolated Langendorff heart.

Langendorff Heart Preparation—New Zealand rabbits of either sex were sacrificed with a blow on the head, and the heart was rapidly removed and placed in a dish containing Feigen's solution (composition: 154.00 m*M* NaCl, 5.63 m*M* KCl, 0.82 m*M* $CaCl_2 \cdot 2H_2O$, 23.81 m*M* $NaHCO_3$, and 11.10 m*M* dextrose). This preparation was essentially the same as described by Long and Chiou (14), except that perfusion pressure and heart rate and force were continuously displayed on a recorder[4].

Parallel Line Assay—In this type of assay, several different compounds are compared to a standard compound for their ability to cause the test responses. The purpose of this assay is to define as precisely as possible the potency of the test compound in terms of the standard compound. This assay was particularly suitable since the major interest was in comparing the activities of the adenosine analogs with adenosine.

[1] Zellstoff-fabrik, Waldorf, Germany.
[2] Sigma.
[3] Gift of Dr. Saburo Fukui, Kyoto University, Kyoto, Japan.
[4] Beckman.

Table II—Relative Potencies of Adenosine and Analogs

Compound	n	Potency[a] (95% Confidence Interval)	Significance[b]
Adenosine	15	1.00	
I*b*	9	0.85[c] (0.36–1.88)	NS
	9	2.28[d] (0.99–8.37)	NS
II	10	1.59[c] (0.81–3.56)	NS
	10	2.32[d] (1.05–7.23)	*
III	8	0.18[c] (0.04–0.38)	*
	8	0.51[d] (0.06–1.69)	NS

[a] Potency relative to adenosine; 100.0 μg of adenosine caused coronary perfusion pressure to decrease 59.5 ± 3.8 mm Hg (mean ± *SEM*, n = 15). The high dose of adenosine (243 μg) had a duration of action of 0.76 ± 0.07 min. [b] Significance was determined from the 95% confidence interval. For details, see *Experimental*. NS = not significantly different from adenosine. * = significantly different from adenosine. [c] Relative vasodilator potency. [d] Relative duration of action.

This method is better than using the ratio of ED_{50}'s since at least two or three doses of each compound are used in the analysis.

For optimal results, dose–response curves are constructed for the test compounds and adenosine. From these curves, doses of the test drug that approximate the same response as adenosine are then used for the assay. In the interpretation of the analysis of variance and potency estimations, F values at the 0.05 level are always used. In calculating the fiducial limits, a tabulated t value at the 0.05 level was used. By definition, any potency estimation along with the 95% confidence limit (same as fiducial) is significantly different from the standard compound if the interval does not contain 1.00.

RESULTS AND DISCUSSION

Table I shows the potencies relative to adenosine in the hindlimb preparation. With the exception of 5′-deoxy-5′-chloroadenosine (I*b*), 5′-deoxy-5′-bromoadenosine (II), and 2′,3′,5′-trideoxy-3′,5′-dichloroadenosine (III), the compounds were much less potent than adenosine. Compound IV, the *ara*-analog of I*b*, was almost inactive. Compounds V and VII, the saturated and unsaturated homologs of the potent ethyl esters of adenosine-5′-carboxylic acids VI and VIII, respectively, were inactive.

Extension of the 5′-position of adenosine by two carbon atoms as in IX led to a considerable drop in activity. Introduction of a nitromethyl or aminomethyl moiety in the 5′-position of adenosine by two carbon atoms as in X–XII was detrimental to vasodilator activity. Similarly, the introduction of a methyl group in the 5′-position of adenosine as in XIII and XIV led to decreased activity. 5′-Iodoadenosine (XV) was virtually inactive compared to the 5′-chloro (I*b*) and 5′-bromo (II) analogs. Compound XVIII, which contains an 8-bromo substituent in the adenine moiety, was the least active compound. The low order of activity of XVIII could, in part, be attributed to its *syn*- rather than *anti*-conformation (15).

Table II shows the coronary vasodilator potencies and duration of action of I*b*, II, and III relative to adenosine in the Langendorff heart preparation. The activity and duration of action of I*b* and II confirm earlier reports (16, 17). This study and an earlier report (17) showed that both 2′-deoxyadenosine (XVII) and 3′-deoxyadenosine are relatively weak vasodilators. It is, therefore, interesting that III, which lacks both 2′- and 3′-hydroxyl groups and has a chloro substituent in the 3′-position, was significantly more potent than IV–XVIII.

REFERENCES

(1) A. N. Drury and A. Szent-Gyorgi, *J. Physiol. (London)*, **68,** 213 (1929).

(2) A. Fleish and I. Sibul, *Arch. Physiol.*, **231,** 787 (1933).

(3) B. Issekutz, Jr., *Arch. Exp. Pathol. Pharmakol.*, **199,** 233 (1942).

(4) R. M. Berne, *Am. J. Physiol.*, **204,** 317 (1963).

(5) H. P. Baer, G. I. Drummond, and E. L. Duncan, *Mol. Pharmacol.*, **2,** 67 (1966).

(6) H. H. Stein, *J. Med. Chem.*, **16,** 1306 (1973).

(7) H. H. Stein, P. Somani, and R. N. Prasad, *Ann. N.Y. Acad. Sci.*, **255,** 380 (1975).

(8) K. Kikugawa and M. Ichino, *Tetrahedron Lett.*, **1971,** 87.

(9) H. P. C. Hogenkamp, *Biochemistry*, **13,** 2736 (1974).

(10) T. E. Walker, H. Follmann, and H. P. C. Hogenkamp, *Carbohydr. Res.*, **27,** 225 (1973).

(11) T. E. Walker and H. P. C. Hogenkamp, *ibid.*, **32,** 413 (1974).

(12) K. J. Ryan and E. M. Acton, in "Synthetic Procedures in Nucleic Acid Chemistry," vol. 1, W. W. Zorbach and R. S. Tipson Eds., Interscience, New York, N.Y., 1968, pp. 163, 167.

(13) D. Finney, "Statistical Methods in Biological Assay," Charles Griffin & Co. Ltd., London, England, 1952, pp. 139, 148.

(14) J. P. Long and C. Y. Chiou, *J. Pharm. Sci.*, **59,** 133 (1970).

(15) P. O. P. Ts'O, in "Basic Principles of Nucleic Acid Chemistry," vol. 1, P. O. P. Ts'O, Ed., Academic, New York, N.Y., 1974, pp. 454, 517.

(16) W. Jahn, *Naunyn-Schmiedebergs Arch. Pathol. Pharmakol.*, **251,** 95 (1965).

(17) L. B. Cobbin, R. Einstein, and M. H. Maguire, *Br. J. Pharmacol.*, **50,** 25 (1974).

ACKNOWLEDGMENTS

Supported by U.S. Public Health Grant GM-20307 from the National Institutes of Health.

The technical assistance of Andrew J. Penziner is gratefully acknowledged. The authors thank Dr. John P. Long for helpful suggestions and Dr. Harold E. Williamson for helpful comments in the preparation of the manuscript.

Anhydrocannabisativine, a New Alkaloid from *Cannabis sativa* L.

MAHMOUD A. ELSOHLY *x, CARLTON E. TURNER *, CHARLES H. PHOEBE, Jr. ‡, JOSEPH E. KNAPP ‡, PAUL L. SCHIFF, Jr. ‡, and DAVID J. SLATKIN ‡

Received February 7, 1977, from the **Research Institute of Pharmaceutical Sciences, School of Pharmacy, University of Mississippi, University, MS 38677,* and the [1]*Department of Pharmacognosy, School of Pharmacy, University of Pittsburgh, Pittsburgh, PA 15261.* Accepted for publication March 30, 1977.

Abstract □ Ethanol extracts of the leaves and roots of a Mexican variant of *Cannabis sativa* L. (marijuana) afforded, after partitioning and chromatography, the new spermidine alkaloid, anhydrocannabisativine. The structure was determined by spectral analysis and semisynthesis.

Keyphrases □ Anhydrocannabisativine—isolated from ethanol extract of leaves and roots of *Cannabis sativa*, structure determined □ *Cannabis sativa*—ethanol extract of leaves and roots, anhydrocannabisativine isolated, structure determined □ Alkaloids—anhydrocannabisativine isolated from ethanol extract of leaves and roots of *Cannabis sativa*, structure determined

The occurrence of nitrogen-containing substances in *Cannabis sativa* L. was presented recently (1). The most novel compound is the spermidine alkaloid, cannabisativine (I), isolated from the leaves and roots (2–4). The isolation of I represented the first occurrence of the spermidine (pyrido[2,1-*d*][1,5,9]triazacyclotridecine) nucleus in a higher plant. This investigation dealt with the isolation of a related alkaloid, anhydrocannabisativine (II), from the roots and leaves of a Mexican variant of *C. sativa* L.

DISCUSSION

The plant was defatted with hexane and extracted with ethanol, and the extract residue was partitioned between chloroform and 2% citric acid. The acidic layer was made basic with concentrated ammonium hydroxide and extracted with chloroform. This chloroform extract, when chromatographed on a silica gel G column and eluted with 2% ammonium hydroxide in methanol, afforded II. Numerous attempts to crystallize the alkaloid or its salts failed, so spectral data were obtained on the residue.

The IR spectrum showed absorptions at 1715 (C=O), 1661 (amide C=O), and 1615 (C=C) cm^{-1}. The mass spectrum showed a molecular ion at *m/e* 363 for $C_{21}H_{37}N_3O_2$ [18 amu (H_2O) less than I]. A comparison of the mass spectral fragmentations of I and II showed great similarities, except for fragments arising from the C-7 side chain. Peaks at *m/e* 292 ($M - C_5H_{11}$) and 264 ($M - C_5H_{11}CO$) indicated that II was an analog of I with a keto group on C-2 of the side chain.

Direct comparison of the alkaloid with a dehydration product of I confirmed the structure, and the compound was named anhydrocannabisativine (II) [13-(2-oxoheptanyl)-1,4,5,6,7,8,9,10,11,13,16,16a-dodecahydropyrido[2,1-*d*][1,5,9]triazacyclotridecine-2(3*H*)-one].

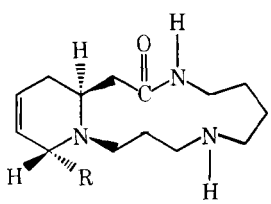

I: R =

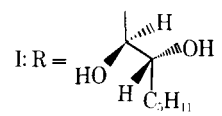

II: R =

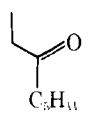

EXPERIMENTAL[1]

Plant Material—Leaves and roots of a Mexican variant of *C. sativa* L. were used[2].

Extraction—Air-dried ground leaves (5 kg) were first defatted by percolation with hexane (60 liters) and then extracted with ethanol (100 liters) at room temperature. The extract was evaporated *in vacuo* at 40° to leave a dark-green syrup (645 g) (12.9%).

Isolation of II—The ethanol extract was partitioned between chloroform (2 liters) and 2% citric acid (3 × 700 ml). The acidic layer was then made alkaline (pH 9) with concentrated ammonium hydroxide and partitioned with chloroform (3 × 2 liters). The combined chloroform layers were dried over anhydrous sodium sulfate and evaporated *in vacuo* at 40° to yield a dark yellowish-brown residue of the crude alkaloidal fraction (0.7 g) (0.014%). This residue was chromatographed over a 1.8 × 30-cm silica gel G column[3] (40 g).

Elution with 2% concentrated ammonium hydroxide in methanol afforded II (23 mg); $[\alpha]_D^{22}$ + 18.7° (c 0.1, methanol); IR: ν_{max} (film on potassium bromide) 3290, 3020, 2925, 2860, 1715, 1661, 1642, 1615, 1540, 1460, 1365, 1210, 1124, 1100, and 1050 cm^{-1}; NMR: δ 5.8 (2H, m, vinyl) and 9.6 (1H, s, broad, CONH) ppm; mass spectrum: M^+ *m/e* 363 (12%), 348 (1), 292 (4), 264 (22), 250 (68), 208 (55), 198 (60), 192 (25), 171 (20), 84 (60), 80 (40), 70 (100), and 43 (60).

Following this same isolation procedure, additional quantities of II (20 mg) were isolated from air-dried ground roots (66 kg) of this species.

Preparation of II from I—Compound I (5 mg) was dissolved in a saturated aqueous solution of oxalic acid (0.3 ml). The solution was evaporated to dryness, and the reaction flask was flushed with nitrogen and then attached to a drying tube. The reaction mixture was heated (180–185°) for 2 min and left to cool to room temperature. The mixture was dissolved in water (5 ml), made alkaline with concentrated ammonium hydroxide (pH 9), and extracted with chloroform (3 × 5 ml).

The combined layers were dried with anhydrous sodium sulfate and evaporated *in vacuo* at 40° to leave a residue (4 mg). This residue was chromatographed on a 0.9 × 12-cm silica gel G column[3] (10 g). Elution with 2% concentrated ammonium hydroxide in methanol afforded II (2 mg), identical (TLC, $[\alpha]_D$, and mass spectrum) with the natural product.

REFERENCES

(1) M. A. ElSohly and C. E. Turner, *Pharm. Weekbl.*, **111**, 1069 (1976).

(2) C. E. Turner, M. H. Hsu, J. E. Knapp, P. L. Schiff, Jr., and D. J. Slatkin, *J. Pharm. Sci.*, **65**, 1084 (1976).

(3) H. L. Lotter, D. J. Abraham, C. E. Turner, J. E. Knapp, P. L. Schiff, Jr., and D. J. Slatkin, *Tetrahedron Lett.*, **33**, 2815 (1975).

(4) F. S. El-Feraly and C. E. Turner, United Nations Secretariat Document No. ST/SOA/Ser.S/52, 1975.

ACKNOWLEDGMENTS

Supported in part by Grant DA-00928-01 from the National Institute on Drug Abuse, Research Grant 5S01RR05455-10 from the National Institutes of Health, and the Research Institute of Pharmaceutical Sciences, School of Pharmacy, University of Mississippi.

[1] Melting points were determined on a Thomas-Hoover Uni-Melt melting-point apparatus and are corrected. IR spectra were run in potassium bromide using a Perkin-Elmer 257 spectrophotometer. Optical rotations were determined on a Perkin-Elmer 241 polarimeter. UV spectra were run on a Perkin-Elmer 202 spectrophotometer. NMR spectra were obtained in deuterated chloroform on a Hitachi Perkin-Elmer R-24 spectrometer, with tetramethylsilane as the internal standard. Mass spectra were recorded on a E. I. du Pont de Nemours 21-492 spectrometer.

[2] Lot CMEF-72ME-A(2)C-69; voucher specimens were deposited in the herbarium of the School of Pharmacy, University of Mississippi.

[3] Silica gel G–water (1:2) slurried and dried at 100° (3 hr), passed through 100-mesh sieve, and packed in an elution solvent system.

Synthesis and Local Anesthetic Activity of Benzo[*b*]furan Derivatives

A. SHAFIEE *x, F. SAVABI *, A. REZVANI ‡, M. FARROKHSIAR ‡, and A. KHOYI ‡

Received January 17, 1977, from the **Department of Chemistry, College of Pharmacy, and the* ‡*Department of Experimental Medicine and Pharmacology, Faculty of Medicine, Tehran University, Tehran, Iran.* Accepted for publication March 29, 1977.

Abstract □ Several 2-dialkylaminoethyl 3-methyl-2-benzo[*b*]furancarboxylates, 2-dialkylaminoethyl 3-methyl-2-benzo[*b*]furancarbamates, and 3-methyl-2-benzo[*b*]furancarboxamide derivatives were prepared and tested for local anesthetic activity. Piperidinoethyl 3-methyl-2-benzo[*b*]furancarbamate, 2-diethylaminoethyl 3-methyl-2-benzo[*b*]furancarboxylate, and *N*-(2-diethylaminoethyl)-3-methyl-2-benzo[*b*]furancarboxamide were the most potent.

Keyphrases □ Benzo[*b*]furan derivatives—synthesized, local anesthetic activity evaluated □ Anesthetic activity, local—various benzo[*b*]furan derivatives evaluated □ Structure–activity relationships—various benzo[*b*]furan derivatives evaluated for local anesthetic activity

Diethylaminoethyl 3-methyl-2-benzo[*b*]furancarboxylate (3-methylcoumarilate) has been reported to have spasmolytic activity (1). Some carbamic acids having the benzo[*b*]furan moiety showed antifungal activity (2). It also has been demonstrated that benzoic acid derivatives having the dialkylaminoethyl moiety and dialkylaminoacetanilides have potent local anesthetic activity with low toxicity (3, 4).

In a continuing effort to find a potent local anesthetic compound with low toxicity, a series of dialkylaminoethyl 3-methyl-2-benzo[*b*]furancarboxylates, 2-dialkylaminoethyl 3-methyl-2-benzo[*b*]furancarbamates, and 3-methyl-2-benzo[*b*]furancarboxamide derivatives was prepared and efficacy was determined.

RESULTS AND DISCUSSION

Chemistry—Dialkylaminoethyl 3-methyl-2-benzo[*b*]furancarboxylates were synthesized using readily available 3-methyl-2-benzo[*b*]furancarboxylic acid (I) (5). Reaction of I with thionyl chloride and subsequent reaction of the acyl halide with dialkylaminoethanol gave the desired compound (Scheme I).

3-Methyl-2-benzo[*b*]furancarbamic acid esters (V) were obtained through the reaction of 3-methyl-2-benzo[*b*]furancarboxazide (IV) (2) with 2-dialkylaminoethanol (Scheme II).

Finally, 3-methyl-2-benzo[*b*]furancarboxamide derivatives (VII or VIII) were obtained through the reaction of either IV or 3-methyl-2-benzo[*b*]furancarboxyl chloride (II) with 2-dialkylaminoethylamine or *N*-methylpiperazine (VI) (Scheme III).

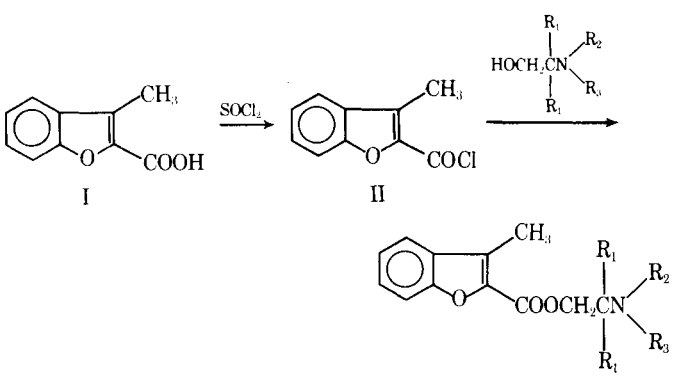

Scheme I

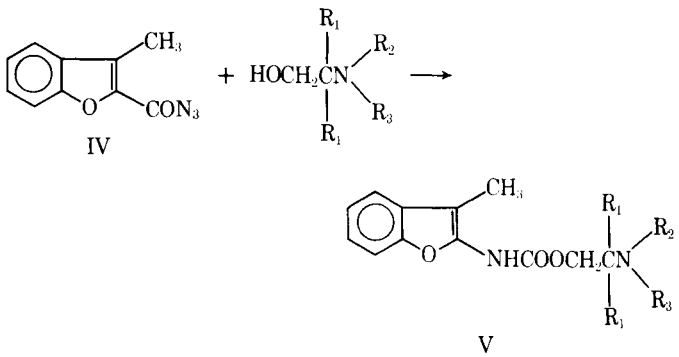

Scheme II

The physical data for the prepared compounds are summarized in Tables I–III.

Pharmacological Assay—The compounds listed in Tables I–III were screened for surface anesthetic activity. The conjunctival sac of rabbits was kept filled with the aqueous solution of the hydrochloride salt of the compounds for 60 sec. The cornea was tested once every minute, and the duration of anesthesia was followed for 18 min. Cocaine was used for comparison.

The results are presented in Table IV.

Compounds III*b*, V*e*, and VII*b* were the most potent. The LD_{50} values of III*b* and V*e* in mice, estimated by the moving average method (6), were 240.8 (204–289.3) and 59.1 (55–63.5) mg/kg, respectively, when injected intraperitoneally. Animals tolerated all substances locally. Apart from a transient irritation, no conjunctival intolerance or corneal opalescence was observed 24 and 48 hr and 1 week after drug application.

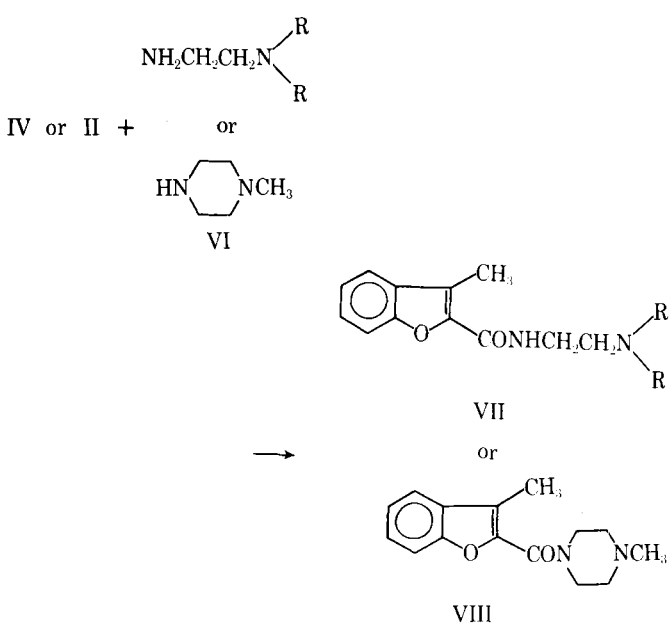

Scheme III

Table I—Physical Constants of 2-Dialkylaminoethyl 3-Methyl-2-benzo[*b*]furancarboxylates

Compound	R_1	R_2	R_3	Yield, %	Melting Point[a]	Formula[b]	Analysis, % Calc.	Found
III*a*	H	CH_3	CH_3	90	189–190°	$C_{14}H_{18}ClNO_3$	C 59.26	59.42
							H 6.35	6.12
							N 4.94	4.81
III*b*	H	C_2H_5	C_2H_5	94	180–181°	$C_{16}H_{22}ClNO_3$	C 61.64	61.51
							H 7.06	7.12
							N 4.49	4.32
III*c*	H	C_4H_9	C_4H_9	80	140–141°	$C_{20}H_{30}ClNO_3$	C 65.31	65.45
							H 8.16	8.23
							N 3.81	3.91
III*d*	H	CH_3	$CH_2C_6H_5$	78	170–171°	$C_{20}H_{22}ClNO_3$	C 66.76	66.55
							H 6.12	6.01
							N 3.89	3.95
III*e*	H	—$(CH_2)_4$—		91	194–195°	$C_{16}H_{20}ClNO_3$	C 62.04	62.22
							H 6.46	6.57
							N 4.52	4.63
III*f*	H	—$(CH_2)_5$—		95	120–121°	$C_{17}H_{22}ClNO_3$	C 63.06	63.14
							H 6.80	6.92
							N 4.33	4.16
III*g*	H	—$(CH_2CH_2)_2O$		85	200–201°	$C_{16}H_{20}ClNO_3$	C 58.99	58.81
							H 6.14	6.02
							N 4.30	4.15
III*h*	CH_3	CH_3	CH_3	65	209–210°	$C_{16}H_{22}ClNO_3$	C 61.64	61.51
							H 7.06	7.01
							N 4.49	4.38

[a] Unless otherwise indicated, the recrystallization solvent was ethanol–ethyl acetate. [b] IR, NMR, and mass spectra of all compounds were as expected.

Table II—Physical Constants of 2-Dialkylaminoethyl 3-Methyl-2-benzo[*b*]furancarbamates

Compound	R_1	R_2	R_3	Yield, %	Melting Point	Formula[a]	Analysis, % Calc.	Found
V*a*	H	CH_3	CH_3	65	134–135°[b]	$C_{14}H_{18}N_2O_3$	C 64.12	64.25
							H 6.87	6.93
							N 10.69	10.73
V*b*	H	C_2H_5	C_2H_5	70	173–174°[c]	$C_{16}H_{22}N_2O_3$	C 66.21	66.05
							H 7.59	7.41
							N 9.66	9.50
V*c*	H	C_4H_9	C_4H_9	75	—[d]	$C_{20}H_{30}N_2O_3$	C 69.36	69.16
							H 8.67	8.48
							N 8.09	8.26
V*d*	H	CH_3	$CH_2C_6H_5$	68	—[d]	$C_{20}H_{22}N_2O_3$	C 71.00	71.18
							H 6.51	6.32
							N 8.28	8.46
V*e*	H	—$(CH_2)_5$—		70	200–201°	$C_{17}H_{22}N_2O_3$	C 67.55	67.66
							H 7.28	7.15
							N 9.27	9.14
V*f*	H	—$(CH_2CH_2)_2O$		70	194–195°	$C_{16}H_{20}N_2O_4$	C 63.16	63.01
							H 6.58	6.64
							N 9.21	9.40
V*g*	CH_3	CH_3	CH_3	67	—[d]	$C_{16}H_{22}N_2O_3$	C 66.21	66.35
							H 7.59	7.72
							N 9.66	9.82

[a] IR, NMR, and mass spectra of all compounds were as expected. [b] This compound was crystallized as a picrate from ethanol. [c] This compound was crystallized as a hydrochloride from absolute ethanol. [d] This compound resisted crystallization as a free base or as a salt.

Table III—Physical Constants of *N*-(2-Dialkylaminoethyl)-3-methyl-2-benzo[*b*]furancarboxamide

Compound	R	Yield, %	Melting Point[a]	Formula[b]	Analysis, % Calc.	Found
VII*a*	CH_3	84	69–70°	$C_{14}H_{18}N_2O_2$	C 68.29	68.43
					H 7.32	7.45
					N 11.38	11.26
VII*b*	C_2H_5	90	45–46°	$C_{16}H_{22}N_2O_2$	C 70.07	70.24
					H 8.03	8.12
					N 10.22	10.18
VII*c*	—$(CH_2)_4$—	88	72–73°	$C_{16}H_{20}N_2O_2$	C 70.59	70.75
					H 7.35	7.12
					N 10.29	10.18
VII*d*	—$(CH_2)_2O(CH_2)_2$—	90	55–56°	$C_{16}H_{20}N_2O_3$	C 66.67	66.49
					H 6.94	6.81
					N 9.72	9.55
VIII	—	98	258–260°[c]	$C_{15}H_{18}N_2O_2$	C 69.77	69.65
					H 6.97	6.99
					N 10.85	10.74

[a] Unless otherwise indicated, the crystallization solvent was petroleum ether and the compound was prepared by Method A (see *Experimental*). [b] IR, NMR, and mass spectra of all compounds were as expected. [c] This compound was crystallized as a hydrochloride from absolute ethanol; it was synthesized by Method B (see *Experimental*).

Table IV—Local Anesthetic Activity of Benzo[*b*]furan Derivatives[a]

Compound[b]	Concentration, %	Potency	Duration, min
IIIa	1	0.85 (0.75–0.95)	13–18
IIIb	1	1.0	Over 18
	0.5	0.96 (0.91–1.0	16–18
	0.25	0.41 (0.30–0.53)	6–8
IIIc	1	0.75 (0.65–0.85)	10–15
IIId	1	0.85 (0.76–0.93)	13–17
IIIe	1	0.62 (0.51–0.74)	9–15
IIIf	1	1.0	Over 18
	0.5	0.68 (0.57–0.79)	11–13
IIIg	1	0.82 (0.73–0.91)	12–18
IIIh	1	0	0
Vb	1	0.72 (0.61–0.83)	13–15
Ve	1	1.0	Over 18
	0.25	0.75 (0.64–0.85)	11–15
Vf	1	0.97 (0.93–1.0)	17–18
VIIa	1	0	0
VIIb	1	0.96 (0.91–1.0)	16–18
	0.50	0.84 (0.75–0.93)	14–16
	0.25	0.57 (0.45–0.68)	10–14
VIIc	1	0.84 (0.76–0.92)	13–16
VIId	1	0	0
VIII	1	0	0
Cocaine	0.25	1.0	Over 18
	0.125	0.89 (0.82–0.96)	11–18

[a] Surface anesthesia was tested according to the method of M. R. A. Chance and H. J. Lobstein, *J. Pharmacol. Exp. Ther.*, **82**, 203 (1944). Anesthetic potency was calculated for the first 18 min [A. H. Campbell, J. A. Strasse, G. H. Lord, and J. E. Willson, *J. Pharm. Sci.*, **57**, 2045 (1968)]. A potency of 1.00 indicates an onset of anesthesia in 1 min and a duration of at least 18 min. [b] Compounds of Tables I–III not included in this table could not be dissolved in water and were not tested.

EXPERIMENTAL[1]

Compound II—A mixture of I (17.68 g, 0.01 mole) (5) in 100 ml of thionyl chloride was refluxed for 4 hr. The excess of thionyl chloride was evaporated under reduced pressure, and the residue was distilled to give II (16 g, 82%), bp 114–116°/6 mm Hg, mp 64–65° (hexane).

Anal.—Calc. for $C_{10}H_7ClO_2$: C, 61.70, H, 3.60. Found: C, 61.85; H, 3.79.

2-Dimethylaminoethyl 3-Methyl-2-benzo[*b*]furancarboxylate (IIIa)—A solution of 2-dimethylaminoethanol (0.89 g, 0.01 mole) and II (1.945 g, 0.01 mole) in 20 ml of benzene was refluxed for 4 hr. The solvent was evaporated, and the residue was crystallized from ethanol–ethyl acetate to give IIIa (2.55 g, 90%), mp 189–190°; IR (potassium bromide): 1715 cm^{-1} (ester); NMR (deuterochloroform, as free base): δ 7.66–7.17 (m, 4H, aromatic), 4.43 (t, 2H, OCH_2), 2.66 (t, 2H, CH_2N), 2.53 (s, 3H, CH_3), and 2.33 (s, 6H, NCH_3) ppm; *m/e* 247.

Compounds IIIb–IIIh were prepared similarly (Table I).

2-Dimethylaminoethyl 3-Methyl-2-benzo[*b*]furancarbamate (Va)—A solution of IV (2.01 g, 0.01 mole) (2) and 2-dimethylaminoethanol (0.89 g, 0.01 mole) in 20 ml of benzene was refluxed for 4 hr. The solvent was evaporated, and the residue was crystallized as a picrate, mp 134–135°; IR (potassium bromide, as free base): 1720 and 1249 cm^{-1} (ester); NMR (deuterochloroform, as free base): δ 7.50–7.00 (m, 5H, aromatic and NH), 4.23 (t, 2H, OCH_2), 2.56 (t, 2H, CH_2N), 2.23 (s, 6H, NCH_3), and 2.07 (s, 3H, CH_3) ppm; *m/e* 262.

Compounds Vb–Vg were prepared similarly (Table II).

***N*-(2-Diethylaminoethyl)-3-methyl- 2- benzo[*b*]furancarboxamide (VIIb)**—*Method A*—A solution of IV (2.01 g, 0.01 mole) and 2-diethylaminoethylamine (1.16 g, 0.01 mole) in 30 ml of benzene was refluxed for 2 hr, and the solvent was evaporated. The residue was crystallized from petroleum ether to give VIIb (2.5 g, 91%), mp 45–46°; IR (potassium bromide): 3300 (NH) and 1650 (amide) cm^{-1}; NMR (deuterochloroform): δ 7.73–7.00 (m, 5H, aromatic and NH), 3.5 (unresolved t, $CONCH_2$), 2.69 (t, 2H, CH_2N), 2.66 (s, 3H, CH_3), 2.54 (q, 4H, NCH_2), and 1.60 (t, 6H, CH_3) ppm; *m/e* 274.

Method B—A solution of II (1.945 g, 0.01 mole) and 2-diethylaminoethylamine (1.16 g, 0.01 mole) in 30 ml of benzene was refluxed for 2 hr. The solvent was evaporated, and the residue was crystallized from ethyl acetate to give VIIb as the hydrochloride (2.8 g, 90%), mp 129–130°, and as a free base, mp 45–46° (petroleum ether).

Compounds VIIa, VIIc, VIId, and VIII were prepared similarly (Table III).

[1] Melting points were taken on a Kofler hot-stage microscope and are uncorrected. IR spectra were recorded using a Perkin-Elmer 267 spectrophotometer. Mass spectra were recorded on a Varian Mat III instrument. NMR spectra were determined with a Varian T-60A instrument.

REFERENCES

(1) A. Szadowska, *Acta Physiol. Polon.*, **17**, 571 (1966).

(2) F. Ghabgharan, H. Kooshkabadi, M. Emami, A. Rashidbaigi, and A. Shafiee, *J. Pharm. Sci.*, **65**, 1085 (1976).

(3) N. Sharghi, I. Lalezari, G. Niloofari, and H. Golgolab, *J. Med. Chem.*, **12**, 696 (1969).

(4) I. Lalezari and A. Shafiee, *ibid.*, **15**, 113 (1972).

(5) W. R. Boehme, *Org. Syn.*, **33**, 43 (1953).

(6) C. S. Weil, *Biometrics*, **8**, 243 (1952).

ACKNOWLEDGMENTS

Supported by a grant from the Tehran University Research Council.

Determination of Ionization Constants in Mixed Aqueous Solvents of Varying Composition by a Single Titration

JEF PEETERS

Received February 14, 1977, from *Physico-Chemistry Department, Janssen Pharmaceutica, 2340 Beerse, Belgium.* Accepted for publication April 8, 1977.

Abstract □ A potentiometric titration method is proposed in which only one titration is necessary to obtain pK'a values for different solvent compositions. The method allows the results to be extrapolated to the value for pure water. Examples are given, and the advantages and disadvantages of the method are discussed.

Keyphrases □ Ionization constants—potentiometric determination in mixed aqueous solvents of various composition □ Potentiometry—determination of ionization constants in mixed aqueous solvents of various composition

The use of mixed aqueous solvents for the potentiometric determination of ionization constants has disadvantages and should be avoided if possible. However, the solubility requirements for aqueous titrations are often too demanding, and many compounds are not suited for spectrophotometric analysis. Although Albert and Serjeant

Table IV—Local Anesthetic Activity of Benzo[*b*]furan Derivatives[a]

Compound[b]	Concentration, %	Potency	Duration, min
IIIa	1	0.85 (0.75–0.95)	13–18
IIIb	1	1.0	Over 18
	0.5	0.96 (0.91–1.0	16–18
	0.25	0.41 (0.30–0.53)	6–8
IIIc	1	0.75 (0.65–0.85)	10–15
IIId	1	0.85 (0.76–0.93)	13–17
IIIe	1	0.62 (0.51–0.74)	9–15
IIIf	1	1.0	Over 18
	0.5	0.68 (0.57–0.79)	11–13
IIIg	1	0.82 (0.73–0.91)	12–18
IIIh	1	0	0
Vb	1	0.72 (0.61–0.83)	13–15
Ve	1	1.0	Over 18
	0.25	0.75 (0.64–0.85)	11–15
Vf	1	0.97 (0.93–1.0)	17–18
VIIa	1	0	0
VIIb	1	0.96 (0.91–1.0)	16–18
	0.50	0.84 (0.75–0.93)	14–16
	0.25	0.57 (0.45–0.68)	10–14
VIIc	1	0.84 (0.76–0.92)	13–16
VIId	1	0	0
VIII	1	0	0
Cocaine	0.25	1.0	Over 18
	0.125	0.89 (0.82–0.96)	11–18

[a] Surface anesthesia was tested according to the method of M. R. A. Chance and H. J. Lobstein, *J. Pharmacol. Exp. Ther.*, **82**, 203 (1944). Anesthetic potency was calculated for the first 18 min [A. H. Campbell, J. A. Strasse, G. H. Lord, and J. E. Willson, *J. Pharm. Sci.*, **57**, 2045 (1968)]. A potency of 1.00 indicates an onset of anesthesia in 1 min and a duration of at least 18 min. [b] Compounds of Tables I–III not included in this table could not be dissolved in water and were not tested.

EXPERIMENTAL[1]

Compound II—A mixture of I (17.68 g, 0.01 mole) (5) in 100 ml of thionyl chloride was refluxed for 4 hr. The excess of thionyl chloride was evaporated under reduced pressure, and the residue was distilled to give II (16 g, 82%), bp 114–116°/6 mm Hg, mp 64–65° (hexane).

Anal.—Calc. for $C_{10}H_7ClO_2$: C, 61.70, H, 3.60. Found: C, 61.85; H, 3.79.

2-Dimethylaminoethyl 3-Methyl-2-benzo[*b*]furancarboxylate (IIIa)—A solution of 2-dimethylaminoethanol (0.89 g, 0.01 mole) and II (1.945 g, 0.01 mole) in 20 ml of benzene was refluxed for 4 hr. The solvent was evaporated, and the residue was crystallized from ethanol–ethyl acetate to give IIIa (2.55 g, 90%), mp 189–190°; IR (potassium bromide): 1715 cm^{-1} (ester); NMR (deuterochloroform, as free base): δ 7.66–7.17 (m, 4H, aromatic), 4.43 (t, 2H, OCH_2), 2.66 (t, 2H, CH_2N), 2.53 (s, 3H, CH_3), and 2.33 (s, 6H, NCH_3) ppm; *m/e* 247.

Compounds IIIb–IIIh were prepared similarly (Table I).

2-Dimethylaminoethyl 3-Methyl-2-benzo[*b*]furancarbamate (Va)—A solution of IV (2.01 g, 0.01 mole) (2) and 2-dimethylaminoethanol (0.89 g, 0.01 mole) in 20 ml of benzene was refluxed for 4 hr. The solvent was evaporated, and the residue was crystallized as a picrate, mp 134–135°; IR (potassium bromide, as free base): 1720 and 1249 cm^{-1} (ester); NMR (deuterochloroform, as free base): δ 7.50–7.00 (m, 5H, aromatic and NH), 4.23 (t, 2H, OCH_2), 2.56 (t, 2H, CH_2N), 2.23 (s, 6H, NCH_3), and 2.07 (s, 3H, CH_3) ppm; *m/e* 262.

Compounds Vb–Vg were prepared similarly (Table II).

***N*-(2-Diethylaminoethyl)-3-methyl- 2- benzo[*b*]furancarboxamide (VIIb)**—*Method A*—A solution of IV (2.01 g, 0.01 mole) and 2-diethylaminoethylamine (1.16 g, 0.01 mole) in 30 ml of benzene was refluxed for 2 hr, and the solvent was evaporated. The residue was crystallized from petroleum ether to give VIIb (2.5 g, 91%), mp 45–46°; IR (potassium bromide): 3300 (NH) and 1650 (amide) cm^{-1}; NMR (deuterochloroform): δ 7.73–7.00 (m, 5H, aromatic and NH), 3.5 (unresolved t, $CONCH_2$), 2.69 (t, 2H, CH_2N), 2.66 (s, 3H, CH_3), 2.54 (q, 4H, NCH_2), and 1.60 (t, 6H, CH_3) ppm; *m/e* 274.

Method B—A solution of II (1.945 g, 0.01 mole) and 2-diethylaminoethylamine (1.16 g, 0.01 mole) in 30 ml of benzene was refluxed for 2 hr. The solvent was evaporated, and the residue was crystallized from ethyl acetate to give VIIb as the hydrochloride (2.8 g, 90%), mp 129–130°, and as a free base, mp 45–46° (petroleum ether).

Compounds VIIa, VIIc, VIId, and VIII were prepared similarly (Table III).

[1] Melting points were taken on a Kofler hot-stage microscope and are uncorrected. IR spectra were recorded using a Perkin-Elmer 267 spectrophotometer. Mass spectra were recorded on a Varian Mat III instrument. NMR spectra were determined with a Varian T-60A instrument.

REFERENCES

(1) A. Szadowska, *Acta Physiol. Polon.*, **17**, 571 (1966).

(2) F. Ghabgharan, H. Kooshkabadi, M. Emami, A. Rashidbaigi, and A. Shafiee, *J. Pharm. Sci.*, **65**, 1085 (1976).

(3) N. Sharghi, I. Lalezari, G. Niloofari, and H. Golgolab, *J. Med. Chem.*, **12**, 696 (1969).

(4) I. Lalezari and A. Shafiee, *ibid.*, **15**, 113 (1972).

(5) W. R. Boehme, *Org. Syn.*, **33**, 43 (1953).

(6) C. S. Weil, *Biometrics*, **8**, 243 (1952).

ACKNOWLEDGMENTS

Supported by a grant from the Tehran University Research Council.

Determination of Ionization Constants in Mixed Aqueous Solvents of Varying Composition by a Single Titration

JEF PEETERS

Received February 14, 1977, from *Physico-Chemistry Department, Janssen Pharmaceutica, 2340 Beerse, Belgium.* Accepted for publication April 8, 1977.

Abstract □ A potentiometric titration method is proposed in which only one titration is necessary to obtain pK'a values for different solvent compositions. The method allows the results to be extrapolated to the value for pure water. Examples are given, and the advantages and disadvantages of the method are discussed.

Keyphrases □ Ionization constants—potentiometric determination in mixed aqueous solvents of various composition □ Potentiometry—determination of ionization constants in mixed aqueous solvents of various composition

The use of mixed aqueous solvents for the potentiometric determination of ionization constants has disadvantages and should be avoided if possible. However, the solubility requirements for aqueous titrations are often too demanding, and many compounds are not suited for spectrophotometric analysis. Although Albert and Serjeant

Table I—Titration Data for 1-Methyl-1*H*-imidazole [a]

NaOH Added, ml	pH	Methanol, %	pK'a Value
1.6	5.47	60.34	6.455
2.0	5.71	58.33	6.480
2.4	5.90	56.45	6.512
2.8	6.05	54.69	6.532
3.2	6.19	53.03	6.560
3.6	6.31	51.47	6.578
4.0	6.42	50.00	6.593
4.4	6.53	48.61	6.612
4.8	6.64	47.30	6.632
5.2	6.74	46.05	6.643
5.6	6.85	44.87	6.661
6.0	6.96	43.75	6.675
6.4	7.08	42.68	6.691
6.8	7.21	41.67	6.706
7.2	7.35	40.70	6.713
7.6	7.52	39.77	6.717
8.0	7.76	38.89	6.726

[a] Product (6.5 mg) is converted to its acidic form with 0.85 ml of 0.1 *N* HCl. Then 7 ml of methanol is added and brought to 10 ml with water. The solution is titrated with aqueous 0.01 *N* NaOH. Number of points $n = 17$, regression coefficient $r = -0.9985$, slope $m = -0.013$, intercept $b = 7.235$, F value = 5152, and variance of intercept $s^2 = 7.551 \times 10^{-5}$.

(1) condemned the results obtained in mixed aqueous solvents as being of doubtful value, the method is rather popular, especially for the comparison of closely related compounds.

In a recent review, Cookson (2) discussed the advantages and disadvantages of mixed solvents. The purpose of this note is not to justify the method nor to condemn it; many workers have no alternative and prefer to obtain less accurate results rather than to get entangled in experimental difficulties and time-consuming methods (3–5).

This paper presents a relatively simple titration procedure in which only one titration is necessary to obtain pK'a[1] values for different solvent compositions. Consequently, the method allows the results to be extrapolated to the value for pure water. The method has been applied routinely in this laboratory for about 3 years.

In the conventional method, solutions with different solvent composition are titrated, and the results are extrapolated, mostly by graphical techniques. This method is rather time consuming, since at least three solutions with different solvent composition are titrated with three different titer solutions having compositions equal to the titrated solution. In the proposed method, this step can be avoided.

THEORETICAL

If a compound dissolved in a binary mixture, with a stated ratio in volumes of both constituent solvents, is titrated with a titer solution having another, also stated, ratio in volumes of both constituent solvents, the composition of the resulting solution is continuously changing during the titration. The exact composition can be calculated at each step of the titration:

$$P = \frac{(P_i{}^p V_p) + (P_i{}^t V_t)}{V_p + V_t} \qquad \text{(Eq. 1)}$$

where P is the percent of nonaqueous solvent; $P_i{}^p$ and $P_i{}^t$ are the initial percentages of nonaqueous solvent in the solution and the titrant, respectively; and V_p and V_t are the volumes of the solution and the titrant, respectively. Since, on the other hand, the pK'a can be calculated by well-known formulas (1), an extrapolation of pK'a to the value for pure water can be done with as many points as necessary, provided the titration curve (pH *versus* milliliters of titrant) is available.

During the titration of a compound, *e.g.*, BH^+, with a strong base, the ratio of concentration of BH^+ and B is expressed as:

$$\frac{[BH^+]}{[B]} = \frac{EP}{V_t} - 1 \qquad \text{(Eq. 2)}$$

where EP is the equivalence point indicating the end of the titration.

Substitution of Eq. 2 in the well-known formulas (1) allows calculation of the pK'a at any point of a titration curve and, in combination with Eq. 1, the necessary data pairs are obtained for extrapolation.

Slightly differing expressions are obtained when a base is converted into its acidic form by addition of an excess strong acid prior to titration:

$$P = \frac{(P_i{}^p V_p) + (P_i{}^t V_t) + (P_i{}^a V_a)}{V_p + V_t + V_a} \qquad \text{(Eq. 3)}$$

$$\frac{[BH^+]}{[B]} = \frac{EP_2 - EP_1}{V_t - EP_1} - 1 \qquad \text{(Eq. 4)}$$

where index a indicates the added acid solution; EP_1 is the first equivalence point, indicating the end of the neutralization of the excess acid; and EP_2 is the second equivalence point, indicating the end of the titration.

EXPERIMENTAL

Materials—The following materials were used without further purification: 1-methyl-1*H*-imidazole[2], cinnarizine[3], seperidol hydrochloride[4], diphenoxylate hydrochloride[5], etomidate sulfate[6], and miconazole nitrate[7]. The solvents used were analytical grade.

Water was distilled and deionized by being passed through an intimate mixture of acidic cation- and basic anion-exchange resins[8] before use. Sodium hydroxide and hydrochloric acid solutions were prepared by dilution of concentrated reagents, commercially available[9].

Equipment—Titration curves were recorded with an automatic titration setup[10], equipped with glass and calomel electrodes[11]. The electrode system was standardized with the standard buffer[12] 0.025 *M* KH_2PO_4–0.025 *M* Na_2HPO_4.

Method—If the compound is available as a salt, an appropriate amount is dissolved in the organic solvent and water is added to obtain the desired mixture. If the compound is a free base, the appropriate amount is converted to its acidic form by addition of a small excess of 0.1 *N* HCl; then the organic solvent and water are added.

The solutions are thermostated in a water-jacketed vessel, and 0.01 *N* NaOH is added from a 25-ml buret. After the titration, the pH and the corresponding milliliters of titrant are read from the recorded titration curve. The calculations are performed on a small desk calculator.

RESULTS AND DISCUSSION

Table I illustrates the use of the method for 1-methyl-1*H*-imidazole. This compound was chosen for comparison purposes. The first and the last points of the titration curve were not used for the calculation because equilibrium conditions were not reached at these stages of the titration with the automatic equipment.

The pK'a value in pure water, obtained after extrapolation of the data, was 7.24; 6.95 and 7.20 are given in Ref. 6. A determination using the more conventional technique and extrapolation of data obtained in separate single titrations with 5, 10, 20, 30, 40, and 50% methanol yielded the value of 7.16.

A collection of data obtained with the proposed method and comparison with values determined by other methods are given in Table II. Etomidate is included in the table to demonstrate that very weak bases

[1] The symbol pK'a indicates that the ionization constants are uncorrected values (concentration constants).

[2] Ninety-nine percent, Aldrich-Europe.

[3] USAN for (*E*)-1-(diphenylmethyl)-4-(3-phenyl-2-propenyl)piperazine; Janssen Pharmaceutica, Beerse, Belgium.

[4] USAN for 4-[4-[4-chloro-3-(trifluoromethyl)phenyl]-4-hydroxy-1-piperidinyl]-1-(4-fluorophenyl)-1-butanone hydrochloride; Janssen Pharmaceutica, Beerse, Belgium.

[5] USP and RINN for ethyl 1-(3-cyano-3,3-diphenylpropyl)-4-phenyl-4-piperidinecarboxylate monohydrochloride; Janssen Pharmaceutica, Beerse, Belgium.

[6] USAN for (*R*)-(+)-ethyl 1-(1-phenylethyl)-1*H*-imidazole-5-carboxylate; Janssen Pharmaceutica, Beerse, Belgium.

[7] USAN for 1-[2-(2,4-dichlorophenyl)-2-[(2,4-dichlorophenyl)methoxy]ethyl]-1*H*-imidazole mononitrate; Janssen Pharmaceutica, Beerse, Belgium.

[8] Elgacan B 114, The Elga Group, England.

[9] Dilut-It, Baker Chemicals, Deventer, Holland.

[10] Radiometer titrator TTT 2, autoburet ABU 12 b, and titrigraph REA 300.

[11] Radiometer glass electrode G 202 C and calomel electrode K 401.

[12] NBS.

Table II—pK'a Values Determined by the Proposed Method and Comparison with Values Determined by Other Methods

Compound	Proposed Method	Comparison Value
Seperidol	8.43	8.44[a]
Cinnarizine	7.47	7.60[a]
Diphenoxylate	7.07	—
Etomidate	Not applicable	4.24[b]
Miconazole	6.91	6.65[a]

[a] Determined by conventional titration method and extrapolation to pure water. [b] Determined by potentiometric titration and UV spectrophotometry.

(pKa < 5) are not suited for the method. Indeed, the addition of methanol to the solution reduced the pH of the medium so that it fell outside the measurable range.

The method yields results comparable with results from the conventional method of performing various titrations in differently composed mixtures and extrapolating to pure water. Moreover, the method is fast and saves a great deal of manipulation time.

In dealing with the determination of pK'a values for insoluble compounds, one commonly uses a binary solvent mixture with a fixed ratio, *e.g.*, methanol–water (1:1), and compares the dissociation constant in that medium. This approach is reasonable as long as the compounds are structurally similar, differing only by some substituents or substituent position. However, when the pKa values of compounds with different structures are to be compared, as in structure–activity relationship studies, not all of the compounds may be soluble in the chosen binary mixture. Furthermore, the influence of the solvent will not be the same on each compound. With the proposed method, the influence of the solvent is extrapolated at least to some extent.

From a fundamental point of view, the method has serious shortcomings: (*a*) linearity over a small composition range does not necessarily justify extrapolation over a considerable distance, (*b*) a single titration does not permit estimation of the precision of individual points on the curve, and (*c*) the method only works for compounds in a narrow pK'a range. In spite of these shortcomings, the method is useful in situations where only approximate pK'a values are necessary for many water-insoluble compounds and where a comparison is to be made between closely related compounds. In comparison with the conventional titration procedure, the proposed method is rapid, easily applicable, and yields good results. Moreover, it is possible to delay the precipitation of a free base during titration by choosing the experimental conditions in such a way that the percentage of organic cosolvent increases together with the concentration of free base.

The method should also be of interest to people studying the influence of mixtures of water and organic solvent on the dissociation behavior of weak acids and weak bases. Indeed, a range of different percentages of the cosolvent is covered by a single titration; consequently, the amount of experimental manipulation could be greatly reduced.

REFERENCES

(1) A. Albert and E. P. Serjeant, "The Determination of Ionization Constants," 2nd ed., Chapman and Hall, London, England, 1971.

(2) R. F. Cookson, *Chem. Rev.*, **74,** 5 (1974).

(3) R. H. Levy and M. Rowland, *J. Pharm. Sci.*, **60,** 1155 (1971).

(4) I. Setnikar, *ibid.*, **55,** 1190 (1966).

(5) D. J. Glover, *J. Am. Chem. Soc.*, **87,** 5275, 5279 (1965).

(6) D. D. Perrin, "Dissociation Constants of Organic Bases in Aqueous Solutions," Butterworths, London, England, 1965.

ACKNOWLEDGMENTS

The author thanks Mr. A. Jacobs for performing some titrations.

l-Bunolol Metabolism in Rats: Identification of Urinary Metabolites

FRANZ-JOSEF LEINWEBER *, JOSEPH M. SZPIECH, and FREDERICK J. DI CARLO ‡x

Received January 24, 1977, from the *Department of Drug Metabolism, Warner-Lambert Research Institute, Morris Plains, NJ 07950.* Accepted for publication March 31, 1977.

*Present address: Department of Biochemistry and Drug Metabolism, Hoffmann-La Roche Inc., Nutley, NJ 07110. ‡Present address: Office of Toxic Substances (WH-557), U.S. Environmental Protection Agency, Washington, DC 20460.

Abstract □ Urine collected for 24 hr from rats given a single oral dose of ^{3}H-*l*-bunolol (10 mg/kg) was found to contain only 25.8% of the dose and more than 30 labeled compounds. Nine compounds were identified and quantified as follows: bunolol (0.35% of urinary tritium), bunolol glucuronide (5.12%), bunolol sulfate (0.08%), dihydrobunolol (0.08%), dihydrobunolol glucuronide (0.74%), dihydrobunolol sulfate (0.12%), hydroxydihydrobunolol (0.58%), β-(5-oxytetralonyl)lactic acid (0.74%), and (5-oxytetralonyl)acetic acid glucuronide (1.12%). The total quantity of identified labeled compounds was only 2.3% of the dose and 8.9% of the urinary radioactivity.

Keyphrases □ *l*-Bunolol—metabolism in rats, urinary metabolites identified □ Metabolism—*l*-bunolol in rats, urinary metabolites identified □ Antiadrenergic agents—*l*-bunolol, metabolism in rats, urinary metabolites identified

The β-adrenoceptor blocking activity of *l*-bunolol is now being evaluated by clinical trials. Earlier studies on bunolol metabolism were conducted in dogs (1–3) and *in vitro* (4, 5) with the *dl*-form. The present report is the first to describe the metabolism of the *l*-isomer, which is approximately 2.5 times more potent than the *dl*-preparation in inhibiting isoproterenol tachycardia in conscious dogs (6).

EXPERIMENTAL

Reference Compounds—Isotopically labeled *l*-bunolol hydrochloride contained tritium in the 7-position of the naphthalenone ring (69.3 μCi/mg, 99.9% radiochemical purity, 99.3% chemical purity). Synthetic nonradioactive dihydrobunolol, β-(5-oxytetralonyl)lactic acid, (5-oxytetralonyl)acetic acid, and ^{14}C-labeled hydroxybunolol and hydroxydihydrobunolol isolated from dog urine (3) were used.

Radioactivity Counting—Quantitative assays of urine for tritium were performed with a liquid scintillation spectrometer[1]. The external standardization method was employed for quench corrections. Feces were assayed for tritium after combustion in an oxidizer[2].

Animals, Dosing, and Collection of Excreta—Male Wistar rats[3], 270–290 g, were dosed by gavage with an aqueous solution of ^{3}H-*l*-bunolol hydrochloride (10 mg/kg). The animals were housed in individual glass

[1] Packard Tri-Carb model 3320.
[2] Oxymat JA-101, Teledyne Intertechnique, Westwood, N.J.
[3] Marland Breeding Farms, Hewitt, N.J.

Table II—pK'a Values Determined by the Proposed Method and Comparison with Values Determined by Other Methods

Compound	Proposed Method	Comparison Value
Seperidol	8.43	8.44[a]
Cinnarizine	7.47	7.60[a]
Diphenoxylate	7.07	—
Etomidate	Not applicable	4.24[b]
Miconazole	6.91	6.65[a]

[a] Determined by conventional titration method and extrapolation to pure water. [b] Determined by potentiometric titration and UV spectrophotometry.

(pKa < 5) are not suited for the method. Indeed, the addition of methanol to the solution reduced the pH of the medium so that it fell outside the measurable range.

The method yields results comparable with results from the conventional method of performing various titrations in differently composed mixtures and extrapolating to pure water. Moreover, the method is fast and saves a great deal of manipulation time.

In dealing with the determination of pK'a values for insoluble compounds, one commonly uses a binary solvent mixture with a fixed ratio, *e.g.*, methanol–water (1:1), and compares the dissociation constant in that medium. This approach is reasonable as long as the compounds are structurally similar, differing only by some substituents or substituent position. However, when the pKa values of compounds with different structures are to be compared, as in structure–activity relationship studies, not all of the compounds may be soluble in the chosen binary mixture. Furthermore, the influence of the solvent will not be the same on each compound. With the proposed method, the influence of the solvent is extrapolated at least to some extent.

From a fundamental point of view, the method has serious shortcomings: (*a*) linearity over a small composition range does not necessarily justify extrapolation over a considerable distance, (*b*) a single titration does not permit estimation of the precision of individual points on the curve, and (*c*) the method only works for compounds in a narrow pK'a range. In spite of these shortcomings, the method is useful in situations where only approximate pK'a values are necessary for many water-insoluble compounds and where a comparison is to be made between closely related compounds. In comparison with the conventional titration procedure, the proposed method is rapid, easily applicable, and yields good results. Moreover, it is possible to delay the precipitation of a free base during titration by choosing the experimental conditions in such a way that the percentage of organic cosolvent increases together with the concentration of free base.

The method should also be of interest to people studying the influence of mixtures of water and organic solvent on the dissociation behavior of weak acids and weak bases. Indeed, a range of different percentages of the cosolvent is covered by a single titration; consequently, the amount of experimental manipulation could be greatly reduced.

REFERENCES

(1) A. Albert and E. P. Serjeant, "The Determination of Ionization Constants," 2nd ed., Chapman and Hall, London, England, 1971.

(2) R. F. Cookson, *Chem. Rev.*, **74,** 5 (1974).

(3) R. H. Levy and M. Rowland, *J. Pharm. Sci.*, **60,** 1155 (1971).

(4) I. Setnikar, *ibid.*, **55,** 1190 (1966).

(5) D. J. Glover, *J. Am. Chem. Soc.*, **87,** 5275, 5279 (1965).

(6) D. D. Perrin, "Dissociation Constants of Organic Bases in Aqueous Solutions," Butterworths, London, England, 1965.

ACKNOWLEDGMENTS

The author thanks Mr. A. Jacobs for performing some titrations.

l-Bunolol Metabolism in Rats: Identification of Urinary Metabolites

FRANZ-JOSEF LEINWEBER *, JOSEPH M. SZPIECH, and FREDERICK J. DI CARLO ‡x

Received January 24, 1977, from the *Department of Drug Metabolism, Warner-Lambert Research Institute, Morris Plains, NJ 07950.* Accepted for publication March 31, 1977.

*Present address: Department of Biochemistry and Drug Metabolism, Hoffmann-La Roche Inc., Nutley, NJ 07110. ‡Present address: Office of Toxic Substances (WH-557), U.S. Environmental Protection Agency, Washington, DC 20460.

Abstract □ Urine collected for 24 hr from rats given a single oral dose of ^{3}H-*l*-bunolol (10 mg/kg) was found to contain only 25.8% of the dose and more than 30 labeled compounds. Nine compounds were identified and quantified as follows: bunolol (0.35% of urinary tritium), bunolol glucuronide (5.12%), bunolol sulfate (0.08%), dihydrobunolol (0.08%), dihydrobunolol glucuronide (0.74%), dihydrobunolol sulfate (0.12%), hydroxydihydrobunolol (0.58%), β-(5-oxytetralonyl)lactic acid (0.74%), and (5-oxytetralonyl)acetic acid glucuronide (1.12%). The total quantity of identified labeled compounds was only 2.3% of the dose and 8.9% of the urinary radioactivity.

Keyphrases □ *l*-Bunolol—metabolism in rats, urinary metabolites identified □ Metabolism—*l*-bunolol in rats, urinary metabolites identified □ Antiadrenergic agents—*l*-bunolol, metabolism in rats, urinary metabolites identified

The β-adrenoceptor blocking activity of *l*-bunolol is now being evaluated by clinical trials. Earlier studies on bunolol metabolism were conducted in dogs (1–3) and *in vitro* (4, 5) with the *dl*-form. The present report is the first to describe the metabolism of the *l*-isomer, which is approximately 2.5 times more potent than the *dl*-preparation in inhibiting isoproterenol tachycardia in conscious dogs (6).

EXPERIMENTAL

Reference Compounds—Isotopically labeled *l*-bunolol hydrochloride contained tritium in the 7-position of the naphthalenone ring (69.3 μCi/mg, 99.9% radiochemical purity, 99.3% chemical purity). Synthetic nonradioactive dihydrobunolol, β-(5-oxytetralonyl)lactic acid, (5-oxytetralonyl)acetic acid, and ^{14}C-labeled hydroxybunolol and hydroxydihydrobunolol isolated from dog urine (3) were used.

Radioactivity Counting—Quantitative assays of urine for tritium were performed with a liquid scintillation spectrometer[1]. The external standardization method was employed for quench corrections. Feces were assayed for tritium after combustion in an oxidizer[2].

Animals, Dosing, and Collection of Excreta—Male Wistar rats[3], 270–290 g, were dosed by gavage with an aqueous solution of ^{3}H-*l*-bunolol hydrochloride (10 mg/kg). The animals were housed in individual glass

[1] Packard Tri-Carb model 3320.
[2] Oxymat JA-101, Teledyne Intertechnique, Westwood, N.J.
[3] Marland Breeding Farms, Hewitt, N.J.

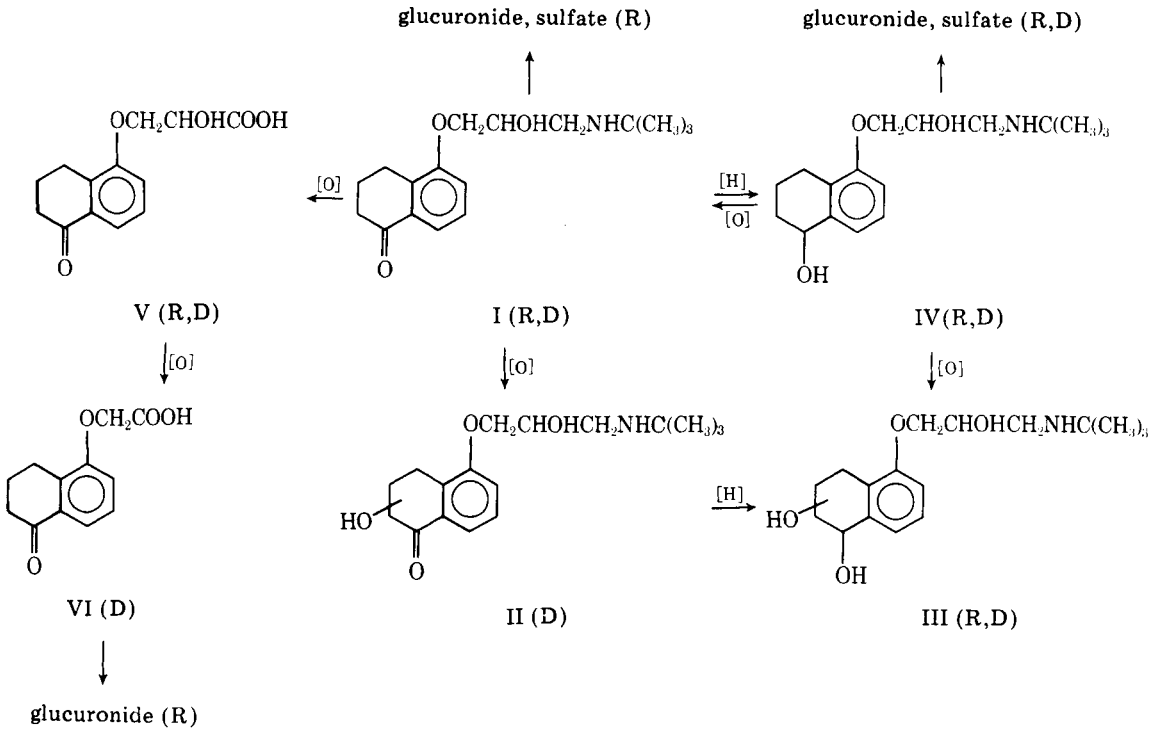

Scheme I—Pathways of bunolol biotransformation in the rat and dog; (R) and (D) signify the identification of the compound in rat and dog urine, respectively.

metabolic units and were offered a synthetic liquid diet[4] *ad libitum*. Urine and feces were collected from each rodent for 24 hr and assayed for tritium.

Chromatography—After developing the silica gel G[5] TLC plates in chloroform–acetic acid–methanol (15:1:4), radioactive bands were located with a radiochromatogram scanner[6]. For most purposes, areas under radioactive peaks were measured with a compensating planimeter[7].

Fractionation of Urine—The urine from the three rats was adjusted to pH 2 and extracted eight times with 500-ml volumes of ether to collect unconjugated acids. Unconjugated bases were extracted with ether (15 × 500 ml) after adjusting the pH of the aqueous phase to 10. Then the aqueous phase was brought to pH 5, freed of ether with a nitrogen stream, and incubated at 37° for 7 hr with β-glucuronidase[8] (0.2 IU/ml). Fresh enzyme (0.2 IU/ml) was added, and incubation was resumed for 17 hr.

After the solution was brought to pH 2, deconjugated acids were extracted with ether (5 × 500 ml). Basic aglycones were obtained by adjusting the aqueous phase to pH 10 and extracting eight times with ether. A nitrogen stream was used to remove ether from the aqueous phase before incubation at pH 6 with aryl sulfatase[9] (0.7 IU/ml), first for 6 hr and then for 18 hr, after adding the same quantity of fresh enzyme. Deconjugated acids were collected at pH 2 with ether, and deconjugated bases were extracted at pH 10. The remaining aqueous solution contained unclassified polar metabolites.

Fractionation of Bunolol and Metabolites—A 1.5 × 82-cm column of Sephadex G-10 was used for the fractionation of bunolol and its basic metabolites. After the column was equilibrated with 20 m*M* sodium phosphate buffer (pH 7.0), calibration was performed by applying 1-ml solutions of bunolol (0.1 μmole), dihydrobunolol (0.3 μmole), and hydroxydihydrobunolol (0.1 μmole) in phosphate. Effluents of radioactive samples were monitored for tritium, and those of nonradioactive compounds were evaluated by UV spectrometry (bunolol at 254 nm, dihydrobunolol at 272 nm).

After the separation of urinary components, the fractions eluted from ~75 to 108 ml were pooled and subsequently analyzed for dihydrobunolol. Similarly, according to the precalibration data with reference compounds (3), the fractions eluted from ~108 to 140 ml were pooled for the subsequent quantitative determination of bunolol. Each pool was reduced to dryness *in vacuo*. and the residues were taken up in methanol.

Aliquots from each pool were chromatographed on 20 × 20-cm silica gel G plates flanked by reference compounds. Each pool representing the eluate from ~75 to 108 ml was chromatographed in parallel with reference dihydrobunolol; each pool representing the eluate from ~108 to 140 ml was chromatographed in parallel with reference bunolol (10 μg/spot). After development of the plates, bunolol was visualized under UV light and dihydrobunolol was visualized by exposure to iodine vapor. The bands between the reference spots were scraped from the plates, and the tritium was eluted with methanol.

RESULTS

The mean excretion of the isotope in 24 hr was 39.0% of the orally administered ^{3}H-*l*-bunolol (13.2% in feces and 25.8% in urine). Solvent extraction and TLC indicated that the urine contained at least 31 labeled compounds (Table I). More than half of the urinary radioactivity consisted of unclassified polar metabolites. Base glucuronides comprised the largest classified fraction and represented 26.9% of the excreted radioactivity.

Table II shows the nine labeled compounds identified in rat urine and the quantities of each. The level of unchanged bunolol was very low, but bunolol glucuronide was present in the largest amount and some bunolol sulfate was detected. Dihydrobunolol showed a similar pattern; *i.e.*, it was present in the same three forms and predominantly as the glucuro-

Table I—Classification and Quantification of Labeled Components in Rat Urine after a Single Oral Dose of ^{3}H-*l*-Bunolol Hydrochloride (10 mg/kg)

Fraction	Labeled Components, Minimum Number	Percent of Dose	Percent of Urinary Tritium
Unconjugated acids	3	1.04	4.0
Unconjugated bases	12	2.58	10.0
Acid glucuronides	2	0.37	1.4
Base glucuronides	5	6.94	26.9
Acid sulfates	3	0.28	1.1
Base sulfates	5	0.92	3.6
Polar metabolites	1	13.70	53.1
Total	31	25.8	100

[4] Carnation Slender.
[5] Analtech.
[6] Packard model 7201.
[7] Keuffel and Esser.
[8] Ketodase, Warner-Chilcott.
[9] Calbiochem.

Table II—Quantities of Labeled Compounds Identified in the Urine of Rats after a Single Oral Dose of ^{3}H-*l*-Bunolol Hydrochloride (10 mg/kg)

Compound	Unconjugated		Glucuronide		Sulfate	
	% of Dose	% of Urinary Tritium	% of Dose	% of Urinary Tritium	% of Dose	% of Urinary Tritium
Bunolol	0.09	0.35	1.32	5.12	0.02	0.08
Dihydrobunolol	0.02	0.08	0.19	0.74	0.03	0.12
Hydroxybunolol	N.D.[a]	—	N.D.	—	N.D.	—
Hydroxydihydrobunolol	0.15	0.58	N.D.	—	N.D.	—
β-(5-Oxytetralonyl)lactic acid	0.19	0.74	N.D.	—	N.D.	—
(5-Oxytetralonyl)acetic acid	N.D.	—	0.29	1.12	N.D.	—

[a] Not detected.

nide. Hydroxydihydrobunolol was found, but hydroxybunolol was absent. The other metabolites were unconjugated β-(5-oxytetralonyl)lactic acid and (5-oxytetralonyl)acetic acid glucuronide. The total quantity of identified labeled compounds was only 2.3% of the dose and 8.9% of the urinary radioactivity.

DISCUSSION

It is very improbable that the great differences between bunolol biotransformation in the rat and dog (3) are attributable to the administration of the *l*-isomer to rats and the *dl*-form to dogs. Additionally, dogs excreted 62% of the dose in urine in the same period (1) as rats excreted only 26%; the slow excretion by the rat probably results from the extensive enterohepatic recirculation of bunolol metabolites[10]. More than half of the bunolol metabolites in rat urine are unclassified polar metabolites; such unknown compounds represent only 23% of the metabolites in dog urine (3). Whereas base glucuronides constitute the major classified fraction of bunolol metabolites in rat urine, they contribute much less to the radioactivity of dog urine where unconjugated acids and bases account for 61% of the isotope (3).

There are several qualitative differences in bunolol (I) biotransformation by rats and dogs. The most interesting is the presence of hydroxybunolol (II) in dog urine and its absence in rat urine. This finding implies that hydroxydihydrobunolol (III) is formed from dihydrobunolol (IV), not from hydroxybunolol, at least in the rat (Scheme I). Also, β-(5-oxytetralonyl)lactic acid (V) was present in both rat and dog urine, while (5-oxytetralonyl)acetic acid (VI) was detected only in dog urine.

[10] M. C. Crew, R. J. St. Hilaire, R. L. Gala, and F. J. Di Carlo, unpublished data.

The quantitative differences may have greater pharmacological significance. Dihydrobunolol has approximately the same β-adrenergic blocking potency as bunolol (4). The total quantities of unconjugated bunolol and dihydrobunolol were 0.7% of the dose in dog urine and only 0.1% in rat urine. These data suggested that bunolol might express its activity more readily in dogs than in rats, an interpretation verified experimentally (7).

REFERENCES

(1) F.-J. Leinweber, L. J. Haynes, M. C. Crew, and F. J. Di Carlo, *J. Pharm. Sci.*, **60**, 1512 (1971).

(2) F.-J. Leinweber, R. C. Greenough, C. F. Schwender, L. J. Haynes, and F. J. Di Carlo, *ibid.*, **60**, 1516 (1971).

(3) F.-J. Leinweber, R. C. Greenough, and F. J. Di Carlo, *ibid.*, **66**, 1570 (1977).

(4) F.-J. Leinweber, R. C. Greenough, C. F. Schwender, H. R. Kaplan, and F. J. Di Carlo, *Xenobiotica*, **2**, 191 (1972).

(5) F.-J. Leinweber and F. J. Di Carlo, *J. Pharmacol. Exp. Ther.*, **189**, 271 (1974).

(6) M. A. Commarato, E. C. Giardino, G. A. Kopia, and H. R. Kaplan, *Pharmacologist*, **18**, 227 (1976).

(7) H. R. Kaplan, M. A. Commarato, and E. C. Lattime, *J. Pharm. Sci.*, **67**, 132 (1978).

ACKNOWLEDGMENTS

The authors are indebted to their colleague and friend, the late Mr. Edward J. Merrill of the Warner-Lambert Research Institute, for the synthesis of ^{3}H-labeled *l*-bunolol.

l-Bunolol and Propranolol: Oral and Intravenous β-Adrenoceptor Blocking Activity in Rats Compared to Dogs and Humans

H. R. KAPLAN *[x], M. A. COMMARATO [‡], and E. C. LATTIME [§]

Received January 27, 1977, from the *Department of Pharmacology, Warner-Lambert Research Institute, Morris Plains, NJ 07950.* Accepted for publication March 31, 1977. *Present address: Department of Pharmacology, Pharmaceutical Research Division, Warner-Lambert/Parke-Davis, Ann Arbor, MI 48106. ‡Present address: Food and Drug Administration, Bureau of Drugs, Rockville, MD 20857. §Present address: Department of Zoology/Physiology, Rutgers—the State University, Newark, NJ 08903.

Abstract □ To determine the pharmacological significance of reported differences between species in *l*-bunolol metabolism, oral and intravenous β-adrenoceptor blocking activity against an isoproterenol-induced tachycardia was compared in dogs, rats, and humans. Propranolol was similarly studied in rats and dogs. Species differences in intravenous potency were minimal for both compounds in contrast to oral dose studies. Oral to intravenous ratios of doses causing a comparable degree of β-adrenoceptor blockade after *l*-bunolol were: rat, 212; dog, 4; and human, 5. For propranolol, the oral to intravenous dose ratios were 210 and 32 for the rat and dog, respectively. These pharmacological findings show major differences in the rat compared to dogs and humans and may be explained in part by differences in the urinary excretion patterns of *l*-bunolol in the various species.

Keyphrases □ *l*-Bunolol—β-adrenoceptor blocking activity compared in dogs, rats, and humans, oral and intravenous dosage □ Propranolol—β-adrenoceptor blocking activity compared in dogs and rats, oral and intravenous dosage □ β-Adrenoceptor blocking activity—*l*-bunolol and propranolol compared in dogs, rats, and humans, oral and intravenous dosage □ Antiadrenergic agents—*l*-bunolol, β-adrenoceptor blocking activity compared in dogs, rats, and humans, oral and intravenous dosage

l-Bunolol is a potent β-adrenoceptor antagonist undergoing extensive clinical investigation for treatment of hypertension, angina, and arrhythmia. There are major differences in the urinary excretion patterns of *l*- (and *dl*-) bunolol and its metabolites after oral dosing in the rat (1, 2), dog (1, 3), and human (1, 4, 5). The presence of recognized active metabolites in rat urine is substantially reduced as compared to the dog and human. These observations suggest that the rat, because of its unique metabolism, may be more resistant to the β-adrenoceptor blocking activity of orally administered *l*-bunolol than are the other two species. Therefore, the β-adrenoceptor blocking dose of *l*-bunolol after intravenous and oral administrations to the rat was determined, and the data were compared to those previously reported for the dog (6) and human[1]. Similar comparisons were also made with propranolol[2].

EXPERIMENTAL

Oral Dose Studies—Two hours prior to the induction of pentobarbital (58 mg/kg ip) anesthesia, separate groups of 24-hr fasted, male Sprague–Dawley rats[3], 260–388 g, were dosed by gavage with aqueous solutions of *l*-bunolol (0.1, 0.3, 1, and 3 mg of base/kg), propranolol (1, 3, 10, and 30 mg of base/kg), or lactose (0.1 mg/kg) (control). Drugs and lactose were dissolved in distilled water, and the volume of administration was 0.1 ml/100 g of body weight. After anesthesia, heart rate was recorded[4] from a cardiotachometer, which was triggered by the R wave of the lead II electrocardiograph.

Isoproterenol (0.025 μg total dose) was injected *via* a catheterized tail vein 2.5, 3, and 3.5 hr after oral drug or lactose administration. The isoproterenol dose selected caused reproducible, submaximal tachycardic responses of 87 ± 12 (*SEM*) beats/min in the control group of animals. Potency values were calculated at 3 hr after drug administration since maximal inhibition of isoproterenol usually occurred at this time.

Intravenous Dose Studies—Inhibition of isoproterenol-induced tachycardia also was determined after single intravenous doses of *l*-bunolol (3, 10, and 30 μg/kg) and propranolol (10, 30, and 100 μg/kg) to separate groups of anesthetized rats. The standard intravenous isoproterenol challenge was given before and 10 min after drug administration.

Potency values in the oral dose study were based on the average heart rate response to isoproterenol produced in the control (lactose) group of animals; in the intravenous dose study, each animal served as its own control. Data were analyzed using a weighted linear regression format and the Student *t* test (7). A *p* value of <0.05 was regarded as significant.

Table I—*l*-Bunolol and Propranolol: Intravenous and Oral β-Adrenoceptor Blocking Doses in Rats

Route	*l*-Bunolol, μg/kg		Propranolol, μg/kg	
	ID_{50}[a]	Relative Activity[b]	ID_{50}	Relative Activity
Intravenous	11 (8–17)		41 (32–55)	
		212[c] (134–338)		210[c] (146–297)
Oral	2390 (1749–4590)		8688 (6720–11,083)	

[a] Dose (micrograms per kilogram) required to cause a 50% inhibition of the tachycardic response to 0.025 μg of isoproterenol (95% confidence limits). Each value represents results from at least four animals. [b] Oral to intravenous dose ratio (95% confidence limits). [c] $p < 0.05$.

RESULTS AND DISCUSSION

The intravenous and oral doses of *l*-bunolol and propranolol in rats required to inhibit an isoproterenol-induced tachycardia by 50% are presented in Table I. Large multiples (>200) of the intravenous ID_{50} dose of *l*-bunolol and propranolol were required orally to cause comparable pharmacological effects in rats. For comparison, oral to intravenous dose ratios also were computed for the dog and human (Table II). Clinical data for propranolol were derived from the literature (8–11). Factors other than absorption apparently are involved, since both *l*-bunolol (1–5, 12) and propranolol (10, 13, 14) are virtually completely absorbed after oral administration in each species.

The rat, unlike the dog or human, was highly resistant to β-adrenergic receptor blockade by oral treatment with *l*-bunolol. One explanation could be a rapid and extensive biotransformation of *l*-bunolol (and other β-adrenergic blockers) to inactive or conjugated polar metabolites. The large separation in oral to intravenous milligram potency is not unique to *l*-bunolol but was also observed for propranolol (this study, 15), me-

[1] Unpublished observations by Dr. John W. Wallace (Cardiology Division, Department of Internal Medicine, University of Texas Medical Branch at Galveston, Galveston, TX 77550) on file at Warner-Lambert Research Institute, Morris Plains, NJ 07950.

[2] All references to propranolol used throughout the text refer to the *dl* or racemic form of the compound.

[3] Charles River.

[4] Beckman type R dynograph.

Table II—*l*-Bunolol and Propranolol: Comparative Oral to Intravenous Dose Ratios in Rats, Dogs, and Humans

Species	*l*-Bunolol	Propranolol
Rat	212 (Table I)[a]	210 (Table I)
Dog	4 (6)	32 (6)
Human	5[b]	8–20 (8–11)

[a] Appropriate reference citations are in parentheses. [b] Unpublished observations.

toprolol (16), labetalol (17), and other β-blockers (18) and has been ascribed in part to unique metabolism in the rat.

Other factors such as presystemic (first-pass) elimination (*e.g.*, hepatic extraction) warrant consideration. Previous studies in the dog (19) showed that *l*-bunolol underwent relatively little presystemic inactivation compared to propranolol. These results are consistent with the large differences in oral to intravenous dose ratios reported in the dog and human for propranolol compared to *l*-bunolol (Table II). In the rat, the oral to intravenous dose ratios for *l*-bunolol and propranolol were virtually identical, 212 and 210, respectively. Therefore, some presystemic or extrahepatic mechanism may be operative for *l*-bunolol in the rat (unlike the dog), as was reported for propranolol in this species (20, 21).

Based on the urinary excretion patterns of *l*-bunolol and its active metabolite dihydrobunolol in the rat and dog (22) (Table III), the observed oral to intravenous potency differences between the two species were greater than expected. Therefore, other undefined differences must account for the low oral potency of *l*-bunolol in the rat. Comparative pharmacological studies on hydroxydihydrobunolol (Table III) (2, 3), which is expected to be an active metabolite, have not been performed. Such a study would be of interest; however, the compound is presently unavailable in adequate quantities.

These studies indicate that large oral doses of *l*-bunolol, propranolol, and, presumably, most other β-blockers are required to achieve β-adrenoceptor blockade in the rat. Failure to recognize this species difference could result in the misinterpretation of experimental data when oral doses of β-blockers are used in the rat.

Table III—Identified Active Compounds of Oral Bunolol in Pooled Urine[a] (0–24-hr Collection)

Species	Oral Dose, mg/kg	Percent of Dose Excreted		
		Bunolol	Dihydrobunolol	Hydroxydihydrobunolol[b]
Rat	10	0.09	0.02	0.15
Dog	10	0.4	0.3	6.0
Human	~0.04[c]	12.9	23.7	1.8

[a] Values were obtained from Di Carlo *et al.* (1). [b] Hydroxydihydrobunolol has not been evaluated pharmacologically; whether or not pharmacological data on this urinary metabolite will account for the low oral potency in the rat remains to be established. [c] A 3-mg total dose. The mean body weight of subjects was 74.1 ± 6.6 kg.

REFERENCES

(1) F. J. Di Carlo, I. W. F. Davidson, J. M. Szpiech, and F.-J. Leinweber, *Fed. Proc.*, **36,** 1031 (1977).

(2) F.-J. Leinweber, J. M. Szpiech, and F. J. Di Carlo, *J. Pharm. Sci.*, **67,** 129 (1978).

(3) F.-J. Leinweber, R. C. Greenough, and F. J. Di Carlo, *ibid.*, **66,** 1570 (1977).

(4) F. J. Di Carlo, F.-J. Leinweber, J. M. Szpiech, R. L. Burt, and I. W. F. Davidson, *Fed. Proc.*, **35,** 566 (1976).

(5) F. J. Leinweber, J. M. Szpiech, and F. J. Di Carlo, *Pharmacology*, in press.

(6) R. D. Robson and H. R. Kaplan, *J. Pharmacol. Exp. Ther.*, **175,** 157 (1970).

(7) D. J. Finney, "Statistical Methods in Biological Assay," 2nd ed., Hafner, New York, N.Y., 1964.

(8) H. Kesteloot, R. Sluyts, A. Floor-Wieringa, and R. Van Strik, *Eur. J. Pharmacol.*, **10,** 303 (1970).

(9) I. Brick, K. J. Hutchison, D. G. McDevitt, I. C. Roddie, and R. G. Shanks, *Br. J. Pharmacol.*, **34,** 127 (1968).

(10) C. T. Dollery, D. S. Davies, and M. E. Conolly, *Ann. N.Y. Acad. Sci.*, **179,** 108 (1971).

(11) C. R. Cleaveland, R. E. Rangno, and D. G. Shand, *Arch. Intern. Med.*, **130,** 47 (1972).

(12) F.-J. Leinweber, L. J. Haynes, M. C. Crew, and F. J. Di Carlo, *J. Pharm. Sci.*, **60,** 1512 (1971).

(13) A. Hayes and R. G. Cooper, *J. Pharmacol. Exp. Ther.*, **176,** 302 (1971).

(14) J. W. Paterson, M. E. Conolly, *et al.*, *Pharmacol. Clin.*, **2,** 127 (1970).

(15) D. R. Lee, E. L. Phelan, and F. O. Simpson, "Proceedings of the Second Symposium on the Spontaneously Hypertensive Rat," U. S. Department of Health, Education and Welfare Publication 77-1179, 1977.

(16) N. O. Bodin, K. O. Borg, R. Johansson, C.-H. Ramsay, and I. Skånberg, *Acta Pharmacol. Toxicol., Suppl. 5,* **36,** 116 (1975).

(17) R. T. Brittain and G. P. Levy, *Br. J. Clin. Pharmacol., Suppl. 3,* **3,** 681 (1976).

(18) J. V. Levy, *Am. J. Med.*, **61,** 779 (1976).

(19) H. R. Kaplan and M. A. Commarato, *J. Pharmacol. Exp. Ther.*, **185,** 395 (1973).

(20) D. G. Shand, R. E. Rangno, and G. H. Evans, *Pharmacology*, **8,** 344 (1972).

(21) D. G. Shand, R. A. Branch, G. H. Evans, A. S. Nies, and G. R. Wilkinson, *Drug Metab. Disp.*, **1,** 679 (1973).

(22) F.-J. Leinweber, R. C. Greenough, C. F. Schwender, H. R. Kaplan, and F. J. Di Carlo, *Xenobiotica* **2,** 191 (1972).

ACKNOWLEDGMENTS

The authors thank Mr. N. Stasilli for assistance with statistical analyses.

Solvent Deposition Method for Enhancement of Dissolution Rate: Importance of Drug-to-Excipient Ratio

HANS JOHANSEN * **and NIELS MØLLER** ‡x

Received November 24, 1975, from the *DAK-Laboratories, Lergravsvej 59, DK-2300 Copenhagen S, Denmark, and the ‡Royal Danish School of Pharmacy, Institute of Pharmaceutics, Universitetsparken 2, DK-2100 Copenhagen Ø, Denmark. Accepted for publication April 6, 1977.

Abstract □ Dissolution rates and particle sizes of phenylbutazone solvent deposited on lactose, starch, and silicon dioxide, separately, and of norethindrone and digoxin deposited on lactose were investigated. Microparticulate dispersed drugs on the surface of excipients result when drug-to-excipient ratios are low. Fast dissolution rates are observed for such systems. This effect can be extended to higher ratios when silicon dioxide is used as the excipient. Because of adsorption, however, the release from silicon dioxide is more or less limited.

Keyphrases □ Dissolution rate—enhanced by solvent deposition method, effect of drug-to-excipient ratio □ Solvent deposition method—enhancement of dissolution rate, effect of drug-to-excipient ratio □ Dosage forms, solid—enhancement of dissolution rate by solvent deposition method, effect of drug-to-excipient ratio

A solvent deposition system is a solid preparation in which a drug is deposited from a solvent on the surface of a matrix. This step is usually done by simple evaporation of the solvent used for distribution of the drug onto the matrix. Biopharmaceutical aspects of this technique were considered by Termansen (1), who stated that the purpose of preparing a formulation of linguets of methyltestosterone in this way was to obtain small methyltestosterone particles having satisfactory absorption.

Solvent deposition systems were described and characterized previously (2, 3). The term "minuscular form" was introduced to describe "that the drug has undergone molecular micronization when it is dispersed on the extensive surface of a microparticulate adsorbent." It was concluded (2, 3) that fast drug dissolution is obtained from solvent deposition systems.

The purpose of the present report is to emphasize the importance of a low drug-to-excipient weight ratio when the solvent deposition technique must be considered as an optimal method of increasing dissolution rates of slightly soluble drugs.

EXPERIMENTAL

Materials—Soluble, swelling, and adsorptive excipients were used. The specific surface areas, determined by the gas adsorption technique (4), were: lactose (particles less than 50 μm), 0.50 m^2/g; lactose (particles less than 150 μm), 0.20 m^2/g; potato starch, 0.20 m^2/g; and silicon dioxide[1], 190 m^2/g.

A polyethylene 12-tridecyl ether urea complex[2] (I) was used. All solvents and other substances were pharmacopeial or analytical grade.

Solvent Deposition Systems—The preparations were made in 10–50-g portions by wetting the excipients with solutions of the drug in organic solvents. The solvents were evaporated at room temperature with frequent stirring, and the mixtures were passed through a 200-μm sieve (70 mesh).

To avoid phenylbutazone undergoing fast air-oxidation during excipient application, these systems were prepared in a nitrogen atmosphere (4). The solvent was acetone. The size of the lactose particles was less than 50 μm.

For norethindrone, the solvent was chloroform and the size of the lactose particles was less than 150 μm. For digoxin, the solvent was chloroform–methanol (1:1) and the size of the lactose particles was less than 150 μm. Aggregates of digoxin preparations were broken by passage through a 150-μm sieve (100 mesh).

Dissolution Rate—Determinations of dissolution rates, at the indicated wavelengths, of the preparations used samples equivalent to 8 mg of phenylbutazone (237 nm), 8 mg of norethindrone (248 nm), and 20 mg of digoxin (222 nm). Tests were conducted at 37 ± 0.2° in a beaker apparatus with a magnetic stirrer (3 × 0.6 cm) at 509 rpm. The dissolution medium was 1000 ml of 0.1 *N* HCl containing 0.05% of I.

Establishment of reproducible wettability, *etc.*, was done as described previously (4). The dissolution profiles given in the figures are means of six tests. On the average, the relative standard deviation was about 2%, varying from 0.6 to 4.0%.

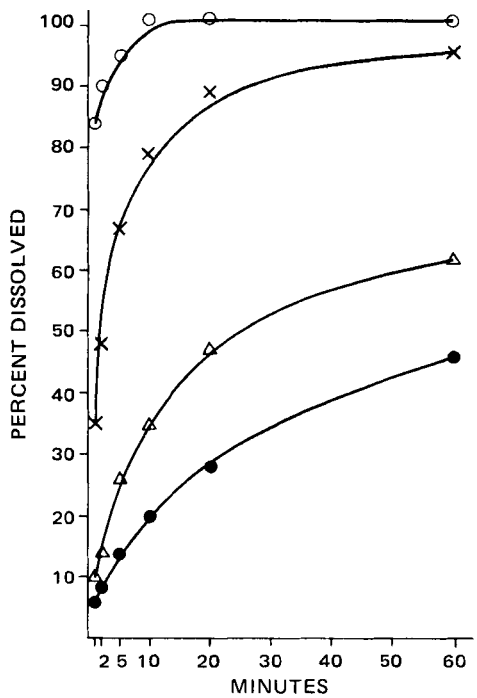

Figure 1—*Dissolution profiles of phenylbutazone solvent deposited on lactose (particle size less than 50 μm). Key: ○, 2% phenylbutazone; ×, 10% phenylbutazone; △, 50% phenylbutazone; and ●, 75% phenylbutazone.*

RESULTS AND DISCUSSION

Figures 1–3 show the influence of the drug-to-excipient ratio on the dissolution rate of systems using phenylbutazone as a model substance. It is almost insoluble in 0.1 *N* HCl (14 mg/liter, 37°), and it crystallizes into needles easily identifiable by microscopy. Figure 4 shows some typical scanning electron micrographs of the systems, indicating crystallization processes with crystals and aggregates of sizes that increase with an increasing drug content. The starch systems are preferred for the illustration since the differentiation of drug and excipient is clear. Similar

[1] Aerosil 200.
[2] Renex 35, Atlas Powder Co.

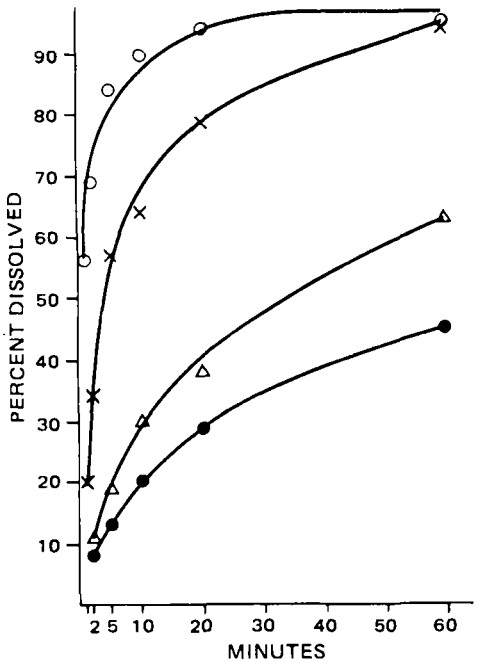

Figure 2—*Dissolution profiles of phenylbutazone solvent deposited on potato starch. Key: ○, 2% phenylbutazone; ×, 10% phenylbutazone; △, 50% phenylbutazone; and ●, 75% phenylbutazone.*

micrographs of the silicon dioxide systems show that pure minuscular preparations are obtained at the drug-to-excipient ratios of 2 and 10%, while large phenylbutazone crystals are predominant in the 50 and 75% systems.

The very extensive surface of silicon dioxide makes it possible to prepare systems with the drug present as small submicrometer particles or as a molecular coating at higher drug-to-excipient ratios than are found for lactose and starch. However, phenylbutazone adsorption onto the insoluble silicon dioxide surface takes place (Fig. 3) most evidently for the low drug-to-excipient ratio. Similar drug adsorption to silicon dioxide in 0.1 *N* HCl was observed for several drugs, particularly for diethylstilbestrol and polythiazide. Therefore, the use of silicon dioxide as an excipient in solvent deposition systems is somewhat limited.

The conclusions based on the experiments with phenylbutazone (Figs. 1–3) are valid for any drug being dissolution rate tested at varying drug-to-excipient ratios. Examples using lactose as the excipient are shown in Figs. 5 and 6. Official tablets of norethindrone or digoxin are usually prepared by solvent deposition techniques to achieve a satisfactory content uniformity for the solid dosage forms of low dosages. Both drugs are very slightly soluble in 0.1 *N* HCl, but drugs of higher water

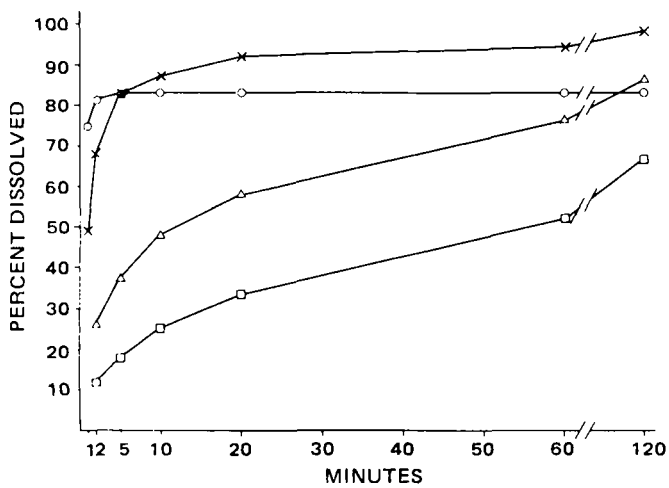

Figure 3—*Dissolution profiles of phenylbutazone solvent deposited on silicon dioxide. Key: ○, 2% phenylbutazone; ×, 10% phenylbutazone; △, 50% phenylbutazone; and □, 75% phenylbutazone.*

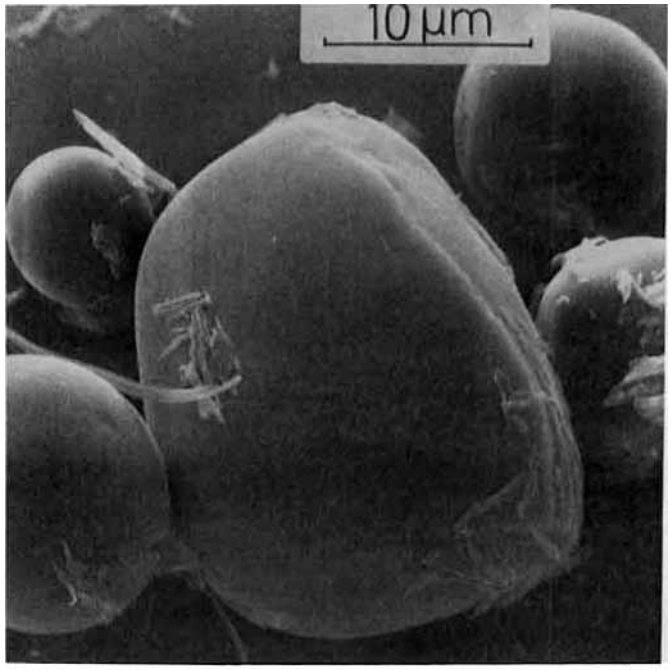

a

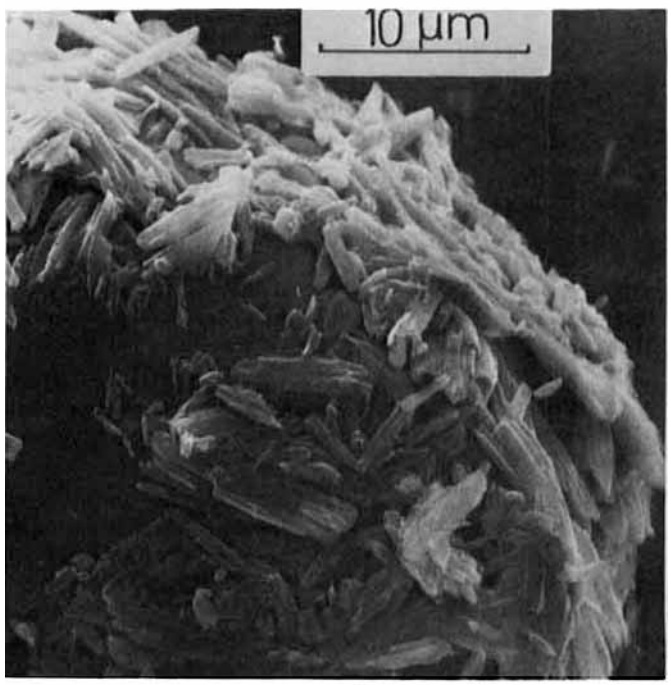

b

Figure 4—*Scanning electron micrographs of phenylbutazone solvent deposited on 90% (a) and 50% (b) potato starch.*

solubility also have been examined, *e.g.*, aspirin. However, because of the higher solubility and good wettability of such solvent-deposited drugs, the dissolution rates of the systems become rather fast; even large particles of 100–200 μm are prevalent when higher drug-to-excipient ratios are used.

Results of dissolution studies on solvent-deposited digoxin and hydrocortisone on lactose were reported and compared to frictionally deposited triturations and to simple blends using a rotating-basket apparatus (60 rpm) (5, 6). The investigators found that the solvent-deposited triturations dissolved more rapidly than the simple blends but slower than the frictionally deposited triturations, although the drug-to-excipient ratio was rather low (1:20).

The dissolution profiles of solvent-deposited and frictionally deposited digoxin and hydrocortisone on lactose (1:20) gave no significant differ-

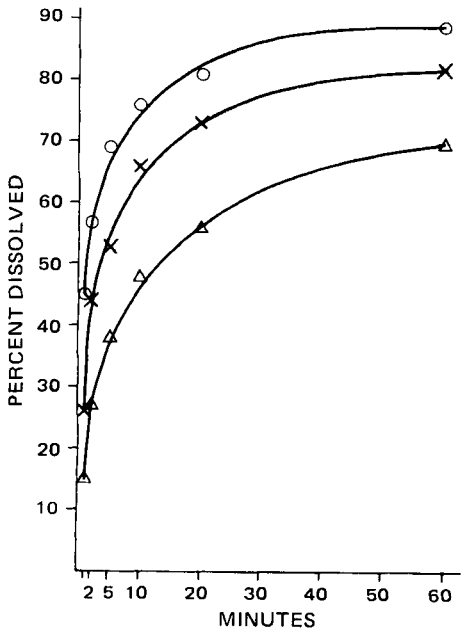

Figure 5—*Dissolution profiles of norethindrone solvent deposited on lactose (particle size less than 150 μm). Key: ○, 2% norethindrone; ×, 10% norethindrone; and △, 20% norethindrone.*

ences when the experiments were carried out in the present beaker apparatus. This result points to the need for caution in interpreting experimental data, because factors such as hydrodynamics and granule size may determine the distinguishability of different formulations.

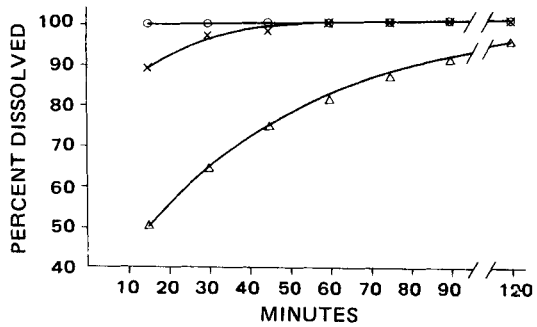

Figure 6—*Dissolution profiles of digoxin solvent deposited on lactose (particle size less than 150 μm). Key: ○, 1% digoxin; ×, 5% digoxin; and △, 25% digoxin.*

REFERENCES

(1) J. B. Termansen, *Arch. Pharm. Chemi*, **66**, 1214 (1959).

(2) D. C. Monkhouse and J. L. Lach, *J. Pharm. Sci.*, **61**, 1430 (1972).

(3) *Ibid.*, **61**, 1435 (1972).

(4) H. Johansen and N. Møller, *Arch. Pharm. Chemi Sci. Ed.*, **4**, 114 (1976).

(5) C. Ampolsuk, J. V. Mauro, A. A. Nyhuis, N. Shah, and C. I. Jarowski, *J. Pharm. Sci.*, **63**, 117 (1974).

(6) N. Shah, R. Pytelewski, H. Eisen, and C. I. Jarowski, *ibid.*, **63**, 339 (1974).

New *In Vivo* Evidence for Narcotic Agonistic Property of Leucine-Enkephalin

HEMENDRA N. BHARGAVA

Received February 28, 1977, from the *Department of Pharmacognosy and Pharmacology, College of Pharmacy, University of Illinois at the Medical Center, Chicago, IL 60612.* Accepted for publication April 7, 1977.

Abstract □ Administration of leucine-enkephalin or morphine to mice rendered dependent on morphine by pellet implantation inhibited the naloxone-precipitated abstinence syndrome. The withdrawal jumping response was inhibited by morphine or leucine-enkephalin; however, both failed to inhibit withdrawal defecation and rearing behavior. On a molar basis, leucine-enkephalin was half as potent as morphine in inhibiting the abstinence syndrome. New *in vivo* pharmacological evidence for narcotic agonist-like activity of leucine-enkephalin is provided.

Keyphrases □ Leucine-enkephalin—narcotic agonist activity evaluated, mice □ Narcotic activity—leucine-enkephalin evaluated, mice

The discovery of specific opiate receptors in brain and other opiate-sensitive tissues suggested the possible existence of endogenous ligands (1–3). Two pentapeptides, methionine-enkephalin and leucine-enkephalin, were identified (4) and postulated to be endogenous ligands for the opiate receptors in mammalian brain (5–8). Both peptides mimic the ability of morphine to inhibit electrically induced contractions of the guinea pig ileum and mouse vas deferens. These inhibitory effects are antagonized by the opiate antagonist, naloxone (4). Enkephalins also inhibit the stereospecific receptor binding of naloxone in brain homogenate (4). The binding of enkephalins to the opiate receptor is inhibited by a high sodium-ion concentration and enhanced by a high manganese-ion concentration, a response characteristic for opiate agonists (9).

Enkephalins also produce analgesia when administered into the lateral ventricles of rats (10, 11). It has been suggested that enkephalin and morphine receptor sites for analgesia may be similar or identical (12, 13). Recently, methionine-enkephalin was shown to suppress antagonist-induced morphine abstinence in morphine-dependent mice (14). The present report presents new *in vivo* evidence for the similarity of action of morphine and leucine-enkephalin.

EXPERIMENTAL

Male Swiss-Webster mice[1], 25–30 g, were maintained on food and water *ad libitum* in a room maintained on 12-hr light–dark cycles at an ambient temperature of 23 ± 1° and a humidity of 65 ± 2%. Mice were rendered

[1] Scientific Small Laboratories, Arlington Heights, Ill.

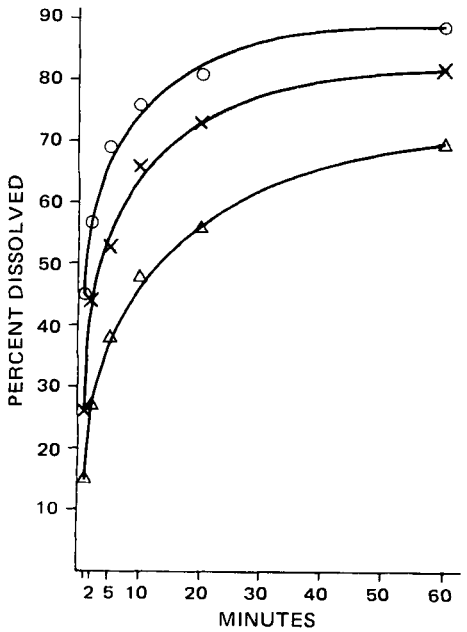

Figure 5—*Dissolution profiles of norethindrone solvent deposited on lactose (particle size less than 150 μm). Key: ○, 2% norethindrone; ×, 10% norethindrone; and △, 20% norethindrone.*

ences when the experiments were carried out in the present beaker apparatus. This result points to the need for caution in interpreting experimental data, because factors such as hydrodynamics and granule size may determine the distinguishability of different formulations.

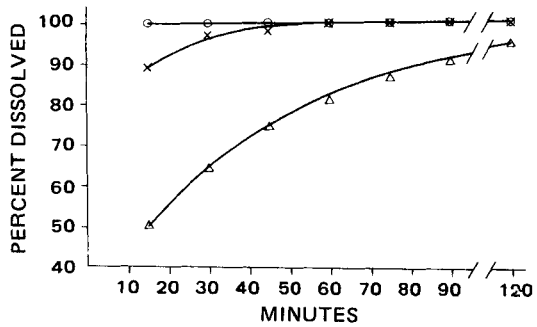

Figure 6—*Dissolution profiles of digoxin solvent deposited on lactose (particle size less than 150 μm). Key: ○, 1% digoxin; ×, 5% digoxin; and △, 25% digoxin.*

REFERENCES

(1) J. B. Termansen, *Arch. Pharm. Chemi*, **66**, 1214 (1959).

(2) D. C. Monkhouse and J. L. Lach, *J. Pharm. Sci.*, **61**, 1430 (1972).

(3) *Ibid.*, **61**, 1435 (1972).

(4) H. Johansen and N. Møller, *Arch. Pharm. Chemi Sci. Ed.*, **4**, 114 (1976).

(5) C. Ampolsuk, J. V. Mauro, A. A. Nyhuis, N. Shah, and C. I. Jarowski, *J. Pharm. Sci.*, **63**, 117 (1974).

(6) N. Shah, R. Pytelewski, H. Eisen, and C. I. Jarowski, *ibid.*, **63**, 339 (1974).

New *In Vivo* Evidence for Narcotic Agonistic Property of Leucine-Enkephalin

HEMENDRA N. BHARGAVA

Received February 28, 1977, from the *Department of Pharmacognosy and Pharmacology, College of Pharmacy, University of Illinois at the Medical Center, Chicago, IL 60612.* Accepted for publication April 7, 1977.

Abstract □ Administration of leucine-enkephalin or morphine to mice rendered dependent on morphine by pellet implantation inhibited the naloxone-precipitated abstinence syndrome. The withdrawal jumping response was inhibited by morphine or leucine-enkephalin; however, both failed to inhibit withdrawal defecation and rearing behavior. On a molar basis, leucine-enkephalin was half as potent as morphine in inhibiting the abstinence syndrome. New *in vivo* pharmacological evidence for narcotic agonist-like activity of leucine-enkephalin is provided.

Keyphrases □ Leucine-enkephalin—narcotic agonist activity evaluated, mice □ Narcotic activity—leucine-enkephalin evaluated, mice

The discovery of specific opiate receptors in brain and other opiate-sensitive tissues suggested the possible existence of endogenous ligands (1–3). Two pentapeptides, methionine-enkephalin and leucine-enkephalin, were identified (4) and postulated to be endogenous ligands for the opiate receptors in mammalian brain (5–8). Both peptides mimic the ability of morphine to inhibit electrically induced contractions of the guinea pig ileum and mouse vas deferens. These inhibitory effects are antagonized by the opiate antagonist, naloxone (4). Enkephalins also inhibit the stereospecific receptor binding of naloxone in brain homogenate (4). The binding of enkephalins to the opiate receptor is inhibited by a high sodium-ion concentration and enhanced by a high manganese-ion concentration, a response characteristic for opiate agonists (9).

Enkephalins also produce analgesia when administered into the lateral ventricles of rats (10, 11). It has been suggested that enkephalin and morphine receptor sites for analgesia may be similar or identical (12, 13). Recently, methionine-enkephalin was shown to suppress antagonist-induced morphine abstinence in morphine-dependent mice (14). The present report presents new *in vivo* evidence for the similarity of action of morphine and leucine-enkephalin.

EXPERIMENTAL

Male Swiss-Webster mice[1], 25–30 g, were maintained on food and water *ad libitum* in a room maintained on 12-hr light–dark cycles at an ambient temperature of 23 ± 1° and a humidity of 65 ± 2%. Mice were rendered

[1] Scientific Small Laboratories, Arlington Heights, Ill.

morphine dependent by the subcutaneous implantation (15) of a morphine pellet containing 75 mg of morphine base. Three days after implantation, either saline or various doses of leucine-enkephalin[2] in saline were injected intracerebrally (16) in volumes such that each mouse received 0.5 μl/g. Intracerebral injections of India ink were made in 10 mice, and the brain sections revealed that the injection sites were the ventricles.

To precipitate withdrawal, naloxone hydrochloride was injected subcutaneously immediately after the administration of saline or leucine-enkephalin. Three signs of morphine withdrawal—*viz.*, stereotyped jumping behavior, withdrawal defecation, and rearing behavior, were monitored. Stereotyped jumping was used as a quantal response for estimating the median effective dose of naloxone (ED_{50}). After naloxone administration, the mice were placed on a circular platform and the percentage of mice jumping off the platform, the number of fecal boli, and the number of rearings in 15 min were noted for each dose of naloxone.

Eight mice were used for each of the three doses of naloxone to calculate the naloxone ED_{50}, the potency ratio, their 95% confidence limits, and the statistical significance (p values) (17). Similar experiments were conducted with various doses of morphine sulfate substituting for leucine-enkephalin.

RESULTS AND DISCUSSION

Leucine-enkephalin inhibited the naloxone-precipitated abstinence syndrome in morphine-dependent mice. Stereotyped jumping behavior was significantly ($p < 0.05$) inhibited by all doses used. An inverse relationship previously was observed between the degree of dependence and naloxone ED_{50} (18–21). As shown in Table I, leucine-enkephalin increased the naloxone ED_{50} by more than twofold at three different doses (1.75, 3.5, and 7.0 μmoles/kg). With increasing doses of leucine-enkephalin, an apparent increase in the naloxone ED_{50} was noted. However, no significant differences could be seen between the three doses. Earlier investigators (10) also failed to obtain dose–effect data with leucine-enkephalin in determining its analgesic activity.

Leucine-enkephalin was inactive in inhibiting other abstinence signs like withdrawal defecation or rearing behavior. This effect on withdrawal defecation can perhaps be explained by the fact that the drug is active for only 5–10 min when administered intracerebrally, as is evident by its analgesic activity (10). Presumably, it is inactivated rapidly by the proteolytic enzymes in the brain. Also, the solubility of enkephalin may be such that it cannot enter the bloodstream from the brain in sufficient concentrations to affect the intestinal movements.

Administration of morphine also inhibited the withdrawal jumping response. A dose of 0.875 μmole of morphine sulfate/kg increased the naloxone ED_{50}; however, this value was not statistically significant from that for the saline controls. The higher dose of morphine sulfate (1.75 μmoles/kg) significantly inhibited the jumping response, as evidenced by a 4.5-fold increase in naloxone ED_{50} over the saline control. Both doses of morphine sulfate did not produce a significant effect on withdrawal defecation or rearing during the 15-min observation. Comparison of the ED_{50} of naloxone at the same dose (1.75 μmoles/kg) of leucine-enkephalin and morphine showed that morphine sulfate was twice as effective on a molar basis as leucine-enkephalin in inhibiting the morphine abstinence syndrome.

Leucine-enkephalin can inhibit a specific sign of naloxone-precipitated withdrawal in morphine-dependent mice. The withdrawal jumping is a highly characteristic response and is widely used (18–21) for determining the degree of dependence and the intensity of the narcotic abstinence syndrome. In these studies, leucine-enkephalin was half as active as morphine on a molar basis (at 1.75 μmoles/kg) in inhibiting the jumping response. For analgesic activity, morphine was more potent than enkephalin by an order of magnitude (10) or equipotent (11) in the rat. At the doses tested, both leucine-enkephalin and morphine were inactive in producing an inhibitory effect on withdrawal defecation and rearing behavior.

There is strong evidence suggesting morphine and enkephalins behave similarly *in vitro;* however, *in vivo* evidence for similarity is less abundant. The present investigation provides new *in vivo* pharmacological evidence of the narcotic agonistic property of leucine-enkephalin.

[2] Bachem, Inc., Marina Del Rey, Calif.

Table I—Comparison of the Effects of Leucine-Enkephalin and Morphine Sulfate, Administered Intracerebrally, on the Naloxone ED_{50} in Morphine-Dependent Mice[a]

Treatment	Dose, μmoles/kg	Naloxone ED_{50}, μg/kg	Potency Ratio[b]
Saline	—	166 (109–255)	—
Morphine sulfate	0.875	200 (117–341)	1.20 (0.62–2.34)
	1.75	729 (476–1117)	4.39 (2.47–7.81)[c]
Leucine-enkephalin	1.75	366 (239–561)	2.20 (1.20–3.96)[c]
	3.50	387 (242–620)	2.33 (1.23–4.31)[c]
	7.00	409 (261–643)	2.46 (1.37–4.43)[c]

[a] The figures in parentheses represent the 95% confidence limits. [b] Potency ratios were calculated according to Ref. 17 for comparison of ED_{50} values in drug-treated groups with the saline control. [c] $p < 0.05$ *versus* saline controls.

REFERENCES

(1) A. Goldstein, L. I. Lowney, and B. K. Pal, *Proc. Natl. Acad. Sci. USA,* **68,** 1742 (1971).

(2) E. J. Simon, J. M. Hiller, and I. Edelman, *ibid.,* **70,** 1947 (1973).

(3) C. B. Pert and S. H. Snyder, *ibid.,* **70,** 2243 (1973).

(4) J. Hughes, T. W. Smith, H. W. Kosterlitz, L. A. Fothergill, B. A. Morgan, and H. R. Morris, *Nature,* **258,** 577 (1975).

(5) L. Terenius and A. Wahlstrom, *Acta Pharmacol. Toxicol.,* **35,** 55 (1974).

(6) J. Hughes, *Brain Res.,* **88,** 295 (1975).

(7) G. W. Pasternak, R. Goodman, and S. H. Snyder, *Life Sci.,* **16,** 1765 (1975).

(8) H. Teschemacher, K. E. Opheim, B. M. Cox, and A. Goldstein, *ibid.,* **16,** 1771 (1975).

(9) R. Simantov and S. H. Snyder, *ibid.,* **18,** 781 (1976).

(10) J. D. Belluzzi, N. Grant, V. Garsky, D. Sarantakis, C. D. Wise, and L. Stein, *Nature,* **260,** 625 (1976).

(11) J. B. Malick and J. M. Goldstein, *Pharmacologist,* **18,** 120 (1976).

(12) H. W. Kosterlitz and J. Hughes, *Life Sci.,* **17,** 91 (1975).

(13) H. Akil and J. C. Liebeskind, *Brain Res.,* **94,** 279 (1975).

(14) H. N. Bhargava, *Eur. J. Pharmacol.,* **41,** 81 (1977).

(15) *Ibid.,* **36,** 259 (1976).

(16) T. J. Haley and W. G. McCormick, *Br. J. Pharmacol.,* **12,** 12 (1957).

(17) J. T. Litchfield and F. Wilcoxon, *J. Pharmacol. Exp. Ther.,* **96,** 99 (1949).

(18) E. L. Way, H. H. Loh, and F. H. Shen, *ibid.,* **167,** 1 (1969).

(19) Y. Maruyama and A. E. Takemori, *ibid.,* **185,** 602 (1973).

(20) D. L. Francis and F. Schneider, *Br. J. Pharmacol.,* **41,** 424p (1971).

(21) H. N. Bhargava, *Psychopharmacology,* **52,** 55 (1977).

ACKNOWLEDGMENTS

The author thanks Dr. Norman R. Farnsworth for his interest, Mr. George Matwyshyn for technical assistance, and Ms. Dorothy Wilson for help in the preparation of this manuscript.

Enhancement of Ampicillin Partition Behavior

A. R. HURWITZ ˣ and C. F. CARNEY

Received October 19, 1976, from the *Pharmacy Research and Development Department, Ayerst Laboratories, Inc., Rouses Point, NY 12979.* Accepted for publication April 12, 1977.

Abstract □ Several ion-pair or adduct forming additives that enhanced ampicillin partition behavior were identified and evaluated. At pH 3, picric acid and trichloroacetic acid increased the ampicillin aqueous–octanol partition coefficient 250 and 30 times, respectively. At pH 7, quaternary compounds gave the most significant increases in the partition coefficient. Values for an aqueous pH 7 chloroform system increased from zero in the absence of additives to 2.28, 1.86, 1.82, and 1.70 for equimolar amounts of benzalkonium, tetraheptylammonium, benzethonium, and cetalkonium chlorides, respectively. Extraction of ampicillin from aqueous pH 7 solution was possible by adding a quaternary agent in an equimolar amount. However, extraction of ampicillin from plasma required large molar excesses. Tetraheptylammonium chloride was added at a molar concentration 10^3 times greater than that of the ampicillin. Plasma samples spiked at the 3-μg/ml level gave 93% recovery (*CV* 6.7%, $n = 16$) when extracted three times. The extracts were quantitated by TLC.

Keyphrases □ Ampicillin—aqueous–octanol partition coefficient, effect of various ion-pair or adduct forming additives □ Partition coefficients, aqueous–octanol—ampicillin, effect of various ion-pair or adduct forming additives □ Ion-pair forming agents—effect on aqueous–octanol partition coefficient of ampicillin □ Adduct forming agents—effect on aqueous–octanol partition coefficient of ampicillin □ Antibacterials—ampicillin, aqueous–octanol partition coefficient, effect of various ion-pair or adduct forming additives

The aqueous–octanol pH partition profile of ampicillin in the pH 3–8 range was determined previously (1). The apparent partition coefficient was <0.01 and independent of pH because of the ampholytic character of the drug.

Common anionic penicillins usually have been extracted as the acids at pH ~2 with solvents such as chloroform (2). In some cases, solutions at pH up to 5 have been extracted after the addition of ammonium sulfate for its salting-out effect (3). An improved extraction was obtained by adding ion-pair or adduct forming agents (4). However, there has been no apparent attempt to enhance the partition behavior of ampholytic penicillins, such as ampicillin, with ion-pair or adduct forming agents.

Several acids and quaternary ammonium compounds were identified and evaluated for their ability to enhance ampicillin partitioning. The results were used to develop a specific chemical determination of plasma ampicillin levels.

EXPERIMENTAL

Materials—Ampicillin trihydrate[1] and tetradecylamine[2], practical grade, were used as received. All other reagents and solvents were analytical reagent, reagent, or compendial grade and were used directly. Phosphate (0.1 *M*) buffer solutions were prepared at pH 7.0.

Additives to Enhance Partitioning—Equimolar amounts (5.7×10^{-3} *M*) of picric acid or trichloroacetic acid and ampicillin were combined in a buffer solution before extraction with octanol. After separation, the octanol phase was extracted three times with a buffer solution. The ampicillin content of the combined extracts was determined by a colorimetric assay (5).

Solutions of quaternary additives were prepared in chloroform or ethyl acetate and shaken with buffer solutions of ampicillin. Quaternary additives and ampicillin were used in equimolar quantities (5.7×10^{-3} *M*). This procedure gave higher distribution ratios than when the quaternary additive was dissolved in the buffer prior to extraction. After equilibration, an aliquot of the organic phase was evaporated to dryness and reconstituted with buffer. This extract and the aqueous phase were assayed by a colorimetric method (5).

Preparation of Tetraheptylammonium Acetate—Equimolar amounts of silver acetate and tetraheptylammonium iodide were added to water and shaken with a known volume of chloroform for 30 min. The mixture was centrifuged, and the chloroform phase was withdrawn.

Preparation of Tetraheptylammonium Hydroxide—A small, analytical, straight glass column was packed with anion-exchange resin[3] and washed extensively with 0.1 *N* NaOH until a portion of the eluate acidified with nitric acid showed no precipitate when silver nitrate solution was added. The column was then washed with 500 ml of water. An aqueous solution of tetraheptylammonium chloride was added to the column and eluted with more water. The acidified eluate yielded no precipitate with silver nitrate. The eluate was shaken with chloroform to transfer the tetraheptylammonium hydroxide into the chloroform layer.

Assay of Quaternary Cation Concentration—An aliquot of chloroform or the aqueous phase was transferred to a glass-stoppered erlenmeyer flask. Fifteen milliliters of 6 *N* H_2SO_4 was added, and the water and chloroform volumes were each adjusted to 30 ml. Finally, 1 ml of 0.01% methyl yellow in alcohol was added. The quaternary ammonium compound was titrated with sodium lauryl sulfate solution to a salmon-pink color in the chloroform layer.

The titrant was standardized in the same fashion with known amounts of the individual quaternary ammonium compounds. Calculations of concentrations in each case were based on this standardization.

Spiked Plasma Extraction Procedure—A 12-μl aliquot of a 1-mg/ml ampicillin aqueous solution was added to 4 ml of plasma in a small separator and mixed to give a concentration of 3 μg/ml of plasma. Four milliliters of a 6–10-mg/ml tetraheptylammonium chloride in chloroform solution was added, and the separators were stoppered and gently shaken by hand for 3 min. After the phases separated, the organic phase was drained into a 35-ml conical centrifuge tube. This procedure was repeated twice with 4-ml portions of the chloroform solution, and the pooled chloroform was evaporated to dryness with the aid of a nitrogen stream. The residue was transferred to a 1-ml volumetric flask and diluted to volume with chloroform.

TLC Assay—Any GLC, TLC, or high-pressure liquid chromatographic (HPLC) procedure with adequate specificity and sensitivity could be applied to the extraction residues. In this study, extracts were analyzed by a TLC method based on a previously developed procedure[4]. Ampicillin standard solution and reconstituted extracts were applied to separate labeled channels of a silica gel plate. The developing solvent was ethyl acetate–acetone–water–formic acid (65:15:13:9).

RESULTS AND DISCUSSION

Additives to Enhance Partitioning—At low pH, the ampicillin amine cation (pKa = 7.25) is present while at high pH the carboxylic anion (pKa = 2.66) is present. At pH 4.9, the compound exists almost completely as the zwitterion. It has been claimed that the anionic species is the most efficiently partitioned (6). Since ampicillin exists either in ionized or zwitterion forms at common pH values, the search for compounds to enhance its partition behavior centered on potential ion-pair formers.

Modin and Schroder-Nielsen (4) reported ion-pair partitioning for penicillin V, penicillin G, and other anionic penicillins. To determine if

[1] USP grade.

[2] Eastman.

[3] Dowex 1-X8, J. T. Baker Chemical Co.

[4] G. Krol, R. Anstey, and J. Gurak, Analytical Research and Development Department, Ayerst Laboratories, Rouses Point, NY 12979.

Table I—Aqueous Chloroform or Aqueous Ethyl Acetate Apparent Partition Coefficient Values for Ampicillin with the Addition of Several Quaternary Ammonium Chlorides at pH 7.0 ([Ampicillin]$_i$ and [Quaternary Ammonium Chloride]$_i$ = 5.7×10^{-3} *M*)

Quaternary Compound	Partition Coefficient, Chloroform	Partition Coefficient, Ethyl Acetate
Benzalkonium	2.28	—
Benzethonium	1.82	1.45
Tetraheptyl-ammonium	1.86[a]	0.67[a]
Cetalkonium	1.70	0.30[a]
Cetylpyridinium	0.62	—

[a] Two or more determinations.

Table II—Chloroform Apparent Partition Coefficient Values of Ampicillin at pH 7.0 with Tetraheptylammonium and Various Anionic Counterions ([Ampicillin]$_i$ and [Tetraheptylammonium]$_i$ = 5.7×10^{-3} *M*)

Anion	Partition Coefficient[a]
Acetate	4.78
Hydroxide	1.74
Chloride	1.80
Bromide	0.46
Iodide	0.016

[a] Average of two determinations except iodide.

ion-pair partitioning of ampicillin would be possible, many candidate cationic and anionic compounds were screened.

At pH 3, the anionic compounds trichloroacetic acid, a carboxylic acid (pKa = 0.70), and picric acid, a phenol (pKa = 0.38), increased the apparent partition coefficient in octanol about 30 and 250 times, respectively. Pamoic, 1,2-ethanedisulfonic, bromoacetic, 3-bromopropionic, chloroacetic, benzilic, and diphenylacetic acids offered no enhanced extraction of ampicillin into octanol at pH 3. Trichloroacetic and picric acids increased the aqueous–chloroform partition coefficient from 0 to 0.010 and 0.011, respectively, and the aqueous–ethyl acetate partition coefficient from 0 to 0.062 and 4.64, respectively.

Several long chain (>six carbons) alkylammonium cationic compounds were evaluated at pH 7. The apparent partition coefficient values determined upon quaternary compound addition to aqueous chloroform and aqueous ethyl acetate systems are shown in Table I. The apparent slight variation in chloroform partition coefficients compared to the fivefold difference in ethyl acetate partition coefficients between cetalkonium and benzethonium is not understood at this time. Chloroform, a good solvent for ion-pairs, may have had a leveling effect.

Aqueous chloroform partition coefficient values increased when the concentration of quaternary compound added to the organic phase was increased while the ampicillin concentration in the aqueous phase was kept constant. When the ratio of the initial tetraheptylammonium chloride concentration to the initial ampicillin concentration was increased from 1 to 2.08 to 3.30, the aqueous chloroform partition coefficient increased from 1.85 to 4.90 to 6.77. Similarly, when the ratio of tetraheptylammonium acetate to ampicillin was increased from 0.95 to 1.85 to 2.76, aqueous ethyl acetate partition coefficient values increased from 3.0 to 7.5 to 8.9.

No significant increase in the partition coefficient in octanol, chloroform, or ethyl acetate systems was found for urea; proline; guanosine; hexadecylamine; tetradecylamine; tetrabutylammonium hydroxide, chloride, bromide, and iodide; nonyltrimethylammonium bromide; and tridodecylammonium acetate. For example, with added nonyltrimethylammonium bromide, the aqueous–chloroform and the aqueous–ethyl acetate partition coefficient values were only 0.05 and 0.04, respectively. With added tridodecylammonium acetate, the aqueous–chloroform partition coefficient value was 0.07.

Effect of Quaternary Counterion—Tetraheptylammonium was purchased or prepared with various counterions. The water–chloroform partition coefficient values as a function of the associated anion are shown in Table II. Although the largest partition coefficient was observed with acetate, a two-order of magnitude increase in the partition coefficient occurred as the halogen molecular weight decreased.

A similar variation with the halogen species was previously reported (7) in the dye extraction of long chain amines. Anion interference was observed for the analysis of long chain amines by the dye extraction method because of competition between the anions and the dye for extraction into the organic phase. Acetate did not interfere. For the other anions studied, the degree of interference followed the order $I^- > Br^- > Cl^-$. This order correlated with that for the extraction of the anions into chloroform by ammonium ions (8). Since a similar interference occurs for ampicillin–tetraheptylammonium chloride extraction, the observed partition coefficient values in the presence of different anions are in the anticipated order.

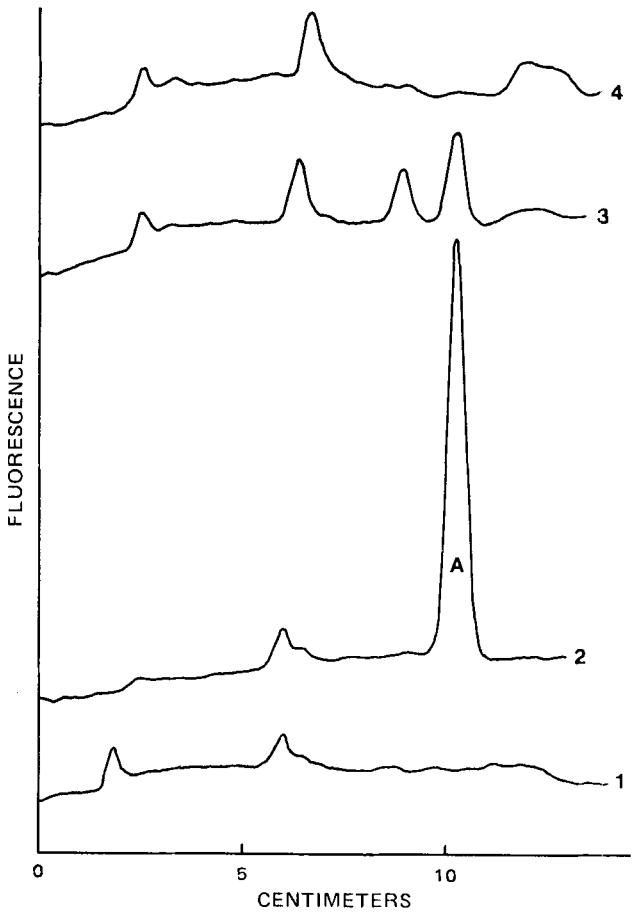

Figure 1—*Thin-layer chromatograms of ampicillin (A). Key: 1, extract of blank human plasma; 2, ampicillin standard spotted from water; 3, extract from plasma of ampicillin partially degraded in acid before spiking; and 4, extract from plasma of ampicillin totally degraded in base before spiking.*

Extraction of Ampicillin from Plasma—Human plasma and dog plasma and serum were spiked at the 3-μg/ml level. Tetraheptylammonium chloride at a molar ratio of about 2000:1 ampicillin was the optimum level for extractions from human plasma. No apparent advantage occurred when the tetraheptylammonium chloride concentration was raised above this level. However, below this level, recoveries of ampicillin fell off quickly. Neither cetalkonium nor benzalkonium at molar ratios up to 2000:1 aided plasma ampicillin extraction. Tetraheptylammonium acetate showed a partition coefficient 2.5 times greater than that of tetraheptylammonium chloride in aqueous systems. It could be considered for plasma extraction, but it is not commercially available.

The percent recovery from human plasma was 60% after a single extraction, 88% after two extractions, and 93% after three extractions. The coefficient of variation for three extractions (n = 16) was 6.7%. After three extractions, recovery was 92% from dog serum and 84% from dog plasma. Possibly more interfering substances are present in plasma than in serum. However, the dog serum and plasma data were from single determinations. With the outlined procedure, quantitation of a concentration of 0.5 μg of ampicillin/ml of plasma was possible. By suitable alterations of the procedure, this quantitation limit might be lowered by a factor of two or three.

Extractions of decomposed samples of ampicillin gave anticipated recoveries of the intact species. Some decomposition products were also extracted but not quantitatively (Fig. 1).

Analysis of Plasma Ampicillin Extracts—GLC, TLC, HPLC, and adsorption chromatographic procedures have been developed for ampicillin. However, these methods cannot be adapted for the detection and quantitation of ampicillin and its metabolites in plasma since sensitivities are not adequate. The best sensitivity attained was 10 μg/ml by HPLC (9). Fluorescence methods with a sensitivity at 0.1 μg/ml have been used (10–12). However, these methods at best are specific for intact ampicillin but do not measure decomposition products or metabolites. Enhanced extraction with tetraheptylammonium chloride followed by chromatography offers the possibility of quantitating plasma ampicillin levels in the 1-μg/ml range.

Metabolites could also be extracted, followed by identification and quantitation. The procedure could be modified for the separation of ampicillin from its prodrugs. For example, pivampicillin could be easily separated with a prior chloroform extraction. Ampicillin would then be quantitated using the described procedure.

REFERENCES

(1) C. Carney and A. Hurwitz, *J. Pharm. Sci.*, **66**, 294 (1977).

(2) G. Boxer and P. Everett, *Anal. Chem.*, **21**, 670 (1949).

(3) S. Pan, *ibid.*, **26**, 1438 (1954).

(4) R. Modin and M. Schroder-Nielsen, *Acta Pharm. Suec.*, **8**, 573 (1971).

(5) J. Smith, G. Degrey, and V. Patel, *Analyst*, **92**, 247 (1967).

(6) E. Purich, J. Colaizzi, and R. Poust, *J. Pharm. Sci.*, **62**, 545 (1973).

(7) H. Biswas and B. Mandal, *Anal. Chem.*, **44**, 1636 (1972).

(8) W. Muller and R. Diamond, *J. Phys. Chem.*, **70**, 3469 (1966).

(9) K. Tsuji and J. Robertson, *J. Pharm. Sci.*, **64**, 1542 (1975).

(10) K. Miyazaki, O. Ogino, and T. Arita, *Chem. Pharm. Bull.*, **22**, 1910 (1974).

(11) A. Dverr and H. Schatzmann, *Experientia*, **31**, 503 (1975).

(12) W. Jusko, *J. Pharm. Sci.*, **60**, 728 (1971).

ACKNOWLEDGMENTS

Presented at the Pharmaceutical Analysis Section, APhA Academy of Pharmaceutical Sciences, Orlando meeting, November 1976.

The authors gratefully acknowledge the technical assistance of Mr. F. DiBernardo, Mr. Y. Garceau, and Mr. R. Anstey and the helpful discussions with Dr. J. Hasegawa and Dr. G. Krol.

COMMUNICATIONS

Spectrophotometric Analysis of Binary Mixtures of Antazoline and Naphazoline

Keyphrases □ Antazoline hydrochloride—spectrophotometric analysis simultaneously with naphazoline nitrate in pharmaceutical formulations □ Naphazoline nitrate—spectrophotometric analysis simultaneously with antazoline hydrochloride in pharmaceutical formulations □ Spectrophotometry—analyses, antazoline hydrochloride and naphazoline nitrate, simultaneously in pharmaceutical formulations □ Antihistaminics—antazoline hydrochloride, spectrophotometric analysis simultaneously with naphazoline nitrate in pharmaceutical formulations □ Adrenergic agents—naphazoline nitrate, spectrophotometric analysis simultaneously with antazoline hydrochloride in pharmaceutical formulations

To the Editor:

Two-component spectrophotometric analysis (1) is based on solving a set of two linear equations. Glenn (2) formulated the solution of the two linear equations in terms of absorbance ratios that are independent of concentration. Pernarowski *et al.* (3) used absorbance ratios for the analysis of binary mixtures and derived an equation similar to Glenn's equation. However, these authors (3) assumed that an isoabsorptive point must be chosen to apply their equation. The equation published by Cho and Pernarowski (4) to obtain absolute concentration was derived under the impression that an isoabsorptive point must be present to apply the equation of Pernarowski *et al.* (3). The three published equations (2–4) are consistent with each other and can be applied using any suitably chosen pair of wavelengths. None of the selected wavelengths needs to be an isoabsorptive point.

According to Glenn's limitations (2), if the contribution of one component to the absorption curve of the total mixture is low, erroneous results are obtained whenever the two-wavelength method of analysis is applied. In this connection, we suggest the use of least squares (5) to minimize the instrumental errors during the analysis of the minor component in binary mixtures.

These methods were applied to the determination of antazoline hydrochloride (I) (0.5% w/v) and naphazoline nitrate (II) (0.025% w/v) in nasal drops (6–8) also containing chlorobutanol (0.5% w/v) and sodium chloride (0.6% w/v). Thus, by diluting 1 ml of the nasal drop solution to 50 ml with 0.1 *N* H_2SO_4, measuring the absorbances of 1-cm pathlengths at 281 and 295 nm[1], and applying the Glenn and Cho and Pernarowski equations, the mean percentage recoveries for I were 99.5 ± 1.05 and 99.7 ± 1.24, respectively, for 10 samples; for II, they were 107.1 ± 2.35 and 107.1 ± 2.64, respectively, for 10 samples. The recoveries obtained using the two equations were consistent. The relatively high percentage recoveries obtained for II were due to its low contribution to the absorption curve of the total mixture at the concentration used.

To improve the accuracy and precision for the determination of II, the method of least squares (5) was applied. Fifteen absorbances measured at the wavelengths of 267–295 nm at 2-nm intervals gave the best results (mean ± *SD* = 100.7 ± 1.10) for the determination of II in the same 10 samples. The final wavelengths used covered the peak characteristics of II (8). Neither chlorobutanol nor sodium chloride interfered with the determinations.

(1) H. Heilmeyer, "Spectrophotometry in Medicine," Adam Hilger Ltd., London, England, 1943, p. 7.

(2) A. L. Glenn, *J. Pharm. Pharmacol.*, **12**, 595 (1960).

(3) M. Pernarowski, A. M. Knevel, and J. E. Christian, *J. Pharm. Sci.*, **50**, 943 (1961).

(4) M. J. Cho and M. Pernarowski, *ibid.*, **59**, 1333 (1970).

(5) B. W. Madsen, D. Herbison-Evans, and J. S. Robertson, *J. Pharm. Pharmacol.*, **26**, 629 (1974).

[1] Prolabo spectrophotometer, Jean & Constant, Paris, France.

Analysis of Plasma Ampicillin Extracts—GLC, TLC, HPLC, and adsorption chromatographic procedures have been developed for ampicillin. However, these methods cannot be adapted for the detection and quantitation of ampicillin and its metabolites in plasma since sensitivities are not adequate. The best sensitivity attained was 10 μg/ml by HPLC (9). Fluorescence methods with a sensitivity at 0.1 μg/ml have been used (10–12). However, these methods at best are specific for intact ampicillin but do not measure decomposition products or metabolites. Enhanced extraction with tetraheptylammonium chloride followed by chromatography offers the possibility of quantitating plasma ampicillin levels in the 1-μg/ml range.

Metabolites could also be extracted, followed by identification and quantitation. The procedure could be modified for the separation of ampicillin from its prodrugs. For example, pivampicillin could be easily separated with a prior chloroform extraction. Ampicillin would then be quantitated using the described procedure.

REFERENCES

(1) C. Carney and A. Hurwitz, *J. Pharm. Sci.*, **66**, 294 (1977).

(2) G. Boxer and P. Everett, *Anal. Chem.*, **21**, 670 (1949).

(3) S. Pan, *ibid.*, **26**, 1438 (1954).

(4) R. Modin and M. Schroder-Nielsen, *Acta Pharm. Suec.*, **8**, 573 (1971).

(5) J. Smith, G. Degrey, and V. Patel, *Analyst*, **92**, 247 (1967).

(6) E. Purich, J. Colaizzi, and R. Poust, *J. Pharm. Sci.*, **62**, 545 (1973).

(7) H. Biswas and B. Mandal, *Anal. Chem.*, **44**, 1636 (1972).

(8) W. Muller and R. Diamond, *J. Phys. Chem.*, **70**, 3469 (1966).

(9) K. Tsuji and J. Robertson, *J. Pharm. Sci.*, **64**, 1542 (1975).

(10) K. Miyazaki, O. Ogino, and T. Arita, *Chem. Pharm. Bull.*, **22**, 1910 (1974).

(11) A. Dverr and H. Schatzmann, *Experientia*, **31**, 503 (1975).

(12) W. Jusko, *J. Pharm. Sci.*, **60**, 728 (1971).

ACKNOWLEDGMENTS

Presented at the Pharmaceutical Analysis Section, APhA Academy of Pharmaceutical Sciences, Orlando meeting, November 1976.

The authors gratefully acknowledge the technical assistance of Mr. F. DiBernardo, Mr. Y. Garceau, and Mr. R. Anstey and the helpful discussions with Dr. J. Hasegawa and Dr. G. Krol.

COMMUNICATIONS

Spectrophotometric Analysis of Binary Mixtures of Antazoline and Naphazoline

Keyphrases □ Antazoline hydrochloride—spectrophotometric analysis simultaneously with naphazoline nitrate in pharmaceutical formulations □ Naphazoline nitrate—spectrophotometric analysis simultaneously with antazoline hydrochloride in pharmaceutical formulations □ Spectrophotometry—analyses, antazoline hydrochloride and naphazoline nitrate, simultaneously in pharmaceutical formulations □ Antihistaminics—antazoline hydrochloride, spectrophotometric analysis simultaneously with naphazoline nitrate in pharmaceutical formulations □ Adrenergic agents—naphazoline nitrate, spectrophotometric analysis simultaneously with antazoline hydrochloride in pharmaceutical formulations

To the Editor:

Two-component spectrophotometric analysis (1) is based on solving a set of two linear equations. Glenn (2) formulated the solution of the two linear equations in terms of absorbance ratios that are independent of concentration. Pernarowski *et al.* (3) used absorbance ratios for the analysis of binary mixtures and derived an equation similar to Glenn's equation. However, these authors (3) assumed that an isoabsorptive point must be chosen to apply their equation. The equation published by Cho and Pernarowski (4) to obtain absolute concentration was derived under the impression that an isoabsorptive point must be present to apply the equation of Pernarowski *et al.* (3). The three published equations (2–4) are consistent with each other and can be applied using any suitably chosen pair of wavelengths. None of the selected wavelengths needs to be an isoabsorptive point.

According to Glenn's limitations (2), if the contribution of one component to the absorption curve of the total mixture is low, erroneous results are obtained whenever the two-wavelength method of analysis is applied. In this connection, we suggest the use of least squares (5) to minimize the instrumental errors during the analysis of the minor component in binary mixtures.

These methods were applied to the determination of antazoline hydrochloride (I) (0.5% w/v) and naphazoline nitrate (II) (0.025% w/v) in nasal drops (6–8) also containing chlorobutanol (0.5% w/v) and sodium chloride (0.6% w/v). Thus, by diluting 1 ml of the nasal drop solution to 50 ml with 0.1 *N* H_2SO_4, measuring the absorbances of 1-cm pathlengths at 281 and 295 nm[1], and applying the Glenn and Cho and Pernarowski equations, the mean percentage recoveries for I were 99.5 ± 1.05 and 99.7 ± 1.24, respectively, for 10 samples; for II, they were 107.1 ± 2.35 and 107.1 ± 2.64, respectively, for 10 samples. The recoveries obtained using the two equations were consistent. The relatively high percentage recoveries obtained for II were due to its low contribution to the absorption curve of the total mixture at the concentration used.

To improve the accuracy and precision for the determination of II, the method of least squares (5) was applied. Fifteen absorbances measured at the wavelengths of 267–295 nm at 2-nm intervals gave the best results (mean ± *SD* = 100.7 ± 1.10) for the determination of II in the same 10 samples. The final wavelengths used covered the peak characteristics of II (8). Neither chlorobutanol nor sodium chloride interfered with the determinations.

(1) H. Heilmeyer, "Spectrophotometry in Medicine," Adam Hilger Ltd., London, England, 1943, p. 7.

(2) A. L. Glenn, *J. Pharm. Pharmacol.*, **12**, 595 (1960).

(3) M. Pernarowski, A. M. Knevel, and J. E. Christian, *J. Pharm. Sci.*, **50**, 943 (1961).

(4) M. J. Cho and M. Pernarowski, *ibid.*, **59**, 1333 (1970).

(5) B. W. Madsen, D. Herbison-Evans, and J. S. Robertson, *J. Pharm. Pharmacol.*, **26**, 629 (1974).

[1] Prolabo spectrophotometer, Jean & Constant, Paris, France.

(6) P. F. G. Boon and W. Sudds, *ibid.*, **19**, 88S (1967).
(7) J. Molina and R. D. Poe, *ibid.*, **20**, 481 (1968).
(8) H. Abdine, A. M. Wahbi, and M. A. Korany, *ibid.*, **24**, 522 (1972).

A. M. Wahbi ˣ
H. Abdine
M. A. Korany
F. A. El-Yazbi
Faculty of Pharmacy
University of Alexandria
Alexandria, Egypt

Received February 23, 1977.
Accepted for publication September 14, 1977.

Simplified Method to Study Stability of Pharmaceutical Systems

Keyphrases □ Stability—pharmaceutical preparations, criticism of previously reported method relating plot of log $t_{0.9}$ and reciprocal of absolute temperature to shelflife □ Shelflife—pharmaceutical preparations, criticism of previously reported method of prediction by relating to plot of log $t_{0.9}$ and reciprocal of absolute temperature

To the Editor:

A recent study (1) reported a simplified method to study the stability of pharmaceutical preparations. According to this method, shelflife or $t_{0.9}$, the time required for 10% degradation, is determined at elevated temperatures, and, by plotting log $t_{0.9}$ against the reciprocal of the absolute temperature, the shelflife at room temperature can be calculated by extrapolation of the apparent straight line. This approach is suggested (1) to be applicable to all orders of reactions since the initial decay of up to 10% can be fitted by a first-order equation regardless of the actual order of reaction.

Although some limited academic applications of this method (1) can be demonstrated, it has little utility because of erroneous assumptions inherent in the approach and the unfeasible experimental methods suggested.

This study suggests the use of the Arrhenius approach for all orders of reactions, an erroneous assumption. In fitting a straight line through a log $t_{0.9}$ and reciprocal absolute temperature profile, the intercept on log $t_{0.9}$ can be obtained only if $1/T$ approaches zero or T approaches infinity. Thus, no significance should be attached to such intercepts since they represent only a mathematical treatment parameter.

Although Amirjahed (1) tried to prove that, for up to 10% degradation, the concentrations can be fitted by straight lines, no correlation was made between the calculated rate constants reported in the literature. For example, no correlation exists between the rate constants calculated for zero-order reactions ($r = 0.078$) as reported in Table VI of Ref. 1.

Even in those instances where a straight line can be fitted to the log $t_{0.9}$–temperature profile, the slope of the line will be highly dependent on the initial concentration except for a first-order reaction. For example, an allowable (±5%) content variation will result in a 10% variation in the calculated shelflife of a zero-order reaction. Thus, the statement made by the author that "the present method does not depend on x and k" is misleading. Briefly, therefore, a shelflife obtained at one concentration level cannot be extrapolated to other levels and is only valid for the sample studied, making it an evasive method with little practical utility.

The conclusions drawn (1) were based on either theoretically generated curves or published data obtained by more rigorous methods. It would have been more convincing if the author had used actual laboratory data for decompositon up to 10% to calculate the stability at room temperature, since this approach will require extremely sensitive analytical techniques to obtain concentration profiles. Generally, the techniques available for the analysis of dosage forms are not sensitive enough to detect small variations accurately. Thus, unless appropriate analytical techniques are available, the suggested method (1) has little utility, especially in "small laboratories and hospital pharmacy manufacturing units" as recommended by the author (1).

(1) A. K. Amirjahed, *J. Pharm. Sci.*, **66**, 785 (1977).

S. Bakar
S. Niazi ˣ
Department of Pharmacy
College of Pharmacy
University of Illinois at the Medical Center
Chicago, IL 60612

Received July 1, 1977.
Accepted for publication September 29, 1977.

Use of Area under the Curve to Estimate Absolute Bioavailability of Digoxin

Keyphrases □ Digoxin—bioavailability estimated using area under the curve from 0 to 24 and 0 to 72 hr and 0 to infinity □ Bioavailability—digoxin, estimated using area under the curve from 0 to 24 and 0 to 72 hr and 0 to infinity □ Cardiotonic agents—digoxin, bioavailability estimated using area under the curve from 0 to 24 and 0 to 72 hr and 0 to infinity

To the Editor:

The absolute bioavailability of digoxin from tablets has been discussed widely with respect to the actual numerical value as well as the most appropriate method of measurement. Reported values are based on the use of the area under the serum digoxin concentration–time curve from 0 to a finite time, such as 24 or 72 hr, and range from 55 to 65% (1–6). These areas for a finite time approximate the theoretically correct area from zero to infinity (7). This communication compares the approximate method of estimating the absolute bioavailability of a digoxin tablet[1] using the area under the curve from 0 to 24 hr and from 0 to 72 hr and the theoretically correct method using the area under the curve from 0 to infinity.

The absolute bioavailability of a digoxin tablet[1] was measured in 12 normal volunteer subjects. The tablet was given at doses of 0.5 and 1.0 mg (two or four 0.25-mg tab-

[1] Lanoxin Tablet, 0.25 mg, lot 022-1, Burroughs Wellcome and Co.

(6) P. F. G. Boon and W. Sudds, *ibid.*, **19**, 88S (1967).
(7) J. Molina and R. D. Poe, *ibid.*, **20**, 481 (1968).
(8) H. Abdine, A. M. Wahbi, and M. A. Korany, *ibid.*, **24**, 522 (1972).

A. M. Wahbi ˣ
H. Abdine
M. A. Korany
F. A. El-Yazbi
Faculty of Pharmacy
University of Alexandria
Alexandria, Egypt

Received February 23, 1977.
Accepted for publication September 14, 1977.

Simplified Method to Study Stability of Pharmaceutical Systems

Keyphrases □ Stability—pharmaceutical preparations, criticism of previously reported method relating plot of log $t_{0.9}$ and reciprocal of absolute temperature to shelflife □ Shelflife—pharmaceutical preparations, criticism of previously reported method of prediction by relating to plot of log $t_{0.9}$ and reciprocal of absolute temperature

To the Editor:

A recent study (1) reported a simplified method to study the stability of pharmaceutical preparations. According to this method, shelflife or $t_{0.9}$, the time required for 10% degradation, is determined at elevated temperatures, and, by plotting log $t_{0.9}$ against the reciprocal of the absolute temperature, the shelflife at room temperature can be calculated by extrapolation of the apparent straight line. This approach is suggested (1) to be applicable to all orders of reactions since the initial decay of up to 10% can be fitted by a first-order equation regardless of the actual order of reaction.

Although some limited academic applications of this method (1) can be demonstrated, it has little utility because of erroneous assumptions inherent in the approach and the unfeasible experimental methods suggested.

This study suggests the use of the Arrhenius approach for all orders of reactions, an erroneous assumption. In fitting a straight line through a log $t_{0.9}$ and reciprocal absolute temperature profile, the intercept on log $t_{0.9}$ can be obtained only if $1/T$ approaches zero or T approaches infinity. Thus, no significance should be attached to such intercepts since they represent only a mathematical treatment parameter.

Although Amirjahed (1) tried to prove that, for up to 10% degradation, the concentrations can be fitted by straight lines, no correlation was made between the calculated rate constants reported in the literature. For example, no correlation exists between the rate constants calculated for zero-order reactions ($r = 0.078$) as reported in Table VI of Ref. 1.

Even in those instances where a straight line can be fitted to the log $t_{0.9}$–temperature profile, the slope of the line will be highly dependent on the initial concentration except for a first-order reaction. For example, an allowable (±5%) content variation will result in a 10% variation in the calculated shelflife of a zero-order reaction. Thus, the statement made by the author that "the present method does not depend on x and k" is misleading. Briefly, therefore, a shelflife obtained at one concentration level cannot be extrapolated to other levels and is only valid for the sample studied, making it an evasive method with little practical utility.

The conclusions drawn (1) were based on either theoretically generated curves or published data obtained by more rigorous methods. It would have been more convincing if the author had used actual laboratory data for decompositon up to 10% to calculate the stability at room temperature, since this approach will require extremely sensitive analytical techniques to obtain concentration profiles. Generally, the techniques available for the analysis of dosage forms are not sensitive enough to detect small variations accurately. Thus, unless appropriate analytical techniques are available, the suggested method (1) has little utility, especially in "small laboratories and hospital pharmacy manufacturing units" as recommended by the author (1).

(1) A. K. Amirjahed, *J. Pharm. Sci.*, **66**, 785 (1977).

S. Bakar
S. Niazi ˣ
Department of Pharmacy
College of Pharmacy
University of Illinois at the Medical Center
Chicago, IL 60612

Received July 1, 1977.
Accepted for publication September 29, 1977.

Use of Area under the Curve to Estimate Absolute Bioavailability of Digoxin

Keyphrases □ Digoxin—bioavailability estimated using area under the curve from 0 to 24 and 0 to 72 hr and 0 to infinity □ Bioavailability—digoxin, estimated using area under the curve from 0 to 24 and 0 to 72 hr and 0 to infinity □ Cardiotonic agents—digoxin, bioavailability estimated using area under the curve from 0 to 24 and 0 to 72 hr and 0 to infinity

To the Editor:

The absolute bioavailability of digoxin from tablets has been discussed widely with respect to the actual numerical value as well as the most appropriate method of measurement. Reported values are based on the use of the area under the serum digoxin concentration–time curve from 0 to a finite time, such as 24 or 72 hr, and range from 55 to 65% (1–6). These areas for a finite time approximate the theoretically correct area from zero to infinity (7). This communication compares the approximate method of estimating the absolute bioavailability of a digoxin tablet[1] using the area under the curve from 0 to 24 hr and from 0 to 72 hr and the theoretically correct method using the area under the curve from 0 to infinity.

The absolute bioavailability of a digoxin tablet[1] was measured in 12 normal volunteer subjects. The tablet was given at doses of 0.5 and 1.0 mg (two or four 0.25-mg tab-

[1] Lanoxin Tablet, 0.25 mg, lot 022-1, Burroughs Wellcome and Co.

(6) P. F. G. Boon and W. Sudds, *ibid.*, **19**, 88S (1967).
(7) J. Molina and R. D. Poe, *ibid.*, **20**, 481 (1968).
(8) H. Abdine, A. M. Wahbi, and M. A. Korany, *ibid.*, **24**, 522 (1972).

A. M. Wahbi ˣ
H. Abdine
M. A. Korany
F. A. El-Yazbi
Faculty of Pharmacy
University of Alexandria
Alexandria, Egypt

Received February 23, 1977.
Accepted for publication September 14, 1977.

Simplified Method to Study Stability of Pharmaceutical Systems

Keyphrases □ Stability—pharmaceutical preparations, criticism of previously reported method relating plot of log $t_{0.9}$ and reciprocal of absolute temperature to shelflife □ Shelflife—pharmaceutical preparations, criticism of previously reported method of prediction by relating to plot of log $t_{0.9}$ and reciprocal of absolute temperature

To the Editor:

A recent study (1) reported a simplified method to study the stability of pharmaceutical preparations. According to this method, shelflife or $t_{0.9}$, the time required for 10% degradation, is determined at elevated temperatures, and, by plotting log $t_{0.9}$ against the reciprocal of the absolute temperature, the shelflife at room temperature can be calculated by extrapolation of the apparent straight line. This approach is suggested (1) to be applicable to all orders of reactions since the initial decay of up to 10% can be fitted by a first-order equation regardless of the actual order of reaction.

Although some limited academic applications of this method (1) can be demonstrated, it has little utility because of erroneous assumptions inherent in the approach and the unfeasible experimental methods suggested.

This study suggests the use of the Arrhenius approach for all orders of reactions, an erroneous assumption. In fitting a straight line through a log $t_{0.9}$ and reciprocal absolute temperature profile, the intercept on log $t_{0.9}$ can be obtained only if $1/T$ approaches zero or T approaches infinity. Thus, no significance should be attached to such intercepts since they represent only a mathematical treatment parameter.

Although Amirjahed (1) tried to prove that, for up to 10% degradation, the concentrations can be fitted by straight lines, no correlation was made between the calculated rate constants reported in the literature. For example, no correlation exists between the rate constants calculated for zero-order reactions ($r = 0.078$) as reported in Table VI of Ref. 1.

Even in those instances where a straight line can be fitted to the log $t_{0.9}$–temperature profile, the slope of the line will be highly dependent on the initial concentration except for a first-order reaction. For example, an allowable (±5%) content variation will result in a 10% variation in the calculated shelflife of a zero-order reaction. Thus, the statement made by the author that "the present method does not depend on x and k" is misleading. Briefly, therefore, a shelflife obtained at one concentration level cannot be extrapolated to other levels and is only valid for the sample studied, making it an evasive method with little practical utility.

The conclusions drawn (1) were based on either theoretically generated curves or published data obtained by more rigorous methods. It would have been more convincing if the author had used actual laboratory data for decompositon up to 10% to calculate the stability at room temperature, since this approach will require extremely sensitive analytical techniques to obtain concentration profiles. Generally, the techniques available for the analysis of dosage forms are not sensitive enough to detect small variations accurately. Thus, unless appropriate analytical techniques are available, the suggested method (1) has little utility, especially in "small laboratories and hospital pharmacy manufacturing units" as recommended by the author (1).

(1) A. K. Amirjahed, *J. Pharm. Sci.*, **66**, 785 (1977).

S. Bakar
S. Niazi ˣ
Department of Pharmacy
College of Pharmacy
University of Illinois at the Medical Center
Chicago, IL 60612

Received July 1, 1977.
Accepted for publication September 29, 1977.

Use of Area under the Curve to Estimate Absolute Bioavailability of Digoxin

Keyphrases □ Digoxin—bioavailability estimated using area under the curve from 0 to 24 and 0 to 72 hr and 0 to infinity □ Bioavailability—digoxin, estimated using area under the curve from 0 to 24 and 0 to 72 hr and 0 to infinity □ Cardiotonic agents—digoxin, bioavailability estimated using area under the curve from 0 to 24 and 0 to 72 hr and 0 to infinity

To the Editor:

The absolute bioavailability of digoxin from tablets has been discussed widely with respect to the actual numerical value as well as the most appropriate method of measurement. Reported values are based on the use of the area under the serum digoxin concentration–time curve from 0 to a finite time, such as 24 or 72 hr, and range from 55 to 65% (1–6). These areas for a finite time approximate the theoretically correct area from zero to infinity (7). This communication compares the approximate method of estimating the absolute bioavailability of a digoxin tablet[1] using the area under the curve from 0 to 24 hr and from 0 to 72 hr and the theoretically correct method using the area under the curve from 0 to infinity.

The absolute bioavailability of a digoxin tablet[1] was measured in 12 normal volunteer subjects. The tablet was given at doses of 0.5 and 1.0 mg (two or four 0.25-mg tab-

[1] Lanoxin Tablet, 0.25 mg, lot 022-1, Burroughs Wellcome and Co.

lets), and the intravenous bolus dose[2] was 1.0 mg. Serum samples were collected through 72 (oral) or 96 (intravenous) hr and analyzed by radioimmunoassay (8). The area under each curve from 0 to 24 or 72 hr was calculated using the trapezoidal method. Areas under the curve from 0 to infinity were calculated using the trapezoidal method from 0 to the final data point and by extrapolation from the final point to infinity (9). Absolute bioavailability (B) was calculated for each subject according to:

$$B = \frac{(AUC_{0\to t}/D)_{\text{oral}}}{(AUC_{0\to t}/D)_{\text{iv}}} 100\% \qquad \text{(Eq. 1)}$$

where AUC is the area under the serum digoxin concentration–time curve from 0 to t = 24 or 72 hr and D is dose; B also was calculated according to:

$$B = \frac{(AUC_{0\to\infty} \times \beta/D)_{\text{oral}}}{(AUC_{0\to\infty} \times \beta/D)_{\text{iv}}} 100\% \qquad \text{(Eq. 2)}$$

where β is the apparent terminal log–linear slope. The values for β varied randomly between the intravenous and oral treatments. Therefore, the areas under the curve, from 0 to infinity, were corrected for these changes (9).

The estimates of the absolute bioavailability of digoxin calculated using the areas under the curve from 0 to 24 hr (Eq. 1), from 0 to 72 hr (Eq. 1), and from 0 to infinity (Eq. 2) were 59.0, 72.6, and 79.7%, respectively, for the 0.5-mg oral dose and 49.4, 59.8, and 85.8%, respectively, for the 1.0-mg oral dose (numbers are the means of individual values for the 12 subjects). Use of the truncated areas underestimated bioavailability by 26 and 9% (0.5-mg dose) and by 42 and 30% (1.0-mg dose) for the 24- and 72-hr areas, respectively.

These results indicate that the estimation of the absolute bioavailability of digoxin from serum level measurements is dependent on the extent of time that sampling is carried out and that the calculation probably becomes more accurate as time approaches infinity. These differences, particularly between the 24-hr and infinity calculations, may be due to slow or prolonged absorption of drug over a portion of the first 24 hr. Consequently, the area under the curve from 0 to 24 hr for the oral preparation may represent a smaller fraction of the area to infinity than that for the intravenous dose, yielding an apparently low estimate of absolute bioavailability. The error introduced by use of a finite area is, naturally, reduced as the final sampling time is increased.

The absolute bioavailability of digoxin tablets may be underestimated by the use of finite areas under the curve and may actually exceed 80% for the brand tested rather than the much lower values previously accepted.

[2] Lanoxin Injection, lot 644-G, Burroughs Wellcome and Co.

(1) D. J. Greenblatt, D. W. Duhme, J. Koch-Weser, and T. W. Smith, *N. Engl. J. Med.*, **289,** 651 (1973).

(2) D. H. Huffman and D. L. Azarnoff, *J. Am. Med. Assoc.*, **222,** 957 (1972).

(3) D. H. Huffman, C. V. Manion, and D. L. Azarnoff, *Clin. Pharmacol. Ther.*, **16,** 310 (1974).

(4) D. H. Huffman, C. V. Manion, and D. L. Azarnoff, *J. Pharm. Sci.*, **64,** 433 (1975).

(5) J. G. Wagner, M. Christensen, E. Sakmar, D. Blair, J. D. Yates, P. W. Willis, III, A. J. Sedman, and R. G. Stoll, *J. Am. Med. Assoc.*, **224,** 199 (1973).

(6) F. Bochner, D. H. Huffman, D. D. Shen, and D. L. Azarnoff, *J. Pharm. Sci.*, **66,** 644 (1977).

(7) M. Gibaldi and D. Perrier, "Pharmacokinetics," Dekker, New York, N.Y., 1975, p. 146.

(8) W. G. Kramer, A. J. Kolibash, M. S. Bathala, J. A. Visconti, R. P. Lewis, and R. H. Reuning, *J. Pharm. Sci.*, **66,** 1720 (1977).

(9) J. G. Wagner, "Biopharmaceutics and Relevant Pharmacokinetics," Drug Intelligence Publications, Hamilton, Ill., 1971, pp. 297–301.

William G. Kramer ˣ

Department of Pharmaceutics
College of Pharmacy
University of Houston
Houston, TX 77004

Richard H. Reuning

Division of Pharmaceutics and Pharmaceutical Chemistry
College of Pharmacy
Ohio State University
Columbus, OH 43210

Received June 13, 1977.
Accepted for publication September 26, 1977.

REVIEWS

Foreign Compound Metabolism in Mammals, Vol. 4. A Specialist Periodical Report. Edited by D. E. HATHWAY, *et al.* The Chemical Society, Burlington House, London, W1V OBN, England. 1977. 411 pp. 14 × 22 cm. Price $55.00. Available from Special Issues Sales, American Chemical Society, 1155 16th St., N.W., Washington, DC 20036.

This book, which continues the excellent literature reviews previously assembled by Dr. Hathway and associates in former volumes of this series, covers the period 1974–1975. The material is organized into four chapters: Drug Kinetics; Biotransformations; Mechanisms of Biotransformation; and Species, Strain, and Sex Differences in Metabolism. As may be deduced from these headings, the major portion of the book is devoted to the biotransformation of foreign compounds. In addition to drugs, the compounds covered include food additives and contaminants, carcinogens, toxins, and agricultural and industrial chemicals.

An interesting feature of the book's format is the manner in which the elements of a reference and textbook are combined. The first two chapters are organized by classes of compound so that one can readily learn what has been published on specific compounds of interest. The latter two chapters are built along conceptual lines in that the material is segregated into discussions of the reported mechanisms of various metabolic reactions and of the species differences found for selected biotransformations.

An outstanding accomplishment of the authors is the clarity of writing. One error noted, the more specific placement of a hydroxyl group on a fluorinated phenyl ring (p. 115) than was published in the original article, is an important reminder of the need to check back to the original sources.

This volume is considered an essential item in the library of every serious student of drug disposition. Furthermore, the purchase of this book is one direct way we may encourage Dr. Hathway and his colleagues to continue their very useful contributions to this somewhat nebulous discipline.

Reviewed by Morton A. Schwartz
Department of Biochemistry and Drug Metabolism
Hoffmann-La Roche Inc.
Nutley, NJ 07110

International Symposium on Marine Natural Products. Edited by R. H. THOMPSON. Pergamon, Maxwell House, Fairview Park, Elmsford, NY 10523, 1976. 44 pp. 19 × 28 cm. Price $8.00.

This publication contains five plenary lectures presented at the International Symposium on Marine Natural Products held in Aberdeen, Scotland, September 8–11, 1975, under the auspices of the International Union of Pure and Applied Chemistry (Organic Chemistry Division) in conjunction with the Chemical Society, Perkin Division. The book is a handy, compact reproduction of the lectures, which originally appeared as a series of articles in *Pure and Applied Chemistry*, vol. 48, pp. 1–44, in 1976.

B. Tursch reviews in the first lecture the recent developments in the chemistry of Alcyonaceans or soft corals which are abundant in the Indo-Pacific region. A series of sesquiterpenes, diterpenes, and sterols isolated from this group of organisms is reviewed. The origin of the compounds in these coelenterates is discussed, with particular reference to organisms living in symbiosis with them—*viz.*, intracellular dinoflagellate algae known as zooxanthellae. These latter organisms are suspected of being responsible for the synthesis of terpenoids encountered in the Alcyonaria. The biological significance of the symbiosis is discussed in particular reference to the obvious protection of Alcyonaceans by toxic terpenoids produced by the zooxanthellae.

In the second paper, L. Minale reviews the natural product chemistry of the marine sponges. He reports that over 100 new compounds have been derived from marine sponges, particularly bromo compounds, terpenes, diterpenes, and sterols. In some cases, the origin of the compounds is discussed as, for example, with the brominated compounds. Here the author states that it appears possible that the brominated compounds isolated from sponges, like the bromoterpenes from molluscs, were originally fabricated by algae symbionts. The author also provides data showing that sponges often have terpenes in large amounts, most of which possess unique structural features without parallel in terrestrial sources.

The third paper deals with the biomimetic synthesis of marine natural products. Dr. D. J. Faulkner presents extensive chemical evidence that the biosynthetic pathways to many halogenated marine natural products are based on bromonium-ion-initiated cyclization reactions. The synthesis of 10-bromochamigrene is used to illustrate the efficacy of biomimetic synthesis.

Paper four by Dr. Y. Kato and Dr. P. J. Scheuer deals with the aplysiatoxins and their structure determination. These authors report that under the influence of ethanolic acetic acid the aplysiatoxins rearrange with retention of all carbon atoms. Furthermore, an osmate of the anhydrotoxins was able to be reduced to a glycol that resists oxidative cleavage but loses water and rearranges with acid. These reactions and others coupled with consideration of PMP data lead to partial assignment of the relative stereochemistry of the toxins.

The fifth and final paper by Dr. J. T. Baker provides an excellent review of the natural product research on Australian marine organisms for 1959–1975. The overview is thorough and complete, citing all authors, organisms studied, compounds isolated, and structures elucidated.

This book is highly recommended as a valuable reference source for all scientists interested in the progress of marine chemistry and pharmacology.

Reviewed by Ara Der Marderosian
Philadelphia College of Pharmacy and Science
Philadelphia, PA 19104

Alicyclic Chemistry. Vol. 5. A Specialist Periodical Report. Edited by W. PARKER *et al.* The Chemical Society, Burlington House, London W1V OBN, England, 1977. ix + 438 pp. 14 × 22 cm. Price $56.00. Available from Special Issues Sales, American Chemical Society, 1155 Sixteenth St., N.W., Washington, DC 20036.

This volume is the fifth in a series of literature summaries dealing with alicyclic chemistry including such topics as synthesis, reactions, stereochemistry, physical properties, and spectroscopy of small, medium, and large carbocyclic systems. The literature published during 1975 is covered. The book is divided into five chapters, each of which is authored by scientists having authoritative expertise in a given area of alicyclic chemistry.

Chapter 1 (B. Halton, New Zealand, 100 pages) discusses the chemistry of three-membered ring systems. Previous volumes in this series discussed three- and four-membered rings in a single chapter. Chapter 2 (I. Watt, Scotland, 91 pages) describes four-membered rings. Chapter 3 (N. M. D. Brown and D. J. Cowley, Northern Ireland, 31 pages) discusses five- and six-membered rings and related fused systems. Medium- and large-ring compounds are described in Chapter 4 (E. J. Thomas, England, 70 pages), and the bridged and caged carbocyclics are discussed in Chapter 5 (G. B. Gill, England, 126 pages).

Discussion of the literature of 1975 dealing with three-membered rings and bridged carbocyclics is enhanced by bibliographies of books, reviews, and discussions relevant to the chemistry of these systems. Each chapter usually begins with a review of theory and structure of the individual alicyclic systems. Major emphasis on the preparation and reactions of each ring system is provided. In addition to discussion of the parent saturated ring system in each class, the authors provide literature surveys of the unsaturated members as well as functional analogs such as ketone, alcohol, and amine derivatives. The text is well illustrated with structures, mechanisms, and reactions. Arabic numerals are used to denote specific structures and, in certain chapters, these numbers total 500 or more. Fortunately, Roman numbers are not employed.

In the introduction, the editor attempts to answer previous critical reviews of this series regarding the lack of a subject index. Professor

REVIEWS

Foreign Compound Metabolism in Mammals, Vol. 4. A Specialist Periodical Report. Edited by D. E. HATHWAY, *et al.* The Chemical Society, Burlington House, London, W1V OBN, England. 1977. 411 pp. 14 × 22 cm. Price $55.00. Available from Special Issues Sales, American Chemical Society, 1155 16th St., N.W., Washington, DC 20036.

This book, which continues the excellent literature reviews previously assembled by Dr. Hathway and associates in former volumes of this series, covers the period 1974–1975. The material is organized into four chapters: Drug Kinetics; Biotransformations; Mechanisms of Biotransformation; and Species, Strain, and Sex Differences in Metabolism. As may be deduced from these headings, the major portion of the book is devoted to the biotransformation of foreign compounds. In addition to drugs, the compounds covered include food additives and contaminants, carcinogens, toxins, and agricultural and industrial chemicals.

An interesting feature of the book's format is the manner in which the elements of a reference and textbook are combined. The first two chapters are organized by classes of compound so that one can readily learn what has been published on specific compounds of interest. The latter two chapters are built along conceptual lines in that the material is segregated into discussions of the reported mechanisms of various metabolic reactions and of the species differences found for selected biotransformations.

An outstanding accomplishment of the authors is the clarity of writing. One error noted, the more specific placement of a hydroxyl group on a fluorinated phenyl ring (p. 115) than was published in the original article, is an important reminder of the need to check back to the original sources.

This volume is considered an essential item in the library of every serious student of drug disposition. Furthermore, the purchase of this book is one direct way we may encourage Dr. Hathway and his colleagues to continue their very useful contributions to this somewhat nebulous discipline.

Reviewed by Morton A. Schwartz
Department of Biochemistry and Drug Metabolism
Hoffmann-La Roche Inc.
Nutley, NJ 07110

International Symposium on Marine Natural Products. Edited by R. H. THOMPSON. Pergamon, Maxwell House, Fairview Park, Elmsford, NY 10523, 1976. 44 pp. 19 × 28 cm. Price $8.00.

This publication contains five plenary lectures presented at the International Symposium on Marine Natural Products held in Aberdeen, Scotland, September 8–11, 1975, under the auspices of the International Union of Pure and Applied Chemistry (Organic Chemistry Division) in conjunction with the Chemical Society, Perkin Division. The book is a handy, compact reproduction of the lectures, which originally appeared as a series of articles in *Pure and Applied Chemistry*, vol. 48, pp. 1–44, in 1976.

B. Tursch reviews in the first lecture the recent developments in the chemistry of Alcyonaceans or soft corals which are abundant in the Indo-Pacific region. A series of sesquiterpenes, diterpenes, and sterols isolated from this group of organisms is reviewed. The origin of the compounds in these coelenterates is discussed, with particular reference to organisms living in symbiosis with them—*viz.*, intracellular dinoflagellate algae known as zooxanthellae. These latter organisms are suspected of being responsible for the synthesis of terpenoids encountered in the Alcyonaria. The biological significance of the symbiosis is discussed in particular reference to the obvious protection of Alcyonaceans by toxic terpenoids produced by the zooxanthellae.

In the second paper, L. Minale reviews the natural product chemistry of the marine sponges. He reports that over 100 new compounds have been derived from marine sponges, particularly bromo compounds, terpenes, diterpenes, and sterols. In some cases, the origin of the compounds is discussed as, for example, with the brominated compounds. Here the author states that it appears possible that the brominated compounds isolated from sponges, like the bromoterpenes from molluscs, were originally fabricated by algae symbionts. The author also provides data showing that sponges often have terpenes in large amounts, most of which possess unique structural features without parallel in terrestrial sources.

The third paper deals with the biomimetic synthesis of marine natural products. Dr. D. J. Faulkner presents extensive chemical evidence that the biosynthetic pathways to many halogenated marine natural products are based on bromonium-ion-initiated cyclization reactions. The synthesis of 10-bromochamigrene is used to illustrate the efficacy of biomimetic synthesis.

Paper four by Dr. Y. Kato and Dr. P. J. Scheuer deals with the aplysiatoxins and their structure determination. These authors report that under the influence of ethanolic acetic acid the aplysiatoxins rearrange with retention of all carbon atoms. Furthermore, an osmate of the anhydrotoxins was able to be reduced to a glycol that resists oxidative cleavage but loses water and rearranges with acid. These reactions and others coupled with consideration of PMP data lead to partial assignment of the relative stereochemistry of the toxins.

The fifth and final paper by Dr. J. T. Baker provides an excellent review of the natural product research on Australian marine organisms for 1959–1975. The overview is thorough and complete, citing all authors, organisms studied, compounds isolated, and structures elucidated.

This book is highly recommended as a valuable reference source for all scientists interested in the progress of marine chemistry and pharmacology.

Reviewed by Ara Der Marderosian
Philadelphia College of Pharmacy and Science
Philadelphia, PA 19104

Alicyclic Chemistry. Vol. 5. A Specialist Periodical Report. Edited by W. PARKER *et al.* The Chemical Society, Burlington House, London W1V OBN, England, 1977. ix + 438 pp. 14 × 22 cm. Price $56.00. Available from Special Issues Sales, American Chemical Society, 1155 Sixteenth St., N.W., Washington, DC 20036.

This volume is the fifth in a series of literature summaries dealing with alicyclic chemistry including such topics as synthesis, reactions, stereochemistry, physical properties, and spectroscopy of small, medium, and large carbocyclic systems. The literature published during 1975 is covered. The book is divided into five chapters, each of which is authored by scientists having authoritative expertise in a given area of alicyclic chemistry.

Chapter 1 (B. Halton, New Zealand, 100 pages) discusses the chemistry of three-membered ring systems. Previous volumes in this series discussed three- and four-membered rings in a single chapter. Chapter 2 (I. Watt, Scotland, 91 pages) describes four-membered rings. Chapter 3 (N. M. D. Brown and D. J. Cowley, Northern Ireland, 31 pages) discusses five- and six-membered rings and related fused systems. Medium- and large-ring compounds are described in Chapter 4 (E. J. Thomas, England, 70 pages), and the bridged and caged carbocyclics are discussed in Chapter 5 (G. B. Gill, England, 126 pages).

Discussion of the literature of 1975 dealing with three-membered rings and bridged carbocyclics is enhanced by bibliographies of books, reviews, and discussions relevant to the chemistry of these systems. Each chapter usually begins with a review of theory and structure of the individual alicyclic systems. Major emphasis on the preparation and reactions of each ring system is provided. In addition to discussion of the parent saturated ring system in each class, the authors provide literature surveys of the unsaturated members as well as functional analogs such as ketone, alcohol, and amine derivatives. The text is well illustrated with structures, mechanisms, and reactions. Arabic numerals are used to denote specific structures and, in certain chapters, these numbers total 500 or more. Fortunately, Roman numbers are not employed.

In the introduction, the editor attempts to answer previous critical reviews of this series regarding the lack of a subject index. Professor

REVIEWS

Foreign Compound Metabolism in Mammals, Vol. 4. A Specialist Periodical Report. Edited by D. E. HATHWAY, *et al.* The Chemical Society, Burlington House, London, W1V OBN, England. 1977. 411 pp. 14 × 22 cm. Price $55.00. Available from Special Issues Sales, American Chemical Society, 1155 16th St., N.W., Washington, DC 20036.

This book, which continues the excellent literature reviews previously assembled by Dr. Hathway and associates in former volumes of this series, covers the period 1974–1975. The material is organized into four chapters: Drug Kinetics; Biotransformations; Mechanisms of Biotransformation; and Species, Strain, and Sex Differences in Metabolism. As may be deduced from these headings, the major portion of the book is devoted to the biotransformation of foreign compounds. In addition to drugs, the compounds covered include food additives and contaminants, carcinogens, toxins, and agricultural and industrial chemicals.

An interesting feature of the book's format is the manner in which the elements of a reference and textbook are combined. The first two chapters are organized by classes of compound so that one can readily learn what has been published on specific compounds of interest. The latter two chapters are built along conceptual lines in that the material is segregated into discussions of the reported mechanisms of various metabolic reactions and of the species differences found for selected biotransformations.

An outstanding accomplishment of the authors is the clarity of writing. One error noted, the more specific placement of a hydroxyl group on a fluorinated phenyl ring (p. 115) than was published in the original article, is an important reminder of the need to check back to the original sources.

This volume is considered an essential item in the library of every serious student of drug disposition. Furthermore, the purchase of this book is one direct way we may encourage Dr. Hathway and his colleagues to continue their very useful contributions to this somewhat nebulous discipline.

Reviewed by Morton A. Schwartz
Department of Biochemistry and Drug Metabolism
Hoffmann-La Roche Inc.
Nutley, NJ 07110

International Symposium on Marine Natural Products. Edited by R. H. THOMPSON. Pergamon, Maxwell House, Fairview Park, Elmsford, NY 10523, 1976. 44 pp. 19 × 28 cm. Price $8.00.

This publication contains five plenary lectures presented at the International Symposium on Marine Natural Products held in Aberdeen, Scotland, September 8–11, 1975, under the auspices of the International Union of Pure and Applied Chemistry (Organic Chemistry Division) in conjunction with the Chemical Society, Perkin Division. The book is a handy, compact reproduction of the lectures, which originally appeared as a series of articles in *Pure and Applied Chemistry*, vol. 48, pp. 1–44, in 1976.

B. Tursch reviews in the first lecture the recent developments in the chemistry of Alcyonaceans or soft corals which are abundant in the Indo-Pacific region. A series of sesquiterpenes, diterpenes, and sterols isolated from this group of organisms is reviewed. The origin of the compounds in these coelenterates is discussed, with particular reference to organisms living in symbiosis with them—*viz.*, intracellular dinoflagellate algae known as zooxanthellae. These latter organisms are suspected of being responsible for the synthesis of terpenoids encountered in the Alcyonaria. The biological significance of the symbiosis is discussed in particular reference to the obvious protection of Alcyonaceans by toxic terpenoids produced by the zooxanthellae.

In the second paper, L. Minale reviews the natural product chemistry of the marine sponges. He reports that over 100 new compounds have been derived from marine sponges, particularly bromo compounds, terpenes, diterpenes, and sterols. In some cases, the origin of the compounds is discussed as, for example, with the brominated compounds. Here the author states that it appears possible that the brominated compounds isolated from sponges, like the bromoterpenes from molluscs, were originally fabricated by algae symbionts. The author also provides data showing that sponges often have terpenes in large amounts, most of which possess unique structural features without parallel in terrestrial sources.

The third paper deals with the biomimetic synthesis of marine natural products. Dr. D. J. Faulkner presents extensive chemical evidence that the biosynthetic pathways to many halogenated marine natural products are based on bromonium-ion-initiated cyclization reactions. The synthesis of 10-bromochamigrene is used to illustrate the efficacy of biomimetic synthesis.

Paper four by Dr. Y. Kato and Dr. P. J. Scheuer deals with the aplysiatoxins and their structure determination. These authors report that under the influence of ethanolic acetic acid the aplysiatoxins rearrange with retention of all carbon atoms. Furthermore, an osmate of the anhydrotoxins was able to be reduced to a glycol that resists oxidative cleavage but loses water and rearranges with acid. These reactions and others coupled with consideration of PMP data lead to partial assignment of the relative stereochemistry of the toxins.

The fifth and final paper by Dr. J. T. Baker provides an excellent review of the natural product research on Australian marine organisms for 1959–1975. The overview is thorough and complete, citing all authors, organisms studied, compounds isolated, and structures elucidated.

This book is highly recommended as a valuable reference source for all scientists interested in the progress of marine chemistry and pharmacology.

Reviewed by Ara Der Marderosian
Philadelphia College of Pharmacy and Science
Philadelphia, PA 19104

Alicyclic Chemistry. Vol. 5. A Specialist Periodical Report. Edited by W. PARKER *et al.* The Chemical Society, Burlington House, London W1V OBN, England, 1977. ix + 438 pp. 14 × 22 cm. Price $56.00. Available from Special Issues Sales, American Chemical Society, 1155 Sixteenth St., N.W., Washington, DC 20036.

This volume is the fifth in a series of literature summaries dealing with alicyclic chemistry including such topics as synthesis, reactions, stereochemistry, physical properties, and spectroscopy of small, medium, and large carbocyclic systems. The literature published during 1975 is covered. The book is divided into five chapters, each of which is authored by scientists having authoritative expertise in a given area of alicyclic chemistry.

Chapter 1 (B. Halton, New Zealand, 100 pages) discusses the chemistry of three-membered ring systems. Previous volumes in this series discussed three- and four-membered rings in a single chapter. Chapter 2 (I. Watt, Scotland, 91 pages) describes four-membered rings. Chapter 3 (N. M. D. Brown and D. J. Cowley, Northern Ireland, 31 pages) discusses five- and six-membered rings and related fused systems. Medium- and large-ring compounds are described in Chapter 4 (E. J. Thomas, England, 70 pages), and the bridged and caged carbocyclics are discussed in Chapter 5 (G. B. Gill, England, 126 pages).

Discussion of the literature of 1975 dealing with three-membered rings and bridged carbocyclics is enhanced by bibliographies of books, reviews, and discussions relevant to the chemistry of these systems. Each chapter usually begins with a review of theory and structure of the individual alicyclic systems. Major emphasis on the preparation and reactions of each ring system is provided. In addition to discussion of the parent saturated ring system in each class, the authors provide literature surveys of the unsaturated members as well as functional analogs such as ketone, alcohol, and amine derivatives. The text is well illustrated with structures, mechanisms, and reactions. Arabic numerals are used to denote specific structures and, in certain chapters, these numbers total 500 or more. Fortunately, Roman numbers are not employed.

In the introduction, the editor attempts to answer previous critical reviews of this series regarding the lack of a subject index. Professor

Parker indicates that inclusion of such an index would entail too great an expenditure of time, money, and administrative effort and points out that the detailed table of contents might suffice in this regard. The book retains an extensive author index, and each chapter has comprehensive references to literature citations. These references are provided in close proximity to their citation in the text.

Overall, this publication is very readable and should prove to be valuable to scientists having research and/or academic interest in alicyclic chemistry. This volume should be purchased by institutional libraries. The relatively high cost of the book will prevent all but the specialist from investing in its purchase. The editors are aware of the cost factor and indicate that they are examining methods for producing a less expensive publication.

Reviewed by Thomas N. Riley
Department of Medicinal Chemistry
School of Pharmacy
University of Mississippi
University, MS 38677

USAN and the USP Dictionary of Drug Names. Edited by MARY C. GRIFFITHS, MARIE J. DICKERMAN, and LLOYD C. MILLER. U. S. Pharmacopeial Convention, 12601 Twinbrook Parkway, Rockville, MD 20852. 1977. 382 pp. 21 × 28 cm. Price $18.50.

The 1977 edition of this now standard reference source lists more than 11,000 entries, including 1616 USAN (all U.S. Adopted Names selected and released from June 1961 through June 1977), 2239 investigational drug code designations, USP and NF official names, FDA established names, brand names, abbreviations, and trivial names. Each entry includes a pronunciation guide, the pharmacological category, and reference to sources of additional information.

The book contains a cross-index of names by pharmacologic–therapeutic categories and three appendixes: Guiding Principles for Coining U.S. Adopted Names, Molecular Formulas and Corresponding USAN, and Names and Addresses of Domestic Firms.

Staff Review

NOTICES

NMR: An Introduction to Proton Nuclear Magnetic Resonance Spectroscopy. By ADDISON AULT and GERALD O. DUDEK. Holden-Day, 500 Sansome St., San Francisco, CA 94111, 1976. 142 pp. 15 × 21 cm. Price $4.95.

Intended as a comprehensive nontheoretical introduction to NMR spectroscopy, the text covers both the interpretation of NMR spectra and the practical, experimental aspects of preparing the sample and obtaining the spectrum. Particular attention is given to the central concepts of magnetic equivalence and the requirements for observing a first-order spectrum. A large number of illustrative proton NMR spectra of high quality are presented and interpreted. The book is suitable as a supplementary text in organic chemistry courses. Understanding of the text requires no mathematics or advanced chemistry.

Infrared Absorption Spectroscopy, Second Ed. By KOJI NAKANISHI and PHILIPPA H. SOLOMON. Holden-Day, 500 Sansome St., San Francisco, CA 94111, 1977. 287 pp. 17 × 25 cm. Price $10.95.

This book is intended to be an introduction to IR spectroscopy for students and a reference source for practicing researchers. It includes a general discussion of the IR spectrum, tables of characteristic frequencies for different classes of organic compounds, a discussion of band position and intensity, and an introduction to Raman spectroscopy. Many problems and their solutions are given, enhancing the self-teaching utility of the book.

Modern Practice of Gas Chromatography. Edited by ROBERT L. GROB. Wiley, 605 Third Ave., New York, NY 10016, 1977. 654 pp. 16 × 24 cm. Price $22.50.

This book is organized into three parts. Part 1 is for readers interested in the theory and basics of GC, Part 2 is for those desiring information about the techniques and instrumentation, and Part 3 is for readers who are already knowledgeable about GC and want to familiarize themselves with applications.

Atlas of Cell Biology. By JEAN-CLAUDE ROLAND, ANNETTE SZÖLLÖSI, and DANIEL SZÖLLÖSI. Little, Brown, Boston, MA 02106, 1977. 117 pp. 20 × 25 cm.

Directed at students of introductory cell biology, this book contains nearly 250 illustrations that simplify and enhance the fundamental aspects of this discipline. By grouping photomicrographs with simple functional diagrams, it shows the structure of various kinds of cells and illustrates exactly how cells work. An appendix explains when to use the various methods of cell examination, how to prepare a sample, and how the laboratory instruments work.

The Essential Guide to Prescription Drugs: What You Need to Know for Safe Drug Use. By JAMES W. LONG. Harper & Row, 10 East 53rd St., New York, NY 10022, 1977. 752 pp. 16 × 23.5 cm. Price $8.95.

Advances in Chromatography, Vol. 14. Edited by J. CALVIN GIDDINGS, ELI GRUSHKA, JACK CAZES, and PHYLLIS R. BROWN. Dekker, 270 Madison Ave., New York, NY 10016, 1976. 459 pp. 15.5 × 23.5 cm. Price $34.50.

British Pharmacopoeia 1973 Addendum 1977. Her Majesty's Stationery Office (PMIC), Atlantic House, Holborn Viaduct, London, ECIP 1BN, England, 1977. 51 pp. 21 × 30 cm.

Actinomycetes: The Boundary Microorganisms. Edited by TADASHI ARAI. University Park Press, Chamber of Commerce Bldg., Baltimore, MD 21202, 1976. 651 pp. 17 × 26 cm. Price $98.60.

Clinical Toxicology, Vol. XVIII. Edited by W. A. M. DUNCAN and B. J. LEONARD. Excerpta Medica, 305 Keizersgracht, P.O. Box 1126, Amsterdam, The Netherlands, 1977. 348 pp. 16 × 24 cm. Price $35.75. Available from Elsevier North-Holland, 52 Vanderbilt Ave., New York, NY 10017.

The Molecular Biology of Animal Viruses, Vol. 1. Edited by DEBI PROSAD NAYAK. Dekker, 270 Madison Ave., New York, NY 10016, 1977. 542 pp. 18 × 24 cm. Price $49.75.

Proceedings Of The First Cleveland Symposium On Macromolecules. Edited by A. G. WALTON. Elsevier North-Holland, 52 Vanderbilt Ave., New York, NY 10017, 1977. 309 pp. 18 × 24 cm. Price $97.50.

Antibiotics In Clinical Practice, Third Ed. by HILLAS SMITH. University Park Press, Chamber of Commerce Bldg., Baltimore, MD 21202, 1977. 413 pp. 14 × 22 cm. Price $19.50.

Prolactin and Human Reproduction. Edited by P. G. CROSIGNANI and C. ROBYN. Academic (London), 24–28 Oval Road, London, NW1 7DX, England, 1977. 305 pp. 15 × 23 cm. Price $20.50.

NEW JOURNALS

Drug and Chemical Toxicology: An International Journal for Rapid Communication. Edited by JOHN G. KELLER. Dekker, 270 Madison Ave., New York, NY 10016. Price for Vol. 1 (1977–1978) $40.00 (four issues).

Leukemia Research. Edited by SVEN-AAGE KILLMANN, C. N. MULLER-BERAT, JEAN BERNARD, and EUGENE P. CRONKITE. Pergamon, Maxwell House, Fairview Park, Elmsford, NY 10523. Price $50.00 (four issues).

Parker indicates that inclusion of such an index would entail too great an expenditure of time, money, and administrative effort and points out that the detailed table of contents might suffice in this regard. The book retains an extensive author index, and each chapter has comprehensive references to literature citations. These references are provided in close proximity to their citation in the text.

Overall, this publication is very readable and should prove to be valuable to scientists having research and/or academic interest in alicyclic chemistry. This volume should be purchased by institutional libraries. The relatively high cost of the book will prevent all but the specialist from investing in its purchase. The editors are aware of the cost factor and indicate that they are examining methods for producing a less expensive publication.

Reviewed by Thomas N. Riley
Department of Medicinal Chemistry
School of Pharmacy
University of Mississippi
University, MS 38677

USAN and the USP Dictionary of Drug Names. Edited by MARY C. GRIFFITHS, MARIE J. DICKERMAN, and LLOYD C. MILLER. U. S. Pharmacopeial Convention, 12601 Twinbrook Parkway, Rockville, MD 20852. 1977. 382 pp. 21 × 28 cm. Price $18.50.

The 1977 edition of this now standard reference source lists more than 11,000 entries, including 1616 USAN (all U.S. Adopted Names selected and released from June 1961 through June 1977), 2239 investigational drug code designations, USP and NF official names, FDA established names, brand names, abbreviations, and trivial names. Each entry includes a pronunciation guide, the pharmacological category, and reference to sources of additional information.

The book contains a cross-index of names by pharmacologic–therapeutic categories and three appendixes: Guiding Principles for Coining U.S. Adopted Names, Molecular Formulas and Corresponding USAN, and Names and Addresses of Domestic Firms.

Staff Review

NOTICES

NMR: An Introduction to Proton Nuclear Magnetic Resonance Spectroscopy. By ADDISON AULT and GERALD O. DUDEK. Holden-Day, 500 Sansome St., San Francisco, CA 94111, 1976. 142 pp. 15 × 21 cm. Price $4.95.

Intended as a comprehensive nontheoretical introduction to NMR spectroscopy, the text covers both the interpretation of NMR spectra and the practical, experimental aspects of preparing the sample and obtaining the spectrum. Particular attention is given to the central concepts of magnetic equivalence and the requirements for observing a first-order spectrum. A large number of illustrative proton NMR spectra of high quality are presented and interpreted. The book is suitable as a supplementary text in organic chemistry courses. Understanding of the text requires no mathematics or advanced chemistry.

Infrared Absorption Spectroscopy, Second Ed. By KOJI NAKANISHI and PHILIPPA H. SOLOMON. Holden-Day, 500 Sansome St., San Francisco, CA 94111, 1977. 287 pp. 17 × 25 cm. Price $10.95.

This book is intended to be an introduction to IR spectroscopy for students and a reference source for practicing researchers. It includes a general discussion of the IR spectrum, tables of characteristic frequencies for different classes of organic compounds, a discussion of band position and intensity, and an introduction to Raman spectroscopy. Many problems and their solutions are given, enhancing the self-teaching utility of the book.

Modern Practice of Gas Chromatography. Edited by ROBERT L. GROB. Wiley, 605 Third Ave., New York, NY 10016, 1977. 654 pp. 16 × 24 cm. Price $22.50.

This book is organized into three parts. Part 1 is for readers interested in the theory and basics of GC, Part 2 is for those desiring information about the techniques and instrumentation, and Part 3 is for readers who are already knowledgeable about GC and want to familiarize themselves with applications.

Atlas of Cell Biology. By JEAN-CLAUDE ROLAND, ANNETTE SZÖLLÖSI, and DANIEL SZÖLLÖSI. Little, Brown, Boston, MA 02106, 1977. 117 pp. 20 × 25 cm.

Directed at students of introductory cell biology, this book contains nearly 250 illustrations that simplify and enhance the fundamental aspects of this discipline. By grouping photomicrographs with simple functional diagrams, it shows the structure of various kinds of cells and illustrates exactly how cells work. An appendix explains when to use the various methods of cell examination, how to prepare a sample, and how the laboratory instruments work.

The Essential Guide to Prescription Drugs: What You Need to Know for Safe Drug Use. By JAMES W. LONG. Harper & Row, 10 East 53rd St., New York, NY 10022, 1977. 752 pp. 16 × 23.5 cm. Price $8.95.

Advances in Chromatography, Vol. 14. Edited by J. CALVIN GIDDINGS, ELI GRUSHKA, JACK CAZES, and PHYLLIS R. BROWN. Dekker, 270 Madison Ave., New York, NY 10016, 1976. 459 pp. 15.5 × 23.5 cm. Price $34.50.

British Pharmacopoeia 1973 Addendum 1977. Her Majesty's Stationery Office (PMIC), Atlantic House, Holborn Viaduct, London, ECIP 1BN, England, 1977. 51 pp. 21 × 30 cm.

Actinomycetes: The Boundary Microorganisms. Edited by TADASHI ARAI. University Park Press, Chamber of Commerce Bldg., Baltimore, MD 21202, 1976. 651 pp. 17 × 26 cm. Price $98.60.

Clinical Toxicology, Vol. XVIII. Edited by W. A. M. DUNCAN and B. J. LEONARD. Excerpta Medica, 305 Keizersgracht, P.O. Box 1126, Amsterdam, The Netherlands, 1977. 348 pp. 16 × 24 cm. Price $35.75. Available from Elsevier North-Holland, 52 Vanderbilt Ave., New York, NY 10017.

The Molecular Biology of Animal Viruses, Vol. 1. Edited by DEBI PROSAD NAYAK. Dekker, 270 Madison Ave., New York, NY 10016, 1977. 542 pp. 18 × 24 cm. Price $49.75.

Proceedings Of The First Cleveland Symposium On Macromolecules. Edited by A. G. WALTON. Elsevier North-Holland, 52 Vanderbilt Ave., New York, NY 10017, 1977. 309 pp. 18 × 24 cm. Price $97.50.

Antibiotics In Clinical Practice, Third Ed. by HILLAS SMITH. University Park Press, Chamber of Commerce Bldg., Baltimore, MD 21202, 1977. 413 pp. 14 × 22 cm. Price $19.50.

Prolactin and Human Reproduction. Edited by P. G. CROSIGNANI and C. ROBYN. Academic (London), 24–28 Oval Road, London, NW1 7DX, England, 1977. 305 pp. 15 × 23 cm. Price $20.50.

NEW JOURNALS

Drug and Chemical Toxicology: An International Journal for Rapid Communication. Edited by JOHN G. KELLER. Dekker, 270 Madison Ave., New York, NY 10016. Price for Vol. 1 (1977–1978) $40.00 (four issues).

Leukemia Research. Edited by SVEN-AAGE KILLMANN, C. N. MULLER-BERAT, JEAN BERNARD, and EUGENE P. CRONKITE. Pergamon, Maxwell House, Fairview Park, Elmsford, NY 10523. Price $50.00 (four issues).

Parker indicates that inclusion of such an index would entail too great an expenditure of time, money, and administrative effort and points out that the detailed table of contents might suffice in this regard. The book retains an extensive author index, and each chapter has comprehensive references to literature citations. These references are provided in close proximity to their citation in the text.

Overall, this publication is very readable and should prove to be valuable to scientists having research and/or academic interest in alicyclic chemistry. This volume should be purchased by institutional libraries. The relatively high cost of the book will prevent all but the specialist from investing in its purchase. The editors are aware of the cost factor and indicate that they are examining methods for producing a less expensive publication.

Reviewed by Thomas N. Riley
Department of Medicinal Chemistry
School of Pharmacy
University of Mississippi
University, MS 38677

USAN and the USP Dictionary of Drug Names. Edited by MARY C. GRIFFITHS, MARIE J. DICKERMAN, and LLOYD C. MILLER. U. S. Pharmacopeial Convention, 12601 Twinbrook Parkway, Rockville, MD 20852. 1977. 382 pp. 21 × 28 cm. Price $18.50.

The 1977 edition of this now standard reference source lists more than 11,000 entries, including 1616 USAN (all U.S. Adopted Names selected and released from June 1961 through June 1977), 2239 investigational drug code designations, USP and NF official names, FDA established names, brand names, abbreviations, and trivial names. Each entry includes a pronunciation guide, the pharmacological category, and reference to sources of additional information.

The book contains a cross-index of names by pharmacologic–therapeutic categories and three appendixes: Guiding Principles for Coining U.S. Adopted Names, Molecular Formulas and Corresponding USAN, and Names and Addresses of Domestic Firms.

Staff Review

NOTICES

NMR: An Introduction to Proton Nuclear Magnetic Resonance Spectroscopy. By ADDISON AULT and GERALD O. DUDEK. Holden-Day, 500 Sansome St., San Francisco, CA 94111, 1976. 142 pp. 15 × 21 cm. Price $4.95.

Intended as a comprehensive nontheoretical introduction to NMR spectroscopy, the text covers both the interpretation of NMR spectra and the practical, experimental aspects of preparing the sample and obtaining the spectrum. Particular attention is given to the central concepts of magnetic equivalence and the requirements for observing a first-order spectrum. A large number of illustrative proton NMR spectra of high quality are presented and interpreted. The book is suitable as a supplementary text in organic chemistry courses. Understanding of the text requires no mathematics or advanced chemistry.

Infrared Absorption Spectroscopy, Second Ed. By KOJI NAKANISHI and PHILIPPA H. SOLOMON. Holden-Day, 500 Sansome St., San Francisco, CA 94111, 1977. 287 pp. 17 × 25 cm. Price $10.95.

This book is intended to be an introduction to IR spectroscopy for students and a reference source for practicing researchers. It includes a general discussion of the IR spectrum, tables of characteristic frequencies for different classes of organic compounds, a discussion of band position and intensity, and an introduction to Raman spectroscopy. Many problems and their solutions are given, enhancing the self-teaching utility of the book.

Modern Practice of Gas Chromatography. Edited by ROBERT L. GROB. Wiley, 605 Third Ave., New York, NY 10016, 1977. 654 pp. 16 × 24 cm. Price $22.50.

This book is organized into three parts. Part 1 is for readers interested in the theory and basics of GC, Part 2 is for those desiring information about the techniques and instrumentation, and Part 3 is for readers who are already knowledgeable about GC and want to familiarize themselves with applications.

Atlas of Cell Biology. By JEAN-CLAUDE ROLAND, ANNETTE SZÖLLÖSI, and DANIEL SZÖLLÖSI. Little, Brown, Boston, MA 02106, 1977. 117 pp. 20 × 25 cm.

Directed at students of introductory cell biology, this book contains nearly 250 illustrations that simplify and enhance the fundamental aspects of this discipline. By grouping photomicrographs with simple functional diagrams, it shows the structure of various kinds of cells and illustrates exactly how cells work. An appendix explains when to use the various methods of cell examination, how to prepare a sample, and how the laboratory instruments work.

The Essential Guide to Prescription Drugs: What You Need to Know for Safe Drug Use. By JAMES W. LONG. Harper & Row, 10 East 53rd St., New York, NY 10022, 1977. 752 pp. 16 × 23.5 cm. Price $8.95.

Advances in Chromatography, Vol. 14. Edited by J. CALVIN GIDDINGS, ELI GRUSHKA, JACK CAZES, and PHYLLIS R. BROWN. Dekker, 270 Madison Ave., New York, NY 10016, 1976. 459 pp. 15.5 × 23.5 cm. Price $34.50.

British Pharmacopoeia 1973 Addendum 1977. Her Majesty's Stationery Office (PMIC), Atlantic House, Holborn Viaduct, London, ECIP 1BN, England, 1977. 51 pp. 21 × 30 cm.

Actinomycetes: The Boundary Microorganisms. Edited by TADASHI ARAI. University Park Press, Chamber of Commerce Bldg., Baltimore, MD 21202, 1976. 651 pp. 17 × 26 cm. Price $98.60.

Clinical Toxicology, Vol. XVIII. Edited by W. A. M. DUNCAN and B. J. LEONARD. Excerpta Medica, 305 Keizersgracht, P.O. Box 1126, Amsterdam, The Netherlands, 1977. 348 pp. 16 × 24 cm. Price $35.75. Available from Elsevier North-Holland, 52 Vanderbilt Ave., New York, NY 10017.

The Molecular Biology of Animal Viruses, Vol. 1. Edited by DEBI PROSAD NAYAK. Dekker, 270 Madison Ave., New York, NY 10016, 1977. 542 pp. 18 × 24 cm. Price $49.75.

Proceedings Of The First Cleveland Symposium On Macromolecules. Edited by A. G. WALTON. Elsevier North-Holland, 52 Vanderbilt Ave., New York, NY 10017, 1977. 309 pp. 18 × 24 cm. Price $97.50.

Antibiotics In Clinical Practice, Third Ed. by HILLAS SMITH. University Park Press, Chamber of Commerce Bldg., Baltimore, MD 21202, 1977. 413 pp. 14 × 22 cm. Price $19.50.

Prolactin and Human Reproduction. Edited by P. G. CROSIGNANI and C. ROBYN. Academic (London), 24–28 Oval Road, London, NW1 7DX, England, 1977. 305 pp. 15 × 23 cm. Price $20.50.

NEW JOURNALS

Drug and Chemical Toxicology: An International Journal for Rapid Communication. Edited by JOHN G. KELLER. Dekker, 270 Madison Ave., New York, NY 10016. Price for Vol. 1 (1977–1978) $40.00 (four issues).

Leukemia Research. Edited by SVEN-AAGE KILLMANN, C. N. MULLER-BERAT, JEAN BERNARD, and EUGENE P. CRONKITE. Pergamon, Maxwell House, Fairview Park, Elmsford, NY 10523. Price $50.00 (four issues).

Parker indicates that inclusion of such an index would entail too great an expenditure of time, money, and administrative effort and points out that the detailed table of contents might suffice in this regard. The book retains an extensive author index, and each chapter has comprehensive references to literature citations. These references are provided in close proximity to their citation in the text.

Overall, this publication is very readable and should prove to be valuable to scientists having research and/or academic interest in alicyclic chemistry. This volume should be purchased by institutional libraries. The relatively high cost of the book will prevent all but the specialist from investing in its purchase. The editors are aware of the cost factor and indicate that they are examining methods for producing a less expensive publication.

Reviewed by Thomas N. Riley
Department of Medicinal Chemistry
School of Pharmacy
University of Mississippi
University, MS 38677

USAN and the USP Dictionary of Drug Names. Edited by MARY C. GRIFFITHS, MARIE J. DICKERMAN, and LLOYD C. MILLER. U. S. Pharmacopeial Convention, 12601 Twinbrook Parkway, Rockville, MD 20852. 1977. 382 pp. 21 × 28 cm. Price $18.50.

The 1977 edition of this now standard reference source lists more than 11,000 entries, including 1616 USAN (all U.S. Adopted Names selected and released from June 1961 through June 1977), 2239 investigational drug code designations, USP and NF official names, FDA established names, brand names, abbreviations, and trivial names. Each entry includes a pronunciation guide, the pharmacological category, and reference to sources of additional information.

The book contains a cross-index of names by pharmacologic–therapeutic categories and three appendixes: Guiding Principles for Coining U.S. Adopted Names, Molecular Formulas and Corresponding USAN, and Names and Addresses of Domestic Firms.

Staff Review

NOTICES

NMR: An Introduction to Proton Nuclear Magnetic Resonance Spectroscopy. By ADDISON AULT and GERALD O. DUDEK. Holden-Day, 500 Sansome St., San Francisco, CA 94111, 1976. 142 pp. 15 × 21 cm. Price $4.95.

Intended as a comprehensive nontheoretical introduction to NMR spectroscopy, the text covers both the interpretation of NMR spectra and the practical, experimental aspects of preparing the sample and obtaining the spectrum. Particular attention is given to the central concepts of magnetic equivalence and the requirements for observing a first-order spectrum. A large number of illustrative proton NMR spectra of high quality are presented and interpreted. The book is suitable as a supplementary text in organic chemistry courses. Understanding of the text requires no mathematics or advanced chemistry.

Infrared Absorption Spectroscopy, Second Ed. By KOJI NAKANISHI and PHILIPPA H. SOLOMON. Holden-Day, 500 Sansome St., San Francisco, CA 94111, 1977. 287 pp. 17 × 25 cm. Price $10.95.

This book is intended to be an introduction to IR spectroscopy for students and a reference source for practicing researchers. It includes a general discussion of the IR spectrum, tables of characteristic frequencies for different classes of organic compounds, a discussion of band position and intensity, and an introduction to Raman spectroscopy. Many problems and their solutions are given, enhancing the self-teaching utility of the book.

Modern Practice of Gas Chromatography. Edited by ROBERT L. GROB. Wiley, 605 Third Ave., New York, NY 10016, 1977. 654 pp. 16 × 24 cm. Price $22.50.

This book is organized into three parts. Part 1 is for readers interested in the theory and basics of GC, Part 2 is for those desiring information about the techniques and instrumentation, and Part 3 is for readers who are already knowledgeable about GC and want to familiarize themselves with applications.

Atlas of Cell Biology. By JEAN-CLAUDE ROLAND, ANNETTE SZÖLLÖSI, and DANIEL SZÖLLÖSI. Little, Brown, Boston, MA 02106, 1977. 117 pp. 20 × 25 cm.

Directed at students of introductory cell biology, this book contains nearly 250 illustrations that simplify and enhance the fundamental aspects of this discipline. By grouping photomicrographs with simple functional diagrams, it shows the structure of various kinds of cells and illustrates exactly how cells work. An appendix explains when to use the various methods of cell examination, how to prepare a sample, and how the laboratory instruments work.

The Essential Guide to Prescription Drugs: What You Need to Know for Safe Drug Use. By JAMES W. LONG. Harper & Row, 10 East 53rd St., New York, NY 10022, 1977. 752 pp. 16 × 23.5 cm. Price $8.95.

Advances in Chromatography, Vol. 14. Edited by J. CALVIN GIDDINGS, ELI GRUSHKA, JACK CAZES, and PHYLLIS R. BROWN. Dekker, 270 Madison Ave., New York, NY 10016, 1976. 459 pp. 15.5 × 23.5 cm. Price $34.50.

British Pharmacopoeia 1973 Addendum 1977. Her Majesty's Stationery Office (PMIC), Atlantic House, Holborn Viaduct, London, ECIP 1BN, England, 1977. 51 pp. 21 × 30 cm.

Actinomycetes: The Boundary Microorganisms. Edited by TADASHI ARAI. University Park Press, Chamber of Commerce Bldg., Baltimore, MD 21202, 1976. 651 pp. 17 × 26 cm. Price $98.60.

Clinical Toxicology, Vol. XVIII. Edited by W. A. M. DUNCAN and B. J. LEONARD. Excerpta Medica, 305 Keizersgracht, P.O. Box 1126, Amsterdam, The Netherlands, 1977. 348 pp. 16 × 24 cm. Price $35.75. Available from Elsevier North-Holland, 52 Vanderbilt Ave., New York, NY 10017.

The Molecular Biology of Animal Viruses, Vol. 1. Edited by DEBI PROSAD NAYAK. Dekker, 270 Madison Ave., New York, NY 10016, 1977. 542 pp. 18 × 24 cm. Price $49.75.

Proceedings Of The First Cleveland Symposium On Macromolecules. Edited by A. G. WALTON. Elsevier North-Holland, 52 Vanderbilt Ave., New York, NY 10017, 1977. 309 pp. 18 × 24 cm. Price $97.50.

Antibiotics In Clinical Practice, Third Ed. by HILLAS SMITH. University Park Press, Chamber of Commerce Bldg., Baltimore, MD 21202, 1977. 413 pp. 14 × 22 cm. Price $19.50.

Prolactin and Human Reproduction. Edited by P. G. CROSIGNANI and C. ROBYN. Academic (London), 24–28 Oval Road, London, NW1 7DX, England, 1977. 305 pp. 15 × 23 cm. Price $20.50.

NEW JOURNALS

Drug and Chemical Toxicology: An International Journal for Rapid Communication. Edited by JOHN G. KELLER. Dekker, 270 Madison Ave., New York, NY 10016. Price for Vol. 1 (1977–1978) $40.00 (four issues).

Leukemia Research. Edited by SVEN-AAGE KILLMANN, C. N. MULLER-BERAT, JEAN BERNARD, and EUGENE P. CRONKITE. Pergamon, Maxwell House, Fairview Park, Elmsford, NY 10523. Price $50.00 (four issues).

FEBRUARY 1978
VOLUME 67 NUMBER 2

JOURNAL OF PHARMACEUTICAL SCIENCES

MARY H. FERGUSON
Editor

SHELLY ELLIOTT
Production Editor

JANET D. SHOFF
Copy Editor

EDWARD G. FELDMANN
Contributing Editor

SAMUEL W. GOLDSTEIN
Contributing Editor

BELLE R. BECK
Editorial Secretary

DAVID BOHARDT
Director of Publications

L. LUAN CORRIGAN
Assistant Director of Publications

EDITORIAL ADVISORY BOARD

JOHN AUTIAN	HERBERT A. LIEBERMAN
NORMAN R. FARNSWORTH	DAVID E. MANN, JR.
WILLIAM O. FOYE	GERALD J. PAPARIELLO
WILLIAM J. JUSKO	EDWARD G. RIPPIE

The *Journal of Pharmaceutical Sciences* is published monthly by the American Pharmaceutical Association at 2215 Constitution Ave., N.W., Washington, DC 20037. Second-class postage paid at Washington, D.C., and at additional mailing office.

All expressions of opinion and statements of supposed fact appearing in articles or editorials carried in this journal are published on the authority of the writer over whose name they appear and are not to be regarded as necessarily expressing the policies or views of the American Pharmaceutical Association.

Offices—Editorial, Advertising, and Subscription Offices: 2215 Constitution Ave., N.W., Washington, DC 20037. Printing Offices: 20th & Northampton Streets, Easton, PA 18042.

Annual Subscriptions—United States and foreign, industrial and government institutions $50, educational institutions $50, individuals *for personal use only* $30; single copies $5. All foreign subscriptions add $5 for postage. Subscription rates are subject to change without notice. Members of the American Pharmaceutical Association may elect to receive the *Journal of Pharmaceutical Sciences* as a part of their annual $70 (foreign $75) APhA membership dues.

Claims—Missing numbers will not be supplied if dues or subscriptions are in arrears for more than 60 days or if claims are received more than 60 days after the date of the issue, or if loss was due to failure to give notice of change of address. The Association cannot accept responsibility for foreign delivery when its records indicate shipment has been made.

Change of Address—Members and subscribers should notify at once both the Post Office and the American Pharmaceutical Association, 2215 Constitution Ave., N.W., Washington, DC 20037, of any change of address.

Microfilm—Microfilm volumes are available from University Microfilms International, 300 N. Zeeb Road, Ann Arbor, MI 48106.

© Copyright 1978, American Pharmaceutical Association, 2215 Constitution Ave., N.W., Washington, DC 20037; all rights reserved.

WHY A CONSIDERATION FEE?

Publish or perish are familiar words and the meaning is clear. Publish if you want to qualify for a raise, a promotion, tenure, or a new position. Publish as many papers as possible from each research project because it is the number of papers that is important. Publish or perish is familiar now; publish until scientific journals perish is becoming familiar.

I have listened to your problems with budgets, grants, and reviewers who do not recognize how important it is for your paper to be published. Now will you take a minute and listen to mine?

Last year the cost of publishing the Journal was approximately $45,000 greater than Journal income. On January 1, 1978, there was an 8% increase in the cost of printing, and there has been a 20% increase in the cost of paper. The number of Journal subscriptions is steadily decreasing as libraries stop multiple subscriptions and institutions stop paying for employee subscriptions. Approximately 40,000 people read the Journal; less than 10,000 subscribe. It may be less expensive to make photocopies of two or three articles of particular interest than to subscribe, but it violates the Journal copyright. Most importantly, it directly cuts into the primary source of income upon which the Journal is dependent for its operating revenue. Three out of four people reading this issue will not read from personal copies. One out of 20 reprint requests to authors will be filled with reprints obtained with perfectly valid institution purchase orders that the institutions then refuse to honor or will pay only after repeated billing and collection efforts. Page charges are not paid for approximately 40% of the articles published in the Journal, although it would appear that publication costs should be an integral part of a research budget.

In an effort to reduce Journal losses and offset some of the expense of considering manuscripts for publication, a nonrefundable $25.00 consideration fee is now required for all manuscripts submitted to the Journal. If the manuscript is published, page charges will be reduced by $25.00, the full amount of the consideration fee. Clearly, the consideration fee is an expense only for those authors whose manuscripts are not of acceptable quality or whose sponsoring institutions require them to publish but refuse to accept any responsibility for publication expense. In addition to reducing publication losses, the manuscript consideration fee should improve the quality of manuscripts submitted to the Journal on the basis that authors would not pay the fee if, in their own opinion, their manuscripts are of marginal quality.

Who receives the most benefit from the publication of papers? It cannot be the reader because 75% of Journal readers are unwilling to pay reasonable subscription costs for personal copies; it cannot be the Journal since we operate at a deficit and do not even recoup publishing costs. The major benefit must accrue to authors and their sponsoring institutions because even a publish or perish paper brings recognition and a certain prestige to the authors and their sponsors. If readers are not willing to pay subscription fees to read the articles, and authors are being forced to publish for their professional survival, it appears that authors and their sponsors should be willing to share some of the responsibility for publication expense. This is exactly what is happening in many cases.

Many authors and their sponsoring institutions are supporting the consideration fee, recognizing that (*a*) it is not an additional expense since it is subtracted from page charges, (*b*) it may help reduce the backlog of manuscripts, making faster publication possible, and (*c*) an effort is being made to contain Journal losses arising from manuscripts from sources that are unwilling to assume any publication expense responsibility. There are, of course, other journals that will publish these latter papers now, but they have the same problems as *J. Pharm. Sci.* Unless authors, readers, and journals begin working out solutions to their mutual problems now, publish until the scientific journals perish will become a grim reality.

FEBRUARY 1978
VOLUME 67 NUMBER 2

JOURNAL OF PHARMACEUTICAL SCIENCES

MARY H. FERGUSON
Editor

SHELLY ELLIOTT
Production Editor

JANET D. SHOFF
Copy Editor

EDWARD G. FELDMANN
Contributing Editor

SAMUEL W. GOLDSTEIN
Contributing Editor

BELLE R. BECK
Editorial Secretary

DAVID BOHARDT
Director of Publications

L. LUAN CORRIGAN
Assistant Director of Publications

EDITORIAL ADVISORY BOARD

JOHN AUTIAN	HERBERT A. LIEBERMAN
NORMAN R. FARNSWORTH	DAVID E. MANN, JR.
WILLIAM O. FOYE	GERALD J. PAPARIELLO
WILLIAM J. JUSKO	EDWARD G. RIPPIE

The *Journal of Pharmaceutical Sciences* is published monthly by the American Pharmaceutical Association at 2215 Constitution Ave., N.W., Washington, DC 20037. Second-class postage paid at Washington, D.C., and at additional mailing office.

All expressions of opinion and statements of supposed fact appearing in articles or editorials carried in this journal are published on the authority of the writer over whose name they appear and are not to be regarded as necessarily expressing the policies or views of the American Pharmaceutical Association.

Offices—Editorial, Advertising, and Subscription Offices: 2215 Constitution Ave., N.W., Washington, DC 20037. Printing Offices: 20th & Northampton Streets, Easton, PA 18042.

Annual Subscriptions—United States and foreign, industrial and government institutions $50, educational institutions $50, individuals *for personal use only* $30; single copies $5. All foreign subscriptions add $5 for postage. Subscription rates are subject to change without notice. Members of the American Pharmaceutical Association may elect to receive the *Journal of Pharmaceutical Sciences* as a part of their annual $70 (foreign $75) APhA membership dues.

Claims—Missing numbers will not be supplied if dues or subscriptions are in arrears for more than 60 days or if claims are received more than 60 days after the date of the issue, or if loss was due to failure to give notice of change of address. The Association cannot accept responsibility for foreign delivery when its records indicate shipment has been made.

Change of Address—Members and subscribers should notify at once both the Post Office and the American Pharmaceutical Association, 2215 Constitution Ave., N.W., Washington, DC 20037, of any change of address.

Microfilm—Microfilm volumes are available from University Microfilms International, 300 N. Zeeb Road, Ann Arbor, MI 48106.

© Copyright 1978, American Pharmaceutical Association, 2215 Constitution Ave., N.W., Washington, DC 20037; all rights reserved.

WHY A CONSIDERATION FEE?

Publish or perish are familiar words and the meaning is clear. Publish if you want to qualify for a raise, a promotion, tenure, or a new position. Publish as many papers as possible from each research project because it is the number of papers that is important. Publish or perish is familiar now; publish until scientific journals perish is becoming familiar.

I have listened to your problems with budgets, grants, and reviewers who do not recognize how important it is for your paper to be published. Now will you take a minute and listen to mine?

Last year the cost of publishing the Journal was approximately $45,000 greater than Journal income. On January 1, 1978, there was an 8% increase in the cost of printing, and there has been a 20% increase in the cost of paper. The number of Journal subscriptions is steadily decreasing as libraries stop multiple subscriptions and institutions stop paying for employee subscriptions. Approximately 40,000 people read the Journal; less than 10,000 subscribe. It may be less expensive to make photocopies of two or three articles of particular interest than to subscribe, but it violates the Journal copyright. Most importantly, it directly cuts into the primary source of income upon which the Journal is dependent for its operating revenue. Three out of four people reading this issue will not read from personal copies. One out of 20 reprint requests to authors will be filled with reprints obtained with perfectly valid institution purchase orders that the institutions then refuse to honor or will pay only after repeated billing and collection efforts. Page charges are not paid for approximately 40% of the articles published in the Journal, although it would appear that publication costs should be an integral part of a research budget.

In an effort to reduce Journal losses and offset some of the expense of considering manuscripts for publication, a nonrefundable $25.00 consideration fee is now required for all manuscripts submitted to the Journal. If the manuscript is published, page charges will be reduced by $25.00, the full amount of the consideration fee. Clearly, the consideration fee is an expense only for those authors whose manuscripts are not of acceptable quality or whose sponsoring institutions require them to publish but refuse to accept any responsibility for publication expense. In addition to reducing publication losses, the manuscript consideration fee should improve the quality of manuscripts submitted to the Journal on the basis that authors would not pay the fee if, in their own opinion, their manuscripts are of marginal quality.

Who receives the most benefit from the publication of papers? It cannot be the reader because 75% of Journal readers are unwilling to pay reasonable subscription costs for personal copies; it cannot be the Journal since we operate at a deficit and do not even recoup publishing costs. The major benefit must accrue to authors and their sponsoring institutions because even a publish or perish paper brings recognition and a certain prestige to the authors and their sponsors. If readers are not willing to pay subscription fees to read the articles, and authors are being forced to publish for their professional survival, it appears that authors and their sponsors should be willing to share some of the responsibility for publication expense. This is exactly what is happening in many cases.

Many authors and their sponsoring institutions are supporting the consideration fee, recognizing that (*a*) it is not an additional expense since it is subtracted from page charges, (*b*) it may help reduce the backlog of manuscripts, making faster publication possible, and (*c*) an effort is being made to contain Journal losses arising from manuscripts from sources that are unwilling to assume any publication expense responsibility. There are, of course, other journals that will publish these latter papers now, but they have the same problems as *J. Pharm. Sci.* Unless authors, readers, and journals begin working out solutions to their mutual problems now, publish until the scientific journals perish will become a grim reality.

pH Effect on Chromatographic Column

In the article "High-Speed Liquid Chromatographic Determination of Pilocarpine in Pharmaceutical Dosage Forms," which appeared in the November Journal[1], I noticed that the author used a mobile phase whose pH was 9.2. The author used this mobile phase with two columns (octadecylsilane and cyanopropylsilane). According to my information, the pH of the mobile phase should not be more than 8; otherwise, the bonds in these two columns get hydrolyzed, which destroys the columns rather fast. These two columns cost about $600.

V. Das Gupta
Department of Pharmaceutics
College of Pharmacy
University of Houston
Houston, TX 77004

Received November 28, 1977.

[1] S. K. W. Khalil, *J. Pharm. Sci.*, **66**, 1625 (1977).

Measurement of Iodochlorhydroxyquin/Clioquinol

In his recent paper, "TLC Determination of Iodochlorhydroxyquin and Its Conjugate in Plasma," Del Soldato[1] claimed that no method existed until then for the measurement of these compounds in biological fluids. This is simply not true. Two GLC methods were published in 1973, one a study of patients with subacute myelo-optico-neuropathy[2] and the other a pharmacokinetic study using healthy volunteers[3]. Since then, two further GLC methods, using extractive alkylation, were reported[4,5].

No doubt some confusion arises from the fact that the compound 5-chloro-7-iodo-8-hydroxyquinoline is called iodochlorhydroxyquin in the United States while the name clioquinol is used in Europe and Japan. This usage, however, does not excuse the statement of Del Soldato since, of the two papers published in 1973, one used the name clioquinol in its title while the other used iodochlorhydroxyquin.

David B. Jack
Biochemistry Department
Western Infirmary
Glasgow G11 6NT
Scotland

Received December 12, 1977.

[1] P. Del Soldato, *J. Pharm. Sci.*, **66**, 1334 (1977).
[2] Z. Tamura, M. Yoshioka, T. Imanari, J. Fukaya, J. Kusaka, and K. Samejima, *Clin. Chim. Acta*, **47**, 13 (1973).
[3] D. B. Jack and W. Riess, *J. Pharm. Sci.*, **62**, 1929 (1973).
[4] P. H. Degen, W. Schneider, P. Vuillard, U. P. Geiger, and W. Riess, *J. Chromatogr.*, **117**, 407 (1976).
[5] P. Hartvig and C. Fagerlund, *ibid.*, **140**, 170 (1977).

Dragendorff's Reagent Research Acknowledged

This letter is intended to correct an omission under *Acknowledgments* in the recent article: "TLC Sensitivity of Six Modifications of Dragendorff's Reagent"[1]. Dr. G. R. Padmanabhan, currently at Ciba-Geigy Corp., Suffern, N.Y., and Dr. J. E. Heveran of Hoffmann–La Roche Inc., Nutley, N.J., were instrumental in the selection of some of the compounds used in the study, namely trimethylsulfonium iodide, edrophonium chloride, and benzyltriphenylphosphonium chloride, and they provided technical assistance in the initial stages of the experiment. In addition, in an unpublished study, several other compounds, not included in our work, were examined by them using a somewhat different procedure than ours. Their names were inadvertently omitted from the original manuscript.

Ralph Gomez
Linda Rubia
Research Products Section
Quality Control Department
Hoffmann–La Roche Inc.
Nutley, NJ 07110

Received December 2, 1977.

[1] L. B. Rubia and R. Gomez, *J. Pharm. Sci.*, **66**, 1656 (1977).

pH Effect on Chromatographic Column

In the article "High-Speed Liquid Chromatographic Determination of Pilocarpine in Pharmaceutical Dosage Forms," which appeared in the November Journal[1], I noticed that the author used a mobile phase whose pH was 9.2. The author used this mobile phase with two columns (octadecylsilane and cyanopropylsilane). According to my information, the pH of the mobile phase should not be more than 8; otherwise, the bonds in these two columns get hydrolyzed, which destroys the columns rather fast. These two columns cost about $600.

V. Das Gupta
Department of Pharmaceutics
College of Pharmacy
University of Houston
Houston, TX 77004

Received November 28, 1977.

[1] S. K. W. Khalil, *J. Pharm. Sci.*, **66**, 1625 (1977).

Measurement of Iodochlorhydroxyquin/Clioquinol

In his recent paper, "TLC Determination of Iodochlorhydroxyquin and Its Conjugate in Plasma," Del Soldato[1] claimed that no method existed until then for the measurement of these compounds in biological fluids. This is simply not true. Two GLC methods were published in 1973, one a study of patients with subacute myelo-optico-neuropathy[2] and the other a pharmacokinetic study using healthy volunteers[3]. Since then, two further GLC methods, using extractive alkylation, were reported[4,5].

No doubt some confusion arises from the fact that the compound 5-chloro-7-iodo-8-hydroxyquinoline is called iodochlorhydroxyquin in the United States while the name clioquinol is used in Europe and Japan. This usage, however, does not excuse the statement of Del Soldato since, of the two papers published in 1973, one used the name clioquinol in its title while the other used iodochlorhydroxyquin.

David B. Jack
Biochemistry Department
Western Infirmary
Glasgow G11 6NT
Scotland

Received December 12, 1977.

[1] P. Del Soldato, *J. Pharm. Sci.*, **66**, 1334 (1977).
[2] Z. Tamura, M. Yoshioka, T. Imanari, J. Fukaya, J. Kusaka, and K. Samejima, *Clin. Chim. Acta*, **47**, 13 (1973).
[3] D. B. Jack and W. Riess, *J. Pharm. Sci.*, **62**, 1929 (1973).
[4] P. H. Degen, W. Schneider, P. Vuillard, U. P. Geiger, and W. Riess, *J. Chromatogr.*, **117**, 407 (1976).
[5] P. Hartvig and C. Fagerlund, *ibid.*, **140**, 170 (1977).

Dragendorff's Reagent Research Acknowledged

This letter is intended to correct an omission under *Acknowledgments* in the recent article: "TLC Sensitivity of Six Modifications of Dragendorff's Reagent"[1]. Dr. G. R. Padmanabhan, currently at Ciba-Geigy Corp., Suffern, N.Y., and Dr. J. E. Heveran of Hoffmann–La Roche Inc., Nutley, N.J., were instrumental in the selection of some of the compounds used in the study, namely trimethylsulfonium iodide, edrophonium chloride, and benzyltriphenylphosphonium chloride, and they provided technical assistance in the initial stages of the experiment. In addition, in an unpublished study, several other compounds, not included in our work, were examined by them using a somewhat different procedure than ours. Their names were inadvertently omitted from the original manuscript.

Ralph Gomez
Linda Rubia
Research Products Section
Quality Control Department
Hoffmann–La Roche Inc.
Nutley, NJ 07110

Received December 2, 1977.

[1] L. B. Rubia and R. Gomez, *J. Pharm. Sci.*, **66**, 1656 (1977).

pH Effect on Chromatographic Column

In the article "High-Speed Liquid Chromatographic Determination of Pilocarpine in Pharmaceutical Dosage Forms," which appeared in the November Journal[1], I noticed that the author used a mobile phase whose pH was 9.2. The author used this mobile phase with two columns (octadecylsilane and cyanopropylsilane). According to my information, the pH of the mobile phase should not be more than 8; otherwise, the bonds in these two columns get hydrolyzed, which destroys the columns rather fast. These two columns cost about $600.

V. Das Gupta
Department of Pharmaceutics
College of Pharmacy
University of Houston
Houston, TX 77004

Received November 28, 1977.

[1] S. K. W. Khalil, *J. Pharm. Sci.*, **66**, 1625 (1977).

Measurement of Iodochlorhydroxyquin/Clioquinol

In his recent paper, "TLC Determination of Iodochlorhydroxyquin and Its Conjugate in Plasma," Del Soldato[1] claimed that no method existed until then for the measurement of these compounds in biological fluids. This is simply not true. Two GLC methods were published in 1973, one a study of patients with subacute myelo-optico-neuropathy[2] and the other a pharmacokinetic study using healthy volunteers[3]. Since then, two further GLC methods, using extractive alkylation, were reported[4,5].

No doubt some confusion arises from the fact that the compound 5-chloro-7-iodo-8-hydroxyquinoline is called iodochlorhydroxyquin in the United States while the name clioquinol is used in Europe and Japan. This usage, however, does not excuse the statement of Del Soldato since, of the two papers published in 1973, one used the name clioquinol in its title while the other used iodochlorhydroxyquin.

David B. Jack
Biochemistry Department
Western Infirmary
Glasgow G11 6NT
Scotland

Received December 12, 1977.

[1] P. Del Soldato, *J. Pharm. Sci.*, **66**, 1334 (1977).
[2] Z. Tamura, M. Yoshioka, T. Imanari, J. Fukaya, J. Kusaka, and K. Samejima, *Clin. Chim. Acta*, **47**, 13 (1973).
[3] D. B. Jack and W. Riess, *J. Pharm. Sci.*, **62**, 1929 (1973).
[4] P. H. Degen, W. Schneider, P. Vuillard, U. P. Geiger, and W. Riess, *J. Chromatogr.*, **117**, 407 (1976).
[5] P. Hartvig and C. Fagerlund, *ibid.*, **140**, 170 (1977).

Dragendorff's Reagent Research Acknowledged

This letter is intended to correct an omission under *Acknowledgments* in the recent article: "TLC Sensitivity of Six Modifications of Dragendorff's Reagent"[1]. Dr. G. R. Padmanabhan, currently at Ciba-Geigy Corp., Suffern, N.Y., and Dr. J. E. Heveran of Hoffmann–La Roche Inc., Nutley, N.J., were instrumental in the selection of some of the compounds used in the study, namely trimethylsulfonium iodide, edrophonium chloride, and benzyltriphenylphosphonium chloride, and they provided technical assistance in the initial stages of the experiment. In addition, in an unpublished study, several other compounds, not included in our work, were examined by them using a somewhat different procedure than ours. Their names were inadvertently omitted from the original manuscript.

Ralph Gomez
Linda Rubia
Research Products Section
Quality Control Department
Hoffmann–La Roche Inc.
Nutley, NJ 07110

Received December 2, 1977.

[1] L. B. Rubia and R. Gomez, *J. Pharm. Sci.*, **66**, 1656 (1977).

JOURNAL OF PHARMACEUTICAL SCIENCES

FEBRUARY 1978
VOLUME 67 NUMBER 2

RESEARCH ARTICLES

Kinetics of Plasma Coagulation and Lysis I: Basic Kinetic Model for Time Course of Coagulation–Lysis Systems and Its Potential Application to Clinical Studies

EDWARD R. GARRETT *x, **JEAN DAVER** §, **PIERRE DESNOYERS** ‡, **MARTINE KOSSER** ‡, and **MICHEL VINCENT** ‡

Received February 22, 1977, from the *Beehive, College of Pharmacy, University of Florida, Gainesville, FL 32610, the ‡Servier Research Institute, F. 92150 Suresnes, France, and the §Biomedical Laboratory, F. 81100 Castres, France. Accepted for publication April 29, 1977.

Abstract □ The time courses of coagulation and coagulation–lysis were spectrophotometrically monitored after the addition of thrombin or thrombin–streptokinase to plasma, diluted 1:5 with normal saline, obtained from normal and presumably abnormal subjects. The kinetics of clotting, after an initial lag period of 0.5–1.5 min, demonstrated essentially first-order dependence on the amount of fibrinogen available to form the clot, and the asymptotic absorbance was independent of thrombin concentration. The rate of clotting was a function of added thrombin, and the ratios of the rate constants at 2.5 and 1.25 units of thrombin/ml of undiluted plasma were 1.65 ± 0.03 *SEM*. At early times, the coagulation–lysis curve with thrombin–streptokinase could be superimposed on the clotting curve with thrombin alone for a given plasma with minor compensation for variable lag times. Subsequently, the curves diverged; lysis was monitored by the decrease in absorbance of the coagulation–lysis system. The rate of fibrinolysis increased with streptokinase concentration and was a function of the extent of lysis, and it permitted the description of the kinetics of lysis by a pseudoautocatalytic mechanism where the bimolecular rate constant appears proportional to streptokinase concentration. Ranges of clotting and lytic parameters for the plasma of normal subjects are given, and their potential use in diagnosing abnormalities is described.

Keyphrases □ Coagulation and coagulation–lysis—time courses after addition of thrombin or thrombin–streptokinase to plasma, kinetic model developed □ Models, kinetic—coagulation and coagulation–lysis, time courses after addition of thrombin or thrombin–streptokinase to plasma □ Kinetic models—coagulation and coagulation–lysis, time courses after addition of thrombin or thrombin–streptokinase to plasma

The effects of pathological states on the rates of plasma coagulation and lysis are well recognized. Measurements of coagulation parameters such as partial thromboplastin time, prothrombin time, Howell time, and whole blood coagulation time are often employed to adjust dosage regimens of anticoagulant drugs and to diagnose certain liver dysfunctions, circulatory disorders, and other diseases. Nevertheless, quantitative information on the kinetics of blood coagulation and lysis is scarce (1–5). In fact, the parameter normally used to estimate lytic rates is a one-value response, the lysis time, a time taken as the interval between the addition of thrombin and an empirical observation of dissolution of the fibrin network. Prior postulated kinetic models have been based on this one-value response (1–8).

These present investigations are a continuation of prior studies on coagulation–lysis system kinetics, with the ultimate objective of searching for "normocoagulating" drugs (8) that could maintain the equilibrium of such systems. The results of kinetic studies of plasma coagulation and lysis of diluted plasma from various normal subjects are given as a function of various concentrations of thrombin and streptokinase. The continuously spectrophotometrically monitored time courses of formation and lysis of the clot, a method proposed by Bouvier and colleagues (9–11), were used to determine the pertinent kinetic parameters and to establish kinetic models. The potential use of these derived kinetic parameters to diagnose abnormalities is described.

EXPERIMENTAL

Platelet-poor plasmas were obtained from whole citrated blood[1] from presumed normal subjects[1] and subjects with possible thromboembolic diseases[2] by centrifugation at 4° for 10 min at 1500×*g*. They were then frozen at −20° and thawed in a water bath at 37° when used. The monitoring of the time course of clotting and lysis at 350 min was similar to that previously reported (9–11); details of effects of storage time and treatment of blood and plasma were given (9–11).

[1] Nancy Regional Blood Transfusion Center, Nancy, France.
[2] Hotel Dieu Hospital, Paris, France.

Table I—Reproducibility of Parameters of Blood Clotting Model (Eq. 1) at a Fixed Concentration of Plasma (20%) and Varying Concentrations of Thrombin [a]

	Thrombin, Units/ml of Undiluted Plasma						
	1.25			2.5			
Replicate	k_c, min^{-1}	10^2A_∞	t_{lag}, sec	k_c, min^{-1}	10^2A_∞	t_{lag}, sec	$\frac{k_c\ (2.5)}{k_c\ (1.25)}$
1	0.94	53	62	1.42	55	27	1.51
2	1.15	49	55	1.60	51	26	1.39
3	0.97	53	58	1.48	55	27	1.53
4	1.00	53	65	1.51	54	28	1.51
5	0.95	52	76	1.37	55	30	1.44
6	0.93	51	54	1.51	57	29	1.62
7	1.02	54	56	1.56	52	31	1.53
8	1.01	49	67	1.54	52	27	1.52
9	0.99	51	59	1.33	50	32	1.34
10	1.00	48	68	1.40	54	34	1.40
Mean	1.00	53	66	1.5	55	28	1.48
SD	0.084	2	7.8	0.09	2	2	0.08

[a] Data fitted by a Wang digital computer and the Simplex program to $A = A_\infty[1 - e^{-k_c(t-t_{lag})}]$, where A is the absorbance at time t. The plasma was from an individual subject.

A 2-ml aliquot of each diluted plasma, previously diluted 1:5 with normal saline (0.9%), was added to a 1 × 1-cm 25° thermostated quartz cell. The coagulation was initiated by adding 0.1 ml of Michaelis buffer and 0.1 ml of thrombin[3] solution in Michaelis buffer containing 1.25 or 2.5 units of thrombin/ml of undiluted plasma by calibrated syringes and immediately mixing on a vortex mixer.

The Michaelis buffer was prepared from a mixture of 1 volume of a stock buffer solution (I) and 4 volumes of 0.85% NaCl, which was adjusted to pH 7.42. The stock buffer solution (I) at pH 7.42 contained 5 volumes of a solution prepared to contain 9.714 g of sodium acetate trihydrate and 14.714 g of barbital sodium in 500 ml of freshly boiled distilled water, 5 volumes of 0.1 *N* HCl, 2 volumes of 8.5% NaCl, and 15 volumes of distilled water. The increasing absorbance due to coagulation was monitored as a function of time against a similarly treated blank in a continuously recording UV spectrophotometer[4].

The 2.0 ml of diluted plasma was also mixed in the cell with the same amount of thrombin solution (0.1 ml) and with 0.1 ml of a streptokinase[5] solution in isotonic saline containing 25 or 50 Christensen units/ml of undiluted plasma. The initially increasing and subsequent decreasing absorbances due to coagulation and lysis were monitored spectrophotometrically as a function of time. The thrombin and streptokinase solutions were kept refrigerated prior to use.

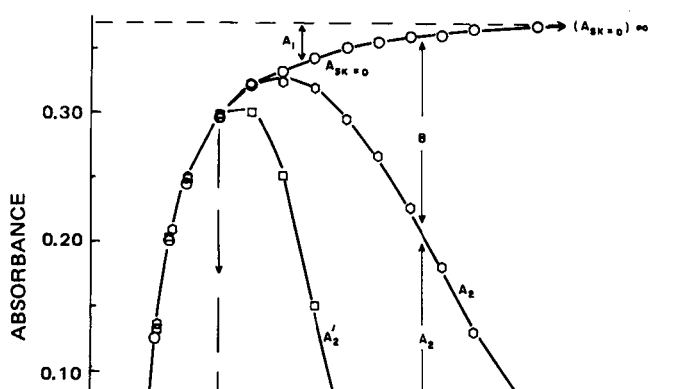

Figure 1—*Typical plots of the observed absorbance of clots from 20% human plasma in isotonic saline with time with 2.5 units of thrombin/ml of undiluted plasma (○) and with 25 (○), and 50 (□) units of streptokinase added per milliliter of undiluted plasma. The initial portions of the curves were superimposed so as to be independent of slightly variable t_{lag} times. The values of* B *for Eq. 5 can be determined from the difference between the values at a specific time of* $A_{SK=0}$ *and* A_2 *(or* A_2'*). The values of* A *can be determined from the sum of* A_2 *(or* A_2'*) and* A_1*, the difference between the asymptotic value of* $(A_{SK=0})_\infty$ *and* $A_{SK=0}$ *at the same time. The arrow at* t_s *represents the limit of coincidence among the various absorbance–time curves.*

RESULTS AND DISCUSSION

Kinetics of Clotting—A typical spectrophotometric absorbance, A, against time plot for the clotting of isotonic saline-diluted plasma at a thrombin concentration of 2.5 units of undiluted plasma/ml is given in Fig. 1. A lag time, t_{lag}, was observed before significant clotting was apparent as monitored by absorbance. The increase in thrombin concentration appeared to lessen this lag time but had no significant effect on the final magnitude of the absorbance. Qualitatively, the curve, on correction for lag time, appeared to be generated by a first-order process, where the rate of absorbance increase appeared to be proportional to the concentration of a precursor, P. Apparently, the amount of this precursor diminished with time and was directly related to the amount of clot yet to be formed, $A_\infty - A$. It follows that:

$$-dA/dt = k_cP = k_c(A_\infty - A) \qquad \text{(Eq. 1)}$$

Thus, for $t > t_{lag}$:

$$\ln (A_\infty - A) = \ln A_\infty - k_c(t - t_{lag}) \qquad \text{(Eq. 2)}$$

Various models for the clotting time curves, A *versus* time, t (Fig. 1), were challenged by fitting them by nonlinear regression with digital computerization to the models $P \rightarrow A$ (with compensation for lag where $A = 0$ at $t = t_{lag}$) and $P' \rightarrow P \rightarrow A$ (where lag time was and was not considered). Appropriate fitting was satisfactorily obtained by the former model in accordance with Eqs. 1 and 2.

As expected, the absorbance data at the very early times (<0.5 min) showed slight deviations from the semilogarithmic plot of the data in accordance with Eq. 2. This result is a consequence of the inability to monitor technologically the absorbance accurately during the initial fast rates of clot formation. The validity of Eq. 2 depends on the accurate determination of the final values, A_∞, of the absorbance on cessation of clotting. The clotting system is a heterogeneous one, and secondary and tertiary cross-linking of fibrin polymer may give a consistently elevating final absorbance for longer periods of time.

Such slight elevations were observed, and the appropriate A_∞ was chosen to give complete linearity of the semilogarithmic plots of $A_\infty - A$ against time. Actually, only minor decreases of 2–5% in the experimentally observed A_∞ values were necessary to obtain complete linearity in such plots. The clotting rate constant, k_c, was obtained from the slope. Although graphical methods are applicable to determine the clotting parameters t_{lag}, A_∞, and k_c from Eq. 2, it was more practical to fit the nonlogarithmic transformation of this equation:

$$A = A_\infty[1 - e^{-k_c(t-t_{lag})}] \qquad \text{(Eq. 3)}$$

by nonlinear regression to the data of Fig. 1 using a digital computer[6] and

[3] Thrombin (Hoffmann-La Roche), vial of 100 mg at 45 NIH units/mg, Batch B 938 K 91 A.

[4] Beckman (Acta III), Fullerton, Calif.

[5] Kabikinase (AB Kabi, Stockholm), vials of 5000 Christensen units.

[6] Wang.

Table II—Plasma (Diluted 1:5 with Isotonic Saline) Clotting Parameters [a] for Clinically Appraised Normals of Set A

Subject	Thrombin, Units/ml of Undiluted Plasma: 1.25 t_{lag}, sec	1.25 $100\,A_\infty$	1.25 k_c, min^{-1}	1.25 $t_{1/2}$, min	2.5 t_{lag}, sec	2.5 $100\,A_\infty$	2.5 k_c, min^{-1}	2.5 $t_{1/2}$, min	$\frac{k_c\ (2.5)}{k_c\ (1.25)}$
1	30	35.7	0.91	0.75	15	32.1	1.51	0.45	1.66
2	40	32.5	0.93	0.74	118	34.3	1.83	0.37	1.97
3	15	33.8	0.79	0.87	40	34.4	1.53	0.45	1.94
4	63	43.6	0.75	0.92	30	45.1	1.26	0.54	1.68
5	83	41.3	0.73	0.94	0	39.9	1.18	0.58	1.62
6	84	32.7	0.77	0.89	55	32.9	1.45	0.47	1.88
7	60	37.7	0.55	1.25	27	37.7	0.84	0.81	1.52
8	80	38.2	0.78	0.87	34	40.8	1.38	0.49	1.77
9	80	38	0.64	1.07	45	39.9	1.00	0.69	1.56
10	93	36.6	0.59	1.16	28	37.3	1.08	0.63	1.83
Average *SD*	62.80 ± 26.35	37.07 ± 3.40	0.74 ± 0.12	0.94 ± 0.16	69.20 ± 31.62	37.44 ± 4.08	1.30 ± 0.29	0.56 ± 0.13	1.74 ± 0.15
Average ± *SD* with 7 and 10 omitted	59.37 ± 27.34	36.97 ± 4.05	0.78 ± 0.094	0.88 ± 0.10	42.12 ± 35.17	34.92 ± 7.57	1.39 ± 0.25	0.50 ± 0.09	1.76 ± 0.15

[a] Obtained by a Wang digital computer and the Simplex program fitting to the equation $A = A_\infty[1 - e^{-k_c(t-t_{lag})}]$, where A is the absorbance at time t.

a Simplex algorithm (12). Some terminal absorbance values were ignored in obtaining the best fit.

Reproducibility of Parameters of Clotting Rates—The reproducibilities of the clotting rate constants, k_c, the lag times, t_{lag}, for the same plasma diluted to 20% by isotonic saline, and the estimated infinite clotting absorbances are demonstrated in Table I for 10 replicate studies of the same plasma from a particular individual for two thrombin concentrations. There was a significant difference between the t_{lag} of the two thrombin concentrations; the lag time at twice the thrombin concentration was practically halved. There was no significant difference in the A_∞ values at the two thrombin concentrations, but the ratio of the clotting rate constants was 1.5 for the higher thrombin concentration to the lower.

Two sets (Tables II and III) of plasma from normal subjects were kinetically evaluated with respect to clotting parameters. The sets differ in that their studies were conducted 6 months apart. Table II presents the data for the plasma of the 10 presumed normal subjects of Set A. Mean k_c rate constants for plasma at 1:5 dilution were 0.74 min^{-1} ± 0.12 *SD* ($t_{1/2}$ 0.94 min) with a range of 0.55–0.93, the average t_{lag} was 63 sec ± 26 *SD*, and the average A_∞ value was 0.371 ± 0.034 *SD* at 1.25 units of thrombin/ml of undiluted plasma. The average k_c was 1.30 min^{-1} ± 0.29 *SD* ($t_{1/2}$ 0.52 min) with a range of 0.84–1.83, the average t_{lag} was 39 sec ± 32 *SD*, and the average A_∞ value was 0.374 ± 0.041 *SD* at 2.5 units of thrombin/ml. The average of the individual ratios of the k_c values at the two thrombin concentrations was 1.74 ± 0.15, whereas the ratio of the average k_c values was 1.76.

Of course, Subjects 7 and 10 may not be representative of the normal population. Subjects classified as normal by the classical tests of coagulation and lysis could be considered abnormal when their blood properties are subjected to careful kinetic analysis (13).

Table III presents the data for the plasma of 20 presumed normal subjects of Set B where the clotting parameters were obtained similarly. The mean k_c rate constant at 1.25 units of thrombin/ml of undiluted plasma was 0.85 min^{-1} ± 0.14 *SD* ($t_{1/2}$ 0.84 min) with a range of 0.54–1.04, the average t_{lag} was 90 sec ± 19 *SD*, and the average A_∞ value was 0.367 ± 0.028 *SD*. The mean k_c rate constant at 2.5 units of thrombin/ml of undiluted plasma was 1.37 min^{-1} ± 0.22 *SD* ($t_{1/2}$ 0.52 min) with a range of 1.02–1.67, the average t_{lag} was 50 sec ± 8 *SD*, and the average A_∞ value was 0.375 ± 0.039 *SD*. The average of the individual ratios of the k_c values at the two thrombin concentrations was 1.62 ± 0.17 *SD*, whereas the ratio of the average k_c values was 1.61.

Kinetics of Fibrinolysis—The absorbance, A, of plasma diluted with isotonic saline and with both thrombin and streptokinase added was monitored with time; typical plots of the data obtained are given in Fig. 1. The possibilities that such coagulation–lysis data could be fit to various kinetic models were challenged graphically and by digital computer estimates. They included:

$$P \xrightarrow{k_1} A \xrightarrow{k_2} B$$

Scheme I

$$P_1 \xrightarrow{k_1} P_2 \xrightarrow{k_2} A \xrightarrow{k_3} B$$

Scheme II

Table III—Plasma (Diluted 1:5 with Isotonic Saline) Clotting Parameters [a] for Clinically Appraised Normals of Set B

Subject	Thrombin, Units/ml of Undiluted Plasma: 1.25 t_{lag}, sec	1.25 $100\,A_\infty$	1.25 k_c, min^{-1}	1.25 $t_{1/2}$, min	2.5 t_{lag}, sec	2.5 $100\,A_\infty$	2.5 k_c, min^{-1}	2.5 $t_{1/2}$, min	$\frac{k_c\ (2.5)}{k\ (1.25)}$
1	52	35.5	0.97	0.71	38	32.2	1.67	0.41	1.72
2	64	32.0	1.04	0.67	37	36.0	1.58	0.44	1.52
3	68	37.2	0.84	0.83	38	33.2	1.51	0.46	1.80
4	61	36.2	0.92	0.75	42	34.6	1.50	0.46	1.63
5	99	40.7	0.99	0.70	52	44.6	1.48	0.47	0.49
6	90	37.4	1.00	0.69	47	38.5	1.44	0.48	1.44
7	78	39.5	0.94	0.74	43	40.3	1.11	0.62	1.18
8	88	32.7	1.00	0.69	48	32.2	1.58	0.44	1.58
9	91	39.1	0.87	0.80	53	37.8	1.57	0.44	1.80
10	94	34.8	0.91	0.76	55	35.3	1.56	0.44	1.71
11	100	38.9	0.73	0.95	57	42.4	1.12	0.62	1.53
12	103	33.3	0.84	0.83	59	34.8	1.50	0.46	1.79
13	119	42.1	0.83	0.83	52	44.7	1.53	0.45	1.84
14	85	38.6	0.92	0.75	52	39.4	1.34	0.52	1.46
15	84	32.1	0.80	0.87	54	33.0	1.37	0.51	1.71
16	89	36.2	0.67	1.03	54	36.6	1.03	0.67	1.54
17	101	37.8	0.82	0.85	52	41.8	1.26	0.55	1.54
18	103	37.2	0.63	1.10	69	39.3	1.02	0.68	1.62
19	124	37.1	0.54	1.28	53	36.8	1.03	0.67	1.91
20	118	35.5	0.68	1.02	49	36.3	1.12	0.62	1.65
Mean ± *SD*	90 ± 19	36.7 ± 2.8	0.85 ± 0.14	0.84 ± 0.16	50 ± 8	37.5 ± 3.9	1.37 ± 0.22	0.52 ± 0.09	1.62 ± 0.17

[a] Based on nonlinear fitting by a Wang digital computer using a Simplex algorithm to the equation $A = A_\infty[1 - e^{-k_c(t-t_{lag})}]$, where A is the absorbance at time t.

Table IV—Reproducibility of Coagulation–Lysis Parameters [a] at a Fixed Plasma Concentration of 20% and a Thrombin Concentration of 2.5 Units/ml of Undiluted Plasma

	Streptokinase, Units/ml of Undiluted Plasma					
	25			50		
	$10^2 k_1$	A_0	$10^2 B_0$	$10^2 k_1$	A_0	$10^2 B_0$
	2.95	0.61	0.12	4.49	0.61	0.086
	3.0	0.56	0.3	4.83	0.56	0.12
	2.1	0.61	0.32	3.76	0.61	0.17
	2.34	0.59	0.34	4.19	0.59	0.19
	1.89	0.6	0.63	3.71	0.6	0.19
	2.27	0.63	0.44	4.12	0.63	0.14
	2.64	0.58	0.33	4.76	0.58	0.12
	2.63	0.6	0.37	4.23	0.6	0.14
	2.21	0.56	0.47	3.73	0.57	0.21
	2.36	0.6	0.38	4.23	0.61	0.13
Mean ± *SD*	2.44 ± 0.36	0.59 ± 0.02	0.37 ± 0.13	4.21 ± 0.4	0.59 ± 0.02	0.15 ± 0.04
Range	1.9–3.0	0.56–0.63	0.12–0.63	3.7–4.8	0.56–0.63	0.09–0.21

[a] Obtained from slope and intercept of appropriate plots in accordance with $\ln A/B = -(A_0 + B_0)k_1 t + \ln A_0/B_0$.

$$P \xrightarrow{k_1} A \cdots\cdots \xrightarrow[\text{lag}]{k_2} C$$

Scheme III

$$P \xrightarrow{k_1} A \underset{k_{-2}}{\overset{k_2}{\rightleftharpoons}} C \cdots\cdots \xrightarrow[\text{lag}]{k_3} D$$

Scheme IV

All of these rate constants were considered to be first order, and a delay or lag time was introduced into Schemes III and IV. Scheme IV also considered an equilibrium between the extent of clotting as represented by the absorbance, A, and a nonobservable equilibration with a reversible product, C. None of these kinetic models was properly applicable to fit the data.

When the coagulation–lysis curves with added streptokinase were superimposed on the coagulation curve, where compensation was made for the time of commencement of the coagulation process, *i.e.*, A was plotted against $t - t_{lag}$ for the same plasma (Fig. 1), some striking features were apparent. For most of the streptokinase concentrations, the curves of absorbance were superimposable on the clotting curve for plasma without streptokinase for a considerable length of time. Only subsequent to this point did the absorbance due to the clot decrease. This result implied a delay or lag in the lytic action of streptokinase. Since the rate of lysis initially increased and then decreased, it was hypothesized that the kinetics of lysis simulated an autocatalytic reaction that could be expressed by:

$$A + B \xrightarrow{k_1} C$$

Scheme V

so that:

$$-dA/dt = k_1 AB \qquad \text{(Eq. 4)}$$

and:

$$\ln A/B = -(A_0 + B_0)k_1 t + \ln A_0/B_0 \qquad \text{(Eq. 5)}$$

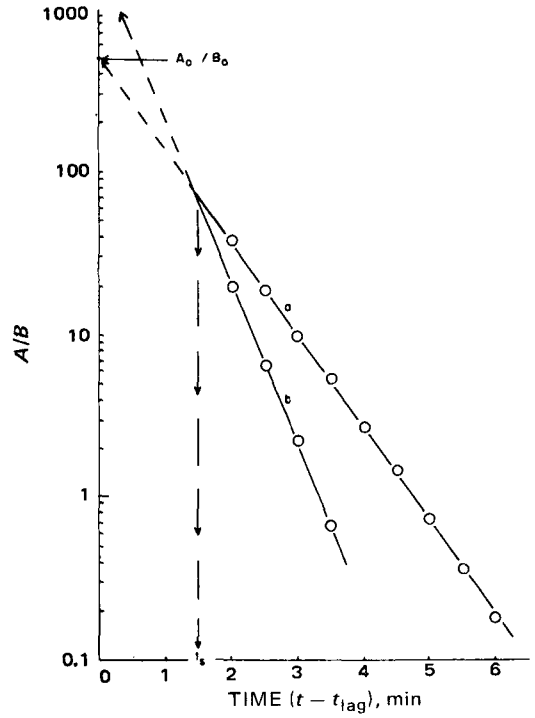

Figure 2—*Example of the linearity of semilogarithmic plots in accordance with Eq. 5, where the slopes are* $-[(A_0 + B_0)k_1]/2.303$ *and the intercept is ln* A_0/B_0. *Time* t_s *is that of coincidence of the plots of absorbance* versus *time for the thrombin plus plasma with and without streptokinase. Curves a and b are for 20% plasma in isotonic saline containing 2.5 units of thrombin/ml of undiluted plasma and 25 and 50 units of streptokinase/ml of undiluted plasma, respectively.*

after some period of time, t_s, when the absorbance, A, deviates from the clotting time curve obtained for $A_{SK=0}$ *versus* time, *i.e.*, the curve without any added streptokinase given by Eqs. 1–3. These same equations are presumed to be valid for any streptokinase concentration up to time t_s.

It was initially presumed that A in Scheme V and Eqs. 4 and 5 represented the observed absorbance, A_2 (or A_2') (Fig. 1), at any streptokinase concentration and was directly proportional to the extent of clotting. If this absorbance with added streptokinase, $A_2 = A_{SK>0}$, were proportional to the amount of clot yet to be lysed at any time, the product B that catalyzes the lysis could be obtained from:

$$B = A_{SK=0} - A_2 \qquad \text{(Eq. 6)}$$

Thus, a plot of ln A/B *versus* time, t, should give a slope of $-(A_0 + B_0)k_1$ and an intercept of ln A_0/B_0 in accordance with Eq. 5. Obviously, specific values of A_0, B_0, and k_1 cannot be obtained by this method. The $A = A_2$ and B values could be obtained from plots similar to those shown in Fig. 1. Unfortunately such plots, although linear for data in the terminal

Table V—Plasma (Diluted 1:5 with Isotonic Saline and with 2.5 Units of Thrombin/ml of Undiluted Plasma) Fibrinolytic Kinetic Parameters [a] for the Clinically Appraised Normals [b] of Set A

	Streptokinase, Units/ml of Undiluted Plasma						
	25			50			
Subject	$10^2 k_1$	$10^2 A_0$	$10^2 B_0$	$10^2 k_1$	$10^2 A_0$	$10^2 B_0$	$\frac{k_{SK50}}{k_{SK25}}$
1	4.07	34.3	0.76	8.36	34.1	0.90	2.05
2	2.52	38.5	0.46	4.84	38.3	0.68	1.92
3	1.51	36.8	1.75	4.03	37.6	0.90	2.67
4	2.35	47.1	0.87	4.46	47.2	0.79	1.90
5	3.35	42.5	0.49	5.88	42.6	0.37	1.76
6	3.40	36.5	0.49	6.52	36.5	0.54	1.92
7	2.50	38.1	1.36	6.58	38.0	1.52	2.63
8	0.76	43.0	2.97	3.25	45.3	0.67	4.28
9	2.70	42.5	0.48	5.80	42.5	0.52	2.15
10	2.62	39.6	0.40	4.77	39.3	0.68	1.82
Average ± *SD*	2.58 ± 0.94	39.9 ± 3.9	1.00 ± 0.82	5.50 ± 1.49	40.1 ± 4.1	0.76 ± 0.32	2.31 ± 0.76[c,d]
Range	1.51–3.96[e]	34–47	0.40–1.75[e]	3.25–7.50[e]	34.–47.	0.37–1.52	1.8–2.7[e]

[a] $\ln A/B = -(A_0 + B_0)k_1 t + \ln A_0/B_0$. [b] Same set as in Table II. [c] 2.09 ± 0.33 when Subject 8 was omitted. [d] $\bar{k}_{SK50}/\bar{k}_{SK25} = 2.11$. [e] Subject 8 was omitted.

Table VI—Plasma (Diluted 1:5 with Isotonic Saline and with 2.5 Units of Thrombin/ml of Undiluted Plasma) Fibrinolytic Kinetic Parameters [a] for the Clinically Appraised Normals [b] of Set B

Subject	Streptokinase, Units/ml of Undiluted Plasma: 25 $10^2 k_1$	25 $10^2 A_0$	25 $10^2 B_0$	50 $10^2 k_1$	50 $10^2 A_0$	50 $10^2 B_0$	$\frac{k_{SK50}}{k_{SK25}}$
1	3.97	33.8	1.25	8.38	34.1	0.88	2.11
2	2.46	38.5	0.54	5.39	38.7	0.34	2.19
3	4.05	34.9	0.08	9.21	35.0	0.03	2.27
4	3.06	35.8	1.16	8.14	36.5	0.49	2.66
5	0.74	46.8	3.23	2.39	48.6	1.43	3.24
6	1.69	43.7	1.32	3.60	44.4	0.62	2.13
7	1.47	46.3	1.68	2.72	46.6	1.37	1.85
8	1.69	35.3	1.68		No available data		
9	2.51	41.9	1.08	5.20	42.3	0.69	2.07
10		No available data		3.47	39.0	0.95	
11	1.81	48.3	1.70	3.57	48.8	1.25	1.97
12	1.40	38.0	2.00	3.46	39.0	0.95	2.47
13	2.19	48.4	1.64	3.96	48.3	1.70	1.81
14	2.83	44.0	1.02	4.94	43.9	1.13	1.75
15	3.16	39.4	0.62	5.63	39.5	0.46	1.78
16	2.29	40.1	1.87	6.20	40.8	1.17	2.71
17	0.63	46.0	4.00	2.63	48.6	1.39	4.20
18	2.71	44.3	0.75	5.41	44.7	0.32	2.00
19	3.10	39.8	1.20	6.15	39.5	1.46	1.98
20	2.84	39.3	0.69	6.56	39.6	0.43	2.31
Average ± *SD*	2.35 ± 0.95	41.3 ± 4.6	1.45 ± 0.92	5.11 ± 2.00	42.0 ± 4.7	0.90 ± 0.48	2.31 ± 0.61[c,d]
Range	1.4–4.0[e]	33.8–48.4	0.08–2.0[e]	2.4–9.2	34.1–48.8	0.032–1.7	1.8–2.7[e]

[a] $\ln A/B = -(A_0 + B_0)k_1 t + \ln A_0/B_0$. [b] Same subjects as in Table III. [c] 2.13 ± 0.30 when Subjects 5 and 17 were omitted. [d] $\bar{k}_{SK50}/\bar{k}_{SK25} = 2.17$. [e] Subjects 5 and 17 were omitted.

phase, were not linear in the phase after time t_s to the time shown by the double-headed vertical arrows.

However, linear semilogarithmic plots against time were obtained for essentially the entire time course after t_s in accordance with Eq. 5 (Fig. 2) when the A value was taken as the amount of total clotting capacity that had not yet been lysed. This value was determined from the difference between the absorbance of the final total clot formed without streptokinase, $(A_{SK=0})_\infty$, and the deficit absorbance that could be assigned to the lytic product, B (Fig. 1), as in:

$$A = (A_{SK=0})_\infty - B = A_1 + A_2 = a(\alpha_1 + \alpha_2) = a\alpha \qquad \text{(Eq. 7)}$$

where α is the total concentration of clotting sites, both yet to be clotted ($\alpha_1 = A_1/a$) and already clotted ($\alpha_2 = A_2/a$), and a is a proportionality constant.

This sum, A, is proportional to an amount of material in the plasma, available both prior to and after clotting, that is consumed during lysis. It would be presumed that the initial amount of this material, A_0, is directly proportional to the plasma content but is diminished by lysis. The intercept of plots (Fig. 2) in accordance with Eq. 5 and the definitions of B and A in Eqs. 6 and 7, respectively, is $\ln A_0/B_0$. The A_0 values were estimated from the asymptotic absorbance in the absence of streptokinase, and the B_0 values were calculated from this value and the intercept. The k_1 values were determined from the quotient of the negative of the slope and $A_0 + B_0$.

Thus, A_0 is the same as A_∞ in Eqs. 1–3 when there is no streptokinase added and:

$$A_0 = a\alpha_0 = (A_{SK=0})_\infty \qquad \text{(Eq. 8)}$$

where α_0 is the total concentration of yet-to-be-clotted clotting sites at time zero and is equivalent to the number of clotted sites at infinite time, A_∞/a, when streptokinase is not added.

The concentration of lytic cofactor β at any time is the sum of an intrinsic concentration of lytic agent β_0, initially in the plasma, and that concentration produced from the apparent concentration of lysed clotting sites:

$$\beta = \beta_0 - (\alpha_0 - \alpha) = \beta_0 + [\alpha_0 - (\alpha_1 + \alpha_2)] \qquad \text{(Eq. 9)}$$

Thus, the actual bimolecular reaction monitored by application of Eq. 5 is between unlysed clotting sites α (whether clotted, α_2, or yet to be clotted, α_1) and a lytic cofactor, β, either inherent in the plasma as β or derived from the lysed clot: $\alpha + \beta \rightarrow \gamma$.

Thus, if $\beta = aB$, *i.e.*, each unit of lysed clotting site α resulted in a unit of cofactor β:

$$-d\alpha/dt = k_1'\alpha\beta = \frac{dA/a}{dt} = k_1'AB/a^2 \qquad \text{(Eq. 10)}$$

so that:

$$-dA/dt = \frac{k_1'}{a}AB \qquad \text{(Eq. 11)}$$

when the observed k_1 of Scheme V and Eqs. 4 and 5 is equivalent to k_1'/a and the observed $B_0 = a\beta_0$ where the proportionality factor a is unobtainable from the given data.

Reproducibility of Parameters of Fibrinolytic Rates—The reproducibilities of the lytic rate constants, k_1, and the A_0 and B_0 pa-

Table VII—Estimated Normal Parameters

Parameter	Average	Normal Range	Presumed Normals Outside Range: Lower	Higher	Range to Include All Presumed Normals[a]
t_{lag}, sec at 1.25 units of thrombin/ml[b]	81	37–110	2/30	3/30	30–125
t_{lag}, sec at 2.50 units of thrombin/ml[b]	57	27–60	2/30	1/30	15–90
k_c, min^{-1} at 1.25	0.80	0.59–1.05	2/30	0/30	0.4–1.20
k_c, min^{-1} at 2.5	1.35	1.0–1.7	1/30	1/30	0.7–2.0
(k_c at 2.5)/(k_c at 1.25)	1.65	1.4–2.0	1/30	0/30	1.1–2.3
$10^2 A_\infty$ and $10^2 A_0$	37	32–45	0/30	0/30	26–52
$10^2 k_1$ (conc.-min)$^{-1}$ at 25 units of streptkinase/ml[b,c]	2.43	1.4–3.5	3/30	3/30	0.6–4.2
$10^2 k_1$ (conc.-min)$^{-1}$ at 50 units of streptokinase/ml[b,c]	5.24	3.0–8.4	3/30	1/30	2.0–12.0
(k_1 at 50)/(k_1 at 25)	2.3	1.7–2.9	0/30	3/30	1.1–4.3
$10^2 B_0$ at 25 units of streptokinase/ml[b,c]	1.3	0.4–3.0	1/30	2/30	0–5.0
$10^2 B_0$ at 50 units of streptokinase/ml[b,c]	0.8	0.3–1.6	1/30	1/30	0–2.4

[a] Estimated to cover more than 95% confidence limits. Except for t_{lag} at both thrombin concentrations where 1/30 was less than the given ranges, none of the presumed normals out of 30 was outside the ranges given for the parameters. [b] Per milliliter of undiluted plasma. [c] At a thrombin concentration of 2.5 units/ml of undiluted plasma.

Table VIII—Plasma (Diluted 1:5 with Isotonic Saline) Clotting Factors [a] for Subjects Treated with Heparin and 2.5 Units of Thrombin/ml of Undiluted Plasma [b]

Set	t_{lag}, sec	$100\,A_\infty$	k_c, min^{-1}	$t_{1/2}$, min
A	240	69.7	0.095	7.22
B	235	62.7	0.038	17.90

[a] Based on fitting to the equation $A = A_\infty[1 - e^{-k(t-t_{lag})}]$. [b] Clotting rates were too slow at 1.25 units of thrombin/ml of undiluted plasma to be determined satisfactorily.

rameters for the same plasma as considered in Table I are summarized in Table IV. The wide variation in B_0 is anticipated since it is a small number and is derived from extrapolation to obtain the intercept of plots in accordance with Eq. 5. The B values at the initial times are subject to the error obtained when one takes small differences of large numbers (Eq. 6). Nevertheless, the B_0 values for the two concentrations of streptokinase were significantly different and decreased with increasing streptokinase concentration. The lytic rate constant, k_1, increased 1.7 times for an apparent doubling of the streptokinase concentration.

The two sets of plasma from the normal subjects considered with respect to clotting rates in Tables II and III were kinetically evaluated for fibrinolysis in Tables V and VI, respectively. Table V gives the data for the plasma of 10 presumed normal subjects and shows mean lytic constants, k_1, for plasma at 1:5 dilution and 2.5 units of thrombin/ml of undiluted plasma of 2.58 ± 0.94 *SD* and 5.45 ± 1.5 *SD* (ratio 2.11) at the concentrations of streptokinase of 25 and 50 units/ml of undiluted plasma, respectively. There were no significant statistical differences between the means of the A_0 and B_0 parameters, respectively, for the two streptokinase concentrations. The only anomalous ratios of k_{SK50}/k_{SK25} and $B_{0(SK50)}/B_{0(SK25)}$ were in Subject 8. Subject 1 had inconsistently high lytic constants.

Table VI lists the data for the plasma of 20 presumed normal subjects and shows mean lytic constants, k_1, for similarly treated plasmas of 2.35 ± 0.95 *SD* and 5.11 ± 2.0 *SD* (ratio 2.17) at the concentrations of streptokinase of 25 and 50 units/ml of undiluted plasma, respectively. Similar to the results of Table V, there were no statistically significant differences between the means of the A_0 and B_0 parameters for the two streptokinase concentrations. The parameters for this set of normals (Table VI) were not consistently different from those of Table V; Subjects 5 and 17 showed anomalous ratios of k_{SK50}/k_{SK25}. Subjects 1 and 3 had inconsistently high lytic constants, whereas Subjects 5, 7, and 17 had inconsistently low lytic constants.

Characterization of Subjects on Basis of Established Normal Ranges for Clotting and Lytic Parameters—On the basis of the evaluated parameters for presumed normals of Set A (Tables II and V) and Set B (Tables III and VI), Table VII was constructed to give estimated averages, normal ranges, and possible extended ranges for the designated parameters of clotting and lysis under the described conditions. The normal ranges given cover the entire population of 30 presumed normals with exceptions of one to three individuals in several categories. The extended ranges included all, with a minor exception, of the values from the 30 presumed normals.

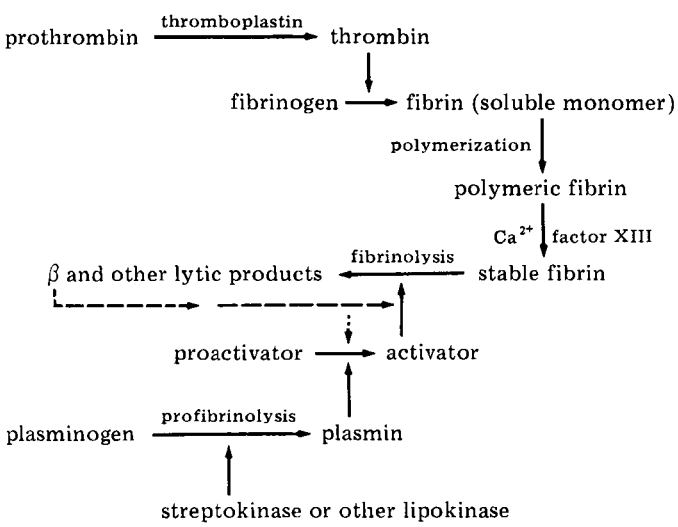

Scheme VI—Accepted scheme of blood coagulation and lysis is given by solid arrows.

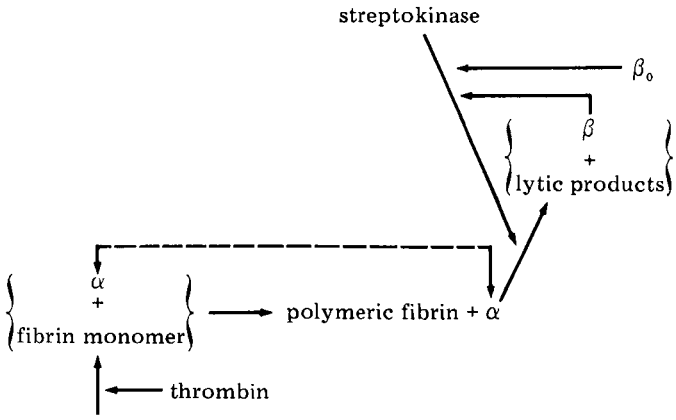

Scheme VII—Simplistic scheme of blood coagulation and lysis that incorporates the observed kinetic dependencies. Arrows perpendicular to the coagulation–lysis process or to a catalytic action represent catalytic or cofactor action and can be mediated by sequential processes. The α produced by thrombin action is considered the same as that consumed in the lytic process. The kinetic information is insufficient to state whether the β formed on lysis or the intrinsic β_0 is a necessary catalyst or cofactor in the ultimate sequence of streptokinase action or is consumed by the lytic process.

The clotting parameters of two cardiovascular risk subjects treated with heparin are given in Table VIII. The lag times and final absorbances on clotting were greatly in excess of normals. The clotting rate constants were extremely low, 1:10 or less that of the normals. Three other subjects, diagnosed as high cardiovascular risks and on moderate heparin therapy, had final absorbances on clotting that were also greatly in excess of normals, *i.e.*, 77, 64, and 170.

Studies are in progress to correlate the results of kinetic appraisals with the careful diagnoses of clinically appraised subjects.

Relation of Established Mechanisms to Observed Kinetics—It is generally recognized that blood clotting and lysis mechanisms are complex and intricate. However, Scheme VI is widely employed to illustrate the probable mechanisms.

The present studies showed that the rate of formation of polymeric or stable fibrin as monitored by the spectrophotometric absorbance of clot formation is generally dependent on the concentration of thrombin.

The rate of fibrinolysis ultimately depends on the concentration of added streptokinase. However, fibrinolysis does not occur immediately after the addition of streptokinase. Thus, streptokinase action on lysis must be mediated by other processes such as the formation of activator. Apparently, a cofactor or catalyst for these processes must be released by the phenomenon of lysis. This pathway is indicated by the dashed arrow in Scheme VI. It may catalyze the activator action on lysis or may be a necessary cofactor for activator production. Either a small concentration of β, β_0, can be present at zero time or a slow rate of spontaneous lysis can occur to promote the accumulation of β that significantly catalyzes lysis at the time, t_s, when the absorbances of the coagulation and lytic curves diverge (Fig. 1).

The kinetics of lysis (Fig. 2 and Eq. 5) depend not only on β but the apparent concentration of some factor, α, that accompanies and is proportional to unlysed fibrin, whether soluble or polymerized. This factor can be rationalized as a concentration of proactivator or derived activator, which is consumed during the lytic process.

A simplification of Scheme VI that incorporates these observations is given in Scheme VII.

The procedures and kinetic analyses described in this paper may be useful in diagnosing abnormalities in clinical subjects and in monitoring the effect of therapy. They may also be found to correlate the time course of drug action with the concomitantly studied pharmacokinetics of administered therapeutic agents in subjects. These *in vitro* studies might serve as screens for possible agents that inhibit coagulation and enhance fibrinolysis, actions that may be favored in proper therapeutic treatment of cardiovascular disease.

REFERENCES

(1) W. Berg, *Acta Med. Scand., Suppl.* 478, 47 (1967).

(2) W. Berg, K. Korsan-Bengsten, and J. Ygge, *Thromb. Diath. Haemorrh.*, **19**, 169 (1968).
(3) R. J. Merrills and J. T. B. Shaw, *Biochem. J.*, **106**, 101 (1968).
(4) W. Liniger and P. Ruegsegger, *Math. Biosci.*, **1**, 263 (1967).
(5) W. Liniger and P. Ruegsegger, *Thromb. Diath. Haemorrh.*, **17**, 412 (1967).
(6) J. Daver, E. Edmond, E. Panak, and M. Ricoeur, *Rev. Eur. Etudes Clin. Biol.*, **15**, 333 (1970).
(7) J. Daver, P. Desnoyers, and M. Ricoeur, in "Synthetic Fibrinolytic Thrombolytic Agents," K. N. Von Kaulla and J. F. Davidson, Eds., Charles C Thomas, Springfield, Ill., 1975, pp. 245–264.
(8) P. Desnoyers, J. Daver, J. Labaume, and J. Sebastien, in *ibid.*, pp. 265–275.
(9) C. A. Bouvier and J. Gründlinger, *Schweiz. Med. Wochenschr.*, **93** (41), 1451 (1963).
(10) J. Gründlinger and C. A. Bouvier, *Thromb. Diath. Haemorrh.*, **12**, 425 (1964).
(11) C. A. Bouvier, M. Beretta-Piccoli, and M. Giacometti, in "Progress in Chemical Fibrinolysis and Thrombolysis," J. F. Davidson, M. Samama, and P. Desnoyers, Eds., Raven, New York, N.Y., 1975, pp. 281–288.
(12) L. A. Nelder and R. Mead, *Computer J.*, **7**, 308 (1965).
(13) R. Bierme, J. Daver, B. Boneu, M. Ricoeur, and M. Verry, "Third Congress of International Society on Thrombosis and Haemostasis," Washington, D.C., Aug. 22–26, 1972, Abstr. p. 276.

ACKNOWLEDGMENTS

The authors are grateful to Dr. Kwang Eun Kim and Mlle. Francoise Chamboine for assistance in evaluating the data and to Dr. Richard Süverkrup for the programming of the Simplex algorithm on the computer. Appreciation is also expressed to Dr. Jean Claude Arnaud, Director of Research of the Servier Research Laboratories, whose support and encouragement made this collaborative endeavor possible.

Physicochemical Properties of Glycyrrhizic Acid in Aqueous Media II: Effect on Flocculation–Deflocculation Behavior of Suspensions of Sulfathiazole and Graphite

AKINOBU OTSUKA ˣ, YORINOBU YONEZAWA, and YASUHIKO NAKAMURA

Received January 19, 1977, from the *Faculty of Pharmacy, Meijo University, Tempaku-ku, Nagoya, Japan.* Accepted for publication April 22, 1977.

Abstract □ The flocculation–deflocculation behavior of sulfathiazole and graphite in aqueous solutions of glycyrrhizic acid was studied by measuring the sedimentation volume and turbidity of supernates. The dispersing effect of glycyrrhizic acid on suspensions of sulfathiazole showed a maximum in the pH 3–4 region, the same pH region where the ζ-potential of sulfathiazole particles showed a negative maximum. The results were explained by the variation of degrees of ionization of glycyrrhizic acid and sulfathiazole with pH. With graphite suspensions, the pH region where the dispersing effect of glycyrrhizic acid showed a maximum shifted to a higher pH compared with sulfathiazole. This result can be attributed to the fact that graphite is a nonpolar substance so the surface properties are not affected by a pH change. Hence, the adsorption of glycyrrhizic acid occurs even in a fairly high pH range.

Keyphrases □ Glycyrrhizic acid—effect on flocculation–deflocculation behavior of sulfathiazole and graphite, aqueous solutions, various pH values □ Sulfathiazole—flocculation–deflocculation behavior, effect of glycyrrhizic acid, aqueous solutions, various pH values □ Graphite—flocculation–deflocculation behavior, effect of glycyrrhizic acid, aqueous solutions, various pH values □ Flocculation–deflocculation behavior—sulfathiazole and graphite, effect of glycyrrhizic acid, aqueous solutions, various pH values □ Antibacterials—sulfathiazole, flocculation–deflocculation behavior, effect of glycyrrhizic acid, aqueous solutions, various pH values

A previous report from this laboratory (1) dealt with the surface-active properties and the formation of molecular aggregates of glycyrrhizic acid, a triterpenoid acidic glucoside extracted from *Glycyrrhiza glabra* L. This paper describes the dispersing effect of this substance on aqueous suspensions of sulfathiazole and graphite. While the use of natural products for suspending agents or emulsifying agents has attracted special interest recently, studies of this kind on glycyrrhizic acid have not been published.

EXPERIMENTAL

Materials—Monopotassium glycyrrhizinate[1] was used as received. Graphite[2] and sulfathiazole[3] were obtained as commercial samples. The specific surface area of the graphite determined by the air permeation method[4] was 0.25 m^2/g. The sulfathiazole was finely ground, and the sample with a specific surface area of 0.62 m^2/g was used. All other reagents were analytical grade.

Sedimentation Measurements—To 2.50 g of sulfathiazole or 2.00 g of graphite in a 50-ml graduated test tube was added 50 ml of an aqueous solution of monopotassium glycyrrhizinate whose pH had been adjusted with hydrochloric acid or potassium hydroxide solutions. The mixture was shaken in a constant-temperature bath at 25° for 24 hr and subsequently allowed to stand for 24 hr at the same temperature; the sedimentation volume was then measured.

Turbidity Tests—After the measurements of sedimentation volume, the turbidity of the cloudy liquid phase above the sediment was measured at 500 nm according to:

$$\tau = -\ln T/l \qquad \text{(Eq. 1)}$$

where τ is the turbidity, T is the transmittance, and l is the cell path length.

Adsorption Measurements—After the sedimentation measurements and/or the turbidity tests, the suspensions were centrifuged quickly. The glycyrrhizic acid concentration in the supernate was determined as follows. For the sulfathiazole–glycyrrhizic acid system, 10 ml of supernate was transferred into a test tube, and then 1 ml of concentrated hydrochloric acid and 5 ml of water were added. The mixture was heated to 95° and then allowed to cool. The formed precipitate was dissolved in 5 ml of chloroform, and the absorbance was measured at 258 nm.

For the graphite–glycyrrhizic acid system, the absorbance of the su-

[1] Maruzen Seiyaku Co., Tokyo, Japan.
[2] Yoneyama Chemical Industries, Osaka, Japan.
[3] Sankyo Co., Tokyo, Japan.
[4] Model SS-100, Shimadzu Seisakusho, Kyoto, Japan.

(2) W. Berg, K. Korsan-Bengsten, and J. Ygge, *Thromb. Diath. Haemorrh.*, **19**, 169 (1968).
(3) R. J. Merrills and J. T. B. Shaw, *Biochem. J.*, **106**, 101 (1968).
(4) W. Liniger and P. Ruegsegger, *Math. Biosci.*, **1**, 263 (1967).
(5) W. Liniger and P. Ruegsegger, *Thromb. Diath. Haemorrh.*, **17**, 412 (1967).
(6) J. Daver, E. Edmond, E. Panak, and M. Ricoeur, *Rev. Eur. Etudes Clin. Biol.*, **15**, 333 (1970).
(7) J. Daver, P. Desnoyers, and M. Ricoeur, in "Synthetic Fibrinolytic Thrombolytic Agents," K. N. Von Kaulla and J. F. Davidson, Eds., Charles C Thomas, Springfield, Ill., 1975, pp. 245–264.
(8) P. Desnoyers, J. Daver, J. Labaume, and J. Sebastien, in *ibid.*, pp. 265–275.
(9) C. A. Bouvier and J. Gründlinger, *Schweiz. Med. Wochenschr.*, **93** (41), 1451 (1963).
(10) J. Gründlinger and C. A. Bouvier, *Thromb. Diath. Haemorrh.*, **12**, 425 (1964).
(11) C. A. Bouvier, M. Beretta-Piccoli, and M. Giacometti, in "Progress in Chemical Fibrinolysis and Thrombolysis," J. F. Davidson, M. Samama, and P. Desnoyers, Eds., Raven, New York, N.Y., 1975, pp. 281–288.
(12) L. A. Nelder and R. Mead, *Computer J.*, **7**, 308 (1965).
(13) R. Bierme, J. Daver, B. Boneu, M. Ricoeur, and M. Verry, "Third Congress of International Society on Thrombosis and Haemostasis," Washington, D.C., Aug. 22–26, 1972, Abstr. p. 276.

ACKNOWLEDGMENTS

The authors are grateful to Dr. Kwang Eun Kim and Mlle. Francoise Chamboine for assistance in evaluating the data and to Dr. Richard Süverkrup for the programming of the Simplex algorithm on the computer. Appreciation is also expressed to Dr. Jean Claude Arnaud, Director of Research of the Servier Research Laboratories, whose support and encouragement made this collaborative endeavor possible.

Physicochemical Properties of Glycyrrhizic Acid in Aqueous Media II: Effect on Flocculation–Deflocculation Behavior of Suspensions of Sulfathiazole and Graphite

AKINOBU OTSUKA ˣ, YORINOBU YONEZAWA, and YASUHIKO NAKAMURA

Received January 19, 1977, from the *Faculty of Pharmacy, Meijo University, Tempaku-ku, Nagoya, Japan.* Accepted for publication April 22, 1977.

Abstract □ The flocculation–deflocculation behavior of sulfathiazole and graphite in aqueous solutions of glycyrrhizic acid was studied by measuring the sedimentation volume and turbidity of supernates. The dispersing effect of glycyrrhizic acid on suspensions of sulfathiazole showed a maximum in the pH 3–4 region, the same pH region where the ζ-potential of sulfathiazole particles showed a negative maximum. The results were explained by the variation of degrees of ionization of glycyrrhizic acid and sulfathiazole with pH. With graphite suspensions, the pH region where the dispersing effect of glycyrrhizic acid showed a maximum shifted to a higher pH compared with sulfathiazole. This result can be attributed to the fact that graphite is a nonpolar substance so the surface properties are not affected by a pH change. Hence, the adsorption of glycyrrhizic acid occurs even in a fairly high pH range.

Keyphrases □ Glycyrrhizic acid—effect on flocculation–deflocculation behavior of sulfathiazole and graphite, aqueous solutions, various pH values □ Sulfathiazole—flocculation–deflocculation behavior, effect of glycyrrhizic acid, aqueous solutions, various pH values □ Graphite—flocculation–deflocculation behavior, effect of glycyrrhizic acid, aqueous solutions, various pH values □ Flocculation–deflocculation behavior—sulfathiazole and graphite, effect of glycyrrhizic acid, aqueous solutions, various pH values □ Antibacterials—sulfathiazole, flocculation–deflocculation behavior, effect of glycyrrhizic acid, aqueous solutions, various pH values

A previous report from this laboratory (1) dealt with the surface-active properties and the formation of molecular aggregates of glycyrrhizic acid, a triterpenoid acidic glucoside extracted from *Glycyrrhiza glabra* L. This paper describes the dispersing effect of this substance on aqueous suspensions of sulfathiazole and graphite. While the use of natural products for suspending agents or emulsifying agents has attracted special interest recently, studies of this kind on glycyrrhizic acid have not been published.

EXPERIMENTAL

Materials—Monopotassium glycyrrhizinate[1] was used as received. Graphite[2] and sulfathiazole[3] were obtained as commercial samples. The specific surface area of the graphite determined by the air permeation method[4] was 0.25 m^2/g. The sulfathiazole was finely ground, and the sample with a specific surface area of 0.62 m^2/g was used. All other reagents were analytical grade.

Sedimentation Measurements—To 2.50 g of sulfathiazole or 2.00 g of graphite in a 50-ml graduated test tube was added 50 ml of an aqueous solution of monopotassium glycyrrhizinate whose pH had been adjusted with hydrochloric acid or potassium hydroxide solutions. The mixture was shaken in a constant-temperature bath at 25° for 24 hr and subsequently allowed to stand for 24 hr at the same temperature; the sedimentation volume was then measured.

Turbidity Tests—After the measurements of sedimentation volume, the turbidity of the cloudy liquid phase above the sediment was measured at 500 nm according to:

$$\tau = -\ln T/l \qquad \text{(Eq. 1)}$$

where τ is the turbidity, T is the transmittance, and l is the cell path length.

Adsorption Measurements—After the sedimentation measurements and/or the turbidity tests, the suspensions were centrifuged quickly. The glycyrrhizic acid concentration in the supernate was determined as follows. For the sulfathiazole–glycyrrhizic acid system, 10 ml of supernate was transferred into a test tube, and then 1 ml of concentrated hydrochloric acid and 5 ml of water were added. The mixture was heated to 95° and then allowed to cool. The formed precipitate was dissolved in 5 ml of chloroform, and the absorbance was measured at 258 nm.

For the graphite–glycyrrhizic acid system, the absorbance of the su-

[1] Maruzen Seiyaku Co., Tokyo, Japan.
[2] Yoneyama Chemical Industries, Osaka, Japan.
[3] Sankyo Co., Tokyo, Japan.
[4] Model SS-100, Shimadzu Seisakusho, Kyoto, Japan.

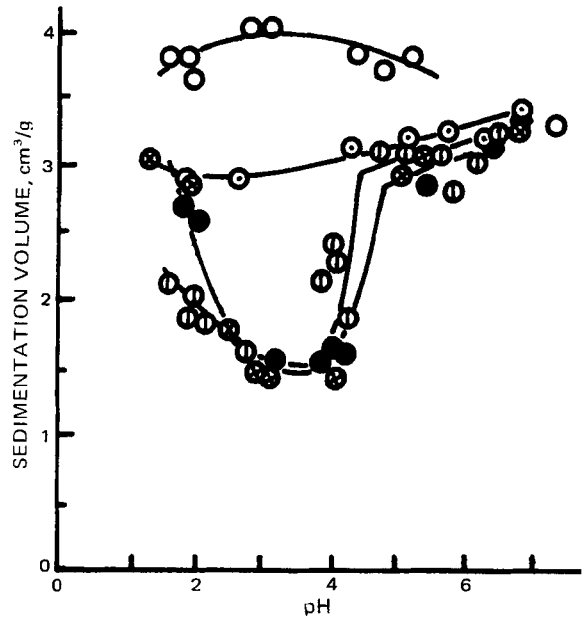

Figure 1—*Relationship between sedimentation volume and pH for sulfathiazole suspensions in the absence and presence of glycyrrhizic acid. Key [concentration of glycyrrhizic acid (mM)]: ○, 0; ⊙, 0.10; ⊕, 0.30; ●, 0.50; and ⊗, 0.75.*

pernate at 258 nm was measured directly. The amount of glycyrrhizic acid adsorbed was calculated from the difference in the concentrations before and after adsorption.

ζ-Potential Measurements—The ζ-potential was measured using a streaming potential measuring apparatus, which was an improvement on the Hazel type (2). The ζ-potential was calculated from the Helmholtz–Smoluchowski equation:

$$\zeta = 4\pi\eta\kappa H/PD \qquad \text{(Eq. 2)}$$

where H is the streaming potential, P is the pressure that drives the liquid through a powder bed, η is the viscosity, κ is the specific conductance, and D is the dielectric constant of the liquid.

RESULTS

The relationship between the sedimentation volume and the pH for sulfathiazole is given in Fig. 1. Figures 2 and 3 show the turbidity of the liquid phase against the pH for sulfathiazole and graphite, respectively. In each case, the parameter is the glycyrrhizic acid concentration present.

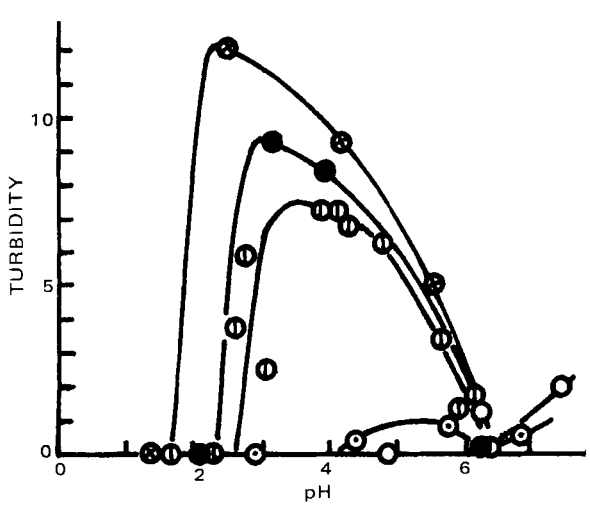

Figure 2—*Relationship between turbidity of the liquid phase above the sediment and pH for sulfathiazole suspensions in the absence and presence of glycyrrhizic acid. Key [concentration of glycyrrhizic acid (mM)]: ○, 0; ⊙, 0.10; ⊕, 0.30; ●, 0.50; and ⊗, 0.75.*

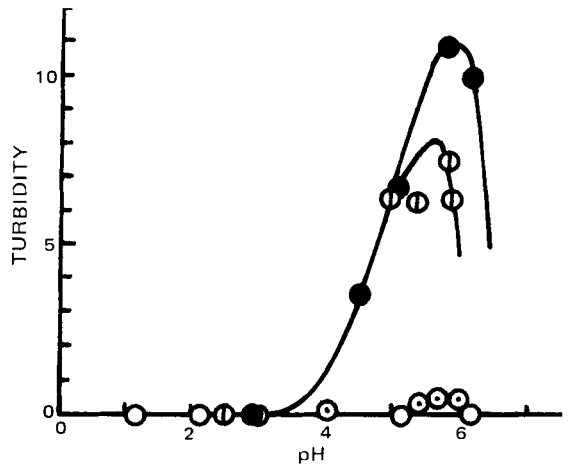

Figure 3—*Relationship between turbidity of the liquid phase above the sediment and pH for graphite suspensions in the absence and presence of glycyrrhizic acid. Key [concentration of glycyrrhizic acid (mM)]: ○, 0; ⊙, 0.10; ⊕, 0.30; and ●, 0.50.*

In the absence of glycyrrhizic acid, the sedimentation volume of sulfathiazole was extremely large, leaving a clear layer of liquid above a sediment. This result means that sulfathiazole particles were in a flocculated state. In the presence of sufficient glycyrrhizic acid, the sedimentation volume decreased as the pH rose to 3–4, but it increased with a further rise in pH. The turbidity of the liquid phase showed a maximum in the same pH range. These results indicate that the dispersibility of sulfathiazole in aqueous solution of glycyrrhizic acid was optimal in this pH range.

The results for graphite suspensions were qualitatively similar to those for sulfathiazole except that the pH range in which there was a marked increase in dispersibility of suspensions shifted to 4–6. The dispersibility of sulfathiazole or graphite in aqueous solutions of glycyrrhizic acid decreased as the ionic strength increased. Figure 4 illustrates that the sedimentation volume increased when potassium chloride was added to suspensions. Moreover, the addition of the salt caused the complete disappearance of turbidity in the liquid phase above the sediment layer of graphite.

Figure 5 shows the effect of pH on the amount of glycyrrhizic acid adsorbed by sulfathiazole. The parameter here is the initial concentration of glycyrrhizic acid. Figure 6 presents the adsorption isotherms drawn on the basis of the data in Fig. 5. The amount adsorbed was large in a low pH range and decreased with rising pH. At any pH above 4.5, virtually

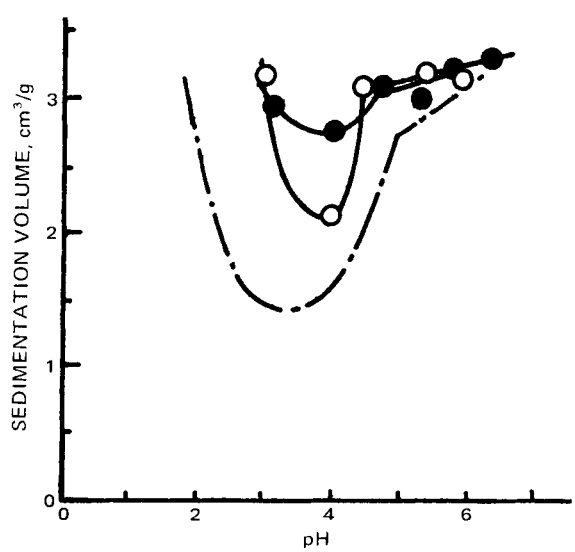

Figure 4—*Effect of potassium chloride addition on the sedimentation volume of sulfathiazole in the solution of glycyrrhizic acid. Key [concentration of potassium chloride (M)]: — · —, 0; ○, 0.10; and ●, 0.50. Concentration of glycyrrhizic acid is 0.50 mM.*

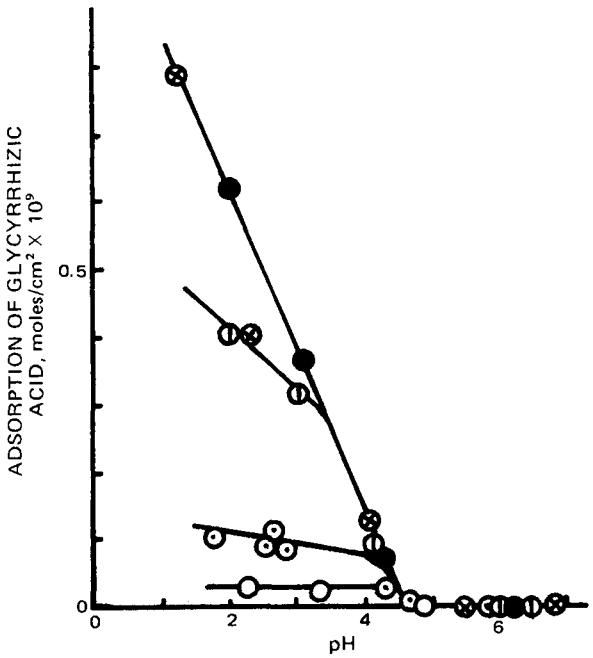

Figure 5—*Amount of adsorption of glycyrrhizic acid on sulfathiazole* versus *pH. Key [initial concentration of glycyrrhizic acid (mM)]:* ○, *0.05;* ⊙, *0.10;* ⊕, *0.30;* ●, *0.50; and* ⊗, *0.75.*

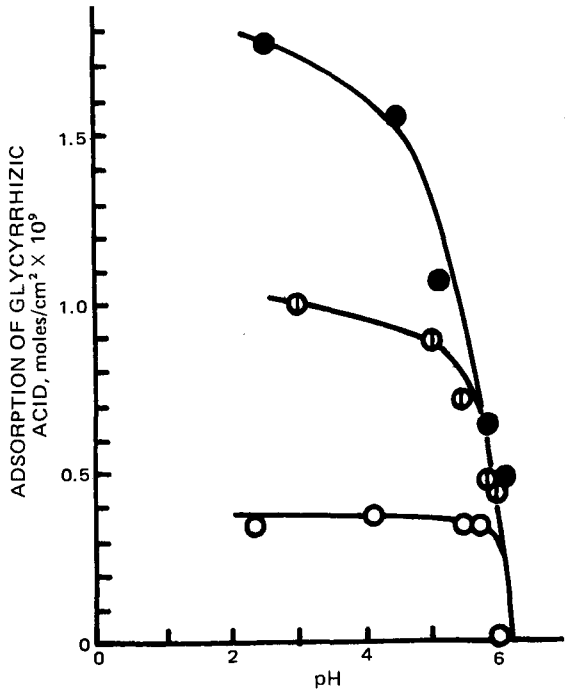

Figure 7—*Amount of adsorption of glycyrrhizic acid on graphite* versus *pH. Key [initial concentration of glycyrrhizic acid (mM)]:* ○, *0.10;* ⊕, *0.30; and* ●, *0.50.*

no adsorption occurred. With graphite (Figs. 7 and 8), the amount of glycyrrhizic acid adsorbed fell to practically zero above pH 6.5.

The addition of potassium chloride caused an increase in the amount of glycyrrhizic acid adsorbed on sulfathiazole whereas the adsorption on graphite was hardly affected (Fig. 9).

The curves of ζ-potential against pH for sulfathiazole are given in Fig. 10. In the absence of glycyrrhizic acid, a gradual reduction in the ζ-potential with rising pH was observed. In the presence of glycyrrhizic acid, the ζ-potential dropped rapidly with an increase in pH and reached negative maxima in the pH 3–4 region.

DISCUSSION

When discussing the effects of pH on the adsorption of glycyrrhizic acid by sulfathiazole or graphite and on the flocculation–deflocculation behavior of these suspensions, the variation of the charge on both the powder surface and the glycyrrhizic acid molecule with pH should be considered. Although glycyrrhizic acid is a tribasic acid, it is impossible to detect the first and second end-points in the titration curve of its aqueous solution by a strong base. The titration curve, however, yields the apparent average dissociation constant.

The variation of the degree of ionization of carboxyl groups with pH is shown in Fig. 11*a*. The distribution of the various forms of sulfathiazole as a function of pH was calculated from literature values of its dissociation constants (3, 4) and is given in Fig. 11*b*, which explains the variation of the ζ-potential with pH in the absence of glycyrrhizic acid.

When glycyrrhizic acid is added to the suspensions, glycyrrhizinate anions are adsorbed on the surface of sulfathiazole; the negative charge of particles then becomes higher than in the absence of glycyrrhizic acid.

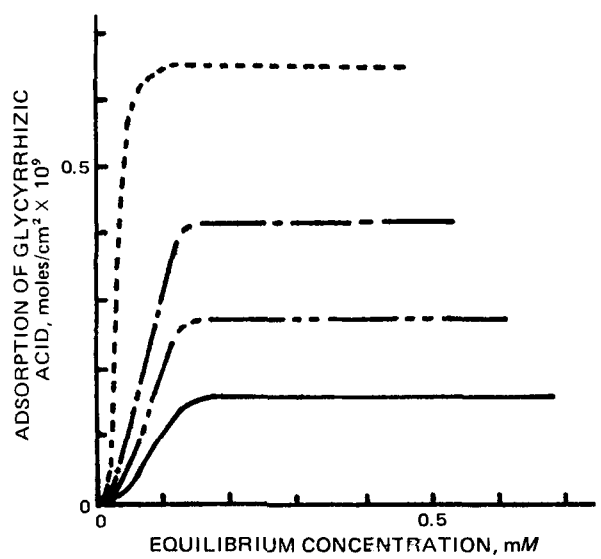

Figure 6—*Adsorption isotherms for sulfathiazole at various pH values. Key: - - -, pH 2.0; – – –, pH 3.0; – - – -, pH 3.5; and —, pH 4.0.*

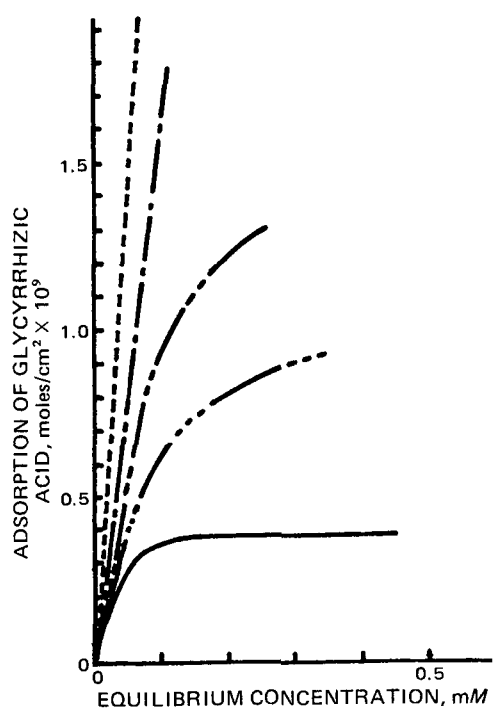

Figure 8—*Adsorption isotherms for graphite at various pH values. Key: - - -, pH 3.0; – – –, pH 4.0; – - – -, pH 5.0; – - – - –, pH 5.5; and —, pH 6.0.*

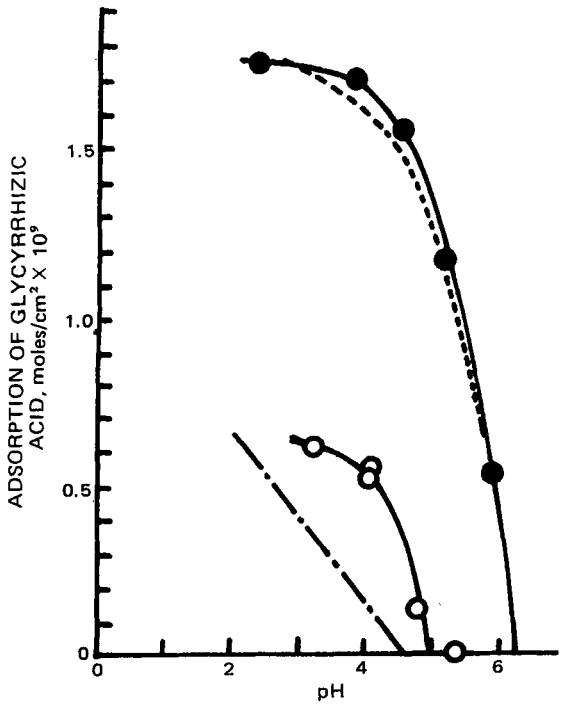

Figure 9—*Effect of the addition of potassium chloride on the amount of adsorption of glycyrrhizic acid. Key:* - - -, *in the absence of potassium chloride for sulfathiazole;* ○, *in 0.5* M *KCl solution for sulfathiazole;* - - -, *in the absence of potassium chloride for graphite; and* ●, *in 0.5* M *KCl solution for graphite. Initial concentration of glycyrrhizic acid was 0.50 m*M.

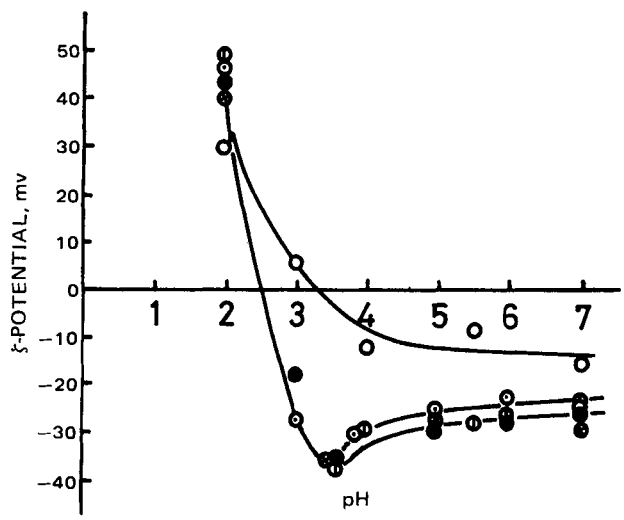

Figure 10—*ζ-Potential of sulfathiazole in the absence and presence of glycyrrhizic acid* versus *pH. Key* [*concentration of glycyrrhizic acid* (*m*M)]: ○, *0;* ⊙, *0.10;* ⊕, *0.30;* ●, *0.50; and* ⊗, *0.75.*

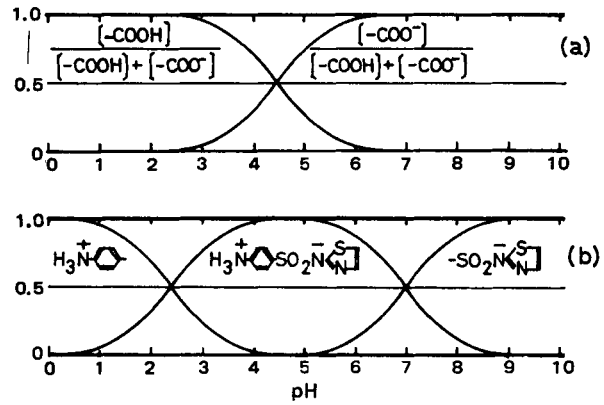

Figure 11—*Distribution of various forms of glycyrrhizic acid* (a) *and sulfathiazole* (b) *as functions of pH.*

As a result, negative maxima appear in the ζ-potential–pH relationship. This result may be due to two effects which counteract each other:

1. With rising pH, the degree of ionization of adsorbed glycyrrhizic acid increases, which causes an increase in the negative charge of particles.
2. An increase in the negative charge of particles and glycyrrhizic acid molecules increases the escaping tendency of the molecules into the liquid phase and, hence, the amount of adsorption decreases.

The dispersibility of sulfathiazole in the presence of glycyrrhizic acid increases in the pH region over which an increase in the negative charge on particles occurs, and the optimum pH for dispersibility agrees with the pH where the ζ-potential shows negative maxima.

The existence of an optimum pH region is also known for the dispersibility of graphite in the solutions of glycyrrhizic acid. There is no essential difference between sulfathiazole and graphite regarding the stabilization mechanism of suspensions. However, graphite is a nonpolar substance; therefore, the surface properties of graphite are not affected by a pH change, and glycyrrhizic acid adsorption occurs even at a fairly high pH. As a result, the pH region where the dispersibility of graphite shows maxima shifts to a higher pH compared with sulfathiazole.

With the addition of electrolytes to the sulfathiazole–glycyrrhizic acid system, the electrostatic repulsive forces between negatively charged sulfathiazole surfaces and glycyrrhizinate anions are diminished. Consequently, glycyrrhizic acid adsorption increases. However, as the salt concentration increases, the repulsive force between particles decreases, resulting in the flocculation of suspensions.

With graphite, the electrostatic repulsion between particles and anions may be ignored; electrolyte addition does not produce such a marked increase in adsorption as in the case of sulfathiazole. The lowering of dispersibility of graphite by electrolytes can be explained in the same manner as for sulfathiazole.

REFERENCES

(1) A. Otsuka, Y. Yonezawa, K. Iba, T. Tatsumi, and H. Sunada, *Yakugaku Zasshi*, **96**, 203 (1976).

(2) M. Nakagaki and Y. Nakamura, *ibid.*, **92**, 1000 (1972).

(3) M. Nakagaki, N. Koga, and H. Terada, *ibid.*, **83**, 586 (1963).

(4) T. Koizumi, T. Arita, and K. Kakemi, *Chem. Pharm. Bull.*, **12**, 413 (1964).

Plasma Concentrations of Thioridazine Metabolites and ECG Abnormalities

LOUIS A. GOTTSCHALK ˣ, EUGENE DINOVO, ROBERT BIENER, and BINA R. NANDI

Received February 14, 1977, from the *Department of Psychiatry and Human Behavior, College of Medicine, University of California, Irvine, CA 92717*, and the *University of California Irvine Medical Center, Orange, CA 92668.* Accepted for publication April 25, 1977.

Abstract □ Five acute schizophrenic patients were given a standard thioridazine dose (4 mg/kg/day po). Their plasma concentrations of thioridazine and its metabolites were determined by GLC, and their ECG's were recorded routinely. In four of the five patients, abnormal ECG's (malformation of the T-wave or lengthening of the repolarization time) were found whenever plasma concentrations of the thioridazine ring sulfoxide were elevated. No relationship could be detected between the appearance of ECG abnormalities and the concentrations of thioridazine and its other metabolites.

Keyphrases □ Thioridazine and metabolites—plasma concentrations and ECG abnormalities, relationship evaluated, humans □ ECG abnormalites—relationship to plasma concentrations of thioridazine and metabolites evaluated, humans □ Tranquilizers—thioridazine and metabolites, plasma concentrations and ECG abnormalities, relationship evaluated, humans

Abnormal electrocardiograms (ECG's) have been reported as an effect of thioridazine (1–6). This study explored the relationship of the plasma concentration of thioridazine and its metabolites during chronic thioridazine administration (4 mg/kg po) to the appearance of ECG abnormalities in schizophrenic patients. This investigation was one facet of ongoing studies on the pharmacokinetics of thioridazine (7) and mesoridazine (8) and clinical responses in acute schizophrenic patients.

EXPERIMENTAL

Subjects—The acute schizophrenic patients[1] selected were 21–55 years of age. None had a significant history of hepatic or cardiorenal disease, chronic alcoholism, or drug abuse. All subjects were drug free for at least 4 weeks prior to the study.

The selection of subjects was based on the independent diagnosis of schizophrenia by three psychiatrists. High scores on the major features of schizophrenia from three psychiatric rating scales, the Overall–Gorham brief psychiatric rating scale (9), the Hamilton depression rating scale (10), and the Wittenborn scale (10), and from an objective speech content analysis measure (11) corroborated the diagnosis of severe acute schizophrenia. Details of these methods for selecting subjects were reported previously (7).

Procedures—This was a placebo–drug, single oral dose, noncrossover study followed by daily drug administration. A liquid placebo was administered on Day 1. On Day 6, a single oral dose of thioridazine (4 mg/kg) was given. Starting on Day 10, thioridazine (4 mg/kg/day) was given in divided doses for 4–6 weeks. Generally, no neuroleptic other than thioridazine was administered to the patients.

Violent and unmanageable behavior, insomnia, or severe pain occasionally occurred in some subjects; these reactions were treated, when necessary, by supplementing the thioridazine with other medicaments. Specifically, chloral hydrate and meperidine were given to one patient and aspirin was given to another.

Blood was drawn for a drug screen and automated chemistry analysis[2] before thioridazine administration. On Day 6, blood was drawn for drug level determinations before and at 1, 4, 8, 24, 48, 72, and 96 hr after the initial oral thioridazine dose. After the 10th day, blood was drawn twice weekly for analysis.

Plasma thioridazine levels were measured by the GLC method of Dinovo *et al.* (12), which allows individual measurements for thioridazine and its metabolites.

ECG's, taken before and during drug administration, were read by members of the Cardiology Division, University of California Irvine Medical Center, having no knowledge of the nature of the study. The ECG's were reported to be abnormal if there was malformation of the T-wave or lengthening of the repolarization time. The morphology of the T-wave varied from blunting to inversion. The prolongation of repolarization appeared as a hypertrophy pattern, ST segment shifts, and abnormal QRST angles. Small Q-waves were reported as well as elevated ST segments. Occasionally, the ST segments became convex and U-waves appeared.

RESULTS AND DISCUSSION

Figures 1–5 show the variations in plasma levels of thioridazine and its metabolites following the continuous dose of thioridazine in five schizophrenic patients. The plasma level variations following the single dose of thioridazine on Day 6 are omitted in these figures and not considered in the results because no ECG abnormalities were noted for the 4 days following this single dose, probably because the plasma concentration of the metabolites of thioridazine did not reach sufficient levels for a necessary duration.

The fluctuations in plasma concentrations of thioridazine and its metabolites (mesoridazine, sulforidazine, and the thioridazine ring sulfoxide) can be accounted for on some occasions. Figure 1 (Patient C. K.) shows fluctuations in thioridazine, mesoridazine, and thioridazine ring sulfoxide plasma levels while the patient was receiving oral thioridazine at a dose of 4 mg/kg; some of these variations were possibly related to interruptions in the continuous oral administration of thioridazine. On the two occasions when abnormal ECG's were noted, the levels of thioridazine ring sulfoxide were close to 0.9 μg/ml; when normal ECG's were reported, the levels of thioridazine ring sulfoxide were lower, as were the levels of thioridazine and mesoridazine.

Figure 2 (Patient G. S.) also shows the plasma concentrations of thioridazine and its metabolites after the initiation on Day 10 of the continuous daily oral dosage of thioridazine (300 mg) at 4 mg/kg. The patient interrupted daily dosage of thioridazine on Days 25 and 39, and plasma measurements of drug level were not done between Days 22 and 29 and Days 36 and 43. ECG's were reported to be abnormal on two occasions when the plasma thioridazine ring sulfoxide levels were 1.4 μg/ml or above. Plasma thioridazine and mesoridazine concentrations were all below 0.6 μg/ml.

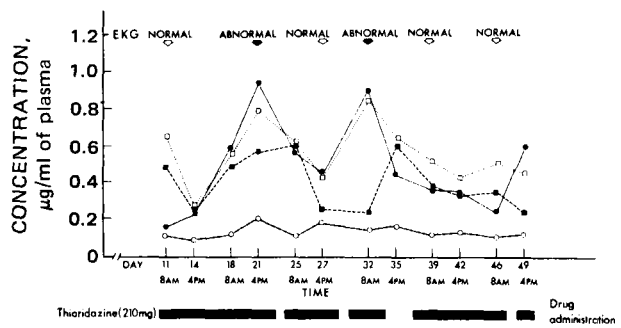

Figure 1—*GLC analysis of plasma concentrations of thioridazine and metabolites during standard daily oral dose (4 mg/kg) in Patient C. K. Key:* ■, *thioridazine;* □, *mesoridazine;* ○, *sulforidazine; and* ●, *thioridazine ring sulfoxide.*

[1] Adult Psychiatric Service, University of California Irvine Medical Center.
[2] SMA-6 and SMA-12.

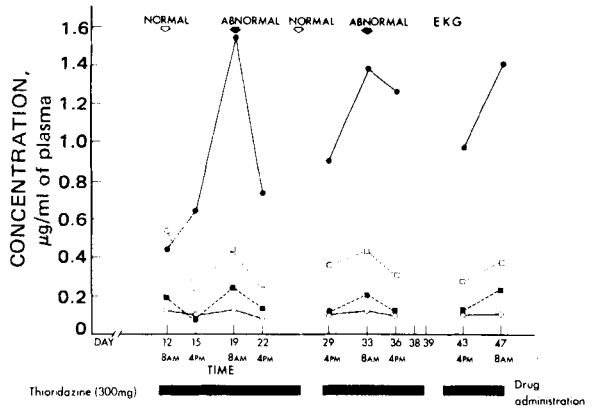

Figure 2—*GLC analysis of plasma concentrations of thioridazine and metabolites during standard daily oral dose (4 mg/kg) in Patient G. S. Key: ■, thioridazine; □, mesoridazine; ○, sulforidazine; and ●, thioridazine ring sulfoxide.*

Figure 3 (Patient R. R.) shows fairly steady-state plasma levels for thioridazine and its metabolites after Day 13 during the daily continuous oral dosage of 290 mg of thioridazine, except for Days 37–43 when there was a notable unexplained drop in plasma drug levels. On Days 22 and 34, abnormal ECG's were reported; the plasma levels of the thioridazine ring sulfoxide on these days were among the highest for this patient, namely, 2.2 μg/ml or above (the diagrammed levels for this metabolite are half the recorded value in Fig. 3).

With Patient S. C. (Fig. 4), continuous daily oral dosage of 300 mg of thioridazine was started on Day 10. Thioridazine, mesoridazine, and sulforidazine built up to a peak about Day 29, dropped off moderately about Day 33, and continued at a steady level until Day 50, except for the thioridazine ring sulfoxide which varied widely. These fluctuations are perhaps related to the activation of hepatic microsomal enzymes induced by the thioridazine and the other medication (chloral hydrate and meperidine) administered to this patient. Abnormal ECG's appeared when the plasma thioridazine ring sulfoxide levels exceeded 1.0 μg/ml.

Figure 5 (Patient H. D.) shows plasma drug concentrations after the patient was started on a continuous daily oral dose of 240 mg of thioridazine on Day 10. Although the thioridazine ring sulfoxide levels exceeded 1.0 μg/ml on several occasions, no abnormal ECG's were observed.

Of specific interest here are the relatively high plasma levels of the thioridazine ring sulfoxide and the fact that ECG changes were frequently, but not always, noted when these plasma levels reached or exceeded 0.9 μg/ml.

These findings suggest that the thioridazine ring sulfoxide metabolite of thioridazine induces ECG abnormalities in susceptible patients. The thioridazine ring sulfoxide was reported elsewhere[3] (13) to be pharmacologically inactive. The relationship of this metabolite to evidence of

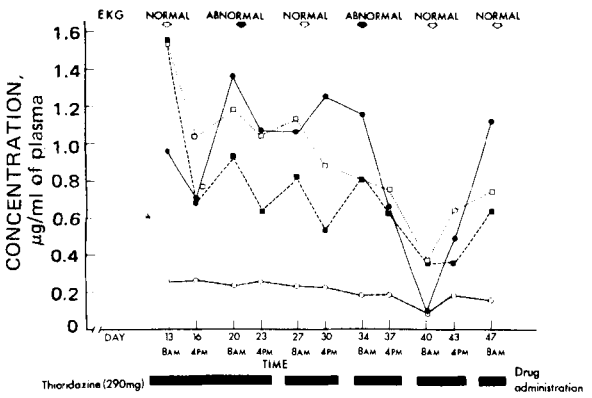

Figure 3—*GLC analysis of plasma concentrations of thioridazine and metabolites during standard daily oral dose (4 mg/kg) in Patient R. R. Key: ■, thioridazine; □, mesoridazine; ○, sulforidazine; and ●, thioridazine ring sulfoxide (half recorded level).*

[3] R. G. Muusze, unpublished Ph.D. dissertation, University of Amsterdam, Amsterdam, The Netherlands, 1975.

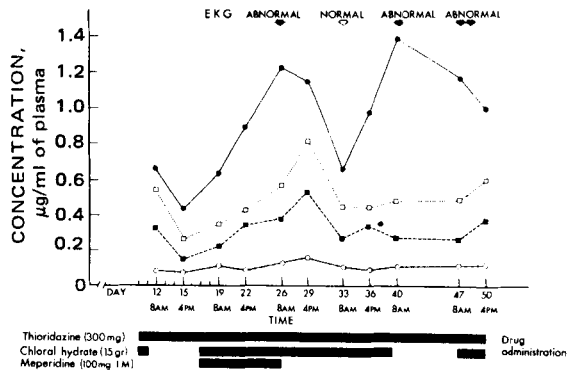

Figure 4—*GLC analysis of plasma concentrations of thioridazine and metabolites during standard oral dose (4 mg/kg) in Patient S. C. Key: ■, thioridazine; □, mesoridazine; ○, sulforidazine; and ●, thioridazine ring sulfoxide.*

interferences in myocardial conductance points to an interesting mechanism in the variety of biochemical pathways leading to a physiological adverse side effect.

If sufficient amounts of this metabolite had been readily available, the effects of the thioridazine ring sulfoxide on the heart in animals would have been studied. Unfortunately, only enough to serve as a standard in the GLC assays could be obtained. Therefore, it has not been possible to pursue the desirable definitive studies of the cardiotoxic effect of this specific metabolite.

The effect of thioridazine and its metabolites on the ECG has been reported essentially as changes in the T-wave morphology or interference with repolarization. The malformation of the T-wave can range from a simple apex blunting to broadening to notching to an actual inversion of the deflection (1, 2, 4). Investigation suggests that thioridazine treatment, alone or in combination with other phenothiazines or alcohol, may result in a lengthening of the time of repolarization to the extreme of ventricular arrhythmias, heart block, and death (2, 14–16). The abnormal repolarization category has included ECG patterns of hypertrophy, ST-segment shifts, abnormal QRST angles, and prolonged QT intervals.

The factors that bring about the ECG effects have not yet been clarified. Hypokalemia has been considered (3, 16), but deviations in serum electrolytes have not always been present (3, 17). The incidence of ECG T-wave abnormalities has been found to increase with the amount of thioridazine consumed per day (4, 18). The incidence of such abnormalities appears to be related to dose size, whereas the severity has been reported to be related to chronological age (4). The duration of treatment with thioridazine is not considered to be a factor in either the incidence or severity of these ECG changes (4).

Previous findings that dose size and chronological age are related to the incidence and/or severity of ECG abnormalities occurring with thioridazine are not inconsistent with the findings that high plasma concentrations of the thioridazine ring sulfoxide are frequently associated

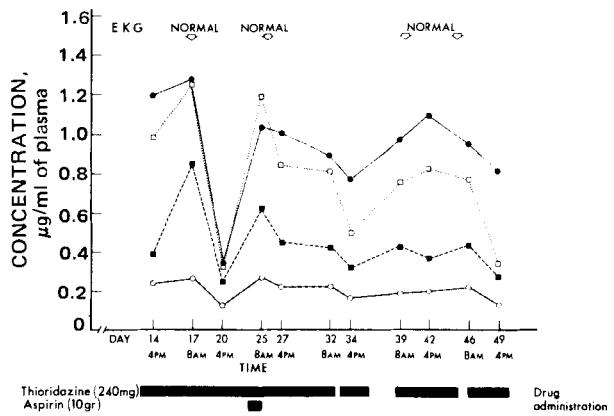

Figure 5—*GLC analysis of plasma concentrations of thioridazine and metabolites during standard daily oral dose (4 mg/kg) in Patient H. D. Key: ■, thioridazine; □, mesoridazine; ○, sulforidazine; and ●, thioridazine ring sulfoxide.*

with abnormal electroencephalographic changes. The pathogenic mechanism involved remains unknown, however, and it is hoped that this report will stimulate research in this area.

REFERENCES

(1) A. G. Kelly, J. E. Fay, and S. G. Laverty, *Can. Med. Assoc. J.*, **89**, 546 (1963).

(2) J. R. Huston and G. E. Bell, *J. Am. Med. Assoc.*, **198**, 16 (1966).

(3) R. J. Rosenquist, W. W. Brauer, and J. N. Mark, *Minn. Med.*, **54**, 877 (1971).

(4) C. Thornton and M. H. Wendkos, *Dis. Nerv. Syst.*, **32**, 320 (1971).

(5) D. M. Gallant and M. P. Bishop, *Curr. Ther. Res.*, **14**, 10 (1972).

(6) J. M. Samet and B. Surawicz, *J. Clin. Pharmacol.*, **14**, 588 (1974).

(7) L. A. Gottschalk, R. Biener, E. P. Noble, H. Birch, D. E. Wilbert, and J. F. Heiser, *Comp. Psychiat.*, **16**, 323 (1975).

(8) L. A. Gottschalk, E. C. Dinovo, R. Biener, H. Birch, M. Syben, and E. P. Noble, in "Pharmacokinetics of Psychoactive Drugs: Blood Levels and Clinical Response," L. A. Gottschalk and S. Merlis, Eds., Spectrum, New York, N.Y., 1976, pp. 177, 189.

(9) J. E. Overall and D. P. Gorham, *Psychol. Rep.*, **10**, 799 (1962).

(10) W. Guy and R. R. Bonato, "Manual for the ECDEU Assessment Battery," 2nd rev., National Institute of Mental Health, U.S. Department of Health, Education, and Welfare, Chevy Chase, Md., 1970.

(11) L. A. Gottschalk and G. C. Gleser, "The Measurement of Psychological States Through the Content Analysis of Verbal Behavior," University of California Press, Berkeley, Calif., 1969.

(12) E. C. Dinovo, L. A. Gottschalk, B. R. Nandi, and P. G. Geddes, *J. Pharm. Sci.*, **65**, 667 (1976).

(13) R. G. Muusze and J. F. K. Huber, *J. Chromatogr.*, **83**, 405 (1973).

(14) S. Desautels, G. Filteau, and A. St. Jean, *Can. Med. Assoc. J.*, **90**, 1030 (1964).

(15) H. Bachman and R. Elosuo, *Ann. Med. Intern. Fenn.*, **53**, 1 (1964).

(16) M. A. Sydney, *Br. Med. J.*, **4**, 467 (1973).

(17) T. A. Ban and A. St. Jean, *Can. Med. Assoc. J.*, **91**, 537 (1964).

(18) M. H. Wendkos and C. C. Thornton, *Behav. Neuropsychiatry*, **1**, 18 (1969).

ACKNOWLEDGMENTS

Supported in part by Research Project Grant MH-20174 from the Psychopharmacology Branch, National Institute of Mental Health, and by a grant-in-aid from Sandoz Pharmaceuticals.

Potential CNS Antitumor Agents—Phenothiazines II: Fluphenazine Analogs

TADASHI HIRATA *, GEOFFREY PENG ‡, and JOHN S. DRISCOLL ×

Received February 28, 1977, from the *Drug Design and Chemistry Section, Laboratory of Medicinal Chemistry and Biology, Drug Research and Development Program, Division of Cancer Treatment, National Cancer Institute, National Institutes of Health, Bethesda, MD 20014.* Accepted for publication April 19, 1977.

*Present address: Kyowa Hakko Kogyo Co. Ltd., Tokyo, Japan. ‡Present address: University of Illinois at the Medical Center, Chicago, IL 60680.

Abstract □ Fluphenazine was found to possess moderate, reproducible activity against the intraperitoneal L-1210 and P-388 leukemia murine tumor models. Seven ether derivatives of fluphenazine and eight compounds in which the terminal side-chain hydroxyl group was replaced by an amine function were prepared and evaluated in the intraperitoneal L-1210, P-388, and B16 melanoma systems as well as the intracerebral L-1210 and ependymoblastoma brain tumor models. While no substantial intracerebral activity was observed, seven derivatives possessed reproducible activity in the intraperitoneal L-1210 or P-388 system. Several gave T/C values of 150%. No B16 melanoma activity was observed. These compounds were also tested for their cytotoxic properties in culture against L-1210, P-388, and KB cells. The amine isosteres, while possessing little *in vivo* activity, were the most cytotoxic of the compounds prepared, with several having ED_{50} values <1 μg/ml.

Keyphrases □ Fluphenazine and various analogs—synthesized, CNS antitumor and cytotoxic activity evaluated □ Phenothiazines, various—synthesized, CNS antitumor and cytotoxic activity evaluated □ Antitumor activity, CNS—fluphenazine and various analogs evaluated □ Cytotoxic activity—fluphenazine and various analogs evaluated □ Structure-activity relationships—fluphenazine and various analogs evaluated for CNS antitumor and cytotoxic activity

Brain tumors and other cancers of the central nervous system (CNS) continue to constitute a difficult clinical problem. Approximately 8500 patients per year die from brain tumors. CNS cancer is the second most common type in children under 15 years old (1). Secondary CNS tumors are encountered among leukemia patients (2), who are often treated prophylactically with irradiation of the CNS or with intrathecal methotrexate administration (3, 4).

Drugs able to enter the CNS are obvious candidates as potential CNS antitumor agents. Psychotropic drugs in general (5–8) and phenothiazine derivatives in particular (5–20) have been investigated for their antitumor properties. The possibility that phenothiazine derivatives may have had a favorable effect on human carcinomas has been discussed (19).

Although some activity has been observed with phenothiazines in animal tumor models when the tumor was intraperitoneally or subcutaneously implanted, no CNS antitumor activity was found when an intracerebral tumor model was studied using phenothiazine nitrogen mustard derivatives (20). At the time the phenothiazine mustard investigation (20) was initiated, a second, parallel, attempt to produce a CNS antitumor agent based on a nonalkylating phenothiazine system was started. This work was based on the intraperitoneal murine leukemia activity observed during the initial testing of trifluoperazine (I), fluphenazine (II), and the hydroxyethyl ether of fluphenazine (III). Compounds I and II are known to penetrate the blood–brain barrier and to have significant CNS activity in humans. It appeared that if a compound of this type could be discovered that had high intraperitoneal

with abnormal electroencephalographic changes. The pathogenic mechanism involved remains unknown, however, and it is hoped that this report will stimulate research in this area.

REFERENCES

(1) A. G. Kelly, J. E. Fay, and S. G. Laverty, *Can. Med. Assoc. J.*, **89**, 546 (1963).

(2) J. R. Huston and G. E. Bell, *J. Am. Med. Assoc.*, **198**, 16 (1966).

(3) R. J. Rosenquist, W. W. Brauer, and J. N. Mark, *Minn. Med.*, **54**, 877 (1971).

(4) C. Thornton and M. H. Wendkos, *Dis. Nerv. Syst.*, **32**, 320 (1971).

(5) D. M. Gallant and M. P. Bishop, *Curr. Ther. Res.*, **14**, 10 (1972).

(6) J. M. Samet and B. Surawicz, *J. Clin. Pharmacol.*, **14**, 588 (1974).

(7) L. A. Gottschalk, R. Biener, E. P. Noble, H. Birch, D. E. Wilbert, and J. F. Heiser, *Comp. Psychiat.*, **16**, 323 (1975).

(8) L. A. Gottschalk, E. C. Dinovo, R. Biener, H. Birch, M. Syben, and E. P. Noble, in "Pharmacokinetics of Psychoactive Drugs: Blood Levels and Clinical Response," L. A. Gottschalk and S. Merlis, Eds., Spectrum, New York, N.Y., 1976, pp. 177, 189.

(9) J. E. Overall and D. P. Gorham, *Psychol. Rep.*, **10**, 799 (1962).

(10) W. Guy and R. R. Bonato, "Manual for the ECDEU Assessment Battery," 2nd rev., National Institute of Mental Health, U.S. Department of Health, Education, and Welfare, Chevy Chase, Md., 1970.

(11) L. A. Gottschalk and G. C. Gleser, "The Measurement of Psychological States Through the Content Analysis of Verbal Behavior," University of California Press, Berkeley, Calif., 1969.

(12) E. C. Dinovo, L. A. Gottschalk, B. R. Nandi, and P. G. Geddes, *J. Pharm. Sci.*, **65**, 667 (1976).

(13) R. G. Muusze and J. F. K. Huber, *J. Chromatogr.*, **83**, 405 (1973).

(14) S. Desautels, G. Filteau, and A. St. Jean, *Can. Med. Assoc. J.*, **90**, 1030 (1964).

(15) H. Bachman and R. Elosuo, *Ann. Med. Intern. Fenn.*, **53**, 1 (1964).

(16) M. A. Sydney, *Br. Med. J.*, **4**, 467 (1973).

(17) T. A. Ban and A. St. Jean, *Can. Med. Assoc. J.*, **91**, 537 (1964).

(18) M. H. Wendkos and C. C. Thornton, *Behav. Neuropsychiatry*, **1**, 18 (1969).

ACKNOWLEDGMENTS

Supported in part by Research Project Grant MH-20174 from the Psychopharmacology Branch, National Institute of Mental Health, and by a grant-in-aid from Sandoz Pharmaceuticals.

Potential CNS Antitumor Agents—Phenothiazines II: Fluphenazine Analogs

TADASHI HIRATA *, GEOFFREY PENG ‡, and JOHN S. DRISCOLL ×

Received February 28, 1977, from the *Drug Design and Chemistry Section, Laboratory of Medicinal Chemistry and Biology, Drug Research and Development Program, Division of Cancer Treatment, National Cancer Institute, National Institutes of Health, Bethesda, MD 20014.* Accepted for publication April 19, 1977.

*Present address: Kyowa Hakko Kogyo Co. Ltd., Tokyo, Japan. ‡Present address: University of Illinois at the Medical Center, Chicago, IL 60680.

Abstract □ Fluphenazine was found to possess moderate, reproducible activity against the intraperitoneal L-1210 and P-388 leukemia murine tumor models. Seven ether derivatives of fluphenazine and eight compounds in which the terminal side-chain hydroxyl group was replaced by an amine function were prepared and evaluated in the intraperitoneal L-1210, P-388, and B16 melanoma systems as well as the intracerebral L-1210 and ependymoblastoma brain tumor models. While no substantial intracerebral activity was observed, seven derivatives possessed reproducible activity in the intraperitoneal L-1210 or P-388 system. Several gave T/C values of 150%. No B16 melanoma activity was observed. These compounds were also tested for their cytotoxic properties in culture against L-1210, P-388, and KB cells. The amine isosteres, while possessing little *in vivo* activity, were the most cytotoxic of the compounds prepared, with several having ED_{50} values <1 μg/ml.

Keyphrases □ Fluphenazine and various analogs—synthesized, CNS antitumor and cytotoxic activity evaluated □ Phenothiazines, various—synthesized, CNS antitumor and cytotoxic activity evaluated □ Antitumor activity, CNS—fluphenazine and various analogs evaluated □ Cytotoxic activity—fluphenazine and various analogs evaluated □ Structure-activity relationships—fluphenazine and various analogs evaluated for CNS antitumor and cytotoxic activity

Brain tumors and other cancers of the central nervous system (CNS) continue to constitute a difficult clinical problem. Approximately 8500 patients per year die from brain tumors. CNS cancer is the second most common type in children under 15 years old (1). Secondary CNS tumors are encountered among leukemia patients (2), who are often treated prophylactically with irradiation of the CNS or with intrathecal methotrexate administration (3, 4).

Drugs able to enter the CNS are obvious candidates as potential CNS antitumor agents. Psychotropic drugs in general (5–8) and phenothiazine derivatives in particular (5–20) have been investigated for their antitumor properties. The possibility that phenothiazine derivatives may have had a favorable effect on human carcinomas has been discussed (19).

Although some activity has been observed with phenothiazines in animal tumor models when the tumor was intraperitoneally or subcutaneously implanted, no CNS antitumor activity was found when an intracerebral tumor model was studied using phenothiazine nitrogen mustard derivatives (20). At the time the phenothiazine mustard investigation (20) was initiated, a second, parallel, attempt to produce a CNS antitumor agent based on a nonalkylating phenothiazine system was started. This work was based on the intraperitoneal murine leukemia activity observed during the initial testing of trifluoperazine (I), fluphenazine (II), and the hydroxyethyl ether of fluphenazine (III). Compounds I and II are known to penetrate the blood–brain barrier and to have significant CNS activity in humans. It appeared that if a compound of this type could be discovered that had high intraperitoneal

Table I—Physical and Chemical Data

Compound	Melting Point	Yield, %	Formula	Number of Hydrochlorides	Analysis, %		
						Calc.	Found
V	73.5–74.5°	55	$C_{16}H_{13}ClF_3NS$	0	C	56.06	56.09
					H	3.82	3.78
					Cl	10.34	10.39
					N	4.09	4.08
					S	9.35	9.51
VII	194–197°	85	$C_{24}H_{32}Cl_2F_3N_3OS$	2	C	53.53	53.14
					H	5.99	6.14
					Cl	13.17	12.71
					N	7.80	7.69
					S	5.95	5.97
VIII	192–195°	63	$C_{26}H_{36}Cl_2F_3N_3OS$	2	C	55.12	55.47
					H	6.41	6.09
					Cl	12.52	12.14
					N	7.42	7.28
					S	5.66	5.95
IX	171–173°	58	$C_{24}H_{31}Cl_3F_3N_3OS \cdot \frac{1}{2}H_2O$	2	C	49.53	49.38
					H	5.54	5.57
					Cl	18.28	18.30
					N	7.22	7.16
					S	5.51	5.43
X	154–155°	67	$C_{25}H_{34}Cl_2F_3N_3O_2S \cdot H_2O$	2	C	51.19	50.89
					H	6.19	6.01
					Cl	12.09	11.92
					N	7.16	7.02
					S	5.47	5.50
XI	188–191°	63	$C_{25}H_{32}Cl_2F_3N_3OS \cdot \frac{1}{2}H_2O$	2	C	53.66	53.27
					H	5.94	5.97
					Cl	12.67	12.75
					N	7.51	7.30
					S	5.73	5.86
XII	181–183°	77	$C_{27}H_{38}Cl_2F_3N_3OS$	2	C	55.89	55.82
					H	6.55	6.81
					Cl	12.22	12.27
					N	7.24	7.00
					S	5.53	5.31
XIII	192–195°	77	$C_{28}H_{40}Cl_2F_3N_3OS$	2	C	56.59	56.34
					H	6.73	6.85
					Cl	11.93	12.21
					N	7.07	6.90
					S	5.40	5.28
XIV	205–207°	84	$C_{28}H_{32}Cl_2F_3N_3OS$	2	C	57.36	57.13
					H	5.46	5.66
					Cl	12.09	11.82
					N	7.16	6.95
					S	5.47	5.41
XV	181–185°	63	$C_{24}H_{34}Cl_3F_3N_4OS \cdot \frac{1}{2}H_2O$	3	C	47.41	47.16
					H	5.80	5.88
					Cl	17.50	17.38
					N	9.22	9.03
					S	5.27	5.43
XVI	217–219°	69	$C_{25}H_{36}Cl_3F_3N_4OS$	3	C	49.71	49.39
					H	6.01	6.31
					Cl	17.61	17.60
					N	9.28	9.19
					S	5.31	5.23
XVII	207–210°	61	$C_{25}H_{34}Cl_3F_3N_4S \cdot \frac{1}{2}H_2O$	3	C	50.42	50.05
					H	5.93	5.67
					Cl	17.88	17.78
					N	9.42	9.12
					S	5.39	5.57
XVIII	204–206°	74	$C_{28}H_{38}Cl_3F_3N_4S$	3	C	53.72	53.83
					H	6.12	6.46
					Cl	16.99	16.80
					N	8.95	8.82
					S	5.12	5.14
XIX	253–256°	73	$C_{27}H_{38}Cl_3F_3N_4S$	3	C	52.81	52.53
					H	6.24	5.98
					Cl	17.32	16.88
					N	9.12	9.20
					S	5.22	5.13
XX	255–257°	63	$C_{26}H_{36}Cl_3F_3N_4OS \cdot \frac{1}{2}H_2O$	3	C	49.96	49.98
					H	5.97	5.93
					Cl	17.02	17.17
					N	8.96	8.84
					S	5.13	5.50
XXI	202–205°	38	$C_{24}H_{35}Cl_3F_3N_5S \cdot 2H_2O$	3	C	46.12	46.43
					H	6.29	5.91
					Cl	17.02	17.20
					N	11.21	11.10
					S	5.13	5.32

Table I— *(Continued)*

Compound	Melting Point	Yield, %	Formula	Number of Hydrochlorides	Analysis, %	Calc.	Found
XXII	135–137°	47	$C_{34}H_{37}F_3N_4O_3S_2$	0	C	60.87	60.92
					H	5.56	5.41
					N	8.35	8.04
					S	9.56	9.29
XXIII	238–240°	13	$C_{24}H_{29}ClF_3N_3OS \cdot H_2O$	0	C	55.65	56.06
					H	5.99	5.91
					Cl	6.86	7.02
					N	8.12	8.33
					S	6.18	6.18

antitumor activity (*e.g.*, T/C 200%)[1], it might also possess a degree of CNS antitumor activity. Therefore, an investigation was started to explore the effect on the antitumor activity of altering the hydroxyethyl side chain of II.

CHEMISTRY

Since III had antitumor activity equal to or better than the parent compound, the effect of modifying the terminal hydroxyl group in the II side chain was investigated. To provide as much nonlinearity as possible among the physicochemical parameters, σ^* was plotted against π (21), and these data were used as much as possible for the selection of candidate R groups (Scheme I). An attempt also was made to provide some steric differences among the various R groups. The effect of replacing the terminal hydroxyl group by an amine function (XV–XXII) also was investigated.

The synthetic procedure used is shown in Scheme I. Compound IV was alkylated in the 10-position to give V, using the general procedure employed by Jackson and Shirley (13) to produce the corresponding β-chloroethyl compound. The reaction of V with piperazineethanol provided II, which was chlorinated to produce the key intermediate (VI). Compound VI then was reacted with the appropriate sodium alkoxide or amine to give the desired analogs. Physical and chemical properties of these materials are listed in Table I.

When III was reacted with thionyl chloride (Scheme II), an intramolecular alkylation product (XXIII) was isolated in addition to the desired product (IX). If the reaction mixture was chromatographed on alumina, XXIII was produced exclusively. Chromatography under less basic conditions (silica gel) retarded the intramolecular reaction and gave IX and XXIII in yields of 58 and 13%, respectively.

The NMR spectra of these phenothiazines as free bases in deuterochloroform were similar to the spectrum of the parent compound (II), which had the following resonance characteristics: aromatic protons as a multiplet at δ 7.0 ppm and methylene groups attached to the phenothiazine nitrogen, to the hydroxyl group, and at the middle of the propyl chain at δ 3.9 (t), 3.6 (t), and 1.9 (t) ppm, respectively; the methylene groups in and attached to the piperazine ring gave a broad singlet or partially resolved triplet at δ 2.4 ppm while the hydroxyl proton gave a singlet at δ 2.9 ppm. These data are in agreement with those reported earlier for II (22). The major differences in the spectra of XXII and XXIII were the resonance frequencies of the methylene groups attached to the quaternary nitrogen atoms. They occurred at δ 5.1 and 3.8 ppm for these two compounds, respectively.

The elemental analytical values for several compounds (Table I) indicated that they were hemihydrates. While this is not uncommon for derivatives of this type (23), the mass spectra of two such compounds (XV and XVII) were run to confirm their structures. Compound XVII gave a molecular ion at *m/e* 476 while the spectrum of XV showed a peak at *m/e* 462 corresponding to M − H_2O. Both compounds gave strong peaks

I: R = CH_3
II: R = CH_2CH_2OH
III: R = $CH_2CH_2OCH_2CH_2OH$

[1] T/C = (treated survival ÷ control survival) × 100%.

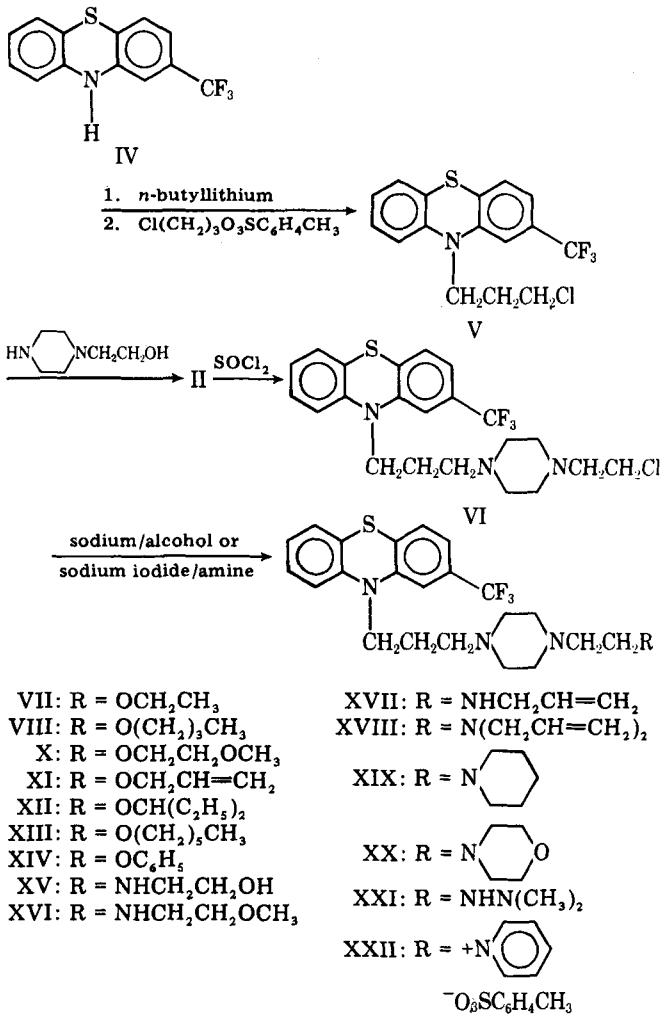

VII: R = OCH_2CH_3
VIII: R = $O(CH_2)_3CH_3$
X: R = $OCH_2CH_2OCH_3$
XI: R = $OCH_2CH{=}CH_2$
XII: R = $OCH(C_2H_5)_2$
XIII: R = $O(CH_2)_5CH_3$
XIV: R = OC_6H_5
XV: R = $NHCH_2CH_2OH$
XVI: R = $NHCH_2CH_2OCH_3$

XVII: R = $NHCH_2CH{=}CH_2$
XVIII: R = $N(CH_2CH{=}CH_2)_2$
XIX: R = N⬡
XX: R = N⬡O
XXI: R = $NHN(CH_3)_2$
XXII: R = $+N$⬡ $^-O_3SC_6H_4CH_3$

Scheme I

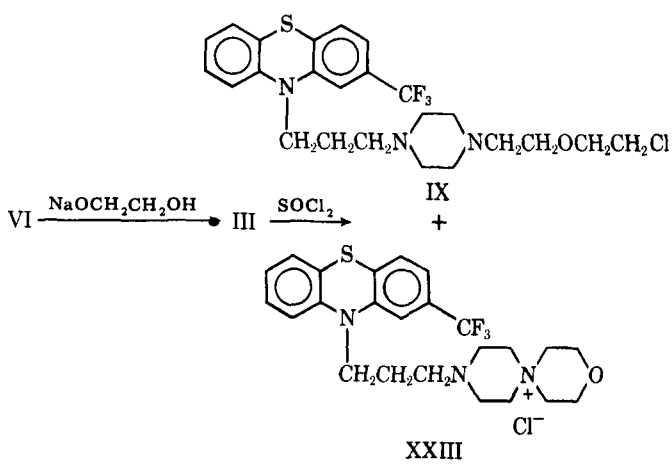

Scheme II

Table II—Antitumor Activity[a]

Compound	L-1210 Lymphoid Leukemia[b] OD[d]	T/C	P-388 Lymphocytic Leukemia[b] OD	T/C	Ependymoblastoma[c] OD	T/C
I	66	142	100	150	75	115
	37	137	100	163	75	110
II	50	164	25	148	30	110
	25	130	25	145	15	126
III	50	150	25	150	50	106
	120	150	25	126		
V	100	118	200	104		
VI	25	110	25	115		
VII	35	136	12.5	116	37.5	97
	50	132	12.5	138		
VIII	50	122	50	153		
	25	116	50	129		
IX	25	122	25	141		
			50	134		
X	50	151	6.2	161		
	50	138	25	127	37.5	125
XI	35	148	20	144		
	35	129	5	125	50	130
XII	6.2	112	40	131		
	12.5	97	20	109		
XIII	12.5	106	12.5	130		
			12.5	129		
XIV	12.5	126	25	122		
	12.5	104	25	124		
XV	6.2	104	12.5	135		
			12.5	110		
XVI	6.2	110	80	120		
	50	108	40	113		
XVII	6.2	106	50	144	37.5	92
			50	116	50	130
XVIII	25	112	25	112		
			25	111		
XIX	25	96	12.5	118		
XX	25	116	50	112		
			50	104		
XXI	25	104				
XXII	12.5	101	20	126		
			20	122		
XXIII	12.5	114				

[a] Protocols and test systems were described in Ref. 24. The results from two separate experiments are given when available. [b] Day 1, 5, and 9 treatment schedule. Intraperitoneal treatment of intraperitoneal tumor. [c] QD 1–5 treatment schedule. Intraperitoneal treatment of intracerebral tumor. [d] Optimum dose (milligrams per kilogram per injection).

at *m/e* 406 corresponding to M − CH_2NHR. No evidence for the presence of sulfoxide was observed in either sample.

BIOLOGY

Tumor Models Employed—Compounds were tested according to standard National Cancer Institute (NCI) protocols (24). The every 4th day (Q4D-1,5,9) treatment schedule was determined to be superior to the chronic (QD 1–9) or Day 1 only schedule for these compounds in the L-1210 and P-388 tumor systems. Intraperitoneal treatment of intraperitoneally implanted tumor was employed with these two tumor models (Table II).

The compounds with reproducible intraperitoneal L-1210 activity (I–III, VII, X, and XI) were tested in the intracerebral L-1210 and intracerebral ependymoblastoma tumor models (intracerebral tumor implantation and intraperitoneal drug administration). The criterion for statistically significant activity has been established (24) as a T/C value of ≥ 125% in these tumor systems.

Because chlorpromazine had been reported to have significant activity in the B16 melanocarcinoma tumor system (14), all compounds except IV–VI were tested against the intraperitoneal B16 tumor. No significant activity (T/C ≥ 140%) was observed for any compound.

In vitro cytotoxicity data were also obtained using the L-1210, P-388, and KB cell lines (24) (Table III).

***In Vivo* Studies**—Compounds I–III had reproducible, moderate antitumor activity against the intraperitoneal L-1210 and the P-388 tumor systems (Table II). There was not much difference in the activity of the three compounds, each producing T/C values of about 150% (*i.e.*, an increase in lifespan of 50%). Replacing the terminal hydroxyl group of III by a proton gave VII, which retained activity in both systems but at a somewhat lower level. Replacement by a methoxyl group gave X, in which equivalent activity was found; and replacement by an olefin methylene group gave XI, which was approximately as active as III in both tumor systems. Replacement of the hydroxyl group in III by a butyl group (XIII) abolished the L-1210 activity. This compound, however, retained marginal P-388 activity. Nonreproducible P-388 and L-1210 activity was obtained with the 3-pentyl (XII) and phenyl (XIV) ethers of fluphenazine.

Little *in vivo* activity was observed among the amino derivatives. Some marginal P-388 activity was observed with XV (the nitrogen analog of III), the vinyl compound XVII, and the *unsym*-dimethylhydrazine analog XXII.

Because of their activity in one or both intraperitoneal tumor systems, seven fluphenazine analogs were tested in the murine L-1210 and ependymoblastoma (EM) brain tumor models. No activity was seen in the intracerebral L-1210 tests. Although statistically significant activity (T/C ≥ 125%) (24) was observed with II, X, XI, and XVII, this activity was so marginal that for practical purposes it can be concluded that none of the L-1210 intraperitoneal active compounds investigated possesses antitumor activity in either of the two intracerebral model systems studied.

***In Vitro* Studies**—While the simple phenothiazines IV and V are essentially inactive in the three cell culture systems studied (L-1210, P-388, and KB), many II analogs prepared possessed substantial cytotoxicity. While II was moderately cytotoxic, I, III, X, XX, and XXI appeared to be about eight times as cytotoxic as II in the L-1210 and P-388 systems. Most active of all were the nitrogen isosteres XV–XVII with ED_{50} values <1 μg/ml (Table III).

Table III—Cell Culture Activity (Micrograms per Milliliter)[a]

Compound	L-1210	P-388	KB
I	6	6	18
II	49	40	13
III	6	5	11
IV		>100	>100
V	>100	>100	>100
VI		17	7
VII	5	49	18
VIII	56	40	>100
IX	36	7	21
X	6	4	8
XI	25	5	7
XII	>100	54	59
XIII	>100	88	>100
XIV	69	52	>100
XV	0.6	0.4	2
XVI	4	0.5	2.5
XVII	0.9	0.5	6
XVIII	54	44	>100
XIX	2.3	0.39	2.9
XX	5	4	2.5
XXI	6	5	23
XXII	58	43	8
XXIII	59	51	51

[a] Concentration required to inhibit cell growth to 50% that of the control.

For the oxygen analogs prepared (I–III and VII–XIV), *in vitro* cytotoxicity tended to parallel *in vivo* activity. Compounds I, III, VII, X, and XI possessed *in vivo* activity in both the L-1210 and P-388 systems. These compounds also had *in vitro* ED_{50} activities in the 5–20-μg/ml range. Fluphenazine (II), which had substantial intraperitoneal L-1210 and P-388 activity, also was active *in vitro* but at a higher ED_{50} value (40 μg/ml). While VII, the ethyl ether of II, was relatively toxic, the butyl ether (VIII) was less so and the hexyl ether (XIII) was essentially noncytotoxic, suggesting a possible dependence on the lipophilicity of these compounds. It is not possible to determine *in vivo versus in vitro* relationships for the nitrogen analogs because of the generally poor *in vivo* activity of these compounds. These materials, however, were the most cytotoxic compounds prepared.

DISCUSSION

Phenothiazines of the type described here clearly have reproducible, moderate *in vivo* antitumor activity in the intraperitoneal L-1210 and P-388 tumor models and are cytotoxic in cell culture, but the possible utility of the activity observed is presently unclear. CNS agents in general (25) and phenothiazines, such as chlorpromazine, in particular (25, 26) can reduce body temperature (hypothermia) in mice. The apparent an-

titumor activity of reserpine has been attributed to hypothermic effects (27). However, the compounds described in the present study are definitely cytotoxic.

Moreover, materials of this type are known to be surface-active agents (9, 28) capable of modifying cell surface characteristics. They produce numerous other physiological effects (9, 29). The similarity in activity of the best compounds in this series could conceivably be related to metabolic similarities (30). More needs to be known about their mechanism of intraperitoneal antitumor action before the possible usefulness of these compounds can be assessed.

Based on the intracerebral tumor models employed in this study, these phenothiazines show little promise as single agents for therapy against brain tumors. However, phenothiazines are known to enhance the activity of certain other drugs (7, 9). The very reasonable intraperitoneal antitumor activity of these compounds might suggest a possible use in combination with other agents if the action of the phenothiazines is compatible with a synergistic mechanism.

EXPERIMENTAL[2]

2-Trifluoromethylphenothiazine, 3-chloroethyl-*p*-toluenesulfonate, and 1-piperazineethanol were obtained commercially. When several compounds were prepared by comparable procedures, only one representative example is discussed. Reference should be made to Table I for supplementary information.

Fluphenazine [4-[3-[2-(Trifluoromethyl)phenothiazin-10-yl]-propyl]-1-piperazineethanol] (II)—A stirred mixture of V (52.0 g, 0.15 mole), sodium iodide (22.5 g, 0.15 mole), and 1-piperazineethanol (33.8 g, 0.3 mole) was refluxed in 2-butanone (260 ml) for 20 hr (Scheme I). The mixture was concentrated *in vacuo*, and the residue was poured into a mixture of concentrated hydrochloric acid (40 ml), water (300 ml), and ether (150 ml). After thorough shaking, the aqueous layer was isolated, made basic with 40% aqueous potassium hydroxide, saturated with potassium carbonate, and extracted with three 200-ml portions of ether.

The ether extracts were washed with a saturated sodium chloride solution, dried over sodium sulfate, and concentrated to a dark oil, which was distilled to give 27.2 g (41%) of an oil, bp 260–270°/0.4 torr [lit. (31) bp 268–274°/0.5 torr]. This material was used without further purification for the preparation of VI.

2-[2-[4-[3-[2 - (Trifluoromethyl)phenothiazin-10-yl]propyl]-1-piperazinyl]ethoxy]ethanol Dihydrochloride (III)—Small pieces of sodium (2.3 g, 0.1 mole) were dissolved in ethylene glycol (40 ml) with warming, when necessary, over 3 hr. Compound VI dihydrochloride (9.0 g, 0.017 mole) was added in small portions, and the solution was heated at 105° for 6 hr. After cooling, water (300 ml) was added, and the resulting mixture was extracted with benzene.

The extracts were combined, washed with water, dried over sodium sulfate, and evaporated to a brown oil. The oil was dissolved in dry ether, the solution was filtered, and hydrogen chloride gas was added to yield 8.52 g (90%) of the dihydrochloride salt. Recrystallization from 2-propanol gave a tan solid, mp 222–224° [lit. (23) mp 220–222°].

10-(3-Chloropropyl)-2-(trifluoromethyl)phenothiazine (V)—This compound, mp 73–74° [lit. (32) mp 70–71°], was prepared in a 55% yield on a 35-g scale by the general method of Jackson and Shirley (13).

10-[3-[4-(2-Chloroethyl) -1- piperazinyl]propyl]-2-(trifluoromethyl)phenothiazine Dihydrochloride (VI)—A solution of II (4.58 g, 0.01 mole) in alcohol-free chloroform (100 ml) was saturated with hydrogen chloride gas (Scheme I). To this stirred solution was added dropwise thionyl chloride (2.9 g, 0.02 mole) in purified chloroform (60 ml). A gray precipitate resulted. The stirred reaction mixture was refluxed for 3 hr and then poured into dry ether (300 ml). The resulting fine solid was washed with dry ether and dried to give 5.0 g (95%) of product as a dihydrochloride, mp 208–211° [lit. (23) mp 209–211°].

General Procedure for Phenothiazine Ethers (VII, VIII, and X-XIV)—To a solution of sodium metal (0.23 g, 10 mmoles) in 15 ml of the appropriate alcohol was slowly added 1.22 g (2 mmoles) of VI (Scheme I). The reaction mixture was stirred at reflux for 4 hr. Excess alcohol was removed *in vacuo*, and the residue was treated with water and then extracted with ether. The extracts were washed with saturated aqueous sodium carbonate and then dried over anhydrous sodium carbonate.

Removal of the solvent gave a viscous oil, which was dissolved in benzene and filtered to remove any insoluble material. The benzene was evaporated, the residue was dissolved in dry ether, and hydrogen chloride gas was added. The resulting precipitate was purified by solution in a small amount of methanol and treatment with activated charcoal[3]. After filtration, dry ether was added carefully to reprecipitate the dihydrochloride salt.

General Procedures for Phenothiazine Amines—*Method A (XVI-XVIII)*—A mixture of VI (4.0 g, 7.6 mmoles), sodium iodide (1.0 g, 6.7 mmoles), and 30 ml of the appropriate amine was heated at reflux for 3–6 hr (Scheme I). The excess amine was evaporated *in vacuo*, the residue was treated with aqueous sodium carbonate, and this solution was extracted with benzene. The extracts were dried with sodium sulfate and evaporated to an oily residue, which was dissolved in dry ether. Hydrogen chloride gas was added to precipitate a crude trihydrochloride salt, which was purified by recrystallization from methanol–ether.

Method B (XIX and XX)—A mixture of VI (4.0 g, 7.6 mmoles), sodium iodide (1.0 g, 6.7 mmoles), 50 ml of the appropriate amine, and *N,N*-dimethylformamide (50 ml) was heated at 65–90° for 5 hr (Scheme I). Workup and purification were as described in Method A.

10-[3-[4-[2 - (2-Chloroethoxy)ethyl]-1-piperazinyl]propyl]-2-(trifluoromethyl)-10*H*-phenothiazine Dihydrochloride (IX)—A solution of III (3.2 g, 5.8 mmoles) in purified chloroform (100 ml) was saturated with hydrogen chloride gas. To this stirred, gently heated solution was added dropwise 1.1 g (9.2 mmoles) of thionyl chloride in 25 ml of purified chloroform over 90 min (Scheme II). The mixture was refluxed for an additional 3 hr, treated with activated charcoal, and filtered. The solvent was evaporated and the residue was treated with saturated sodium bicarbonate solution to produce the free base which was extracted with ether. The extracts were dried over anhydrous sodium carbonate.

Addition of hydrogen chloride gas gave 3.4 g of a crude hydrochloride salt. This material was purified by conversion to the free base, which was chromatographed on silica gel with benzene–acetone (1:1) to give 2.2 g (66%) of IX after conversion to the dihydrochloride salt. Recrystallization from methanol–ether gave fine crystals, mp 170.5–173°. The spiro compound XXIII was isolated from a second chromatographic fraction (see XXIII).

10-[3-[4-[2-(2,2-Dimethylhydrazino)ethyl -1- piperazinyl]propyl]-2-(trifluoromethyl)]-10*H*-phenothiazine Trihydrochloride Dihydrate (XXI)—A solution of VI (1.5 g, 2.8 mmoles) in benzene (100 ml) was added to a suspension of sodium iodide (2.0 g, 12.4 mmoles) in 1,1-dimethylhydrazine (40 g, 670 mmoles), and the resulting mixture was refluxed for 5 hr (Scheme I). Evaporation of the solvent gave an oil, which was treated with water and extracted with benzene and chloroform. Upon removal of the combined solvents *in vacuo*, an oil resulted and was then converted into a trihydrochloride salt with hydrogen chloride gas in methanol. Recrystallization from methanol–ether gave 0.6 g (38%) of product, mp 202–205°.

1-[2-[4-[3-[2-(Trifluoromethyl) -10*H*-phenothiazin-10-yl]propyl]-1-piperazinyl]ethyl]pyridinium *p*-Toluenesulfonate (XXII)—*p*-Toluenesulfonyl chloride (1.0 g, 5.25 mmoles) was added portionwise to a cold solution of II (1.6 g, 3.6 mmoles) in dry pyridine (30 ml). After 18 hr at 4°, the mixture was poured into ice water and extracted with ether. The ether extracts were washed first with a 5% sodium bicarbonate solution and then several times with cold water. The ether solution was dried (sodium sulfate) and evaporated to yield an oil; this oil solidified to give 1.4 g of crude product after trituration with ether and benzene. Three recrystallizations from benzene gave colorless crystals, mp 135–137°.

9-[3-[2-(Trifluoromethyl) -10*H*-phenothiazin- 10-yl]propyl]-3-oxa-9-aza-6-azoniaspiro[5.5]undecane Chloride (XXIII)—Continued chromatographic elution of the sample described for IX gave a second fraction containing 0.45 g (13%) of XXIII, mp 238–240°.

REFERENCES

(1) M. D. Walker, *Ca*, **25**, 114 (1975).

(2) A. H. Pearson, *Conn. Med.*, **38**, 513 (1974).

(3) J. M. Walsh, J. R. Cassady, E. Frei, P. L. Kornblith, and K. Welch, *Arch. Surg.*, **110**, 692 (1975).

(4) S. Thunold and P. J. Moe, *Acta Pathol. Microbiol. Scand. Sect. A Suppl.*, **236**, 84 (1973).

(5) F. Kanzawa, A. Hoshi, and K. Kuretani, *Gann*, **61**, 529 (1970).

[2] All melting points were recorded on a Thomas-Hoover capillary melting-point apparatus and are uncorrected. Elemental analyses were performed by the National Institute of Arthritis, Metabolism, and Digestive Diseases, National Institutes of Health, Bethesda, Md. New compounds were characterized by NMR and IR spectroscopy, using Varian T-60 and Perkin-Elmer 621 instruments. Mass spectra were obtained with a duPont 21-492 instrument.

[3] Norite.

(6) A. Hoshi, F. Kanzawa, and K. Kuretani, *Chem. Pharm. Bull.*, **17**, 848 (1969).
(7) M. H. Cohen, *J. Pharmacol. Exp. Ther.*, **194**, 475 (1975).
(8) J. S. Driscoll, N. R. Melnick, F. R. Quinn, N. Lomax, J. P. Davignon, R. Ing, B. J. Abbott, G. Congleton, and L. Dudeck, *Cancer Treat. Rep.*, in press.
(9) "Psychopharmacological Agents," vol. II, M. Gordon, Ed., Academic, New York, N.Y., 1967.
(10) L. S. Gottlieb, M. Hazel, S. Broitman, and N. Zamcheck, *Fed. Proc.*, **19**, 181 (1960).
(11) I. K. Cohen and C. G. Thomas, *Proc. Am. Assoc. Cancer Res.*, **4**, 11 (1963).
(12) L. W. Wattenberg and J. L. Leong, *Cancer Res.*, **25**, 365 (1965).
(13) T. G. Jackson and D. A. Shirley, *J. Med. Chem.*, **11**, 622 (1968).
(14) M. H. Van Woert and S. H. Palmer, *Cancer Res.*, **29**, 1952 (1969).
(15) R. Hilf, C. Bell, H. Goldenberg, and I. Michel, *ibid.*, **31**, 1111 (1971).
(16) A. M. Pamukcu, L. W. Wattenberg, J. M. Price, and G. T. Bryan, *J. Natl. Cancer Inst.*, **47**, 155 (1971).
(17) A. Polliack and I. S. Levij, *Cancer Res.*, **32**, 1912 (1972).
(18) F. Kanzawa, A. Hoshi, and K. Kuretani, *Gann*, **63**, 225, 375 (1972).
(19) W.-J. Eicke, *Med. Klin.*, **68**, 1015 (1973).
(20) T. Hirata and J. S. Driscoll, *J. Pharm. Sci.*, **65**, 1699 (1976).
(21) P. N. Craig, *J. Med. Chem.*, **14**, 680 (1971).
(22) H. L. Yale, A. I. Cohen, and F. Sowinski, *ibid.*, **6**, 347 (1963).
(23) E. L. Anderson, G. B. Bellinzona, P. N. Craig, G. E. Jaffe, *et al.*, *Arzneim.-Forsch.*, **12**, 937 (1962).
(24) R. I. Geran, N. H. Greenberg, M. M. MacDonald, A. M. Schumacher, and B. J. Abbott, *Cancer Chemother. Rep., Part 3*, **3**, 1 (1972).
(25) J. P. Long, A. M. Lands, and B. L. Zenitz, *J. Pharmacol. Exp. Ther.*, **119**, 479 (1957).
(26) C. M. Gooley, H. Keyzer, and F. Setchell, *Nature*, **223**, 80 (1969).
(27) T. P. Fondy, K. L. Karker, C. Calcagnino, and C. A. Emlich, *Cancer Chemother. Rep.*, **58**, 317 (1974).
(28) A. Felmeister, *J. Pharm. Sci.*, **61**, 151 (1972).
(29) E. W. Baur, *J. Pharmacol. Exp. Ther.*, **177**, 219 (1971).
(30) U. Bruyer, H. J. Gaertner, and A. Prox, *Biochem. Pharmacol.*, **23**, 313 (1974).
(31) "The Merck Index," 8th ed., Merck & Co., Rahway, N.J., 1968, p. 466.
(32) H. L. Yale and F. Sowinski, *J. Am. Chem. Soc.*, **82**, 2039 (1960).

ACKNOWLEDGMENTS

All biological test data were obtained under contracts administered by the Drug Evaluation Branch, National Cancer Institute. The authors thank Mr. Leo Dudeck and Mr. George Congleton, Hazleton Laboratories, for the *in vivo* antitumor results and Mr. Wolf Lichter and Mr. Larry Welham, University of Miami, for the *in vitro* data. Dr. James A. Kelley, National Cancer Institute, National Institutes of Health, determined the mass spectra. The authors also thank the Smith Kline and French Laboratories for their permission to use biological data obtained with samples of I and III which they supplied. The authors also thank E. R. Squibb and Sons for permission to use the biological data obtained with a sample of II supplied by them.

T. Hirata was a National Institutes of Health Visiting Postdoctoral Fellow, 1971–1973. G. Peng was a National Institutes of Health Visiting Postdoctoral Fellow, 1972–1974.

GLC Determination of the Polyvalent Saluretic Uricosuric Agent (2-Cyclopentyl-6,7-dichloro-2-methyl-1-oxo-5-indanyloxy)acetic Acid in Biological Fluids

ANTHONY G. ZACCHEI ˣ and THEODORE I. WISHOUSKY

Received February 2, 1977, from the *Merck Institute for Therapeutic Research, West Point, PA 19486.* Accepted for publication April 20, 1977.

Abstract □ A specific and quantitative GLC method was developed for the determination of (2-cyclopentyl-6,7-dichloro-2-methyl-1-oxo-5-indanyloxy)acetic acid, a novel saluretic uricosuric agent, in biological fluids. The procedure involves the addition of an internal standard to the biological specimens followed by extraction of the acids into benzene at pH 1. The extracted acids, following back-extraction into base and reextraction into methylene chloride at an acidic pH, are converted to the respective methyl esters by reaction with ethereal diazomethane. The sensitivity of the method is such that 2 μg of material can be detected per aliquot of plasma or urine. In the 2.5–50-μg/ml range, recoveries were 98.1 ± 9.6% (plasma, n = 157) and 99.3 ± 6.4% (urine, n = 181). GLC–mass spectrometric techniques established analysis specificity.

Keyphrases □ (2-Cyclopentyl -6,7- dichloro-2-methyl-1-oxo-5-indanyloxy)acetic acid—GLC analysis in biological fluids □ GLC—analysis, (2-cyclopentyl-6,7-dichloro-2-methyl-1-oxo-5-indanyloxy)acetic acid in biological fluids □ Uricosuric agents—(2-cyclopentyl-6,7-dichloro-2-methyl-1-oxo-5-indanyloxy)acetic acid, GLC analysis in biological fluids □ Indanyloxyacetic acid, substituted—GLC analysis in biological fluids

(2-Cyclopentyl-6,7-dichloro -2-methyl-1-oxo-5-indanyloxy)acetic acid (I) is a new nonsulfonamide saluretic agent with uricosuric and antihypertensive activities. The chemical syntheses of this agent and other similar analogs were described recently (1–3). To investigate the physiological disposition of this compound in several species, it was essential that an analytical method for I in biological fluids be developed.

This report describes a specific and sensitive GLC method for the determination of I using a related com-

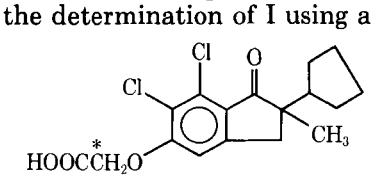

1

(6) A. Hoshi, F. Kanzawa, and K. Kuretani, *Chem. Pharm. Bull.*, **17**, 848 (1969).
(7) M. H. Cohen, *J. Pharmacol. Exp. Ther.*, **194**, 475 (1975).
(8) J. S. Driscoll, N. R. Melnick, F. R. Quinn, N. Lomax, J. P. Davignon, R. Ing, B. J. Abbott, G. Congleton, and L. Dudeck, *Cancer Treat. Rep.*, in press.
(9) "Psychopharmacological Agents," vol. II, M. Gordon, Ed., Academic, New York, N.Y., 1967.
(10) L. S. Gottlieb, M. Hazel, S. Broitman, and N. Zamcheck, *Fed. Proc.*, **19**, 181 (1960).
(11) I. K. Cohen and C. G. Thomas, *Proc. Am. Assoc. Cancer Res.*, **4**, 11 (1963).
(12) L. W. Wattenberg and J. L. Leong, *Cancer Res.*, **25**, 365 (1965).
(13) T. G. Jackson and D. A. Shirley, *J. Med. Chem.*, **11**, 622 (1968).
(14) M. H. Van Woert and S. H. Palmer, *Cancer Res.*, **29**, 1952 (1969).
(15) R. Hilf, C. Bell, H. Goldenberg, and I. Michel, *ibid.*, **31**, 1111 (1971).
(16) A. M. Pamukcu, L. W. Wattenberg, J. M. Price, and G. T. Bryan, *J. Natl. Cancer Inst.*, **47**, 155 (1971).
(17) A. Polliack and I. S. Levij, *Cancer Res.*, **32**, 1912 (1972).
(18) F. Kanzawa, A. Hoshi, and K. Kuretani, *Gann*, **63**, 225, 375 (1972).
(19) W.-J. Eicke, *Med. Klin.*, **68**, 1015 (1973).
(20) T. Hirata and J. S. Driscoll, *J. Pharm. Sci.*, **65**, 1699 (1976).
(21) P. N. Craig, *J. Med. Chem.*, **14**, 680 (1971).
(22) H. L. Yale, A. I. Cohen, and F. Sowinski, *ibid.*, **6**, 347 (1963).
(23) E. L. Anderson, G. B. Bellinzona, P. N. Craig, G. E. Jaffe, *et al.*, *Arzneim.-Forsch.*, **12**, 937 (1962).
(24) R. I. Geran, N. H. Greenberg, M. M. MacDonald, A. M. Schumacher, and B. J. Abbott, *Cancer Chemother. Rep., Part 3*, **3**, 1 (1972).
(25) J. P. Long, A. M. Lands, and B. L. Zenitz, *J. Pharmacol. Exp. Ther.*, **119**, 479 (1957).
(26) C. M. Gooley, H. Keyzer, and F. Setchell, *Nature*, **223**, 80 (1969).
(27) T. P. Fondy, K. L. Karker, C. Calcagnino, and C. A. Emlich, *Cancer Chemother. Rep.*, **58**, 317 (1974).
(28) A. Felmeister, *J. Pharm. Sci.*, **61**, 151 (1972).
(29) E. W. Baur, *J. Pharmacol. Exp. Ther.*, **177**, 219 (1971).
(30) U. Bruyer, H. J. Gaertner, and A. Prox, *Biochem. Pharmacol.*, **23**, 313 (1974).
(31) "The Merck Index," 8th ed., Merck & Co., Rahway, N.J., 1968, p. 466.
(32) H. L. Yale and F. Sowinski, *J. Am. Chem. Soc.*, **82**, 2039 (1960).

ACKNOWLEDGMENTS

All biological test data were obtained under contracts administered by the Drug Evaluation Branch, National Cancer Institute. The authors thank Mr. Leo Dudeck and Mr. George Congleton, Hazleton Laboratories, for the *in vivo* antitumor results and Mr. Wolf Lichter and Mr. Larry Welham, University of Miami, for the *in vitro* data. Dr. James A. Kelley, National Cancer Institute, National Institutes of Health, determined the mass spectra. The authors also thank the Smith Kline and French Laboratories for their permission to use biological data obtained with samples of I and III which they supplied. The authors also thank E. R. Squibb and Sons for permission to use the biological data obtained with a sample of II supplied by them.

T. Hirata was a National Institutes of Health Visiting Postdoctoral Fellow, 1971–1973. G. Peng was a National Institutes of Health Visiting Postdoctoral Fellow, 1972–1974.

GLC Determination of the Polyvalent Saluretic Uricosuric Agent (2-Cyclopentyl-6,7-dichloro-2-methyl-1-oxo-5-indanyloxy)acetic Acid in Biological Fluids

ANTHONY G. ZACCHEI ˣ and THEODORE I. WISHOUSKY

Received February 2, 1977, from the *Merck Institute for Therapeutic Research, West Point, PA 19486.* Accepted for publication April 20, 1977.

Abstract □ A specific and quantitative GLC method was developed for the determination of (2-cyclopentyl-6,7-dichloro-2-methyl-1-oxo-5-indanyloxy)acetic acid, a novel saluretic uricosuric agent, in biological fluids. The procedure involves the addition of an internal standard to the biological specimens followed by extraction of the acids into benzene at pH 1. The extracted acids, following back-extraction into base and reextraction into methylene chloride at an acidic pH, are converted to the respective methyl esters by reaction with ethereal diazomethane. The sensitivity of the method is such that 2 μg of material can be detected per aliquot of plasma or urine. In the 2.5–50-μg/ml range, recoveries were 98.1 ± 9.6% (plasma, n = 157) and 99.3 ± 6.4% (urine, n = 181). GLC–mass spectrometric techniques established analysis specificity.

Keyphrases □ (2-Cyclopentyl -6,7- dichloro-2-methyl-1-oxo-5-indanyloxy)acetic acid—GLC analysis in biological fluids □ GLC—analysis, (2-cyclopentyl-6,7-dichloro-2-methyl-1-oxo-5-indanyloxy)acetic acid in biological fluids □ Uricosuric agents—(2-cyclopentyl-6,7-dichloro-2-methyl-1-oxo-5-indanyloxy)acetic acid, GLC analysis in biological fluids □ Indanyloxyacetic acid, substituted—GLC analysis in biological fluids

(2-Cyclopentyl-6,7-dichloro -2-methyl-1-oxo-5-indanyloxy)acetic acid (I) is a new nonsulfonamide saluretic agent with uricosuric and antihypertensive activities. The chemical syntheses of this agent and other similar analogs were described recently (1–3). To investigate the physiological disposition of this compound in several species, it was essential that an analytical method for I in biological fluids be developed.

This report describes a specific and sensitive GLC method for the determination of I using a related com-

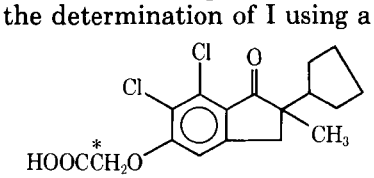

1

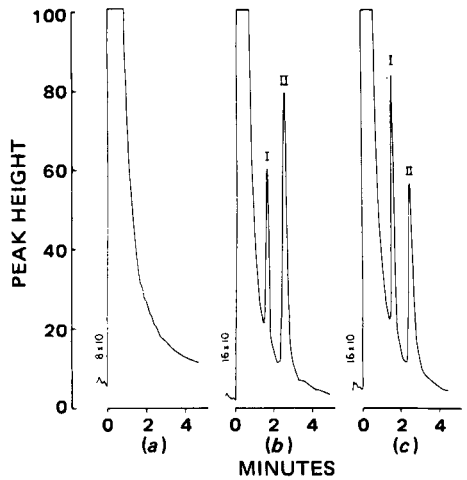

Figure 1—*Gas chromatograms of: control dog plasma* (a), *control dog plasma to which I (5 μg) and II (10 μg) were added* (b), *and dog plasma obtained 30 min after dosing* (c). *All samples were analyzed as described. Aliquots of 5 μl out of a 100-μl final volume were injected on a 1% QF-1 column.*

pound as an internal standard, derivatization with diazomethane, and a flame-ionization detector. Biological specimens from dogs, baboons, and monkeys were used to demonstrate the applicability of the assay following pharmacological I doses. The method also can be used to estimate the levels of the major cyclopentyl ring-hydroxylated metabolites.

EXPERIMENTAL

Reagents and Chemicals—The reagents and chemicals used were I, (2-cyclohexyl-6,7-dichloro-1-oxo-5-indanyloxy)acetic acid (II) as the internal standard, benzene, methylene chloride, ethyl acetate, and freshly prepared 0.5 *M* diazomethane (generated from *N*-nitroso-*N*-methylurea[1]).

Instrumentation—*GLC*—The gas chromatograph[2] was equipped with a flame-ionization detector and a 183-cm × 4-mm (i.d.) glass column packed with either 1% QF-1 or 1% OV-210 on 80–100-mesh Chromosorb W-AW. However, better results with respect to metabolite peaks were obtained when the derivatized extracts were analyzed on a 122-cm × 4-mm (i.d.) glass column packed with 3% OV-210[3]. The column temperature was maintained isothermally between 240 and 250°, depending on the column employed. The detector and injection port temperatures were about 30° higher than the column temperature. Helium was used as the carrier gas with flow rates between 40 and 52 ml/min, depending on the column used.

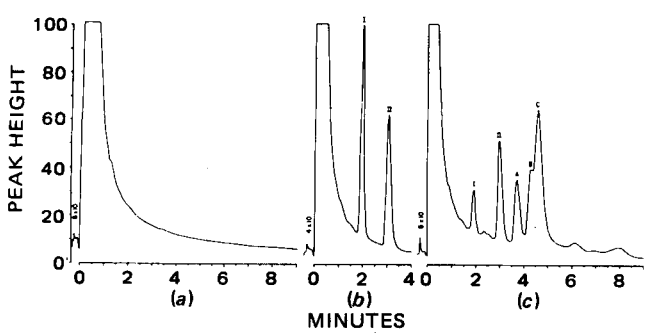

Figure 2—*Gas chromatograms of: control baboon urine* (a), *control baboon urine to which I (10 μg) and II (10 μg) were added* (b), *and baboon urine (0–24 hr)* (c). *Aliquots of 5 μl were analyzed on a 3% OV-210 column.*

[1] K & K Laboratories, Plainview, N.Y.
[2] Hewlett-Packard model 5750.
[3] OV-210 on 80–100-mesh Chromosorb W-HP, Supelco, Inc., and OV-210 on 100–120-mesh Gas Chrom Q, Applied Science Laboratories.

Table I—Recovery of I from Plasma and Urine Using GLC Method

Amount of I Added, μg		Amount Recovered[a] Plasma n	Plasma Mean ± SD	Urine n	Urine Mean ± SD
50.0	A	22	50.49 ± 2.00	19	50.48 ± 2.76
	B		100.97 ± 4.03[b]		100.99 ± 5.52
40.0	A	22	40.30 ± 2.20	28	40.62 ± 1.45
	B		100.71 ± 5.51		101.56 ± 3.63
30.0	A	20	30.61 ± 1.60	18	30.08 ± 0.96
	B		102.02 ± 5.36		100.28 ± 3.22
20.0	A	25	20.26 ± 1.26	30	20.41 ± 1.07
	B		101.29 ± 6.28		102.02 ± 5.29
10.0	A	21	9.90 ± 0.78	29	9.78 ± 0.47
	B		99.00 ± 7.81		97.80 ± 4.66
5.0	A	25	4.62 ± 0.55	31	4.80 ± 0.34
	B		93.23 ± 10.58		95.80 ± 6.85
2.5	A	22	2.28 ± 0.39	26	2.45 ± 0.25
	B		90.74 ± 15.44		97.71 ± 9.97
2.5–50	B	157	98.06 ± 9.60	181	99.31 ± 6.39

[a] Values in A rows represent micrograms recovered; values in B rows represent percent recovery.

GLC–Mass Spectrometry—All mass spectra were obtained on a mass spectrometer[4] with a GLC inlet system. A 122-cm × 3-mm (i.d.) glass column packed with 3% OV-210 (80–100-mesh Chromosorb W-HP) was used. The gas chromatograph was operated isothermally at 240° with a helium flow rate of 30 ml/min. The mass spectrometer ionizing and accelerating potentials were 20 ev and 3.5 kv, respectively. The source, separator, and injection port temperatures were 270, 250 and 245°, respectively.

Measurement of I in Biological Samples—The concentration of I in biological specimens was determined as follows. To an appropriate aliquot (usually 1.0 ml) of plasma or urine in a 50-ml glass-stoppered centrifuge tube were added 10.0 μg of II in 1 ml of pH 8 phosphate buffer, 1 ml of 2 *N* HCl, and 25 ml of benzene. The tube was shaken for 10 min and centrifuged, and at least 20 ml of the organic phase was transferred to a similar tube containing 2 ml of 0.1 *N* NaOH. After the tube was shaken for 10 min, it was centrifuged and the organic phase was removed by aspiration.

The pH of the aqueous phase was adjusted to 1 by the addition of 0.2 ml of 2 *N* HCl, and the free acids were extracted into 5 ml of methylene chloride (vortex, 1 min). After centrifugation, the methylene chloride phase was transferred to a 13-ml centrifuge tube and then reacted with 100 μl of ethereal diazomethane. The content of the tube was evaporated to dryness under nitrogen in a warm water bath (~50°). The residue was subsequently dissolved in 50 μl of ethyl acetate, and appropriate aliquots, usually 5 μl, were injected into the gas chromatograph. The retention times of I and II as the methyl ester derivatives on a 3% OV-210 column were 2.0 and 3.0 min, respectively.

Standard plasma and urine curves were constructed by plotting the peak height ratios (I to II) *versus* weight ratios (I to II). A linear relationship was obtained in the 2.5–50-μg/sample range. The peak height ratio obtained from an unknown sample was then used to determine the amount of I initially present in the sample. The standard recovery sam-

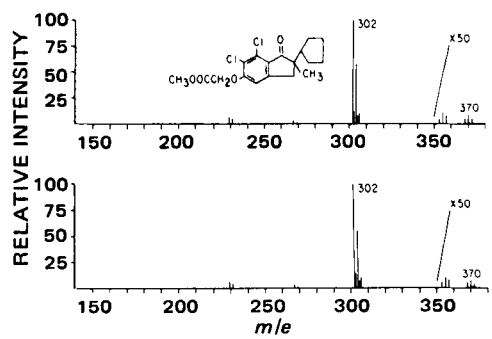

Figure 3—*Comparison of the mass spectrum of I (top) carried through the GLC method with the mass spectrum of material (bottom) obtained from monkey urine. The mass spectra were obtained as the material emerged from the GLC column.*

[4] LKB-9000S.

Table II—Comparison of the Plasma Radioactivity with Plasma I Levels following Administration of ^{14}C-I to Monkeys at 5 mg/kg

	Plasma I Level, μg/ml							
	Monkey 1, Intravenous		Monkey 2, Intravenous		Monkey 3, Oral		Monkey 4, Oral	
Hours	A[a]	B[b]	A	B	A	B	A	B
0.12	77.7	82.3	60.1	59.1	—	—	—	—
0.25	68.9	68.9	49.5	51.1	16.4	16.4	12.1	11.4
0.5	59.7	59.9	40.0	42.3	27.9	30.8	22.5	20.5
1.0	47.3	51.3	31.0	32.3	35.4	37.4	31.8	31.1
1.5	—	—	—	—	37.8	41.9	31.6	30.9
2	38.8	38.9	23.8	23.1	38.0	41.5	31.2	31.0
4	26.9	26.3	15.9	13.6	29.6	27.8	28.1	27.4
6	19.7	16.9	13.0	11.1	23.7	21.1	23.5	21.3
24	12.8	5.4	9.1	3.4	12.7	4.6	18.4	7.6
48	3.0	1.8	1.9	1.0	3.0	2.0	4.0	2.6
72	1.7	1.4	1.2	0.7	1.9	—	2.3	2.1

[a] Determined as I equivalents using radioactivity data. [b] Determined as unchanged I using GLC method.

ples were run concurrently with the unknown specimens as previously described.

Biological Studies—Four beagle dogs (10.5–11.6 kg), four Rhesus monkeys (3.7–4.7 kg), and four anubis baboons (6.2–7.5 kg) received 5 mg of I/kg po or iv. In each instance, the administered drug was ^{14}C-radiolabeled in the methylene carbon (asterisk in Structure I). The details of the radiochemical synthesis and metabolism studies will be reported elsewhere.

The animals were fasted overnight prior to drug administration. Blood specimens were collected in heparinized tubes, plasma was separated by centrifugation, and aliquots were removed for analysis. Urine specimens were immediately frozen upon collection and kept frozen until analyzed. The samples were analyzed for I using the described procedure.

RESULTS AND DISCUSSION

The developed method is similar to that described previously for a related indanyloxyacetic acid compound (4). GLC analysis of I (as the methyl ester) provided a quantitative analysis of intact drug in urine and plasma. Figure 1 shows gas chromatograms of the following samples using flame-ionization detection: (*a*) control dog plasma, (*b*) I and II added to control dog plasma, and (*c*) dog plasma obtained 30 min after dosing. The retention times of I and II were 1.6 and 2.6 min, respectively. Gas chromatograms of control samples (dog, monkey, or baboon) did not exhibit any extraneous peaks with retention times similar to either I or II as the methyl esters. A typical GLC tracing from a control sample is illustrated in Fig. 1*a*.

A linear relationship was obtained when peak height (or peak area) was plotted *versus* the amount of I injected. Linear curves also were obtained following the analysis of various amounts of I (2.5–50.0 μg) and II (10.0 μg) added to control dog, monkey, or baboon plasma and urine samples (Table I). These data were obtained from analyses performed on the 1% QF-1, 1% OV-210, and 3% OV-210 GLC columns. All analyses were performed over 1 year. As indicated, the mean recoveries of I added to control plasma varied from 90.7 to 102% with a mean recovery of 98.1 ± 9.6% (n = 157) over the entire concentration range. Mean recoveries of I added to control urine in amounts of 2.5–50.0 μg ranged from 95.8 to 102.0% with a mean value of 99.3 ± 6.4% (n = 181). As is evident, the GLC method for determining the levels of I in biological specimens is sensitive and exhibits a high degree of accuracy and precision.

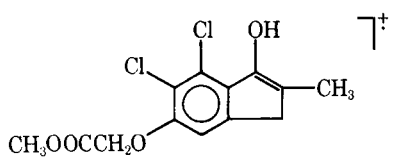

III

Typical levels of I in monkey plasma following a 5-mg/kg dose are presented in Table II. Total radioactivity levels, calculated as I equivalents, are also presented for comparative purposes. As indicated, peak plasma levels of I and radioactivity occurred about 2 hr after oral administration. Furthermore, essentially all radioactivity in the plasma (0–6 hr) following either intravenous or oral administration was intact I. At 48 hr, about half of the plasma radioactivity was attributed to metabolites. Extensive metabolism was observed in the baboon, as illustrated by the results obtained from the GLC analysis of 0–24-hr baboon urine (Fig. 2). The large peaks at 3.5–5 min are attributed to the hydroxylated metabolites. GLC–mass spectral studies showed that hydroxylation occurred on the 2-cyclopentyl moiety, giving rise to several stereochemical isomers (5).

Confirmation of method specificity was obtained when several representative biological specimens (after GLC analysis) were analyzed by combined GLC–mass spectrometry using the aforementioned conditions. A comparison of the mass spectrum of authentic I carried through the GLC procedure with material isolated from monkey urine is presented in Fig. 3. The mass spectra, which were obtained as the material emerged from the GLC column, were identical. The relative intensity of the molecular ion (m/e 370) was less than 0.2% of the intensity of the base peak (m/e 302). The peak at m/e 302 resulted from a McLafferty rearrangement mechanism to form ion III.

REFERENCES

(1) E. J. Cragoe, Jr., E. M. Schultz, J. D. Schneeberg, G. E. Stokker, O. W. Woltersdorf, Jr., G. M. Fanelli, Jr., and L. S. Watson, *J. Med. Chem.*, **18**, 225 (1975).

(2) O. W. Woltersdorf, Jr., E. J. Cragoe, Jr., and L. S. Watson, paper presented at the 169th National American Chemical Society Meeting, Philadelphia, Pa., Apr. 1975, Medicinal Chemistry Division Paper 48.

(3) O. W. Woltersdorf, Jr., J. D. Schneeberg, E. M. Schultz, G. E. Stokker, E. J. Cragoe, Jr., L. S. Watson, and G. M. Fanelli, Jr., paper presented at the 169th National American Chemical Society Meeting, Philadelphia, Pa., Apr. 1975, Medicinal Chemistry Division Paper 49.

(4) A. G. Zacchei and T. Wishousky, *J. Pharm. Sci.*, **65**, 1770 (1976).

(5) A. G. Zacchei and T. Wishousky, paper presented at the 23rd Annual Conference on Mass Spectrometry and Allied Topics, Houston, Tex., May 1975, Paper J-7.

ACKNOWLEDGMENTS

The authors thank Mr. O. Woltersdorf, Ms. J. Schneeberg, and Dr. E. J. Cragoe, Jr., for supplies of I and related compounds.

Molecular Complexing Ability of Quinoline and Its Simple Derivatives

N. E. WEBB * **and C. C. THOMPSON** ‡x

Received December 17, 1976, from the *Department of Chemistry, Memphis State University, Memphis, TN 38152.* Accepted for publication April 20, 1977. *Present address: Department of Chemistry, Christian Brothers College, Memphis, TN 38104. ‡Present address: School of Science and Technology, Southwest Missouri State University, Springfield, MO 65802.

Abstract □ Electron donor–acceptor complexes for a group of quinolines and naphthalenes with 9-(dicyanomethylene)-2,4,7-trinitrofluorene in 1,2-dichloroethane were studied by optical absorption methods. Association constants, molar absorptivities, and charge-transfer transition energies were evaluated for each system, together with theoretically calculated orbital energies and complex geometries. In contrast to the association constants and structures reported for *N*-heterocycle–halogen complexes, these studies indicate that, with a moderately large π-electron acceptor, quinolines function as π- rather than *n*- (lone-pair) donors. These results support intercalation models for drug–receptor interactions involving the quinoline moiety.

Keyphrases □ Molecular complexing—various quinoline and naphthalene derivatives with 9-(dicyanomethylene)-2,4,7-trinitrofluorene, mechanism of π-electron donation □ Complexing, molecular—various quinoline and naphthalene derivatives with 9-(dicyanomethylene)-2,4,7-trinitrofluorene, mechanism of π-electron donation □ Quinolines, various—mechanism of π-electron donation in molecular complexing with 9-(dicyanomethylene)-2,4,7-trinitrofluorene □ Naphthalenes, various—mechanism of π-electron donation in molecular complexing with 9-(dicyanomethylene)-2,4,7-trinitrofluorene □ 9-(Dicyanomethylene)-2,4,7-trinitrofluorene—mechanism of π-electron donation by various quinolines and naphthalenes in molecular complexing

The possible role of electron donor–acceptor complexes in drug–receptor binding processes as well as in many other biological reactions has been widely discussed (1–5). For example, in the intercalation model (6–8) of antimalarial drug interactions, the parallel planar arrangement of DNA base pairs and the quinoline moiety of drugs such as pamaquine and chloroquine almost certainly involves some degree of π-electron interaction.

The ubiquitous occurrence of *N*-heterocyclic compounds in living systems has prompted several investigations into the nature of their complexes with various compounds (9–13). Although molecules such as pyridine and quinoline may function as either *n*- or π-electron donors, with σ-acceptors, particularly iodine and iodine monochloride, binding is through the nitrogen lone-pair electrons (11, 13–17). However, with π-acceptors, the results are by no means as certain; conflicting interpretations have been reported (18–21).

This study was initiated to: (*a*) discover the mode of binding of quinoline and its simple derivatives to a moderately large π-electron acceptor, (*b*) determine the effects of different substituents on the complexing ability of quinoline, and (*c*) examine the implications of the resulting donor–acceptor model in drug–receptor interactions. The present report describes optical absorption studies combined with theoretical calculations for complexes of amino- and hydroxyquinolines and their naphthalene analogs with 9-(dicyanomethylene)-2,4,7-trinitrofluorene (I).

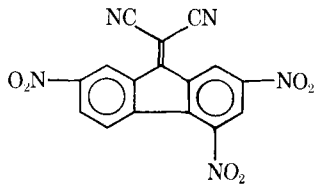

I

EXPERIMENTAL

Materials—Quinoline[1] was dried over potassium hydroxide and fractionally distilled at reduced pressure. 8-Hydroxyquinoline[1] was recrystallized from toluene. 8-Aminoquinoline[2], 5-aminoquinoline[1], 1-hydroxynaphthalene[2], and 1-aminonaphthalene[1] were purified by vacuum sublimation. Naphthalene[1] was twice recrystallized from absolute ethanol. Isoquinoline[1] was fractionally distilled at reduced pressure. 9-(Dicyanomethylene)-2,4,7-trinitrofluorene[2] was twice recrystallized from acetonitrile. 1,2-Dichloroethane[3] was purged with dry nitrogen (dew point less than −40°) immediately before use.

Spectroscopic Measurements—Optical absorption spectra for solutions with a fixed concentration of I and different donor concentrations were recorded[4] at 20 and 40°. Spectral data were collected using 1-, 2-, or 5-cm matched quartz cells with either the pure solvent or an equimolar solution of I as reference. Absorption, if any, of the free donor was subtracted from the measured absorbance during the data analysis step. For each system, absorbance measurements were reproducible to ±0.002 absorbance unit.

Data Analysis—The reversible association of an electron donor, *D*, with an electron acceptor, *A*, to form a 1:1 molecular complex, *AD*, may be written as $A + D \rightleftharpoons AD$. The association constant, *K*, for this reaction is given by:

$$K = \frac{[AD]}{([A]_0 - [AD])([D]_0 - [AD])} \qquad \text{(Eq. 1)}$$

where $[A]_0$ and $[D]_0$ represent initial concentrations of *A* and *D*, respectively; and $[AD]$ is the equilibrium concentration of *AD*. If Beer's law is obeyed by *AD* in a wavelength region where free donor and acceptor do not absorb or where their contributions have been subtracted, the complex absorbance, A_{AD}, will be:

$$A_{AD} = [AD]\epsilon_{AD}b \qquad \text{(Eq. 2)}$$

where ϵ_{AD} is the molar absorptivity of the complex and *b* is the pathlength. Equations 1 and 2 can be combined to yield a modification of the Scatchard (22) equation:

$$\frac{A_{AD}}{[A]_0[D]_0b} = -K\left[\frac{A_{AD}([A]_0 + [D]_0 - [AD])}{[A]_0[D]_0b}\right] + K\epsilon_{AD} \qquad \text{(Eq. 3)}$$

In this work, association constants and molar absorptivities for each donor–acceptor complex were computed[5] by means of an iterative least-squares curve-fitting procedure (23). For each system, a Scatchard plot was generated from eight or more data sets, which consisted of initial donor and acceptor concentrations along with the absorbances at the charge-transfer band maximum. Values of *K* and ϵ_{AD} were determined from the slopes and intercepts of these linear plots.

Theoretical Calculations—The Hückel molecular orbital (HMO) method (24) was applied to I and to each aromatic donor molecule. Heteroatom parameters used in this work followed closely the values recommended by Streitwieser (25). The HMO atomic orbital coefficients and π-orbital energies were then used in a second-order perturbation

[1] Aldrich Chemical Co., Milwaukee, Wis.
[2] Eastman Organic Chemicals, Rochester, N.Y.
[3] Spectral grade, Eastman Organic Chemicals, Rochester, N.Y.
[4] Cary model 14 spectrophotometer.
[5] XDS Sigma 9 computer.

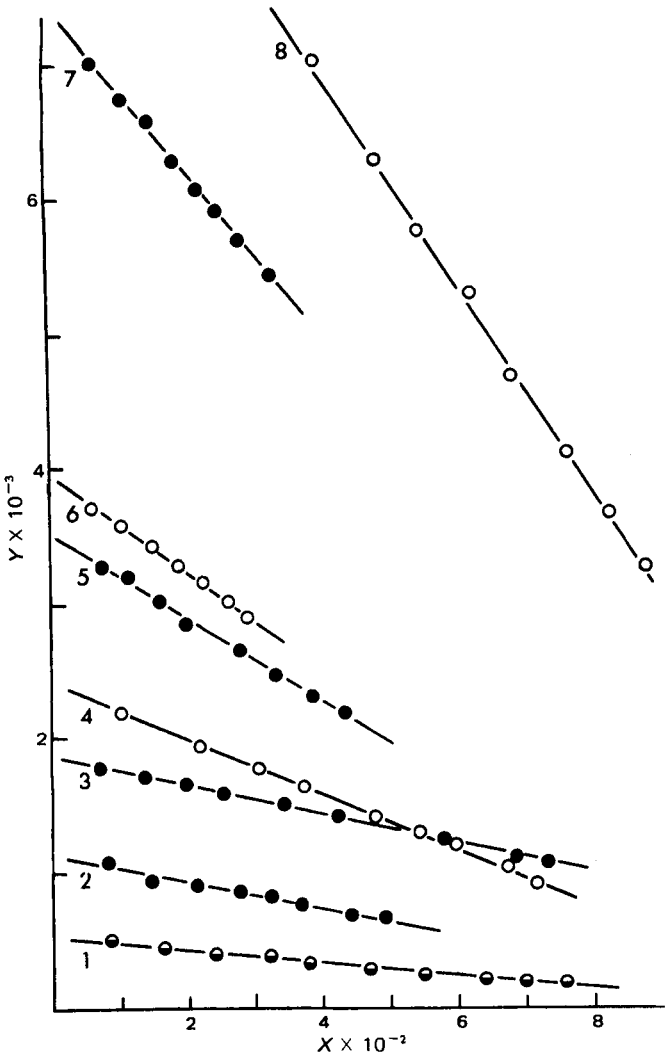

Figure 1—*Scatchard plots with* $X = A_{AD}([A]_0 + [D]_0 - [AD])/([A]_0[D]_0b)$ *and* $Y = A_{AD}/([A]_0[D]_0b)$ *for complexes of I with isoquinoline (1), quinoline (2), 8-hydroxyquinoline (3), naphthalene (4), 5-aminoquinoline (5), 1-hydroxynaphthalene (6), 8-aminoquinoline (7), and 1-aminonaphthalene (8) in 1,2-dichloroethane at 20°.*

treatment (26) to obtain binding energies and the most favorable geometries for the different complexes.

RESULTS AND DISCUSSION

Intensely colored mixtures are formed immediately upon combining 1,2-dichloroethane solutions of the quinolines or naphthalenes with I.

Table II—Association Constants for Iodine and Iodine Monochloride Complexes

Complex	Solvent	Temperature	K, M^{-1}	Reference
Benzene–iodine	Carbon tetrachloride	25°	0.15	16
Naphthalene–iodine	Carbon tetrachloride	25°	0.25	16
Pyridine–iodine	Carbon tetrachloride	25°	101	17
	Cyclohexane	25°	107	27
	Heptane	25°	140	14
	Heptane	16.7°	290	11
	Chloroform	28°	43.7	15
2,6-Lutidine–iodine	Chloroform	28°	26.2	15
Quinoline–iodine	Heptane	25°	114.6	28
	Chloroform	28°	69	15
Benzene–iodine monochloride	Carbon tetrachloride	25°	0.54	16
Naphthalene–iodine monochloride	Carbon tetrachloride	25°	1.39	16
Pyridine–iodine monochloride	Carbon tetrachloride	25°	483,000	17
2,6-Lutidine–iodine monochloride	Carbon tetrachloride	25°	89,000	17

Visible absorption spectra of these mixtures are characterized by broad featureless absorption bands, typical of electron donor–acceptor complexes. For each complex system, absorption data were collected near the wavelength maximum of the charge-transfer band for solutions covering a reasonably wide donor concentration range. From these absorbance values, association constants, K, and molar absorptivities, ϵ, were computed using Eq. 3. Figure 1 shows typical Scatchard plots for several complex systems. Donor and acceptor concentrations, absorption maxima, and computed K and ϵ values are given in Table I.

For comparison, association constants previously reported for aromatic hydrocarbon and N-heterocyclic donors with iodine and iodine monochloride are listed in Table II. The large variations in K for the halogen complexes are readily attributable to different modes of binding for the two donor types. X-ray diffraction studies (29, 30) of the N-heterocyclic complexes have shown a planar colinear arrangement of the interatomic axis of halogen acceptors with the nitrogen atom of the donors. This configuration is due to a relatively strong interaction of the nitrogen lone-pair electrons with an antibonding σ-orbital of the acceptor. In the case of the hydrocarbons, only the comparatively less favorable π-electron donation is possible.

In contrast to the marked increase in K for halogen–heterocycle over halogen–aromatic hydrocarbon complexes, association constants for interactions of the quinolines with I are somewhat lower than those of their naphthalene analogs. These results immediately suggest that, with I, both quinolines and naphthalenes form sandwich-type π–π complexes and that the presence of a nitrogen atom reduces slightly the donor ability of the π-system. This interpretation is further substantiated by other similarities between the two classes of donors.

Substitution of both quinoline and naphthalene by electron-releasing groups is accompanied by increased association constants and by shifts in the charge-transfer absorption maxima to longer wavelengths. Effects of the amino group on both K and λ_{max} are more pronounced than for the

Table I—Experimental Details, Association Constants, and Molar Absorptivities of I[a] Complexes in 1,2-Dichloroethane

Donor	Donor Concentration, M	Temperature	λ_{max}, nm	K, M^{-1}	ϵ, M^{-1} cm^{-1}
Naphthalene	0.05–0.72	20°	488	1.98 ± 0.03	1150 ± 60
		40°	485	1.52 ± 0.04	1150 ± 70
Quinoline	0.08–0.72	20°	440[b]	0.90 ± 0.04	1500 ± 40
Isoquinoline	0.02–1.90	20°	475[b]	0.54 ± 0.006	1130 ± 100
1-Hydroxynaphthalene	0.02–0.09	20°	560	3.64 ± 0.04	1060 ± 30
		40°	555	3.28 ± 0.11	910 ± 40
8-Hydroxyquinoline	0.02–0.83	20°	495	1.03 ± 0.07	1570 ± 120
		40°	490	0.77 ± 0.08	1600 ± 50
1-Aminonaphthalene	0.03–0.27	20°	660	7.95 ± 0.12	1280 ± 10
		40°	665	5.56 ± 0.09	1220 ± 10
5-Aminoquinoline	0.02–0.20	20°	600	3.02 ± 0.06	1130 ± 10
		40°	595	2.70 ± 0.16	1000 ± 50
8-Aminoquinoline	0.007–0.05	20°	645	5.94 ± 0.07	1230 ± 20
		40°	640	4.03 ± 0.11	1200 ± 20

[a] Concentrations of I are 0.001 M for all systems except 8-aminoquinoline for which the concentration is 0.003 M. [b] Shoulder.

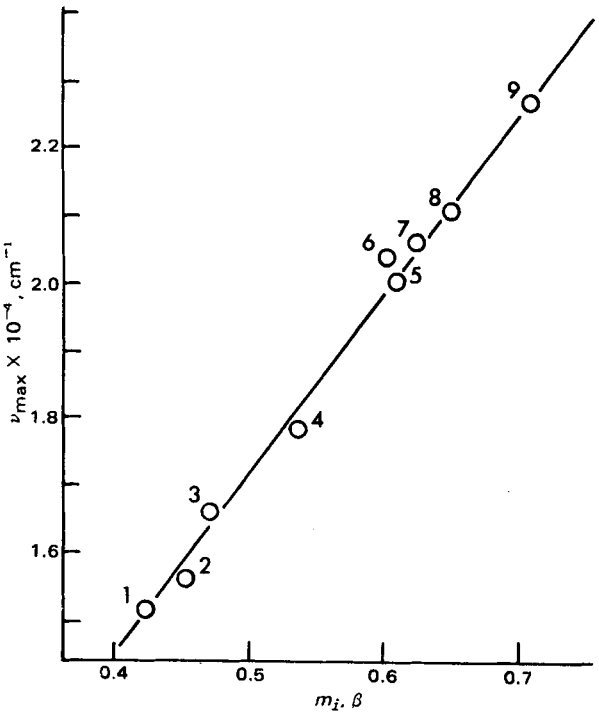

Figure 2—*Charge-transfer transition energies* versus *energies (in β units from the Hückel molecular orbital method) of the highest occupied donor orbitals for complexes of I with 1-aminonaphthalene (1), 8-aminoquinoline (2), 5-aminoquinoline (3), 1-hydroxynaphthalene (4), 5-hydroxyquinoline (5), 8-hydroxyquinoline (6), naphthalene (7), isoquinoline (8), and quinoline (9).*

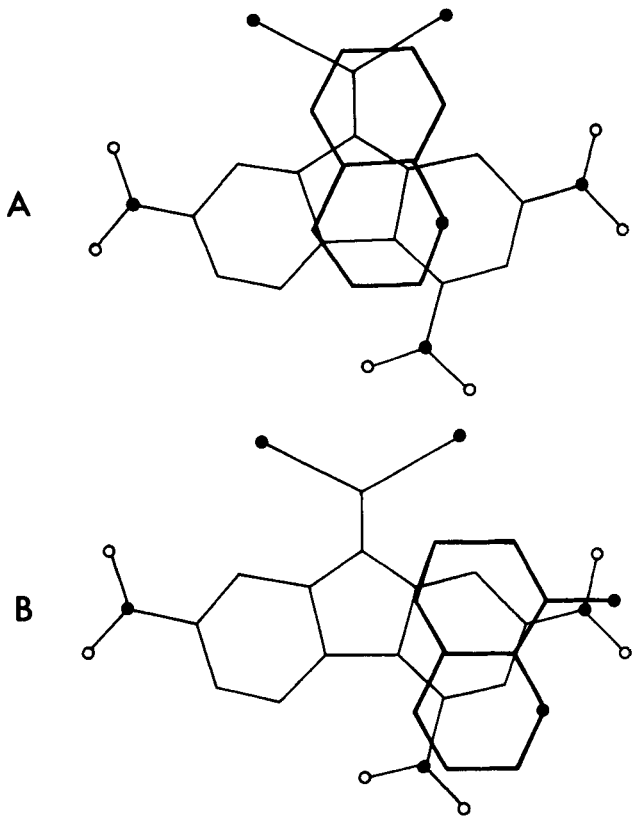

hydroxyl group. These trends are consistent with a greater electron-releasing tendency of the amino group as reflected by the respective Hammett σ constants, $\sigma_{NH_2} = -0.660$ and $\sigma_{OH} = -0.357$. Molecular orbital calculations for amino- and hydroxyquinolines also show a greater electron-releasing effect for the amino derivatives, thereby making them better electron donors.

Association constants for complexes of 8- and 5-aminoquinoline (Table I) indicate that the position of substitution also has a significant influence on donor strength. If, as a first approximation, the energy of the highest occupied π-molecular orbital is taken as a measure of donor ability, HMO calculations predict electron donor strengths in the order: 8 > 5 > 6 > 3 > 4 > 7 > 2 > 0 for aminoquinolines and 8 > 5 > 4 > 6 > 3 > 7 > 2 > 0 for hydroxyquinolines.

Linear relationships between ionization potentials or orbital energies for a series of donors with a common acceptor were found in numerous cases (3). Figure 2 shows a plot of highest occupied donor orbital energies *versus* charge-transfer transition energies for the complexes in this work. Points for both the quinolines and naphthalenes fall on a single straight line, indicating that the same mode of electron donation is operative in the two systems.

Although molar absorptivities for the quinoline and 8-hydroxyquinoline complexes show some enhancement, no systematic variations are apparent throughout the series. This behavior again differs from that of the halogen complexes, which show greatly increased absorptivities with *N*-heterocyclic donors. For example, a value of ϵ_{max} approaching 50,000 M^{-1} cm^{-1} was reported for the pyridine–iodine complex (11).

Since electron donor–acceptor complexes of the type discussed here involve weak interactions, typically 5–6 kcal/mole or less, even a moderate amount of steric hindrance near the binding site can lead to substantially reduced association constants. For complexes of iodine with methyl-substituted pyridines and quinolines, a two- to fivefold decrease between *K*'s for the parent compound and 2,6-lutidine and complete suppression of complex formation with 7,8-benzoquinoline were reported (15, 17). If complexation through the nitrogen lone pair is important, substitution at the 8-position of quinoline would sterically hinder the approach of an acceptor, especially a molecule as large as I. Association constants for the complexes in the present work show no evidence of steric hindrance by substituents in the 8-position. In fact, just the reverse trend is noted (Table I).

Stabilization energies computed by a second-order perturbation method (26) indicate that the most favorable geometry occurs for each complex system when donor and acceptor molecules are stacked in parallel planes at an intermolecular distance of 3.3–3.4 Å. Theoretical binding energies ranged from −3.7 kcal/mole for quinoline–I to −8.5 kcal/mole for 5-aminoquinoline–I. Minimum energy configurations for the quinoline and 8-aminoquinoline complexes with I are shown in Structures A and B, respectively, where dark circles represent nitrogen and open circles represent oxygen. The intermolecular distance is 3.35 Å in both cases, and the binding energies are −3.7 kcal/mole for Complex A and −5.7 kcal/mole for Complex B. Calculations for both in-plane and perpendicular orientations of the interacting species result in net positive binding energies.

CONCLUSIONS

Molecular complexation through the π-electron system of quinolines is indicated by the following evidence.

Association constants and molar absorptivities for quinoline complexes with I are of the same order of magnitude as those for naphthalenes where only π-donation is possible.

A linear correlation is found between the highest occupied molecular orbital (HOMO) energies and charge-transfer band energies for each complex. Such correlations are characteristic of π–π complexes.

A decrease in charge-transfer transition energies and an increase in association constants result from substitution of the quinoline or naphthalene ring with electron-releasing groups.

Little, if any, steric hindrance to complex formation is experienced on substitution at the 8-position in quinoline.

Perturbation calculations favor a stacking of donor and acceptor molecules in parallel planes separated by 3.3–3.4 Å.

The π-complexing mode of quinolines in their interaction with the acceptor lends support to intercalation models of drug activity of quinoline-based compounds (6–8). However, caution must be exercised in assigning mechanistic importance to these interactions until more substantive evidence for the role of charge-transfer complexes in biological systems is demonstrated.

REFERENCES

(1) A. Szent-Györgyi, "Introduction to a Submolecular Biology," Academic, New York, N.Y., 1960.

(2) "Molecular Association in Biology," B. Pullman, Ed., Academic, New York, N.Y., 1968.
(3) R. Foster, "Organic Charge Transfer Complexes," Academic, New York, N.Y., 1969, pp. 335–373.
(4) M. A. Slifkin, "Charge Transfer Interactions of Biomolecules," Academic, New York, N.Y., 1971.
(5) L. B. Kier, "Molecular Orbital Theory in Drug Research," Academic, New York, N.Y., 1971, pp. 86–89.
(6) F. E. Hahn, R. L. O'Brien, J. Ciak, J. L. Allison, and J. G. Olenick, *Mil. Med. Suppl.*, **131**, 1071 (1966).
(7) R. L. O'Brien, J. G. Olenick, and F. E. Hahn, *Proc. Natl. Acad. Sci. USA*, **55**, 1511 (1966).
(8) R. L. O'Brien, J. L. Allison, and F. E. Hahn, *Biochim. Biophys. Acta*, **129**, 622 (1966).
(9) G. Cilento and P. Giusti, *J. Am. Chem. Soc.*, **81**, 3801 (1959).
(10) I. Isenberg and A. Szent-Györgyi, *Proc. Natl. Acad. Sci. USA*, **44**, 857 (1958).
(11) C. Reid and R. S. Mulliken, *J. Am. Chem. Soc.*, **76**, 3869 (1954).
(12) E. M. Kosower, *ibid.*, **78**, 3497 (1956).
(13) E. M. Kosower and P. E. Klinedinst, Jr., *ibid.*, **78**, 3493 (1958).
(14) H. D. Bist and W. B. Person, *J. Phys. Chem.*, **71**, 2750 (1967).
(15) J. N. Chaudhuri and S. Basu, *Trans. Faraday Soc.*, **55**, 898 (1959).
(16) L. J. Andrews and R. M. Keefer, *J. Am. Chem. Soc.*, **74**, 4500 (1952).
(17) A. I. Popov and R. H. Rygg, *ibid.*, **79**, 4622 (1957).
(18) D. R. Kearnes, P. Gardner, and J. Carmody, *J. Phys. Chem.*, **71**, 931 (1967).
(19) M. Chowdhury and S. Basu, *Trans. Faraday Soc.*, **56**, 335 (1959).
(20) M. Chowdhury, *J. Phys. Chem.*, **65**, 1899 (1961).
(21) A. R. Cooper, C. W. P. Crowne, and P. G. Farrell, *Trans. Faraday Soc.*, **63**, 447 (1967).
(22) G. Scatchard, *Ann. N.Y. Acad. Sci.*, **51**, 660 (1949).
(23) P. A. D. de Maine and R. D. Seawright, "Digital Computer Programs for Physical Chemistry," vols. I and II, Macmillan, New York, N.Y., 1963.
(24) E. Hückel, *Z. Phys.*, **76**, 628 (1932).
(25) A. Streitwieser, Jr., "Molecular Orbital Theory for Organic Chemists," Wiley, New York, N.Y., 1961.
(26) M. J. S. Dewar, "The Molecular Orbital Theory of Organic Chemistry," McGraw-Hill, New York, N.Y., 1969.
(27) A. G. Maki and E. K. Plyler, *J. Phys. Chem.*, **66**, 766 (1962).
(28) V. G. Krishna and B. Bhowmik, *J. Am. Chem. Soc.*, **90**, 1700 (1968).
(29) O. Hassel, C. Rømming, and T. Tufts, *Acta Chem. Scand.*, **10**, 696 (1956).
(30) *Ibid.*, **15**, 967 (1961).

ACKNOWLEDGMENTS

The authors thank the Memphis State University Computer Center for technical assistance and for a grant of computer time.

Kinetics and Mechanism of Oxidation of Promazine and Promethazine by Ferric Perchlorate

M. R. GASCO ˣ and M. E. CARLOTTI

Received January 17, 1977, from the *Istituto di Chimica Farmaceutica dell'Università di Torino, Torino, Italy.* Accepted for publication April 26, 1977.

Abstract □ The equilibrium constants, kinetics, and mechanism of promazine and promethazine oxidation by ferric perchlorate were investigated at different temperatures and acidities using a stopped-flow spectrophotometric technique. The overall reaction can be represented as follows:

$$\mathrm{Fe(III)} + \mathrm{P} \underset{k_{-1}}{\overset{k_1}{\rightleftharpoons}} \mathrm{Fe(II)} + \mathrm{P}^{\cdot+}$$

where $\mathrm{P}^{\cdot+}$ represents the radical cation corresponding to the phenothiazine derivative. The equilibrium quotients were evaluated at 1.00 *M* $HClO_4$, 25.0°, and ionic strength 1.0 *M*. The kinetics of reaction follow the equation:

$$-\frac{d[\mathrm{P}]}{dt} = k_1[\mathrm{Fe}^{3+}][\mathrm{P}] - k_{-1}[\mathrm{Fe}^{2+}][\mathrm{P}^{\cdot+}]$$

The rate constants k_1 and k_{-1} are independent of acidity and are related to the corresponding equilibrium quotients.

Keyphrases □ Promazine—kinetics and mechanism of oxidation by ferric perchlorate, various temperatures and pH values □ Promethazine—kinetics and mechanism of oxidation by ferric perchlorate, various temperatures and pH values □ Phenothiazines—promazine and promethazine, kinetics and mechanism of oxidation by ferric perchlorate, various temperatures and pH values □ Oxidation—kinetics and mechanism, promazine and promethazine by ferric perchlorate, various temperatures and pH values □ Ferric perchlorate—oxidation of promazine and promethazine, kinetics and mechanism, various temperatures and pH values

Free radicals of dialkylaminoalkylphenothiazine derivatives have been found in the urine of patients receiving phenothiazine drugs (1). Studies were carried out to elucidate both the role of such free radicals in biotransformation and structure–activity relationships.

Using electron spin resonance, Fenner (2, 3) noted the influence of the electron-donating and electron-withdrawing groups on the ring, as well as that of the side chain bonded to the nitrogen (in position 10), on radical formation. Investigation of the oxidation by inorganic agents also showed the large influence of the side chain (4, 5). In particular, the oxidation of the two isomers promazine[1] [10-(3-dimethylaminopropyl)phenothiazine] (I) and promethazine[2] [10-(2-dimethylaminopropyl)phenothiazine] (II), both with ammonium persulfate and ceric sulfate in aqueous solution at different pH values, gave different oxidation products (6, 7). Moreover, I and II show different pharmacodynamic properties; I is an antidepressant and II is an antihistaminic.

The differences in the behavior of these compounds toward oxidation suggested an investigation of the kinetics

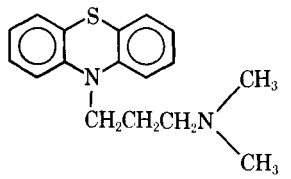

I

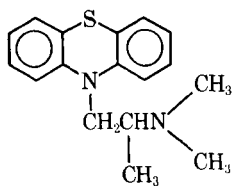

II

(2) "Molecular Association in Biology," B. Pullman, Ed., Academic, New York, N.Y., 1968.
(3) R. Foster, "Organic Charge Transfer Complexes," Academic, New York, N.Y., 1969, pp. 335–373.
(4) M. A. Slifkin, "Charge Transfer Interactions of Biomolecules," Academic, New York, N.Y., 1971.
(5) L. B. Kier, "Molecular Orbital Theory in Drug Research," Academic, New York, N.Y., 1971, pp. 86–89.
(6) F. E. Hahn, R. L. O'Brien, J. Ciak, J. L. Allison, and J. G. Olenick, *Mil. Med. Suppl.*, **131**, 1071 (1966).
(7) R. L. O'Brien, J. G. Olenick, and F. E. Hahn, *Proc. Natl. Acad. Sci. USA*, **55**, 1511 (1966).
(8) R. L. O'Brien, J. L. Allison, and F. E. Hahn, *Biochim. Biophys. Acta*, **129**, 622 (1966).
(9) G. Cilento and P. Giusti, *J. Am. Chem. Soc.*, **81**, 3801 (1959).
(10) I. Isenberg and A. Szent-Györgyi, *Proc. Natl. Acad. Sci. USA*, **44**, 857 (1958).
(11) C. Reid and R. S. Mulliken, *J. Am. Chem. Soc.*, **76**, 3869 (1954).
(12) E. M. Kosower, *ibid.*, **78**, 3497 (1956).
(13) E. M. Kosower and P. E. Klinedinst, Jr., *ibid.*, **78**, 3493 (1958).
(14) H. D. Bist and W. B. Person, *J. Phys. Chem.*, **71**, 2750 (1967).
(15) J. N. Chaudhuri and S. Basu, *Trans. Faraday Soc.*, **55**, 898 (1959).
(16) L. J. Andrews and R. M. Keefer, *J. Am. Chem. Soc.*, **74**, 4500 (1952).
(17) A. I. Popov and R. H. Rygg, *ibid.*, **79**, 4622 (1957).
(18) D. R. Kearnes, P. Gardner, and J. Carmody, *J. Phys. Chem.*, **71**, 931 (1967).
(19) M. Chowdhury and S. Basu, *Trans. Faraday Soc.*, **56**, 335 (1959).
(20) M. Chowdhury, *J. Phys. Chem.*, **65**, 1899 (1961).
(21) A. R. Cooper, C. W. P. Crowne, and P. G. Farrell, *Trans. Faraday Soc.*, **63**, 447 (1967).
(22) G. Scatchard, *Ann. N.Y. Acad. Sci.*, **51**, 660 (1949).
(23) P. A. D. de Maine and R. D. Seawright, "Digital Computer Programs for Physical Chemistry," vols. I and II, Macmillan, New York, N.Y., 1963.
(24) E. Hückel, *Z. Phys.*, **76**, 628 (1932).
(25) A. Streitwieser, Jr., "Molecular Orbital Theory for Organic Chemists," Wiley, New York, N.Y., 1961.
(26) M. J. S. Dewar, "The Molecular Orbital Theory of Organic Chemistry," McGraw-Hill, New York, N.Y., 1969.
(27) A. G. Maki and E. K. Plyler, *J. Phys. Chem.*, **66**, 766 (1962).
(28) V. G. Krishna and B. Bhowmik, *J. Am. Chem. Soc.*, **90**, 1700 (1968).
(29) O. Hassel, C. Rømming, and T. Tufts, *Acta Chem. Scand.*, **10**, 696 (1956).
(30) *Ibid.*, **15**, 967 (1961).

ACKNOWLEDGMENTS

The authors thank the Memphis State University Computer Center for technical assistance and for a grant of computer time.

Kinetics and Mechanism of Oxidation of Promazine and Promethazine by Ferric Perchlorate

M. R. GASCO ˣ and M. E. CARLOTTI

Received January 17, 1977, from the *Istituto di Chimica Farmaceutica dell'Università di Torino, Torino, Italy.* Accepted for publication April 26, 1977.

Abstract □ The equilibrium constants, kinetics, and mechanism of promazine and promethazine oxidation by ferric perchlorate were investigated at different temperatures and acidities using a stopped-flow spectrophotometric technique. The overall reaction can be represented as follows:

$$\mathrm{Fe(III)} + \mathrm{P} \underset{k_{-1}}{\overset{k_1}{\rightleftharpoons}} \mathrm{Fe(II)} + \mathrm{P}^{\cdot+}$$

where $\mathrm{P}^{\cdot+}$ represents the radical cation corresponding to the phenothiazine derivative. The equilibrium quotients were evaluated at 1.00 *M* $HClO_4$, 25.0°, and ionic strength 1.0 *M*. The kinetics of reaction follow the equation:

$$-\frac{d[\mathrm{P}]}{dt} = k_1[\mathrm{Fe}^{3+}][\mathrm{P}] - k_{-1}[\mathrm{Fe}^{2+}][\mathrm{P}^{\cdot+}]$$

The rate constants k_1 and k_{-1} are independent of acidity and are related to the corresponding equilibrium quotients.

Keyphrases □ Promazine—kinetics and mechanism of oxidation by ferric perchlorate, various temperatures and pH values □ Promethazine—kinetics and mechanism of oxidation by ferric perchlorate, various temperatures and pH values □ Phenothiazines—promazine and promethazine, kinetics and mechanism of oxidation by ferric perchlorate, various temperatures and pH values □ Oxidation—kinetics and mechanism, promazine and promethazine by ferric perchlorate, various temperatures and pH values □ Ferric perchlorate—oxidation of promazine and promethazine, kinetics and mechanism, various temperatures and pH values

Free radicals of dialkylaminoalkylphenothiazine derivatives have been found in the urine of patients receiving phenothiazine drugs (1). Studies were carried out to elucidate both the role of such free radicals in biotransformation and structure–activity relationships.

Using electron spin resonance, Fenner (2, 3) noted the influence of the electron-donating and electron-withdrawing groups on the ring, as well as that of the side chain bonded to the nitrogen (in position 10), on radical formation. Investigation of the oxidation by inorganic agents also showed the large influence of the side chain (4, 5). In particular, the oxidation of the two isomers promazine[1] [10-(3-dimethylaminopropyl)phenothiazine] (I) and promethazine[2] [10-(2-dimethylaminopropyl)phenothiazine] (II), both with ammonium persulfate and ceric sulfate in aqueous solution at different pH values, gave different oxidation products (6, 7). Moreover, I and II show different pharmacodynamic properties; I is an antidepressant and II is an antihistaminic.

The differences in the behavior of these compounds toward oxidation suggested an investigation of the kinetics

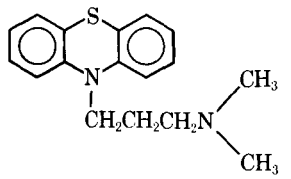

I

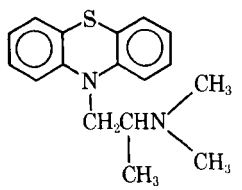

II

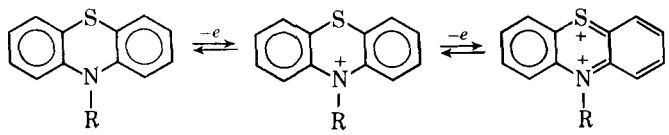

III IV

Scheme I

and mechanism of the oxidation reaction; no data were available on the oxidation of these heteroaromatic nuclei in aqueous solution. The redox properties of the *N*-dialkylaminoalkylphenothiazine derivatives are characterized by two successive monoelectron steps (8); one step yields the free radical (III), and the other step yields the bivalent cation (IV) (Scheme I). This last species is unstable in water, giving rise to a sulfoxide (8).

The present work evaluates the equilibrium data and the kinetics and mechanism of oxidation of I and II to the first-step oxidation product, *i.e.*, the free radical (III). Ferric perchlorate was used as an oxidant; the formal reduction potential of the Fe(III)–Fe(II) couple does not allow I and II to be oxidized further to cation IV.

EXPERIMENTAL

Reagents—Compounds I[1] and II[2] were employed as chlorhydrates. Iron(III) perchlorate[3] was a reagent grade product. Iron(II) perchlorate was prepared by dissolution of pure iron[3] in perchloric acid. Perchloric acid[4] and lithium perchlorate[4] were used to bring the solutions to the proper acidity and ionic strength.

Procedure—Solutions of I and II were prepared daily and stored in the dark. Ferric perchlorate solutions were standardized by complexometric titration. The ferrous perchlorate content was determined with cerium(IV) sulfate titration. The spectra and equilibrium measurements were performed spectrophotometrically[5].

The kinetic runs were carried out with a stopped-flow spectrophotometer[6] at the wavelength of maximum absorption of free radicals (III) (path length of the cell was 2.00 cm).

The variations of transmittance as a function of time were stored on an oscilloscope screen[7] and photographed (Fig. 1).

RESULTS AND DISCUSSION

Spectrophotometric and Equilibrium Data—For I, the experiments

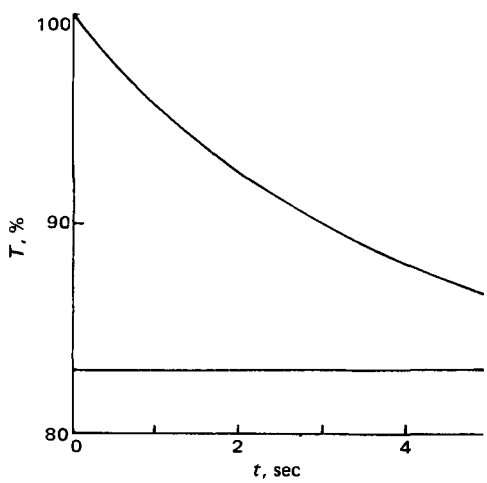

Figure 1—*Plot of transmittance as a function of time for a typical run [2 × 10⁻⁵ M I; 1 × 10⁻³ M Fe(ClO₄)₃; 2 × 10⁻⁴ M Fe(ClO₄)₂; 1.00 M HClO₄] at ionic strength 1.0 M and 25.0°.*

[1] Promazine, Rhône-Poulenc.
[2] Prometazine, Rhône-Poulenc.
[3] C. Erba reagent grade.
[4] Merck reagent grade.
[5] Perkin-Elmer EPS-3T spectrophotometer.
[6] Durrum-Gibson, Palo Alto, Calif.
[7] Tektronix 564.

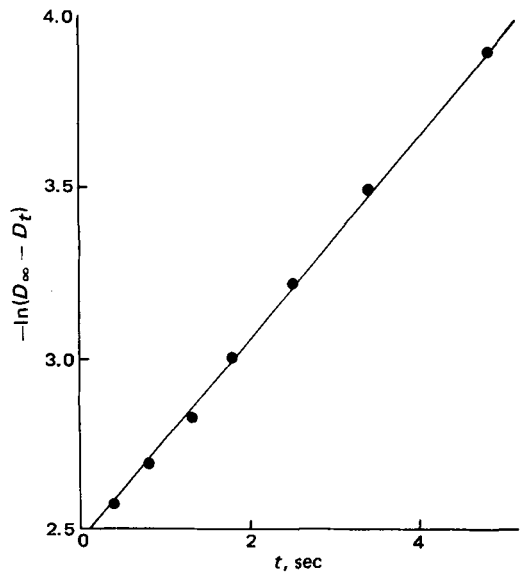

Figure 2—*Plot of ln* $(D_\infty - D_t)$ *versus time corresponding to the run of Fig. 1.*

were performed in solution with an excess of Fe(III) [4.0×10^{-5} *M* of I, $\geq 5.0 \times 10^{-5}$ *M* $Fe(ClO_4)_3$]. In the initial absence of Fe(II), the formation of a product with an absorbance maximum at λ 513 nm was observed; the absorbance did not increase further when $\geq 2 \times 10^{-4}$ *M* $Fe(ClO_4)_3$ was used. The molar absorptivity, ϵ_{513} $(1.00 \pm 0.05) \times 10^4$ M^{-1} cm^{-1}, was determined for this reaction product, which, according to literature data (8), is the radical cation (III).

The reaction can be depicted as follows:

$$Fe(III) + P \underset{k_{-1}}{\overset{k_1}{\rightleftarrows}} Fe(II) + P^{\cdot+}$$

Scheme II

where P represents the phenothiazine derivative and $P^{\cdot+}$ is the corresponding cation radical (III).

By running the experiments in different concentrations of ferric and ferrous perchlorate (at constant concentration of I), the equilibrium quotient corresponding to Scheme II was determined to be 1.4 ± 0.2 (1.00 *M* $HClO_4$ at 25.0° and ionic strength 1.0 *M*).

With II, the formation of a product with an absorbance maximum around 515 nm was observed. With a constant concentration of II, the absorbance increases by increasing the excess of ferric perchlorate (up to 1.0×10^{-2} *M*), thus suggesting that Scheme II has a low equilibrium quotient in this case. Then the molar absorptivity of the oxidation

Table I—Values of Pseudo-First-Order Rate Constants (k_{obs}, $seconds^{-1}$) for the Reaction of I (2.0×10^{-5} *M*) and Excess of Fe^{3+} at Different Experimental Conditions (at Ionic Strength 1.0 *M* and 1.00 *M* $HClO_4$, Except Where Stated)

$Fe(ClO_4)_3$, *mM*	$Fe(ClO_4)_2$, *mM*			
	0.50	1.00	1.50	2.00
		25.0°		
2.0	0.066	0.13_5[a] 0.14[b] 0.13[c] 0.13	0.19	0.24
4.0	0.084	0.16_5[a] 0.17[b] 0.16[c] 0.16	0.21	0.26_5
6.0	0.105	0.20[a] 0.19_5[b] 0.19[c] 0.18_5	0.23	0.27_5
8.0	0.125	0.22[a] 0.23[b] 0.22[c] 0.21_5	0.25_5	0.29_5
10.0	0.25	0.24_5[a] 0.24_5[b] 0.24[c] 0.25_5	0.27_5	0.31
		37.0°		
2.0	0.12	0.20	0.28	0.36_5
4.0	0.17	0.25_5	0.33	0.40
6.0	0.22_5	0.30_5	0.39_5	0.46
8.0	0.25	0.37_5	0.45_5	0.50
10.0	0.31	0.42_5	0.51	0.56
		10.0°		
2.0	0.042	0.073	0.093	0.12
4.0	0.048	0.081	0.10_5	0.13
6.0	0.055	0.091	0.11_5	0.13
8.0	0.063	0.103	0.13	0.15
10.0	0.068	0.11	0.14	0.16_5

[a] With 0.050 *M* $HClO_4$. [b] With 0.20 *M* $HClO_4$. [c] With 0.50 *M* $HClO_4$.

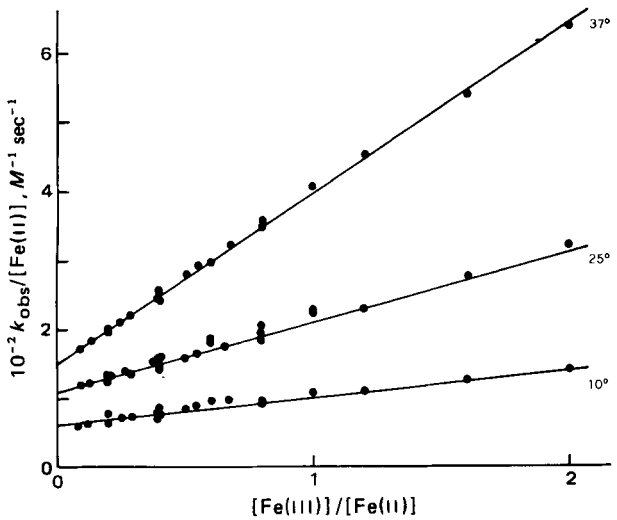

Figure 3—*Plots of* $k_{obs}/[Fe(II)]$ *as a function of* $[Fe(III)]/[Fe(II)]$ *for the reaction of I at different temperatures.*

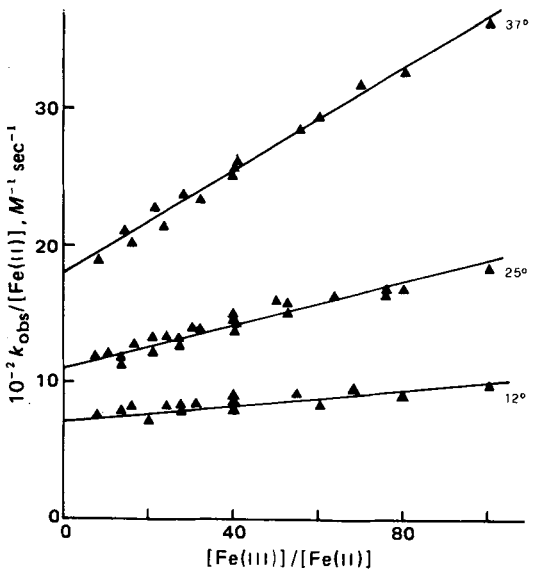

Figure 4—*Plots of* $k_{obs}/[Fe(II)]$ *as a function of* $[Fe(III)]/[Fe(II)]$ *for the reaction of II at different temperatures.*

product was evaluated by adopting an oxidizing agent with a higher formal redox potential, potassium hexachloroiridate(IV) (9) (E^0 0.96 v); ϵ_{515} (9.0 ± 0.7) × 10^3 M^{-1} cm^{-1} was obtained. By performing measurements at different concentrations of ferric and ferrous perchlorate, the equilibrium quotient of Scheme II for II was determined to be K_1 = (7.8 ± 1.3) × 10^{-3} (1.00 *M* $HClO_4$ at 25.0° and ionic strength 1.0 *M*).

Kinetics of Reaction—According to Scheme II, the kinetic law can be formulated as follows:

$$-\frac{d[P]}{dt} = \frac{d[P^{\cdot+}]}{dt} = k_1[P][Fe(III)] - k_{-1}[P^{\cdot+}][Fe(II)] \quad \text{(Eq. 1)}$$

In the presence of large excesses (>10-fold) of both ferric and ferrous perchlorate with respect to the organic substrate, it can be assumed that $k_1' = k_1[Fe(III)]$ and $k_{-1}' = k_{-1}[Fe(II)]$. Hence:

$$\frac{d[P^{\cdot+}]}{dt} = k_1'[P] - k_{-1}'[P^{\cdot+}] \quad \text{(Eq. 2)}$$

By substituting $[P]_0 = [P] + [P^{\cdot+}]$ and $[P^{\cdot+}]_0 = 0$ and integrating, it follows that:

$$\ln \frac{k_1'[P]_0}{k_1'([P]_0 - [P^{\cdot+}]) - k_{-1}'[P^{\cdot+}]} = (k_1' + k_{-1}')t \quad \text{(Eq. 3)}$$

Because $[P^{\cdot+}]_\infty/[P]_0 = k_1'/(k_1' + k_{-1}')$, where $[P^{\cdot+}]_\infty$ represents the radical concentration at equilibrium, it follows that:

$$\ln \frac{[P^{\cdot+}]_\infty}{[P^{\cdot+}]_\infty - [P^{\cdot+}]} = (k_1' + k_{-1}')t \quad \text{(Eq. 4)}$$

Table II—Values of Pseudo-First-Order Rate Constants (k_{obs}, seconds^{-1}) for Reaction of II (2.0 × 10^{-5} *M*) and Excess of Fe^{3+} at Different Experimental Conditions (Ionic Strength 1.0 *M* and 1.00 *M* $HClO_4$ Except Where Stated)

$Fe(ClO_4)_3$, *mM*	$Fe(ClO_4)_2$, m*M*			
	0.10	0.15	0.20	0.25
		25.0°		
2.0	0.118	0.18[a]	0.17_5	0.24	0.30
4.0	0.132	0.19_5[a]	0.18	0.26_5	0.32
6.0	0.15_5	0.20_5[a]	0.21	0.27_5	0.33
8.0	0.16_5	0.23_5[a]	0.23	0.31	0.34_5
10.0	0.18_5	0.24_5[a]	0.25	0.32_5	0.36
		37.0°		
2.0	0.23	0.32			0.47
4.0	0.26_5	0.36			0.49
6.0	0.29	0.38_5			0.53
8.0	0.31_5	0.42			0.57
10.0	0.35_5	0.47			0.63_5
		12.0°		
2.0	0.072	0.115			0.18_5
4.0	0.078	0.12			0.20
6.0	0.084	0.13			0.20_5
8.0	0.091	0.13_5			0.21
10.0	0.098	0.14			0.21_5

[a] With 0.50 *M* $HClO_4$.

Then the slopes of plots $\ln(D_\infty - D_t)$ (where D_∞ and D_t represent the absorbances for $P^{\cdot+}$ at equilibrium and at time t, respectively) as a function of time allow estimation of the observed rate constants (Fig. 2), given by the expression:

$$k_{obs} = k_1[Fe(III)] + k_{-1}[Fe(II)] \quad \text{(Eq. 5)}$$

The kinetic runs were carried out in the presence of excesses of both ferric perchlorate (2.0–10.0 × 10^{-4} *M* for I and 2.0–10.0 × 10^{-3} *M* for II) and ferrous perchlorate (0.50–2.0 × 10^{-3} *M* for I and 1.0–2.5 × 10^{-4} *M* for II) with respect to the phenothiazine derivatives (2.0 × 10^{-5} *M*). Measurements were performed at different acidities (0.050–1.00 *M* $HClO_4$) with a constant ionic strength (1.0 *M* $LiClO_4$) and at different temperatures (10.0, 25.0, and 37.0°). The rate constants were evaluated by means of the least-squares method, and the standard deviation of the single measurement ranged between 2 and 4% of the mean (Tables I and II).

According to Eq. 5, a plot of $k_{obs}/[Fe(II)]$ as a function of $[Fe(III)]/[Fe(II)]$ gives the value of k_{-1} from the intercept and of k_1 from the slope. Such plots are shown in Figs. 3 and 4 for I and II, respectively; the corresponding values of k_1, k_{-1}, and K_1 are listed in Table III along with the related thermodynamic activation parameters.

The equilibrium quotients from the kinetic data agree satisfactorily with the ones evaluated by spectrophotometric data. Such values allow one to estimate, from the E^0 value of the Fe(III)/Fe(II) couple in 1.0 *M* $HClO_4$ at 25.0° (0.738 v) (10), the formal reduction potentials of the couples $P^{\cdot+}/P$. The calculated values, 0.74 v for I and 0.865 v for II, correspond rather well with the half-wave potentials ($E_{1/2}$) determined by a polarographic technique (11).

Table III—Specific Rate Constants (M^{-1}/sec^{-1}) for the Reaction of I and II with Fe^{3+} (1.00 *M* $HClO_4$ and Ionic Strength 1.0 *M*) at Different Temperatures

	k_1	k_{-1}	K_1
		I	
10.0°	40 ± 2	61 ± 3	0.66
25.0°	(1.0 ± 0.05) × 10^2	(1.1 ± 0.05) × 10^2	0.91
37.0°	(2.5 ± 0.1) × 10^2	(1.5 ± 0.1) × 10^2	1.7
$\Delta H^{\neq}$, kcal mole^{-1}	11.2 ± 0.8	5.3 ± 0.9	
$\Delta S^{\neq}$, cal deg^{-1} mole^{-1}	−12 ± 3	−32 ± 3	
		II	
12.0°	3.2 ± 0.2	(7.1 ± 0.4) × 10^2	4.5 × 10^{-3}
25.0°	8.3 ± 0.4	(1.1 ± 0.1) × 10^3	7.5 × 10^{-3}
37.0°	19.0 ± 1.0	(1.8 ± 0.1) × 10^3	1.1 × 10^{-2}
$\Delta H^{\neq}$, kcal mole^{-1}	12.0 ± 1.0	6.0 ± 1.2	
$\Delta S^{\neq}$, cal deg^{-1} mole^{-1}	−14 ± 3	−25 ± 4	

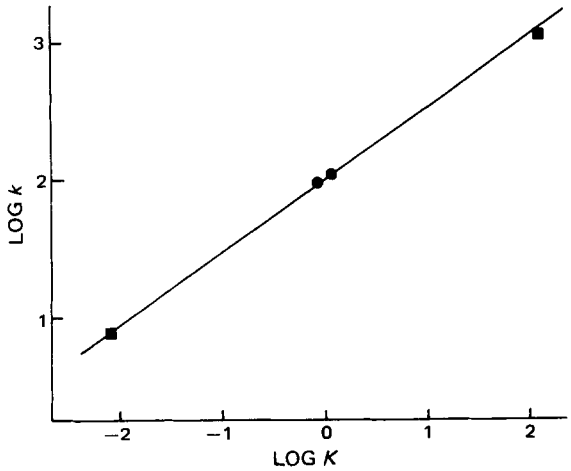

Figure 5—*Plot of log* k *against log* K *for the reactions corresponding to Scheme II for I (●) and II (■) at ionic strength 1.0* M *and 25.0°.*

Table III shows that the enthalpies of activation are higher for the forward reaction (involving Fe^{3+} and phenothiazines) than for the reverse reaction (involving Fe^{2+} and cation radicals); such low values for reactions involving radicals were found in other cases (12).

The reaction rates are independent of the acidity; it can be suggested that the reactive species, in the present conditions, is Fe^{3+}_{aq}. But in several other reactions involving Fe(III), *e.g.*, complexation (13) and redox (14), the reactive species is $FeOH^{2+}_{aq}$, which derives from the hydrolytic equilibrium:

$$Fe^{3+}_{aq} \rightleftarrows FeOH^{2+}_{aq} + H^+$$

Scheme III

with $K_7 = 1.63 \times 10^{-3}$ *M* (15). It follows that, in the present acidity range, the predominant species is Fe^{3+}_{aq}. This behavior can be ascribed to a mechanism involving a simple electron transfer rather than a hydrogen atom transfer, probably operating when $FeOH^{2+}_{aq}$ is the active species (16).

When the mechanism of the redox reaction is an electron transfer, a relationship between the free energy of activation and the overall free energy of reaction should hold. According to the Marcus (17) theory, a plot of log *k versus* log *K* is linear with a slope of about 0.50. Figure 5 shows that this expectation is satisfied in the present reactions. Such relationships have been found to be applicable in the redox reactions involving some relevant biological systems, such as cytochrome c, some catecholamines, and ascorbic acid (18).

The present findings suggest the possibility of correlating the oxidation rates of phenothiazines with thermodynamic and structural data of these systems.

REFERENCES

(1) J. S. Forrest, F. M. Forrest, and M. Berger, *Biochim. Biophys. Acta*, **29**, 441 (1958).

(2) H. Fenner, *Arch. Pharm.*, **304**, 36 (1971).

(3) *Ibid.*, **304**, 47 (1971).

(4) G. M. Nano, P. Sancin, and G. Tappi, *Pharm. Acta Helv.*, **38**, 263 (1963).

(5) M. R. Gasco, *Atti Accad. Sci. Torino*, **100**, 509 (1965–66).

(6) M. R. Gasco and R. Calvino, *ibid.*, **102**, 237 (1967–68).

(7) *Ibid.*, **102**, 1 (1967–68).

(8) J. P. Billon, *Ann. Chim. (Paris)*, **7**, 183 (1962).

(9) W. N. Latimer, "The Oxidation States of the Elements and Their Potentials in Aqueous Solution," 2nd ed., Prentice-Hall, New York, N.Y., 1952.

(10) L. B. Magnusson and J. R. Huizenga, *J. Am. Chem. Soc.*, **75**, 2242 (1953).

(11) P. Kabasakalian and J. M. Glotten, *Anal. Chem.*, **31**, 43 (1959).

(12) E. Collison, F. S. Dainton, B. Mill, S. Tazuka, and D. R. Smith, *Nature*, **198**, 26 (1963).

(13) S. Ganger and S. Stuher, *Inorg. Chem.*, **13**, 379 (1974). J. H. Espenson and S. R. Helzes, *ibid.*, **8**, 1051 (1969).

(14) J. H. Baxendale, H. R. Hardy, and L. H. Sutcliffe, *Trans. Faraday Soc.*, **47**, 963 (1951). J. H. Thomas, G. Trudel, and S. Bywater, *J. Phys. Chem.*, **64**, 51 (1960).

(15) R. M. Milburn, *J. Am. Chem. Soc.*, **79**, 537 (1957).

(16) W. L. Reynolds and R. W. Lumry, "Mechanisms of Electron Transfer," Ronald Press, New York, N.Y., 1966.

(17) R. A. Marcus, *Ann. Rev. Phys. Chem.*, **15**, 155 (1964).

(18) J. M. Yandell, D. P. Fay, and N. Sutin, *J. Am. Chem. Soc.*, **95**, 1131 (1973). J. C. Cassatt and C. P. Marini, *Biochemistry*, **13**, 5323 (1974). E. Pelizzetti, E. Mentasti, E. Pramauro, and G. Giraudi, *Inorg. Chim. Acta*, **15**, L 1 (1975). E. Pelizzetti, E. Mentasti, and E. Pramauro, *ibid.*, **15**, 2898 (1976).

ACKNOWLEDGMENTS

The authors thank Professor G. Saini (Istituto di Chimica Analitica) for use of the stopped-flow spectrophotometer.

Alkaloids of *Strychnos dolichothyrsa* Gilg ex Onochie et Hepper

R. VERPOORTE ˣ and A. BAERHEIM SVENDSEN

Received February 23, 1977, from the *Department of Pharmacognosy, Gorlaeus Laboratories, Wassenaarseweg 76, Leiden, The Netherlands.* Accepted for publication April 22, 1977.

Abstract □ Three alkaloids of the stem bark of *Strychnos dolichothyrsa* Gilg ex Onochie et Hepper (Loganiaceae) were isolated and identified as caracurine V and its mono- and di-*N*-oxide by comparison with synthesized compounds. ^{13}C-NMR was used to confirm the structure of the *N*-oxides. The muscle relaxant activity and the toxicity of the *N*-oxides were less than those of caracurine V.

Keyphrases □ *Strychnos dolichothyrsa*—stem bark alkaloids isolated and identified, muscle relaxant activity evaluated □ Alkaloids—from stem bark of *Strychnos dolichothyrsa* isolated and identified, muscle relaxant activity evaluated □ Caracurine V and *N*-oxides—isolated from stem bark of *Strychnos dolichothyrsa*, muscle relaxant activity evaluated □ Relaxant activity, muscle—alkaloids isolated from stem bark of *Strychnos dolichothyrsa* evaluated

Extracts of the stem bark of *Strychnos dolichothyrsa* Gilg ex Onochie et Hepper showed a strong muscle relaxant effect in pharmacological screenings (1, 2), especially in the tertiary alkaloid fractions. The isolation and identification of bisnordihydrotoxiferine, one main alkaloid of this species, and some minor alkaloids derived from

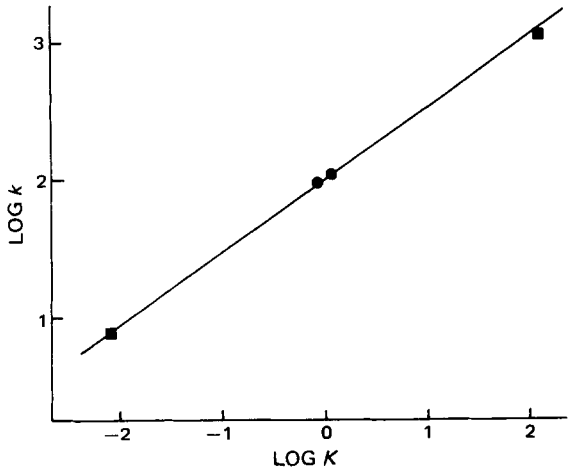

Figure 5—*Plot of log* k *against log* K *for the reactions corresponding to Scheme II for I (●) and II (■) at ionic strength 1.0* M *and 25.0°.*

Table III shows that the enthalpies of activation are higher for the forward reaction (involving Fe^{3+} and phenothiazines) than for the reverse reaction (involving Fe^{2+} and cation radicals); such low values for reactions involving radicals were found in other cases (12).

The reaction rates are independent of the acidity; it can be suggested that the reactive species, in the present conditions, is Fe^{3+}_{aq}. But in several other reactions involving Fe(III), *e.g.*, complexation (13) and redox (14), the reactive species is $FeOH^{2+}_{aq}$, which derives from the hydrolytic equilibrium:

$$Fe^{3+}_{aq} \rightleftarrows FeOH^{2+}_{aq} + H^+$$

Scheme III

with $K_7 = 1.63 \times 10^{-3}$ *M* (15). It follows that, in the present acidity range, the predominant species is Fe^{3+}_{aq}. This behavior can be ascribed to a mechanism involving a simple electron transfer rather than a hydrogen atom transfer, probably operating when $FeOH^{2+}_{aq}$ is the active species (16).

When the mechanism of the redox reaction is an electron transfer, a relationship between the free energy of activation and the overall free energy of reaction should hold. According to the Marcus (17) theory, a plot of log *k versus* log *K* is linear with a slope of about 0.50. Figure 5 shows that this expectation is satisfied in the present reactions. Such relationships have been found to be applicable in the redox reactions involving some relevant biological systems, such as cytochrome c, some catecholamines, and ascorbic acid (18).

The present findings suggest the possibility of correlating the oxidation rates of phenothiazines with thermodynamic and structural data of these systems.

REFERENCES

(1) J. S. Forrest, F. M. Forrest, and M. Berger, *Biochim. Biophys. Acta*, **29**, 441 (1958).

(2) H. Fenner, *Arch. Pharm.*, **304**, 36 (1971).

(3) *Ibid.*, **304**, 47 (1971).

(4) G. M. Nano, P. Sancin, and G. Tappi, *Pharm. Acta Helv.*, **38**, 263 (1963).

(5) M. R. Gasco, *Atti Accad. Sci. Torino*, **100**, 509 (1965–66).

(6) M. R. Gasco and R. Calvino, *ibid.*, **102**, 237 (1967–68).

(7) *Ibid.*, **102**, 1 (1967–68).

(8) J. P. Billon, *Ann. Chim. (Paris)*, **7**, 183 (1962).

(9) W. N. Latimer, "The Oxidation States of the Elements and Their Potentials in Aqueous Solution," 2nd ed., Prentice-Hall, New York, N.Y., 1952.

(10) L. B. Magnusson and J. R. Huizenga, *J. Am. Chem. Soc.*, **75**, 2242 (1953).

(11) P. Kabasakalian and J. M. Glotten, *Anal. Chem.*, **31**, 43 (1959).

(12) E. Collison, F. S. Dainton, B. Mill, S. Tazuka, and D. R. Smith, *Nature*, **198**, 26 (1963).

(13) S. Ganger and S. Stuher, *Inorg. Chem.*, **13**, 379 (1974). J. H. Espenson and S. R. Helzes, *ibid.*, **8**, 1051 (1969).

(14) J. H. Baxendale, H. R. Hardy, and L. H. Sutcliffe, *Trans. Faraday Soc.*, **47**, 963 (1951). J. H. Thomas, G. Trudel, and S. Bywater, *J. Phys. Chem.*, **64**, 51 (1960).

(15) R. M. Milburn, *J. Am. Chem. Soc.*, **79**, 537 (1957).

(16) W. L. Reynolds and R. W. Lumry, "Mechanisms of Electron Transfer," Ronald Press, New York, N.Y., 1966.

(17) R. A. Marcus, *Ann. Rev. Phys. Chem.*, **15**, 155 (1964).

(18) J. M. Yandell, D. P. Fay, and N. Sutin, *J. Am. Chem. Soc.*, **95**, 1131 (1973). J. C. Cassatt and C. P. Marini, *Biochemistry*, **13**, 5323 (1974). E. Pelizzetti, E. Mentasti, E. Pramauro, and G. Giraudi, *Inorg. Chim. Acta*, **15**, L 1 (1975). E. Pelizzetti, E. Mentasti, and E. Pramauro, *ibid.*, **15**, 2898 (1976).

ACKNOWLEDGMENTS

The authors thank Professor G. Saini (Istituto di Chimica Analitica) for use of the stopped-flow spectrophotometer.

Alkaloids of *Strychnos dolichothyrsa* Gilg ex Onochie et Hepper

R. VERPOORTE ˣ and A. BAERHEIM SVENDSEN

Received February 23, 1977, from the *Department of Pharmacognosy, Gorlaeus Laboratories, Wassenaarseweg 76, Leiden, The Netherlands.* Accepted for publication April 22, 1977.

Abstract □ Three alkaloids of the stem bark of *Strychnos dolichothyrsa* Gilg ex Onochie et Hepper (Loganiaceae) were isolated and identified as caracurine V and its mono- and di-*N*-oxide by comparison with synthesized compounds. ^{13}C-NMR was used to confirm the structure of the *N*-oxides. The muscle relaxant activity and the toxicity of the *N*-oxides were less than those of caracurine V.

Keyphrases □ *Strychnos dolichothyrsa*—stem bark alkaloids isolated and identified, muscle relaxant activity evaluated □ Alkaloids—from stem bark of *Strychnos dolichothyrsa* isolated and identified, muscle relaxant activity evaluated □ Caracurine V and *N*-oxides—isolated from stem bark of *Strychnos dolichothyrsa*, muscle relaxant activity evaluated □ Relaxant activity, muscle—alkaloids isolated from stem bark of *Strychnos dolichothyrsa* evaluated

Extracts of the stem bark of *Strychnos dolichothyrsa* Gilg ex Onochie et Hepper showed a strong muscle relaxant effect in pharmacological screenings (1, 2), especially in the tertiary alkaloid fractions. The isolation and identification of bisnordihydrotoxiferine, one main alkaloid of this species, and some minor alkaloids derived from

Table I—Low-Field Region of the ^{13}C-NMR Spectra of Caracurine V, Strychnine, and Their *N*-Oxides[a]

Carbon	Ia	Ib			Ic	$\Delta(\delta_{Ia} - \delta_{Ic})$	III	IV	$\Delta(\delta_{III} - \delta_{IV})$
		N_b-Tertiary (A)	N_b-Oxide (B)	$\Delta(\delta_A - \delta_B)$					
C-8	133.59	133.29	130.62	(+2.67)	130.69	(+2.90)	132.62	129.35	(+3.27)
C-9	119.52	120.31	120.74	(−0.43)	121.22	(−1.70)	122.31	122.67	(−0.36)
C-10	121.70	121.76	121.76	(0)	121.95	(−0.25)	124.25	125.10	(−0.85)
C-11	128.25	128.62	129.59	(−0.97)	129.65	(−1.40)	128.62	129.95	(−1.33)
C-12	110.17	110.72	111.51	(−0.79)	111.63	(−1.46)	116.24	116.60	(−0.36)
C-13	152.34	152.10	151.92	(+0.18)	151.62	(+0.72)	142.21	141.60	(+0.61)
C-19	127.34	128.14	133.77	(−5.63)	133.78	(−6.44)	127.65	134.44	(−6.79)
C-20	141.24	140.69	135.96	(+4.73)	136.20	(+5.04)	140.27	135.05	(+5.22)
C-23	—	—	—	—	—	—	169.39	169.27	(+0.12)

[a] The chemical shifts, in parts per million, are relative to tetramethylsilane.

bisnordihydrotoxiferine were reported previously (3).

Further work on the stem bark alkaloids of *S. dolichothyrsa* showed the presence of a quite polar alkaloid as well as two chemically related minor alkaloids. This paper describes the isolation of these alkaloids and their structure elucidation based on comparisons with synthesized compounds and ^{13}C-NMR studies.

EXPERIMENTAL

Plant Material—The stem bark of *S. dolichothyrsa* Gilg ex Onochie et Hepper was collected[1] near Kribi, Cameroun, in June and July 1970.

^{13}C-NMR Spectroscopy—The spectra were recorded at 25.15 MHz in the Fourier-transform mode. The alkaloids were dissolved in deuterochloroform; for the *N*-oxides of caracurine V, 30% deuteromethanol was added. Tetramethylsilane was used as the internal standard. Both proton-noise decoupled and off-resonance spectra were recorded.

TLC—The following solvents were used in saturated tanks: A, ethyl acetate–2-propanol–25% ammonia (45:35:5); B, ethanol–ether–diethylamine (10:80:10); C, chloroform–cyclohexane–diethylamine (30:60:10); D, 1-butanol–water–acetic acid (60:15:15); E, ethyl acetate–2-propanol–25% ammonia (45:35:10); and F, methanol–2 *M* ammonia–1 *M* ammonium nitrate (70:20:10).

TLC aluminum sheets[2], precoated with silica gel 60 F_{254}, were used. A 1% ceric sulfate solution in 10% sulfuric acid was the spray reagent used to locate the alkaloids.

Isolation—Caracurine V (*Ia*) was obtained pure by column chromatography of the collected fractions as described previously (3). For the final separation, a column of 250 g of basic aluminum oxide[3] (activity III) was used with cyclohexane–chloroform (1:1), gradually changed *via* chloroform to chloroform–methanol (1:1).

Characterization of Caracurine V—From the collected fractions, 10 mg of pure caracurine V as a crystalline hydrochloride (mp >300° dec.) and 20 mg as the amorphous base were isolated. The UV spectrum of the base showed maxima at 259 and 299 nm (in methanol). The IR spectrum of the hydrochloride (potassium bromide disk) showed major peaks at 3400, 2900, 2700, 1600, 1480, 1465, 1400, 1340, 1300, 1230, 1190, 1100, 1020, 960, 920, 890, 860, and 755 cm^{-1}.

The major fragments observed in the mass spectrum of the base (160°, 70 ev) were *m/e* 585 (37), 584 (100) (M^+), 566 (10), 322 (10), 321 (10), 293 (15), 292 (14), 263 (15), 180 (29), 144 (92), 143 (54), and 137 (25). The R_f values in the TLC systems were: A, 0.24; B, 0.23; C, 0.16; and D, 0.25. A purple color was obtained with the ceric sulfate spray reagent.

Characterization of Caracurine V *N*-Oxide (*Ib*) and Caracurine V Di-*N*-oxide (Ic)—Compounds *Ib* and Ic were obtained from the column chromatography fractions as described previously (3) by preparative TLC. The UV spectra and color reactions of both alkaloids were similar to those of caracurine V. The R_f values were 0.40 and 0.18 in TLC System E and 0.45 and 0.72 in TLC System F for *Ib* and Ic, respectively. These data correspond with those found for the *N*-oxides obtained during the synthesis of caracurine V.

Synthesis of Wieland–Gumlich Aldehyde (II) and Ia–Ic—*Preparation of 23-Isonitrososstrychnine*—Strychnine (III) (50 g) was dissolved in 300 ml of ethanol (98%) in a three-necked round-bottom flask equipped with a funnel, a reflux condenser, and a stirrer. Isoamyl nitrite (90 ml) was added with stirring, and then a solution of 13.9 g of sodium in 375 ml of ethanol (98%) was added over 1 hr. The temperature was gradually increased from 60 to 90° and then kept at 90° for 4 hr.

After evaporation to dryness under reduced pressure, to remove excess isoamyl nitrite, 75 ml of water was added to the residue and it was again evaporated to dryness. The procedure was then repeated again. Finally, the residue was mixed with 450 ml of water, 80 ml of acetic acid, and 3 g of activated carbon and filtered. To the filtrate, 3 g of activated carbon was added; after filtration and addition of 37.5 ml of concentrated hydrochloric acid, the filtrate was kept at 0° for 24 hr.

The precipitate that formed was filtered off and recrystallized from methanol, mp >220° dec. The UV spectrum of the product showed maxima at 234, 290, and 315 nm. The IR spectrum (potassium bromide disk) showed maxima at 3440, 3100, 2900, 1660, 1590, 1480, 1410, 1285, 1100, 1035, 980, 880, and 755 cm^{-1}. These data correspond with those of 23-isonitrososstrychnine hydrochloride according to Hymon *et al.* (4). The yield was 80%.

Preparation of II from 23-Isonitrososstrychnine—23-Isonitrososstrychnine hydrochloride (5.5 g) was added to 10 ml of thionyl chloride at 20° with stirring and left for 1 hr. Then the solution was added dropwise to 50 g of ice over 5 min and allowed to stand for 6 hr at 20° with stirring. The N_a-cyanoformyl Wieland–Gumlich aldehyde hydrochloride was filtered off and washed with 5 ml of water. On suspension in 50 ml of water, the pH was adjusted to 3 with 1 *M* sodium carbonate, the mixture was heated gently, and steam was passed through the solution until no more hydrogen cyanide could be detected in the vapors.

The solution was then cooled, the pH was brought to 9 with 1 *M* sodium carbonate, and the solution was extracted five times with ether and five times with chloroform. The ether extract gave 1.076 g of an amorphous product, and the chloroform extract gave another 80 mg of an amorphous product. From the filtrate of the N_a-cyanoformyl Wieland–Gumlich aldehyde hydrochloride, another 25 mg of II was recovered after basification to pH 9 and extraction with ether. The reaction products were identified as II by means of TLC properties, melting point (210–212°), UV and IR spectra, and comparison with data for the authentic sample of II.

The UV spectrum showed maxima at 244 and 298 nm. The IR spectrum (potassium bromide disk) showed major peaks at 3400, 2920, 2860, 1720, 1650, 1600, 1490, 1460, 1390, 1310, 1255, 1145, 1070, 1040, 940, 870, 800, and 745 cm^{-1}. The R_f values in the TLC systems were: A, 0.22; B, 0.33; C, 0.10; and D, 0.31. The color reaction with the ceric sulfate spray reagent was orange.

Preparation of Ia from II—Compound II (300 mg), together with 4 ml of pivalic acid, was heated at 120° for 8 hr in an evacuated sealed tube. After removal of pivalic acid under reduced pressure, water was added. The solution was basified with 1 *M* sodium hydroxide and extracted five times with chloroform. The products obtained were purified by column chromatography. The column, comprised of 25 g of basic aluminum oxide[3] (activity IV), was eluted with benzene–chloroform (9:1) followed by pure chloroform, chloroform–methanol (98:2), and chloroform–methanol (1:1). Pure caracurine V (60 mg) was obtained and identified by its physical data, which were in accordance with those found in the literature (5–8) and similar to those found for the alkaloid isolated from *S. dolichothyrsa*.

Compounds *Ib* and Ic were eluted from the column with chloroform–methanol (98:2) after the elution of caracurine V. Their R_f values, color reactions, and UV spectra were similar to those of the alkaloids isolated from *S. dolichothyrsa*. The color reactions and UV and IR spectra were also similar to those of caracurine V.

[1] By Dr. A. J. M. Leeuwenberg and Professor Dr. F. Sandberg. The identification of the plant material was made by Dr. A. J. M. Leeuwenberg, Laboratory of Plant taxonomy and Plant Geography, Agricultural University, Wageningen, The Netherlands, where a herbarium specimen, collection number Lg 7870, was deposited.

[2] Merck, Darmstadt, Germany.

[3] M. Woelm, Eschwege, Germany.

Table II—High-Field Region of the ^{13}C-NMR Spectra of Caracurine V, Strychnine, and Their *N*-Oxides[a]

Carbon	Ia	Ib			Ic	$\Delta(\delta_{Ia} - \delta_{Ic})$	III	IV	$\Delta(\delta_{III} - \delta_{IV})$
		N_b-Tertiary (A)	N_b-Oxide (B)	$\Delta(\delta_A - \delta_B)$					
C-2	56.84	56.91	55.82	(+1.09)	55.76	(+1.08)	60.06	58.48	(+1.58)
C-3	59.94	59.94	82.63	(−22.69)	82.57	(−22.63)	60.06	82.63	(−22.57)
C-5	51.20	51.27	68.68	(−17.41)	68.68	(−17.48)	50.23	67.70	(−17.47)
C-6	40.77	40.71	37.25	(+3.46)	37.25	(+3.52)	42.83[b]	39.31	(+3.52)
C-7	55.51	55.82	56.91	(−1.09)	56.91	(−1.40)	51.93	53.26	(−1.33)
C-14	26.14	25.91	24.45	(+1.46)	24.39	(+1.75)	26.81	25.11	(+1.70)
C-15	34.03	33.85	32.46	(+1.39)	32.40	(+1.63)	31.54	30.33	(+1.21)
C-16	52.54	52.42	52.15	(+0.27)	51.99	(+0.55)	48.17	47.56	(+0.61)
C-17	98.89	98.95	98.53	(+0.42)	98.59	(+0.30)	77.53	77.29	(+0.24)
C-18	66.49	66.37	65.95	(+0.42)	65.89	(+0.60)	64.55	64.43	(+0.12)
C-21	53.32	53.03	70.50	(−17.47)	70.50	(−17.18)	52.66	70.49	(−17.83)
C-22	—	—	—	—	—	—	42.34[b]	42.22	(+0.12)

[a] The chemical shifts, in parts per million, are relative to tetramethylsilane. [b] These signals may be reversed.

Reaction of Caracurine V with Hydrogen Peroxide—Caracurine V (1 mg) was suspended in 0.5 ml of 5% hydrogen peroxide solution and left for 30 min. TLC showed the presence of about equal amounts of Ia–Ic. When the suspension was heated on a water bath, only Ic was present.

Reaction of Ib with Hydrogen Peroxide—Compound Ib (1 mg) was suspended in 0.5 ml of 5% hydrogen peroxide solution and heated on a water bath. TLC showed the presence of one main component; it had the same R_f values and a similar UV spectrum as Ic.

Reaction of Ib and Ic with Sulfurous Acid—The *N*-oxide (1 mg) was suspended in 0.5 ml of 5% sulfurous acid solution and left for 10 min. TLC showed the presence of one major product; it had the same R_f values, color reactions, and UV spectrum as caracurine V.

RESULTS AND DISCUSSION

A previous investigation (3) of the stem bark alkaloids of *S. dolichothyrsa* showed the presence of bisnordihydrotoxiferine and some minor alkaloids derived from this alkaloid. Further investigation on the alkaloid mixture by means of column chromatography led to the isolation of a polar alkaloid and two minor alkaloids derived from this alkaloid. Based on UV, IR, and mass spectra, the alkaloids were thought to belong to the caracurine V series. The identity of the alkaloids was established by comparison with synthesized alkaloids, Ia–Ic (Scheme I).

The synthesis of caracurine V was described by several investigators (5, 9, 10). Battersby and Hodson (9) obtained a relatively higher yield than did Bernauer *et al.* (5) by using pivalic acid instead of acetic acid for the condensation of two molecules of II (Scheme II). By this synthesis, small amounts of bisnortoxiferine also were formed. The method of Battersby and Hodson was used in this investigation; II was obtained according to the synthesis described by Hymon *et al.* (4).

The products obtained from the dimerization of II were separated by column chromatography. Caracurine V, which was obtained by this procedure, gave identical UV, IR, and mass spectra as the polar alkaloid isolated from *S. dolichothyrsa;* the spectral data were also in agreement with those reported in literature (5–8). Moreover, TLC confirmed the identification.

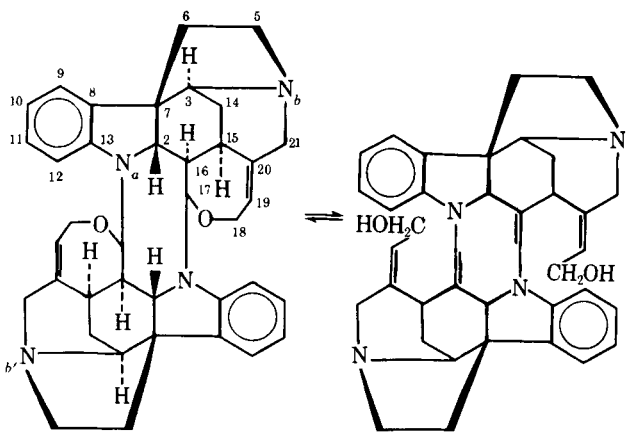

Ia: caracurine V
Ib: N_b^+-O^-
Ic: N_b^+-O^-, N_b^+-O^-

bisnortoxiferine

Scheme I

Two by-products, obtained by the synthesis of caracurine V, were isolated after the column chromatographic separation. Their UV spectra, TLC behavior, and color reactions corresponded with the two minor alkaloids isolated from *S. dolichothyrsa.* Although the spectra and color reactions were very similar to those of caracurine V, the two compounds had a more polar character on TLC. Mass spectrometry failed to give an M^+ peak for the most polar compound. For the other compound, a very small peak was observed at *m/e* 584 and an even smaller peak was observed *m/e* 600.

Treatment of both compounds with sulfurous acid yielded caracurine V according to TLC and color reactions. Oxidation of caracurine V with 5% hydrogen peroxide for 30 min yielded two main products which, on TLC, corresponded with the unknown compounds. Heating caracurine V with hydrogen peroxide solution yielded the most polar compound.

Based on these facts, the two compounds were identified as Ib and Ic (Scheme I), analogous to the occurrence of the *N*-oxides of bisnordihydrotoxiferine (3). Further evidence for these structures was obtained by means of ^{13}C-NMR spectroscopy, which, in contrast to UV, IR, and proton NMR spectroscopy, showed distinct and readily interpretable differences in the spectra.

The chemical shifts recorded for Ia–Ic are summarized in Tables I and II. The assignments were made with the aid of off-resonance decoupled spectra and by comparison of the spectra with the chemical shifts recorded for a number of *Strychnos* alkaloids (11). To permit direct comparison of the shifts resulting from the *N*-oxidation of caracurine V and strychnine (III), the data for strychnine and strychnine *N*-oxide (IV) are also summarized in Tables I and II.

The carbons adjacent to the nitrogen, which is oxidized, were affected most (Table I). The shifts of C-3, C-5, and C-21, as observed for strychnine, were 22.57, 17.47, and 17.83 ppm, respectively, downfield upon *N*-oxidation. The shifts observed for caracurine V upon *N*-oxidation for those three carbons were very similar: 22.63, 17.48, and 17.18 ppm, respectively. The other carbons in caracurine V di-*N*-oxide that shifted

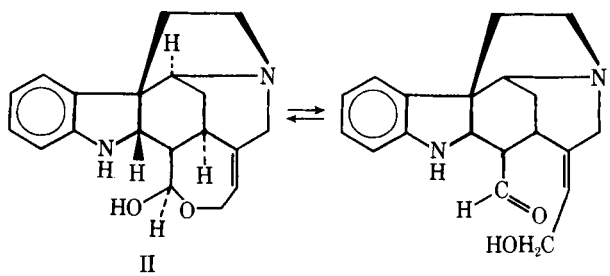

II

Scheme II

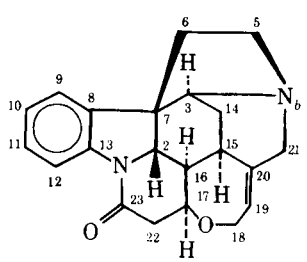

III: strychnine
IV: N_b^+-O^-

Table III—Muscle Relaxant Effect of Caracurine V and Its *N*-Oxides in Mice[a]

Compound	Dose, mg/kg	Screen Grip Test
Ia	6	–
	10	++
	13	++++(lethal)
Ib	10	–
	18	++
	25	++(lethal)
Ic	25	–
	40	+++
	60	++++(lethal)

[a] The activity was determined with the screen grip test as it was used in the screening of *Strychnos* plant material (1, 2). The loss of screen grip is rated as follows: ++++, the mouse falls off as the screen is tilted to a 45° angle; +++, the mouse falls off as the screen is tilted to a 90° angle; ++, the mouse falls off as the screen is inverted; and +, the mouse falls off at the first gentle shake.

considerably were C-20 and C-19, 5.04 ppm downfield and 6.44 ppm upfield, respectively. These shifts agree with those observed for strychnine *N*-oxide. The shifts of the signals of the other carbons, although not as large as those mentioned, are also in good agreement for both caracurine V and strychnine (Tables I and II).

The spectrum of Ib obviously results from the addition of the spectra of Ia and Ic. Whether or not the *N*-oxides are artifacts is difficult to say. The *N*-oxides are readily formed, for example, in chloroform solution (3). However, on TLC of a freshly prepared 1% acetic acid in water extract of the stem bark of *S. dolichothyrsa*, the *N*-oxides were observed. The *N*-oxides were tested in the pharmacological screening as described in investigations of African *Strychnos* species (1, 2). Both compounds proved to be less toxic and less active as muscle relaxants than caracurine V (Table III).

REFERENCES

(1) F. Sandberg, E. Lunnell, and K. J. Ryrberg, *Acta Pharm. Suec.*, **6**, 79 (1969).

(2) F. Sandberg, R. Verpoorte, and A. Cronlund, *ibid.*, **8**, 341 (1971).

(3) R. Verpoorte and A. Baerheim Svendsen, *Lloydia*, **39**, 357 (1976).

(4) J. R. Hymon, H. Schmid, P. Karrer, A. Boller, H. Els, P. Fahrni, and A. Fürst, *Helv. Chim. Acta*, **52**, 1564 (1969).

(5) K. Bernauer, F. Berlage, W. v. Philipsborn, H. Schmid, and P. Karrer, *ibid.*, **41**, 2293 (1958).

(6) A. R. Battersby, D. A. Yeowell, L. M. Jackman, H. D. Schroeder, M. Hesse, H. Hiltebrand, W. v. Philipsborn, H. Schmid, and P. Karrer, *Proc. Chem. Soc.*, **1961**, 413.

(7) M. Hesse, "Indolakaloide, Teil 1 und 2, Fortschritte der Massenspektrometrie," vol. 1, Verlag Chemie, Weinheim, West Germany, 1974.

(8) H. Asmis, H. Schmid, and P. Karrer, *Helv. Chim. Acta*, **37**, 1983 (1954).

(9) A. R. Battersby and H. F. Hodson, *J. Chem. Soc.*, **1960**, 736.

(10) H. A. Hiltebrand, Dissertation, Zurich, Switzerland, 1964.

(11) R. Verpoorte, P. J. Hylands, and N. G. Bisset, *Org. Magn. Reson.*, **9**, 567 (1977).

ACKNOWLEDGMENTS

The authors thank Dr. A. J. M. Leeuwenberg, Laboratory of Plant Taxonomy and Plant Geography, Agricultural University, Wageningen, The Netherlands, and Professor Dr. F. Sandberg, Department of Pharmacognosy, Uppsala University, Sweden, for collecting and identifying the plant material.

Light-Scattering Studies on Bile Acid Salts I: Pattern of Self-Association of Sodium Cholate, Sodium Glycocholate, and Sodium Taurocholate in Aqueous Electrolyte Solutions

YUNIK CHANG and JOHN R. CARDINAL ˣ

Received March 4, 1977, from the *College of Pharmacy, University of Utah, Salt Lake City, UT 84112.* Accepted for publication May 10, 1977.

Abstract □ The pattern of association of the trihydroxy bile salts in aqueous electrolyte solutions was investigated utilizing the light-scattering technique. The turbidity of the bile salts sodium cholate, sodium taurocholate, and sodium glycocholate was determined over the concentration range of 0–25 mg/ml at 25°. For sodium cholate, the concentration of the supporting electrolyte was varied from 0.15 to 0.5 *M*. For all bile salts in 0.15 *M* electrolyte, the turbidity was determined in sodium fluoride, sodium chloride, sodium bromide, and sodium iodide. Comparison of the light-scattering data with a monomer–micellar model showed that qualitative agreement was obtained; however, quantitative agreement could not be achieved. Further examination of the data showed that the light-scattering results were in good agreement with a model that includes dimers, trimers, and a higher aggregate containing approximately eight monomeric units.

Keyphrases □ Sodium cholate—pattern of association in aqueous electrolyte solutions, light-scattering study □ Sodium glycocholate—pattern of association in aqueous electrolyte solutions, light-scattering study □ Sodium taurocholate—pattern of association in aqueous electrolyte solutions, light-scattering study □ Association—sodium cholate, glycocholate, and taurocholate, pattern in aqueous electrolyte solutions, light-scattering study □ Light scattering—study of pattern of association of sodium cholate, glycocholate, and taurocholate in aqueous electrolyte solutions □ Bile acid salts—pattern of association in aqueous electrolyte solutions, light-scattering study

The mechanism by which bile salts solubilize various solutes such as steroids, fat-soluble vitamins, and drugs has often been described following the model for detergent micelles (1). In this model, it is assumed that a reversible equilibrium exists between monomeric species and micelles. The polydispersity of the micelle is assumed to be quite small. The micelle size is dependent on the nature of the bile salt, *i.e.*, the number of hydroxyl groups and conjugation, as well as on temperature, pH, ionic strength, *etc.* (2).

Table III—Muscle Relaxant Effect of Caracurine V and Its *N*-Oxides in Mice[a]

Compound	Dose, mg/kg	Screen Grip Test
Ia	6	–
	10	++
	13	++++(lethal)
Ib	10	–
	18	++
	25	++(lethal)
Ic	25	–
	40	+++
	60	++++(lethal)

[a] The activity was determined with the screen grip test as it was used in the screening of *Strychnos* plant material (1, 2). The loss of screen grip is rated as follows: ++++, the mouse falls off as the screen is tilted to a 45° angle; +++, the mouse falls off as the screen is tilted to a 90° angle; ++, the mouse falls off as the screen is inverted; and +, the mouse falls off at the first gentle shake.

considerably were C-20 and C-19, 5.04 ppm downfield and 6.44 ppm upfield, respectively. These shifts agree with those observed for strychnine *N*-oxide. The shifts of the signals of the other carbons, although not as large as those mentioned, are also in good agreement for both caracurine V and strychnine (Tables I and II).

The spectrum of Ib obviously results from the addition of the spectra of Ia and Ic. Whether or not the *N*-oxides are artifacts is difficult to say. The *N*-oxides are readily formed, for example, in chloroform solution (3). However, on TLC of a freshly prepared 1% acetic acid in water extract of the stem bark of *S. dolichothyrsa*, the *N*-oxides were observed. The *N*-oxides were tested in the pharmacological screening as described in investigations of African *Strychnos* species (1, 2). Both compounds proved to be less toxic and less active as muscle relaxants than caracurine V (Table III).

REFERENCES

(1) F. Sandberg, E. Lunnell, and K. J. Ryrberg, *Acta Pharm. Suec.*, **6**, 79 (1969).

(2) F. Sandberg, R. Verpoorte, and A. Cronlund, *ibid.*, **8**, 341 (1971).

(3) R. Verpoorte and A. Baerheim Svendsen, *Lloydia*, **39**, 357 (1976).

(4) J. R. Hymon, H. Schmid, P. Karrer, A. Boller, H. Els, P. Fahrni, and A. Fürst, *Helv. Chim. Acta*, **52**, 1564 (1969).

(5) K. Bernauer, F. Berlage, W. v. Philipsborn, H. Schmid, and P. Karrer, *ibid.*, **41**, 2293 (1958).

(6) A. R. Battersby, D. A. Yeowell, L. M. Jackman, H. D. Schroeder, M. Hesse, H. Hiltebrand, W. v. Philipsborn, H. Schmid, and P. Karrer, *Proc. Chem. Soc.*, **1961**, 413.

(7) M. Hesse, "Indolakaloide, Teil 1 und 2, Fortschritte der Massenspektrometrie," vol. 1, Verlag Chemie, Weinheim, West Germany, 1974.

(8) H. Asmis, H. Schmid, and P. Karrer, *Helv. Chim. Acta*, **37**, 1983 (1954).

(9) A. R. Battersby and H. F. Hodson, *J. Chem. Soc.*, **1960**, 736.

(10) H. A. Hiltebrand, Dissertation, Zurich, Switzerland, 1964.

(11) R. Verpoorte, P. J. Hylands, and N. G. Bisset, *Org. Magn. Reson.*, **9**, 567 (1977).

ACKNOWLEDGMENTS

The authors thank Dr. A. J. M. Leeuwenberg, Laboratory of Plant Taxonomy and Plant Geography, Agricultural University, Wageningen, The Netherlands, and Professor Dr. F. Sandberg, Department of Pharmacognosy, Uppsala University, Sweden, for collecting and identifying the plant material.

Light-Scattering Studies on Bile Acid Salts I: Pattern of Self-Association of Sodium Cholate, Sodium Glycocholate, and Sodium Taurocholate in Aqueous Electrolyte Solutions

YUNIK CHANG and JOHN R. CARDINAL ˣ

Received March 4, 1977, from the *College of Pharmacy, University of Utah, Salt Lake City, UT 84112.* Accepted for publication May 10, 1977.

Abstract □ The pattern of association of the trihydroxy bile salts in aqueous electrolyte solutions was investigated utilizing the light-scattering technique. The turbidity of the bile salts sodium cholate, sodium taurocholate, and sodium glycocholate was determined over the concentration range of 0–25 mg/ml at 25°. For sodium cholate, the concentration of the supporting electrolyte was varied from 0.15 to 0.5 *M*. For all bile salts in 0.15 *M* electrolyte, the turbidity was determined in sodium fluoride, sodium chloride, sodium bromide, and sodium iodide. Comparison of the light-scattering data with a monomer–micellar model showed that qualitative agreement was obtained; however, quantitative agreement could not be achieved. Further examination of the data showed that the light-scattering results were in good agreement with a model that includes dimers, trimers, and a higher aggregate containing approximately eight monomeric units.

Keyphrases □ Sodium cholate—pattern of association in aqueous electrolyte solutions, light-scattering study □ Sodium glycocholate—pattern of association in aqueous electrolyte solutions, light-scattering study □ Sodium taurocholate—pattern of association in aqueous electrolyte solutions, light-scattering study □ Association—sodium cholate, glycocholate, and taurocholate, pattern in aqueous electrolyte solutions, light-scattering study □ Light scattering—study of pattern of association of sodium cholate, glycocholate, and taurocholate in aqueous electrolyte solutions □ Bile acid salts—pattern of association in aqueous electrolyte solutions, light-scattering study

The mechanism by which bile salts solubilize various solutes such as steroids, fat-soluble vitamins, and drugs has often been described following the model for detergent micelles (1). In this model, it is assumed that a reversible equilibrium exists between monomeric species and micelles. The polydispersity of the micelle is assumed to be quite small. The micelle size is dependent on the nature of the bile salt, *i.e.*, the number of hydroxyl groups and conjugation, as well as on temperature, pH, ionic strength, *etc.* (2).

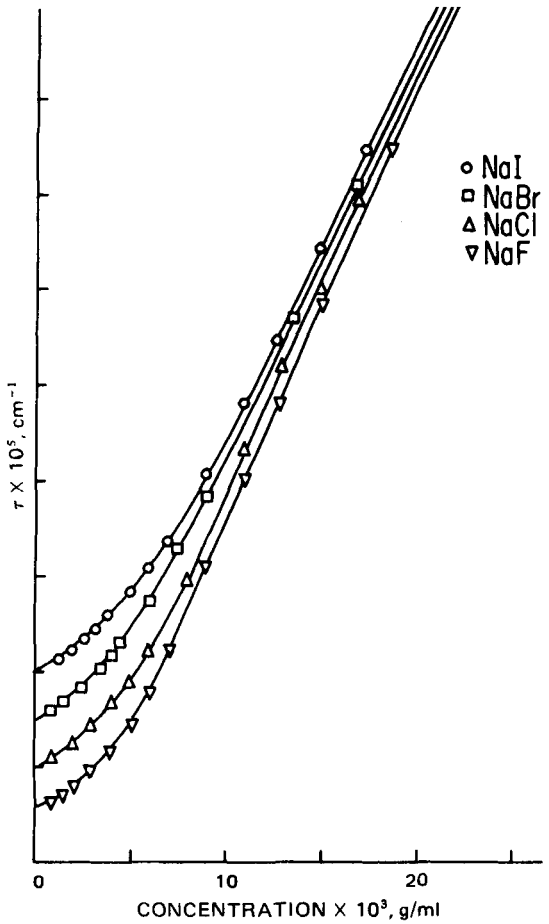

Figure 1—*Plots of the turbidity, τ,* versus *concentration of sodium cholate in 0.15* M *sodium halides. Each division on the ordinate represents 5 × 10^{-5} cm^{-1}. The intercepts representing the turbidity of the solvent are: sodium iodide, 5.98 × 10^{-5} cm^{-1}; sodium bromide, 5.32 × 10^{-5} cm^{-1}; sodium chloride, 5.07 × 10^{-5} cm^{-1}; and sodium fluoride, 4.85 × 10^{-5} cm^{-1}.*

In contrast, other studies (3–6) suggested that the self-association of the bile salts occurs in a stepwise fashion and that various concentration limits for the association process can be defined. The concentration limits are approximately the same for all trihydroxy bile salts, while different limits exist for all dihydroxy bile salts. These concentration limits define regions over which the association process remains relatively constant. Discrete changes in both the nature of the association and the aggregation number are thought to occur at these concentration limits.

Recently, Mukerjee and Cardinal (7) investigated the self-association of the bile salt sodium cholate in water in the absence of added electrolytes. An attempt was made to explain the variation in total naphthalene solubility as a function of the sodium cholate concentration on the basis of various self-association models. Comparison of the sodium cholate solubilization data with solubilization data from a typical micelle-forming system, sodium decanesulfonate, showed clearly that the solubilization process for sodium cholate does not resemble a micellar system. In addition, the solubility data were inconsistent with the reported concentration limit model (3–6).

Mukerjee and Cardinal (7) also concluded that the solubilization data were consistent with a model that requires the existence of dimers and some higher oligomers. More definite conclusions could not be reached because of uncertainties of the assumed models. A similar conclusion about the concentration limit model was also reached by Vitello (8) based on the analysis of light-scattering data.

The purpose of the present study was to examine the self-association pattern of the bile salts. The variation of the light scattered as a function of concentration was obtained for sodium cholate, sodium glycocholate, and sodium taurocholate in 0.15 *M* sodium halides. The effect of electrolyte concentration was determined for sodium cholate. The light-scattering curves were examined in terms of various association models.

EXPERIMENTAL

Materials—Cholic acid[1] was recrystallized according to the method of Hofmann (9). Taurocholic acid and glycocholic acid were synthesized from cholic acid according to the method of Lack *et al.* (10). All bile acids were found to be free of other bile acids by TLC (100-μg spot). In addition, the conjugated acids were found to be free of glycine ethyl ester or taurine by TLC.

In all cases, the sodium salts were obtained by titration of the free acid with sodium hydroxide to pH 10.0 in water. The solid salts were obtained by solvent removal in a flash evaporator followed by overnight drying in a vacuum oven at 45°. All inorganic salts were used as received, except sodium fluoride which was recrystallized from water.

All water was obtained as follows: laboratory distilled water was passed through an ion-exchange column[2], distilled twice from an all-glass still, and stored in all-glass containers.

Apparatus—Light-scattering measurements were made with a light-scattering photometer[3] using the small dissymmetry cell[4] centered in the light beam with four polymer pieces of equal width. These pieces were utilized to align the cell in the light beam by the scored markings on the cell table supplied with the instrument.

Refractive index measurements[5] also were obtained. Temperature control[6] of the refractometer was maintained at 25 ± 0.2°. The pH measurements were made with a digital pH meter[7].

Light-Scattering Measurements—Solutions for the light-scattering measurements were made either by dilution or by direct weighing of the required quantities. All dilutions were made from initial stock solutions adjusted to pH 10.0.

The usual methods employed for the removal of particulate matter from solutions for the light-scattering measurements, such as repeat filtration or ultracentrifugation, were inadequate for this investigation. However, the following procedure yielded particulate-free solutions. A syringe was filled with 50 ml of the solution for measurement, approximately 25 ml of this solution was filtered (0.22-μm filter[8] pore diameter) and saved for future use, and, without removal of the applied pressure, the final portion of the solution was filtered directly into the light-scattering cell. The scattering cell had been cleaned previously in an apparatus of the type designed by Schipmann and Farber (11).

With this technique, scattering ratios reproducible within the ability to read the galvanometer deflection were obtained. This reproducibility was found for both repeat measurements of the same sample and for successive portions of a sample of a given concentration.

The light-scattering measurements were obtained at 436 nm at room temperature, which was close to 25°. The instrument was calibrated routinely with water according to the method of Huisman (12). The value of 4.79 × 10^{-5} cm^{-1} was accepted for the turbidity of water (12). As a check on this calibration method, the turbidity of benzene and carbon tetrachloride was measured using the instrument constant from the described procedure. A value of 2.50 × 10^{-4} cm^{-1} was found for carbon tetrachloride, and 7.71 × 10^{-4} cm^{-1} was obtained for benzene. These values compare very well with those of Coumou (13), who reported 2.48

[1] J. T. Baker Chemical Co., Phillipsburg, N.J.
[2] Model LD-2a, Corning Glass Works, Corning, N.Y.
[3] Brice-Phoenix model BP-2000, Virtis Co., Gardiner, N.Y.
[4] Catalog No. D105, Virtis Co., Gardiner, N.Y.
[5] Brice-Phoenix differential refractometer, model BP-2000-V, Virtis Co., Gardiner, N.Y.
[6] Lauda circulating water bath, model K2-R, Brinkmann Instruments, Westbury, N.Y.
[7] Model 110, Corning Glass Works, Corning, N.Y.
[8] Millipore Filter Corp., Bedford, Mass.

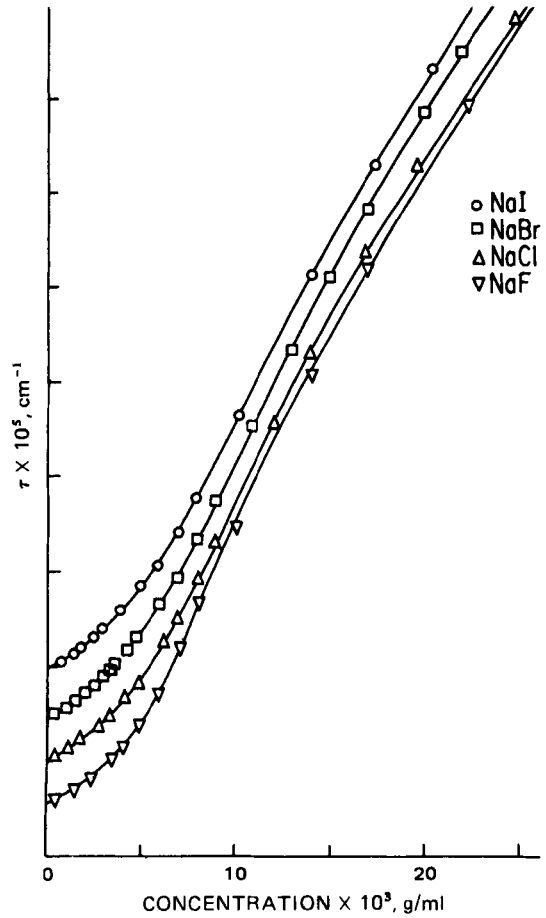

Figure 2—*Plots of the turbidity, τ,* versus *concentration of sodium taurocholate in 0.15* M *sodium halides. The units of the ordinate and the intercepts are the same as in Fig. 1.*

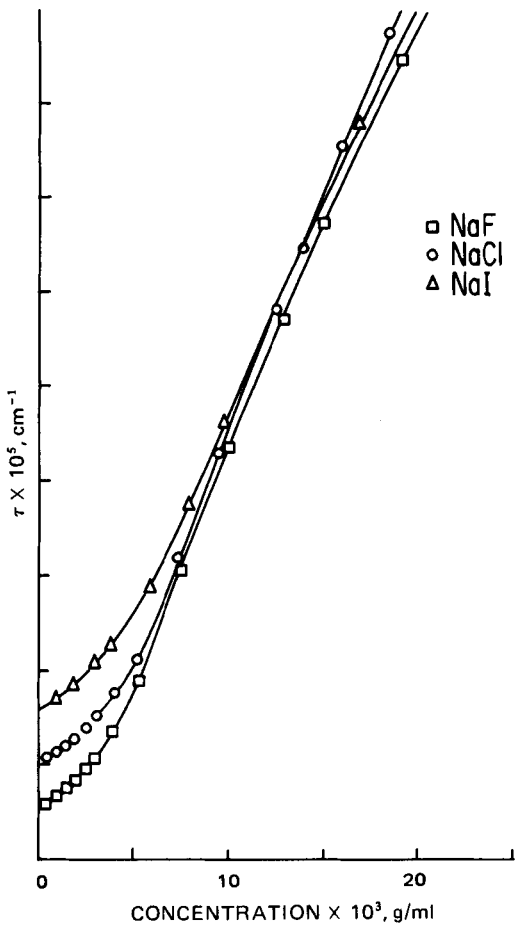

Figure 3—*Plots of the turbidity, τ,* versus *concentration of sodium glycocholate in 0.15* M *sodium halides. The units of the ordinate and the intercepts are the same as in Fig. 1.*

$\times 10^{-4}$ cm^{-1} for carbon tetrachloride and 7.64 $\times 10^{-4}$ cm^{-1} for benzene.

All solutions were checked for dissymmetry, and only solutions showing a dissymmetry of less than 1.03 were utilized. Depolarization and fluorescence of the scattered light were negligible.

RESULTS

The turbidity, τ (in centimeters^{-1}), as a function of the bile salt concentration (in grams per milliliter) for various trihydroxy bile salts in 0.15 *M* sodium halides is shown in Figs. 1–3. Figure 4 is a similar plot for sodium cholate in 0.3 and 0.5 *M* sodium chloride. The refractive increments, *dn/dc*, at a constant electrolyte concentration for the various systems studied are given in Table I. A comparison of the *dn/dc* values reported by previous workers is also included.

DISCUSSION

The results shown in Figs. 1–4 are in qualitative agreement with those found previously (2, 4, 8, 14, 15). The turbidity increased slowly at low concentrations, followed by a relatively rapid increase at higher concentrations. This relatively rapid increase is usually attributed to micelle formation. However, no "kinks" or "breaks" appear in the plots. Thus, as pointed out by Vitello (8), the light-scattering data appear to be inconsistent with the concentration limit model of Ekwall *et al.* (3) and Fontell (4–6).

In the following sections, these data will be compared with the monomer–micelle equilibrium model. It will be shown that these data are in relatively poor agreement with this model. A new model will be described for the association process which yields substantially better agreement with the experimental results.

Monomer–Micelle Equilibrium Model—The usual method for investigating the self-association of the bile salts by light scattering has followed the techniques outlined by Debye (16). This method assumes the existence of a critical micelle concentration (CMC). The concentration of the monomer unit is assumed to increase linearly with concentration below this value and to remain nearly equal to this value above the CMC. These assumptions permitted Debye to derive the following equations, which permit the determination of the molecular weight, M, and the second virial coefficient, B, for the micelle:

$$\frac{H(c - c_0)}{(\tau - \tau_0)} = \frac{1}{M} + 2B(c - c_0) \qquad \text{(Eq. 1}a\text{)}$$

where:

$$H = \frac{32\pi^3 n^2 (dn/dc)^2}{3\lambda_0^4 N_A} \qquad \text{(Eq. 1}b\text{)}$$

and c represents the total concentration (in grams per milliliter), τ represents the total turbidity at concentration c, c_0 and τ_0 are the respective

Table I—Summary of Refractive Index Increments for the Trihydroxy Bile Salts

Solvent	*dn/dc* at 436 nm, ml/g: Sodium Cholate, Present Work	Sodium Taurocholate, Present Work	Sodium Taurocholate, Ref. 8	Sodium Glycocholate, Present Work
0.15 *M* Sodium fluoride	0.191	0.167	0.168	0.189
0.15 *M* Sodium chloride	0.193	0.166	0.172	0.184
0.15 *M* Sodium bromide	0.194	0.164	0.172	—
0.15 *M* Sodium iodide	0.193	0.173	0.165	0.189
0.3 *M* Sodium chloride	0.196	—	—	—
0.5 *M* Sodium chloride	0.197[a]	—	—	—

[a] Vitello (8) found 0.186.

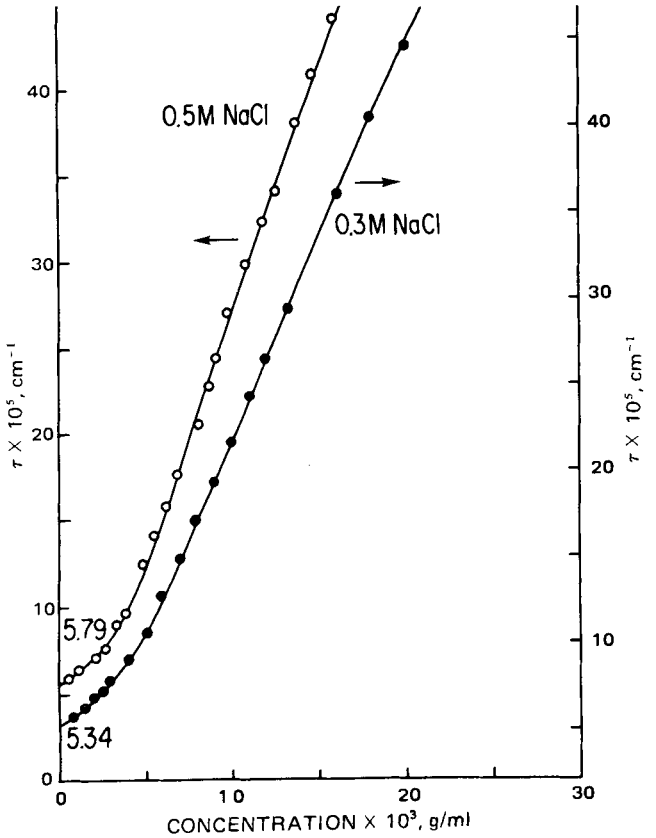

Figure 4—*Plots of the turbidity, τ, as a function of the concentration of sodium cholate in 0.3 and 0.5* M *sodium chloride.*

values at the CMC, n is the refractive index of the solution, dn/dc is the refractive increment at a constant concentration of the supporting electrolyte, λ_0 is the wavelength of light in vacuum, and N_A is Avogadro's number. The micelle molecular weight and the second virial coefficient are obtained from the intercept and slope of a plot of $H(\Delta c/\Delta\tau)$ *versus* Δc.

The equation of Debye is valid for a two-component system containing solvent and uncharged colloidal particles. However, in a three-component system containing, for example, solvent, salt, and charged colloidal particles, the approach of Debye is not totally applicable. Vrij and Overbeek (17) showed that the problem arises from the negative adsorption of the salt on the colloidal particles and that the true molecular weight of the aggregate and the true second virial coefficient can be obtained from the following equations:

$$\frac{H'\,\Delta c}{\Delta\tau} = \frac{1}{\mathrm{M}} + 2B\,\Delta c \qquad \text{(Eq. 2}a\text{)}$$

where:

$$H' = \frac{H(dn/dc_1)^2\mu_s}{(dn/dc_1)^2c_2} \qquad \text{(Eq. 2}b\text{)}$$

where $(dn/dc_1)c_2$ is the same as the refractive increment used in Eq. 1*b* and $(dn/dc_1)\mu_s$ is the refractive increment for the colloid at a constant chemical potential of the supporting electrolyte. For micellar systems, the monomeric surfactant ions are assumed to be a part of the supporting electrolyte (12). The value of $(dn/dc_1)\mu_s$ can be obtained from:

$$\left(\frac{dn}{dc_1}\right)_{\mu_s} = \left(\frac{dn}{dc_1}\right)_{c_2}\left[1 + \frac{(dn/dc_2)c_1}{(dn/dc_1)c_2}\left(\frac{dc_2}{dc_1}\right)_{\mu_s}\right] \qquad \text{(Eq. 3)}$$

where $(dn/dc_2)c_1$ is the refractive increment of the supporting electrolyte and $(dc_2/dc_1)\mu_s$ represents the negative adsorption of the supporting electrolyte on the micellar aggregate. Vrij and Overbeek (17) showed that this latter quantity can be obtained from:

$$\mathrm{M_1}^* = \mathrm{M_1}\left[1 + \frac{(dn/dc_2)c_1}{(dn/dc_1)c_2}\left(\frac{dc_2}{dc_1}\right)_{\mu_s}\right]^2 \qquad \text{(Eq. 4)}$$

where $\mathrm{M_1}^*$ represents the apparent molecular weight of the micelle obtained from Eq. 1*a*. The true molecular weight of the micelle $\mathrm{M_1}$ can be obtained from the intercept of a plot of $\mathrm{M_1}^*$ *versus* $(dn/dc_2)c_1$ according to Eq. 4. This procedure assumes that the negative adsorption is independent of the nature of the co-ion found in solution (12). The usual procedure for obtaining $\mathrm{M_1}$ is to determine $\mathrm{M_1}^*$ from Eq. 1*a* for various halides at a given electrolyte concentration and to plot according to Eq. 4.

Table II—CMC Values for Sodium Taurocholate in 0.15 *M* Sodium Halides at 25°

Salt	CMC, g/ml		
	Present Work	Ref. 8	Ref. 18[a]
Sodium fluoride	0.0040	0.0045	—
Sodium chloride	0.0048	0.0039	0.00141
Sodium bromide	0.0044	0.0045	—
Sodium iodide	0.0047	0.0040	—

[a] At 20°.

Huisman (12) utilized the approach outlined to investigate the micelle molecular weights of sodium alkyl sulfates as a function of electrolyte concentration and showed that the neglect of the negative adsorption effect as in the Debye approach leads to micelle molecular weights that are too low. In addition, Huisman showed (12) that excellent agreement between experimental results and calculated curves can be obtained from Eq. 2*a* and from the following equation, which gives the concentrations of the monomer and micelle:

$$\beta = \frac{f_q c_q}{f_1{}^q c_1{}^q} \qquad \text{(Eq. 5)}$$

where f_q is the activity coefficient of the micelle (assumed to be unity), c_q is the concentration of micelles, f_1 is the activity coefficient of the monomer, c_1 is the monomer concentration, q is the aggregation number, and β is the equilibrium constant. This equation neglects counterion effects on the equilibrium process; however, for the systems investigated here, the concentration of the counterion is large and effectively constant. Therefore, this equation should hold for the systems of interest.

In the present study, the necessary data for application of Eqs. 2*a*–5 to the systems of sodium cholate, sodium taurocholate, and sodium glycocholate in 0.15 *M* sodium halides were obtained. However, for comparison of these systems with the monomer–micelle model, only data for sodium taurocholate will be utilized; the results for the other systems are qualitatively the same.

As discussed previously (7), the value obtained for the CMC in bile salt solutions cannot be defined precisely but largely depends on the range of concentrations utilized in the extrapolation. For example, these investigators (7) found CMC values that differ by almost a factor of two from sodium cholate solubilization data, depending on the range of concentrations used in the extrapolation. This same phenomenon was found for the light-scattering data. This result is due to the high degree of curvature found in the CMC region.

However, if the extrapolations are made using only the lowest concentrations and the concentration range greater than about 8×10^{-3} g/ml, then a fairly consistent set of CMC values for sodium taurocholate can be obtained from the data shown in Fig. 2. These values are given in Table II, along with values obtained by other workers for the same systems. The results obtained in this work are slightly higher than those of Vitello (8) but are within the error of the extrapolation.

With the values obtained for the CMC shown in Table II, the apparent aggregation number and the apparent second virial coefficient for sodium taurocholate micelles were obtained according to Eq. 1*a*. These values are shown in Table III, together with a comparison of values obtained by previous workers. The results obtained in the present study appear to be consistent with those obtained previously.

To determine the extent to which the monomer–micelle model represents the nature of the association of sodium taurocholate, a comparison

Table III—Summary of Aggregation Numbers and Second Virial Coefficients for Sodium Taurocholate Micelles in 0.15 *M* Sodium Halides at 25°

Salt	Aggregation Number		$B \times 10^4$, ml mole/g^2
	Present Work	Ref. 8	
Sodium fluoride	6.0	7.6	0.62
Sodium chloride	5.7	7.1, 4.6[a], 7[b]	0.83
Sodium bromide	5.6	6.7	0.81
Sodium iodide	4.7	5.4	0.75

[a] Reference 2. [b] Reference 19.

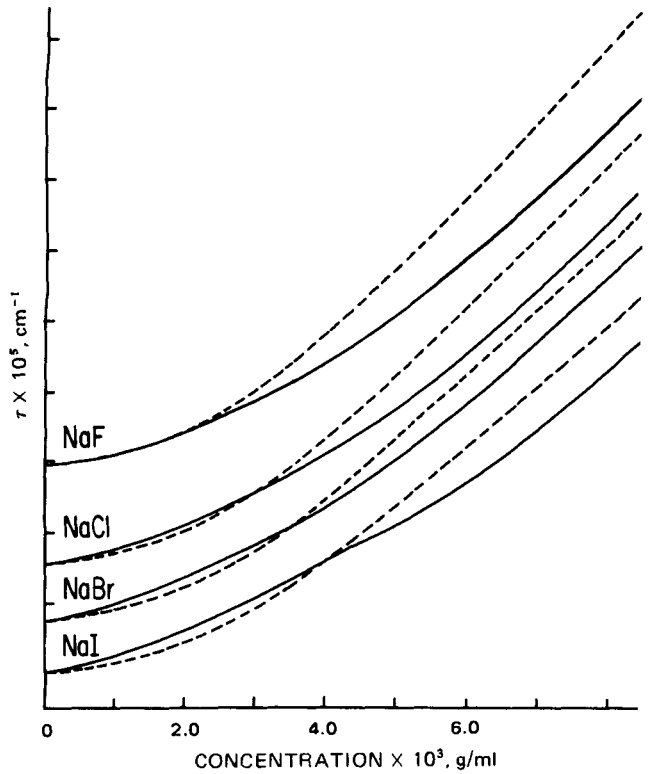

Figure 5—*Comparison of the calculated turbidity (- - -) for sodium taurocholate based on the monomer–micellar model with the experimental curve (—) in the low concentration region. Each division on the ordinate represents* 2×10^{-5} *cm*$^{-1}$.

between the experimental curves and those obtained by calculation according to Eqs. 2*a*–5 was made. The true micelle molecular weight was 3490 according to Eq. 4. This value corresponds to a true aggregation number of 6.49. With the value of $(dc_2/dc_1)\mu_s$ obtained from the plot of Eq. 4, the value of H' for each of the four salt systems was found from Eqs. 2*b* and 3. For the monomer–micelle model, the total concentration of the bile salt is given by:

$$C_T = C_{mon} + q\beta[C_{mon}]^q \qquad \text{(Eq. 6)}$$

where C_{mon} is the concentration of the monomer unit in molar units, q is the aggregation number, and β is the equilibrium constant. The total turbidity for the system is given by:

$$\tau_T = \tau_0 + \tau_{mon} + \tau_{mic} \qquad \text{(Eq. 7)}$$

where τ_0 is the total turbidity of the solvent (water plus electrolyte), τ_{mon} is the turbidity due to the monomer, and τ_{mic} is the turbidity due to the micelle. To calculate the total turbidity at any concentration, C_T, it is only necessary to combine the values obtained from Eqs. 2*a*–6 together with the experimentally measured value for τ_0. The value of β is obtained by fitting one experimental curve. Then all of the remaining values for the various halides can be calculated. It is assumed that the activity coefficient of the monomer is constant in 0.15 *M* sodium halides.

Figure 5 gives a comparison of the experimental and calculated curves for the various halides at a low concentration. Figure 6 shows the comparison for the entire concentration range from 0 to 25×10^{-3} g/ml. In this calculation, 6.5 was taken as the aggregation number, 7.5×10^{-4} mole ml/g^2 was used for the second virial coefficient (average value of those shown in Table III), and 1.23×10^{11} was found for the association constant. Therefore, the only variable among the four different halide systems was the value of H', which was obtained as outlined above.

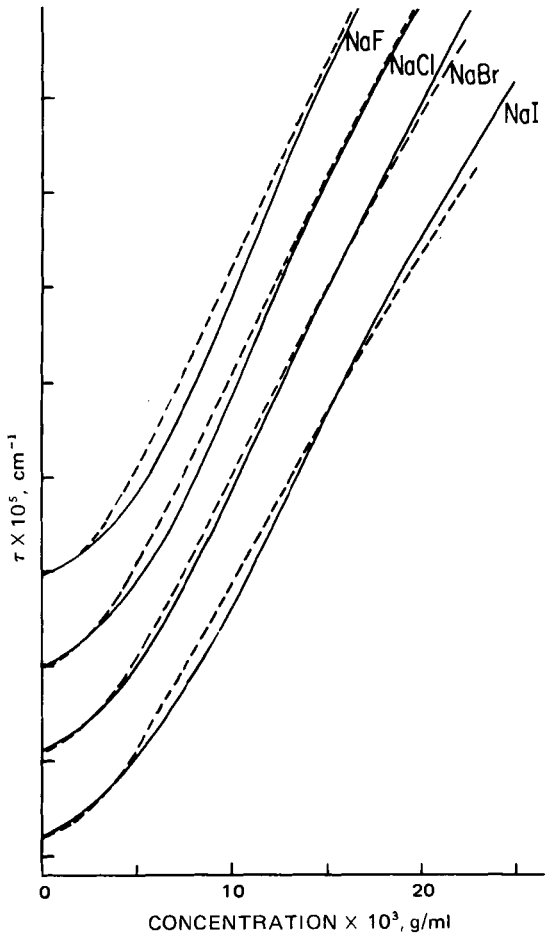

Figure 6—*Comparison of the calculated turbidity (- - -) for sodium taurocholate with the experimental values (—) for the entire concentration range from 0 to* 25×10^{-3} *g/ml. The units of the ordinate are the same as in Fig. 1.*

From Figs. 5 and 6, it can be seen that at very low concentrations, the calculated curves fall below the experimental curves; at intermediate concentrations, the calculated curves are substantially above the experimental values. If other consistent values are chosen for B, q, and β, the regions of disagreement between the calculated and experimental curves will vary. However, it was not possible to obtain a consistent set of parameters that would reproduce the experimental curve assuming the existence of only monomers and a higher oligomer.

This type of comparison between the experimental results and the calculated curves was also made for sodium cholate and sodium glycocholate. A similar trend was obtained in these systems.

Based on these results, it is concluded that qualitative agreement between the calculated curves and the experimental values can be obtained with the monomer–micelle model. That is, the shape of the calculated

Table IV—Equilibrium Constants, Second Virial Coefficients, Molecular Weights, and Aggregation Numbers for Sodium Cholate in 0.15 *M* Sodium Halides

Salt	K_2, liters/mole	K_3, liters/mole	Second Virial Coefficient, ml mole/g^2	Molecular Weight	Aggregation Number
Sodium fluoride	8.5	300	4.0×10^{-3}	3170	7.4
Sodium chloride	6.9	260	5.3×10^{-3}	3110	7.2
Sodium bromide	7.0	300	3.5×10^{-3}	2600	6.0
Sodium iodide	6.5	320	4.6×10^{-3}	2780	6.5
Average or extrapolated values	7.2	293	4.38×10^{-3}	3240	7.63

Table V—Equilibrium Constants, Second Virial Coefficients, Molecular Weights, and Aggregation Numbers for Sodium Taurocholate in 0.15 *M* Sodium Halides

Salt	K_2, liters/mole	K_3, liters/mole	Second Virial Coefficient, ml mole/g^2	Molecular Weight	Aggregation Number
Sodium fluoride	20	240	1.2×10^{-3}	3950	7.4
Sodium chloride	35	310	1.2×10^{-3}	3620	6.7
Sodium bromide	33	350	1.3×10^{-3}	3370	6.3
Sodium iodide	31	240	1.2×10^{-3}	3200	5.9
Average or extrapolated values	30	290	1.22×10^{-3}	4120	7.67

Table VI—Equilibrium Constants, Second Virial Coefficients, Molecular Weights, and Aggregation Numbers for Sodium Glycocholate in 0.15 *M* Sodium Halides

Salt	K_2, liters/mole	K_3, liters/mole	Second Virial Coefficient, ml mole/g^2	Molecular Weight	Aggregation Number
Sodium fluoride	34	240	2.4×10^{-3}	3900	8.0
Sodium chloride	34	200	2.2×10^{-3}	3490	7.2
Sodium iodide	35	190	2.4×10^{-3}	3370	6.9
Average or extrapolated values	34.2	210	2.32×10^{-3}	3930	8.05

curves follows the same trend as the experimental values in that the turbidity increases slowly at low concentrations, followed by a region with curvature, and then increases nearly linearly with concentration. However, with this model, it is not possible to obtain calculated curves that reproduce the experimental results quantitatively throughout the concentration range investigated. This result can only mean that the monomer–micelle equilibrium model does not adequately describe the self-association of the trihydroxy bile salts in aqueous solution. The conclusion is similar to that reached in earlier work based on the solubilization of naphthalene by sodium cholate (7).

Stepwise Association Models—Attwood and Udeala (21, 22) showed that the method of Steiner (20) can be utilized to differentiate between various association models for the self-association of various antihistamines by light-scattering techniques. In the present study, the method of Steiner was applied to gain insight into the self-association of the bile salts.

In this model, aggregate growth is assumed to occur by stepwise addition of monomers to existing monomers or aggregates. The simplest of such schemes is dimerization, which can be represented by:

$$2b_1 \overset{K_2}{\rightleftarrows} b_2$$

Scheme I

and:

$$K_2 = \frac{b_2}{b_1^2} \qquad \text{(Eq. 8)}$$

where b_1 is the monomer concentration, b_2 is the dimer concentration, and K_2 is the association constant for dimerization. Further steps in this process can be written as:

$$b_2 + b_1 \overset{K_3}{\rightleftarrows} b_3$$

$$b_3 + b_1 \overset{K_4}{\rightleftarrows} b_4$$

$$b_{q-1} + b_1 \overset{K_q}{\rightleftarrows} b_q$$

Scheme II

The total equivalent concentration is given by:

$$C_T = b_1 + 2K_2[b_1]^2 + 3K_2K_3[b_1]^3 + \cdots q \prod_2^q K_q[b_1]^q \qquad \text{(Eq. 9a)}$$

$$C_T = \sum q b_q \qquad \text{(Eq. 9b)}$$

The various association constants K_2, K_3, *etc.*, can be obtained by the method developed by Steiner (20). According to this method of analysis, the weight-average molecular weight of the aggregates is related to weight concentration, c (grams per milliliter), by:

$$M/M_w = 1 + d \ln x/d \ln c \qquad \text{(Eq. 10)}$$

where M is the molecular weight of the monomer and x is the weight

Table VII—Equilibrium Constants, Second Virial Coefficients, Association Constants, and Aggregation Numbers for Sodium Cholate in Various Concentrations of Sodium Chloride

Concentration of Sodium Chloride, mole/liter	K_2, liters/mole	K_3, liters/mole	β_q	Second Virial Coefficient, ml mole/g^2	Aggregation Number
0.15	6.9	206	5.2×10^{11}	5.4×10^{-3}	7.2
0.30	16	400	8.3×10^{11}	1.4×10^{-3}	6.4
0.50	10	330	7.2×10^{11}	2×10^{-3}	8.9

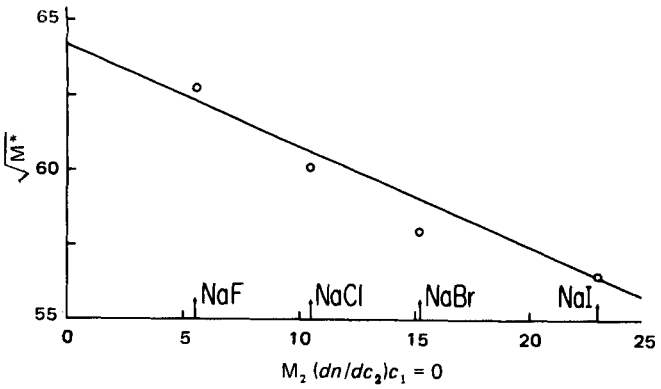

Figure 7—*Plot for the determination of true molecular weight of the high aggregate for sodium taurocholate.*

fraction of species existing as monomeric units. The value of M_w is obtained by application of the equation:

$$\frac{Hc}{\Delta\tau} = \frac{1}{M_w} + 2Bc \qquad \text{(Eq. 11)}$$

in which it is assumed that the second virial coefficient can be neglected. The parameter $\Delta\tau$ represents the excess turbidity of the solution over the solvent. The weight fraction of the monomer can be obtained by graphical integration according to:

$$\ln x = \int_0^c [(M/M_w) - 1] d \ln c \qquad \text{(Eq. 12)}$$

The equilibrium constants can be obtained from:

$$\frac{[(M_w/xM) - 1]}{(xc/M)} = 4K_2 + 9K_2K_3(xc/M) \cdots + q^2 \prod_2^q K_q(xc/M)^{q-2} \qquad \text{(Eq. 13)}$$

where K_2 is obtained from the intercept and K_3 is obtained from the slope of the plot of the data according to Eq. 13. Higher association constants can be obtained by successive application of this equation.

Application of Eq. 13 to the light-scattering data for the bile salts sodium cholate, sodium taurocholate, and sodium glycocholate in 0.15 *M* sodium halides leads to a consistent set of values for K_2 and K_3 (Tables IV–VI). For each bile salt in the various halides, the values of K_2 and K_3

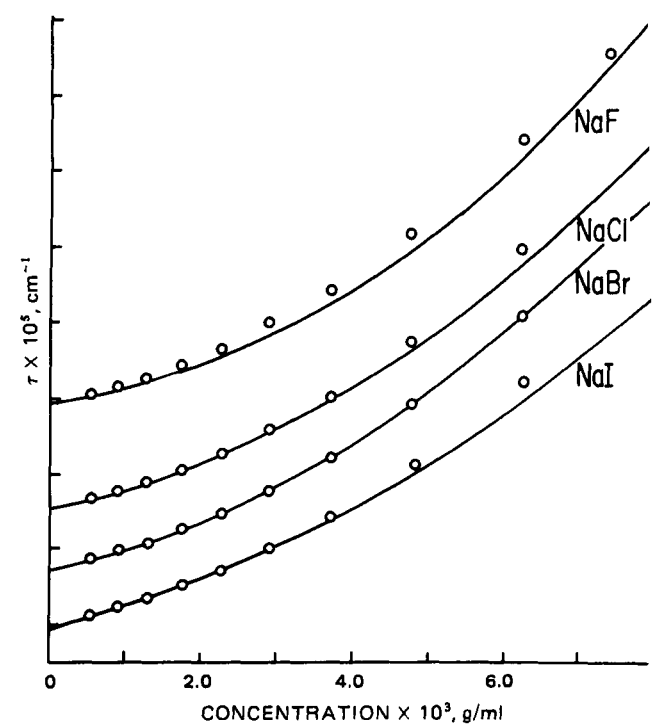

Figure 8—*Comparison of the experimental curves (—) for sodium taurocholate with the calculated values (O) based on the model depicted by Eq. 14b. The units of the ordinate are the same as in Fig. 5.*

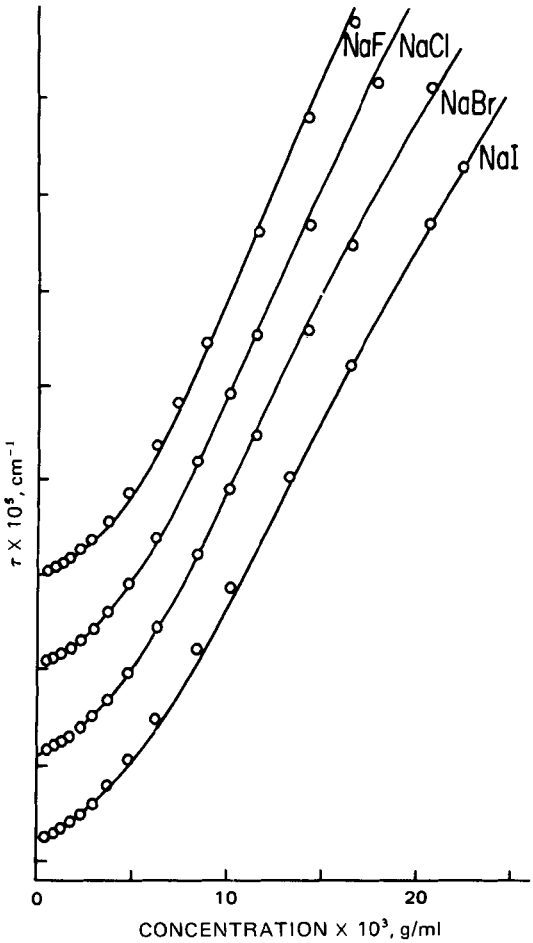

Figure 9—*Comparison of the experimental curves (—) for sodium taurocholate with the calculated values (O) based on the model depicted by Eq. 14b for the entire concentration range from 0 to 25 × 10^{-3} g/ml. The units of the ordinate are the same as in Fig. 1.*

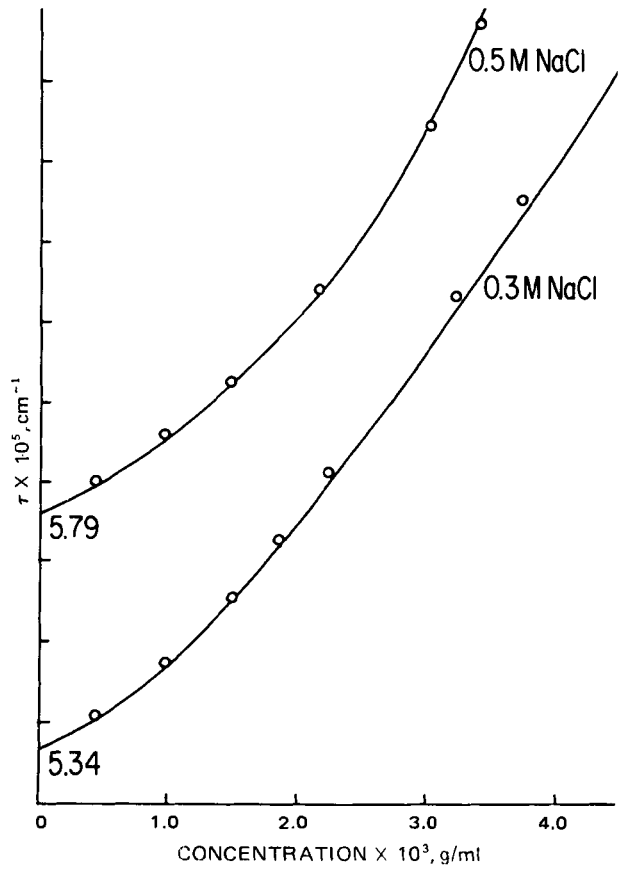

Figure 10—*Comparison of the experimental curves (—) for sodium cholate in 0.3 and 0.5 M sodium chloride with the calculated values (O) based on the stepwise association model depicted by Eq. 14b. Each division of the ordinate represents 1 × 10^{-5} cm^{-1}.*

are nearly the same. However, when Eq. 13 was extended to obtain a value for K_4, the initial slopes of these plots were always nearly zero. At higher values of xc/M, the plots tend to increase rapidly. This result was interpreted to indicate that the value of K_4 must be small relative to the lower association constants and, therefore, that the stability of the tetramer is small with respect to that of the dimer and trimer. On the other hand, the rapid increase of the plots at higher values of xc/M suggests that aggregates larger than the trimer must exist in solution.

To determine the size and association constants for these higher aggregates, the procedure as outlined is not applicable since reliable estimates of K_4, K_5, *etc.*, cannot be obtained. However, based on the qualitative agreement between the experimental results and the monomer–micellar model discussed previously, as well as the results mentioned here, it seems reasonable to assume that higher aggregates must exist. This assumption suggests that the total equivalent concentration, C_T, for the trihydroxy bile salts may follow a model given by:

$$C_T = b_1 + 2b_2 + 3b_3 + qb_q \qquad \text{(Eq. 14a)}$$

$$C_T = b_1 + 2K_2b_1^2 + 3K_2K_3b_1^3 + q\beta_q b_1^q \qquad \text{(Eq. 14b)}$$

where b_1, b_2, b_3, and b_q represent the concentrations of monomer, dimer, trimer, and higher aggregate at the total concentration C_T, respectively; q is the average aggregation number of the higher aggregate; and β_q is the average overall association constant for the formation of b_q as defined by Eq. 9a. The concentration of intermediate-sized aggregates is assumed to be small.

To test this model against the experimental results, it was necessary to develop a method by which the average size of this higher aggregate could be determined. A somewhat similar question was addressed previously by Mysels and Princen (23) in their considerations of light scattering by sodium lauryl sulfate. For this system, the monomeric ions of sodium lauryl sulfate were thought to exist in equilibrium with lauryl sulfate dimers below the CMC (24). To take this effect into account, Mysels and Princen utilized the Debye treatment to obtain the apparent micelle molecular weight. However, it was assumed that the turbidity at the CMC could be calculated to be that due to the solvent, monomers, and dimers.

In the analysis of the light-scattering data for the bile salts according to the model depicted by Eq. 14*b*, a procedure similar to that of Mysels and Princen (23) was followed. However, because of the expected low aggregation number of the higher aggregate, certain alternatives were adopted. An assumption inherent in the law of mass action when applied to micellar systems (Eq. 5) is that the monomer activity must increase with an increase in total concentration (25). This increase in activity is related to the weight average degree of association and would be expected to be significant for aggregates as small as 7–8-mers (25).

In the present systems, this increase in activity can be obtained directly from application of Eq. 12, assuming that the activity coefficients are constant. Therefore, at any C_T, the concentration of monomer is known, allowing calculation of the total turbidity due to monomers, dimers, and trimers at that C_T according to Eq. 11. In the same way, the total concentration of these species at any given C_T can be calculated. Thus, the apparent molecular weight of the higher aggregate can be obtained from:

$$\frac{H(c - c_0')}{(\tau - \tau_0')} = \frac{1}{M} + 2B(c - c_0') \qquad \text{(Eq. 15)}$$

where $c_0' = b_1 + 2K_2b_1^2 + 3K_2K_3b_1^3$ and $\tau_0' = \tau_0 + \tau_{mon} + \tau_{dimer} + \tau_{trimer}$.

Application of Eq. 15 to the light-scattering results leads to the aggregation numbers and second virial coefficients for the higher aggregates (Tables IV–VI).

To apply the corrections suggested by Vrij and Overbeek (17) to this analysis, it is necessary to assume that all low molecular weight aggregates can be taken to be a part of the supporting electrolyte in the same way as the monomers are assumed to be a part of the supporting electrolyte in the treatment of the micellar model (12). This assumption seems justifiable since the small aggregates are of the same charge as the micelles and, therefore, should be excluded effectively from the double layer of

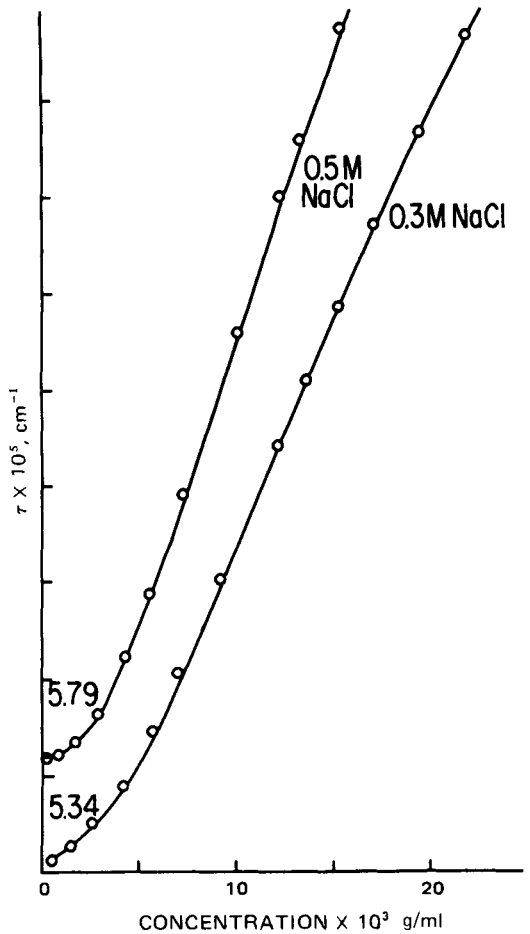

Figure 11—*A plot similar to Fig. 10 for the entire concentration range of 0–25 × 10^{-3} g/ml. The units of the ordinate are the same as in Fig. 1.*

the micelle. This implies that the concentration fluctuations of these aggregates should be independent of micellar fluctuations. Based on this assumption, the true micelle molecular weight was obtained according to Eq. 4. A plot of these data for sodium taurocholate is shown in Fig. 7. The true molecular weights and aggregation numbers obtained for all three bile salts studied are given in Tables IV–VI.

A comparison of the experimental results for sodium taurocholate with the values calculated according to Eqs. 14*b* and 15 is shown in Figs. 8 and 9. For this calculation, the turbidity of the low aggregates was obtained as described earlier. The turbidity of the higher aggregates was obtained in an analogous manner to that used for the high aggregate in the monomer–micelle model. The value of $q\beta_q$ used in fitting the data was 5.5 × 10^{14}. By comparison with Figs. 5 and 6, which give model calculations for the monomer–micelle model, it can be seen that the correlation of this model with the experimental results has improved substantially. In contrast to the monomer–micelle model, no systematic variations exist between the calculated values and the experimental results.

Calculations performed in this manner represent a severe test of the model since average values of K_2, K_3, $q\beta_q$, and B obtained from all four halides were utilized. If, for example, the individual values for each system shown in Table V are utilized, the agreement between the experimental and the calculated curves is much better. This point is further proof of the validity of the assumed model.

Similar correlations between experimental results and calculated values can be obtained for sodium cholate and sodium glycocholate. The values used are shown in Tables IV and VI.

Based on these results, it can be concluded that the self-association of the trihydroxy bile salts in 0.15 *M* sodium halides is best described by a model that assumes the existence of monomers, dimers, trimers, and a higher aggregate containing approximately eight monomeric units. The size of the higher aggregate is not markedly dependent on the bile salt. The only marked difference between the three bile salts appears to be in the value of the dimerization constant, the value for sodium cholate being substantially smaller than that for sodium taurocholate and sodium glycocholate. This result could arise from a decrease in the degree of overlap of the electrical double layers because of the increased length of the side chain of the conjugated bile salts. On the other hand, these effects are not noted in the trimerization constants where charge repulsion would be expected to be greater. This effect may be due to the particular arrangement of the various species in the trimer, which is not known at present.

Effects of Ionic Strength—The effects of ionic strength on the self-association of sodium cholate were studied to a limited extent. For this study, light-scattering curves for sodium cholate in 0.3 and 0.5 *M* sodium chloride were obtained. These results were analyzed according to the methods outlined. However, since data were obtained only in sodium chloride, the more complete analysis according to the method of Vrij and Overbeek (17) cannot be applied. Therefore, the molecular weights and aggregation numbers obtained must be considered to be apparent values, uncorrected for effects due to negative adsorption. The values obtained for K_2, K_3, and the aggregation numbers are shown in Table VII. The calculated values, together with the experimental curves, are shown in Figs. 10 and 11. The agreement between the calculated curves and the experimental values is excellent.

Based on these results, it appears that the pattern of association of sodium cholate is relatively unaffected by changes in the ionic strength of the medium. A comparison of these results with those obtained in 0.15 *M* sodium chloride suggests that the average size of the aggregate might increase slightly with an increase in the ionic strength. This effect is difficult to confirm, however, since the aggregation number is smaller in 0.3 *M* sodium chloride as compared to 0.15 *M* salt. This result may, however, be due to the relatively high values of K_2 and K_3 obtained in 0.3 *M* sodium chloride. This latter result is probably related to experimental difficulties.

REFERENCES

(1) D. M. Small, in "The Bile Acids," vol. 1, P. P. Nair and D. Kritchevsky, Eds., Plenum, New York, N.Y., 1971, chap. 8.

(2) D. M. Small, *Adv. Chem. Ser.*, **84**, 31 (1968).

(3) P. Ekwall, K. Fontell, and A. Sten, *Proc. Int. Congr. Surf. Act., 2nd*, **1957**, 397.

(4) K. Fontell, *Kolloid Z.-Z. Polym.*, **244**, 246 (1971).

(5) *Ibid.*, **244**, 253 (1971).

(6) *Ibid.*, **250**, 333 (1972).

(7) P. Mukerjee and J. R. Cardinal, *J. Pharm. Sci.*, **65**, 882 (1976).

(8) L. B. Vitello, Ph.D. thesis, Clarkson College of Technology, Potsdam, N.Y., 1973.

(9) A. F. Hofmann, *Acta Chem. Scand.*, **17**, 173 (1963).

(10) L. Lack, F. O. Dorrity, Jr., T. Walker, and G. D. Singletary, *J. Lipid Res.*, **14**, 367 (1973).

(11) R. H. Schipmann and E. Farber, *J. Polym. Sci.*, **B1**, 65 (1963).

(12) H. F. Huisman, *Konik. Ned. Akad. Wetenschap. Proc. Ser.*, **B67**, 367, 376, 388, 407 (1964).

(13) D. J. Coumou, *J. Colloid Sci.*, **15**, 408 (1960).

(14) J. P. Kratohvil and H. T. DelliColli, *Can. J. Biochem.*, **46**, 945 (1968).

(15) P. DeMoerloose and R. Ruyssen, *J. Pharm. Belg.*, **14**, 95 (1959).

(16) P. Debye, *J. Phys. Colloid Chem.*, **51**, 18 (1947).

(17) A. Vrij and J. T. G. Overbeek, *J. Colloid Sci.*, **17**, 570 (1962).

(18) M. C. Carey and D. M. Small, *J. Colloid Interface Sci.*, **31**, 382 (1969).

(19) T. Furasawa, *Fukuoka Acta Med.*, **53**, 124 (1962).

(20) R. F. Steiner, *Arch. Biochem. Biophys.*, **39**, 333 (1952).

(21) D. Attwood and O. K. Udeala, *J. Phys. Chem.*, **79**, 889 (1975).

(22) D. Attwood and O. K. Udeala, *J. Pharm. Sci.*, **65**, 1053 (1976).

(23) K. J. Mysels and L. H. Princen, *J. Phys. Chem.*, **63**, 1649 (1959).

(24) P. Mukerjee, K. J. Mysels, and C. I. Dulin, *ibid.*, **62**, 1390 (1958).

(25) P. Mukerjee, *J. Pharm. Sci.*, **63**, 972 (1974).

ACKNOWLEDGMENTS

Abstracted in part from a dissertation submitted by Y. Chang to the University of Utah in partial fulfillment of the Doctor of Philosophy degree requirements.

Financial support by the University of Utah Research Committee is gratefully acknowledged.

Simple, Rapid, and Micro High-Pressure Liquid Chromatographic Determination of Endogenous "True" Creatinine in Plasma, Serum, and Urine

WIN L. CHIOU ˣ, M. A. F. GADALLA, and GEOFFREY W. PENG

Received February 4, 1977, from the *Clinical Pharmacokinetics Laboratory and Department of Pharmacy, College of Pharmacy, University of Illinois at the Medical Center, Chicago, IL 60612.* Accepted for publication June 1, 1977.

Abstract □ Previously published methods for endogenous creatinine levels in plasma, serum, or urine lack specificity or are subject to interferences from endogenous or exogenous substances. The developed simple, rapid, and specific high-pressure liquid chromatographic method includes the novel deproteinization and extraction of 1 volume of plasma or serum with 2.5 volumes of acetonitrile and also of 1 volume of urine with 40 volumes of a 20% water–80% acetonitrile solution. An aliquot of the supernate is then injected directly into the chromatograph. A cation-exchange column and acidified (0.02% of 85% phosphoric acid) 0.1 *M* ammonium phosphate solution as the mobile phase, with a flow rate of 2 ml/min, were used. Creatinine, with a retention time of 3.8 min, was monitored *via* its UV absorption at 215 nm. Both peak height and integrated area methods of quantitation yielded the same results. Several methods were employed to show that the "suspected" creatinine peak from plasma samples was due entirely to the "true" creatinine. No interference was found in samples obtained from normal and renal patients. The day-to-day variation in the detector response was small. Each assay requires only about 5 min for completion. Ten microliters of plasma or serum or 1 μl of urine is sufficient for analysis.

Keyphrases □ Creatinine—high-pressure liquid chromatographic analysis in biological fluids □ High-pressure liquid chromatography—analysis, creatinine in biological fluids

Accurate measurements of endogenous creatinine levels in plasma, serum, or urine are important in the monitoring of renal function and dosage regimen modifications in patients with renal insufficiency (1–16). Although determinations of creatinine levels have been performed routinely in hospitals and clinics for decades, attempts to improve the assay have appeared continuously since the introduction of the Jaffe alkaline picrate reaction (17).

BACKGROUND

The Jaffe alkaline picrate method, with various modifications, is still the most widely used procedure for creatinine quantitation (18–23). Its nonspecificity and interferences by endogenous and exogenous noncreatinine chromogens have been well documented (24–27). It has been recommended that a factor of 0.7 be used to calculate the measured "apparent" creatinine value so as to obtain the "true" endogenous creatinine value (1, 2, 28). The degree of such interferences by noncreatinine chromogens was reported to be decreased as the creatinine level increased (29).

In attempting to measure directly the true creatinine in plasma or serum and to avoid interferences by other chromogens, Yatzidis (27, 30) recently developed a method based on the absorbance difference measured at 500 nm of plasma or serum samples after reaction with picrate reagents buffered at pH 9.65 and 11.50. The sample required for the assay is 0.1 or 0.2 ml. One obvious drawback is that the reaction with the picrate reagents alone takes 45–60 min. The author's claim of noninterferences, however, could not be substantiated in this laboratory since absorbances or recoveries of the spiked creatinine in 5% (w/v) human albumin solution and normal plasma were lower than the predicted values based on the standard curve constructed from aqueous creatinine solutions (31). Further studies in this laboratory on plasma samples from eight renal patients showed that the interferences ranged from 20 to 44%.

Another method involves the use of a cation-exchange membrane to remove proteins and interfering substances from serum samples and the subsequent reaction of creatinine desorbed from the membrane with the alkaline picrate (32). This method requires 0.4 ml of serum and would probably take about 30 min for each assay. Acetoacetate and possibly some other interfering substances are not removed. Therefore, interferences occur at least in samples from ketotic patients (32).

A reaction kinetic assay for serum and urine creatinine, using the Jaffe reaction but without deproteinization, was reported to be simple and reliable and to require only 0.5–2 min (33). The serum sample required per test is 0.2 ml. One drawback is that the interference from compounds with a similar or identical reaction rate cannot be detected. Furthermore, accuracy for samples from renal patients has not been demonstrated.

A kinetic enzymatic method for the determination of serum creatinine was recently reported (34). It requires 0.25 ml of serum and takes about 10 min for each assay. It was claimed to be subject to few or no interferences. Preparation and stability (34) of the reagent, which consisted of nine components, appear to be the disadvantages. The applicability of the method to plasma and urine samples was not studied. Furthermore, the accuracy and reproducibility of measurements for concentrations below 1 mg % were not reported. Serum creatinine levels in normal infants often might be as low as 0.5 mg %.

Apparently, none of these cited investigations presented convincing experimental evidence that the absorbances measured after reaction with various reagents were indeed entirely due to the true creatinine. Presence of interfering substances, endogenous or exogenous, can hardly be detected by the specific assays employed during analysis.

Accuracy and precision in measurements of creatinine levels in plasma, serum, and/or urine are critical to the correlation between renal function and renal clearance or biological drug half-life. It is reasonable to speculate that the poor or unpredictable correlation of certain drugs (35, 36) may be caused partly by the creatinine assay problem.

This paper reports a simple, rapid, specific, reliable, and micro high-pressure liquid chromatographic (HPLC) method developed for the determination of the endogenous "true" creatinine in plasma, serum, and urine. The method also is likely to be subject to fewer interferences by other noncreatinine substances than any other creatinine assay published previously. Evidence that the concentration measured was due entirely to the true creatinine also will be presented.

EXPERIMENTAL

Materials—Creatinine[1], ammonium phosphate[1], and phosphoric acid (85%) were reagent grade and were used without further purification. Glass-distilled acetonitrile[2], methanol[2], and distilled water were used.

Preliminary Spectrophotometric Studies—To study the feasibility of using the UV detector directly for creatinine quantitation by the HPLC method, the UV spectra of creatinine in possible mobile phases such as water and acidified 0.1 *M* ammonium phosphate (pH 2.6) containing 0.02% (v/v) phosphoric acid were obtained with a UV–visible recording spectrophotometer[3].

HPLC System—The system consisted of a solvent delivery pump[4], a sample injection valve[5], a variable wavelength detector[6], a variable span potentiometric 12.7-cm (5-in.) recorder[7], and an electronic integrator[8]. Unless otherwise specified, a 30-cm cation-exchange column[9], acidified 0.1 *M* ammonium phosphate as the mobile phase, a wavelength of 215 nm for the absorbance monitoring, and a chart paper speed of 30.5 cm

[1] Fisher Scientific Co., Fair Lawn, N.J.
[2] Burdick and Jackson Laboratories, Muskegon, Mich.
[3] Model 200, Perkin-Elmer Corp., Norwalk, Conn.
[4] Model M-6000 A, Waters Associates, Milford, Mass.
[5] U6K injector, Waters Associates, Milford, Mass.
[6] Model LC-55, Perkin-Elmer Corp., Norwalk, Conn.
[7] Laboratory Data Control, Riviera Beach, Fla.
[8] Autolab Minigrator, Spectra-Physics, Santa Clara, Calif.
[9] Partisil PXS 10/25 SCX, Whatman Inc., Clinton, N.J.

(12 in.)/hr were used. Short sections of the narrow diameter stainless steel tubing and Swageloks connected the column to the injection valve and the detector. The flow rate was set at 2 ml/min, and the study was conducted at ambient temperature.

Peak heights and relative areas under the curves obtained from the digital integrator were used to construct standard curves and to measure creatinine concentrations in biological samples. Degassing of the mobile phases was unnecessary. The retention times of creatinine from aqueous creatinine solutions and plasma or urine samples spiked with creatinine after treatment with acetonitrile (to be described later) were all identical (3.8 min). Unspiked plasma, serum, and urine samples from human subjects also yielded creatinine peaks with the identical retention time.

Standard Curves of Creatinine in Water—Because of the large difference of creatinine levels in plasma (or in serum) and urine, slightly different methods were used to prepare samples for the HPLC study. To study the recovery of the spiked creatinine in plasma and urine, it was necessary to establish standard curves of creatinine in water with the same procedures used for the plasma and urine creatinine analysis.

For the plasma creatinine study, the following standard solutions of creatinine in water were prepared: 0.5, 1.0, 2.0, 4, 6, 8, 10, 15, and 20 mg %. In a 13 × 100-mm culture tube, 0.2 ml of the standard solution was mixed with 0.5 ml of acetonitrile, and 50 μl of the mixture (solution) was then injected directly into the chromatograph.

For the urine creatinine study, the following standard creatinine solutions in water were prepared: 50, 100, 200, 300, and 400 mg %. In the same type of culture tube, 0.1 ml of the standard solution was mixed with 4 ml of 20% (v/v) water–80% acetonitrile solution in a vortex mixer[10]; 10 μl of the resultant solution was then injected directly into the chromatograph for creatinine determination.

Standard Curves of Creatinine in Spiked Plasma—Aliquots of 0.2 ml of plasma[11] were pipetted into 13 × 100-mm culture tubes and spiked with concentrated aqueous creatinine stock solutions (100, 200, and 1000 mg %) to yield 2, 4, 6, 8, 10, 15, and 20 mg % of the spiked creatinine in the plasma. To each tube, 0.5 ml of acetonitrile was added (mainly for deproteinization). Then the mixture was vortexed for a few seconds and centrifuged at 2000 rpm for about 1 min. Fifty microliters of the supernate was injected directly into the chromatograph for creatinine analysis. A plasma sample without the spiking of additional creatinine also was analyzed similarly as a control.

Standard Curves of Creatinine in Spiked Urine—Aliquots of 0.1 ml of freshly voided urine from a normal adult were pipetted into 13 × 100-mm culture tubes and spiked with various volumes of the aqueous creatinine stock solution (1 g %) to obtain concentrations of 50, 100, 200, 300, and 400 mg % of the spiked creatinine. To each tube, 4 ml of the 20% water–80% acetonitrile solution was added. Then the mixture was vortexed for a few seconds and centrifuged, and 10 μl of the supernate was injected into the chromatograph. One urine sample without spiking of additional creatinine also was studied as a control.

Evidence of Creatinine in Plasma as Measured by HPLC Assay—Several tests were performed to show that the HPLC peak with a retention time of 3.8 min obtained from human plasma samples was attributed to creatinine alone: (*a*) comparison of HPLC peak characteristics obtained from the aqueous creatinine solution and plasma sample using a reversed-phase-type column[12] and various combinations of methanol–water as the mobile phase, (*b*) comparison of HPLC peak characteristics obtained from the aqueous creatinine solution and plasma sample using the cation-exchange column[9] and acidified 0.1 *M* ammonium phosphate as the mobile phase, and (*c*) comparison of HPLC peak heights and areas obtained at 215 and 233 nm from the aqueous creatinine solution and plasma sample using the cation-exchange column and acidified 0.1 *M* ammonium phosphate as the mobile phase.

Reproducibility Studies—Plasma samples from one normal and two renal patients and urine samples from three normal subjects were assayed for creatinine concentrations in six duplicates at the same time, using 0.2 ml of plasma and 0.1 ml of urine. A plasma sample also was analyzed seven times during 3 weeks. The sample was frozen between analyses.

RESULTS AND DISCUSSION

In all previously published methods, creatinine levels in biological samples, with or without further isolation and purification, were not measured directly by spectrophotometry. Such a quantitation method is obviously the simplest one in any HPLC method. The UV spectrum of 2 mg % creatinine in water was run (Fig. 1), and peak absorption wavelengths at 234 and 201 nm were found.

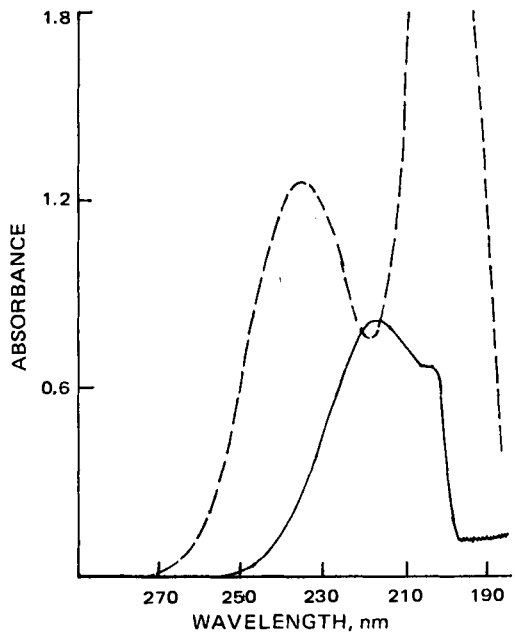

Figure 1—*UV spectra of 2 mg % creatinine in water (- - -) and in acidified 0.1* M *ammonium phosphate (—).*

In the preliminary studies using the reversed-phase column[12] and various combinations of the methanol–water system as the mobile phase, injections of aqueous creatinine solutions with concentrations clinically encountered all resulted in distinct peaks on chromatograms when monitored at 234 nm. Unfortunately, the resolution was not satisfactory with the plasma samples deproteinized with acetonitrile as described under *Experimental.* The best resolution was obtained when 50% methanol–50% water was used as a mobile phase. A typical chromatogram is shown in Fig. 2. It is possible that other solvent systems or other types of the reversed-phase column may yield satisfactory resolution.

Since creatinine is a weak base with a K_b value of 3.57×10^{-11} at 40° (37), it seems logical to use a cation-exchange column[9]. A pH of 2.6 was chosen for the aqueous mobile phase since most creatinine would be in the ionic form. As expected, water acidified with phosphoric acid [about 0.02% (v/v)] as a mobile phase resulted in an almost total retention of creatinine. Addition of ammonium phosphate to the acidified mobile phase reduced the creatinine retention time. Acidified 0.1 *M* ammonium phosphate produced satisfactory resolution with a reasonably short retention time (3.8 min). Chromatograms from the spiked and unspiked plasma of a normal subject and from unspiked plasma of two renal patients are shown in Fig. 3.

Creatinine is very soluble in water and insoluble in most water-immiscible organic solvents (37). Therefore, purification and isolation by the classical extraction method appear to be impossible. The use of the water-miscible acetonitrile with an acetonitrile–plasma or serum ratio of 2.5, as employed in the present study, serves three major functions: (*a*) solubilization of creatinine in the supernate, (*b*) deproteinization of plasma or serum samples, and (*c*) salting out of inorganic or organic salts from plasma or serum samples.

Although creatinine is not soluble in pure acetonitrile, creatinine from concentrated aqueous solutions would not precipitate after mixing with 2.5 volumes of acetonitrile. The efficiency of deproteinization was tested by mixing the supernate with equal or larger volumes of 15% trichloroacetic acid. In no case was precipitation observed, indicating the completeness of the deproteinizing process.

To study the possible precipitation problem that might take place in the column and subsequently damage or block the column (38), 100 μl of the supernate was injected into the mobile phase in beakers. Again, no precipitation was visible, indicating the decreased likelihood of precipitation and column clogging after prolonged use. In fact, the resolution and retention time of creatinine remained unchanged after more than 1000 injections. The postulation of possible salting out or precipitation of organic or inorganic salts from biological samples after treatment with acetonitrile is supported by the fact that precipitation occurred after

[10] Vortex Genie, Fisher Scientific Co., Fair Lawn, N.J.
[11] Obtained from the University Hospital Blood Bank.
[12] ODS Sil-X-1, Perkin-Elmer Corp., Norwalk, Conn.

Table I—Linearity of Creatinine in Plasma Based on Peak Area and Peak Height Methods

Number[a]	Spiked Creatinine Concentration, mg %	Peak Area (Arbitrary Units)	Response Factor[b]	Peak Height, cm	Response Factor[c]
1	0	2.438	—	1.30	—
2	0.5	3.443	2.01	1.90	1.20
3	1.0	4.464	2.03	2.45	1.15
4	1.5	5.341	1.94	3.00	1.13
5	2.0	6.171	1.88	3.59	1.15
6	0	1.757	—	1.05	—
7	2.0	5.588	1.92	3.35	1.15
8	4.0	10.315	2.14	5.65	1.15
9	6.0	14.022	2.04	7.35	1.05
10	8.0	17.616	1.98	10.25	1.15
11	10.0	21.702	2.00	13.00	1.19
12	15.0	33.472	2.01	19.25	1.21
13	20.0	41.907	2.01	24.10	1.15
		Average	2.00		1.15
		SD	0.07		0.04
		CV	3.44%		3.70%

[a] Two sources of plasma samples were used for Numbers 1–5 and 6–13, respectively. [b] Response factor = (peak area from spiked samples − peak area from unspiked samples)/(spiked creatinine concentration). [c] Response factor = (peak height from spiked samples − peak height from unspiked samples)/(spiked creatinine concentration).

mixing the normal phosphate buffer solution (pH 7.4) with the same ratio of acetonitrile. Trichloroacetic acid is probably the most widely used deproteinizing agent. After the addition of the concentrated aqueous solution (10–30%) to the plasma or serum sample, the mixture is usually centrifuged or filtered and the supernate or filtrate is then neutralized with a certain amount of base. Plasma or serum samples also are commonly deproteinized by the addition of sodium tungstate solution and subsequent neutralization with acid.

Compared with these two common methods, the acetonitrile method is much simpler and faster. Acetonitrile is chemically much more inert and is also expected to cause less interferences in quantitation by the various analytical detection methods. Furthermore, plasma or serum samples after treatment with trichloroacetic acid or tungstate and acid were very turbid. Centrifugation at 2000 rpm for 1 min in both methods failed to produce a clear supernate. On the other hand, addition of acetonitrile and subsequent vortexing for a few seconds resulted in a clear supernate, with precipitates settling in the bottom of the tube and forming a hard cake. Centrifugation for 1 min would ensure the supernate to be free of particles, and the supernate could then easily be poured to another tube if required.

Therefore, it is concluded that acetonitrile is an ideal deproteinizing agent. Its use in deproteinization for the direct HPLC study appears not to have been previously reported. Such a method of deproteinization was also successful for assays of gentamicin and other drugs in plasma or serum samples. Results of extensive studies will be reported later.

The linearity of typical standard curves based on peak height and integrated area measurements of creatinine spiked in human plasma samples is summarized in Table I. The concentrations of spiked creatinine, ranging from 0 to 20 mg %, were investigated using plasma samples from two different sources. The excellent linearity of the standard curves was indicated by the consistency of the response factors obtained at all concentrations in both sources of plasma samples.

The response factors were obtained as the ratios of the corrected responses divided by the spiked creatinine concentrations. The corrected responses were the peak heights or peak areas from spiked plasma samples minus the blank values of the plasma from the same source. The blank values were due to the creatinine already present in the plasma samples. In using the peak heights for quantitation, it is recommended

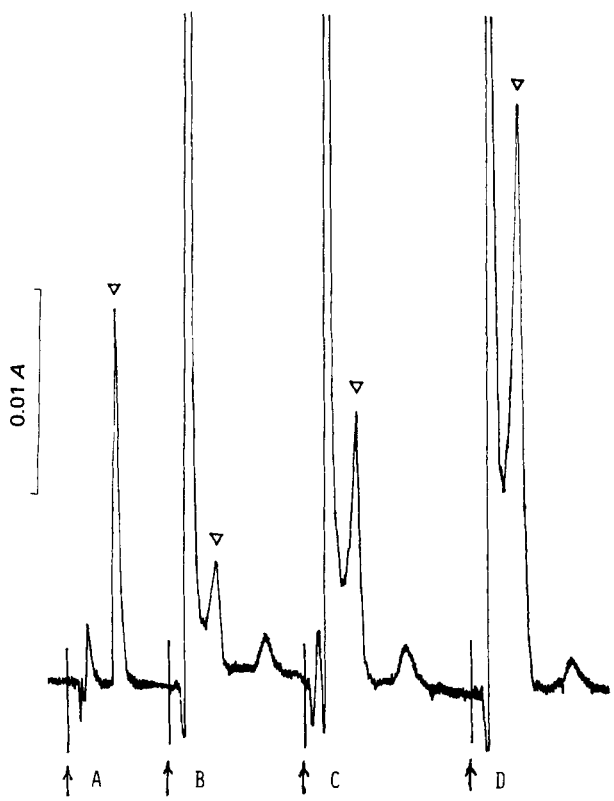

Figure 2—*Chromatograms of creatinine in water (A), creatinine in plasma (B), 2 mg % creatinine spiked in plasma (C), and 4 mg % creatinine spiked in plasma (D). The (▽) and (↑) indicate the peak of creatinine and the point of injection, respectively. Column = reversed phase (ODS Sil-X-1). Mobile phase = water–methanol (1:1, v/v). Sensitivity = 0.05 A (full-scale deflection). Creatinine retention time = 3 min.*

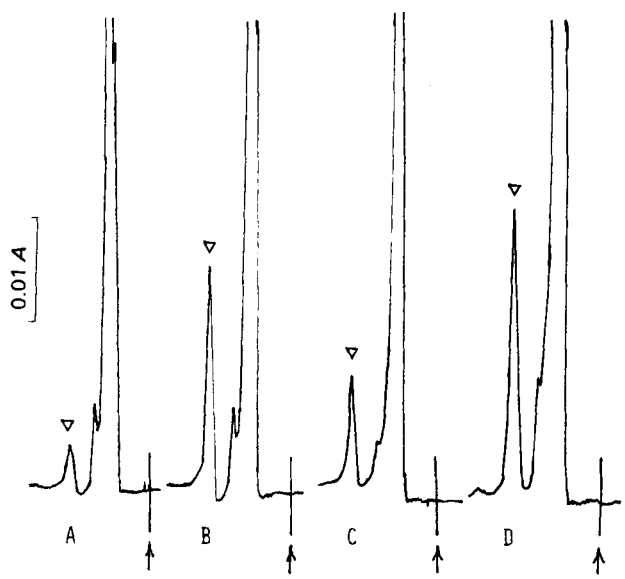

Figure 3—*Chromatograms of creatinine from normal subject plasma (A), the same plasma spiked with 4 mg % creatinine (B), and plasma from two renal patients (C and D). The (▽) and (↑) indicate the peak of creatinine and the point of injection, respectively. Column = cation exchange (Partisil SCX). Sensitivity = 0.05 A (full-scale deflection). Creatinine retention time = 3.8 min.*

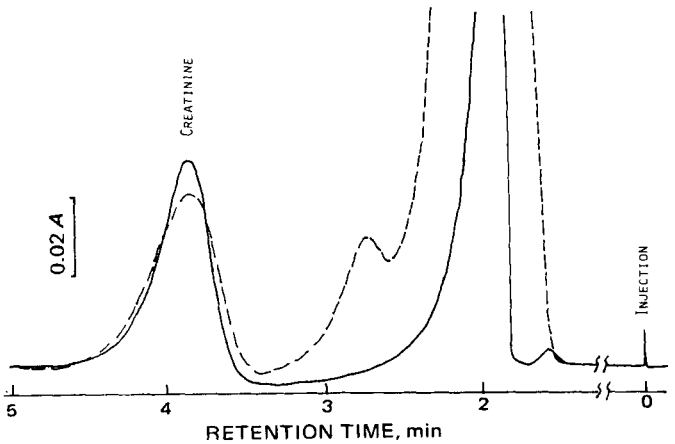

Figure 4—*Chromatograms of creatinine in water (—) and plasma (- - -). Column = cation exchange (Partisil SCX). Sensitivity = 0.1 A (full-scale deflection). Chart speed = 5.1 cm (2 in.)/min.*

that a 25.4-cm (10-in.) [instead of 12.7-cm (5-in.)] recorder be used for easier and more accurate measurement.

The standard curves based on the peak area measurements of aqueous creatinine solutions also showed excellent linearity, with the slopes identical to those based on peak area measurement of creatinine-spiked plasma samples. This result indicates the complete recovery of the spiked creatinine in the deproteinized supernate and shows that aqueous creatinine solutions can be used to establish the standard curves based on the area method for plasma creatinine assays and also for the routine calibration of the instrument. However, when peak height measurements were used, the standard curves from aqueous creatinine solutions had steeper slopes than those from spiked plasma samples despite excellent linearity in both cases. At the same concentration of creatinine in water and in plasma, the peak heights from the aqueous solutions were higher (16.4%) than those obtained from the plasma samples, but the integrated peak areas were the same for the aqueous solutions and the plasma samples.

The lower peak height with the same integrated area under the curve from the spiked plasma can be explained by the widening of the peak. The peak-widening phenomenon was clearly demonstrated when the two types of samples with similar creatinine concentration were studied using a faster recorder chart speed of 5.1 cm (2 in.)/min. The chromatograms obtained are shown in Fig. 4. The creatinine retention times from both samples were essentially the same.

The exact cause of such peak widening is unknown. The pH factor was ruled out since creatinine dissolved in pH 7.4 phosphate buffer did not

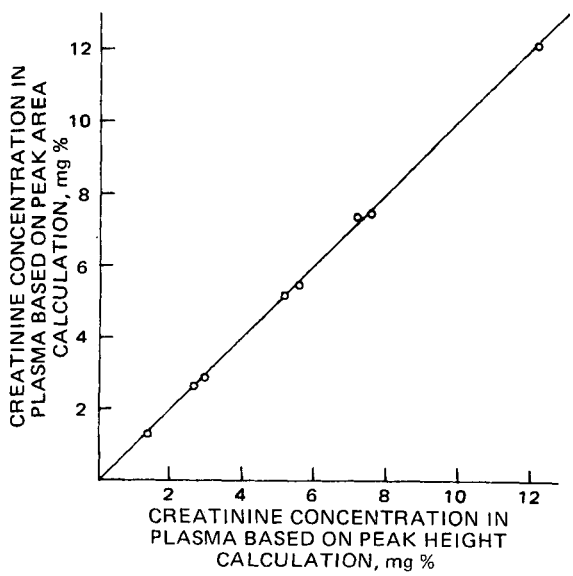

Figure 5—*Correlation between peak height and peak area calculations for creatinine levels in plasma in eight subjects. The line has a slope of one.*

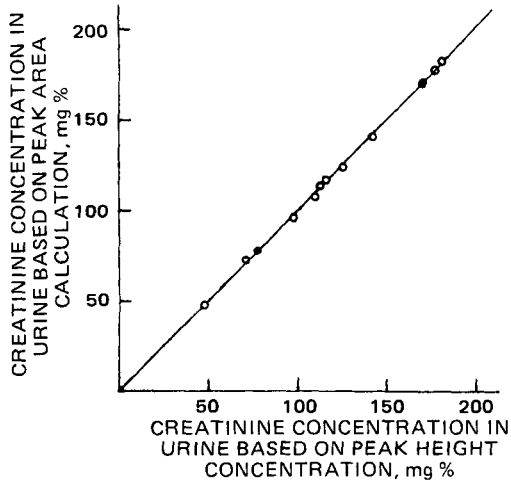

Figure 6—*Correlation between peak height and peak area calculations for creatinine in urine in 12 subjects. The line has a slope of one.*

manifest such a property. Some basic organic compounds present in plasma might interfere with the interaction between the creatinine cation and the cation-exchange column. Since the slopes from the aqueous creatinine and the spiked plasma samples were different when the peak height method was employed, the slope from the spiked plasma study should be used to estimate creatinine levels of unknown plasma samples.

Plasma creatinine levels from one normal subject and seven renal patients were estimated by both the peak height and area methods. The results are plotted in Fig. 5. All data points are on or close to the line with a slope of one, indicating that both methods can be used for quantitation.

No assay published to date has shown that the creatinine levels measured were due entirely to creatinine; interference from other endogenous or exogenous (such as drugs or diet) substances on the assay accuracy could not be eliminated entirely, nor could it be detected with assurance during the assay. The suspected creatinine peak from the plasma samples in the present HPLC study is concluded to be caused entirely by the true creatinine, and such a conclusion is supported by the following findings.

The retention times of the suspected creatinine peak from the plasma, spiked plasma, and aqueous creatinine solution in the reversed-phase column (methanol–water mobile phase system) and the cation-exchange column (acidified ammonium phosphate mobile phase system) were all identical for each particular system studied. Some typical chromatograms are shown in Figs. 2 and 3. These results indicate that the suspected creatinine has partition or solubility and adsorption properties identical to those of the pure creatinine. The results from the cation-exchange column studies also indicate that both suspected and pure creatinines have identical ionic dissociation properties. The identical peak height or area ratio (3.3 in both cases) between 215 and 233 nm from both aqueous creatinine and renal patient plasma samples also indicates that both suspected and pure creatinines have the identical UV absorption property at these two wavelengths and that the suspected peak is entirely from the true creatinine. The same UV absorption property also was found in the methanol–water system.

One important advantage of the present HPLC method over all the previously published methods is that the presence of an interfering substance in plasma can most likely be detected by its influence on the sharpness and resolution of the creatinine peak. The excellence of the present HPLC method also is demonstrated by the fact that no interference was found in the analyses of plasma samples from seven renal patients who were maintained on various kinds of drugs.

The excellent linearity of typical standard curves based on peak area and height measurements of creatinine-spiked urine samples, in concentrations ranging from 0 to 400 mg %, is summarized in Table II. When comparing these standard curves with those from an aqueous creatinine solution, a pattern similar to that found in the plasma analysis was observed; the slopes of standard curves from urine samples and from aqueous solutions were identical using the peak area method, but the aqueous solutions gave steeper slopes using the peak height method. The peak height from the urine sample for the same spiked creatinine concentration was only 10.8% lower than that from the aqueous creatinine

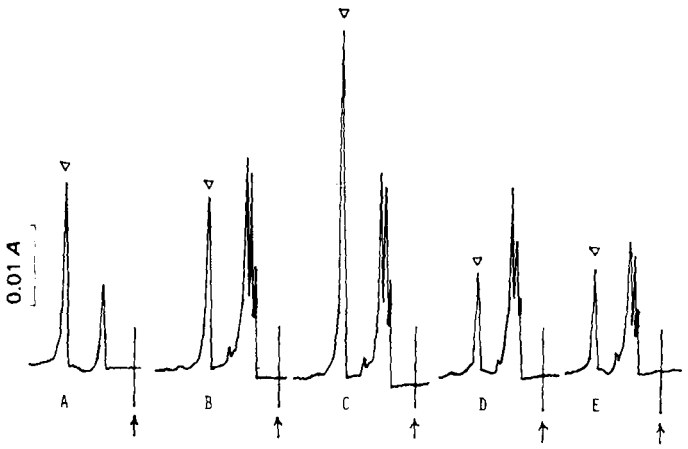

Figure 7—*Chromatograms of creatinine from water (A), urine of a normal subject (B), the same urine sample spiked with creatinine (C), and urine of two normal subjects (D and E). The (▽) and (↑) indicate the peak of creatinine and the point of injection, respectively. Column = cation exchange (Partisil SCX). Sensitivity = 0.05 A (full-scale deflection). Creatinine retention time = 3.8 min.*

solution. This result might be explained by the greater dilution used in the urine study (41 *versus* 3.5 times).

Creatinine concentrations of urine samples from 12 normal subjects analyzed by both the peak height and area methods are plotted in Fig. 6. The two methods of calculation gave essentially the same results. In spite of the large amount of complex substances present in the urine samples, chromatograms from all urine samples were remarkably well resolved and no interference with the creatinine peak was found. Typical chromatograms from urine samples of three normal subjects are shown in Fig. 7.

Reproducibility is important in any assay developed. Results of six duplicate studies on three plasma and three urine samples are summarized in Table III. Excellent reproducibility of the proposed HPLC method is clearly demonstrated by the low coefficients of variation. The excellent day-to-day reproducibility also is demonstrated by the results of the plasma study on one normal subject in which the same plasma sample was analyzed seven times during 3 weeks. These analyses gave an average creatinine concentration of 1.28 mg % with a standard deviation of 0.03 mg % and a coefficient of variation of 2.34%. Since the sample preparation is extremely simple and the day-to-day instrumental variation is minimal, it is concluded that no internal standard is necessary for the proposed method.

The ratio of 2.5 between the volume of acetonitrile and the volume of plasma or serum was satisfactory. It is likely that other ratios also may give satisfactory results. In the urine analysis also, other reagent to urine ratios or other strengths of acetonitrile (80% in the present study) probably could be used. With the same acetonitrile ratios used in the present study, 10 μl of the plasma or serum sample and 1 μl of the urine sample could be analyzed for creatinine with the same degree of accuracy. The study for the plasma or serum sample, in this case, can be conducted in a tapered tube, and only 25 μl of the deproteinized supernate must be injected into the chromatograph. Use of the different initial volumes of

Table II—Linearity of Creatinine in Urine Samples Based on Peak Area and Peak Height Methods

Spiked Creatinine Concentration, mg %	Peak Area (Arbitrary Units)	Response Factor[a]	Peak Height, cm	Response Factor[b]
0	57.27	—	4.45	—
50	73.92	3.33	5.45	2.00
100	88.59	3.13	6.45	2.00
200	121.11	3.14	8.50	2.03
300	153.82	3.22	10.60	2.05
400	186.53	3.23	12.55	2.03
	Average	3.21		2.02
	SD	0.08		0.02
	CV	2.52%		1.00%

[a] Response factor = (peak area from spiked samples − peak area from unspiked samples) × 10/(spiked creatinine concentration). [b] Response factor = (peak height from spiked samples − peak height from unspiked samples) × 100/(spiked creatinine concentration).

Table III—Reproducibility Studies in the Determinations of Creatinine Levels in Plasma and Urine of Three Subjects by the Integrated Area Method

	Plasma Creatinine Concentrations Found, mg %			Urine Creatinine Concentrations Found, mg %		
	Subject 1	Subject 2	Subject 3	Subject 1	Subject 2	Subject 3
	2.455	5.213	1.283	70.26	191.12	166.25
	2.599	5.344	1.217	72.38	185.03	172.18
	2.438	5.520	1.174	69.30	192.55	169.40
	2.460	5.532	1.276	74.93	186.25	172.25
	2.594	5.675	1.212	68.97	187.61	173.21
	2.369	5.457	1.228	73.27	184.37	171.45
Average	2.49	5.46	1.23	71.5	187.8	170.8
SD	0.09	0.16	0.04	2.38	3.33	2.56
CV	3.86%	2.95%	3.35%	3.33%	1.77%	1.50%

the same plasma sample such as 10, 30, 100, and 200 μl all resulted in the same creatinine value.

The proposed method for the true creatinine analysis is reliable, simple, and rapid. Each separate analysis of a sample takes only about 5 min. Another major advantage of this method is the ease of preparation and the economy of the mobile phase used. The microsize of the plasma or serum sample required for analysis is particularly valuable to the monitoring of the renal function in premature and mature infants, children, and adults with collapsed vascular veins. In these patients, the sample required can be obtained easily from the fingertip or the heel in the case of tiny, premature infants.

With the use of this novel assay for creatinine, it is possible that different findings or conclusions regarding the clinical pharmacokinetics of creatinine and its relationship with the pharmacokinetics of drugs and the renal function may be arrived at when they are reevaluated.

REFERENCES

(1) W. L. Chiou and F. H. Hsu, *Res. Commun. Chem. Pathol. Pharmacol.*, **10**, 315 (1975).

(2) W. L. Chiou and F. H. Hsu, *J. Clin. Pharmacol.*, **15**, 427 (1975).

(3) "Clinical Pharmacokinetics: A Symposium," G. Levy, Ed., APhA Academy of Pharmaceutical Sciences, Washington, D.C., 1974, p. 1.

(4) M. Gibaldi and D. Perrier, "Pharmacokinetics," Dekker, New York, N.Y., 1975.

(5) M. Gibaldi and G. Levy, *J. Am. Med. Assoc.*, **235**, 1864 (1976).

(6) J. G. Wagner, "Fundamentals of Clinical Pharmacokinetics," Drug Intelligence Publications, Hamilton, Ill., 1976.

(7) S. Riegelman and W. Sadee, in "Clinical Pharmacokinetics: A Symposium," G. Levy, Ed., APhA Academy of Pharmaceutical Sciences, Washington, D.C., 1974, p. 169.

(8) R. E. Notari, "Biopharmaceutics and Pharmacokinetics: An Introduction," 2nd ed., Dekker, New York, N.Y., 1975.

(9) R. W. Jelliffe, *Am. J. Med.*, **57**, 63 (1974).

(10) P. G. Welling, W. A. Craig, and C. M. Kunin, *Clin. Pharmacol. Ther.*, **18**, 45 (1975).

(11) W. M. Bennett, I. Singer, and C. H. Coggins, *J. Am. Med. Assoc.*, **223**, 991 (1973).

(12) M. Kristensen, J. M. Hansen, J. Kampmann, B. Lumholtz, and K. S. Nielsen, *J. Clin. Pharmacol.*, **14**, 307 (1974).

(13) T. N. Tozer, *J. Pharmacokinet. Biopharm.*, **2**, 13 (1974).

(14) D. L. Giusti and L. Hayton, *Drug Intell. Clin. Pharmacol.*, **7**, 382 (1973).

(15) J. R. Koup, W. J. Jusko, C. M. Elwood, and R. K. Kohli, *Clin. Pharmacol. Ther.*, **18**, 9 (1975).

(16) "The Effect of Disease States on Drug Pharmacokinetics," L. Z. Benet, Ed., American Pharmaceutical Association, Washington, D.C., 1976.

(17) O. Folin, *J. Biol. Chem.*, **17**, 475 (1914).

(18) O. M. Edwards, R. I. S. Bayliss, and S. Millen, *Lancet*, **2**, 1165 (1969).

(19) J. Brochner-Mortensen and P. Rodbro, *Scand. J. Clin. Lab. Invest.*, **36**, 35 (1976).

(20) M. C. Crim, D. H. Calloway, and S. Margen, *J. Nutr.*, **105**, 428 (1975).

(21) W. J. Turner and S. Cohn, *Clin. Pharmacol. Ther.*, **18**, 405 (1975).

(22) J. D. Jones and P. C. Burnett, *Clin. Chem.*, **20,** 1204 (1974).
(23) E. J. Sampson, D. D. Derck, and L. M. Demers, *ibid.*, **22,** 346 (1976).
(24) R. J. Henry, "Clinical Chemistry: Principles and Technics," Hoeber, New York, N.Y., 1964, p. 297.
(25) P. J. Watkins, *Clin. Chim. Acta,* **18,** 191 (1967).
(26) L. Sadilek, *ibid.*, **12,** 436 (1965).
(27) H. Yatzidis, *Clin. Chem.*, **20,** 1131 (1974).
(28) E. D. Frohlich, "Pathophysiology: Altered Regulatory Mechanisms in Disease," Lippincott, Philadelphia, Pa., 1972, p. 270.
(29) I. Davidsohn and J. B. Henry, "Clinical Diagnosis by Laboratory Methods," 15th ed., Saunders, Philadelphia, Pa., 1974, p. 596.
(30) H. Yatzidis, *Clin. Chem.*, **21,** 1848 (1975).
(31) F.-H. Hsu, MS thesis, University of Illinois, Chicago, Ill., 1976.
(32) S. Vedso, C. Rud, and J. F. Place, *Scand. J. Clin. Lab. Invest.*, **34,** 275 (1974).
(33) K. Larsen, *Clin. Chim. Acta,* **41,** 209 (1972).
(34) G. A. Moss, R. J. L. Bondar, and D. M. Buzzelli, *Clin. Chem.*, **21,** 1422 (1975).
(35) M. Barza, R. B. Brown, D. Sheu, M. Gibaldi, and L. Weinstein, *J. Infect. Dis.*, **132,** 165 (1975).
(36) G. H. McCracken, Jr., *Am. J. Dis. Child.*, **124,** 884 (1972).
(37) "The Merck Index," 9th ed., Merck & Co., Rahway, N.J., 1976, p. 334.
(38) G. W. Peng, V. Smith, A. Peng, and W. L. Chiou, *Res. Commun. Chem. Pathol. Pharmacol.*, **15,** 341 (1976).

ACKNOWLEDGMENTS

Supported in part by Special Project Grant PHS-05D 619-02 from the Department of Health, Education, and Welfare.

General Treatment of Linear Pharmacokinetics

PETER VENG PEDERSEN

Received December 20, 1976, from the *Department of Pharmacy, University of Sydney, N.S.W. 2006 Australia.* Accepted for publication April 28, 1977. Present address: Department of Pharmacy, University of California, San Francisco, CA 94143.

Abstract □ A general treatment of linear pharmacokinetics that enables equations to be obtained simply for all linear compartmental models, with input in one or more compartments, is presented. Two approaches are described: one based on a full Laplace transformation and one that avoids transformation of the input functions and the use of convolution integrals. The latter approach is of particular interest when dealing with complex input functions not having a simple Laplace transform. The concept of acceptor and donor subsystems is introduced. It is demonstrated that disposition in certain models may be simplified and analyzed in terms of disposition in subsystems of simpler composition. The treatment presented is illustrated with several examples.

Keyphrases □ Pharmacokinetics—general treatment for derivation of equations for all linear compartmental models □ Models, pharmacokinetic—general treatment for derivation of equations for all linear compartmental models

Mathematical modeling in pharmacokinetics is commonly based on linear models in which it is assumed that the rate of transfer from any compartment is proportional to the amount in that compartment (1–5). Benet (6) presented a general treatment of linear mammillary models that considers elimination from any compartment but allows input into the central compartment only. Other investigators (7, 8) extended Benet's approach to include input into a peripheral compartment, but they only considered mammillary models. This paper presents a general treatment of any linear pharmacokinetic model with input in one or more compartments.

Two approaches are presented: one requires a Laplace transformation of the input functions, and one avoids such a transformation. The concept of subsystems is introduced. It is demonstrated that certain models can be simplified and analyzed in terms of the disposition of the subsystems.

THEORY

Every possible model having n compartments is a subset of the dense n-compartmental system, defined as a system with reversible transfer between all n compartments and elimination and input in every compartment (*e.g.*, Scheme I). A description of the dense system will describe all compartmental models when the domains of the rate constants and input functions are defined as $k_{ij} \geq 0$ and $f_i(t) \geq 0$, $t > 0$, respectively.

The linear differential equations that describe the kinetics in a dense system are given by[1]:

$$\mathbf{x}' = (\mathbf{K}^T - \mathbf{\Sigma})\mathbf{x} + \mathbf{f} \qquad \text{(Eq. 1)}$$

$$\mathbf{\Sigma} = \text{diag}(E_1, E_2, \ldots, E_n) \qquad \text{(Eq. 2)}$$

$$E_i = \sum_{j=0}^{n} k_{ij} \qquad \text{(Eq. 3)}$$

The ith component of vector $\mathbf{x}$ is the amount in the ith compartment at time t. The ith diagonal element, E_i, of the diagonal matrix, $\mathbf{\Sigma}$, is the sum of the exit rate constants of the ith compartment; $\mathbf{K}^T$ is the transpose of the $n \times n$ matrix, $\mathbf{K} = k_{ij}$, which contains the intercompartmental rate constants. The diagonal elements of $\mathbf{K}$ and $\mathbf{K}^T$ are always zero.

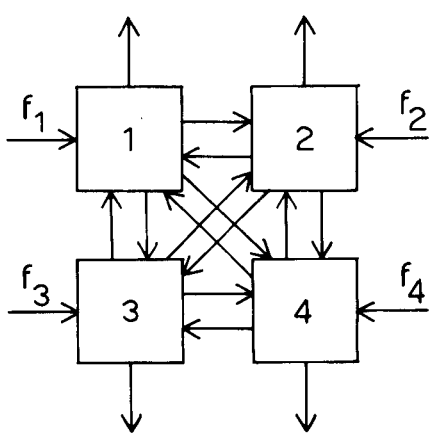

Scheme I—Dense four-compartmental system with reversible transfer between all compartments and elimination and input in every compartment.

[1] Boldface capital letters denote $n \times n$ matrixes, and boldface lower case letters denote vectors of corresponding dimension.

(22) J. D. Jones and P. C. Burnett, *Clin. Chem.*, **20,** 1204 (1974).
(23) E. J. Sampson, D. D. Derck, and L. M. Demers, *ibid.*, **22,** 346 (1976).
(24) R. J. Henry, "Clinical Chemistry: Principles and Technics," Hoeber, New York, N.Y., 1964, p. 297.
(25) P. J. Watkins, *Clin. Chim. Acta,* **18,** 191 (1967).
(26) L. Sadilek, *ibid.*, **12,** 436 (1965).
(27) H. Yatzidis, *Clin. Chem.*, **20,** 1131 (1974).
(28) E. D. Frohlich, "Pathophysiology: Altered Regulatory Mechanisms in Disease," Lippincott, Philadelphia, Pa., 1972, p. 270.
(29) I. Davidsohn and J. B. Henry, "Clinical Diagnosis by Laboratory Methods," 15th ed., Saunders, Philadelphia, Pa., 1974, p. 596.
(30) H. Yatzidis, *Clin. Chem.*, **21,** 1848 (1975).
(31) F.-H. Hsu, MS thesis, University of Illinois, Chicago, Ill., 1976.
(32) S. Vedso, C. Rud, and J. F. Place, *Scand. J. Clin. Lab. Invest.*, **34,** 275 (1974).
(33) K. Larsen, *Clin. Chim. Acta,* **41,** 209 (1972).
(34) G. A. Moss, R. J. L. Bondar, and D. M. Buzzelli, *Clin. Chem.*, **21,** 1422 (1975).
(35) M. Barza, R. B. Brown, D. Sheu, M. Gibaldi, and L. Weinstein, *J. Infect. Dis.*, **132,** 165 (1975).
(36) G. H. McCracken, Jr., *Am. J. Dis. Child.*, **124,** 884 (1972).
(37) "The Merck Index," 9th ed., Merck & Co., Rahway, N.J., 1976, p. 334.
(38) G. W. Peng, V. Smith, A. Peng, and W. L. Chiou, *Res. Commun. Chem. Pathol. Pharmacol.*, **15,** 341 (1976).

ACKNOWLEDGMENTS

Supported in part by Special Project Grant PHS-05D 619-02 from the Department of Health, Education, and Welfare.

General Treatment of Linear Pharmacokinetics

PETER VENG PEDERSEN

Received December 20, 1976, from the *Department of Pharmacy, University of Sydney, N.S.W. 2006 Australia.* Accepted for publication April 28, 1977. Present address: Department of Pharmacy, University of California, San Francisco, CA 94143.

Abstract □ A general treatment of linear pharmacokinetics that enables equations to be obtained simply for all linear compartmental models, with input in one or more compartments, is presented. Two approaches are described: one based on a full Laplace transformation and one that avoids transformation of the input functions and the use of convolution integrals. The latter approach is of particular interest when dealing with complex input functions not having a simple Laplace transform. The concept of acceptor and donor subsystems is introduced. It is demonstrated that disposition in certain models may be simplified and analyzed in terms of disposition in subsystems of simpler composition. The treatment presented is illustrated with several examples.

Keyphrases □ Pharmacokinetics—general treatment for derivation of equations for all linear compartmental models □ Models, pharmacokinetic—general treatment for derivation of equations for all linear compartmental models

Mathematical modeling in pharmacokinetics is commonly based on linear models in which it is assumed that the rate of transfer from any compartment is proportional to the amount in that compartment (1–5). Benet (6) presented a general treatment of linear mammillary models that considers elimination from any compartment but allows input into the central compartment only. Other investigators (7, 8) extended Benet's approach to include input into a peripheral compartment, but they only considered mammillary models. This paper presents a general treatment of any linear pharmacokinetic model with input in one or more compartments.

Two approaches are presented: one requires a Laplace transformation of the input functions, and one avoids such a transformation. The concept of subsystems is introduced. It is demonstrated that certain models can be simplified and analyzed in terms of the disposition of the subsystems.

THEORY

Every possible model having n compartments is a subset of the dense n-compartmental system, defined as a system with reversible transfer between all n compartments and elimination and input in every compartment (*e.g.*, Scheme I). A description of the dense system will describe all compartmental models when the domains of the rate constants and input functions are defined as $k_{ij} \geq 0$ and $f_i(t) \geq 0$, $t > 0$, respectively.

The linear differential equations that describe the kinetics in a dense system are given by[1]:

$$\mathbf{x}' = (\mathbf{K}^T - \mathbf{\Sigma})\mathbf{x} + \mathbf{f} \qquad \text{(Eq. 1)}$$

$$\mathbf{\Sigma} = \text{diag}(E_1, E_2, \ldots, E_n) \qquad \text{(Eq. 2)}$$

$$E_i = \sum_{j=0}^{n} k_{ij} \qquad \text{(Eq. 3)}$$

The ith component of vector $\mathbf{x}$ is the amount in the ith compartment at time t. The ith diagonal element, E_i, of the diagonal matrix, $\mathbf{\Sigma}$, is the sum of the exit rate constants of the ith compartment; $\mathbf{K}^T$ is the transpose of the $n \times n$ matrix, $\mathbf{K} = k_{ij}$, which contains the intercompartmental rate constants. The diagonal elements of $\mathbf{K}$ and $\mathbf{K}^T$ are always zero.

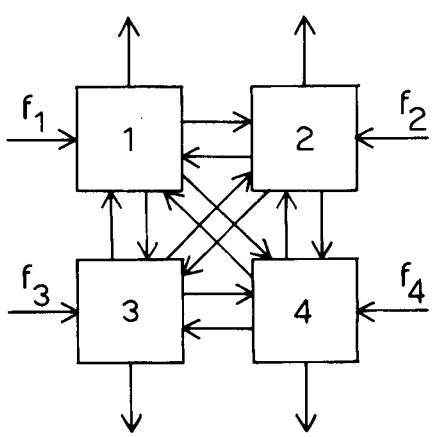

Scheme I—Dense four-compartmental system with reversible transfer between all compartments and elimination and input in every compartment.

[1] Boldface capital letters denote $n \times n$ matrixes, and boldface lower case letters denote vectors of corresponding dimension.

Full Transformation Approach—The Laplace transform of Eq. 1 yields (bars denote transformed quantities):

$$s\bar{\mathbf{x}} - \mathbf{x}(0) = (\mathbf{K}^T - \boldsymbol{\Sigma})\bar{\mathbf{x}} + \bar{\mathbf{f}} \qquad \text{(Eq. 4)}$$

which can be rearranged to:

$$\bar{\mathbf{x}} = [-\mathbf{K}^T + (s\mathbf{I} + \boldsymbol{\Sigma})]^{-1}[\mathbf{x}(0) + \bar{\mathbf{f}}] \qquad \text{(Eq. 5)}$$

where $\mathbf{I}$ is the identity matrix and $\mathbf{x}(0)$ is the vector $\mathbf{x}$ at time $t = 0$.

It is convenient to introduce a matrix, $\mathbf{S}$, defined as:

$$\mathbf{S} = -\mathbf{K} + \text{diag}(s + E_1, s + E_2, \ldots, s + E_n) \qquad \text{(Eq. 6)}$$

Then the solution of Eq. 1 by Eq. 5 simply becomes:

$$\mathbf{x} = L^{-1}(\mathbf{Dv}) \qquad \text{(Eq. 7)}$$

where L^{-1} is the inverse Laplace transform operator. The matrix:

$$\mathbf{D} = (\mathbf{S}^T)^{-1} \qquad \text{(Eq. 8)}$$

will be called the disposition matrix. The vector:

$$\mathbf{v} = \mathbf{x}(0) + \bar{\mathbf{f}} \qquad \text{(Eq. 9)}$$

will be called the input vector.

Equation 7 describes the simultaneous and complete solution of all compartments in any linear pharmacokinetic model. Thus, the solution is simply stated as the inverse transform of the product of the disposition matrix and the input vector.

The ith row of the disposition matrix, $\mathbf{d}_i = (d_{i1}, d_{i2}, \ldots, d_{in})$, will be called the disposition vector for the ith compartment.

It then follows from Eq. 7 that:

$$x_i = L^{-1}(\mathbf{d}_i\mathbf{v}) \qquad \text{(Eq. 10)}$$

i.e., the solution for any compartment is the inverse transform of the scalar product of its disposition vector and the input vector of the system.

The elements of the disposition matrix, $\mathbf{D}$, are simply expressed in terms of $\mathbf{S}$ by:

$$d_{ij} = |\mathbf{S}|_{ij}/|\mathbf{S}| \qquad \text{(Eq. 11)}$$

where $\mathbf{S}$ is the determinant of $\mathbf{S}$ and $\mathbf{S}_{ij}$ is the cofactor corresponding to the ijth element.

Equation 10 can thus be written more specifically as:

$$x_i = L^{-1}\sum_{j=1}^{n}\frac{|\mathbf{S}|_{ij}}{|\mathbf{S}|}[x_j(0) + \bar{f}_j] \qquad \text{(Eq. 12)}$$

or:

$$x_i = L^{-1}\sum_{j=1}^{n}\frac{|-\mathbf{K} + \text{diag}(s + E_1, s + E_2, \ldots, s + E_n)|_{ij}}{|-\mathbf{K} + \text{diag}(s + E_1, s + E_2, \ldots, s + E_n)|} \times [x_j(0) + \bar{f}_j] \qquad \text{(Eq. 13)}$$

Subsystems—A compartmental system can be divided into various subsystems by "pulling it apart," with exit arrows remaining fixed to their respective compartments (*e.g.*, Scheme II).

A subsystem not receiving input from other subsystems may be called a donor system and is said to be irreversibly connected (Scheme II, System D). An acceptor system is a subsystem receiving input from other subsystems (Scheme II, Systems A, B, and C).

The usefulness of subsystems arises from the fact that a compartmental system that can be divided into one or more irreversibly connected subsystems can be analyzed in terms of the disposition of subsystems treated as isolated systems. Therefore, the system can be analyzed in a section of simpler composition. For example, consider a system that can be divided into an acceptor and a donor system, denoted [1] and [2], respectively (Scheme III, Systems A and B). Disposition in the donor system is independent of the remainder of the system so that:

$$\mathbf{x}^{[2]} = L^{-1}(\mathbf{D}^{[2]}\mathbf{v}^{[2]}) \qquad \text{(Eq. 14)}$$

where $\mathbf{D}^{[2]}$ and $\mathbf{v}^{[2]}$ are the $n^{[2]} \times n^{[2]}$ disposition matrix and the input vector for the donor system treated as an isolated system, respectively (Scheme III, System B).

Similarly, disposition in the isolated acceptor system (Scheme III, System A) is given by $\mathbf{x}^{[1]} = L^{-1}(\mathbf{D}^{[1]}\mathbf{v}^{[1]})$. In contrast to a donor system, however, this disposition will not be the same as when the system is connected to the other subsystem because it receives input from it. However, the correct disposition is obtained by adding an additional

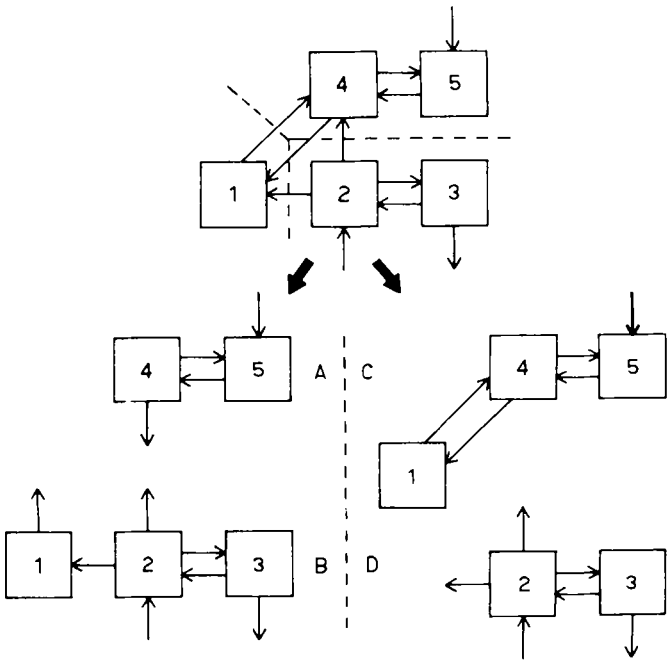

Scheme II—Five compartmental system that can be "pulled apart" to form various subsystems, of which only four are shown. D is a donor system irreversibly connected to the acceptor System C. Partitioning into A and B produces only acceptor systems.

input element, $\bar{f}_j$ (Scheme III, System B), to the jth element of the vector $\mathbf{v}^{[1]}$. This additional element is related to disposition in the donor system and the connector constant, k_{ij}, by:

$$\bar{f}_j = k_{ij}\bar{x}_i^{[2]} = k_{ij}(\mathbf{d}_i^{[2]}\mathbf{v}^{[2]}) \qquad \text{(Eq. 15)}$$

Thus, the general case with N donor systems, each connected to an acceptor system (denoted [1]) by one or more connector constants, is described by:

$$\mathbf{x}^{[1]} = L^{-1}\left(\mathbf{D}^{[1]}\left[\mathbf{v}^{[1]} + \sum_{i=2}^{N}\mathbf{C}^{[i]}\mathbf{D}^{[i]}\mathbf{v}^{[i]}\right]\right) \qquad \text{(Eq. 16)}$$

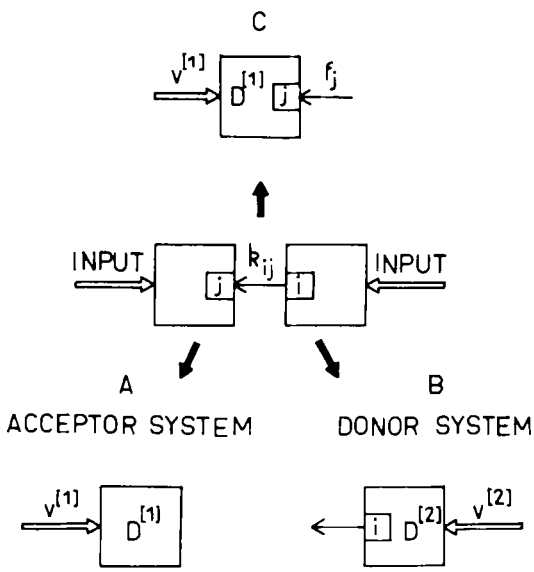

Scheme III—Simple illustration of the subsystem approach. Disposition in the donor system, B, is unaffected by disposition in the acceptor system, A, so that it can be analyzed separately in terms of the simpler disposition matrix, $\mathbf{D}^{[2]}$, and the input vector, $\mathbf{v}^{[2]}$. The isolated acceptor system, A, can be analyzed similarly; but an additional input element, $\bar{f}_j$, must be added to the input vector, $\mathbf{v}^{[1]}$, to account for the fact that the acceptor system receives input from the donor system (C). The additional input element is simply related to disposition in the donor system via the connector constant, k_{ij} (Eq. 15).

and:

$$\mathbf{x}^{[i]} = L^{-1}(\mathbf{D}^{[i]}\mathbf{v}^{[i]}) \qquad i \neq 1 \qquad \text{(Eq. 17)}$$

where the $n^{[1]} \times n^{[i]}$ matrix $\mathbf{C}^{[i]}$ in Eq. 16 will be called the connector matrix for the ith donor system. The j,kth element of the connector matrix, $C^{[i]}$, contains the connector constant that connects the jth compartment in the acceptor system with the kth compartment in donor system [i].

The ith compartment in a subsystem in this context is defined as the compartment corresponding to the ith row of the disposition matrix of the subsystem. This definition allows arbitrary numbers to be assigned to the compartments so that Eqs. 16 and 17 still apply.

Partial Transformation Approach—The described approach is based on a Laplace transformation of both the disposition and the input kinetics. Its use is convenient in cases where the input functions are simple such that an inverse transformation can be obtained without the use of complex inversion formulas or convolution integrals.

If the input function(s) is not simple, it may be useful to apply the following approach, which does not require transformation of the input functions. According to Eq. 9, Eq. 7 can be written:

$$\mathbf{x} = L^{-1}[\mathbf{D}\mathbf{x}(0) + \mathbf{D}\bar{\mathbf{f}}] \qquad \text{(Eq. 18)}$$

By application of the convolution theorem, this equation becomes:

$$\mathbf{x} = \mathbf{\Phi}(t)\mathbf{x}(0) + \int_0^t \mathbf{\Phi}(t-\tau)\mathbf{f}(\tau)\,d\tau \qquad \text{(Eq. 19)}$$

where the inverse transform of the disposition matrix, given by:

$$\mathbf{\Phi}(t) = L^{-1}\mathbf{D} \qquad \text{(Eq. 20)}$$

is the normalized fundamental matrix of the complementary homogeneous equation $\mathbf{x}' - (\mathbf{K}^T - \mathbf{\Sigma})\mathbf{x} = \mathbf{0}$. The elements of this matrix are readily obtained according to Eq. 11 by:

$$\Phi_{ij}(t) = L^{-1}(d_{ij}) = L^{-1}(|\mathbf{S}|_{ij}/|\mathbf{S}|) \qquad \text{(Eq. 21)}$$

Equation 19 is of little practical interest because it involves a convolution integral. However, the following remarkable property of the fundamental matrix (9):

$$\mathbf{\Phi}(t-\tau) = e^{(\mathbf{K}^T-\mathbf{\Sigma})(t-\tau)} = e^{(\mathbf{K}^T-\mathbf{\Sigma})t}e^{(\mathbf{K}^T-\mathbf{\Sigma})(-\tau)} = \mathbf{\Phi}(t)\mathbf{\Phi}(-\tau) \qquad \text{(Eq. 22)}$$

enables the convolution integral to be converted into an ordinary integral so that Eq. 19 may be written as:

$$\mathbf{x} = \mathbf{\Phi}(t)\left[\mathbf{x}(0) + \int_0^t \mathbf{\Phi}(-t)\mathbf{f}(t)\,dt\right] \qquad \text{(Eq. 23)}$$

RESULTS AND DISCUSSION

Equation 12 describes any compartment of any linear pharmacokinetic model with input in one or more compartments. It is of interest to consider the following commonly applied system.

Special Case: Input in Central Compartment Only—In this case [with $x_{i>1}(0) = 0$], Eq. 12 reduces to:

$$x_i = L^{-1}\left[\frac{|\mathbf{S}|_{i1}}{|\mathbf{S}|}[x_1(0) + \bar{f}_1]\right] = L^{-1}(d_{i1}v_1) \qquad \text{(Eq. 24)}$$

More specifically, when $i = 1$, Eq. 24 describes the central compartment. Benet (6) presented a general treatment of mammillary systems with central input that represents a special case within this category. A mammillary model consists specifically of a central compartment connected to a number of peripheral compartments that are themselves unconnected. Benet's approach (6) can be summarized by:

$$x_1 = L^{-1}[(d_{s,1})(in_s)] \qquad \text{(Eq. 25)}$$

where in_s was called the input function and $d_{s,1}$ was called the disposition function for Compartment 1, the central compartment. An elaborate expression (Eq. 1 of Ref. 6) was presented for the disposition function $d_{s,1}$, and examples were given of various input functions, in_s. It is evident from these examples that the vector element, $v_1 = x_1(0) + \bar{f}_1$, in Eq. 24 agrees with the input function, in_s, in Eq. 25.

However, although $d_{s,1}$ as defined by Benet (Eq. 1 of Ref. 6) and the disposition element, $d_{11} = |\mathbf{S}|_{11}/|\mathbf{S}|$ (Eq. 24, $i = 1$), may seem identical from comparison of Eqs. 24 and 25, they are in general not the same. For example, the expression presented (6) for $d_{s,1}$ is not directly applicable to a system if it contains compartments connected in ring arrangement

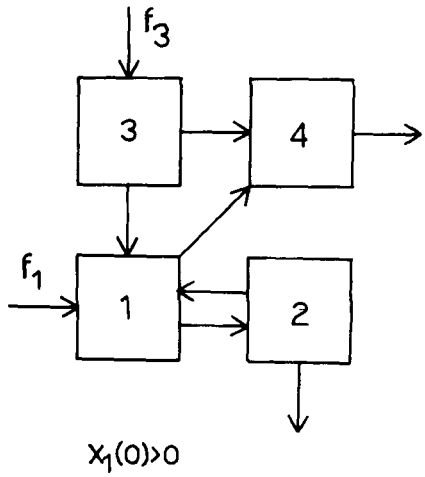

Scheme IV—Arbitrary linear pharmacokinetic model used to demonstrate the application of Eq. 12.

(*e.g.*, Scheme IV of Ref. 6). Although such systems can sometimes be "broken down" into separate mammillary systems and analyzed in terms of these systems (6), this is not always the case.

Vaughan and coworkers (7, 8) extended Benet's approach to account for cases with input into peripheral compartments. However, their equations (Eqs. 20 and 22 in Ref. 7) are limited to mammillary systems only. In contrast, Eq. 12 describes any linear pharmacokinetic system. Furthermore, this equation is a simpler representation than those presented previously (6–8) and has the additional advantage that the solution for a peripheral compartment can be found as readily as for the central compartment.

Simultaneous Noncentral Input—The applicability of Eq. 12 can be demonstrated using the system in Scheme IV. The **S** matrix (Eq. 6) may be readily assembled so that:

$$|\mathbf{S}| = \begin{vmatrix} (s+E_1) & -k_{12} & 0 & -k_{14} \\ -k_{21} & (s+E_2) & 0 & 0 \\ -k_{31} & 0 & (s+E_3) & -k_{34} \\ 0 & 0 & 0 & (s+E_4) \end{vmatrix}$$
$$= (s+E_3)[(s+E_1)(s+E_2) - k_{12}k_{21}] \qquad \text{(Eq. 26)}$$

where $E_{1-4} = k_{12} + k_{14}, k_{21} + k_{20}, k_{31} + k_{34}$, and k_{40} (Eq. 3). If the solution for Compartment 1 is sought, Eq. 12 gives:

$$x_1 = L^{-1}\left(\frac{|\mathbf{S}|_{11}}{|\mathbf{S}|}[x_1(0) + f_1] + \frac{|\mathbf{S}|_{13}}{|\mathbf{S}|}f_3\right) \qquad \text{(Eq. 27)}$$

where:

$$|\mathbf{S}|_{11} = (-1)^{1+1}\begin{vmatrix} (s+E_2) & 0 & 0 \\ 0 & (s+E_3) & -k_{34} \\ 0 & 0 & (s+E_4) \end{vmatrix}$$
$$= (s+E_4)(s+E_2)(s+E_3) \qquad \text{(Eq. 28)}$$

and:

$$|\mathbf{S}|_{13} = (-1)^{1+3}\begin{vmatrix} -k_{21} & (s+E_2) & 0 \\ -k_{31} & 0 & -k_{34} \\ 0 & 0 & (s+E_4) \end{vmatrix}$$
$$= (s+E_4)k_{31}(s+E_2) \qquad \text{(Eq. 29)}$$

It is convenient to write the determinant in "factor form" as $|\mathbf{S}| = (s + \lambda_1)(s + \lambda_2)(s + \lambda_3)(s + \lambda_4)$ where λ_{1-4}, the eigenvalues of the matrix $\mathbf{K} - \mathbf{\Sigma}$, are obtained from Eq. 26. Equation 27 thus becomes:

$$x_1 = L^{-1}\left[\frac{(s+E_2)(s+E_3)(s+E_4)}{(s+\lambda_1)(s+\lambda_2)(s+\lambda_3)(s+\lambda_4)}[x_1(0) + f_1] + \frac{k_{31}(s+E_2)(s+E_4)}{(s+\lambda_1)(s+\lambda_2)(s+\lambda_3)(s+\lambda_4)}\bar{f}_3\right] \qquad \text{(Eq. 30)}$$

The inverse transform can then be obtained as demonstrated previously when f_1 and f_3 are given (6–8, 10–12).

The input functions f_1 and f_3 may be any continuous or discontinuous

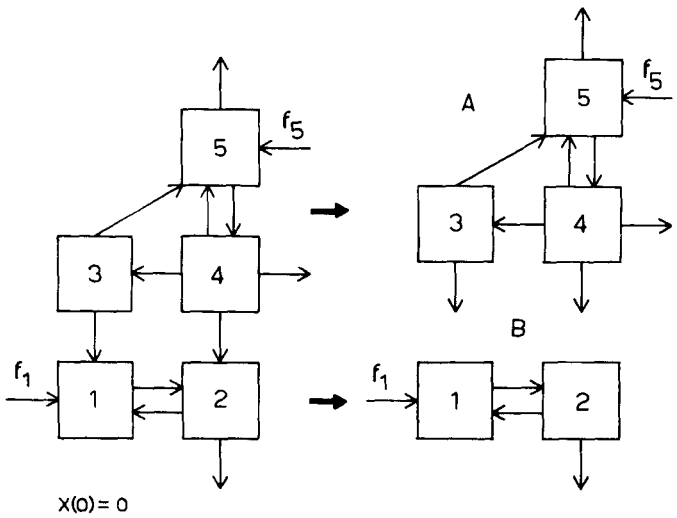

Scheme V—Arbitrary linear pharmacokinetic model used to demonstrate the subsystem approach. A is a donor system and B is an acceptor system.

functions. For example, the input function describing an instantaneous input in Compartment 1 of the amounts m_1, m_2, and m_3 at times t_1, t_2, and t_3, respectively, is:

$$f_1 = m_1\delta(t - t_1) + m_2\delta(t - t_2) + m_3\delta(t - t_3) \qquad \text{(Eq. 31)}$$

where δ is the unit impulse function (12). The Laplace transform of Eq. 31 is then:

$$\bar{f}_1 = m_1e^{-t_1s} + m_2e^{-t_2s} + m_3e^{-t_3s} \qquad \text{(Eq. 32)}$$

Specifically, when $t_1 = 0$, this equation becomes:

$$\bar{f}_1 = x_1(0) + m_2e^{-t_2s} + m_3e^{-t_3s} \qquad \text{(Eq. 33)}$$

Equation 9 shows that the input vector **v** is the sum of the initial condition and the transform of the input. However, the last example demonstrates that the initial conditions can also be considered as the transforms of certain input functions. Therefore, when a full transformation approach is applied, the initial conditions can be included in the input functions, f_i, to give a simpler representation. Therefore, the $x_j(0)$ term in Eqs. 12 and 13 can be omitted, and **v** can be replaced by $\bar{\mathbf{f}}$ in Eqs. 7 and 10 without loss of generality.

A Subsystem Approach—*Solution for Donor System*—The system in Scheme V can be divided into a donor subsystem (Scheme V, System A) and an acceptor subsystem (Scheme V, System B). If the disposition of the donor system is of interest, then Eq. 17 can be used:

$$\begin{bmatrix} x_3 \\ x_4 \\ x_5 \end{bmatrix} = L^{-1}\begin{bmatrix} d_{11} & d_{12} & d_{13} \\ d_{21} & d_{22} & d_{23} \\ d_{31} & d_{32} & d_{33} \end{bmatrix}^{[2]}\begin{bmatrix} 0 \\ 0 \\ \bar{f}_5 \end{bmatrix} \qquad \text{(Eq. 34)}$$

where the superscript, [2], of the disposition elements is placed outside the matrix frame for simplicity. The $d_{ij}^{[2]}$ elements are obtained using Eq. 11 from:

$$|\mathbf{S}|^{[2]} = \begin{array}{c} \\ (3) \\ (4) \\ (5) \end{array}\begin{array}{c} \begin{array}{ccc} (3) & (4) & (5) \end{array} \\ \begin{vmatrix} (s+E_3) & 0 & -k_{35} \\ -k_{43} & (s+E_4) & -k_{45} \\ 0 & -k_{54} & (s+E_5) \end{vmatrix} \end{array} \qquad \text{(Eq. 35)}$$

In applying Eqs. 10–13, it is important to realize that the i and j are independent of the numbers assigned to the compartments. It is completely arbitrary how such a numbering is made. The order in which the elements of the **x** vector are written is also arbitrary as long as the order of the elements of the respective input vector, **v**, corresponds and the **s** matrix is composed accordingly. For example, the **x** vector in Eq. 34 could have been written as $\mathbf{x}^{[2]} = (x_3,x_5,x_4)^T$, which corresponds to $\mathbf{v}^{[2]} = (0,\bar{f}_5,0)^T$ and:

$$|\mathbf{S}|^{[2]} = \begin{array}{c} \\ (3) \\ (5) \\ (4) \end{array}\begin{array}{c} \begin{array}{ccc} (3) & (5) & (4) \end{array} \\ \begin{vmatrix} (s+E_3) & -k_{35} & 0 \\ 0 & (s+E_5) & -k_{54} \\ -k_{43} & -k_{45} & (s+E_4) \end{vmatrix} \end{array} \qquad \text{(Eq. 36)}$$

The solution for Compartment 4 corresponds to element 3 of the $\mathbf{x}^{[2]}$ vector in the latter case. Thus, according to Eq. 12:

$$x_{i=3} = x_4 = L^{-1}\left(\frac{|\mathbf{S}|_{32}^{[2]}}{|\mathbf{S}|^{[2]}}\bar{f}_5\right) \qquad \text{(Eq. 37)}$$

where $|\mathbf{S}|^{[2]}$ is given by Eq. 36. In the other case, one obtains:

$$x_{i=2} = x_4 = L^{-1}\left(\frac{|\mathbf{S}|_{23}^{[2]}}{|\mathbf{S}|^{[2]}}\bar{f}_5\right) \qquad \text{(Eq. 38)}$$

where $|\mathbf{S}|^{[2]}$ is given by Eq. 35, which yields the same solution as Eq. 37.

Solution for Acceptor System—Let the **x** vectors for systems [1] and [2] (Scheme V, Systems B and A) be written arbitrarily as $\mathbf{x}^{[1]} = (x_1,x_2)^T$ and $\mathbf{x}^{[2]} = (x_3,x_4,x_5)^T$, respectively; then Eq. 16 can be written as:

$$\begin{bmatrix} x_1 \\ x_2 \end{bmatrix} = L^{-1}\begin{bmatrix} d_{11} & d_{12} \\ d_{21} & d_{22} \end{bmatrix}^{[1]} \times\left(\begin{bmatrix} \bar{f}_1 \\ 0 \end{bmatrix} + \begin{bmatrix} k_{31} & 0 & 0 \\ 0 & k_{42} & 0 \end{bmatrix}\begin{bmatrix} d_{11} & d_{12} & d_{13} \\ d_{21} & d_{22} & d_{23} \\ d_{31} & d_{32} & d_{33} \end{bmatrix}^{[2]}\begin{bmatrix} 0 \\ 0 \\ \bar{f}_3 \end{bmatrix}\right) \qquad \text{(Eq. 39)}$$

The disposition elements $d_{ij}^{[1]}$ and $d_{ij}^{[2]}$ are given by Eq. 11, where **S** is composed as discussed; *i.e.*, $d_{ij}^{[1]}$ is obtained from:

$$|\mathbf{S}|^{[1]} = \begin{vmatrix} (s+E_1) & -k_{12} \\ -k_{21} & (s+E_2) \end{vmatrix} \qquad \text{(Eq. 40)}$$

and $d_{ij}^{[2]}$ is obtained from Eq. 35. The connector constant k_{42} connects the second element of the $\mathbf{x}^{[1]}$ vector with the second element of the $\mathbf{x}^{[2]}$ vector; it is thus placed in the 2,2-position of the connector matrix in Eq. 39. The connector constant k_{31} is placed in the 1,1-position by the same reasoning. The compartments can be numbered arbitrarily as before, but the composition of the **S** and **C** matrices and the input vectors must correspond to the arbitrary order of the elements in the **x** vectors.

For Compartment 1, Eqs. 39 and 11 give:

$$x_1 = L^{-1}\left[\frac{|\mathbf{S}|_{11}^{[1]}}{|\mathbf{S}|^{[1]}}\bar{f}_1 + \frac{k_{31}|\mathbf{S}|_{11}^{[1]}|\mathbf{S}|_{13}^{[2]} + k_{42}|\mathbf{S}|_{12}^{[1]}|\mathbf{S}|_{23}^{[2]}}{|\mathbf{S}|^{[1]}|\mathbf{S}|^{[2]}}\bar{f}_3\right] \qquad \text{(Eq. 41)}$$

from which x_1 can be obtained when f_1 and f_3 are given (6–8, 10–12).

There is always an advantage in using a subsystem approach to solve for a donor system compartment because of the simplification of the system. If the solution for an acceptor system compartment is sought, it will also often be convenient to apply such an approach. The number of algebraic operations required to evaluate a determinant is of the order n^3. With large systems, it should be an advantage to work with the smaller determinants and cofactors of the subsystems.

Partial Transform Approach—Equation 23, which defines the unique time domain solution of Eq. 1, has an advantage over Eq. 12 in that it does not require transformation of the input functions. The elements of the fundamental matrix are always readily found according to Eq. 21 by the method of partial fractions using Heaviside's expansion formula in its extended form (10, 12) because the ratio $|\mathbf{S}|_{ij}/|\mathbf{S}|$ is always of the form $P(s)/Q(s)$, where P and Q are polynomials in s with Q of a higher degree (n) than P. Equation 23, however, has the disadvantage that the input functions, f_i, must be continuous in the time interval of interest. If this is not the case, the approach is still applicable, but the system must be analyzed in sections of time where the input is continuous.

However, in the special case with multiple instantaneous (bolus) inputs into the central compartment, the solution may readily be obtained as:

$$x_j = \sum_{i=1} \Phi_{j1}(t - t_i)m_i \qquad t_i < t \qquad \text{(Eq. 42)}$$

where t_i and m_i are as defined previously (Eq. 31) and the summation is to be taken to the highest integer value of i for which $t_i < t$ is satisfied.

For simplicity, consider the two-compartment system in Scheme VI where the continuous input functions, f_1, is of a form that does not have a simple Laplace transform. For Compartment 1 of this system, Eq. 23 yields directly:

$$x_1 = \Phi_{11}(t)\left[x_1(0) + \int_0^t \Phi_{11}(-t)f_1(t)\,dt\right] + \Phi_{12}(t)\int_0^t \Phi_{21}(-t)f_1(t)\,dt \qquad \text{(Eq. 43)}$$

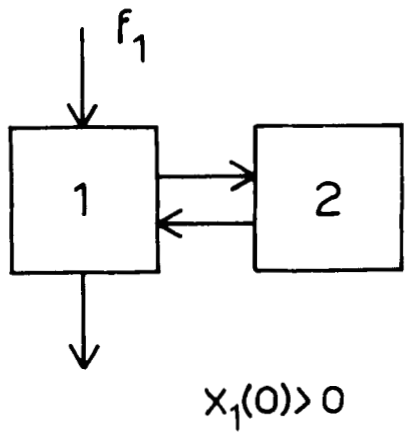

Scheme VI—Two-compartmental linear pharmacokinetic model used to demonstrate the partial transformation approach that does not require Laplace transformation of the input function f_1.

where, according to Eq. 21:

$$\Phi_{11}(t) = \frac{\alpha - E_2}{\alpha - \beta} e^{-\alpha t} + \frac{E_2 - \beta}{\alpha - \beta} e^{-\beta t} \quad \text{(Eq. 44)}$$

$$\Phi_{12}(t) = \frac{-k_{21}}{\alpha - \beta} e^{-\alpha t} + \frac{k_{21}}{\alpha - \beta} e^{-\beta t} \quad \text{(Eq. 45)}$$

$$\Phi_{21}(t) = \frac{-k_{12}}{\alpha - \beta} e^{-\alpha t} + \frac{k_{12}}{\alpha - \beta} e^{-\beta t} \quad \text{(Eq. 46)}$$

and $\alpha\beta = E_1E_2 - k_{12}k_{21}$ and $\alpha + \beta = E_1 + E_2$.

Equation 43 becomes, after substitution:

$$x_1 = \frac{\alpha - E_2}{\alpha - \beta} e^{-\alpha t} \left[x_1(0) + \int_0^t e^{\alpha t} f_1(t)\, dt \right] + \frac{E_2 - \beta}{\alpha - \beta} e^{-\beta t} \left[x_1(0) + \int_0^t e^{\beta t} f_1(t)\, dt \right] \quad \text{(Eq. 47)}$$

As an example, input f_1 may be in the form of a dissolution rate-limited release from an injected depot of slightly soluble crystalline drug. If it is assumed that *in vivo* dissolution follows the Hixson–Crowell relationship (13), then the input function may be written:

$$f_1(t) = -\frac{d}{dt} m_0(1 - k_d t)^3 = 3k_d m_0(1 - k_d t)^2 \qquad t < 1/k_d \quad \text{(Eq. 48)}$$

where m_0 is the dose injected and k_d is the *in vivo* dissolution constant. Substitution of this equation into Eq. 47 yields, after integration:

$$x_1 = \frac{3k_d m_0(\alpha - E_2)}{\alpha(\alpha - \beta)} \left[k_d{}^2 t^2 - \frac{2k_d{}^2 + 2\alpha k_d}{\alpha} t + \frac{2k_d{}^2 + 2\alpha k_d + \alpha^2}{\alpha^2} \right] + \frac{3k_d m_0(E_2 - \beta)}{\beta(\alpha - \beta)} \left[k_d{}^2 t^2 - \frac{2k_d{}^2 + 2\beta k_d}{\beta} t + \frac{2k_d{}^2 + 2\beta k_d + \beta^2}{\beta^2} \right] + \frac{\alpha - E_2}{\alpha - \beta} \left[x_1(0) - \frac{3k_d m_0(2k_d{}^2 + 2\alpha k_d + \alpha^2)}{\alpha^3} \right] e^{-\alpha t} + \frac{E_2 - \beta}{\alpha - \beta} \times \left[x_1(0) - \frac{3k_d m_0(2k_d{}^2 + 2\beta k_d + \beta^2)}{\beta^3} \right] e^{-\beta t} \qquad t < 1/k_d \quad \text{(Eq. 49)}$$

Equation 49 could have been obtained using a full transformation approach but that would require a somewhat larger derivation. The advantage of using a partial transform approach becomes particularly significant for more complex input functions.

REFERENCES

(1) T. Teorell, *Arch. Int. Pharmacodyn. Ther.*, **57**, 205 (1937).

(2) F. H. Dost, "Der Blutspiegel," Georg Thieme, Stuttgart, Germany, 1968, chap. 5.

(3) A. Rescigno and G. Serge, "Drug and Tracer Kinetics," Blaisdell, New York, N.Y., 1966, chap. 4.

(4) D. S. Riggs, "Control Theory and Physiological Feedback Mechanism," Williams & Wilkins, Baltimore, Md., 1970, chap. 3.

(5) J. G. Wagner, "Biopharmaceutics and Relevant Pharmacokinetics," Drug Intelligence Publications, Hamilton, Ill., 1971, chap. 35.

(6) L. Z. Benet, *J. Pharm. Sci.*, **61**, 536 (1972).

(7) D. P. Vaughan and A. Trainor, *J. Pharmacokinet. Biopharm.*, **3**, 203 (1975).

(8) D. P. Vaughan, D. J. H. Mallard, A. Trainor, and M. Mitchard, *Eur. J. Clin. Pharmacol.*, **8**, 141 (1975).

(9) J. L. Goldberg and A. J. Schwartz, "System of Ordinary Differential Equations," Harper & Row, San Francisco, Calif., 1972, p. 211.

(10) L. Z. Benet and J. S. Turi, *J. Pharm. Sci.*, **60**, 1592 (1971).

(11) G. Doetsch, "Handbuch der Laplace-Transformation," vols. I–III, Birkhauser Verlag, Basel, Switzerland, 1971.

(12) M. R. Spiegel, "Laplace Transforms," McGraw-Hill, San Francisco, Calif., 1965, p. 8.

(13) A. W. Hixson and J. H. Crowell, *Ind. Eng. Chem.*, **23**, 923 (1931).

Physiological Perfusion Model for Cephalosporin Antibiotics I: Model Selection Based on Blood Drug Concentrations

D. S. GREENE *x, R. QUINTILIANI, and C. H. NIGHTINGALE ‡

Received December 2, 1976, from the *School of Pharmacy, University of Connecticut, Storrs, CT 06268,* and the *Department of Medicine, Hartford Hospital, Hartford, CT 06115.* Accepted for publication May 2, 1977. *Present address: College of Pharmacy, University of Rhode Island, Kingston, RI 02881. ‡Present address: School of Pharmacy, State University of New York at Buffalo, Amherst, NY 14260.

Abstract □ Various cephalosporins with different degrees of protein binding were administered to human volunteers. Blood samples were collected as a function of time and were assayed for drug content by a microbiological assay. A pharmacokinetic analysis of the data was performed using a two-compartment model with and without protein binding in the central compartment and a perfusion model. Both the two-compartment model without protein binding and the physiological perfusion model adequately described the blood levels of all three cephalosporins.

Keyphrases □ Cephalosporins, various—pharmacokinetic analysis using two-compartment and perfusion models □ Antibiotics, various cephalosporin—pharmacokinetic analysis using two-compartment and perfusion models □ Models, pharmacokinetic—two-compartment and perfusion, for various cephalosporins

Compartmental models are a "black box" approach to predicting blood levels. The model consists of a central compartment, usually considered to be the plasma compartment, and possibly one or more tissue compartments. The compartments and the associated volumes and rate constants have no physiological meaning; *i.e.*, the plasma

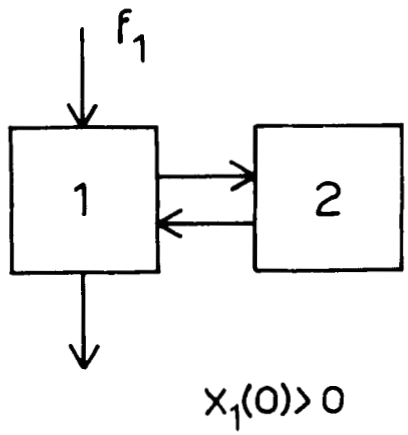

Scheme VI—Two-compartmental linear pharmacokinetic model used to demonstrate the partial transformation approach that does not require Laplace transformation of the input function f_1.

where, according to Eq. 21:

$$\Phi_{11}(t) = \frac{\alpha - E_2}{\alpha - \beta} e^{-\alpha t} + \frac{E_2 - \beta}{\alpha - \beta} e^{-\beta t} \quad \text{(Eq. 44)}$$

$$\Phi_{12}(t) = \frac{-k_{21}}{\alpha - \beta} e^{-\alpha t} + \frac{k_{21}}{\alpha - \beta} e^{-\beta t} \quad \text{(Eq. 45)}$$

$$\Phi_{21}(t) = \frac{-k_{12}}{\alpha - \beta} e^{-\alpha t} + \frac{k_{12}}{\alpha - \beta} e^{-\beta t} \quad \text{(Eq. 46)}$$

and $\alpha\beta = E_1E_2 - k_{12}k_{21}$ and $\alpha + \beta = E_1 + E_2$.

Equation 43 becomes, after substitution:

$$x_1 = \frac{\alpha - E_2}{\alpha - \beta} e^{-\alpha t} \left[x_1(0) + \int_0^t e^{\alpha t} f_1(t)\, dt \right] + \frac{E_2 - \beta}{\alpha - \beta} e^{-\beta t} \left[x_1(0) + \int_0^t e^{\beta t} f_1(t)\, dt \right] \quad \text{(Eq. 47)}$$

As an example, input f_1 may be in the form of a dissolution rate-limited release from an injected depot of slightly soluble crystalline drug. If it is assumed that *in vivo* dissolution follows the Hixson–Crowell relationship (13), then the input function may be written:

$$f_1(t) = -\frac{d}{dt} m_0(1 - k_d t)^3 = 3k_d m_0(1 - k_d t)^2 \qquad t < 1/k_d \quad \text{(Eq. 48)}$$

where m_0 is the dose injected and k_d is the *in vivo* dissolution constant. Substitution of this equation into Eq. 47 yields, after integration:

$$x_1 = \frac{3k_d m_0(\alpha - E_2)}{\alpha(\alpha - \beta)} \left[k_d{}^2 t^2 - \frac{2k_d{}^2 + 2\alpha k_d}{\alpha} t + \frac{2k_d{}^2 + 2\alpha k_d + \alpha^2}{\alpha^2} \right] + \frac{3k_d m_0(E_2 - \beta)}{\beta(\alpha - \beta)} \left[k_d{}^2 t^2 - \frac{2k_d{}^2 + 2\beta k_d}{\beta} t + \frac{2k_d{}^2 + 2\beta k_d + \beta^2}{\beta^2} \right] + \frac{\alpha - E_2}{\alpha - \beta} \left[x_1(0) - \frac{3k_d m_0(2k_d{}^2 + 2\alpha k_d + \alpha^2)}{\alpha^3} \right] e^{-\alpha t} + \frac{E_2 - \beta}{\alpha - \beta} \times \left[x_1(0) - \frac{3k_d m_0(2k_d{}^2 + 2\beta k_d + \beta^2)}{\beta^3} \right] e^{-\beta t} \qquad t < 1/k_d \quad \text{(Eq. 49)}$$

Equation 49 could have been obtained using a full transformation approach but that would require a somewhat larger derivation. The advantage of using a partial transform approach becomes particularly significant for more complex input functions.

REFERENCES

(1) T. Teorell, *Arch. Int. Pharmacodyn. Ther.*, **57**, 205 (1937).

(2) F. H. Dost, "Der Blutspiegel," Georg Thieme, Stuttgart, Germany, 1968, chap. 5.

(3) A. Rescigno and G. Serge, "Drug and Tracer Kinetics," Blaisdell, New York, N.Y., 1966, chap. 4.

(4) D. S. Riggs, "Control Theory and Physiological Feedback Mechanism," Williams & Wilkins, Baltimore, Md., 1970, chap. 3.

(5) J. G. Wagner, "Biopharmaceutics and Relevant Pharmacokinetics," Drug Intelligence Publications, Hamilton, Ill., 1971, chap. 35.

(6) L. Z. Benet, *J. Pharm. Sci.*, **61**, 536 (1972).

(7) D. P. Vaughan and A. Trainor, *J. Pharmacokinet. Biopharm.*, **3**, 203 (1975).

(8) D. P. Vaughan, D. J. H. Mallard, A. Trainor, and M. Mitchard, *Eur. J. Clin. Pharmacol.*, **8**, 141 (1975).

(9) J. L. Goldberg and A. J. Schwartz, "System of Ordinary Differential Equations," Harper & Row, San Francisco, Calif., 1972, p. 211.

(10) L. Z. Benet and J. S. Turi, *J. Pharm. Sci.*, **60**, 1592 (1971).

(11) G. Doetsch, "Handbuch der Laplace-Transformation," vols. I–III, Birkhauser Verlag, Basel, Switzerland, 1971.

(12) M. R. Spiegel, "Laplace Transforms," McGraw-Hill, San Francisco, Calif., 1965, p. 8.

(13) A. W. Hixson and J. H. Crowell, *Ind. Eng. Chem.*, **23**, 923 (1931).

Physiological Perfusion Model for Cephalosporin Antibiotics I: Model Selection Based on Blood Drug Concentrations

D. S. GREENE *x, R. QUINTILIANI, and C. H. NIGHTINGALE ‡

Received December 2, 1976, from the *School of Pharmacy, University of Connecticut, Storrs, CT 06268,* and the *Department of Medicine, Hartford Hospital, Hartford, CT 06115.* Accepted for publication May 2, 1977. *Present address: College of Pharmacy, University of Rhode Island, Kingston, RI 02881. ‡Present address: School of Pharmacy, State University of New York at Buffalo, Amherst, NY 14260.

Abstract □ Various cephalosporins with different degrees of protein binding were administered to human volunteers. Blood samples were collected as a function of time and were assayed for drug content by a microbiological assay. A pharmacokinetic analysis of the data was performed using a two-compartment model with and without protein binding in the central compartment and a perfusion model. Both the two-compartment model without protein binding and the physiological perfusion model adequately described the blood levels of all three cephalosporins.

Keyphrases □ Cephalosporins, various—pharmacokinetic analysis using two-compartment and perfusion models □ Antibiotics, various cephalosporin—pharmacokinetic analysis using two-compartment and perfusion models □ Models, pharmacokinetic—two-compartment and perfusion, for various cephalosporins

Compartmental models are a "black box" approach to predicting blood levels. The model consists of a central compartment, usually considered to be the plasma compartment, and possibly one or more tissue compartments. The compartments and the associated volumes and rate constants have no physiological meaning; *i.e.*, the plasma

Table I—Plasma Flows and Organ Weights for Perfusion Model Calculations

Tissue	Total Volume, liters	Extracellular[a] Volume, liters	Plasma[b] Flow, liters/hr
Bone	3.60[c]	—[d]	6.48[c]
Skin	3.00[c]	0.45	7.60[c]
RET	0.60[c]	0.09	57.60[e]
Muscle	33.00[e]	4.95	43.20[e]
Liver	3.90[e]	0.59	54.00
Blood	5.40[c]	3.24[b]	168.88[f]

[a] Calculated by multiplying total volume by 0.15, the fraction of tissue weight that is extracellular water (18). [b] Calculated by multiplying blood flow or blood volume by (1 − hematocrit), using an hematocrit of 0.40 (18). [c] From W. W. Mapleson, *J. Appl. Physiol.*, 18, 197 (1963). [d] Extracellular water not assumed for bone compartment. [e] Reference 9. [f] Calculated as sum of all plasma flows to listed tissues.

compartment does not consist of solely the plasma but also contains all well-perfused tissues. The number of compartments and the tissues in each compartment vary with different drugs, depending on the physical characteristics and binding of the drug. There are cases, however, where a physiological interpretation of parameters or compartments may be applicable (1).

Although the physiological interpretation of parameters obtained from compartmental analysis is limited, these models are useful for the prediction of blood levels and for the development of dosage regimens (1). The compartment models, however, have a very limited ability for predicting tissue levels.

The compartmental model approach does not address directly the serum protein binding of drugs. Although the shape and height of a serum level *versus* time curve are altered by protein binding and the resultant pharmacokinetic constants obtained from compartmental analysis reflects this change, specific information regarding the binding processes is usually not available.

A physiological perfusion model was proposed (2) to describe the uptake of thiopental by various tissues of the body. The model was revolutionary because it used physiological volumes and blood flows instead of black box compartments. The perfusion model was used to describe the pharmacokinetics of methotrexate (3–5) and cytarabine (6, 7). Other studies using the perfusion model also have appeared (8–10). The predictions that have been made of tissue and plasma levels have generally agreed well with experimental data.

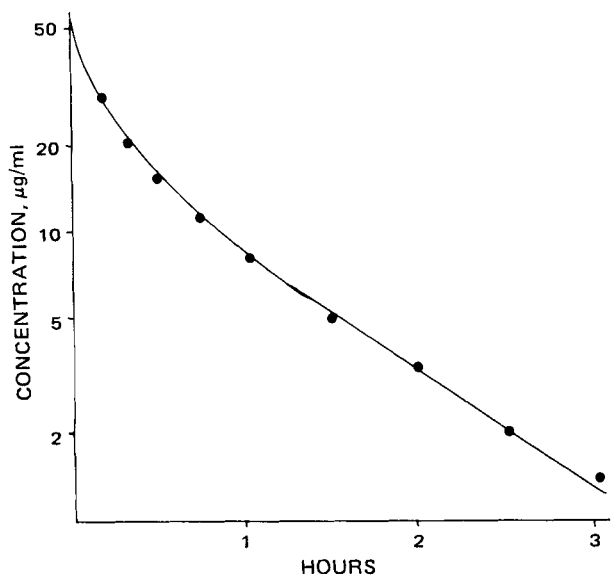

Figure 1—*Serum cephalexin concentration* versus *time after a 1-g iv dose.*

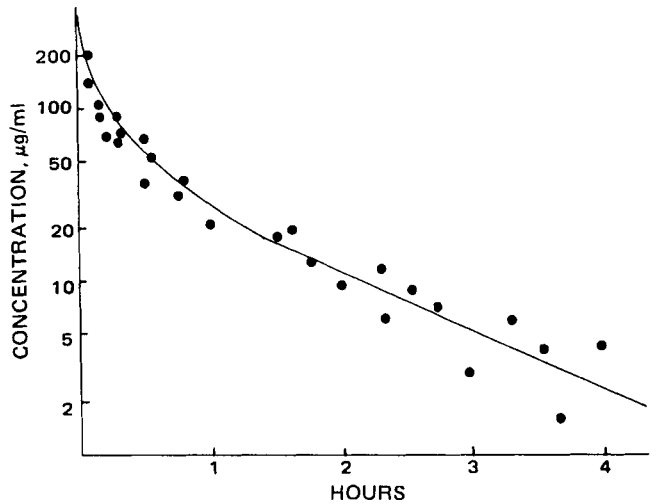

Figure 2—*Serum cephradine concentration* versus *time after a 2-g iv dose.*

The pharmacokinetics of the cephalosporins previously were studied using a compartmental analysis (11–14). Physiological blood flow models have not been investigated for these drugs. The purpose of this study was to evaluate the pharmacokinetics of cefazolin (highly bound) and cephradine and cephalexin (negligibly bound) using a variety of models to describe the data.

EXPERIMENTAL

The cephalosporins selected for study, *i.e.*, cefazolin, cephalexin, and cephradine, were reported to be 88, 10, and 15% bound to human plasma proteins at normal therapeutic concentrations, respectively. One gram of cefazolin, 0.5 g of cephalexin, and 2.0 g of cephradine were administered intravenously to five healthy human volunteers. Blood samples were collected as a function of time for 4 hr after administration.

Several weeks lapsed between the administration of each drug. Serum was separated from blood and frozen until assayed, using a disk diffusion microbiological technique (15).

PHARMACOKINETIC MODELING

Three models were used to fit the data: a two-compartment model, a two-compartment model with protein binding, and a perfusion model. The two-compartment model without protein binding (Scheme I) was modified by the addition of binding within the central (plasma) compartment (Scheme II). The following assumptions were made in the development of the model:

1. Binding is present only in the central compartment; all drug in the tissue compartment is in the free form.
2. Distribution and elimination are linear processes.
3. Only free drug is able to distribute to the tissue compartment; *i.e.*, the rate of distribution is proportional to the free drug concentration.
4. The binding equilibrium in the central compartment occurs in-

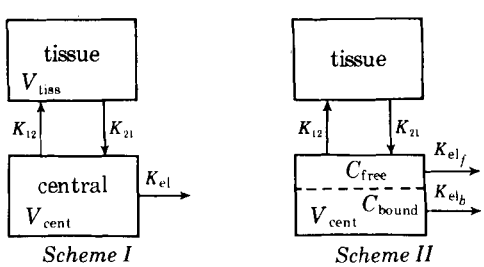

Scheme I *Scheme II*

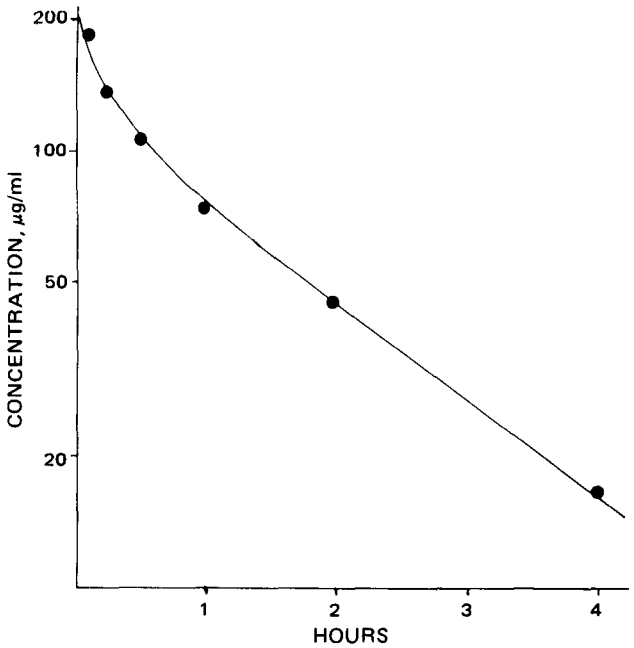

Figure 3—*Serum cefazolin concentration* versus *time after a 1-g iv dose.*

stantaneously, the concentrations of free and bound drugs being defined by:

$$C_B = \frac{n_1 K_{a_1} P C_f}{1 + K_{a_1} C_f} + \frac{n_2 K_{a_2} P C_f}{1 + K_{a_2} C_f} \qquad \text{(Eq. 1)}$$

where C_B and C_f represent the bound and free concentrations of drug, respectively; n_1 and n_2 and K_{a_1} and K_{a_2} represent the numbers of binding sites and affinity constants, respectively, for each type of binding site; and P represents the concentration of protein in the central compartment.

The concentration of protein is assumed to be constant throughout the central compartment. It is expected that the fitted volume of the central compartment approaches the plasma volume (3.2 liters).

5. Elimination of both free and bound drug occurs. The rate constant for the elimination of the drug is a sum of the elimination rate constants of free and bound drug.

The differential equations used to fit the serum concentrations of cefazolin were:

$$\frac{d(C_t)}{dt} = K_{21} C_2 - K_{12} C_f - K_{el_b} C_b - K_{el_f} C_f \qquad \text{(Eq. 2)}$$

$$\frac{d(C_2)}{dt} = K_{12} C_f - K_{21} C_2 \qquad \text{(Eq. 3)}$$

where C_2 represents the concentration of drug in the tissue compartment, and C_f and C_t represent the free and total concentrations of drug in the central compartment, respectively. The rate constants K_{12}, K_{21}, K_{el_b}, and K_{el_f} are defined in Scheme II.

All data were fit using an overall rate constant, K_{el}, which represented the sum of K_{el_b} and K_{el_f}. All serum level data were in the form of the total concentration of cefazolin in the plasma. The free concentration of cefazolin in the plasma was calculated by solving Eq. 1 for C_f. The initial conditions for the integration of these equations were C_t = dose/V_c and $C_2 = 0$ at time = 0 for Eqs. 2 and 3, respectively, where V_c represents the volume of the central compartment.

A perfusion model similar to that by Benowitz *et al.* (9) was developed for the cephalosporin antibiotics using the following assumptions:

1. The equilibrium between free and bound drug is an instantaneous process, the free and bound drug concentrations being described by the Scatchard equation (Eq. 1).

2. Only free drug is able to leave the plasma and enter the tissue; the bound drug is retained in the plasma.

3. The distribution of drug between the plasma and tissues is blood flow limited.

4. Drug does not enter the cells of the tissues; all drug is contained within the extracellular water of the tissues.

5. Drug in the blood is restricted to the plasma water; the drug is unable to enter the erythrocytes.

6. Elimination of drug occurs by: (*a*) glomerular filtration—only the free drug is filtered in the glomerulus, and (*b*) tubular secretion—both free and bound drug are removed by active secretion.

7. Since bone is largely porous mineral substance, the drug is assumed to distribute through the entire tissue.

Assumptions 4 and 5 follow from the work of Okui *et al.* (16) and Kornguth and Kunin (17). These independent studies showed that erythrocytes are relatively impermeable to the cephalosporins. Since the membranes of cells in various tissues are very similar to the membranes of the erythrocytes, cephalosporins probably cannot penetrate into these tissues; *i.e.*, the drug will be restricted to the extracellular water.

For the purpose of characterizing cephalosporin distribution in the body, the following tissue compartments were chosen: skin, which has a large volume compartment and low blood flow; rapidly equilibrating tissues (RET), including the heart and kidneys, which have small volumes and high blood flows; muscle tissue, which has moderate blood flow and intermediate mass; liver, which has large blood flow and intermediate mass; and bone, which is a relatively high-volume, poorly perfused tissue.

The brain was not included in this model because of the lack of penetration of the cephalosporins into the cerebral spinal fluid (18). The fat tissue was also excluded because of the poor lipid solubility of the cephalosporins.

The perfusion model used for the calculation of blood and tissue levels appears in Scheme III. The values used for the blood flows and organ volumes appear in Table I. The contribution of glomerular filtration to

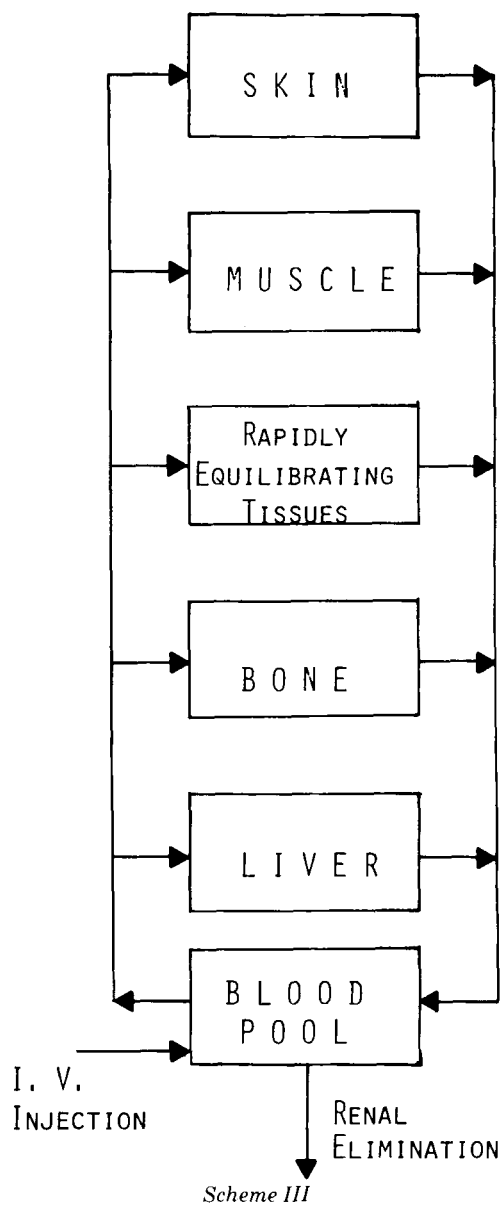

Scheme III

Table II—Pharmacokinetic Parameters for Cephalexin, Cefazolin, and Cephradine Using Two-Compartment Model Analysis

Parameter	Cefazolin	Cephradine	Cephalexin
Dose, g	1.0	2.0	0.5
α, hr^{-1}	4.83 ± 1.78	6.23 ± 1.57	4.64 ± 0.09
β, hr^{-1}	0.57 ± 0.12	0.88 ± 0.13	0.93 ± 0.09
K_{12}, hr^{-1}	1.96 ± 0.94	2.39 ± 0.84	1.27 ± 0.13
K_{21}, hr^{-1}	2.15 ± 0.91	1.73 ± 0.38	2.68 ± 0.22
K_{el}, hr^{-1}	1.30 ± 0.23	2.12 ± 0.63	1.62 ± 0.14
$T_{1/2_\alpha}$, hr	0.17 ± 0.08	0.12 ± 0.03	0.15 ± 0.01
$T_{1/2_\beta}$, hr	1.25 ± 0.26	0.81 ± 0.11	0.75 ± 0.07
V_c, liters	3.48 ± 0.36	10.20 ± 2.01	10.90 ± 0.80
$V_{d_{ss}}$, liters	6.79 ± 1.87	19.02 ± 2.00	16.40 ± 1.20
V_{d_β}, liters	8.15 ± 2.61	23.65 ± 1.25	19.60 ± 1.10
$V_{d_{ext}}$, liters	10.11 ± 3.76	30.70 ± 0.97	24.70 ± 2.00

drug elimination from the body was calculated by assuming a glomerular filtration rate of 120 ml/min for free drug (19) and by calculating the clearance of total drug with the assumption that only free drug is filtered. The active secretion rates, calculated by subtracting the contribution of glomerular filtration from the total drug clearance, were 53, 170, and 240 ml/min for cefazolin, cephalexin, and cephradine, respectively.

A differential equation describing the concentration of drug in a tissue compartment can be written as:

$$V_{\text{tiss}} \frac{d(C_{\text{tiss}})}{dt} = Q_{\text{tiss}}(C_f - C_{\text{tiss}}) \qquad \text{(Eq. 4)}$$

where V_{tiss} and Q_{tiss} represent the volumes of the tissue and plasma flow to the tissue, respectively; and C_f and C_{tiss} represent the free concentrations of drug in the plasma and tissue, respectively. A differential equation for the total drug concentration, C_t, in the plasma can be written as:

$$V_P \frac{d(C_t)}{dt} = \Sigma Q_{\text{tiss}_i}(C_{\text{tiss}_i} - C_f) - \text{GFR}C_f - \text{AS}C_t \qquad \text{(Eq. 5)}$$

where V_P and Q_{tiss_i} represent the plasma volume and plasma flow to the ith tissue, respectively; and C_f represents the free concentration of drug in the plasma. Elimination of drug from the body is included in the terms GFR and AS, the glomerular filtration and active secretion rates, respectively. Equation 5, a differential equation describing the rate of change of total drug in plasma, can be transformed (see *Appendix*) to give a differential equation for the free concentration of drug in the plasma:

$$V_P \frac{d(C_f)}{dt} = \frac{\Sigma Q_{\text{tiss}_i}(C_{\text{tiss}_i} - C_f) - \text{GFR}C_f - \text{AS}C_t}{1 + \dfrac{n_1 K_{a_1} P}{(1 + K_{a_1} C_f)^2} + \dfrac{n_2 K_{a_2} P}{(1 + K_{a_2} C_f)^2}} \qquad \text{(Eq. 6)}$$

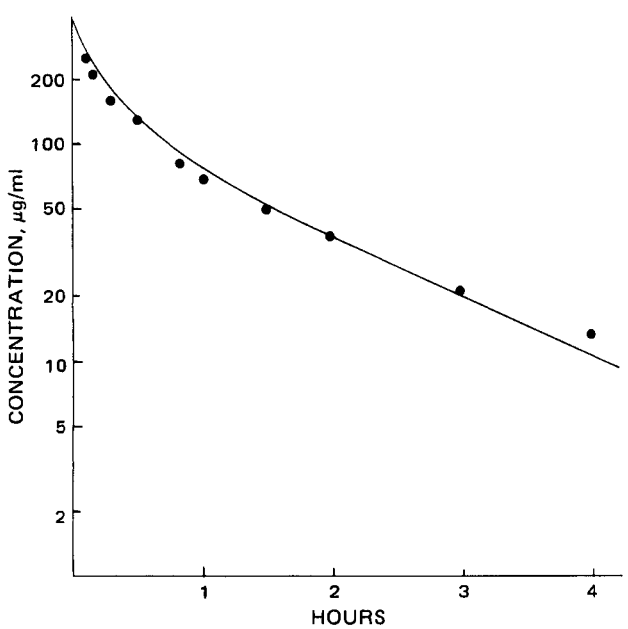

Figure 4—*Serum cefazolin concentration* versus *time fit using two-compartment open model with protein binding.*

Table III—Pharmacokinetic Parameters for Cefazolin Using Two-Compartment Model with Protein Binding

Parameter	Value
K_{12}, hr^{-1}	7.25 ± 23.50
K_{21}, hr^{-1}	1.00 ± 16.09
K_{el}, hr^{-1}	1.15 ± 145.11
V_c, liters	4.04 ± 51.07

in which C_{tiss} represents the free concentration of drug in the tissue.

Differential equations in the form of Eq. 4 were written for each tissue compartment, and Eq. 6 was used to describe the free plasma concentration of drug. The values for protein binding parameters for cefazolin obtained from continuous ultrafiltration experiments were 0.1 and 0.85 mole for n_1 and n_2, respectively. The 0.1-mole value of n_1 may indicate that this binding site represents binding to a protein species less abundant than serum albumin. The affinity constants K_{a_1} and K_{a_2} were 2.67×10^5 and 2.4×10^4 liters/mole, respectively. An albumin concentration of 5.97×10^{-4} M was assumed for all calculations. Both cephalexin and cephradine were assumed to be completely in the free form since the binding was less than 10% at normal therapeutic concentrations.

RESULTS AND DISCUSSION

Two-Compartment Model Analysis of Cephalosporin Data—Semilog plots of the serum concentration of cephalexin (Fig. 1), cephradine (Fig. 2), and cefazolin (Fig. 3) *versus* time all were nonlinear, indicating that a one-compartment model would not adequately describe the pharmacokinetics of these cephalosporins (11). Therefore, a two-compartment model (Scheme I) was used.

All two-compartment model analyses were performed using the NONLIN nonlinear least-squares regression program (20). The integrated forms of the two-compartment model equations were used for all data fitting (1). It was assumed that elimination and distribution were first-order processes, the rate being proportional to the total drug concentration. All serum levels were in terms of total levels, and no attempt was made to correct for any form of drug binding.

The parameters obtained for the fits of the two-compartment model equations to the blood level data from cefazolin, cephalexin, and cephradine after intravenous doses appear in Table II. All correlation

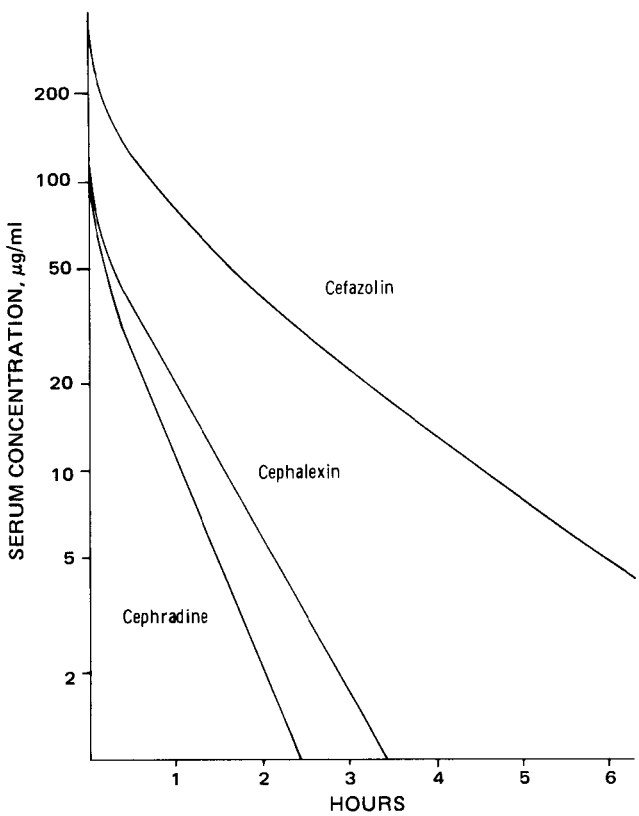

Figure 5—*Calculated serum levels for cefazolin, cephradine, and cephalexin using perfusion model after a 1-g iv dose.*

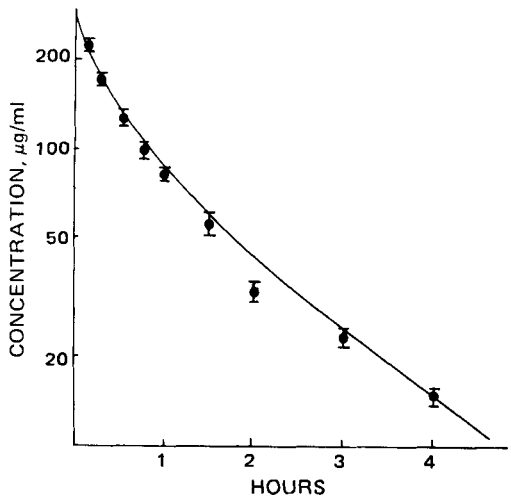

Figure 6—*Serum cefazolin levels in humans after a 1-g iv dose. Key:—, calculated levels of cefazolin using perfusion model; and ●, experimental serum drug levels.*

coefficients exceeded 0.98, indicating excellent fits of the model to the experimental data. A comparison of the volume of distribution for cefazolin with cephradine and cephalexin demonstrates the effect of protein binding on this parameter. The decreased volume of distribution of cefazolin accounts for the higher serum levels that have been found for this drug.

The clearance of these cephalosporins was calculated using the formula:

$$\text{clearance} = K_{el}V_c \qquad \text{(Eq. 7)}$$

The clearances for cefazolin, cephalexin, and cephradine were 75.4, 294, and 364 ml/min, respectively. The low value reported for the clearance of cefazolin in comparison to the other cephalosporins may be due to the high fraction of the drug present in the bound form.

Two-Compartment Model with Protein Binding for Cefazolin—The two-compartment model without protein binding adequately described the blood levels of all of the cephalosporins studied. However, since cefazolin is approximately 80–90% protein bound at normal therapeutic concentrations, a two-compartment model with protein binding was investigated. Because of problems associated with obtaining fits of Eq. 2 to the experimental data, it was possible to fit data from only one of the five subjects. The parameters obtained from this fit are listed in Table III. The NONLIN program was unable to converge to suitable

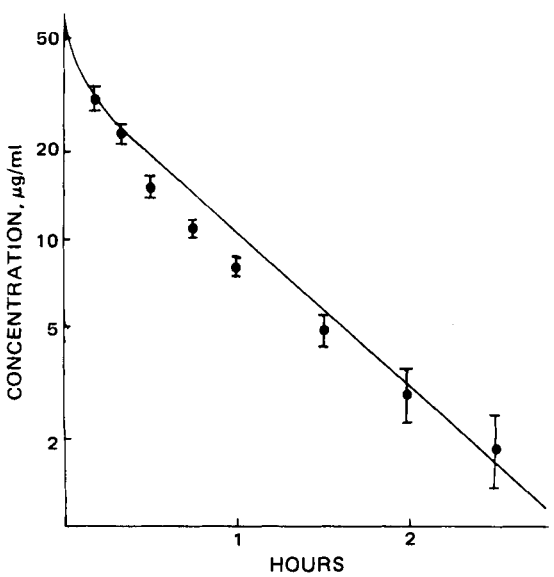

Figure 7—*Serum cephalexin levels in humans after a 0.5-g iv dose. Key: —, calculated levels of cephalexin using perfusion model; and ●, experimental serum drug levels.*

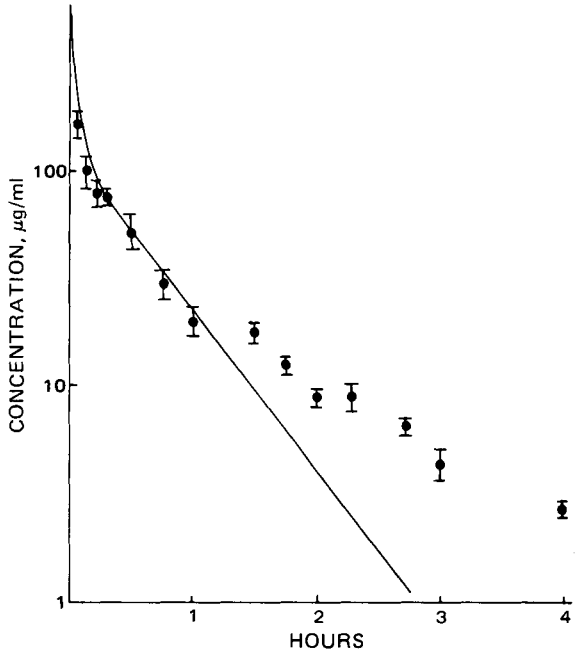

Figure 8—*Serum cephradine levels in humans after a 2-g iv dose. Key: —, calculated levels of cephradine using perfusion model; and ●, experimental serum drug levels.*

estimates for the parameters within 20 iterations for the other four subjects. Adjustment of the initial estimates did little to improve the fit of the equation to the data. A plot of calculated and experimental data for the subject fit by this model appears in Fig. 4. The parameters n_1, n_2, K_{a_1}, and K_{a_2} represent protein binding parameters and were not fitted parameters. The parameters K_{12}, K_{21}, K_{el}, and V_c were fitted to the data.

Examination of Table III shows that the parameters have extremely large standard deviations. Since only one set of data was fit and the standard deviations were unacceptably large, it was concluded that this model could not adequately fit the data using the NONLIN (20) program.

Perfusion Model Predictions of Cephalosporin Levels—The calculated serum levels for a 1-g dose of cefazolin, cephradine, and cephalexin appear in Fig. 5. Comparison of the calculated serum levels using the perfusion model with actual data for cefazolin (Fig. 6) and cephalexin (Fig. 7) demonstrates that this model adequately predicts the serum levels for these drugs.

The perfusion model also predicted the levels for cephradine (Fig. 8) for the first 1.5 hr after administration. However, after 1.5 hr, the experimental data were consistently higher than the predicted line. This deviation between the two curves may be attributable to an overestimate of cephradine clearance in the perfusion model.

The perfusion model was designed for any drug with the characteristics outlined in the previously stated assumptions. For cefazolin, the model was adjusted to account for protein binding. The excellent fit of the data to the predicted curve suggests that these drugs are basically "handled" in a similar fashion by the body and that their different pharmacokinetic profiles are mainly a function of protein binding.

The results of this study show that the two-compartment model with protein binding could not adequately describe the data, probably because the model is a complex nonlinear model.

The two-compartment model and the flow model were equally effective in describing the serum data.

APPENDIX

The equation for the change in total drug as a function of time is Eq. 5. The change in total drug as a function of time can be written as:

$$\frac{d(C_t)}{dt} = \frac{d(C_B)}{dt} + \frac{d(C_f)}{dt} \qquad \text{(Eq. A1)}$$

since:

$$C_t = C_B + C_f \qquad \text{(Eq. A2)}$$

where C_t, C_B, and C_f represent the concentrations of total, bound, and free drug, respectively. The concentration of bound drug can be written as shown in Eq. 1. Differentiation of Eq. 1 yields:

$$\frac{d(C_B)}{dt} = \left[\frac{n_1 K_{a_1} P}{(1 + K_{a_1} C_f)^2} + \frac{n_2 K_{a_2} P}{(1 + K_{a_2} C_f)^2}\right] \frac{d(C_f)}{dt} \qquad \text{(Eq. A3)}$$

Substitution of Eqs. A3 and A2 into Eq. 5 yields Eq. 6.

REFERENCES

(1) J. G. Wagner, "Fundamentals of Clinical Pharmacokinetics," Drug Intelligence Publications, Hamilton, Ill., 1976.

(2) H. L. Price, P. J. Kovnat, J. Safer, E. H. Conner, and M. L. Price, *Clin. Pharmacol. Ther.*, **1**, 16 (1960).

(3) R. L. Dedrick, D. S. Zaharko, and R. J. Lutz, *J. Pharm. Sci.*, **62**, 882 (1973).

(4) K. B. Bischoff, R. L. Dedrick, D. S. Zaharko, and J. S. Longstreth, *ibid.*, **60**, 1128 (1971).

(5) K. B. Bischoff, R. L. Dedrick, and D. S. Zaharko, *ibid.*, **59**, 149 (1970).

(6) R. L. Dedrick, D. D. Forester, and D. H. W. Ho, *Biochem. Pharmacol.*, **21**, 1 (1972).

(7) R. L. Dedrick, D. D. Forester, J. N. Cannon, S. M. El Dareen, and L. B. Mellett, *ibid.*, **22**, 2405 (1972).

(8) C. N. Chen and J. D. Andrade, *J. Pharm. Sci.*, **65**, 717 (1976).

(9) N. Benowitz, R. P. Forsyth, K. L. Melmon, and M. Rowland, *Clin. Pharmacol. Ther.*, **16**, 87 (1974).

(10) A. Zwart, N. T. Smith, and J. E. W. Beneken, *Comp. Biomed. Res.*, **5**, 228 (1972).

(11) D. S. Greene, D. R. Flanagan, R. Quintiliani, and C. H. Nightingale, *J. Clin. Pharmacol.*, **16**, 257 (1976).

(12) C. H. Nightingale, D. S. Greene, and R. Quintiliani, *J. Pharm. Sci.*, **64**, 1899 (1975).

(13) C. Simon, V. Malerczyk, E. Brahnstaedt, and W. Toeller, *Dtsch. Med. Wochenschr.*, **98**, 2448 (1973).

(14) J. Kosmidis, J. M. T. Hamilton-Miller, J. N. G. Gilchrist, D. W. Kerry, and W. Brumfitt, *Br. Med. J.*, **4**, 653 (1973).

(15) D. C. Grove and W. A. Randall, "Assay Methods of Antibiotics, A Laboratory Manual," Medical Encyclopedia, New York, N.Y., 1955.

(16) M. Okui, T. Matsubara, M. Nishida, and J. Kozatani, *Adv. Antimicrob. Antineoplast. Chemother.*, **1**, 915 (1972).

(17) M. L. Kornguth and C. M. Kunin, *J. Infect. Dis.*, **133**, 175 (1976).

(18) H. P. Bassaris, R. Quintiliani, E. G. Maderazo, R. C. Tilton, and C. H. Nightingale, *Curr. Ther. Res.*, **19**, 110 (1976).

(19) "Scientific Tables," K. Diem and C. Lenter, Eds., Ciba-Geigy, Basel, Switzerland, 1970.

(20) C. M. Metzler, G. L. Elfring, and A. J. McEwen, "A Users Manual for NONLIN and Associated Programs," Upjohn Co., Kalamazoo, Mich., 1974.

Stabilization of Sulfisomidine Tablets by Use of Film Coating Containing UV Absorber: Protection of Coloration and Photolytic Degradation from Exaggerated Light

YOSHIHISA MATSUDA ˣ, HIROMI INOUYE, and REIKO NAKANISHI

Received February 17, 1977, from *Kobe Women's College of Pharmacy, Higashinada, Kobe 658, Japan.* Accepted for publication April 28, 1977.

Abstract □ The effect of model polymer coating films of vinyl acetate, containing oxybenzone as a UV absorber, on the coloration and photolytic degradation of simple sulfisomidine tablets was examined to attempt stabilization of photosensitive solid dosage forms. Coloration of the tablet surface was followed by the tristimulus colorimetric method in the fading tester equipped with a mercury vapor lamp. Photolytic degradation in the UV region was investigated by a new method for measuring the absorption spectra of a crystal sample in the gas phase, *i.e.*, the semi-integral *attenuance spectra*. Two parameters of a film, thickness and concentration of the UV absorber, were varied at every exposure. These physical and chemical changes are discussed in relation to light transmission properties of films.

Keyphrases □ Sulfisomidine tablets—effect of film coating containing UV absorber on coloration and photolytic degradation □ Film coating—containing UV absorber, effect on coloration and photolytic degradation of sulfisomidine tablets □ UV absorber—contained in film coating, effect on coloration and photolytic degradation of sulfisomidine tablets □ Coloration—sulfisomidine tablets, effect of film coating containing UV absorber □ Photolytic degradation—sulfisomidine tablets, effect of film coating containing UV absorber □ Degradation, photolytic—sulfisomidine tablets, effect of film coating containing UV absorber □ Tablets—sulfisomidine, coloration and photolytic degradation, effect of film coating containing UV absorber

Many solid pharmaceutical medicaments exhibit physical or chemical changes because of the radiant energy of light. Light irradiation can cause color development or color fading. From pharmaceutical and therapeutic standpoints, physical changes can be as serious as chemical instability of the active ingredient. Therefore, protection of solid dosage forms under storage from the deleterious effects of light is one problem in quality control.

Pharmaceutical products can be adequately protected by the use of special glass containers, *i.e.*, light-resistant containers specified in pharmacopeias. The protective effect of colored glass on the fading of tablets containing colorants (1, 2) and on the coloration and photolytic degradation of photolabile sulfisomidine tablets (3) has been investigated.

Coating tablets with a polymer film containing UV absorbers may be another method for protection from light. Along with the use of light-resistant containers, this approach should increase the protective effect since the coating is applied to individual tablets. The effect of the protective coating on the photostability of colorants used in the tablet coating also was studied (4–6), but no report dealt with organic active ingredients. One interesting point in such studies of solid-state stability is the relationship shown to exist (3) between the apparent and chemical changes.

The purpose of the present work was to investigate the

where C_t, C_B, and C_f represent the concentrations of total, bound, and free drug, respectively. The concentration of bound drug can be written as shown in Eq. 1. Differentiation of Eq. 1 yields:

$$\frac{d(C_B)}{dt} = \left[\frac{n_1 K_{a_1} P}{(1 + K_{a_1} C_f)^2} + \frac{n_2 K_{a_2} P}{(1 + K_{a_2} C_f)^2}\right] \frac{d(C_f)}{dt} \qquad \text{(Eq. A3)}$$

Substitution of Eqs. A3 and A2 into Eq. 5 yields Eq. 6.

REFERENCES

(1) J. G. Wagner, "Fundamentals of Clinical Pharmacokinetics," Drug Intelligence Publications, Hamilton, Ill., 1976.

(2) H. L. Price, P. J. Kovnat, J. Safer, E. H. Conner, and M. L. Price, *Clin. Pharmacol. Ther.*, **1**, 16 (1960).

(3) R. L. Dedrick, D. S. Zaharko, and R. J. Lutz, *J. Pharm. Sci.*, **62**, 882 (1973).

(4) K. B. Bischoff, R. L. Dedrick, D. S. Zaharko, and J. S. Longstreth, *ibid.*, **60**, 1128 (1971).

(5) K. B. Bischoff, R. L. Dedrick, and D. S. Zaharko, *ibid.*, **59**, 149 (1970).

(6) R. L. Dedrick, D. D. Forester, and D. H. W. Ho, *Biochem. Pharmacol.*, **21**, 1 (1972).

(7) R. L. Dedrick, D. D. Forester, J. N. Cannon, S. M. El Dareen, and L. B. Mellett, *ibid.*, **22**, 2405 (1972).

(8) C. N. Chen and J. D. Andrade, *J. Pharm. Sci.*, **65**, 717 (1976).

(9) N. Benowitz, R. P. Forsyth, K. L. Melmon, and M. Rowland, *Clin. Pharmacol. Ther.*, **16**, 87 (1974).

(10) A. Zwart, N. T. Smith, and J. E. W. Beneken, *Comp. Biomed. Res.*, **5**, 228 (1972).

(11) D. S. Greene, D. R. Flanagan, R. Quintiliani, and C. H. Nightingale, *J. Clin. Pharmacol.*, **16**, 257 (1976).

(12) C. H. Nightingale, D. S. Greene, and R. Quintiliani, *J. Pharm. Sci.*, **64**, 1899 (1975).

(13) C. Simon, V. Malerczyk, E. Brahnstaedt, and W. Toeller, *Dtsch. Med. Wochenschr.*, **98**, 2448 (1973).

(14) J. Kosmidis, J. M. T. Hamilton-Miller, J. N. G. Gilchrist, D. W. Kerry, and W. Brumfitt, *Br. Med. J.*, **4**, 653 (1973).

(15) D. C. Grove and W. A. Randall, "Assay Methods of Antibiotics, A Laboratory Manual," Medical Encyclopedia, New York, N.Y., 1955.

(16) M. Okui, T. Matsubara, M. Nishida, and J. Kozatani, *Adv. Antimicrob. Antineoplast. Chemother.*, **1**, 915 (1972).

(17) M. L. Kornguth and C. M. Kunin, *J. Infect. Dis.*, **133**, 175 (1976).

(18) H. P. Bassaris, R. Quintiliani, E. G. Maderazo, R. C. Tilton, and C. H. Nightingale, *Curr. Ther. Res.*, **19**, 110 (1976).

(19) "Scientific Tables," K. Diem and C. Lenter, Eds., Ciba-Geigy, Basel, Switzerland, 1970.

(20) C. M. Metzler, G. L. Elfring, and A. J. McEwen, "A Users Manual for NONLIN and Associated Programs," Upjohn Co., Kalamazoo, Mich., 1974.

Stabilization of Sulfisomidine Tablets by Use of Film Coating Containing UV Absorber: Protection of Coloration and Photolytic Degradation from Exaggerated Light

YOSHIHISA MATSUDA ˣ, HIROMI INOUYE, and REIKO NAKANISHI

Received February 17, 1977, from *Kobe Women's College of Pharmacy, Higashinada, Kobe 658, Japan.* Accepted for publication April 28, 1977.

Abstract □ The effect of model polymer coating films of vinyl acetate, containing oxybenzone as a UV absorber, on the coloration and photolytic degradation of simple sulfisomidine tablets was examined to attempt stabilization of photosensitive solid dosage forms. Coloration of the tablet surface was followed by the tristimulus colorimetric method in the fading tester equipped with a mercury vapor lamp. Photolytic degradation in the UV region was investigated by a new method for measuring the absorption spectra of a crystal sample in the gas phase, *i.e.*, the semi-integral *attenuance spectra*. Two parameters of a film, thickness and concentration of the UV absorber, were varied at every exposure. These physical and chemical changes are discussed in relation to light transmission properties of films.

Keyphrases □ Sulfisomidine tablets—effect of film coating containing UV absorber on coloration and photolytic degradation □ Film coating—containing UV absorber, effect on coloration and photolytic degradation of sulfisomidine tablets □ UV absorber—contained in film coating, effect on coloration and photolytic degradation of sulfisomidine tablets □ Coloration—sulfisomidine tablets, effect of film coating containing UV absorber □ Photolytic degradation—sulfisomidine tablets, effect of film coating containing UV absorber □ Degradation, photolytic—sulfisomidine tablets, effect of film coating containing UV absorber □ Tablets—sulfisomidine, coloration and photolytic degradation, effect of film coating containing UV absorber

Many solid pharmaceutical medicaments exhibit physical or chemical changes because of the radiant energy of light. Light irradiation can cause color development or color fading. From pharmaceutical and therapeutic standpoints, physical changes can be as serious as chemical instability of the active ingredient. Therefore, protection of solid dosage forms under storage from the deleterious effects of light is one problem in quality control.

Pharmaceutical products can be adequately protected by the use of special glass containers, *i.e.*, light-resistant containers specified in pharmacopeias. The protective effect of colored glass on the fading of tablets containing colorants (1, 2) and on the coloration and photolytic degradation of photolabile sulfisomidine tablets (3) has been investigated.

Coating tablets with a polymer film containing UV absorbers may be another method for protection from light. Along with the use of light-resistant containers, this approach should increase the protective effect since the coating is applied to individual tablets. The effect of the protective coating on the photostability of colorants used in the tablet coating also was studied (4–6), but no report dealt with organic active ingredients. One interesting point in such studies of solid-state stability is the relationship shown to exist (3) between the apparent and chemical changes.

The purpose of the present work was to investigate the

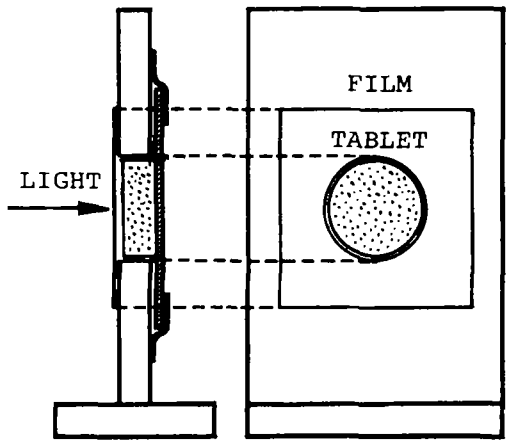

Figure 1—*Sample holder for exposure test.*

possibility of protection of dosage forms from physical and chemical changes by applying films containing a commercially available UV absorber. The solution of this problem may indicate ways to improve photolabile solid dosage forms. In examining solid-state stability, it is desirable to follow the change of samples in the solid rather than liquid state since they may exhibit different behavior in solution due to the effect of a solvent. To satisfy this requirement, a new method for measuring the absorption spectra of a crystal in the gas phase was employed, and solid-state stability was quantitated.

EXPERIMENTAL

Preparation of Tablets—One gram of sulfisomidine JP, <100 mesh in size, was filled into a single set of flat-faced punches and die, which was equipped with a compression–tension testing machine[1]. Tablets of 15-mm diameter and 4.5-mm thickness were prepared. To unify the surface condition of each tablet, a constant compression force of 2000 kg was used. Each tablet was adhered to a glass plate with an epoxide resin. Samples were stored over silica gel in a desiccator in the dark until the exposure test.

Preparation and Application of Polymer Films—Films containing a UV absorber were prepared according to the following formula: vinyl acetate (50% polymer), 10–25 g; 1,1,1-trichloroethane, 47.8–39.4 g; ethanol, 37.2–30.6 g; 2-ethoxyethanol, 5 g; and oxybenzone, *q.s.* for a total of 100 g.

Five grams of 2-ethoxyethanol, a given amount of vinyl acetate of a film base, and oxybenzone[2] (2-hydroxy-4-methoxybenzophenone) as a UV absorber were added to a mixed solvent of 1,1,1-trichloroethane and ethanol in the ratio of 54:42 (w/w) and then thoroughly dispersed and dissolved with a homogenizer. Each 5 ml of these solutions was spread over a flat horizontal glass plate and dried for 7 days at room temperature. Then the completely polymerized and transparent films were peeled, and sample films of 3 × 3 cm were prepared.

The thickness of films was varied from 18 to 110 μm by changing the amount of vinyl acetate and mixed solvent; it was obtained as a mean of the measured values at the four fixed points on a film using an electromagnetic thickness meter[3]. The concentrations of oxybenzone added were 0.5–10% of the weight of the dried film. These films were fixed on the front side of the holders for sample tablets as a case model of film-coated dosage forms.

Exposure Test—The sample holders (Fig. 1) were placed in the rack of a fading tester[4] with a 400-w mercury vapor lamp[5], as reported previously (2), and exposed to UV rays. The spectral energy distribution of this lamp included 13 line spectra with a high proportion of radiation (highest intensity at 365 and 577 nm) and a continuous spectrum with low intensity within the range of 280–720 nm. The distance between the light source and the sample was 30 cm.

The irradiation energy (300–400 nm) and illumination at the surface of a sample tablet were 3.47×10^3 μw/cm^2 and 1.74×10^4 lx, as measured with a UV intensity meter[6] and an illumination meter[7], respectively. Samples were withdrawn from the fading tester at designated time intervals for colorimetry. Elevation of temperature in the fading tester was prevented by a constantly operating fan; the temperature was maintained below 27°.

Colorimetric Measurements—To obtain a quantitative color measurement related to human color perception, the surface color of the tablets in the *Lab* system was measured with an integrating sphere-type color and color difference meter[8] equipped with a halogen lamp as the light source. A barium sulfate plate was used as the reflectance standard. The Hunter color difference formula employed to evaluate the degree of coloration is expressed by (7):

$$\Delta E(Lab) = [(\Delta L)^2 + (\Delta a)^2 + (\Delta b)^2]^{1/2} \qquad \text{(Eq. 1)}$$

where $\Delta E(Lab)$ is the color difference in National Bureau of Standards (NBS) units in the *Lab* system, and ΔL, Δa, and Δb are the differences between two lightness values, L, and those between chromaticity coordinates a and b in the *Lab* system.

Fluctuations in the values of L, a, and b of one sample fell within 0.1 NBS unit. After the measurement, samples were returned into the fading tester, and exposure was continued.

Absorption Measurements—To follow changes in the absorption spectra of sample powders in the gas phase, a drop of acetone solution of pure sulfisomidine was placed on a quartz glass plate. The sample particles (particle size of 2–5 μm) were allowed to recrystallize on it by evaporating the solvent thoroughly and were exposed to light in the same manner as the tablets. At every exposure, they were placed in the attachment unit for semitransparent samples of a multipurpose recording spectrophotometer[9]; the absorption spectra (more precisely, the semi-integral attenuance spectra) were measured in the UV region with air as the absorption control. The semi-integral attenuance, ${}_pE_t$, is defined by (8):

$${}_pE_t = \log(I_o/I_t) \qquad \text{(Eq. 2)}$$

where $I_o = I_t + I_a + I_r$; $I_t = I_p + I_d$; $I_r = I_{sr} + I_{dr}$; I_o, I_t, and I_r are the energies of incident, transmitted, and reflected light, respectively; and the subscripts a, p, d, sr, and dr indicate absorbed, parallel transmitted, diffusely transmitted, specularly reflected, and diffusely reflected light, respectively. The transmission spectra of films were also measured, using the same spectrophotometer.

RESULTS AND DISCUSSION

Effects of Film Thickness and Concentration of Oxybenzone on Coloration—The previous study (3) with glass color filters, which have a variety of light transmission properties, showed that the photostability of sulfisomidine tablets was significantly affected by the amount of UV rays and that their coloration best fit an apparent second-order degradation equation with respect to colorimetric values.

Figure 2 gives the color changes of tablet surfaces protected with films containing oxybenzone. The result where the chromaticity coordinates, a and b, are close to zero and lightness L is nearly 100 before exposure demonstrates that the surface color of a tablet is nearly white. Characteristic changes in the values of L, a, and b were observed in the earlier stage of exposure, as in the previous work. After these marked changes, the color development followed a definite trend which was a function of time. The trajectory of the point (a_t, b_t), where t is exposure time, on the chromaticity diagram (not presented in this paper) showed that the surface color became gradually yellow tan as the exposure time proceeded.

Changes in these colorimetric values were affected by thickness of the film; the thicker the film, the more effective was its protection from coloration. The fact that the protective effect was remarkable, especially in both L and b, suggests that the yellowness of tablets was controlled by film coating.

The plots of the reciprocal of colorimetric values against time in Fig. 3 gave a good linear relation except in the early stage. It was confirmed

[1] Autograph model IS-5000, Shimadzu Co., Kyoto, Japan.
[2] Uvinul-M40, Ogawa Perfume Co., Tokyo, Japan.
[3] Permascope type ES-8, Helmut Fischer GMBH & Co., Maichingen, West Germany.
[4] Model MH-1, Mitsubishi Electric Co., Tokyo, Japan.
[5] JIS C 7604, high-pressure mercury lamps for color fading.
[6] Model UVR-365, Tokyo Optical Instruments Co., Tokyo, Japan.
[7] Model SPI-5, Tokyo Optical Instruments Co., Tokyo, Japan.
[8] Model ND-101, Nippon Denshoku Co., Tokyo, Japan.
[9] Model MPS-50L, Shimadzu Co., Kyoto, Japan.

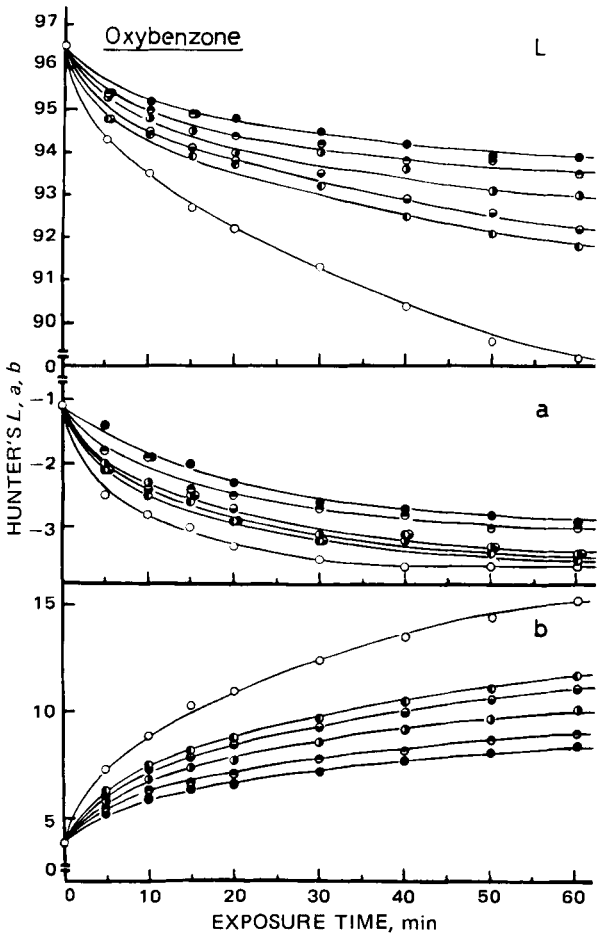

Figure 2—*Effect of exposure time and film thickness on Hunter's colorimetric values. Key:* ○, *control;* ◐, *20 μm;* ◒, *30 μm;* ◑, *50 μm;* ◓, *67 μm; and* ●, *85 μm.*

that the coloration kinetics were apparent second order also in the presence of the UV absorber, and the following equations may be applied:

$$1/L = k_L t + 1/L_0 \qquad \text{(Eq. 3}a\text{)}$$

$$1/a = k_a t + 1/a_0 \qquad \text{(Eq. 3}b\text{)}$$

$$1/b = -k_b t + 1/b_0 \qquad \text{(Eq. 3}c\text{)}$$

where k_L, k_a, and k_b are second-order rate constants with respect to L, a, and b, respectively; and L_0, a_0, and b_0 are values of L, a, and b extrapolated to the zero time. The values of L_0, a_0, and b_0 did not agree with those observed initially. This fact indicates that the complex coloration reaction is in progress in the early stage of exposure.

To examine the effect of film thickness in detail, the initial coloration rate and the rate of stabilization were defined for the first portion that deviated from the straight line and for the subsequent straight portion in Fig. 3, respectively.

The colorimetric values, L, a, and b, are scalars in themselves; however, if they are given as point A (L, a, b) in three-dimensional color space, the movement of point A should be expressed as a vector quantity. When the magnitude and direction of vector **A** vary continuously, accompanying the change of a variable, t (time), **A** should be a continuous function of t. Therefore, Eq. 4, the differential coefficient at $t = 0$ of the vector **A**, may be given as the initial coloration rate:

$$\left|\frac{d\mathbf{A}}{dt}\right|_{t=0} = \sqrt{\left(\frac{d\mathbf{A}_L}{dt}\right)^2_{t=0} + \left(\frac{d\mathbf{A}_a}{dt}\right)^2_{t=0} + \left(\frac{d\mathbf{A}_b}{dt}\right)^2_{t=0}} \qquad \text{(Eq. 4)}$$

where $\mathbf{A}_L$, $\mathbf{A}_a$, and $\mathbf{A}_b$ are components of the vectors L, a, and b, respectively, and t is exposure time. On calculating Eq. 4, $d\mathbf{A}_L/dt$, $d\mathbf{A}_a/dt$, and $d\mathbf{A}_b/dt$ were obtained by numerical differentiation of the smoothed curves in Fig. 2.

The rate of stabilization (R.S.) was calculated using:

$$\text{R.S.} = (k_{L_0} - k_L)/k_{L_0} \times 100\ (\%) \qquad \text{(Eq. 5)}$$

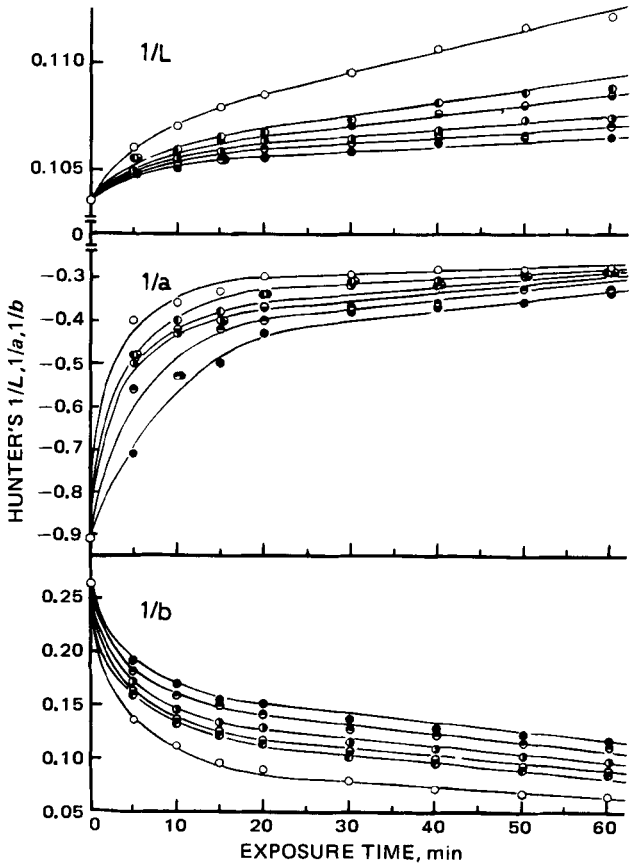

Figure 3—*Reciprocal plots of Hunter's colorimetric values in Fig. 2. Key:* ○, *control;* ◐, *20 μm;* ◒, *30 μm;* ◑, *50 μm;* ◓, *67 μm; and* ●, *85 μm.*

where k_{L_0} is the value of k_L obtained from the control without any film. Equation 5 is based on the result that, among the values of k_L, k_a, and k_b calculated from the regression lines in the portion of the second-order kinetics, the thickness of films affected mostly the k_L value but hardly affected the others.

The effects of film thickness on the initial coloration rate and on the rate of stabilization are shown in Figs. 4 and 5, respectively. The initial coloration rate was reduced significantly with increasing thickness at every concentration, and its effect increased with a decreasing concentration of oxybenzone in the range of great thickness. The values of the initial coloration rate for higher concentrations of oxybenzone were re-

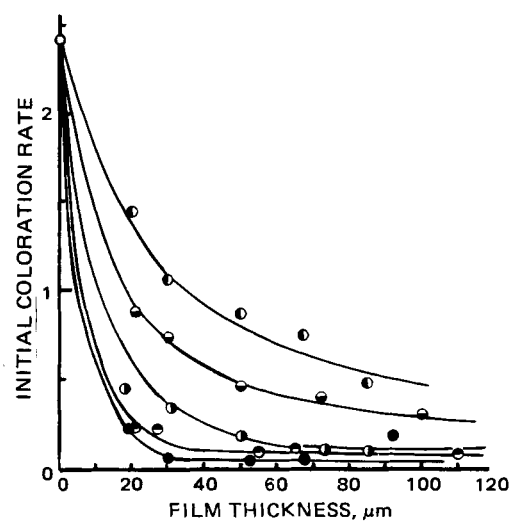

Figure 4—*Effect of film thickness and concentration of oxybenzone on initial coloration rate. Key:* ○, *control;* ◐, *0.5%;* ◒, *1%;* ◑, *2%;* ◓, *5%; and* ●, *10%.*

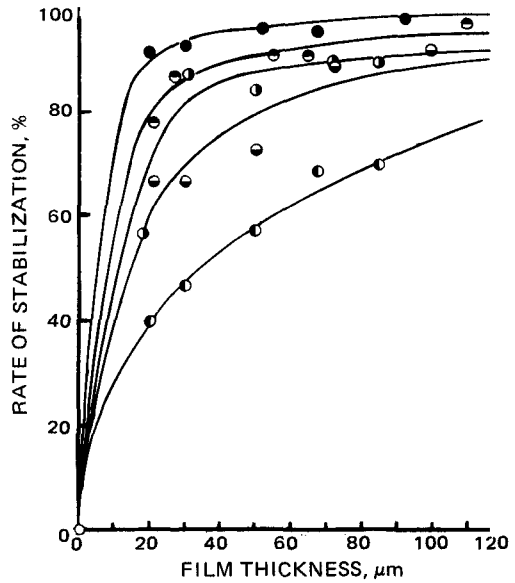

Figure 5—*Effect of film thickness and concentration of oxybenzone on rate of stabilization. Key:* ○, *control;* ◐, *0.5%;* ◒, *1%;* ◑, *2%;* ◓, *5%; and* ●, *10%.*

duced nearly to zero with a small film thickness, and the rate remained constant with additional increases in film thickness. Therefore, the protective effectiveness of a 10% addition of oxybenzone against initial coloration is almost wholly attained with about a 30-μm film thickness and is saturated in the greater thickness.

The dependency of rates of stabilization on the additive concentration of oxybenzone and film thickness in Fig. 5 showed good correspondence to that of the initial coloration rates; the rate of stabilization increased with an increase of both parameters, exhibiting a rapid initial rise and reaching values of more than 90% of stabilization above 5% addition of oxybenzone. The results illustrated in Figs. 4 and 5 indicate that if initial coloration can be protected, control of subsequent coloration also should be satisfactory.

This evidence on coloration is summarized in Fig. 6 as the color difference, ΔE, before and after 60-min exposure *versus* film thickness. At a 10% concentration of oxybenzone, ΔE remained nearly 1 NBS unit, even after such an exaggerated exposure. It was confirmed (9) that two colors less than 1 NBS unit in color difference could not be distinguished visually. Therefore, apparent coloration probably did not occur for this concentration. For a 0.5% concentration, the color difference became less than 6 NBS units for more than 80-μm film thickness. Consequently, coloration was visually "appreciable," whereas it was "very much" for the control on comparison with the relationship between visual perception and color difference (10).

Light Transmission Properties of Films—The bonding strength between atoms of photosensitive medicinal substances is usually smaller than that of ordinary organic compounds. When such substances are

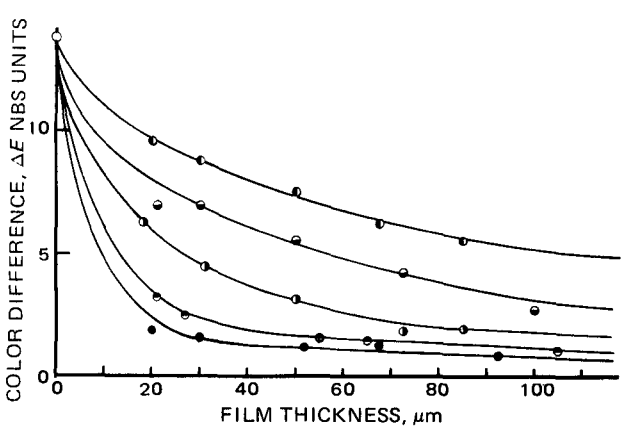

Figure 6—*Effect of film thickness and concentration of oxybenzone on coloration after a 60-min exposure. Key:* ○, *control;* ◐, *0.5%;* ◒, *1%;* ◑, *2%;* ◓, *5%; and* ●, *10%.*

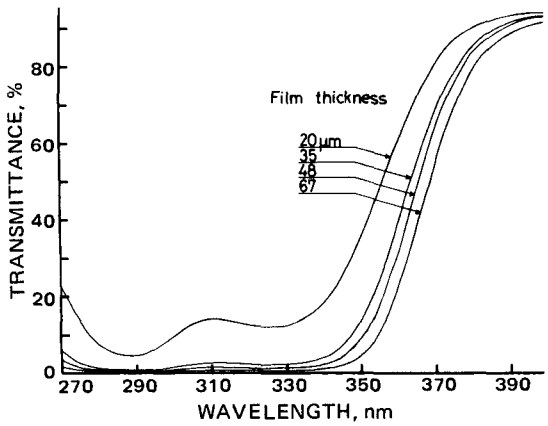

Figure 7—*Transmission curves of films containing 0.5% oxybenzone.*

exposed to light, dissociation of the bonds, *i.e.*, photolytic degradation, can occur only if the energy of light absorbed by the molecule is equal to or greater than the bonding energy. According to the quantum theory, the radiant energy of light is in inverse proportion to the wavelength. Thus, the contribution of UV rays is of prime importance in this study. Results presented previously suggest that the difference in the behavior of coloration must depend on the light transmission properties of a film.

Figure 7 shows transmission curves of films containing 0.5% oxybenzone. These films showed no change in the character of the transmission curves on 60 min of exposure to light, thus indicating that oxybenzone is photostable and will not decompose. The film without oxybenzone was virtually transparent to light above 270 nm; it did not show any absorption band, and its thickness did not affect the transmission curve in this region.

The percentage transmission of each curve in the shorter wavelength region was much lower than that in the visible region, exhibiting the maximum transmission at 310 nm and decreasing with increasing film thickness over the UV region. For more than 35-μm thickness, the shielding effect against light in the UV region was almost complete, and the films showed an excellent protective effect. Calculation of the "Sunscreen Index" according to Kumler (11) gave oxybenzone a high index of approximately 14.4. While the transmission properties in the visible region above 400 nm were little affected by film thickness, the wavelength at which the curve rose shifted to longer wavelengths and the

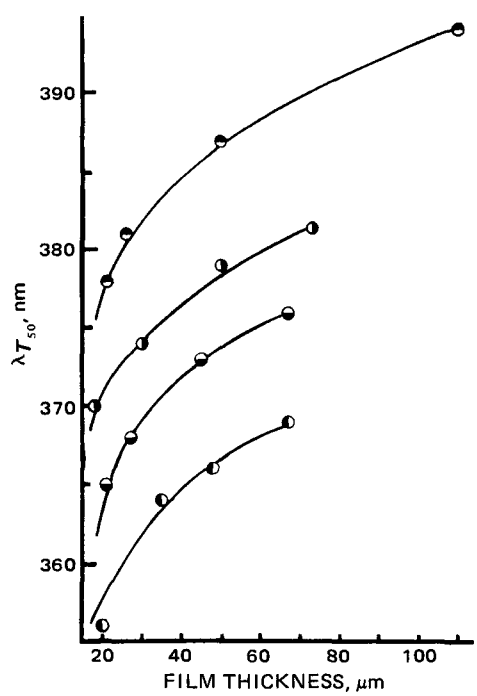

Figure 8—*Effect of film thickness and concentration of oxybenzone on* $\lambda_{T_{50}}$. *Key:* ◐, *0.5%;* ◒, *1%;* ◑, *2%; and* ◓, *5%.*

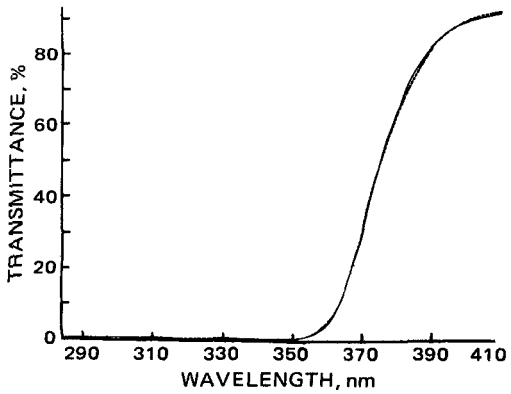

Figure 9—*Transmission properties of films having a similar* CL *value. Key* (CL *value*): —, *67.0 (1%, 67 μm); and - - -, 62.0 (2%, 31 μm).*

slope of the curve became steeper with increasing thickness. The same tendency was found when the additive concentration was varied for one thickness. From these characteristics, the film containing oxybenzone can be considered to play the role of a sharp-cut filter.

The effect of addition of oxybenzone on the cut wavelength of a film, λ_{T50}, at which the percentage transmission corresponds to 50% on the transmission curve, is shown in Fig. 8. The intensity of more than 50% of the line spectrum at 365 nm, which was the highest in the UV region, was shut out even for a 0.5% film of 50-μm thickness and most of the UV rays for a 5% film of 110 μm. It was proved from this finding and the data shown in Fig. 7 that visible light could not take part in the coloration.

According to the Lambert–Beer law, the absorbance of a solution is in proportion to the product of its concentration, C, and the length of the light path, L. Therefore, films having the same value of this product should give the same transmission curve if this law holds. The transmission curves of two films having a similar *CL* value are shown in Fig. 9; the transmission properties of both curves coincide precisely over the whole wavelength range, indicating that this law is applicable to a solid film. Consequently, a 0.5% film of 40-μm thickness, for example, would have as much protective effectiveness as a 2% film of 10 μm. The validity of this statement is supported by the fact that plots having a similar *CL* value in Figs. 4 and 5 gave approximately equal values of two parameters for coloration. In any case, the protective effectiveness of films from light should be evaluated not only by cut wavelengths but also by steepness of the transmission curve.

Photolytic Degradation—The mechanism of coloration of solid materials by light has not been fully understood because of its complex reaction system. Thus, it is not well known whether coloration has some connection with decomposition. However, photolytic degradation of materials in solid dosage forms is essentially a surface phenomenon. In such a case, to study the effect of light properly, microscopic crystal particles of sample materials should be exposed to light so that they uniformly absorb the energy of light and then should be analyzed spectrophotometrically.

Typical absorption spectra for the control and 0.5% film of 20 μm are given in Figs. 10 and 11, respectively. The spectrum of the original state before exposure gave an absorption maximum and minimum at 266 and 232 nm, respectively. As the exposure time proceeded, the absorption curve showed a flattening tendency, increasing the minimum and decreasing the maximum. The isosbestic points were confirmed at 219, 253, and 317 nm; for a 0.5% film, however, these points were not obtained and

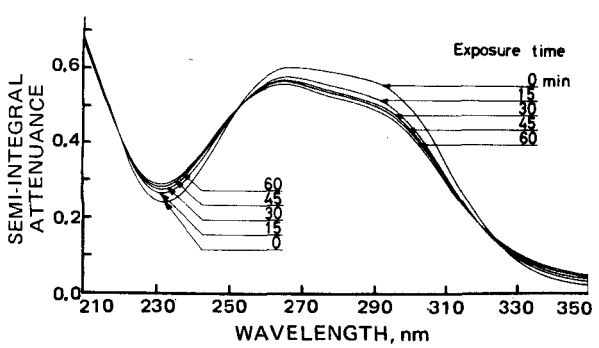

Figure 10—*Effect of exposure time on absorption spectrum for control.*

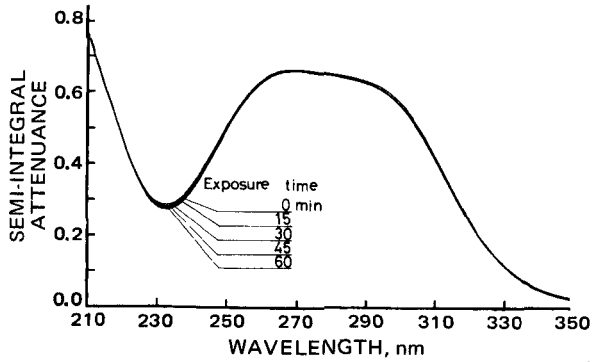

Figure 11—*Effect of exposure time on absorption spectrum for 0.5% film of 20 μm.*

the absorption curve gradually decreased without intersecting the original curve in any wavelength region. The photolytic degradation was not apparently observed for films with more than 1% addition. The presence and absence of isosbestic points may suggest induction of a photooxidation reaction on the crystal surface, which has a selectivity with respect to wavelength.

The changes in the nondimensionalized absorbance at 266 nm, E_t/E_0, with time (3) indicated that the degradation followed apparent zero-order kinetics, accompanying an induction period, and that the kinetic equation might be applied as follows:

$$d(E_t/E_0)/dt = -k \qquad \text{(Eq. 6}a\text{)}$$

or:

$$E_t/E_0 = 1 - kt \qquad \text{(Eq. 6}b\text{)}$$

where k is the apparent zero-order rate constant and the subscripts t and 0 are exposure time and initial time, respectively. From these degradation kinetics, it was confirmed that even a 0.5% film of 20-μm thickness, which permitted the transmission of UV rays the most among the films used, was less than 2% degraded after the 60-min exposure whereas the control was 8% degraded. This fact demonstrates that a lower concentration of addition gives sufficient protection from degradation.

It was stated (12) that the color change not indicative of significant degradation might be visually unacceptable. However, the result illustrated in Fig. 6 suggests that an evident correlation does not always exist between coloration and photolytic degradation. For films with more than 1% addition, sulfisomidine tablets under ordinary storage conditions will be sufficiently stable and remain unchanged; the tablets were hardly changed in spite of their coloration, even under intense UV irradiation. These films are expected to have a better protective effectiveness for degradation than for coloration.

SUMMARY AND CONCLUSIONS

The photolabile sulfisomidine tablets protected by a polymer film containing oxybenzone were exposed to exaggerated UV rays in a fading tester. Coloration of these tablet surfaces was significantly controlled by a film coating, and the coloration kinetics were apparent second order, accompanying an induction period with respect to colorimetric values. Two variables to evaluate the protective effectiveness of the film, the initial coloration rate and the rate of stabilization, showed a good correspondence and were improved with increasing film thickness or concentration of oxybenzone. The visible light apparently could not be responsible for these coloration processes.

From the light transmission properties of the films, they could be considered as sharp-cut filters. The cut wavelength, which permitted the transmission of 50% of the light, shifted to longer wavelengths with increasing film thickness, indicating improvement of the shielding effect of UV energy.

Photolytic degradation, examined by a spectrophotometric method, followed apparent zero-order kinetics, accompanying a similar induction period as the coloration, presumably due to photooxidation on the surface of crystal particles. However, photolytic degradation was not observed with higher concentrations of oxybenzone. Results obtained from coloration and photolytic degradation suggested that an evident correlation did not necessarily exist between them.

In conclusion, a UV absorber, if nonpoisonous for the additive amount in the ordinary dosage administration, is expected to be an excellent additive for the protection of photolabile solid dosage forms.

REFERENCES

(1) C. J. Swartz, L. Lachman, T. Urbanyi, and J. Cooper, *J. Pharm. Sci.*, **50**, 145 (1961).

(2) Y. Matsuda and Y. Minamida, *J. Pharm. Soc. Jpn.*, **96**, 425 (1976).

(3) Y. Matsuda and Y. Minamida, *Chem. Pharm. Bull.*, **24**, 2229 (1976).

(4) B. R. Hajratwala, *J. Pharm. Sci.*, **63**, 129 (1974).

(5) *Ibid.*, **63**, 1927 (1974).

(6) B. R. Hajratwala and A. J. Hennig, *J. Pharm. Sci.*, **66**, 107 (1977).

(7) R. S. Hunter, *J. Opt. Soc. Am.*, **38**, 661 (1948).

(8) K. Shibata, "Spectrophotometry and Spectrophotometer," Kohdansha Co., Tokyo, Japan, 1974, p. 159.

(9) G. Kawakami, *Acta Chromat.*, **3**, 54 (1977).

(10) E. I. Stearms, *Am. Dyestuff Rep.*, **40**, 563 (1951).

(11) W. D. Kumler, *J. Am. Pharm. Assoc., Sci. Ed.*, **41**, 492 (1952).

(12) S. S. Kornblum, *Drug Cosmet. Ind.*, **106**, 42 (1970).

ACKNOWLEDGMENTS

Presented at the 26th Kinki-Branch Meeting of the Pharmaceutical Society of Japan, Higashi-Osaka, Japan, October 1976.

The authors are indebted to Miss M. Mihara for technical assistance.

Electron-Capture Detector GLC Technique for Estimating Tocainide in Biological Fluids

R. VENKATARAMANAN and J. E. AXELSON ˣ

Received September 20, 1976, from the *Faculty of Pharmaceutical Sciences, University of British Columbia, Vancouver, British Columbia, Canada.* Accepted for publication May 2, 1977.

Abstract □ A sensitive and specific electron-capture detector GLC method capable of detecting picogram quantities of tocainide, a lidocaine analog, in biological fluids was developed. This method consists of extracting the compound into methylene chloride and derivatizing with heptafluorobutyric anhydride to form the monoheptafluorobutyryl derivative. The derivative formation was confirmed by GLC–mass spectrometry. Quantitative estimation was performed using 1-bromonaphthalene as an internal standard. The minimum detectable level by the electron-capture method was approximately 30 pg/injection as opposed to approximately 3 ng/injection with a flame-ionization detector. Linear response was observed in the range from 50 pg to 3 ng using an electron-capture detector. No interference from endogenous substances was observed.

Keyphrases □ Tocainide—electron-capture GLC analysis in biological fluids □ GLC, electron capture—analysis, tocainide in biological fluids □ Cardiac depressants—tocainide, electron-capture GLC analysis in biological fluids

Lidocaine (I), a commonly used drug in acute coronary care for the treatment of acute myocardial infarction (1), has a prompt onset of action and elicits minimal hemodynamic disturbances (2). In spite of these advantages over other commonly used antiarrhythmic agents such as propranolol, procainamide, and quinidine (3), lidocaine is not an ideal antiarrhythmic agent. Its undesirable features include a short biological half-life ($t_{1/2}$ = 90 min) (4), inactivation by first-pass metabolism (5), and formation of toxic metabolites (6).

Tocainide[1,2], 2-amino-*N*-(2,6-dimethylphenyl)propanamide (II) hydrochloride, a primary amine analog of lidocaine, has antiarrhythmic activity without the disadvantages of lidocaine therapy. Tocainide exhibits a biological half-life of approximately 11 hr in normal healthy volunteers (7), oral effectiveness (8), and total availability after oral administration (9).

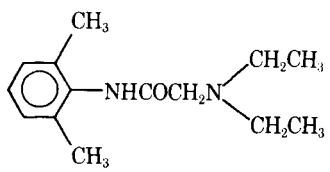

I

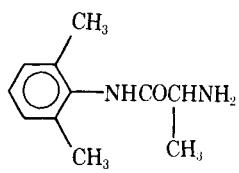

II

A flame-ionization detector GLC assay method was developed for the separation and quantitation of this compound in biological fluids[3]. Flame-ionization detectors are inherently less sensitive than electron-capture or nitrogen-specific detectors and, as a consequence, relatively large volumes of biological samples (1–5 ml of blood) are required for quantitation of compounds. Unfortunately, the sample volume required for the flame-ionization detector method is greater than what can be routinely obtained from small animals when serial samples are taken.

The limitations of the flame-ionization detector assay technique necessitated the development of a more sensitive assay method for the quantitative analysis of II. It was desirable to convert II to a suitable derivative that is highly electronegative and amenable to electron-capture detection. Several derivatizing agents have been used in the quantitative analysis of primary amines (10). In the present study, heptafluorobutyric anhydride satisfied the requirements.

EXPERIMENTAL

Materials—The hydrochloride salt of II was used. The solvents, methylene chloride[4], hexane[4], and benzene[4], were either pesticide grade[5] or distilled in glass.

[1] Astra Pharmaceutical Products, Framingham, Mass.

[2] Previous publications referred to this compound as W36095-HCL.

[3] Dr. David Lalka, Astra Pharmaceutical Products, Framingham, Mass., personal communication.

[4] Caledon, Georgetown, Ontario, Canada.

[5] Nanograde, Mallinckrodt Chemical Works, St. Louis, Mo.

REFERENCES

(1) C. J. Swartz, L. Lachman, T. Urbanyi, and J. Cooper, *J. Pharm. Sci.*, **50**, 145 (1961).

(2) Y. Matsuda and Y. Minamida, *J. Pharm. Soc. Jpn.*, **96**, 425 (1976).

(3) Y. Matsuda and Y. Minamida, *Chem. Pharm. Bull.*, **24**, 2229 (1976).

(4) B. R. Hajratwala, *J. Pharm. Sci.*, **63**, 129 (1974).

(5) *Ibid.*, **63**, 1927 (1974).

(6) B. R. Hajratwala and A. J. Hennig, *J. Pharm. Sci.*, **66**, 107 (1977).

(7) R. S. Hunter, *J. Opt. Soc. Am.*, **38**, 661 (1948).

(8) K. Shibata, "Spectrophotometry and Spectrophotometer," Kohdansha Co., Tokyo, Japan, 1974, p. 159.

(9) G. Kawakami, *Acta Chromat.*, **3**, 54 (1977).

(10) E. I. Stearms, *Am. Dyestuff Rep.*, **40**, 563 (1951).

(11) W. D. Kumler, *J. Am. Pharm. Assoc., Sci. Ed.*, **41**, 492 (1952).

(12) S. S. Kornblum, *Drug Cosmet. Ind.*, **106**, 42 (1970).

ACKNOWLEDGMENTS

Presented at the 26th Kinki-Branch Meeting of the Pharmaceutical Society of Japan, Higashi-Osaka, Japan, October 1976.

The authors are indebted to Miss M. Mihara for technical assistance.

Electron-Capture Detector GLC Technique for Estimating Tocainide in Biological Fluids

R. VENKATARAMANAN and J. E. AXELSON ˣ

Received September 20, 1976, from the *Faculty of Pharmaceutical Sciences, University of British Columbia, Vancouver, British Columbia, Canada.* Accepted for publication May 2, 1977.

Abstract □ A sensitive and specific electron-capture detector GLC method capable of detecting picogram quantities of tocainide, a lidocaine analog, in biological fluids was developed. This method consists of extracting the compound into methylene chloride and derivatizing with heptafluorobutyric anhydride to form the monoheptafluorobutyryl derivative. The derivative formation was confirmed by GLC–mass spectrometry. Quantitative estimation was performed using 1-bromonaphthalene as an internal standard. The minimum detectable level by the electron-capture method was approximately 30 pg/injection as opposed to approximately 3 ng/injection with a flame-ionization detector. Linear response was observed in the range from 50 pg to 3 ng using an electron-capture detector. No interference from endogenous substances was observed.

Keyphrases □ Tocainide—electron-capture GLC analysis in biological fluids □ GLC, electron capture—analysis, tocainide in biological fluids □ Cardiac depressants—tocainide, electron-capture GLC analysis in biological fluids

Lidocaine (I), a commonly used drug in acute coronary care for the treatment of acute myocardial infarction (1), has a prompt onset of action and elicits minimal hemodynamic disturbances (2). In spite of these advantages over other commonly used antiarrhythmic agents such as propranolol, procainamide, and quinidine (3), lidocaine is not an ideal antiarrhythmic agent. Its undesirable features include a short biological half-life ($t_{1/2}$ = 90 min) (4), inactivation by first-pass metabolism (5), and formation of toxic metabolites (6).

Tocainide[1,2], 2-amino-*N*-(2,6-dimethylphenyl)propanamide (II) hydrochloride, a primary amine analog of lidocaine, has antiarrhythmic activity without the disadvantages of lidocaine therapy. Tocainide exhibits a biological half-life of approximately 11 hr in normal healthy volunteers (7), oral effectiveness (8), and total availability after oral administration (9).

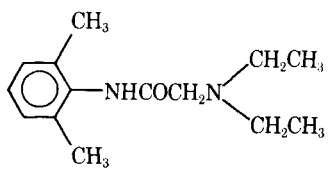

I

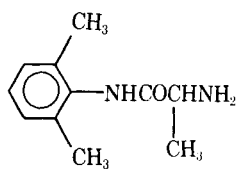

II

A flame-ionization detector GLC assay method was developed for the separation and quantitation of this compound in biological fluids[3]. Flame-ionization detectors are inherently less sensitive than electron-capture or nitrogen-specific detectors and, as a consequence, relatively large volumes of biological samples (1–5 ml of blood) are required for quantitation of compounds. Unfortunately, the sample volume required for the flame-ionization detector method is greater than what can be routinely obtained from small animals when serial samples are taken.

The limitations of the flame-ionization detector assay technique necessitated the development of a more sensitive assay method for the quantitative analysis of II. It was desirable to convert II to a suitable derivative that is highly electronegative and amenable to electron-capture detection. Several derivatizing agents have been used in the quantitative analysis of primary amines (10). In the present study, heptafluorobutyric anhydride satisfied the requirements.

EXPERIMENTAL

Materials—The hydrochloride salt of II was used. The solvents, methylene chloride[4], hexane[4], and benzene[4], were either pesticide grade[5] or distilled in glass.

[1] Astra Pharmaceutical Products, Framingham, Mass.

[2] Previous publications referred to this compound as W36095-HCL.

[3] Dr. David Lalka, Astra Pharmaceutical Products, Framingham, Mass., personal communication.

[4] Caledon, Georgetown, Ontario, Canada.

[5] Nanograde, Mallinckrodt Chemical Works, St. Louis, Mo.

Table I—Recovery of II in Rat Plasma as Determined by the Electron-Capture Detector GLC Analysis

Amount of II Added to 0.1 ml of Plasma, ng	*n*	Amount of II Recovered after Extraction, ng	Mean Recovery, %	*SD* of Percent Recovery
0.1751	1	0.1262	72.1	—
0.3501	6	0.2237	63.90	10.596
0.7002	5	0.4607	65.79	4.984
1.0503	6	0.7333	69.82	7.794
1.4004	6	0.9118	65.11	2.400
1.7505	3	1.0181	58.16	0.675
2.1006	2	1.3299	63.31	2.200
2.4507	6	1.8767	76.58	1.855
2.8008	4	1.9303	68.92	0.728
Mean recovery			67.08	5.43

Heptafluorobutyric anhydride[6] was stored in tightly stoppered bottles at 5° in a refrigerator. Once an ampul of heptafluorobutyric anhydride was opened, the contents were used within 3 days or discarded.

The internal standard solution consisted of 1-bromonaphthalene[7] in benzene when the electron-capture detector was used and an aqueous solution of glycinexylidide[1] when the flame-ionization detector was used.

Sodium hydroxide[8] (1 *N*) was used to alkalinize the solution prior to extraction.

GLC—All routine analyses were conducted using a reporting gas chromatograph equipped with a ^{63}Ni-electron-capture detector[9] or dual flame-ionization detectors[10]. The glass column, 1.8 m × 2 mm i.d., contained 3% OV-17 coated on 80–100-mesh Chromosorb W (HP).

All columns were conditioned for 24 hr at 100°, and then the oven temperature was programmed to increase by 0.1°/min up to 280°. The oven temperature was allowed to remain at 280° for approximately 24 hr to complete the conditioning process. The flow of carrier gas during the conditioning period was 7 ml/min.

The electron-capture detector method was developed using a 95% argon–5% methane carrier gas mixture; helium was used as the carrier gas for the flame-ionization detectors. The gas flow rates for the flame-ionization detector were: carrier gas, 40 ml/min; hydrogen, 40 ml/min; and air, ~300 ml/min. For the electron-capture detector, the carrier gas flow rate was 40 ml/min.

The operating conditions with both procedures were: injection port temperature, 200°; oven, 180°; and detector, 300°.

Mass Spectrometry—A GLC–mass spectrometer[11] (electron impact) was used under the following conditions: energy of the ionization beam, 70 ev; electron multiplier voltage, 2 kv; analyzer temperature, 75°; and separator oven temperature, 180°. Sample introduction was carried out by a GLC procedure on a glass column, 1.8 m × 2 mm i.d., packed with 3% OV-17 on 80–100-mesh Chromosorb W (HP) under the following conditions: injection temperature, 180°; oven temperature, 160°; and helium (carrier gas) flow rate, 25 ml/min.

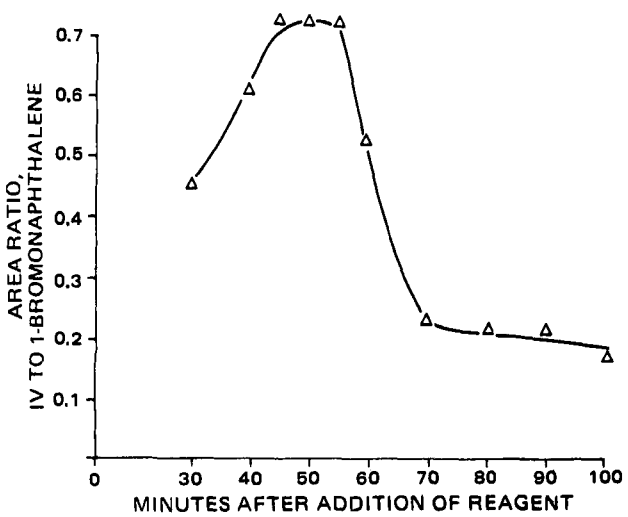

Figure 1—*Reaction kinetics of II at 55°. Plot of area ratio of the derivative formed (IV) to 1-bromonaphthalene as a function of time using 2.53 ng of II and 1.83 ng of 1-bromonaphthalene.*

[6] Pierce Chemical Co., Rockford, Ill.
[7] ICN Pharmaceuticals Inc., Plainview, N.Y.
[8] Mallinckrodt Chemical Works, St. Louis, Mo.
[9] Hewlett-Packard model 5833A reporting gas chromatograph.
[10] Hewlett-Packard model 5830A reporting gas chromatograph.
[11] Finnigan 9500 automated GC/MS, Finnigan, Palo Alto, Calif.

Table II—Plasma Levels of II Using 0.05 ml of Plasma in a Rat that Received 20 mg/kg iv

Minutes	Plasma Level, μg/ml
30	2.697
60	1.831
90	1.664
150	1.528
180	1.097

Extraction Procedure—To 0.1 ml of plasma or aqueous solution containing the drug, 1 ml of 1 *N* sodium hydroxide was added. The total volume was then made up to 2 ml with distilled water. A 10-ml volume of methylene chloride was added, and the tubes were shaken in a wrist-action shaker[12] for 15 min. After centrifugation to separate the layers, 7 ml of organic phase was transferred to a 15-ml centrifuge tube. The organic layer was evaporated to dryness under a low stream of nitrogen.

The residue was dissolved in 1 ml of hexane, and 10 μl of the derivatizing agent, heptafluorobutyric anhydride, was added. Then the tube was shaken thoroughly in a vortex mixer. The mixture was then incubated at 55° for 50 min in a constant-temperature oven. After completion of the reaction, the tube was cooled to room temperature and the solution was evaporated to dryness under a low stream of nitrogen.

The residue was dissolved in 100–200 μl of benzene containing the internal standard (0.63 ng/μl). A 3-μl aliquot of the sample was then injected into the gas–liquid chromatograph, and the response was noted.

Recovery Studies—A known amount of II was added to 0.05 or 0.1 ml of rat plasma and extracted by the described procedure. The base was obtained from the hydrochloride salt by extraction with benzene after the addition of sodium hydroxide. The solvent was then carefully evaporated, and the base remained as a solidifying oil. The base was dried in a vacuum oven at 30° for a minimum of 24 hr before use.

The purity of the base so obtained was determined by differential scanning calorimetry[13] and by a melting-point determination using a hot-stage microscope. Percentage recoveries were calculated from the standard curve of the base, which was derivatized without any extraction. The recovery values are given in Table I.

Biological Measurements of II in Plasma—The application of the technique developed for the determination of *in vivo* levels of II was demonstrated by studying the elimination of the compound in the rat. A freshly prepared solution of II was injected into a male Wistar rat (300 g) through the tail artery as a single bolus of 20 mg/kg.

Blood samples were taken at regular intervals of time through a jugular vein cannula, and the plasma obtained was used for the analysis of II. Representative plasma level data obtained are listed in Table II.

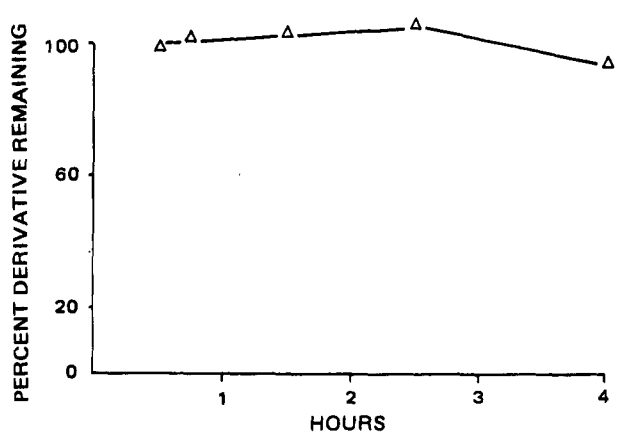

Figure 2—*Stability of IV at room temperature.*

[12] Burrell Corp., Pittsburgh, Pa.
[13] Model 1B differential scanning calorimeter, Perkin-Elmer, Norwalk, Conn.

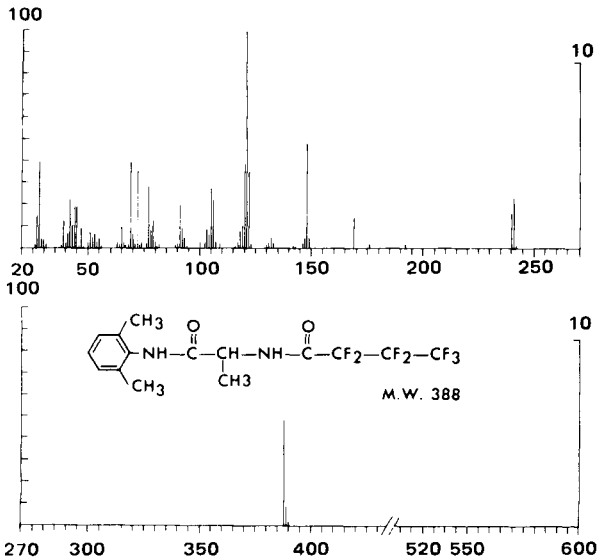

Figure 3—*Mass spectra of IV obtained by GLC–mass spectrometry after extraction from plasma of rat dosed with 20 mg of II/kg.*

RESULTS AND DISCUSSION

Selection of Derivatizing Agent and Solvent—Heptafluorobutyric imidazole[6], heptafluorobutyric anhydride, and pentafluorobenzoyl chloride[6] were examined as potential derivatizing agents. With pentafluorobenzoyl chloride, a low area ratio was obtained in the absence of a catalyst. Even though the addition of a catalyst (pyridine) did improve the yield of the derivative, it led to a number of background peaks in the chromatogram.

With heptafluorobutyric imidazole, precipitation of the reaction product occurred when hexane was used as the solvent; when methylene chloride was used, interfering peaks appeared preventing quantitation. Heptafluorobutyric anhydride was the most suitable and was used in later studies.

Careful selection of the solvent for the reaction is important for obtaining the optimum yield of the derivative. The choice, however, is limited to solvents that are inert to derivatization and that elute rapidly from the column. With a fixed concentration of II, various solvents were investigated for their suitability. The use of hexane resulted in a quantitatively higher area ratio of the derivative to the internal standard than did benzene or methylene chloride. Therefore, hexane was used as the solvent for the derivatization reaction.

Evaluation of Optimum Conditions—Both the temperature and time of the reaction are important in derivative formation. While the temperature was kept constant at 55°, the time for the reaction was varied from 0 to 100 min and the yield of the derivative, as observed by the area ratio of the derivative to the internal standard, was monitored. From Fig. 1, it is clear that the optimum yield was obtained around 45–55 min; 50 min was taken to be the optimum time in later studies.

Figure 2 shows that the derivative formed was stable over 4 hr at 21.1°. In subsequent studies, the sample was injected into the gas chromatograph 30 min after the completion of the reaction time.

Under suboptimal conditions, the yield of the derivative was low and the peak obtained was not sharp and symmetrical, indicating incomplete derivative formation.

Confirmation of Derivative Structure—Plasma samples from rats administered tocainide were pooled, extracted, and analyzed by GLC–mass spectrometry after derivatization. Mass spectra corresponding to tocainide were compared to spectra obtained from the analysis of pure derivatized compound and were identical. As shown in Scheme I, heptafluorobutyric anhydride (III) reacts with II to form a monoheptafluorobutyryl derivative (IV) and heptafluorobutyric acid (V).

The postulated fragmentation pattern is shown in Scheme II and was consistent with the formation of IV. The peak at *m/e* 388 corresponds to the molecular ion peak; other abundant ions were observed at *m/e* 240, 192, 176, 169, 147, 120, 119, 105, and 69 (Fig. 3). These observations confirm that intact II, devoid of any plasma interference, was measured in the assay.

Removal of Excess Reagent—The presence of even trace amounts of the strongly electron-withdrawing heptafluorobutyric anhydride in the sample gave rise to severe disturbances in the chromatogram. Therefore, it was essential to remove the excess reagent as well as the by-product of the reaction, heptafluorobutyric acid. Walle and Ehrsson (11) suggested a method of water addition to hydrolyze the anhydride, followed by the addition of ammonium hydroxide to remove the acid into

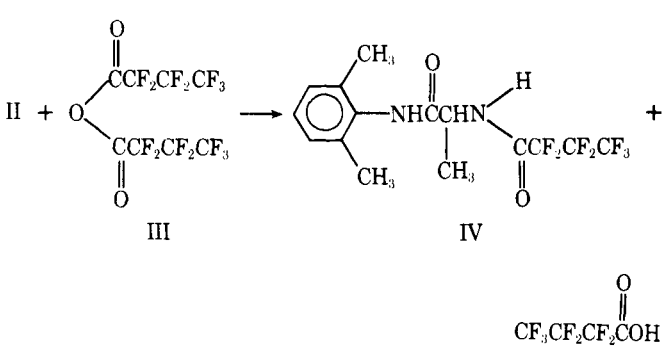

Scheme I

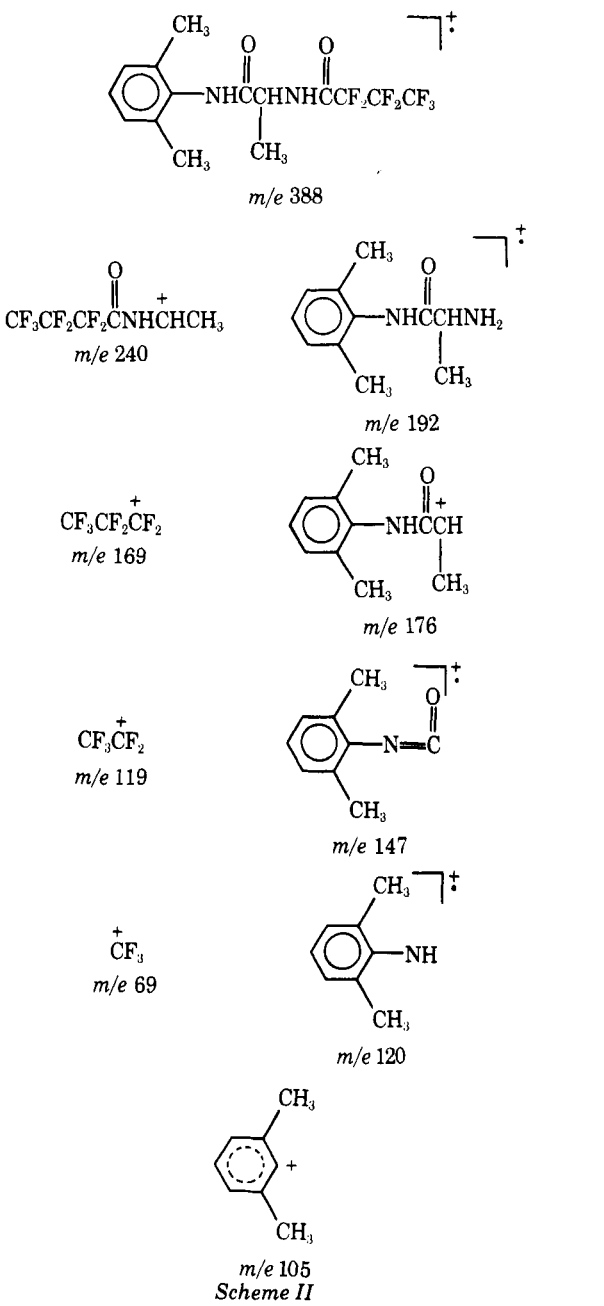

Scheme II

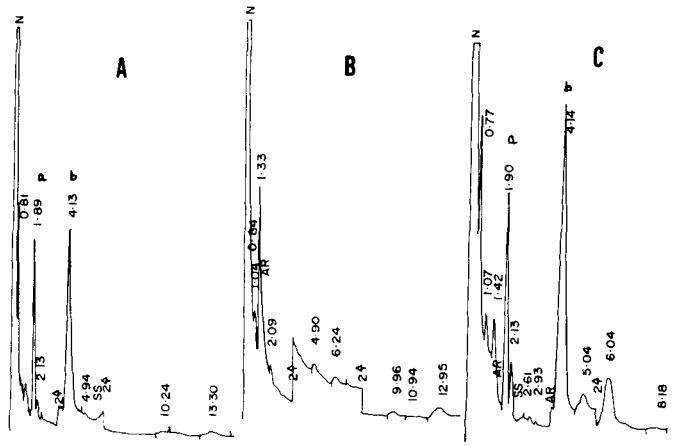

Figure 4—*Gas–liquid chromatograms of extracts by using an electron-capture detector. Key: A, extraction from an aqueous solution; B, blank plasma extract; C, extraction from rat plasma spiked with II; a, 1-bromonaphthalene; and b, derivative of tocainide. All other peaks present in the chromatograms were due to endogenous substances present in plasma or to solvents used for the analysis.*

the aqueous layer. However, after such a treatment, the derivative deteriorated rapidly. Evaporation of the mixture to remove the excess reagent resulted in a derivative that was stable over 4 hr, so this latter method was employed in all other studies.

Figure 4A shows a typical chromatogram obtained by extraction of an aqueous solution of tocainide. The chromatogram obtained after extraction of blank plasma is shown in Fig. 4B. The extraneous peaks at about 10 and 13 min in Figs. 4A and 4B resulted from concentration of the solvent used for extraction and were not readily removed by normal purification procedures. These peaks, as well as the peak at 1.3 min in Fig. 4B, clearly do not interfere with the analysis of II and the internal standard.

Figure 4C shows a chromatogram obtained when the extraction procedure described under *Experimental* was applied to rat plasma spiked with II. This chromatogram was identical to that observed after extraction of rat plasma in animals receiving II by intravenous administration. The peak at 4.14 min corresponds to the monoheptafluorobutyryl derivative of II, and that at 1.90 min is consistent with the internal standard, 1-bromonaphthalene.

A typical chromatogram as obtained from the flame-ionization detector

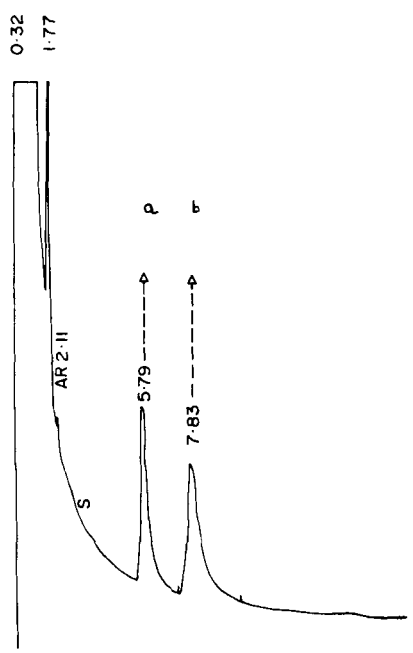

Figure 5—*Typical chromatogram of II (74 ng) and the internal standard (glycinexylidide) (80 ng) using the flame-ionization detector (attenuation 4).*

Table III—Estimation of II Added to Plasma by Flame-Ionization Detector GLC Analysis

Amount Added, ng	Mean Area Ratio[a]	*SE*
2.637	0.048	0.0133
5.273	0.098	0.0046
10.546	0.216	0.0029
15.313	0.313	0.0067
21.092	0.437	0.0031
52.731	1.188	0.0518
105.462	2.250	0.0187
158.193	3.850	0.0980
210.924	4.960	0.2571
527.343	11.969	0.1577
791.015	15.413	0.0824
1054.812	19.484	0.3786

[a] Mean of three values; $y = mx + c$, where $m = 0.229$ and $c = -0.0056$.

Table IV—Estimation of II Added to Plasma by Electron-Capture Detector GLC Analysis

Amount Added, ng	*n*	Mean Area Ratio[a]	*SE*
0.1751	1	0.0336	—
0.3501	6	0.0720	0.0020
0.7002	5	0.1611	0.0024
1.0503	6	0.2633	0.0049
1.4004	6	0.3316	0.0020
1.7505	3	0.3731	0.0015
2.1006	2	0.4899	0.0085
2.4507	6	0.6938	0.0028
2.8008	4	0.7155	0.0019

[a] With $y = mx + c$, where $m = 0.264$ and $c = -0.027$.

is shown in Fig. 5. The peak at 5.79 min corresponds to II, and that at 7.83 min corresponds to the internal standard, glycinexylidide. The area ratio of the derivative of II and the internal standard was used as the index of detector performance and the overall efficiency of the analytical procedure developed. The total recovery of II by the extraction procedure followed was 67.08 ± 5.43% (Table I).

Comparison of Electron-Capture and Flame-Ionization Detectors—Meaningful pharmacokinetic analysis necessitates frequent and extensive blood sampling to characterize drug disposition adequately. The precision of the GLC assay for II using a flame-ionization detector is illustrated in Table III. The results are based on at least three determinations at each II concentration, ranging from 0.35 to 82 μg/ml. The calibration curve obtained by plotting the area ratio of II to the internal standard was linear over a range of 2.6–600 ng (corresponding to 0.35–82 μg/ml). When the equation $y = mx + c$ was used for curve fitting, the slope value obtained was 0.0229 ($r^2 = 0.999$) while the intercept was $c = -0.0056$. This analysis, however, required 1–2 ml of plasma (approximately 2–4 ml of blood). In spite of this extensive linear range, this method could not be applied to animal experimentation using the rat because of the limitation in the frequency and volume of blood samples required.

In contrast, the electron-capture detector method permits detection of picogram levels of II, thereby permitting the use of substantially smaller sample volumes and more frequent blood collection. The reproducibility of the electron-capture assay technique is demonstrated in Table IV. The observed results are based on four determinations at each concentration of II, ranging from 0.39 to 4.0 μg/ml of plasma. All analyses by the electron-capture detector required only 50–100 μl of rat plasma to quantitate II adequately. The regression line obtained after electron-capture detector GLC analysis of II was $y = mx + c$, where m was 0.264 and $c = -0.027$ ($r^2 = 0.988$).

REFERENCES

(1) B. K. Yeh and A. J. Gosselin, *Ration. Drug Ther.*, **9**, 1 (1975).

(2) A. J. Moss and R. D. Patton, "Antiarrhythmic Agents," Charles C Thomas, Springfield, Ill., 1973, p. 50.

(3) F. H. N. Spracklen, J. J. Kimberling, E. M. M. Besterman, and J. W. Litchfield, *Br. Med. J.*, **1**, 89 (1968).

(4) R. N. Boyes, D. B. Scott, P. J. Jebson, M. J. Godman, and D. G. Julian, *Clin. Pharmacol. Ther.*, **12**, 105 (1971).

(5) R. N. Boyes, H. J. Adams, and B. R. Duce, *J. Pharmacol. Exp. Ther.*, **174**, 1 (1970).

(6) J. M. Strong and A. J. Atkinson, Jr., *Anal. Chem.*, **44**, 2287 (1972).
(7) M. B. Meyer, D. Lalka, B. R. Duce, and A. T. Elvin, *Clin. Pharmacol. Ther.*, **17**, 204 (1975) (abstract).
(8) D. G. McDevitt, A. S. Nies, G. R. Wilkinson, R. F. Smith, R. L. Woosley, and J. A. Oates, *ibid.*, **19**, 396 (1976).
(9) D. Lalka, M. B. Meyer, B. R. Duce, and A. T. Elvin, *ibid.*, **19**, 757 (1976).
(10) S. Ahiya, *J. Pharm. Sci.*, **65**, 172 (1976).
(11) T. Walle and H. Ehrsson, *Acta Pharm. Suec.*, **7**, 389 (1970).

ACKNOWLEDGMENTS

Presented in part to the 23rd Canadian Conference on Pharmaceutical Research, Saskatoon, Saskatchewan, Canada, May 1976.

Supported by B.C. Heart Foundation Grant 65-0566.

The authors are grateful to Dr. D. Lalka and Mr. B. R. Duce of Astra Pharmaceutical Products, Framingham, Mass., Dr. D. Hasman of Cantest Ltd., Vancouver, B.C., and Dr. F. Abbott of the Faculty of Pharmaceutical Sciences, University of British Columbia, Vancouver, B.C., for their help and assistance.

Bilirubin Dynamics in the Gunn Rat during Phototherapy

R. T. CALVERT *, A. HULSHOFF, R. G. BUICE ‡, and H. B. KOSTENBAUDER ˣ

Received March 28, 1977, from the *College of Pharmacy, University of Kentucky, Lexington, KY 40506.* Accepted for publication May 9, 1977. *Present address: Department of Pharmacy, University of Manchester, Manchester M13 9PL, England. ‡Present address: School of Pharmacy, Northeast Louisiana University, Monroe, LA 71201.

Abstract □ Bilirubin dynamics were studied in homozygous Gunn rats under normal room lighting conditions and under conditions simulating phototherapy. A kinetic model was developed for the formation, distribution, and elimination of bilirubin. The decrease in plasma bilirubin concentration during illumination with low intensity [300 footcandles (fc)] and high intensity (1000–1100 fc) light was studied. The plasma bilirubin concentration in the rats decreased under phototherapy until a new steady-state concentration was reached, the decline being more rapid under high intensity light conditions. Gunn rats were also injected with a tracer dose of ^{14}C-bilirubin following a period during which the rats were illuminated with low or high intensity light. The distribution and elimination of the labeled bilirubin were followed under continuous illumination. The chosen kinetic model, when adapted to the set of data under investigation, fit all of the data concerning bilirubin kinetics in Gunn rats under continuous illumination.

Keyphrases □ Bilirubin—kinetics of formation, distribution, and elimination in rats, effect of phototherapy □ Kinetics—bilirubin formation, distribution, and elimination in rats, effect of phototherapy □ Phototherapy—effect on kinetics of bilirubin formation, distribution, and elimination, rats

Phototherapy was first described by Cremer *et al.* (1) and has since become a popular procedure for the treatment of neonatal hyperbilirubinemia. The efficacy of phototherapy is well established (2–7), but reservations have been expressed regarding the exposure of infants to blue or visible light intensities of 300–500 footcandles (fc), often continuously for as long as 3–5 days (8–14). It has been suggested that the generalized acceptance of this mode of therapy for neonatal hyperbilirubinemia has occurred without standardization of technique or individualization of application (15). Considerations of effects of variables such as light intensity and duration of exposure have been based primarily on clinical response following empirical selection of such parameters.

The present study was designed to investigate bilirubin kinetics in Gunn rats under normal room lighting conditions and under light exposure simulating phototherapy, with the objective of developing a kinetic model to predict the relative effectiveness of various phototherapy procedures. Gunn rats lack glucuronyltransferase activity for bilirubin conjugation and thus cannot excrete the pigment normally (16). Since Gunn rats show a markedly increased plasma bilirubin level, they are frequently used as a model in bilirubin studies.

Bilirubin kinetics previously were studied in humans (17–23) and in Gunn rats (17, 24–26). The effect of light on the catabolism of labeled bilirubin was studied in Gunn rats (27) and in infants with severe unconjugated hyperbilirubinemia (28), but in no report to date has a kinetic model been described that explains the change in the plasma bilirubin concentration due to phototherapy.

The approach used in the current study was based on the determination of the plasma level–time course of an intravenously injected tracer dose of ^{14}C-bilirubin in Gunn rats maintained under conditions of normal room lighting and under various conditions of illumination simulating phototherapy and on the determination of the rate at which the bilirubin plasma pool approaches a new steady-state level when Gunn rats are exposed to varying conditions of illumination.

EXPERIMENTAL

Reagents—Bilirubin[1] and riboflavin 5′-phosphate monosodium salt[2] were used as received from the supplier. All other solvents and reagents were analytical reagent grade.

Preparation of ^{14}C-Bilirubin Injections—This preparation was carried out in subdued light, as were all assays. Crystalline ^{14}C-bilirubin was prepared by a modification of the biosynthetic method of Barrett *et al.* (29), using Sprague–Dawley rats instead of dogs, and purified by the method of Ostrow *et al.* (30). After recrystallization (twice) from methanol, an aliquot was examined for radiochemical purity by TLC, using chloroform–acetic acid (99:1) on silica gel sheets[3], and by paper chromatography[4] with pyridine–ethyl acetate–water (1:2:1). The chromatograms were cut into 1-cm strips, and the amount of radioactivity on each strip was measured.

Ninety-five percent of the total activity was located in the bilirubin

[1] Lot 9324, Nutritional Biochemicals Corp., Cleveland, OH 44128.
[2] Mann Research, Orangeburg, NY 10962.
[3] ITLC type SG, Gelman Instrument Co., Ann Arbor, Mich.
[4] Whatman Grade 1, Scientific Products, Columbus, OH 43207.

(6) J. M. Strong and A. J. Atkinson, Jr., *Anal. Chem.*, **44**, 2287 (1972).
(7) M. B. Meyer, D. Lalka, B. R. Duce, and A. T. Elvin, *Clin. Pharmacol. Ther.*, **17**, 204 (1975) (abstract).
(8) D. G. McDevitt, A. S. Nies, G. R. Wilkinson, R. F. Smith, R. L. Woosley, and J. A. Oates, *ibid.*, **19**, 396 (1976).
(9) D. Lalka, M. B. Meyer, B. R. Duce, and A. T. Elvin, *ibid.*, **19**, 757 (1976).
(10) S. Ahiya, *J. Pharm. Sci.*, **65**, 172 (1976).
(11) T. Walle and H. Ehrsson, *Acta Pharm. Suec.*, **7**, 389 (1970).

ACKNOWLEDGMENTS

Presented in part to the 23rd Canadian Conference on Pharmaceutical Research, Saskatoon, Saskatchewan, Canada, May 1976.

Supported by B.C. Heart Foundation Grant 65-0566.

The authors are grateful to Dr. D. Lalka and Mr. B. R. Duce of Astra Pharmaceutical Products, Framingham, Mass., Dr. D. Hasman of Cantest Ltd., Vancouver, B.C., and Dr. F. Abbott of the Faculty of Pharmaceutical Sciences, University of British Columbia, Vancouver, B.C., for their help and assistance.

Bilirubin Dynamics in the Gunn Rat during Phototherapy

R. T. CALVERT *, A. HULSHOFF, R. G. BUICE ‡, and H. B. KOSTENBAUDER ˣ

Received March 28, 1977, from the *College of Pharmacy, University of Kentucky, Lexington, KY 40506.* Accepted for publication May 9, 1977. *Present address: Department of Pharmacy, University of Manchester, Manchester M13 9PL, England. ‡Present address: School of Pharmacy, Northeast Louisiana University, Monroe, LA 71201.

Abstract □ Bilirubin dynamics were studied in homozygous Gunn rats under normal room lighting conditions and under conditions simulating phototherapy. A kinetic model was developed for the formation, distribution, and elimination of bilirubin. The decrease in plasma bilirubin concentration during illumination with low intensity [300 footcandles (fc)] and high intensity (1000–1100 fc) light was studied. The plasma bilirubin concentration in the rats decreased under phototherapy until a new steady-state concentration was reached, the decline being more rapid under high intensity light conditions. Gunn rats were also injected with a tracer dose of ^{14}C-bilirubin following a period during which the rats were illuminated with low or high intensity light. The distribution and elimination of the labeled bilirubin were followed under continuous illumination. The chosen kinetic model, when adapted to the set of data under investigation, fit all of the data concerning bilirubin kinetics in Gunn rats under continuous illumination.

Keyphrases □ Bilirubin—kinetics of formation, distribution, and elimination in rats, effect of phototherapy □ Kinetics—bilirubin formation, distribution, and elimination in rats, effect of phototherapy □ Phototherapy—effect on kinetics of bilirubin formation, distribution, and elimination, rats

Phototherapy was first described by Cremer *et al.* (1) and has since become a popular procedure for the treatment of neonatal hyperbilirubinemia. The efficacy of phototherapy is well established (2–7), but reservations have been expressed regarding the exposure of infants to blue or visible light intensities of 300–500 footcandles (fc), often continuously for as long as 3–5 days (8–14). It has been suggested that the generalized acceptance of this mode of therapy for neonatal hyperbilirubinemia has occurred without standardization of technique or individualization of application (15). Considerations of effects of variables such as light intensity and duration of exposure have been based primarily on clinical response following empirical selection of such parameters.

The present study was designed to investigate bilirubin kinetics in Gunn rats under normal room lighting conditions and under light exposure simulating phototherapy, with the objective of developing a kinetic model to predict the relative effectiveness of various phototherapy procedures. Gunn rats lack glucuronyltransferase activity for bilirubin conjugation and thus cannot excrete the pigment normally (16). Since Gunn rats show a markedly increased plasma bilirubin level, they are frequently used as a model in bilirubin studies.

Bilirubin kinetics previously were studied in humans (17–23) and in Gunn rats (17, 24–26). The effect of light on the catabolism of labeled bilirubin was studied in Gunn rats (27) and in infants with severe unconjugated hyperbilirubinemia (28), but in no report to date has a kinetic model been described that explains the change in the plasma bilirubin concentration due to phototherapy.

The approach used in the current study was based on the determination of the plasma level–time course of an intravenously injected tracer dose of ^{14}C-bilirubin in Gunn rats maintained under conditions of normal room lighting and under various conditions of illumination simulating phototherapy and on the determination of the rate at which the bilirubin plasma pool approaches a new steady-state level when Gunn rats are exposed to varying conditions of illumination.

EXPERIMENTAL

Reagents—Bilirubin[1] and riboflavin 5′-phosphate monosodium salt[2] were used as received from the supplier. All other solvents and reagents were analytical reagent grade.

Preparation of ^{14}C-Bilirubin Injections—This preparation was carried out in subdued light, as were all assays. Crystalline ^{14}C-bilirubin was prepared by a modification of the biosynthetic method of Barrett *et al.* (29), using Sprague–Dawley rats instead of dogs, and purified by the method of Ostrow *et al.* (30). After recrystallization (twice) from methanol, an aliquot was examined for radiochemical purity by TLC, using chloroform–acetic acid (99:1) on silica gel sheets[3], and by paper chromatography[4] with pyridine–ethyl acetate–water (1:2:1). The chromatograms were cut into 1-cm strips, and the amount of radioactivity on each strip was measured.

Ninety-five percent of the total activity was located in the bilirubin

[1] Lot 9324, Nutritional Biochemicals Corp., Cleveland, OH 44128.
[2] Mann Research, Orangeburg, NY 10962.
[3] ITLC type SG, Gelman Instrument Co., Ann Arbor, Mich.
[4] Whatman Grade 1, Scientific Products, Columbus, OH 43207.

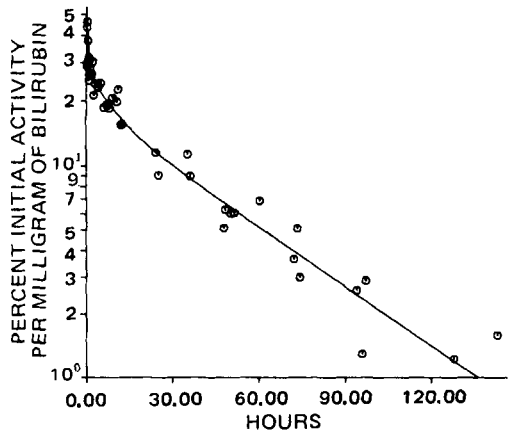

Figure 1—*Composite plasma ^{14}C-bilirubin data from six Gunn rats under normal room lighting conditions. The solid line represents a computer fit of data to a three-compartment model (Model 2).*

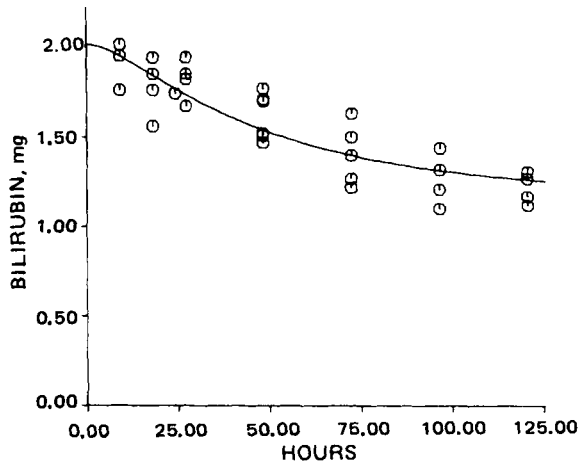

Figure 2—*Plasma bilirubin decline in six Gunn rats during continuous low intensity (300 fc) illumination. The solid line represents a computer fit of data to a three-compartment model (Model 11).*

region marked by the yellow-orange color and corresponding to the R_f value of an authentic bilirubin sample. The UV spectra of the crystalline ^{14}C-bilirubin in chloroform and in ethyl acetate showed no characteristics other than those of the authentic sample.

To prepare the injections, crystalline ^{14}C-bilirubin was further purified by TLC as described and eluted with ethyl acetate. The dried crystals were dissolved in a known volume of chloroform. A volume containing the required radioactivity was removed, and the solvent was evaporated under nitrogen. Crystalline ^{14}C-bilirubin was dissolved in 0.2 ml of 1% sodium carbonate, and 0.8 ml of freshly isolated rat plasma was added. An aliquot of the injection was assayed for activity and bilirubin content by the method described for the determination of plasma bilirubin specific activity. Each rat received an intravenous ^{14}C-bilirubin dose of 200,000–660,000 dpm.

Gunn Rat Studies—Adult homozygous male Gunn rats, 300–400 g, were shaved just prior to use. Six control rats were kept under normal room lighting after receiving intravenous injections of ^{14}C-bilirubin. Blood samples were taken periodically from the tail artery of the ether-anesthetized rats using 0.37-ml micro-blood-collecting tubes[5] fitted with disposable 20-gauge hypodermic needles.

Blood samples were centrifuged for 20 min at 5000×*g* and stored in the dark at −20° prior to ^{14}C-bilirubin specific activity determination. Rats used for phototherapy studies were placed in metabolism cages under a light canopy equipped with four daylight fluorescent tubes[6].

The cage to canopy distance was adjusted to allow the desired light intensity to reach the backs of the rats. Six rats were exposed to continuous low intensity (300 fc)[7] illumination[8], three rats received intravenous riboflavin 5′-phosphate injections of 75 mg/kg every 9 hr while being exposed continuously to low intensity illumination, and four rats were illuminated continuously with high intensity (1000–1100 fc)[7] light[8]. The plasma bilirubin concentration of all rats was followed for several days. The same sampling procedure as for the control rats was used.

In the third series of experiments, rats were illuminated for many hours before being injected with an intravenous tracer dose of ^{14}C-bilirubin. In the period following the injection, illumination was continued; blood samples were taken periodically and treated as in the control rat studies. Five rats were exposed to continuous low intensity illumination for 48 hr prior to injection, four rats received intravenous riboflavin 5′-phosphate injections (75 mg/kg every 9 hr) during the entire experiment while being illuminated continuously with low intensity light from 20 hr prior to the ^{14}C-bilirubin injection onwards, and four rats were exposed to continuous high intensity light for 12 hr prior to injection.

Each rat was used in only one experiment, since it was considered that the stress accompanying the prolonged light exposure studies was incompatible with a crossover design. All animals were produced by the same breeding colony.

Determination of Specific Activity of Plasma Bilirubin—Plasma bilirubin was isolated and purified by a two-stage process. The bilirubin was extracted from the plasma using a literature method (31) shown to separate bilirubin from its more polar degradation products. The lower phase, containing the bilirubin, was then further purified by TLC. A 0.1-ml plasma sample was added to a test tube containing 0.6 ml of ethyl acetate–lactic acid–water (62:36:2), and the mixture was shaken for 5 min. After the addition of 0.2 ml of chloroform, the tube was shaken for 5 min and centrifuged for 20 min.

The lower layer was transferred to a 5 × 20-cm thin-layer plate[3], which was then developed with chloroform–acetic acid (99:1). The yellow bilirubin band (R_f 0.7) was transferred to a screw-capped tube containing 1.5 ml of ethyl acetate, shaken for 1 min, and centrifuged for 20 min. After washing with water, the absorbance of the ethyl acetate layer was measured[9] at 445 nm, and the bilirubin concentration was determined using a standard curve. The UV spectrum of the isolated bilirubin was identical to that of an authentic sample, indicating that little or no degradation occurred.

The amount of radioactivity in an aliquot of the ethyl acetate solution was counted using a liquid scintillation counter[10] (about 50–1000 dpm/vial). Each vial was counted until 10,000 counts were made. The efficiency of counting was determined by automatic external standardization and was 75–85%. The activity of the bilirubin could then be expressed as disintegrations per minute per microgram.

Data were normalized to express each data point as a percent of dose per milligram of bilirubin for a 300-g rat with an initial plasma bilirubin level of 6 mg/100 ml, as described by Shipley and Clark (32):

$$\%\ \text{dose/mg of bilirubin at time } t = 10^5 \frac{(\text{dpm}/\mu\text{g})_t \times \text{rat weight (g)} \times \text{initial bilirubin concentration (mg/100 ml)}}{\text{dose (dpm)} \times 300 \times 6} \qquad \text{(Eq. 1)}$$

Determination of Plasma Bilirubin Concentration—In all studies not involving injections of tracer doses of ^{14}C-bilirubin, plasma bilirubin levels were determined by coupling bilirubin with diazotized sulfanilic acid, using caffeine and sodium benzoate as accelerators, as described by Jendrassik and Grof (33) and modified by Nosslin (34). The absorbance was measured[9] at 600 nm.

Data Analysis—The kinetic models used to describe the disappearance of ^{14}C-bilirubin from the plasma and the changes in the plasma bilirubin concentration were each defined by a series of differential equations or as the sum of exponentials. Least-squares estimates of the model parameters were obtained using a NONLIN program (35) and a digital computer[11]. All data points were given relative weight equal to the number of determinations per data point.

RESULTS

Control Data Studies—Individual rat data showed that the specific

[5] Caraway, Fisher Scientific Co., Louisville, KY 40299.
[6] F 40D, General Electric Co., Cleveland, OH 44117.
[7] One footcandle = 10.76 lux.
[8] Under the experimental condition, 300-fc illumination resulted in a radiant flux of 3.8 μw/cm^2/nm and 1100-fc illumination resulted in a radiant flux of 15 μw/cm^2/nm, as determined in the wavelength range of 425–475 nm with an Olympic Mark II Bili-meter, Olympic Medical Corp., Seattle, WA 98108.
[9] Cary 15 spectrophotometer, Cary Instruments, Monrovia, CA 91016.
[10] Packard Tri-Carb model 3375, Packard Instrument Co., Downers Grove, Ill.
[11] IBM 370 computer at the University of Kentucky.

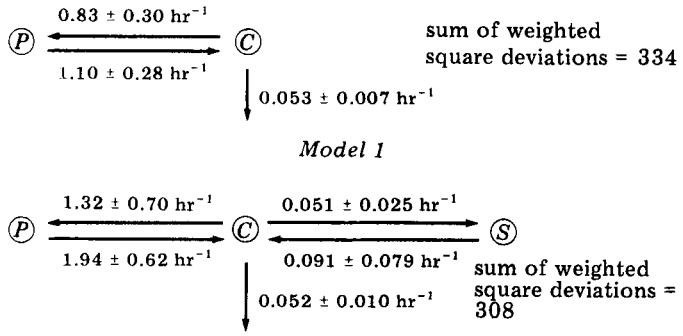

activity declined exponentially after a distribution phase of a few hours, suggesting that bilirubin confers the characteristics of a multicompartment model on the Gunn rat. This result also was reported by other investigators (17, 26). Between 6 and 12 hr, the plasma bilirubin activity–time curves exhibited small secondary peaks, characteristic of a recycling process and similar to that noted for certain drugs (36). When averaging all of the data, this apparent recycling phenomenon is masked by rather large interanimal variations; this complexity was, therefore, ignored in subsequent data-fitting computations.

Plasma ^{14}C-bilirubin disappearance data from rats kept under normal lighting conditions were fitted to a two-compartment model (Model 1) and to a three-compartment model (Model 2). The data points are shown in Fig. 1.

Models 1 and 2 are characterized by a central compartment (C), which contains the plasma and the other fluids and tissues in rapid equilibrium with plasma, and a (rapidly) miscible peripheral compartment (P). The three-compartment model also includes a slowly miscible compartment (S). The elimination rate constants and all intercompartmental rate constants are of first order. The analysis of the sums of squares by the F ratio test (37) indicates that there is no significant improvement at the 5% significance level when fitting the data to a three-compartment model compared with the two-compartment model fitting. However, it will be shown that the decrease in the plasma bilirubin concentration due to the illumination with low intensity light can best be described by a three-compartment model. From the initial value of percent dose per milligram of bilirubin at zero time, the amount of bilirubin in the central compartment under normal steady-state conditions was calculated to be 2.01 mg. The biological half-life, $t_{1/2}$, in the postdistributive phase was 23 hr, and the bilirubin production rate was 0.105 mg/hr.

Estimates of $t_{1/2}$ and the bilirubin production rate were also obtained by describing the disappearance of ^{14}C-bilirubin by:

$$Y = Ae^{-\alpha t} + Be^{-\beta t} \qquad \text{(Eq. 2)}$$

where Y = percent dose per milligram at time t, and A, B, α, and β are parameters for which least-squares estimates were calculated (Table I).

Decrease of Plasma Bilirubin Concentration during Illumination—During the continuous illumination with low or high intensity light,

Table I—Data Obtained following Intravenous Injection of ^{14}C-Bilirubin to Gunn Rats under Varying Conditions of Illumination; $Y = Ae^{-\alpha t} + Be^{-\beta t}$ (Y = % dose/mg of Bilirubin at Time t)

Illumination	A, % dose/mg of Bilirubin	α, hr^{-1}	B, % dose/mg of Bilirubin	β, hr^{-1}	$t_{1/2}$, hr (0.693/β)	Bilirubin Production Rate[a], mg/hr
Controls (normal room light)	20.2 (4.4)[b]	1.94 (0.63)	25.4 (1.1)	0.0297 (0.0037)	23.3	0.116
300 fc	12.1 (3.4)	1.24 (0.65)	40.1 (1.8)	0.0371 (0.0039)	18.7	0.092
1100 fc	14.0 (2.3)	1.18 (0.36)	37.6 (1.2)	0.0522 (0.0034)	13.3	0.137

[a] Calculated as $100/(A/\alpha + B/\beta)$. [b] Standard deviations of the parameters are shown in parentheses.

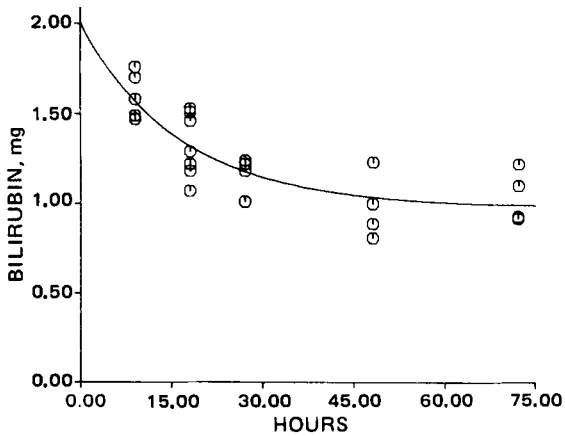

Figure 3—*Plasma bilirubin decline in seven Gunn rats during continuous severe phototherapy. The light intensity was either 1000–1100 fc or 300 fc with riboflavin as an adjunct. The solid line represents a computer fit of data to a two-compartment model (Model 3).*

the amount of bilirubin in the plasma decreased until a new steady-state level was reached (Figs. 2 and 3). No difference was detectable in the rates of decline of the plasma bilirubin concentration of rats illuminated with low intensity light while simultaneously receiving riboflavin 5′-monophosphate injections and of rats illuminated with high intensity light. Consequently, the data of these rats were pooled for analysis (Fig. 3).

On visual inspection of the graphs of Figs. 2 and 3, it appears that the new steady-state level of the amount of bilirubin in the plasma was approximately 60% of the initial value for rats illuminated with low intensity light and 50% for rats exposed to high intensity light. Any model used to describe the data must be compatible with these observations. The data were fitted to Models 3–12 (Fig. 4). Due to the restricted number of data points, it was not possible to obtain a computer solution if all of the parameters in the model under investigation were to be estimated in one computer run. Therefore, only the bilirubin production rate and the rate constant for the elimination process due to the phototherapy were introduced as adjustable parameters in Models 3–12. All other rate constants were given the values as obtained in the control rat studies.

The resulting values for the parameters, sums of weighted square de-

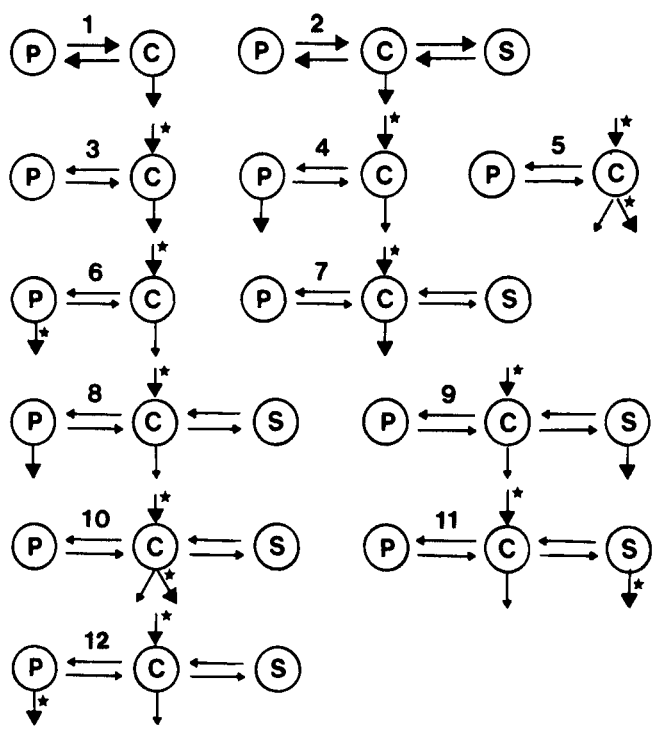

Figure 4—*Survey of kinetic models used in the data analysis. Zero-order rate constants are denoted by ★. Thick-lined arrows represent rate constants used as adjustable parameters in the computer fittings.*

Table II—Values of Characteristic Properties of the Models Used in the Computer Fit of the Data on the Decrease of the Plasma Bilirubin Level of Gunn Rats Due to Illumination

Model	Illumination Intensity, fc	*SWSD*[a]	Bilirubin Production Rate, mg/hr ± *SD*	Bilirubin[b] Excretion Rate ± *SD*	New Steady-State Level, % Initial Value
3	300	0.0472	0.00515 ± 0.00034	0.0105 ± 0.0012 hr^{-1}	<25
	1100	0.00487	0.102 ± 0.005	0.104 ± 0.006 hr^{-1}	48.3
4	300	0.121	0.0765 ± 0.0035	$0.157 \times 10^{-4} \pm 0.21 \times 10^{-5}$ hr^{-1}	65.0
	1100	0.00484	0.118 ± 0.003	0.0808 ± 0.0028 hr^{-1}	45.7
5	300	0.121	0.114 ± 0.005	0.0376 ± 0.0039 mg/hr	66.2
	1100	0.103	0.187 ± 0.030	0.149 ± 0.026 mg/hr	32.9
6	300	0.0545	0.115 ± 0.005	0.0475 ± 0.0039 mg/hr	58.4
	1100	6.11	0.12 ± 0.60	29.9 ± 133 mg/hr	<15
7	300	0.0150	0.0134 ± 0.0049	0.0182 ± 0.0050 hr^{-1}	<36
	1100	0.00851	0.113 ± 0.006	0.120 ± 0.004 hr^{-1}	47.3
8	300	0.0736	0.0663 ± 0.0029	$0.442 \times 10^{-4} \pm 0.56 \times 10^{-5}$ hr^{-1}	63.2
	1100	0.00762	0.116 ± 0.004	0.108 ± 0.006 hr^{-1}	47.3
9	300	0.0717	0.0728 ± 0.0028	0.00851 ± 0.00086 hr^{-1}	64.2
	1100	0.00506	0.0983 ± 0.0026	3.23 ± 0.27 hr^{-1}	47.5
10	300	0.0731	0.109 ± 0.006	0.0433 ± 0.0036 mg/hr	63.7
	1100	0.104	0.229 ± 0.058	0.273 ± 0.056 mg/hr	24.9
11	300	0.0248	0.105 ± 0.002	0.0431 ± 0.0019 mg/hr	59.2
	1100	0.00488	0.101 ± 0.002	1.27 ± 0.09 mg/hr or	48.3
				44.0 ± 2.8 mg/hr	48.3
12	300	0.0688	0.123 ± 0.006	0.0568 ± 0.0057 mg/hr	65.0
	1100	0.118	0.138 ± 0.030	0.114 ± 0.020 mg/hr	<35

[a] Sum of weighted square deviations. [b] Due to illumination.

viations, and the new steady-state plasma bilirubin levels as predicted by the models are shown in Table II.

^{14}C-Bilirubin Disappearance from Plasma under Phototherapy Conditions—Bilirubin kinetics were studied in rats that had been illuminated for a considerable period prior to the injection of labeled bilirubin. Ideally, the disappearance of the radioactive compound would be studied after the new steady state has been reached. This approach would require an illumination period of about 150 hr with low intensity light or 90 hr with high intensity light before injection of the labeled bilirubin. The illumination must be continued for a few more days after injection. When exposed to such prolonged periods of illumination, many of the Gunn rats died before the end of the experiment. Therefore, the rats were exposed for a shorter period to low or high intensity light before the injection, and the data were normalized as follows:

$$(\%\ \text{dose/mg of bilirubin})_{\text{time } t} = (\%\ \text{dose/mg of bilirubin})_{\text{observed}} \times \frac{(\text{amount plasma bilirubin})_{\text{time } t}}{(\text{amount plasma bilirubin})_{\text{new steady state}}} \quad \text{(Eq. 3)}$$

The amounts of bilirubin in plasma at time t were read from the graphs in Figs. 2 and 3. The new steady-state bilirubin levels for the low and high intensity light data were those predicted by Models 11 and 3, respectively (Table II). As before, the data from the rats illuminated with low intensity light while receiving riboflavin 5′-monophosphate injections were pooled with the high intensity light data, since there was no detectable difference between these two groups of data.

The decrease of the amount of radioactivity in the plasma of rats exposed to 300- (40 data points) and 1000–1100- (40 data points) fc light is shown in Figs. 5 and 6, respectively. The normalized plasma bilirubin specific activities (Eq. 1) could again be expressed as a simple two-exponential equation (Eq. 2). Values for A, B, α, and β, as well as for $t_{1/2}$ and the bilirubin production rate, are presented in Table I.

DISCUSSION

Since the products produced during the photocatabolism of bilirubin in the Gunn rat are not known (38), it was decided that bilirubin should not only be separated from its more polar degradation products by the much used extraction method of Weber and Schalm (31) but should subsequently be separated by TLC from unknown and possibly interfering products that might be present after the extraction in the organic layer.

In a previous report (39), it was established that riboflavin 5′-monophosphate administered intravenously to Gunn rats kept under low intensity light (300 fc) caused the plasma bilirubin level to decline to a new steady-state level at a faster rate than was achieved with low intensity light alone. These observations were confirmed in this study. Furthermore, no difference in the rate with which bilirubin was removed from the plasma was observed between the high intensity light data and the low intensity light data with simultaneous riboflavin 5′-monophosphate injections.

As is apparent from the numbers in Table II, none of the two-compartment models in Fig. 4 describes both the low and high intensity light data entirely satisfactorily, with the possible exception of Model 4. However, a significantly better fit (at the 5% significance level) was obtained with Model 11 when fitting the 300-fc data.

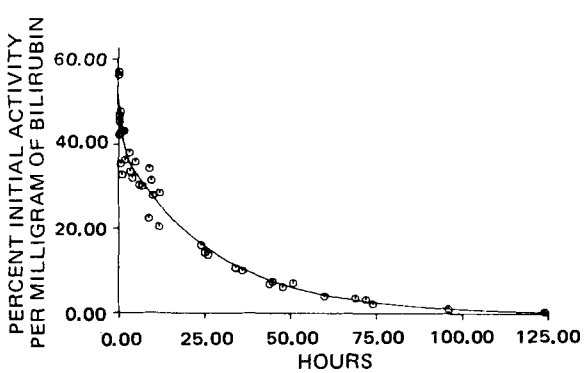

Figure 5—*Composite plasma ^{14}C-bilirubin data from five Gunn rats exposed to continuous low intensity (300 fc) illumination prior to and following the injection of the tracer dose. The solid line represents a computer fit of data for Eq. 2.*

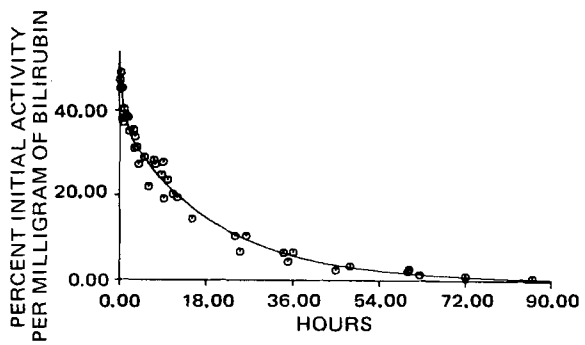

Figure 6—*Composite ^{14}C-plasma bilirubin data from eight Gunn rats exposed to continuous severe conditions of illumination (1000–1100 fc or 300 fc with riboflavin 5′-monophosphate as an adjunct) prior to and following the injection of the tracer dose. The solid line represents a computer fit of data to Eq. 2.*

Although Model 11 showed, for the low intensity light data, no significant improvement over Model 9 at the 5% significance level, Model 11 must still be preferred to Model 9 for several reasons. The bilirubin production rate as generated by the use of Model 11 is in better agreement with the value from the control rat studies than is the value obtained with Model 9; the coefficients of variation of the adjustable parameters are smaller for Model 11 than for Model 9, and the predicted new steady-state plasma bilirubin level is closer to the observed value (60%) when using Model 11. Consequently, Model 11 was considered the best possible model (of those in Fig. 4) to describe both the low and high intensity light data.

The high intensity light data could be fitted almost equally well to Models 3, 4, and 7–9. Depending on the initial value of the zero-order rate constant fed to the computer, very different estimates of that parameter were obtained for the high intensity light data; yet the bilirubin production rate, sum of weighted square deviations, and new steady-state values remained essentially unchanged. Once the zero-order elimination rate constant has exceeded a certain value under the influence of severe illumination conditions, the depletion of the slowly miscible compartment (S) occurs so rapidly that the model can be considered to collapse into the two-compartment Model 3 (Fig. 4).

It must be realized that, when searching for the best possible model as described here, a number of assumptions were made:

1. Only first-order and zero-order rate constants were considered.
2. The bilirubin production rate, as well as the intercompartmental rate constants, remained constant during phototherapy. The values in Table I suggest that, for the duration of the experiments, the bilirubin production rate remains essentially unaffected by illumination. The plasma levels in some rats tended to increase after prolonged periods of illumination (80–100 hr). These data points were not included in the analyses.
3. The rate of excretion of bilirubin from the central compartment, under control conditions, remained unaffected by subsequent illumination. When fitting the high intensity light data to Model 3, the obtained first-order elimination rate constant (0.104 hr^{-1}) was in excellent agreement with the expected value of 0.103 hr^{-1}, this value being the sum of the elimination rate constant (0.052 hr^{-1}) and the intercompartmental rate constant from C to S (0.051 hr^{-1}) from the control rat studies (Model 1), thus supporting this assumption.
4. In the jaundiced rat, bilirubin and its degradation products were reported to be partly excreted in the bile (17, 27).

There is no evidence that the liver in the Gunn rat is a separate compartment kinetically distinguishable from the central compartment, as has been suggested in reports concerning bilirubin kinetics in humans (20, 23). It was assumed that bilirubin was excreted solely from the central compartment under normal conditions. Obviously, this may be an oversimplification. On the basis of the present data, however, it was impossible to decide whether elimination under normal conditions occurs from one or more than one compartment; if elimination occurs from more than one compartment, it would be impossible to calculate the model constants independently (40).

5. Similarly, the degradation and elimination of bilirubin under phototherapy conditions might occur in more than one compartment.

Despite these and other possible complications, the chosen three-compartment model with zero-order elimination from the slowly miscible peripheral compartment has been shown to be excellently suited for the description of the changes in the plasma bilirubin concentration of the Gunn rat under continuous illumination with different light intensities.

REFERENCES

(1) R. J. Cremer, P. W. Perryman, and D. H. Richards, *Lancet*, **1**, 1094 (1958).

(2) J. Lucey, M. Ferreiro, and J. Hewitt, *Pediatrics*, **41**, 1047 (1968).

(3) S. O. Porto, R. S. Pildes, and H. Goodman, *J. Pediatr.*, **75**, 1045 (1969).

(4) J. E. Hodgman and A. Schwartz, *Am. J. Dis. Child.*, **119**, 473 (1970).

(5) F. Giunta and J. Rath, *Pediatrics*, **44**, 162 (1969).

(6) F. Giunta, *ibid.*, **47**, 123 (1971).

(7) P. C. Bajpai, P. K. Misra, V. K. Das, T. K. Tripathi, and C. L. Kapoor, *Indian J. Med. Res.*, **61**, 1658 (1973).

(8) T. R. C. Sisson, S. C. Glauser, E. M. Glauser, W. Tasman, and T. Kuwabara, *J. Pediatr.*, **77**, 221 (1970).

(9) R. J. Wurtman and R. M. Neer, *N. Engl. J. Med.*, **282**, 394 (1970).

(10) G. Ente and S. W. Klein, *ibid.*, **283**, 544 (1970).

(11) J. E. Hodgman and A. Teberg, *Birth Defects, Orig. Artic. Ser.*, **6**, 75 (1972).

(12) A. E. Kopelman, R. S. Brown, and G. B. Odell, *J. Pediatr.*, **81**, 466 (1972).

(13) G. B. Odell, R. S. Brown, and A. E. Kopelman, *ibid.*, **81**, 473 (1972).

(14) W. Oh and H. Karecki, *Am. J. Dis. Child.*, **124**, 230 (1972).

(15) R. E. Behrman and D. Y. Y. Hsia, *J. Pediatr.*, **75**, 718 (1969).

(16) R. Schmid, J. Axelrod, L. Hammaker, and R. L. Schwamm, *J. Clin. Invest.*, **37**, 1123 (1958).

(17) R. Schmid and L. Hammaker, *ibid.*, **42**, 1720 (1963).

(18) J. L. Cameron, R. M. Filler, F. L. Iber, T. Abei, and J. G. Randolph, *N. Engl. J. Med.*, **274**, 231 (1966).

(19) P. V. D. Barrett, P. D. Berk, M. Menken, and N. I. Berlin, *Ann. Intern. Med.*, **68**, 355 (1968).

(20) P. D. Berk, R. B. Howe, J. R. Bloomer, and N. I. Berlin, *J. Clin. Invest.*, **48**, 2176 (1969).

(21) M. Schmidt, J. Eisenburg, and W. Stich, *Klin. Wochenschr.*, **49**, 345 (1971).

(22) M. Black, J. Fevery, D. Parker, J. Jacobsen, B. H. Billing, and E. R. Carson, *Clin. Sci. Mol. Med.*, **46**, 1 (1974).

(23) G. Kirshenbaum, D. M. Shames, and R. Schmid, *J. Pharmacokinet. Biopharm.*, **4**, 115 (1976).

(24) L. H. Bernstein, J. B. Ezzer, L. Gartner, and I. M. Arias, *J. Clin. Invest.*, **45**, 1194 (1966).

(25) S. H. Robinson, *Proc. Soc. Exp. Biol. Med.*, **138**, 281 (1971).

(26) B. F. Scharschmidt, P. H. Plotz, P. D. Berk, J. G. Waggoner, and J. Vergalla, *J. Clin. Invest.*, **53**, 786 (1974).

(27) J. D. Ostrow, *ibid.*, **50**, 707 (1971).

(28) E. W. Callahan, M. M. Thaler, M. Karon, K. Bauer, and R. Schmid, *Pediatrics*, **46**, 841 (1970).

(29) P. V. D. Barrett, F. X. Mullins, and N. I. Berlin, *J. Lab. Clin. Med.*, **68**, 905 (1966).

(30) J. D. Ostrow, L. Hammaker, and R. Schmid, *J. Clin. Invest.*, **40**, 1442 (1961).

(31) A. P. Weber and L. Schalm, *Clin. Chim. Acta*, **7**, 805 (1962).

(32) R. A. Shipley and R. E. Clark, "Tracer Methods for In Vivo Kinetics," Academic, New York, N.Y., 1972, p. 23.

(33) L. Jendrassik and P. Grof, *Biochem. Z.*, **297**, 81 (1938).

(34) B. Nosslin, *Scand. J. Clin. Lab. Invest., Suppl. 49*, **12**, 54 (1960).

(35) C. M. Metzler, G. L. Elfring, and A. J. McEwen, "A Users Manual for NONLIN and Associated Programs," Research Biostatistics, Upjohn Co., Kalamazoo, Mich., 1974.

(36) H. B. Kostenbauder, R. P. Rapp, J. P. McGovren, T. S. Foster, D. G. Perrier, H. M. Blacker, W. C. Hulon, and A. W. Kinkel, *Clin. Pharmacol. Ther.*, **18**, 449 (1975).

(37) J. Mandel, "The Statistical Analysis of Experimental Data," Interscience, New York, N.Y., 1964, p. 164.

(38) A. F. McDonagh, *Ann. N. Y. Acad. Sci.*, **244**, 533 (1975).

(39) H. B. Kostenbauder and D. R. Sanvordeker, *Experientia*, **29**, 282 (1973).

(40) L. Z. Benet, *J. Pharm. Sci.*, **61**, 536 (1972).

ACKNOWLEDGMENTS

Supported by research Grant 5R01HD05745-02 from the National Institute of Child Health and Human Development.

Effect of Intensity of Agitation on Disintegration Time of Tablets

P. L. MADAN

Received November 22, 1976, from the *Department of Allied Health and Industrial Sciences, College of Pharmacy and Allied Health Sciences, St. John's University, Jamaica, NY 11439.* Accepted for publication May 5, 1977.

Abstract □ The effect of the intensity of agitation on the disintegration time of tablets was studied. Preliminary results obtained using tablets fabricated under controlled conditions and selected commercial tablets revealed that the intensity of agitation produced in the test apparatus was not reproducible with fixed geometry for successive runs when the settings were maintained constant. The disintegration times increased at a lower intensity of agitation. The intertablet range values obtained were rather large at the start and increased with a corresponding decrease in the intensity of agitation. The results showed that the measurement of disintegration times with the existing apparatus may not serve as a guide to the pharmaceutical formulator in the preparation of optimal dosage forms of drugs for clinical trial and may not ensure lot-to-lot uniformity of the pharmaceutical product.

Keyphrases □ Tablets—disintegration time, effect of intensity of agitation, specially fabricated and commercial formulations □ Disintegration time—tablets, specially fabricated and commercial, effect of intensity of agitation □ Agitation intensity—effect on disintegration time of specially fabricated and commercial tablets □ Dosage forms—tablets, specially fabricated and commercial, effect of intensity of agitation on disintegration time

The disintegration test is an essential attribute of tablets intended for oral administration, except those intended to exhibit extended release of their active ingredient(s). The rate at which a drug dissolves from its fragmented dosage form in the human GI tract often partially or completely controls the rate at which the drug appears in the blood (1). Therefore, measurement of disintegration time not only serves as a guide to the pharmaceutical formulator in the preparation of optimal dosage forms of drugs for clinical trial but also ensures that a given pharmaceutical product is essentially uniform from lot to lot.

The tablet disintegration apparatus has been official since USP IX and consists of a basket-rack assembly attached to a device for raising and lowering the basket in the immersion fluid through a distance of 5.5 ± 0.5 cm and at a constant frequency rate of 30 ± 2 complete cycles/min (cpm) (2, 3).

Some drawbacks of the disintegration test apparatus include:

1. The intensity of agitation produced in the apparatus is relatively much higher than that produced in the stomach. Therefore, the *in vivo* disintegration times may be much greater than the *in vitro* results (4).
2. The primary agitation intensity produced in the apparatus results from the turbulence of fluid flowing through the basket chamber, making the apparatus incapable of reproducing a given intensity of agitation with fixed geometry for successive runs when the settings are maintained constant.
3. The apparatus has only one speed, and the high degree of agitation introduced in the test may make it difficult to discriminate between a physiologically available product and a physiologically unavailable product[1] (5, 6).
4. The apparatus fails to simulate *in vivo* conditions (7).

While it may be difficult, if not impossible, to simulate *in vivo* conditions, the other drawbacks are primarily related to the single-speed agitation of the apparatus. This investigation reports the effect of agitation intensity on the disintegration time of tablets.

Table I—Tablet Formulations

Ingredient, % (w/w)	Formulation I	II	III	IV
Sodium salicylate	20	20	—	—
Magnesium trisilicate	—	—	20	20
Corn starch	5	5	5	5
Magnesium stearate	0.75	0.75	0.75	0.75
Lactose	74.25	—	74.25	—
Dibasic calcium phosphate	—	74.25	—	74.25

EXPERIMENTAL

Fabrication of Tablets—The tablets used in the preliminary investigation were made by direct compression using a water-insoluble and a water-soluble active ingredient, each incorporated into a water-soluble and water-insoluble matrix. Table I shows the composition of the formulations studied.

The active ingredient and the diluent were mixed in a planetary type mixer[2] for 5 min. Then the mixture was passed through a No. 30 bolting cloth and remixed for 5 min in the same mixer. The disintegrant (corn starch) was then passed through a No. 60 bolting cloth, added to the mixture, and blended for 5 min with a twin-shell V blender[3].

The lubricant (magnesium stearate) was passed through a No. 60 bolting cloth and sprinkled directly on the mixture, which had been spread as a thin layer on a waxed paper. The mixture then was blended for 3 min using the twin-shell V blender. The blends were then compressed into tablets on a single-punch press[4] equipped with a round, flat-faced punch and operated at a speed to produce 60 tablets/min. The characteristics of the tablets obtained were: weight, 500 ± 10 mg; hardness, 8.0 ± 0.5 kg; friability, <2.5%; and thickness, sufficient to give desired hardness.

Determination of Disintegration Time—The disintegration times were determined with the official test apparatus[5] (2, 3); water, maintained at 37 ± 1°, was the immersion fluid.

Effect of Intensity of Agitation—The effect of the intensity of agitation on the disintegration time of the tablets was determined by replacing the constant-speed motor used in the official test apparatus with similar constant-speed motors[6] having frequencies of 4 and 12 cpm. Thus, the basket-rack assembly could be raised and lowered in the immersion fluid at a constant frequency of 4, 12, or 30 cpm.

RESULTS AND DISCUSSION

Fabrication of Tablets—To eliminate the influence of unknown excipients, the investigation was restricted initially to the tablets fabri-

[1] P. L. Madan, unpublished results.
[2] Model 80 N, Hobart Manufacturing Co., Troy, Ohio.
[3] Patterson Kelley Co., East Stroudsburg, Pa.
[4] Model A-3, Stokes Division, Pennwalt Corp., Philadelphia, Pa.
[5] Van-Kel Industries, Chatham, N.J.
[6] Merkle-Korff Gear Co., Chicago, Ill.

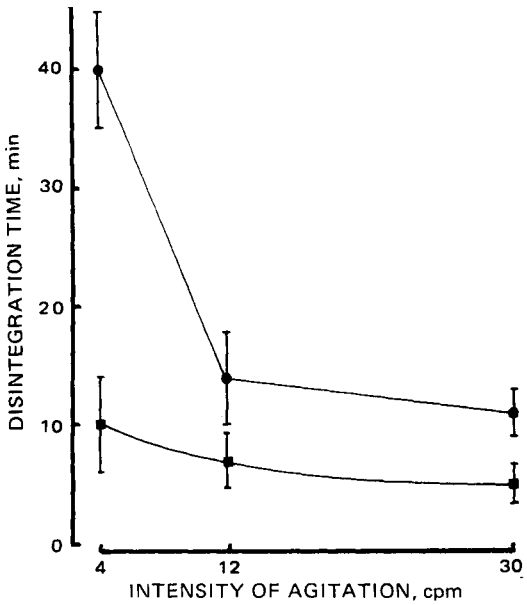

Figure 1—*Disintegration time of sodium salicylate tablets as a function of the intensity of agitation. Key: ●, Formulation II; and ■, Formulation I.*

cated under controlled conditions. The tablets were fabricated using a single-punch machine under conditions that would ensure minimum intertablet variability in the disintegration times due to manufacturing variables (*e.g.*, type and concentration of excipients and compression force employed).

Formulations—Two formulations, both known to compress directly into tablets, were selected. The basic difference between the two formulations was in terms of their water-solubility characteristics. One formulation was made primarily of lactose and was, therefore, considered essentially water soluble. The other formulation was made primarily of dibasic calcium phosphate and thus considered essentially water insoluble.

Since the active ingredient may influence disintegration, especially when present in a significant proportion, two types of active ingredients were selected for incorporation into each of the two formulations: water-soluble sodium salicylate and water-insoluble magnesium trisilicate.

Determination of Disintegration Time—The disintegration times were determined at three speeds: 4, 12, and 30 cpm. Figure 1 shows the disintegration times and the range values obtained with the water-soluble sodium salicylate in each of the two matrixes at the three agitation intensities. As expected, the disintegration times obtained at the lower speeds were higher than those obtained at 30 cpm. However, in spite of fabricating the tablets under controlled conditions, the intertablet range values obtained at 30 cpm were rather large. This result suggests the lack of reproducibility of the intensity of agitation produced in the apparatus at the speed specified in the official compendia (2, 3).

Even at less than half the speed specified in the official compendia, the agitation intensity was not reproducible (Fig. 1). The disintegration times as well as the range values obtained at 12 cpm were higher than those obtained at 30 cpm. A further reduction in the intensity of agitation apparently worsened the situation since there was a significant increase in the disintegration times as well as in the intertablet range values at 4 cpm.

The disintegration times as well as the intertablet range values were lower for tablets made with the water-soluble matrix. One possible explanation for this difference may be the hydrophilic character of the lactose used in the water-soluble matrix. Apparently, the immersion fluid penetrated the water-soluble matrix somewhat rapidly and, in doing so, it dissolved in part the matrix as well as the water-soluble drug contained within the tablet. Due to the dissolution of portions of the tablet, its entire structure would weaken and it would tend to fall apart even in the absence of agitation.

To test this hypothesis, an experiment was conducted using an aqueous solution of a water-soluble dye as the tracer. The tablets were soaked in the dye solution, and the migration of the dye in the tablets was examined. Tablets soaked in the dye solution for short time periods were completely covered with the dye externally but exhibited a spotty appearance when examined sectionally. The spots were located only near the periphery of the tablet and appeared dense at some points.

An increase in the soaking time increased not only the number and the density but also the distance of the spots from the surface of the tablets. Further increases in the soaking time resulted in the erosion of portions of the tablets, both externally and internally. However, the tablets were not completely spotted on the inside. An attempt was made to soak the tablets for longer periods to achieve spottiness throughout the inside, but such efforts were not very successful. The tablets became soft and soggy, and any attempt to obtain a section of the tablets only resulted in their being crushed.

The experiments were repeated using harder tablets, and the sequence of results obtained was identical to that found with the experimental ones.

It is, therefore, reasonable to assume that the disintegration of the hydrophilic tablets was due to the rapid penetration and dissolution of the tablet components. Thus, in the presence of agitation, the dissolution process of the water-soluble components of the tablets will be hastened and, at the same time, the disintegration of the tablet will be accelerated. Depending on the characteristics of the tablet formulation, the effect of the intensity of agitation on both the disintegration time and the range values could vary from negligible to enormous.

Apparently, the characteristics of the lactose-based tablets used in this study were such that the immersion fluid penetrated the tablets easily, weakening the tablet structure and causing disintegration soon thereafter. This result would also explain the similarity in the range values observed at 12 and 30 cpm. It is possible that the penetration of the immersion fluid resulting in the weakening of the tablet structure was a function of the agitation intensity, but the extent of weakening was more or less similar. At 4 cpm, however, the intensity of agitation was much slower and, therefore, accounted for an increase in the range values at this speed.

For tablets made with the water-insoluble matrix, the disintegration times as well as the range values increased at the lower speed of agitation. While the increase in the disintegration time was significantly higher at 4 cpm than at 12 cpm, the increase in the range values at these two speeds was only modest and more or less similar. Apparently, the hydrophobic nature of the dibasic calcium phosphate retarded the penetration of the immersion fluid through the tablet, thus resulting in increased disintegration times, the effect being more pronounced at the lower intensity of agitation.

However, once the immersion fluid penetrated the tablets and contacted the hydrophilic components, the tablet structure began to weaken and the tablet started to disintegrate. Apparently the disintegration of the water-insoluble based tablet was a function of the weakening of the tablet structure (Fig. 1). Thus, a reduction in the speed of agitation only increased the time of weakening of the tablet structure but did not significantly affect the range values.

Figure 2 shows the disintegration times and the range values obtained with the tablets containing the hydrophobic active ingredient, magnesium trisilicate. The results are similar to those found for tablets containing sodium salicylate, except that the disintegration times as well as the range values were somewhat higher. These results were even more apparent for tablets made with the water-insoluble matrix than for those made with the water-soluble matrix, supporting the view that the penetration of the immersion fluid was slower through the water-insoluble matrix, thus resulting in not only delayed disintegration but also in higher range values. For the tablets made with the water-soluble matrix, although the active ingredient was hydrophobic, the hydrophilic nature of the matrix may have aided in the penetration of the immersion fluid through the tablet, resulting in relatively faster disintegration and thus giving relatively lower disintegration times and lower range values.

It has been argued that the lack of reproducibility of the intensity of agitation in the disintegration apparatus may result from the turbulance of the fluid flowing through the basket chamber when the apparatus is operated at 30 cpm (8). If such is the case, then reducing the speed should reduce the turbulance, which, in turn, should produce a relatively reproducible intensity of agitation. Reducing the speed of the apparatus apparently did not result in a corresponding reduction of the turbulance (Figs. 1 and 2). Possibly there was some reduction in the degree of turbulance, but it was not sufficient to cause appreciable reproducibility in the intensity of agitation.

The coefficient of variation of the disintegration times (Fig. 3) was largest for the essentially water-soluble tablet (Formulation I) at all three speeds but was smaller for the three formulations that contained one or more hydrophobic components. At 30 cpm, the coefficients of variation followed the order: Formulation I > Formulation III > Formulation II > Formulation IV. At 12 cpm, the order was: Formulation I > Formula-

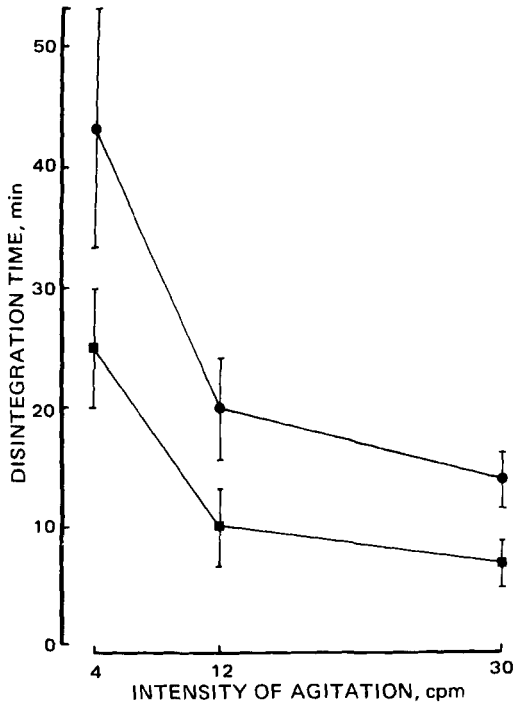

Figure 2—*Disintegration time of magnesium trisilicate tablets as a function of intensity of agitation. Key: ●, Formulation IV; and ■, Formulation III.*

tion III ≈ Formulation II > Formulation IV. And at 4 cpm, the order was: Formulation I > Formulation IV > Formulation III > Formulation II.

The rank order shows some similarity at the two higher speeds but lacks consistency at the lowest speed. However, it is interesting to note the linear relationship between the coefficient of variation and the intensity of agitation for the essentially water-insoluble tablet (Formulation IV) and the lack of such a relationship for the three formulations containing one or more water-soluble components.

These results suggest that a reduction in the speed of agitation apparently did not correspondingly reduce the turbulance in the apparatus. Had such been the case, the water-soluble components of the formulations would have been affected by the disintegration fluid relative to the speed of agitation and the results would have been reversed. That is, there would have been a direct relationship between the coefficient of variation and the speed of agitation for the formulations containing the water-soluble components but not for the formulations containing the water-insoluble components; the penetration of the disintegrating fluid in the tablets and the dissolution of the water-soluble components would have been a function of the intensity of agitation produced in the apparatus.

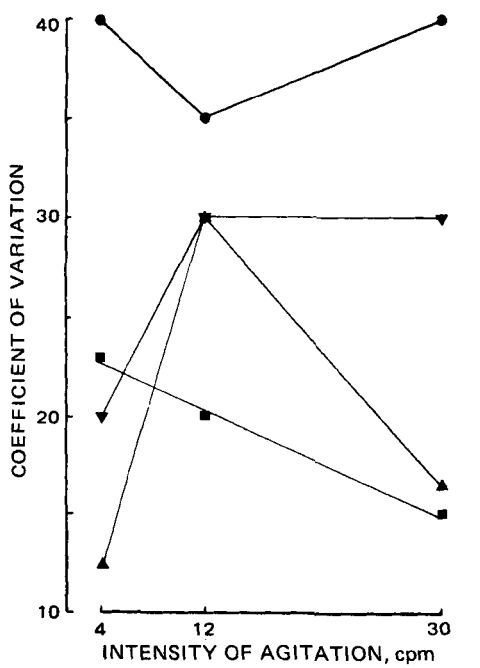

Figure 3—*Coefficient of variation as a function of intensity of agitation. Key: ●, Formulation I; ▲, Formulation II; ▼, Formulation III; and ■, Formulation IV.*

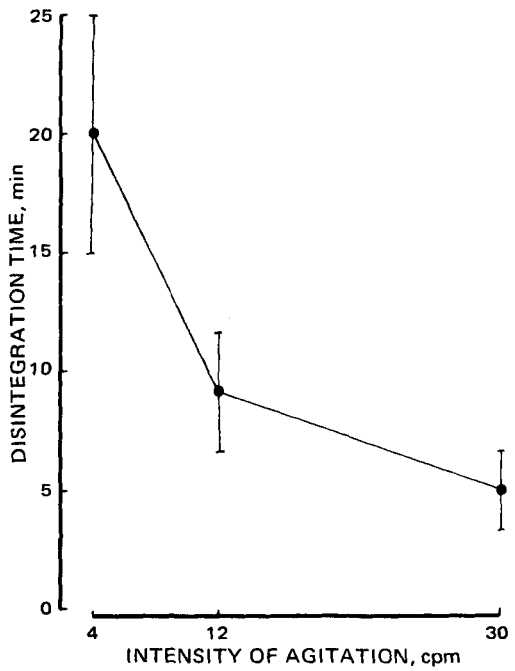

Figure 4—*Disintegration time of a commercial formulation as a function of the intensity of agitation.*

To determine the effect of the intensity of agitation on commercial formulations, several of them were studied at the three disintegration speeds. In most cases, the results showed that the disintegration times followed the order: 30 < 12 < 4 cpm. The intertablet range values increased significantly at lower speeds. Figure 4 shows the results obtained with a typical commercial formulation.

In the few cases where the commercial tablet formulations did not show

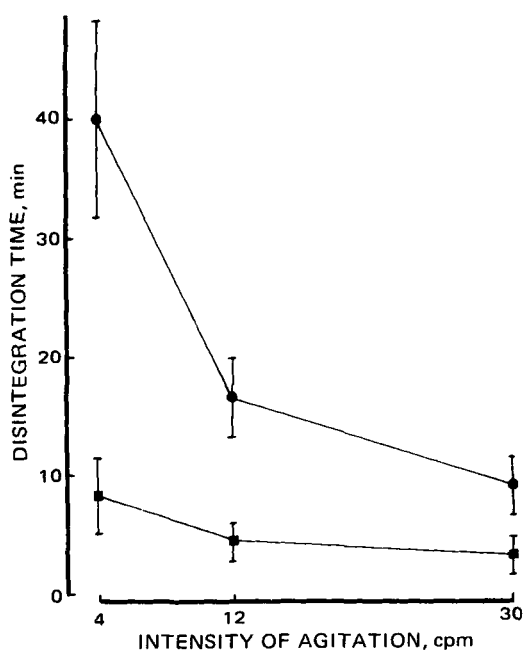

Figure 5—*Effect of disks on the disintegration time of tablets. Key: ●, Formulation IV; and ■, Formulation I.*

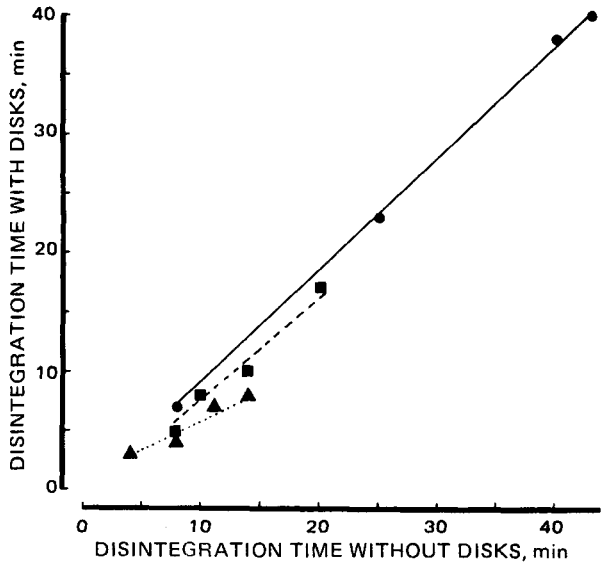

Figure 6—*Disintegration time with disks as a function of the disintegration time without disks. Key: ●, 4 cpm; ■, 12 cpm; and ▲, 30 cpm.*

significant variations in the disintegration times and the intertablet range values at the three agitation intensities, their disintegration time was less than 2 min. These tablets appeared to start breaking apart as soon as they were placed in the immersion fluid. In contrast, tablets that gave higher disintegration times did not exhibit any disintegration sign during the first few minutes. After a lapse of time, which varied from one brand to the other, the tablets started to disintegrate slowly. Visual observation indicated that the rate of disintegration of the slow-disintegrating tablets appeared to slow down as the disintegration process progressed. That is, the rate of breakdown of the tablet into larger fragments was faster than the rate of breakdown of the larger fragments into smaller particles.

Possibly, the commercial formulations that did not show variations in the disintegration times and intertablet range values at the three agitation intensities may have contained a component that approximated an erupting type of a disintegrant. In such a case, the agitation intensity would be expected to have little, if any, effect on the disintegration time. To test the validity of this hypothesis, the disintegration times of these formulations were determined in the absence of any externally applied agitation, and the results approximated the disintegration times obtained at 4, 12, and 30 cpm.

Effect of Disks—Disks are used in the disintegration apparatus to prevent the tablets from floating in the assembly (2, 3). It has been reported that the presence of disks causes a high degree of abrasion, resulting in rapid tablet disintegration (9).

The effect of disks on the disintegration time of the tablets is shown in Fig. 5. The disintegration times as well as the intertablet range values obtained at the three speeds were indeed reduced in the presence of disks. However, the reduction in the disintegration time was greater at 12 or 30 cpm than at 4 cpm. This result may be due to an increased degree of abrasion caused at the higher speed of agitation because of the more frequent abrasive contact of the disks with the tablets.

Visual observation during disintegration experimentation showed that the movement of disks in the apparatus at 4 cpm was relatively negligible; the disks appeared to be stationary most of the time. Even if the disks did have any abrasive action, it was only negligible. This view is supported by the excellent correlation found between the disintegration times obtained in the presence and absence of disks (Fig. 6).

Table II—Parameters of Correlation between Disintegration Times in the Presence and Absence of Disks

Intensity of Agitation, cpm	Correlation Coefficient[a]	Slope	Equation of Straight Line
4	0.99895	0.9535	$y = 0.9535x - 0.6516$
12	0.9700	0.8334	$y = 0.8334x - 0.8342$
30	0.9874	0.5346	$y = 0.5346x + 0.6886$

[a] Theoretical value at a probability level of 0.05 = 0.95.

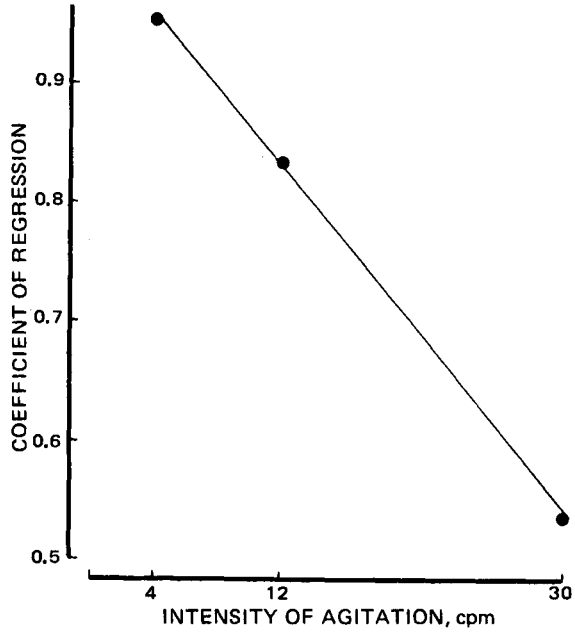

Figure 7—*Coefficient of regression as a function of the intensity of agitation.*

The results shown in Fig. 6 are summarized in Table II. These results indicate that the correlation between the disintegration times in the presence and absence of the disks followed the order 4 > 30 > 12 cpm. Apparently, the abrasive action of the disks was minimal at 4 cpm and, therefore, the value of the correlation coefficient was closest to unity. At 30 cpm, the abrasive action was much greater, and the disintegration times of all formulations studied appear to have been affected more or less similarly.

At 12 cpm, however, the correlation coefficient was the lowest of the three values, probably because the presence of disks affected different formulations differently at this intensity of agitation. This result may have been due to the nonreproducibility of the agitation intensity in successive runs because of the unpredictable nature of the turbulance, resulting in the smaller value of the correlation coefficient. However, at all three speeds, the calculated values of the correlation coefficient were greater than 0.95, the theoretical value of the correlation coefficient at a probability level of 0.05, indicating that the correlation between the disintegration times obtained in the presence and absence of disks was significant.

The three equations in Table II indicate that the straight lines do not pass through the origin. In all cases, the magnitude of the y-intercept was small (less than 1 min) and deviated from zero in the order 4 < 30 < 12 cpm. The rank order observed here was similar to that observed for the correlation coefficients.

The slope (coefficient of regression) followed the order 4 > 12 > 30 cpm (Table II), indicating that the influence of the disks on the disintegration times of the tablets was a function of the intensity of agitation. The coefficient of regression was closest to unity at the lowest intensity of agitation and declined sharply with an increasing intensity of agitation. That the coefficient of regression was directly related to the intensity of agitation is evidenced by the linear plot shown in Fig. 7.

Extrapolation of the linear plot yields a value of 63 cpm for the regression coefficient to be 0, *i.e.*, no correlation between the disintegration times in the presence and absence of disks. For the coefficient of regression to be unity, the graph in Fig. 7 predicts a value of 1.5 cpm, apparently the minimum intensity of agitation needed to keep the disks afloat but not sufficiently turbulant to have any abrasive action.

REFERENCES

(1) J. G. Wagner, "Biopharmaceutics and Relevant Pharmacokinetics," Drug Intelligence Publications, Hamilton, Ill., 1971, chap. 10.

(2) "The United States Pharmacopeia," 19th rev., Mack Publishing Co., Easton, Pa., 1975, p. 650.

(3) "The National Formulary," 14th ed., Mack Publishing Co., Easton, Pa., 1975, p. 978.

(4) W. H. Steinberg, G. H. Frey, J. N. Masci, and H. H. Hutchins, *J.*

Pharm. Sci., **54**, 747 (1965).
(5) G. Levy and L. E. Hollister, *N.Y. J. Med.*, **64**, 3002 (1964).
(6) P. L. Madan and M. Minisci, *Drug Intell. Clin. Pharm.*, **10**, 588 (1976).
(7) G. Levy, *J. Pharm. Sci.*, **52**, 1039 (1963).
(8) P. L. Madan, in "Manual for Pharmacy Technicians," 2nd ed., J. M. Durgin, Z. I. Hanan, and C. O. Ward, Eds., C. V. Mosby, St. Louis, Mo., in press.
(9) E. L. Knoechel, C. C. Sperry, and C. J. Lintner, *J. Pharm. Sci.*, **56**, 116 (1967).

Microsealed Drug Delivery Systems I: *In Vitro–In Vivo* Correlation on Subcutaneous Release of Desoxycorticosterone Acetate and Prolonged Hypertensive Animal Model for Cardiovascular Studies

YIE W. CHIEN *x, LEONARD F. ROZEK ‡, and HOWARD J. LAMBERT *

Received October 18, 1976, from the **Pharmaceutical Research Group, Development Department, and the* ‡*Cardiovascular Group, Biological Research Department, Searle Laboratories, G. D. Searle & Co., Skokie, IL 60076.* Accepted for publication May 2, 1977.

Abstract □ A new generation drug delivery system, named the Microsealed Drug Delivery (MDD) system, was developed. Subcutaneous implantation of MDD's in rats for up to 129 days resulted in a constant release profile of desoxycorticosterone acetate. Three formulations were examined. An excellent *in vitro–in vivo* correlation was established on both the mechanism and the rate of controlled release of desoxycorticosterone acetate from MDD's. A significant degree of hypertension was reproducibly produced within 21 days after implantation and successfully sustained through Day 98. Comparative studies were conducted on MDD's and a previously developed matrix-type silicone device. The elevation of systolic blood pressure initiated by either MDD's or the matrix-type silicone device was essentially the same in pattern, and the difference in the hypertensive responses between these polymeric drug delivery systems was statistically insignificant, although a higher dose, which is time dependent, was administered to rats through the matrix-type silicone device than through MDD's. The bioavailability of desoxycorticosterone acetate and its dose–response relationship apparently were accomplished more effectively *via* the constant drug delivery mechanism of MDD's.

Keyphrases □ Drug delivery systems, microsealed—subcutaneous release of desoxycorticosterone acetate in rats, *in vitro–in vivo* correlation, *compared to matrix-type silicone device* □ Desoxycorticosterone acetate—subcutaneous release from microsealed drug delivery system in rats, *in vitro–in vivo* correlation, compared to matrix-type silicone device □ Dosage forms—microsealed drug delivery system, subcutaneous release of desoxycorticosterone acetate in rats, *in vitro–in vivo* correlation, compared to matrix-type silicone device □ Adrenocortical steroids—desoxycorticosterone acetate, subcutaneous release from microsealed drug delivery system in rats, *in vitro–in vivo* correlation, compared to matrix-type silicone device

Metacorticoid hypertension, induced by the chronic administration of desoxycorticosterone acetate to rats in conjunction with saline loading, simulates, both pathologically and physiologically, the syndrome of essential hypertension in humans (1). A close relationship was observed between salt metabolism and many forms of experimental and clinical hypertension. An increase in total sodium, due in large part to an increase in intracellular sodium, and a fall in intracellular potassium, were reported to occur during the development of hypertension induced by desoxycorticosterone acetate (2).

Induction of experimental hypertension in rats to evaluate the antihypertensive activity of various drugs requires either daily injections of a desoxycorticosterone acetate suspension or implantation of a desoxycorticosterone acetate-containing wax pellet (3) while the rats are maintained on saline. The first technique consistently initiates onset of metacorticoid hypertension within 21–28 days, but the required daily injections are time consuming and may be hazardous for the animals. The second technique, because of inconsistent release rates of desoxycorticosterone acetate from the wax matrix, results in wide variations in hypertensive onset.

Recent reports (4, 5) demonstrated that experimental hypertension could be reproducibly induced in rats and successfully maintained for a prolonged period of time, *e.g.*, 100 days, by subcutaneous delivery of desoxycorticosterone acetate through a long-acting matrix-type silicone device. The release of desoxycorticosterone acetate was substantially prolonged by homogeneously impregnating the desoxycorticosterone acetate in a silicone polymer matrix. The same drug delivery system was also applied for the intravaginal administration of ethynodiol diacetate to rabbits for sustained contraceptive activity (6). Both the *in vitro* and *in vivo* releases of desoxycorticosterone acetate from silicone devices followed a matrix-controlled process, as defined by Q *versus* $t^{1/2}$ release kinetics (4, 6–11). The release profile of a drug from the matrix-type polymeric devices is high initially and then decreases with time.

In this investigation, a new generation drug delivery system, named the Microsealed Drug Delivery (MDD) system (12), was developed to provide a means for the constant (zero-order) release of desoxycorticosterone acetate. Both the *in vitro–in vivo* release profiles of desoxycorticosterone acetate from MDD's were studied, and their relationship was analyzed. The differences between MDD's and matrix-type silicone devices on the modes of desoxycorticosterone acetate release were examined. The time courses for the production of metacorticoid hypertension in rats also were explored.

Pharm. Sci., **54**, 747 (1965).
(5) G. Levy and L. E. Hollister, *N.Y. J. Med.*, **64**, 3002 (1964).
(6) P. L. Madan and M. Minisci, *Drug Intell. Clin. Pharm.*, **10**, 588 (1976).
(7) G. Levy, *J. Pharm. Sci.*, **52**, 1039 (1963).
(8) P. L. Madan, in "Manual for Pharmacy Technicians," 2nd ed., J. M. Durgin, Z. I. Hanan, and C. O. Ward, Eds., C. V. Mosby, St. Louis, Mo., in press.
(9) E. L. Knoechel, C. C. Sperry, and C. J. Lintner, *J. Pharm. Sci.*, **56**, 116 (1967).

Microsealed Drug Delivery Systems I: *In Vitro–In Vivo* Correlation on Subcutaneous Release of Desoxycorticosterone Acetate and Prolonged Hypertensive Animal Model for Cardiovascular Studies

YIE W. CHIEN *x, LEONARD F. ROZEK ‡, and HOWARD J. LAMBERT *

Received October 18, 1976, from the **Pharmaceutical Research Group, Development Department, and the* ‡*Cardiovascular Group, Biological Research Department, Searle Laboratories, G. D. Searle & Co., Skokie, IL 60076.* Accepted for publication May 2, 1977.

Abstract □ A new generation drug delivery system, named the Microsealed Drug Delivery (MDD) system, was developed. Subcutaneous implantation of MDD's in rats for up to 129 days resulted in a constant release profile of desoxycorticosterone acetate. Three formulations were examined. An excellent *in vitro–in vivo* correlation was established on both the mechanism and the rate of controlled release of desoxycorticosterone acetate from MDD's. A significant degree of hypertension was reproducibly produced within 21 days after implantation and successfully sustained through Day 98. Comparative studies were conducted on MDD's and a previously developed matrix-type silicone device. The elevation of systolic blood pressure initiated by either MDD's or the matrix-type silicone device was essentially the same in pattern, and the difference in the hypertensive responses between these polymeric drug delivery systems was statistically insignificant, although a higher dose, which is time dependent, was administered to rats through the matrix-type silicone device than through MDD's. The bioavailability of desoxycorticosterone acetate and its dose–response relationship apparently were accomplished more effectively *via* the constant drug delivery mechanism of MDD's.

Keyphrases □ Drug delivery systems, microsealed—subcutaneous release of desoxycorticosterone acetate in rats, *in vitro–in vivo* correlation, *compared to matrix-type silicone device* □ Desoxycorticosterone acetate—subcutaneous release from microsealed drug delivery system in rats, *in vitro–in vivo* correlation, compared to matrix-type silicone device □ Dosage forms—microsealed drug delivery system, subcutaneous release of desoxycorticosterone acetate in rats, *in vitro–in vivo* correlation, compared to matrix-type silicone device □ Adrenocortical steroids—desoxycorticosterone acetate, subcutaneous release from microsealed drug delivery system in rats, *in vitro–in vivo* correlation, compared to matrix-type silicone device

Metacorticoid hypertension, induced by the chronic administration of desoxycorticosterone acetate to rats in conjunction with saline loading, simulates, both pathologically and physiologically, the syndrome of essential hypertension in humans (1). A close relationship was observed between salt metabolism and many forms of experimental and clinical hypertension. An increase in total sodium, due in large part to an increase in intracellular sodium, and a fall in intracellular potassium, were reported to occur during the development of hypertension induced by desoxycorticosterone acetate (2).

Induction of experimental hypertension in rats to evaluate the antihypertensive activity of various drugs requires either daily injections of a desoxycorticosterone acetate suspension or implantation of a desoxycorticosterone acetate-containing wax pellet (3) while the rats are maintained on saline. The first technique consistently initiates onset of metacorticoid hypertension within 21–28 days, but the required daily injections are time consuming and may be hazardous for the animals. The second technique, because of inconsistent release rates of desoxycorticosterone acetate from the wax matrix, results in wide variations in hypertensive onset.

Recent reports (4, 5) demonstrated that experimental hypertension could be reproducibly induced in rats and successfully maintained for a prolonged period of time, *e.g.*, 100 days, by subcutaneous delivery of desoxycorticosterone acetate through a long-acting matrix-type silicone device. The release of desoxycorticosterone acetate was substantially prolonged by homogeneously impregnating the desoxycorticosterone acetate in a silicone polymer matrix. The same drug delivery system was also applied for the intravaginal administration of ethynodiol diacetate to rabbits for sustained contraceptive activity (6). Both the *in vitro* and *in vivo* releases of desoxycorticosterone acetate from silicone devices followed a matrix-controlled process, as defined by Q *versus* $t^{1/2}$ release kinetics (4, 6–11). The release profile of a drug from the matrix-type polymeric devices is high initially and then decreases with time.

In this investigation, a new generation drug delivery system, named the Microsealed Drug Delivery (MDD) system (12), was developed to provide a means for the constant (zero-order) release of desoxycorticosterone acetate. Both the *in vitro–in vivo* release profiles of desoxycorticosterone acetate from MDD's were studied, and their relationship was analyzed. The differences between MDD's and matrix-type silicone devices on the modes of desoxycorticosterone acetate release were examined. The time courses for the production of metacorticoid hypertension in rats also were explored.

Table I—Independence of the *In Vitro* Release Rates of Desoxycorticosterone Acetate on Drug Content in the Medicated Core Matrix of Microsealed Delivery Devices

Drug Content, mg/cm³	Release Rates[a], μg/cm²/day
21.2	50.8 (±2.1)
36.3	56.9 (±3.2)
64.9	53.5 (±1.2)

[a] Mean (± *SD*) of three determinations.

EXPERIMENTAL

Preparation of MDD's—MDD's were fabricated, following the methodology and process outlined earlier (12), to contain 21.1–64.9 mg of desoxycorticosterone acetate[1] in a unit volume of a medicated core matrix. After inspection by photomicrography, UV and IR spectrophotometry, and differential scanning calorimetry, desoxycorticosterone acetate chemical was used as obtained.

***In Vitro* Drug Release Studies**—The *in vitro* drug elution system used in characterizing the mechanism and rates of release of desoxycorticosterone acetate from MDD's was essentially the same as that reported previously (4, 7). Lengths of 16 cm of the MDD were mounted in a circular shape in the arms of a Plexiglas holder. The holder was then rotated at a constant speed (81 rpm) in an elution medium [150 ml of 75% (v/v) polyethylene glycol 400[2] in distilled water] at 37°.

A 50-ml sample of the elution medium was withdrawn each day and was replaced with the same quantity of drug-free elution medium, which was also thermostated at 37°. The sample was then assayed spectrophotometrically at λ_{max} 240 nm. The amount of desoxycorticosterone acetate released daily was calculated and followed for 8 days, and the mechanisms as well as the rates of drug release from MDD's were then analyzed.

***In Vivo* Drug Release Studies**—Sixty male Charles River CD strain rats (with an average weight of 130–190 g and an age of 4–6 weeks) were assigned to three studies. In each study, a control group (implanted with placebo MDD's) was examined in parallel with the treated group (implanted with medicated MDD's). The systolic blood pressure of each rat was indirectly determined using a programmed electrosphygmomanometer[3] at the onset of the study and at weekly intervals thereafter.

Following the determination of initial blood pressure, the rats were anesthetized with ether. A 1-cm cutaneous incision was made in the dorsal thoracic area of each rat. After the formation of a subcutaneous tunnel with forceps, a 3-cm length of the MDD was inserted. The incision was closed with wound clips, and the rats were then returned to their cages for recovery.

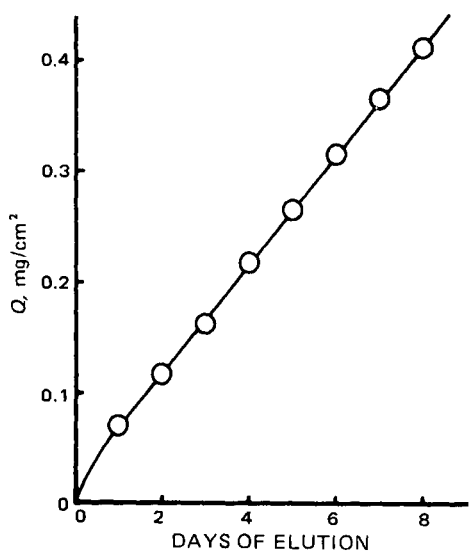

Figure 1—*Time course for the* in vitro *release of oxycorticosterone acetate from MDD 603 in 75% (v/v) aqueous polyethylene glycol 400 solution at 37°. The rate of* in vitro *release, Q/t, was calculated from the slope as 49.34 μg/cm²/day.*

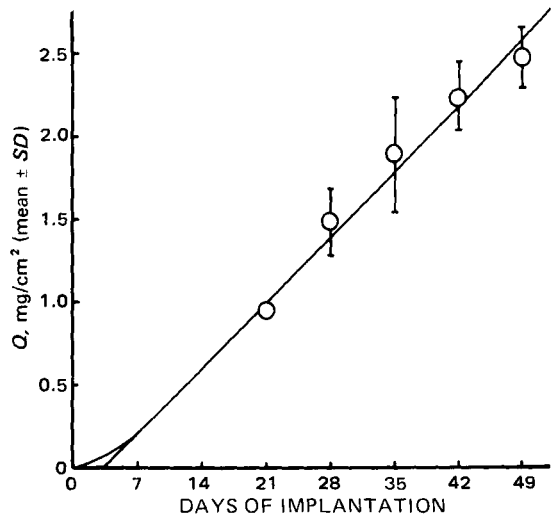

Figure 2—*Time course for the subcutaneous release of desoxycorticosterone acetate from MDD 603 in rats. The rate of* in vivo *release, Q/t, was calculated from the slope as 53.7 μg/cm²/day. Each data point represents the mean* (±SD) *of three to five determinations.*

Both the control and treated groups were maintained on a normal laboratory rat diet with a fluid ration of 1% saline solution throughout the study.

At scheduled intervals, five rats were randomly selected from the treated group for removal of the MDD's. After measurement of the systolic blood pressure, the MDD's were removed. Their residual desoxycorticosterone acetate content was thoroughly extracted with methanol and assayed spectrophotometrically.

The placebo MDD's were removed from the control group at the end of each study following the final reading of systolic blood pressure.

RESULTS AND DISCUSSION

***In Vitro* Release of Desoxycorticosterone Acetate from MDD's**—A typical set of data on the *in vitro* release of desoxycorticosterone acetate from an MDD is illustrated in Fig. 1. The cumulated amount, *Q*, of desoxycorticosterone acetate released from a unit surface area of the MDD was linearly proportional to the duration (in days) of elution in the elution solution. Apparently, a constant (zero-order) release profile is achieved using the MDD.

The release profile shown in Fig. 1 was generated from an MDD containing 64.9 mg of desoxycorticosterone acetate/cm³. From the slope of the linear *Q versus t* plot, the rate of release, *Q/t*, of desoxycorticosterone acetate was calculated to be 49.34 μg/cm²/day. The magnitude of the desoxycorticosterone acetate release rates, *Q/t*, was independent of the desoxycorticosterone acetate content in the medicated core matrix of the MDD (Table I). This observation provides additional evidence that release of desoxycorticosterone acetate from MDD's follows a zero-order rate process.

***In Vivo* Release of Desoxycorticosterone Acetate from MDD's in Rats**—Subcutaneous implantation of MDD's in the dorsal thoracic area of rats for various lengths of time also resulted in a constant (zero-order) release of desoxycorticosterone acetate (Fig. 2). This constant release rate was in agreement with the *in vitro* observations. From the slope of the linear *Q versus t* relationship, the *in vivo* release rate, *Q/t*, was computed to be 53.7 μg/cm²/day. This magnitude of the *in vivo* release rate was very close to the value of the *in vitro* release rate (49.3 μg/cm²/day) obtained from the same MDD formulation (MDD 603).

Several MDD formulations were developed to give a range of *in vitro* release rates for desoxycorticosterone acetate. Three were used for the subcutaneous drug release study in rats to establish their *in vitro–in vivo* correlation (Fig. 3). The *in vivo* release rates of desoxycorticosterone acetate were well correlated to their *in vitro* release rates for the corresponding MDD formulations. The establishment of this correlation allows one to predict the mechanisms and rates of long-term drug release in *in vivo* conditions (up to 129 days) on the basis of the data generated from a short-term (8-day) *in vitro* drug release study.

Induction of Prolonged Experimental Hypertension by

[1] Searle Chemicals, Chicago, Ill.
[2] MC/B Manufacturing Chemists, Norwood, Ohio.
[3] Model PE-300, Narco Biosystems, Houston, Tex.

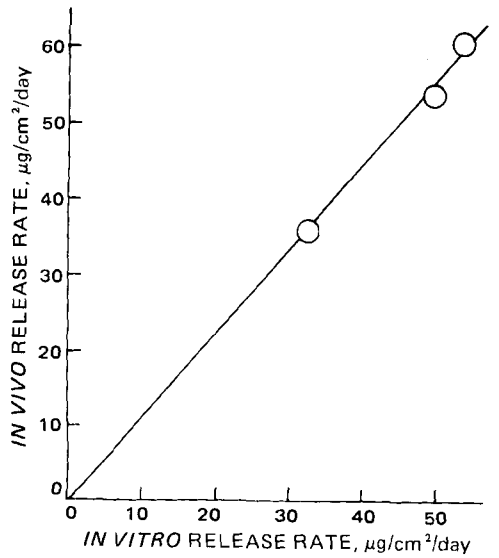

Figure 3—*Linear correlation of* in vivo *with* in vitro *release rates of desoxycorticosterone acetate (64.9 mg/cm³) from three MDD formulations. An* in vivo–in vitro *correlation factor of 1.13 was estimated.*

MDD's—The final objective of this investigation was to examine the possibility of producing a reproducible, prolonged metacorticoid hypertension in experimental animals by continuous administration of a constant, low dose of desoxycorticosterone acetate *via* long-term subcutaneous implantation of an MDD formulation. Figure 4 shows a typical result.

The mean systolic blood pressure of both the treated and control groups increased following implantation of the devices. This increase is normally seen following control subcutaneous injections or implantation in rats maintained on a 1% NaCl fluid ration (4). These effects are thought to occur as a result of the increased sodium intake and the growth of the animals. Blood pressure normally will plateau as the animals reach maturity (as seen in the control group in Fig. 4).

At Day 21, the elevation of systolic blood pressure in the treated rats was significantly greater than that in the control group. This hypertensive state was maintained and sustained up to Day 98. The development of such a prolonged experimental hypertensive animal model should facilitate the routine evaluation program of antihypertensive drugs.

The long-acting hypertensive state (Fig. 4) resulted from the subcutaneous implantation of an MDD, which continuously released to each rat a dose of desoxycorticosterone acetate as low as only 168.1 μg/day for 129 days. This dose level is significantly lower than the minimum effective

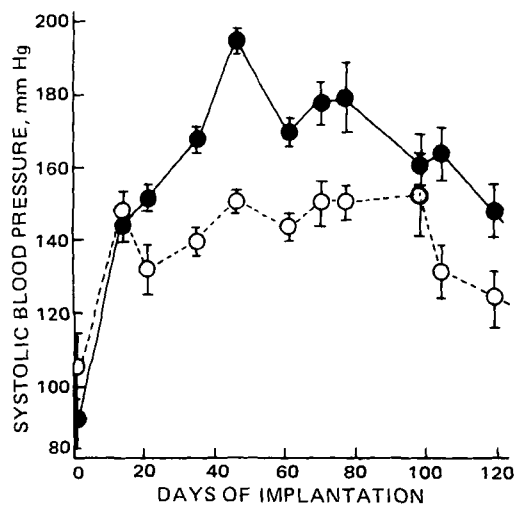

Figure 4—*Time course for the prolonged elevation of systolic blood pressure (mean ± SD) in rats after the long-term subcutaneous implantation of MDD 603-1 (3 cm long). Key: ●, medicated MDD (with an* in vivo *release rate of 168.1 μg/day or 35.9 μg/cm²/day); and ○, placebo MDD. The implants were inserted on Day 0 and removed on Days 59, 70, 104, or 129 after implantation.*

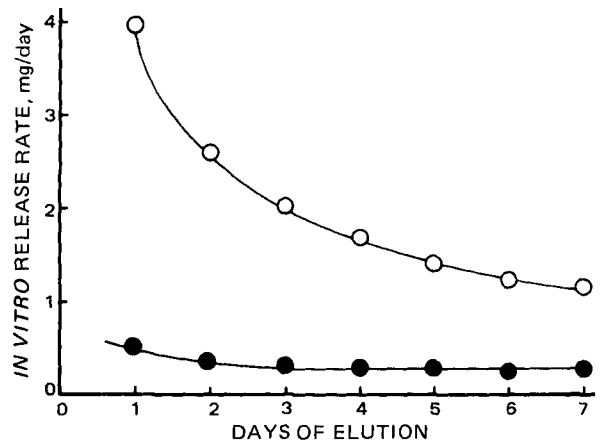

Figure 5—*Comparison of the 7-day* in vitro *release rates of desoxycorticosterone acetate (146.9 mg/cm³) from the matrix-type silicone device (4.845 cm²) (○) and the MDD (4.686 cm²) (●).*

dose of 400 μg/day/rat established earlier by a study of subcutaneous bolus injection (4). This observation indicates that the administration of the MDD with a constant drug release profile optimizes the bioavailability and dose–response relationship of desoxycorticosterone acetate. It also appears that the concept of constant drug availability, or input, substantially minimizes the dose requirement of a treatment.

Comparative Studies between MDD's and Matrix-Type Silicone Device—Recently, the authors examined the possibility of producing a sustained metacorticoid hypertension in rats by the continuous administration of desoxycorticosterone acetate through a 3-cm implant of a matrix-type silicone device subcutaneously implanted in the dorsal thoracic area (4). The dose–response relationship was also investigated. The dose dependency of the differential systolic blood pressure was essentially the same as that exhibited by daily bolus injection, although the modes of administration of desoxycorticosterone acetate between silicone device implantation and daily bolus injection were not identical.

For comparison, the release profiles of desoxycorticosterone acetate from both an MDD and a matrix-type silicone device were investigated under identical conditions. The results of the short-term *in vitro* and long-term *in vivo* release profiles of desoxycorticosterone acetate are compared in Figs. 5 and 6, respectively. The data clearly demonstrated that the release of desoxycorticosterone acetate from the matrix-type silicone device was not constant but was time dependent. Both the *in vitro* and *in vivo* release profiles of desoxycorticosterone acetate were high initially and then decreased with time. This release pattern was best described by a Q *versus* $t^{1/2}$ relationship (4, 6–11). On the other hand,

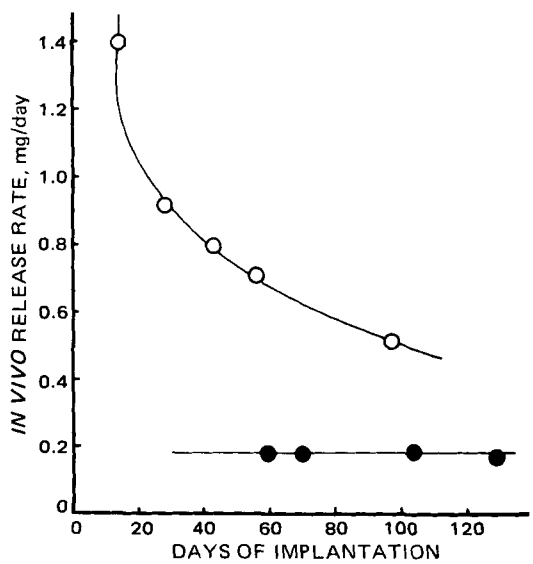

Figure 6—*Comparison of the long-term* in vivo *release rates of desoxycorticosterone acetate (146.9 mg/cm³) from the matrix-type silicone device (4.845 cm²) (○) and the MDD (4.686 cm²) (●).*

Table II—Time Course for the Elevation of Systolic Blood Pressure in Rats following Prolonged Administration of Desoxycorticosterone Acetate *via* Two Drug Delivery Systems

Days	Systolic Blood Pressure, Mean ± *SEM*		
		Treatment Groups	
	Control Group[a]	MSD[b]	MDD[c]
0	105 ± 13	110 ± 8	91 ± 9
14	148 ± 4	149 ± 6	144 ± 4
21	132 ± 7	163 ± 7	152 ± 3
35	140 ± 4	160 ± 5	168 ± 4
46	151 ± 3	210 ± 10	195 ± 3
61	144 ± 4	178 ± 3	170 ± 4
70	151 ± 7	182 ± 4	178 ± 6
77	151 ± 5	197 ± 5	179 ± 10
98	153 ± 12	158 ± 5	161 ± 9
104	132 ± 8	155 ± 5	164 ± 7
119	125 ± 9	160 ± 6	148 ± 7

[a] Each value is a mean (± *SE*) of four measurements in rats implanted with control (placebo) device. [b] Each value is a mean (± *SE*) of five measurements in rats implanted with the matrix-type silicone device (MSD). [c] Each value is a mean (± *SE*) of four measurements in rats implanted with the MDD.

the release rate profiles of desoxycorticosterone acetate from MDD's with identical dimensions were constant and independent of time.

The time courses for the evaluation of systolic blood pressure in rats following the long-term (120-day) administration of desoxycorticosterone acetate *via* MDD's and the matrix-type silicone device are compared in Table II along with the control group. The statistical significance of the difference in systolic blood pressures between treatment groups and the control group as well as between these two treatment groups was analyzed using the Student *t* test (Table III). The systolic blood pressure in both treatment groups was statistically greater than that in the control group after Day 21, with the exception of Day 98.

Table III—Results of Student *t* Statistic

Days	Unpaired *t* Values[a]		
	T-1/C[b]	T-2/C[c]	T-1/T-2
0	0.37	−0.90	1.62
14	0.15	−0.61	0.61
21	3.33*	2.64*	1.45
35	2.76*	4.96**	−1.17
46	5.12**	9.85**	1.26
61	6.55**	4.09**	1.57
70	3.80**	2.84*	0.52
77	6.36**	2.48*	1.78
98	0.41	0.55	−0.35
104	2.38*	2.93*	−1.06
119	3.33*	2.07	1.29

[a] The asterisks shown on the *t* value denote that the difference in the systolic blood pressure between groups is statistically significant: *, $p < 0.05$; and **, $p < 0.01$. [b] T-1 represents the treatment group tested with the matrix-type silicone device. [c] T-2 represents the treatment group treated with the MDD.

The difference in systolic blood pressure between the treatment groups was not significant statistically (Table III), although the daily dose of desoxycorticosterone acetate delivered to each rat by the matrix-type silicone device was substantially higher than that administered by MDD's (Figs. 5 and 6). The results suggested that the dose–response relationship of desoxycorticosterone acetate in the initiation of metacorticoid hypertension was optimized by the constant drug delivery mechanism of MDD's.

REFERENCES

(1) H. C. Stanton and J. B. White, *Arch. Int. Pharmacodyn. Ther.*, **154,** 351 (1965).

(2) S. M. Friedman, M. Nakashima, and C. L. Friedman, *Proc. Soc. Exp. Biol. Med.*, **150,** 171 (1975).

(3) F. M. Sturdevant, *Ann. Intern. Med.*, **49,** 1281 (1958).

(4) Y. W. Chien, L. F. Rozek, and H. J. Lambert, in "Controlled Release Polymeric Formulations," D. R. Paul and F. W. Harris, Eds., ACS Symposium Series, vol. 33, American Chemical Society, Washington, D.C., 1976, pp. 72–86.

(5) H. F. Ormsbee, III, and C. F. Ryan, *J. Pharm Sci.*, **62,** 255 (1973).

(6) Y. W. Chien, S. E. Mares, J. Berg, S. Huber, H. J. Lambert, and K. F. King, *ibid.*, **64,** 1776 (1975).

(7) Y. W. Chien, H. J. Lambert, and D. E. Grant, *ibid.*, **63,** 365 (1974).

(8) Y. W. Chien and H. J. Lambert, *ibid.*, **63,** 515 (1974).

(9) Y. W. Chien, H. J. Lambert, and T. K. Lin, *ibid.*, **64,** 1643 (1975).

(10) Y. W. Chien and E. P. K. Lau, *ibid.*, **65,** 488 (1976).

(11) Y. W. Chien, in "Controlled Release Polymeric Formulations," D. R. Paul and F. W. Harris, Eds., ACS Symposium Series, vol. 33, American Chemical Society, Washington, D.C., 1976, pp. 53–71.

(12) Y. W. Chien and H. J. Lambert, U.S. pat. 3,946,106 (Mar. 23, 1976).

ACKNOWLEDGMENTS

The authors express their appreciation to Ms. D. M. Jefferson and Ms. L. Zeitlin for technical assistance, to Ms. B. Sullivan, Ms. D. Warren, and Ms. M. L. Sachen for manuscript preparation, and to Dr. David T. K. Lin for helpful discussions.

Thermal Degradation of Gelatin as Applied to Processing of Gel Mass

WILFRED C. LING

Received January 13, 1977, from *Pharmaceutical Research and Development, Pharmaceutical Products Division, Abbott Laboratories, North Chicago, IL 60064.* Accepted for publication May 13, 1977.

Abstract □ The rheological parameters of rigidity and viscosity were studied for gelatin, both as a 6% solution and a 38% gel mass containing glycerin, sorbitol, and water. A compressive test for rigidity and a rotational shear method for viscosity were used to characterize the thermal degradation of several lots of alkali-processed calf-skin gelatin. The objective of this study was to use kinetic data for process predictions in the manufacturing of the gel mass for soft gelatin capsules. Empirical equations relating degradation to time, temperature, and pH were derived for dilute gelatin solutions. Through parallel studies with a concentrated gel mass, other empirical equations were developed to predict degradation of the gel mass based on dilute solution data and processing conditions. Analysis of the kinetic data and empirical equations have generally confirmed earlier observations on degradation, except on quantitative aspects. While these equations are adequate for the intended use in process predictions, the study revealed substantial variability both within and among lots of commercial gelatin. These variabilities of uncertain causes contributed to inexact characterization of degradation, as demonstrated by the generally approximate results of process predictions.

Keyphrases □ Gelatin—thermal degradation, solution and gel mass, rigidity and viscosity, applied to processing predictions □ Degradation, thermal—gelatin solution and gel mass, rigidity and viscosity, applied to processing predictions □ Thermal degradation—gelatin solution and gel mass, rigidity and viscosity, applied to processing predictions □ Rigidity—gelatin solution and gel mass, thermal degradation, applied to processing predictions □ Viscosity—gelatin solution and gel mass, thermal degradation, applied to processing predictions

Rigidity in a gelatin gel is generally attributed to the helical structure of the macromolecules (1, 2). Whereas solution viscosity is a function of molecular weight, gel rigidity for dilute gelatin is independent of the molecular weight of the gelatin (3). Therefore, both rigidity and viscosity parameters are necessary to define the mechanical properties of the gelatin properly. The purpose of this study was to characterize gelatin degradation with respect to rigidity and viscosity to provide a degree of predictability to the manufacturing process for soft gelatin capsules.

Among reported studies on thermal degradation of gelatin, only a few (4, 5) have sufficiently detailed analysis for possible application. Most are limited to the study of dilute gelatin solutions, with little or no quantitative treatment of the degradation process. The approach taken for this study was to examine the thermal degradation of both the dilute gelatin and a concentrated gel mass containing glycerin and sorbitol, thus establishing a correlation between the two processes with respect to rheological parameters.

The empirical kinetic approach taken was similar to that recommended for complex catalytic reactions (6) where a theoretical approach is either impossible or too complicated to be practical. The importance of the kinetic treatment is, therefore, not to elucidate the degradation mechanism but to provide a quantitative basis for predictive applications.

Table I—Characteristics of Gelatin Used

Lot	Nominal Bloom, g	Rigidity Index, g	Viscosity, mps	pH	Moisture, %
A	150	63.5	34.0	5.50	10.5
B	150	62.4	38.3	6.10	10.0
C	130	59.4	35.4	5.80	9.7
D	170	71.0	40.1	5.30	9.4
E	150	63.5	34.6	5.45	8.9
F	150	62.9	37.7	6.20	9.7

EXPERIMENTAL

Material—*Gelatin*—Pharmaceutical grade gelatin USP, <16–>60-mesh size, six lots, from alkali-processed calf skin was used (Table I). Preparation of the gel mass included the use of glycerin USP and 76% sorbitol[1].

Kinetic Procedures—*Thermal Degradation of Dilute Gelatin Solution*—The preparation of gelatin solution followed the standard procedures used in the testing of gel strength and viscosity (7). The gelatin was allowed to hydrate in distilled water at room temperature for 2 hr. The mixture was then heated to 61° in a 65° water bath for no more than 15 min until completely dissolved. The solution was pipetted immediately into several 50-ml glass ampuls and flame sealed. The sealed ampuls were then placed in a constant-temperature bath[2] controlled to ±0.2°. The time at which complete dissolution was achieved was taken as time zero. At different intervals, the ampuls were removed for later testing.

At each sampling, 28 ml of the ampul solution was poured into a glass ointment jar, measuring approximately 38 mm diameter × 28 mm deep, and covered tightly. The jar sample, as well as the remaining solution in an erlenmeyer flask, was stored at 5° for later testing.

All samples were tested for rigidity and viscosity by methods to be described. In addition, the pH[3] of the 6% gelatin solutions was determined at 24°.

Thermal Degradation of Gel Mass—The gel mass was a specific formulation used in making a soft gelatin capsule product. The approximate composition, on a dry basis, is 38% (w/w) gelatin, 13% glycerin, 13% sorbitol, 1% dye and preservatives, and 35% water.

All ingredients were mixed in a beaker until uniform and then transferred to a filtering flask where the mixture was deaerated at an absolute pressure of 1000 torr. The gel mass, while still held in a closed vacuum, was heated in a 75° water bath for 30 min. Then the vacuum was released, and the melt was poured into several 125-ml erlenmeyer flasks. The flasks were stoppered and submerged completely in a constant-temperature bath controlled to within ±0.2°.

Zero time was taken as the time when the gel mass was removed from the melting bath but before placement into the constant-temperature bath. At predetermined intervals, the flasks were removed from the bath and the gel mass was poured into a 30-ml ointment jar for rigidity testing. A portion of the gel mass was molded into strips for moisture determination as described later. A cylindrical rod of gel mass, molded simultaneously with the strips, was kept in a closed bottle for use in the viscosity determination.

Rigidity Determination—The procedure involved subjecting a sample of gelatin or gel mass to penetrative compression by a flat-ended cylindrical plunger, 6.35 mm in diameter, at a constant speed, using a material testing machine equipped with simultaneous recording of force and displacement[4].

[1] I.C.I. United States, Wilmington, Del.
[2] Model 6566, Precision Scientific Co., Chicago, Ill.
[3] Zeromatic pH meter, Beckman Instruments Corp., Fullerton, Calif.
[4] Instron floor model TT Universal testing instrument, model 1115, Instron Corp., Canton, Mass.

Table II—Parameters of Rigidity Index Testing

Sample	Rigidity Index Symbol	Plunger Compression Rate, mm/min	Plunger Compression Depth, mm	Pretest Aging Hours	Pretest Aging Temperature
Dilute gelatin	*f*	50.8	2.00	70	0°
Gel mass	*F*	5.08	1.27	96	23°

Each test sample was poured into a 38-mm diameter ointment jar to a depth of 22 ± 2 mm and allowed to cool on a level surface until gelation and then was kept for a designated aging period prior to testing. Samples in the gel state were heated to 45–50° prior to pouring into the jars. The specific aging period and depth of compression are defined in Table II for both dilute gelatin and the concentrated gel mass.

Viscosity Determination—The viscosities of the gelatin solution and the gel mass were determined with a rotational viscometer equipped with programmable shear rate control and simultaneous recording of shear rate and shear stress[5]. For standardization, all determinations were made at 60 ± 0.2° with viscosity computed at shear rates of 3234 and 36 sec^{-1} for the 6% gelatin solution and 38% gel mass, respectively. Each sample was allowed to equilibrate in the temperature-controlled sensing cup for 15 min prior to the run. The repeatability of viscosity determinations was within ±5% (95% of all cases, 95% confidence level).

Moisture Determination for Gel Mass and Gelatin—The moisture of the gel mass was determined by drying strips extruded from the molten gel mass. The strips, measuring 1 × 2 × 33 mm long, were weighed[6] and dried for 20 hr in a vacuum oven[7] maintained at 60 ± 0.5°/10–20 torr. The weight loss divided by the initial weight was taken as the moisture content.

RESULTS AND DISCUSSION

Many methods of gel strength have been reported (8–11). None, however, was suitable for this study from the standpoint of accuracy and convenience.

The linear force–displacement curve (Fig. 1) characterizes the gelatin rigidity in a form analogous to the stress–strain diagram of an elastic body, confirming earlier observations (12). However, the lack of a well-defined dimensional relation with respect to the force, area, and deformation in the penetrative type of compression precluded the calculation of rigidity or shear modulus. The term "rigidity index" expresses relative rigidity and is defined as the force required to depress the gelatin surface a fixed distance when tested within a specific set of parameters. It is similar to the Bloom gelometer test commonly used in the gelatin industry. One difference is the strain rate. In this method, the strain rate is constant and independent of stress. In the Bloom test, the stress rate is constant but only to the extent that the flow rate of the lead shots is regulated.

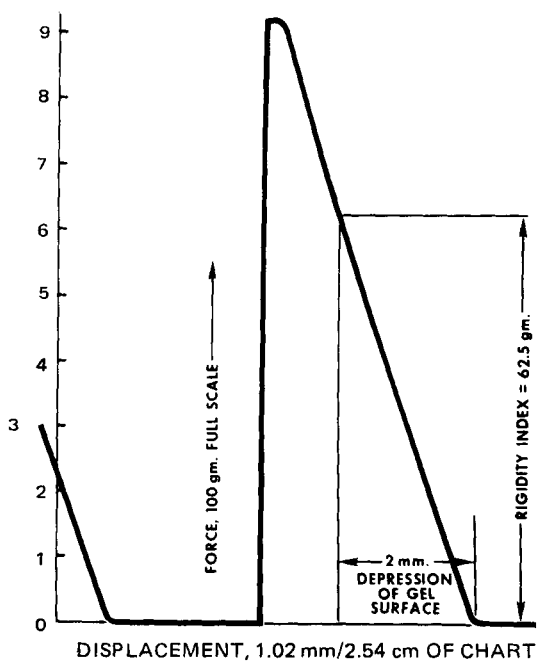

Figure 1—*Typical force–displacement curve of rigidity testing for 6% gelatin at 0°.*

[5] Rotovisco model RV-3, Haake Instruments, Rochelle Park, N.J.
[6] Sartorius model 2462, Brinkmann Instruments, Westbury, N.Y.
[7] Model 634 vacuum oven, Hotpack Corp., Philadelphia, Pa.

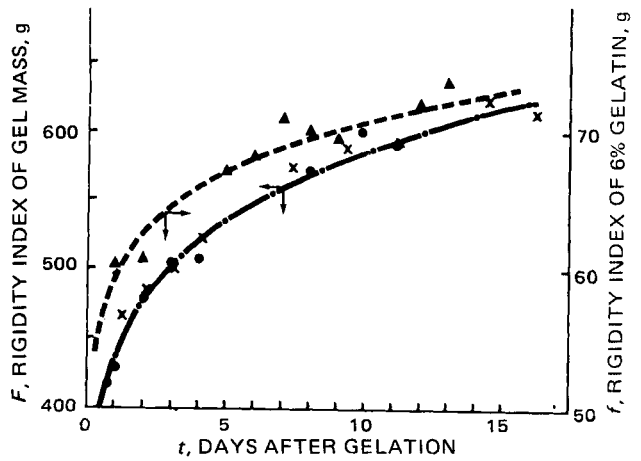

Figure 2—*Effect of aging on rigidity of 6% gelatin and gel mass containing 38% gelatin. Key: ▲, 6% gelatin (Lot 01); ●, 38% gel mass containing Lot 01 gelatin; and ×, 38% gel mass containing Lot 02 gelatin. Dotted curves are transposed from linear regression curves of log* F versus *log* t *and log* f versus *log* t.

The advantages of a constant strain rate and relative freedom from human error were the reasons for using the standard material testing machine instead of the gelometer. In view of the wide difference in rigidity between dilute gelatin and gel mass, two sets of standard test parameters were used as defined in Table II. The repeatability of the rigidity index determination was within ±3% (95% of all cases, 95% confidence level) for the 6% gelatin and ±6% for the 38% gel mass. The decrease of reproducibility in the case of the gel mass is believed to be due more to compositional variations than instrument error.

Effect of Aging—The phenomenon of progressive rigidity increase after gelation is well known. Figure 2 shows the effect of aging on the rigidity of both dilute gelatin and the gel mass. The selection of 70 and 96 hr for aging of the dilute gelatin and gel mass, respectively, in the standard test procedure (Table II) was dictated primarily by convenience of test scheduling and the reduced sensitivity of rigidity change with time. A 10 times faster compression rate for the dilute gelatin was selected to

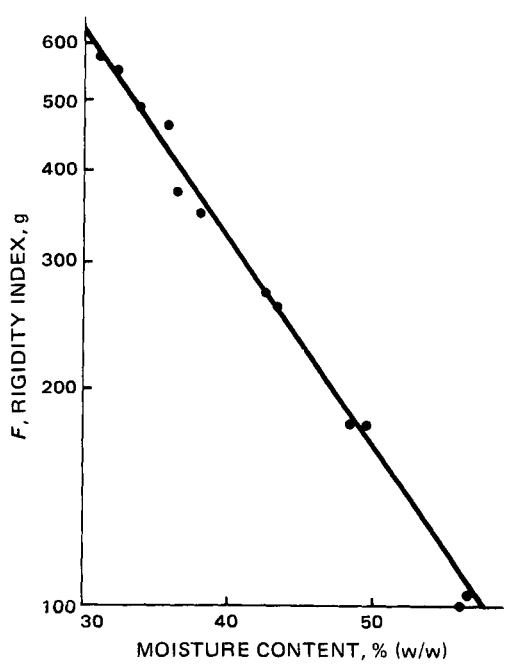

Figure 3—*Effect of moisture content on rigidity of gel mass.*

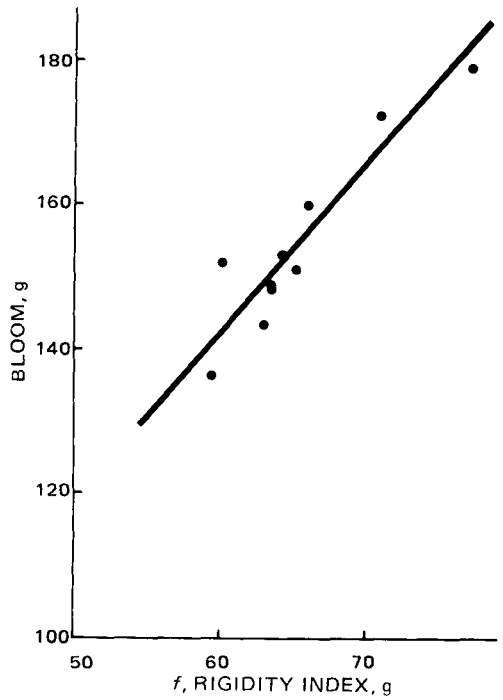

Figure 4—*Relation between bloom and rigidity index of 6% gelatin.*

shorten the test duration and thereby minimize the effect of ambient temperature.

Effect of Gelatin Concentration—The gelatin solution was prepared as a 6.67% solution based on the weight of the commercial gelatin. For an average moisture content of 10% in the commercial gelatin, the gelatin concentration in the solution was about 6% on the dry basis. No attempt was made to make all gelatin solutions at precisely 6%. Ferry (13) found that rigidity was proportional to the square of the gelatin concentration for dilute gelatin. By using this relationship, it can be calculated that a maximum error of 4.6% in rigidity may be encountered due to the normal variation of gelatin moisture between 10 and 12%.

The effect of moisture on rigidity variation, however, is much greater for the gel mass. Figure 3 shows the effect of moisture on the rigidity index of a gel mass sample. Based on this relationship, each percent moisture change represents a rigidity change of 6.8%. It follows, therefore, that any

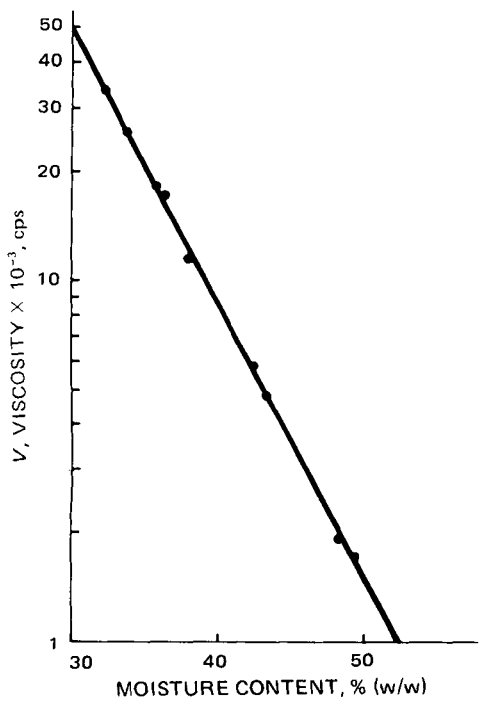

Figure 5—*Effect of moisture content on viscosity of gel mass.*

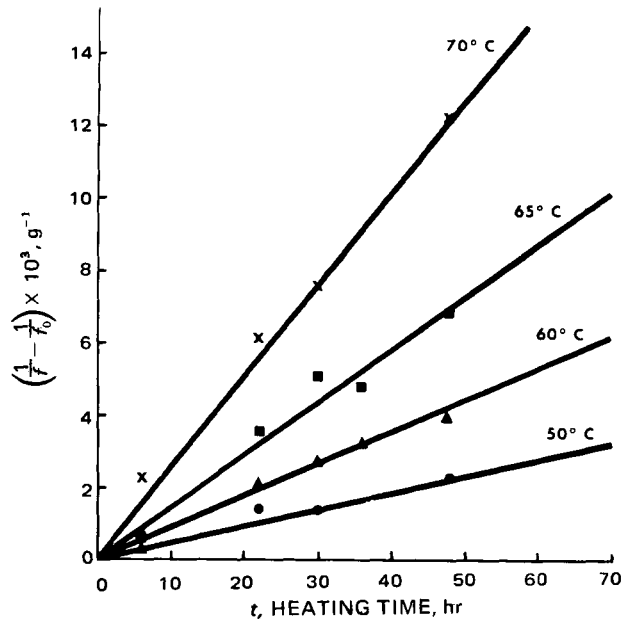

Figure 6—*Rigidity degradation of 6% gelatin at different temperatures (gelatin Lot A).*

rigidity measurement of gelatin degradation must be based on a standard moisture content. All results of rigidity determination were corrected to a standard moisture content of 35% by means of:

$$\log F_2 = \log F_1 + 0.0287M_1 - 1.0045 \qquad \text{(Eq. 1)}$$

where F_1 is the rigidity index of the gel mass at moisture M_1, F_2 is the rigidity index at 35% standard moisture, and M_1 is the percent moisture of the gel mass sample. Equation 1 is derived by incorporating the 35% standard moisture into the regression equation of Fig. 3, which is significant at $p < 0.001$.

Although based on experimental data of only one lot of material, Eq. 1 should be applicable for all gelatin lots for moisture correction within the 30–40% range. By differentiating the regression equation, it can be seen that the slope of 0.0287 relates to fractional rather than absolute change of rigidity with respect to moisture change.

Correlation of Rigidity Index to Bloom Reading—Although the rigidity index method was used in the testing of the 6% gelatin, each gelatin also was tested for rigidity by the Bloom gelometer method (7). Figure 4 shows the correlation of the two methods by testing 10 different gelatin lots. The linear correlation is significant at $p < 0.001$.

Viscosity Determination—Figure 5 shows the effect of moisture on the viscosity of a gel mass identical in formulation to the gel mass used for the degradation studies. Based on this correlation, the results of every viscosity determination were adjusted to a standard moisture of 35% for analysis of viscosity degradation. The following equation was used:

$$\log V_2 = \log V_1 + 0.0757M_1 - 2.6495 \qquad \text{(Eq. 2)}$$

where V_1 is the viscosity of the gel mass at moisture M_1 in centipoises, V_2 is the viscosity at 35% moisture in centipoises, and M_1 is the percent moisture of the gel mass sample. Equation 2 shows that moisture in the 30–40% range has a much more pronounced effect on viscosity than on rigidity. A 1% change in moisture creates a viscosity change of 19% for the particular gel mass under study.

Treatment of Kinetic Data—A total of 20 runs was made in the study of rigidity and viscosity degradation of 6% gelatin solutions (12 runs) and the 38% gel mass (eight runs). The experimental data were treated empirically to fit simple kinetic models. The apparent order of reaction was arrived at by trying integral increments of the exponent, n, in the following equation:

$$\frac{-dx}{dt} = kx^n \qquad \text{(Eq. 3)}$$

where $-dx/dt$ is the rate of loss of the rheological parameter of either rigidity or viscosity, k is the rate constant, x is the value of the rheological parameter at time t after heating begins, and n is the apparent reaction order. The experimental data were used to fit the integrated forms of Eq. 3.

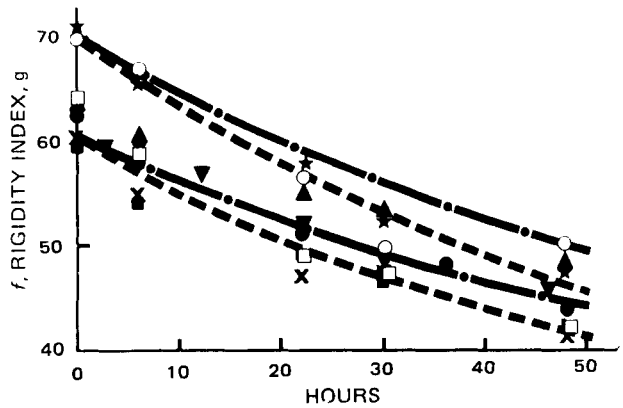

Figure 7—*Rigidity–time profile of 6% gelatin heated at 65°. Key: ●, gelatin Lot A; ▲, Lot B; ■, ×, Lot C; ○, ★, Lot D; □, Lot E; ▼, Lot F; - · -, pH 6.20; and - - -, pH 5.35. Curves were calculated from Eqs. 5 and 14 using* f_0 *of 60 and 70.*

Degradation of 6% Gelatin Solution—*Kinetic Models*—An apparent second-order model represented by:

$$\frac{-df}{dt} = k_f f^2 \qquad \text{(Eq. 4)}$$

and the integral form:

$$\frac{1}{f} - \frac{1}{f_0} = k_f t \qquad \text{(Eq. 5)}$$

gave the best fit of the rigidity degradation data, where f is the rigidity index of 6% gelatin at time t in grams, f_0 is the rigidity index at $t = 0$ in grams, k_f is the rate constant (reciprocal of gram hours), and t is the heating time in hours.

Figure 6 shows the degradation function, $(1/f - 1/f_0)$, plotted against heating time at four different temperatures. The solid lines are based on linear regression forced through zero. The rate constant for each temperature was obtained from the slope of the lines. Figure 7 shows the rigidity profile for eight runs at 65° using six lots of gelatin. Dotted curves are based on calculations using equations developed later.

The viscosity loss proceeded much more rapidly than rigidity loss during the initial period of heating, confirming several earlier observations (5, 14). The best fitting model for the viscosity degradation, following the approach of Eq. 3, was:

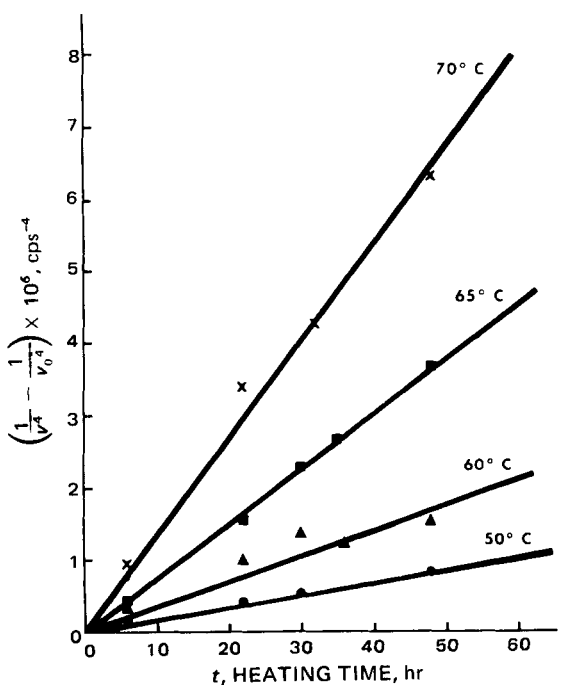

Figure 8—*Viscosity degradation of 6% gelatin at different temperatures (gelatin Lot A).*

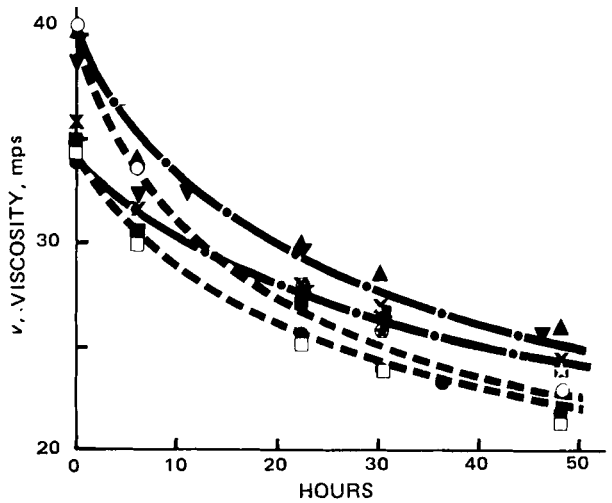

Figure 9—*Viscosity–time profile of 6% gelatin heated at 65°. Key: ●, gelatin Lot A; ▲, Lot B; ■, ×, Lot C; ○, ★, Lot D; □, Lot E, ▼, Lot F; - · -, pH 6.20; and - - -, pH 5.35. Curves were calculated from Eqs. 7 and 15 using* v_0 *of 34 and 40.*

$$\frac{-dv}{dt} = k_v v^5 \qquad \text{(Eq. 6)}$$

which, upon integration within limits, gives:

$$\frac{1}{v^4} - \frac{1}{v_0^4} = 4k_v t \qquad \text{(Eq. 7)}$$

where v is the viscosity of the 6% gelatin solution (60°) at time t in millipoises, v_0 is the viscosity of the 6% gelatin solution at $t = 0$ in millipoises (mps), k_v is the rate constant (mps^{-4} hr^{-1}), and t is the heating time in hours.

Figure 8 shows the plot of $(1/v^4 - 1/v_0^4)$ *versus* t for the degradation of a 6% gelatin at four temperatures. The viscosity profile of eight gelatin solutions, sampled during thermal degradation at 65°, was plotted in Fig. 9, corresponding in time scale to the rigidity degradation of the same eight gelatin solutions as shown in Fig. 7.

It is apparent from Figs. 6 and 8 that the actual degradation reactions were more complex than represented by Eqs. 5 and 7. The presence of complex curves, showing periods of increasing and decreasing rates, seems to be characteristic of most runs. The irregularities cannot all be explained as experimental errors.

Effect of Temperature—The rate constant, k_f, for rigidity degradation was plotted against the reciprocal of absolute temperature in Fig. 10. The equation of the k_f regression line, expressed in exponential form, becomes:

$$k_f = 5.9031 \times 10^7 e^{-9025.56/T} \qquad \text{(Eq. 8)}$$

Equation 8, which is significant at $p < 0.05$, is in the familiar form of the Arrhenius equation as:

$$k = Ae^{-\Delta H_a/RT} \qquad \text{(Eq. 9)}$$

where ΔH_a is the activation energy for the degradation reaction, T is the absolute temperature, A is a constant, and R is the gas constant. The term ΔH_a may be taken as the activation energy for rigidity degradation. When equating the exponential terms of Eqs. 8 and 9, ΔH_a was determined to be about 17,900 cal/g mole.

The rate constants k_v for viscosity degradation at the four temperatures were obtained as 0.25 of the slopes of the regression lines of Fig. 8. The plots of k_v *versus* $1/T$ and k_f *versus* $1/T$ are both shown in Fig. 10. The equation of the k_v regression line, after transformation to the exponential form, becomes:

$$k_v = 1.3471 \times 10^7 e^{-11573/T} \qquad \text{(Eq. 10)}$$

The experimental fit of Eq. 10 is significant at $p < 0.05$. When equating the exponential term of Eq. 10 to $\Delta H_a/RT$ of Eq. 9, the activation energy, ΔH_a, for viscosity degradation was calculated to be about 23,000 cal/g mole, which, when compared at the probability level of 0.1, is not significantly different from the ΔH_a of 17,900 for rigidity degradation.

Effect of pH—An appropriate mathematical relationship can be de-

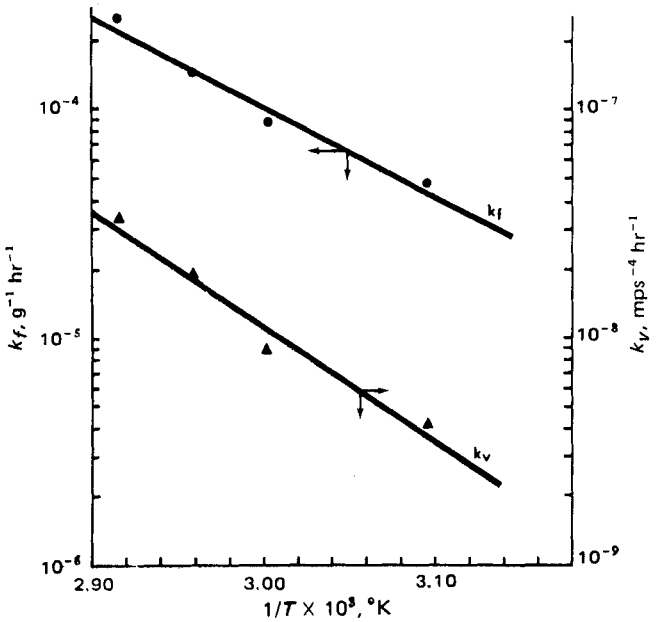

Figure 10—*Semilogarithmic plot of degradation rate constants,* k_f *and* k_v, *versus reciprocal absolute temperature (pH 5.5).*

rived, showing the rate constants k_f and k_v for the degradation of six different gelatin solutions at 65°, as a function of the initial pH of the solutions. The following equations represent the least-squares lines for k_f and k_v *versus* pH:

$$k_f = (36.1851 - 3.9596\ \text{pH}) \times 10^{-5} \quad \text{(Eq. 11)}$$

$$k_v = (55.243 - 7.2414\ \text{pH}) \times 10^{-9} \quad \text{(Eq. 12)}$$

Both linear correlations are significant at $p < 0.1$. The weak correlations suggest that other undefined factors might contribute to variations in the degradation rates.

The final equation to predict the average rate constant, k_f, was obtained by combining the separate equations relating to temperature (Eq. 8) and pH (Eq. 11). The combined equation is:

$$k_f = c(590.31)(36.1851 - 3.9596\ \text{pH})e^{-9025.56/T} \quad \text{(Eq. 13)}$$

The value of c was calculated as 6787.3 by substituting experimental values of pH, T, and k_f in Eq. 13 and calculating the average. In this treatment, any interaction of pH on the activation energy within the pH 5–7 range was assumed to be negligible. Equation 13 is thus reduced to:

$$k_f = (1.4498 \times 10^8 - 1.5865 \times 10^7\ \text{pH})e^{-9025.56/T} \quad \text{(Eq. 14)}$$

Similar consolidation of temperature (Eq. 10) and pH (Eq. 12) effects yields the following equation for viscosity degradation:

$$k_v = (4.3172 \times 10^7 - 5.6591 \times 10^6\ \text{pH})e^{-11573/T} \quad \text{(Eq. 15)}$$

Degradation of Gel Mass—*Kinetic Models*—The degradation of the rigidity index for the 38% gel mass fits the second-order model as follows:

$$\frac{1}{F} - \frac{1}{F_0} = K_F t \quad \text{(Eq. 16)}$$

where F is the rigidity index of the gel mass at time t in grams, F_0 is the rigidity index of the gel mass at time 0, K_F is the rate constant (reciprocal of gram hours), and t is the heating time in hours.

The viscosity degradation of the gel mass differs substantially from that of the dilute gelatin; instead of a fifth-order decay, the kinetic data follow more closely a second-order model as defined by:

$$\frac{1}{V} - \frac{1}{V_0} = K_v t \quad \text{(Eq. 17)}$$

where V is the viscosity of the gel mass at time t in centipoises, V_0 is the viscosity of the gel mass at $t = 0$ in centipoises, K_V is the rate constant (reciprocal of centipoise hours), and t is the heating time in hours.

Estimating Initial Values, F_0 *and* V_0, *of Gel Mass*—Rigidity and viscosity measurements of most gel mass samples at time zero showed lower than expected values based on extrapolation. Due to uncertainties of complete dissolution of the gelatin particles in the concentrated gel mass, the actual rigidity and viscosity at time zero were not used in the data treatment. Instead, F_0 was obtained by extrapolating the $1/F$ *versus* t regression line to $t = 0$. The value V_0 was obtained by extrapolating the $1/V$ regression line to $t = 0$.

Earlier work had shown that the rigidity of the gel mass was higher than that of the dilute gelatin not only because of the increased gelatin concentration but also because of the additional rigidity contributed by molecular interactions with plasticizers such as glycerin (12, 15). For a specific composition of the gel mass, however, the rigidity is expected to be proportional to the rigidity of the dilute gelatin in the standard 6% concentration. The rigidity indexes of six lots of gelatin were correlated to those of the gel mass made from the respective lots as follows:

$$F_0 = 147.9 + 7.93 f_0 \quad \text{(Eq. 18)}$$

where f_0 and F_0 are, respectively, the rigidity index of the 6% gelatin and that of the gel mass made from the same lot of gelatin prior to heating. The correlation of Eq. 18 is significant at $p < 0.01$.

In a like manner, the initial viscosities, V_0, for six runs were correlated to the respective initial viscosity, v_0, of the dilute gelatin. The resulting regression equation is:

$$V_0 = -42019 + 1915.05 v_0 \quad \text{(Eq. 19)}$$

Equation 19 gave a significant fit to the data at $p < 0.001$.

Relating Gel Mass Degradation to Dilute Gelatin Degradation—The rate constants K_f and K_V for gel mass degradation were determined for eight runs at 60 and 65° utilizing gelatin lots previously evaluated for thermal degradation at identical conditions as 6% gelatin solutions. The objective of these parallel runs was to relate the rate constants K_f to k_f and K_V to k_v so that Eqs. 16 and 17 may be used to predict gel mass degradation based on the kinetics of the 6% gelatin solution.

Another commonly used approach for predicting gel mass degradation is to assume that fractional degradation of the dilute gelatin is the same as that of the gel mass at any given time. This assumption may be represented by Eqs. 20 and 21 for rigidity and viscosity, respectively:

$$F = f\left(\frac{F_0}{f_0}\right) \quad \text{(Eq. 20)}$$

$$V = v\left(\frac{V_0}{v_0}\right) \quad \text{(Eq. 21)}$$

Experimental data, however, have not supported these assumptions fully. Thus, even though the initial rheological parameters of the gel mass and that of the 6% gelatin were related according to Eqs. 18 and 19, the relation changed as heating progressed, depending upon the initial pH of the solution.

The following empirical equation shows how the ratio of the two rate constants, K_F/k_f, is dependent on the pH of the 6% gelatin solution:

$$\phi_F = \frac{K_F}{k_f} = -0.2757 + 0.06166\ \text{pH} \quad \text{(Eq. 22)}$$

The experimental fit of Eq. 22 is significant at $p < 0.001$.

The rate constant ratio for viscosity, K_V/k_v, is related to the pH of the 6% gelatin solution as follows:

$$\phi_V = \frac{K_V}{k_v} = -165.02 + 39.12\ \text{pH} \quad \text{(Eq. 23)}$$

Although the correlation of ϕ_V and pH is weaker than that developed for ϕ_F, it is significant, nonetheless, at $p < 0.1$.

By combining Eqs. 14, 16, 18, and 22, an overall expression is obtained for estimating the rigidity index of the specific gel mass from data of rigidity and pH of the 6% gelatin:

$$\frac{1}{F} = \frac{1}{147.9 + 7.93 f_0} - (3.996 - 1.3313\ \text{pH} + 0.09782\ \text{pH}^2) \times 10^7 t e^{-9025.56/T} \quad \text{(Eq. 24)}$$

Similarly, by combining Eqs. 15, 17, 19, and 23, the following overall equation is obtained for calculating gel mass viscosity:

$$\frac{1}{V} = \frac{1}{-42019 + 1915.05 v_0} - (7.1241 - 2.6229\ \text{pH} + 0.2214\ \text{pH}^2) \times 10^9 t e^{-11573/T} \quad \text{(Eq. 25)}$$

Equation 25 allows the estimation of gel mass viscosity on the basis of the initial viscosity and pH of the 6% gelatin, heating time, and temperature.

Table III—Comparison of Calculated and Actual Data

Calculated Parameter	Input Parameter	Equations Used	Estimated Limits[a] of Error[b], %
Rigidity index for 6% gelatin, f	f_0	5, 14	−7.2 to +9.7
Rigidity index for gel mass, F	f_0	24	−12.9 to +8.7
Rigidity index for gel mass, F	f_0	5, 14, 18, 20	−19.8 to +9.6
Rigidity index for gel mass, F	f_0, V	18, 19, 27	−15.4 to +15.8
Viscosity for 6% gelatin, v	v_0	7, 15	−7.5 to +8.9
Viscosity for gel mass, V	v_0	25	−28.8 to +18.9
Viscosity for gel mass, V	v_0	7, 15, 19, 21	−26.6 to +51.3

[a] Estimated to include at least 95% of all cases at 95% confidence level. [b] Error = (calculated − actual)/actual, compared with 33 actual data points, except the first and fifth items where there were 47 points.

Estimating Rigidity Degradation Based on Viscosity Degradation—Dividing Eq. 16 by Eq. 17 and rearranging result in:

$$\frac{1}{F} - \frac{1}{F_0} = \frac{K_F}{K_V}\left(\frac{1}{V} - \frac{1}{V_0}\right) \qquad \text{(Eq. 26)}$$

When substituting the equivalents of K_F and K_V in Eqs. 22 and 23, the following results:

$$\frac{1}{F} = \frac{1}{F_0} + \left(\frac{1}{V} - \frac{1}{V_0}\right) \times \left(\frac{3.9966 - 1.3313\ \text{pH} + 0.09782\ \text{pH}^2}{712.41 - 262.29\ \text{pH} + 22.14\ \text{pH}^2}\right) e^{2547.44/T} \qquad \text{(Eq. 27)}$$

By using Eq. 27, the rigidity index of a gel mass may be computed based on the experimental values of gel mass viscosity, provided that the initial values of the 6% gelatin rigidity, viscosity, and pH and the heating temperatures are known. Such an equation is useful if the rigidity of the gel mass cannot be determined either due to the nonavailability of the test facilities or the lack of time necessary for proper aging of the test sample.

Equation 27 may be rearranged into the following form:

$$\frac{[(F_0 - F)/F_0]}{[(V_0 - V)/V_0]} = \frac{F}{V}\psi e^{2547.44/T} \qquad \text{(Eq. 28)}$$

where ψ is a function of pH as indicated by the term in parentheses in Eq. 27.

The left-hand side of Eq. 28 represents the ratio of fractional degradation of rigidity to viscosity. It can be shown that, for the gelatin lots studied, within the normal pH range of 5–6.5 and temperature range 50–70°, the percentage degradation of viscosity is always greater than that of rigidity. Furthermore, as pH increases, the rigidity loss tends to increase more than the increase of the viscosity loss. As temperature increases, however, viscosity loss tends to increase more than rigidity loss. Both the pH and temperature effects confirm observations made by Ames (5).

Test of Empirical Equations against Actual Data—The usefulness of the empirical equations was tested by computing the rheological parameters and comparing them with the experimental values. Estimated limits of errors were then computed based on the application of tolerance limits (16).

Table III summarizes the limits of error in using the various equations. In general, the thermal degradation of the 6% gelatins is predicted with better accuracy than that of the 38% gel mass. This statement is true for both the rigidity index and viscosity. The largest error is in the estimation of gel mass viscosity (Eq. 25). The larger prediction error with gel mass is probably due, in part, to increased nonhomogeneity with concentrated gel mass. Such things as presence of air bubbles and undetected moisture differences possibly contribute to errors in the rigidity and viscosity determinations. Other errors might appear through interactions between viscosity and rigidity of the concentrated gel mass, even though rigidity was reported to be independent of viscosity in dilute solutions (*e.g.*, 6%) (13).

The premise of Eqs. 20 and 21 was that the conditions producing a given percentage degradation of the dilute gelatin will cause the same percentage degradation of the concentrated gel mass. Comparison of errors associated to the use of Eqs. 24 and 25 *versus* Eqs. 20 and 21 in Table III shows that Eqs. 20 and 21 are oversimplified and that more accurate predictions are possible using Eqs. 24, 25, and 27.

REFERENCES

(1) J. W. Janus, "Recent Advances in Gelatin and Glue Research," G. Stainby, Ed., Pergamon, New York, N.Y., 1956.

(2) A. Todd, *Nature*, **191**, 567 (1961).

(3) G. Stainby, P. R. Saunders, and A. G. Ward, *J. Polym. Sci.*, **12**, 325 (1954).

(4) P. J. Tiemstra, *Food Technol.*, **22**, 1151 (1968).

(5) W. M. Ames, *J. Soc. Chem. Ind. (London)*, **66**, 279 (1947).

(6) S. Weller, *A.I.Ch.E. J.*, **2**, 59 (1956).

(7) "Standard Methods for Sampling and Testing of Gelatins," Gelatin Manufacturers Institute of America, New York, N.Y., 1964.

(8) C. E. Sheppard, S. S. Sweet, and J. W. Scott, Jr., *J. Ind. Eng. Chem.*, **12**, 1007 (1920).

(9) M. Briefer and J. H. Cohen, *Ind. Eng. Chem.*, **19**, 252 (1927).

(10) J. D. Ferry, *Rev. Sci. Instrum.*, **12**, 79 (1941).

(11) P. R. Saunders and A. G. Ward, in *Proc. 2nd Int. Congr. Rheol., Oxford*, 1954, p. 284.

(12) S. E. Sheppard and S. S. Sweet, *J. Am. Chem. Soc.*, **43**, 539 (1921).

(13) J. D. Ferry, *ibid.*, **70**, 2244 (1948).

(14) P. R. Saunders and A. G. Ward, *Nature*, **176**, 26 (1955).

(15) J. E. Carless and J. R. Nixon, *J. Soc. Cosmet. Chem.*, **21**, 427 (1970).

(16) A. Hald, "Statistical Theory with Engineering Applications," Wiley, New York, N.Y., 1952.

ACKNOWLEDGMENTS

The author expresses appreciation to Dr. J. A. Seitz for comments and suggestions, to Dr. Saul Borodkin for assistance and suggestions in data treatment, and to Mr. Roy Hill for experimental assistance.

Ascorbate Stimulation of Salicylate Absorption in Isolated Rat Intestine

GENE BARNETT *x, THOMAS LOCKWOOD, AQUILES ARANCIBIA ‡, and LESLIE Z. BENET

Received March 2, 1977, from the *School of Pharmacy, University of California, San Francisco, CA 94143.* Accepted for publication April 20, 1977. *Present address: Division of Research, National Institute on Drug Abuse, Rockville, MD 20857. ‡Present address: Facultad de Ciencias Químicas, Universidad de Chile, Vicuña Mackenna 20, Santiago, Chile.

Abstract □ Salicylate transport across the rat intestine was measured using both *in vitro* and *in vivo* procedures. After the steady state for labeled salicylate was reached, the addition of ascorbate stimulated tracer flux with the establishment of a new steady state. The tissue permeability had a saturable dependence on ascorbate concentration. Also, ascorbate stimulated the tissue short-circuit current.

Keyphrases □ Ascorbate—effect on GI absorption of salicylate, rat intestine *in vivo* and *in vitro* □ Salicylate—GI absorption, effect of ascorbate, rat intestine *in vivo* and *in vitro* □ Absorption, GI—salicylate, effect of ascorbate, rat intestine *in vivo* and *in vitro* □ GI absorption—salicylate, effect of ascorbate, rat intestine *in vivo* and *in vitro*

Ascorbic acid effects on metabolic activity as well as on nutrition are the subject of substantial scientific activity (1). The effect of sex on metabolic availability of ascorbic acid is just one example of the basic questions under study (2). Recently, the modification of salicylamide metabolism in the male by ascorbic acid taken orally was reported (3). Followup work with crossover studies on rats using oral and intramuscular administrations demonstrated that the ascorbic acid interaction was strongest for oral drug administration. This interaction may occur during the first pass of the drugs through both the liver and the intestinal tissue.

Ascorbate interaction with salicylate transport across the isolated rat intestine is reported here as determined by *in vitro* and *in vivo* techniques. The absorption is clearly stimulated, and the *in vitro* experiment also demonstrates an increase in the tissue short-circuit current.

EXPERIMENTAL

In vitro salicylate flux across the rat jejunum was measured by a reported procedure (4) using the technique of Ussing and Zerhan (5) as modified by Schultz and Zalusky (6). The tissue chamber[1] consisted of two conical half chambers with a 1.13-cm^2 cross-sectional area. Each half chamber was connected to a gas lift perfusion apparatus containing 10 ml of buffer solution and was heated to 37° by water jackets.

The composition of the buffer, in milliequivalents per liter, was: Na, 143.3; K, 6; Mg, 2.4; Ca, 5; Cl, 128.3; HCO_3, 25; H_2PO_4, 1.2; SO_4, 2.4; and glucose, 25. The pH was adjusted to 7.4 with carbon dioxide, and solution mixing was effected by 95% O_2–5% CO_2. Salt bridges, consisting of 4% agar in buffer solution, were connected to silver–silver chloride electrodes located approximately 22 mm from the mounted tissue while calomel electrodes were placed *via* salt bridges at about 2 mm from the tissue.

Sprague–Dawley male rats, 300–400 g, were sacrificed by decapitation. Four tissue sections were excised from each animal for mounting on the cells by cutting along the mesenteric line from the segment of intestine 25–50 cm distal to the stomach. ^{14}C-Salicylic acid, 2 μCi and 0.1 m*M*, was introduced on the mucosal side of the tissue; the increasing concentration in the serosal bathing solution was measured at 10-min intervals from 20 min after the label was added until 110 min. The ascorbate solution, made fresh with buffer and pH adjusted with sodium hydroxide and carbon dioxide, was added to the serosal solution at 50 min.

The salicylate flux before ascorbate addition, J, was determined by a linear least-squares fit to the data points from 20 to 50 min. The flux after ascorbate treatment, J^c, was determined by a fit to the data from 70 to 110 min. The spontaneous potential difference across the tissue was continuously recorded. External current was applied periodically to determine the current needed to force the tissue potential to zero.

In vivo salicylate absorption was measured using the same animals and buffer. The labeled salicylic acid was 7 μ*M*, and the ascorbate was initially 28 m*M*. The procedure of Schanker *et al.* (7), as modified (8), was used. The small intestine was cannulated, using polyethylene 320 tubing, at the ligament of Trietz and at a point 10 cm proximal to the ileocecal junction to form an *in situ* loop of intestine. Perfusion of the loop at a rate of 1.5 ml/min was carried out in the direction of normal GI flow by means of a peristaltic pump.

At the end of the experiment, the animal was sacrificed, the intestine was separated from the mesentery, and the length of perfused intestine was measured. Samples were removed from the reservoir at fixed times during the experiment and were assayed by liquid scintillation spectrometry. Apparent absorption rate constants, calculated as the disappearance rate per centimeter of perfused intestine, were measured before, k_a, and after, $k_a{}^c$, ascorbate administration, thus allowing each animal to serve as its own control.

RESULTS AND DISCUSSION

The flux data from the *in vitro* studies are presented in Table I. The flux of labeled salicylate from the mucosal to the serosal side of the tissue was measured before, J, and after, J^c, ascorbate, [C], was added to the serosal solution. Salicylate reached a new steady-state flux after ascorbate addition over a concentration range of 1–57 m*M*. For example, for [C] = 6 m*M*, the average salicylate flux, $\bar{J}$, before ascorbate addition was 6.69 nmoles/cm^2/hr with a standard error of the mean of ±0.59, using 14 separate tissues taken from seven different animals. The stimulatory effect of ascorbate resulted in an average salicylate flux ratio, $\overline{(J^c/J)}$, of 1.24 for these 14 tissues, thus showing an average 24% increase in the transport rate at this concentration. The paired t-test applied to these data showed that the $\overline{(J^c/J)}$ was different from unity at a significance level of 99.95%. For the studies reported in Table I, five different concentrations of ascorbate were used on 42 tissues from 11 animals. The difference in the $\bar{J}$ values is a reflection of the large range of flux values usually found in this type of measurement. It was imperative, therefore, to use each tissue as its own control, thus allowing application of paired t-test statistics, to observe the flux change due to ascorbate. In 39 out of the 42 cases, the treatment with ascorbate resulted in an increased flux. At [C] = 57 m*M*, one tissue had no flux change; at 6 m*M*, two of the 14 tissues had a 4% decrease. From J averaged over all 42 tissues and for the salicylate concentration of 0.1 m*M*, the average permeability of the jejunum for salicylate transport from the mucosal to the serosal side of the tissue was P_{ms} = 0.592 cm/hr.

Table I—Average Salicylate Flux[a] before and after Addition of Serosal Ascorbate

[C], m*M*	$\bar{J}$	$\overline{(J^c/J)}$	$p<$	Tissues, Animals
1	6.50 ± 0.38	1.19 ± 0.05	0.0025	8, 4
6	6.69 ± 0.59	1.24 ± 0.05	0.0005	14, 7
17	6.00 ± 0.65	1.34 ± 0.05	0.0005	8, 4
28	4.80 ± 0.85	1.67 ± 0.14	0.0025	6, 3
57	5.59 ± 1.08	1.60 ± 0.22	0.01	6, 3
				42, 11

[a] Flux units are nanomoles per square centimeter per hour ± *SEM*.

[1] E. W. Wright, Inc., New Haven, Conn.

Table II—Effect of Ascorbate on Apparent Absorption Rate Constants for Salicylate

	k_a, $\times 10^6$ cm^{-1} hr^{-1}	$k_a{}^c$, $\times 10^6$ cm^{-1} hr^{-1}
	1.76	2.82
	1.56	2.21
	1.90	2.49
	1.41	1.86
Mean	1.66	2.34[a]

[a] $p < 0.01$.

The average flux ratios are plotted in Fig. 1 as a function of the ascorbate concentration. With the average tissue permeability to salicylate, P_{ms}, and fitting of the data in Fig. 1, the permeability as a function of ascorbate concentration, $P_{ms}{}^c$, is reported for a salicylate concentration of 0.1 m*M*. The computer fit was forced to unity for no added ascorbate and fits well to the "best" experimental point at [*C*] = 6 m*M*. While fitting is not precise, it does allow an estimate to be reported:

$$P_{ms}{}^c = P_{ms}\{1 + V[C]/(K + [C])\} \qquad \text{(Eq. 1)}$$

where $V = 0.74 \pm 0.17$ (*SD*) and $K = 10.5 \pm 7.9$. *In vivo* studies (9) showed that P_{ms} has a linear dependence on the salicylate concentration over a considerable range but nothing is yet known about the dependence for $P_{ms}{}^c$.

The tissue potential difference, V_t, was recorded continuously throughout each experiment. At frequent set intervals, the tissue potential was forced to zero by applying an external current momentarily to obtain, in addition to V_t, the tissue resistance, R, and the short-circuit current, I_{sc} (10). In Fig. 2, the top graph shows a normal monotonically decreasing tissue potential, V_t, as a function of time. The ascorbate was introduced at 50 min but showed no perceptible perturbation to V_t.

The tissue electrical resistance, R, the middle graph in Fig. 2, showed usual behavior as compared to earlier work and responded to the ascorbate treatment at 50 min with a substantial decrease. The short-circuit current, I_{sc}, is the electrical parameter often used to characterize biological tissues. The bottom graph of Fig. 2 shows a 13% increase in I_{sc}, with onset immediately after ascorbate was added, which leveled to a constant value at 70 min.

The electrical effect of ascorbate is different than that observed with either theophylline[2] or ouabain[3] on the same type of tissue. For ascorbate, the increase in I_{sc} was essentially due to the decrease in R. For theophylline, I_{sc} increased due to both an increase in V_t and a decrease in R. For ouabain, I_{sc} decreased because of a decrease in V_t and an increase in R. With the continuous recording of V_t, it was possible to ascertain a more rapid, distinct response for both ouabain and theophylline when added to the serosal solution, thus supporting the claim that the serosal side of the tissue is the more responsive for the action of both drugs.

In vivo absorption studies were carried out to determine if the effect of ascorbate on salicylate flux was an *in vitro* artifact or a biological phenomenon. Table II gives apparent absorption rate constants before,

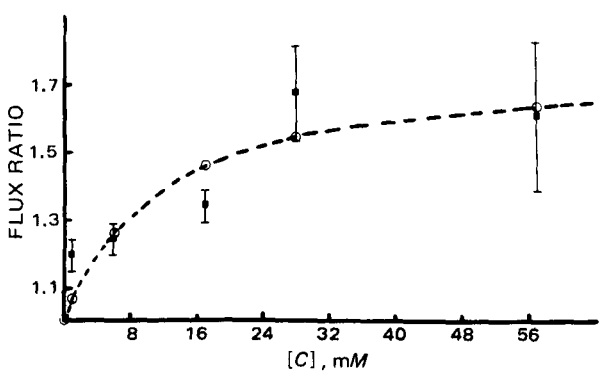

Figure 1—*Averaged individual tissue flux ratios as a function of ascorbate concentration. The solid squares are the average values, and the bars are the standard errors of the mean for each ascorbate concentration. The circles connected by the dotted curve is the mathematical fit to the experimental data by the BMD nonlinear computer program (11).*

[2] G. Barnett, unpublished work.

[3] D. W. Adair, doctoral dissertation, University of California, San Francisco, Calif., in preparation.

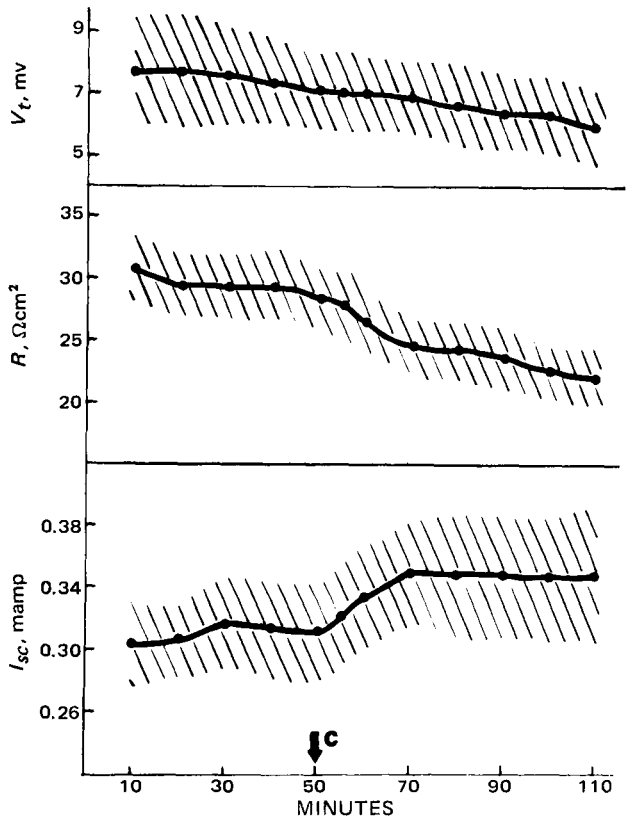

Figure 2—*Tissue electrical parameters as a function of time. The top graph is the tissue potential difference,* V_t; *the middle graph is the tissue resistance,* R; *and the bottom graph is the tissue short-circuit current,* I_{sc}. *Each point is an average of 13 tissues, reported in Table I for the case* [C] = 6 m*M*, *where the shaded region extends over ± 1* SEM. *Ascorbate, 6 m*M, *was added to the serosal bathing solution at 50 min, as noted by the arrow.*

k_a, and after, $k_a{}^c$, the introduction of ascorbate into the solution which perfused the mucosal tissue surface. Each of the four experiments showed increased absorption, while the mean value gave a 40% increase in the rate constant; by the paired t-test, this increase is significant at a 99% level. From Fig. 1, it is observed that the *in vitro* procedures gave roughly a similar result.

Clinical work has indicated that ascorbic acid affects both the absorption rate and various metabolic processes. In this precisely defined, and thus rather theoretical, system, ascorbate enhanced the absorption of tracer quantities of salicylate across the intestine of the laboratory rat. Tissue electrical resistance decreased for the 6 m*M* ascorbate treatment and, based on these tentative results, showed the same effect at higher ascorbate levels as well. The electrical response is considerably different than that due to treatment with the metabolic inhibitor ouabain or the antidiuretic hormone-like behavior of theophylline.

The estimate of the salicylate tissue permeability reported here suggests a saturable dependence on the ascorbate concentration. The average flux after ascorbate treatment, $\bar{J}^c$, appears to be independent of either the ascorbate concentration or the initial average flux, $\bar{J}$. The range for $\bar{J}^c$ was 7.6–8.0, while the average for all 42 tissues was 7.82 ± 0.27 nmoles/cm^2/hr. This constant, or perhaps maximum, salicylate flux in the presence of exogenous ascorbate, observed in averaged data, is not explained, although it has been suggested that perhaps the treatment results in a return of each tissue to a state of preexperimental integrity[4].

REFERENCES

(1) "Second Conference on Vitamin C," C. G. King and J. J. Burns, Eds., Annals of the New York Academy of Sciences, vol. 258, 1975.

(2) H. S. Loh, A. Odumosu, and C. W. M. Wilson, *Clin. Pharmacol. Ther.*, **6**, 390 (1974).

[4] L. Pauling, Pauling Institute of Science and Medicine, Palo Alto, Calif., personal communication.

(3) J. B. Houston and G. Levy, *Nature*, **255**, 78 (1975). J. B. Houston and G. Levy, "Abstracts of the 123rd Annual Meeting," vol. 6, American Pharmaceutical Association, Washington, D.C., 1976, p. 136.
(4) G. Barnett and V. Licko, *Biochim. Biophys. Acta*, **464**, 276 (1977).
(5) H. H. Ussing and K. Zerhan, *Acta Physiol. Scand.*, **23**, 110 (1951).
(6) S. G. Schultz and R. J. Zalusky, *Gen. Physiol.*, **47**, 567 (1964).
(7) L. S. Schanker, D. J. Tocco, B. B. Brodie, and C. A. M. Hogben, *J. Pharmacol. Exp. Ther.*, **123**, 81 (1958).
(8) J. M. Orr and L. Z. Benet, *Am. J. Digest. Dis.*, **20**, 858 (1975).
(9) H. Kunze, G. Rehbock, and W. Vogt, *Naunyn-Schmiedebergs Arch. Pharmacol.*, **273**, 331 (1972).
(10) T. W. Clarkson and S. R. Toole, *Am. J. Physiol.*, **206**, 658 (1964).
(11) W. Dixon, "BMD Biomedical Computer Programs," University of California Press, Los Angeles, Calif., 1974.

ACKNOWLEDGMENTS

The authors acknowledge Dr. Dennis Adair for expert advice and assistance.

Metabolic Studies of the Nonnutritive Sweeteners Cyclopentylmethylsulfamate and Cyclopentylsulfamate: Determination of Metabolites in Rat Urine

WILLIAM J. SPILLANE ˣ and G. ANTHONY BENSON

Received December 22, 1976, from the *Department of Chemistry, University College, Galway, Ireland.* Accepted for publication May 5, 1977.

Abstract □ The *nonnutritive* sweetener sodium cyclopentylmethylsulfamate was fed to Wistar albino rats. The urine was collected for 3 days, combined, and examined (GLC) for the metabolites cyclopentylmethylamine and cyclopentylmethanol. The percent conversion to these metabolites was 0.077 and 0.0102, respectively. The percent conversion to cyclopentylmethylamine was the lowest conversion to amine observed when compared to the metabolism of three other sweet sulfamates, cyclopentylsulfamate, cycloheptylsulfamate, and cyclooctylsulfamate, previously administered to rats. The average excretion of unmetabolized sulfamate was 15.4%. Sodium cyclopentylsulfamate was fed to rats over 9 days, and an analysis was carried out for the metabolites cyclopentylamine, cyclopentanone, and cyclopentanol. A decrease in the level of metabolites occurred after the first 3 days.

Keyphrases □ Cyclopentylsulfamate and cyclopentylmethylsulfamate—metabolism in rats □ Metabolism—various sulfamates in rats □ Sulfamates, various—metabolism in rats compared □ Sweeteners, nonnutritive—various sulfamates, metabolism in rats compared

The artificial sweetener cyclamate (*N*-cyclohexylsulfamate) has been the subject of many investigations, including the feeding of the compound to different animal species to study its distribution and metabolism (1–4). Until 1966, it was generally considered that the compound, whether administered orally, intravenously, or intraperitoneally, was excreted entirely unchanged. However, in 1966, Kojima and Ichibagase (5) found cyclohexylamine in the urine of dogs and humans who had been fed cyclamate. Various toxicological studies (6–9) then showed that certain animals fed cyclamate developed lesions, chromceromal breaks, and tumors of the urinary bladder. The presence of cyclohexylamine as a metabolite and the possibility of cyclamate being a carcinogen resulted in the sweetener being banned in 1969 in the United States and Britain.

The purposes of this investigation were to study the level of excretion of sweet-tasting sulfamates related to cyclamate, to determine whether metabolic breakdown occurs, and, if so, to compare the levels of breakdown with the levels reported for cyclamate. Cycloheptylsulfamate and cyclopentylsulfamate were administered to rats and rabbits, and the results were reported previously (10, 11). The recent surprising finding (12) that sodium cyclopentylmethylsulfamate is sweet and the suggestion that its amine metabolite may be less carcinogenic than, for example, cyclohexylamine prompted study of this compound.

This paper describes the results of *in vivo* administration of cyclopentylmethylsulfamate to rats and the extended feeding of cyclopentylsulfamate to rats.

EXPERIMENTAL

Reagents and Chemicals—Cyclopentylmethylamine, bp 140–143°, was prepared by the following route: cyclopentanone[1] → cyclopentanol (13) → cyclopentylbromide (14) → cyclopentylcyanide (15) → cyclopentylmethylamine (16). This amine was sulfamated by the method of Audrieth and Sveda (1) and recrystallized (twice) from ethanol.

Anal.—Calc. for $C_6H_{12}NNaO_3S$: C, 35.82; H, 5.97; N, 6.96. Found: C, 35.85; H, 5.45; N, 6.81.

Sodium cyclopentylsulfamate was prepared as previously described (10). Cyclopentylmethylamine, cyclopentylamine[1], cyclopentylmethanol[1], cyclopentanol[1], cyclopentanone[1], and dichloromethane[2] were redistilled before use. *p*-Benzoquinone was sublimed; *n*-dodecane[3], analytical reagent grade sulfosalicylic acid[4], chloroform, ethanol, and 1,4-dioxane (reagent grade) were used as obtained.

Feeding Experiments—Female Wistar albino rats, ~300 g, were kept on solid food and water in metabolism cages[5]. Prior to feeding, the urine of each rat was collected and monitored using both detection methods (described later), and the rats were then starved of water for 24 hr. Sodium cyclopentylmethylsulfamate (1450 mg/kg) was administered orally in aqueous solution (25–30 ml of water). The extended feeding of sodium cyclopentylsulfamate was carried out over 9 days as follows: 200 mg in 20 ml of water was fed for the first 5 days, sulfamate was not given for the 6th and 7th days, and feeding was resumed for the 8th and 9th days.

The urine of the rats fed cyclopentylmethylsulfamate was collected

[1] Aldrich Chemical Co.
[2] May and Baker.
[3] British Drug Houses.
[4] AnalaR grade, May and Baker.
[5] NKP cages, Kent, England.

(3) J. B. Houston and G. Levy, *Nature*, **255**, 78 (1975). J. B. Houston and G. Levy, "Abstracts of the 123rd Annual Meeting," vol. 6, American Pharmaceutical Association, Washington, D.C., 1976, p. 136.
(4) G. Barnett and V. Licko, *Biochim. Biophys. Acta*, **464**, 276 (1977).
(5) H. H. Ussing and K. Zerhan, *Acta Physiol. Scand.*, **23**, 110 (1951).
(6) S. G. Schultz and R. J. Zalusky, *Gen. Physiol.*, **47**, 567 (1964).
(7) L. S. Schanker, D. J. Tocco, B. B. Brodie, and C. A. M. Hogben, *J. Pharmacol. Exp. Ther.*, **123**, 81 (1958).
(8) J. M. Orr and L. Z. Benet, *Am. J. Digest. Dis.*, **20**, 858 (1975).
(9) H. Kunze, G. Rehbock, and W. Vogt, *Naunyn-Schmiedebergs Arch. Pharmacol.*, **273**, 331 (1972).
(10) T. W. Clarkson and S. R. Toole, *Am. J. Physiol.*, **206**, 658 (1964).
(11) W. Dixon, "BMD Biomedical Computer Programs," University of California Press, Los Angeles, Calif., 1974.

ACKNOWLEDGMENTS

The authors acknowledge Dr. Dennis Adair for expert advice and assistance.

Metabolic Studies of the Nonnutritive Sweeteners Cyclopentylmethylsulfamate and Cyclopentylsulfamate: Determination of Metabolites in Rat Urine

WILLIAM J. SPILLANE ˣ and G. ANTHONY BENSON

Received December 22, 1976, from the *Department of Chemistry, University College, Galway, Ireland.* Accepted for publication May 5, 1977.

Abstract □ The *nonnutritive* sweetener sodium cyclopentylmethylsulfamate was fed to Wistar albino rats. The urine was collected for 3 days, combined, and examined (GLC) for the metabolites cyclopentylmethylamine and cyclopentylmethanol. The percent conversion to these metabolites was 0.077 and 0.0102, respectively. The percent conversion to cyclopentylmethylamine was the lowest conversion to amine observed when compared to the metabolism of three other sweet sulfamates, cyclopentylsulfamate, cycloheptylsulfamate, and cyclooctylsulfamate, previously administered to rats. The average excretion of unmetabolized sulfamate was 15.4%. Sodium cyclopentylsulfamate was fed to rats over 9 days, and an analysis was carried out for the metabolites cyclopentylamine, cyclopentanone, and cyclopentanol. A decrease in the level of metabolites occurred after the first 3 days.

Keyphrases □ Cyclopentylsulfamate and cyclopentylmethylsulfamate—metabolism in rats □ Metabolism—various sulfamates in rats □ Sulfamates, various—metabolism in rats compared □ Sweeteners, nonnutritive—various sulfamates, metabolism in rats compared

The artificial sweetener cyclamate (*N*-cyclohexylsulfamate) has been the subject of many investigations, including the feeding of the compound to different animal species to study its distribution and metabolism (1–4). Until 1966, it was generally considered that the compound, whether administered orally, intravenously, or intraperitoneally, was excreted entirely unchanged. However, in 1966, Kojima and Ichibagase (5) found cyclohexylamine in the urine of dogs and humans who had been fed cyclamate. Various toxicological studies (6–9) then showed that certain animals fed cyclamate developed lesions, chromceromal breaks, and tumors of the urinary bladder. The presence of cyclohexylamine as a metabolite and the possibility of cyclamate being a carcinogen resulted in the sweetener being banned in 1969 in the United States and Britain.

The purposes of this investigation were to study the level of excretion of sweet-tasting sulfamates related to cyclamate, to determine whether metabolic breakdown occurs, and, if so, to compare the levels of breakdown with the levels reported for cyclamate. Cycloheptylsulfamate and cyclopentylsulfamate were administered to rats and rabbits, and the results were reported previously (10, 11). The recent surprising finding (12) that sodium cyclopentylmethylsulfamate is sweet and the suggestion that its amine metabolite may be less carcinogenic than, for example, cyclohexylamine prompted study of this compound.

This paper describes the results of *in vivo* administration of cyclopentylmethylsulfamate to rats and the extended feeding of cyclopentylsulfamate to rats.

EXPERIMENTAL

Reagents and Chemicals—Cyclopentylmethylamine, bp 140–143°, was prepared by the following route: cyclopentanone[1] → cyclopentanol (13) → cyclopentylbromide (14) → cyclopentylcyanide (15) → cyclopentylmethylamine (16). This amine was sulfamated by the method of Audrieth and Sveda (1) and recrystallized (twice) from ethanol.

Anal.—Calc. for $C_6H_{12}NNaO_3S$: C, 35.82; H, 5.97; N, 6.96. Found: C, 35.85; H, 5.45; N, 6.81.

Sodium cyclopentylsulfamate was prepared as previously described (10). Cyclopentylmethylamine, cyclopentylamine[1], cyclopentylmethanol[1], cyclopentanol[1], cyclopentanone[1], and dichloromethane[2] were redistilled before use. *p*-Benzoquinone was sublimed; *n*-dodecane[3], analytical reagent grade sulfosalicylic acid[4], chloroform, ethanol, and 1,4-dioxane (reagent grade) were used as obtained.

Feeding Experiments—Female Wistar albino rats, ~300 g, were kept on solid food and water in metabolism cages[5]. Prior to feeding, the urine of each rat was collected and monitored using both detection methods (described later), and the rats were then starved of water for 24 hr. Sodium cyclopentylmethylsulfamate (1450 mg/kg) was administered orally in aqueous solution (25–30 ml of water). The extended feeding of sodium cyclopentylsulfamate was carried out over 9 days as follows: 200 mg in 20 ml of water was fed for the first 5 days, sulfamate was not given for the 6th and 7th days, and feeding was resumed for the 8th and 9th days.

The urine of the rats fed cyclopentylmethylsulfamate was collected

[1] Aldrich Chemical Co.
[2] May and Baker.
[3] British Drug Houses.
[4] AnalaR grade, May and Baker.
[5] NKP cages, Kent, England.

for 3 days after feeding. The urine samples were refrigerated, and the samples were bulked and analyzed at the end of 3 days. The urine of the rats fed cyclopentylsulfamate was collected and refrigerated each day for 9 days. The samples were then analyzed as described below.

GLC Analysis and Standardization—Cyclopentylmethylamine and cyclopentylmethanol were determined by a GLC procedure described previously (10). The conditions for this separation were: column temperature, 120°; carrier (nitrogen) flow rate, 60 ml/min; and internal standard, *n*-dodecane. Under these conditions, the retention times of cyclopentylmethylamine, *n*-dodecane, and cyclopentylmethanol were 4.8, 7.8, and 12.4 min, respectively (Fig. 1).

A standard curve was prepared by injecting microliter portions of the amine and the alcohol into 5-ml samples of urine. Details of the extraction from urine and the injection of samples were similar to those previously described for cyclopentylsulfamate metabolites (10). Urine samples taken before and after feeding were similarly analyzed. To estimate the percent recovery, varying amounts of amine and alcohol were determined by the established procedure (10); the results are given in Table I. GLC analysis of the metabolites of cyclopentylsulfamate and percent recovery data were reported previously (10).

Visible Spectrophotometic Analysis and Standardization—The details for the analysis of cyclopentylsulfamate were reported previously[6] (10). A similar procedure was used for cyclopentylmethylsulfamate, except that the hydrolysis in dioxane solution took 4.5 hr at 95° for completion. A calibration graph was prepared by injecting microliter quantities of cyclopentylmethylamine into 25-ml samples of chloroform. The amine was subsequently reacted with *p*-benzoquinone according to the published procedure (10). The plot of absorbance *versus* concentration was linear over the 20–100-μg/ml range.

Stability of Cyclopentylmethylsulfamate and Cyclopentylsulfamate during Storage in Urine and Sampling Procedure for GLC—The possibility of sulfamate conversion to one or more of the metabolites while refrigerated in urine or during the sampling procedure was checked by adding the two sulfamates individually to rat urine at levels of 5, 10, and 15 mg/ml. The urine samples were then refrigerated for 3 days. After basification and extraction with dichloromethane, GLC analysis showed that neither sulfamate had been converted to any of its metabolites.

RESULTS AND DISCUSSION

By using different sweet sulfamates, the effect of structural modification of the cyclamate nucleus on the stability of the compound in the body was studied. By elucidating the stability of various sulfamates *in vivo*, it may be possible to predict and prepare a sweet sulfamate resistant to metabolic breakdown and, therefore, less likely to cause cancer.

Table II summarizes the results of feeding cyclopentylmethylsulfamate to five rats at a level of 1450 mg/kg. Three rats excreted cyclopentylmethylamine and cyclopentylmethanol. No attempt was made to search for other metabolites, since it is clear from the work on cyclamate that the amine, alcohol, and ketone (where it exists) are the principal metabolites. The average conversion of cyclopentylmethylsulfamate to its corresponding amine was 0.011%.

Previously (17), the conversion of cyclamate to cyclohexylamine, cyclohexanone, and cyclohexanol in rats was reported to be 0.0068, 0.0005, and 0.0003%, respectively. These data point to the fact that cyclopentylmethylsulfamate is cleaved to a greater extent than its cyclohexyl analog in rats. In another study (17) with rats, the average conversion to cyclamate was 0.006%, again showing the greater stability of the cyclamate compound over that of cyclopentylmethylsulfamate.

The results of feeding cyclopentylsulfamate (10) and cycloheptylsulfamate (11) to rats and rabbits were also reported. In the rat, the percentage conversion of cyclopentylsulfamate and cycloheptylsulfamate to cyclopentylamine and cycloheptylamine was 0.57 and 0.064, respectively[7]. These figures are significantly greater than those found previously (17) for the conversion of cyclamate to cyclohexylamine and suggest that cyclamate is more stable than cyclopentylsulfamate and cycloheptylsulfamate. The results for cyclopentylmethylsulfamate are presented in Table II; it was more stable than cyclopentylsulfamate, cycloheptylsulfamate, and cyclooctylsulfamate in the rat but was metabolized more easily than cyclamate.

Table II also shows the percentage unmetabolized sulfamate recovered in the urine for the five rats; the average recovery of cyclopentylmethylsulfamate was 15.4%. Previous studies showed that the percent of cyclopentylsulfamate (10) and cycloheptylsulfamate (11) recovered in the urine was 15.17 and 35.06, respectively. This result could indicate that the main excretory pathway for sulfamates in rats is through the feces, with the level of absorption from the intestine being small. Evidence for this possibility was provided by the study of Derse and Daun (18); in rats administered cyclamate, about 17% of it was excreted in the urine and about 70% was excreted in the feces. Bickel *et al.* (19) administered cyclamate at a level of 2500 mg/kg to rats and observed that 32% was excreted in the urine. The present results for other sweet sulfamates support the idea that the main excretory pathway for sulfamates is *via* the feces.

Cyclopentylsulfamate was also fed to rats over 9 days to ascertain if a pattern of metabolic breakdown was observable; the results are shown in Table III. In some rats, metabolic breakdown of the sulfamate occurred to cyclopentylamine, cyclopentanone, and cyclopentanol. However, no trend or increase was observed in the level of metabolites due to continued administration of the compound for 5 days. The rats did not receive a dose

Table I—Percent Recovery of Cyclopentylmethylamine and Cyclopentylmethanol from Urine

Amine		Alcohol	
μg	%	μg	%
348.0	97.41	1111.2	91.79
348.0	95.68	740.8	90.71
174.0	103.4	370.4	100.43
104.0	104.5	296.3	106.31
69.6	110.3	222.2	101.26
Mean ± *SE*	102.2 ± 4.58		98.10 ± 5.48

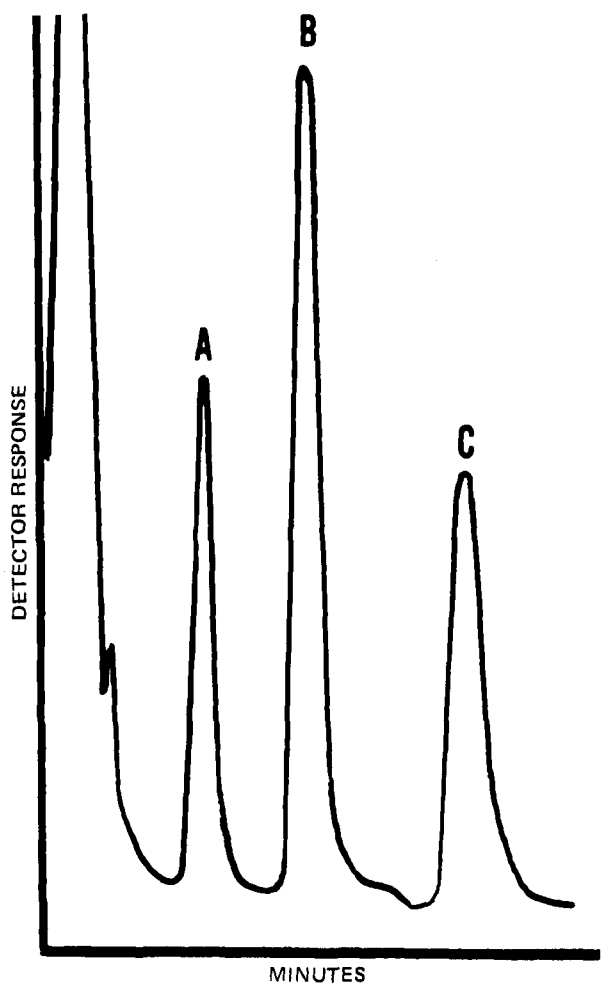

Figure 1—*Gas chromatogram of the urine metabolites of cyclopentylmethylsulfamate. Key: A, cyclopentylmethylamine (4.8 min); B, n-dodecane (7.8 min) (internal standard); and C, cyclopentylmethanol (12.4 min).*

[6] Perkin-Elmer 124 double-beam spectrophotometers.

[7] In similar feeding experiments, cyclooctylsulfamate was converted to the extent of 0.21% on the average in rats.

Table II—Metabolism of Cyclopentylmethylsulfamate in Rats

Animal	Recovered Sulfamate, Visible Spectrophotometry		Metabolites, GLC				Total Metabolites, %
			Cyclopentylmethylamine		Cyclopentylmethanol		
	mg	%	mg	%	mg	%	
1	160.3	32.0	0.0347	0.013	0.037	0.015	0.028
2	35.7	7.1	0.0178	0.007	0.017	0.006	0.013
3	43.5	8.6	0.0384	0.015	0.040	0.016	0.031
4	100.5	20.1	None	—	None	—	—
5	47.4	9.4	None	—	None	—	—
Mean ± *SE*	77.4 ± 42.3	15.4 ± 8.4	0.029 ± 0.009	0.011 ± 0.004	0.031 ± 0.009	0.012 ± 0.004	0.024 ± 0.007

Table III—Metabolism of Cyclopentylsulfamate after Prolonged Administration to Rats (200 mg/Animal)

Rat	Metabolite	1[a]	2	3	4	5	6	7	8	9
	Cyclopentylamine	14[b] (0.015)	—[c]	34 (0.037)	23 (0.025)	37 (0.040)	T[d]	47 (0.052)	T	T
1	Cyclopentanone	T	T	8 (0.009)	T	T	—	—	—	—
	Cyclopentanol	81 (0.089)	T	6 (0.006)	T	6 (0.006)	4 (0.04)	—	—	—
	Cyclopentylamine	52 (0.05)	24 (0.05)	15 (0.011)	T	T	T	10 (0.011)	T	T
2	Cyclopentanone	—	T	T	T	—	—	—	—	—
	Cyclopentanol	16 (0.017	T	—	T	—	T	—	—	—
	Cyclopentylamine	12 (0.013)	T	28 (0.03)	T	T	T	10 (0.11)	T	T
3	Cyclopentanone	T	11 (0.012)	T	8 (0.009)	—	—	T	T	—
	Cyclopentanol	T	6 (0.007)	—	T	—	T	T	T	—
	Cyclopentylamine	39 (0.042)	42 (0.046)	25 (0.027)	—	T	T	T	T	T
4	Cyclopentanone	T	T	T	4 (0.004)	T	T	T	—	—
	Cyclopentanol	T	T	1 (0.001)	T	26 (0.028)	—	—	—	—
	Cyclopentylamine	56 (0.061)	21 (0.023)	14 (0.015)	—	38 (0.042)	13 (0.014)	17 (0.018)	T	T
5	Cyclopentanone	—	T	—	5 (0.006)	T	—	—	—	—
	Cyclopentanol	—	—	16 (0.017)	48 (0.052)	—	48 (0.052)	—	—	—

[a] Days are numbered consecutively. [b] Amount excreted (micrograms) and, in parentheses, percent conversion. [c] Indicates that no metabolites were observed. [d] The conversion was too low to be measurable.

of sulfamate on Days 6 and 7 but were again administered the compound on Days 8 and 9. No increase in the level of metabolites was observed, and in all cases the levels dropped below those found for the first 3 days.

Cyclopentylamine was the principal metabolite excreted by the five rats. The average conversion to the amine for the results given in Table III is 0.027%. Furthermore, Rat 5 excreted cyclopentylamine regularly for 6 days before the level finally dropped. The other metabolites, cyclopentanone and cyclopentanol, were excreted in an irregular pattern for the five animals. The average conversion of cyclopentylsulfamate in rats to the ketone and alcohol was 0.008 and 0.026%, respectively. These *in vivo* studies will be continued with other sweet sulfamates.

REFERENCES

(1) L. F. Audrieth and M. Sveda, *J. Org. Chem.*, **9**, 89 (1944).

(2) S. Kojima, H. Ichibagase, and S. Iguchi, *Chem. Pharm. Bull.*, **14**, 965 (1966).

(3) J. A. Schoenberger, D. M. Rix, A. Sakamoto, J. D. Taylor, and R. M. Kark, *Am. J. Med. Sci.*, **255**, 555 (1953).

(4) J. D. Taylor, R. K. Richards, and J. C. Davin, *Proc. Soc. Exp. Biol. Med.*, **78**, 530 (1951).

(5) S. Kojima and H. Ichibagase, *Chem. Pharm. Bull.*, **14**, 971 (1966).

(6) E. Bajusz, *Nature*, **223**, 406 (1969).

(7) M. S. Legator, K. A. Palmer, S. Greer, and K. W. Petersen, *Science*, **165**, 1139 (1969).

(8) G. T. Bryan and E. Ertürk, *ibid.*, **167**, 996 (1970).

(9) J. M. Price, C. G. Biava, B. L. Oser, E. E. Vogin, J. Steinfeld, and H. L. Ley, *ibid.*, **167**, 1131 (1970).

(10) G. A. Benson and W. J. Spillane, *J. Pharm. Sci.*, **65**, 1841 (1976).

(11) *Ibid.*, **66**, 881 (1977).

(12) C. Nofre and F. Pautet, *Naturwissenschaften*, **62**, 97 (1975).

(13) S. W. Chaikin and W. G. Brown, *J. Am. Chem. Soc.*, **71**, 122 (1949).

(14) A. I. Vogel, "Practical Organic Chemistry," Longman, New York, N.Y., 1956, p. 277.

(15) M. T. Rogers and J. D. Roberts, *J. Am. Chem. Soc.*, **68**, 844 (1946).

(16) R. F. Nyson and W. J. Brown, *ibid.*, **70**, 3738 (1948).

(17) A. Suenga, S. Kojima, and H. Ichibagase, *Chem. Pharm. Bull.*, **20**, 1357 (1972).

(18) P. H. Derse and R. J. Daun, *J. Assoc. Off. Anal. Chem.*, **49**, 1090 (1966).

(19) M. H. Bickel, B. Burkard, E. Meir-Strasser, and M. Van Der Borek. Boot, *Xenobiotica*, **4**, 425 (1974).

ACKNOWLEDGMENTS

The authors thank the Department of Education (Ireland) for a grant to G. A. Benson and the Chemical Society (London) and van't Hoff Fund (Amsterdam) for grants.

Comparative Pharmacokinetics of Coumarin Anticoagulants XXXII: Interindividual Differences in Binding of Warfarin and Dicumarol in Rat Liver and Implications for Physiological Pharmacokinetic Modeling

GERHARD LEVY ˣ, CHII-MING LAI, and AVRAHAM YACOBI

Received January 27, 1977, from the *Department of Pharmaceutics, School of Pharmacy, State University of New York at Buffalo, Amherst, NY 14260.* Accepted for publication May 6, 1977.

Abstract □ This investigation was designed to determine the *in vivo* binding of racemic warfarin and dicumarol in the liver of individual adult male rats. The animals received single injections of one or the other drug. They were sacrificed after a period of time equivalent to several times the biological half-life of the drug, at plasma concentrations of 0.40 ± 0.10 (warfarin) or 7.7 ± 1.1 (dicumarol) μg/ml. Drug concentrations in the liver, serum, and serum water (*i.e.*, unbound drug in serum) were determined, and the concentration of unbound drug in the liver was calculated on the basis of the assumption that the concentrations of unbound drug in the serum and in liver water are equal. The free fraction of warfarin in the liver of 13 rats ranged from 0.06×10^{-2} to 0.6×10^{-2} and was substantially smaller than the warfarin free fraction in the serum. The free fraction of dicumarol in the liver of 10 rats ranged from 3.5×10^{-4} to 14×10^{-4} and was larger than the dicumarol free fraction in the serum. However, there was a statistically significant positive correlation between the serum and liver free fraction values of both drugs. Physiologically based pharmacokinetic modeling of protein-bound drugs, which requires estimation of protein-binding parameters in serum and tissues, must take account of the possibility of pronounced intersubject differences in the binding of such drugs in serum as well as tissues. With warfarin and dicumarol, tissue to plasma distribution ratios for liver and kidneys are much less variable (and, therefore, more suitable for pharmacokinetic modeling) than are the ratios of unbound to total concentration.

Keyphrases □ Warfarin—*in vivo* binding in rat liver, implications for pharmacokinetic modeling □ Dicumarol—*in vivo* binding in rat liver, implications for pharmacokinetic modeling □ Pharmacokinetics—warfarin and dicumarol, *in vivo* binding in rat liver, implications for modeling □ Coumarin anticoagulants—warfarin and dicumarol, *in vivo* binding in rat liver, implications for pharmacokinetic modeling □ Anticoagulants—warfarin and dicumarol, *in vivo* binding in rat liver, implications for pharmacokinetic modeling

The distribution of a drug in the body is affected by its binding to proteins in plasma as well as by its binding to tissues. Physiologically based pharmacokinetic models for drugs that are subject to such binding must incorporate parameters that relate the concentrations of free and bound drug in the various compartments (1, 2). While there is a large body of knowledge about the binding of drugs in plasma or serum, little is known about the binding of drugs in tissues (2).

One reason for this lack of knowledge is the virtual impossibility of performing meaningful tissue binding studies *in vitro*. It is unrealistic to equate the drug binding characteristics of tissue proteins with those of plasma albumin, and it is incorrect to assume that the binding parameters obtained with dilute protein solutions apply to high "concentrations" of proteins found in tissues (2). Even in the qualitative sense, *in vitro* studies of drug binding to tissues can be misleading. For example, phenylbutazone displaces dicumarol from plasma proteins but has no apparent effect on the *in vivo* liver to plasma concentration ratio of dicumarol in rats (3). This result indicates that phenylbutazone displaces dicumarol equally from plasma and tissue binding sites, yet *in vitro* studies with liver homogenate did not reveal any displacing effect of phenylbutazone on dicumarol (3).

Warfarin and dicumarol are very extensively protein bound in plasma or serum (4–6). They must also be extensively bound in tissues such as the liver, since their liver to serum concentration ratios can exceed unity (3, 7). Since these anticoagulants are eliminated almost entirely by biotransformation in the liver, the binding of the drugs in the liver is of particular interest. There are pronounced interindividual differences in the serum protein binding of warfarin and dicumarol in rats (4) and of warfarin in humans (5, 8). The interindividual variation of dicumarol serum protein binding has not been studied in humans but may be expected to be of similar magnitude as that of warfarin.

In view of this variability, there arises the question of whether the binding of these drugs in tissues is similarly variable. This question was addressed in the investigation described here. For physiologically based pharmacokinetic modeling, one may elect to use tissue to serum distribution ratios (9, 10). Therefore, the variability of these ratios for the two anticoagulants with respect to the liver and kidneys was also assessed.

EXPERIMENTAL

The experimental data reported here were obtained in conjunction with other investigations, and the protocols and experimental procedures already were described (7, 11, 12). Briefly, adult male Sprague–Dawley rats were selected by suitable screening tests to obtain groups of animals with a relatively wide distribution of warfarin or dicumarol free fraction values in serum. They received a single injection of warfarin, 0.6 mg/kg iv, or dicumarol, 6 or 8 mg/kg iv.

Blood samples were obtained periodically, and drug concentrations in plasma were determined promptly by specific and sensitive methods. These data were used to predict the time when warfarin concentrations had decreased by about 90% and dicumarol concentrations had decreased by about 80%. At the indicated time, the animals were exsanguinated from the aorta and the liver and kidneys were removed. These organs were blotted and pressed lightly to remove most of the remaining blood.

Drug concentrations were determined in the tissues after homogenization and extraction and in serum. The free fraction of warfarin or dicumarol in serum was determined by equilibrium dialysis. Duplicate serum free fraction determinations differed, on the average, by 6.4% for warfarin (13) and 14% for dicumarol (11).

The liver of an adult rat contains about 70% water (14). It was assumed that the concentration of free (unbound) drug in this tissue water is equal to the concentration of free drug in plasma or serum water. Therefore, the free fraction of warfarin or dicumarol in the liver may be estimated by dividing (0.7 × serum free fraction × total concentration in serum) by the total concentration of the drug in the liver. The free fraction ratio, liver to serum, is then 0.7 × total concentration in serum divided by the total concentration in the liver.

Table I—Binding of Warfarin in Rat Liver and Serum

Rat Number	Concentration, g or μg/ml		Free Fraction × 10^2		Free Fraction Ratio, Liver to Serum
	Liver	Serum	Liver	Serum	
1-I	0.977	0.288	0.417	2.02	0.206
2-I	0.976	0.590	0.614	1.45	0.423
3-I	0.764	0.244	0.422	1.89	0.223
4-I	1.31	0.517	0.365	1.32	0.277
5-I	0.863	0.494	0.469	1.17	0.401
6-I	0.933	0.408	0.306	1.00	0.306
7-I	0.895	0.313	0.358	1.46	0.245
8-I	0.897	0.297	0.121	0.523	0.231
9-I	0.851	0.491	0.183	0.455	0.402
10-I	1.07	0.369	0.0952	0.396	0.240
11-I	0.710	0.380	0.0980	0.261	0.375
12-I	1.13	0.393	0.0613	0.252	0.243
13-I	0.942	0.375	0.0632	0.227	0.278
Mean	0.948	0.397	0.275[a]	0.956[a]	0.296
SD	0.156	0.102	—	—	0.077

[a] The correlation between the liver and serum free fraction values is statistically significant ($r = 0.867$, $p < 0.001$).

Table II—Binding of Dicumarol in Rat Liver and Serum

Rat Number	Concentration, g or μg/ml		Free Fraction × 10^4		Free Fraction Ratio, Liver to Serum
	Liver	Serum	Liver	Serum	
1-II	2.36	7.78	3.47	1.50	2.31
2-II	3.22	7.60	5.61	3.39	1.65
3-II	2.59	9.08	5.22	2.13	2.45
4-II	4.37	9.08	5.41	3.72	1.45
5-II	2.79	7.85	12.3	6.25	1.97
6-II	3.86	7.35	5.06	3.79	1.34
7-II	3.35	8.58	13.9	7.79	1.78
8-II	4.91	7.38	8.33	7.90	1.05
19-II	3.81	5.24	5.71	5.94	0.961
10-II	4.88	6.88	7.21	7.30	0.988
Mean	3.61	7.68	7.22[a]	4.97[a]	1.59
SD	0.91	1.13	—	—	0.53

[a] The correlation between the liver and serum free fraction values is statistically significant ($r = 0.741$, $p < 0.02$).

RESULTS

The concentrations of warfarin in the liver and serum of 13 rats at the time when they were killed are listed in Table I. Also listed are the warfarin free fraction values in the liver and serum. The serum warfarin concentration was similar in all animals and averaged 0.397 ± 0.101 μg/ml (mean ± *SD*). Warfarin concentrations in the liver averaged about 2.5 times higher. The serum free fraction values ranged over almost one order of magnitude. The liver free fraction values ranged as widely, from 0.000613 to 0.00614, but were about 70% smaller than the free fraction values in serum. There is a statistically significant positive correlation between the liver and serum free fraction values.

The concentration and free fraction data for dicumarol are listed in Table II. The animals were killed when the dicumarol concentration in serum was 7.68 ± 1.13 μg/ml (mean ± *SD*). The concentration in the liver at that time was about one-half the concentration in serum. There was a fivefold range in serum free fraction values and a fourfold range in liver free fraction values. The liver and serum free fraction values show a statistically significant positive correlation.

Liver to serum and kidney to serum concentration ratios for warfarin were reported previously in tabular form (7) and are presented here in Fig. 1, plotted against total clearance. The same type of information for dicumarol (12) is presented in Fig. 2. In both cases, the liver to serum concentration ratios are considerably less variable than the free fraction values. There is no statistically significant correlation between the liver to serum concentration ratios and the serum free fraction values of either warfarin ($r = 0.27$, $p > 0.4$) or dicumarol ($r = 0.60$, $p > 0.1$).

The kidney to serum concentration ratios are considerably lower than the liver to serum concentration ratios and are also much less variable than the free fraction values. However, the kidney to serum concentration ratio of warfarin (Fig. 1) and the liver to serum concentration ratio of dicumarol (Fig. 2) increase slightly with increasing total clearance.

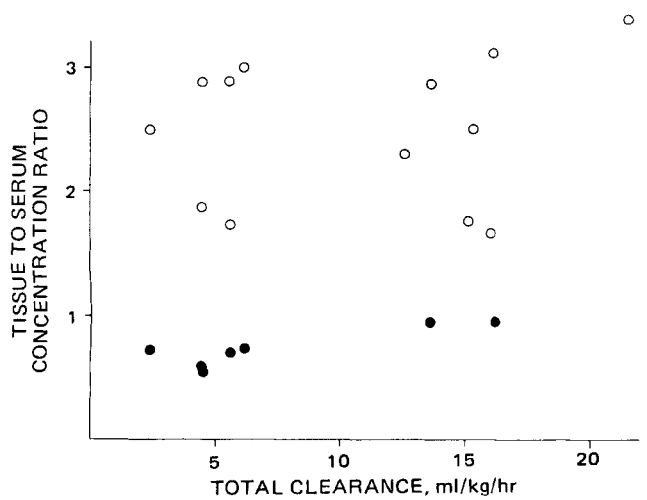

Figure 1—*Liver to serum* (○) *and kidney to serum* (●) *concentration ratios of warfarin in individual adult male rats, plotted as a function of the total clearance of the drug. Correlation coefficients are:* ○, r = *0.159* (p > *0.6*); *and* ●, r = *0.884* (p < *0.01*). *Kidney to serum concentration ratios were not determined in six animals.*

DISCUSSION

Almost one-half of the total amount of warfarin in the body is located in the liver (7). It is essential, therefore, to consider the binding of warfarin in the liver in the development of physiologically based pharmacokinetic models. The results of this study show that there are pronounced interindividual differences in the free fraction of warfarin in the liver. Interestingly, there is a positive correlation between liver and serum free fraction values. This causes the liver to serum concentration ratios of total (free and bound) warfarin to be relatively constant. Thus, these ratios are more suitable for pharmacokinetic modeling than are binding parameters derived from the free fraction values.

Before attempting a mechanistic explanation of the correlation of free fraction values in the liver and serum, the term "liver binding" should be amplified. Unlike plasma or serum, the liver cannot be viewed as an aqueous solution of proteins (plus various other components). Binding of drugs in the liver may involve some partitioning into lipoid phases and association with structural proteins that are hydrated but can hardly be considered to be in solution. In view of these complexities, the correlation of liver and serum free fraction values is helpful in that it permits some speculation concerning the reason(s) for the pronounced interindividual differences in these values.

These differences with respect to serum are not due to differences in the concentrations of albumin or total protein (7). They may be due to structural differences in the protein or (and this appears more likely) to qualitative and/or quantitative differences in endogenous inhibitors of

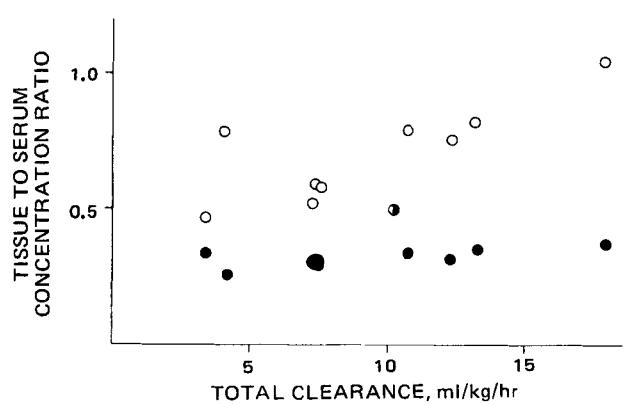

Figure 2—*Liver to serum* (○) *and kidney to serum* (●) *concentration ratios of dicumarol in individual adult male rats, plotted as a function of the total clearance of the drug. Correlation coefficients are:* ○, r = *0.718* (p < *0.02*); *and* ●, r = *0.425* (p > *0.2*).

protein binding. Such inhibitors exist in normal subjects and accumulate in patients with impaired or absent renal function (15, 16). It is not unreasonable to assume that these inhibitors compete with and, therefore, reduce the protein binding of certain drugs in serum as well as in tissues such as the liver. If that is so, a correlation of serum and liver free fraction values for a drug is to be expected.

The results obtained with dicumarol are consistent with those for warfarin: pronounced intersubject differences in liver free fraction values, a positive correlation of these values with the serum free fraction values, and, consequently, relatively little variation of liver to serum concentration ratios. It would be inappropriate to ascribe the lower liver to serum concentration ratios of dicumarol, as compared to those of warfarin, to the more extensive serum protein binding of the former. Obviously, tissue to serum concentration ratios depend on the relative binding of the drug in both phases.

In the case of dicumarol, there exists a pronounced concentration dependence of liver to serum concentration ratios at serum concentrations below about 7 μg/ml (3). At the lowest concentration studied, that ratio was about 5. The decrease in the liver to serum concentration ratio of dicumarol with increasing concentration (in the low serum concentration range) may be due to saturation of certain binding sites in the liver; it could also be a consequence of a cooperative effect of dicumarol binding on serum albumin at concentrations below 10 μg/ml (17, 18). Above that concentration, the serum free fraction of dicumarol remains essentially constant over a wide concentration range (11). Tissue to serum concentration ratios above unity can also occur if there exists an active "uphill" transport process from blood to the liver or within the liver. If that were the case, it would be impossible to calculate liver free fraction values as done here. It is unlikely that there would be a correlation between serum free fraction values and liver free fraction values if the latter were only apparent values, reflecting the kinetic parameters of a specialized transport process (unless, of course, the endogenous inhibitors presumed to be responsible for interindividual differences in free fraction values compete with warfarin and dicumarol for binding sites on serum proteins as well as for sites in the transport process).

The experimental studies required to resolve these frustrating uncertainties are very formidable and technically complex. However, until the resolution of these open questions, so-called physiologically based pharmacokinetic models for protein-bound drugs provide only limited capability for describing and predicting the characteristics of drug distribution processes in the body.

REFERENCES

(1) K. B. Bischoff and R. L. Dedrick, *J. Pharm. Sci.*, **57**, 1346 (1968).

(2) D. Shen and M. Gibaldi, *ibid.*, **63**, 1698 (1974).

(3) E. Jähnchen, L. B. Wingard, Jr., and G. Levy, *J. Pharmacol. Exp. Ther.*, **187**, 176 (1973).

(4) A. Yacobi, C.-M. Lai, and G. Levy, *J. Pharm. Sci.*, **64**, 1995 (1975).

(5) A. Yacobi, J. A. Udall, and G. Levy, *Clin. Pharmacol. Ther.*, **19**, 552 (1976).

(6) H. B. Hucker, S. C. Stauffer, and S. E. White, *J. Pharm. Sci.*, **61**, 1490 (1972).

(7) A. Yacobi and G. Levy, *ibid.*, **64**, 1660 (1975).

(8) A. Yacobi, R. G. Stoll, A. R. DiSanto, and G. Levy, *Res. Commun. Chem. Pathol. Pharmacol.*, **14**, 743 (1976).

(9) K. B. Bischoff, R. L. Dedrick, and D. S. Zaharko, *J. Pharm. Sci.*, **59**, 149 (1970).

(10) K. B. Bischoff, R. L. Dedrick, D. S. Zaharko, and J. A. Longstreth, *ibid.*, **60**, 1128 (1971).

(11) C.-M. Lai and G. Levy, *ibid.*, **66**, 1739 (1977).

(12) C.-M. Lai, A. Yacobi, and G. Levy, *J. Pharmacol. Exp. Ther.*, **199**, 74 (1976).

(13) A. Yacobi, J. A. Udall, and G. Levy, *Clin. Pharmacol. Ther.*, **20**, 300 (1976).

(14) S. Solomon, P. Wise, and A. Ratner, *Proc. Soc. Exp. Biol. Med.*, **153**, 359 (1976).

(15) I. Sjöholm, A. Kober, I. Odar-Cederlöf, and O. Borgå, *Biochem. Pharmacol.*, **25**, 1205 (1976).

(16) G. Levy, T. Baliah, and J. A. Procknal, *Clin. Pharmacol. Ther.*, **20**, 512 (1976).

(17) R. Nagashima, G. Levy, and E. Nelson, *J. Pharm. Sci.*, **57**, 58 (1968).

(18) R. Nagashima, G. Levy, and E. J. Sarcione, *ibid.*, **57**, 1881 (1968).

ACKNOWLEDGMENTS

Supported in part by Grant GM 20852 from the National Institute of General Medical Sciences, National Institutes of Health.

Previous paper in this series: A. Yacobi, C.-M. Lai, and G. Levy, *J. Pharm. Sci.*, **66**, 1741 (1977).

Fenoprofen: Drug Form Selection and Preformulation Stability Studies

CLARENCE A. HIRSCH ˣ, RALPH J. MESSENGER, and JAMES L. BRANNON

Received September 17, 1976, from *Lilly Research Laboratories, Indianapolis, IN 46206.* Accepted for publication May 13, 1977.

Abstract □ Several fenoprofen salts were prepared to obtain the most acceptable form for an oral dosage formulation. Thermal analysis techniques were used to compare stabilities of the water of hydration in different salt forms and to assess the effects of the water of hydration on compatibility with propoxyphene and codeine salts. Photodegradation products of fenoprofen were isolated and identified, and their relevance to product formulation was evaluated.

Keyphrases □ Fenoprofen—various salts synthesized, evaluated as oral dosage forms, stability studies □ Dosage forms, oral—various fenoprofen salts evaluated, stability studies □ Stability—various fenoprofen salts evaluated as oral dosage forms □ Anti-inflammatory agents—fenoprofen, various salts synthesized, evaluated as oral dosage forms, stability studies

Fenoprofen, (±)-α-methyl-3-phenoxybenzeneacetic acid (I), is a nonsteroidal, anti-inflammatory, analgesic, and antipyretic agent[1]. The pharmacology of fenoprofen was described previously (1), and absorption, metabolism, and excretion patterns in humans were reported (2, 3). Fenoprofen is safe and effective in the symptomatic treatment of rheumatoid arthritis (4–6) and is also useful for its analgesic (7) and antipyretic (8) effects.

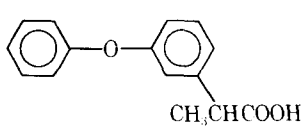

I

[1] Nalfon, fenoprofen calcium, developed by Lilly Research Laboratories.

protein binding. Such inhibitors exist in normal subjects and accumulate in patients with impaired or absent renal function (15, 16). It is not unreasonable to assume that these inhibitors compete with and, therefore, reduce the protein binding of certain drugs in serum as well as in tissues such as the liver. If that is so, a correlation of serum and liver free fraction values for a drug is to be expected.

The results obtained with dicumarol are consistent with those for warfarin: pronounced intersubject differences in liver free fraction values, a positive correlation of these values with the serum free fraction values, and, consequently, relatively little variation of liver to serum concentration ratios. It would be inappropriate to ascribe the lower liver to serum concentration ratios of dicumarol, as compared to those of warfarin, to the more extensive serum protein binding of the former. Obviously, tissue to serum concentration ratios depend on the relative binding of the drug in both phases.

In the case of dicumarol, there exists a pronounced concentration dependence of liver to serum concentration ratios at serum concentrations below about 7 μg/ml (3). At the lowest concentration studied, that ratio was about 5. The decrease in the liver to serum concentration ratio of dicumarol with increasing concentration (in the low serum concentration range) may be due to saturation of certain binding sites in the liver; it could also be a consequence of a cooperative effect of dicumarol binding on serum albumin at concentrations below 10 μg/ml (17, 18). Above that concentration, the serum free fraction of dicumarol remains essentially constant over a wide concentration range (11). Tissue to serum concentration ratios above unity can also occur if there exists an active "uphill" transport process from blood to the liver or within the liver. If that were the case, it would be impossible to calculate liver free fraction values as done here. It is unlikely that there would be a correlation between serum free fraction values and liver free fraction values if the latter were only apparent values, reflecting the kinetic parameters of a specialized transport process (unless, of course, the endogenous inhibitors presumed to be responsible for interindividual differences in free fraction values compete with warfarin and dicumarol for binding sites on serum proteins as well as for sites in the transport process).

The experimental studies required to resolve these frustrating uncertainties are very formidable and technically complex. However, until the resolution of these open questions, so-called physiologically based pharmacokinetic models for protein-bound drugs provide only limited capability for describing and predicting the characteristics of drug distribution processes in the body.

REFERENCES

(1) K. B. Bischoff and R. L. Dedrick, *J. Pharm. Sci.*, **57**, 1346 (1968).

(2) D. Shen and M. Gibaldi, *ibid.*, **63**, 1698 (1974).

(3) E. Jähnchen, L. B. Wingard, Jr., and G. Levy, *J. Pharmacol. Exp. Ther.*, **187**, 176 (1973).

(4) A. Yacobi, C.-M. Lai, and G. Levy, *J. Pharm. Sci.*, **64**, 1995 (1975).

(5) A. Yacobi, J. A. Udall, and G. Levy, *Clin. Pharmacol. Ther.*, **19**, 552 (1976).

(6) H. B. Hucker, S. C. Stauffer, and S. E. White, *J. Pharm. Sci.*, **61**, 1490 (1972).

(7) A. Yacobi and G. Levy, *ibid.*, **64**, 1660 (1975).

(8) A. Yacobi, R. G. Stoll, A. R. DiSanto, and G. Levy, *Res. Commun. Chem. Pathol. Pharmacol.*, **14**, 743 (1976).

(9) K. B. Bischoff, R. L. Dedrick, and D. S. Zaharko, *J. Pharm. Sci.*, **59**, 149 (1970).

(10) K. B. Bischoff, R. L. Dedrick, D. S. Zaharko, and J. A. Longstreth, *ibid.*, **60**, 1128 (1971).

(11) C.-M. Lai and G. Levy, *ibid.*, **66**, 1739 (1977).

(12) C.-M. Lai, A. Yacobi, and G. Levy, *J. Pharmacol. Exp. Ther.*, **199**, 74 (1976).

(13) A. Yacobi, J. A. Udall, and G. Levy, *Clin. Pharmacol. Ther.*, **20**, 300 (1976).

(14) S. Solomon, P. Wise, and A. Ratner, *Proc. Soc. Exp. Biol. Med.*, **153**, 359 (1976).

(15) I. Sjöholm, A. Kober, I. Odar-Cederlöf, and O. Borgå, *Biochem. Pharmacol.*, **25**, 1205 (1976).

(16) G. Levy, T. Baliah, and J. A. Procknal, *Clin. Pharmacol. Ther.*, **20**, 512 (1976).

(17) R. Nagashima, G. Levy, and E. Nelson, *J. Pharm. Sci.*, **57**, 58 (1968).

(18) R. Nagashima, G. Levy, and E. J. Sarcione, *ibid.*, **57**, 1881 (1968).

ACKNOWLEDGMENTS

Supported in part by Grant GM 20852 from the National Institute of General Medical Sciences, National Institutes of Health.

Previous paper in this series: A. Yacobi, C.-M. Lai, and G. Levy, *J. Pharm. Sci.*, **66**, 1741 (1977).

Fenoprofen: Drug Form Selection and Preformulation Stability Studies

CLARENCE A. HIRSCH ˣ, RALPH J. MESSENGER, and JAMES L. BRANNON

Received September 17, 1976, from *Lilly Research Laboratories, Indianapolis, IN 46206.* Accepted for publication May 13, 1977.

Abstract □ Several fenoprofen salts were prepared to obtain the most acceptable form for an oral dosage formulation. Thermal analysis techniques were used to compare stabilities of the water of hydration in different salt forms and to assess the effects of the water of hydration on compatibility with propoxyphene and codeine salts. Photodegradation products of fenoprofen were isolated and identified, and their relevance to product formulation was evaluated.

Keyphrases □ Fenoprofen—various salts synthesized, evaluated as oral dosage forms, stability studies □ Dosage forms, oral—various fenoprofen salts evaluated, stability studies □ Stability—various fenoprofen salts evaluated as oral dosage forms □ Anti-inflammatory agents—fenoprofen, various salts synthesized, evaluated as oral dosage forms, stability studies

Fenoprofen, (±)-α-methyl-3-phenoxybenzeneacetic acid (I), is a nonsteroidal, anti-inflammatory, analgesic, and antipyretic agent[1]. The pharmacology of fenoprofen was described previously (1), and absorption, metabolism, and excretion patterns in humans were reported (2, 3). Fenoprofen is safe and effective in the symptomatic treatment of rheumatoid arthritis (4–6) and is also useful for its analgesic (7) and antipyretic (8) effects.

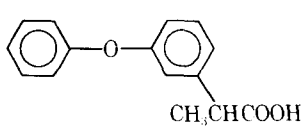

I

[1] Nalfon, fenoprofen calcium, developed by Lilly Research Laboratories.

Table I—Salts of Fenoprofen

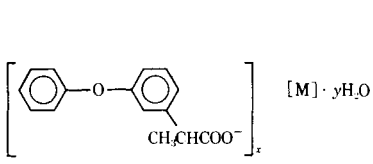

Compound	M	x	y	Physical[a] Form	Water Solubility, mg/ml	Humidity Stability
II	Na^+	1	2	C	>200	Fair
III	Na^+	1	0	A	>200	Very poor
IV	K^+	1	?	C	>200	Very poor
V	Ca^{2+}	2	2	C	2.5	Very good
VI	Ca^{2+}	2	1	A	2.5	Poor
VII	Ca^{2+}	2	0	A	2.5	Poor
VIII	Mg^{2+}	2	0	—	>200	—
IX	$Al(OH)^{2+}$	2	0	A	0.1	Very good
X	$Al(OH)_2^+$	1	0	A	0.1	Very good
XI	NH_4^+	1	0	C	>200	Very poor
XII	$HOCH_2CH_2N^+H(CH_3)_2$	1	0	O	—	—
XIII	$HOCH_2CH_2N^+(CH_3)_3$	1	0	C	>200	Very poor
XIV	$C_6H_5CH_2N^+H_3$	1	0	C	5	Very good
XV		1	0	C	100	Very good
XVI	$H_2NC_6H_5COOCH_2CH_2N^+H(C_2H_5)_2$	1	0	C	6	—
XVII	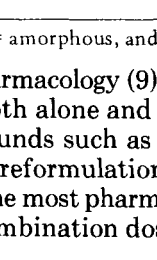	2	0	C	0.1	Very good
XVIII	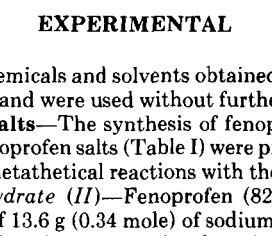	1	0	O	—	—
XIX	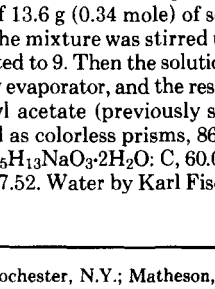	1	0	C	10	—

[a] C = crystalline, A = amorphous, and O = oil. Crystallinity, or lack thereof, was determined by X-ray diffraction patterns.

Preclinical pharmacology (9) indicated the utility of oral dosage forms, both alone and in combination with other analgesic compounds such as propoxyphene or codeine. In this study, a preformulation stability program was designed to select the most pharmaceutically acceptable form for single and combination dosage.

EXPERIMENTAL

Reagents—All chemicals and solvents obtained commercially[2] were reagent (ACS) grade and were used without further purification.

Preparation of Salts—The synthesis of fenoprofen was described by Marshall (10). Fenoprofen salts (Table I) were prepared directly from the free acid or *via* metathetical reactions with the sodium salt.

Sodium Salt Dihydrate (II)—Fenoprofen (82.0 g, 0.34 mole) was added to a solution of 13.6 g (0.34 mole) of sodium hydroxide in 350 ml of deionized water. The mixture was stirred until solution was attained, and the pH was adjusted to 9. Then the solution was evaporated at 10 mm of pressure on a rotary evaporator, and the residue was recrystallized from 200 ml of "wet" ethyl acetate (previously saturated with water). The product was obtained as colorless prisms, 86.6 g, mp 80°.

Anal.—Calc. for $C_{15}H_{13}NaO_3 \cdot 2H_2O$: C, 60.00; H, 5.75; Na, 7.66. Found: C, 59.82; H, 6.12; Na, 7.52. Water by Karl Fischer titration: calc., 12.00%; found, 11.9%.

[2] Eastman Kodak, Rochester, N.Y.; Matheson, Coleman and Bell, Norwood, Ohio.

Anhydrous Sodium Salt (III)—All efforts to prepare crystalline anhydrous fenoprofen sodium failed. Dehydration of the dihydrate under vacuum at 50° gave an amorphous form, which rehydrated at 20% relative humidity (RH) or above.

Anal.—Calc. for $C_{15}H_{13}NaO_3$: C, 68.17; H, 4.95. Found: C, 67.94; H, 5.25.

Potassium Salt (IV)—The procedure used for the sodium salt was followed using potassium hydroxide. Crystallization from ethyl acetate gave colorless needles of the potassium salt, which were, however, very hygroscopic under ambient conditions.

Anal.—Calc. for $C_{15}H_{13}KO_3$: C, 64.25; H, 4.67. Found: C, 63.82; H, 5.08.

Calcium Salt Dihydrate (V)—A solution of 60.0 g (0.2 mole) of fenoprofen sodium dihydrate in 300 ml of deionized water was treated dropwise with a solution of 11.1 g (0.1 mole) of calcium chloride in 100 ml of water. After stirring for 2 hr, the precipitated fenoprofen calcium was filtered off and air dried, 56.0 g, mp 105–110°. Recrystallization from 50% ethanol–water gave colorless needles, 45 g, mp 105–110°.

Anal.—Calc. for $C_{30}H_{26}CaO_6 \cdot 2H_2O$: C, 64.49; H, 5.41. Found: C, 64.41; H, 5.47. Water by Karl Fischer titration: calc., 6.45%; found, 6.43%.

Anhydrous Calcium Salt (VII)—All efforts to obtain a crystalline anhydrous calcium salt failed. Dehydration of the dihydrate under vacuum at 75° gave an amorphous anhydrous material, which rehydrated to the dihydrate at 60% RH or above.

Anal.—Calc. for $C_{30}H_{26}CaO_6$: C, 68.94; H, 5.01. Found: C, 69.10; H, 5.22.

Trituration of the dihydrate with absolute methanol gave what seemed to be fenoprofen calcium monohydrate (VI) (3.2% water by Karl Fischer titration), but the compound was amorphous and rehydrated at ambient conditions to crystalline dihydrate.

Table II—Stability of Fenoprofen Salts to Relative Humidity

Relative Humidity, %[a]	Percent Weight Change							
	II[b]	III	V[c]	VI	VII	IX	XIV	XVII
1	−11.4	−0.5	0.0	—	0.5	0.0	0.0	−0.3
20	+0.3	+10.7	0.0	+0.3	+1.7	—	0.0	−0.3
40	+0.4	+12.5	0.0	+0.2	+2.9	0.0	0.0	−0.2
60	—	—	—	+0.7	+3.7	—	—	—
70	+2.5	+15.8	0.0	—	—	—	0.0	−0.1
80	—	—	—	+3.3	—	—	—	—
93	+9.3	+36.5	0.0	—	+6.3	0.0	0.0	0.0

[a] Controlled humidity chambers were attained by means of saturated solutions of appropriate inorganic salts in closed containers. [b] Theory for dihydrate is 12.0% water. [c] Theory for dihydrate is 6.4% water.

Magnesium Salt (VIII)—The procedure used for fenoprofen calcium was followed with magnesium sulfate instead of calcium chloride. No precipitation occurred, and all efforts to crystallize the magnesium salt failed.

Hydroxyaluminum Salt (IX)—A solution of 16.0 g (0.053 mole) of fenoprofen sodium dihydrate and 2.01 g (0.024 mole) of sodium bicarbonate in 200 ml of deionized water was stirred and treated with a solution of 9.40 g (0.025 mole) of aluminum nitrate nonahydrate in 100 ml of water. Stirring was continued for 1 hr. Then the precipitated product was filtered off, washed with water, and dried at 75° (3 mm of pressure) for 12 hr.

Anal.—Calc. for $C_{30}H_{27}AlO_7$: C, 68.40; H, 5.20. Found: C, 67.90; H, 5.62.

Dihydroxyaluminum Salt (X)—A solution of 8.0 g (0.027 mole) of fenoprofen sodium dihydrate and 4.2 g (0.050 mole) of sodium bicarbonate in 150 ml of deionized water was stirred and treated with a solution of 9.40 g (0.025 mole) of aluminum nitrate nonahydrate in 100 ml of water. The precipitated product was filtered off and dried at 70° (3 mm of pressure) for 12 hr.

Anal.—Calc. for $C_{15}H_{15}AlO_5$: C, 59.60; H, 5.00. Found: C, 59.44; H, 5.07.

Preparation of Amine Salts of Fenoprofen—The preparations of numerous amine salts were attempted. Many gave oils or extremely hygroscopic solids. In general, an equivalent amount of the amine was added to fenoprofen acid dissolved in anhydrous ether. Crystallization of the salt was induced (when necessary) by addition of petroleum ether.

Ammonium Salt (XI)—Needles from ethyl acetate–petroleum ether were extremely hygroscopic.

N,N-*Dimethyl*-N-*(2-hydroxyethyl)ammonium Salt (XII)*—Compound XII was an oil.

Choline Salt (XIII)—Extremely hygroscopic crystals were obtained.

Benzylammonium Salt (XIV)—Colorless needles from ethyl acetate–petroleum ether were obtained, mp 107–108°.

Anal.—Calc. for $C_{22}H_{23}NO_3$: C, 75.62; H, 6.63; N, 4.01. Found: C, 75.33; H, 6.88; N, 3.93.

Morpholine Salt (XV)—Compound XV was obtained as colorless crystals from ethyl acetate–petroleum ether, mp 96–98°.

Anal.—Calc. for $C_{19}H_{23}NO_4$: C, 69.28; H, 7.04; N, 4.25. Found: C, 69.14; H, 6.82; N, 4.25.

Procaine Salt (XVI)—Colorless prisms from ethyl acetate–hexane were prepared, mp 85°.

Anal.—Calc. for $C_{28}H_{34}N_2O_5$: C, 70.27; H, 7.16; N, 5.85. Found: C, 70.07; H, 7.06; N, 6.14.

N,N′-*Dibenzylethylenediamine Salt (XVII)*—Colorless crystals from ethanol were prepared, mp 103°.

Anal.—Calc. for $C_{46}H_{48}N_2O_6$: C, 76.22; H, 6.67; N, 3.87. Found: C, 76.28; H, 6.66; N, 3.91.

d-*Propoxyphene Salt (XVIII)*—This compound was a viscous oil.

Codeine Salt (XIX)—Compound XIX was obtained as light-tan crystals from ethyl acetate, mp 103–105°.

Anal.—Calc. for $C_{33}H_{35}NO_6$: C, 73.13; H, 6.51; N, 2.59. Found: C, 73.01; H, 6.61; N, 2.58.

Solubility Measurements—The UV absorption spectrum of fenoprofen sodium exhibited an absorption maximum at 270 nm. A standard absorbance–concentration curve was determined and used to estimate equilibrium solubilities of the inorganic salts of fenoprofen. The solubilities of amine salts were obtained by comparison with UV absorption curves of standard solutions of the respective salts. Saturated solutions were prepared by vigorous agitation of a mixture of a 2-g sample in 10 ml of deionized water at 25° for 24 hr followed by filtration. No attempt was made to determine solubilities above 200 mg/ml.

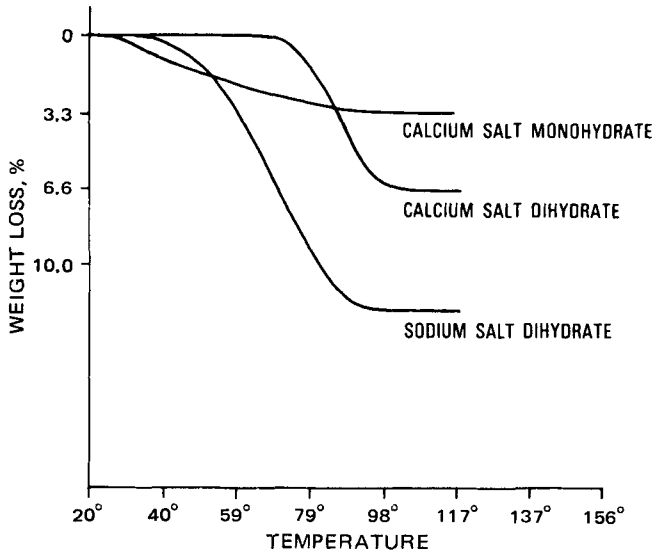

Figure 1—*Hydrate stability of fenoprofen salts by thermal gravimetric analysis.*

Humidity Stability Measurements—Preweighed samples were equilibrated in controlled humidity chambers for 48 hr at 25° and then reweighed to determine the gain or loss of weight. Samples were stored at several relative humidities ranging from 1 to 93% (Table II).

Thermal Gravimetric Analyses (TGA)—*Hydrate Stability*—Thermograms were obtained on a thermogravimetric analyzer under a controlled atmosphere (nitrogen sweep, 40 cm³/min) and a constant heating rate (5°/min)[3]. The temperature at which the weight loss began was taken as a relative measure of hydrate stability (Fig. 1).

Compatibility with Analgesic Amine Salts—Fenoprofen calcium dihydrate was triturated in a mortar with an equal amount of propoxyphene hydrochloride[4], propoxyphene napsylate (2-naphthalenesulfonate)[5], and codeine sulfate in separate experiments. Thermograms were obtained initially and after storage for comparison (Fig. 2).

Differential Thermal Analysis (DTA)—Thermal analysis curves were obtained using a differential scanning calorimeter[6]. Samples for analysis were prepared by trituration of the fenoprofen salt with the appropriate amine salt in a mortar. In one instance, a mixture of fenoprofen calcium dihydrate and propoxyphene hydrochloride was treated with a few drops of water, triturated, and allowed to dry under ambient conditions (Fig. 3). Analyses were carried out under a nitrogen atmosphere with a heating rate of 20°/min and a sensitivity of 5 mcal/sec. Samples were stored at 25° (45–60% RH), 37°(20–30% RH), and 50° (10–20% RH) and analyzed periodically for comparison (Figs. 3–5).

Simultaneous differential thermal and thermal gravimetric analyses[7] were carried out under nitrogen (40 cm³/min) and at a heating rate of 5°/min (Figs. 6 and 7).

Photodegradation—*Low-Pressure Mercury Lamp*[8]—An aqueous solution of fenoprofen sodium (25 mg/ml) was purged with nitrogen and exposed to the mercury lamp in a quartz immersion well with a filter[9]. In this apparatus, the exposed solution surrounds the lamp at an average distance of 5 cm. Samples were taken periodically, and fenoprofen was quantitated by GLC using a 0.61-m (2-ft) column of 3% methylphenyl silicone on Chromosorb G at 195°. The percentage decomposition ($t_{\%}$) with exposure time was: t_{10}, 2 hr; t_{25}, 8 hr; and t_{40}, 40 hr.

Exposed samples were subjected to TLC; spots were developed with benzene–acetic acid (10:1) on silica gel F-254 plates and visualized by short wavelength UV light or iodine vapors. Major components were observed with R_f values of 0.15, 0.21, 0.25, 0.32, and 0.44 (fenoprofen). Minor components had R_f values of 0.54 and 0.62. The minor components were neutral and were removed by extraction, separated by preparative TLC, and identified as *m*-phenoxyacetophenone (R_f 0.54) and *m*-phenoxystyrene (R_f 0.62) by comparison of spectral (IR and mass) characteristics with authentic samples. Two major components were isolated

[3] DuPont model 950.
[4] Darvon, Lilly.
[5] Darvon-N, Lilly.
[6] Perkin-Elmer DSC-2.
[7] Rigaku DT-TGA.
[8] Hanovia lamp (200-w).
[9] Vycor.

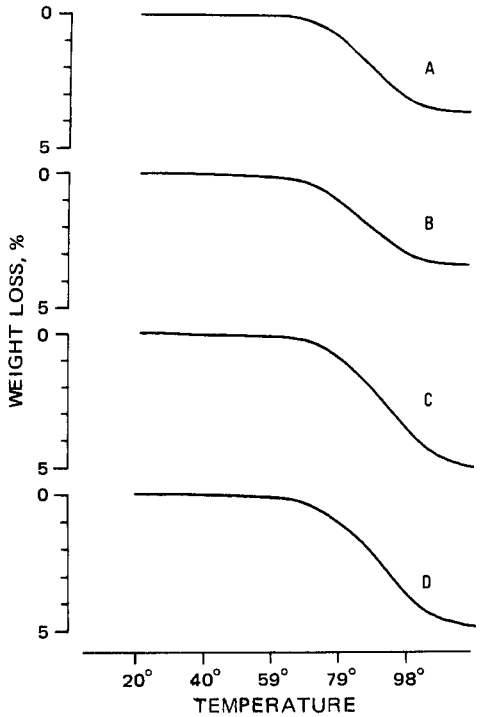

Figure 2—*Thermal gravimetric analysis curves of mixtures of fenoprofen calcium dihydrate with propoxyphene salts. Key: A, 1:1 mixture of fenoprofen calcium dihydrate and propoxyphene hydrochloride; B, sample of A stored 5 years at 25°; C, 1:1 mixture of fenoprofen calcium dihydrate and propoxyphene napsylate monohydrate; and D, sample of C stored 5 years at 25°.*

by column chromatography [silica gel, elution with benzene–acetic acid (10:1)] and analyzed by IR, NMR, and mass spectra. Identification of both components as isomeric hydroxybiphenylpropionic acids is detailed in the *Discussion* section.

Similar degradation occurred when a solution of fenoprofen (25 mg/ml) in isopropyl alcohol was exposed to the mercury lamp.

Carbon-Arc Lamp[10]—Aqueous solutions of fenoprofen sodium (25 mg/ml) were exposed in both Pyrex and quartz containers, and the absence of degradation was revealed by GLC. The percentage decomposition ($t_{\%}$) with time was $t_{0.5} > 96$ hr in either container. Although no quantitative degradation was seen by GLC, trace amounts of *m*-phenoxyacetophenone (R_f 0.54) were detected by TLC. Spectral characteristics (IR and mass spectra) were the same as those of an authentic sample.

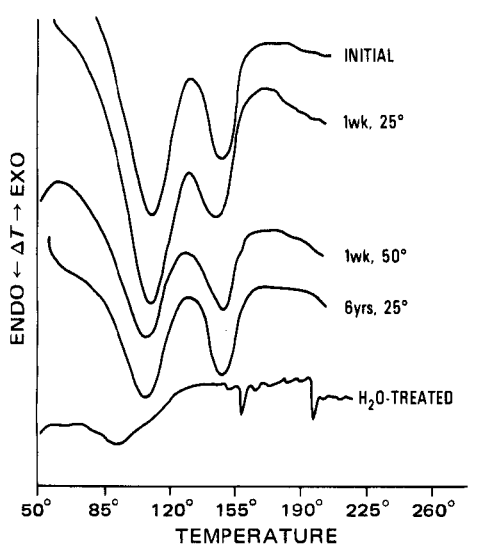

Figure 3—*Differential thermal analysis curves of fenoprofen calcium dihydrate–propoxyphene hydrochloride mixture showing effects of storage and of added water.*

[10] Fadeometer (5000 $\mu w/cm^2$).

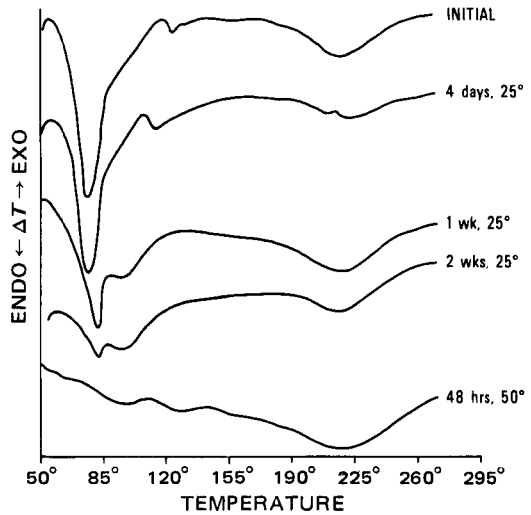

Figure 4—*Differential thermal analysis curves of fenoprofen sodium dihydrate–propoxyphene napsylate monohydrate mixture showing effect of storage.*

Direct Sunlight—A solution of fenoprofen (25 mg/ml) in isopropyl alcohol in a quartz container was exposed to direct sunlight for 1 week. IR analysis and TLC revealed no degradation.

DISCUSSION

Fenoprofen free acid is unacceptable as an oral dosage form because of its low melting point (40°). A relatively high melting compound would avoid frictional heat problems associated with mechanical handling and eutectic melts in combination dosage forms. Therefore, salt forms of fenoprofen were prepared (Table I) and evaluated in terms of their physical characteristics, compatibility with propoxyphene and codeine salts, and chemical stability. Light stability and oxidation were specifically noted.

In many instances, fenoprofen salts could not be induced to crystallize. The sodium salt (II) was obtained as a crystalline dihydrate, but the anhydrous form (III) was amorphous. The potassium salt (IV) was crystalline but very hygroscopic. The calcium salt was crystalline as the dihydrate (V), whereas both the monohydrate (VI) and the anhydrous form (VII) were amorphous. Efforts to crystallize sodium and calcium derivatives from anhydrous solvents failed; crystallization occurred only when sufficient water was present to form dihydrates. The magnesium compound (VIII) could not be crystallized, and both aluminum deriva-

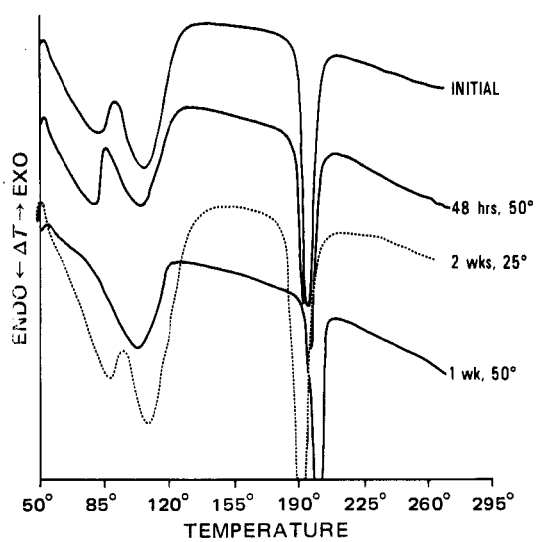

Figure 5—*Differential thermal analysis curves of fenoprofen calcium dihydrate–codeine sulfate pentahydrate mixture showing effect of storage.*

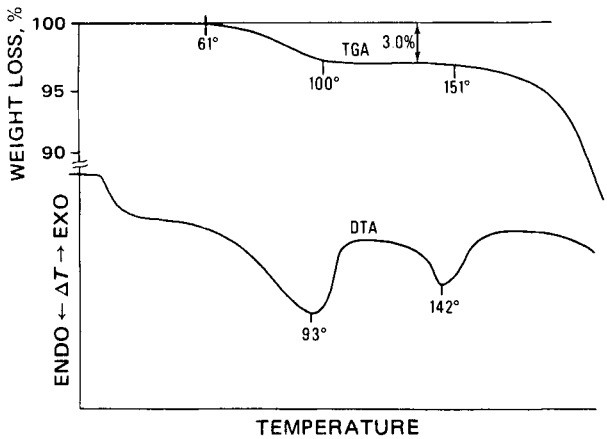

Figure 6—*Simultaneous differential thermal and gravimetric analyses of fenoprofen calcium dihydrate–propoxyphene hydrochloride mixture.*

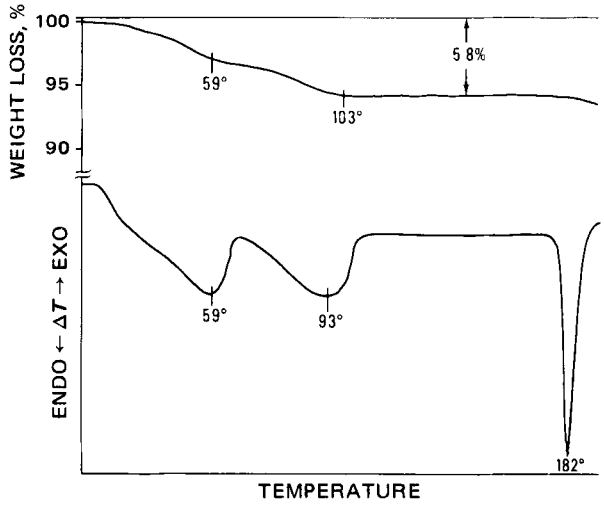

Figure 7—*Simultaneous differential thermal and gravimetric analyses of fenoprofen calcium dihydrate–codeine sulfate pentahydrate mixture.*

tives (IX and X) were amorphous and insoluble in water. Although initially considered too insoluble for capsule or tablet formulation, the aluminum salts were later found useful for oral suspension formulation (11).

A number of amine salts were prepared (Table I), but no advantages over sodium and calcium compounds were found. Organic amine salts were, therefore, excluded from further consideration because of the extensive toxicology studies and production costs involved. Preliminary data indicated the sodium salt dihydrate (II) and calcium salt dihydrate (V) to have the most suitable physical characteristics, *i.e.*, crystallinity and appreciable water solubility.

In evaluating drug form candidates for solid dosage formulations, the possible effects of changes in relative humidity upon physical stability must be considered. Table II demonstrates the sensitivities of several fenoprofen salts to changes in relative humidity. The sodium salt dihydrate lost both moles of water at 25° and 1% RH, but the calcium salt dihydrate was stable under these conditions. The anhydrous, amorphous sodium salt absorbed excessive amounts of water at high relative humidity, whereas both amorphous forms of fenoprofen calcium absorbed only enough water to form the crystalline dihydrate. Compounds IX, XIV, and XVII were stable over the humidity range studied but were not considered further for reasons already discussed.

Thermal gravimetric analysis was used to compare relative stabilities of the water of hydration. Samples were heated at a controlled rate in a defined atmosphere, and the percent weight losses were recorded as a function of temperature. The temperature at which weight loss began was taken as a measure of hydrate stability. Thermograms in Fig. 1 show that crystalline sodium salt dihydrate lost water at or near room temperature, but crystalline calcium salt dihydrate was stable to 70°. Amorphous calcium salt monohydrate, however, lost water at room temperature. These results indicated that the water of hydration was more tightly bound in calcium salt crystals than in sodium salt crystals. The integrity of the crystal structure of calcium salt dihydrate allows greater flexibility in formulation considerations.

Preclinical pharmacology indicated the potential utility of an oral dosage form combining fenoprofen with analgesic amines such as propoxyphene or codeine. Furthermore, it was desirable to mix the drugs in the formulation. Attempts to formulate fenoprofen sodium dihydrate with either propoxyphene salts (hydrochloride or napsylate) or codeine salts (sulfate or phosphate) failed. These combinations were chemically and physically incompatible. Intimate mixing caused eutectic melts and/or acid–base reactions in all instances.

In contrast, mixtures of fenoprofen calcium dihydrate with propoxyphene salts remained free-flowing powders indefinitely. Mixtures with codeine salts were also compatible. Although its relatively low water solubility contributed to this compatibility, the stability of the bound water of hydration of the calcium salt compared to that of the sodium salt was more significant. The integrity of crystalline structure of fenoprofen calcium dihydrate in the presence of propoxyphene or codeine salts is shown by both thermal gravimetric analysis and differential thermal analysis. Thermograms in Fig. 2 show that the crystallinity was unchanged after storage of mixtures of fenoprofen calcium dihydrate with either propoxyphene hydrochloride or propoxyphene napsylate. Similarly, mixtures of fenoprofen calcium dihydrate and codeine sulfate pentahydrate showed no change in crystallinity when stored for 8 months at 25°.

Differential thermal analysis is a useful technique for studying drug–drug interactions or drug–excipient interactions (12–14). In this study, differential thermal analysis proved useful in demonstrating the absence of an interaction between fenoprofen calcium dihydrate and propoxyphene salts. In Fig. 3, the endotherm peaking at 109° is due to the loss of crystallinity and volatilization of the water of hydration; the endotherm at 147° suggests a eutectic melt. Any acid–base reaction that could occur is not evident in the thermogram. Interaction did occur in aqueous systems to form a viscous oil at room temperature. The effect on the thermogram of adding excess water to the sample to force interaction is seen in the bottom curve of Fig. 3.

Data shown in Fig. 6 were obtained using an instrument[7] that simultaneously performs thermal gravimetric and differential thermal analyses. The top curve (thermal gravimetric analysis) shows a weight loss corresponding to the first endotherm in the lower curve (differential thermal analysis). The second endotherm is not associated with a weight loss and is consistent with a eutectic melt.

Figure 3 reveals the stability of stored samples by the unchanged characteristic endotherms. By comparison, the incompatibility of fenoprofen sodium dihydrate with propoxyphene hydrochloride was apparent, since mixtures became viscous oils after only a few hours of storage. Although somewhat more compatible with propoxyphene napsylate, fenoprofen sodium did interact over short periods (Fig. 4).

Thermal analyses of mixtures of fenoprofen calcium dihydrate with codeine sulfate pentahydrate indicated compatibility. The endotherm at 80° (Fig. 5) suggests the volatilization of the water of hydration of codeine sulfate pentahydrate; the endotherm at 105° is due to the volatilization of the water of hydration of fenoprofen calcium dihydrate; and the endotherm at 190° is a eutectic melt of the anhydrous components. This result is verified by the simultaneous differential thermal and thermal gravimetric analysis data in Fig. 7. Storage at room temperature did not alter the physical integrity of the mixture. However, thermograms reveal that the water of hydration of codeine sulfate was lost when stored at 50° for 1 week (Fig. 5).

The relative constancy of the eutectic melt of 190° suggests no interaction even when water was lost. Interaction of fenoprofen sodium dihydrate with codeine sulfate pentahydrate was visually apparent after a few hours. A crystalline, anhydrous, nonhygroscopic form of fenoprofen sodium might be compatible with propoxyphene or codeine salts. However, such a form could not be prepared, and the amorphous form is hygroscopic.

Thus, from a pharmaceutical point of view, fenoprofen calcium is clearly superior to fenoprofen sodium. Bioequivalence has been shown (2) by comparable blood levels from either fenoprofen calcium or fenoprofen sodium in similar oral dosage formulations.

Sodium and calcium salts of fenoprofen are basic salts and, therefore, potentially reactive toward acids or acidic salts. Otherwise, fenoprofen has no particularly labile functional groups prone to alteration in typical pharmaceutical formulations. Routine preformulation stability studies

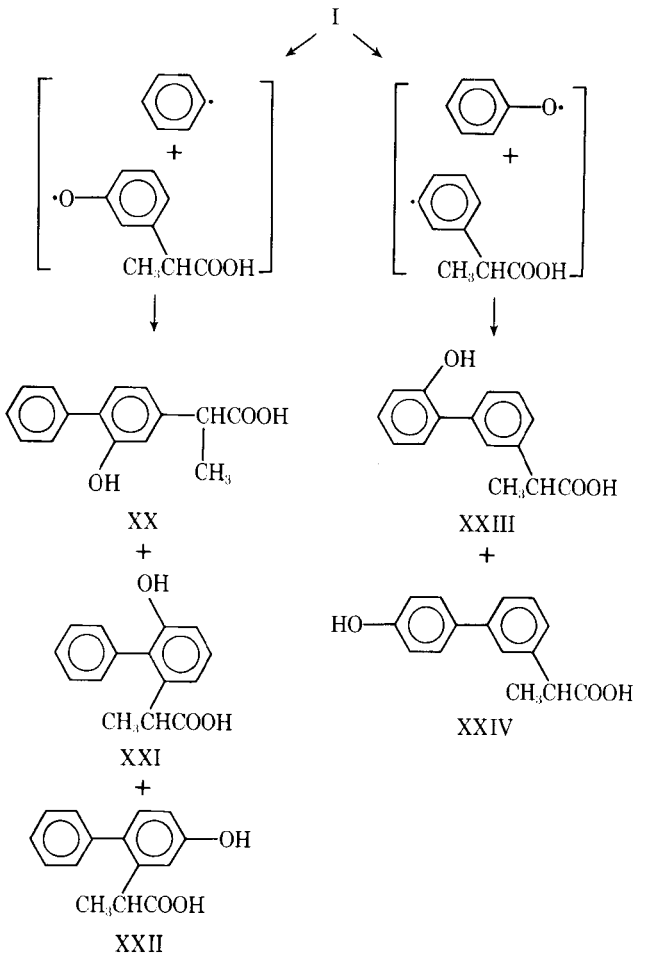

Scheme I

with the sodium and calcium salts revealed no significant degradation in the presence of formulative adjuncts.

However, aqueous solutions of fenoprofen sodium exposed to high-intensity short wavelength UV light[8] degraded slowly, but significantly, to several compounds more polar than fenoprofen, as shown by TLC (R_f values given under *Experimental*). Major degradation products, A (R_f 0.32) and B (R_f 0.21), were isolated by column chromatography and characterized by IR, NMR, and mass spectrometry. Both compounds gave mass spectra virtually identical to the spectrum of fenoprofen, *i.e.*,

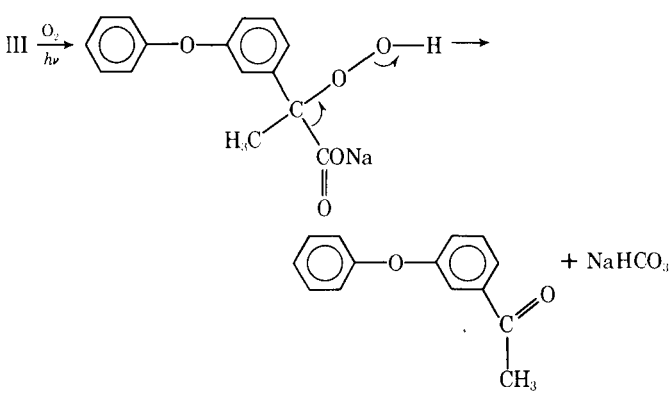

XXV

Scheme II

a molecular ion of *m/e* 242 and the major fragment of *m/e* 197. NMR spectra were similar in proton count and splitting patterns to fenoprofen. However, whereas fenoprofen has one deuterium-exchangeable proton, these compounds both exchanged two protons. Furthermore, IR spectra showed the presence of hydroxyl and carboxyl groups.

The same degradation was observed when isopropyl alcohol solutions of fenoprofen acid were exposed. These data provided strong evidence that fenoprofen had undergone a photochemically induced Claisen rearrangement as shown in Scheme I. Photo-Claisen rearrangements of diphenyl ethers have been studied (15, 16). The products isolated in the present study are two of the five possible isomeric α-methyl(phenyl)-hydroxybenzeneacetic or α-methyl(hydroxyphenyl)benzeneacetic acids (XX–XXIV). Comparison of UV spectra of A and B with *o*- and *p*-phenylphenols indicates that A is either XX or XXIII and that B is either XXII or XXIV[11]. No effort was made to identify the specific isomers by unambiguous synthesis.

To determine the relevance of such degradation to product stability, solutions of fenoprofen were exposed to both a carbon-arc lamp and direct sunlight. Prolonged exposure caused no detectable photo-Claisen rearrangement in either experiment. However, solutions exposed to the carbon-arc lamp formed trace amounts of *m*-phenoxyacetophenone (XXV), which was identified by comparison of spectral characteristics with an authentic sample. Although the mechanism is not certain, this ketone is most likely formed by hydroperoxide formation at the α-carbon followed by decarboxylation (Scheme II). However, GLC assays revealed that this mode of degradation was not quantitatively significant.

Direct sunlight exposure caused no detectable degradation when analyzed using TLC or mass spectrometry. Whereas the photo-Claisen mode of degradation can occur in the absence of oxygen but requires high energy irradiation, formation of the ketone requires oxygen. Neither reaction occurs to an extent that is detrimental to the product.

REFERENCES

(1) R. C. Nickander, R. J. Kraay, and W. S. Marshall, *Fed. Proc.*, **30,** 563 (1971).

(2) A. Rubin, B. E. Rodda, P. Warrick, A. S. Ridolfo, and C. M. Gruber, *J. Pharm. Sci.*, **60,** 1797 (1971).

(3) *Ibid.*, **61,** 739 (1972).

(4) A. S. Ridolfo, W. M. Mikulaschek, C. M. Gruber, Jr., and N. E. Scholz, *Am. J. Med. Sci.*, **265** (5), 375 (1973).

(5) P. M. G. Reynolds and P. J. Whorwell, *Curr. Med. Res. Opin.*, **2,** 461 (1974).

(6) I. F. Anderson, *S. Afr. Med. J.*, **48,** 899 (1974).

(7) A. Sunshine and E. Laska, *Clin. Pharmacol. Ther.*, **12,** 302 (1971).

(8) C. M. Gruber, Jr., *J. Clin. Pharm.*, **215** (Apr. 1974).

(9) J. A. Miller, Jr., and T. A. Bromstrup, *Fed. Proc.*, **30,** 564 (1971).

(10) W. S. Marshall, U.S. pat. 3,600,437 (Aug. 17, 1971).

(11) C. H. Fields and C. A. Hirsch, Belg. pat. 811,810 (Apr. 9, 1974).

(12) J. K. Guillory, S. C. Hwang, and J. L. Lach, *J. Pharm. Sci.*, **58,** 301 (1969).

(13) H. Jacobson and G. Reier, *ibid.*, **58,** 631 (1969).

(14) D. C. Monkhouse and J. L. Leek, *ibid.*, **61,** 1435 (1972).

(15) W. Nudenborg, *Science*, **116,** 309 (1952).

(16) F. L. Bach and J. C. Borclox, "Abstracts of Papers Presented at the 150th Meeting, American Chemical Society, Atlantic City, N.J.," American Chemical Society, Washington, D.C., 1965, p. 95.

ACKNOWLEDGMENTS

The authors thank Mr. Thomas Cole for assistance in obtaining thermal analysis data and Dr. John Becker for useful discussions of thermal analysis techniques. They also thank Dr. Alan Dinner for elucidation of isomeric structures of degradation products *via* UV spectra.

[11] Dr. A. Dinner, Lilly Research Laboratories, Indianapolis, IN 46206, personal communication.

Analysis of the Prodrug 7-Acetylacroninium Perchlorate in Presence of the Parent Compound Acronine

ANNE BAGGER HANSEN *, BO KREILGÅRD *x, CHONG-HENG HUANG ‡§, and A. J. REPTA ‡

Received February 21, 1977, from the **Department of Pharmaceutics, The Royal Danish School of Pharmacy, Universitetsparken 2, DK-2100 Copenhagen Ø, Denmark,* and the ‡*Department of Pharmaceutical Chemistry, School of Pharmacy, University of Kansas, Lawrence, KS 66044.* Accepted for publication April 22, 1977. §Present address: Central Research, Pfizer, Inc., Groton, CT 06340.

Abstract □ Analysis of acronine and the prodrug acetylacroninium perchlorate in parenteral solutions is described. The unstable prodrug reacts quantitatively with the nucleophilic agent aniline by an unusual mechanism to form a phenylimino derivative of acronine. This derivative and acronine itself were determined by a spectrophotometric two-component method.

Keyphrases □ 7-Acetylacroninium perchlorate—two-component spectrophotometric analysis with acronine in parenteral solutions □ Acronine—two-component spectrophotometric analysis with 7-acetylacroninium perchlorate in parenteral solutions □ Spectrophotometry—two-component analysis, acronine and 7-acetylacroninium perchlorate in parenteral solutions □ Prodrugs—7-acetylacroninium perchlorate, two-component spectrophotometric analysis with acronine in parenteral solutions □ Antineoplastic agents—acronine, two-component spectrophotometric analysis with 7-acetylacroninium perchlorate in parenteral solutions

Clinical evaluation of parenteral administration of the water-insoluble cytotoxic agent acronine[1] (I) (1, 2) resulted in the preparation of the prodrug acetylacroninium perchlorate (II) (3). The formulation of a suitable parenteral solution of the prodrug was described previously (4).

Since it has not been possible to prepare samples of acetylacroninium perchlorate free from unreacted acronine perchlorate (3) and since the prodrug is not stable ($t_{1/2} \sim$ 25 min at 25° in water), problems were encountered in analysis of the prodrug. In a previous report, a method was described (4) by which the prodrug was extracted into chloroform, presumably as an ion-pair with gentisate ion, and the absorptivity was measured at 520 nm. The molar absorptivity of this ion-pair was estimated by an indirect method (4).

This report deals with a direct measurement of the ester and parent compound by utilizing the ester's high reactivity with the nucleophile aniline. The reaction product (III), which is essentially the Schiff base of acronine and aniline, and acronine itself were determined by two-component visible spectrophotometry. The method is compared with the previously published methods.

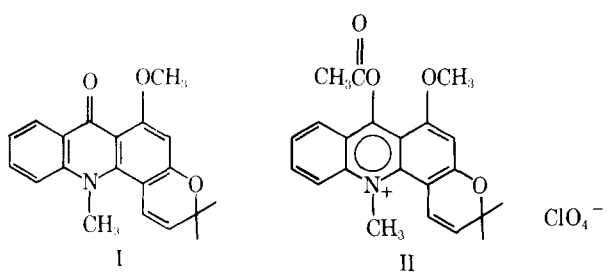

I II

[1] NSC 403169; referred to as acronycine in previous publications.

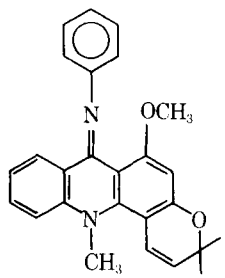

III

EXPERIMENTAL

Materials—Acronine was used as obtained[2]. The purity of the sample was examined by a phase solubility analysis procedure similar to the general method described by Mader (5). The solvent was methanol–water (3:1), and the sample was equilibrated for 44 hr at 25.0 ± 0.1° and protected from light.

Calculations based on the solubility diagram (5) showed a content of 100.5% acronine in the sample, indicating no significant amounts of impurities. This result was in agreement with the fact that TLC experiments revealed no secondary spots (<0.5%) with detection by iodine vapor or UV light at 254 nm. Acetylacroninium perchlorate was prepared as described by Bourne *et al.* (3).

The chloroform was purified by distillation. Aniline was purified by distillation *in vacuo* and stored under nitrogen in a refrigerator. All other chemicals were reagent grade and were used without further purification. The TLC plates were 0.25-mm silica gel 60 F_{254} precoated plates[3]. The mobile phase in TLC was ethyl acetate–cyclohexane–25% ammonia (40:10:1). Silica gel[4], 0.05–0.2 mm, was used for column chromatography.

Synthesis and Characterization of III—Preliminary experiments showed that the same reaction between the prodrug and aniline took place (*i.e.*, the same reaction product was formed and to the same extent) in aqueous solution and in organic solvents. Compound III was prepared by dissolving 680 mg of II in 50 ml of chloroform and then adding 1.0 ml of aniline. The reaction was complete within a few seconds, and the chloroform solution was extracted with 50 ml of 1 *N* HCl to remove excess aniline quantitatively.

Conversion of the salt of III into the corresponding base, which is more readily chromatographed, was accomplished by shaking the chloroform solution with 50 ml of 2 *M* ammonia. Residual water in the organic layer was removed by filtration through anhydrous sodium sulfate, and the chloroform was removed under reduced pressure at 30°. The residue was crystallized from water–methanol to yield a yellow product (580 mg), a mixture of I and III.

Isolation of III was by column chromatography on 80 g of silica gel. The column (2 cm i.d.) was eluted by cyclohexane–ethyl acetate–25% ammonia (50:50:1), the fractions containing III were collected, and the organic solvent was removed under reduced pressure. The product thus obtained was recrystallized twice from hot methanol and dried *in vacuo* at 40° for 18 hr (yield of 410 mg).

The suggested structure of the compound, mp 219–220° (uncorrected), obtained from the reaction between II and aniline is shown as III. The elemental analysis[5] for carbon, hydrogen, and nitrogen of III (mol.

[2] National Cancer Institute, Bethesda, Md.
[3] Merck No. 5715.
[4] Merck No. 7734.
[5] Performed by Microchemical Laboratory, University of Copenhagen.

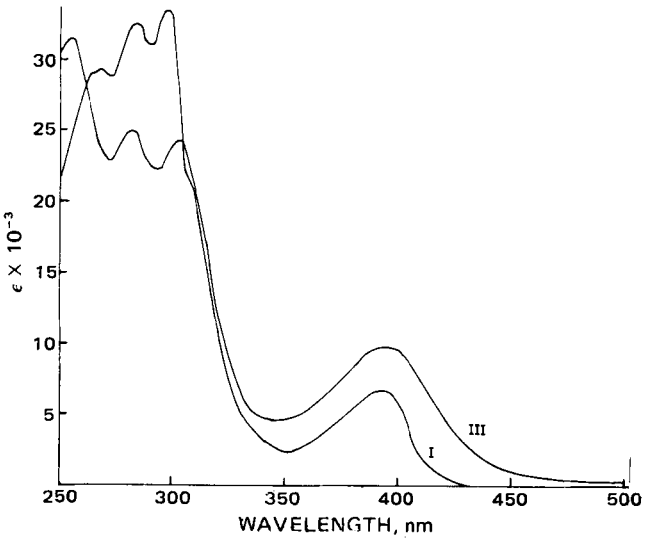

Figure 1—*Absorption spectra in chloroform of I and the product (III) formed by reaction between II and aniline.*

wt. 396.5) was ±0.3% of the calculated figures. The NMR spectrum of III was similar to that of I (3) with the exception of five aromatic protons at δ 6.8–7.4 ppm (multiplet). The mass spectrum supports the structure of III with a parent ion of *m/e* 396 (27%) and a base peak of *m/e* 395 ($M^+ - 1$).

The acid dissociation constant, pKa, for protonated III was determined at 25° and an ionic strength of 0.05 by the spectrophotometric method described by Albert and Sergeant (6). Due to the very low solubility of III in water, 10% methanol was added to the buffer solutions. The analytical wavelength was 292 nm, and 1.00-cm cells were used. The pKa, 8.7, is of an order of magnitude expected for compounds with a protonated imino nitrogen (7).

Preparation of Samples for Analysis—A solution of sodium gentisate (0.8 *M*, pH 6) was prepared by mixing the necessary quantity of gentisic acid, 10% sodium hydroxide, and water (4). To 400 ml of the gentisate solution was added 950 mg of II. The sample was placed in an ultrasonic bath for 10 min, removed, and vigorously agitated for an additional 10 min. The resulting clear solution was frozen in sealed ampuls and stored at −40° in an air thermostat. The samples were kept for 0.5–3 hr at room temperature prior to analysis.

Two samples (c and d) were prepared by extracting most of I from the sample described above with ether, removing the ether under reduced pressure, and shaking the sample thus obtained with excess of solid II (containing I as an impurity). These mixtures were finally filtered to obtain a clear solution.

Analytical Procedure—*Method A: Aniline Reaction, Two-Component Spectrophotometry*—A solution containing an aliquot (2.00 ml) of the test solution, water (7.00 ml), and aniline (0.1 ml) was extracted with three 7.0-ml portions of chloroform. The combined chloroform extracts were shaken with 1 *N* HCl (15.0 ml) to remove excess aniline. Removal of aniline was necessary to avoid the possible interference of colored products formed by oxidation of aniline.

Finally, the chloroform extracts were shaken with borate buffer, pH 10.5 (20 ml), filtered through anhydrous sodium sulfate, and diluted with chloroform to 25 ml. The absorbance of the solution was measured at 440 nm and, after a fivefold dilution, at 393 nm. Calculations of the content of I and III were done according to general equations for two-component systems (8).

Method B: Spectrophotometry of 7-Acetylacroninium Ion (II)—The intact prodrug was analyzed as previously described (4) with the following minor modification. It was found that the decrease of A_{520} in chloroform solutions of the prodrug ion proceeded with a variable rate and that this decrease followed pseudo-zero-order kinetics. Therefore, the value of A_{520} for the chloroform extract was read at ~10-min intervals for ~40 min after the first reading and extrapolated to the time of initiation of the extraction. Since it was not possible to prepare a pure sample of II and since II is extremely unstable in aqueous and nonaqueous solvents, it was not possible to determine the accuracy or precision of the method.

Method C: Spectrophotometry of Total Acronine (I)—The total content of free and esterified acronine was analyzed after complete hydrolysis of the prodrug as described previously (4). The blank solution was prepared from a 0.8 *M* solution of sodium gentisate treated as the test solution. The relative standard deviation of the method was 0.9% ($n = 10$).

Table I—Analytical Results for II (Calculated as I) and I in Various Parenteral Solutions[a]

Sample	Compound	Method A	Method B	Method C
a	II	77.2	69.2	—
	I	25.1	—	—
	I + II	102.3	—	100 (1.67)
b	II	67.7	64.8	—
	I	35.9	—	—
	I + II	103.6	—	100 (1.67)
c	II	52.2	49.0	—
	I	44.3	—	—
	I + II	96.5	—	100 (2.52)
d	II	39.5	39.8	—
	I	53.8	—	—
	I + II	93.3	—	100 (2.53)
e	II	72.8	69.6	—
	I	29.9	—	—
	I + II	102.7	—	100 (1.66)
f	II	58.8	58.1	—
	I	41.9	—	—
	I + II	100.7	—	100 (1.68)
g	II	73.3	71.9	—
	I	27.9	—	—
	I + II	101.2	—	100 (1.67)
h	II	61.8	58.5	—
	I	37.6	—	—
	I + II	99.4	—	100 (1.64)

[a] The values stated are expressed in percentage of the total concentration of free and esterified I determined by Method C and are the mean of a duplicate analysis. The values in parentheses are the actual values of I plus II in milligrams of I per milliliter determined using Method C.

RESULTS

***In Situ* TLC Qualitative Studies on Aniline Reaction**—Qualitative studies on the reaction between II and aniline were performed using *in situ* reflectance measurements of TLC plates as described elsewhere (9). With the described TLC system, acetanilide, a possible reaction product between aniline and 7-acetylacroninium perchlorate (II), was well separated from I and III. Experiments using 242 nm (reflectance minimum of acetanilide) as the analytical wavelength showed that acetanilide was not formed (detection limit ~1% of II) in a sample of II to which excess aniline was added. The only reaction product detected was III (range of analytical wavelength was from 220 to 400 nm with 10-nm increments). Furthermore, aniline did not react with I.

Two-Component Spectrophotometry—The absorption spectra of I and III are shown in Figure 1. The wavelengths for analysis were 393 nm, where both I and III showed maximum absorbance, and 440 nm, where the absorbance of I was small compared to that of III. The molar absorptivities determined from Beer law-type plots were $\epsilon_{393} = 6700\ M^{-1}\ cm^{-1}$ [this value was previously reported to be $6950\ M^{-1}\ cm^{-1}$ (4)] and $\epsilon_{440} \sim 15\ M^{-1}\ cm^{-1}$ for I and $\epsilon_{393} = 9910\ M^{-1}\ cm^{-1}$ and $\epsilon_{440} = 1710\ M^{-1}\ cm^{-1}$ for III.

To examine the precision of the method, nine determinations were made on a test solution containing approximately 1.5 mg of 7-acetylacroninium perchlorate and 0.5 mg of acronine/ml. The relative standard deviations were 1.0 and 4.3%, respectively.

Comparison of Three Methods—Table I shows the results of analysis, using the described methods, of eight samples containing unknown amounts of I and II (see *Experimental*).

DISCUSSION

A possible reaction between aniline and the acetyl ester (II) might be expected to be the aminolysis of II with the formation of acetanilide (10). However, acetanilide was not formed, and III was the only reaction product found. The mechanism for the formation of III from aniline and II appears to involve direct and rapid attack of the nucleophile at the 7-carbon and displacement of the acyl group. This mechanism may be rationalized on the basis of the electrodeficient character of the nitrogen and the resonance between the quaternary nitrogen and the carbon in the 7-position. This carbon is electropositive, and a nucleophilic attack at C-7 is possible. This is in agreement with the fact that aryl oxygen

cleavage was shown (11) to be a significant reaction in the hydrolysis of II in water.

Samples were analyzed using the three methods described (Table I). The total of I plus II calculated as I determined using Method A agrees with the total content of I determined after complete hydrolysis. This fact, together with the observation that III is the only reaction product formed from II and aniline, strongly indicates that Method A provides an accurate measurement of I and II. With the exception of Sample a, only small deviations can be observed between the content of II determined by Methods A and B. This result may indicate that the value of $\epsilon_{520} = 6200$ M^{-1} cm^{-1} for II (4) is not correct and that using a value of $\epsilon_{520} = 6020$ M^{-1} cm^{-1} leads to improved agreement between the results of Methods A and B.

The methods described are intended to be applied to II and I in a 0.8 *M* solution of sodium gentisate (4). The present work shows that the reaction between II and aniline is applicable for the determination of a mixture of I and II in parenteral solutions and that spectrophotometric analysis of the reaction mixture appears to be a simple and reliable method of analysis.

REFERENCES

(1) G. H. Svoboda, G. A. Poore, P. J. Simpson, and G. B. Boder, *J. Pharm. Sci.*, **55**, 758 (1966).

(2) G. H. Svoboda, M. J. Sweeney, and W. D. Walkling, *ibid.*, **60**, 333 (1971).

(3) D. W. A. Bourne, T. Higuchi, and A. J. Repta, *ibid.*, **66**, 628 (1977).

(4) C.-H. Huang, B. Kreilgård, and A. J. Repta, *Bull. Parenteral Drug Assoc.*, **30**, 1 (1976).

(5) W. J. Mader, *CRC Crit. Rev. Anal. Chem.*, **1**, 193 (1970).

(6) A. Albert and E. P. Sergeant, "Ionization Constants of Acids and Bases," Methuen, London, England, 1962.

(7) A. C. Capomacchia, J. Casper, and S. G. Schulman, *J. Pharm. Sci.*, **63**, 1272 (1974).

(8) H. H. Willard, L. L. Merritt, Jr., and J. A. Dean, "Instrumental Methods of Analysis," 5th ed., Van Nostrand, New York, N.Y., 1974, p. 92.

(9) A. B. Hansen and S. S. Larsen, *Dan. Tidsskr. Farm.*, **46**, 105 (1972).

(10) K. A. Conners, "Reaction Mechanisms in Organic Analytical Chemistry," Wiley, New York, N.Y., 1973, p. 516 ff.

(11) A. J. Repta, J. R. Dimmock, B. Kreilgård, and J. J. Kaminski, *J. Pharm. Sci.*, **66**, 1501 (1977).

ACKNOWLEDGMENTS

Supported in part by Contract N01-CM-23217 from the Division of Cancer Treatment, National Cancer Institute, National Institutes of Health, and from the Danish Medical Research Council.

Comparison of Solid and Solution Conformations of Hydroxyurea and 3-Ethyl-1-hydroxyurea Utilizing IR–X-Ray Method

GEORGE R. PARKER *[x] **and JAMES D. KORP** [‡]

Received February 10, 1977, from the *Department of Medicinal Chemistry, College of Pharmacy, and the Department of Chemistry, Crystallography Laboratory, University of Houston, Houston, TX 77004.* Accepted for publication May 12, 1977.

*Present address: College of Pharmacy, University of Oklahoma, Oklahoma City, OK 73190. [‡]Present address: Department of Chemistry, Crystallography Laboratory, Baylor University, Waco, Tex.

Abstract □ The IR–X-ray method for determining solution conformation was used to compare the conformations of the antitumor agents hydroxyurea and its 3-ethyl analog in solutions with conformations in the solid state. X-ray crystal analysis data for hydroxyurea obtained from the literature and the 3-ethyl analog data determined experimentally indicated that similar conformations are present in both compounds, with a carbonyl bond of mostly double bond character and intermolecular hydrogen bonding. The ethyl analog also possessed inter- and intramolecular hydrogen bonding involving the 1- and 3-hydrogens and the carbonyl and hydroxyl oxygens. Comparison of IR spectra (1780–1550 cm^{-1}) of the solid state (mineral oil mulls) with solution spectra (taken in dry octanol, in octanol equilibrated with water and dried, and in wet and dry acetonitrile) indicated that only in dry acetonitrile did the spectrum of hydroxyurea resemble that of the solid. The ethyl analog possessed absorptions similar to the solid only in dry octanol, while spectra of all other solutions for both compounds had strong C=N character and diminished C=O double bond character. The IR solution data were rationalized according to the conformational system of hydroxyureas, which is represented by canonical forms possessing a C=O bond or strong C=N bonds and a CO bond. Hydroxyurea appears to prefer hydrogen bonding to a solvent (water) to bonding with itself, while the ethyl analog possesses internal hydrogen bonding which changes the conformational preferences and conformational equilibrium. In solvents where this inter- or intramolecular hydrogen bonding competes with bonding with the solvent, interconversion of conformers takes place; but this interconversion cannot occur when strong hydrogen bonding (with solvate formation) exists with water. Hydroxyurea tends to exhibit this behavior only when hydrogen bonding to solvent or water is not possible, allowing interconversion through a form possessing a C=O bond. Hydroxyurea and its 3-ethyl analog thus have different solution conformational equilibria depending on the solvent.

Keyphrases □ Hydroxyurea and 3-ethyl analog—comparison of solid and solution conformations □ Conformations—solid and solution compared, hydroxyurea and 3-ethyl analog □ Antineoplastic agents—hydroxyurea and 3-ethyl analog, comparison of solid and solution conformations

The structure or conformation of drugs in solution is a significant property to scientists studying the molecular dynamics involved in absorption, *in vivo* transport, site of action, and enzymatic biotransformations of biologically active compounds (1). Knowledge concerning the actual or potential structure or conformation of drug molecules becomes even more relevant to the molecular pharmacologist or medicinal chemist if a particular structure or conformation is essential for a biological process and that particular molecular species is one of many possible species that may be present *in vivo*.

While the structure of molecules in the solid state can be ascertained with a high degree of accuracy *via* X-ray crystallography, the structure and conformation of molecules in simple solutions are continually being studied and are topics of rigorous debate (2). Various methods have

cleavage was shown (11) to be a significant reaction in the hydrolysis of II in water.

Samples were analyzed using the three methods described (Table I). The total of I plus II calculated as I determined using Method A agrees with the total content of I determined after complete hydrolysis. This fact, together with the observation that III is the only reaction product formed from II and aniline, strongly indicates that Method A provides an accurate measurement of I and II. With the exception of Sample a, only small deviations can be observed between the content of II determined by Methods A and B. This result may indicate that the value of $\epsilon_{520} = 6200$ M^{-1} cm^{-1} for II (4) is not correct and that using a value of $\epsilon_{520} = 6020$ M^{-1} cm^{-1} leads to improved agreement between the results of Methods A and B.

The methods described are intended to be applied to II and I in a 0.8 *M* solution of sodium gentisate (4). The present work shows that the reaction between II and aniline is applicable for the determination of a mixture of I and II in parenteral solutions and that spectrophotometric analysis of the reaction mixture appears to be a simple and reliable method of analysis.

REFERENCES

(1) G. H. Svoboda, G. A. Poore, P. J. Simpson, and G. B. Boder, *J. Pharm. Sci.*, **55**, 758 (1966).

(2) G. H. Svoboda, M. J. Sweeney, and W. D. Walkling, *ibid.*, **60**, 333 (1971).

(3) D. W. A. Bourne, T. Higuchi, and A. J. Repta, *ibid.*, **66**, 628 (1977).

(4) C.-H. Huang, B. Kreilgård, and A. J. Repta, *Bull. Parenteral Drug Assoc.*, **30**, 1 (1976).

(5) W. J. Mader, *CRC Crit. Rev. Anal. Chem.*, **1**, 193 (1970).

(6) A. Albert and E. P. Sergeant, "Ionization Constants of Acids and Bases," Methuen, London, England, 1962.

(7) A. C. Capomacchia, J. Casper, and S. G. Schulman, *J. Pharm. Sci.*, **63**, 1272 (1974).

(8) H. H. Willard, L. L. Merritt, Jr., and J. A. Dean, "Instrumental Methods of Analysis," 5th ed., Van Nostrand, New York, N.Y., 1974, p. 92.

(9) A. B. Hansen and S. S. Larsen, *Dan. Tidsskr. Farm.*, **46**, 105 (1972).

(10) K. A. Conners, "Reaction Mechanisms in Organic Analytical Chemistry," Wiley, New York, N.Y., 1973, p. 516 ff.

(11) A. J. Repta, J. R. Dimmock, B. Kreilgård, and J. J. Kaminski, *J. Pharm. Sci.*, **66**, 1501 (1977).

ACKNOWLEDGMENTS

Supported in part by Contract N01-CM-23217 from the Division of Cancer Treatment, National Cancer Institute, National Institutes of Health, and from the Danish Medical Research Council.

Comparison of Solid and Solution Conformations of Hydroxyurea and 3-Ethyl-1-hydroxyurea Utilizing IR–X-Ray Method

GEORGE R. PARKER *[x] **and JAMES D. KORP** [‡]

Received February 10, 1977, from the *Department of Medicinal Chemistry, College of Pharmacy, and the Department of Chemistry, Crystallography Laboratory, University of Houston, Houston, TX 77004.* Accepted for publication May 12, 1977.

*Present address: College of Pharmacy, University of Oklahoma, Oklahoma City, OK 73190. [‡]Present address: Department of Chemistry, Crystallography Laboratory, Baylor University, Waco, Tex.

Abstract □ The IR–X-ray method for determining solution conformation was used to compare the conformations of the antitumor agents hydroxyurea and its 3-ethyl analog in solutions with conformations in the solid state. X-ray crystal analysis data for hydroxyurea obtained from the literature and the 3-ethyl analog data determined experimentally indicated that similar conformations are present in both compounds, with a carbonyl bond of mostly double bond character and intermolecular hydrogen bonding. The ethyl analog also possessed inter- and intramolecular hydrogen bonding involving the 1- and 3-hydrogens and the carbonyl and hydroxyl oxygens. Comparison of IR spectra (1780–1550 cm^{-1}) of the solid state (mineral oil mulls) with solution spectra (taken in dry octanol, in octanol equilibrated with water and dried, and in wet and dry acetonitrile) indicated that only in dry acetonitrile did the spectrum of hydroxyurea resemble that of the solid. The ethyl analog possessed absorptions similar to the solid only in dry octanol, while spectra of all other solutions for both compounds had strong C=N character and diminished C=O double bond character. The IR solution data were rationalized according to the conformational system of hydroxyureas, which is represented by canonical forms possessing a C=O bond or strong C=N bonds and a CO bond. Hydroxyurea appears to prefer hydrogen bonding to a solvent (water) to bonding with itself, while the ethyl analog possesses internal hydrogen bonding which changes the conformational preferences and conformational equilibrium. In solvents where this inter- or intramolecular hydrogen bonding competes with bonding with the solvent, interconversion of conformers takes place; but this interconversion cannot occur when strong hydrogen bonding (with solvate formation) exists with water. Hydroxyurea tends to exhibit this behavior only when hydrogen bonding to solvent or water is not possible, allowing interconversion through a form possessing a C=O bond. Hydroxyurea and its 3-ethyl analog thus have different solution conformational equilibria depending on the solvent.

Keyphrases □ Hydroxyurea and 3-ethyl analog—comparison of solid and solution conformations □ Conformations—solid and solution compared, hydroxyurea and 3-ethyl analog □ Antineoplastic agents—hydroxyurea and 3-ethyl analog, comparison of solid and solution conformations

The structure or conformation of drugs in solution is a significant property to scientists studying the molecular dynamics involved in absorption, *in vivo* transport, site of action, and enzymatic biotransformations of biologically active compounds (1). Knowledge concerning the actual or potential structure or conformation of drug molecules becomes even more relevant to the molecular pharmacologist or medicinal chemist if a particular structure or conformation is essential for a biological process and that particular molecular species is one of many possible species that may be present *in vivo*.

While the structure of molecules in the solid state can be ascertained with a high degree of accuracy *via* X-ray crystallography, the structure and conformation of molecules in simple solutions are continually being studied and are topics of rigorous debate (2). Various methods have

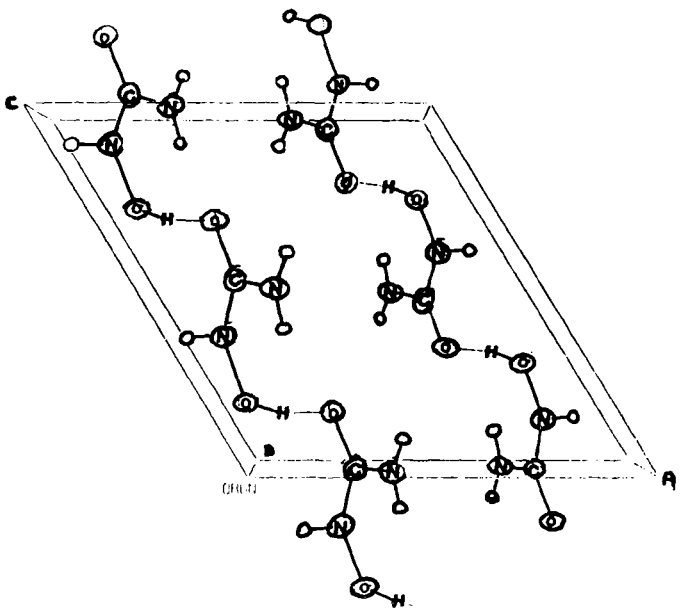

Figure 1—*X-ray crystal structure of hydroxyurea showing hydrogen bonding between hydroxyl of one molecule and carbonyl oxygen of another.*

been utilized to correlate known structure in the solid state (from X-ray crystal data) to structure and conformation in solution *via* the combination of instrumental methods of analysis such as X-ray crystallography with NMR spectroscopy (3), dipole moments (4), and circular dichroism (5).

This paper reports: (*a*) the correlation of solid and solution conformations in the hydroxyurea series of antitumor agents (hydroxyurea and 3-ethyl-1-hydroxyurea) utilizing the literature and experimentally determined X-ray crystal structures in combination with the IR spectra of solids and solutions according to the method of Byrn *et al.* (6), and (*b*) assumptions concerning the structure and conformations of these compounds in solution. The hydroxyurea class was studied since it exhibits

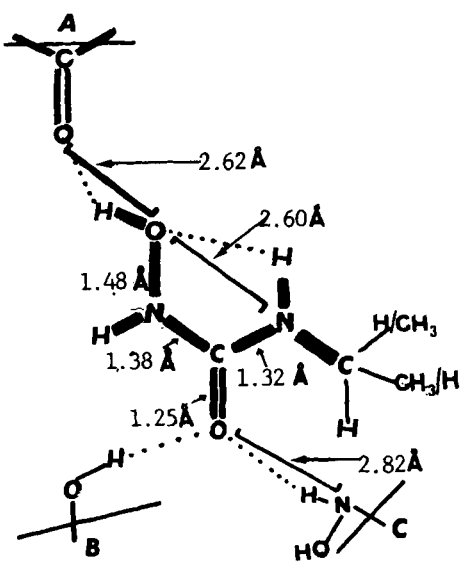

Figure 2—*X-ray crystal structure of 3-ethyl-1-hydroxyurea showing bond distances and inter- and intramolecular hydrogen bonds [estimated standard deviation = ±0.04 Å]. Thermodynamic disorder was observed in the terminal methyl group.*

Table I—IR Absorptions in Carbonyl–Nitrogen Region of Hydroxyurea and 3-Ethyl-1-hydroxyurea in the Solid State (Mineral Oil Mulls) and in Various Solution Conditions

Sample Obtained in	Absorptions in Carbonyl Nitrogen Absorption Region (1780–1550 cm^{-1}), cm^{-1}	
	Hydroxyurea	3-Ethyl-1-hydroxyurea
Mull	1625, 1570	1635, 1580–1560
Octanol (dry)	1655	1680, 1560
Octanol (after water equilibration and drying)	1650	1640
Acetonitrile (wet)	1690	1680
Acetonitrile (dry)	1740, 1640	1680

a solvent conformational dependency which may influence the biological action (7, 8).

EXPERIMENTAL

Compounds—3-Ethyl-1-hydroxyurea was synthesized according to the method of Dresler and Stein (9) with modifications (10, 11). Hydroxyurea[1] was used as received.

X-Ray Crystal Analysis of 3-Ethyl-1-hydroxyurea—A clear, tabular crystal of 3-ethyl-1-hydroxyurea was mounted on an automatic diffractometer[2] equipped with an MoK$\bar{\alpha}$ X-ray source (K$\bar{\alpha}$ = 0.71073 Å) monochromatized by a dense graphite crystal. All measurements were made at ambient room temperature. The crystal symmetry was established as 2/m, space group I2/a. Unit cell parameters were a = 9.981, b = 8.011, c = 14.003 Å, β = 103.32°, and Z = 8 molecules/cell. The calculated density was 1.29 g/cm^3. Using the θ–2θ scan technique in the range $6° < 2\theta < 60°$, 413 independent reflections with $I > 3\sigma$ (I) were measured.

The structure was solved by application of the multiple-entry tangent formula program MULTAN (12). The ethyl moiety was highly disordered; however, the remainder of the molecule refined well. The three hydrogens not associated with the ethyl group were located. The final R value [$R = (\Sigma||F_o| - |F_c||)/\Sigma|F_o|$] of 11% was a disappointingly high value caused by the disorder problem. Since the ethyl portion of the structure was not involved in the hydrogen bonding between C=O and OH, no attempt was made to sort out and clarify the disorder.

This relatively crude crystallographic determination revealed that the title compound has a structure quite similar to that of hydroxyurea itself (Fig. 1), with an analogous intermolecular hydrogen-bonding scheme between the hydroxyl oxygens and the keto oxygens *via* the hydroxyl hydrogens. The approximate distance between oxygens involved in the hydrogen bonding is 2.62 Å (4). There also appears to be hydrogen bonding between the 3-hydrogen and oxygen of the hydroxyl group (intramolecular) and between the 1-hydrogen and carbonyl oxygen of another molecule. No unusual features were noted in the hydroxyurea portion of the molecule. The structure with interatomic bond distances and hydrogen bonds is shown in Fig. 2.

IR Spectra—Spectral data were obtained on double-beam IR spectrophotometers[3], utilizing liquid plates for solutions and mulls[4] for solids taken between sodium chloride plates. Solution spectra were taken of hydroxyurea and 3-ethyl-1-hydroxyurea in octanol[5] (dry), in octanol after water equilibration for 24 hr and drying over sodium sulfate (anhydrous), in acetonitrile[6] (wet), and in acetonitrile dried over sodium sulfate.

Spectra were taken with the solvents as the blank. All spectra were taken with the same instrument readings and at 90% transmission. The spectral data of the compounds in solution and taken as mulls are shown in Table I.

DISCUSSION

The X-ray crystal structure of hydroxyurea, a clinically effective antitumor agent and the most potent member of the hydroxyurea class, was first determined concurrently by two groups (13, 14). The initial reports were recently confirmed and corrected after reinvestigation at liquid nitrogen temperature (−140°), indicating the crystal structure as shown in Fig. 1 from the atomic coordinate data of Armagan *et al.* (15). Hy-

[1] Squibb Institute of Medical Research.
[2] Enraf-Nonius CAD-4.
[3] Beckman 4250 and Perkin-Elmer 700.
[4] Nujol.
[5] Fisher certified, dried over anhydrous sodium sulfate for 24 hr.
[6] Aldrich 99%, not less than 0.03% water.

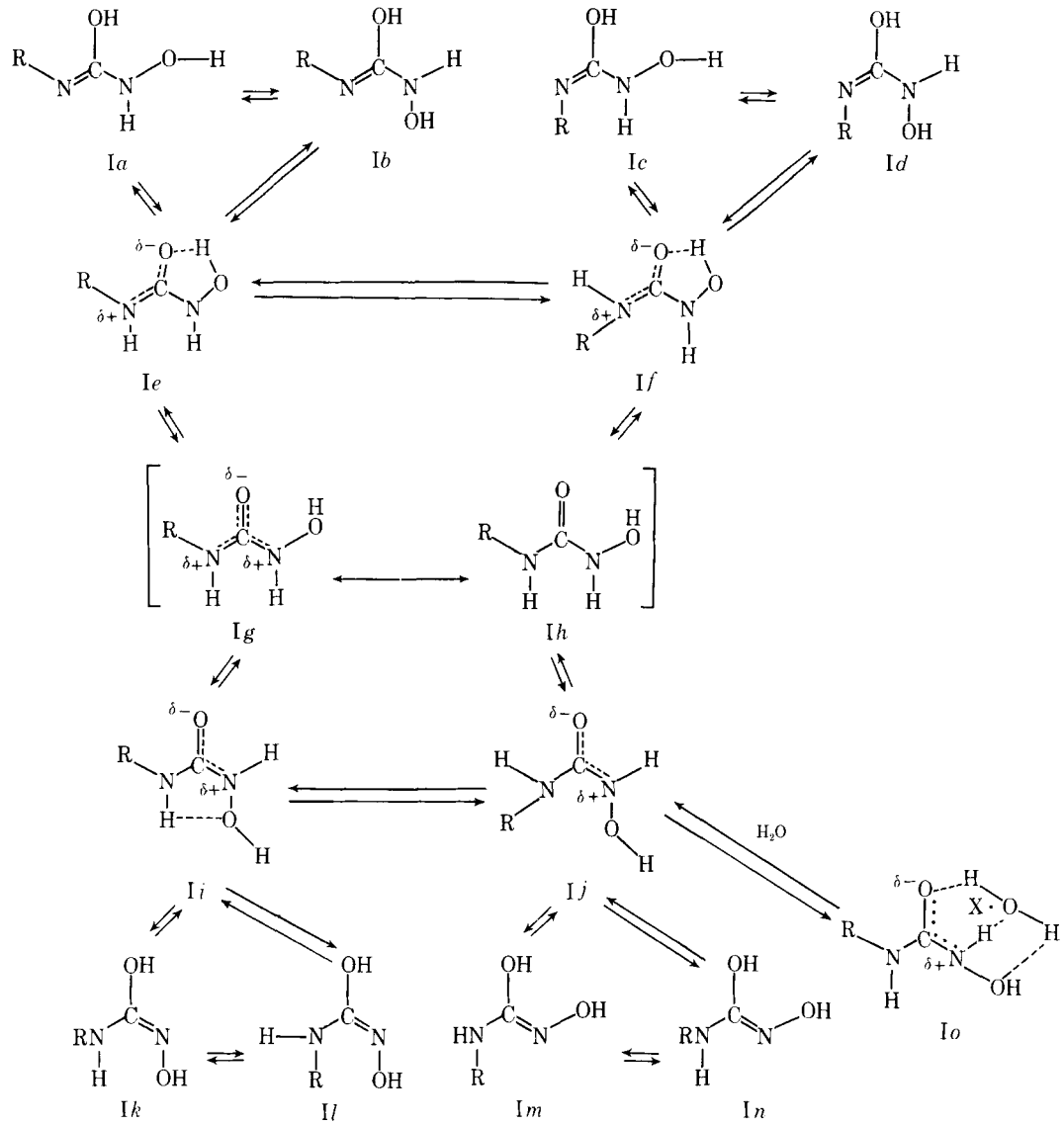

Scheme I—Conformational and tautomeric system of hydroxyureas. Canonical forms Ig and Ih represent electronic species where the π bond is localized in the C=O bond (Ih) or distributed across the NCN system (Ig). Conformers Ie, If, and Ii are possible because of internal hydrogen bonding, and conformer Ij can hydrogen bond to solvent or water (Io). Tautomers are possible (Ia–Id and Ik–In) if bond breaking and bond making occur.

droxyurea appears as chains of molecules with hydrogen bonding between the hydroxyl of one molecule and the carbonyl oxygen of another with four molecules in a unit cell. From the bond lengths and bond angles and with Pauling's method of determining bond order from bond length (16), the C=O bond was found to be about 80% double bond in character and both the N^1–C and C–N^2 bonds were found to be about 10% double bond in character.

With the method of Byrn *et al.* (6), the IR spectrum of solid hydroxyurea (a mineral oil mull) was compared to spectra taken in solutions. This method compares the important absorptions in IR spectra of solids of known structure with spectra in solution to evaluate the equivalence of conformation in the two systems. Since hydroxyurea can best be evaluated by the absorptions in the carbonyl–nitrogen region (1780–1550 cm^{-1}), only absorptions in this region were analyzed and compared. A powder diffraction X-ray analysis indicated that no phase change occurs on grinding, and thus the IR spectra of the mull represented the structure of hydroxyurea in the solid state.

The IR spectrum of solid hydroxyurea appeared as a broad band from 1650 to 1540 cm^{-1}, with peaks at 1625 and 1570 cm^{-1} representing the amide I and II bands of hydroxyurea. The amide I band (1625 cm^{-1}) is primarily C=O stretching vibrations, while the amide II band (1570 cm^{-1}) is due to NH bending and CN stretching (17). Spectra of hydroxyurea in solution were limited by poor solubility in solvents such as chloroform, benzene, ether, tetrahydrofuran, ethyl acetate, and cyclohexane, but spectra could be obtained in alcohols such as 1-octanol. The IR spectrum of hydroxyurea in dry octanol showed a broad band at 1635–1680 cm^{-1} with the peak at 1655 cm^{-1}. When hydroxyurea in octanol was equilibrated with water and dried with anhydrous sodium sulfate, an identical absorption was observed which peaked at 1645–1655 cm^{-1}.

It is assumed from these data that the structure or apparent conformation(s) (which can be represented by canonical forms Ig and Ih, conformers Ie, If, Ii, and Ij, and/or tautomers Ia–Id and Ik–In in Scheme I) present in solution is different than that present in the solid crystal, but the structure present in dry octanol is the same as that present in octanol equilibrated with water and dried.

Since hydrogen bonding with the solvent can affect the conformations present in solution, IR spectral analysis with a solvent that could not hydrogen bond to hydroxyurea was desirable. Since hydroxyurea was not soluble in most solvents that would not hydrogen bond (benzene, cyclohexane, and alkanes), acetonitrile was selected as a suitable alternative. Because of its miscibility with water, however, the equilibration step (as with octanol) with an aqueous phase was not possible. Therefore, IR spectra were taken in wet and anhydrous acetonitrile (dried over sodium sulfate); absorptions were found at 1690 cm^{-1} in wet acetonitrile and at 1640 and 1740 cm^{-1} in the anhydrous solvent.

Analysis and comparison of the IR spectral data in the solid state *versus* solutions, for hydroxyurea indicate that the conformational or structural species in solution is similar to that of the solid state in solvents that cannot hydrogen bond (dry acetonitrile). In the solid state, the amide I

and II bands are of equal intensity; in dry acetonitrile, the amide I band is more intense and at a lower wavelength, indicating a C=O bond is of greater double bond character and with less hydrogen bonding occurring with the carbonyl oxygen. This finding might be accounted for by the fact that hydroxyurea molecules in the solid state possess intermolecular hydrogen bonding (at a distance of 2.627 Å from C=O to HO) whereas hydrogen bonding of this type in a nonbonding, dry solution is less likely.

In the presence of water or in solvents that can hydrogen bond (such as octanol), the predominant structural or conformational species has minimal double bond CO character because of strong hydrogen bonding with water or solvent and maximal C=N bond character as observed by the intense absorption at 1650 cm^{-1}. This type of structural species could be represented (Scheme I) by tautomers *Ia–Id* and *Ik–In* or by a conformer such as *Ij*, which would hydrogen bond strongly to water or solvent. Tautomeric forms were ruled out through an NMR study[7]. This study showed that the NH protons exchanged slowly in deuterium oxide, which would not occur if tautomeric species were present in solution.

The substitution of groups on the hydroxyurea molecule, such as alkyl addition at the 1- or 3-nitrogen, produced analogs with appreciably less antitumor activity than hydroxyurea (18). It was of interest to determine if substituted analogs exhibit similar or different structural or conformational characteristics in comparison with hydroxyurea. Since no literature reports of X-ray crystal studies of 1- or 3-alkyl-substituted hydroxyureas could be found, an X-ray crystal analysis of a representative member of the class was initiated.

The physical properties of some substituted hydroxyureas precluded routine crystallographic analysis. For example, the 1-substituted methyl and ethyl analogs have low melting points and require low temperature analysis; and while the methyl analog produces suitable crystals for analysis, the ethyl analog is an amorphous powder unsuitable for crystallographic study. With the higher melting 3-substituted analogs, which could be analyzed at room temperatures, difficulties arose in finding a solvent for optimal growth of suitable crystals. Crystals grown from most solvents (methanol, ether, tetrahydrofuran, and acetone) produced plates or flakes that were too thin for X-ray analysis, as was the case with the biologically inactive 3-*n*-butyl analog. The 3-ethyl analog could be crystallized from acetone, producing crystals suitable for X-ray analysis; the derived data indicate that the structure is remarkably similar to that of hydroxyurea.

The crystal structure of 3-ethyl-1-hydroxyurea indicated hydrogen bonding between the hydroxyl hydrogen of one molecule and the carbonyl oxygen of another at a distance of about 2.62 Å[8] and internal hydrogen bonding between the 3-hydrogen and the hydroxyl oxygen at a distance of about 2.60 Å[8] (distances calculated between heavy atoms). The carbonyl bond was shorter in length than the bond in hydroxyurea crystals (1.25 Å[8] compared to 1.267 Å), which indicated a double bond character approaching 90%. However, with the relatively high estimated standard deviations[8] accompanying the ethyl disorder, little weight can be given to this figure. The CN^1 bond was slightly longer, indicating that any double bond character in this region was most likely between the CN^3 bond.

The IR spectrum of the ethyl analog in the solid state (taken as a mineral oil mull) showed absorptions at 1635 cm^{-1} (amide I) and in the 1540–1580-cm^{-1} range (amide II), with peaks at 1560 and 1580 and a shoulder peak at 1540 cm^{-1}. The intensity of the amide I band was slightly stronger than that of the amide II band, and the peak at 1560 cm^{-1} was the strongest in the amide II range.

Comparison of the crystal structure of the ethyl analog and its IR spectrum with the data for hydroxyurea indicates a good correlation with theoretical principles. The amide I band was shifted to a higher frequency in the ethyl analog, and this compound possessed a greater double bond character in the C=O bond. The amide II band was shifted to a lower frequency, indicative of the lower amount of C=N character in the ethyl analog. Differences in the observed hydrogen bonding of the 3-hydrogen (intramolecular) and 1-hydrogen (intermolecular) in the two compounds might explain the complex absorption in the amide II region (two peaks plus a shoulder peak) in comparison to a broad single absorption for hydroxyurea (with a slight shoulder ridge at 1550 cm^{-1}).

The IR spectra of solutions of the ethyl analog in solvents that could hydrogen bond to the molecules (dry octanol) showed two characteristic peaks observed in all substituted hydroxyurea analogs in dry octanol (8). For the 3-ethyl analog, the two absorptions peaks were at 1680 and 1560 cm^{-1}, with the absorption at the lower frequency being significantly more intense. These absorptions in dry octanol indicated an identifiable amide I band (for C=O) besides a strong amide II band and thus indicate that the structure(s) or conformation(s) present in dry octanol is different than that of hydroxyurea in the same solvent (a single intense absorption at 1650 cm^{-1}).

It also can be deduced from these data that the structure in dry octanol is similar to that observed in the solid state for the ethyl-substituted analog in that it has a definite degree of C=O character (although less than in the solid state). When the ethyl analog in octanol was equilibrated with water and separated and then the octanol was dried with anhydrous sodium sulfate, the IR spectrum showed only a single absorption (similar to that observed with hydroxyurea in dry octanol) at 1640 cm^{-1}. Spectra taken of the ethyl analog in wet acetonitrile showed a broad band with the peak at 1680 cm^{-1} and a distinct shoulder at 1630 cm^{-1}. When the spectra was taken in dry acetonitrile, the peak remained at 1680 cm^{-1} but the shoulder disappeared.

From these IR spectral data, it is assumed that, for the 3-ethyl analog, the structural or conformational species present (with a definite C=O character) is different in dry octanol from that present in dry acetonitrile (which lacks C=O character) but that the species present does not change appreciably in wet acetonitrile as was observed with hydroxyurea. The species present in the octanol solution after water equilibration, observed *via* the IR spectra, also appears to resemble the form(s) present in acetonitrile whether water is present or not.

It is apparent from these IR spectral data that, while the structural forms of hydroxyurea and its 3-ethyl analog are quite similar in the solid state, the species present in solutions differ appreciably. The spectral data can be visualized as due to changes in the equilibrium proportions of *Ie*, *If*, *Ii*, and *Ij* and canonical forms *Ig* and *Ih*. These canonical forms depict the extreme structural forms where C=O character is 100% and the CN bonds are single bond in character, allowing free rotation and thus fast interconversion through conformers *Ie*, *If*, *Ii*, and *Ij* (form *Ih*), or where the CO bond is substantially single bond in character and the remaining electron density is distributed across the CN bonds, producing restriction of rotation and separation of charge (form *Ig*).

For hydroxyurea (where R = H), a structural form similar to *Ig* is present in octanol regardless of whether the solvent is dry or has been equilibrated with water and dried. In dry acetonitrile, a form similar to *Ih* appears to be present; but when water is added, the structural form reverts back to a species similar to *Ig*. With the ethyl analog (where R = C_2H_5), the equilibrium is shifted in the direction of *Ih* in dry octanol; but after contact with water (water equilibration), the equilibrium is shifted to a form resembling *Ig*. In acetonitrile, a form similar to *Ig* is present whether water is present or not.

This behavior could be attributed to the ability of the ethyl analog to have strong enough inter- or intramolecular hydrogen bonding when hydrogen bonding is not possible with the solvent (dry acetonitrile) so that the species present is similar to *Ig* and, therefore, the addition of water would not change the species present. With respect to the IR results, hydroxyurea does not seem to possess the internal hydrogen bonding seen in the ethyl analog, and interactions with octanol and/or water predominate (form *Ig*). In solvents that do not hydrogen bond (dry acetonitrile), interconversions through the conformers *via* a form such as *Ih* would occur; this process would not continue when strong hydrogen bonding with water occurred (wet acetonitrile). Another possible explanation is that differences in solvation of hydroxyurea and the 3-ethyl derivative exist and change the relative stability of the conformers.

In conclusion, it is apparent that the addition of an ethyl group to the hydroxyurea molecule adds a property that influences the conformational preferences in solutions besides the added lipophilicity and bulk expected. The effect could influence the species present *in vivo* at various biological sites (at membranes, at site of action, *etc.*) and thus influence the process involved, depending on which species is stabilized due to the ability of hydrogen bonding with the hydroxyurea molecule by macromolecules or water.

[7] Unpublished data.
[8] Estimated standard deviation = ±0.04 Å.

REFERENCES

(1) E. J. Ariens, *Farmaco*, **24**, 6 (1969).

(2) I. W. Mathison, W. E. Solomons, P. H. Morgan, and R. R. Tidwell, in "Principles of Medicinal Chemistry," W. O. Foye, Ed., Lea & Febiger, Philadelphia, Pa., 1974, pp. 89–92.

(3) B. Pullman, P. Courriere, and H. Berthod, *J. Med. Chem.*, **17**, 439 (1974).

(4) I. J. Borowitz, S. Liverles, K. Megerle, and R. D. Rapp, *Tetrahedron*, **30**, 4209 (1974).

(5) V. Cody, W. L. Duax, K. Yasuda, Y. Osawa, and D. A. Noeton, *ibid.*, **28**, 5683 (1972).
(6) S. R. Byrn, C. W. Graber, and S. L. Midland, *J. Org. Chem.*, **41**, 2283 (1976).
(7) G. R. Parker, N. K. Hilgendorf, and J. G. Lindberg, *J. Pharm. Sci.*, **65**, 585 (1976).
(8) G. R. Parker and E. C. Moore, *ibid.*, **66**, 1040 (1977).
(9) W. Dresler and R. Stein, *Justus Liebigs Ann. Chem.*, **150**, 242 (1869).
(10) R. E. Harmon, J. C. Dabrowiak, D. J. Brown, S. K. Gupta, M. Herbert, and D. Chitharanjan, *J. Med. Chem.*, **13**, 577 (1970).
(11) G. Clifton, S. R. Bryant, and C. G. Skinner, *ibid.*, **13**, 377 (1970).
(12) G. Germain, P. Main, and M. M. Woolfson, *Acta Crystallogr.*, **A27**, 368 (1971).
(13) I. K. Larsen and B. Jerslev, *Acta Chem. Scand.*, **20**, 983 (1966).
(14) H. Berman and S. H. Kim, *Acta Crystallogr.*, **23**, 180 (1967).
(15) N. Armagan, J. P. G. Richards, and A. A. Uraz, *ibid.*, **B32**, 1042 (1976).
(16) L. Pauling, "The Nature of the Chemical Bond," 3rd ed., Cornell University Press, Ithaca, N.Y., 1960, p. 281.
(17) N. L. Alpert, W. E. Keiser, and H. A. Szymanski, "The Theory and Practice of Infrared Spectroscopy," Plenum, New York, N.Y., 1970, p. 281.
(18) R. H. Adamson, *Proc. Soc. Exp. Biol. Med.*, **119**, 456 (1965).

ACKNOWLEDGMENTS

The authors thank Miss Barbara Stearns, Squibb Institute of Medical Research, for supplying the hydroxyurea.

GLC Determination of Phenylbutazone in Human Plasma

ANTOINE SIOUFI ˣ, FRANÇOISE CAUDAL, and FRANÇOISE MARFIL

Received March 1, 1977, from *Ciba-Geigy Biopharmaceutical Research Center, 92506 Rueil-Malmaison Cedex, France.* Accepted for publication May 11, 1977.

Abstract □ A GLC method for phenylbutazone at concentrations down to 10 ng/ml in human plasma is described. After addition of an internal standard, phenylbutazone is extracted at pH 5 into benzene. The dry extract is dissolved in benzene, and phenylbutazone is determined by GLC using a ^{63}Ni-electron-capture detector.

Keyphrases □ Phenylbutazone—GLC analysis in human plasma □ GLC—analysis, phenylbutazone in human plasma □ Antirheumatic agents—phenylbutazone, GLC analysis in human plasma

Many methods have been proposed for the quantitative assay of phenylbutazone[1] (I) in biological fluids. The first UV method (1, 2) (extraction of phenylbutazone with heptane in acidic medium) was modified (3, 4) and automated (5), for the serial determination of phenylbutazone in human plasma. The UV determination of phenylbutazone after oxidation to azobenzene by alkaline permanganate was described (6) and applied to small-volume samples (7). The method of Burns (1, 2) was also applied to 1 drop of capillary blood (8). Stevens (9) determined phenylbutazone by UV absorption after fast extraction in hexane from an acidic medium.

Several investigators studied the determination of phenylbutazone by GLC. McGilveray *et al.* (10) described a procedure using 1 *N* HCl and heptane for extraction and diphenyl phthalate as the external standard. Midha *et al.* (11) published an elaborated method for determining phenylbutazone and oxyphenbutazone. These two compounds were derivatized by flash-heater methylation with trimethylanilinium hydroxide, but each yielded two peaks.

A GLC technique was also used to determine phenylbutazone and oxyphenbutazone in the plasma and urine of horses and dogs (12). The extraction was performed with 2 *N* H_2SO_4 and 3 × 20 ml of benzene. Phenylbutazone was assayed by GLC without derivatization, but oxyphenbutazone was separated as its heptafluorobutyryl derivative.

Tanimura *et al.* (13) determined phenylbutazone, oxyphenbutazone, and γ-hydroxyphenylbutazone in human or rabbit plasma, using fluoranthene as the internal standard and *N,O*-bis(trimethylsilyl)trifluoroacetamide as the silylating reagent. A GLC method in rat serum or urine, using promethazine as the external standard, was also described (14). The retention times were between 15 and 18 min. This method was checked for its specificity. Finally, a high-pressure liquid chromatographic (HPLC) technique was recently reported (15).

The GLC method described here is simple and fast, and it specifically determines phenylbutazone in human plasma with a high sensitivity. A phenylbutazone analog, 4-butyl-1,2-bis(*p*-tolyl)-3,5-pyrazolidine (II), is used as the internal standard.

EXPERIMENTAL

Reagents—A pH 5 buffer[2] was prepared by diluting the contents of seven vials with 1000 ml of water. Benzene was analytical grade[3]. The

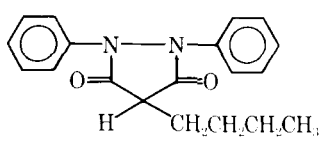

I

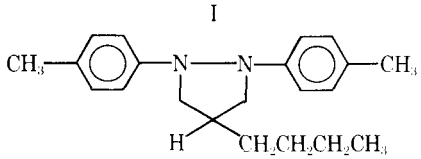

II

[1] Active ingredient of Butazolidin (Geigy).

[2] Titrisol, Merck.
[3] Mallinckrodt.

(5) V. Cody, W. L. Duax, K. Yasuda, Y. Osawa, and D. A. Noeton, *ibid.*, **28**, 5683 (1972).
(6) S. R. Byrn, C. W. Graber, and S. L. Midland, *J. Org. Chem.*, **41**, 2283 (1976).
(7) G. R. Parker, N. K. Hilgendorf, and J. G. Lindberg, *J. Pharm. Sci.*, **65**, 585 (1976).
(8) G. R. Parker and E. C. Moore, *ibid.*, **66**, 1040 (1977).
(9) W. Dresler and R. Stein, *Justus Liebigs Ann. Chem.*, **150**, 242 (1869).
(10) R. E. Harmon, J. C. Dabrowiak, D. J. Brown, S. K. Gupta, M. Herbert, and D. Chitharanjan, *J. Med. Chem.*, **13**, 577 (1970).
(11) G. Clifton, S. R. Bryant, and C. G. Skinner, *ibid.*, **13**, 377 (1970).
(12) G. Germain, P. Main, and M. M. Woolfson, *Acta Crystallogr.*, **A27**, 368 (1971).
(13) I. K. Larsen and B. Jerslev, *Acta Chem. Scand.*, **20**, 983 (1966).
(14) H. Berman and S. H. Kim, *Acta Crystallogr.*, **23**, 180 (1967).
(15) N. Armagan, J. P. G. Richards, and A. A. Uraz, *ibid.*, **B32**, 1042 (1976).
(16) L. Pauling, "The Nature of the Chemical Bond," 3rd ed., Cornell University Press, Ithaca, N.Y., 1960, p. 281.
(17) N. L. Alpert, W. E. Keiser, and H. A. Szymanski, "The Theory and Practice of Infrared Spectroscopy," Plenum, New York, N.Y., 1970, p. 281.
(18) R. H. Adamson, *Proc. Soc. Exp. Biol. Med.*, **119**, 456 (1965).

ACKNOWLEDGMENTS

The authors thank Miss Barbara Stearns, Squibb Institute of Medical Research, for supplying the hydroxyurea.

GLC Determination of Phenylbutazone in Human Plasma

ANTOINE SIOUFI ˣ, FRANÇOISE CAUDAL, and FRANÇOISE MARFIL

Received March 1, 1977, from *Ciba-Geigy Biopharmaceutical Research Center, 92506 Rueil-Malmaison Cedex, France.* Accepted for publication May 11, 1977.

Abstract □ A GLC method for phenylbutazone at concentrations down to 10 ng/ml in human plasma is described. After addition of an internal standard, phenylbutazone is extracted at pH 5 into benzene. The dry extract is dissolved in benzene, and phenylbutazone is determined by GLC using a ^{63}Ni-electron-capture detector.

Keyphrases □ Phenylbutazone—GLC analysis in human plasma □ GLC—analysis, phenylbutazone in human plasma □ Antirheumatic agents—phenylbutazone, GLC analysis in human plasma

Many methods have been proposed for the quantitative assay of phenylbutazone[1] (I) in biological fluids. The first UV method (1, 2) (extraction of phenylbutazone with heptane in acidic medium) was modified (3, 4) and automated (5), for the serial determination of phenylbutazone in human plasma. The UV determination of phenylbutazone after oxidation to azobenzene by alkaline permanganate was described (6) and applied to small-volume samples (7). The method of Burns (1, 2) was also applied to 1 drop of capillary blood (8). Stevens (9) determined phenylbutazone by UV absorption after fast extraction in hexane from an acidic medium.

Several investigators studied the determination of phenylbutazone by GLC. McGilveray *et al.* (10) described a procedure using 1 *N* HCl and heptane for extraction and diphenyl phthalate as the external standard. Midha *et al.* (11) published an elaborated method for determining phenylbutazone and oxyphenbutazone. These two compounds were derivatized by flash-heater methylation with trimethylanilinium hydroxide, but each yielded two peaks.

A GLC technique was also used to determine phenylbutazone and oxyphenbutazone in the plasma and urine of horses and dogs (12). The extraction was performed with 2 *N* H_2SO_4 and 3 × 20 ml of benzene. Phenylbutazone was assayed by GLC without derivatization, but oxyphenbutazone was separated as its heptafluorobutyryl derivative.

Tanimura *et al.* (13) determined phenylbutazone, oxyphenbutazone, and γ-hydroxyphenylbutazone in human or rabbit plasma, using fluoranthene as the internal standard and *N,O*-bis(trimethylsilyl)trifluoroacetamide as the silylating reagent. A GLC method in rat serum or urine, using promethazine as the external standard, was also described (14). The retention times were between 15 and 18 min. This method was checked for its specificity. Finally, a high-pressure liquid chromatographic (HPLC) technique was recently reported (15).

The GLC method described here is simple and fast, and it specifically determines phenylbutazone in human plasma with a high sensitivity. A phenylbutazone analog, 4-butyl-1,2-bis(*p*-tolyl)-3,5-pyrazolidine (II), is used as the internal standard.

EXPERIMENTAL

Reagents—A pH 5 buffer[2] was prepared by diluting the contents of seven vials with 1000 ml of water. Benzene was analytical grade[3]. The

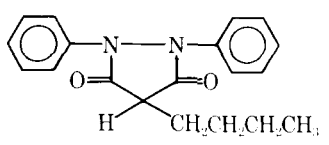

I

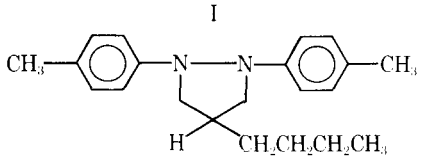

II

[1] Active ingredient of Butazolidin (Geigy).

[2] Titrisol, Merck.
[3] Mallinckrodt.

Table I—Precision and Accuracy of the Assay Applied to Spiked Human Plasma Samples (1 ml and 100 μl)

Amount Added, ng/ml	Amount Found[a]		CV, %	
	1 ml	100 μl	1 ml	100 μl
10	10	—	3.1	—
25	25	—	5.7	—
50	51[b]	—	2.6	—
100	—	100	—	6.2
150	150	—	1.1	—
500	509	503	2.2	2.6
1,000	988	—	2.5	—
1,500	—	1,515	—	1.5
5,000	4914	4,769	3.3	1.0
10,000	—	10,214	—	4.4
25,000	—	25,069	—	3.6
50,000	—	50,389	—	1.0

[a] Average of six assays. [b] Four assays only.

benzene internal standard solution contained 1 μg of II[4]/ml.

Materials—The glassware was dried at 100° and immersed for 0.5 hr in an ultrasonic bath, first in water and then in methanol. A gas chromatograph[5] equipped with a linear 15-mCi ^{63}Ni-electron-capture detector[6] was used.

The peak areas were given by an electronic integrator[7]. The column was operated at 250°, the injector was at 300°, and the detector was at 300° with an argon–methane (90:10) flow rate of 70 ml/min. Glass columns were washed with 1 *N* HCl, distilled water, acetone, and benzene and then silanized with a 1% (v/v) solution of hexamethyldisilazane in benzene.

After this treatment, the columns were washed again with benzene and dried at 100°. The column packing was 5% OV-17[8] on 80–100-mesh Chromosorb WHP[8]. The filled column was flushed with the carrier gas at 50° for 30 min and then gradually heated to 300° at 1°/min with a flow rate of 30 ml/min. The column temperature was held overnight at 300°. The temperature was then repeatedly increased at 8°/min from 150 to 300° over 24 hr. During the five last cycles, 20 μl of silylating reagent[9] was injected between 150 and 220°.

Extraction—A 500-μl aliquot of the internal standard solution was added to a stoppered glass tube, and the solution was taken to dryness under a nitrogen stream. Then 100 μl of the sample, 1 ml of pH 5 buffer, and 4 ml of benzene were introduced in the tube; the tube was shaken mechanically[10] for 20 min at 400 rpm and centrifuged at 5000 rpm for 10 min.

An aliquot volume of the benzene phase was transferred to another tube and taken to dryness under a nitrogen stream in a water bath at 37°.

GLC—Benzene, 500 μl, was added to the dry residue, and the tube was shaken on a mixer[11]. A 3-μl portion of the benzene solution was then injected into the gas chromatograph using the solvent-flush technique.

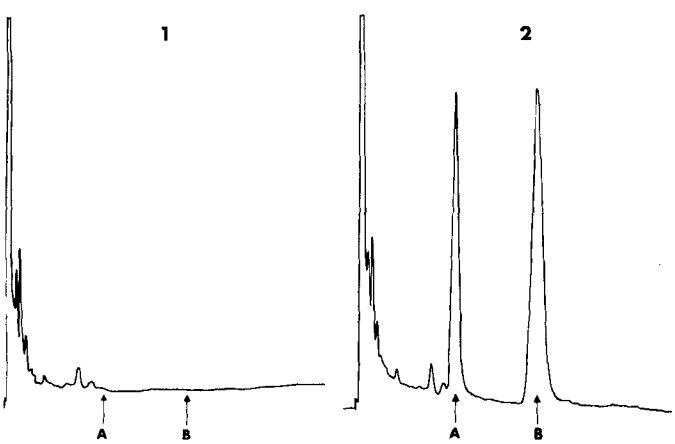

Figure 1—*Chromatograms of a human plasma blank (1) and 150 ng of phenylbutazone/ml (A) and 500 ng of internal standard/ml (B) in human plasma (2).*

[4] Ciba-Geigy, Basel, Switzerland.
[5] Hewlett-Packard 5710 A.
[6] Hewlett-Packard 18 713 A.
[7] Hewlett-Packard 3380 A.
[8] Applied Science Laboratories.
[9] Silyl 8, Pierce.
[10] Infors.

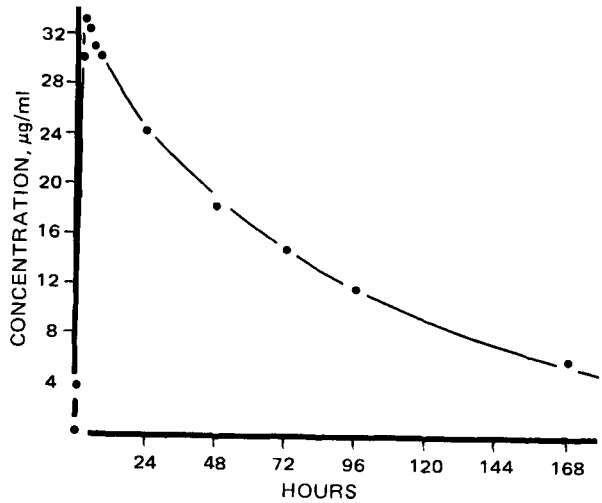

Figure 2—*Plasma phenylbutazone concentrations after oral administration of 300 mg (mean of six subjects).*

The phenylbutazone content was calculated from the peak area ratio by reference to a calibration curve. This curve was plotted on the basis of a benzene solution containing 1 μg of I/ml. Aliquot parts of this solution were taken to dryness, and plasma was added to yield plasma solutions containing 100–50,000 ng/ml.

The phenylbutazone and internal standard solutions were stable for 1 week at 4°. After 5–7 days, there was a progressive change in the peak area ratio of the two compounds, indicating some degradation.

Experiment in Humans—Six healthy volunteers were given 300 mg of phenylbutazone in a cachet. Blood samples were withdrawn 0.5, 1, 2, 3, 4, 6, 8, 24, 48, 72, 96, and 168 hr after administration, transferred to heparinized tubes, and centrifuged immediately. Plasma was removed and stored at −20° until analysis.

RESULTS AND DISCUSSION

Analytical Yield—Extraction was studied at several acidic pH values with a 1-μg/ml plasma ^{14}C-phenylbutazone solution. Acidic pH solutions were: 2 *N* HCl; 1 *N* HCl; and pH 1, 2, 3, 4, 5, and 6 buffers (seven vials[2] diluted with 1000 ml of water). At all of these pH values, phenylbutazone recovery was 88 ± 6% (average of five assays). When the plasma was simply diluted with distilled water, the pH was 7.2 and the average extraction yield of five assays was 50 ± 4%.

Phenylbutazone is a carbon acid with a pKa of 4.5–4.7 (16), and it may appear surprising that it is extracted with a high recovery at pH 5. Stella (17) showed that phenylbutazone has a hindered dissolution at pH values greater than its pKa because of noninstantaneous ionization kinetics.

Sensitivity and Accuracy—Table I gives the results obtained when the described procedure was applied to spiked plasma samples of different volumes.

The coefficients of variation were calculated on the basis of six replicate analyses of each sample. With a 100-μl sample, concentrations down to 100 ng/ml can be determined accurately. If a 1-ml sample is used, the assay limit is lowered to 10 ng/ml, and even smaller concentrations can be detected.

Phenylbutazone and the internal standard do not contain functional groups commonly associated with high electron-capture ability. Nevertheless, both are well detected.

Plasma Interference—Figure 1 shows the chromatograms of a human plasma extract and of the same plasma spiked with 150 ng of phenylbutazone and 500 ng of the internal standard. No interference by the normal plasma components was recorded.

Specificity—Three unconjugated metabolites of phenylbutazone have been described (18): oxyphenbutazone (III), γ-hydroxyphenylbutazone (IV), and *p*,γ-dihydroxyphenylbutazone (V). These metabolites account for 23, 2, and 0.5%, respectively, of the total radioactivity in the plasma after administration of ^{14}C-labeled drug.

The proposed technique was applied to plasma solutions containing

[11] Vortex.

50 μg of III/ml and 5 μg of IV and V/ml. These concentrations greatly exceed those expected in plasma. None of the three metabolites was recorded.

Application—The technique was applied to study phenylbutazone elimination after oral administration to humans. The mean plasma phenylbutazone concentration–time curve is depicted in Fig. 2. The mean elimination half-life was 68.5 hr.

The technique has been applied in studying the pharmacokinetics of phenylbutazone in humans after the administration of single and multiple doses[12].

REFERENCES

(1) J. J. Burns, *J. Pharmacol. Exp. Ther.*, **109**, 346 (1953).

(2) *Ibid.*, **113**, 481 (1955).

(3) B. Herrmann, *Med. Exp.*, **1**, 170 (1960).

(4) G. R. Van Petten, H. Feng, R. J. Withey, and H. F. Lettau, *J. Clin. Pharmacol.*, **11**, 177 (1971).

(5) B. G. Lukas, C. B. Borman, and S. B. Zak, *J. Pharm. Sci.*, **65**, 86 (1976).

(6) G. E. Wallace, *ibid.*, **57**, 2053 (1968).

(7) E. Jähnchen and G. Levy, *Clin. Chem.*, **18**, 984 (1972).

(8) M. W. Fuchs, *Rhumatologie*, **16**, 489 (1964).

(9) H. M. Stevens, *Clin. Chem.*, **16**, 437 (1970).

(10) I. J. McGilveray, K. K. Midha, R. Brien, and L. Wilson, *J. Chromatogr.*, **89**, 17 (1974).

(11) K. K. Midha, I. J. McGilveray, and C. Charette, *J. Pharm. Sci.*, **63**, 1234 (1974).

(12) R. B. Bruce, W. R. Maynard, and L. K. Dunning, *ibid.*, **63**, 446 (1974).

(13) Y. Tanimura, Y. Saitoh, F. Nakagawa, and T. Suzuki, *Chem. Pharm. Bull.*, **23**, 651 (1974).

(14) R. Perego, E. Martinelli, and P. C. Vanoni, *J. Chromatogr.*, **54**, 280 (1971).

(15) N. J. Pound and R. W. Sears, *J. Pharm. Sci.*, **64**, 284 (1975).

(16) J. J. Burns, T. F. Yu, P. Dayton, L. Berger, A. B. Gutman, and B. B. Brodie, *Nature*, **182**, 1162 (1958).

(17) V. J. Stella, *J. Pharm. Sci.*, **64**, 706 (1975).

(18) W. Dieterle, J. W. Faigle, F. Früh, H. Mory, W. Theobald, K. O. Alt, and W. J. Richter, *Arzneim.-Forsch.*, **26**, 572 (1976).

[12] A. Sioufi, F. Caudal, and D. Grimault, to be published.

ACKNOWLEDGMENTS

The authors thank Dr. J. W. Faigle and Dr. W. Dieterle (Pharmacological Chemistry Department, Ciba-Geigy, Basel, Switzerland) for information on phenylbutazone metabolism. They are also grateful to Dr. W. Theobald (Medical Department, Ciba-Geigy, Basel, Switzerland) and to Dr. J. P. Schoeller (Medical Department, Ciba-Geigy, Rueil, France) for performing the clinical experiments.

Effect of Enzyme-Inducing and Enzyme-Inhibiting Agents on Drug Absorption I: 3-*O*-Methylglucose Transport in Rats

WILLIAM R. RAVIS and STUART FELDMAN ˣ

Received February 22, 1977, from the *Department of Pharmaceutics, University of Houston, Houston, TX 77004.* Accepted for publication May 26, 1977.

Abstract □ The influence of preadministration of phenobarbital, benzo[*a*]pyrene, and proadifen hydrochloride on 3-*O*-methylglucose transfer across the everted rat small intestine was examined. The active and passive components of the sugar transport mechanism were evaluated using phlorizin, a potent inhibitor of active transport of sugars. Pretreatment of the animals with phenobarbital did not alter 3-*O*-methylglucose transfer characteristics. Pretreatment with intraperitoneally administered benzo[*a*]pyrene increased mucosal to serosal transfer of the sugar at low (0.1 m*M*) sugar concentrations. Enhancement of the active transfer of 3-*O*-methylglucose by pretreatment with proadifen hydrochloride was noted at low sugar concentrations. The passive transfer of the sugar was reduced after pretreatment with proadifen hydrochloride.

Keyphrases □ 3-*O*-Methylglucose—transfer across everted rat small intestine, effect of preadministration of phenobarbital, benzo[*a*]pyrene, and proadifen hydrochloride □ Transport, drug—3-*O*-methylglucose, transfer across everted rat small intestine, effect of preadministration of phenobarbital, benzo[*a*]pyrene, and proadifen hydrochloride □ Enzyme inducers—phenobarbital, benzo[*a*]pyrene, and proadifen hydrochloride, effect on transfer of 3-*O*-methylglucose across everted rat small intestine □ Phenobarbital—effect of preadministration on transfer of 3-*O*-methylglucose across everted rat small intestine □ Benzo[*a*]pyrene—effect of preadministration on transfer of 3-*O*-methylglucose across everted rat small intestine □ Proadifen hydrochloride—effect of preadministration on transfer of 3-*O*-methylglucose across everted rat small intestine

Intestinal glucose absorption is an active energy-expending process (1) believed to be controlled enzymatically and susceptible to alteration by chemical agents known to affect cell metabolism (2–4). The structural specificity of this particular mechanism has been well documented (5, 6). The 3-*O*-methyl derivative possesses transport characteristics similar to glucose; however, it is not metabolized by animal tissue (7). Thus, this sugar is useful for studying the sugar transport process across intestinal tissue.

Recent investigations showed the ability of various hepatic enzyme-inducing agents to enhance drug metabolism in the intestinal mucosa (8). Phenobarbital produced a striking hypertrophy of the small intestinal endoplasmic reticulum with an increase in this tissue's *N*-demethylase activity (9). However, no difference in mucosal to serosal transfer of ^{14}C-3-*O*-methylglucose or ^{14}C-palmitic acid was observed compared to controls. Previously, evidence that phenobarbital pretreatment heightened the mucosal transfer rate of ^{59}Fe-iron sulfate in duodenal rat intestinal sacs was reported (10). That effect may be due, in part, to an increased synthesis of a carrier molecule. In addition, subcutaneous phenobarbital injections enhanced active bile salt ileal transport (11).

It was of interest, therefore, to examine the possible effect of pretreatment with known hepatic enzyme-inducing agents on the active transport of 3-*O*-methylglucose

50 μg of III/ml and 5 μg of IV and V/ml. These concentrations greatly exceed those expected in plasma. None of the three metabolites was recorded.

Application—The technique was applied to study phenylbutazone elimination after oral administration to humans. The mean plasma phenylbutazone concentration–time curve is depicted in Fig. 2. The mean elimination half-life was 68.5 hr.

The technique has been applied in studying the pharmacokinetics of phenylbutazone in humans after the administration of single and multiple doses[12].

REFERENCES

(1) J. J. Burns, *J. Pharmacol. Exp. Ther.*, **109**, 346 (1953).

(2) *Ibid.*, **113**, 481 (1955).

(3) B. Herrmann, *Med. Exp.*, **1**, 170 (1960).

(4) G. R. Van Petten, H. Feng, R. J. Withey, and H. F. Lettau, *J. Clin. Pharmacol.*, **11**, 177 (1971).

(5) B. G. Lukas, C. B. Borman, and S. B. Zak, *J. Pharm. Sci.*, **65**, 86 (1976).

(6) G. E. Wallace, *ibid.*, **57**, 2053 (1968).

(7) E. Jähnchen and G. Levy, *Clin. Chem.*, **18**, 984 (1972).

(8) M. W. Fuchs, *Rhumatologie*, **16**, 489 (1964).

(9) H. M. Stevens, *Clin. Chem.*, **16**, 437 (1970).

(10) I. J. McGilveray, K. K. Midha, R. Brien, and L. Wilson, *J. Chromatogr.*, **89**, 17 (1974).

(11) K. K. Midha, I. J. McGilveray, and C. Charette, *J. Pharm. Sci.*, **63**, 1234 (1974).

(12) R. B. Bruce, W. R. Maynard, and L. K. Dunning, *ibid.*, **63**, 446 (1974).

(13) Y. Tanimura, Y. Saitoh, F. Nakagawa, and T. Suzuki, *Chem. Pharm. Bull.*, **23**, 651 (1974).

(14) R. Perego, E. Martinelli, and P. C. Vanoni, *J. Chromatogr.*, **54**, 280 (1971).

(15) N. J. Pound and R. W. Sears, *J. Pharm. Sci.*, **64**, 284 (1975).

(16) J. J. Burns, T. F. Yu, P. Dayton, L. Berger, A. B. Gutman, and B. B. Brodie, *Nature*, **182**, 1162 (1958).

(17) V. J. Stella, *J. Pharm. Sci.*, **64**, 706 (1975).

(18) W. Dieterle, J. W. Faigle, F. Früh, H. Mory, W. Theobald, K. O. Alt, and W. J. Richter, *Arzneim.-Forsch.*, **26**, 572 (1976).

[12] A. Sioufi, F. Caudal, and D. Grimault, to be published.

ACKNOWLEDGMENTS

The authors thank Dr. J. W. Faigle and Dr. W. Dieterle (Pharmacological Chemistry Department, Ciba-Geigy, Basel, Switzerland) for information on phenylbutazone metabolism. They are also grateful to Dr. W. Theobald (Medical Department, Ciba-Geigy, Basel, Switzerland) and to Dr. J. P. Schoeller (Medical Department, Ciba-Geigy, Rueil, France) for performing the clinical experiments.

Effect of Enzyme-Inducing and Enzyme-Inhibiting Agents on Drug Absorption I: 3-*O*-Methylglucose Transport in Rats

WILLIAM R. RAVIS and STUART FELDMAN ˣ

Received February 22, 1977, from the *Department of Pharmaceutics, University of Houston, Houston, TX 77004.* Accepted for publication May 26, 1977.

Abstract □ The influence of preadministration of phenobarbital, benzo[*a*]pyrene, and proadifen hydrochloride on 3-*O*-methylglucose transfer across the everted rat small intestine was examined. The active and passive components of the sugar transport mechanism were evaluated using phlorizin, a potent inhibitor of active transport of sugars. Pretreatment of the animals with phenobarbital did not alter 3-*O*-methylglucose transfer characteristics. Pretreatment with intraperitoneally administered benzo[*a*]pyrene increased mucosal to serosal transfer of the sugar at low (0.1 m*M*) sugar concentrations. Enhancement of the active transfer of 3-*O*-methylglucose by pretreatment with proadifen hydrochloride was noted at low sugar concentrations. The passive transfer of the sugar was reduced after pretreatment with proadifen hydrochloride.

Keyphrases □ 3-*O*-Methylglucose—transfer across everted rat small intestine, effect of preadministration of phenobarbital, benzo[*a*]pyrene, and proadifen hydrochloride □ Transport, drug—3-*O*-methylglucose, transfer across everted rat small intestine, effect of preadministration of phenobarbital, benzo[*a*]pyrene, and proadifen hydrochloride □ Enzyme inducers—phenobarbital, benzo[*a*]pyrene, and proadifen hydrochloride, effect on transfer of 3-*O*-methylglucose across everted rat small intestine □ Phenobarbital—effect of preadministration on transfer of 3-*O*-methylglucose across everted rat small intestine □ Benzo[*a*]pyrene—effect of preadministration on transfer of 3-*O*-methylglucose across everted rat small intestine □ Proadifen hydrochloride—effect of preadministration on transfer of 3-*O*-methylglucose across everted rat small intestine

Intestinal glucose absorption is an active energy-expending process (1) believed to be controlled enzymatically and susceptible to alteration by chemical agents known to affect cell metabolism (2–4). The structural specificity of this particular mechanism has been well documented (5, 6). The 3-*O*-methyl derivative possesses transport characteristics similar to glucose; however, it is not metabolized by animal tissue (7). Thus, this sugar is useful for studying the sugar transport process across intestinal tissue.

Recent investigations showed the ability of various hepatic enzyme-inducing agents to enhance drug metabolism in the intestinal mucosa (8). Phenobarbital produced a striking hypertrophy of the small intestinal endoplasmic reticulum with an increase in this tissue's *N*-demethylase activity (9). However, no difference in mucosal to serosal transfer of ^{14}C-3-*O*-methylglucose or ^{14}C-palmitic acid was observed compared to controls. Previously, evidence that phenobarbital pretreatment heightened the mucosal transfer rate of ^{59}Fe-iron sulfate in duodenal rat intestinal sacs was reported (10). That effect may be due, in part, to an increased synthesis of a carrier molecule. In addition, subcutaneous phenobarbital injections enhanced active bile salt ileal transport (11).

It was of interest, therefore, to examine the possible effect of pretreatment with known hepatic enzyme-inducing agents on the active transport of 3-*O*-methylglucose

Table I—3-*O*-Methylglucose Transfer across the Everted Rat Small Intestine as a Function of Concentration and Time

Concentration, m*M*	*n*	Cumulative 3-*O*-Methylglucose Transferred with Time, m*M* × 10^3			
		30 min	60 min	90 min	120 min
1	10	1.40	2.92	4.42	5.81
2	6	2.31	4.74	6.72	8.29
3.5	3	3.00	7.41	11.7	15.7
5	8	5.54	11.1	15.7	19.7
6.25	3	5.00	11.0	16.4	21.4
7.5	10	5.27	13.0	19.8	26.3
8.5	2	5.28	12.2	19.4	27.1
10	8	7.56	17.3	25.8	33.9
		With Phlorizin (0.08 m*M*)			
1	4	0.42	0.61	0.86	1.22
2	4	0.51	0.95	1.61	2.69
5	4	0.61	1.74	3.57	6.08
10	3	2.25	6.09	10.73	15.78

across rat jejunal sacs. The agents examined were phenobarbital, proadifen hydrochloride (I), and benzo[*a*]pyrene (II); all previously were found to alter hepatic drug metabolism. The experimental drug, I, is well documented as a rather nonspecific enzyme inhibitor (12) but also was found to induce microsomal enzyme activity at later periods following administration (13).

EXPERIMENTAL

Animals and Treatment—Male Sprague–Dawley rats[1], 176–250 g, were maintained on regular rat chow and water *ad libitum*. The rats were fasted 24 hr prior to the experiment. The animals were given 80 mg of phenobarbital sodium[2]/kg ip or po for 3 consecutive days before the experiment.

Compound II[3] was administered intraperitoneally or orally dissolved in corn oil at a dosage of 20 mg/kg 48 hr prior to the experiment. The last group received I[4] either orally or intraperitoneally dissolved in water at a dose of 100 mg/kg 24 hr prior to the experiment. Control animals were dosed similarly with the appropriate vehicle.

Preparation of Jejunal Sacs—Under ether anesthesia, a midline incision was made and the entire small intestine was removed. The intestine was immediately rinsed with cold saline, and the first 15 cm distal to the pylorus was discarded. The remaining intestine was everted over a glass rod. Either the Wilson and Wiseman (14) technique of everted sacs or a method described by Feldman and Gibaldi (15) utilizing cannulated sacs was used.

For both preparations, the mucosal bathing solution and the serosal solution consisted of pH 7.4 Krebs–Henseleit buffer. The buffer pH was checked at the beginning and end of the experiments. Prior to use, all serosal solutions were bubbled with 95% oxygen–5% carbon dioxide; the mucosal solutions were bubbled continuously throughout the experiments. In all studies, the temperature of the preparations was maintained at 37 ± 0.2°.

Serosal to Mucosal Concentration Ratio Experiment—For these studies, 5-cm sacs were prepared as described by Wilson and Wiseman (14). After filling the sacs with 0.5 ml of buffer containing 0.78 m*M* 3-*O*-methylglucose[5], the sacs were incubated in 15 ml of mucosal buffer of the same sugar concentration for 0.5 hr. After incubation, the contents of the everted intestinal sacs and mucosal solution were analyzed for the sugar.

Cannulated Everted Intestinal Sacs—Everted intestinal segments, 10 cm, were hung from glass cannulas, as described by Feldman and Gibaldi (15), and were suspended in 60 ml of mucosal buffer containing varying concentrations of 3-*O*-methylglucose. After placement, 2 ml of buffer, free of the sugar, was instilled into the sacs. The serosal fluid was withdrawn at predetermined intervals, followed by rinsing of the serosa with 2 ml of buffer which was then combined with the initial sample for that time period. Another 2 ml was then placed into the sac for the next interval. Intervals were chosen such that the accumulated serosal concentration of 3-*O*-methylglucose never exceeded 30% of that of the mucosal solution.

Table II—Estimates of the Transfer Rate Constant for 3-*O*-Methylglucose Transport

	Graphical Analysis	Computer Fit
K_D, liters/min	8.8×10^{-6}	9.26×10^{-6}
K_m, m*M*	5.45	5.32
V_{max}, m*M*/min	2.50×10^{-4}	2.44×10^{-4}

In certain experiments, 0.08 m*M* phlorizin[6] was dissolved in both serosal and mucosal buffers. Phlorizin is a potent inhibitor of active sugar absorption (16). This concentration of phlorizin completely inhibited active sugar transport as determined by transfer experiments at a 10 m*M* sugar concentration.

Tissue Uptake and Transfer of ^{14}C-3-*O*-Methylglucose—Mucosal solutions were prepared such that they contained 0.03 μCi of ^{14}C-3-*O*-methylglucose[7] with appropriate addition of unlabeled sugar to assure a final concentration of 0.1 m*M*. Everted ligated sacs, 10 cm, prepared according to Wilson and Wiseman (14), were filled with 1.0 ml of buffer free of sugar and incubated for 10 min in 15 ml of mucosal solution. The sac contents and mucosal fluid were saved for liquid scintillation analysis. The sac tissue was rinsed quickly with 2 ml of water and then homogenized[8] in 2 ml of methanol. The homogenate was then centrifuged, and the methanol supernate was counted. Approximately 89% of all labeled compound added to the preparation was accounted for.

Assay—A colorimetric method (17) was employed for the quantitation of unlabeled 3-*O*-methylglucose. All solutions were then filtered[9] and analyzed spectrophotometrically[10] at 500 nm. The 3-*O*-methylglucose concentration was calculated using standard curves, taking into account blank tissue values.

Final solutions from ^{14}C-3-*O*-methylglucose experiments were analyzed for radioactivity with a liquid scintillation spectrometer[11]. From volume-adjusted samples, 0.2-ml aliquots were combined with 11 ml of scintillation cocktail[12] for counting both the aqueous and methanol solutions.

Data Evaluation—Transfer rates for each segment were calculated by averaging the amounts appearing in the serosal fluid for each time interval or from the slope of the cumulative amount as a function of time plot. With repeated experiments, rate determinations by either method yielded identical values. Statistical analysis of the data was evaluated by the Student *t* test (18). In all experiments, the two intestinal sacs prepared from each animal revealed no significant difference in transfer capabilities.

RESULTS AND DISCUSSION

To ensure the integrity of the transport mechanism and to characterize this process under the experimental conditions, sugar transfer rates were determined at various mucosal drug concentrations. Table I lists the average cumulative millimoles of 3-*O*-methylglucose transferred at the end of each time period with respect to the mucosal concentration. The amounts in the lower portion of the table are cumulative millimoles of 3-*O*-methylglucose transferred for experiments performed in the presence of 0.08 m*M* phlorizin. Sugar transfer with phlorizin would be indicative of the passive transfer rate of 3-*O*-methylglucose across the everted rat small intestine. Inspection of the rates for each concentration during each individual time period shows that the fluxes were similar up to 90 min, thus giving reason to believe that a steady state was obtained and that the integrity of the active transport process was maintained.

The 90–120-min interval is somewhat inconclusive because of the accelerated passive component at higher 3-*O*-methylglucose concentrations (Table I). The low calculated passive clearance may suggest a membrane-limited passive diffusion process as reported (19) for drugs with similarly low clearance values across rat intestinal sacs. Such drugs would display increases in their diffusion in the later stages of incubation, resulting from a loss of the functional integrity of the epithelial mucosal barrier. However, a tissue accumulation phenomenon as described for

[1] Texas Inbred Mice Co.
[2] Merck and Co., Rahway, N.J.
[3] Eastman-Kodak Co., Rochester, N.Y.
[4] Smith Kline and French Laboratories, Philadelphia, Pa.
[5] Calbiochem, Los Angeles, Calif.
[6] Sigma Chemical Co., St. Louis, Mo.
[7] New England Nuclear, Boston, Mass.
[8] Polytron model 125-C, Brinkmann Instruments.
[9] Type HA, 0.45 μm, Millipore Corp., Bedford, Mass.
[10] Coleman model 124.
[11] Packard model 3326 Tri-Carb.
[12] PCS, Amersham/Searle Corp., Arlington Heights, Ill.

Table III—Ratio of Serosal to Mucosal (S/M) Concentration of 3-*O*-Methylglucose[a] after 30 min of Incubation

Treatment	*n*	Ratio (S/M)[b]
Control	44	1.57 ± 0.25
Phenobarbital[c]	20	1.58 ± 0.23
II[d]	16	1.53 ± 0.32
I[e]	8	1.95 ± 0.29[f]

[a] Initial mucosal and serosal concentration = 0.78 m*M*. [b] Mean ± *SD*. [c] Given 80 mg/kg ip for 3 days prior to experiment. [d] Given 20 mg/kg ip for 48 hr prior to experiment. [e] Given 100 mg/kg ip for 24 hr prior to experiment. [f] $p < 0.05$.

methyl orange (20) cannot be ruled out. For this reason, only data up to 90 min were considered for the calculation of transfer rates.

Figure 1 shows the relationship between transfer rates obtained from the data in Table I and the 3-*O*-methylglucose mucosal concentration. The total active and passive transfer and the passive diffusion are illustrated separately.

The apparent active component can be evaluated from the observed differences in comparing the two sets of data. The application of Michaelis–Menten kinetics to a number of active intestinal transport systems was documented (21, 22) and yielded useful information regarding the characteristics of these transport processes. This fairly simple model was imposed on the apparent active transport, thus allowing estimation of the parameters descriptive of this treatment. Values for V_{max} of 2.50 $\times 10^{-4}$ m*M*/min and for K_m of 5.45 m*M* were calculated from linear regression analysis under the conditions of the experiments, and the representative Lineweaver–Burke plot is illustrated in Fig. 2.

For purposes of comparison, overall transfer rates for the case where the inhibitor was not present were again utilized for reestimation of parameters by a nonlinear least-squares computer program. The equation for the iterations was:

$$R = K_D[C] + \frac{V_{max}[C]}{K_m + [C]} \qquad \text{(Eq. 1)}$$

where R refers to the observed sugar transfer rate, K_D is the constant for passive clearance, C is the 3-*O*-methylglucose concentration in the mucosal buffer, and V_{max} and K_m are Michaelis–Menten kinetic constants. Computer estimates of V_{max}, K_m, and K_D appear in Table II. Original estimates were determined from linear regression analysis and the passive rate (from data presented in Fig. 1 and Table I). Data points at each concentration were weighted with the reciprocal of the variances. Comparatively, both methods of approximation gave fairly similar values for the parameters for the experiments (Table II).

The results of studies employing the Wilson and Wiseman (14) technique for comparing differences in intestinal sugar transport in treated and control animals appear in Table III. All segments were incubated for 1 hr, and pretreatments were performed as described under *Experimental*. These experiments were designed to provide a means for preliminary screening for the effects of pretreatment. Segments from control animals had final serosal to mucosal concentration ratios of 1.57 ± 0.25.

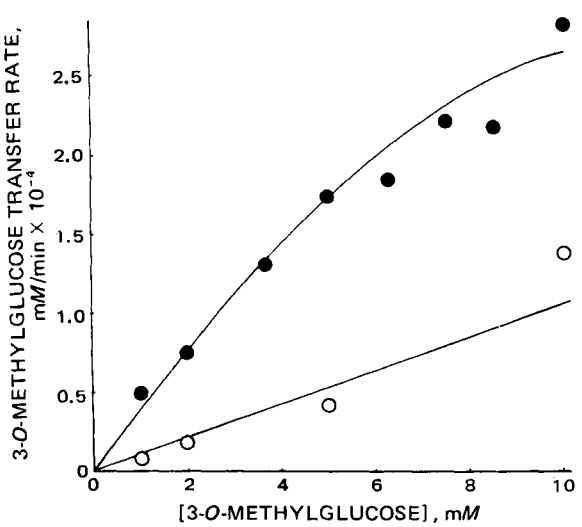

Figure 1—*Plot of the 3-O-methylglucose transfer rate across the everted rat small intestine* versus *3-O-methylglucose concentration alone (●) and in the presence of 0.08 m*M *phlorizin (○).*

Table IV—Effect of Pretreatment on the Rate and Amount of 3-*O*-Methylglucose[a] Transferred across the Everted Rat Small Intestine

Treatment	*n*	Rate of 3-*O*-Methylglucose Transfer, m*M*/min × 10^{-6} ± *SD*	Amount Transferred in 2 hr, m*M*
Control	10	49.2 ± 10.1	5.81 ± 0.99
Phenobarbital, oral	2	44.3	5.67
Phenobarbital, intraperitoneal	4	40.7 ± 5.4	4.73 ± 0.76
II, oral	4	45.2 ± 10.6	5.63 ± 1.07
II, intraperitoneal	4	37.5 ± 3.7	5.09 ± 0.59
I, oral	8	45.9 ± 12.8	5.49 ± 1.46
I, intraperitoneal	8	42.3 ± 9.4	5.37 ± 1.04

[a] Initial mucosal concentration = 1 m*M*.

Intestinal sacs prepared from animals pretreated with phenobarbital and II had ratios of 1.58 ± 0.23 and 1.53 ± 0.32, respectively, and showed no significant differences compared to controls. However, pretreatment with I resulted in significant increases in the final ratios, 1.95 ± 0.29. Nevertheless, this 24% increase may not be justification to assume that active transport was enhanced. Effects such as a decrease in serosal to mucosal flux in pretreated animals may result in misleading effects.

For this reason, experiments were performed with cannulated hanging sacs from segments of pretreated animals to compare transfer rates. In contrast to the ratio studies, the serosal solutions were free of the sugar, so transfer rates reflect both active and passive transfer. Table IV summarizes the rates observed after oral and intraperitoneal dosing of the inducing agents and demonstrate no significant differences between control and treated animals. As in the case of previous experiments with this technique, steady state was maintained throughout the 2-hr experiment. Comparing the total amounts of sugar transferred for each treatment showed no difference from control values.

These data appear to contradict the previous studies in that no increase in mucosal to serosal transport occurred with I treatment. It was apparent that further experiments would be necessary to separate the active component to examine pretreatment effects. To interpret the previous data better, investigations were conducted with ligated everted sacs containing buffer free of the sugar. Information obtained from short-time tissue uptake studies and transfer of 3-*O*-methylglucose at a low concentration (0.1 m*M*) would be more reflective of the active component.

Table V contains the millimoles of the sugar present in the sac tissue and in the serosal fluid after 10 min of incubation. Intraperitoneal pretreatment with II enhanced labeled sugar transfer; however, the amount in the tissue, although somewhat higher, was not significantly different than control values. Both oral and intraperitoneal administration of I resulted in enhanced 3-*O*-methylglucose transfer, but the tissue levels were increased significantly only for intraperitoneal administration. Phenobarbital pretreatment had no observed effect on either quantitative measurement compared to control experiments.

It is difficult to interpret why the effects of II were not noted in the two previous experiments performed at high sugar concentrations, and this

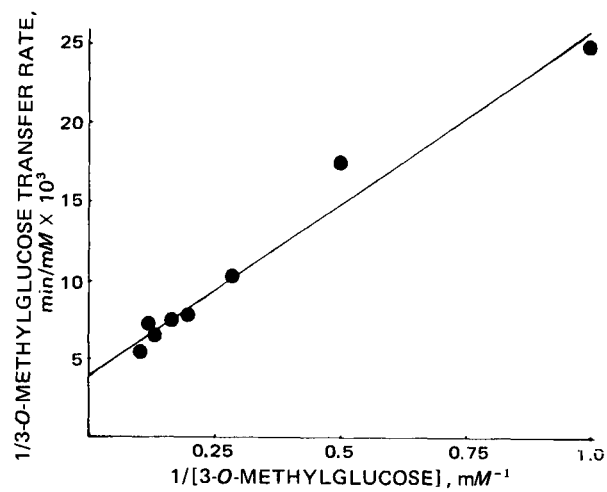

Figure 2—*Plot of the reciprocal of the 3-O-methylglucose transfer rate* versus *the reciprocal of the sugar concentration.*

Table V—Effect of Pretreatment on Transfer and Tissue Uptake of ^{14}C-3-*O*-Methylglucose[a] across the Everted Rat Small Intestine

Treatment	*n*	Amount Transferred to Serosal Fluid in 10 min, m*M* × 10^{-5}	10-min Tissue Uptake, m*M* × 10^{-5}
Control	28	0.38 ± 0.06	1.90 ± 0.32
Phenobarbital, oral	12	0.35 ± 0.06	2.09 ± 0.39
Phenobarbital, intraperitoneal	12	0.39 ± 0.08	1.89 ± 0.32
II, oral	12	0.36 ± 0.10	1.97 ± 0.21
II, intraperitoneal	12	0.58 ± 0.14[c]	2.22 ± 0.37[b]
I, oral	12	0.50 ± 0.09[c]	2.16 ± 0.50
I, intraperitoneal	12	0.60 ± 0.11[c]	2.64 ± 0.28[c]
Phlorizin	4	0.143 ± 0.004[c]	0.52 ± 0.13[c]

[a] Initial 3-*O*-methylglucose concentration = 0.1 m*M*. [b] $p < 0.1$. [c] $p < 0.001$.

result deserves further study. These experiments again demonstrate that everted intestinal sacs from I-treated animals appear to enhance abilities to transfer and uptake sugar. The fact that serosal accumulation of 3-*O*-methylglucose is not a complicating factor in these experiments points to a possible explanation of opposing effects of I on active and passive transport. This would explain the apparent lack of effect of I pretreatment in the cannulated everted intestinal sac experiments.

The present investigations demonstrated that pretreating rats with I, an enzyme-inducing agent, results in alteration of 3-*O*-methylglucose transfer across everted rat small intestinal sacs. Comparisons of results from several studies suggest that pretreatment with I may produce changes in both active and passive transfer. Alterations in the *in vitro permeability of red blood cells* by I were documented (23) and were believed to result from stability changes in the biological membrane, which were found to depend on the drug concentration in the suspension.

With regard to the active transport enhancement, the literature (10, 11) describes such changes with pretreatment of known liver microsomal-inducing agents. However, consideration must be given to visual observations made on the appearance and condition of the intestine removed from animals treated with I. As reported by Levy and Hayton (24), this drug has an inhibitory effect on GI motility. Their studies were performed at a lower dose (40 mg/kg), and their observations were made shortly afterward (40 *min*) compared to the present pretreatment. However, food material and bile were consistently noted in the small intestine of the treated animals in the present study.

Bile salts alone inhibit or depress active absorption of various substrates through intestinal tissue (25). On the other hand, bile salts are capable of altering the permeability of the intestinal membrane to drugs (26). Measurements of sac tissue weight showed an approximate 10–13% increase in the wet tissue weight of the sac prepared from treated rats. Twenty-four-hour fasting was reported to result in a loss in the intestinal tissue weight (27); however, the effects on active absorption were inconclusive after this fast period. The complexity of the situation existing in treated animals requires additional studies before a single conclusion can be reached. Further investigations are currently underway.

REFERENCES

(1) E. Anselmi, R. Jordana, and J. Larralde, *Rev. Esp. Fisiol.*, **25,** 211 (1969).

(2) *Ibid.*, **26,** 325 (1970).

(3) J. Larralde, M. J. Ruano, J. Bolafer, and R. Jordana, *Int. Physiol. Biochim.*, **83,** 271 (1975).

(4) S. Saleh, M. T. Khayyal, A. M. El Musri, and A. M. Ghazal, *Metabolism*, **18,** 599 (1969).

(5) T. Wilson and B. R. Landau, *Am. J. Physiol.*, **198,** 99 (1960).

(6) J. E. G. Barnett, A. Ralph, and K. A. Munday, *Biochem. J.*, **114,** 569 (1969).

(7) T. Z. Csaky, *Fed. Proc.*, **22,** 3 (1963).

(8) B. G. Lake, R. Hopkins, J. Chakraborty, J. W. Bridges, and D. V. W. Parke, *Drug Metab. Disp.*, **1,** 342 (1973).

(9) F. B. Thomas, N. Baba, N. J. Greenberger, and D. Salsburey, *J. Lab. Clin. Med.*, **80,** 548 (1972).

(10) F. B. Thomas, F. S. McCullough, and N. J. Greenberger, *Gastroenterology*, **62,** 590 (1972).

(11) V. S. Ostrower, P. Coan, and F. Kern, *ibid.*, **67,** 1162 (1974).

(12) B. B. Brodie, *J. Pharm. Pharmacol.*, **8,** 1 (1956).

(13) M. W. Anders and G. J. Mannering, *Mol. Pharmacol.*, **2,** 341 (1966).

(14) T. H. Wilson and G. Wiseman, *J. Physiol.*, **123,** 116 (1954).

(15) S. Feldman and M. Gibaldi, *J. Pharm. Sci.*, **58,** 425 (1969).

(16) H. Newey, B. J. Parsons, and D. H. Smyth, *J. Physiol.*, **148,** 83 (1959).

(17) N. Nelson, *J. Biol. Chem.*, **153,** 735 (1944).

(18) G. W. Snedecor and W. G. Cochran, "Statistical Methods," Iowa State University Press, Ames, Iowa, 1967, chap. 2.

(19) M. Gibaldi and B. Grundhofer, *Proc. Soc. Exp. Biol. Med.*, **141,** 564 (1972).

(20) M. Gibaldi and B. Grundhofer, *J. Pharm. Sci.*, **61,** 116 (1972).

(21) R. B. Fisher and D. S. Parsons, *J. Physiol.*, **119,** 210 (1953).

(22) E. L. Jervis and D. H. Smyth, *ibid.*, **149,** 433 (1959).

(23) I. P. Lee, H. I. Yamamura, and R. L. Dixon, *Biochem. Pharmacol.*, **17,** 1671 (1968).

(24) G. Levy and W. L. Hayton, *Life Sci.*, **10,** 691 (1971).

(25) T. M. Parkinson and J. A. Olson, *ibid.*, **6,** 393 (1963).

(26) S. Feldman and M. Gibaldi, *J. Pharm. Sci.*, **58,** 967 (1969).

(27) J. P. A. McManus and K. J. Isselbacher, *Gastroenterology*, **59,** 214 (1970).

Plant Anticancer Agents V: New Bisindole Alkaloids from *Tabernaemontana johnstonii* Stem Bark

DAVID G. I. KINGSTON ˣ, B. B. GERHART, F. IONESCU, M. M. MANGINO, and S. M. SAMI

Received December 22, 1976, from the *Department of Chemistry, Virginia Polytechnic Institute and State University, Blacksburg, VA 24061.* Accepted for publication May 13, 1977.

Abstract □ The isolation and structure elucidation of the three new bisindole alkaloids, gabunamine, tabernamine, and 19,20-epoxyconoduramine, from *Tabernaemontana johnstonii* stem bark are described. The isolation of the seven known alkaloids, conodurine, conoduramine, gabunine, isovoacangine, ibogamine, pericyclivine, and perivine, from the same source also is noted. The alkaloids gabunamine, gabunine, and tabernamine showed significant cytotoxicity against the P-388 cell culture system.

Keyphrases □ Alkaloids, various—isolated from *Tabernaemontana johnstonii* stem bark, structures elucidated, cytotoxic activity evaluated □ *Tabernaemontana johnstonii*—stem bark, various alkaloids isolated, structures elucidated, cytotoxic activity evaluated □ Cytotoxic activity—various alkaloids isolated from *Tabernaemontana johnstonii* stem bark evaluated

As part of a systematic survey of botanical sources for anticancer activity, an aqueous alcoholic extract of the stems and bark of *Tabernaemontana johnstonii* Pichon (Apocynaceae) was examined and gave reproducible activity against the cell culture (KB) of human carcinoma of the nasopharynx and against lymphocytic leukemia of the mouse (P-388). No previous studies on the constituents of this plant have been reported, but plants classified in the Tabernaemontaneae tribe are a rich source of indole alkaloids (1).

The tribe is almost the sole plant source of the iboga-type alkaloids, the related voacamine group of bisalkaloids, and the vobtusine group of bisalkaloids; it is also an important source of the 2-acylindole alkaloids and has afforded other types of indole alkaloids (1–3). The plant *T. holstii*, a close relative of *T. johnstonii*, was shown to contain the bisindole alkaloids conodurine, conoduramine, and gabunine and the indole alkaloids coronaridine, 19-oxocoronaridine, pericyclivine, perivine, and vobasine (4).

The purpose of the present work was to isolate the components of *T. johnstonii* responsible for the observed cytotoxicity and/or antileukemic activity.

EXPERIMENTAL

Materials and methods were generally the same as those previously described (4).

Plant Material—The air-dried stems and bark[1] of *T. johnstonii* Pichon (Apocynaceae) were collected in Kenya during 1971.

Extraction and Initial Separation of Alkaloids—plant material (10.3 kg) was extracted, and the crude alkaloid fraction (232 g) was subjected to chromatography on alumina as previously described (4). It yielded a benzene eluate, A (130 g), which was used in all subsequent work. Column chromatography of Fraction A on TLC grade silica gel[2,3] with elution by a chloroform–methanol gradient, yielded 14 fractions, B–O.

Isovoacangine (I)—Chromatographic separation of the combined Fractions C and D (14 g) on a silica gel column, with elution by chloroform, yielded a brown oil (3 g) in one group of fractions. Crystallization from methanol gave isovoacangine (I) as colorless crystals, mp 156–157°, undepressed in admixture with authentic material (5). The spectroscopic properties (IR, UV, and NMR) of the isolated material were consistent with this structural assignment.

Conodurine (II) and Conoduramine (III)—Fraction G (13.5 g) deposited crystals on standing in methanol at 0°. Purification of the crystalline material by preparative TLC, with development by ether–hexane–methanol (4:5:1) followed by final crystallization from methanol, yielded II. Fraction I (19 g) was subjected to column chromatography on TLC grade silica gel, with elution by ether–hexane–methanol (4:5:1), to yield a major fraction; this fraction gave pure III on crystallization from methanol. Both alkaloids were identical with the samples previously described (4).

Ibogamine (IV), Pericyclivine, and 19,20-Epoxyconoduramine (V)—Chromatographic separation of Fraction J on silica gel, with elution by benzene–dichloromethane–ether (10:8:5), yielded 14 major fractions. Purification of fraction 3 (1.2 g) by preparative TLC, with development

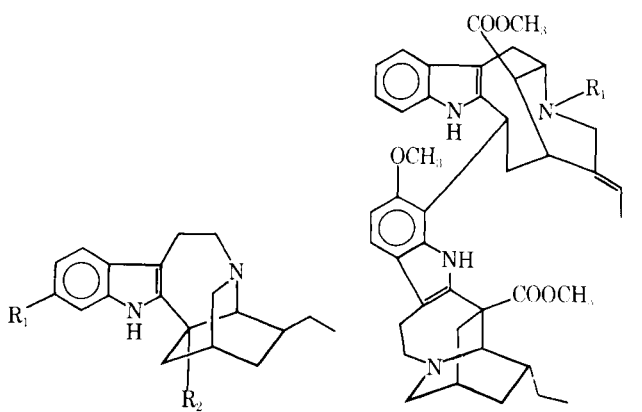

I: $R_1 = OCH_3$, $R_2 = COOCH_3$
IV: $R_1 = R_2 = H$

II: $R_1 = CH_3$
VI: $R_1 = H$

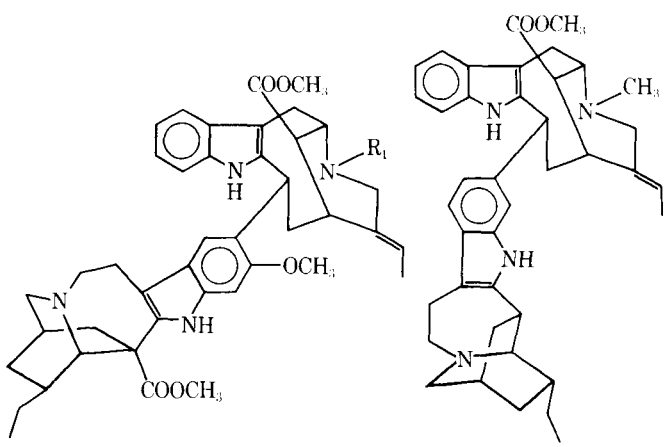

III: $R_1 = CH_3$
VII: $R_1 = H$

VIII

[1] Voucher specimens are on deposit at the U.S. Department of Agriculture, Beltsville, Md.

[2] Silica gel PF-254, EM Laboratories, Inc.

[3] R. L. Lyon, H. H. S. Fong, and N. R. Farnsworth, Department of Pharmacognosy and Pharmacology, University of Illinois at the Medical Center, Chicago, IL 60612, personal communication.

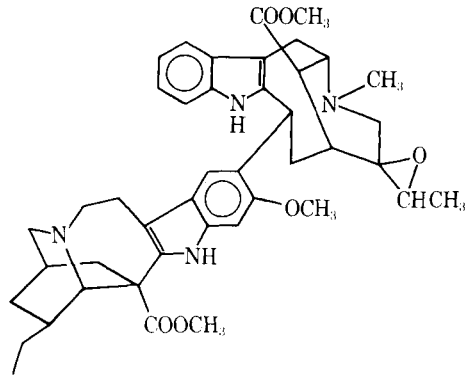

V

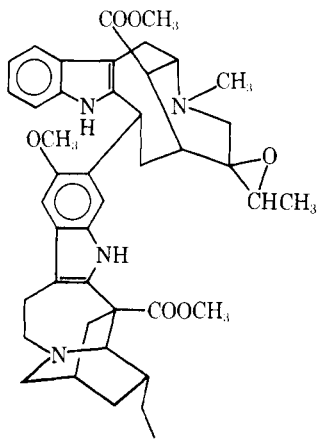

IX

by benzene–ether (5:1), yielded ibogamine (IV) as the major product, mp 159–161°, undepressed in admixture with authentic material (6, 7). Its IR spectrum was superimposable on that of authentic material. Fraction 7 (0.22 g) was purified by preparative TLC, with development by ether, to yield pericyclivine as the major component, mp 222–223° (after crystallization from methanol), undepressed in admixture with authentic material (4).

Fraction 10 (0.96 g) was subjected to preparative TLC in benzene–dichloromethane–ether–methanol (25:20:25:7). The center band was eluted and subjected to repeated preparative TLC in benzene–dichloromethane–ether–methanol (20:16:20:3) to yield 19,20-epoxyconoduramine (V) as colorless crystals (10 mg). The material had an R_f of 0.75 in the second solvent system and gave a brown color with the ceric sulfate spray reagent. The UV spectrum of the isolate showed λ_{max} 228 (log ϵ 4.72), 288 (4.12), and 295 (4.16) nm; its IR spectrum showed a strong band at λ_{max} 1730 cm^{-1}.

Perivine, Gabunine (VI), and Gabunamine (VII)—Fractions L and M were combined (10 g) and subjected to chromatography on silica gel, with elution by benzene–dichloromethane–ether (5:4:3) containing between 1 and 10% methanol, to yield 25 fractions. Fraction 5 (600 mg) was purified by preparative TLC in chloroform–methanol (90:10) to give perivine (280 mg) and gabunine (VI, 90 mg), identical with the samples previously described.

Fraction 8 (680 mg) was purified by preparative TLC in chloroform–methanol (95:5) to give gabunamine (VII, 84 mg). The isolated material was homogeneous on TLC, with R_f 0.35 in benzene–dichloromethane–ether–methanol (25:20:15:6), and gave an orange-brown color with the ceric sulfate spray reagent. Its IR spectrum showed several similarities to that of gabunine, with major absorptions at λ_{max} 3430, 1715, and 740 cm^{-1}. Its mass spectrum showed principal ions at m/e 704 (4), 690 (M^+, 2), 646 (6), 525 (3), 510 (4), 451 (4), 394 (4), 352 (10), 338 (21), 336 (20), 310 (12), 225 (43), 194 (60), 183 (22), 182 (36), 181 (26), 180 (40), 172 (40), 166 (100), 158 (47), 136 (35), and 122 (50). Its NMR spectrum showed signals at δ 0.90 (3H, triplet), 1.70 (3H, doublet), 2.48 (3H, singlet), 3.70 (3H, singlet), 3.96 (3H, broad singlet), 6.80 (1H, singlet), and 7.08 (4H, broad peak) ppm.

Chemical Modifications of VII—Compound VII (5 mg) was heated under reflux with 10% HCl–methanol (1:1) (5 ml) for 12 hr (8). Standard workup gave a crude product containing I (identified by TLC and its color with ceric sulfate) as the major component. Methylation of VII by a literature method (9) gave a compound identified as III by its TLC characteristics.

Synthesis of VI and VII—Compound I (60 mg) was heated under reflux in a nitrogen atmosphere with 1.5% methanolic hydrogen chloride; perivinol (120 mg) (10) was added in small portions over 1 hr. Reflux was continued for an additional 1.5 hr, and the mixture was cooled, made basic with sodium carbonate, and extracted with dichloromethane. The extracts were washed, dried, and evaporated to yield a crude product (165 mg), which was purified by preparative TLC in benzene–dichloromethane–ether–methanol (25:20:15:6). Elution of the band with R_f 0.35 yielded VII, identical with the sample isolated; elution of the band with R_f 0.50 yielded VI.

Isolation of Tabernamine (VIII)—Fraction N (9.7 g) was subjected to chromatography on TLC grade silica gel, with elution by ethyl acetate containing increasing amounts of ethanol, to give 11 fractions. The fifth fraction, which showed the greatest cytotoxicity, was subjected to preparative TLC in dichloromethane–methanol (85:15). The major component was eluted and purified further by high-pressure liquid chromatography (HPLC) on a silica gel column, 0.7 × 30 cm, with elution by ethyl acetate–hexane (9:1). The major fraction from this procedure was obtained as a white amorphous solid, homogeneous on TLC in two solvent systems and on HPLC, and was named tabernamine. The physical properties of tabernamine were described previously (11).

DISCUSSION

Tabernamine (VIII)—The major evidence for the structure of this new bisindole alkaloid was presented previously (11). It is of some importance, however, to assign unambiguously the position of attachment of the vobasane ring system to the ibogamine moiety. Therefore, the original arguments are amplified as follows.

The basic question concerns the assignment of the signals of the indole protons in the NMR spectrum of tabernamine. In deuterochloroform, tabernamine shows a doublet at δ 7.45 (1H) ppm and what appears to be a portion of another doublet at 7.03 (1H) ppm. One part of this second signal is obscured, however, by a large complex signal centered at δ 7.1 ppm because of the aromatic protons of the vobasane indole ring. In methanol, an *AB* quartet is clearly visible as two doublets at δ 6.88 and 7.28 ppm.

In simple indoles, the 4-proton (corresponding to the 11′-proton of tabernamine) absorbs downfield of the 5-, 6-, and 7-protons; for indole itself in acetone, for example, these resonances occur at δ 7.55, 7.00, 7.08, and 7.40 ppm, respectively (12). In various methyl indoles, the 4-proton absorbs downfield from the remaining protons at about δ 7.4–7.5 (chloroform) or 7.2 (acetone) ppm (13). On this basis, it is possible to assign the doublet observed at δ 7.45 (chloroform) or 7.28 (methanol) ppm to the 11′-proton in tabernamine, coupled with a coupling constant of 8 Hz to the 12′-proton whose resonance is observed at δ 7.03 (chloroform) or 6.88 (methanol) ppm. Since the 12′-proton shows no further coupling, the 13′-position must be occupied by the vobasane moiety, as indicated in Structure VIII.

Furthermore, it is known that the 7-proton of indole frequently shifts downfield when a more polar solvent is employed (14), while the 4-proton frequently shifts upfield under the same conditions (13). The observed upfield shift of the signal at δ 7.45 ppm in chloroform to 7.28 ppm in methanol is consistent only with its assignment to the 11′-proton, corresponding to the 4-proton of indole.

A further argument in favor of Structure VIII for tabernamine comes from studies of the position of electrophilic substitution in indole. Although electrophilic substitution on the benzene ring of indoles occurs in both the 5- and 6-positions, the 6-position is usually the major site of attack (15). In particular, electrophilic substitution on indoles containing a basic side chain occurs almost exclusively in the 6-position; tryptophan nitrate, for example, undergoes nitration in the 6-position to yield 6-nitrotryptophan (16). Therefore, it is most likely that ibogamine, containing a basic side chain, undergoes substitution in the 13′-position, corresponding to the 6-position of indole, to yield tabernamine of Structure VIII.

19,20-Epoxyconoduramine (V)—The evidence for the structure of this compound, isolated in very small yield from one specific fraction only, is entirely spectroscopic. The structural assignment should be regarded as tentative unless or until a larger sample can be made available for degradative studies.

The UV spectrum of the compound showed typical indole absorption, and its mass spectrum showed peaks typical of bisindole alkaloids of the conoduramine type. The parent ion was 16 mass units higher than that

Table I—Cytotoxicity of Certain Fractions and Pure Alkaloids from *T. johnstonii*[a]

Fraction or Alkaloid	ED_{50}, μg/ml P-388	KB
C	5.7	
D	16	
Isovoacangine (I)	18	59
E	18	
F	27	
G	19	
Conodurine (II)	26	31
Conoduramine (III)	20	19
H	13	
I	2.6	
J	3.0	
Ibogamine (IV)	–	>100
Pericyclivine	13	>100
K	2.6	
L	2.6	
M	2.7	
Perivine	20	70
Gabunine (VI)	3.2	–
Gabunamine (VIII)	1.3	5.8
N	2.3	
Tabernamine (VIII)	2.1	–
O	2.4	

[a] Bioassays were performed by the A. D. Little Co., Cambridge, Mass., using established protocols.

of conoduramine, requiring the placement of an additional oxygen in the molecule. A careful analysis of the mass spectrum indicated that the additional oxygen atom must be situated on the vobasane moiety of the bisalkaloid. Thus, the normal peaks derived from the alicyclic portion of the iboga moiety were observed at *m/e* 122, 136, and 148 (17). The peaks at *m/e* 180, 182, and 194, however, which would be expected from the alicyclic portion of the vobasane moiety (17), were shifted largely to *m/e* 196, 198, and 210; the small intensity peaks remaining at *m/e* 180, 182, and 194 presumably arise from the $(M - 16)^{+\cdot}$ ion discussed later.

Two important ions indicate that the additional oxygen atom is located as an epoxide function in the 19,20-position of the vobasane moiety. An intense peak at *m/e* 676 is due to loss of 44 mass units from the parent ion; the fragment lost in this process can also bear the charge and, in this case, appears as an ion at *m/e* 44. Loss of 44 mass units is a relatively uncommon process in mass spectrometry and is not observed from normal bisindole alkaloids of this type. It can be explained adequately, however, by the 19,20-epoxide structure proposed, since epoxides undergo transannular cleavage, leading in this case to the loss of a C_2H_4O fragment (18). The observation of a fragment ion at *m/e* 704 (M − 16) is also consistent with the epoxide formulation, since loss of oxygen has been observed from other alkaloidal epoxides (17).

The NMR spectrum of the new compound fully supports the structure proposed. In particular, the three-proton doublet at δ 1.34 ppm may be assigned to the 18-methyl group (19), and three-proton singlets at δ 2.42, 2.60, and 3.66 ppm occur at essentially the same chemical shift as the corresponding signals in conoduramine. The observation of a broadened three-proton signal at δ 3.92 ppm is also significant, because a similarly broadened signal occurs in the NMR spectrum of conoduramine and may be assigned to the hydrogen-bonded methoxyl group of the isovoacangine ring. Finally, the aromatic region of the spectrum of the new compound shows a similar pattern of peaks to conoduramine, establishing that the vobasane unit is linked to the 12′-position of the isovoacangine moiety.

The preceding evidence establishes the major features of the structure of the new compound as being those of 19,20-epoxyconoduramine (V) or 19,20-epoxyvoacamine (IX). Since no voacangine-derived bisalkaloids have been detected in *T. johnstonii*, Structure V probably may be assigned to the new compound. Study of the details of the stereochemistry of the epoxy substituent and definitive proof of this structural assignment await the isolation of a further quantity of material.

This is the first report of the isolation of any alkaloid of the vobasane skeleton containing a 19,20-epoxy function, although a recent report (20) described such a function in an alkaloid with the dihydroakuammiline skeleton.

Gabunamine (VII)—The structure of this new compound is established by its degradation to isovoacangine, by its synthesis from isovoacangine and perivinol, and by its conversion to conoduramine. The spectroscopic data for the compound are entirely consistent with the assigned structure. In particular, the mass spectrum indicated its relationship to conoduramine and related molecules, while the NMR spectrum indicated that it differed from conoduramine only in the lack of an *N*-methyl group. The name gabunamine is assigned to the compound since it is related to conoduramine in the same way that gabunine is related to conodurine.

Cytotoxic Activities—The isolation of the alkaloids described was undertaken on the basis of the cytotoxicity of the various fractions investigated; the cytotoxicities of Fractions C–O, and of the alkaloids isolated therefrom, are given in Table I. The cytotoxicity of 19,20-epoxyconodurine could not be determined because of the scarcity of material.

The P-388 *in vitro* assay system appears to be more sensitive to most indole alkaloids tested than does the KB assay, and it thus might prove to be a generally useful screen for compounds of this type. The alkaloids isolated also largely account for the cytotoxicity of the fractions from which they were isolated, although the possibility cannot be excluded that other, unknown compounds also contribute to the cytotoxicities of the crude fractions.

REFERENCES

(1) R. Hegnauer, "Chemotaxonomie der Pflanzen," vol. 3, Birkhäuser, Basel, Switzerland, 1964, pp. 124–163, 632–637.

(2) M. Hesse, "Indolalkaloide in Tabellen," Springer-Verlag, Berlin, Germany, 1964 and 1968.

(3) "The Alkaloids," vols. 8 and 11, R. H. F. Manske, Ed., Academic, New York, N.Y., 1965 and 1968.

(4) D. G. I. Kingston, B. T. Li, and F. Ionescu, *J. Pharm. Sci.*, **66,** 1135 (1977).

(5) U. Renner, D. A. Prins, and W. G. Stoll, *Helv. Chim. Acta*, **42,** 1572 (1959).

(6) D. F. Dickel, C. L. Holden, R. C. Maxfield, L. E. Paszek, and W. I. Taylor, *J. Am. Chem. Soc.*, **80,** 123 (1958).

(7) M. F. Bartlett, D. F. Dickel, and W. I. Taylor, *ibid.*, **80,** 126 (1958).

(8) W. Winkler, *Naturwissenschaften*, **48,** 694 (1961).

(9) M. P. Cava, S. K. Talapatra, J. A. Weisbach, B. Douglas, R. F. Raffauf, and J. L. Beal, *Tetrahedron Lett.*, **1965,** 931.

(10) M. Gorman and J. Sweeny, *ibid.*, **1964,** 3105.

(11) D. G. I. Kingston, B. B. Gerhart, and F. Ionescu, *ibid.*, **1976,** 649.

(12) P. J. Black and M. L. Heffernan, *Aust. J. Chem.*, **18,** 353 (1965).

(13) J.-Y. Lallemand and T. Bernath, *Bull. Soc. Chim. Fr.*, **1970,** 4091.

(14) M. G. Reinecke, H. W. Johnson, Jr., and J. F. Sebastian, *J. Am. Chem. Soc.*, **91,** 3817 (1969).

(15) R. J. Sundberg, "The Chemistry of Indoles," Academic, New York, N.Y., 1970.

(16) R. de Fazi, G. Berti, and A. Da Settimo, *Gazz. Chim. Ital.*, **87,** 2238 (1959).

(17) M. Hesse, "Indolalkaloide," Verlag Chemie, Weinheim, West Germany, 1974.

(18) H. Budzikiewicz, C. Djerassi, and D. H. Williams, "Mass Spectrometry of Organic Compounds," Holden-Day, San Francisco, Calif., 1967.

(19) L. M. Jackman and S. Sternhell, "Applications of Nuclear Magnetic Resonance Spectroscopy in Organic Chemistry," 2nd ed., Pergamon, Oxford, England, 1969.

(20) S. Mamatas-Kalamaras, T. Sévenet, C. Thal, and P. Potier, *Phytochemistry*, **14,** 1849 (1975).

ACKNOWLEDGMENTS

Supported by Research Grant CA-12831 from the National Cancer Institute, U.S. Department of Health, Education, and Welfare, Bethesda, MD. 20014.

The authors thank Dr. U. Renner for a sample of isovoacangine, Dr. D. F. Dickel (Ciba-Geigy) and Mr. E. S. Rump (Smith Kline and French Laboratories) for samples of ibogamine, Dr. M. P. Cava for samples of conodurine, conoduramine, and gabunine, Dr. G. H. Svoboda (Lilly Research Laboratories) for a generous sample of perivine, and Dr. R. E. Perdue, Jr., of the U.S. Department of Agriculture, Beltsville, Md., for plant material (Collection PR-25267).

Previous paper: D. G. I. Kingston, F. Ionescu, and B. T. Li, *Lloydia*, **40,** 215 (1977).

Bioavailability of Acetazolamide Tablets

GERALD J. YAKATAN ˣ, EDWARD L. FROME, ROBERT G. LEONARD, ASHOK C. SHAH *, and JAMES T. DOLUISIO

Received April 4, 1977, from the *Drug Dynamics Institute, College of Pharmacy, University of Texas at Austin, Austin, TX 78712.* Accepted for publication May 26, 1977. *Present address: The Upjohn Co., Kalamazoo, MI 49001.

Abstract □ Plasma acetazolamide levels were measured by an enzymatic assay following single 250-mg oral tablet doses to 20 healthy volunteers; five different lots of acetazolamide tablets from a single manufacturer were used in a balanced incomplete block design. From the measured plasma levels, estimates of the bioavailability parameters (area under the plasma concentration *versus* time curve, time to peak plasma concentration, and peak plasma concentration) were obtained by least-squares digital computer fitting. No significant differences among the tablets were observed ($\alpha = 0.05$) for the analysis of variance of the area under the curve or time to peak parameters. Two tablets, however, provided statistically higher peak plasma concentrations than the other three. Thus, lot-to-lot bioinequivalence of acetazolamide tablets was observed. Some *in vitro* tests employed showed general trends for correlation with the *in vivo* data. However, considerable refinement of these techniques appears necessary for *in vitro* prediction of the observed lot-to-lot bioinequivalence.

Keyphrases □ Acetazolamide—bioavailability of various tablet lots compared in humans □ Bioavailability—acetazolamide, various tablet lots compared in humans □ Carbonic anhydrase inhibitors—acetazolamide, bioavailability of various tablet lots compared in humans

Acetazolamide is a potent carbonic anhydrase inhibitor and finds its primary use in the management of chronic simple and secondary glaucoma. The drug has been reported to be quantitatively absorbed from the human GI tract and to have a plasma half-life of about 100 min (1, 2). About 80% of the drug is excreted by tubular secretion of the anionic species, and 70–90% of the administered dose is recovered unchanged within 24 hr (3). The apparent volume of distribution in humans is about 20% of body weight (4).

Lehmann *et al.* (4) reported that acetazolamide was absorbed with an apparent half-life of approximately 0.5 hr and eliminated with an apparent half-life of 4.1 hr (range of 2.4–5.8 hr). Peak plasma levels were seen in 2 hr (range of 1.25–3 hr); however, the drug was taken soon after a meal. One subject showed poor absorption and had a flat plasma concentration–time curve with concentrations never exceeding 1.4 μg/ml after a 500-mg oral dose. Other investigators observed a lack of response in a patient given acetazolamide orally who responded to intramuscular therapy (5). Maren and Robinson (2) also reported variable acetazolamide absorption but only at high doses.

Variations in the bioavailability of acetazolamide dosage forms possibly may result from formulation factors or aging. Another sulfonamide-type diuretic, hydrochlorothiazide, has shown variable dissolution characteristics for tablet formulations (6, 7). Tannenbaum *et al.* (8) showed that product formulation could affect the bioavailability of hydrochlorothiazide dosage forms, although recently (9, 10) several groups showed that possible differences in dissolution may not be reflective of significant differences in the bioavailability of commercial products. These studies were based on urinary excretion data only, however.

Therefore, there may be variability in dissolution and/or bioavailability with low solubility sulfonamides in tablet formulations. The possibility that such variations may occur with acetazolamide prompted the present study.

The objectives of this study were to establish a methodology for determining the biological equivalency of acetazolamide tablets in humans, to determine whether lot-to-lot variability in bioavailability occurs, to provide *in vitro* dissolution rate data capable of indicating potential lot-to-lot variability in acetazolamide tablets, and to correlate *in vitro* dissolution parameters with *in vivo* bioavailability data.

EXPERIMENTAL

Materials—Acetazolamide powder[1] was used to prepare standards. The 250-mg acetazolamide tablets[2] (designated A–E) used in the human studies were representative of tablets found in normal channels of distribution. All other chemicals were analytical reagent grade.

Disintegration and Dissolution Studies—Disintegration and dissolution measurements on the 250-mg acetazolamide tablets were carried out utilizing the USP XIX methods. The conditions were as follows: temperature, 37°; dissolution media, distilled water, simulated gastric fluid without pepsin, and pH 10 carbonate buffer; volume of dissolution medium, 900 or 1500 ml; and stirring speed, 50 or 100 rpm.

Filtered samples were withdrawn from the dissolution flasks at various times up to 1 hr, and the absorbance of the solution was determined at 265 nm. Where necessary to maintain the absorbance readings in the region from 1 to 2 units, the samples were quantitatively diluted.

Dissolution rate measurements also were obtained utilizing the rotating-filter-stationary basket apparatus (11).

Assay of Plasma Acetazolamide—Plasma acetazolamide levels were determined by a modified enzymatic method based on the inhibition of carbonic anhydrase activity. The method was originally developed by Maren (12) to evaluate the relative activity of compounds that inhibit carbonic anhydrase. Although little information on the sensitivity or reproducibility of the assay was available, the ease and rapidity of the technique indicated that it would be advantageous for the large number of samples generated in bioavailability studies. The Maren technique was modified to provide a rapid, accurate, and precise method for determining plasma acetazolamide; the procedure was described in detail previously (13).

Bioavailability Studies in Humans—*Selection of Subjects*—Normal, healthy, adult males, who were within 10% of their ideal body weight (14) and 21–40 years of age, were admitted to the study. Informed signed consent was obtained from each subject. One week prior to initiation of the study, the subjects were given a thorough physical examination including extensive laboratory tests. Subjects with test results outside normal limits were excluded, as were any individuals showing a history of any significant organ abnormality or disease.

Study Design—The basic experimental design employed to determine relative bioavailability of the five acetazolamide dosage forms was a balanced incomplete block design. The 20 subjects were randomly assigned to 10 different groups (two subjects per group), and each subject received three of the five possible treatments. The treatments were separated by a 1-week washout period, and the design balanced over weeks. The balanced incomplete block design utilized is shown in Table I.

Administration of Dosage Forms—The subjects were fasted overnight prior to and for 4 hr immediately after administration of a 250-mg

[1] Diamox (CL 6063, Batch D3235), Lederle Laboratories, Pearl River, N.Y.
[2] Diamox (Lot Nos.: A, 396-341; B, 401-351; C, 4469-680; D, 4469-324; and E, 4469-475), Lederle Laboratories, Pearl River, N.Y.

Table I—Balanced Incomplete Block Design for Acetazolamide Bioavailability Study

Group	Subject	Treatment[a] Week 1	Week 2	Week 3
I	1	A	B	C
	2	A	B	C
II	3	A	E	B
	4	A	E	B
III	5	B	C	D
	6	B	C	D
IV	7	B	D	E
	8	B	D	E
V	9	C	D	E
	10	C	D	E
VI	11	C	E	B
	12	C	E	B
VII	13	D	B	A
	14	D	B	A
VIII	15	D	C	A
	16	D	C	A
IX	17	E	A	C
	18	E	A	C
X	19	E	A	D
	20	E	A	D

[a] Treatments on different lots of 250-mg acetazolamide tablets.

acetazolamide tablet. The tablet was administered with 240 ml of water. Four hours postadministration, the subjects were given a meal and were allowed to eat and drink normally during the rest of the day.

The subjects were ambulatory throughout each 12-hr treatment day and were permitted to proceed with their normal daily routine inasmuch as was possible considering their availability for blood sampling. The subjects were not permitted to engage in any strenuous or athletic activities on the day of drug administration.

Blood Collection Schedule—The following blood samples were collected: 6-ml samples were drawn at 0, 0.5, 1.0, 1.5, 2.0, 3.0, 4.0, 6.0, 8.0, 10.0, 12.0, and 24.0 hr following drug administration.

The blood samples were drawn through an indwelling 19-gauge scalp vein needle into heparinized specimen tubes. The samples were centrifuged immediately, and the plasma was removed and frozen until assayed.

RESULTS AND DISCUSSION

Disintegration and Dissolution Studies—The results of the disintegration studies are shown in Table II. The data are generally internally consistent; *i.e.*, the rank order for disintegration is reasonably well maintained over the different disintegration media employed. Tablet E stands out significantly as the slowest disintegrating form tested.

The USP dissolution apparatus was utilized for most dissolution studies since it was readily available. The studies were run for 1 hr, and the times to achieve dissolution of different percentages of the acetazolamide present in a tablet were determined from plots of percent of dose dissolved *versus* time. The values obtained for the five tablets used in the human bioavailability studies are given in Table III. The dissolution data obtained using distilled water or simulated gastric fluid do not show any gross differences among the dosage forms under the conditions employed, although Tablets C and D dissolved faster than the other three products in gastric fluid.

In carbonate buffer, however, Tablet E shows markedly different dissolution characteristics (less than 20% in solution in 1 hr *versus* 20% in solution in generally less than 10 min for the other dosage forms). Thus, a nonphysiological dissolution medium detects differences in dissolution behavior of acetazolamide tablets not observable with more traditional

Table II—Disintegration Time (Seconds) of Different Lots of Acetazolamide Tablets by USP XIX Method

Tablet	Disintegration Medium: Gastric Fluid[a]	Distilled Water[a]	Carbonate Buffer[b]
A	45.0 ± 5.0	82.3 ± 9.8	543 ± 240
B	37.7 ± 2.5	49.7 ± 8.4	374 ± 230
C	30.3 ± 3.1	24.0 ± 2.0	180 ± 13.4
D	65.0 ± 5.6	42.3 ± 3.2	388 ± 120
E	112.0 ± 15.2	124.0 ± 21.0	2169 ± 465

[a] Mean ± *SD*, $n = 3$. [b] Mean ± *SD*, $n = 6$.

Table III—Dissolution Behavior of Different Lots of Acetazolamide Tablets Using the USP Apparatus

Medium	Tablet	Dissolution Time[a], min T_{10}	T_{20}	T_{25}	T_{30}	T_{40}	T_{50}	T_{75}
Water	A	12	25	32	39	52		
	B	13	27	34	42	58		
	C	11	33	51	>60	>60		
	D	9	25	34	45	>60		
	E	12	25	33	42	60		
Gastric fluid	A	11	24	31	37	55		
	B	12	25	33	40	58		
	C	12	23	28	32	42	54	
	D	8	20	25	32	44		
	E	10	23	32	41	60		
Carbonate buffer	A	6	12	14	17	23	30	44
	B	3	7	8	10	14	18	32
	C	2	3	4	5	9	15	46
	C	2	3	3	5	10	18	38
	D	3	4	5	6	9	12	30
	D	3	5	6	7	9	12	30
	E	26	>60					
	E	32	>60					

[a] Dissolution measurements were carried out under the following conditions: 900-ml dissolution volumes, 37°, 1-hr total time, and 50 rpm.

dissolution media.

The dissolution data obtained with the rotating-filter–stationary basket apparatus (Table IV) appear to show greater sensitivity to possible differences in the tablets. Although dissolution was relatively rapid under the conditions employed, greater percentage differences were observed between Tablets C and D and the others with this dissolution procedure than with the USP method.

Bioavailability Studies in Humans—The plasma samples obtained were assayed as outlined under *Experimental*. The plasma concentration *versus* time curves for each subject were analyzed according to a one-compartment open model with a lag time of the form shown in Scheme I:

$$\xrightarrow{\text{lag}} G \xrightarrow{k_a} B \xrightarrow{k_e} U$$

Scheme I

where G, B, and U represent the amounts of drug in the GI tract, total body, and the amount excreted, respectively; and k_a and k_e represent the overall first-order rate constants associated with the loss of drug from the GI tract and the body, respectively. Since measurements of drug concentrations were made in the central or total body compartment, the acetazolamide levels in this compartment as a function of time can be described by:

$$b = \frac{\gamma_a D_0 k_a}{(k_a - k_e)V_B}\{\exp[-k_e(t - L)] - \exp[-k_a(t - L)]\} \quad \text{(Eq. 1)}$$

where b represents the concentration of acetazolamide in the body compartment at any time, t; γ_a is the fraction of the dose, D_0, absorbed; V_B is the volume of distribution for the body compartment; and L is the time lag accounting for dosage form or physiological factors delaying drug absorption.

If y_i, $i = 1 \ldots, n$, denotes the concentration measured at time x_i, the model that is to be fit is:

$$E(y_i) = \frac{\alpha_1\alpha_3}{(\alpha_1 - \alpha_2)}\{\exp[-\alpha_2(x_i - \alpha_4)] - \exp[-\alpha_1(x_i - \alpha_4)]\} \quad \text{(Eq. 2)}$$

Table IV—Dissolution Behavior of Different Lots of Acetazolamide Tablets Using the Rotating-Filter–Stationary Basket Apparatus

Tablet	Dissolution Time[a], min T_{30} Average	Range	T_{50} Average	Range	T_{90} Average	Range
A	4.1	4.5–3.6	5.9	5.1–6.9	9.00	7.8–10.9
B	1.9	1.6–2.3	2.7	2.3–2.8	5.7	5.2–6.1
C	1.1	1.0–1.2	1.48	1.4–1.6	3.0	2.5–4.0
D	1.6	1.3–2.0	2.16	1.7–2.9	3.96	3.4–4.4
E	4.0	3.1–4.7	5.25	4.0–6.9	8.03	6.7–9.6

[a] Experimental conditions: observations made on six tablets; medium = 1000 ml, pH 7.2 phosphate buffer; 37°; and 400 rpm.

Table V—Maximum Plasma Concentration Achieved (Micrograms per Milliliter) as a Function of Tablet Lot, Study Day, and Subject after Administration of 250-mg Acetazolamide Tablets

	Study Day 1		Study Day 2		Study Day 3	
Tablet	Subject	C_{max}	Subject	C_{max}	Subject	C_{max}
A	1	6.10	17	4.88	13	6.50
	2	8.11	18	10.13	14	Dropped
	3	6.02	19	5.71	15	8.76
	4	5.81	20	6.48	16	6.32
B	5	5.10	1	4.51	3	8.67
	6	12.11	2	10.31	4	13.10
	7	8.67	13	6.29	11	8.04
	8	10.52	14	Dropped	12	8.90
C	9	9.66	5	9.51	1	6.49
	10	8.40	6	17.94	2	13.46
	11	6.90	15	17.27	17	12.60
	12	12.86	16	11.43	18	12.99
D	13	9.57	7	15.63	5	9.43
	14	10.16	8	17.15	6	12.78
	15	14.12	9	11.25	19	8.07
	16	10.84	10	10.03	20	5.63
E	17	11.03	3	8.08	7	5.64
	18	7.79	4	11.12	8	9.23
	19	4.89	11	12.29	9	9.60
	20	9.01	12	4.91	10	9.20

where α_1 represents the rate constant k_a; α_2 represents k_e; α_3 represents the absorbed dose/apparent volume of distribution, $\gamma_a D_0/V_B$; and α_4 is the delay time, L.

The computational problem is to:

$$\underset{\alpha}{\text{minimize}} \sum_{i=1}^{n} [y_i - E(y_i)]^2$$

i.e., to find the least-squares estimates of the parameters $\alpha = \alpha_1, \alpha_2, \alpha_3$, and α_4. Gradient methods, which lead to iterative least-squares algorithms, are often unstable and fail to converge. For this reason, the Nelder–Mead (15) simplex algorithm, NELMIN, as coded by O'Neil (16), was employed to obtain the least-squares estimates. O'Neil's FORTRAN subroutine requires the FORTRAN function for the minimization problem described[3]. The initial estimates of the α values were determined graphically for each curve.

A FORTRAN program, CTCNM, utilizing the Nelder–Mead procedure, was then developed and run on a digital computer[4]. After obtaining the least-squares estimates, $\hat{\alpha}$, CTCNM computes estimates of time to maximum concentration, maximum concentration, and area under the concentration–time curve. Output also includes a table with the input data, fitted values, residuals, and the minimum sum of squares evaluated at $\hat{\alpha}$.

The estimates of maximum concentration, time to maximum concentration, and the area under the concentration–time curve for each subject and tablet studies are given in Tables V–VII, respectively. Figure 1 shows the mean plasma concentration–time curves for each tablet and the computer fits of the data according to Eq. 2. Visual interpretation of the concentration–time curves shown should be made with the understanding that a complete crossover design was not employed.

Statistical Analysis of Data—The analysis of variance was utilized to determine whether the bioavailability of the five tablets studied was different. Each bioavailability parameter, area under the plasma concentration–time curve (AUC), time to peak concentration (t_{max}), and maximum concentration achieved (C_{max}), was treated as the response in a univariate analysis of variance. The statistical analysis was complicated by the loss of some data which occurred when one subject withdrew from the study. Since the design was no longer balanced, it was necessary to utilize regression methods to obtain the analysis of variance. The statistical model employed was:

$$Y_{ijk} = \mu + \beta_{ij} + \rho_j + \tau_k + \epsilon_{ijk} \qquad \text{(Eq. 3)}$$

where μ is the overall mean; β represents subject effects; τ represents treatment effects; ρ represents a replication effect; $i = 1, 2, \ldots, 10$; $j = 1, 2$; and $k = 1, 2, \ldots, 5$. The ϵ's are assumed to behave as independent, random, normal variables with mean zero and constant variance. The parameters are subject to the usual constraints: $\sum_{i=1}^{10}\beta_{ij} = 0$ for $j = 1, 2$; $\sum_{k=1}^{5}\tau_k = 0$; and $\rho_1 = -\rho_2$. The model (Eq. 3) was expressed in matrix notation, and the computations were performed using the FIT command in Omnitab II (17). This program provides all of the results required in the subsequent analysis, including estimates of the parameters, the residual sum of squares, and estimates of the parameter variance–covariance matrix.

This approach permitted the construction of an analysis of variance table for the unbalanced incomplete block design data to determine whether bioavailability differences existed among the tablets studied. Analysis of the data in Table VII for the area under the plasma concentration–time curve (AUC) showed no significant differences among tablets at the 0.05 level. The ranked treatment means for the five tablets studied were (micrograms per milliliter × hours): A, 87.2; D, 88.1; E, 89.0; C, 91.9; and B, 103.1.

The analysis of variance table for the AUC data showed:

source	*df*	*SS*	*MS*	*F*
treatments (adjusted)	4	1716.77	429.19	1.51
residual	34	9686.33	284.89	
critical value: $F_{0.05}(4,34) = 2.65$				

Table VI—Time to Maximum Plasma Concentration (Hours) as a Function of Tablet Lot, Study Day, and Subject after Administration of 250-mg Acetazolamide Tablets

	Study Day 1		Study Day 2		Study Day 3	
Tablet	Subject	t_{max}	Subject	t_{max}	Subject	t_{max}
A	1	6.53	17	4.87	13	2.38
	2	1.33	18	1.36	14	Dropped
	3	7.89	19	0.97	15	3.30
	4	5.83	20	4.54	16	6.77
B	5	4.84	1	4.28	3	2.71
	6	2.24	2	1.56	4	2.06
	7	1.71	13	5.70	11	2.18
	8	2.66	14	Dropped	12	2.71
C	9	3.83	5	5.28	1	5.25
	10	0.86	6	0.22	2	0.26
	11	5.29	15	1.55	17	0.67
	12	1.83	16	0.18	18	1.18
D	13	2.93	7	1.06	5	2.56
	14	0.20	8	0.67	6	0.70
	15	1.03	9	2.33	19	3.22
	16	3.60	10	2.52	20	2.58
E	17	0.65	3	7.74	7	4.19
	18	2.68	4	2.16	8	4.02
	19	0.68	11	0.35	9	1.86
	20	4.00	12	0.71	10	1.06

Analysis of the data in Table VI for the time to achieve peak concentration (t_{max}) also showed no significant differences among the tablets tested. The ranked treatment means (hours) for the dosage forms studied were: D, 2.06; C, 2.38; E, 2.51; B, 2.52; and A, 3.96.

The analysis of variance table for the time to peak data showed:

source	*df*	*SS*	*MS*	*F*
treatments (adjusted)	4	19.71	4.93	1.74
residual	34	96.25	2.83	
critical value: $F_{0.05}(4,34) = 2.65$				

Although no statistically significant differences could be noted, the mean data show that Tablet A took almost twice as long as Tablet D to reach peak plasma levels.

The peak plasma concentration data (C_{max}) presented in Table V show that statistically significant differences existed among the tablets tested. The ranked treatment means (micrograms per milliliter) for the five dosage forms were: A, 6.90; B, 8.55; E, 8.60; D, 11.28; and C, 11.44.

The analysis of variance table for the peak plasma concentration data showed:

source	*df*	*SS*	*MS*	*F*
treatments (adjusted)	4	143.21	35.80	6.21
residual	34	196.13	5.77	
critical value: $F_{0.05}(4,34) = 2.65$				

To determine which of the tablets differed from one another, the standard deviation for the difference between two treatment means was calculated. The value calculated was that which yielded the largest value for the standard deviation from the variance–covariance matrix. Thus, the most conservative estimate available was used to test for differences among tablets.

[3] Available on request from the authors.
[4] CDC 6600-6400.

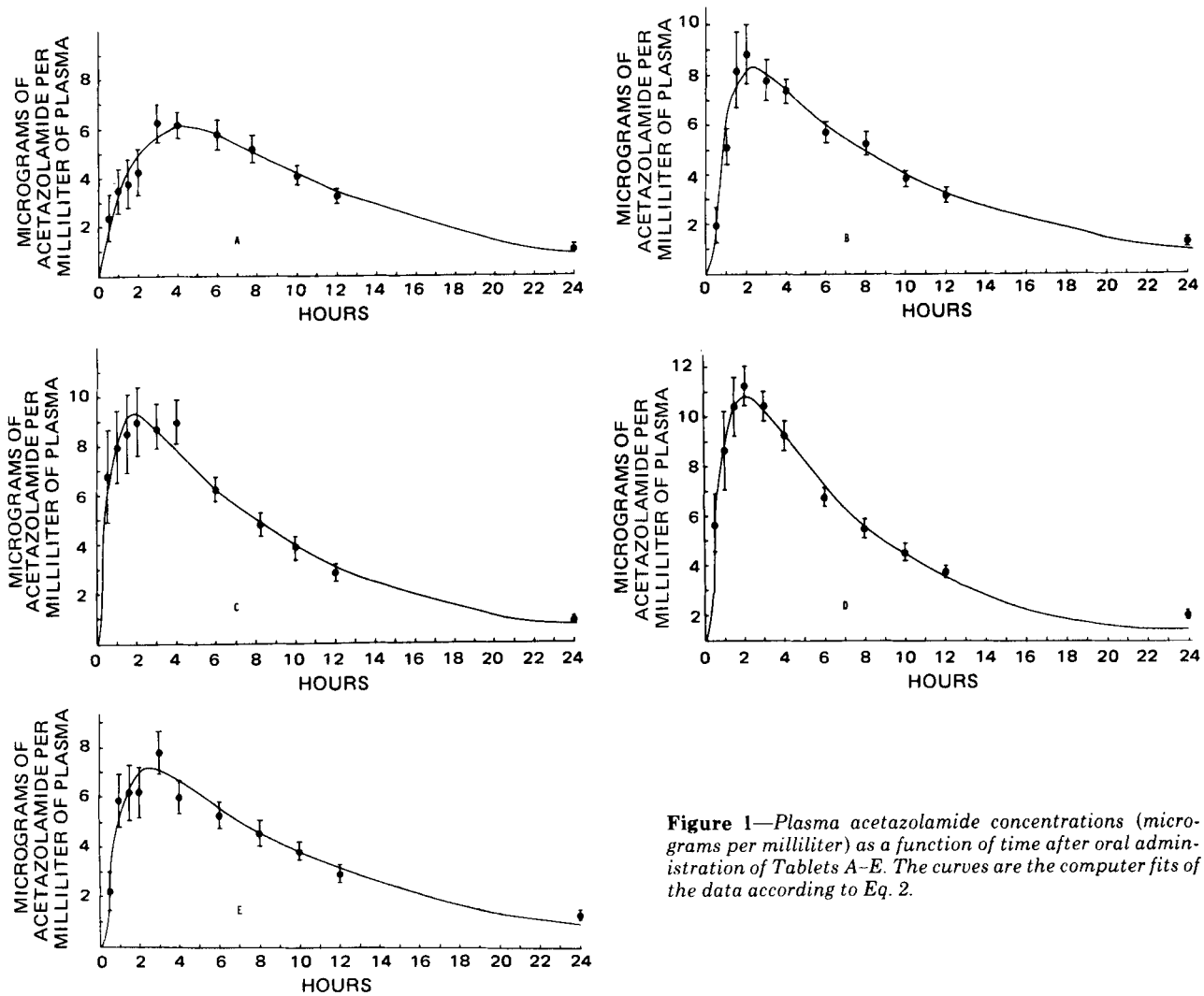

Figure 1—*Plasma acetazolamide concentrations (micrograms per milliliter) as a function of time after oral administration of Tablets A–E. The curves are the computer fits of the data according to Eq. 2.*

The standard deviation between treatment means was 1.13. The critical value from the t distribution at the 0.05 level for 34 degrees of freedom is 1.69. Thus, if the difference between any two treatment means was greater than 1.91 ($SD \times t_{\alpha=0.05}$), the treatments (tablets) were considered to be statistically different. According to this method of analysis, the peak plasma concentrations from Tablets C and D were different from A, B, and E.

Table VII—Area under the Plasma Level–Time Curve (Micrograms per Milliliter × Hours) as a Function of Tablet Lot, Study Day, and Subject after Administration of 250-mg Acetazolamide Tablets

	Study Day 1		Study Day 2		Study Day 3	
Tablet	Subject	Area	Subject	Area	Subject	Area
A	1	91.06	17	52.89	13	128.29
	2	72.95	18	98.42	14	Dropped
	3	116.05	19	49.07	15	122.42
	4	84.22	20	70.38	16	102.92
B	5	167.65	1	131.28	3	137.77
	6	69.07	2	97.64	4	92.61
	7	57.79	13	114.95	11	69.44
	8	108.59	14	Dropped	12	85.83
C	9	91.14	5	120.26	1	79.69
	10	76.69	6	63.50	2	80.62
	11	86.20	15	142.16	17	61.45
	12	83.08	16	104.94	18	101.50
D	13	105.51	7	74.63	5	88.69
	14	131.44	8	89.80	6	51.85
	15	127.2	9	98.48	19	70.94
	16	88.61	10	68.14	20	70.41
E	17	76.16	3	148.05	7	55.16
	18	98.32	4	90.49	8	84.13
	19	45.21	11	67.50	9	98.40
	20	91.08	12	153.74	10	59.94

The rank order of the tablets on the basis of peak concentration attained was exactly the same as from the data on time to peak. This internal consistency from parameters that should be related lends support to the inference that differences exist among the tablets tested, at least in terms of the rate of availability.

***In Vitro–In Vivo* Correlations**—The *in vivo* data indicate that while all of the tablets tested were equivalent in terms of the extent of absorption, C and D provided significantly higher peak plasma concentrations than A, B, and E. Analysis of the *in vitro* USP dissolution data showed that the same general trends held in gastric fluid and pH 10 carbonate buffer, although the observed differences did not appear to be of a sufficient magnitude to make the dissolution test discriminatory except for Tablet E in carbonate buffer. With water as the dissolution medium, there was no discrimination among tablets; in fact, C and D performed slightly more poorly than the others.

The poor performance of Tablet E in the carbonate buffer dissolution test was probably due more to its disintegration characteristics than to any discrimination by the dissolution test. Tablet E had an extremely long disintegration time in carbonate buffer, which contributed to its very slow dissolution.

A better *in vitro* correlation with the *in vivo* data was obtained with the rotating-filter–stationary basket apparatus. A much greater percentage difference was observed between the tablets giving the highest blood levels (C and D) and the other three tablets than was seen with the USP apparatus. The rank correlation between the T_{90} for dissolution and the mean C_{max} values was excellent, indicating that this dissolution procedure may eventually provide a method for monitoring lot-to-lot variations in acetazolamide bioavailability. More extensive evaluation of the spin filter technique was limited by the number of tablets available.

While trends for a correlation between disintegration and/or dissolution test and *in vivo* bioavailability exist, the apparent *in vitro* test procedures would have to be refined considerably to increase their ability

to discriminate accurately among acetazolamide tablets. That considerable refinement would be necessary is accentuated by the fact that the *in vivo* data show statistical differences among tablets tested in only one bioequivalence parameter. Detection of this inequivalence by *in vitro* testing would require highly sensitive and statistically validated methodology.

REFERENCES

(1) T. H. Maren, E. Mayer, and B. C. Wadsworth, *Bull. Johns Hopkins Hosp.*, **95**, 199 (1954).

(2) T. H. Maren and B. Robinson, *ibid.*, **106**, 1 (1960).

(3) T. H. Maren, *Physiol. Rev.*, **47**, 595 (1967).

(4) B. Lehmann, E. Linner, and P. J. Wistrand, *Adv. Biosci.*, **5**, 197 (1969).

(5) B. Becker and W. H. Middleton, *AMA Arch. Ophthalmol.*, **54**, 1 (1955).

(6) D. Cooke, H. S. Changard, and C. A. Mainville, *Can. J. Pharm. Sci.*, **1**, 69 (1969).

(7) P. Seth, *Pharm. Acta Helv.*, **47**, 457 (1972).

(8) P. J. Tannenbaum, E. Rosen, T. Flanagan, and A. P. Crosley, *Clin. Pharmacol. Ther.*, **9**, 598 (1968).

(9) M. C. Meyer, A. P. Melikian, P. L. Whyatt, and G. W. A. Slyka, *Curr. Ther. Res.*, **17**, 570 (1975).

(10) R. D. Hossie, G. L. Mattok, and I. J. McGilveray, *Rev. Can. Biol., Suppl.*, **32**, 85 (1973).

(11) A. C. Shah, C. G. Peot, and J. F. Ochs, *J. Pharm. Sci.*, **62**, 671 (1973).

(12) T. Maren, *J. Pharmacol. Exp. Ther.*, **130**, 26 (1960).

(13) G. J. Yakatan, R. V. Smith, and C. A. Martin, *Anal. Chim. Acta*, **84**, 173 (1976).

(14) "Desirable Weights of Adults," Statistical Bull. 40, Metropolitan Life Insurance, New York, N.Y., Nov.-Dec. 1959.

(15) J. A. Nelder and R. Mead, *Computer J.*, **7**, 308 (1965).

(16) R. O'Neil, *Appl. Stat.*, **20**, 338 (1971).

(17) D. Hogben, S. T. Peavy, and R. N. Varner, "Omnitab II Users Reference Manual," NBS Technical Note 552, Washington, D.C., 1971, pp. 110–165.

ACKNOWLEDGMENTS

Supported in part by Contract 74-139 from the Food and Drug Administration.

The authors gratefully acknowledge the excellent technical assistance of Ms. Carol Martin.

NOTES

Hydrolytic Degradation of 2,6-Dichlorobenzylthiopseudourea Hydrochloride

J. J. ZALIPSKY ˣ, D. M. PATEL, and N. H. REAVEY-CANTWELL

Received October 18, 1976, from the *Analytical and Physical Chemistry Department, Research Division, William H. Rorer, Inc., Fort Washington, PA 19034.* Accepted for publication April 12, 1977.

Abstract □ Degradation of 2,6-dichlorobenzylthiopseudourea hydrochloride was followed in basic medium (pH 7.5) to isolate and characterize all possible degradation products. IR, Raman, and NMR spectroscopy, TLC, and elemental analysis were used to identify the products. Degradation of base-hydrolyzed 2,6-dichlorobenzylthiopseudourea hydrochloride produced 2,6-dichlorobenzylthiol and cyanamide and was followed by oxidation (air) to produce bis(2,6-dichlorobenzyl) disulfide, dimerization to give cyanoguanidine, and hydrolysis to yield urea. The kinetics of hydrolysis at 22.5° (pH 7.0 and 7.5) and at 37° (pH 7.0) revealed a pseudo-first-order reaction with respect to the substrate. Apparent first-order rate constants and energy of activation, entropy of activation, and half-life values were determined.

Keyphrases □ 2,6-Dichlorobenzylthiopseudourea—hydrolytic degradation in basic medium, products isolated and identified □ Degradation, hydrolytic—2,6-dichlorobenzylthiopseudourea in basic medium, products isolated and identified □ Hydrolysis—2,6-dichlorobenzylthiopseudourea in basic medium, products isolated and identified □ Thiopseudourea, substituted—hydrolytic degradation in basic medium, products isolated and identified

The novel thiopseudourea analogs exhibited gastric, antisecretory, spasmolytic, and antiulcerogenic activities in laboratory animals. 2,6-Dichlorobenzylthiopseudourea (I) was selected as a candidate for exhaustive pharmacological and chemical studies.

Thiopseudourea is chemically susceptible to hydrolytic degradation and scission of the sulfur–carbon bond in strongly basic solutions (1). Limited information is available on solution stability and on the degradation products resulting from base hydrolysis. Zuman and Fedoreňko (2) investigated the kinetic hydrolysis of several substituted thiopseudoureas at pH 11, using a polarographic method to detect thiols as degradation products. No reference was made of the formation of the disulfide as one major resultant product. The homogeneous base-catalyzed oxidation of *n*-butylthiol to form disulfide with molecular oxygen has been studied in aprotic (3) and aqueous (4) solutions.

The objectives of this investigation were to isolate all possible degradation products resulting from the base hydrolysis of I at pH 7.5 and to follow the hydrolysis kinetics of this entity in a neutral medium and a weakly basic buffered medium at pH 7.0 and 7.5 at 22.5° and at pH 7.0 at 37°. This study was also conducted to characterize the

to discriminate accurately among acetazolamide tablets. That considerable refinement would be necessary is accentuated by the fact that the *in vivo* data show statistical differences among tablets tested in only one bioequivalence parameter. Detection of this inequivalence by *in vitro* testing would require highly sensitive and statistically validated methodology.

REFERENCES

(1) T. H. Maren, E. Mayer, and B. C. Wadsworth, *Bull. Johns Hopkins Hosp.*, **95**, 199 (1954).

(2) T. H. Maren and B. Robinson, *ibid.*, **106**, 1 (1960).

(3) T. H. Maren, *Physiol. Rev.*, **47**, 595 (1967).

(4) B. Lehmann, E. Linner, and P. J. Wistrand, *Adv. Biosci.*, **5**, 197 (1969).

(5) B. Becker and W. H. Middleton, *AMA Arch. Ophthalmol.*, **54**, 1 (1955).

(6) D. Cooke, H. S. Changard, and C. A. Mainville, *Can. J. Pharm. Sci.*, **1**, 69 (1969).

(7) P. Seth, *Pharm. Acta Helv.*, **47**, 457 (1972).

(8) P. J. Tannenbaum, E. Rosen, T. Flanagan, and A. P. Crosley, *Clin. Pharmacol. Ther.*, **9**, 598 (1968).

(9) M. C. Meyer, A. P. Melikian, P. L. Whyatt, and G. W. A. Slyka, *Curr. Ther. Res.*, **17**, 570 (1975).

(10) R. D. Hossie, G. L. Mattok, and I. J. McGilveray, *Rev. Can. Biol., Suppl.*, **32**, 85 (1973).

(11) A. C. Shah, C. G. Peot, and J. F. Ochs, *J. Pharm. Sci.*, **62**, 671 (1973).

(12) T. Maren, *J. Pharmacol. Exp. Ther.*, **130**, 26 (1960).

(13) G. J. Yakatan, R. V. Smith, and C. A. Martin, *Anal. Chim. Acta*, **84**, 173 (1976).

(14) "Desirable Weights of Adults," Statistical Bull. 40, Metropolitan Life Insurance, New York, N.Y., Nov.-Dec. 1959.

(15) J. A. Nelder and R. Mead, *Computer J.*, **7**, 308 (1965).

(16) R. O'Neil, *Appl. Stat.*, **20**, 338 (1971).

(17) D. Hogben, S. T. Peavy, and R. N. Varner, "Omnitab II Users Reference Manual," NBS Technical Note 552, Washington, D.C., 1971, pp. 110–165.

ACKNOWLEDGMENTS

Supported in part by Contract 74-139 from the Food and Drug Administration.

The authors gratefully acknowledge the excellent technical assistance of Ms. Carol Martin.

NOTES

Hydrolytic Degradation of 2,6-Dichlorobenzylthiopseudourea Hydrochloride

J. J. ZALIPSKY ˣ, D. M. PATEL, and N. H. REAVEY-CANTWELL

Received October 18, 1976, from the *Analytical and Physical Chemistry Department, Research Division, William H. Rorer, Inc., Fort Washington, PA 19034.* Accepted for publication April 12, 1977.

Abstract □ Degradation of 2,6-dichlorobenzylthiopseudourea hydrochloride was followed in basic medium (pH 7.5) to isolate and characterize all possible degradation products. IR, Raman, and NMR spectroscopy, TLC, and elemental analysis were used to identify the products. Degradation of base-hydrolyzed 2,6-dichlorobenzylthiopseudourea hydrochloride produced 2,6-dichlorobenzylthiol and cyanamide and was followed by oxidation (air) to produce bis(2,6-dichlorobenzyl) disulfide, dimerization to give cyanoguanidine, and hydrolysis to yield urea. The kinetics of hydrolysis at 22.5° (pH 7.0 and 7.5) and at 37° (pH 7.0) revealed a pseudo-first-order reaction with respect to the substrate. Apparent first-order rate constants and energy of activation, entropy of activation, and half-life values were determined.

Keyphrases □ 2,6-Dichlorobenzylthiopseudourea—hydrolytic degradation in basic medium, products isolated and identified □ Degradation, hydrolytic—2,6-dichlorobenzylthiopseudourea in basic medium, products isolated and identified □ Hydrolysis—2,6-dichlorobenzylthiopseudourea in basic medium, products isolated and identified □ Thiopseudourea, substituted—hydrolytic degradation in basic medium, products isolated and identified

The novel thiopseudourea analogs exhibited gastric, antisecretory, spasmolytic, and antiulcerogenic activities in laboratory animals. 2,6-Dichlorobenzylthiopseudourea (I) was selected as a candidate for exhaustive pharmacological and chemical studies.

Thiopseudourea is chemically susceptible to hydrolytic degradation and scission of the sulfur–carbon bond in strongly basic solutions (1). Limited information is available on solution stability and on the degradation products resulting from base hydrolysis. Zuman and Fedoreňko (2) investigated the kinetic hydrolysis of several substituted thiopseudoureas at pH 11, using a polarographic method to detect thiols as degradation products. No reference was made of the formation of the disulfide as one major resultant product. The homogeneous base-catalyzed oxidation of *n*-butylthiol to form disulfide with molecular oxygen has been studied in aprotic (3) and aqueous (4) solutions.

The objectives of this investigation were to isolate all possible degradation products resulting from the base hydrolysis of I at pH 7.5 and to follow the hydrolysis kinetics of this entity in a neutral medium and a weakly basic buffered medium at pH 7.0 and 7.5 at 22.5° and at pH 7.0 at 37°. This study was also conducted to characterize the

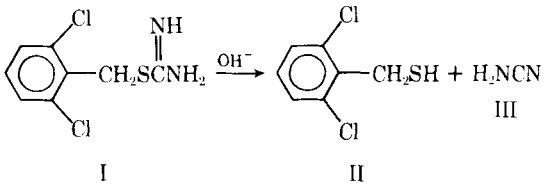

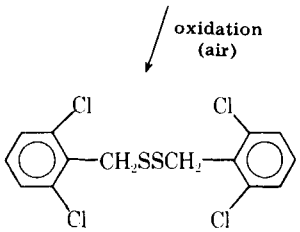

IV

Scheme I

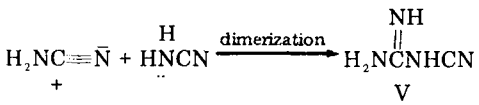

Scheme II

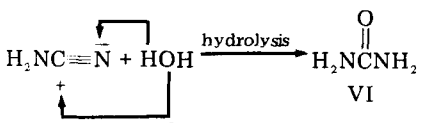

Scheme III

structures of the major degradation products by IR, Raman, and NMR spectroscopy, melting points, TLC, and elemental analysis.

The methods of isolation of the degradation products were liquid–liquid extraction and column chromatography. The hydrolysis kinetics of I were followed by the UV method. In addition, a limited study was carried out on solution stability of I at pH 1.5 and 4.0 in water and methanol.

EXPERIMENTAL

Materials—All chemicals were reagent grade. Compound I was synthesized by a reported method (5). The identity and purity of I were confirmed by IR[1], UV[2], and NMR[3] spectra, potentiometric titration[4], melting-point[5] (132–134°) determination, elemental analysis[6] for $C_8H_9Cl_3N_2S$ (calc.: C, 35.37; H, 3.34; Cl, 39.16; N, 10.31; S, 11.81; found: C, 35.77; H, 3.35; Cl, 39.48; N, 10.30; S, 11.58), and TLC using 250-μm aluminum oxide[7] plates (Type T) eluted with methanol–chloroform (50:50) (R_f 0.72). Cyanoguanidine[8] and urea[9] were obtained commercially.

Base Hydrolysis Degradation Products—A solution of I, 300 mg in 100 ml of pH 7.5 phosphate buffer, was incubated for 3 days at 37° in a constant-temperature water bath. During incubation, a white precipitate was formed and some needle-like crystals accumulated in the flask neck. After incubation, the contents were analyzed as follows.

The long, colorless needles were removed and dried over phosphorus pentoxide. IR spectroscopy, melting-point determination, and elemental analysis were carried out to identify the sublimed crystals. The entire contents of the flask were transferred to a 250-ml separator to which 20 ml of chloroform was added to extract insoluble material. The chloroform extract, after evaporation of the solvent, yielded a white solid, which was crystallized two times with ethanol and dried at 55° for 5 hr under vacuum. IR, UV, NMR, and Raman spectra, melting-point determination, elemental analysis, and TLC [250-μm alumina plate (acidic) using cyclohexane–chloroform (90:10) and methanol–chloroform (30:70) and visualized under UV light] were used to identify the product (R_f 0.63 and 0.75, respectively).

The aqueous phase was evaporated to dryness. The resultant solid was triturated with 2 ml of ethanol, and the ethanol solution was passed through an alumina column (neutral, 10 × 1 cm). The ethanol-eluted fractions (~4 ml) were collected. The fourth fraction contained most of the solid after solvent evaporation. The solid was examined by IR spectroscopy, melting-point determination, and TLC[10] [alumina plate (acidic) using methanol–chloroform–ammonia (40:60:5 drops)]. Similar analyses were carried out on authentic cyanoguanidine.

The ethanol-insoluble solid was mixed with a few milliliters of methanol, and this solution was passed through an alumina column (a methanol–chloroform mixture was used to elute fractions). A small amount of solid was obtained on solvent evaporation. IR spectra and TLC, using an alumina acidic plate and solvents consisting of ethanol–chloroform (30:70) and methanol–chloroform (40:60), were obtained to identify the product. The spot was visualized using bromcresol green spray reagent. Similar analyses were performed on authentic urea.

Kinetics—Three solutions (10^{-3} *M*) of I were prepared in phosphate buffers at an ionic strength of 0.1 with potassium chloride in a 100-ml

Table I—Apparent Rate Constants and Activation Parameters for the Hydrolysis of I

Temperature	pH	$10^{-4}k$, hr^{-1}	E_a, kcal	$\Delta S^{\ddagger}$, eu	$t_{1/2}$, days
22.5°	7.0	4.55	19.0	−25.7	63.4
22.5°	7.5	8.79	—	—	32.8
37.0°	7.0	20.72	—	—	14.0

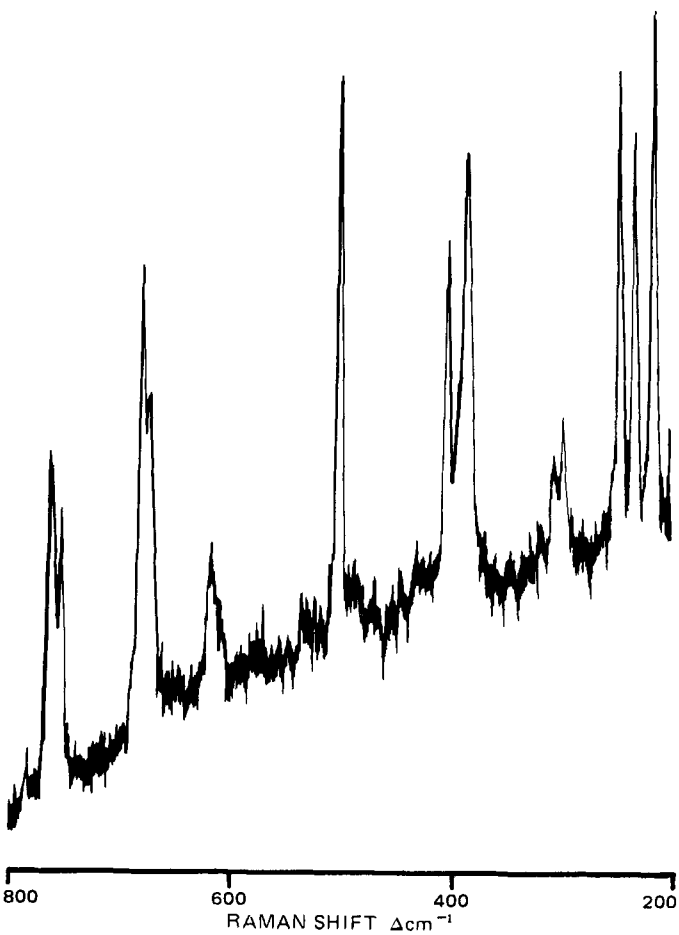

Figure 1—*Raman spectrum of bis(2,6-dichlorobenzyl) disulfide.*

[1] Perkin-Elmer model 221 spectrophotometer (potassium bromide disk).
[2] Cary model 14 spectrophotometer.
[3] Varian spectrometer model T-60.
[4] Brinkmann instruments pH meter.
[5] Thomas-Hoover capillary melting-point apparatus.
[6] Micro-Analysis, Wilmington, Del.
[7] Brinkmann Instruments, Westbury, N.Y.
[8] Eastman Kodak Co., Rochester, N.Y.
[9] J. T. Baker Chemical Co., Phillipsburg, N.J.

[10] Spray reagent was 10% aqueous sodium hydroxide, 10% aqueous sodium nitroprusside, 10% aqueous potassium ferricyanide, and water (1:1:1:3). The mixture is mixed with an equal volume of acetone before use.

volumetric flask at pH 7.0 and 7.5. Two solutions at pH 7.0 and 7.5 were equilibrated at a reaction temperature of 22.5°; the third solution at pH 7.0 was equilibrated at a reaction temperature of 37°. An aliquot was withdrawn periodically and filtered[11] (5-μm pore size), and the maximum absorbance at λ 275 nm was measured by running a UV spectrum from 400 to 260 nm. A plot of log concentration I remaining in solution *versus* time was constructed.

RESULTS AND DISCUSSION

Degradation Products—This study shows that I undergoes degradation in an aqueous medium (pH 7.0 and 7.5). The degradation of I and the formation of the degradation products are depicted in Schemes I–III. The major degradation product isolated by chloroform extraction from the reaction was bis(2,6-dichlorobenzyl) disulfide (IV). The identity of this new compound, mp 107–108°, was confirmed by IR spectroscopy: 3060, 2950, 1580, 1439, 1090, 897, 885, 781, and 759 cm^{-1}; NMR (carbon tetrachloride plus tetramethylsilane): δ 4.3 (CH_2) and 7.42 (aromaticity) ppm; and TLC, one spot visualized under UV light after fluorescein spray. In addition, a Raman spectrum[12] was obtained to confirm the S–S stretching vibration at 502 cm^{-1} of IV (Fig. 1).

Anal.—Calc. for $C_{14}H_{10}Cl_4S_2$: C, 43.77; H, 2.62; Cl, 36.91; S, 16.69. Found: C, 43.56; H, 2.52; Cl, 37.37; S, 17.27.

The crystals that accumulated above the solution at pH 7.5 were identified as 2,6-dichlorobenzylthiol (II). The identity of this new product, mp 38°, was confirmed by IR spectroscopy (2550, 1580, 1560, 1437, 1090, 975, 775, and 755 cm^{-1}).

Anal.—Calc. for $C_7H_6Cl_2S$: C, 43.54; H, 3.13. Found: C, 43.43; H, 2.90.

This compound had a very disagreeable odor.

[11] Millipore.
[12] Model 82 laser-Raman spectrophotometer, Cary Instruments.

Cyanoguanidine (V) was isolated as the ethanol-soluble fraction and was shown to be comparable with the authentic compound by IR, melting point (206–208°), and TLC (R_f 0.57). The presence of urea (VI) as the methanol-soluble fraction was confirmed by IR and TLC and was comparable with authentic urea (R_f 0.16 and 0.43). The schemes thus indicate the formation path of the degradation products as evidenced by the experimental data.

Kinetics—The hydrolytic degradation of I in solution at pH 7.0 and 7.5 at 22.5° and at pH 7.0 at 37° has been shown to be a pseudo-first-order reaction with respect to substrate. A linear relationship was obtained when the log concentration of I was plotted against time. Apparent first-order rate constants were calculated from the slope by least-squares regression, with a correlation coefficient of 0.99. Table I shows apparent rate constants and energy of activation, entropy of activation, and half-life values of I under the conditions studied. Increasing the temperature from 22.5 to 37° accelerated the degradation rate of I 4.5-fold, as expected.

Limited experimental data also were obtained on I stability in water (pH 5.86) and in solutions at pH 1.5 and 4 at 22.5°. The compound was stable up to 76, 39, and 17 days, respectively. A methanolic solution of I (9.48×10^{-4} *M*) showed degradation of 15.10 and 49.82% in 2 and 10 days, respectively.

REFERENCES

(1) L. F. Fieser and M. Fieser, "Organic Chemistry," 3rd ed., Reinhold, New York, N.Y., 1956, p. 139.

(2) P. Zuman and M. Fedoreňko, *Z. Phys. Chem. (Leipzig)*, **209**, 376 (1958).

(3) T. J. Wallace and A. Schriesheim, *J. Org. Chem.*, **27**, 1514 (1962).

(4) J. Xan, E. A. Wilson, L. D. Roberts, and N. H. Horton, *J. Am. Chem. Soc.*, **63**, 1139 (1941).

(5) J. Diamond, U.S. pat. 3,891,704 (1975).

Polynitro Aromatic Compounds in Analytical Chemistry II: Reaction of Menadione with 2,4-Dinitrophenylhydrazine

L. B. BURNS, R. J. STEDMAN, and M. M. TUCKERMAN ˣ

Received January 15, 1976, from the *School of Pharmacy, Temple University, Philadelphia, PA 19140.* Accepted for publication April 13, 1977.

Abstract □ The intense blue color formed in the official assay of menadione injection by treatment of the sample with 2,4-dinitrophenylhydrazine and ammonia is shown by data from visible light spectra and mass spectra and by comparison of the pKa value with that of the corresponding reaction product of acetone to be due to proton abstraction from a monohydrazone.

Keyphrases □ Menadione—blue-colored product of reaction with 2,4-dinitrophenylhydrazine identified □ 2,4-Dinitrophenylhydrazine—blue-colored product of reaction with menadione identified □ Spectrophotometry—analysis, menadione, blue-colored product of reaction with 2,4-dinitrophenylhydrazine identified □ Vitamins—menadione, blue-colored product of reaction with 2,4-dinitrophenylhydrazine identified

The NF (1) assay for menadione (I) consists of heating menadione in alcohol–ether with an acidic solution of 2,4-dinitrophenylhydrazine to give an orange precipitate, followed by the addition of alcoholic ammonia to produce an intense blue color. The absorbance in the visible at 635 nm is proportional to the menadione concentration. The orange precipitate has been assigned Structure II, in which hydrazone formation has taken place at the less hindered carbonyl (2), but no definitive information seems to be available about the blue material.

In the present work, the composition of the precipitate II was confirmed by mass spectrometry. Since menadione contains a methyl group capable of losing a proton to form an anion, it is possible that Meisenheimer complex formation with the nitro aromatic ring might be responsible for the blue color formation. However, spectrophotometric comparison of the pKa value of menadione 2,4-dinitrophenylhydrazone with that of a simple model compound, acetone 2,4-dinitrophenylhydrazone, suggested that *N*-deprotonation rather than Meisenheimer complexation was taking place.

EXPERIMENTAL[1]

Menadione 2,4-Dinitrophenylhydrazone (II)—This compound was obtained as orange crystals according to the NF procedure (1). The ma-

[1] Mass spectral data were obtained on a Hitachi Perkin-Elmer RMU 6E instrument. UV–visible spectra were run on a Cary model 15 spectrophotometer. Measurements of pH were made with an ionalyzer, Orion Research model 801 digital pH meter, using a glass–silver–silver chloride combination electrode.

volumetric flask at pH 7.0 and 7.5. Two solutions at pH 7.0 and 7.5 were equilibrated at a reaction temperature of 22.5°; the third solution at pH 7.0 was equilibrated at a reaction temperature of 37°. An aliquot was withdrawn periodically and filtered[11] (5-μm pore size), and the maximum absorbance at λ 275 nm was measured by running a UV spectrum from 400 to 260 nm. A plot of log concentration I remaining in solution *versus* time was constructed.

RESULTS AND DISCUSSION

Degradation Products—This study shows that I undergoes degradation in an aqueous medium (pH 7.0 and 7.5). The degradation of I and the formation of the degradation products are depicted in Schemes I–III. The major degradation product isolated by chloroform extraction from the reaction was bis(2,6-dichlorobenzyl) disulfide (IV). The identity of this new compound, mp 107–108°, was confirmed by IR spectroscopy: 3060, 2950, 1580, 1439, 1090, 897, 885, 781, and 759 cm^{-1}; NMR (carbon tetrachloride plus tetramethylsilane): δ 4.3 (CH_2) and 7.42 (aromaticity) ppm; and TLC, one spot visualized under UV light after fluorescein spray. In addition, a Raman spectrum[12] was obtained to confirm the S–S stretching vibration at 502 cm^{-1} of IV (Fig. 1).

Anal.—Calc. for $C_{14}H_{10}Cl_4S_2$: C, 43.77; H, 2.62; Cl, 36.91; S, 16.69. Found: C, 43.56; H, 2.52; Cl, 37.37; S, 17.27.

The crystals that accumulated above the solution at pH 7.5 were identified as 2,6-dichlorobenzylthiol (II). The identity of this new product, mp 38°, was confirmed by IR spectroscopy (2550, 1580, 1560, 1437, 1090, 975, 775, and 755 cm^{-1}).

Anal.—Calc. for $C_7H_6Cl_2S$: C, 43.54; H, 3.13. Found: C, 43.43; H, 2.90.

This compound had a very disagreeable odor.

[11] Millipore.
[12] Model 82 laser-Raman spectrophotometer, Cary Instruments.

Cyanoguanidine (V) was isolated as the ethanol-soluble fraction and was shown to be comparable with the authentic compound by IR, melting point (206–208°), and TLC (R_f 0.57). The presence of urea (VI) as the methanol-soluble fraction was confirmed by IR and TLC and was comparable with authentic urea (R_f 0.16 and 0.43). The schemes thus indicate the formation path of the degradation products as evidenced by the experimental data.

Kinetics—The hydrolytic degradation of I in solution at pH 7.0 and 7.5 at 22.5° and at pH 7.0 at 37° has been shown to be a pseudo-first-order reaction with respect to substrate. A linear relationship was obtained when the log concentration of I was plotted against time. Apparent first-order rate constants were calculated from the slope by least-squares regression, with a correlation coefficient of 0.99. Table I shows apparent rate constants and energy of activation, entropy of activation, and half-life values of I under the conditions studied. Increasing the temperature from 22.5 to 37° accelerated the degradation rate of I 4.5-fold, as expected.

Limited experimental data also were obtained on I stability in water (pH 5.86) and in solutions at pH 1.5 and 4 at 22.5°. The compound was stable up to 76, 39, and 17 days, respectively. A methanolic solution of I (9.48×10^{-4} *M*) showed degradation of 15.10 and 49.82% in 2 and 10 days, respectively.

REFERENCES

(1) L. F. Fieser and M. Fieser, "Organic Chemistry," 3rd ed., Reinhold, New York, N.Y., 1956, p. 139.

(2) P. Zuman and M. Fedoreňko, *Z. Phys. Chem. (Leipzig)*, **209**, 376 (1958).

(3) T. J. Wallace and A. Schriesheim, *J. Org. Chem.*, **27**, 1514 (1962).

(4) J. Xan, E. A. Wilson, L. D. Roberts, and N. H. Horton, *J. Am. Chem. Soc.*, **63**, 1139 (1941).

(5) J. Diamond, U.S. pat. 3,891,704 (1975).

Polynitro Aromatic Compounds in Analytical Chemistry II: Reaction of Menadione with 2,4-Dinitrophenylhydrazine

L. B. BURNS, R. J. STEDMAN, and M. M. TUCKERMAN ˣ

Received January 15, 1976, from the *School of Pharmacy, Temple University, Philadelphia, PA 19140.* Accepted for publication April 13, 1977.

Abstract □ The intense blue color formed in the official assay of menadione injection by treatment of the sample with 2,4-dinitrophenylhydrazine and ammonia is shown by data from visible light spectra and mass spectra and by comparison of the pKa value with that of the corresponding reaction product of acetone to be due to proton abstraction from a monohydrazone.

Keyphrases □ Menadione—blue-colored product of reaction with 2,4-dinitrophenylhydrazine identified □ 2,4-Dinitrophenylhydrazine—blue-colored product of reaction with menadione identified □ Spectrophotometry—analysis, menadione, blue-colored product of reaction with 2,4-dinitrophenylhydrazine identified □ Vitamins—menadione, blue-colored product of reaction with 2,4-dinitrophenylhydrazine identified

The NF (1) assay for menadione (I) consists of heating menadione in alcohol–ether with an acidic solution of 2,4-dinitrophenylhydrazine to give an orange precipitate, followed by the addition of alcoholic ammonia to produce an intense blue color. The absorbance in the visible at 635 nm is proportional to the menadione concentration. The orange precipitate has been assigned Structure II, in which hydrazone formation has taken place at the less hindered carbonyl (2), but no definitive information seems to be available about the blue material.

In the present work, the composition of the precipitate II was confirmed by mass spectrometry. Since menadione contains a methyl group capable of losing a proton to form an anion, it is possible that Meisenheimer complex formation with the nitro aromatic ring might be responsible for the blue color formation. However, spectrophotometric comparison of the pKa value of menadione 2,4-dinitrophenylhydrazone with that of a simple model compound, acetone 2,4-dinitrophenylhydrazone, suggested that *N*-deprotonation rather than Meisenheimer complexation was taking place.

EXPERIMENTAL[1]

Menadione 2,4-Dinitrophenylhydrazone (II)—This compound was obtained as orange crystals according to the NF procedure (1). The ma-

[1] Mass spectral data were obtained on a Hitachi Perkin-Elmer RMU 6E instrument. UV–visible spectra were run on a Cary model 15 spectrophotometer. Measurements of pH were made with an ionalyzer, Orion Research model 801 digital pH meter, using a glass–silver–silver chloride combination electrode.

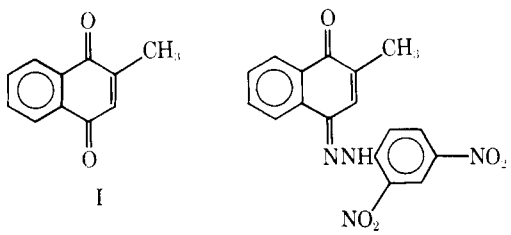

I

II

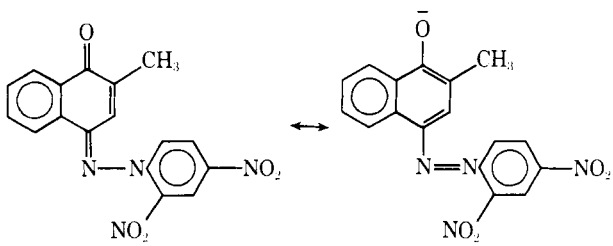

III

terial was collected by centrifugation and washed with ethanol. The mass spectrum (electron-impact ionization) showed the expected molecular ion ($M^{+\cdot}$) at *m/e* 352. The isotope peaks at 353 and 354 had intensities of 21 and 4% of $M^{+\cdot}$, respectively ($C_{17}H_{12}N_4O_5$ requires M + 1 = 20.1% and M + 2 = 2.7%).

Acetone 2,4-Dinitrophenylhydrazone—This compound was prepared as orange crystals according to the method of Brady (3) and was recrystallized from ethanol.

Determination of Apparent pKa Values for Dinitrophenylhydrazones[2]—Portions of 2 mg of the dinitrophenylhydrazones were dissolved in 50.0 ml of dimethyl sulfoxide. To 1-ml aliquots of these solutions were added 3 ml of dimethyl sulfoxide, varying amounts of hydrochloric acid or potassium hydroxide, and enough water to bring the volume to 10.00 ml. The apparent pH of each solution was measured using a standardized pH meter. The UV–visible absorption spectra were run between 250 and 650 nm using an appropriate blank.

The positions and intensities of absorption maxima under strongly acid and strongly alkaline conditions were: menadione 2,4-dinitrophenylhydrazone, λ_{max} 405 nm (ϵ 28,400) (acid) and 630 nm (ϵ 86,800) (alkali); and acetone 2,4-dinitrophenylhydrazone, λ_{max} 370 nm (ϵ 22,700) (acid) and 430 (ϵ 22,200) and 530 (ϵ 14,200) nm (alkali).

The families of curves at a range of pH values for both compounds showed an isosbestic point, consistent with the presence of only two absorbing species.

The pKa values were calculated from the proportions of the two forms present at an intermediate pH (4, 5). For either compound, the spectrum at high pH showed a long wavelength maximum, which could be used to estimate the anionic form without interference from the neutral species. Therefore, it was possible to use a single absorbance measurement to determine the fraction of anionic form present at any pH.

Menadione 2,4-Dinitrophenylhydrazone—At pH 10.76, the mole fraction of the anionic form was 0.31; therefore, the pKa was 11.10. Measurement was at 630 nm.

Acetone 2,4-Dinitrophenylhydrazone—At pH 11.28, the mole fraction of the anionic form was 0.33; therefore, the pKa was 11.58. Measurement was at 530 nm.

[2] All pH and pKa values are apparent.

DISCUSSION

The mass spectrometric molecular weight and the intensities of the isotope peaks support the view that the orange precipitate formed initially in the menadione assay has Structure II; it seems unlikely that reaction would take place at the other, more hindered carbonyl group to give the isomeric hydrazone.

A possibility initially entertained was that the color obtained on basifying II was due to formation of a Meisenheimer complex. The nearly instantaneous production of the color argued against this interpretation, which would require dissociation of II to menadione and 2,4-dinitrophenylhydrazone followed by recombination to give the Meisenheimer complex. This process was expected to be relatively slow.

Acetone 2,4-dinitrophenylhydrazone was chosen as a model compound because the modest change in absorbance it shows on basification is not consistent with Meisenheimer complex formation but only with simple *N*-deprotonation. The finding that II has an apparent pKa value similar to that of the acetone derivative suggests that it too is undergoing *N*-deprotonation. The somewhat greater acidity of II is attributable to the more extensive charge delocalization in the anion; two mesomeric representations are illustrated in Structure III. The very intense long wavelength absorption of III is appropriate for a chromophore conjugated over both the dinitrophenyl and the menadione moieties.

In summary, the evidence supports the view that the mesomeric structure of the type shown by III represents the blue-colored species used in the menadione assay.

REFERENCES

(1) "The National Formulary," 13th ed., Mack Publishing Co., Easton, Pa., 1970, p. 404.

(2) K. Fickentscher, *Dtsch. Apoth.-Ztg.*, **108**, 1545 (1968).

(3) J. Brady, *J. Chem. Soc.*, **1931**, 756.

(4) M. E. Caserio, "Experimental Organic Chemistry," Benjamin, New York, N.Y., 1967, p. 158.

(5) H. H. Jaffe and M. Orchin, "Theory and Application of U.V. Spectroscopy," Wiley, New York, N.Y., 1964, pp. 560–571.

ACKNOWLEDGMENTS

Abstracted in part from a thesis submitted by L. Burns to Temple University in partial fulfillment of the Doctor of Philosophy degree requirements.

Quantitation of Etorphine in Urine by Selective Ion Monitoring Using Tritiated Etorphine as an Internal Standard

SATYA P. JINDAL [x] **and PER VESTERGAARD**

Received November 29, 1976, from the *Rockland Research Institute, Orangeburg, NY 10962.* Accepted for publication April 25, 1977.

Abstract □ Selective ion monitoring combined with GLC was used for the assay of etorphine in urine. Commercially available tritiated etorphine was added as an internal standard. The advantage of the methodology using this internal standard is higher sensitivity by a factor of about 20 when compared with ordinary GLC.

Keyphrases □ Etorphine—GLC-selective ion mass spectrometric analysis, urine □ GLC-selective ion mass spectrometry—analysis, etorphine in urine □ Narcotic analgesics—etorphine, GLC-selective ion mass spectrometric analysis in urine

Etorphine, 6,14-*endo*-etheno-7-[1-(*R*)-hydroxy-1-methylbutyl]-6,7,8,14-tetrahydroripavine, as synthesized by Bentley and Hardy (1), is an analgesic approximately 1000 times as potent as morphine (2, 3). The fact that it works sublingually and has abuse potential (4) raises the possibility that it may become a future threat in the drug abuse field. Its extreme potency makes it a valuable tool for the study of narcotic receptors (5) but makes it difficult to detect after administration of pharmacologically effective doses.

Etorphine could not be detected in the urine with commonly available methods, including GLC, after the administration of high euphoronigenic doses in humans (6). Therefore, a sensitive and specific analytical method for this compound is needed.

Selective ion monitoring, the technique built on combined GLC–mass spectrometry with selective focusing on suitable fragments of the molecular ion (mass fragmentography) or the molecular ion itself, is used widely in pharmacology and biology (7, 8). This technique was used to develop a very sensitive and specific method for the analysis of etorphine in rabbit urine with commercially available $^3H_2$-etorphine as an internal standard.

EXPERIMENTAL

Nonlabeled etorphine[1], 15,16(*n*)-$^3H_2$-etorphine (specific activity[2] 41 Ci/mmole), and *N,O*-bis(trimethylsilyl)trifluoroacetamide[3] were obtained commercially and were used as received.

All animals were male, New Zealand White rabbits.

Extraction of Etorphine from Urine—To 2 ml of fresh urine was added an appropriate amount (36,000 cpm) of tritiated etorphine as an internal standard. The urine was saturated with sodium chloride, adjusted to pH 9.0 with 1 *N* NH_4OH, and extracted twice with 5 ml of butyl chloride. The organic fractions were combined, 1 ml of 0.1 *N* HCl was added, and the solution was shaken for 20 min. Then the organic layer was discarded, and the aqueous phase was adjusted to pH 9 with 0.4 *N* NH_4OH and extracted twice with 5 ml of butyl chloride. The organic layers were combined and dried, and the solvent was evaporated under nitrogen at 40°.

Recovery of etorphine added to control rabbit urine was studied using $^3H_2$-etorphine, 36,000 cpm.

Formation of Derivatives—Trimethylsilyl derivatives were formed by reacting the residue with 100 μl of *N,O*-bis(trimethylsilyl)trifluoroacetamide (9) at 60° for 0.5 hr. Different amounts of a mixture of etorphine and tritiated etorphine were taken and derivatized similarly. The reaction mixtures were taken to dryness under a nitrogen stream and then dissolved in 20 μl of benzene. An aliquot of this solution was injected in the gas chromatograph–mass spectrometer for the mass fragmentographic assay.

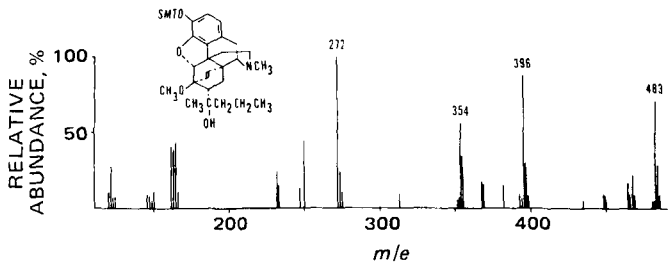

Figure 1—*Mass spectrum of etorphine trimethylsilyl (SMT) ether.*

Instrumentation—A magnetic sector, single focusing mass spectrometer[4] interfaced with a gas chromatograph and equipped with a multiple-ion detector/peak matcher accessory was used (7, 8).

GLC was performed on a 1.8-m × 2-mm i.d. column silanized before packing with 5% dimethylchlorosilane in toluene[3] and packed with 1% OV-1 on 100–120-mesh Gas Chrom Q[5]. The column was conditioned for 24 hr at 280° with a flow rate of 20 ml of helium/min. The column temperature was 230°, the flash heater was at 250°, the separator was at 250°, the ion source was at 270°, and the trap current was at 60 μamp.

In the scan mode, the accelerating voltage was 3.5 kv and the ionization potential was 70 ev. The magnetic field was kept constant by focusing the background peak at *m/e* 429, and the voltages were 3082 and 3108 v for measuring the ion intensities at *m/e* 487 and 483, respectively. The retention time was 5.5 min.

RESULTS

Recovery of etorphine added to control urine was studied using $^3H_2$-etorphine. In a typical experiment, $^3H_2$-etorphine (36,000 cpm) was added to control urine and extracted as described; 23,240 cpm was recovered. Based on 10 determinations, a mean recovery of 68 ± 6% (*SD*) was obtained for $^3H_2$-etorphine added to urine. On treatment with *N,O*-bis(trimethylsilyl)trifluoroacetamide under the experimental conditions,

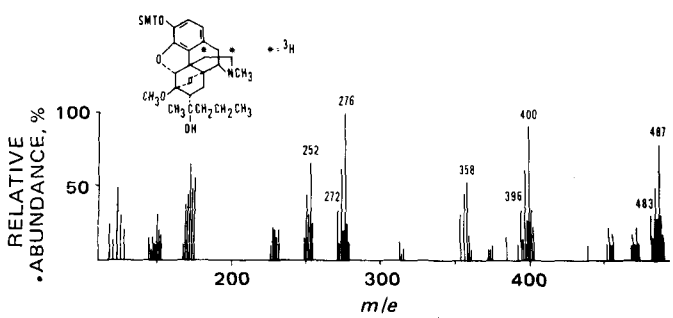

Figure 2—*Mass spectrum of tritiated etorphine trimethylsilyl (SMT) ether. The molecular ion at* m/e *487, with two tritium atoms, shows the highest relative intensity and was used for the mass fragmentographic assay.*

[1] Research Triangle Institute, Research Triangle Park, N.C.
[2] Amersham/Searle, Amersham, England.
[3] Pierce Chemical Co., Rockford, Ill.
[4] LKB model 9000.
[5] Applied Science Laboratories, State College, Pa.

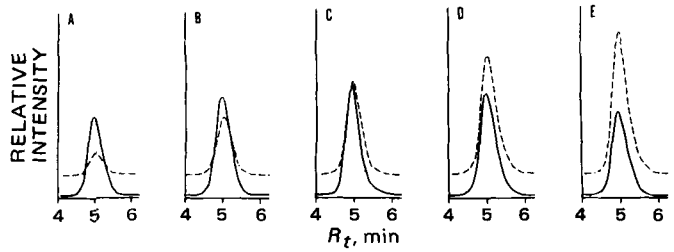

Figure 3—*Mass fragmentograms obtained by injecting approximately 5% (1 μl) of a solution containing 0, 8, 16, 24, and 40 ng of etorphine (A–D, respectively). Each solution contained 25 ng of $^3H_2$-etorphine. Key: - - -, etorphine trimethylsilyl ether, m/e 483; and —, $^3H_2$-etorphine trimethylsilyl ether, m/e 487.*

etorphine yielded a single trimethylsilyl derivative. The mass spectrum (Fig. 1) showed a molecular ion at *m/e* 483, and the fragmentation pattern is consistent with the structure.

The spectrum of tritiated etorphine derivative (Fig. 2) showed a molecular ion at *m/e* 487 and ions at *m/e* 483 and 485. The ion at *m/e* 487, corresponding to two tritium atoms, showed the maximum relative intensity and was used for quantitation. Known mixtures of etorphine, 0–40 ng per "fixed" amount (25 ng) of internal standard, were each added to 2 ml of control urine. Samples were extracted, derivatized, and analyzed on the gas chromatogram–mass spectrometer focused on ions 483 and 487. Figure 3 illustrates the mass fragmentograms, showing linear increase in the ion intensity ratio 483/487 with an increasing amount of etorphine.

The calibration curve was calculated from the data presented in Fig. 3 and was used for quantitation of etorphine present in the urine, with correction for the presence of small amounts of cold etorphine in the internal standard (10). The assay was reproducible to ±7% at the 5-ng level, and the reproducibility was much better at higher levels. The practical sensitivity of the assay in its current form is about 5 ng/ml of urine, which compares with a sensitivity of 100 ng/ml for GLC (6). Obviously, with ordinary GLC, the sensitivity would have been inadequate in the present experiments, since the maximum concentrations found were 50 ng/ml.

A number of experiments were performed on rabbits to determine urinary excretion after the subcutaneous administration of varying doses of etorphine. Figures 4 and 5 show the urinary etorphine excretion after the subcutaneous administration of 25 μg of etorphine hydrochloride in water to a 6-kg rabbit. Urine was collected by catherization periodically at 2-hr intervals for 8 hr after the dose was given. The last sample was collected 24 hr after the injection.

DISCUSSION

The specific activity of commercially available etorphine makes it possible to establish a mass fragmentographic assay for etorphine without

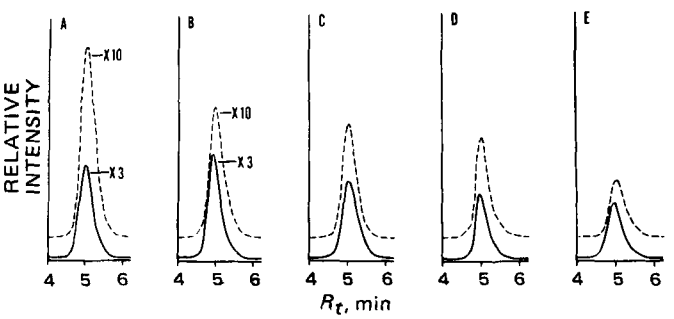

Figure 4—*Mass fragmentograms obtained from 2-ml aliquots of each urine sample collected over 24 hr and processed as described. Mass fragmentogram A represents 12% of total urine volume; B, C, and D each represent 33% of total urine volume; and E represents 25% of total urine volume. Key: - - -, rabbit urine etorphine trimethylsilyl ether, m/e 483; and —, $^3H_2$-etorphine trimethylsilyl ether, m/e 487.*

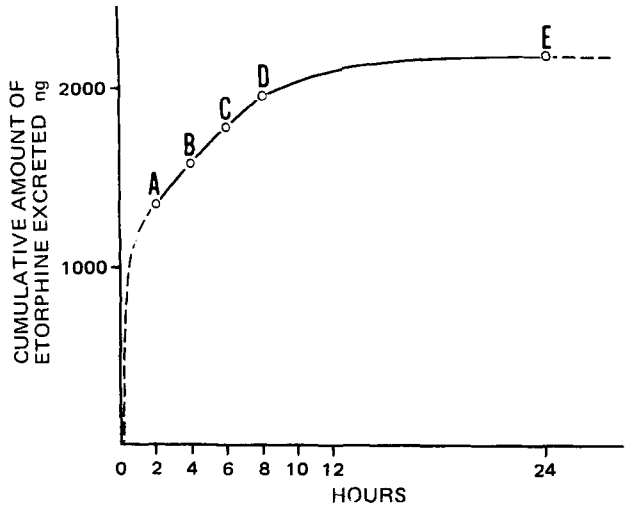

Figure 5—*Cumulative urinary excretion of etorphine over 24 hr.*

synthesis of a deuterated standard. The method could possibly be twice as sensitive if a fully deuterated standard can be obtained. This method does have the advantage that it can be immediately established by any laboratory having a gas chromatograph–mass spectrometer.

The fact that a radioisotope is used made it possible, during method development, to monitor each step of the analytical procedure. The use of small amounts of tritiated compounds in the mass spectrometer poses no problem if reasonable safety procedures are followed with proper exhaustion from the vacuum lines and proper precautions when oil is changed in the vacuum pumps. The advantage of an isotopically labeled internal standard otherwise chemically identical to the substance to be assayed is that it can be expected to pass through the different physicochemical steps of the analysis in a way similar to the compound itself to compensate for losses.

The sensitivity of the selective ion monitoring assay can probably be improved by prepurification of the biological sample or by purification and concentration by liquid chromatography of the trimethylsilyl derivative just prior to GLC–mass spectrometry.

REFERENCES

(1) K. W. Bentley and D. G. Hardy, *Proc. Chem. Soc.*, **1963**, 220.

(2) R. E. Lister, *J. Pharm. Pharmacol.*, **16**, 364 (1964).

(3) G. F. Blane, A. L. A. Boura, A. E. Fitzgerald, and R. E. Lister, *Br. J. Pharmacol. Chemother.*, **30**, 11 (1967).

(4) D. R. Jasinski, J. D. Griffith, and C. B. Carter, *Clin. Pharmacol. Ther.*, **17**, 267 (1975).

(5) S. J. Mule, G. Casella, and D. H. Clouet, *Psychopharmacology*, **44**, 125 (1975).

(6) C. W. Gordetzky and M. P. Kullberg, *Clin. Pharmacol. Ther.*, **17**, 273 (1975).

(7) C.-G. Hammar, B. Holmstedt, and R. Ryhage, *Anal. Biochem.*, **25**, 532 (1968).

(8) B. Holmstedt and L. Palmer, *Adv. Biochem. Psychopharmacol.*, **7**, 1 (1973).

(9) C. W. Gehrke and K. Leimer, *J. Chromatogr.*, **57**, 219 (1971).

(10) L. Bertilsson and F. Sjoqvist, *Adv. Biochem. Psychopharmacol.*, **7**, 147 (1973).

ACKNOWLEDGMENTS

Supported by the Office of Research of the Department of Mental Hygiene of the State of New York and by Grant DA-00327 from the National Institute on Drug Abuse.

Mrs. Theresa Lutz and Mr. Sidney Bernstein who helped with the illustrations are gratefully acknowledged.

Drug Partitioning: Relationships between Forward and Reverse Rate Constants and Partition Coefficient

HUGO KUBINYI

Received February 28, 1977, from the *Research Institute of KNOLL AG, D-6700 Ludwigshafen/Rhein, Germany.* Accepted for publication April 18, 1977.

Abstract □ The rate constant, k_1, of drug transport from an aqueous phase to an organic phase and the rate constant, k_2, of the reverse process can be described as functions of the partition coefficient, P: $\log k_1 = \log P - \log(\beta P + 1) + c'$ and $\log k_2 = -\log(\beta P + 1) + c'$. In a homologous series, where $\log P$ is a simple function of the number of CH_2 groups, $\log k_1$ and $\log k_2$ also can be described as functions of the number of CH_2 groups. The relationships between these equations and current physicochemical models of drug absorption are discussed.

Keyphrases □ Partition coefficients—relationship to forward and reverse rate constants and number of CH_2 groups in a homologous series □ Drug partitioning—relationship of partition coefficients to forward and reverse rate constants and number of CH_2 groups in a homologous series

The partition coefficient, P, of a drug is an equilibrium constant defined in terms of the ratio of k_1, the rate constant of drug transport from the aqueous phase to the organic phase, and k_2, the rate constant of the reverse process, according to:

$$P = \frac{k_1}{k_2} \qquad \text{(Eq. 1)}$$

It is possible to assess the individual rate constants, as shown by Lippold and Schneider (1–3), who determined k_1 and k_2 in homologous series using a three-compartment model (Table I).

THEORETICAL

From the data of Table I, it is evident that there must be additional relationships between k_1 and k_2 beside that expressed in Eq. 1. Examination of the data indicates that k_2 is linearly related to k_1 for the homologs previously studied (1–3); *i.e.*:

$$k_2 = -\beta k_1 + c \qquad \text{(Eq. 2)}$$

Equations 3 and 4 can be derived for the dependence of either k_1 or k_2 on the partition coefficient, P, by substitution of Eq. 2 into Eq. 1, solving first for k_1 (Eq. 3) and then for k_2 (Eq. 4):

$$k_1 = \frac{cP}{\beta P + 1} \qquad \text{(Eq. 3)}$$

$$k_2 = \frac{c}{\beta P + 1} \qquad \text{(Eq. 4)}$$

If Eqs. 3 and 4 are written in the logarithmic form, then Eqs. 5 and 6 result:

$$\log k_1 = \log P - \log(\beta P + 1) + c' \qquad \text{(Eq. 5)}$$

$$\log k_2 = -\log(\beta P + 1) + c' \qquad \text{(Eq. 6)}$$

where the term c' has been substituted for the constant, $\log c$.

Since, in homologous series, $\log P$ is a function of the number of CH_2 groups, N (4):

$$\log P = aN + b \qquad \text{(Eq. 7)}$$

Eqs. 5 and 6 can be rewritten in terms of the relationship expressed in Eq. 7:

$$\log k_1 = aN - \log(\beta' 10^{aN} + 1) + b' \qquad \text{(Eq. 8)}$$

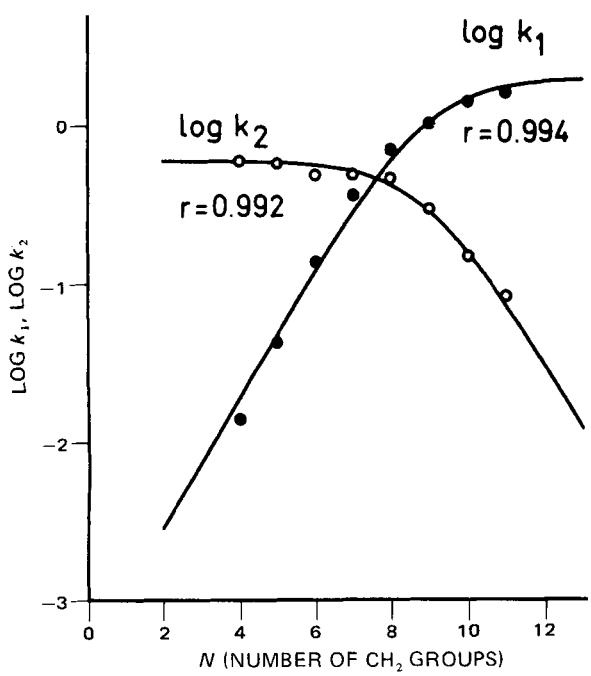

Figure 1—*Rate constants* k_1 *and* k_2 *of the partitioning of homologous quaternary alkylammonium bromides; comparison of experimental values from a three-compartment system (no salt added) (1) and values calculated from Eqs. 8 and 9* (a, b, β, *and* c *values from Table II).*

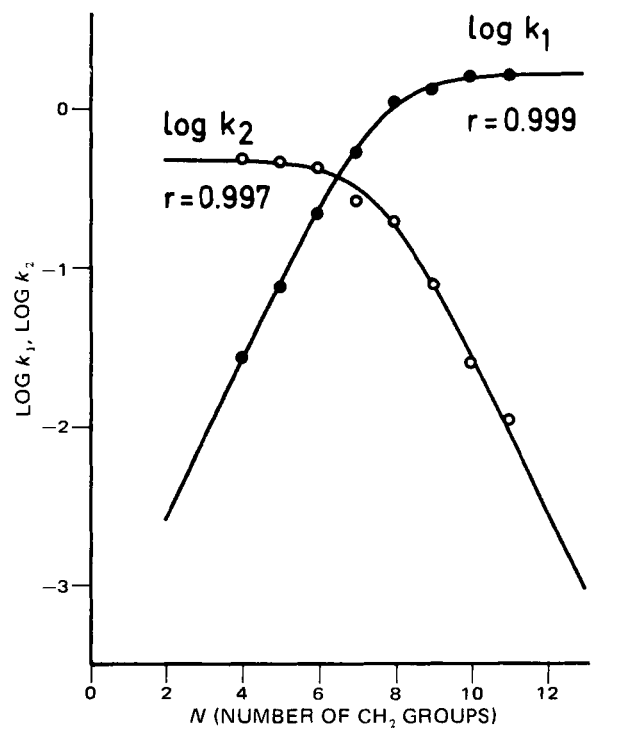

Figure 2—*Rate constants* k_1 *and* k_2 *of the partitioning of homologous quaternary alkylammonium bromides; comparison of experimental values from a three-compartment system (sodium bromide added) (2) and values calculated from Eqs. 8 and 9* (a, b, β, *and* c *values from Table II).*

Table I—Experimental k_1 and k_2 Values from Lippold and Schneider (1–3) for Quarternary Alkylammonium Bromides and *n*-Alkylsulfonates Using Three-Phase Model (Water–1-Octanol–Water)

	Quaternary Alkylammonium Bromides									
	No Salt Added		Plus Sodium Bromide		Plus Sodium Butanesulfonate		Plus Sodium Trichloroacetate		Benzilonium *n*-Alkylsulfonates	
N^a	k_1	k_2	k_1	k_2	k_1	k_2	k_1	k_2	k_1	k_2
2	—	—	—	—	—	—	0.057	1.130	—	—
3	—	—	—	—	—	—	0.115	0.940	—	—
4	0.014	0.600	0.027	0.490	0.055	0.920	0.224	0.824	—	—
5	0.043	0.578	0.076	0.470	0.143	0.640	0.435	0.585	—	—
6	0.140	0.490	0.217	0.425	0.345	0.360	0.930	0.396	0.095	0.635
7	0.370	0.500	0.534	0.264	0.808	0.276	1.200	0.198	—	—
8	0.715	0.471	1.112	0.196	1.140	0.128	1.244	0.076	0.63	0.425
9	1.064	0.300	1.340	0.078	—	—	1.560	0.042	—	—
10	1.440	0.149	1.620	0.025	—	—	—	—	1.33	0.15
11	1.648	0.084	1.650	0.011	—	—	—	—	—	—
12	—	—	—	—	—	—	—	—	1.46	0.02

[a] Number of CH_2 groups.

Table II—*a*, *b*, β, and *c* Values[a], Calculated from k_1 and k_2 Values of Table I, Using Eqs. 2 and 7

	Quaternary Alkylammonium Bromides				
Parameter	No Salt Added	Plus Sodium Bromide	Plus Sodium Butanesulfonate	Plus Sodium Trichloroacetate	Benzilonium *n*-Alkylsulfonates
$k_2 = -\beta k_1 + c$ (Eq. 2)					
β	0.296 (±0.07)	0.286 (±0.04)	0.612 (±0.56)	0.688 (±0.16)	0.430 (±0.15)
c	0.598 (±0.06)	0.480 (±0.04)	0.770 (±0.36)	1.020 (±0.14)	0.686 (±0.16)
n	8	8	5	8	4
r	0.975	0.989	0.896	0.975	0.994
s	0.047	0.032	0.161	0.100	0.038
F	115	267	12.3	114	153
$\log \frac{k_1}{k_2} = aN + b$ (Eq. 7)					
a	0.412 (±0.04)	0.501 (±0.02)	0.546 (±0.06)	0.420 (±0.02)	0.442 (±0.06)
b	−3.146 (±0.31)	−3.265 (±0.15)	−3.373 (±0.35)	−2.179 (±0.10)	−3.440 (±0.57)
n	8	8	5	8	4
r	0.996	0.999	0.998	0.999	0.999
s	0.103	0.051	0.057	0.045	0.063
F	672	4036	918	3674	974

[a] The 95% confidence limits are given in parentheses.

$$\log k_2 = -\log(\beta' 10^{aN} + 1) + c' \qquad \text{(Eq. 9)}$$

where b' has been substituted for the constant $b + c'$ and β' has been substituted for $\beta \times 10^b$.

RESULTS AND DISCUSSION

If Eqs. 2 and 7 are applied to k_1 and k_2 values of Table I, the *a*, *b*, β, and *c* values given in Table II result. Log k_1 and log k_2 values can be calculated from these values using Eqs. 8 and 9; a comparison of observed and calculated log k_1 and log k_2 values is given in Table III and Figs. 1 and 2.

Either Eqs. 3 and 4 or Eqs. 8 and 9 are generally applicable for the quantitative description of k_1 and k_2 values. Equation 3 corresponds to previous drug absorption models (5–14). However, all β values differ significantly from one, giving strong evidence for the validity of the diffusion models (6–12); other models (5, 13, 14) predict $\beta = 1$ for the *in vitro* system used by Lippold and Schneider (1–3). In all cases, the influence of molecular size effects on diffusion coefficients is negligible.

Equations 5 and 6 are special forms of the bilinear model (15, 16) derived recently for the quantitative description of the dependence of biological activity of drugs on their hydrophobic character.

Table III—Comparison of Observed and Calculated log k_1 and log k_2 Values (*a*, *b*, β, and *c* Values of Table II Were Used to Calculate log k_1 and log k_2 from Eqs. 8 and 9, Respectively)

	Quaternary Alkylammonium Bromides				
	No Salt Added	Plus Sodium Bromide	Plus Sodium Butanesulfonate	Plus Sodium Trichloroacetate	Benzilonium *n*-Alkylsulfonates
log k_1 values: r	0.994	0.999	0.995	0.993	0.997
log k_2 values: r	0.992	0.997	0.955	0.996	0.999
log k_1 and log k_2 values[a]					
n	16	16	10	16	8
r	0.994	0.999	0.984	0.995	0.998
s[b]	0.068	0.040	0.092	0.060	0.047
F[b]	335	1414	63	377	429

[a] Log k_1 and log k_2 values were combined because both values are predicted by Eqs. 8 and 9 using the same *a*, *b*, β, and *c* values. [b] The $(n - 4)$ degrees of freedom; F values are only rough estimates because Eqs. 8 and 9 are nonlinear.

REFERENCES

(1) B. C. Lippold and G. F. Schneider, *Arzneim.-Forsch.*, **25**, 843 (1975).

(2) *Ibid.*, **25**, 1683 (1975).

(3) B. C. Lippold and G. F. Schneider, *Pharmazie*, **31**, 237 (1976).

(4) A. Leo, C. Hansch, and D. Elkins, *Chem. Rev.*, **71**, 525 (1971).

(5) T. Koizumi, T. Arita, and K. Kakemi, *Chem. Pharm. Bull.*, **12**, 413 (1964).

(6) R. G. Stehle and W. I. Higuchi, *J. Pharm. Sci.*, **56**, 1367 (1967).

(7) A. Suzuki, W. I. Higuchi, and N. F. H. Ho, *ibid.*, **59**, 644 (1970).

(8) *Ibid.*, **59**, 651 (1970).

(9) R. G. Stehle and W. I. Higuchi, *J. Pharm. Sci.*, **61**, 1922 (1972).

(10) *Ibid.*, **61**, 1931 (1972).

(11) G. L. Flynn and S. H. Yalkowsky, *J. Pharm. Sci.*, **61**, 838 (1972).

(12) S. H. Yalkowsky and G. L. Flynn, *ibid.*, **62**, 210 (1973).

(13) J. G. Wagner and A. J. Sedman, *J. Pharmacokinet. Biopharm.*, **1**, 23 (1973).

(14) J. G. Wagner, "Fundamentals of Clinical Pharmacokinetics," Drug Intelligence Publications, Hamilton, Ill., 1975, p. 203 ff.

(15) H. Kubinyi, *Arzneim.-Forsch.*, **26**, 1991 (1976).

(16) H. Kubinyi, *J. Med. Chem.*, **20**, 625 (1977).

Physiologically Active Substances from Marine Sponges V: Isolation of Physiologically Active Compounds from the Sponge *Verongia archeri*

JOGINDER S. CHIB ˣ, MARTIN F. STEMPIEN, Jr., RONALD A. MIERZWA, GEORGE D. RUGGIERI, and ROSS F. NIGRELLI

Received November 26, 1976, from the *Osborn Laboratories of Marine Sciences, New York Aquarium, New York Zoological Society, Brooklyn, NY 11224.* Accepted for publication April 19, 1977.

Abstract □ Methanolic extracts of hard and soft varieties of the sponge *Verongia archeri* were found to contain similar compounds. An isolation procedure and the structures of 2-(3′,5′-dibromo-4′-hydroxyphenyl)-acetamide, 1-(3′,5′-dibromo-1′,6′-dihydroxy-4′-methoxycyclohexa-2′,4′-diene)acetonitrile, and 2-oxo-5,7-dibromo-6-methoxy-9-hydroxy-8,9-dihydrocoumarin from one variety are described.

Keyphrases □ *Verongia archeri*—methanolic extracts of hard and soft sponges, various compounds isolated and identified, antibacterial activity evaluated □ Antibacterial activity—evaluated in various compounds isolated from methanolic extracts of hard and soft sponge *Verongia archeri*

Sponges of the genus *Verongia* have attracted considerable attention because of the strong antibacterial activity of their chemical constituents. The sponges *V. aerophobia* (1–3), *V. cauliformis* (4, 5), *V. fistularis* (6), *V. thiona* (7–9), and *Ianthella ardis* (10, 11) have yielded several antibiotics (I–VI). A 3,4-dihydroxyquinoline derivative (VII) was also identified as one metabolite in *V. aerophobia* (12).

In a continuing investigation (13, 14) of marine natural resources, the sponges *V. archeri* (hard and soft) were studied. The isolation and identification of various antibiotics from these two species are reported.

EXPERIMENTAL[1]

Materials—The hard form of *V. archeri*[2] was collected as isolated cylinders from the north shore of Jamaica. The soft form was collected either as isolated cylinders or as groups of anastomosing cylinders, up to 40 cm in height, from the British Virgin Islands. Both varieties lose their antibiotic activity after freeze drying, but the activity is retained when the sponges are oven dried at 60–80°. A similar phenomenon was observed with the sponge *V. fistularis*.

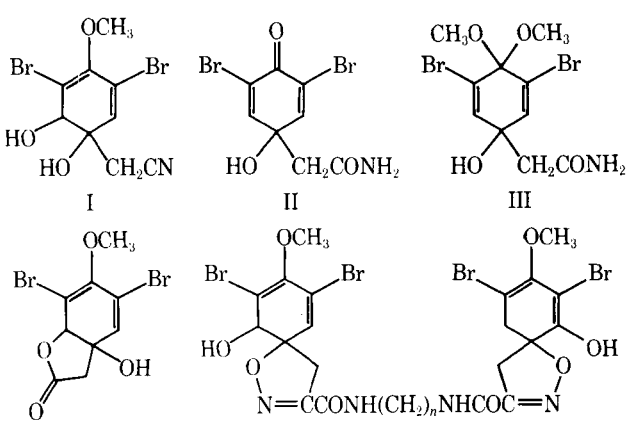

Both varieties of *V. archeri* exhibit the same antibiotic profile, and the same active compounds were isolated from each species. The methods described in this report are for the hard species of *V. archeri*.

Preparation of Crude Antibiotic Fraction—Powdered sponge (7 kg) was extracted repeatedly with methanol (3 × 5 liters) at room temperature until the extract showed no antibiotic activity. A total of 1580 g was obtained after solvent removal. This product was extracted with ethyl acetate to obtain 278 g of ethyl acetate-soluble material and then was extracted with ether to obtain 240 g of material.

The ether-soluble material was partitioned between acetonitrile and petroleum ether (1:1). The acetonitrile-soluble fraction (210 g) contained the antibiotic active substances, while the petroleum ether-soluble material was inactive against *Escherichia coli*. The acetonitrile-soluble fraction was then extracted with chloroform. Evaporation of the chloroform yielded 30 g of an antibiotic-containing mixture. The purification of Compounds A, B, and C from this mixture is outlined in Scheme I.

RESULTS AND DISCUSSION

Compound A—This compound from pooled fractions 101–134 (40 mg) was first crystallized from 95% ethanol and then recrystallized from chloroform–methyl ethyl ketone.

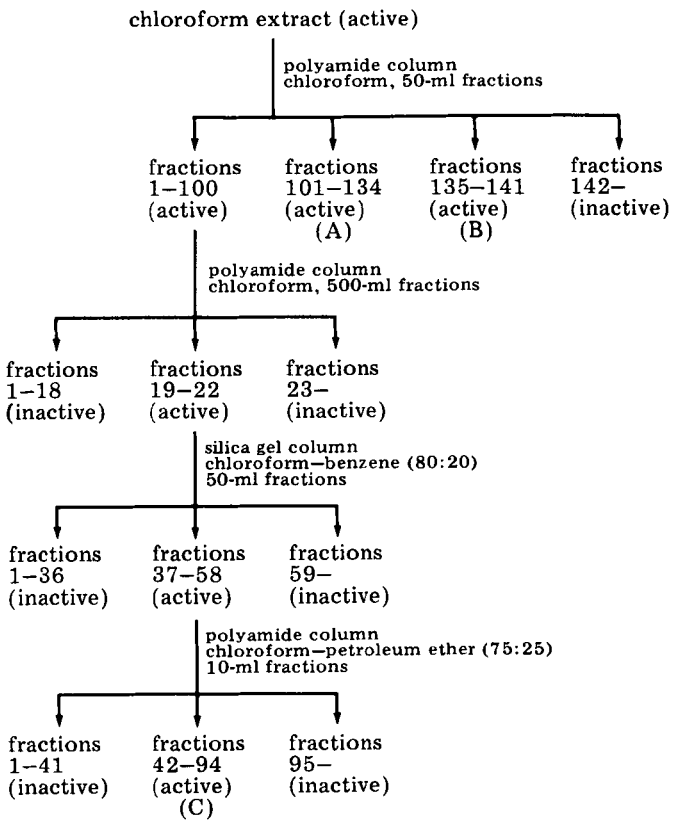

Scheme I

[1] The following instruments were used: a Perkin-Elmer model 421 grating IR spectrometer, a Cary 14 UV spectrophotometer, a Perkin-Elmer model 141 polarimeter, an A-60A Varian NMR spectrometer, and a Hitachi Perkin-Elmer model 107 mass spectrometer. Microanalyses were performed by Schwarzkopf Microanalytical Laboratories, Woodside, N.Y.

[2] The sponge was identified by Dr. Willard D. Hartman, Department of Zoology, Yale University, New Haven, Conn.

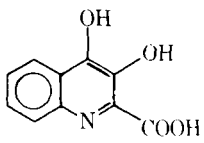

VII

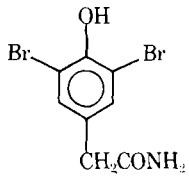

VIII

The IR spectrum in a potassium bromide pellet showed absorbances at 3425 (amine, hydroxyl) and 1625 (amide carbonyl) cm^{-1}. The spectrum in deuterated dimethyl sulfoxide gave proton resonances at δ 7.45 (s, 2H), 7.1–6.80 (broad, 3H), and 3.31 (s, 2H) ppm. The mass spectrum had molecular ions at *m/e* 307, 309, and 311 (1:2:1 ratio) and prominent peaks at 263, 265, and 267 (1:2:1 ratio, $M^+ - 44$). The compound, mp 190–191°, gave an elemental analysis of: C, 31.31; H, 2.17; and N, 4.67.

These data are indicative of Structure VIII, 2-(3′,5′-dibromo-4′-hydroxyphenyl)acetamide, with a molecular formula of $C_8H_7Br_2NO_2$. Confirmation of this structure for Compound A was achieved by treatment with diazomethane followed by a study of the mass spectrum of the resulting methyl ether. This spectrum showed the molecular ion peak at *m/e* 321, 323, and 325 (1:2:1 ratio) and another prominent triplet at 277, 279, and 281 (1:2:1 ratio, $M^+ - 44$). The identity was also established by synthesis from *p*-hydroxyphenylacetic acid (5).

Compound B—Evaporation of solvent from pooled fractions 135–141 gave 6.1 g of a white crystalline substance, which was crystallized from chloroform–methyl ethyl ketone as an analytically pure compound (5.5 g), mp 120–122°.

The IR spectrum in a potassium bromide pellet showed absorptions at 3370 (hydroxyl) and 2265 (nitrile) cm^{-1}. The NMR spectrum in deuterated dimethyl sulfoxide gave proton resonances at δ 6.49 (s, 1H), 6.12 (d, 1H, J = 7 Hz), 6.05 (s, 1H), 3.96 (d, 1H, J = 7 Hz), 3.66 (s, 3H), and 2.77 (s, 2H) ppm and an optical rotation of $[\alpha]_D$ +186° (c, 0.5 g/liter in methanol). The mass spectrum had molecular ions at *m/e* 337, 339, and 341 (1:2:1 ratio). The compound gave an elemental analysis of: C, 31.50; H, 2.82, Br, 46.94; and N, 4.23.

On the basis of its spectral and elemental analysis, this component was identified as 1-(3′,5′-dibromo-1′,6′-dihydroxy-4′-methoxycyclohexa-2,4-diene)acetonitrile (I), previously isolated (1) from *V. cauliformis*.

Compound C—This compound was crystallized from hexane–ethyl acetate as an analytically pure substance (92 mg), mp 129–130°.

The IR spectrum in a potassium bromide pellet gave absorbances at 3310 (hydroxyl) and 1760 cm^{-1}, and the UV spectrum had the λ_{max} at 282.2 nm (ϵ 4680). The NMR spectrum in deuterated chloroform gave proton resonances at δ 6.3 (s, 1H), 5.17 (s, 1H), 3.77 (s, 3H), 3.50 (broad, 1H), and 2.9 (s, 2H) ppm. The mass spectrum had molecular ions at *m/e* 338, 340, and 342 (1:2:1 ratio) and peaks at 320, 322, and 324 (1:2:1 ratio, $M^+ - H_2O$), indicating the presence of two bromine atoms in the compound. The compound gave an elemental analysis of: C, 31.76; H, 2.35; and Br, 47.06.

The data suggest that this antibiotic is 2-oxo-5,7-dibromo-6-methoxy-9-hydroxy-8,9-dihydrocoumarin (aeroplysinin-2) (IV), described by Minale *et al.* (3).

Biological Activity—The natural products were tested for their antibacterial activity against *E. coli*[3] in the following manner. The compound, 0.003 g, was applied to a paper disk and incubated for 18 hr at 35°. Zones of bacterial inhibition were measured and indicated by: +, less than 15 mm; 2+, 15–18 mm; 3+, 18–22 mm; and 4+, greater than 22 mm. The results were: I, 4+; IV, +; and VIII, 3+.

REFERENCES

(1) E. Fattorusso, L. Minale, and G. Sodano, *Chem. Commun.*, **1970,** 751.

(2) E. Fattorusso, L. Minale, and G. Sodano, *J. Chem. Soc. Perkin I*, **1972,** 16.

(3) L. Minale, G. Sodano, W. R. Chan, and A. M. Chen, *J. Chem. Soc. Chem. Commun.*, **1972,** 674.

(4) G. M. Sharma and P. R. Burkholder, *J. Antibiot., Ser. A*, **20,** 200 (1967).

(5) G. M. Sharma and P. R. Burkholder, *Tetrahedron Lett.*, **1967,** 4147.

(6) G. M. Sharma, B. Vig, and P. R. Burkholder, *J. Org. Chem.*, **35,** 2823 (1970).

(7) E. Fattorusso, L. Minale, K. Moody, G. Sodano, and R. H. Thomson, *Gazz. Chim. Ital.*, **101,** 61 (1971).

(8) K. Moody, R. H. Thomson, E. Fattorusso, L. Minale, and G. Sodano, *J. Chem. Soc. Perkin I*, **1972,** 18.

(9) R. J. Anderson and D. J. Faulkner, *Tetrahedron Lett.*, **1973,** 1175.

(10) W. Fulmor, G. E. V. Lear, G. O. Morton, and R. D. Mills, *ibid.*, **1970,** 4551.

(11) D. B. Cosulich and F. M. Lovell, *J. Chem. Soc. Chem. Commun.*, **1971,** 397.

(12) E. Fattorusso, S. Forenza, L. Minale, and G. Sodano, *Gazz. Chim. Ital.*, **101,** 104 (1971).

(13) M. F. Stempien, Jr., J. S. Chib, R. F. Nigrelli, and R. A. Mierzwa, in "Food-Drugs from the Sea Proceedings, Marine Technology Society," L. R. Worthen, Ed., Marine Technology Society, Washington, D.C., 1972, pp. 110–115.

(14) J. S. Chib, R. A. Mierzwa, R. F. Nigrelli, and M. F. Stempien, Jr., paper presented at the National Conference of Indian Science Congress, Chandigarh, India, 1973, p. 124.

ACKNOWLEDGMENTS

Supported by Sea Grant Project Grant 1-35263 to the New York Zoological Society.

The authors thank Professor A. K. Bose of Stevens Institute of Technology, Hoboken, N.J., for helpful discussions during this work and for providing facilities for the recording of mass and NMR spectra.

[3] The American Type Cuture Collection, *Escherichia coli* 4157 ← NC TC 86 (original *Escherichia* strain) containing both smooth and rough colonies.

High-Pressure Liquid Chromatographic Determination of Camphor and Parachlorophenol in Camphorated Parachlorophenol

JOSEPH D. MUSTO, JAYANT N. SANE, and VICTOR D. WARNER ˣ

Received December 27, 1976, from the *Department of Medicinal Chemistry and Pharmacology, College of Pharmacy and Allied Health Professions, Northeastern University, Boston, MA 02115.* Accepted for publication April 18, 1977.

Abstract □ Quantitative analyses of both camphor and parachlorophenol in camphorated parachlorophenol by high-pressure liquid chromatography is described. A 5% solution of phenol in the mobile phase (heptane–chloroform, 3:2) served as the internal standard; the assay involved addition of this phenol solution to the camphorated parachlorophenol, followed by further dilution using the mobile phase (heptane–chloroform, 3:2) and injection into the instrument.

Keyphrases □ Camphor—high-pressure liquid chromatographic analysis in pharmaceutical formulations of camphorated parachlorophenol □ Parachlorophenol—high-pressure liquid chromatographic analysis in pharmaceutical formulations of camphorated parachlorophenol □ High-pressure liquid chromatography—analyses, camphor and parachlorophenol in pharmaceutical formulations of camphorated parachlorophenol □ Anti-infectives, topical—camphorated parachlorophenol, high-pressure liquid chromatographic analyses of camphor and parachlorophenol, pharmaceutical formulations

Quantitative determinations of phenolic compounds (1–5) include bromination (1), bromination–UV spectroscopy (2), GLC (4, 5), and NMR spectroscopy (6).

None of these methods has been adapted to the simultaneous assay of the components of camphorated parachlorophenol. The USP XIX procedure involves separate assays for the two components. Parachlorophenol is assayed by oxidation followed by silver chloride formation, while the camphor assay involves hydrazone formation.

This paper reports the simultaneous quantitative determination of camphor and parachlorophenol in camphorated parachlorophenol by high-pressure liquid chromatography (HPLC) using heptane–chloroform (3:2).

EXPERIMENTAL

Reagents and Chemicals—All chemicals and reagents used were USP, NF, ACS, or chromatographic grade.

Preparation of Solutions—A 5.0% (w/v) phenol solution was prepared in the mobile phase (heptane–chloroform, 3:2). A standard stock solution of camphorated parachlorophenol was prepared according to the USP. All dilutions were done on a weight per volume basis, using the mobile phase as the diluent.

Preparation of Linearity Curve—A standard stock solution containing 65.0% (w/w) camphor and 35.0% (w/w) parachlorophenol was prepared. To varying amounts of this stock solution, 2.50, 5.00, 7.50, and 10.00 g, was added 10 ml of a 5.0% phenol solution (internal standard). The solution was then diluted to 100 ml with the mobile phase. Each standard solution was injected (10 μl), and the peak height ratios of camphor to phenol and parachlorophenol to phenol were calculated. When the peak height ratios were plotted *versus* percent known concentration of camphor or parachlorophenol, the chromatographic response was linear for the tested concentrations of both camphor and parachlorophenol.

Assay—The camphorated parachlorophenol (5 g) was added to 10 ml of the 5.0% phenol solution (internal standard), and this solution was then diluted to 100 ml with the mobile phase. A 10-μl standard septum injection was made with a 25-μl syringe[1]. The 1:20 dilution of the standard stock solution of camphorated parachlorophenol served as the standard for determining concentrations. This solution contained 3.25% camphor and 1.75% parachlorophenol.

Table I—Assay Results on USP Camphorated Parachlorophenol

Assay	Camphor, %	Parachlorophenol, %
1	64.3	34.7
2	65.6	34.9
3	65.0	35.4
4	64.6	35.6
SD	0.56	0.42
CV	0.86	1.19
Average deviation	0.43	0.35

Calculations—The following formula was used for calculating concentrations:

$$\% \text{ sample} = \frac{R_S}{R_{std}} \% \text{ std} \times D \qquad \text{(Eq. 1)}$$

where % sample is the percent camphor or parachlorophenol in the sample, % std is the percent camphor or parachlorophenol in the standard, R_{std} is the peak height ratio of standard camphor and phenol or standard parachlorophenol and phenol, R_S is the peak height ratio of camphor sample and phenol or parachlorophenol sample and phenol, and D is the dilution factor equal to 20.

Instrument Parameters—A high-pressure liquid chromatograph[2] was used with a solvent system of 60% heptane and 40% chloroform. A UV detector at 254 nm was used at an attenuation of ×8 for camphor and ×64 for parachlorophenol and phenol. The flow rate was 2.5 ml/min at an inlet pressure of 0.131 Nm^{-2}. The chart speed was 0.5 cm/min. The column[3] was 0.64 cm o.d. × 15 cm long, packed with 5-μm silica gel[4]. The injection volume was 7–15 μl, and the elution order was camphor (2.76 min), parachlorophenol (10.64 min), and phenol (12.61 min).

DISCUSSION

The results in Table I indicate that camphor and parachlorophenol can be simultaneously assayed by simple dilution of the sample and injection into a high-pressure liquid chromatograph. The linearity curve indicated that the components being analyzed gave a linear response well beyond the limits expected in the sample.

This method allows for a much more rapid assay compared to the USP XIX procedure—only 20 min compared to approximately 5 hr.

REFERENCES

(1) "The United States Pharmacopeia," 19th rev., Mack Publishing Co., Easton, Pa., 1975, pp. 67, 375.

(2) D. G. Garrett, "The Quantitative Analysis of Drugs," 3rd ed., Chapman and Hall, London, England, 1964, pp. 513–518, 550.

(3) P. Rozza, *Acta Pharm. Hung.*, **37**, 145 (1967).

(4) P. A. Hedin, J. P. Minyard, Jr., and A. C. Thompson, *J. Chromatogr.*, **30**, 43 (1967).

(5) V. Kusy, *ibid.*, **57**, 132 (1971).

(6) D. Gupta and L. A. Cates, *J. Pharm. Sci.*, **63**, 93 (1974).

ACKNOWLEDGMENTS

Supported in part by National Institutes of Health Grant RR07143.

[1] Hamilton.

[2] Waters Associates model ALC 202.

[3] Hi-Eff Micropart.

[4] Applied Science Laboratories.

Validity of Oral Bioavailability Estimates of Phenolsulfonphthalein Based on Total Urinary Excretion from Rats

S. T. HORHOTA and HO-LEUNG FUNG ˣ

Received April 11, 1977, from the *Department of Pharmaceutics, School of Pharmacy, State University of New York at Buffalo, Amherst, NY 14260.* Accepted for publication May 5, 1977.

Abstract □ Urinary recovery of phenolsulfonphthalein from rats was determined after intracardial (0.075 mg) and oral (1.5 mg) doses. Although trace quantities of conjugated metabolites could be identified by TLC, the levels present did not introduce significant error into estimates of total phenolsulfonphthalein excretion if samples were assayed directly by colorimetric methods for only unchanged dye. The absolute availability of phenolsulfonphthalein based on urinary recovery under the present experimental conditions was estimated at 10.6%.

Keyphrases □ Phenolsulfonphthalein—urinary excretion from rats, validity of oral bioavailability estimates □ Excretion, urinary—phenolsulfonphthalein in rats, validity of oral bioavailability estimates □ Bioavailability, oral—phenolsulfonphthalein in rats, based on urinary excretion data □ Dyes—phenolsulfonphthalein, urinary excretion from rats, validity of oral bioavailability estimates

Phenolsulfonphthalein (I), a strong acid, is completely ionized at a pH above 1. Because of its ionic nature and poor lipid solubility, the absorption of this dye from the rat small intestine is relatively poor (1). Mechanistically, I is absorbed from the rat small intestine in part by an active transport process of low capacity (2, 3); its percentage of absorption from the perfused rat intestine was found to decrease as the dye concentration was increased (4).

Because I can be easily detected in urine by simple colorimetric methods (5, 6) and its absorption characteristics are well known, the dye is often used as a marker to monitor absorption changes in the small intestine. The effects of surfactants (7, 8), vehicle viscosity, and an anticholinergic agent (9) on absorption were studied using I. Conclusions regarding absorption differences were based on the total urinary excretion and/or the excretion rate of I as determined by direct colorimetry.

Recently, Conway *et al.* (10) reported the identification of I sulfate and glucuronide conjugates in the urine and bile of rats after 15-mg/kg iv administration. No estimate of the amounts of metabolites excreted was given. Since conjugation of the phenolic moiety suppresses the acid–base color change that is the basis of the colorimetric assay used in all absorption studies, urinary excretion of I in rats may be underestimated by not accounting for both free and conjugated materials.

The purpose of this study was to investigate the potential for error in analyzing only unconjugated I as an estimate of total oral absorption. The absolute oral bioavailability of I in the rat based on total urinary excretion also was determined.

Table I—Percent of Administered I Recovered in the Urine of Rats (0–24 hr) before and after Hydrolysis Treatment

	Unhydrolyzed		Hydrolyzed	
Rat	Oral	Intracardiac	Oral	Intracardiac
1	8.8	66.6	8.9	58.6
2	4.3	64.5	3.8	72.6
3	6.1	50.4	7.0	68.0
4	7.7	81.2	6.3	51.9
5	7.3	78.5	5.4	61.1
6	5.5	43.1	6.0	54.1
Mean (*SD*)	6.6 (1.6)	64.1 (15.1)	6.2 (1.7)	61.1 (8.0)
Paired *t* test	n.s. ($p > 0.80$)			
			n.s. ($p > 0.75$)	

EXPERIMENTAL

Materials—All chemicals were reagent grade. Solutions were prepared with distilled water. Compound I was obtained commercially as the sodium salt[1]. Silica gel plates[2] were used for TLC analysis.

Animal Experiments—Male Sprague–Dawley rats[3], 290–350 g, were fasted overnight (16–18 hr) with free access to water. Compound I was administered either intracardially (0.5 ml of 0.15 mg/ml equivalent free acid) or by gastric intubation (1 ml of 1.5 mg/ml equivalent free acid) to each rat in a randomized crossover design.

A 1-week recovery period was allowed between administrations. Animals were placed in metabolism cages with free access to water only. Urine was collected from 0 to 24 hr and centrifuged to remove stray hair contamination, and the volume was recorded.

Analysis of Unconjugated I in Urine—Aliquots of 2.0 ml of urine were pipetted into each of two test tubes; 3.0 ml of 0.1 *N* HCl was added to one tube, and 3.0 ml of 1 *N* NaOH was added to the second. Both tubes were centrifuged, and the supernates were decanted into 1-cm glass spectrophotometer cells. The acid solution served as the reference material.

The absorbance of the basic solution *versus* the reference was recorded on a double-beam spectrophotometer[4] from 530 to 650 nm. The absorbance value at the maximum of 560 nm was noted, and the concentration of I in the sample was calculated. Standard solutions were prepared by adding 1.0 ml of a known I solution (2.4–20 μg/ml) to 2.0 ml of blank urine and 2.0 ml of 1 *N* NaOH or 0.1 *N* HCl.

Analysis of Free and Conjugated I in Urine—Aliquots of 5.0 ml of urine were pipetted into test tubes with polytef-lined screw caps followed by the addition of 0.5 ml of concentrated hydrochloric acid. Loosely capped tubes were heated in an oil bath at 96–97° for 90 min, removed, and allowed to cool to room temperature. After centrifugation, 2.0 ml of urine was transferred to each of two 10-ml volumetric flasks. Samples were neutralized by dropwise addition of 10 *N* NaOH. Solutions were brought to volume with either 0.1 *N* HCl or 1 *N* NaOH. After centrifugation, absorbance values were recorded as described.

Standards were prepared by adding 1.0 ml of a known I solution (20–80 μg/ml) to 4.0 ml of blank urine and 0.5 ml of concentrated hydrochloric acid and were treated in an identical manner.

Qualitative TLC Analysis—Aliquots of 50 μl of sample were spotted on silica gel plates. Elution was carried out in 1-butanol–acetic acid–water (40:12:34) as described by Hart and Schanker (11). Compound I was visualized by exposing the plates to ammonia vapor.

RESULTS

Table I shows the percent of administered I recovered in the 0–24-hr urine samples of rats after oral or intracardiac administration and the

[1] Lot 323607, J. T. Baker, Phillipsburg, N.J.
[2] No. 5762-9H, E. M. Laboratories; supplied through VWR Scientific, Buffalo, N.Y.
[3] Blue Spruce Farms, Altamont, N.Y.
[4] Hitachi Perkin-Elmer model 124.

Table II—Percent Oral Availability of I in Rats Based on Total Urinary Excretion

Rat	Unhydrolyzed	Hydrolyzed
1	13.2	15.2
2	6.7	5.3
3	12.1	10.3
4	9.5	12.1
5	9.3	8.8
6	12.8	11.8
Mean for pooled data	10.6%	
95% confidence interval	5.5–18.1%	

effect of hydrolysis treatment. Qualitative TLC of unhydrolyzed urine revealed two spots with R_f values similar to those reported previously (12) for free and conjugated I, but the latter spot was present only in trace quantities. Only one spot corresponding to unconjugated I was detected in hydrolyzed urine.

Hart and Schanker (11) previously demonstrated the effectiveness of the hydrolytic procedure by comparison with results after glucuronidase treatment. Preliminary studies also indicated no loss of I as a result of the deconjugation process. No drug was found in the 24–48-hr urine samples, in agreement with findings by Feldman *et al.* (7) at the same oral dosage level.

Paired t test comparison of the unhydrolyzed *versus* hydrolyzed samples showed no significant difference for oral ($p > 0.80$) or intracardiac ($p > 0.75$) administrations. It can be concluded that no substantial error is introduced in measuring only free I in the urine of rats after oral or intracardiac administration at doses used in this study. The absolute oral availability, A, of I based on total urinary excretion was calculated as:

$$A = \frac{\%\text{ of oral dose recovered}}{\%\text{ of intracardiac dose recovered}} \times 100 \qquad \text{(Eq. 1)}$$

The results are shown in Table II. Data from unhydrolyzed and hydrolyzed samples were also pooled since the two treatments were not different from each other. The 95% confidence interval for the ratio of two normally distributed variables was calculated using Fieller's theorem as outlined by Colquhoun (13).

DISCUSSION

Compound I is a sulfonic acid dye with pKa's of 1 (sulfonic acid) and 7.9 (phenolic) and is completely ionized at gastric and intestinal pH's. A characteristic yellow (acid) to red (base) color change makes it widely used as an acid–base indicator. The development of simple assays in biological fluids based on this color change has made I an attractive compound to study in animal species (7, 8, 10–12) as well as in humans (6, 9). About 3–5% of orally administered solutions are recovered as unchanged drug in the 0–24-hr urine of rats (7, 8).

Conway *et al.* (10) identified conjugated metabolites of I in the urine and bile of rats after intravenous administration of a dose 3.3 times higher than the dose used in absorption studies. The fraction of the dose excreted as metabolites was not given. If metabolites are present in sufficient amounts, it is possible that the recovery of I reported previously may be an underestimate of total urinary excretion. Results reported here show this not to be the case after either oral (1.5 mg) or intracardiac (0.075 mg) administrations; there is no significant difference in the recovery of I in urine before and after hydrolysis.

The absolute oral availability of I based on total urinary excretion was estimated to be 10.6% (95% confidence interval of 5.5–18.1%). This information has not been reported previously.

An average of only 62.6% of an intracardiac dose was recovered in the urine. Hart and Schanker (11) reported the active secretion of I in the bile of rats. This interpretation is complicated by the fact that urinary excretion was prevented by ligation of the renal pedicles. Feldman *et al.* (7) recovered about 42% of an intraperitoneal dose of I as unchanged drug in rat urine. If biliary excretion is an important pathway for the elimination of I in rats, the potential for saturation of this pathway must be considered in interpreting urinary excretion data at different dose levels. An example of this phenomenon was reported by Axelson and Gibaldi (14), who showed that the biliary excretion of riboflavin in rats increases disproportionately with increasing body levels, thus affecting the total urinary recovery of the vitamin.

REFERENCES

(1) R. C. Lanman, C. E. Stremsterfer, and L. S. Schanker, *Xenobiotica*, **1**, 613 (1971).

(2) H. Kunze and W. Vogt, *Arch. Exp. Pathol. Pharmakol.*, **256**, 139 (1967).

(3) H. Kunze, *ibid.*, **259**, 260 (1968).

(4) K. Kakemi, H. Sezaki, R. Konishi, T. Kimura, and M. Murakami, *Chem. Pharm. Bull.*, **18**, 275 (1970).

(5) S. Feldman and M. Gibaldi, *Gastroenterology*, **514**, 918 (1968).

(6) G. M. McLeod, A. B. French, C. J. Good, and F. S. Wright, *J. Lab. Clin. Med.*, **71**, 192 (1968).

(7) S. Feldman, M. Salvino, and M. Gibaldi, *J. Pharm. Sci.*, **59**, 705 (1970).

(8) S. Malik, D. Canaham, and M. W. Gouda, *ibid.*, **64**, 987 (1975).

(9) J. J. Ashley and G. Levy, *ibid.*, **62**, 688 (1973).

(10) W. D. Conway, V. K. Batra, and A. Abramowitz, *ibid.*, **62**, 1810 (1973).

(11) L. G. Hart and L. S. Schanker, *Proc. Soc. Exp. Biol. Med.*, **123**, 433 (1966).

(12) A. M. Guarino and J. B. Anderson, *Xenobiotica*, **6**, 1 (1976).

(13) D. Colquhoun, "Lectures on Biostatistics," Clarendon, Oxford, England, 1971.

(14) J. E. Axelson and M. Gibaldi, *J. Pharm. Sci.*, **61**, 404 (1972).

ACKNOWLEDGMENTS

Supported in part by Grant 5S07RR05454-14.

S. T. Horhota is a Fellow of the American Foundation for Pharmaceutical Education.

The authors acknowledge John Lettieri for technical assistance.

Rapid High-Pressure Liquid Chromatographic Determination of Quinidine and Dihydroquinidine in Plasma Samples

ROBERT E. KATES ˣ, DOUGLAS W. McKENNON, and THOMAS J. COMSTOCK

Received February 14, 1977, from the *College of Pharmacy, Ohio State University, Columbus, OH 43210.* Accepted for publication May 3, 1977.

Abstract □ A high-pressure liquid chromatographic assay for quinidine and dihydroquinidine was developed. A cation-exchange column was utilized with an eluting solvent pH of about 9. The internal standard was cinchonine. The reproducibility and precision of this method were evaluated by analyzing replicate samples and by comparing results with those obtained from a TLC–fluorometric procedure. In addition, several drugs were evaluated to ascertain whether they interfered with the analysis of quinidine and dihydroquinidine.

Keyphrases □ Quinidine—high-pressure liquid chromatographic analysis in plasma □ Dihydroquinidine—high-pressure liquid chromatographic analysis in plasma □ High-pressure liquid chromatography—analyses, quinidine and dihydroquinidine in plasma □ Cardiac depressants—quinidine, high-pressure liquid chromatographic analysis in plasma

Measuring plasma quinidine concentrations has proven to be a valuable aid in the evaluation and management of patients on quinidine therapy (1, 2). The first procedure for determining plasma quinidine levels was published in 1943 (3). Since that time, modifications of the original method have been proposed (4, 5), and new and improved analytical methodologies have been developed (6–9). The improvements in the analysis of quinidine relate both to increased sensitivity and better specificity.

While several procedures provide adequate sensitivity, only two are truly specific for quinidine (8, 9). These procedures allow for the separation of quinidine from dihydroquinidine and permit the quantitation of both compounds. However, these procedures involve a TLC separation followed by fluorometric analysis and are both extremely tedious and time consuming.

Since dihydroquinidine has been reported to represent as much as 24% of the total alkaloid present in some quinidine preparations (10), a rapid and simple procedure for separating and measuring both compounds concurrently would be of value for research and patient care. This report describes a new high-pressure liquid chromatographic (HPLC) procedure that facilitates the separation and analysis of both quinidine and dihydroquinidine in plasma samples.

EXPERIMENTAL

Chemicals and Reagents—Quinidine[1], dihydroquinidine[2], and cinchonine[3] were obtained as the free bases and used without further purification.

Glass-distilled benzene[4] and methanol[4] were used. A 0.01 *M* solution of trimethylamine was prepared by dissolving trimethylamine hydrochloride[3] in double-distilled water. Potassium hydroxide[5] was used in the preparation of the mobile phase, and a 5 *N* solution of sodium hydroxide[5] was prepared for the extraction.

Instrumentation—A dual-piston reciprocating pump[6] with a variable UV wavelength detector system was used[7]. Samples were injected onto the column *via* a 50-μl valve loop[8]. The column employed was a 25-cm × 4.6-mm cation-exchange column[9]. The system was operated at room temperature with a flow rate of 2 ml/min, which developed a pressure of approximately 2000 psi. The detector was set to read absorbance at 230 nm.

Mobile Phase Preparation—Trimethylamine hydrochloride (0.01 mole) was dissolved in approximately 100 ml of water. Potassium hydroxide (0.001 mole) was then added, and the solution was diluted to 1 liter with water. The pH of this solution was approximately 9. The mobile phase was then prepared by mixing this aqueous solution with methanol in a ratio of 1:4 (water–alcohol). The mobile phase was routinely degassed by application of a vacuum.

Procedure—To 1 ml of plasma was added 200 ng of cinchonine (100 μl of a methanolic solution). A 0.1-ml aliquot of 5 *N* sodium hydroxide and 3 ml of benzene were then added. The tube was shaken for 5 min and centrifuged to separate the aqueous and organic layers.

The benzene was then transferred to a clean tube and evaporated to dryness at 55° under nitrogen. The residue was dissolved in 200 μl of the mobile phase, and 50 μl was injected. All samples were analyzed in triplicate. Peak areas were determined by means of an integrating recorder[10].

RESULTS AND DISCUSSION

The described procedure is sufficiently sensitive to measure quinidine and dihydroquinidine levels as low as 100 ng/ml. To measure levels in the low nanogram region, only minor modifications are necessary. They include reducing the amount of internal standard to 100 ng, using a 100-μl injection loop, and operating at a lower attenuation. As was reported (11), the extraction of quinidine from plasma at a high pH is essentially 100% efficient. Likewise, at a high pH, dihydroquinidine is readily extracted from plasma into benzene (12).

Several compounds were evaluated for use as internal standards including cinchonidine, chloroquine, primaquine, brucine, and quinine. All of these compounds were unsuitable because of poor separation from

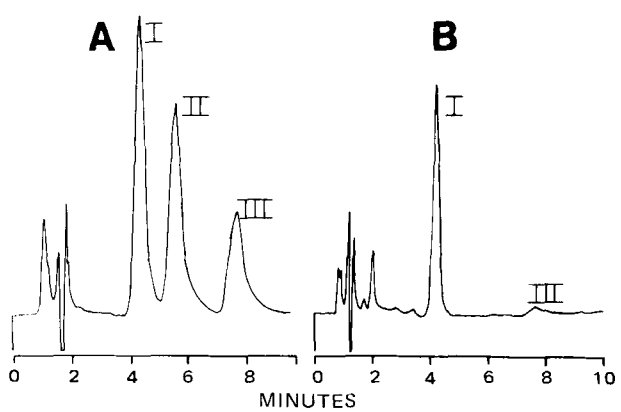

Figure 1—*Chromatograms of a plasma sample (A) spiked with 2 μg of quinidine/ml (I), 200 ng of cinchonine/ml (II), and 1 μg of dihydroquinidine/ml (III), and a sample from a patient (B) without any cinchonine added.*

[1] Supplied by C. T. Ueda, College of Pharmacy, Omaha, Neb.
[2] Tridom Chemical, Inc., Hauppauge, N.Y.
[3] Aldrich Chemical Co., Milwaukee, Wis.
[4] Burdick and Jackson Labs., Muskegon, Mich.
[5] ACS grade, Fisher Scientific, Fairlawn, N.J.
[6] Tracor model 995.
[7] Tracor model 970.
[8] Rheodyne model 7120.
[9] Partisil 10 SCX, Reeve Angel, Clifton, N.J.
[10] Houston Instruments model 5221-15.

Table I—Evaluation of Assay Precision and Accuracy for Quinidine (n = 7)

Quinidine Added, μg/ml	Mean Quinidine Measured, μg/ml	*SD* of Measured Concentration
1	0.96	0.07
5	4.90	0.46
10	11.0	1.0

quinidine or too long retention times. Cinchonine was selected because it eluted fairly rapidly and was readily separated from quinidine and dihydroquinidine.

Figure 1A shows a chromatogram of a spiked plasma sample containing quinidine (2 μg/ml), cinchonine (200 ng/ml), and dihydroquinidine (1 μg/ml). The retention times were 4.4, 5.7, and 7.8 min, respectively. Chromatograms of extracted blank plasma samples showed no peaks. No plasma constituents eluted with retention times near those of the compounds being measured.

Figure 1B shows a chromatogram from a patient sample without any cinchonine added and demonstrates that none of the metabolites of quinidine eluted under the cinchonine peak. The small amount of dihydroquinidine detected is typical of what has been observed with most patient samples. The concentration of quinidine measured in the sample shown was 1.2 μg/ml, while the concentration of dihydroquinidine was estimated to be 50 ng/ml. The dihydroquinidine detected here represented approximately 4% of the total alkaloid measured. This result agrees with the percentage of the impurity found in the drug product administered. It has been reported that the disposition kinetics of quinidine and dihydroquinidine are essentially the same (12). Therefore, one would anticipate that the ratio of quinidine to dihydroquinidine in the plasma would not change with time.

Standard curves were prepared by adding known amounts of drug to blank plasma samples with known concentrations of quinidine and dihydroquinidine and then determining the peak area ratios, relative to the internal standard, at various concentrations. Either water or plasma could be used for preparing the standard curves. The relative extraction efficiencies of these two compounds and the internal standard were not affected by plasma components.

The quinidine standard curve was linear over a range of 0.5–10 μg/ml and extrapolated through the origin. The slope of the regression line was 0.62 with a correlation coefficient of 0.99. The standard curve for dihydroquinidine was linear over a range of 0.5–5.0 μg/ml and also extrapolated through the origin. The slope of the regression line was 0.62 with a correlation coefficient of 0.99.

The precision and accuracy of this assay procedure were evaluated by analyzing several plasma samples with known concentrations of quinidine and dihydroquinidine. Quinidine was evaluated at three concentrations, and dihydroquinidine was evaluated at four levels. The results of the quinidine samples are summarized in Table I. The standard deviations ranged from 7% at 1 μg/ml to 9% at 10 μg/ml.

The results from the evaluation of the dihydroquinidine measurements are reported in Table II. The standard deviations ranged from 15% at 0.5 μg/ml to 3% at 5 μg/ml. To facilitate more accurate measurements of smaller quantities of dihydroquinidine, it is necessary to utilize a smaller quantity of the internal standard and to operate the detector at a lower attenuation.

The procedure was further evaluated by comparing the results of the analysis of patient samples by both the HPLC method and a TLC–fluorometric procedure (8). Blood samples were obtained from six patients who were receiving oral quinidine sulfate for ventricular arrhythmias.

Table II—Evaluation of Assay Precision and Accuracy for Dihydroquinidine

Dihydroquinidine Added, μg/ml	n	Mean Dihydroquinidine Measured, μg/ml	*SD* of Measured Concentration
0.5	6	0.53	0.08
1.0	7	0.98	0.08
3.0	7	3.0	0.22
5.0	7	4.9	0.17

Table III—Comparison of HPLC and TLC–Fluorometric Assay Procedures Using Patient Samples

Patient	Quinidine Concentration, μg/ml	
	HPLC	TLC–Fluorometric[a]
C.K.	0.90	1.0
B.M.	1.8	1.8
J.M.	1.9	2.0
J.M.	2.2	2.3
W.G.	0.90	1.0
D.F.	0.57	0.66
R.T.	0.84	0.88

[a] Reference 8.

Samples were drawn using heparinized syringes to avoid possible problems with commercially available blood-drawing tubes (13). The results are shown in Table III. The two methods agree quite favorably with only minor variability, which ranged from 0.1 to 0.4 μg/ml.

The samples analyzed by the TLC–fluorometric procedure were inadvertently thawed and left at room temperature for approximately 48 hr. They were then refrozen and stored for several days before analysis. The observed results indicate that plasma samples containing quinidine are stable at room temperature for at least 48 hr.

Since patients receiving quinidine usually are concurrently taking other medications, it was necessary to evaluate the possible interference by other drugs with the assay procedure. Plasma samples were obtained from patients on various medications and were then extracted and analyzed according to the described protocol. No interfering peaks were observed when plasma samples containing the following drugs were analyzed: propranolol, lidocaine, procainamide, digoxin, warfarin, chlorothiazide, spironolactone, furosemide, isoniazid, allopurinol, flurazepam, triamterene, and dipyridamole. All of these drugs were being administered in therapeutic doses, and blood samples were drawn, when possible, to reflect peak levels.

In summary, an HPLC procedure for measuring plasma concentrations of quinidine and dihydroquinidine has been developed. The procedure is sufficiently rapid to provide clinical usefulness in that it requires, on the average, only 20 min to extract and analyze a sample. However, it is sufficiently sensitive to be of value for research purposes.

REFERENCES

(1) J. Koch-Weser, *N. Engl. J. Med.*, **287**, 227 (1972).

(2) I. R. Edwards, B. W. Hancock, and R. Saynor, *Br. J. Clin. Pharmacol.*, **1**, 455 (1974).

(3) B. B. Brodie and S. Undenfriend, *J. Pharmacol. Exp. Ther.*, **73**, 154 (1943).

(4) A. L. Edgar and M. Sokolaw, *Lab. Clin. Med.*, **36**, 474 (1950).

(5) G. Cramer and B. Isaksson, *J. Clin. Lab. Invest.*, **15**, 553 (1963).

(6) K. K. Midha and C. Charette, *J. Pharm. Sci.*, **63**, 1244 (1974).

(7) J. L. Valentine, P. Driscoll, E. L. Hamburg, and E. D. Thompson, *ibid.*, **65**, 96 (1976).

(8) C. T. Ueda, B. J. Williamson, and B. S. Dzindzio, *Clin. Pharmacol. Ther.*, **20**, 260 (1976).

(9) G. Hartel and A. Korhonen, *J. Chromatogr.*, **37**, 70 (1968).

(10) F. Alexander, H. Gold, L. N. Katz, R. Scott, and P. D. White, *J. Pharmacol. Exp. Ther.*, **90**, 191 (1947).

(11) G. Hartel and A. Harjanne, *Clin. Chim. Acta*, **23**, 289 (1969).

(12) C. T. Ueda, B. J. Williamson, and B. S. Dzindzio, *Res. Commun. Chem. Pathol. Pharmacol.*, **14**, 215 (1976).

(13) D. Fremstad, *Clin. Pharmacol. Ther.*, **20**, 120 (1976).

ACKNOWLEDGMENTS

Supported in part by Health Professions Special Projects Grant 05D000714-010 from the Department of Health, Education, and Welfare.

The authors thank Dr. C. T. Ueda for analyzing patient samples by the TLC–fluorometric procedure, Ms. Linda Rodgers for excellent laboratory assistance, and Ms. Suzanne Hessler for assistance in manuscript preparation.

Plant Anticancer Agents VI: Isolation of Voacangine, Voacamine, and Epivoacorine from *Tabernaemontana arborea* Sap

DAVID G. I. KINGSTON

Received December 22, 1976, from the *Department of Chemistry, Virginia Polytechnic Institute and State University, Blacksburg, VA 24061.* Accepted for publication May 13, 1977.

Abstract □ Fractionation of the sap of *Tabernaemontana arborea*, guided by cytotoxicity against the P-388 lymphocytic leukemia, yielded the known indole alkaloids voacangine, voacamine, and epivoacorine as the major cytotoxic constituents.

Keyphrases □ Alkaloids, various—isolated from *Tabernaemontana arborea* sap, cytotoxic activity evaluated □ *Tabernaemontana arborea*—sap, various alkaloids isolated, cytotoxic activity evaluated □ Cytotoxic activity—various alkaloids isolated from *Tabernaemontana arborea* sap evaluated

Previously (1–4), the isolation of various indole and bisindole alkaloids from *Tabernaemontana johnstonii* and *T. holstii* was described. In all cases, the bisindole alkaloids isolated were derived from isovoacangine coupled to a vobasane moiety, and no evidence for the presence of voacangine-derived bisalkaloids was found.

During a systematic search for novel anticancer agents of plant origin, dried extracts of the sap of *T. arborea* J. N. Rose ex J. D. Smith became available. In this investigation, the major cytotoxic components were isolated.

EXPERIMENTAL

Methods and materials were identical to those described previously (2, 4).

Plant Material—Samples of dried water-displaced extracts of the trunk sections of two trees of the species *T. arborea* J. N. Rose ex J. D. Smith were obtained from Costa Rica.

Initial Fractionation and Chromatography—A 1000-g sample of the dried extract was subjected to partition between water (2.5 liters) and chloroform (4 × 3 liters). The cytotoxic chloroform fraction (107 g) was separated from the inactive water fraction and subjected to a further partition between 90% aqueous methanol (3 liters) and hexane (3 liters). The cytotoxic aqueous methanol extract (45 g) was separated from the hexane fraction and from some insoluble material and subjected to chromatography on 2.5 kg of TLC grade silica gel. Elution was carried out with ethyl acetate containing increasing amounts of ethanol; 10 fractions, A–J, were collected.

Voacangine (I)—Fraction A (6.3 g) was recrystallized from methanol to yield I as colorless needles, mp 136–137° [lit. (5) mp 136–137°]. The sample had identical IR and UV spectra to those reported for I (6) and had an $[\alpha]_D^{22}$ of −42° (c 3.7, chloroform) [lit. $[\alpha]_D^{22}$ −42° (6) and −37° (5)]. The mass spectrum was identical with that reported (7), except for minor variations in peak intensities, and the NMR spectrum was entirely consistent with a voacangine structural formulation.

Voacamine (II)—A portion of Fraction E (1.2 g) was subjected to preparative TLC with benzene–dichloromethane–ether–methanol (38:30:22:10) with three developments. The UV-absorbing central band was scraped and eluted to yield 260 mg of a fraction which was crystallized from methanol to yield II (35 mg), mp 222–237° dec. [lit. (6) mp 223°], $[\alpha]_D^{22}$−46° (c 1.4, chloroform). Its UV spectrum showed λ_{max} 226 (log ϵ 4.60), 288 (4.13), and 295 (4.15) nm; its IR spectrum in chloroform was identical with that published for II (6).

Its mass spectrum also was identical with that published for II (7), except for minor variations in peak intensities, and its NMR spectrum was in agreement with published spectral data for II (8, 9). The observation of one-proton aromatic singlets at δ 6.82 and 6.96 ppm established the structure as being either of the conoduramine or voacamine types.

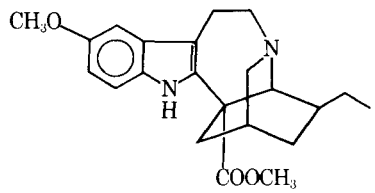

I

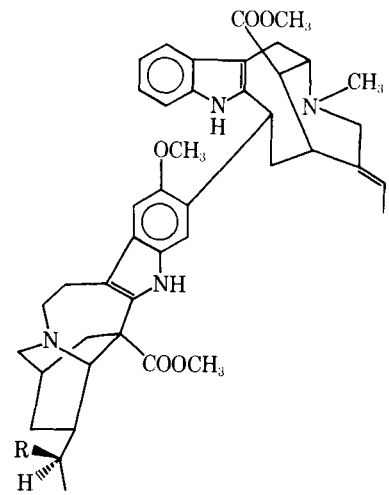

II: R = H
III: R = OH

The remote possibility that the compound could be conoduramine was excluded by a direct high-pressure liquid chromatographic (HPLC) comparison of samples, which showed that they were different.

Epivoacorine (III)—A portion of Fraction I (0.1 g) was subjected to preparative TLC with benzene–dichloromethane–ether–methanol (37:29:22:12) with three developments. The UV absorbing band, R_f ~0.25, was scraped and eluted to yield a fraction from which III was obtained

Table I—Cytotoxicity of Certain Fractions and Pure Alkaloids from *T. arborea*[a]

Fraction or Alkaloid	P-388 ED_{50}, μg/ml
Aqueous methanol extract	8.0
A	6.8
B	14
C	8.6
D	7.8
E	9.0
F	23
G	18
H	7.1
I	2.7
J	9.0
Voacangine	6.8
Voacamine	2.6
Epivoacorine	1.7

[a] Bioassays were performed by the A. D. Little Co., Cambridge, Mass., using established protocols.

by crystallization from methanol, mp 260–270° dec. [lit. (10) mp 265°], $[\alpha]_D^{22}$ −51° (c 2.2, chloroform). Its UV absorption spectrum showed λ_{max} 226 (log ε 4.63), 288 (4.17), and 295 (4.18) nm, and its IR spectrum was identical to that published for III (6).

Its NMR spectrum was consistent with this structural formulation; in particular, the aromatic region and the methyl signals were essentially identical to those recorded for II, except that the triplet at δ 0.92 ppm in II was replaced by a doublet at δ 1.26 ppm. Its mass spectrum also was consistent with this structural formulation (7). Finally, chromatographic comparison with an authentic sample established the identity of the isolated material as III.

Cytotoxic Activities—The cytotoxicities of Fractions A–J and of the three isolated alkaloids are given in Table I.

REFERENCES

(1) D. G. I. Kingston, B. B. Gerhart, and F. Ionescu, *Tetrahedron Lett.*, **1976**, 649.

(2) D. G. I. Kingston, B. T. Li, and F. Ionescu, *J. Pharm. Sci.*, **66**, 1135 (1977).

(3) D. G. I. Kingston, F. Ionescu, and B. T. Li, *Lloydia*, **40**, 215 (1977).

(4) D. G. I. Kingston, B. B. Gerhart, F. Ionescu, M. M. Mangino, and S. M. Sami, *J. Pharm Sci.*, **67**, 249 (1978).

(5) D. F. Dickel, C. L. Holden, R. C. Maxfield, L. E. Paszek, and W. I. Taylor, *J. Am. Chem. Soc.*, **80**, 123 (1958).

(6) N. Neuss, "Physical Data of Indole and Dihydroindole Alkaloids," Lilly Research Laboratories, Indianapolis, Ind., vol. I, 1964, and vol. II, 1964–1968.

(7) H. Budzikiewicz, C. Djerassi, F. Pusieux, F. Percheron, and J. Poisson, *Bull. Soc. Chim. Fr.*, **1963**, 1899.

(8) G. Büchi, R. E. Manning, and S. A. Monti, *J. Am. Chem. Soc.*, **85**, 1893 (1963).

(9) *Ibid.*, **86**, 4631 (1964).

(10) J. Poisson, F. Puisieux, C. Miet, and M. B. Patel, *Bull. Soc. Chim. Fr.*, **1965**, 3549.

ACKNOWLEDGMENTS

Supported by Research Grant CA-12831 from the National Cancer Institute, U.S. Department of Health, Education, and Welfare, Bethesda, MD 20014.

The author thanks Professor J. Poisson for a sample of epivoacorine, Professor G. Büchi for a sample of voacorine, and Dr. M. S. Hudson of Hudson Research, Tropical Science Center, for the dried plant extracts. Technical assistance was provided by Mrs. D. Davis and Mrs. A. A. Yousten.

Plant Anticancer Agents VII: Structural Effects on Cytotoxicity of Bisindole Alkaloids of Voacamine Type

DAVID G. I. KINGSTON

Received December 22, 1976, from the *Department of Chemistry, Virginia Polytechnic Institute and State University, Blacksburg, VA 24061.* Accepted for publication May 26, 1977.

Abstract □ Structural effects on the cytotoxicity of bisindole alkaloids of the voacamine series were investigated with compounds isolated from various *Tabernaemontana* species and compounds synthesized specifically for this purpose. Activity is sensitive both to the position of attachment of the vobasane unit on the iboga moiety and to the presence of an *N*-methyl group on the vobasane unit.

Keyphrases □ Alkaloids—isolated from various *Tabernaemontana* species or synthesized, structural effects on cytotoxicity evaluated □ *Tabernaemontana* alkaloids, various—structural effects on cytotoxicity evaluated □ Cytotoxicity—alkaloids isolated from various *Tabernaemontana* species or synthesized, structural effects evaluated □ Structure-activity relationships—alkaloids isolated from various *Tabernaemontana* species or synthesized, cytotoxicity evaluated

During studies on the isolation and structure elucidation of naturally occurring anticancer agents, some bisindole alkaloids of the voacamine type were isolated from various species of the genus *Tabernaemontana* and their structure and cytotoxicity were determined (1–5). This paper presents a preliminary account of the structure–activity relationships observed.

Table I—Cytotoxicity of the Simple Indole Alkaloids from which the Bisindoles Are Formed

Alkaloid		Cytotoxicity (ED_{50}), μg/ml P-388	KB
XI	Voacangine	6.8	>100
XII	Isovoacangine	18	59
XIII	Ibogamine	—	>100
XIV	Perivine	20	70
XV	Vobasine	—	>100

Table II—Cytotoxicity of Bisindole Alkaloids as a Function of the Presence of a Methyl Group on the Vobasane Ring

Alkaloid	R	Cytotoxicity (ED_{50}), μg/ml P-388	KB
II	H	1.3	5.8
III	CH_3	20	19
IX	H	3.2	—
X	CH_3	26	31

RESULTS AND DISCUSSION

Cytotoxicity data for the bisindole alkaloids I–X and for the simple indole alkaloids XI–XV are given in Tables I–IV. All bisindole alkaloids tested were of the voacamine type and may be considered to be composed of an iboga unit coupled to a vobasane unit. Data are given for two com-

Table III—Cytotoxicity of Bisindole Alkaloids as a Function of the Position of Attachment of the Vobasane Unit to the Iboga Moiety

Alkaloid		Position of Attachment	Cytotoxicity (ED_{50}), μg/ml P-388	KB
I	Voacamidine	11′	14	—
III	Conoduramine	12′	20	19
VI	Voacamine	13′	2.6	—
VII	Epivoacorine	13′	1.7	—
VIII	Tabernamine	13′	2.1	—
X	Conodurine	14′	26	31

by crystallization from methanol, mp 260–270° dec. [lit. (10) mp 265°], $[\alpha]_D^{22}$ −51° (c 2.2, chloroform). Its UV absorption spectrum showed λ_{max} 226 (log ε 4.63), 288 (4.17), and 295 (4.18) nm, and its IR spectrum was identical to that published for III (6).

Its NMR spectrum was consistent with this structural formulation; in particular, the aromatic region and the methyl signals were essentially identical to those recorded for II, except that the triplet at δ 0.92 ppm in II was replaced by a doublet at δ 1.26 ppm. Its mass spectrum also was consistent with this structural formulation (7). Finally, chromatographic comparison with an authentic sample established the identity of the isolated material as III.

Cytotoxic Activities—The cytotoxicities of Fractions A–J and of the three isolated alkaloids are given in Table I.

REFERENCES

(1) D. G. I. Kingston, B. B. Gerhart, and F. Ionescu, *Tetrahedron Lett.*, **1976**, 649.

(2) D. G. I. Kingston, B. T. Li, and F. Ionescu, *J. Pharm. Sci.*, **66**, 1135 (1977).

(3) D. G. I. Kingston, F. Ionescu, and B. T. Li, *Lloydia*, **40**, 215 (1977).

(4) D. G. I. Kingston, B. B. Gerhart, F. Ionescu, M. M. Mangino, and S. M. Sami, *J. Pharm Sci.*, **67**, 249 (1978).

(5) D. F. Dickel, C. L. Holden, R. C. Maxfield, L. E. Paszek, and W. I. Taylor, *J. Am. Chem. Soc.*, **80**, 123 (1958).

(6) N. Neuss, "Physical Data of Indole and Dihydroindole Alkaloids," Lilly Research Laboratories, Indianapolis, Ind., vol. I, 1964, and vol. II, 1964–1968.

(7) H. Budzikiewicz, C. Djerassi, F. Pusieux, F. Percheron, and J. Poisson, *Bull. Soc. Chim. Fr.*, **1963**, 1899.

(8) G. Büchi, R. E. Manning, and S. A. Monti, *J. Am. Chem. Soc.*, **85**, 1893 (1963).

(9) *Ibid.*, **86**, 4631 (1964).

(10) J. Poisson, F. Puisieux, C. Miet, and M. B. Patel, *Bull. Soc. Chim. Fr.*, **1965**, 3549.

ACKNOWLEDGMENTS

Supported by Research Grant CA-12831 from the National Cancer Institute, U.S. Department of Health, Education, and Welfare, Bethesda, MD 20014.

The author thanks Professor J. Poisson for a sample of epivoacorine, Professor G. Büchi for a sample of voacorine, and Dr. M. S. Hudson of Hudson Research, Tropical Science Center, for the dried plant extracts. Technical assistance was provided by Mrs. D. Davis and Mrs. A. A. Yousten.

Plant Anticancer Agents VII: Structural Effects on Cytotoxicity of Bisindole Alkaloids of Voacamine Type

DAVID G. I. KINGSTON

Received December 22, 1976, from the *Department of Chemistry, Virginia Polytechnic Institute and State University, Blacksburg, VA 24061.* Accepted for publication May 26, 1977.

Abstract □ Structural effects on the cytotoxicity of bisindole alkaloids of the voacamine series were investigated with compounds isolated from various *Tabernaemontana* species and compounds synthesized specifically for this purpose. Activity is sensitive both to the position of attachment of the vobasane unit on the iboga moiety and to the presence of an *N*-methyl group on the vobasane unit.

Keyphrases □ Alkaloids—isolated from various *Tabernaemontana* species or synthesized, structural effects on cytotoxicity evaluated □ *Tabernaemontana* alkaloids, various—structural effects on cytotoxicity evaluated □ Cytotoxicity—alkaloids isolated from various *Tabernaemontana* species or synthesized, structural effects evaluated □ Structure-activity relationships—alkaloids isolated from various *Tabernaemontana* species or synthesized, cytotoxicity evaluated

During studies on the isolation and structure elucidation of naturally occurring anticancer agents, some bisindole alkaloids of the voacamine type were isolated from various species of the genus *Tabernaemontana* and their structure and cytotoxicity were determined (1–5). This paper presents a preliminary account of the structure–activity relationships observed.

Table I—Cytotoxicity of the Simple Indole Alkaloids from which the Bisindoles Are Formed

Alkaloid		Cytotoxicity (ED_{50}), μg/ml P-388	KB
XI	Voacangine	6.8	>100
XII	Isovoacangine	18	59
XIII	Ibogamine	—	>100
XIV	Perivine	20	70
XV	Vobasine	—	>100

Table II—Cytotoxicity of Bisindole Alkaloids as a Function of the Presence of a Methyl Group on the Vobasane Ring

Alkaloid	R	Cytotoxicity (ED_{50}), μg/ml P-388	KB
II	H	1.3	5.8
III	CH_3	20	19
IX	H	3.2	—
X	CH_3	26	31

RESULTS AND DISCUSSION

Cytotoxicity data for the bisindole alkaloids I–X and for the simple indole alkaloids XI–XV are given in Tables I–IV. All bisindole alkaloids tested were of the voacamine type and may be considered to be composed of an iboga unit coupled to a vobasane unit. Data are given for two com-

Table III—Cytotoxicity of Bisindole Alkaloids as a Function of the Position of Attachment of the Vobasane Unit to the Iboga Moiety

Alkaloid		Position of Attachment	Cytotoxicity (ED_{50}), μg/ml P-388	KB
I	Voacamidine	11′	14	—
III	Conoduramine	12′	20	19
VI	Voacamine	13′	2.6	—
VII	Epivoacorine	13′	1.7	—
VIII	Tabernamine	13′	2.1	—
X	Conodurine	14′	26	31

Table IV—Cytotoxicity of 13′-Perivoacangine (IV) and 13′-Peribogamine (V)

Alkaloid	Cytotoxicity (ED_{50}), μg/ml P-388	KB
IV	0.39	0.35
V	0.44	2.1

mon cell culture systems, the P-388 lymphocytic leukemia and Eagle's carcinoma of the nasopharynx (KB). Inspection of the data in Tables I–IV indicates that the P-388 system was slightly more sensitive in most cases to the alkaloids tested, giving cytotoxicities that were greater by a factor between 1 and 5 but usually close to 1.

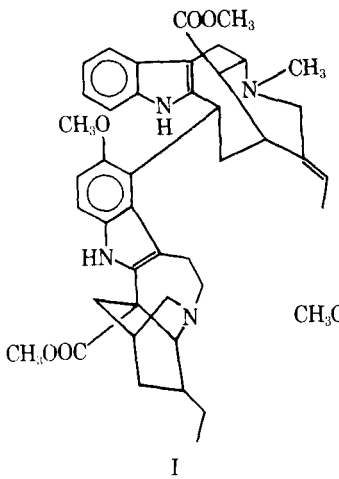

I

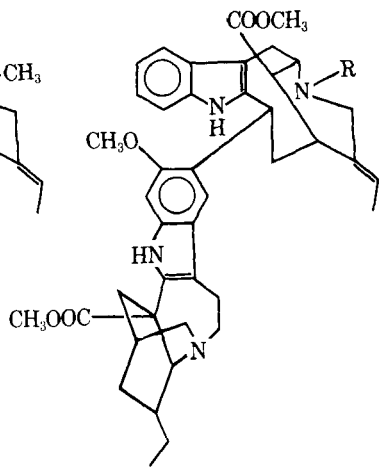

II: R = H
III: R = CH_3

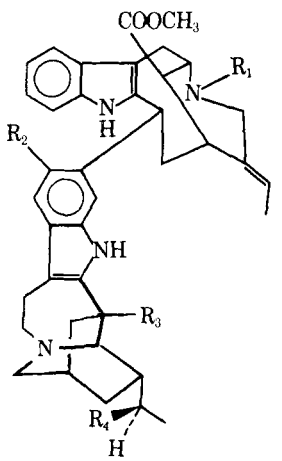

IV: R_1 = H, R_2 = OCH_3, R_3 = $COOCH_3$, R_4 = H
V: R_1 = R_2 = R_3 = R_4 = H
VI: R_1 = CH_3, R_2 = OCH_3, R_3 = $COOCH_3$, R_4 = H
VII: R_1 = CH_3, R_2 = OCH_3, R_3 = $COOCH_3$, R_4 = OH
VIII: R_1 = CH_3, R_2 = R_3 = R_4 = H

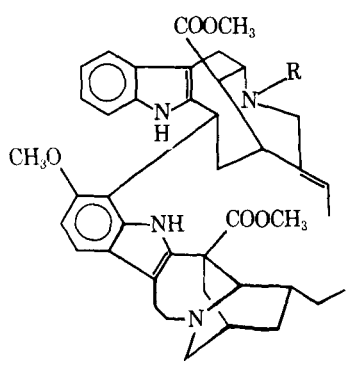

IX: R = H
X: R = CH_3

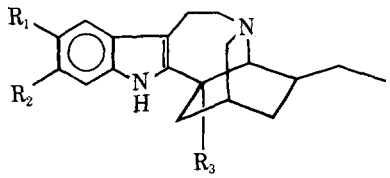

XI: R_1 = OCH_3, R_2 = H, R_3 = $COOCH_3$
XII: R_1 = H, R_2 = OCH_3, R_3 = $COOCH_3$
XIII: R_1 = R_2 = R_3 = H

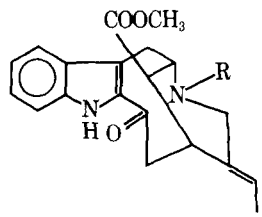

XIV: R = H
XV: R = CH_3

Table I lists the cytotoxicities of XI–XV. These alkaloids may be considered to be the components from which the bisindole alkaloids are formed, although it is recognized that perivine and vobasine are not exact models for the vobasane part of a voacamine-type bisalkaloid. Nevertheless, these simple alkaloids were largely inactive in both systems, and voacangine was the only alkaloid showing activity approaching the arbitrary figure of 4 μg/ml that justifies further screening by the National Cancer Institute[1].

The cytotoxicities of the bisindole alkaloids gabunamine (II), conoduramine (III), gabunine (IX), and conodurine (X) are presented in Table II. The first conclusion that may be drawn from these data is that the bisindole alkaloids show significantly greater cytotoxicity than would be expected from the cytotoxicities of the component parts. Thus, a simple mixture of vobasine and isovoacangine would be expected to have an ED_{50} in the KB system no less than 80 μg/ml, while conoduramine and conodurine had ED_{50} values of 19 and 31 μg/ml, respectively, in this system. Similar results were found with the P-388 system; thus a mixture of perivine and isovoacangine would be exected to have an ED_{50} of about 19 μg/ml, while gabunamine and gabunine had ED_{50} values of 1.3 and 3.2 μg/ml, respectively.

A second conclusion is based on a comparison of the cytotoxicities of conoduramine and conodurine derived from vobasine with those of the alkaloids gabunamine and gabunine derived from perivine. In each case, the perivine-derived alkaloid, lacking an *N*-methyl group in the vobasane moiety, was significantly more active than the corresponding vobasine-derived alkaloid. This finding suggests that the presence of a free alicyclic NH group in the vobasane moiety of a bisindole alkaloid of this type is necessary for significant cytotoxicity.

Cytotoxicities are presented in Table III for bisindole alkaloids that differ in the point of attachment of the vobasane unit to the iboga moiety. In each case, the vobasane unit in question bears an *N*-methyl group so as to eliminate the effects due to this group. Of the six alkaloids tested, only those linked between the 13′-position of the iboga moiety and the vobasane system showed significant cytotoxicity, and all alkaloids linked at the 13′-position showed about the same level of cytotoxicity in the P-388 system. These findings are the more striking when consideration is given to the fact that the iboga moieties of VI–VIII linked at the 13′-position are quite different in many respects. Thus, voacangine (XI) showed modest cytotoxicity, while ibogamine (XIII) did not; yet the bisalkaloids derived from these simple iboga alkaloids, voacamine (VI) and tabernamine (VIII), respectively, showed very similar cytotoxicities.

The presence or absence of methoxyl, methoxycarbonyl, and hydroxyl substituents on various parts of the iboga moiety seems to make little difference to the cytotoxicity of these bisindole alkaloids, and the dominant feature giving rise to activity appears to be the position of linkage between the vobasane and iboga units. It would be interesting to see whether this finding carried over into other classes of bisindole alkaloids, particularly those related to vincaleukoblastine, since recent synthetic work may make such systems accessible (6–8).

[1] Drug Research and Development Program, Division of Cancer Treatment, National Cancer Institute.

The major conclusion regarding the naturally occurring bisalkaloids shown in Tables II and III is that activity is increased both by the absence of the *N*-methyl group of the vobasane unit and by the presence of a linkage to the 13′-position of the iboga unit. To test this conclusion and to determine whether both effects operate together, two new alkaloids, 13′-perivoacangine (IV) and 13′-peribogamine (V), were prepared from perivinol and voacangine or ibogamine, respectively.

The structure of IV follows from its method of synthesis by analogy with the synthesis of voacamine from vobasinol and voacangine (9). The spectroscopic properties of the isolated material fully support the assigned structure: in particular, the NMR spectrum of IV differed from that of VI only in that the latter showed a three-proton singlet at δ 2.62 ppm, which was absent in the former. The mass spectrum of IV also corroborated its structure, being completely in accord with expectations for this class of compound (10).

The structure of V could also be assigned by analogy with that of tabernamine (4). The NMR spectrum of V showed a pair of doublets centered at δ 6.88 and 7.31 ppm, which could be assigned to the 12′- and 11′-protons of the ibogamine moiety, respectively, thus indicating that coupling had occurred in the 13′-position as with tabernamine. The mass spectrum of V also supported the structural assignment proposed, being entirely consistent with expectations (10).

After this work was completed, the isolation of *N*-demethylvoacamine from *Tabernaemontana accedens* was reported (11); its physical properties appear to be identical with those of perivoacangine within normal experimental error.

The cytotoxicity data for IV and V are given in Table IV. The expected synergistic effect of the two structural variations did, in fact, occur, and both alkaloids showed a greater cytotoxicity than any other alkaloid of this class tested. The cytotoxicity of IV is particularly noteworthy because it is of approximately equal potency in both the P-388 and KB systems, thus giving an increased chance that this substance or related compounds will be active in other tumor systems, including *in vivo* systems.

In summary, the results presented provide a first attempt to correlate the structure and cytotoxicity of a well-defined group of bisindole alkaloids. Some initial correlations were made and tested successfully by the synthesis of compounds with increased cytotoxicity. Further studies along these lines should eventually lead to compounds with significant *in vivo* activity. Such studies are currently in progresss.

EXPERIMENTAL

Materials, methods, and bioassays were identical to those described previously (2, 4).

13′-Perivoacangine (IV)—Perivinol (250 mg) and voacangine (170 mg) were heated under reflux in 20 ml of 1.5% hydrogen chloride in methanol for 12 hr under nitrogen. Workup as previously described (4), followed by purification of the major product by preparative TLC [ethyl acetate and then benzene–ether–methanol (10:10:2)], yielded IV as an off-white amorphous powder, homogeneous on TLC (two systems). The isolated material had R_f 0.45 in chloroform–methanol (95:5) and 0.37 in benzene–ether–methanol (10:10:2). It had $[\alpha]_D$ − 83° (c 2.3, $CHCl_3$); UV: λ_{max} 227 (log ϵ 4.62), 286 (4.18), and 294 (4.18) nm. Its IR spectrum showed ν_{max} 1725 cm^{-1}.

Its PMR spectrum was almost identical to that of voacamine (VI), except that it lacked one three-proton singlet at δ 2.62 ppm, attributable to the *N*-methyl group of the vobasane ring in voacamine. Its mass spectrum showed ions at *m/e* 718 (M^+ + 28, 2), 704 (M^+ + 14, 8), 690 (M^+, 2), 646 (16), 614 (5), 451 (13), 225 (43), 194 (42), 183 (26), 182 (47), 181 (12), 180 (28), 166 (22), 149 (24), 148 (12), 139 (11), 136 (82), 135 (45), 124 (13), 123 (10), 122 (145), and 43 (100).

13′-Peribogamine (V)—Perivinol (164 mg) and ibogamine (179 mg) were condensed as described for IV; workup followed by preparative TLC (dichloromethane–methanol, 88:12) yielded peribogamine (V, 57 mg) as an amorphous white powder, homogeneous on TLC (three systems) and high-pressure liquid chromatography. It had λ_{max} 235 (log ϵ 4.55), 287 (4.08), and 295 (4.03) nm; its IR spectrum showed ν_{max} 1715 cm^{-1}.

Its PMR spectrum (methanol) showed peaks at δ 0.98 (3H, t), 1.75 (3H, d), 2.52 (3H, s), 5.45 (1H, m), 6.88 (1H, d, J = 8 Hz), and 7.31 (1H, d, J = 8 Hz) ppm. Its mass spectrum showed ions at *m/e* 616 (M^+ + 14, 2), 602 (M^+, 10), 181 (30), 169 (45), 149 (42), 136 (100), 122 (42), and 119 (55).

Anal.—Calc. for $C_{39}H_{46}N_4O_2$: C, 77.74; H, 7.64; N, 9.30. Found: C, 78.31; H, 7.74; N, 9.53.

REFERENCES

(1) D. G. I. Kingston, B. B. Gerhart, and F. Ionescu, *Tetrahedron Lett.*, **1976**, 649.

(2) D. G. I. Kingston, B. T. Li, and F. Ionescu, *J. Pharm. Sci.*, **66**, 1135 (1977).

(3) D. G. I. Kingston, F. Ionescu, and B. T. Li, *Lloydia*, **40**, 215 (1977).

(4) D. G. I. Kingston, B. B. Gerhart, F. Ionescu, M. M. Mangino, and S. M. Sami, *J. Pharm. Sci.*, **67**, 249 (1978).

(5) D. G. I. Kingston, *ibid.*, **67**, 271 (1978).

(6) N. Langlois, F. Guéritte, Y. Langlois, and P. Potier, *J. Am. Chem. Soc.*, **98**, 7017 (1976).

(7) J. P. Kutney, A. H. Ratcliffe, A. M. Treasurywala, and S. Wunderly, *Heterocycles*, **3**, 639 (1975).

(8) G. H. Büchi (unpublished results), cited by G. A. Cordell and N. R. Farnsworth in *Heterocycles*, **4**, 393 (Ref. 30) (1976).

(9) G. Büchi, R. E. Manning, and S. A. Monti, *J. Am. Chem. Soc.*, **86**, 4631 (1964).

(10) M. Hesse, "Indolalkaloide," Verlag Chemie, Weinheim, West Germany, 1974.

(11) H. Achenbach and E. Schaller, *Chem. Ber.*, **109**, 3527 (1976).

ACKNOWLEDGMENTS

Supported by Research Grant CA-12831 from the National Cancer Institute, U.S. Department of Health, Education, and Welfare, Bethesda, MD 20014.

The author thanks Mr. B. B. Gerhart and Dr. F. Ionescu for assistance in the preparation of samples and Dr. U. Renner for a sample of voacamidine.

Differential Borohydride Assay for Conjugated Ketosteroids: Improvement with Propylene Glycol

JOEL KIRSCHBAUM

Received March 3, 1977, from the *Squibb Institute for Medical Research, New Brunswick, NJ 08903.* Accepted for publication May 5, 1977.

Abstract □ A previously developed differential UV assay for 3-one-4-ene steroids involving reduction with sodium borohydride was frequently found to be less than 100% complete. Such incomplete reduction can be mimicked by additions of sodium metaborate, a product of the hydrolysis of sodium borohydride, to the reaction system. Complete reduction can be achieved by adding propylene glycol to the reduction system. The phenomenon was studied using halcinonide as a model.

Keyphrases □ Steroids, 3-one-4-ene—effect of added propylene glycol on differential UV analysis □ UV spectrophotometry, differential—analysis of various 3-one-4-ene steroids, effect of added propylene glycol □ Propylene glycol—effect of addition on differential UV analysis of various 3-one-4-ene steroids

While developing a differential UV assay for the 3-one-4-ene steroid halcinonide[1] (I), a topical anti-inflammatory agent, sodium borohydride reagent frequently gave incomplete reduction of the steroid. The method was adapted from the procedure of Görög (1), as modified by Chafetz *et al.* (2), for quantitating conjugated 3-ketosteroids. This differential assay involves measuring the absorbance of an aliquot of methanolic steroid solution containing sodium borohydride, decomposed prior to the addition of steroid. Its absorbance is determined against a methanolic reference solution of steroid reduced by sodium borohydride. This simple procedure eliminates many interferences from excipients and other unconjugated steroids that may be present in the sample.

Sodium borohydride solutions prepared from some bottles of the reducing agent gave incomplete reduction of halcinonide. This paper reports that such incomplete reductions can be mimicked by the addition of sodium metaborate ($NaBO_2$) to the reaction system. Sodium metaborate is a known product of the hydrolysis of sodium borohydride (3). Complete reduction can be obtained when glycols, especially propylene glycol, are present in the reaction mixture.

EXPERIMENTAL

Reagents—Reagent grade anhydrous methanol was used. Sodium borohydride–propylene glycol reagent was prepared by adding 460 mg of sodium borohydride to a flask containing 8 ml of methanol, 2 ml of 1 *N* sodium hydroxide, and 0.5 ml of propylene glycol and mixing. This reagent was used not less than 45 min after preparation and was prepared fresh daily.

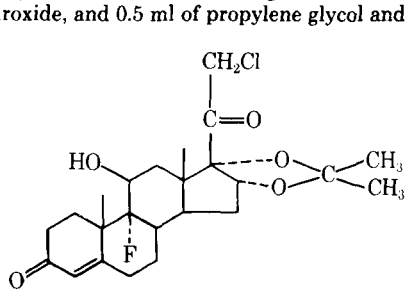

I

Methanolic 1 *N* HCl was prepared by diluting 8.5 ml of concentrated acid to 100 ml with methanol. To prepare the halcinonide standard, approximately 25 mg of steroid was dissolved in 100 ml of methanol, with the aid of an ultrasonic bath when necessary. This solution was diluted fivefold with methanol.

Differential Assay—Pipet 5.0-ml aliquots of standard or assay solution into the bottom of 25-ml volumetric flasks, designated standard blank or sample blank, followed by 1.0 ml of the sodium borohydride reagent. Wash down the sides of the flasks with about 1 ml of methanol and then gently swirl the flasks to mix the contents. After permitting the flasks to stand for 30–35 min with occasional swirling, destroy the excess borohydride by adding 2.0 ml of 1 *N* methanolic hydrochloric acid. Place the flasks briefly in an ultrasonic bath to hasten the removal of dissolved gases, dilute to volume with methanol, and then mix.

Pipet 1.0-ml aliquots of the same sodium borohydride reagent solution into the bottom of 25-ml volumetric flasks, designated sample or standard, followed by 2.0 ml of methanolic hydrochloric acid. Wash down the sides and rims with methanol and then swirl the flasks. After about 15 min, pipet 5.0 ml of sample or standard solution into its respective flask, dilute to volume with methanol, and mix.

Determine the absorbance of each sample or standard against its respective reduced reference blank at 350 nm and at the peak maximum at about 239 nm, using matched 1-cm cells and a suitable spectrophotometer. If the absorbance at 350 nm exceeds ±0.003, wash the outside of the cells with methanol to remove any contamination with the sodium borohydride–hydrochloric acid reaction mixture. Use the algebraic difference between absorbances at 239 and 350 nm to calculate the halcinonide content of the sample based on the concentration and absorbances of the standard. Formulations of halcinonide can be extracted or diluted with methanol prior to the assay.

TLC—The amount of sodium metaborate in various lots of sodium borohydride was estimated by a TLC procedure (4). Plates[2], 250 μm thick, were developed with 0.1 *N* aqueous hydrochloric acid and dried for 2 hr at 125°. Samples of 25 μl of borohydride (prepared by following the recommended procedure), standards (1, 2, or 3% in methanolic sodium hydroxide; the last concentration spotted one to four times), and blank (methanolic sodium hydroxide) were spotted on several plates with 25-μl syringes[3]. The developing solvent was methanol–1-butanol–water (3:1:1). After development and warm air drying, the plates were sprayed with stabilized starch solution[4], redried, and then sprayed with 0.1 *N* iodine in potassium iodide (5).

RESULTS AND DISCUSSION

Sodium borohydride reduces the carbonyl function in the 3-one-4-ene steroid A ring of halcinonide to a hydroxyl group, thus destroying the chromophore and eliminating steroid UV peak absorbance. The extent of reduction is determined by comparing the absorbance of an aliquot of steroid diluted with methanol with the absorbance of a similarly diluted aliquot of differentially reduced steroid (1). Incomplete reduction was often found with various bottles of sodium borohydride from different lots.

Since sodium borohydride is readily hydrolyzed to sodium metaborate (Scheme I) (3), the simplest working hypothesis is that sodium metaborate, or a compound related to it, replaces or affects the active borohydride.

$$NaBH_4 + 2H_2O \rightarrow NaBO_2 + 4H_2$$

Scheme I

[1] Halog Cream, E. R. Squibb and Sons.

[2] Mallinckrodt Chromar.

[3] Hamilton.

[4] Fisher.

Experimentally, adding metaborate to sodium borohydride reagent or replacing borohydride with metaborate results in diminished reduction. Since sufficient borohydride is present in control experiments to give complete reduction, this incomplete or inhibited reduction may be caused by metaborate (or a related compound), perhaps *via* complexation with the enol form of the 3-one.

Evidence for decomposition of the borohydride at the surface comes from iodometric titrations (6) of sodium borohydride solutions. Material taken from the surface of three bottles of borohydride showed 1% less borohydride content by titration than material taken from the bottom of the bottle. When used in the differential assay, such material removed from the surface also gave 1–4% less halcinonide reduction than did material from the bottom of the bottles. Sodium metaborate itself may not be responsible for the inhibition of reduction; such a compound as sodium borinate ($NaBH_2O$) may be the inhibitor in borohydride solutions.

As determined by TLC, the content of metaborate (R_f 0.11) was equal to or less than 1%, as estimated by visual comparison with standards, for borohydride giving 99% reduction. Borohydride appeared to remain near the origin (R_f 0.02). Light spots were visible against a dark background. Approximately 2% metaborate was found in borohydride solution giving 97% reduction, and ~10% metaborate was found in borohydride reducing 82% of the halcinonide present. This final value may be erroneously low because of the presence of an insoluble suspension in the borohydride solution. The sodium metaborate content of these three lots of sodium borohydride was inversely related to their reducing ability.

Glycols and other compounds containing vicinal hydroxyl groups sequester borate ions (7). Mannitol or glucose added to halcinonide gave increased differential absorbances, indicative of greater reduction. Glycerol additions permitted 100% reduction over 30–35 min. However, propylene glycol gave 100% reduction over a wider range of conditions and did not contribute to the absorbance of the differential reduction (*cf.*, discussion of variables below).

Propylene glycol blocks inhibition of reduction by sodium metaborate, as was seen when propylene glycol was added to halcinonide standard. Reduction of 100% was found with 0–5% sodium metaborate added to sodium borohydride solution containing propylene glycol, 99% reduction was found with 10% added metaborate, and 95% reduction resulted with 15% added metaborate.

Sodium borohydride, supplied by three vendors, gave reductions that were 92–98% complete when powder from the surface was used. Following the recommended addition of propylene glycol, reductions were 100 ± 0.5% complete. Borohydride that was solidified to the extent that scraping the surface dislodged only a few milligrams at a time gave 82% reduction without added propylene glycol and 88% with the recommended quantity. Such solidified, rock-like borohydride should be discarded.

The recommended molar ratio of sodium borohydride to halcinonide is approximately 2100:1. In spite of the large excess, an iodometric assay (6) showed that the quantity of sodium borohydride remaining after the 30-min reduction of halcinonide solution was similar, within a 1% experimental error, to the borohydride content of solutions unreacted with borohydride. This result indicates that the excess borohydride was not decomposed and was necessary for quantitative reduction.

Table I shows that other 3-one-4-ene and 3-one-4,6-diene steroids are reduced to the same extent as halcinonide with the recommended procedure. 3-One-1,4-diene steroids are less than 10% reduced, limiting this procedure. The procedure of Chafetz *et al.* (2), using lithium borohydride, also reduces 1,4-diene steroids. Two samples of 3–5-year-old lithium borohydride gave incomplete reductions of halcinonide and triamcinolone after the recommended procedure was modified for equimolar lithium borohydride. The addition of propylene glycol increased the extent of reduction. Such use of propylene glycol could be of general utility in increasing yields during large-scale reductions with borohydrides. The concentration of glycol may have to be adjusted for each reaction, since too much propylene glycol inhibits reduction, as shown in the following discussion of variables.

Complete reduction, using either propylene glycol added to solutions of halcinonide standard or to borohydride reduction reagent, was found between 25 and 45 min. The reaction is judged complete when the absorbance of aliquots of halcinonide standard carried through the recommended procedure is equal to the differential absorbance of an aliquot of halcinonide diluted in methanol and read *versus* a methanol blank. Recoveries averaged 100.1% (n = 11), with a coefficient of variation of 0.42.

Table I—Differential Sodium Borohydride Reduction of Other 3-One-4-ene Steroids

Name	Structural Feature	Without Propylene Glycol, %	With Propylene Glycol, %
Hydrocortisone	3-One-4-ene	93	100
Progesterone	3-One-4-ene	98	100
Fluoxymesterone	3-One-4-ene	96	100
Triamcinolone	3-One-1,4-diene	2	3
Dexamethasone	3-One-1,4-diene	3	3
Betamethasone	3-One-1,4-diene	3	3
Prednisolone	3-One-1,4-diene	6	6
Chlormadinone	3-One-4,6-diene	99	100

Reductions without propylene glycol added to standards were 94–98% complete, depending on the lot of borohydride used. Using 1.0–4.0 ml of propylene glycol/50 ml of standard solution yielded 100% reduction within 25 of the recommended 30 min. Five milliliters of propylene glycol gave 95–99% reduction, and 10 ml gave 92% reduction. Several different grades of purity of propylene glycol, including glass distilled, were used and gave identical results. Three milliliters of propylene glycol in the absence of halcinonide had negligible absorbance.

Complete reduction of halcinonide was obtained using methanolic sodium hydroxide solution, with final sodium hydroxide normalities ranging from 0.30 to 0.02 N, which provides a buffer against possible contaminating acid.

Volumes of sodium borohydride reagent (from a lot that appeared to be free of metaborate) between 0.7 ml (31 mg) and 2.0 ml (88 mg) gave 100 ± 0.5% reduction. The percentage of halcinonide reduced with the recommended 1.0 ml of sodium borohydride reagent ranged between 99 and 101% in all studies. Below 0.6 ml, reduction was incomplete; concentrations above 2.0 ml were not investigated.

The procedures described here give results that are within 1% of anticipated steroid content in contrast to the previous, generally low-biased results.

REFERENCES

(1) S. Görög, *J. Pharm. Sci.*, **57**, 1137 (1968).

(2) L. Chafetz, D. C. Tsilifonis, and J. M. Riedl, *ibid.*, **61**, 148 (1972).

(3) J. A. Gardiner and J. W. Collat, *J. Am. Chem. Soc.*, **87**, 1692 (1965).

(4) K. Kawanabe, S. Takitani, M. Miyazaki, and Z. Tamura, *Bunseki Kagaku*, **13**, 976 (1964); through *Chem. Abstr.*, **62**, 4592c (1965).

(5) "The United States Pharmacopeia," 19th rev., Mack Publishing Co., Easton, Pa., 1975, p. 770.

(6) D. A. Lyttle, E. H. Jensen, and W. A. Struck, *Anal. Chem.*, **24**, 1843 (1952).

(7) I. M. Kolthoff and E. B. Sandell, "Textbook of Quantitative Analysis," 3rd ed., Macmillan, New York, N.Y., 1952, p. 534.

ACKNOWLEDGMENTS

Presented at the Federation of Analytical Chemistry and Spectroscopy Societies, Philadelphia meeting, November 1976.

The author thanks Dr. G. Brewer, Dr. L. Chafetz (Warner-Lambert), Dr. J. Dunham, Dr. K. Florey, Mr. H. Kadin, and Mr. R. Poet for their helpful comments and suggestions. Also acknowledged are the typing of Mrs. C. Saloom and the illustrative and photographic work of Mr. S. Meloni and Mr. A. Warade.

Quantitative Structure–Activity Relationships and Carminative Activity

BRIAN K. EVANS *, KENNETH C. JAMES ˣ, and DAVID K. LUSCOMBE

Received February 15, 1977, from the *Welsh School of Pharmacy, University of Wales Institute of Science and Technology, Cardiff, CFI 3NU, United Kingdom.* Accepted for publication May 13, 1977. *Present address: Department of Pharmacy, University Hospital of Wales, Cardiff, United Kingdom.

Abstract □ Carminative activities of 34 alcohols, esters, ethers, phenols, and carbonyl compounds were determined using the guinea pig isolated ileum preparation and are expressed as the ability to produce a 50% inhibition (ID_{50}) of a standard response to carbachol. Aqueous solubilities were measured at 37° using either UV absorption or GLC. The ratios of solubility to ID_{50} were reasonably constant, suggesting nonspecific biological activity, similar to that previously observed with general anesthetics. Hansch analysis indicated that carminative activities were largely controlled by solubility, as indicated by octanol–water distribution coefficients. The principal remaining factor appeared to be the steric availability of the oxygen atom in the functional group of the compound.

Keyphrases □ Carminative activity—various classes of compounds, related to solubility □ Solubility—various classes of compounds, related to carminative activity □ Structure–activity relationships—various classes of compounds, carminative activity related to solubility

Ferguson (1) investigated various groups of compounds, each having a common pharmacological action; while the biologically effective concentrations of the compounds varied over 1000-fold, the ratios C/C_s for nonvolatile compounds and p/p_s for vapors varied only 10-fold. The symbols C and p represent the biologically active concentration and vapor pressure, respectively; C_s is the aqueous solubility, and p_s is the saturated vapor pressure. Ferguson equated these ratios with thermodynamic activity. This behavior was observed almost exclusively in homologous series, in which biological activity changes with molecular weight, and groups of chemically related molecules such as phenols (2) or quaternary ammonium compounds (3).

Until recently, anesthetics were the only pharmacological group in which molecules of widely different structure had been observed to follow Ferguson's principle. However, Evans *et al.* (4) suggested that the carminatives could fit a similar situation. These substances have a common pharmacological action but no characteristic chemical feature. Since their physical properties are similar (they are all volatile liquids, mainly lipophilic in character but having significant aqueous solubilities), it was considered that their biological activities may be primarily dependent on their physical properties.

In a preliminary investigation (4), the antispasmodic activities of seven compounds, camphor, carvone, cineole, cinnamaldehyde, eugenol, linalol, and thymol, were evaluated and related to their aqueous solubilities. This paper is an extension of that work, in which a larger range of compounds was examined.

EXPERIMENTAL

Materials—All materials were the purest products commercially available and were used without further purification.

Solubility Determinations—Solubilities were taken from Seidell (5) when available. For the remaining compounds, a moderate excess of solute was stirred continuously with water for up to 10 hr in a sealed conical flask immersed in a thermostatically controlled water bath at 37°. The method of sampling varied with the solute.

Saturated solutions of solid solutes were sampled by pipet and immediately passed through a 0.45-μm membrane filter. Mixtures containing liquid solutes were immersed overnight in a water bath at 37° to allow complete separation. When the solute was lighter than water, the solution and excess solute were first transferred to a separator and subsequently sampled through the tap.

Compounds containing conjugated chromophores were assayed by UV spectrophotometry. Samples of saturated solutions were diluted to suitable volumes with spectroscopic ethanol, and absorptions were measured at the appropriate λ_{max}. Wavelength maxima and adherence to Beer's law were established in preliminary experiments.

The remaining compounds were determined by GLC using a hydrogen flame-ionization detection system. Two columns were used, one consisting of 10% Apiezon L on 80–100-mesh Chromosorb W and the other consisting of Poropak Q polymer beads. The columns were conditioned before use for 48 hr at 210–220° with a nitrogen flow rate of 60 ml/min.

Octanol–water distribution coefficients were obtained or calculated (6).

Carminative Activity—The biological activity of each carminative was determined using the guinea pig isolated ileum preparation suspended in aerated Tyrode physiological solution at 37°. A standard submaximal response to the agonist carbachol was first obtained, and then the activity of the carminative was determined by its ability to inhibit the standard response to carbachol.

Three doses of carminative were selected that inhibited the response to the agonist by 20–80%, and six determinations were performed at each dose level. The percentage inhibition of the standard agonist response was plotted against the log of the corresponding dose of carminative. From this plot, the carminative concentration required to inhibit the agonist response by 50% (ID_{50}) was estimated.

The carminative solution was maintained at 37° throughout each investigation.

RESULTS AND DISCUSSION

The traditional carminatives are all essential oils. These complex mixtures, because of their natural origin, are of variable composition and are difficult to standardize. Therefore, known constituents of essential oils and pure chemical compounds of established carminative activity were selected.

Thirty-four compounds, including alcohols, esters, ethers, phenols, and carbonyl compounds, were examined. Their biological activities and solubilities are presented in Table I together with the ratios C/C_s. These ratios are more scattered than those given by Ferguson (1) for general anesthetics, although most of them lie between 0.1 and 1.0; the corresponding ID_{50} values vary over 100-fold. Ferguson's assumptions were criticized recently (7), and the present distribution of "thermodynamic activities" are of the same order as the recalculated values for general anesthetics.

The classical examples of nonspecific biological activity (1–3) represent systems in which equilibrium would be expected to be established rapidly between the site of action and the surrounding environment, a necessary criterion for this concept. Hansch *et al.* (8) suggested that equilibrium is not established in most cases of nonspecific biological action and that biological activity is dependent on the probability of a given molecule reaching the site of action. It was further shown that such a model could be expressed in the general form:

$$\log BR = a \log P + b(\log P)^2 + c \qquad \text{(Eq. 1)}$$

where BR represents biological response; P is the partition coefficient

Table I—Physical and Biological Data

Compound	ID_{50}[a], $M \times 10^3$	Solubility, C_s, at 37°, $M \times 10^3$	Thermodynamic Activity, C_s/ID_{50}	log P
Benzaldehyde	54.4 (0.3)	21.1	2.57	1.48
Butyl acetate	43.4 (0.6)	50.2	0.86	1.74
Camphor	6.1 (0.6)	16.3	0.37	—
Carvone	10.5 (0.4)	11.0	0.96	—
Catechol	94.8 (0.7)	1966[b]	0.05	0.95
Cineole	13.9 (0.3)	9.1	1.54	—
Cinnamaldehyde	12.1 (0.5)	9.1	1.33	—
Citral	7.6 (0.5)	8.8	0.86	—
o-Cresol	22.8 (0.3)	285[b]	0.08	1.95
m-Cresol	28.9 (0.3)	231[b]	0.12	1.99
p-Cresol	28.8 (0.3)	209[b]	0.14	1.93
Dibutyl ether	58.5 (1.5)	17.2	3.40	3.06
Diethyl ether	260 (2.6)	712	0.37	0.80
Diethyl malonate	62.0 (0.6)	145	0.43	—
Diisopropyl ether	196 (2.1)	79.2	0.93	1.63
3,4-Dimethylphenol	12.4 (0.4)	25.3	0.49	2.42
Di-*n*-propyl ether	99.3 (0.7)	107	2.47	2.03
Ethyl acetate	260 (3.1)	817	0.32	0.70
Ethyl vinyl ether	62.2 (0.7)	139	0.45	1.04
Eugenol	3.7 (0.5)	40.2	0.09	2.99
1-Hexanol	33.8 (0.5)	41.0[b]	0.82	2.03
Isopropyl acetate	110 (0.7)	193	0.58	1.02
Linalol	4.7 (0.7)	38.0	0.12	—
Menthol	7.4 (0.3)	8.6	0.86	3.31
o-Methoxyphenol	54.4 (0.5)	10.6	5.12	1.90
p-Methoxyphenol	47.5 (0.3)	4.0	11.8	1.34
1-Pentanol	77.3 (0.4)	213	0.36	1.16
2-Phenoxyethanol	126 (1.1)	261	0.48	1.16
n-Propyl acetate	114 (0.7)	196	0.57	1.50
Quinol	123 (0.7)	193[b]	0.64	0.55
Resorcinol	89.3 (1.2)	6609[b]	0.01	0.79
Salicylaldehyde	20.0 (0.7)	208[b]	0.10	1.76
Thymol	2.2 (0.4)	59.9	0.04	3.30

[a] Figures in parentheses represent confidence limits ($p' = 0.05$). [b] Taken from Ref. 6.

between octanol and water; and a, b, and c are constants. The Ferguson effect was considered a special case, where $b(\log P)^2$ is very small in comparison with the other terms. In the present work, when most of the 34 compounds were considered, Eq. 2 was found to be the best correlation between biological activity, expressed as log $1/ID_{50}$, and log P:

$$\log 1/ID_{50} = 0.632 + 0.447(0.081) \log P \qquad (5.51)$$

n	r	s
31	0.715	0.353

(Eq. 2)

where $F_{1,29} = 31\ \alpha(0.001) = 13.4$. The heading n represents the number of compounds considered, r is the correlation coefficient, and s is the standard deviation. Three compounds were omitted because octanol–water distribution coefficients were not available. The figure in parentheses following the coefficient in log P represents its standard error ($p' = 0.05$), and the figure in parentheses below the coefficient represents the ratio of the coefficient to the standard error. Comparison of this value with the t value obtained from statistical tables indicates that the probability that the relationship is coincidental is negligible. This finding is confirmed by the figures following the equation, which are results of analysis of variance of the observed results about the regression followed by an F test and which indicate a highly significant correlation. Consideration of a term in $(\log P)^2$ did not improve the relationship significantly.

Carminative activity thus appears to be dependent on the balance between aqueous and nonaqueous solubilities; but since Eq. 2 accounts for only 50% of the variation, other factors must also be important. Equation 3 expresses the relationship between ID_{50} and log P when only alcohols and phenols are considered; it accounts for 90% of the variation:

$$\log 1/ID_{50} = 0.429 + 0.598(0.052) \log P$$

n	r	s
17	0.947	0.175

(Eq. 3)

where $F_{1,15} = 131\ \alpha(0.001) = 16.6$. Therefore, the factors causing the additional variation in Eq. 2 must be linked to the nature of the functional groups in the molecule, *i.e.*, hydroxyl, carbonyl, and ester and ether oxygen, since the correlation is considerably improved when compounds containing one specific functional group are considered as in Eq. 3.

The success of Eq. 3 is somewhat surprising because some of the compounds involved contain more than one functional group (*e.g.*, catechol and methoxyphenol). Therefore, the inference is that only one hydroxyl group is required and that hydroxyl has a considerably greater influence on carminative activity than the ether group. The relationship obtained when compounds containing one hydroxyl only are considered is not significantly better than Eq. 3, supporting this view.

Neither esters nor ethers followed Eq. 3, but each group of compounds yielded its own analogous correlation between ID_{50} and P. Since alcohols, which are weakly charged in comparison with phenols, fitted smoothly into the same correlation as the phenols (Eq. 3), it is unlikely that the effect of hydroxyl on carminative activity is influenced by the electronic charge on the group. Similarly, the failure of the ethers to fit the same relationship as the hydroxyl compounds is more likely to result from hindrance to ether oxygen than from electronic considerations, and the group that replaces the hydrogen of hydroxyl to form an ether would be expected to bring about this hindrance.

The contribution of the carbonyl group to carminative activity must be greater than either hydroxyl or ether, because the ID_{50} values of this group were lower. Therefore, it was assumed that the carbonyl oxygen of esters, rather than the ether oxygen, was the center of biological activity. Octanol–water distribution coefficients were available for only two of the carbonyl compounds. This number was not sufficient to submit this group to a similar treatment to that described.

In summary, the carminative activities of alcohols, esters, ethers, and phenols are largely due to their solubilities, as indicated by their octanol–water distribution coefficients. Other factors are involved, the principal one being the nature of the oxygenated groups in the molecule, probably arising from the steric availability of the oxygen therein. Where two such groups are present in one molecule, carminative activity is almost exclusively influenced by only one of them. The order of increasing influence is O < OH < C=O.

REFERENCES

(1) J. Ferguson, *Proc. Roy. Soc.*, **127B**, 387 (1939).

(2) N. A. Allawala and S. Riegelman, *J. Am. Pharm. Assoc., Sci. Ed.*, **43**, 93 (1954).

(3) B. Ecanow and F. P. Siegel, *J. Pharm. Sci.*, **52**, 812 (1963).

(4) B. K. Evans, K. C. James, and D. K. Luscombe, *J. Pharm. Pharmacol., Suppl.*, **24**, 173P (1972).

(5) A. Seidell, "Solubilities of Organic Compounds," vol. II, 3rd ed., van Nostrand, New York, N.Y., 1941.

(6) A. Leo, C. Hansch, and D. Elkins, *Chem. Rev.*, **71**, 525 (1971).

(7) A. Cammarata, *J. Pharm. Sci.*, **64**, 2025 (1975).

(8) C. Hansch, R. M. Muir, T. Fujita, P. P. Maloney, F. Geiger, and M. Streich, *J. Am. Chem. Soc.*, **85**, 2817 (1963).

GLC Determination of Plasma Concentrations of γ-Oxo Metabolite of Phenylbutazone

K. K. MIDHA ˣ, I. J. McGILVERAY, and J. K. COOPER

Received March 24, 1977, from the *Drug Research Laboratories, Health Protection Branch, National Health & Welfare, Ottawa, Ontario K1A 0L2, Canada.* Accepted for publication May 19, 1977.

Abstract □ A quantitative method for the γ-oxo metabolite of phenylbutazone from plasma is described. The procedure involved an ethylene dichloride extraction of acidified plasma to which an internal standard, acenocoumarol, had been added. The extracted γ-oxo metabolite and the internal standard were methylated and analyzed by GLC. Determination of 0.25 μg of γ-oxo metabolite/ml with a relative standard deviation of 6.5% was accomplished.

Keyphrases □ Phenylbutazone γ-oxo metabolite—GLC analysis in plasma □ Metabolites—γ-oxo derivative of phenylbutazone, GLC analysis in plasma □ γ-Oxo metabolite of phenylbutazone—GLC analysis in plasma □ GLC—analysis, phenylbutazone γ-oxo metabolite in plasma □ Antirheumatic agents—phenylbutazone, γ-oxo metabolite, GLC analysis in plasma

Phenylbutazone, an antirheumatic agent, undergoes biotransformation in humans to oxyphenbutazone; the γ-hydroxy, *p*,γ-dihydroxy, and γ-oxo derivatives; the C-4 glucuronides of phenylbutazone and the γ-hydroxy derivative; and, possibly, the γ-oxo derivative of oxyphenbutazone (1–5). Oxyphenbutazone and the γ-oxo metabolite (I) of phenylbutazone are both antirheumatic agents.

GLC (6–9) and high-speed liquid chromatography (10, 11) have been used to determine plasma levels of phenylbutazone, oxyphenbutazone, and the γ-hydroxy derivative of phenylbutazone, but methods for I have not been reported. A GLC procedure for the quantitative determination of plasma I concentrations is reported here; it is suitable for pharmacokinetic studies.

EXPERIMENTAL

Ethylene dichloride[1] and ether[2] were distilled in glass prior to use. Stock solutions containing 100 μg of I[3]/ml were prepared weekly in 0.1 *N* NaOH. Appropriate dilutions (0.25–20.0 μg/ml) were made immediately before use. Solutions containing 100 μg of the internal standard acenocoumarol[4] (II)/ml were prepared daily in 0.1 *N* NaOH (aqueous) and diluted to 8 μg/ml with distilled water. An ethereal solution of diazomethane was synthesized from *N*-methyl-*N*-nitroso-*p*-toluenesulfonamide[5].

Plasma Level Study—Compound I (200 mg) was administered orally in solution, as described by McGilveray *et al.* (6) for phenylbutazone, to a healthy 85.6-kg male volunteer. Blood samples (10 ml) were withdrawn from the cubital vein, using heparinized evacuated tubes[6], before and at

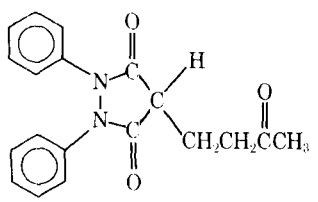

I

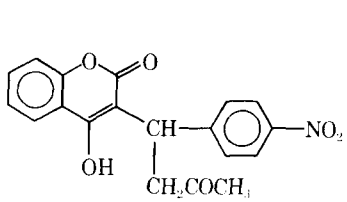

II

[1] Caledon Laboratories Ltd., Georgetown, Ontario, Canada.
[2] Mallinckrodt Chemical Works Ltd., Montreal, Quebec, Canada.
[3] United Pharmaceutical Works, Prague, Czechoslovakia.
[4] Geigy Pharmaceuticals, Dorval, Quebec, Canada.
[5] Diazald, Aldrich Chemical Co., Milwaukee, Wis.
[6] Vacutainers, Becton Dickinson Co., Mississauga, Ontario, Canada.

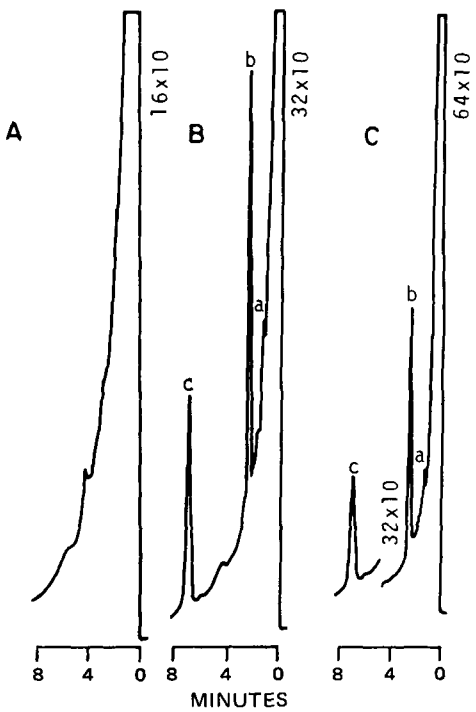

Figure 1—*Gas chromatograms of human plasma. Key: A, control plasma; B, spiked plasma containing 3 μg of I/ml and 8 μg of II/ml; and C, plasma from a dosed volunteer (55 hr) containing 7.75 μg of I/ml and 8 μg of II/ml. Peaks a and b are due to methylated I, and peak c is due to methylated acenocoumarol.*

18 appropriate time intervals over 223 hr following the dose. The blood samples were centrifuged, and the separated plasma was stored at −15° before analysis.

Extraction of I—To a 1-ml plasma sample ("spiked" or from dosed volunteers) in a glass-stoppered centrifuge tube[7] (50 ml) were added 1 ml of II (8 μg/ml), 3 ml of 3 *N* HCl, and 20 ml of ethylene dichloride. The samples were extracted and derivatized with diazomethane as previously described (12), except that the organic extract was not dried.

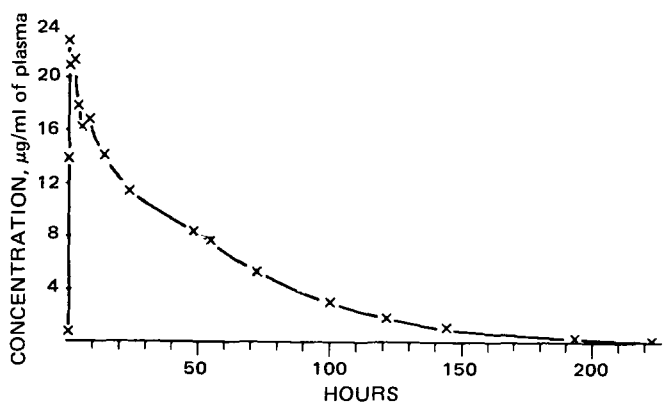

Figure 2—*Plasma profile of an 85.6-kg volunteer who received a 200-mg solution of I orally.*

[7] Fisher Scientific Co., Montreal, Quebec, Canada.

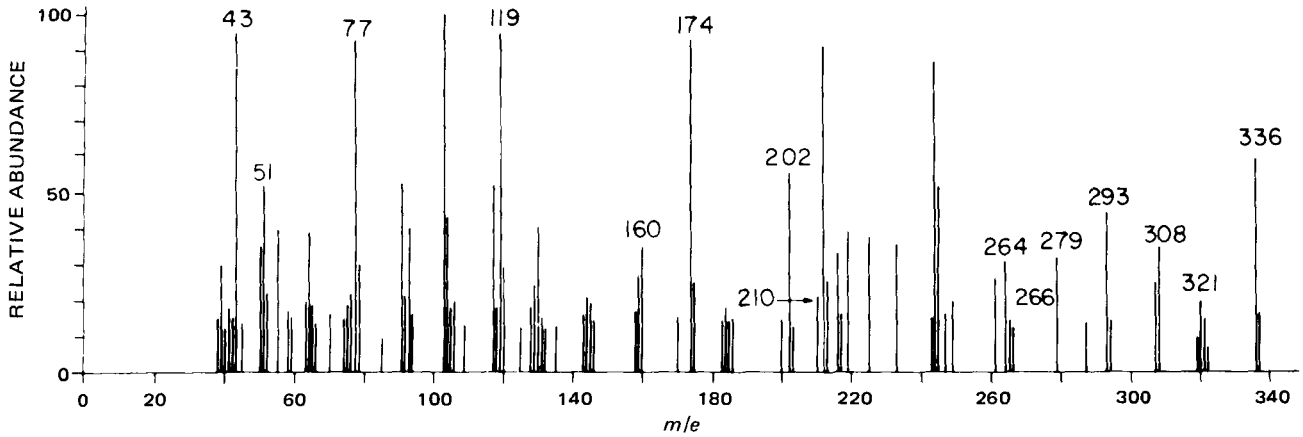

Figure 3—*GLC–mass spectrum (normalized) of the compound giving rise to the peak for methylated I from pooled plasma extracts from the dosed human volunteer.*

GLC—A gas chromatograph[8] equipped with a flame-ionization detector was employed. The column was a spiral glass tube, 180 × 0.25-cm i.d., packed with 3% phenyl methyl dimethyl silicone[9] coated on acid-washed, dimethylchlorosilane-treated, 80–100-mesh, high-performance flux-calcined diatomite support[10].

The column was conditioned by maintaining it at 340° for 18 hr with a low nitrogen flow. For the analyses, the injection port, detector, and column oven temperatures were maintained at 300, 310, and 285°, respectively. The nitrogen carrier gas flow rate was maintained at 70 ml/min. Hydrogen and compressed air flow rates were adjusted to give maximum response.

Calculations—Peak height ratios were calculated by dividing the height of the peak due to methylated I (retention time of 2.6 min) by that from methylated II (7.1 min). Calibration curves were constructed from the results of spiked control plasma samples by plotting the peak height ratios against the concentration of I (micrograms per milliliter of plasma).

RESULTS AND DISCUSSION

Methylation of I with diazomethane gave two peaks with retention times of 1.5 and 2.6 min (peaks a and b, Fig. 1B) on GLC analysis. The heights of the respective peaks were in the ratio 1:6.5. This ratio was independent of oven temperature, instrument, and sample size. Therefore, the major peak, with a retention time of 2.6 min, was used for quantitation. GLC–mass spectrometry[11] of peaks a and b gave a molecular ion at *m/e* 336 and other diagnostic ions at *m/e* 321, 308, 293, 279, 264, 202, 177, 160, 119, 77, 51, and 43.

It was demonstrated[12] by preparative TLC and subsequent PMR characterization that the major product of diazomethane-methylated phenylbutazone is 1,2-diphenyl-4-methyl-4-*n*-butyl-3,5-pyrazolidinedione and the minor product is 1,2-diphenyl-3-methoxy-4-*n*-butyl-3,5-pyrazolinedione. On this basis, the compound giving rise to peak b (retention time of 2.6 min) was tentatively assigned the structure 1,2-diphenyl-4-methyl-4-(2-oxo-*n*-butyl)-3,5-pyrazolidinedione; the compound giving rise to peak a was tentatively assigned the structure 1,2-diphenyl-3-methoxy-4-(2-oxo-*n*-butyl)-5-pyrazolinone.

Methylation of II with diazomethane gave one peak on GLC analysis with a retention time of 7.1 min (peak c, Fig. 1B). The methylated derivative of II has the structure 3-(α-acetonyl-*p*-nitrobenzyl)-4-methoxycoumarin (12).

Attempts to prepare derivatives of I by the safer flash-heater methylation technique using trimethylanilinium hydroxide gave irreproducible results. Several other liquid phases such as saturated hydrocarbon lubricant[13], methyl silicone gum[14], phenyl methyl silicone fluid[15], and phenyl methyl dimethyl silicone fluid[16] were tested, but the major peak for I exhibited either tailing or interference from plasma constituents.

Carbon disulfide, employed as the injection solvent, rendered a very small solvent peak. Plasma extracts reacted with diazomethane but not dissolved in carbon disulfide were stable for up to 12 hr at room temperature; however, in the unreacted plasma extracts, I was much less stable.

Figure 1A shows a typical chromatogram obtained by processing fresh blank plasma from humans as described under *Experimental.* No extraneous peaks were observed in any chromatograms from human plasma samples. A chromatogram obtained when the method was applied to spiked plasma containing 3.0 μg of I/ml and 8.0 μg of II/ml is shown in Fig. 1B. Figure 1C shows a chromatogram obtained from a 55-hr sample (1 ml) from the human volunteer who ingested a 200-mg dose of I as described under *Experimental.*

The overall recoveries of I (47.42 ± 1.64%) and II (99.9 ± 1.25%) from plasma were identical to those reported earlier for the analysis of II using I as the internal standard (12). The accuracy and precision of the GLC assay are demonstrated in Table I. Results were based on at least five determinations at each I concentration, ranging from 0.25 to 20.0 μg/ml. The overall relative standard deviation was 3.55%.

The calibration curve was linear ($y = mx$) over the concentration range of 0.25–20.0 μg of I/ml of plasma. A mean slope value of 0.617 ± 0.005 ($p = 0.05$; $r^2 = 0.999$) was obtained. During the analysis, the peak height ratio of the drug and the internal standard was used as the index of detector performance and overall efficiency.

Application of the method to plasma level determinations in a human male is demonstrated in Fig. 2. Plasma profiles observed over 223 hr indicate that the half-life of this drug (~32 hr) was approximately half that of phenylbutazone (~70 hr) in the same subject (6). The specificity of the analytical procedure was determined by pooling the remaining plasma from the dosed volunteer, extracting without the addition of II, and derivatizing as described under *Experimental.* A GLC–mass spectrum (Fig. 3) of the compound giving rise to the resultant peak for I was obtained and compared with that of authentic methylated I. No ions other than those for methylated I were observed in the mass spectrum of the peak from pooled plasma samples, indicating virtually no interference.

The described GLC procedure is sensitive and specific for the determination of I following single doses of I.

Table I—Estimation of I Added to Plasma by GLC[a]

Added I, μg	*n*	Mean Peak Height Ratio, I/II	*SD*	*CV*
0.25	5	0.170	0.011	6.50
1.0	5	0.684	0.016	5.35
2.0	6	1.440	0.053	3.65
3.0	7	2.026	0.092	4.56
5.0	5	3.052	0.043	1.42
10.0	5	6.076	0.106	1.74
20.0	5	12.328	0.207	1.68
			Mean *CV* =	3.56

[a] The equation is $y = mx$, where $m = 0.617 \pm 0.005$ ($r^2 = 0.999$).

[8] *Model 3920,* Perkin-Elmer, Montreal, Quebec, Canada.
[9] OV-11, Chromatographic Specialties, Brockville, Ontario, Canada.
[10] Chromosorb W, Chromatographic Specialties, Brockville, Ontario, Canada.
[11] Perkin-Elmer model 900 gas chromatograph attached to a Hitachi Perkin-Elmer model RMSU mass spectrometer through a jet separator.
[12] Dr. D. V. C. Awang, Drug Research Laboratories, Health Protection Branch, National Health & Welfare, Ottawa, Ontario, Canada K1A 0L2, personal communication.
[13] Apiezon-L, Chromatographic Specialties, Brockville, Ontario, Canada.
[14] SE-30, Chromatographic Specialties, Brockville, Ontario, Canada.
[15] OV-17, Chromatographic Specialties, Brockville, Ontario Canada.
[16] OV-7, Chromatographic Specialties, Brockville, Ontario, Canada.

REFERENCES

(1) J. J. Burns, R. K. Rose, T. Chenkin, A. Goldman, A. Schulert, and B. B. Brodie, *J. Pharmacol. Exp. Ther.*, **109**, 346 (1953).

(2) J. J. Burns, R. K. Rose, S. Goodwin, J. Reichenthal, E. C. Horning, and B. B. Brodie, *ibid.*, **113**, 481 (1955).

(3) O. M. Bakke, G. H. Draffan, and D. S. Davies, *Xenobiotica*, **4**, 237 (1974).

(4) W. Dieterle, J. W. Faigle, F. Fruh, H. Mory, W. Theobald, K. O. Alt, and W. J. Richer, *Arzneim.-Forsch.*, **26**, 572 (1976).

(5) I. J. McGilveray, K. K. Midha, and N. Mousseau, *Pharmacologist*, **16**, 218 (1974).

(6) I. J. McGilveray, K. K. Midha, R. Brien, and L. Wilson, *J. Chromatogr.*, **89**, 17 (1974).

(7) K. K. Midha, I. J. McGilveray, and C. Charette, *J. Pharm. Sci.*, **63**, 1234 (1974).

(8) *Ibid.*, **63**, 1751 (1974).

(9) Y. Tanimura, Y. Saitoh, F. Nakagawa, and T. Suzuki, *Chem. Pharm. Bull.*, **23**, 651 (1975).

(10) N. J. Pound, I. J. McGilveray, and R. Sears, *J. Chromatogr.*, **89**, 23 (1974).

(11) N. J. Pound and R. W. Sears, *J. Pharm. Sci.*, **64**, 284 (1975).

(12) K. K. Midha and J. K. Cooper, *ibid.*, **66**, 799 (1977).

ACKNOWLEDGMENTS

The authors thank United Pharmaceutical Works, National Corp., Prague, Czechoslovakia, for the gift of I and Mr. J.-C. Ethier for the mass spectra.

Synthesis and Antibacterial Evaluation of 2-(Substituted Phenylureido)-4-thiocyanatobenzothiazoles

ROBERT J. ALAIMO ˣ, STANFORD S. PELOSI, and RAYMOND FREEDMAN

Received March 14, 1977, from the *Chemistry Division and Pharmacometrics Division, Norwich-Eaton Pharmaceuticals, Division of Morton-Norwich Products, Inc., Norwich, NY 13815.* Accepted for publication May 2, 1977.

Abstract □ The synthesis and antibacterial evaluation of a number of 2-(substituted phenylureido)-4-thiocyanatobenzothiazoles are described. The more active compounds against the test organisms *in vitro* generally were those substituted with halogens on the phenyl and benzothiazole rings.

Keyphrases □ Benzothiazoles, various substituted—synthesized, evaluated for antibacterial activity □ Antibacterial activity—evaluated for various substituted benzothiazoles □ Structure–activity relationships—various substituted benzothiazoles evaluated for antibacterial activity

Previously, the synthesis and antiparasitic screening of a series of thiocyanatobenzothiazoles were reported (1). These compounds exhibited significant anthelmintic and antifungal activities. As an extension of this work, the synthesis of some 2-(substituted phenylureido)-4-thiocyanatobenzothiazoles is reported here. These compounds possess a high degree of *in vitro* activity against the Gram-positive bacteria *Staphylococcus aureus* and *Corynebacterium liquefaciens*.

DISCUSSION

The method of preparation of the 2-(substituted phenylureido)-4-thiocyanatobenzothiazoles (V–XII) (Table I) involved the reaction of the appropriate 2-amino-4-thiocyanatobenzothiazole (I–IV) with a phenyl isocyanate. The synthesis of I, II, and IV was reported previously (1, 2); the synthesis of III is reported here. The general procedure for the preparation of V–XII is shown in Scheme I. The assignment of structures for other compounds of the V–XII type was discussed previously (1).

The compounds were tested for antibacterial activity against *S. aureus* and *C. liquefaciens* using *in vitro* serial dilution techniques (3). Compounds V–XII exhibited activity against the test organisms at levels of from 0.048 to 6.25 μg/ml of test media. The test results for V–XII and the reference standard, nifuradene[1] (XIII) (4), are shown in Table I.

[1] U.S. Adopted Name for 1-[(5-nitrofurfurylidene)amino]-2-imidazolidinone.

Table I—Antibacterial Evaluation of Phenylureidothiocyanatobenzothiazoles

Compound	R_1	R_2	R_3	Minimal Inhibitory Concentration, μg/ml	
				S. aureus[a]	*C. liquefaciens*[b]
V	CH_3	H	4-NO_2	0.75	0.75
VI	Cl	H	H	0.38	3.1
VII	Cl	H	4-Cl	0.19	0.75
VIII	*n*-Bu	H	4-Br	6.25	6.25
IX	Cl	Cl	4-Cl	0.19	1.5
X	Cl	Cl	4-Br	0.38	0.048
XI	Cl	Cl	3,4-$(Cl)_2$	3.1	6.25
XII	Cl	Cl	4-F	0.38	1.5
XIII	Nifuradene			3.10	12.5

[a] Strain No. Mi-12, Norwich Pharmacal Co. [b] Strain No. Co-11, ATCC 11828.

In general, the compounds possessing the highest degree of antibacterial activity against the test organisms were substituted with halogen atoms on both the phenyl and benzothiazole rings (VII and IX–XII). However, no other structure–activity trends were apparent among the eight compounds tested.

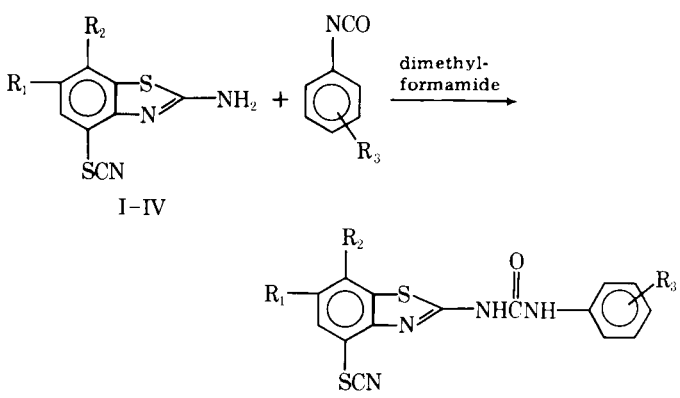

Scheme I

REFERENCES

(1) J. J. Burns, R. K. Rose, T. Chenkin, A. Goldman, A. Schulert, and B. B. Brodie, *J. Pharmacol. Exp. Ther.*, **109**, 346 (1953).

(2) J. J. Burns, R. K. Rose, S. Goodwin, J. Reichenthal, E. C. Horning, and B. B. Brodie, *ibid.*, **113**, 481 (1955).

(3) O. M. Bakke, G. H. Draffan, and D. S. Davies, *Xenobiotica*, **4**, 237 (1974).

(4) W. Dieterle, J. W. Faigle, F. Fruh, H. Mory, W. Theobald, K. O. Alt, and W. J. Richer, *Arzneim.-Forsch.*, **26**, 572 (1976).

(5) I. J. McGilveray, K. K. Midha, and N. Mousseau, *Pharmacologist*, **16**, 218 (1974).

(6) I. J. McGilveray, K. K. Midha, R. Brien, and L. Wilson, *J. Chromatogr.*, **89**, 17 (1974).

(7) K. K. Midha, I. J. McGilveray, and C. Charette, *J. Pharm. Sci.*, **63**, 1234 (1974).

(8) *Ibid.*, **63**, 1751 (1974).

(9) Y. Tanimura, Y. Saitoh, F. Nakagawa, and T. Suzuki, *Chem. Pharm. Bull.*, **23**, 651 (1975).

(10) N. J. Pound, I. J. McGilveray, and R. Sears, *J. Chromatogr.*, **89**, 23 (1974).

(11) N. J. Pound and R. W. Sears, *J. Pharm. Sci.*, **64**, 284 (1975).

(12) K. K. Midha and J. K. Cooper, *ibid.*, **66**, 799 (1977).

ACKNOWLEDGMENTS

The authors thank United Pharmaceutical Works, National Corp., Prague, Czechoslovakia, for the gift of I and Mr. J.-C. Ethier for the mass spectra.

Synthesis and Antibacterial Evaluation of 2-(Substituted Phenylureido)-4-thiocyanatobenzothiazoles

ROBERT J. ALAIMO ˣ, STANFORD S. PELOSI, and RAYMOND FREEDMAN

Received March 14, 1977, from the *Chemistry Division and Pharmacometrics Division, Norwich-Eaton Pharmaceuticals, Division of Morton-Norwich Products, Inc., Norwich, NY 13815.* Accepted for publication May 2, 1977.

Abstract □ The synthesis and antibacterial evaluation of a number of 2-(substituted phenylureido)-4-thiocyanatobenzothiazoles are described. The more active compounds against the test organisms *in vitro* generally were those substituted with halogens on the phenyl and benzothiazole rings.

Keyphrases □ Benzothiazoles, various substituted—synthesized, evaluated for antibacterial activity □ Antibacterial activity—evaluated for various substituted benzothiazoles □ Structure–activity relationships—various substituted benzothiazoles evaluated for antibacterial activity

Previously, the synthesis and antiparasitic screening of a series of thiocyanatobenzothiazoles were reported (1). These compounds exhibited significant anthelmintic and antifungal activities. As an extension of this work, the synthesis of some 2-(substituted phenylureido)-4-thiocyanatobenzothiazoles is reported here. These compounds possess a high degree of *in vitro* activity against the Gram-positive bacteria *Staphylococcus aureus* and *Corynebacterium liquefaciens*.

DISCUSSION

The method of preparation of the 2-(substituted phenylureido)-4-thiocyanatobenzothiazoles (V–XII) (Table I) involved the reaction of the appropriate 2-amino-4-thiocyanatobenzothiazole (I–IV) with a phenyl isocyanate. The synthesis of I, II, and IV was reported previously (1, 2); the synthesis of III is reported here. The general procedure for the preparation of V–XII is shown in Scheme I. The assignment of structures for other compounds of the V–XII type was discussed previously (1).

The compounds were tested for antibacterial activity against *S. aureus* and *C. liquefaciens* using *in vitro* serial dilution techniques (3). Compounds V–XII exhibited activity against the test organisms at levels of from 0.048 to 6.25 μg/ml of test media. The test results for V–XII and the reference standard, nifuradene[1] (XIII) (4), are shown in Table I.

[1] U.S. Adopted Name for 1-[(5-nitrofurfurylidene)amino]-2-imidazolidinone.

Table I—Antibacterial Evaluation of Phenylureidothiocyanatobenzothiazoles

Compound	R_1	R_2	R_3	Minimal Inhibitory Concentration, μg/ml	
				S. aureus[a]	*C. liquefaciens*[b]
V	CH_3	H	4-NO_2	0.75	0.75
VI	Cl	H	H	0.38	3.1
VII	Cl	H	4-Cl	0.19	0.75
VIII	*n*-Bu	H	4-Br	6.25	6.25
IX	Cl	Cl	4-Cl	0.19	1.5
X	Cl	Cl	4-Br	0.38	0.048
XI	Cl	Cl	3,4-$(Cl)_2$	3.1	6.25
XII	Cl	Cl	4-F	0.38	1.5
XIII	Nifuradene			3.10	12.5

[a] Strain No. Mi-12, Norwich Pharmacal Co. [b] Strain No. Co-11, ATCC 11828.

In general, the compounds possessing the highest degree of antibacterial activity against the test organisms were substituted with halogen atoms on both the phenyl and benzothiazole rings (VII and IX–XII). However, no other structure–activity trends were apparent among the eight compounds tested.

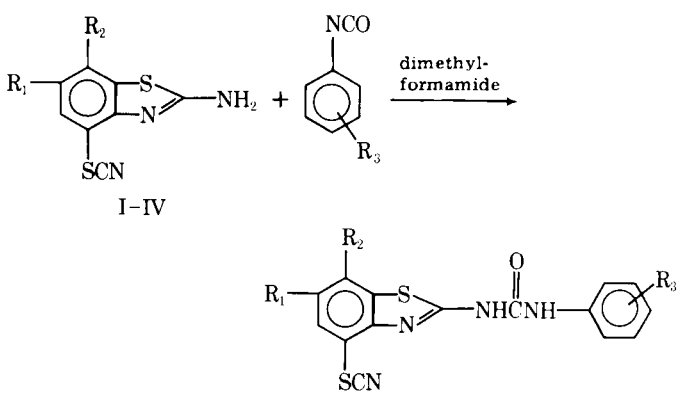

Scheme I

Table II—Analytical and Physical Data for New Compounds

Compound	Melting Point	Yield, %	Recrystallization Solvent	Formula		Analysis, % Calc.	Found
V	283–284°	65	Ethanol–dimethylformamide	$C_{16}H_{11}N_5O_3S_2$	C	49.86	49.73
					H	2.88	2.90
					N	18.17	18.12
VI	329–330°	79	Methanol–dimethylformamide	$C_{15}H_9ClN_4OS_2$	C	49.93	49.60
					H	2.51	2.51
					N	15.53	15.75
VII	239–240°	67	Nitromethane–dimethylformamide	$C_{15}H_8Cl_2N_4OS_2$	C	45.57	45.25
					H	2.04	2.07
					N	14.18	14.41
VIII	259–260°	99	Methanol–dimethylformamide	$C_{19}H_{17}BrN_4OS_2$	C	49.46	49.17
					H	3.71	3.77
					N	12.14	11.91
IX	238–239°	51	Ethanol	$C_{15}H_7Cl_3N_4OS_2$	C	41.92	41.70
					H	1.64	1.66
					N	13.04	12.96
X	243–245°	50	Ethanol	$C_{15}H_7BrCl_2N_4OS_2$	C	37.99	37.60
					H	1.49	1.45
					N	11.82	11.77
XI	313–320°	50	Ethanol	$C_{15}H_6Cl_4N_4OS_2$	C	38.81	38.66
					H	1.30	1.35
					N	12.07	12.13
XII	308–310°	63	Nitromethane	$C_{15}H_7Cl_2FN_4OS_2$	C	43.59	43.23
					H	1.70	1.77
					N	13.56	13.55

EXPERIMENTAL[2]

2-Amino-6-(*n*-butyl)-4-thiocyanatobenzothiazole (III) was prepared as follows. A solution of sodium thiocyanate (81 g, 1.0 mole) in methanol (300 ml) was chilled to −7° in an ice–salt bath. The stirred solution was treated dropwise with bromine (90 g, 0.57 mole) in sodium bromide-saturated methanol (150 ml).

After all of the bromine had been added, *p*-butylaniline (30 g, 0.2 mole) was poured into the reaction mixture. The mixture was stirred for 4.5 hr and was then filtered and poured into 400 ml of water. After neutralization with ammonium hydroxide, the product was removed by filtration and recrystallized from methanol to give cream-colored needles (37 g, 71% yield), mp 167–169°.

Anal.—Calc. for $C_{12}H_{13}N_3S_2$: C, 54.72; H, 4.97; N, 15.96. Found: C, 54.43; H, 4.97; N, 15.89.

6-Methyl-2-{1-[3-(*p*-nitrophenyl)ureido]}-4-thiocyanatobenzothiazole (V) was prepared in the following manner. A solution of 2-amino-6-methyl-4-thiocyanatobenzothiazole (I) (35 g, 0.16 mole) in dimethylformamide (250 ml) was treated portionwise with *p*-nitrophenyl isocyanate (27 g, 0.16 mole). The stirred reaction mixture was heated on a steam bath for 5 hr and then diluted with water to precipitate 40 g (65% yield) of off-white solid.

Recrystallization from ethanol–dimethylformamide provided an analytical sample, mp 283–284°.

Anal.—Calc. for $C_{16}H_{11}N_5O_3S_2$: C, 49.86; H, 2.88; N, 18.17. Found: C, 49.73; H, 2.90; N, 18.12.

Compounds VI–XII were prepared in a similar fashion. Spectral data for V–XII are consistent with the structure assignments. Two characteristic features of the IR spectra of V–XII are absorptions at 2150 (SCN) and 1700 (C=O) cm^{-1}. NMR spectra for V–XII in dimethyl sulfoxide-d_6 were as expected and readily interpretable. The analytical and physical data for V–XII are shown in Table II.

[2] Melting points were determined in open capillary tubes using a Mel-Temp melting-point apparatus and are uncorrected. IR spectra were recorded on a Perkin-Elmer model 137 Infracord (Nujol). NMR spectra were obtained on a Varian A-60A instrument in dimethyl sulfoxide-d_6, using tetramethylsilane as an internal standard.

REFERENCES

(1) R. J. Alaimo, S. S. Pelosi, C. J. Hatton, and J. E. Gray, *J. Med. Chem.*, **17**, 775 (1974).

(2) H. P. Kaufmann, *Arch. Pharm.*, **266**, 197 (1928).

(3) R. Freedman and R. E. Chamberlain, *Antimicrob. Agents Chemother.*, **1967**, 502.

(4) H. R. Snyder, Jr., and R. Freedman, *J. Med. Chem.*, **18**, 524 (1975).

Total Synthesis of 1,11- and 3,11-Diazasteroids

I. Y. C. TAO and R. T. BLICKENSTAFF ˣ

Received March 31, 1977, from the *Veterans Administration Hospital and Biochemistry Department, Indiana University School of Medicine, Indianapolis, IN 46202.* Accepted for publication May 11, 1977.

Abstract □ The 2- and 6-methoxy derivatives of 8-aminoquinoline, as well as 5-aminoisoquinoline, condensed with 2-ethoxycarbonylcyclopentanone to give tricyclic intermediates in 86–90% yield. These secosteroids were cyclized in 35–69% yield with polyphosphoric acid to 2-methoxy-1,11-diaza-, 7-methoxy-1,11-diaza-, and 3,11-diaza-1,3,5,7,9,13-gonahexaen-12-ones, respectively. The latter exhibits slight antileukemic activity.

Keyphrases □ Diazasteroids, various—synthesized, antitumor activity evaluated □ Steroids, various diaza—synthesized, antitumor activity evaluated □ Antitumor activity—evaluated in various diazasteroids □ Structure–activity relationships—various diazasteroids evaluated for antitumor activity

1,11-Diaza-8,14-seco-1,3,5,7,9-gonapentaene-12,14-dione (III, Scheme I) was cyclized (1) with polyphosphoric acid in 75% yield to 1,11-diaza-1,3,5,7,9,13-gonahexaen-12-one (IV), contrary to an earlier report that it would not cyclize (2). The synthesis has now been extended to the isomeric secosteroid (XIV) and to two methoxy derivatives of III. These diazasteroids were of interest for evaluation as antitumor agents in light of the reported activity of 2-azaestradiol 17-acetate 3-methyl ether (3). Consequently, the new diazasteroids, as well as *N*-oxides of two of them, were submitted to the National Institutes of Health for antitumor assay.

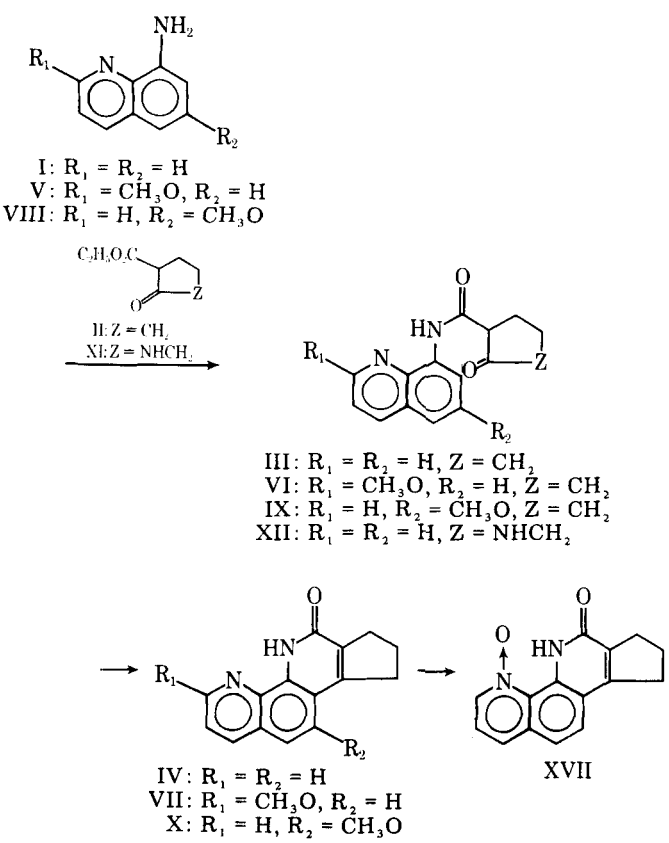

Scheme I

EXPERIMENTAL[1]

3,11-Diaza-8,14-seco-1,3,5,7,9-gonapentaene-12,14-dione (XIV)—An equimolar mixture of 5-aminoisoquinoline (XIII, 2.88 g, 0.02 mole) and 2-ethoxycarbonylcyclopentanone (II, 3.12 g) was dissolved in 45 ml of xylene, and the resulting orange solution was heated at reflux for 1 hr (Scheme II). Most of the xylene was distilled off, and the residue was solidified upon cooling. Filtration gave a light-orange cake, 4.62 g (0.018 mole), 90% yield of crude XIV, mp 112–115° [lit. (2) mp 120–122°]; IR: 1720 (keto C=O) and 1670 (amide C=O) cm^{-1}.

Since this intermediate was difficult to crystallize, a portion of it was converted to the corresponding methiodide salt for identification purposes. A solution of 0.5 g of crude XIV and 6 ml of methyl iodide in 10 ml of methanol was heated at reflux for 2 hr and then concentrated to a few milliliters. Orange plates were filtered and recrystallized from water, mp 217–219° [lit. (4) mp 206–207.5°].

Anal.—Calc. for $C_{16}H_{17}IN_2O_2$: C, 48.50; H, 4.32; I, 32.03; N, 7.07. Found: C, 48.10; H, 4.36; I, 32.27; N, 6.97.

3,11-Diaza-1,3,5,7,9,13-gonahexaen-12-one (XV)—The secosteroid XIV (3.44 g, 13.5 mmoles) was added to 35 g of polyphosphoric acid at 100–115° in 15 min. The reaction was exothermic with foaming. The mixture was kept at 100–115° for 1 hr with occasional stirring and then was poured onto crushed ice and brought to pH 6 with aqueous sodium hydroxide. Filtration gave 2.2 g of a yellow powder (XV) in 69% yield. The filtrate was made alkaline and extracted three times with chloroform to give 29% of recovered 5-aminoisoquinoline. Recrystallization of XV from methanol gave the analytical sample, mp >290°; IR: 1630 and 1610 cm^{-1}.

Anal.—Calc. for $C_{15}H_{12}N_2O$: C, 76.25; H, 5.12; N, 11.86. Found: C, 76.06; H, 5.08; N, 11.75.

3,11-Diaza-1,3,5,7,9,13-gonahexaen-12-one 1-*N*-Oxide (XVI)—A solution of 3.54 g (15 mmoles) of XV in 20 ml of chloroform was added at room temperature to a stirred solution of 3.05 g of *m*-chloroperbenzoic acid in 100 ml of chloroform. The resulting suspension was stirred for 48 hr and then filtered to give 2.65 g of a yellow powder. This powder was treated with cold methanol, and filtering gave 2.19 g of crude XVI. The methanol solution contained unreacted XV. Recrystallization of crude XVI from aqueous methanol gave a powder, mp >290°. The IR spectrum

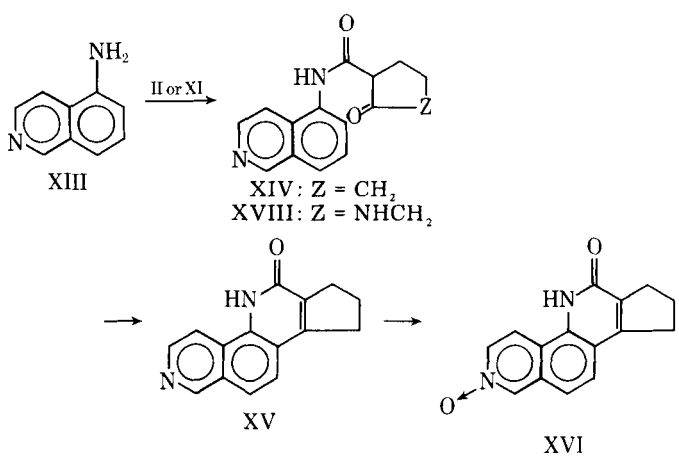

Scheme II

[1] Melting points were obtained on a Thomas-Hoover melting-point apparatus and are corrected. IR spectra were taken as smears or mineral oil mulls on a Perkin-Elmer 247 spectrophotometer. PMR spectra were obtained in deuterodimethyl sulfoxide on a Varian HA-100 spectrophotometer with tetramethylsilane as an internal standard. Microanalyses were performed by Galbraith Laboratories, Knoxville, Tenn. The 2-ethoxycarbonylcyclopentanone is actually a 1:1 mixture of methyl and ethyl esters.

Table I—Synthesis of 1,11-Diazasteroids

Number	Compound Name	Yield, %	Melting Point	Mass Spectrum, *m/e*	IR, cm^{-1}	Formula	Analysis, %	Calc.	Found
VI	2-Methoxy-1,11-diaza-8,14-seco-1,3,5,7,9-gonapentaene-12,14-dione[a]	86	143–144.5°[b]	—	1735, 1660	$C_{16}H_{16}N_2O_3$	C	67.59	67.55
							H	5.67	5.69
							N	9.85	9.71
VII	2-Methoxy-1,11-diaza-1,3,5,7,9,13-gonahexaen-12-one	35	275–276°	266	3360, 1660, 1600	$C_{16}H_{14}N_2O_2 \cdot CH_3OH$	C	68.44	68.45
							H	6.08	5.88
							N	9.37	9.88
IX	7-Methoxy-1,11-diaza-8,14-seco-1,3,5,7,9-gonapentaene-12,14-dione[a]	89	116–118°	—	1720, 1670	$C_{16}H_{16}N_2O_3$	C	67.59	67.40
							H	5.67	5.76
							N	9.85	9.95
X	7-Methoxy-1,11-diaza-1,3,5,7,9,13-gonahexaen-12-one[e]	39	247–249.5° dec.[c,d]	266	1620, 1610	$C_{16}H_{14}N_2O_2$	C	72.16	72.09
							H	5.30	5.35
							N	10.52	10.52
XII	1,11,15-Triaza-8,14-seco-D-homo-1,3,5,7,9-gonapentaene-12,14-dione	77	220–221.5°[d]	—	3320, 3160	$C_{15}H_{15}N_3O_2$	C	66.90	67.11
							H	5.61	5.45
							N	15.60	15.38
XVII	1,11-Diaza-1,3,5,7,9,13-gonahexaen-12-one 1-*N*-oxide	14	242.5–244° dec.[f]	252	3325, 1270, 850	$C_{15}H_{12}N_2O_2 \cdot H_2O$	C	66.66	66.89
							H	5.22	5.19
							N	10.36	10.42
XVIII	3,11,15-Triaza-8,14-seco-D-homo-1,3,5,7,9-gonapentaene-12,14-dione	83	186.5–188°[d]	—	1680, 1650, 1630	$C_{15}H_{15}N_3O_2$	C	66.90	66.81
							H	5.61	5.46
							N	15.60	15.56

[a] These condensations were carried out as in the preparation of XIV (see *Experimental*), except that the amine was added dropwise to a 10% excess of the keto ester over 40–60 min. [b] Crystallized from acetone–water. [c] After chromatography on Florisil. [d] Crystallized from acetone–chloroform. [e] NMR: δ 8.65 (1H, d, $J_{2,3}$ = 4 Hz, $J_{2,4}$ = 1.5 Hz, H_2), 7.99 (1H, d, $J_{3,4}$ = 8 Hz, $J_{2,4}$ = 1.5 Hz, H_4), 7.44 (1H, d, $J_{3,4}$ = 8 Hz, $J_{2,3}$ = 4 Hz, H_3), 6.71 (1H, s, H_6), 4.03 (3H, s, CH_3O), 3.00 (4H, m, $H_{15,17}$), and 2.30 (2H, m, H_{16}) ppm. [f] Crystallized from water.

exhibited *N*-oxide bands at 1240 and 850 cm^{-1}; the mass spectrum showed *m/e* 252 (also indicated the presence of water).

Anal.—Calc. for $C_{15}H_{12}N_2O_2 \cdot H_2O$: C, 66.66; H, 5.22; N, 10.36. Found: C, 66.27; H, 5.16; N, 10.26.

RESULTS AND DISCUSSION

8-Amino-2-methoxyquinoline, prepared by a minor modification of the method of Mislow and Koepeli (5), condensed with II to give an 86% yield of the secosteroid VI, which cyclized to 2-methoxy-1,11-diaza-1,3,5,7,9,13-gonahexaen-12-one in 35% yield (VII, Table I). Similarly, 8-amino-6-methoxyquinoline (VIII) and II reacted to produce IX (89%), which was cyclized to 7-methoxy-1,11-diaza-1,3,5,7,9,13-gonahexaen-12-one (X) (39%). 5-Aminoisoquinoline (XIII) and II gave XIV (90%), which was cyclized to the 3,11-diazasteroid XV (69%, see *Experimental*). Both I and XIII condensed with 3-ethoxycarbonyl-2-piperidone (XI) to give the secosteroids XII and XVIII, respectively, neither of which could be cyclized to steroids. *N*-Oxides of IV and XV were prepared by oxidation with *m*-chloroperbenzoic acid.

Diazasteroids IV, VII, X, XVI, and XVII were inactive in the National Cancer Institute screen against P-388 leukemia in mice. However, XV (NSC 265959) exhibited slight activity at 12.5–50 mg/kg; at higher dose levels, it was toxic[2].

REFERENCES

(1) I. Y. C. Tao and R. T. Blickenstaff, *Steroids*, **27**, 205 (1976).

(2) D. G. Bew and G. R. Clemo, *J. Chem. Soc.*, **1955**, 1775.

(3) R. J. Chorvat and R. Pappo, *Tetrahedron Lett.*, **1975**, 623.

(4) F. D. Popp, W. R. Schleigh, P. M. Froehlich, R. J. Dubois, and A. C. Casey, *J. Org. Chem.*, **33**, 833 (1968).

(5) K. Mislow and J. B. Koepeli, *J. Am. Chem. Soc.*, **68**, 1553 (1946).

[2] *Note added in proof:* Dr. Chinan Fan, Department of Biochemistry, Scripps Clinic and Research Foundation, La Jolla, Calif., found that XV exhibits a modest inhibitory activity ($K_i = 1.3 \times 10^{-5}$ *M*) against the L-1210 dihydrofolate reductase; 1,2,3,4,13,14-hexahydro-IV (1) and 1-methyl-1,2,3,4-tetrahydro-XII (1) were inactive against P-388 and against dihydrofolate reductase.

Structures of Silver Sulfonamides

AUKE BULT ˣ and HUUB B. KLASEN

Received June 7, 1976, from the *Laboratory for Pharmaceutical and Analytical Chemistry, State University of Groningen, Antonius Deusinglaan 2, Groningen 8004, The Netherlands.* Accepted for publication May 24, 1977.

Abstract □ The structures of silver sulfonamides were found to depend highly on the substituent at the amide nitrogen of the sulfonamide. Silver is coordinated to that nitrogen and the sulfonamide is in the amido form if no substituent is present or if the substituent is a phenyl, acetyl, or 2-pyrimidyl group. If the substituent is a 2-thiazolyl or 2-pyridinyl group, the sulfonamide is in the imido form and silver coordinates to the nitrogen of the substituent. Depending on the number of suitable donor atoms per sulfonamide, the silver compounds are charged or uncharged and the primary amino group may be involved in complexation.

Keyphrases □ Silver—coordinating properties with various sulfonamides, structures of complexes studied □ Sulfonamides, various—coordination with silver, structures of complexes studied □ Complexes—various silver sulfonamides, coordination properties and structures studied □ Anti-infectives, topical—various silver sulfonamides, coordination properties and structures studied

Interest in silver sulfadiazine as an antibacterial agent in the treatment of extensive burns has increased steadily. IR (1) and NMR (1) studies as well as X-ray analysis (2, 3) of the structure of silver sulfadiazine have been reported. The bactericidal action *in vivo* of silver sulfadiazine is superior to the related silver sulfonamides. Because the

Table I—Synthesis of 1,11-Diazasteroids

Number	Compound Name	Yield, %	Melting Point	Mass Spectrum, *m/e*	IR, cm^{-1}	Formula	Analysis, %	Calc.	Found
VI	2-Methoxy-1,11-diaza-8,14-seco-1,3,5,7,9-gonapentaene-12,14-dione[a]	86	143–144.5°[b]	—	1735, 1660	$C_{16}H_{16}N_2O_3$	C	67.59	67.55
							H	5.67	5.69
							N	9.85	9.71
VII	2-Methoxy-1,11-diaza-1,3,5,7,9,13-gonahexaen-12-one	35	275–276°	266	3360, 1660, 1600	$C_{16}H_{14}N_2O_2 \cdot CH_3OH$	C	68.44	68.45
							H	6.08	5.88
							N	9.37	9.88
IX	7-Methoxy-1,11-diaza-8,14-seco-1,3,5,7,9-gonapentaene-12,14-dione[a]	89	116–118°	—	1720, 1670	$C_{16}H_{16}N_2O_3$	C	67.59	67.40
							H	5.67	5.76
							N	9.85	9.95
X	7-Methoxy-1,11-diaza-1,3,5,7,9,13-gonahexaen-12-one[e]	39	247–249.5° dec.[c,d]	266	1620, 1610	$C_{16}H_{14}N_2O_2$	C	72.16	72.09
							H	5.30	5.35
							N	10.52	10.52
XII	1,11,15-Triaza-8,14-seco-D-homo-1,3,5,7,9-gonapentaene-12,14-dione	77	220–221.5°[d]	—	3320, 3160	$C_{15}H_{15}N_3O_2$	C	66.90	67.11
							H	5.61	5.45
							N	15.60	15.38
XVII	1,11-Diaza-1,3,5,7,9,13-gonahexaen-12-one 1-*N*-oxide	14	242.5–244° dec.[f]	252	3325, 1270, 850	$C_{15}H_{12}N_2O_2 \cdot H_2O$	C	66.66	66.89
							H	5.22	5.19
							N	10.36	10.42
XVIII	3,11,15-Triaza-8,14-seco-D-homo-1,3,5,7,9-gonapentaene-12,14-dione	83	186.5–188°[d]	—	1680, 1650, 1630	$C_{15}H_{15}N_3O_2$	C	66.90	66.81
							H	5.61	5.46
							N	15.60	15.56

[a] These condensations were carried out as in the preparation of XIV (see *Experimental*), except that the amine was added dropwise to a 10% excess of the keto ester over 40–60 min. [b] Crystallized from acetone–water. [c] After chromatography on Florisil. [d] Crystallized from acetone–chloroform. [e] NMR: δ 8.65 (1H, d, $J_{2,3}$ = 4 Hz, $J_{2,4}$ = 1.5 Hz, H_2), 7.99 (1H, d, $J_{3,4}$ = 8 Hz, $J_{2,4}$ = 1.5 Hz, H_4), 7.44 (1H, d, $J_{3,4}$ = 8 Hz, $J_{2,3}$ = 4 Hz, H_3), 6.71 (1H, s, H_6), 4.03 (3H, s, CH_3O), 3.00 (4H, m, $H_{15,17}$), and 2.30 (2H, m, H_{16}) ppm. [f] Crystallized from water.

exhibited *N*-oxide bands at 1240 and 850 cm^{-1}; the mass spectrum showed *m/e* 252 (also indicated the presence of water).

Anal.—Calc. for $C_{15}H_{12}N_2O_2 \cdot H_2O$: C, 66.66; H, 5.22; N, 10.36. Found: C, 66.27; H, 5.16; N, 10.26.

RESULTS AND DISCUSSION

8-Amino-2-methoxyquinoline, prepared by a minor modification of the method of Mislow and Koepeli (5), condensed with II to give an 86% yield of the secosteroid VI, which cyclized to 2-methoxy-1,11-diaza-1,3,5,7,9,13-gonahexaen-12-one in 35% yield (VII, Table I). Similarly, 8-amino-6-methoxyquinoline (VIII) and II reacted to produce IX (89%), which was cyclized to 7-methoxy-1,11-diaza-1,3,5,7,9,13-gonahexaen-12-one (X) (39%). 5-Aminoisoquinoline (XIII) and II gave XIV (90%), which was cyclized to the 3,11-diazasteroid XV (69%, see *Experimental*). Both I and XIII condensed with 3-ethoxycarbonyl-2-piperidone (XI) to give the secosteroids XII and XVIII, respectively, neither of which could be cyclized to steroids. *N*-Oxides of IV and XV were prepared by oxidation with *m*-chloroperbenzoic acid.

Diazasteroids IV, VII, X, XVI, and XVII were inactive in the National Cancer Institute screen against P-388 leukemia in mice. However, XV (NSC 265959) exhibited slight activity at 12.5–50 mg/kg; at higher dose levels, it was toxic[2].

REFERENCES

(1) I. Y. C. Tao and R. T. Blickenstaff, *Steroids*, **27**, 205 (1976).

(2) D. G. Bew and G. R. Clemo, *J. Chem. Soc.*, **1955**, 1775.

(3) R. J. Chorvat and R. Pappo, *Tetrahedron Lett.*, **1975**, 623.

(4) F. D. Popp, W. R. Schleigh, P. M. Froehlich, R. J. Dubois, and A. C. Casey, *J. Org. Chem.*, **33**, 833 (1968).

(5) K. Mislow and J. B. Koepeli, *J. Am. Chem. Soc.*, **68**, 1553 (1946).

[2] *Note added in proof:* Dr. Chinan Fan, Department of Biochemistry, Scripps Clinic and Research Foundation, La Jolla, Calif., found that XV exhibits a modest inhibitory activity ($K_i = 1.3 \times 10^{-5}$ *M*) against the L-1210 dihydrofolate reductase; 1,2,3,4,13,14-hexahydro-IV (1) and 1-methyl-1,2,3,4-tetrahydro-XII (1) were inactive against P-388 and against dihydrofolate reductase.

Structures of Silver Sulfonamides

AUKE BULT ˣ and HUUB B. KLASEN

Received June 7, 1976, from the *Laboratory for Pharmaceutical and Analytical Chemistry, State University of Groningen, Antonius Deusinglaan 2, Groningen 8004, The Netherlands.* Accepted for publication May 24, 1977.

Abstract □ The structures of silver sulfonamides were found to depend highly on the substituent at the amide nitrogen of the sulfonamide. Silver is coordinated to that nitrogen and the sulfonamide is in the amido form if no substituent is present or if the substituent is a phenyl, acetyl, or 2-pyrimidyl group. If the substituent is a 2-thiazolyl or 2-pyridinyl group, the sulfonamide is in the imido form and silver coordinates to the nitrogen of the substituent. Depending on the number of suitable donor atoms per sulfonamide, the silver compounds are charged or uncharged and the primary amino group may be involved in complexation.

Keyphrases □ Silver—coordinating properties with various sulfonamides, structures of complexes studied □ Sulfonamides, various—coordination with silver, structures of complexes studied □ Complexes—various silver sulfonamides, coordination properties and structures studied □ Anti-infectives, topical—various silver sulfonamides, coordination properties and structures studied

Interest in silver sulfadiazine as an antibacterial agent in the treatment of extensive burns has increased steadily. IR (1) and NMR (1) studies as well as X-ray analysis (2, 3) of the structure of silver sulfadiazine have been reported. The bactericidal action *in vivo* of silver sulfadiazine is superior to the related silver sulfonamides. Because the

Table I—Analytical Data of the Silver Sulfonamides

Compound	% Ag		% C		% H		% N		% S	
	Calc.	Found	Calc.	Found	Calc.	Found	Calc.	Found	Calc.	Found
I Silver benzenesulfonamide	40.86	40.3	27.27	27.2	2.29	2.3	5.31	5.2	12.14	12.0
II Silver benzenesulfonamidobenzene	31.73	31.6	42.35	42.4	2.96	2.9	4.12	4.1	9.43	9.5
III Silver 2-(benzenesulfonamido)pyrimidine	31.54	31.1	35.08	34.9	2.36	2.2	12.29	12.5	9.89	9.3
IV Silver 2-(benzenesulfonamido)thiazole	31.07	30.8	31.12	31.3	2.03	2.0	8.07	7.9	18.47	18.3
V Silver sulfanilamide	38.65	38.5	25.80	25.8	2.53	2.5	10.04	10.2	11.49	11.6
VI Silver sulfanilamidobenzene	30.13	29.1	40.56	40.9	3.12	3.2	7.89	8.1	9.03	9.0
VII Silver sulfadiazine	30.22	29.4	33.62	33.4	2.54	2.4	15.70	15.7	8.98	9.0
VIII Silver sulfathiazole	29.70	28.3	29.83	30.1	2.23	2.3	11.61	11.6	17.71	17.7
IX Silver sulfapyridine	30.29	31.5	37.07	36.8	2.83	2.7	11.80	11.8	9.00	8.9
X Silver sulfacetamide	33.60	34.0	29.90	29.8	2.82	2.7	8.73	8.9	9.99	9.9

bactericidal action is related quantitatively to the binding of silver to microbial DNA, the dissociation of the silver sulfonamide is a prerequisite. The unique property of silver sulfadiazine seems to be its moderate initial dissociation coupled with its continual release of silver (4).

This investigation systematically studied the coordinating properties of silver with sulfonamides and obtained insight into the structures of the silver compounds. A difference in structure is one factor that influences the silver release and contributes to the different biological activities of the silver sulfonamides.

EXPERIMENTAL

Equipment and Analyses—A double-beam grating spectrophotometer[1], an IR spectrophotometer[2], and a conductivity meter[3] were used. The silver was analyzed by the Volhard titration after decomposition of the compound with 65% HNO_3. Elemental analyses also were performed[4].

Materials and Reagents—All chemicals were analytical or reagent grade. The sulfanilamides and benzenesulfonamides were obtained commercially.

Synthesis—*Benzenesulfonamides*—2 - (Benzenesulfonamido)py - rimidine and 2-(benzenesulfonamido)thiazole were prepared according to literature methods (5).

Benzenesulfonamidobenzene—Benzenesulfonyl chloride, 20 g, was added dropwise, with stirring, to a cooled solution of 10 g of aniline in 80 ml of dry pyridine. After standing overnight at room temperature, the solvent was partly removed under reduced pressure to a small volume. Addition of water separated the crude product, which was isolated by filtration, washed with water, and recrystallized from ethanol–water, yielding 20 g, mp 102–103.1°.

Anal.—Calc. for $C_{12}H_{11}N_1O_2S_1$: C, 61.76; H, 4.76; N, 6.01; S, 13.75. Found: C, 61.5; H, 4.7; N, 6.0; S, 13.6.

Sulfanilamidobenzene—A solution of 15 g of aniline in 50 ml of dry pyridine was added dropwise, with stirring, to a cooled solution of 20 g of *N*-acetylsulfanilyl chloride in 50 ml of dry pyridine. The mixture was then heated for 1 hr at 80°. After the solvent was removed under reduced pressure to half volume, the mixture was poured into 4 *N* HCl; the separated product was filtered off and dissolved in 200 ml of 10% (w/v) NaOH. Then the mixture was refluxed for 1 hr and acidified. The separated product was filtered off, washed with water, and recrystallized from ethanol–water, yielding 13.2 g, mp 188.1–188.9°.

Anal.—Calc. for $C_{12}H_{12}N_2O_2S_1$: C, 58.02; H, 4.87; N, 11.29; S, 12.92. Found: C, 57.9; H, 4.8; N, 11.3; S, 12.9.

Silver Sulfonamides—The sulfonamide, 0.03 mole, was dissolved in 30 ml of 1.0 *N* NaOH and 70 ml of water. After dissolution, in some cases with gentle heating, the solution was diluted with water to 300 ml. A solution of 0.03 mole of silver nitrate in 100 ml of water was then added dropwise with stirring. The white precipitate was separated, washed with water, and dried at 120°.

The elemental analyses are given in Table I. For purification, a quantity of silver sulfadiazine (VII) was dissolved in 25% NH_3 solution and again isolated by: (*a*) the partial evaporation of the solvent in air, from which a crystalline product (A) was formed (1); and (*b*) acidifying to pH 7 with 4 *N* HNO_3, after which the precipitate (B) was filtered off, washed with water, and dried at 120°.

The elemental analyses of VII and Products A and B were nearly identical, but the IR spectra were slightly different. The spectrum of B was the most regular and well defined and closely resembled the spectrum of a commercial sample of VII[5].

RESULTS AND DISCUSSION

Silver prefers the formation of two and four coordinate complexes with linear and tetrahedral geometry, respectively (6). With the anionic ligand, L, the formation of the anionic complexes $[AgL_2]^-$ and $[AgL_4]^{3-}$ is possible (6–8). The effective formation of these complexes depends on the number of suitable donor atoms per L. One donor atom per L favors the formation of the anionic complexes; more donor atoms per L favor the formation of uncharged, polymeric complexes $(AgL)_n$.

Table II summarizes the results of the physical measurements. The IR spectra of the silver compounds II, III, and IV show that the introduction of silver in the sulfonamide is attended with the deprotonation of the amide nitrogen (^{1}N); ν(NH) is absent. The remaining stretching frequency ^{1}NH of I decreases by 70 cm^{-1}.

Comparison of $\nu^*(^4NH_2)$ [$\nu^* = (\nu_s + \nu_{as})/2$] of the silver compounds with that of the parent compounds (sulfonamides) gives information about the involvement of this group in complexation. The values of $\Delta^*\nu = \nu^*_{\text{sulfonamide}} - \nu^*_{\text{silver compound}}$ are: V = +100 cm^{-1}, VI = +155 cm^{-1}, VII = +25 cm^{-1}, VIII = −90 cm^{-1}, IX = −5 cm^{-1}, and X = +70 cm^{-1}. These results make reliable conclusions difficult because of the possible interference by hydrogen bonding. Considering the magnitude of the shift of the stretching frequency ^{1}NH in I, the involvement of $^4NH_2$ in silver complexation is possible in V, VI, and X. In VII, $^4NH_2$ is not involved in coordination (2, 3).

Of great value are the results of an IR study of sulfonamides (10). The value of ν^*(SO), the weighted average value of ν_s(SO) and ν_{as}(SO), depends on the character of the groups attached to SO_2 (Table II). If R_3 is H, the value of ν^*(SO) is about 1230–1255 cm^{-1} (the amido form) except when R_2 is 2-thiazole or 2-pyridine. In that case, ν^*(SO) is about 1200 cm^{-1} and these sulfonamides are in the imido form (5, 11). The proton R_3 = H is located on the nitrogen of R_2. These results are also supported by X-ray analysis of sulfathiazole (12).

The introduction of $^4NH_2$ in the sulfonamide (R_1 in Table II) lowers ν^*(SO) by about 15–16 cm^{-1}. When R_3 is Na, the compound is the anion of the sulfonamide. The value of ν^*(SO) is lowered to 1160–1200 cm^{-1}. The divergency of the values can be ascribed to the different possibilities of delocalization of the negative charge dependent on the nature of R_2. The lowering of ν^*(SO) correlates with the quantity of negative charge on the amide nitrogen and is the largest when R_2 is H, *i.e.*, 1156 cm^{-1} (10).

Thus, when R_3 is Ag, the value of ν^*(SO) can give information about the electronic environment of the amide nitrogen. By using the values of ν^*(SO), the silver compounds can be divided into two groups. Group A consists of I–III, V–VII, and X. The substitution of the R_3 H by Ag lowers ν^*(SO) by 50–75 cm^{-1}; ν^*(SO) of R_3 = Ag and R_3 = Na have about the same value. Group B consists of IV, VIII, and IX. The substitution of the R_3 H by Ag hardly changes ν^*(SO); the value of ν^*(SO) for R_3 = Ag is over 30 cm^{-1} higher as for R_3 = Na.

For Group B compounds, the small change of ν^*(SO) by silver substitution indicates that the electronic environment of the amide nitrogen

[1] Perkin-Elmer 124.
[2] Beckman Accu Lab 2.
[3] Radiometer type CDM^{2d} and conductivity cell type CDC104.
[4] Analytical Department of the Chemical Laboratories, University of Groningen, Groningen, The Netherlands.
[5] Philips-Duphar B. V., Weesp, The Netherlands.

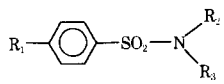

Table II—Physical Data of the Silver Sulfonamides

Compound				Λ_M, Ω^{-1} cm^2/mole[a]			ν^*(SO)[b], cm^{-1}
Number	R_1	R_2	R_3	Acetonitrile	*N,N*-Dimethylformamide	Dimethyl Sulfoxide	
—	H	H	H	—	—	—	1243
I	H	H	Ag	—	—	13.6	1168
—	H	H	Na	—	—	—	1155
—	H	Benzene	H	—	—	—	1248
II	H	Benzene	Ag	87.4	36.5	15.9	1190
—	H	2-Pyrimidine	H	—	—	—	1256
III	H	2-Pyrimidine	Ag	—	—	3.7	1204
—	H	2-Thiazole	H	—	—	—	1213
IV	H	2-Thiazole	Ag	—	5.2	8.15	1212
—	NH_2	H	H	—	—	—	1228
V	NH_2	H	Ag	—	—	7.6	1158
—	NH_2	H	Na	—	—	—	1156
—	NH_2	Benzene	H	—	—	—	1232
VI	NH_2	Benzene	Ag	—	12.4	14.9	1171
—	NH_2	Benzene	Na	—	—	—	1171
—	NH_2	2-Pyrimidine	H	—	—	—	1241
VII	NH_2	2-Pyrimidine	Ag	—	—	2.2	1178
—	NH_2	2-Pyrimidine	Na	—	—	—	1186
—	NH_2	2-Thiazole	H	—	—	—	1197
VIII	NH_2	2-Thiazole	Ag	—	5.2	7.25	1199
—	NH_2	2-Thiazole	Na	—	—	—	1166
—	NH_2	2-Pyridine	H	—	—	—	1190
IX	NH_2	2-Pyridine	Ag	—	6.6	9.75	1192
—	NH_2	2-Pyridine	Na	—	—	—	1159
—	NH_2	Acetyl	H	—	—	—	1238
X	NH_2	Acetyl	Ag	75.6	33.2	18.75	1174
—	NH_2	Acetyl	Na	—	—	—	1206

[a] Measured at 10^{-3} *M*. The Λ_M values are calculated for $[AgL_2]Ag$ (see text). Standard ranges of 1:1 electrolyte (9): acetonitrile, 120–160; *N,N*-dimethylformamide, 65–90; and dimethyl sulfoxide, 23–42. [b] Potassium bromide pellets; $\nu^*(SO) = \sqrt{[\nu_s(SO)^2 + \nu_{as}(SO)^2]/2}$.

remains almost unchanged. These sulfonamides are in the imido form and maintain that form in the silver compounds. The silver is bound to the substituent R_1 = 2-thiazole or 2-pyridine. The donor atom is the nitrogen in R_2. The same method of coordination is found with cobalt in sulfathiazole (13).

The resemblance in lowering of ν^*(SO) in Group A as a result of substitution of the R_3 H by Ag or Na indicates a similarity in the type of bonding for sodium and silver. The conclusion that silver is ionically bound like sodium cannot be correct because almost all compounds are nonconducting and the UV spectra are different. In addition, it has been shown (3) that VII has coordinative bonding. The results can be interpreted as follows. In the compounds of Group A, a coordinative bond between the amide nitrogen and silver is formed. The formation of that bond has been proved for VII (2, 3); it is very likely for I and II (the amide nitrogen is the only donor atom) and likely for III, V, VI, and X. A fraction of the lowering of ν^*(SO) may be caused by an SO···Ag interaction, but this interaction will be weak (2, 3, 6).

Conductivity—The values of Λ_M given in Table II are based on the assumption of the formation of the complex $[AgL_2]Ag$ (L is the anion of the sulfonamide). The values indicate that only II and X may have that composition. The Λ_M values of these compounds in the three solvents agree with the values found for the complex $[AgL_2]Ag$ (L is the anion of a barbiturate) (7). The Λ_M values of IV, VI, VIII, and IX in *N,N*-dimethylformamide are indicative of uncharged compounds.

All silver compounds are soluble in dimethyl sulfoxide. However, the values of Λ_M are rather variable. This variation can be attributed to the strong dissociative and solvolytic effects of dimethyl sulfoxide. This explanation is supported by the fact that Λ_M of IV, VI, VIII, and IX is larger in dimethyl sulfoxide than *N,N*-dimethylformamide, and this result is unlike the theoretical expectation (the standard ranges of *N,N*-dimethylformamide have higher values than of dimethyl sulfoxide; see footnote *a* of Table II). The values of Λ_M in dimethyl sulfoxide of III, V, and VII indicate the presence of uncharged compounds. From Λ_M, it is difficult to draw a conclusion about the electrolyte type of I, but the insolubility in acetonitrile and *N,N*-dimethylformamide indicates an uncharged compound.

UV—The UV spectra of the sulfonamides and their silver compounds in methanol are similar (III and VIII are insoluble in methanol). In general, the spectra of the sodium sulfonamides are different from the former spectra and confirm the difference in the interaction of silver and sodium with the sulfonamides.

From the results discussed so far, the following conclusions about the structures of the individual compounds can be derived: I, silver coordinates with the amide nitrogen (^{1}N); II, silver coordinates with ^{1}N, and the compound has the composition $[AgL_2]Ag$; III, silver coordinates with ^{1}N and is uncharged, and the involvement in coordination of the two nitrogen atoms of 2-pyrimidine is likely (resemblance with VII); IV, silver coordinates to the nitrogen atom of 2-thiazole and is uncharged; V, silver coordinates with ^{1}N and the primary amino group and is uncharged; VI, silver coordinates with ^{1}N and the primary amino group and is uncharged; VII, silver coordinates with ^{1}N and is uncharged, and the two nitrogen atoms of 2-pyrimidine are involved in coordination (2, 3); VIII, silver coordinates to the nitrogen atom of 2-thiazole and is uncharged; IX, silver coordinates to the nitrogen atom of 2-pyridine and is uncharged; and X, silver coordinates with ^{1}N and possibly the primary amino group, and the composition of the compound is $[AgL_2]Ag$.

The composition $[AgL_2]Ag$ of II and X indicates the presence of one suitable donor atom per L. For II, this structure agrees with expectation; for X, this structure is uncertain because of the possible involvement of the primary amino group. In the uncharged compounds (III and V–VII), at least two suitable donor atoms per L are needed. In IV, VIII, and IX, with the nitrogen of 2-thiazole or 2-pyridine as a donor atom, the second donor atom of L is uncertain. Possibly ^{1}N is the second donor atom, but the imido form must be maintained (sulfur of 2-thiazole and oxygen of SO are less probable).

The variation in structure of the silver compounds and the resulting differences in stability constants and silver release can at least partly explain the different bacterial action.

REFERENCES

(1) B. J. Sandmann, R. U. Nesbitt, Jr., and R. A. Sandmann, *J. Pharm. Sci.*, **63**, 948 (1974).

(2) A. W. Struss, *Diss. Abstr. Int. B*, **35**, 5808 (1975).

(3) D. S. Cook and M. F. Turner, *J. Chem. Soc. Perkin II*, **1975**, 1021.

(4) C. L. Fox and S. M. Modak, *Antimicrob. Agents Chemother.*, **5**, 582 (1974).

(5) T. Uno, K. Machida, K. Hanai, M. Ueda, and S. Sasaki, *Chem. Pharm. Bull.*, **11**, 704 (1963).

(6) F. A. Cotton and G. W. Wilkinson, "Advanced Inorganic Chemistry," 3rd ed., Interscience, New York, N.Y., 1972, p. 1044.

(7) A. Bult and H. B. Klasen, *Pharm. Weekbl.*, **110**, 533 (1975).
(8) J. R. Demember and F. A. Wallace, *J. Am. Chem. Soc.*, **97**, 6240 (1975).
(9) W. J. Geary, *Coord. Chem. Rev.*, **7**, 81 (1971).
(10) A. Rastelli, P. G. de Benedetti, A. Albasini, G. Vampa, and M. Melegari, *Farmaco, Ed. Sci.*, **29**, 654 (1974).
(11) P. G. de Benedetti, A. Rastelli, A. Albasini, M. Melegari, and G. Vampa, *Atti Soc. Nat. Mat. Modena*, **105**, 73 (1974).
(12) G. J. Kruger and G. Gafner, *Acta Crystallogr., B*, **27**, 326 (1971).
(13) A. Bult, *Pharm. Weekbl.*, **111**, 385 (1976).

ACKNOWLEDGMENTS

The authors are indebted to Professor Dr. D. A. Doornbos and Dr. A. S. Horn for their help.

In Vitro Uptake of Oral Contraceptive Steroids by Magnesium Trisilicate

SALEH A. H. KHALIL *x and M. IWUAGWU

Received March 12, 1977, from the *School of Pharmacy, University of Benin, Benin City, Nigeria.* Accepted for publication May 27, 1977. *Present address: Department of Pharmaceutics, Faculty of Pharmacy, Alexandria University, Alexandria, Egypt.

Abstract □ Some steroids used in oral contraceptives were adsorbed significantly by magnesium trisilicate. The adsorption affinity followed the sequence: ethindrone > mestranol > norethindrone > ethinyl estradiol. Adsorption data obtained at relatively low initial concentrations fitted a Langmuir plot; the values for monolayer adsorption ranged between 0.24 and 0.32 mg/g. At higher concentrations of the steroids, multilayer adsorption occurred. The results of desorption experiments made at 37° in water and 0.05 *N* HCl suggested that desorption was incomplete and depended on the amount of steroid adsorbed. During the dissolution testing of a brand of contraceptive tablets containing norethindrone acetate, the presence of 0.5% (w/v) magnesium trisilicate in the medium resulted in almost complete reduction in the amount of the steroid remaining in solution after 1 hr.

Keyphrases □ Magnesium trisilicate—*in vitro* adsorption of various progestins, estrogens, and commercial contraceptive tablets □ Adsorption, *in vitro*—various progestins, estrogens, and commercial contraceptive tablets by magnesium trisilicate □ Progestins—ethindrone and norethindrone, *in vitro* adsorption by magnesium trisilicate □ Estrogens—ethinyl estradiol and mestranol, *in vitro* adsorption by magnesium trisilicate □ Contraceptives, oral—commercial product, *in vitro* adsorption by magnesium trisilicate □ Antacids—magnesium trisilicate, *in vitro* adsorption of various progestins, estrogens, and commercial contraceptive tablets

The adsorption of steroids at oil–water interfaces (1, 2) and at lipid surfaces (3) has been reported. In view of the adsorption on magnesium trisilicate of such drugs as prednisolone (4), digoxin (5), and digitoxin (5), the possible uptake of contraceptive steroids on this antacid cannot be ruled out.

Wagner (6) reported that the presence of a solid adsorbent interferes with drug absorption. The bioavailability of some drugs decreased when coadministered with antacids possessing adsorptive properties (7, 8). A recent report (9) confirmed the previously reported *in vitro* findings (5) that concurrent administration of digoxin with some antacids (including magnesium trisilicate) results in a significant reduction in digoxin bioavailability.

Table I—Equilibrium Aqueous Solubilities at 37 ± 0.1° of the Steroids and Monolayer Adsorption Values on 1% (w/v) Magnesium Trisilicate

Steroid	Aqueous Solubility, μmoles/liter	Monolayer Adsorption Value, mg/g
Ethindrone	2.9	0.32
Mestranol	4.8	0.25
Norethindrone	28.2	0.24
Ethinyl estradiol	33.7	—

The objective of the present work was to examine the *in vitro* adsorption on magnesium trisilicate of two progestins, norethindrone and its 10-methyl derivative ethindrone, and two estrogens, ethinyl estradiol and mestranol, of closely related chemical structure.

EXPERIMENTAL

Materials—Magnesium trisilicate powder BP[1] of 11.2-μm mean surface volume diameter was used. Ethindrone[2], ethinyl estradiol[3], mestranol[4], and norethindrone[5] were used as supplied. A batch of contraceptive tablets[6] was used in the dissolution studies. Chloroform and ethanol were analytical reagent grade[7].

Methods—*Adsorption Experiments*—Adsorption experiments were carried out at 37 ± 0.2° using 1% (w/v) magnesium trisilicate, as previously reported (5). After centrifugation, the steroid concentration remaining in the supernate was determined spectrophotometrically[8] at 240 nm (for ethindrone and norethindrone) and 280 nm (for ethinyl estradiol and mestranol) against a blank. A preextraction step with chloroform was necessary to eliminate the interference due to leachable materials from magnesium trisilicate.

Three replicate runs were made, and the results were averaged. Reproducibility was within ±3.0%.

Desorption Rates—The desorption rates of adsorbed ethindrone were determined at 37 ± 0.2° in both water and 0.05 *N* HCl over 3 hr as previously reported (5). The amount of steroid desorbed at a specified time was determined in the supernate after centrifugation as described earlier.

For ethindrone, the effect of the amount adsorbed on the extent of desorption after 3 hr was investigated.

Dissolution Testing—The dissolution rate of a brand of contraceptive tablets[6] was tested using the USP rotating-basket dissolution apparatus[9]. Two media were used: water and 0.5% (w/v) magnesium trisilicate in water. The dissolution medium (800 ml) was maintained at 37 ± 0.1°, and two tablets were used; the speed of rotation of the basket was 100 rpm. Samples were withdrawn after 0.5, 1, 2, and 3 hr. Fresh aliquots of water were added each time to maintain a constant volume.

The percentage of steroid in solution was calculated with reference to the labeled norethindrone acetate content. Determinations of the concentration of norethindrone acetate in solution were made in the aliquot withdrawn after centrifugation and extraction. Measurements were made at 240 nm.

[1] Evans Medical Ltd., England.
[2] Control No. 167017, WHO Centre for Chemical Reference Substances, Solna 3, Sweden.
[3] Batch 50187, Schering AG.
[4] Batch A 5365, Organon Laboratories Ltd., United Kingdom.
[5] Reference No. 1253, Organon Laboratories Ltd., United Kingdom.
[6] Anovlar 21, Batch 05-73-1070, Schering. Each tablet contained 4 mg of norethindrone acetate and 50 μg of ethinyl estradiol.
[7] British Drug Houses Ltd., Poole, England.
[8] Unicam SP 500 series 2 spectrophotometer.
[9] Erweka, Apparatebau GMBH, D-6056 Heusenstamm, West Germany.

(7) A. Bult and H. B. Klasen, *Pharm. Weekbl.*, **110**, 533 (1975).
(8) J. R. Demember and F. A. Wallace, *J. Am. Chem. Soc.*, **97**, 6240 (1975).
(9) W. J. Geary, *Coord. Chem. Rev.*, **7**, 81 (1971).
(10) A. Rastelli, P. G. de Benedetti, A. Albasini, G. Vampa, and M. Melegari, *Farmaco, Ed. Sci.*, **29**, 654 (1974).
(11) P. G. de Benedetti, A. Rastelli, A. Albasini, M. Melegari, and G. Vampa, *Atti Soc. Nat. Mat. Modena*, **105**, 73 (1974).
(12) G. J. Kruger and G. Gafner, *Acta Crystallogr., B*, **27**, 326 (1971).
(13) A. Bult, *Pharm. Weekbl.*, **111**, 385 (1976).

ACKNOWLEDGMENTS

The authors are indebted to Professor Dr. D. A. Doornbos and Dr. A. S. Horn for their help.

In Vitro Uptake of Oral Contraceptive Steroids by Magnesium Trisilicate

SALEH A. H. KHALIL *x and M. IWUAGWU

Received March 12, 1977, from the *School of Pharmacy, University of Benin, Benin City, Nigeria.* Accepted for publication May 27, 1977. *Present address: Department of Pharmaceutics, Faculty of Pharmacy, Alexandria University, Alexandria, Egypt.

Abstract □ Some steroids used in oral contraceptives were adsorbed significantly by magnesium trisilicate. The adsorption affinity followed the sequence: ethindrone > mestranol > norethindrone > ethinyl estradiol. Adsorption data obtained at relatively low initial concentrations fitted a Langmuir plot; the values for monolayer adsorption ranged between 0.24 and 0.32 mg/g. At higher concentrations of the steroids, multilayer adsorption occurred. The results of desorption experiments made at 37° in water and 0.05 *N* HCl suggested that desorption was incomplete and depended on the amount of steroid adsorbed. During the dissolution testing of a brand of contraceptive tablets containing norethindrone acetate, the presence of 0.5% (w/v) magnesium trisilicate in the medium resulted in almost complete reduction in the amount of the steroid remaining in solution after 1 hr.

Keyphrases □ Magnesium trisilicate—*in vitro* adsorption of various progestins, estrogens, and commercial contraceptive tablets □ Adsorption, *in vitro*—various progestins, estrogens, and commercial contraceptive tablets by magnesium trisilicate □ Progestins—ethindrone and norethindrone, *in vitro* adsorption by magnesium trisilicate □ Estrogens—ethinyl estradiol and mestranol, *in vitro* adsorption by magnesium trisilicate □ Contraceptives, oral—commercial product, *in vitro* adsorption by magnesium trisilicate □ Antacids—magnesium trisilicate, *in vitro* adsorption of various progestins, estrogens, and commercial contraceptive tablets

The adsorption of steroids at oil–water interfaces (1, 2) and at lipid surfaces (3) has been reported. In view of the adsorption on magnesium trisilicate of such drugs as prednisolone (4), digoxin (5), and digitoxin (5), the possible uptake of contraceptive steroids on this antacid cannot be ruled out.

Wagner (6) reported that the presence of a solid adsorbent interferes with drug absorption. The bioavailability of some drugs decreased when coadministered with antacids possessing adsorptive properties (7, 8). A recent report (9) confirmed the previously reported *in vitro* findings (5) that concurrent administration of digoxin with some antacids (including magnesium trisilicate) results in a significant reduction in digoxin bioavailability.

Table I—Equilibrium Aqueous Solubilities at 37 ± 0.1° of the Steroids and Monolayer Adsorption Values on 1% (w/v) Magnesium Trisilicate

Steroid	Aqueous Solubility, μmoles/liter	Monolayer Adsorption Value, mg/g
Ethindrone	2.9	0.32
Mestranol	4.8	0.25
Norethindrone	28.2	0.24
Ethinyl estradiol	33.7	—

The objective of the present work was to examine the *in vitro* adsorption on magnesium trisilicate of two progestins, norethindrone and its 10-methyl derivative ethindrone, and two estrogens, ethinyl estradiol and mestranol, of closely related chemical structure.

EXPERIMENTAL

Materials—Magnesium trisilicate powder BP[1] of 11.2-μm mean surface volume diameter was used. Ethindrone[2], ethinyl estradiol[3], mestranol[4], and norethindrone[5] were used as supplied. A batch of contraceptive tablets[6] was used in the dissolution studies. Chloroform and ethanol were analytical reagent grade[7].

Methods—*Adsorption Experiments*—Adsorption experiments were carried out at 37 ± 0.2° using 1% (w/v) magnesium trisilicate, as previously reported (5). After centrifugation, the steroid concentration remaining in the supernate was determined spectrophotometrically[8] at 240 nm (for ethindrone and norethindrone) and 280 nm (for ethinyl estradiol and mestranol) against a blank. A preextraction step with chloroform was necessary to eliminate the interference due to leachable materials from magnesium trisilicate.

Three replicate runs were made, and the results were averaged. Reproducibility was within ±3.0%.

Desorption Rates—The desorption rates of adsorbed ethindrone were determined at 37 ± 0.2° in both water and 0.05 *N* HCl over 3 hr as previously reported (5). The amount of steroid desorbed at a specified time was determined in the supernate after centrifugation as described earlier.

For ethindrone, the effect of the amount adsorbed on the extent of desorption after 3 hr was investigated.

Dissolution Testing—The dissolution rate of a brand of contraceptive tablets[6] was tested using the USP rotating-basket dissolution apparatus[9]. Two media were used: water and 0.5% (w/v) magnesium trisilicate in water. The dissolution medium (800 ml) was maintained at 37 ± 0.1°, and two tablets were used; the speed of rotation of the basket was 100 rpm. Samples were withdrawn after 0.5, 1, 2, and 3 hr. Fresh aliquots of water were added each time to maintain a constant volume.

The percentage of steroid in solution was calculated with reference to the labeled norethindrone acetate content. Determinations of the concentration of norethindrone acetate in solution were made in the aliquot withdrawn after centrifugation and extraction. Measurements were made at 240 nm.

[1] Evans Medical Ltd., England.
[2] Control No. 167017, WHO Centre for Chemical Reference Substances, Solna 3, Sweden.
[3] Batch 50187, Schering AG.
[4] Batch A 5365, Organon Laboratories Ltd., United Kingdom.
[5] Reference No. 1253, Organon Laboratories Ltd., United Kingdom.
[6] Anovlar 21, Batch 05-73-1070, Schering. Each tablet contained 4 mg of norethindrone acetate and 50 μg of ethinyl estradiol.
[7] British Drug Houses Ltd., Poole, England.
[8] Unicam SP 500 series 2 spectrophotometer.
[9] Erweka, Apparatebau GMBH, D-6056 Heusenstamm, West Germany.

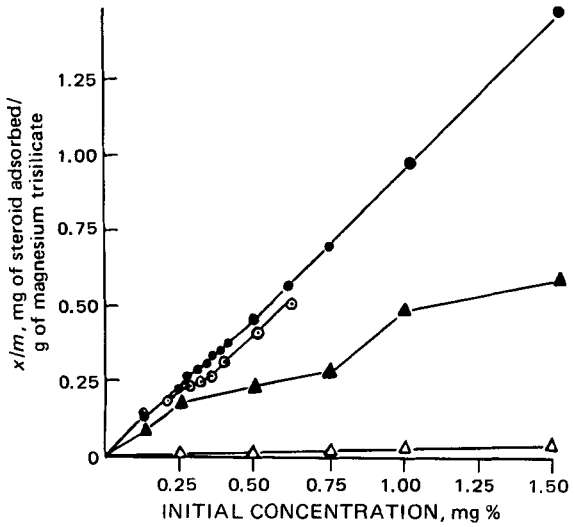

Figure 1—*Adsorption plots of some contraceptive steroids on 1% (w/v) magnesium trisilicate at 37°. Key: ●, ethindrone; ⊙, mestranol; ▲, norethindrone; and △, ethinyl estradiol.*

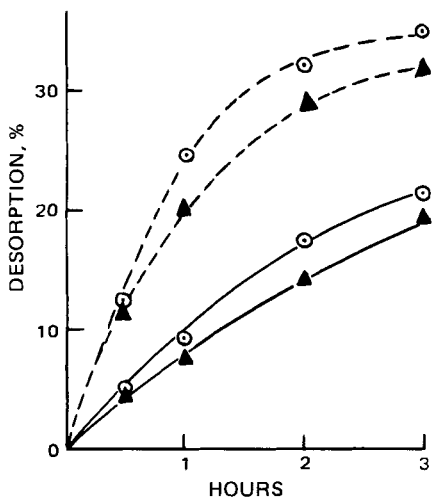

Figure 2—*Desorption rate at 37° in 0.05 N HCl (- - -) and water (—) for norethindrone (⊙) and ethindrone (▲). Amount of adsorbed steroid = 0.25 mg/g.*

Equilibrium Solubilities—The equilibrium solubilities of the steroids in water were determined by equilibrating excess steroid in glass-stoppered flasks at 37 ± 0.1° for 24 hr. Samples were filtered through a membrane filter[10] (0.2-μm mean pore diameter), which had been shown not to adsorb the steroids. The filtered samples were assayed by measurements at either 240 or 280 nm.

RESULTS AND DISCUSSION

Preliminary experiments showed that equilibrium was attained within 3–12 hr, depending on the steroid used and its initial concentrations. Figure 1 shows the adsorption plots for the four steroids. The extent of adsorption followed the sequence: ethindrone > mestranol > norethindrone > ethinyl estradiol.

Ethinyl estradiol was very slightly adsorbed (<6.5%) over the concentrations used. Unlike the norethindrone adsorption plot, the plots of both ethindrone and mestranol showed relatively less extended plateau regions over which monolayer adsorption occurred. At relatively low initial concentrations, the adsorption data fitted a Langmuir plot. Values of the monolayer adsorption, calculated from the reciprocal of slopes of the linear plots, are shown in Table I together with the equilibrium aqueous solubilities determined at 37 ± 0.1°.

The insignificant adsorption of ethinyl estradiol on the antacid was believed to be due to the partial ionization of the phenolic group of ring A at the pH 9.6 of the medium. When the pH of the medium was preadjusted to 4.5–9.0, no significant change in the extent of adsorption was observed. Only a slight increase from 6.5 to 9.0% occurred for an initial concentration of 1.0 mg % of the steroid.

[10] Sartorius, GMBH, 34 Göttingen, West Germany.

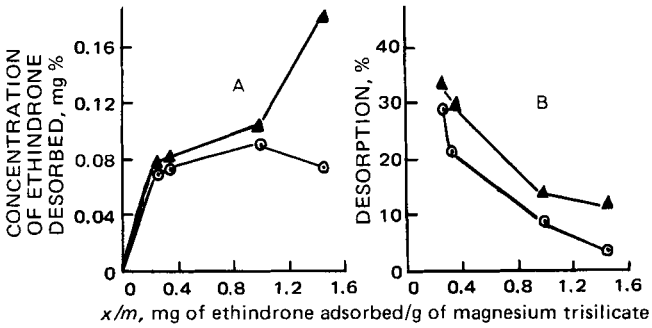

Figure 3—*Results of desorption of ethindrone after 3 hr as a function of amount of adsorbed steroid in 0.05 N HCl (▲) and water (⊙).*

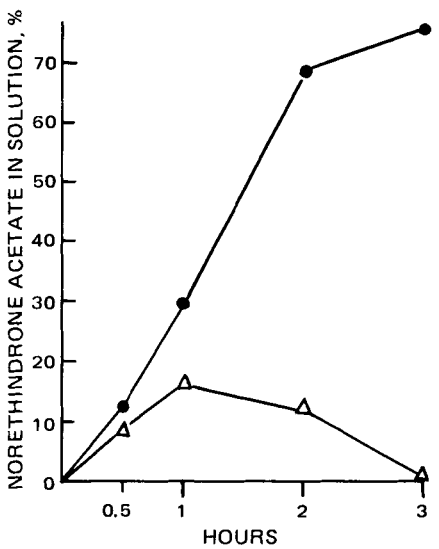

Figure 4—*Results of dissolution testing of a brand of contraceptive tablets at 37° in water (●) and in water containing 0.5% (w/v) magnesium trisilicate (△).*

The minor differences in the chemical structure of the four steroids were probably responsible for the observed variation in the extent of adsorption. While ethinyl estradiol was insignificantly adsorbed over the concentrations used, its 3-methyl ether, mestranol, was adsorbed significantly. Similarly, norethindrone was relatively less adsorbed than its 10-methyl derivative, ethindrone. That a slight change in the chemical structure of a drug affects the extent of its adsorption on magnesium trisilicate was previously shown for digoxin and digitoxin (5) and atropine and hyoscine (10).

The four steroids examined possess varying relative polarity, as reflected by the equilibrium solubilities in water (Table I). With the more polar steroids, the extent of adsorption was decreased. This result is in agreement with the findings of Patrick and Eberman (11) who concluded that, for a given solvent, the more soluble solutes are generally less strongly adsorbed than the less soluble solutes.

The results of desorption experiments using ethindrone and norethindrone are shown in Fig. 2. In the two media, norethindrone was relatively more desorbed than ethindrone. Because of the decomposition of the antacid in 0.05 *N* HCl, desorption rates in this medium were relatively higher than in water. However, in spite of the extensive decomposition of the antacid in 0.05 *N* HCl [about 82%, as was determined from the amount of magnesium ions released (5)], desorption was incomplete and did not exceed 35%. This result is probably due to readsorption on the silica gel formed from decomposition of the antacid in an acid medium.

The effect of the amount of ethindrone adsorbed (*x/m* values) on the extent of desorption after 3 hr was studied (Fig. 3). In water, variations

in the x/m values from 0.25 to 1.44 mg/g produced from 0.07 to 0.09 mg % of desorbed ethindrone (Fig. 3A). In 0.05 N HCl, the amounts of ethindrone desorbed were relatively higher. When the amounts of steroid desorbed were converted to percentages desorption (with reference to the x/m values), a gradual decrease occurred as the x/m values were increased (Fig. 3B).

The results of dissolution testing of the brand of contraceptive tablets in both water and 0.5% (w/v) magnesium trisilicate are shown in Fig. 4. The presence of the antacid in the medium drastically decreased the concentration of norethindrone acetate in solution. After 3 hr, the concentration of steroid in solution was less than 2%, compared with 75.2% in water. The reduction in concentration of steroid was a direct result of the adsorption onto the antacid particles.

It is suggested that the concurrent administration of magnesium trisilicate and oral contraceptive tablets containing the steroids tested might interfere with the steroid absorption. A recent report (9) that confirmed the decreased bioavailability in humans of digoxin in the presence of magnesium trisilicate lends supporting evidence to this suggestion.

REFERENCES

(1) A. Munck, *Biochim. Biophys. Acta*, **24**, 507 (1957).

(2) J. F. Baret and R. Roux, *C. R. Acad. Sci., Sci. Ser. C*, **266**, 243 (1968).

(3) A. T. Florence and R. Rahman, *J. Pharm. Pharmacol.*, **25**, 942 (1973).

(4) T. Chulski and A. A. Forist, *J. Am. Pharm. Assoc., Sci. Ed.*, **47**, 553 (1958).

(5) S. A. H. Khalil, *J. Pharm. Pharmacol.*, **26**, 961 (1974).

(6) J. G. Wagner, *Can. J. Pharm. Sci.*, **1**, 55 (1966).

(7) G. J. L. Hall and A. E. Davis, *Med. J. Aust.*, **2**, 95 (1969).

(8) F. M. Forrest, I. S. Forrest, and M. T. Serra, *Biol. Psychiat.*, **2**, 53 (1970).

(9) D. D. Brown and R. P. Juhl, *N. Engl. J. Med.*, **295**, 1034 (1976).

(10) S. El-Masry and S. A. H. Khalil, *J. Pharm. Pharmacol.*, **26**, 243 (1974).

(11) W. A. Patrick and N. F. Eberman, *J. Phys. Chem.*, **29**, 220 (1925).

ACKNOWLEDGMENTS

Presented in part at the 113th British Pharmaceutical Conference, St. Andrews, Scotland, September 1976.

Improved Colorimetric Determination of Aspirin and Salicylic Acid Concentrations in Human Plasma

I. A. MUNI *, J. L. LEELING ˣ, R. J. HELMS, N. JOHNSON, Jr., J. J. BARE, and B. M. PHILLIPS

Received April 4, 1977, from the *Toxicology Department, Miles Laboratories, Inc., Elkhart, IN 46514.* Accepted for publication May 26, 1977. *Present address: J. T. Baker Diagnostics, Bethlehem, PA 18017.

Abstract □ An improvement in a previously described method for the determination of plasma salicylic acid and aspirin levels in humans is described. The procedure was simplified by employing only one plasma sample for both salicylates. More accurate estimation of salicylates, particularly aspirin, was achieved by using two different calibration curves. Salicylic acid was estimated by reaction with an aqueous solution of the Folin–Ciocalteu phenol reagent. Absorbance of the blue-colored complex, which formed on addition of sodium hydroxide, was measured at 670 nm. The influence of alkalinity in the formation of the colored complex is discussed. The average recovery of aspirin added to plasma was 94.61%; it was 214.72% by the previous method.

Keyphrases □ Aspirin—colorimetric analysis in human plasma □ Salicylic acid—colorimetric analysis in human plasma □ Colorimetry—analyses, aspirin and salicylic acid in human plasma □ Analgesics—aspirin and salicylic acid, colorimetric analyses in human plasma

Aspirin is hydrolyzed rapidly *in vivo* to salicylic acid (1–3). Determination of blood levels of both salicylates is of considerable pharmaceutical and clinical interest. Several spectrometric procedures are available (4–6) for the estimation of these salicylates after aspirin ingestion.

The colorimetric method of Smith (4), utilizing Folin–Ciocalteu phenol reagent, is used commonly to quantitate salicylates in plasma (Scheme I). The absorbance density of the colored complex formed in alkaline solution is read at 670 nm, and the salicylic acid concentration is obtained from a standard calibration curve. The aspirin concentration is estimated from the difference between free (nonhydrolyzed) and total (hydrolyzed) salicylates.

Table I—Typical Recoveries of Salicylic Acid

Added, μg[a]	Found, μg[b] Nonhydrolyzed Curve[c]	Found, μg[b] Hydrolyzed Curve[d]
5	5.25 ± 0.63	3.08 ± 0.55
10	10.50 ± 0.90	7.00 ± 0.66
20	21.67 ± 2.04	15.92 ± 1.67
25	23.90 ± 0.85	17.33 ± 1.04
40	42.33 ± 0.50	32.25 ± 0.43

[a] Amounts of salicylic acid in distilled water added per milliliter of human plasma sample. [b] n = 3. [c] Free curve, approximate pH 9.6 (Smith method, improved method). [d] Approximate pH 10.4 (improved method; used for total salicylates and aspirin determination).

When this general procedure was applied in this laboratory in bioavailability studies of various aspirin dosage forms in human volunteers, the absorbance intensity of the colored complex was extremely pH dependent. Furthermore, the Smith method (nonhydrolyzed standard curve) resulted in much higher recoveries of total salicylates and aspirin from human plasma because the final pH values of the colored solutions read at 670 nm are different for free (pH 9.6) and total (pH 10.4) samples. The average difference in pH values, about 0.8 unit higher in total (hydrolyzed) samples, is due to an additional amount of 0.5 ml of 1.5 N NaOH in the final test solution. As far as could be determined, the correlation between the alkalinity of a test solution and the absorbance of the colored complex has not been reported. Such a pH influence could be important in the estimation of salicylates, particularly aspirin.

The present report describes a modification of the Smith

in the x/m values from 0.25 to 1.44 mg/g produced from 0.07 to 0.09 mg % of desorbed ethindrone (Fig. 3A). In 0.05 N HCl, the amounts of ethindrone desorbed were relatively higher. When the amounts of steroid desorbed were converted to percentages desorption (with reference to the x/m values), a gradual decrease occurred as the x/m values were increased (Fig. 3B).

The results of dissolution testing of the brand of contraceptive tablets in both water and 0.5% (w/v) magnesium trisilicate are shown in Fig. 4. The presence of the antacid in the medium drastically decreased the concentration of norethindrone acetate in solution. After 3 hr, the concentration of steroid in solution was less than 2%, compared with 75.2% in water. The reduction in concentration of steroid was a direct result of the adsorption onto the antacid particles.

It is suggested that the concurrent administration of magnesium trisilicate and oral contraceptive tablets containing the steroids tested might interfere with the steroid absorption. A recent report (9) that confirmed the decreased bioavailability in humans of digoxin in the presence of magnesium trisilicate lends supporting evidence to this suggestion.

REFERENCES

(1) A. Munck, *Biochim. Biophys. Acta*, **24**, 507 (1957).

(2) J. F. Baret and R. Roux, *C. R. Acad. Sci., Sci. Ser. C*, **266**, 243 (1968).

(3) A. T. Florence and R. Rahman, *J. Pharm. Pharmacol.*, **25**, 942 (1973).

(4) T. Chulski and A. A. Forist, *J. Am. Pharm. Assoc., Sci. Ed.*, **47**, 553 (1958).

(5) S. A. H. Khalil, *J. Pharm. Pharmacol.*, **26**, 961 (1974).

(6) J. G. Wagner, *Can. J. Pharm. Sci.*, **1**, 55 (1966).

(7) G. J. L. Hall and A. E. Davis, *Med. J. Aust.*, **2**, 95 (1969).

(8) F. M. Forrest, I. S. Forrest, and M. T. Serra, *Biol. Psychiat.*, **2**, 53 (1970).

(9) D. D. Brown and R. P. Juhl, *N. Engl. J. Med.*, **295**, 1034 (1976).

(10) S. El-Masry and S. A. H. Khalil, *J. Pharm. Pharmacol.*, **26**, 243 (1974).

(11) W. A. Patrick and N. F. Eberman, *J. Phys. Chem.*, **29**, 220 (1925).

ACKNOWLEDGMENTS

Presented in part at the 113th British Pharmaceutical Conference, St. Andrews, Scotland, September 1976.

Improved Colorimetric Determination of Aspirin and Salicylic Acid Concentrations in Human Plasma

I. A. MUNI *, J. L. LEELING ˣ, R. J. HELMS, N. JOHNSON, Jr., J. J. BARE, and B. M. PHILLIPS

Received April 4, 1977, from the *Toxicology Department, Miles Laboratories, Inc., Elkhart, IN 46514.* Accepted for publication May 26, 1977. *Present address: J. T. Baker Diagnostics, Bethlehem, PA 18017.

Abstract □ An improvement in a previously described method for the determination of plasma salicylic acid and aspirin levels in humans is described. The procedure was simplified by employing only one plasma sample for both salicylates. More accurate estimation of salicylates, particularly aspirin, was achieved by using two different calibration curves. Salicylic acid was estimated by reaction with an aqueous solution of the Folin–Ciocalteu phenol reagent. Absorbance of the blue-colored complex, which formed on addition of sodium hydroxide, was measured at 670 nm. The influence of alkalinity in the formation of the colored complex is discussed. The average recovery of aspirin added to plasma was 94.61%; it was 214.72% by the previous method.

Keyphrases □ Aspirin—colorimetric analysis in human plasma □ Salicylic acid—colorimetric analysis in human plasma □ Colorimetry—analyses, aspirin and salicylic acid in human plasma □ Analgesics—aspirin and salicylic acid, colorimetric analyses in human plasma

Aspirin is hydrolyzed rapidly *in vivo* to salicylic acid (1–3). Determination of blood levels of both salicylates is of considerable pharmaceutical and clinical interest. Several spectrometric procedures are available (4–6) for the estimation of these salicylates after aspirin ingestion.

The colorimetric method of Smith (4), utilizing Folin–Ciocalteu phenol reagent, is used commonly to quantitate salicylates in plasma (Scheme I). The absorbance density of the colored complex formed in alkaline solution is read at 670 nm, and the salicylic acid concentration is obtained from a standard calibration curve. The aspirin concentration is estimated from the difference between free (nonhydrolyzed) and total (hydrolyzed) salicylates.

Table I—Typical Recoveries of Salicylic Acid

Added, μg[a]	Found, μg[b] Nonhydrolyzed Curve[c]	Found, μg[b] Hydrolyzed Curve[d]
5	5.25 ± 0.63	3.08 ± 0.55
10	10.50 ± 0.90	7.00 ± 0.66
20	21.67 ± 2.04	15.92 ± 1.67
25	23.90 ± 0.85	17.33 ± 1.04
40	42.33 ± 0.50	32.25 ± 0.43

[a] Amounts of salicylic acid in distilled water added per milliliter of human plasma sample. [b] n = 3. [c] Free curve, approximate pH 9.6 (Smith method, improved method). [d] Approximate pH 10.4 (improved method; used for total salicylates and aspirin determination).

When this general procedure was applied in this laboratory in bioavailability studies of various aspirin dosage forms in human volunteers, the absorbance intensity of the colored complex was extremely pH dependent. Furthermore, the Smith method (nonhydrolyzed standard curve) resulted in much higher recoveries of total salicylates and aspirin from human plasma because the final pH values of the colored solutions read at 670 nm are different for free (pH 9.6) and total (pH 10.4) samples. The average difference in pH values, about 0.8 unit higher in total (hydrolyzed) samples, is due to an additional amount of 0.5 ml of 1.5 N NaOH in the final test solution. As far as could be determined, the correlation between the alkalinity of a test solution and the absorbance of the colored complex has not been reported. Such a pH influence could be important in the estimation of salicylates, particularly aspirin.

The present report describes a modification of the Smith

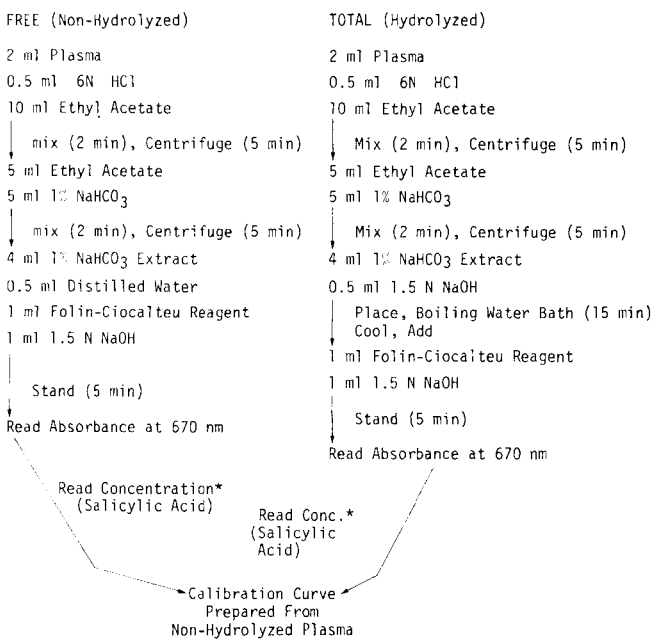

*Scheme I—Flow chart of the Smith (4) method. *Blank plasma absorbance is subtracted before the concentration of salicylic acid is read.*

*Scheme II—Flow chart of the improved method. *Blank plasma absorbance is subtracted before the concentration of salicylic acid is read.*

method (4); it is simpler and gives more accurate results in the assay of salicylic acid, total salicylates, and aspirin in human plasma. Recoveries of salicylates from human plasma, as determined by the Smith method and by the modified method, are also reported.

EXPERIMENTAL

Chemicals—Pure salicylic acid[1], mp 157–159°, and aspirin[1], mp 135–137°, were used. All solvents were analytical grade. Folin–Ciocalteu phenol reagent[2] (diluted 1:3 with distilled water) was used for the colorimetric determination of salicylates.

Apparatus—A spectrophotometer[3] with an optical system providing a wavelength range from 220 to 1000 nm was used. The alkalinity of various samples was measured with a pH meter[4].

Plasma Extraction—Plasma samples, including blanks, were extracted according to Schemes I and II.

Colorimetric Analysis—All samples were read at 670 nm. A distilled water solution containing 1% $NaHCO_3$ was used as a reference. The samples were read 7–20 min after the addition of 1 ml of 1.5 *N* NaOH. In each instance, the pH of the final solution was measured before the absorbance was read.

pH Studies—The effect of varying pH on the absorbance intensity of the colored complex was studied using different concentrations of salicylic acid in 4 ml of 1% $NaHCO_3$ solutions (Scheme II). The total volume of each test sample at the time of the absorbance measurement was kept constant (6.5 ml). The pH was varied from 8.9 to 11.7 by adding different volumes of sodium hydroxide solutions of various normalities. The final volumes were adjusted to 6.5 ml by adding appropriate volumes of distilled water.

Preparation of Calibration Curves—Various concentrations of salicylic acid and aspirin in distilled water were added to plasma samples, which were processed as shown in Scheme II. The concentrations of salicylic acid *versus* their respective absorbances (aspirin was hydrolyzed to salicylic acid) were plotted on coordinate graph paper.

Recovery Studies—Several different concentrations of salicylates (mixtures of salicylic acid and aspirin in distilled water) were added to human plasma, and the samples were processed as shown in Schemes I and II. Recoveries of salicylates were calculated, after subtracting blank values, by employing only one calibration curve, free (nonhydrolyzed) or by using both the free (nonhydrolyzed) and total (hydrolyzed) calibration curves.

RESULTS AND DISCUSSION

Smith (4) used two different plasma samples (2 ml each), one for the analysis of salicylic acid and the other for aspirin analysis. The present simplified method employs only one plasma sample (2 ml); the sodium bicarbonate extract is divided into halves, one for salicylic acid analysis and the other for aspirin assay (Schemes I and II). This step reduces the

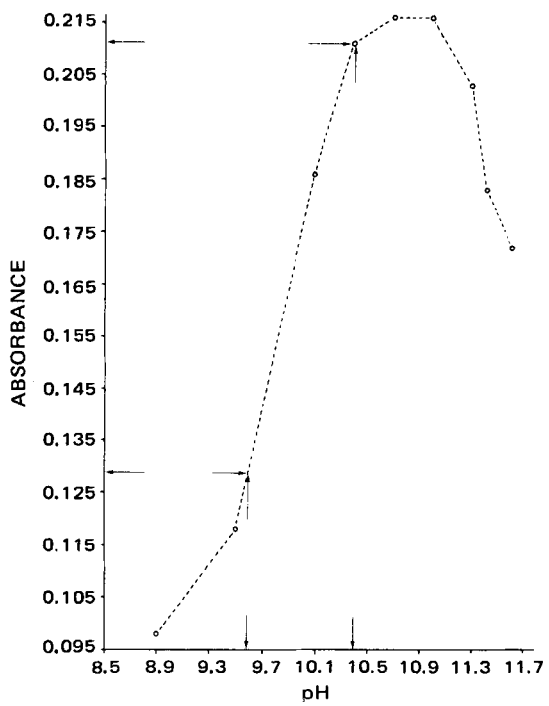

Figure 1—*Absorbance at various pH values.*

[1] Dow Chemical Co., Midland, Mich.
[2] Fisher Scientific Co., Fair Lawn, N.J.
[3] DU model 2400, Beckman Instruments, Fullerton, Calif.
[4] Zeromatic II, Beckman Instruments, Fullerton, Calif.

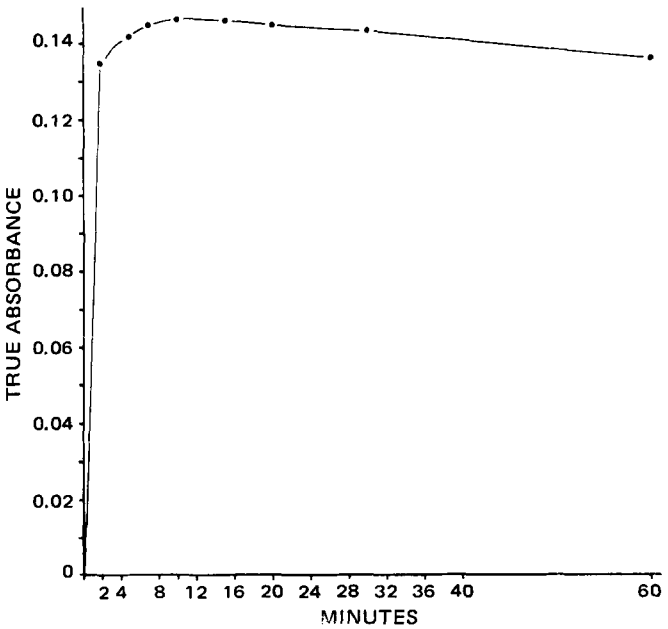

Figure 2—*Folin–Ciocalteu reagent color formation.*

volume of plasma needed for the complete analysis and eliminates two additional extraction steps. Improved accuracy was achieved by using two (nonhydrolyzed and hydrolyzed) calibration curves for the estimation of salicylic acid and total salicylate and, by difference, aspirin.

The reason for using two calibration curves is as follows. The absorbance intensity of the colored complex (a reduced form of molybdenum and tungsten) is extremely pH dependent. The final pH of the colored complex solution from nonhydrolyzed plasma (Smith referred to it as "free") was 9.61 ± 0.01 (n = 50), while the average pH of the hydrolyzed test samples (Smith's "total salicylates") was 10.41 ± 0.01 (n = 50). This result is probably due to the excess amount of 1.5 N NaOH added to the test samples for aspirin hydrolysis. Absorbance intensities of colored solutions containing similar concentrations of salicylic acid are markedly different at pH 9.6 and 10.4 (Fig. 1). Therefore, reading the values of both salicylic acid and total salicylate from a single curve prepared either at pH 9.6, as described by Smith, or at pH 10.4 gives erroneous results.

Tables I and II summarize the salicylate recovery data obtained. Average recoveries of aspirin (total salicylates − free salicylic acid/0.767) from human plasma were 214.72 ± 9.66, 169.71 ± 8.22, or 94.61 ± 11.68%

Table II—Typical Recoveries of Aspirin

Added, μg[a]	Found, μg[b]		
	Both Curves[c]	Nonhydrolyzed Curve[d]	Hydrolyzed Curve[e]
2.5	2.06 ± 1.46	5.00 ± 2.74	3.91 ± 2.17
5.0	3.26 ± 0.99	10.00 ± 1.21	7.82 ± 0.82
10.0	8.15 ± 2.54	19.99 ± 2.46	15.65 ± 2.07
12.5	14.67 ± 1.49	28.25 ± 2.33	23.22 ± 1.27
20.0	25.32 ± 0.76	49.54 ± 0.68	38.70 ± 0.77

[a] Amounts of aspirin in distilled water added per milliliter of human plasma sample. [b] n = 3. [c] Nonhydrolyzed curve and hydrolyzed curve (recommended for salicylic acid, total salicylates, and aspirin estimations). [d] Approximate pH 9.6 (recommended for salicylic acid estimation). [e] Approximate pH 10.4 (improved method; recommended for total salicylates and aspirin determination).

using a nonhydrolyzed curve (prepared as described by Smith and represented by $y = 0.0033x + 0.0017$), a hydrolyzed curve ($y = 0.0042x + 0.0073$), or both calibration curves, respectively. It is readily apparent from these data that the results obtained with two curves are more reliable than with either curve separately.

Figure 2 illustrates the rate of development and fading of the Folin–Ciocalteu blue color at room temperature. This finding was in general agreement with Smith's observation, and the time interval of 7–20 min was selected for measuring the absorbance of test samples.

In conclusion, the presently reported procedure, which is a modification of Smith's method for the estimation of plasma levels of salicylic acid and aspirin, is simpler and more accurate.

REFERENCES

(1) D. Lester, G. Lolli, and L. A. Greenberg, *J. Pharmacol. Exp. Ther.*, **87**, 329 (1946).

(2) P. K. Smith, H. L. Gleason, C. G. Stoll, and S. Ogorzalek, *ibid.*, **87**, 237 (1946).

(3) J. R. Leonards, *Proc. Soc. Exp. Biol. Med.*, **110**, 304 (1962).

(4) M. J. H. Smith, *J. Pharm. Pharmacol.*, **3**, 409 (1951).

(5) W. E. Lange and S. A. Bell, *J. Pharm. Sci.*, **55**, 386 (1966).

(6) K. O'Dean, J. Pütler, and F. Hoffmeister, *Arzneim.-Forsch.*, **25**, 801 (1975).

ACKNOWLEDGMENTS

Presented in part at the 10th Great Lakes Regional American Chemical Society Meeting, Evanston, Ill., June 1976.

The authors gratefully acknowledge the assistance of Mr. Larry Craigo, Mr. Rick Minegar, and Mr. Carl Myers.

Comparison of Plasma Creatinine Levels in Patients Determined by High-Pressure Liquid Chromatography, Automated Analysis, and Boiling Alkaline Picrate Method

Keyphrases □ Creatinine—analyses by high-pressure liquid chromatography, automated analysis, and alkaline picrate method compared, human plasma □ High-pressure liquid chromatography—analysis, creatinine in human plasma, compared to automated analysis and alkaline picrate method □ Automated analysis—creatinine in human plasma, compared to high-pressure liquid chromatography and alkaline picrate method □ Alkaline picrate—analysis, creatinine in human plasma, compared to high-pressure liquid chromatography and automated analysis method

To the Editor:

Accurate determinations of endogenous creatinine levels in plasma or serum are important to the diagnosis of renal function and the modification of dosage regimens in patients with renal diseases (1, 2). The potential interference problems associated with many presently used procedures have been reviewed (3, 4).

This communication reports findings on the plasma creatinine levels as determined by three different methods using the same batch of plasma samples from some 30 patients with various degrees of renal function. These creatinine assays included an automated analysis[1] routinely performed in many hospitals, a boiling alkaline picrate method (5), and a rapid, micro high-pressure liquid chromatographic (HPLC) method recently developed in this laboratory (4).

The HPLC method involves vortex mixing of plasma with acetonitrile (1:2.5 v/v) and chromatographing the supernate on an ion-exchange column, using acidified 0.1 *M* ammonium phosphate as the mobile phase. Although ammonium chloride was used in earlier studies, ammonium phosphate offers the same separation and is superior in inertness toward the HPLC system.

The results are summarized in Table I. In general, the values obtained from the boiling alkaline picrate method were higher than those from automated analysis which, in turn, were greater than those from HPLC. The average creatinine levels of these plasma samples assayed by the automated analysis and the boiling alkaline picrate method were 14.55% (n = 30) and 32.41% (n = 28), respectively, greater than the level obtained by HPLC. The differences ranged from −12.8 to +45.2% for the automated analysis and from −15.3 to +101.6% for the boiling alkaline picrate method.

Table I—Comparison of Plasma Creatinine Levels of Patients Determined by Three Different Methods

	Creatinine Levels, mg % Determined by			Percent Deviation from HPLC	
Patient	HPLC	Automated Analysis	Boiling Alkaline Picrate	Automated Analysis	Boiling Alkaline Picrate
1	2.16	2.2	2.63	+1.85	+21.76
2	2.62	3.2	3.70	+22.14	+41.22
3	2.79	3.8	3.90	+36.20	+39.78
4	5.79	7.4	7.43	+27.81	+28.32
5	1.63	2.2	2.43	+34.97	+49.08
6	2.42	3.3	4.10	+36.36	+69.42
7	2.21	2.7	2.82	+2.17	+27.60
8	0.65	0.7	1.25	+7.69	+92.31
9	0.68	0.8	1.16	+17.65	+70.59
10	0.62	0.9	1.25	+45.16	+101.61
11	0.91	1.0	1.45	+9.89	+59.34
12	1.88	2.2	2.53	+17.02	+34.57
13	1.90	2.3	3.02	+21.05	+58.95
14	2.10	2.6	3.12	+23.81	+48.57
15	2.92	3.2	3.61	+9.59	+23.63
16	3.00	3.3	3.51	+10.00	+17.00
17	4.08	4.1	4.29	+0.49	+5.15
18	4.35	4.4	4.98	+1.15	+14.48
19	4.95	4.6	5.47	−7.07	+10.51
20	4.29	4.6	5.27	+7.23	+22.84
21	6.08	5.3	5.67	−12.83	−6.74
22	5.35	5.8	5.96	+8.41	+11.40
23	8.46	8.7	8.70	+2.84	+2.84
24	9.50	10.2	9.29	+7.37	−2.21
25	13.33	12.9	11.35	−3.22	−14.85
26	12.92	14.1	13.51	+9.13	+4.57
27	18.50	18.6	15.67	+0.54	−15.30
28	10.67	12.3	12.24	+15.28	+12.83
29	9.67	10.2	—	+5.48	—
30	15.00	16.8	—	+12.00	—
				Mean ± SD 14.55 ± 11.87	32.41 ± 27.26

The overestimation of plasma or serum creatinine levels determined by either the automated analysis or manual method using the principle of complexation between creatinine and picric acid is well documented (4). This overestimation is due to the presence of endogenous substances (pseudocreatinine), which also can react with the picrate reagent. The results of the present study are consistent with these previous findings, since the HPLC method is

[1] SAM-6, Technicon Instruments Corp., Tarrytown, N.Y.

free of these interferences and only measures the "true" creatinine.

The boiling alkaline picrate method has been claimed to measure the true creatinine (5). The results of the present study do not support the claim. In a previous study (3), the "apparent" recovery of the spiked creatinine in plasma was only 81% and, after heat treatment, certain components in plasma were thought to suppress the creatinine–picrate complex reaction or to interfere with the color formation. Thus, the reason for the higher creatinine values by the boiling alkaline picrate method remains to be determined.

(1) W. L. Chiou and F. H. Hsu, *J. Clin. Pharmacol.*, **15**, 427 (1975).
(2) W. L. Chiou and F. H. Hsu, *Res. Commun. Chem. Pathol. Pharmacol.*, **9**, 315 (1975).
(3) W. L. Chiou, F. H. Hsu, and G. W. Peng, *Clin. Chem.*, **23**, 1374 (1977).
(4) W. L. Chiou, M. A. F. Gadalla, and G. W. Peng, *J. Pharm. Sci.*, **67**, 182 (1978).
(5) H. Yatzids, *Clin. Chem.*, **21**, 1848 (1975).

Win L. Chiou ˣ
Geoffrey W. Peng
M. A. F. Gadalla
Clinical Pharmacokinetics Laboratory
College of Pharmacy
University of Illinois at the Medical Center
Chicago, IL 60612
Samuel T. Nerenberg
Department of Pathology
College of Medicine
University of Illinois at the Medical Center
Chicago, IL 60612

Received October 7, 1977.
Accepted for publication November 8, 1977.

BOOKS

REVIEWS

Practical Clinical Pharmacy. Edited by CHARLES A. WALKER and JOHN R. FOXX. Stratton, 381 Park Avenue South, New York, NY 10016. 1977. x + 142 pp. 15 × 23 cm. Price $16.95.

The reader approaches a book called "Practical Clinical Pharmacy" with expectations of gaining insight into techniques of monitoring drug therapy, strategies for improving pharmacist–prescriber and pharmacist–patient communications, and data on the clinical pharmacology and therapeutic use of drugs. What the reader receives in lieu of this critical information is a collection of philosophical discussions on the role and potential for clinical pharmacy practice.

The book contains 14 presentations delivered at the "First Annual Symposium on a Clinical Pharmacy Program" sponsored by the School of Pharmacy at Florida A & M University; the date of the symposium is not disclosed. The presentations are organized under three themes: (*a*) the clinical curricula, (*b*) the role and liabilities of a clinical pharmacist, and (*c*) other health professionals' view of clinical pharmacy. The most informative discussions are by Roger Palmer on "The Role of Clinical Pharmacology and Pharmacokinetics in a Clinical Pharmacy Program" and by Charles Walker and Karam Soliman on "The Clinical Pharmacist's Role in Research and Therapeutics."

Perhaps the book is an appropriate addition to health professions libraries. It is an unlikely choice for personal purchase.

Reviewed by Gerald E. Schumacher
College of Pharmacy and Allied Health Professions
Wayne State University
Detroit, MI 48202

Design of Biopharmaceutical Properties through Prodrugs and Analogs. Edited by EDWARD B. ROCHE. American Pharmaceutical Association, 2215 Constitution Avenue, N.W., Washington, DC 20037. 1977. 455 pp. 16 × 23 cm. Price $20.00, $13.00 Member Rate.

This series of 15 papers was presented at Orlando in November 1976 and published less than 1 year later! Congratulations to the editor, authors, and APhA.

Papers of particular interest are "Structural Aspects of Selective Distribution" by Roche with 34 references, which provides a good background for "Structural Effects of Partitioning Behavior of Drugs" by Dunn (13 references), and "Correlation Analysis in the Design of Pharmacodynamic Properties of Drugs" by Hansch (12 references). Also of special interest are "Alteration of Pharmacokinetics through Structural Modification" by Notari (34 references), "Novel Approaches for the Design of Membrane Transport Properties of Drugs" by Bodor (38 references), and "Physical Model Approach to the Design of Drugs with Improved Intestinal Absorption" by Ho, Park, Morozowich, and W. Higuchi. The latter, with 91 pages (89 references), is well worth the price of the book. It should be of particular value to students.

"The Prediction of Chemical Liability through Substituent Effects" by Charton (68 references) contains a wealth of tabulated data and constants. In "Alteration of Drug Metabolism through Structural Modification" by Nelson is a very useful list of 112 pertinent references. Finally, Morozowich, Cho, and Kezdy put it all together in "Application of Physical Organic Principles to Prodrug Design" (93 references).

Considering the applied nature of this approach to designing useful agents, the editor might have given greater emphasis to the practical consideration that such modifications result in new compounds in the sense of requiring extensive and costly safety studies and provide no short cut in this critical area of testing. Also, it would have been helpful for those interested in this general approach to have at least listed the related approaches of molecular complexes, alternate salts, solid solutions, liposomal transport, *etc.*, as means of achieving useful drug modification.

Reviewed by Henry C. Caldwell
Research and Development
Smith Kline & French Laboratories
Philadelphia, PA 19101

Aspirin and Related Drugs: Their Actions and Uses. Edited by K. D. RAINSFORD, K. BRUNE, and M. W. WHITEHOUSE. Birkhauser Verlag, P. O. Box 34, CH-4010 Basel, Switzerland. 1977. 118 pp. 17 × 24 cm.

The 11 papers and introductory comments contained in this volume comprise the Symposium on Aspirin and Related Drugs held in conjunction with the Physiology Section, 47th Congress of the Australian and New Zealand Association for the Advancement of Science, on May 14, 1976 at the University of Tasmania, Hobart, Australia. The compilation of these papers provides a useful overview of the current research trends in Australia in the areas of salicylate pharmacology and toxicology.

While this book is not a comprehensive review of the pharmacology of nonsteroidal anti-inflammatory agents, it does provide insight into some current theories of anti-inflammatory and gastrotoxic mechanisms of action. Theories of anti-inflammatory modes of action discussed in this book include both the inhibition and stimulation of microsomal

free of these interferences and only measures the "true" creatinine.

The boiling alkaline picrate method has been claimed to measure the true creatinine (5). The results of the present study do not support the claim. In a previous study (3), the "apparent" recovery of the spiked creatinine in plasma was only 81% and, after heat treatment, certain components in plasma were thought to suppress the creatinine–picrate complex reaction or to interfere with the color formation. Thus, the reason for the higher creatinine values by the boiling alkaline picrate method remains to be determined.

(1) W. L. Chiou and F. H. Hsu, *J. Clin. Pharmacol.*, **15**, 427 (1975).
(2) W. L. Chiou and F. H. Hsu, *Res. Commun. Chem. Pathol. Pharmacol.*, **9**, 315 (1975).
(3) W. L. Chiou, F. H. Hsu, and G. W. Peng, *Clin. Chem.*, **23**, 1374 (1977).
(4) W. L. Chiou, M. A. F. Gadalla, and G. W. Peng, *J. Pharm. Sci.*, **67**, 182 (1978).
(5) H. Yatzids, *Clin. Chem.*, **21**, 1848 (1975).

Win L. Chiou ˣ
Geoffrey W. Peng
M. A. F. Gadalla
Clinical Pharmacokinetics Laboratory
College of Pharmacy
University of Illinois at the Medical Center
Chicago, IL 60612
Samuel T. Nerenberg
Department of Pathology
College of Medicine
University of Illinois at the Medical Center
Chicago, IL 60612

Received October 7, 1977.
Accepted for publication November 8, 1977.

BOOKS

REVIEWS

Practical Clinical Pharmacy. Edited by CHARLES A. WALKER and JOHN R. FOXX. Stratton, 381 Park Avenue South, New York, NY 10016. 1977. x + 142 pp. 15 × 23 cm. Price $16.95.

The reader approaches a book called "Practical Clinical Pharmacy" with expectations of gaining insight into techniques of monitoring drug therapy, strategies for improving pharmacist–prescriber and pharmacist–patient communications, and data on the clinical pharmacology and therapeutic use of drugs. What the reader receives in lieu of this critical information is a collection of philosophical discussions on the role and potential for clinical pharmacy practice.

The book contains 14 presentations delivered at the "First Annual Symposium on a Clinical Pharmacy Program" sponsored by the School of Pharmacy at Florida A & M University; the date of the symposium is not disclosed. The presentations are organized under three themes: (*a*) the clinical curricula, (*b*) the role and liabilities of a clinical pharmacist, and (*c*) other health professionals' view of clinical pharmacy. The most informative discussions are by Roger Palmer on "The Role of Clinical Pharmacology and Pharmacokinetics in a Clinical Pharmacy Program" and by Charles Walker and Karam Soliman on "The Clinical Pharmacist's Role in Research and Therapeutics."

Perhaps the book is an appropriate addition to health professions libraries. It is an unlikely choice for personal purchase.

Reviewed by Gerald E. Schumacher
College of Pharmacy and Allied Health Professions
Wayne State University
Detroit, MI 48202

Design of Biopharmaceutical Properties through Prodrugs and Analogs. Edited by EDWARD B. ROCHE. American Pharmaceutical Association, 2215 Constitution Avenue, N.W., Washington, DC 20037. 1977. 455 pp. 16 × 23 cm. Price $20.00, $13.00 Member Rate.

This series of 15 papers was presented at Orlando in November 1976 and published less than 1 year later! Congratulations to the editor, authors, and APhA.

Papers of particular interest are "Structural Aspects of Selective Distribution" by Roche with 34 references, which provides a good background for "Structural Effects of Partitioning Behavior of Drugs" by Dunn (13 references), and "Correlation Analysis in the Design of Pharmacodynamic Properties of Drugs" by Hansch (12 references). Also of special interest are "Alteration of Pharmacokinetics through Structural Modification" by Notari (34 references), "Novel Approaches for the Design of Membrane Transport Properties of Drugs" by Bodor (38 references), and "Physical Model Approach to the Design of Drugs with Improved Intestinal Absorption" by Ho, Park, Morozowich, and W. Higuchi. The latter, with 91 pages (89 references), is well worth the price of the book. It should be of particular value to students.

"The Prediction of Chemical Liability through Substituent Effects" by Charton (68 references) contains a wealth of tabulated data and constants. In "Alteration of Drug Metabolism through Structural Modification" by Nelson is a very useful list of 112 pertinent references. Finally, Morozowich, Cho, and Kezdy put it all together in "Application of Physical Organic Principles to Prodrug Design" (93 references).

Considering the applied nature of this approach to designing useful agents, the editor might have given greater emphasis to the practical consideration that such modifications result in new compounds in the sense of requiring extensive and costly safety studies and provide no short cut in this critical area of testing. Also, it would have been helpful for those interested in this general approach to have at least listed the related approaches of molecular complexes, alternate salts, solid solutions, liposomal transport, *etc.*, as means of achieving useful drug modification.

Reviewed by Henry C. Caldwell
Research and Development
Smith Kline & French Laboratories
Philadelphia, PA 19101

Aspirin and Related Drugs: Their Actions and Uses. Edited by K. D. RAINSFORD, K. BRUNE, and M. W. WHITEHOUSE. Birkhauser Verlag, P. O. Box 34, CH-4010 Basel, Switzerland. 1977. 118 pp. 17 × 24 cm.

The 11 papers and introductory comments contained in this volume comprise the Symposium on Aspirin and Related Drugs held in conjunction with the Physiology Section, 47th Congress of the Australian and New Zealand Association for the Advancement of Science, on May 14, 1976 at the University of Tasmania, Hobart, Australia. The compilation of these papers provides a useful overview of the current research trends in Australia in the areas of salicylate pharmacology and toxicology.

While this book is not a comprehensive review of the pharmacology of nonsteroidal anti-inflammatory agents, it does provide insight into some current theories of anti-inflammatory and gastrotoxic mechanisms of action. Theories of anti-inflammatory modes of action discussed in this book include both the inhibition and stimulation of microsomal

free of these interferences and only measures the "true" creatinine.

The boiling alkaline picrate method has been claimed to measure the true creatinine (5). The results of the present study do not support the claim. In a previous study (3), the "apparent" recovery of the spiked creatinine in plasma was only 81% and, after heat treatment, certain components in plasma were thought to suppress the creatinine–picrate complex reaction or to interfere with the color formation. Thus, the reason for the higher creatinine values by the boiling alkaline picrate method remains to be determined.

(1) W. L. Chiou and F. H. Hsu, *J. Clin. Pharmacol.*, **15**, 427 (1975).
(2) W. L. Chiou and F. H. Hsu, *Res. Commun. Chem. Pathol. Pharmacol.*, **9**, 315 (1975).
(3) W. L. Chiou, F. H. Hsu, and G. W. Peng, *Clin. Chem.*, **23**, 1374 (1977).
(4) W. L. Chiou, M. A. F. Gadalla, and G. W. Peng, *J. Pharm. Sci.*, **67**, 182 (1978).
(5) H. Yatzids, *Clin. Chem.*, **21**, 1848 (1975).

Win L. Chiou ˣ
Geoffrey W. Peng
M. A. F. Gadalla
Clinical Pharmacokinetics Laboratory
College of Pharmacy
University of Illinois at the Medical Center
Chicago, IL 60612
Samuel T. Nerenberg
Department of Pathology
College of Medicine
University of Illinois at the Medical Center
Chicago, IL 60612

Received October 7, 1977.
Accepted for publication November 8, 1977.

BOOKS

REVIEWS

Practical Clinical Pharmacy. Edited by CHARLES A. WALKER and JOHN R. FOXX. Stratton, 381 Park Avenue South, New York, NY 10016. 1977. x + 142 pp. 15 × 23 cm. Price $16.95.

The reader approaches a book called "Practical Clinical Pharmacy" with expectations of gaining insight into techniques of monitoring drug therapy, strategies for improving pharmacist–prescriber and pharmacist–patient communications, and data on the clinical pharmacology and therapeutic use of drugs. What the reader receives in lieu of this critical information is a collection of philosophical discussions on the role and potential for clinical pharmacy practice.

The book contains 14 presentations delivered at the "First Annual Symposium on a Clinical Pharmacy Program" sponsored by the School of Pharmacy at Florida A & M University; the date of the symposium is not disclosed. The presentations are organized under three themes: (*a*) the clinical curricula, (*b*) the role and liabilities of a clinical pharmacist, and (*c*) other health professionals' view of clinical pharmacy. The most informative discussions are by Roger Palmer on "The Role of Clinical Pharmacology and Pharmacokinetics in a Clinical Pharmacy Program" and by Charles Walker and Karam Soliman on "The Clinical Pharmacist's Role in Research and Therapeutics."

Perhaps the book is an appropriate addition to health professions libraries. It is an unlikely choice for personal purchase.

Reviewed by Gerald E. Schumacher
College of Pharmacy and Allied Health Professions
Wayne State University
Detroit, MI 48202

Design of Biopharmaceutical Properties through Prodrugs and Analogs. Edited by EDWARD B. ROCHE. American Pharmaceutical Association, 2215 Constitution Avenue, N.W., Washington, DC 20037. 1977. 455 pp. 16 × 23 cm. Price $20.00, $13.00 Member Rate.

This series of 15 papers was presented at Orlando in November 1976 and published less than 1 year later! Congratulations to the editor, authors, and APhA.

Papers of particular interest are "Structural Aspects of Selective Distribution" by Roche with 34 references, which provides a good background for "Structural Effects of Partitioning Behavior of Drugs" by Dunn (13 references), and "Correlation Analysis in the Design of Pharmacodynamic Properties of Drugs" by Hansch (12 references). Also of special interest are "Alteration of Pharmacokinetics through Structural Modification" by Notari (34 references), "Novel Approaches for the Design of Membrane Transport Properties of Drugs" by Bodor (38 references), and "Physical Model Approach to the Design of Drugs with Improved Intestinal Absorption" by Ho, Park, Morozowich, and W. Higuchi. The latter, with 91 pages (89 references), is well worth the price of the book. It should be of particular value to students.

"The Prediction of Chemical Liability through Substituent Effects" by Charton (68 references) contains a wealth of tabulated data and constants. In "Alteration of Drug Metabolism through Structural Modification" by Nelson is a very useful list of 112 pertinent references. Finally, Morozowich, Cho, and Kezdy put it all together in "Application of Physical Organic Principles to Prodrug Design" (93 references).

Considering the applied nature of this approach to designing useful agents, the editor might have given greater emphasis to the practical consideration that such modifications result in new compounds in the sense of requiring extensive and costly safety studies and provide no short cut in this critical area of testing. Also, it would have been helpful for those interested in this general approach to have at least listed the related approaches of molecular complexes, alternate salts, solid solutions, liposomal transport, *etc.*, as means of achieving useful drug modification.

Reviewed by Henry C. Caldwell
Research and Development
Smith Kline & French Laboratories
Philadelphia, PA 19101

Aspirin and Related Drugs: Their Actions and Uses. Edited by K. D. RAINSFORD, K. BRUNE, and M. W. WHITEHOUSE. Birkhauser Verlag, P. O. Box 34, CH-4010 Basel, Switzerland. 1977. 118 pp. 17 × 24 cm.

The 11 papers and introductory comments contained in this volume comprise the Symposium on Aspirin and Related Drugs held in conjunction with the Physiology Section, 47th Congress of the Australian and New Zealand Association for the Advancement of Science, on May 14, 1976 at the University of Tasmania, Hobart, Australia. The compilation of these papers provides a useful overview of the current research trends in Australia in the areas of salicylate pharmacology and toxicology.

While this book is not a comprehensive review of the pharmacology of nonsteroidal anti-inflammatory agents, it does provide insight into some current theories of anti-inflammatory and gastrotoxic mechanisms of action. Theories of anti-inflammatory modes of action discussed in this book include both the inhibition and stimulation of microsomal

free of these interferences and only measures the "true" creatinine.

The boiling alkaline picrate method has been claimed to measure the true creatinine (5). The results of the present study do not support the claim. In a previous study (3), the "apparent" recovery of the spiked creatinine in plasma was only 81% and, after heat treatment, certain components in plasma were thought to suppress the creatinine–picrate complex reaction or to interfere with the color formation. Thus, the reason for the higher creatinine values by the boiling alkaline picrate method remains to be determined.

(1) W. L. Chiou and F. H. Hsu, *J. Clin. Pharmacol.*, **15**, 427 (1975).
(2) W. L. Chiou and F. H. Hsu, *Res. Commun. Chem. Pathol. Pharmacol.*, **9**, 315 (1975).
(3) W. L. Chiou, F. H. Hsu, and G. W. Peng, *Clin. Chem.*, **23**, 1374 (1977).
(4) W. L. Chiou, M. A. F. Gadalla, and G. W. Peng, *J. Pharm. Sci.*, **67**, 182 (1978).
(5) H. Yatzids, *Clin. Chem.*, **21**, 1848 (1975).

Win L. Chiou ˣ
Geoffrey W. Peng
M. A. F. Gadalla
Clinical Pharmacokinetics Laboratory
College of Pharmacy
University of Illinois at the Medical Center
Chicago, IL 60612
Samuel T. Nerenberg
Department of Pathology
College of Medicine
University of Illinois at the Medical Center
Chicago, IL 60612

Received October 7, 1977.
Accepted for publication November 8, 1977.

BOOKS

REVIEWS

Practical Clinical Pharmacy. Edited by CHARLES A. WALKER and JOHN R. FOXX. Stratton, 381 Park Avenue South, New York, NY 10016. 1977. x + 142 pp. 15 × 23 cm. Price $16.95.

The reader approaches a book called "Practical Clinical Pharmacy" with expectations of gaining insight into techniques of monitoring drug therapy, strategies for improving pharmacist–prescriber and pharmacist–patient communications, and data on the clinical pharmacology and therapeutic use of drugs. What the reader receives in lieu of this critical information is a collection of philosophical discussions on the role and potential for clinical pharmacy practice.

The book contains 14 presentations delivered at the "First Annual Symposium on a Clinical Pharmacy Program" sponsored by the School of Pharmacy at Florida A & M University; the date of the symposium is not disclosed. The presentations are organized under three themes: (*a*) the clinical curricula, (*b*) the role and liabilities of a clinical pharmacist, and (*c*) other health professionals' view of clinical pharmacy. The most informative discussions are by Roger Palmer on "The Role of Clinical Pharmacology and Pharmacokinetics in a Clinical Pharmacy Program" and by Charles Walker and Karam Soliman on "The Clinical Pharmacist's Role in Research and Therapeutics."

Perhaps the book is an appropriate addition to health professions libraries. It is an unlikely choice for personal purchase.

Reviewed by Gerald E. Schumacher
College of Pharmacy and Allied Health Professions
Wayne State University
Detroit, MI 48202

Design of Biopharmaceutical Properties through Prodrugs and Analogs. Edited by EDWARD B. ROCHE. American Pharmaceutical Association, 2215 Constitution Avenue, N.W., Washington, DC 20037. 1977. 455 pp. 16 × 23 cm. Price $20.00, $13.00 Member Rate.

This series of 15 papers was presented at Orlando in November 1976 and published less than 1 year later! Congratulations to the editor, authors, and APhA.

Papers of particular interest are "Structural Aspects of Selective Distribution" by Roche with 34 references, which provides a good background for "Structural Effects of Partitioning Behavior of Drugs" by Dunn (13 references), and "Correlation Analysis in the Design of Pharmacodynamic Properties of Drugs" by Hansch (12 references). Also of special interest are "Alteration of Pharmacokinetics through Structural Modification" by Notari (34 references), "Novel Approaches for the Design of Membrane Transport Properties of Drugs" by Bodor (38 references), and "Physical Model Approach to the Design of Drugs with Improved Intestinal Absorption" by Ho, Park, Morozowich, and W. Higuchi. The latter, with 91 pages (89 references), is well worth the price of the book. It should be of particular value to students.

"The Prediction of Chemical Liability through Substituent Effects" by Charton (68 references) contains a wealth of tabulated data and constants. In "Alteration of Drug Metabolism through Structural Modification" by Nelson is a very useful list of 112 pertinent references. Finally, Morozowich, Cho, and Kezdy put it all together in "Application of Physical Organic Principles to Prodrug Design" (93 references).

Considering the applied nature of this approach to designing useful agents, the editor might have given greater emphasis to the practical consideration that such modifications result in new compounds in the sense of requiring extensive and costly safety studies and provide no short cut in this critical area of testing. Also, it would have been helpful for those interested in this general approach to have at least listed the related approaches of molecular complexes, alternate salts, solid solutions, liposomal transport, *etc.*, as means of achieving useful drug modification.

Reviewed by Henry C. Caldwell
Research and Development
Smith Kline & French Laboratories
Philadelphia, PA 19101

Aspirin and Related Drugs: Their Actions and Uses. Edited by K. D. RAINSFORD, K. BRUNE, and M. W. WHITEHOUSE. Birkhauser Verlag, P. O. Box 34, CH-4010 Basel, Switzerland. 1977. 118 pp. 17 × 24 cm.

The 11 papers and introductory comments contained in this volume comprise the Symposium on Aspirin and Related Drugs held in conjunction with the Physiology Section, 47th Congress of the Australian and New Zealand Association for the Advancement of Science, on May 14, 1976 at the University of Tasmania, Hobart, Australia. The compilation of these papers provides a useful overview of the current research trends in Australia in the areas of salicylate pharmacology and toxicology.

While this book is not a comprehensive review of the pharmacology of nonsteroidal anti-inflammatory agents, it does provide insight into some current theories of anti-inflammatory and gastrotoxic mechanisms of action. Theories of anti-inflammatory modes of action discussed in this book include both the inhibition and stimulation of microsomal

prostaglandin synthetase systems and their subsequent effects on smooth muscle, and the nonclassical concept of unspecific interference with physiological membrane function, similar to the barbiturates, resulting in both anti-inflammatory response and GI irritation. The latter theory accounts for the fact that all attempts, to date, to develop acidic nonsteroidal anti-inflammatory agents without gastrotoxicity have met with limited success.

Four chapters are devoted to studies on GI side effects of aspirin and related drugs, with emphasis on postulated biochemical mechanisms resulting in subsequent physiological damage. Additional findings are presented concerning the pharmacokinetics of salicylates in rheumatoid arthritis; drug interactions; naturally occurring salicylates as alternatives to aspirin; and copper–salicylate complexes with enhanced anti-inflammatory potency.

As expected with any work by 12 different authors, the writing style is far from uniform; little effort was made to organize the varied papers into standard book form. However, pharmacologists interested in nonsteroidal anti-inflammatory drug research will find this book a useful addition to their technical library.

Reviewed by William P. Heilman
Diamond Shamrock Corporation
T. R. Evans Research Center
Painesville, OH 44077

Cannabinoid Assays in Humans. NIDA Research Monograph 7. Edited by ROBERT E. WILLETTE. National Institute on Drug Abuse, 11400 Rockville Pike, Rockville, MD 20852. 1976. 120 pp. 21 × 27 cm. Price $6.00. Available from National Technical Information Service, Springfield, VA 22161.

This seventh monograph of the continuing series on drug abuse research describes recent developments in the determination of the levels of cannabinoids in the human body. The monograph consists of 12 papers dealing with three major methods of cannabinoid assay: immunoassay techniques, chromatographic (gas–liquid and high-pressure liquid) methods, and mass spectrometric techniques.

This monograph is highly recommended for a wide range of marijuana researchers. The techniques described would be useful for marijuana screening procedures, forensic toxicology, and pharmacokinetic and pharmacological research.

Reviewed by David J. Slatkin
University of Pittsburgh
School of Pharmacy
Pittsburgh, PA 15261

Testing and Screening for Drugs of Abuse: Techniques, Issues and Clinical Implications. By G. G. De ANGELIS. Dekker, 270 Madison Ave., New York, NY 10016, 1976. 152 pp. 15 × 23 cm. Price $17.50.

Urine analysis has become an integral part of our society. Its results affect the private sector as well as the Governmental sector, but its greatest impact is in the treatment centers for drug abuse. "Testing and Screening for Drugs of Abuse" takes a hard look at the issues and clinical implications of urine analysis. The chemical techniques are superficially discussed so that the nonscientific person is able to obtain a fair understanding of the methodologies used in drug screening laboratories.

The book is divided into three main sections. The first section deals with general considerations, such as the rationale behind the choice of urine over blood as the body fluid for drug screening. Other nonchemical tests such as the Himmelsbach test and the pupilary test are discussed and compared to urine analysis. The author also discusses the use of diagnostic tests such as serum amylase, serum glutamic–oxaloacetic transaminase, 17-ketosteroids, serum uric acid, blood sugar, and cholesterol for determining whether or not a drug abuse problem exists. The author suggests that this type of testing would be much more effective in determining whether a patient is a beginner or chronic drug user.

The second section deals with the analytical methodologies employed by drug screening laboratories. Techniques such as TLC, spectrophotofluorometry, GLC, and the immunoassays (FRAT, EMIT, RIA, and HI) are briefly discussed. These analytical methods are compared for sensitivity, specificity, false positives, false negatives, productivity, and cost. The concepts of sensitivity, specificity, false positives, and false negatives are developed so that the nonscientific individual can follow the comparisons. Possible sources of analytical error are investigated, and methods of recognizing and correcting them are mentioned.

The third section deals with the clinical implications of urine screening. Problems related to the stigmatism of urine analysis with illegal behavior are revealed. Urine analysis scheduling is also discussed. The author refers to Goldstein and Brown who published a thorough analysis of testing schedules. The sociological effects of urine analysis are investigated. The author discusses various parallel studies involving treatment with and without urine screening. Based on the results of these studies, he evaluates the effects of urine screening and the manner in which urine screening data should be utilized. The idea of urine surveillance *versus* urine screening is also developed. Other important factors such as the client's rights, vocational screening, the role of the drug user in the testing program, and the community role are presented.

"Testing and Screening for Drugs of Abuse" is written with a nonscientific reader in mind. It translates technical language into simple terms, making the book valuable to program directors, clinicians, staff members, and any other nontechnical personnel. The problems associated with drug screening are accurately presented and possible solutions are suggested, thus making this book worthwhile reading for the technical staff as well. In my opinion, this book is a valuable reading experience for students and personnel involved in drug treatment programs irrespective of their position.

Reviewed by Thomas Catalano
Scientific Research Division
New York City Police Department
New York, NY 10003

NOTICES

Handbook of Injectable Drugs. By LAWRENCE A. TRISSEL. American Society of Hospital Pharmacists, 4630 Montgomery Ave., Washington, DC 20014. 1977. 431 pp. 15 × 23 cm. Price $15.00.

Narcotic Antagonists: Naltrexone Progress Report. NIDA Research Monograph 9. Edited by DEMETRIOS JULIUS and PIERRE RENAULT. National Institute on Drug Abuse, 11400 Rockville Pike, Rockville, MD 20852. 1976. 181 pp. 20 × 27 cm. Price $7.50. Available from National Technical Information Service, Springfield, VA 22161.

Rx· 3X/Week LAAM: Alternative to Methadone. NIDA Research Monograph 8. Edited by JACK D. BLAINE and PIERRE F. RENAULT. National Institute on Drug Abuse, 11400 Rockville Pike, Rockville, MD 20852. 1976. 127 pp. 20 × 27 cm. Price $6.00. Available from National Technical Information Service, Springfield, VA 22161.

Effects of Labeling the "Drug-Abuser": An Inquiry. NIDA Research Monograph 6. By JAY R. WILLIAMS. National Institute on Drug Abuse, 11400 Rockville Pike, Rockville, MD 20852. 1976. 39 pp. 20 × 27 cm. Price $1.05. Available from Superintendent of Documents, U.S. Government Printing Office, Washington, DC 20402.

Young Men and Drugs—A Nationwide Survey. NIDA Research Monograph 5. By JOHN A. O'DONNELL, HARWIN L. VOSS, RICHARD R. CLAYTON, GERALD T. SLATIN, and ROBIN G. W. ROOM. National Institute on Drug Abuse, 11400 Rockville Pike, Rockville, MD 20852. 1976. 144 pp. 20 × 27 cm. Price $2.25. Available from Superintendent of Documents, U.S. Government Printing Office, Washington, DC 20402.

Aminergic Hypotheses of Behavior: Reality Or Cliche? NIDA Research Monograph 3. Edited by BRUCE KENNETH BERNARD. National Institute on Drug Abuse, 11400 Rockville Pike, Rockville, MD 20852. 1975. 148 pp. 20 × 27 cm. Price $2.25. Available from Superintendent of Documents, U.S. Government Printing Office, Washington, DC 20402.

Operational Definitions in Socio-Behavioral Drug Use Research 1975. NIDA Research Monograph 2. Edited by JACK ELINSON and DAVID NURCO. National Institute on Drug Abuse, 11400 Rockville Pike, Rockville, MD 20852. 1975. 58 pp. 20 × 27 cm. Price $2.50. Available from Superintendent of Documents, U.S. Government Printing Office, Washington, DC 20402.

prostaglandin synthetase systems and their subsequent effects on smooth muscle, and the nonclassical concept of unspecific interference with physiological membrane function, similar to the barbiturates, resulting in both anti-inflammatory response and GI irritation. The latter theory accounts for the fact that all attempts, to date, to develop acidic nonsteroidal anti-inflammatory agents without gastrotoxicity have met with limited success.

Four chapters are devoted to studies on GI side effects of aspirin and related drugs, with emphasis on postulated biochemical mechanisms resulting in subsequent physiological damage. Additional findings are presented concerning the pharmacokinetics of salicylates in rheumatoid arthritis; drug interactions; naturally occurring salicylates as alternatives to aspirin; and copper–salicylate complexes with enhanced anti-inflammatory potency.

As expected with any work by 12 different authors, the writing style is far from uniform; little effort was made to organize the varied papers into standard book form. However, pharmacologists interested in nonsteroidal anti-inflammatory drug research will find this book a useful addition to their technical library.

Reviewed by William P. Heilman
Diamond Shamrock Corporation
T. R. Evans Research Center
Painesville, OH 44077

Cannabinoid Assays in Humans. NIDA Research Monograph 7. Edited by ROBERT E. WILLETTE. National Institute on Drug Abuse, 11400 Rockville Pike, Rockville, MD 20852. 1976. 120 pp. 21 × 27 cm. Price $6.00. Available from National Technical Information Service, Springfield, VA 22161.

This seventh monograph of the continuing series on drug abuse research describes recent developments in the determination of the levels of cannabinoids in the human body. The monograph consists of 12 papers dealing with three major methods of cannabinoid assay: immunoassay techniques, chromatographic (gas–liquid and high-pressure liquid) methods, and mass spectrometric techniques.

This monograph is highly recommended for a wide range of marijuana researchers. The techniques described would be useful for marijuana screening procedures, forensic toxicology, and pharmacokinetic and pharmacological research.

Reviewed by David J. Slatkin
University of Pittsburgh
School of Pharmacy
Pittsburgh, PA 15261

Testing and Screening for Drugs of Abuse: Techniques, Issues and Clinical Implications. By G. G. De ANGELIS. Dekker, 270 Madison Ave., New York, NY 10016, 1976. 152 pp. 15 × 23 cm. Price $17.50.

Urine analysis has become an integral part of our society. Its results affect the private sector as well as the Governmental sector, but its greatest impact is in the treatment centers for drug abuse. "Testing and Screening for Drugs of Abuse" takes a hard look at the issues and clinical implications of urine analysis. The chemical techniques are superficially discussed so that the nonscientific person is able to obtain a fair understanding of the methodologies used in drug screening laboratories.

The book is divided into three main sections. The first section deals with general considerations, such as the rationale behind the choice of urine over blood as the body fluid for drug screening. Other nonchemical tests such as the Himmelsbach test and the pupilary test are discussed and compared to urine analysis. The author also discusses the use of diagnostic tests such as serum amylase, serum glutamic–oxaloacetic transaminase, 17-ketosteroids, serum uric acid, blood sugar, and cholesterol for determining whether or not a drug abuse problem exists. The author suggests that this type of testing would be much more effective in determining whether a patient is a beginner or chronic drug user.

The second section deals with the analytical methodologies employed by drug screening laboratories. Techniques such as TLC, spectrophotofluorometry, GLC, and the immunoassays (FRAT, EMIT, RIA, and HI) are briefly discussed. These analytical methods are compared for sensitivity, specificity, false positives, false negatives, productivity, and cost. The concepts of sensitivity, specificity, false positives, and false negatives are developed so that the nonscientific individual can follow the comparisons. Possible sources of analytical error are investigated, and methods of recognizing and correcting them are mentioned.

The third section deals with the clinical implications of urine screening. Problems related to the stigmatism of urine analysis with illegal behavior are revealed. Urine analysis scheduling is also discussed. The author refers to Goldstein and Brown who published a thorough analysis of testing schedules. The sociological effects of urine analysis are investigated. The author discusses various parallel studies involving treatment with and without urine screening. Based on the results of these studies, he evaluates the effects of urine screening and the manner in which urine screening data should be utilized. The idea of urine surveillance *versus* urine screening is also developed. Other important factors such as the client's rights, vocational screening, the role of the drug user in the testing program, and the community role are presented.

"Testing and Screening for Drugs of Abuse" is written with a nonscientific reader in mind. It translates technical language into simple terms, making the book valuable to program directors, clinicians, staff members, and any other nontechnical personnel. The problems associated with drug screening are accurately presented and possible solutions are suggested, thus making this book worthwhile reading for the technical staff as well. In my opinion, this book is a valuable reading experience for students and personnel involved in drug treatment programs irrespective of their position.

Reviewed by Thomas Catalano
Scientific Research Division
New York City Police Department
New York, NY 10003

NOTICES

Handbook of Injectable Drugs. By LAWRENCE A. TRISSEL. American Society of Hospital Pharmacists, 4630 Montgomery Ave., Washington, DC 20014. 1977. 431 pp. 15 × 23 cm. Price $15.00.

Narcotic Antagonists: Naltrexone Progress Report. NIDA Research Monograph 9. Edited by DEMETRIOS JULIUS and PIERRE RENAULT. National Institute on Drug Abuse, 11400 Rockville Pike, Rockville, MD 20852. 1976. 181 pp. 20 × 27 cm. Price $7.50. Available from National Technical Information Service, Springfield, VA 22161.

Rx· 3X/Week LAAM: Alternative to Methadone. NIDA Research Monograph 8. Edited by JACK D. BLAINE and PIERRE F. RENAULT. National Institute on Drug Abuse, 11400 Rockville Pike, Rockville, MD 20852. 1976. 127 pp. 20 × 27 cm. Price $6.00. Available from National Technical Information Service, Springfield, VA 22161.

Effects of Labeling the "Drug-Abuser": An Inquiry. NIDA Research Monograph 6. By JAY R. WILLIAMS. National Institute on Drug Abuse, 11400 Rockville Pike, Rockville, MD 20852. 1976. 39 pp. 20 × 27 cm. Price $1.05. Available from Superintendent of Documents, U.S. Government Printing Office, Washington, DC 20402.

Young Men and Drugs—A Nationwide Survey. NIDA Research Monograph 5. By JOHN A. O'DONNELL, HARWIN L. VOSS, RICHARD R. CLAYTON, GERALD T. SLATIN, and ROBIN G. W. ROOM. National Institute on Drug Abuse, 11400 Rockville Pike, Rockville, MD 20852. 1976. 144 pp. 20 × 27 cm. Price $2.25. Available from Superintendent of Documents, U.S. Government Printing Office, Washington, DC 20402.

Aminergic Hypotheses of Behavior: Reality Or Cliche? NIDA Research Monograph 3. Edited by BRUCE KENNETH BERNARD. National Institute on Drug Abuse, 11400 Rockville Pike, Rockville, MD 20852. 1975. 148 pp. 20 × 27 cm. Price $2.25. Available from Superintendent of Documents, U.S. Government Printing Office, Washington, DC 20402.

Operational Definitions in Socio-Behavioral Drug Use Research 1975. NIDA Research Monograph 2. Edited by JACK ELINSON and DAVID NURCO. National Institute on Drug Abuse, 11400 Rockville Pike, Rockville, MD 20852. 1975. 58 pp. 20 × 27 cm. Price $2.50. Available from Superintendent of Documents, U.S. Government Printing Office, Washington, DC 20402.

prostaglandin synthetase systems and their subsequent effects on smooth muscle, and the nonclassical concept of unspecific interference with physiological membrane function, similar to the barbiturates, resulting in both anti-inflammatory response and GI irritation. The latter theory accounts for the fact that all attempts, to date, to develop acidic nonsteroidal anti-inflammatory agents without gastrotoxicity have met with limited success.

Four chapters are devoted to studies on GI side effects of aspirin and related drugs, with emphasis on postulated biochemical mechanisms resulting in subsequent physiological damage. Additional findings are presented concerning the pharmacokinetics of salicylates in rheumatoid arthritis; drug interactions; naturally occurring salicylates as alternatives to aspirin; and copper–salicylate complexes with enhanced anti-inflammatory potency.

As expected with any work by 12 different authors, the writing style is far from uniform; little effort was made to organize the varied papers into standard book form. However, pharmacologists interested in nonsteroidal anti-inflammatory drug research will find this book a useful addition to their technical library.

Reviewed by William P. Heilman
Diamond Shamrock Corporation
T. R. Evans Research Center
Painesville, OH 44077

Cannabinoid Assays in Humans. NIDA Research Monograph 7. Edited by ROBERT E. WILLETTE. National Institute on Drug Abuse, 11400 Rockville Pike, Rockville, MD 20852. 1976. 120 pp. 21 × 27 cm. Price $6.00. Available from National Technical Information Service, Springfield, VA 22161.

This seventh monograph of the continuing series on drug abuse research describes recent developments in the determination of the levels of cannabinoids in the human body. The monograph consists of 12 papers dealing with three major methods of cannabinoid assay: immunoassay techniques, chromatographic (gas–liquid and high-pressure liquid) methods, and mass spectrometric techniques.

This monograph is highly recommended for a wide range of marijuana researchers. The techniques described would be useful for marijuana screening procedures, forensic toxicology, and pharmacokinetic and pharmacological research.

Reviewed by David J. Slatkin
University of Pittsburgh
School of Pharmacy
Pittsburgh, PA 15261

Testing and Screening for Drugs of Abuse: Techniques, Issues and Clinical Implications. By G. G. De ANGELIS. Dekker, 270 Madison Ave., New York, NY 10016, 1976. 152 pp. 15 × 23 cm. Price $17.50.

Urine analysis has become an integral part of our society. Its results affect the private sector as well as the Governmental sector, but its greatest impact is in the treatment centers for drug abuse. "Testing and Screening for Drugs of Abuse" takes a hard look at the issues and clinical implications of urine analysis. The chemical techniques are superficially discussed so that the nonscientific person is able to obtain a fair understanding of the methodologies used in drug screening laboratories.

The book is divided into three main sections. The first section deals with general considerations, such as the rationale behind the choice of urine over blood as the body fluid for drug screening. Other nonchemical tests such as the Himmelsbach test and the pupilary test are discussed and compared to urine analysis. The author also discusses the use of diagnostic tests such as serum amylase, serum glutamic–oxaloacetic transaminase, 17-ketosteroids, serum uric acid, blood sugar, and cholesterol for determining whether or not a drug abuse problem exists. The author suggests that this type of testing would be much more effective in determining whether a patient is a beginner or chronic drug user.

The second section deals with the analytical methodologies employed by drug screening laboratories. Techniques such as TLC, spectrophotofluorometry, GLC, and the immunoassays (FRAT, EMIT, RIA, and HI) are briefly discussed. These analytical methods are compared for sensitivity, specificity, false positives, false negatives, productivity, and cost. The concepts of sensitivity, specificity, false positives, and false negatives are developed so that the nonscientific individual can follow the comparisons. Possible sources of analytical error are investigated, and methods of recognizing and correcting them are mentioned.

The third section deals with the clinical implications of urine screening. Problems related to the stigmatism of urine analysis with illegal behavior are revealed. Urine analysis scheduling is also discussed. The author refers to Goldstein and Brown who published a thorough analysis of testing schedules. The sociological effects of urine analysis are investigated. The author discusses various parallel studies involving treatment with and without urine screening. Based on the results of these studies, he evaluates the effects of urine screening and the manner in which urine screening data should be utilized. The idea of urine surveillance *versus* urine screening is also developed. Other important factors such as the client's rights, vocational screening, the role of the drug user in the testing program, and the community role are presented.

"Testing and Screening for Drugs of Abuse" is written with a nonscientific reader in mind. It translates technical language into simple terms, making the book valuable to program directors, clinicians, staff members, and any other nontechnical personnel. The problems associated with drug screening are accurately presented and possible solutions are suggested, thus making this book worthwhile reading for the technical staff as well. In my opinion, this book is a valuable reading experience for students and personnel involved in drug treatment programs irrespective of their position.

Reviewed by Thomas Catalano
Scientific Research Division
New York City Police Department
New York, NY 10003

NOTICES

Handbook of Injectable Drugs. By LAWRENCE A. TRISSEL. American Society of Hospital Pharmacists, 4630 Montgomery Ave., Washington, DC 20014. 1977. 431 pp. 15 × 23 cm. Price $15.00.

Narcotic Antagonists: Naltrexone Progress Report. NIDA Research Monograph 9. Edited by DEMETRIOS JULIUS and PIERRE RENAULT. National Institute on Drug Abuse, 11400 Rockville Pike, Rockville, MD 20852. 1976. 181 pp. 20 × 27 cm. Price $7.50. Available from National Technical Information Service, Springfield, VA 22161.

Rx· 3X/Week LAAM: Alternative to Methadone. NIDA Research Monograph 8. Edited by JACK D. BLAINE and PIERRE F. RENAULT. National Institute on Drug Abuse, 11400 Rockville Pike, Rockville, MD 20852. 1976. 127 pp. 20 × 27 cm. Price $6.00. Available from National Technical Information Service, Springfield, VA 22161.

Effects of Labeling the "Drug-Abuser": An Inquiry. NIDA Research Monograph 6. By JAY R. WILLIAMS. National Institute on Drug Abuse, 11400 Rockville Pike, Rockville, MD 20852. 1976. 39 pp. 20 × 27 cm. Price $1.05. Available from Superintendent of Documents, U.S. Government Printing Office, Washington, DC 20402.

Young Men and Drugs—A Nationwide Survey. NIDA Research Monograph 5. By JOHN A. O'DONNELL, HARWIN L. VOSS, RICHARD R. CLAYTON, GERALD T. SLATIN, and ROBIN G. W. ROOM. National Institute on Drug Abuse, 11400 Rockville Pike, Rockville, MD 20852. 1976. 144 pp. 20 × 27 cm. Price $2.25. Available from Superintendent of Documents, U.S. Government Printing Office, Washington, DC 20402.

Aminergic Hypotheses of Behavior: Reality Or Cliche? NIDA Research Monograph 3. Edited by BRUCE KENNETH BERNARD. National Institute on Drug Abuse, 11400 Rockville Pike, Rockville, MD 20852. 1975. 148 pp. 20 × 27 cm. Price $2.25. Available from Superintendent of Documents, U.S. Government Printing Office, Washington, DC 20402.

Operational Definitions in Socio-Behavioral Drug Use Research 1975. NIDA Research Monograph 2. Edited by JACK ELINSON and DAVID NURCO. National Institute on Drug Abuse, 11400 Rockville Pike, Rockville, MD 20852. 1975. 58 pp. 20 × 27 cm. Price $2.50. Available from Superintendent of Documents, U.S. Government Printing Office, Washington, DC 20402.

prostaglandin synthetase systems and their subsequent effects on smooth muscle, and the nonclassical concept of unspecific interference with physiological membrane function, similar to the barbiturates, resulting in both anti-inflammatory response and GI irritation. The latter theory accounts for the fact that all attempts, to date, to develop acidic nonsteroidal anti-inflammatory agents without gastrotoxicity have met with limited success.

Four chapters are devoted to studies on GI side effects of aspirin and related drugs, with emphasis on postulated biochemical mechanisms resulting in subsequent physiological damage. Additional findings are presented concerning the pharmacokinetics of salicylates in rheumatoid arthritis; drug interactions; naturally occurring salicylates as alternatives to aspirin; and copper–salicylate complexes with enhanced anti-inflammatory potency.

As expected with any work by 12 different authors, the writing style is far from uniform; little effort was made to organize the varied papers into standard book form. However, pharmacologists interested in nonsteroidal anti-inflammatory drug research will find this book a useful addition to their technical library.

Reviewed by William P. Heilman
Diamond Shamrock Corporation
T. R. Evans Research Center
Painesville, OH 44077

Cannabinoid Assays in Humans. NIDA Research Monograph 7. Edited by ROBERT E. WILLETTE. National Institute on Drug Abuse, 11400 Rockville Pike, Rockville, MD 20852. 1976. 120 pp. 21 × 27 cm. Price $6.00. Available from National Technical Information Service, Springfield, VA 22161.

This seventh monograph of the continuing series on drug abuse research describes recent developments in the determination of the levels of cannabinoids in the human body. The monograph consists of 12 papers dealing with three major methods of cannabinoid assay: immunoassay techniques, chromatographic (gas–liquid and high-pressure liquid) methods, and mass spectrometric techniques.

This monograph is highly recommended for a wide range of marijuana researchers. The techniques described would be useful for marijuana screening procedures, forensic toxicology, and pharmacokinetic and pharmacological research.

Reviewed by David J. Slatkin
University of Pittsburgh
School of Pharmacy
Pittsburgh, PA 15261

Testing and Screening for Drugs of Abuse: Techniques, Issues and Clinical Implications. By G. G. De ANGELIS. Dekker, 270 Madison Ave., New York, NY 10016, 1976. 152 pp. 15 × 23 cm. Price $17.50.

Urine analysis has become an integral part of our society. Its results affect the private sector as well as the Governmental sector, but its greatest impact is in the treatment centers for drug abuse. "Testing and Screening for Drugs of Abuse" takes a hard look at the issues and clinical implications of urine analysis. The chemical techniques are superficially discussed so that the nonscientific person is able to obtain a fair understanding of the methodologies used in drug screening laboratories.

The book is divided into three main sections. The first section deals with general considerations, such as the rationale behind the choice of urine over blood as the body fluid for drug screening. Other nonchemical tests such as the Himmelsbach test and the pupilary test are discussed and compared to urine analysis. The author also discusses the use of diagnostic tests such as serum amylase, serum glutamic–oxaloacetic transaminase, 17-ketosteroids, serum uric acid, blood sugar, and cholesterol for determining whether or not a drug abuse problem exists. The author suggests that this type of testing would be much more effective in determining whether a patient is a beginner or chronic drug user.

The second section deals with the analytical methodologies employed by drug screening laboratories. Techniques such as TLC, spectrophotofluorometry, GLC, and the immunoassays (FRAT, EMIT, RIA, and HI) are briefly discussed. These analytical methods are compared for sensitivity, specificity, false positives, false negatives, productivity, and cost. The concepts of sensitivity, specificity, false positives, and false negatives are developed so that the nonscientific individual can follow the comparisons. Possible sources of analytical error are investigated, and methods of recognizing and correcting them are mentioned.

The third section deals with the clinical implications of urine screening. Problems related to the stigmatism of urine analysis with illegal behavior are revealed. Urine analysis scheduling is also discussed. The author refers to Goldstein and Brown who published a thorough analysis of testing schedules. The sociological effects of urine analysis are investigated. The author discusses various parallel studies involving treatment with and without urine screening. Based on the results of these studies, he evaluates the effects of urine screening and the manner in which urine screening data should be utilized. The idea of urine surveillance *versus* urine screening is also developed. Other important factors such as the client's rights, vocational screening, the role of the drug user in the testing program, and the community role are presented.

"Testing and Screening for Drugs of Abuse" is written with a nonscientific reader in mind. It translates technical language into simple terms, making the book valuable to program directors, clinicians, staff members, and any other nontechnical personnel. The problems associated with drug screening are accurately presented and possible solutions are suggested, thus making this book worthwhile reading for the technical staff as well. In my opinion, this book is a valuable reading experience for students and personnel involved in drug treatment programs irrespective of their position.

Reviewed by Thomas Catalano
Scientific Research Division
New York City Police Department
New York, NY 10003

NOTICES

Handbook of Injectable Drugs. By LAWRENCE A. TRISSEL. American Society of Hospital Pharmacists, 4630 Montgomery Ave., Washington, DC 20014. 1977. 431 pp. 15 × 23 cm. Price $15.00.

Narcotic Antagonists: Naltrexone Progress Report. NIDA Research Monograph 9. Edited by DEMETRIOS JULIUS and PIERRE RENAULT. National Institute on Drug Abuse, 11400 Rockville Pike, Rockville, MD 20852. 1976. 181 pp. 20 × 27 cm. Price $7.50. Available from National Technical Information Service, Springfield, VA 22161.

Rx· 3X/Week LAAM: Alternative to Methadone. NIDA Research Monograph 8. Edited by JACK D. BLAINE and PIERRE F. RENAULT. National Institute on Drug Abuse, 11400 Rockville Pike, Rockville, MD 20852. 1976. 127 pp. 20 × 27 cm. Price $6.00. Available from National Technical Information Service, Springfield, VA 22161.

Effects of Labeling the "Drug-Abuser": An Inquiry. NIDA Research Monograph 6. By JAY R. WILLIAMS. National Institute on Drug Abuse, 11400 Rockville Pike, Rockville, MD 20852. 1976. 39 pp. 20 × 27 cm. Price $1.05. Available from Superintendent of Documents, U.S. Government Printing Office, Washington, DC 20402.

Young Men and Drugs—A Nationwide Survey. NIDA Research Monograph 5. By JOHN A. O'DONNELL, HARWIN L. VOSS, RICHARD R. CLAYTON, GERALD T. SLATIN, and ROBIN G. W. ROOM. National Institute on Drug Abuse, 11400 Rockville Pike, Rockville, MD 20852. 1976. 144 pp. 20 × 27 cm. Price $2.25. Available from Superintendent of Documents, U.S. Government Printing Office, Washington, DC 20402.

Aminergic Hypotheses of Behavior: Reality Or Cliche? NIDA Research Monograph 3. Edited by BRUCE KENNETH BERNARD. National Institute on Drug Abuse, 11400 Rockville Pike, Rockville, MD 20852. 1975. 148 pp. 20 × 27 cm. Price $2.25. Available from Superintendent of Documents, U.S. Government Printing Office, Washington, DC 20402.

Operational Definitions in Socio-Behavioral Drug Use Research 1975. NIDA Research Monograph 2. Edited by JACK ELINSON and DAVID NURCO. National Institute on Drug Abuse, 11400 Rockville Pike, Rockville, MD 20852. 1975. 58 pp. 20 × 27 cm. Price $2.50. Available from Superintendent of Documents, U.S. Government Printing Office, Washington, DC 20402.

MARCH 1978
VOLUME 67 NUMBER 3

JOURNAL OF PHARMACEUTICAL SCIENCES

MARY H. FERGUSON
Editor

SHELLY ELLIOTT
Production Editor

JANET D. SHOFF
Copy Editor

EDWARD G. FELDMANN
Contributing Editor

SAMUEL W. GOLDSTEIN
Contributing Editor

BELLE R. BECK
Editorial Secretary

DAVID BOHARDT
Director of Publications

L. LUAN CORRIGAN
Assistant Director of Publications

EDITORIAL ADVISORY BOARD

JOHN AUTIAN
HERBERT A. LIEBERMAN
NORMAN R. FARNSWORTH
DAVID E. MANN, JR.
WILLIAM O. FOYE
GERALD J. PAPARIELLO
WILLIAM J. JUSKO
EDWARD G. RIPPIE

The *Journal of Pharmaceutical Sciences* is published monthly by the American Pharmaceutical Association at 2215 Constitution Ave., N.W., Washington, DC 20037. Second-class postage paid at Washington, D.C., and at additional mailing office.

All expressions of opinion and statements of supposed fact appearing in articles or editorials carried in this journal are published on the authority of the writer over whose name they appear and are not to be regarded as necessarily expressing the policies or views of the American Pharmaceutical Association.

Offices—Editorial, Advertising, and Subscription Offices: 2215 Constitution Ave., N.W., Washington, DC 20037. Printing Offices: 20th & Northampton Streets, Easton, PA 18042.

Annual Subscriptions—United States and foreign, industrial and government institutions $50, educational institutions $50, individuals *for personal use only* $30; single copies $5. All foreign subscriptions add $5 for postage. Subscription rates are subject to change without notice. Members of the American Pharmaceutical Association may elect to receive the *Journal of Pharmaceutical Sciences* as a part of their annual $70 (foreign $75) APhA membership dues.

Claims—Missing numbers will not be supplied if dues or subscriptions are in arrears for more than 60 days or if claims are received more than 60 days after the date of the issue, or if loss was due to failure to give notice of change of address. The Association cannot accept responsibility for foreign delivery when its records indicate shipment has been made.

Change of Address—Members and subscribers should notify at once both the Post Office and the American Pharmaceutical Association, 2215 Constitution Ave., N.W., Washington, DC 20037, of any change of address.

Microfilm—Microfilm volumes are available from University Microfilms International, 300 N. Zeeb Road, Ann Arbor, MI 48106.

© Copyright 1978, American Pharmaceutical Association, 2215 Constitution Ave., N.W., Washington, DC 20037; all rights reserved.

A PROFESSION IN TRANSITION

Pharmacy's present condition can be summed up rather cryptically: *It's a mess!*

But before our readers get unhappy with us for making this blunt assessment, we would hasten to point out that such a condition is not inherently bad or objectionable, provided that it is only temporary.

Let us explain it this way. Improvement in any program, activity, project, or what have you, requires some sort of change to occur. During that period in which the change is being implemented or effectuated, there is going to be disorder and disruption. To cite an example from everyday life, most of us at one time or another have decided that our living room would benefit from a different furniture arrangement. In going from one state of orderliness to another, we must endure a temporary and brief period when the room looks like a disaster area.

Consequently, if we agree that improvements are desirable in pharmacy education, practice, and regulation, then change is required and, in turn, that automatically means a degree of disorder.

Now let us take our analogy one step further. The rearrangement of the living room furniture will proceed successfully and happily only on two conditions. First, there must be some sort of advance "master plan" even if it is only very informal in nature; and second, there must be general agreement or concurrence on that master plan on the part of all the family members. Given these conditions—plus some muscle, some determination, and a couple of strong backs—the project will proceed to satisfactory completion with a minimum of disorder and inconvenience.

This brings us to the point of this editorial. From our perspective, we are not certain that the changes presently in process in pharmacy are following any distinct master plan or that they enjoy the support of a majority of people within the profession.

On the subject of regulation, we continually hear comments on the one hand that "there ought to be a law . . .," but at the same time we hear protests about all of the red tape, paperwork, and government interference. Some of our people advocate increased regulation at the federal level, some hold out for a resurgence of state regulation, and others want a return to voluntary self-regulation. Mandatory continuing education and mandatory patient medication records are only two issues about which there is sharply divided opinion as to the desirability of a regulatory approach.

With regard to the nature of pharmacy practice, we have an equally broad spectrum of apparent viewpoints. At one extreme, there are mail order pharmacies where the pharmacist performs only the dispensing function, working exclusively with drug products and having zero contact with the patient. At the other extreme, there are office-type practices in which certain pharmacists spend their entire time with the patient, taking drug histories, advising on drug compliance, monitoring therapeutic results, and so on, resulting in no immediate contact with drug products. In between there are all variations as to the proportion of patient contact or "clinical" involvement, and this holds in the institutional environment as well as the community environment. Pharmacists in some hospitals are still relegated to a corner in the basement, while in others they make daily rounds with the medical staff.

Turning to pharmacy education, we find an even greater diversity of opinion. One degree *versus* two degrees, four-year programs to six-year programs, internships *versus* externships, are just a few of the unsettled issues. At least as fundamental, if not more so, is the nature or thrust of the curriculum. Voices are heard advocating less emphasis on the basic sciences, while others argue for a return to basics; some voices urge more clinical exposure, while others say that the classroom should be emphasized; some that want more clinical training say it should be in an institutional environment, while others want more exposure in the community environment; and yet other voices are pushing for more or less business training, more or less courses in the humanities, more or less emphasis on communicative skills, and so on, seemingly *ad infinitum*.

Clearly, pharmacy needs to "get its act together" and settle on where it wants to go. Short of doing so, there will be further splintering and deterioration, perhaps to a point beyond retrieval.

This is not to say that responsible pharmacy organizations have been negligent in addressing these questions. On the contrary. The APhA policy committees and the House of Delegates have had some very spirited sessions in recent years wrestling with these controversial matters. The American Association of Colleges of Pharmacy has had some equally emotional sessions, and in late February conducted a special open hearing, inviting views from all interested segments on the subject of the types of pharmacy personnel necessary to meet society's needs.

Pharmacy in America is now at a point where its people must begin to arrive at some sort of consensus as to what pharmacy is; in turn, this means we need to reach general agreement on the issues of how pharmacists should be trained, how they should practice, and how they should be regulated.

We have already pulled all the pieces apart, and unless we begin the job of putting them back together—and pursue the task to its successful completion—we shall be inviting pharmacy's eventual demise. —EGF

MARCH 1978
VOLUME 67 NUMBER 3

JOURNAL OF PHARMACEUTICAL SCIENCES

MARY H. FERGUSON
Editor

SHELLY ELLIOTT
Production Editor

JANET D. SHOFF
Copy Editor

EDWARD G. FELDMANN
Contributing Editor

SAMUEL W. GOLDSTEIN
Contributing Editor

BELLE R. BECK
Editorial Secretary

DAVID BOHARDT
Director of Publications

L. LUAN CORRIGAN
Assistant Director of Publications

EDITORIAL ADVISORY BOARD

JOHN AUTIAN
HERBERT A. LIEBERMAN
NORMAN R. FARNSWORTH
DAVID E. MANN, JR.
WILLIAM O. FOYE
GERALD J. PAPARIELLO
WILLIAM J. JUSKO
EDWARD G. RIPPIE

The *Journal of Pharmaceutical Sciences* is published monthly by the American Pharmaceutical Association at 2215 Constitution Ave., N.W., Washington, DC 20037. Second-class postage paid at Washington, D.C., and at additional mailing office.

All expressions of opinion and statements of supposed fact appearing in articles or editorials carried in this journal are published on the authority of the writer over whose name they appear and are not to be regarded as necessarily expressing the policies or views of the American Pharmaceutical Association.

Offices—Editorial, Advertising, and Subscription Offices: 2215 Constitution Ave., N.W., Washington, DC 20037. Printing Offices: 20th & Northampton Streets, Easton, PA 18042.

Annual Subscriptions—United States and foreign, industrial and government institutions $50, educational institutions $50, individuals *for personal use only* $30; single copies $5. All foreign subscriptions add $5 for postage. Subscription rates are subject to change without notice. Members of the American Pharmaceutical Association may elect to receive the *Journal of Pharmaceutical Sciences* as a part of their annual $70 (foreign $75) APhA membership dues.

Claims—Missing numbers will not be supplied if dues or subscriptions are in arrears for more than 60 days or if claims are received more than 60 days after the date of the issue, or if loss was due to failure to give notice of change of address. The Association cannot accept responsibility for foreign delivery when its records indicate shipment has been made.

Change of Address—Members and subscribers should notify at once both the Post Office and the American Pharmaceutical Association, 2215 Constitution Ave., N.W., Washington, DC 20037, of any change of address.

Microfilm—Microfilm volumes are available from University Microfilms International, 300 N. Zeeb Road, Ann Arbor, MI 48106.

© Copyright 1978, American Pharmaceutical Association, 2215 Constitution Ave., N.W., Washington, DC 20037; all rights reserved.

A PROFESSION IN TRANSITION

Pharmacy's present condition can be summed up rather cryptically: *It's a mess!*

But before our readers get unhappy with us for making this blunt assessment, we would hasten to point out that such a condition is not inherently bad or objectionable, provided that it is only temporary.

Let us explain it this way. Improvement in any program, activity, project, or what have you, requires some sort of change to occur. During that period in which the change is being implemented or effectuated, there is going to be disorder and disruption. To cite an example from everyday life, most of us at one time or another have decided that our living room would benefit from a different furniture arrangement. In going from one state of orderliness to another, we must endure a temporary and brief period when the room looks like a disaster area.

Consequently, if we agree that improvements are desirable in pharmacy education, practice, and regulation, then change is required and, in turn, that automatically means a degree of disorder.

Now let us take our analogy one step further. The rearrangement of the living room furniture will proceed successfully and happily only on two conditions. First, there must be some sort of advance "master plan" even if it is only very informal in nature; and second, there must be general agreement or concurrence on that master plan on the part of all the family members. Given these conditions—plus some muscle, some determination, and a couple of strong backs—the project will proceed to satisfactory completion with a minimum of disorder and inconvenience.

This brings us to the point of this editorial. From our perspective, we are not certain that the changes presently in process in pharmacy are following any distinct master plan or that they enjoy the support of a majority of people within the profession.

On the subject of regulation, we continually hear comments on the one hand that "there ought to be a law . . .," but at the same time we hear protests about all of the red tape, paperwork, and government interference. Some of our people advocate increased regulation at the federal level, some hold out for a resurgence of state regulation, and others want a return to voluntary self-regulation. Mandatory continuing education and mandatory patient medication records are only two issues about which there is sharply divided opinion as to the desirability of a regulatory approach.

With regard to the nature of pharmacy practice, we have an equally broad spectrum of apparent viewpoints. At one extreme, there are mail order pharmacies where the pharmacist performs only the dispensing function, working exclusively with drug products and having zero contact with the patient. At the other extreme, there are office-type practices in which certain pharmacists spend their entire time with the patient, taking drug histories, advising on drug compliance, monitoring therapeutic results, and so on, resulting in no immediate contact with drug products. In between there are all variations as to the proportion of patient contact or "clinical" involvement, and this holds in the institutional environment as well as the community environment. Pharmacists in some hospitals are still relegated to a corner in the basement, while in others they make daily rounds with the medical staff.

Turning to pharmacy education, we find an even greater diversity of opinion. One degree *versus* two degrees, four-year programs to six-year programs, internships *versus* externships, are just a few of the unsettled issues. At least as fundamental, if not more so, is the nature or thrust of the curriculum. Voices are heard advocating less emphasis on the basic sciences, while others argue for a return to basics; some voices urge more clinical exposure, while others say that the classroom should be emphasized; some that want more clinical training say it should be in an institutional environment, while others want more exposure in the community environment; and yet other voices are pushing for more or less business training, more or less courses in the humanities, more or less emphasis on communicative skills, and so on, seemingly *ad infinitum*.

Clearly, pharmacy needs to "get its act together" and settle on where it wants to go. Short of doing so, there will be further splintering and deterioration, perhaps to a point beyond retrieval.

This is not to say that responsible pharmacy organizations have been negligent in addressing these questions. On the contrary. The APhA policy committees and the House of Delegates have had some very spirited sessions in recent years wrestling with these controversial matters. The American Association of Colleges of Pharmacy has had some equally emotional sessions, and in late February conducted a special open hearing, inviting views from all interested segments on the subject of the types of pharmacy personnel necessary to meet society's needs.

Pharmacy in America is now at a point where its people must begin to arrive at some sort of consensus as to what pharmacy is; in turn, this means we need to reach general agreement on the issues of how pharmacists should be trained, how they should practice, and how they should be regulated.

We have already pulled all the pieces apart, and unless we begin the job of putting them back together—and pursue the task to its successful completion—we shall be inviting pharmacy's eventual demise. —EGF

Need for Urine Drug Testing

We are very concerned to learn about the proposed elimination of all mandatory urine testing, with the exception of the initial drug screening urinalysis. This proposal holds the potential for both counterproduction and retrogression against the worthy goals of addict rehabilitation. The proposal has been made apparently on the following grounds: (*a*) mandated weekly urine testing on all patients is a waste of time, and the money saved could be utilized more effectively by hiring additional counseling staff or meeting other program needs; (*b*) controlled blind proficiency testing has shown that a percentage of reported results are inaccurate, raising questions about the validity of urine testing; (*c*) some clinics make only minimum use of urine test results because of the questionable validity factor; and (*d*) delays between urine collection and the receipt of urinalysis reports are sometimes excessive.

The advantages of mandatory urine testing are many:

1. A continuity of observation is established on a uniform basis.
2. As differentiated from "soft subjective" indicators, urinalysis is a solid, objective measure of the progress of clients.
3. It is an extremely useful tool for client confrontation in clinical management and is vital in penetrating the veil of self-deception developed by addicts.
4. It exposes the real behavior of a client and thus generates an honest basis between the client and the clinician[1,2].
5. It is a valuable psychological aid and deterrent, both in breaking the individual's drug-using habit and in keeping the client away from harmful street drugs of unknown identity.
6. In certain legal situations, it may well prove beneficial to the client's situation.
7. It can provide a sound basis for rational statistical determinations concerning individual treatment plans or the performance of modalities and/or programs.
8. It can be of *sine qua non* value in the therapeutic community or residential setting where weekend passes, peer level changes, responsibility assignment, and job readiness decisions must be made.
9. It has indispensible deterrent value in avoiding methadone diversion.
10. It provides visibility regarding epidemiological potential of illicit drugs of different types "sold on the street."

The relative cost of mandatory urine testing is not excessive. Urinalysis costs have been estimated at about 12 million of the 262 million total (about 5%). The view that a reduction in costs of urinalysis will permit the expenditure of those funds to increase the counseling staff is a defective argument. A counselor prepared with urinalysis data is in a position to be more efficient in his or her approach; conversely, a counselor not so prepared can be expected to be less efficient because of the time-consuming and less reliable techniques he or she must employ to determine what the client is really doing. It would seem paradoxical, at the minimum, to increase staff level and at the same time to take a course of action that would make every counselor less efficient. We believe that the abandonment of mandatory urinalysis for the purpose of increasing social services to the clients will open a pandora's box where performance cannot be rationally measured. A fear that programs will deteriorate to mere amusement centers appears reasonable.

Urinalysis credibility, if that is an issue, can be increased by providing guidance to laboratories in the establishment of effective quality control systems and the semiautomatic revalidation of challenged results. The U.S. Center for Disease Control ought to increase its minimum sensitivity requirements. It is not practical to abandon mandatory urinalysis because certain laboratories do not provide consistent, high quality results. Physicians faced with an analogous diagnostic situation can be expected to request test(s) while recognizing the inherent probability of a controllable level of error. There are so many options open to a well-trained counselor when error is suspected, including even recollection of specimens, that abandonment of the visibility provided by mandatory urinalysis cannot be justified on this ground.

The delay factor between urine collection and the reports of urinalysis is another argument offered by urine testing antagonists. However, an emergency treatment situation, as in the case of a hospitalized patient, is not analogous to the long-term methadone treatment situation. This argument, therefore, is also invalid.

Regarding the argument that the current mandatory urine testing does not give any choice to the clinician and/or the program or medical director according to the needs of their clients, we propose several "sets" of tests of alleged drugs of abuse. The clinician and /or program or medical director can select one set according to the individual needs of clients and also according to the drug abuse pattern of the geographical location of the treatment unit.

The proposed sets are:

A. Morphine, codeine, heroin adulterant optional, drugs used in treatment such as methadone and LAAM, amphetamines including methamphetamine (Desoxyn and Methedrine), phenmetrazine (Preludin), barbiturates, and propoxyphene (Darvon).

B. Morphine, codeine, heroin adulterant optional, and drugs used in treatment such as methadone and LAAM.

C. Amphetamines including methamphetamine (Desoxyn and Methedrine), phenmetrazine (Preludin), barbiturates, and drugs used in treatment such as methadone and LAAM.

D. Cocaine as its metabolite benzoylecgonine.

E. Benzodiazepine-type drugs of high abuse potential such as diazepam (Valium), oxazepam (Serax), and chlordiazepoxide (Librium).

F. Pentazocine (Talwin), antihistaminic-type drugs such as tripelennamine (Pyribenzamine), and phenothiazine-type tranquilizers.

G. Requests for special testing of drugs not listed above having a recognized abuse potential and a feasible qualitative and specific test. These drugs might include sedative–hypnotics like meprobamate (Miltown and Equanil) and ethchlorvynol (Placidyl), opiates such as hydromorphone (Dilaudid) and hydrocodone, hallucinogenic drugs such as phencyclidine (PCP), and antidepressants such as doxepin (Sinequan).

The following mandatory urine testing is viewed as minimally acceptable:

1. Provision for continued weekly analysis for any new or readmitted client and for those clients who have failed to have a clean urinalysis for a consecutive 3 months, with the clinician's choice of one of the above sets of tests according to the individual need of the client.
2. Provision for continued weekly analysis for parolees and other clients subject to the Criminal Justice System.
3. Provision for monthly urinalysis for all clients who were not tested on the weekly schedule.

In conclusion, we believe it is fair to observe that *all* aspects of drug abuse treatment at all levels need improvement. Scrapping of mandatory urinalysis cannot be justified for any of the grounds set forth in the first paragraph. In the lofty name of providing flexibility to the clinician, the proposed regulation sets up a clearly predictable abandonment of minimum urinalysis by insincere programs. Sincere programs surrounded by programs that abandon even minimum urinalysis will experience major difficulties in staff morale and retention because of the predictable attitude that they are being unfairly burdened with an unnecessary task.

The net result of the proposed elimination of mandatory urine testing will be a deterioration in methadone program effectiveness.

K. K. Kaistha
Rahmeh Tadrus
State of Illinois
Dangerous Drugs Commission
Toxicology Division
c/o I.I.T. Research
10 W. 35th Street
Chicago, IL 60616

Received December 19, 1977.

[1] E. C. Senay and P. F. Renault, *J. Psychedelic Drugs*, **3**, 47 (1971).
[2] K. K. Kaistha, *J. Chromatogr.*, **141** (2) (1977); *Chromatogr. Rev.*, **21** (2), 145 (1977).

JOURNAL OF PHARMACEUTICAL SCIENCES

MARCH 1978
VOLUME 67 NUMBER 3

RESEARCH ARTICLES

Pharmacokinetic Profile of Clonazepam in Rhesus Monkeys

ALLEN A. LAI and RENÉ H. LEVY ˣ

Received March 3, 1977, from the *Departments of Pharmaceutical Sciences and Neurological Surgery, Schools of Pharmacy and Medicine, University of Washington, Seattle, WA 98195.* Accepted for publication June 7, 1977.

Abstract □ The pharmacokinetic profile of clonazepam was studied in five chronically catheterized male rhesus monkeys using short-term intravenous infusion and oral administration in a Latin-square design. Clonazepam in a 40% polyethylene glycol 400 solution was infused at a constant rate over 25 hr into each monkey. Steady-state plasma levels in the ranges of 20, 40, 60, and 80 ng/ml were achieved with infusion rates of 15, 30, 45, and 60 μg/hr/kg, respectively. An oral dose of 0.5 mg of clonazepam also was administered to each monkey by intranasal gastric intubation. Plasma levels were assayed by electron-capture GLC. The intravenous and oral kinetics of clonazepam could be described in terms of a one-compartment open model with first-order elimination. The mean (±*SE*) parameters from short-term infusion studies were: total body clearance, 0.86 ± 0.03 liter/hr/kg; elimination half-life, 5.6 ± 0.6 hr; and volume of distribution, 6.8 ± 0.5 liters/kg. Intra- and interindividual variability in these parameters was prevalent, implying that dosing of monkeys during efficacy testing requires individual adjustments. Long-term (7–10-day) infusion studies revealed a small, but significant, decrease in clearance as well as diurnal oscillation in "steady-state" plasma levels.

Keyphrases □ Clonazepam—pharmacokinetics in rhesus monkeys □ Pharmacokinetics—clonazepam in rhesus monkeys □ Anticonvulsants—clonazepam, pharmacokinetics in rhesus monkeys

Clonazepam, 5-(2-chlorophenyl)-1,3-dihydro-7-nitro-2*H*-1,4-benzodiazepin-2-one, has shown anticonvulsant properties in several animal species (1). It was used for several years in Europe in the treatment of petit mal epilepsy prior to its recent approval for use in the United States. Clinically, the oral formulation is particularly effective in controlling petit mal at doses of 1–2 mg/day (2). In Europe and Australia, the intravenous formulation also has been found effective in suppressing status epilepticus (3, 4).

Clonazepam will be evaluated in an epileptic monkey model specific to motor seizures (5, 6). The present study was undertaken to determine the pharmacokinetic profile in the rhesus monkey and to design an optimum dosage regimen.

Earlier studies[1] in monkeys indicated that rapid intravenous injection of clonazepam (in 10% propylene glycol) in the femoral vein produced irregularities in the early time points of the plasma concentration–time curve. These irregularities were attributed to *in vivo* drug precipitation. As a result, intravenous bolus injections were replaced by short-term (1-day) constant-rate infusions in the present study design. The preliminary studies[1] also indicated that the clonazepam elimination half-life is short, precluding a once a day oral administration regimen. This situation suggested chronic intravenous administration (through indwelling catheters) for efficacy evaluation. Consequently, long-term (7–10-day) infusion studies also were included in the experimental design.

EXPERIMENTAL

Animal Preparation—Five male rhesus monkeys were chair adapted for 1 month prior to the study and maintained in a three-level restraining chair during each individual experiment. The monkeys were given cage rest at appropriate intervals. The jugular and femoral veins of each monkey were catheterized chronically to enable withdrawal of venous blood samples and drug infusion, respectively. Patency of catheters was assured by a slow, continuous saline infusion.

All monkeys were maintained on monkey chow and fresh fruit in the Vivarium at the University of Washington.

Protocol—Four short-term (25-hr) intravenous infusion studies and one oral study were planned for each monkey using a randomized 5 × 5 Latin-square design. For the short-term infusions, clonazepam in a sterile polyethylene glycol 400–water mixture (40:60 v/v) was infused at a constant rate[2] of 1 ml/hr over 25 hr. Steady-state levels of 20, 40, 60, and 80 ng/ml were achieved with infusion rates of approximately 15, 30, 45, and 60 μg/hr/kg. The oral dose was an aqueous suspension of a 0.5-mg clonazepam tablet[3]/monkey, administered by intranasal gastric intubation.

[1] R. H. Levy, J. S. Lockard, and H. J. Kupferberg, unpublished results.
[2] Holter infusion pump, Extracorporeal Medical Specialties, King of Prussia, Pa.
[3] Clonopin, Roche Laboratories, Nutley, N.J.

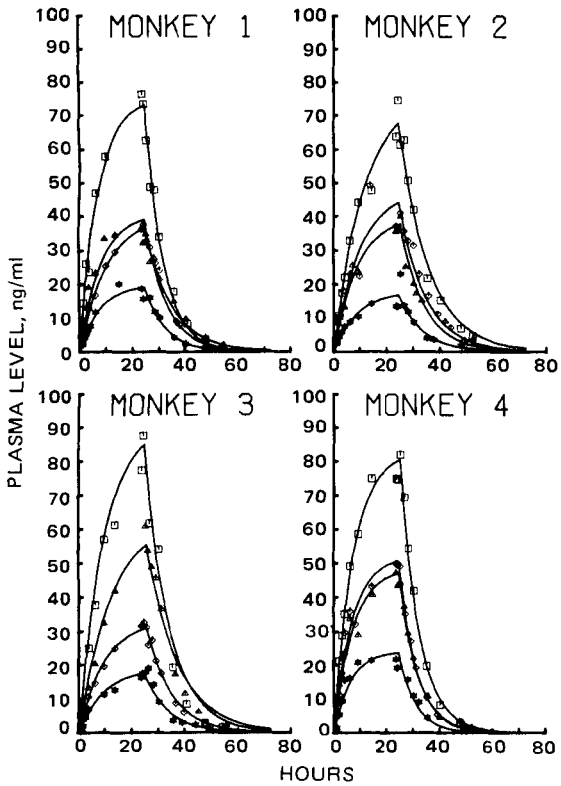

Figure 1—*Plots of plasma clonazepam concentrations* versus *time for the four 25-hr infusions in Monkeys 1–4. The continuous lines were obtained by a least-squares fit of experimental data points.*

Long-term (7–10-day) intravenous infusions, designed to achieve a steady-state plasma level of 40 ng/ml, also were performed (one per monkey).

Blood samples were collected at predetermined times into 3-ml tubes containing edetate potassium as an anticoagulant. The blood specimens were centrifuged immediately, and plasma samples were separated and frozen. Plasma samples generally were assayed on the day following the end of a study. All studies in the Latin-square design were completed, except for two short-term infusions and one oral study in Monkey 5 (technical difficulties with catheters). For the long-term infusion, Monkey 5 was replaced by Monkey 6.

Analytical Procedures—Plasma samples were analyzed for clonazepam using the electron-capture GLC assay of de Silva and Bekersky (7) with the following modifications. Since plasma was used in place of whole blood, the blood denaturation step was eliminated. Moreover, 80–100-mesh Chromosorb W-HP[4] replaced 60–80-mesh Gas Chrom Q. The gas chromatograph[5] was equipped with a 15-mCi ^{63}Ni-electron-capture detector. The operating conditions were as follows: injection port, 300°; oven, 260°; detector, 300°; and argon–methane (90:10) carrier gas flow, 20 ml/min. The reliability of the determinations was monitored by assaying one control sample with each run. The percent standard deviation of multiple assays over 1 year was 7.7%.

Data Analysis—Experimental data points were fitted to appropriate model equations using the BMDX85 nonlinear least-squares program on a digital computer[6]. All plasma concentrations were assigned equal weights. Experimental concentrations during the infusion and postinfusion periods were fitted to Eqs. 1 and 2, respectively. The computer output yielded two parameters, total body clearance(s) and elimination rate constant(s). Values for the volume of distribution were calculated from these parameters (ratio of total body clearance and elimination rate constant) as well as from area measurements (Eq. 3).

Bioavailability of the oral formulation was calculated as the ratio of the area under the plasma concentration–time curves after oral and intravenous administrations, with correction for dosage (Eq. 4) as well as intrasubject variation in half-life (Eq. 5).

[4] Supelco, Bellefonte, Pa.
[5] HP model 5710A, Hewlett-Packard, Avondale, Pa.
[6] CDC 6400, Control Data Corp., Minneapolis, Minn.

Table I—Pharmacokinetic Parameters of Clonazepam in Rhesus Monkeys Obtained from Short-Term (25-hr) Intravenous Infusion Studies

Monkey	Mean Elimination Half-Life, hr (*SD*)	Mean Volume of Distribution, liters/kg (*SD*)	Mean Total Body Clearance, liter/hr/kg (*SD*)
1	5.7 (1.0)	7.0 (1.0)	0.86 (0.18)
2	6.7 (0.7)	7.7 (0.7)	0.83 (0.16)
3	7.0 (0.8)	7.9 (1.1)	0.78 (0.16)
4	4.7 (0.3)	6.5 (0.3)	0.96 (0.05)
5	4.0 (0.2)	5.0 (0.8)	0.86 (0.10)
Mean (*SE*)	5.6 (0.6)	6.8 (0.5)	0.86 (0.03)

RESULTS AND DISCUSSION

Short-Term Infusion Kinetics—Figure 1 shows the plasma concentration–time curves obtained for the four 25-hr infusions in Monkeys 1–4. In most cases, steady-state plasma levels were nearly achieved by 25 hr; on the following day, plasma concentrations decayed to less than 10% of the 25-hr levels. The experimental concentrations during infusion (C_i) and postinfusion (C_p) were fitted to the following equations (8), respectively:

$$C_i = \frac{R}{Cl}(1 - e^{-K_E t}) \qquad \text{(Eq. 1)}$$

$$C_p = \frac{R}{Cl}(1 - e^{-K_E t_i})e^{-K_E(t - t_i)} \qquad \text{(Eq. 2)}$$

where R represents the zero-order infusion rate, t is the time since the beginning of the infusion, t_i is the time at which infusion is stopped, Cl is the total body clearance, and K_E is the first-order rate constant for elimination by all processes.

The least-squares fitting procedure involved a simultaneous fit of the data points to both equations, yielding a single set of parameters[7]. The results of curve fitting are shown by the continuous lines in Fig. 1. The agreement between data points and the least-squares lines suggests that, as a first approximation, a one-compartment open model with first-order elimination is appropriate to describe the short-term infusion kinetics of clonazepam in monkeys.

A summary of pharmacokinetic parameters obtained by least-squares regression analysis in all five monkeys is given in Table I. The uniqueness of the parameters obtained from the regression analysis of each set of experimental data can be assessed from the corresponding standard deviations. The mean percent standard deviations for half-life ($T_{1/2}$) and total body clearance in the 18 infusion studies were 8.1 and 3.3%, respectively.

The mean half-life in individual monkeys ranged from 4.0 to 7.0 hr. The overall mean half-life (±*SE*) was 5.6 ± 0.6 hr. A half-life of 4.8 hr reported for one squirrel monkey given an intravenous bolus dose is within the range of values found in this study (9). The clonazepam elimination half-life in humans is longer, ranging from 17 to 60 hr (9–12). In the present study, the intrasubject variability in half-life, expressed as percentage standard deviation, ranged from 5 to 18%. Data on intrasubject variability in the clonazepem biological half-life in humans are scarce. Knop *et al.* (9) found half-life values of 17 and 22 hr in the same volunteer given a 2-mg iv infusion 3 months apart.

Mean total body clearance in individual monkeys ranged between 0.78 and 0.96 liter/hr/kg with an overall mean (±*SE*) of 0.86 ± 0.03 liter/hr/kg. The intrasubject variability (5–21%) was of the same order of magnitude as that found with the half-life. The clearance values found in this study are larger than the values reported in one squirrel monkey (9) and the range of values (0.02–0.09 liter/hr/kg) found in humans (9, 10).

The volume of distribution (V_d) was calculated by two methods: from the ratio of the total body clearance and the elimination rate constant (Method I) and by Eq. 3 (Method II):

$$V_d = \frac{(D)_{iv}}{AUC\ K_E} \qquad \text{(Eq. 3)}$$

where AUC is the area under the plasma concentration–time curve (from $t = 0$ to $t = \infty$) calculated by the trapezoidal rule, $(D)_{iv}$ is the total dose infused, and K_E is as previously defined. The mean ratio (±*SD*) of 18 sets

[7] The infusion (C_i) and postinfusion (C_p) concentrations were fitted to Eqs. 1 and 2 separately and yielded almost identical sets of parameters, indicating that the simultaneous fitting approach is valid.

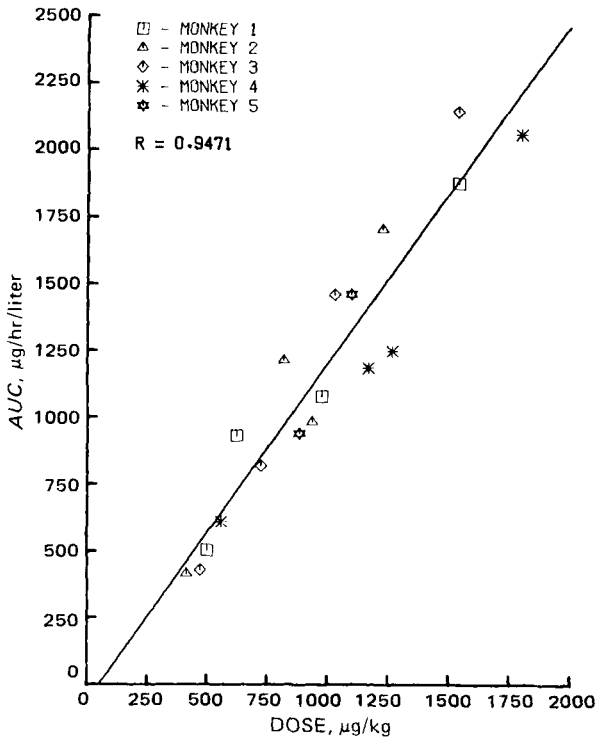

Figure 2—*Plots of* AUC versus *dose following 25-hr infusions in Monkeys 1–5.*

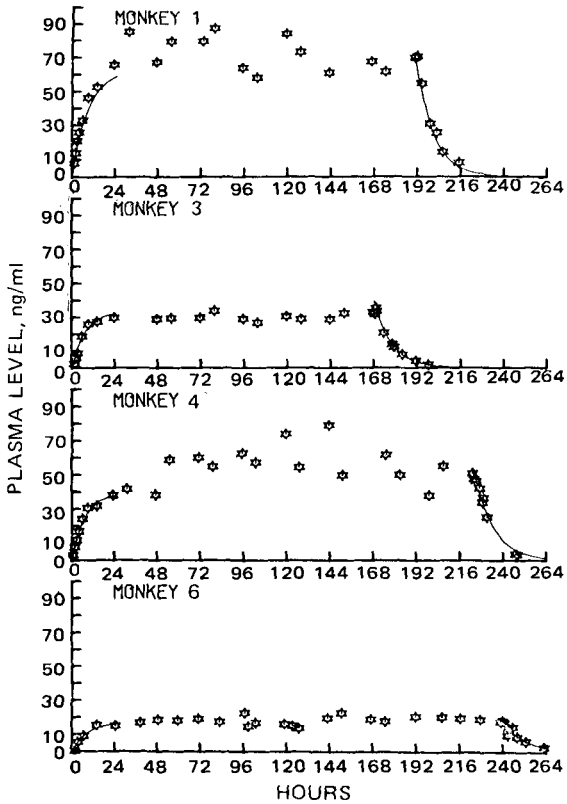

Figure 3—*Plots of plasma clonazepam concentrations* versus *time following a 7–10-day continuous zero-order intravenous infusion in Monkeys 1, 3, 4, and 6. The continuous lines were obtained by a least-squares fit of experimental data points.*

of values of volume of distribution calculated by these two methods was 1.02 ± 0.05, indicating that Methods I and II are equivalent.

The values listed in Table I (obtained by Method I) ranged from 5.0 to 7.9 liters/kg with an overall mean (±*SE*) of 6.8 (±0.5) liters/kg. These values are larger than those reported for any other species, suggesting that, in monkeys, clonazepam partitions extensively outside of the total body water compartment. Knop *et al.* (9) found a volume of distribution of 2.1 liters/kg in one squirrel monkey. The values of this parameter ranged from 1.5 to 4.4 liters/kg in humans (9–12) and from 2.4 to 3.5 liters/kg in dogs (9, 11). The intrasubject variability (5–21%) was of the same magnitude as that found for other parameters.

A plot of the area under the plasma concentration–time curve *versus* dose (Fig. 2) shows a linear relationship with a correlation coefficient of 0.94. This result suggests that the kinetics of clonazepam in monkeys are linear in the 400–1800-μg/kg range. The slope of this plot yields a total body clearance value very close to the overall mean of individual studies. The presence of kinetic linearity further supports the use of a one-compartment open model with first-order elimination to describe clonazepam kinetics in monkeys.

A urinary excretion study was performed in one monkey (Monkey 3) given a 15.39-mg dose of clonazepam by intravenous infusion over 48 hr. Urine samples were collected at 24-hr intervals for 4 days. Analysis of these samples yielded a total of 122.35 μg of clonazepam excreted unchanged, *i.e.*, 0.8% of the dose. This value is close to the values reported by Kaplan *et al.* (11) for dogs and humans, 0.1 and 0.5%, respectively. Thus, it appears that clonazepam is almost completely metabolized in all species investigated so far.

Long-Term Infusion Kinetics—Figure 3 shows experimental plasma concentrations as a function of time following a 7–10-day continuous zero-order infusion of clonazepam in Monkeys 1, 3, 4, and 6. The 0–25-hr data were fitted to Eq. 1, and the postinfusion data were fitted to Eq. 2; the resulting pharmacokinetic parameters (Table II) were subjected to statistical comparison (paired *t*-test). The results indicated that there is a significant difference in half-life and total body clearance between the 0–25-hr period and the postinfusion decay. The postinfusion clearances were, on the average, 14.4% smaller than the 0–25-hr values, and the postinfusion half-lives were 29.7% longer.

Table II—Pharmacokinetic Parameters of Clonazepam in Rhesus Monkeys Obtained from the 0–25-hr and Postinfusion Data during Long-Term (7–10-day) Intravenous Infusion Studies

	Elimination Half-Life, hr		Total Body Clearance, liters/hr/kg	
Monkey	0–25 hr	Post-infusion	0–25 hr	Post-infusion
1	6.3	6.3	0.67	0.60
2	—	11.6	—	0.42
3	5.4	6.6	1.06	0.91
4	5.0	7.7	0.98	0.72
6	6.1	8.7	1.19	1.13
	$p < 0.05$		$p < 0.05$	

The shorter apparent half-life obtained in the 0–25-hr period could be the result of simultaneous distribution and elimination if clonazepam exhibits a prolonged distribution phase. A lengthening of the tetracycline half-life when going from single to multiple dosing was reported by Doluisio and Dittert (13). Subsequent studies[8] suggested that the shorter initial tetracycline half-life is due to a prolonged distribution phase. An alternative explanation for the longer postinfusion clonazepam half-lives at the end of long-term infusions could be metabolite(s) inhibition of metabolism, as suggested for diazepam (14). A decrease in total body clearance and an increase in half-life after 6 days of administration of diazepam to seven volunteers were attributed to the accumulation of desmethyldiazepam, the major metabolite.

The clearances and half-lives obtained in the long-term infusions were compared to the corresponding values obtained in the short-term studies. There was no significant differences ($p \leq 0.05$) between the short-term infusion parameters and either the 0–25-hr or postinfusion values.

Fluctuations in steady-state plasma levels during long-term infusions (from Days 2 to 7–10) were present in all monkeys. The degree of oscillation within a 24-hr period was measured by the ratio C^*_{max}/C^*_{min}, where C^*_{max} and C^*_{min} represent the highest and lowest "steady-state" concentrations, respectively. These ratios ranged from 1.01 to 1.64 (mean ± *SD* = 1.21 ± 0.17) in five monkeys; consequently, the infusion data from Day 2 onward were not fitted to Eq. 1. Fluctuations in steady-state plasma levels could be caused by variations in experimental factors such as drug assay and/or infusion pump rotational speed. However, in the present study, appropriate steps were taken to ensure that these factors would not contribute to the observed oscillations.

[8] W. G. Crouthamel, School of Pharmacy, University of Maryland, Baltimore, MD 21201, personal communication.

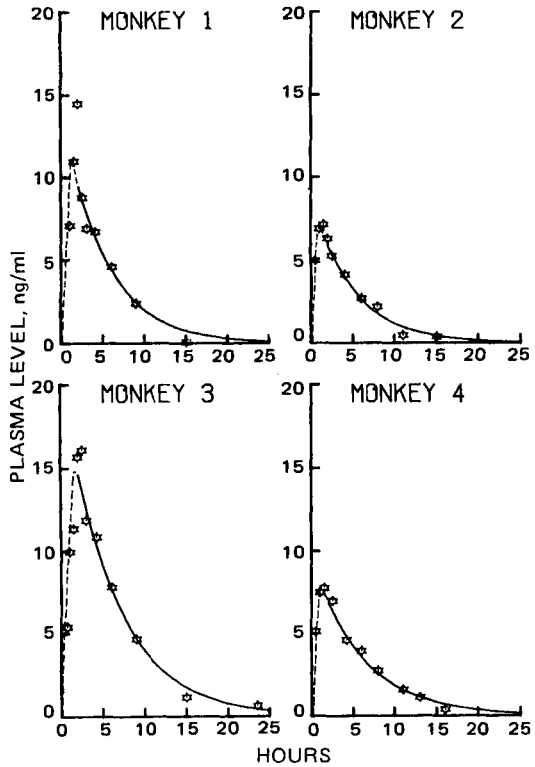

Figure 4—*Plots of plasma clonazepam concentrations* versus *time following oral administration of 0.5 mg of clonazepam to Monkeys 1–4. The continuous lines were obtained by a least-squares fit of postabsorption experimental data points.*

A similar type of time dependency was observed for two other anticonvulsants, ethosuximide (15) and valproic acid (16, 17), during chronic infusion in rhesus monkeys. Twenty-four-hour monitoring of plasma concentrations under controlled environmental conditions showed that the fluctuations in steady-state plasma levels of these two drugs could be attributed to diurnal oscillations in total body clearance (14–16). Such a phenomenon may also be present with clonazepam.

Oral Kinetics—Plasma concentration–time profiles following oral administration of 0.5 mg of clonazepam to Monkeys 1–4 are shown in Fig. 4. The peak time (t_{max}) was generally between 1 and 2 hr, suggesting that the broken tablet was rapidly absorbed. However, the absorption half-life could not be determined because of an insufficient number of data points during the absorption phase. The experimental data points at times larger than t_{max} were fitted to a monoexponential equation, and postabsorption half-lives were obtained (Table III). These values were much shorter than the corresponding mean intravenous half-lives. Statistical comparison (paired t-test) showed that the difference is significant ($p < 0.025$).

Apparent elimination half-lives obtained following oral administration can be longer than the corresponding intravenous half-lives in the presence of prolonged absorption. However, decreases in apparent half-lives following oral administration have not been reported. As discussed earlier, if a prolonged distribution phase is present, a shorter half-life would be expected from the decay curve starting at 2 hr after oral administration than after 25 hr of constant-rate infusion. Similarly, if metabolism is inhibited by metabolites, the latter would be expected to reach higher levels after 25 hr of constant-rate infusion than at 2 hr after a single oral dose. Another difference between the two experimental conditions is the presence of polyethylene glycol 400 in the intravenous studies, and its potential role in the observed phenomenon cannot be excluded.

Ronfeld and Benet (18) showed that the intravenous kinetics of phenytoin in rhesus monkeys were not altered following prolonged infusion of polyethylene glycol 400. The possible effect of polyethylene glycol on the oral kinetics of clonazepam is presently being investigated.

Bioavailability (F) was assessed using the following two equations:

$$F = \frac{(AUC)_{oral}(D)_{iv}}{(AUC)_{iv}(D)_{oral}} \quad \text{(Eq. 4)}$$

$$F = \frac{(AUC)_{oral}(D)_{iv}(K_E)_{oral}}{(AUC)_{iv}(D)_{oral}(K_E)_{iv}} \quad \text{(Eq. 5)}$$

Table III—Pharmacokinetic Parameters of Clonazepam in Rhesus Monkeys Obtained after Oral Administration

Monkey	Elimination Half-Life, hr	Bioavailability, % With Elimination Constant Adjustment	Bioavailability, % Without Adjustment
1	3.5	90	57
2	3.5	91	48
3	4.3	156	97
4	4.3	50	46
Mean (*SD*)	3.9 (0.5)	97 (44)	62 (24)

where F, AUC, K_E, and $(D)_{iv}$ are as previously defined; $(D)_{oral}$ is the oral dose; and subscripts iv and oral stand for the modes of administration. Equation 4 makes the assumption that total body clearance during the oral study was identical to the mean value obtained in the short-term infusion studies. This method gave values ranging between 46% (Monkey 4) and 97% (Monkey 3) with a mean of 62%. Calculation of bioavailability using Eq. 5 (19) makes the assumption that the volume of distribution of each animal during the oral study was the same as the mean value obtained in the short-term infusion studies. This method gave values ranging between 50% (Monkey 4) and 156% (Monkey 3) with a mean value of 97%.

In view of the substantial intrasubject variability in the volume of distribution observed in the intravenous studies (both short and long term), even the values obtained from Eq. 5 may not represent an accurate assessment of the fraction of dose absorbed. Other factors may contribute to the wide range of bioavailability values obtained. The possibility of a first-pass effect exists since clonazepam is almost totally metabolized and its total body clearance represents over 30% of the liver blood flow (20) in the monkey. Metabolism by microorganisms of the GI flora is another possibility (21) since a major pathway of clonazepam metabolism involves reduction of the aromatic nitro group to 7-aminoclonazepam.

REFERENCES

(1) L. D. Randall and B. Kappell, in "The Benzodiazepines," S. Garattini, E. Mussini, and L. O. Randall, Eds., Raven, New York, N.Y., 1973, pp. 27–51.

(2) R. Kruse, *Epilepsia*, **12**, 179 (1971).

(3) H. Gastaut, J. Courjon, R. Poire, and M. Weber, *ibid.*, **12**, 197 (1971).

(4) P. F. Bladin, *Med. J. Aust.*, **1**, 683 (1973).

(5) J. S. Lockard, W. L. Wilson, and V. Uhlir, *Epilepsia*, **13**, 437 (1972).

(6) A. A. Ward, in "Experimental Models of Epilepsy," D. P. Purpura, J. K. Penry, D. Tower, D. M. Woodbury, and R. Walter, Eds., Raven, New York, N.Y., 1972, pp. 13–35.

(7) J. A. F. de Silva and I. Bekersky, *J. Chromatogr.*, **99**, 447 (1974).

(8) E. M. P. Widmark, *Acta Med. Scand.*, **52**, 87 (1919).

(9) H. J. Knop, E. Van der Kleijn, and L. C. Edmunds, in "Clinical Pharmacology of Anti-Epileptic Drugs," H. Schneider, D. Janz, C. Gardner-Thorpe, H. Meinardi, and A. L. Sherwin, Eds., Springer-Verlag, New York, N.Y., 1975, pp. 247–260.

(10) A. Berlin and H. Dahlstrom, *Eur. J. Clin. Pharmacol.*, **9**, 155 (1975).

(11) S. A. Kaplan, K. Alexander, M. J. Jack, C. V. Puglisi, J. A. F. de Silva, T. L. Lee, and R. E. Weinfeld, *J. Pharm. Sci.*, **63**, 527 (1974).

(12) O. Sjö, E. F. Hvidberg, J. Naestoft, and M. Lund, *Eur. J. Clin. Pharmacol.*, **8**, 249 (1975).

(13) J. T. Doluisio and L. W. Dittert, *Clin. Pharmacol. Ther.*, **10**, 690 (1969).

(14) U. Klotz, K. H. Antonin, and P. R. Bieck, *Eur. J. Clin. Pharmacol.*, **10**, 121 (1976).

(15) I. H. Patel, R. H. Levy, and J. S. Lockard, *J. Pharm. Sci.*, **66**, 650 (1977).

(16) R. H. Levy, J. S. Lockard, I. H. Patel, and W. C. Congdon, *ibid.*, **66**, 1154 (1977).

(17) J. S. Lockard, R. H. Levy, L. L. DuCharme, W. C. Congdon, and I. H. Patel, *Epilepsia*, **18**, 183 (1977).

(18) R. Ronfeld and L. Z. Benet, "Abstracts," Vol. 2, No. 2, APhA Academy of Pharmaceutical Sciences, Chicago meeting, 1972.

(19) J. G. Wagner, *J. Pharm. Sci.*, **56**, 652 (1967).

(20) R. P. Forsyth, A. S. Nies, F. Wyle, J. Hentze, and K. L. Melmon, *J. Appl. Physiol.*, **25**, 736 (1968).

(21) P. K. Zachariah and M. R. Juchau, *Drug Metab. Disp.*, **2**, 74 (1974).

ACKNOWLEDGMENTS

Presented at the Basic Pharmaceutics Section, APhA Academy of Pharmaceutical Sciences, Orlando meeting, November 1976.

Supported by NIH Research Contract NOI-NS-1-2282 and Research Grant NS-04053 awarded by the National Institute of Neurological and Communicative Disorders and Strokes, Public Health Service.

The authors thank Hoffmann–La Roche for the generous supply of clonazepam and nitrazepam. They also thank Ms. Barbara J. Oyloe, Mr. Douglas J. Ng, and Mr. James L. Cook for technical assistance.

Effect of Vehicles and Other Active Ingredients on Stability of Hydrocortisone

V. DAS GUPTA

Received December 23, 1976, from the *College of Pharmacy, University of Houston, Houston, TX 77004.* Accepted for publication May 10, 1977.

Abstract □ The stability of hydrocortisone in various types of vehicles, aqueous, water-washable (polyethylene glycol ointment base), and oil in water or water in oil-type emulsified vehicles, and in the presence of other ingredients, iodochlorhydroxyquin, menthol, and phenol, was studied under normal conditions (room temperature and weakly acidic pH). The study was conducted using a stability-indicating assay method, high-pressure liquid chromatography. The hydrocortisone was very unstable in water and water-washable ointment base. The addition of alcohol and glycerin to water had a stabilizing effect. Under drastic conditions (very acidic or very basic pH), hydrocortisone proved to be unstable only on the basic side. The data at higher temperatures confirmed that the decomposition in water and polyethylene glycol was pseudo-first order. The decomposition process appears to be different in the highly basic solution *versus* weakly acidic media or in water *versus* polyethylene glycol ointment base.

Keyphrases □ Hydrocortisone—stability in various types of vehicles, effect of other active ingredients □ Stability—hydrocortisone in various types of vehicles, effect of other active ingredients □ Vehicles, various types—effect on stability of hydrocortisone, effect of other active ingredients □ Dosage forms—hydrocortisone in various types of vehicles, effect of other active ingredients on stability □ Glucocorticoids—hydrocortisone, stability in various types of vehicles, effect of other active ingredients

Hydrocortisone (I) is widely used in topical dosage forms that often contain other active ingredients such as iodochlorhydroxyquin, menthol, and phenol. Many different types of vehicles have been used to incorporate the active ingredients, *i.e.*, aqueous, water washable, water in oil or oil in water emulsion, and nonpolar vehicles. No comprehensive study on the stability of hydrocortisone in various vehicles and in the presence of other ingredients has been reported.

The degradation of the C-17 side chain (Structure I) of certain corticosteroids was studied (1–3) using base-catalyzed degradation, and it was suggested that the reaction was complex pseudo-first order. The degradation of hydrocortisone hemisuccinate at 70° was studied (4) over a narrow pH range and found to be a first-order reaction. Various factors influencing the stability of corticosteroids in aqueous suspensions and solutions were investigated (5), and it was concluded that prednisolone should not be exposed to materials capable of producing an elevated pH during formulation. Prednisolone in anhydrous form was considered to be stable (6) in liquid paraffin but not in water.

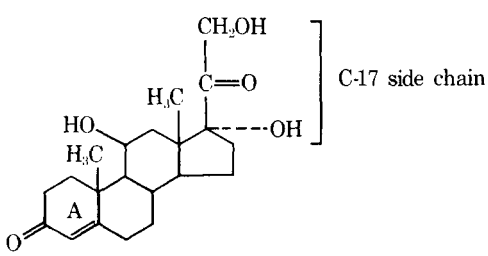

I

The stability of cortisone and hydrocortisone was investigated (7, 8) using the UV spectrophotometric and phenylhydrazine methods to detect alterations in ring A (Structure I); the blue tetrazolium method was used to detect deterioration of the C-17 side chain. One such study (8) determined the shelflife of hydrocortisone in polyethylene glycol base to be approximately 6 months.

Only recently have better methods of analysis (from a stability point of view) become available (9, 10). The purpose of this study was to evaluate the effect of various vehicles and other active ingredients (iodochlorhydroxyquin, menthol, and phenol) on the stability of hydrocortisone. The other bases studied were water, polyethylene glycol ointment base USP (11), cold cream[1] USP (12), petrolatum[2], and three commercial bases[3]. The study was conducted using a stability-indicating assay method by high-pressure liquid chromatography (HPLC).

EXPERIMENTAL

Chemicals and Reagents—All chemicals and reagents were USP, NF, or ACS grade and were used without further purification.

Apparatus—A high-pressure liquid chromatograph[4] capable of operating at an inlet pressure of 6000 psig was used.

Column—The column consisted of a monomolecular layer of cyano-

[1] E. Fougera & Co., Hicksville, NY 11802.
[2] McKesson Laboratories, Bridgeport, Conn.
[3] Aquaphore, Duke Laboratories, Norwalk, Conn.; HEB, Barnes-Hind Pharmaceuticals, Sunnyvale, Calif.; and Dermovan, Texas Pharmacal Co., San Antonio, TX 78296.
[4] Waters ALC 202 equipped with a U6K universal liquid chromatograph injector and a UV detector (254-nm fixed wavelength), Waters Associates, Milford, Mass.

(21) P. K. Zachariah and M. R. Juchau, *Drug Metab. Disp.*, **2**, 74 (1974).

ACKNOWLEDGMENTS

Presented at the Basic Pharmaceutics Section, APhA Academy of Pharmaceutical Sciences, Orlando meeting, November 1976.

Supported by NIH Research Contract NOI-NS-1-2282 and Research Grant NS-04053 awarded by the National Institute of Neurological and Communicative Disorders and Strokes, Public Health Service.

The authors thank Hoffmann–La Roche for the generous supply of clonazepam and nitrazepam. They also thank Ms. Barbara J. Oyloe, Mr. Douglas J. Ng, and Mr. James L. Cook for technical assistance.

Effect of Vehicles and Other Active Ingredients on Stability of Hydrocortisone

V. DAS GUPTA

Received December 23, 1976, from the *College of Pharmacy, University of Houston, Houston, TX 77004.* Accepted for publication May 10, 1977.

Abstract □ The stability of hydrocortisone in various types of vehicles, aqueous, water-washable (polyethylene glycol ointment base), and oil in water or water in oil-type emulsified vehicles, and in the presence of other ingredients, iodochlorhydroxyquin, menthol, and phenol, was studied under normal conditions (room temperature and weakly acidic pH). The study was conducted using a stability-indicating assay method, high-pressure liquid chromatography. The hydrocortisone was very unstable in water and water-washable ointment base. The addition of alcohol and glycerin to water had a stabilizing effect. Under drastic conditions (very acidic or very basic pH), hydrocortisone proved to be unstable only on the basic side. The data at higher temperatures confirmed that the decomposition in water and polyethylene glycol was pseudo-first order. The decomposition process appears to be different in the highly basic solution *versus* weakly acidic media or in water *versus* polyethylene glycol ointment base.

Keyphrases □ Hydrocortisone—stability in various types of vehicles, effect of other active ingredients □ Stability—hydrocortisone in various types of vehicles, effect of other active ingredients □ Vehicles, various types—effect on stability of hydrocortisone, effect of other active ingredients □ Dosage forms—hydrocortisone in various types of vehicles, effect of other active ingredients on stability □ Glucocorticoids—hydrocortisone, stability in various types of vehicles, effect of other active ingredients

Hydrocortisone (I) is widely used in topical dosage forms that often contain other active ingredients such as iodochlorhydroxyquin, menthol, and phenol. Many different types of vehicles have been used to incorporate the active ingredients, *i.e.*, aqueous, water washable, water in oil or oil in water emulsion, and nonpolar vehicles. No comprehensive study on the stability of hydrocortisone in various vehicles and in the presence of other ingredients has been reported.

The degradation of the C-17 side chain (Structure I) of certain corticosteroids was studied (1–3) using base-catalyzed degradation, and it was suggested that the reaction was complex pseudo-first order. The degradation of hydrocortisone hemisuccinate at 70° was studied (4) over a narrow pH range and found to be a first-order reaction. Various factors influencing the stability of corticosteroids in aqueous suspensions and solutions were investigated (5), and it was concluded that prednisolone should not be exposed to materials capable of producing an elevated pH during formulation. Prednisolone in anhydrous form was considered to be stable (6) in liquid paraffin but not in water.

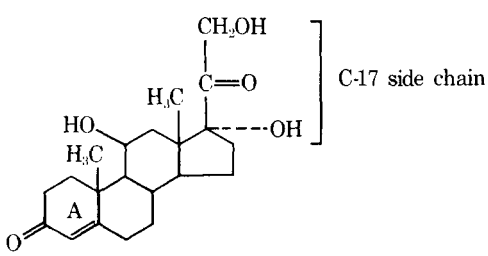

I

The stability of cortisone and hydrocortisone was investigated (7, 8) using the UV spectrophotometric and phenylhydrazine methods to detect alterations in ring A (Structure I); the blue tetrazolium method was used to detect deterioration of the C-17 side chain. One such study (8) determined the shelflife of hydrocortisone in polyethylene glycol base to be approximately 6 months.

Only recently have better methods of analysis (from a stability point of view) become available (9, 10). The purpose of this study was to evaluate the effect of various vehicles and other active ingredients (iodochlorhydroxyquin, menthol, and phenol) on the stability of hydrocortisone. The other bases studied were water, polyethylene glycol ointment base USP (11), cold cream[1] USP (12), petrolatum[2], and three commercial bases[3]. The study was conducted using a stability-indicating assay method by high-pressure liquid chromatography (HPLC).

EXPERIMENTAL

Chemicals and Reagents—All chemicals and reagents were USP, NF, or ACS grade and were used without further purification.

Apparatus—A high-pressure liquid chromatograph[4] capable of operating at an inlet pressure of 6000 psig was used.

Column—The column consisted of a monomolecular layer of cyano-

[1] E. Fougera & Co., Hicksville, NY 11802.
[2] McKesson Laboratories, Bridgeport, Conn.
[3] Aquaphore, Duke Laboratories, Norwalk, Conn.; HEB, Barnes-Hind Pharmaceuticals, Sunnyvale, Calif.; and Dermovan, Texas Pharmacal Co., San Antonio, TX 78296.
[4] Waters ALC 202 equipped with a U6K universal liquid chromatograph injector and a UV detector (254-nm fixed wavelength), Waters Associates, Milford, Mass.

Table I—Data on the Dosage Forms Studied [a]

Lot	Base	Type of Base	pH[b]	Ingredient(s)
A	Polyethylene glycol	Water washable	5.9	1% Hydrocortisone
B	Petrolatum	Nonpolar	5.8	1% Hydrocortisone
C	Cold cream	Water in oil emulsion	6.4	1% Hydrocortisone
D	Commercial	Water in oil	5.9	1% Hydrocortisone
E	Commercial	Oil in water emulsion	5.9	1% Hydrocortisone
F	Commercial	Oil in water emulsion	6.6	1% Hydrocortisone plus 3% iodochlorhydroxyquin
G	Commercial	Oil in water emulsion	5.9	1% Hydrocortisone, 0.25% menthol, and 0.25% phenol
H	Water with 10% (v/v) glycerin	Aqueous	6.6[c]	1% Hydrocortisone, 10% zinc oxide, and 10% talc

[a] For ingredients of commercial bases, see Ref. 13. Commercial base F contained cetyl alcohol, glycerin, synthetic spermaceti, mineral oil, water, and preservatives. [b] From Ref. 13. [c] The pH of the decanted aqueous phase.

propylsilane permanently bonded to silica (30 cm × 4 mm i.d.). It was purchased[5] and used without further treatment.

Recorder and Integrator—The chromatograph was attached to a recorder[6] and a digital integrator[7].

Chromatographic Conditions—The chromatographic solvent was 0.02 *M* KH_2PO_4 in water containing 20% (v/v) methanol. The temperature was ambient. The flow rate was 2.0 ml/min (at an inlet pressure of approximately 2300 psig), and the chart speed was 30.5 cm/hr. The absorbance unit for full-scale deflection was 0.08.

Preparation of Ointments—All ointments were prepared by a trituration method as reported earlier (13). Zinc oxide shake lotion with 1% hydrocortisone was prepared by making a smooth paste of hydrocortisone with 10% each of talc, zinc oxide, and glycerin (the latter by volume). The paste was then brought to volume with water with continous stirring. All necessary data on the dosage forms are listed in Table I.

After preparation, all lots (ointments as well as shake lotion) were assayed for hydrocortisone using the HPLC method. They were then stored at room temperature and assayed again. The results, ages of the samples, and methods of analysis are presented in Table II.

Preparation of Standard Solutions—A 50.0-mg quantity of hydrocortisone was dissolved in about 70 ml of alcohol and brought to volume (100.0 ml) in a volumetric flask. Aliquots of 4.0 ml of this solution were diluted with either alcohol or water to 100.0 ml and labeled as alcoholic or aqueous standard solutions (20 μg/ml), respectively.

Preparation of Assay Solution—A 200.0-mg portion of each lot was weighed accurately (zinc oxide shake lotion was thoroughly shaken before weighing) and transferred to a 150-ml beaker. Approximately 40 ml of

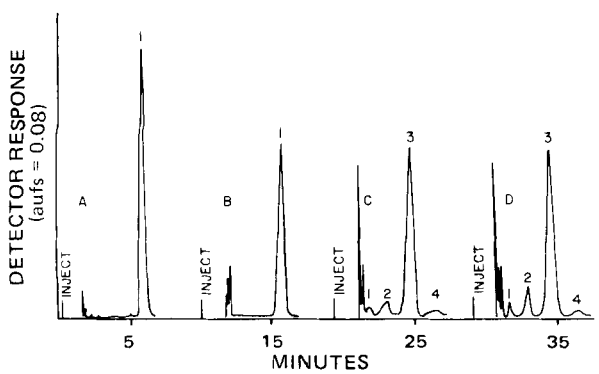

Figure 1—*Chromatograms of standard hydrocortisone (I) solutions and Lots F and G of dosage forms. Key: peak 1 in A, standard solution of I in water; peak 1 in B, standard solution of I in alcohol; peak 3 in C, I from Lot F; peak 2 in C, iodochlorhydroxyquin; other peaks in C, the base; peak 3 in D, I from Lot G; peak 1 in D, phenol; and other peaks in D, the base.*

[5] Waters catalog No. 84042.
[6] Omniscribe model 5213-12, Houston Instruments, Austin, Tex.
[7] Autolab Minigrator, Spectra-Physics, Santa Clara, Calif.

Table II—Assay Results on Various Dosage Forms

Lot	Day 0 Results by USP Method[a], % of Claim	Age of Sample, months	Assay Results, % Retained		
			USP Method	HPLC	UV
A	99.6	54	59.6	29.6	64.3
B	97.2	41	96.2	96.8	—
C	99.3	14	98.8	98.6	—
D	101.0	40	100.3	99.7	—
E	99.2	30	98.7	98.0	—
F	99.2	12	98.7	99.1	—
G	100.6	30	100.6	99.7	—
H	98.5	15	47.3	45.2	59.1

[a] It was confirmed that both the USP and HPLC methods give similar results on Day 0.

alcohol was added, and the mixture was heated to boiling on a hot plate, except that no heat was used for Lot A. The mixture was then cooled and brought to volume (100.0 ml) with alcohol. The solution was filtered[8] if necessary.

HPLC Procedure—A 30.0-μl sample of the standard solution was injected into the chromatograph. After its elution, an identical volume of the assay solution was injected.

Since preliminary investigations indicated that the area of the peak was directly related to the concentration of hydrocortisone (range of 0.2–0.8 μg), the results were calculated using:

$$\frac{A_a}{A_s} \times 100 = \text{percent of label claim} \qquad \text{(Eq. 1)}$$

where A_a is the area of the assay sample and A_s is the area of the standard sample.

Although the peak of the standard solution in water was sharper (Fig. 1A) than the one in alcohol (Fig. 1B), their areas were the same. Based on five readings, a standard deviation of ±0.54% was determined (Table II). All lots were also assayed by the USP method (14) (Table II). For these studies, only the alcoholic standard solution was used. Lots A and H were also assayed by UV spectroscopy at 242 nm using the alcoholic standard solution for comparison of absorbance values (Table II).

Stability Tests on Hydrocortisone under Drastic Conditions of Storage and pH—Since the data at room temperature indicated that hydrocortisone was unstable in Lots A (polyethylene glycol base) and H (aqueous with 10% by volume of glycerin), these systems were studied under drastic conditions using the newly developed stability-indicating HPLC assay procedure. The following samples were prepared, assayed initially, stored at 65 ± 2°, and reassayed periodically: (*a*) 20 μg of hydrocortisone/ml in various mixtures of alcohol and water (100, 50, and 0% alcohol), (*b*) 20 μg of hydrocortisone/ml in a water–glycerin (10% v/v) mixture, and (*c*) 1 and 0.5% ointment of hydrocortisone in polyethylene glycol base USP (11). The results are presented in Figs. 2–5 and Table III.

The following two experiments were conducted at room temperature:

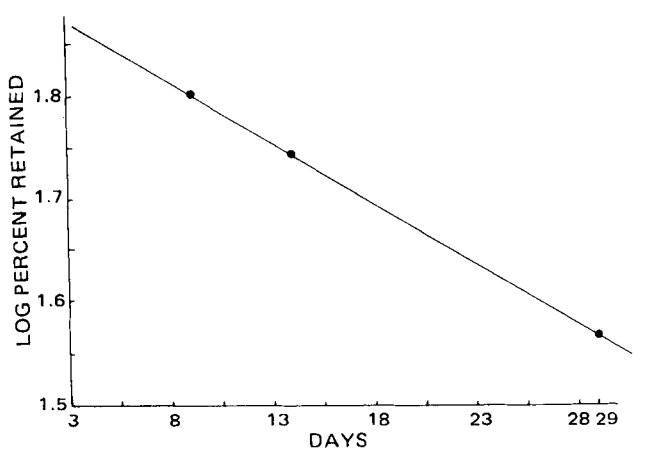

Figure 2—*Pseudo-first-order plot of log percent retained* versus *time when hydrocortisone in water (initial concentration of 20 μg/ml) was stored at 65°.*

[8] Whatman No. 1 filter paper.

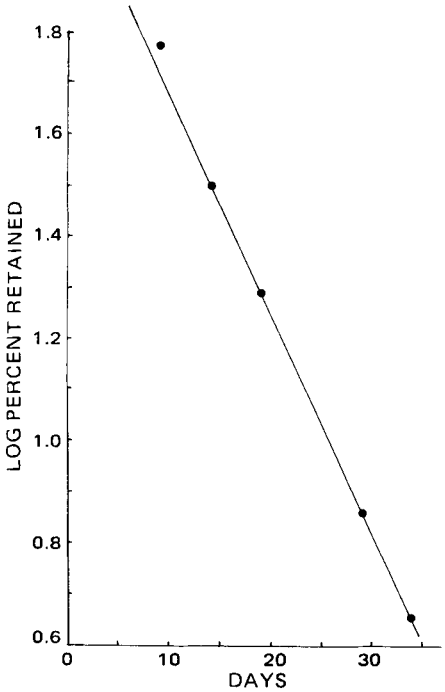

Figure 3—*Pseudo-first-order plot of log percent retained* versus *time when Lot A was stored at 65°.*

1. A 1.0-ml quantity of an alcoholic solution of hydrocortisone (1 mg/ml) was mixed with 1.0 ml of approximately 0.05 *N* NaOH and stored at room temperature for 72 hr. The mixture was then neutralized with approximately 0.05 *N* HCl, brought to volume (50.0 ml) with alcohol, and assayed by HPLC as well as by the USP method.
2. A 1.0-ml quantity of the alcoholic solution of hydrocortisone (1 mg/ml) was mixed with 2.0 ml of approximately 0.05 *N* HCl and stored at room temperature for 140 hr. The mixture was then neutralized with approximately 0.05 *N* NaOH, brought to volume (50.0 ml) with alcohol, and assayed by HPLC.

The results of Experiment 1 are presented in Fig. 5C. In Experiment 2, no decomposition or new peaks were recorded.

DISCUSSION

Hydrocortisone appeared to be stable at room temperature in all three commercial vehicles[3] (Tables I and II), and the presence of other ingredients (iodochlorhydroxyquin, menthol, and phenol) did not affect its stability (Table II). All bases studied had a weakly acidic pH (Table I). Petrolatum did not affect the stability of hydrocortisone for 41 months at room temperature.

Hydrocortisone appeared to be unstable at room temperature in both water and polyethylene glycol ointment base (Tables II and III). In both water and polyethylene glycol, the order of reaction appeared to be complex pseudo-first order (Figs. 2 and 3 and Table III). This study was

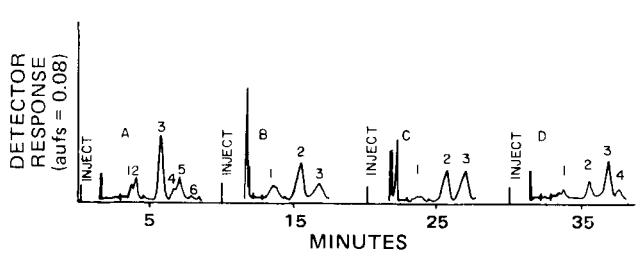

Figure 4—*Chromatograms of Lot A. Key: peak 3 in A, hydrocortisone (I) when the lot was stored at room temperature for 4.5 years and solution for assay was made in water; peak 2 in B, I under conditions identical to A except that the solution was made in alcohol; all other peaks in A and B, decomposition products; peak 2 in C, I when sample was stored at 65° for 19 days (alcohol was used to make the solution); peak 2 in D, same as in C except that the sample was 29 days old; and all other peaks in C and D, decomposition products.*

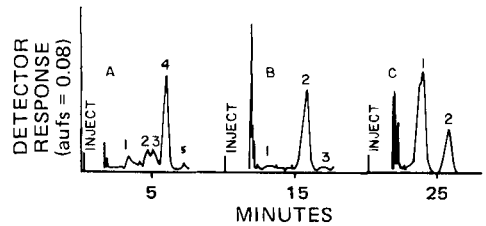

Figure 5—*Chromatograms of various hydrocortisone (I) samples. Key: peak 4 in A, I from a solution in water (20 μg/ml) stored at 65° for 29 days; peak 2 in B, I from Lot H stored for 15 months at room temperature (alcohol was used to make the solution); peak 2 in C, I after it was allowed to decompose under basic conditions for 72 hr at room temperature; and all other peaks in A, B, and C, decomposition products.*

needed to confirm an earlier report (8) in which a stability-indicating assay method had not been used. The developed method appears to be stability indicating since the hydrocortisone in Lot A had almost completely decomposed (4.4 *versus* 54.3% by the USP method) after 29 days of storage at 65° (Fig. 4D).

The developed method is very sensitive; only 0.2 μg of hydrocortisone is required for the assay. The sensitivity can be improved further by reducing the absorbance units for full-scale deflection from 0.08 (used in these studies) to 0.02. The method appears to be accurate and precise (standard deviation based on five readings was 0.54%). The commercial bases and other ingredients did not interfere (Figs. 1C and 1D) in the assay procedure. On the other hand, the USP method (14) and UV spectroscopy do not appear to be stability indicating (Tables II and III).

Studies under drastic conditions (higher temperature of 65° and highly acidic and basic pH values) indicated that the decomposition process of hydrocortisone was complex (parallel) pseudo-first order, as reported previously (8) (Scheme I).

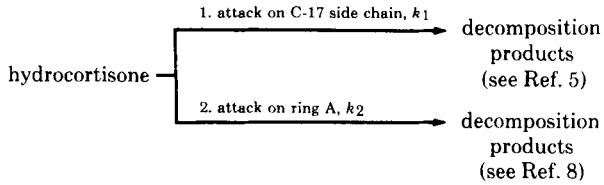

Scheme I

In the chromatograms, it appears that the decomposition products from Pathway 1 have shorter retention times than hydrocortisone and that the products from Pathway 2 have longer retention times than hydrocortisone.

Some of the following discussion will confirm these observations. Under basic conditions at room temperature, only 25.1% of the hydrocortisone remained intact after 72 hr (Table III). The decomposition appeared to be according to Pathway 1 (Fig. 5C) since similar results were obtained by the USP method (Table III), which detects changes in the C-17 side chain. Moreover, no peak was recorded after the hydrocortisone peak (Fig. 5C).

Under highly acidic conditions at room temperature for 140 hr, there was no decomposition of hydrocortisone.

In water at 65°, the decomposition appeared to be according to both pathways (Fig. 5A). Both alcohol and glycerin had a stabilizing effect when mixed with water (Table III). This stabilizing effect was due to a decrease in Pathway 1 degradation; under identical conditions, both alcohol and glycerin reduced the peak heights appearing before hydrocortisone (peaks 1–3 in Fig. 5A). The peak appearing after hydrocortisone had the same height (peak 5 in Fig. 5A). It was not possible to assay water solutions by the USP method since the system must be essentially free of water.

Decomposition *via* Pathway 2 appeared to be predominant in polyethylene glycol base (Figs. 4B and 4C). At a higher temperature, Pathway 2 accelerated more than Pathway 1. This result was confirmed by comparing the assay results by the developed method and the USP method (14). For example, at room temperature the results were 29.6 *versus* 59.6% by the USP method. At higher temperature after 14 days of storage, the results were 31.6 *versus* 76.8% by the USP method. Since ring A is involved in Pathway 2, it was expected that the USP method results would be higher. This acceleration at higher temperature was probably due to a phase change since the base is a semisolid at room temperature and a liquid at 65°.

Table III—Assay Results [a] on Hydrocortisone Stored at 65°

Vehicle	Initial Concentration	Number of Days Stored	Percent Retained by HPLC	Percent Retained by USP Method
Water	20 μg/ml	14	54.9	—[b]
Water with 50% alcohol	20 μg/ml	14	71.2	—[b]
Alcohol	20 μg/ml	14	92.6	93.7
Water with 10% (v/v) glycerin	20 μg/ml	14	84.8	—[b]
Polyethylene glycol	10 mg/g	9	59.2	—
Polyethylene glycol	10 mg/g	14	13.6[c]	76.8[c]
Polyethylene glycol	5 mg/g	9	47.2	
Under basic conditions[d]	1 mg/ml	3	25.1	24.7

[a] Some other results are presented in Figs. 2 and 3. [b] It was not possible to assay by the USP method since the system must be essentially free of water. [c] There was no interference from the base even after storing at 65° for 10 days. [d] See text for details.

It is apparent that the USP method is not a stability-indicating assay method. In fact, it proved to be stability indicating only under abnormal conditions of a highly basic pH, which is rarely found in practice. The data on Lot A were further analyzed using the following relationship:

$$\frac{X_1}{C_0} = \frac{k_1}{k}(1 - e^{-Kt}) \qquad \text{(Eq. 2)}$$

where C_0 is the initial concentration of hydrocortisone in Lot A; $X_1 = (C_0 - C)$ and is the concentration of the decomposition products according to Pathway 1 since C at time t could be determined by the USP method; k_1 is the decomposition constant according to Pathway 1; and $K = k_1 + k_2$, where k_2 is the decomposition constant according to Pathway 2. The K value was determined from Fig. 4 to be 0.0988/day. By using Eq. 2, the values for k_1 and k_2 in Lot A at higher temperature were estimated to be 0.0908 and 0.008/day, respectively.

The chromatogram of Lot H at room temperature (Fig. 5B) did not indicate much decomposition because of the small peaks from the decomposition products. The low percent of hydrocortisone (55%) found may be the result of its adsorption onto the plastic container in which it was compounded. The other possibility is the adsorption of decomposition products onto the container or the other ingredients (talc and zinc oxide). None of these observations was confirmed. The ointments were compounded in a stainless steel mixer and stored in ointment jars made of opal glass.

REFERENCES

(1) H. L. Mason, *Proc. Staff Meet. Mayo Clin.*, **13**, 235 (1938).

(2) L. Velluz, A. Petit, and R. Berret, *Bull. Soc. Chim. Fr.*, **1947**, 123.

(3) D. E. Guttman and P. D. Meister, *J. Am. Pharm. Assoc., Sci. Ed.*, **47**, 773 (1958).

(4) J. W. Mauger, A. N. Paruta, and R. J. Gerraughty, *J. Pharm. Sci.*, **58**, 574 (1969).

(5) T. Chulski and A. A. Forist, *J. Am. Pharm. Assoc., Sci. Ed.*, **47**, 553 (1958).

(6) A. O. Weis-Fogh and C. F. Wiese, *Arch. Pharm. Chemi*, **71**, 835 (1964).

(7) T. Takubo, T. Tadaoka, and T. Sawai, *Yakuzaigaku*, **22**, 66 (1962).

(8) A. E. Allen and V. D. Gupta, *J. Pharm. Sci.*, **63**, 107 (1974).

(9) W. C. Landgraf and E. C. Jennings, *ibid.*, **62**, 278 (1973).

(10) M. C. Olson, *ibid.*, **62**, 2001 (1973).

(11) "The United States Pharmacopeia," 19th rev., Mack Publishing Co., Easton, Pa., 1975, p. 566.

(12) *Ibid.*, p. 103.

(13) V. D. Gupta and A. N. Deleon, *Indian J. Hosp. Pharm.*, **10**, 141 (1973).

(14) "The United States Pharmacopeia," 19th rev., Mack Publishing Co., Easton, Pa., 1975, p. 238.

Demonstration of Penicillamine as a Product in Benzylpenicillenic Acid Degradation in Neutral Media Using Differential Pulse Polarography

MOHAMMED JEMAL *, STANLEY L. HEM ‡, and ADELBERT M. KNEVEL *x

Received February 28, 1977, from the **Department of Medicinal Chemistry and Pharmacognosy and the* ‡*Department of Industrial and Physical Pharmacy, Purdue University, West Lafayette, IN 47907.* Accepted for publication May 25, 1977.

Abstract □ During the study of the temporal changes of benzylpenicillenic acid in aqueous buffers using differential pulse polarography, penicillamine was found to be a degradation product at neutral pH. Since this result was not previously reported, the effects of pH and buffer concentration on penicillamine formation were investigated. The amount of penicillamine produced was greatest under conditions producing maximum benzylpenicillenic acid stability. Penicillamine was not obtained from benzylpenicilloic acid, the reported degradation product of benzylpenicillenic acid at neutral pH. Penicillamine also was detected in penicillin G solutions of neutral pH. Therefore, it is suggested that penicillamine found in penicillin G solutions arises from benzylpenicillenic acid degradation which, in turn, is produced from penicillin G isomerization. A pathway is proposed to show that penicillamine originates from the UV-absorbing isomer of benzylpenicillenic acid.

Keyphrases □ Benzylpenicillenic acid—degradation in neutral media, differential pulse polarographic study, penicillamine demonstrated as product □ Degradation—benzylpenicillenic acid in neutral media, differential pulse polarographic study, penicillamine demonstrated as product □ Differential pulse polarography—study of benzylpenicillenic acid degradation in neutral media, penicillamine demonstrated as product □ Penicillamine—demonstrated as product of benzylpenicillenic acid degradation in neutral media, differential pulse polarographic study □ Antibacterials—benzylpenicillenic acid degradation in neutral media, differential pulse polarographic study, penicillamine demonstrated as product

Benzylpenicillenic acid, which forms spontaneously from penicillin G (benzylpenicillin), has been implicated in penicillin allergy (1). Benzylpenicillenic acid reacts with nucleophiles and has been proposed as the intermediate in the reaction of penicillin G with proteins (2, 3). The penicillamine moiety is an antigenic determinant in penicillin allergy, and penicillamine cross reacts with both penicillin G and benzylpenicillenic acid (1, 4).

It has been suggested (5–8) that benzylpenicillenic acid (I) in aqueous solutions is in equilibrium with a thiazoli-

Table III—Assay Results [a] on Hydrocortisone Stored at 65°

Vehicle	Initial Concentration	Number of Days Stored	Percent Retained by HPLC	Percent Retained by USP Method
Water	20 μg/ml	14	54.9	—[b]
Water with 50% alcohol	20 μg/ml	14	71.2	—[b]
Alcohol	20 μg/ml	14	92.6	93.7
Water with 10% (v/v) glycerin	20 μg/ml	14	84.8	—[b]
Polyethylene glycol	10 mg/g	9	59.2	—
Polyethylene glycol	10 mg/g	14	13.6[c]	76.8[c]
Polyethylene glycol	5 mg/g	9	47.2	
Under basic conditions[d]	1 mg/ml	3	25.1	24.7

[a] Some other results are presented in Figs. 2 and 3. [b] It was not possible to assay by the USP method since the system must be essentially free of water. [c] There was no interference from the base even after storing at 65° for 10 days. [d] See text for details.

It is apparent that the USP method is not a stability-indicating assay method. In fact, it proved to be stability indicating only under abnormal conditions of a highly basic pH, which is rarely found in practice. The data on Lot A were further analyzed using the following relationship:

$$\frac{X_1}{C_0} = \frac{k_1}{k}(1 - e^{-Kt}) \qquad \text{(Eq. 2)}$$

where C_0 is the initial concentration of hydrocortisone in Lot A; $X_1 = (C_0 - C)$ and is the concentration of the decomposition products according to Pathway 1 since C at time t could be determined by the USP method; k_1 is the decomposition constant according to Pathway 1; and $K = k_1 + k_2$, where k_2 is the decomposition constant according to Pathway 2. The K value was determined from Fig. 4 to be 0.0988/day. By using Eq. 2, the values for k_1 and k_2 in Lot A at higher temperature were estimated to be 0.0908 and 0.008/day, respectively.

The chromatogram of Lot H at room temperature (Fig. 5B) did not indicate much decomposition because of the small peaks from the decomposition products. The low percent of hydrocortisone (55%) found may be the result of its adsorption onto the plastic container in which it was compounded. The other possibility is the adsorption of decomposition products onto the container or the other ingredients (talc and zinc oxide). None of these observations was confirmed. The ointments were compounded in a stainless steel mixer and stored in ointment jars made of opal glass.

REFERENCES

(1) H. L. Mason, *Proc. Staff Meet. Mayo Clin.*, **13**, 235 (1938).

(2) L. Velluz, A. Petit, and R. Berret, *Bull. Soc. Chim. Fr.*, **1947**, 123.

(3) D. E. Guttman and P. D. Meister, *J. Am. Pharm. Assoc., Sci. Ed.*, **47**, 773 (1958).

(4) J. W. Mauger, A. N. Paruta, and R. J. Gerraughty, *J. Pharm. Sci.*, **58**, 574 (1969).

(5) T. Chulski and A. A. Forist, *J. Am. Pharm. Assoc., Sci. Ed.*, **47**, 553 (1958).

(6) A. O. Weis-Fogh and C. F. Wiese, *Arch. Pharm. Chemi*, **71**, 835 (1964).

(7) T. Takubo, T. Tadaoka, and T. Sawai, *Yakuzaigaku*, **22**, 66 (1962).

(8) A. E. Allen and V. D. Gupta, *J. Pharm. Sci.*, **63**, 107 (1974).

(9) W. C. Landgraf and E. C. Jennings, *ibid.*, **62**, 278 (1973).

(10) M. C. Olson, *ibid.*, **62**, 2001 (1973).

(11) "The United States Pharmacopeia," 19th rev., Mack Publishing Co., Easton, Pa., 1975, p. 566.

(12) *Ibid.*, p. 103.

(13) V. D. Gupta and A. N. Deleon, *Indian J. Hosp. Pharm.*, **10**, 141 (1973).

(14) "The United States Pharmacopeia," 19th rev., Mack Publishing Co., Easton, Pa., 1975, p. 238.

Demonstration of Penicillamine as a Product in Benzylpenicillenic Acid Degradation in Neutral Media Using Differential Pulse Polarography

MOHAMMED JEMAL *, STANLEY L. HEM ‡, and ADELBERT M. KNEVEL *x

Received February 28, 1977, from the **Department of Medicinal Chemistry and Pharmacognosy and the* ‡*Department of Industrial and Physical Pharmacy, Purdue University, West Lafayette, IN 47907.* Accepted for publication May 25, 1977.

Abstract □ During the study of the temporal changes of benzylpenicillenic acid in aqueous buffers using differential pulse polarography, penicillamine was found to be a degradation product at neutral pH. Since this result was not previously reported, the effects of pH and buffer concentration on penicillamine formation were investigated. The amount of penicillamine produced was greatest under conditions producing maximum benzylpenicillenic acid stability. Penicillamine was not obtained from benzylpenicilloic acid, the reported degradation product of benzylpenicillenic acid at neutral pH. Penicillamine also was detected in penicillin G solutions of neutral pH. Therefore, it is suggested that penicillamine found in penicillin G solutions arises from benzylpenicillenic acid degradation which, in turn, is produced from penicillin G isomerization. A pathway is proposed to show that penicillamine originates from the UV-absorbing isomer of benzylpenicillenic acid.

Keyphrases □ Benzylpenicillenic acid—degradation in neutral media, differential pulse polarographic study, penicillamine demonstrated as product □ Degradation—benzylpenicillenic acid in neutral media, differential pulse polarographic study, penicillamine demonstrated as product □ Differential pulse polarography—study of benzylpenicillenic acid degradation in neutral media, penicillamine demonstrated as product □ Penicillamine—demonstrated as product of benzylpenicillenic acid degradation in neutral media, differential pulse polarographic study □ Antibacterials—benzylpenicillenic acid degradation in neutral media, differential pulse polarographic study, penicillamine demonstrated as product

Benzylpenicillenic acid, which forms spontaneously from penicillin G (benzylpenicillin), has been implicated in penicillin allergy (1). Benzylpenicillenic acid reacts with nucleophiles and has been proposed as the intermediate in the reaction of penicillin G with proteins (2, 3). The penicillamine moiety is an antigenic determinant in penicillin allergy, and penicillamine cross reacts with both penicillin G and benzylpenicillenic acid (1, 4).

It has been suggested (5–8) that benzylpenicillenic acid (I) in aqueous solutions is in equilibrium with a thiazoli-

dinyloxazolone isomer (II) that does not possess absorbance at λ_{max} 322 nm as does I (Scheme I, reaction 1). The hydrolysis of I at various pH conditions was studied, and the hydrolysis products were reported (6). Benzylpenicilloic acid (III) was the main I hydrolysis product in 0.1 *M* phosphate buffer, pH 7.5 (9).

During the study of the electrochemical behavior of I using differential pulse polarography in buffers of different pH values, a new polarographic wave was observed as the wave height of I decreased with time. The appearance of this new wave in solutions of neutral pH was of special interest since most parenteral penicillin solutions are prepared at neutral pH. The new wave that developed as the result of I degradation is penicillamine (IV). A pathway for the formation of IV from I near neutral pH is proposed.

EXPERIMENTAL

Materials—Benzylpenicillenic acid (I) was obtained commercially[1] as prepared from penicillin G by Levine's method (9).

Benzylpenicilloic acid (III) was prepared fresh as needed (10). For a 0.004 *M* benzylpenicilloic acid solution, exactly 0.143 g of penicillin G sodium was added to a 100-ml volumetric flask containing 2 ml of water. Exactly 0.8 ml of 1.0 *N* NaOH was added, and the solution was allowed to stand for 2 hr at room temperature. Then 0.8 ml of 1.0 *N* HCl was added, and the solution was diluted to volume with Sorensen pH 7.0 phosphate buffer.

Benzylpenaldic acid (V) was prepared from benzylpenicilloic acid (11). Fifty milliliters of 4×10^{-3} *M* benzylpenicilloic acid in Sorensen pH 7.0 phosphate buffer was mixed with 50 ml of 2×10^{-3} *M* mercuric chloride. The reaction was followed by UV spectrophotometry. The absorption at 277 nm decreased steadily, and benzylpenaldic acid production was taken to be complete when the absorption had disappeared completely. Only fresh solutions of benzylpenaldic acid were used.

DL-Penicillamine[2] was obtained commercially and was labeled 99+%.

Apparatus—The polarographic analyzer[3] was used in conjunction with a drop timer[4]. The polarographic cell bottom[5] was provided with a cell top[6]. A three-electrode system was used with dropping mercury as the working electrode, saturated calomel electrode[7] (SCE) as the reference electrode, and platinum wire as the counter electrode. The mercury capillary had the following characteristics. In 0.056 *M* citrate buffer, pH 6.45 (with 5% alcohol USP), at open circuit, the mercury flow rate was 2.57 mg/sec and the natural drop time was 3.0 sec at a mercury reservoir height of 78.6 cm.

Prepurified nitrogen was used to remove oxygen from the polarographic solutions and to provide a blanket against the intrusion of air. An *x–y* recorder[8] was used to record polarographic waves.

Procedure—Common buffers were made in a standard way (12). A 0.056 *M* citrate buffer, pH 6.45, was prepared using 16.0 g of trisodium citrate dihydrate and 0.51 g of citric acid monohydrate/liter.

Because I is unstable in aqueous solutions (6, 7), stock solutions were prepared in absolute alcohol. Such stock solutions degraded slowly. Their concentrations were checked before use by measuring UV absorbance at 322 nm. Stock solutions of 5×10^{-3} *M* deteriorated at the rate of about 1%/hr at room temperature.

Penicillamine (IV) stock solutions were prepared in double-distilled water. Their concentrations changed upon aging and were checked before use by differential pulse polarography in 0.1 *M* sodium potassium phosphate buffer, pH 6.8. Penicillamine solutions of 5×10^{-3} *M* deteriorated at the rate of 0.5%/hr at room temperature.

All polarographic and UV data were obtained at 22 ± 1°. The polarographic data were secured as follows. The appropriate amount of I stock solution was transferred quantitatively to a 10-ml volumetric flask.

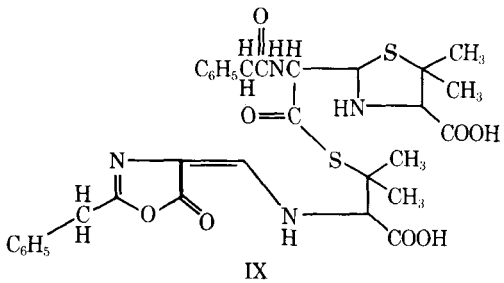

IX

Sufficient alcohol was added to make the final solution 5% in alcohol. Then the appropriate buffer was added to volume, and the time of buffer addition was recorded. The solution was immediately transferred to a polarographic cell, and a stream of prepurified nitrogen was bubbled through it for about 5 min. Nitrogen flow was then directed so that it formed a blanket over the solution, and recording of the polarogram was begun immediately. Recording was repeated as required, with the solution kept under a nitrogen blanket.

To estimate the amount of IV produced from the I solution in the polarographic cell, a known concentration of IV was added to the polarographic cell solution while gently bubbling with nitrogen. Bubbling was continued for about 2 min before recording of the IV wave was initiated.

Solutions of I for UV[9] studies were prepared in 10-ml volumetric flasks under a nitrogen atmosphere. Deaerated buffer was mixed with sufficient deaerated alcohol to produce a solution 5% in alcohol, and a sample of deaerated I stock solution was added to the mixture. The resulting solution was immediately transferred under a nitrogen atmosphere to a UV cell[10] provided with ground-glass stoppers.

RESULTS AND DISCUSSION

The commercial I used gave a molar absorptivity of 21,000 at λ_{max} of 322 nm, which is lower than the 30,500 value reported for the pure compound (7). The low value was attributed in part to the presence of water of hydration. A trace amount of III was detected in the product using TLC [silica gel[11]: 1-butanol–water–acetic acid (66:17:17); with R_f values of 0.39 for III and 0.70 for I]. Compound IV, however, was not detected in fresh samples using either TLC or differential pulse polarography.

Derivatives of I such as the benzylpenicilloylpenicillenic acid derivative (IX), absorbing at λ_{max} 322 nm, have been proposed (7). Because these derivatives do not possess the sulfhydryl group, they are more stable than I in solution (5–7). To determine if these compounds were present in the samples of I, solutions were prepared in pH 2.32 McIlvaine buffer and studied using UV spectrophotometry. The UV absorbance decreased rapidly due to I degradation. A stable absorbance at λ_{max} 350 nm was observed, however, and this absorbance was attributed to a compound (X) proposed previously (6). The absorbance of this compound in the product used in this research was established at 6% of the total absorbance at 322 nm.

The I concentrations reported are corrected values. All were calculated on the basis that the molar absorptivity of pure I was 30,500. Correction for the presence of X was made by subtracting 6% of the total absorbance at 322 nm in absolute alcohol.

Compound I gave an anodic wave due to its sulfhydryl group in buffers at various pH values. The electrode reaction of a sulfhydryl group involves oxidation of mercury in the presence of the sulfhydryl into mercury mercaptide (13, 14). Compound I was studied using three modes of po-

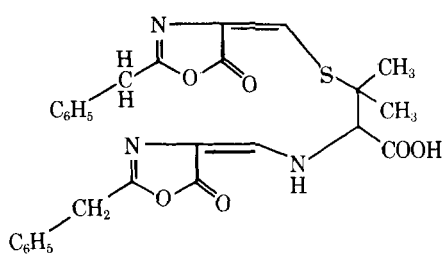

X

[1] Sigma Chemical Co., St. Louis, Mo.
[2] Aldrich Chemical Co., Milwaukee, Wis.
[3] PAR model 174A, Princeton Applied Research Corp., Princeton, N.J.
[4] PAR model 174/70.
[5] PAR model 9301.
[6] PAR model 9300.
[7] Model 3-712, Coleman Instruments, Oak Brook, Ill.
[8] Model 2000, Omnigraphic, Houston Instruments, Bellaire, Tex.
[9] Cary 17 spectrophotometer, Cary Instruments, Monrovia, Calif.
[10] Model 193-QS Hellma cells, Hellma Cells Inc., Jamaica, N.Y.
[11] Precoated TLC silica gel plates, E. M. Laboratories, Elmsford, N.Y.

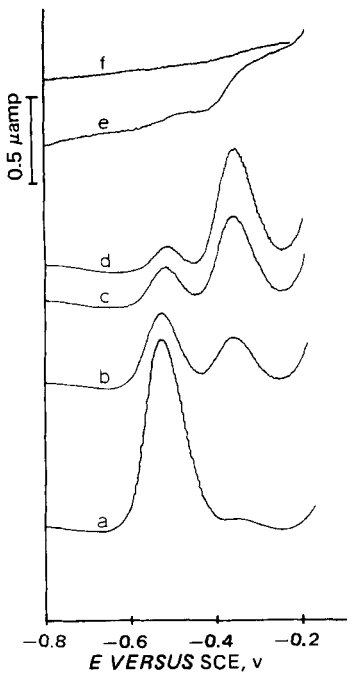

Figure 1—*Polarograms of 7.10 × 10^{-5} M I in 0.1 M sodium potassium phosphate buffer, pH 6.80. The age of solution when recording started (in seconds) was: a, 900; b, 2700; c, 4500; d, 6300; e, 6750; and f, 7150. Polarograms a–d were recorded in the differential pulse mode, e was recorded in the pulse mode, and f was recorded in the dc mode. The drop time was 2 sec, the scan rate was 2 mv/sec, and the pulse amplitude was 25 mv. The low-pass filter was at off for differential pulse and pulse modes but was at 3.0 for the dc mode.*

larography: dc polarography, pulse polarography, and differential pulse polarography. Well-defined waves were observed in all three modes, but differential pulse polarography was the most sensitive. One or two waves were observed depending on the concentration of I taken, the mercury electrode capillary, the height of the mercury reservoir, and the drop time used (with the drop timer used, various automatic drop times could be used for the same capillary and the same mercury reservoir height).

The objective of this study was not to present a detailed account of the electrochemical properties of I but rather to investigate changes in the polarograms of I solutions during aging in aqueous buffer preparations and to report on the development of a new polarographic wave that appeared as the wave of I decreased. To follow the development of the new wave with time, it was necessary to select concentrations of I giving only a single wave because the second wave of I and the IV wave were not resolvable, as will be shown.

When a I polarogram at pH 6.80 was followed during aging, the wave due to I decreased with time and a new wave developed on the anodic side of the I wave. Typical polarograms of a I solution during aging are shown in Fig. 1; polarograms e and f demonstrate that the differential pulse mode is a more sensitive technique than either the pulse mode or the direct current mode.

The polarographic peak that appeared during the aging of I was due to the appearance of IV and not to the formation of III, the reported degradation product of I at neutral pH (6, 9). Polarographic analyses of III solutions did not exhibit a wave at the potential of the I wave or at the potential of the second increasing wave. When the polarography of a penicillin G solution at neutral pH was undertaken, two waves were seen immediately after solution preparation: one at the potential of the I wave and the other at the potential of the second wave of the I polarogram. In the penicillin G solution polarograms, both polarographic peak heights increased with time.

When IV was added to either the I or the penicillin G solution, the IV wave appeared at exactly the same peak potential as the second wave of I or penicillin G. The peak potential of IV in a given buffer changed slightly with its concentration and also with the presence of adsorbents. The peak potential of IV shifted in the anodic direction when it was added to a I or penicillin G solution, probably because of some adsorbing impurities in the preparations. The I used was prepared from penicillin G, and common penicillin products contain impurities of protein origin that act as adsorbents (15). Thus, to compare the peak potential of an authentic sample of IV and the peak potential of the second wave, IV must be added to the I or penicillin G solution.

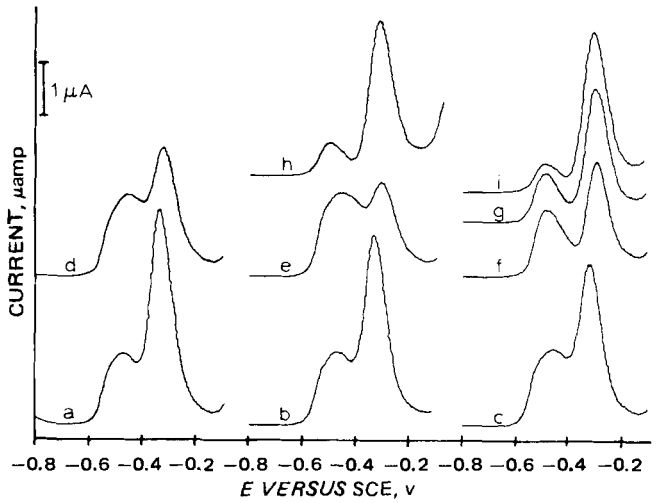

Figure 2—*Change of differential pulse polarogram of 2.0 × 10^{-4} M I in 0.056 M citrate buffer, pH 6.45, giving two peaks with time. The age of solution when recording started (in seconds) was: a, 400; b, 900; c, 1600; d, 2600; e, 4600; f, 7500; g, 9400; h, 11,700; and i, 12,300. Instrument settings were as in Fig. 1.*

When TLC was used with I solutions that showed the second wave, no IV spot could be detected. However, IV spots on TLC could be seen with concentrated penicillin G solutions (about 3 × 10^{-1} *M*) aged for several days and showing IV waves. TLC of such penicillin G solutions also showed V [silica gel[12], 1-butanol–water–acetic acid (66:17:17); R_f 0.48 for IV and 0.31 for V]. The I solutions used for polarography were too dilute to show IV by TLC. It was not possible to achieve concentrated I solutions because of the limited solubility of the compound in aqueous buffers of neutral pH. Based on the polarographic and TLC results, the second wave seen in I solutions and also in penicillin G solutions is believed to be due to IV.

When a sufficiently high concentration (above 1.0 × 10^{-4} *M*) of I was employed, two waves were obtained for I. The first wave was the one seen in low concentrations, and the second wave was due to the additional I. Once the second wave started to show, the height of the first wave remained unchanged with increases in concentration. The potential of the second wave of I was very close to the potential of IV, and the two could not be resolved. Therefore, it was difficult to follow the production of IV in such concentrated I solutions (Fig. 2).

In polarogram a of Fig. 2, the two waves belong to I. From polarograms a through e, the second wave decreased while the first remained unchanged. From f through i, the first wave of I started to decrease, indicating that the second wave of I had all disappeared. The second peak seen in this case was due to IV produced from I and, thus, was increasing while the I was decreasing. Up to the time that the first wave of I started to decrease, the second wave was due to both IV and I; it would be difficult to measure the amount of IV in this period.

It was known from the literature that phosphate buffer species accelerate I degradation (6, 7). Hence, the effect of acceleration of I degradation of IV production was studied. The production of IV from I in pH 6.8 sodium potassium phosphate buffers of concentrations ranging from 0.1 to 1.0 *M* was determined. The amount of IV produced increased with time and then leveled off. As expected from the difference in the rate of I degradation, IV production in the 1.0 *M* phosphate buffer leveled off earlier than in the 0.1 *M* buffer.

The amounts of IV produced in different concentrations of pH 6.8 phosphate buffer after practically all I had disappeared are shown in Fig. 3 (the I solutions were followed until about 95% of the I had disappeared; at this time, the variation of IV concentration with time was negligible). For a given concentration of I, the amount of IV produced decreased with an increase in phosphate concentration, which, therefore, means that the amount of IV produced was less under conditions in which I was least stable.

Compound I is most stable at about pH 6.0, and its degradation rate increases as the pH is lowered or raised from this value (6, 7). It was of

[12] Precoated silica gel 1B, J. T. Baker Chemical Co., Phillipsburg, N.J.

Table I—Variation of Penicillamine Produced, Expressed as the Mole Fraction of the Initial Concentration (6.5×10^{-5} *M*) of Benzylpenicillenic Acid, with pH

Buffer	pH	Mole Fraction of Penicillamine
Sorensen's glycine	8.7	0
McIlvaine	7.5	0.13
	5.8	0.37
	3.8	0.07
	2.3	0

interest to determine the effect of pH on IV production. Among the buffers listed in Table I, I was most stable in pH 5.8 McIlvaine buffer; the amount of IV produced was the largest in this buffer. The amount decreased as the pH was lowered or raised. These results, coupled with those presented in Fig. 3, show that the conditions favoring I stability also favor IV production.

The finding that IV was produced from I near neutral pH was interesting and was not reported previously (6, 9). Longridge and Timms (6) studied I degradation products in a wide range of pH values and reported III as the only degradation product at neutral pH. Since these workers used TLC for identification of non-UV-absorbing substances, the insensitivity of the detection method probably failed to show the presence of the non-UV-absorbing substance IV.

Levine (9) also reported III as a I degradation product in 0.1 *M* phosphate buffer, pH 7.5, and did not mention the presence of IV. Compound III was identified by converting it to IV and benzylpenilloaldehyde (VIII) (α-decarboxylation product of V, Scheme I) in the presence of mercuric chloride. The yield of III was based on the estimation of VIII. The IV produced directly from I (and also the resulting VIII) would be confounded by that obtained through conversion of III.

To determine whether IV came directly from I or from its major degradation product, III, polarograms of III were studied during aging under

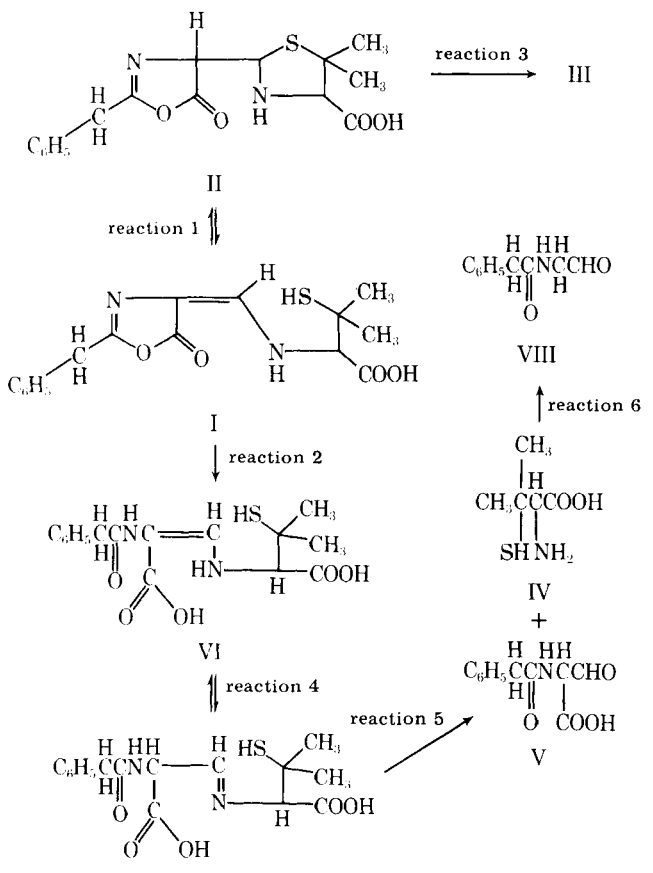

Scheme I

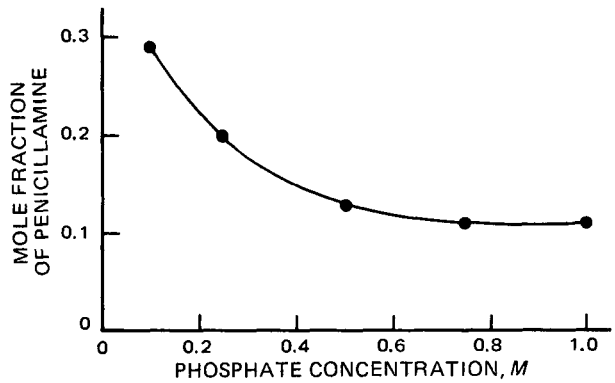

Figure 3—*Penicillamine produced during degradation of* 6.5×10^{-5} M *I in sodium potassium phosphate buffer, pH 6.8, as a function of phosphate concentration. Penicillamine is expressed as a mole fraction of the I concentration at* t = 0.

the same conditions as for I. A IV wave did not develop in III solutions, which means that IV was obtained from I or II. This result suggests that, in addition to the pathway normally proposed for I degradation at neutral pH (6, 7), another pathway involves IV production.

In Scheme I, the main pathway as reported starts with reaction 1. An additional pathway appears to exist; it starts with reaction 2 to produce benzylpenamaldic acid (VI) from the UV-absorbing isomer of I. Reactions 4 and 5 of VI are well known (10, 16). Since development of a UV band at 280 nm due to VI was not observed, it is believed that the rate of reaction 5 is much faster than the rate of reaction 2 and that there is no significant accumulation of VI.

This research has shown that IV found in penicillin G solutions arises from I formed from penicillin G. Parenteral penicillin G solutions containing I also are likely to contain IV. Since IV is reported to have a role in penicillin allergy, it is recommended that quality control procedures of such penicillin preparations include tests not only for the presence of I but also for IV. This testing could be accomplished by using differential pulse polarography.

REFERENCES

(1) M. A. Schwartz, *J. Pharm. Sci.*, **58**, 643 (1969).

(2) B. B. Levine and Z. Ovary, *J. Exp. Med.*, **114**, 875 (1961).

(3) E. S. Wagner, W. W. Davis, and M. Gorman, *J. Med. Chem.*, **12**, 483 (1969).

(4) G. A. Caron, *Immunology*, **6**, 81 (1963).

(5) J. L. Longridge and D. Timms, *J. Chem. Soc. B*, **1971**, 848.

(6) *Ibid.*, **1971**, 852.

(7) K. H. Dudley, T. C. Butler, and D. Johnson, *J. Pharmacol. Exp. Ther.*, **179**, 505 (1971).

(8) H. Bundgaard, *J. Pharm. Sci.*, **60**, 1273 (1971).

(9) B. B. Levine, *Arch. Biochem. Biophys.*, **93**, 50 (1961).

(10) M. A. Schwartz and A. J. Delduce, *J. Pharm. Sci.*, **58**, 1137 (1969).

(11) E. V. Brown, in "The Chemistry of Penicillin," H. T. Clarke, J. R. Johnson, and B. Robinson, Eds., Princeton University Press, Princeton, N.J., 1949, pp. 473–534.

(12) "Scientific Tables," 7th ed., K. Diem and C. Lentner, Eds., Ciba-Geigy Ltd., Basel, Switzerland, 1970, pp. 280–282.

(13) W. Stricks and I. M. Kolthoff, *J. Am. Chem. Soc.*, **74**, 4646 (1952).

(14) F. Peter and R. Rosset, *Anal. Chim. Acta*, **79**, 47 (1975).

(15) G. T. Stewart, *Lancet*, **1**, 1177 (1967).

(16) R. B. Woodward, A. Neuberger, and N. R. Trenner, in "The Chemistry of Penicillin," H. T. Clarke, J. R. Johnson, and B. Robinson, Eds., Princeton University Press, Princeton, N.J., 1949, pp. 415–439.

ACKNOWLEDGMENTS

Supported in part by the African-American Institute and General Research Support Grant 5S01RR05586-07.

Pharmacokinetics of Aryldihydro-*s*-triazines with Antifolate Activity I: Metabolism and Excretion by Rats

A. J. RYAN, J. J. ASHLEY, and R. A. UPTON ˣ

Received June 3, 1976, from the *Department of Pharmacy, University of Sydney, Sydney, Australia, 2006.* Accepted for publication June 7, 1977.

Abstract □ The metabolism and excretion of three aryldihydro-*s*-triazines were studied using rats. The compounds investigated were 4,6-diamino-1,2-dihydro-2,2-dimethyl-1-phenyl-*s*-triazine (I), the prototype of the series; 4,6-diamino-1-(3,4-dichlorophenyl)-1,2-dihydro-2,2-dimethyl-*s*-triazine (II); and *N*-(*m*-tolyl)-*p*-(4,6-diamino-1,2-dihydro-2,2-dimethyl-*s*-triazin-1-yl)hydrocinnamide (III). All three compounds were excreted rapidly. Urinary excretion was favored by a lower molecular weight, and biliary excretion was favored by a higher molecular weight. The overall elimination rates of I and III were similar, I being excreted predominantly in urine and III (considerably metabolized) in bile. The overall elimination rate of II, excreted mainly in urine, was lower than for the other two triazines. A large percentage (and probably all) of the dose of I and II was unmetabolized. Metabolism of III does not appear to involve the phenyldihydrotriazine moiety. This broad view of the metabolism and excretion of the three triazines gives no particular insight into why II, although a more potent inhibitor of dihydrofolate reductase and of L-1210 tumor cell cultures, has been found to compare very poorly with III in its *in vivo* antineoplastic activity in rats.

Keyphrases □ Triazines, various substituted—metabolism and excretion in rats □ Metabolism—various substituted triazines in rats □ Excretion—various substituted triazines in rats

Clinical use of methotrexate has demonstrated that dihydrofolate reductase enzyme inhibitors can curb development of certain human neoplasms. The clinical effect derives from mitosis inhibition, which, apparently, is dependent on this enzyme. Since methotrexate exhibits little tissue specificity in its enzyme inhibition, most cells with rapid mitosis rates are affected, whether normal or neoplastic. As a result, clinical use of methotrexate is accompanied by serious toxic manifestations.

Isoenzyme selectivity favoring dihydrofolate reductase inhibition specifically from neoplastic tissue has been obtained *in vitro* with active-site-directed irreversible inhibitors based on 4,6-diamino-1,2-dihydro-2,2-dimethyl-1-phenyl-*s*-triazine (I) (1, 2). However, while many isoenzyme-selective compounds exhibited impressive ability to prolong survival of experimental animals bearing tumors, they also displayed considerable toxicity. Furthermore, the relative *in vivo* antineoplastic potencies of the aryldihydrotriazines did not always correlate with their relative potencies against the enzyme or against tumor cell cultures *in vitro*.

Despite the antineoplastic activity of many aryldihydrotriazines, little information is available on their metabolism or pharmacokinetics. To gain insight into why certain aspects of their *in vitro* behavior are not translated into the anticipated *in vivo* effects, a pharmacokinetic investigation was conducted. Metabolism and excretion data are presented.

EXPERIMENTAL

Synthetic Methods—1-(Substituted-phenyl)-4,6-diamino-1,2-dihydro-2,2-dimethyl-*s*-triazines were prepared by the three-component synthesis of Modest (3). 4,6-Diamino-1,2-dihydro-2,2-dimethyl-1-phenyl-*s*-triazine (I) as the hydrochloride was recrystallized from water, mp 200–204° (uncorrected) [lit. (3) mp 200–203°]. 4,6-Diamino-1-(3,4-dichlorophenyl)-1,2-dihydro-2,2-dimethyl-*s*-triazine (II) as the hydrochloride was recrystallized from water, mp 207–212° [lit. (3) mp 207–212°].

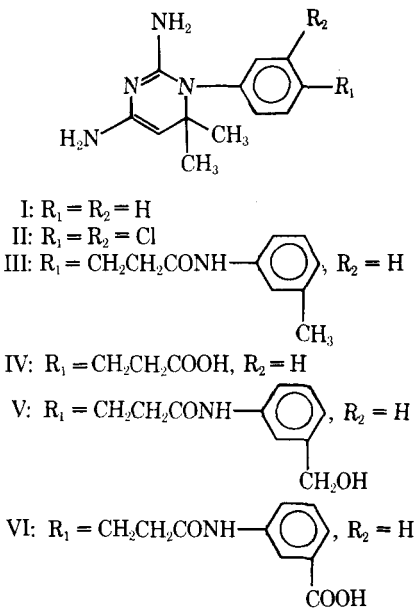

N - (*m*-Tolyl)-*p*-(4,6-diamino-1,2-dihydro-2,2-dimethyl-*s*-triazin-1-yl)hydrocinnamide (III) was synthesized as the *p*-toluenesulfonate salt in a manner similar to that for synthesis of the ethanesulfonate salt (2), mp 210–213° (recrystallized from ethanol). The product and its intermediates had appropriate NMR and UV spectra.

Anal.—Calc. for $C_{28}H_{34}N_6O_4S$: C, 61.1; H, 6.2; N, 15.3. Found: C, 61.6; H, 6.4; N, 14.9.

p - (4,6-Diamino-1,2-dihydro-2,2-dimethyl-*s*-triazin-1-yl)hydrocinnamic acid (IV) was prepared as the ethanesulfonate salt from methanolic acetone, mp 191–193° [lit. (4) mp 191–193°].

N - (*m*-Carboxyphenyl)-*p*-(4,6-diamino-1,2-dihydro-2,2-dimethyl-*s*-triazin-1-yl)hydrocinnamide (VI) was synthesized as the hydrochloride. *m*-Aminobenzoic acid was esterified by refluxing in an ethanolic solution of hydrogen chloride. Ethyl *m*-aminobenzoate was refluxed with *p*-nitrocinnamoyl chloride in toluene. The resultant ethyl *N*-(4-nitrocinnamoyl)-3-aminobenzoate was hydrogenated under 1900 psi of hydrogen using platinum oxide catalyst. Ethyl *N*-[3-(4-aminophenyl)propionyl]-3-aminobenzoate was hydrolyzed (85 hr in a solution of 1% NaOH in 80% methanol under nitrogen), giving *N*-[3-(4-aminophenyl)propionyl]-3-aminobenzoic acid. This was converted to VI, which was recrystallized from water, mp 184°. All IR, NMR, and UV spectra and elemental analyses of the product and intermediates were consistent with the assigned structures. Overall yield was 43%.

Anal.—Calc. for $C_{21}H_{25}ClN_6O_3 \cdot H_2O$: C, 54.5; H, 5.9; N, 18.2. Found: C, 54.3; H, 6.1; N, 17.8.

The radiolabel for I was derived from ^{3}H-aniline[1]; for the other triazines, it was derived from ^{14}C-dicyanodiamide[2]. Radioactive triazines were recrystallized to constant specific activity and gave one radioactive peak[3] by TLC on silica gel GF, corresponding to the sole UV-detectable spot (specific activities in disintegrations per minute per milligram: I,

[1] Radiochemical Center, Amersham, United Kingdom.
[2] International Chemical and Nuclear Corp.
[3] Nuclear Chicago Actigraph III radioscanner, G. D. Searle and Co.

8.02×10^6; II, 1.42×10^6; III, 2.04×10^6; IV, 1.82×10^5; and VI, 1.60×10^5).

Radiotracer Techniques—Radioisotope levels were measured by liquid scintillation spectrometry[4] using Bray's scintillation solution (5). Aliquots (300 mg) of dried feces, ground with sand, were digested for 1 hr at 40° in 1 ml of 1 *M* KOH (aqueous) before 10 ml of Bray's solution was added; counting was done 24 hr later.

Reverse isotope dilutions were performed by adding known amounts of nonradioactive aryldihydrotriazine to aliquots of radioactive urine or bile. The solutions were evaporated to dryness *in vacuo* below 40°, and the residues were crystallized to constant specific activity from the appropriate solvents. Prior elution with methanol from an ion-exchange column[5] aided crystallization from samples containing II.

GLC Techniques—A GLC assay was devised to differentiate and quantitate potential metabolites of III after hydrolysis of the amide bond common to these compounds.

Hydrolysis of Triazines—Bile was collected in a 5-ml ampul and diluted to 1.5 ml with water. Internal standard solution[6] (200 μl) and then 1.0 ml of methanolic potassium hydroxide solution (10 *N*) were added. The walls of the ampul were washed down with 0.5 ml of methanol before sealing under nitrogen. After shaking, the ampul was stored at 40° for 7 days.

Extraction of m-*Toluidine and* m-*Aminobenzyl Alcohol*—After cooling, the contents of the ampul were transferred to a 15-ml graduated glass centrifuge tube, followed by ethereal (2 × 5 ml) and aqueous (0.5 ml) washings from the ampul. The centrifuge tube was agitated and then centrifuged. The ether phase (Extract 1) was transferred to a 15-ml tapered evaporation tube.

Extraction of m-*Aminobenzoic Acid*—The aqueous phase was cooled in an ice bath. After addition of 1.5 ml of 10 *N* HCl and sufficient water (to 5 ml) to redissolve the resultant potassium chloride precipitate, it was extracted with ether (5 ml) and the ether was discarded. Then the aqueous phase was diluted to 7 ml with water, and 1.0 ml of a sodium oxalate solution (20 mg/ml) and 0.5 ml of 10 *N* NaOH were added. The pH was then adjusted to 3.8–4.1. The resulting solution was extracted twice with 5 ml of ether, and the ether extracts were combined (Extract 2) in an evaporation tube.

Preparation of Ether Extracts—The volume of each ether extract was reduced to about 100 μl on a water bath at 40°. (Superheating was prevented by use of a fine-glass boiling stick.) Fresh ether (10 ml) was immediately added. After agitation of the tube, the ether volume was reduced to about 20 μl and the tube was stoppered and placed directly in ice.

Prior to chromatography, Extract 1 was centrifuged (~2000×*g* for 5 min). To Extract 2, 200 μl of an ethereal solution of diazomethane (6) was added and the extract was restoppered. After a minimum of 30 min, the volume of ether was again reduced to about 20 μl. The tube was stoppered and placed in ice until sample analysis.

GLC—All analyses were performed under isothermal conditions using the chromatograph[7] in the single-column mode. The Pyrex glass column (1.5-m length, 4-mm bore) was packed with 3% OV-17 on 100–120-mesh Gas Chrom Q[8]. Gas flow rates were: carrier gas (nitrogen), 40 ml/min; hydrogen, 40 ml/min; and air, 550 ml/min.

Column temperatures and retention times were: *m*-toluidine, 102°, 4.25 min (internal standard, 2,4-dimethylaniline, 6.75 min); *m*-aminobenzyl alcohol, 143°, 4.75 min (2,4,6-trichloroaniline, 5.75 min); and *m*-aminobenzoic acid, 143°, 8.0 min (*o*-aminobenzoic acid, 4.25 min; both acids chromatographed as their methyl esters). The flame-ionization detector was coupled to a recorder[9] equipped with an integrator[10].

Standard curves were constructed after known amounts of triazines added to blank bile samples were processed. Since an authentic sample of *N*-[*m*-(hydroxymethyl)phenyl]-*p*-(4,6-diamino-1,2-dihydro-2,2-dimethyl-*s*-triazin-1-yl)hydrocinnamide (V) was not available, the assay for this metabolite was based on a standard curve for *m*-aminobenzyl alcohol carried through the entire procedure. Since III underwent complete hydrolysis, allowing virtually total recovery of *m*-toluidine (95, 97, or 101% recovery from 109, 210, or 1920 μg of III added to bile, respectively), it was assumed that V would similarly yield stoichiometric proportions of *m*-aminobenzyl alcohol.

Table I—Excretion of Aryldihydrotriazines after Intraperitoneal Dosage in Rats [a] (Expressed as Percent of Dose ± *SE*)

Sample	I	II	III
Urine			
0–24 hr	85 ± 2.0	57 ± 1.5	27 ± 1.0
24–48 hr	0.8 ± 0.2	3.3 ± 0.4	0.6 ± 0.1
48–72 hr	0.3 ± 0.1	0.8 ± 0.1	0.31 ± 0.02
72–100 hr	—	—	0.24 ± 0.04
Feces			
0–24 hr	9.6 ± 2.2	19 ± 1.9	37 ± 5.5
24–48 hr	2.0 ± 1.0	5.1 ± 1.3	20 ± 4.6
48–72 hr	0.1 ± 0.08	1.9 ± 0.4	1.8 ± 0.4
72–100 hr	—	—	0.6 ± 0.2
Total recovered	98	87	88

[a] Five milligrams of radiolabeled compound was given to each rat. Three rats received I, three rats received II, and six rats received III.

GLC–Mass Spectrometry—Bile samples were prepared as for GLC, except that internal standards were not used. A quadrupole instrument[11] was employed to scan chemical-ionization spectra of components of interest. The GLC column (glass, 1.5-m length, 2-mm bore) was packed with 3% OV-225 on 100–120-mesh Gas Chrom Q[7]. Methane was the carrier gas (flow rate of 20 ml/min). Column temperatures of 140° for *m*-toluidine and 200° for both *m*-aminobenzyl alcohol and methyl *m*-aminobenzoate resulted in retention times of 1–2 min. The source temperature was 50°, and the ionization energy was 165 ev.

Animal Techniques—Male Wistar rats[12], 250–300 g and 3–6 months old, were used after maintenance for 1–4 months in an environment untreated with insecticides. They received a commercial diet formulated for laboratory mice and rats. No animal was used for experimentation more than once.

Samples of urine and feces were collected from animals housed in cages equipped with a urine–feces separator. They were fed daily, and water was available *ad libitum*. When serial urine samples were required as frequently as every 2 hr, rats were water loaded intraperitoneally with 2 ml of saline 1 hr prior to dosage, immediately after dosage, and after collection of each urine sample. Rats were induced to urinate by compelling them to inhale ether fumes at specified times (7).

Bile was collected from cannulated rats under urethan anesthesia.

RESULTS

Gross Excretion Pattern—A dose[13] of 5 mg ip of I, II, or III was given to each of 12 rats (Table I). All three compounds were excreted rapidly, with 95, 76, and 64% of the radioactivity from a dose of I, II, and III, respectively, being collected in the first 24 hr. Moreover, an additional amount of III, as much as 20% of the dose, may have already been excreted *via* the bile into the GI tract at the time of collection of the 24-hr feces.

The well-documented trend toward excretion of larger molecules in the bile and feces (8) was in evidence with this series of compounds; 12, 26, and 60% of the radioactive dose were excreted in the 72-hr feces of animals dosed with I, II, and III, respectively (having molecular weights of 217, 286, and 378, respectively).

Urinary Excretion—Representative urinary excretion rate plots in Fig. 1 show that, initially, the urinary excretion of all three compounds was rapid, in accordance with the considerable polarity of the common triazine moiety (pKa of about 11) (3). Within 1 hr, 50% of the injected I appeared in the urine; within 2 hr, 70–75% appeared in the urine. The less polar II and III were excreted in the urine at a rate initially less than that of I. Thus, in the 2 hr following injection, only 30% of the dose of II and 20% of III were excreted in the urine.

Biliary Excretion–The greater susceptibility of the high molecular weight triazine to biliary excretion, inferred from the fecal data (Table I), is confirmed by biliary excretion rate plots (Fig. 2) derived from anesthetized animals dosed intravenously with 1 mg of triazine[14]. A high

[4] Tri-Carb model 3314 with automatic external standardization, model 3950, Packard Instrument Co.

[5] XAD-2, BDH Chemicals Ltd.

[6] 2,4-Dimethylaniline (270 μg/ml), 2,4,6-trichloroaniline (25 μg/ml), and *o*-aminobenzoic acid (115 μg/ml) in 0.1 *N* HCl.

[7] Pye Series 104, model 64, W. G. Pye and Co. Ltd.

[8] Applied Science Laboratories.

[9] Speedomax type G, model S, 60000 series, Leeds and Northrup Co.

[10] Model 203, Disc Instruments Inc.

[11] A 3200E gas chromatograph–mass spectrometer (9500 gas chromatograph) with MS data system 6000 and digital (zeta) plotter, Finnigan Corp.

[12] University of Sydney Animal House, Castle Hill, New South Wales.

[13] All triazines were injected in a 10-mg/ml solution in 60% dimethyl sulfoxide in water.

[14] Reliable intraperitoneal dosage was not possible after the abdominal operation for biliary cannulation, and the lethal dose of any of the triazines by the intravenous route was little more than 1 mg.

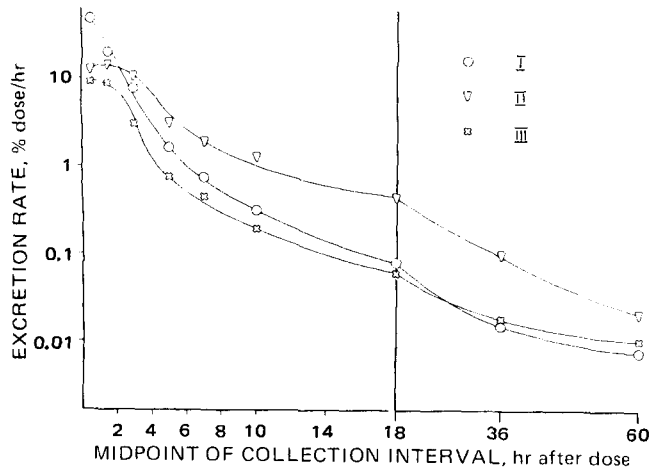

Figure 1—*Representative urinary excretion curves for aryldihydrotriazines I–III after a 5-mg ip dose.*

rate of excretion of III was achieved early after injection but rapidly subsided shortly afterward. Whereas 50% of the III dose appeared in the 3-hr bile, only 11% was excreted over the next 7 hr. The lower molecular weight I and II were excreted in the bile at lower, but more consistent, rates; 12% of the dose of I and 10% of II appeared in the 8-hr biles.

Extrapolation of the biliary excretion profiles indicated that I and II, particularly, may ultimately be excreted in the bile to a slightly greater extent than is reflected by their appearance in the feces. Furthermore, 28% of an oral dose of I and 9% of an oral dose of II were found in the 72-hr urine. The possibility of reabsorption of biliary excreted triazines from the GI tract was investigated by arranging that the bile of a dosed rat flowed into the duodenum of an undosed acceptor rat. From a comparison of the biliary excretion from acceptor rats with that from rats receiving an intravenous bolus dose directly, reabsorption of approximately 13, 24, and 3% of the biliary radioactivity from I, II, and III, respectively, was calculated. No allowance was made, of course, for involvement of metabolites.

Metabolism—Metabolism of the dosed triazines was investigated by reverse isotope dilution analysis of the excretion fluid containing the major part of the injected radioactivity. After a 5-mg ip dose of I, only the unchanged triazine (99% unchanged in one rat, 98% in another) was found in 24-hr urine containing 80% of the dose. It thus seems unlikely that any of the 90% of the dose eventually excreted in the urine was metabolized. Even if all of the compound excreted in the feces had been metabolized, which seems improbable by comparison with III (discussed later), this amount would represent only a minor fraction of the original dose.

In the 12 hr following a 5-mg ip dose of II, 52% was excreted in the urine, all as unmetabolized II (95 and 100% unchanged in two rats). The urine

Table II—Mass Spectral Data for Aromatic Amines Derived from Hydrolysis of Bile Containing Metabolites of III[a]

GLC Peak	m/e	Percent of Base Peak	Authentic Sample: Percent of Base Peak	Assignment[b]
1			*m*-Toluidine	
	108	100	100	$P + H^+$
	136	10	9	$P + C_2H_5^+$
	122	2	2	
	148	2	2	$P + C_3H_5^+$
2			*m*-Aminobenzyl Alcohol	
	106	100	100	$P + H^+ - H_2O$
	124	36	42	$P + H^+$
	94	5	7	
	134	3	3	$P + C_2H_5^+ - H_2O$
	152	1	1	$P + C_2H_5^+$
	164	0.5	Minute	$P + C_3H_5^+$
3			Methyl *m*-Aminobenzoate	
	152	100	100	$P + H^+$
	120	8	14	$P + H^+ - CH_3OH$
	180	4	2	$P + C_2H_5^+$
	166	2	10	
	192	1.5	0.5	$P + C_3H_5^+$

[a] Bile was obtained from anesthetized rats for 3 hr after a 1-mg iv dose of III. [b] P = parent compound.

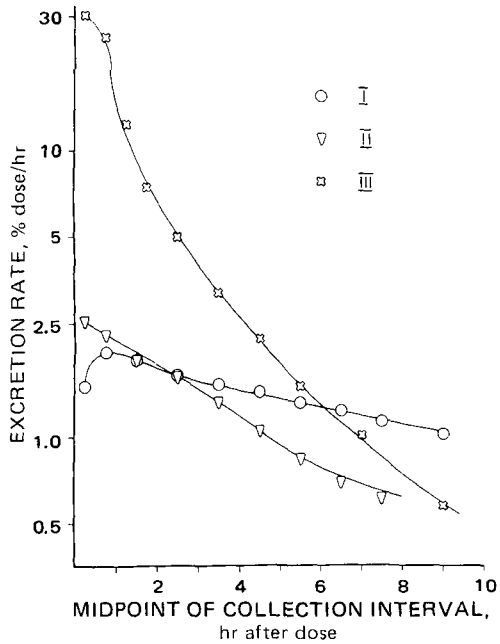

Figure 2—*Representative biliary excretion curves for aryldihydrotriazines I–III after a 1-mg iv dose.*

accumulated ultimately 65% of the dose. The chemical relationship of I and II would suggest that, if I was not metabolized, metabolism of II was not likely.

Only 59% of the radioactivity excreted in the bile in the 3 hr following a 1-mg iv dose of III was in the form of the unchanged compound.

Compound IV might be expected as a metabolite if the amide bond of III was to split. A 5-mg ip dose of IV given to each of four rats was excreted rapidly in urine (average of 83% of the dose in 2 hr, all as unmetabolized IV), with very little appearing in the feces (6.3% in 72 hr). When four rats (anesthetized) were each dosed with 1 mg iv of IV, only an average 5.3% of the radioactivity was excreted in the 3-hr bile, in contrast to 55% following injections of III. Therefore, it was not likely that IV was a major metabolite in the bile of rats receiving III.

GLC techniques were devised to identify and assay amines liberated by hydrolyzing the amide bond of III or potential metabolites. *m*-Toluidine, *m*-aminobenzyl alcohol, and *m*-aminobenzoic acid (chromatographed as the methyl ester) were verified in the hydrolysate of a 3-hr bile sample by GLC–mass spectrometry (Table II). Since I, II, and IV apparently are not metabolized, metabolism of III is probably confined to the terminal phenyl ring. In that case, *m*-toluidine, *m*-aminobenzyl alcohol, and *m*-aminobenzoic acid would be in the hydrolysate derived from III, V, and VI, respectively, in the bile.

Of the radioactive content of 3-hr bile, 99% could be accounted for in terms of these three compounds: 57% as unchanged III, 25% as V, and 17% as VI (Table III). In light of the low level of biliary excretion of I, II, and IV, the close correspondence between the amount of the chromatographed species in bile and its radioactivity[15] indicates that the chromatographed species derived exclusively from triazines excreted with the amide bond intact.

Since the extreme hydrolysis conditions used should cleave conjugates also, the GLC data indicate the biliary content of the respective triazines plus their conjugates, if present. Reverse isotope dilution analyses, however, were performed under conditions such that a measure of the diluting species only was expected. The parity in the proportion of triazine as VI in the bile, whether determined by GLC (17%) or by dilution analysis (20%) after a dose of III, suggests that VI was probably not conjugated.

Four animals dosed with 1 mg iv of VI excreted in 3-hr bile an average 46 ± 2 (*SE*) % of the dose. This excretion rate could certainly account for 9% of the dose of III as VI in 3-hr bile (Table III).

Thus, V and VI appear to be the only significant metabolites (unless V is conjugated) in the bile of rats dosed with III. There was more V than VI, but neither of these metabolites was excreted in as great a quantity as the unchanged III. It must be considered probable that V is an intermediate in the metabolism of III to VI.

[15] The triazine ring contains the ^{14}C-label of III.

Table III—Quantitative Assay of Metabolites of III in Bile [a]

Animal	III	V	VI	Total Recovery by GLC	Total Recovery by Liquid Scintillation Counting (LSC)	Percent Recovery, 100 × GLC/LSC
1	272	151	163	586	550	107
2	287	153	61	501	530	95
3	308	106	97	512	521	98
4	346	124	77	547	569	96
5	343	146	61	550	565	97
Mean	311	136	92	539	547	99
As percent biliary excretion	57	25	17	99	—	—
As percent dose	30	13	9	—	53	—

[a] Content of III, V, and VI in the 3-hr bile of anesthetized rats dosed with 1.03 mg iv of III. Data are expressed as micrograms of III equivalent to each metabolite. Assay was by GLC after alkaline hydrolysis.

DISCUSSION

Of the three triazines chosen for study, two were among folate antagonists previously tested (2) for *in vivo* antineoplastic activity; III was reported to prolong considerably the survival of rats bearing Walker 256 ascites tumor; II was a more potent inhibitor of dihydrofolate reductase and of L-1210 tumor cell cultures but, nevertheless, compared very poorly with III in its *in vivo* antineoplastic efficacy. It was anticipated that adverse pharmacokinetic properties may have been responsible for the comparative lack of *in vivo* activity by II. Thus, to investigate triazines with molecular weights both lower and higher than the molecular weight of II, the prototype of the series, I, was included.

The radioactive contents of bile and urine samples, although not giving direct information on III as the unchanged species, do indicate minimum amounts of the dose of this compound eliminated or maximum amounts excreted as this compound *per se*. The relationship between the biliary and urinary excretion data presented is then consistent with the standard pharmacokinetic assumption that urinary and biliary excretion are parallel first-order processes dependent on the blood concentration of the compound. If this model is valid, the urinary excretion rate profiles can be used to project the shape of blood concentration–time curves.

Following injection, the urinary excretion of all three triazines (or their metabolites) was initially rapid, I being the most rapidly excreted and III the least. Urinary excretion subsequently slowed as the bloodstream was depleted of these compounds. Despite an initial urinary output rate of I as much as five times that of III, the urinary excretion of these compounds (in terms of percentage of the dose) decelerated similarly. Excretion of II in the urine, however, was far more persistent than for the other two compounds (at 18 hr the urinary excretion rate of II was about five times that of the other triazines).

If the blood was being depleted of radioactivity at similar rates following injections of either I or III, it seems that biliary excretion favoring III (and its metabolites) was countering the imbalance in their urinary excretion rates. By superimposition of the biliary and urinary data, a coarse estimate of the total excretion is obtainable. In the first 2 hr after injection, 74% of the dose of I (70% in urine and 4% in bile) and 60% of the dose of III (20 and 40%) were excreted. In contrast, in the first 2 hr after injection of II, only 34% (30% in urine and 4% in bile) of the dose was excreted. By allowing for an amount of the metabolites of III being formed but not excreted in the first 2 hr, closer elimination rates of I and III and a greater discrepancy between those of II and III may be assumed.

Biliary excretion, however, appears to have been operating by a more complex mechanism than the direct first-order transfer of triazine from the bloodstream to bile. Although dosed by the intravenous (femoral) route, many animals displayed an early period of increasing biliary excretion rate. Furthermore, the biliary excretion rate of a 1-mg iv dose of I varied only two- to threefold over the first 9 hr after injection, while urinary excretion (at least by unanesthetized rats dosed with 5 mg ip) in this period accounted for 90% of the dose. It seems likely that an additional physiological compartment was intervening between blood and bile, as previously found (9).

Under these circumstances, the initial removal rate from the blood of any triazine by the biliary route would have been greater than its initial appearance rate in the bile. Thus, the approximate extent of the 2-hr elimination of III calculated above may be even more an underestimate than previously considered.

Thus, the overall elimination rates of I and III appear to be similar, I being excreted predominantly in urine and III (extensively metabolized) in bile. While all three compounds are eliminated rapidly, the overall elimination rate for II, excreted mainly in urine, is lower than for the other two triazines. Compound II, like I, does not seem to be metabolized. Metabolism of III apparently does not involve the phenyldihydrotriazine moiety.

This broad view of the metabolism and excretion of the three triazines gives no particular insight into the antineoplastic superiority of III over II *in vivo* (2). Conceivably, one metabolite of III is considerably more active as an inhibitor of dihydrofolate reductase than III itself. On the other hand, the relative pharmacokinetic properties of II and III, on the basis of their elimination behavior, appear to favor the superior activity of the more persistent II rather than explain its relative inactivity *in vivo*. Studies on blood levels of these triazines have been commenced.

REFERENCES

(1) B. R. Baker, "Design of Active-Site-Directed Irreversible Enzyme Inhibitors," Wiley, New York, N.Y., 1967.

(2) B. R. Baker, N. M. J. Vermeulen, W. T. Ashton, and A. J. Ryan, *J. Med. Chem.*, **13**, 1130 (1970).

(3) E. J. Modest, *J. Org. chem.*, **21**, 1 (1956).

(4) A. J. Ryan, N. M. J. Vermeulen, and B. R. Baker, *J. Med. Chem.*, **13**, 1140 (1970).

(5) G. A. Bray, *Anal. Biochem.*, **1**, 279 (1960).

(6) K. Hammarstrand and E. J. Bonelli, "Derivative Formation in Gas Chromatography," Varian Aerograph Applications Laboratory, Palo Alto, Calif., 1968, p. 9.

(7) E. Nelson, M. Hanano, and G. Levy, *J. Pharmacol. Exp. Ther.*, **153**, 159 (1966).

(8) P. Millburn, in "Metabolic Conjugation and Metabolic Hydrolysis," W. H. Fishman, Ed., Academic, New York, N.Y., 1970, p. 1.

(9) K. Takada, S. Muranishi, and H. Sezaki, *J. Pharmacokinet. Biopharm.*, **2**, 495 (1974).

ACKNOWLEDGMENTS

Supported in part by grants from the University of Sydney Cancer Fund and the Australian Research Grants Committee.

The authors are grateful to Dr. G. M. Holder for advice and assistance.

Pharmacokinetics of Aryldihydro-*s*-triazines with Antifolate Activity II: Blood Levels and Their Relevance to Antineoplastic Activity in Rats

R. A. UPTON ˣ, J. J. ASHLEY, and A. J. RYAN

Received June 3, 1976, from the *Department of Pharmacy, University of Sydney, Sydney, Australia, 2006.* Accepted for publication June 7, 1977.

Abstract □ Blood levels of three aryldihydro-*s*-triazines in rats were followed: 4,6-diamino-1,2-dihydro-2,2-dimethyl-1-phenyl-*s*-triazine (I), the prototype of the series; 4,6-diamino-1-(3,4-dichlorophenyl)-1,2-dihydro-2,2-dimethyl-*s*-triazine (II); and *N*-(*m*-tolyl)-*p*-(4,6-diamino-1,2-dihydro-2,2-dimethyl-*s*-triazin-1-yl)hydrocinnamide (III). The blood profiles obtained provide substantial evidence that III, but not II, was precipitated in the peritoneal cavity where it was injected. Precipitation after intraperitoneal injection may explain why III and similar triazines with long nonpolar chains have been reported to be more active against intraperitoneal Walker 256 tumor than is II, even though the latter compound is a far more potent inhibitor of Walker 256 dihydrofolate reductase and of tumor cell cultures *in vitro*. Precipitation in the peritoneal cavity also may be involved in the difficulty of obtaining the toxicity-free antineoplastic activity expected from certain aryldihydrotriazines selectively inhibiting neoplastic dihydrofolate reductase.

Keyphrases □ Triazines, various substituted—blood levels related to antineoplastic activity, rats □ Blood levels—various substituted triazines, related to antineoplastic activity, rats □ Antineoplastic activity—various substituted triazines, related to blood levels, rats

To produce cancer chemotherapeutic agents with less toxicity than that accompanying the clinical use of methotrexate, antifolate compounds selectively inhibiting dihydrofolate reductase from neoplastic tissues have been sought (1, 2). However, while many of these compounds exhibit impressive ability to prolong survival of animals bearing tumors, their isoenzyme selectivity has not given rise to a demonstrable protection from toxicity. Furthermore, no certain relationship between the antifolate and the antineoplastic potencies of these and related compounds has been found.

In a previous study (3), the metabolism and excretion of two test compounds provided no positive explanation for the reversal in their relative antifolate and relative antineoplastic potencies. In another approach to understanding this anomaly, a study of the blood levels of these aryldihydro-*s*-triazines is now described.

EXPERIMENTAL

Synthetic Methods—The triazines studied were: 4,6-diamino-1,2-dihydro-2,2-dimethyl-1-phenyl-*s*-triazine (I), 4,6-diamino-1-(3,4-dichlorophenyl)-1,2-dihydro-2,2-dimethyl-*s*-triazine (II), and *N*-(*m*-tolyl)-*p*-(4,6-diamino-1,2-dihydro-2,2-dimethyl-*s*-triazin-1-yl)hydrocinnamide (III). Their syntheses were described previously (3).

Radiotracer Techniques—Radioisotope levels were measured with a liquid scintillation spectrometer[1]. Bray's scintillation solution was used for counting the activity of injections (4). Whole blood (0.2 ml) was mixed thoroughly with 1.5 ml of a digestant solution[2] in a preweighed scintillation vial. Aqueous hydrogen peroxide solution (0.5 ml, 27.5% w/w) was then incorporated. After at least 30 min, a scintillation solution[3] (15 ml) was added; the vial was shaken well and stored in the counter for at least 2 hr before counting.

Animal Techniques—Male Wistar rats[4], 250–300 g and 3–6 months old, were used after maintenance for 1–4 months in an environment untreated with insecticides. They received a commercial diet formulated for laboratory mice and rats. Blood was sampled no sooner than 12 hr after implantation of a jugular cannula (5). No animal was used for experimentation more than once.

RESULTS

A 5-mg ip dose[5] of I, II, or III was given to each of eight animals. Representative blood level curves are shown in Fig. 1. The concentrations of all three compounds in blood were low, indicating high volumes of distribution. At its peak, the blood I concentration was only 0.17% of the dose/g of blood. [A 250-g rat has about 20 g of blood (6).] Concentrations of II in the blood were even lower, while III reached radioactivity levels in the blood only about one-seventh those attained by I.

Following peaks close to 15 min after dosing, blood concentrations of both I and II declined rapidly. The blood levels from a dose of III showed a broad peak, which yielded to a (log) rate of decline similar to those of the other triazines after about 1 hr. The comparative long-term persistence of II in blood predicted from urinary excretion rate plots (3) was confirmed.

All blood level curves presented show the radioactivity in blood resulting from a dose of labeled triazine. Previous data (3) indicated that I and II were not metabolized; therefore, radioactivity levels in blood reflect the concentrations of these administered species. (The persistent tail of the blood profile for II might reflect some very minor, enduring metabolite.) Compound III, in contrast, was significantly metabolized. Blood radioactivity, therefore, gives no direct information on unchanged III.

Additional uncertainty arises in that metabolites may be distributed differently from their parent compounds (7). If the volumes of distribution are appreciably different, irregularities in blood curves based on total radioactivity in the sampled volume may occur. These irregularities could be especially noticeable if emerging metabolites have considerably lower volumes of distribution than their parent and, thus, the influence of metabolism on the total concentration (radioactivity) is counter to that of excretion.

Unusual Absorption Peak for III—Compared to the absorption peaks obtained with I and II, the peak due to III was low and of an unusual and broad shape. The lower radioactivity in blood than that succeeding a dose of either I or II may have been due to a considerably greater volume of distribution of III. In such a situation, the production of metabolites with lower volumes of distribution than that of III may have led to peaks subsequent to the absorption peak, which, if sufficiently close, may have been misinterpreted as an extension of the absorption peak.

More frequent monitoring of blood early after a 5-mg ip injection of III showed that consistent decay of blood levels might not commence until about 2 hr after dosing. If, however, the extended plateau observed was in some way due to peaks in total blood radioactivity caused by the production of metabolites, these peaks were not in evidence following a 1-mg iv (jugular) dose[6] to three rats (Fig. 2). Given the minor chemical differences between III and its two metabolites (3), close similarity in their biological distributions should not be surprising.

Slow first-order absorption of III may have been expected to lead to slow attainment of a peak blood level and then decay, *i.e.*, a broad but definite peak. Characteristically, however, in the first sample after intraperitoneal dosage, the 5-min sample, maximum blood levels or a little

[1] Tri-Carb model 3314, with automatic external standardization, model 3950, Packard Instrument Co.
[2] A 1:1 mixture of 2-propanol and Soluene 100 (Packard).
[3] A 1:9 mixture of 0.5 *N* HCl and Insta-gel (Packard).
[4] University of Sydney Animal House, Castle Hill, New South Wales.
[5] Unless otherwise specified, all triazines were injected in a 10-mg/ml solution in 60% dimethyl sulfoxide in water.
[6] The lethal dose of any of the triazines by the intravenous route was little more than 1 mg.

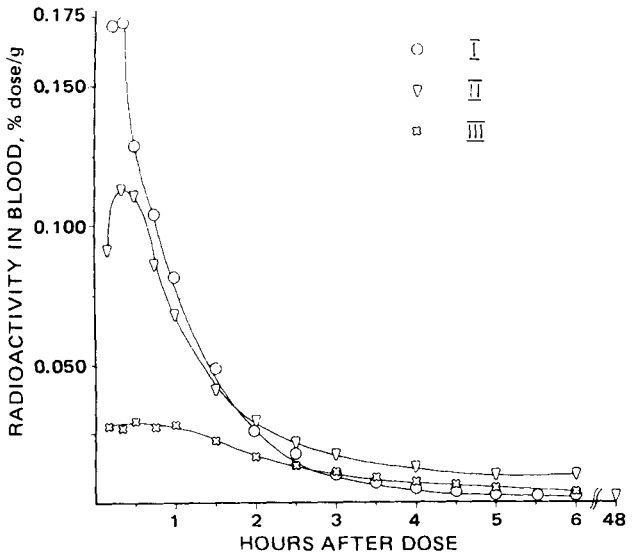

Figure 1—*Representative blood level curves after 5 mg ip of I, II, or III.*

less had already been achieved. A slight drop in level in the 10-min sample and a subsequent return toward the level of the 5-min sample were followed by relatively steady levels. A consistent decline in blood levels commenced only about 60–120 min after dosage.

The profile to this point, a plateau rather than a peak, was similar to that obtained when steady-state blood levels are generated by an intravenous bolus dose followed by a constant intravenous infusion (8–10). An approximately analogous situation might have been expected if the administered compound, injected in a nonaqueous solvent, had precipitated in the peritoneal cavity because of dilution of the solvent with peritoneal fluid or because of more rapid absorption of the solvent than the dosed compound (11). Precipitation by either or a combination of these mechanisms may have abruptly terminated the initial rapid rate of first-order absorption following intraperitoneal injection.

A later phase of constant low level absorption may have been driven by the low concentration in the aqueous peritoneal fluid, constant at saturation level unless further limited by the redissolution rate of the precipitate. Following complete redissolution, however, a consistent decline in the content of the peritoneal fluid, the absorption rate, and the blood level could have been expected.

Testing Precipitation Model—The III injection solution (0.5 ml, 10 mg/ml in 60% dimethyl sulfoxide) was diluted with 1 ml of water. Within 2 hr, some opalescence was apparent; after overnight standing, large crystals (still growing) were observed. The supernate, probably still a colloidal suspension, held about one-third of the radioactivity. In contrast, I and II were soluble at 10 mg/ml of pure water. Not surprisingly, precipitate was not visible upon opening the peritoneal cavity shortly after injecting III.

Varying Volume of Injection Solvent—If the initial peak in blood levels of III was due to an initial rapid first-order absorption terminated by the precipitation of this compound upon dilution or absorption of the injection solvent, an increase in the solvent volume injected should increase the duration and height of the initial peak. Furthermore, this increase should curtail the subsequent plateau since, with increased early absorption, less compound should precipitate, thereby shortening the time required for its complete redissolution. In the limiting situation, it can be envisaged that the initial peak should not be delayed or augmented further by increased solvent injection since all of the compound would be absorbed before it could precipitate and no trailing plateau would be observed; *i.e.*, the conventional profile should result.

Fifteen animals were dosed with 5 mg ip of III in 0.5, 1.0, or 2.0 ml of 60% dimethyl sulfoxide (Fig. 3). The predicted increase in height and width of the initial peak was seen after increasing the solvent volume from 0.5 to 1.0 ml (height changed from 0.029 to 0.050% of the dose/g of blood; $p < 0.05$ by two-tailed t test). Dosing in 2.0 ml of solvent also produced a greater peak than dosing in 0.5 ml (0.047% of the dose/g of blood; $p < 0.05$), but, in agreement with the prediction of a limit to the increase, the peak after dosing in 2.0 ml was no greater than that after dosing in 1.0 ml of solvent.

The blood profiles obtained with the larger dose volumes, however, were not always ideal; periods of stationary blood levels or after-peaks

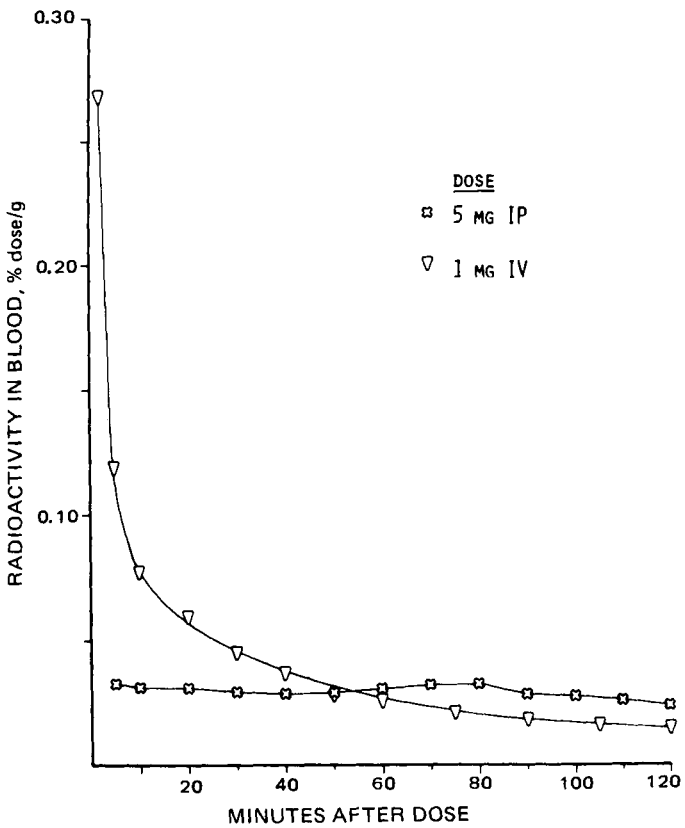

Figure 2—*Representative blood level curves after 1 mg iv or 5 mg ip of III.*

were particularly noticeable in profiles exhibiting smaller initial peaks, as would be expected if the compound was still precipitating in these cases.

A dose of 2.5 mg ip of III in 0.25, 0.5, or 1.0 ml of 60% dimethyl sulfoxide was given to 15 animals (Fig. 4). All profiles except one showed plateaus or large secondary peaks. No significant difference was found by a t test between the heights of initial peaks after 2.5-mg doses in the three injection volumes. This result, however, could have been due to the considerable variability observed. Variability, which is not a surprising

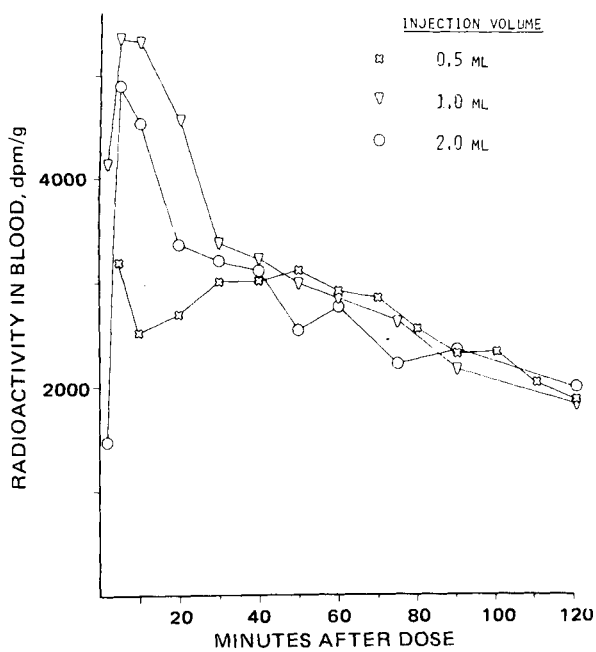

Figure 3—*Representative blood level curves after 5 mg ip of III in 0.5, 1.0, or 2.0 ml of 60% dimethyl sulfoxide.*

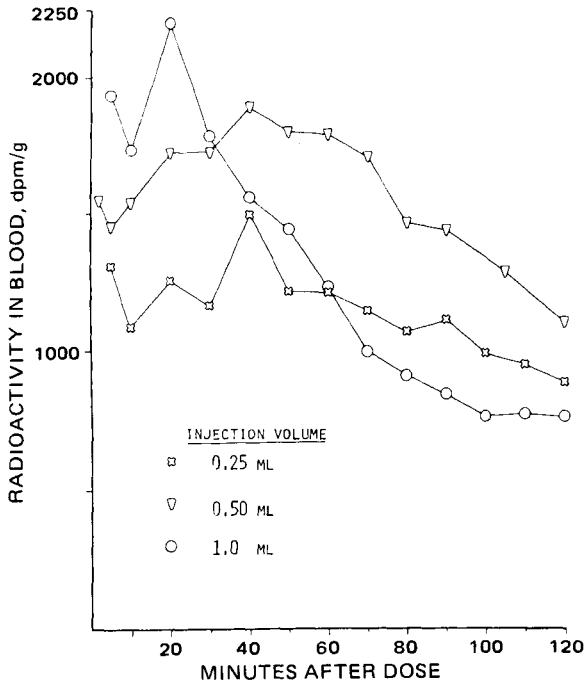

Figure 4—*Representative blood level curves after 2.5 mg ip of III in 0.25, 0.5, or 1.0 ml of 60% dimethyl sulfoxide.*

consequence of the complexity of factors that might impinge on precipitation in the peritoneal cavity, appears to have diminished with an increase in dose volume. The average height of initial peaks was 0.029 ± 0.007 (*SE*), 0.028 ± 0.004, or 0.039 ± 0.003% of the 2.5-mg dose/g of blood after dosing in 0.25, 0.5, or 1.0 ml (five rats per injection volume).

Varying Dose—Doses of 2.5, 5, or 10 mg ip of III were given in the same injection volume of 1.0 ml of 60% dimethyl sulfoxide. In Fig. 5, profiles with few irregularities have been chosen as examples for 2.5- and 5-mg dosing. All five animals dosed with 10 mg in 1.0 ml had irregular blood profiles. The comparatively smooth curves resulting from the lower two doses in 1.0 ml had an interrelationship approximately that expected if no precipitation had occurred. The irregular profile representing the 10-mg dose, however, had an initial peak of similar magnitude to that

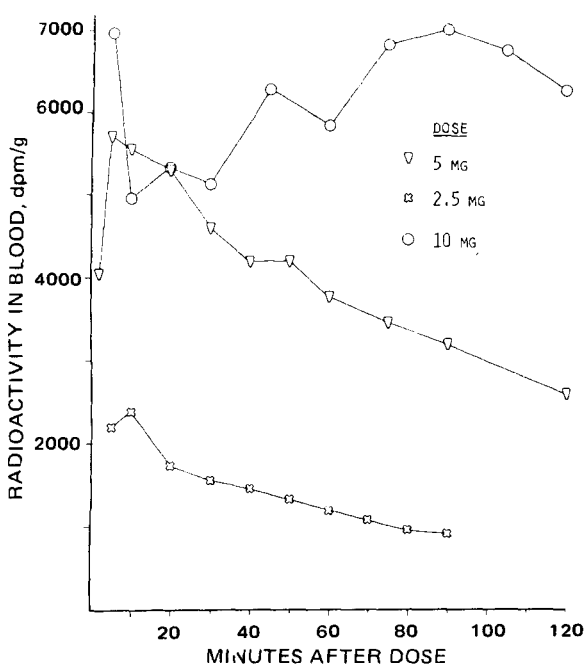

Figure 5—*Representative blood level curves after intraperitoneal dose of 1.0 ml of 60% dimethyl sulfoxide containing 2.5, 5.0, or 10 mg of III.*

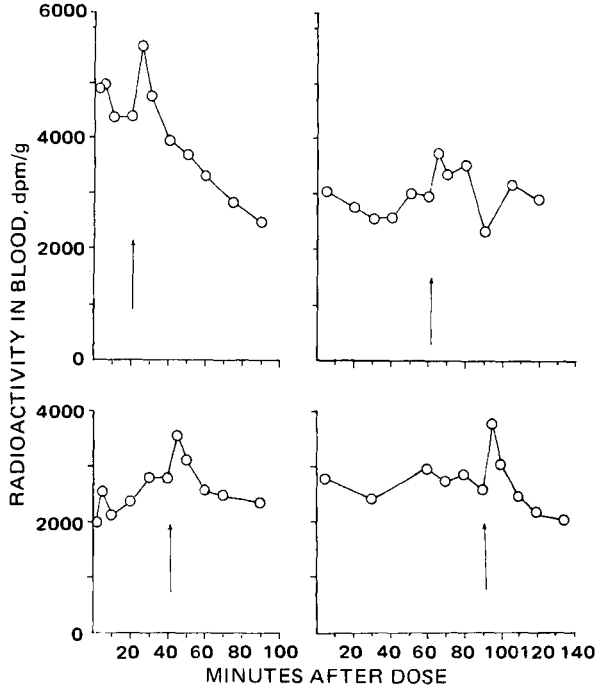

Figure 6—*Representative blood level curves showing the effect of a 60% dimethyl sulfoxide chase injection approximately 20, 40, 60, or 90 min after 5 mg ip of III.*

following a dose of only 5 mg in the same volume of solvent. In the very early period after either dose, similar amounts of III possibly were absorbed from the peritoneal cavity because the absorption rate was controlled more by the concentration of dimethyl sulfoxide than by the concentration of III in the cavity.

Varying Both Dose and Solvent Volume—The interrelationship between some doses was not adequately explained by a simple precipitation model alone. Plateaus at very different levels were seen in blood profiles resulting from injection of different volumes of the one solution, *e.g.*, 2.5 mg in 0.25 ml, 5 mg in 0.5 ml, and 10 mg in 1.0 ml of a 10-mg/ml solution of III (Figs. 3, 4, and 5). This result may have been expected if the plateau level was dependent on the dimethyl sulfoxide concentration in the peritoneal fluid and if this concentration was constant after injection. However, if dimethyl sulfoxide was rapidly absorbed, the blood plateau level should have been governed by the saturation concentration of III in the aqueous peritoneal fluid and would have thus been independent of dose or injection volume. In the event of precipitation, however, many additional factors may have influenced the plateau level in the blood profile, factors such as the volume of peritoneal fluid and the relative rates of precipitation, redissolution, and absorption of III.

Injecting Solvent after Dose—It might be proposed that dimethyl sulfoxide improved absorption not by influencing the solubility of III but by some physiological action, *e.g.*, on the peritoneal membrane. Therefore, a 5-mg ip dose of III in 0.5 ml of 60% dimethyl sulfoxide was followed after about 20, 40, 60, 90, or 150 min by an intraperitoneal injection of 1.0 ml of 60% dimethyl sulfoxide (Fig. 6). A peak in the blood curve occurred immediately after the dimethyl sulfoxide "chase" injection, irrespective of the time at which it was given. With the baseline of each peak thus induced, taken as a straight line joining the point immediately (1.5 min) prior to the dimethyl sulfoxide chase with that about 20 min later, the heights of these peaks were expressed as a percentage of the current baseline blood levels (Table I).

Where conventional first-order absorption applies, around 90% of the dose has usually been absorbed by the time maximum blood levels are reached. The initial peak after a 5-mg ip dose of III was almost always observed before 10 min. On fairly conservative grounds then, if normal first-order kinetics had been operating, only 0.0001% of the dose would have remained in the peritoneal cavity 60 min after dosing. It is highly improbable that the stimulation of even complete absorption of this percentage of the original dose could lead to the 17% enhancement ($p < 0.01$) of blood level caused by dimethyl sulfoxide administration 61.5 min after the III dose. While these data are not consistent with a physiological effect of dimethyl sulfoxide on conventional absorption, they confirm the precipitation model that predicts that dimethyl sulfoxide momen-

Table I—Effect of Dimethyl Sulfoxide Solvent Injected after III

Animal	Time of Solvent Injection, min	Time of Peak, min	Enhancement by Solvent Injection, %	
1	21.5	25	6.7	
2	21.5	25	29.6	
3	21.5	25	43.5	
4	21.5	25	32.5	
5	21.5	25	25.9	
6	21.5	25	29.1	
			Mean	27.9
7	41.5	45	29.2	
8	41.5	45	36.8	
			Mean	33.0
9	61.5	65	15.8	
10	61.5	65	13.6	
11	61.5	65	15.5	
12	61.5	65	17.2	
13	61.5	65	20.8	
			Mean	16.6
14	91.5	95	18.4	
15	91.5	95	48.4	
16	91.5	95	17.3	
			Mean	28.0
17	151.5	155	15.2	
18	241.5	250	8.5	
19	241.5	245	5.7	
20	241.5	245	6.9	
21	241.5	245	11.2	
22	241.5	250	10.3	
			Mean	8.5

tarily increases the solubility of precipitated triazine in the peritoneal cavity.

Dimethyl sulfoxide injection 241.5 min after the triazine dose produced significantly less ($p < 0.01$) percentage enhancement of blood levels than did dimethyl sulfoxide 61.5 min after the triazine. A decline with time in the capacity of dimethyl sulfoxide to enhance blood levels of III is not likely if enhancement is due to some systemic (rather than absorptive) physiological action of dimethyl sulfoxide. This decline, however, confirms again the precipitation model that allows that the precipitate in the peritoneal cavity is progressively redissolved and thus provides a diminishing basis for the influence of a secondary dimethyl sulfoxide injection on the blood profile.

Dimethyl sulfoxide (60%) was administered either 61.5 or 121.5 min after dosing five rats with 5 mg ip of II, a water-soluble compound. Minor enhancement of blood II levels was noticed at both times (4.4 and 2.9% after 61.5 min; 0, 5.4, and 10.7% after 121.5 min) but was even less than enhancement of III levels after the 241.5-min dimethyl sulfoxide administration. Moreover, with II, blood level enhancement did not appear to follow dimethyl sulfoxide administration as closely as with III.

DISCUSSION

Of the three aryldihydro-*s*-triazines chosen for study, two were among folate antagonists previously tested (2) for *in vivo* antineoplastic activity; III was reported to be the most effective of a series of long chain substituted phenyldihydrotriazines in prolonging survival of rats bearing Walker 256 ascites tumor; II, without long chain substitution, was a more potent antifolate and inhibitor of L-1210 tumor cultures but, nevertheless, compared very poorly with more complex inhibitors such as III in its *in vivo* antineoplastic efficacy. Since adverse pharmacokinetic properties may have been responsible for the comparative lack of *in vivo* activity by II, the prototype of the series I was included in the present study to provide triazines with molecular weights both lower and higher than that of II.

The relative elimination characteristics of the triazines (3) do not explain the relative inactivity *in vivo* of the more slowly eliminated II. Moreover, in the present study, blood II concentrations were shown to reach five times the concentrations attainable with III and to be more persistent.

The shape of the blood profiles observed after intraperitoneal injection of III indicates that the blood levels attained are comparatively low, largely because of slower absorption. However, action is not required in the bloodstream so much as in the peritoneal cavity which accommodates the Walker 256 tumor in free-cell form. With compounds as rapidly excreted (3) and having as large volumes of distribution as these triazines, it seems unlikely that concentrations in the peritoneal cavity anywhere near those resulting initially from the intraperitoneal injection itself can be achieved or maintained by return of the drug *via* the bloodstream. Thus, the drug level in the blood might be regarded as an index not of the rate of arrival of the drug at its site of action but rather of the rate of its loss from that site. A significant delay in absorption might then confer an advantage for activity.

Simulation of II distribution according to a two-compartment model suggests that only about 1% of an intraperitoneal dose remains in the peritoneal cavity after 30 min (without allowing for return of triazine *via* the bloodstream). On the other hand, after apparent precipitation of III following its intraperitoneal injection, the concentration in peritoneal fluid may, for about 90 min at least, approximate the aqueous saturation level, although unexplained phenomena make the actual concentration uncertain. (Any estimate of peritoneal concentrations from present kinetic information must also be judged speculative.)

Furthermore, although the concentration might commence to decline after 90 min, the precipitate may persist for as long as 240 min (dimethyl sulfoxide chase experiments), leading to less than expected rates of decline between 90 and 240 min. Thus, it seems that precipitation may be a mechanism whereby concentrations well in excess of the ED_{50} (3.8×10^{-6} mg/ml for III against L-1210 cultures) are considerably sustained at the site of action.

As a result of this mechanism, apparently, an intraperitoneal dose of III was effective against peritoneal Walker 256 but not against Walker 256 in the leg muscle (2). Furthermore, all aryldihydrotriazines in this series that were active against Walker 256 ascites were substituted on the phenyl ring with long nonpolar side chains that probably permitted no greater solubility than III. Given intraperitoneally, none was as active against Walker 256 in leg muscle as they were against the ascites tumor.

Equivalent solubility could be expected also from a series of irreversible, isoenzyme-selective inhibitors (identical but bearing a sulfonyl fluoride substituent). These compounds were similarly active against Walker 256 ascites, but their chemotherapeutic indexes did not match their isoenzyme selectivities (2). Since precipitation in the peritoneal cavity might reasonably be expected both to increase antineoplastic efficacy and to decrease systemic toxicity, it should not be surprising that these compounds might have chemotherapeutic indexes reflecting their relative solubilities as much as their relative isoenzyme selectivities.

Two factors complicate these findings. The antineoplastic study (2) employed III as the ethanesulfonate salt, but only the *p*-toluenesulfonate was available during the pharmacokinetic study. In addition, rats used for pharmacokinetic studies did not carry ascites tumors.

Baker and Ashton (12) advanced the desirability of administering III "by intravenous infusion, so that administration could be discontinued at once should toxicity develop." They reported that III (ethanesulfonate) "was not soluble enough to achieve a toxic dose intravenously." Although their findings are not stated in detail, it is inferred that the compound was not only nontoxic but also ineffective by this route (otherwise the sought-after specificity would have been attained). Not only does their statement once again indicate that the antineoplastic activity of III was dependent on the injection route and the tumor sharing the peritoneal cavity but that insolubility was similarly a characteristic with the ethanesulfonate as with the *p*-toluenesulfonate salt of III. In contrast to the ethanesulfonate, the *p*-toluenesulfonate was soluble enough to achieve, as indicated before, a consistently lethal intravenous dose at little more than 4 mg/kg.

It is, nevertheless, difficult to reconcile these observations with the approximate solubility of III ethanesulfonate given by Baker and Ashton (12, 13) at 10 mg/ml (these authors indicated that the solubility given was approximate but did not state how it was determined). At this solubility, a large and surprising discrepancy would exist between the solubilities of the ethanesulfonate and the *p*-toluenesulfonate salts of III, and it is questionable whether precipitation would occur from the volume of peritoneal fluid of an animal bearing an ascites tumor. Solubilities (<0.5–5 mg/ml) given for other triazines effective *in vivo* are consistent with their probable precipitation in the peritoneal cavity, as observed for III *p*-toluenesulfonate.

Data from a precipitating compound are, at this stage, too complex to fit satisfactorily to mathematical models. Preliminary compartmental modeling with soluble I and II, however, indicates that II is absorbed from the peritoneal cavity more slowly than I. If this trend continues toward III and other higher molecular weight triazines, a slower inherent absorption may, in addition to precipitation, contribute to their efficacy against the peritoneal tumor. This slower inherent absorption may be particularly relevant to the antiascites activity of a later series of water-

soluble, but high molecular weight, aryldihydro-*s*-triazines synthesized by Baker and Ashton (12).

REFERENCES

(1) B. R. Baker, "Design of Active-Site-Directed Irreversible Enzyme Inhibitors," Wiley, New York, N.Y., 1967.

(2) B. R. Baker, N. M. J. Vermeulen, W. T. Ashton, and A. J. Ryan, *J. Med. Chem.*, **13**, 1130 (1970).

(3) A. J. Ryan, J. J. Ashley, and R. A. Upton, *J. Pharm. Sci.*, **67**, 306 (1978).

(4) G. A. Bray, *Anal. Biochem.*, **1**, 279 (1960).

(5) R. A. Upton, *J. Pharm. Sci.*, **64**, 112 (1975).

(6) A. J. Creskoff, T. Fitz-Hugh, Jr., and E. J. Farris, in "The Rat in Laboratory Investigation," E. J. Farris and J. Q. Griffith, Jr., Eds., Hafner, New York, N.Y., 1949, p. 406.

(7) S. Riegelman, M. Rowland, and L. Z. Benet, *J. Pharmacokin. Biopharm.*, **1**, 83 (1973).

(8) R. N. Boyes, D. B. Scott, P. J. Jebson, M. J. Godman, and D. G. Julian, *Clin. Pharmacol. Ther.*, **12**, 105 (1971).

(9) P. A. Mitenko and R. I. Ogilvie, *ibid.*, **13**, 329 (1972).

(10) J. G. Wagner, *ibid.*, **16**, 691 (1974).

(11) H. B. Hucker, P. M. Ahmad, and E. A. Miller, *J. Pharmacol. Exp. Ther.*, **154**, 176 (1966).

(12) B. R. Baker and W. T. Ashton, *J. Med. Chem.*, **16**, 209 (1973).

(13) B. R. Baker, *Ann. N.Y. Acad. Sci.*, **186**, 214 (1971).

ACKNOWLEDGMENTS

Supported in part by grants from the University of Sydney Cancer Fund and the Australian Research Grants Committee.

Synthesis, Toxicity, and Cardiovascular Properties of *N*-Aralkyl- and *N*-Acyl-5-aminoethylindans

WILLIAM E. SOLOMONS *, IAN W. MATHISON ‡x, RAYMOND H. JONES, NORBERT J. WOJCIECHOWSKI §, and JAMES W. LAWSON §

Received March 8, 1977, from the **Department of Chemistry, University of Tennessee at Martin, Martin, TN 38237*, the ‡*School of Pharmacy, Ferris State College, Big Rapids, MI 49307*, and the §*Department of Molecular Biology, College of Pharmacy, University of Tennessee Center for the Health Sciences, Memphis, TN 38163.* Accepted for publication June 7, 1977.

Abstract □ Secondary amines and amides of 5-aminoethyl-6-methoxyindan and 5-aminoethyl-6-methylindan were synthesized, and the blood pressure lowering effects and accompanying changes in heart rate were evaluated in the unanesthetized desoxycorticosterone acetate hypertensive rat. The acute toxicities of the compounds were determined in mice. The amines were significantly more potent than the amides as antihypertensive agents and also were more toxic. 5-(3,4-Dimethoxybenzyl)aminoethyl-6-methylindan produced the greatest depression in systolic blood pressure at the dose level studied. Structure–activity relationships relevant to blood pressure lowering, heart rate, and toxicity are discussed.

Keyphrases □ Indans, various substituted—synthesized, cardiovascular properties and toxicity evaluated, rats □ Cardiovascular properties—various substituted indans evaluated □ Toxicity—various substituted indans evaluated □ Structure–activity relationships—various substituted indans evaluated for toxicity and cardiovascular properties

The recent synthesis of cyclopentanoisoquinolines (1, 2) is a continuation of interest in the cardiovascular activity of substituted and reduced isoquinolines (3–6). During the synthesis of the novel cyclopentano[*h*]- and [*f*]-1,2,3,4-tetrahydroisoquinolines (1, 2), some previously unreported substituted aminoethylindans (1) were produced as intermediates to the desired products.

In an attempt to search exhaustively for antihypertensive agents, these intermediates were screened in the desoxycorticosterone acetate hypertensive rat for their blood pressure lowering effects. The hypotensive properties noted with the few intermediates in this screening test prompted preparation of derivatives of the aminoethylindan nucleus in the hope that blood pressure lowering activity might be enhanced and some structure–activity relationships could be developed. This approach was further encouraged by the report of Troxler and Hofmann (7) that certain *N*-substituted aminoethylindans possessed significant hypotensive activity.

The synthesis of eight compounds is reported here, together with the mouse approximate LD_{50} (ALD_{50}) and the effects of the compounds on systolic blood pressure and heart rate in the hypertensive rat.

EXPERIMENTAL

Chemistry—The synthesis of the precursor molecules (5-aminoethyl-6-methoxyindan and 5-aminoethyl-6-methylindan) for the current series was reported previously in connection with the synthesis of the cyclopentano-1,2,3,4-tetrahydroisoquinolines (1, 2). The amide derivatives were synthesized from the precursor aminoethylindans by the classic acylation with the appropriate acyl chloride in the presence of a base. Compound VIII was prepared from the aminoethylindan by condensation with 3,4-dimethoxybenzaldehyde, followed by catalytic hydrogenation of the resulting Schiff base. The synthetic pathway for the preparation of the compounds is shown in Schemes I–III.

Physical properties and analytical data of the synthesized compounds are shown in Table I. All melting points were determined on a melting-point apparatus[1] and are uncorrected. IR spectra were determined[2] in potassium bromide and were characteristic of the compounds reported. Elemental analyses[3] were within ±0.4% of the theoretical values.

Biological Methods—Acute toxicity determinations were performed in female Swiss-Webster mice, 15–24 g. Compounds were administered

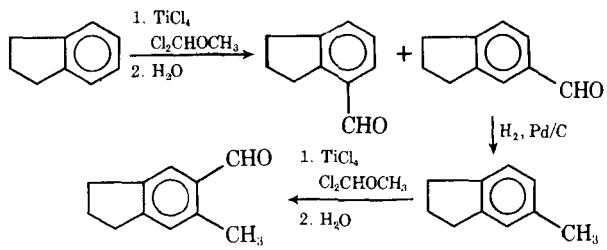

Scheme I

[1] Swissco.

[2] Beckman IR 33.

[3] Galbraith Laboratories, Knoxville, Tenn., and Chemalytics, Inc., Tempe, Ariz.

soluble, but high molecular weight, aryldihydro-*s*-triazines synthesized by Baker and Ashton (12).

REFERENCES

(1) B. R. Baker, "Design of Active-Site-Directed Irreversible Enzyme Inhibitors," Wiley, New York, N.Y., 1967.

(2) B. R. Baker, N. M. J. Vermeulen, W. T. Ashton, and A. J. Ryan, *J. Med. Chem.*, **13**, 1130 (1970).

(3) A. J. Ryan, J. J. Ashley, and R. A. Upton, *J. Pharm. Sci.*, **67**, 306 (1978).

(4) G. A. Bray, *Anal. Biochem.*, **1**, 279 (1960).

(5) R. A. Upton, *J. Pharm. Sci.*, **64**, 112 (1975).

(6) A. J. Creskoff, T. Fitz-Hugh, Jr., and E. J. Farris, in "The Rat in Laboratory Investigation," E. J. Farris and J. Q. Griffith, Jr., Eds., Hafner, New York, N.Y., 1949, p. 406.

(7) S. Riegelman, M. Rowland, and L. Z. Benet, *J. Pharmacokin. Biopharm.*, **1**, 83 (1973).

(8) R. N. Boyes, D. B. Scott, P. J. Jebson, M. J. Godman, and D. G. Julian, *Clin. Pharmacol. Ther.*, **12**, 105 (1971).

(9) P. A. Mitenko and R. I. Ogilvie, *ibid.*, **13**, 329 (1972).

(10) J. G. Wagner, *ibid.*, **16**, 691 (1974).

(11) H. B. Hucker, P. M. Ahmad, and E. A. Miller, *J. Pharmacol. Exp. Ther.*, **154**, 176 (1966).

(12) B. R. Baker and W. T. Ashton, *J. Med. Chem.*, **16**, 209 (1973).

(13) B. R. Baker, *Ann. N.Y. Acad. Sci.*, **186**, 214 (1971).

ACKNOWLEDGMENTS

Supported in part by grants from the University of Sydney Cancer Fund and the Australian Research Grants Committee.

Synthesis, Toxicity, and Cardiovascular Properties of *N*-Aralkyl- and *N*-Acyl-5-aminoethylindans

WILLIAM E. SOLOMONS *, IAN W. MATHISON ‡x, RAYMOND H. JONES, NORBERT J. WOJCIECHOWSKI §, and JAMES W. LAWSON §

Received March 8, 1977, from the **Department of Chemistry, University of Tennessee at Martin, Martin, TN 38237*, the ‡*School of Pharmacy, Ferris State College, Big Rapids, MI 49307*, and the §*Department of Molecular Biology, College of Pharmacy, University of Tennessee Center for the Health Sciences, Memphis, TN 38163.* Accepted for publication June 7, 1977.

Abstract □ Secondary amines and amides of 5-aminoethyl-6-methoxyindan and 5-aminoethyl-6-methylindan were synthesized, and the blood pressure lowering effects and accompanying changes in heart rate were evaluated in the unanesthetized desoxycorticosterone acetate hypertensive rat. The acute toxicities of the compounds were determined in mice. The amines were significantly more potent than the amides as antihypertensive agents and also were more toxic. 5-(3,4-Dimethoxybenzyl)aminoethyl-6-methylindan produced the greatest depression in systolic blood pressure at the dose level studied. Structure–activity relationships relevant to blood pressure lowering, heart rate, and toxicity are discussed.

Keyphrases □ Indans, various substituted—synthesized, cardiovascular properties and toxicity evaluated, rats □ Cardiovascular properties—various substituted indans evaluated □ Toxicity—various substituted indans evaluated □ Structure–activity relationships—various substituted indans evaluated for toxicity and cardiovascular properties

The recent synthesis of cyclopentanoisoquinolines (1, 2) is a continuation of interest in the cardiovascular activity of substituted and reduced isoquinolines (3–6). During the synthesis of the novel cyclopentano[*h*]- and [*f*]-1,2,3,4-tetrahydroisoquinolines (1, 2), some previously unreported substituted aminoethylindans (1) were produced as intermediates to the desired products.

In an attempt to search exhaustively for antihypertensive agents, these intermediates were screened in the desoxycorticosterone acetate hypertensive rat for their blood pressure lowering effects. The hypotensive properties noted with the few intermediates in this screening test prompted preparation of derivatives of the aminoethylindan nucleus in the hope that blood pressure lowering activity might be enhanced and some structure–activity relationships could be developed. This approach was further encouraged by the report of Troxler and Hofmann (7) that certain *N*-substituted aminoethylindans possessed significant hypotensive activity.

The synthesis of eight compounds is reported here, together with the mouse approximate LD_{50} (ALD_{50}) and the effects of the compounds on systolic blood pressure and heart rate in the hypertensive rat.

EXPERIMENTAL

Chemistry—The synthesis of the precursor molecules (5-aminoethyl-6-methoxyindan and 5-aminoethyl-6-methylindan) for the current series was reported previously in connection with the synthesis of the cyclopentano-1,2,3,4-tetrahydroisoquinolines (1, 2). The amide derivatives were synthesized from the precursor aminoethylindans by the classic acylation with the appropriate acyl chloride in the presence of a base. Compound VIII was prepared from the aminoethylindan by condensation with 3,4-dimethoxybenzaldehyde, followed by catalytic hydrogenation of the resulting Schiff base. The synthetic pathway for the preparation of the compounds is shown in Schemes I–III.

Physical properties and analytical data of the synthesized compounds are shown in Table I. All melting points were determined on a melting-point apparatus[1] and are uncorrected. IR spectra were determined[2] in potassium bromide and were characteristic of the compounds reported. Elemental analyses[3] were within ±0.4% of the theoretical values.

Biological Methods—Acute toxicity determinations were performed in female Swiss-Webster mice, 15–24 g. Compounds were administered

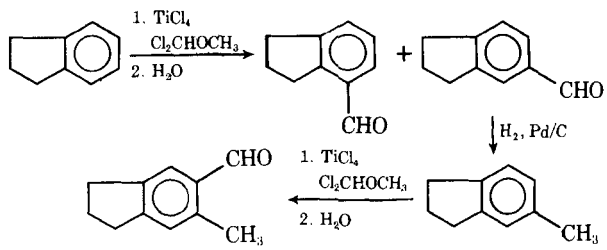

Scheme I

[1] Swissco.

[2] Beckman IR 33.

[3] Galbraith Laboratories, Knoxville, Tenn., and Chemalytics, Inc., Tempe, Ariz.

Table I—Physical Data of *N*-Substituted Aminoethylindans

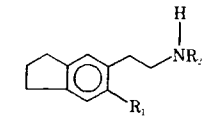

Compound	R_1	R_2	Formula	Melting Point	Yield, %	Basic Catalyst	Recrystallization Solvent	Analysis, %	Calc.	Found
I	CH_3O	C_6H_5CO	$C_{19}H_{21}NO_2$	104-106°	23	Sodium carbonate	Ether	C	77.26	77.42
								H	7.17	7.26
								N	4.74	4.70
II	CH_3O	$3,4,5\text{-}(CH_3O)_3C_6H_2CO$	$C_{22}H_{27}NO_5$	144-145°	27	Sodium carbonate	Ethyl acetate	C	68.55	68.71
								H	7.06	6.93
								N	3.63	3.61
III	CH_3O	$C_6H_5CH_2CO$	$C_{20}H_{23}NO_2$	135°	54	Potassium bicarbonate	Ether	C	77.63	77.48
								H	7.51	7.55
								N	4.52	4.49
IV	CH_3O	$3,4\text{-}(CH_3O)_2C_6H_3CH_2CO$	$C_{22}H_{27}NO_4$	115°	42	Potassium bicarbonate	Ethanol	C	71.51	71.52
								H	7.38	7.45
								N	3.79	3.78
V	CH_3	H·HCl	$C_{12}H_{18}ClN$	229-231°	89	—	Cold dilute hydrochloric acid	C	68.07	68.15
								H	8.56	8.48
								Cl	16.74	16.61
								N	6.62	6.02
VI	CH_3	$C_6H_5CH_2CO$	$C_{20}H_{23}NO$	125.5-127°	42	Triethylamine	Benzene	C	81.87	81.68
								H	7.90	8.07
								N	4.77	5.08
VII	CH_3	$3,4\text{-}(CH_3O)_2C_6H_3CH_2CO$	$C_{22}H_{27}NO_3$	144-145°	48	Triethylamine	Benzene	C	74.75	74.53
								H	7.69	7.46
								N	3.69	3.90
VIII	CH_3	$3,4\text{-}(CH_3O)_2C_6H_3CH_2\cdot HCl$	$C_{21}H_{28}ClNO_2$	223-224°	60	—	Acetonitrile-ethanol	C	69.69	69.63
								H	7.79	7.96
								Cl	9.97	9.75
								N	3.87	3.87

Table II—Acute Toxicity in Mice and Cardiovascular Activity in Desoxycorticosterone Hypertensive Rats of *N*-Substituted Aminoethylindans

Compound	*n* (Mice)	Mouse ALD_{50}, mg/kg ip	Cardiovascular Activity: Dose, mg/kg ip	*n* (Rats)	Controls[a]	Mean Change in Pressure and Heart Rate from Control ± *SE*[b]: 1 hr	2 hr	4 hr	24 hr
I	10	>1000[c]	100[c]	6	200 ± 8 (393 ± 23)	−18 ± 8[d] (−20 ± 23)	−24 ± 7[d] (+9 ± 30)	−12 ± 6 (−14 ± 18)	−13 ± 4[d] (−67 ± 22[d])
II	10	>1000[c]	100[c]	6	210 ± 14 (353 ± 12)	−27 ± 8[d] (+23 ± 28)	−35 ± 13[d] (+10 ± 28)	−12 ± 8 (+47 ± 29)	−16 ± 4 (−4 ± 10)
III	12	1000–1500[c]	100[c]	6	206 ± 11 (382 ± 19)	−32 ± 7[d] (+13 ± 12)	−24 ± 5[d] (+54 ± 25)	−21 ± 4[d] (+19 ± 21)	−13 ± 4[d] (+61 ± 12[d])
IV	15	500–1000[c]	100[c]	6	202 ± 8 (389 ± 29)	−10 ± 4[d] (+23 ± 29)	−10 ± 2[d] (+57 ± 31)	−19 ± 3[d] (+14 ± 12)	−19 ± 4[d] (−27 ± 24)
V	43	79–89[e]	10[e]	6	181 ± 6 (299 ± 13)	−24 ± 8[d] (+32 ± 17)	−24 ± 4[d] (+34 ± 14)	−15 ± 5[d] (+25 ± 11)	−6 ± 4 (−4 ± 11)
			25[e]	6	185 ± 6 (349 ± 22)	—[f]	—[f]	−18 ± 4[d] (+20 ± 21)	−11 ± 2[d] (−26 ± 14)
VI	6	>1000[c]	100[c]	5	179 ± 10 (325 ± 7)	−7 ± 7 (+17 ± 17)	−2 ± 6 (+24 ± 11)	−1 ± 7 (+23 ± 13)	−3 ± 10 (+2 ± 17)
VII	6	>1000[c]	100[c]	6	195 ± 8 (354 ± 19)	−2 ± 6 (+43 ± 10[d])	−4 ± 9 (+47 ± 12[d])	+2 ± 5 (+37 ± 15[d])	−3 ± 7 (+22 ± 12)
VIII	20	140–178[c]	100[c]	6	186 ± 6 (366 ± 16)	−58 ± 4[d] (−55 ± 17[d])	−60 ± 7[d] (0 ± 14)	−47 ± 2[d] (+4 ± 8)	−17 ± 2[d] (−14 ± 10)
0.9% NaCl	—	—	1 ml/kg	12	183 ± 8 (351 ± 14)	+5 ± 4 (+18 ± 12)	+4 ± 3 (+25 ± 14)	−2 ± 3 (+6 ± 6)	0 ± 3 (0 ± 14)
Methyldopa	—	—	50[c]	6	205 ± 9 (378 ± 22)	−31 ± 4[d] (+106 ± 26[d])	−50 ± 4[d] (+104 ± 28[d])	−48 ± 6[d] (+31 ± 39)	−16 ± 5[d] (−19 ± 12)
Guanethidine	—	—	10[e]	5	197 ± 11 (427 ± 27)	−25 ± 8[d] (−67 ± 28[d])	−46 ± 9[d] (−101 ± 24[d])	−44 ± 6[d] (−95 ± 22[d])	−27 ± 6[d] (−81 ± 26[d])

[a] Mean systolic blood pressure (mm Hg) ± *SE*. Numbers in parentheses represent mean heart rate (beats per minute) ± *SE*. [b] Mean difference in systolic blood pressure from control (mm Hg) ± *SE*. Numbers in parentheses represent mean difference in heart rate from control (beats per minute) ± *SE*. [c] Administered as a suspension in 1% tragacanth. [d] Significant change from control, $p < 0.05$, by Newman–Keuls *a posteriori* test. [e] Administered as a solution in distilled water. [f] No readings possible at this time period, no perceptible pulse; respiration and movement artifacts.

in aqueous solutions or as suspensions in 1% tragacanth by the intraperitoneal route to groups of three or more mice. The LD_{50} values were estimated from the results obtained by administering two or more dose levels of each compound, usually spaced 0.3 logarithmic interval or less, to these groups of mice. Animals were observed for up to 72 hr following injection, but the toxicity values reported in Table II represent the outcome 24 hr after administration.

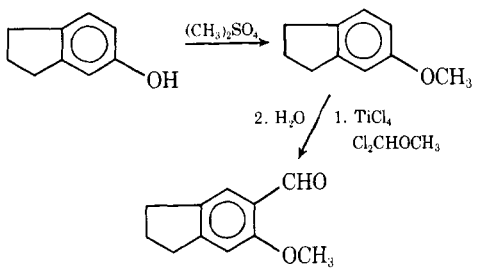

Scheme II

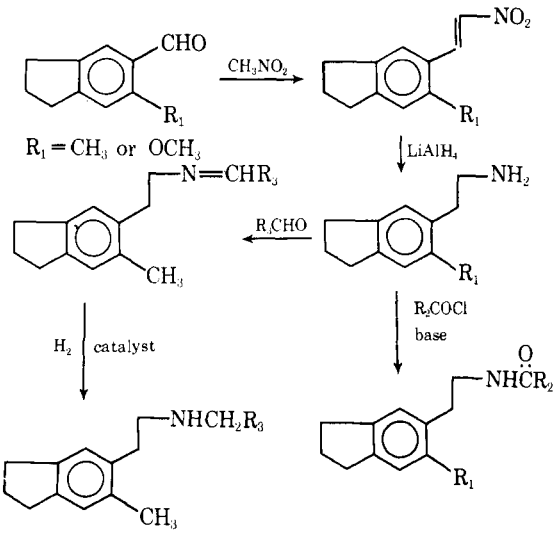

Scheme III

The indirect measurements of blood pressure and heart rate were determined in male Charles River rats made hypertensive (systolic blood pressure >150 mm Hg) by subcutaneously implanting a wax-formulated pellet containing 10 mg of desoxycorticosterone acetate as previously described (8, 9). Systolic blood pressure was measured in the caudal arteries of prewarmed (40°), unanesthetized, restrained animals by a pneumatic pulse transducer placed distal to an automated tail pressure cuff and was recorded on a physiograph[4]. Heart rate was determined from the amplified pulse waves recorded during the blood pressure measurements. Prior to the actual experiments, animals were accustomed to the measurement handling procedure several times during the preceding weeks.

Control systolic blood pressure and heart rates were determined in a group of usually six hypertensive rats on each day. A compound for evaluation was administered by intraperitoneal injection either in solution or as a suspension at 24-hr intervals following injection. Mean values of the group for these parameters at a particular measurement period were calculated, and then the mean difference from control, along with its associated standard error, was calculated for each period. The statistical significance of the changes produced by a compound was tested by an analysis of variance and the Newman–Keuls *a posteriori* test (10) when *F* was significant. A probability level of 0.05 or less was accepted as a significant change (Table II).

All compounds synthesized in this series, except V, were tested at a dosage level of 100 mg/kg. Compound V was relatively more toxic in the mouse, and it was evaluated at two lower dosage levels, 10 and 25 mg/kg. Methyldopa and guanethidine sulfate, two known antihypertensive agents, were included as reference standards. Another group of hypertensive rats was injected with 0.9% NaCl in a dose of 1 ml/kg. The latter group was included as a placebo group for the entire study.

RESULTS AND DISCUSSION

The pharmacological data in Table II show that, with two exceptions (VI and VII), the compounds synthesized significantly lowered systolic blood pressure in the unanesthetized desoxycorticosterone hypertensive rat. The duration of action and time of suggested maximum effect varied somewhat. The greatest hypotensive response generally occurred within 1–2 hr following administration. In some instances (*e.g.*, I and II), this suggested peak response time also was the only time during which the blood pressure was significantly lower than the control value, but other

[4] Narco Bio-Systems Inc., Houston, Tex.

compounds (*e.g.*, III–V and VIII) produced significant lowering of blood pressure which persisted throughout the 24-hr measurement period.

Hypertensive rats receiving a placebo injection of 0.9% NaCl showed no significant changes in systolic blood pressure or heart rate at any time. Methyldopa and guanethidine sulfate, as expected, produced significant depressions in mean systolic blood pressure from control levels.

Group 1—Examination of the amides I–IV, VI, and VII from a structure–activity viewpoint revealed some interesting features. Amides possessing a methoxy group in the 6-position on the indan nucleus (I–IV) clearly exhibited significant antihypertensive activity for varying periods following drug administration. The amides substituted at the 6-position with a methyl group (VI and VII), however, were devoid of hypotensive properties at the dose level studied (100 mg/kg).

This trend is best seen by comparing IV and VII, in which the only difference in structure is the 6-substituent. The methoxy compound (IV) possessed significant blood pressure lowering activity throughout 24 hr, whereas its methyl analog (VII) was inactive as an antihypertensive agent. Significant acceleration in heart rate was noted with VII, and this acceleration may have obviated any significant blood pressure depression. In general, however, significant acceleration of heart rate was not observed and did not appear to be a factor among the other members of this group.

In this group of compounds, III and IV demonstrated the longest duration of action, producing significant depressions in blood pressure over 24 hr. However, differences in the magnitude of the antihypertensive response between III and IV were observed during the 1st and 2nd hr, with III being the most potent during this time. Additionally, the peak hypotensive response of III appeared to be reached at the 1- and 2-hr readings while that of IV was reached during the 4–24-hr observation period.

The decrease in lipid solubility of IV, as a result of the addition of the methoxy groups to the phenylacetamide moiety of III, may explain the differences in the time of onset of the blood pressure lowering effects between these two compounds. The correlation of optimal blood pressure lowering activity with greater lipophilicity was noted previously in studies on antihypertensive decahydroisoquinolines (9). The reflex increase in heart rate that one might anticipate as a result of the hypotensive response was not observed with these compounds; indeed, at the 24-hr time period, significant depression in heart rate was noted with III.

The insertion of a methylene group between the phenyl moiety and the amide group (I and III and II and IV) did not appear to influence the antihypertensive activity.

With the exception of IV, where the LD_{50} was estimated to lie in the 500–1000-mg/kg range, the toxicity results showed that the approximate LD_{50} values were not markedly different from one another and that the compounds were relatively nontoxic.

Group 2—This group comprises amines V and VIII. Antihypertensive activity was noted with both compounds; indeed, VIII produced the greatest depression in blood pressure of the entire series. These two amines were significantly more toxic than their amide counterparts, which neccessitated, in the case of V, the use of much smaller doses for antihypertensive evaluation. Compound VIII, however, was studied at the same dosage level as the Group 1 amides.

The primary amine, V, produced significant depressions in systolic pressure through 4 hr at the low dose of 10 mg/kg. No measurements were possible at the 1- and 2-hr time periods with a high dosage of V (25 mg/kg) due to the inability to detect a tail pulse as well as a greater incidence of movement artifacts in the physiograph recordings with this group of rats. Significant depression of blood pressure, however, was observed at the 4- and 24-hr periods, but data obtained at these points in time showed that there was no difference in the magnitude of the blood pressure response between the two dose levels of V. The blood pressure data show that V appears to be five to seven times more potent than amides I–IV as an antihypertensive agent.

Compound VIII produced substantial depression of blood pressure over 24 hr, which was accompanied at the 1-hr reading by a significant heart rate decrease. The heart rate depression is apparently independent of the blood pressure lowering ability of VIII. This effect is suggested by the fact that, at the 2- and 4-hr measurements, heart rate was not depressed whereas the mean changes in systolic blood pressure were still significantly less than control values and approximately of the same magnitude as the changes observed at the 1-hr period. Like V, the antihypertensive activity of VIII was significantly greater than amides I–IV.

It is evident from the toxicity data that the presence of the aralkyl group in VIII (a secondary amine) decreases the toxicity relative to V (a primary amine). Compound VIII possessed an approximate LD_{50} in the 140–178-mg/kg range, while V was markedly more toxic with a value in the 79–89-mg/kg range.

REFERENCES

(1) I. W. Mathison, W. E. Solomons, and R. H. Jones, *J. Org. Chem.*, **39**, 2852 (1974).

(2) I. W. Mathison, R. H. Jones, and W. E. Solomons, *J. Heterocycl. Chem.*, **12**, 165 (1975).

(3) I. W. Mathison, R. C. Gueldner, J. W. Lawson, S. J. Fowler, and E. R. Peters, *J. Med. Chem.*, **11**, 997 (1968).

(4) I. W. Mathison and J. W. Lawson, *Chim. Ther.*, **3**, 438 (1968).

(5) I. W. Mathison and P. H. Morgan, *J. Med. Chem.*, **17**, 1136 (1974).

(6) I. W. Mathison and R. R. Tidwell, *ibid.*, **18**, 1227 (1975).

(7) F. Troxler and A. Hofmann (to Sandoz Ltd.), British pat. 1,133,457 (1968).

(8) I. W. Mathison, K. C. Fowler, P. H. Morgan, R. R. Tidwell, E. R. Peters, N. J. Wojciechowski, J. W. Lawson, and F. K. Hetzer, *J. Med. Chem.*, **16**, 332 (1973).

(9) I. W. Mathison, P. H. Morgan, N. J. Wojciechowski, and J. W. Lawson, *Eur. J. Med. Chem.*, **11**, 247 (1976).

(10) B. J. Winer, "Statistical Principles in Experimental Design," 2nd ed., McGraw-Hill, New York, N.Y., 1971, p. 191.

ACKNOWLEDGMENTS

The authors express their appreciation to Marion Laboratories, Inc., Kansas City, Mo., for support. The technical assistance of Mrs. Frances Hetzer, Mrs. Ann Lewis, Mrs. Kathleen Fowler, Mrs. Mary Tidwell, and Miss Dana Lynch is gratefully acknowledged.

Flavin-Catalyzed Photooxidation of an Acridan Drug: A Reinvestigation

W.-R. KNAPPE

Received January 18, 1977, from the *Department of Biology, University of Konstanz, D-7750 Konstanz, German Federal Republic.*
Accepted for publication June 7, 1977.

Abstract □ Anaerobic irradiation of flavin derivatives (IIa and IIb) in the presence of 2-chloro-9-(3-dimethylaminopropyl)acridan phosphate (Ia) resulted in the reduction of the flavins to IVa and IVb and oxidation of an equimolar amount of Ia to IIIa. This photoreduction occurred from the first excited triplet state of IIa and IIb and proceeded *via* a covalent intermediate (V) between flavin and the acridan derivative. If the N-10 of the acridan was blocked by a methyl group, *e.g.*, Ic, V could be observed spectrophotometrically at −40°, decomposing homolytically on warming. With N-10 unsubstituted acridan derivatives, *e.g.*, Ia and Ib, V could not be observed because of fast heterolytic decomposition, yielding IVa, IVb, and the acridine compounds IIIa and IIIb. All photoreactions showed a kinetic isotope effect between 1.50 and 2.20 when position 9 of the acridan compounds was substituted by deuterium instead of hydrogen.

Keyphrases □ Acridan, substituted—mechanism of anaerobic flavin-catalyzed photooxidation □ Flavin-catalyzed photooxidation–substituted acridan, mechanism studied □ Photooxidation, flavin catalyzed—substituted acridan, mechanism studied

Recently, the anaerobic photodecomposition of an acridan drug, 2-chloro-9-(3-dimethylaminopropyl)acridan phosphate (Ia)[1], was studied in the presence of riboflavin 5′-phosphate (IIa) (1, 2). It was postulated that the photooxidation of the acridan derivative Ia to its acridine derivative IIIa does not involve a photoreduction of the flavin IIa but proceeds as follows (2).

The flavin is photoexcited to the first excited singlet state, which, on intersystem crossing, yields the triplet state (Scheme I).

$$\text{IIa} \xrightarrow{h\nu} {}^1\text{IIa}^* \xrightarrow{\text{intersystem crossing}} {}^3\text{IIa}^*$$

Scheme I

The flavin transfers its energy to the acridan, with generation of the acridan triplet and flavin ground state (Scheme II).

$${}^3\text{IIa}^* + \text{Ia} \rightarrow {}^1\text{IIa}^\circ + {}^3\text{Ia}^*$$

Scheme II

The acridan triplet decomposes to IIIa and hydrogen (Scheme III).

$${}^3\text{Ia}^* \rightarrow \text{IIIa} + \text{H}_2$$

Scheme III

Since the triplet state of acridan lies 292 kJ/mole above the ground state (3) (and the energy of the triplet of Ia should be almost the same) and the flavin triplet has only an energy of 209 kJ/mole (4), such an energy transfer is not possible. Energy transfer reactions from the flavin triplet to low lying ground states of substituted olefins (*e.g.*, stilbene or retinol), resulting in *cis–trans*-isomerization (5), or to triplet oxygen, yielding singlet oxygen (6), are known, but the energy transfer must be thermodynamically possible in all cases.

The flavin triplet is known to oxidize substrates, however, yielding reduced flavin (7); in this respect, it resembles the flavin in flavoenzymes (7). In these redox reactions, 4a-substituted 4a,5-dihydroflavin derivatives presumably are the first intermediates, as was shown recently (8).

EXPERIMENTAL

Reagents—Compounds Ia[1] and IIa[2] were used as supplied. 3-Methyllumiflavin (IIb) (9), acridan (Ib) (10), *N*-methylacridan (Ic) (11), 9,9-dimethylacridan (Id) (12), 9,9,10-trimethylacridan (Ie) (13), and *N,N′*-dimethyl-9,9′-diacridanyl (Ii) (14) were synthesized according to literature procedures.

9,9-Dideuterioacridan (If) (≈98% 9,9-D_2 from ^{1}H-NMR) was prepared from 9-deuterioacridine (15) by reduction with lithium aluminum deuteride; 9,9-dideuterio-*N*-methylacridan (Ig) (≈98%, 9,9-D_2 from ^{1}H-NMR) was obtained by reduction of *N*-methylacridone with sodium in *O*-D-butanol (16). Compound 9-D-Ia (Ih) (≈96% 9-D) was synthesized from IIIa (2). The acetonitrile used was freshly distilled from phosphorus(V) oxide.

Spectroscopy[3]—The anaerobic irradiations were performed in 1-cm quartz cells of the Thunberg type after argon (<1 ppm O_2) was bubbled through the solutions for 30 min. The light source was a 250-w medium pressure mercury arc with a 300-nm cutoff filter, a 250-w/24-v tungsten halogen lamp with a 442-nm narrow band interference filter[4] (8 nm half-width, B-40), or a broad band interference filter[4] (K 2), transparent from 420 to 480 nm. The quantum yields were calculated from the light intensities measured bolometrically (17).

RESULTS AND DISCUSSION

When an aqueous solution of Ia (6.67×10^{-4} *M*) and 3-methyllumiflavin (IIb, 1×10^{-4} *M*) at pH 9 was irradiated under strictly anaerobic conditions with light of 442 nm, a slow reduction of the flavin occurred, giving 3-methyl-1,5-dihydrolumiflavin (IVb) with a quantum yield of 0.012. This photoreduction was accompanied by the oxidation of an equimolar amount of Ia to its acridine analog IIIa as shown by the increased absorbance at 360 nm and by TLC comparison with an authentic sample. The same reaction was observed using light of a medium pressure mercury arc with a cutoff filter at 300 nm. Spectra are shown in Fig. 1.

Upon admission of oxygen, IVb was reoxidized instantaneously nearly quantitatively. The loss of 10% was due to some side reactions, presumably with the dimethylaminopropyl side chain of Ia and, more probably, due to the prolonged short wavelength irradiation. With filtered light (420–480 or 442 nm), IIb was recovered quantitatively upon admission of oxygen.

The same results were obtained using riboflavin 5′-phosphate (IIa) instead of IIb; the photodestruction of IIa (intramolecular reaction with its side chain) proceeded at pH 9 with a very small quantum yield and was quenched by the Ia present, presumably *via* formation of a hydrophobic complex (18).

The well-known dihydroflavin derivatives IVa and IVb (8) were identified by their characteristic, very fast reoxidation with air, yielding the oxidized flavins IIa and IIb. Further proof of structure was obtained by subtraction of the spectra of IIa and IIb from the spectra of the reaction mixture, resulting in the spectra of IVa and IVb.

The observation (1, 2) that IIa was not reduced under these conditions is probably due to nonanaerobic conditions. Therefore, the main reactions can be formulated in the following way.

The flavin is photoexcited by the long wavelength light and yields, *via* intersystem crossing its triplet state, ^{3}IIb*, according to Scheme I. The

[1] Smith Kline and French, Philadelphia, PA 19101.
[2] Hoffmann-La Roche, Basel, Switzerland.
[3] UV spectra were recorded with a Varian 635 M spectrophotometer.
[4] Balzers.

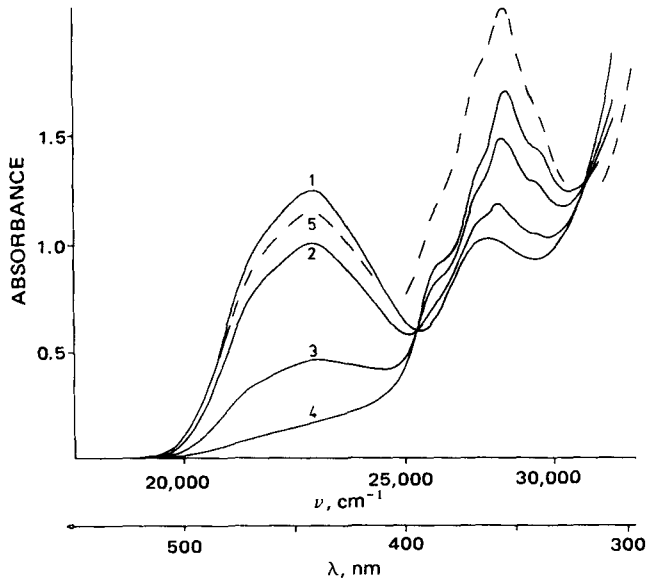

Figure 1—*Spectral course of the photoreduction of IIb (1×10^{-4} M) with Ia (6.67×10^{-4} M) in pH 9 aqueous phosphate buffer under strictly anaerobic conditions. The light source was a 250-w medium pressure mercury arc with a 300-nm cutoff filter. Key: 1, starting material; 2, 3, and 4, after illumination for 3, 13, and 43 min, respectively; and 5, after admission of oxygen.*

reported quenching experiments with iodide (1, 2) could be verified. All intermolecular photoreactions of flavin derivatives, except with solvent molecules, start from the triplet state (7).

The electron-deficient flavin triplet then attacks the acridan substrate, yielding in an overall reaction the reduced flavin IV*b* and the acridine III*a* (Scheme IV).

$$^3\text{II}b^* + \text{I}a \rightarrow \text{IV}b + \text{III}a$$

Scheme IV

On admission of oxygen, IV*b* is reoxidized to II*b*, accompanied by formation of water and hydrogen peroxide (Scheme V).

$$\text{IV}b + O_2 \rightarrow \text{II}b + H_2O_{(2)}$$

Scheme V

Under aerobic conditions, no IV*b* could be detected, since it is reoxidized instantaneously [half time of 6.1 sec (19, 20)] according to Scheme IV. Only the oxidation of I*a* to III*a* was observed, proceeding with a quantum yield of 0.10. This higher quantum yield, compared to the value of 0.012 in the anaerobic case, might be explained by the fact that singlet oxygen, which can be produced by energy transfer from the flavin triplet to the oxygen triplet (6), oxidizes I*a* with a higher efficiency than does the flavin triplet itself.

To gain further insight into the mechanism of this flavin-catalyzed photooxidation of I*a*, simpler acridan derivatives were investigated; 9,9-dimethylacridan (I*d*) and 9,9,10-trimethylacridan (I*e*) were not attacked by the flavin triplet. Therefore, the attack of the flavin triplet on I*a* does not occur at the N-10 position but at position 9 of the acridan nucleus. This finding was proved by the fact that acridan (I*b*) and *N*-methylacridan (I*c*) showed an even higher reactivity toward the flavin triplet than I*a*. The photoreaction of II*b* proceeds with quantum yields of 0.039 and 0.18 in acetonitrile at +25° (Table I).

When the photoreaction of II*b* with I*c* was performed at −40°, a new maximum at 368 nm (log ε 3.87) was observed in the UV spectrum (8), which is characteristic for a 4a-substituted 4a,5-dihydroflavin of type V (Scheme VI). Upon warming the solution to +25°, this intermediate decomposed homolytically, yielding the flavin radical, which disproportionated to 50% II*b* and 50% IV*b*, and the acridanyl radical, which dimerized to I*i*. Compound I*i* could be identified by TLC as the only oxidation product of I*c* (8).

When performing the same reaction with the N-10 unsubstituted I*b*, no intermediate adduct could be detected spectroscopically at −40° (8). Only a reduction of II*b* to IV*b* and an oxidation of an equimolar amount of I*b* to III*b*, identified by TLC comparison with acridine, was observed. In this case, the adduct of type V split heterolytically in a thermodynamically favored manner, yielding the oxidized aromatic substrate (III*b*) and the 1,5-dihydroflavin (IV*b*).

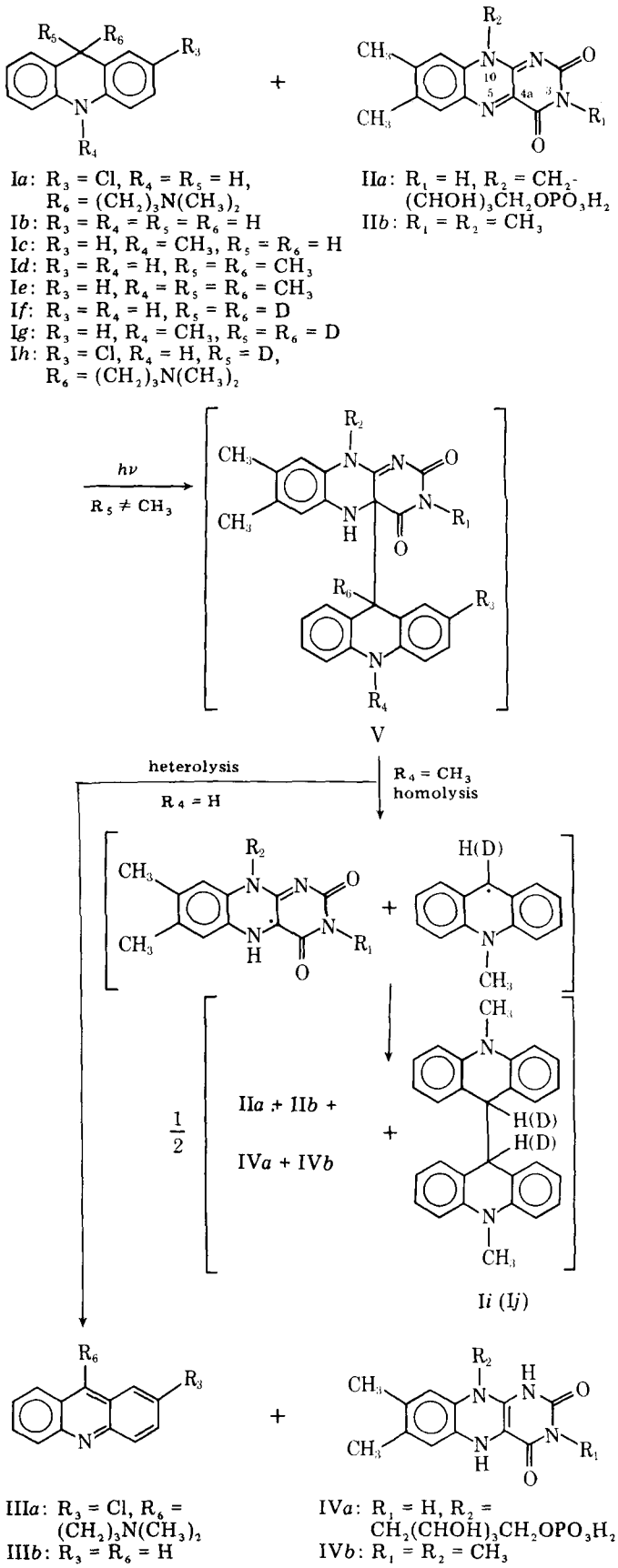

Scheme VI

In the first reaction step yielding the 4a-adduct (V), a CH bond is split, and a primary kinetic isotope effect should be observable when I*b* is

Table I—Quantum Yields (Φ) of the Anaerobic Photoreduction of IIb (1×10^{-4} M) in the Presence of Acridan Derivatives (6.67×10^{-4} M)

Acridan Derivative	Φ	Solvent
Ia	0.012	pH 9 phosphate buffer, anaerobic
Ia	0.10[a]	pH 9 phosphate buffer, aerobic
Ib	0.039	Acetonitrile, anaerobic
If	0.018	Acetonitrile, anaerobic, $\alpha_{H/D} = 2.17$
Ic	0.18	Acetonitrile, anaerobic
Ig	0.12	Acetonitrile, anaerobic, $\alpha_{H/D} = 1.50$
Id	0.000	Acetonitrile, anaerobic
Ie	0.000	Acetonitrile, anaerobic

[a] Quantum yield for the IIb-sensitized oxidation of Ia.

compared to its deuterated analog (If). A primary isotope effect of 2.20 ± 0.10 was found, and the N-10 methylated derivatives (Ic and Ig) showed a smaller isotope effect of 1.50 (Table I).

Therefore, the oxidation of Ia by flavin, which proceeds not only on illumination but even very slowly (0.21 M^{-1} sec^{-1} at pH 4) in the dark, is likely to proceed *via* intermediate formation of an adduct of Structure V, which decomposes heterolytically as pointed out for acridan. This proposal is confirmed on repeating the isotope effect measurements of Digenis *et al.* (2). Compound Ih, prepared according to their method (2), showed a primary isotope effect of 2.1 ± 0.20 when compared to Ia. For inexplicable reasons, Digenis *et al.* (2) found no isotope effects.

Therefore, it can be concluded that Ia as well as other acridan derivatives is photooxidized by the flavin triplet *via* covalent intermediates, which split heterolytically when the N-10 position is not blocked by an alkyl group. If the N-10 position is blocked, *e.g.*, in Ic, the covalent intermediate of type V can be observed spectroscopically at low temperatures, splitting homolytically upon heating.

REFERENCES

(1) M. A. Miyamoto, H. B. Kostenbauder, D. Walstad, and G. A. Digenis, *FEBS Lett.*, **7**, 101 (1970).

(2) G. A. Digenis, S. Shakshir, M. A. Miyamoto, and H. B. Kostenbauder, *J. Pharm. Sci.*, **65**, 247 (1976).

(3) V. Zanker and B. Schneider, *Z. Phys. Chem.*, **68**, 19 (1969).

(4) R. W. Chambers and D. R. Kearns, *Photochem. Photobiol.*, **10**, 215 (1969).

(5) A. Gordon-Walker and G. K. Radda, *Biochem. J.*, **120**, 673 (1970).

(6) D. R. Kearns, R. A. Hollins, A. U. Khan, and P. Radlick, *J. Am. Chem. Soc.*, **89**, 5456 (1967).

(7) P. Hemmerich, *Prog. Chem. Org. Nat. Prod.*, **33**, 451 (1976), and references cited therein.

(8) W.-R. Knappe, *Z. Naturforsch.*, **32b**, 434 (1977).

(9) P. Hemmerich, *Helv. Chim. Acta*, **47**, 464 (1964).

(10) C. Graebe and H. Caro, *Justus Liebigs Ann. Chem.*, **158**, 265 (1871).

(11) H. Decker and G. Dunant, *Ber. Dtsch. Chem. Ges.*, **39**, 2720 (1906).

(12) D. Craig, *J. Am. Chem. Soc.*, **57**, 195 (1935).

(13) W. L. Semon and D. Craig, *ibid.*, **58**, 1278 (1936).

(14) F. Mader and V. Zanker, *Chem. Ber.*, **97**, 2418 (1964).

(15) R. M. Acheson, R. T. Aplin, and R. G. Bolton, *Org. Mass Spectrom.*, **8**, 95 (1974).

(16) F. Ullmann and R. Maag, *Ber. Dtsch. Chem. Ges.*, **40**, 2515 (1907).

(17) W.-R. Knappe, *Chem. Ber.*, **108**, 2422 (1975).

(18) G. Tollin, in "Molecular Associations in Biology," B. Pullman, Ed., Academic, New York, N.Y., 1968, p. 393.

(19) H. Gutfreund, *Biochem. J.*, **74**, 17 P (1960).

(20) Q. H. Gibson and J. W. Hastings, *ibid.*, **83**, 368 (1972).

ACKNOWLEDGMENTS

Supported in part by Deutsche Forschungsgemeinschaft.

The technical assistance of Miss K. Bluhme is gratefully acknowledged. Compound Ia was a gift of Smith Kline and French.

Effect of Ionization on Absorption of Cephalosporins

JOYCE L. DeYOUNG ˣ, HETTY G. H. TAN, H. E. HUBER, and M. A. ZOGLIO

Received January 3, 1977, from *Merrell-National Laboratories, Division of Richardson-Merrell Inc., Cincinnati, OH 45215.* Accepted for publication June 9, 1977.

Abstract □ To explore the relative absorbabilities of different ionic forms of cephalosporins, the absorption rates of four compounds were measured in the pH 5–9 region using an *in situ* rat gut technique. Cephalexin, cephradine, and cephaloglycin have some oral activity, while 3-[(acetyloxy)methyl]-8-oxo-7-[[(4-oxo-1(4*H*)-pyridinyl)acetyl]-amino]-5-thia-1-azabicyclo[4.2.0]oct-2-ene-2-carboxylic acid (I) has insignificant oral activity. The pH–species profiles calculated from their ionization constants showed that cephalexin, cephradine, and cephaloglycin have a large proportion of uncharged molecules plus zwitterions in the pH range of the small intestine, while I exists as the anion throughout this range. When the species profiles are compared with the pH–absorption rate profiles for cephalexin, cephradine, and I, the results are consistent with a model in which the zwitterionic and/or uncharged forms of the molecules are well absorbed, whereas the anions show little or no absorption. Although it has a pH profile for zwitterions plus uncharged molecules similar to cephalexin, cephaloglycin shows poor absorption, suggesting that the ratio of uncharged molecules to zwitterions may be important in absorption.

Keyphrases □ Absorption, GI—various cephalosporins, effect of ionization, rats □ Cephalosporins, various—GI absorption, effect of ionization, rats □ Ionization—effect on GI absorption of various cephalosporins, rats □ Antibacterials—various cephalosporins, GI absorption, effect of ionization, rats

There has been very little published concerning the mechanism of cephalosporin absorption. Some cephalosporins are known to be actively secreted into the renal tubules (1), suggesting that an active process could also be important in absorption. Penzotti and Poole (2) investigated this possibility using everted rat intestinal sacs; for some penicillins and cephalosporins, including cephalexin and cephaloglycin, they found no evidence for a specialized transport mechanism.

If these compounds are passively absorbed, the extent of their ionization in the pH region of the GI tract could determine partly the ease with which they are absorbed. Therefore, the absorption rates of cephalexin, cephradine, cephaloglycin, and 3-[(acetyloxy)methyl]-8-oxo-7-[[(4-

Table I—Quantum Yields (Φ) of the Anaerobic Photoreduction of IIb (1×10^{-4} M) in the Presence of Acridan Derivatives (6.67×10^{-4} M)

Acridan Derivative	Φ	Solvent
Ia	0.012	pH 9 phosphate buffer, anaerobic
Ia	0.10[a]	pH 9 phosphate buffer, aerobic
Ib	0.039	Acetonitrile, anaerobic
If	0.018	Acetonitrile, anaerobic, $\alpha_{H/D} = 2.17$
Ic	0.18	Acetonitrile, anaerobic
Ig	0.12	Acetonitrile, anaerobic, $\alpha_{H/D} = 1.50$
Id	0.000	Acetonitrile, anaerobic
Ie	0.000	Acetonitrile, anaerobic

[a] Quantum yield for the IIb-sensitized oxidation of Ia.

compared to its deuterated analog (If). A primary isotope effect of 2.20 ± 0.10 was found, and the N-10 methylated derivatives (Ic and Ig) showed a smaller isotope effect of 1.50 (Table I).

Therefore, the oxidation of Ia by flavin, which proceeds not only on illumination but even very slowly (0.21 M^{-1} sec^{-1} at pH 4) in the dark, is likely to proceed *via* intermediate formation of an adduct of Structure V, which decomposes heterolytically as pointed out for acridan. This proposal is confirmed on repeating the isotope effect measurements of Digenis *et al.* (2). Compound Ih, prepared according to their method (2), showed a primary isotope effect of 2.1 ± 0.20 when compared to Ia. For inexplicable reasons, Digenis *et al.* (2) found no isotope effects.

Therefore, it can be concluded that Ia as well as other acridan derivatives is photooxidized by the flavin triplet *via* covalent intermediates, which split heterolytically when the N-10 position is not blocked by an alkyl group. If the N-10 position is blocked, *e.g.*, in Ic, the covalent intermediate of type V can be observed spectroscopically at low temperatures, splitting homolytically upon heating.

REFERENCES

(1) M. A. Miyamoto, H. B. Kostenbauder, D. Walstad, and G. A. Digenis, *FEBS Lett.*, **7**, 101 (1970).

(2) G. A. Digenis, S. Shakshir, M. A. Miyamoto, and H. B. Kostenbauder, *J. Pharm. Sci.*, **65**, 247 (1976).

(3) V. Zanker and B. Schneider, *Z. Phys. Chem.*, **68**, 19 (1969).

(4) R. W. Chambers and D. R. Kearns, *Photochem. Photobiol.*, **10**, 215 (1969).

(5) A. Gordon-Walker and G. K. Radda, *Biochem. J.*, **120**, 673 (1970).

(6) D. R. Kearns, R. A. Hollins, A. U. Khan, and P. Radlick, *J. Am. Chem. Soc.*, **89**, 5456 (1967).

(7) P. Hemmerich, *Prog. Chem. Org. Nat. Prod.*, **33**, 451 (1976), and references cited therein.

(8) W.-R. Knappe, *Z. Naturforsch.*, **32b**, 434 (1977).

(9) P. Hemmerich, *Helv. Chim. Acta*, **47**, 464 (1964).

(10) C. Graebe and H. Caro, *Justus Liebigs Ann. Chem.*, **158**, 265 (1871).

(11) H. Decker and G. Dunant, *Ber. Dtsch. Chem. Ges.*, **39**, 2720 (1906).

(12) D. Craig, *J. Am. Chem. Soc.*, **57**, 195 (1935).

(13) W. L. Semon and D. Craig, *ibid.*, **58**, 1278 (1936).

(14) F. Mader and V. Zanker, *Chem. Ber.*, **97**, 2418 (1964).

(15) R. M. Acheson, R. T. Aplin, and R. G. Bolton, *Org. Mass Spectrom.*, **8**, 95 (1974).

(16) F. Ullmann and R. Maag, *Ber. Dtsch. Chem. Ges.*, **40**, 2515 (1907).

(17) W.-R. Knappe, *Chem. Ber.*, **108**, 2422 (1975).

(18) G. Tollin, in "Molecular Associations in Biology," B. Pullman, Ed., Academic, New York, N.Y., 1968, p. 393.

(19) H. Gutfreund, *Biochem. J.*, **74**, 17 P (1960).

(20) Q. H. Gibson and J. W. Hastings, *ibid.*, **83**, 368 (1972).

ACKNOWLEDGMENTS

Supported in part by Deutsche Forschungsgemeinschaft.

The technical assistance of Miss K. Bluhme is gratefully acknowledged. Compound Ia was a gift of Smith Kline and French.

Effect of Ionization on Absorption of Cephalosporins

JOYCE L. DeYOUNG ˣ, HETTY G. H. TAN, H. E. HUBER, and M. A. ZOGLIO

Received January 3, 1977, from *Merrell-National Laboratories, Division of Richardson-Merrell Inc., Cincinnati, OH 45215.* Accepted for publication June 9, 1977.

Abstract □ To explore the relative absorbabilities of different ionic forms of cephalosporins, the absorption rates of four compounds were measured in the pH 5–9 region using an *in situ* rat gut technique. Cephalexin, cephradine, and cephaloglycin have some oral activity, while 3-[(acetyloxy)methyl]-8-oxo-7-[[(4-oxo-1(4*H*)-pyridinyl)acetyl]-amino]-5-thia-1-azabicyclo[4.2.0]oct-2-ene-2-carboxylic acid (I) has insignificant oral activity. The pH–species profiles calculated from their ionization constants showed that cephalexin, cephradine, and cephaloglycin have a large proportion of uncharged molecules plus zwitterions in the pH range of the small intestine, while I exists as the anion throughout this range. When the species profiles are compared with the pH–absorption rate profiles for cephalexin, cephradine, and I, the results are consistent with a model in which the zwitterionic and/or uncharged forms of the molecules are well absorbed, whereas the anions show little or no absorption. Although it has a pH profile for zwitterions plus uncharged molecules similar to cephalexin, cephaloglycin shows poor absorption, suggesting that the ratio of uncharged molecules to zwitterions may be important in absorption.

Keyphrases □ Absorption, GI—various cephalosporins, effect of ionization, rats □ Cephalosporins, various—GI absorption, effect of ionization, rats □ Ionization—effect on GI absorption of various cephalosporins, rats □ Antibacterials—various cephalosporins, GI absorption, effect of ionization, rats

There has been very little published concerning the mechanism of cephalosporin absorption. Some cephalosporins are known to be actively secreted into the renal tubules (1), suggesting that an active process could also be important in absorption. Penzotti and Poole (2) investigated this possibility using everted rat intestinal sacs; for some penicillins and cephalosporins, including cephalexin and cephaloglycin, they found no evidence for a specialized transport mechanism.

If these compounds are passively absorbed, the extent of their ionization in the pH region of the GI tract could determine partly the ease with which they are absorbed. Therefore, the absorption rates of cephalexin, cephradine, cephaloglycin, and 3-[(acetyloxy)methyl]-8-oxo-7-[[(4-

Table I—Composition of Buffer Solutions Used in Absorption Experiments

Buffer[a]	Components	pH[b]
A	0.095 *M* Na_2HPO_4 0.046 *M* Citric acid 0.003 *M* NaCl	5.1
B	0.072 *M* Na_2HPO_4 0.018 *M* Citric acid 0.049 *M* NaCl	6.0
C	0.012 *M* Na_2HPO_4 0.088 *M* NaH_2PO_4 0.048 *M* NaCl	6.0
D	0.020 *M* Na_2HPO_4 0.047 *M* NaH_2PO_4 0.084 *M* NaCl	6.5
E	0.087 *M* Na_2HPO_4 0.006 *M* Citric acid 0.039 *M* NaCl	7.0
F	0.061 *M* Na_2HPO_4 0.039 *M* NaH_2PO_4 0.030 *M* NaCl	7.0
G	0.171 *M* Tromethamine[c]	7.3
H	0.176 *M* Tromethamine	7.8
I	0.200 *M* Tromethamine 0.020 *M* NaCl	8.2
J	0.200 *M* Tromethamine 0.240 *M* NaCl	8.7

[a] All except C are based on published buffer systems (4) adjusted to isotonicity. When necessary, the pH was adjusted with sodium hydroxide or hydrochloric acid. [b] At 37°. [c] Tris(hydroxymethyl)aminomethane.

oxo-1(4*H*)-pyridinyl)acetyl]amino]-5-thia-1-azabicyclo-[4.2.0]oct-2-ene-2-carboxylic acid[1] (I) were studied in the pH 5–9 region using the *in situ* rat gut technique described previously (3). The pH–rate profiles obtained were compared with pH–species profiles calculated from the ionization constants of the compounds.

EXPERIMENTAL

Reagents and Solutions—All commercially available chemicals were reagent or spectrophotometric grade. Cephalexin monohydrate[2], cephaloglycin dihydrate[2], and cephradine[3] were used as received. Drug solutions for absorption experiments were prepared at concentrations of 1–3 mg/ml in the isotonic buffer solutions described in Table I or in isotonic saline.

Test Animals—Male Sprague–Dawley rats, 200–300 g, were fasted 12–14 hr before surgery. Drinking water was allowed.

Analytical Methods—Samples (0.1 ml) of cephalexin, cephradine, and I removed from the rat intestine were diluted with 2–10 ml of 0.1 *M* phosphate buffer, pH 7.5, the volume depending on the concentration of the starting solution and the absorptivity of the compound. The UV spectra of these solutions were measured using a recording spectrophotometer[4]. Rate constants for the disappearance of drug from the lumen were calculated using the wavelengths of maximum absorbance: cephalexin and cephradine, 262 nm; and I, 264 nm.

Because of instability, cephaloglycin solutions were assayed using a high-pressure liquid chromatographic (HPLC) method that separates starting material from degradation products. A 15-μl aliquot of undiluted

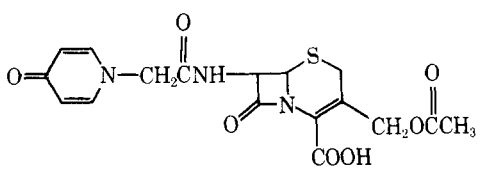

I

[1] RMI 15,307.
[2] Eli Lilly and Co.
[3] E. R. Squibb and Sons.
[4] Beckman Acta III.

Table II—Experimental Conditions and Apparent First-Order Rate Constants for Loss of Cephaloglycin

pH[a]	Buffer[b]	$10^3 k_{deg}$[c], min^{-1}	$10^3 k_{obs}$[d], min^{-1}	$10^3 k_{ab}$, min^{-1}
5.1	A	1.25	2.9	1.6
6.0	B	3.3	2.9	−0.4
6.1[e]	Isotonic saline	~0[f]	~0[f]	0
7.3	G	4.4	6.2	1.8

[a] Initial pH, except 6.1. See text. [b] See Table I for composition. [c] Obtained *in vitro*. [d] Average of results from two rats. [e] See Table III. [f] No significant changes in concentration seen in at least 1 hr.

sample (1.3 mg/ml) from the gut or from a stability test was injected onto a reversed-phase, high efficiency column[5] and eluted[6] using a flow rate of 80 ml/hr. The elution solvent was acetonitrile–formate buffer. The effluent from the column was monitored at 254 nm. Cephaloglycin had a retention time of about 5.5 min. Peak areas and/or heights were used in the calculation of rate constants.

Elution Solvent—A solvent containing 15% acetonitrile in a 0.05 *M* formate buffer was prepared as follows. A solution of 26 ml of 88% formic acid in 800 ml of water was adjusted to pH 3.2 by the addition of triethylamine and then diluted to 1 liter. One hundred milliliters of the concentrate was mixed with 150 ml of acetonitrile and diluted to 1 liter with water to give the elution solvent.

Stability of Cephaloglycin Solutions—Solutions containing approximately 1.3 mg of cephaloglycin/ml in the buffers listed in Table I were held in a 37° water bath for 3–5 hr. They were sampled at appropriate times and assayed by HPLC.

Animal Preparation—The method of studying absorption from the small intestine was the same as that used by Doluisio *et al.* (3). The animals were anesthetized by 1.25 mg of urethan/g ip. Samples were removed every 10 or 15 min for 1–1.5 hr and assayed as described. The pH was measured at the beginning and end of an experiment and, in some instances, at intervals throughout the experiment.

RESULTS

Stability of Cephalosporin Solutions—The HPLC studies indicated that cephaloglycin degradation was occurring in all buffers. Only when cephaloglycin was dissolved in isotonic saline (pH 6) was there no significant degradation in the time period studied. Degradation rate constants were calculated from plots of:

$$\ln X = \ln X_0 - k_{deg}t \qquad \text{(Eq. 1)}$$

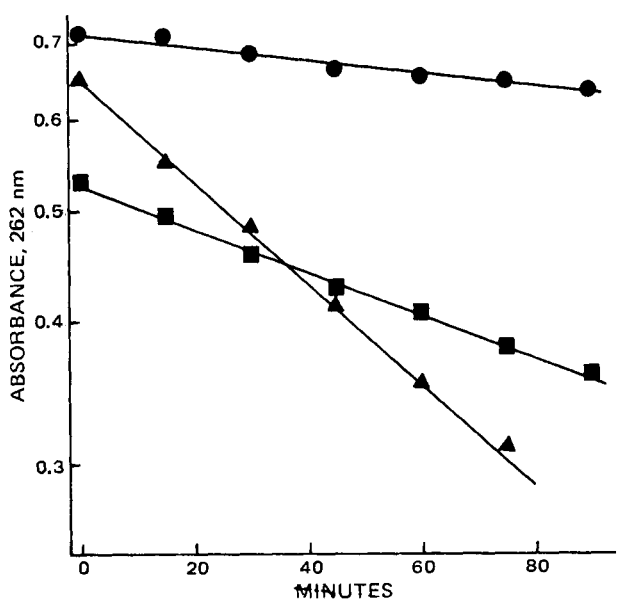

Figure 1—*First-order plots of data for cephalexin in the* in situ *rat gut model. Key:* ●, *pH 8.2;* ■, *pH 7.3; and* ▲, *pH 5.1.*

[5] μBondapak C_{18}, Waters Associates.
[6] Varian model 8500 liquid chromatograph equipped with a Variscan UV-visible detector.

Table III—Experimental Conditions and Apparent First-Order Rate Constants for Loss of Cephalexin from Rat Small Intestine

pH[a]	Buffer[b]	$10^3 k_{ab}$, min^{-1}
5.1	A	10.7[c]
6.0	C	9.0[d]
6.1[e]	Isotonic saline	11.4[c]
6.5	D	10.2[c]
7.0	E	9.1[f]
7.3	G	4.1[f]
7.8	H	3.2[f]
8.2	I	1.8[f]
8.7	J	0.5[f]

[a] Initial pH, except 6.1. See text. [b] See Table I for composition. [c] Average of results from three rats. [d] Average of results from four rats. [e] Final pH. Initial pH of ~5.3 changed to final value within 20 min. See text. [f] Average of results from two rats.

where X is either peak height or peak area and X_0 represents the values at time zero. Graphs of peak heights or peak areas obtained in the same experiment gave k_{deg} values in good agreement. The k_{deg} values obtained using least-squares linear regression on the data are given in Table II.

Previous stability experiments indicated that no significant I decomposition would occur in the pH range used in the time needed for a rat gut study. The adequate stability of cephalexin and cephradine was established using literature data (5, 6).

Loss of Cephalexin, Cephradine, and I from Small Intestine—Absorbance data gave linear plots when graphed according to:

$$\ln A = \ln A_0 - k_{ab}t \qquad \text{(Eq. 2)}$$

where A is the absorbance at time t at the wavelength used for the particular cephalosporin (see *Experimental*), A_0 is the initial absorbance, and k_{ab} is the apparent first-order rate constant for disappearance of drug from the lumen and is assumed to represent absorption. The k_{ab} values for cephalexin and cephradine are listed in Tables III and IV. Typical plots are shown in Fig. 1. Compound I gave no evidence of being absorbed in the pH 5.1–7.3 range. The pH values usually changed by less than 0.5 pH unit during an experiment, except at pH 5 and above pH 8, where changes of about 0.8 unit were seen. Even when a relatively large pH change took place, the first-order plots did not show a deviation from linearity.

As a check for buffer effects on absorption, several experiments were run using a solution of cephalexin in isotonic saline. Measurements at 10-min intervals showed that the pH adjusted rapidly in the rat to a stable value of about 6.1. The average rate constant obtained was not significantly different from the constants obtained in buffers in the same pH region (Table III).

Loss of Cephaloglycin from Small Intestine—HPLC data were plotted according to Eq. 1. The rate constants obtained, k_{obs}, are equal to the sum of the rate constants for loss due to absorption and degradation

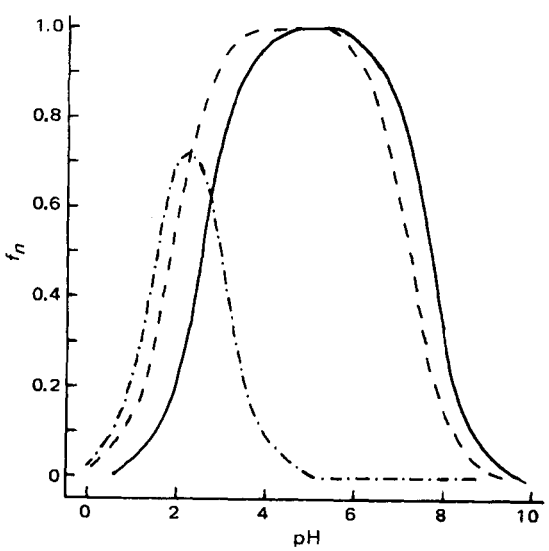

Figure 2—*Plots of* f_n, *fraction of molecules present as zwitterions plus uncharged molecules, as a function of pH for cephalexin (—), cephaloglycin (– –), and I (-·-).*

Table IV—Experimental Conditions and Apparent First-Order Rate Constants for Loss of Cephradine from Rat Small Intestine

pH[a]	Buffer[b]	$10^3 k_{ab}$, min^{-1} [c]
5.1	A	10.6
6.0	C	8.9
6.5	D	11.5
7.0	F	8.7
7.3	G	7.4
7.8	H	4.2
8.2	I	1.8
8.7	J	0.9

[a] Initial pH. [b] See Table I for composition. [c] Average of results from two rats, except at pH 6.5 when four rats were used.

(7). Therefore, k_{ab} values in Table II were calculated by subtracting k_{deg} from k_{obs}. Since the composition of the buffer undoubtedly changes while in the rat gut, the effective values for k_{deg} must be somewhat different from those found *in vitro*. For this reason, the k_{ab} values obtained should be viewed as approximations, indicating only that cephaloglycin has relatively poor absorption characteristics.

DISCUSSION

Work by Penzotti and Poole (2) suggests that, like most drugs, cephalosporins are absorbed by passive diffusion. A number of more or less complex models have been proposed to explain the behavior of passively absorbed drugs (8–13). In general, these theories agree that the neutral drug form will be absorbed more easily than charged species because of its greater ability to penetrate the lipoidal intestinal membranes.

In a series of related compounds, such as the cephalosporins, it is therefore reasonable to suppose that one criterion for a well-absorbed compound is a pH–species profile in which a large fraction of the molecules are present in a neutral form in the pH range of the intestinal tract. The importance of ionization in cephalosporin absorption was investigated using two well-absorbed cephalosporins, cephalexin and cephradine; a relatively poorly absorbed oral compound, cephaloglycin; and I, which has insignificant oral activity.

All of these compounds are amphoteric and can exist in four forms: the cation, zwitterion, uncharged molecule, and anion. Since the zwitterion

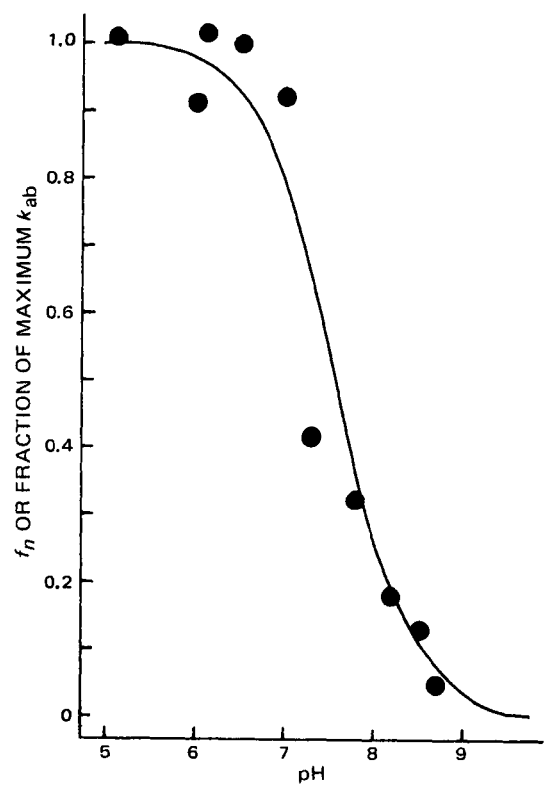

Figure 3—*Absorption rate constants for cephalexin (Table III) expressed as fractions of the average rate constant at pH 5 and 6 plotted on the same scale with* f_n. *(See Fig. 2.)*

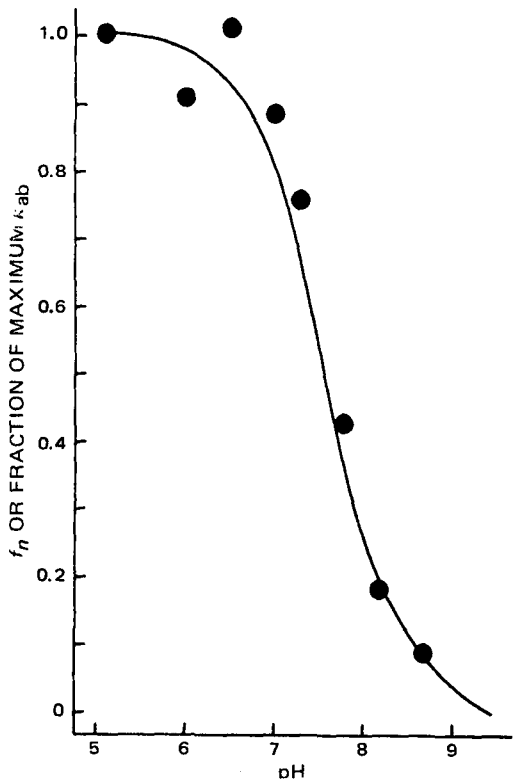

Figure 4—*Absorption rate constants for cephradine (Table IV) expressed as fractions of the average rate constant at pH 5 and 6 plotted on the same scale with f_n for cephalexin. (See Fig. 2.)*

and uncharged molecule, which exist together in a fixed ratio, have no net charge, they should be the best absorbed species. The ionization constants for I (14), cephalexin, and cephaloglycin were used to construct plots of zwitterions plus uncharged molecules as a function of pH[7] (Fig. 2). The pKa values for cephradine were assumed to be essentially the same as those for cephalexin because of their close structural similarity. Based on these profiles, cephalexin, cephradine, and cephaloglycin have significant numbers of molecules with no net charge present in the pH range of the small intestine (about pH 6–8). Compound I, however, is present only as the anion in the pH range in question and might be expected to be poorly absorbed.

At pH 5.1 and 6, essentially all cephalexin and cephradine molecules are present as zwitterions and uncharged molecules. If the rate constants in Tables III and IV are expressed as fractions of the average rate constants in this region and are plotted on the same graph with the fraction of molecules present as zwitterions plus uncharged molecules, the correlation is good (Figs. 3 and 4). This result is in accord with:

$$k_{ab} = k_n f_n \qquad \text{(Eq. 3)}$$

where k_n is the intrinsic rate constant for absorption of neutral species (zwitterions and uncharged molecules) and f_n is the fraction of molecules present as neutral species. The data for I also fit this equation, since there are no neutral species present and no measurable absorption takes place.

Cephaloglycin, although it has a species profile very similar to cephalexin and differs structurally only in the replacement of a hydrogen atom on the C-3 methyl group of cephalexin by an acetate group, shows very poor absorption. One contributing factor could be the different ratios of uncharged molecules to zwitterions in the two compounds. If these species are absorbed differently, Eq. 3 may be rewritten as:

$$k_{ab} = k_u f_u + k_z f_z \qquad \text{(Eq. 4)}$$

where k_z and k_u are the intrinsic absorption rate constants for the zwitterion and uncharged molecule, respectively, and f_z and f_u are the fractions of molecules present in these forms. Equation 4 can be rearranged to:

$$k_{ab}/f_z = k_u(f_u/f_z) + k_z \qquad \text{(Eq. 5)}$$

The ratio f_u/f_z is independent of pH and can be calculated from K_a values (14). For cephalexin, it is 10.5×10^{-5}; for cephaloglycin, it is 2.09×10^{-5}. At any pH values where f_z is the same for both compounds, the ratio of observed absorption rate constants is:

$$\frac{k_{ab}^{cx}}{k_{ab}^{cg}} = \frac{k_u^{cx}(10.5 \times 10^{-5}) + k_z^{cx}}{k_u^{cg}(2.09 \times 10^{-5}) + k_z^{cg}} \qquad \text{(Eq. 6)}$$

where superscripts cx and cg refer to cephalexin and cephaloglycin, respectively. If k_z for both compounds is small enough that virtually no zwitterions are absorbed and if k_u values are equal, Eq. 6 predicts that cephalexin will be absorbed about five times as fast as cephaloglycin. However, if k_z is assumed to be about zero, k_u^{cx} can be calculated from:

$$k_{ab}^{cx} = k_u^{cx} f_u^{cx} \qquad \text{(Eq. 7)}$$

In the pH 5–6 range, the average k_{ab}^{cx} is 10.4×10^{-3} min^{-1} and f_u^{cx} equals 10.5×10^{-5}. These values give k_u^{cx} equal to 99 min^{-1}, which is an exceedingly fast and probably unrealistic rate. This result suggests that properties of these molecules other than ionization are also important in their absorption behavior.

[7] A manuscript describing the calculation of pKa values for cephalexin and cephaloglycin is now in preparation; W. H. Streng, Merrell-National Laboratories.

REFERENCES

(1) C. H. Nightingale, D. S. Greene, and R. Quintiliani, *J. Pharm. Sci.*, **64**, 1899 (1975).

(2) S. C. Penzotti, Jr., and J. W. Poole, *ibid.*, **63**, 1803 (1974).

(3) J. T. Doluisio, N. F. Billups, L. W. Dittert, E. T. Sugita, and J. V. Swintosky, *ibid.*, **58**, 1196 (1969).

(4) G. Gomori, in "Methods in Enzymology," vol. I, S. P. Colowick and N. E. Kaplan, Eds., Academic, New York, N.Y., 1955, pp. 138 ff.

(5) T. Yamana, A. Tsuji, K. Kanayama, and O. Nokano, *J. Antibiot.*, **27**, 1000 (1974).

(6) T. Yamana and A. Tsuji, *J. Pharm. Sci.*, **65**, 1563 (1976).

(7) A. A. Frost and R. G. Pearson, "Kinetics and Mechanism," 2nd ed., Wiley, New York, N.Y., 1961, pp. 160–162.

(8) L. S. Schanker, D. J. Tocco, B. B. Brodie, and C. A. M. Hogben, *J. Pharmacol. Exp. Ther.*, **123**, 81 (1958).

(9) C. A. M. Hogben, D. J. Tocco, B. B. Brodie, and L. S. Schanker, *ibid.*, **125**, 275 (1959).

(10) J. G. Wagner and A. J. Sedman, *J. Pharmacokinet. Biopharm.*, **1**, 23 (1973).

(11) A. Suzuki, W. I. Higuchi, and N. F. H. Ho, *J. Pharm. Sci.*, **59**, 644 (1970).

(12) *Ibid.*, **59**, 651 (1970).

(13) N. F. H. Ho, W. I. Higuchi, and J. Turi, *J. Pharm. Sci.*, **61**, 192 (1972).

(14) W. H. Streng, H. E. Huber, J. L. DeYoung, and M. A. Zoglio, *ibid.*, **65**, 1034 (1976).

ACKNOWLEDGMENTS

Presented in part at the Basic Pharmaceutics Section, APhA Academy of Pharmaceutical Sciences, New York meeting, May 1977.

Structural Survey of Carbonate-Containing Antacids

CARLOS J. SERNA [1], JOE L. WHITE *, and STANLEY L. HEM ‡x

Received February 28, 1977, from the *Department of Agronomy and the ‡Industrial and Physical Pharmacy Department, School of Pharmacy and Pharmacal Sciences, Purdue University, West Lafayette, IN 47907. Accepted for publication June 10, 1977.

Abstract □ A series of carbonate-containing antacids was examined by IR and X-ray analysis to establish the role of carbonate and to compare the structure of the antacids to naturally occurring carbonate minerals. Based on IR analysis, the relative degree of perturbation of carbonate increases in the order calcium carbonate, carbonate-containing aluminum hydroxide gel, and dihydroxyaluminum sodium carbonate. The crystalline carbonate-containing antacids were poorly organized forms of the minerals calcite, $CaCO_3$; dawsonite, $NaAl(OH)_2CO_3$; and hydrotalcite, $Mg_6Al_2CO_3(OH)_{16}{\cdot}4H_2O$. Amorphous carbonate-containing aluminum hydroxide gel can be classified mineralogically as amorphous aluminum hydroxycarbonate. IR and X-ray evidence indicates that magaldrate has a hydrotalcite-like structure with sulfate as the major interlayer anion and carbonate also present in the interlayer space.

Keyphrases □ Antacids, various carbonate containing—IR and X-ray structural analysis, compared to naturally occurring carbonate minerals □ Carbonate-containing antacids, various—IR and X-ray structural analysis, compared to naturally occurring carbonate minerals □ Structural analysis, IR and X-ray—various carbonate-containing antacids, compared to naturally occurring carbonate minerals

An examination of the composition of the most widely used antacids indicates that carbonate is a common component. Crystalline carbonates are exemplified by calcium carbonate, dihydroxyaluminum sodium carbonate, and magnesium aluminum hydroxycarbonate (1), while amorphous carbonates are represented by carbonate-containing aluminum hydroxide gel. Although the name aluminum hydroxide gel does not suggest the presence of carbonate, the USP recently recognized that carbonate may be present in aluminum hydroxide gel (2).

Recent reports showed that carbonate is covalently bonded to aluminum in aluminum hydroxide gel (3) and that carbonate plays an important role in acid neutralization (4) as well as in stabilization of the gel (5). These carbonate-containing antacids were studied by IR spectroscopy and X-ray diffraction to examine the role of carbonate in these diverse antacid compounds and to compare the structure of carbonate-containing antacids to naturally occurring carbonate minerals.

EXPERIMENTAL

Commercial antacid dosage forms were used. Aluminum hydroxide gel was examined in a suspension dosage form[2] labeled as a magnesia and alumina oral suspension. Calcium carbonate was studied in a tablet[3] containing 500 mg of calcium carbonate. Dihydroxyaluminum sodium carbonate was obtained as a tablet[4] containing 334 mg of dihydroxyaluminum sodium carbonate. An antacid suspension[5] was the source of magaldrate.

A commercial sample of aluminum hydroxide[6] was examined.

Mineralogical specimens were studied to establish the structure of the carbonate-containing antacids. Naturally occurring samples of dawsonite[7], $NaAl(OH)_2CO_3$, and hydrotalcite[8], $Mg_6Al_2CO_3(OH)_{16}{\cdot}4H_2O$, were included. The X-ray diffractograms of all mineral specimens were compared to the ASTM Diffraction Data File and found to be of high purity.

The commercial antacids were examined as purchased by X-ray diffraction, using the Debye–Scherrer method, and by IR spectroscopy, using potassium bromide pellets containing 1–7 mg of sample/300 mg of potassium bromide.

The calcium carbonate, dihydroxyaluminum sodium carbonate, and magaldrate dosage forms were examined after several washings with water to remove excipients. Magaldrate suspension was studied by IR spectroscopy under vacuum (10^{-4} mm Hg) and after deuterium exchange under vacuum (10^{-4} mm Hg) at 25°.

RESULTS AND DISCUSSION

Aluminum Hydroxide Gel—IR and X-ray analysis of the aluminum hydroxide gel–magnesium hydroxide gel antacid indicates that the product is a physical mixture of amorphous carbonate-containing aluminum hydroxide gel and crystalline magnesium hydroxide. A comparison of the IR spectrum of the product with synthetic magnesium hydroxide (brucite) and amorphous carbonate-containing aluminum hydroxide gel is shown in Fig. 1.

The broad absorption band centered at 3440 cm^{-1} is due to the hydroxyl stretching vibrations of aluminum hydroxide. The diffuse nature of this band indicates that the hydroxyls are in many different environments. The two bands at 1500 and 1435 cm^{-1} are due to the splitting of the carbonate band that appears at 1415 cm^{-1} when carbonate is unperturbed (3). This finding is corroborated by the presence of the absorption band at 1090 cm^{-1}, which only becomes IR active when the symmetry of the carbonate anion is lowered.

The magnitude of the splitting of the degenerate ν_3 vibration of the carbonate anion in the aluminum hydroxide gel, 65 cm^{-1}, indicates a unidentate coordination with the aluminum hydroxide polycations (6). The band at 850 cm^{-1} is the ν_2 vibration of the carbonate anion and is shifted from its unperturbed frequency of 879 cm^{-1}.

Absorption bands in the IR spectrum of aluminum hydroxide gel at 1640 and 600 cm^{-1} can be assigned to molecular water and Al–O vibrations, respectively (7).

No reported minerals are amorphous and possess the same IR spectrum as carbonate-containing aluminum hydroxide gel. However, Duffin and Goodyear (8) reported on scarbroite, a crystalline aluminum hydroxycarbonate with the formula $Al_2(CO_3)_3{\cdot}12Al(OH)_3$. The IR spectrum of scarbroite is similar to that of carbonate-containing aluminum hydroxide gel (Fig. 1C); the difference between carbonate-containing aluminum hydroxide gel and scarbroite probably is particle size. Scarbroite has been found associated with gibbsite, which is the final crystalline form in the aging of aluminum hydroxide gel.

The remaining bands observed in the IR spectrum of the aluminum hydroxide gel–magnesium hydroxide gel dosage form arise from magnesium hydroxide (Fig. 1B). The IR spectrum of the magnesium hydroxide gel identifies it as crystalline magnesium hydroxide, $Mg(OH)_2$, known mineralogically as brucite. The well-ordered crystalline lattice is indicated by sharp absorption bands, especially for the stretching and libration vibrations of the hydroxyls at 3700 and 360 cm^{-1}, respectively, which indicate the electrostatic nature of the hydroxyl groups (9). Absorption bands at 565 and 445 cm^{-1} can be assigned to Mg–O vibrations (10).

The X-ray diffractogram of the aluminum hydroxide gel–magnesium hydroxide gel dosage form (Table I) is identical to brucite, indicating that the product is a physical mixture of amorphous aluminum hydroxide gel and crystalline magnesium hydroxide.

Calcium Carbonate—The IR spectrum of the calcium carbonate tablet is quite complex (Fig. 2). However, after the water-soluble excipients are removed by washing, the characteristic IR spectrum of the mineral calcite, $CaCO_3$, is observed. Absorption bands due to the carbonate ion occur at 1440, 870, and 710 cm^{-1}. A lattice vibration is seen at 325 cm^{-1} (11).

[1] On leave from Instituto de Edafologia, C.S.I.C., Madrid, Spain.
[2] Maalox, lot 26370, William H. Rorer, Fort Washington, Pa.
[3] Tums, lot 30N, Lewis/Howe Co., St. Louis, Mo.
[4] Rolaids, lot 2806T, Warner-Lambert Co., Morris Plains, N.J.
[5] Riopan, lot 6075RL, Ayerst Laboratories, New York, N.Y.
[6] Lot A 05176-109, Barcroft Co., Lewes, Del.
[7] Tanzania.
[8] Snarum, Norway.

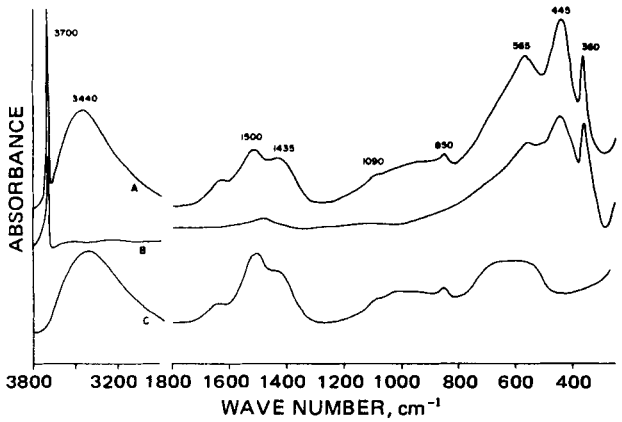

Figure 1—*IR spectra of: A, magnesia and alumina oral suspension washed with water to remove excipients (2 mg/300 mg of potassium bromide); B, synthetic brucite, $Mg(OH)_2$ (2 mg/300 mg of potassium bromide); and C, aluminum hydroxide gel (2 mg/300 mg of potassium bromide).*

There are two other crystal forms of calcium carbonate: aragonite and vaterite. These forms can be distinguished easily from calcite by IR spectroscopy since the carbonate ion is asymmetrically distorted in both polymorphs. However, the carbonate ion in calcite is symmetrically perturbed by the electrostatic field generated by the nearest-neighbor environment. This symmetrical crystal field accounts for the difference in the IR spectra of the undistorted carbonate ion in solution and of calcite (Table II).

The X-ray diffractogram (Table I) clearly establishes that the mineral calcite is the form of calcium carbonate present in the antacid tablet.

Dihydroxyaluminum Sodium Carbonate—The IR spectrum (Fig. 3) of the dihydroxyaluminum sodium carbonate dosage form is identical to the IR spectrum of the mineral dawsonite, $NaAl(OH)_2CO_3$, except that the bands are broader for the dihydroxyaluminum sodium carbonate, which indicates a relatively less ordered structure or a smaller particle size. The relationship between dihydroxyaluminum sodium carbonate and dawsonite is also seen by X-ray diffraction (Table I).

Some confusion exists concerning dihydroxyaluminum sodium carbonate. Lewin (12) claimed to have synthesized an antacid with Structure I.

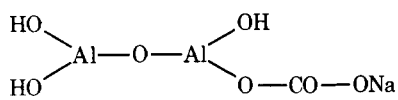

I

However, Lewin's IR spectra indicate that the synthetic compound is dawsonite. Lewin's material probably contained some amorphous aluminum hydroxide because the product had an aluminum to carbonate ratio greater than 1.

Seiyama *et al.* (13) showed that the hydrolysis of sodium aluminate with carbon dioxide is accompanied by the formation of dawsonite. However, because dawsonite was deposited below a critical pH at which

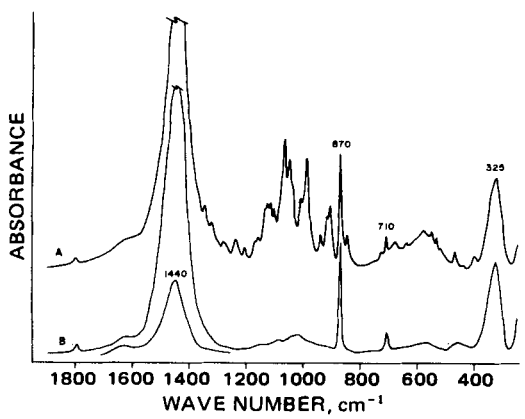

Figure 2—*IR spectra of: A, calcium carbonate tablet (1.5 mg/300 mg of potassium bromide); and B, calcium carbonate tablet washed with water to remove excipients (1.5 mg/300 mg of potassium bromide).*

Table I—X-Ray Data of Carbonate-Containing Antacids and Carbonate-Containing Minerals

Magnesia and Alumina Oral Suspension		Brucite[a] $Mg(OH)_2$	
d_{hkl}	Intensity[b]	d_{hkl}	I/I_1
4.78	s	4.77	90
2.74	w	2.72	6
2.36	vs	2.36	100
Calcium Carbonate Tablet		**Calcite[a] $CaCO_3$**	
d_{hkl}	Intensity[b]	d_{hkl}	I/I_1
3.86	vw	3.86	12
3.04	vs	3.035	100
2.49	vw	2.495	14
2.29	w	2.28	18
2.09	w	2.09	18
1.91	w	1.91	17
1.87	w	1.87	17
Dihydroxyaluminum Sodium Carbonate		**Dawsonite[a] $NaAl(OH)_2CO_3$**	
d_{hkl}	Intensity[b]	d_{hkl}	I/I_1
5.7	vs	5.7	100
3.39	m	3.38	70
2.79	vs	2.79	90
2.50	m	2.50	50
2.15	m	2.15	60
1.98	m	1.98	80
Magaldrate Suspension		**Magaldrate[c]**	
d_{hkl}	Intensity[b]	d_{hkl}	I/I_1
7.75	vs		
3.83	s		
2.57	m	2.57	95
2.32	m	2.30	55
1.95	w	1.97	33
		1.52	100
		1.49	65
		1.41	10
		1.31	10
		1.265	12
		0.992	6
		0.973	8
		0.876	10

Hydrotalcite[a] $Mg_6Al_2CO_3(OH)_{16}{\cdot}4H_2O$

d_{hkl}	I/I_1
7.84	100
3.90	60
2.60	40
2.33	25
1.990	30
1.541	35
1.498	25
1.419	8
1.302	6
1.265	10
0.994	4
0.976	6

[a] Taken from ASTM Diffraction Data File. [b] Estimated intensity from diffractogram: vs = very strong, s = strong, m = medium, w = weak, and vw = very weak. [c] From Ref. 20.

the bicarbonate-ion concentration in solution begins to increase, the formula NaAlOOH HCO_3 was assigned. The IR spectrum of dawsonite does not agree with the presence of bicarbonate ion. Rather the IR spectrum indicates the presence of distorted carbonate ion.

The crystal structure of dawsonite, as determined by Frueh and Golightly (14), places carbonate in a lower site of symmetry than the unperturbed carbonate ion (D_3h). Consequently, the absorption bands at 1575 and 1390 cm^{-1} are due to the removal of the degeneracy of the ν_3 mode of carbonate; this finding is supported by the appearance of the ν_1 mode at 1095 cm^{-1}, which is IR inactive in unperturbed carbonate. The other vibrations of carbonate in dawsonite are indicated in Table II.

The absence of the characteristic water vibration at 1640 cm^{-1} from the IR spectra of both dihydroxyaluminum sodium carbonate and dawsonite indicates that molecular water is not present. This result is in disagreement with the formula of dihydroxyaluminum sodium carbonate

Table II—IR Absorption Bands of Carbonate Ion in Different Carbonate-Containing Antacids

	Wave Number, cm^{-1}				
	Carbonate Ion in Solution	Calcium Carbonate (Calcite)	Aluminum Hydroxide Gel	Dihydroxyaluminum Sodium Carbonate (Dawsonite)	Hydrotalcite
$\upsilon_1(A_1')$, R	—	—	1090	1095	1105[a]
$\upsilon_2(A_2'')$, IR	879	870	850	842	—[b]
$\upsilon_3(E')$, IR, R	1415	1440	1435	1390	1390[c]
			1500	1575	(1640)[d]
$\upsilon_4(E')$, IR, R	680	710	—[b]	727	—[b]
			—[b]	—[b]	

[a] In magaldrate, this absorption is very intense due to the presence of sulfate. [b] Not observed. [c] May be observed as a doublet. [d] Due to bicarbonate ion.

given in the NF (15). Furthermore, the formula $CH_2AlNaO_5 \cdot xH_2O$ given in the NF does not clearly indicate the presence of carbonate and is not as useful as the mineralogical formula, $NaAl(OH)_2CO_3$.

Other crystalline hydroxycarbonates similar to dawsonite have been prepared. Potassium aluminum hydroxycarbonate and ammonium aluminum hydroxycarbonate were shown to have excellent antacid properties (16, 17).

Hydrotalcite—Hydrotalcite is a variety of the pyroaurite–sjögrenite group of minerals with the general formula $M^{2+}{}_6M^{3+}{}_2(OH)_{16}CO_3 \cdot 4H_2O$ in which the divalent cation is magnesium and the trivalent cation is aluminum (18). Three-dimensional structural analysis has not been performed on hydrotalcite; however, a one-dimensional structural analysis was interpreted in terms of a structure consisting of brucite layers alternating with hydrous aluminum layers bearing carbonate (19).

A somewhat different structure, proposed by Brown and Gastuche (20), consists of positively charged brucite-like layers in which aluminum replaces magnesium up to a maximum of about one in three sites. The positive charge is balanced by an interlayer sheet containing carbonate ion and water molecules. This structure seems more probable and can explain the differences in the d_{hkl} values found in several hydrotalcites (1, 19, 20). In addition, hydrotalcite-like structures in which the carbonate ion is totally or partially replaced by other anions such as nitrate, sulfate, perchlorate, or chloride were synthesized (21, 22).

The X-ray diffractogram of natural hydrotalcite is presented in Table I, and the IR spectrum is given in Fig. 4A. The absorption band at 1640 cm^{-1} is not due solely to molecular water since it is not significantly affected by deuterium exchange. This finding indicates that absorption bands at 1640 and 1400 cm^{-1} are due to the vibrations of carbonate groups. Since the carbonate anions are between layers in the Brown–Gastuche structure, it seems unlikely that a splitting in the ν_3 vibration of greater magnitude than that observed in dawsonite will occur. Therefore, it is suggested that bicarbonate ions may be present together with carbonate ions in hydrotalcite. The absorption bands at 1640 and 1400 cm^{-1} may be due to bicarbonate and carbonate, respectively. A slight splitting (1400–1360 cm^{-1}) of the carbonate ν_3 vibration occurred when hydrotalcite was evacuated, which may be due to an interaction of carbonate with the Mg–Al sheets.

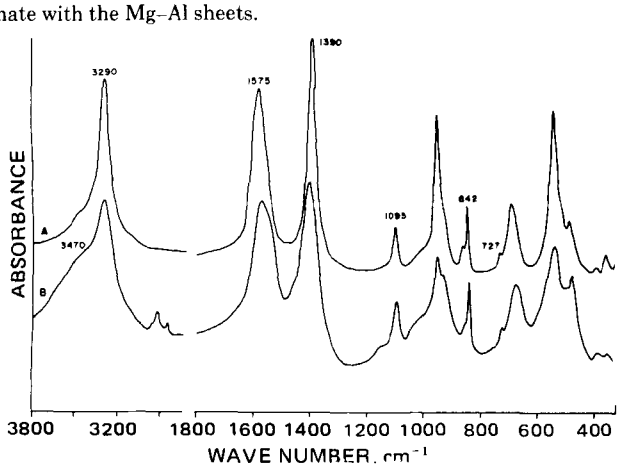

Figure 3—*IR spectra of: A, natural dawsonite, $NaAl(OH)_2CO_3$ (2 mg/300 mg of potassium bromide); and B, dihydroxyaluminum sodium carbonate tablet washed with water to remove excipients (2 mg/300 mg of potassium bromide).*

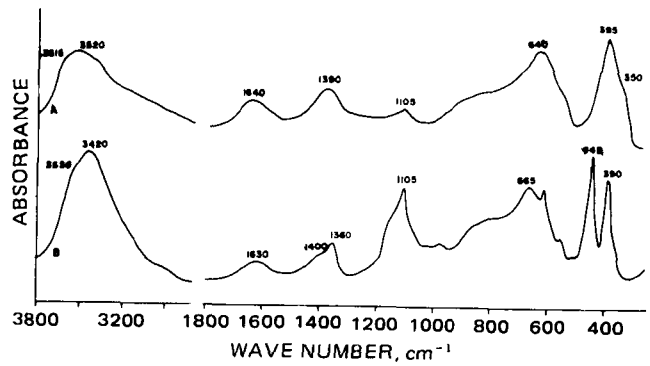

Figure 4—*IR spectra of: A, natural hydrotalcite, $Mg_6Al_2CO_3(OH)_{16} \cdot 4H_2O$ (2 mg/300 mg of potassium bromide); and B, magaldrate suspension washed with water to remove excipients (2 mg/300 mg of potassium bromide).*

Figure 5 shows a schematic representation of the hydrotalcite structure. The positive charge created by the substitution of aluminum for magnesium is compensated by the negatively charged interlayer carbonate, bicarbonate, and hydroxyl ions.

Hydrotalcite, $Mg_6Al_2(OH)_{16}CO_3 \cdot 4H_2O$, was synthesized (1) and its antacid properties were investigated (23).

The USP (24) defines magaldrate as a chemical combination of aluminum hydroxide and magnesium hydroxide, corresponding approximately to the formula $Al_2H_{14}Mg_4O_{14} \cdot 2H_2O$. The USP does not contain X-ray diffraction data on magaldrate, although a table of *d*-spacings was included in NF XIII (25). The NF diffraction pattern is given in Table I along with the diffractograms of the magaldrate dosage form and a natural hydrotalcite.

It is surprising that the two strong reflections at 7.75 and 3.83 Å present in the magaldrate dosage form are not included in the NF reference standard. The other reflections match up very well and would do so in terms of relative intensity if the reflection at 7.75 Å were taken as 100. A comparison of the X-ray spacing of the magaldrate dosage form and hydrotalcite clearly indicates that magaldrate has a hydrotalcite-like structure.

The IR spectra of several synthetic and natural hydrotalcite-type minerals were reported (1, 19, 26, 27), although no band assignments were made. Figure 4 presents the IR spectra of magaldrate and a natural hydrotalcite. Although the IR spectra of both samples are similar, some differences appear in the 1400- and 800–350-cm^{-1} regions. The differences in the 800–350-cm^{-1} region may be understood based on the structure proposed by Brown and Gastuche (20). Hydrotalcite-like structures can accommodate different aluminum to magnesium ratios, which could result in the observed spectral differences since vibrations in the 800–350-cm^{-1} region are probably due to Al–O and Mg–O vibrations of the octahedral sheets.

The differences between magaldrate and natural hydrotalcite at 1400 cm^{-1} are more apparent than real since evacuation of the natural hydrotalcite produced the splitting observed in the magaldrate sample.

A significant difference between the IR spectrum of magaldrate and natural hydrotalcite is the strong absorption band at 1105 cm^{-1} in magaldrate. Absorption bands in this spectral region are characteristic of sulfate anion, which may be the major interlayer anion in magaldrate.

SUMMARY

The carbonate-containing antacids present a wide spectrum of structural arrangements of carbonate. This is seen most clearly if the IR car-

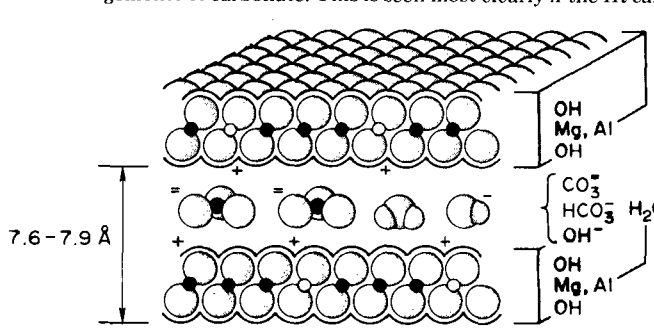

Figure 5—*Schematic representation of hydrotalcite.*

bonate bands are compared (Table II). The carbonate bands observed in the calcium carbonate antacid are very similar to those of the unperturbed carbonate ion, indicating a symmetrical arrangement of carbonate in the crystal structure.

A significant perturbation of the carbonate IR absorption bands was observed in carbonate-containing aluminum hydroxide gel, reflecting the coordination of carbonate to aluminum in the amorphous structure. The splitting of the ν_3 vibration suggests a unidentate interaction with aluminum. Carbonate is perturbed to a greater degree in dihydroxyaluminum sodium carbonate, suggesting a bidentate coordination for the carbonate ion. This is in good agreement with the crystal structure of dawsonite.

IR evidence suggests that both carbonate and bicarbonate are interlayer anions in hydrotalcite.

Based on IR and X-ray analysis, magaldrate has a hydrotalcite-like structure with sulfate as the major interlayer anion and carbonate present in the interlayer space. The evidence does not support the present identification of magaldrate as a magnesium aluminum hydroxide.

The relationship between the carbonate-containing compounds used as antacids and natural minerals is also apparent based on this study. Amorphous carbonate-containing aluminum hydroxide gel can be classified mineralogically as amorphous aluminum hydroxycarbonate. The crystalline carbonate-containing antacids are somewhat poorly organized forms of the minerals calcite, $CaCO_3$; dawsonite, $NaAl(OH)_2CO_3$; and hydrotalcite, $Mg_6Al_2CO_3(OH)_{16}{\cdot}4H_2O$.

Based on these findings, it is suggested that the official definitions should recognize that: (*a*) carbonate is coordinated to aluminum in the aluminum hydroxide gel structure; (*b*) dihydroxyaluminum sodium carbonate is a synthetic form of the mineral dawsonite and the mineralogical formula $NaAl(OH)_2CO_3$ should be used rather than the present official formula, $CH_2AlNaO_5{\cdot}xH_2O$, since no molecular water is present and the official formula does not clearly indicate that the compound is a hydroxycarbonate; and (*c*) magaldrate has a hydrotalcite-like structure.

It is believed that an understanding of the structural relationship between carbonate-containing antacids will lead to improved methods for the production and control of the antacids and will provide a useful framework for the development of new antacids.

REFERENCES

(1) B. Kobo, S. Miyata, T. Kumura, and T. Shimada, *Yakuzai Gaku*, **29**, 55 (1964).

(2) "The United States Pharmacopeia," 19th rev., Mack Publishing Co., Easton, Pa., 1975, p. 21.

(3) J. L. White and S. L. Hem, *J. Pharm. Sci.*, **64**, 468 (1975).

(4) N. J. Kerkhof, J. L. White, and S. L. Hem, *ibid.*, **66**, 1533 (1977).

(5) S. L. Hem, E. J. Russo, S. M. Bahal, and R. S. Levi, *ibid.*, **59**, 317 (1970).

(6) J. Fujita, A. E. Martell, and K. Nakamoto, *J. Chem. Phys.*, **36**, 339 (1962).

(7) P. Tarte, *Spectrochim. Acta*, **23A**, 2127 (1967).

(8) M. A. Duffin and J. Goodyear, *Min. Mag.*, **32**, 352 (1962).

(9) R. A. Buchanan, H. H. Cespers, and H. R. Marlin, *J. Chem. Phys.*, **40**, 1125 (1963).

(10) F. Freund, *Spectrochim. Acta*, **26A**, 195 (1970).

(11) C. K. Huang and P. F. Kerr, *Am. Mineral.*, **45**, 311 (1960).

(12) S. Z. Lewin, U. S. pat. 3,115,387 (Dec. 24, 1963).

(13) T. Seiyama, M. Egashira, E. Sakamoto, and M. Kono, *J. Chem. Soc. Jpn.*, **70**, 264 (1967).

(14) A. J. Frueh and J. P. Golightly, *Can. Mineral.*, **9**, 51 (1967).

(15) "The National Formulary," 14th ed., Mack Publishing Co., Easton, Pa., 1975, pp. 215–217.

(16) H. Besson, S. Caillère, S. Hénin, and R. Prost, *C.R., 277 Ser. D*, **1973**, 261.

(17) S. L. Hem and J. L. White, U. S. pat. 3,911,090 (Oct. 7, 1975).

(18) H. F. W. Taylor, *Mineral. Mag.*, **39**, 377 (1973).

(19) G. J. Ross and H. Kodama, *Am. Mineral.*, **52**, 1036 (1967).

(20) G. Brown and M. C. Gastuche, *Clay Miner.*, **7**, 193 (1967).

(21) D. M. Roy, R. Roy, and E. F. Osborn, *Am. J. Sci.*, **251**, 337 (1953).

(22) S. Miyata, *Clays Clay Miner.*, **23**, 369 (1975).

(23) A. C. Playle, S. R. Gunning, and A. F. Llewellyn, *Pharm. Acta Helv.*, **49**, 298 (1974).

(24) "The United States Pharmacopeia," 19th rev., Mack Publishing Co., Easton, Pa., 1975, pp. 290, 291.

(25) "The National Formulary," 13th ed., Mack Publishing Co., Easton, Pa., 1970, pp. 396, 397.

(26) F. A. Mumpton, H. W. Jaffe, and C. S. Thompson, *Am. Mineral.*, **50**, 1893 (1965).

(27) M. C. Gastuche, G. Brown, and M. M. Mortland, *Clay Miner.*, **7**, 177 (1967).

ACKNOWLEDGMENTS

Supported in part by the Barcroft Co. and a National Institutes of Health Biomedical Research Support Grant.

Carlos J. Serna acknowledges a Fellowship from the Ministerio de Educacion y Ciencia, Madrid, Spain.

This report is Journal Paper 6621, Purdue University Agricultural Experiment Station, West Lafayette, IN 47907.

Kinetics of Digoxin Stability in Aqueous Solution

LARRY A. STERNSON *x and RICHARD D. SHAFFER ‡

Received October 18, 1976, from the **Department of Pharmaceutical Chemistry, McCollum Laboratories, University of Kansas, Lawrence, KS 66044*, and the ‡*INTERx Research Corporation, Lawrence, KS 66044.* Accepted for publication June 13, 1977.

Abstract □ Digoxin hydrolysis was studied as a function of pH. Conversion of digoxin to digoxigenin was followed by high-pressure liquid chromatography and shown to proceed by the initial loss of one, two, or three sugars. The hydrolysis rate was directly proportional to parent drug concentration and hydrogen-ion activity. The individual hydrolysis rate constants of digoxin, digoxigenin bisdigitoxoside, and digoxigenin monodigitoxoside were determined by a simplex fitting procedure. Data are presented suggesting that at least some variation in the bioavailability of orally administered digoxin arises from observed variations in gastric pH; these variations influence the extent to which hydrolysis occurs and, thus, modify the composition of digoxin species available for absorption.

Keyphrases □ Digoxin—hydrolysis, kinetic study, effect of pH □ Hydrolysis—digoxin, kinetic study, effect of pH □ Kinetics—digoxin hydrolysis, effect of pH □ Stability—digoxin in aqueous solution, kinetic study of hydrolysis, effect of pH □ Cardiotonic agents—digoxin, hydrolysis, kinetic study, effect of pH

Digoxin is a widely prescribed glycoside used in the maintenance therapy of cardiac patients. Significant variability has been observed in the efficiency with which digoxin is absorbed from the GI tract among patients given the drug orally. Moreover, significant variations in bioavailability were noted within individual patients (1, 2).

bonate bands are compared (Table II). The carbonate bands observed in the calcium carbonate antacid are very similar to those of the unperturbed carbonate ion, indicating a symmetrical arrangement of carbonate in the crystal structure.

A significant perturbation of the carbonate IR absorption bands was observed in carbonate-containing aluminum hydroxide gel, reflecting the coordination of carbonate to aluminum in the amorphous structure. The splitting of the ν_3 vibration suggests a unidentate interaction with aluminum. Carbonate is perturbed to a greater degree in dihydroxyaluminum sodium carbonate, suggesting a bidentate coordination for the carbonate ion. This is in good agreement with the crystal structure of dawsonite.

IR evidence suggests that both carbonate and bicarbonate are interlayer anions in hydrotalcite.

Based on IR and X-ray analysis, magaldrate has a hydrotalcite-like structure with sulfate as the major interlayer anion and carbonate present in the interlayer space. The evidence does not support the present identification of magaldrate as a magnesium aluminum hydroxide.

The relationship between the carbonate-containing compounds used as antacids and natural minerals is also apparent based on this study. Amorphous carbonate-containing aluminum hydroxide gel can be classified mineralogically as amorphous aluminum hydroxycarbonate. The crystalline carbonate-containing antacids are somewhat poorly organized forms of the minerals calcite, $CaCO_3$; dawsonite, $NaAl(OH)_2CO_3$; and hydrotalcite, $Mg_6Al_2CO_3(OH)_{16}{\cdot}4H_2O$.

Based on these findings, it is suggested that the official definitions should recognize that: (*a*) carbonate is coordinated to aluminum in the aluminum hydroxide gel structure; (*b*) dihydroxyaluminum sodium carbonate is a synthetic form of the mineral dawsonite and the mineralogical formula $NaAl(OH)_2CO_3$ should be used rather than the present official formula, $CH_2AlNaO_5{\cdot}xH_2O$, since no molecular water is present and the official formula does not clearly indicate that the compound is a hydroxycarbonate; and (*c*) magaldrate has a hydrotalcite-like structure.

It is believed that an understanding of the structural relationship between carbonate-containing antacids will lead to improved methods for the production and control of the antacids and will provide a useful framework for the development of new antacids.

REFERENCES

(1) B. Kobo, S. Miyata, T. Kumura, and T. Shimada, *Yakuzai Gaku*, **29**, 55 (1964).

(2) "The United States Pharmacopeia," 19th rev., Mack Publishing Co., Easton, Pa., 1975, p. 21.

(3) J. L. White and S. L. Hem, *J. Pharm. Sci.*, **64**, 468 (1975).

(4) N. J. Kerkhof, J. L. White, and S. L. Hem, *ibid.*, **66**, 1533 (1977).

(5) S. L. Hem, E. J. Russo, S. M. Bahal, and R. S. Levi, *ibid.*, **59**, 317 (1970).

(6) J. Fujita, A. E. Martell, and K. Nakamoto, *J. Chem. Phys.*, **36**, 339 (1962).

(7) P. Tarte, *Spectrochim. Acta*, **23A**, 2127 (1967).

(8) M. A. Duffin and J. Goodyear, *Min. Mag.*, **32**, 352 (1962).

(9) R. A. Buchanan, H. H. Cespers, and H. R. Marlin, *J. Chem. Phys.*, **40**, 1125 (1963).

(10) F. Freund, *Spectrochim. Acta*, **26A**, 195 (1970).

(11) C. K. Huang and P. F. Kerr, *Am. Mineral.*, **45**, 311 (1960).

(12) S. Z. Lewin, U. S. pat. 3,115,387 (Dec. 24, 1963).

(13) T. Seiyama, M. Egashira, E. Sakamoto, and M. Kono, *J. Chem. Soc. Jpn.*, **70**, 264 (1967).

(14) A. J. Frueh and J. P. Golightly, *Can. Mineral.*, **9**, 51 (1967).

(15) "The National Formulary," 14th ed., Mack Publishing Co., Easton, Pa., 1975, pp. 215–217.

(16) H. Besson, S. Caillère, S. Hénin, and R. Prost, *C.R., 277 Ser. D*, **1973**, 261.

(17) S. L. Hem and J. L. White, U. S. pat. 3,911,090 (Oct. 7, 1975).

(18) H. F. W. Taylor, *Mineral. Mag.*, **39**, 377 (1973).

(19) G. J. Ross and H. Kodama, *Am. Mineral.*, **52**, 1036 (1967).

(20) G. Brown and M. C. Gastuche, *Clay Miner.*, **7**, 193 (1967).

(21) D. M. Roy, R. Roy, and E. F. Osborn, *Am. J. Sci.*, **251**, 337 (1953).

(22) S. Miyata, *Clays Clay Miner.*, **23**, 369 (1975).

(23) A. C. Playle, S. R. Gunning, and A. F. Llewellyn, *Pharm. Acta Helv.*, **49**, 298 (1974).

(24) "The United States Pharmacopeia," 19th rev., Mack Publishing Co., Easton, Pa., 1975, pp. 290, 291.

(25) "The National Formulary," 13th ed., Mack Publishing Co., Easton, Pa., 1970, pp. 396, 397.

(26) F. A. Mumpton, H. W. Jaffe, and C. S. Thompson, *Am. Mineral.*, **50**, 1893 (1965).

(27) M. C. Gastuche, G. Brown, and M. M. Mortland, *Clay Miner.*, **7**, 177 (1967).

ACKNOWLEDGMENTS

Supported in part by the Barcroft Co. and a National Institutes of Health Biomedical Research Support Grant.

Carlos J. Serna acknowledges a Fellowship from the Ministerio de Educacion y Ciencia, Madrid, Spain.

This report is Journal Paper 6621, Purdue University Agricultural Experiment Station, West Lafayette, IN 47907.

Kinetics of Digoxin Stability in Aqueous Solution

LARRY A. STERNSON *x and RICHARD D. SHAFFER ‡

Received October 18, 1976, from the **Department of Pharmaceutical Chemistry, McCollum Laboratories, University of Kansas, Lawrence, KS 66044*, and the ‡*INTERx Research Corporation, Lawrence, KS 66044.* Accepted for publication June 13, 1977.

Abstract □ Digoxin hydrolysis was studied as a function of pH. Conversion of digoxin to digoxigenin was followed by high-pressure liquid chromatography and shown to proceed by the initial loss of one, two, or three sugars. The hydrolysis rate was directly proportional to parent drug concentration and hydrogen-ion activity. The individual hydrolysis rate constants of digoxin, digoxigenin bisdigitoxoside, and digoxigenin monodigitoxoside were determined by a simplex fitting procedure. Data are presented suggesting that at least some variation in the bioavailability of orally administered digoxin arises from observed variations in gastric pH; these variations influence the extent to which hydrolysis occurs and, thus, modify the composition of digoxin species available for absorption.

Keyphrases □ Digoxin—hydrolysis, kinetic study, effect of pH □ Hydrolysis—digoxin, kinetic study, effect of pH □ Kinetics—digoxin hydrolysis, effect of pH □ Stability—digoxin in aqueous solution, kinetic study of hydrolysis, effect of pH □ Cardiotonic agents—digoxin, hydrolysis, kinetic study, effect of pH

Digoxin is a widely prescribed glycoside used in the maintenance therapy of cardiac patients. Significant variability has been observed in the efficiency with which digoxin is absorbed from the GI tract among patients given the drug orally. Moreover, significant variations in bioavailability were noted within individual patients (1, 2).

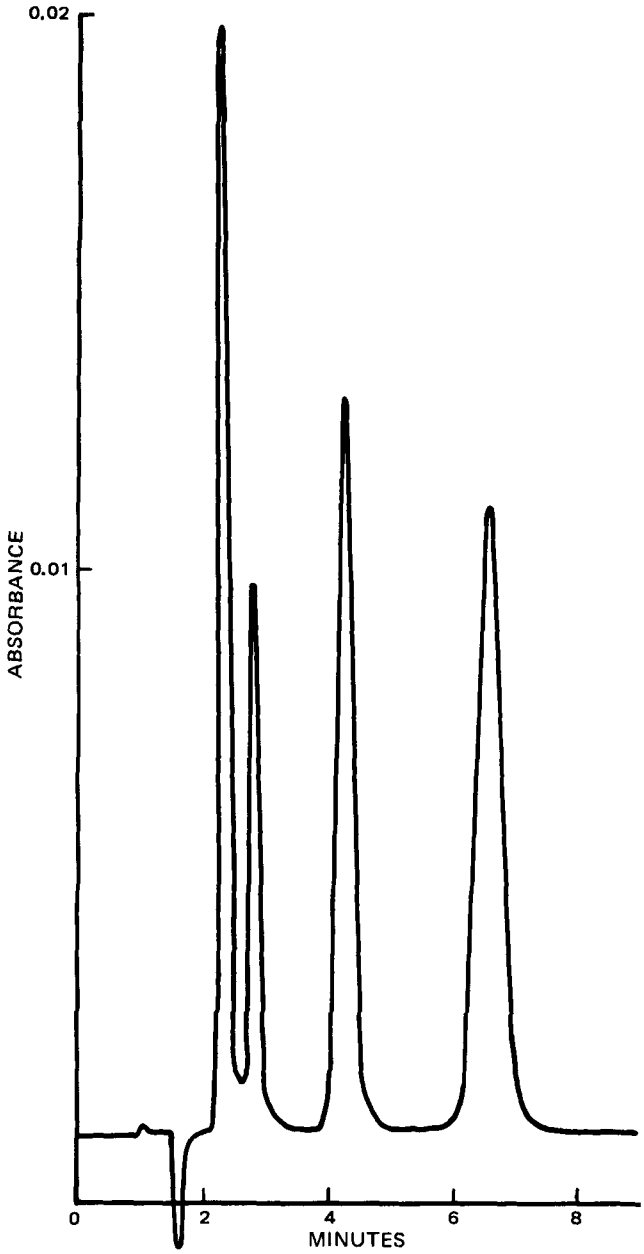

Figure 1—*Chromatogram of digoxigenin species separated by reversed-phase HPLC, obtained from an aqueous solution containing IV (t_R = 2.2 min; 12.2 μg/ml), III (t_R = 2.6 min; 10.2 μg/ml), II (t_R = 4.1 min; 30 μg/ml), and I (t_R = 6.4 min; 4.16 μg/ml).*

Potential sources for this variability have been postulated to involve dosage formulation and inconsistencies in administration (3–7). However, investigations of these parameters have failed to explain many observations associated with oral digoxin absorption.

The glycosidic nature of the digoxin molecule makes it susceptible to hydrolysis, especially in the acidic environment of the stomach. If hydrolysis is rapid enough to compete with absorption, fluctuations in bioavailability may reflect alterations in the amount and composition of the absorbed species. The hydrolysis products have been shown (8) to exhibit different pharmacological and toxicological activity than digoxin but are not distinguished from the parent drug using presently available clinical analytical methods.

Therefore, a study was initiated to determine if the

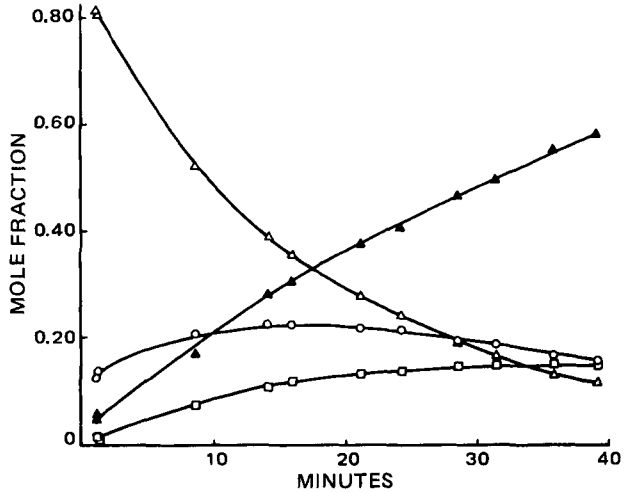

Figure 2—*Time-concentration profile of digoxigenin species [I (△), II (○), III (□), and IV (▲)] present in an aqueous solution of I at pH 1 incubated at 37°.*

variability in digoxin absorption could arise from variations in the extent to which hydrolysis occurs among patients and, thus, competes with drug absorption. An analytical method was developed to quantitate digoxin and its three potential hydrolysis products simultaneously. This method was used to study the hydrolysis kinetics of digoxin species under acid conditions, similar to those found during oral absorption.

RESULTS AND DISCUSSION

Digoxin (digoxigenin trisdigitoxoside) hydrolysis was studied at 37° at pH 1, 2, 4, and 7. At pH 7, no appreciable hydrolysis was observed over 48 hr. In all other media, four-component mixtures were generated, corresponding to the cleavage of one, two, or three digitoxose residues. Separation and simultaneous quantitation of each of the four components in the hydrolysis mixtures were affected by reversed-phase high-pressure liquid chromatography (HPLC) (Fig. 1). Twenty-five nanograms of digoxigenin species could be determined by monitoring the eluent spectrophotometrically at the λ_{max} (225 nm) for digoxin species.

Digoxin (I) hydrolysis is a complex combination of parallel reactions that can proceed initially by three alternative pathways to yield digoxigenin (IV), which is unreactive, and the bisglycoside (II) and monoglycoside (III), which may undergo further hydrolysis (Scheme I). Figures 2 and 3 show the variation in the composition of digoxin hydrolysis mixtures as a function of time at pH 1 and 2, respectively. Each possible hydrolysis product is observed in the hydrolysate. In a series of parallel experiments, the hydrolysis of the reactive products, II and III was studied similarly.

As shown in Fig. 4, for reactions carried out at pH 1, substrate (I, II, or III) disappearance follows pseudo-first-order kinetics. The magnitude of the pseudo-first-order rate constants obtained from these graphs is shown in Table I and reflects the number of alternative pathways available for hydrolysis. These rate constants represent the sum of the individual rate constants describing the disappearance of parent species, and their magnitude increases as the number of available degradation pathways increases. Therefore, I, which can react by three alternative paths ($k_D = k_1 + k_2 + k_3 = 0.053\ min^{-1}$) has a shorter half-life (13.5 min) than II (16.5 min), which can be consumed *via* two pathways ($k_B = k_4 + k_5 = 0.040\ min^{-1}$); III is the most stable ($t_{1/2}$ = 24.3 min) species, since there is only one route available for its breakdown ($k_M = k_6$). Thus, differences in disappearance rates for I–III appear to reflect both probability factors

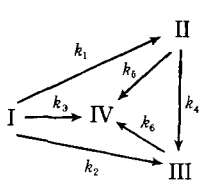

Scheme I

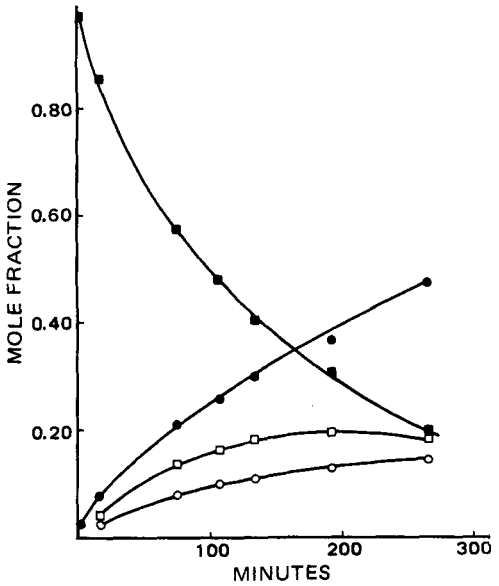

Figure 3—*Time-concentration profile of digoxigenin species [I (△), II (○), III (□), and IV (▲)] present in an aqueous solution of I at pH 2 incubated at 37°.*

as well as variations in stereochemical restrictions imposed at specific glycosidic linkages. Over the pH range studied (1–4), disappearance of substrate showed a first-order dependence on a_{H^+} (Fig. 4). At pH 2, k_D (0.0053 min^{-1}) is one-tenth the magnitude observed at pH 1.

The digoxin hydrolysis mixture was further analyzed to determine which reaction pathways (Scheme I) were operative and to get an indication of the significance of each route. In the experiments in which digoxin was the parent, its disappearance can be described as a pseudo-first-order process, expressed by:

$$-\frac{dD}{dt} = (k_1 + k_2 + k_3)D = k_D D \qquad \text{(Eq. 1)}$$

where k_D is the sum of k_1, k_2, and k_3. Rate expressions describing the appearance of bisglycoside (B), monoglycoside (M), and genin (G) take similar forms, expressed by:

$$\frac{dB}{dt} = k_1 D - (k_4 + k_5)B \qquad \text{(Eq. 2)}$$

$$\frac{dM}{dt} = k_2 D + k_4 B - k_6 M \qquad \text{(Eq. 3)}$$

$$\frac{dG}{dt} = k_3 D + k_5 B + k_6 M \qquad \text{(Eq. 4)}$$

These differential equations can be solved[1] and the amount of each component in the mixture can be expressed as the mole fraction of all digoxin species present:

$$D/D_0 = e^{-k_D t} \qquad \text{(Eq. 5)}$$

$$\frac{B}{D_0} = Ae^{-k_D t} + \left(\frac{B_0}{D_0} - A\right) e^{-\alpha t} \qquad \text{(Eq. 6)}$$

where $A = k_1/(\alpha - k_D)$ and $\alpha = k_4 + k_5$, and:

$$\frac{M}{D_0} = A\left\{Fe^{-k_D t} + \left(1 - \frac{B_0}{D_0 A}\right)Ce^{-\alpha t} - \left[F + \left(1 - \frac{B_0}{D_0 A}\right)C - \frac{M_0}{D_0 A}\right] e^{-k_6 t}\right\} \qquad \text{(Eq. 7)}$$

where $F = [k_4 + (k_2/A)]/(k_6 - k_D)$ and $C = k_4/(\alpha - k_6)$, and:

$$\frac{G}{D_0} = \frac{G_0}{D_0} + \frac{1}{k_D}(k_3 + k_5 A + k_6 AF)(1 - e^{-k_D t}) + \frac{1}{\alpha}\left[k_5\left(\frac{B_0}{D_0} - A\right) + k_6 A\left(1 - \frac{B_0}{D_0 A}\right)C\right](1 - e^{-\alpha t}) + \frac{1}{k_6}\left\{k_6 A\left[\frac{M_0}{D_0 A} - F - C\left(1 - \frac{B_0}{D_0 A}\right)\right]\right\}(1 - e^{-k_6 t}) \qquad \text{(Eq. 8)}$$

[1] Complete derivation of all equations is available from the authors on request.

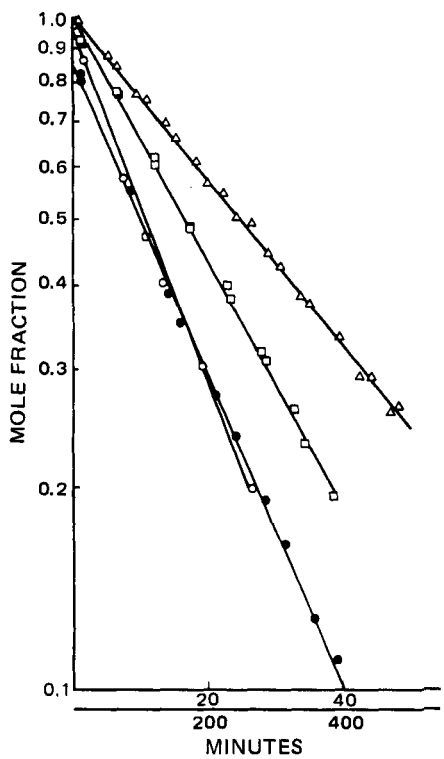

Figure 4—*Disappearance of digoxigenin species from acid solution as a function of time. In the pH 1 (0–60-min time scale) solution, the parent compound was III (▲), II (□), or I (○). In the pH 2 (0–600-min time scale) solution, the parent compound was I (●).*

Initial conditions were defined such that at $t = 0$, the amount of component J present in the mixture was J_0.

Imposing these boundary conditions provides general expressions in which the concentration of digoxin species can be determined in samples initially containing more than one digoxigenin component. Such manipulations were necessary because samples contained small amounts of impurities formed from prior hydrolysis of the parent compound.

From the HPLC tracings obtained during hydrolysis experiments, the amount of each component in the mixture could be expressed as the mole fraction of all digoxin species present as a function of time. Expressing the composition in this form eliminates error due to variations in the HPLC injection volume. When digoxin was the parent compound, these data were fit simultaneously to Eqs. 5–8 by an adaptive simplex procedure similar to that proposed by Nelder and Mead (9).

The quality of the fit at each iteration was determined by using Eqs. 5–8 to predict concentrations for each component at each time point, calculating the difference between these theoretical concentrations and the experimentally determined levels, and then summing the squares of all differences. In this way, all six rate constants were evaluated in one fitting procedure (Table I). The accuracy of this procedure is demonstrated by comparing the pseudo-first-order rate constant (k_D), determined experimentally for digoxin disappearance, with the sum of the individual rate constants (k_1, k_2, and k_3) it represents, determined by computer fit (Table I).

Table I—Rate Constants for Digoxin Hydrolysis at pH 1 [a]

Constant	Time, min^{-1}
k_1	0.0263
k_2	0.0089
k_3	0.0193
k_4	0.0207
k_5	0.0211
k_6	0.0301
k_M [b]	0.029
$(k_4 + k_5)$ [c]	0.042
k_B [b]	0.040
$(k_1 + k_2 + k_3)$ [d]	0.0545
k_D [b]	0.053

[a] Determined by the simplex fitting procedure as described in the text. [b] Determined experimentally from pseudo-first-order plots (Fig. 4). [c] Sum equivalent to k_B. [d] Sum equivalent to k_D.

Table II—Rate Constants for Hydrolysis of II and III at pH 1

Constant	Time, min^{-1}
k_4[a]	0.0232
k_5[a]	0.0165
k_6[a]	0.0368
$k_4 + k_5$[a,b]	0.040
k_B[c]	0.040
k_M[c]	0.029
k_6[d]	0.0290

[a] Determined from the simplex fit of data obtained for II hydrolysis. [b] Sum equivalent to k_B. [c] Determined experimentally from pseudo-first-order plots (Fig. 4). [d] Determined from the simplex fit of data obtained for III hydrolysis.

In experiments where II served as a substrate, kinetics can be described by the differential Eqs. 9–11 which are integrated to give Eqs. 12–14:

$$-\frac{dB}{dt} = (k_4 + k_5)B \quad \text{(Eq. 9)}$$

$$\frac{dM}{dt} = k_4B - k_6M \quad \text{(Eq. 10)}$$

$$\frac{dG}{dt} = k_5B + k_6M \quad \text{(Eq. 11)}$$

$$\frac{B}{B_0} = e^{-\alpha t} \quad \text{(Eq. 12)}$$

$$\frac{M}{B_0} = -Ce^{-\alpha t} + \left(\frac{M_0}{B_0} + C\right)e^{-k_6t} \quad \text{(Eq. 13)}$$

$$\frac{G}{B_0} = \frac{1}{\alpha}(k_5 - k_6C)(1 - e^{-\alpha t}) + \frac{1}{k_6}\left[k_6\left(\frac{M_0}{B_0} + C\right)\right](1 - e^{-k_6t}) + \frac{G_0}{B_0} \quad \text{(Eq. 14)}$$

Similar treatment for III hydrolysis yields:

$$-\frac{dM}{dt} = k_6M = \frac{dG}{dt} \quad \text{(Eq. 15)}$$

$$\frac{M}{M_0} = e^{-k_6t} \quad \text{(Eq. 16)}$$

$$\frac{G}{M_0} = \left(\frac{1}{M_0} - e^{-k_6t}\right) \quad \text{(Eq. 17)}$$

Simplex fit of the data obtained from II and III hydrolysis to Eqs. 12–14 and 16 and 17, respectively, gave the results shown in Table II. The goodness of fit is shown by comparison of k_B and k_M, determined experimentally, with the individual rate constants [$(k_4 + k_5)$ and k_6, respectively] they represent.

These results suggest that all possible hydrolysis routes are operative and approximately equally weighted, except for the direct cleavage of two digitoxose residues from digoxin (k_2) to form III, which occurs to a lesser extent. This observation may reflect stereochemical restrictions imposed at the glycosidic linkage or could be an artifact of the computer-fitting procedure.

The results presented also suggest that the variation in digoxin bioavailability after oral administration may be explained by the pH dependence of its hydrolysis. The digoxin half-life decreased from 131 min at pH 2 to 13.5 min at pH 1. Thus, the composition and amount of digoxin species available for absorption from the stomach should vary significantly with gastric acidity. The stomach pH varies widely among individuals (pH 0.5–4) and also within a patient as influenced by emotional and physical stresses, diet, and other factors (10). Thus, the variability in oral digoxin absorption may arise from variations in gastric pH, which influence the extent to which hydrolysis occurs and effectively competes with absorption of the active drug.

EXPERIMENTAL

Kinetic Experiments—The parent compound was dissolved in aqueous solution of appropriate pH and adjusted to an ionic strength of 1.0 with solid potassium chloride. The final concentration of substrate in all solutions was approximately 10 γ/ml. Ten milliliters of solution was incubated at 37°. At timed intervals, 25-μl samples were withdrawn[2] and subjected directly to HPLC analysis.

HPLC Analysis—Chromatography was performed on a component system[3]; the eluent was monitored spectrophotometrically at 225 nm. The separation utilized a column[4] (4 mm × 30 cm) operating at 2.0 ml/min with methanol-water (55:45) as the mobile phase. The retention volumes for IV, III, II, and I were 4.4, 4.2, 8.2, and 12.8 ml, respectively. The practical detection limit for digoxin was 25 ng from 25-λ injections. Components were quantitated by measuring peak heights and comparing the height with an external standard containing a mixture of known amounts of the four components.

REFERENCES

(1) J. Lindenbaum, M. H. Mellow, M. D. Blackstone, and V. P. Butler, *N. Engl. J. Med.*, **283**, 1344 (1971).

(2) D. H. Huffman and D. L. Azarnoff, *J. Am. Med. Assoc.*, **222**, 957 (1972).

(3) B. F. Johnson, J. McCrerie, A. Fowle, H. Greer, and C. Bye, *Lancet*, **1**, 1473 (1973).

(4) D. L. Sorby and T. N. Tozer, *Drug Intel. Clin. Pharm.*, **1**, 78 (1973).

(5) T. R. D. Shaw, M. R. Howard, and J. Hamer, *Lancet*, **2**, 303 (1972).

(6) D. H. Huffman, C. Y. Manion, and D. L. Azarnoff, *J. Pharm. Sci.*, **64**, 433 (1975).

(7) N. Sanchez, L. B. Sheiner, H. Halkin, and K. L. Melmon, *Br. Med. J.*, **4**, 132 (1973).

(8) K. K. Chen, E. B. Robbin, and H. Worth, *J. Am. Pharm. Assoc., Sci. Ed.*, **27**, 189 (1938).

(9) J. A. Nelder and R. Mead, *Comput. J.*, **7**, 308 (1965).

(10) C. H. Best and N. B. Taylor, "The Physiological Basis of Medical Practice," Williams & Wilkins, Baltimore, Md., 1955, p. 514.

ACKNOWLEDGMENTS

The authors are indebted to Dr. Richard L. Schowen for help with kinetic interpretations and to Dr. Wesley White for aid in developing the computer simulation techniques.

[2] Hamilton syringe.

[3] The chromatographic system consisted of a Waters M6000A solvent delivery system and a U6K universal injector coupled with a Varian Vari-Chrom detector.

[4] μBondapak C_{18}, Waters Associates, Inc.

Treatment of Neuroblastoma in Mice with Bromoacetylcholine and Bromoacetate

CHUNG Y. CHIOU

Received May 2, 1977, from the *Department of Pharmacology and Therapeutics, College of Medicine, University of Florida, Gainesville, FL 32610.* Accepted for publication June 15, 1977.

Abstract □ Bromoacetylcholine (30 mg/kg intratumor one to three times per day) and bromoacetate (12 mg/kg intratumor two times per day) inhibited neuroblastoma in A/J mice efficiently and prolonged the lifespan of these animals at least 200%. Since the neuroblastoma-inoculated A/J mice are considered to be comparable to human neuroblastoma, the cytolytic action of bromoacetylcholine and bromoacetate on murine neuroblastoma warrants further studies on patients. The fact that these tumors were cured in adult mice is very important because older children and adults with neuroblastoma have the poorest prognosis.

Keyphrases □ Bromoacetylcholine—effect on neuroblastoma in mice □ Bromoacetate—effect on neuroblastoma in mice □ Antitumor activity—bromoacetylcholine and bromoacetate, effect on neuroblastoma in mice

Except for leukemia and brain tumors, neuroblastoma is the most common malignancy seen in children. Because metastasis has occurred in over two-thirds of the patients by the time of diagnosis, definitive surgical treatment is not possible in most cases. Similarly, radiation therapy has had very limited success in patients with disseminated disease and has most often been only palliative (1). Treatment, therefore, frequently emphasizes a chemotherapeutic approach, although all three modes of therapy are used in many cases.

A regimen consisting of vincristine, cyclophosphamide, and daunorubicin has shown the best results in clinical trials, but these drugs are far from satisfactory because of their short duration of action and low tumor remission rate (1–4). Newer, more effective drugs are urgently needed to treat this highly malignant disease, which is responsible for at least 8% of childhood deaths by cancer.

Recently, it was shown that bromoacetylcholine is an effective agent for killing murine C-1300 neuroblastoma cells in culture at concentrations as low as 1×10^{-5} *M* (5, 6). It was also noted that moderate doses (10–30 mg/kg) of this compound suppressed the growth of tumors resulting from subcutaneous implantation of the C-1300 cells in A/J mice (6). Since the LD_{50} of bromoacetylcholine in tumor-free A/J mice was found to be 250 mg/kg, the therapeutic index appears to be reasonably high. These results strongly suggest a possible role for this drug in the chemotherapy of neuroblastoma.

Since bromoacetate, the hydrolysis product of bromoacetylcholine, was found early in the present study to inhibit neuroblastoma in cell culture, its effects on subcutaneous neuroblastomas in A/J mice were also investigated.

Generally, the major problem hindering the use of chemotherapeutic agents in cancer treatment is intolerable toxicity and other side effects. To reduce the possible parasympathomimetic side effects of bromoacetylcholine, atropine was included in some regimens in the hope that the combination might provide potent antitumor activity with few undesirable side effects. This use presumed that the cytotoxic effects of bromoacetylcholine were not somehow mediated by its parasympathomimetic action.

Table I—Effects of Doses and Frequencies of Injection on Neuroblastoma Inhibition by Bromoacetylcholine *In Vivo*

Bromoacetylcholine	Frequency of Injection per Day	*n*	Range, days	Mean ± *SE*, days	CLS[a], %	Median Lifespan, days
Control	3	10	11–38	23.9 ± 3.1	—	25
Control	2	10	11–38	24.3 ± 2.9	—	25
Control	1	10	11–38	21.2 ± 3.3	—	18
1 mg/kg	3	7	28–40	33.9 ± 1.7	+42	35
10 mg/kg	3	7	14–150[b]	52.9 ± 16.9	+121	38
30 mg/kg	3	10	30–150[b]	73.4 ± 17.1	+207	53
30 mg/kg	2	8	14–150[b]	60.1 ± 20.2	+147	38
30 mg/kg	1	7	25–150[b]	67.1 ± 21.6	+217	35
60 mg/kg	3	11	4–150[b]	36.0 ± 11.9	+51	32
60 mg/kg	3	13	2–150[b]	35.5 ± 10.7	+49	28
for 1 week; then 30 mg/kg for 2 weeks; then 10 mg/kg for 3 weeks	3					

[a] Percent change of lifespan calculated from mean lifespan. [b] Many mice survived beyond 150 days after drug treatments began; 150 days was chosen arbitrarily as the cutoff date for the purpose of performing statistical analysis.

EXPERIMENTAL

Materials—Bromoacetylcholine perchlorate was synthesized according to a previously published method (7). Bromoacetic acid, atropine sulfate, choline iodide, acetylcholinesterase[1], and butyrylcholinesterase[1] were obtained commercially. Murine C-1300 neuroblastoma cells were obtained from a collection institute[2] and had been maintained in culture in this laboratory for 12 months.

Cell Culture Experiments—Conditions and culture media were described previously in detail (5, 6). To determine whether the hydrolysis products of bromoacetylcholine are capable of inhibiting neuroblastoma, choline and bromoacetate were added to murine C-1300 neuroblastoma cells in culture and their cell growth inhibitory activity was compared with that of the parent compound.

Inhibition of Cholinesterases by Bromoacetate—The enzyme activities of acetylcholinesterase and butyrylcholinesterase were determined spectrophotometrically[3] using the method of Ellman *et al.* (8). The reaction mixture contained 3.0 ml of pH 8 phosphate buffer, 0.017 U of butyrylcholinesterase/ml or 0.083 U of acetylcholinesterase/ml, and 1.32 mg of 5,5-dithiobis(2-nitrobenzoate)/ml in a final volume of 3.135 ml. Various concentrations of bromoacetate were added to the incubation mixture to determine the I_{50} for each enzyme. The cell was shaken and allowed to stand at 25° for 15 min, followed by addition of acetylthiocholine (5.9×10^{-4} *M*).

The yellow anion, 5-thio-2-nitrobenzoate, formed in the reaction was measured at 412 nm. The reversibility of the enzyme inhibition was determined with various concentrations (noted in the *Results* section) of the enzymes and bromoacetate. The initial acetylthiocholine hydrolysis rate was expressed in terms of change in absorbance per minute.

[1] ICN Life Sciences Group, Cleveland, Ohio.
[2] American Type Culture Collection, Rockville, Md.
[3] Gilford automatic recording spectrophotometer, model 2400, Gilford Instrument Laboratories, Oberlin, Ohio.

Table II—Effects of Doses and Frequencies of Injection on Neuroblastoma Inhibition by Bromoacetate *In Vivo*

Bromoacetate	Frequency of Injection per Day	*n*	Range, days	Mean ± *SE*, days	CLS[a], %	Median Lifespan, days
Control	1	10	11–38	21.1 ± 3.3	—	18
Control	2	10	11–38	24.3 ± 2.9	—	25
Control	3	10	11–38	23.9 ± 3.1	—	25
12 mg/kg	1	10	25–150[a]	63.2 ± 14.7	+200	45
12 mg/kg	2	7	28–150[a]	62.4 ± 15.2	+157	57
12 mg/kg	3	8	8–150[a]	45.1 ± 15.9	+89	41
30 mg/kg	3	10	18–150[a]	54.4 ± 16.0	+128	32

[a] See Table I.

***In Vivo* Experiments**—Adult, male A/J mice, 16–18 g, were obtained commercially[4]. A suspension of 1×10^6 murine C-1300 neuroblastoma cells was injected subcutaneously in the interscapular area of these mice and allowed 10 days to develop a measurable tumor. Animals with tumors were then divided into control and treatment groups. Saline (0.9% NaCl) injections were given directly into the tumors of the control mice on a daily schedule, except weekends, for 6 weeks. Treatment animals were injected according to the dosage schedules shown in Tables I–IV. All solutions injected were adjusted to a volume of 30 μl.

Solutions of bromoacetylcholine and bromoacetate were prepared fresh each day and stored on ice to prevent hydrolysis and decomposition. Solutions containing bromoacetic acid were adjusted to approximately pH 7.4 with 5 *M* NaOH to prevent irritation of tissues at the injection sites. Since bromoacetylcholine is a salt, its solutions needed no such adjustment. These solutions also were injected directly into the tumors, except in experiments testing the effects of intraperitoneal administration. Atropine was given intramuscularly. Thirty milligrams of bromoacetylcholine/kg is equimolar with 12 mg of bromoacetate/kg.

RESULTS

Inhibition of Neuroblastoma Cells in Culture by Hydrolysis Products of Bromoacetylcholine—Since bromoacetylcholine is hydrolyzed both enzymatically and chemically to choline and bromoacetate (7), the effect of these compounds was first examined on neuroblastoma growing in culture (Fig. 1). Although cell growth was not significantly inhibited by choline concentrations as high as 1×10^{-4} *M*, bromoacetate at 1×10^{-5} and 1×10^{-4} *M* did decrease the number of viable cells compared to the control. The cytotoxic potency of bromoacetate is thus similar to that of bromoacetylcholine on an equimolar basis.

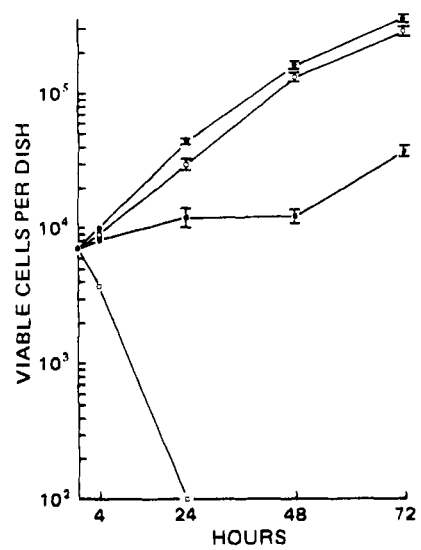

Figure 1—*Effects of bromoacetate and choline, hydrolysis products of bromoacetylcholine, on the cell growth of neuroblastoma* in vitro. *Key:* ●, *control;* ○, *1* × 10^{-4} M *choline;* ■, *1* × 10^{-5} M *bromoacetate; and* □, *1* × 10^{-4} M *bromoacetate. Each point represents the mean of four values, and bars represent the standard error of the mean.*

[4] Jackson Laboratories, Bar Harbor, Me.

Table III—Effect of Atropine on the Neuroblastoma Inhibition by Bromoacetylcholine (I) *In Vivo*

Drugs and Doses	Frequency of Injection per Day	*n*	Range, days	Mean ± *SE*, days	CLS[a], %	Median Lifespan, days
Control	3	5	9–30	22.2 ± 3.7	—	35
Atropine, 1 mg/kg	1	9	18–51	31.8 ± 3.7	+43	28
I, 10 mg/kg	3	7	14–150[a]	52.9 ± 16.9	+121[b]	38
Atropine, 1 mg/kg, plus I, 10 mg/kg	1 3	6	9–32	26.2 ± 3.5	+18	30
I, 30 mg/kg	3	10	30–150[a]	73.4 ± 17.1	+207[b]	53
Atropine, 1 mg/kg, plus I, 30 mg/kg	1 3	7	16–56	28.7 ± 5.3	+29	28

[a] See Table I. [b] These data were transferred here from Table I for comparison.

Inhibition of Cholinesterases by Bromoacetate—Although the cholinesterases are inhibited irreversibly by bromoacetylcholine (9), they were inhibited reversibly by bromoacetate (Fig. 2). Fifty percent inhibition of acetylcholinesterase and of butyrylcholinesterase occurred with $2.96 \pm 0.16 \times 10^{-3}$ *M* and $4.18 \pm 0.38 \times 10^{-3}$ *M* bromoacetate, respectively. These concentrations are about 100-fold higher than those required for inhibition of neuroblastoma in culture. It is thus unlikely that cholinesterase inhibition plays a significant role in the control of neuroblastoma growth.

Inhibition of Neuroblastoma in Mice—Tables I–IV summarize the effects of various therapy regimens on survival rates of A/J mice with implanted neuroblastoma tumors. For bromoacetylcholine, 30 mg/kg injected into the tumors one to three times per day gave the highest success rate, with an average prolongation of life of 147–217% (Table I). Comparatively, bromoacetate (12 mg/kg) given once or twice a day also increased the average survival time 200 and 157%, respectively (Table II).

Atropine (1 mg/kg) given with 30 mg of bromoacetylcholine/kg reduced the survival time to that of control mice (no drug) (Table III). This result is in contrast to its effect upon the cells in culture where it had no effect on bromoacetylcholine inhibition.

Experiments designed to test the effectiveness of bromoacetylcholine and bromoacetate by the intraperitoneal route showed no significant enhancement of survival time (Table IV). Poor absorption, because of the permanent charge in the molecule, and dilution of drug at the tumor site may have contributed to these results.

Mice given bromoacetylcholine or bromoacetate directly into the tumor showed significant reductions in tumor growth (Figs. 3 and 4). Those surviving more than 150 days were free of tumors and had no recurrence of neuroblastoma during the remainder of their natural lives.

DISCUSSION

With the advent of chemotherapy, a marked improvement was made in the treatment of Wilm's tumor, a less common solid tumor in children. No such advances have been made in the chemotherapy of neuroblastoma (1). Several agents, including vincristine, cyclophosphamide, and daunorubicin, have been tried without significant improvement in the overall survival rate of treated patients. Following an initial slowing of tumor growth, there appears to be an escape from the effects of these noncell-specific antineoplastic agents. Remission rates remain low, and the duration of drug effectiveness is relatively short (1–4).

The present work demonstrated the remarkable effectiveness of bromoacetylcholine and bromoacetate in reducing neuroblastoma growth

Table IV—Effects of Intraperitoneal Injection of Bromoacetate (II) and Bromoacetylcholine (I) on Neuroblastoma Inhibition

Drugs	Frequency of Injection per Day	*n*	Range, days	Mean ± *SE*, days	CLS[a], %	Median Lifespan, days
Control	3	9	8–49	30.3 ± 4.0	—	35
I, 30 mg/kg	3	8	31–45	34.3 ± 1.7	+13	35
II, 12 mg/kg	3	8	31–47	38.0 ± 1.9	+25	38

[a] See Table I.

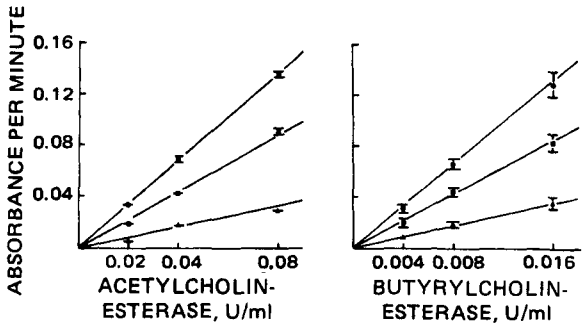

Figure 2—*Inhibition of acetylcholinesterase and butyrylcholinesterase by bromoacetate. Key: ●, control; ■, 3 × 10⁻³ M bromoacetate; and ▲, 1 × 10⁻² M bromoacetate. Each point represents the mean of four values, and bars represent the standard error of the mean. All plotted lines passed through the origin, and the lines obtained with bromoacetate treatments had slopes that were smaller than those of uninhibited ones. These results indicate a reversible inhibition of cholinesterases by bromoacetate.*

both *in vitro* and *in vivo*. Since the murine C-1300 neuroblastoma A/J mouse model has been noted to be comparable to the human disease (10), the present findings open the possibility of an important advance in chemotherapy. They are even more significant in light of the fact that these tumors have been cured in adult mice. Older children and adults with neuroblastoma have a much poorer prognosis than do babies less than 1 year old.

Following the observations of cytotoxicity of these two bromo compounds, preliminary investigations of possible mechanisms of action were made. The results have been presented here and in an earlier paper (6). One proposed mechanism involves the binding of bromoacetylcholine irreversibly to cholinergic receptors and/or cholinesterases. It was speculated that such binding might be responsible for the specific cytotoxicity of this compound. That cholinesterase inhibition is not part of the mechanism can be derived from the fact that 100-fold higher concentrations of bromoacetylcholine and bromoacetate are needed to inhibit these enzymes than to inhibit neuroblastoma cell growth. The irreversible binding of these bromo compounds to the cholinergic receptor on neuroblastoma cell membrane seems to be responsible for their cytolytic effect[5].

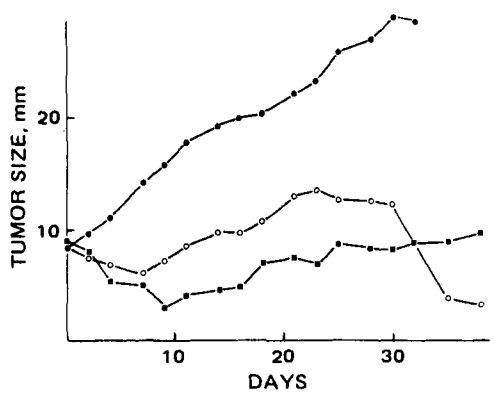

Figure 3—*Effects of bromoacetate and bromoacetylcholine on the tumor size of A/J mice inoculated with 1 × 10⁶ cells of neuroblastoma. Key: ●, control; ■, treated with bromoacetate, 12 mg/kg, twice a day; and ○, treated with bromoacetylcholine, 30 mg/kg, once a day. Note a significant depression of tumor growth in treated* versus *control animals.*

[5] Based on recent findings to be published shortly.

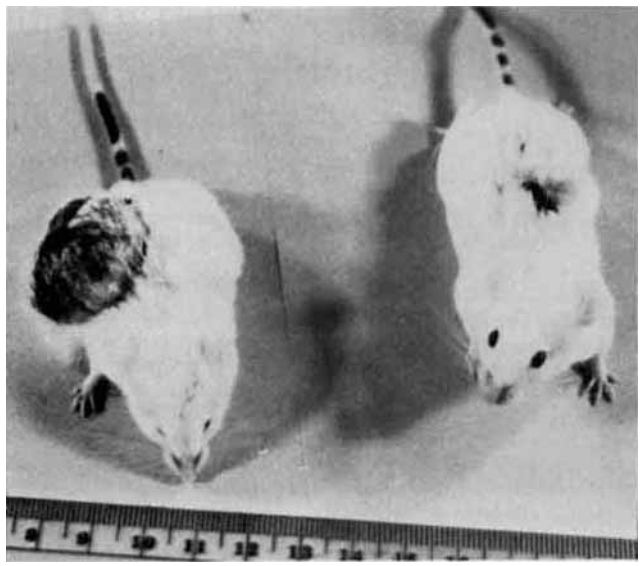

Figure 4—*Treatment of neuroblastoma-inoculated A/J mice with bromoacetylcholine. Left: Mouse inoculated with 1 × 10⁶ cells of neuroblastoma and injected with saline three times daily, except weekends, for 5 weeks as control. Right: Mouse treated with 30 mg of bromoacetylcholine/kg three times daily, except for weekends, for 5 weeks.*

In conclusion, the simple organic compounds bromoacetylcholine and bromoacetate are potent drugs in the inhibition of neuroblastoma growth. The optimal regimen was 30 mg of bromoacetylcholine/kg injected one to three times daily or 12 mg of bromoacetate/kg injected once daily, except weekends, for 6 weeks. Compared to untreated controls, the tumors were significantly reduced in size and the average lifespan was increased 200%. These drugs should be given by intravenous injection to patients with metastatic neuroblastoma since GI absorption is poor, as shown by the experiments utilizing intraperitoneal injections.

REFERENCES

(1) C. Pochedly, "Neuroblastoma," Public Science Group, Acton, Mass., 1976.

(2) A. E. Evans, R. M. Heyn, W. A. Newton, Jr., and S. L. Leiken, *J. Am. Med. Assoc.*, **207**, 1325 (1967).

(3) D. H. James, Jr., O. Histu, E. L. Wren, Jr., and D. Pinkel, *ibid.*, **194**, 123 (1965).

(4) M. P. Sullivan, A. H. Nora, P. Kulapongs, D. M. Lane, J. Windmiller, and W. G. Thurman, *Pediatrics*, **44**, 685 (1969).

(5) C. Y. Chiou, *J. Pharm. Sci.*, **64**, 469 (1975).

(6) *Ibid.*, **66**, 837 (1977).

(7) C. Y. Chiou and B. V. R. Sastry, *Biochem. Pharmacol.*, **17**, 805 (1968).

(8) G. L. Ellman, K. C. Courtney, V. Andres, Jr., and R. M. Featherstone, *ibid.*, **7**, 88 (1961).

(9) C. Y. Chiou, *Eur. J. Pharmacol.*, **26**, 268 (1964).

(10) J. Z. Finklestein, E. Arima, P. E. Byfield, J. E. Byfield, and E. W. Fonkalsrud, *Cancer Chemother. Rep.*, **57**, 405 (1973).

ACKNOWLEDGMENTS

Supported in part by Research Grants CA-17584 from the National Cancer Institute and CH-81 from the American Cancer Society.

The author is grateful to Ms. Marilyn Martin for technical assistance and to Dr. Norman Liddell for assistance in manuscript preparation.

Spectroscopic Approach to Estimation of Microequilibrium Constants of Prototropic Reactions of Aminobenzoic Acids

STEPHEN G. SCHULMAN ˣ, LEONARD S. ROSENBERG, and ROY J. STURGEON *

Received April 29, 1977, from the *College of Pharmacy, University of Florida, Gainesville, FL 32610.* Accepted for publication June 22, 1977. *Present address: College of Pharmacy, University of South Carolina, Columbia, SC 29206.

Abstract □ The microequilibrium constants of protolytic dissociation of diprotic acids, dihydric bases, or ampholytes such as the aminobenzoic acids, with dissimilar ionizing groups, can be estimated by spectrophotometric titration and measurement of the molar absorptivity at the long wavelength absorption maximum of simple alkylated derivatives. The method is applicable when the long wavelength absorption spectral bands of the tautomeric species are well resolved. Compared to the traditional method of estimating microequilibrium constants using the dissociation constants of alkylated derivatives, the proposed method is simpler, faster, and more accurate.

Keyphrases □ Aminobenzoic acids, various—microequilibrium constants of protolytic dissociation estimated spectrophotometrically □ Microequilibrium constants—various aminobenzoic acids, protolytic dissociation, estimated spectrophotometrically □ Spectrophotometry—estimation, microequilibrium constants of protolytic dissociation of various aminobenzoic acids □ Protolytic dissociation—various aminobenzoic acids, microequilibrium constants estimated spectrophotometrically

The purpose of this study was to show that for acids demonstrating tautomeric equilibria and absorbing visible or UV light in such a way that the long wavelength absorption bands of the tautomeric species are well resolved, the tautomeric equilibrium constant and, therefore, the microscopic prototropic equilibrium constants can be determined with greater accuracy than is presently available by using Ebert's method (1). In this approach, it is necessary to determine the molar absorptivity of an alkylated derivative, such as an ester, at its absorption maximum, as well as to determine the macroequilibrium constants of the acid of interest by spectrophotometric titration.

The aminobenzoic acids were chosen as test compounds because their dissociation constants are already well established (2), permitting concentration on the spectroscopic aspects of the study.

BACKGROUND

The aminobenzoic acids undergo prototropic dissociation according to Scheme I. Because of the proximity of the macroequilibrium constants K_1 and K_2, dissociation of the cation, C, may result in formation of a

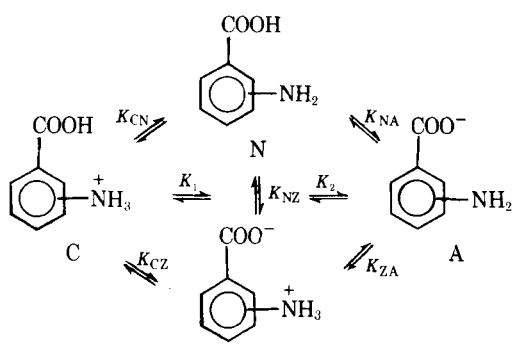

Scheme I

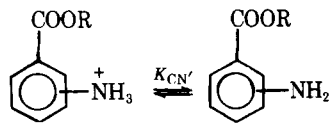

Scheme II

neutral molecule, N, or a zwitterion, Z (3). The respective microequilibrium constants for these dissociations are K_{CN} and K_{CZ} and are related to K_1 (3) by:

$$K_1 = K_{CN} + K_{CZ} \quad \text{(Eq. 1)}$$

Either uncharged species (N or Z) can then dissociate to form the anion, A. The microequilibrium constants for these processes are K_{NA} and K_{ZA} and are related to K_2 (3) by:

$$K_2^{-1} = K_{NA}^{-1} + K_{ZA}^{-1} \quad \text{(Eq. 2)}$$

The tautomeric ratio K_{NZ} is related to the microequilibrium constants by:

$$K_{NZ} = \frac{K_{CN}}{K_{CZ}} = \frac{K_{ZA}}{K_{NA}} \quad \text{(Eq. 3)}$$

For the aminobenzoic acids, K_1 and K_2 were determined potentiometrically (2). The microequilibrium constants K_{CN}, K_{CZ}, K_{NA}, and K_{ZA} were estimated (1) by determining the dissociation constants K_{CN}' for the dissociations of the cations derived from the methyl or ethyl esters of the aminobenzoic acids (4, 5) to form the neutral esters (Scheme II) and equating K_{CN}' to K_{CN}. This approach enables the estimation of K_{CZ} from:

$$K_{CZ} \approx K_1 - K_{CN}' \quad \text{(Eq. 4)}$$

K_{NZ} from:

$$K_{NZ} \approx \frac{K_{CN}'}{K_{CZ}} \quad \text{(Eq. 5)}$$

and, ultimately, K_{NA} and K_{ZA} from:

$$K_{NA} \approx K_2(1 + K_{NZ}^{-1}) \quad \text{(Eq. 6)}$$

and:

$$K_{ZA} = K_2(1 + K_{NZ}) \quad \text{(Eq. 7)}$$

The accuracy of this approach depends on the accuracy of the assumption that $K_{CN}' = K_{CN}$. This assumption was shown for several *N*-arylglycines to be justifiable to about 0.2 pKa unit (6). This value is an acceptable error for the comparison of pKa's (standard free energies of proton exchange) of related compounds. However, if species distributions are important, an error of 0.2 pKa unit translates into an error of 58% in the estimated value of K_{CN}. Moreover, in compounds in which the proton replaced by an alkyl group is involved in an intramolecular or a strong intermolecular hydrogen bond, the error is far more serious. For example, the pKa of salicylic acid is 3.0 while that of *O*-methoxybenzoic acid is 4.1 (7). The discrepancy of 1.1 pKa units would translate into an error of ~1.2 × 10^3% if the K_a of *O*-methoxybenzoic acid was used to represent that of salicylic acid.

EXPERIMENTAL

The *o*-, *m*-, and *p*-aminobenzoic acids, methyl *o*-aminobenzoate, methyl *m*-aminobenzoate, and ethyl *p*-aminobenzoate were purchased[1] as the highest quality analytical reagents and were used without further purification. Salicylic acid, *m*-hydroxybenzoic acid, *p*-hydroxybenzoic

[1] Aldrich Chemical Co., Milwaukee, Wis.

Table I—Molar Absorptivities of the Pertinent Species at the Chosen Analytical Wavelengths and Macroequilibrium Constants of the Aminobenzoic Acids and Their Esters

	ϵ_C	$\epsilon_{N'}$	ϵ_A	$K_{CN'}$[a]	K_1[b]	K_2[b]	ϵ_U
o-Aminobenzoic acid (λ = 327 nm)	0	—	1.76×10^3	—	7.77×10^{-3}	1.12×10^{-5}	$1.75 \pm 0.02 \times 10^3$
Methyl ester (λ = 328 nm)	—	3.63×10^3	—	6.90×10^{-3}	—	—	—
m-Aminobenzoic acid (λ = 311 nm)	0	—	1.40×10^3	—	7.60×10^{-4}	1.82×10^5	$5.68 \pm 0.48 \times 10^2$
Methyl ester (λ = 322 nm)	—	2.06×10^3	—	2.75×10^{-4}	—	—	—
p-Aminobenzoic acid (λ = 285 nm)	1.1×10^2	—	8.00×10^3	—	3.90×10^{-3}	1.42×10^5	$1.48 \pm 0.02 \times 10^4$
Ethyl ester (λ = 285 nm)	—	1.60×10^4	—	4.17×10^{-3}	—	—	—

[a] From Refs. 4 and 5. [b] From Ref. 2.

acid, and the methyl ethers and methyl esters of the hydroxybenzoic acids were also purchased[2] and used without further purification.

Absorption spectra were taken on a grating-type spectrophotometer[3] at 25° in 1-cm cells. The solutions whose spectra were taken were ~1×10^{-4} *M* in the *o*- and *m*-aminobenzoic acids and their esters and ~1×10^{-5} *M* in *p*-aminobenzoic acid and its ester. The pH of these solutions was adjusted with perchloric acid[4] using a pH meter[5] with a combination glass silver–silver chloride electrode. The spectrum of each aminobenzoic acid was scanned for 18 values of pH between pH 7.5 and H_0 − 0.36. From these absorptiometric titrations, plots of absorbance *versus* pH were constructed in which the absorbance was measured at the longest wavelength absorption maximum observable in each set of spectra.

Absorption spectra of the hydroxybenzoic acids at H_0 − 0.36 (neutral molecules), pH 7.0 (singly charged anions), and pH 14.2 (doubly charged anions) were recorded. For salicylic acid, it was necessary to take the spectrum in more concentrated (8.0 *M*) sodium hydroxide (H_- = 15.8) to isolate the doubly charged anion. The absorption spectra of the aminobenzoic esters at pH 7.0 (neutral molecules) and 0.2 (singly charged cations) and of the hydroxybenzoic ethers and esters at pH 1.0 (neutral molecules) and pH 12.0 (singly charged anions) were also recorded.

RESULTS AND DISCUSSION

The absorptiometric titrations of the aminobenzoic acids are represented graphically in Figs. 1 and 2. Pertinent long wavelength absorption maxima and macroequilibrium constants, taken from the literature (4, 5), of the aminobenzoic acids and their esters are listed in Table I. Those of the hydroxybenzoic acids and their ethers and esters are listed in Table II. The tautomeric and microequilibrium constants of the aminobenzoic acids are presented in Tables III and IV.

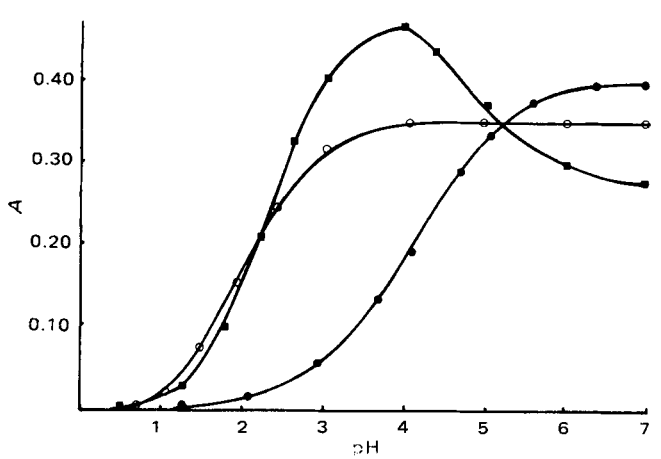

Figure 1—*Variations of absorbance, with pH, of* o*-aminobenzoic acid* (○) (λ_{abs} = *327 nm),* m*-aminobenzoic acid* (●) (λ_{abs} = *311 nm), and* p*-aminobenzoic acid* (■) (λ_{abs} = *285 nm). The analytical wavelength in each case was the absorption maximum of the neutral molecule (longest wavelength absorbing species).*

[2] Pfaltz and Bauer, Flushing, N.Y.
[3] Beckman model DB-GT.
[4] Mallinckrodt Chemical Works, St. Louis, Mo.
[5] Orion model 801.

The protolytic equilibrium constants K_1 and K_2 of a diprotic acid with equivalent ionizing groups (*e.g.*, phthalic acid) may be calculated from the solution of:

$$(a - \epsilon_D C_T l)[H^+]^2 + (a - \epsilon_M C_T l)K_1[H^+] + (a - \epsilon_A C_T l)K_1K_2 = 0 \quad \text{(Eq. 8)}$$

for several different values of a, the absorbance at the analytical wavelength, and the corresponding values of $[H^+]$ in the absorptiometric titration. In Eq. 8, ϵ_D, ϵ_M, and ϵ_A are the molar absorptivities of the diprotic acids, its conjugate base (the monoprotic acid), and the conjugate base of the monoprotic acid, respectively; C_T is the formal concentration of diprotic acid; and l is the optical depth of the sample. If the successive prototropic equilibria appreciably overlap (*i.e.*, if $K_1/K_2 < 1 \times 10^3$), ϵ_M cannot be determined independently because the monoprotic species cannot be isolated. However, ϵ_M can be treated as a unknown parameter along with K_1 and K_2 if Eq. 8 is solved for at least three points in the absorptiometric titration.

Now, consider the spectrophotometric determination of K_1 and K_2 for diprotic acids with dissimilar ionizing groups, such as the aminobenzoic acids. For the latter compounds, K_2 and K_1 are related only to the total proton uptake by anion A and uncharged species U (U represents both the neutral species and zwitterion), respectively, and are independent

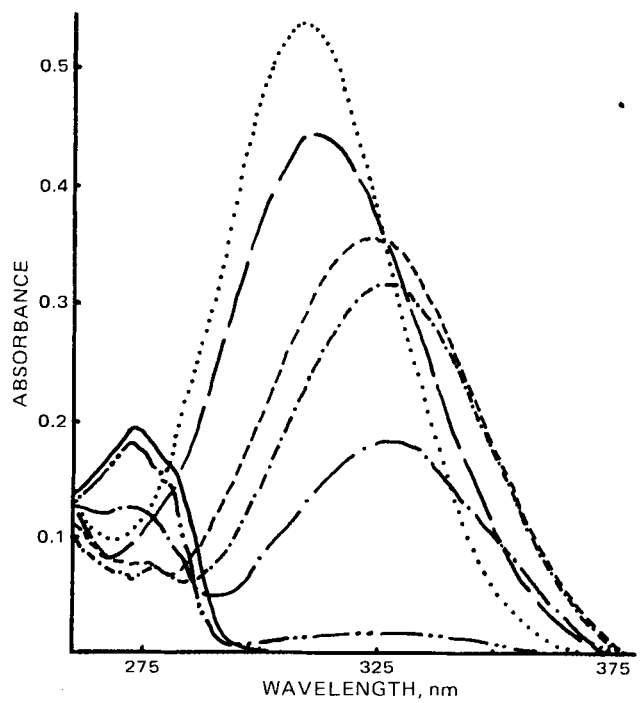

Figure 2—*The pH dependence of the absorption spectrum of* o*-aminobenzoic acid, demonstrating the red shifting and subsequent blue shifting of the spectrum, with decreasing pH as the anion is converted partially to the neutral molecule and then to the cation. Key:* . . . , *pH 11.04 and 7.03;* – – –, *pH 5.05;* – · – , *pH 4.08;* ·····, *pH 3.05;* ——·——, *pH 2.11; and* —··—··—, *pH 1.07.*

Table II—Longest Wavelength Absorption Maxima in Water of the Various Species Derived from the Hydroxybenzoic Acids and Their Ethers and Esters

	Neutral Molecule		Monoanion		Dianion	
	λ_{max}, nm	ϵ_{max}	λ_{max}, nm	ϵ_{max}	λ_{max}, nm	ϵ_{max}
Salicylic acid	302	3.68×10^3	295	3.57×10^3	309	4.09×10^3
Methyl ether	295	3.29×10^3	280	2.03×10^3		
Methyl ester	302	3.12×10^3	333	4.21×10^3		
m-Hydroxybenzoic acid	297	2.60×10^3	287	2.30×10^3	312	2.99×10^3
Methyl ether	301	2.58×10^3	286	2.21×10^3		
Methyl ester	296	2.80×10^3	322	2.90×10^3		
p-Hydroxybenzoic acid	256	1.47×10^4	246	1.25×10^4	281	1.75×10^4
Methyl ether	257	1.46×10^4	250	1.29×10^4		
Methyl ester	256	1.60×10^4	296	2.44×10^4		

of the tautomeric composition of U. Therefore, it is permissible to write Eq. 8 as:

$$(a - \epsilon_C C_T l)[H^+]^2 + (a - \epsilon_U C_T l)K_1[H^+] + (a - \epsilon_A C_T l)K_1K_2 = 0 \quad \text{(Eq. 9)}$$

where ϵ_C and ϵ_A are the molar absorptivities of the cation and anion, respectively, and ϵ_U may pragmatically be taken as the molar absorptivity of the uncharged species. The actual significance of ϵ_U may be explained as follows. At the analytical wavelength:

$$A = \epsilon_C[C]l + \epsilon_N[N]l + \epsilon_Z[Z]l + \epsilon_A[A]l \quad \text{(Eq. 10)}$$

where [C], [N], [Z], and [A] are the equilibrium concentrations of cation, neutral molecule, zwitterion, and anion, respectively, and ϵ_N and ϵ_Z are the molar absorptivities of the neutral molecule and the zwitterion, respectively. If the total absorbance of uncharged species U is given by:

$$\epsilon_U[U]l = \epsilon_N[N]l + \epsilon_Z[Z]l \quad \text{(Eq. 11)}$$

where [U] is the total concentration of uncharged species, then:

$$\epsilon_U = \frac{\epsilon_N[N] + \epsilon_Z[Z]}{[U]} \quad \text{(Eq. 12)}$$

but:

$$[U] = [N] + [Z] \quad \text{(Eq. 13)}$$

so:

$$\epsilon_U = \frac{\epsilon_N[N] + \epsilon_Z[Z]}{[N] + [Z]} \quad \text{(Eq. 14)}$$

Consequently, ϵ_U may be defined as the composite molar absorptivity, at the analytical wavelength, of both uncharged species, weighted for the relative contributions of the neutral and zwitterionic species to this composite. The solution of Eq. 10 for at least three values of $[H^+]$ and the corresponding values of a in the spectrophotometric titration gives the values of K_1, K_1K_2, and ϵ_U satisfying these simultaneous equations (8).

Equation 14 may be rearranged to give:

$$\frac{[N]}{[Z]} = \frac{\epsilon_U - \epsilon_Z}{\epsilon_N - \epsilon_U} = K_{NZ} \quad \text{(Eq. 15)}$$

The value of K_{NZ} obtained in this manner could be used to resolve K_1 and K_2 into the component microequilibrium constants. However, because the uncharged species cannot be isolated, ϵ_N and ϵ_Z are generally unknown. In some cases, notably when one ionizing group is intimately coupled to the π-system of the chromophore and one is not, it is possible to equate ϵ_Z or ϵ_N to ϵ_C and the other to ϵ_A. Since ϵ_C and ϵ_A can be determined directly, K_{NZ} can be evaluated (9, 10).

In molecules like the aminobenzoic acids, however, both ionizing groups are intimately coupled to the chromophoric part of the molecule and this approach is not possible. However, in some molecules such as the aminobenzoic acids, the dissociation of one functional group (*e.g.*, the carboxyl group) produces a blue shift and the dissociation of the other group (*e.g.*, the amino group) produces a red shift of the absorption spectrum. The spectral maxima of the neutral and zwitterionic forms may then be sufficiently separated that an analytical wavelength may be chosen where the molar absorptivity of one uncharged species will be appreciable while that of the other will be negligible.

In the aminobenzoic acids, if the analytical wavelength is chosen as the long wavelength absorption maximum of the neutral molecule, $\epsilon_Z = 0$ in all three isomers. Hence, Eq. 15 reduces to:

$$K_{NZ} = \frac{\epsilon_U}{\epsilon_N - \epsilon_U} \quad \text{(Eq. 16)}$$

The molar absorptivity of a substituted aromatic molecule is determined by the degree of electronic interaction of the substituents with the aromatic π-system. The greater the degree of interaction, the greater is the extent to which the selection rules governing the probability of electronic transition in the unsubstituted aromatic nucleus break down. In the longer wavelength absorptions of benzenoid molecules, the electronic transitions are forbidden by the angular momentum selection rule (11). Hence, the presence of strongly interacting substituents on a benzene ring tends to intensify the long wavelength absorption bands. This action is illustrated in the hydroxybenzoic acids (Table II), where the species having the neutral carboxyl groups and the most highly dissociated hydroxyl groups have the highest absorptivities.

In the aminobenzoic acids, the neutrality of the amino and carboxyl groups results in the strongest coupling of the functional groups with the ring and, hence, the most intense absorption bands. Protonation of the amino group or dissociation of the carboxyl group destroys electronic coupling with the aromatic ring and, therefore, results in weaker absorption bands than in the neutral molecule. For this reason, ϵ_C and ϵ_A would be poor substitutes for ϵ_N in Eq. 16. The esters of the aminobenzoic acids, however, have electronic configurations that should closely approximate those of the neutral aminobenzoic acids. This theory is supported by the fact that the neutral hydroxybenzoic acids have molar absorptivities, at their absorption maxima, similar to those of their uncharged ethers and esters at their absorption maxima (the maximum relative deviation is 15%). Moreover, the singly charged anions of the hydroxybenzoic acids (ionized at the carboxyl groups) have molar absorptivities similar to those of the anions derived from the methoxybenzoic acids (also ionized at the carboxyl groups).

Consequently, it is permissible to equate $\epsilon_{N'}$, the molar absorptivity of the neutral aminobenzoic ester at its absorption maximum, with ϵ_N, the molar absorptivity of the corresponding neutral aminobenzoic acid at its absorption maximum. Equation 16 then becomes:

$$K_{NZ'} = \frac{\epsilon_U}{\epsilon_{N'} - \epsilon_U} \quad \text{(Eq. 17)}$$

Table III—Microequilibrium Constants for the Protolytic Dissociations of the Aminobenzoic Acids Calculated from the Macroequilibrium Constants K_1 and K_2 and the Spectroscopic Data in Table I

Isomer	$K_{NZ'}$	K_{CN}	K_{CZ}	K_{NA}	K_{ZA}
ortho	0.93	3.7×10^{-3}	4.0×10^{-3}	2.3×10^{-5}	2.2×10^{-5}
meta	0.38	2.1×10^{-4}	5.5×10^{-4}	6.6×10^{-5}	2.5×10^{-5}
para	12.3	3.60×10^{-3}	3.0×10^{-4}	1.54×10^{-5}	1.89×10^{-4}

Table IV—Microequilibrium Constants for the Protolytic Dissociations of the Aminobenzoic Acids Calculated from the Macroequilibrium Constants K_1 and K_2 and the Dissociation Constants of Their Methyl Esters ($K_{CN'}$)

Isomer	K_{NZ}	$K_{CN'}$[a]	K_{CZ}	K_{NA}	K_{ZA}
ortho	7.9	6.90×10^{-3}	8.7×10^{-4}	1.3×10^{-5}	1.0×10^{-4}
meta	0.57	2.75×10^{-4}	4.9×10^{-4}	5.0×10^{-5}	2.9×10^{-5}
para	−16	4.17×10^{-3}	-2.7×10^{-4}	-1.5×10^{-5}	-2.3×10^{-4}
	8.5	3.49×10^{-3} (ethyl ester)[b]	4.1×10^{-4}	1.6×10^{-5}	1.3×10^{-4}

[a] From Refs. 4 and 5. [b] Determined spectrophotometrically in this work.

Since the maximum error in substituting ϵ_N' for ϵ_N is ~15% for the hydroxybenzoic acids, it may be assumed that this value is the order of maximum error in substituting ϵ_N' for ϵ_N for the aminobenzoic acids.

In the present study, the literature values of the macroequilibrium constants K_1 and K_2 (2) are used and Eq. 9 is rearranged to solve for ϵ_U for each of the aminobenzoic acids, using the absorptiometric titration data represented in Fig. 1, according to:

$$\epsilon_U = \frac{(a - \epsilon_C C_T l)[H^+]^2 + (a - \epsilon_A C_T l)K_1K_2 + aK_1[H^+]}{C_T l K_1[H^+]} \quad \text{(Eq. 18)}$$

The values of ϵ_U thus obtained are presented in Table I. These values, along with those of ϵ_N' (Table I), are employed in Eq. 17 to calculate the value of K_{NZ}' which approximates the true tautomeric equilibrium ratio K_{NZ} of each aminobenzoic acid. The values of K_{NZ}', calculated in this manner, as well as those calculated from the literature K_1, K_2, and K_{CN}' values, are also presented in Tables III and IV for comparison.

The agreement between the microequilibrium constants calculated by both methods is quite good for the *meta*-isomer. However, in the *ortho*-isomer, the spectroscopic method indicates that the neutral molecule and the zwitterion comprise almost equal fractions of the population of uncharged molecules, while the method using the K_{CN}' of the ester suggests that the neutral molecule is predominant over the zwitterion by about 8:1. Although it is difficult to establish unequivocally which approach is more accurate, the disparity between the results obtained in this case for the *para*-isomer is more definitive. The spectroscopic method indicates that the neutral molecule predominates over the zwitterion in *p*-aminobenzoic acid by 12.3:1. However, the K_{CN}' of the methyl ester yields a negative value for the tautomeric ratio, a result that is physically impossible and is transmitted into the calculations of the remaining microconstants.

The K_{CN}' of the ethyl ester of *p*-aminobenzoic acid was determined. Use of this value to calculate the microconstants of the *para*-isomer gives microconstants in reasonably good agreement with those obtained by the spectroscopic method. Hence, the microconstants obtained by using the K_{CN}' of the ester are substantially dependent on the inductive effect (and other chemical effects) of the esterifying group. The absorptivities of the methyl and ethyl esters of *p*-aminobenzoic acid are, however, virtually identical; therefore, the spectroscopic method is, barring unusual steric interferences, free of uncertainties imposed by the nature of the esterifying group.

It is concluded, therefore, that the spectroscopic method described in this paper for estimating microequilibrium constants of prototropic reactions is, when applicable, simpler, faster, and more accurate than the conventional method, employing the dissociation constant of an alkylated derivative as equivalent to one microequilibrium constant of interest.

REFERENCES

(1) L. Ebert, *Z. Phys. Chem.*, **121**, 385 (1926).

(2) P. Lumme, *Suom. Kemistil.*, **30B**, 173 (1957).

(3) E. Q. Adams, *J. Am. Chem. Soc.*, **38**, 1503 (1916).

(4) J. Johnson and A. C. Cummings, *Z. Phys. Chem.*, **57**, 557 (1907).

(5) *Ibid.*, **57**, 574 (1907).

(6) A. Bryson, M. Davies, and E. P. Serjeant, *J. Am. Chem. Soc.*, **85**, 1933 (1963).

(7) J. F. J. Dippy, *Chem. Rev.*, **25**, 151 (1939).

(8) R. Robinson and A. I. Biggs, *Aust. J. Chem.*, **10**, 128 (1957).

(9) J. T. Edsall, R. B. Martin, and B. R. Hollingsworth, *Proc. Natl. Acad. Sci. USA*, **44**, 505 (1958).

(10) R. J. Sturgeon and S. G. Schulman, *J. Pharm. Sci.*, **66**, 958 (1977).

(11) J. N. Murrell, "The Theory of the Electronic Spectra of Organic Molecules," Wiley, New York, N.Y., 1963, chap. 6.

ACKNOWLEDGMENTS

The authors are grateful to Ms. Rebecca McKinley for typing the manuscript.

Comparative Pharmacokinetics of Coumarin Anticoagulants XXXIII: Frequency Distribution of Dicumarol Total Clearance in Rats

CHII-MING LAI and GERHARD LEVY ˣ

Received March 31, 1977, from the *Department of Pharmaceutics, School of Pharmacy, State University of New York at Buffalo, Amherst, NY 14260.* Accepted for publication May 12, 1977.

Abstract □ The total clearance of dicumarol was determined in 172 adult male Sprague–Dawley rats. Clearance values ranged from 1.46 to 27.0 ml/hr/kg. Statistical analysis of a histogram of the total clearance values indicated a trimodal distribution, with modes at 6.28, 14.8, and 23.7 ml/hr/kg. The percentage of animals in each of these components was 60.5, 33.7, and 5.8. A previous study had shown that the total clearance of dicumarol was proportional to the fraction of nonprotein-bound drug in serum (serum free fraction) and that interindividual differences in total clearance of dicumarol in rats were due almost entirely to corresponding differences in the serum free fraction. Therefore, it is likely that the observed trimodal frequency distribution of total clearance values reflects a similar distribution of serum free fraction values of dicumarol. The frequency distribution curve for dicumarol total clearance is very similar to the trimodal frequency distribution curve for warfarin serum free fraction values in rats. This observation is consistent with the previously demonstrated strong correlation of serum free fraction values of dicumarol and warfarin in individual animals.

Keyphrases □ Dicumarol—total clearance in rats, frequency distribution □ Clearance, total—dicumarol in rats, frequency distribution □ Pharmacokinetics—total clearance of dicumarol in rats, frequency distribution □ Coumarin anticoagulants—dicumarol, total clearance in rats, frequency distribution □ Anticoagulants—dicumarol, total clearance in rats, frequency distribution

Pronounced differences exist in the elimination kinetics of dicumarol in animals and humans. Vesell and Page (1) found that the dicumarol biological half-life ($t_{1/2}$) in 28 healthy adult humans not taking other drugs ranged from 7 to 74 hr and that these values were reproducible upon subsequent administration of a second dose. Studies in this laboratory revealed a $t_{1/2}$ range of 5.1–27.9 hr and a total clearance range of 2.6–24.0 ml/hr/kg in 30 adult male Sprague–Dawley rats (2). Such differences have been found repeatedly and are also well reproducible (2, 3).

The dicumarol $t_{1/2}$ was determined in human subjects after administration of a standard oral dose, and these

Since the maximum error in substituting ϵ_N' for ϵ_N is ~15% for the hydroxybenzoic acids, it may be assumed that this value is the order of maximum error in substituting ϵ_N' for ϵ_N for the aminobenzoic acids.

In the present study, the literature values of the macroequilibrium constants K_1 and K_2 (2) are used and Eq. 9 is rearranged to solve for ϵ_U for each of the aminobenzoic acids, using the absorptiometric titration data represented in Fig. 1, according to:

$$\epsilon_U = \frac{(a - \epsilon_C C_T l)[H^+]^2 + (a - \epsilon_A C_T l)K_1K_2 + aK_1[H^+]}{C_T l K_1[H^+]} \quad \text{(Eq. 18)}$$

The values of ϵ_U thus obtained are presented in Table I. These values, along with those of ϵ_N' (Table I), are employed in Eq. 17 to calculate the value of K_{NZ}' which approximates the true tautomeric equilibrium ratio K_{NZ} of each aminobenzoic acid. The values of K_{NZ}', calculated in this manner, as well as those calculated from the literature K_1, K_2, and K_{CN}' values, are also presented in Tables III and IV for comparison.

The agreement between the microequilibrium constants calculated by both methods is quite good for the *meta*-isomer. However, in the *ortho*-isomer, the spectroscopic method indicates that the neutral molecule and the zwitterion comprise almost equal fractions of the population of uncharged molecules, while the method using the K_{CN}' of the ester suggests that the neutral molecule is predominant over the zwitterion by about 8:1. Although it is difficult to establish unequivocally which approach is more accurate, the disparity between the results obtained in this case for the *para*-isomer is more definitive. The spectroscopic method indicates that the neutral molecule predominates over the zwitterion in *p*-aminobenzoic acid by 12.3:1. However, the K_{CN}' of the methyl ester yields a negative value for the tautomeric ratio, a result that is physically impossible and is transmitted into the calculations of the remaining microconstants.

The K_{CN}' of the ethyl ester of *p*-aminobenzoic acid was determined. Use of this value to calculate the microconstants of the *para*-isomer gives microconstants in reasonably good agreement with those obtained by the spectroscopic method. Hence, the microconstants obtained by using the K_{CN}' of the ester are substantially dependent on the inductive effect (and other chemical effects) of the esterifying group. The absorptivities of the methyl and ethyl esters of *p*-aminobenzoic acid are, however, virtually identical; therefore, the spectroscopic method is, barring unusual steric interferences, free of uncertainties imposed by the nature of the esterifying group.

It is concluded, therefore, that the spectroscopic method described in this paper for estimating microequilibrium constants of prototropic reactions is, when applicable, simpler, faster, and more accurate than the conventional method, employing the dissociation constant of an alkylated derivative as equivalent to one microequilibrium constant of interest.

REFERENCES

(1) L. Ebert, *Z. Phys. Chem.*, **121**, 385 (1926).

(2) P. Lumme, *Suom. Kemistil.*, **30B**, 173 (1957).

(3) E. Q. Adams, *J. Am. Chem. Soc.*, **38**, 1503 (1916).

(4) J. Johnson and A. C. Cummings, *Z. Phys. Chem.*, **57**, 557 (1907).

(5) *Ibid.*, **57**, 574 (1907).

(6) A. Bryson, M. Davies, and E. P. Serjeant, *J. Am. Chem. Soc.*, **85**, 1933 (1963).

(7) J. F. J. Dippy, *Chem. Rev.*, **25**, 151 (1939).

(8) R. Robinson and A. I. Biggs, *Aust. J. Chem.*, **10**, 128 (1957).

(9) J. T. Edsall, R. B. Martin, and B. R. Hollingsworth, *Proc. Natl. Acad. Sci. USA*, **44**, 505 (1958).

(10) R. J. Sturgeon and S. G. Schulman, *J. Pharm. Sci.*, **66**, 958 (1977).

(11) J. N. Murrell, "The Theory of the Electronic Spectra of Organic Molecules," Wiley, New York, N.Y., 1963, chap. 6.

ACKNOWLEDGMENTS

The authors are grateful to Ms. Rebecca McKinley for typing the manuscript.

Comparative Pharmacokinetics of Coumarin Anticoagulants XXXIII: Frequency Distribution of Dicumarol Total Clearance in Rats

CHII-MING LAI and GERHARD LEVY ˣ

Received March 31, 1977, from the *Department of Pharmaceutics, School of Pharmacy, State University of New York at Buffalo, Amherst, NY 14260.* Accepted for publication May 12, 1977.

Abstract □ The total clearance of dicumarol was determined in 172 adult male Sprague–Dawley rats. Clearance values ranged from 1.46 to 27.0 ml/hr/kg. Statistical analysis of a histogram of the total clearance values indicated a trimodal distribution, with modes at 6.28, 14.8, and 23.7 ml/hr/kg. The percentage of animals in each of these components was 60.5, 33.7, and 5.8. A previous study had shown that the total clearance of dicumarol was proportional to the fraction of nonprotein-bound drug in serum (serum free fraction) and that interindividual differences in total clearance of dicumarol in rats were due almost entirely to corresponding differences in the serum free fraction. Therefore, it is likely that the observed trimodal frequency distribution of total clearance values reflects a similar distribution of serum free fraction values of dicumarol. The frequency distribution curve for dicumarol total clearance is very similar to the trimodal frequency distribution curve for warfarin serum free fraction values in rats. This observation is consistent with the previously demonstrated strong correlation of serum free fraction values of dicumarol and warfarin in individual animals.

Keyphrases □ Dicumarol—total clearance in rats, frequency distribution □ Clearance, total—dicumarol in rats, frequency distribution □ Pharmacokinetics—total clearance of dicumarol in rats, frequency distribution □ Coumarin anticoagulants—dicumarol, total clearance in rats, frequency distribution □ Anticoagulants—dicumarol, total clearance in rats, frequency distribution

Pronounced differences exist in the elimination kinetics of dicumarol in animals and humans. Vesell and Page (1) found that the dicumarol biological half-life ($t_{1/2}$) in 28 healthy adult humans not taking other drugs ranged from 7 to 74 hr and that these values were reproducible upon subsequent administration of a second dose. Studies in this laboratory revealed a $t_{1/2}$ range of 5.1–27.9 hr and a total clearance range of 2.6–24.0 ml/hr/kg in 30 adult male Sprague–Dawley rats (2). Such differences have been found repeatedly and are also well reproducible (2, 3).

The dicumarol $t_{1/2}$ was determined in human subjects after administration of a standard oral dose, and these

Table I—Evaluation of Different Types of Frequency Distribution Curves for Dicumarol Total Clearance in Rats

Type of Distribution	Means, ml/hr/kg	*SD*'s	Number of Rats in Each Component	χ^2	Degrees of Freedom	*p*
Normal	9.97	5.75	172	54.0	11	<0.00001
Log-normal	8.51	+6.51, −3.69	172	18.0	10	≃0.055
Bimodal	6.28	2.07	96	16.3	9	≃0.057
	16.7	3.65	76			
Log-bimodal	6.27	+2.25, −1.65	108[a]	7.34	6	≃0.285
	14.7	+4.51, −3.44	63			
Trimodal	6.28	2.07	104	4.46	7	≃0.709
	14.8	2.67	58			
	23.7	1.45	10			

[a] One rat with a total clearance of 1.46 ml/hr/kg was excluded due to a large discontinuity in the histogram.

values were corrected for presumed differences in dicumarol absorption since its elimination kinetics are dose dependent in humans (4). A histogram of these $t_{1/2}$ values is apparently unimodal. Solomon and Schrogie (5) reported that the frequency distribution of dicumarol $t_{1/2}$ values in rabbits is apparently bimodal, but details were not provided. On the other hand, Millar *et al.* (6) found that rabbits can be divided arbitrarily into four groups on the basis of the change in prothrombin time produced by a standard dicumarol dose. However, it appears that the prothrombin times in that study may be trimodally distributed.

The $t_{1/2}$ and total clearance of dicumarol in 172 rats were determined in this laboratory over the last several years as a screening procedure for the selection of animals for studies of dicumarol and warfarin pharmacokinetics. The frequency distribution of the dicumarol total clearance in these rats has now been characterized and related to other relevant information obtained previously in this series of investigations.

EXPERIMENTAL

Five groups of adult male Sprague–Dawley rats[1], 187–280 g, were given unrestricted access to food[2] and water before and during the pharmacokinetic study. None received any drugs previously. The studies were carried out in different seasons between 1973 and 1975.

A single dose of ^{14}C-dicumarol, 8 mg/kg iv, was injected, and 0.45-ml blood samples were obtained from the tail artery every 3–6 hr for 24 hr. Plasma was separated and extracted, and the extract was analyzed for total (free and bound) unmetabolized dicumarol as previously described (7, 8). The total dicumarol clearance, *i.e.*, the product of the apparent first-order elimination rate constant and the apparent volume of distribution, was calculated from the slope and intercept of the least-squares regression line of a plot of log dicumarol concentration *versus* time.

Histograms to describe the frequency distribution of the total clearance or log total clearance values were constructed by iteratively changing the class interval to maximize the number of bars in the respective histogram while minimizing the number of regional reversals (modes and antimodes), as suggested by Martin *et al.* (9). For the multimodal characterizations, the mean values, standard deviations, and percentages of the total number of animals in each Gaussian component were estimated as described by Bhattacharya (10). The logarithm of the clearance values was used in these calculations when indicated. Distribution curves were fitted to the histograms (11), and the expected frequencies for overlapping components were summed prior to evaluating the agreement of the distribution model with the histogram by χ^2 test.

RESULTS

The total clearance of dicumarol in the 172 rats ranged from 1.46 to 27.0 ml/hr/kg. These determinations were made at different times of the year, between May 1973 and March 1975, on groups of 26–56 animals. Histograms of the results obtained from each of the five groups are shown in Fig. 1. There was no statistically significant difference between the frequency distribution of the data from each group of animals, as determined by the Kruskall–Wallis nonparametric one-way analysis of variance (12). Consequently, all data were combined for determination of the frequency distribution characteristics of the total clearance values.

The characteristics of the different types of frequency distribution curves fitted to the data and the results of their statistical evaluation are summarized in Table I. There was a highly statistically significant difference between the normal distribution curve and the histogram and a borderline difference between the log normal and bimodal curves and the respective histograms. A reasonably good fit was obtained with the log-bimodal distribution curve, but the best fit was obtained with the trimodal distribution curve.

According to the trimodal distribution model, 60.5% of the animals were in the component with the lowest clearance (mean ± *SD* = 6.28 ± 2.07 ml/hr/kg), 33.7% were in the component with intermediate clearance (14.8 ± 2.67 ml/hr/kg), and 5.8% were in the component with the highest clearance (23.7 ± 1.45 ml/hr/kg). The combined histogram for all 172 animals and the trimodal distribution curve fitted to the data are shown in Fig. 2.

There was no statistically significant correlation between the total clearance and either the apparent volume of distribution of dicumarol (*milliliters per kilogram*) or the body weight (indicative of age) of the animals.

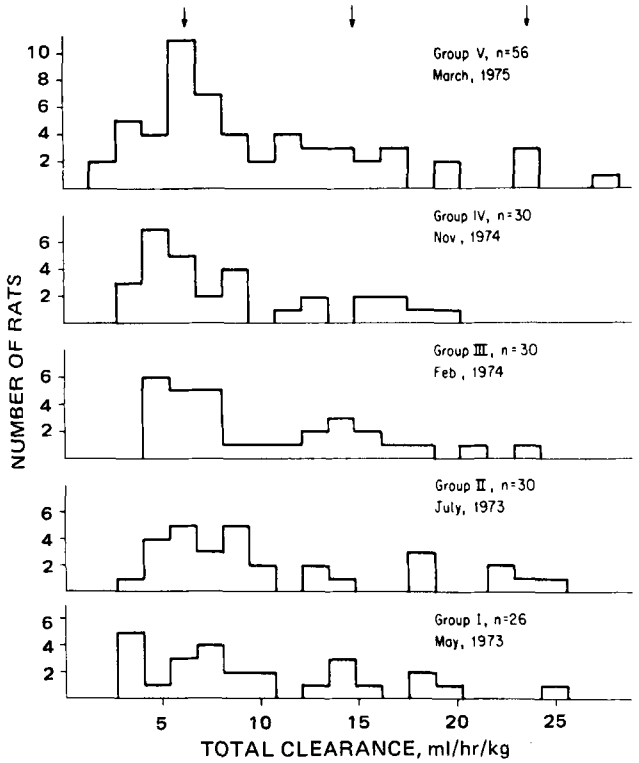

Figure 1—*Frequency distribution of dicumarol total clearance values in each of five groups of adult male Sprague–Dawley rats. The arrows on the abscissa indicate the means of the Gaussian components of the trimodal distribution curve shown in Fig. 2.*

[1] Blue Spruce Farms, Altamont, N.Y.
[2] Charles River Formula 4RF.

Table II—Comparison of the Frequency Distribution Characteristics of Dicumarol Total Clearance and Serum Free Fraction of Warfarin in Rats

Parameter	Relative Mean of Each Component[a]			Percentage of Animals in Each Component		
	Component I	Component II	Component III	Component I	Component II	Component III
Total clearance of dicumarol	0.265	0.624	1.0	60.5	33.7	5.8
Serum free fraction of warfarin[b]	0.239	0.675	1.0	53.6	27.2	19.2

[a] Relative to the mean of Component III. [b] From Ref. 17.

DISCUSSION

The total clearance of dicumarol in rats is proportional to the serum free fraction of the drug (13). This result is consistent with theoretical considerations (14) and was demonstrated previously with respect to warfarin in rats (15) and humans (16). Intersubject differences in serum protein binding are largely responsible for the observed differences in the total clearance of these anticoagulants (13–16). Thus, it is reasonable to assume that the frequency distribution characteristics of dicumarol total clearance determined in this investigation reflect a corresponding frequency distribution of serum free fraction values of dicumarol.

Since there is a strong correlation between the serum free fraction values of dicumarol and warfarin in individual rats (2), it may be expected that the frequency distribution characteristics of dicumarol total clearance and warfarin serum free fraction are quite similar in the same strain of rats. The frequency distribution of serum free fraction values of warfarin determined in this laboratory in rats from the same strain and source as those used in the present investigation was trimodal (17). A quantitative comparison of the dicumarol and warfarin frequency distribution characteristics is presented in Table II. Considering the fact that these studies were performed with different animals and by different investigators, the similarity of the frequency distribution characteristics is striking[3].

Multimodal frequency distribution characteristics can occur as artifacts caused by combining different groups of animals. These groups may differ in age, environmental history (*e.g.*, exposure to enzyme-inducing pesticides), or physiological status related to the season of the year. These types of artifacts were ruled out to the best of our ability in this investigation.

If the trimodal frequency distribution of dicumarol total clearance values in rats is a genetic effect, it would be ideal to carry out multigeneration studies. Motulsky (4) pointed out that when a population can be categorized into clearly distinct classes by some measurement and a multimodal frequency distribution curve is obtained, the involvement of a single gene may be suspected. The trimodality of the dicumarol total clearance data in rats suggests the existence of three genotypic classes, consisting of two homozygous groups and one heterozygous group and representing small, intermediate, and large clearance phenotypes. Since the large intersubject variation of dicumarol and warfarin serum free fraction values cannot be explained by corresponding variations in the concentration of serum albumin or total proteins, it may be due to quantitative differences in the serum concentration of endogenous inhibitor(s) of drug binding to proteins or qualitative differences in albumin (15, 18). Intersubject variations in the serum concentration of endogenous inhibitors could be due to genetically determined differences in the formation rate or clearance of these compounds.

The results of studies in rabbits performed more than 30 years ago were interpreted to indicate that recessive genes play a role in the biotransformation of dicumarol (19). More recently, Motulsky (4) found a sibling–sibling correlation of dicumarol half-life values, but no parent–offspring correlation, and concluded that these findings are indicative of the operation of recessive genes in the elimination of dicumarol. Subsequently, Vesell and Page (1) determined the dicumarol biological half-life in seven sets of identical twins and seven sets of fraternal twins who were not taking other drugs. The half-life values were almost identical in each set of identical twins but significantly different in each set of fraternal twins. These investigators concluded that the dicumarol biological half-life is under genetic control.

None of these studies revealed the biochemical site of the genetic effect, and in none was the serum free fraction of the drug determined. On the other hand, some rats in this study were used to determine the serum free fraction value of dicumarol, and a linear relationship between this parameter and the total clearance of dicumarol was found (13). Vesell and Page (1) observed a strong correlation between the half-life values of the extensively (>99%) serum protein-bound drugs dicumarol and phenylbutazone in the same subjects and no apparent correlation between the half-life values of either of these drugs and that of the poorly (<10%) serum protein-bound drug antipyrine. They speculated that the correlation of dicumarol and phenylbutazone half-life values may be related to their extensive serum protein binding. It would be of interest, therefore, to determine the serum protein binding of dicumarol and phenylbutazone in the same sets of identical and fraternal twins. One such twin study, carried out with nortriptyline, revealed that the plasma protein binding of this drug in humans is partly under genetic control (20).

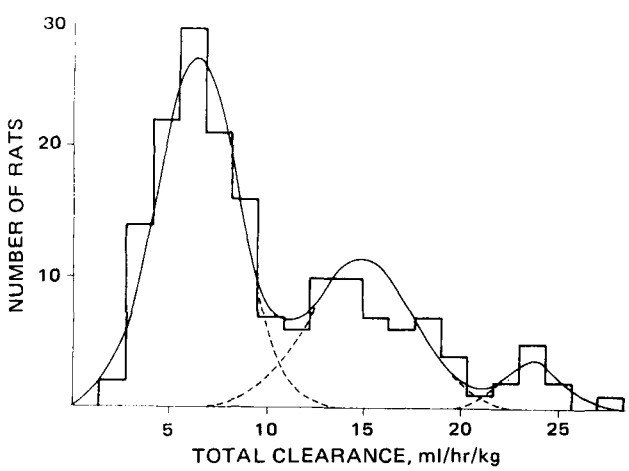

Figure 2—*Composite histogram showing the frequency distribution of dicumarol total clearance values for all 172 rats. Also shown is the trimodal distribution curve fitted to the data, with the dotted lines indicating the overlapping portions of the individual Gaussian components.*

[3] An explanation for the use of total clearance as a screening parameter for dicumarol studies and serum free fraction as a screening parameter for warfarin experiments is in order. Theoretically, either parameter is suitable. We know now (but did not know when these investigations were started) that either drug can be used to screen for rapid and slow eliminators of one or the other anticoagulant. It is technically easier, and more rapid, to determine serum free fraction values, but the dicumarol free fraction is so small that these determinations are relatively imprecise. Therefore, total clearance was used as a screening parameter for dicumarol.

REFERENCES

(1) E. S. Vesell and J. G. Page, *J. Clin. Invest.*, **47**, 2657 (1968).

(2) A. Yacobi, C.-M. Lai, and G. Levy, *J. Pharm. Sci.*, **64**, 1995 (1975).

(3) C.-M. Lai, A. Yacobi, and G. Levy, *J. Pharmacol. Exp. Ther.*, **199**, 74 (1976).

(4) A. G. Motulsky, *Progr. Med. Genet.*, **3**, 49 (1964).

(5) H. M. Solomon and J. J. Schrogie, *Clin. Pharmacol. Ther.*, **8**, 65 (1967).

(6) G. J. Millar, L. B. Jaques, and M. Henriet, *Arch. Int. Pharmacodyn. Ther.*, **150**, 197 (1964).

(7) L. B. Wingard, Jr., and G. Levy, *J. Pharmacol. Exp. Ther.*, **184**, 253 (1973).

(8) E. Jähnchen, L. B. Wingard, Jr., and G. Levy, *ibid.*, **187**, 176 (1973).

(9) H. F. Martin, B. J. Gudzinowicz, and H. Fanger, "Normal Values in Clinical Chemistry; A Guide to Statistical Analysis of Laboratory Data," Dekker, New York, N.Y., 1975, pp. 142–154.

(10) C. G. Bhattacharya, *Biometrics*, **23**, 115 (1967).

(11) I. M. Chakravarti, R. G. Laha, and J. Roy, "Handbook of Methods of Applied Statistics, Vol. I: Techniques of Computation, Descriptive Methods and Statistical Inference," Wiley, New York, N.Y., 1967, p. 152.

(12) D. Colquhoun, "Lectures on Biostatistics: An Introduction to Statistics with Applications in Biology and Medicine," Clarendon, Oxford, England, 1971, pp. 191–195.
(13) C.-M. Lai and G. Levy, *J. Pharm. Sci.*, **66**, 1739 (1977).
(14) G. Levy and A. Yacobi, *ibid.*, **63**, 805 (1974).
(15) A. Yacobi and G. Levy, *ibid.*, **64**, 1660 (1975).
(16) A. Yacobi, J. A. Udall, and G. Levy, *Clin. Pharmacol. Ther.*, **19**, 552 (1976).
(17) J. T. Slattery, A. Yacobi, and G. Levy, *Life Sci.*, **19**, 447 (1976).
(18) A. Yacobi, J. T. Slattery, and G. Levy, *J. Pharm. Sci.*, in press.
(19) K. P. Link, *Harvey Lect.*, **39**, 162 (1943–1944). (Quoted in Ref. 4.)
(20) B. Alexanderson and O. Borgå, *Eur. J. Clin. Pharmacol.*, **4**, 196 (1972).

ACKNOWLEDGMENTS

Supported in part by Grant GM 20852 from the National Institute of General Medical Sciences, National Institutes of Health.

Previous paper in this series: G. Levy, C.-M. Lai, and A. Yacobi, *J. Pharm. Sci.*, **67**, 229 (1978).

Comparison of Two Methods for Obtaining Size Distribution Characteristics of Particulate Matter in Large-Volume Parenterals

JAMES BLANCHARD ˣ, JOHN A. SCHWARTZ, DALE M. BYRNE *, and DAVID B. MARX ‡

Received October 4, 1976, from the *Department of Pharmaceutical Sciences, College of Pharmacy, University of Arizona, Tucson, AZ 85721.* Accepted for publication June 21, 1977. *Present address: Optical Sciences Center, University of Arizona, Tucson, AZ 85721. ‡Present address: College of Agriculture, University of Arizona, Tucson, AZ 85721.

Abstract □ The size distributions of the particulate matter present in six types of large-volume parenteral solutions, as determined by an automatic particle counter and a microscopic counting technique, were compared by plotting log $N_{>D}$ *versus* log D. The resulting data were analyzed individually and also as averages. The data showed a linear relationship between log $N_{>D}$ and log D over the 1–100-μm particle-size range, indicating that both methods determine a similar particle-size distribution. The data also indicated that the particle-size distributions were largely independent of the type of solution and obeyed a power law of the form $N_{>D} = N_{>1}D^K$. These observations suggest that the major source of contamination is air-borne dust particles, which fall into a solution randomly, and that it may be possible to monitor the smaller, more abundant particles with the automatic particle counter to obtain a rapid estimate of parenteral cleanliness. The automatic particle counter thus appears to be a viable alternative to the microscopic counting technique for assessing the particulate matter content of parenterals.

Keyphrases □ Size distribution—particulate matter in six large-volume parenteral solutions, automatic particle counter and microscopic techniques compared □ Distribution, size—particulate matter in six large-volume parenteral solutions, automatic particle counter and microscopic techniques compared □ Particles—size distribution in six large-volume parenteral solutions, automatic particle counter and microscopic techniques compared □ Parenterals, large volume—six types, size distribution of particulate matter, automatic particle counter and microscopic techniques compared □ Dosage forms—large-volume parenterals, six types, size distribution of particulate matter, automatic particle counter and microscopic techniques compared

Particulate matter has been defined as "extraneous, mobile, undissolved substances, other than gas bubbles, unintentionally present in parenteral solutions" (1). The problem of particulate matter has plagued the preparers of parenterals since their introduction. Although the clinical significance of particulate matter is still somewhat controversial, it is generally accepted that the safest approach is to minimize particulate matter as much as possible (2–4).

Standards set by the USP–NF (1), based on a microscopic counting procedure, limit the allowable levels of particulate contamination. While this method is the accepted standard, it suffers from several shortcomings since it is subjective, tedious, and time consuming and requires a considerable amount of practice before the operator becomes proficient. In addition, the method is destructive and, therefore, not ideally suited for the in-line monitoring of production batches of parenterals. It is highly desirable to find an alternative method that will overcome these limitations.

In a previous study (5), the ability of several methods to monitor the levels of particulate matter in parenterals was compared. The automatic particle counter warranted further investigation since it offered some advantages over the other methods tested. This instrument was first mentioned by Draftz and Graf (6) who described its characteristics. One apparent limitation of this instrument is its inability to count accurately small numbers of particles since the minimum detectable concentration is only 1 particle/ml. This limitation could be a serious drawback when monitoring particles larger than approximately 5 μm in diameter since sufficiently high counts to obtain statistically reliable data are not normally found in the relatively clean solutions available commercially.

This limitation does not necessarily preclude the use of the automatic particle counter in monitoring the particulate matter content of these solutions provided that the number of larger, less abundant particles (upon which the present compendial standard is based) can be determined from the number of smaller, more abundant particles. The major goals of this study were to determine if such a relationship exists and, if so, to characterize its nature.

EXPERIMENTAL

Large-volume parenteral solutions[1] (1000 ml) were inspected by two methods: an instrumental technique using an automatic particle counter[2]

[1] McGaw Laboratories, Glendale, CA 91201.
[2] Prototron model ILI 1000, Spectrex Corp., Redwood City, CA 94063.

(12) D. Colquhoun, "Lectures on Biostatistics: An Introduction to Statistics with Applications in Biology and Medicine," Clarendon, Oxford, England, 1971, pp. 191–195.
(13) C.-M. Lai and G. Levy, *J. Pharm. Sci.*, **66**, 1739 (1977).
(14) G. Levy and A. Yacobi, *ibid.*, **63**, 805 (1974).
(15) A. Yacobi and G. Levy, *ibid.*, **64**, 1660 (1975).
(16) A. Yacobi, J. A. Udall, and G. Levy, *Clin. Pharmacol. Ther.*, **19**, 552 (1976).
(17) J. T. Slattery, A. Yacobi, and G. Levy, *Life Sci.*, **19**, 447 (1976).
(18) A. Yacobi, J. T. Slattery, and G. Levy, *J. Pharm. Sci.*, in press.
(19) K. P. Link, *Harvey Lect.*, **39**, 162 (1943–1944). (Quoted in Ref. 4.)
(20) B. Alexanderson and O. Borgå, *Eur. J. Clin. Pharmacol.*, **4**, 196 (1972).

ACKNOWLEDGMENTS

Supported in part by Grant GM 20852 from the National Institute of General Medical Sciences, National Institutes of Health.

Previous paper in this series: G. Levy, C.-M. Lai, and A. Yacobi, *J. Pharm. Sci.*, **67**, 229 (1978).

Comparison of Two Methods for Obtaining Size Distribution Characteristics of Particulate Matter in Large-Volume Parenterals

JAMES BLANCHARD ˣ, JOHN A. SCHWARTZ, DALE M. BYRNE *, and DAVID B. MARX ‡

Received October 4, 1976, from the *Department of Pharmaceutical Sciences, College of Pharmacy, University of Arizona, Tucson, AZ 85721.* Accepted for publication June 21, 1977. *Present address: Optical Sciences Center, University of Arizona, Tucson, AZ 85721. ‡Present address: College of Agriculture, University of Arizona, Tucson, AZ 85721.

Abstract □ The size distributions of the particulate matter present in six types of large-volume parenteral solutions, as determined by an automatic particle counter and a microscopic counting technique, were compared by plotting log $N_{>D}$ *versus* log D. The resulting data were analyzed individually and also as averages. The data showed a linear relationship between log $N_{>D}$ and log D over the 1–100-μm particle-size range, indicating that both methods determine a similar particle-size distribution. The data also indicated that the particle-size distributions were largely independent of the type of solution and obeyed a power law of the form $N_{>D} = N_{>1}D^K$. These observations suggest that the major source of contamination is air-borne dust particles, which fall into a solution randomly, and that it may be possible to monitor the smaller, more abundant particles with the automatic particle counter to obtain a rapid estimate of parenteral cleanliness. The automatic particle counter thus appears to be a viable alternative to the microscopic counting technique for assessing the particulate matter content of parenterals.

Keyphrases □ Size distribution—particulate matter in six large-volume parenteral solutions, automatic particle counter and microscopic techniques compared □ Distribution, size—particulate matter in six large-volume parenteral solutions, automatic particle counter and microscopic techniques compared □ Particles—size distribution in six large-volume parenteral solutions, automatic particle counter and microscopic techniques compared □ Parenterals, large volume—six types, size distribution of particulate matter, automatic particle counter and microscopic techniques compared □ Dosage forms—large-volume parenterals, six types, size distribution of particulate matter, automatic particle counter and microscopic techniques compared

Particulate matter has been defined as "extraneous, mobile, undissolved substances, other than gas bubbles, unintentionally present in parenteral solutions" (1). The problem of particulate matter has plagued the preparers of parenterals since their introduction. Although the clinical significance of particulate matter is still somewhat controversial, it is generally accepted that the safest approach is to minimize particulate matter as much as possible (2–4).

Standards set by the USP–NF (1), based on a microscopic counting procedure, limit the allowable levels of particulate contamination. While this method is the accepted standard, it suffers from several shortcomings since it is subjective, tedious, and time consuming and requires a considerable amount of practice before the operator becomes proficient. In addition, the method is destructive and, therefore, not ideally suited for the in-line monitoring of production batches of parenterals. It is highly desirable to find an alternative method that will overcome these limitations.

In a previous study (5), the ability of several methods to monitor the levels of particulate matter in parenterals was compared. The automatic particle counter warranted further investigation since it offered some advantages over the other methods tested. This instrument was first mentioned by Draftz and Graf (6) who described its characteristics. One apparent limitation of this instrument is its inability to count accurately small numbers of particles since the minimum detectable concentration is only 1 particle/ml. This limitation could be a serious drawback when monitoring particles larger than approximately 5 μm in diameter since sufficiently high counts to obtain statistically reliable data are not normally found in the relatively clean solutions available commercially.

This limitation does not necessarily preclude the use of the automatic particle counter in monitoring the particulate matter content of these solutions provided that the number of larger, less abundant particles (upon which the present compendial standard is based) can be determined from the number of smaller, more abundant particles. The major goals of this study were to determine if such a relationship exists and, if so, to characterize its nature.

EXPERIMENTAL

Large-volume parenteral solutions[1] (1000 ml) were inspected by two methods: an instrumental technique using an automatic particle counter[2]

[1] McGaw Laboratories, Glendale, CA 91201.
[2] Prototron model ILI 1000, Spectrex Corp., Redwood City, CA 94063.

Table I—Comparison of the Particle-Size Distribution Characteristics of Large-Volume Parenteral Solutions by Two Methods

Type of Solution	Method of Measurement[a]	Average Number of Particles per Milliliter[b] >1 μm	>10 μm	>25 μm	Average Slope (K) of Log–Log Plot ± SE	Average Correlation Coefficient between Log $N_{>D}$ and Log D
Dextrose, 5% in half-strength normal saline[c]	I	255.7	0.100	0.004	−3.4070 ± 0.2052	−0.9906
	M	76.6	0.473	0.062	−2.2094 ± 0.1327	−0.9800
Normal saline[d]	I	559.1	0.205	0.009	−3.4361 ± 0.4385	−0.9900
	M	306.7	0.967	0.098	−2.5012 ± 0.2512	−0.9906
Dextrose, 5% in multiple-electrolyte solution[e]	I	425.8	2.826	0.384	−2.1781 ± 0.2843	−0.9711
	M	148.2	1.386	0.216	−2.0291 ± 0.1358	−0.9909
Dextrose, 5% in normal saline[f]	I	1414.6	2.842	0.240	−2.6970 ± 0.4357	−0.9819
	M	252.7	0.966	0.105	−2.4177 ± 0.1787	−0.9908
Dextrose, 5% in water[g]	I	1284.1	6.784	0.842	−2.2771 ± 0.1500	−0.9920
	M	12.3	0.174	0.032	−1.8490 ± 0.1769	−0.9800
Dextrose, 5% in lactated Ringer's solution[h]	I	2084.8	2.409	0.163	−2.9372 ± 0.1672	−0.9881
	M	228.2	1.302	0.167	−2.2438 ± 0.2627	−0.9862

[a] I = instrumental; M = microscopic counting. [b] Average of six bottles. [c] Lot A5D324B. [d] Lot A5J450A. [e] Dextrose, 5% in Isolyte M, Lot A5J223C. [f] Lot A5J512B. [g] Lot A5H142B. [h] Lot A5K015C.

and a membrane filtration and microscopic technique. Six types of solutions were chosen on the basis of their extensive clinical use (Table I). Prior to examination, each container was assigned a code number; labels were removed by soaking to eliminate investigator bias. Before each container was examined by either method, it was inverted 20 times to resuspend any particulate matter in accordance with USP–NF recommendations (1).

Instrumental Method—The automatic particle counter employs a revolving laser beam to measure automatically the number of particles larger than a selected threshold setting using the principle of light scattering. This instrument is capable of detecting particles as small as 1 μm in diameter. Solutions were examined using the particle counter in the manner previously described (5). The number of particles per milliliter exceeding the following diameters was determined: 1.000, 1.259, 1.585, 1.995, 2.512, 3.162, 3.981, 5.012, and 6.310 μm. These diameters were chosen to facilitate data analysis since their logarithms are equally spaced.

Starting at 1 μm, particle counts were recorded at successively increasing threshold settings until a given setting produced 10 readings whose average was less than 10 particles/ml. This value was chosen to limit the instrumental error resulting from the fact that the automatic particle counter displays the truncated, rather than the rounded, version of the number of particles counted (5).

Membrane Filtration and Microscopic Method—All cleaning, collecting, and counting procedures were performed in a laminar flow hood[3] using a modification of a reported procedure (7). Blank analyses of membrane filters were run periodically to determine the efficiency of the cleaning procedure. The blanks were negligible in relation to the total particles counted in any sample tested. This method was used to count particles in the following size ranges: 10–25, 25–50, 50–100, and greater than 100 μm. To compare these results with those obtained using the instrumental method, the particle counts per milliliter exceeding the following diameters were calculated: 10, 25, 50, and 100 μm.

The data were analyzed using a general linear model employing a weighted least-squares regression. The differences among the intercepts for solution types, methods, and bottles were examined statistically. Differences among slopes were examined similarly after adjusting for intercept differences. The results are summarized in the form of an analysis of variance (ANOVA) table (Table II).

RESULTS AND DISCUSSION

Cadle (8) noted that particulate materials present in the atmosphere exhibit a particle-size distribution that obeys a power law of the form:

$$N_{>D} = N_{>1}D^{K} \qquad \text{(Eq. 1)}$$

where $N_{>D}$ is the number of particles per milliliter with a diameter larger than D, $N_{>1}$ is the number of particles per milliliter with a diameter larger than 1 μm, D is the particle diameter in micrometers, and K is a constant. Equation 1 can be expressed in the following logarithmic form:

$$\log N_{>D} = K \log D + \log N_{>1} \qquad \text{(Eq. 2)}$$

which is useful for expressing the particle-size distributions in parenterals in the form of a log–log plot (9). When expressed in this manner, K is the slope and $\log N_{>1}$ is the y-intercept of a plot of $\log N_{>D}$ *versus* $\log D$.

Linearity of Log–Log Plots—The data shown in Fig. 1 indicate that the particle-size distributions obtained in both the <10-μm region (using the automatic particle counter) and the >10-μm region (using the microscope) appear to be linear when plotted on a log–log scale. A weighted least-squares program executed on a digital computer[4] was used to fit the automatic particle counter data. The weighting factor was the reciprocal of the variance (10) since each data point represented the average of 10 readings.

This weighting procedure was used because the variances of the 10 readings recorded at each threshold setting were not equal since the numbers of particles exceeding the given threshold setting were not uniformly distributed in the volume of fluid examined. This phenomenon has been referred to as "schooling," analogous to the schooling of fish. Data obtained using the microscopic counting technique were fitted using an unweighted least-squares program because no precise statistical

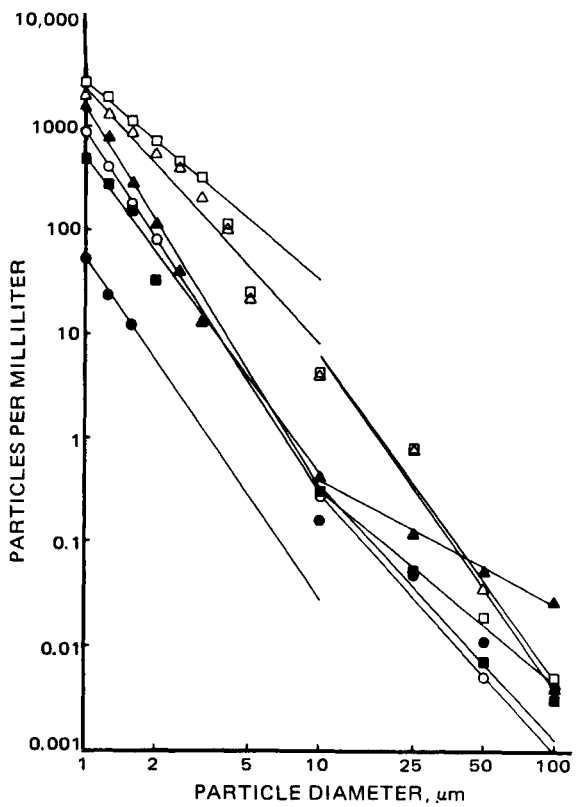

Figure 1—*Particle-size distributions for individual samples of three types of large-volume parenteral solutions. The two samples denoted by the open and closed symbols represent extremes of the slope* (K) *within a given solution type. Key:* ○ *and* ●, *dextrose, 5% in half-strength normal saline;* □ *and* ■, *dextrose, 5% in normal saline; and* △ *and* ▲, *dextrose, 5% in lactated Ringer's solution.*

[3] Model B-D 048, Envirco, Albuquerque, NM 87107.

[4] CDC 6400.

Table II—ANOVA to Test the Effects of Bottles, Methods, and Solution Types on the Slopes and Intercepts of the Log–Log Plots

Source of Variation[a]	*df*	*SS*	*MS*	*F*
S_α	5	15.026	3.005	4.03[b]
B/S_α	27	20.126	0.745	27.90[b]
M_α	1	7.600	7.600	13.35[b]
MS_α	5	13.032	2.606	4.58[b]
BM/S_α	27	15.364	0.569	21.30[b]
S_β	5	0.962	0.192	1.70
B/S_β	27	3.056	0.113	4.24[b]
M_β	1	0.077	0.077	3.50
MS_β	5	0.053	0.011	0.48
BM/S_β	27	0.596	0.022	0.83
Residual	191	5.103	0.027	—

[a] α = intercept, β = slope, S = solution type, B = bottle, and M = method. [b] Significant at the 0.05 level.

weighting factor was calculated since each filter was only counted once.

The correlation coefficients varied from −0.9561 to −0.9991 for the weighted instrumental data and from −0.9431 to −0.9998 for the unweighted microscopic data. These values justify the use of Eq. 2 to describe the particle-size distributions observed. The linear nature of this relationship is further exemplified in Fig. 1.

Intercepts of Log–Log Plots (log $N_{>1}$)—As previously indicated, the intercept of the log–log plot described by Eq. 2 equals the logarithm of the number of particles per milliliter exceeding 1 μm in diameter. As derived from data obtained using the automatic particle counter, the intercepts imply a variation of 53.20–2853 particles/ml among the individual bottles tested. The statistical analyses demonstrated that the intercepts for data obtained from individual bottles of a given solution type differed significantly ($F_{27,191}$ = 27.90) and also exhibited a significant method by bottle interaction ($F_{27,191}$ = 21.30). This variation in the intercept values (Fig. 1) is merely indicative of the different levels of contamination (>1 μm) in each individual bottle of a given solution type.

The intercepts for each type of solution were then averaged to minimize this sample-to-sample variation. The resulting average values for the intercepts, as determined by the automatic particle counter, imply a range of 255.7–2084.8 particles/ml (Fig. 2). The values indicate that the number of particles exceeding 1 μm based on an average of six samples varies with the type of solution examined. The statistical analyses demonstrated that the intercepts for data pertaining to the six solution types differed significantly ($F_{5,27}$ = 4.03) as determined by both methods. In addition, the differences in the intercepts from method to method were not constant (*i.e.*, varied in magnitude) between solution types ($F_{5,27}$ = 4.58). These differences are not surprising in view of the temporal variations in air quality likely to exist during the filling operation. All solutions appeared relatively clean in relation to the USP–NF standard (1), which implies an intercept of 16,280 particles/ml >1 μm.

Slopes of Log–Log Plots (K)—The slopes of the least-squares-fitted lines of the individual samples, as determined using either instrumental data or microscopic counting data, varied from −1.6616 to −4.8293 and from −1.1595 to −3.7303, respectively. These ranges are consistent with those previously reported (9, 11). These observations, together with Fig. 1, indicate that the value of K in Eqs. 1 and 2 varies from bottle to bottle. This result implies that the particle-size distributions differ among individual bottles and that the log–log plots of these distributions may not be parallel to one another.

The statistical analyses demonstrated that the slopes for data obtained from individual bottles of a given solution type were significantly different ($F_{27,191}$ = 4.24). However, for an individual bottle of a given solution type, the slopes were not significantly different from method to method ($F_{27,191}$ = 0.83). The data presented in Fig. 1 were chosen to illustrate the wide variability between particle-size distributions that is possible and represent extreme cases of the individual samples tested. The range of slopes observed also seems to indicate that the variation in the particle-size distributions determined by the automatic particle counter (in the 1–10-μm range) is greater than that determined microscopically (in the 10–100-μm range).

A possible explanation for the wider particle-size distribution observed using the automatic particle counter may result from the fact that, for the relatively clean solutions utilized, most of the usable instrumental readings (*i.e.*, those with sufficiently high counts to ensure accuracy) fell in the 1–3-μm range; therefore, only about 50% of the 1–10-μm logarithmic

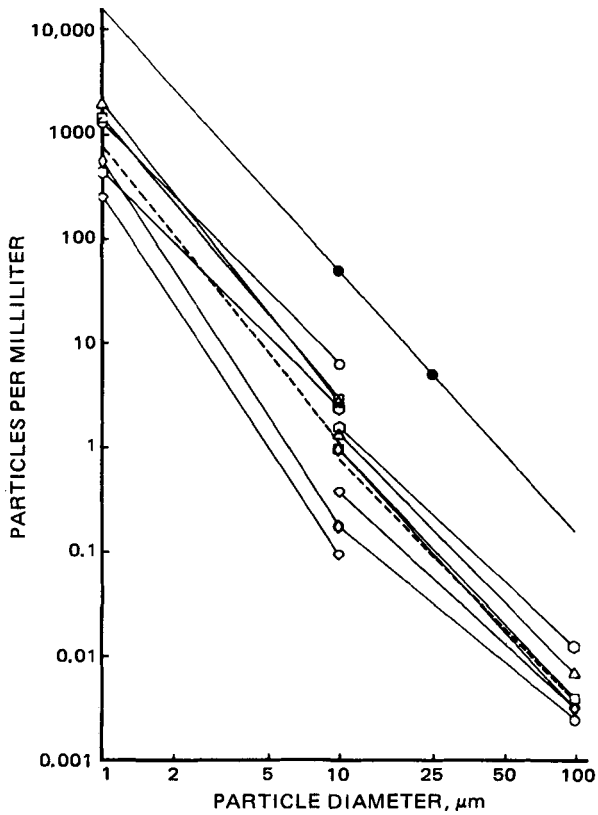

Figure 2—*Average particle-size distributions of six types of large-volume parenteral solutions as determined by the automatic particle counter (1–10-μm region) and the microscope (10–100-μm region). Key:* ▽, *dextrose, 5% in half-strength normal saline;* ◇, *normal saline;* ○, *dextrose, 5% in multiple electrolyte solution;* □, *dextrose, 5% in normal saline;* ○, *dextrose, 5% in water;* △, *dextrose, 5% in lactated Ringer's solution; - - -, overall average; and* ●, *USP–NF standard.*

interval was used. Thus, when determining the least-squares fit of such data, a greater degree of variability was possible.

The automatic particle counter may underestimate the number of particles counted at the larger particle diameters, *i.e.*, where the counts become relatively low and the error due to the truncated display becomes larger. This error could increase the slope of the least-squares fit of the instrumental data. For two out of every three individual solutions examined, the slope of the instrumental data exceeded the slope of the microscopic data.

The automatic particle counter requires a calibration (12) and is, therefore, a relative measuring technique whereas the microscope provides an absolute measurement. An error may arise because the particle counter is calibrated using a monodisperse set of latex spheres that have uniform, well-defined optical properties and are suspended in a halomethane–alcohol mixture. In contrast, the particles in parenterals are primarily quartz in composition (*i.e.*, dust), nonuniform in their optical properties, irregular in shape, and suspended in water. The microscopic counting technique is not subject to this potential source of variation. Possibly a calibration standard consisting of quartz particles suspended in water (not presently available) would permit a better correlation between the two techniques.

In addition to these possible explanations for the variability between the two measuring techniques is the fundamental difference that the automatic particle counter utilizes a nondestructive technique whereas the microscopic counting procedure is destructive. The ramifications of this difference are that the counts obtained using the particle counter are dependent on the combined properties of the countainer, the contaminants, and the solution itself and how they mutually interact. In other words, the laser beam of the instrument must penetrate the glass container and then detect and count particles in the environment of the solution. In the destructive microscopic counting technique, the solution is removed from the bottle and then filtered. Thus, only the particulates to be counted remain on the collecting filter, thereby eliminating any variations in counts due to differences in the properties or position of the container (13).

In contrast to Fig. 1, which shows data for individual samples, Fig. 2 displays averaged data. From Fig. 2, it appears that the log–log plots for each type of solution are essentially parallel to one another in both the 1–10- and 10–100-μm size ranges. In fact, the statistical analyses demonstrated that the slopes for data pertaining to the six solution types were not significantly different ($F_{5,27} = 1.70$) as determined by both methods. In addition, as expected, there was no significant method by solution-type interaction ($F_{5,27} = 0.48$). This parallelism of the log–log plots indicates that each measurement method produces a similar value for K in Eq. 2. This result means that each method determines approximately the same relative number of particles exceeding a given size. However, as indicated by the different intercepts of the log–log plots, the absolute number of particles counted may vary.

Alignment of Log–Log Plots—Austin (14) noted that air-borne dust present in a clean room exhibits a particle-size distribution that obeys a power law identical in form to Eq. 2. Since air-borne dust is believed to be one primary source of parenteral contamination, it has been suggested (15) that a similar power law relationship might be observed in parenterals. If, indeed, there is a single particle-size distribution extending over the 1–100-μm range that can be described by Eqs. 1 and 2, then both counting methods theoretically should produce linear log–log plots with equal slopes and equal intercepts, subject to the limitations previously discussed.

The extreme examples shown in Fig. 1 indicate that there may be a rather poor alignment between the size distributions in the 1–10- and 10–100-μm regions in individual bottles. However, the averaged data in Fig. 2 indicate a much improved agreement between the distributions measured by the two methods. This apparent misalignment can be resolved partially by noting that the two measuring techniques size and count particles differently. The microscopic counting technique sizes particles according to their "longest dimension"; the automatic particle counter sizes particles in terms of their "equivalent spherical diameter." Therefore, it was not surprising that a perfect alignment of the two particle-size distributions was not observed since they were obtained by two methods utilizing different types of size estimation (16).

This problem probably would be magnified when comparing a destructive technique with a nondestructive technique as in this study. The destructive microscopic counting technique requires that the parenteral solution be removed from the container and collected on a filter. During this filtration procedure, the solution was passed through an infusion set, thereby exerting an additional shear force on the particles, which could alter the observed particle-size distribution (17). In contrast, the instrumental measurements were obtained from solutions not subjected to this additional shear force. The effects of different degrees of shear force on the particle-size distributions of parenterals recently were observed (11, 18).

The alignment of the particle-size distributions recorded in the 1–10- and 10–100-μm regions is obviously dependent on the linearity, slopes, and intercepts of the log–log plots. Therefore, all previously mentioned differences existing between the two measuring techniques also could be cited here to account for the imperfect alignment.

As previously noted, the average slopes for the six types of solutions shown in Fig. 2 are essentially parallel to one another, both within each size range examined and between the two size ranges. These results indicate that the relative distribution of particles was largely independent of the solution composition. This observation recently was made by other investigators (17, 19). Thus, it seemed appropriate to average the data over all solutions examined, without regard to solution type.

The dashed line in Fig. 2 shows the overall average particle-size distribution for all bottles tested as determined by the two methods. The alignment, parallelism, and slopes of the overall average data are in better agreement than the data for any of the individual solutions or the six solution types previously averaged. This result would be anticipated solely on the basis that a larger number of readings was averaged; any differences would likely be minimized when averaged over a greater number of readings provided that there was no true difference between the two techniques. If a true difference existed, it would have been magnified by averaging a greater number of readings. The statistical analyses obtained by pooling the data from all bottles tested indicated that the intercepts were significantly different from method to method ($F_{1,27} = 13.35$) whereas the slopes did not differ from method to method ($F_{1,27} = 3.50$).

The solid circles shown in Fig. 2 represent the levels of particulate matter allowed under the recently proposed USP–NF standard (1). The log–log plots representing the averages for the six types of solutions, as determined by either method, were well below the levels represented by the linear extrapolation of this standard. Thus, the solutions tested were relatively clean in relation to this standard.

SUMMARY AND CONCLUSIONS

The results of this study indicate a linear relationship between log $N_{>D}$ and log D over the 1–100-μm size range using averaged data. The data not only substantiate previous work (9) concerning particle-size distributions of parenterals but also extend the range of 1–30 μm over which this relationship had previously been observed using a particle counter[5] operating on the light-blockage principle (20). These previous studies used destructive counting techniques that can reportedly alter particle-size distributions. In this study, both a destructive and a nondestructive technique were utilized to determine the particle-size distributions over the 1–100-μm range. The observed linearity of this relationship over this extended range indicates that the two methods are broadly comparable in their ability to determine the particle-size distribution.

The apparent adherence of the particle-size distribution to a single power law (Eq. 1) indicates that it may be possible, at least with averaged data, to extrapolate particle counts obtained in the 1–10-μm region with the automatic particle counter to particle counts obtained in the 10–100-μm region using the microscopic counting technique. The significance of this observation is that one could monitor the smaller, more abundant particles with the automatic particle counter (or other suitable instrumental techniques) and thereby obtain a rapid estimate of the quality of the solution. Furthermore, since the method is nondestructive, the actual bottle tested can be administered to the patient.

Since the average slopes for the various types of solutions examined were essentially parallel, it can be concluded that the average particle-size distributions of the contaminants were independent of the contents of the solution. This conclusion implies that each solution contained contaminants of similar origin. If, in fact, different solutions do contain similar contaminants, then the use of averaged data appears to be both valid and highly desirable when examining the levels of particulate contamination in parenterals for quality control purposes. Since the particle-size distributions appear to be independent of solution type, the major source of contamination normally found in parenterals probably is air-borne dust particles, which contaminate the parenterals according to a power law similar to one used by Cadle (8) to describe air-borne dust particles.

In spite of the previously listed potential differences between the two methods of measurement, the automatic particle counter and the microscopic counting technique apparently are broadly comparable in their ability to characterize the particle-size distributions of large-volume parenterals. Therefore, the automatic particle counter, when used in the manner described, is a reasonably accurate device for determining particle-size distributions and appears to be a viable alternative to the microscopic counting technique for assessing the cleanliness of large-volume parenterals. More elaborate studies involving samples of various lots of parenterals from different manufacturers are needed to establish unequivocally the utility of the automatic particle counter in assessing parenteral cleanliness.

REFERENCES

(1) "First Supplement to USP XIX–NF XIV," Mack Publishing Co., Easton, Pa., July 1975, pp. 56, 57.

(2) J. M. Garvan and B. W. Gunner, *Med. J. Aust.*, **2**, 140 (1963).

(3) M. A. Gross, *Drug Intel. Clin. Pharm.*, **1**, 12, 21 (1967).

(4) S. J. Turco and N. M. Davis, *J. Am. Med. Assoc.*, **217**, 81 (1971).

(5) J. Blanchard, C. M. Thompson, and J. A. Schwartz, *Am. J. Hosp. Pharm.*, **33**, 144 (1976).

(6) R. G. Draftz and J. Graf, *Bull. Parenteral Drug Assoc.*, **28**, 35 (1974).

(7) "Analysis of Intravenous Solutions for Particulate Matter," Application Report AR-2, Millipore Corp., Bedford, Mass., 1967.

(8) R. D. Cadle, "Particle Size; Theory and Applications," Reinhold, New York, N.Y., 1965, p. 37.

(9) M. J. Groves, *Analyst*, **94**, 992 (1969).

(10) P. R. Bevington, "Data Reduction and Error Analysis for the Physical Sciences," McGraw-Hill, New York, N.Y., 1969, pp. 102–108.

(11) L. Ernerot, *Sv. Farm. Tidskr.*, **78**, 129 (1974).

[5] High Accuracy Products Corp., Claremont, CA 91711.

(12) "Instruction Manual, Prototron In Situ Liquid Inspection Station, Model ILI 1000," Spectrex Corp., Redwood City, Calif., 1974.
(13) M. Porter, *Bull. Parenteral Drug Assoc.*, **29**, 169 (1975).
(14) P. R. Austin, "Design and Operation of Clean Rooms," Business News Publishing, Detroit, Mich., 1970, chap. 2.
(15) M. J. Groves, "Parenteral Products," William Heinemann Medical Books, London, England, 1973, p. 232.
(16) G. H. Hopkins and R. W. Young, *Bull. Parenteral Drug Assoc.*, **28**, 15 (1974).
(17) S. M. Blaug and R. E. Sarabia, *ibid.*, **29**, 74 (1975).
(18) J. Blanchard, J. A. Schwartz, and D. M. Byrne, *J. Pharm. Sci.*, **66**, 935 (1977).
(19) L. Ernerot, I. Helmstein, and E. Sandell, *Acta Pharm. Suec.*, **7**, 501 (1970).
(20) L. D. Carver, *Ann. N.Y. Acad. Sci.*, **158**, 710 (1969).

ACKNOWLEDGMENTS

The authors thank Mr. William T. Fink for constructive criticism of the manuscript and Mr. John Hoyte for the use of the Prototron particle counter. Financial support from the University of Arizona Foundation and the University of Arizona Alumni Association is gratefully acknowledged.

Autoradiographic Distribution Studies of 2-^{14}C-Fluorouracil following Oral or Intravenous Administration in Mice Bearing Solid Sarcoma-180

JASHOVAM SHANI, JEFFREY A. BERMAN, and WALTER WOLF ˣ

Received September 16, 1976, from the *Radiopharmacy Program, School of Pharmacy and Cancer Research Center, University of Southern California, Los Angeles, CA 90033.* Accepted for publication June 21, 1977.

Abstract □ 2-^{14}C-Fluorouracil was injected or fed to mice bearing sarcoma-180, a tumor sensitive to fluorouracil, and the fate and localization of the label were followed for 2 hr. The disappearance of the label from the blood and its localization in the tumor and organs of these mice were studied by autoradiography as a model for scintigraphic localization. In tumor-bearing mice, the tumor, kidney, liver, and bladder were visualized 10 min after intravenous injection of 2-^{14}C-fluorouracil; 2 hr after the injection, the activity in the tumor and bone marrow was still noticeable. The localization in the tumor and the liver appeared visually to be rapid, and the retention of the label in the liver of the tumor-bearing animals was noticeably greater than in the control mice by visual observation. There seemed to be no difference in the distribution of 2-^{14}C-fluorouracil when the drug was administered orally to starved or to fed mice. The tumor was visualized equally after oral administration as well as after intravenous injection, except for a somewhat faster clearance from most organs in the intravenous group. There was no difference in uptake and excretion if additional carrier was added, which doubled the administered dose of fluorouracil per mouse. Inasmuch as most of the activity viewed in the sarcoma-180 bearing mice is known to be due to the metabolite floxuridine monophosphate, a correlation between the tissue localization of the drug and its clinical efficacy may lead to a method for predicting the chemotherapeutic regimen in patients. The present work attempted to determine animal data relevant to a nuclear medicine observation.

Keyphrases □ 2-^{14}C-Fluorouracil—tissue distribution in mice after oral or intravenous administration, autoradiographic determination □ Autoradiography—determination, 2-^{14}C-fluorouracil, tissue distribution in mice after oral or intravenous administration □ Distribution, tissue—2-^{14}C-fluorouracil in mice after oral or intravenous administration, autoradiographic determination □ Antineoplastic agents—2-^{14}C-fluorouracil, tissue distribution in mice after oral or intravenous administration, autoradiographic determination

Fluorouracil[1] has been indicated since 1958 for treatment of patients with primary carcinoma of the breast, stomach, or colon with metastases to the liver (1). However, there are different views on its optimal chemotherapeutic regimens, *i.e.*, acute loading *versus* weekly therapy, rapid *versus* slow infusion, oral *versus* intra-arterial administration, and regional infusion *versus* radiological adjunct therapy (2).

BACKGROUND

Due to the inconsistency and variability of the clinical response to fluorouracil, the regimen of its systemic administration is controversial. For the past 12 years, the following regimens have been tested. Oral daily administration proved effective in patients with liver metastases due to the high concentration in the portal system (3–5). In cases of rectal carcinoma, oral administration was replaced by rectal instillation (6). Intravenous weekly administration (without a loading dose) maintained antitumor effectiveness and reduced toxicity in studies with 437 patients (7–9) and in a cumulative study of 548 patients with disseminated cancer (10). Intra-arterial infusion, through a catheter into the external carotid artery, the hepatic artery, or the bronchial artery, exhibited improvement in over 50% of patients (11, 12). Intralymphatic injection was tested for lymphoreticulosarcoma and lymph node metastases (13). Intralumenal infusion into sequestered intestinal lumen prior to surgery (14) and intramuscular and intraperitoneal (15) injections also were evaluated.

In the first comprehensive study of a regimen of choice in cancer patients, Mukherjee *et al.* (15) administered 2-^{14}C-fluorouracil by oral, intravenous, intramuscular, and intraperitoneal routes. They measured the radioactivity in the plasma, respiratory carbon dioxide, and urine and observed that the unchanged drug was detected in the urine following intravenous administration longer than after administration by any other route.

Since the intravenous and oral routes remained the preferred methods for administering fluorouracil, most recent studies compared those two routes. Bateman *et al.* (16) found a clinically useful response rate in 21% of the intravenous group and in 40% of the oral group. Although the response duration for both groups was not significantly different, great variability in peak plasma level and decay was observed after oral administration, while the range of peak levels and plasma decay in the intravenously administered patients was relatively uniform (17). Cohen *et al.* (18) reported that patients receiving intravenous doses showed consistent and rapid plasma clearance, while patients demonstrated widely varying peak plasma concentrations after oral ingestion.

Comparison of therapy regimens after intraperitoneal administration of fluorouracil to mice bearing L-1210 solid lymphocytic leukemia demonstrated essentially no schedule dependency; this finding is consistent with the effectiveness of weekly doses (19). It was suggested that the optimal treatment might be injections of fluorouracil every 2 days

[1] 5-Fluorouracil.

(12) "Instruction Manual, Prototron In Situ Liquid Inspection Station, Model ILI 1000," Spectrex Corp., Redwood City, Calif., 1974.
(13) M. Porter, *Bull. Parenteral Drug Assoc.*, **29**, 169 (1975).
(14) P. R. Austin, "Design and Operation of Clean Rooms," Business News Publishing, Detroit, Mich., 1970, chap. 2.
(15) M. J. Groves, "Parenteral Products," William Heinemann Medical Books, London, England, 1973, p. 232.
(16) G. H. Hopkins and R. W. Young, *Bull. Parenteral Drug Assoc.*, **28**, 15 (1974).
(17) S. M. Blaug and R. E. Sarabia, *ibid.*, **29**, 74 (1975).
(18) J. Blanchard, J. A. Schwartz, and D. M. Byrne, *J. Pharm. Sci.*, **66**, 935 (1977).
(19) L. Ernerot, I. Helmstein, and E. Sandell, *Acta Pharm. Suec.*, **7**, 501 (1970).
(20) L. D. Carver, *Ann. N.Y. Acad. Sci.*, **158**, 710 (1969).

ACKNOWLEDGMENTS

The authors thank Mr. William T. Fink for constructive criticism of the manuscript and Mr. John Hoyte for the use of the Prototron particle counter. Financial support from the University of Arizona Foundation and the University of Arizona Alumni Association is gratefully acknowledged.

Autoradiographic Distribution Studies of 2-^{14}C-Fluorouracil following Oral or Intravenous Administration in Mice Bearing Solid Sarcoma-180

JASHOVAM SHANI, JEFFREY A. BERMAN, and WALTER WOLF ˣ

Received September 16, 1976, from the *Radiopharmacy Program, School of Pharmacy and Cancer Research Center, University of Southern California, Los Angeles, CA 90033.* Accepted for publication June 21, 1977.

Abstract □ 2-^{14}C-Fluorouracil was injected or fed to mice bearing sarcoma-180, a tumor sensitive to fluorouracil, and the fate and localization of the label were followed for 2 hr. The disappearance of the label from the blood and its localization in the tumor and organs of these mice were studied by autoradiography as a model for scintigraphic localization. In tumor-bearing mice, the tumor, kidney, liver, and bladder were visualized 10 min after intravenous injection of 2-^{14}C-fluorouracil; 2 hr after the injection, the activity in the tumor and bone marrow was still noticeable. The localization in the tumor and the liver appeared visually to be rapid, and the retention of the label in the liver of the tumor-bearing animals was noticeably greater than in the control mice by visual observation. There seemed to be no difference in the distribution of 2-^{14}C-fluorouracil when the drug was administered orally to starved or to fed mice. The tumor was visualized equally after oral administration as well as after intravenous injection, except for a somewhat faster clearance from most organs in the intravenous group. There was no difference in uptake and excretion if additional carrier was added, which doubled the administered dose of fluorouracil per mouse. Inasmuch as most of the activity viewed in the sarcoma-180 bearing mice is known to be due to the metabolite floxuridine monophosphate, a correlation between the tissue localization of the drug and its clinical efficacy may lead to a method for predicting the chemotherapeutic regimen in patients. The present work attempted to determine animal data relevant to a nuclear medicine observation.

Keyphrases □ 2-^{14}C-Fluorouracil—tissue distribution in mice after oral or intravenous administration, autoradiographic determination □ Autoradiography—determination, 2-^{14}C-fluorouracil, tissue distribution in mice after oral or intravenous administration □ Distribution, tissue—2-^{14}C-fluorouracil in mice after oral or intravenous administration, autoradiographic determination □ Antineoplastic agents—2-^{14}C-fluorouracil, tissue distribution in mice after oral or intravenous administration, autoradiographic determination

Fluorouracil[1] has been indicated since 1958 for treatment of patients with primary carcinoma of the breast, stomach, or colon with metastases to the liver (1). However, there are different views on its optimal chemotherapeutic regimens, *i.e.*, acute loading *versus* weekly therapy, rapid *versus* slow infusion, oral *versus* intra-arterial administration, and regional infusion *versus* radiological adjunct therapy (2).

BACKGROUND

Due to the inconsistency and variability of the clinical response to fluorouracil, the regimen of its systemic administration is controversial. For the past 12 years, the following regimens have been tested. Oral daily administration proved effective in patients with liver metastases due to the high concentration in the portal system (3–5). In cases of rectal carcinoma, oral administration was replaced by rectal instillation (6). Intravenous weekly administration (without a loading dose) maintained antitumor effectiveness and reduced toxicity in studies with 437 patients (7–9) and in a cumulative study of 548 patients with disseminated cancer (10). Intra-arterial infusion, through a catheter into the external carotid artery, the hepatic artery, or the bronchial artery, exhibited improvement in over 50% of patients (11, 12). Intralymphatic injection was tested for lymphoreticulosarcoma and lymph node metastases (13). Intralumenal infusion into sequestered intestinal lumen prior to surgery (14) and intramuscular and intraperitoneal (15) injections also were evaluated.

In the first comprehensive study of a regimen of choice in cancer patients, Mukherjee *et al.* (15) administered 2-^{14}C-fluorouracil by oral, intravenous, intramuscular, and intraperitoneal routes. They measured the radioactivity in the plasma, respiratory carbon dioxide, and urine and observed that the unchanged drug was detected in the urine following intravenous administration longer than after administration by any other route.

Since the intravenous and oral routes remained the preferred methods for administering fluorouracil, most recent studies compared those two routes. Bateman *et al.* (16) found a clinically useful response rate in 21% of the intravenous group and in 40% of the oral group. Although the response duration for both groups was not significantly different, great variability in peak plasma level and decay was observed after oral administration, while the range of peak levels and plasma decay in the intravenously administered patients was relatively uniform (17). Cohen *et al.* (18) reported that patients receiving intravenous doses showed consistent and rapid plasma clearance, while patients demonstrated widely varying peak plasma concentrations after oral ingestion.

Comparison of therapy regimens after intraperitoneal administration of fluorouracil to mice bearing L-1210 solid lymphocytic leukemia demonstrated essentially no schedule dependency; this finding is consistent with the effectiveness of weekly doses (19). It was suggested that the optimal treatment might be injections of fluorouracil every 2 days

[1] 5-Fluorouracil.

after tumor inoculation (19). These data suggest single weekly doses of fluorouracil rather than intensive monthly courses.

These variations, plus the fact that fluorouracil remains the drug of choice for a significant number of neoplasms, led to a study of the distribution of ^{18}F-fluorouracil to optimize and individualize chemotherapeutic regimens.

Naturally, no disposition or organ distribution after intravenous or oral administration can be studied in a large number of humans. Therefore, the distribution of 2-^{14}C-fluorouracil as a function of these two administration routes was studied in a model animal bearing a tumor responsive to the drug: a solid sarcoma-180. The goals of this research were to: (*a*) evaluate the time course of distribution of fluorouracil in fluorouracil-responsive tumor-bearing mice, (*b*) evaluate the intravenous *versus* oral route of administration, (*c*) determine whether there is any difference if fluorouracil is given before or after meals, (*d*) decide whether or not a loading dose is necessary for fluorouracil absorption and distribution in the two groups tested, and (*e*) study drug distribution in the organs.

An autoradiographic method was chosen so that ^{14}C-visualization could be related to subsequent ^{18}F-localization by scintigraphic methods. While this technique is of interest for total body visualization of organs, it is also the closest analogy to the manner in which the nuclear medicine scan "sees" the body and its organs. Indeed, the same arguments concerning quantitation (or lack of it) can be leveled against both procedures; but to determine if a given agent can be "visualized" by a scan, it is useful to determine if it can be visualized by an autoradiographic tomographic cut. In addition, the present development of positron emission tomographic procedures make autoradiography the logical model of such animal model studies[2].

EXPERIMENTAL

Sixty male Swiss-Webster mice[3], 18–22 g, were implanted subcutaneously with sarcoma-180 cell suspension. Seven days later, they were divided into three equal groups: a, b, and c. Sixty additional control male mice were divided into three additional groups: a, b, and c. All 120 mice received 2-^{14}C-fluorouracil[4], 10 μCi/0.15 mg. Group a received the drug intravenously; Group b was given the drug orally while on a regular feeding diet; Group c was given the drug orally after 18 hr of fasting.

The mice in each group were divided into five equal subgroups and were rapidly sacrificed and frozen in dry ice–hexane at 10, 15, 30, 70, or 120 min after the drug was administered. Twenty-four additional mice (12 transplanted and 12 controls) received, in addition to the same regimen, 0.15 mg of unlabeled fluorouracil as carrier and were sacrificed and frozen 2 hr after injection. These procedures follow a standard whole-body autoradiographic methodology (21).

The mice were placed overnight in a freezer (−20°). The legs and tail were dissected, and each mouse was mounted sagitally on an aluminum block and covered with carboxymethylcellulose. These procedures must be carried out below 0°. The embedded mice were then placed in the freezer for 10–30 hr to allow the carboxymethylcellulose to harden. The animals were cut into 30-μm sections, and every 10th section was placed on a cellulose tape. The sections were freeze dried on glass plates; they were then exposed to a photographic film[5] for 10–14 days, developed in an X-omat system, and analyzed.

For a semiquantitative analysis of the whole-body autoradiograms, a 0–6 scale was established. The higher the figure, the higher is the electron density of the organ evaluated on the film. This scale is based on standard radiological procedures. Each film was evaluated by two experienced technicians; to minimize intraexperimental variations, all films were read *en bloc* at the end of the experiment. The liver, stomach, intestine, kidney (cortex and medulla), bladder, bone, tumor (periphery and center), and blood were evaluated. All animals were manipulated under the same experimental conditions, and all evaluations were given absolute readings.

RESULTS

Intravenous Administration—The first organ that visually showed concentrations of the radioactivity of 2-^{14}C-fluorouracil in the control mice was the kidney, where the activity appeared to be significant 10 min postinjection, followed 5 min later by observable concentrations in the bladder and liver. Forty-five minutes postinjection, significant radioactivity was visualized in the liver, the bladder showed a heavy concentration, and significant kidney uptake was seen, especially in the renal medulla.

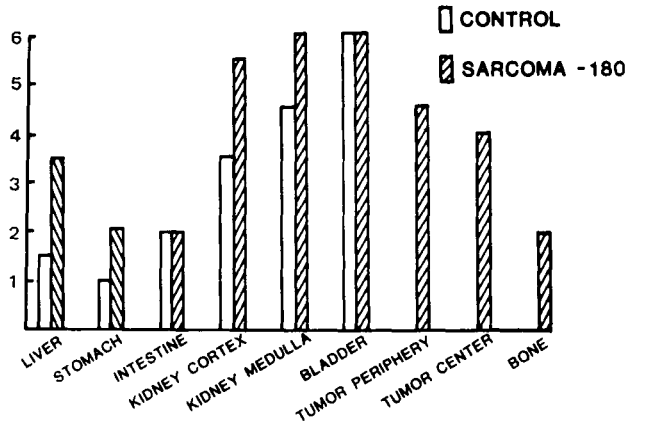

Figure 1—*Distribution of radioactivity following administration of 10 μCi of 2-^{14}C-fluorouracil. Both the control mice and the mice bearing sarcoma-180 were sacrificed 30 min after the intravenous administration of the radioactive drug.*

In the tumor-bearing group, the tumor, kidney, liver, and bladder were visualized as early as 10 min after injection. The observable concentration in the tumor remained steady, but the activity in the kidney decreased with time. Two hours after injection, there was only slight liver and kidney visualization, but the activity in the tumor and bone marrow was still significant. In the tumor-bearing animals, there apparently was an early (10-min) liver and tumor concentration of radioactivity, and the retention in the liver was noticeably greater than in control mice. The bladder activity in the tumor-bearing mice was not substantial until 30 min after injection. Representative readings for the intravenous results are shown in Figs. 1 and 2.

Oral Administration—There was considerable localization in the stomach, intestine, kidney, and bladder 15 min after oral administration. There was no significant visual difference in uptake between the fed and starved animals, except for an earlier clearance from the empty stomachs of the starved mice. The tumor was visualized 10 min after drug administration at the same rate and intensity as following intravenous administration, with a peak 30 min postinjection. The tumor was still visualized 2 hr after oral drug administration; however, its level of localization was significantly less than in the intravenously injected animals.

There was essentially no significant difference in the uptake of the orally administered drug between the fed and starved groups or, at 2 hr postinjection, between the groups with or without additional fluorouracil carrier. Activity in the nasal mucosa was observed in most animals, corresponding to similar findings in humans. Representative values for the

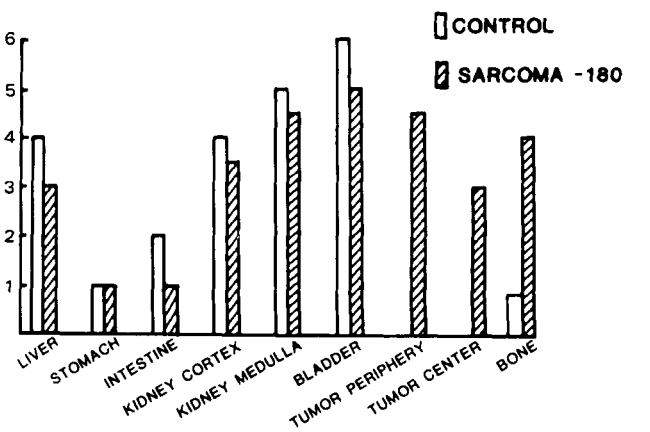

Figure 2—*Distribution of radioactivity following administration of 10 μCi of 2-^{14}C-fluorouracil. Both the control mice and the mice bearing sarcoma-180 were sacrificed 70 min after the intravenous administration of the radioactive drug.*

[2] Preliminary results of this study were presented at the 1975 meeting of the Society of Nuclear Medicine (20).
[3] Jackson Laboratories, Bar Harbor, Me.
[4] Biochemical and Nuclear Corp., Burbank, Calif.
[5] Kodak RP-54.

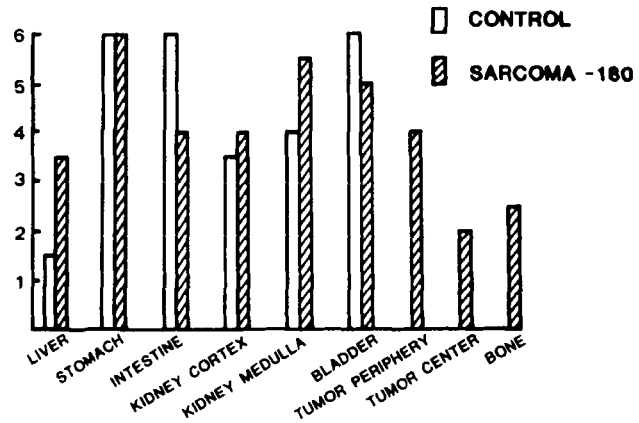

Figure 3—*Distribution of radioactivity following administration of 10 μCi of 2-^{14}C-fluorouracil. Both the control mice and the mice bearing sarcoma-180 were fed* ad libitum *and sacrificed 30 min after oral administration of the radioactive drug.*

fed mice are given in Figs. 3 and 4; the retention capacity of the label, with time, in the tumor periphery of all three groups is shown in Fig. 5. Figure 6 shows the variation in the tumor periphery/center as a function of time.

DISCUSSION

The solid tumor sarcoma-180 in Swiss mice was chosen due to consistent reports about its responsiveness to fluorouracil. This drug was reported to cause significant inhibition of the tumor (22) as well as morphological changes (23). In one study, the sarcoma-180 tumor had the highest observable retention of 2-^{14}C-fluorouracil of all tissues examined (24), and it showed high conversion of fluorouracil into nucleotides (25). It suited the present study because there was maximal observable tumor localization 70 min after intravenous injection, which decreased slowly during the 2nd hr, and this decrease was within a reasonable experimental time period.

The 0.5–2-hr plateau in tumor activity had been noticed before (26), but there is a difference in visual binding dynamics between the center and the periphery. The persistence of fluorouracil in this tumor appears to be consistent with the clinical effectiveness of the drug against some slow-growing human tumors, especially due to the fact that much of its activity was concentrated in the cortex, rather than in the medulla of the tumor, as could be expected due to the necrotic nature of the tumor (Fig. 6). Higher ratios between outer and inner areas of the tumor were reported in prolonged (3-day) experiments (27). By 72 hr, floxuridine (2′-deoxy-5-fluorouridine) monophosphate was the metabolite present in most tissues in the highest concentrations (27).

The bone marrow revealed its peak activity in the present experiments 2 hr after injection. In the animals that were mounted obliquely so that the spinal column was noticeable, marrow localization appeared to be

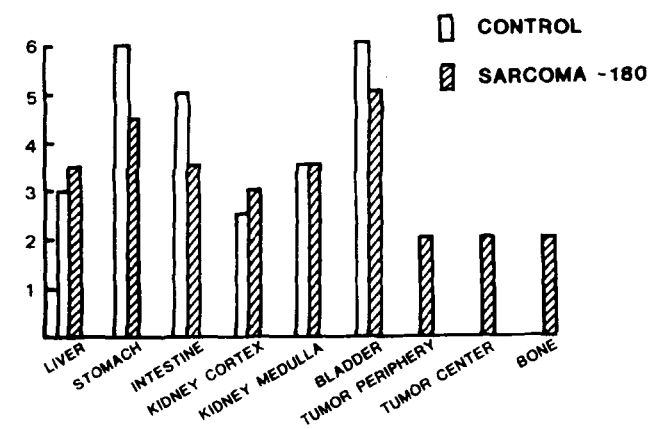

Figure 4—*Distribution of radioactivity following administration of 10 μCi of 2-^{14}C-fluorouracil. Both the control mice and the mice bearing sarcoma-180 were fed* ad libitum *and sacrificed 70 min after oral administration of the radioactive drug.*

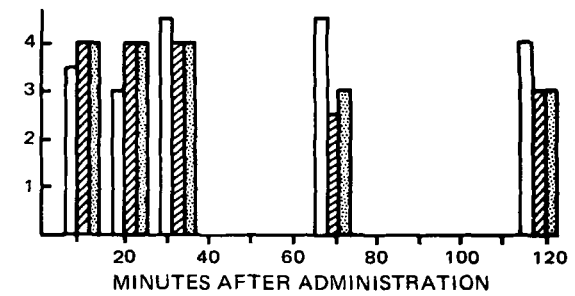

Figure 5—*Retention of radioactivity from 2-^{14}C-fluorouracil in the tumor periphery of mice bearing sarcoma-180 at various intervals after oral or intravenous administration of 10 μCi of the radioactive drug. Key:* □, *intravenous;* ▨, *oral to fed; and* ■, *oral to starved.*

more intense in tumor-bearing animals after intravenous administration. This result correlates to marrow uptake after fluorouracil administration in humans.

The brain did not concentrate any activity during the experimental period. Prolonged studies of 24 hr and more demonstrated specific localization in the granulosa layer of the cerebellum (27). A similar situation was seen in the pancreas, which concentrates the drug with time, but no pancreatic activity could be noticed in the present studies.

Blood clearance was rapid and in agreement with a one-compartment kinetic model in humans (18). In humans, plasma clearance after oral administration is much slower than after intravenous administration; the plasma peak is in approximately 1 hr as compared to the intravenous $T_{1/2}$ of 10 min (18). Although the differences in the plasma time course of free fluorouracil after oral or intravenous administration do not reflect the difference in clinical response associated with those routes (16), it might be a reliable parameter for the availability and metabolism in each patient.

The liver is apparently the main site of fluorouracil degradation. In humans, there is more extensive catabolism when the drug is administered orally rather than intravenously (25). There was a significant delay in liver uptake in tumor-bearing mice as well as a rapid clearance in the control mice, probably due to impaired metabolism in the tumor-bearing animals. It is suggested that the delayed concentration in the bladder of the tumor-bearing animals is another result of this high liver uptake and slow metabolism. The concentration in the kidney is an outcome of this relationship, and fluorouracil is concentrated in the kidney's medulla.

CONCLUSIONS

It is apparent that intravenous injections of fluorouracil localize more specifically in the tumor and bone marrow sites, as noted by visual observation, and that the apparent drug retention at these sites is greater than after oral administration. The fact that the bladder activity in an injected animal occurs at a later time than in the orally administered animal, and considering the interrelationship between toxicity and degradation, it seems that fluorouracil toxicity is diminished by an increase in its degradation. There was less degradation after the continuous intravenous infusion of 5-fluorodesoxyribose than after a single intravenous dose, and 5-fluorodesoxyribose toxicity was increased greatly when injected as a continuous intravenous drip (28). A study to determine the optimal chemotherapeutic dose and regimen of fluorouracil administration, using γ-emitting 5-^{18}F-fluorouracil, is now being conducted;

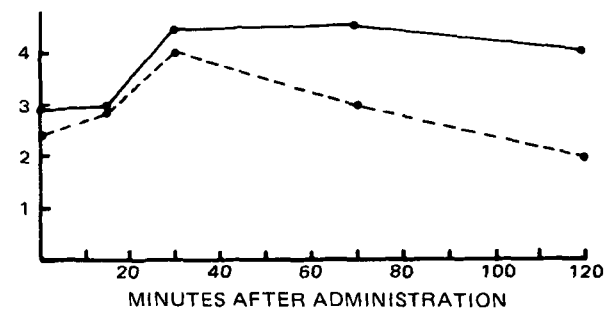

Figure 6—*Distribution of radioactivity from 2-^{14}C-fluorouracil in the sarcoma-180 tumor tissue of mice during the first 2 hr following intravenous administration of 10 μCi of the radioactive drug. Key:* ●—●, *tumor periphery; and* ●- -●, *tumor center.*

results comparing the localization of a responsive *versus* a nonresponsive tumor were published elsewhere (29).

The present study also models the observations made by a nuclear medicine scan, where visual differences of film contrast (scales of gray) are the bases for clinical diagnosis. Thus, because visual differences are observable, it is expected that similar visual differences may be observable in the human. In addition, the use of ^{18}F-fluorouracil-labeled material in conjunction with tomographic cuts obtained with the new positron emission tomographic scanners is likely to produce scans whose interpretation can be correlated closely to the present work.

Although the question of whether localization and utilization of chemotherapeutic agents are an indication of their pharmacological activity is a matter of controversy, studies correlating these factors will help in predicting a more appropriate fluorouracil chemotherapeutic regimen.

REFERENCES

(1) L. F. Humphrey, *Am. Surg.*, **38**, 725 (1972).

(2) F. Ansfield, S. MacMan, and G. Ramirez, *Oncology*, **26**, 114 (1972).

(3) C. L. Khung, T. C. Hall, and A. J. Piro, *Clin. Pharmacol. Ther.*, **7**, 527 (1966).

(4) S. H. Nadler, *Arch. Surg.*, **97**, 654 (1968).

(5) C. J. Staley, J. T. Hart, F. Van Hagen, and F. W. Preston, *Cancer Chemother. Rep.*, **20**, 107 (1962).

(6) R. Cluzan, P. Arnavon, O. LeBlaye, E. Lehn, A. Lefesvre, and R. Levillain, *Therapie*, **26**, 1121 (1971).

(7) E. M. Jacobs, J. R. Bateman, J. K. Luce, and D. A. Wood, *Proc. Am. Assoc. Cancer Res.*, **8**, 34 (abstract) (1967).

(8) E. M. Jacobs, W. J. Reeves, Jr., R. Pugh, and J. R. Bateman, *Proc. Xth Int. Cancer Congr.*, **1970**, 480 (abstract).

(9) J. Horton, K. B. Olson, and J. Sullivan, *Ann. Intern. Med.*, **73**, 897 (1970).

(10) E. M. Jacobs, W. J. Reeves, D. A. Wood, R. Pugh, J. Braunwald, and J. R. Bateman, *Cancer*, **27**, 1302 (1971).

(11) J. M. Anderson, R. S. Patrick, D. W. Short, and W. A. Mackey, *Br. Med. J.*, **3**, 954 (1972).

(12) J. Couture and L. Deschenes, *Cancer*, **29**, 1632 (1972).

(13) S. Daufman, *N. Engl. J. Med.*, **288**, 199 (1973).

(14) L. M. Rousselot, D. R. Cole, and C. E. Grossi, *Dis. Colon Rectum*, **15**, 169 (1972).

(15) K. L. Mukherjee, J. Boohar, D. Wentland, F. J. Ansfield, and C. Heidelberger, *Cancer Res.*, **23**, 49 (1963).

(16) J. R. Bateman, R. P. Pugh, F. R. Cassidy, G. J. Marshall, and L. E. Irwin, *Cancer*, **28**, 907 (1971).

(17) J. R. Bateman, L. E. Irwin, J. R. Pugh, F. R. Cassidy, and J. Weiner, *Proc. 11th Annual Meeting, Am. Soc. Clin. Oncol.* (Abstract WCG-106), **16**, 1087 (1975).

(18) J. L. Cohen, L. E. Irwin, G. J. Marshall, H. Harvey, and J. R. Bateman, *Cancer Chemother. Rep.*, **58**, 723 (1974).

(19) M. Chadwick and W. I. Rogers, *Cancer Res.*, **32**, 1045 (1972).

(20) W. Wolf, J. A. Berman, and J. Shani, *J. Nucl. Med.*, **10**, 582 (1975).

(21) L. Roth, in "Radiopharmacy," M. Tubis and W. Wolf, Eds., Wiley–Interscience, New York, N.Y., 1976.

(22) C. Heidelberger, N. K. Chaudhuri, P. Danenberg, D. Mooren, and L. Griesbach, *Nature*, **179**, 663 (1957).

(23) K. Kaziwara, H. Kawaji, and M. Arakawa, *Oncology 1970*, **II**, 10 (1971).

(24) N. K. Chaudhuri, B. J. Montag, and C. Heidelberger, *Cancer Res.*, **18**, 318 (1958).

(25) N. I. Chaudhuri, K. L. Mukherjee, and C. Heidelberger, *Biochem. Pharmacol.*, **1**, 328 (1958).

(26) C. Heidelberger, K. C. Leibman, E. Harbers, and P. M. Bhargava, *Cancer Res.*, **17**, 399 (1957).

(27) R. H. Liss and M. Chadwick, *Cancer Chemother. Rep.*, **58**, 777 (1976).

(28) C. Heidelberger, *Cancer Res.*, **30**, 1549 (1970).

(29) J. Shani and W. Wolf, *ibid.*, **37**, 2306 (1077).

ACKNOWLEDGMENTS

Supported in part by NCI Grants 5-P01-CA-14089 and 1-P01-CA-19438. The authors gratefully acknowledge the gift of a sample of 2-^{14}C-fluorouracil from Mr. Gary Balekjian, Biochemical Nuclear Corp., Burbank, Calif., and of fluorouracil from Dr. Ing, National Cancer Institute. Discussion of this work with Dr. J. Bateman, Dr. L. Irwin, and Dr. M. Chadwick is gratefully acknowledged.

Jashovam Shani is a recipient of a fellowship from the International Atomic Energy Agency.

Isolation and Characterization of the Sesquiterpene Lactones Costunolide, Parthenolide, Costunolide Diepoxide, Santamarine, and Reynosin from *Magnolia grandiflora* L.

FAROUK S. EL-FERALY ˣ and YEE-MING CHAN

Received February 7, 1977, from the *Pharmacognosy Department, School of Pharmacy, University of Mississippi, University, MS 38677.* Accepted for publication June 27, 1977.

Abstract □ The germacranolide sesquiterpene lactones costunolide, parthenolide, and costunolide diepoxide were isolated from the leaves of *Magnolia grandiflora* L. Costunolide diepoxide might be, at least in part, an artifact derived from air oxidation of parthenolide. The root bark yielded only costunolide together with the two eudesmanolides, santamarine and reynosin. In an attempt to synthesize costunolide diepoxide, the action of *m*-chloroperbenzoic acid on parthenolide and on costunolide was studied. The products were costunolide diepoxide from parthenolide and the two cyclized derivatives, santamarine and reynosin, from costunolide. The elusive costunolide 1,10-epoxide was obtained by epoxidizing costunolide using a biphasic system containing sodium bicarbonate. Under these conditions, epoxidation of costunolide took place without cyclization.

Keyphrases □ *Magnolia grandiflora* L.—leaves, isolation and characterization of various sesquiterpene lactones □ Lactones, various sesquiterpene—isolated and characterized from leaves of *Magnolia grandiflora* L.

Numerous cytotoxic sesquiterpene lactones have been isolated from plants belonging to the Magnoliaceae family (1–4). *Magnolia grandiflora* L., a member of this family, is commonly known as Southern Magnolia (5). This large evergreen ornamental tree is widespread throughout the United States (5).

Only the sesquiterpene parthenolide (I) was reported to occur in this plant (4). The present studies revealed the presence of additional sesquiterpenes in the leaves and root bark. These studies were carried out as a part of a random screening program of local flora for biologically active compounds.

results comparing the localization of a responsive *versus* a nonresponsive tumor were published elsewhere (29).

The present study also models the observations made by a nuclear medicine scan, where visual differences of film contrast (scales of gray) are the bases for clinical diagnosis. Thus, because visual differences are observable, it is expected that similar visual differences may be observable in the human. In addition, the use of ^{18}F-fluorouracil-labeled material in conjunction with tomographic cuts obtained with the new positron emission tomographic scanners is likely to produce scans whose interpretation can be correlated closely to the present work.

Although the question of whether localization and utilization of chemotherapeutic agents are an indication of their pharmacological activity is a matter of controversy, studies correlating these factors will help in predicting a more appropriate fluorouracil chemotherapeutic regimen.

REFERENCES

(1) L. F. Humphrey, *Am. Surg.*, **38**, 725 (1972).

(2) F. Ansfield, S. MacMan, and G. Ramirez, *Oncology*, **26**, 114 (1972).

(3) C. L. Khung, T. C. Hall, and A. J. Piro, *Clin. Pharmacol. Ther.*, **7**, 527 (1966).

(4) S. H. Nadler, *Arch. Surg.*, **97**, 654 (1968).

(5) C. J. Staley, J. T. Hart, F. Van Hagen, and F. W. Preston, *Cancer Chemother. Rep.*, **20**, 107 (1962).

(6) R. Cluzan, P. Arnavon, O. LeBlaye, E. Lehn, A. Lefesvre, and R. Levillain, *Therapie*, **26**, 1121 (1971).

(7) E. M. Jacobs, J. R. Bateman, J. K. Luce, and D. A. Wood, *Proc. Am. Assoc. Cancer Res.*, **8**, 34 (abstract) (1967).

(8) E. M. Jacobs, W. J. Reeves, Jr., R. Pugh, and J. R. Bateman, *Proc. Xth Int. Cancer Congr.*, **1970**, 480 (abstract).

(9) J. Horton, K. B. Olson, and J. Sullivan, *Ann. Intern. Med.*, **73**, 897 (1970).

(10) E. M. Jacobs, W. J. Reeves, D. A. Wood, R. Pugh, J. Braunwald, and J. R. Bateman, *Cancer*, **27**, 1302 (1971).

(11) J. M. Anderson, R. S. Patrick, D. W. Short, and W. A. Mackey, *Br. Med. J.*, **3**, 954 (1972).

(12) J. Couture and L. Deschenes, *Cancer*, **29**, 1632 (1972).

(13) S. Daufman, *N. Engl. J. Med.*, **288**, 199 (1973).

(14) L. M. Rousselot, D. R. Cole, and C. E. Grossi, *Dis. Colon Rectum*, **15**, 169 (1972).

(15) K. L. Mukherjee, J. Boohar, D. Wentland, F. J. Ansfield, and C. Heidelberger, *Cancer Res.*, **23**, 49 (1963).

(16) J. R. Bateman, R. P. Pugh, F. R. Cassidy, G. J. Marshall, and L. E. Irwin, *Cancer*, **28**, 907 (1971).

(17) J. R. Bateman, L. E. Irwin, J. R. Pugh, F. R. Cassidy, and J. Weiner, *Proc. 11th Annual Meeting, Am. Soc. Clin. Oncol.* (Abstract WCG-106), **16**, 1087 (1975).

(18) J. L. Cohen, L. E. Irwin, G. J. Marshall, H. Harvey, and J. R. Bateman, *Cancer Chemother. Rep.*, **58**, 723 (1974).

(19) M. Chadwick and W. I. Rogers, *Cancer Res.*, **32**, 1045 (1972).

(20) W. Wolf, J. A. Berman, and J. Shani, *J. Nucl. Med.*, **10**, 582 (1975).

(21) L. Roth, in "Radiopharmacy," M. Tubis and W. Wolf, Eds., Wiley–Interscience, New York, N.Y., 1976.

(22) C. Heidelberger, N. K. Chaudhuri, P. Danenberg, D. Mooren, and L. Griesbach, *Nature*, **179**, 663 (1957).

(23) K. Kaziwara, H. Kawaji, and M. Arakawa, *Oncology 1970*, **II**, 10 (1971).

(24) N. K. Chaudhuri, B. J. Montag, and C. Heidelberger, *Cancer Res.*, **18**, 318 (1958).

(25) N. I. Chaudhuri, K. L. Mukherjee, and C. Heidelberger, *Biochem. Pharmacol.*, **1**, 328 (1958).

(26) C. Heidelberger, K. C. Leibman, E. Harbers, and P. M. Bhargava, *Cancer Res.*, **17**, 399 (1957).

(27) R. H. Liss and M. Chadwick, *Cancer Chemother. Rep.*, **58**, 777 (1976).

(28) C. Heidelberger, *Cancer Res.*, **30**, 1549 (1970).

(29) J. Shani and W. Wolf, *ibid.*, **37**, 2306 (1077).

ACKNOWLEDGMENTS

Supported in part by NCI Grants 5-P01-CA-14089 and 1-P01-CA-19438. The authors gratefully acknowledge the gift of a sample of 2-^{14}C-fluorouracil from Mr. Gary Balekjian, Biochemical Nuclear Corp., Burbank, Calif., and of fluorouracil from Dr. Ing, National Cancer Institute. Discussion of this work with Dr. J. Bateman, Dr. L. Irwin, and Dr. M. Chadwick is gratefully acknowledged.

Jashovam Shani is a recipient of a fellowship from the International Atomic Energy Agency.

Isolation and Characterization of the Sesquiterpene Lactones Costunolide, Parthenolide, Costunolide Diepoxide, Santamarine, and Reynosin from *Magnolia grandiflora* L.

FAROUK S. EL-FERALY ˣ and YEE-MING CHAN

Received February 7, 1977, from the *Pharmacognosy Department, School of Pharmacy, University of Mississippi, University, MS 38677.* Accepted for publication June 27, 1977.

Abstract □ The germacranolide sesquiterpene lactones costunolide, parthenolide, and costunolide diepoxide were isolated from the leaves of *Magnolia grandiflora* L. Costunolide diepoxide might be, at least in part, an artifact derived from air oxidation of parthenolide. The root bark yielded only costunolide together with the two eudesmanolides, santamarine and reynosin. In an attempt to synthesize costunolide diepoxide, the action of *m*-chloroperbenzoic acid on parthenolide and on costunolide was studied. The products were costunolide diepoxide from parthenolide and the two cyclized derivatives, santamarine and reynosin, from costunolide. The elusive costunolide 1,10-epoxide was obtained by epoxidizing costunolide using a biphasic system containing sodium bicarbonate. Under these conditions, epoxidation of costunolide took place without cyclization.

Keyphrases □ *Magnolia grandiflora* L.—leaves, isolation and characterization of various sesquiterpene lactones □ Lactones, various sesquiterpene—isolated and characterized from leaves of *Magnolia grandiflora* L.

Numerous cytotoxic sesquiterpene lactones have been isolated from plants belonging to the Magnoliaceae family (1–4). *Magnolia grandiflora* L., a member of this family, is commonly known as Southern Magnolia (5). This large evergreen ornamental tree is widespread throughout the United States (5).

Only the sesquiterpene parthenolide (I) was reported to occur in this plant (4). The present studies revealed the presence of additional sesquiterpenes in the leaves and root bark. These studies were carried out as a part of a random screening program of local flora for biologically active compounds.

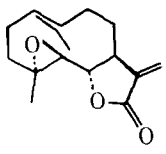

I

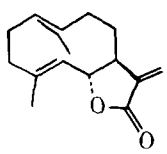

II

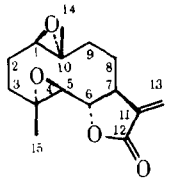

III

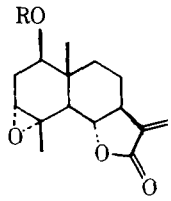

IV: R = H
V: R = CCH_3 (=O)

EXPERIMENTAL[1]

Isolation of Parthenolide (I), Costunolide (II), and Costunolide Diepoxide (III)—The dried and powdered leaves[2] (2.25 kg) were exhaustively extracted by percolation with 95% ethanol. The residue (438 g) remaining after solvent evaporation *in vacuo* at 40° was partitioned between chloroform and water. The chloroform residue (161 g) was partitioned between hexane and 10% aqueous methanol to give methanol-soluble material (74 g). Chromatography of the methanol fraction (22 g) on silica gel 60 (1.2 kg), with chloroform as the eluting solvent, gave 2.19 g of the first band, which crystallized spontaneously, and showed one major spot (R_f 0.80) when subjected to TLC.

This fraction was purified by recrystallization from ether–hexane to give II (0.371 g), mp 105–106°, $[\alpha]_D^{22}$ +117° (*c*, 0.200 in $CHCl_3$); UV: end absorbance 210 nm, log ϵ = 4.05; IR ($CHCl_3$): ν_{max} 1765, 1667, 1285, 1136, 995, and 930 cm^{-1}; PMR ($CDCl_3$): δ 1.70 and 1.42 (each 3H, br s, C_4CH_3 and $C_{10}CH_3$), 4.57 (1H, t, J = 10 Hz, C_6H), 4.79 (1H, m, C_5H), 4.9 (1H, m, C_1H), 5.54 (1H, d, J = 3 Hz, $C_{13}H$), and 6.27 (1H, d, J = 4 Hz, $C_{13}H$) ppm; mass spectrum: M^+ at *m/e* 232 (57%).

Anal.—Calc. for $C_{15}H_{20}O_2$: C, 77.55; H, 8.68. Found: C, 77.39; H, 8.45.

The IR and PMR spectra were superimposable on those of II (6).

The band following the II fraction from the silica gel 60 column provided 5.7 g of crude I and gave one major spot on TLC (R_f 0.65). The material was crystallized twice from absolute ethanol–ether to give prisms or plates of I (4.11 g), mp 115–116°, $[\alpha]_D^{22}$ −71.4° (*c*, 0.220 in CH_2Cl_2); UV: end absorbance 210 nm, log ϵ = 3.97; IR ($CHCl_3$): ν_{max} 1777, 1670, 1287, 1137, and 982 cm^{-1}; PMR ($CDCl_3$): δ 1.30 (3H, s, C_4CH_3), 1.73 (3H, s, $C_{10}CH_3$), 2.78 (1H, d, J = 9 Hz, C_5H), 3.88 (1H, t, J = 8 Hz, C_6H), 5.25 (1H, m, C_1H), 5.65 (1H, d, J = 3 Hz, $C_{13}H$), and 6.33 (1H, d, J = 3.5 Hz, $C_{13}H$) ppm; mass spectrum: M^+ at *m/e* 248 (11%).

Anal.—Calc. for $C_{15}H_{20}O_3$: C, 72.55; H, 8.12. Found: C, 72.38; H, 8.19.

The compound was identical in all regards to an authentic sample of parthenolide[3] (R_f, melting point, mixed melting point, and superimposable IR and PMR spectra).

The band following the parthenolide fraction was much less colored than the preceding band and gave one spot (R_f 0.50) on TLC. It was crystallized from absolute ethanol–ether to give needles (0.91 g) of III, mp 168–169°, $[\alpha]_D^{22}$ −30° (*c*, 0.200 in CH_2Cl_2); UV: end absorbance 210 nm, log ϵ = 3.89; IR ($CHCl_3$): ν_{max} 1777, 1670, 1386, 1287, and 1132 cm^{-1}; PMR ($CDCl_3$): δ 1.32 and 1.38 (each 3H, s, C_4CH_3 and $C_{10}CH_3$), 2.85 (1H, d, J = 8.0 Hz, C_5H), 3.87 (1H, t, J = 8.5 Hz, C_6H), 5.47 (1H, d, J = 3.0 Hz, $C_{13}H$), and 6.18 (1H, d, J = 3.5 Hz, $C_{13}H$) ppm; mass spectrum: M^+ at *m/e* 264 (less than 1%).

Anal.—Calc. for $C_{15}H_{20}O_4$: C, 68.16; H, 7.63. Found: C, 68.37; H, 7.69.

Epoxidation of I—Compound I (100 mg) was dissolved in 10 ml of chloroform. Then 1.0 equivalent (82 mg) of *m*-chloroperbenzoic acid (85%) was added, and the solution was allowed to stand at 5° for 2 hr. The reaction mixture was diluted with 100 ml of chloroform and was then washed with 5% Na_2SO_3 (30 ml), 5% $NaHCO_3$ (30 ml), and then water (10 ml). The chloroform phase was dried over anhydrous sodium sulfate and evaporated to leave 120 mg of a crystalline residue. This residue was recrystallized from absolute ethanol–ether to give 100 mg of a product identical in all respects to the isolated material (same R_f, melting point, mixed melting point, specific rotation, and superimposable IR and PMR spectra).

Epoxidation of II—Compound II (100 mg) was epoxidized with 2.0 equivalents of *m*-chloroperbenzoic acid (180 mg), as described for I, and yielded 154 mg of a crystalline residue. This residue was recrystallized from absolute ethanol–ether to give needles (53 mg) of IV, mp 243–246°, $[\alpha]_D^{22}$ +73° (*c*, 0.140 in C_2H_5OH); UV: end absorbance 210 nm, log ϵ = 4.16; IR (KBr): ν_{max} 3430, 1767, 1677, 1131, and 994 cm^{-1}; PMR (dimethyl sulfoxide-d_6): δ 0.80 (3H, s, $C_{10}CH_3$), 1.35 (3H, s, C_4CH_3), 2.96 (1H, d, J = 3.5 Hz, C_5H), 3.24 (1H, m, CH), 4.08 (1H, t, J = 11.0 Hz, C_6H), 4.64 (1H, exchangeable, d, J = 5.0 Hz, C_1OH), 5.53 (1H, d, J = 3.0 Hz, $C_{13}H$), and 5.96 (1H, d, J = 3.5 Hz, $C_{13}H$) ppm; mass spectrum: M^+ at *m/e* 264 (15%).

Anal.—Calc. for $C_{15}H_{20}O_4$: C, 68.16; H, 7.63. Found: C, 68.05; H, 7.64.

This compound was characterized as epoxysantamarine (IV) by comparing its physical and spectral data to those published (7). Acetylation of IV following the previously reported procedure (7) gave needles of V, mp 183–185°; $[\alpha]_D^{22}$ +64° (*c*, 0.14 in absolute ethanol); UV: end absorbance 210 nm, log ϵ = 3.92; IR ($CHCl_3$): ν_{max} 1772, 1734, 1674, 1127, 997, and 957 cm^{-1}; PMR ($CDCl_3$): δ 1.02 (3H, s, $C_{10}CH_3$), 1.50 (3H, s, C_4CH_3), 2.06 (3H, s, $CH_3C{=}O$), 3.00 (1H, d, J = 3.5 Hz, C_5H), 3.93 (1H, dd, J = 10 and 11 Hz, C_6H), 4.75 (1H, dd, J = 9.5 and 6.0 Hz, C_1H), 5.45 (1H, d, J = 3.0 Hz, $C_{13}H$), and 6.14 (1H, d, J = 3.0 Hz, $C_{13}H$) ppm; mass spectrum: M^+ at *m/e* 306 (11%).

Anal.—Calc. for $C_{17}H_{22}O_5$: C, 66.65; H, 7.24. Found: C, 66.47; H, 7.26.

The physical and spectral characteristics of V were identical to those reported for acetylepoxysantamarine (7).

In another run, 300 mg of II was dissolved in 20 ml of chloroform, and 1 equivalent (263 mg) of *m*-chloroperbenzoic acid was added. The reaction mixture was worked up as already described to yield 320 mg of a residue. This residue, when treated with a chloroform–ether mixture, deposited 81 mg of pure santamarine (VII), mp 134–135°, $[\alpha]_D^{22}$ +72.8° (*c*, 0.180 in absolute ethanol); UV: end absorbance 210 nm, log ϵ = 4.30; IR (KBr): ν_{max} 3380, 1773, 1673, 1128, and 995 cm^{-1}; PMR ($CDCl_3$): δ 0.86 (3H, s, $C_{10}CH_3$), 1.85 (3H, s, C_4CH_3), 3.70 (1H, dd, J = 6.0 and 9.5 Hz, C_1H), 3.98 (1H, t, J = 10 Hz, C_6H), 5.43 (1H, d, J = 3.0 Hz, $C_{13}H$), and 6.10 (1H, d, J = 3.0 Hz, $C_{13}H$) ppm; mass spectrum: M^+ at *m/e* 248 (64%).

Anal.—Calc. for $C_{15}H_{20}O_3$: C, 72.55; H, 8.12. Found: C, 72.45; H, 8.22.

The identity of VII was further confirmed by comparison with an authentic sample of santamarine[4]; the two compounds proved to be identical in all respects.

The mother liquor (239 mg) gave two spots with R_f values of 0.52 (santamarine; major) and 0.40 (reynosin; minor) when chromatographed on silver nitrate-impregnated silica gel G plates[5]. Separation of the two compounds of the mother liquor was achieved by chromatography on a column of 10 g of silver nitrate-impregnated silica gel G[6] with ether as a solvent. The separation was monitored by TLC. A mixture of unreacted

[1] Melting points were determined on a Thomas-Hoover Uni-Melt melting-point apparatus and are uncorrected. Elemental analyses were performed by Scandinavian Microanalytical Laboratories, Herlev, Denmark. IR spectra were run in potassium bromide or chloroform using a Perkin-Elmer 257 or Beckman IR-33 IR spectrometer. ^{1}H-NMR (PMR) spectra were recorded on a Jeolco C-60-HL spectrometer using deuterated chloroform as the solvent (unless otherwise specified) and tetramethylsilane as the internal standard; chemical shifts were reported in δ (parts per million) units. UV spectra were obtained in methanol on a Beckman Acta III spectrophotometer. Optical rotations were determined on a Perkin-Elmer 141 automatic polarimeter. Mass spectral data were obtained on a DuPont CEC 492 spectrometer. TLC was performed on Merck silica gel G plates using absolute ethanol–chloroform (6:94) as the eluent. The spots were visualized by spraying with 0.3% aqueous potassium permanganate.

[2] The plant material was collected at Tupelo, Miss., in June 1976; a voucher specimen has been deposited in the Herbarium, Department of Pharmacognosy, School of Pharmacy, University of Mississippi.

[3] Provided by Dr. G. Cordell, Department of Pharmacognosy and Pharmacology, University of Illinois.

[4] Provided by Dr. T. Mabry, Department of Botany, University of Texas.

[5] Silver nitrate impregnation was done by spraying silica gel G precoated plates with a 5% aqueous solution of silver nitrate and then drying the plates at 110° for 30 min. The plates were then spotted and developed with ether.

[6] Silver nitrate silica gel G for column separations was prepared by suspending 50 g of the TLC-grade silica gel G in 100 ml of 5% aqueous silver nitrate. The mixture was dried at 110° for 6 hr, passed through a 60–80-mesh sieve, and stored in amber-colored jars.

II and VII was obtained first, followed by 64 mg of pure VII and then 33 mg of reynosin (VIII), mp 145–146°, $[\alpha]_D^{22}$ +122° (*c*, 0.100 in absolute ethanol); UV: end absorbance at 210 nm, log ϵ = 3.96; IR ($CHCl_3$): ν_{max} 3610, 1772, 1653, 1410, 1127, and 1082 cm^{-1}; PMR ($CDCl_3$): δ 0.83 (3H, s, $C_{10}CH_3$), 3.55 (1H, dd, J = 4 and 10.5 Hz, C_1H), 4.06 (1H, t, J = 11.0 Hz, C_6H), 4.90 and 5.03 (1H each, br s, $C_4{=}CH_2$), 5.45 (1H, d, J = 3.0 Hz, $C_{13}H$), and 6.12 (1H, d, J = 3.5 Hz, $C_{13}H$) ppm; mass spectrum: M^+ at *m/e* 248 (4.7%).

Anal.– Calc. for $C_{15}H_{20}O_3$: C, 72.55; H, 8.12. Found: C, 72.51; H, 8.02.

The physical and spectral properties were identical to those reported for reynosin (7).

Controlled Epoxidation of II to Costunolide 1,10-Epoxide (VI)—Compound II (100 mg) was dissolved in 30 ml of methylene chloride, and the solution was stirred with 30 ml of 0.5 *M* aqueous sodium bicarbonate. One equivalent of *m*-chloroperbenzoic acid (96 mg) was then added slowly, and the two-phase system was stirred for 1 hr. The organic phase was separated and washed successively with 30 ml of 1.0 *M* sodium sulfite, 60 ml of 1.0 *M* NaOH, and finally with 30 ml of water. The methylene chloride layer was dried over anhydrous sodium sulfate and then evaporated under reduced pressure to leave a residue.

This residue readily crystallized from ether–absolute ethanol to give 66 mg of colorless needles, mp 123–125°, $[\alpha]_D^{22}$ +14° (*c*, 0.15 in methylene chloride); UV: end absorbance at 210 nm, log ϵ = 4.07; IR ($CHCl_3$): ν_{max} 1767, 1667, 1437, 1379, 1278, 1236, 1066, and 948 cm^{-1}; PMR ($CDCl_3$): δ 1.15 (3H, s, $C_{10}CH_3$), 1.85 (3H, s, C_4CH_3), 4.63 (1H, t, J = 10 Hz, C_6H), 5.32 (1H, br d, J = 10.0 Hz, C_5H), 5.48 (1H, d, J = 3.5 Hz, $C_{13}H$), and 6.25 (1H, d, J = 3.5 Hz, $C_{13}H$) ppm; mass spectrum: M^+ at *m/e* 248 (19%).

Since the compound started to cyclize within a few hours after it had been prepared, no attempts were made to submit it for elemental analysis.

Epoxidation of II using the two-phase system described, but in the presence of excess *m*-chloroperbenzoic acid for several days, produced III.

Cyclization of VI—Compound VI (80 mg) was dissolved in 15 ml of chloroform, which was preshaken with 1 ml of concentrated hydrochloric acid. The reaction was monitored by TLC; after 20 min, all of the VI was converted to a mixture of reynosin and santamarine. The solvent was then removed by evaporation, and the residue was chromatographed on a 1.0 × 10.0-cm column packed with 7 g of 5% silver nitrate-impregnated silica gel. The column was eluted with ether, and the separation was monitored by TLC. The first band yielded 59 mg of VII, followed by another band which provided 15 mg of VIII; the identity of these compounds was established by comparison with the compounds described earlier.

Compound VI underwent facile cyclization to VII and VIII upon storage, even in the solid form.

Air Oxidation of I—Parthenolide (I; 20 mg) was dissolved in three drops of chloroform, and the solution was allowed to stand at room temperature for 4 weeks. Evaporated solvent was replaced as needed, and the composition of the solution was monitored daily by TLC. After 4 weeks, most I was oxidized to II, but some of it underwent polymerization. The reaction mixture was dissolved in chloroform and filtered. The oily material obtained (10 mg) was crystallized from an absolute ethanol–ether mixture, and the product was identical in all regards to III.

Isolation of II, VII, and VIII from Root Bark—The root bark (1.0 kg) was exhaustively extracted by percolation with chloroform at room temperature. Then the solvent was evaporated *in vacuo* to leave 61 g of a crystalline residue, which was partitioned between 10% aqueous methanol (100 ml) and hexane (3 × 100 ml). The methanol solubles (43 g) were chromatographed on 1200 g of silica gel 60 with chloroform as a solvent. Costunolide (II; 29 g) was eluted first, followed by an orange band (200 mg) which deposited crystals (74 mg) of santamarine (VII) upon standing.

The fractions next to the orange band were combined, based on TLC, and evaporated to leave 1.0 g of a colorless residue. A portion of this residue (500 mg) was chromatographed on 40 g of silica gel G with chloroform as a solvent. The separation was monitored by TLC, and the column yielded 56 mg of crystalline reynosin (VIII). The identity of the isolated VII and VIII was established by comparison to those compounds prepared by treatment of II with 1 equivalent of *m*-chloroperbenzoic acid, as described earlier.

RESULTS AND DISCUSSION

An alcoholic extract of the leaves of *M. grandiflora* L. yielded a number of sesquiterpene lactones upon solvent partitioning and chromatography on silica gel with chloroform as a solvent. The two germacranolide sesquiterpenes[7], costunolide (II) and parthenolide (I), were obtained from the first and the second chromatographic bands[8], respectively. They were characterized by direct comparison with authentic samples.

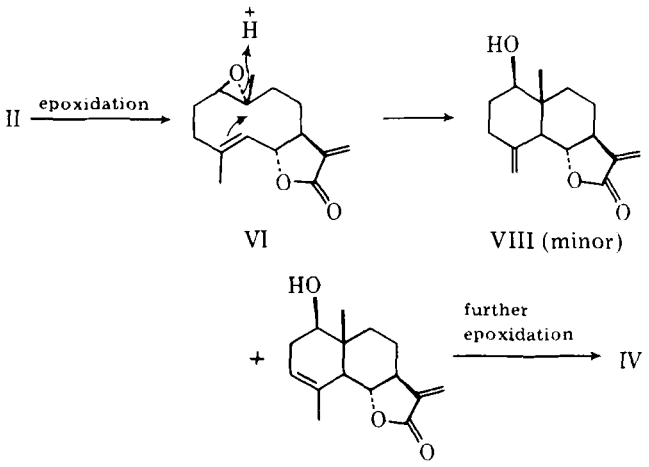

Scheme I

Costunolide diepoxide (III), $C_{15}H_{20}O_4$, was eluted next to the parthenolide band and was crystallized from an absolute ethanol–ether mixture to give needles, mp 168–169°. Its IR spectrum exhibited no hydroxyl absorption and still showed the characteristic α,β-unsaturated-γ-lactone carbonyl band at ν_{max} ($CHCl_3$) 1777 cm^{-1} with the C=C absorption band at 1670 cm^{-1}. This result suggested that the remaining two oxygen atoms must be in the form of ether groups.

The PMR spectrum of III exhibited two three-proton singlets at δ 1.32 and 1.38 ppm, which were assigned to a pair of methyl groups on oxygenated carbon atoms (1). Except for the absence of the signal for the olefinic C-1 proton, other resonances in the spectrum were similar to those of I.

The spectral data obtained for III suggested a 1,10-epoxyparthenolide structure. To confirm this assignment, epoxidation of I was undertaken using 1 equivalent of *m*-chloroperbenzoic acid. The exclusive product was III, so its structure was secured. It followed that the absolute stereochemistry of C-4, C-5, C-6, and C-7 should be the same as for I (8). The chirality at C-1 and C-10 will be discussed later in connection with the structure and stereochemistry of VI.

Chloroform solutions of I were found to contain III when stored at room temperature for a few days. The transformation of I to III became nearly complete in 4 weeks. This finding indicated that III might be, at least in part, an artifact obtained by air oxidation of I. This type of air oxidation was reported previously (9) with other sesquiterpenes.

This is the first report of costunolide diepoxide (III), although compounds of similar type, *e.g.*, epitulipinolide diepoxide (1) and agerol diepoxide (10), were reported previously.

Unexpectedly, epoxidation of II using 2 equivalents of *m*-chloroperbenzoic acid did not yield III. Instead, the major product, mp 243–246°, was identified as the hydroxylated eudesmanolide, epoxysantamarine (IV). The structure of IV was established by comparing its physical and spectral data and those of its acetate derivative (V) to the data reported (7) for epoxysantamarine and acetylepoxysantamarine, respectively.

The formation of IV during the attempted epoxidation of II can be best explained by assuming that epoxidation first involves the less hindered 1,10-double bond of II to produce VI. The latter compound could then cyclize under the acidic conditions of epoxidation to give VII. Further epoxidation of VII by more of the peracid should then produce IV (Scheme I). To confirm this mechanism, II was treated with only 1 equivalent of the peracid. As expected, the major product under these conditions was characterized as VII; a small amount of its β-isomer, VIII, was also obtained.

The role played by VI in the cyclization of II during attempted epoxidation made it both interesting and challenging to try to synthesize it.

[7] Both parthenolide (4) and costunolide (6) were reported to possess cytotoxic activity in KB cells with ED_{50} values of 23 and 0.26 μg/ml, respectively.

[8] The costunolide band yielded, in addition to costunolide, a novel sesquiterpene hydroperoxide; similarly, the parthenolide band yielded another novel sesquiterpene hydroperoxide. The structures of both compounds were discussed recently by El-Feraly *et al.* (*Tetrahedron Lett.*, 1977, 1973).

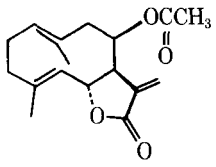

IX

This synthesis was accomplished by epoxidizing II in a two-phase system containing sodium bicarbonate (11). The presence of the latter prevented any cyclization and provided VI as the only product. As expected, VI underwent facile acid-catalyzed cyclization to VII and VIII. Moreover, it could be further epoxidized to III in the presence of excess peracid.

Since the absolute stereochemistry of C-1 in VII is *R* (7), it then followed that C-1 in VI must have the same absolute configuration. Also, the epoxide group of VI, being derived from the *trans*-1,10-double bond of II, must also have a *trans*-geometry. Therefore, the absolute stereochemistry of costunolide 1,10-epoxide should be as depicted in Structure VI. Consequently, III, which could be obtained by further epoxidation of VI, as mentioned before, must have similar chirality at C-1 and C-10.

Dihydrocostunolide was reported (12) to undergo epoxidation with perbenzoic acid to dihydrocostunolide diepoxide. In other words, epoxidation of dihydrocostunolide proceeded without cyclization. This behavior can be explained in terms of the poor acidity of perbenzoic acid and its reduction product, benzoic acid, relative to *m*-chloroperbenzoic acid and *m*-chlorobenzoic acid. However, there may be another explanation. The germacranolide sesquiterpene epitulipinolide (IX) can be epoxidized (1) with *m*-chloroperbenzoic acid to epitulipinolide 1,10-epoxide without cyclization. It appears, therefore, that the conformational factors affecting the transannular system of double bonds must play a significant role in deciding whether facile cyclization is to take place or not.

The root bark of *M. grandiflora* L. yielded, in addition to II, the two eudesmanolides VII and VIII. In view of the above discussion, these compounds must have been derived by the cyclization of biogenetically formed VI.

REFERENCES

(1) R. W. Doskotch, S. L. Keely, Jr., C. D. Hufford, and F. S. El-Feraly, *Phytochemistry*, **14**, 769 (1975), and references cited therein.

(2) R. W. Doskotch, F. S. El-Feraly, E. H. Fairchild, and C. Huang, *J. Chem. Soc. Chem. Commum.*, **1976**, 402.

(3) M. Fujita, H. Itokawa, and Y. Sashida, *Yakugaku Zasshi*, **93**, 422 (1973).

(4) R. M. Wiedhopf, M. Young, E. Bianchi, and J. R. Cole, *J. Pharm. Sci.*, **62**, 345 (1973).

(5) R. A. Vines, "Trees, Shrubs and Woody Vines of the Southwest," University of Texas Press, Austin, Tex., 1960.

(6) R. W. Doskotch and F. S. El-Feraly, *J. Pharm. Sci.*, **58**, 877 (1969).

(7) H. Yoshioka, T. J. Mabry, and B. N. Timmermann, "Sesquiterpene Lactones, Chemistry, NMR and Plant Distribution," University of Tokyo Press, Tokyo, Japan, 1973.

(8) A. Quick and D. Rogers, *J. Chem. Soc. Perkin II*, **1976**, 465.

(9) Y. Sashida, H. Itokawa, Y. Akita, and M. Fujita, *Yakugaku Zasshi*, **96**, 218 (1976).

(10) F. Bellesia, R. Grandi, A. Marchesini, U. M. Pagoni, and R. Trave, *Phytochemistry*, **14**, 1737 (1975).

(11) W. K. Anderson and T. Veysoglu, *J. Org. Chem.*, **38**, 2267 (1973).

(12) A. S. Bawdekur, C. R. Kelkar, and S. C. Bhattacharyya, *Tetrahedron Lett.*, **1966**, 1225.

ACKNOWLEDGMENTS

Supported in part by the Research Institute of Pharmaceutical Sciences, School of Pharmacy, University of Mississippi, University, Miss.

The authors are indebted to Dr. Stephen Billets, Research Institute of Pharmaceutical Sciences, University, Miss., for the mass spectra.

Sustained Release from Inert Wax Matrixes I: Drug–Wax Combinations

HANS G. SCHROEDER *, ADNAN DAKKURI ‡, and PATRICK P. DeLUCA ˣ

Received July 9, 1976, from the *College of Pharmacy, University of Kentucky, Lexington, KY 40506.* Accepted for publication August 3, 1977.

*Present address: The Upjohn Co., Kalamazoo, MI 49001. ‡Present address: School of Pharmacy, Ferris State College, Big Rapids, MI 49307.

Abstract □ The melting and energy characteristics of several drug–wax combinations were investigated using differential scanning calorimetry. The phase diagrams of binary mixtures of tripelennamine hydrochloride and tolazoline hydrochloride with carnauba wax and castor wax showed no eutectic formation and gave no indication that a significant interaction was involved. However, in tripelennamine mixtures, a slight depression in the drug melting point was observed at around 50% concentration. For ternary systems, *i.e.*, drug, carnauba wax, and stearyl alcohol, thermograms of samples prepared by a fusion method differed slightly from those obtained with mixtures formulated by dissolving all ingredients in chloroform and evaporating the solvent. However, the location of the peak of each component remained essentially the same. A plot of melting point *versus* concentration of each compound showed insignificant changes in melting point and indicated that no interaction was occurring. The phase diagrams suggested that the combinations are strictly physical and that it is the physical characteristics, such as the hardness and composition of the core and drug particle size, that influence the release or dissolution of the drug from the waxy matrix.

Keyphrases □ Wax matrixes, inert—release of tripelennamine hydrochloride or tolazoline hydrochloride from mixtures with carnauba wax or castor wax □ Tripelennamine hydrochloride—release from inert carnauba or castor wax matrixes □ Tolazoline hydrochloride—release from inert carnauba or castor wax matrixes □ Dosage forms—inert wax matrixes, release of tripelennamine hydrochloride or tolazoline hydrochloride from mixtures with carnauba or castor wax □ Antihistaminics—tripelennamine hydrochloride, release from inert carnauba or castor wax matrixes □ Vasodilators, peripheral—tolazoline hydrochloride, release from inert carnauba or castor wax matrixes

The major factors influencing drug distribution in a sustained-release matrix (core) and drug release from the core include the particle size and drug solubility as well as core hardness and composition. Generally, the drug is physically incorporated into a wax matrix and compressed.

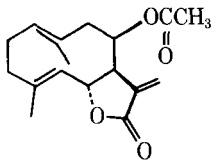

IX

This synthesis was accomplished by epoxidizing II in a two-phase system containing sodium bicarbonate (11). The presence of the latter prevented any cyclization and provided VI as the only product. As expected, VI underwent facile acid-catalyzed cyclization to VII and VIII. Moreover, it could be further epoxidized to III in the presence of excess peracid.

Since the absolute stereochemistry of C-1 in VII is *R* (7), it then followed that C-1 in VI must have the same absolute configuration. Also, the epoxide group of VI, being derived from the *trans*-1,10-double bond of II, must also have a *trans*-geometry. Therefore, the absolute stereochemistry of costunolide 1,10-epoxide should be as depicted in Structure VI. Consequently, III, which could be obtained by further epoxidation of VI, as mentioned before, must have similar chirality at C-1 and C-10.

Dihydrocostunolide was reported (12) to undergo epoxidation with perbenzoic acid to dihydrocostunolide diepoxide. In other words, epoxidation of dihydrocostunolide proceeded without cyclization. This behavior can be explained in terms of the poor acidity of perbenzoic acid and its reduction product, benzoic acid, relative to *m*-chloroperbenzoic acid and *m*-chlorobenzoic acid. However, there may be another explanation. The germacranolide sesquiterpene epitulipinolide (IX) can be epoxidized (1) with *m*-chloroperbenzoic acid to epitulipinolide 1,10-epoxide without cyclization. It appears, therefore, that the conformational factors affecting the transannular system of double bonds must play a significant role in deciding whether facile cyclization is to take place or not.

The root bark of *M. grandiflora* L. yielded, in addition to II, the two eudesmanolides VII and VIII. In view of the above discussion, these compounds must have been derived by the cyclization of biogenetically formed VI.

REFERENCES

(1) R. W. Doskotch, S. L. Keely, Jr., C. D. Hufford, and F. S. El-Feraly, *Phytochemistry*, **14**, 769 (1975), and references cited therein.

(2) R. W. Doskotch, F. S. El-Feraly, E. H. Fairchild, and C. Huang, *J. Chem. Soc. Chem. Commum.*, **1976**, 402.

(3) M. Fujita, H. Itokawa, and Y. Sashida, *Yakugaku Zasshi*, **93**, 422 (1973).

(4) R. M. Wiedhopf, M. Young, E. Bianchi, and J. R. Cole, *J. Pharm. Sci.*, **62**, 345 (1973).

(5) R. A. Vines, "Trees, Shrubs and Woody Vines of the Southwest," University of Texas Press, Austin, Tex., 1960.

(6) R. W. Doskotch and F. S. El-Feraly, *J. Pharm. Sci.*, **58**, 877 (1969).

(7) H. Yoshioka, T. J. Mabry, and B. N. Timmermann, "Sesquiterpene Lactones, Chemistry, NMR and Plant Distribution," University of Tokyo Press, Tokyo, Japan, 1973.

(8) A. Quick and D. Rogers, *J. Chem. Soc. Perkin II*, **1976**, 465.

(9) Y. Sashida, H. Itokawa, Y. Akita, and M. Fujita, *Yakugaku Zasshi*, **96**, 218 (1976).

(10) F. Bellesia, R. Grandi, A. Marchesini, U. M. Pagoni, and R. Trave, *Phytochemistry*, **14**, 1737 (1975).

(11) W. K. Anderson and T. Veysoglu, *J. Org. Chem.*, **38**, 2267 (1973).

(12) A. S. Bawdekur, C. R. Kelkar, and S. C. Bhattacharyya, *Tetrahedron Lett.*, **1966**, 1225.

ACKNOWLEDGMENTS

Supported in part by the Research Institute of Pharmaceutical Sciences, School of Pharmacy, University of Mississippi, University, Miss.

The authors are indebted to Dr. Stephen Billets, Research Institute of Pharmaceutical Sciences, University, Miss., for the mass spectra.

Sustained Release from Inert Wax Matrixes I: Drug–Wax Combinations

HANS G. SCHROEDER *, ADNAN DAKKURI ‡, and PATRICK P. DeLUCA ˣ

Received July 9, 1976, from the *College of Pharmacy, University of Kentucky, Lexington, KY 40506.* Accepted for publication August 3, 1977.

*Present address: The Upjohn Co., Kalamazoo, MI 49001. ‡Present address: School of Pharmacy, Ferris State College, Big Rapids, MI 49307.

Abstract □ The melting and energy characteristics of several drug–wax combinations were investigated using differential scanning calorimetry. The phase diagrams of binary mixtures of tripelennamine hydrochloride and tolazoline hydrochloride with carnauba wax and castor wax showed no eutectic formation and gave no indication that a significant interaction was involved. However, in tripelennamine mixtures, a slight depression in the drug melting point was observed at around 50% concentration. For ternary systems, *i.e.*, drug, carnauba wax, and stearyl alcohol, thermograms of samples prepared by a fusion method differed slightly from those obtained with mixtures formulated by dissolving all ingredients in chloroform and evaporating the solvent. However, the location of the peak of each component remained essentially the same. A plot of melting point *versus* concentration of each compound showed insignificant changes in melting point and indicated that no interaction was occurring. The phase diagrams suggested that the combinations are strictly physical and that it is the physical characteristics, such as the hardness and composition of the core and drug particle size, that influence the release or dissolution of the drug from the waxy matrix.

Keyphrases □ Wax matrixes, inert—release of tripelennamine hydrochloride or tolazoline hydrochloride from mixtures with carnauba wax or castor wax □ Tripelennamine hydrochloride—release from inert carnauba or castor wax matrixes □ Tolazoline hydrochloride—release from inert carnauba or castor wax matrixes □ Dosage forms—inert wax matrixes, release of tripelennamine hydrochloride or tolazoline hydrochloride from mixtures with carnauba or castor wax □ Antihistaminics—tripelennamine hydrochloride, release from inert carnauba or castor wax matrixes □ Vasodilators, peripheral—tolazoline hydrochloride, release from inert carnauba or castor wax matrixes

The major factors influencing drug distribution in a sustained-release matrix (core) and drug release from the core include the particle size and drug solubility as well as core hardness and composition. Generally, the drug is physically incorporated into a wax matrix and compressed.

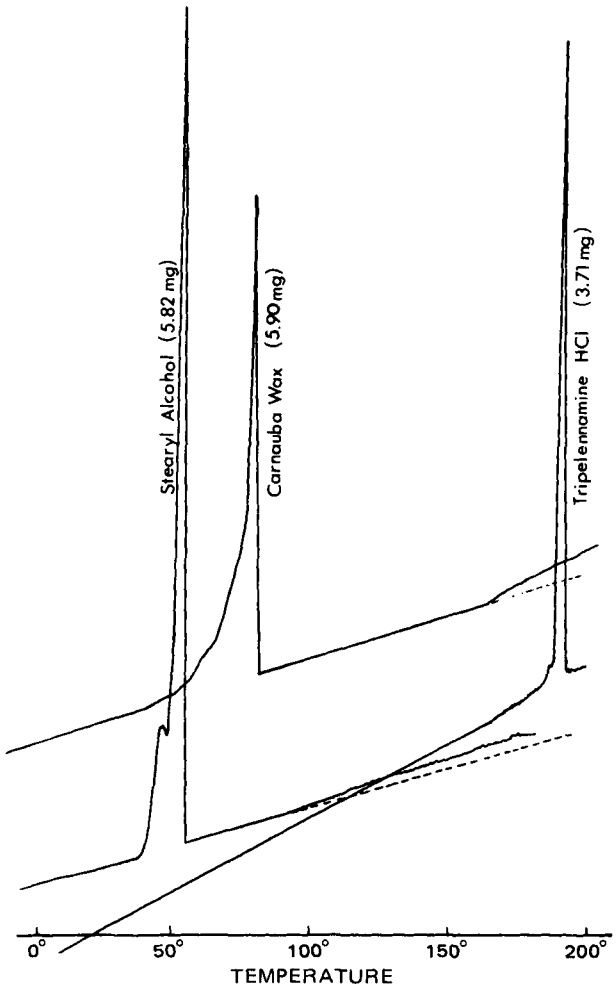

Figure 1—*DSC thermograms of tripelennamine hydrochloride, carnauba wax, and stearyl alcohol.*

BACKGROUND

Phase studies with sulfathiazole–urea combinations revealed that a eutectic mixture is formed (1) and that its physical properties differed significantly from the properties of mixtures at other compositions. The particle size of the drug crystals was smaller, and the increased surface area resulted in faster absorption and higher blood levels. A fused conglomerate of chloramphenicol and urea at the eutectic composition manifested no enhancement in the chloramphenicol dissolution rate as compared with the pure drug (2). However, in the presence of excess urea, a significant increase in drug release was reported.

Other investigators, after raising some theoretical questions concerning the proposed mechanism (2), postulated that the enhanced dissolution rate was attributable to the presence of solid solutions in the system rather than simple eutectic formation (3). This study (3) showed that dissolution rates from fused systems were greater than those from physical mixtures or pure drug. For example, evaluation of the dissolution rates of some griseofulvin–succinic acid samples indicated that the solid solution dissolved six to seven times faster than the pure material (4). Recently, the *in vitro* dissolution of tolbutamide was reported to be considerably increased by fusion with polyethylene glycol 6000 (5); enhanced bioavailability from such samples also was demonstrated (6).

Eutectic transformation, interactions resulting in the formation of monotectic or peritective compounds, formation of solid solution, and, possibly, stoichiometric compounds might be associated with a matrix solid dispersion system such as the drug–wax combination. The properties of a eutectic mixture would be expected to differ from those of a simple physical mixture. If the particle size and solubility of the drug were altered, then the dissolution characteristics and the *in vivo* availability could be influenced. Therefore, an investigation of the matrix-type sustained-release dosage form should commence with some basic phase studies to determine whether a drug–wax interaction occurs and at what composition a eutectic mixture exists.

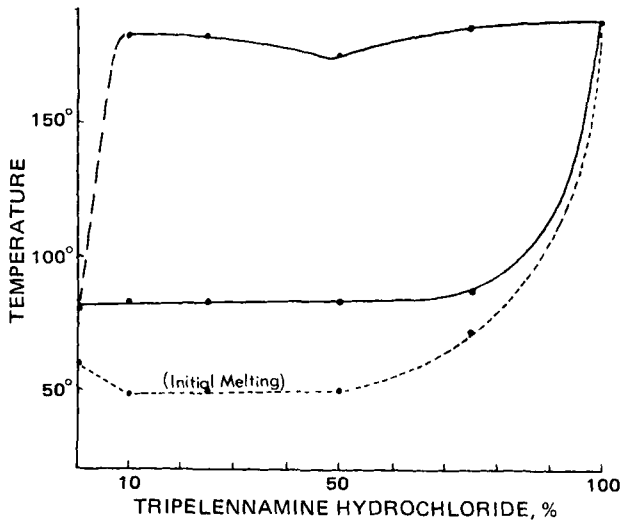

Figure 2—*Phase diagram for tripelennamine–carnauba wax binary system. The upper and lower solid curves correspond to the peak temperatures of the drug and wax, respectively. The broken line represents the temperature at which the initial deviation from the baseline in the thermogram occurred.*

In the present report, differential scanning calorimetry (DSC) was employed to investigate the melting and energy characteristics of various mixtures of drug (tripelennamine and tolazoline) and wax (carnauba wax, castor wax, and stearyl alcohol). A change in the these parameters would be indicative of component interactions. The information might be used to formulate a core with a better control of drug release.

EXPERIMENTAL

Materials[1]—Tripelennamine hydrochloride and tolazoline hydrochloride were used without further purification. Carnauba wax, castor wax, and stearyl alcohol were the wax bases used.

Fused Mixtures—The fused drug–wax binary mixtures were prepared by melting carnauba wax or castor wax to approximately 90°. Tripelennamine hydrochloride or tolazoline hydrochloride, after passing through a 40-mesh screen, was added in small portions while the mass was mixed. With constant stirring, the mixture was allowed to cool slowly to about 75°, and the entire mass was then immediately cast on cold glass plates. Subsequently, the congealed mass was crushed into a finely divided state and screened (40 mesh).

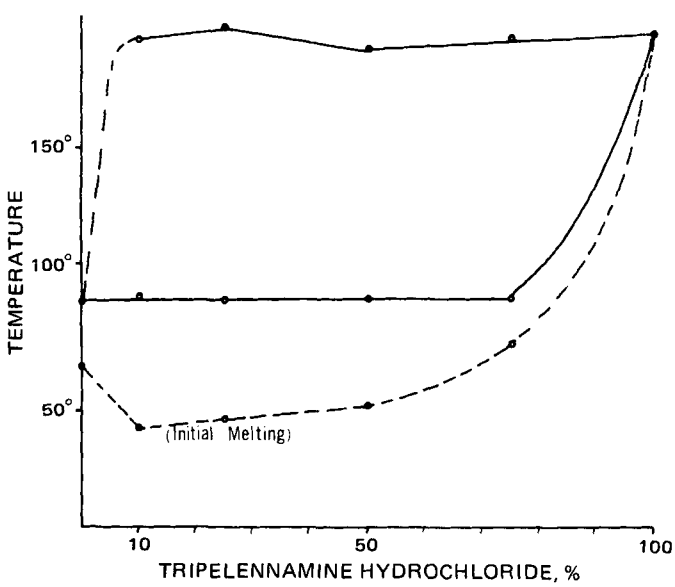

Figure 3—*Phase diagram for tripelennamine–castor wax binary system.*

[1] Supplied by Ciba-Geigy Corp., Summit, N.J.

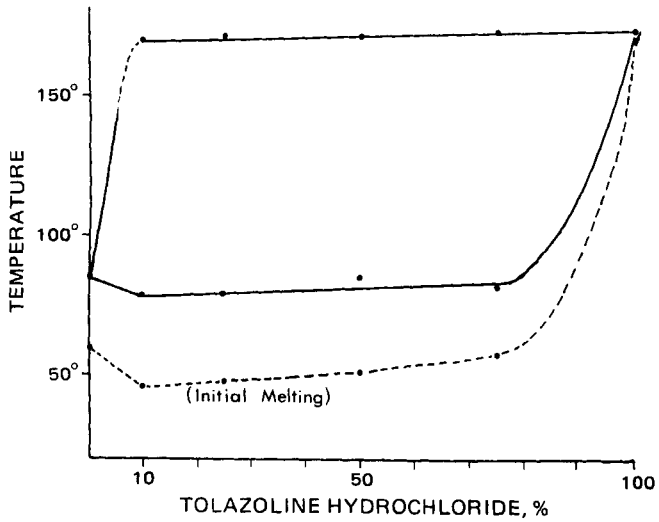

Figure 4—*Phase diagram for tolazoline–carnauba wax binary system.*

For the fused drug–carnauba wax–stearyl alcohol ternary mixtures, carnauba wax was first melted to approximately 90° and stearyl alcohol was then added. When a homogeneous mixture was attained, the drug was added. The mass was allowed to congeal and then powdered, following essentially the same procedure as already outlined.

Evaporated Mixtures—Carnauba wax and stearyl alcohol were dissolved in chloroform. A solution of the drug in the same vehicle was then added to the wax solution. After the system was mixed thoroughly, it was gently heated to evaporate the solvent. Subsequently, the solidified mass was crushed and passed through a 40-mesh screen.

Thermal Analysis—A differential scanning calorimeter[2] was used to determine the energy changes. The samples were placed in aluminum pans and scanned from 0 to 200° at 5°/min. To scan in the 0–40° range, the sample cover was filled with a methanol–dry ice mixture. Nitrogen purge at a rate of 30 ml/min was used constantly. Observed temperature values were corrected by using reference melting-point standards for calibration.

RESULTS AND DISCUSSION

One-Component Systems—The thermal stability of some individual substances was investigated. The DSC thermograms in Fig. 1 indicate that stearyl alcohol (mp 50–52°) and carnauba wax (mp 76–79°) undergo sublimation or degradation at elevated temperatures. Deviation from the baseline occurred at slightly above 100° for stearyl alcohol and at around 160° for carnauba wax. Tripelennamine hydrochloride (mp 188–190°) showed no sign of thermal decomposition in the 0–200° range.

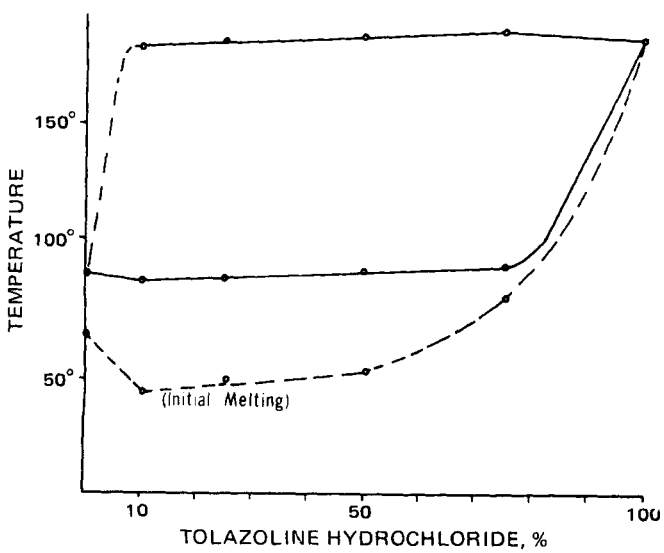

Figure 5—*Phase diagram for tolazoline–castor wax binary system.*

[2] Perkin-Elmer model DSC-1B.

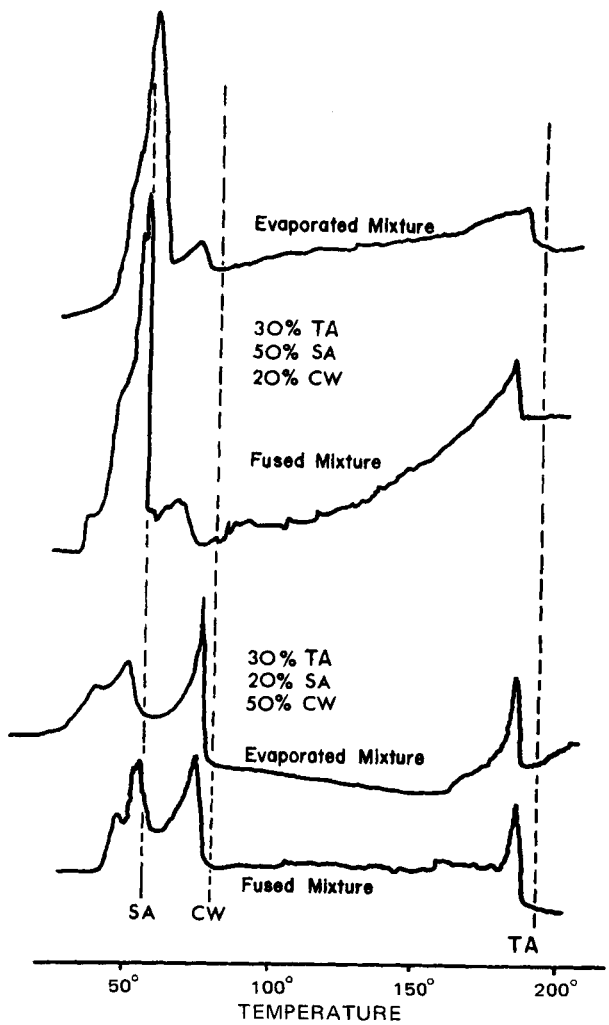

Figure 6—*DSC thermograms for two compositions of tripelennamine–carnauba wax–stearyl alcohol. Samples of each composition were prepared by dispersing tripelennamine in a melt of carnauba wax and stearyl alcohol (fused mixture) and by dissolving all ingredients in chloroform and evaporating the solvent (evaporated mixture). Key: SA, stearyl alcohol; CW, carnauba wax; and TA, tripelennamine hydrochloride.*

The fact that stearyl alcohol and carnauba wax undergo degradation or sublimation at elevated temperatures should be of no consequence since the preparation of the fused mixtures involved heating the components only to approximately 85–90°.

Two-Component Systems—Drug–wax mixtures were prepared at 0, 10, 25, 50, 75, and 100% (w/w) drug concentrations, and samples of these mixtures were heated in the differential scanning calorimeter. The locations of the peaks in each thermogram were plotted against the drug concentration to construct a phase diagram for each system. The tripelennamine–carnauba wax phase diagram is shown in Fig. 2. There was no indication of interaction or eutectic formation at above 10% drug concentration. The slight depression in the melting point of tripelennamine observed in the 50:50 combination is not unusual; it is well known that a slight change in the melting behavior of a substance occurs in the presence of another component.

Figure 3 shows the phase diagram for the tripelennamine–castor wax system. It is quite similar to that obtained for the tripelennamine–carnauba wax mixtures; once again, a slight depression in the melting point for the drug occurred at around 50% drug concentration. However, there was no indication that an interaction or eutectic formation was involved since the melting characteristics of the two components remained essentially unchanged.

For the tolazoline–carnauba wax and tolazoline–castor wax systems, the slight lowering in the melting point of the drug observed in the 50:50

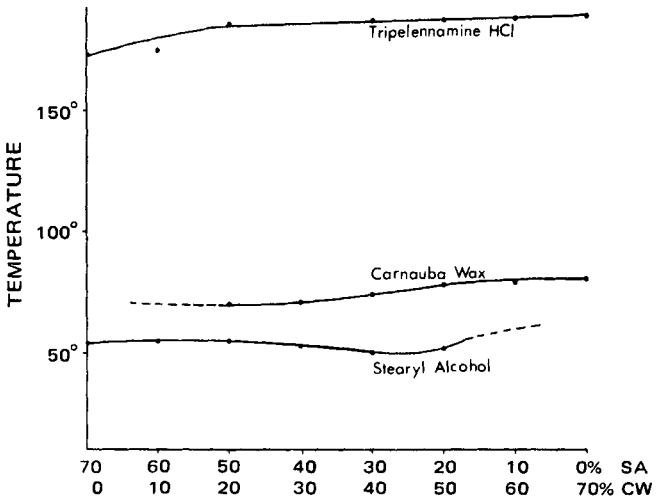

Figure 7—*Plot of the melting point (location of peak in the DSC thermogram) for each material in the tripelennamine–carnauba wax (CW)–stearyl alcohol (SA) system at various compositions. Tripelennamine concentration was kept constant at 30%, and the concentrations of the other two components were varied between 0 and 70%.*

tripelennamine–wax systems was absent. As shown in Figs. 4 and 5, the phase diagrams clearly indicated that an interaction between tolazoline and the waxes was nonexistent, although a slight decrease in the tolazoline melting point occurred as the wax composition increased.

Three-Component Systems—Ternary mixtures of tripelennamine, carnauba wax, and stearyl alcohol were prepared by two different methods to assess the effect of the preparation method on thermal behavior. The evaporated mixtures were selected for investigation to determine if the components would interact if combined in the dissolved state. Compounds that exhibit solid-state interactions frequently demonstrate interaction in solution. This phenomenon was observed with *N*-acetyl-*p*-aminophenol and urea (7) and niacinamide and ascorbic acid (8) and in griseofulvin–succinic acid (4) and chloramphenicol–urea (9) systems.

The concentration of tripelennamine hydrochloride was held constant at 30% (w/w), and the carnauba wax and stearyl alcohol concentrations were varied between 0 and 70%. Samples of the fused and evaporated mixtures were scanned. Thermograms for two compositions are shown in Fig. 6. While the curves for the evaporated samples differed slightly from thermograms of fused samples, the locations of the peak for each component remained essentially the same. From these results, it appears that an interaction between the components of the system does not occur even if they are dispersed at the molecular level.

Figure 7 shows a plot of the melting point *versus* concentration for each component. The slight variation in the melting points of the various components was considered to be insignificant. In addition, no interaction occurred in the three-component system.

REFERENCES

(1) K. Sekiguchi and N. Obi, *Chem. Pharm. Bull.*, **9**, 866 (1961).

(2) K. Sekiguchi, N. Obi, and Y. Ueda, *ibid.*, **12**, 134 (1964).

(3) A. H. Goldberg, M. Gibaldi, and J. L. Kanig, *J. Pharm. Sci.*, **54**, 1145 (1965).

(4) *Ibid.*, **55**, 487 (1966).

(5) S. A. Said, H. M. El-Fatatry, and A. S. Geneidi, *Aust. J. Pharm. Sci.*, **NS3**, 42 (1974).

(6) S. A. Said and S. F. Saad, *ibid.*, **NS4**, 121 (1975).

(7) A. H. Goldberg, M. Gibaldi, and J. L. Kanig, *J. Pharm. Sci.*, **55**, 482 (1966).

(8) D. E. Guttman and D. Brooke, *ibid.*, **52**, 941 (1963).

(9) A. H. Goldberg, M. Gibaldi, J. L. Kanig, and M. Mayersohn, *ibid.*, **55**, 581 (1966).

ACKNOWLEDGMENTS

Presented at the Basic Pharmaceutics Section, APhA Academy of Pharmaceutical Sciences, New Orleans meeting, April 1976.

Supported in part by a grant from the Ciba-Geigy Corp., Summit, N.J.

Sustained Release from Inert Wax Matrixes II: Effect of Surfactants on Tripelennamine Hydrochloride Release

ADNAN DAKKURI *, HANS G. SCHROEDER ‡, and PATRICK P. DeLUCA ˣ

Received July 9, 1976, from the *College of Pharmacy, University of Kentucky, Lexington, KY 40506.* Accepted for publication August 3, 1977. *Present address: School of Pharmacy, Ferris State College, Big Rapids, MI 49307. ‡Present address: The Upjohn Co., Kalamazoo, MI 49001.

Abstract □ The influence of several surfactants on the *in vitro* release of tripelennamine hydrochloride from a wax matrix was investigated. The congealed mass, obtained by dispersing the drug and surfactant in a molten mixture of carnauba wax and stearyl alcohol, was granulated and compressed into cores. While controlling particle-size distribution, tablet hardness, and weight, dissolution in simulated intestinal fluid was measured with the rotating-basket method. Water-insoluble surfactants such as glyceryl monostearate had no effect on the dissolution rate; slightly soluble or slowly soluble agents, such as sodium stearate, ammonium stearate, triethanolamine, and dioctyl sodium sulfosuccinate moderately increased dissolution. However, the water-soluble hydrophilic polyoxyethylene 23 lauryl ether considerably increased the dissolution rate; *i.e.*, about 80% of drug was released by a zero-order process over 4 hr. Since only a few surfactants were investigated, it is difficult to explain the difference in dissolution rate on the basis of ionic character. The profound effect of polyoxyethylene 23 lauryl ether could be attributed to both its hydrophilic nature and wetting action in an aqueous environment at the liquid–solid interface. Only with polyoxyethylene 23 lauryl ether was more than 50% released over 8 hr. With no surfactant present, approximately 38% was released, and release in the 1st hr was most rapid. The data suggest that a surfactant may make more channels available for the dissolution fluid to leach out the drug. Thus, the effective porosity of the matrix is increased. Furthermore, wetting is an important factor that controls matrix permeability.

Keyphrases □ Wax matrixes, inert—release of tripelennamine hydrochloride, effect of various surfactants □ Tripelennamine hydrochloride—release from inert wax matrixes, effect of various surfactants □ Surfactants, various—effect on release of tripelennamine hydrochloride from inert wax matrixes □ Antihistaminics—tripelennamine hydrochloride, release from inert wax matrixes, effect of various surfactants □ Tablets—tripelennamine hydrochloride in inert wax matrixes, effect of various surfactants on drug release □ Dosage forms—tablets of tripelennamine hydrochloride in inert wax matrixes, effect of various surfactants on drug release

A method of rapidly achieving and adequately maintaining a desired plasma drug level involves fabrication of a core tablet in which the instantly available portion of the drug is contained in an outer coating and the maintenance dosage is incorporated in a sustained-release wax matrix or core (1, 2). If it is assumed that the drug is readily available from the coating to achieve sufficient absorption to produce a rapid therapeutic response, the release of the balance of the drug from the core is dependent on drug particle size and solubility and core hardness and composition. Since the first three factors have been studied extensively, this investigation focused on the composition of the core. Many compositions have been suggested for sustaining drug release over a long period (3–5).

BACKGROUND

Surfactants have been used successfully as binders in solid formulations; they also function as lubricants during tablet compression. Although these functions are believed to have little connection with surface activity, it is this wetting action that promotes the drug release from the matrix (6). Therefore, surfactant incorporation into the matrix should give rise to two distinct phenomena: (*a*) a wetting action that promotes uniform distribution of the drug in the substrate, and (*b*) a wetting action in an aqueous environment at the liquid–solid interface that promotes uniform release of the drug from the substrate.

The role of wetting on the drug release rate from inert matrixes was emphasized by Singh *et al.* (6), who found that matrix permeability and permeation rates of the matrix by the solvent individually limit drug release. The determining factors were the pore-size distribution of the matrix and the permeation pressure of the contacting fluid defined by its surface tension and contact angle.

The purpose of this investigation was to study the effect of several surfactants individually incorporated in an inert solid matrix on drug release in an *in vitro* system; it is believed that drug distribution will be improved and that the drug release will be controlled more easily. Since drug solubility influences the release rate, drugs of varying solubility in water will be selected for eventual study with cationic, anionic, and nonionic surfactants. This report is limited to tripelennamine with several surfactants.

The surfactants were selected on a somewhat arbitrary basis, but all are pharmaceutically accepted compounds and have been used principally as dispersing and emulsifying agents in topical preparations. The stearates were selected because of their lubricant characteristics and their slight or slow solubility in water. Dioctyl sodium sulfosuccinate, polyoxyethylene 23 lauryl ether, and triethanolamine were selected as representatives of anionic, nonionic, and cationic agents, respectively.

EXPERIMENTAL

Materials—Tripelennamine hydrochloride, carnauba wax, and stearyl alcohol were used as received[1]. The surfactants were glyceryl monostearate[2], sodium stearate[2], ammonium stearate[3], dioctyl sodium sulfosuccinate[4], triethanolamine[5], and polyoxyethylene 23 lauryl ether[6].

Core Preparation—Three methods of incorporating the drug and surfactant into the matrix were explored:

1. The drug and surfactant were physically dispersed into the molten wax matrix.
2. The drug and surfactant were dissolved in a vehicle, the solution was incorporated into the molten wax phase, and the solvent was subsequently evaporated.
3. The ingredients were dry blended and compressed into a slug and then granulated and compressed into a core.

The first method was selected because it produced a more uniform matrix.

The granulations for compression into cores were prepared by melting the carnauba wax to approximately 90° and adding the stearyl alcohol. When a homogeneous melt was attained, the surfactant was added. Stirring was continued until an even distribution was reached. Then tripelennamine hydrochloride was added in small portions while the mass was mixed. With constant stirring, the mixture was allowed to cool slowly to about 75°, and the entire mass was then immediately poured onto cold glass plates and allowed to congeal. The solid mass was then granulated.

Equal quantities of carnauba wax, stearyl alcohol, and tripelennamine were used to prepare the surfactant-free formulation. In the other for-

[1] Supplied by Ciba-Geigy Corp., Summit, N.J.
[2] Fisher Scientific, Fair Lawn, N.J.
[3] Matheson, Coleman and Bell, Rutherford, N.J.
[4] Aerosol OT, Fisher Scientific, Fair Lawn, N.J.
[5] Ransdell Co., Louisville, Ky.
[6] Brij 35, J. T. Baker Chemical Co., Phillipsburg, N.J.

Table I—Tripelennamine Hydrochloride Content, Hardness, and Weight of Cores

Formulation	Tripelennamine Hydrochloride in Granulations[a], %	Hardness[b]	Weight[c], mg	Tripelennamine Hydrochloride Core[d], mg
Experimental control[e]	35.7 ± 1.1	9.6	202.6	71.17
Commercial control	—	10.5	199.6	67.22
Glyceryl monostearate, 2 mg	35.1 ± 0.6	9.9	216.7	71.42
Glyceryl monostearate, 5 mg	33.5 ± 0.7	10.1	205.4	71.68
Glyceryl monostearate, 10 mg	35.1 ± 0.5	9.4	212.0	74.43
Sodium stearate, 5 mg	33.8 ± 0.6	9.8	207.6	67.58
Ammonium stearate, 5 mg	35.5 ± 0.8	9.4	197.0	71.42
Triethanolamine, 5 mg	34.4 ± 0.5	8.9	198.0	66.24
Dioctyl sodium sulfosuccinate, 5 mg	34.3 ± 0.6	10.0	207.3	71.74
Polyoxyethylene 23 lauryl ether, 5 mg	32.7 ± 0.4	9.6	196.7	64.83

[a] Average of six determinations of 1-g samples. Theoretical = 33.3%. [b] Pfizer hardness tester (lb/in.^{2}). Average of 10 determinations. [c] Average of 10 determinations. [d] Average of three determinations from powder obtained from 10 cores. [e] No surfactant present.

mulations, equal quantities of carnauba wax and stearyl alcohol were replaced with the amount of surfactant added.

The granulation was screened and separated into four fractions: >1200, 750–1200, 300–750, and <300 μm. The particle-size distribution of the granulation was held constant for all formulations and was controlled by recombining a fixed amount of granules in each size range: 20, 30, 30, and 20% (w/w) for the four size ranges, respectively.

Magnesium stearate, 1%, was added to the granulation, which was then compressed[7] into 200-mg cores using 9.5-mm (0.38-in.) punches and die. Considerable effort was expended to ensure a uniform tablet weight and a consistent tablet hardness. Every effort was made to make the cores comparable to the commercial cores[8]. It was necessary to compress the cores to the same hardness as the commercial cores, which had been subjected to double compression: first when the cores were prepared and then when the outer coating was applied.

Since the purpose was the determination of drug release from the sustained-release portion, the outer coating of the tablet was washed off with water and the resultant cores were used as controls in the preparation of the experimental cores, as previously mentioned. Therefore, the results should be equally valid when applied to the slow-release core of timed-release tablets.

Dissolution Procedure—The USP XIX rotating-basket method (7) was employed for investigating drug release from the cores. Three tablets were placed in the basket, which was immersed in 600 ml of simulated intestinal fluid[9] previously warmed to 37°. The basket was rotated at 50 rpm, and the water bath was maintained at 37 ± 0.5° for 8 hr.

At 1-hr intervals, a 2-ml sample was withdrawn from the vessel for assay with a pipet fitted with a glass wool prefilter and immediately replaced with an equivalent volume of dissolution medium. The remaining portions of the tablets were assayed at the termination of each dissolution experiment to determine the amount of drug remaining. Duplicate runs were made on each batch.

Tripelennamine Hydrochloride Assay—Aliquots of the dissolution medium were assayed for tripelennamine hydrochloride content by diluting to an appropriate volume with methanol, filtering the sample, and measuring its absorbance[10] at 244 nm against a methanol blank containing the same volume of dissolution medium as the sample. A standard Beer's law plot was constructed, and an absorptivity of 52.08 ml/mg (1-cm cell) was calculated. This factor was used to determine the tripelennamine concentration in the sample. The cumulative drug released was computed from the sample assays using the Wurster and Taylor equation (8).

The presence of the surfactants did not interfere with the drug assay. Intact cores, remains of cores, and granulations were analyzed by extracting the tripelennamine with methanol in a blender[11]. An aliquot was removed and diluted to an appropriate volume with methanol, and the absorbance was read at 244 nm using a methanol blank.

RESULTS AND DISCUSSION

Table I shows the values for tripelennamine hydrochloride contents in the granulations and intact cores as well as the hardness and weight of the cores of all batches. The consistency of the drug percentage in the various granulations indicates that the drug was uniformly distributed, and the lower standard deviations for the surfactant-containing granulations suggest improved drug distribution.

Since the outer coating of commercial tablets readily disintegrates and releases tripelennamine hydrochloride in the gastric fluid, this study was concerned only with drug release from the slow-release wax matrix designed to resist attack in gastric fluid. However, preliminary studies showed that some dissolution occurred within 20 min in simulated gastric fluid. This dissolution can be attributed to surface drug. Any additional drug release was negligible until the core was transferred to the intestinal fluid.

In Fig. 1, tripelennamine release from commercial cores[8] is plotted along with the release from the prepared surfactant-free cores. The two release patterns are similar. Therefore, all comparisons should be valid, and the results obtained using surfactants in the formulations should be representative of what would be expected if such surfactants were incorporated into the commercial cores. The lower initial drug release from these cores can be attributed to the lower concentration of surface drug as a result of washing off the outer coating. Nevertheless, this release can be ignored because the similarity between the two release patterns is clearly evident.

Commercial cores (no outer coating) subjected to single compression only were much softer (5–6 lb/in.^{2}) than the cores obtained by removing the outer coating of the commercial tablet. The increased hardness in the latter cores was due to the second compression step in adding the coating. While the incremental drug release was much faster (between 2 and 5 hr) for the single-compression cores, the incremental release of drug before and after this period was similar to the other two cores (Fig. 1). The abrupt drug release was due to core disintegration, which increased the surface area significantly, particularly in the 2–3-hr interval. This result emphasizes the need for controlled core disintegration. The desired drug dissolution from the sustained-release portion over 10 hr, assuming no initial release, is depicted by the dotted line in Fig. 1.

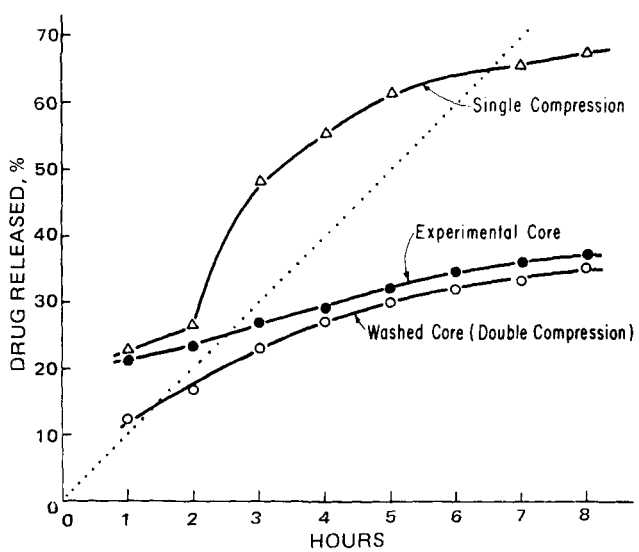

Figure 1—*Tripelennamine hydrochloride release from a wax matrix in the absence of surfactants. Key: △, commercial single-compression cores; ●, experimental cores (no surfactant present); and ○, cores obtained by washing off the outer coating of commercial tablets.*

[7] Stokes model E single-punch tablet press.
[8] Cores of Pyribenzamine Lontabs, Ciba Pharmaceutical Co., Summit, N.J.
[9] Pancreatin NF, 7.44 g; sodium bicarbonate, 120.0 g; and distilled water, sufficient quantity to make 8000 ml; pH 8.0 ± 0.1.
[10] Gilford model 240 spectrophotometer.
[11] Waring.

Table II—Incremental Release (Milligrams) of Tripelennamine Hydrochloride from Cores [a]

Formulation	First 20 min	1st hr	2nd hr	3rd hr	4th hr	5th hr	6th hr	7th hr	8th hr	Remains	Total Recovered mg	Total Recovered %
Commercial control	—	8.93	3.17	4.60	2.97	1.60	1.50	1.40	1.39	40.99	65.55	97.5
Experimental control [b]	—	15.39	1.00	3.03	1.59	2.01	1.56	1.23	1.12	38.06	64.99	91.3
Glyceryl monostearate, 2 mg	—	13.93	1.85	2.95	1.56	2.11	1.19	1.58	2.22	43.56	70.95	99.3
Glyceryl monostearate, 5 mg	—	12.57	2.56	2.81	1.84	0.94	1.30	1.26	1.32	41.20	65.80	91.7
Glyceryl monostearate, 10 mg	8.27	12.86	4.00	3.00	2.60	1.21	1.05	0.95	1.39	42.96	70.02	94.1
Sodium stearate, 5 mg	8.98	14.24	3.52	4.75	2.69	2.25	2.87	2.96	0.57	33.28	67.13	99.3
Ammonium stearate, 5 mg	8.93	13.31	3.84	3.38	2.62	2.77	1.97	2.30	2.09	32.52	64.80	90.7
Triethanolamine, 5 mg	8.29	13.11	3.66	3.62	3.08	2.08	2.49	1.84	0.84	32.36	63.08	95.2
Dioctyl sodium sulfosuccinate, 5 mg	8.36	12.82	4.62	3.70	2.72	2.37	1.51	2.28	2.72	32.56	65.30	91.0
Polyoxyethylene 23 lauryl ether, 5 mg	9.40	19.08	14.86	9.30	8.79	3.65	0.17	0.56	—	6.11	62.52	96.3

[a] Values reported are the average of duplicate samples, three cores each. [b] No surfactant present.

The effect of glyceryl monostearate on the tripelennamine release rate is shown in Fig. 2; the data for three levels of surfactant are plotted. There was very little difference from the release pattern without surfactant present. The fact that glyceryl monostearate did not affect the drug dissolution rate can probably be attributed to its water insolubility.

However, as shown in Fig. 3, when sodium stearate or ammonium stearate was used, the release pattern was improved; sodium stearate gave better results when compared with ammonium stearate. Between 1 and 8 hr, there was a strong ($r = 0.988$) and statistically highly significant correlation ($p < 0.001$) between the amount of drug released and time. The linearity of the relationship and the resulting high correlation coefficient suggest that the drug was released by a zero-order process within the specified time period. Sodium stearate dissolves slowly in water but is more readily soluble in intestinal fluid; this property is probably the reason for it having a greater effect on the dissolution rate than either glyceryl monostearate or ammonium stearate. The latter surfactant is slightly soluble in water and, consequently, the dissolution rate obtained with it lies between the rates obtained with sodium stearate and glyceryl monostearate.

Figure 4 illustrates the effect of three different surfactants on the dissolution rate. While both the cationic surfactant triethanolamine and the anionic agent dioctyl sodium sulfosuccinate increased the release rate, the nonionic agent polyoxyethylene 23 lauryl ether showed a profound effect. Over 4 hr, about 80% of the drug appeared to be released by a zero-order process, as suggested by the linear relationship between the amount of drug released and time. However, very little additional tripelennamine was released thereafter, and less than 90% was in solution following 8 hr.

It is difficult to explain the difference in the dissolution rate on the basis of ionic type since only a few surfactants were investigated. The greater rate with the core containing polyoxyethylene 23 lauryl ether could be attributed, in addition to surface activity, to greater water solubility and hydrophilicity. Triethanolamine is a good wetting agent and shows good miscibility with water, while dioctyl sodium sulfosuccinate is slowly soluble in water.

The incremental drug release with various surfactants is shown in Table II. Only with polyoxyethylene 23 lauryl ether did more than a 50% release occur over 8 hr. With no surfactant present, only 38% was released over the same period, and half of that occurred in the 1st hr.

The desired situation for the tripelennamine core would be the release of its entire content in 10 hr. To maintain sustained release and subsequently to attain a constant blood drug level over such a period, an average of 6.67 mg (66.7 mg/200-mg core) of drug should be released each hour. While polyoxyethylene 23 lauryl ether, sodium stearate, and triethanolamine show promise in improving the release profile, an *in vivo* study is needed to correlate with the *in vitro* dissolution method. The dissolution method utilized is by no means indicative or predictive of the attainable blood levels, and some correlation between *in vitro* drug release and *in vivo* performance is required.

Drug release is principally *via* a leaching mechanism, and drug diffusion through the matrix is either nonexistent or insignificant (4). Either the core must be slowly and continually eroding so that new surfaces are being exposed or channels must be continually forming in the core so that the intestinal fluid penetrates the core and leaches out the drug. Spontaneous core disintegration has a deleterious effect because it only provides an instantaneous drug release and any further release from the resultant small particles is negligible.

The data in Table II show that total release is not possible. A certain percentage of drug will always be coated very effectively with a wax film impermeable to the dissolution fluid. Consequently, total release may be difficult to achieve. The same phenomenon was observed with slowly eroding, timed-release tablets prepared with a swellable gum, carbomer 934P (9). The lubricant magnesium stearate might exert a slight retardant

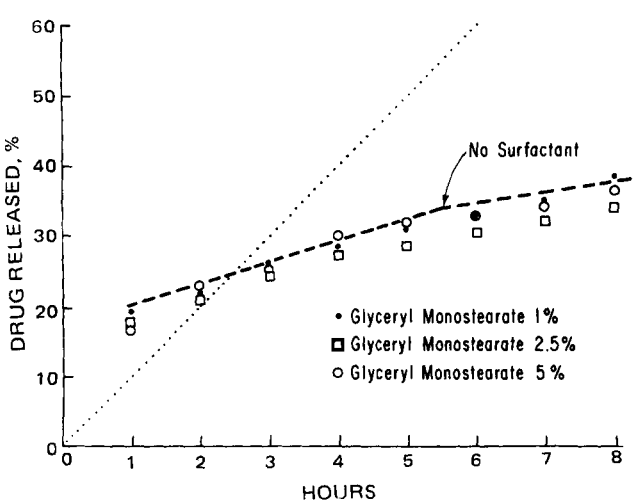

Figure 2—*Tripelennamine hydrochloride release from a wax matrix containing different levels of glyceryl monostearate. Key: ●, 1%; □, 2.5%; and ○, 5%. The broken line represents drug release from a surfactant-free core.*

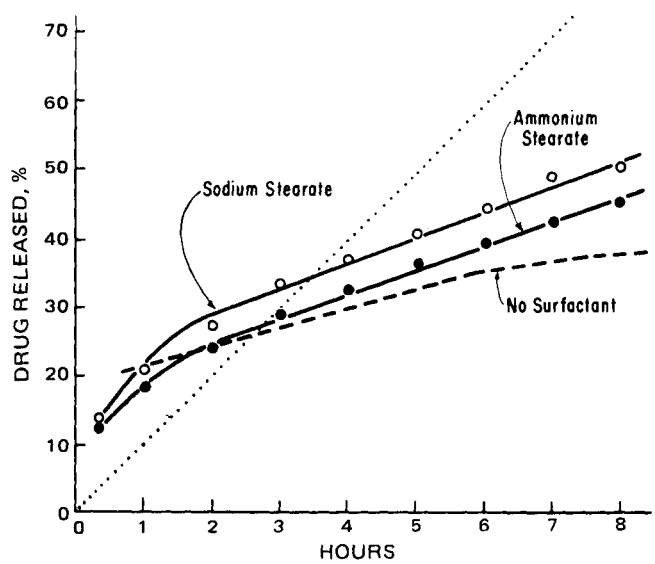

Figure 3—*Effect of stearates on the release of tripelennamine hydrochloride from a wax matrix. Key (surfactant in cores): ●, 2.5% ammonium stearate; and ○, 2.5% sodium stearate. The broken line represents drug release from a surfactant-free core.*

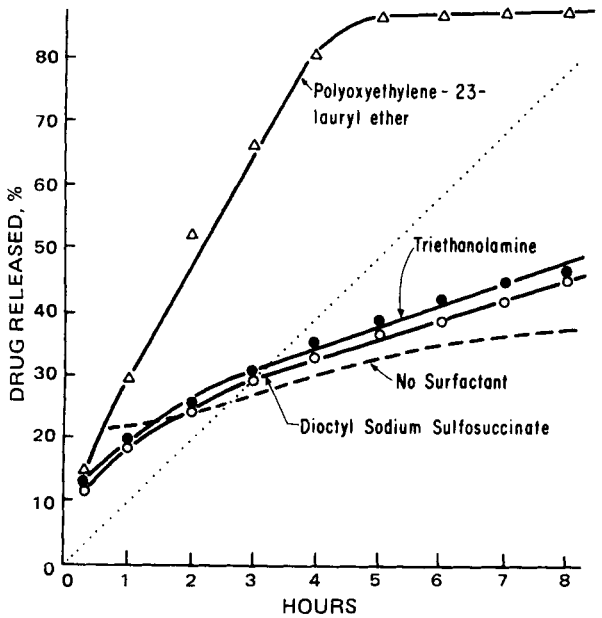

Figure 4—*Effect of surfactants of varying types on tripelennamine hydrochloride release from a wax matrix. The cores contained 2.5% surfactant. The broken line represents drug release from a surfactant-free core.*

effect on core dissolution; it possibly can be replaced with magnesium lauryl sulfate, but its toxicity has not yet been established (10).

The data suggest that a surfactant may make more channels available for the dissolution fluid to leach out the drug. Thus, the effective porosity of the matrix is increased. Wetting is an important factor that controls matrix permeability. It may be of interest to measure the degree of wetting of the various surfactants selected for this study.

REFERENCES

(1) J. Cooper and J. J. Windheuser, U.S. pat. 2,887,438 (1959).

(2) F. W. Goodhart, F. W. McCoy, and F. C. Ninger, *J. Pharm. Sci.*, **63**, 1748 (1974).

(3) E. Stempel, *Drug Cosmet. Ind.*, **98** (1), 44 (1966).

(4) *Ibid.*, **98** (2), 36 (1966).

(5) J. C. Johnson, "Tablet Manufacture," Noyes Data Corp., Park Ridge, N.J., 1974.

(6) P. Singh, S. J. Desai, A. P. Simonelli, and W. I. Higuchi, *J. Pharm. Sci.*, **57**, 217 (1968).

(7) "The United States Pharmacopeia," 19th rev., Mack Publishing Co., Easton, Pa., 1975, p. 651.

(8) D. E. Wurster and P. W. Taylor, *J. Pharm. Sci.*, **54**, 670 (1965).

(9) N. H. Choulis and H. Papadopoulos, *ibid.*, **64**, 1033 (1975).

(10) H. C. Caldwell and W. J. Westlake, *ibid.*, **61**, 984 (1972).

ACKNOWLEDGMENTS

Presented at the Basic Pharmaceutics Section, APhA Academy of Pharmaceutical Sciences, New Orleans meeting, April 1976.

Sustained Release from Inert Wax Matrixes III: Effect of Povidone on Tripelennamine Hydrochloride Release

ADNAN DAKKURI *, L. DAVID BUTLER, and PATRICK P. DeLUCA ˣ

Received October 13, 1976, from the *College of Pharmacy, University of Kentucky, Lexington, KY 40506.* Accepted for publication February 16, 1977. *Present address: School of Pharmacy, Ferris State College, Big Rapids, MI 49307.

Abstract □ The utilization of povidone as a channeling agent in the formulation of a sustained-release tripelennamine hydrochloride core significantly influenced drug release over 10 hr. Povidone was incorporated into a mixture of carnauba wax and stearyl alcohol by fusion and subsequent congealing in concentrations of 5, 10, and 20% (w/w); the stearyl alcohol concentration was altered to maintain a constant tripelennamine content. Tablet hardness and weight were also held constant. With the povidone-free formulation as a control, the addition of 5% of the channeling agent increased the release by 37% over 8 hr; at the 20% level, the increase was 55%. Between 0.5 and 8 hr, the drug appeared to be released by a zero-order process and a plateau was then approached. Over this interval, the dissolution pattern approached the optimum situation of 10% release/hr with 10–20% povidone. The results obtained from cores made by double compression of the dry-blended ingredients indicated that fusion is essential for channel formation. There was no evidence of complexation between tripelennamine and povidone. A decrease in the release rate was obtained when the polymer was included in the dissolution medium. It appears that channel formation is the mechanism underlying the increase in the drug dissolution rate from cores containing the polymer.

Keyphrases □ Povidone—effect on tripelennamine hydrochloride release from inert wax matrix tablets □ Wax matrixes, inert—effect of povidone on tripelennamine hydrochloride release, tablets □ Tripelennamine hydrochloride—release from inert wax matrix tablets, effect of povidone □ Polymers—povidone, effect on tripelennamine hydrochloride release from inert wax matrix tablets □ Antihistaminics—tripelennamine hydrochloride, release from inert wax matrix tablets, effect of povidone □ Tablets—containing inert wax matrix, effect of povidone on tripelennamine hydrochloride release □ Dosage forms—tablets containing inert wax matrix, effect of povidone on tripelennamine hydrochloride release

The mechanism of drug release from the wax matrix-type core involves leaching by the intestinal fluid that contacts the imbedded drug. In addition to dissolving "surface" drug, the fluid can enter the core through pores, cracks, and intergranular spaces and dissolve the drug. Drug diffusion through the matrix is either nonexistent or insignificant (1).

Higuchi (2) theoretically treated the matrix model and showed that the porosity and degree of tortuosity (a measure of diffusional path) in the capillary system influence the dissolution rate. Since the amount of drug per unit of matrix volume decreases with time as dissolution occurs, the porosity should increase and tortuosity should decrease to maintain a constant dissolution rate, in ac-

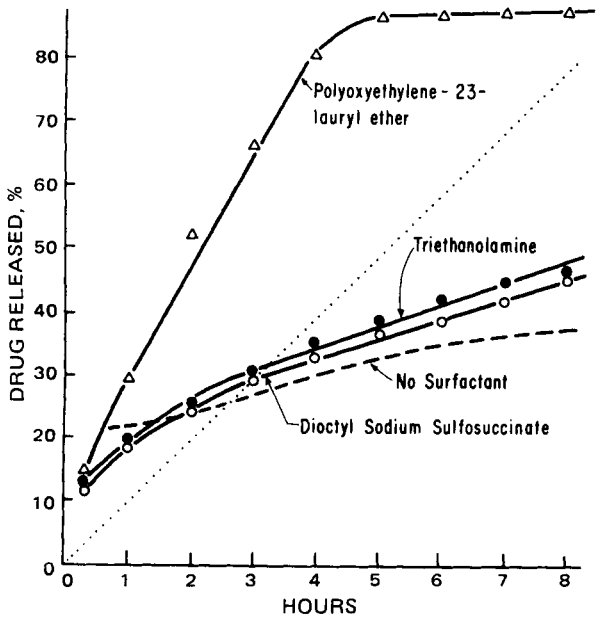

Figure 4—*Effect of surfactants of varying types on tripelennamine hydrochloride release from a wax matrix. The cores contained 2.5% surfactant. The broken line represents drug release from a surfactant-free core.*

effect on core dissolution; it possibly can be replaced with magnesium lauryl sulfate, but its toxicity has not yet been established (10).

The data suggest that a surfactant may make more channels available for the dissolution fluid to leach out the drug. Thus, the effective porosity of the matrix is increased. Wetting is an important factor that controls matrix permeability. It may be of interest to measure the degree of wetting of the various surfactants selected for this study.

REFERENCES

(1) J. Cooper and J. J. Windheuser, U.S. pat. 2,887,438 (1959).

(2) F. W. Goodhart, F. W. McCoy, and F. C. Ninger, *J. Pharm. Sci.*, **63**, 1748 (1974).

(3) E. Stempel, *Drug Cosmet. Ind.*, **98** (1), 44 (1966).

(4) *Ibid.*, **98** (2), 36 (1966).

(5) J. C. Johnson, "Tablet Manufacture," Noyes Data Corp., Park Ridge, N.J., 1974.

(6) P. Singh, S. J. Desai, A. P. Simonelli, and W. I. Higuchi, *J. Pharm. Sci.*, **57**, 217 (1968).

(7) "The United States Pharmacopeia," 19th rev., Mack Publishing Co., Easton, Pa., 1975, p. 651.

(8) D. E. Wurster and P. W. Taylor, *J. Pharm. Sci.*, **54**, 670 (1965).

(9) N. H. Choulis and H. Papadopoulos, *ibid.*, **64**, 1033 (1975).

(10) H. C. Caldwell and W. J. Westlake, *ibid.*, **61**, 984 (1972).

ACKNOWLEDGMENTS

Presented at the Basic Pharmaceutics Section, APhA Academy of Pharmaceutical Sciences, New Orleans meeting, April 1976.

Sustained Release from Inert Wax Matrixes III: Effect of Povidone on Tripelennamine Hydrochloride Release

ADNAN DAKKURI *, L. DAVID BUTLER, and PATRICK P. DeLUCA ˣ

Received October 13, 1976, from the *College of Pharmacy, University of Kentucky, Lexington, KY 40506.* Accepted for publication February 16, 1977. *Present address: School of Pharmacy, Ferris State College, Big Rapids, MI 49307.

Abstract □ The utilization of povidone as a channeling agent in the formulation of a sustained-release tripelennamine hydrochloride core significantly influenced drug release over 10 hr. Povidone was incorporated into a mixture of carnauba wax and stearyl alcohol by fusion and subsequent congealing in concentrations of 5, 10, and 20% (w/w); the stearyl alcohol concentration was altered to maintain a constant tripelennamine content. Tablet hardness and weight were also held constant. With the povidone-free formulation as a control, the addition of 5% of the channeling agent increased the release by 37% over 8 hr; at the 20% level, the increase was 55%. Between 0.5 and 8 hr, the drug appeared to be released by a zero-order process and a plateau was then approached. Over this interval, the dissolution pattern approached the optimum situation of 10% release/hr with 10–20% povidone. The results obtained from cores made by double compression of the dry-blended ingredients indicated that fusion is essential for channel formation. There was no evidence of complexation between tripelennamine and povidone. A decrease in the release rate was obtained when the polymer was included in the dissolution medium. It appears that channel formation is the mechanism underlying the increase in the drug dissolution rate from cores containing the polymer.

Keyphrases □ Povidone—effect on tripelennamine hydrochloride release from inert wax matrix tablets □ Wax matrixes, inert—effect of povidone on tripelennamine hydrochloride release, tablets □ Tripelennamine hydrochloride—release from inert wax matrix tablets, effect of povidone □ Polymers—povidone, effect on tripelennamine hydrochloride release from inert wax matrix tablets □ Antihistaminics—tripelennamine hydrochloride, release from inert wax matrix tablets, effect of povidone □ Tablets—containing inert wax matrix, effect of povidone on tripelennamine hydrochloride release □ Dosage forms—tablets containing inert wax matrix, effect of povidone on tripelennamine hydrochloride release

The mechanism of drug release from the wax matrix-type core involves leaching by the intestinal fluid that contacts the imbedded drug. In addition to dissolving "surface" drug, the fluid can enter the core through pores, cracks, and intergranular spaces and dissolve the drug. Drug diffusion through the matrix is either nonexistent or insignificant (1).

Higuchi (2) theoretically treated the matrix model and showed that the porosity and degree of tortuosity (a measure of diffusional path) in the capillary system influence the dissolution rate. Since the amount of drug per unit of matrix volume decreases with time as dissolution occurs, the porosity should increase and tortuosity should decrease to maintain a constant dissolution rate, in ac-

Table I—Formulas (in Milligrams) per Core

Ingredient	I Concentration 0%	5%	10%	20%
Tripelennamine hydrochloride	66.7	66.7	66.7	66.7
Carnauba wax	66.7	66.7	66.7	66.7
Stearyl alcohol	66.7	56.7	46.7	26.7
Povidone	—	10.0	20.0	40.0
Magnesium stearate	2.0	2.0	2.0	2.0

Table II—Hardness and Weight of Dry-Blended Cores Containing Various Amounts of I (mol. wt. 10,000)

I, %	Weight[a], mg	Hardness[b], kg. (lb)/in.^{2}
0	204	4.1 (9.1)
5	201	4.3 (9.5)
10	205	4.4 (9.6)
20	210	4.3 (9.5)

[a] Average of 12 determinations. [b] Average of six determinations.

cordance with the Higuchi equation.

Drug dissolution from time-released tablets results from slow and continuous core erosion in which new surfaces are being exposed (3), or channels must be continually forming in the core so that the intestinal fluid penetrates the core and leaches out the drug. A polymer like povidone (I) might fulfill the requirement as a channeling agent to improve the release from a wax matrix core.

This investigation studied the effect of two types of I, individually incorporated in an inert solid matrix, on drug release in an *in vitro* system. The effects of the core preparation method and the influence of I in the dissolution medium on drug release from polymer-free cores also are evaluated.

EXPERIMENTAL

Materials—Tripelennamine hydrochloride, stearyl alcohol, and carnauba wax were used as received[1], except that the first two materials were passed through a 40-mesh screen. Two types of povidone USP, having average molecular weights of 10,000 and 40,000, were employed[2].

Core Preparation—Two methods of incorporating the drug and I into the matrix were explored, *i.e.*, double compression and fusion. In the first method, the materials were blended in a rotary mixer[3]. The mixture was compressed[4] into slugs, which were then passed through an oscillating granulator[5] using a No. 14 screen. The tablets were finally compressed[4] utilizing a 0.95-cm (3/8-in.) standard concave punch and die set.

In the fusion method, the granulations to be compressed into cores were prepared by melting carnauba wax to approximately 90° and adding stearyl alcohol. When a homogeneous melt was attained, I was added; stirring was continued until an even distribution was obtained. Then tripelennamine hydrochloride was added in small portions while the mass was mixed.

With constant stirring, the mixture was allowed to cool slowly to about 75–85°, depending on the concentration and type of I. The entire mass was then immediately cast on cold glass plates and allowed to congeal. Subsequently, the mass was granulated (14 mesh); 1% magnesium stearate was added before compression into cores.

Equal quantities of tripelennamine hydrochloride, carnauba wax, and stearyl alcohol were used to prepare the polymer-free formulation (Table I). In the other formulations, the stearyl alcohol concentration was reduced to accommodate polymer addition (Table I). Considerable effort was expended to ensure a uniform tablet weight (200 mg) and a consistent tablet hardness of 4.1–4.5 kg[6] (9–10 lb)/in.^{2}.

Dissolution Procedure—The USP rotating-basket method (4) was used to investigate drug release from the cores at 37°. Three tablets were placed in the basket, which was immersed in 600 ml of simulated intestinal fluid USP. The basket was rotated at 50 rpm for 10 hr. At 1-hr intervals, a 2-ml sample was withdrawn from the vessel for assay with a pipet fitted with a glass wool prefilter and immediately replaced with an equivalent volume of dissolution medium. Two to four runs were made on each batch.

Table III—Effect of Method of Preparation, Concentration, and Type of I on Disintegration Time of Tripelennamine Hydrochloride Cores[a]

I, %	Disintegration Time, min
Double Compression, I mol. wt. 10,000	
0	60
5	48
10	42
20	31
Fusion, I mol. wt. 10,000	
0	284
5	164
10	152
20	86
Fusion, I mol. wt. 40,000	
0	284
5	230
10	128
20	93

[a] Average of six determinations in simulated intestinal fluid USP.

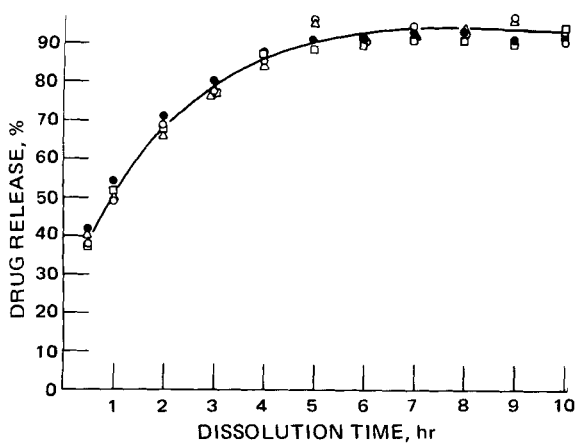

Figure 1—*Effect of I (mol. wt. 10,000) on tripelennamine hydrochloride release from cores prepared by double compression. Key (polymer concentration): ○, 0%; △, 5%; □, 10%; and ●, 20%.*

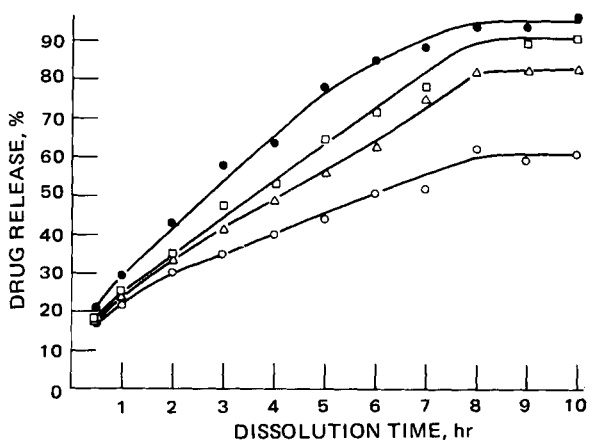

Figure 2—*Effect of I (mol. wt. 10,000) on tripelennamine hydrochloride release from fused cores. Key (polymer concentration): ○, 0%; △, 5%; □, 10%; and ●, 20%.*

[1] Supplied by Ciba-Geigy Corp., Summit, N.J.
[2] Plasdone C-15 and Plasdone C-30, GAF Corp., New York, N.Y.
[3] Model C-100, Hobart Manufacturing Co., Troy, Ohio.
[4] Stokes model E single-punch tablet press.
[5] Type TG-2S, Erweka-Apparatebau GMBH, Frankfurt (Main), West Germany.
[6] Pfizer hardness tester.

Table IV—Percent Cumulative Release of Tripelennamine Hydrochloride from Fused Cores Containing Various Amounts of I (mol. wt. 10,000) [a]

I, %	Dissolution Time, hr										
	0.5	1	2	3	4	5	6	7	8	9	10
0	16.2	21.4	30.4	34.9	40.1	44.1	50.8	51.2	62.4	59.4	60.7
5	16.6	23.1	33.2	41.3	48.5	55.8	62.9	74.4	82.1	81.7	82.8
10	17.7	24.6	34.7	47.2	53.0	64.6	71.6	78.0	88.9	89.2	90.8
20	20.9	29.5	42.8	57.4	63.2	78.1	85.0	88.4	94.0	93.7	96.4

[a] Values reported are the average of duplicate samples, three cores each.

Modified intestinal fluid[7] also was used for the cores containing the higher molecular weight I. Furthermore, to determine the effect of I when present in the dissolution medium on drug release from polymer-free cores, dissolution of these cores in intestinal fluid containing 0.005, 0.05, 0.5, 1.0, and 2.0% I (mol. wt. 40,000) was investigated. The 0.005% represents the I concentration in the dissolution medium if all polymer in the cores dissolves. Samples were withdrawn from the vessel after 0.5, 1, 4, 8, and 10 hr.

Disintegration Time—The USP apparatus and procedure with disks were used to determine tablet disintegration time in simulated intestinal fluid at 37° (4). The reported value is an average of six tablets.

Tripelennamine Hydrochloride Assay—Aliquots (0.5 or 1.0 ml) of the dissolution medium were acidified with 10% HCl (0.1 or 0.2 ml), diluted to 10 ml with methanol, and assayed for tripelennamine hydrochloride content by measuring absorbance[8] at 240 nm against a methanol blank containing the same volumes of dissolution medium and acid as the sample. The drug concentration in the sample was calculated from a standard Beer's law plot. The cumulative drug released was computed from the sample assay using the Wurster and Taylor equation (5).

RESULTS AND DISCUSSION

Table II shows the values for the hardness and weight of the cores prepared by double compression. The values obtained for the fused formulations are similar to those obtained with the dry-blended batches.

Figure 1 shows the release of tripelennamine from the cores prepared by double compression. These dissolution profiles clearly indicate that the incorporation of I in the core had no significant effect on drug release. The lack of cohesiveness in these cores is evident from the relatively short disintegration time of the polymer-free cores (Table III) when compared with the time (about 5 hr) for the fused cores.

The failure of I to improve the release profile from a wax matrix, when the cores are prepared by the slugging method, probably can be attributed to the absence of channels in the dry-blended cores and the extensive diffusive blending of the water-soluble I throughout the tablet matrix. The fusion process apparently is necessary to prevent core disintegration and subsequent rapid drug release. In other words, fusion is essential for channel formation within the core. The apparent lack of cohesiveness in such cores is also evident from the fact that a 90% plateau was approached within 5 hr. The high initial release within the first 30 min (Fig. 1) was due to the drug on the surface being released more rapidly than the drug in the matrix, as well as to rapid penetration of the medium in the cores.

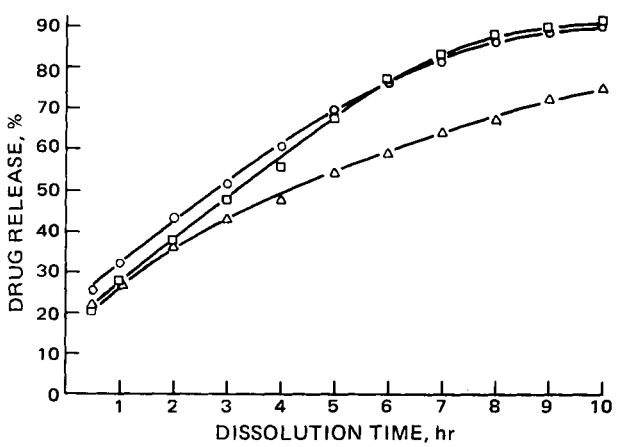

Figure 3—*Effect of I (mol. wt. 40,000) on tripelennamine hydrochloride release in simulated intestinal fluid USP from fused cores. Key (polymer concentration): △, 5%; □, 10%; and ○, 20%.*

[7] Simulated intestinal fluid USP without pancreatin.
[8] Gilford model 240 spectrophotometer.

The effect of I content in the fused cores on dissolution rate is illustrated in Fig. 2. The polymer appears to influence significantly drug release when incorporated in the wax matrix by the fusion method. The dissolution rate increased significantly with an increase in I concentration, suggesting a concomitant increase in porosity within the matrix. Between 0.5 and 8 hr, the drug appeared to be released by a zero-order process; *i.e.*, the correlation coefficient was higher by linear regression analysis for the zero-order process.

The amount of tripelennamine released is listed in Table IV. The increase in total drug release at the end of each run with an increase in I content (61% for 0% and 96% for 20% polymer) shows that the amount of drug effectively coated with wax decreased as the amount of I in the core increased. The amount of stearyl alcohol in the formulation was reduced to accommodate polymer addition. Furthermore, channel formation increased with an increase in polymer.

The effect of I (mol. wt. 40,000) on drug release from fused cores is shown in Fig. 3. As with the lower molecular weight I, an increase in drug release was observed with an increase in polymer content. However, in contrast to I (mol. wt. 10,000), there was no significant difference ($p > 0.001$) between the release profiles of 10 and 20% polymer cores. Furthermore, the plateau was approached only after a 9-hr interval, and it was not as well defined as in the case of I (mol. wt. 10,000).

More drug was released at the end of 10 hr when the lower rather than the higher molecular weight I at the same concentration was used. As the molecular weight of the polymer increases, the channeling effect in the granules that are effectively coated with wax probably decreases, thus making it more difficult for the medium to leach drug out. Furthermore, the difference observed with the lower and higher molecular weights may relate to a difference in their aqueous solubility.

The dissolution profiles of the fused cores containing I in intestinal fluid are shown in Fig. 4. These profiles are similar to those in Fig. 3; there was a noticeable increase as the polymer level was increased from 0 to 5% and from 5 to 10% but no significant difference between 10 and 20% levels. However, the presence of pancreatin in the dissolution medium caused about a 5% decrease in drug release at the end of 10 hr.

These results indicate that I acts as a channeling agent within the wax matrix. If complexation between tripelennamine and I is the mechanism underlying the increase in the drug dissolution rate from cores containing

Table V—Percent Decrease in Dissolution of Tripelennamine Hydrochloride from Polymer-Free Cores in Modified Intestinal Fluid Containing Various Amounts of I (mol. wt. 40,000) [a]

I, %	Dissolution Time, hr				
	0.5	1	4	8	10
0.005	—	—	—	—	0.4
0.05	1.9	—	—	—	2.7
0.5	3.8	—	—	1.1	4.9
1.0	3.8	0.4	0.4	4.4	5.4
2.0	6.0	3.9	3.9	8.8	8.0

[a] Using dissolution in intestinal fluid (simulated intestinal fluid USP without pancreatin) as control.

Table VI—Slope and Correlation Coefficient of the Zero-Order Component of the Release Profile of Fused Cores Containing Various Amounts of I (mol. wt. 10,000)

I, %	Slope, %/hr	Correlation Coefficient
0	5.56	0.988
5	8.42	0.998
10	9.23	0.996
20	9.85	0.982

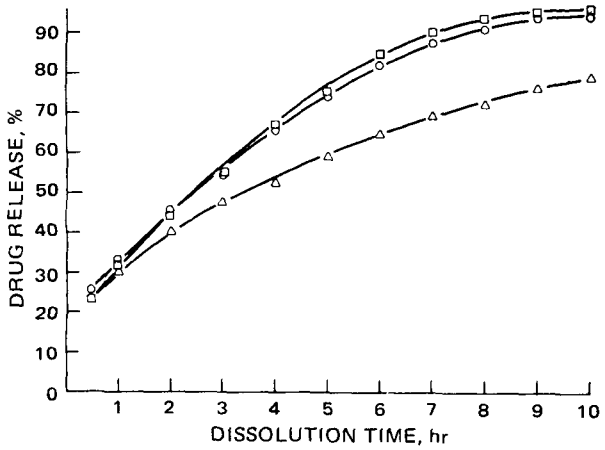

Figure 4—*Effect of I (mol. wt. 40,000) on tripelennamine hydrochloride release in modified intestinal fluid from fused cores. Key (polymer concentration):* △, *5%;* □, *10%; and* ○, *20%.*

the polymer, then the same effect should be expected when I is included in the medium. This was not the case, because there was a decrease in the drug release rate (Table V). The decrease in dissolution became more pronounced as the polymer concentration in the medium was increased. The apparent decrease was probably due to the increasing viscosity of the medium as the polymer concentration increased.

This conclusion was further substantiated by an IR study. Tripelennamine and low and high molecular weight I were dissolved in ethanol, the solvent was evaporated on a boiling water bath, and the mixture was dried under vacuum. The high frequency region of the IR spectrum[9] of the drug–polymer system was simply the summation of the spectra of the two components; there was no evidence of complexation between the two compounds. This result was not unexpected, because the tripelennamine molecule cannot hydrogen bond with the carbonyl group of I. Such bonding is possible with, for example, tolbutamide (6).

The optimum situation for the tripelennamine core would be the release of its entire content in 10 hr. Therefore, an average of 6.67 mg (66.7 mg/200-mg core) of drug should be released each hour. Table VI shows the slope and correlation coefficient for the zero-order component of the release profile of cores having various levels of I (mol. wt. 10,000) and prepared by fusion. At the 10–20% I level, the drug was released in a fashion approaching the optimum situation, at least in the 0.5–8-hr interval, with a total release of 89% for the 10% level and 94% for the 20% level over 10 hr.

Table III shows the effect of the method of preparation, concentration, and type of I on the core disintegration time. There was a rank correlation between the disintegration time and polymer concentration for both types. It appears that I acts as a disintegrant through channel formation. The data also clearly indicate the lack of cohesiveness in the cores prepared by double compression in comparison with the fused cores. While in the dissolution apparatus, the fused polymer-free and 5% I cores remained intact with a smooth surface at the end of 10 hr. On the other hand, cores containing higher concentrations of I appeared to have fissures as dissolution proceeded. The occurrence of the latter phenomenon was probably due to the I reducing the interparticle bonding of the drug–wax granules during compression.

The higher release of drug initially (0.5–8 hr) suggests that it may be possible to incorporate 100 mg of tripelennamine hydrochloride into a sustained-release matrix and to design the formulation in such a manner that 30–40% of the drug would be released in the first 2 hr in the stomach, with the remaining 60–70% released over the following 8 hr in the intestinal tract.

While it might be possible to design a sustained-release form as described, a certain percentage of the drug, about 10%, probably will always be coated very effectively with a wax film that is impermeable to GI fluids. Consequently, total drug release may be difficult to achieve.

[9] Perkin-Elmer model 567 grating IR spectrophotometer.

REFERENCES

(1) A. Dakkuri, H. G. Schroeder, and P. P. DeLuca, *J. Pharm. Sci.*, **67**, 354 1978).

(2) T. Higuchi, *ibid.*, **52**, 1145 (1963).

(3) N. H. Choulis and H. Papadopoulous, *ibid.*, **64**, 1033 (1975).

(4) "The United States Pharmacopeia," 19th rev., Mack Publishing Co., Easton, Pa., 1975, pp. 650, 651.

(5) D. E. Wurster and P. W. Taylor, *J. Pharm. Sci.*, **54**, 670 (1965).

(6) S. A. Said, H. M. El-Fatatry, and A. S. Geneidi, *Aust. J. Pharm. Sci.*, **NS3**, 42 (1974).

ACKNOWLEDGMENTS

Presented at the Basic Pharmaceutics Section, APhA Academy of Pharmaceutical Sciences, New Orleans meeting, April 1976.

Analysis of Betamethasone and Its Organic Esters in Pharmaceutical Products

R. E. GRAHAM *ˣ, E. R. BIEHL ‡, and C. T. KENNER ‡

Received March 28, 1977, from the **Food and Drug Administration, Dallas District, Dallas, TX 75204,* and the ‡*Department of Chemistry, Southern Methodist University, Dallas, TX 75275.* Accepted for publication July 1, 1977.

Abstract □ A rapid, quantitative analysis for betamethasone and its organic esters at room temperature is described. The method is similar to the official blue tetrazolium reaction for corticosteroids, except that methylene chloride is used as the solvent. The reaction is complete in 27–69 min, and the formazans produced are stable for at least 90 min after the addition of tetramethylammonium hydroxide. The results of the analysis of 13 different pharmaceutical formulations by the proposed method are reported. The degradation of betamethasone and its esters caused by strong bases is a pseudo-first-order reaction in methylene chloride. The average half-life of the corticosteroids studied is 56 min under the basic conditions described.

Keyphrases □ Betamethasone and various esters—spectrophotometric analyses in pharmaceutical products □ Spectrophotometry—analyses, betamethasone and various esters in pharmaceutical products □ Glucocorticoids—betamethasone and various esters, spectrophotometric analyses in pharmaceutical products

Betamethasone and its esters are synthetic corticosteroids which are included in several types of pharmaceutical preparations. Chafetz *et al.* (1) reported a colorimetric procedure for betamethasone benzoate in topical gel preparations that utilized preliminary oxidation of the 17-keto function, followed by reaction with phenylhy-

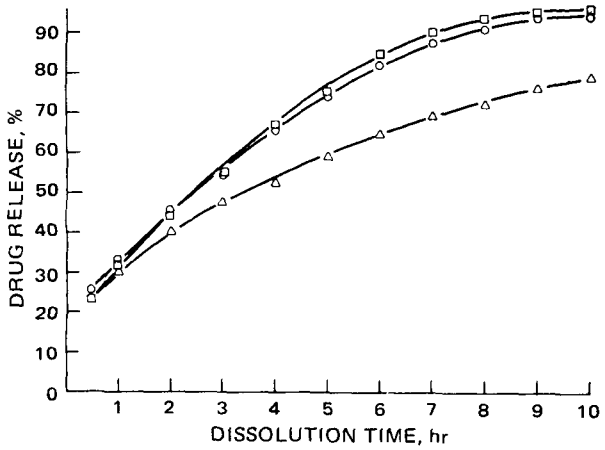

Figure 4—*Effect of I (mol. wt. 40,000) on tripelennamine hydrochloride release in modified intestinal fluid from fused cores. Key (polymer concentration):* △, *5%;* □, *10%; and* ○, *20%.*

the polymer, then the same effect should be expected when I is included in the medium. This was not the case, because there was a decrease in the drug release rate (Table V). The decrease in dissolution became more pronounced as the polymer concentration in the medium was increased. The apparent decrease was probably due to the increasing viscosity of the medium as the polymer concentration increased.

This conclusion was further substantiated by an IR study. Tripelennamine and low and high molecular weight I were dissolved in ethanol, the solvent was evaporated on a boiling water bath, and the mixture was dried under vacuum. The high frequency region of the IR spectrum[9] of the drug–polymer system was simply the summation of the spectra of the two components; there was no evidence of complexation between the two compounds. This result was not unexpected, because the tripelennamine molecule cannot hydrogen bond with the carbonyl group of I. Such bonding is possible with, for example, tolbutamide (6).

The optimum situation for the tripelennamine core would be the release of its entire content in 10 hr. Therefore, an average of 6.67 mg (66.7 mg/200-mg core) of drug should be released each hour. Table VI shows the slope and correlation coefficient for the zero-order component of the release profile of cores having various levels of I (mol. wt. 10,000) and prepared by fusion. At the 10–20% I level, the drug was released in a fashion approaching the optimum situation, at least in the 0.5–8-hr interval, with a total release of 89% for the 10% level and 94% for the 20% level over 10 hr.

Table III shows the effect of the method of preparation, concentration, and type of I on the core disintegration time. There was a rank correlation between the disintegration time and polymer concentration for both types. It appears that I acts as a disintegrant through channel formation. The data also clearly indicate the lack of cohesiveness in the cores prepared by double compression in comparison with the fused cores. While in the dissolution apparatus, the fused polymer-free and 5% I cores remained intact with a smooth surface at the end of 10 hr. On the other hand, cores containing higher concentrations of I appeared to have fissures as dissolution proceeded. The occurrence of the latter phenomenon was probably due to the I reducing the interparticle bonding of the drug–wax granules during compression.

The higher release of drug initially (0.5–8 hr) suggests that it may be possible to incorporate 100 mg of tripelennamine hydrochloride into a sustained-release matrix and to design the formulation in such a manner that 30–40% of the drug would be released in the first 2 hr in the stomach, with the remaining 60–70% released over the following 8 hr in the intestinal tract.

While it might be possible to design a sustained-release form as described, a certain percentage of the drug, about 10%, probably will always be coated very effectively with a wax film that is impermeable to GI fluids. Consequently, total drug release may be difficult to achieve.

[9] Perkin-Elmer model 567 grating IR spectrophotometer.

REFERENCES

(1) A. Dakkuri, H. G. Schroeder, and P. P. DeLuca, *J. Pharm. Sci.*, **67**, 354 1978).

(2) T. Higuchi, *ibid.*, **52**, 1145 (1963).

(3) N. H. Choulis and H. Papadopoulous, *ibid.*, **64**, 1033 (1975).

(4) "The United States Pharmacopeia," 19th rev., Mack Publishing Co., Easton, Pa., 1975, pp. 650, 651.

(5) D. E. Wurster and P. W. Taylor, *J. Pharm. Sci.*, **54**, 670 (1965).

(6) S. A. Said, H. M. El-Fatatry, and A. S. Geneidi, *Aust. J. Pharm. Sci.*, **NS3**, 42 (1974).

ACKNOWLEDGMENTS

Presented at the Basic Pharmaceutics Section, APhA Academy of Pharmaceutical Sciences, New Orleans meeting, April 1976.

Analysis of Betamethasone and Its Organic Esters in Pharmaceutical Products

R. E. GRAHAM *ˣ, E. R. BIEHL ‡, and C. T. KENNER ‡

Received March 28, 1977, from the **Food and Drug Administration, Dallas District, Dallas, TX 75204,* and the ‡*Department of Chemistry, Southern Methodist University, Dallas, TX 75275.* Accepted for publication July 1, 1977.

Abstract □ A rapid, quantitative analysis for betamethasone and its organic esters at room temperature is described. The method is similar to the official blue tetrazolium reaction for corticosteroids, except that methylene chloride is used as the solvent. The reaction is complete in 27–69 min, and the formazans produced are stable for at least 90 min after the addition of tetramethylammonium hydroxide. The results of the analysis of 13 different pharmaceutical formulations by the proposed method are reported. The degradation of betamethasone and its esters caused by strong bases is a pseudo-first-order reaction in methylene chloride. The average half-life of the corticosteroids studied is 56 min under the basic conditions described.

Keyphrases □ Betamethasone and various esters—spectrophotometric analyses in pharmaceutical products □ Spectrophotometry—analyses, betamethasone and various esters in pharmaceutical products □ Glucocorticoids—betamethasone and various esters, spectrophotometric analyses in pharmaceutical products

Betamethasone and its esters are synthetic corticosteroids which are included in several types of pharmaceutical preparations. Chafetz *et al.* (1) reported a colorimetric procedure for betamethasone benzoate in topical gel preparations that utilized preliminary oxidation of the 17-keto function, followed by reaction with phenylhy-

Table I—Absorbance [a] Replication of Proposed Procedure

Number	Betamethasone	Betamethasone Acetate	Betamethasone Valerate	Betamethasone Benzoate	Betamethasone 21-Benzoate
1	0.510	0.592	0.535	0.484	0.496
2	0.530	0.594	0.533	0.488	0.490
3	0.515	0.595	0.537	0.489	0.491
4	0.518	0.589	0.533	0.509	0.492
5	0.511	0.590	0.531	0.487	0.494
6	0.510	0.591	0.530	0.489	0.492
7	0.507	0.586	0.528	0.482	0.496
8	0.519	0.580	0.544	0.486	0.490
9	0.516	0.587	0.530	0.484	0.499
10	0.505	0.596	0.528	0.481	0.494
Average	0.514	0.590	0.533	0.488	0.493
SD [b]	0.008	0.005	0.005	0.009	0.003
RSD, %	1.6	0.9	0.9	0.8	0.6

[a] Solutions were kept in the dark except when being measured. [b] Calculated from the range by the method of Dean and Dixon (8).

drazine. NF XIV (2) includes monographs for betamethasone, betamethasone acetate, and betamethasone valerate in 11 different formulations.

The final determinative step for all of these products is the blue tetrazolium reaction at elevated temperatures (45 or 50°) for either 30 or 90 min, followed by quenching with acetic acid. The elevated temperatures help offset the steric interference of the C-16 β-methyl group (3) of the betamethasone molecule in the blue tetrazolium reaction. Possible problems in these methods arise from evaporative concentration, incomplete color development, and less specificity of the oxidation–reduction reaction for the C-17 α-keto function. The blue tetrazolium reaction with betamethasone and certain of its organic esters is quantitative when run at room temperature in methylene chloride (4).

This paper reports a quantitative analytical procedure for betamethasone and its organic esters utilizing the blue tetrazolium reaction at room temperature in methylene chloride. The results of the analyses of 13 different pharmaceutical formulations by the proposed method are given.

EXPERIMENTAL

Apparatus—The following were used: UV–visible recording spectrophotometers[1] with 1-cm stoppered quartz cells, glass chromatographic columns for partition chromatography (2.2 × 25 cm constricted at one end to 0.4 × 5 cm), an aluminum tamping rod, an electrobalance[2], and TLC equipment[3].

Materials—Alcohol USP, analytical reagent grade absolute ethanol, and distilled-in-glass grade acetonitrile, chloroform, *n*-heptane, absolute methanol, and methylene chloride were used. Blue tetrazolium[4], 10% aqueous tetramethylammonium hydroxide[5], and acid-washed diatomaceous earth[6] were also used. NF reference standard betamethasone, betamethasone acetate, and betamethasone valerate were used as well as betamethasone benzoate[7] and betamethasone 21-benzoate[7].

Reagents—A 1% solution of tetramethylammonium hydroxide was prepared by diluting 5.00 ml of the 10% aqueous solution to 50.0 ml with absolute ethanol. Blue tetrazolium, 5 mg/ml, was prepared by dissolving 50.0 mg in 10.0 ml of absolute methanol. Standard corticosteroid solutions were prepared to contain 0.012 mg of the steroid/ml in methylene chloride unless otherwise indicated.

Acetonitrile–n-Heptane (Mutually Saturated)—Acetonitrile, 25 ml, was mixed with 300 ml of *n*-heptane (sufficient for two determinations) in a separator, agitated vigorously for 2 min, and allowed to stand until both layers were clear. These mutually saturated solutions were used whenever acetonitrile or *n*-heptane was called for in these directions.

Chloroform (Water Saturated)—Water, 50 ml, was added to 250 ml of chloroform in a separator. The separator was agitated vigorously for 2 min, and both layers were allowed to clarify before use. The water-saturated reagent was used only when aqueous trap layers were inserted in the column.

Proposed Procedure: Sample Preparation—*Tablets*—Twenty tablets were weighed, ground to pass a 60-mesh sieve, and mixed thoroughly. Then a sample containing approximately 1.2 mg of the steroid was weighed accurately into a 100-ml beaker. Absolute methanol, 3 ml, was added and allowed to set for about 5 min, and the entire contents were washed into a separator with 1 ml of dilute hydrochloric acid USP, 75 ml of water, and 25 ml of methylene chloride.

After agitation, the methylene chloride extract was passed through cotton (previously washed with methylene chloride and dried) into a beaker, and the extraction procedure was repeated five times. The volume of the combined extracts was reduced to about 75 ml under air on the steam bath. The solution was cooled to room temperature, transferred to a 100-ml volumetric flask, adjusted to volume with methylene chloride, and mixed thoroughly for determination as described under *Determinative Procedures*.

Creams, Lotions, Gels, and Ointments—Water-soluble interferences found in several samples necessitated the use of a preliminary aqueous acid extraction. For this type of sample, a composite of several containers was prepared, and a sample containing approximately 1.2 mg of the steroid (0.6 mg for the more dilute creams) was weighed accurately. If the product showed interference, the sample was dissolved in 150 ml of water plus 5 ml of dilute hydrochloric acid USP and transferred to a separator.

Anhydrous sodium sulfate was added when necessary to break emulsions, and the sample was extracted six times with 25-ml portions of chloroform. The extracts were filtered through cotton (previously washed with chloroform and dried), and the combined extracts were taken just to dryness under air on the steam bath. The residue (or the unextracted sample for products that did not show interferences) was dissolved in 1.5 ml of acetonitrile plus 1.5 ml of *n*-heptane with slight warming on the steam bath. The procedure was continued as directed under *Column Preparation*.

Aerosols—The container was placed in dry ice and acetone for about 10 min, the top was removed carefully, and the container was allowed to sit overnight at room temperature. The nonvolatile residue was washed into a 100-ml volumetric flask and made to volume with chloroform. Aliquots containing approximately 1.0 mg of the steroid were evaporated under air on the steam bath just to dryness. The residue was dissolved in 1.5 ml of acetonitrile plus 1.5 ml of *n*-heptane, and the procedure was continued as directed under *Column Preparation*.

Suspensions—After the suspension was mixed well, duplicate samples were taken immediately with 1-ml (T.C.) pipets and drained into separate 100-ml beakers. The pipets were washed three times with 0.5-ml portions of acetonitrile and three times with 0.5-ml portions of *n*-heptane into the

Table II—Reaction Time and Stability of Formazan in Methylene Chloride

Steroid	Time to Attain Maximum Absorbance, min	Absorbance			Absorbance [a] per Micromole
		Original [b] Maximum	After 70 min	After 90 min	
Betamethasone	27	0.518	0.519	0.520	1.017
Betamethasone acetate	27	0.489	0.490	0.476	1.036
Betamethasone valerate	69	0.519	0.519	0.520	1.043
Betamethasone benzoate	57	0.499	0.500	0.501	1.022
Betamethasone 21-benzoate	44	0.491	0.493	0.491	1.004

[a] See Ref. 3 for definition. The average is 1.024. [b] The absorbance noted at the time specified in the preceding column.

[1] Cary models 15 and 17.
[2] Cahn model G-2.
[3] Eastman No. 6060 silica gel with fluorescent indicator.
[4] Dajac Laboratories.
[5] Eastman Organic Chemicals.
[6] Celite 545, Johns-Manville Product Corp., New York, NY 10016.
[7] Warner-Lambert, Morris Plains, NJ 07950.

Table III—Analyses of Typical Pharmaceutical Formulations

Number and Type of Sample	Steroid[a]	Amount Declared,	Amount Found, % of Declared			
			By Proposed Method		By Isoniazid Method	
1 Tablets[b]	I	0.6 mg/tablet	106.2	106.9	106.3	105.6
2 Cream[c]	I	0.2%	114.3	113.4	113.6	112.3
3 Cream[c]	II	0.1%	131.6	132.5	116.8	116.9
4 Cream[d]	III	0.025%	93.2	91.5	93.0	93.5
5 Cream[c]	III	0.025%	108.6	NR[e]	99.5	NR[e]
6 Cream[d]	II	0.01%	112.2	113.8	108.8	109.7
7 Lotion[c]	II	0.1%	117.8	115.9	117.8	118.6
8 Lotion[f]	III	0.025%	96.7	NR[e]	96.9	NR[e]
9 Gel[f]	III	0.025%	94.6	90.6	89.5	93.7
10 Gel[b]	III	0.025%	106.1	109.6	106.8	107.4
11 Ointment[c]	II	0.1%	111.7	110.8	113.6	114.4
12 Aerosol[c]	II	0.15%	96.7	95.6	96.9	95.3
13 Suspension[c]	IV	3 mg/ml	107.8	108.4	109.3	109.3
	V	3 mg/ml	ND[g]	ND[g]	95.2	97.3

[a] Compound I is betamethasone, II is betamethasone valerate, III is betamethasone benzoate, IV is betamethasone acetate, and V is betamethasone sodium phosphate. [b] These samples required aqueous acid extraction but no column separation. [c] These samples required only the column separation. [d] These samples required an aqueous acid extraction plus the column separation. [e] NR means that these samples were not run in duplicate. [f] These samples required sodium sulfate saturated aqueous acid extraction but no column separation. [g] ND means not determined by this method.

beakers, and the procedure was continued as directed under *Column Preparation*.

Standards—A sample of about 1.2 mg of the desired corticosteroid standard was weighed accurately into a 100-ml beaker and dissolved in 1.5 ml of acetonitrile plus 1.5 ml of *n*-heptane. The procedure was then continued as directed under *Column Preparation*.

Column Preparation—*Acetonitrile Layer*—A glass wool plug was inserted into the bottom of a chromatographic column, and a 4.0-g portion of diatomaceous earth was mixed with 4.0 ml of acetonitrile, transferred to the column, and packed firmly with a tamping rod.

Trap Layer—When needed, a neutral aqueous trap layer was prepared and inserted in the column as directed by Graham *et al.* (5).

Sample Layer—The dissolved sample, standard, or residue, prepared as directed under *Sample Preparation*, was mixed thoroughly with 3–4 g of diatomaceous earth to yield a light fluffy mixture. This mixture was transferred to the column above the trap or acetonitrile layer and packed firmly. The sample beaker, tamping rod, spatula, and funnel were dry washed with about 1 g of diatomaceous earth, which was added to the column and packed firmly. The same equipment was dry washed with glass wool, which was placed on top of the sample layer plus washings and packed firmly. The beaker was retained and washed with the *n*-heptane and chloroform used during the column elution step.

Column Elution—The beaker was washed with 150 ml of *n*-heptane in small portions and transferred to the column to maintain a liquid head approximately 12 cm above the column bed. The last wash was allowed to drain completely from the column, the tip was rinsed with alcohol USP, and the entire effluent was discarded. A new beaker was placed under the column, and the sample beaker was washed with 125 ml of chloroform in small portions, which were added to the column to maintain the liquid level close to the top of the column. The last portion was allowed to drain completely, and the tip was rinsed with alcohol USP.

The effluent was evaporated carefully just to dryness on a steam bath under a hood to ensure complete removal of the acetonitrile. The residue was dissolved in methylene chloride and diluted accurately with methylene chloride to a volume that contained approximately 0.012 mg of corticosteroid/ml.

Betamethasone sodium phosphate, if present, was eluted from the neutral aqueous trap layer following the chloroform elution with 125 ml of alcohol USP. The effluent was diluted accurately to a volume that contained approximately 0.015 mg of corticosteroid salt/ml and retained for determination by the isoniazid method as directed under *Determinative Procedures*.

Determinative Procedures—*Isoniazid Method*—The procedure of Umberger (6) was used, except that the concentration of hydrochloric acid was doubled to increase the sensitivity.

Blue Tetrazolium Method—Aliquots of 20 ml were run by the procedure given in USP XIX (7), except that: (*a*) the tetramethylammonium hydroxide reagent was diluted with absolute ethanol instead of alcohol USP, (*b*) the blue tetrazolium reagent was prepared with absolute methanol in place of alcohol USP, (*c*) the photometric scans from 720 to 490 nm were made against methylene chloride as the reference instead of the reagent blank, and (*d*) the scans were started 70 min after the addition of the tetramethylammonium hydroxide. The scans were always made in the order of reagent blank, standard, samples, and reagent blank; the reagent blank was kept in the dark between the original and final scans. The absorbance was read from the absorbance maximum at 525 nm.

Each measured absorbance value had to be corrected for the continuously increasing reagent blank absorbance. The correction for each reading was obtained by dividing the increase in absorbance of the reagent blank by the number of scans (omitting the original reagent blank scan) to obtain an average increase per scan. This average was then multiplied by the scan number and added to the original reagent blank absorbance. The net absorbance was then calculated by subtracting the corrected reagent blank absorbance from the measured absorbance for that scan.

Base Degradation of Betamethasone—Approximately 2.4 mg of each of the five reference standards was weighed accurately, dissolved in methylene chloride, and made to volume in a 200-ml volumetric flask with methylene chloride. Two milliliters of 1% tetramethylammonium hydroxide was added to each of five 20-ml aliquots taken from each steroid solution, 2.00 ml of blue tetrazolium reagent was immediately added to one aliquot of each set, and the absorbance was determined 70 min after the addition of the blue tetrazolium. At specified successive time intervals covering 430 min, 2.00 ml of blue tetrazolium reagent was added to the remaining aliquots of each set and the absorbance produced during 70 min was determined.

METHOD DEVELOPMENT

Recovery Studies—The five standards of betamethasone and its esters were put through the column cleanup and the determinative procedures of the proposed method. Comparison of the absorbances obtained from the steroid standards run through the column separation procedures with those obtained by direct determination on the identical standard solutions without the column procedure showed recoveries of 100.8% for betamethasone, 99.5% for betamethasone acetate, 100.5% for betamethasone valerate, 101.5% for betamethasone benzoate, and 101.8% for betamethasone 21-benzoate. The overall average recovery was 100.8%.

Replication Studies of Absorbances Produced by Proposed Blue Tetrazolium Method—Accurately weighed portions of each of the five corticosteroid standards were dissolved and diluted to 500 ml with methylene chloride to yield solutions containing approximately 0.012 mg/ml. Ten 20-ml aliquots of each were developed by the proposed blue tetrazolium determinative procedure, and the absorbances were determined (Table I). All solutions were kept in the dark during the color development period. The relative standard deviation, calculated from the range (8), varied from 0.6 to 1.8% with an overall average of 1.2%.

This experiment was repeated, except that the solutions were exposed to laboratory light during the color development period. The absorbance of the reagent blank increased an average of 0.161 absorbance unit compared to the reagent blank kept in the dark. The average relative standard deviation in this study was 2.6%.

Beer's Law Study—More concentrated solutions (up to 3.2 mg/100 ml) were prepared for each of the five standards in methylene chloride. Aliquots of 2.00, 5.00, 10.0, 15.0, and 20.0 ml of each of these solutions were taken, diluted to 20.0 ml with methylene chloride, and put through the proposed blue tetrazolium determinative procedure. Absorbances ranged from 0.070 to 1.200, and correlation coefficients of 0.9999 or better were obtained for each steroid using a least-squares fitting program.

Table IV—Decrease of Absorbance with Time due to Degradation by Base in Methylene Chloride

Drug		Absorbance (A)[a] and Time (T, min)[b]					Rate of Decrease of Absorbance with Time, A/min
Betamethasone	A	0.631	0.218	0.113	0.030	0.011	4.7×10^{-3}
	T	70	130	190	310	370	
Betamethasone acetate	A	0.558	0.292	0.143	0.043	0.017	3.0×10^{-3}
	T	70	120	180	300	420	
Betamethasone valerate	A	0.528	0.318	0.109	0.020	0.010	5.0×10^{-3}
	T	70	130	190	310	430	
Betamethasone benzoate	A	0.630	0.349	0.155	0.054	0.028	3.4×10^{-3}
	T	70	120	180	300	360	
Betamethasone 21-benzoate	A	0.605	0.360	0.140	0.009	ND[c]	3.7×10^{-3}
	T	70	130	190	310		

[a] Absorbance was always measured 70 min after the addition of the blue tetrazolium reagent. [b] These time periods were measured from the addition of the tetramethylammonium hydroxide and include the final 70 min after the addition of the blue tetrazolium reagent. [c] Not determined.

Color Development Time and Stability of Formazan Produced—A 20.00-ml aliquot of each of the five standards was treated according to the proposed blue tetrazolium determinative procedure, except that the solution was transferred to a cell immediately after the addition of the tetramethylammonium hydroxide. Readings were taken every minute *versus* a reagent blank for 90 min, and the time necessary to reach maximum absorption was noted for each steroid. The results (Table II) show that the completion of the reaction required from 27 min for betamethasone to 69 min for betamethasone valerate and that the formazan was stable for at least 90 min after the addition of the reagents.

Methylene Chloride Volatility Study—Five 100-ml aliquots of methylene chloride were pipetted into five separate 500-ml glass-stoppered volumetric flasks, the stoppers were inserted, and the flasks were weighed immediately and reweighed each day for 7 days. The average weight loss per day was equivalent to a decrease of 0.12% in volume. The experiment was repeated using four 100-ml flasks for 5 days with the stoppers sealed with masking tape. The average weight loss per day in this experiment was equivalent to a volume decrease of 0.06%/day.

Water Effect Study—An accurately weighed sample of approximately 1.2 mg of betamethasone acetate was dissolved and diluted to 100 ml with water-saturated methylene chloride, which was prepared by vigorous agitation with water in a separator for 2 min and then filtered through chloroform-washed cotton. A second similar sample was prepared with dry methylene chloride, and three 20.0-ml aliquots of each were run by the proposed blue tetrazolium determinative procedure. The average absorbance of the samples prepared with the water-saturated solvent was 100.6% of the average absorbance of the samples prepared with the dry solvent.

RESULTS AND DISCUSSION

The results of the analyses of 13 different pharmaceutical preparations containing either betamethasone or an organic ester of betamethasone by the proposed procedure are shown in Table III. The isoniazid method (6), which measures the amount of conjugated ketone in the A ring, gave comparable results and showed that there was essentially no decomposition in the samples examined. Interference with the blue tetrazolium reaction was noted with Samples 3 and 5 and was confirmed by the method of variation of absorbance with time previously reported (9). TLC of the betamethasone acetate fraction of the suspension (Sample 13) did not reveal the presence of betamethasone.

The data in Table IV show that base degradation of betamethasone and its organic esters proceeded rapidly in methylene chloride. The decomposition was a pseudo-first-order reaction, which showed decreases of from 3.0×10^{-3} to 5.0×10^{-3} (overall average 4.0×10^{-3}) absorbance unit/min. The half-life of the five corticosteroids under the conditions used varied from 51 min for betamethasone to 62.5 min for betamethasone benzoate with an overall average of 56 min.

Due to the low solubility of water in methylene chloride, it is necessary to dilute the tetramethylammonium hydroxide and to prepare the blue tetrazolium reagent with water-free solvents that are miscible with methylene chloride. As an example of the effect of water, the substitution of alcohol USP for both solvents increased the water content from 0.9 to 1.2% and changed the time necessary to reach maximum absorbance from 13 to 90 min for hydrocortisone (4).

Beer's law was obeyed for concentrations between 0.05 and 0.50 mg/24 ml for all five corticosteroids.

Methylene chloride underwent evaporative concentration in glass-stoppered volumetric flasks at a daily average rate of approximately 0.1% (v/v). This finding indicates that the same standard could be used for several days without significant change. In this study, however, the standards were used only on the day of preparation.

The rate studies listed in Table II show that the reaction of blue tetrazolium with betamethasone and its organic esters in methylene chloride was complete at room temperature in relatively short periods—from 27 to 69 min. Once the reaction was complete, the formazan was stable for at least 90 min from the time of the addition of the tetramethylammonium hydroxide. The calculated values of the absorbance per micromole (3) shown in Table II indicate that the reaction had gone to completion in the specified time. The average absorbance per micromole for the five standards was 1.024, which agrees favorably with the value of 1.031 previously reported (3) for 21 different corticosteroids not including betamethasone.

While the blue tetrazolium reaction with the steroids was complete in the specified times and the formazans produced were stable, the absorption of the blank continued to increase. However, the rate of increase of absorbance in the light-protected blank was slower than the rate of increase of absorbance of the blank in the reference cell when a long series of scans was necessary. As a consequence, the procedure described in the USP XIX (7), which requires that the samples be scanned *versus* the reagent blank, will cause an error of approximately 0.001 absorbance unit/min when a long series of scans is made. The correct net absorbance for the samples can only be obtained by scanning against the solvent and calculating the corrected net absorbance as described under *Determinative Procedures*.

REFERENCES

(1) L. Chafetz, D. C. Tsilifonis, and C. Moran, *J. Pharm. Sci.*, **63**, 1771 (1974).

(2) "The National Formulary," 14th ed., Mack Publishing Co., Easton, Pa., 1975.

(3) R. E. Graham, E. R. Biehl, C. T. Kenner, G. H. Luttrell, and D. L. Middleton, *J. Pharm. Sci.*, **64**, 226 (1975).

(4) R. E. Graham, E. R. Biehl, and C. T. Kenner, *ibid.*, **65**, 1048 (1976).

(5) R. E. Graham, P. A. Williams, and C. T. Kenner, *ibid.*, **59**, 1472 (1970).

(6) E. J. Umberger, *Anal. Chem.*, **27**, 768 (1955).

(7) "The United States Pharmacopeia," 19th rev., Mack Publishing Co., Easton, Pa., 1975, p. 622.

(8) R. B. Dean and W. J. Dixon, *Anal. Chem.*, **23**, 636 (1951).

(9) R. E. Graham, P. A. Williams, and C. T. Kenner, *J. Pharm. Sci.*, **59**, 1152 (1970).

Equilibrium Penetration of Monolayers IV: Dipalmitoyllecithin–Cetrimonium Bromide System

MARYLYN A. McGREGOR and G. T. BARNES ˣ

Received March 3, 1977, from the *Department of Chemistry, University of Queensland, Brisbane, Australia.* Accepted for publication June 9, 1977.

Abstract □ Equilibrium surface pressure–area isotherms of dipalmitoyllecithin monolayers were measured on substrates containing various concentrations of the surfactant, cetrimonium (hexadecyltrimethylammonium) bromide. From these isotherms, the saturation adsorptions of surfactant for various surface lecithin concentrations were calculated. Plotting of these adsorptions against the inverse of the area per lecithin molecule, as required for the "accessible area" theory, revealed two linear segments, corresponding to penetration at high and at low monolayer areas. At both high and low areas, the adsorption into the accessible areas of the surface was similar to adsorption at a monolayer-free surface. The effective cross-sectional area of the monolayer molecule in the low area region was equal to the collapse area; in the high area region, it was equal to an area corresponding to the co-area, as calculated from the Amagat equation. The change in cross-sectional area corresponded to the transition in the monolayer from a liquid condensed state to a liquid expanded state.

Keyphrases □ Cetrimonium bromide—equilibrium penetration of dipalmitoyllecithin monolayers, surface pressure–area isotherms measured □ Dipalmitoyllecithin monolayers—equilibrium penetration by cetrimonium bromide, surface pressure–area isotherms measured □ Adsorption—cetrimonium bromide on dipalmitoyllecithin monolayers, calculated from surface pressure–area isotherms □ Surfactants—cetrimonium bromide, equilibrium penetration of dipalmitoyllecithin monolayers, surface pressure–area isotherms measured □ Monolayers—dipalmitoyllecithin, equilibrium penetration by cetrimonium bromide, surface pressure–area isotherms measured

The penetration of insoluble monolayers by surfactants injected into the aqueous subphase has been of interest since the work of Schulman and Hughes (1). Much interest has stemmed from the biological implications of penetration experiments involving biologically significant material (2–7), excited particularly by analogies between the monolayer and membrane structures (8). However, understanding of the penetration process has been slow to develop. To a large extent, this lack is a consequence of the early emphasis on kinetic studies and the neglect of equilibrium measurements that could provide essential adsorption data (9).

BACKGROUND

Using the little equilibrium penetration data available (10), Fowkes (11) and McGregor and Barnes (12) proposed theoretical treatments based on the osmotic approach to monolayer properties and on the concept of accessible areas, respectively. Equilibrium penetration can be regarded as the equilibrium adsorption of surfactant molecules at a monolayer-covered surface. In the accessible area theory, this adsorption is considered to occur in the spaces between monolayer molecules. Therefore, the adsorption, Γ_f, is a function of the area per monolayer molecule, $\hat{A}_M$:

$$\Gamma_f = \Gamma_w - a_M \Gamma_w (1/\hat{A}_M) \qquad \text{(Eq. 1)}$$

where Γ_w is the surface concentration of surfactant in the accessible area and a_M is the apparent cross-sectional area of the monolayer molecule. According to the theory, a plot of Γ_f against $1/\hat{A}_M$ should give a straight line and physically reasonable values for Γ_w and a_M.

Such linear plots have been reported for several systems (12–14). Usually, these plots consist of two or more straight lines, yielding different values for Γ_w and/or a_M and showing that the characteristics of penetration may differ for different conditions.

In this paper, data on the equilibrium penetration of dipalmitoyllecithin monolayers by cetrimonium (hexadecyltrimethylammonium) bromide are presented and analyzed in terms of the accessible area theory. Both compounds are available in a highly purified condition and, thus, fulfill one main experimental criterion for this type of study. Both also have some biological importance as representatives of their class: dipalmitoyllecithin as a model lecithin representing lecithins of biological origin and uncertain composition (15) and cetrimonium bromide as typical of the quaternary ammonium compounds used as antibacterial agents and thought to act by modifying the cell membrane (16).

EXPERIMENTAL

The monolayer-forming substance was β,γ-dipalmitoyl-L-α-lecithin[1]. The spreading solvent was *n*-hexane[2]–absolute ethanol[3] (9:1). A lecithin solution was made, sealed in 1-ml ampuls, and stored in a freezer. The surface pressure–area (π–$\hat{A}_M$) isotherm of the lecithin is shown in Fig. 1. This isotherm is in reasonable agreement with the isotherms given by Cadenhead and Kellner (17) for various spreading solvent mixtures.

The surfactant, cetrimonium bromide[4], was tested by mass spectrometry and GLC; no impurities or homologs were detected, indicating a purity of >99.9%. The critical micelle concentration (CMC) found by surface tension measurements was 0.96 m*M*, which is within the literature range of 0.90–1.0 m*M* (13). Triple-distilled water was used for all subphases and surfactant solutions.

Penetration experiments were performed on a film balance, consisting of a trough and barriers of polytef; a Wilhelmy plate and strain gauge were used to detect surface tension variations (13). The apparatus for injecting the surfactant into the subphase was described previously (13, 18). Briefly, two perforated glass tubes were immersed in the trough and attached by polytef tubing to a pumping system (all polytef or glass parts) and a glass injection chamber. With this arrangement, it was possible to place the surfactant solution in the injection chamber and then to circulate and mix the subphase without appreciably disturbing a monolayer spread on the surface.

Penetration experiments were carried out as follows. The surface tension of the clean water surface was recorded, and then the monolayer was spread at a high area. Because of solvent loss when opening the ampuls, the concentration of the monolayer solution was not known accurately and the amount of monolayer delivered to the surface had to be determined by using the surface pressure–area isotherm for the lecithin (Fig. 1). Therefore, the monolayer was compressed to approximately 5 mN/m surface pressure, and the area was noted and compared with the isotherm.

After the monolayer had been expanded back to maximum area, a known amount of a concentrated surfactant solution was placed in the injection chamber and the pump was switched on. In about 10 min, the subphase concentration was homogeneous, as indicated by a constant value for the surface pressure. The monolayer was then compressed in a stepwise manner, with increases in surface pressure of about 5 mN/m for each step; it was allowed to stand after each compression until equilibrium had been reached, as shown by a steady value on the recorder output. This equilibration time varied from about 5 min to 2 hr as the pressure was raised. The stepwise compression was continued until the monolayer collapsed or overflow occurred. The π–$\hat{A}_M$ isotherm was calculated from the equilibrium surface pressure data.

With lower concentrations of surfactant, an alternative technique was used in which the monolayer was spread on a subphase containing the surfactant. At low surfactant concentrations, the results agreed well with

[1] A grade, Calbiochem.
[2] Spectroscopic grade, BDH Chemicals Ltd.
[3] Spectroscopic grade, E. Merck.
[4] Pro analysis grade, E. Merck.

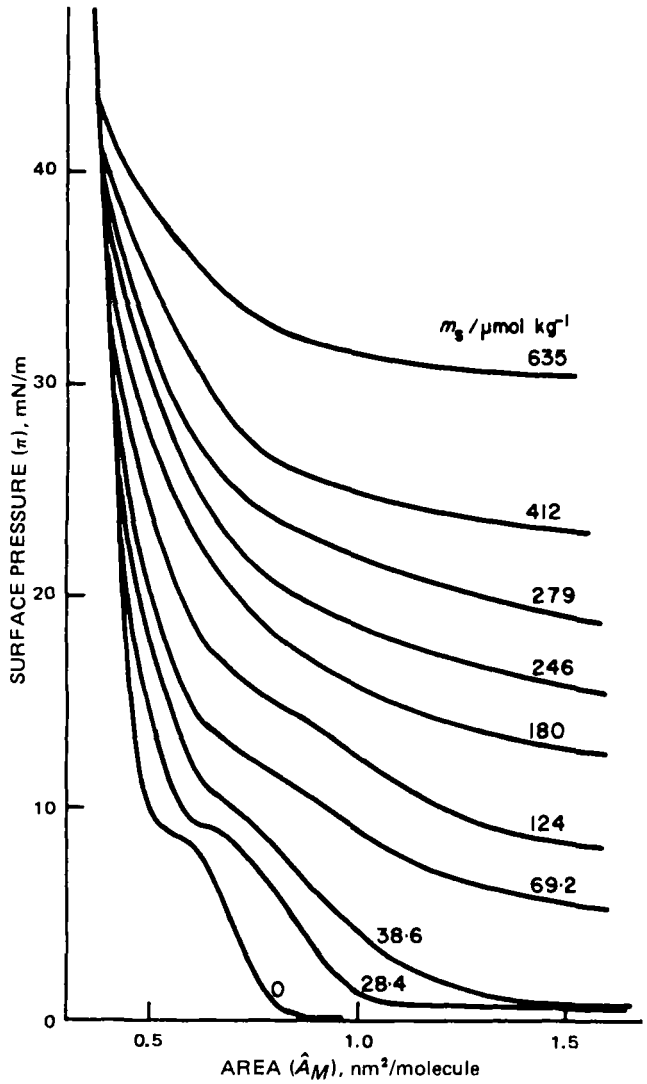

Figure 1—*Surface pressure-area isotherms of dipalmitoyllecithin monolayers on cetrimonium bromide solutions of the various concentrations shown (T = 298° K).*

those obtained by injection; but at high surfactant concentrations, the monolayer could not be spread satisfactorily.

After an experimental run, the monolayer was removed by sweeping; a surface tension reading was then taken for the clean surface. This surface tension was used to determine the concentration of the subphase from a calibration curve (13).

RESULTS

The equilibrium surface pressure–area isotherms for dipalmitoyllecithin monolayers on subphases containing various surfactant concentrations are given in Fig. 1. From these curves, plots of π against log m_S (molality of surfactant) for selected values of $\hat{A}_M$ were prepared (Fig. 2). These plots show considerably more scatter at low areas where the isotherms are steeper than at high areas. All curves are approximately linear at surface pressures greater than 15 mN/m, indicating saturation adsorption. The slopes of these linear sections are shown in Fig. 3.

Figure 3 has two significant features. First, at high areas, the slopes tend toward the slope for a monolayer-free surface, as expected. Second, an inflection point at approximately 0.6 nm²/molecule corresponds to the transition between the liquid-expanded and liquid-condensed states of the lecithin monolayers on water shown in the isotherm in Fig. 1.

The data of Fig. 3 were used to calculate the saturation adsorptions of surfactant in the monolayer-covered surface. For these calculations, the Gibbs equation must be modified to allow for the presence of the monolayer. The equation takes the form derived by Pethica (10):

$$\Gamma = \frac{1}{\Phi\Psi RT}\frac{d\pi}{d\ln m_S} \qquad \text{(Eq. 2)}$$

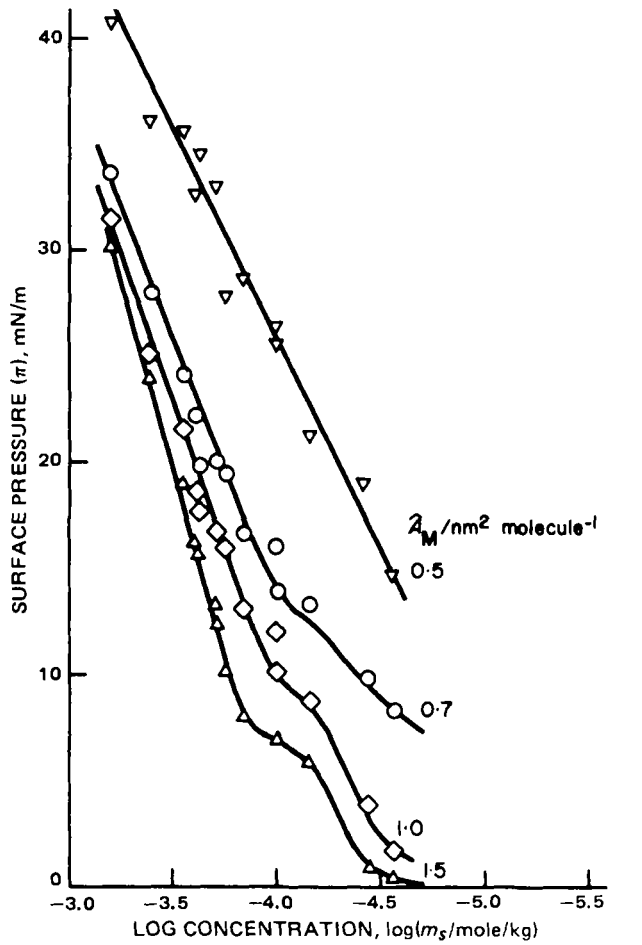

Figure 2—*Surface pressures of cetrimonium bromide solutions under dipalmitoyllecithin monolayers as a function of surfactant concentration. Curves were calculated from the data of Fig. 1 for the areas per dipalmitoyllecithin molecule,* $\hat{A}_M$.

where Γ is the relative adsorption of surfactant with reference to water. The factor Φ arises from the presence of the monolayer and, following Pethica (10), is calculated from:

$$\Phi = \hat{A}_M/(\hat{A}_M - \bar{\bar{A}}_M) \qquad \text{(Eq. 3)}$$

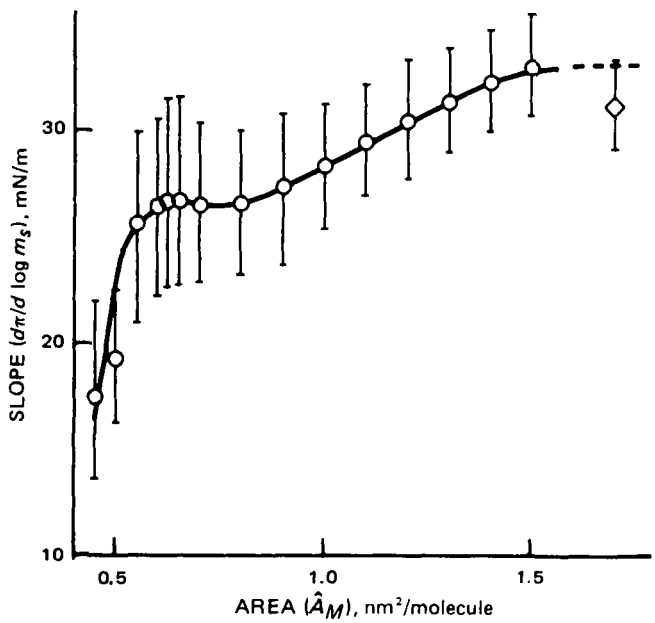

Figure 3—*Slopes of the π–log* m_S *curves in the region of saturation adsorption for cetrimonium bromide solutions under dipalmitoyllecithin monolayers (○) and with no monolayer present (◇).*

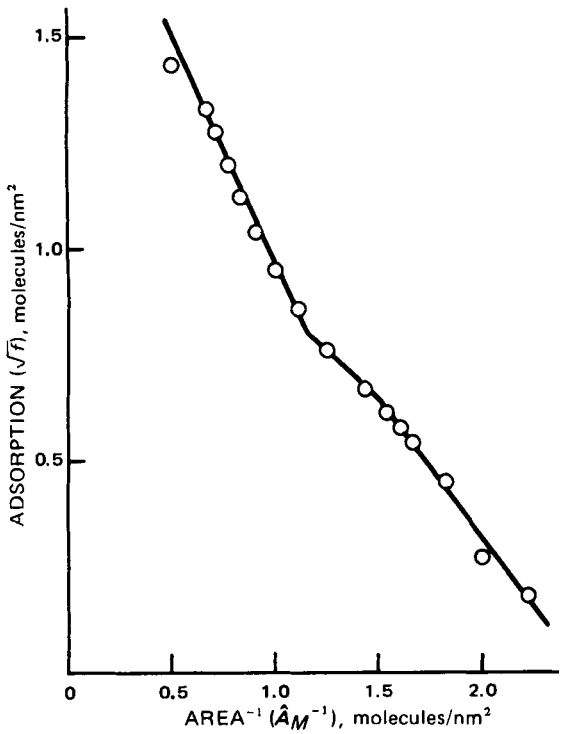

Figure 4—*Adsorptions of cetrimonium bromide into dipalmitoyllecithin monolayers plotted according to Eq. 1.*

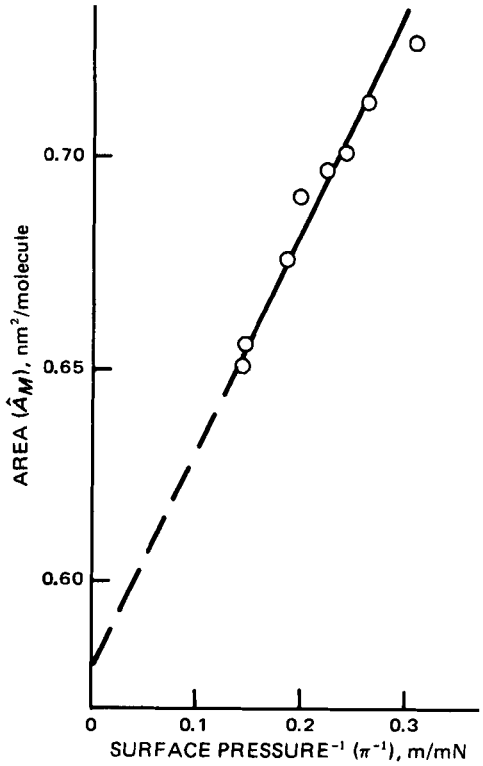

Figure 5—*Monolayer area, $\hat{A}_M$, plotted against the inverse of surface pressure in the high area region of the dipalmitoyllecithin isotherm.*

where $\bar{\bar{A}}_M$ is the partial molecular area of the monolayer substance. The factor Ψ, arising from the presence of the counterion, is to allow for the ionization of the surfactant and was given a value of 2 for the present experimental situation: an ionic surfactant, with no other salt added to the subphase solution (13). The adsorption values are shown in Fig. 4.

DISCUSSION

There are no adsorption data in the literature for direct comparison with the results in Fig. 4. Hendrikx and Ter-Minassian-Saraga (19, 20) measured the penetration of egg lecithin monolayers by radiolabeled cetrimonium bromide. At comparable areas per molecule, their adsorption values are lower than the present values, but the differences possibly could be attributed to the different lecithins used and the presence of buffer ions in their system. It is not possible to extract any adsorption values from the published results of Vilallonga *et al.* (21).

When the saturation adsorption values are plotted against the inverse of the area per monolayer molecule, as required by the accessible area theory (Eq. 1), two distinct linear sections can be seen (Fig. 4). A third middle section or transition region corresponds to the transition in the monolayer state from liquid condensed to liquid expanded (Fig. 1).

By using the accessible area approach, values for the two parameters Γ_w and a_M were determined for the two linear sections (Table I). There is no significant difference between the values of Γ_w for the low and high area regions, and both agree with the value for adsorption on a monolayer-free surface of 1.71 ± 0.20 molecules/nm^2.

There is a substantial difference, however, between the values for a_M in the low and high area regions. At low areas, the value obtained for a_M, 0.41 ± 0.06 nm^2/molecule, agrees well with the collapse area of the lecithin, 0.37 ± 0.01 nm^2/molecule. At high areas, a rearrangement of the equation used by Schofield and Rideal (22), the Amagat equation:

$$\hat{A}_M = \hat{A}_0 + qkt/\pi \qquad \text{(Eq. 4)}$$

Table I—Analysis of the Equilibrium Penetration of Dipalmitoyllecithin Monolayers by Cetrimonium Bromide in Terms of Eq. 1

	Γ_w, molecule/nm^2 (π = 30 mN/m)	a_M, nm^2/molecule (π = 30 mN/m)
Low $\hat{A}_M$	1.70 ± 0.19	0.41 ± 0.06
High $\hat{A}_M$	1.97 ± 0.19	0.51 ± 0.07
No monolayer	1.71 ± 0.20	—

where q is a measure of the lateral adhesion of the molecules in the film, was used to find an estimate, $\hat{A}_0$, for the effective cross-sectional area of a lecithin molecule in the liquid-expanded state. The fit of the experimental data to Eq. 4 is good, as shown by the linear plot of $\hat{A}_M$ against $1/\pi$ in Fig. 5. From the intercept of the linear plot, a value of 0.58 ± 0.07 nm^2/molecule is obtained from $\hat{A}_0$. This value agrees within the experimental error with the value for a_M, 0.51 ± 0.07 nm^2/molecule, in the high area region.

Hence, the transition in the lecithin monolayer from the liquid-condensed state to the liquid-expanded state accounts for the two linear regions in the adsorption curve (Fig. 4). In the low area region, the monolayer is in a condensed state with the polar head groups anchored on the surface and the long chain tails upright. In this condensed state, the collapse area of the lecithin is a good estimate of the effective cross-sectional area of a dipalmitoyllecithin molecule and, therefore, is the appropriate area to be used for the accessible area theory.

However, in the high area region, the monolayer is in an expanded state with its polar heads anchored on the surface and the long chain tails slightly bent and disordered and probably divergent because of a higher proportion of *gauche*-conformers (15). Thus, a lecithin molecule in the expanded state would occupy a larger area on the surface. This area was estimated by calculating the co-area, $\hat{A}_0$, (using Eq. 4), which represents a correction to the ideal two-dimensional gas equation for the effective area of the molecules. Therefore, the co-area is the same as the area required. In both regions, the surfactant molecules are adsorbing into available spaces between the clusters of monolayer molecules. Hence, the value obtained for adsorption is similar to that on a monolayer-free surface.

In the octadecanol–cetrimonium bromide system, there are also two distinct linear sections joined by a transition region (13). However, in this system, the value for Γ_w changes from the low area region to the high area region and the value for a_M is constant over the entire range. In the high area region, the surfactant adsorbs into large areas of free surface between the clusters of close-packed monolayer molecules; the value obtained for Γ_w, therefore, is for a monolayer-free surface. In the low area region, the value for Γ_w is significantly higher than the adsorption into a monolayer-free surface. The surfactant apparently adsorbs into small holes in the monolayer, with only one surfactant molecule per hole. Since the surface concentration of surfactant is small, the surfactant ions are too widely separated for electrostatic effects to be apparent, and it is the size of the surfactant ion that is important. In this region, the inverse of the

value obtained for Γ_w, 0.37 nm^2/molecule, is in good agreement with the estimated cross-sectional area of the surfactant ion (13).

There is no similar region in the present system. The explanation of this difference appears to concern the ionic nature of the choline group in comparison with the nonionic nature of the alcohol. With octadecanol monolayers, the surfactant ion is being adsorbed into holes in an uncharged matrix of octadecanol molecules; with the lecithin monolayers, the matrix consists of the zwitterionic phosphatidyl choline. The positively charged quaternary ammonium part of the lecithin molecule apparently dominates the penetration process so that, even when the adsorption of surfactant ions is small, the ionic environment is roughly similar to that found with the higher adsorption at a monolayer-free surface. Hence, in both situations, the adsorption is limited by electrostatic effects and not by the size of the surfactant ion.

The shape of the surface pressure–area isotherms of the penetrated lecithin monolayers is interesting (Fig. 1). At very low areas, all surfactant molecules are squeezed out of the surface, as indicated by the tendency of the isotherms of penetrated monolayers to join up with the surface pressure–area isotherm for the lecithin monolayer on water. Unfortunately, there was too much scatter in the data to allow adsorptions to be calculated at areas per molecule lower than 0.45 nm^2/molecule, but qualitatively the ejection of surfactant is clearly shown by the isotherms in Fig. 1.

CONCLUSION

Analysis of the equilibrium penetration of dipalmitoyllecithin monolayers by cetrimonium bromide according to Eq. 1, derived from the accessible area theory (12), shows that: (*a*) good straight lines are obtained, as required by the theory; and (*b*) the values of the parameters a_M and Γ_w obtained from these analyses are physically reasonable in that they correspond to the effective molecular areas of the lecithin in the various monolayer states and to the adsorption of the surfactant at a monolayer-free surface, respectively.

It is concluded that the accessible area theory provides a satisfactory description of equilibrium penetration in the present system. Alternatively, the theory could have been used to predict equilibrium penetrations from the surface pressure–area isotherm of dipalmitoyllecithin and the adsorption of cetrimonium bromide at a monolayer-free surface.

REFERENCES

(1) J. H. Schulman and A. H. Hughes, *Biochem. J.*, **29,** 1243 (1935).

(2) J. H. Schulman and E. K. Rideal, *Proc. Roy. Soc.*, **B122,** 29, 46 (1937).

(3) E. D. Goddard and J. H. Schulman, *J. Colloid Sci.*, **8,** 309 (1953).

(4) N. L. Gershfeld, *J. Phys. Chem.*, **66,** 1923 (1962).

(5) G. Colacicco, *Lipids*, **5,** 636 (1970).

(6) M. C. Phillips, M. T. A. Evans, and H. Hauser, in "Monolayers," Advances in Chemistry Series No. 144, American Chemical Society, Washington, D.C., 1975, p. 217.

(7) M. C. Phillips, D. E. Graham, and H. Hauser, *Nature*, **254,** 154 (1975).

(8) H. Davson and J. F. Danielli, "The Permeability of Natural Membranes," 2nd ed., Cambridge University Press, Cambridge, England, 1952.

(9) G. L. Gaines, Jr., "Insoluble Monolayers at Liquid–Gas Interfaces," Interscience, New York, N.Y., 1966, p. 310.

(10) B. A. Pethica, *Trans. Faraday Soc.*, **51,** 1402 (1955).

(11) F. M. Fowkes, *J. Phys. Chem.*, **65,** 355 (1961).

(12) M. A. McGregor and G. T. Barnes, *J. Colloid Interface Sci.*, **49,** 362 (1974).

(13) *Ibid.*, **54,** 439 (1976).

(14) *Ibid.*, **62,** 213 (1977).

(15) M. C. Phillips, *Progr. Surface Membrane Sci.*, **5,** 139 (1972).

(16) "The Pharmacological Basis of Therapeutics," 5th ed., L. S. Goodman and A. Gilman, Eds., Macmillan, New York, N.Y., 1975, p. 1001.

(17) D. A. Cadenhead and B. M. J. Kellner, *J. Colloid Interface Sci.*, **49,** 143 (1974).

(18) M. A. McGregor and G. T. Barnes, *ibid.*, **60,** 408 (1977).

(19) Y. Hendrikx and L. Ter-Minassian-Saraga, *C.R. Acad. Sci. Paris*, **269,** 880 (1969).

(20) Y. Hendrikx and L. Ter-Minassian-Saraga, *J. Chim. Phys.*, **67,** 1620 (1970).

(21) F. A. Vilallonga, E. R. Garrett, and M. Cereijido, *J. Pharm. Sci.*, **61,** 1720 (1972).

(22) R. K. Schofield and E. K. Rideal, *Proc. Roy. Soc.*, **A109,** 57 (1925).

Effects of Paper on Performance of Antibiotic-Impregnated Disks

ROBERT A. RIPPERE

Received February 7, 1977, from the *Antibiotic Residue Branch, National Center for Antibiotics Analysis, Food and Drug Administration, Washington, DC 20204.* Accepted for publication June 23, 1977.

Abstract □ Grades of paper used in the manufacture and assay of antibiotic susceptibility disks have significant effects on the diffusion of antibiotics from the paper when compared to a control grade of paper. The papers also evoke different microbiological responses to changing concentrations of some antibiotics. Regulatory implications and the need for further standardization of assays among control laboratories are explored. Grades of paper generally used for assay and control of susceptibility disks, on the other hand, appear to be comparable to each other in both respects.

Keyphrases □ Antibiotic susceptibility disks—effect of various grades of paper on performance □ Paper, various grades—effect on performance of antibiotic susceptibility disks □ Disks, paper—effect of various grades on performance in antibiotic susceptibility tests

That different grades of paper affect diameters of zones of inhibition produced by known antibiotic concentrations has been recognized for some time (1, 2). One study (1) compared two grades of paper[1] to a control grade. One grade produced inhibition zones somewhat larger than the standard disk for each of four antibiotics; the other grade produced either significantly smaller zones or none at all.

Marth *et al.* (2) determined that use of 6.35- and 12.7-mm disks of the same grade of paper permitted detection of the same low levels of penicillin in milk but that 6.35-mm disks of another grade were generally able to detect only higher concentrations of antibiotic under the same conditions.

[1] Whatman.

value obtained for Γ_w, 0.37 nm^2/molecule, is in good agreement with the estimated cross-sectional area of the surfactant ion (13).

There is no similar region in the present system. The explanation of this difference appears to concern the ionic nature of the choline group in comparison with the nonionic nature of the alcohol. With octadecanol monolayers, the surfactant ion is being adsorbed into holes in an uncharged matrix of octadecanol molecules; with the lecithin monolayers, the matrix consists of the zwitterionic phosphatidyl choline. The positively charged quaternary ammonium part of the lecithin molecule apparently dominates the penetration process so that, even when the adsorption of surfactant ions is small, the ionic environment is roughly similar to that found with the higher adsorption at a monolayer-free surface. Hence, in both situations, the adsorption is limited by electrostatic effects and not by the size of the surfactant ion.

The shape of the surface pressure–area isotherms of the penetrated lecithin monolayers is interesting (Fig. 1). At very low areas, all surfactant molecules are squeezed out of the surface, as indicated by the tendency of the isotherms of penetrated monolayers to join up with the surface pressure–area isotherm for the lecithin monolayer on water. Unfortunately, there was too much scatter in the data to allow adsorptions to be calculated at areas per molecule lower than 0.45 nm^2/molecule, but qualitatively the ejection of surfactant is clearly shown by the isotherms in Fig. 1.

CONCLUSION

Analysis of the equilibrium penetration of dipalmitoyllecithin monolayers by cetrimonium bromide according to Eq. 1, derived from the accessible area theory (12), shows that: (*a*) good straight lines are obtained, as required by the theory; and (*b*) the values of the parameters a_M and Γ_w obtained from these analyses are physically reasonable in that they correspond to the effective molecular areas of the lecithin in the various monolayer states and to the adsorption of the surfactant at a monolayer-free surface, respectively.

It is concluded that the accessible area theory provides a satisfactory description of equilibrium penetration in the present system. Alternatively, the theory could have been used to predict equilibrium penetrations from the surface pressure–area isotherm of dipalmitoyllecithin and the adsorption of cetrimonium bromide at a monolayer-free surface.

REFERENCES

(1) J. H. Schulman and A. H. Hughes, *Biochem. J.*, **29,** 1243 (1935).

(2) J. H. Schulman and E. K. Rideal, *Proc. Roy. Soc.*, **B122,** 29, 46 (1937).

(3) E. D. Goddard and J. H. Schulman, *J. Colloid Sci.*, **8,** 309 (1953).

(4) N. L. Gershfeld, *J. Phys. Chem.*, **66,** 1923 (1962).

(5) G. Colacicco, *Lipids*, **5,** 636 (1970).

(6) M. C. Phillips, M. T. A. Evans, and H. Hauser, in "Monolayers," Advances in Chemistry Series No. 144, American Chemical Society, Washington, D.C., 1975, p. 217.

(7) M. C. Phillips, D. E. Graham, and H. Hauser, *Nature*, **254,** 154 (1975).

(8) H. Davson and J. F. Danielli, "The Permeability of Natural Membranes," 2nd ed., Cambridge University Press, Cambridge, England, 1952.

(9) G. L. Gaines, Jr., "Insoluble Monolayers at Liquid–Gas Interfaces," Interscience, New York, N.Y., 1966, p. 310.

(10) B. A. Pethica, *Trans. Faraday Soc.*, **51,** 1402 (1955).

(11) F. M. Fowkes, *J. Phys. Chem.*, **65,** 355 (1961).

(12) M. A. McGregor and G. T. Barnes, *J. Colloid Interface Sci.*, **49,** 362 (1974).

(13) *Ibid.*, **54,** 439 (1976).

(14) *Ibid.*, **62,** 213 (1977).

(15) M. C. Phillips, *Progr. Surface Membrane Sci.*, **5,** 139 (1972).

(16) "The Pharmacological Basis of Therapeutics," 5th ed., L. S. Goodman and A. Gilman, Eds., Macmillan, New York, N.Y., 1975, p. 1001.

(17) D. A. Cadenhead and B. M. J. Kellner, *J. Colloid Interface Sci.*, **49,** 143 (1974).

(18) M. A. McGregor and G. T. Barnes, *ibid.*, **60,** 408 (1977).

(19) Y. Hendrikx and L. Ter-Minassian-Saraga, *C.R. Acad. Sci. Paris*, **269,** 880 (1969).

(20) Y. Hendrikx and L. Ter-Minassian-Saraga, *J. Chim. Phys.*, **67,** 1620 (1970).

(21) F. A. Vilallonga, E. R. Garrett, and M. Cereijido, *J. Pharm. Sci.*, **61,** 1720 (1972).

(22) R. K. Schofield and E. K. Rideal, *Proc. Roy. Soc.*, **A109,** 57 (1925).

Effects of Paper on Performance of Antibiotic-Impregnated Disks

ROBERT A. RIPPERE

Received February 7, 1977, from the *Antibiotic Residue Branch, National Center for Antibiotics Analysis, Food and Drug Administration, Washington, DC 20204.* Accepted for publication June 23, 1977.

Abstract □ Grades of paper used in the manufacture and assay of antibiotic susceptibility disks have significant effects on the diffusion of antibiotics from the paper when compared to a control grade of paper. The papers also evoke different microbiological responses to changing concentrations of some antibiotics. Regulatory implications and the need for further standardization of assays among control laboratories are explored. Grades of paper generally used for assay and control of susceptibility disks, on the other hand, appear to be comparable to each other in both respects.

Keyphrases □ Antibiotic susceptibility disks—effect of various grades of paper on performance □ Paper, various grades—effect on performance of antibiotic susceptibility disks □ Disks, paper—effect of various grades on performance in antibiotic susceptibility tests

That different grades of paper affect diameters of zones of inhibition produced by known antibiotic concentrations has been recognized for some time (1, 2). One study (1) compared two grades of paper[1] to a control grade. One grade produced inhibition zones somewhat larger than the standard disk for each of four antibiotics; the other grade produced either significantly smaller zones or none at all.

Marth *et al.* (2) determined that use of 6.35- and 12.7-mm disks of the same grade of paper permitted detection of the same low levels of penicillin in milk but that 6.35-mm disks of another grade were generally able to detect only higher concentrations of antibiotic under the same conditions.

[1] Whatman.

Three grades of paper from the same manufacturer were specified for use in assays and in collaborative studies of methods designed to detect penicillin in milk (3–6). The three were found to be comparable in absorptivity, purity, and performance.

The Code of Federal Regulations, §460.6(d) (7), requires that control disks be 6.35 mm in diameter with a basis weight of 26–34 mg/cm^2. Control disks must also be able to absorb 2.5 times their weight of distilled water. In addition, the paper used must neither buffer nor affect the pH of any solution placed on it. The paper can neither enhance nor diminish the activity of any antibiotic solution incorporated into it.

The Code of Federal Regulations, §460.1(a) (7), also requires that the paper used to produce susceptibility disks be capable of complete absorption of 20 μl of solution/31.67 mm^2 of paper (0.25-in. diameter round disk). In addition, the absorbent paper and the dye or ink used must not influence either bacterial growth or activity of the antibiotic.

Kramer and Kirshbaum (1) concluded that control disks in all laboratories should be prepared from the same specified grade of paper to eliminate interlaboratory variation due to papers. The laboratories that control the disks sold in the United States have used various grades to prepare standard disks. Each disk manufacturer punches antibiotic disks from its own proprietary grade of paper. These proprietary grades are represented by the paper manufacturer[2] to be of essentially the same composition and to perform similarly.

The present study compared the performances of disks of all four grades of paper currently used for manufacture or control of disks to the performance of a lot of control disks. In addition, the performance of a second lot of control disks is discussed.

EXPERIMENTAL

Antibiotics selected for the study generally were those listed in the "Standardized Disc Susceptibility Test" described in §460.1 (7), with the exception of clindamycin and oleandomycin. For each antibiotic tested, one or more weighings of the appropriate Food and Drug Administration (FDA) working standard were dissolved in the solvent indicated in §460.6(d) (7). In each instance, the concentration of the initial stock solution was the highest concentration of the standard curve. Two dilutions in the same solvent were made from each stock solution to provide three doses that were equally spaced logarithmically. Interdose ratios varied from 2:1 to 4:1.

Blank disks of various grades of paper from three suppliers[3] and two lots of blank A-740-E[4] disks were used. All disks were 6.35 mm in diameter.

Disks of grades B-126[5], B-225[5], B-676[5], A-470[6], and lots 7810 and 9996 of A-740-E were placed on a 10-mesh stainless steel screen mounted on a wooden frame. Aliquots (20 μl) of each solution were dispensed to all disks being tested at one time with a syringe[7] mounted in a repeating dispenser[8]. Disks were then dried in circulating air at ambient temperature (24–28°) for a minimum of 3 hr.

Except as specified below, 150 × 15-mm assay dishes were prepared according to directions in §460.6(c) (7). Gentamicin and tobramycin plates contained a 42-ml base layer of neomycin assay agar (Antibiotic Medium 11) overlaid with 8 ml of neomycin assay agar inoculated with 0.1% of a suspension of *Staphylococcus aureus* (ATCC 13150), which had been grown for 24 hr at 37° on a Roux bottle containing 250 ml of seed agar (Antibiotic Medium 1) and washed off with 50 ml of sterile USP saline TS. Carbenicillin plates contained a 42-ml base layer of Antibiotic Medium 1 overlaid with 8 ml of 1.5% agar, which had been inoculated with 5% of a suspension of *Pseudomonas aeruginosa* (ATCC 25619) prepared according to §460.6(b) (12) (7).

Assays were performed, and the results were calculated according to the 3 × 3 factorial design of USP XIX (8). Lot 7810 of A-740-E paper was designated as the standard. All other papers were considered as unknowns. Each dose was replicated nine times on each lot of paper for each assay. Twelve disks, two of each content of antibiotic on both the standard and one test lot of paper, were placed in a circle in each plate. Five plates thus were used for each assay. All plates were incubated for 16–18 hr at 34 or 37°.

After incubation, zone diameters were estimated to the nearest 0.1 mm by projecting images onto a calibrated screen with an overhead projector[9] (12.5× magnification). Assay potencies and validity and slope values were calculated with a programmable calculator[10].

Table I—Relative Potencies of Antibiotic Solutions Obtained from Various Absorbent Papers Using 3 × 3 Assay Design [a]

Antibiotic	A-740-E, Lot 9996	A-470	B-126	B-225	B-676
Ampicillin	—[b]	106	108	123	96
	95	105	110	—	89
Bacitracin	100	97	113	109	92
Carbenicillin	98	104	100	109	99
Cephalothin	—	106	113	141	89
	95	106	117	—	87
Chloramphenicol	97	105	109	115	95
Colistin	—	93	98	80	55
	—	—	—	76	54
	95	92	103	—	—
Erythromycin	101	100	99	101	92
Gentamicin	99	99	97	107	60
Kanamycin	—	97	93	94	69
	99	98	90	—	70
Methicillin	104	101	99	111	98
Neomycin	105	99	80	86	53
Novobiocin	98	99	102	113	93
Penicillin G	100	102	103	129	82
Polymyxin B	94	98	115	120	69
Rifampin	—	107	96	122	71
	98	106	99	120	—
Streptomycin	96	99	92	105	69
Tetracycline	—	91	—	100	85
	—	97	138	—	94
	100	93	119	102	89
Tobramycin	—	106	—	96	52
	101	—	—	108	59
	110	107	91	—	—
Vancomycin	98	96	97	118	84

[a] Expressed as percentages of the standard, which is A-740-E, lot 7810. [b] Each line for an antibiotic represents assays done on a single day; dashes indicate that no assay was performed with the particular paper on that day.

RESULTS AND DISCUSSION

Relative potency results obtained from 3 × 3 assays for each grade of paper are presented in Table I. Each value represents one assay of 27 disks of the test lot of paper compared to 27 disks of the standard. All values given on a single line in Table I were derived from disks of the various papers prepared consecutively by one analyst from the three solutions of antibiotic.

It is apparent from the data that the performances of A-470 and lot 9996 of A-740-E papers were comparable to the performance of the standard. Of 47 assays performed with the two papers, only one test of lot 9996 yielded a result differing from the standard by >10%. Under the conditions followed in this study, an assay result that deviates by >±10% from the standard of comparison is considered significant.

Papers used for commercial production of disks generally do not release antibiotics comparably either to another manufacturer's papers or to each other. Grade B-676 released less antibiotic than any other paper tested.

[2] Eaton-Dikeman, Mount Holly Springs, PA 17065, personal communication.
[3] BBL Division of BioQuest, Cockeysville, MD 21030; Difco Laboratories, Detroit, MI 48232; and Pfizer Disks, Inc., Barceloneta, PR 00617.
[4] Grade 740-E paper, Schleicher & Schuell, Keene, NH 03431.
[5] Paper grades 126, 225, and 676, Eaton-Dikeman, Mount Holly Springs, PA 17065.
[6] Grade 470 paper, Schleicher & Schuell, Keene, NH 03431.
[7] Model 1001, Hamilton Co., Reno, NV 89502.
[8] Model PB 600-1, Hamilton Co.
[9] Balopticon, Bausch & Lomb, Rochester, NY 14602.
[10] Model 9830-A, Hewlett-Packard, Loveland, CO 80537.

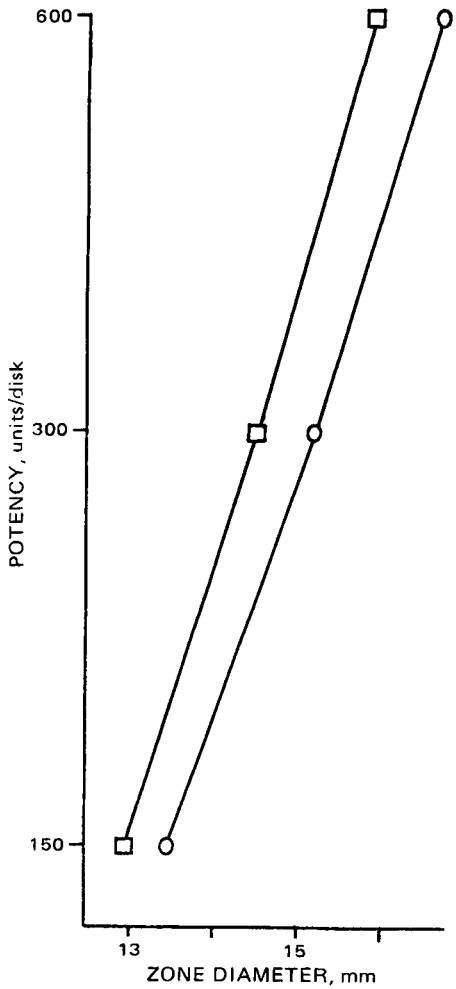

Figure 1—*Graph showing the parallel and valid response lines promoted by B-676 (□) and A-740-E (○) paper disks impregnated with polymyxin B. Grade B-676 paper appeared to adsorb or bind a significant quantity of several antibiotic solutions applied to it. In most instances, the loss of activity was proportional to the initial concentration of solution so that the slope of the dose response was not affected.*

Of all drugs studied, B-676 performed similarly to A-740-E only for bacitracin, carbenicillin, chloramphenicol, erythromycin, methicillin, and novobiocin. Grade B-676 paper appeared to bind, either physically or chemically, a particularly high proportion of the oligosaccharide and polypeptide antibiotics. This binding effect tied up 30–50% of the antibiotic loaded onto the disk compared to the standard paper.

Of the production papers studied, the performance of B-126 was the most similar to that of the A-740-E disks. This paper produced results differing by more than 10% from the standard only for bacitracin, cephalothin, neomycin, polymyxin, and tetracycline. In every instance, B-126 promoted greater diffusion than did B-676 paper. Grade B-126 generally indicated lower potencies than did B-225; higher potencies were obtained from B-126 only for bacitracin, colistin, and tetracycline. The result obtained for tetracycline with B-126 was significantly higher than for B-225 and B-676.

Relative potencies obtained with B-225 paper frequently differed significantly from the standard. Assays of colistin and neomycin were 14–24% lower than the standard, while relative potencies of ampicillin, cephalothin, chloramphenicol, methicillin, novobiocin, penicillin G, polymyxin B, rifampin, and vancomycin exceeded the standard by 10–41%. Ampicillin, penicillin G, and cephalothin results were particularly high. With few exceptions, this paper resulted in higher assays than any other paper tested, but B-126 gave higher recoveries of colistin and tetracycline than did B-225.

The regulations, §460.1(a) (7), state: "The absorbent paper and dye or ink used (to produce antibiotic susceptibility discs) must not affect either bacterial growth or the antibiotic." The data presented here strongly suggest that the grades of paper used in the manufacture of commercial susceptibility disks do affect the diffusibility of all antibiotics studied except carbenicillin and erythromycin. The widely disparate relative potencies obtained from one or more of the production papers for each of the other antibiotics shown in Table I indicate that antibiotic activity is influenced by the respective papers. This influence may be either negative or positive.

All official microbiological assays of antibiotics in the United States involve use of multiple doses of standard to define a response line and a single dose of sample, the response of which is compared to the standard curve. This assay design requires three basic assumptions: the response line must be statistically linear throughout the range of contents covered by the standard curve, the standard and sample must produce parallel response lines, and a given quantity of antibiotic in a sample must cause the *same* response as a like quantity of standard.

Antibiotic disks are certified by FDA on the basis of their performance under specified conditions rather than on actual content of antibiotic in the disks. Potency assays only determine that commercial disks produce inhibition zones of similar diameter and definition as disks made from official FDA antibiotic standards. As long as standard and manufactured disks exhibit parallel dose responses, determinations of potency by this means are accurate and valid.

Dose responses evoked by the papers for each antibiotic were studied with the USP 3 × 3 factorial design (8). Since disks of all papers were prepared by hand from the same solutions of antibiotic standards, any influences of formulation and/or manufacturing processes were eliminated. As expected, most assays demonstrated parallel responses by the different papers. The A-470 and A-740-E papers performed similarly to each other in this regard. The majority of the very low relative potencies obtained from B-676 paper (Table I) were valid because of the parallelism of the dose responses (Fig. 1). As Fig. 1 clearly shows, however, a quantity of polymyxin on B-676 paper did not produce the same response as the same quantity on the standard paper. The paper caused the same effect with cephalothin, kanamycin, penicillin, rifampin, streptomycin, tetracycline, tobramycin, and vancomycin. The assays of colistin, gentamicin, and neomycin on B-676 paper, which produced exceptionally low results, were not valid because of a lack of parallelism between the respective dose responses and those of the standard.

Standard control disks are prepared for each antibiotic subject to certification by FDA from blank disks of A-740-E paper. Thus, in the certification procedure, the quantity of antibiotic loaded onto a commercial disk is tested in combination with the commercial paper against a known quantity of drug loaded onto, and acting in concert with, A-740-E paper. Within limits specified in the regulations, §460.6(f) (7), the antibiotic and paper of production disks must perform similarly to the FDA working standards and the A-740-E paper.

In some instances, the various grades of production paper appeared to influence markedly the dose response of the test organism to varying amounts of antibiotic. Grade B-126 paper seemed to diminish the dose response to tetracycline, producing a slope (defined as the change in zone diameter caused by a 10-fold increase in antibiotic content, *i.e.*, a logarithmic cycle, as determined by the zone diameters produced by the lowest and highest doses of antibiotic) of approximately 4.5 mm while the other grades, including A-470 and A-740-E papers, resulted in slopes of about 6.5 mm.

More frequently, however, these papers tended to enhance the dose response to the antibiotics. Grades B-225 and B-676 both appeared to produce a significantly greater dose response to colistin and gentamicin than did the other papers. With gentamicin, A-470, A-740-E, and B-126 produced slopes of approximately 4 mm, whereas the B-225 and B-676 values were closer to 6 mm. These two papers promoted slopes of essentially 7.5 mm with colistin, whereas the other papers each evoked about a 5.5-mm response. These increased responses (Fig. 2) cause invalid assays because of the lack of parallelism of the response lines. Since the two papers do not meet the requirement of parallel dose responses for a valid assay, potency assays of the two drugs on B-225 and B-676 paper are inaccurate.

For the same reasons, *i.e.*, increased dose responses and, therefore, not parallel response lines, assays of neomycin on B-676 paper and tobramycin on B-126 paper are of no value. Grade B-676 caused a response of 6 mm to neomycin while the other papers resulted in slopes closer to 5 mm. Slopes of essentially 4.5 mm were observed for tobramycin except with B-126, which caused a response of 6 mm. The diminished response to tetracycline on B-126 paper, discussed earlier, similarly renders assay of this product worthless, because a significantly greater quantity of this antibiotic is released from the paper at the low dose, compared with A-740-E, than is released at the higher levels. This results in a nonparallel response line and a nonlinear line from the B-126 paper.

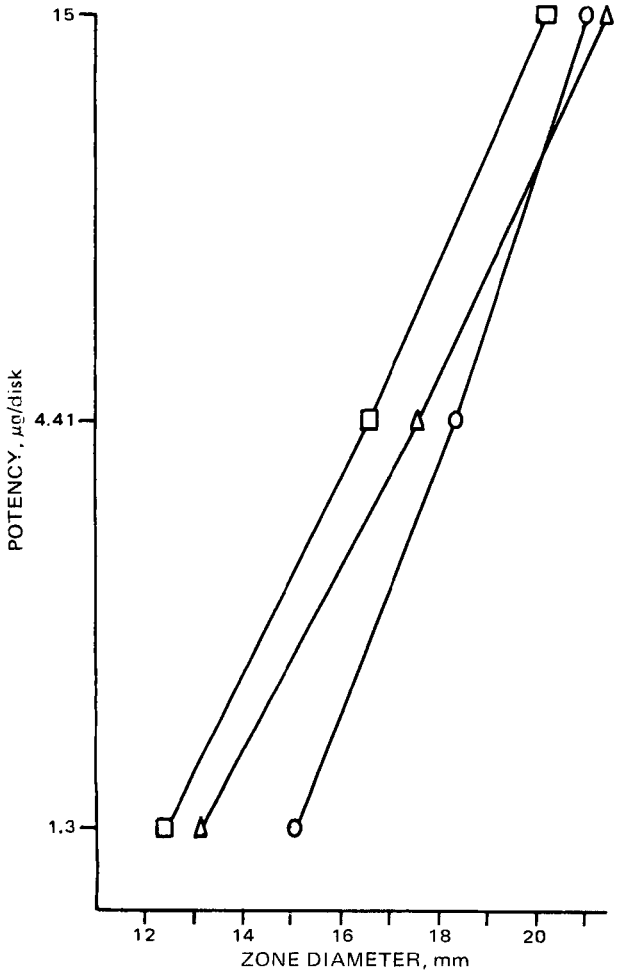

Figure 2—*Graph showing intersecting response lines due to enhanced dose response of* Bordetella bronchiseptica *to colistin on B-225 (△) and B-676 (□) papers compared with the response evoked by A-740-E (○). The same effect was noticed for aminoglycoside antibiotics with one or another of all commercial production papers. None of these assays produces meaningful results because of the lack of parallelism of the respective response lines produced by the production papers compared to the responses from the standard A-740-E paper.*

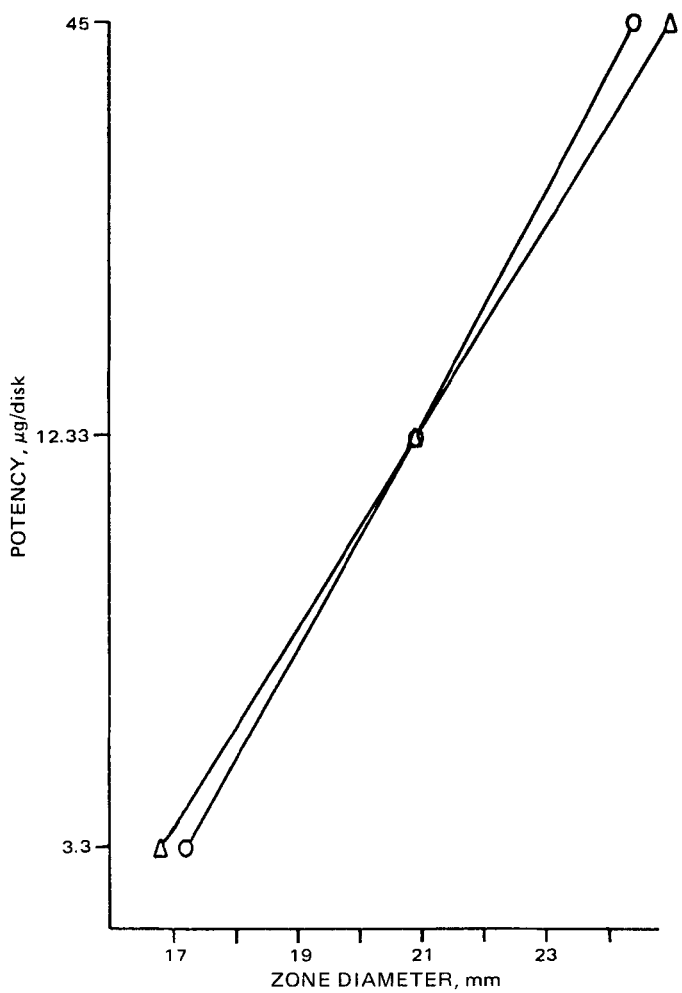

Figure 3—*Graph of valid assay of tetracycline on B-225 (△) paper against* Sarcina lutea. *Penicillin on B-126 paper showed the same relationship to A-740-E (○) standard disks. The respective response lines are not sufficiently divergent to invalidate the assay, but an assay of any batch of disks with antibiotic concentration close to either end of the standard curve will result in a potency value quite dissimilar to the actual content of antibiotic.*

The significant changes in slope of these respective dose responses reflect effects of the papers on bacterial growth. Thus, H-126 masks the effectiveness of tetracycline against the test organism. The opposite effect is caused by one or more of all three commercial papers in combination with colistin, gentamicin, neomycin, and tobramycin.

When analyzed by the statistical methods presented in USP XIX (8), penicillin assays on B-126 paper and tetracyline assays on B-225 paper are both valid. In these instances (Fig. 3), the slope from the B-126 paper for penicillin was approximately 6.5 mm while the slope of the standard A-740-E paper line was about 5.5 mm. The slope generated by B-225 paper with tetracycline was close to 7.5 mm, while the standard paper created a response of about 6.5 mm. The two response lines intersected nearly at the center. Thus, a lot of disks made with this paper and formulated at a potency near the center of the curve will assay in close agreement with theory. However, if the lot is formulated closer to either end of the response line to achieve the labeled content, assay potency will diverge proportionately from theory.

Tetracycline susceptibility disks are marketed in the United States with labeled concentrations of 5, 10, and 30 μg. The Code of Federal Regulations, §460.6(f) (7), requires the potency of a batch to be between 67 and 150% of the labeled strength to be certified for use. With the differences in dose response of the test organism promoted by B-225 and A-740-E papers impregnated with this antibiotic, a 5-μg disk produced on B-225 paper that actually contains 3.8 μg of tetracycline will act as though it only holds 3.3 μg when tested beside A-740-E paper. Conversely, a 30-μg disk of grade B-225 paper formulated to contain 37 μg of drug can be expected to produce the same response by the test organism as an A-740-E disk containing 45 μg.

Thus, a commercial disk of the B-225 paper that actually contains 3.8 μg of tetracycline is apt to fail the performance test as being subpotent; a disk containing 37 μg, well within legal requirements for a 30-μg disk, is likely to fail the performance test as superpotent. Such results tend to confound both production and analytical departments.

The differences in the diffusion characteristics of the various grades of paper clearly outline the need for one specified paper for the preparation of standard control disks. Data presented here indicate that the two lots of A-740-E paper act similarly with regard to diffusion of all currently used concentrations of each antibiotic studied, as Kramer and Kirshbaum (1) previously reported. The performance of the single lot of A-470 paper was also comparable to that of the A-740-E papers. Since A-740-E paper is readily available as punched 6.35-mm disks, the use of such disks could help fulfill the need for uniform standard disks by control laboratories.

Because paper is, in essence, a natural product and subject to certain variation in both the source fiber and the manufacturing process, it might be advisable for all control laboratories, insofar as possible, to use the same lot of paper for the preparation of standard disks. In this way, analytical discrepancies due to possible variations in lots of the same grade of paper would be reduced to the greatest extent, at least for the majority of assays that are valid in design.

SUMMARY

Three grades of papers used in the production of antibiotic susceptibility disks and two grades of papers used by control laboratories to assay

susceptibility disks were compared for performance. Grades A-740-E, A-470, and B-126 papers perform in the same manner. Grade B-676 paper appears to bind a high percentage of most antibiotic solutions applied to it. This binding is particularly pronounced with polypeptide and aminoglycoside drugs. Grade B-225 paper, on the other hand, frequently releases antibiotics at greater rates than the A-470 and A-740-E papers.

Analysis of slopes of dose–response lines did not show the same effects on classes of antibiotics from one paper to another. Again, the A-470 and A-740-E papers were generally equivalent for each drug. In a few instances, one or another of the production papers appeared to enhance the dose response compared to the slopes produced by A-740-E paper. Grade B-126 decreased the dose response to tetracycline. These types of differences in dose responses between papers nullify the concept of the design of the performance test used to certify production lots of the respective disks, rendering assay of these products quite inaccurate. Thus, it has been shown that, contrary to the intent of the Code of Federal Regulations, §460.1(a) (7), each grade of paper used in the manufacture of antibiotic susceptibility disks affects bacterial growth and/or the antibiotic in one or more instances.

Most potency assays are statistically valid. However, since sample disks of production papers frequently do not evoke the same response as a like quantity of antibiotic on a standard disk, universal agreement among control laboratories as to the type of paper to be used to prepare standard control disks is highly desirable. Such agreement could extend to the use of a common lot of paper by those laboratories and would greatly enhance the likelihood of interlaboratory concurrence in potency values of commercial lots of antibiotic disks.

REFERENCES

(1) J. Kramer and A. Kirshbaum, *Appl. Microbiol.*, **9**, 334 (1961).

(2) E. H. Marth, F. J. Alexander, and R. V. Hussong, *J. Milk Food Technol.*, **26**, 150 (1963).

(3) A. Kirshbaum, J. Kramer, and B. Arret, *Antibiot. Chemother.*, **10**, 249 (1960).

(4) B. Arret and A. Kirshbaum, *J. Milk Food Technol.*, **22**, 329 (1959).

(5) W. W. Wright, *J. Assoc. Offic. Anal. Chem.*, **45**, 301 (1962).

(6) *Ibid.*, **45**, 307 (1962).

(7) "Code of Federal Regulations," Title 21, Superintendent of Documents, U.S. Government Printing Office, Washington, D.C., 1976.

(8) "The United States Pharmacopeia," 19th rev., Mack Publishing Co., Easton, Pa., 1975, pp. 601–611.

ACKNOWLEDGMENTS

The author expresses his appreciation to Blondell Anderson for technical assistance and to Ira Zimmerman for writing calculator programs for statistical analyses of the data.

Microdetermination of Procainamide in Human Serum

T. M. LUDDEN *‡ˣ, D. LALKA ‡, M. G. WYMAN §, B. N. GOLDREYER §, K. D. HAEGELE ‡, D. T. BROOKS *‡, I. DAVILA ‡, and J. E. WALLACE ¶

Received March 25, 1977, from the **College of Pharmacy, University of Texas–Austin, Austin, TX 78712; the* ‡*Departments of Pharmacology,* ¶*Pathology, and the* ‡*Division of Clinical Pharmacology, Department of Medicine, University of Texas Health Science Center at San Antonio, San Antonio, TX 78284* (where inquiries should be directed); and the §*Division of Cardiology, San Pedro and Peninsula Hospital, San Pedro, CA 90732.* Accepted for publication July 1, 1977.

Abstract □ An electron-capture GLC method to measure procainamide (0.1–1 μg/sample) in human serum was developed. An internal standard, *p*-amino-*N*-[2-(dipropylamino)ethyl]benzamide, is added to the serum before the sample is alkalinized with pH 10.5 phosphate buffer and extracted with ethyl acetate. The ethyl acetate phase is evaporated to dryness, and the residue is reacted with pentafluoropropionic anhydride. *N*-Pentafluoropropionyl derivatives of the drug and the internal standard had retention times of 5 and 8 min, respectively, when chromatographed at 235° on a 1-m (4-mm i.d.) glass column packed with 5% OV-17 (carrier gas flow of 40 ml/min). The coefficient of variation was less than 5% for spiked standards. Furthermore, *N*-acetylprocainamide added to samples did not interfere. One hundred and eighty-six samples from 16 patients receiving procainamide intravenously were assayed by this GLC procedure and by a standard colorimetric method. Linear regression analysis yielded a correlation coefficient of 0.985 (slope, 1.040; intercept, 0.015).

Keyphrases □ Procainamide—electron-capture GLC analysis in human serum □ GLC, electron capture—analysis, procainamide in human serum □ Cardiac depressants—procainamide, electron-capture GLC analysis in human serum

Procainamide has been used clinically over the last 25 years for the prevention and treatment of ventricular arrhythmias. Several studies (1–4) demonstrating the utility of plasma procainamide concentrations in dosage regimen design have stimulated interest in procainamide assays.

The colorimetric technique of Mark *et al.* (5) is commonly used to determine procainamide in biological fluids. However, Gibson *et al.* (6) reported that *N*-acetylprocainamide, a major metabolite of procainamide in humans (7), may be hydrolyzed to procainamide under certain conditions. Recently, it was found (8) that the colorimetric method (5) as modified by Sitar *et al.* (9) did not result in the hydrolysis of *N*-acetylprocainamide. A specific flame-ionization detection GLC assay for procainamide was developed (10) and gave results similar to those of the colorimetric analysis.

Several GLC techniques (10–13) and a high-pressure liquid chromatographic (HPLC) procedure (14) were described for procainamide analysis, but these methods require at least 0.5–1 ml of serum. This report describes an electron-capture GLC determination of procainamide that requires as little as 0.1 ml of plasma. In addition, the results of this new procedure are compared to those obtained using the modified colorimetric procedure (9).

EXPERIMENTAL

Reagents—Stock solutions of procainamide hydrochloride[1], *N*-acetylprocainamide hydrochloride[2], and the internal standard, *p*-

[1] ICN Pharmaceuticals, Plainview, N.Y.

[2] Astra Pharmaceutical Products, Worcester, Mass.

susceptibility disks were compared for performance. Grades A-740-E, A-470, and B-126 papers perform in the same manner. Grade B-676 paper appears to bind a high percentage of most antibiotic solutions applied to it. This binding is particularly pronounced with polypeptide and aminoglycoside drugs. Grade B-225 paper, on the other hand, frequently releases antibiotics at greater rates than the A-470 and A-740-E papers.

Analysis of slopes of dose–response lines did not show the same effects on classes of antibiotics from one paper to another. Again, the A-470 and A-740-E papers were generally equivalent for each drug. In a few instances, one or another of the production papers appeared to enhance the dose response compared to the slopes produced by A-740-E paper. Grade B-126 decreased the dose response to tetracycline. These types of differences in dose responses between papers nullify the concept of the design of the performance test used to certify production lots of the respective disks, rendering assay of these products quite inaccurate. Thus, it has been shown that, contrary to the intent of the Code of Federal Regulations, §460.1(a) (7), each grade of paper used in the manufacture of antibiotic susceptibility disks affects bacterial growth and/or the antibiotic in one or more instances.

Most potency assays are statistically valid. However, since sample disks of production papers frequently do not evoke the same response as a like quantity of antibiotic on a standard disk, universal agreement among control laboratories as to the type of paper to be used to prepare standard control disks is highly desirable. Such agreement could extend to the use of a common lot of paper by those laboratories and would greatly enhance the likelihood of interlaboratory concurrence in potency values of commercial lots of antibiotic disks.

REFERENCES

(1) J. Kramer and A. Kirshbaum, *Appl. Microbiol.*, **9**, 334 (1961).

(2) E. H. Marth, F. J. Alexander, and R. V. Hussong, *J. Milk Food Technol.*, **26**, 150 (1963).

(3) A. Kirshbaum, J. Kramer, and B. Arret, *Antibiot. Chemother.*, **10**, 249 (1960).

(4) B. Arret and A. Kirshbaum, *J. Milk Food Technol.*, **22**, 329 (1959).

(5) W. W. Wright, *J. Assoc. Offic. Anal. Chem.*, **45**, 301 (1962).

(6) *Ibid.*, **45**, 307 (1962).

(7) "Code of Federal Regulations," Title 21, Superintendent of Documents, U.S. Government Printing Office, Washington, D.C., 1976.

(8) "The United States Pharmacopeia," 19th rev., Mack Publishing Co., Easton, Pa., 1975, pp. 601–611.

ACKNOWLEDGMENTS

The author expresses his appreciation to Blondell Anderson for technical assistance and to Ira Zimmerman for writing calculator programs for statistical analyses of the data.

Microdetermination of Procainamide in Human Serum

T. M. LUDDEN *‡ˣ, D. LALKA ‡, M. G. WYMAN §, B. N. GOLDREYER §, K. D. HAEGELE ‡, D. T. BROOKS *‡, I. DAVILA ‡, and J. E. WALLACE ¶

Received March 25, 1977, from the **College of Pharmacy, University of Texas–Austin, Austin, TX 78712; the* ‡*Departments of Pharmacology,* ¶*Pathology, and the* ‡*Division of Clinical Pharmacology, Department of Medicine, University of Texas Health Science Center at San Antonio, San Antonio, TX 78284* (where inquiries should be directed); and the §*Division of Cardiology, San Pedro and Peninsula Hospital, San Pedro, CA 90732.* Accepted for publication July 1, 1977.

Abstract □ An electron-capture GLC method to measure procainamide (0.1–1 μg/sample) in human serum was developed. An internal standard, *p*-amino-*N*-[2-(dipropylamino)ethyl]benzamide, is added to the serum before the sample is alkalinized with pH 10.5 phosphate buffer and extracted with ethyl acetate. The ethyl acetate phase is evaporated to dryness, and the residue is reacted with pentafluoropropionic anhydride. *N*-Pentafluoropropionyl derivatives of the drug and the internal standard had retention times of 5 and 8 min, respectively, when chromatographed at 235° on a 1-m (4-mm i.d.) glass column packed with 5% OV-17 (carrier gas flow of 40 ml/min). The coefficient of variation was less than 5% for spiked standards. Furthermore, *N*-acetylprocainamide added to samples did not interfere. One hundred and eighty-six samples from 16 patients receiving procainamide intravenously were assayed by this GLC procedure and by a standard colorimetric method. Linear regression analysis yielded a correlation coefficient of 0.985 (slope, 1.040; intercept, 0.015).

Keyphrases □ Procainamide—electron-capture GLC analysis in human serum □ GLC, electron capture—analysis, procainamide in human serum □ Cardiac depressants—procainamide, electron-capture GLC analysis in human serum

Procainamide has been used clinically over the last 25 years for the prevention and treatment of ventricular arrhythmias. Several studies (1–4) demonstrating the utility of plasma procainamide concentrations in dosage regimen design have stimulated interest in procainamide assays.

The colorimetric technique of Mark *et al.* (5) is commonly used to determine procainamide in biological fluids. However, Gibson *et al.* (6) reported that *N*-acetylprocainamide, a major metabolite of procainamide in humans (7), may be hydrolyzed to procainamide under certain conditions. Recently, it was found (8) that the colorimetric method (5) as modified by Sitar *et al.* (9) did not result in the hydrolysis of *N*-acetylprocainamide. A specific flame-ionization detection GLC assay for procainamide was developed (10) and gave results similar to those of the colorimetric analysis.

Several GLC techniques (10–13) and a high-pressure liquid chromatographic (HPLC) procedure (14) were described for procainamide analysis, but these methods require at least 0.5–1 ml of serum. This report describes an electron-capture GLC determination of procainamide that requires as little as 0.1 ml of plasma. In addition, the results of this new procedure are compared to those obtained using the modified colorimetric procedure (9).

EXPERIMENTAL

Reagents—Stock solutions of procainamide hydrochloride[1], *N*-acetylprocainamide hydrochloride[2], and the internal standard, *p*-

[1] ICN Pharmaceuticals, Plainview, N.Y.

[2] Astra Pharmaceutical Products, Worcester, Mass.

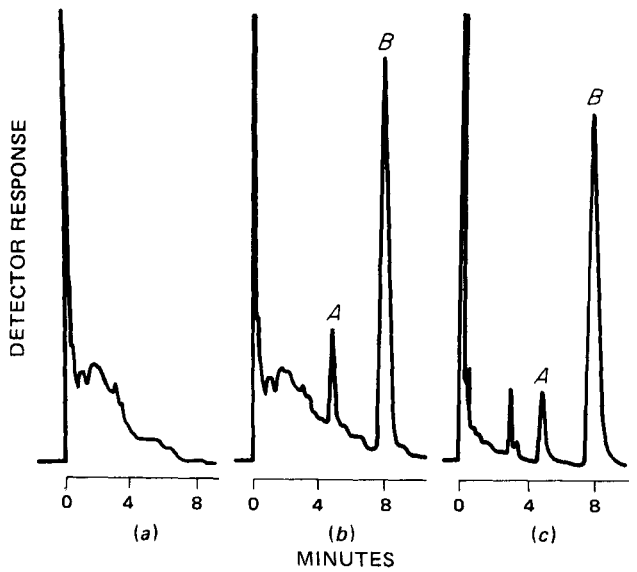

Figure 1—*Gas chromatogram of derivatized extract of 1 ml of pooled serum containing no procainamide or internal standard (a), 1 ml of pooled serum containing 0.1 μg of procainamide and 0.63 μg of internal standard (b), and 0.1 ml of pooled serum containing 0.1 μg of procainamide and 0.63 μg of internal standard (c). Key: A, N-pentafluoropropionyl procainamide; and B, N-pentafluoropropionyl derivative of the internal standard.*

amino-*N*-[2-(dipropylamino)ethyl]benzamide hydrochloride[3], were prepared in absolute methanol. The *N*-acetylprocainamide contained 1.1% procainamide. Pentafluoropropionic anhydride[4] was used as received. All other chemicals were reagent grade.

Phosphate buffer, pH 10.5, was prepared by dissolving 17.5 g of anhydrous dibasic potassium phosphate and 4 g of tribasic sodium phosphate dodecahydrate in a total volume of 100 ml of distilled, deionized water.

Extraction of Serum and Preparation of Serum Standards—To 15-ml culture tubes fitted with polytef-lined screw caps were added 1–10 μl (0.1–1 μg of base) of the procainamide stock solution and 7 μl (0.63 μg of base) of the internal standard stock solution. To determine if *N*-acetylprocainamide is hydrolyzed by extraction or derivatization, 100 μg of this metabolite was added to several tubes in place of procainamide. Methanol was removed by evaporation, and either 0.1 or 1 ml of pooled human serum was added. One gram of sodium chloride and 1 ml of pH 10.5 phosphate buffer (2 g of sodium chloride and 2 ml of buffer for 1-ml serum samples) were then added, and each sample was extracted with 5.5 ml of ethyl acetate.

Samples were shaken for 10 min at low speed on a reciprocating shaker[5] and then centrifuged for 10 min at 1500×*g*. Approximately 5 ml of the ethyl acetate was then transferred to a clean culture tube and evaporated to dryness at 40° in a stream of dry air. At this point, 100 μl of absolute methanol was added to each sample and then evaporated at 40°. This step was necessary to remove traces of moisture that could interfere with the derivatization reaction.

Extraction efficiencies for several concentrations of procainamide were determined by adding the internal standard to a known volume of the ethyl acetate after extraction instead of to the serum sample before extraction. Standards representing 100% extraction were prepared by adding both procainamide, at several concentrations, and the internal standard to the ethyl acetate extracts of blank serum samples.

Preparation of Pentafluoropropionyl Derivatives—Derivatization was accomplished by adding 20 μl of pentafluoropropionic anhydride to each residue, tightly capping the tube, and heating at 40° for 25 min. Subsequently, excess derivatizing reagent was removed by evaporation at 40° in a stream of dry air. Evaporation was facilitated by the addition and evaporation of two 100-μl portions of absolute methanol. The derivatized samples were then diluted with 100 μl of ethyl acetate, and 1–3 μl was injected into the gas chromatograph.

Assay of Patient Serum Samples—Aliquots (0.1–1 ml) of 186 serum samples from 16 patients receiving procainamide intravenously were placed in 15-ml siliconized culture tubes containing 0.63 μg of internal standard and were extracted, derivatized, and injected onto the gas chromatograph as described for serum standards. These serum samples were also assayed by the modified colorimetric assay of Sitar *et al.* (9).

Table I—Standard Curve and Precision Data for Electron-Capture GLC Assay of Procainamide in Human Plasma

Plasma Volume, ml	Procainamide Added, μg/ml	Mean Peak Height Ratio	Procainamide Found, μg/ml
1.0	0.10[a]	0.245	0.101 ± 0.005[b]
	0.30	0.754	0.304 ± 0.005
	0.50	1.23	0.514 ± 0.015
	0.70	1.74	0.720 ± 0.015
	1.00	2.50	1.015 ± 0.023
0.1	1.0	0.244	1.05 ± 0.04
	3.0	0.708	3.09 ± 0.06
	5.0	1.15	5.03 ± 0.10
	7.0	1.60	7.01 ± 0.09
	10.0	2.27	9.96 ± 0.31

[a] $n = 5$. [b] Mean ± *SD*.

GLC—A gas chromatograph[6] equipped with a ^{63}Ni-electron-capture detector was utilized. Glass columns, 1 m long and 4 mm i.d., were packed with 5% OV-17 on 100–120-mesh Gas Chrom Q[7]. The oven temperature was 235° with the injector at 250° and the detector at 350°. Argon–methane (95:5) carrier gas was maintained at a flow rate of 40 ml/min. Prior to attachment to the detector, the packed column was conditioned for 18 hr at 280° with a gas flow of 40 ml/min and was then treated with 3 × 20 μl of silylating agent[8] at 200°.

The pentafluoropropionyl derivatives of procainamide and internal standard had retention times of approximately 5 and 8 min, respectively (Fig. 1).

Calculations—Peak height ratios were calculated by dividing the height of the procainamide peak by the height of the internal standard peak. Standard curves were obtained from data obtained for freshly prepared serum standards and from serum standards kept frozen for up to 3 weeks. The peak height ratios were plotted against the concentration of procainamide base, and the least-squares regression line of best fit was calculated. The concentrations of procainamide in patient samples were derived from the peak height ratios and the regression equation for the standard curve.

The absolute recoveries for several concentrations of procainamide were calculated by dividing the peak height ratio obtained for the serum samples containing a known amount of procainamide, to which the internal standard had been added to the ethyl acetate extract, by the peak height ratio obtained for the serum samples to which both the known amount of procainamide and the internal standard had been added to the ethyl acetate extract.

Mass Spectrometry—A mass spectrometer[9] was used to establish the identity of the pentafluoropropionyl derivatives of both procainamide and the internal standard.

RESULTS AND DISCUSSION

Figure 1 shows typical chromatograms obtained after derivatization of blank serum and serum containing procainamide and the internal standard. Verification by combined GLC–mass spectrometry confirmed these compounds to be the *N*-pentafluoropropionyl derivatives. Since *N*-acetylprocainamide does not react with pentafluoropropionic anhydride and has very poor intrinsic electron-capturing ability, it is not detectable at usual serum concentrations. In addition, *N*-acetylprocainamide added to serum, 100 μg/ml, and taken through the extraction and derivatization procedures did not give rise to any additional procainamide above that originally present as a contaminant (1.1%). However, at significantly higher derivatization temperatures (>60°) or at incubation times longer than 1 hr, a partial hydrolysis of *N*-acetylprocainamide to procainamide was observed.

Adsorption of procainamide on chromatographic columns and/or

[3] Dr. T. Q. Spitzer, E. R. Squibb and Sons, New Brunswick, N.J.
[4] PCR, Inc., Gainesville, Fla.
[5] Eberbach Corp., Ann Arbor, Mich.
[6] Model 5710A, Hewlett-Packard, Avondale, Pa.
[7] Supelco, Bellefonte, Pa.
[8] Silyl-8, Pierce Chemical Co., Rockford, Ill.
[9] Model 5980A GLC–mass spectrometer equipped with a 5933A data system, Hewlett-Packard, Avondale, Pa.

Table II—Efficiency of Extraction of Procainamide from Human Serum

Plasma Volume, ml	Procainamide Added, μg/ml[a]	Mean Procainamide Found, μg/ml	Mean Recovery, %
1.0	0.10	0.0602	60.2
	0.30	0.188	62.6
	0.50	0.339	67.8
	0.70	0.446	63.7
	1.0	0.683	68.3
0.1	1.0	0.928	92.8
	3.0	2.58	86.0
	5.0	4.26	85.3
	7.0	6.26	89.4
	10.0	9.00	90.0

[a] $n = 4$.

supports was a problem in several previous GLC methods (10–12). With the current procedure, there was no apparent problem with adsorption (Table I); standard curves were reproducible from day to day, provided the chromatographic column was properly conditioned and silanized. It was necessary to replace the first 4–6 cm of the column with fresh packing and to resilanize the entire column monthly.

In preliminary studies, 5% OV-17 proved to be superior to 3 or 10% OV-1 and 3% OV-17. Stationary phases other than 5% OV-17 resulted in significant adsorption and unsymmetrical peak shape for the pentafluoropropionyl derivatives of procainamide and the internal standard.

The proposed procedure has the advantage of requiring a single extraction step instead of the extraction and back-extraction necessary for GLC with flame-ionization detection (13). Preliminary studies indicated that the use of less than 1 ml of phosphate buffer for 0.1-ml serum samples (less than 2 ml for 1-ml serum samples) resulted in the extraction of unacceptable amounts of extraneous material. The amount of sodium chloride was not critical, provided that saturation of the aqueous phase was achieved. It is important that serum standards and not mere aqueous standards be used for calibration curves. The extraction efficiencies of the internal standard from serum and water are different (11). There were no differences among calibration curves prepared from human serum from different sources.

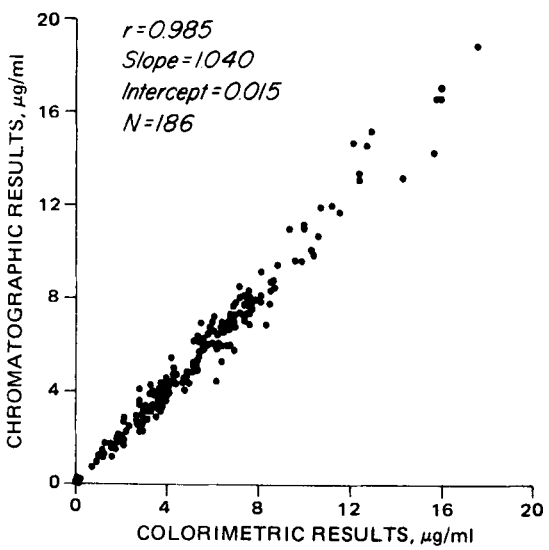

Figure 2—*Graph of procainamide concentration as measured by the electron-capture GLC procedure* versus *that measured by the modified colorimetric procedure (9) in serum samples of patients receiving procainamide.*

Extraction of procainamide from serum resulted in an average absolute recovery of 64.5% for 1-ml samples and of 88.7% for 0.1-ml samples (Table II). Although actual recoveries were quite variable, the inclusion of an internal standard resulted in precise standard curves (Table I).

Comparison of this new GLC technique with the modified colorimetric technique (9) using 186 samples from 16 patients receiving procainamide by long-term intravenous infusion (Fig. 2) yielded a correlation coefficient of 0.985. The results of duplicate GLC analyses of several patient samples gave an average coefficient of variation of 4.5%.

N-Acetylprocainamide has antiarrhythmic activity similar to that of procainamide (12, 15, 16). Therefore, it is important that both procainamide and *N*-acetylprocainamide be measured when evaluating procainamide therapy. The analytical procedure described here would, of course, not be appropriate for that purpose. However, for bioavailability studies requiring several blood samples from the same individual over a relatively short time, the electron-capture GLC technique offers the distinct advantage of requiring very small serum samples. The sensitivity of the method permits the use of very small sample volumes at times of high drug concentration, allowing more blood to be drawn at times of low drug concentration. In addition, the precision of the method is well within the limits necessary for sophisticated pharmacokinetic studies.

REFERENCES

(1) J. Koch-Weser, S. W. Klein, L. L. Foo-Canto, J. A. Kaster, and R. W. DeSanctis, *N. Engl. J. Med.*, **281**, 1253 (1969).

(2) J. Koch-Weser and S. W. Klein, *J. Am. Med. Assoc.*, **215**, 1454 (1971).

(3) P. Collste and E. Karlsson, *Acta Med. Scand.*, **194**, 405 (1973).

(4) T. R. D. Shaw, C. R. Kumana, R. B. Royds, C. M. Padglam, and J. Hamer, *Br. Heart J.*, **36**, 265 (1974).

(5) L. C. Mark, H. J. Hayden, J. M. Steele, J. R. Cooper, I. Berlin, E. A. Rovenstine, and B. B. Brodie, *J. Pharmacol. Exp. Ther.*, **102**, 5 (1951).

(6) T. P. Gibson, D. T. Lowenthal, H. A. Nelson, and W. A. Briggs, *Clin. Pharmacol. Ther.*, **17**, 321 (1975).

(7) J. Dreyfuss, J. T. Bigger, Jr., A. J. Cohen, and E. C. Schrieber, *ibid.*, **13**, 366 (1972).

(8) C. V. Manion, D. Lalka, D. Baer, and M. B. Meyer, *J. Pharm. Sci.*, **66**, 981 (1977).

(9) D. S. Sitar, D. N. Graham, R. E. Rangno, L. R. Dusfresne, and R. I. Ogilvie, *Clin. Chem.*, **22**, 379 (1976).

(10) J. Sterling, S. Cox, and W. G. Haney, *J. Pharm. Sci.*, **63**, 1744 (1974).

(11) K. Frislid, J. E. Bredesen, and P. K. M. Lunde, *Clin. Chem.*, **21**, 1180 (1975).

(12) J. Elson, J. M. Strong, W. K. Lee, and A. J. Atkinson, Jr., *Clin. Pharmacol. Ther.*, **17**, 134 (1975).

(13) K. J. Simons and R. H. Levy, *J. Pharm. Sci.*, **64**, 1967 (1975).

(14) K. Carr, R. L. Woosley, and J. A. Oates, *J. Chromatogr.*, **129**, 363 (1976).

(15) D. E. Drayer, M. M. Reidenberg, and R. W. Sevy, *Proc. Soc. Exp. Biol. Med.*, **146**, 358 (1974).

(16) E. Karlsson, G. Aberg, P. Collste, L. Molin, B. Norlander, and F. Sjoqvist, *Eur. J. Clin. Pharmacol.*, **8**, 79 (1975).

ACKNOWLEDGMENTS

Supported by a research grant from the University of Texas Research Institute, by U.S. Public Health Service Training Grant 06-D-000-197, and by a grant from the American Heart Association, Texas Affiliate, Inc.

The authors thank Mrs. Mary Hill and Mrs. Barbara Boyle for their help in the preparation of this manuscript.

Sheabutter V: Effect of Particle Size on Release of Medicament from Ointment

G. H. KONNING * **and H. C. MITAL** [‡x]

Received December 22, 1976, from the *Faculty of Pharmacy, University of Science and Technology, Kumasi, Ghana, and the ‡Department of Pharmacy, University of Nigeria, Nsukka, Nigeria. Accepted for publication June 9, 1977.

Abstract □ An ointment prepared from fat (sheabutter) obtainable from an indigenous (African) fruit released medicaments faster than either of the two ointment bases recommended by the British Pharmacopoeia. Reduction in particle size of crystalline medicaments incorporated in ointments increased surface area and transfer from the ointment to the substrate, possibly due to greater dissolution in the base, and, therefore, increased the availability of medicament at the ointment–substrate interface.

Keyphrases □ Sheabutter ointment—drug release compared to other ointments effect of particle size □ Drug release—sheabutter ointment compared to others, effect of particle size □ Particle size—effect on drug release from sheabutter ointment, compared to other ointments □ Ointments—sheabutter compared to others, drug release, effect of particle size

The aim of any formulation is to produce a finished product that is not only elegant and acceptable to the consumer but also possesses maximal therapeutic efficacy. An ointment may be intended to act solely on the skin surface to produce a local effect or to penetrate the skin. Regardless of its intended site of action, the ultimate desire is the rapid release of the active medicament from the base. The development of an ointment must include tests for medicament release in addition to product stability, washability, *etc.*

Ointments consist primarily of the excipients (base) and the active medicament. In the current work, the physicochemical forms of both the base and medicament were varied, and the influence of such variations on release was studied.

Agar diffusion (1), dialysis (2), and radiometry (3) have been used to evaluate release from ointments. Since the *in vitro* agar diffusion technique is reputed to correlate fairly well with adsorption through the skin (4), it was used in these studies.

EXPERIMENTAL

Ointment Bases—White soft paraffin BP, simple ointment BP, and sheabutter ointment prepared from sheabutter (75% w/w), arachis oil (25% w/w), and hard paraffin BP (10% w/w) were used. Sheabutter (5) is a fat obtained from the fruit of an indigenous (African) tree, *Butyrospermum parkii.* The arachis oil used was a local product; it complied with the BP monograph on a weight per milliliter basis. Hard paraffin BP was incorporated in the base to increase consistency.

Medicaments—Salicylic acid[1] and benzoic acid[1] were recrystallized from water and then dried in a desiccator for 24 hr prior to use.

Fractionation of Medicament—The medicament was dried at 70° for 1 hr and the dry crystals were sieved mechanically through a set of brass sieves, 420–75 μm. The collected fractions were stored for ointment preparation.

Preparation of Medicated Ointments—An appropriate amount of medicament that passed through a specific sieve was triturated with the base. The finished product was packed in previously sterilized collapsible tubes and stored at 28–30° until required.

[1] Laboratory chemical grade, May & Baker.

Table I—Size of Crystals Recovered from Ointments

Sieve Number	Sieve Size, μm	Crystal Size, μm: Benzoic Acid: Paraffin	Benzoic Acid: Simple	Benzoic Acid: Sheabutter	Salicylic Acid: Paraffin	Salicylic Acid: Simple	Salicylic Acid: Sheabutter
36	420	251	234	207	270	250	205
60	250	150	146	132	150	148	129
100	150	123	116	105	130	120	110
200	75	67	65	64	66	66	62

Microorganisms—*Escherichia coli* (NCTC 5938) and *Staphylococcus aureus* (NCTC 8532) were subcultured as previously described (6) and standardized nephelometrically to contain ~10^9 organisms/ml. The suspension was stored at 4° and used for a maximum of 2 weeks.

Size of Crystals Recovered from Ointments—The particle size of medicament in each ointment was determined. To recover the crystals from the finished ointment, the solvent should dissolve away the base without affecting the medicament. The solvent selected by experimentation, turpentine oil for salicylic acid and *n*-hexane for benzoic acid, was first shaken mechanically with excess medicament for 1 hr to presaturate the solvent and was then filtered.

An aliquot of the medicated ointment (1 g) was then shaken together with 20 ml of the presaturated solvent as before. Presaturation ensured little dissolution, if any, of the medicament being recovered from the ointment. The crystals were then filtered off from the solution and dried on filter paper. Crystal samples were mounted under a calibrated microscope, and the size of 20 crystals was measured.

Release of Medicament from Ointment—*Through Seeded Agar*—Portions of 1 ml of the standardized bacterial suspension were thoroughly mixed with nutrient agar at 42° and poured into petri dishes to set. Circular holes of uniform diameter and depth were cut into the agar; sufficient ointment containing medicament of a specific particle size was squeezed out to fill the cups.

The petri dishes were first kept in a refrigerator for 1 hr to minimize the growth of the microorganisms and to allow the ointment to diffuse through the agar. They were finally incubated at 37° for 24 hr.

Through Agar Containing Chemical Indicator—The medicaments, benzoic and salicylic acids, give color reactions with bromcresol purple and ferric chloride solutions, respectively. A 1-ml aliquot of the solution was added to 20 ml of nutrient agar, mixed, and poured into petri dishes to set. The ointment was extruded to fill cups made of the agar, and the dishes were stored at 37°.

As the medicament diffused through the agar, the pH of the medium changed from alkaline to acid and was manifested by a perceptible change in color. Since the color change was rapid, it was possible to follow the release rate by measuring the zone showing a change in color against time.

RESULTS

Size of Crystals Recovered from Ointments—Microscopic examination showed all particles recovered from the various ointments to be much smaller than the particles that originally passed through a specific

Table II—Solubility of Benzoic and Salicylic Acid Ointment Bases

Ointment	Medicament Solubility, % (w/w): Benzoic Acid: 70°	Benzoic Acid: 80°	Benzoic Acid: 100°	Salicylic Acid: 70°	Salicylic Acid: 80°	Salicylic Acid: 100°
Paraffin	6.0	8.0	20.0	0.5	1.0	6.0
Simple	10.0	12.5	25.0	1.0	1.5	8.0
Sheabutter	12.5	14.5	36.0	5.0	7.0	12.5

Table III—Influence of Particle Size on Release Rate of Benzoic and Salicylic Acids from Ointments Determined by Microbial Method

Sieve Size, μm	Inhibition Zone, mm					
	Paraffin		Simple		Sheabutter	
	E. coli	*S. aureus*	*E. coli*	*S. aureus*	*E. coli*	*S. aureus*
	Benzoic Acid					
75	17.4	17.7	17.9	18.9	18.0	19.0
125	17.4	17.8	17.6	18.8	17.8	18.9
150	17.0	17.7	17.3	18.7	17.7	18.9
250	16.5	17.5	17.0	18.7	17.5	18.7
420	16.5	17.3	16.3	18.2	17.0	18.4
	Salicylic Acid					
75	16.0	17.5	17.5	18.0	18.0	19.0
125	15.8	17.3	17.4	17.4	18.0	18.5
150	15.7	17.0	17.0	17.0	18.0	18.5
250	15.5	16.0	16.2	16.3	17.5	18.2
420	15.0	16.0	16.0	16.0	17.0	17.5

sieve aperture (Table I). This observation led to the speculation that the ointment bases probably exerted some solvent action.

If it is assumed that all particles that pass through a specific sieve are spherical and uniform in diameter, the surface area of the particles equals $4\pi r^3/3$ or $\pi D^3/6$, where r and D are the radius and diameter of the particle, respectively, and π is a constant. The ratio of the surface area of the particle in the ointment and the surface area of the same particle passing through a specific sieve is given by:

$$\frac{\pi D_2{}^3/6}{\pi D_1{}^3/6} = D_2{}^3/D_1{}^3 \qquad \text{(Eq. 1)}$$

where D_1 is the diameter of the aperture through which a particle passes and D_2 is the diameter of the same particle after recovery from the ointment.

The percentage ratio equals $D_2{}^3/D_1{}^3 \times 100$. By plotting the log percentage ratio against the particle size, a straight line was obtained. Since the pattern was the same for both benzoic and salicylic acids, only the plot for benzoic acid is presented in Fig. 1. Linearity of the regression indicated that the medicament dissolved in the bases, dissolution being proportional to the surface area of the particles; *i.e.*, the finer the particles, the greater was their dissolution rate in all of the ointment bases studied.

Particles of the same original size incorporated in the ointments and subsequently recovered from them differed markedly in size from one ointment base to another (Table I and Fig. 1). For instance, benzoic acid crystals recovered from white soft paraffin were larger than those from either the simple or sheabutter ointment. Although differences in size were less marked with salicylic acid ointments, the results indicated that the crystals were larger in both white soft paraffin and simple ointments than they were in sheabutter.

Determination of solubility of the medicaments in the three ointment bases (Table II) seems to explain the differences observed in the crystal size in the different ointments.

Effect of Particle Size on Release of Medicaments from Ointments by Biological and Colorimetric Methods—Sizes of inhibition

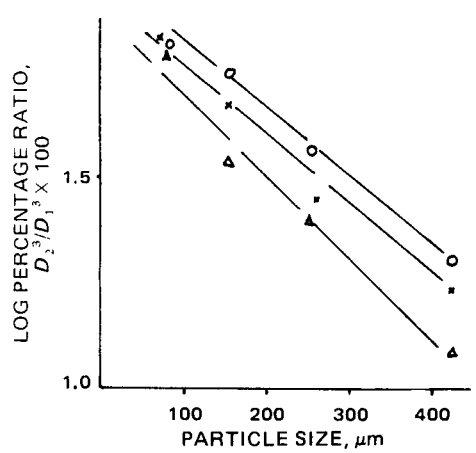

Figure 1—*Relationship between particle size and percentage diameter ratio (log) of benzoic acid crystals. Key: O, white soft paraffin; ×, simple ointment; and Δ, sheabutter ointment.*

Table IV—Influence of Particle Size on Release Rate of Benzoic and Salicylic Acids from Ointments Determined by Color Zones

Ointment	Sieve Size, μm	Color Zone, mm			
		0	8	16	24
	Benzoic Acid				
Paraffin	420	10.0	22.8	27.8	31.0
	75	10.0	27.8	32.6	35.4
Simple	420	10.0	25.6	29.4	30.0
	75	10.0	29.4	33.6	34.8
Sheabutter	420	10.0	28.0	36.2	38.8
	75	10.0	31.8	40.0	44.0
	Salicylic Acid				
Paraffin	420	10.0	23.6	29.0	32.0
	75	10.0	27.0	33.4	36.6
Simple	420	10.0	28.0	33.4	36.0
	75	10.0	30.0	36.4	40.6
Sheabutter	420	10.0	30.5	38.4	44.0
	75	10.0	35.4	44.7	50.4

zones produced by drug diffusion against microorganisms were determined (Table III). All ointments containing larger crystals of either benzoic or salicylic acid released their medicaments poorly; those containing smaller particles showed increasingly better release.

The colorimetric method was quicker and more sensitive than the biological procedure, so it was practically possible to follow the release rate over time. At any specified time over the experiment, release from ointments containing smaller crystals was relatively better than that from ointments containing larger crystals. This observation corroborated the results obtained using the biological approach. Since the pattern was the same for all three ointments, only that for sheabutter ointment is illustrated in Fig. 2; the overall results are summarized in Table IV.

DISCUSSION

The degree of fineness of solid medicaments incorporated in ointments may affect the grittiness and the aesthetic appearance of the final product. The BP recognizes this fact and recommends the use of finely sifted powder in ointments.

The current work shows that the ultimate fineness of crystalline par-

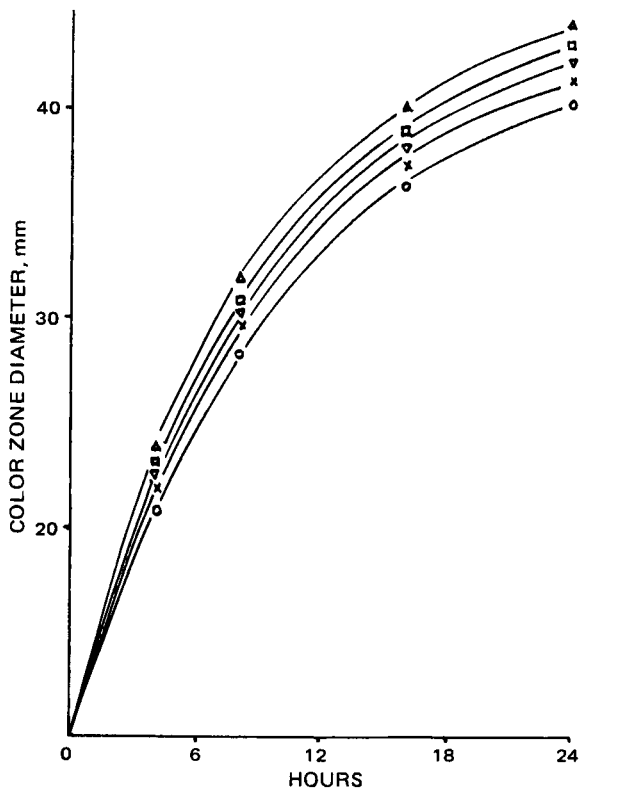

Figure 2—*Release of benzoic acid of different particle sizes from sheabutter ointment. Key (sizes in micrometers): Δ, 75; □, 120; ▽, 150; ×, 250; and O, 420.*

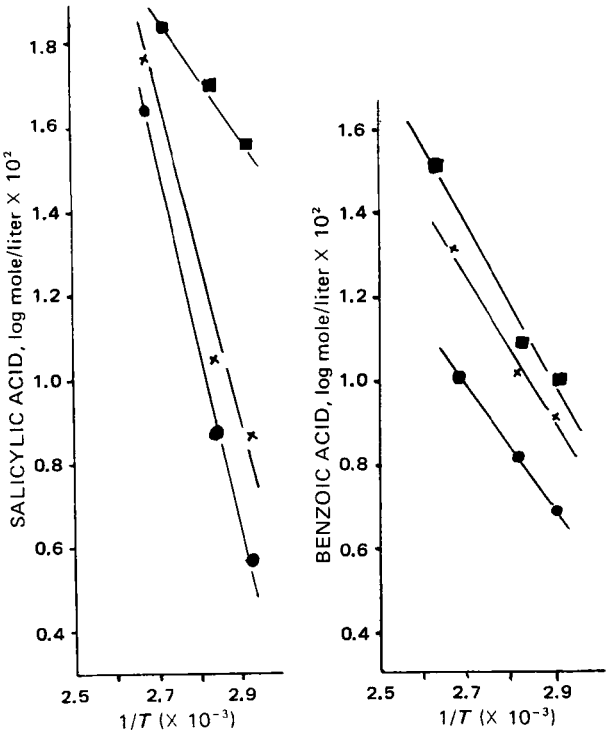

Figure 3—*Plots of logarithm of molar solubility of salicylic acid (left) and benzoic acid (right) in ointment bases* versus *the reciprocal of absolute temperature. Key:* ■, *sheabutter ointment;* ×, *simple ointment; and* ●, *paraffin ointment.*

ticles in a formulated ointment may differ from that originally incorporated. Medicaments recovered from white soft paraffin, simple, and sheabutter ointments were far smaller than they were before incorporation (Table I). Since the medicaments were incorporated in the bases by trituration, it may be argued that the diminution in particle size resulted from the mechanical process of mixing the base and medicament together, a process that may, indeed, produce some comminution. While trituration may account in part for the observation, the particles recovered from the ointments were not only smaller than they were when originally added but they varied in size from one base to another, suggesting the influence of the base.

Subsequent investigation (Table II) showed both benzoic and salicylic acids to be partially soluble in the three ointment bases. While it was practically impossible to determine the solubility of the medicaments in paraffin ointments at temperatures below 70° because the bases are semisolid, results recorded at all temperatures where the bases were completely melted established both acids to be less soluble in paraffin than in either simple or sheabutter ointment. The solubilities of benzoic acid and salicylic acid in the bases at elevated temperatures when plotted (on the log axis) against temperature ($1/T$) gave straight lines (Fig. 3), indicating the same order of solubilities in the ointment bases at room temperature as at the elevated temperatures. Therefore, this result confirms that the particle size was greater in the base in which it is least soluble and smaller in the one in which it is most soluble: that the particle size in the sheabutter ointment is smaller than the particle size in the simple ointment, which is smaller than the particle size in the paraffin ointment.

Particle size and, therefore, the surface area of medicament incorporated in the ointments increased the release rate markedly. Efficacies of both benzoic and salicylic acid ointments increased persistently, albeit slightly, as the particles became smaller (Table III). These observations were confirmed by a colorimetric method devised to detect the release rate, the superior sensitivity of the latter technique making the influence of particle size on release appear even more pronounced than was possible to observe using the microbial technique (Table IV and Fig. 2).

The reason for the observed differences in efficacies of ointments containing the same amount of medicament but of different particle size is not clear, but the cause seems to be linked with biological availability. Availability itself may be related to the transfer rate of medicament from an ointment base to the biological substrate under treatment, represented in this *in vitro* technique by nutrient agar. Medicament transfer across the ointment–substrate interface only occurs in solution; with solid medicaments, transfer depends on the amount of medicament in solution at the interface. Since smaller particles with larger surface areas dissolve much more readily than larger particles (Fig. 1), the smaller crystals conceivably dissolve in the oleaginous ointment bases and build up relatively higher concentrations at the interface for partitioning to the substrate. The current work suggests that when the total amount of particulate medicament incorporated in ointments is fixed, then efficacy depends primarily upon availability, which is itself controlled by particle size and surface area.

Besides the influence of the physical state of the medicament, the ointment bases contributed significantly to efficacy. For instance, similar amounts of medicament of the same degree of fineness showed much greater activity in sheabutter ointments than in either simple or paraffin ointments (Tables III and IV). The present finding corroborates an earlier report (6) that sheabutter ointments containing chloramphenicol, ammoniated mercury, *etc.*, were far more efficacious than simple or paraffin ointments containing the same medicaments.

REFERENCES

(1) H. Sheinaus and C. O. Lee, *J. Am. Pharm. Assoc., Sci. Ed.*, **44**, 7 (1955).

(2) W. C. Friedler and G. J. Sperandio, *ibid.*, **46**, 47 (1957).

(3) D. L. Sorby and E. M. Plein, *ibid.*, **48**, 308 (1959).

(4) E. M. Plein and J. B. Plein, *ibid.*, **46**, 705 (1957).

(5) H. C. Mital and F. R. Dove, *Planta Med.*, **20**, 283 (1971).

(6) G. H. Konning and H. C. Mital, *Pharm. Acta Helv.*, **49**, 192 (1974).

Influence of Cobalt (Dietary), Cobalamins, and Inorganic Cobalt Salts on Phenytoin- and Cortisone-Induced Teratogenesis in Mice

JOSEPH J. MITALA *, DAVID E. MANN, Jr. ˣ, and RONALD F. GAUTIERI

Received April 27, 1977, from the *Department of Pharmacology, School of Pharmacy and School of Dentistry, Temple University, Philadelphia, PA 19140.* Accepted for publication July 8, 1977. *Present address: Department of Pharmacology, School of Pharmacy, Ferris State College, Big Rapids, MI 49307.

Abstract □ Various cobalt-containing agents (cyanocobalamin, sodium cobaltinitrite, and cobaltous chloride), which formerly had been shown to prevent the onset of cleft palate in CF-1 mice injected with cortisone, were studied to determine whether they would afford similar protection against phenytoin. Phenytoin, however, failed to cause cleft palate in the mouse fetus when given to pregnant animals alone; and cortisone, on the contrary, induced this anomaly in the presence of the so-called cobalt antagonists as well as when administered in their absence. It is suggested from these results that high dietary intake of cobalt prevents cleft palate caused by phenytoin challenge and also negates the protective effects associated with the acute administration of cobalt compounds. Therefore, it is concluded that these well-known teratogens inhibit palatal closure in mice by different mechanisms.

Keyphrases □ Cobalt-containing agents, various—effect on phenytoin- and cortisone-induced teratogenesis in mice □ Teratogenesis, phenytoin and cortisone induced—effect of various cobalt-containing agents in mice □ Phenytoin-induced teratogenesis—effect of various cobalt-containing agents in mice □ Cortisone-induced teratogenesis—effect of various cobalt-containing agents in mice

Phenytoin (diphenylhydantoin) was first used therapeutically to palliate the seizures of *grand mal* epilepsy and later was used to mitigate the cortical dysrhythmias associated with psychomotor forms of this disease (1). Its clinical use has been extended to the treatment of the schizophrenias (2), delirium tremens (3), peripheral neuropathies (4), and ventricular dysrhythmias (5). Such diversification eventually brought attention to previously unrecognized side effects including megaloblastic anemia (6), osteomalacia (7), gingival hyperplasia (8), and various congenital malformations such as hare-lip and cleft palate (9).

Kuenssberg and Knox (10), after reviewing the findings of a prospective study involving more than 15,000 pregnancies, noted that five offspring of 48 deliveries were born with anomalies (hydrocephalus, hypospadias, and anal defects) to mothers who had received antiepileptic therapy (phenytoin and/or other drugs) during their gestation periods. Massey (11) reported the appearance of cleft palate in A/Jax mice after phenytoin was employed unsuccessfully as an antagonist to cortisone-induced cleft palate. Gibson and Becker (12), assuming that Massey's results might have been due to strain specificity, gave phenytoin to Swiss-Webster mice and succeeded in causing cleft palate along with decreased fetal weight, increased resorptions, and long bone deformities. Coincident with Massey's work with phenytoin and cortisone, Kasirsky *et al.* (13, 14) injected cobalt salts in CF-1 mice and produced a low incidence of this anomaly. However, when a cobalt salt was injected simultaneously with teratogenic doses of cortisone, the occurrence of the palatal defect was significantly inhibited.

Mann and Gautieri (15) reported a decreased incidence of cortisone-induced cleft palate with another cobalt-containing agent, cyanocobalamin (vitamin B_{12}). They proposed that other agents with a cobalt moiety might also inhibit the onset of the most prominent teratological manifestation associated with phenytoin administration in mice and humans, cleft palate. Therefore, the principal objectives of this study were to ascertain: (*a*) if cyanocobalamin and its congener, hydroxycobalamin, could prevent this and other anomalies from arising after phenytoin administration in mice, and (*b*) if cobaltous chloride and sodium cobaltinitrite could protect against phenytoin teratogenesis as each agent did against cortisone challenge under comparable experimental conditions. The latter observation, if affirmative, would substantiate the pharmacological similarities presumed to exist between the steroidal hormone and phenytoin at fundamental levels of activity.

Finally, the clinical benefit to be derived from this investigation, if indeed cortisone and phenytoin proved to be alike in this respect, is that pregnant patients who require phenytoin therapy can minimize the likelihood of giving birth to malformed children through the simultaneous administration of either cyanocobalamin or its congener, hydroxycobalamin, during their gestation periods.

EXPERIMENTAL

Animals—CF-1 albino mice[1] were utilized. The females were confined in groups of 10–15 to aggregate cages and were not mated until they weighed at least 20 g. Males were placed individually in metal cages (12.5 × 15 × 10 cm) with a wire-mesh front and floor[2]. All mice were maintained on a mouse/rat diet[3] (6% fat) and tap water *ad libitum*. The room housing the mice was protected from exposure to natural sunlight and was equipped with an electrical lighting system[4], which allowed 12 hr of light (7:00 am–7:00 pm) and 12 hr of darkness. The temperature was maintained between 22 and 26°.

Breeding Procedure and Dosage Regimen—The breeding procedure was described previously (16). Gravid mice were assigned to 29 experimental groups, each consisting of a minimum of six animals. The various groups employed are listed in Table I according to treatment regimen.

Suspected phenytoin antagonists were given intramuscularly in a fixed volume of 0.42 ml, except for the cobalt salts (cobaltous chloride and sodium cobaltinitrite) which were injected intraperitoneally in a volume according to body weight. The cobalt salts were prepared in distilled water in concentrations of 0.25% (cobaltous chloride) and 0.5% (sodium cobaltinitrite), which permitted delivery of the required milligrams per kilogram dose in a volume of 0.01 ml/g. Thus, each animal received a volume of solution no greater than 0.42 ml/injection.

Phenytoin was administered subcutaneously in a volume that corre-

[1] Charles River Breeding Laboratories, Wilmington, Mass.
[2] RD-T unit, Norwich Wire Works, Inc., Norwich, N.Y.
[3] Teklad Standard Diets, Division of ARS/Sprague-Dawley, Monmouth, Ill.
[4] Astronomic dial time switch with "skipper," model V-45073, International Register Co., Spring Grove, Ill.

sponded to the volume required for delivery of the estimated dose of this agonist (50-mg/kg dose as 0.005 ml of a 1.0% solution/g). At a single injection, each animal received a volume of this agonist no greater than 0.26 ml. Cortisone acetate[5] was given intramuscularly in a fixed dose of 2.5 mg (0.1 ml of a 2.5% suspension). All doses given subcutaneously were made beneath the loose skin of the back, while intramuscular doses were injected in close proximity to the semimembranous muscle. When multiple injections were required, alternate leg sites were used and an aspiration was performed to avoid intravenous administration.

The three dosage regimens were as follows:

1. According to volume per gram of body weight: physiological saline[6], 0.005 ml/g, and propylene glycol[7], 70% in saline, 0.005 ml/g.
2. In a fixed dose in a volume of 0.42 ml: physiological saline and cyanocobalamin[8], 0.25% (1.05 mg), 0.5% (2.1 mg), and 1.0% (4.2 mg); and hydroxycobalamin[9], 0.25% (1.05 mg), 0.5% (2.1 mg), and 1.0% (4.2 mg). In a volume of 0.1 ml: cortisone acetate, 2.5% (2.5 mg).
3. On a milligram per kilogram basis: cobaltous chloride[10], 0.25% (25 mg/kg); sodium cobaltinitrite[11], 0.5% (50 mg/kg); and phenytoin[12], 1.0% (50 mg/kg).

Preparation of Solutions—A 70% concentration of propylene glycol (in saline) was chosen as the solvent for phenytoin, because it was less irritating than higher concentrations when given parenterally[13] and the lower pH (9.39–9.95), approaching the physiological range, was less likely to cause fetal anomalies because of extreme alkalinity compared to the commercial preparation (pH 12).

The phenytoin solution was freshly prepared prior to injection by agitating the drug in the propylene glycol vehicle for approximately 20 min[14]. Because agitation causes an exothermic reaction, the solution was allowed to equilibrate before administration. Determinations of pH were made prior to injection[15].

Cyanocobalamin and hydroxycobalamin solutions were freshly prepared by weighing[16] and dissolving each agent in physiological saline. Cobaltous chloride and sodium cobaltinitrite were similarly weighed and dissolved in distilled water immediately before injection. Cortisone acetate was available as a commercially prepared suspension in a multiple-dose vial. All injections were accomplished with a glass syringe[17].

Examination of Fetuses—Following treatment, which ended on Day 14, gestation was allowed to continue to Day 18, 12–24 hr prior to expected delivery. At this time, each pregnant mouse was weighed[18] and sacrificed by cervical dislocation. A laparotomy was performed extending from the vaginal orifice to an area just below the xiphoid process along the linea alba to expose the uterine horns. The number and position of fetuses and resorption sites (metrial glands) were determined and recorded. The fetuses were removed and stimulated mechanically with a blunt probe to determine viability. Then they were blotted dry, weighed to the nearest hundredth of a gram[18], examined for gross external defects, and sexed on the basis of gross observations.

The specimens were then prepared for macroscopic examination. Because it was desirable to evaluate structural changes of bone and soft tissues, two methods of preparation were employed. For skeletal examination, every third fetus was prepared according to the method of Staples and Schnell (17). The other fetuses were fixed and decalcified in Bouin's solution in preparation of freehand razor blade sectioning according to the technique of Wilson (18). This method permits the evaluation of a large number of animals quickly and efficiently. All specimens were examined for bone and soft tissue defects[19].

Statistical Methods and Analysis—The degree of significance of observed variations among the experimental groups was determined by the Student t test and the uncorrected χ^2 test for binomial populations (19). All t values and χ^2 calculations were performed on a computer[20].

[5] Cortone, lot 0772N, Merck Sharp and Dohme, West Point, Pa.
[6] 0.9% Sodium Chloride Injection USP, lots G261A3 and G282X8, Baxter Laboratories, Division of Travenol Laboratories, Deerfield, Ill.
[7] Lot 766340, Fisher Scientific Co., Fair Lawn, N.J.
[8] Code 28625, courtesy of Dr. Walter J. Bagdon, Merck Sharp and Dohme, West Point, Pa.
[9] Lot E85428/70444, courtesy of Dr. Walter J. Bagdon, Merck Sharp and Dohme, West Point, Pa.
[10] Lot 713262, Fisher Scientific Co., Fair Lawn, N.J.
[11] Lot 22658, J. T. Baker Chemical Co., Phillipsburg, N.J.
[12] Dilantin sodium, lots W508K and PE338, Parke-Davis Co., Detroit, Mich.
[13] As determined from a pilot study.
[14] Vortex Genie mixer, model S8223.
[15] Beckman Expandomatic SS-2 pH meter.
[16] Ainsworth substitution balance, type 28N.
[17] B-D 1-ml tuberculin syringe with 1.27-cm, 26-gauge needle.
[18] Torbal torsion balance, model PL-800.
[19] Bausch & Lomb stereoscopic dissecting microscope, model ASZ30L2.
[20] Wang 2200.

Table I—Treatment Regimen of Experimental Groups

Group	Treatment[a] (Day)
1	Untreated controls
2	Saline (11) + saline (11–14)
3	Saline (11) + 70% I in saline (11–14)
4	Saline (11) + II (11–14)
5	III, 4.2 mg (11), + II (11–14)
6	III, 2.1 mg (11), + II (11–14)
7	III, 1.05 mg (11), + II (11–14)
8	Saline (10) + saline (11–14)
9	Saline (10) + 70% I in saline (11–14)
10	Saline (10) + II (11–14)
11	III, 4.2 mg (10), + II (11–14)
12	III, 2.1 mg (10), + II (11–14)
13	III, 1.05 mg (10), + II (11–14)
14	IV (11) + II (11–14)
15	V (11) + II (11–14)
16	IV (11) + cortisone (11–14)
17	V (11) + cortisone (11–14)
18	IV (11) + saline (11–14)
19	V (11) + saline (11–14)
20	VI, 4.2 mg (11), + II (11–14)
21	VI, 2.1 mg (11), + II (11–14)
22	VI, 1.05 mg (11), + II (11–14)
23	VI, 4.2 mg (11), + saline (11–14)
24	VI, 2.1 mg (11), + saline (11–14)
25	VI, 1.05 mg (11), + saline (11–14)
26	III, 2.1 mg (11), + saline (11–14)
27	III, 4.2 mg (11), + saline (11–14)
28	Saline (11) + cortisone (11–14)
29	III, 4.2 mg (10), + saline (11–14)

[a] I is propylene glycol, II is phenytoin, III is cyanocobalamin, IV is cobaltous chloride, V is sodium cobaltinitrite, and VI is hydroxycobalamin.

The probability, p, was determined for the t and χ^2 values using standard probability tables.

RESULTS AND DISCUSSION

Maternal Effects of Drugs—Injections of cobaltous chloride, sodium cobaltinitrite, and cortisone elicited slight lethargic responses in gravid mice that lasted approximately 5 min after each administration. This reaction is in agreement with the responses of malaise, weakness, and fatigue previously observed following the administration of cobalt salts (20). Spontaneous seizures caused by increased brain excitability attributed to cortisone were not seen (21). Physiological saline, propylene glycol, phenytoin, and the cobalamins did not induce central stimulation, although, according to Massey (11), a dose of 50 mg of phenytoin/kg produced restlessness and agitation in mice followed by lethargy.

Although previous studies utilizing propylene glycol (100%) as the solvent for phenytoin did not report skin reactions (11), this investigation revealed that the minimal concentration of this vehicle (70%) required to dissolve the antiepileptic agent caused local irritation, alopecia, and epidermal lesions in some mice several days after the initial subcutaneous injection. No deaths in gravid animals resulted from drug administration.

Table II presents the mean values for maternal and fetal deviations of the test groups in relation to their respective saline controls. Each group contained a minimum of six litters and approximately 120 fetuses.

Maternal Weights—Significantly higher mean terminal weights occurred in Groups 3, 4, 7, 9, 21, and 22 whose animals received low and intermediate doses of the cobalamins or saline followed by propylene glycol.

Fetal Ratio—Minor variations in the fetal ratio (the number of fetuses in the right uterine horn *versus* the number of fetuses in the left horn) were noted in eight groups; the occurrence appeared to be of a random nature.

Fetal Resorptions and Sex Ratios—There were no differences in the fetal resorption and sex ratios among the various groups.

Mean Fetal Weight—A significant decrease in mean fetal weight was observed in Groups 16 and 17 compared to the saline control. This response is in disagreement with that observed by Kasirsky *et al.* (13), who reported that cobaltous chloride prevented the reduction in mean fetal weight caused by cortisone. The decrease in mean fetal weight was significant when either saline control value (Group 2 or 8) was compared to that of the untreated group. This effect was probably due to injection trauma.

A significant increase in mean fetal weight occurred when cyanoco-

Table II—Mean Values of Test Groups

Treatment Group[a]	Maternal Weight Ratio, Start/Terminal	Fetal Ratio, Right/Left	Resorption Ratio, Right/Left	$\bar{X}$ Fetal Weight, g	Sex Ratio, Male/Female	Soft Tissue Abnormalities	Skeletal Abnormalities
1	27.5/50.4	6.4[b]/4.3[b]	0.4/0.1	1.24	5.4/5.3	2.4	0.5
2	27.9/44.9	4.2/7.6	0.2/0.2	1.05[b]	6.0/5.5	2.5	0.7
3	29.8/53.1[b]	5.7/6.9	0.0/0.0	1.13	6.7/5.7	7.7[b]	0.9
4	30.9/51.8[b]	5.3/6.7	0.7/0.0	1.07	6.3/5.7	2.0	0.7
5	29.7/51.2	5.9/5.3[b]	0.4/0.0	1.17	6.1/4.8	3.0	1.1
6	30.6/43.9	6.7[b]/5.2	0.0/0.0	0.95	6.0/5.5	10.0[b]	1.0
7	28.4/51.5[b]	5.2/6.2	0.0/0.1	1.23[b]	5.9/5.5	6.0	1.5[b]
8	25.3/42.9	4.8/5.0	0.3/0.0	1.01[b]	5.5/4.2	9.3	1.5
9	30.6[b]/51.3[b]	5.0/4.8	0.2/0.5	1.18[b]	4.7/5.2	8.2	1.7
10	25.8/45.7	6.0/5.2	0.2/0.0	1.06	6.2/5.0	10.3	0.5
11	26.2/47.1	5.2/5.7	0.2/0.0	1.19[b]	6.0/4.8	8.0	1.0
12	27.1/47.9	5.3/6.0	0.3/0.3	1.16[b]	6.3/5.0	10.1	1.1
13	26.1/44.0	5.7/5.2	0.3/0.2	1.06	6.0/4.8	4.0	0.8
14	25.4/43.7	3.8/4.8	0.2/0.5	1.18	4.3/4.3	2.8	0.3
15	27.0/45.8	4.1/5.3	1.1/0.9	1.16	4.0/5.4	4.7	0.1[b]
16	29.2/40.9	3.8/3.4[b]	1.0/0.5	0.87[b]	4.8/4.2	8.2[b-d]	2.8[b]
17	28.0/43.7	4.3/5.0	0.4/1.0	0.86[b]	5.8/5.2	11.4[b-d]	5.0[b]
18	27.6/49.5	3.7/5.5	0.7/0.7	1.18	4.8/4.3	1.3	1.2
19	27.0/48.1	4.2/6.3	0.0/0.7	1.11	5.5/5.0	3.2	1.3
20	30.6/49.1	4.5/4.0[b]	0.2/0.0	1.25[b]	3.8/4.3	2.5	1.0
21	29.8/51.8[b]	4.3/7.0	0.3/0.0	1.13	5.5/5.8	2.3	0.2
22	28.9/51.7[b]	5.3/6.8	0.2/0.0	1.17	6.3/5.8	1.5	0.7
23	27.1/47.5	5.2/4.8[b]	0.3/0.5	1.13	5.7/4.3	1.2	0.7
24	28.9/50.6	5.2/5.7	0.8/0.5	1.18	5.0/5.8	1.2	0.5
25	29.3/50.2	4.7/6.5	0.3/0.5	1.14	6.2/5.0	1.7	0.5
26	25.7/50.4	5.3/5.3[b]	0.3/0.2	1.25[b]	5.2/5.5	2.8	0.5
27	26.7/48.4	4.7/5.0[b]	0.2/0.7	1.27[b]	5.3/4.3	1.7	0.2
28	29.9/44.0	3.3/4.2[b]	1.2/0.6	0.90	4.0/5.0	6.4[b-d]	3.6[b]
29	30.5[b]/53.8[b]	6.0/6.7	0.3/0.0	1.18[b]	7.2/5.5	2.2[b]	1.7

[a] See Table I. [b] As compared to saline (Day 10 or 11) + saline (Days 11–14), p less than 0.05 (minimum of six litters per group). [c] Litter incidence of cleft palate. [d] Fetal incidence of cleft palate.

balamin was substituted for saline before the phenytoin administration. With this treatment regimen, doubling or halving the 2.1-mg dose of the vitamin given on Day 11 or 10 of gestation prior to phenytoin caused this response in Group 7 or 11, respectively. Intermediate and large doses of the cobalamins followed by saline (Groups 26, 27, and 29) also caused significantly greater mean fetal weights than those of their saline counterparts. Groups 9, 12, and 20 likewise showed significantly greater mean fetal weights than did the saline group.

Production of Soft Tissue and Skeletal Anomalies—The various soft tissue and skeletal malformations representing significant deviations from their respective saline groups in their occurrence and nature are presented in Tables III and IV, respectively.

It was assumed at the onset of this study that cortisone and phenytoin produced cleft palate by a similar mechanism, because both agents had been shown to cause this defect in several strains of mice (11, 12, 22). Also, because cortisone induced cleft palate in CF-1 mice (13, 14), it was presumed that phenytoin would elicit similar results in this strain and that the prophylactic administration of cobalt salts would prevent the appearance of this anomaly in response to phenytoin challenge. However, in this study, the antiepileptic agent did not cause the palatal defect in either the cobalt salt- or saline-pretreated groups, whereas cleft palate occurred after cortisone administration in both of these pretreated groups, contrary to previous findings (13, 14).

A plausible explanation for these unexpected results may be the factor of diet, a major variable that could explain the earlier observations of Massey (11) and Kasirsky *et al.* (13, 14). The former investigator may have inadvertently revealed the important effect of food in her teratogenic studies when she reported the results of using two different kinds of diet in two otherwise similar experiments. The incidence of cleft palate among the fetuses of phenytoin-treated gravid mice fed a diet rich in cobalt and cyanocobalamin was lower than that among fetuses of such mice fed a diet poor in these constituents. Even greater amounts of cobalt and cyanocobalamin were contained in the diet utilized in this study than in that employed by Massey, and all animals received this enriched regimen immediately upon arrival at this facility.

Therefore, with all other factors being equal, it is suggested that the chronic intake of large quantities of dietary cobalt is the principal means by which cleft palate production caused by phenytoin is inhibited. In fact, when gravid animals were given this diet, neither cobaltous chloride nor sodium cobaltinitrite injection alone produced this anomaly in the offspring or, in conjunction with challenge by cortisone, prevented its onset as previously described by Kasirsky *et al.* (13, 14). Consequently, it is concluded that a relatively high dietary intake of cobalt is the principal means by which phenytoin-induced cleft palate is prevented in CF-1 mice and that, because cortisone teratogenesis referable to the appearance of this palatal defect remains unaltered under these dietary conditions,

Table III—Significant Occurrence and Nature of Soft Tissue Anomalies

Treatment Group[a]	Number of Litters	Number of Fetuses with Defects[b]									
		C.P.	Mal. P.	C.T.T.	Hyd.	Cryp.	Ano.	6 D	Ex.	EcO.	C. Tpa.
2	6	0	4	4	0	0	4	0	0	0	0
3	7	0	18	11	1	2	0	3	0	0	0
6	6	0	10	1	3	4	0	0	0	0	5
16	6	24	0	8	0	4	0	1	1	1	0
17	6	29	0	11	8	2	0	2	0	0	0
28	6	22	0	2	3	3	0	1	0	0	0
8	6	0	3	17	1	6	0	8	0	0	6
29	6	0	0	3	0	6	0	3	0	0	0

[a] See Table I. [b] C.P. = cleft palate, Mal.P. = malformed palate, C.T.T. = connective tissue beneath temporal lobe(s), Hyd. = hydronephrosis (uni- or bilateral), Cryp. = uni- or bilateral cryptorchidism, Ano. = anophthalmia (uni- or bilateral), 6 D = sixth digit on forepaw(s), Ex. = exencephaly, EcO = ectopic ovary, and C.Tpa. = connective tissue in pelvic area.

Table IV—Significant Occurrence and Nature of Skeletal Anomalies

Treatment Group[a]	Number of Litters	Number of Fetuses with Defects[b]						
		Mal.St.	F.St.	Cr.St.	Rud.St.	D.O.St.	ExR.	S.O.
2	6	2	1	0	0	0	1	0
7	11	6	0	1	2	6	2	0
15	7	0	1	0	0	0	0	0
16	6	0	1	1	0	0	1	11
17	6	0	6	0	0	0	2	17
28	6	0	1	2	0	3	0	12

[a] See Table I. [b] Mal.St. = malformed sternebrae, F.St. = fused sternebrae, Cr.St. = crankshaft sternebrae, Rud.St. = rudimentary sternebrae, D.O.St. = delayed ossification of sternebrae, ExR. = extra rib, and S.O. = split occiput.

different mechanisms of action for cortisone and phenytoin must be involved in the inhibition of palate closure in this strain of mice. Additional studies involving high and low dietary intake of cobalt to confirm this hypothesis are being contemplated.

REFERENCES

(1) H. H. Merritt and T. J. Putnam, *J. Am. Med. Assoc.*, **111**, 1068 (1938).

(2) L. B. Kalinowsky and T. J. Putnam, *Arch. Neurol. Psychiat.*, **49**, 414 (1943).

(3) P. J. F. Walsh, *Am. J. Psychiat.*, **119**, 262 (1962).

(4) M. Ellenberg, *N.Y. State J. Med.*, **68**, 2653 (1968).

(5) A. S. Harris and R. H. Kokernot, *Am. J. Physiol.*, **163**, 505 (1950).

(6) C. F. Hawkins and M. J. Meynell, *Lancet*, **2**, 737 (1954).

(7) A. Richens and D. J. F. Rowe, *Br. Med. J.*, **4**, 73 (1970).

(8) H. J. Panuska, R. J. Gorlin, J. E. Bearman, and D. F. Mitchell, *J. Periodontol.*, **32**, 15 (1961).

(9) B. D. Speidel and S. R. Meadow, *Lancet*, **2**, 839 (1972).

(10) E. V. Kuenssberg and J. D. E. Knox, *ibid.*, **1**, 198 (1973).

(11) K. M. Massey, *J. Oral Ther. Pharmacol.*, **2**, 380 (1966).

(12) J. E. Gibson and B. A. Becker, *Proc. Soc. Exp. Biol. Med.*, **128**, 908 (1968).

(13) G. Kasirsky, R. F. Gautieri, and D. E. Mann, Jr., *J. Pharm. Sci.*, **56**, 1330 (1967).

(14) G. Kasirsky, W. T. Sherman, R. F. Gautieri, and D. E. Mann, Jr., *ibid.*, **58**, 766 (1969).

(15) D. E. Mann, Jr., and R. F. Gautieri, *Lancet*, **1**, 1451 (1973).

(16) R. S. Thompson and R. F. Gautieri, *J. Pharm. Sci.*, **58**, 406 (1969).

(17) R. E. Staples and V. L. Schnell, *Stain Technol.*, **39**, 61 (1964).

(18) J. G. Wilson, in "Teratology Principles and Techniques," J. G. Wilson and J. Warkany, Eds., University of Chicago Press, Chicago, Ill., 1965, p. 267.

(19) G. G. Simpson, A. Roe, and R. C. Lewontin, "Quantitative Zoology," Harcourt, Brace, New York, N.Y., 1960, pp. 176, 186.

(20) "The Pharmacological Basis of Therapeutics," 5th ed., L. S. Goodman and A. Gilman, Eds., Macmillan, New York, N.Y., 1975, pp. 1320, 1332.

(21) *Ibid.*, p. 1485.

(22) H. Kalter, *Am. J. Physiol.*, **185**, 65 (1956).

ACKNOWLEDGMENTS

Adapted in part from a dissertation submitted by J. J. Mitala to Temple University in partial fulfillment of the Doctor of Philosophy degree requirements.

Supported by the Craniofacial Anomalies Program of the National Institutes of Dental Research, Grant 1 R01 NS 11821-01.

The authors are indebted to Dr. Theodore S. Kallelis, Dr. Robert S. Thompson, Mr. Peter M. Lemke, Mr. Ray Brooke, and Mr. John Zellers for their technical and surgical assistance.

Differences in Antibacterial Activity of Benzalkonium Chloride

R. M. E. RICHARDS*x and LYNETTE M. MIZRAHI

Received March 21, 1977, from the *Department of Pharmacy, Medical Faculty, University of Rhodesia, Salisbury, Rhodesia.* Accepted for publication July 11, 1977. *Present address: Department of Pharmaceutical Technology, University of Strathclyde, Glasgow G1 1XW, Scotland.

Abstract □ Benzalkonium solutions obtained from different manufacturers were shown to have different activities. This difference in activity was related to the composition of the benzalkonium chloride. The potential seriousness of this situation is emphasized, and a recommendation is made that the official monographs on benzalkonium chloride be amended appropriately, noting the apparently superior antibacterial activity of the tetradecyl (C_{14}) homolog.

Keyphrases □ Benzalkonium chloride—various commercial solutions, antibacterial activity evaluated and related to composition □ Antibacterial activity—evaluated in various commercial solutions of benzalkonium chloride, related to composition

The International Pharmacopoeia (IP 1967) (1) allows the alkyl chain of benzalkonium chloride to be a mixture of the alkyls from C_8H_{17} to $C_{18}H_{37}$. USP XIX (2) states that the alkyl chain may represent a mixture including all or some of the group beginning with C_8H_{17} and extending through higher homologs, with the $C_{12}H_{25}$ homolog representing not less than 40%, on the anhydrous basis, and the $C_{14}H_{29}$ homolog representing not less than 20% of the total alkylbenzyldimethylammonium chloride content; the two homologs together must comprise not less than 70% of the total alkylbenzyldimethylammonium chloride content.

BP 1973 (3) allows a mixture of alkylbenzyldimethylammonium chlorides, without specifying any particular homolog or percentage composition.

This permitted variation in the alkyl chain length may contribute to the variation in benzalkonium chloride activity (compare Refs. 4 and 5 and Refs. 6 and 7). Therefore, the comparative antibacterial activity of four commercial benzalkonium solutions was investigated to determine whether differences occur in the antibacterial activity due to variations in the number of carbon atoms in the alkyl radical and the relative percentage of particular chain lengths in a given benzalkonium chloride. Such investigations should also indicate whether a given formulation preserved with benzalkonium chloride might have different preservative capacities, depending on the commercial source of benzalkonium chloride.

Two benzalkonium solutions had approximately 50% tetradecyl (C_{14}) derivative, and the other two products had approximately 65% dodecyl (C_{12}). Therefore, with respect to the proportion of the C_{12} and C_{14} homologs, the four products were divided into two pairs. Other differences in composition, however, also existed among the four solutions.

different mechanisms of action for cortisone and phenytoin must be involved in the inhibition of palate closure in this strain of mice. Additional studies involving high and low dietary intake of cobalt to confirm this hypothesis are being contemplated.

REFERENCES

(1) H. H. Merritt and T. J. Putnam, *J. Am. Med. Assoc.*, **111**, 1068 (1938).

(2) L. B. Kalinowsky and T. J. Putnam, *Arch. Neurol. Psychiat.*, **49**, 414 (1943).

(3) P. J. F. Walsh, *Am. J. Psychiat.*, **119**, 262 (1962).

(4) M. Ellenberg, *N.Y. State J. Med.*, **68**, 2653 (1968).

(5) A. S. Harris and R. H. Kokernot, *Am. J. Physiol.*, **163**, 505 (1950).

(6) C. F. Hawkins and M. J. Meynell, *Lancet*, **2**, 737 (1954).

(7) A. Richens and D. J. F. Rowe, *Br. Med. J.*, **4**, 73 (1970).

(8) H. J. Panuska, R. J. Gorlin, J. E. Bearman, and D. F. Mitchell, *J. Periodontol.*, **32**, 15 (1961).

(9) B. D. Speidel and S. R. Meadow, *Lancet*, **2**, 839 (1972).

(10) E. V. Kuenssberg and J. D. E. Knox, *ibid.*, **1**, 198 (1973).

(11) K. M. Massey, *J. Oral Ther. Pharmacol.*, **2**, 380 (1966).

(12) J. E. Gibson and B. A. Becker, *Proc. Soc. Exp. Biol. Med.*, **128**, 908 (1968).

(13) G. Kasirsky, R. F. Gautieri, and D. E. Mann, Jr., *J. Pharm. Sci.*, **56**, 1330 (1967).

(14) G. Kasirsky, W. T. Sherman, R. F. Gautieri, and D. E. Mann, Jr., *ibid.*, **58**, 766 (1969).

(15) D. E. Mann, Jr., and R. F. Gautieri, *Lancet*, **1**, 1451 (1973).

(16) R. S. Thompson and R. F. Gautieri, *J. Pharm. Sci.*, **58**, 406 (1969).

(17) R. E. Staples and V. L. Schnell, *Stain Technol.*, **39**, 61 (1964).

(18) J. G. Wilson, in "Teratology Principles and Techniques," J. G. Wilson and J. Warkany, Eds., University of Chicago Press, Chicago, Ill., 1965, p. 267.

(19) G. G. Simpson, A. Roe, and R. C. Lewontin, "Quantitative Zoology," Harcourt, Brace, New York, N.Y., 1960, pp. 176, 186.

(20) "The Pharmacological Basis of Therapeutics," 5th ed., L. S. Goodman and A. Gilman, Eds., Macmillan, New York, N.Y., 1975, pp. 1320, 1332.

(21) *Ibid.*, p. 1485.

(22) H. Kalter, *Am. J. Physiol.*, **185**, 65 (1956).

ACKNOWLEDGMENTS

Adapted in part from a dissertation submitted by J. J. Mitala to Temple University in partial fulfillment of the Doctor of Philosophy degree requirements.

Supported by the Craniofacial Anomalies Program of the National Institutes of Dental Research, Grant 1 R01 NS 11821-01.

The authors are indebted to Dr. Theodore S. Kallelis, Dr. Robert S. Thompson, Mr. Peter M. Lemke, Mr. Ray Brooke, and Mr. John Zellers for their technical and surgical assistance.

Differences in Antibacterial Activity of Benzalkonium Chloride

R. M. E. RICHARDS*x and LYNETTE M. MIZRAHI

Received March 21, 1977, from the *Department of Pharmacy, Medical Faculty, University of Rhodesia, Salisbury, Rhodesia.* Accepted for publication July 11, 1977. *Present address: Department of Pharmaceutical Technology, University of Strathclyde, Glasgow G1 1XW, Scotland.

Abstract □ Benzalkonium solutions obtained from different manufacturers were shown to have different activities. This difference in activity was related to the composition of the benzalkonium chloride. The potential seriousness of this situation is emphasized, and a recommendation is made that the official monographs on benzalkonium chloride be amended appropriately, noting the apparently superior antibacterial activity of the tetradecyl (C_{14}) homolog.

Keyphrases □ Benzalkonium chloride—various commercial solutions, antibacterial activity evaluated and related to composition □ Antibacterial activity—evaluated in various commercial solutions of benzalkonium chloride, related to composition

The International Pharmacopoeia (IP 1967) (1) allows the alkyl chain of benzalkonium chloride to be a mixture of the alkyls from C_8H_{17} to $C_{18}H_{37}$. USP XIX (2) states that the alkyl chain may represent a mixture including all or some of the group beginning with C_8H_{17} and extending through higher homologs, with the $C_{12}H_{25}$ homolog representing not less than 40%, on the anhydrous basis, and the $C_{14}H_{29}$ homolog representing not less than 20% of the total alkylbenzyldimethylammonium chloride content; the two homologs together must comprise not less than 70% of the total alkylbenzyldimethylammonium chloride content.

BP 1973 (3) allows a mixture of alkylbenzyldimethylammonium chlorides, without specifying any particular homolog or percentage composition.

This permitted variation in the alkyl chain length may contribute to the variation in benzalkonium chloride activity (compare Refs. 4 and 5 and Refs. 6 and 7). Therefore, the comparative antibacterial activity of four commercial benzalkonium solutions was investigated to determine whether differences occur in the antibacterial activity due to variations in the number of carbon atoms in the alkyl radical and the relative percentage of particular chain lengths in a given benzalkonium chloride. Such investigations should also indicate whether a given formulation preserved with benzalkonium chloride might have different preservative capacities, depending on the commercial source of benzalkonium chloride.

Two benzalkonium solutions had approximately 50% tetradecyl (C_{14}) derivative, and the other two products had approximately 65% dodecyl (C_{12}). Therefore, with respect to the proportion of the C_{12} and C_{14} homologs, the four products were divided into two pairs. Other differences in composition, however, also existed among the four solutions.

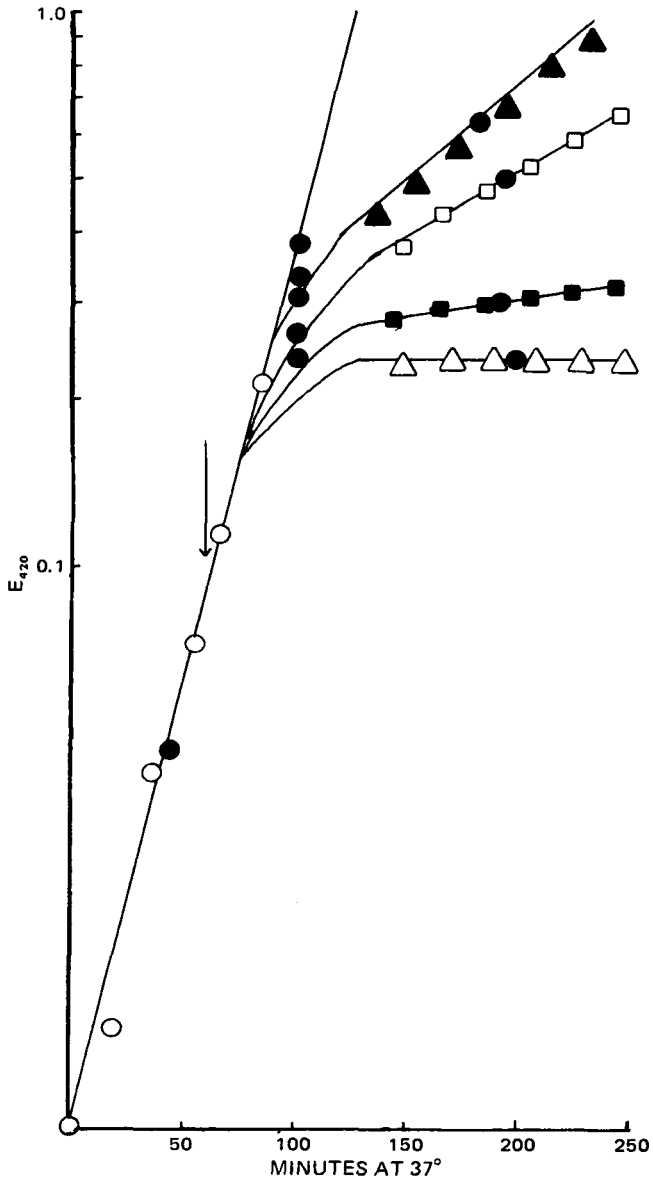

Figure 1—*Effect of a final concentration of 3 μg/ml of Solutions A, B, C, and D, separately, on the growth rate of* E. coli. *Key:* ○, *control culture (no benzalkonium added);* ■, *Solution A;* □, *Solution B;* △, *Solution C;* ▲, *Solution D; and* ●, E_{420} *values at given times calculated from the experimentally determined* E_{420} *values at known times for each culture. Addition of benzalkonium was made at the time indicated by the arrow.*

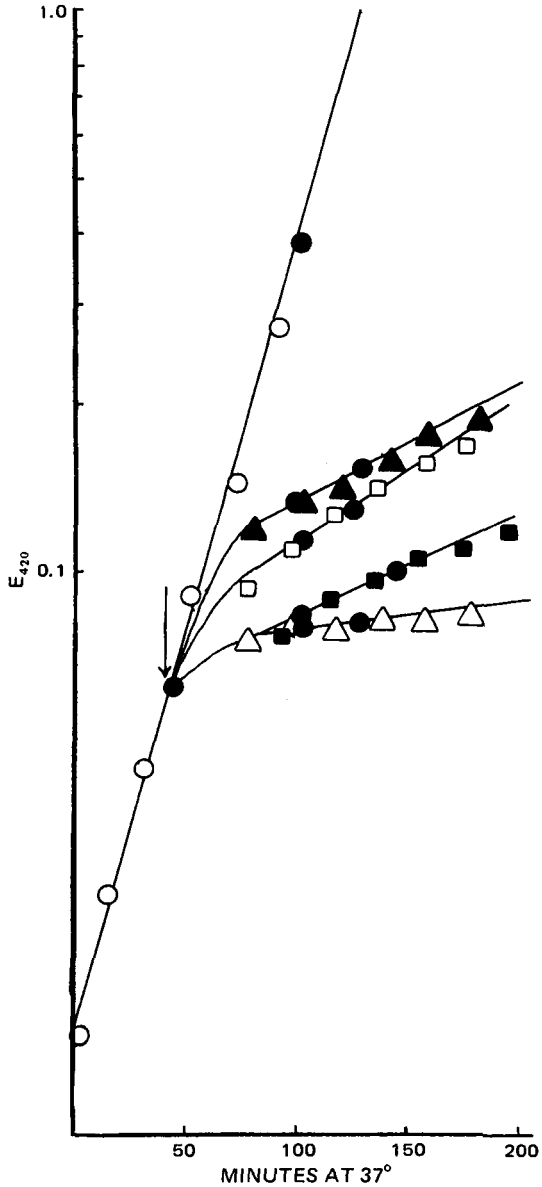

Figure 2—*Effect of a final concentration of 0.8 μg/ml of Solutions A, B, C, and D, separately, on the growth rate of* S. aureus. *Key:* ○, *control culture (no benzalkonium added);* ■, *Solution A;* □, *Solution B;* △, *Solution C;* ▲, *Solution D; and* ●, E_{420} *values at given times calculated from the experimentally determined* E_{420} *values at known times for each culture. Additions of benzalkonium was made at the time indicated by the arrow.*

EXPERIMENTAL

Chemicals, Organisms, and Media—The properties of the four solutions of benzalkonium chloride (A, B, C, and D) are given in Table I. Solutions B, C, and D comply with USP specifications, and all four comply with the BP and IP. *Escherichia coli*[1], *Staphylococcus aureus*[2], and *Pseudomonas aeruginosa*[3] were the test organisms. Nutrient broth No. 2[4] was the growth medium for liquid cultures, and nutrient agar[4] was the growth medium for solid cultures.

Methods—The evaluations used either log phase cultures for growth rate studies or 16-hr cultures for determinations of killing times. Cell numbers were determined by colony counts, and the cultures were maintained as already described (8).

Effect on Growth Rate—Log phase cultures were prepared, and the effects of 3 μg/ml of Solutions A, B, C, and D were determined on the growth rate of *E. coli* by the method described for determining the effect of three aromatic alcohols on log phase *P. aeruginosa* (9). The results are illustrated in Fig. 1.

The procedure was repeated using 0.8 μg/ml of Solutions A, B, C, and D against log phase *S. aureus* (Fig. 2).

The effects of equimolar concentrations of each solution against log phase *E. coli* and *S. aureus* cultures were determined, and the results were again expressed graphically (Figs. 3 and 4).

Effect on Cell Death—Tubes containing 9.9 ml of the aqueous solutions under test were equilibrated in a water bath at 22–23°. Then 0.1 ml of a 16-hr culture of either *P. aeruginosa, S. aureus,* or *E. coli* was added to give a final inoculum of approximately 2×10^6 cells/ml. At intervals of 15, 30, 45, 60, 90, 120, 150, 180, 240, 300, and 360 min after inoculum addition, 0.5-ml samples were aseptically transferred to 4.5 ml of inactivating recovery medium [of the composition already described

[1] NCTC 8196, National Collection of Type Cultures, Colindale, London, England.
[2] NCTC 6571, National Collection of Type Cultures, Colindale, London, England.
[3] NCTC 6750, National Collection of Type Cultures, Colindale, London, England.
[4] Oxoid, Oxo Ltd., London, England.

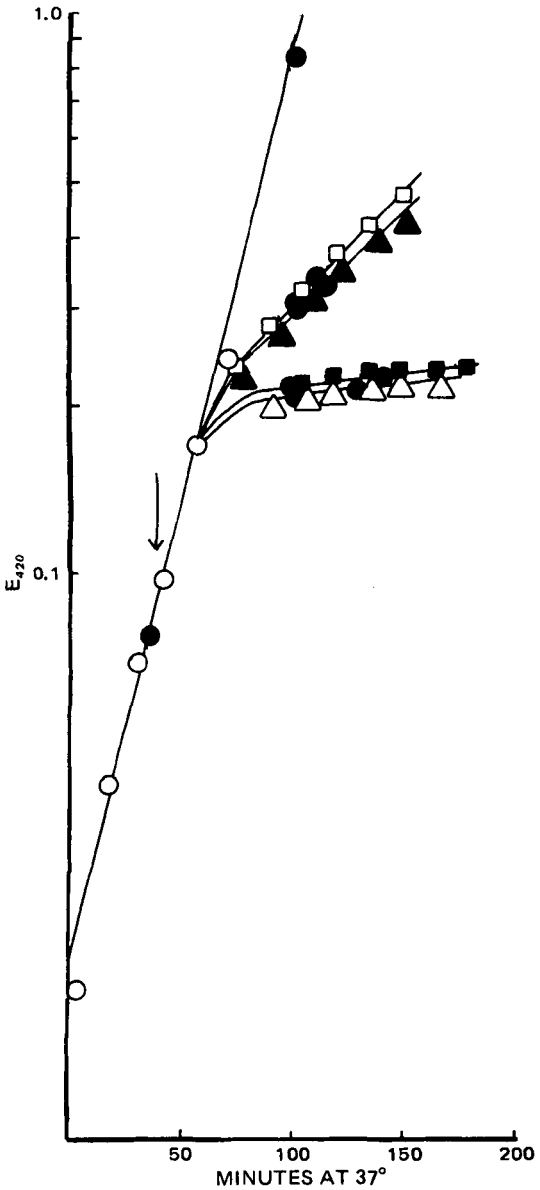

Figure 3—*Comparison of effect of equimolar concentrations of Solutions A, B, C, and D, separately, on the growth rate of* E. coli. *Key:* ○, *control culture (no benzalkonium added);* ■, *Solution A (3.12-μg/ml final concentration of benzalkonium);* □, *Solution B (2.91 μg/ml);* △, *Solution C (3.00 μg/ml);* ▲, *Solution D (2.96 μg/ml); and* ●, E_{420} *values of given times calculated from the experimentally determined* E_{420} *values at known times for each culture. Addition of benzalkonium was made at the time indicated by the arrow.*

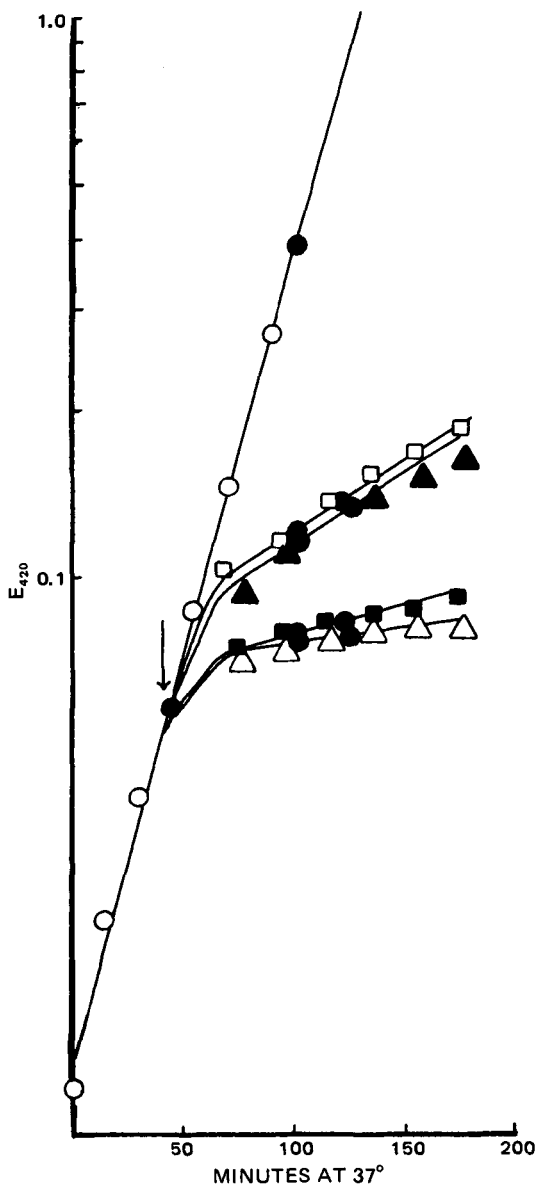

Figure 4—*Comparison of effect of equimolar concentrations of Solutions A, B, C, and D, separately, on the growth rate of* S. aureus. *Key:* ○, *control culture (no benzalkonium added);* ■, *Solution A (0.83-μg/ml final concentration of benzalkonium);* □, *Solution B (0.78 μg/ml);* △, *Solution C (0.80 μg/ml);* ▲, *Solution D (0.79 μg/ml); and* ●, E_{420} *values at given times calculated from the experimentally determined* E_{420} *values at known times for each culture. Addition of benzalkonium was made at the time indicated by the arrow.*

(5) but without the added agar] and incubated at 37° for 48 hr. Controls were carried out as described (9). The results are given in Table II.

RESULTS AND DISCUSSION

The addition of the same concentration of Solutions A, B, C, and D in subinhibitory amounts to log phase cultures of *E. coli* or *S. aureus* resulted in varying depressions of the growth rate (Figs. 1 and 2). When equimolar concentrations of A, B, C, and D were used, A and C produced a similar response and B and D had similar activity to each other (Figs. 3 and 4).

The results show that altering the composition of benzalkonium does result in different antibacterial activity and that solutions containing predominantly the tetradecyl (C_{14}) homolog apparently have greater activity than solutions consisting mainly of the dodecyl (C_{12}) homolog.

Further growth rate experiments with *S. aureus* cultures showed that Solutions B and D had to be added at twice the concentration as that of Solutions A and C to produce the same degree of inhibition on the growth rate. Thus, Solutions A and C were approximately twice as active as B and D against log phase *S. aureus* cultures.

Killing times for the four solutions against an inoculum of approximately 2×10^6 cells/ml of 16-hr cultures of *E. coli* or *S. aureus* showed a similar pattern (Table II). The concentration of A, B, C, and D used in these determinations was chosen to demonstrate the differences in activity. At high concentrations, all solutions would have a rapid killing time. However, low concentrations may have to be used in pharmaceutical preservation because of the constraints of the formulation, as in certain contact lens solutions, or the original concentration of the antibacterial may be depleted because of interactions with the container or other formulation components. The different levels of activity obtained with A, B, C, and D could have practical importance; at a concentration where two solutions exhibited fair antibacterial activity, the other two solutions were not able to kill the test inoculum of *S. aureus* during the 6-hr evaluation.

Minimum inhibitory concentration determinations and minimum bactericidal concentration determinations of the benzalkonium solutions

Table I—Properties of Four Benzalkonium Chloride Solutions as Supplied by Manufacturers

Property	Solution A	Solution B	Solution C	Solution D
Composition of alkyl chain	—	C_{10}, 3.5%	—	—
	C_{12}, 25–30%[a]	C_{12}, 67.5%	C_{12}, 40%	C_{12}, 60–65%
	C_{14}, 50–55%	C_{14}, 24.0%	C_{14}, 50%	C_{14}, 25–30%
	C_{16}, 15–20%	C_{16}, 5.0%	C_{16}, 10%	C_{16}, 10–15%
Molecular weight	375–382	348.04	359.6	355–362
Active matter, %	50.0–50.5	50 ± 1.5 (w/v)	50–52 (v/v)	50.0–50.5
Inert ingredients	3% maximum solubilizing agents/cloud-point modifiers	—	10% (w/v) ethyl alcohol 40% (w/v) water	2% maximum solubilizing agents/cloud-point modifiers
pH	7.0–7.5	8.0 ± 1.0 (5% v/v)	10.3–10.7	7.0–7.5
Free amine, %	0.5 maximum	0.3 maximum	Not given	0.5 maximum

[a] All percentages in this table are w/w unless otherwise specified.

in nutrient broth inoculated with *S. aureus* showed the same pattern of results. Solutions A and C were active at lower concentrations than Solutions B and D.

The problem was even greater with *P. aeruginosa* (Table II). At a concentration of benzalkonium chloride widely recommended for use in preserving multidose ophthalmic solutions, Solution C inactivated approximately 2×10^6 *P. aeruginosa* cells/ml in less than 15 min but Solution B required more than 4 hr to achieve the same result. Each solution had a different activity against this test organism, but the solutions containing mainly the C_{14} homolog were more active.

The pH of all reaction mixtures tested was similar (7.30–7.75), so differences in benzalkonium activity due to differences in pH were discounted.

Prior to 1956 (5), many misleading results were obtained in evaluating the antibacterial activity of benzalkonium chloride because of inadequate techniques, particularly in failing to inactivate the benzalkonium carried over with the bacteria sample to be tested for viability or death. Moreover, the previous history of the test organism, the inoculum size, the spacing of the contact times, the homogeneous mixing of organisms in the antibacterial solution, the pH and temperature of the bacteria–antibacterial reaction mixtures, the presence of other chemicals, the size of the test sample withdrawn in proportion to the volume of the reaction mixture sampled, the time period and temperature of incubation of the test sample, and the nutritional capacity of the culture medium used for culturing the damaged bacteria all influence the assessments of antibacterial activity.

When all of these factors have been understood and adequately provided for in the experimental technique, however, it appears that an investigator may be unwittingly deceived in any overall assessment of the activity of benzalkonium chloride based on the results obtained with one particular product. The inconsistencies existing in the literature due to this factor may be quite impossible to unravel. However, in the future the official monographs describing benzalkonium chloride should specify a product that has a much more precise composition and also note the apparently superior antibacterial activity of the C_{14} homolog.

Table II—Killing Times at 22–23° for Solutions A, B, C, and D, 0.0025% against 16-hr *S. aureus* and *E. coli* Cultures and 0.01% against 16-hr *P. aeruginosa*

Organism[a]	Antibacterial	Killing Time, min
S. aureus	A	90–120
	B	>360
	C	60–90
	D	>360
E. coli	A	150–180
	B	300–360
	C	120–150
	D	>360
P. aeruginosa	A	45–60
	B	240–300
	C	<15
	D	90–120

[a] Initial bacterial concentration in antibacterial solution was approximately 2×10^6/ml. The pH of all solutions was in the 7.30–7.75 range.

REFERENCES

(1) "International Pharmacopoeia," World Health Organization, Geneva, Switzerland, 1967 (also known as "Specifications for the Quality Control of Pharmaceutical Preparations").

(2) "The United States Pharmacopeia," 19th rev., Mack Publishing Co., Easton, Pa., 1975.

(3) "The British Pharmacopoeia," Her Majesty's Stationery Office, London, England, 1973.

(4) C. A. Lawrence, *J. Am. Pharm. Assoc., Sci. Ed.*, **44**, 457 (1955).

(5) S. Riegelman, D. G. Vaughan, and M. Okumoto, *ibid.*, **45**, 93 (1956).

(6) D. A. Norton, D. J. G. Davies, M. E. Richardson, B. J. Meakin, and A. Keall, *J. Pharm. Pharmacol.*, **26**, 841 (1974).

(7) R. M. E. Richards, *ibid.*, **27**, 381 (1975).

(8) M. R. W. Brown and R. M. E. Richards, *ibid.*, **16**, 41T (1964).

(9) R. M. E. Richards and R. J. McBride, *J. Pharm. Sci.*, **62**, 585 (1973).

Relationship between Osmolality and Osmolarity

W. H. STRENG ˣ, H. E. HUBER, and J. T. CARSTENSEN *

Received November 10, 1976, from *Merrell-National Laboratories, Division of Richardson-Merrell Inc., Cincinnati, OH 45215.* Accepted for publication June 23, 1977. *Present address: School of Pharmacy, University of Wisconsin, Madison, WI 53706.

Abstract □ Since the compendia require the osmolarity of certain parenterals to be labeled and since experimentally only the osmolality can be measured, it is necessary to obtain the relationship between these two quantities. This relationship was determined by considering fundamental physical-chemical definitions. The osmolality of a solution was found to be simply related to the osmotic coefficient. The conversion to osmolarity requires the use of the partial molal volume(s) of the solute(s). A single conversion factor is required for a particular solute system; *i.e.*, the conversion factor is independent of the solution concentration.

Keyphrases □ Osmolality—converted to osmolarity using partial molal volume of solute at infinite dilution □ Osmolarity—converted from osmolality using partial molal volume of solute at infinite dilution □ Physicochemical properties—solutions, osmolality converted to osmolarity using partial molal volume of solute at infinite dilution

According to USP XIX (1), labeling on sodium chloride injection must include the osmolarity of the solution. This requirement presents some difficulty since the quantity measured experimentally is the osmolality. Therefore, it is necessary to determine the relationship between osmolality and osmolarity to make the conversion. Clear and concise definitions showing the relationship between these two quantities are not readily available. However, common usage and consistency with the well-established definitions for molality and molarity require that the definition for osmolality be "that mass of solute which, when dissolved in 1 kg of water, will exert an osmotic pressure equal to that exerted by a gram-molecular weight of an ideal unionized substance dissolved in 1 kg of water," and that the definition for osmolarity be "that mass of solute which, when dissolved in 1 liter of solution, will exert an osmotic pressure equal to that exerted by a gram-molecular weight of an ideal unionized substance dissolved in 1 liter of solution."

Murty *et al.* (2) recently found that the conversion necessitated the measurement of the solution density. It will be shown in this paper that, instead, the partial molal volume of the solute at infinite dilution is needed.

DISCUSSION

Single-Solute System—The relationship between the osmotic pressure and solvent activity can be found in many texts (3–5). It is assumed in the derivation that the vapor pressure of the solvent behaves as an ideal gas and that the solution is incompressible. This relationship is:

$$\Pi\bar{v}_1 = RT \ln \frac{p_1^0}{p_1} = -RT \ln \frac{p_1}{p_1^0} = -RT \ln a_1 \qquad \text{(Eq. 1)}$$

where Π is the osmotic pressure; $\bar{v}_1$ is the partial molal volume of the solvent; R is the gas law constant; T is temperature in degrees Kelvin; p_1^0 and p_1 are the vapor pressure of the pure solvent and the solution, respectively; and a_1 is the solvent activity.

Solving for Π yields:

$$\Pi = -\frac{RT}{\bar{v}_1} \ln a_1 \qquad \text{(Eq. 2)}$$

Since, by definition (5):

$$\ln a_1 \equiv -\frac{\nu m W_1}{1000} \varphi \qquad \text{(Eq. 3)}$$

where m is the molality of the solution, W_1 is the molecular weight of the solvent, ν is the number of ions into which the solute dissociates, and φ is the osmotic coefficient, the osmotic pressure is related to the osmotic coefficient according to:

$$\Pi = \left\{\frac{RT}{\bar{v}_1}\right\} \left\{\frac{\nu m W_1}{1000}\right\} \varphi \qquad \text{(Eq. 4)}$$

According to the definition, osmolality can be expressed as:

$$\xi_m = \frac{\Pi}{\epsilon_m} \qquad \text{(Eq. 5)}$$

where ξ_m is the osmolality and ϵ_m is the osmotic pressure exerted by a gram-molecular weight of an ideal unionized substance dissolved in 1 kg of water.

The value of ϵ_m can be calculated by substituting the following into Eq. 4:

$$m = \nu = \varphi = 1 \qquad \text{(Eq. 6)}$$

These substitutions can be made since the reference state is, by necessity, ideal and the substance is unionized.

Therefore:

$$\epsilon_m = \left\{\frac{RT}{\bar{v}_1}\right\} \left\{\frac{W_1}{1000}\right\} \qquad \text{(Eq. 7)}$$

Inserting Eqs. 7 and 4 into Eq. 5 results in[1]:

$$\xi_m = \nu m \varphi \qquad \text{(Eq. 8)}$$

Similar to osmolality, osmolarity can be expressed as:

$$\xi_c = \frac{\Pi}{\epsilon_c} \qquad \text{(Eq. 9)}$$

where ξ_c is the osmolarity and ϵ_c is the osmotic pressure exerted by a gram-molecular weight of an ideal unionized substance dissolved in a total solution volume of 1 liter.

To evaluate Eq. 9, the osmotic pressure as given according to Eq. 4 must be expressed in terms of molarities:

$$\Pi = \left\{\frac{RT}{\bar{v}_1}\right\} \left\{\frac{\nu W_1}{1000} \varphi\right\} \left\{\frac{c}{d - 0.001 c W_2}\right\} \qquad \text{(Eq. 10)}$$

where c is the molarity of the solution, d is the density of the solution, and W_2 is the molecular weight of the solute.

The value for ϵ_c can then be determined by substituting the following into Eq. 10:

$$c = \nu = \varphi = 1 \qquad \text{(Eq. 11)}$$

These substitutions can be made since the reference state is ideal and the substance is unionized.

Therefore:

$$\epsilon_c = \left\{\frac{RT}{\bar{v}_1}\right\} \left\{\frac{W_1}{1000}\right\} \left\{\frac{1}{d - 0.001 c W_2}\right\} \qquad \text{(Eq. 12)}$$

The last term on the right in Eq. 12 can be simplified since the total volume, V_T, is:

$$V_T = n_1\bar{v}_1 + n_2\bar{v}_2 \qquad \text{(Eq. 13)}$$

where n_1 and n_2 are the numbers of moles of the solvent and the solute, respectively, and $\bar{v}_2$ is the partial molal volume of the solute. Then:

$$d - 0.001 c W_2 = \frac{n_1 W_1 + n_2 W_2}{n_1\bar{v}_1 + n_2\bar{v}_2} - \frac{n_2 W_2}{n_1\bar{v}_1 + n_2\bar{v}_2} \qquad \text{(Eq. 14)}$$

$$d - 0.001 c W_2 = \frac{n_1 W_1}{V_T} = \frac{w t_1}{V_T} = d_1 \qquad \text{(Eq. 15)}$$

[1] The osmolality should be expressed as $\xi_m = (\nu m \varphi)(\bar{v}_1^0/\bar{v}_1)$, where $\bar{v}_1^0/\bar{v}_1$ is the ratio of the partial molal volumes for the solvent at infinite dilution and in the solution. This ratio usually has a value close to one for the concentration ranges normally considered.

where wt_1 is the weight of the solvent in the reference solution and d_1 is the density of the solvent in the reference solution.

The determination of the solvent density in the reference solution can be made by utilizing the partial molal volumes at infinite dilution. Since the reference solution is ideal, the total volume in Eq. 13 can be expressed as (6):

$$V_T = n_1\bar{v}_1^0 + n_2\bar{v}_2^0 \qquad \text{(Eq. 16)}$$

where $\bar{v}_i^0$ is the partial molal volume at infinite dilution.

The densities of the solvent for the reference solution and at infinite dilution are given by Eqs. 17*a* and 17*b*, respectively:

$$d_1 = \frac{wt_1}{V_T} = \frac{n_1W_1}{V_T} \qquad \text{(Eq. 17a)}$$

$$d_1^0 = \frac{wt_1^0}{V_T} = \frac{n_1^0W_1}{V_T} \qquad \text{(Eq. 17b)}$$

With the same volume, V_T, the ratio of the densities equals:

$$\frac{d_1}{d_1^0} = \frac{wt_1}{wt_1^0} = \frac{n_1}{n_1^0} \qquad \text{(Eq. 18a)}$$

or:

$$d_1 = d_1^0\frac{n_1}{n_1^0} \qquad \text{(Eq. 18b)}$$

It is possible to determine the value of n_1 in the reference state by rearranging Eq. 16 and realizing that n_2 is equal to one:

$$n_1 = \frac{V_T - \bar{v}_2^0}{\bar{v}_1^0} \qquad \text{(Eq. 19)}$$

Furthermore, at infinite dilution, n_2 equals zero and, therefore:

$$n_1^0 = \frac{V_T}{\bar{v}_1^0} \qquad \text{(Eq. 20)}$$

Combining Eqs. 19 and 20 with Eq. 18*b* results in:

$$d_1 = d_1^0\left\{\frac{V_T - \bar{v}_2^0}{V_T}\right\} = d_1^0\left\{1 - \frac{\bar{v}_2^0}{V_T}\right\} \qquad \text{(Eq. 21)}$$

Finally, since the molar concentration scale is being used, the total volume equals 1000 ml and Eq. 21 becomes:

$$d_1 = d_1^0(1 - 0.001\bar{v}_2^0) \qquad \text{(Eq. 22)}$$

Therefore, the ideal reference state osmotic pressure is equal to:

$$\epsilon_c = \left\{\frac{RT}{\bar{v}_1}\right\}\left\{\frac{W_1}{1000}\right\}\left\{\frac{1}{d_1^0(1 - 0.001\bar{v}_2^0)}\right\} \qquad \text{(Eq. 23)}$$

Inserting Eqs. 23 and 10 into Eq. 9 results in:

$$\xi_c = \nu\varphi\left\{\frac{c}{d - 0.001cW_2}\right\}\{d_1^0(1 - 0.001\bar{v}_2^0)\} \qquad \text{(Eq. 24)}$$

or:

$$\xi_c = \nu m\varphi\{d_1^0(1 - 0.001\bar{v}_2^0)\} \qquad \text{(Eq. 25)}$$

Combining Eq. 8 with Eq. 25 results in the relationship between osmolarity and osmolality[2]:

$$\xi_c = \xi_m\{d_1^0(1 - 0.001\bar{v}_2^0)\} \qquad \text{(Eq. 26)}$$

The fact that the partial molal volume of the solute is included in Eq. 23 implies that the reference state is dependent on the compound. The conversion from osmolality to osmolarity does not require knowing the density of the solution but rather the density of the pure solvent and the partial molal volume of the solute at infinite dilution.

Multisolute System—Equation 26 is only applicable to two-component systems, *i.e.*, a solvent and one solute. If there is more than one solute, then the concentrations need to be replaced by summations over all solute species. The osmotic pressure expressed according to Eq. 4 then becomes:

$$\Pi = \left\{\frac{RT}{\bar{v}_1}\right\}\left\{\frac{W_1\varphi}{1000}\right\}\left\{\sum_i \nu_i m_i\right\} \qquad \text{(Eq. 27)}$$

The osmolality is still expressed as given in Eq. 5, and the evaluation of ϵ_m remains the same since the conditions given in Eq. 6 are changed to:

$$\sum_i m_i = \nu_i = \varphi = 1 \qquad \text{(Eq. 28)}$$

Inserting Eqs. 7 and 27 into Eq. 5 results in[3]:

$$\xi_m = \sum_i \nu_i m_i\varphi \qquad \text{(Eq. 29)}$$

A similar approach to the osmolarity results in:

$$\Pi = \left\{\frac{RT}{\bar{v}_1}\right\}\left\{\frac{W_1\varphi}{1000}\right\}\left\{\sum_i \frac{\nu_i c_i}{d - 0.001\sum_n c_nW_n}\right\} \qquad \text{(Eq. 30)}$$

In Eq. 30, the summation $\Sigma_n c_n W_n$ is the sum of the weights of all solute species per unit volume.

For multisolute systems, the reference state needs to be defined as having 1 mole of particles dissolved in 1 liter of solution. Expressing the reference state this way is identical to saying a gram-molecular weight of solute for the two-component system. Evaluation of the osmotic pressure for the reference state, ϵ_c, utilizes the condition:

$$\sum_i c_i = \nu_i = \varphi = 1 \qquad \text{(Eq. 31)}$$

for which Eq. 12 becomes:

$$\epsilon_c = \left\{\frac{RT}{\bar{v}_1}\right\}\left\{\frac{W_1}{1000}\right\}\left\{\sum_i \frac{c_i}{d - 0.001\sum_n c_nW_n}\right\} \qquad \text{(Eq. 32)}$$

The last term on the right in Eq. 32 can be simplified since the total volume is:

$$V_T = n_1\bar{v}_1 + \sum_i n_i\bar{v}_i \qquad \text{(Eq. 33)}$$

where the summation is over all solute species; then:

$$d - 0.001\sum_n c_nW_n = \frac{n_1W + \sum_i n_iW_i}{n_1\bar{v}_1 + \sum_i n_i\bar{v}_i} - \frac{\sum_i n_iW_i}{n_1\bar{v}_1 + \sum_i n_i\bar{v}_i} \qquad \text{(Eq. 34)}$$

$$d - 0.001\sum_n c_nW_n = \frac{n_1W_1}{V_T} = \frac{wt_1}{V_T} = d_1 \qquad \text{(Eq. 35)}$$

The determination of the solvent density in the reference solution can be made by utilizing the partial molal volumes at infinite dilution. Since the reference solution is ideal, the total volume in Eq. 33 can be expressed as:

$$V_T = n_1\bar{v}_1^0 + \sum_i n_i\bar{v}_i^0 \qquad \text{(Eq. 36)}$$

As before, the densities of the solvent in the reference solution and at infinite dilution are related according to Eq. 18*b*. Evaluation of n_1 is somewhat more complex, giving:

$$n_1 = \frac{V_T - \sum_i n_i\bar{v}_i^0}{\bar{v}_1^0} \qquad \text{(Eq. 37)}$$

The infinite dilution value is expressed according to Eq. 20, and Eq. 21 becomes:

$$d_1 = d_1^0\left\{\frac{V_T - \sum_i n_i\bar{v}_i^0}{V_T}\right\} = d_1^0\left\{1 - \frac{\sum_i n_i\bar{v}_i^0}{V_T}\right\} \qquad \text{(Eq. 38)}$$

and since V_T = 1000 ml:

$$d_1 = d_1^0\left(1 - 0.001\sum_i n_i\bar{v}_i^0\right) \qquad \text{(Eq. 39)}$$

Therefore, the ideal reference state osmotic pressure is:

$$\epsilon_c = \left\{\frac{RT}{\bar{v}_1}\right\}\left\{\frac{W_1}{1000}\right\}\left\{\frac{1}{d_1^0\left(1 - 0.001\sum_i n_i\bar{v}_i^0\right)}\right\} \qquad \text{(Eq. 40)}$$

[2] As mentioned, the ratio $\bar{v}_1^0/\bar{v}_1$ has not been included in Eq. 8. This same ratio should be in Eqs. 24 and 25. Equation 26 is correct as written.

[3] The osmolality should be expressed as $\xi_m = \Sigma_i\nu_i m_i\varphi(\bar{v}_1^0/\bar{v}_1)$, in accordance with footnote 1.

Table I—Relationship between Osmolality and Osmolarity of Sodium Chloride Solutions

Weight-Volume Percent	Weight Percent	Molarity	Molality	φ	II, atm	ξ_m, mOsm/kg	ξ_c, mOsm/liter
0.04	0.04	0.0064	0.0064	0.974	0.30	12.5	12.2
0.15	0.15	0.026	0.026	0.955	1.19	48.9	47.9
0.34	0.34	0.058	0.058	0.941	2.65	108	106
0.50	0.50	0.086	0.086	0.942	3.95	162	159
0.59	0.59	0.102	0.102	0.932	4.66	191	187
0.9	0.9	0.15	0.15	0.928	6.97	286	280
1.01	1.00	0.172	0.173	0.928	7.83	321	315
1.51	1.50	0.259	0.261	0.923	11.8	482	473
2.02	2.00	0.346	0.349	0.921	15.7	643	630
2.54	2.50	0.435	0.439	0.920	19.7	808	792
3.06	3.00	0.523	0.529	0.922	23.8	975	956
3.58	3.50	0.613	0.621	0.924	28.0	1150	1130
4.11	4.00	0.703	0.713	0.926	32.2	1320	1290
4.64	4.50	0.793	0.806	0.929	36.5	1500	1470
5.17	5.00	0.885	0.901	0.932	41.0	1680	1650
5.71	5.50	0.976	0.995	0.936	45.4	1860	1820

Substituting Eqs. 40 and 30 into Eq. 9 results in:

$$\xi_c = \varphi \left\{ \sum_i \frac{\nu_i c_i}{d - 0.001 \sum_n c_n W_n} \right\} \left\{ d_1{}^0 \left(1 - 0.001 \sum_i n_i \bar{v}_i{}^0 \right) \right\} \quad \text{(Eq. 41)}$$

or:

$$\xi_c = \sum_i \nu_i m_i \varphi \left\{ d_1{}^0 \left(1 - 0.001 \sum_i n_i \bar{v}_i{}^0 \right) \right\} \quad \text{(Eq. 42)}$$

Combining Eq. 29 with Eq. 42 results in the relationship between the osmolarity and osmolality of solutions having any number of solutes[4]:

$$\xi_c = \xi_m \left\{ d_1{}^0 \left(1 - 0.001 \sum_i n_i \bar{v}_i{}^0 \right) \right\} \quad \text{(Eq. 43)}$$

The fact that the partial molal volumes of the solutes are included in Eq. 40 implies that the reference state using a molarity concentration scale is dependent on the composition of the solution. Equation 43 reduces to Eq. 26 when there is one solute since n_i then equals one. It should be reemphasized that the values for n_i used in Eq. 43 are the reference state values and not those for the actual solution being measured.

It is possible to select any number of states that will satisfy the conditions for the reference state in Eqs. 31 and 43 because the sum of the molar concentrations equals one in the reference state and nothing is specified concerning the individual concentrations. One possible reference state would maintain the same mole fractions of all solutes and adjust the weights so that the total concentration is one, as shown in Eq. 44:

$$wt_i = \left[\frac{\frac{wt_x}{W_x}}{\sum \frac{wt_n}{W_n}} \right] \{ W_x \sum c_i \} = \frac{wt_x \sum c_i}{\sum \frac{wt_n}{W_n}} = \frac{wt_x}{\sum \frac{wt_n}{W_n}} \quad \text{(Eq. 44)}$$

where:

wt_i = weight of solute in reference state
wt_x = weight of solute in sample solution
W_n, W_x = molecular weight of solute
$\sum \frac{wt_n}{W_n}$ = total number of moles in sample solution
$\sum c_i = 1$ = total concentration in reference state
$\left[\frac{\frac{wt_x}{W_x}}{\sum \frac{wt_n}{W_n}} \right]$ = mole fraction of solute X in sample solution

[4] Similar to the single-solute system, the ratio $\bar{v}_1{}^0/\bar{v}_1$ has not been included in Eqs. 41 and 42. Equation 43 is correct as written.

Table II—Conversion Factors for Several Compounds

Salt	$\bar{v}_2{}^0$, ml/mole	$d_1{}^0(1 - 0.001\bar{v}_2{}^0)$[a]
Potassium chloride[b]	26.74	0.97041
Potassium bromide[b]	33.97	0.96320
Potassium sulfate[b]	32.28	0.96488
Sodium chloride[c]	16.63	0.98049

[a] $d_1{}^0 = 0.99707$ g/ml at 25°. [b] Reference 10. [c] Reference 9.

The weights of each solute in the reference state can be calculated according to Eq. 44 and these weights can be inserted into Eq. 45:

$$n_i = \frac{wt_i}{W_i} \quad \text{(Eq. 45)}$$

to find the number of moles that would then be inserted into Eq. 43. Whether this is the best reference state needs to be investigated.

CALCULATIONS

Table I gives the relationships between osmolality (milliosmoles per kilogram) and osmolarity (milliosmoles per liter) for sodium chloride solutions. This calculation utilized Eq. 26 for which the conversion factor $d_1{}^0(1 - 0.001\bar{v}_2{}^0)$ is equal to 0.9805. The data were obtained from Refs. 7–9, and the partial molal volume, $\bar{v}_2{}^0$, is equal to the apparent molal volume at infinite dilution. Table II lists the conversion factors for several compounds at 25°.

REFERENCES

(1) "The United States Pharmacopeia," 19th rev., Mack Publishing Co., Easton, Pa., 1975.

(2) B. S. R. Murty, J. N. Kapoor, and P. P. DeLuca, *Am. J. Hosp. Pharm.*, **33**, 546 (1976).

(3) S. Glasstone and D. Lewis, "Elements of Physical Chemistry," 2nd ed., Van Nostrand, New York, N.Y., 1960, p. 252.

(4) G. N. Lewis, M. Randall, K. S. Pitzer, and L. Brewer, "Thermodynamics," 2nd ed., McGraw-Hill, New York, N.Y., 1961, p. 323.

(5) R. A. Robinson and R. H. Stokes, "Electrolyte Solutions," 2nd ed. (rev.), Butterworths, London, England, 1970, p. 30.

(6) G. N. Lewis, M. Randall, K. S. Pitzer, and L. Brewer, "Thermodynamics," 2nd ed., McGraw-Hill, New York, N.Y., 1961, p. 226.

(7) "CRC Handbook of Chemistry and Physics," 49th ed., Chemical Rubber Co., Cleveland, Ohio, 1968, p. D-174.

(8) R. A. Robinson and R. H. Stokes, "Electrolyte Solutions," 2nd ed. (rev.), Butterworths, London, Eng' ..d, 1970, p. 483.

(9) G. N. Lewis, M. Randall, K. S ..itzer, and L. Brewer, "Thermodynamics," 2nd ed., McGraw-Hill, New York, N.Y., 1961, p. 205.

(10) H. E. Wirth, *J. Am. Chem. Soc.*, **59**, 2549 (1937).

Characterization of Impurities in Sulfasalazine

J. J. ZALIPSKY ˣ, D. M. PATEL, and N. H. REAVEY-CANTWELL

Received January 27, 1977, from the *Analytical and Physical Chemistry Department, Research Division, William H. Rorer, Inc., Fort Washington, PA 19034.* Accepted for publication June 21, 1977.

Abstract □ The chemical structures of four impurities isolated from sulfasalazine were determined. Three impurities are the by-products of the reaction process in drug synthesis, *i.e.*, during diazotization of sulfapyridine and during coupling with salicylic acid. Only one contaminant was identified as a starting material, sulfapyridine, in the drug synthesis. The four impurities were characterized as 2-[[*p*-(2-pyridylsulfamoyl)-phenyl]azo]hydroxybenzene (I), 3-[[*p*-(2-pyridylsulfamoyl)phenyl]-azo]salicylic acid (II), 5-[[*p*-[4-(2-pyridylanilino)]-*N*-phenyl]azo]salicylic acid (III), and sulfapyridine (IV). Compounds I–III are novel molecules, and IV is the precursor of sulfasalazine. The isolation of the impurities was accomplished by TLC and liquid extraction procedures. The methods used to characterize the impurities were a combination of IR, UV, and NMR spectroscopy, mass spectrometry, and TLC. For I and III, comparisons also were made with the synthesized materials to supplement the evaluation.

Keyphrases □ Sulfasalazine—various impurities isolated and characterized □ Impurities, various—isolated and characterized in sulfasalazine □ Antibacterials—sulfasalazine, various impurities isolated and characterized

The nature and number of impurities associated with the synthesis of sulfasalazine NF (1), 5-[[*p*-(2-pyridylsulfamoyl)phenyl]azo]salicylic acid, are of considerable interest to the regulatory agencies, the USP–NF, and the manufacturers of the drug substance. The drug product is used for treatment of arthritis (2) and ulcerative colitis (3).

Sulfasalazine is prepared by diazotizing sulfapyridine and coupling the diazotized intermediate with salicylic acid (4, 5). The common analytical procedures used for sulfasalazine are titration with titanium trichloride (6), polarography (7), spectrophotometry (6), and high-speed liquid chromatography (8). All procedures are specific for pure sulfasalazine; but in the presence of unknown impurities, these methods are questionable. Therefore, knowledge of the impurities is essential to interpret analytical results.

A recent quantitative analysis (9) of sulfasalazine utilized TLC and spectrophotometry, a modified version of which is official in NF XIV (1). Reference was also made (9) to the number of impurities (10–12) associated with sulfasalazine; however, none of them was identified except sulfapyridine by TLC.

A column chromatographic method was developed (10) to separate the impurities, and three impurities were characterized partially: a polymer, an undiazotized sulfamide, and a positional isomer of sulfasalazine. In spite of early attempts to gain information on the impurities, there is no conclusive evidence as to their identity and structure.

The purposes of this study were to isolate the impurities, to elucidate their structures by mass spectrometry, and to explain the similarities and differences of their structures with respect to sulfasalazine. A combination of other methods (UV, NMR, and IR spectroscopy and TLC) and comparison with authentic synthetic materials also were used.

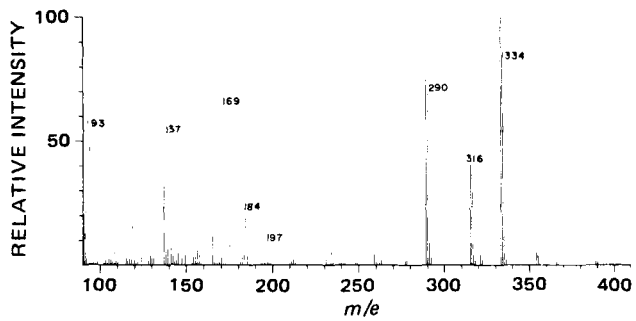

Figure 1—*Electron-impact mass spectrum of sulfasalazine.*

EXPERIMENTAL

Materials and Equipment—All chemicals were reagent grade. Silica gel[1] and aluminum oxide[2] TLC plates (0.250 and 0.500 mm) were prepared in this laboratory. IR spectra were obtained on a spectrophotometer[3] using potassium bromide pellets. UV spectra were determined on a recording spectrophotometer[4]. Mass spectra[5] were obtained at various temperatures using electron impact at 70 ev and chemical ionization with isobutane or methane gas. NMR spectra[6] also were obtained.

Isolation and Analyses of Impurities—The impurities in sulfasalazine were selectively separated and isolated from TLC preparative plates. The drug in dimethylformamide was spotted on the plate, the solvent was evaporated using forced air, and the plate was developed in different solvents. The separated zones containing impurity components were scraped from the plate, eluted with the same solvent, and filtered. The solvent was evaporated, and the residue was dried at 90° for 2 hr. The separated spots also were visualized (red-yellow color) by spraying the plate with ferric chloride solution (1 g in 50 ml of 10% HCl) and heating at 100° for a few minutes.

Impurity component I was isolated from a silica gel HR plate using chloroform–acetone–acetic acid (90:5:5) (R_f 0.83). This impurity traveled ahead of sulfasalazine. This yellow material (I) was compared by TLC with the synthesized compound 2-[[*p*-(2-pyridylsulfamoyl)phenyl]azo]-hydroxybenzene, a by-product obtained from the reaction of diazotized sulfapyridine and phenol. In addition, impurity I was extracted into ether from a sodium bicarbonate solution of a commercial sample of sulfasalazine. IR, NMR, UV, and mass spectra were obtained on this impurity.

Impurity component II was isolated from an aluminum oxide plate,

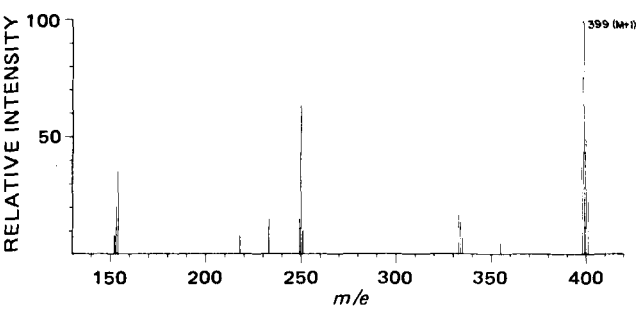

Figure 2—*Chemical-ionization mass spectrum of sulfasalazine.*

[1] EM. Laboratories.
[2] Brinkmann Instruments.
[3] Perkin-Elmer model 221.
[4] Cary model 140.
[5] MS30 AEI mass spectrometer with DS30 data system, RMU6D mass spectrometer, and Finnigan 3300 mass spectrometer.
[6] Varian model T-60.

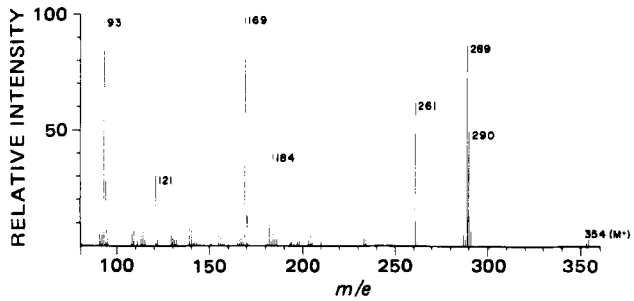

Figure 3—*Electron-impact mass spectrum of I.*

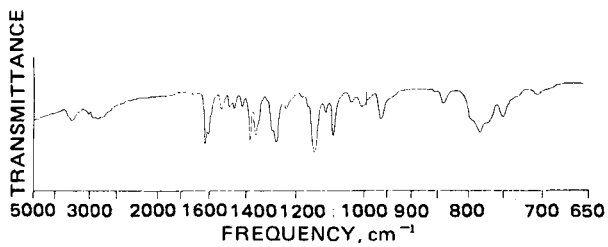

Figure 4—*IR spectrum of I.*

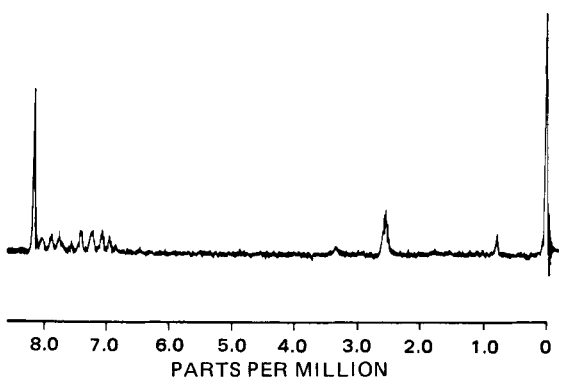

Figure 5—*The 60-MHz spectrum of I.*

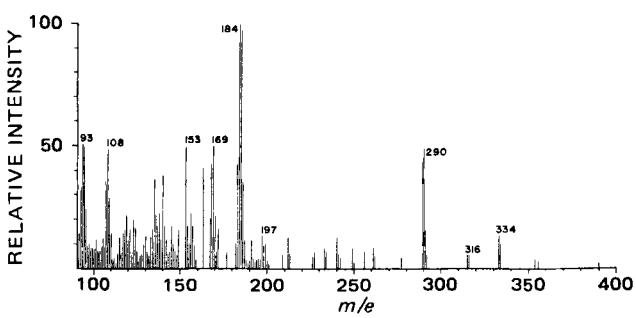

Figure 6—*Electron-impact mass spectrum of II.*

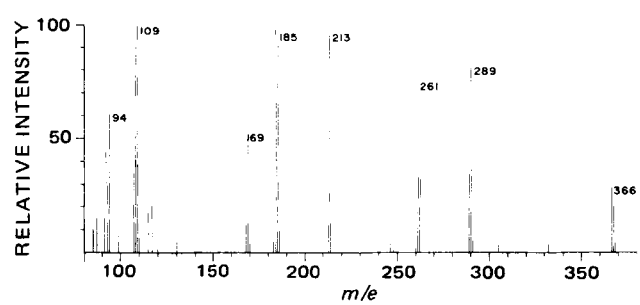

Figure 7—*Electron-impact mass spectrum of III.*

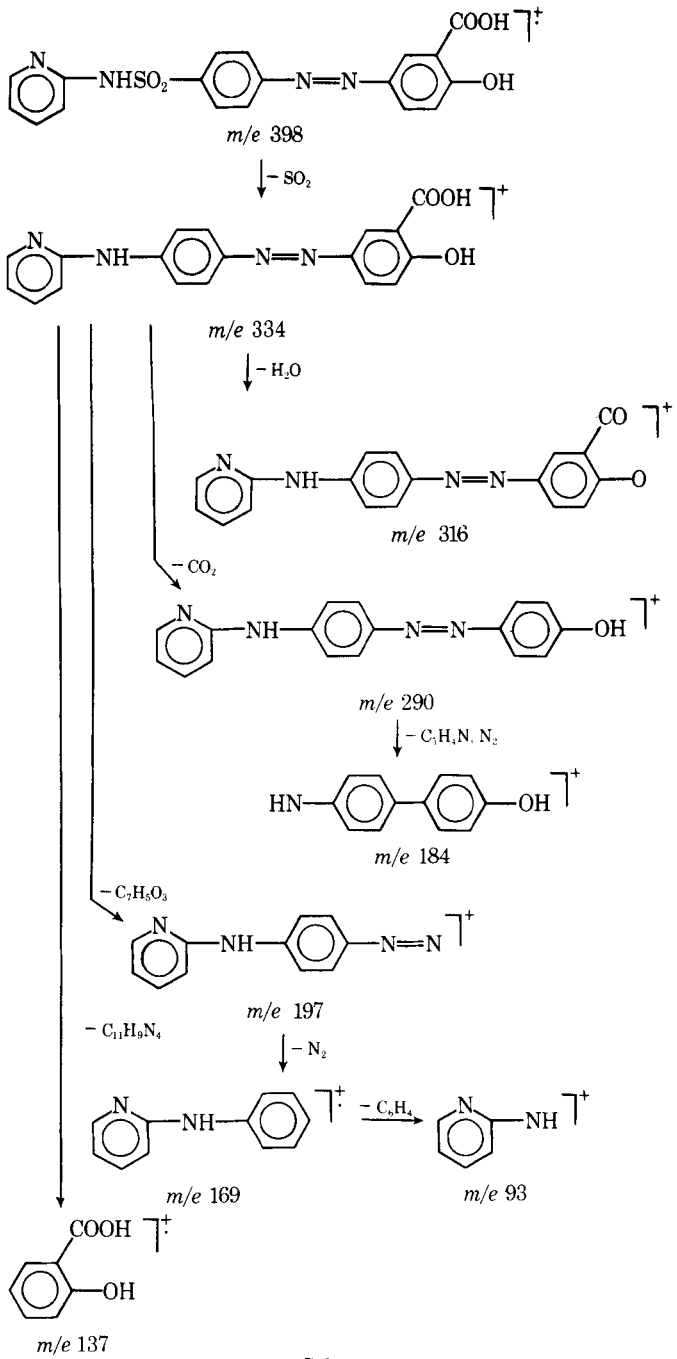

Scheme I

traveling behind sulfasalazine, using chloroform–methyl ethyl ketone–formic acid (70:15:10) (R_f 0.48). Its mass spectrum was obtained.

Impurity component III was isolated from a silica gel plate, traveling below II, using chloroform–methyl ethyl ketone–formic acid (30:50:20) (R_f 0.45). Compound III was also compared with an authentic material synthesized as follows. About 1 g of sulfapyridine was cautiously heated in a beaker until a dark mass resulted and the evolution of sulfur dioxide subsided. The dark mass was triturated with 30 ml of chloroform to extract the soluble fraction. The chloroform was evaporated, and the residue obtained was chromatographed on a TLC plate (silica gel HR) using ether as the solvent system.

Three yellow zones (A, B, and C) were separated on the plate and eluted with ether. The residue from each zone was diazotized and coupled with salicylic acid, and the resultant product was dried at 90° for 1 hr. TLC, IR, and mass spectra of the synthesized material from zone A (origin) was compared with impurity component III. Material isolated from zone A was also analyzed by mass spectrometry.

Impurity components IV and V (R_f 0.40 and 0.35, respectively) traveled below III in the same TLC system. Their mass spectra were obtained.

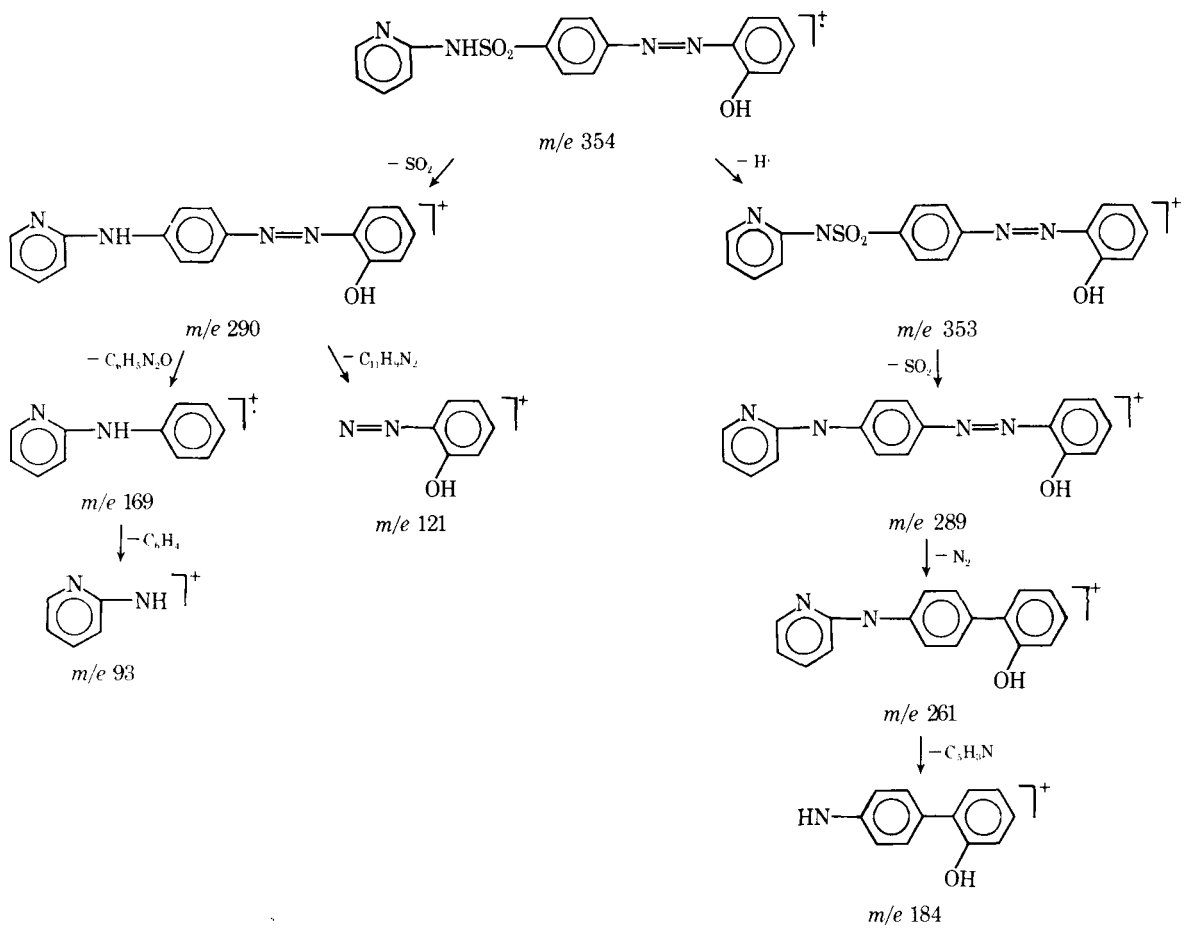

Scheme II

RESULTS AND DISCUSSION

The isolation and identification of four impurities associated with sulfasalazine were accomplished by TLC and mass spectral analyses. Chemical-ionization and electron-impact mass spectra were obtained to determine molecular ions and to follow the mass fragmentation pattern of the components. It was evident from the electron-impact mass spectra that the impurity components and sulfasalazine were unstable since no measurable molecular ion was detected. The electron-impact and chemical-ionization mass spectra of sulfasalazine isolated from an alumina TLC plate (R_f 0.76) in a pure form are shown in Figs. 1 and 2. The mass fragmentation pattern is shown in Scheme I.

Impurity I, isolated by TLC, was a yellow material characterized as 2-[[*p*-(2-pyridylsulfamoyl)phenyl]azo]hydroxybenzene. The electron-impact mass spectrum of I is shown in Fig. 3 with the molecular ion *m/e* 354. The mass fragmentation pattern is shown in Scheme II. The synthesized material, a by-product of the phenol reaction with diazotized sulfapyridine, and the ether-soluble material extracted from sodium bicarbonate solution of sulfasalazine showed the same TLC characteristics (R_f 0.85), UV spectrum (in methanol, λ_{max} 243 and 326 nm), and principal IR bands (2825, 1620, 1600, 1380, 1355, 1270, 1135, 1082, 962, 784, and 750 cm^{-1}) (Fig. 4). The NMR spectrum (Fig. 5) of I in dimethyl sulfoxide showed a multiplet (6.9–8.2 ppm) characteristic of substituted aromatic rings. No carboxylic proton was detected.

Impurity II was a pink color, and its electron-impact mass spectrum is shown in Fig. 6. This impurity was characterized as an isomer of sulfasalazine, 3-[[*p*-(2-pyridylsulfamoyl)phenyl]azo]salicylic acid. The mass spectrum of II was similar to that of sulfasalazine, except for two additional peaks at *m/e* 108 and 153. In addition, a peak at *m/e* 137 is of small abundance as compared to sulfasalazine fragmentation. The occurrence of fragment ions *m/e* 153 and 108 and a low abundance of *m/e* 137 ion can be best explained by possible electron-impact-induced rearrangement of *m/e* 334 ion of II to generate an intermediate (*a*), which can fragment as shown in Scheme III.

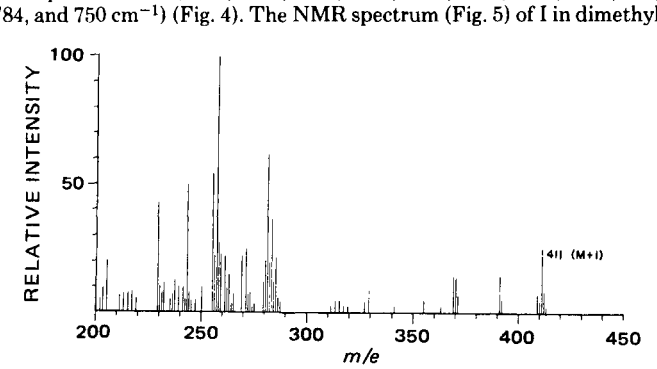

Figure 8—*Chemical-ionization mass spectrum of III.*

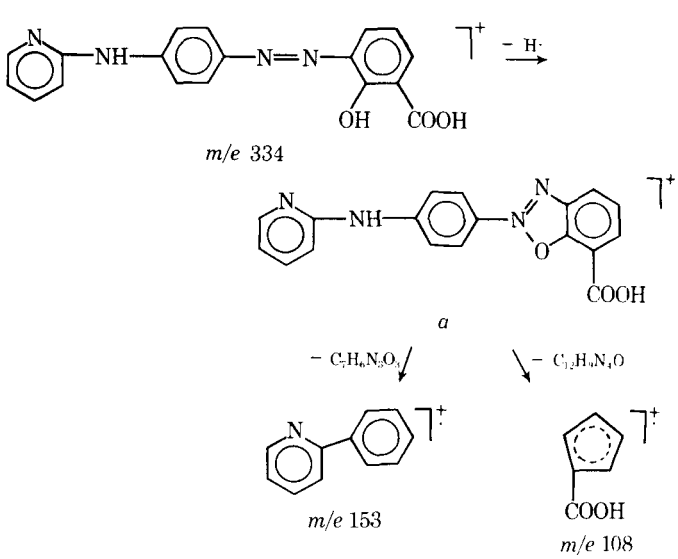

Scheme III

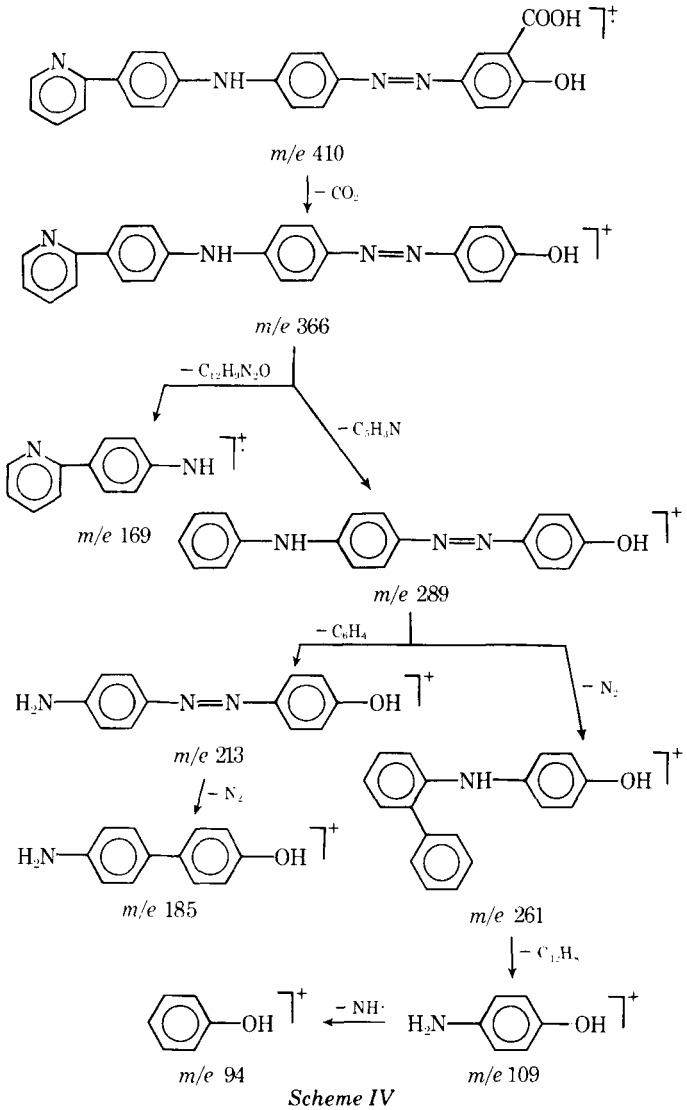

Scheme IV

If an intermediate of type *a* through skeletal rearrangement can be postulated, then the cleavage of the azobenzene bond and the expulsion of carbon monoxide would lead to the formation of the five-membered ring species at *m/e* 108. This type of rearrangement would also explain the small abundance of the *m/e* 137 ion in II as compared to a relatively large abundent ion in sulfasalazine where a cyclic intermediate of type *a* is not possible. The UV spectrum of II in methanol was similar to that of the parent drug.

Impurity III isolated from the TLC plate was characterized as 5-[[*p*-[4-(2-pyridylanilino)]-*N*-phenyl]azo]salicylic acid. The electron-impact and chemical-ionization mass spectra are shown in Figs. 7 and 8. The molecular ion was at *m/e* 410. The proposed mass fragmentation pattern is shown in Scheme IV, and the computer-produced data are listed in Table I. The difference in 12 mass units between sulfasalazine (*m/e* 398) and III (*m/e* 410) accounts for the replacement of SO_2 in the former with the disubstituted aromatic ring, C_6H_4. Furthermore, no sulfur was found in III by a standard microanalytical method.

Table I—Mass Fragmentation Ions of III

Calculated Mass	Measured Mass	Formula	*m/e*
—	—	$C_{24}H_{18}N_4O_3$	410[a]
366.1481	366.1335	$C_{23}H_{18}N_4O$	366
289.1215	289.1100	$C_{18}H_{15}N_3O$	298
261.1153	261.1129	$C_{18}H_{15}NO$	261
213.0901	213.0905	$C_{12}H_{11}N_3O$	213
185.0839	185.0898	$C_{12}H_{11}NO$	185
169.0765	169.0764	$C_{11}H_9N_2$	169
109.0527	109.0526	C_6H_7NO	109
94.0418	94.0432	C_6H_6O	94

[a] Molecular ion from chemical ionization.

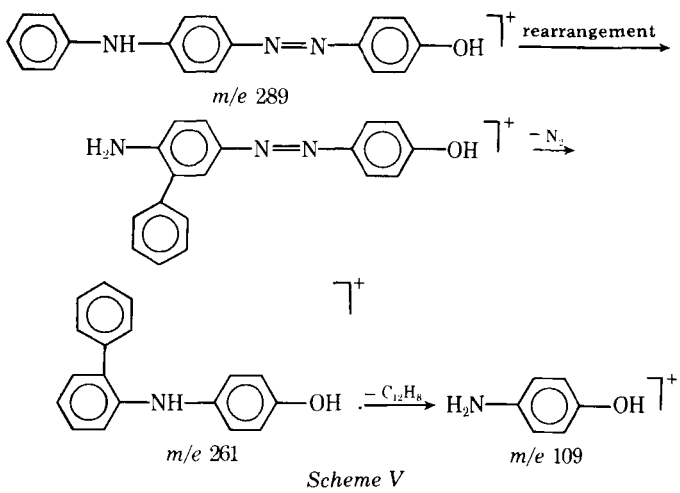

Scheme V

The appearance of an intense peak at *m/e* 109 in III can be explained by the promoted rearrangement of the diphenylamine group in the *m/e* 289 ion by electron impact and the subsequent loss of N=N and a biphenyl group to give *p*-hydroxyaniline (Scheme V). A similar type of rearrangement was proposed (11) for diaryl ethers. The absence or very low intensity of the *m/e* 109 peak in sulfasalazine and in components I and II supports the presence of a diphenylamine group in III.

The chemical-ionization mass spectrum of product A, which resulted from heated sulfapyridine and was isolated by TLC (zone A, R_f 0.0), is shown in Fig. 9. This material had molecular ion *m/e* 261 and was characterized as 4-amino-4′-(2-pyridyl)diphenylamine. Zone A material, when

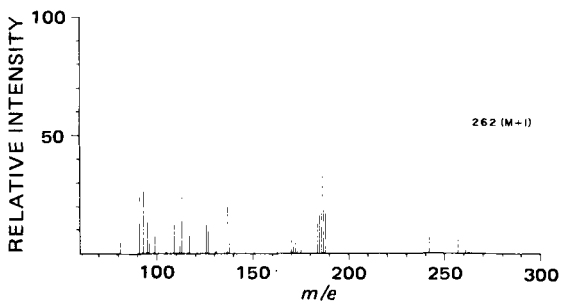

Figure 9—*Chemical-ionization mass spectrum of product A isolated from heated IV.*

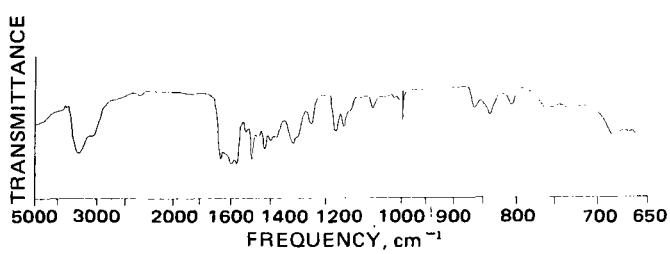

Figure 10—*IR spectrum of III.*

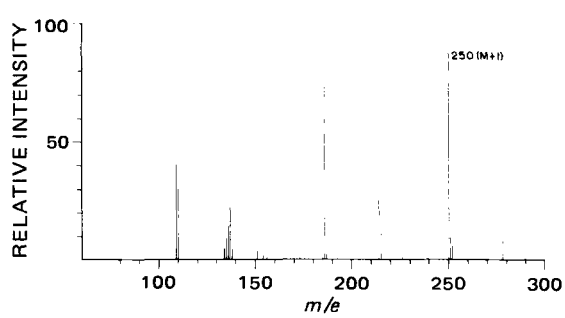

Figure 11—*Chemical-ionization mass spectrum of IV.*

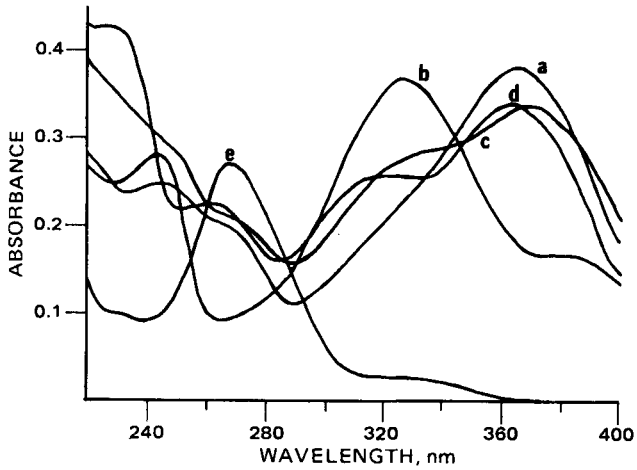

Figure 12—*UV spectra of sulfasalazine (a), I (b), II (c), III (d), and IV (e). Spectra were obtained in methanol (10^{-5} M).*

diazotized and coupled with salicylic acid, gave a product corresponding to impurity III. The sequence of synthetic steps is shown in Scheme VI. The synthesized material was found to be comparable with impurity III by TLC, mass spectrometry, and IR spectrophotometry (3400, 3100, 1660, 1595, 1485, 1429, 1308, 1249, 1168, 836, 758, and 683 cm^{-1}) (Fig. 10).

The mass spectrum of IV, isolated by TLC, is shown in Fig. 11 and was identified as sulfapyridine, *m/e* 249. The presence of sulfapyridine as an impurity in sulfasalazine was also confirmed by TLC. Impurity V, isolated from the TLC plate, was not fully characterized. The chemical-ionization mass spectrum showed a molecular ion, *m/e* 390.

Four lots of sulfasalazine from different manufacturers showed all impurities described; impurity III was the major one. The UV spectra of I–IV and sulfasalazine are shown in Fig. 12. Compounds I–III are the novel compounds, and their structures reveal some characteristic properties similar to sulfasalazine. Thus, the presence of these impurities in the drug will interfere in analytical methods such as UV spectroscopy,

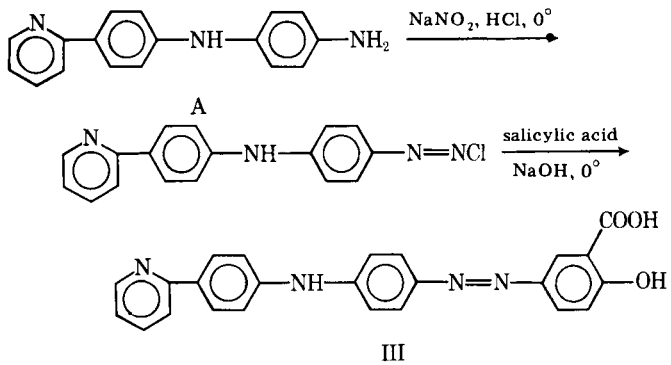

Scheme VI

polarography, and nonaqueous titration. Identification of other impurities in sulfasalazine will be reported in the near future.

REFERENCES

(1) "The National Formulary," 14th ed., Mack Publishing Co., Easton, Pa., 1975, p. 667.

(2) N. Svartz, *Acta Med. Scand., Suppl. 341,* **162,** 247 (1958).

(3) "Physician's Desk Reference," 27th ed., Medical Economics Co., Oradell, N.J., 1973, p. 1117.

(4) E. E. A. Askelof, N. Svartz, and H. C. Willstaedt, U.S. pat. 2,396,145 (Mar. 5, 1946); through *Chem. Abstr.,* **40,** 3472 (1946).

(5) A. Korkuczanski, *Przemy. Chem.,* **37,** 162 (1958); through *Chem. Abstr.,* **52,** 13727c (1958).

(6) A. Berggren and S. Hansen, *Farm. Rev.,* **34,** 537 (1952).

(7) B. Nygard, J. Olofason, and M. Sandberg, *Acta Pharm. Suec.,* **3,** 343 (1966).

(8) L. D. Bighley and P. McDonnell, *J. Pharm. Sci.,* **64,** 1549 (1975).

(9) D. R. Powell and B. A. Burton, *ibid.,* **63,** 1290 (1974).

(10) J. C. Stone and R. Gorby, *ibid.,* **63,** 1296 (1974).

(11) J. H. D. Eland and C. J. Danby, *J. Chem. Soc.,* **1965,** 5935.

Solid-State Dispersions Employing Urethan

H. V. MAULDING

Received December 21, 1970, from the *Pharmacy Research and Development Department, Sandoz Pharmaceuticals, Hanover, NJ 07936.* Accepted for publication May 24, 1971. (Publication delayed at the request of the author.)

Abstract □ The dissolution rates of a number of drug–urethan solid-state dispersion systems were studied. A marked enhancement of the initial dissolution rates of several poorly water-soluble drugs was found when they were incorporated into a urethan matrix by heat fusion. These differences were considerable when pure substances such as griseofulvin, hydrocortisone, chloramphenicol, and acetaminophen were compared to the urethan–drug solid dispersion. Physical mixtures of the medicinal agents with urethan also gave a marked increase in the amount of drug in solution, with the value in most cases being over one-half that of the solid-state dispersion. Data are given, comparing ultrafiltration with samples filtered through cotton, regarding drug content remaining in solution.

Keyphrases □ Solid-state dispersions—various drug–urethan systems, dissolution rates compared to pure drug substances and physical mixtures □ Dissolution rates—various drug–urethan solid-state dispersions, compared to pure drug substances and physical mixtures □ Urethan—solid-state dispersions with various drugs, dissolution rates compared to pure drug substances and physical mixtures

The application of relatively soluble and nontoxic substances as vehicles for difficultly soluble medicinal agents in the form of solid-state dispersions is well documented (1–7). Dialkylamides and polyethylene glycols were shown to increase absorption of steroids and griseofulvin, respectively (8, 9).

Drugs may be poorly soluble in GI fluids, leading to difficult and erratic absorption when administered orally. Absorption of insoluble medicaments is sometimes a function of the dissolution rate of these substances in aqueous solutions (10–12). Solid solutions or dispersions may function to increase dissolution rates by breaking

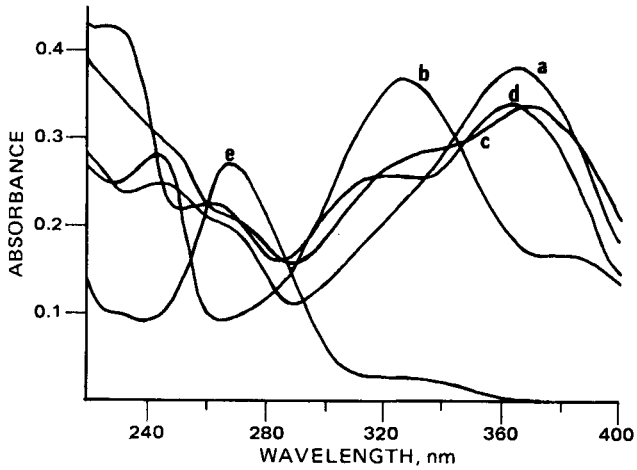

Figure 12—*UV spectra of sulfasalazine (a), I (b), II (c), III (d), and IV (e). Spectra were obtained in methanol (10^{-5} M).*

diazotized and coupled with salicylic acid, gave a product corresponding to impurity III. The sequence of synthetic steps is shown in Scheme VI. The synthesized material was found to be comparable with impurity III by TLC, mass spectrometry, and IR spectrophotometry (3400, 3100, 1660, 1595, 1485, 1429, 1308, 1249, 1168, 836, 758, and 683 cm^{-1}) (Fig. 10).

The mass spectrum of IV, isolated by TLC, is shown in Fig. 11 and was identified as sulfapyridine, *m/e* 249. The presence of sulfapyridine as an impurity in sulfasalazine was also confirmed by TLC. Impurity V, isolated from the TLC plate, was not fully characterized. The chemical-ionization mass spectrum showed a molecular ion, *m/e* 390.

Four lots of sulfasalazine from different manufacturers showed all impurities described; impurity III was the major one. The UV spectra of I–IV and sulfasalazine are shown in Fig. 12. Compounds I–III are the novel compounds, and their structures reveal some characteristic properties similar to sulfasalazine. Thus, the presence of these impurities in the drug will interfere in analytical methods such as UV spectroscopy,

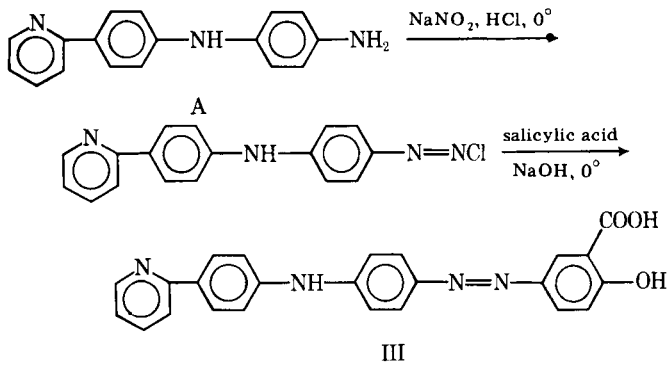

Scheme VI

polarography, and nonaqueous titration. Identification of other impurities in sulfasalazine will be reported in the near future.

REFERENCES

(1) "The National Formulary," 14th ed., Mack Publishing Co., Easton, Pa., 1975, p. 667.

(2) N. Svartz, *Acta Med. Scand., Suppl. 341,* **162,** 247 (1958).

(3) "Physician's Desk Reference," 27th ed., Medical Economics Co., Oradell, N.J., 1973, p. 1117.

(4) E. E. A. Askelof, N. Svartz, and H. C. Willstaedt, U.S. pat. 2,396,145 (Mar. 5, 1946); through *Chem. Abstr.,* **40,** 3472 (1946).

(5) A. Korkuczanski, *Przemy. Chem.,* **37,** 162 (1958); through *Chem. Abstr.,* **52,** 13727c (1958).

(6) A. Berggren and S. Hansen, *Farm. Rev.,* **34,** 537 (1952).

(7) B. Nygard, J. Olofason, and M. Sandberg, *Acta Pharm. Suec.,* **3,** 343 (1966).

(8) L. D. Bighley and P. McDonnell, *J. Pharm. Sci.,* **64,** 1549 (1975).

(9) D. R. Powell and B. A. Burton, *ibid.,* **63,** 1290 (1974).

(10) J. C. Stone and R. Gorby, *ibid.,* **63,** 1296 (1974).

(11) J. H. D. Eland and C. J. Danby, *J. Chem. Soc.,* **1965,** 5935.

Solid-State Dispersions Employing Urethan

H. V. MAULDING

Received December 21, 1970, from the *Pharmacy Research and Development Department, Sandoz Pharmaceuticals, Hanover, NJ 07936.* Accepted for publication May 24, 1971. (Publication delayed at the request of the author.)

Abstract □ The dissolution rates of a number of drug–urethan solid-state dispersion systems were studied. A marked enhancement of the initial dissolution rates of several poorly water-soluble drugs was found when they were incorporated into a urethan matrix by heat fusion. These differences were considerable when pure substances such as griseofulvin, hydrocortisone, chloramphenicol, and acetaminophen were compared to the urethan–drug solid dispersion. Physical mixtures of the medicinal agents with urethan also gave a marked increase in the amount of drug in solution, with the value in most cases being over one-half that of the solid-state dispersion. Data are given, comparing ultrafiltration with samples filtered through cotton, regarding drug content remaining in solution.

Keyphrases □ Solid-state dispersions—various drug–urethan systems, dissolution rates compared to pure drug substances and physical mixtures □ Dissolution rates—various drug–urethan solid-state dispersions, compared to pure drug substances and physical mixtures □ Urethan—solid-state dispersions with various drugs, dissolution rates compared to pure drug substances and physical mixtures

The application of relatively soluble and nontoxic substances as vehicles for difficultly soluble medicinal agents in the form of solid-state dispersions is well documented (1–7). Dialkylamides and polyethylene glycols were shown to increase absorption of steroids and griseofulvin, respectively (8, 9).

Drugs may be poorly soluble in GI fluids, leading to difficult and erratic absorption when administered orally. Absorption of insoluble medicaments is sometimes a function of the dissolution rate of these substances in aqueous solutions (10–12). Solid solutions or dispersions may function to increase dissolution rates by breaking

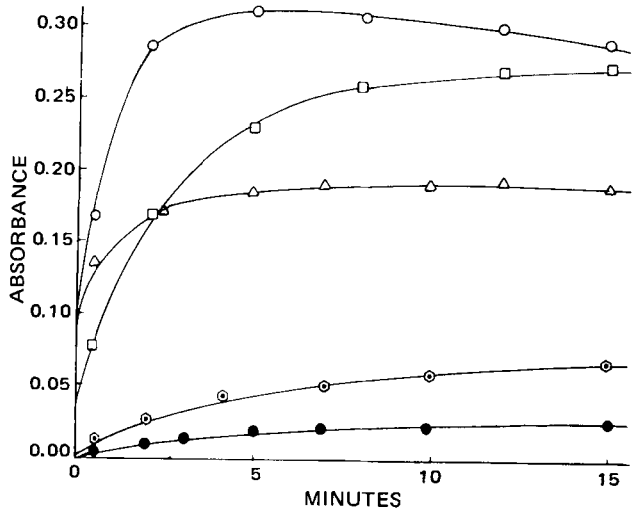

Figure 1—*Griseofulvin dissolution in pH 6.65 phosphate buffer (500 ml) at 37° and 60 rpm. Key: ●, wetted, nonmicronized griseofulvin powder, 25 mg; △, 5% griseofulvin solid-state dispersion in urethan, 500 mg total, 25 mg of griseofulvin; □, 5% griseofulvin solid-state dispersion in polyethylene glycol 4000, 500 mg total, 25 mg of griseofulvin; ⊙, 5% physical mixture of griseofulvin and urethan, 500 mg total, 25 mg of griseofulvin; and ○, 5% griseofulvin solid-state dispersion in urethan, 1 g total, 50 mg of griseofulvin.*

down crystal lattice energy, concomitantly decreasing the size of the medicament theoretically to the colloidal and even the molecular level. Thus, there is a subsequent increase in the rate of solution which is inversely proportional to particle size (3). If the dissolution process is the rate-limiting step in absorption, the greater the surface area a drug has, the faster and more complete should be the absorption. Levy (13) considered methods by which finely divided drugs may be presented to the GI tract.

The comparatively simple molecule, urethan, was utilized in these studies for several reasons. It is readily water soluble, has little tendency to form insoluble complexes with drugs, possesses a low melting point (important with heat-sensitive compounds), and is an efficient solvent for many organic molecules.

Urethan possesses the disadvantage of weak pharmacological activity, being used primarily in relatively large doses as a sedative. The compound also exhibits an ease of sublimation at relatively mild conditions.

EXPERIMENTAL

Chemicals—The following chemicals were used: urethan[1] (ethylcarbamate), mp 48–50°, reagent grade; hydrocortisone[2], micronized; griseofulvin[3], nonmicronized; chloramphenicol[4]; and polyethylene glycol 4000[5], powdered.

Dissolution Rates—A 60-rpm stirrer motor, fitted with a 2.54-cm propeller blade placed 4 cm from the bottom of an 800-ml beaker containing 500 ml of pH 6.65 phosphate buffer, was used in determining these rates. The phosphate buffer was prepared by adjusting the pH of 0.1 *M* KH_2PO_4 with sodium hydroxide solution. The drug, drug–urethan solid dispersion, or drug–urethan physical mixture was placed into a stirred solution from a height of about 1.5 cm. The temperature of the dissolution rate media was kept at 37 ± 0.1° by immersing the beaker in a constant-temperature bath.

Five-milliliter samples were periodically withdrawn for analyses by means of serological pipets with cotton filters attached[6] or by serological pipets followed by ultrafiltration utilizing 0.22-μm filters[7]. Spectrophotometric analyses[8] were carried out following dilution of the 5-ml samples. The compounds were read at the following wavelengths: chloramphenicol, 278 nm; griseofulvin, 295 nm; hydrocortisone, 274 nm; and acetaminophen, 250 nm.

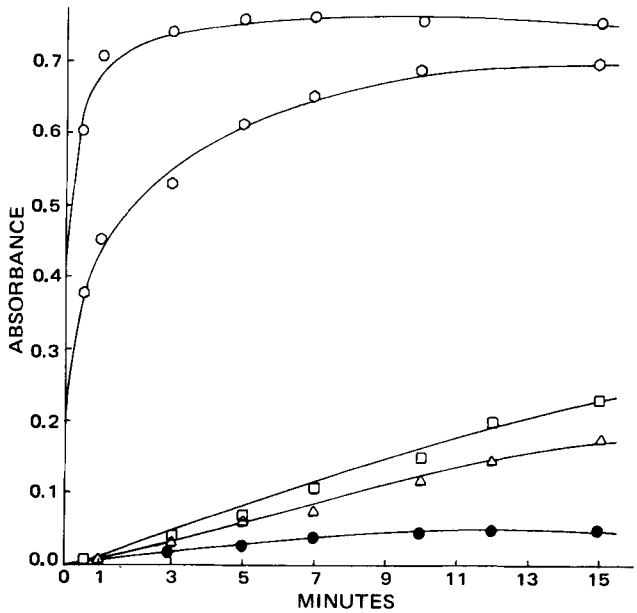

Figure 2—*Dissolution studies of hydrocortisone in pH 6.65 phosphate buffer (500 ml) at 37° and 60 rpm. Key: ●, micronized hydrocortisone, 50 mg; △, micronized hydrocortisone, 50 mg, added to dissolution media which previously had 950 mg of urethan dissolved in it; □, micronized hydrocortisone, 50 mg added to dissolution media which previously had 1.95 g of urethan dissolved in it; ○, 5% physical mixture of micronized hydrocortisone in urethan, 500 mg total, 50 mg of hydrocortisone; and ○, 5% solid-state dispersion of micronized hydrocortisone in urethan, 500 mg total, 50 mg of hydrocortisone.*

Preparation of Solid Dispersions—Solutions were produced by dissolution of 500 mg (5%) of the drug in 9.5 g of molten urethan, heated on a hot plate, and stirred magnetically. All substances exhibited miscibility under these conditions. The molten solution was poured onto a cold surface (metal pan), where it immediately congealed, and was then scraped up with a microspatula. This material was ground with mortar and pestle, if needed. A sample was used for dissolution rate studies with no further sizing. Higher percentages of actives were incorporated into urethan by the same procedure. Physical mixtures were prepared by carefully mixing the medicament with urethan in a mortar. Dissolution studies were run on an aliquot of this material.

Solubility Determinations—An excess of the substance under scrutiny was added to screw-capped vials (18-ml capacity) containing 15 ml of solvent, and varying amounts of urethan were added. The flasks were clamped on a motor-driven shaft and rotated vertically at 6 rpm in a constant-temperature bath at 37 ±0.1° until equilibrium was established. Samples were withdrawn, passed through filters[7] (0.22 μm), and analyzed spectrophotometrically for solubility.

RESULTS AND DISCUSSION

Several classes of drugs were incorporated into solid dispersion systems by dissolution in liquid urethan (mp 48–50°) followed by rapid chilling to solidify the solution. No difficulties were encountered with the procedure in concentrations up to 25% (w/w) drug–urethan. The resultant solid-state dispersion was examined for its ability to accelerate the dissolution rates of the relatively insoluble medicinal agents examined.

Properties of urethan such as a low melting point, solubility, and lack of assay interference favor its use as a carrier for drug molecules in spite of the fact that its low molecular weight does not fulfill the molecular size criterion for a host molecule of an interstitial molecular solution (9). Solid

[1] Fisher Scientific Co., Fair Lawn, N.J.
[2] Merck Sharp & Dohme, West Point, Pa.
[3] Schering Corp., Bloomfield, N.J.
[4] Mann Research Laboratories, New York, N.Y.
[5] Carbowax, Union Carbide, New York, N.Y.
[6] Kimble Products, Owens-Illinois, Toledo, Ohio.
[7] Millipore Corp., Bedford, Mass.
[8] Cary 14 recording spectrophotometer.

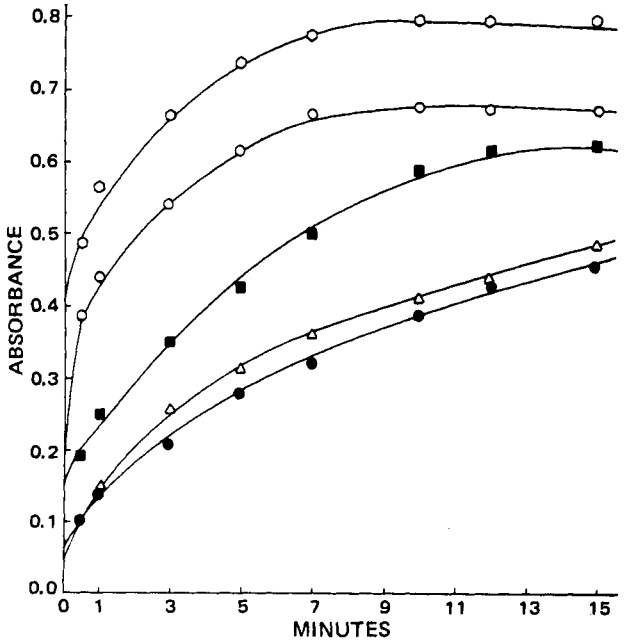

Figure 3—*Dissolution studies involving various percentage strengths solid-state dispersions of hydrocortisone in urethan (all equivalent to 50 mg of hydrocortisone). Key: ○, 5% hydrocortisone; ○, 10% hydrocortisone; ■, 15% hydrocortisone; △, 20% hydrocortisone; and ●, 25% hydrocortisone. Studies were carried out in pH 6.65 buffer at 37° and 60 rpm.*

dispersions prepared in matrixes of urethan are easy to work with because of their rather crystalline nature. For this reason, they are somewhat advantageous over polymeric matrixes, which are sometimes difficult to solidify.

Of the compounds studied, only a few are reported in this article for the sake of brevity. These compounds cover the spectrum, from the reasonably soluble acetaminophen to the relatively insoluble griseofulvin. Unfortunately, the data given are not as orderly as might be hoped when one compound is compared to another. The question may frequently arise as to whether one is visualizing a "dilution" effect or phenomena brought about by decreasing the particle size of the drug in the urethan matrix. The other matrixes examined, such as niacinamide, polyethylene glycols, urea, and urea–urethan mixtures, produced essentially the same qualitative results.

The solvent selected was pH 6.65 phosphate buffer, which was previously utilized in work with the ergot alkaloids (14). Few compounds studied ionized appreciably in this solvent system. Other conditions employed were those found acceptable in prior studies on differences in rates of solution (14).

No appreciable degradation of the drugs used was noted by TLC methods, as was reported (9) for griseofulvin. Such light-sensitive ergot alkaloids as dihydroergocristine showed no visible decomposition under the mild conditions of the process. Neither alterations nor shifts in UV spectra were noted.

Figure 1 illustrates a considerable enhancement of the amount of griseofulvin in solution upon incorporation of the antifungal into a 5% solid dispersion in urethan relative to the prewet nonmicronized griseofulvin itself. Polyethylene glycol 4000 containing 5% griseofulvin, prepared essentially after the method of Chiou and Riegelman (9), exhibited an even greater amount in solution than the 5% griseofulvin–urethan, although initially the latter showed higher levels in solution. This situation was characteristic of urethan as a carrier because exceptionally high levels of drug in solution were attained in the first 5–30 sec.

Figure 1 also indicates that a twofold increase in the quantity of solid dispersion used brings about an approximate doubling of the amount of griseofulvin in solution, as if it were a function of the quantity of dispersion added. The physical mixture was appreciably slower to dissolve than the solid dispersion, but this was not the situation with all drugs investigated.

Micronized hydrocortisone gave a great deal less in solution at times up to 15 min relative to the 5% solid dispersion (Fig. 2). However, the physical mixture, prepared by mixing in a mortar, gave values approaching those of the solid dispersion after 15 min. Some evidence of

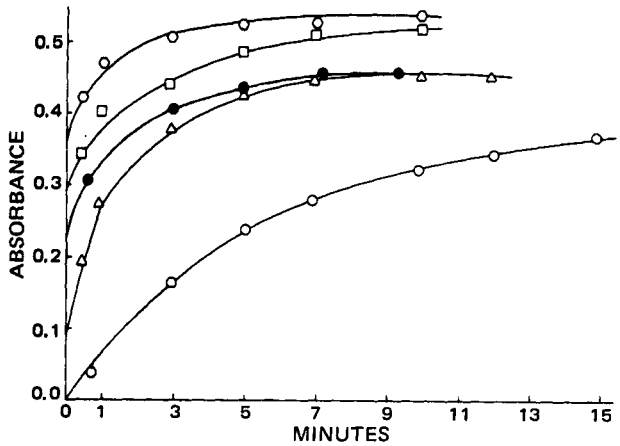

Figure 4—*Dissolution profile of chloramphenicol in pH 6.65 phosphate buffer (500 ml) at 37° and 60 rpm. Key: ○, chloramphenicol, 50 mg; △, 5% solid-state dispersion, chloramphenicol in polyethylene glycol 4000, 1 g; ●, 5% physical mixture, chloramphenicol in polyethylene glycol 4000, 1 g; ○, 5% solid-state dispersion, chloramphenicol in urethan, 1 g; and □, 5% physical mixture, chloramphenicol in urethan, 1 g.*

interaction between the steroid and urethan was indicated by the quantity of hydrocortisone in solution being doubled or tripled at elapsed times of 3 min or more when the drug was added to dissolution media containing previously dissolved urethan. This situation indicates that another variable is apparently operative in systems of this sort and complicates analysis.

The amounts of hydrocortisone in solution at a given time were inversely proportional to the percentage of steroid incorporated when equivalent amounts of hydrocortisone (50 mg of drug) were investigated (Fig. 3); this result is explainable from the standpoint of less isolation of colloidial particles by the soluble carrier. The more dilute the system, the larger is the amount of compound in solution. As the drug concentration is increased, one may think of the dissolution properties of the pure substance being approached, although this is probably not strictly correct.

The more soluble chloramphenicol exhibited an increase in the amount of compound in solution for the 5% solid dispersion, with all drug dissolved at 7 min (Fig. 4). The physical mixture of urethan and chloramphenicol showed more total drug in solution relative to the 5% physical mixture in polyethylene glycol 4000, which was greater than the solid solution (5%) of chloramphenicol in the polyethylene glycol. This finding illustrates the inconsistencies encountered from compound to compound, since the physical mixture was superior to the solid dispersion.

Acetaminophen was run in the same general manner as the other substances (150 mg of drug, 10% solid dispersion, and 1.5 g of total mixture), using distilled water (500 ml) as reported earlier (5). This compound, which possesses relatively good solubility properties comparable to griseofulvin, showed complete solution of both the 5% physical mixture and solid dispersion after 30 sec at 37°. At 27°, the solid dispersion was dissolved after 30 sec and the physical mixture was dissolved after 3 min, but the drug did not go into solution after 15 min.

Figure 5 demonstrates the differences in total drug found when samples were simply filtered through the cotton of serological pipets in contrast to aliquots being filtered serologically followed by ultrafiltration. An almost constant difference may be noted in the examples cited, possibly the consequence of entrapment of some compound on the ultrafilter[7] (0.22 μm) or other variables. This figure illustrates an almost direct relationship between milligrams of hydrocortisone added to the dissolution media and the elevation of total drug in solution at a given time. This occurrence was characteristic of many compounds examined.

Solubility studies were carried out with the more insoluble compounds and urethan, with no evidence of interaction up to 8 mg of urethan/ml.

The results represented in the figures were usually reproducible, ±15% or better, from day to day. The sequences presented in the figures were run on a given day.

Chloramphenicol palmitate[9] was run in 5% solid dispersions with

[9] Chloromycetin Palmitate, supplied by Dr. H. E. Machamer, Parke-Davis & Co.

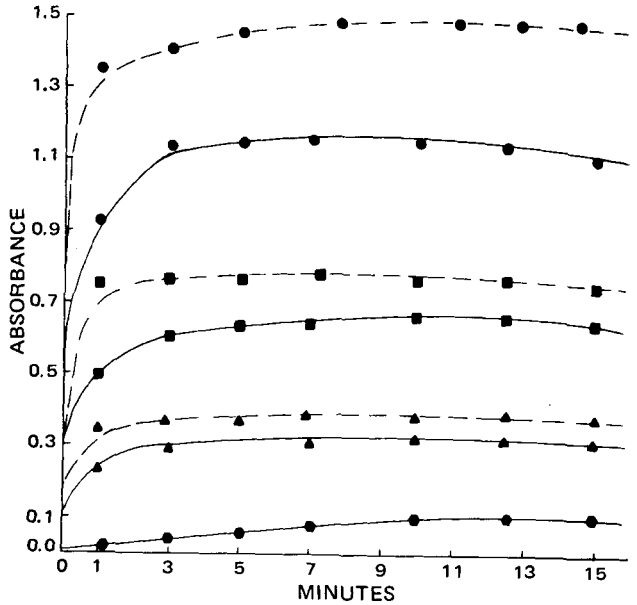

Figure 5—*Comparison of dissolution results of hydrocortisone filtered through serological pipets with cotton filters to samples filtered serologically followed by ultrafiltration with 0.22-μm filters. Key: - - -, serologically filtered; —, ultrafiltered; ▲, 5% solid-state dispersion in urethan, 500 mg, 25 mg of steroid; ■, 5% solid-state dispersion in urethan, 1 g, 50 mg of steroid; ●, 5% solid-state dispersion in urethan, 2 g, 100 mg of steroid; and ●, micronized hydrocortisone, 50 mg. Studies were carried out in pH 6.65 phosphate buffer (500 ml) at 37° and 60 rpm.*

urethan and polyethylene glycol 4000. A 5% physical mixture in urethan was also utilized. None of these systems gave an appreciable elevation in the dissolution rate over the pure drug. The amount solubilized was extremely low in all cases, indicating almost the absence of an appreciable effect.

SUMMARY

Many variables are present in these dissolution studies, rendering analysis a complicated matter, and typical results should not be inferred as general from one substance to another. As with any system of this nature, animal testing is imperative before reconciliation of the *in vitro* data can be completed. This testing was done by Chiou and Riegelman (9) with griseofulvin and polyethylene glycols.

When various medicinal agents are prepared in 5% solid-state dispersions in urethan, a large augmentation of the amount in solution at time periods up to 15 min is observed relative to the pure drug. This result is likely a partial consequence of diminution of particle sizes to the colloidal level in the freely water-soluble urethan.

The probability of some change in the crystalline state of the medicament in the solid-state dispersion cannot be discounted. This change could lead to supersaturated solutions along with the concomitant decrease in particle size.

Simple admixture of the drug with urethan and other diluents leads to an increase in the drug in solution. For this reason, care must be taken in ascribing observed effects entirely to a particle-size decrease rather than partially to simple dilution.

REFERENCES

(1) S. Feldman and M. Gibaldi, *J. Pharm. Sci.*, **56**, 370 (1967).

(2) M. Mayersohn and M. Gibaldi, *ibid.*, **55**, 1323 (1966).

(3) A. H. Goldberg, M. Gibaldi, and J. L. Kanig, *ibid.*, **54**, 1145 (1965).

(4) A. H. Goldberg, M. Gibaldi, J. L. Kanig, and M. Mayersohn, *ibid.*, **55**, 581 (1966).

(5) A. H. Goldberg, M. Gibaldi, and J. L. Kanig, *ibid.*, **55**, 482 (1966).

(6) *Ibid.*, **55**, 487 (1966).

(7) W. L. Chiou and S. Riegelman, *J. Pharm. Sci.*, **58**, 1505 (1969).

(8) W. L. Hayton, D. E. Guttman, and G. Levy, *ibid.*, **59**, 575 (1970).

(9) W. L. Chiou and S. Riegelman, *ibid.*, **59**, 937 (1970).

(10) L. J. Edwards, *Trans. Faraday Soc.*, **47**, 1191 (1951).

(11) E. Nelson, *J. Am. Pharm. Assoc., Sci. Ed.*, **48**, 96 (1959).

(12) E. Nelson and I. Schaldemose, *ibid.*, **48**, 489 (1959).

(13) G. Levy, *Am. J. Pharm.*, **135**, 78 (1963).

(14) H. V. Maulding and M. A. Zoglio, *J. Pharm. Sci.*, **59**, 384 (1970).

Synthesis and Evaluation of *N*-Deacetyl-*N*-glycosylalkylthiocolchicines as Antileukemic Agents

GEORGE T. SHIAU, KALYAN K. DE, and ROBERT E. HARMON ˣ

Received February 17, 1977, from the *Department of Chemistry, Western Michigan University, Kalamazoo, MI 49008.* Accepted for publication June 10, 1977.

Abstract □ A series of *N*-deacetyl-*N*-glycosylalkylthiocolchicines (glucosyl, galactosyl, mannosyl, ribosyl, and arabinosyl) was prepared by heating *N*-deacetylalkylthiocolchicines with the appropriate monosaccharides in methanol. Some compounds (glucosyl-, mannosyl-, and ribosylalkylthiocolchicines) were per-*O*-acetylated in dry pyridine with acetic anhydride. The compounds were tested against leukemia L-1210 and P-388 systems. Preliminary results showed that the antileukemic activity of the glycosyl compounds *in vitro* is similar to that of the *N*-deacetylalkylthiocolchicines used for their preparation. However, the presence of a glycosyl moiety in the molecule gives the advantage of greater solubility in water. Of the results obtained to date in lymphoid leukemia screening *in vivo*, five glycosyl compounds showed promising activity levels and have now reached confirmed active status.

Keyphrases □ *Thiocolchicines, various substituted*—synthesized, antileukemic and cytotoxic activity evaluated □ Antileukemic activity—various substituted thiocolchicines evaluated □ Cytotoxic activity—various substituted thiocolchicines evaluated □ Structure-activity relationships—various substituted thiocolchicines evaluated for antileukemic and cytotoxic activity

Thiocolchicoside (β-D-glucopyranosylmethylthiocolchicine) (Ic), prepared from acetyldemethylcolchicine by the action of methyl mercaptan followed by ether cleavage and condensation with acetobromoglucose (1), has shown muscle relaxant activity (2) and found clinical application (3). In a program to prepare new derivatives of colchicine

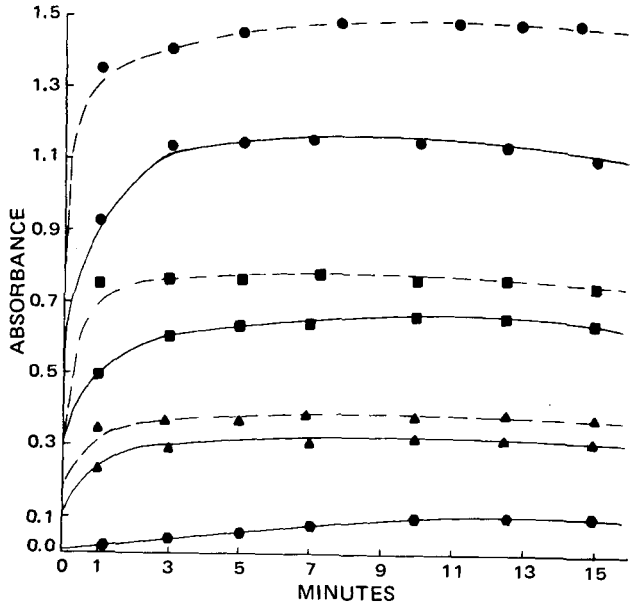

Figure 5—*Comparison of dissolution results of hydrocortisone filtered through serological pipets with cotton filters to samples filtered serologically followed by ultrafiltration with 0.22-μm filters. Key: - - -, serologically filtered; —, ultrafiltered; ▲, 5% solid-state dispersion in urethan, 500 mg, 25 mg of steroid; ■, 5% solid-state dispersion in urethan, 1 g, 50 mg of steroid; ●, 5% solid-state dispersion in urethan, 2 g, 100 mg of steroid; and ●, micronized hydrocortisone, 50 mg. Studies were carried out in pH 6.65 phosphate buffer (500 ml) at 37° and 60 rpm.*

urethan and polyethylene glycol 4000. A 5% physical mixture in urethan was also utilized. None of these systems gave an appreciable elevation in the dissolution rate over the pure drug. The amount solubilized was extremely low in all cases, indicating almost the absence of an appreciable effect.

SUMMARY

Many variables are present in these dissolution studies, rendering analysis a complicated matter, and typical results should not be inferred as general from one substance to another. As with any system of this nature, animal testing is imperative before reconciliation of the *in vitro* data can be completed. This testing was done by Chiou and Riegelman (9) with griseofulvin and polyethylene glycols.

When various medicinal agents are prepared in 5% solid-state dispersions in urethan, a large augmentation of the amount in solution at time periods up to 15 min is observed relative to the pure drug. This result is likely a partial consequence of diminution of particle sizes to the colloidal level in the freely water-soluble urethan.

The probability of some change in the crystalline state of the medicament in the solid-state dispersion cannot be discounted. This change could lead to supersaturated solutions along with the concomitant decrease in particle size.

Simple admixture of the drug with urethan and other diluents leads to an increase in the drug in solution. For this reason, care must be taken in ascribing observed effects entirely to a particle-size decrease rather than partially to simple dilution.

REFERENCES

(1) S. Feldman and M. Gibaldi, *J. Pharm. Sci.*, **56**, 370 (1967).

(2) M. Mayersohn and M. Gibaldi, *ibid.*, **55**, 1323 (1966).

(3) A. H. Goldberg, M. Gibaldi, and J. L. Kanig, *ibid.*, **54**, 1145 (1965).

(4) A. H. Goldberg, M. Gibaldi, J. L. Kanig, and M. Mayersohn, *ibid.*, **55**, 581 (1966).

(5) A. H. Goldberg, M. Gibaldi, and J. L. Kanig, *ibid.*, **55**, 482 (1966).

(6) *Ibid.*, **55**, 487 (1966).

(7) W. L. Chiou and S. Riegelman, *J. Pharm. Sci.*, **58**, 1505 (1969).

(8) W. L. Hayton, D. E. Guttman, and G. Levy, *ibid.*, **59**, 575 (1970).

(9) W. L. Chiou and S. Riegelman, *ibid.*, **59**, 937 (1970).

(10) L. J. Edwards, *Trans. Faraday Soc.*, **47**, 1191 (1951).

(11) E. Nelson, *J. Am. Pharm. Assoc., Sci. Ed.*, **48**, 96 (1959).

(12) E. Nelson and I. Schaldemose, *ibid.*, **48**, 489 (1959).

(13) G. Levy, *Am. J. Pharm.*, **135**, 78 (1963).

(14) H. V. Maulding and M. A. Zoglio, *J. Pharm. Sci.*, **59**, 384 (1970).

Synthesis and Evaluation of *N*-Deacetyl-*N*-glycosylalkylthiocolchicines as Antileukemic Agents

GEORGE T. SHIAU, KALYAN K. DE, and ROBERT E. HARMON ˣ

Received February 17, 1977, from the *Department of Chemistry, Western Michigan University, Kalamazoo, MI 49008.* Accepted for publication June 10, 1977.

Abstract □ A series of *N*-deacetyl-*N*-glycosylalkylthiocolchicines (glucosyl, galactosyl, mannosyl, ribosyl, and arabinosyl) was prepared by heating *N*-deacetylalkylthiocolchicines with the appropriate monosaccharides in methanol. Some compounds (glucosyl-, mannosyl-, and ribosylalkylthiocolchicines) were per-*O*-acetylated in dry pyridine with acetic anhydride. The compounds were tested against leukemia L-1210 and P-388 systems. Preliminary results showed that the antileukemic activity of the glycosyl compounds *in vitro* is similar to that of the *N*-deacetylalkylthiocolchicines used for their preparation. However, the presence of a glycosyl moiety in the molecule gives the advantage of greater solubility in water. Of the results obtained to date in lymphoid leukemia screening *in vivo*, five glycosyl compounds showed promising activity levels and have now reached confirmed active status.

Keyphrases □ *Thiocolchicines, various substituted*—synthesized, antileukemic and cytotoxic activity evaluated □ Antileukemic activity—various substituted thiocolchicines evaluated □ Cytotoxic activity—various substituted thiocolchicines evaluated □ Structure-activity relationships—various substituted thiocolchicines evaluated for antileukemic and cytotoxic activity

Thiocolchicoside (β-D-glucopyranosylmethylthiocolchicine) (Ic), prepared from acetyldemethylcolchicine by the action of methyl mercaptan followed by ether cleavage and condensation with acetobromoglucose (1), has shown muscle relaxant activity (2) and found clinical application (3). In a program to prepare new derivatives of colchicine

Table I—Physical Constants of *N*-Deacetyl-*N*-glycosylalkylthiocolchicines and Their Per-*O*-acetyl Derivatives

Compound	Yield, %	Recrystallization Solvent	Melting Point		Specific Rotation		Formula	Analysis, %			
			Present	Reported[a]	Present[b]	Reported[a]		C	H	N	S
IIa	87	Ethanol–water	161–162°	190°	−220°	−505° (0.5% H_2O)	$C_{26}H_{33}NO_9S\cdot C_2H_5OH$	57.81 58.08	6.75 6.86	2.41 2.34	5.51[c] 5.59[d]
IIb	84	Ethanol–water	152–153°	184°	−204°	−445° (0.2% H_2O)	$C_{26}H_{33}NO_9S\cdot C_2H_5OH$	57.81 57.70	6.75 6.54	2.41 2.30	5.51 5.32
IIc	85	Methanol	153–155°	—	−244°	—	$C_{26}H_{33}NO_9S\cdot H_2O$	56.41 56.67	6.37 6.28	2.53 2.58	5.79 5.51
IId	77	Methanol	151–153°	175°	−233°	−345° (0.2% H_2O)	$C_{25}H_{31}NO_8S\cdot CH_3OH$	58.09 58.61	6.56 6.53	2.61 2.36	5.97 6.44
IIe	87	Ethanol	123–125°	159°	−207°	−220° (0.2% CH_3OH)	$C_{25}H_{31}NO_8S\cdot C_2H_5OH$	58.79 58.59	6.76 6.67	2.54 2.68	5.81 5.77
IIf	70	—[e]	—	—	—	—	—	—	—	—	—
IIIa	90	Methanol	230–231°	—	−183°	—	$C_{34}H_{41}NO_{13}S$	58.03 58.16	5.87 5.98	1.99 1.95	
IIIb	85	Methanol–water	140–142°	—	—	—	—	—	—	—	—
IIIc	70	Water	135°[e]	—	—	—	—	—	—	—	—
IIId	82	Ethanol	161–163°	—	−189°	—	$C_{35}H_{43}NO_{13}S$	58.57 58.72	6.04 6.14	1.95 1.90	

[a] Reference 4. [b] Sample of 0.10 g in 100 ml of 95% ethanol solution. [c] Calculated. [d] Found. [e] An amorphous powder.

as potential anticancer agents, a series of compounds of this type was prepared for evaluation of intracranial antileukemic activity.

RESULTS AND DISCUSSION

The preparation of *N*-deacetyl-*N*-glycosylalkylthiocolchicines by heating *N*-deacetylalkylthiocolchicine with monosaccharide in methanol was reported (4). The same procedure was followed, for example, for the preparation of *N*-deacetyl-*N*-(D-glucosyl)methylthiocolchicine (IIa). The product crystallized from methanol. Although it had the same melting point, ~190°, as reported (4), it turned out to be a mixture of the starting material and the product expected as based on TLC, IR, and NMR evidence. However, the required Compound IIa, mp 161–162°, was separated from the filtrate and recrystallized from aqueous 85% ethanol.

Other glycosyl analogs were prepared in good yield (Table I). Some compounds were per-*O*-acetylated with excess acetic anhydride in dry pyridine at 0° (5). The products were recrystallized from either methanol or ethanol. Yields were in excess of 80% (Table I).

All compounds were examined by TLC (Table II) and characterized by IR, NMR, and mass spectrometry, specific rotation, melting point, and elemental analysis (Table I). Compounds IIa–IIe in water had identical UV spectra to the spectrum of Ia in water, *i.e.*, λ_{max} 380 (ε 18,200), λ_{min} 315, λ_{max} 285 (ε 11,000), and λ_{max} 260 (ε 21,700) nm.

N-Deacetyl-*N*-glycosylalkylthiocolchicines were not sufficiently volatile for mass spectrometry; but, as expected (6), the trimethylsilyl derivatives had much greater volatility. Peaks corresponding to the molecular ions of trimethylsilyl derivatives were weak, but their per-*O*-acetylated analogs (IIIa–IIId) gave very intense peaks of molecular ions. This result strongly indicates that the coupling of compounds (Ia and Ib) with monosaccharide has taken place. Compounds IIa–IIf had very strong and wide IR absorptions at 1750 cm^{-1} due to OH and NH stretching, respectively. On the other hand, the per-*O*-acetylated analogs, IIIa–IIId, gave weak absorptions at 3350 cm^{-1} and very strong absorptions at 1750 cm^{-1}, as expected, due to NH stretching and acetyl C=O stretching, respectively.

In the IR spectra of IIa–IIf and IIIa–IIId, there was no absorption at the 1620–1700-cm^{-1} region due to the Schiff base C=N stretching (7). Therefore, the suspected structure of a Schiff base was eliminated. The 100-MHz spectrum of IIIa showed that the coupling constants were $J_{1,2} = J_{2,3} = 9$ Hz, suggesting that H-1, H-2, and H-3 of the glucosyl moiety were *ax*, indicating the β-configuration. The specific rotation data also supported this configuration.

The compounds were tested[1] in an *in vitro* assay against L-1210 (mouse leukemia) and were also examined by the National Cancer Institute's screening service against L-1210 and P-388 leukemia cell cultures (Tables III–V).

These preliminary results show that the antileukemia activity of IIa–IIf, *in vitro*, is similar to that of compounds used for their preparation. However, the presence of a glycosyl moiety in the molecule gives the advantage of greater solubility in water (Table VI).

Compound IIa was active against KB cells with an ED_{50} of 2.6×10^{-3} μg/ml (4.8×10^{-9} *M*). Thus, its activity was confirmed in cell culture. In the lymphoid leukemia screen *in vivo*, all compounds tested, except IIb,

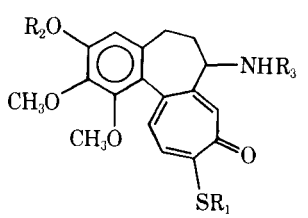

Ia: $R_1 = R_2 = CH_3$, $R_3 = H$
Ib: $R_1 = C_2H_5$, $R_2 = CH_3$, $R_3 = H$
Ic: $R_1 = CH_3$, R_2 = D-glucosyl, $R_3 = COCH_3$
IIa: $R_1 = R_2 = CH_3$, R_3 = D-glucosyl
IIb: $R_1 = R_2 = CH_3$, R_3 = D-galactosyl
IIc: $R_1 = R_2 = CH_3$, R_3 = D-mannosyl
IId: $R_1 = R_2 = CH_3$, R_3 = D-ribosyl
IIe: $R_1 = R_2 = CH_3$, R_3 = L-arabinosyl
IIf: $R_1 = C_2H_5$, $R_2 = CH_3$, R_3 = D-glucosyl
IIIa: $R_1 = R_2 = CH_3$, R_3 = per-*O*-acetyl-D-glucosyl
IIIb: $R_1 = R_2 = CH_3$, R_3 = per-*O*-acetyl-D-mannosyl
IIIc: $R_1 = R_2 = CH_3$, R_3 = per-*O*-acetyl-D-ribosyl
IIId: $R_1 = C_2H_5$, $R_2 = CH_3$, R_3 = per-*O*-acetyl-D-glucosyl

Table II—R_f Value of *N*-Deacetyl-*N*-glycosylmethylthiocolchicines

Solvent	Compound					
	Ia	IIa	IIb	IIc	IId	IIe
Ethanol–ethyl acetate, 1:4 (v/v)	0.41	0.32	0.31	0.37	0.50	0.45
Acetone	0.73	0.22	0.19	0.28	0.49	0.25

Table III—Antileukemic Activities of *N*-Deacetyl-*N*-glycosylalkylthiocolchicines and Their Per-*O*-acetyl Analogs

Compound	L-1210 Tube Dilution *In Vitro* Assay, μg/ml	
	ID_{50}	ID_{90}
Ia	0.0070	0.011[a]
Ib	0.069	0.098[a]
IIa	0.016	0.023
IIb	0.017	0.023
IIc	0.017	0.023
IId	0.0092	0.013
IIe	0.017	0.024
IIf	0.069	0.098
IIIa	0.1	0.1
IIIb	0.1	0.1
IIIc	0.1	0.1
IIId	0.1	0.1

[a] Reference 8.

[1] At The Upjohn Co., Kalamazoo, Mich.

Table IV—Evaluation of *N*-Deacetylalkylthiocolchicines and *N*-Deacetyl-*N*-glycosylalkylthiocolchicines against Lymphoid Leukemia L-1210 *In Vivo* [a]

Compound		Dose[b], mg/kg	Toxicity on Day 5[c]	Control Body Weight Change[d]	Weight Difference (T − C)[e]	Tumor Evaluation[f]		Percent T/C[g]
Number	NSC Number					Test	Control	
I*a*	9170	400	5/6	−2.2	0.8	8.8	9.3	94
		200	6/6	−2.2	0.7	9.7	9.3	104
		100	6/6	−2.2	0.7	9.5	9.3	102
I*b*	186306	50.0	3/3	−0.5	0.5	10.0	10.2	98
		25.0	3/3	−0.5	0.0	9.7	10.2	95
		12.5	3/3	−0.5	1.0	11.0	10.2	107
II*b*	225332	50.0	4/4	−1.8	1.0	11.5	10.2	112
		25.0	4/4	−1.8	−1.5	10.3	10.2	100
		12.5	4/4	−1.8	1.5	10.3	10.2	100
II*c*	221659	200	6/6	0.3	−0.1	6.8	9.9	
		100	6/6	0.3	−0.5	13.5	9.9	136
		50.0	6/6	0.3	0.1	13.0	9.9	131
		150	4/6	−1.8	−2.0	12.3	10.2	120
		100	6/6	−1.8	0.2	13.2	10.2	129
		50.0	6/6	−1.8	0	13.0	10.2	127
		25.0	6/6	−1.8	0	10.5	10.2	102
II*d*	221660	200	0/4	0.0	0	0.0	9.9	—
		100	1/4	0.0	−3.0	6.0	9.9	—
		50.0	3/4	0.0	−5.7	6.0	9.9	—
		25.0	4/4	−1.8	0.3	12.5	10.2	122
		12.5	3/4	−1.8	−0.1	13.3	10.2	130
		6.25	4/4	−1.8	0.1	11.0	10.2	107
		3.12	3/4	−1.8	1.1	11.3	10.2	110
II*f*	186309	400	6/6	2.1	−2.1	14.0	9.0	155
		200	6/6	2.1	−1.1	12.0	9.0	133
		100	6/6	2.1	−1.1	10.4	9.0	115
		50.0	6/6	2.1	0.2	10.0	9.0	111
II*e*	248896	96.0	6/6	1.4	−3.6	11.5	9.0	127
		48.0	6/6	1.4	−2.4	12.2	9.0	135
		24.0	6/6	1.4	−1.9	11.3	9.0	125
		12.0	6/6	1.4	−0.9	10.8	9.0	120
		6.0	6/6	1.4	−0.1	9.2	9.0	102
II*a*	186308	200	0/6	−0.3	0.3	0.0	9.5	—
		100	5/6	−0.3	−5.0	6.2	9.5	—
		50.0	6/6	−0.3	−2.0	14.0	9.5	147
		75.0	5/6	1.1	−4.3	9.4	9.8	95
		50.0	6/6	1.1	−2.2	14.7	9.8	150
		35.0	6/6	1.1	−3.0	13.7	9.8	139
		100	2/6	0.1	−3.0	8.0	8.5	—
		50.0	6/6	0.1	−3.3	11.5	8.5	135
		25.0	6/6	0.1	−1.1	12.0	8.5	141
		12.5	6/6	1.0	−0.8	12.0	8.5	141
		6.25	6/6	0.1	−0.7	10.7	8.5	125
		3.13	6/6	0.1	−0.6	10.0	8.5	117

[a] Mice were implanted intraperitoneally with 1×10^5 L-1210 cells. [b] Dose per injection; nine doses. [c] Number of survivors/total number of mice on Day 5 in survival systems as a measure of drug toxicity. [d] Average weight change of control animals in grams (toxicity minus initial day). [e] Average weight of test group minus average weight of control animals in grams. [f] Survival time in days. [g] Ratio of survival time of treated animals to control animals expressed as a percentage; a compound is considered active if it has a T/C of ≥125%.

Table V—Evaluation of *N*-Deacetyl-*N*-glycosylalkylthiocolchicines against P-388 Lymphocytic Leukemia *In Vivo* [a]

Compound	Dose[b], mg/kg	Toxicity on Day 5[c]	Control Body Weight Change[d]	Weight Difference (T − C)[e]	Tumor Evaluation[f]		Percent T/C[g]
					Test	Control	
II*a*	200	0/6	0.3	−0.3	4.7	11.1	—
	100	3/6	0.3	−4.3	6.0	11.1	—
	50.0	6/6	0.3	−1.0	17.3	11.1	155
II*e*	48.0	5/6	1.2	−2.6	17.1	11.0	155
	36.0	6/6	1.2	−2.7	16.3	11.0	148
	24.0	6/6	1.2	−0.2	16.8	11.0	152
	12.0	6/6	1.2	−1.3	16.0	11.0	145
II*f*	400	6/6	2.1	−2.1	14.0	9.0	155
	200	6/6	2.1	−1.1	12.0	9.0	133
	100	6/6	2.1	−1.1	10.4	9.0	115
	50.0	6/6	2.1	0.2	10.0	9.0	111
III*a* (NSC 251700)	192	6/6	2.0	−3.1	16.4	10.9	150
	96.0	6/6	2.0	−3.4	14.0	10.9	128
	48.0	6/6	2.0	−2.5	14.1	10.9	129
	24.0	6/6	2.0	−1.3	13.1	10.9	120
	12.0	6/6	2.0	−1.0	12.8	10.9	117
	6.0	6/6	2.0	−0.2	11.7	10.9	107

[a] Mice were implanted intraperitoneally with 1×10^6 P-388 cells. [b] Dose per injection; nine injections. The first injection was given 1 day after tumor was implanted. [c–g] See Table IV.

Table VI—Solubility of *N*-Deacetyl-*N*-glycosylmethylthiocolchicines in Water at 25°

Compound	Solubility, *M*
I*a*	2.9×10^{-4}
II*a*	1.7×10^{-2}
II*b*	$>3.0 \times 10^{-1}$
II*c*	4.3×10^{-2}
II*d*	5.2×10^{-3}
II*e*	3.2×10^{-2}

showed much better activity than the compounds (I*a* and I*b*) used for their preparation and have now reached confirmed active status.

EXPERIMENTAL[2]

***N*-Deacetyl-*N*-(D-glucosyl)methylthiocolchicine (II*a*)**—To a solution of 11.2 g of *N*-deacetylmethylthiocolchicine (8) in 200 ml of methanol was added 5.4 g of D-(+)-glucose. The mixture was heated at 70° for 2 hr and then concentrated to about 100 ml. On standing overnight at room temperature, some solid deposited. The mixture was filtered, and the filtrate was further concentrated to about 70 ml and stored at 10°.

Over several days, it gave a pale-yellow solid, which was washed with cold methanol to yield 14.8 g (87%) of II*a*, mp 157–159°. Recrystallization from aqueous 85% ethanol gave pale-yellow rectangular prisms, mp 161–162°. This compound was characterized as containing one molecule of ethanol by elemental analyses and NMR spectroscopy.

***N*-Deacetyl-*N*-(D-galactosyl)methylthiocolchicine (II*b*)**—A mixture of 2.00 g of I*a* and 1.00 g of D-(+)-galactose in 60 ml of methanol was refluxed for 2 hr. The clear solution was concentrated to 10 ml and then stored at 10°. The crystals were filtered and washed with ethanol, yielding 2.48 g (84%). For further purification, 0.70 g of the product was dissolved in 50 ml of ethanol by heating. On cooling slowly to room temperature, the solution gave 0.56 g of II*b* as pale-yellow rectangular prisms, mp 152–153°.

A similar procedure was used to obtain IIc–II*f*.

***N*-Deacetyl-*N*-(tetra-*O*-acetyl-D-glucosyl)methylthiocolchicine (III*a*)**—To a stirred ice-cold solution of acetic anhydride (10 ml) in anhydrous pyridine (20 ml) was slowly added II*a* (5.8 g, 10 mmoles). The solution was left overnight at room temperature and then slowly poured into ice water (200 ml) with stirring. The precipitate was filtered, washed with water, and dried by pressing on a porous plate. Recrystallization from methanol gave 6.3 g (90%) of yellow fine needles of III*a*, mp 230–231°.

A similar procedure was used to obtain III*b*–III*d*.

Solubility Measurement—To 100 mg of each sample in small test tubes was added distilled water (0.5 ml). The test tubes were kept in a constant-temperature bath at 37° for 3 hr and then at 25° overnight so that some dissolved material crystallized out. The mixture was then filtered. The concentrations of the filtrates were measured at 380 nm. An average extinction coefficient of 18,200 at 380 nm was used in the calculation. The experimental error was within ±5%. The results are listed in Table VI.

[2] Melting points were measured with a Thomas-Hoover Uni-melt apparatus and are uncorrected. IR spectra were obtained on Beckman IR-8 and Perkin-Elmer 457 spectrophotometers. UV spectra were recorded with a Beckman model 24 spectrophotometer. NMR spectra were measured on Varian A-60 and Varian XL-100 spectrometers using tetramethylsilane as the internal standard and dimethyl sulfoxide-d_6 or deuterochloroform as the solvent. Mass spectra were recorded at 70 ev on an LKB 9000 SN mass spectrometer. Elemental analyses were performed by Midwest Microlab, Inc., Indianapolis, Ind. Eastman chromagram sheet 6061 silica gel was used for TLC, and the chromatograms were examined with UV light.

REFERENCES

(1) L. Vellez and G. Muller, *Bull. Soc. Chim. Fr.*, **1954**, 755; **1955**, 194.

(2) G. Plotka and R. Jequir, *Arch. Int. Pharmacodyn. Ther.*, **109**, 386 (1957).

(3) R. Pluvinage, D. Lemoine, and H. Gros, *Sem. Hop. Paris*, **33**, 3602 (1957).

(4) L. Velluz and G. Muller, French pat. 1, 175. 407 (1955). L. Velluz and G. Muller, British pat. 733, 729 (1957).

(5) M. L. Wolfrom and A. Thompson, in "Methods in Carbohydrate Chemistry," R. L. Whistler and M. L. Wolfrom, Eds., Academic, New York, N.Y., 1963, p. 211.

(6) T. Radford and D. C. Dejongh, in "Biochemical Applications of Mass Spectrometry," G. R. Waller, Ed., Wiley–Interscience, New York, N.Y., 1972, p. 318.

(7) N. B. Colthup, L. H. Daly, and S. E. Wiberly, "Introduction to Infrared and Raman Spectroscopy," Academic, New York, N.Y., 1964, p. 282.

(8) G. T. Shiau, K. K. De, and R. E. Harmon, *J. Pharm. Sci.*, **64**, 646 (1975).

ACKNOWLEDGMENTS

Presented in part at the 168th American Chemical Society National Meeting, Atlantic City, N.J., September 1974.

Supported by Grant CA 13119-02A1 from the National Institutes of Health.

The authors thank Mr. V. K. Sood and Miss S. L. Kuentzel, The Upjohn Co., Kalamazoo, Mich., for mass spectral measurements and antileukemic activity determinations, respectively.

Ambiguities in IR and X-Ray Characterization of Amphotericin B

G. SCHWARTZMAN *x, I. ASHER ‡, V. FOLEN §, W. BRANNON §, and J. TAYLOR ¶

Received April 14, 1977, from **Pharmaceutical Research and Testing, Food and Drug Administration, U.S. Department of Health, Education, and Welfare, Washington, D.C.*; the ‡*Office of Science, Food and Drug Administration, U.S. Department of Health, Education, and Welfare, Rockville, Md.*; the §*Division of Drug Chemistry, Food and Drug Administration, U.S. Department of Health, Education, and Welfare, Washington, D.C.*; and the ¶*National Center for Antibiotics Analysis, Food and Drug Administration, U.S. Department of Health, Education, and Welfare, Washington, D.C.* Accepted for publication June 22, 1977.

Abstract □ Two distinct IR spectra of amphotericin B have been reported. These differences can be obtained from the same sample by surprisingly small changes in the method of sample preparation. Type I spectra (hand-ground samples) are characterized by a sharp C=O stretching band at 1692 cm^{-1}, and Type II spectra (vibrator-ground samples) are characterized by a broad C=O stretching band near 1710 cm^{-1}. X-ray powder diffraction demonstrates that vibrator grinding promotes a transition from a crystalline to an amorphous phase. The two phases are not bioequivalent. Differential thermal analysis reveals a transition near 157°, and samples heated to 158° give only Type II IR spectra. However, a marked color change accompanies such heating (*i.e.*, structural changes affecting the chromophore have been thermally induced), while X-ray spectra show an increase of only about 30% in amorphous content. Furthermore, hand-ground samples heated to 120° still display only Type I IR spectra. Thus, the vibrator-induced transition is not solely a static thermal effect. Many observed spectral lines can be assigned to specific functional groups.

Keyphrases □ Amphotericin B—different IR spectra attributed to method of sample preparation □ IR spectroscopy—amphotericin B, different spectra attributed to method of sample preparation □ Antifungal agents, topical—amphotericin B, different IR spectra attributed to method of sample preparation

IR absorption spectroscopy is an essential technique in constructing the analytical profile of a drug. Its use depends on comparison of sample spectra to reliable standard spectra. It is disconcerting, therefore, that conflicting IR spectra of amphotericin B have been reported (1, 2). Evidence given in this paper demonstrates that both spectra can be obtained from the same sample at "room temperature," depending on the mode of preparation. Complete IR spectra of both forms are presented and analyzed, and they are supplemented by data obtained by other techniques. Thermally induced changes in amphotericin B (near 157°) also are discussed.

Amphotericin B ($C_{47}H_{73}NO_{17}$) is a mycosamine-containing, macrocyclic, polyene antibiotic, widely used as a fungicide. A proposed structure (I) is based on the X-ray work of Ganis *et al.* (3). This structure is consistent with mass spectroscopic measurements (4) but not with an earlier proposed partial structure (5). ^{13}C-NMR spectra confirm the presence of the hemiketal ring in dimethyl sulfoxide solution (6). Amphotericin B is soluble in dimethyl sulfoxide and, to a lesser extent, in methanol but is virtually insoluble in carbon tetrachloride, chloroform, and neutral water (7, 8).

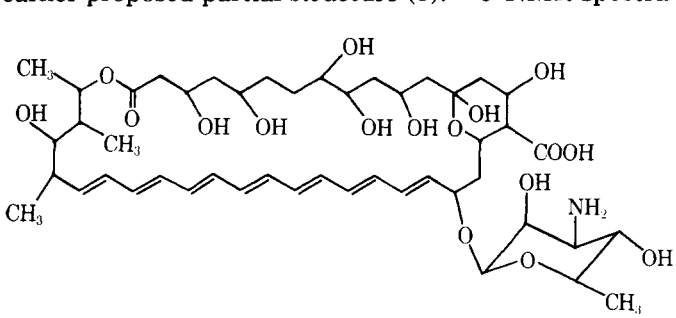

I

EXPERIMENTAL

Samples of the Food and Drug Administration amphotericin B[1] working standard powder[2] were used without further purification. Samples were ground either by hand or in a vibrator[3] and then made into potassium bromide disks or a liquid paraffin mull[4].

Spectra were taken using several different IR spectrometers[5]. Some disks were made from 1 mg of amphotericin and 200 mg of potassium bromide, hand ground in a 65-mm (o.d.) agate mortar with an agate pestle for 2 min. The disks were machine pressed under vacuum, using a 13-mm die for 2 min at 9080 kg (20,000 lb). Other samples were ground in a vibrator[3] for 2 min in a metal capsule with one steel ball, rather than hand ground, before being pressed into disks.

Mulls were made in the mortar by adding a few drops of mineral oil to fresh amphotericin and hand grinding for 2 min. Mulls were squeezed between sodium chloride plates for observation. Saturated dimethyl sulfoxide solutions (approximately 40 mg/ml) were made from unground samples.

In thermal studies, unground samples were heated in glass test tubes immersed in an oil bath (158°) prior to processing. X-ray powder diffraction spectra were taken with a wide angle X-ray diffractometer[6] with a theta compensating slit and focusing monochromator. Differential thermal analysis and thermal gravimetric analysis data also were obtained[7]. Such heat-treated samples were made into disks and mulls for IR measurements.

DISCUSSION

IR Spectra at Room Temperature—IR spectra of amphotericin B powder at room temperature seem to represent a mixture of two distinct forms, Types I and II. Type I predominates in hand-ground samples (Fig. 1A), whereas Type II usually predominates in vibrator-ground samples (Fig. 1B). Some vibrator-ground samples display a more equal mixture of forms (Fig. 1C). Since mulls are usually hand ground and samples for disks are often vibrated along with potassium bromide, this effect can cause considerable confusion. However, when prepared under identical conditions (*i.e.*, hand ground or vibrator ground), potassium bromide disks and liquid paraffin mulls give the same spectra.

Type I spectra are characterized by a sharp C=O stretching band at 1692 cm^{-1} (with a high frequency shoulder), a 1556-cm^{-1} C=C stretching band, and considerably more detail in the CH band and stretching regions (*e.g.*, near 850, 1380, and 2860 cm^{-1}). Type II spectra typically display broader, less resolved bands, including a broad C=O stretching band (width of approximately 50 cm^{-1} rather than approximately 10 cm^{-1})

[1] Lot Ampho B-2, E. R. Squibb & Sons, New Brunswick, N.J.
[2] Supplied by the National Center for Antibiotics Analysis.
[3] WIG-L-BUG, Crescent Dental Manufacturing Co., Chicago, Ill.
[4] Nujol.
[5] Models 521, 567, and 621, Perkin-Elmer Corp., Norwalk, Conn.
[6] Generator XRG-3000, goniometer 15U10021, and electronic panel 3005/220, Phillips Electronics Instruments, Mount Vernon, N.Y.
[7] Model 990 thermal analyzer with a model 950 thermogravimetric attachment, E. I. du Pont de Nemours & Co., Wilmington, Del.

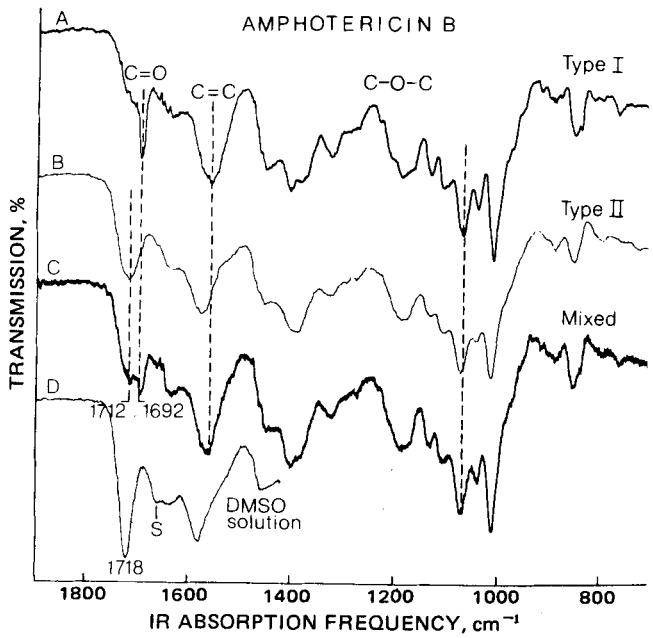

Figure 1—*IR spectra of amphotericin B powder, showing differences between hand-ground (A) and vibrator-ground (B) samples, some vibrator-ground samples displaying mixed forms (C), and samples in dimethyl sulfoxide (D).*

at 1712 cm^{-1}, and a 1566-cm^{-1} C=C stretching band. Other differences are found near 900, 1233, 2930, and 2970 cm^{-1}.

Spectra of amphotericin B in dimethyl sulfoxide (Fig. 1D) have C=O and C=C stretching bands near 1718 and 1580 cm^{-1}, respectively, and tend to resemble Type II. The observed absorption frequencies are listed in Table I. Many peaks can be tentatively assigned to specific structural features (9–11), using such model compounds as glucosamine.

Microscopic examination showed the FDA amphotericin B working standard powder to consist of thin, irregularly shaped fragments, which tended to clump together into approximately 80-μm clusters. The fragments were roughly 5–15 μm long in hand-ground or untreated samples and 1–5 μm long in vibrator-ground samples; they were less than 0.3 μm thick. The irregular, shattered appearance of untreated samples indicates considerable grinding and other comminution as part of the working standard's final processing by the manufacturer. This treatment could account for the broad 1710-cm^{-1} band (typical of Type II grinding) seen as a shoulder in all spectra of hand-ground or even untreated samples, both disks and mulls.

Nonetheless, the observed spectral differences between hand-ground and vibrator-ground samples do not appear to be a size effect (12, 13) since: (*a*) the differences in particle sizes are not very great; (*b*) if a difference does exist, Type II spectra should be of higher resolution since the particle size of Type II is smaller (yet compare, for example, the 800–950-cm^{-1} regions of Figs. 1A and 1B); (*c*) the observed differences

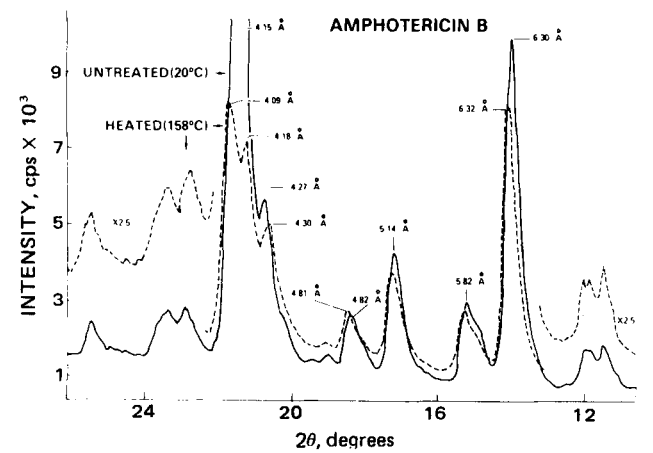

Figure 2—*X-ray diffraction spectrum of unground and unheated amphotericin B powder.*

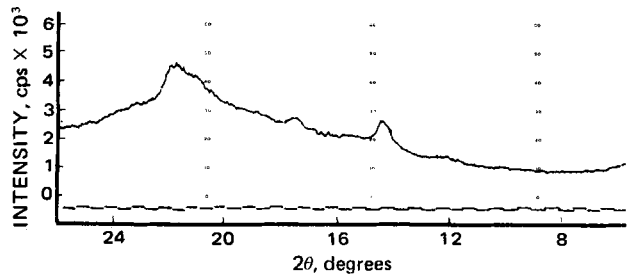

Figure 3—*X-ray diffraction spectrum of vibrator-ground amphotericin B powder.*

involve both frequency shifts and changes in the width of the bands; and (*d*) the powders are somewhat fine for an appreciable Christiansen effect, and no marked asymmetries are seen.

X-Ray Powder Diffraction—The X-ray powder diffraction spectrum of untreated (unground and unheated) amphotericin B (solid line, Fig. 2) demonstrates that the substance has a definite crystal structure. Material heated to 158° produces a pattern with less intense peaks, small shifts in *d*-spacings, and increased background. These changes show that some strain has been introduced in the crystal lattice and that the amorphous fraction of the powder has increased. The diffraction pattern of vibrator-ground powder (ground in 2-mg aliquots, 2 min each; Fig. 3) has only a few broad peaks of very low intensity and much higher background, characteristic of patterns obtained from almost completely amorphous powders.

This result demonstrates that the original crystalline sample has undergone a transition to an amorphous form. There is no change in color, but the transition is associated with a 40% loss in biological activity, as measured by the CFR *Saccharomyces cerevisiae* assay (14). Since the first step of the assay is to dissolve the sample, an accompanying irreversible chemical change is indicated.

The phase transition is apparently the physical basis for the observed changes in the IR spectrum; a similar effect was observed in the Cinchona alkaloids (15). Spectra of amphotericin B heated 15 min at 120° and then ground by hand are still Type I, which suggests that the elevated temperatures in the vibrator capsule during grinding are not themselves sufficient to induce the observed phase transition. Nor is salt complexation responsible, since samples ground with and without potassium bromide have identical IR spectra. However, if mulls are made by adding liquid paraffin directly to the vibrator capsule before grinding, the spectra are of Type I. This result suggests that pressure effects, probably aided by elevated temperatures, may be important.

The broad 1710-cm^{-1} shoulder in Type I spectra could represent the presence of some amorphous material (Type II) in the original standard. Indeed, about 30–40% of the area in the C=O stretch band of Fig. 1A may have such an origin (the absorption efficiencies of the two forms may differ, however).

Thermal Transitions above 157°—Differential thermal analysis of amphotericin B (14) shows a sharp drop beginning near 140°, with a minimum near 157°. Thermal gravimetric analysis reveals no corresponding weight loss, and sample decomposition occurs only above 200°. Amphotericin B heated at 158° for 15 min irreversibly changes color from bright yellow to orange brown. Such samples display a loss of about 30% in antifungal effectiveness (14), a 20–25% decrease in UV absorbance (14), a 25–30% decrease in crystalline peak scattering intensities in powder X-ray diffraction spectra (Fig. 2), and Type II (or mixed type) IR spectra.

Such results suggest that irreversible chemical changes occur near 158°. Heating amphotericin B to 120° for approximately 15 min has little effect on its IR spectrum, although heating for a longer period may affect the 1712- and 1692-cm^{-1} bands. The X-ray results confirm that heating to 158° can partially increase the amorphous fraction of amphotericin B; slight shifts (0.38 Å) in several peaks of the X-ray powder diffraction spectrum (Fig. 2) further suggest some additional strain in the remaining crystalline fraction. However, lack of a complete transition to the amorphous form and the presence of a color change indicate that the effects of static heating cannot totally account for those observed upon grinding with a vibrator. Neither process markedly affects the resonance Raman spectrum[8].

Evidently, sample preparation can be very important in obtaining

[8] I. M. Asher, M. Bunow, and I. Levin, unpublished data.

Table I—IR Spectra of Amphotericin B [a]

Type I	Type II	Dimethyl Sulfoxide	Tentative Assignment
(625)			
664		(661)	OH out-of-plane bend
697			
(732)			
762	(sh)	758	Pyranose ring breathing
795	(792)	791	
812	(804) sh	(s1)	
818			
(837) sh			
851	850	850	CH bend (G)
(878)			
889	888	888	CH bend, CH_3 rock
(898) sh		(900) sh	
916		(915) sh	Pyranose ring vibration
(931) sh			
(953) sh			
(972) sh		(970) sh	
(981) sh	(s1)		CH out-of-plane bend (*trans*-polyene)
1009	1010	1010	
1041	1040	(1036) sh	
1070	1068	1069	
1109	1106	1106 sh	CO asymmetric stretching (COC, OOH)
1132	1130	1132	
1164 sh	(1173)		
1186	(1188)	1183	COC asymmetric stretching (COC=O)
1210 sh			
1233 sh	(1230) sh	(1232) sh	
1272 sh	1269	1273	CH_2 wag, bend (skeletal)
(sh)	(1291)	1292	
1324	1322	1321	
(1338) sh			
(1371) sh			
1381	(1385)	(1380)	CH_3 symmetric bend
1401	(1400)	(1402)	CH in-plane bend (polyene)
1448	1449	1452 sh	CH_2, CH_3 asymmetric bend
1556*	1566*	1565	Polyene C=C stretching
(1628)	1628 sh	S	NH_2 in-plane bend
1692*			
(1710) sh	1712*	1716	
(sh)	2859*	S	CH_2, CH_3 symmetric stretching
2918			CH_2, asymmetric stretching
	2925		
2940			
(2960) sh			CH_3 asymmetric stretching
2978	(2979) sh		
3009	3015		CH stretching (polyene)
(3370)			OH stretching
3390	3390	3350	(Strongly H-bonded)

[a] B = broad; sh = shoulder; sl = slant; S = solvent peaks; () = weak, frequency uncertain; * = frequency characteristic of Type I or II; and + = may arise from slight admixture of Type II.

consistent IR spectra of pharmaceuticals. Ideally, both samples and standards should be prepared by identical techniques at the same time. In general, hand-ground samples seem preferable.

REFERENCES

(1) J. Vandeputte, J. L. Wachtel, and E. T. Stiller, *Antibiot. Annu.*, **1955–56**, 579 (1956). "Index of Antibiotics from Actinomycetes," H. Umezawa, Ed., University Park Press, State College, Pa., 1967, p. 133.

(2) L. Wayland and P. J. Weiss, in "IR and UV Spectra of Some Compounds of Pharmaceutical Interest," Association of Official Analytical Chemists, Washington, D.C., 1972, p. 235.

(3) P. Ganis, G. Avitabile, W. Mechlinski, and C. P. Shaffner, *J. Am. Chem. Soc.*, **93**, 4560 (1971).

(4) K. D. Maegele and D. M. Desiderio, *Biomed. Mass Spectrom.*, **1**, 20 (1974).

(5) A. C. Cope, U. Axen, E. P. Burrows, and J. Weinlich, *J. Am. Chem. Soc.*, **88**, 4228 (1966).

(6) R. C. Pandey and K. L. Rinehart, Jr., *J. Antibiot.*, **29**, 1035 (1976).

(7) "The Merck Index," 8th ed., Merck & Co., Rahway, N.J., 1968, p. 75.

(8) M. L. Andrew and P. J. Weiss, *Antibiot. Chemother.*, **9**, 277 (1959).

(9) L. J. Bellamy, "Advances in Infrared Group Frequencies," Methuen, London, England, 1968.

(10) K. Nakanishi, "Infrared Absorption Spectroscopy," Holden-Day, San Francisco, Calif., 1966.

(11) M. Avram and G. D. Mateescu, "Infrared Spectroscopy Applications in Organic Chemistry," Wiley–Interscience, New York, N.Y., 1966, p. 475.

(12) G. Duyckaerts, *Analyst*, **84**, 201 (1959).

(13) C. N. R. Rao, "Chemical Applications of Infrared Spectroscopy," Academic, New York, N.Y., 1963, pp. 586–591.

(14) I. M. Asher, G. Schwartzman, and the U.S. Standard Antibiotics Research Group, in "Analytical Profiles of Drug Substances," vol. 6, K. Florey, Ed., Academic, New York, N.Y., 1977.

(15) A. L. Hayden and O. R. Sammul, *J. Am. Pharm. Assoc., Sci. Ed.*, **49**, 497 (1960).

ACKNOWLEDGMENTS

The authors thank Dr. M. Maienthal, Division of Drug Chemistry, Food and Drug Administration, for the differential thermal analysis and thermal gravimetric analysis data.

Synthesis of Diastereoisomeric 4-Dimethylamino-3-phenyl-2-butanols and Related Esters for Antimicrobial Evaluation

J. R. DIMMOCK *x, D. K. KOWAL *, W. A. TURNER *, P. J. SMITH ‡, L. M. NOBLE ‡, and W. J. PANNEKOEK ‡

Received May 23, 1977, from the *College of Pharmacy and the ‡Department of Chemistry and Chemical Engineering, University of Saskatchewan, Saskatoon, Saskatchewan, Canada, S7N 0W0. Accepted for publication June 29, 1977.

Abstract □ 4-Dimethylamino-3-phenyl-2-butanone was reduced to the corresponding diastereoisomeric alcohols, which were separated by fractional crystallization of the corresponding hydrochloride salts. The configuration of the diastereoisomeric alcohols was determined by PMR spectroscopy. The assignments were confirmed by a consideration of the mass spectral data obtained for the two alcohols. Acylation of the alcohols gave the corresponding esters. Antimicrobial evaluation of the compounds prepared showed that 4-dimethylamino-3-phenyl-2-butanone had a promising level of antifungal activity while the other derivatives showed either a low level of potency or were inactive.

Keyphrases □ 4-Dimethylamino-3-phenyl-2-butanols—diastereoisomers and related esters, synthesized, antimicrobial activity evaluated □ Antimicrobial activity—evaluated in diastereoisomeric 4-dimethylamino-3-phenyl-2-butanols and related esters □ Structure–activity relationships—diastereoisomeric 4-dimethylamino-3-phenyl-2-butanols and related esters evaluated for antimicrobial activity

Various Mannich bases (β-aminoketones) have antimicrobial activity (1–4); reduction of the keto group in this series of compounds to the corresponding alcohol has been accompanied by an increase in pharmacological activity (5). The bioactivities of such alcohols may be improved by esterification, thereby masking the polar hydroxyl group and, consequently, facilitating transportation to a site of action.

With benzoate esters of alcohols derived from Mannich bases, the hydrolysis rates are influenced by the Hammett and Taft values of the nuclear substituents, and correlations between the hydrolysis rates and antimicrobial activity may emerge. Furthermore, acylation of these alcohols to the antifungal agent phenoxyacetic acid to produce esters capable of hydrolysis was of interest. As a continuation of a program on the synthesis and antimicrobial evaluation of various acyclic and cycloaliphatic Mannich bases and the related alcohols and esters (6–8), II–V (Scheme I) were prepared.

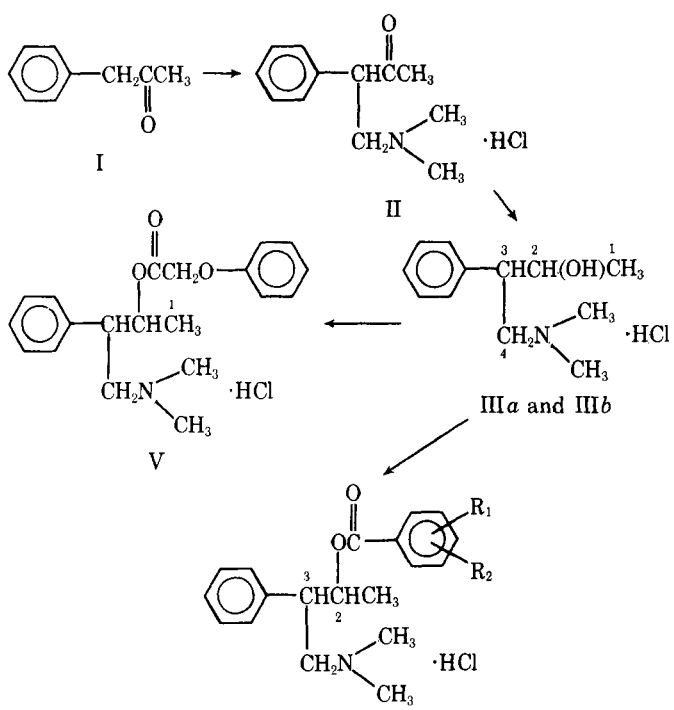

Scheme I

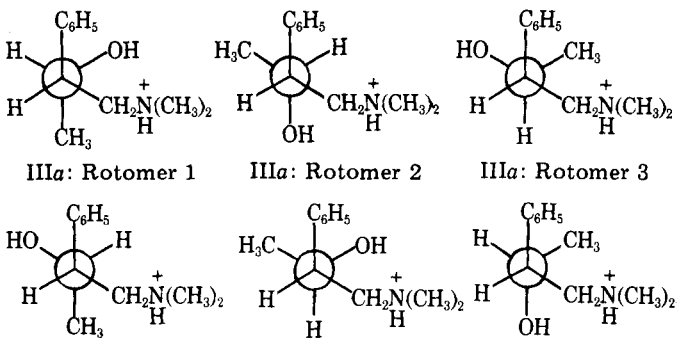

RESULTS AND DISCUSSION

The Mannich reaction between phenylacetone, paraformaldehyde, and dimethylamine hydrochloride occurs either at the methylene or methyl group of the ketone. The compound obtained gave the expected product, namely, the Mannich base II, as shown by PMR spectroscopy. Reduction of II with lithium aluminum hydride gave diastereoisomers III*a*, mp 142–143°, and III*b*, mp 93°. PMR spectroscopy of the crude reduction product showed that the ratio of III*a* to III*b* was approximately 60:40.

The elucidation of the relative stereochemistry of III*a* and III*b* was achieved by PMR spectroscopy. In diastereoisomers bearing a proton at both asymmetric centers, the vicinal coupling constants will be the average value for the various rotomer contributions. If, in the preferred conformation, the vicinal protons are *trans* to each other, the coupling constant of the adjacent protons is 8–12 Hz; with *gauche*-oriented protons, the average reported values are 1–4 Hz (9, 10).

An examination of the conformational free energy differences[1] of the groups at carbons 2 and 3 allows a prediction of the preferred rotomer. At carbon 2, the conformational free energy differences of methyl and hydroxyl groups are 1.7 and 0.7 kcal/mole, respectively (11, 12). At carbon 3, the conformational free energy difference of the phenyl ring is 3.1 kcal/mole (12). Although the literature appears to be deficient in assigning a value to the dimethylaminomethyl group, it is known that the

[1] The conformational free energy difference is defined as the negative of the free energy difference $\Delta G_x°$ corresponding to the conformational equilibrium constant K for a monosubstituted cyclohexane with the substituent, x, axial or equatorial.

Table I—Physical Properties of Benzoate Esters of 4-Dimethylamino-3-phenyl-2-butanol Hydrochloride

Compound	Yield, %	Melting Point	Molecular Formula	Analysis, % Calc.	Analysis, % Found	Mass Spectrum[a] P Calc.	Mass Spectrum[a] P Found	IR Spectra, cm^{-1} (C=O)
IV*a*	40	145–147°	$C_{19}H_{24}ClNO_2$	C 68.35 H 7.25	68.40 7.47	297	297	1715 (s)
IV*b*	69	204–205°	$C_{20}H_{26}ClNO_3$	C 66.01 H 7.20	65.80 7.40	327	327	1700 (s)
IV*c*	78	192–193°	$C_{19}H_{23}Cl_2NO_2$	C 61.96 H 6.29	61.70 6.59	331	331	1725 (s)
IV*d*	65	200–201°	$C_{19}H_{23}Cl_2NO_2$	C 61.96 H 6.29	61.60 6.62	331	331	1720 (s)
IV*e*	83	179–180°	$C_{19}H_{23}ClN_2O_4$	C 60.23 H 6.12	60.30 6.29	342	342	1725 (s)
IV*f*	81	207–209°	$C_{19}H_{22}ClN_3O_6$	C 53.84 H 5.23	53.50 5.52	387	387	1730 (s)

[a] Parent peak (P) represents the free base.

conformational free energy difference of the dimethylamino function is 2.4 kcal/mole (12). Therefore, if it is assumed that a methylene group between carbon 3 and the dimethylamino group lowers the conformational free energy difference [*e.g.*, $-\Delta G_x°$ values for $C(CH_3)_2$ and $CH_2C(CH_3)_3$ are 5.0 and 2.0 kcal/mole, respectively (12)], then at carbon 3 the phenyl ring will have the larger conformational free energy difference than the dimethylaminomethyl. Thus, the rotomer in which the C_6H_5–CH_3 interaction is minimal, *i.e.*, Rotomers 1 of III*a* and III*b*, predominate.

PMR spectroscopy (100 Hz) showed III*a* to have a coupling constant of 3.2 Hz between H_2 and H_3; hence a *gauche*-orientation is indicated between these hydrogens, and III*a* is considered to be the *threo*-isomer (13). Similarly, III*b*, with a coupling constant of 9.2 Hz, has a *trans*-coupling of hydrogens and is the *erythro*-isomer (13).

Examination of the mass spectra of the isomeric alcohols is consistent with the assignment of *threo*- and *erythro*-diastereoisomers to III*a* and III*b*, respectively, if the minor isomer (*erythro*) is more sterically crowded. The intensity of the molecular ion of the more crowded *erythro*-isomer would be predicted to be smaller than the less crowded *threo*-isomer (14), and the percent Σ_{25} values for the parent ions of III*a* and III*b* are 0.32 and 0.23%, respectively. The only significant fragment ion observed in the mass spectrum of either III*a* or III*b* is $CH_2{=}N^+(CH_3)_2$ (%Σ_{25} = 67.5%), *m/e* 58, formed by cleavage of the carbon–carbon bond next to the nitrogen (Scheme II).

Acylation of a mixture of III*a* and III*b* with either a substituted benzoyl chloride or phenoxyacetyl chloride afforded the corresponding ester series IV (Table I) and V in yields ranging from 20 to 83%. Examination of the PMR spectrum of V showed that the 1-methyl signals were downfield by approximately 1.7 ppm compared to IV*a*–IV*f*. For the phenoxyacetyl ester but not the benzoate esters, models revealed that it is possible for the phenoxyacetyl aromatic ring to assume a position perpendicular to the C-1 methyl group, which could account for the increased deshielding of the methyl protons. However, temperature-dependent studies did not alter the position of the 1-methyl signals, so alternative explanations for this phenomenon are required.

The evaluation of II–V against a wide range of microorganisms is shown in Table II. Mannich base II showed a promising level of activity against four fungi and two yeasts and had a spectrum of activity similar to the cyclic analog 2-dimethylaminomethyl-6-phenylcyclohexanone (7). The antimicrobial activity of II may be due to its structure *per se* or, alternatively, this β-aminoketone may deaminate, producing the corresponding α,β-unsaturated ketone (15, 16). Reduction of II led to abolition of antimicrobial activity in the screens chosen. Deamination of III*a*–III*b* to an α,β-unsaturated ketone would be unlikely, which may account for its inactivity, or the polar hydroxyl group may permit facile metabolism and detoxification to occur.

Masking of the polar hydroxyl groups produced the esters IV*a*–IV*f* and V. In series IV, there were different substituents in the acyl aromatic ring, but there appeared to be no correlation between the predicted hydrolysis rate and antimicrobial activity. Thus, while IV*b*, containing the electron-donating *p*-methoxy group, was four times as active as the unsubstituted ester, compounds containing the electron-withdrawing chlorine atoms were also more active than IV*a*. Furthermore, the nitro esters, IV*e* and IV*f*, for which the greatest hydrolysis would be predicted, were virtually devoid of antimicrobial activity. The nature of the substituents in the acyl aromatic ring in IV*a*–IV*f* seemed more important than the hydrolysis rate, and antimicrobial activity possibly was due to the esters *per se*. This possibility was strengthened by the observation that V was devoid of antifungal activity, suggesting that hydrolysis to phenoxyacetic acid did not occur.

The antimicrobial results obtained parallel the results obtained for related series of Mannich bases and the corresponding alcohols and esters (7, 8). In general, the Mannich bases showed good levels of activity against fungi, while the corresponding alcohols were often bereft of antimicrobial potency. The esters containing chlorine as the nuclear acyl substituents were more active than esters whose nuclear substituents were methoxy or methyl; in turn, these esters displayed higher bioactivity than the unsubstituted esters, while nitro esters were almost invariably inactive.

In addition, in comparing the screening results of series VI and VII (R = H, CH_3, Cl, or NO_2), it was seen that a dimethylene chain (n = 2) between the phenyl ring and the carbon bearing the acyloxy function gave higher potency than when n = 0 (8). In series IV, in which one methylene group separated the aromatic ring from carbon 2, the average antimicrobial activity (8) was intermediate between series VI and VII.

Both II and III*a* were evaluated in the L-1210 lymphoid leukemia screen in mice and shown to be toxic at 400 mg/kg in the Q4D and QD1-9 protocols, respectively (17). In the dose range of 12.5–200 mg/kg for II (QD1-9 protocol) and 100–200 mg/kg (QD1-9 protocol) for III*a*, in which cases murine toxicity was absent, the compounds were inactive. The alcohol III*a* was also screened against P-388 lymphocytic leukemia in mice in a dose range of 50–200 mg/kg (Q4D protocol) and shown to be nontoxic and inactive.

EXPERIMENTAL

Melting points are uncorrected. Organic extracts were washed with water and dried with anhydrous magnesium sulfate, and the solvent was removed using a water aspirator. Elemental analyses were performed[2]. Mass spectra[3] were determined at 70 ev. IR spectra[4] were determined

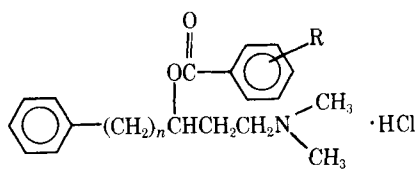

VI: n = 2
VII: n = 0

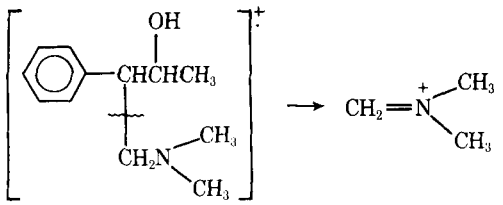

Scheme II

[2] R. M. Smith, College of Pharmacy, and R. E. Teed, Department of Chemistry and Chemical Engineering, University of Saskatchewan.

[3] AEI MS-12 mass spectrometer, Picker X-Ray Engineering Ltd., determined by D. R. Bain, Department of Chemistry and Chemical Engineering, University of Saskatchewan.

[4] Unicam SP 200 G spectrophotometer, Canlab Ltd., and IR 8 spectrophotometer, Beckman Instruments.

Table II—Screening of 4-Dimethylamino-3-phenyl-2-butanone Hydrochloride and Related Alcohols and Esters against Various Microorganisms[a]

Microorganisms[b]	II	III[c]	IV*a*[c]	IV*b*[d]	IV*c*[d]	IV*d*[e]	IV*e*[e]	IV*f*[d]	V[d]
Streptococcus faecalis	200	>200	>200	>200	>200	>200	>200	>200	>200
Staphylococcus aureus (*R*)[f]	200	>200	>200	>200	>200	>200	>200	>200	>200
Staphylococcus aureus (*S*)[g]	200	>200	>200	>200	>200	>200	>200	>200	>200
Klebsiella pneumoniae	200	>200	>200	>200	>200	>200	>200	>200	>200
Pseudomonas aeruginosa	>200	>200	>200	>200	>200	>200	>200	>200	>200
Escherichia coli	200	>200	>200	>200	>200	>200	>200	>200	>200
Salmonella typhimurium	200	>200	>200	>200	>200	>200	>200	>200	>200
Trichophyton mentagrophytes	<12	>200	200	200	50	50	>200	>200	>200
Mycobacterium smegmatis	50	>200	200	200	50	50	>200	200	>200
Candida albicans	200	>200	>200	>200	>200	200	>200	>200	>200
Bacillus subtilis	200	>200	>200	>200	200	200	>200	>200	>200
Fusarium oxysporum	<12	>200	>200	200	200	200	>200	>200	>200
Penicillium citrinium	<12	>200	>200	200	200	200	>200	>200	>200
Aspergillus niger	<12	>200	>200	200	200	200	>200	>200	>200
Cryptococcus neoformans	<12	>200	>200	200	200	200	>200	>200	>200
Blastomyces dermatitides	<12	>200	>200	200	200	200	>200	>200	>200
Xanthomonas vesicatoria	200	>200	>200	>200	200	200	>200	>200	>200
Streptococcus pyogenes	200	>200	>200	>200	>200	>200	>200	>200	>200
Sarcina lutea	200	>200	>200	>200	200	200	>200	>200	>200
Average antimicrobial activity[h]	584	0	11	37	84	89	0	6	0

[a] Figures in this table are the minimum inhibitory concentrations of the compounds in micrograms per milliliter. [b] The strains of microorganisms in this table are identified by the following numbers: ATCC 9790, SKF 24390, SKF 23390, SKF 4200, SKF 11320, SKF 12140, SKF 11350, SKF 17410, ATCC 101, SKF 3470, ATCC 6633, ATCC 9848, ATCC 16040, SKF 330, EK1, EK2, ATCC 11551, ATCC 8668, and ATCC 9341, respectively. [c] Screened as a mixture of equal amounts of *threo*- and *erythro*-isomers. [d] Pure *erythro*-isomer. [e] Configuration of screening sample not determined. [f] Strain resistant to penicillin G. [g] Strain sensitive to penicillin G. [h] Figures were evaluated from the following expression: (combined antimicrobial activity × 100)/number of microorganisms in screen. The combined antimicrobial activity was determined by giving the following scores at the highest potency of the compound against the microorganism: 200 μg = 1, 50 μg = 4, and <12 μg = 16.

as potassium bromide disks unless otherwise stated. NMR spectra[5] (60 Hz) were carried out in deuterochloroform using tetramethylsilane as the internal standard unless otherwise stated. The 100-Hz NMR spectra[6] also were determined.

4-Dimethylamino-3-phenyl-2-butanone Hydrochloride (II)—A mixture of phenylacetone (22.4 g, 0.167 mole), paraformaldehyde (8.0 g, 0.265 mole), dimethylamine hydrochloride (21.6 g, 0.265 mole), hydrochloric acid (1 ml), and ethanol (100 ml) was heated under reflux with stirring for 4 hr. On cooling, the solvent was removed to give a pale-yellow oil. This oil solidified on trituration with dry ether, yielding a pale-yellow powder (32 g). Recrystallization of the solid from 2-propanol gave II as colorless cubes (23.3 g, 61%), mp 145–146° [lit. (18) mp 145–146°]; NMR (D_2O): δ 2.15 (s, 3H, CH_3), 2.95 [s, 6H, $N(CH_3)_2$], 3.70 (m, 2H, CH_2), 4.55 (t, 1H, CH), and 7.50 (m, 5H, C_6H_5) ppm.

Anal.—Calc. for $C_{12}H_{18}ClNO$: C, 63.29; H, 7.97. Found: C, 63.00; H, 8.12.

Reduction of 4-Dimethylamino-3-phenyl-2-butanone with Lithium Aluminum Hydride—4-Dimethylamino-3-phenyl-2-butanone (94.4 g, 0.493 mole) in dry ether (200 ml) was added dropwise to a stirring suspension of lithium aluminum hydride (9.40 g, 0.247 mole) in dry ether (300 ml). The reaction mixture was heated under reflux for 4 hr, cooled, and decomposed by the dropwise addition of water (25 ml). The inorganic material was removed by filtration, and a pale-yellow syrup consisting of a mixture of *erythro*- and *threo*-4-dimethylamino-1-phenyl-2-butanols (76.7 g, 81%) was obtained from the organic extract; IR (smear); 3400 s (OH) and 1705 s (C=O) cm^{-1} (absent).

The NMR (CD_2Cl_2) spectrum showed that the ratio of *erythro*- and *threo*-isomers was 40:60 by integration of the methyl doublets. A small quantity of the reaction mixture (5.0 g) was dissolved in dry acetone (25 ml) and acidified with ethanolic hydrochloric acid (20% v/v). The colorless crystals (4.1 g) that deposited were fractionally crystallized from dry acetone to give III*a* (1.8 g) as colorless needles, mp 142–143°; NMR (CD_2Cl_2): δ 7.3 (m, 5H, C_6H_5), 4.35 (m, 1H, C-2 H), 3.9 (m, 1H, C-4 H), 3.2 (m, 2H, C-4 H, C-3 H), 2.36 [s, 6H, $N(CH_3)_2$], and 0.90 (d, 3H, C-1 H_3) ppm.

Anal.—Calc. for $C_{12}H_{20}ClNO$: C, 62.73; H, 8.77; N, 6.10. Found: C, 62.75; H, 8.80; N, 6.12.

From the acetone mother liquor, the second isomer was obtained. It was recrystallized from dry acetone to give III*b* (1.6 g) as colorless shiny plates, mp 93°; NMR (CD_2Cl_2): δ 7.3 (m, 5H, C_6H_5), 4.0 (m, 1H, C-2 H), 3.8 (m, 1H, C-4 H), 3.2 (m, 1H, C-4 H), 3.1 (m, 1H, C-3 H), 2.32 [s, 6H, $N(CH_3)_2$], and 1.05 (d, 3H, C-1 H_3) ppm.

Anal.—Calc. for $C_{12}H_{20}ClNO$: C, 62.73; H, 8.77. Found: C, 62.60; H, 8.98.

Esters of 4-Dimethylamino-3-phenyl-2-butanol (IV*a*–IV*f*)—These compounds were prepared by the following general method. A solution of the acid chloride (0.025 mole) in dry ether (35 ml) was added dropwise to a stirring solution of 4-dimethylamino-3-phenyl-2-butanol (crude reaction mixture, 0.025 mole) in dry ether (35 ml). The temperature of the reaction mixture was maintained at 0–5° during addition, and then the solution was stirred at room temperature for at least 8 hr. The precipitate was removed by filtration and recrystallized from ether–ethanol to give colorless crystals, except in the case of the nitro esters which were pale yellow in color.

The physical data of the esters are summarized in Table I. NMR spectra of available esters indicated that IV*b*, IV*c*, and IV*f* consisted of only the *erythro*-isomer ($JH_{2,3}$ = 8.0, 8.1, and 6.9 Hz, respectively) while IV*a* consisted of a 50:50 mixture of the *erythro* ($JH_{2,3}$ = 8.0 Hz) and *threo* ($JH_{2,3}$ = 2.4 Hz) isomers.

4-Dimethylamino-3-phenyl-2-butanol Phenoxyacetate Hydrochloride (V)—The general esterification described earlier was employed, except that dry benzene was used as the solvent. The desired ester hydrochloride (5%) was obtained as colorless prisms, mp 170–172°; mass spectrum: 327 (M^+ − HCl).

Anal.—Calc. for $C_{20}H_{26}ClNO_3$: C, 66.01; H, 7.20. Found: C, 65.50; H, 7.47.

Screening of Compounds—The antimicrobial evaluations were undertaken according to the published procedure[7] (7, 8). The antineoplastic screens were accomplished using the reported protocols (17).

REFERENCES

(1) E. D. Taylor and W. L. Nobles, *J. Am. Pharm. Assoc., Sci. Ed.*, **49**, 317 (1960).

(2) W. L. Nobles and T. Blackburn, *J. Pharm. Sci.*, **53**, 1554 (1964).

(3) C. D. Blanton and W. L. Nobles, *ibid.*, **51**, 878 (1962).

(4) R. S. Varma and W. L. Nobles, *J. Med. Chem.*, **11**, 195 (1968).

(5) J. J. Denton, V. A. Lawson, W. B. Neier, and R. J. Turner, *J. Am. Chem. Soc.*, **71**, 2052 (1949).

(6) J. R. Dimmock and W. A. Turner, *Can. J. Pharm. Sci.*, **9**, 33 (1974).

(7) J. R. Dimmock, W. A. Turner, and H. A. Baker, *J. Pharm. Sci.*, **64**, 995 (1975).

(8) J. R. Dimmock, A. M. Qureshi, L. M. Noble, P. J. Smith, and H. A. Baker, *ibid.*, **65**, 38 (1976).

(9) C. A. Kingsbury and W. B. Thornton, *J. Org. Chem.*, **31**, 1000 (1966).

(10) G. G. Lyle and M. L. Durand, *ibid.*, **32**, 3295 (1967).

[5] WP 60 spectrophotometer, Brucker Spectrospin (Canada) Ltd., and T60 spectrophotometer, Varian Associates of Canada Ltd.

[6] HA 100-12 spectrophotometer, Varian Associates of Canada Ltd. Determined in the Chemistry Department, University of Alberta.

[7] Carried out by Dr. J. F. Pagano and staff at Smith Kline and French Laboratories, Philadelphia, PA 16101.

(11) J. A. Husch, "Topics in Stereochemistry," vol. 1, N. L. Allinger and E. L. Eliel, Eds., Interscience, New York, N.Y., 1967, p. 199.
(12) E. L. Eliel, N. L. Allinger, S. J. Angyal, and G. A. Morrison, "Conformational Analysis," Interscience, New York, N.Y., 1965, p. 44.
(13) A. F. Casy, "PMR Spectroscopy in Medicinal and Biological Chemistry," Academic, New York, N.Y., 1971, p. 104.
(14) K. Biemann, "Mass Spectrometry, Organic Chemical Applications," McGraw-Hill, New York, N.Y., 1962, p. 145.
(15) P. N. Gordon, J. D. Johnston, and A. R. English, *Antimicrob. Agents Chemother.*, **1965**, 165.
(16) H. Schoenenberger, T. Bastug, L. Bindl, A. Adam, D. Adam, A. Petter, and W. Zwez, *Pharm. Acta Helv.*, **44**, 691 (1969).
(17) R. I. Geran, N. H. Greenberg, M. M. MacDonald, A. M. Schumacher, and B. J. Abbott, *Cancer Chemother. Rep. (Part 3)*, **3**(2) (Sept. 1972).
(18) W. Wilson and Z.-Y. Kyi, *J. Chem. Soc.*, **1952**, 1321.

ACKNOWLEDGMENTS

The authors thank the Medical Research Council of Canada for providing a Studentship to W. A. Turner and the Government of Saskatchewan for providing funds under the Students Temporary Employment Programme (1971) for D. K. Kowal. Dr. Harry B. Wood, Jr., Drug Research and Development Division, National Cancer Institute, Bethesda, Md., kindly arranged for two compounds to be screened against the L-1210 and P-388 tumor systems.

Simple High-Pressure Liquid Chromatographic Determination of Trisulfapyrimidines in Human Serum

THOMAS J. GOEHL *x, LALIT K. MATHUR ‡, JEFFREY D. STRUM ‡, JAMES M. JAFFE ‡, WILLIAM H. PITLICK ‡, VINOD P. SHAH §, ROLLAND I. POUST ‡, and JOHN L. COLAIZZI ‡

Received April 19, 1977, from the **Departments of Medicinal Chemistry and* ‡*Pharmaceutics, School of Pharmacy, University of Pittsburgh, Pittsburgh, PA 15261,* and the §*Division of Biopharmaceutics, Food and Drug Administration, Washington, DC 20204.* Accepted for publication June 30, 1977.

Abstract □ A simple and rapid high-pressure liquid chromatographic method was developed for the determination of sulfadiazine, sulfamerazine, and sulfamethazine in human serum. After the trichloroacetic acid precipitation of the serum proteins, an aliquot of the supernate is injected into a high-pressure liquid chromatograph equipped with a reversed-phase microparticulate column and a fixed wavelength UV detector. For each of the three components of trisulfapyrimidines, a linear calibration curve was observed in the 1–30-μg/ml range, with the precision of the assay estimated to be ±2% (*RSD*). Preliminary pharmacokinetic data are also presented.

Keyphrases □ Sulfadiazine—high-pressure liquid chromatographic analysis in human serum □ Sulfamethazine—high-pressure liquid chromatographic analysis in human serum □ Sulfamerazine—high-pressure liquid chromatographic analysis in human serum □ High-pressure liquid chromatography—analyses, sulfadiazine, sulfamethazine, and sulfamerazine in human serum □ Antibacterials—sulfadiazine, sulfamethazine, and sulfamerazine, high-pressure liquid chromatographic analyses in human serum □ Trisulfapyrimidines—high-pressure liquid chromatographic analyses in human serum

The antibacterial properties of the sulfonamides were first recognized with the discovery of sulfamidochrysoidine (1), and these drugs are still frequently used in the treatment of urinary tract infections. Unfortunately, kidney damage has been associated with sulfonamide therapy, resulting from the crystallization in the renal tubules of the N^4-acetylated metabolites of many sulfonamides. To overcome this problem, combinations of sulfa drugs are commonly utilized. One such combination is the trisulfapyrimidines: sulfadiazine, sulfamerazine, and sulfamethazine.

A colorimetric method based on a diazotization reaction, as proposed by Bratton and Marshall (2), is commonly employed for quantitating sulfonamides. However, when applied to biological fluids, interferences from metabolites possessing a free amino group was observed. To overcome this lack of specificity, Rieder (3) introduced an extraction step.

Many other spectrophotometric and TLC methods subsequently were proposed for the determination of sulfonamides in biological fluids (4–12). GLC of the sulfa drugs also was attempted (13–15). However, derivatization must be performed to eliminate adsorption of these compounds to the chromatographic support. The separation and quantitation of sulfa drugs, alone (16–18) and in pharmaceutical preparations (19, 20), by high-pressure liquid chromatography (HPLC) were described. Recently, methods were proposed for sulfamethazine residues in bovine tissue (21) and for sulfamethazine, sulfamerazine, sulfathiazole, and their metabolites in cattle urine (22).

A study relating dissolution and bioavailability profiles of triple sulfa suspensions required a specific and sensitive method for the individual trisulfapyrimidine components. This report describes a simple, rapid, specific, and sensitive HPLC method devised for this purpose.

EXPERIMENTAL

Apparatus—A modular high-pressure liquid chromatograph consisted of a constant-flow pump[1], a valve-type injector[2], a fixed wavelength (254 nm) UV detector[3], and a strip-chart recorder[4]. A stainless steel column (3.9 mm × 30 cm) packed with fully porous 10-μm silica particles, to which is chemically bonded a monomolecular layer of octadecylsilane[5], was obtained commercially.

Chromatographic Conditions—The mobile phase consisted of acetonitrile–1% acetic acid (13:87). A flow rate of 1.5 ml/min was established (1100 psi). The column was maintained at 29.6° by inserting it into a glass sleeve which was then immersed in a constant-temperature water bath[6].

[1] Chromatography pump model M-6000A, Serial No. SDS-5235, Waters Associates, Milford, Mass.
[2] Universal injector model U6K, Serial No. U6K-6065, large capacity, Waters Associates, Milford, Mass.
[3] Model 440 absorbance detector, Serial No. 440-01249, Waters Associates, Milford, Mass.
[4] A-25 dual channel, Varian Associates, Walnut Creek, Calif.
[5] Waters Associates prepacked μBondapak C_{18} column.
[6] B. Braun Thermomix II (No. 26394), Bronwill Scientific Co., Rochester, N.Y.

(11) J. A. Husch, "Topics in Stereochemistry," vol. 1, N. L. Allinger and E. L. Eliel, Eds., Interscience, New York, N.Y., 1967, p. 199.
(12) E. L. Eliel, N. L. Allinger, S. J. Angyal, and G. A. Morrison, "Conformational Analysis," Interscience, New York, N.Y., 1965, p. 44.
(13) A. F. Casy, "PMR Spectroscopy in Medicinal and Biological Chemistry," Academic, New York, N.Y., 1971, p. 104.
(14) K. Biemann, "Mass Spectrometry, Organic Chemical Applications," McGraw-Hill, New York, N.Y., 1962, p. 145.
(15) P. N. Gordon, J. D. Johnston, and A. R. English, *Antimicrob. Agents Chemother.*, **1965**, 165.
(16) H. Schoenenberger, T. Bastug, L. Bindl, A. Adam, D. Adam, A. Petter, and W. Zwez, *Pharm. Acta Helv.*, **44**, 691 (1969).
(17) R. I. Geran, N. H. Greenberg, M. M. MacDonald, A. M. Schumacher, and B. J. Abbott, *Cancer Chemother. Rep. (Part 3)*, **3**(2) (Sept. 1972).
(18) W. Wilson and Z.-Y. Kyi, *J. Chem. Soc.*, **1952**, 1321.

ACKNOWLEDGMENTS

The authors thank the Medical Research Council of Canada for providing a Studentship to W. A. Turner and the Government of Saskatchewan for providing funds under the Students Temporary Employment Programme (1971) for D. K. Kowal. Dr. Harry B. Wood, Jr., Drug Research and Development Division, National Cancer Institute, Bethesda, Md., kindly arranged for two compounds to be screened against the L-1210 and P-388 tumor systems.

Simple High-Pressure Liquid Chromatographic Determination of Trisulfapyrimidines in Human Serum

THOMAS J. GOEHL *x, LALIT K. MATHUR ‡, JEFFREY D. STRUM ‡, JAMES M. JAFFE ‡, WILLIAM H. PITLICK ‡, VINOD P. SHAH §, ROLLAND I. POUST ‡, and JOHN L. COLAIZZI ‡

Received April 19, 1977, from the **Departments of Medicinal Chemistry and* ‡*Pharmaceutics, School of Pharmacy, University of Pittsburgh, Pittsburgh, PA 15261,* and the §*Division of Biopharmaceutics, Food and Drug Administration, Washington, DC 20204.* Accepted for publication June 30, 1977.

Abstract □ A simple and rapid high-pressure liquid chromatographic method was developed for the determination of sulfadiazine, sulfamerazine, and sulfamethazine in human serum. After the trichloroacetic acid precipitation of the serum proteins, an aliquot of the supernate is injected into a high-pressure liquid chromatograph equipped with a reversed-phase microparticulate column and a fixed wavelength UV detector. For each of the three components of trisulfapyrimidines, a linear calibration curve was observed in the 1–30-μg/ml range, with the precision of the assay estimated to be ±2% (*RSD*). Preliminary pharmacokinetic data are also presented.

Keyphrases □ Sulfadiazine—high-pressure liquid chromatographic analysis in human serum □ Sulfamethazine—high-pressure liquid chromatographic analysis in human serum □ Sulfamerazine—high-pressure liquid chromatographic analysis in human serum □ High-pressure liquid chromatography—analyses, sulfadiazine, sulfamethazine, and sulfamerazine in human serum □ Antibacterials—sulfadiazine, sulfamethazine, and sulfamerazine, high-pressure liquid chromatographic analyses in human serum □ Trisulfapyrimidines—high-pressure liquid chromatographic analyses in human serum

The antibacterial properties of the sulfonamides were first recognized with the discovery of sulfamidochrysoidine (1), and these drugs are still frequently used in the treatment of urinary tract infections. Unfortunately, kidney damage has been associated with sulfonamide therapy, resulting from the crystallization in the renal tubules of the N^4-acetylated metabolites of many sulfonamides. To overcome this problem, combinations of sulfa drugs are commonly utilized. One such combination is the trisulfapyrimidines: sulfadiazine, sulfamerazine, and sulfamethazine.

A colorimetric method based on a diazotization reaction, as proposed by Bratton and Marshall (2), is commonly employed for quantitating sulfonamides. However, when applied to biological fluids, interferences from metabolites possessing a free amino group was observed. To overcome this lack of specificity, Rieder (3) introduced an extraction step.

Many other spectrophotometric and TLC methods subsequently were proposed for the determination of sulfonamides in biological fluids (4–12). GLC of the sulfa drugs also was attempted (13–15). However, derivatization must be performed to eliminate adsorption of these compounds to the chromatographic support. The separation and quantitation of sulfa drugs, alone (16–18) and in pharmaceutical preparations (19, 20), by high-pressure liquid chromatography (HPLC) were described. Recently, methods were proposed for sulfamethazine residues in bovine tissue (21) and for sulfamethazine, sulfamerazine, sulfathiazole, and their metabolites in cattle urine (22).

A study relating dissolution and bioavailability profiles of triple sulfa suspensions required a specific and sensitive method for the individual trisulfapyrimidine components. This report describes a simple, rapid, specific, and sensitive HPLC method devised for this purpose.

EXPERIMENTAL

Apparatus—A modular high-pressure liquid chromatograph consisted of a constant-flow pump[1], a valve-type injector[2], a fixed wavelength (254 nm) UV detector[3], and a strip-chart recorder[4]. A stainless steel column (3.9 mm × 30 cm) packed with fully porous 10-μm silica particles, to which is chemically bonded a monomolecular layer of octadecylsilane[5], was obtained commercially.

Chromatographic Conditions—The mobile phase consisted of acetonitrile–1% acetic acid (13:87). A flow rate of 1.5 ml/min was established (1100 psi). The column was maintained at 29.6° by inserting it into a glass sleeve which was then immersed in a constant-temperature water bath[6].

[1] Chromatography pump model M-6000A, Serial No. SDS-5235, Waters Associates, Milford, Mass.
[2] Universal injector model U6K, Serial No. U6K-6065, large capacity, Waters Associates, Milford, Mass.
[3] Model 440 absorbance detector, Serial No. 440-01249, Waters Associates, Milford, Mass.
[4] A-25 dual channel, Varian Associates, Walnut Creek, Calif.
[5] Waters Associates prepacked μBondapak C_{18} column.
[6] B. Braun Thermomix II (No. 26394), Bronwill Scientific Co., Rochester, N.Y.

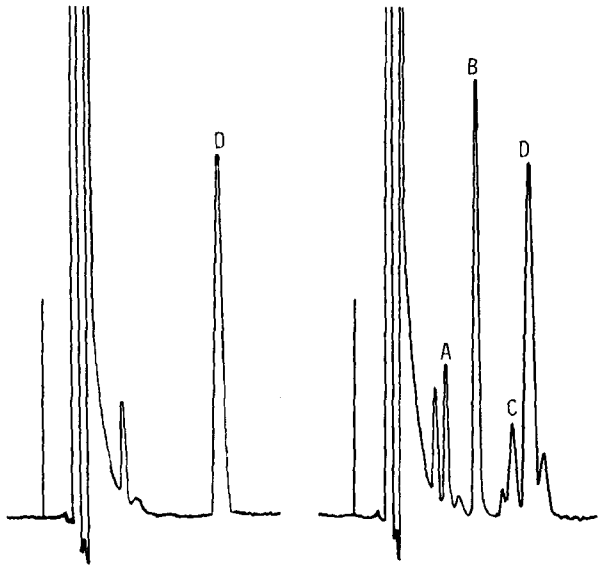

Figure 1—*Chromatogram obtained from HPLC assay of control human serum spiked with internal standard (left) and serum from a volunteer who had received a single dose of a trisulfapyrimidines suspension (right). Key: A, sulfadiazine (4.3 μg/ml); B, sulfamerazine (18.6 μg/ml); C, sulfamethazine (5.2 μg/ml); and D, sulfamethizole (25 μg/ml).*

Reagents and Materials—Samples of sulfadiazine[7], sulfamerazine[8], sulfamethazine[9], and sulfamethizole[10] were used as received. All other materials were reagent grade. A stock solution of trisulfapyrimidines was prepared by dissolving 100 mg each of sulfadiazine, sulfamerazine, and sulfamethazine in 0.1 *N* NaOH and adjusting the volume to 50 ml in a volumetric flask. The internal standard stock solution was prepared by dissolving 50 mg of sulfamethizole in 1 *N* NaOH and adjusting to volume in a 100-ml volumetric flask. Plasma standards were prepared by taking appropriate small volumes of the stock solutions and adding these to control plasma[11].

HPLC Assay—To 0.2 ml of serum or citrated plasma in a 1-ml capacity vial[12] was added 10 μl of the internal standard solution, followed by 0.1 ml of a 14% solution of trichloroacetic acid. The samples were mixed[13] and then centrifuged[14] at 2500 rpm for 15 min. A 5-μl aliquot of the clear supernate was then injected onto the column.

Calculations—Peak height ratios were calculated by dividing the peak height corresponding to the sulfa drug by the peak height corresponding to the internal standard. Calibration curves were constructed daily from results obtained from spiked control plasma samples containing equal amounts of each trisulfapyrimidine in the 1–30-μg/ml range by plotting peak height ratios *versus* concentration of the individual sulfa drug.

Colorimetric Assay—A modification of the Bratton–Marshall method (2) was used. To 0.5 ml of serum was added 0.5 ml of a 14% trichloroacetic acid solution. The samples were vortexed and centrifuged, and 300 μl of the supernate was transferred to a 12-ml centrifuge tube containing 3.0 ml of 0.1 *N* HCl. To each tube were added 0.5 ml of 0.1% sodium nitrate, 0.5 ml of 0.5% ammonium sulfamate, and 0.5 ml of 0.1% *N*-(1-naphthyl)ethylenediamine dihydrochloride. The absorbance was then determined at 544 nm. Calibration curves were constructed for each batch of samples from spiked control plasma containing equal amounts of each trisulfapyrimidine in the 1–30-μg/ml range.

Human Study Protocol—To establish the usefulness of the HPLC method for bioavailability studies, a 10-ml dose of a trisulfapyrimidines oral suspension (providing 0.33 g of each trisulfapyrimidine) was administered to a normal human volunteer; 15 blood samples of approximately 5 ml each were collected. Each sample was assayed in duplicate by both HPLC and the conventional Bratton–Marshall method.

[7] Lot R02114, Eli Lilly and Co., Indianapolis, Ind.
[8] Lot M07059, Eli Lilly and Co., Indianapolis, Ind.
[9] Lot R02011, Eli Lilly and Co., Indianapolis, Ind.
[10] Lot R159178, Ayerst Laboratories, New York, N.Y.
[11] Citrated plasma obtained from the Central Blood Bank, Pittsburgh, Pa.
[12] Reacti-Vials No. 13261, Pierce, Inc., Rockford, Ill.
[13] Vortex-Genie, Catalog No. 12-812-VI, Fisher Scientific Industries, Springfield, Mass.
[14] IEC EXD centrifuge 460G, Damon/IEC Division, Needham Heights, Mass.

Table I—Precision and Accuracy of the HPLC Method for the Estimation of the Trisulfapyrimidines in Serum

Concentration, Theoretical, μg/ml	Concentration, Experimental, Mean[a] (Range)	*CV*	Relative Error, %
	Sulfadiazine		
1	1.0 (0.9–1.0)	3.0	4.0
2	2.0 (1.9–2.1)	3.9	3.0
5	5.1 (5.0–5.1)	1.5	1.7
10	9.7 (9.4–10.0)	2.6	2.7
15	15.3 (15.1–15.4)	0.8	2.0
20	20.2 (19.9–20.3)	0.9	1.1
25	24.7 (24.5–25.0)	1.0	1.4
30	30.1 (29.4–30.9)	2.1	1.6
	Sulfamerazine		
1	1.0 (0.9–1.1)	5.3	4.3
2	2.0 (1.9–2.1)	3.6	2.8
5	5.0 (5.0–5.1)	1.1	1.0
10	9.7 (9.4–9.9)	2.0	3.5
15	15.3 (15.3–15.4)	0.4	2.1
20	20.3 (20.3–20.4)	0.2	1.7
25	24.6 (24.4–25.0)	1.0	1.5
30	30.0 (29.4–30.8)	2.1	1.5
	Sulfamethazine		
1	1.0 (0.9–1.0)	5.6	4.3
2	2.0 (2.0–2.2)	2.8	3.3
5	5.0 (5.0–5.1)	0.5	0.6
10	9.6 (9.3–9.9)	2.4	3.8
15	15.2 (15.1–15.3)	0.6	1.4
20	20.3 (20.2–20.4)	0.3	1.5
25	24.8 (24.6–25.0)	0.7	1.0
30	30.0 (29.5–30.9)	2.0	1.4

[a] $n = 4$.

RESULTS AND DISCUSSION

A method that was capable of distinguishing among the trisulfapyrimidines and their metabolites in serum at suitably low concentrations was desired. Because of the large number of blood samples expected in a planned bioavailability–dissolution study, the total time required for each analysis also posed a critical limitation. HPLC seemed to offer the best approach for solving these problems because of its great versatility. To separate the various sulfa drugs, several column packings have been tried (16–22). In this present study, a reversed-phase microparticulate column was chosen. This type of column offered the possibility of minimum sample preparation prior to actual injection into the chromatograph.

Initial work with pure solutions of the trisulfapyrimidines showed good separation on the reversed-phase column using an acetonitrile–dilute acetic acid mobile phase. This result suggested the possibility of precipitating the serum proteins with acetonitrile and the subsequent direct injection of the supernate onto the column. At first, this approach appeared satisfactory since no interfering peaks were noted in the chromatogram. Within a short time, however, column back-pressure increased; on inspection of the column inlet frit, it seemed obvious that precipitation was not complete. Trichloroacetic acid precipitation was tried next and proved satisfactory.

The chromatogram obtained from the analysis of serum from a volunteer who had ingested a single dose of a triple sulfa suspension showed the peaks for the trisulfapyrimidines plus other peaks that were probably metabolites. These additional peaks were not resolved from the parent drug peaks. Adjustment of both the polarity of the mobile phase and the column temperature was again required to resolve the drug peaks.

Heparin, when used as an anticoagulant, interfered, whereas citrate did not. A peak for caffeine also interfered, requiring further refinement of the polarity of the mobile phase and the column temperature.

For the determination of the stability of sulfadiazine, sulfamerazine, and sulfamethazine in plasma, citrated plasma was spiked with a solution of the trisulfapyrimidines to produce concentrations of 5, 10, and 20 μg of each sulfa drug/ml. These samples were divided into 15 smaller portions, and then the vials were sealed and frozen. The samples were assayed immediately and then at weekly intervals. No appreciable decomposition was noted over at least 3 weeks. Repeated analysis of selected clinical samples at weekly intervals showed similar results.

Chromatograms obtained on the analysis of control human serum and human serum from a volunteer who had received a single dose of a triple sulfa suspension are shown in Fig. 1. The chromatogram of control serum showed no interfering peaks. In the other chromatogram, peaks corre-

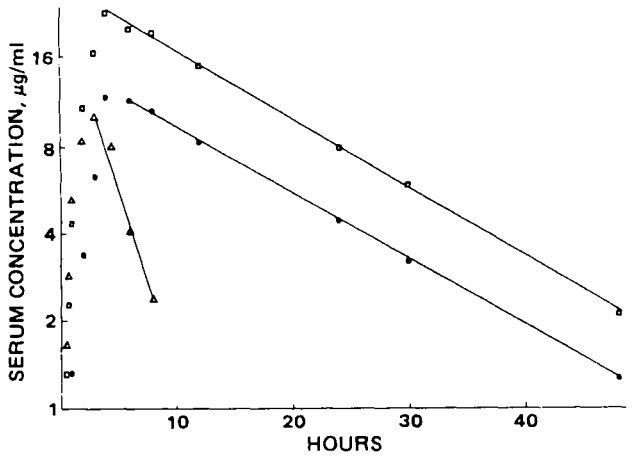

Figure 2—*Plot of serum concentrations of sulfadiazine* (●), *sulfamerazine* (□), *and sulfamethazine* (△) versus *time obtained after a dose of a trisulfapyrimidines suspension.*

sponding to sulfadiazine (retention time of 4.85 min), sulfamerazine (retention time of 6.43 min), sulfamethazine (retention time of 8.37 min), and the internal standard (retention time of 9.23 min) were observed. In addition, two peaks corresponding to metabolites (under investigation) were seen.

Verification that these peaks corresponded to the three unchanged drugs was obtained by comparing their retention times and peak width at half-height with standards and by using the standard addition technique. These methods confirmed that all three drugs were present in the clinical serum samples examined and that no hidden peaks were interfering in the assay.

On administration of sulfadiazine alone, at a dose three times higher than that given in the triple sulfa suspension study, a metabolite was found that had a retention time similar to sulfamerazine. The peak, however, was small even at this higher dose. Thus, this size would account for the inability to detect the peak in the blood samples obtained in the triple sulfa study.

The standard curves for the assay of all three trisulfapyrimidines were linear in the 1–30-μg/ml range, and the precision and accuracy of the method were studied. To control human plasma were added known amounts of the three compounds, and then these samples were assayed as described. The mean percent relative standard deviation (*CV*) and the mean relative error for each compound are reported in Table I. Virtually complete recovery was found with this method.

The utility of this new HPLC method was shown by assaying serum samples obtained from a human volunteer who had ingested a 10-ml dose of a trisulfapyrimidines suspension. In addition, these same samples were assayed by the conventional Bratton–Marshall method.

Since it was possible to separate unchanged drug from metabolites using HPLC, the concentrations of the individual components in these serum samples were determined. Serum concentrations for sulfadiazine, sulfamerazine, and sulfamethazine *versus* time are shown in Fig. 2. Elimination half-lives were 13.0, 12.7, and 2.3 hr, respectively. However, the spectrophotometric analysis of trisulfapyrimidines by the Bratton–Marshall method measures total sulfa concentrations and other primary

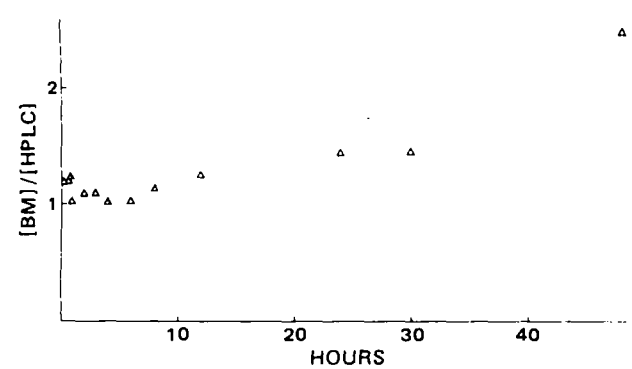

Figure 3—*Plot of ratio of total drug concentrations obtained by the Bratton–Marshall method to that determined by the HPLC method* versus *time (see text).*

Table II—Mean Total Sulfa Serum Concentrations Determined by HPLC and Bratton–Marshall Methods in a Single Subject after Administration of a Single Dose of a Trisulfapyrimidines Suspension

Time	Total Sulfa Drug Concentration, μg/ml: HPLC Method	Total Sulfa Drug Concentration, μg/ml: Bratton–Marshall Method
10 min	<1	1.0
20 min	1.2	1.5
30 min	3.4	4.1
45 min	5.9	7.3
60 min	10.6	10.8
2 hr	22.7	24.6
3 hr	33.3	36.1
4 hr	43.0	43.8
6 hr	35.8	36.8
8 hr	32.6	36.9
12 hr	24.1	30.2
24 hr	12.4	17.8
30 hr	9.1	13.2
48 hr	3.4	8.3

amines. Mean total sulfa concentrations obtained from duplicate analysis of the volunteer's serum samples by both the Bratton–Marshall and HPLC methods are shown in Table II. For the HPLC method, total sulfa concentrations were obtained by summing the mean values for each component at each time period. The two methods showed differences in concentrations probably because of interference by metabolites in the Bratton–Marshall method. These differences became more marked at later sampling times, as indicated by a plot of the ratio of drug concentrations obtained by the Bratton–Marshall method to concentrations determined by HPLC (Fig. 3).

In conclusion, a simple, specific, and sensitive HPLC method has been described; it can be used for bioavailability determination of the trisulfapyrimidines.

REFERENCES

(1) G. Donagk, *Dtsch. Med. Wochenschr.*, **61**, 250 (1935).

(2) A. C. Bratton and E. K. Marshall, *J. Biol. Chem.*, **128**, 537 (1939).

(3) J. Rieder, *Chemotherapy*, **17**, 1 (1972).

(4) F. M. Kunze, *J. Assoc. Offic. Anal. Chem.*, **47**, 474 (1964).

(5) M. P. Gruber and R. W. Klein, *J. Pharm. Sci.*, **57**, 1212 (1968).

(6) J. T. Stewart, A. B. Ray, and W. B. Fackler, *ibid.*, **58**, 1261 (1969).

(7) E. Schleider, D. M. Eno, J. A. Feldman, and A. M. Galinsky, *ibid.*, **58**, 1258 (1969).

(8) H. M. Miller, *J. Assoc. Offic. Anal. Chem.*, **53**, 1100 (1970).

(9) D. Banes and O. H. Riggleman, *ibid.*, **54**, 1195 (1971).

(10) U. G. Cieri, *ibid.*, **56**, 1475 (1973).

(11) C. W. Sigel, J. T. Woolley, Jr., and C. A. Nichol, *J. Pharm. Sci.*, **64**, 973 (1975).

(12) P. E. Flinn, *J. Chromatogr. Sci.*, **13**, 580 (1975).

(13) R. J. Daun, *J. Assoc. Offic. Anal. Chem.*, **54**, 1277 (1971).

(14) O. Gyllehnaal and H. Ehrsson, *J. Chromatogr.*, **107**, 327 (1975).

(15) N. Nose, K. Susumu, H. Akiko, and A. Watanabe, *ibid.*, **123**, 167 (1976).

(16) T. C. Kram, *J. Pharm. Sci.*, **61**, 254 (1972).

(17) S. C. Su, A. V. Hartkopf, and B. L. Karger, *J. Chromatogr.*, **119**, 523 (1976).

(18) P. H. Cobb and G. T. Hill, *ibid.*, **123**, 444 (1976).

(19) R. B. Poet and H. H. Pu, *J. Pharm. Sci.*, **62**, 809 (1973).

(20) M. H. Penner, *ibid.*, **64**, 1017 (1975).

(21) C. L. Johnson, D. T. Jeter, and R. C. Clairborne, *ibid.*, **64**, 1657 (1975).

(22) J. P. Sharma, E. G. Perkins, and R. F. Bevill, *ibid.*, **65**, 1606 (1976).

ACKNOWLEDGMENTS

Supported by Food and Drug Administration Contract 223-76-3010.

The authors thank Mr. Chan-Loi Yong and Mrs. Kathy Weyant for technical assistance, and Mr. Jack Korpi, Waters Associates, Inc., Millford, Mass., for helpful suggestions.

Synthesis and Biological Activities of 10-Substituted Benzo[*b*][1,5]naphthyridines

BIRANDRA K. SINHA *x and **RONALD I. SATO** ‡

Received March 22, 1977, from the *Organic Chemistry Division, Microbiological Associates, Bethesda, MD 20016.* Accepted for publication May 11, 1977. *Present address: Laboratory of Environmental Biophysics, National Institute of Environmental Health Sciences, Research Triangle Park, NC 27709. ‡Present address: Frederick Cancer Research Center, Frederick, MD 21701.

Abstract □ Eight 10-substituted benzo[*b*][1,5]naphthyridine derivatives containing *N*-(pyrrolidino)alkylamines, methanesulfonanilides, and aminoacetanilides were prepared, and their binding with DNA was studied by (*a*) T_m measurements and (*b*) the effect on DNA-dependent RNA polymerase *in vitro*. In addition, they were evaluated as antineoplastic agents in the P-388 test. None of the compounds exhibited anticancer activity.

Keyphrases □ Benzo[*b*][1,5]naphthyridines, substituted—synthesized, binding with DNA studied, antitumor activity evaluated □ Binding—DNA to various substituted benzo[*b*][1,5]naphthyridines □ DNA—binding to various substituted benzo[*b*][1,5]naphthyridines □ Antitumor activity—various benzo[*b*][1,5]naphthyridines evaluated □ Structure–activity relationships—various substituted benzo[*b*][1,5]naphthyridines, binding with DNA studied, antitumor activity evaluated

The biological properties of acridine derivatives are well documented (1–5). These effects are believed to result from the intercalation of the acridine derivatives into DNA, inhibiting the ability of DNA to act as a template in DNA replication and RNA synthesis (6). Azacrin (I), structurally related to acridines and regarded as a combination of an 8-aminoquinoline and a 4-aminoquinoline, was synthesized (7) as an antimalarial. It was shown that I is an effective schizontocide in *Plasmodium falciparum* infection (8).

Although a large number of benzo[*b*][1,5]naphthyridine derivatives have been prepared (9, 10) and screened as antimalarial, antibacterial, and antineoplastic agents, the mechanism of action of these drugs remains poorly defined. Therefore, some 10-substituted benzo[*b*][1,5]naphthyridines (VI–XIII) were prepared and their ability to bind to DNA was studied by the evaluation of T_m (the temperature at which 50% hyperchromicity is attained owing to heat denaturation of native DNA) and their effect on *Escherichia coli* DNA-dependent RNA polymerase. In addition, these compounds were screened as potential antineoplastic agents.

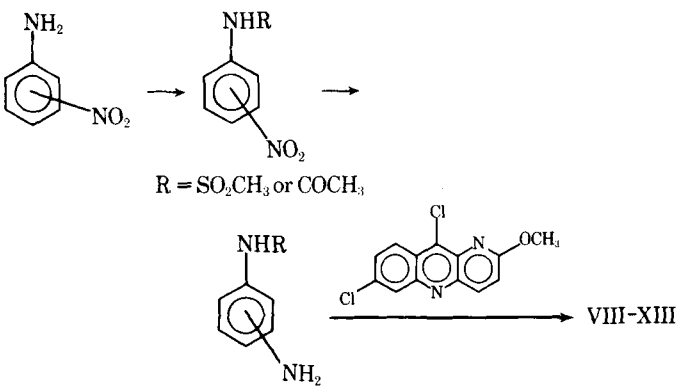

Scheme I

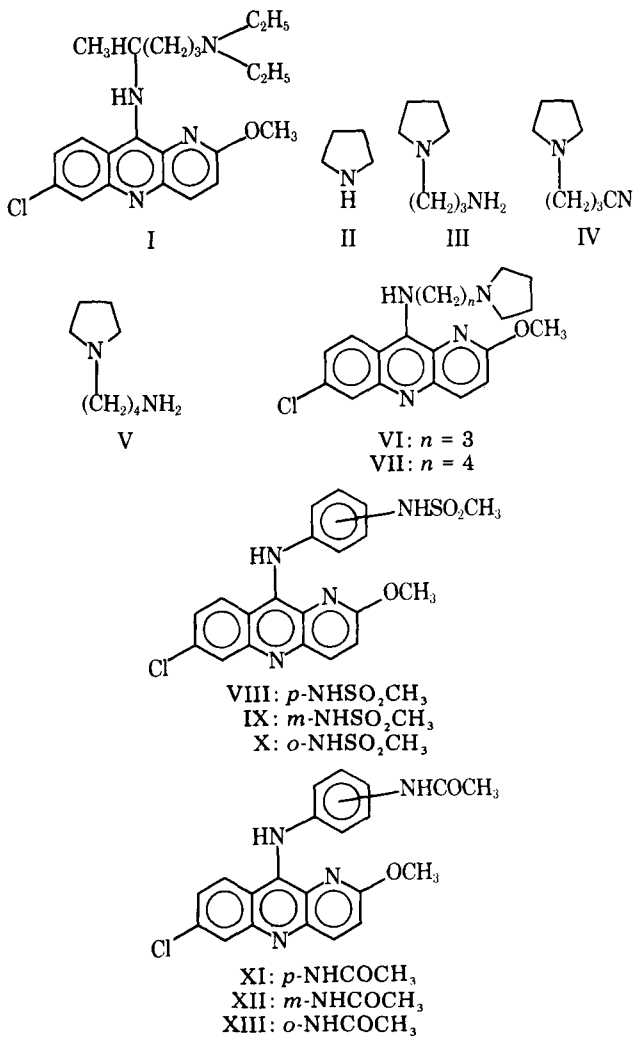

RESULTS AND DISCUSSION

Chemistry—The intermediate *N*-(δ-aminopropyl)pyrrolidine (III) for the synthesis of VI was prepared from pyrrolidine by a cyanoethylation reaction with acrylonitrile, followed by reduction with lithium aluminum hydride. The intermediate V was prepared from II and 4-chlorobutyronitrile according to the method of Burckhalter *et al.* (11), followed by lithium aluminum hydride reduction (12) of the nitrile (IV).

The intermediates, aminomethanesulfonanilides for VIII–X and aminoacetanilides for XI–XIII, were prepared in excellent yields from the corresponding nitroanilines by standard chemical reactions. The desired target compounds, VIII–XIII, were then prepared (Scheme I) by reacting the appropriate amines with 7,10-dichloro-2-methoxypyrido[3,2-*b*]quinoline according to the method of Besly and Goldberg (7).

Biological Activity—The T_m studies were carried out according to

Table I—T_m Determination[a]

Compound	T_m	ΔT_m
DNA	68.5°	—
DNA + VI	83.5°	15.0°
DNA + VII	87.5°	19.0°
DNA + VIII	70.5°	2.0°
DNA + IX	70.0°	1.5°
DNA + X	70.5°	2.0°
DNA + XI	72.5°	4.0°
DNA + XII	68.5°	0
DNA + XIII	69.0°	0.5°

[a] The drugs were used at a concentration of 1×10^{-5} *M* in a solution containing 30 μg of calf thymus DNA/ml in 5 m*M* phosphate buffer at pH 7.4; the melting temperatures were determined at 260 nm by means of a Gilford 250 recording spectrophotometer with a thermoprogrammer 2527 programmed for a temperature rise of 1.0°/min.

Table II—Effect of 10-Substituted Benzo[*b*][1,5]naphthyridine on *E. coli* DNA-Primed RNA Polymerase

Drug Concentration, μg/ml	RNA Polymerase Activity[a], % Control							
	VI	VII	VIII	IX	X	XI	XII	XIII
400	0	0	111	116	145	153	178	186
200	1	0	134	145	113	190	153	182
100	10	1	135	119	153	143	112	173
50	23	19	111	128	140	138	139	163
25	42	30	126	147	150	124	123	126

[a] RNA polymerase activity was assayed as described under *Experimental*. All assays were run in triplicate. The results represent the average of two separate experiments that did not differ by more than 5%.

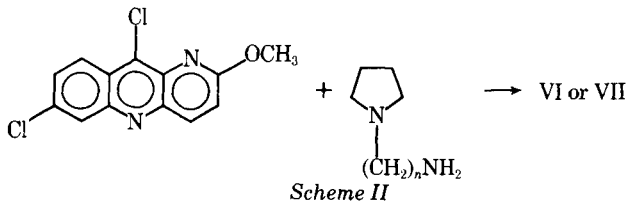

Scheme II

literature methods (13–15); results are presented in Table I. The T_m data show that the 10-substituted aminoalkyl derivatives (VI and VII) bind and stabilize the DNA helix toward the thermal denaturation, while the anilino derivatives (VIII–XIII) have little or no effect on the T_m of the DNA molecule.

The effect of benzonaphthyridine derivatives (VI–XIII) on *E. coli* DNA-dependent RNA polymerase *in vitro* is presented in Table II. While VI and VII are strong inhibitors, VIII–XIII exhibited a stimulation of DNA-dependent RNA polymerase. The inhibition of RNA polymerase by VI and VII appears to result from the binding of these derivatives to DNA by intercalation (indicated by T_m data), followed by an obstruction of the minor groove by the side chains, limiting the approach of the enzyme. The stimulation of RNA polymerase, on the other hand, may result from the binding of these anilino derivatives (VIII–XIII) to RNA, as has been shown for polyamines (16), which, in turn, may relieve product inhibition of the polymerase.

Compounds VI–XIII were tested against the lymphocytic leukemia P-388 test system according to the standard protocol (17) of the Division of Cancer Treatment, National Cancer Institute, National Institutes of Health. None of the compounds screened exhibited anticancer activity patterns considered adequate to justify expanded testing (T/C = 95–110%). Activity is defined as a percent T/C of 125 or greater.

EXPERIMENTAL[1]

7-Chloro-10-[3′-(*N*-pyrrolidino)propylamine]-2-methoxybenzo[*b*][1,5]naphthyridine (VI) Trihydrochloride (General Method)—The following reaction is typical for the preparation of benzonaphthyridine derivatives (VI–XIII) listed in Table III utilizing 7,10-dichloro-2-methoxybenzo[*b*][1,5]naphthyridine (Scheme II).

To a solution of the 7,10-dichloro compound (3.35 g, 12 mmoles) in 20.0 g of phenol (previously dried at 130° for 1 hr) was added 1.84 g (14 mmoles) of III. The reaction mixture was heated to 110° for 2.5 hr with stirring and cooled. Then the reaction mixture was poured into 700 ml of dry ether saturated with hydrochloric acid gas. The yellow salt was filtered and washed well with ether and acetone. Crystallization from absolute methanol–acetone afforded 3.72 g (65%) of analytically pure VI, mp 260–261° dec., as the trihydrochloride.

RNA Polymerase Assay—Calf thymus DNA[2], *E. coli* RNA polymerase[2], the nucleoside triphosphate[2], and 8-^{14}C-ATP (50 mCi/mmole)[3] were purchased. The activity of RNA polymerase was determined by measuring the amount of ^{14}C-ATP rendered acid insoluble, as determined by the filter disk assay of Bollum (18). The incubation mixture contained, in 0.125 ml of 5 μ*M* tris(hydroxymethyl)aminomethane–hydrochloric acid buffer, pH 8.0, 1.25 μmoles of magnesium chloride, 1.25 μmoles of β-mercaptoethanol, 0.019 μmole of cytidine 5′-triphosphate (CTP), 0.019 μmole of uridine 5′-triphosphate (UTP), 0.019 μmole of guanosine 5′-triphosphate (GTP), 0.019 μmole (65,000 cpm) of 8-^{14}C-ATP, and 3.65 μg of calf thymus.

The compounds to be tested were dissolved in dimethyl sulfoxide, and 5 μl of the solution was added to the incubation mixture just prior to the

Table III—Physical Characteristics of 10-Substituted Benzo[*b*][1,5]naphthyridines

Compound	Melting Point	Yield, %	Formula	*m/e* (Relative Intensity)	Analysis, % Calc.	Found
VI	260–261° dec.	65	$C_{20}H_{23}ClN_4O \cdot 3HCl$	370 (M^+, 9), 286 (9), 84 (100)	C 50.01	50.29
					N 5.45	5.53
					N 11.66	11.74
VII	264–265° dec.	53	$C_{21}H_{25}ClN_4O \cdot 3HCl$	384 (M^+, 9) 300 (9), 84 (100)	C 51.03	51.22
					H 5.71	5.90
					N 12.04	11.92
VIII	289.5–290.5°	88	$C_{20}H_{17}ClN_4O_3 \cdot HCl$	428 (M^+, 26), 349 (100)	C 51.62	51.31
					H 3.90	3.86
					N 12.04	11.92
IX	298–300° dec.	99	$C_{20}H_{17}ClN_4O_3S \cdot HCl$	428 (M^+, 100), 349 (37)	C 51.62	51.45
					H 3.90	3.78
					N 12.04	11.86
X	286–287° dec.	75	$C_{20}H_{17}ClN_4O_3S \cdot HCl$	428 (M^+, 42), 349 (100)	C 51.62	51.26
					H 3.90	4.00
					N 12.04	11.87
XI	289–290° dec.	80	$C_{21}H_{17}ClN_4O_2 \cdot HCl$	392 (M^+, 100), 349 (25)	C 58.75	58.69
					H 4.23	4.29
					N 13.05	12.90
XII	274–275° dec.	65	$C_{21}H_{17}ClN_4O_2 \cdot HCl$	392 (M^+, 100), 377 (15)	C 58.75	58.52
					H 4.23	4.30
					N 13.05	12.85
XIII	228–229° dec.	72	$C_{21}H_{17}ClN_4O_2 \cdot HCl$	392 (M^+, 100), 377 (42), 349 (47)	C 58.75	58.62
					H 4.23	4.14
					N 13.05	12.84

[1] Melting points were obtained with a Thomas-Hoover melting-point apparatus and are uncorrected. All elemental analyses were performed by Galbraith Laboratories, Inc., Knoxville, Tenn., and are within ±0.4% of theoretical values, except where indicated. All mass spectra were taken on an LKB 9000 spectrometer with a source temperature of ~290°.

[2] Sigma Chemical Co.

[3] New England Nuclear.

addition of enzyme. Controls contained 5 μl of dimethyl sulfoxide. The reaction mixtures were incubated for 10 min at 37°. The acid-insoluble material from an aliquot (100 μl) of each incubation mixture was isolated by the procedure of Bollum (18), placed in 18 ml of scintillation fluid (6.0 g of 2,5-diphenyloxazole, 0.2 g of 1,4-bis[2-(5-phenyloxazolyl)]benzene, 1400 ml of toluene, and 600 ml of methanol), and counted in a liquid scintillation spectrometer[4]. In the absence of added drug, 1.05 nmoles of 8-^{14}C-ATP was incorporated into DNA during the 10-min incubation period.

REFERENCES

(1) C. H. Browning and W. Gilmour, *J. Pathol. Bacteriol.*, **18**, 144 (1913).

(2) A. Albert, "The Acridines," 2nd ed., Arnold, London, England, 1966, p. 431.

(3) A. Ledóchowski, in "Advances in Antimicrobial and Antineoplastic Chemotherapy," vol. II (Proceedings of the VIIth International Congress of Chemotherapy, Prague, 1971), University Park Press, Baltimore, Md., p. 133.

(4) C. Radzikowski, A. Ledóchowski, M. Hrabowska, B. Stefańska, B. Horowska, J. Konopa, E. Morawska, and M. Urbańska, *Arch. Immunol. Ther. Exp.*, **17**, 99 (1969).

(5) B. F. Cain, R. N. Seelye, and G. J. Atwell, *J. Med. Chem.*, **17**, 922 (1974).

(6) A. R. Peacocke, in "Acridine," R. H. Acheson, Ed., Wiley, New York, N.Y., 1976, p. 723.

(7) D. M. Besly and A. A. Goldberg, *J. Chem. Soc.*, **1954**, 2448.

(8) J. F. B. Edeson, *Ann. Trop. Med. Parasitol.*, **48**, 160 (1954).

(9) E. F. Elslager and D. F. Worth, *J. Med. Chem.*, **12**, 955 (1969).

(10) E. F. Elslager, S. C. Perricone, and D. F. Worth, *J. Hererocycl. Chem.*, **7**, 543 (1970).

(11) J. H. Burckhalter, W. S. Brinigar, and P. E. Thompson, *J. Org. Chem.*, **26**, 4070 (1961).

(12) A. Terada and A. Hassner, *Bull. Chem. Soc. Jpn.*, **42**, 2666 (1969).

(13) E. Marquez, J. W. Cranston, R. W. Ruddon, and J. H. Burckhalter, *J. Med. Chem.*, **17**, 856 (1974).

(14) F. E. Hahn, R. L. O'Brien, J. Ciak, J. L. Allison, and J. G. Olenick, *Mil. Med. Suppl.*, **131**, 1071 (1966).

(15) J. L. Allison, R. L. O'Brien, and F. E. Hahn, *Science*, **149**, 1111 (1965).

(16) J. S. Krakow, *Biochim. Biophys. Acta*, **72**, 566 (1963).

(17) R. I. Geran, N. H. Greenberg, M. M. Macdonald, A. M. Schumacher, and B. J. Abbot, *Cancer Chemother. Rep., Part 3* (2), 3 (1972).

(18) F. J. Bollum, in "Proceedings in Nucleic Acid Research," vol. I, J. L. Cantoni and D. R. Davies, Eds., Harper and Row, New York, N.Y., 1966, p. 296.

[4] Model LS230, Beckman Instruments.

ACKNOWLEDGMENTS

Supported by Contract N01-CM-43761 from the National Cancer Institute, National Institutes of Health, Department of Health, Education, and Welfare.

The authors thank Dr. R. L. Cysyk of the Laboratory of Chemical Pharmacology, National Cancer Institute, for performing the RNA polymerase studies.

New Method of Preparing Gelatin Microcapsules of Soluble Pharmaceuticals

P. L. MADAN ˣ, R. K. JANI *, and A. J. BARTILUCCI

Received February 4, 1977, from the *College of Pharmacy and Allied Health Professions, St. John's University, Jamaica, NY 11439.* Accepted for publication June 13, 1977. *Present address: New Product Development, Alcon Laboratories, Fort Worth, TX 76101.

Abstract □ A new method of preparing gelatin microcapsules of soluble pharmaceuticals is described. Spherical droplets of a gelatin dispersion prepared in the drug solution were produced by the capillary method, and the droplets were congealed rapidly to yield discrete units in the form of a free-flowing powder. The microcapsules obtained were spherical in shape and showed no tendency to form agglomerates. Hardening of the microcapsules resulted in a significant reduction of the release rate without altering the reproducibility. The results indicated that the process of microencapsulation described is simple, reproducible, economical, and amenable to industrial application.

Keyphrases □ Gelatin microcapsules—method of preparation with soluble pharmaceuticals □ Microcapsules, gelatin—method of preparation with soluble pharmaceuticals □ Dosage forms—gelatin microcapsules, method of preparation with soluble pharmaceuticals

In recent years, microencapsulation has found increased use in pharmaceuticals from both clinical and therapeutic aspects.

Among the methods available for microencapsulation, the gelatin encapsulation process is the oldest and perhaps the most commonly used (1–4). Gelatin microcapsules have been prepared by complex coacervation (1, 2, 5), simple coacervation (3, 6), and emulsification (4). The emulsification process is the simplest technique, but apparently the microcapsules thus produced tend to adhere together and show poor flow properties (7). In addition, they are difficult to wet and display physical characteristics unsuitable for formulation purposes (7).

The process of encapsulation reported here makes use of the fact that aqueous dispersions of gelatin set to a gel when cooled (8).

EXPERIMENTAL

Materials—All materials were USP grade and were used as received without further purification or recrystallization. The gelatin[1] had the following specifications as provided by the manufacturer: type, B, edible; bloom, 303 g; viscosity, 58.4 mps; pH, 6.30; and moisture, 10.00%.

Microcapsule Preparation—A 30% dispersion of gelatin was prepared in a 5% aqueous solution of sodium salicylate by first soaking the gelatin in the sodium salicylate solution and then heating to about 50° to effect a homogeneous dispersion. The dispersion was maintained at 50° to prevent the gelation of gelatin, and small spherical droplets of the dispersion were prepared by a method similar to the capillary method reported previously (6).

The droplets leaving the capillary were gelled by collecting them in mineral oil USP, maintained at 5° in an ice bath. Visual observation

[1] P. Leiner and Sons, America Inc., St. Claire Shores, Mich.

addition of enzyme. Controls contained 5 μl of dimethyl sulfoxide. The reaction mixtures were incubated for 10 min at 37°. The acid-insoluble material from an aliquot (100 μl) of each incubation mixture was isolated by the procedure of Bollum (18), placed in 18 ml of scintillation fluid (6.0 g of 2,5-diphenyloxazole, 0.2 g of 1,4-bis[2-(5-phenyloxazolyl)]benzene, 1400 ml of toluene, and 600 ml of methanol), and counted in a liquid scintillation spectrometer[4]. In the absence of added drug, 1.05 nmoles of 8-^{14}C-ATP was incorporated into DNA during the 10-min incubation period.

REFERENCES

(1) C. H. Browning and W. Gilmour, *J. Pathol. Bacteriol.*, **18**, 144 (1913).

(2) A. Albert, "The Acridines," 2nd ed., Arnold, London, England, 1966, p. 431.

(3) A. Ledóchowski, in "Advances in Antimicrobial and Antineoplastic Chemotherapy," vol. II (Proceedings of the VIIth International Congress of Chemotherapy, Prague, 1971), University Park Press, Baltimore, Md., p. 133.

(4) C. Radzikowski, A. Ledóchowski, M. Hrabowska, B. Stefańska, B. Horowska, J. Konopa, E. Morawska, and M. Urbańska, *Arch. Immunol. Ther. Exp.*, **17**, 99 (1969).

(5) B. F. Cain, R. N. Seelye, and G. J. Atwell, *J. Med. Chem.*, **17**, 922 (1974).

(6) A. R. Peacocke, in "Acridine," R. H. Acheson, Ed., Wiley, New York, N.Y., 1976, p. 723.

(7) D. M. Besly and A. A. Goldberg, *J. Chem. Soc.*, **1954**, 2448.

(8) J. F. B. Edeson, *Ann. Trop. Med. Parasitol.*, **48**, 160 (1954).

(9) E. F. Elslager and D. F. Worth, *J. Med. Chem.*, **12**, 955 (1969).

(10) E. F. Elslager, S. C. Perricone, and D. F. Worth, *J. Hererocycl. Chem.*, **7**, 543 (1970).

(11) J. H. Burckhalter, W. S. Brinigar, and P. E. Thompson, *J. Org. Chem.*, **26**, 4070 (1961).

(12) A. Terada and A. Hassner, *Bull. Chem. Soc. Jpn.*, **42**, 2666 (1969).

(13) E. Marquez, J. W. Cranston, R. W. Ruddon, and J. H. Burckhalter, *J. Med. Chem.*, **17**, 856 (1974).

(14) F. E. Hahn, R. L. O'Brien, J. Ciak, J. L. Allison, and J. G. Olenick, *Mil. Med. Suppl.*, **131**, 1071 (1966).

(15) J. L. Allison, R. L. O'Brien, and F. E. Hahn, *Science*, **149**, 1111 (1965).

(16) J. S. Krakow, *Biochim. Biophys. Acta*, **72**, 566 (1963).

(17) R. I. Geran, N. H. Greenberg, M. M. Macdonald, A. M. Schumacher, and B. J. Abbot, *Cancer Chemother. Rep., Part 3* (2), 3 (1972).

(18) F. J. Bollum, in "Proceedings in Nucleic Acid Research," vol. I, J. L. Cantoni and D. R. Davies, Eds., Harper and Row, New York, N.Y., 1966, p. 296.

[4] Model LS230, Beckman Instruments.

ACKNOWLEDGMENTS

Supported by Contract N01-CM-43761 from the National Cancer Institute, National Institutes of Health, Department of Health, Education, and Welfare.

The authors thank Dr. R. L. Cysyk of the Laboratory of Chemical Pharmacology, National Cancer Institute, for performing the RNA polymerase studies.

New Method of Preparing Gelatin Microcapsules of Soluble Pharmaceuticals

P. L. MADAN ˣ, R. K. JANI *, and A. J. BARTILUCCI

Received February 4, 1977, from the *College of Pharmacy and Allied Health Professions, St. John's University, Jamaica, NY 11439.* Accepted for publication June 13, 1977. *Present address: New Product Development, Alcon Laboratories, Fort Worth, TX 76101.

Abstract □ A new method of preparing gelatin microcapsules of soluble pharmaceuticals is described. Spherical droplets of a gelatin dispersion prepared in the drug solution were produced by the capillary method, and the droplets were congealed rapidly to yield discrete units in the form of a free-flowing powder. The microcapsules obtained were spherical in shape and showed no tendency to form agglomerates. Hardening of the microcapsules resulted in a significant reduction of the release rate without altering the reproducibility. The results indicated that the process of microencapsulation described is simple, reproducible, economical, and amenable to industrial application.

Keyphrases □ Gelatin microcapsules—method of preparation with soluble pharmaceuticals □ Microcapsules, gelatin—method of preparation with soluble pharmaceuticals □ Dosage forms—gelatin microcapsules, method of preparation with soluble pharmaceuticals

In recent years, microencapsulation has found increased use in pharmaceuticals from both clinical and therapeutic aspects.

Among the methods available for microencapsulation, the gelatin encapsulation process is the oldest and perhaps the most commonly used (1–4). Gelatin microcapsules have been prepared by complex coacervation (1, 2, 5), simple coacervation (3, 6), and emulsification (4). The emulsification process is the simplest technique, but apparently the microcapsules thus produced tend to adhere together and show poor flow properties (7). In addition, they are difficult to wet and display physical characteristics unsuitable for formulation purposes (7).

The process of encapsulation reported here makes use of the fact that aqueous dispersions of gelatin set to a gel when cooled (8).

EXPERIMENTAL

Materials—All materials were USP grade and were used as received without further purification or recrystallization. The gelatin[1] had the following specifications as provided by the manufacturer: type, B, edible; bloom, 303 g; viscosity, 58.4 mps; pH, 6.30; and moisture, 10.00%.

Microcapsule Preparation—A 30% dispersion of gelatin was prepared in a 5% aqueous solution of sodium salicylate by first soaking the gelatin in the sodium salicylate solution and then heating to about 50° to effect a homogeneous dispersion. The dispersion was maintained at 50° to prevent the gelation of gelatin, and small spherical droplets of the dispersion were prepared by a method similar to the capillary method reported previously (6).

The droplets leaving the capillary were gelled by collecting them in mineral oil USP, maintained at 5° in an ice bath. Visual observation

[1] P. Leiner and Sons, America Inc., St. Claire Shores, Mich.

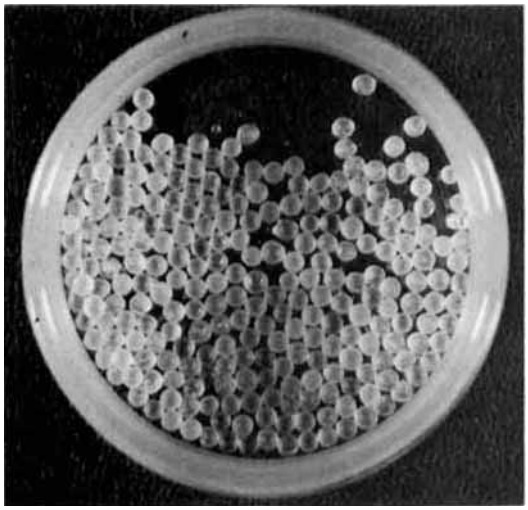

Figure 1—*Photomicrograph of microcapsules recovered as the final product.*

showed that the droplets collecting in the mineral oil exhibited no tendency to agglomerate. About 15 min was required to cause the gelling of the droplets; however, to ensure complete gelling, the droplets were allowed to remain in the mineral oil for 30 min.

After 30 min, the gelled droplets were removed and the excess mineral oil adhering to the droplets was removed by washing with acetone. A portion of the droplets was treated with formaldehyde solution USP to harden the capsules; the gelled, washed capsules were then air dried at room temperature. The final product obtained after washing and drying was in the form of discrete spherical units, recovered as a free-flowing powder. The microcapsules showed no tendency to agglomerate and displayed excellent flow properties.

Release from Microcapsules—Release of sodium salicylate from the microcapsules was determined by examining duplicate samples, containing approximately 25 mg of the drug, using the modified flask dissolution method. A 500-ml, three-necked, round-bottom flask had a 6-cm hole cut in the center to accommodate the entrance of the 40-mesh screen basket assembly used in the USP dissolution method. A 300-ml quantity of the dissolution medium (0.1 *N* HCl), preheated to 37°, was added to the flask immersed in a water bath maintained at 37 ± 0.5°. The basket containing the microcapsules was immersed in the dissolution medium, centered, and rotated at 100 rpm using a constant-speed motor.

Samples of the dissolution medium were withdrawn at predetermined intervals using a pipet fitted with a cotton plug. A constant volume of the dissolution medium was maintained by the addition of an equal volume of the dissolution medium after each sample was withdrawn. In each case, the cotton plug was added to the dissolution mixture. Concentrations were determined spectrophotometrically[2] at 304 nm after appropriate dilutions.

RESULTS AND DISCUSSION

Microcapsule Preparation—Sodium salicylate was used as the model drug because it lends itself conveniently to the spectrophotometric analysis.

This microencapsulation process makes use of the fact that aqueous dispersions of gelatin set to a gel when such dispersions are cooled (8). Various concentrations of gelatin dispersions were investigated; at concentrations below 30%, gelation was incomplete. The droplets tended to soften at room temperature and became sticky. Increasing the concentration above 30% did not decrease gelation, but the dispersion had to be maintained at higher temperatures to prevent gelation in the capillary which could result in gelatin degradation (8). At 30% and 50°, the gelatin dispersion did not gel in the capillary and the gelled droplets did not soften at room temperature.

Microscopic examination revealed that most of the microcapsules (>90%) were monodisperse, having a diameter of 185 μm (Fig. 1). The deviation of the microcapsules from monodispersity may be attributed to slight temperature fluctuations, which may have altered the viscosity of the gelatin dispersion, resulting in variations in the droplet size.

[2] Beckman model DB-GT.

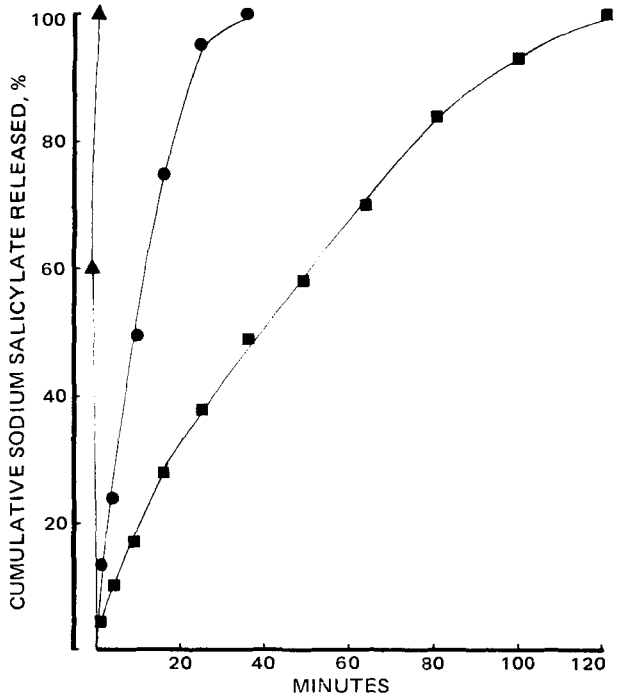

Figure 2—*Dissolution of sodium salicylate from unencapsulated drug (▲), unhardened microcapsules (●), and hardened microcapsules (■).*

The total recovery of the microcapsules from a given batch was almost 100%. Except for the last traces of the starting material, which tended to stick to the capillary apparatus, every single droplet collected in the mineral oil was recovered as a microcapsule. The drug content of the microcapsules, as determined by extracting the drug from the microcapsules (2), was 13.7% (w/w), in good agreement with the theoretically calculated value of 14.3% (w/w).

Release from Microcapsules—The release characteristics of the microcapsules are shown in Fig. 2. Included for comparison purposes is the dissolution pattern of the unencapsulated drug particles. Figure 2 shows that the encapsulation process produced microcapsules with controlled release of sodium salicylate. The unencapsulated drug particles dissolved completely in less than 2 min, but it took about 20 min for drug release from the unhardened microcapsules. Hardening the microcapsules

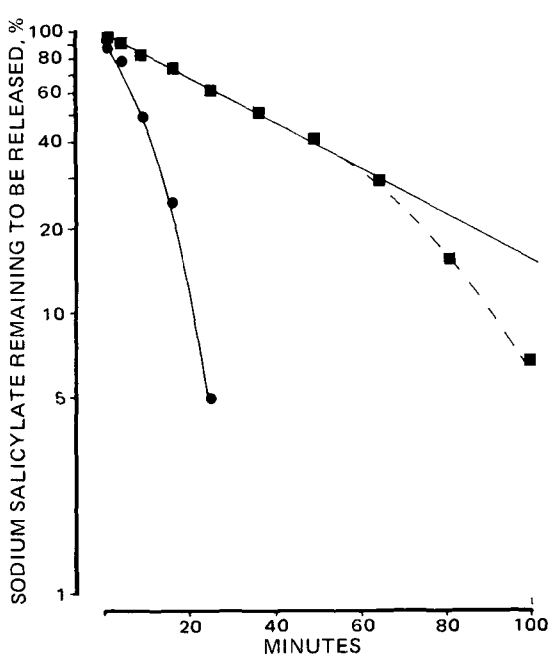

Figure 3—*Release of sodium salicylate from unhardened microcapsules (●) and hardened microcapsules (■).*

Table I—Salicylate Release from Microcapsules

Minutes	Salicylate Released[a], % Batch I[b]	Batch II[b]	Batch III[b]
1	4.5 (0.5)	4.0 (0.5)	3.9 (0.4)
5	10.0 (0.3)	10.1 (0.2)	10.2 (0.3)
10	18.1 (0.7)	17.0 (0.5)	17.5 (0.7)
15	27.5 (1.2)	28.3 (0.8)	28.0 (0.8)
25	38.0 (0.6)	37.7 (0.9)	38.1 (0.7)
35	47.5 (1.0)	48.0 (0.7)	48.2 (0.5)
50	58.3 (0.7)	58.9 (1.2)	58.5 (0.4)
65	70.0 (0.9)	71.0 (0.5)	71.0 (1.4)
80	83.5 (1.1)	84.1 (0.9)	83.7 (0.8)
100	93.1 (1.2)	92.5 (0.9)	93.5 (0.4)
120	100.0	100.0	100.0

[a] Each value is an average of at least two experiments. Values in parentheses indicate the ± range. [b] Each batch was prepared at a different time.

slowed the release significantly, increasing the time for complete drug release to about 2 hr.

Since sodium salicylate is readily water soluble, this amount of time corresponds to about a 103-fold increase in the time required for the complete dissolution of the drug particles.

The dissolution characteristics (Fig. 2) indicate that the release of sodium salicylate from the unhardened microcapsules approaches zero-order kinetics throughout much of the extraction process. For the hardened microcapsules, the dissolution shows essentially zero-order kinetics from about 30 to about 85% sodium salicylate release.

One aim with microencapsulation is to obtain zero-order drug release from the microcapsules (8). Unfortunately, experience shows that most microcapsule formulations release the drug at roughly a first-order rather than a zero-order rate (9). Figure 3 shows a first-order plot of sodium salicylate release from the microcapsules. While the unhardened microcapsules do not appear to follow first-order kinetics, the hardened microcapsules show a first-order release up to about 70% sodium salicylate released.

In most microencapsulation processes, microcapsule recovery involves a drying step that may influence the microcapsule integrity. For example, solvent evaporation during drying may cause shrinkage of the shell wall, thus creating coating defects, flaws, and/or deposition of a portion of the drug on the microcapsule surface due to the solvent migration effect. Because of these effects, either singly or in combination, the release patterns of the drug from the microcapsules may show an initial rapid drug release, which has been reported to range from about 10–20% (6) to as high as 50% (3). Since the microencapsulation process reported here uses gelation rather than drying, this effect was minimal in drug release from the microcapsules.

The microencapsulation process used in this investigation gave good reproducibility. Release rates obtained with the microcapsules from the same batch were within a narrow range, the maximum range observed being 3% (Table I). Duplicate batches of the microcapsules prepared at various times were identical to the original batch in terms of batch yield, microcapsule size and size distribution, and release rate profile. In addition, the process described is simple, economical, and amenable to industrial application.

REFERENCES

(1) P. L. Madan, J. C. Price, and L. A. Luzzi, in "Microencapsulation: Processes and Applications," Plenum, New York, N.Y., 1974, p. 39.

(2) P. L. Madan, L. A. Luzzi, and J. C. Price, *J. Pharm. Sci.*, **63,** 280 (1974).

(3) J. R. Nixon, S. A. H. Khalil, and J. E. Carless, *J. Pharm. Pharmacol.*, **20,** 528 (1968).

(4) N. Tanaka, S. Takino, and I. Utsumi, *J. Pharm. Sci.*, **52,** 664 (1963).

(5) P. L. Madan, L. A. Luzzi, and J. C. Price, *ibid.*, **61,** 1586 (1972).

(6) P. L. Madan, D. K. Madan, and J. C. Price, *ibid.*, **65,** 1476 (1976).

(7) J. W. McGinity, A. B. Combs, and A. N. Martin, *ibid.*, **64,** 889 (1975).

(8) P. L. Madan, D. K. Madan, and J. C. Price, *Can. J. Pharm. Sci.*, **11,** 21 (1976).

(9) J. R. Robinson and S. P. Eriksen, *J. Pharm. Sci.*, **55,** 1254 (1966).

Synthesis of Methaqualone and Its Diphasic Titration in Pure and Tablet Forms

FARID S. G. SOLIMAN ˣ, RAGAB M. SHAFIK, and ELSAYED A. ELNENAEY

Received April 4, 1977, from the *Departments of Pharmaceutical and Pharmaceutical Analytical Chemistry, Faculty of Pharmacy, University of Alexandria, Alexandria, A.R. Egypt.* Accepted for publication June 13, 1977.

Abstract □ A one-step synthesis of methaqualone from *N*-acetylanthranilic acid and *o*-toluidine in the absence of a catalyst is described. A rapid diphasic titration procedure for its microestimation in pure and tablet forms, using dioctyl sodium sulfosuccinate and dimethyl yellow screened with oracet blue B, is proposed. The data were compared with those obtained from nonaqueous titration methods.

Keyphrases □ Methaqualone—one-step synthesis, diphasic titration analysis in bulk drug and tablets □ Titration, diphasic—analysis, methaqualone in bulk drug and tablets □ Hypnotic–sedatives—methaqualone, one-step synthesis, diphasic titration analysis in bulk drug and tablets

Methaqualone, 2-methyl-3-*o*-tolyl-4(3*H*)-quinazolinone (I), is marketed both as a sedative–hypnotic and as an anticonvulsant (1). Several methods have been reported for its synthesis and evaluation as the base or hydrochloride in bulk drug and dosage forms.

Methaqualone has been synthesized by: (*a*) refluxing a solution of *N*-acetylanthranilic acid with *o*-toluidine in toluene in the presence of different catalysts (2–5); (*b*) by heating anthranilic acid, *o*-toluidine, acetic acid, and polyphosphoric acid (6); (*c*) by condensing 2-methyl-3,1,4-benzoxazone with *o*-toluidine (7, 8); or (*d*) by heating methyl anthranilate with *o*-toluidine *N*-(magnesium bromide) and acetylating the intermediate amide, which subsequently cyclizes (9). The hydrochloride of I was prepared by heating *N*-acetylanthranilic acid with *o*-toluidine hydrochloride (10).

For the estimation of I or its hydrochloride salt, diazometric (11), colorimetric (12), spectrophotometric (13, 14), complexometric (15), and nonaqueous titration (16–18) methods have been proposed.

In the present investigation, I was prepared by heating *N*-acetylanthranilic acid with *o*-toluidine in bromobenzene in the absence of a catalyst. This report also describes a

Table I—Salicylate Release from Microcapsules

Minutes	Salicylate Released[a], % Batch I[b]	Batch II[b]	Batch III[b]
1	4.5 (0.5)	4.0 (0.5)	3.9 (0.4)
5	10.0 (0.3)	10.1 (0.2)	10.2 (0.3)
10	18.1 (0.7)	17.0 (0.5)	17.5 (0.7)
15	27.5 (1.2)	28.3 (0.8)	28.0 (0.8)
25	38.0 (0.6)	37.7 (0.9)	38.1 (0.7)
35	47.5 (1.0)	48.0 (0.7)	48.2 (0.5)
50	58.3 (0.7)	58.9 (1.2)	58.5 (0.4)
65	70.0 (0.9)	71.0 (0.5)	71.0 (1.4)
80	83.5 (1.1)	84.1 (0.9)	83.7 (0.8)
100	93.1 (1.2)	92.5 (0.9)	93.5 (0.4)
120	100.0	100.0	100.0

[a] Each value is an average of at least two experiments. Values in parentheses indicate the ± range. [b] Each batch was prepared at a different time.

slowed the release significantly, increasing the time for complete drug release to about 2 hr.

Since sodium salicylate is readily water soluble, this amount of time corresponds to about a 103-fold increase in the time required for the complete dissolution of the drug particles.

The dissolution characteristics (Fig. 2) indicate that the release of sodium salicylate from the unhardened microcapsules approaches zero-order kinetics throughout much of the extraction process. For the hardened microcapsules, the dissolution shows essentially zero-order kinetics from about 30 to about 85% sodium salicylate release.

One aim with microencapsulation is to obtain zero-order drug release from the microcapsules (8). Unfortunately, experience shows that most microcapsule formulations release the drug at roughly a first-order rather than a zero-order rate (9). Figure 3 shows a first-order plot of sodium salicylate release from the microcapsules. While the unhardened microcapsules do not appear to follow first-order kinetics, the hardened microcapsules show a first-order release up to about 70% sodium salicylate released.

In most microencapsulation processes, microcapsule recovery involves a drying step that may influence the microcapsule integrity. For example, solvent evaporation during drying may cause shrinkage of the shell wall, thus creating coating defects, flaws, and/or deposition of a portion of the drug on the microcapsule surface due to the solvent migration effect. Because of these effects, either singly or in combination, the release patterns of the drug from the microcapsules may show an initial rapid drug release, which has been reported to range from about 10–20% (6) to as high as 50% (3). Since the microencapsulation process reported here uses gelation rather than drying, this effect was minimal in drug release from the microcapsules.

The microencapsulation process used in this investigation gave good reproducibility. Release rates obtained with the microcapsules from the same batch were within a narrow range, the maximum range observed being 3% (Table I). Duplicate batches of the microcapsules prepared at various times were identical to the original batch in terms of batch yield, microcapsule size and size distribution, and release rate profile. In addition, the process described is simple, economical, and amenable to industrial application.

REFERENCES

(1) P. L. Madan, J. C. Price, and L. A. Luzzi, in "Microencapsulation: Processes and Applications," Plenum, New York, N.Y., 1974, p. 39.

(2) P. L. Madan, L. A. Luzzi, and J. C. Price, *J. Pharm. Sci.*, **63,** 280 (1974).

(3) J. R. Nixon, S. A. H. Khalil, and J. E. Carless, *J. Pharm. Pharmacol.*, **20,** 528 (1968).

(4) N. Tanaka, S. Takino, and I. Utsumi, *J. Pharm. Sci.*, **52,** 664 (1963).

(5) P. L. Madan, L. A. Luzzi, and J. C. Price, *ibid.*, **61,** 1586 (1972).

(6) P. L. Madan, D. K. Madan, and J. C. Price, *ibid.*, **65,** 1476 (1976).

(7) J. W. McGinity, A. B. Combs, and A. N. Martin, *ibid.*, **64,** 889 (1975).

(8) P. L. Madan, D. K. Madan, and J. C. Price, *Can. J. Pharm. Sci.*, **11,** 21 (1976).

(9) J. R. Robinson and S. P. Eriksen, *J. Pharm. Sci.*, **55,** 1254 (1966).

Synthesis of Methaqualone and Its Diphasic Titration in Pure and Tablet Forms

FARID S. G. SOLIMAN ˣ, RAGAB M. SHAFIK, and ELSAYED A. ELNENAEY

Received April 4, 1977, from the *Departments of Pharmaceutical and Pharmaceutical Analytical Chemistry, Faculty of Pharmacy, University of Alexandria, Alexandria, A.R. Egypt.* Accepted for publication June 13, 1977.

Abstract □ A one-step synthesis of methaqualone from *N*-acetylanthranilic acid and *o*-toluidine in the absence of a catalyst is described. A rapid diphasic titration procedure for its microestimation in pure and tablet forms, using dioctyl sodium sulfosuccinate and dimethyl yellow screened with oracet blue B, is proposed. The data were compared with those obtained from nonaqueous titration methods.

Keyphrases □ Methaqualone—one-step synthesis, diphasic titration analysis in bulk drug and tablets □ Titration, diphasic—analysis, methaqualone in bulk drug and tablets □ Hypnotic–sedatives—methaqualone, one-step synthesis, diphasic titration analysis in bulk drug and tablets

Methaqualone, 2-methyl-3-*o*-tolyl-4(3*H*)-quinazolinone (I), is marketed both as a sedative–hypnotic and as an anticonvulsant (1). Several methods have been reported for its synthesis and evaluation as the base or hydrochloride in bulk drug and dosage forms.

Methaqualone has been synthesized by: (*a*) refluxing a solution of *N*-acetylanthranilic acid with *o*-toluidine in toluene in the presence of different catalysts (2–5); (*b*) by heating anthranilic acid, *o*-toluidine, acetic acid, and polyphosphoric acid (6); (*c*) by condensing 2-methyl-3,1,4-benzoxazone with *o*-toluidine (7, 8); or (*d*) by heating methyl anthranilate with *o*-toluidine *N*-(magnesium bromide) and acetylating the intermediate amide, which subsequently cyclizes (9). The hydrochloride of I was prepared by heating *N*-acetylanthranilic acid with *o*-toluidine hydrochloride (10).

For the estimation of I or its hydrochloride salt, diazometric (11), colorimetric (12), spectrophotometric (13, 14), complexometric (15), and nonaqueous titration (16–18) methods have been proposed.

In the present investigation, I was prepared by heating *N*-acetylanthranilic acid with *o*-toluidine in bromobenzene in the absence of a catalyst. This report also describes a

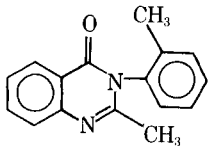

I

rapid diphasic titration analysis of I. The procedure is analogous to that applied for the microdetermination of secondary and tertiary organic bases and their salts (19).

The new method employed a previously standardized aqueous solution of dioctyl sodium sulfosuccinate (II) against a reference sample of I. The titration was conducted in a water–chloroform diphase at pH 1.09, using dimethyl yellow screened with oracet blue B dye as indicator. The method was used for methaqualone base and its tablet form, and the results were compared with those obtained from nonaqueous titration procedures (17, 18).

EXPERIMENTAL[1]

Synthesis of Methaqualone (I)—*N*-Acetylanthranilic acid (3.6 g, 0.02 mole) and freshly distilled *o*-toluidine (2.14 g, 0.02 mole) in bromobenzene (10 ml) were refluxed for 2.5 hr. Subsequently, nearly half of the volume of the solvent was distilled, and the dark reaction solution was mixed with benzene (30 ml). The solution was filtered, and the filtrate was extracted with 3 × 10 ml of hydrochloric acid (1:1). The acidic layer was purified by extraction with ether and then made alkaline (pH 8) with sodium hydroxide (25%). The crude semisolid product that solidified on standing was filtered, washed with water, and dried.

An analytically pure sample was obtained [yield of 2.3 g (48.4%)] by recrystallization from benzene–light petroleum (bp 40–60°) as colorless crystals, mp 112.5–113° [lit. mp 115–116° (2, 7), mp 120° (3), mp 113–115° (4, 5), and mp 113–114° (10)]; IR: 3100–2700 (CH_3) and 1670 (C=O) cm^{-1} and a band split at 1600, 1590, and 1560 cm^{-1} (C=N, C=C, and aromatics); ^{1}H-NMR: δ 2.02 (3H, s, CH_3 at C-2), 2.08 (3H, s, CH_3-*N*-tolyl), and 7.18–8.1 (8H, m, C-5, C-6, C-7, C-8, and *N*-tolyl) ppm; mass spectrum: *m/e* (relative intensity) 251 (10) (M + 1), 250 (50) (M^+), 249 (8) (M − 1), 236 (18), 235 (100), 234 (8), 233 (32), 239 (9), 206 (7), 167 (5), 166 (10), 165 (5), 152 (5), 143 (9), 132 (19), 125 (6), 124 (6), 117 (7), 116 (6), 109 (5), 104 (6), 103 (6), 102 (6), 92 (5), 91 (41), 90 (9), 89 (9), 85 (9), 83 (5), 77 (12), 76 (16), 75 (5), 69 (6), 68 (6), 67 (6), 65 (23), 63 (7), 51 (9), and 50 (11).

Anal.—Calc. for $C_{16}H_{14}N_2O$: N, 11.19. Found: N, 11.0.

Evaluation of Methaqualone (I) by Proposed Diphasic Titration Method—*Equipment*—Conventional laboratory glassware and a 10-ml microburet graduated to 0.02 ml were used.

Materials and Solutions—The following were used: methaqualone[2] dried in a vacuum desiccator to constant weight; methaqualone tablets[3]; a solution of dioctyl sodium sulfosuccinate[4] (II) (2.25 g) in distilled water (500 ml), prepared by gentle warming; chloroform[5]; pH 1.09 buffer, prepared by mixing 1 *N* sodium acetate[6] (200 ml) with 1 *N* HCl[6] (280 ml) and diluting to 1 liter with distilled water; and dimethyl yellow indicator[6] (15 mg) screened with oracet blue B dye (15 mg) in chloroform (500 ml).

Operational Parameters—The reference methaqualone base was the same microanalytically checked and spectroscopically studied sample. The aqueous solution of II was standardized by titration against the reference methaqualone following the procedure described later. For comparison purposes, the nonaqueous titration procedure of BP 1973 (17) for pure methaqualone and the literature (18) nonaqueous titration method for methaqualone tablets were performed.

Determination of Methaqualone Base—An accurately weighed amount of I (1–10 mg), contained in a 500-ml conical flask, was dissolved in 50 ml of chloroform. Distilled water (20 ml), pH 1.09 buffer (5 ml), and screened dimethyl yellow indicator (5 ml) were added, and the mixture was titrated against II with vigorous swirling. Toward the end-point, the titrant was added dropwise; the two phases were allowed to separate, and the mixture was swirled gently for 5 sec (the color of the end-point tended to concentrate between the two phases). The end-point was detected by a color change from green to pinkish gray in the bulk of the chloroform layer.

A blank determination was carried out. The percent recovery was calculated using:

$$\% \text{ recovery} = \frac{(V)(E)(100)}{\text{wt}} \qquad \text{(Eq. 1)}$$

where V is the milliliters of II used in the titration, E is the milligrams of I equivalent to 1 ml of the used II solution, and wt is the weight of I in milligrams.

Determination of Tablets—Twenty tablets were weighed and finely powdered. A quantity of the powder equivalent to about 8.0 mg of I was accurately weighed. Chloroform (50 ml), distilled water (20 ml), pH 1.09 buffer (5 ml), and screened dimethyl yellow indicator (5 ml) were added, and the mixture was titrated against II following the same procedure described for methaqualone in pure form. The content of the tablet was then calculated using:

$$\text{recovery of I per tablet} = \frac{(V)(E)(W_a)}{W_b} \qquad \text{(Eq. 2)}$$

where W_a is the average weight of the tablet and W_b is the weight of powdered tablets used in the assay.

RESULTS AND DISCUSSION

The synthetic route utilized in the preparation of I is believed to proceed *via* the initial formation of the intermediate *o*-acetamidobenz-*o*-tolylamide and subsequent loss of water. The structure of I was confirmed by elemental analysis, mass peak, and spectroscopic data. The predominant fragmentation process of I in the mass spectrum indicates the loss of a methyl radical from C-2, giving *m/e* 235 (III), which then fragments to *m/e* 91 ($CH_3C_6H_4$+) (IV) and 102 ($C_6H_4N^+{\equiv}C\cdot$) (V). The latter loses a cyanide radical to form the benzyne radical ion (*m/e* 76) (VI), which loses a hydrogen radical to give the benzyne cation (*m/e* 75) (VII).

The proposed diphasic titration procedure involves titration of I with II where a water-soluble complex is formed. When all I has reacted, any excess of II at pH 1.09 partitions into the chloroform phase as dioctyl hydrogen sulfosuccinate. The latter forms a chloroform-soluble colored complex with the screened dimethyl yellow indicator.

Comparative study of the results obtained using the proposed diphasic titration method with those using the compendial nonaqueous titration procedure of BP 1973 (17) for pure I was performed. The mean percent recoveries and standard deviations found were 99.9 ± 1.9 (average of 10 determinations) for the proposed diphasic method and 97.3 ± 2.4 (average of five determinations) for the BP 1973 procedure. This result revealed that the diphasic titration data were precise and could be satisfactorily used for the routine analysis of I. The described diphasic titration process was also advantageous because it excluded the limitation of working in nonaqueous media and was convenient for the microdetermination of I.

For the analysis of methaqualone tablets using the diphasic titration method, the mean recovery obtained (average of six determinations) was 148.9 ± 4.4 mg/tablet. For comparative study, the same tablets were determined using the potentiometric nonaqueous titration process described previously (18); and the mean recovery (average of five determinations) was 146.3 ± 2.5 mg/tablet. This nonaqueous titration method required preliminary separation of I from the tablets. In the present diphasic titration method, no previous isolation of I is necessary since ordinary tablet excipients and lubricants do not interfere. Moreover, the diphasic titration is timesaving when applied to the routine analysis of methaqualone tablets.

REFERENCES

(1) "The Merck Index," 8th ed., Merck and Co., Rahway, N.J., 1968, p. 672.

[1] Melting points were determined in open glass capillaries and are uncorrected. The IR spectrum was recorded on a Perkin-Elmer 421 spectrometer using potassium bromide pellets. The NMR spectrum was determined on a Varian A-60A spectrometer using deuterated dimethyl sulfoxide as the solvent. Mass spectral analysis was performed on an Organic MS 20 AEI (70 ev); peaks of relative intensity below 5% of the base peak have been omitted. Microanalysis for a sample dried over phosphorus pentoxide under reduced pressure was carried out at the Microanalytical Unit, Faculty of Science, University of Cairo, Cairo, A.R. Egypt.

[2] Prepared by the described new method.

[3] Especially made, for the present investigation, to contain 150 mg of I/tablet and calcium carbonate, starch, magnesium stearate, and talc as diluent and lubricant ingredients.

[4] Cyanamid Co.

[5] Prolabo, France.

[6] BDH, England.

(2) I. K. Kacker and S. H. Zaheer, *J. Indian Chem. Soc.*, **28**, 344 (1951).
(3) G. Serventi and R. Marchesi, *Boll. Sci. Fac. Chim. Ind. Bologna*, **15**, 117 (1957).
(4) J. Klosa, *Prakt. Chem.*, **14**, 84 (1961).
(5) J. Klosa and H. Starke, East German pat. 35,123 (1965); through *Chem. Abstr.*, **63**, 8377f (1965).
(6) D. Stefanova, L. Daleva, R. Kolchagova, and L. Zehyazkov, *Khim. Farm. Zh.*, **7**, 19 (1973); through *Chem. Abstr.*, **80**, 14891e (1974).
(7) S. H. Zaheer and I. Kacker, Indian pat. 69,698 (1962); through *Chem. Abstr.*, **57**, 12443h (1962).
(8) H. Froemmel and H. Foken, East German pat. 37,239 (1965); through *Chem. Abstr.*, **63**, 8378b (1965).
(9) P. A. Petyunin and Y. V. Kozhevnikov, *Biol. Akt. Soedin. Akad. Nauk SSSR*, **1965**, 152; through *Chem. Abstr.*, **63**, 16348h (1965).
(10) N. Droge, Kemikolieforretning AIS. Neth., 295, 501 (1965); through *Chem. Abstr.*, **63**, 18113g (1965).
(11) E. Maggiorelli and G. Gangemi, *Boll. Chim. Farm.*, **103**, 748 (1964).
(12) H. Hoehlein, *Pharmazie*, **21**, 464 (1966).
(13) E. Maggiorelli and G. Gangemi, *Boll. Chim. Farm.*, **105**, 128 (1966).
(14) N. M. Sanghavi and A. V. Katdare, *Indian J. Pharm.*, **34**, 159 (1972).
(15) N. M. Sanghavi and M. G. Pai, *ibid.*, **36**, 71 (1974).
(16) W. Schnellbach and H. Houta, *Pharm. Acta Helv.*, **47**, 75 (1972).
(17) "British Pharmacopoeia 1973," British Pharmacopoeia Commission, London, England, 1973, p. 296.
(18) L. G. Chatten, R. E. Moskalyk, R. A. Locock, and F. J. Schaefer, *J. Pharm. Sci.*, **63**, 1294 (1974).
(19) I. M. Roushdi and R. M. Shafik, *J. Pharm. Sci. U.A.R.*, **9**, 65 (1968).

ACKNOWLEDGMENTS

The authors are grateful to Professor Dr. Thomas Kappe, Institut für Organische Chemie der Universität Graz, A-8010 Graz, Austria, for the IR, NMR, and mass spectral determinations.

S-(4-Chlorophenyl) 3-Aryl-3-hydroxypropanethioates as Antibacterial Agents

HARRY R. SNYDER, Jr.[x], STANLEY E. BURROUS, RAYMOND FREEDMAN, and THEADOR J. HEBERT

Received March 14, 1977, from the *Research and Development Department, Norwich-Eaton Pharmaceuticals Division of Morton-Norwich Products, Inc., Norwich, NY 13815.* Accepted for publication June 1, 1977.

Abstract □ A series of *S*-(4-chlorophenyl) 3-aryl-3-hydroxypropanethioates was prepared and shown to have *in vitro* activity against several selected bacterial species.

Keyphrases □ 3-Hydroxypropanethioates, 3-aryl—series synthesized, antibacterial activity evaluated □ Antibacterial activity—3-aryl-3-hydroxypropanethioates evaluated □ Structure-activity relationships—3-aryl-3-hydroxypropanethioates evaluated for antibacterial activity

The usual pathway for fatty acid (both saturated and unsaturated) synthesis in bacteria is *via* thiol esters of coenzyme A intermediates (1–3). The enzyme responsible for the introduction of the double bond into the fatty acids of *Escherichia coli* is β-hydroxydecanoylthiol ester dehydrase (2, 3). This enzyme is vital for the growth of *E. coli* (2); its inhibition completely stops the growth of the bacterium (4, 5).

The required substrate for dehydrase preferably contains β-hydroxydecanoate as a thiol ester (2–4), which is dehydrated to a β,γ-unsaturated ester. It was postulated that a reasonable structure for a dehydrase inhibitor would possess a thiol ester of a β-hydroxy acid in which the γ-carbon is tertiary and, therefore, incapable of forming a β,γ-double bond. Therefore, a series of *S*-(4-chlorophenyl) 3-aryl-3-hydroxypropanethioates (I*a*–I*g*, Table I) was prepared and tested for activity *in vitro* against several selected bacterial species.

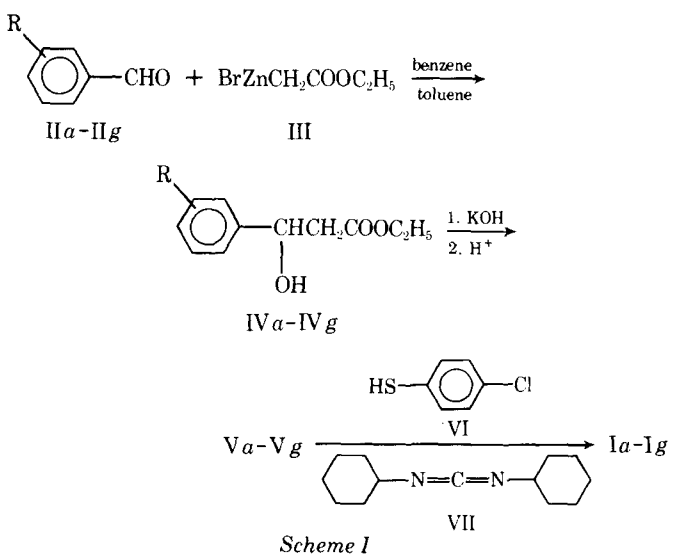

Scheme I

DISCUSSION

Chemistry—The title compounds were prepared by the following reaction sequence (Scheme I). The appropriately substituted benzaldehyde (II*a*–II*g*) was reacted with the zinc complex (III) formed by ethyl bromoacetate and zinc under the conditions of the Reformatsky reaction (6). The resulting crude ethyl 3-aryl-3-hydroxypropanoates (IV*a*–IV*g*) were hydrolyzed directly with alcoholic potassium hydroxide solution to yield the 3-aryl-3-hydroxypropanoic acids (V*a*–V*g*, Table II). The hydroxy acids were coupled with 4-chlorobenzenethiol (VI) using dicyclohexylcarbodiimide (VII) in dichloromethane to yield the desired products. All thiol esters showed a strong OH peak at 2.8–3.0 μm in their IR spectra (mineral oil mull).

Biological Activity—The propanethioates were screened *in vitro*

(2) I. K. Kacker and S. H. Zaheer, *J. Indian Chem. Soc.*, **28**, 344 (1951).
(3) G. Serventi and R. Marchesi, *Boll. Sci. Fac. Chim. Ind. Bologna*, **15**, 117 (1957).
(4) J. Klosa, *Prakt. Chem.*, **14**, 84 (1961).
(5) J. Klosa and H. Starke, East German pat. 35,123 (1965); through *Chem. Abstr.*, **63**, 8377f (1965).
(6) D. Stefanova, L. Daleva, R. Kolchagova, and L. Zehyazkov, *Khim. Farm. Zh.*, **7**, 19 (1973); through *Chem. Abstr.*, **80**, 14891e (1974).
(7) S. H. Zaheer and I. Kacker, Indian pat. 69,698 (1962); through *Chem. Abstr.*, **57**, 12443h (1962).
(8) H. Froemmel and H. Foken, East German pat. 37,239 (1965); through *Chem. Abstr.*, **63**, 8378b (1965).
(9) P. A. Petyunin and Y. V. Kozhevnikov, *Biol. Akt. Soedin. Akad. Nauk SSSR*, **1965**, 152; through *Chem. Abstr.*, **63**, 16348h (1965).
(10) N. Droge, Kemikolieforretning AIS. Neth., 295, 501 (1965); through *Chem. Abstr.*, **63**, 18113g (1965).
(11) E. Maggiorelli and G. Gangemi, *Boll. Chim. Farm.*, **103**, 748 (1964).
(12) H. Hoehlein, *Pharmazie*, **21**, 464 (1966).
(13) E. Maggiorelli and G. Gangemi, *Boll. Chim. Farm.*, **105**, 128 (1966).
(14) N. M. Sanghavi and A. V. Katdare, *Indian J. Pharm.*, **34**, 159 (1972).
(15) N. M. Sanghavi and M. G. Pai, *ibid.*, **36**, 71 (1974).
(16) W. Schnellbach and H. Houta, *Pharm. Acta Helv.*, **47**, 75 (1972).
(17) "British Pharmacopoeia 1973," British Pharmacopoeia Commission, London, England, 1973, p. 296.
(18) L. G. Chatten, R. E. Moskalyk, R. A. Locock, and F. J. Schaefer, *J. Pharm. Sci.*, **63**, 1294 (1974).
(19) I. M. Roushdi and R. M. Shafik, *J. Pharm. Sci. U.A.R.*, **9**, 65 (1968).

ACKNOWLEDGMENTS

The authors are grateful to Professor Dr. Thomas Kappe, Institut für Organische Chemie der Universität Graz, A-8010 Graz, Austria, for the IR, NMR, and mass spectral determinations.

S-(4-Chlorophenyl) 3-Aryl-3-hydroxypropanethioates as Antibacterial Agents

HARRY R. SNYDER, Jr.[x], STANLEY E. BURROUS, RAYMOND FREEDMAN, and THEADOR J. HEBERT

Received March 14, 1977, from the *Research and Development Department, Norwich-Eaton Pharmaceuticals Division of Morton-Norwich Products, Inc., Norwich, NY 13815.* Accepted for publication June 1, 1977.

Abstract □ A series of *S*-(4-chlorophenyl) 3-aryl-3-hydroxypropanethioates was prepared and shown to have *in vitro* activity against several selected bacterial species.

Keyphrases □ 3-Hydroxypropanethioates, 3-aryl—series synthesized, antibacterial activity evaluated □ Antibacterial activity—3-aryl-3-hydroxypropanethioates evaluated □ Structure-activity relationships—3-aryl-3-hydroxypropanethioates evaluated for antibacterial activity

The usual pathway for fatty acid (both saturated and unsaturated) synthesis in bacteria is *via* thiol esters of coenzyme A intermediates (1–3). The enzyme responsible for the introduction of the double bond into the fatty acids of *Escherichia coli* is β-hydroxydecanoylthiol ester dehydrase (2, 3). This enzyme is vital for the growth of *E. coli* (2); its inhibition completely stops the growth of the bacterium (4, 5).

The required substrate for dehydrase preferably contains β-hydroxydecanoate as a thiol ester (2–4), which is dehydrated to a β,γ-unsaturated ester. It was postulated that a reasonable structure for a dehydrase inhibitor would possess a thiol ester of a β-hydroxy acid in which the γ-carbon is tertiary and, therefore, incapable of forming a β,γ-double bond. Therefore, a series of *S*-(4-chlorophenyl) 3-aryl-3-hydroxypropanethioates (I*a*–I*g*, Table I) was prepared and tested for activity *in vitro* against several selected bacterial species.

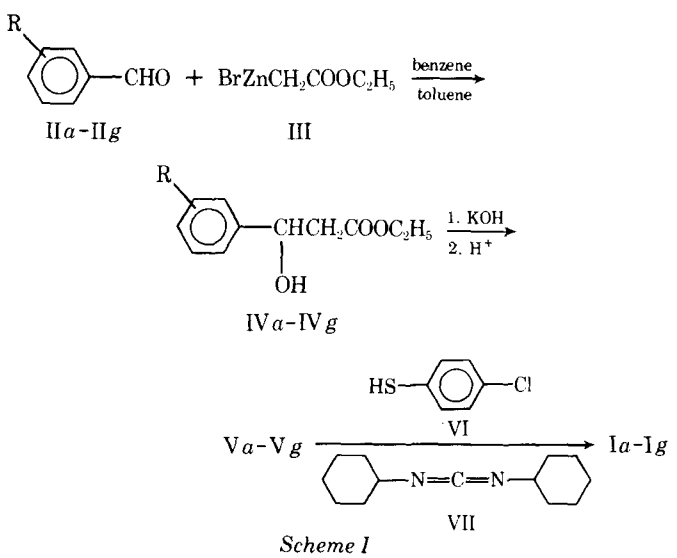

Scheme I

DISCUSSION

Chemistry—The title compounds were prepared by the following reaction sequence (Scheme I). The appropriately substituted benzaldehyde (II*a*–II*g*) was reacted with the zinc complex (III) formed by ethyl bromoacetate and zinc under the conditions of the Reformatsky reaction (6). The resulting crude ethyl 3-aryl-3-hydroxypropanoates (IV*a*–IV*g*) were hydrolyzed directly with alcoholic potassium hydroxide solution to yield the 3-aryl-3-hydroxypropanoic acids (V*a*–V*g*, Table II). The hydroxy acids were coupled with 4-chlorobenzenethiol (VI) using dicyclohexylcarbodiimide (VII) in dichloromethane to yield the desired products. All thiol esters showed a strong OH peak at 2.8–3.0 μm in their IR spectra (mineral oil mull).

Biological Activity—The propanethioates were screened *in vitro*

Table I—*S*-(4-Chlorophenyl) 3-Aryl-3-hydroxypropanethioates

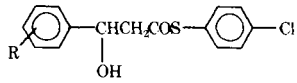

Compound	R	Melting Point	Yield, %	Recrystallization Solvent	Formula	Analysis, % Calc.	Found
I*a*	H	103–105°	60	Benzene–hexane	$C_{15}H_{13}ClO_2S$	C 61.53	61.86
						H 4.48	4.54
						Cl 12.11	12.08
I*b*	4-CH_3	113–114°	74	Benzene–hexane	$C_{16}H_{15}ClO_2S$	C 62.64	62.92
						H 4.93	4.97
						Cl 11.56	11.66
I*c*	4-C_2H_5	121–123°	60	Methanol	$C_{17}H_{17}ClO_2S$	C 63.64	63.36
						H 5.34	5.22
						Cl 11.05	11.12
I*d*	4-Cl	93–94°	66	Benzene–hexane	$C_{15}H_{12}Cl_2O_2S$	C 55.06	55.45
						H 3.70	3.84
						Cl 21.51	21.50
I*e*	2,4-Cl_2	78–79°	42	Methanol	$C_{15}H_{11}Cl_3O_2S$	C 49.81	49.74
						H 3.07	3.03
						Cl 29.41	29.54
I*f*	3,4-Cl_2	74–75°	77	Benzene–hexane	$C_{15}H_{11}Cl_3O_2S$	C 49.81	50.21
						H 3.07	3.18
						Cl 29.41	29.11
I*g*	3-Cl, 4-CH_3	85–86°	68	Benzene–hexane	$C_{16}H_{14}Cl_2O_2S$	C 56.31	56.35
						H 4.12	4.22
						Cl 20.78	20.81

Table II—3-Aryl-3-hydroxypropanoic Acids

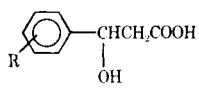

Compound	R	Melting Point	Yield[a], %	Recrystallization Solvent	Formula	Analysis, % Calc.	Found
V*a*	H	89–91°	23	Hexane–benzene	$C_9H_{10}O_3$	C 65.06	65.09
						H 6.07	6.13
						Cl —	—
V*b*	4-CH_3	88–90°	70	Benzene–hexane	$C_{10}H_{12}O_3$	C 66.65	66.53
						H 6.71	6.66
						Cl —	—
V*c*	4-C_2H_5	74–75°	45	Benzene–hexane	$C_{11}H_{14}O_3$	C 68.02	68.11
						H 7.27	7.25
						Cl —	—
V*d*	4-Cl[b]	75–77°	65	Benzene–hexane	$C_9H_9ClO_3$	C —	—
						H —	—
						Cl —	—
V*e*	2,4-Cl_2	124–125°	68	Benzene	$C_9H_8Cl_2O_3$	C 45.98	46.07
						H 3.43	3.55
						Cl 30.17	30.15
V*f*	3,4-Cl_2	74–75°	77	Benzene–hexane	$C_9H_8Cl_2O_3$	C 45.98	45.98
						H 3.43	3.43
						Cl 30.17	30.37
V*g*	3-Cl, 4-CH_3	85–86°	67	Benzene–hexane	$C_{10}H_{11}ClO_3$	C 55.95	56.12
						H 5.17	5.22
						Cl 16.52	16.32

[a] Yield calculated from aldehyde. [b] See Ref. 10.

Table III—*In Vitro* Antibacterial Activity of *S*-(4-Chlorophenyl) 3-Aryl-3-hydroxypropanethioates

Compound	Minimal Inhibitory Concentration Values, μg/ml *Staphylococcus aureus*	*Corynebacterium liquefaciens*	*Haemophilis vaginalis*	*Streptococcus agalactiae*	*Pasteurella multocida*	*Escherichia coli*
I*a*	6.25	6.25	12.50	3.10	6.25	>50
I*b*	12.50	12.50	3.10	3.10	3.10	>50
I*c*	6.25	6.25	6.25	3.10	6.25	>50
I*d*	12.50	6.25	3.10	6.25	6.25	>50
I*e*	6.25	3.10	12.50	12.50	25.00	>50
I*f*	25.00	12.50	25.00	12.50	25.00	>50
I*g*	12.50	12.50	25.00	12.50	25.00	>50

against *Staphylococcus aureus* (Mi-12)[1], *Corynebacterium liquefaciens* (Co-11)[1], *Haemophilis vaginalis* (He-127)[1], *Streptococcus agalactiae* (VStB-1)[1], *Pasteurella multocida* (VPa-6)[1], and *Escherichia coli* (Es-2)[1] according to procedures described previously (7, 8). Compounds I*a*–I*g* possess *in vitro* antibacterial properties against several selected bacterial species (Table III). However, the compounds were ineffective against *E. coli* at the level used.

[1] Eaton Laboratories strain numbers.

EXPERIMENTAL[2]

Crystallization solvents, yields, melting points, and analyses of the compounds synthesized are reported in Tables I and II. All spectra were

[2] The melting points were taken in open capillary tubes on a Mel-Temp melting-point apparatus and are uncorrected. IR spectra (Nujol mull) were obtained on a Perkin-Elmer Infracord model 137, and NMR spectra (deuterated dimethyl sulfoxide using tetramethylsilane as an internal standard) were obtained on a Varian model A-60A spectrometer.

consistent with the assigned structures. Compounds Ia–Ig gave a strong qualitative test for sulfur using the oxygen flask ignition procedure.

The general procedure for the synthesis of the 3-aryl-3-hydroxypropanoic acids (Va–Vg) is illustrated by the preparation of 3-(3-chloro-4-methylphenyl)-3-hydroxypropanoic acid (Vg). The Reformatsky reaction was carried out as described (6) using 3-chloro-4-methylbenzaldehyde (9) (154 g, 1.0 mole), ethyl bromoacetate (150 ml, 1.3 moles), and zinc dust (90 g, 1.35 g-atoms). The crude ester was treated with a solution of 85% potassium hydroxide (80 g, 1.2 moles) in 95% ethanol (1500 ml). The mixture was refluxed for 4 hr and was then evaporated *in vacuo*.

The residue was dissolved in water (1500 ml) and extracted with ether. The aqueous layer was acidified with concentrated hydrochloric acid and extracted with chloroform (2 × 700 ml). The chloroform extracts were combined and dried over anhydrous magnesium sulfate. The drying agent was removed by filtration, and the solvent was removed *in vacuo* to leave the solid product (Vg).

The general procedure for the synthesis of the *S*-(4-chlorophenyl) 3-aryl-3-hydroxypropanethioates (Ia–Ig) is illustrated by the preparation of *S*-(4-chlorophenyl) 3-(3-chloro-4-methylphenyl)-3-hydroxypropanethioate (Ig). A solution of Vg (43 g, 0.2 mole) and VI (29 g, 0.2 mole) in dichloromethane (~600 ml) was stirred at room temperature. A solution of VII (41 g, 0.2 mole) in a small amount of dichloromethane was added in one portion. There was an immediate, very exothermic, reaction with the formation of a white precipitate. After the initial reaction had subsided, the reaction mixture was stirred for 4 hr at room temperature and then filtered. The filtrate was evaporated to dryness under reduced pressure to leave a white, solid product (Ig).

REFERENCES

(1) G. Scheurbrandt and K. Bloch, *J. Biol. Chem.*, **237**, 2064 (1962).

(2) A. T. Voris, S. Matsumura, and K. Bloch, *ibid.*, **239**, 3653 (1964).

(3) D. Brock, L. Kass, and K. Bloch, *ibid.*, **242**, 4432 (1967).

(4) G. Helmkamp, Jr., R. Rando, D. Brock, and K. Bloch, *ibid.*, **243**, 3229 (1968).

(5) L. Kass, *ibid.*, **243**, 3223 (1968).

(6) R. Adams, "Organic Reactions," vol. I, Wiley, New York, N.Y., 1947, p. 16.

(7) R. Freedman and R. E. Chamberlain, in "Antimicrobial Agents and Chemotherapy," G. L. Hobby, Ed., Ann Arbor, Mich., 1967, p. 502.

(8) H. R. Snyder, Jr., C. F. Spencer, and R. Freedman, *J. Pharm. Sci.*, **66**, 1204 (1977).

(9) R. J. Alaimo and C. J. Hatton, *J. Med. Chem.*, **19**, 349 (1976).

(10) D. S. Noyce, P. A. King, C. A. Lane, and W. L. Reed, *J. Am. Chem. Soc.*, **84**, 1638 (1962).

ACKNOWLEDGMENTS

The authors are indebted to Mrs. Christina Kinney, Mr. Patrick Moynihan, Mrs. V. Borchers, Mr. Warren Smith, Mr. Gerald Lawton, and Mr. Alex Winterstein for technical assistance and to Mr. Grant Gustin and Mr. Marvin Tefft for the analytical data. Mrs. Patricia Curtis obtained the NMR spectra.

Assessment of Enterohepatic Circulation of ^{3}H-Digoxin with a Minimal Interruption Technique

JAMES H. CALDWELL ˣ, NEIL R. THOMFORD, and YOICHIRO KAKUMOTO

Received March 14, 1977, from the *Departments of Medicine and Surgery, College of Medicine, Ohio State University, Columbus, OH 43210.* Accepted for publication June 8, 1977.

Abstract □ The biliary excretion of ^{3}H-digoxin in rats prepared for bile sampling with minimal interruption of the enterohepatic circulation was compared with that in rats with complete interruption after intraduodenal or intravenous administration. Following dosage by either route, significantly more radioactivity was recovered from animals with nearly intact enterohepatic circulation. The method described allows direct measurement of this cycle in unanesthetized animals without the consequences of bile depletion.

Keyphrases □ ^{3}H-Digoxin—biliary excretion measured by enterohepatic circulation minimal interruption technique, rats □ Excretion, biliary—^{3}H-digoxin, measured by enterohepatic circulation minimal interruption technique, rats □ Enterohepatic circulation—minimal interruption technique used to measure biliary excretion of ^{3}H-digoxin, rats □ Cardiotonic agents—digoxin, biliary excretion measured by enterohepatic circulation minimal interruption technique, rats

The enterohepatic cycle plays a major role in the biotransformation and disposition of some drugs. This aspect of cardiac glycoside metabolism has received considerable attention since it was suggested (1) that enterohepatic recycling is a major determinant of the half-life of these compounds. Direct measurement of the enterohepatic cycle is not usually done; instead, conclusions are drawn from data on fecal excretion or bile fistula preparations.

While these methods are useful for estimating the hepatobiliary contribution to total drug disposition, they allow only indirect conclusions about the extent of recycling. A model previously used for studies of biliary responses to partial hepatectomy and hypoxia (2–4) was adopted to compare the biliary excretion of digoxin in rats with minimal and total interruption of the enterohepatic circulation.

EXPERIMENTAL

^{3}H-Digoxin[1] (specific activity of 1.0 mCi/1.33 μg) was 96% radiochemically pure. Solutions of a specific activity of 0.25 μCi/μg/0.01 ml were prepared by diluting the stock solution with unlabeled digoxin. Aliquots of standards and samples were assayed for radioactivity in a liquid scintillation spectrometer after addition to 10 ml of scintillation medium[2], using automatic external standardization.

Twenty-four female Wistar rats, 250–300 g, were anesthetized with ether, and a midline incision was made. The proximal bile duct was cannulated with polyethylene No. 50 tubing[3]. A duodenostomy was constructed with polyethylene No. 160 tubing, and both duodenal and biliary cannulas were brought through a skin incision in the right flank. The two tubes were connected with a short length of flexible tubing (1.5 mm i.d., 2.4 mm o.d.), the skin was closed with a single suture, and the midline wound was closed.

The animals were allowed to recover in individual metabolic cages; they were observed and allowed free access to food and water for at least 48

[1] New England Nuclear Corp., Boston, Mass.
[2] Scintisol-Complete, Isolab, Akron, Ohio.
[3] Intramedic, Becton, Dickinson and Co., Parsippany, N.J.

consistent with the assigned structures. Compounds Ia–Ig gave a strong qualitative test for sulfur using the oxygen flask ignition procedure.

The general procedure for the synthesis of the 3-aryl-3-hydroxypropanoic acids (Va–Vg) is illustrated by the preparation of 3-(3-chloro-4-methylphenyl)-3-hydroxypropanoic acid (Vg). The Reformatsky reaction was carried out as described (6) using 3-chloro-4-methylbenzaldehyde (9) (154 g, 1.0 mole), ethyl bromoacetate (150 ml, 1.3 moles), and zinc dust (90 g, 1.35 g-atoms). The crude ester was treated with a solution of 85% potassium hydroxide (80 g, 1.2 moles) in 95% ethanol (1500 ml). The mixture was refluxed for 4 hr and was then evaporated *in vacuo*.

The residue was dissolved in water (1500 ml) and extracted with ether. The aqueous layer was acidified with concentrated hydrochloric acid and extracted with chloroform (2 × 700 ml). The chloroform extracts were combined and dried over anhydrous magnesium sulfate. The drying agent was removed by filtration, and the solvent was removed *in vacuo* to leave the solid product (Vg).

The general procedure for the synthesis of the *S*-(4-chlorophenyl) 3-aryl-3-hydroxypropanethioates (Ia–Ig) is illustrated by the preparation of *S*-(4-chlorophenyl) 3-(3-chloro-4-methylphenyl)-3-hydroxypropanethioate (Ig). A solution of Vg (43 g, 0.2 mole) and VI (29 g, 0.2 mole) in dichloromethane (~600 ml) was stirred at room temperature. A solution of VII (41 g, 0.2 mole) in a small amount of dichloromethane was added in one portion. There was an immediate, very exothermic, reaction with the formation of a white precipitate. After the initial reaction had subsided, the reaction mixture was stirred for 4 hr at room temperature and then filtered. The filtrate was evaporated to dryness under reduced pressure to leave a white, solid product (Ig).

REFERENCES

(1) G. Scheurbrandt and K. Bloch, *J. Biol. Chem.*, **237**, 2064 (1962).

(2) A. T. Voris, S. Matsumura, and K. Bloch, *ibid.*, **239**, 3653 (1964).

(3) D. Brock, L. Kass, and K. Bloch, *ibid.*, **242**, 4432 (1967).

(4) G. Helmkamp, Jr., R. Rando, D. Brock, and K. Bloch, *ibid.*, **243**, 3229 (1968).

(5) L. Kass, *ibid.*, **243**, 3223 (1968).

(6) R. Adams, "Organic Reactions," vol. I, Wiley, New York, N.Y., 1947, p. 16.

(7) R. Freedman and R. E. Chamberlain, in "Antimicrobial Agents and Chemotherapy," G. L. Hobby, Ed., Ann Arbor, Mich., 1967, p. 502.

(8) H. R. Snyder, Jr., C. F. Spencer, and R. Freedman, *J. Pharm. Sci.*, **66**, 1204 (1977).

(9) R. J. Alaimo and C. J. Hatton, *J. Med. Chem.*, **19**, 349 (1976).

(10) D. S. Noyce, P. A. King, C. A. Lane, and W. L. Reed, *J. Am. Chem. Soc.*, **84**, 1638 (1962).

ACKNOWLEDGMENTS

The authors are indebted to Mrs. Christina Kinney, Mr. Patrick Moynihan, Mrs. V. Borchers, Mr. Warren Smith, Mr. Gerald Lawton, and Mr. Alex Winterstein for technical assistance and to Mr. Grant Gustin and Mr. Marvin Tefft for the analytical data. Mrs. Patricia Curtis obtained the NMR spectra.

Assessment of Enterohepatic Circulation of ^{3}H-Digoxin with a Minimal Interruption Technique

JAMES H. CALDWELL ˣ, NEIL R. THOMFORD, and YOICHIRO KAKUMOTO

Received March 14, 1977, from the *Departments of Medicine and Surgery, College of Medicine, Ohio State University, Columbus, OH 43210.* Accepted for publication June 8, 1977.

Abstract □ The biliary excretion of ^{3}H-digoxin in rats prepared for bile sampling with minimal interruption of the enterohepatic circulation was compared with that in rats with complete interruption after intraduodenal or intravenous administration. Following dosage by either route, significantly more radioactivity was recovered from animals with nearly intact enterohepatic circulation. The method described allows direct measurement of this cycle in unanesthetized animals without the consequences of bile depletion.

Keyphrases □ ^{3}H-Digoxin—biliary excretion measured by enterohepatic circulation minimal interruption technique, rats □ Excretion, biliary—^{3}H-digoxin, measured by enterohepatic circulation minimal interruption technique, rats □ Enterohepatic circulation—minimal interruption technique used to measure biliary excretion of ^{3}H-digoxin, rats □ Cardiotonic agents—digoxin, biliary excretion measured by enterohepatic circulation minimal interruption technique, rats

The enterohepatic cycle plays a major role in the biotransformation and disposition of some drugs. This aspect of cardiac glycoside metabolism has received considerable attention since it was suggested (1) that enterohepatic recycling is a major determinant of the half-life of these compounds. Direct measurement of the enterohepatic cycle is not usually done; instead, conclusions are drawn from data on fecal excretion or bile fistula preparations.

While these methods are useful for estimating the hepatobiliary contribution to total drug disposition, they allow only indirect conclusions about the extent of recycling. A model previously used for studies of biliary responses to partial hepatectomy and hypoxia (2–4) was adopted to compare the biliary excretion of digoxin in rats with minimal and total interruption of the enterohepatic circulation.

EXPERIMENTAL

^{3}H-Digoxin[1] (specific activity of 1.0 mCi/1.33 μg) was 96% radiochemically pure. Solutions of a specific activity of 0.25 μCi/μg/0.01 ml were prepared by diluting the stock solution with unlabeled digoxin. Aliquots of standards and samples were assayed for radioactivity in a liquid scintillation spectrometer after addition to 10 ml of scintillation medium[2], using automatic external standardization.

Twenty-four female Wistar rats, 250–300 g, were anesthetized with ether, and a midline incision was made. The proximal bile duct was cannulated with polyethylene No. 50 tubing[3]. A duodenostomy was constructed with polyethylene No. 160 tubing, and both duodenal and biliary cannulas were brought through a skin incision in the right flank. The two tubes were connected with a short length of flexible tubing (1.5 mm i.d., 2.4 mm o.d.), the skin was closed with a single suture, and the midline wound was closed.

The animals were allowed to recover in individual metabolic cages; they were observed and allowed free access to food and water for at least 48

[1] New England Nuclear Corp., Boston, Mass.
[2] Scintisol-Complete, Isolab, Akron, Ohio.
[3] Intramedic, Becton, Dickinson and Co., Parsippany, N.J.

hr. Twenty animals in good condition were then fasted overnight; on the morning of experiment, they were placed in a restraint cage but allowed continued access to water. The flank incision was opened by cutting the single suture, and the bile and duodenal cannulas were disconnected.

Experiments began with the intraduodenal or intravenous administration of ^{3}H-digoxin in a dose of 2.5 μCi/10 μg/100 g. For intraduodenal administration, the dose was instilled into the duodenal cannula and the tubing was clamped. Intravenous doses were given over 1 min into a tail vein. Five rats in each group (minimally or totally interrupted) received drug by either the intraduodenal or intravenous route. Collection of bile began at the same time. Hourly bile volume was measured by collection in a graduated centrifuge tube.

In minimally interrupted enterohepatic cycle experiments (10 animals), duplicate 0.025-ml aliquots of each bile sample were immediately removed for assay, and the remainder of the collected bile was returned to the intestine through the duodenal cannula. Since hourly bile volumes were approximately 1.0 ml or more, the removal of 0.05 ml for assay resulted in no more than a 5% interruption of the cycle. For interrupted enterohepatic cycle experiments (10 animals), similar aliquots were taken for assay, but the total hourly bile volume was replaced by fresh donor rat bile containing no drug. Thus, in the latter group of animals, bile salt depletion was prevented while total removal of drug *via* the bile fistula was achieved.

Collections were continued for 12 hr. Total radioactivity over 12 hr was calculated as the sum of the product of hourly bile volume and disintegrations per minute per milliliter for each sample and expressed as a percent of the dose.

RESULTS

Significantly more radioactivity was recovered in bile from animals with minimally interrupted enterohepatic circulation when compared with those with total biliary drainage. After intravenous dosing, 90.2 ± 18.5 and 60.5 ± 21.1% ($p < 0.05$) were recovered from intact and interrupted animals, respectively. Following intraduodenal dosing, 77.1 ± 22.9 and 42.9 ± 2.9% ($p < 0.025$) were recovered. Since neither group was depleted of bile, the results reflect the recycling of tritium-labeled drug and metabolites during the study period.

Characterization of the recovered radioactivity was not carried out in order not to remove more bile from the intact animals than the minimum required for assay. Previously (5), the majority of the radioactivity recovered from bile fistula rats 12 hr after dosing was unchanged ^{3}H-digoxin plus its principal metabolites.

DISCUSSION

The results of this study are in good agreement with those of other investigations. Rietbrock *et al.* (6) reported 71 and 45% excretion of ^{3}H-digoxin 12 hr after intravenous and intraduodenal administrations, respectively, in anesthetized rats with bile fistulas receiving donor bile replacement. Russell and Klaassen (7), using bile fistula rats without donor bile, found 59% biliary excretion of ^{3}H-digoxin 12 hr after intravenous dosing.

Abshagen *et al.* (5), using a method similar to that described here, found in anesthetized rats that interruption of the enterohepatic circulation reduced the blood half-life of total radioactivity by 50% and that the principal metabolites of ^{3}H-digoxin, bis- and monodigitoxoside, were extensively recycled along with the parent glycoside. Since the percent excretion of dose in intact rats was not compared with that reported for bile fistula animals, the present investigation was conducted to assess, by direct comparison, the contribution of reabsorbed digoxin and metabolites to total hepatobiliary disposition. The principal metabolites of digoxin possess positive inotropic activity (8). Therefore, it seems reasonable to relate the biological duration of action to the retention of both the parent drug and metabolites as estimated by total radioactivity assay.

Several methods are available for estimating the role of biliary excretion and intestinal reabsorption in drug disposition. The determination of fecal excretion does not allow direct measurement of biliary excretion or whether recycling occurs. Bile fistula studies allow measurement of biliary output but do not assess recycling. Refeeding bile from dosed animals to other recipient animals demonstrates that recycling can occur but does not permit its quantitation in the presence of the original dose. Demonstration of a reduced $T_{1/2}$ in bile fistula animals confirms that biliary excretion plays a considerable role in total body drug disposition but does not predict the extent of recycling. The present method allows continuous sampling of biliary excretion while imposing minimal interruption of the enterohepatic circulation in unanesthetized animals.

This principle previously was applied to an existing method for assessing biliary physiology in humans. With double-lumen tubes for duodenal perfusion of a nonabsorbable marker and correction for incomplete recovery of aspirated bile, 30% of a single parenteral dose of ^{3}H-digoxin was found in the bile of normal volunteers in 24 hr (9). This result contrasts with a calculated total percent enterohepatic cycling of 6.5% from studies of postoperative patients with bile fistulas (10). The results of the present study and previous findings suggest that underestimation of the enterohepatic cycle is likely when methods that interrupt this cycle are employed.

REFERENCES

(1) G. T. Okita, *Fed. Proc.*, **26,** 1125 (1967).

(2) N. R. Thomford and P. T. Butterfield, *Surgery,* **66,** 1073 (1969).

(3) P. T. Butterfield, G. M. Penn, and N. R. Thomford, *ibid.*, **68,** 651 (1970).

(4) Y. Kakumoto, R. C. Gardner, K. J. Isselbacher, and R. A. Malt, *Surg. Forum,* **22,** 47 (1971).

(5) U. Abshagen, K. V. Bergmann, and N. Rietbrock, *Naunyn-Schmiedebergs Arch. Pharmacol.,* **275,** 1 (1972).

(6) N. Rietbrock, U. Abshagen, K. V. Bergmann, and H. Kewitz, *ibid.*, **274,** 171 (1972).

(7) J. Q. Russell and C. D. Klaassen, *J. Pharmacol. Exp. Ther.,* **186,** 455 (1973).

(8) P. M. Stephen, S. Dutta, and B. H. Marks, *Naunyn-Schmiedebergs Arch. Pharmacol.,* **292,** 251 (1976).

(9) J. H. Caldwell and C. T. Cline, *Clin. Pharmacol. Ther.,* **19,** 410 (1976).

(10) J. E. Doherty, W. F. Flanigan, M. L. Murphy, R. T. Bullock, G. L. Dalrymple, O. W. Beard, and W. H. Perkins, *Circulation,* **42,** 867 (1970).

ACKNOWLEDGMENTS

Supported in part by a grant from the Central Ohio Heart Chapter, the American Heart Association, and by Grant 1 R01 AM 1255301 from the National Institutes of Health.

GLC Determination of Floxuridine in Plasma Using a Thermionic Nitrogen Detector

A. P. De LEENHEER [x] **and C. F. GELIJKENS**

Received March 18, 1977, from the *Laboratoria voor Medische Biochemie en voor Klinische Analyse, Faculteit van de Farmaceutische Wetenschappen, Rijksuniversiteit, Academisch Ziekenhuis, 135 De Pintelaan, 9000-Gent, Belgium.* Accepted for publication June 24, 1977.

Abstract □ A specific GLC method was developed for the determination of floxuridine in plasma using the thermionic nitrogen detector. The method involves the isolation of the compound and internal standard from plasma on a strong anion-exchange column at pH 10, followed by elution with 0.3 *M* acetic acid in methanol. The eluate is evaporated to dryness, and the residue is dissolved in dimethyl sulfoxide and permethylated with potassium *tert*-butoxide and methyl iodide. The permethylated compounds are reextracted from the reaction mixture with cyclohexane–methylene dichloride (9:1). The organic solution is evaporated to dryness, the residue is dissolved in ethyl acetate, and an aliquot is analyzed by GLC on a 3% OV-17 column. The extraction recovery from spiked plasma was 93.2 ± 2.1% (*SD*), whereas linearity for the overall procedure was in the 0–1-μg/ml range. The detection limit of the thermionic nitrogen detector was 50 ng/ml. The within-run and within-days precision (*CV*) were 4.0 and 6.2%, respectively, at 300 ng/ml.

Keyphrases □ Floxuridine—GLC analysis in plasma □ GLC—analysis, floxuridine in plasma □ Antineoplastic–antiviral agents—floxuridine, GLC analysis in plasma

Biochemical studies (1) have shown floxuridine (5-fluoro-2′-deoxyuridine) (I) to be an intermediate in the formation of 5-fluoro-2′-deoxyuridine 5′-monophosphate, a potent inhibitor of thymidylate synthetase (2), a well-known target enzyme in cancer chemotherapy. This conversion takes place either directly by the action of deoxythymidine kinase (3) or indirectly by pathways in which I is first degraded to fluorouracil by nucleoside phosphorylase (4) and subsequently converted to 5-fluorouridine 5′-monophosphate (5, 6), which is finally metabolized to 5-fluoro-2′-deoxyuridine 5′-monophosphate by ribonucleotide reductase (7).

Cohen (8) identified I among the metabolites formed after administration of 1-(tetrahydrofuran-2-yl)-5-fluorouracil to rats. Several investigators (9–11) studied the physiological disposition of I and its metabolites after administration to patients. Therapeutic responses to this fluorinated nucleoside have been reported in various cancers (12–15).

Although several methods (16–22) were developed for fluorouracil analysis in biological fluids, few methods exist for the determination of I. Clarkson *et al.* (11) described a sensitive microbiological assay, which, however, is unable to differentiate between fluorouracil and I. Pantarotto *et al.* (18) published a mass fragmentographic method.

The present report describes a sensitive and simple GLC method for the measurement of I levels in human plasma; a thermionic nitrogen detector is used.

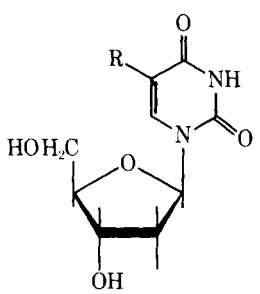

I: R = F
II: R = Cl

EXPERIMENTAL

Reagents—The potassium *tert*-butoxide[1] stock solution (6 g/100 ml) was prepared as reported previously (23) and diluted prior to use with an equal volume of dry dimethyl sulfoxide[2].

A carbonate buffer of pH 10 and ionic strength 0.1 was prepared by dissolving 2.1 g of sodium bicarbonate and 2.7 g of sodium carbonate in 1000 ml of double-distilled water.

The liquid scintillation cocktail consisted of 4 g of 2,5-diphenyloxazole[3], 50 mg of 1,4-bis[2-(5-phenyloxazolyl)]benzene[3], and 100 g of naphthalene[2]/liter of dioxane[2] (all scintillation grade).

All other inorganic and organic chemicals used were analytical grade, except methanol[2] (fluorometric quality).

Extraction Procedure—Pipet 1.0 ml of plasma, 100 μl of internal standard solution [2.1 mg of 5-chloro-2′-deoxyuridine[4] (II)/100 ml of distilled water], and 5.0 ml of carbonate buffer in a 15-ml centrifuge tube. Transfer the sample quantitatively (two subsequent washings with 1.0 ml of carbonate buffer) to a 2.0-cm × 6-mm i.d. glass column loosely packed with anion-exchange resin[5], plugged with glass wool, and fitted with a polytef tap and a 15-ml reservoir on top.

Allow the sample to pass through the resin bed and wash consecutively with 15 ml of distilled water and 15 ml of methanol; elute the compound and internal standard with 10 ml of 0.3 *M* acetic acid in methanol. Then evaporate the collected eluate to dryness in a water bath at 50° under a nitrogen stream.

Derivatization—Dissolve the residue of the column eluate in 200 μl of dry dimethyl sulfoxide. Add 50 μl of potassium *tert*-butoxide reagent, wait 10 sec, and then add 100 μl of methyl iodide. After 1 hr, add 5.0 ml of 0.05 *N* H_2SO_4; extract twice with 5.0 ml of cyclohexane–methylene dichloride (9:1). Evaporate the combined extracts to dryness in a heating block[6] at 50° under a nitrogen stream and dissolve the residue in 50 μl of ethyl acetate with the aid of a whirl mixer[7].

Parameters for GLC Analysis—A gas chromatograph[8] equipped with dual nitrogen–phosphorus thermionic detectors[9] was used for single-column operation. The stationary liquid phase, 3% OV-17[10], was coated on 100–120-mesh Gas Chrom Q[11] and packed into a 1.6-m × 2-mm i.d. spiral silanized glass column. The temperature settings were: oven, 205°; injection port, 250°; and detector, 300°.

Helium was used as a carrier gas at a linear velocity, $\bar{u}_0$, of 10 cm/sec; hydrogen and air flows were adjusted to 4 and 130 ml/min, respectively. The voltage controlling the temperature of the rubidium salt bead was set to obtain 30% of full-scale recorder deflection with an electrometer setting of 1 × 32, the zero control being turned fully counterclockwise.

The electrometer setting employed was 1 × 16. A 0–1-mv range recorder[12] was used. All injections were made on-column with a 10-μl sy-

[1] Fluka A. G., Buchs, Switzerland.
[2] E. Merck A. G., Darmstadt, West Germany.
[3] Packard Instrument Co., Downers Grove, Ill.
[4] Calbiochem A. G., Lucerne, Switzerland.
[5] AG 1-X4 (Cl^-), 100–200 mesh, Bio-Rad, Richmond, Va.
[6] Dri-Bath, Thermolyne, Dubuque, Iowa.
[7] Vortex Supermixer, Lab-Line Instruments, Melrose Park, Ill.
[8] Hewlett-Packard model 5710A.
[9] Hewlett-Packard model 18789A.
[10] Hewlett-Packard, Avondale, Pa.
[11] Supelco Inc., Bellefonte, Pa.
[12] Hewlett-Packard model 7123B.

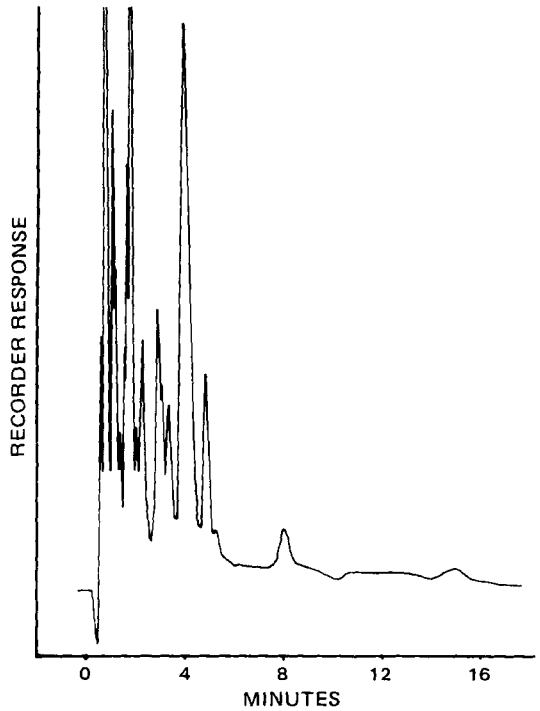

Figure 1—*Gas chromatogram of a drug-free plasma sample. The column was 3% OV-17 (oven temperature = 205°, $\bar{u}_0$ = 10 cm/sec).*

ringe[13], using an injection volume of 1 μl.

Linearity Experiments—Solutions of I[14] in citrate plasma of human origin were made containing 0.1, 0.2, 0.4, 0.6, 0.8, and 1.0 μg/ml. Samples (1.0 ml) were treated as described in the extraction and derivatization procedures and analyzed by GLC. Peak height ratios of I to the internal standard were plotted *versus* the concentration of I (micrograms per milliliter).

Recovery Experiments—To 1.0-ml plasma samples containing 1.0 μg of I/ml, 11 ng of 6-^{3}H-I[15] (specific activity of 2.3 Ci/mmole) was added. Dilutions with blank plasma were made to obtain 0.1, 0.2, 0.4, 0.6, 0.8, and 1.0 μg of I/ml (corresponding to 1.1, 2.2, 4.4, 6.6, 8.8, and 11 ng of 6-^{3}H-I/ml, respectively). Aliquots of 1.0 ml were then taken through the extraction procedure but without adding internal standard.

Column eluates were collected separately in polyethylene counting vials[3] and evaporated to dryness in a sand bath at 50° under a nitrogen stream. The residues were dissolved in 0.5 ml of distilled water, and 10 ml of liquid scintillation cocktail was added. Polyethylene vials containing 0.5-ml aliquots of original plasma samples and 10 ml of liquid scintillation cocktail were used as references to estimate extraction recoveries. All vials were counted for 5 min in a liquid scintillation counter[16]. The internal standard method, *i.e.*, adding 100 μl of tritiated water (specific activity of 0.94 μCi/g) to each counting vial, was used to correct for quenching.

Recovery values were calculated as follows:

$$\text{recovery (\%)} = \frac{\text{dpm of extract}}{(\text{dpm of reference sample}) \times 2} \times 100 \quad \text{(Eq. 1)}$$

RESULTS AND DISCUSSION

Due to its highly polar character, the I molecule is poorly extracted from aqueous solutions using double-phase extraction procedures. In addition, the required high polarity of the organic solvent system always causes many endogenous impurities to be coextracted from plasma, resulting in interfering peaks. Therefore, an on-column extraction technique (22) was developed.

Being a weak acid (pKa = 7.66) (24), I is present almost entirely as a monoanionic species (99.55%) at pH 10 and is quantitatively adsorbed on the anion-exchange resin employed. Other plasma constituents are removed with a water–methanol wash. Subsequent quantitative elution of I is performed with 0.3 *M* acetic acid in methanol. No apparent denaturation of plasma proteins occurs. The isolation of I from plasma was quantitative. Recovery experiments showed a mean of 93.2 ± 2.1% (*SD*) in the 0–1-μg/ml range.

The permethylation reaction was shown earlier (23) to yield stable low molecular weight permethylated nucleosides suitable for quantitative GLC. Initially, columns prepared with 3% OV-17[10], 3% SP-2250[11], 3% OV-25[10], and 1% STAP[11] (reaction product of Carbowax 20 M and succinic acid) were found to be superior in terms of selectivity and peak symmetry. Under the conditions described and with the 3% OV-17 column, the retention times, R_t, of I and the internal standard, 5-chloro-2′-deoxyuridine (II), were 6.4 and 12.0 min, respectively.

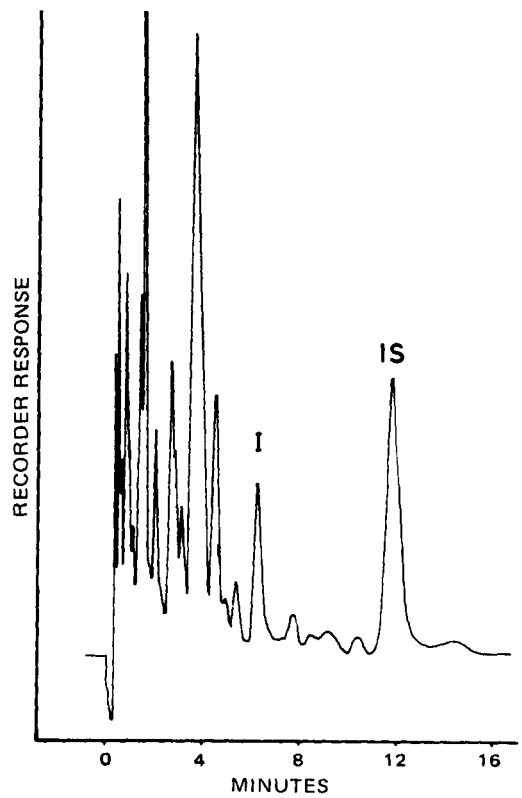

Figure 2—*Gas chromatogram of a plasma sample spiked with 500 ng of I/ml. The column was 3% OV-17 (oven temperature = 205°, $\bar{u}_0$ = 10 cm/sec). IS = internal standard.*

Table I—Precision of the I Assay

Long-Term Precision		12 Replicate
Day	ng/ml	Analyses, ng/ml
1	271	290
2	298	314
3	301	292
4	299	287
5	269	292
6	273	288
7	295	304
8	277	291
9	299	290
10	294	321
11	317	285
12	306	308
13	289	Mean 297
14	330	*SD* 12
15	299	*CV*, % 4.0
16	294	
17	268	
18	335	
19	285	
20	294	
	Mean 295	
	SD 18	
	CV, % 6.2	

[13] Hamilton 701, Reno, Nev.
[14] Sigma Chemical Co., St. Louis, Mo. (or Produits Roche N.V., Brussels, Belgium).
[15] Radiochemical Centre, Amersham, England.
[16] Tri-Carb 3390, Packard Instrument Co.

Compound II was chosen on the basis of its structural similarity to I. Due to its similar pKa (7.90) (25), II can be added directly to the plasma sample. Compound II also is easily and quantitatively permethylated with the method described. The derivative obtained is well extracted from the reaction mixture before GLC and yields excellent chromatographic characteristics on the 3% OV-17 column system. The chromatograms (Figs. 1 and 2) showed no major interfering peaks eluting in the regions corresponding to I and II.

The use of the thermionic nitrogen detector (26) provides higher sensitivity and better specificity for nitrogen-containing compounds. A linear relationship between peak height ratios of I to II and plasma concentrations of I was demonstrated in the 0–1-μg/ml range (regression line: $y = 1.02x - 0.01$, $r = 0.996$). A detection limit of 50 ng of I/ml was obtained by injecting 1.0 μl of the 50 μl of ethyl acetate from the reconstituted sample residues, using 1.0 ml of plasma for analysis.

The within-run precision of the overall procedure was determined by analyzing 12 plasma samples spiked with 300 ng of I/ml. A standard deviation and a coefficient of variation of 12 ng/ml and 4.0%, respectively, were found. Analysis of 20 plasma samples, also spiked with 300 ng of I/ml, over 3 weeks yielded some indication of the long-term precision, namely, 18 ng/ml (*SD*) and 6.2% (*CV*). These data on replicate analysis and long-term precision are presented in Table I and are acceptable for an analysis at the submicrogram level.

The described procedure is an example of the superiority of the thermionic nitrogen detector because of its selectivity for nitrogen-containing compounds. Although interference from other endogenous substances was expected, blank plasma samples and plasma samples spiked with I at the submicrogram level were taken through the procedure and gave no significant peaks that might interfere. Besides this increased selectivity, sensitivity is increased approximately 20 times compared to the flame-ionization detector.

The applicability of this method for plasma samples collected from patients treated with I was not demonstrated because I is not used as a chemotherapeutic agent to treat cancer cases in our medical environment. Since I occurs as a metabolite in humans treated with the antineoplastic agent fluorouracil, development of the described procedure is important. Therefore, we propose to extend our method for the assay of I in urine and tumorous tissue.

REFERENCES

(1) C. Heidelberger, *Prog. Nucleic Acid Res. Mol. Biol.*, **4**, 1 (1965).

(2) K. U. Hartman and C. Heidelberger, *J. Biol. Chem.*, **236**, 3006 (1961).

(3) E. Bresnick and U. B. Thompson, *ibid.*, **240**, 3967 (1965).

(4) G. D. Birnie, H. Kroeger, and C. Heidelberger, *Biochemistry*, **2**, 566 (1963).

(5) E. Harbers, N. K. Chaudhuri, and C. Heidelberger, *J. Biol. Chem.*, **234**, 1255 (1959).

(6) P. Reyes, *Biochemistry*, **8**, 2057 (1969).

(7) R. J. Kent and C. Heidelberger, *Mol. Pharmacol.*, **8**, 465 (1972).

(8) A. M. Cohen, *Drug Metab. Disp.*, **3**, 303 (1975).

(9) K. L. Mukherjee, J. Boohar, D. Wentland, F. J. Ansfield, and C. Heidelberger, *Cancer Res.*, **23**, 49 (1963).

(10) K. L. Mukherjee, A. R. Curreri, M. Javid, and C. Heidelberger, *ibid.*, **23**, 67 (1963).

(11) B. Clarkson, A. O'Connor, L. R. Winston, and D. Hutchison, *Clin. Pharmacol. Ther.*, **5**, 581 (1964).

(12) A. R. Curreri and F. J. Ansfield, *Cancer Chemother. Rep.*, **2**, 8 (1959).

(13) C. W. Young *et al.*, *ibid.*, **6**, 17 (1960).

(14) C. Heidelberger and F. J. Ansfield, *Cancer Res.*, **23**, 1226 (1963).

(15) R. J. Reitemeier, C. G. Moertel, and R. G. Hahn, *Cancer Chemother. Rep.*, **44**, 39 (1965).

(16) J. J. Windheuser, J. L. Sutter, and E. Auen, *J. Pharm. Sci.*, **61**, 301 (1972).

(17) J. L. Cohen and J. P. Brennan, *ibid.*, **62**, 572 (1973).

(18) C. Pantarotto, A. Martini, G. Belvedere, A. Bossi, M. G. Donelli, and A. Frigerio, *J. Chromatogr.*, **99**, 519 (1974).

(19) K. V. Rao, K. Killion, and Y. Taurikut, *J. Pharm. Sci.*, **63**, 1328 (1974).

(20) C. Finn and W. Sadée, *Cancer Chemother. Rep.*, **59**, 279 (1975).

(21) B. L. Hillcoat, M. Kawai, P. B. McCullogh, J. Rosenfeld, and C. K. Williams, *Br. J. Clin. Pharmacol.*, **3**, 135 (1976).

(22) A. P. De Leenheer, M. Cl. Cosyns-Duyck, C. F. Gelijkens, and J. V. Huys, "Abstracts, 2nd European Congress on Clinical Chemistry," Prague, Czechoslovakia, Oct. 3–8, 1976.

(23) A. P. De Leenheer and C. F. Gelijkens, *Anal. Chem.*, **14**, 2203 (1976).

(24) I. Wempen, R. Duschinsky, L. Kaplan, and J. J. Fox, *J. Am. Chem. Soc.*, **83**, 4755 (1961).

(25) K. Berens and D. Shugar, *Acta Biochim. Polon.*, **10**, 25 (1963).

(26) B. Kolb and J. Bischoff, *J. Chromatogr. Sci.*, **12**, 625 (1974).

ACKNOWLEDGMENTS

Supported by the National Medical Research Foundation (F.G.W.O.) through Grants 20452 and 3.004.76.

The authors are indebted to Produits Roche N.V., Brussels, Belgium, for their gift of I.

GLC Determination of Pemoline in Biological Fluids

JEAN-CLAUDE LIBEER and PAUL SCHEPENS ˣ

Received October 26, 1976, from the *Department of Pharmacy, University of Antwerp, Antwerp, Belgium.* Accepted for publication June 22, 1977.

Abstract □ A specific GLC method for the determination of microgram quantities of the central stimulant pemoline in biological fluids is described. Extraction problems due to the low solubility of pemoline are avoided by acid hydrolysis of the drug to 5-phenyl-2,4-oxazolidinedione, which then can be easily isolated by two-phase extraction with dichloromethane, ether, or chloroform. Amide–imide tautomerism enables a cleanup of the extract. Quantitative determination at the microgram level is done on a methylated fraction of the dichloromethane extract by GLC using a suitable internal standard. For supporting evidence of the GLC method's specificity, the compound is also identified by examining an aliquot of the final dichloromethane extract by TLC.

Keyphrases □ Pemoline—GLC analysis in biological fluids □ GLC—analysis, pemoline in biological fluids □ Stimulants, central—pemoline, GLC analysis in biological fluids

The synthesis of a series of oxazolidinones was reported (1), and later (2) the central stimulant activity of pemoline (2-imino-5-phenyl-4-oxazolidinone) was noted. Its pharmacology also was reviewed (3, 4).

Compound II was chosen on the basis of its structural similarity to I. Due to its similar pKa (7.90) (25), II can be added directly to the plasma sample. Compound II also is easily and quantitatively permethylated with the method described. The derivative obtained is well extracted from the reaction mixture before GLC and yields excellent chromatographic characteristics on the 3% OV-17 column system. The chromatograms (Figs. 1 and 2) showed no major interfering peaks eluting in the regions corresponding to I and II.

The use of the thermionic nitrogen detector (26) provides higher sensitivity and better specificity for nitrogen-containing compounds. A linear relationship between peak height ratios of I to II and plasma concentrations of I was demonstrated in the 0–1-μg/ml range (regression line: $y = 1.02x - 0.01$, $r = 0.996$). A detection limit of 50 ng of I/ml was obtained by injecting 1.0 μl of the 50 μl of ethyl acetate from the reconstituted sample residues, using 1.0 ml of plasma for analysis.

The within-run precision of the overall procedure was determined by analyzing 12 plasma samples spiked with 300 ng of I/ml. A standard deviation and a coefficient of variation of 12 ng/ml and 4.0%, respectively, were found. Analysis of 20 plasma samples, also spiked with 300 ng of I/ml, over 3 weeks yielded some indication of the long-term precision, namely, 18 ng/ml (*SD*) and 6.2% (*CV*). These data on replicate analysis and long-term precision are presented in Table I and are acceptable for an analysis at the submicrogram level.

The described procedure is an example of the superiority of the thermionic nitrogen detector because of its selectivity for nitrogen-containing compounds. Although interference from other endogenous substances was expected, blank plasma samples and plasma samples spiked with I at the submicrogram level were taken through the procedure and gave no significant peaks that might interfere. Besides this increased selectivity, sensitivity is increased approximately 20 times compared to the flame-ionization detector.

The applicability of this method for plasma samples collected from patients treated with I was not demonstrated because I is not used as a chemotherapeutic agent to treat cancer cases in our medical environment. Since I occurs as a metabolite in humans treated with the antineoplastic agent fluorouracil, development of the described procedure is important. Therefore, we propose to extend our method for the assay of I in urine and tumorous tissue.

REFERENCES

(1) C. Heidelberger, *Prog. Nucleic Acid Res. Mol. Biol.*, **4**, 1 (1965).

(2) K. U. Hartman and C. Heidelberger, *J. Biol. Chem.*, **236**, 3006 (1961).

(3) E. Bresnick and U. B. Thompson, *ibid.*, **240**, 3967 (1965).

(4) G. D. Birnie, H. Kroeger, and C. Heidelberger, *Biochemistry*, **2**, 566 (1963).

(5) E. Harbers, N. K. Chaudhuri, and C. Heidelberger, *J. Biol. Chem.*, **234**, 1255 (1959).

(6) P. Reyes, *Biochemistry*, **8**, 2057 (1969).

(7) R. J. Kent and C. Heidelberger, *Mol. Pharmacol.*, **8**, 465 (1972).

(8) A. M. Cohen, *Drug Metab. Disp.*, **3**, 303 (1975).

(9) K. L. Mukherjee, J. Boohar, D. Wentland, F. J. Ansfield, and C. Heidelberger, *Cancer Res.*, **23**, 49 (1963).

(10) K. L. Mukherjee, A. R. Curreri, M. Javid, and C. Heidelberger, *ibid.*, **23**, 67 (1963).

(11) B. Clarkson, A. O'Connor, L. R. Winston, and D. Hutchison, *Clin. Pharmacol. Ther.*, **5**, 581 (1964).

(12) A. R. Curreri and F. J. Ansfield, *Cancer Chemother. Rep.*, **2**, 8 (1959).

(13) C. W. Young *et al.*, *ibid.*, **6**, 17 (1960).

(14) C. Heidelberger and F. J. Ansfield, *Cancer Res.*, **23**, 1226 (1963).

(15) R. J. Reitemeier, C. G. Moertel, and R. G. Hahn, *Cancer Chemother. Rep.*, **44**, 39 (1965).

(16) J. J. Windheuser, J. L. Sutter, and E. Auen, *J. Pharm. Sci.*, **61**, 301 (1972).

(17) J. L. Cohen and J. P. Brennan, *ibid.*, **62**, 572 (1973).

(18) C. Pantarotto, A. Martini, G. Belvedere, A. Bossi, M. G. Donelli, and A. Frigerio, *J. Chromatogr.*, **99**, 519 (1974).

(19) K. V. Rao, K. Killion, and Y. Taurikut, *J. Pharm. Sci.*, **63**, 1328 (1974).

(20) C. Finn and W. Sadée, *Cancer Chemother. Rep.*, **59**, 279 (1975).

(21) B. L. Hillcoat, M. Kawai, P. B. McCullogh, J. Rosenfeld, and C. K. Williams, *Br. J. Clin. Pharmacol.*, **3**, 135 (1976).

(22) A. P. De Leenheer, M. Cl. Cosyns-Duyck, C. F. Gelijkens, and J. V. Huys, "Abstracts, 2nd European Congress on Clinical Chemistry," Prague, Czechoslovakia, Oct. 3–8, 1976.

(23) A. P. De Leenheer and C. F. Gelijkens, *Anal. Chem.*, **14**, 2203 (1976).

(24) I. Wempen, R. Duschinsky, L. Kaplan, and J. J. Fox, *J. Am. Chem. Soc.*, **83**, 4755 (1961).

(25) K. Berens and D. Shugar, *Acta Biochim. Polon.*, **10**, 25 (1963).

(26) B. Kolb and J. Bischoff, *J. Chromatogr. Sci.*, **12**, 625 (1974).

ACKNOWLEDGMENTS

Supported by the National Medical Research Foundation (F.G.W.O.) through Grants 20452 and 3.004.76.

The authors are indebted to Produits Roche N.V., Brussels, Belgium, for their gift of I.

GLC Determination of Pemoline in Biological Fluids

JEAN-CLAUDE LIBEER and PAUL SCHEPENS ˣ

Received October 26, 1976, from the *Department of Pharmacy, University of Antwerp, Antwerp, Belgium.* Accepted for publication June 22, 1977.

Abstract □ A specific GLC method for the determination of microgram quantities of the central stimulant pemoline in biological fluids is described. Extraction problems due to the low solubility of pemoline are avoided by acid hydrolysis of the drug to 5-phenyl-2,4-oxazolidinedione, which then can be easily isolated by two-phase extraction with dichloromethane, ether, or chloroform. Amide–imide tautomerism enables a cleanup of the extract. Quantitative determination at the microgram level is done on a methylated fraction of the dichloromethane extract by GLC using a suitable internal standard. For supporting evidence of the GLC method's specificity, the compound is also identified by examining an aliquot of the final dichloromethane extract by TLC.

Keyphrases □ Pemoline—GLC analysis in biological fluids □ GLC—analysis, pemoline in biological fluids □ Stimulants, central—pemoline, GLC analysis in biological fluids

The synthesis of a series of oxazolidinones was reported (1), and later (2) the central stimulant activity of pemoline (2-imino-5-phenyl-4-oxazolidinone) was noted. Its pharmacology also was reviewed (3, 4).

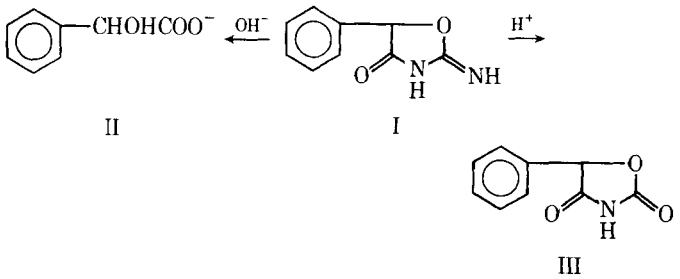

Scheme I

The detection methods for pemoline (I) in biological fluids consist of its conversion to mandelic acid (II) (Scheme I) and subsequent spectrophotometric or GLC determination (5, 6). These methods are not specific because mandelic acid also is produced by metabolism of styrene and other drugs. A major drawback of the spectrophotometric determination is a definite lack of sensitivity. Pemoline is practically insoluble in water, ether, and acetone but is soluble in hot alcohol and dimethyl sulfoxide. Because of its low solubility, extraction from biological fluids is the major problem.

This report concerns the development of a specific extraction procedure and the subsequent determination by TLC and GLC of pemoline in urine samples of athletes suspected of drug abuse.

EXPERIMENTAL

Sample Collection—Twenty-four-hour urine outputs from a male volunteer were collected following a therapeutic pemoline dose (40 mg po). The samples were stored at −22° until analysis. A plasma sample was taken 4 hr after pemoline administration and immediately analyzed.

Pemoline Hydrolysis—A saturated aqueous solution of pemoline[1] was hydrolyzed with an equal volume of 3.6 *N* H_2SO_4 in a boiling water bath for 1 hr. After cooling, the solution was extracted twice with dichloromethane; the combined dichloromethane layers were evaporated to dryness *in vacuo* at 40°. The residue was taken up in hot methanol and quickly filtered, and the methanol was evaporated, yielding a white crystalline powder, mp 107°.

This powder was fairly soluble in methanol, ethanol, ether, and dichloromethane and sparingly soluble in hexane, benzene, toluene, and petroleum ether. It formed water-soluble salts with sodium hydroxide. The structure of the hydrolysis product, 5-phenyl-2,4-oxazolidinedione (III) (Scheme I), was confirmed by IR (potassium bromide), NMR (deuterochloroform), and mass spectral data.

Assay for Pemoline in Urine—Urine (10 ml) was acidified with 1 ml of 36 *N* H_2SO_4 and hydrolyzed in a boiling water bath for 1 hr. After cooling, an amount of phosphotungstic acid, sufficient to discolor the urine and precipitate interfering materials, was added. After centrifugation, the supernate was decanted and extracted.

Assay for Pemoline in Serum or Plasma—Serum or plasma (10 ml) was thoroughly mixed with 10 ml of 10% trichloroacetic acid. After centrifugation, the protein-free supernate was hydrolyzed with 0.5 ml of 36 *N* H_2SO_4 in a boiling water bath for 1 hr and subsequently extracted.

Extraction—The hydrolysis product, III, was extracted with three 20-ml portions of dry dichloromethane, and the combined organic fractions were extracted twice with 5 ml of 0.5 *N* NaOH. The aqueous layers were acidified with 10% H_2SO_4 and reextracted with three 20-ml portions of dichloromethane. The combined dichloromethane layers were evaporated *in vacuo* at 40° to near dryness and derivatized.

Derivatization—A known amount of the internal standard, allobarbital, was added to the remaining dichloromethane solution (about 0.5 ml), which was then treated dropwise with a solution of diazomethane in dry dichloromethane (7) until a yellow color persisted for 1 min. The solution was washed with three 5-ml portions of 0.5 *N* NaOH, dried over anhydrous sodium sulfate, transferred to a 15-ml glass-stoppered silanized vial, and evaporated with a nitrogen stream at room temperature. The derivatization product was 3-methyl-5-phenyl-2,4-oxazolidinedione (IV) according to IR, NMR (deuterochloroform), and mass spectral data.

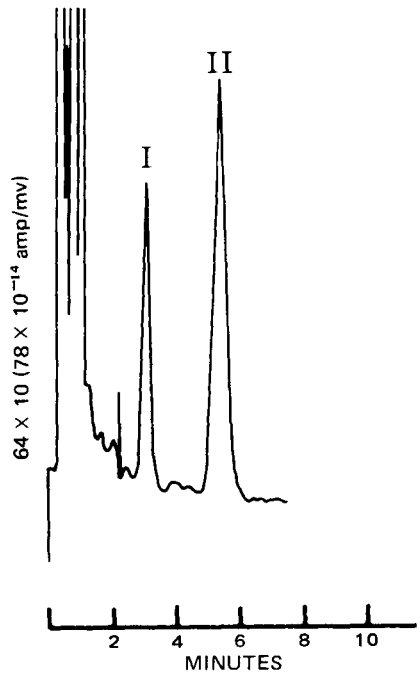

Figure 1—*Gas chromatogram of an extract of 20 ml of urine taken 14 hr after administration of 40 mg of pemoline. Peaks I and II are due to methylated allobarbital and a 2-μg injection of IV, respectively.*

TLC—The extract was dissolved in 100 μl of ethanol, and 20 μl of this solution was spotted on a precoated silica gel 60 F_{254} plate[2], together with known amounts of IV. The plate was run in a developing chamber previously saturated with chloroform–hexane (50:50). After development, the plate was air dried. Then the spots were located with iodoplatinate (Reagent A) or with a freshly prepared solution of 0.5% fast blue salt B[3] in water followed by 1 *N* NaOH (Reagent B).

In the presence of pemoline, a red spot with R_f 0.30 appeared with Reagent A (detection limit = 5 μg) and a yellow spot appeared with Reagent B (detection limit = 3 μg).

GLC—A gas chromatograph[4] equipped with a dual flame-ionization detector was used. The column consisted of 3% phenylmethyl dimethyl silicone[5] coated on 100–120-mesh diatomaceous earth[6] packed in a 2-m × 2.5-mm i.d. silanized Pyrex column. Analyses were carried out isothermally at an oven temperature of 180°; injector and detector temperatures were maintained at 200°. Nitrogen was used as carrier gas at 30 ml/min (bubble flowmeter). All injections were made on-column with a 10-μl syringe[7], and about 1 μl of the extract with allobarbital as the internal standard was injected (Fig. 1). Peak areas were measured using an electronic calculator[8].

RESULTS AND DISCUSSION

The extraction of pemoline from biological fluids presented the major drawback. Acid hydrolysis of pemoline to III, which is very soluble in organic solvents, was the most obvious method. Furthermore, because III is a weak acid, it could be extracted back into alkali for cleanup (amide–imide tautomerism) (8). Interfering material, mainly due to the acid hydrolysis of urine, could be removed almost completely by phosphotungstic acid without a noticeable loss of pemoline.

The use of anhydrous sodium sulfate, even analytical grade, was avoided because it introduced many impurities that interfered in the GLC

[1] Aldrich Chemicals.

[2] Merck.
[3] Fluka AG, Buchs, Switzerland.
[4] Hewlett-Packard 5170 A.
[5] OV-7.
[6] Gas Chrom Q, Applied Science Laboratories.
[7] Hamilton 701 N, Whittier, Calif.
[8] Hewlett-Packard 3380 A.

Table I—Recoveries of Pemoline Added to Human Urine Samples

Pemoline Added to 20 ml of Human Urine, μg	Amount Recovered, μg	Recovery, %
25.5	25.1	98.4
51	49.9	97.8
102	100	98.0
204	203.5	99.8
408	403.5	98.9
	Mean value ± *SD*	98.6 ± 0.80

analysis. Therefore, organic layers were dried by cooling for 15 min; remaining water droplets were removed with filter paper.

Pemoline could not be chromatographed even on nonpolar liquid phases. The product of acid hydrolysis, III, is more volatile, but peaks tend to tail on columns of various polarities. When 40–60-mesh polytetrafluoroethylene polymer[9] was used as support material, some improvement in peak symmetry was observed, but the columns were of low efficiency. Methylation with diazomethane to IV yielded a very volatile compound that demonstrated excellent peak symmetry on fairly nonpolar liquid phases.

Since the *N*-methyl derivative is insoluble in alkali, a final cleanup was possible by extracting the organic layer with sodium hydroxide.

Because of its similarity with the hydrolysis product of pemoline in chemical behavior, allobarbital was chosen as an internal standard. Both drugs are weak acids and can be reextracted into alkali, so allobarbital can be added immediately after hydrolysis. Furthermore, both products form *N*-methyl derivatives with diazomethane, so the final cleanup with sodium hydroxide solution gives no loss.

Recovery studies from urine and plasma were carried out by adding the internal standard before derivatization; in all other experiments, the internal standard was added immediately after hydrolysis. Addition of pemoline to five 20-ml urine samples in the range anticipated for therapeutic levels gave a recovery of 98.6 ± 0.80%. All determinations were carried out in duplicate, the lowest recovery from a single determination being 97.8% (Table I). Although recoveries were high, extreme care had to be taken during evaporation since IV and the methylated allobarbital are extremely volatile.

[9] Chromosorb T, Applied Science Laboratories.

Table II—Recoveries of 10 μg of Pemoline Added to Human Plasma Samples

Amount Recovered[a], μg	Recovery, %
10.20	101.5
9.70	96.3
9.80	97.4
9.90	98.2
9.90	98.6
Mean value ± *SD*	98.4 ± 1.94

[a] Values of the recovered IV without correction to I.

Addition of pemoline to human plasma yielded a recovery of 98.4 ± 1.94% (Table II). Since the normal range of plasma concentrations is 1.0 μg/ml, 10-ml samples were required when using a flame-ionization detector. Efficiency, however, could be improved markedly by using a nitrogen detector[10]. Although pemoline gave no increased nitrogen signal, the extreme stability and high noise-to-signal ratio of the detector allowed quantitative estimation of 20 ng of pemoline, which is sensitive enough to require 1 ml of plasma. Oral intake of 40 mg of pemoline, a therapeutic dose, gives a plasma concentration of 0.8 μg/ml at about 4 hr. Determination in urine is still possible 48 hr after ingestion due to the long elimination time of pemoline.

A complete elimination and metabolism pattern of pemoline is currently being investigated.

REFERENCES

(1) W. Traube and R. Ascher, *Chem. Ber.*, **46**, 2083 (1913).
(2) L. Schmidt, *Arzneim.-Forsch.*, **6**, 423 (1956).
(3) P. Bugard, *Thérapie*, **17**, 63 (1962).
(4) D. Duval and J. Sterne, *ibid.*, **15**, 1250 (1960).
(5) L. M. Cummins and J. E. Perry, *J. Pharm. Sci.*, **58**, 762 (1969).
(6) A. Slob, *Br. J. Ind. Med.*, **30**, 390 (1973).
(7) H. M. Fales and T. M. Jaouni, *Anal. Chem.*, **45**, 2302 (1973).
(8) J. C. Libeer and P. Schepens, *Pharm. Weekbl.*, **112**, 210 (1977).

[10] Hewlett-Packard 18789 A dual N-P-FID.

Synthesis of 4,5-Dimethoxykynuramine and Its *In Vivo* Conversion to 6,7-Dimethoxy-4-quinolinol

THOMAS J. SCHWAN ˣ, LeROY J. HONKOMP, HARRY R. SNYDER, Jr., and EDWARD J. WATSON *

Received November 8, 1976, from the *Research and Development Department, Norwich-Eaton Pharmaceuticals Division of Morton-Norwich Products, Inc., Norwich, NY 13815.* Accepted for publication June 14, 1977. *Present address: Wyeth Laboratories, West Chester, PA 19380.

Abstract □ 4,5-Dimethoxykynuramine was synthesized in a three-step sequence originating with veratrole. Indirect evidence indicates that the drug was converted *in vivo* to the hypotensive agent 6,7-dimethoxy-4-quinolinol by the action of monoamine oxidase.

Keyphrases □ 4,5-Dimethoxykynuramine—synthesized, *in vivo* conversion to 6,7-dimethoxy-4-quinolinol □ 6,7-Dimethoxy-4-quinolinol—formed *in vivo* from 4,5-dimethoxykynuramine □ Antihypertensive agents—6,7-dimethoxy-4-quinolinol, formed *in vivo* from 4,5-dimethoxykynuramine

The hypotensive and antihypertensive activities of 6,7-dimethoxy-4-quinolinol (I) were demonstrated previously (1).

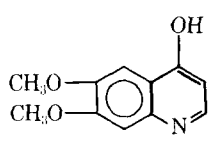

I

Since it had been shown that the *in vitro* incubation of kynuramine (II) with monoamine oxidase gave 4-quinolinol (III) (Scheme I) (2), the possibility of the conversion of 4,5-dimethoxykynuramine (IV) to the aldehyde V and then the quinolinol I (Scheme II) was considered. Should this transformation occur *in vivo*, IV might be considered a useful prodrug for I.

Table I—Recoveries of Pemoline Added to Human Urine Samples

Pemoline Added to 20 ml of Human Urine, μg	Amount Recovered, μg	Recovery, %
25.5	25.1	98.4
51	49.9	97.8
102	100	98.0
204	203.5	99.8
408	403.5	98.9
	Mean value ± *SD*	98.6 ± 0.80

analysis. Therefore, organic layers were dried by cooling for 15 min; remaining water droplets were removed with filter paper.

Pemoline could not be chromatographed even on nonpolar liquid phases. The product of acid hydrolysis, III, is more volatile, but peaks tend to tail on columns of various polarities. When 40–60-mesh polytetrafluoroethylene polymer[9] was used as support material, some improvement in peak symmetry was observed, but the columns were of low efficiency. Methylation with diazomethane to IV yielded a very volatile compound that demonstrated excellent peak symmetry on fairly nonpolar liquid phases.

Since the *N*-methyl derivative is insoluble in alkali, a final cleanup was possible by extracting the organic layer with sodium hydroxide.

Because of its similarity with the hydrolysis product of pemoline in chemical behavior, allobarbital was chosen as an internal standard. Both drugs are weak acids and can be reextracted into alkali, so allobarbital can be added immediately after hydrolysis. Furthermore, both products form *N*-methyl derivatives with diazomethane, so the final cleanup with sodium hydroxide solution gives no loss.

Recovery studies from urine and plasma were carried out by adding the internal standard before derivatization; in all other experiments, the internal standard was added immediately after hydrolysis. Addition of pemoline to five 20-ml urine samples in the range anticipated for therapeutic levels gave a recovery of 98.6 ± 0.80%. All determinations were carried out in duplicate, the lowest recovery from a single determination being 97.8% (Table I). Although recoveries were high, extreme care had to be taken during evaporation since IV and the methylated allobarbital are extremely volatile.

[9] Chromosorb T, Applied Science Laboratories.

Table II—Recoveries of 10 μg of Pemoline Added to Human Plasma Samples

Amount Recovered[a], μg	Recovery, %
10.20	101.5
9.70	96.3
9.80	97.4
9.90	98.2
9.90	98.6
Mean value ± *SD*	98.4 ± 1.94

[a] Values of the recovered IV without correction to I.

Addition of pemoline to human plasma yielded a recovery of 98.4 ± 1.94% (Table II). Since the normal range of plasma concentrations is 1.0 μg/ml, 10-ml samples were required when using a flame-ionization detector. Efficiency, however, could be improved markedly by using a nitrogen detector[10]. Although pemoline gave no increased nitrogen signal, the extreme stability and high noise-to-signal ratio of the detector allowed quantitative estimation of 20 ng of pemoline, which is sensitive enough to require 1 ml of plasma. Oral intake of 40 mg of pemoline, a therapeutic dose, gives a plasma concentration of 0.8 μg/ml at about 4 hr. Determination in urine is still possible 48 hr after ingestion due to the long elimination time of pemoline.

A complete elimination and metabolism pattern of pemoline is currently being investigated.

REFERENCES

(1) W. Traube and R. Ascher, *Chem. Ber.*, **46**, 2083 (1913).
(2) L. Schmidt, *Arzneim.-Forsch.*, **6**, 423 (1956).
(3) P. Bugard, *Thérapie*, **17**, 63 (1962).
(4) D. Duval and J. Sterne, *ibid.*, **15**, 1250 (1960).
(5) L. M. Cummins and J. E. Perry, *J. Pharm. Sci.*, **58**, 762 (1969).
(6) A. Slob, *Br. J. Ind. Med.*, **30**, 390 (1973).
(7) H. M. Fales and T. M. Jaouni, *Anal. Chem.*, **45**, 2302 (1973).
(8) J. C. Libeer and P. Schepens, *Pharm. Weekbl.*, **112**, 210 (1977).

[10] Hewlett-Packard 18789 A dual N-P-FID.

Synthesis of 4,5-Dimethoxykynuramine and Its *In Vivo* Conversion to 6,7-Dimethoxy-4-quinolinol

THOMAS J. SCHWAN ˣ, LeROY J. HONKOMP, HARRY R. SNYDER, Jr., and EDWARD J. WATSON *

Received November 8, 1976, from the *Research and Development Department, Norwich-Eaton Pharmaceuticals Division of Morton-Norwich Products, Inc., Norwich, NY 13815.* Accepted for publication June 14, 1977. *Present address: Wyeth Laboratories, West Chester, PA 19380.

Abstract □ 4,5-Dimethoxykynuramine was synthesized in a three-step sequence originating with veratrole. Indirect evidence indicates that the drug was converted *in vivo* to the hypotensive agent 6,7-dimethoxy-4-quinolinol by the action of monoamine oxidase.

Keyphrases □ 4,5-Dimethoxykynuramine—synthesized, *in vivo* conversion to 6,7-dimethoxy-4-quinolinol □ 6,7-Dimethoxy-4-quinolinol—formed *in vivo* from 4,5-dimethoxykynuramine □ Antihypertensive agents—6,7-dimethoxy-4-quinolinol, formed *in vivo* from 4,5-dimethoxykynuramine

The hypotensive and antihypertensive activities of 6,7-dimethoxy-4-quinolinol (I) were demonstrated previously (1).

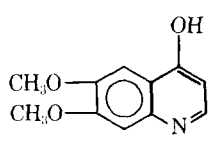

I

Since it had been shown that the *in vitro* incubation of kynuramine (II) with monoamine oxidase gave 4-quinolinol (III) (Scheme I) (2), the possibility of the conversion of 4,5-dimethoxykynuramine (IV) to the aldehyde V and then the quinolinol I (Scheme II) was considered. Should this transformation occur *in vivo*, IV might be considered a useful prodrug for I.

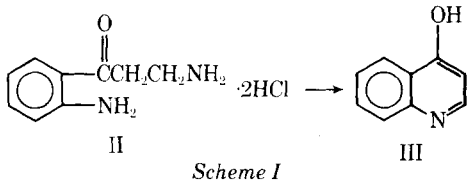

II III

Scheme I

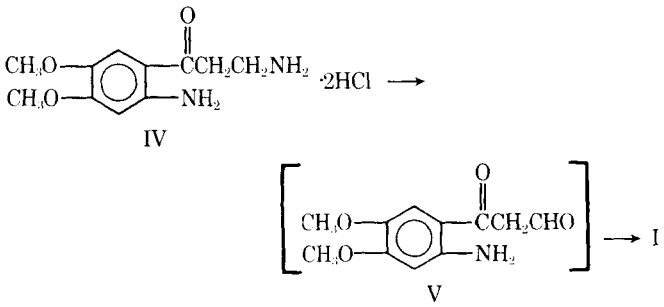

IV V I

Scheme II

This report presents the synthesis and pharmacology of IV as well as a study of its *in vivo* conversion to I.

RESULTS AND DISCUSSION

Friedel–Crafts acylation of veratrole (VI) with β-nitropropionyl chloride (VII) (3) gave 3′,4′-dimethoxy-3-nitropropiophenone (VIII), apparently the first example of the utilization of VII in this type of synthesis (Scheme III). Treatment of VIII with concentrated nitric acid gave the dinitro compound IX.

The NMR spectrum of IX exhibited two aromatic singlets, thereby eliminating the possibility of a 1,2,3,4-arrangement of substituents (an *ortho*-orientation of protons). However, a 1,2,3,5-arrangement containing a *meta*-orientation of protons with an expected J of 2–3 Hz (4) could not be completely ruled out. The lack of any splitting pattern in the aromatic protons of IX prompted assignment of the 1,2,4,5-orientation of substituents to IX. Subsequence demonstration of the conversion of IX → IV → I verified this structural assignment.

Hydrogenation of IX using palladium-on-carbon gave IV, isolated as a dihydrochloride salt.

Preliminary screening of IV *via* the CARDAMAP (5) procedure revealed hypotensive activity of long duration (5 hr) at 50 mg/kg iv, but lower doses (10 mg/kg iv) yielded no effect on blood pressure. Urine from the experimental animals was retained for detection of the presence of I. The results of TLC indicated that I was excreted as a metabolite of IV in the dog and that parent IV was also present in the final extract of dog urine.

This publication presents quantitative estimates of the excretion of I in rat urine following orally administered IV. Additionally, the effects on excretion (and, therefore, presumably conversion) of animals pretreated with a monoamine oxidase inhibitor, pheniprazine[1], are discussed.

With the assumptions of complete absorption of IV from the GI tract and a subsequent 100% conversion to I, on a weight basis 76.7% of an administered dose of IV is available for conversion to I. The percent recovery as presented is calculated on this stoichiometric equivalent dose of I.

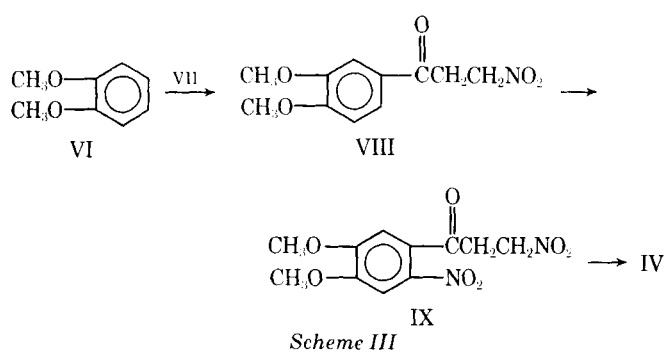

VI VIII IX IV

Scheme III

Urine samples collected up to 2 hr postdrug from the first group (A), who received only IV, contained an average of 0.063 ± 0.015 mg of I, representing 2.2% of the available IV administered. A second group (B), pretreated with pheniprazine prior to administration of IV, did not excrete any urine during the initial 2-hr period, so no values were available for comparison. The 2–4-hr period for Group A yielded 0.131 ± 0.012 mg of I, or 4.5% of the administered dose of IV recoverable as I, compared to 0.005 ± 0.002 mg, or 0.2%, from Group B. This difference was significant (t test) at $p < 0.001$.

The cumulative percentage recoveries over 6 hr following drug administration amounted to 7.9% in Group A as compared to 0.4% in Group B. The urine from the pheniprazine-only treated animals, Group C, averaged 5.3, 7.0, and 13.1 fluorescent units at the 2-, 4-, and 6-hr time periods, respectively. These figures were applied as a correction factor for the Group B animals prior to the determination of the concentration of I.

These results indicated that 6 hr was probably not a sufficient time for near complete excretion of I. Therefore, a second experiment was run, identical to the first, except that urine collections were made at 4 and 24 hr. An additional group (Group D) of animals was included and received only I to obtain data for comparison to groups treated with IV. Four hours following only the administration of IV, an average of 0.173 ± 0.032 mg, or 6.8% of the equivalent dose of I, was recovered in the urine. Twenty hours later, a mean additional 0.0992 ± 0.023 mg (3.9%) was recovered from this group, yielding a cumulative total of 10.7%.

In the animals pretreated with pheniprazine (Group B), no I could be detected in the urine 4 hr after IV administration; at 24 hr, an average of only 0.017 mg (0.7%) of the dose was recovered (this average was supplied by detectable levels in only two of the five animals tested). Group D, which received only I, yielded an average of 0.223 ± 0.045 mg (5.4%) of the administered dose at 4 hr and an additional 0.640 ± 0.066 mg at 24 hr for a total of 21.3%.

The possibility was considered that pheniprazine pretreatment could interfere with excretion and/or detection of I. Therefore, an additional group of animals (Group E) was treated with 20 mg of pheniprazine/kg po 2 hr prior to 10 mg of I/kg po. Urine samples were collected and analyzed at 4 and 24 hr as previously described. At the respective time intervals, urinary excretion of I averaged 0.417 ± 0.084 mg (11.6%) and 1.215 ± 0.085 mg (33.9%), approximately double that of the animals receiving I alone (Group D).

When the two separate studies involving administration of IV are compared to one another, the percentage recoveries as I at the 4-hr level are remarkably similar, adding credence that the values are reliable. The slight difference in the percentage recovery of I in the animals treated with IV as compared to those dosed with I was not significant at the 4-hr interval; however, at 24 hr the percentage recovery was double in the latter group. This result may indicate that IV is rapidly absorbed and partially converted to I, so that blood levels of I may not be distinguishable between the two groups over the relatively short time period of 4 hr. However, over the longer period (24 hr), I is more completely absorbed than IV and/or the rate and degree of conversion of IV → I decreases with time. Since parent IV was found in the urine of dogs treated intravenously with the compound, it would not be surprising to find unconverted compound in the urine of rats in the present study.

Although it has been shown that pheniprazine pretreatment does not block absorption, excretion, or detection of I in rat urine, the possibility still exists that pheniprazine may block or markedly reduce IV absorption. This premise has not been tested.

The 100% increase of I in the urine of animals pretreated with pheniprazine and I as compared to those treated with I alone may suggest one or both of the following: (*a*) pheniprazine pretreatment increases absorption and/or excretion of I and/or (*b*) I is metabolized through enzyme systems susceptible to inactivation by pheniprazine. Additional work is necessary to clarify this finding.

EXPERIMENTAL[2]

Pharmacology—Urine from experimental animals dosed with IV was found to contain I along with IV by TLC in the following solvent systems: 1-butanol–acetic acid–water (5:4:1), methanol–ethyl acetate–water (5:

[1] Catron, Lakeside Laboratories.

[2] The NMR spectrum was determined on a Varian A-60A spectrometer in deuterated dimethyl sulfoxide using tetramethylsilane as an internal standard. IR spectra were determined as mineral oil mulls with a Perkin-Elmer 137B spectrophotometer. Melting points were taken on a Mel-Temp block and are corrected.

4:1), methanol, and 2-propanol–ethyl acetate–water (5:4:1).

In an initial experiment, 15 male Charles River rats, 350–425 g, were divided into three groups of five animals each. Each animal was placed in an individual metabolism cage, and food was withheld for 24 hr prior to dosing. Water was provided *ad libitum*. Group A was dosed with IV, 10 mg/kg po; Group B was pretreated with pheniprazine, 20 mg/kg po, 2 hr prior to the administration of IV, 10 mg/kg po. Group C served as a pheniprazine control; *i.e.*, these animals received 20 mg of pheniprazine/kg po only.

The urine from each animal was collected separately at 2, 4, and 6 hr following IV administration. Each sample was analyzed for I according to a reported spectrophotofluorometric method (6) in which the I concentration is determined from standard curves constructed from fluorescence readings (activating wavelength of 320 nm and fluorescent wavelength of 370 nm) obtained with control urine to which known concentrations of I have been added and subsequently extracted. Compound IV exhibits no fluorescence between 200 and 600 nm.

A second experiment involving 15 rats was conducted as already described, except that urine collections were made at 4 and 24 hr following IV. To this experiment was added, for comparison, a fourth group (D), which was dosed with I (10 mg/kg po).

Chemistry—*β-Nitropropionyl Chloride (VII) (3)*—To a stirred suspension of 70 g (0.59 mole) of β-nitropropionic acid, 0.5 ml of pyridine and 500 ml of chloroform was added slowly, at room temperature, 210 ml (339 g, 2.85 moles) of thionyl chloride. The mixture was stirred and refluxed for 2.5 hr and cooled. The solvents were removed *in vacuo* to give 91 g (>100%) of the crude acid chloride, VII, which was used directly in the next step.

3′,4′-Dimethoxy-3-nitropropiophenone (VIII)—Aluminum chloride (173 g, 1.30 moles) was added quickly to 700 ml of vigorously stirred nitrobenzene. While the temperature was maintained between 10 and 15°, a solution of 91 g (0.59 mole) of VII in 50 ml of nitrobenzene was added followed by a solution of 73 g (0.53 mole) of veratrole (VI) in 50 ml of nitrobenzene. The mixture was stirred at room temperature for 6 hr and then poured cautiously into a mixture of 300 ml of concentrated hydrochloric acid and 2 kg of iced water.

The organic layer was separated, and the aqueous material was extracted with 3 × 200-ml portions of chloroform. The combined organic layers were washed with 300 ml of water, 300 ml of 10% sodium carbonate, and 2 × 300-ml portions of water. After the solution was dried over magnesium sulfate, the solvents were removed *in vacuo* to give the oily product. Crystallization from ethyl acetate gave 45.5 g (36%) of VIII, mp 113–118°. The analytical sample, mp 126–128°, was obtained by recrystallization from ethanol; IR: 6.08 (C=O, ketone), 6.31 (C=C), 6.49, and 7.41 (NO_2) μm.

Anal.—Calc. for $C_{11}H_{13}NO_5$: C, 55.23; H, 5.48; N, 5.86. Found: C, 55.11; H, 5.78; N, 5.59.

3′,4′-Dimethoxy-3,6′-dinitropropiophenone (IX)—To 300 ml of concentrated nitric acid, stirred and maintained at 5–10°, was added 45.5 g (0.19 mole) of VIII in small portions over 20 min. The resulting solution was stirred at 5° for 10 min and then added slowly to 2.5 kg of iced water. The suspension was stirred at room temperature for 20 min and filtered. The solid was washed with 3 × 200-ml portions of water, air dried, and dried at 60° to give 48 g of crude IX, mp 120–127°. Recrystallization from 2 liters of ethanol gave 34 g (63%) of IX, mp 135–140°.

The analytical sample, mp 140–142°, was obtained by recrystallization from alcohol; IR: 5.88 (C=O, ketone), 6.20 (C=C), 6.55–6.70, and 7.35 (NO_2) μm; NMR: δ 7.67 and 7.28 (2 s, 2H, aromatic), 3.68 and 3.43 (2 t, 4H, methylene), 3.98, and 3.96 (2 s, 6H, CH_3O) ppm.

Anal.—Calc. for $C_{11}H_{12}N_2O_7$: C, 46.48; H, 4.26; N, 9.86. Found: C, 46.62; H, 4.39; N, 9.78.

3′,4′-Dimethoxy-3,6′-diaminopropiophenone Dihydrochloride (4,5-Dimethoxykynuramine) (IV)—A 17.3-g (0.61-mole) portion of IX, 500 ml of methanol, 240 ml of methanol saturated with hydrochloric acid, and 22 g of 5% palladium-on-carbon (50% moisture) were shaken on a Parr apparatus at room temperature until the theoretical quantity of hydrogen was consumed (5.5 hr). The catalyst was filtered, and the resulting solution was concentrated to dryness at 35–45° *in vacuo*. The residue was slurried with ethanol, and the solid was filtered to give 13.5 g of the crude product, mp 204–209°.

The material was recrystallized from ethanol, and the solid was washed with 70 ml of ethanol to afford 5.3 g (29%) of the product, mp 208–214°.

The analytical sample, mp 202–207°, was recrystallized from ethanol containing hydrochloric acid; IR: 6.01 (C=O, ketone) and 6.21 (C=C) μm.

Anal.—Calc. for $C_{11}H_{18}N_2O_3 \cdot 2HCl$: C, 44.45; H, 6.10; N, 9.43. Found: C, 44.63; H, 6.35; N, 9.21.

REFERENCES

(1) R. K. Bickerton, R. F. Dailey, W. T. Rockhold, and R. H. Buller, *J. Pharmacol. Exp. Ther.*, **144**, 218 (1964).

(2) H. Weissbach, T. Smith, J. Daly, B. Witkop, and S. Udenfriend, *J. Biol. Chem.*, **235**, 1160 (1960).

(3) G. Barger and F. Tutin, *Biochem. J.*, **12**, 402 (1918).

(4) L. M. Jackman, "Applications of Nuclear Magnetic Resonance Spectroscopy in Organic Chemistry," Pergamon, New York, N.Y., 1959, p. 85.

(5) G. O'Bleness, R. K. Bickerton, and W. T. Rockhold, *Comput. Appl. Serv.*, **4**, 69 (1964).

(6) P. L. Cox, J. P. Heotis, and J. A. Buzard, *Arch. Int. Pharmacodyn. Ther.*, **168**, 450 (1967).

ACKNOWLEDGMENTS

The authors are indebted to Mr. Nelson J. Miles for chemical synthesis, Mr. Grant Gustin and Mr. Marvin Tefft for the microanalyses, Ms. Patricia Curtis for the NMR spectrum, Mr. R. D. Hollifield for the fluorometric work, Ms. M. Chalon and Mr. E. Micalizzi for technical assistance, Mr. Ronald Herrett for TLC work, and Dr. Charles S. Davis for many helpful discussions.

Separation and Quantitation of Possible Degradation Products of Procarbazine Hydrochloride in Its Dosage Form

GARY L. BURCE ˣ and JUDY P. BOEHLERT

Received March 17, 1977, from the *Stability Research Laboratory, Quality Control Department, Hoffmann-La Roche Inc., Nutley, NJ 07110.* Accepted for publication July 13, 1977.

Abstract □ A stability-indicating assay for the degradation products of procarbazine hydrochloride was developed using high-pressure liquid chromatography. The method uses a buffered methanol–water mobile phase on a reversed-phase column. Concentrations of degradation products as low as 0.04 mg/ml, 0.02% degradation, can be quantitated using an internal standard of cinnamyl alcohol. The typical range for degradation products in procarbazine capsules is 0.1–0.5% after as long as 4.5 years.

Keyphrases □ Procarbazine hydrochloride degradation products—high-pressure liquid chromatographic analysis in pharmaceutical formulations □ Degradation products—of procarbazine hydrochloride, high-pressure liquid chromatographic analysis in pharmaceutical formulations □ High-pressure liquid chromatography—analyses, degradation products of procarbazine hydrochloride in pharmaceutical formulations □ Antineoplastic agents—procarbazine hydrochloride, high-pressure liquid chromatographic analysis of degradation products in pharmaceutical formulations

Procarbazine, *N*-(1-methylethyl)-4-[(2-methylhydrazino)methyl]benzamide (I), is an antineoplastic agent used to treat Hodgkin's disease and other diseases involving malignant tumors (1). Procarbazine is capable of undergoing oxidation by atmospheric oxygen or degradation in the presence of moisture to give *N*-(1-methylethyl)-4-[(2-methylazo)methyl]benzamide (II), *N*-(1-methylethyl)-4-[(2-methylamino)hydrazo]benzamide (III), and, to a much lesser extent, *N*-isopropyl-4-formylbenzamide (IV) (2–5).

Procarbazine can be assayed using UV spectroscopy (2, 5), polarography (2, 6), coulometry (2, 7, 8), or direct titration as the hydrochloride salt (2, 5). These methods are applicable to both the pure compound and the dosage forms. TLC on silica gel has been used to separate procarbazine from II and III and to estimate the amount of II and III present (2). However, both oxidation of procarbazine and isomerization between II and III can occur during chromatography, severely lowering the accuracy and precision of this method.

This report presents a method for accurately quantitating small amounts of II–IV in procarbazine hydrochloride capsules using high-pressure liquid chromatography (HPLC).

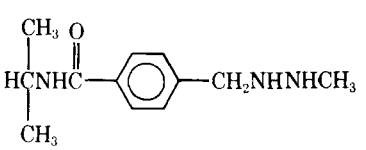

I

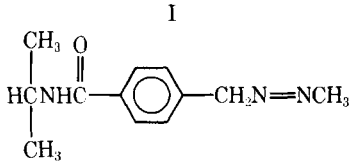

II

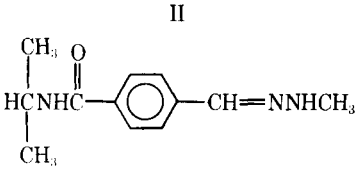

III

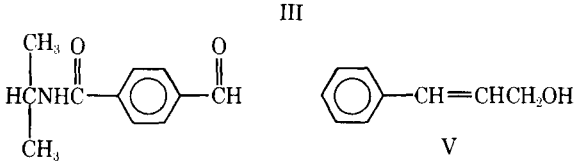

IV V

EXPERIMENTAL

Procarbazine hydrochloride and its degradation products, II–IV, were all reference standard quality[1]. Cinnamyl alcohol[2] (V) and monobasic ammonium phosphate[3] were reagent grade. Certified ACS metol[4] was used to prepare the mobile phase along with distilled, deionized, filtered water. The mobile phase, used for dissolving the drugs in pure form and extracting them from the capsule material as well as for eluting the samples from the column, consisted of 56% water containing the ammonium phosphate and 44% methanol. The final concentration of ammonium phosphate was 0.05 *M* in the mixture, and the pH was 5.5. No pH adjustment was needed after making up the mobile phase.

Instrumentation—The constant-pressure liquid chromatograph[5] was equipped with a 254-nm UV detector and a septum injector. The output signal was measured on a dual-pen recorder[6] with integrator. A 25-cm Partisil PXS 10/25 ODS-2 reversed-phase column[7] with a C_{18}-type bonded phase on silica particles, 10 μm in diameter, was used.

Procedure—The cinnamyl alcohol internal standard was weighed and dissolved in the mobile phase at about 1 mg/ml. This solution, diluted 1:10 with the mobile phase for a final concentration of about 0.1 mg/ml, was used to dissolve the standards and to extract the degradation products from the capsule mixture. Standards were weighed, dissolved in the mobile phase with the internal standard solution, and immediately injected.

The dosage form was assayed by accurately weighing the contents of five capsules[8] of procarbazine hydrochloride (~1.7 g containing approximately 250 mg of procarbazine hydrochloride) into a centrifuge tube. A 10-ml aliquot of the internal standard in the mobile phase was added, and the centrifuge tube was shaken for 15 sec. A small amount of this solution was immediately filtered through a 0.45-μm filter[9] and immediately injected. About 4-μl quantities of standards and samples were injected on the column.

Amber glassware was used throughout this procedure because these compounds are reported to be light sensitive (2). Samples must be chromatographed immediately after dissolution because procarbazine hydrochloride can degrade in these solutions.

RESULTS AND DISCUSSION

Representative chromatograms are shown in Fig. 1. The chromatographic parameters calculated from these chromatograms are listed in

[1] Hoffmann-La Roche, Nutley, NJ 07110.
[2] Eastman Kodak Co., Rochester, NY 14650.
[3] Mallinckrodt Inc., St. Louis, MO 63147.
[4] Fisher Scientific, Fair Lawn, NJ 07410.
[5] Model 848, Instrument Products Division, DuPont Inc., Wilmington, DE 19898.
[6] Model 282, Linear Instruments Corp., Irving, CA 92714.
[7] Whatman Inc., Clifton, NJ 07014.
[8] Matulane, Hoffmann-La Roche Inc., Nutley, NJ 07110.
[9] Millipore Corp., Bedford, MA 01730.

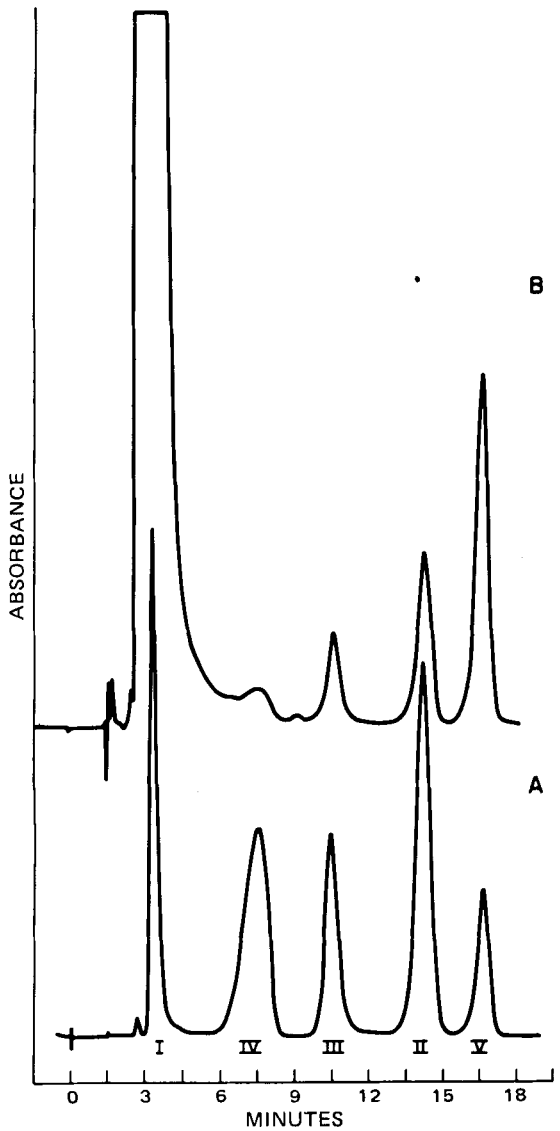

Figure 1—*Chromatograms run with a flow rate of 1.5 ml/min at 1900 psi and 0.04 absorbance full scale. Key: A, set of standards, I = 1.58 mg/ml, II = 0.43 mg/ml, III = 0.81 mg/ml, IV = 1.21 mg/ml, and V = 0.087 mg/ml; and B, typical extraction of procarbazine and degradation products from capsules using the procedure given in the text.*

Table I. All peaks are Gaussian shaped, except for the peak of IV. This peak shows both fronting and excess broadening, resulting in large values of height equivalent to a theoretical plate (HETP).

The method yields baseline separation of procarbazine, its degradation products, and the internal standard. Additionally, since procarbazine is eluted from the column firs., overloading the column with procarbazine should not significantly affect either the retention volumes or resolution of subsequent peaks.

Standard analytical curves were determined for I–IV using their peak

Table I—Chromatographic Characteristics of Procarbazine, Degradation Products, and Cinnamyl Alcohol

Compound	Retention Time, min	Retention Volume, ml[a]	Net Retention Volume, ml[b]	Number of Plates[c]	HETP
I	3.31	4.95	2.70	670	0.37
II	14.21	21.31	19.06	2810	0.089
III	10.61	15.91	13.66	1120	0.22
IV	7.61	11.41	9.16	240	1.04
V	16.85	25.27	23.02	5390	0.046

[a] The flow rate is 1.5 ml/min. [b] The void volume of the column is 2.25 ml. [c] Number of plates was calculated from the equation $N = 5.54$ (retention time/width at half maximum)^2 (9).

Table II—Slopes, Intercepts, and Correlation Coefficients for Procarbazine and the Degradation Products as Pure Compounds and in Capsule Material[a]

Compound	Matrix[b]	Slope, mg/ml[c]	Intercept, mg/ml[c,d]	r
I	None	0.36 (0.01)	0 (0.01)	99.99
II	None	0.43 (0.03)	0 (0.01)	99.88
II	Capsule	0.40 (0.03)	−0.11 (0.05)	99.88
III	None	0.48 (0.02)	0 (0.01)	99.99
III	Capsule	0.52 (0.03)	−0.21 (0.04)	99.98
IV	None	0.24 (0.01)	0 (0.01)	99.97
IV	Capsule	0.22 (0.02)	0.02 (0.02)	99.96

[a] Five data points were used to determine each curve. [b] Analytical curves were determined of either pure compounds dissolved in the mobile phase or compounds added to 1.7 g of capsule material in a standard addition method. These standard addition samples were extracted as described previously. [c] Numbers in parentheses are 95% confidence limits for the slope and intercept. [d] Samples in capsule material have some degradation products in them initially causing the negative intercepts.

heights (PH). The slopes, intercepts, and correlation coefficients are listed in Table II. The values in parentheses listed next to each slope and intercept are the 95% confidence limits. These parameters were calculated using:

$$\text{mg/ml} = \text{slope} \times \frac{\text{PH (sample)}}{\text{PH (internal standard)}} + \text{intercept} \quad \text{(Eq. 1)}$$

The use of an internal standard, cinnamyl alcohol, compensates for any variability in the amount of sample injected. Typically, about 4 μl of sample is injected. Therefore, the amount of sample injected ranges from 1.4 μg to 200 ng. The limit of detection using these chromatographic conditions, as estimated by a signal to noise ratio of 2:1, is approximately 4 μg/ml or 20 ng injected. The limits of quantitation, estimated as 10 times the limit of detection, is 40 μg/ml or 200 mg injected (10). The sensitivity under these conditions is about 0.7 mg/ml for full-scale deflection but can be increased by using less internal standard and raising the sensitivity of the detector from 0.04 to 0.01 absorbance unit. No isomerization between II and III was observed if the standards were chromatographed immediately upon dissolution.

Small amounts of degradation products were added to a sample of procarbazine hydrochloride in capsule material to test whether the extraction was complete and whether the presence of large amounts of procarbazine hydrochloride would interfere with the analysis of the degradation products. The contents of 30 procarbazine hydrochloride capsules were pooled, and 1.7 g of capsule material was added to each centrifuge tube. Small amounts of II–IV were weighed and also added to these tubes. The samples were then extracted as described previously and chromatographed. The analytical curves were determined; the slopes, intercepts, and correlation coefficients, along with their 95% confidence limits, are listed in Table II.

The range of values for the slope of each compound extracted from the capsule matrix corresponds very well with that for the pure compound, confirming that all degradation products are extracted from the capsule matrix into the mobile phase. Complete extraction of these compounds was demonstrated further by extracting the contents of five capsules, filtering off the mobile phase, and reextracting the capsule matrix with the mobile phase. No degradation products were found chromatographically in the second extraction solution. The negative intercepts of the analytical curves for II and III were due to the presence of these

Table III—Typical Values for the Amount of Degradation Products Found in Procarbazine Capsules[a]

Sample[b]	Shelflife, years[c]	Degradation to II[d], %	Degradation to III[d], %	Degradation to IV[d], %
A	4.5	0.29	0.26	0.044
B	4.0	0.31	0.36	0.012
C	4.0	0.31	0.48	0.013
D	2.5	0.29	0.49	0.013
E	1.4	0.25	0.48	0.014
F	0.8	0.27	0.45	0.014

[a] All values are the average of three determinations. [b] A–F represent different lots of material. [c] Number of years since manufacture. All samples were held at 25° over this time. [d] Percent degradation calculated using the equation:

$$\%\ \text{degradation} = \frac{\text{degradation product (mg/ml)}}{\text{25 mg of procarbazine/ml}} \times 100$$

Five capsules, each containing 50 mg of procarbazine (250 mg), were extracted into 10 ml of mobile phase.

degradation products in the capsule mixture itself. Therefore, the extraction with mobile phase removes all degradation products from the capsule matrix.

Representative samples of procarbazine hydrochloride capsules manufactured at various times were assayed for II–IV. A typical chromatogram is shown in Fig. 1B; the values for the percent degradation product found, based on the initial amount of procarbazine being 50 mg/capsule, are given in Table III. These values are all significantly below 0.5% degradation and confirm that II and III are the main degradation products while IV is only seen in a trace amount.

In previous accelerated degradation studies, II and III were found at about the 1% level after 1 month at 55°[10]. Only a very small amount of IV was found at this temperature. Sample A (Table III) had a smaller amount of III and a larger amount of IV than any other sample. This result could, in part, be due to the oxidation of III to IV as described previously (2). Another potential degradation product, *N*-isopropyltoluamide, having a retention volume of 32 ml, was not found in any sample (2–5).

[10] J. Carstensen, Hoffmann-La Roche, unpublished data.

REFERENCES

(1) "Physicians' Desk Reference," 29th ed., Medical Economics Co., Oradell, N.J., 1975, pp. 1248–1250.

(2) R. J. Rucki, in "Analytical Profiles of Drug Substances," vol. 5, K. Florey, Ed., Academic, New York, N.Y., 1976, pp. 403–427.

(3) H. Aebi, B. Dewald, and H. Suter, *Helv. Chim. Acta*, **48**, 656 (1965).

(4) H. Erlenmeyer, R. Zell, H. Brintzinger, and B. Prijs, *ibid.*, **47**, 876 (1964).

(5) "The United States Pharmacopeia," 19th rev., Mack Publishing Co., Easton, Pa., 1975, p. 410.

(6) J. B. Johnson and V. S. Venturella, *Bull. Parenter. Drug Assoc.*, **25**, 239 (1971).

(7) S. Oliveri-Vigh, J. J. Donahue, J. E. Heveran, and B. Z. Senkowski, *J. Pharm. Sci.*, **60**, 1851 (1971).

(8) H. Beral and V. Stoicescu, *Pharm. Zentralh.*, **108**, 469 (1969).

(9) B. L. Karger, L. R. Snyder, and C. Horvath, "An Introduction to Separation Science," Wiley, New York, N.Y., chap. 5.

(10) L. A. Currie, *Anal. Chem.*, **40**, 586 (1968).

In Vitro Evidence for Ipecac Inactivation by Activated Charcoal

DAVID O. COONEY

Received February 9, 1977, from the *Chemical Engineering Department, Clarkson College of Technology, Potsdam, NY 13676.* Accepted for publication June 15, 1977.

Abstract □ The *in vitro* adsorption of the alkaloid emetine, a primary constituent of ipecac, on activated charcoal was studied. The results support the supposition that syrup of ipecac should not be given to counteract poisonings if activated charcoal is also to be administered.

Keyphrases □ Emetine—*in vitro* adsorption on activated charcoal □ Ipecac—*in vitro* adsorption of constituent emetine on activated charcoal □ Adsorption, *in vitro*—emetine on activated charcoal □ Charcoal, activated—*in vitro* adsorption of emetine □ Alkaloids—emetine, *in vitro* adsorption on activated charcoal

Statements occasionally appear in the literature indicating that syrup of ipecac and activated charcoal should not be given together to counteract poisonings. The reasoning is the hypothesis that the alkaloids emetine and cephaeline, which constitute more than 90% of the alkaloids of ipecac, would adsorb to the charcoal and thereby fail to act as desired, but no proof has yet been presented.

The only reference to ipecac adsorption to activated charcoal appears to be that in an 1846 paper by Garrod, which was quoted by Holt and Holz (1). Studies (2–5) on other alkaloids such as strychnine, nicotine, atropine, morphine, yohimbine, veratrine, and aconitine have clearly established a substantial affinity between alkaloids and activated charcoal. However, the extent of binding varies widely, not only with the alkaloid involved but with pH. Since alkaloids are basic, the extent of adsorption is often much less at pH values corresponding to gastric conditions than it is at a neutral pH. This result is due to the well-recognized fact (2) that ionized forms of solutes usually bind much less strongly than their nonionized forms.

In light of the lack of any data concerning the adsorption of alkaloids of ipecac on charcoal, a study of emetine adsorption was performed. Only emetine was studied since it comprises more than half of the total alkaloid content of ipecac (6). Moreover, cephaeline ($C_{28}H_{38}N_2O_4$) differs from emetine ($C_{29}H_{40}N_2O_4$) only by the lack of one methyl group, so it would be expected to behave similarly to emetine in terms of adsorption.

EXPERIMENTAL

Simulated gastric fluid USP (pepsin omitted), pH 1.2, was used for all solutions. Emetine hydrochloride[1] was dissolved to the extent of either 0.2 or 0.4 g/liter in the gastric fluid. Powdered activated charcoal[2] was washed twice with 6 *N* HCl and six times with distilled water and then was dried at 120° for 24 hr.

Various amounts of the charcoal were mixed with 10-ml aliquots of the emetine solutions in capped glass vials and shaken for 6 hr or longer. After most of the charcoal settled, the supernate was filtered through 0.45-μm pore-size microporous membranes[3]. The clear filtrate was analyzed by UV spectrophotometry at 253.6 nm. Samples of emetine solutions of known concentrations, prepared by dilution with the gastric fluid, were treated in the same manner, except that charcoal was omitted.

RESULTS

Figure 1 shows the adsorption isotherm obtained, as represented by a plot of Q^* (grams of emetine adsorbed per gram of charcoal) *versus* C_f (concentration of emetine in grams per liter in the surrounding fluid at equilibrium). The data could be fit well (by eye) with the Freundlich equation $Q^* = 0.249C_f^{0.182}$ in the range from $0 < C_f < 0.03$ and by another Freundlich expression, $Q^* = 0.177C_f^{0.0793}$, in the range of about $0.06 < C_f < 0.400$.

[1] Sigma Chemical Co., St. Louis, Mo.
[2] Norit A, American Norit Co., Jacksonville, Fla.
[3] Amicon Corp., Lexington, Mass.

degradation products in the capsule mixture itself. Therefore, the extraction with mobile phase removes all degradation products from the capsule matrix.

Representative samples of procarbazine hydrochloride capsules manufactured at various times were assayed for II–IV. A typical chromatogram is shown in Fig. 1B; the values for the percent degradation product found, based on the initial amount of procarbazine being 50 mg/capsule, are given in Table III. These values are all significantly below 0.5% degradation and confirm that II and III are the main degradation products while IV is only seen in a trace amount.

In previous accelerated degradation studies, II and III were found at about the 1% level after 1 month at 55°[10]. Only a very small amount of IV was found at this temperature. Sample A (Table III) had a smaller amount of III and a larger amount of IV than any other sample. This result could, in part, be due to the oxidation of III to IV as described previously (2). Another potential degradation product, *N*-isopropyltoluamide, having a retention volume of 32 ml, was not found in any sample (2–5).

[10] J. Carstensen, Hoffmann-La Roche, unpublished data.

REFERENCES

(1) "Physicians' Desk Reference," 29th ed., Medical Economics Co., Oradell, N.J., 1975, pp. 1248–1250.

(2) R. J. Rucki, in "Analytical Profiles of Drug Substances," vol. 5, K. Florey, Ed., Academic, New York, N.Y., 1976, pp. 403–427.

(3) H. Aebi, B. Dewald, and H. Suter, *Helv. Chim. Acta*, **48**, 656 (1965).

(4) H. Erlenmeyer, R. Zell, H. Brintzinger, and B. Prijs, *ibid.*, **47**, 876 (1964).

(5) "The United States Pharmacopeia," 19th rev., Mack Publishing Co., Easton, Pa., 1975, p. 410.

(6) J. B. Johnson and V. S. Venturella, *Bull. Parenter. Drug Assoc.*, **25**, 239 (1971).

(7) S. Oliveri-Vigh, J. J. Donahue, J. E. Heveran, and B. Z. Senkowski, *J. Pharm. Sci.*, **60**, 1851 (1971).

(8) H. Beral and V. Stoicescu, *Pharm. Zentralh.*, **108**, 469 (1969).

(9) B. L. Karger, L. R. Snyder, and C. Horvath, "An Introduction to Separation Science," Wiley, New York, N.Y., chap. 5.

(10) L. A. Currie, *Anal. Chem.*, **40**, 586 (1968).

In Vitro Evidence for Ipecac Inactivation by Activated Charcoal

DAVID O. COONEY

Received February 9, 1977, from the *Chemical Engineering Department, Clarkson College of Technology, Potsdam, NY 13676.* Accepted for publication June 15, 1977.

Abstract □ The *in vitro* adsorption of the alkaloid emetine, a primary constituent of ipecac, on activated charcoal was studied. The results support the supposition that syrup of ipecac should not be given to counteract poisonings if activated charcoal is also to be administered.

Keyphrases □ Emetine—*in vitro* adsorption on activated charcoal □ Ipecac—*in vitro* adsorption of constituent emetine on activated charcoal □ Adsorption, *in vitro*—emetine on activated charcoal □ Charcoal, activated—*in vitro* adsorption of emetine □ Alkaloids—emetine, *in vitro* adsorption on activated charcoal

Statements occasionally appear in the literature indicating that syrup of ipecac and activated charcoal should not be given together to counteract poisonings. The reasoning is the hypothesis that the alkaloids emetine and cephaeline, which constitute more than 90% of the alkaloids of ipecac, would adsorb to the charcoal and thereby fail to act as desired, but no proof has yet been presented.

The only reference to ipecac adsorption to activated charcoal appears to be that in an 1846 paper by Garrod, which was quoted by Holt and Holz (1). Studies (2–5) on other alkaloids such as strychnine, nicotine, atropine, morphine, yohimbine, veratrine, and aconitine have clearly established a substantial affinity between alkaloids and activated charcoal. However, the extent of binding varies widely, not only with the alkaloid involved but with pH. Since alkaloids are basic, the extent of adsorption is often much less at pH values corresponding to gastric conditions than it is at a neutral pH. This result is due to the well-recognized fact (2) that ionized forms of solutes usually bind much less strongly than their nonionized forms.

In light of the lack of any data concerning the adsorption of alkaloids of ipecac on charcoal, a study of emetine adsorption was performed. Only emetine was studied since it comprises more than half of the total alkaloid content of ipecac (6). Moreover, cephaeline ($C_{28}H_{38}N_2O_4$) differs from emetine ($C_{29}H_{40}N_2O_4$) only by the lack of one methyl group, so it would be expected to behave similarly to emetine in terms of adsorption.

EXPERIMENTAL

Simulated gastric fluid USP (pepsin omitted), pH 1.2, was used for all solutions. Emetine hydrochloride[1] was dissolved to the extent of either 0.2 or 0.4 g/liter in the gastric fluid. Powdered activated charcoal[2] was washed twice with 6 *N* HCl and six times with distilled water and then was dried at 120° for 24 hr.

Various amounts of the charcoal were mixed with 10-ml aliquots of the emetine solutions in capped glass vials and shaken for 6 hr or longer. After most of the charcoal settled, the supernate was filtered through 0.45-μm pore-size microporous membranes[3]. The clear filtrate was analyzed by UV spectrophotometry at 253.6 nm. Samples of emetine solutions of known concentrations, prepared by dilution with the gastric fluid, were treated in the same manner, except that charcoal was omitted.

RESULTS

Figure 1 shows the adsorption isotherm obtained, as represented by a plot of Q^* (grams of emetine adsorbed per gram of charcoal) *versus* C_f (concentration of emetine in grams per liter in the surrounding fluid at equilibrium). The data could be fit well (by eye) with the Freundlich equation $Q^* = 0.249C_f^{0.182}$ in the range from $0 < C_f < 0.03$ and by another Freundlich expression, $Q^* = 0.177C_f^{0.0793}$, in the range of about $0.06 < C_f < 0.400$.

[1] Sigma Chemical Co., St. Louis, Mo.
[2] Norit A, American Norit Co., Jacksonville, Fla.
[3] Amicon Corp., Lexington, Mass.

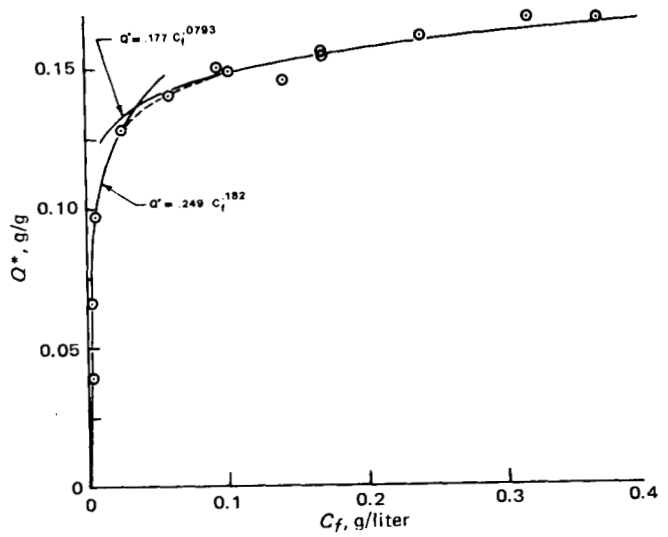

Figure 1—*Adsorption of emetine by powdered activated charcoal from simulated gastric fluid.*

DISCUSSION

On the basis that the usual dose of syrup of ipecac is 1 tablespoonful, or 15 ml (7), and that ipecac syrup yields 123–157 mg of ether-soluble alkaloids/100 ml of syrup (7), an average dose of ipecac syrup would contain about 21 mg of alkaloids. If this dose mixes with V liters of gastric contents upon ingestion, it would produce a concentration, C_0, equal to $0.021/V$ g/liter of alkaloids in the gastric contents. If one were then to administer W g of activated charcoal, adsorption of some of the alkaloids would occur, lowering their concentration to a value of C_f at equilibrium.

One can show by a simple mass balance that $Q^* = V(C_0 - C_f)/W$. If it is assumed that C_f will be lower than 0.03 g/liter (as will nearly always be the case) and if it is assumed that all alkaloids present behave like emetine in terms of adsorption, then $Q^* = 0.249C_f^{0.182}$ will pertain. Therefore, $0.249C_f^{0.182} = V(0.021/V - C_f)/W = (0.021 - VC_f)/W$. Now, it can be shown that for *any* reasonable choices of V and W, C_f will be very small. As one example, for $V = 0.5$ liter and $W = 1$ g, $C_f = 1.25 \times 10^{-6}$ g/liter, or 0.003% of the initial concentration.

This result indicates that the extent of emetine binding by any reasonable dose of activated charcoal is extremely high *in vitro*. Although *in vivo* data on emetine binding are lacking, the present results strongly suggest that there may be no acceptable dose level for syrup of ipecac that would leave enough free alkaloids in solution, after an adsorption equilibrium is attained, to cause emesis. Moreover, since the quantity of charcoal that *should* be administered to counteract poisonings effectively is as high as 120 g (8), even an extremely large dose of ipecac syrup might be inactivated under *in vivo* circumstances.

REFERENCES

(1) L. E. Holt, Jr., and P. H. Holz, *J. Pediatr.*, **63**, 306 (1963).

(2) A. H. Andersen, *Acta Pharmacol. Toxicol.*, **2**, 69 (1946). *Ibid.*, **3**, 199 (1947). *Ibid.*, **4**, 275 (1948).

(3) A. L. Picchioni, L. Chin, H. L. Verhulst, and B. Dieterle, *Toxicol. Appl. Pharmacol.*, **8**, 447 (1966).

(4) A. L. Picchioni, L. Chin, and H. E. Laird, *Clin. Toxicol.*, **7**, 97 (1974).

(5) D. Henschler, *Arh. Hig. Rada*, **21**, 129 (1970).

(6) "The Pharmacological Basis of Therapeutics," 4th ed., L. S. Goodman and A. Gilman, Eds., Macmillan, New York, N.Y., 1970, p. 1128.

(7) "Remington's Pharmaceutical Sciences," 15th ed., Mack Publishing Co., Easton, Pa., 1975, pp. 800, 801.

(8) J. W. Hayden and E. G. Comstock, *Clin. Toxicol.*, **8**, 515 (1975).

Determination of Desmethyldiazepam in Plasma by Electron-Capture GLC: Application to Pharmacokinetic Studies of Clorazepate

DAVID J. GREENBLATT

Received May 20, 1977, from the *Clinical Pharmacology Unit, Massachusetts General Hospital, Boston, MA 02114.* Accepted for publication July 18, 1977.

Abstract □ Plasma desmethyldiazepam concentrations were quantitated by a rapid and sensitive technique using electron-capture GLC. Following addition of diazepam as the internal standard, plasma is extracted at physiological pH into benzene–isoamyl alcohol. The extract is evaporated to dryness and reconstituted with toluene–isoamyl alcohol prior to chromatography. Both diazepam and desmethyldiazepam are quantitatively extracted. The variation of identical samples is 5%, and the sensitivity is 5 ng of desmethyldiazepam/ml of original sample. The method is applicable to pharmacokinetic studies of clorazepate, a benzodiazepine derivative transformed to desmethyldiazepam prior to absorption.

Keyphrases □ Desmethyldiazepam—electron-capture GLC analysis in plasma □ GLC, electron capture—analysis, desmethyldiazepam in plasma □ Clorazepate—pharmacokinetic study by GLC analysis of desmethyldiazepam in plasma □ Tranquilizers—clorazepate, pharmacokinetic study by GLC analysis of desmethyldiazepam in plasma

Clorazepate dipotassium (I) is a 1,4-benzodiazepine derivative extensively used as a sedative and antianxiety agent (1, 2). Previous studies (3) suggested that clorazepate is transformed to desmethyldiazepam (II) by hydrolysis and decarboxylation in the acidic stomach contents (Scheme I). Desmethyldiazepam is subsequently absorbed from the proximal small bowel and appears to account for most or all of the clinical effects attributable to clorazepate.

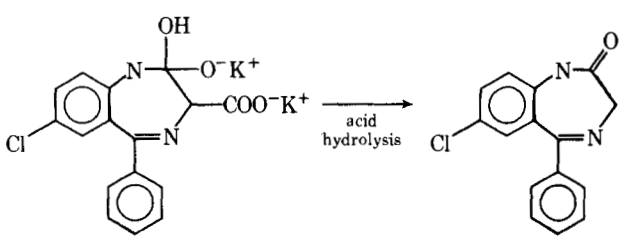

I *Scheme I* II

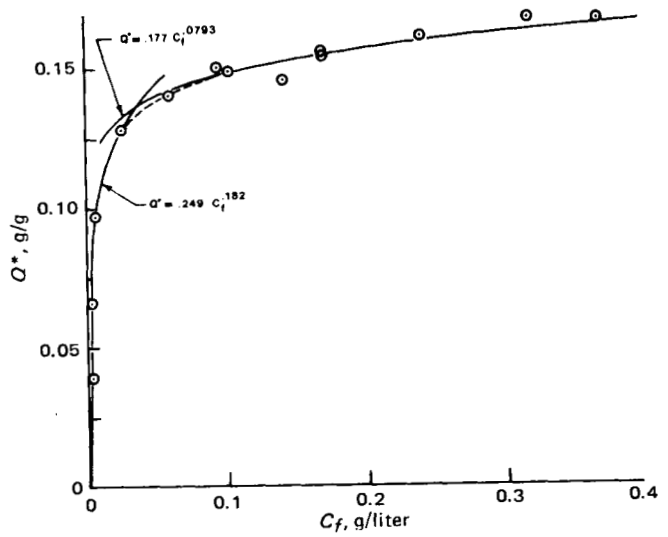

Figure 1—*Adsorption of emetine by powdered activated charcoal from simulated gastric fluid.*

DISCUSSION

On the basis that the usual dose of syrup of ipecac is 1 tablespoonful, or 15 ml (7), and that ipecac syrup yields 123–157 mg of ether-soluble alkaloids/100 ml of syrup (7), an average dose of ipecac syrup would contain about 21 mg of alkaloids. If this dose mixes with V liters of gastric contents upon ingestion, it would produce a concentration, C_0, equal to $0.021/V$ g/liter of alkaloids in the gastric contents. If one were then to administer W g of activated charcoal, adsorption of some of the alkaloids would occur, lowering their concentration to a value of C_f at equilibrium.

One can show by a simple mass balance that $Q^* = V(C_0 - C_f)/W$. If it is assumed that C_f will be lower than 0.03 g/liter (as will nearly always be the case) and if it is assumed that all alkaloids present behave like emetine in terms of adsorption, then $Q^* = 0.249C_f^{0.182}$ will pertain. Therefore, $0.249C_f^{0.182} = V(0.021/V - C_f)/W = (0.021 - VC_f)/W$. Now, it can be shown that for *any* reasonable choices of V and W, C_f will be very small. As one example, for $V = 0.5$ liter and $W = 1$ g, $C_f = 1.25 \times 10^{-6}$ g/liter, or 0.003% of the initial concentration.

This result indicates that the extent of emetine binding by any reasonable dose of activated charcoal is extremely high *in vitro*. Although *in vivo* data on emetine binding are lacking, the present results strongly suggest that there may be no acceptable dose level for syrup of ipecac that would leave enough free alkaloids in solution, after an adsorption equilibrium is attained, to cause emesis. Moreover, since the quantity of charcoal that *should* be administered to counteract poisonings effectively is as high as 120 g (8), even an extremely large dose of ipecac syrup might be inactivated under *in vivo* circumstances.

REFERENCES

(1) L. E. Holt, Jr., and P. H. Holz, *J. Pediatr.*, **63**, 306 (1963).

(2) A. H. Andersen, *Acta Pharmacol. Toxicol.*, **2**, 69 (1946). *Ibid.*, **3**, 199 (1947). *Ibid.*, **4**, 275 (1948).

(3) A. L. Picchioni, L. Chin, H. L. Verhulst, and B. Dieterle, *Toxicol. Appl. Pharmacol.*, **8**, 447 (1966).

(4) A. L. Picchioni, L. Chin, and H. E. Laird, *Clin. Toxicol.*, **7**, 97 (1974).

(5) D. Henschler, *Arh. Hig. Rada*, **21**, 129 (1970).

(6) "The Pharmacological Basis of Therapeutics," 4th ed., L. S. Goodman and A. Gilman, Eds., Macmillan, New York, N.Y., 1970, p. 1128.

(7) "Remington's Pharmaceutical Sciences," 15th ed., Mack Publishing Co., Easton, Pa., 1975, pp. 800, 801.

(8) J. W. Hayden and E. G. Comstock, *Clin. Toxicol.*, **8**, 515 (1975).

Determination of Desmethyldiazepam in Plasma by Electron-Capture GLC: Application to Pharmacokinetic Studies of Clorazepate

DAVID J. GREENBLATT

Received May 20, 1977, from the *Clinical Pharmacology Unit, Massachusetts General Hospital, Boston, MA 02114.* Accepted for publication July 18, 1977.

Abstract □ Plasma desmethyldiazepam concentrations were quantitated by a rapid and sensitive technique using electron-capture GLC. Following addition of diazepam as the internal standard, plasma is extracted at physiological pH into benzene–isoamyl alcohol. The extract is evaporated to dryness and reconstituted with toluene–isoamyl alcohol prior to chromatography. Both diazepam and desmethyldiazepam are quantitatively extracted. The variation of identical samples is 5%, and the sensitivity is 5 ng of desmethyldiazepam/ml of original sample. The method is applicable to pharmacokinetic studies of clorazepate, a benzodiazepine derivative transformed to desmethyldiazepam prior to absorption.

Keyphrases □ Desmethyldiazepam—electron-capture GLC analysis in plasma □ GLC, electron capture—analysis, desmethyldiazepam in plasma □ Clorazepate—pharmacokinetic study by GLC analysis of desmethyldiazepam in plasma □ Tranquilizers—clorazepate, pharmacokinetic study by GLC analysis of desmethyldiazepam in plasma

Clorazepate dipotassium (I) is a 1,4-benzodiazepine derivative extensively used as a sedative and antianxiety agent (1, 2). Previous studies (3) suggested that clorazepate is transformed to desmethyldiazepam (II) by hydrolysis and decarboxylation in the acidic stomach contents (Scheme I). Desmethyldiazepam is subsequently absorbed from the proximal small bowel and appears to account for most or all of the clinical effects attributable to clorazepate.

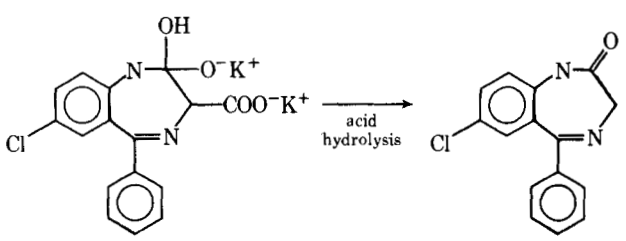

I *Scheme I* II

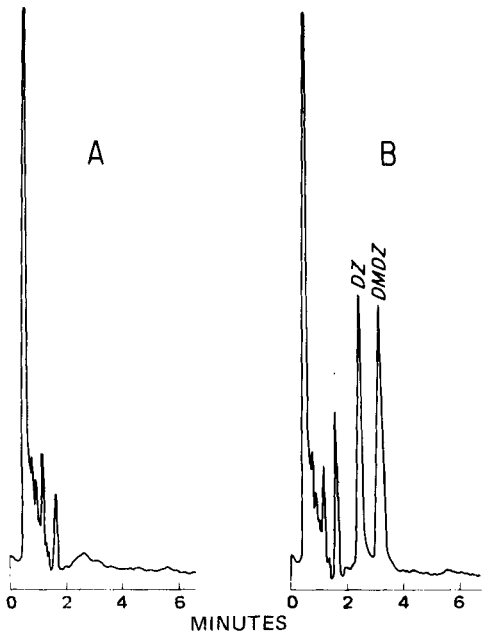

Figure 1—*A: sample chromatogram of a drug-free control plasma extract. B: chromatogram of the same plasma sample to which were added diazepam (DZ) and desmethyldiazepam (DMDZ) in concentrations of 100 ng/ml.*

Reported GLC procedures for desmethyldiazepam in plasma involved chromatography of the intact substance following extensive cleanup procedures (4–7) or acid hydrolysis of the compound to a benzophenone derivative prior to chromatography (8–10). Some studies, however, suggested that desmethyldiazepam may be analyzed using simple extraction without extensive cleanup or derivatization (11–19). The present report describes a rapid and sensitive method for analysis of intact desmethyldiazepam in plasma and illustrates its applicability to clinical pharmacokinetic studies of clorazepate.

EXPERIMENTAL

Instrumental Conditions—The gas chromatograph[1] was equipped with a 2-mCi ^{63}Ni-electron-capture detector operated at 320° in the pulsed mode, with a pulse interval of 150 μsec. The purge gas[2] was argon–methane (95:5) at a flow rate of 80 ml/min. Detector settings were: range, 1; and attenuation, 128.

The column was coiled glass[3], 1.8 m (6 ft) long × 4 mm i.d., packed with 3% OV-17 on 80–100-mesh Chromosorb WHP[3]. Carrier gas[2] was ultrapure helium at a flow rate of 50 ml/min. The column was conditioned at 325° using a low flow of carrier gas for 48 hr prior to its attachment to the detector. Temperature settings during operation were: injection port, 300°; and column, 280°.

Assay—Stock solutions of diazepam and desmethyldiazepam, 1 μg/ml, were prepared in benzene–acetone–methanol (80:15:5) as described previously (13). Diazepam served as the internal standard; a fixed quantity of the diazepam stock solution (usually 100–200 μl) was added to conical 40-ml centrifuge tubes equipped with polytef-lined screw caps. The solution was evaporated to dryness at 40° using a mild vacuum. Calibration standards were prepared by addition of at least four known quantities (usually 100, 200, 300, and 400 ng) of desmethyldiazepam to consecutive tubes. These solutions also were evaporated to dryness.

Drug-free control plasma, 1 ml, was added to each calibration sample, and 1 ml of "unknown" plasma was added to the other tubes. A 7.5-ml aliquot of benzene (containing 1.5% isoamyl alcohol) was added to all tubes, and the mixtures were agitated gently on a vortex mixer for 60 sec.

[1] Model 5750, Hewlett-Packard, Avondale, Pa.
[2] Matheson Gas Products, Gloucester, Mass.
[3] Supelco, Inc., Bellefonte, Pa.

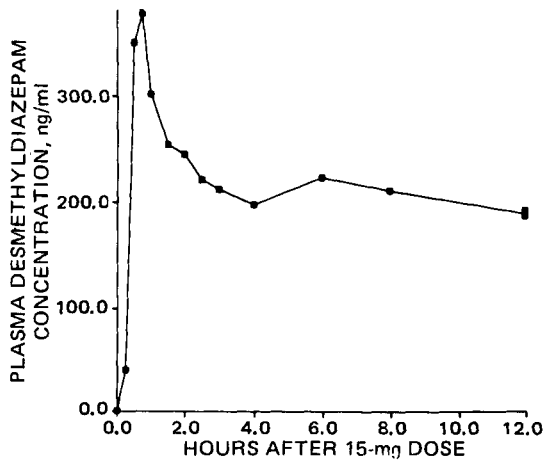

Figure 2—*Plasma desmethyldiazepam concentrations measured in a healthy volunteer during the first 12 hr after ingestion of 15 mg of clorazepate dipotassium.*

The tubes were centrifuged for 10 min at 2500 rpm, and an aliquot of the organic layer (~6 ml) was transferred to a conical 13-ml centrifuge tube.

The organic extracts were evaporated to dryness at 40° using a mild vacuum. The residue was redissolved in 100–200 μl of toluene (containing 15% isoamyl alcohol), of which 1–2 μl was injected into the chromatograph. Under these chromatographic conditions, the retention times were: diazepam, 2.5 min; and desmethyldiazepam, 3.25 min (Fig. 1).

Calculations—Calibration lines were prepared daily using the peak height ratio of desmethyldiazepam to diazepam *versus* the desmethyldiazepam concentration in the calibration samples. Least-squares regression analysis was used to determine the slope of the "best" line passing through the origin. Desmethyldiazepam concentrations in unknown samples were determined from the standard curve using the ratio of the desmethyldiazepam peak height to that of the internal standard.

Clinical Study—A healthy female volunteer ingested 15 mg of clorazepate dipotassium[4] with 100 ml of water after an overnight fast. Venous blood samples were drawn from an indwelling butterfly cannula or by separate venipuncture prior to drug administration and at 0.25, 0.5, 0.75, 1.0, 1.5, 2.0, 2.5, 3, 4, 6, 8, 12, 24, 36, 48, 73, 95, 120, and 144 hr after drug administration. Plasma samples were separated and frozen until analyzed. Desmethyldiazepam concentrations were determined by the described method. Samples drawn from 12 hr after ingestion through the end of the study were analyzed in duplicate.

The time course of plasma desmethyldiazepam concentrations following clorazepate ingestion in this subject appeared consistent with a two-compartment open pharmacokinetic model, with first-order drug absorption from the GI tract into the "central compartment," with a "lag time" prior to drug absorption (20). Accordingly, data points were analyzed with a computer, using iterative nonlinear least-squares regression analysis (21), and fitted to a function of the form:

$$C = -(A + B)e^{-k_a(t-t_0)} + Ae^{-\alpha(t-t_0)} + Be^{-\beta(t-t_0)} \quad \text{(Eq. 1)}$$

where C represents the plasma desmethyldiazepam concentration at time t after the dose; t_0 is the lag time prior to the start of absorption; A and B are "hybrid" intercept terms; and k_a, α, and β are hybrid exponents consistent with the absorption, distribution, and elimination phases, respectively, of the plasma concentration curve (22). The hybrid exponents were used to calculate the apparent first-order rates of drug absorption, $t_{1/2a}$, and elimination, $t_{1/2\beta}$, as follows:

$$t_{1/2a} = (\ln 2)/k_a = 0.693/k_a \quad \text{(Eq. 2)}$$

$$t_{1/2\beta} = (\ln 2)/\beta = 0.693/\beta \quad \text{(Eq. 3)}$$

RESULTS AND DISCUSSION

Assay Reproducibility and Sensitivity—Quantitative recovery of diazepam and desmethyldiazepam is achieved by this procedure. The coefficient of variation for 72 identical samples containing 25 ng of

[4] Tranxene, Abbott Laboratories, North Chicago, Ill.

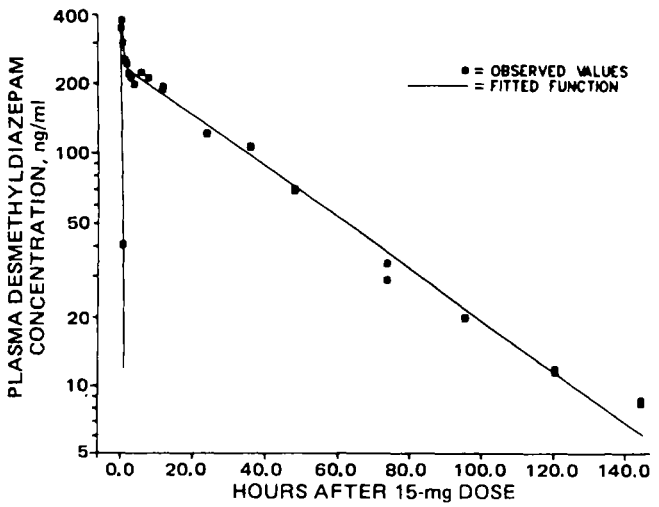

Figure 3—*Plasma desmethyldiazepam concentrations in the same volunteer during 144 hr after ingestion of 15 mg of clorazepate dipotassium. Replicate determinations were performed on samples drawn at 12 hr and thereafter. The solid line is the computer-fitted function.*

desmethyldiazepam/ml was 5.3%. The limits of sensitivity are approximately 5 ng of desmethyldiazepam/ml of original sample.

Pharmacokinetic Results—Following oral administration of 15 mg of clorazepate dipotassium to the healthy volunteer subject, a peak plasma desmethyldiazepam concentration of 379 ng/ml was measured in the sample drawn at 0.75 hr (Fig. 2). Following the achievement of peak levels, concentrations declined with an apparent biexponential pattern. The following function was generated by the computer following 50 iterative steps:

$$C = -2448.2e^{-4.19(t-t_0)} + 2208.0e^{-3.28(t-t_0)} + 240.2e^{-0.0257(t-t_0)} \quad \text{(Eq. 4)}$$

The lag time value, t_0, was 0.24 hr. Apparent half-life values were: $t_{1/2\alpha}$, 9.9 min; and $t_{1/2\beta}$, 27.0 hr (Fig. 3).

The described method enables rapid, reproducible, and sensitive quantitation of desmethyldiazepam in plasma. There is no evidence that desmethyldiazepam undergoes *N*-methylation to form diazepam in humans (2); chromatograms of plasma samples, containing no internal standard, from patients receiving clorazepate reveal no measurable amounts of diazepam. Thus, diazepam serves as a suitable internal standard. Addition of this compound to the original biological sample prior to extraction eliminates the need for precise volumetric measurements during subsequent steps.

Both desmethyldiazepam and diazepam are extracted quantitatively into the organic solvent at physiological pH using a single extraction. Chromatograms of these extracts are consistently free of any interfering peaks having retention times close to those of diazepam and desmethyldiazepam. Therefore, further cleanup procedures are not necessary. Since both compounds yield symmetrical, Gaussian peaks under the described conditions, peak heights rather than peak areas can be used for reliable quantitation of detector response (23). Thus, an electronic integrator is not necessary.

The method is readily adaptable to pharmacokinetic studies of desmethyldiazepam in human blood or plasma following ingestion of therapeutic doses of clorazepate dipotassium.

REFERENCES

(1) D. J. Greenblatt and R. I. Shader, "Benzodiazepines in Clinical Practice," Raven, New York, N.Y., 1974.

(2) D. J. Greenblatt and R. I. Shader, *N. Engl. J. Med.*, **291**, 1011, 1239 (1974).

(3) P. J. Carrigan, G. C. Chao, W. M. Barker, D. J. Hoffman, and A. H. C. Chun, *J. Clin. Pharmacol.*, **17**, 18 (1977).

(4) S. Garattini, F. Marcucci, and E. Mussini, in "Gas Chromatography in Biology and Medicine," R. Porter, Ed., J & A Churchill Ltd., London, England, 1969, p. 161.

(5) J. A. F. deSilva and C. V. Puglisi, *Anal. Chem.*, **42**, 1725 (1970).

(6) P. L. Morselli, N. Principi, G. Tognoni, E. Reali, G. Belvedere, S. M. Standen, and F. Sereni, *J. Perinat. Med.*, **1**, 133 (1973).

(7) R. Brandt, *Arzneim.-Forsch.*, **26**, 454 (1976).

(8) J. A. F. deSilva, M. A. Schwartz, V. Stefanovic, J. Kaplan, and L. D'Arconte, *Anal. Chem.*, **36**, 2099 (1964).

(9) A. Viala, J. P. Cano, C. Dravet, C. A. Tassinari, and J. Roger, *Psychiatr. Neurol. Neurochir.*, **74**, 153 (1971).

(10) D. J. Hoffman and A. H. C. Chun, *J. Pharm. Sci.*, **64**, 1668 (1975).

(11) L. Kangas, A. Pekkarinen, C. Sourander, and E. Raijola, *Ann. Clin. Res., Suppl. 11*, **6**, 12 (1974).

(12) A. Berlin, B. Siwers, S. Agurell, A. Hiort, F. Sjoqvist, and S. Strom, *Clin. Pharmacol. Ther.*, **13**, 733 (1972).

(13) J. A. F. deSilva, I. Bekersky, C. V. Puglisi, M. A. Brooks, and R. E. Weinfeld, *Anal. Chem.*, **48**, 10 (1976).

(14) J. A. S. Gamble, R. A. E. Assaf, J. S. Mackay, M. S. Kennedy, and P. J. Howard, *Anaesthesia*, **30**, 159 (1975).

(15) I. A. Zingales, *J. Chromatogr.*, **75**, 55 (1973).

(16) A. Robin, S. H. Curry, and R. Whelpton, *Psychol. Med.*, **4**, 388 (1974).

(17) E. Arnold, *Acta Pharmacol. Toxicol.*, **36**, 335 (1975).

(18) A. G. Howard, G. Nickless, and D. M. Hailey, *J. Chromatogr.*, **90**, 325 (1974).

(19) S. M. MacLeod, H. G. Giles, G. Patzalek, J. Thiessen, and E. M. Sellers, in "Currents in Alcoholism," vol. 1, F. A. Seixas, Ed., Grune & Stratton, New York, N.Y., 1977, p. 295.

(20) D. J. Greenblatt, R. T. Schillings, A. A. Kyriakopoulos, R. I. Shader, S. E. Sisenwine, J. A. Knowles, and H. W. Ruelius, *Clin. Pharmacol. Ther.*, **20**, 329 (1976).

(21) R. A. Usanis, "NLIN—Nonlinear Least Squares Estimation of Parameters (Library Services Series Document No. LSR-089-1)," Triangle Universities Computation Center, Research Triangle Park, N.C., 1972.

(22) D. J. Greenblatt and J. Koch-Weser, *N. Engl. J. Med.*, **293**, 702, 964 (1975).

(23) A. Janik, *J. Chromatogr. Sci.*, **13**, 93 (1975).

ACKNOWLEDGMENTS

Supported in part by Grant MH-12279 from the U.S. Public Health Service.

The author is grateful for the collaboration of Dr. Richard I. Shader and Dr. Anastasios Georgotas and for the assistance of Marcia Allen, Ann Werner, and Kate Franke.

Alkaloids from *Lupinus argenteus* var. *stenophyllus*

WILLIAM J. KELLER ˣ **and STEVEN G. ZELENSKI**

Received May 5, 1977, from the *School of Pharmacy, Northeast Louisiana University, Monroe, LA 71209.* Accepted for publication June 14, 1977.

Abstract □ TLC and GLC of an alkaloid extract of the aboveground portions of *Lupinus argenteus* Pursh. var. *stenophyllus* (Rydb.) Davis (Leguminosae) suggested the presence of sparteine, β-isosparteine, Δ^5-dehydrolupanine, α-isolupanine, lupanine, thermopsine, and anagyrine. GLC–mass spectrometry confirmed these preliminary findings. Preparative TLC was used to isolate sparteine, and this alkaloid was further characterized by IR spectral analysis and derivatization.

Keyphrases ◘ Alkaloids, various—isolated from aboveground portions of *Lupinus argenteus* var. *stenophyllus* □ *Lupinus argenteus* var. *stenophyllus*—various alkaloids isolated from aboveground portions

The legume genus *Lupinus* is native to the Rocky Mountain states, and several of its species have been reported as being toxic to grazing livestock (1). The age and species of *Lupinus* together with the species of animal contribute to a variation in the symptoms and severity of lupine poisoning (2, 3). It is generally acknowledged that the quinolizidine alkaloid content of the lupine is responsible for acute toxicoses and death in livestock (1–4). It recently was shown that the ingestion of certain lupine species by pregnant cows causes crooked calf disease in the offspring (5). One study (6) suggested that the quinolizidine alkaloid anagyrine is the teratogen responsible for the congenital deformities.

The silvery lupine, *L. argenteus* Pursh., has long been considered to be highly toxic to grazing sheep (7, 8). While investigating possible causes of crooked calf disease, Shupe *et al.* (5) found that this species exhibited marked toxicity in cows. In a later study, Keeler (9) suggested *L. argenteus* to be a nonteratogenic lupine because it did not contain anagyrine and grew in range areas where crooked calf disease was unknown. A search of the chemical literature revealed no other investigation of *L. argenteus* or its variety *stenophyllus*.

The present study was directed at characterizing alkaloids from the aboveground portions of mature, flowering *L. argenteus* Pursh. var. *stenophyllus* (Rydb.) Davis. Data from this investigation explained the acute toxicity associated with this plant but provided questions as to its nonteratogenic nature.

EXPERIMENTAL[1]

Plant Material—The flowering aboveground portions of *L. argenteus* Pursh. var. *stenophyllus* (Rydb.) Davis (Leguminosae) were used[2].

Extraction and Fractionation—The air-dried powdered plant material (235 g) was homogenized with ethanol in a blender[3]. After filtration, the ethanolic extract was concentrated to 20 ml *in vacuo*, acidified with 10% acetic acid, and extracted with two successive 100-ml portions of ether, ethyl acetate, and chloroform. The acidic aqueous solution was made basic with 28% ammonium hydroxide and extracted with four 100-ml portions of chloroform. The combined chloroform extracts were filtered through anhydrous magnesium sulfate and evaporated to give a brown syrup (3 g), which solidified on standing.

TLC—Chloroform–methanol–28% ammonium hydroxide (100:10:1) and cyclohexane–diethylamine (7:3) were the developing solvents during chromatography of the alkaloid fraction over 0.25-mm layers of silica gel G. Dragendorff spray reagent revealed the presence of six alkaloidal substances. Cochromatography with reference standards suggested the presence of α-isolupanine, lupanine, thermopsine, and anagyrine. An Ehrlich-positive chromophore indicated the presence of Δ^5-dehydrolupanine (10). Both TLC systems revealed the presence of an alkaloid that could have been sparteine, β-isosparteine, or genisteine (α-isosparteine) based on identical R_f values.

GLC—With 3% OV-17 on Gas Chrom Q (2-m × 2-mm i.d. glass column) and a program of 4°/min from 125 to 265°, the alkaloid fraction was partially resolved to give peaks corresponding with reference β-isosparteine, Δ^5-dehydrolupanine, α-isolupanine, lupanine, thermopsine, and anagyrine. This GLC system failed to separate sparteine from genisteine.

Combined GLC–Mass Spectrometry—The alkaloid fraction was injected directly into a 2-m × 2-mm i.d. glass column containing 3% OV-17 on Gas Chrom Q. The column temperature was programmed from 160 to 265° at 2°/min. The injection temperature was 230°, and the carrier gas was helium at a flow of 28 ml/min. The effluent from the column entered the mass spectrometer through a glass jet separator maintained at 220°. The ion source temperature was maintained at 220° with the ionizing voltage at 70 ev and accelerating voltages of 12,600–900 ev. Spectra were recorded every 6 sec on the low-resolution mass spectrometer interfaced with a data reduction system.

Identification of β-Isosparteine—The GLC retention time relative to sparteine was 1.29 (standard 1.29); mass spectrum: M^+ *m/e* 234 (29%), 193 (26), 150 (26), 137 (92), 122 (19), 110 (35), and 98 (100) [standard M^+ *m/e* 234 (7%), 193 (9), 150 (13), 137 (96), 122 (17), 110 (25), and 98 (100)].

Identification of Δ^5-Dehydrolupanine—The GLC retention time relative to sparteine was 3.20 (standard 3.20); mass spectrum: M^+ *m/e* 246 (4%), 245 (3), 205 (3), 163 (9), 148 (14), 134 (21), 120 (14), and 98 (100) [standard M^+ *m/e* 246 (34%), 245 (10), 205 (2), 163 (5), 148 (5), 134 (8), 120 (5), and 98 (100)].

Identification of α-Isolupanine—The GLC retention time relative to sparteine was 3.36 (standard 3.36); mass spectrum: M^+ *m/e* 248 (16%), 247 (10), 219 (14), 150 (86), 149 (100), 148 (43), 137 (75), 136 (90), 134 (64), 124 (52), 112 (77), 110 (91), and 96 (37) [standard M^+ *m/e* 248 (89%), 247 (46), 219 (77), 150 (28), 149 (56), 148 (13), 137 (16), 136 (100), 134 (13), 124 (9.7), 112 (10), 110 (20), and 96 (11)].

Identification of Lupanine—The GLC retention time relative to sparteine was 3.76 (standard 3.76); mass spectrum: M^+ *m/e* 248 (3.8%), 247 (3.4), 149 (51), 136 (100), 134 (21), 112 (17), 110 (20), and 98 (36) [standard M^+ *m/e* 248 (7%), 247 (5), 149 (99), 136 (100), 134 (50), 112 (39), 110 (60), and 98 (56)].

Identification of Thermopsine—The GLC retention time relative to sparteine was 5.06 (standard 5.06); mass spectrum: M^+ *m/e* 244 (17%), 243 (6), 229 (6), 160 (47), 146 (84), 136 (46), 134 (30), 122 (47), and 98 (100) [standard M^+ *m/e* 244 (44%), 243 (10), 229 (3), 160 (11), 146 (16), 136 (10), 134 (4), 122 (7), and 98 (100)].

Identification of Anagyrine—The GLC retention time relative to sparteine was 5.61 (standard 5.61); mass spectrum: M^+ *m/e* 244 (1.8%), 161 (6), 160 (5), 146 (15), 136 (10), 122 (7), 117 (5), and 98 (100) [standard M^+ *m/e* 244 (60%), 161 (7), 160 (8), 146 (12), 136 (9), 122 (7), 117 (3), and 98 (100)].

The GLC peak corresponding with both sparteine and genisteine gave the following mass spectrum: M^+ *m/e* 234 (18%), 233 (13), 193 (21), 150 (21), 137 (100), 122 (19), 110 (32), and 98 (94). Under the conditions of

[1] IR spectra were recorded neat using a Perkin-Elmer model 257 spectrophotometer. GLC was conducted using a Hewlett-Packard model 5720A. Combined GLC–mass spectrometry was carried out with a DuPont 321 Dimaspec and 320 data system. The melting-point determinations were made using a Thomas-Hoover capillary melting-point apparatus and are uncorrected.

[2] Collected in Boulder Basin, Blaine County, Idaho, on August 6, 1973, and identified by Dr. Karl Holte, Botany Department, Idaho State University. A voucher specimen (No. 51553) is on deposit at the Idaho State University Herbarium, Pocatello, ID 83201.

[3] Waring.

combined GLC–mass spectrometry, reference sparteine and genisteine gave essentially the same mass spectrum.

Isolation of Sparteine—The entire alkaloid fraction (3 g) was dissolved in ethanol–chloroform (1:1) and streaked onto 12 silica gel PF_{254} plates (1 mm) using a previously described technique (11). The band corresponding with sparteine and genisteine was scraped from the plates, and the alkaloid material was eluted from the silica gel scrapings with three 30-ml portions of methanol. The eluates were combined and processed in the usual fashion (12) to give a light-brown oil. The IR spectrum of this material was the same as that recorded for reference sparteine. The oil was dissolved in benzene and treated with methyl iodide to give sparteine methiodide, mp 235–236° [lit. (13) mp 237–238°].

Quantitation of Alkaloids—The quantity of each identified alkaloid in the extract was determined as previously described (10). Based on the dry weight of the plant, the following levels of alkaloid were found: sparteine, 0.05%; β-isosparteine, 0.005%; Δ^5-dehydrolupanine, 0.04%; α-isolupanine, 0.60%; lupanine, 0.01%; thermopsine, 0.36%; and anagyrine, 0.01%.

DISCUSSION

Crooked calf disease is characterized by congenital malformations in calves born to cows that ingested certain *Lupinus* species during early gestation (9). Symptoms include arthrogryposis or torticollis and scoliosis and, occasionally, cleft palate (5). Keeler (6) suggested that the quinolizidine alkaloid anagyrine may be the teratogen responsible for crooked calf disease because of its high concentration in those species of *Lupinus* shown to induce the disease. In another report, Keeler (9) pointed out that *L. argenteus* is probably nonteratogenic because of a total lack of anagyrine; this report revealed lupanine as the only alkaloid identified in extracts of *L. argenteus*.

The present study of *L. argenteus* var. *stenophyllus* verifies the presence of lupanine in the species but also reveals low concentrations of anagyrine. According to Keeler (9), this situation would suggest nonteratogenicity. However, several alkaloids present in the title plant were apparently not studied by Keeler (6, 9). For instance, the epimer of anagyrine, thermopsine, may also be a potential teratogen.

Furthermore, Keeler (6) stated that the GLC peak associated with extracts of teratogenic lupines is really a mixture of anagyrine and α-isolupanine. Perhaps α-isolupanine is also teratogenic. In view of the large concentrations of α-isolupanine and thermopsine in *L. argenteus* var. *stenophyllus*, further biological testing with whole extracts and individual alkaloids appears necessary before concluding that this plant is nonteratogenic.

REFERENCES

(1) J. M. Kingsbury, "Poisonous Plants of the United States and Canada," Prentice-Hall, Englewood Cliffs, N.J., 1964, pp. 333–341.

(2) O. A. Beath, C. S. Gilbert, H. F. Eppson, and I. Rosenfeld, *Wyo. Agr. Exp. Sta. Bull.*, **1953**, 324.

(3) J. F. Couch, *J. Chem. Educ.*, **14**, 16 (1937).

(4) R. F. Keeler, *Lloydia*, **38**, 56 (1975).

(5) J. L. Shupe, W. Binns, L. F. James, and R. F. Keeler, *J. Am. Vet. Med. Assoc.*, **151**, 198 (1967).

(6) R. F. Keeler, *Teratology*, **7**, 31 (1973).

(7) O. A. Beath, *Wyo. Agr. Exp. Sta. Bull.*, **1920**, 125.

(8) C. D. Marsh, A. B. Clawson, and H. Marsh, *USDA Bull.*, **1916**, 405.

(9) R. F. Keeler, *Teratology*, **7**, 23 (1973).

(10) G. M. Hatfield, L. J. J. Valdez, W. J. Keller, W. L. Merrill, and V. H. Jones, *Lloydia*, **40**, 374 (1977).

(11) W. J. Keller and F. R. Cole, *ibid.*, **32**, 498 (1969).

(12) W. J. Keller, J. L. McLaughlin, and L. R. Brady, *J. Pharm. Sci.*, **62**, 408 (1973).

(13) J. F. Couch, *J. Am. Chem. Soc.*, **59**, 1469 (1937).

ACKNOWLEDGMENTS

The authors thank Dr. G. M. Hatfield for help in collection of plant material and Dr. F. R. Cole for technical assistance. The authors are deeply indebted to Dr. S. I. Goldberg for supplying samples of β-isosparteine, α-isolupanine, and anagyrine.

Simultaneous Salt and Ethanol Removal from Human Serum Albumin

PAUL K. NG ˣ, GAUTAM MITRA, and JOHN L. LUNDBLAD

Received April 8, 1977, from the *Department of Biochemical Development, Cutter Laboratories, Inc., Berkeley, CA 94710.* Accepted for publication June 28, 1977.

Abstract □ Diafiltration of salt and ethanol from human serum albumin was shown to be a competitive alternative to freeze drying. At least 99% of the original alcohol content could be removed in approximately five volume changes. Data on changes in ionic strength, bacteriological buildup, permeate flux, and dimer contents are presented.

Keyphrases □ Albumin, human serum—simultaneous salt and ethanol removal by diafiltration □ Diafiltration—simultaneous salt and ethanol removal from human serum albumin

Albumin is prepared commercially by variation of the low temperature–alcohol methods (1). Method 6 yields albumin as Fraction V upon lowering the pH to 4.7–4.9 at 40% ethanol. Salts are removed by redissolving Fraction V in 10% ethanol and reprecipitating at 40% ethanol.

Most pharmaceutical companies use freeze drying for the removal of ethanol from the albumin paste, but other routes such as gel filtration (2) and thin-layer evaporations under vacuum (3) also are feasible. An alternative process, diafiltration, is proposed for the simultaneous removal of salt and alcohol. The data obtained provide the basis for utilizing this method in the large-scale production of albumin preparations for clinical use.

EXPERIMENTAL

Fraction V is the starting material. An ultrafiltration thin-channel system[1] was employed in the preliminary study. This system streams the process fluid over the membrane (10,000 mol. wt. retentivity) in shallow channels, and smooth laminar flow is produced. The accompanying shear force is regulated by adjusting the fluid velocity with a reversible peristaltic pump. The system is connected with a fluid reservoir pressurized to 25 psig. A hollow fiber unit[2] also was studied for operations greater than

[1] Model TCF10, Amicon, Lexington, Mass.
[2] Model DC-30, Amicon, Lexington, Mass.

combined GLC–mass spectrometry, reference sparteine and genisteine gave essentially the same mass spectrum.

Isolation of Sparteine—The entire alkaloid fraction (3 g) was dissolved in ethanol–chloroform (1:1) and streaked onto 12 silica gel PF_{254} plates (1 mm) using a previously described technique (11). The band corresponding with sparteine and genisteine was scraped from the plates, and the alkaloid material was eluted from the silica gel scrapings with three 30-ml portions of methanol. The eluates were combined and processed in the usual fashion (12) to give a light-brown oil. The IR spectrum of this material was the same as that recorded for reference sparteine. The oil was dissolved in benzene and treated with methyl iodide to give sparteine methiodide, mp 235–236° [lit. (13) mp 237–238°].

Quantitation of Alkaloids—The quantity of each identified alkaloid in the extract was determined as previously described (10). Based on the dry weight of the plant, the following levels of alkaloid were found: sparteine, 0.05%; β-isosparteine, 0.005%; Δ^5-dehydrolupanine, 0.04%; α-isolupanine, 0.60%; lupanine, 0.01%; thermopsine, 0.36%; and anagyrine, 0.01%.

DISCUSSION

Crooked calf disease is characterized by congenital malformations in calves born to cows that ingested certain *Lupinus* species during early gestation (9). Symptoms include arthrogryposis or torticollis and scoliosis and, occasionally, cleft palate (5). Keeler (6) suggested that the quinolizidine alkaloid anagyrine may be the teratogen responsible for crooked calf disease because of its high concentration in those species of *Lupinus* shown to induce the disease. In another report, Keeler (9) pointed out that *L. argenteus* is probably nonteratogenic because of a total lack of anagyrine; this report revealed lupanine as the only alkaloid identified in extracts of *L. argenteus*.

The present study of *L. argenteus* var. *stenophyllus* verifies the presence of lupanine in the species but also reveals low concentrations of anagyrine. According to Keeler (9), this situation would suggest nonteratogenicity. However, several alkaloids present in the title plant were apparently not studied by Keeler (6, 9). For instance, the epimer of anagyrine, thermopsine, may also be a potential teratogen.

Furthermore, Keeler (6) stated that the GLC peak associated with extracts of teratogenic lupines is really a mixture of anagyrine and α-isolupanine. Perhaps α-isolupanine is also teratogenic. In view of the large concentrations of α-isolupanine and thermopsine in *L. argenteus* var. *stenophyllus*, further biological testing with whole extracts and individual alkaloids appears necessary before concluding that this plant is nonteratogenic.

REFERENCES

(1) J. M. Kingsbury, "Poisonous Plants of the United States and Canada," Prentice-Hall, Englewood Cliffs, N.J., 1964, pp. 333–341.

(2) O. A. Beath, C. S. Gilbert, H. F. Eppson, and I. Rosenfeld, *Wyo. Agr. Exp. Sta. Bull.*, **1953**, 324.

(3) J. F. Couch, *J. Chem. Educ.*, **14**, 16 (1937).

(4) R. F. Keeler, *Lloydia*, **38**, 56 (1975).

(5) J. L. Shupe, W. Binns, L. F. James, and R. F. Keeler, *J. Am. Vet. Med. Assoc.*, **151**, 198 (1967).

(6) R. F. Keeler, *Teratology*, **7**, 31 (1973).

(7) O. A. Beath, *Wyo. Agr. Exp. Sta. Bull.*, **1920**, 125.

(8) C. D. Marsh, A. B. Clawson, and H. Marsh, *USDA Bull.*, **1916**, 405.

(9) R. F. Keeler, *Teratology*, **7**, 23 (1973).

(10) G. M. Hatfield, L. J. J. Valdez, W. J. Keller, W. L. Merrill, and V. H. Jones, *Lloydia*, **40**, 374 (1977).

(11) W. J. Keller and F. R. Cole, *ibid.*, **32**, 498 (1969).

(12) W. J. Keller, J. L. McLaughlin, and L. R. Brady, *J. Pharm. Sci.*, **62**, 408 (1973).

(13) J. F. Couch, *J. Am. Chem. Soc.*, **59**, 1469 (1937).

ACKNOWLEDGMENTS

The authors thank Dr. G. M. Hatfield for help in collection of plant material and Dr. F. R. Cole for technical assistance. The authors are deeply indebted to Dr. S. I. Goldberg for supplying samples of β-isosparteine, α-isolupanine, and anagyrine.

Simultaneous Salt and Ethanol Removal from Human Serum Albumin

PAUL K. NG ˣ, GAUTAM MITRA, and JOHN L. LUNDBLAD

Received April 8, 1977, from the *Department of Biochemical Development, Cutter Laboratories, Inc., Berkeley, CA 94710.* Accepted for publication June 28, 1977.

Abstract □ Diafiltration of salt and ethanol from human serum albumin was shown to be a competitive alternative to freeze drying. At least 99% of the original alcohol content could be removed in approximately five volume changes. Data on changes in ionic strength, bacteriological buildup, permeate flux, and dimer contents are presented.

Keyphrases □ Albumin, human serum—simultaneous salt and ethanol removal by diafiltration □ Diafiltration—simultaneous salt and ethanol removal from human serum albumin

Albumin is prepared commercially by variation of the low temperature–alcohol methods (1). Method 6 yields albumin as Fraction V upon lowering the pH to 4.7–4.9 at 40% ethanol. Salts are removed by redissolving Fraction V in 10% ethanol and reprecipitating at 40% ethanol.

Most pharmaceutical companies use freeze drying for the removal of ethanol from the albumin paste, but other routes such as gel filtration (2) and thin-layer evaporations under vacuum (3) also are feasible. An alternative process, diafiltration, is proposed for the simultaneous removal of salt and alcohol. The data obtained provide the basis for utilizing this method in the large-scale production of albumin preparations for clinical use.

EXPERIMENTAL

Fraction V is the starting material. An ultrafiltration thin-channel system[1] was employed in the preliminary study. This system streams the process fluid over the membrane (10,000 mol. wt. retentivity) in shallow channels, and smooth laminar flow is produced. The accompanying shear force is regulated by adjusting the fluid velocity with a reversible peristaltic pump. The system is connected with a fluid reservoir pressurized to 25 psig. A hollow fiber unit[2] also was studied for operations greater than

[1] Model TCF10, Amicon, Lexington, Mass.
[2] Model DC-30, Amicon, Lexington, Mass.

Table I—Changes in Ionic Strength *versus* Volume Changes

Volume Change	Ionic Strength Removed, %	Ionic Strength Predicted, %
1.4	77.0	75.0
2.0	86.0	86.5
2.6	91.0	92.6
4.0	96.0	98.2
5.0	97.0	99.3

0.5 liter. This system can utilize up to three hollow fiber cartridges, each with 9290 cm^2 of membrane surface area.

Protein concentration was determined by the biuret technique. Solution conductivity was monitored by a conductivity meter[3]. Based on dilutions, the percentage of initial ionic strength was related to the percentage of initial conductivity.

Ethanol[4] was assayed by GLC[5]. An internal standard of either distilled or spectroquality grade 1-propanol[6] was used. Ethanol concentration was calculated from both peak height and peak area ratios. Monomer and polymer contents of albumin were quantitated by the method of sodium lauryl sulfate–polyacrylamide electrophoresis (4).

RESULTS AND DISCUSSION

In the experiment illustrated in Fig. 1, diafiltration was carried out with a membrane filter[7] with a nominal molecular weight cutoff value of 10,000. It was freely permeable to low molecular weight solutes such as salt and ethanol but impermeable to albumin (molecular weight of 65,000). Ionic strengths and ethanol concentrations were determined for the samples taken from the retentate side of the membrane. The solid line depicts the theoretical line for zero rejection. It confirms that ethanol falls exponentially with time following a first-order decay curve. Salts, however, are slightly impeded, showing fractional binding with serum albumin.

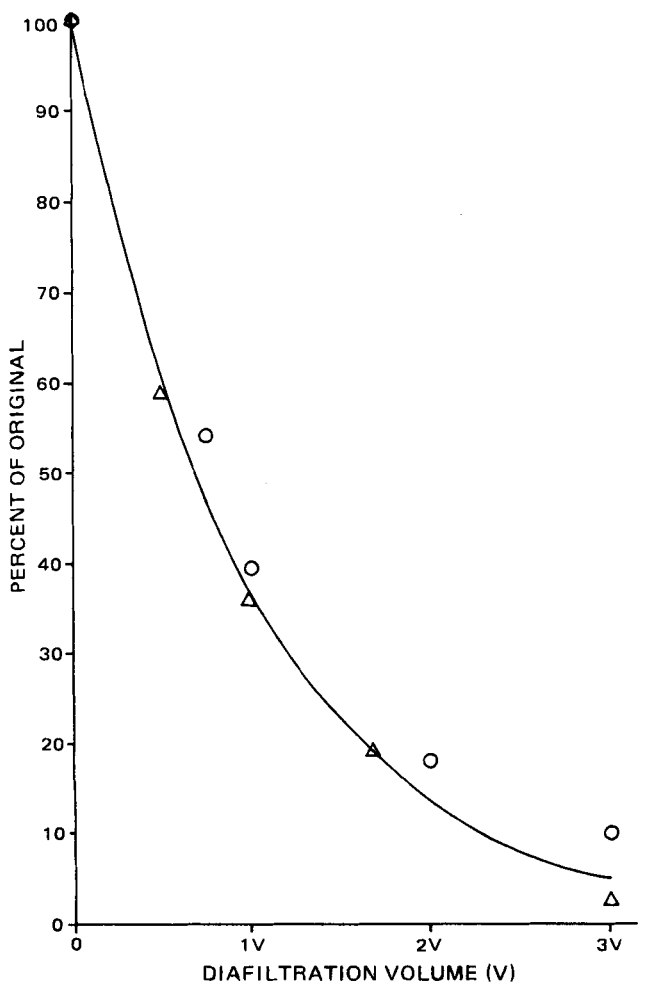

Figure 1—*Salt and alcohol levels during Fraction V diafiltration. Key:* ○, *ionic strength; and* △, *ethanol.*

[3] Radiometer, Copenhagen, Denmark.
[4] Shell, Houston, Tex.
[5] Model 3920, Perkin-Elmer, Norwalk, Conn.
[6] Mallinckrodt, St. Louis, Mo.
[7] PM10 membrane, Amicon, Lexington, Mass.

Table II—Bacteriological Buildup during Processing

Sample	Counts per Milliliter D-2558	D-2561	D-2577
Initial time	17	70	63
After three volume changes	21	30	63
After five volume changes	53	80	84
Distilled water (control)	0	0	—

As a further test of the theoretical consideration, a 10-liter 5% albumin solution was diafiltered against pyrogen-free water in a hollow filter unit. Fluid was circulated through the hollow fibers. Salt and solvent were transported convectively through the walls by a pressure gradient. As shown in Table I, a good correlation was obtained between the experimental and the theoretical removal efficiency.

Ultrafiltration rates of the hollow fiber system are controlled by the average transmembrane pressure and the ambient temperatures. Figure 2 shows the flux of a 5% solution. The observed temperature dependence arises both from the increased diffusivity of the albumin and the lowered viscosity of the solution.

The microbiological aspect of diafiltration at +5° was studied to ascertain the feasibility for commercial fractionation. Pilot-scale preparations of 30–50 liters were attempted. Initial protein concentrations were maintained at 7.5 ± 0.5%. Retentate samples were collected for bacteria plate count, and average numbers for three runs are shown in Table II.

No more than a one order of magnitude increase in colonies was noted

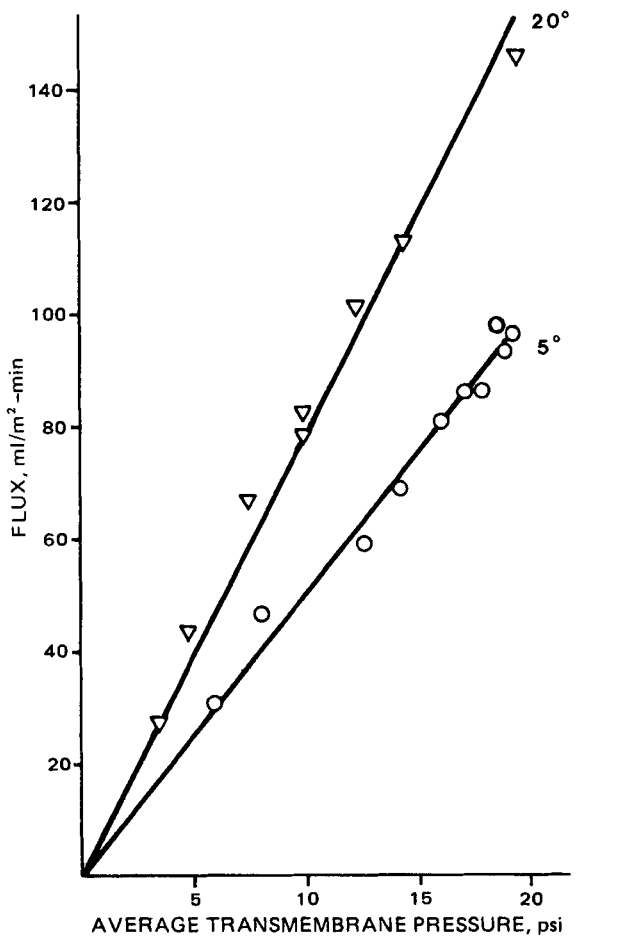

Figure 2—*Effect of pressure and temperature on the permeate flux through a hollow fiber cartridge (10,000 mol. wt. retentivity).*

Table III—Dimer Contents of Freeze-Dried (F) Albumin and Diafiltered (D) Albumin

Sample	Dimer, % (±1%)	Monomer, % (±1%)
F-93	3.8	96.2
F-2541	6.9	93.1
D-64	3.7	96.3
D-2558	3.8	96.2
D-2568	1.2	98.8
D-2573	0.6	99.4

at completion. The data showed that there was slight bacteriological buildup as the alcohol level dropped. The solution after five volume changes was sterile filtered. It passed the USP rabbit pyrogen test, suggesting that the bacteria counts were not dangerously high.

Optimization of this process was considered elsewhere (5). Production of albumin solutions in final containers was attempted and was proven to be feasible. Test results showed all factors to be within specifications with regard to protein composition, pH, protein level, electrolytes, stabilizers, heme content, and heat stability. The monomer concentration of the heat-treated albumin was between 96.3 and 99.4% as measured by sodium lauryl sulfate–polyacrylamide electrophoresis. A comparison of samples prepared by diafiltration and freeze drying is shown in Table III. Statistically, there was no significant difference between the two groups.

Friedli and Kistler (2) showed that albumin containing 10.4 mg of ethanol/g of albumin could be pasteurized without obvious damage to the protein. Similar observations also were reported (6). Conventional freeze drying could presumably achieve a limit of 15 mg of ethanol/g of albumin in the final product (2). Starting from Fraction V, gel filtration effectively reduces ethanol from about 1000 mg/g of albumin to 10–15 mg/g of albumin. With diafiltration, less than 10 mg of ethanol/g of albumin could be obtained in approximately 4.6 volume changes. A constant albumin concentration was maintained throughout the entire process. This procedure has an obvious advantage over gel filtration, which requires acceptance of a more dilute eluate. The capital and running costs of freeze drying are prohibitively high. Diafiltration has the merit of much lower energy consumption since operation proceeds through the pumping of solutions. The process produces salt-poor albumin. Thus, the extra step of Fraction V reprecipitation can be avoided.

REFERENCES

(1) E. J. Cohn, E. L. Strong, W. L. Hughes, D. J. Mulford, J. N. Ashworth, M. Mein, and H. L. Taylor, *J. Am. Chem. Soc.*, **68**, 459 (1946).

(2) H. Friedli and P. Kistler, *Chimia*, **26**, 25 (1972).

(3) J. K. Smith, J. G. Watt, C. M. Watson, and G. G. A. Masterbroek, *Vox Sang.*, **22**, 120 (1972).

(4) M. J. Bertolini, D. D. Schroeder, and D. L. Tankersley, *Anal. Biochem.*, **71**, 6 (1976).

(5) P. Ng, J. Lundblad, and G. Mitra, *Sep. Sci.*, **11**, 499 (1976).

(6) A. J. Dickson and J. K. Smith, *Vox Sang.*, **28**, 90 (1975).

Constituents of West African Medicinal Plants XX: Quindoline from *Cryptolepis sanguinolenta*

DANIEL DWUMA-BADU *, JOHN S. K. AYIM *, NICHOLAS I. Y. FIAGBE *, JOSEPH E. KNAPP ‡, PAUL L. SCHIFF, Jr. ‡, and DAVID J. SLATKIN ‡x

Received March 16, 1977, from the **Faculty of Pharmacy, University of Science and Technology, Kumasi, Ghana, West Africa*, and the ‡*Department of Pharmacognosy, School of Pharmacy, University of Pittsburgh, Pittsburgh, PA 15261.* Accepted for publication June 22, 1977.

Abstract □ An ethanol extract of the roots of *Cryptolepis sanguinolenta* (Asclepidaceae) afforded, after partitioning and chromatography, the alkaloids quindoline and CSA-3. The structural elucidation of CSA-3 is currently in progress. Cryptolepine was also isolated from this species.

Keyphrases □ *Cryptolepis sanguinolenta*—ethanol extract of roots, quindoline and CSA-3 isolated □ Alkaloids—quindoline and CSA-3 isolated from ethanol extract of roots of *Cryptolepis sanguinolenta* □ Quindoline—isolated from ethanol extract of roots of *Cryptolepis sanguinolenta*

Cryptolepis sanguinolenta (Lindl.) Schlecter is a plant native to West Africa used in the treatment of malaria[1]. The indoloquinoline alkaloid, cryptolepine (I), previously was isolated from this species (1). This compound has reported hypotensive activity and causes a marked and prolonged fall in blood pressure in dogs as well as a lowering of body temperature (2, 3).

A systematic phytochemical investigation of this species resulted in the isolation of cryptolepine and two other alkaloids, quindoline (II) and CSA-3 (III), a new alkaloid whose structure will be reported later. Quindoline (II) was

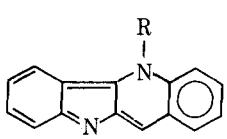

I: R = CH_3
II: R = H

originally synthesized over 70 years ago (4, 5) and was since prepared from cryptolepine (1). This is the first report of the isolation of quindoline from a natural source.

EXPERIMENTAL[2]

Plant Material—Roots of *C. sanguinolenta* (Lindl.) Schlecter (Asclepidaceae) were used[3].

Extraction—Air-dried ground roots (200 g) were extracted by percolation with ethanol (6 liters). The extract was evaporated *in vacuo* at 40° to leave a dark-red syrup (11 g, 5.5%).

[1] Dr. Oku-Ampofo, Centre for Plant Medicine Research, Mampong-Akwapim, Ghana, personal communication.

[2] Melting points were determined on a Thomas-Hoover Uni-Melt melting-point apparatus and are corrected. IR spectra were run in potassium bromide using a Perkin-Elmer 257 spectrophotometer. UV spectra were run on a Perkin-Elmer 202 spectrophotometer. Mass spectra were recorded on an LKB-9000 spectrometer. NMR spectra were obtained on a Hitachi Perkin-Elmer R-24 spectrometer with tetramethylsilane as the internal standard.

[3] Identified by Mr. K. Obeng-Darko; a herbarium specimen is located at the Faculty of Pharmacy, University of Science and Technology, Kumasi, Ghana, West Africa.

Table III—Dimer Contents of Freeze-Dried (F) Albumin and Diafiltered (D) Albumin

Sample	Dimer, % (±1%)	Monomer, % (±1%)
F-93	3.8	96.2
F-2541	6.9	93.1
D-64	3.7	96.3
D-2558	3.8	96.2
D-2568	1.2	98.8
D-2573	0.6	99.4

at completion. The data showed that there was slight bacteriological buildup as the alcohol level dropped. The solution after five volume changes was sterile filtered. It passed the USP rabbit pyrogen test, suggesting that the bacteria counts were not dangerously high.

Optimization of this process was considered elsewhere (5). Production of albumin solutions in final containers was attempted and was proven to be feasible. Test results showed all factors to be within specifications with regard to protein composition, pH, protein level, electrolytes, stabilizers, heme content, and heat stability. The monomer concentration of the heat-treated albumin was between 96.3 and 99.4% as measured by sodium lauryl sulfate–polyacrylamide electrophoresis. A comparison of samples prepared by diafiltration and freeze drying is shown in Table III. Statistically, there was no significant difference between the two groups.

Friedli and Kistler (2) showed that albumin containing 10.4 mg of ethanol/g of albumin could be pasteurized without obvious damage to the protein. Similar observations also were reported (6). Conventional freeze drying could presumably achieve a limit of 15 mg of ethanol/g of albumin in the final product (2). Starting from Fraction V, gel filtration effectively reduces ethanol from about 1000 mg/g of albumin to 10–15 mg/g of albumin. With diafiltration, less than 10 mg of ethanol/g of albumin could be obtained in approximately 4.6 volume changes. A constant albumin concentration was maintained throughout the entire process. This procedure has an obvious advantage over gel filtration, which requires acceptance of a more dilute eluate. The capital and running costs of freeze drying are prohibitively high. Diafiltration has the merit of much lower energy consumption since operation proceeds through the pumping of solutions. The process produces salt-poor albumin. Thus, the extra step of Fraction V reprecipitation can be avoided.

REFERENCES

(1) E. J. Cohn, E. L. Strong, W. L. Hughes, D. J. Mulford, J. N. Ashworth, M. Mein, and H. L. Taylor, *J. Am. Chem. Soc.*, **68**, 459 (1946).

(2) H. Friedli and P. Kistler, *Chimia*, **26**, 25 (1972).

(3) J. K. Smith, J. G. Watt, C. M. Watson, and G. G. A. Masterbroek, *Vox Sang.*, **22**, 120 (1972).

(4) M. J. Bertolini, D. D. Schroeder, and D. L. Tankersley, *Anal. Biochem.*, **71**, 6 (1976).

(5) P. Ng, J. Lundblad, and G. Mitra, *Sep. Sci.*, **11**, 499 (1976).

(6) A. J. Dickson and J. K. Smith, *Vox Sang.*, **28**, 90 (1975).

Constituents of West African Medicinal Plants XX: Quindoline from *Cryptolepis sanguinolenta*

DANIEL DWUMA-BADU *, JOHN S. K. AYIM *, NICHOLAS I. Y. FIAGBE *, JOSEPH E. KNAPP ‡, PAUL L. SCHIFF, Jr. ‡, and DAVID J. SLATKIN ‡x

Received March 16, 1977, from the **Faculty of Pharmacy, University of Science and Technology, Kumasi, Ghana, West Africa*, and the ‡*Department of Pharmacognosy, School of Pharmacy, University of Pittsburgh, Pittsburgh, PA 15261.* Accepted for publication June 22, 1977.

Abstract □ An ethanol extract of the roots of *Cryptolepis sanguinolenta* (Asclepidaceae) afforded, after partitioning and chromatography, the alkaloids quindoline and CSA-3. The structural elucidation of CSA-3 is currently in progress. Cryptolepine was also isolated from this species.

Keyphrases □ *Cryptolepis sanguinolenta*—ethanol extract of roots, quindoline and CSA-3 isolated □ Alkaloids—quindoline and CSA-3 isolated from ethanol extract of roots of *Cryptolepis sanguinolenta* □ Quindoline—isolated from ethanol extract of roots of *Cryptolepis sanguinolenta*

Cryptolepis sanguinolenta (Lindl.) Schlecter is a plant native to West Africa used in the treatment of malaria[1]. The indoloquinoline alkaloid, cryptolepine (I), previously was isolated from this species (1). This compound has reported hypotensive activity and causes a marked and prolonged fall in blood pressure in dogs as well as a lowering of body temperature (2, 3).

A systematic phytochemical investigation of this species resulted in the isolation of cryptolepine and two other alkaloids, quindoline (II) and CSA-3 (III), a new alkaloid whose structure will be reported later. Quindoline (II) was

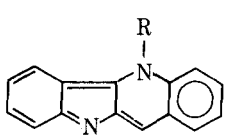

I: R = CH_3
II: R = H

originally synthesized over 70 years ago (4, 5) and was since prepared from cryptolepine (1). This is the first report of the isolation of quindoline from a natural source.

EXPERIMENTAL[2]

Plant Material—Roots of *C. sanguinolenta* (Lindl.) Schlecter (Asclepidaceae) were used[3].

Extraction—Air-dried ground roots (200 g) were extracted by percolation with ethanol (6 liters). The extract was evaporated *in vacuo* at 40° to leave a dark-red syrup (11 g, 5.5%).

[1] Dr. Oku-Ampofo, Centre for Plant Medicine Research, Mampong-Akwapim, Ghana, personal communication.

[2] Melting points were determined on a Thomas-Hoover Uni-Melt melting-point apparatus and are corrected. IR spectra were run in potassium bromide using a Perkin-Elmer 257 spectrophotometer. UV spectra were run on a Perkin-Elmer 202 spectrophotometer. Mass spectra were recorded on an LKB-9000 spectrometer. NMR spectra were obtained on a Hitachi Perkin-Elmer R-24 spectrometer with tetramethylsilane as the internal standard.

[3] Identified by Mr. K. Obeng-Darko; a herbarium specimen is located at the Faculty of Pharmacy, University of Science and Technology, Kumasi, Ghana, West Africa.

Fractionation—The ethanol extract was partitioned between water (1 liter) and chloroform (1 liter) to give fractions of 4.3 (2.2%) and 6.0 (3.0%) g, respectively. The chloroform fraction was then partitioned between petroleum ether (bp 60–90°) (200 ml) and methanol–water (9:1) (200 ml) to yield fractions of 3.5 (18%) and 2.0 (1.0%) g, respectively.

Chromatography—The aqueous methanol fraction was chromatographed on silicic acid[4] (75 g, 2 × 50 cm) in chloroform.

Isolation of II—Elution with 1% methanol–chloroform afforded a residue (233 mg), which was dissolved in chloroform (25 ml) and partitioned with 1% hydrochloric acid (3 × 25 ml). The combined acid layers (75 ml) were made basic to pH 8 with concentrated ammonium hydroxide and partitioned with chloroform (3 × 75 ml). The combined chloroform layers were dried over anhydrous sodium sulfate and evaporated *in vacuo* at 40° to yield a yellowish residue (15 mg).

Repeated attempts at crystallizing quindoline failed, so data were obtained on the amorphous residue; UV: λ_{max} (methanol) 227 (log ϵ 4.30), 269 sh (4.45), 274 (4.46), 330 sh (3.82), and 345 (4.03) nm; λ_{max} (0.01 *N* ethanolic hydrochloric acid) 224 (log ϵ 4.27), 242 sh (3.94), 273 (4.36), 280 (4.38), 350 sh (4.03), and 368 (4.26) nm; IR: ν_{max} (potassium bromide) 1632, 1608, 1487, 1457, 1396, 1370, 1333, 1222, 1150, 1140, 1122, 1105, 1000, 875, 865, 845, 837, 813, 754, 745, 738, 710, and 604 cm^{-1}; mass spectrum (M^+): *m/e* 218 (100%), 217 (8), 190 (8), 109 (12), 95.5 (4), 90 (3), and 89 (5). The alkaloid was found to be identical with an authentic sample of quindoline[5] by direct comparison (UV, IR, and mass spectra and TLC).

Isolation of III—Elution with 2% methanol–chloroform afforded a residue (327 mg), which, when crystallized from methanol, gave III (105 mg), mp > 300°. The structural elucidation of this substance is currently in progress.

Isolation of I—Elution with 30% methanol–chloroform afforded I (300 mg), mp 167–168° dec. [lit. (1) mp 166–169°], hydrochloride mp 263–264° dec. [lit. (1) mp 263–265°], hydroiodide mp 285–287° dec. [lit. (4) mp 284–286°], *methiodide* mp 284–285° dec. [lit. (1) mp 285–288°]; UV: λ_{max} (methanol) 224 (log ϵ 4.11), 246 (3.87), 275 (4.41), 283 (4.43), 355 sh (4.02), 370 (4.33), 4.10 (3.28), and 433 (3.29) nm; λ_{max} (0.01 *N* ethanolic potassium hydroxide) 214 (log ϵ 4.40), 230 sh (4.01), 297 sh (4.38), 307 (4.48), 368 (3.50), and 386 (4.08) nm; IR: ν_{max} (potassium bromide) 1631, 1611, 1585, 1505, 1492, 1460, 1400, 1366, 1357, 1330, 1310, 1300, 1275, 1250, 1160, 1150, 1130, 1040, 900, 887, 875, 850, and 750 cm^{-1}; mass spectrum (M^+): *m/e* 232 (100%), 231 (12), 217 (26), 190 (10), 116 (14), and 89 (15); NMR (trifluoroacetic acid): δ 5.08 (s, 3H, NCH_3), 7.55–8.62 (m, 8H, aromatic), and 8.95 (s, 1H, aromatic) ppm.

[4] Mallinckrodt, 100 mesh.

[5] Reference sample provided by Professor Emery Gellert, Department of Chemistry, University of Wollongong, Wollongong, Australia.

REFERENCES

(1) E. Gellert, Raymond-Hamet, and E. Schlittler, *Helv. Chim. Acta*, **34**, 642 (1951).

(2) Raymond-Hamet, *C.R. Soc. Biol.*, **126**, 768 (1937).

(3) Raymond-Hamet, *C.R. Acad. Sci.*, **207**, 1016 (1938).

(4) F. Fichter and R. Boehringer, *Chem. Ber.*, **39**, 3940 (1906).

(5) F. Fichter and F. Rohner, *ibid.*, **43**, 3490 (1910).

ACKNOWLEDGMENTS

Supported in part by Grant R-15 from the Health Research Services Foundation; Research Grant 5S01RR05455-10 from the National Institutes of Health; and the International Foundation of Science, Stockholm, Sweden. The mass spectrometer facility was supported by Research Grant RR-00273 to the University of Pittsburgh from the National Institutes of Health.

The authors are grateful to Mr. John Naworal, Graduate School of Public Health, University of Pittsburgh, for determining the mass spectra and to Professor Emery Gellert for the reference sample of quindoline.

New Spectrophotofluorometric Assay for Probenecid

R. F. CUNNINGHAM ˣ, Z. H. ISRAILI, and P. G. DAYTON

Received January 24, 1977, from the *Department of Medicine, Clinical Pharmacology Program, Emory University School of Medicine, Atlanta, GA 30322.* Accepted for publication June 15, 1977.

Abstract □ A new spectrophotofluorometric assay for probenecid is presented based on conversion of the drug to a fluorescent anthranilic acid derivative. The assay is especially applicable with "clean" biological fluids such as cerebrospinal fluid and offers severalfold greater sensitivity than the commonly used UV method.

Keyphrases □ Probenecid—spectrophotofluorometric analysis in biological fluids □ Spectrophotofluorometry—analysis, probenecid in biological fluids □ Uricosuric agents—probenecid, spectrophotofluorometric analysis in biological fluids

Recently, several GLC procedures (1–4) and a new radioimmunoassay were developed (5) to measure low probenecid levels in biological fluids. Interest in such assays was stimulated by studies of the accumulation of cyclic adenosine monophosphate (6, 7) and metabolites of biogenic amines (8–11) in cerebrospinal fluid caused by probenecid and the well-known inhibitory effect of this drug on active transport systems in the brain (12).

Based on observations with a fluorescent amino derivative of probenecid (13), it was decided that a fluorometric assay would offer definite advantages over existing methodologies—greater sensitivity than the UV procedure (14) and less cost than GLC. In the present study, reaction conditions for quantitative conversion of probenecid to a fluorescent species were investigated and the fluorescent product was characterized. A method for quantitating probenecid in cerebrospinal fluid and plasma is proposed and evaluated.

EXPERIMENTAL

Probenecid[1], ring-labeled ^{14}C-probenecid[1] (specific activity of 0.8 mCi/mmole), and 2′-nitroprobenecid[1] were used as received. The side-chain metabolites were prepared as previously described (15). Radioactivity was measured in a liquid scintillation spectrometer[2] in a counting fluid prepared as described previously (5). Relative fluorescence intensity was measured in 1.0-cm cells in a spectrophotofluorometer[3].

TLC was carried out on silica gel G glass plates[4] (5 × 20 cm, 250 μm)

[1] Courtesy of Dr. John E. Baer, Merck Sharp and Dohme, West Point, Pa.

[2] Beckman LS-255; efficiency for ^{14}C = 90%.

[3] Aminco-Bowman, equipped with an EMI 9558 QC phototube, a Schoeffel microphotometer model 600 at 1200 v, and a magnetic arc stabilizer accessory; slits were set at 3 mm.

[4] Analabs, New England Nuclear, North Haven, Conn.

Fractionation—The ethanol extract was partitioned between water (1 liter) and chloroform (1 liter) to give fractions of 4.3 (2.2%) and 6.0 (3.0%) g, respectively. The chloroform fraction was then partitioned between petroleum ether (bp 60–90°) (200 ml) and methanol–water (9:1) (200 ml) to yield fractions of 3.5 (18%) and 2.0 (1.0%) g, respectively.

Chromatography—The aqueous methanol fraction was chromatographed on silicic acid[4] (75 g, 2 × 50 cm) in chloroform.

Isolation of II—Elution with 1% methanol–chloroform afforded a residue (233 mg), which was dissolved in chloroform (25 ml) and partitioned with 1% hydrochloric acid (3 × 25 ml). The combined acid layers (75 ml) were made basic to pH 8 with concentrated ammonium hydroxide and partitioned with chloroform (3 × 75 ml). The combined chloroform layers were dried over anhydrous sodium sulfate and evaporated *in vacuo* at 40° to yield a yellowish residue (15 mg).

Repeated attempts at crystallizing quindoline failed, so data were obtained on the amorphous residue; UV: λ_{max} (methanol) 227 (log ϵ 4.30), 269 sh (4.45), 274 (4.46), 330 sh (3.82), and 345 (4.03) nm; λ_{max} (0.01 *N* ethanolic hydrochloric acid) 224 (log ϵ 4.27), 242 sh (3.94), 273 (4.36), 280 (4.38), 350 sh (4.03), and 368 (4.26) nm; IR: ν_{max} (potassium bromide) 1632, 1608, 1487, 1457, 1396, 1370, 1333, 1222, 1150, 1140, 1122, 1105, 1000, 875, 865, 845, 837, 813, 754, 745, 738, 710, and 604 cm^{-1}; mass spectrum (M^+): *m/e* 218 (100%), 217 (8), 190 (8), 109 (12), 95.5 (4), 90 (3), and 89 (5). The alkaloid was found to be identical with an authentic sample of quindoline[5] by direct comparison (UV, IR, and mass spectra and TLC).

Isolation of III—Elution with 2% methanol–chloroform afforded a residue (327 mg), which, when crystallized from methanol, gave III (105 mg), mp > 300°. The structural elucidation of this substance is currently in progress.

Isolation of I—Elution with 30% methanol–chloroform afforded I (300 mg), mp 167–168° dec. [lit. (1) mp 166–169°], hydrochloride mp 263–264° dec. [lit. (1) mp 263–265°], hydroiodide mp 285–287° dec. [lit. (4) mp 284–286°], *methiodide* mp 284–285° dec. [lit. (1) mp 285–288°]; UV: λ_{max} (methanol) 224 (log ϵ 4.11), 246 (3.87), 275 (4.41), 283 (4.43), 355 sh (4.02), 370 (4.33), 4.10 (3.28), and 433 (3.29) nm; λ_{max} (0.01 *N* ethanolic potassium hydroxide) 214 (log ϵ 4.40), 230 sh (4.01), 297 sh (4.38), 307 (4.48), 368 (3.50), and 386 (4.08) nm; IR: ν_{max} (potassium bromide) 1631, 1611, 1585, 1505, 1492, 1460, 1400, 1366, 1357, 1330, 1310, 1300, 1275, 1250, 1160, 1150, 1130, 1040, 900, 887, 875, 850, and 750 cm^{-1}; mass spectrum (M^+): *m/e* 232 (100%), 231 (12), 217 (26), 190 (10), 116 (14), and 89 (15); NMR (trifluoroacetic acid): δ 5.08 (s, 3H, NCH_3), 7.55–8.62 (m, 8H, aromatic), and 8.95 (s, 1H, aromatic) ppm.

[4] Mallinckrodt, 100 mesh.

[5] Reference sample provided by Professor Emery Gellert, Department of Chemistry, University of Wollongong, Wollongong, Australia.

REFERENCES

(1) E. Gellert, Raymond-Hamet, and E. Schlittler, *Helv. Chim. Acta*, **34**, 642 (1951).

(2) Raymond-Hamet, *C.R. Soc. Biol.*, **126**, 768 (1937).

(3) Raymond-Hamet, *C.R. Acad. Sci.*, **207**, 1016 (1938).

(4) F. Fichter and R. Boehringer, *Chem. Ber.*, **39**, 3940 (1906).

(5) F. Fichter and F. Rohner, *ibid.*, **43**, 3490 (1910).

ACKNOWLEDGMENTS

Supported in part by Grant R-15 from the Health Research Services Foundation; Research Grant 5S01RR05455-10 from the National Institutes of Health; and the International Foundation of Science, Stockholm, Sweden. The mass spectrometer facility was supported by Research Grant RR-00273 to the University of Pittsburgh from the National Institutes of Health.

The authors are grateful to Mr. John Naworal, Graduate School of Public Health, University of Pittsburgh, for determining the mass spectra and to Professor Emery Gellert for the reference sample of quindoline.

New Spectrophotofluorometric Assay for Probenecid

R. F. CUNNINGHAM ˣ, Z. H. ISRAILI, and P. G. DAYTON

Received January 24, 1977, from the *Department of Medicine, Clinical Pharmacology Program, Emory University School of Medicine, Atlanta, GA 30322.* Accepted for publication June 15, 1977.

Abstract □ A new spectrophotofluorometric assay for probenecid is presented based on conversion of the drug to a fluorescent anthranilic acid derivative. The assay is especially applicable with "clean" biological fluids such as cerebrospinal fluid and offers severalfold greater sensitivity than the commonly used UV method.

Keyphrases □ Probenecid—spectrophotofluorometric analysis in biological fluids □ Spectrophotofluorometry—analysis, probenecid in biological fluids □ Uricosuric agents—probenecid, spectrophotofluorometric analysis in biological fluids

Recently, several GLC procedures (1–4) and a new radioimmunoassay were developed (5) to measure low probenecid levels in biological fluids. Interest in such assays was stimulated by studies of the accumulation of cyclic adenosine monophosphate (6, 7) and metabolites of biogenic amines (8–11) in cerebrospinal fluid caused by probenecid and the well-known inhibitory effect of this drug on active transport systems in the brain (12).

Based on observations with a fluorescent amino derivative of probenecid (13), it was decided that a fluorometric assay would offer definite advantages over existing methodologies—greater sensitivity than the UV procedure (14) and less cost than GLC. In the present study, reaction conditions for quantitative conversion of probenecid to a fluorescent species were investigated and the fluorescent product was characterized. A method for quantitating probenecid in cerebrospinal fluid and plasma is proposed and evaluated.

EXPERIMENTAL

Probenecid[1], ring-labeled ^{14}C-probenecid[1] (specific activity of 0.8 mCi/mmole), and 2′-nitroprobenecid[1] were used as received. The side-chain metabolites were prepared as previously described (15). Radioactivity was measured in a liquid scintillation spectrometer[2] in a counting fluid prepared as described previously (5). Relative fluorescence intensity was measured in 1.0-cm cells in a spectrophotofluorometer[3].

TLC was carried out on silica gel G glass plates[4] (5 × 20 cm, 250 μm)

[1] Courtesy of Dr. John E. Baer, Merck Sharp and Dohme, West Point, Pa.

[2] Beckman LS-255; efficiency for ^{14}C = 90%.

[3] Aminco-Bowman, equipped with an EMI 9558 QC phototube, a Schoeffel microphotometer model 600 at 1200 v, and a magnetic arc stabilizer accessory; slits were set at 3 mm.

[4] Analabs, New England Nuclear, North Haven, Conn.

Table I—Spectrophotofluorometric Method for Probenecid

Probenecid Reacted, μg	Relative Fluorescence Intensity Units per Microgram[a] Standards	Water (1.0 ml)	Dog Cerebrospinal Fluid[b] (1.0 ml)	Dog Plasma[b] (0.1 ml)
4	120	111	113	117
7	106		116	109
10	95	111		133
15	106	106	111	104
30	110	102	105	118
40	112		102	102
80	101	101	101	102
115	93		102	103
150	94	95	97	93

[a] Corrected for ethylene dichloride aliquots with blanks subtracted. Values represent averages of duplicates (duplicates within averages ±4%). Blanks for water, dog cerebrospinal fluid (1 ml), and dog plasma (0.1 ml) were 111, 121, and 450 relative fluorescence intensity units, respectively. [b] Cerebrospinal fluid samples from two other dogs and plasma samples from two human subjects gave blank values of 310 and 115 for cerebrospinal fluid and 370 and 600 for plasma. When probenecid (100 μg/test) was added to these samples and assayed, the relative fluorescence intensity units per microgram values for probenecid were 76 and 81 for cerebrospinal fluid and 95 and 101 for plasma.

using three solvent systems: A, methanol–ethyl acetate–acetic acid (10:10:1 v/v); B, methanol–ethyl acetate–28% ammonium hydroxide (10:10:1); and C, 95% ethanol–acetone–28% ammonium hydroxide (10:10:1). For radiochromatography, 0.5-cm zones of gel were scraped using a thin-layer plate scraper[5] and transferred into counting vials. Radiochemical purity (>95%) was established by TLC as already described.

Two dogs (mongrel male, 14 kg) were anesthetized with pentobarbital sodium (30 mg/kg ip) and administered ^{14}C-probenecid (140 mg, 20 μCi ip). Blood samples were drawn prior to dosing (5 min) and at 1, 2, 3, and 4 hr. Cerebrospinal fluid was collected at 4 hr by cisternal puncture using a 19-gauge spinal needle. Aliquots of plasma (0.1 ml) or cerebrospinal fluid (1.0 ml) were analyzed for probenecid by the spectrophotofluorometric method. As a check on the method, additional aliquots were analyzed by direct counting and by counting ethylene dichloride extracts (evaporated to dryness prior to mixing with counting fluid).

For the spectrophotofluorometric assay, human and dog plasma (0.1 ml diluted to 1 ml with water) or dog cerebrospinal fluid (1 ml) was acidified with 0.5 ml of 3 *N* HCl and shaken for 30 min with 10 ml of ethylene dichloride. After centrifugation (500×*g*, 10 min; all subsequent centrifugation steps were carried out in the same manner), 8 ml of the organic layer was placed in a 40-ml conical centrifuge tube and evaporated to dryness with an air stream at room temperature. Care was taken to transfer only the organic phase and to dry completely.

To the residue, 1 ml of a mixture of concentrated sulfuric acid–70% nitric acid (100:1 v/v) was added. The tube was sealed with a polyethylene stopper to prevent steam uptake during subsequent heating. A hypodermic needle (18 gauge) was inserted through the stopper and left in place throughout the procedure to allow for vapor expansion. After mixing[6] to dissolve the residue, the solution was heated (boiling water bath, 30–35 min) and then diluted with 2 ml of ice-cold water. Stannous chloride (0.2 ml, 2 *M* in 1 *N* HCl) was added, and the heating was resumed for 20–25 min. Upon cooling to room temperature, charcoal[7] (0.5 ml of a 10% water slurry) was added; the mixture was then shaken for 2 min and centrifuged.

The charcoal residue was resuspended in 1 ml of water, briefly stirred, and recentrifuged. Upon repetition of this step with additional water, the final charcoal residue was suspended in 2 ml of 0.2 *N* NaOH and heated (boiling water bath, 20–25 min). After cooling to room temperature, 2 ml of 95% ethanol was added; the mixture was briefly stirred and then centrifuged. Just prior to fluorescence measurement, 3 ml of the supernate was mixed with 0.2 ml of acetic acid.

Relative fluorescence intensity was measured within 5 min of the addition of acetic acid, after which time the sample became turbid and required recentrifugation. The procedure could be stopped for at least 2 days at any point following the addition of stannous chloride and prior to the addition of acetic acid. Excitation and emission wavelengths were 340 and 415 nm, respectively. The spectrophotofluorometer was standardized with anthranilic acid (1 μg/ml in 95% ethanol, 1200 relative fluorescence intensity units).

[5] Autozonal scraper, New England Nuclear, North Haven, Conn.
[6] Vortex mixer.
[7] Norit A, Matheson, Coleman and Bell.

Table II—Comparison of Spectrophotofluorometric and Radiochemical Assays

Dog[a]	Sample and Time, hr	Probenecid, μg/ml Fluorometric	Radiochemical
1	Plasma 1	28	31.9
	Plasma 2	24	27.2
	Plasma 3	25	25.7
	Plasma 4	18	21.6
	Cerebrospinal fluid 4	1.2	1.5
2	Plasma 1	47	38.5
	Plasma 2	37	40.5
	Plasma 3	35	38.1
	Plasma 4	27	34.3
	Cerebrospinal fluid 4	2.6	2.1

[a] Dose of 10 mg/kg ip.

The relationship between fluorescence and concentration of probenecid was determined by reacting known amounts of the drug (obtained by evaporating aliquots of ethanol stock solution of probenecid). Similar determinations were made with solutions of probenecid (1–150 μg/ml) in water, human and dog plasma, and dog cerebrospinal fluid (obtained from pentobarbital-anesthetized animals). Water, plasma, and cerebrospinal fluid control blanks were analyzed simultaneously.

RESULTS

Various reaction conditions were investigated to maximize fluorescence. Of the several nitrating reagents tested (nitronium tetrafluoroborate, cupric nitrate–acetic anhydride, *etc.*), a mixture of concentrated sulfuric acid and 70% nitric acid (100:1 v/v) was the most effective. Virtually complete nitration was obtained by heating at 100° for 20 min. Increasing the ratio of nitric acid resulted in a more rapid reaction but required a concomitant increase in the amount of reducing agent.

A large quantity of stannous chloride (0.4 mmole/test) was needed for complete conversion of the nitro compound to the fluorescent amine. Dilution with water was necessary to keep salts in solution. Charcoal, 50 mg/test, adsorbed 98–100% of radioactivity in samples containing ^{14}C-probenecid when reacted as described. Two 1-ml water washes of the charcoal removed only negligible amounts (<2%) of carbon-14 but eliminated residual mineral acids and salts. Elution of ^{14}C-labeled fluorescent product from the charcoal with 0.2 *N* NaOH (2 ml heated at 90–100° for 20 min) resulted in greater than 90% recovery of carbon-14. Fluorescence was increased about twofold by the addition of an equal volume of 95% ethanol. A pH range of 3.3–3.9 was optimal for maximum fluorescence of the product in an aqueous solution; the addition of 0.1–0.3 ml of acetic acid/3 ml of the final alkaline–alcoholic supernate resulted in maximum fluorescence.

The interference by metabolites of probenecid in the method was evaluated by adding these compounds at the nitration step of the procedure. The metabolites gave the same relative fluorescence as probenecid on a molar basis. Interference in the method, however, would be minimal since the metabolites of probenecid are poorly extracted by ethylene dichloride (16). Pentobarbital and salicylate (20 μg/test) did not contribute detectable fluorescence.

Typical results are summarized in Table I. A linear relationship was obtained between the relative fluorescence intensity and the amount of probenecid (≤ 100 μg/test). When 10 μg of probenecid was reacted on four separate occasions, 940, 910, 975, and 990 relative fluorescence intensity units were obtained (blanks subtracted). Recoveries from water, cerebrospinal fluid (1.0 ml/test), or plasma (0.1 ml/test) were 80–125%. The water or cerebrospinal fluid blank (1 ml) was 1.1–3.4 μg of probenecid equivalent, while plasma blank (0.1 ml) was 3.6–6.4 μg of probenecid equivalent.

Plasma and cerebrospinal fluid samples from two dogs administered ^{14}C-probenecid were assayed by the fluorescence procedure as well as by ^{14}C-measurement. Results obtained by the two methods are compared in Table II. The ratios of cerebrospinal fluid to plasma concentrations of probenecid were in agreement with results obtained in this laboratory using radioimmunoassay for measurement of probenecid in dogs (17).

After carrying ^{14}C-probenecid through the method, the final product was studied by TLC in Solvent Systems A–C. Radioactivity migrated as a single spot with R_f values identical to those of *p*-sulfoanthranilic acid in each system (R_f 0.67, 0.21, and 0.47 in A–C, respectively). The fluorescent product of probenecid and *p*-sulfoanthranilic acid exhibited the

same maximum activation and emission wavelengths as described for 2′-aminoprobenecid (13).

DISCUSSION

The basis of the fluorescence method is conversion of probenecid to an anthranilic acid derivative. Blanchard *et al.* (13) reduced 2′-nitroprobenecid to 2′-aminoprobenecid and described the fluorescent properties of the latter. This observation was applied to the assay of probenecid by first nitrating the drug and then reducing the nitro group. However, the resulting fluorescent product was not 2′-aminoprobenecid, a relatively nonpolar compound that could be extracted into organic solvents, but the more polar *p*-sulfoanthranilic acid. Consequently, interfering substances such as salts and degradation products of biological origin (blank) were only poorly separated from the fluorescent probenecid derivative. The present method achieves a partial separation of interfering substances by means of a charcoal adsorption–elution step. A more effective separation to maximize fluorescence, such as TLC or high-pressure liquid chromatography, seems indicated.

While the fluorometric method for probenecid has only severalfold greater sensitivity than the spectrophotometric method for assay in cerebrospinal fluid and less sensitivity for plasma, there is no significant interference by drugs such as salicylate, unlike the interference by this compound in the UV assay (14). Since metabolites of probenecid are poorly extracted by ethylene dichloride (16), the method is generally specific for probenecid.

REFERENCES

(1) K. Sabih, C. D. Klaassen, and K. Sabih, *J. Pharm. Sci.*, **60,** 745 (1971).

(2) A. G. Zacchei and L. Weidner, *ibid.*, **62,** 1972 (1973).

(3) E. Watson and S. Wilk, *J. Neurochem.*, **21,** 1569 (1973).

(4) W. D. Conway and S. Melethil, *J. Chromatogr.*, **115,** 222 (1975).

(5) J. Y. Mu, B. A. Faraj, Z. H. Israili, and P. G. Dayton, *Life Sci.*, **14,** 837 (1974).

(6) H. Cramer, L. K. Y. Ng, and T. N. Chase, *J. Neurochem.*, **19,** 1601 (1972).

(7) J. B. Sebens and J. Korf, *Exp. Neurol.*, **46,** 333 (1975).

(8) J. Korf and H. M. Van Praag, *Psychopharmacologia*, **18,** 129 (1970).

(9) R. Sjöström, *ibid.*, **25,** 96 (1972).

(10) C. Gardey-Levassort, G. Olive, D. Sadeghi, and P. Lechat, *Pharmacology*, **9,** 107 (1973).

(11) J. M. Perel, M. Levitt, and D. L. Dunner, *Psychopharmacologia*, **35,** 83 (1974).

(12) H. F. Cserr and D. H. Van Dyke, *Am. J. Physiol.*, **220,** 718 (1971).

(13) K. C. Blanchard, D. Maroske, D. G. May, and I. M. Weiner, *J. Pharmacol. Exp. Ther.*, **180,** 397 (1972).

(14) P. G. Dayton, T. F. Yü, W. Chen, L. Berger, L. A. West, and A. B. Gutman, *ibid.*, **140,** 278 (1963).

(15) Z. H. Israili, J. M. Perel, R. F. Cunningham, P. G. Dayton, T. F. Yü, A. B. Gutman, K. R. Long, R. C. Long, Jr., and J. H. Goldstein, *J. Med. Chem.*, **15,** 709 (1972).

(16) P. G. Dayton, J. M. Perel, R. F. Cunningham, Z. H. Israili, and I. M. Weiner, *Drug Metab. Dispos.*, **1,** 742 (1973).

(17) W. L. Shei, J. Y. Mu, R. F. Cunningham, Z. H. Israili, and P. G. Dayton, *Psychopharmacologia*, **53,** 315 (1977).

ACKNOWLEDGMENTS

Supported by Research Grant GM 14270 from the National Institutes of Health, Bethesda, Md.

Determination of Fluoxymesterone, Norethandrolone, Prednisolone, and Prednisone in Tablets by Differential Pulse Polarography

R. N. YADAV and F. W. TEARE ˣ

Received February 1, 1977, from the *Faculty of Pharmacy, University of Toronto, Toronto, Ontario, Canada, M5S 1A1.* Accepted for publication June 22, 1977.

Abstract □ A differential pulse polarographic method for the determination of fluoxymesterone, norethandrolone, prednisolone, and prednisone in tablets is described. This method is more sensitive than dc polarography, and the measurement of diffusion current is greatly simplified. Sørensen phosphate buffer, pH 5.6, was used as the supporting electrolyte. No apparent interference was observed from tablet excipients; the method is rapid, simple, and relatively precise.

Keyphrases □ Fluoxymesterone—differential pulse polarographic analysis in tablets □ Norethandrolone—differential pulse polarographic analysis in tablets □ Prednisolone—differential pulse polarographic analysis in tablets □ Prednisone—differential pulse polarographic analysis in tablets □ Differential pulse polarography—analyses, fluoxymesterone, norethandrolone, prednisolone, and prednisone in tablets □ Androgens—fluoxymesterone and norethandrolone, differential pulse polarographic analysis in tablets □ Glucocorticoids—prednisolone and prednisone, differential pulse polarographic analysis in tablets □ Steroids—fluoxymesterone, norethandrolone, prednisolone, and prednisone, differential pulse polarographic analyses in tablets

The differential pulse polarographic assay of several Δ^4-3-ketosteroids in parenteral formulations (1) and oral contraceptive tablets (2) recently was reported. In addition, the polarographic reduction of certain other Δ^4-3-ketosteroids is well documented (3–7), and a number of workers reported the dc polarographic assay of steroids having this same α,β-unsaturated keto group in pharmaceutical preparations (8–10). Several reports concerned the application of colorimetric (11, 12), spectrophotometric (13, 14), and titrimetric (15) procedures for the estimation of prednisone, prednisolone, and other corticosteroids in pharmaceutical dosage forms.

This paper reports a simple and rapid differential pulse polarographic method for the analysis of fluoxymesterone (I), norethandrolone (II), prednisolone (III), and prednisone (IV) in commercial tablets.

EXPERIMENTAL

Polarographic Analysis—Assays were performed using a polarographic analyzer[1] equipped with a drop timer[2] in the differential pulse

[1] Princeton Applied Research model 174A.
[2] Princeton Applied Research model 172A.

same maximum activation and emission wavelengths as described for 2′-aminoprobenecid (13).

DISCUSSION

The basis of the fluorescence method is conversion of probenecid to an anthranilic acid derivative. Blanchard *et al.* (13) reduced 2′-nitroprobenecid to 2′-aminoprobenecid and described the fluorescent properties of the latter. This observation was applied to the assay of probenecid by first nitrating the drug and then reducing the nitro group. However, the resulting fluorescent product was not 2′-aminoprobenecid, a relatively nonpolar compound that could be extracted into organic solvents, but the more polar *p*-sulfoanthranilic acid. Consequently, interfering substances such as salts and degradation products of biological origin (blank) were only poorly separated from the fluorescent probenecid derivative. The present method achieves a partial separation of interfering substances by means of a charcoal adsorption–elution step. A more effective separation to maximize fluorescence, such as TLC or high-pressure liquid chromatography, seems indicated.

While the fluorometric method for probenecid has only severalfold greater sensitivity than the spectrophotometric method for assay in cerebrospinal fluid and less sensitivity for plasma, there is no significant interference by drugs such as salicylate, unlike the interference by this compound in the UV assay (14). Since metabolites of probenecid are poorly extracted by ethylene dichloride (16), the method is generally specific for probenecid.

REFERENCES

(1) K. Sabih, C. D. Klaassen, and K. Sabih, *J. Pharm. Sci.*, **60,** 745 (1971).

(2) A. G. Zacchei and L. Weidner, *ibid.*, **62,** 1972 (1973).

(3) E. Watson and S. Wilk, *J. Neurochem.*, **21,** 1569 (1973).

(4) W. D. Conway and S. Melethil, *J. Chromatogr.*, **115,** 222 (1975).

(5) J. Y. Mu, B. A. Faraj, Z. H. Israili, and P. G. Dayton, *Life Sci.*, **14,** 837 (1974).

(6) H. Cramer, L. K. Y. Ng, and T. N. Chase, *J. Neurochem.*, **19,** 1601 (1972).

(7) J. B. Sebens and J. Korf, *Exp. Neurol.*, **46,** 333 (1975).

(8) J. Korf and H. M. Van Praag, *Psychopharmacologia*, **18,** 129 (1970).

(9) R. Sjöström, *ibid.*, **25,** 96 (1972).

(10) C. Gardey-Levassort, G. Olive, D. Sadeghi, and P. Lechat, *Pharmacology*, **9,** 107 (1973).

(11) J. M. Perel, M. Levitt, and D. L. Dunner, *Psychopharmacologia*, **35,** 83 (1974).

(12) H. F. Cserr and D. H. Van Dyke, *Am. J. Physiol.*, **220,** 718 (1971).

(13) K. C. Blanchard, D. Maroske, D. G. May, and I. M. Weiner, *J. Pharmacol. Exp. Ther.*, **180,** 397 (1972).

(14) P. G. Dayton, T. F. Yü, W. Chen, L. Berger, L. A. West, and A. B. Gutman, *ibid.*, **140,** 278 (1963).

(15) Z. H. Israili, J. M. Perel, R. F. Cunningham, P. G. Dayton, T. F. Yü, A. B. Gutman, K. R. Long, R. C. Long, Jr., and J. H. Goldstein, *J. Med. Chem.*, **15,** 709 (1972).

(16) P. G. Dayton, J. M. Perel, R. F. Cunningham, Z. H. Israili, and I. M. Weiner, *Drug Metab. Dispos.*, **1,** 742 (1973).

(17) W. L. Shei, J. Y. Mu, R. F. Cunningham, Z. H. Israili, and P. G. Dayton, *Psychopharmacologia*, **53,** 315 (1977).

ACKNOWLEDGMENTS

Supported by Research Grant GM 14270 from the National Institutes of Health, Bethesda, Md.

Determination of Fluoxymesterone, Norethandrolone, Prednisolone, and Prednisone in Tablets by Differential Pulse Polarography

R. N. YADAV and F. W. TEARE ˣ

Received February 1, 1977, from the *Faculty of Pharmacy, University of Toronto, Toronto, Ontario, Canada, M5S 1A1.* Accepted for publication June 22, 1977.

Abstract □ A differential pulse polarographic method for the determination of fluoxymesterone, norethandrolone, prednisolone, and prednisone in tablets is described. This method is more sensitive than dc polarography, and the measurement of diffusion current is greatly simplified. Sørensen phosphate buffer, pH 5.6, was used as the supporting electrolyte. No apparent interference was observed from tablet excipients; the method is rapid, simple, and relatively precise.

Keyphrases □ Fluoxymesterone—differential pulse polarographic analysis in tablets □ Norethandrolone—differential pulse polarographic analysis in tablets □ Prednisolone—differential pulse polarographic analysis in tablets □ Prednisone—differential pulse polarographic analysis in tablets □ Differential pulse polarography—analyses, fluoxymesterone, norethandrolone, prednisolone, and prednisone in tablets □ Androgens—fluoxymesterone and norethandrolone, differential pulse polarographic analysis in tablets □ Glucocorticoids—prednisolone and prednisone, differential pulse polarographic analysis in tablets □ Steroids—fluoxymesterone, norethandrolone, prednisolone, and prednisone, differential pulse polarographic analyses in tablets

The differential pulse polarographic assay of several Δ^4-3-ketosteroids in parenteral formulations (1) and oral contraceptive tablets (2) recently was reported. In addition, the polarographic reduction of certain other Δ^4-3-ketosteroids is well documented (3–7), and a number of workers reported the dc polarographic assay of steroids having this same α,β-unsaturated keto group in pharmaceutical preparations (8–10). Several reports concerned the application of colorimetric (11, 12), spectrophotometric (13, 14), and titrimetric (15) procedures for the estimation of prednisone, prednisolone, and other corticosteroids in pharmaceutical dosage forms.

This paper reports a simple and rapid differential pulse polarographic method for the analysis of fluoxymesterone (I), norethandrolone (II), prednisolone (III), and prednisone (IV) in commercial tablets.

EXPERIMENTAL

Polarographic Analysis—Assays were performed using a polarographic analyzer[1] equipped with a drop timer[2] in the differential pulse

[1] Princeton Applied Research model 174A.
[2] Princeton Applied Research model 172A.

Table I—Current Peak Height *versus* Steroid Concentration

Steroid	E_p, v (*versus* SCE)	Concentration, μg/ml				
		5	10	20	30	40
		Relative Peak Height				
I	−1.44	4.7	8.9	17.0	25.2	32.8
II	−1.35	10.1	21.4	42.4	57.4	68.9
III	−1.19	7.0	15.0	32.7	44.5	53.7
IV	−1.16	10.6	20.8	37.7	50.9	58.9

mode. A three-electrode polarographic cell containing a dropping mercury electrode (DME) as the analyzer electrode, a saturated calomel electrode (SCE) as the reference electrode, and platinum wire as an auxiliary electrode was used.

The dropping mercury electrode had a drop time of 2 sec and a flow rate of 1.5 mg/sec. The capillary characteristic ($m^{2/3}t^{1/6}$) was 1.471 measured in Sørensen phosphate buffer (16) with an open circuit and at a mercury column height of 95 cm. The current range was either 2 or 5 μamp. Other parameters were: pulse amplitude, 25 mv; and scan rate, 2 mv/sec. The potential range scan in volts for each steroid was: I, from −1.15 to −1.90; II, from −1.11 to −1.86; III, from −1.0 to −1.75; and IV, from −0.95 to −1.70. All polarograms were recorded on an *x–y* recorder[3].

A pH meter[4] fitted with a combination glass–saturated colomel electrode pair was used to measure the pH of all solutions.

Reagents and Chemicals—All chemicals were analytical reagent grade. The pure steroids, obtained from the manufacturers, were used without further purification. The purity of each steroid reported by the manufacturer was: fluoxymesterone[5], 98.5%; norethandrolone[6], 99.26%; prednisolone[7], 99.37%; and prednisone[8], 101.1%.

Calibration Curve—A stock solution was prepared for each steroid by dissolving 20 mg in 100 ml of solvent. Ethanol (95%) was the solvent used for I and IV, while methanol was used for II and III. Suitable aliquots of each stock solution were transferred to separate 25-ml volumetric flasks, and a sufficient quantity of the appropriate organic solvent (ethanol or methanol) was added to produce a volume of 5 ml before the flask was filled to the mark with pH 5.6 Sørensen phosphate buffer.

Triplicate polarograms were recorded for each standard solution in the series, which covered the 5–40-μg/ml range. Aliquots of 20 ml of these solutions were transferred to the cell in turn and deoxygenated with pure nitrogen for 5 min prior to obtaining the polarograms in the quiescent solution while a nitrogen layer was maintained over the solution surface. Polarograms were obtained using the differential pulse mode. Figure 1 shows the actual polarograms of one standard solution of each steroid employed.

Assay of Tablets—Twenty tablets were weighed and finely powdered.

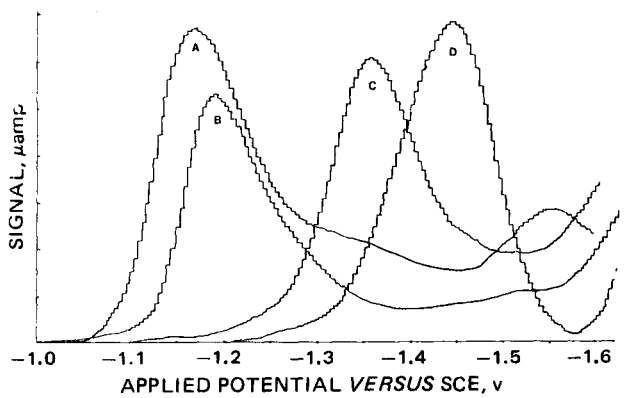

Figure 1—*Differential pulse polarograms for prednisone (A), prednisolone (B), norethandrolone (C), and fluoxymesterone (D). The concentrations of the steroids used were 10, 30, 40, and 50 μg/ml with sensitivities of 0.2, 0.2, 0.5, and 0.5 μamp (full-scale deflection) for C, D, B, and A, respectively.*

[3] Houston Omnigraphic model 2000.
[4] Fisher Accumet model 230 pH/ion meter.
[5] Fluoxymesterone USP, lot R-4185, The Upjohn Co. of Canada Ltd., Don Mills, Ontario, Canada.
[6] Norethandrolone, lot V-183, G. D. Searle & Co., Chicago, Ill.
[7] Prednisolone (anhydrous) USP, batch 508BT, Novopharm Ltd., Scarborough, Ontario, Canada.
[8] Prednisone USP, batch 977ED, Novopharm Ltd., Scarborough, Ontario, Canada.

Table II—Assay Results of Commercial Steroid Tablets

Steroid and Labeled Amount per Tablet	Percent of Labeled Amount Found	
	Polarographic[a] Assay	Manufacturer's Assay
I, 5 mg	92.7 ± 1.6	96.0[b]
II, 10 mg	101.8 ± 0.85	100.3[c]
III, 5 mg	103.7 ± 0.66	103.4[d]
IV, 5 mg	104.7 ± 1.2	103.8[d]

[a] Mean ± %*SD* of five separate determinations with duplicate measurements on each sample solution. [b] High-pressure liquid chromatography, USP XIX. [c] UV spectrophotometric method, NF XIII. [d] Visible spectrophotometric steroid assay, USP XIX.

An amount of tablet powder equivalent to about 7 mg of steroid was accurately weighed and transferred, with the aid of about 50 ml of the appropriate solvent, to a 100-ml volumetric flask. This quantity of steroid should ensure that the peak height value will correspond to the linear portion of the calibration curves plotted from the data in Table I. Then the flask was shaken mechanically[9] for 20 min and diluted to volume with the same solvent.

The flask contents were mixed and excipients were allowed to settle. A 5.0-ml aliquot was pipetted into a 25-ml volumetric flask and diluted to volume with pH 5.6 Sørensen phosphate buffer as the supporting electrolyte. A 20-ml aliquot of this solution was transferred to the polarographic cell. The remainder of the procedure was identical to that described for the calibration curve.

RESULTS AND DISCUSSION

Several investigators reported (17–19) that only those compounds in which the keto group is conjugated with a double bond give rise to a polarographic wave. Kabasakalian and McGlotten (20) studied polarographic reduction of prednisone and prednisolone in well-buffered 50% ethanol solutions and discussed the effects of pH, temperature, concentration, and mercury column height on the polarographic wave. Mixtures of prednisone ($E_{1/2}$ = −1.2 v) and cortisone ($E_{1/2}$ = −1.36 v) can be analyzed with an accuracy within 4% in a 50% methanol solution buffered at pH 5.5 with sodium acetate–acetic acid (21).

Preliminary experiments revealed that all four steroids (I–IV) exhibited well-defined peaks when pH 5.6 Sørensen phosphate buffer was used as a supporting electrolyte (Fig. 1). The peak potentials, E_p, for these steroids are listed in Table I.

The calculation of diffusion current for quantitation is greatly simplified by employing differential pulse polarography rather than dc polarography. The display of the signal in a Gaussian-shaped curve can be measured easily without time-consuming extrapolations for limiting and residual currents as required in classical dc polarography. The instrumental artifacts in differential pulse polarography[10] were discussed by Christie *et al.* (22).

The position of the peak is independent of concentration, and the peak heights are linearly dependent on concentration over the 5–20-μg/ml range for these steroids, with a negative deviation at 30 and 40 μg/ml. Classical dc polarography cannot attain sufficient sensitivity to measure these concentration levels. Table I gives the peak height values for the different steroid concentrations studied. These data were plotted, and the calibration curves were used to determine the steroid concentrations in the sample solutions of the corresponding steroids.

Results obtained by applying the proposed polarographic procedure to the commercially available tablets are presented in Table II. Comparison of the assay results with those obtained by the manufacturers shows a good correlation. The accuracy of the proposed method is evident from the data. The final polarographic assay results for tablets were corrected to account for the percent purity in the reference steroid, using the manufacturer's data for each steroid.

The USP (23) assay of prednisone and prednisolone tablets by the blue tetrazolium procedure is time consuming. Therefore, automated procedures were suggested (24, 25) for single-tablet assays when performing USP content uniformity tests. The procedure involves extraction with chloroform. Aliquots of chloroform are then evaporated, and steroids are redissolved in alcohol. Color is developed by the reduction of blue tetrazolium. The differential pulse polarographic procedure described here is applied directly to the sample extract without additional manipulation

[9] Wrist-action shaker, Burrell Corp., Pittsburgh, Pa.
[10] Princeton Applied Research model 174 polarographic analyzer.

except for dilutions. This procedure is much more convenient than extracting the steroid with a solvent that must be removed before determination. The insoluble constituents in these tablets do not cause any interference and need not be removed before differential pulse polarography. The drug is quantitatively dissolved in the solvent upon shaking for 20 min.

This differential pulse polarographic procedure offers the advantages of sensitivity, speed of analysis, and moderate cost of apparatus. Since the samples are analyzed without prior separation, the procedure results in a considerable saving of time, particularly when a large number of samples are assayed or when a large number of single tablets must be assayed to establish content uniformity.

REFERENCES

(1) L. G. Chatten, R. N. Yadav, and D. K. Madan, *Pharm. Acta Helv.*, **51**, 381 (1976).

(2) L. G. Chatten, R. N. Yadav, S. Binnington, and R. E. Moskalyk, *Analyst*, in press.

(3) M. Brezina and P. Zuman, "Polarography in Medicine, Biochemistry and Pharmacy," Interscience, New York, N.Y., 1958, p. 434.

(4) G. W. C. Milner, "The Principles and Applications of Polarography," Longmans Green, New York, N.Y., 1957, pp. 609–615.

(5) J. I. Spahr and A. M. Knevel, *J. Pharm. Sci.*, **55**, 1020 (1966).

(6) P. Kabasakalian and J. McGlotten, *Anal. Chem.*, **34**, 1440 (1962).

(7) P. Zuman, J. Tenygl, and M. Brezina, *Chem. Listy*, **47**, 1152 (1953); through *Chem. Abstr.*, **48**, 5674f (1954).

(8) M. J. Heasman and A. J. Wood, *J. Pharm. Pharmacol., Suppl.*, **23**, 176S (1971).

(9) P. Gantés and J. P. Juhasz, *Ann. Pharm. Fr.*, **24**, 687 (1966).

(10) L. L. Smith and M. Halwar, *J. Am. Pharm. Assoc., Sci. Ed.*, **48**, 348 (1959).

(11) F. M. Kunze and J. S. Davis, *J. Pharm. Sci.*, **53**, 1259 (1964).

(12) A. L. Woodson, *ibid.*, **60**, 1539 (1971).

(13) G. Steinke and F. Schmidt, *Krankenhaus-Apoth.*, **24**, 20 (1974); through *Chem. Abstr.*, **81**, 96483f (1974).

(14) L. N. Bobkov and N. A. Kazavinov, *Farm. Zh.*, **29**, 59 (1974); through *Chem. Abstr.*, **81**, 68613e (1974).

(15) L. Kurlansik and E. F. Salim, *J. Pharm. Sci.*, **55**, 1457 (1966).

(16) "Scientific Tables," 7th ed., Geigy S. A., Basel, Switzerland, 1970, p. 281.

(17) H. Adkins and F. W. Cox, *J. Am. Chem. Soc.*, **60**, 1151 (1938).

(18) J. Eisenbrand and H. Picher, *Z. Physiol. Chem.*, **260**, 83 (1939); through *Chem. Abstr.*, **33**, 8228[2] (1939).

(19) J. K. Wolfe, E. B. Hershberg, and L. F. Fieser, *J. Biol. Chem.*, **136**, 653 (1940).

(20) P. Kabasakalian and J. McGlotten, *J. Am. Chem. Soc.*, **78**, 5032 (1956).

(21) P. Kabasakalian, S. Delorenzo, and J. McGlotten, *Anal. Chem.*, **28**, 1669 (1956).

(22) J. H. Christie, J. Osteryoung, and R. A. Osteryoung, *ibid.*, **45**, 210 (1973).

(23) "The United States Pharmacopeia," 19th rev., Mack Publishing Co., Easton, Pa., 1975, pp. 398, 403.

(24) W. F. Beyer, *J. Pharm. Sci.*, **55**, 200 (1966).

(25) V. J. Greely, W. W. Hall, T. P. Michaels, and L. P. Sinotte, *Ann. N.Y. Acad. Sci.*, **130**, 545 (1965).

ACKNOWLEDGMENTS

Adapted in part from a thesis submitted by R. N. Yadav to the University of Toronto in partial fulfillment of the Master of Science degree requirements.

The authors are indebted to the pharmaceutical companies for their generous contributions of reference standards and dosage forms.

COMMUNICATIONS

Assay of Amygdalin Dosage Forms from Mexico

Keyphrases □ Amygdalin dosage forms—IR and NMR spectral identification and high-pressure liquid chromatographic analysis of components in various products □ IR spectroscopy—identification, components in various amygdalin dosage forms □ NMR spectroscopy—identification, components in various amygdalin dosage forms □ High-pressure liquid chromatography—analyses, amygdalin and components in various dosage forms

To the Editor:

One controversial topic in cancer treatment today is whether laetrile (1) (amygdalin[1]) is effective as a cancer chemotherapeutic agent. To resolve this complicated issue, the National Cancer Institute (NCI) considered a clinical trial to test the efficacy of amygdalin in cancer treatment. "Available" amygdalin dosage forms were procured and evaluated to determine their suitability for such a trial. Although the question of efficacy in humans may not be answered for a long time, the chemical compositions of the title amygdalin formulations are now known. Because this information has not been previously available to the public[2], it should be of vital interest to current and future users of these dosage forms. For this reason, we are reporting our findings in this communication.

Most amygdalin formulations used by cancer patients in this country are produced in Mexico, and samplings of the products we assayed originated from that country. Our samplings were selected randomly from groupings of these formulations released to NCI by U.S. Customs, which had seized the amygdalin products as they were being transported illegally into the United States. The seized materials consisted of five groups[3] of injectable liquids in amber ampuls and three groups[3] of tablets for oral administration. The amber ampuls had a 10-ml fill volume capacity. A ceramic label indicated the contents as "Amigdalina 3 g." and identified the supplier as Cyto Pharma de Mexico, S.A. The label also stated that the product was an injec-

[1] The trivial names amygdalin, laetrile, nitriloside, vitamin B-17, and 1-mandelonitrile-β-diglycoside have been used synonymously by both the proponents and opponents of laetrile (2). Systematically, laetrile is (*R*)-mandelonitrile-β-glucuronic acid (I) and amygdalin is (*R*)-mandelonitrile-β-D-glucosido-6-β-D-glucoside (II). The drug currently offered as an antitumor agent is amygdalin, which is usually extracted from kernels of apricots and related fruits.

[2] Levi *et al.* (3) described briefly the physicochemical and biochemical properties of two pharmaceutical formulations of amygdalin available in the United States and Canada in the early 1960's. The authors identified neither the manufacturers nor the dosage potencies. However, a comparison of the reported data with those in this article indicates that the earlier products differed from those available today.

[3] According to U.S. Customs records, these groups were seized between 1973 and 1975; all groups, except Group 76-2505-11569, contained at least 1000 dosage units. The seized materials were kept in an air-conditioned vault from the time of seizure to the time of release, July 1977.

except for dilutions. This procedure is much more convenient than extracting the steroid with a solvent that must be removed before determination. The insoluble constituents in these tablets do not cause any interference and need not be removed before differential pulse polarography. The drug is quantitatively dissolved in the solvent upon shaking for 20 min.

This differential pulse polarographic procedure offers the advantages of sensitivity, speed of analysis, and moderate cost of apparatus. Since the samples are analyzed without prior separation, the procedure results in a considerable saving of time, particularly when a large number of samples are assayed or when a large number of single tablets must be assayed to establish content uniformity.

REFERENCES

(1) L. G. Chatten, R. N. Yadav, and D. K. Madan, *Pharm. Acta Helv.*, **51**, 381 (1976).

(2) L. G. Chatten, R. N. Yadav, S. Binnington, and R. E. Moskalyk, *Analyst*, in press.

(3) M. Brezina and P. Zuman, "Polarography in Medicine, Biochemistry and Pharmacy," Interscience, New York, N.Y., 1958, p. 434.

(4) G. W. C. Milner, "The Principles and Applications of Polarography," Longmans Green, New York, N.Y., 1957, pp. 609–615.

(5) J. I. Spahr and A. M. Knevel, *J. Pharm. Sci.*, **55**, 1020 (1966).

(6) P. Kabasakalian and J. McGlotten, *Anal. Chem.*, **34**, 1440 (1962).

(7) P. Zuman, J. Tenygl, and M. Brezina, *Chem. Listy*, **47**, 1152 (1953); through *Chem. Abstr.*, **48**, 5674f (1954).

(8) M. J. Heasman and A. J. Wood, *J. Pharm. Pharmacol., Suppl.*, **23**, 176S (1971).

(9) P. Gantés and J. P. Juhasz, *Ann. Pharm. Fr.*, **24**, 687 (1966).

(10) L. L. Smith and M. Halwar, *J. Am. Pharm. Assoc., Sci. Ed.*, **48**, 348 (1959).

(11) F. M. Kunze and J. S. Davis, *J. Pharm. Sci.*, **53**, 1259 (1964).

(12) A. L. Woodson, *ibid.*, **60**, 1539 (1971).

(13) G. Steinke and F. Schmidt, *Krankenhaus-Apoth.*, **24**, 20 (1974); through *Chem. Abstr.*, **81**, 96483f (1974).

(14) L. N. Bobkov and N. A. Kazavinov, *Farm. Zh.*, **29**, 59 (1974); through *Chem. Abstr.*, **81**, 68613e (1974).

(15) L. Kurlansik and E. F. Salim, *J. Pharm. Sci.*, **55**, 1457 (1966).

(16) "Scientific Tables," 7th ed., Geigy S. A., Basel, Switzerland, 1970, p. 281.

(17) H. Adkins and F. W. Cox, *J. Am. Chem. Soc.*, **60**, 1151 (1938).

(18) J. Eisenbrand and H. Picher, *Z. Physiol. Chem.*, **260**, 83 (1939); through *Chem. Abstr.*, **33**, 8228[2] (1939).

(19) J. K. Wolfe, E. B. Hershberg, and L. F. Fieser, *J. Biol. Chem.*, **136**, 653 (1940).

(20) P. Kabasakalian and J. McGlotten, *J. Am. Chem. Soc.*, **78**, 5032 (1956).

(21) P. Kabasakalian, S. Delorenzo, and J. McGlotten, *Anal. Chem.*, **28**, 1669 (1956).

(22) J. H. Christie, J. Osteryoung, and R. A. Osteryoung, *ibid.*, **45**, 210 (1973).

(23) "The United States Pharmacopeia," 19th rev., Mack Publishing Co., Easton, Pa., 1975, pp. 398, 403.

(24) W. F. Beyer, *J. Pharm. Sci.*, **55**, 200 (1966).

(25) V. J. Greely, W. W. Hall, T. P. Michaels, and L. P. Sinotte, *Ann. N.Y. Acad. Sci.*, **130**, 545 (1965).

ACKNOWLEDGMENTS

Adapted in part from a thesis submitted by R. N. Yadav to the University of Toronto in partial fulfillment of the Master of Science degree requirements.

The authors are indebted to the pharmaceutical companies for their generous contributions of reference standards and dosage forms.

COMMUNICATIONS

Assay of Amygdalin Dosage Forms from Mexico

Keyphrases □ Amygdalin dosage forms—IR and NMR spectral identification and high-pressure liquid chromatographic analysis of components in various products □ IR spectroscopy—identification, components in various amygdalin dosage forms □ NMR spectroscopy—identification, components in various amygdalin dosage forms □ High-pressure liquid chromatography—analyses, amygdalin and components in various dosage forms

To the Editor:

One controversial topic in cancer treatment today is whether laetrile (1) (amygdalin[1]) is effective as a cancer chemotherapeutic agent. To resolve this complicated issue, the National Cancer Institute (NCI) considered a clinical trial to test the efficacy of amygdalin in cancer treatment. "Available" amygdalin dosage forms were procured and evaluated to determine their suitability for such a trial. Although the question of efficacy in humans may not be answered for a long time, the chemical compositions of the title amygdalin formulations are now known. Because this information has not been previously available to the public[2], it should be of vital interest to current and future users of these dosage forms. For this reason, we are reporting our findings in this communication.

Most amygdalin formulations used by cancer patients in this country are produced in Mexico, and samplings of the products we assayed originated from that country. Our samplings were selected randomly from groupings of these formulations released to NCI by U.S. Customs, which had seized the amygdalin products as they were being transported illegally into the United States. The seized materials consisted of five groups[3] of injectable liquids in amber ampuls and three groups[3] of tablets for oral administration. The amber ampuls had a 10-ml fill volume capacity. A ceramic label indicated the contents as "Amigdalina 3 g." and identified the supplier as Cyto Pharma de Mexico, S.A. The label also stated that the product was an injec-

[1] The trivial names amygdalin, laetrile, nitriloside, vitamin B-17, and 1-mandelonitrile-β-diglycoside have been used synonymously by both the proponents and opponents of laetrile (2). Systematically, laetrile is (*R*)-mandelonitrile-β-glucuronic acid (I) and amygdalin is (*R*)-mandelonitrile-β-D-glucosido-6-β-D-glucoside (II). The drug currently offered as an antitumor agent is amygdalin, which is usually extracted from kernels of apricots and related fruits.

[2] Levi *et al.* (3) described briefly the physicochemical and biochemical properties of two pharmaceutical formulations of amygdalin available in the United States and Canada in the early 1960's. The authors identified neither the manufacturers nor the dosage potencies. However, a comparison of the reported data with those in this article indicates that the earlier products differed from those available today.

[3] According to U.S. Customs records, these groups were seized between 1973 and 1975; all groups, except Group 76-2505-11569, contained at least 1000 dosage units. The seized materials were kept in an air-conditioned vault from the time of seizure to the time of release, July 1977.

Table I—Assay Results for the Five Groups of Injectables

U.S. Customs Group (Seizure Date)	Ampul	(*R,S*)-Amygdalin, g/Ampul	Percent Label, 3 g/Ampul
74-2504-10919 (12/28/1973)	1	1.64	54.7
	2	1.64	54.7
	3	1.64	54.7
	4	1.53	51.0
	5	1.65	55.0
Average		1.62	54.0
SD		0.05	1.7
75-2504-10716 (11/09/1974)	1	1.65	55.0
	2	1.68	56.0
	3	1.68	56.0
	4	1.64	54.7
	5	1.65	55.0
Average		1.66	55.3
SD		0.02	0.6
75-2504-11744 (05/21/1975)	1	1.40	46.7
	2	1.39	46.3
	3	1.38	46.0
	4	1.37	45.7
	5	1.38	46.0
Average		1.38	46.1
SD		0.01	0.4
76-2505-11569 (04/11/1975)	1	1.18	39.3
	2	1.19	39.7
	3	1.72	57.3
	4	1.68	56.0
Average		1.44	48.1
SD		0.30	9.9
76-2810-00001 (12/12/1975)	1	1.39	46.3
	2	1.45	48.3
	3	1.42	47.3
	4	1.52	50.7
Average		1.44	48.2
SD		0.06	1.9

table solution. The tablets were uncoated, round, and yellow; they measured approximately 12 × 3 mm. On one side was inscribed "500"; on the other was an outline of a conifer, a logo used by Cyto Pharma de Mexico, S. A. Manufacturing control numbers, expiration dates, and storage recommendations were not apparent on product labeling or packaging.

Injectables—Identification of the "active" component(s) in the injectables was based on spectral and chromatographic evidence. IR data were obtained from the freeze-dried residues of the solutions. IR spectra from all five lots were very similar, showing bands that were rather broad. Absorptions in the 2.8–3.3- and 9–10-μm regions were consistent with those expected for carbohydrates. Bands at 13.2 and 14.3 μm were in agreement with a phenyl; those at ~6.0 and 6.25 μm were suggestive of a primary amide. A very weak band at 4.4 μm was indicative of a nitrile. The proton NMR spectra for all five lots, obtained from the solutions, were comparable and consistent with the structure of amygdalin. However, in the δ 5–6-ppm region, where the benzylic proton was expected, four singlets appeared at δ 5.1, 5.4, 5.9, and 6.2 ppm; in the δ 1.10-ppm region, where no signal was expected, a doublet

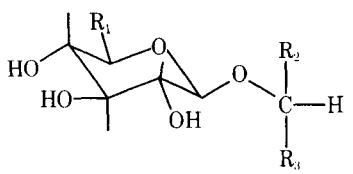

I (laetrile): R_1 = COOH, R_2 = CN, R_3 = C_6H_5

II [(*R*)-amygdalin]: R_1 = CH_2O-β-D-glucoside, R_2 = CN, R_3 = C_6H_5

III [(*S*)-amygdalin]: R_1 = CH_2O-β-D-glucoside, R_2 = C_6H_5, R_3 = CN

appeared. The δ 6.2- and 5.9-ppm resonances were identified as the benzylic proton in (*S*)- and (*R*)-amygdalins, respectively; the δ 5.1- and 5.4-ppm peaks were assigned the benzylic proton in amygdalinamide[4] and amygdalin acid[4], respectively; and the δ 1.10-ppm doublet was assigned to the methyls in 2-propanol[5]. The ratios of (*R*)- to (*S*)-amygdalins in all five batches were 1:1, within experimental error.

GLC–mass spectral analyses of the trimethylsilyl and trifluoroacetyl[6] derivatives of these formulations on methyl silicone (OV-1) and a trichlorophenyl methyl silicone (Versilube F-50)[6] columns, respectively, showed that the (*R*)- and (*S*)-amygdalins were separated; they yielded identical mass spectra. The GLC–mass spectral data also showed amygdalinamide plus another impurity, tentatively identified as 1-*O*-benzylgentiobiose. No evidence of laetrile [(*R*)-mandelonitrile-β-glucuronic acid] was found.

High-pressure liquid chromatographic (HPLC) analysis on a C_8-bonded silica (Lichrosorb RP8) column with aqueous methanol[7] readily separated amygdalin[7], amygdalinamide[7], and amygdalin acid[7]. Aliquots of 1.00 ml from ampuls of each group were each transferred to a 50-ml volumetric flask. After filling to mark with water, 1.00-ml aliquots of the resulting solutions were each mixed with 0.50 ml of an internal standard solution[8] before injection. The concentrations of amygdalin per milliliter were determined by the internal standard method; the amygdalin reference was Pharm-Eco lot PC-0237A[9]. The amount of (*R,S*)-amygdalin per ampul was obtained by multiplying the ampul solution volume[10] times its solution concentration. The results are shown in Table I.

Since these ampuls were not identified by manufacturing control numbers, it is possible that a single seizure group number could contain more than one production batch. The results for Group 76-2505-11569 suggest this possibility.

Tablets—Identification of the "active" component in the tablets was based on spectral and chromatographic evidence. Tablets from each lot were separately ground and extracted with methanol. Then the methanol solutions were evaporated to dryness, and the residues were used for spectral analysis. Recorded as mineral oil[11] mulls, the IR spectra from all three lots were comparable; they were also comparable to those obtained from the injectables. Re-

[4] Amygdalinamide and amygdalin acid are hydrolysis products of amygdalin in which the nitrile is hydrolyzed. They were the major contaminants in all five groups of ampuls. The (*R,S*)-epimers of each have been prepared in our laboratory; estimations of these contaminants in the subject injectables will appear in another report.

[5] 2-Propanol was a significant contaminant in these formulations; its quantitations will appear in another report.

[6] The use of this derivative and column was suggested by Dr. T. Cairns of the Food and Drug Administration.

[7] By varying the methanol–water ratio, epimeric pairs of the respective compounds could be separated. However, the time required to separate the (*R*)- and (*S*)-amygdalins was in excess of 1 hr; for this reason, the HPLC assay conditions were adjusted so that (*R*)- and (*S*)-amygdalins eluted as a single component.

[8] Prepared by dissolving 5 mg of *m*-nitroaniline (EKC) in water in a 50-ml volumetric flask.

[9] This reference was analyzed for 93.0 ± 1.5% (*R,S*)-amygdalin, 2–3% UV-absorbing impurities including ≥0.7% 1-*O*-benzylgentiobiose and ≥0.3% amygdalinamide, and 3.5 ± 0.3% water; the remainder of the sample was not identified. The equivalents of the UV characteristics for (*R*)- and (*S*)-amygdalins have been established.

[10] Each ampul fill volume was determined by carefully scoring the liquid level in each ampul, emptying and drying the ampul, and refilling to the scored mark with water dispensed from a volumetric buret. The average of six ampul volumes was 10.0 ± 0.1 ml.

[11] Nujol.

Table II—Assay Results for the Three Tablet Dosage Forms

U.S. Customs Group 76-2505-11569, Seized 4/11/75			U.S. Customs Group 75-2504-11744, Seized 5/21/75			U.S. Customs Group 75-2501-00107, Seized 6/24/76		
Tablet Weight, mg	Amygdalin per Tablet, mg	% Label[a]	Tablet Weight, mg	Amygdalin per Tablet, mg	% Label[a]	Tablet Weight, mg	Amygdalin per Tablet, mg	% Label[a]
555.0	285	57.0	543.8	423	84.6	548.5	436	87.1
539.1	265	53.0	544.6	457	91.5	554.3	420	84.1
537.6	278	55.6	545.7	419	83.8	553.1	413	82.7
540.5	279	55.8	540.6	439	87.8	545.1	428	85.7
537.2	274	54.9	540.1	428	85.6	554.8	419	83.7
542.3	274	54.9	542.7	453	90.5	553.9	446	89.3
Average 541.1	275.7	55.2	542.9	436.5	87.3	551.6	427.2	85.4
SD 4.7	6.6	1.3	2.2	15.9	3.2	3.9	12.3	2.5

[a] Based on the label amount as 500 mg/tablet.

Table III—Tablet Weights (in Milligrams)

Group	High	Low	Average
76-2505-11569	566.3	525.4	541.5, *SD* = 7.6
75-2504-11744	548.4	528.0	541.9, *SD* = 4.4
75-2501-00107	564.4	545.8	553.4, *SD* = 4.7

corded as solutions in deuterated dimethyl sulfoxide, the proton NMR spectra for all three lots were qualitatively identical to a spectrum of authentic (*R*)-amygdalin[12]. These spectra showed only one singlet, δ 5.9 ppm, in the δ 5–6-ppm region, indicating that the amygdalin in these tablets was the epimerically pure (*R*)-form. The lack of a signal in the δ 5.1–5.4-ppm region indicated the absence of amygdalinamide and amygdalin acid. This indication was verified by HPLC data that showed very minor amounts (~1.0% total[13]) of these two contaminants. Ground tablets were also extracted with deuterium oxide. Proton NMR spectra of these solutions showed little or no 2-propanol in these tablets.

These tablets were assayed by the HPLC method used for the injectables. Six tablets from each group were individually crushed, and each was transferred to a 100-ml volumetric flask with the aid of water. The mixtures were briefly sonicated and then thoroughly agitated. The yellow mixtures were brought to mark with more water and then filtered through 0.45-μm filters[14]. Each 1.00-ml aliquot of the clear yellow filtrates was mixed with 0.50 ml of an internal standard solution[8] before it was injected. Quantifications were based on the internal standard method; the amygdalin reference employed was Pharm-Eco lot PC-0237A III[9]. The results are given in Table II.

In addition, 20 tablets from each group were randomly selected and individually weighed. The results are listed in Table III.

Through this study, analytical methods were developed to assay injectable and oral dosage forms of amygdalin produced in Mexico. The results indicate that all of the dosage forms analyzed were subpotent. The average results for the five groups of injectables ranged from 46 to 55% of label; the three groups of tablets ranged from 55 to 87% of label. In addition, the amygdalin in the injectables was a mixture of (*R*)- and (*S*)-amygdalins; the amygdalin in the tablets was the pure (*R*)-form. The injectable dosage forms were also heavily contaminated by amygdalinamide, amygdalin acid, and 2-propanol.

(1) E. T. Krebs and E. T. Krebs, Jr., U.S. pat. 2,985,664 (1961).
(2) *Fed. Regist.*, **42** (151), Part II, 39770 (Aug. 5, 1977).
(3) L. Levi, W. N. French, J. F. Biokis, and I. W. D. Henderson, *Can. Med. Assoc. J.*, **92**, 1057 (1965).

John Jee
Florence Yoshikawa
Leslie Pont
Andrew Cheung
Peter Lim [x]
Life Sciences Division
SRI International
Menlo Park, CA 94025

Received October 28, 1977.
Accepted for publication January 4, 1978.
Supported by Contract N01-CM-33723 from the National Cancer Institute, National Institutes of Health, Bethesda, MD 20014.
The authors thank E. Shingai and D. Thomas of SRI International for assistance in GLC and mass spectral determinations and J. P. Davignon of NCI for valuable comments and suggestions.

[12] Lot 3634, Aldrich Chemical Co., analyzed for 95 ± 1.5% (*R*)-amygdalin, 1% 1-*O*-benzylgentiobiose, ≤0.4% amygdalinamide and other organic impurities, and 3 ± 0.3% water.
[13] Similar UV spectral characteristics at 254 nm for amygdalin, amygdalinamide, and amygdalin acid were assumed.
[14] Millipore.

REVIEWS

Assay of Drugs and Other Trace Compounds in Biological Fluids. Methodological Developments in Biochemistry. Vol. 5. Edited by ERIC REID. North-Holland, 52 Vanderbilt Ave., New York, NY 10017. 1976. 254 pp. 17 × 25 cm. Price $24.95.

This book consists of the proceedings of a "Techniques Forum" held in September 1975 at the University of Surrey, Guildford, United Kingdom. It is divided into four sections. The first section deals with advances in instrumental techniques and includes GLC–mass spectrometry, polarography, luminescence, quantitative TLC, and high-performance liquid chromatography. The second section deals with general analytical strategy and discusses chromatographic approaches, affinity methods, and ion-pair solvent extraction.

The third section deals with sample preparation and discusses logical approaches one can follow for different biological samples. The fourth section describes methodology for 16 different compounds extracted from biological fluids using the analytical instrumentation and techniques described in the preceding sections.

The first three sections of the book are written in such a general fashion that an experienced researcher may gain some useful knowledge, although a novice may not. The fourth section, however, which comprises most of the book, presents some very useful approaches to the assay of a variety of drugs from biological fluids. This section should definitely help both the novice and experienced researcher concerned with method development.

The ever increasing need to monitor drugs in biological fluids with enhanced sensitivity and specificity makes this book a very practical reference work for the analytical chemist.

Reviewed by Carl V. Puglisi
Department of Biochemistry and Drug Metabolism
Hoffmann–La Roche, Inc.
Nutley, NJ 07110

Drug Disposition and Pharmacokinetics, 2nd Ed. By STEPHEN H. CURRY. Blackwell Scientific Publications, 85 Marylebone High Street, London W1, England. 1977. 275 pp. 15 × 23 cm. Price $18.00. Distributed by Lippincott, East Washington Square, Philadelphia, PA 19105.

The book is primarily a teaching text directed to the undergraduate student. The text covers a wide range of subjects, ranging from the chemical properties of drugs to pharmacological relationships, and does not attempt to treat any one topic in depth.

This edition has similar content and format to the first edition. The only significant changes are the separation of the topic of drug–protein binding into a new chapter, expansion of the chapter on quantitative pharmacological relationships, and inclusion of a small section on nonlinear pharmacokinetics in Chapter 7. Other minor revisions have been made in other parts of the text to include more recent material.

The opening chapter deals with the chemical properties of drugs. Chapters 2–5 are concerned principally with qualitative aspects of drug absorption, distribution, metabolism, and excretion. A brief treatment of drug bioavailability is followed by sections on basic pharmacokinetics and the kinetics associated with urinary drug excretion. The pharmacokinetics chapter deals with the kinetics of the one- and two-compartment models, nonlinear kinetics, and multiple dosing. Some numerical examples are given, but no worked problems.

A chapter on drug interactions precedes an expanded discussion on relationships between drug levels and pharmacological effects. Topics include plasma level–effect relationships of chemotherapeutic agents, chlorpromazine, anticonvulsants, tricyclic antidepressants, and β-blocking agents. Dosage adjustment of antibiotics in patients with renal failure is included as an appendix. Although addressed to antibiotics in particular, the arguments presented there apply equally to all drugs whose effect is related to circulating levels and whose elimination is dependent wholly or partially on kidney function. The very brief treatment afforded this subject is probably justified in view of its extensive coverage by other authors.

In the reviewer's opinion, the book is a useful undergraduate teaching aid for students in pharmacy, pharmacology, medicine, and other related health disciplines and provides sufficient references for further indepth reading in specific subject areas.

Reviewed by Peter G. Welling
School of Pharmacy
University of Wisconsin
Madison, WI 53706

Medicinal Chemistry V. Proceedings of the 5th International Symposium on Medicinal Chemistry. Paris, July 19–22, 1976. Edited by J. MATHIEU. Elsevier Scientific, 52 Vanderbilt Ave., New York, NY 10017. 1977. 456 pp. 17 × 25 cm. Price $52.95.

This volume presents the proceedings of the Fifth International Symposium on Medicinal Chemistry, Paris, July 19–22, 1976. Four types of articles are included: main lectures on fundamental subjects by academicians, brief applied lectures by pharmaceutical industrial researchers, round-table discussion of strategy in drug research directed by Professor E. J. Ariens of Nijmegen, and some miscellaneous topics. The program of the symposium also included poster sessions organized by Professor C. G. Wermuth of Strasbourg.

The main subjects range from the fields of peptides, prodrugs, the central nervous system, cardiovascular agents, and immunology to the fields of organic synthesis, the Hansch approach to drug design, and prevention of aging.

Hypothalamic regulatory hormones and their synthetic analogs are concisely discussed with emphasis on the latest developments in research on synthetic studies and structure–activity relationships. This review was authored by numerous collaborators headed by Nobel Laureate A. V. Schally.

The section on peptides also contains reviews on the identity and mode of action of hypothalamic hypophysiotropic hormones, diverse roles of hypothalamic regulatory peptides, synthetic methodology of bioactive peptides, approaches of peptide chemistry to insulin, and synthesis in the field of 1–34 human parathyroid hormone fragments.

The section on prodrugs begins with A. J. Glazko's presentation of his personal experiences in this area over the last 25 years. This presentation reviews studies of factors affecting metabolic disposition of chloramphenicol and some of its derivatives, 4,4-diacetyldiaminodiphenylsulfone (DADDS), adenine arabinoside, araadenosine monophosphate, and prophenytoin. The second review of this section is on modulation of distribution of efficacy of prodrugs. This discussion is a very interesting review of the conception and synthesis of prodrugs on the basis of metabolic pathways and structure–activity correlation using Hansch's approach.

The third article is on long-chain esters of pipotiazine as long-acting psychotropic prodrugs; these prodrugs are supposed to assure a beneficial continuity in drug distribution at the target level with smaller doses administered by injection than those required by the oral route to achieve the same therapeutic effect. The subsequent review summarizes k_{cat} inhibitors as a new class of enzyme proinhibitors. Finally, this section concludes with an article titled Pro-drugs, Protective Groups and the Medicinal Chemist summarizing that it is possible to design prodrugs on a rational basis.

The section dealing with the central nervous system is in itself a major contribution to the literature of medicinal chemistry and pharmacology. The key article is on brain neurotransmitters and drug receptors and it contains valuable discussions of principles of methodology, the dopamine receptor, antischizophrenic agents, prediction of extrapyramidal and autonomic side effects, and a two-state model of the dopamine receptor. Thereafter, neural inhibition as a tool for research of anticonvulsants is the theme for the discussion of γ-aminobutyric acid, taurine, and glycine. The third paper of this section summarizes recent approaches in psychochemotherapy, including the biochemical classification of antidepressants and stereochemical classifications.

The next presentation is on the effects of neuroleptics on dopamine metabolism in the nigroneostriatal, mesolimbic, and mesocortical dopaminergic systems. Piracetam is characterized as a nootropic agent in the following article. It is noted that this drug does not fit any of the

REVIEWS

Assay of Drugs and Other Trace Compounds in Biological Fluids. Methodological Developments in Biochemistry. Vol. 5. Edited by ERIC REID. North-Holland, 52 Vanderbilt Ave., New York, NY 10017. 1976. 254 pp. 17 × 25 cm. Price $24.95.

This book consists of the proceedings of a "Techniques Forum" held in September 1975 at the University of Surrey, Guildford, United Kingdom. It is divided into four sections. The first section deals with advances in instrumental techniques and includes GLC–mass spectrometry, polarography, luminescence, quantitative TLC, and high-performance liquid chromatography. The second section deals with general analytical strategy and discusses chromatographic approaches, affinity methods, and ion-pair solvent extraction.

The third section deals with sample preparation and discusses logical approaches one can follow for different biological samples. The fourth section describes methodology for 16 different compounds extracted from biological fluids using the analytical instrumentation and techniques described in the preceding sections.

The first three sections of the book are written in such a general fashion that an experienced researcher may gain some useful knowledge, although a novice may not. The fourth section, however, which comprises most of the book, presents some very useful approaches to the assay of a variety of drugs from biological fluids. This section should definitely help both the novice and experienced researcher concerned with method development.

The ever increasing need to monitor drugs in biological fluids with enhanced sensitivity and specificity makes this book a very practical reference work for the analytical chemist.

Reviewed by Carl V. Puglisi
Department of Biochemistry and Drug Metabolism
Hoffmann–La Roche, Inc.
Nutley, NJ 07110

Drug Disposition and Pharmacokinetics, 2nd Ed. By STEPHEN H. CURRY. Blackwell Scientific Publications, 85 Marylebone High Street, London W1, England. 1977. 275 pp. 15 × 23 cm. Price $18.00. Distributed by Lippincott, East Washington Square, Philadelphia, PA 19105.

The book is primarily a teaching text directed to the undergraduate student. The text covers a wide range of subjects, ranging from the chemical properties of drugs to pharmacological relationships, and does not attempt to treat any one topic in depth.

This edition has similar content and format to the first edition. The only significant changes are the separation of the topic of drug–protein binding into a new chapter, expansion of the chapter on quantitative pharmacological relationships, and inclusion of a small section on nonlinear pharmacokinetics in Chapter 7. Other minor revisions have been made in other parts of the text to include more recent material.

The opening chapter deals with the chemical properties of drugs. Chapters 2–5 are concerned principally with qualitative aspects of drug absorption, distribution, metabolism, and excretion. A brief treatment of drug bioavailability is followed by sections on basic pharmacokinetics and the kinetics associated with urinary drug excretion. The pharmacokinetics chapter deals with the kinetics of the one- and two-compartment models, nonlinear kinetics, and multiple dosing. Some numerical examples are given, but no worked problems.

A chapter on drug interactions precedes an expanded discussion on relationships between drug levels and pharmacological effects. Topics include plasma level–effect relationships of chemotherapeutic agents, chlorpromazine, anticonvulsants, tricyclic antidepressants, and β-blocking agents. Dosage adjustment of antibiotics in patients with renal failure is included as an appendix. Although addressed to antibiotics in particular, the arguments presented there apply equally to all drugs whose effect is related to circulating levels and whose elimination is dependent wholly or partially on kidney function. The very brief treatment afforded this subject is probably justified in view of its extensive coverage by other authors.

In the reviewer's opinion, the book is a useful undergraduate teaching aid for students in pharmacy, pharmacology, medicine, and other related health disciplines and provides sufficient references for further indepth reading in specific subject areas.

Reviewed by Peter G. Welling
School of Pharmacy
University of Wisconsin
Madison, WI 53706

Medicinal Chemistry V. Proceedings of the 5th International Symposium on Medicinal Chemistry. Paris, July 19–22, 1976. Edited by J. MATHIEU. Elsevier Scientific, 52 Vanderbilt Ave., New York, NY 10017. 1977. 456 pp. 17 × 25 cm. Price $52.95.

This volume presents the proceedings of the Fifth International Symposium on Medicinal Chemistry, Paris, July 19–22, 1976. Four types of articles are included: main lectures on fundamental subjects by academicians, brief applied lectures by pharmaceutical industrial researchers, round-table discussion of strategy in drug research directed by Professor E. J. Ariens of Nijmegen, and some miscellaneous topics. The program of the symposium also included poster sessions organized by Professor C. G. Wermuth of Strasbourg.

The main subjects range from the fields of peptides, prodrugs, the central nervous system, cardiovascular agents, and immunology to the fields of organic synthesis, the Hansch approach to drug design, and prevention of aging.

Hypothalamic regulatory hormones and their synthetic analogs are concisely discussed with emphasis on the latest developments in research on synthetic studies and structure–activity relationships. This review was authored by numerous collaborators headed by Nobel Laureate A. V. Schally.

The section on peptides also contains reviews on the identity and mode of action of hypothalamic hypophysiotropic hormones, diverse roles of hypothalamic regulatory peptides, synthetic methodology of bioactive peptides, approaches of peptide chemistry to insulin, and synthesis in the field of 1–34 human parathyroid hormone fragments.

The section on prodrugs begins with A. J. Glazko's presentation of his personal experiences in this area over the last 25 years. This presentation reviews studies of factors affecting metabolic disposition of chloramphenicol and some of its derivatives, 4,4-diacetyldiaminodiphenylsulfone (DADDS), adenine arabinoside, araadenosine monophosphate, and prophenytoin. The second review of this section is on modulation of distribution of efficacy of prodrugs. This discussion is a very interesting review of the conception and synthesis of prodrugs on the basis of metabolic pathways and structure–activity correlation using Hansch's approach.

The third article is on long-chain esters of pipotiazine as long-acting psychotropic prodrugs; these prodrugs are supposed to assure a beneficial continuity in drug distribution at the target level with smaller doses administered by injection than those required by the oral route to achieve the same therapeutic effect. The subsequent review summarizes k_{cat} inhibitors as a new class of enzyme proinhibitors. Finally, this section concludes with an article titled Pro-drugs, Protective Groups and the Medicinal Chemist summarizing that it is possible to design prodrugs on a rational basis.

The section dealing with the central nervous system is in itself a major contribution to the literature of medicinal chemistry and pharmacology. The key article is on brain neurotransmitters and drug receptors and it contains valuable discussions of principles of methodology, the dopamine receptor, antischizophrenic agents, prediction of extrapyramidal and autonomic side effects, and a two-state model of the dopamine receptor. Thereafter, neural inhibition as a tool for research of anticonvulsants is the theme for the discussion of γ-aminobutyric acid, taurine, and glycine. The third paper of this section summarizes recent approaches in psychochemotherapy, including the biochemical classification of antidepressants and stereochemical classifications.

The next presentation is on the effects of neuroleptics on dopamine metabolism in the nigroneostriatal, mesolimbic, and mesocortical dopaminergic systems. Piracetam is characterized as a nootropic agent in the following article. It is noted that this drug does not fit any of the

REVIEWS

Assay of Drugs and Other Trace Compounds in Biological Fluids. Methodological Developments in Biochemistry. Vol. 5. Edited by ERIC REID. North-Holland, 52 Vanderbilt Ave., New York, NY 10017. 1976. 254 pp. 17 × 25 cm. Price $24.95.

This book consists of the proceedings of a "Techniques Forum" held in September 1975 at the University of Surrey, Guildford, United Kingdom. It is divided into four sections. The first section deals with advances in instrumental techniques and includes GLC–mass spectrometry, polarography, luminescence, quantitative TLC, and high-performance liquid chromatography. The second section deals with general analytical strategy and discusses chromatographic approaches, affinity methods, and ion-pair solvent extraction.

The third section deals with sample preparation and discusses logical approaches one can follow for different biological samples. The fourth section describes methodology for 16 different compounds extracted from biological fluids using the analytical instrumentation and techniques described in the preceding sections.

The first three sections of the book are written in such a general fashion that an experienced researcher may gain some useful knowledge, although a novice may not. The fourth section, however, which comprises most of the book, presents some very useful approaches to the assay of a variety of drugs from biological fluids. This section should definitely help both the novice and experienced researcher concerned with method development.

The ever increasing need to monitor drugs in biological fluids with enhanced sensitivity and specificity makes this book a very practical reference work for the analytical chemist.

Reviewed by Carl V. Puglisi
Department of Biochemistry and Drug Metabolism
Hoffmann–La Roche, Inc.
Nutley, NJ 07110

Drug Disposition and Pharmacokinetics, 2nd Ed. By STEPHEN H. CURRY. Blackwell Scientific Publications, 85 Marylebone High Street, London W1, England. 1977. 275 pp. 15 × 23 cm. Price $18.00. Distributed by Lippincott, East Washington Square, Philadelphia, PA 19105.

The book is primarily a teaching text directed to the undergraduate student. The text covers a wide range of subjects, ranging from the chemical properties of drugs to pharmacological relationships, and does not attempt to treat any one topic in depth.

This edition has similar content and format to the first edition. The only significant changes are the separation of the topic of drug–protein binding into a new chapter, expansion of the chapter on quantitative pharmacological relationships, and inclusion of a small section on nonlinear pharmacokinetics in Chapter 7. Other minor revisions have been made in other parts of the text to include more recent material.

The opening chapter deals with the chemical properties of drugs. Chapters 2–5 are concerned principally with qualitative aspects of drug absorption, distribution, metabolism, and excretion. A brief treatment of drug bioavailability is followed by sections on basic pharmacokinetics and the kinetics associated with urinary drug excretion. The pharmacokinetics chapter deals with the kinetics of the one- and two-compartment models, nonlinear kinetics, and multiple dosing. Some numerical examples are given, but no worked problems.

A chapter on drug interactions precedes an expanded discussion on relationships between drug levels and pharmacological effects. Topics include plasma level–effect relationships of chemotherapeutic agents, chlorpromazine, anticonvulsants, tricyclic antidepressants, and β-blocking agents. Dosage adjustment of antibiotics in patients with renal failure is included as an appendix. Although addressed to antibiotics in particular, the arguments presented there apply equally to all drugs whose effect is related to circulating levels and whose elimination is dependent wholly or partially on kidney function. The very brief treatment afforded this subject is probably justified in view of its extensive coverage by other authors.

In the reviewer's opinion, the book is a useful undergraduate teaching aid for students in pharmacy, pharmacology, medicine, and other related health disciplines and provides sufficient references for further indepth reading in specific subject areas.

Reviewed by Peter G. Welling
School of Pharmacy
University of Wisconsin
Madison, WI 53706

Medicinal Chemistry V. Proceedings of the 5th International Symposium on Medicinal Chemistry. Paris, July 19–22, 1976. Edited by J. MATHIEU. Elsevier Scientific, 52 Vanderbilt Ave., New York, NY 10017. 1977. 456 pp. 17 × 25 cm. Price $52.95.

This volume presents the proceedings of the Fifth International Symposium on Medicinal Chemistry, Paris, July 19–22, 1976. Four types of articles are included: main lectures on fundamental subjects by academicians, brief applied lectures by pharmaceutical industrial researchers, round-table discussion of strategy in drug research directed by Professor E. J. Ariens of Nijmegen, and some miscellaneous topics. The program of the symposium also included poster sessions organized by Professor C. G. Wermuth of Strasbourg.

The main subjects range from the fields of peptides, prodrugs, the central nervous system, cardiovascular agents, and immunology to the fields of organic synthesis, the Hansch approach to drug design, and prevention of aging.

Hypothalamic regulatory hormones and their synthetic analogs are concisely discussed with emphasis on the latest developments in research on synthetic studies and structure–activity relationships. This review was authored by numerous collaborators headed by Nobel Laureate A. V. Schally.

The section on peptides also contains reviews on the identity and mode of action of hypothalamic hypophysiotropic hormones, diverse roles of hypothalamic regulatory peptides, synthetic methodology of bioactive peptides, approaches of peptide chemistry to insulin, and synthesis in the field of 1–34 human parathyroid hormone fragments.

The section on prodrugs begins with A. J. Glazko's presentation of his personal experiences in this area over the last 25 years. This presentation reviews studies of factors affecting metabolic disposition of chloramphenicol and some of its derivatives, 4,4-diacetyldiaminodiphenylsulfone (DADDS), adenine arabinoside, araadenosine monophosphate, and prophenytoin. The second review of this section is on modulation of distribution of efficacy of prodrugs. This discussion is a very interesting review of the conception and synthesis of prodrugs on the basis of metabolic pathways and structure–activity correlation using Hansch's approach.

The third article is on long-chain esters of pipotiazine as long-acting psychotropic prodrugs; these prodrugs are supposed to assure a beneficial continuity in drug distribution at the target level with smaller doses administered by injection than those required by the oral route to achieve the same therapeutic effect. The subsequent review summarizes k_{cat} inhibitors as a new class of enzyme proinhibitors. Finally, this section concludes with an article titled Pro-drugs, Protective Groups and the Medicinal Chemist summarizing that it is possible to design prodrugs on a rational basis.

The section dealing with the central nervous system is in itself a major contribution to the literature of medicinal chemistry and pharmacology. The key article is on brain neurotransmitters and drug receptors and it contains valuable discussions of principles of methodology, the dopamine receptor, antischizophrenic agents, prediction of extrapyramidal and autonomic side effects, and a two-state model of the dopamine receptor. Thereafter, neural inhibition as a tool for research of anticonvulsants is the theme for the discussion of γ-aminobutyric acid, taurine, and glycine. The third paper of this section summarizes recent approaches in psychochemotherapy, including the biochemical classification of antidepressants and stereochemical classifications.

The next presentation is on the effects of neuroleptics on dopamine metabolism in the nigroneostriatal, mesolimbic, and mesocortical dopaminergic systems. Piracetam is characterized as a nootropic agent in the following article. It is noted that this drug does not fit any of the

classical categories of psychotropic agents but has a positive effect on brain integrative mechanism without affecting limbic and reticular excitability; hence, it is assumed that functional telencephalic selectivity is involved, and on this basis piracetam is characterized as a "nootropic" agent because it affects noetic functions.

The topics on the central nervous system conclude with a discussion of a novel series of annelated benzodiazepines. Noticing that the imine function is not the principal site of metabolism of the benzodiazepines, it was rationalized that appropriate annelations might render the imine function more susceptible to metabolism and inactivation. Some of the compounds reported herein show interesting pharmacological properties.

Cardiovascular agents are reviewed from various standpoints: inhibitors of the renin–angiotensin system, new prospects in coronary theory, β-adrenergic antagonists, and central sites of action in the development of antihypertensive drugs.

The contribution of immunology to medicinal chemistry is the theme of the discussion of natural and synthetic immunostimulants related to the mycobacterial cell wall, immunopharmacology and immunotherapy of residual disease in cancer patients, and the biochemistry of thymic hormones.

Gerontology is surveyed in three articles. First, the pharmaceutical research aspects include illustrations of how biological aging can be studied experimentally and discussion of pharmaceutical aspects of aging based on age-associated deficiencies. Second, molecular and cellular mechanisms of aging of intercellular matrix are outlined. The third paper is organized on the basis of four categories: evidence that free radicals are involved in pathological processes occurring upon exposure to high oxidative stress, evidence that free radicals are involved in normal and abnormal cellular processes under conditions of normal oxidative stress, reactions of radicals expected to proceed *in vivo*, and speculation about the role of radical reactions in human aging and carcinogenesis.

The synthetic methodology included in this volume is another significant contribution to medicinal chemistry; *i.e.*, it emphasizes silyl enol ethers, the transformation of carboxylic acids to heterocycles, and new methods applied to the synthesis of natural products.

The round-table discussion of strategy in drug research is the final section. This discussion proved to be very fruitful because it included, among other topics: a manual method for applying the Hansch approach to drug design, correlation studies with antimycotics and fungicides of the azole group, and a strategy for the design of potent hormones. This section effectively concluded the symposium and provides an excellent finale to an excellent volume.

This reviewer recommends this book to every medicinal chemist and pharmacologist. The coverage of the topics noted is adequate and can serve as the basis for further research of the current literature.

Reviewed by Jaime N. Delgado
College of Pharmacy
University of Texas
Austin, TX 78712

Analytical Profiles of Drug Substances, Vol. 6. Edited by KLAUS FLOREY *et al.* Academic, 111 Fifth Ave., New York, NY 10003. 1977. 16 × 23.5 cm. ix + 600 pp. Price $27.50.

This book is the sixth (although erroneously referred to in the Preface as the fifth) in a series of monograph compilations under the sponsorship of the Pharmaceutical Analysis and Control Section of the APhA Academy of Pharmaceutical Sciences. The objective of this series is to provide, in a single source, information about drug substances not ordinarily included in the official compendia and which may not always be readily retrievable from the literature. The official compendia generally contain tests and specifications for drugs and drug products related to identity, purity, quality, and strength plus other information of greater value to the practitioner than to the pharmaceutical scientist.

In this series, each drug profile presents useful data in the following categories: description, physical properties, synthesis or method of manufacture, stability and degradation, metabolism and pharmacokinetics, analytical methods, and literature references. Included under physical properties are spectral data, melting characteristics, solubility data, crystal properties, and solution characteristics. Analytical methods are thoroughly reviewed and encompass colorimetry, spectrophotometry, fluorometry, titrimetry, chromatography, polarography, coulometry, and also microbiological methods where applicable. Identification tests and elemental analyses are also included. Of particular significance are analytical methods applicable to the drug substance and its metabolities in body fluids.

As noted for the previous volumes, each drug profile is well organized and is presented in a systematic and uniform manner. Each profile is introduced by a table of contents. It would be helpful if each entry of the table of contents were page referenced. This table is followed in orderly sequence by each category covered for that particular drug. The monograph is concluded by a listing of quoted references which, in most cases, is extensive and comprehensive. As is true with the previous volumes of this series, this one is printed clearly and is replete with tables, figures, and graphical presentations. Space is used economically and to maximum advantage.

Volume 6 contains 17 drug profiles which brings to a total of 114 the number of drugs for which profiles are now available. An excellent format has been developed for the presentation of the "vital statistics" on drugs, and hopefully a pattern has been established for a continuous flow of monographs for drug substances currently in the marketplace, drugs in the process of development, and drugs yet to be discovered. Pharmaceutical scientists are reminded of the Editor's standing invitation for the contribution of monographs of drugs in which they have an interest. The continued success of this series will depend on such participation.

"Analytical Profiles" serves well as a companion volume to the official compendia and is an essential addition to the library of those engaged in pharmaceutical research.

Reviewed by Martin I. Blake
College of Pharmacy
University of Illinois
Chicago, IL 60612

NOTICES

Findings of Drug Abuse Research. Vols. 1 and 2. NIDA Research Monograph 1. National Institute on Drug Abuse, 11400 Rockville Pike, Rockville, MD 20852. 1975. 20 × 27 cm. Price $7.00, Vol. 1; $5.05, Vol. 2. Available from Superintendent of Documents, U.S. Government of Printing Office, Washington, DC 20402.

The Epidemiology of Drug Abuse: Current Issues. NIDA Research Monograph 10. Edited by LOUISE G. RICHARDS and LOUISE B. BLEVENS. National Institute on Drug Abuse, 11400 Rockville Pike, Rockville, MD 20852. 1977. 259 pp. 15 × 24 cm. Price $2.60.

Cholesterol. By JOHN R. SABINE. Dekker, 270 Madison Ave., New York, NY 10016. 1977. 489 pp. 15 × 23 cm. Price $25.00.

Immunology Of The Gut. Ciba Foundation Symposium 46 (new series). Elsevier North-Holland, 52 Vanderbilt Ave., New York, NY 10017. 1977. 376 pp. 7 × 25 cm.

Antifungal Compounds. Vol. 1. Edited by MALCOLM R. SIEGEL and HUGH D. SISLER. Dekker, 270 Madison Ave., New York, NY 10016. 1977. 600 pp. 15 × 23 cm. Price $55.00.

Environmental Cancer. Advances in Modern Toxicology Vol. 3. Edited by H. F. KRAYBILL and MYRON A. MEHLMAN. Wiley, 605 Third Ave., New York, NY 10016. 1977. 388 pp. 15 × 23 cm. Price $24.50.

Immunology: A Programmed Text. By J. WAYNE STREILEIN and JOHN D. HUGHES. Little Brown, 34 Beacon St., Boston, MA 02106. 1977. 337 pp. 21 × 28 cm.

Rational Management of Diabetes. By HABEEB BACCHUS. University Park Press, Chamber of Commerce Bldg., Baltimore, MD 21202. 1977. 221 pp. 15 × 23 cm. Price $16.50.

The Fetus and Birth. Ciba Foundation Sympsium 47 (new series). Elsevier Scientific, 52 Vanderbilt Ave., New York, NY 10017. 1977. 481 pp. 17 × 25 cm.

Psychopharmacology: A Biochemical and Behavioral Approach. By LEWIS S. SEIDEN and LINDA A. DYKSTRA. Van Nostrand Reinhold, 450 W. 33rd St., New York, NY 10001. 1977. 451 pp. 15 × 23 cm. Price $19.95.

Reagents for Organic Synthesis. Vol. 6. By MARY FIESER and LOUIS F. FIESER. Wiley, 605 Third Ave., New York, NY 10016. 1977. 765 pp. 15 × 23 cm. Price $29.50.

An Introduction to Clay Colloid Chemistry. 2nd Ed. By H. van OLPHEN. Wiley, 605 Third Ave., New York, NY 10016. 1977. 318 pp. 15 × 23 cm. Price $21.50.

classical categories of psychotropic agents but has a positive effect on brain integrative mechanism without affecting limbic and reticular excitability; hence, it is assumed that functional telencephalic selectivity is involved, and on this basis piracetam is characterized as a "nootropic" agent because it affects noetic functions.

The topics on the central nervous system conclude with a discussion of a novel series of annelated benzodiazepines. Noticing that the imine function is not the principal site of metabolism of the benzodiazepines, it was rationalized that appropriate annelations might render the imine function more susceptible to metabolism and inactivation. Some of the compounds reported herein show interesting pharmacological properties.

Cardiovascular agents are reviewed from various standpoints: inhibitors of the renin–angiotensin system, new prospects in coronary theory, β-adrenergic antagonists, and central sites of action in the development of antihypertensive drugs.

The contribution of immunology to medicinal chemistry is the theme of the discussion of natural and synthetic immunostimulants related to the mycobacterial cell wall, immunopharmacology and immunotherapy of residual disease in cancer patients, and the biochemistry of thymic hormones.

Gerontology is surveyed in three articles. First, the pharmaceutical research aspects include illustrations of how biological aging can be studied experimentally and discussion of pharmaceutical aspects of aging based on age-associated deficiencies. Second, molecular and cellular mechanisms of aging of intercellular matrix are outlined. The third paper is organized on the basis of four categories: evidence that free radicals are involved in pathological processes occurring upon exposure to high oxidative stress, evidence that free radicals are involved in normal and abnormal cellular processes under conditions of normal oxidative stress, reactions of radicals expected to proceed *in vivo*, and speculation about the role of radical reactions in human aging and carcinogenesis.

The synthetic methodology included in this volume is another significant contribution to medicinal chemistry; *i.e.*, it emphasizes silyl enol ethers, the transformation of carboxylic acids to heterocycles, and new methods applied to the synthesis of natural products.

The round-table discussion of strategy in drug research is the final section. This discussion proved to be very fruitful because it included, among other topics: a manual method for applying the Hansch approach to drug design, correlation studies with antimycotics and fungicides of the azole group, and a strategy for the design of potent hormones. This section effectively concluded the symposium and provides an excellent finale to an excellent volume.

This reviewer recommends this book to every medicinal chemist and pharmacologist. The coverage of the topics noted is adequate and can serve as the basis for further research of the current literature.

Reviewed by Jaime N. Delgado
College of Pharmacy
University of Texas
Austin, TX 78712

Analytical Profiles of Drug Substances, Vol. 6. Edited by KLAUS FLOREY *et al.* Academic, 111 Fifth Ave., New York, NY 10003. 1977. 16 × 23.5 cm. ix + 600 pp. Price $27.50.

This book is the sixth (although erroneously referred to in the Preface as the fifth) in a series of monograph compilations under the sponsorship of the Pharmaceutical Analysis and Control Section of the APhA Academy of Pharmaceutical Sciences. The objective of this series is to provide, in a single source, information about drug substances not ordinarily included in the official compendia and which may not always be readily retrievable from the literature. The official compendia generally contain tests and specifications for drugs and drug products related to identity, purity, quality, and strength plus other information of greater value to the practitioner than to the pharmaceutical scientist.

In this series, each drug profile presents useful data in the following categories: description, physical properties, synthesis or method of manufacture, stability and degradation, metabolism and pharmacokinetics, analytical methods, and literature references. Included under physical properties are spectral data, melting characteristics, solubility data, crystal properties, and solution characteristics. Analytical methods are thoroughly reviewed and encompass colorimetry, spectrophotometry, fluorometry, titrimetry, chromatography, polarography, coulometry, and also microbiological methods where applicable. Identification tests and elemental analyses are also included. Of particular significance are analytical methods applicable to the drug substance and its metabolities in body fluids.

As noted for the previous volumes, each drug profile is well organized and is presented in a systematic and uniform manner. Each profile is introduced by a table of contents. It would be helpful if each entry of the table of contents were page referenced. This table is followed in orderly sequence by each category covered for that particular drug. The monograph is concluded by a listing of quoted references which, in most cases, is extensive and comprehensive. As is true with the previous volumes of this series, this one is printed clearly and is replete with tables, figures, and graphical presentations. Space is used economically and to maximum advantage.

Volume 6 contains 17 drug profiles which brings to a total of 114 the number of drugs for which profiles are now available. An excellent format has been developed for the presentation of the "vital statistics" on drugs, and hopefully a pattern has been established for a continuous flow of monographs for drug substances currently in the marketplace, drugs in the process of development, and drugs yet to be discovered. Pharmaceutical scientists are reminded of the Editor's standing invitation for the contribution of monographs of drugs in which they have an interest. The continued success of this series will depend on such participation.

"Analytical Profiles" serves well as a companion volume to the official compendia and is an essential addition to the library of those engaged in pharmaceutical research.

Reviewed by Martin I. Blake
College of Pharmacy
University of Illinois
Chicago, IL 60612

NOTICES

Findings of Drug Abuse Research. Vols. 1 and 2. NIDA Research Monograph 1. National Institute on Drug Abuse, 11400 Rockville Pike, Rockville, MD 20852. 1975. 20 × 27 cm. Price $7.00, Vol. 1; $5.05, Vol. 2. Available from Superintendent of Documents, U.S. Government of Printing Office, Washington, DC 20402.

The Epidemiology of Drug Abuse: Current Issues. NIDA Research Monograph 10. Edited by LOUISE G. RICHARDS and LOUISE B. BLEVENS. National Institute on Drug Abuse, 11400 Rockville Pike, Rockville, MD 20852. 1977. 259 pp. 15 × 24 cm. Price $2.60.

Cholesterol. By JOHN R. SABINE. Dekker, 270 Madison Ave., New York, NY 10016. 1977. 489 pp. 15 × 23 cm. Price $25.00.

Immunology Of The Gut. Ciba Foundation Symposium 46 (new series). Elsevier North-Holland, 52 Vanderbilt Ave., New York, NY 10017. 1977. 376 pp. 7 × 25 cm.

Antifungal Compounds. Vol. 1. Edited by MALCOLM R. SIEGEL and HUGH D. SISLER. Dekker, 270 Madison Ave., New York, NY 10016. 1977. 600 pp. 15 × 23 cm. Price $55.00.

Environmental Cancer. Advances in Modern Toxicology Vol. 3. Edited by H. F. KRAYBILL and MYRON A. MEHLMAN. Wiley, 605 Third Ave., New York, NY 10016. 1977. 388 pp. 15 × 23 cm. Price $24.50.

Immunology: A Programmed Text. By J. WAYNE STREILEIN and JOHN D. HUGHES. Little Brown, 34 Beacon St., Boston, MA 02106. 1977. 337 pp. 21 × 28 cm.

Rational Management of Diabetes. By HABEEB BACCHUS. University Park Press, Chamber of Commerce Bldg., Baltimore, MD 21202. 1977. 221 pp. 15 × 23 cm. Price $16.50.

The Fetus and Birth. Ciba Foundation Sympsium 47 (new series). Elsevier Scientific, 52 Vanderbilt Ave., New York, NY 10017. 1977. 481 pp. 17 × 25 cm.

Psychopharmacology: A Biochemical and Behavioral Approach. By LEWIS S. SEIDEN and LINDA A. DYKSTRA. Van Nostrand Reinhold, 450 W. 33rd St., New York, NY 10001. 1977. 451 pp. 15 × 23 cm. Price $19.95.

Reagents for Organic Synthesis. Vol. 6. By MARY FIESER and LOUIS F. FIESER. Wiley, 605 Third Ave., New York, NY 10016. 1977. 765 pp. 15 × 23 cm. Price $29.50.

An Introduction to Clay Colloid Chemistry. 2nd Ed. By H. van OLPHEN. Wiley, 605 Third Ave., New York, NY 10016. 1977. 318 pp. 15 × 23 cm. Price $21.50.

classical categories of psychotropic agents but has a positive effect on brain integrative mechanism without affecting limbic and reticular excitability; hence, it is assumed that functional telencephalic selectivity is involved, and on this basis piracetam is characterized as a "nootropic" agent because it affects noetic functions.

The topics on the central nervous system conclude with a discussion of a novel series of annelated benzodiazepines. Noticing that the imine function is not the principal site of metabolism of the benzodiazepines, it was rationalized that appropriate annelations might render the imine function more susceptible to metabolism and inactivation. Some of the compounds reported herein show interesting pharmacological properties.

Cardiovascular agents are reviewed from various standpoints: inhibitors of the renin–angiotensin system, new prospects in coronary theory, β-adrenergic antagonists, and central sites of action in the development of antihypertensive drugs.

The contribution of immunology to medicinal chemistry is the theme of the discussion of natural and synthetic immunostimulants related to the mycobacterial cell wall, immunopharmacology and immunotherapy of residual disease in cancer patients, and the biochemistry of thymic hormones.

Gerontology is surveyed in three articles. First, the pharmaceutical research aspects include illustrations of how biological aging can be studied experimentally and discussion of pharmaceutical aspects of aging based on age-associated deficiencies. Second, molecular and cellular mechanisms of aging of intercellular matrix are outlined. The third paper is organized on the basis of four categories: evidence that free radicals are involved in pathological processes occurring upon exposure to high oxidative stress, evidence that free radicals are involved in normal and abnormal cellular processes under conditions of normal oxidative stress, reactions of radicals expected to proceed *in vivo*, and speculation about the role of radical reactions in human aging and carcinogenesis.

The synthetic methodology included in this volume is another significant contribution to medicinal chemistry; *i.e.*, it emphasizes silyl enol ethers, the transformation of carboxylic acids to heterocycles, and new methods applied to the synthesis of natural products.

The round-table discussion of strategy in drug research is the final section. This discussion proved to be very fruitful because it included, among other topics: a manual method for applying the Hansch approach to drug design, correlation studies with antimycotics and fungicides of the azole group, and a strategy for the design of potent hormones. This section effectively concluded the symposium and provides an excellent finale to an excellent volume.

This reviewer recommends this book to every medicinal chemist and pharmacologist. The coverage of the topics noted is adequate and can serve as the basis for further research of the current literature.

Reviewed by Jaime N. Delgado
College of Pharmacy
University of Texas
Austin, TX 78712

Analytical Profiles of Drug Substances, Vol. 6. Edited by KLAUS FLOREY *et al.* Academic, 111 Fifth Ave., New York, NY 10003. 1977. 16 × 23.5 cm. ix + 600 pp. Price $27.50.

This book is the sixth (although erroneously referred to in the Preface as the fifth) in a series of monograph compilations under the sponsorship of the Pharmaceutical Analysis and Control Section of the APhA Academy of Pharmaceutical Sciences. The objective of this series is to provide, in a single source, information about drug substances not ordinarily included in the official compendia and which may not always be readily retrievable from the literature. The official compendia generally contain tests and specifications for drugs and drug products related to identity, purity, quality, and strength plus other information of greater value to the practitioner than to the pharmaceutical scientist.

In this series, each drug profile presents useful data in the following categories: description, physical properties, synthesis or method of manufacture, stability and degradation, metabolism and pharmacokinetics, analytical methods, and literature references. Included under physical properties are spectral data, melting characteristics, solubility data, crystal properties, and solution characteristics. Analytical methods are thoroughly reviewed and encompass colorimetry, spectrophotometry, fluorometry, titrimetry, chromatography, polarography, coulometry, and also microbiological methods where applicable. Identification tests and elemental analyses are also included. Of particular significance are analytical methods applicable to the drug substance and its metabolities in body fluids.

As noted for the previous volumes, each drug profile is well organized and is presented in a systematic and uniform manner. Each profile is introduced by a table of contents. It would be helpful if each entry of the table of contents were page referenced. This table is followed in orderly sequence by each category covered for that particular drug. The monograph is concluded by a listing of quoted references which, in most cases, is extensive and comprehensive. As is true with the previous volumes of this series, this one is printed clearly and is replete with tables, figures, and graphical presentations. Space is used economically and to maximum advantage.

Volume 6 contains 17 drug profiles which brings to a total of 114 the number of drugs for which profiles are now available. An excellent format has been developed for the presentation of the "vital statistics" on drugs, and hopefully a pattern has been established for a continuous flow of monographs for drug substances currently in the marketplace, drugs in the process of development, and drugs yet to be discovered. Pharmaceutical scientists are reminded of the Editor's standing invitation for the contribution of monographs of drugs in which they have an interest. The continued success of this series will depend on such participation.

"Analytical Profiles" serves well as a companion volume to the official compendia and is an essential addition to the library of those engaged in pharmaceutical research.

Reviewed by Martin I. Blake
College of Pharmacy
University of Illinois
Chicago, IL 60612

NOTICES

Findings of Drug Abuse Research. Vols. 1 and 2. NIDA Research Monograph 1. National Institute on Drug Abuse, 11400 Rockville Pike, Rockville, MD 20852. 1975. 20 × 27 cm. Price $7.00, Vol. 1; $5.05, Vol. 2. Available from Superintendent of Documents, U.S. Government of Printing Office, Washington, DC 20402.

The Epidemiology of Drug Abuse: Current Issues. NIDA Research Monograph 10. Edited by LOUISE G. RICHARDS and LOUISE B. BLEVENS. National Institute on Drug Abuse, 11400 Rockville Pike, Rockville, MD 20852. 1977. 259 pp. 15 × 24 cm. Price $2.60.

Cholesterol. By JOHN R. SABINE. Dekker, 270 Madison Ave., New York, NY 10016. 1977. 489 pp. 15 × 23 cm. Price $25.00.

Immunology Of The Gut. Ciba Foundation Symposium 46 (new series). Elsevier North-Holland, 52 Vanderbilt Ave., New York, NY 10017. 1977. 376 pp. 7 × 25 cm.

Antifungal Compounds. Vol. 1. Edited by MALCOLM R. SIEGEL and HUGH D. SISLER. Dekker, 270 Madison Ave., New York, NY 10016. 1977. 600 pp. 15 × 23 cm. Price $55.00.

Environmental Cancer. Advances in Modern Toxicology Vol. 3. Edited by H. F. KRAYBILL and MYRON A. MEHLMAN. Wiley, 605 Third Ave., New York, NY 10016. 1977. 388 pp. 15 × 23 cm. Price $24.50.

Immunology: A Programmed Text. By J. WAYNE STREILEIN and JOHN D. HUGHES. Little Brown, 34 Beacon St., Boston, MA 02106. 1977. 337 pp. 21 × 28 cm.

Rational Management of Diabetes. By HABEEB BACCHUS. University Park Press, Chamber of Commerce Bldg., Baltimore, MD 21202. 1977. 221 pp. 15 × 23 cm. Price $16.50.

The Fetus and Birth. Ciba Foundation Sympsium 47 (new series). Elsevier Scientific, 52 Vanderbilt Ave., New York, NY 10017. 1977. 481 pp. 17 × 25 cm.

Psychopharmacology: A Biochemical and Behavioral Approach. By LEWIS S. SEIDEN and LINDA A. DYKSTRA. Van Nostrand Reinhold, 450 W. 33rd St., New York, NY 10001. 1977. 451 pp. 15 × 23 cm. Price $19.95.

Reagents for Organic Synthesis. Vol. 6. By MARY FIESER and LOUIS F. FIESER. Wiley, 605 Third Ave., New York, NY 10016. 1977. 765 pp. 15 × 23 cm. Price $29.50.

An Introduction to Clay Colloid Chemistry. 2nd Ed. By H. van OLPHEN. Wiley, 605 Third Ave., New York, NY 10016. 1977. 318 pp. 15 × 23 cm. Price $21.50.

APRIL 1978
VOLUME 67 NUMBER 4

JOURNAL OF PHARMACEUTICAL SCIENCES

MARY H. FERGUSON
Editor

SHELLY ELLIOTT
Production Editor

JANET D. SHOFF
Copy Editor

EDWARD G. FELDMANN
Contributing Editor

SAMUEL W. GOLDSTEIN
Contributing Editor

BELLE R. BECK
Editorial Secretary

DAVID BOHARDT
Director of Publications

L. LUAN CORRIGAN
Assistant Director of Publications

EDITORIAL ADVISORY BOARD

JOHN AUTIAN
NORMAN R. FARNSWORTH
WILLIAM O. FOYE
WILLIAM J. JUSKO
HERBERT A. LIEBERMAN
DAVID E. MANN, JR.
GERALD J. PAPARIELLO
EDWARD G. RIPPIE

The *Journal of Pharmaceutical Sciences* is published monthly by the American Pharmaceutical Association at 2215 Constitution Ave., N.W., Washington, DC 20037. Second-class postage paid at Washington, D.C., and at additional mailing office.

All expressions of opinion and statements of supposed fact appearing in articles or editorials carried in this journal are published on the authority of the writer over whose name they appear and are not to be regarded as necessarily expressing the policies or views of the American Pharmaceutical Association.

Offices—Editorial, Advertising, and Subscription Offices: 2215 Constitution Ave., N.W., Washington, DC 20037. Printing Offices: 20th & Northampton Streets, Easton, PA 18042.

Annual Subscriptions—United States and foreign, industrial and government institutions $50, educational institutions $50, individuals *for personal use only* $30; single copies $5. All foreign subscriptions add $5 for postage. Subscription rates are subject to change without notice. Members of the American Pharmaceutical Association may elect to receive the *Journal of Pharmaceutical Sciences* as a part of their annual $70 (foreign $75) APhA membership dues.

Claims—Missing numbers will not be supplied if dues or subscriptions are in arrears for more than 60 days or if claims are received more than 60 days after the date of the issue, or if loss was due to failure to give notice of change of address. The Association cannot accept responsibility for foreign delivery when its records indicate shipment has been made.

Change of Address—Members and subscribers should notify at once both the Post Office and the American Pharmaceutical Association, 2215 Constitution Ave., N.W., Washington, DC 20037, of any change of address.

Microfilm—Microfilm volumes are available from University Microfilms International, 300 N. Zeeb Road, Ann Arbor, MI 48106.

© Copyright 1978, American Pharmaceutical Association, 2215 Constitution Ave., N.W., Washington, DC 20037; all rights reserved.

FRUITLESS NUMBERS GAMES

"At least five," stated one of the group.

"No, no! There could be no more than two," said another.

"You're both wrong," exclaimed a third. "I'm sure that there could be at least five archangels and as many as twenty ordinary type angels!"

With only a bit of imagination and paraphrasing, the above represents the sort of absurdity that took place in arguments among certain theologians during the middle ages. In discussing the attributes of angels, a common point of dispute was how many such spirits could dance at the same time on the head of a pin.

We are reminded of that story every time we hear comments about the so-called "drug lag." Some say it involves this many drugs, while some others say it's half that number and yet others will say it's twice that number. Moreover, at other times, the issue will be argued not in terms of numbers of drugs but in terms of time; for example, that new drug introductions in the United States are a certain number of months behind one country or another with comparable controversy as to whether that estimated time period is overstated or understated.

Statistics pertaining to new drug introductions are very valuable and serve many useful purposes. However, we are of the opinion that their use or application in an effort to prove or disprove the so-called "drug lag" is unfortunate. In our opinion, the question of whether or not there is a drug lag is academic. What really matters is what has been the effect, if any, on health care in the United States.

But it seems that everyone wants to play "the numbers game" in one form or another. Industry representatives and academicians have been doing so repeatedly for at least the past five years. Even the present Commissioner of the Food and Drug Administration seems to have slipped—if not fallen—into that same morass.

In an article over his byline, which appeared in the January 30 issue of the *Journal of the American Medical Association*, FDA Commissioner Donald Kennedy addresses the subject under the title "A Calm Look at 'Drug Lag.' " He starts out by appearing to reject the numbers approach, but then proceeds to draw upon it himself in his effort to defend FDA's record. Predictably, the Pharmaceutical Manufacturers Association, as the principal critic of FDA's performance in the processing of new drug approvals, gave the article poor marks in its initial reaction. And, since Dr. Kennedy chose to buttress his position using the statistical approach, such criticism may have been deserved.

Our own personal view is that a drug lag does exist, and this fact should be conceded without further dispute. But we also believe that—with regard to this subject—it is senseless to haggle over numbers.

In the area of new drug approvals, the drug regulatory process is intended to keep from the market any and all agents until an appropriate determination has been made as to each agent's safety and effectiveness. Hence, the only questions that matter are twofold:

(*a*) Has FDA permitted drugs to be marketed that lack sufficient proof of safety and effectiveness?

(*b*) Has FDA unduly withheld drugs from the market for which adequate evidence has been provided as to their safety and effectiveness?

Whether such agents are permitted to be marketed in some foreign country or another is irrelevant and should not be a factor in assessing either FDA performance or the appropriateness of the drug armamentarium available to health-care practitioners for treating patients in the United States. The sooner everyone can get away from playing the numbers game, the sooner we shall be able to make a meaningful assessment of where this nation stands with respect to the adequacy of drugs approved for marketing.

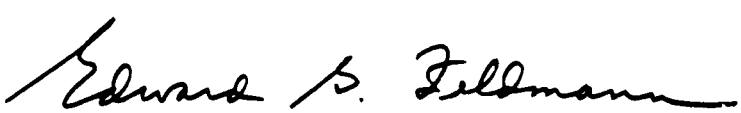

APRIL 1978
VOLUME 67 NUMBER 4

JOURNAL OF PHARMACEUTICAL SCIENCES

MARY H. FERGUSON
Editor

SHELLY ELLIOTT
Production Editor

JANET D. SHOFF
Copy Editor

EDWARD G. FELDMANN
Contributing Editor

SAMUEL W. GOLDSTEIN
Contributing Editor

BELLE R. BECK
Editorial Secretary

DAVID BOHARDT
Director of Publications

L. LUAN CORRIGAN
Assistant Director of Publications

EDITORIAL ADVISORY BOARD

JOHN AUTIAN
NORMAN R. FARNSWORTH
WILLIAM O. FOYE
WILLIAM J. JUSKO
HERBERT A. LIEBERMAN
DAVID E. MANN, JR.
GERALD J. PAPARIELLO
EDWARD G. RIPPIE

The *Journal of Pharmaceutical Sciences* is published monthly by the American Pharmaceutical Association at 2215 Constitution Ave., N.W., Washington, DC 20037. Second-class postage paid at Washington, D.C., and at additional mailing office.

All expressions of opinion and statements of supposed fact appearing in articles or editorials carried in this journal are published on the authority of the writer over whose name they appear and are not to be regarded as necessarily expressing the policies or views of the American Pharmaceutical Association.

Offices—Editorial, Advertising, and Subscription Offices: 2215 Constitution Ave., N.W., Washington, DC 20037. Printing Offices: 20th & Northampton Streets, Easton, PA 18042.

Annual Subscriptions—United States and foreign, industrial and government institutions $50, educational institutions $50, individuals *for personal use only* $30; single copies $5. All foreign subscriptions add $5 for postage. Subscription rates are subject to change without notice. Members of the American Pharmaceutical Association may elect to receive the *Journal of Pharmaceutical Sciences* as a part of their annual $70 (foreign $75) APhA membership dues.

Claims—Missing numbers will not be supplied if dues or subscriptions are in arrears for more than 60 days or if claims are received more than 60 days after the date of the issue, or if loss was due to failure to give notice of change of address. The Association cannot accept responsibility for foreign delivery when its records indicate shipment has been made.

Change of Address—Members and subscribers should notify at once both the Post Office and the American Pharmaceutical Association, 2215 Constitution Ave., N.W., Washington, DC 20037, of any change of address.

Microfilm—Microfilm volumes are available from University Microfilms International, 300 N. Zeeb Road, Ann Arbor, MI 48106.

© Copyright 1978, American Pharmaceutical Association, 2215 Constitution Ave., N.W., Washington, DC 20037; all rights reserved.

FRUITLESS NUMBERS GAMES

"At least five," stated one of the group.

"No, no! There could be no more than two," said another.

"You're both wrong," exclaimed a third. "I'm sure that there could be at least five archangels and as many as twenty ordinary type angels!"

With only a bit of imagination and paraphrasing, the above represents the sort of absurdity that took place in arguments among certain theologians during the middle ages. In discussing the attributes of angels, a common point of dispute was how many such spirits could dance at the same time on the head of a pin.

We are reminded of that story every time we hear comments about the so-called "drug lag." Some say it involves this many drugs, while some others say it's half that number and yet others will say it's twice that number. Moreover, at other times, the issue will be argued not in terms of numbers of drugs but in terms of time; for example, that new drug introductions in the United States are a certain number of months behind one country or another with comparable controversy as to whether that estimated time period is overstated or understated.

Statistics pertaining to new drug introductions are very valuable and serve many useful purposes. However, we are of the opinion that their use or application in an effort to prove or disprove the so-called "drug lag" is unfortunate. In our opinion, the question of whether or not there is a drug lag is academic. What really matters is what has been the effect, if any, on health care in the United States.

But it seems that everyone wants to play "the numbers game" in one form or another. Industry representatives and academicians have been doing so repeatedly for at least the past five years. Even the present Commissioner of the Food and Drug Administration seems to have slipped—if not fallen—into that same morass.

In an article over his byline, which appeared in the January 30 issue of the *Journal of the American Medical Association*, FDA Commissioner Donald Kennedy addresses the subject under the title "A Calm Look at 'Drug Lag.' " He starts out by appearing to reject the numbers approach, but then proceeds to draw upon it himself in his effort to defend FDA's record. Predictably, the Pharmaceutical Manufacturers Association, as the principal critic of FDA's performance in the processing of new drug approvals, gave the article poor marks in its initial reaction. And, since Dr. Kennedy chose to buttress his position using the statistical approach, such criticism may have been deserved.

Our own personal view is that a drug lag does exist, and this fact should be conceded without further dispute. But we also believe that—with regard to this subject—it is senseless to haggle over numbers.

In the area of new drug approvals, the drug regulatory process is intended to keep from the market any and all agents until an appropriate determination has been made as to each agent's safety and effectiveness. Hence, the only questions that matter are twofold:

(*a*) Has FDA permitted drugs to be marketed that lack sufficient proof of safety and effectiveness?

(*b*) Has FDA unduly withheld drugs from the market for which adequate evidence has been provided as to their safety and effectiveness?

Whether such agents are permitted to be marketed in some foreign country or another is irrelevant and should not be a factor in assessing either FDA performance or the appropriateness of the drug armamentarium available to health-care practitioners for treating patients in the United States. The sooner everyone can get away from playing the numbers game, the sooner we shall be able to make a meaningful assessment of where this nation stands with respect to the adequacy of drugs approved for marketing.

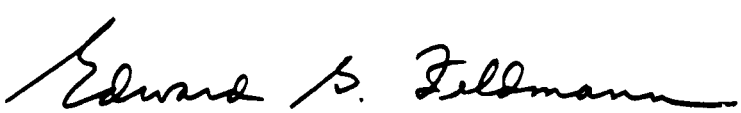

Drug Adsorption by Activated Charcoal

In reference to the recent article "Comparative Drug Adsorption by Activated Charcoal"[1], which appeared in this Journal, I have failed to understand the relevance of Ref. 12. The reference was cited as an explanation for potential errors in the determination of K values in a Langmuir equation. I have found that the reference cited discusses the nonaqueous titration methods for the quantitative determinations of promazine and chlorpromazine. Perhaps the authors can correct this error.

V. Das Gupta
Department of Pharmaceutics
College of Pharmacy
University of Houston
Houston, TX 77004

Received February 21, 1978.

[1] E. M. Sellers, V. Khouw, and L. Dolman, *J. Pharm. Sci.*, **66**, 1640 (1977).

Cytotoxic Agents from Bursera klugii

In the June 1977 issue of the Journal, an article entitled "Cytotoxic Agents from *Bursera klugii* (Burseraceae) I: Isolation of Sapelins A and B" appeared[1]. Since the time of publication, the plant has been reidentified by Dr. Robert E. Perdue and Dr. Arthur S. Barclay of the Beltsville Agricultural Research Center, U.S. Department of Agriculture, Beltsville, Md., as *Trichilia hispida* Penning. ined. (Meliaceae).

Jack R. Cole
College of Pharmacy
University of Arizona
Tucson, AZ 85721

Received December 23, 1977.

[1] S. D. Jolad, R. M. Wiedhopf, and J. R. Cole, *J. Pharm. Sci.*, **66**, 889 (1977).

PHARMACEUTICAL DEVELOPMENT

G.D. Searle & Co., a progressive leader in the health-care field, located in north suburban Chicago, has several outstanding opportunities for scientists with experience in the pharmaceutical industry.

MANAGER
PRODUCT SUPPORT AND IMPROVEMENT

This position is responsible for developing physically and chemically stable and bioavailable formulations for new line extension products and reformulation of marketed products. As manager, this position supervises a small group of professionals. The candidate should have the ability to interact effectively with marketing and production personnel.

The preferred candidate will have a Ph.D. in pharmacy with 3 to 7 years experience in the pharmaceutical industry or an M.S. in pharmacy or chemical engineering with 7 to 10 years experience in the pharmaceutical industry and supervisory experience.

RESEARCH PHARMACIST
ETHICAL PRODUCTS

This position is responsible for the development of formulas and processes for new Searle compounds, the development of line extension products, and the support of production process improvement activities.

The successful candidate will have a B.S. in pharmacy, chemistry, or chemical engineering with at least two years experience in the pharmaceutical industry.

RESEARCH PHARMACIST
CONSUMER PRODUCTS

This position is responsible for developing consumer product dosage forms for Searle's rapidly expanding Consumer Products Division. Duties will include formulation and process development and scale-up.

The successful candidate will have at least a B.S. or a M.S. in pharmacy, chemistry or chemical engineering with 1 to 3 years experience in the pharmaceutical industry, preferably in the areas of liquids and semi-solids.

We are offering excellent salaries and benefit packages, as well as opportunities for personal growth and professional satisfaction.

Your resume and salary history should be submitted to:

A. Abelman, Ph.D.

SEARLE

Searle Laboratories
Box 5110
Chicago, IL 60680

Equal Opportunity M/F . . .
A Practice, Not Just A Policy

Drug Adsorption by Activated Charcoal

In reference to the recent article "Comparative Drug Adsorption by Activated Charcoal"[1], which appeared in this Journal, I have failed to understand the relevance of Ref. 12. The reference was cited as an explanation for potential errors in the determination of K values in a Langmuir equation. I have found that the reference cited discusses the nonaqueous titration methods for the quantitative determinations of promazine and chlorpromazine. Perhaps the authors can correct this error.

V. Das Gupta
Department of Pharmaceutics
College of Pharmacy
University of Houston
Houston, TX 77004

Received February 21, 1978.

[1] E. M. Sellers, V. Khouw, and L. Dolman, *J. Pharm. Sci.*, **66**, 1640 (1977).

Cytotoxic Agents from Bursera klugii

In the June 1977 issue of the Journal, an article entitled "Cytotoxic Agents from *Bursera klugii* (Burseraceae) I: Isolation of Sapelins A and B" appeared[1]. Since the time of publication, the plant has been reidentified by Dr. Robert E. Perdue and Dr. Arthur S. Barclay of the Beltsville Agricultural Research Center, U.S. Department of Agriculture, Beltsville, Md., as *Trichilia hispida* Penning. ined. (Meliaceae).

Jack R. Cole
College of Pharmacy
University of Arizona
Tucson, AZ 85721

Received December 23, 1977.

[1] S. D. Jolad, R. M. Wiedhopf, and J. R. Cole, *J. Pharm. Sci.*, **66**, 889 (1977).

PHARMACEUTICAL DEVELOPMENT

G.D. Searle & Co., a progressive leader in the health-care field, located in north suburban Chicago, has several outstanding opportunities for scientists with experience in the pharmaceutical industry.

MANAGER
PRODUCT SUPPORT AND IMPROVEMENT

This position is responsible for developing physically and chemically stable and bioavailable formulations for new line extension products and reformulation of marketed products. As manager, this position supervises a small group of professionals. The candidate should have the ability to interact effectively with marketing and production personnel.

The preferred candidate will have a Ph.D. in pharmacy with 3 to 7 years experience in the pharmaceutical industry or an M.S. in pharmacy or chemical engineering with 7 to 10 years experience in the pharmaceutical industry and supervisory experience.

RESEARCH PHARMACIST
ETHICAL PRODUCTS

This position is responsible for the development of formulas and processes for new Searle compounds, the development of line extension products, and the support of production process improvement activities.

The successful candidate will have a B.S. in pharmacy, chemistry, or chemical engineering with at least two years experience in the pharmaceutical industry.

RESEARCH PHARMACIST
CONSUMER PRODUCTS

This position is responsible for developing consumer product dosage forms for Searle's rapidly expanding Consumer Products Division. Duties will include formulation and process development and scale-up.

The successful candidate will have at least a B.S. or a M.S. in pharmacy, chemistry or chemical engineering with 1 to 3 years experience in the pharmaceutical industry, preferably in the areas of liquids and semi-solids.

We are offering excellent salaries and benefit packages, as well as opportunities for personal growth and professional satisfaction.

Your resume and salary history should be submitted to:

A. Abelman, Ph.D.

SEARLE

Searle Laboratories
Box 5110
Chicago, IL 60680

Equal Opportunity M/F . . .
A Practice, Not Just A Policy

JOURNAL OF PHARMACEUTICAL SCIENCES

APRIL 1978
VOLUME 67 NUMBER 4

REVIEW ARTICLE

Stability of Pharmaceuticals

JOSEPH A. MOLLICA ˣ, SATINDER AHUJA, and JEROLD COHEN

Received from the *Research and Development Department, Pharmaceuticals Division, Ciba-Geigy Corporation, Suffern, NY 10901.*

Keyphrases ◻ Stability—pharmaceutical formulations, degradation mechanisms, rates, and pathways, evaluation methods, regulatory considerations, review ◻ Degradation—pharmaceutical formulations, rates, mechanisms, and pathways, review ◻ Dosage forms, various—stability, review

CONTENTS

Rates, Mechanisms, and Pathways of Degradation 444
Kinetics 444
Physical Organic Chemistry 445
Hydrolysis 447
Oxidation 447
Miscellaneous Reactions 448
Dosage Forms 448
Preformulation 448
Solutions 448
Semisolids 449
Solids 450
Stability-Indicating Methods 451
Electrometric Methods 451
Solvent Extraction Methods 452
Spectrophotometric Methods 452
Chromatographic Methods 453
Marketed Product Stability 454
Manufacturer's Container: Selection 454
Package Stability: Dispensing and Repackaging 455
Storage Conditions 456
Predictive (Accelerated Testing) 457
Expiration Dating/Shelflife 457
Regulatory Considerations 458
IND/NDA 458
GMP Requirements 458
PPA: Child Resistant Closures 459
Formulation Changes 459
GLP Requirements 459
Computerization/Records/Reports 460
Failure of Drug Product to Meet Required Specifications 460
References 460

Many in-depth articles and seminar proceedings have appeared in the past 2 decades on various aspects of stability (1–10), but no single report has treated the overall subject in an integrated fashion. Investigations into the stability of pharmaceuticals have ranged from fundamental studies on the rates and mechanisms of reactions of the active substance, through evaluation of the influence of the formulation and production processes on the drug and drug product, to, finally, the role of the container and the effect of storage and distribution of the finished packaged article on the integrity of the product.

The objectives of this article are to review the many facets of stability and to outline what a present-day stability program does and should include. We hope to interrelate scientific considerations with regulatory requirements.

It has been recognized that there are legal, moral, economic, and competitive reasons, as well as those of safety and efficacy, to monitor, predict, and evaluate drug product stability (7). However, stability can and does mean different things to different people or to the same people at different times, even those in pharmaceutical science and industry. Although unified nomenclature has been proposed, various terminology is still employed to encompass the what and the how and the why of stability: stability study, kinetic study, compatibility study, stability evaluation, stability-indicating assay, expiration dating, outdating, shelflife, storage legend, preformulation studies, failures of a batch to meet specifications, microbiological stability, stability of the active ingredient, stability of the formulation, stability in the marketed package, stability in sample packages, stability in the dispensing package, and stability in the hands of the consumer. All of these areas have been referred to as stability.

In the pharmaceutical industry, the disciplines primarily involved with stability are pharmaceutical analysis and product development. However, physical and organic chemistry, mathematics, physics, microbiology, toxicology, production, packaging, engineering, quality control, and distribution are all included. Basic subjects for consideration are physical organic chemistry—the evaluation of rates and mechanisms of reactions, kinetics and thermodynamics, and, importantly, organic analysis.

One cannot monitor stability, determine the reaction rate, or investigate any mechanism without an analytical measurement. Hence, the pharmaceutical analyst is pri-

marily involved in stability, because he or she must develop a method that will quantitatively determine the drug in the presence of, or separate from, the transformation product(s). This determination is required to assure that the drug has not undergone change. To select the appropriate method(s), the analyst should have a thorough knowledge of the physicochemical properties of the drug, including an understanding of the routes by which a drug can be degraded or transformed.

The knowledge of the physicochemical properties of the drug is equally important to the development pharmacist in efforts to achieve the optimum drug formulation. Likewise, this knowledge is needed by the package development group so that an appropriate container can be provided.

The stability of this resultant product in various channels of commerce is of concern to the marketing and distribution departments and to the physician, pharmacist, and patient. This concern is manifested by the use of storage legends, expiration dates, protective packaging, and dispensing directions. Furthermore, from a regulatory viewpoint, one should assure that the product is of the "quality, strength, purity, and identity" that it is purported to be throughout the time it is held or offered for sale.

An in-depth discussion on all aspects of this topic is beyond the scope of this review. We intend, however, to highlight the areas involved, with particular attention to recent literature, and to present an integrated overview of a total stability program.

RATES, MECHANISMS, AND PATHWAYS OF DEGRADATION

Kinetics—Two of the main contributors to an understanding of kinetic principles as applied to drug development are T. Higuchi and Garrett (7, 11–13); they brought the principles of chemical kinetics to the evaluation of drug stability. Although the theory was well understood and groundwork in chemical reaction kinetics was underway, only a few papers on drugs appeared in the literature through the 1940's. Detailed studies on drugs were not undertaken until the 1950's. The classical concepts brought to bear were the consideration of factors influencing reactions in solution (14–19), as summarized below.

Most degradation reactions of pharmaceuticals occur at finite rates and are chemical in nature. These reactions are affected by conditions such as solvent, concentration of reactants, temperature, pH of the medium, radiation energy, and presence of catalysts. The manner in which the reaction rate depends on the concentration of reactants describes the order of the reaction. The degradation of most pharmaceuticals can be classified as zero order, first order, or pseudo-first order, even though they may degrade by complicated mechanisms and the true expression may be of higher order or be complex and noninteger.

The quantitative relationship of the specific reaction rate and temperature is the Arrhenius expression:

$$k = Ae^{-\Delta H_a/RT} \qquad \text{(Eq. 1)}$$

where k is the specific rate constant; T is temperature in degrees Kelvin; R is the gas constant; A, the preexponential factor, is a constant associated with the entropy of the reaction and/or collision factors; and ΔH_a is defined as the heat of activation. The equation is usually employed in its logarithmic form:

$$\log k = -(\Delta H_a/2.303RT) + \log A \qquad \text{(Eq. 2)}$$

The slope of a plot of log k against $1/T$ yields the activation energy. This equation provides the underlying basis which allows prediction of stability of pharmaceuticals by extrapolation of rate data obtained at higher temperatures.

An understanding of the limitations of the experimentally obtained heat of activation values is critical in stability prediction; the pitfalls of extrapolation of kinetic data were described (20–22). For example, the apparent heat of activation at a pH value where two or more mechanisms of degradation are involved is not necessarily constant with temperature. Also, the ion product of water, pKw, is temperature dependent, and $-\Delta H_a$ is approximately 12 kcal, a frequently overlooked factor that must be considered when calculating the hydroxide-ion concentration. Therefore, it is necessary to obtain the heats of activation for all bimolecular rate constants involved in a rate–pH profile to predict degradation rates at all pH values for various temperatures.

If photolysis is the rate-determining step of the reaction, most often no predictive advantage is gained by higher temperature studies because the ΔH_a is small and, hence, the effect of temperature is small. Conversely, the heat of activation may be high for pyrolytic reactions, but the degradation rates obtained at elevated temperatures may be of little practical value when extrapolated to room temperature.

Complex reactions, including reversible reactions, consecutive reactions, and parallel reactions, are occasionally encountered in the decomposition of pharmaceuticals. Some of these reactions are discussed under *Physical Organic Chemistry*. A recent review (23) dealt with the kinetics of the most frequently encountered complex drug degradation reactions.

Many drugs are derivatives of carboxylic acids or contain the functional group based on this moiety, *e.g.*, esters, amides, lactones, lactams, imides, and carbamates. The members of this class include many important drugs such as aspirin, penicillin, ascorbic acid, procaine, meperidine, and atropine. This class can illustrate the basic factors affecting the rates of all reactions (24).

The study of hydrolytic reactions as a function of pH yields a rate–pH profile. For an ester, the overall hydrolysis rate of a drug, D, may be expressed as follows:

$$-\frac{dD}{dt} = K_U + K_{H^+}[H^+] + K_{OH^-}[OH^-] + K_N[N] + K_{GB}[GB] + K_{GA}[GA] \qquad \text{(Eq. 3)}$$

where K_U is the rate constant for the uncatalyzed or water-catalyzed reaction, K_{H^+} is the rate constant for the hydrogen-ion-catalyzed hydrolysis, K_{OH^-} is the rate constant for the hydroxide-ion-catalyzed hydrolysis, K_N is the rate constant for nucleophilic catalysis, K_{GB} is the rate constant for general base catalysis, and K_{GA} is the rate constant for general acid catalysis.

The hydrolysis of a compound may be subject to some or all of these terms; however, at any given pH, only one or two terms are significant. The simplest profile is observed when a compound is subjected to only hydrogen-ion

or hydroxide-ion catalysis. The effects of other nucleophiles or general acids or bases are usually studied by varying their concentrations while maintaining the pH constant.

Solvent has a significant effect on the reaction rate. A simplified treatment of solvent effects is presented here. When both reactants are ions in a solvent medium or a continuous dielectric, absolute rate theory gives the following equation:

$$\ln k = \ln k_0 - \frac{N}{RT}\frac{Z_A Z_B e^2}{\epsilon\gamma} \qquad \text{(Eq. 4)}$$

where $\ln k$ is the rate constant at the dielectric constant ϵ, $\ln k_0$ is the rate constant in the medium of infinite dielectric constant, N is Avogadro's number, Z_A is the charge on ion A, Z_B is the charge on ion B, e is the electronic charge, T is absolute temperature, R is the gas constant, ϵ is the dielectric constant, and γ is proportional to the interatomic distance in the activated complex.

This equation predicts a linear relationship between $\ln k$ and $1/\epsilon$. No effect of the dielectric constant would be noted if one of the molecules were neutral because Z_A or Z_B would be zero. The effect of the dielectric constant on the reaction rate between an ion and a neutral molecule is expressed as:

$$\ln k = \ln k_0 + \frac{NZ^2e^2}{2\epsilon RT}\left(\frac{1}{\gamma_1} - \frac{1}{\gamma_2}\right) \qquad \text{(Eq. 5)}$$

where γ is the radius of the reactant ions and the other symbols are as defined in Eq. 4.

Equation 5 predicts that the logarithm of the rate constant will vary linearly with the reciprocal of the dielectric constant. However, many drugs are quite complex and often do not appear to follow theory; *e.g.*, the solvolysis rate of the aspirin anion increases with an increasing ethanol content, but the rates are relatively constant with an increasing dioxane content. Both of these solvents should have produced a decrease in the overall rate. However, based on this type of information, it was concluded that a possible rate-determining step was the attack of water or ethanol on an uncharged cyclic intermediate (25, 26).

For reactions involving two ionic species, the rate constant is dependent on the ionic strength, μ. For aqueous solutions at 25°, Eq. 6 expresses the variation of the rate constant with ionic strength:

$$\log k = \log k_0 + 1.02 Z_A Z_B \sqrt{\mu} \qquad \text{(Eq. 6)}$$

A straight line with a slope equal to $1.02Z_AZ_B$ is obtained when one plots $\log k$ *versus* $\sqrt{\mu}$. Equation 6 would predict no effect on a reaction when one reactant is neutral; but the activity coefficient of a neutral molecule is affected by ionic strength, and one can observe a linear relationship between the logarithm of the rate constant and ionic strength:

$$\ln k = \ln k_0 + b\mu \qquad \text{(Eq. 7)}$$

where b is an empirical constant.

These two ionic effects are commonly called the primary salt effect. In addition, one observes what is called the secondary salt effect, which is the effect of ionic strength on the dissociation constant of a buffer species.

Many pharmaceuticals are subject to general acid, general base, or nucleophilic catalysis in addition to hydrogen-ion or hydroxide-ion catalysis. Several linear free energy relationships quantitate the catalytic rate constant with a property of the species and relate the rate constant for a series of reactions. For acid–base catalysis, this free energy relationship is the Brönsted catalysis law and can be expressed as:

$$k_{GA} = G_A K_A^{\alpha} \qquad \text{(Eq. 8)}$$

and:

$$k_{GB} = G_B K_B^{\beta} \qquad \text{(Eq. 9)}$$

where K_A and K_B are acid and base dissociation constants, respectively; and G_A, G_B, α, and β are constants characteristic of the solvent, temperature, and reaction.

Many drugs have ionizable groups, and the reactions may proceed differently for the ionized and unionized forms. However, analytically one usually measures the total drug concentration, D_T. For a weak base, the contribution of the ionized, D_{H^+}, and unionized, D, drug are related through the pKa of the drug and the pH of the medium; thus:

$$D_T = D + D_{H^+} \qquad \text{(Eq. 10)}$$

The overall reaction rate observed is the sum of both reactions. Two examples, aspirin and barbiturates, that demonstrate the effect of ionization on the rate constant and the mode of degradation are provided in the next section.

The basic kinetic effects are important to an understanding of the reaction and of possible adverse, practical effects. For example, addition of an inert salt such as sodium chloride to adjust isotonicity can affect the reaction rate as a primary salt effect. Buffers used to control pH are also ionic species and can exert a primary salt effect. In addition, they exert a secondary salt effect and also act as catalysts. Sulfite salts are frequently added as antioxidants, but they can form addition products with the active ingredient or act as catalysts.

Organic solvents such as alcohol are generally used for solubilization; the concentration of the organic solvent can affect the dielectric constant of the solvent and thus influence the degradation rate of the active ingredients. The preservatives used to inhibit bacterial growth or other pharmaceutical aids may decompose and their decomposition products may, in turn, influence the decomposition rate of the active ingredients by one or more of the means discussed previously.

Physical Organic Chemistry—The basic kinetic principles outlined are applicable to all chemical systems. However, relatively simple molecules have been used to elucidate a principle or to establish fundamental relationships. A generation ago, physical chemistry and organic chemistry were considered to be two separate nonrelated disciplines. But a number of standard textbooks in the field, ranging from Hammett's (27), through classic works by Bell (28) and Ingold (29), to more recent treatises, relate reaction mechanisms and catalysis to biochemical systems. Most modern textbooks in organic chemistry now integrate physicochemical principles (16–19, 30–36).

Since most modern pharmaceuticals are complex organic molecules, a firm understanding of mechanistic organic chemistry is vital to any detailed study of drug degradation; conversely, degradation studies of many classic drugs have added to an understanding of the mechanism

of many organic reactions. Most widely used drugs have been studied and provide good models for future studies. It is not within the scope of this article to review the myriad studies that have been conducted, but we shall illustrate the complexity and depth through review of two classic examples—aspirin and barbiturates—and highlight the types of reactions that drugs can undergo by a review primarily of the literature of the last few years.

Aspirin is an excellent example of a pharmaceutical compound on which in-depth kinetic studies have been performed and for which reaction mechanisms have been proposed (37–39). The first detailed studies on aspirin hydrolysis were published in 1950 by Edwards (40, 41), 42 years after the first study was reported (42). His work clearly demonstrated specific acid–base catalysis and pH-independent solvolysis of aspirin to salicylic acid. The rate constants for hydrogen-ion and hydroxide-ion catalyses were found to differ with the charge of the molecule. Edwards explained the relationship between the observed rate constant and pH on the assumption that aspirin hydrolysis occurs according to the six simultaneous reactions shown in Scheme I.

$$CH_3COO\cdot C_6H_4COOH + H_3O^+ \xrightarrow{k_1} HOC_6H_4COOH + CH_3COOH + H^+$$

$$CH_3COO\cdot C_6H_4COOH + H_2O \xrightarrow{k_2} HOC_6H_4COOH + CH_3COOH$$

$$CH_3COO\cdot C_6H_4COOH + OH^- \xrightarrow{k_3} HOC_6H_4COOH + CH_3COO^- \text{ or } HOC_6H_4COO^- + CH_3COOH$$

$$CH_3COO\cdot C_6H_4COO^- + H_3O^+ \xrightarrow{k_4} HOC_6H_4COOH + CH_3COOH$$

$$CH_3COO\cdot C_6H_4COO^- + H_2O \xrightarrow{k_5} HOC_6H_4COOH + CH_3COO^- \text{ or } HOC_6H_4COO^- + CH_3COOH$$

$$CH_3COO\cdot C_6H_4COO^- + OH^- \xrightarrow{k_6} HOC_6H_4COO^- + CH_3COO^-$$

Scheme I

The observed overall first-order rate constant, k, can be expressed as a function of the six second-order rate constants and the acid dissociation constant, K, of aspirin:

$$k = \frac{k_1[C_{H^+}] + k_2[C_{H_2O}] + k_3[C_{OH^-}]}{1 + K/[C_{H^+}]} + \frac{k_4[C_{H^+}] + k_5[C_{H_2O}] + k_6[C_{OH^-}]}{1 + [C_{H^+}]/K} \quad \text{(Eq. 11)}$$

Garrett (25, 26) also investigated the pH–rate profile for aspirin hydrolysis, particularly in the pH 4–8 range. Garrett's work pointed to intramolecular nucleophilic catalysis by the ionized carboxyl group. When the carboxylate ion is intramolecular, it catalyzes a number of ester reactions, although it is not a particularly strong nucleophile. As mentioned, the addition of alcohol increases the solvolysis rate, thus strongly suggesting the involvement of a solvent molecule in the transition state. On the basis of the kinetic and isotopic studies, aspirin hydrolysis was shown to be an intramolecular nucleophilic catalyzed hydrolysis involving an anhydride intermediate. It was assumed that the transition state of the reaction involved addition of the carboxylate ion to the carbonyl group of the ester, forming a tetrahedral addition intermediate.

Fersht and Kirby (43, 44) studied the reactivity of a series of substituted aspirins toward hydrolysis. The results show that the most likely mechanism for aspirin hydrolysis was one in which the carboxylate group acted not as a nucleophile but as a general base. The pH–rate profile for aspirin hydrolysis, as determined by Edwards (40, 41), showed that the transition state for hydrolysis in the pH-independent region involved the aspirin anion, either alone in a unimolecular reaction or together with one or more molecules of solvent.

Three mechanisms have been proposed on the basis of the kinetic results for the intramolecular catalytic hydrolysis of aspirin by the carboxyl group: (*a*) a unimolecular process in which the carboxylate group acts as a nucleophile, (*b*) a general acid catalysis in which the undissociated carboxylic acid group reacts with hydroxide ion, and (*c*) a general base catalysis in which the carboxylate anion reacts with a water molecule.

The barbiturates provide another excellent example of the complex mechanisms by which drugs degrade (Scheme II). Early workers (45, 46) assumed that the hydrolysis of barbiturates I*a* and I*b* to the corresponding malonuric acids was irreversible, and various degradation schemes were predicted on that assumption. Garrett *et al.* (47), in the process of further elucidating the hydrolysis kinetics of several important barbiturates, discovered that diethylmalonuric acid (II*a*) in basic solution may cyclize to form barbital (I*a*). Gardner and Goyan (48) confirmed the reversibility of hydrolysis of the barbituric acid nucleus and noted that it may have interesting biological ramifications. Furthermore, they rationalized previous findings (46) in the light of a similar reaction involved in the cyclization of 2-ureidobenzoic acid (49). Thus, the unionized barbiturate (III) could be cleaved at the 1,2-position, leading to production of the bisamide (IV), or at the 1,6- (3,4-) position, leading to the ureide (V); the ionized barbiturate would cleave only at the 1,6- (3,4-) position, leading to the ureide (or malonic acid) exclusively.

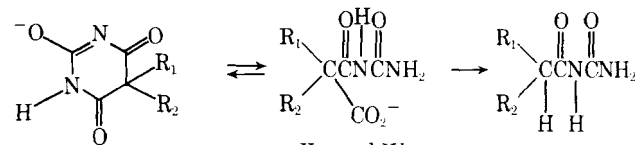

I*a*: $R_1 = R_2 = C_2H_5$
I*b*: $R_1 = C_2H_5$, $R_2 = C_6H_5$

II*a* and II*b*

V

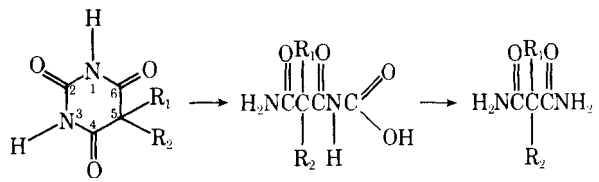

III

IV

Scheme II

Recently, Khan and Khan (50) observed that earlier workers did not kinetically detect the existence of di- and trianionic tetrahedral addition intermediates in the base-catalyzed hydrolysis of barbituric acid because their alkali concentration range was low. At pH values higher than the pKa_2 of barbituric acid, the equilibrium concentration of undissociated barbituric acid was negligible compared to the concentration of mono- and dianionic

barbituric acids. The equations were developed for $k_{1,obs}$ and $k_{2,obs}$ for the following consecutive irreversible first-order reaction path: barbituric acid $\xrightarrow{k_{1,obs}}$ malonuric acid $\xrightarrow{k_{2,obs}}$ ammonia. The rate constants showed three regions of hydroxide-ion dependence:

1. The reciprocals of the rate constants were linearly related to the reciprocal of the hydroxide concentration at low concentration.

2. The rate constants were independent of the hydroxide-ion concentration at higher concentrations of hydroxide ion.

3. The rate constants observed the following relationships at even higher concentrations of hydroxide ion:

$$k_{obs} = a + b[OH^-] + c[OH^-]^2 \qquad \text{(Eq. 12)}$$

The empirical parameters a, b, and c were evaluated using the method of least squares. A trianionic tetrahedral intermediate was proposed to account for the second power of the hydroxide ion in Eq. 12.

Hydrolysis—One common pathway by which drugs degrade is hydrolysis; the two reactions already discussed exemplify this route. Several other examples of drug hydrolysis are included in Table I. Also included in this table are drugs containing other functional groups that can undergo various elimination or addition reactions in an aqueous medium frequently classified as hydrolysis, although the elements of water are not necessarily involved. This list was drawn primarily from the literature of the 1970's; the references listed earlier (1–19) give numerous other examples.

Oxidation—After hydrolysis, the next most common pathway for drug breakdown is oxidation. Many major drugs, such as narcotics, vitamins, antibiotics, and steroids, are prone to undergo this reaction, but there is a dearth of detailed studies on oxidation reactions.

The most common form of oxidative decomposition occurring in pharmaceuticals is autoxidation through a free radical chain process. The free radicals are produced by homolytic bond fission of a covalent bond: $A{:}B \rightarrow A\cdot + B\cdot$. The radicals readily remove electrons from other molecules, and this process is oxidation. The autoxidation of the free radical chain process can be described by the reactions in Scheme III.

$$RH \xrightarrow[\text{catalysis}]{\text{heat, light}} R\cdot + H\cdot$$

$$R\cdot + O_2 \rightarrow RO_2\cdot$$

$$RO_2\cdot + RH \rightarrow ROOH + R\cdot$$

$$ROOH \rightarrow RO\cdot + \cdot OH$$

$$RO_2\cdot + X \rightarrow \text{products}$$

$$RO_2\cdot + RO_2\cdot \rightarrow \text{products}$$

Scheme III

The heavy metals (copper, iron, cobalt, and nickel) catalyze oxidation by shortening the induction period and also affect the oxidation rate by promoting free radical formation.

Oxidations in solution are also subject to specific acid–base catalysis and generally follow first- or second-order kinetics. For example, the oxidative degradation of prednisolone is base catalyzed and exhibits first-order dependency (82). Other solvents may have a catalytic effect on reactions when used alone or in combination with water.

Table I—Hydrolytic Reactions

Compound	Reaction	Reference
Salicylamide	Amide hydrolysis	51
N-Haloacetylphthalimides	Substituted amide hydrolysis	52
1-Acyl-3,5-dimethylpyrazoles	Substituted amide hydrolysis	53
N-Acylphthalimides	Imide hydrolysis	52
Meperidine	Ester hydrolysis	24
Pyridoxine monooctanoate	Ester hydrolysis	54, 55
Trantelinium bromide	Ester hydrolysis	56
Salicylanilide *N*-methylcarbamate	Carbamate hydrolysis	57
4-Biphenyl-*N*-methylcarbamate	Carbamate hydrolysis	57
17α-Acetoxy-6α-methyl-4-pregnen-3,20-dione 3-oximino ester	Hydrolysis of oximino ester	58
Penicillins	Hydrolysis of β-lactam	59–61
Cephalosporins	Hydrolysis of β-lactam Intramolecular aminolysis	62, 63
Clindamycin	Dethiomethylation	64
5-Aminodibenzo[*a*,*d*]cycloheptane derivatives	Deamination	65
Cytarabine (arabinosylcytosine)	Deamination	66
Cytosine	Deamination	67
Cytidine	Deamination	67
5-Azacytidine	Deamination Scission of N–C bond	68
Chlordiazepoxide	Deamination Scission of C=N linkage	69
N-Chlorosuccinimide	Dechlorination	70
N-Chloroquinuclidinium ion	Dechlorination	70
N-Chloro-*N*-methylbenzenesulfonamide	Dechlorination	70
N-Chlorinated piperidines	Dechlorination	71
Iodocytosine	Deiodination Deamination	72
Δ^9-Tetrahydrocannabinol	Hydration and ether solvolysis	73
Antimycin A_1	Hydrolytic ring cleavage Loss of CHO group	74
Dexoxadrol	Hydrolysis of ketal group	75
Hydrochlorothiazide	Ring opening through hydration of free or cationic imine	76, 77
Mazindol	Scission of C=N linkage	78
Methaqualone	Ring cleavage	79
Coumarinic acid	Lactonization	80
Canrenone	Scission of C–S bond Lactonization	81

Ketones, aldehydes, and ethers may also influence free radical reactions, either directly or through trace impurities such as peroxides.

Many drugs are complex molecules and contain multiple functional groups subject to both hydrolysis and oxidation, *e.g.*, ascorbic acid, penicillins, and phenylbutazone. The studies conducted on the latter are summarized here.

The rates and degradation mechanisms of phenylbutazone were studied extensively (83–89). Phenylbutazone can undergo both hydrolysis and oxidation; the initial hydrolytic or oxidative products can be decarboxylated and/or further hydrolyzed or oxidized. On the basis of a detailed study, it was concluded that the equilibrium between phenylbutazone and the carboxylic acid resulting from hydrolysis of the pyrazolidine ring was dependent on solvent but practically independent of pH (86). Slingsby and Zuck (87) noted that oxidation at the C-4 position to produce 4-hydroxyphenylbutazone was the major decomposition route in the solvents they investigated. Awang *et al.* (89) proposed the hydroperoxide at C-4 as an intermediate en route to its formation. They also proposed a mechanism for formation of several other compounds on hydrolysis, decarboxylation, and oxidation of 4-hydroxyphenylbutazone.

Table II—Oxidation

Compound	Site of Oxidation	Reference
Vitamin A esters	Aliphatic chain	90
Amitriptyline hydrochloride	Dimethylamino side chain	91
Hydrocortisone	Dihydroxyacetone side chain	92
Dipyrone	Methanesulfonate	93
Dopa	Phenolic groups	94
Methyldopa	Phenolic groups	95
Ascorbic acid	Hydroxyl groups	96, 97
Methylprednisolone	Hydroxyl at C-21	98
Phenothiazine	5-S in the ring	99
Chloramphenicol	Combination of hydrolysis and oxidation	100

Recent references on oxidation of several drugs are included in Table II.

Miscellaneous Reactions—In addition to hydrolysis and oxidation, many other degradative reactions of drugs have been studied, including addition, elimination, isomerization and epimerization, polymerization, acylation, transesterification, and photolysis. (Most often, light catalysis provides energy to initiate an oxidation reaction.) Some examples of catalysis are included in Table III. Examples of miscellaneous reactions are summarized in Table IV.

DOSAGE FORMS

Preformulation—The excipients employed in pharmaceutical formulations are quite complex and are sometimes even heterogeneous mixtures. To determine the effect of these substances on the drug, it is necessary to conduct semiempirical studies with these excipients as an interface between basic physicochemical evaluation of the substance and final formulation. Preformulation studies are conducted to ascertain the compatibilities of the drug substance with excipients, including biological and chemical preservatives that may be necessary for a given formulation.

Since the selection of a type of dosage form is determined primarily by the preferred route(s) of drug administration, the development pharmacist must provide a relatively stable formulation within these constraints. Consideration also must be given at this time to potential packages for the drug product and their possible effects on stability.

Table III—Catalysis

Compound	Catalyst	Reference
Epinephrine	Sodium metabisulfite Sodium bisulfite Acetone bisulfite	101
Penicillins	Copper(II)–glycine chelate Copper(II)	102, 103
Penicillin G potassium	Monohydrogen and dihydrogen citrate ions	104
Cyclic anhydrides	Perchloric acid	105
Nalidixate sodium	Light	106
9-Aminomethylacridan	Light	107
Phenothiazine	Light	108
Dihydroergotamine mesylate	Light	109
Antipyrine (phenazone)	Light	110
Aminopyrine (aminophenazone)	Light	110
Dipyrone (noramidopyrine methanesulfonate)	Light	110
α-[(Dibutylamino)methyl]-6,8-dichloro-2-(3′,4′-dichlorophenyl)-4-quinolinemethanol	Light	111

Table IV—Miscellaneous Reactions

Compound	Type of Reaction	Reactant	Reference
Morphine	Addition	Sodium bisulfite	112
Dexamethasone phosphate	Addition	Sodium bisulfite	113
Fluorouracil	Addition	Sodium bisulfite	114
Benzylideneanilines	Addition	Diethyl phosphonate	115
Homatropine	Acylation	Aspirin	116
Morphine	Acylation	Aspirin	117
Aspirin	Transesterification	Polyethylene glycol	118, 119
Thiamine	Transamination	Aromatic amines	120
Epitetracycline	Dehydration	Acids	121
Tetracycline	Dehydration	Acids	122
Penicillin	Isomerization	Acids	123, 124
Lincomycin monoesters	Isomerization	Alkalis	125, 126
Tetracyclines	Epimerization	Alkalis	127
Pilocarpine	Epimerization	Alkalis	128
Prostaglandin E_1 and dinoprostone (E_2)	Epimerization	Acids	129
Ampicillin sodium	Dimerization	Self-aminolysis	130
Ampicillin–hetacillin	Interconversion	Acetone	131, 132
Acetaminophen	Complexation	Antipyrine	133
Heterocyclic compounds	Chelation	Copper, aluminum, and iron	134

Preformulation studies are conducted not only to determine the physical and chemical compatibility of the drug substance with other drug substances and several possible excipients, both individually and in combination, but also to forecast the effects of formulation on drug availability.

Akers (135) described the methodology, management, and evaluation of a systematic preformulation program for solid oral dosage forms. He indicated that the development of a stable and effective drug dosage form is determined by the type, quality, and organization of preformulation studies. The interactions among active components and additives, polymorphs, and micelle-forming agents were reviewed (136). Datt (137) also discussed changes that can occur in pharmaceutical preparations and the ways in which they can be circumvented.

The methods used to determine deterioration of drugs, with special attention to evaluating the stability of individual components, were reviewed (138). An approach to the determination of stability in solid pharmaceutical systems during preformulation studies was proposed (139), as were various other approaches for stability evaluations during preformulation studies (140–143). Results of such studies have been applied to proper formulation selection and should be used to design the appropriate subsequent studies for the selected formulation.

Solutions—Unlike heterogeneous systems such as solids and semisolids, the stability of drugs in a homogeneous solution can be predicted with a great degree of accuracy, and the data obtained through basic kinetic studies can often be applied directly to the formulation. However, "extrachemical" or additional reactions can occur to the drug formulated in solution, and they may be overlooked or not considered during the basic studies.

Effect of Additives—The effect of excipients and pharmaceutical aids on stability can be significant. The pH of solutions containing lidocaine hydrochloride changes

in the presence of 5% dextrose in saline solution, normal saline, and lactated Ringer solution (143). Sodium bisulfite can cause precipitation of imipramine hydrochloride. Other examples of the effects of various excipients and pharmaceutical aids on stability of pharmaceuticals in solution are summarized in Table V.

Many parenteral drugs are lyophilized or dry filled into ampuls since they have limited stability in aqueous solution. Therefore, on reconstitution with sterile water or other commonly used diluents or when added to intravenous fluids, degradation often occurs. Detailed stability studies on reconstituted preparations must be undertaken to evaluate the effect of time and storage conditions with commonly used vehicles.

Effect of Container—Branchi and Mecarelli (155) discussed the "chemical inertness" of glass containers from the standpoint of composition of various glasses, leaching of substances from glass by water and other solutions, and the mechanism of such reactions. Other investigators reported on the effect of water at high temperature on borosilicate, soda-lime-treated, and untreated pharmaceutical glass containers (156). For dispensing low pH liquids, surface-treated "parasolvex" flasks were found to provide a marked advantage over flasks of normal glass (157).

Glass was found to be a better container than polyethylene for storage of "cherry laurel" distilled water (158). Stability studies on normal saline solution stored in various glass containers revealed that the materials in certain glass types and stoppers caused a significant pH increase on storage due to material release from the stopper upon autoclaving (159). Sterilization also increased the pH of 5% ephedrine hydrochloride solution; this increase was caused by material leached from the ampul glass (160).

Materials used in production equipment, such as copper and brass, were found to accelerate the decomposition of propazine solutions (161). Interaction of phenylephrine hydrochloride with low density polyethylene containers was reported (162). This interaction was quite significant at room temperature, and the data indicated an apparent binding of phenylephrine hydrochloride to the low density polyethylene bottles. The extent of drug sorption by the plastic materials can be determined by standard methods (163).

Effect of Environment—Discoloration of dosage forms is frequently due to exposure to light and/or oxygen. Light- and oxygen-sensitive promethazine hydrochloride (164) was used to evaluate the effectiveness of plastic (polyethylene) containers compared to those made of glass. Colored plastic or brown glass gave better protection from light than white or clear containers. When light was excluded, a more rapid decrease of drug was observed in plastic than in glass because of oxygen permeation. By using oxygen permeation velocity constants, it could be shown that oxygen saturation was attained after 24 hr.

The use of light-resistant containers was recommended to alleviate the light instability problem for metaproterenol (orciprenaline) sulfate (165), reserpine (166), phenylbutazone sodium (167), and dexamethasone (168). Reserpine degradation can be minimized by using nitrogen atmosphere, an antioxidant such as thiourea, and a chelating agent. Incorporation of a UV absorber in the reserpine solution can also materially reduce degradation (166). The stability of phenylbutazone solution can be enhanced by the use of an antioxidant, sodium metabisulfite, and a chelating agent, diethylenetriaminepentaacetic acid (167).

Table V—Effect of Pharmaceutical Aids on Stability of Active Ingredient

Compound	Other Ingredients	Remarks	Reference
Cholecalciferol (vitamin D_3)	2% Polyoxyethylene ester[a]	Polysorbate 80 and pH mainly responsible for observed decomposition	144
	Surfactant[b]		
	Polysorbate 80[c]		
Pyridoxal 5-phosphate	Thiamine	Increased decomposition rate at pH 6	145
	Thiamine diphosphate	Increased decomposition rate at pH 6	
	Riboflavin phosphate	Increased decomposition rate at pH 6	
	Adenosylcobalamine	Increased decomposition rate at pH 6	
	Pyridoxal	Increased decomposition rate at pH 6	
	Pyridoxine	Increased decomposition rate at pH 6	
Kanamycin	Honey	Loss of activity at room temperature	146
	Sugar syrup	Loss of activity at room temperature	
Bacillin-3	Honey	Loss of activity at room temperature	146
	Sugar syrup	Loss of activity at room temperature	
Cephapirin sodium	Mannitol	Less stable with this component	147
Tetracycline	Calcium	Complexation	147
	Magnesium	Complexation	
Tetracyclines	Urea	Decreased epimerization	148
	Thiourea	Decreased epimerization	
	Polysorbate 20	Decreased epimerization	
	Polyethylene glycol 6000	Decreased epimerization	
Thimerosal	Bromide	Form difficultly soluble halides of cationic mercury compounds	149
	Chloride		
	Iodide		
Menadione	Sodium metabisulfite	Lower pH due to hydrolysis of sodium metabisulfite followed by oxidation of resulting sodium bisulfite	150
Apomorphine hydrochloride	Penicillamine at pH 3.6–4.0	Stabilization	151
Epinephrine (adrenaline)	Boric acid, povidone, erythorbic acid	Stabilization	152
Epinephrine	Sodium hydrogen sulfite	Stabilization	153
Tryptophan	Sodium pyrosulfite, oxygen	Discoloration, precipitation	154

[a] Cremophor EL, derivative of ricinoleic acid. [b] Dupasol X. [c] Tween.

Semisolids—In this category are included all dosage forms that are not true solutions or dry oral solids. Many drugs that would undergo significant degradation, if marketed as a solution, can be stabilized by formulating the active ingredient into a suspension or emulsion. Gels, ointments, suppositories, creams, and lotions are typical semisolid preparations.

In addition to chemical inactivation of the therapeutic agent, these items are subject to a wide variety of physical and chemical changes: separation, sedimentation, creaming, and cracking. Since many excipients are natural

products—fats, oils, waxes, flavoring agents, and perfumes—they are quite subject to oxidation (rancidity) and microbiological contamination.

Effect of Additives—The effect of additives on the kinetics of interconversion of succinylsulfathiazole crystal forms was investigated (169). These investigations showed that a physically stable aqueous pharmaceutical suspension may be achieved by including a suitable transformation retardant. Under these conditions, the suspension keeps its uniformity and ease of resuspension for the expected shelflife of the preparation.

The autoxidation of the oil phase of an oil-in-water emulsion during storage in light was dependent on the emulsifier used (170). The observed differences in the extent of autoxidation might have resulted from different solubilities of oxygen in various emulsifier solutions.

The rheological and penetrometric characteristics of seven vitamin A-containing ointments changed after 14 months of storage. The decrease in vitamin content was a function of the ointment base; the presence of polyethylene glycol and sodium lauryl sulfate in the base enhanced degradation (171). Vitamin A was also unstable in hydrocarbon gels and lipogels (172). Incorporation of an antioxidant, such as α-tocopherol acetate, improved stability.

The effect of different ointment bases on the stability of oxacillin sodium was reported recently (173). In zinc oxide paste, anthralin was converted rapidly into a therapeutically inactive compound (174). Added salicylic acid improved the stability by deactivation of the surface zinc oxide through formation of zinc salicylate.

Four decomposition products were isolated from aminophylline suppositories. Three were identified as amides resulting from reaction of ethylenediamine with constituents of the suppository bases (175). Drofenine (hexahydroadiphenine) hydrochloride in suppositories decomposes to yield the free base and its *N*-oxide. The mechanism of decomposition was independent of the type of suppository base (176).

Effect of Physicochemical Factors—Practical stability considerations of emulsions and suspensions may show an inverse temperature relationship; instead of increased stability under colder or refrigerated conditions, one may encounter irreversible phase changes. Coagulation of particles was observed during freezing–thawing of suspensions. The primary factor involved in the coagulation was the small size of suspended particles (177).

A technique for evaluating the stability of emulsion bases and active components contained within such emulsions was described recently (178). The method, diffuse reflectance spectroscopy, has the capability of detecting changes in particle size or surface properties of emulsions as functions of time without disturbing the system.

The decrease in the acid-consuming capacity of aluminum hydroxide gel during aging, as measured by the USP test, has been found to be due to a decrease in the reaction rate rather than a decrease in equilibrium reactivity. The reactivity profile has three phases related to the structure of the gel (179). Gels containing sorbitol lost less than 10% of their acid-consuming capacity during a 6-month aging period compared with a loss of more than 60% for an identical gel without sorbitol. The mechanism by which sorbitol stabilizes the gel appears to be through inhibition of the secondary polymerization reaction which takes place on aging (180).

The photostability of compounds can be improved by suitable selection of the dosage form. For example, the micellar forms of chlorpromazine, triflupromazine, and homofenazine show greater stability. It has been postulated that, in the colloidal state, these compounds receive better protection in a lyophilic environment than in a hydrophilic environment (181). Ong and Kostenbauder (182) studied the effect of micellar sodium lauryl sulfate on the cupric-ion-promoted hydrolysis of some dicarboxylic acid hemiesters to evaluate the potential of such association of colloids for increasing product lability to metal-ion-promoted hydrolysis. The rate of cupric-ion promoted hydrolysis of sodium *n*-decyl oxalate in the micellar phase is about 50 times as fast as that in bulk solution. However, the hydrolysis rates of hydrocortisone sodium 21-hemisuccinate and hydrocortisone sodium 21-hemi-(3,3-dimethylglutarate) were unaffected by the copper ion.

Solids—Although solid oral dosage forms constitute a large majority of pharmaceutical products, few detailed kinetic studies and studies on rates and mechanisms of drug degradation in the solid state have been published. Most fundamental works on matter in the solid state are on inorganic materials or are from fields other than the pharmaceutical industry. Heterogeneous systems encountered in pharmaceutical dosage forms are often difficult to study and are not as reproducible as a homogeneous solution.

In recent years, Carstensen (1) and coworkers have added a great deal to our understanding in this area. Drug stability in the presence of excipients can be significantly different from that of the neat active ingredient. In the absence of excipients and moisture, topochemical and nucleation-governed reactions occur; some of these approximate first-order reaction rates. The nucleation reactions give rise to sigmoid curves, which are not simple first- or zero-order reactions. In the presence of moisture, the decomposition kinetics should be dictated by the rates in saturated solution and should be zero order.

Carstensen and Pothisiri (183) recently showed that first-order decomposition patterns may be possible in the absence of moisture or when moisture content is low. This effect was demonstrated with *p*-aminosalicylic acid as a model system to approximate the situation encountered in dosage forms. Other recent publications of interest on solid-state decomposition are on *para*-substituted salicylic acids (184), aspirin (185), and digoxin (186).

Although there are not many detailed physical chemistry studies, numerous publications of an empirical or practical nature described incompatibilities or instabilities or other changes in the solid state (187–198). As with liquids and semisolids, numerous "extrachemical" parameters change as a function of time in tablets and capsules. Some of these are discussed here.

Effect of Additives—The discoloration of tablets containing a variety of pharmaceutical compounds, such as 8-hydroxyquinoline sulfate, aminopyrine (amidophenazone), papaverine, theobromine, and salicylamide, was reduced markedly by using carboxymethylcellulose sodium solution during granulation. Carboxymethylcellulose sodium was found to act as a scavenger for trace metals,

which are a causative factor frequently encountered in the discoloration of pharmaceutical tablets (199).

The moisture sorption and volume expansion of anhydrous α- and β-lactose tablets were examined under various relative humidity conditions (200). The moisture adsorption and tablet expansion occurred more readily with α-lactose tablets, leading to the formation of the monohydrate. Lactose was also found to induce the discoloration of several drugs in solid dosage forms (201).

The adsorption of some antirheumatics on antacids was investigated (202). Elution studies showed that salicylates and anthranilic acid derivatives were tenaciously held by magnesium oxide, while magnesium trisilicate showed intermediate retention power for antipyrine and aminopyrine. A marked reduction in the apparent partition coefficient was observed for all drugs tested in the presence of magnesium trisilicate or aluminum hydroxide.

Effect of Container—The intertablet migration of nitroglycerin could be related to the container used for storage. In certain containers, intertablet transfer among a set of nominally equivalent tablets occurred after several months and resulted in decreased content uniformity. The mechanism of intertablet migration involved capillary condensation (203).

Effect of Environment—The fading of colored tablets by light (high-pressure mercury vapor lamp) was tested (204). The intensity of UV rays contributed mainly to the fading, but visible light also was responsible. Eosin and light green SF had poor stability; tartrazine was very stable.

The influence of a protective coating of sunscreening agents on the photostability of FD&C Blue No. 1 and erythrosine sodium (FD&C Red No. 3) was investigated. The tablets were exposed to 1000 footcandles of light, and approximate shelflives of various colored tablets were calculated (205, 206).

The discoloration of reserpine (0.1-mg)–dihydralazine sulfate (10-mg) tablets on prolonged exposure to air was reported (207). Reserpine was responsible for the discoloration of these tablets, and it was recommended that discolored material should not be used clinically.

Alam and Parrott (208) found a close correspondence between the changes occurring in the dissolution rate of hydrochlorothiazide tablets at elevated temperatures and those occurring after prolonged storage at room temperature. The retardation of the dissolution rate also was reported for sodium salicylate tablets (209), and a possible effect with acetaminophen tablets was noted (210). A study on phenylbutazone tablets BP showed a progressive decrease in dissolution with age (211). This effect could be simulated in short periods at elevated temperatures.

STABILITY-INDICATING METHODS

A review article on stability-indicating methods for drugs and their dosage forms (212) concerned itself primarily with a functional group approach to stability evaluation. The functional group analyses discussed were those most commonly finished with a titrimetric or spectrophotometric determination. Siggia (213, 214) wrote two comprehensive texts on analysis *via* functional groups and demonstrated that functional group analysis can be finished with various instrumental methods.

The current trend in stability-indicating methods is based on direct chromatography or derivatization chromatography. These approaches are used extensively in stability evaluation of pharmaceutical products.

Mollica and Lin (215) discussed problems facing an analytical chemist while developing an analytical method that will quantitatively determine the intact drug molecule in the formulation. When it is not possible to determine the intact drug directly because of interfering substances, it is desirable to precede the analytical finish with a separation procedure. This step can be solvent extraction or chromatographic separation.

The USP and NF (216, 217) provide yet another approach to evaluating stability. It entails monitoring the content of a decomposition product, *e.g.*, salicylic acid in aspirin and disulfonamide in hydrochlorothiazide, while utilizing an assay for the drug itself that may not be totally stability indicating. In some ways, this approach provides a more rigorous control of product stability. In the examples cited, the presence of 1–4% of a decomposition product will make the item unsuitable; thus, much tighter limits are being applied to these products as compared to those that must meet the rubric limits for potency. These examples also illustrate that different standards are used to define product stability. Although at times it is necessary to use more rigorous controls, it would be desirable to develop more uniform criteria for stability evaluation.

To select an appropriate method, the analyst should have a thorough knowledge of the physicochemical properties of a drug, degradation products, degradation mechanisms, and degradation reaction rates. (See discussion under *Rates, Mechanisms, and Pathways of Degradation.*) One can then develop a specific method suitable for monitoring the stability of an active ingredient or formulation. The methodology used for kinetic studies (solid state or solution) can generally be considered scientifically suitable for monitoring stability of pharmaceutical formulations if similar modes of decomposition are encountered. However, the method may not satisfy regulatory or compendial needs.

The effect of drug–excipient interactions on analytical methodology cannot be ignored (218). Frequently, these interactions not only lead to low assay values but also affect drug availability to the patient.

A recent review dealt with drug decomposition and analytical methods for the determination of decomposition products (219). Other recent reviews covered the stability of ascorbic acid (vitamin C) tablets (220), shelflife studies on some oral liquid vitamin formulations (221), analysis of polyene antifungal antibiotics (222), study of free salicylic acid and acetylsalicylic anhydride in aspirin-containing drug specialties (223), analytical methods for prostaglandins (224), and stability of stabilized nitroglycerin tablets in typical distribution and administration systems (225).

For the purpose of this article, stability-indicating methods are classified as electrometric methods, solvent extraction methods, spectrophotometric methods, and chromatographic methods.

Electrometric Methods—Titrimetric methods (aqueous or nonaqueous) that can be used for the precise analysis of the active ingredient most often do not offer the desired specificity for the analysis of pharmaceutical

products. However, if the decomposition products do not interfere with the titration, *e.g.*, formation of nonbasic degradation products of an organic amine or amine hydrochloride, then one may be able to utilize titrimetry. Alternatively, by employing suitable extraction procedures for eliminating possible interferences from excipients and/or decomposition products, one can use titrimetry for monitoring the stability of products.

Organic polarography has been used for the analysis of pharmaceutical products because it offers the desired specificity, but its use has been limited by several technical disadvantages (226). The advantage of polarography for the determination of ethacrynic acid in the presence of its principal degradation product, a dimer, was demonstrated (227). Polarography was also found useful for studying acid and base hydrolyses and β-lactamase degradation of several cephalosporins (228). The compounds were polarographically reduced in the acidic medium. A wave believed to be due to two-electron reductive elimination of the C-3 position substituent was found suitable for stability evaluation.

Solvent Extraction Methods—It is possible to extract acidic, neutral, or basic compounds selectively into organic solvents on the basis of the partition behavior of their ionized and unionized species. The compendia (216, 217) utilize a double-extraction procedure as the preferred method of analysis for organic nitrogenous bases. This approach provides some degree of specificity, because it is possible to remove compounds that are neutral or acidic or have more polar substituents that could arise upon degradation. It does not, however, eliminate isomers or other closely related basic substances. Therefore, the validity of this approach for monitoring stability should be demonstrated prior to its utilization.

Spectrophotometric Methods—Direct spectrophotometric determination is widely used in pharmaceutical analysis but generally lacks selectivity. The selectivity or specificity can be improved through separation or by reaction of an appropriate functional group. For example, the reactions that produce a colored product are generally measured in the visible region of the spectrum. Other reactions increase conjugation to permit measurements in the UV region.

Due to its limited sensitivity, IR analysis is primarily used for identification of decomposition products and has found very few quantitative applications in stability evaluation. NMR spectroscopy is finding an increasing number of applications since it offers specificity along with simplicity of operation. But it, too, lacks sensitivity and precision.

Colorimetric Analysis—Carboxylic acid derivatives (anhydrides, halides, lactams, lactones, amides, and esters) are converted to the corresponding hydroxamic acid by reacting with hydroxylamine hydrochloride in an alkaline medium. The hydroxamic acid is then allowed to react with ferric chloride in the presence of dilute acid to produce red-violet ferric hydroxamate (229).

Soloway and Lipschitz (230) reported observations on amides. The hydroxylaminolysis of amides and the formation of colored complexes of the hydroxamic acids so derived with ferric ion afforded a convenient means of determining amides in the presence of their amino compounds and acid constituents. These reactions were used for stability-indicating colorimetric analyses of N^1-acetylsulfanilamide and N^1-acetylsulfisoxazole since their hydrolysis products did not interfere in the analysis (231, 232). A hydroxylamine colorimetric method has been included in the *Code of Federal Regulations* for the analysis of various cephalosporins (233). This method is stability indicating for decomposition of the β-lactam ring.

Le Pedriel *et al.* (234) reported that acetaminophen and nitrous acid react under mild conditions to form 2-nitro-4-acetamidophenol, which can be analyzed by its color in alkaline solution. Furthermore, they found no interference from acetanilide or phenacetin, a hydrolysis product. Inamdar and Kaji (235) used this reaction for dosage form assay but utilized the yellow color of the nitroso derivative in acid solution for measurement instead of the orange-red color of the phenolate ion. A suitable modification of the colorimetric method was utilized for acetaminophen analysis of conventional and sustained-release tablet formulations containing phenacetin, phenylpropanolamine hydrochloride, and phenyltoloxamine dihydrogen citrate (236).

The reaction between homatropine methylbromide and Dragendorff reagent was stabilized so this colorimetric reaction could be employed for stability evaluation of pharmaceutical formulations (237, 238). The method was specific for the parent compound in the presence of its major decomposition product, tropine methylbromide.

A specific method for the determination of ascorbic acid in the presence of dehydroascorbic acid and 2,3-dioxo-*l*-gluconic acid was reported (239). The method is based on the colorimetric reaction of phenylhydrazinium chloride with ascorbic acid in an acidic medium. The reaction of isoproterenol (isoprenaline) with thiosemicarbazide in alkaline medium was utilized as a specific colorimetric reaction for the analysis of pharmaceutical formulations (240). The picric acid reaction was useful for the determination of testosterone in oily injections (241).

UV Analysis—The spectrophotometric determination of ephedrine and other phenylalkanolamine drugs as benzaldehydes after periodate oxidation was specific for compounds with the general structure Ar–CHOHCH(NHR_1)–R_2 (242). Aspirin stability in methoxypolyethylene glycol, polyethylene glycol acetate, or a mixture of polyethylene glycols was monitored by simultaneous UV spectrophotometric determinations (243). The decomposition was primarily transesterification with the vehicle. Isoniazid (isonicotinic acid hydrazide) could be determined spectrophotometrically by formation of the hydroxamic acid in the presence of nickel(II) (244).

A procedure for the measurement of small amounts of ampicillin in hetacillin was reported; the former molecule yields a UV-absorbing compound with nickel(II) in dimethyl sulfoxide (245). Cephalosporin was analyzed by differential UV spectrophotometry after employing β-lactamase for hydrolysis of the β-lactam ring (246).

Mixtures of tetracycline and 4-epitetracycline were assayed utilizing the large difference in their circular dichroism spectra in the UV region (247). The proposed method was specific and required no prior separation of degradation products. The assay was not useful, however, for the determination of anhydrotetracycline; the latter, even at levels of 10%, affects the assay for tetracycline by only 1%.

Fluorometric Analysis—A stability-indicating spectrophotofluorometric method for epinephrine was reported by Prasad *et al.* (248). In this procedure, the drug was oxidized *via* iodine to "adrenochrome" and then cyclized with alkali to "adrenolutin," which is responsible for the fluorescence. The main decomposition product of epinephrine from simulated formulations containing sodium bisulfite, epinephrinesulfonic acid, was found not to interfere in the assay. A similar method was also described for the analysis of partially decomposed isoproterenol solutions (249).

NMR Analysis—Rackham (250) recently reviewed the applications of quantitative NMR spectroscopy in pharmaceutical research. Several other recent publications emphasized the importance of this technique in stability evaluations. A stability assay for amyl nitrite ampuls was proposed by Schirmer *et al.* (251). The percentage of amyl nitrite in an amyl nitrite ampul is determined from the ratio of the area under the CH_2ONO band to the area under the CH_3 band in the NMR spectrum of the sample. Decomposition of amyl nitrite in ampuls produces N_2O, NO, CO, CO_2, and at least 12 liquid components including water, amyl alcohol, isovaleric acid, valeraldehyde, amyl isovalerate, and amyl nitrate.

Recently, Turczan and Medwick (252) observed that this method yielded relative stability information because the α-methylene group is affected by instability whereas the methyl group is not. They recommended a choice of solvent and internal standards to provide absolute results.

NMR spectroscopy also was found useful for the stability evaluation of cocaine hydrochloride in aqueous solution (253).

Chromatographic Methods—A large number of stability-indicating methods entail some form of chromatography: paper, thin-layer (TLC), column, gas (GLC), and liquid (HPLC). The latter two techniques not only offer separation but provide precise methods of quantitation. Recent reviews (254–264) summarized advances in this area, and several examples of these techniques have been included in this review.

Less than a decade ago, paper chromatography was used extensively in pharmaceutical analysis. This technique has rapidly given way to TLC, GLC, and HPLC. Of these three techniques, HPLC is finding the most widespread application today. Instrumentation for HPLC became commercially available approximately 7 years ago, and the rapid growth of this technique is apparent from the literature; it is already included in several USP XIX monographs.

With this technique, a compound can be chromatographed in several ways and, importantly, the volatility that is required for GLC is not a limitation. The problems due to thermal instability are not encountered because most separations are carried out at ambient or low temperatures. Of various chromatographic techniques employed in stability evaluations, GLC and HPLC provide the most useful quantitative information.

Paper Chromatography—An excellent review on applications of paper chromatography was published recently (265). The following discussion is limited to a few recent examples. A paper chromatographic method was found useful for monitoring the stability of tetracycline and its hydrochloride salt (266). The method is based on the complexation of the antibiotic with a mixture of urea and edetate disodium on chromatographic paper at pH 7.4.

Both paper chromatography and TLC were used for stability evaluation of chlorpromazine (aminazine) solution (267). Several degradation products were observed with both techniques; however, paper chromatography showed better resolution.

TLC—The applications of quantitative TLC in pharmaceutical analysis were reviewed recently (268, 269). A few examples from recent literature are provided here to illustrate the usefulness of this technique. Quantitative TLC by direct fluorometry was rapid and specific for the determination of tetracycline hydrochloride and its degradation product or impurities (270). This method was used for stability investigation of liquid pharmaceutical preparations containing tetracycline.

Other applications include the determination of atropine sulfate in the presence of its hydrolytic degradation products (271) and stability studies on androgenic hormones (272).

Column Chromatography—This technique is being replaced by high-pressure liquid chromatography (HPLC). A few recently published methods for stability evaluation (273–276) utilized separation on ion-exchange columns. A partition column chromatographic procedure was found useful for the determination of tetracyclines (277).

GLC—Derivatization in GLC for pharmaceutical analysis was reviewed recently (260). Derivatization provides an additional approach to selectivity if the appropriate derivatization technique is selected. A few recent examples are described here.

A rapid GLC method was proposed for the simultaneous analysis of salicylic acid in aspirin tablets and in codeine–propoxyphene-type capsules and tablets (278, 279). The procedure involved formation of the methyl ester of salicylic acid with diazomethane. Derivatization with diazomethane also was used for analysis of reserpine and rescinnamine (280).

The degradation of terbutaline under oxidative conditions was investigated by GLC of its trimethylsilyl derivative (281). Silylation was found useful for GLC of iodochlorhydroxyquin and related 8-hydroxyquinolines (282) and in analysis of scopolamine in the presence of its degradation products (283). Patel *et al.* (284) noted that silylation provided advantages for aspirin determination over previously published methods. Silylation also was found useful for analysis of levodopa (285), cycloserine (286), and phenylephrine (287).

Direct GLC of several basic drugs was reported in 1974 (288). GLC was found suitable for stability determination of new potential drugs such as *dl*-3-(*p*-trifluoromethylphenoxy)-*N*-methyl-3-phenylpropylamine and *dl*-3-(*o*-methoxyphenoxy)-*N*-methyl-3-phenylpropylamine (289), aprindine [*N*,*N*-diethyl-*N*′-(2-indanyl)-*N*′-phenyl-1,3-propanediamine] (290), and promethazine hydrochloride (291). This technique was also found useful for the determination of meprobamate and related carbamates (292), cyclophosphamide (293), carbamazepine (294), 9-acridine derivatives (295), and ephedrine and phenylalkylamines (296).

The combination of GLC–mass spectrometry provides a valuable tool for the determination of low levels of degradation products. An example of the low sensitivity (200–800 pg) and selectivity possible with this technique

Table VI—HPLC of Pharmaceuticals

Compound	Mode of HPLC	Reference
Prostaglandins A_2 and B_2	Anion exchange	301
Barbiturates	Anion exchange	302
Penicillin G potassium	Anion exchange	303
Ampicillin	Anion exchange	304
Tetracyclines	Cation exchange	305
Xanthines	Cation exchange	306
Trisulfapyrimidines	Cation exchange	307
Sulfa drugs	Cation exchange	308
Imidazolines	Cation exchange	309
Benzodiazepines	Adsorption	310
Riboflavin	Adsorption	311
Sulfacetamide sodium	Adsorption	312
Cholecalciferol	Adsorption	313
Canrenone	Adsorption	314
Carbamazepine	Adsorption	315
Phenytoin (diphenylhydantoin)	Adsorption	316
Phenobarbital	Adsorption	316
Aspirin, phenacetin, and caffeine	Adsorption	317
Corticosteroids	Partition	318
Hydroxysteroids (derivatized)	Partition (reversed phase)	319
Sulfasalazine (salicylazosulfapyridine)	Partition (reversed phase)	320
Procaine	Partition (reversed phase)	321
Tetracyclines	Partition (reversed phase)	322
Synthetic estrogens	Partition (reversed phase)	323
Phenol	Partition (reversed phase)	324
Ergotamine	Partition (reversed phase)	325
Nortriptyline	Partition (reversed phase)	326
Androsterone (derivatized)	Ion exchange and partition (reversed phase)	327
Dehydroepiandrosterone (derivatized)	Ion exchange and partition (reversed phase)	327
Vitamins (water soluble)	Anion and cation exchange	328
Analgesics (aspirin, caffeine, acetaminophen, and salicylamide)	Anion and cation exchange	329

is seen in the analysis of prostaglandin analogs (297).

HPLC—The theory of HPLC was reviewed recently (298). The importance of this technique to the pharmaceutical analyst can be measured by the large number of recent reviews on the applications in pharmaceutical analysis (259, 261–264, 299, 300). Several applications of recent interest are summarized in Table VI.

MARKETED PRODUCT STABILITY

In the section on *Dosage Forms*, factors influencing stability of common formulations—solutions, semisolids, and solids—were considered. However, a modern pharmaceutical product is not only the optimum formulation, it is also the optimum formulation/package combination. Formulations are designed to maintain or enhance the stability of the active ingredient or other component(s) subject to deterioration and to ensure the pharmaceutical elegance of the product. The design is based on physicochemical properties of the active substance(s) and its compatibility with excipients. This information can be derived from kinetic and preformulation studies. Information on the stability of specific compounds is available in the general pharmaceutical literature (2, 330, 331).

Many approaches are used to stabilize or protect formulations, including lyophilization; microencapsulation (332, 333); control of surface area (334); addition of chelating agents, preservatives, and antioxidants; physical separation of incompatible ingredients; coatings (335); and opaque coverings. The need and use of these devices are intrinsic to the dosage form under consideration.

Extrinsic to the stabilization of the dosage form is the stability of the dosage form–container combination. The container is an integral part of such products as topicals and parenterals. Wood (336) indicated that in addition to physical, chemical, bioavailability, and microbiological criteria, container interactions should be monitored in the evaluation of the stability of topicals. In many cases, it is not feasible for evaluation purposes to isolate the dosage form from the intended container. The container becomes an integral part of the drug product. Even though extensive studies have been conducted on the dosage form, additional studies in the container(s) of choice are necessary to obtain a total stability characterization of the product.

During the design of a product, it is essential that storage and end use be considered. "Use tests" may be indicated where the immediate container will be continually disturbed during use, *e.g.*, an elixir or syrup where, upon use, the headspace will increase or the surface to volume ratio will change.

In addition, consideration has to be given to possible requirements or restrictions on storage of the product–container combination to provide adequate assurance that product performance is satisfactory throughout the determined shelflife. Establishment of packages, storage legends, and shelflife are as (or more) important as the basic efforts taken to determine the stability of the active ingredient as presented in previous sections.

Manufacturer's Container: Selection—Esthetics, economics, stability, safety, law, production, and quality control requirements should be considered in the selection of the appropriate container for a pharmaceutical product (6). Stability cannot be separated from any one of the other factors. Poor product stability in a chosen container affects all of the stated factors; hence, it is of primary significance. For purposes of marketed product stability, the manufacturer's container is defined to be all package components in intimate contact with the product or that provide a degree of protection, *e.g.*, closure, seal, or overwrap.

The *Code of Federal Regulations*, Title 21, Section 314.1, requires that, for any New Drug Application, stability data for the dosage form be provided "in the container in which it is to be marketed." The significance of this requirement is highlighted by the problems experienced with nitroglycerin tablets that led to very explicit federal regulations (337) for the packaging and handling of that product. The enactment of this regulation followed the discovery that appreciable evaporation of nitroglycerin from tablets occurred when stored in plastic containers and certain strip packages. Much has been published on the stability of nitroglycerin tablets relative to the container in which they are stored or dispensed (225, 338–341).

The compendia (342, 343) have provided definitions for various types of containers based on their capability to provide protection:

"Light-resistant Container—A light-resistant container protects the contents from the effects of light by virtue of the specific properties of the material of which it is composed, including any coating applied to it. Alternatively, a clear and colorless or a translucent container may be made light-resistant by means of an opaque covering, in which case the label of the container bears a statement that the opaque covering is needed until the contents have been used. Where it is directed to 'pro-

tect from light' in an individual monograph, storage in a light-resistant container is intended.

Well-closed Container—A well-closed container protects the contents from extraneous solids and from loss of the drug under the ordinary or customary conditions of handling, shipment, storage, and distribution.

Tight Container—A tight container protects the contents from contamination by extraneous liquids, solids, or vapors, from loss of the drug, and from efflorescence, deliquescence, or evaporation under the ordinary or customary conditions of handling, shipment, storage, and distribution, and is capable of tight reclosure. Where a tight container is specified, it may be replaced by a hermetic container for a single dose of a drug.

Hermetic Container—A hermetic container is impervious to air or any other gas under the ordinary or customary conditions of handling, shipment, storage, and distribution."

A quantitative test to measure the permeation of a container closure system was included in USP XIX and NF XIV (344, 345). The limits established to define tight and well-closed containers became official on April 1, 1977 (346). These limits supplement the requirements and tests for light-resistant containers that have been in effect for several editions of the USP and NF.

The various properties one should consider in evaluating pharmaceutical containers were summarized by Krueger (347). Pharmaceutical packages are designed to provide not only a means of transport and brand identification but to serve more significant functions: to provide adequate protection and to ensure the stability of the product while in distribution and storage. A necessary prerequisite to the determination of the degree of protection afforded by a package must be the accumulation of information on the drug product itself. Products subject to hydrolysis or deleterious physical changes caused by moisture require containers that restrict moisture transmission. Light-sensitive dosage forms require barriers that screen out the harmful wavelengths. Formulations subject to oxidation that are single-dose sealed units require blanketing with an inert atmosphere prior to sealing, *e.g.*, nitrogen or carbon dioxide flushing.

When the types of protection that the product requires from the package are established, a basic understanding of the properties of package components, the container and closure, is needed for appropriate package selection. Many publications have dealt with the properties of packaging materials, and several conferences have covered the special requirements for containers needed by the pharmaceutical industry. One such conference, "Pharmaceutical Parameters in Container Selection," in 1969, was sponsored by the University of Wisconsin, Extension Services in Pharmacy.

A comprehensive summary of recent advances in packaging pharmaceuticals, including the relationship of the product and the package, packaging materials, and packaging technology, was prepared by Dean (348). Heubner (349), Ross (350), and Spingler (351) also provided extensive information on the relation of the package to the pharmaceutical product.

Information on the properties and applications of various types of package materials, glass (155–157, 352, 353), aluminum tubes (354), aerosols (355, 356), blisters (357), unit packaging (358, 359), elastomeric closures (360), and plastic (163, 361–369), is also available.

In recent years, polymeric materials have become widely used for pharmaceutical packages. Cooper (370) prepared a useful reference on plastic containers which defines the areas of potential problems, discusses the relationship of the containers to dosage forms, reviews the regulatory requirements around the world, and presents the existing standards for plastic containers.

Specialized test procedures have been developed to determine properties of plastic containers such as oxygen permeation (371). A procedure to determine sorption of drugs on low density polyethylene was reported (372). The permeability of packages made from various resins to gas, water vapor, radiation, bacterial penetration, and sorption phenomena was reviewed (373). The numerous publications dealing with plastic packaging components tend to indicate its utility and growing popularity in drug packaging.

The ultimate criterion for the suitability of a particular container is testing of the drug in the container under normal and stress conditions for extended periods. The scope and nature of this testing as it relates to the product were reviewed earlier. Special consideration must be given to interactions between the product and the container that might not be ascertained by the normal testing of the product. These interactions could include migration of one or more components (additives) of the package into the drug, absorption or adsorption of the drug into or onto the package, esthetic changes of the package or drug, actual physical deterioration of the package, and formation of a reaction product at the drug–container interface.

Package Stability: Dispensing and Repackaging—The USP (374) now includes an entire section entitled "Stability Considerations in Dispensing Practice." Included in this section are: an overall definition of stability; various aspects of stability including chemical, physical, microbiological, therapeutic, and toxicological; factors affecting stability including the nature of the container; the process by which manufacturers select the optimum formulation and container; and the responsibilities of the pharmacist with regard to stability. Furthermore, this section directs the pharmacist to dispense pharmaceutical products in the proper container and closure.

If repackaging is necessary, the following guidelines for the pharmacist have been provided by the USP:

"Repackaging—In general, repackaging is inadvisable. However, if repackaging is necessary, the manufacturer should be consulted concerning potential problems. In the filling of prescriptions, it is essential that suitable containers be used. Appropriate storage conditions and an appropriate expiration date should be indicated on the label of the prescription container. Single-unit packaging calls for care and judgment, and for strict observance of the following guidelines: (1) use moisture-proof packaging materials for solids; (2) where stability data on the new package are not available, repackage at any one time only sufficient stock for a limited time (e.g., 30 days); (3) include on the unit-dose label a lot number or the date of repackaging and an appropriate expiration date; (4) where a sterile product is repackaged from a multiple-dose vial into unit-dose (disposable) syringes, discard the latter if not used within 24 hours, unless data are available to support longer storage; (5) where quantities are repackaged in advance of immediate needs, maintain suitable repackaging records showing name of manufacturer, lot number, date, and designation of persons responsible for repackaging and for checking; (6) where safety closures are required, use container closure systems that ensure compliance with compendial and regulatory standards for storage."

At the time of publication of USP XIX, it was indicated that, upon repackaging, the pharmacist might become responsible for the stability of a product. The Second Interim Revision Announcement to USP XIX and NF XIV indicated that as of April 1, 1977, the monograph requirements for tight or well-closed containers for official products must be adhered to upon dispensing of a prescription. Hence, the responsibility for proper repackaging has been placed on the pharmacist.

As mentioned previously, a serious problem in the dispensing of pharmaceuticals concerns nitroglycerin tablets. The problems encountered in repackaging this product were discussed by Shangraw and Contractor (375). Specific regulations (376) issued by the Food and Drug Administration (FDA) restrict the dispensing of nitroglycerin preparations to the original, unopened container. This regulation was based on the stability of the nitroglycerin preparation relative to its container.

Studies have been conducted to determine the stability of pharmaceutical products under prescription (dispensing) conditions. Russell *et al.* (377) reported on the effects of storage on the glyceryl trinitrate content of nitroglycerin tablets in British dispensing containers. Adamski and Socha (378) showed that chloramphenicol decomposed when stored in frequently opened vessels.

Over the past few years, there has been growing concern about the stability of pharmaceuticals repackaged for hospital use. Several recent publications demonstrate the variety of investigations conducted on the stability of product–container combinations prepared for hospital use. These include investigations on amphotericin B in infusion bottles (379), syrups in single-unit polypropene and polythene cups (380), tobramycin sulfate in bottles and bags (381), and sodium bicarbonate injection in disposable polypropylene syringes (382).

Pharmaceutical stability is acknowledged as a complex area that is further complicated by the relationship of the product to the container and the effects on stability, both positive and negative, of the product–container combination. As already indicated, the USP recommends against repackaging pharmaceuticals and advises the pharmacist to take every precaution if repackaging is necessary. Generally, products repackaged at the dispensing level are stored for relatively short periods; but during that interval, the product can be exposed to harsh storage conditions in the hands of the patient (*e.g.*, the proverbial windowsill). The effects of storage in the prescription container are usually not well defined since the bulk of stability testing is done at the manufacturer's level in the manufacturer's container(s). Hence, repackaging of pharmaceuticals at the dispensing level becomes the weakest link in the protection of the product between the manufacturer and the patient.

Storage Conditions—One aspect of stability evaluation is the determination of effects of environmental conditions on the product. The factors most commonly tested are heat, humidity, light, and air. Temperature tends to accelerate all reactions according to rate theory (see *Rates, Mechanisms, and Pathways of Degradation*), and the other factors accelerate, catalyze, or mediate hydrolytic, photolytic, oxidative, *etc.*, reactions (see *Dosage Forms*).

These data also form the basis for establishment of an expiration date. Expiration dates, however, have real significance only when they can be related to specific storage conditions. That a label bears a 5-year expiration date does not ensure that the product will be suitable after storage for 5 years under any conditions. As previously described, packages can provide a degree of protection from some of the elements, but it is still advisable to relate the expiration date to specific storage conditions.

Levi and Benney (383) pointed out that storage of pharmaceutical products can be defined and controlled by the manufacturer through distribution to the wholesale and pharmacy level. Thereafter, the only means of control is the expiration date and storage legend appearing on the product label. These investigators (383) provided a summary of temperatures experienced in some U.S. cities to define the average climate and to relate storage of laboratory samples to actual field conditions.

Haynes (384) proposed that a "virtual temperature" be determined for laboratory storage of stability samples which relates to actual market conditions. This temperature is determined from the Arrhenius relationship and rate constant for degradation at various temperatures. He provided the virtual temperature for several cities in the United States and abroad. Other publications (385–387) discussed actual market conditions for pharmaceuticals and their relation to laboratory testing.

To obtain laboratory data more representative of field conditions, cycling storage units can be used to simulate actual conditions. Feinberg (388) described the Defense Personnel Support Center "Accelerated Aging Test" which employed cycling conditions. Normally one assumes that the greater part of the storage in the field will be at average climatic conditions with limited exposure to stress conditions. A significant number of locations that provide storage for pharmaceutical products, such as hospitals, pharmacies, and wholesalers, are air-conditioned (383). This fact tends to reinforce the position that long-term storage will generally not be at stress conditions. Levi and Benney (383) proposed a scheme for testing and labeling that takes into account the potential for storage at varying conditions.

Compendial monographs (216, 217) provide directions for "Packaging and Storage"; the storage conditions stipulated in the individual monographs are defined as:

> *"Cold—Any temperature not exceeding 8° (46°F). A refrigerator is a cold place in which the temperature is maintained thermostatically between 2° and 8° (36° and 46°F). A freezer is a cold place in which the temperature is maintained thermostatically between −20° and −10° (−4° and 14°F).*
>
> *Cool—Any temperature between 8° and 15° (46° and 59°F). An article for which storage in a cool place is directed may, alternatively, be stored in a refrigerator, unless otherwise specified in the individual monograph.*
>
> *Room Temperature—The temperature prevailing in a working area. Controlled room temperature is a temperature maintained thermostatically between 15° and 30° (59° and 86°F).*
>
> *Warm—Any temperature between 30° and 40° (86° and 104°F).*
>
> *Excessive Heat—Any temperature above 40° (104°F).*
>
> *Protection from Freezing—Where, in addition to the risk of breakage of the container, freezing subjects a product to loss of strength or potency, or to destructive alteration of the dosage form, the container label bears an appropriate instruction to protect the product from freezing."*

In addition, USP XIX and NF XIV require that:

"Where no specific storage directions or limitations are provided in the individual monograph, it is to be understood that the storage conditions include protection from moisture, freezing, and excessive heat."

If no storage legend appears on a product label, can it be assumed that the product is resistant, within acceptable levels, to the deleterious effects of storage for the entire expiration period at the most severe condition allowed, *e.g.*, 40° (excessive heat)? With the vast majority of pharmaceutical dosage forms, this stability cannot be assumed. It would be necessary to test the material for the full expiration period at the most severe condition to provide such assurance.

The Defense Personnel Support Center has acknowledged that at times certain products may not be stored in accordance with required storage legends. They provide guidelines (388) on the maximum number of days an article requiring refrigeration may be stored out of refrigeration.

Kiger (389, 390) and Schumacher (391) discussed the results of environmental factors on the stability of drugs and listed the storage requirements of some prime drug products for maximum efficiency and the most reliable storage time.

Predictive (Accelerated Testing)—To determine the stability of a pharmaceutical product, samples are stored under the anticipated marketed storage conditions, usually ambient temperature, and either the content of intact drug or the content of degradation product is monitored by specific analytical, microbiological, or physical methods at predetermined intervals. The point at which the product degrades to the lower limit of its specifications is considered the shelflife (392). Depending on the stability of the item, the time involved for this test could be very short or quite long. Obviously, it would be to the investigator's advantage to be able, in a relatively short time, to predict the shelflife of the product. Toward this end, various approaches for predicting shelflife have been developed and applied.

Garrett (5) pointed out that predictive methods may be applied to evaluate degradation rates as functions of several magnitudes of stress. Stability at ambient conditions may be predicted from data at higher temperatures by the application of physicochemical laws utilizing the appropriate statistical evaluation. This approach enables one to estimate stability over short test periods, to evaluate quickly variations in batches or components, to select rapidly the optimum formulations from a series, to apply statistical methods, and to minimize the error component in the variation in analytical results.

Carstensen (393) outlined some procedures that can be used in stability extrapolations and predictions and discussed the application of Arrhenius plotting and applicable confidence limits. Graham (394) pointed out that predictive studies require that the degradation rate be studied as a function of an applied stress such as a change in pH, temperature, or ionic strength. Kinetic experiments are much more easily applied to the drug itself than to formulations; for the latter, such studies are more easily interpreted for solution-type products than for solid dosage forms.

The use of a nomographic chart to facilitate the analysis of data from accelerated testing for predictive purpose was presented by Lordi and Scott (395). An optimized stability testing program was outlined. More recently, a new nomogram was proposed (396) that is capable of predicting stability based on two analytical determinations of samples kept at two definite temperatures above room temperature for certain time periods. This method may be applied to zero-, first-, and second-order kinetics.

Several predictive approaches utilizing isothermal and/or nonisothermal methods have been described. Matsuura and Kawamata (197) developed a method for prediction of shelflife under nonisothermal shelf conditions through the use of an analog computer; the calculated results were in good agreement with experimental values. Zoglio *et al.* (196) reported on a continuous nonisothermal–isothermal method for stability prediction. A simple experimental procedure utilizing nonisothermal estimation of the activation energy and preexponential factor for drug decomposition from a single experiment was described by Madsen *et al.* (194). A computer program was written to assist in the computational aspects. Flexible nonisothermal stability studies that eliminate the need for a fixed time–temperature profile were described by Maulding and Zoglio (191).

Through the use of the Arrhenius equation to extrapolate observed changes, an 8-week testing program for predicting tablet stability was described (397). Carstensen and Su (398) presented the statistical aspects of Arrhenius plotting for predictive purposes. The application of the Gauss–Newton method to accelerated data was demonstrated. A scheme was suggested (399) based on short-term stability data at room temperature for obtaining reliable expiration dates.

Prediction of physical changes of drug preparations such as color stability of a liquid multisulfa preparation (400) and of tablet formulations (401) were reported. The disadvantages of accelerated testing of perfume components of products were reported (402), showing a possible lack of correlation between results and actual market performance. A rapid method for accelerated determination of oxidation of cosmetics was described (403). The test material was heated to 120°, and then oxygen was blown into the container; correlation with other methods was very good.

Several other approaches and review articles on accelerated aging and predictive stability are available (404–409).

With all of the available tools for predicting drug stability, in the final analysis the actual long-term data under ambient conditions are required by the FDA.

Expiration Dating/Shelflife—The objective of stability testing is to determine for what time period and under what condition the product is satisfactory. Expiration dates had been used only for problem products with "limited" stability; those that were stable for longer, yet arbitrary periods, went undated. For New Drug Applications, the FDA has required that if no expiration date is proposed, its absence must be justified (see *Regulatory Considerations*). Interest and concern in the use of valid expiration dates have been shown by government, academia, and industry over the last several years, as evidenced by the frequent seminars held on the subject.

The first major conference was the "Seminar on Drug Stability as Affected by Environment and Containers,"

cosponsored by the FDA and the School of Pharmacy, University of Connecticut, in Washington, D.C., in 1967. Other major conferences were held in 1969 by the University Extension, University of Wisconsin, "The Dating of Pharmaceuticals," and in 1972 by the School of Pharmacy and Pharmacal Sciences, Purdue University, "Implementation of Product Expiration Dating Systems in the Pharmaceutical Industry."

Many manufacturers had voluntarily instituted expiration dates for some or all of their products by 1969 (5), even though there was no official requirement. Federal regulations have required expiration dates for products liable to deterioration or for certain classes of drugs and have proposed expiration dates for all drug items (see *Regulatory Considerations*). In addition, the USP (410) had required that:

> *"In the absence of a specific requirement in the individual monograph for a dosage form, the label shall bear an expiration date assigned for the particular formulation and package of the article. This date identifies the time during which the article may be expected to meet the requirements of the Pharmacopeial monograph provided it is kept under the prescribed storage conditions. The expiration date limits the time during which the product may be dispensed or used."*

The same requirement appears in the latest edition of the NF (411).

The preamble to the proposed CGMP (412) justifies the requirement for expiration dating for all drug products as follows:

> *"Consumers of pharmaceuticals have a vital interest in having those products maintain the identity, strength, quality, and purity essential to render them safe and effective for use. The stability of a drug product during the period of time between its manufacture and its delivery to the patient can have a major influence on such identity, strength, quality, and purity. Many factors affect drug product stability. These include the stability of the active ingredients, the interaction of active and inactive ingredients, the manufacturing process, the storage conditions, the dosage form, the container closure system, the conditions under which the drug product is shipped, stored, and handled by wholesalers and retailers, and the length of time between initial manufacture and final use. Although some of these factors are not within the direct control of the manufacturer, the use of expiration dating by the manufacturer will encourage the removal of outdated or aged stocks."*

It is further stated that: "The appropriate expiration date for each drug product must be determined by suitable stability studies."

Johnson (5) indicated that expiration date intervals reflect the length of time required for: (*a*) the least stable active component to degrade to about 90% of the label claim, (*b*) some aspect of pharmaceutical elegance to become unacceptable, or (*c*) a maximum of 5 years.

Many definitions and uses of the terms normally associated with stability testing and expiration dating have been evident in the literature. Carstensen and Nelson (413) proposed a nomenclature for the various phrases (shelflife, outdate, expiration, and label date) to make scientific and technological dialog more precise in this area.

The USP (414) directs dispensing pharmacists to rotate stocks based on age and states that the expiration date is guaranteed by the manufacturer only if the product is stored in the original container at the recommended conditions.

REGULATORY CONSIDERATIONS

The multitude of recently promulgated governmental regulations concerning the stability of pharmaceutical preparations emphasizes the importance of this subject. These regulations include specific requirements for stability testing on which expiration dating is to be based. The most noteworthy of these regulations are discussed here.

IND/NDA—The Federal Food, Drug, and Cosmetic Act and its amendments require that a manufacturer demonstrate the safety and efficacy of a new drug prior to introducing it into interstate commerce. This requirement is more clearly defined in the Notice of Claimed Investigational Exemption for a New Drug (IND) (415) and the New Drug Application (NDA) (416).

IND's require "a statement of the methods, facilities, and controls used for the manufacturing, processing, and packing of the new drug to establish and maintain appropriate standards of identity, strength, quality, and purity as needed for safety and to give significance to clinical investigations made with the drug." Based on this regulation, available stability data on the new drug substance and dosage forms concerned with a particular IND are required by the FDA.

The requirements for stability information under the regulations for NDA's are more specific and detailed than those for IND's. They require:

> *"a complete description of, and data derived from studies of the stability of the drug, including information showing the suitability of the analytical methods used. Describe any additional stability studies underway or contemplated. Stability data should be submitted for any new-drug substance, for the finished dosage form of the drug in the container in which it is to be marketed, including any proposed multiple-dose container, and if it is to be put into solution at the time of dispensing, for the solution prepared as directed. State the expiration date(s) that will be used on the label to preserve the identity, strength, quality, and purity of the drug until it is used. (If no expiration date is proposed, the applicant must justify its absence.)"*

Under the regulations for Antibiotic Drugs (417), an expiration date is required for the product label of any antibiotic drug. These regulations are detailed in the Antibiotic Application, FD Form 1675 (1/71):

> *"h) A complete description of, and data derived from stability studies of the potency and physical characteristics of the drug, including information showing the suitability of the analytical methods used. Describe any additional stability studies underway or contemplated. Stability data should be submitted for any new antibiotic, for the finished dosage form of the drug in the container including a multiple-dose container in which it is to be marketed, and if it is to be put into solution at the time of dispensing, for the solution prepared as directed.*
>
> *i) The expiration date needed to preserve the identity, strength, quality, and purity of the drug until it is used."*

Guidelines (418) were published to assist drug sponsors and applicants in developing information required by the FDA for IND's and NDA's. These guidelines detail the many factors involved in the stability evaluation of a drug, indicating what is necessary for a stability profile and what is required to satisfy the regulations. Further clarification of the Federal requirements for stability of new drugs was provided by Silk (419) of the FDA.

GMP Requirements—Good Manufacturing Practice

in Manufacture, Processing, Packing, or Holding of Drugs was first promulgated in 1963. In 1969, revisions of these regulations were proposed (420); in 1971, a final revised version of Current Good Manufacturing Practice (421) was implemented. Section 133.13—Stability provided for the assurance of the stability of the finished drug product, requiring that it be:

"a) Determined by reliable, meaningful, and specific test methods.
b) Determined on products in the same container—closure systems in which they are marketed.
c) Determined on any dry drug product that is to be reconstituted at the time of dispensing (as directed in its labeling), as well as, on the reconstituted product.
d) Recorded and maintained in such a manner that the stability data may be utilized in establishing product expiration dates."

Section 133.14—Expiration dating provided:

"assurance that drug products liable to deterioration meet appropriate standards of identity, strength, quality, and purity at the time of use, the label of all such drugs shall have suitable expiration dates which relate to stability tests performed on the product.
a) Expiration dates appearing on the drug labeling shall be justified by readily available data from stability studies such as described in Section 133.13.
b) Expiration dates shall be related to appropriate storage conditions stated on the labeling wherever the expiration date appears.
c) When the drug is marketed in the dry state for use in preparing a liquid product, the labeling shall bear expiration information for the reconstituted product, as well as, expiration date for the dry product."

Revisions of these regulations have been proposed (422) to expand the current regulations for stability testing (Section 211.166) by requiring that a written testing program designed to assess the stability characteristics of drug products and used to establish storage conditions and expiration dates be followed. Additional proposed requirements include:

"1) Statistical criteria, including sample size and test intervals, for each attribute examined to assure statistically valid estimates of stability;
2) Storage conditions for samples tested."

The proposal also requires:

"an adequate number of batches of each drug product shall be tested to determine an appropriate expiration date and a record of such dates shall be maintained. Accelerated studies, combined with basic stability information on the components, drug products, and container–closure system, may be used to support tentative expiration dates provided adequate shelf life studies are not available and are being conducted. Where data from accelerated studies are used to project a tentative expiration date that is beyond a date supported by actual shelf life studies, there must be stability studies conducted, including drug product testing at appropriate intervals, until the tentative expiration date is verified or the appropriate expiration date determined."

The regulation proposed for expiration dating (Section 211.137) requires that the date be statistically valid and that it be applied to all drug products, not only to products liable to deterioration. Thus revision requiring dates for all products is in line with the current compendial policy (410, 411): "in the absence of a specific requirement in the individual monograph for a dosage form, that the label bear an expiration date assigned for the particular formulation and package of the article."

PPA: Child Resistant Closures—To emphasize the concern for the stability of pharmaceutical products in alternate packaging, the rules and regulations for Special Packaging (423) pursuant to Section 3 of the Poison Prevention Packaging Act of 1970 required that for "immediately effective supplemental applications" to qualify child resistant containers, the container and closure composition and the torque of the container be consistent with those provided for in the approved new drug application. Stability commitments to test the stability of initially marketed batches of the drug and to report the results to the FDA quarterly the 1st year, semiannually the 2nd year, and annually thereafter through the expiration date of the article were required. The law also required a commitment to withdraw from the market any batch falling outside the approved specifications for the drug. In cases where the container composition and the composition of the closure component in contact with the drug varied from those in the approved new drug application, appropriate submissions for approval had to be made to the new drug application.

In place of data showing the package to be a satisfactory barrier to moisture and gas transmission, stability data obtained at conditions of exaggerated temperatures and humidity for 3 months could be submitted. This provision again emphasizes the importance of actual stability determinations on the product in the container–closure combination.

It is obvious that great importance is placed on any change in packaging components and its possible effect on drug product stability.

Formulation Changes—Significant formulation changes are normally accompanied by appropriate stability evaluation to determine any untoward effect on the product. However, minor formulation changes, required by government action, have stipulated the need for stability studies. Examples of these changes are: termination of provisional listing and certification of amaranth (FD&C Red No. 2) (424), elimination of chloroform as an ingredient of human drug and cosmetic products (425), and termination of provisional listing of carbon black (426).

Each regulation required essentially the same information and/or commitment, namely that manufacturers of new drugs who either deleted or replaced the delisted component submit data to establish the stability of the revised formulation. If the data were too limited to support a conclusion that the drug would retain its declared potency for a reasonable marketing period, then an alternate three-part commitment was required:

1. Commit to test the stability of marketed batches at reasonable intervals.
2. Submit data as they become available.
3. Recall from the market any batch found to fall outside the approved specifications for the drug.

The formulation change required to conform to these regulations could involve a simple deletion of the item or a replacement of the component; however, the regulations apply equally to all changes. The item may have been an intimate part of the product composition or used only on the surface as an ingredient of printing inks. The regulations do not consider the extent of the formulation change.

GLP Requirements—Recently, guidelines (427) for

good laboratory practices in nonclinical studies of pharmaceutical compounds were adopted by the Pharmaceutical Manufacturers Association, and regulations for such guidelines were proposed by the FDA (428). The FDA-proposed regulations indicate that: "identity, strength, quality, and purity of each batch of a test or control substance should be determined and documented."

The FDA proposal also requires that the stability of the test substance will, where possible, be established by the testing facility under circumstances of the intended study. Where it is not feasible to determine accurately the stability of the test substances prior to study initiation, periodic reanalysis is indicated. Since nonclinical work is basic to the investigation and evaluation of possible medicinal agents, the integrity of the test substance is critical for proper evaluation of test results.

Computerization/Records/Reports—The increasing regulatory requirements outlined above generate additional stability studies which, in turn, produce voluminous data. Since most data accumulated on dosage forms are eventually submitted to a regulatory agency as part of a submission for a new drug application, for a supplemental application, to fulfill regulatory commitments, or in periodic reports, a means of collating and reporting these data is essential. The obvious course of action when multitudes of numbers are concerned is computerization.

Many manufacturers currently utilize computers from the initial stages of stability determination for statistical evaluation of kinetic data to the preparation of reports on dosage forms for submission to the FDA. Computers allow for the design of more complex models, which would be impractical and tedious by manual calculations. (See *Predictive* under *Marketed Product Stability.*)

One of the first approaches to the use of a computer system for processing stability data was a system that aids in the planning, interpretation, and submission of stability data (5). It was noted that data processing is in a dynamic state, and system efficiencies change with new equipment and programs. Blanco *et al.* (429) reported on a computerized stability program permitting maximal use of development and analytical manpower. This system includes capabilities to schedule, to flag exceptional behavior, to interpret data, and to prepare reports for filing with government authorities. The implementation of a computer program involving nearly 400 products was described by Newman (430); other applications of computer uses in stability programs have been reported (431, 432).

With appropriate design, a computer program for dosage form stability evaluation can provide for the control of sample storage at given conditions, control inventory, schedule test intervals, sample at prescribed intervals, delineate test requirements for each sample, review data, highlight untoward results, provide numerous administrative lists and search capability, interpret data, and prepare reports. As automation in the laboratory enables the analyst to perform more determinations, computerization allows for the efficient handling of complex administrative functions and the coordination of voluminous amounts of data by technical personnel which would otherwise require more personnel and increase the potential for human error. Human error is not eliminated by computerization; but with appropriate edit programs and design, it can be minimized.

Several programs specifically for pharmaceutical stability are commercially available from within the pharmaceutical industry and from consultants.

Failure of Drug Product to Meet Required Specifications—A stable product can be legally defined as a product that meets the required specifications for the indicated shelflife. A drug product that does not meet this definition creates significant problems for both the consumer and the manufacturer.

The FDA may initiate action, under the Food and Drug Act, to cause removal of a product from the market. Or, as noted previously, there is provision for the manufacturer to recall batches voluntarily from the marketplace that do not meet established specifications. With instability, there is a potential for the product to be rendered unsafe and ineffective through formation of toxic degradation products or loss of activity. If the instability does not pose a health hazard but, nevertheless, causes the material to be outside established specifications, then a recall results in the possible unavailability of medication to the consumer which would otherwise be adequate. Secondary consequences of an economic nature are incurred due to the expense of a recall and the intangible expense associated with damage to the manufacturer's reputation. The legal, economic, moral, and safety problems that could be incurred by instability are obvious and should further emphasize the need for the manufacturer to provide for a sound program that will ensure that the product is satisfactory throughout its useful life.

A modern, effective stability program, therefore, must encompass basic mechanistic studies on drug degradation, followed by appropriate preformulation studies and a thorough evaluation of the product–container combination to establish a valid expiration date and storage requirements to maintain the integrity of the drug.

REFERENCES

(1) J. T. Carstensen, *J. Pharm. Sci.*, **63**, 1 (1974).

(2) C. J. Lintner, "Quality Control in the Pharmaceutical Industry," vol. 2, M. S. Cooper, Ed., Academic, New York, N.Y., 1973, p. 142.

(3) Conference on Implementation of Product Expiration Dating Systems in the Pharmaceutical Industry, Purdue University, West Lafayette, Ind., 1972.

(4) L. Lachman and P. DeLuca, in "The Theory and Practice of Industrial Pharmacy," L. Lachman, H. A. Lieberman, and J. L. Kanig, Eds., Lea & Febiger, Philadelphia, Pa., 1970, p. 669.

(5) "The Dating of Pharmaceuticals," J. J. Windheuser and W. L. Blockstein, Eds., University of Wisconsin, Madison, Wis., 1970.

(6) Seminar on Drug Stability as Affected by Environment and Containers, FDA/University of Connecticut School of Pharmacy, Washington D.C., Nov. 1967.

(7) E. R. Garrett, in "Advances in Pharmaceutical Sciences," vol. 2, H. S. Bean, A. H. Beckett, and J. E. Carless, Eds., Academic, New York, N.Y., 1967, p. 2.

(8) L. Lachman, *J. Pharm. Sci.*, **54**, 1519 (1965).

(9) E. R. Garrett, *ibid.*, **51**, 811 (1962).

(10) S. A. Schou, *Am. J. Hosp. Pharm.*, **17**, 5 (1960).

(11) T. Higuchi, A. Havinga, and L. W. Busse, *J. Am. Pharm. Assoc., Sci. Ed.*, **39**, 405 (1950).

(12) T. Higuchi and L. W. Busse, *ibid.*, **39**, 411 (1950).

(13) E. R. Garrett, *J. Pharm. Sci.*, **51**, 911 (1962).

(14) A. A. Frost and R. G. Pearson, "Kinetics and Mechanisms," Wiley, New York, N.Y., 1961.

(15) S. W. Benson, "The Foundation of Chemical Kinetics," McGraw-Hill, New York, N.Y., 1960.

(16) K. J. Laidler, "Chemical Kinetics," McGraw-Hill, New York, N.Y., 1965.

(17) W. P. Jencks, "Catalysis in Chemistry and Enzymology," McGraw-Hill, New York, N.Y., 1969.
(18) M. L. Bender, "Mechanism of Homogeneous Catalysis from Protons to Proteins," Wiley, New York, N.Y., 1971.
(19) K. A. Connors, "Reaction Mechanisms in Organic Analytical Chemistry," Wiley, New York, N.Y., 1973.
(20) D. L. Bentley, *J. Pharm. Sci.*, **59,** 464 (1970).
(21) J. T. Carstensen and K. E. Su, *Bull. Parenter. Drug Assoc.*, **25,** 287 (1971).
(22) E. R. Garrett, Seminar on Drug Stability as Affected by Environment and Containers, FDA/University of Connecticut School of Pharmacy, Washington D.C., Nov. 1967, p. 45.
(23) T. Hermann, *Farm. Pol.*, **31,** 369 (1975); through *Chem. Abstr.*, **83,** 152238k (1975).
(24) J. Anschel, J. A. Mollica, and K. S. Lin, *Bull. Parenter. Drug Assoc.*, **26,** 271 (1972).
(25) E. R. Garrett, *J. Am. Chem. Soc.*, **79,** 3401 (1957).
(26) E. R. Garrett, *J. Org. Chem.*, **26,** 3660 (1961).
(27) L. P. Hammett, "Physical Organic Chemistry," McGraw-Hill, New York, N.Y., 1940.
(28) R. P. Bell, "The Proton in Chemistry," Cornell University Press, Ithaca, N.Y., 1959.
(29) C. K. Ingold, "Structure and Mechanism in Organic Chemistry," Cornell University Press, Ithaca, N.Y., 1953.
(30) E. S. Gould, "Mechanisms and Structure in Organic Chemistry," Holt, New York, N.Y., 1959.
(31) R. Breslow, "Organic Reaction Mechanism," Benjamin Press, New York, N.Y., 1965.
(32) J. Hine, "Physical Organic Chemistry," McGraw-Hill, New York, N.Y., 1962.
(33) J. E. Leffler and E. Grunwald, "Rates and Equilibria of Organic Reactions," Wiley, New York, N.Y., 1963.
(34) K. B. Wiberg, "Physical Organic Chemistry," Wiley, New York, N.Y., 1964.
(35) A. Lieberless, "Introduction to Theoretical Organic Chemistry," Macmillan, New York, N.Y., 1968.
(36) V. Gold and D. Bethell, "Advances in Physical Organic Chemistry," vols. 1–13, Academic, New York, N.Y., 1976.
(37) C. A. Kelly, *J. Pharm. Sci.*, **59,** 1053 (1970).
(38) T. Stozek, *Farm. Pol.*, **28,** 771 (1971); through *Chem. Abstr.*, **77,** 168516m (1972).
(39) L. Thomasini, D. Naplatanova, and M. Zakharieva, *Farmatsiya*, **24,** 57 (1974); through *Chem. Abstr.*, **82,** 7566r (1975).
(40) L. J. Edwards, *Trans. Faraday Soc.*, **46,** 723 (1950); through C. A. Kelly, *J. Pharm. Sci.*, **59,** 1053 (1970).
(41) *Ibid.*, **48,** 696 (1952); through C. A. Kelly, *J. Pharm. Sci.*, **59,** 1053 (1970).
(42) J. Rath, *Ann.*, **358,** 98 (1908); through C. A. Kelly, *J. Pharm. Sci.*, **59,** 1053 (1970).
(43) A. R. Fersht and A. J. Kirby, *J. Am. Chem. Soc.*, **89,** 4853 (1967).
(44) *Ibid.*, **89,** 4857 (1967).
(45) J. Hasegawa, K. Ikeda, and T. Matsugawa, *Chem. Pharm. Bull.*, **6,** 36 (1958).
(46) F. Tishler, J. E. Sinsheimer, and J. E. Goyan, *J. Pharm. Sci.*, **51,** 214 (1962).
(47) E. R. Garrett, J. T. Bojarski, and G. J. Yakatan, *ibid.*, **60,** 1145 (1971).
(48) L. A. Gardner and J. E. Goyan, *ibid.*, **62,** 1026 (1973).
(49) A. F. Hegarty and T. C. Brucie, *J. Am. Chem. Soc.*, **92,** 6575 (1970).
(50) M. N. Khan and A. A. Khan, *J. Chem. Soc., Perkin II*, **1976,** 1009.
(51) T. L. Grimes, *Diss. Abstr. Int.*, **35,** 2859-B (1974).
(52) V. Stella and T. Higuchi, *J. Pharm. Sci.*, **62,** 968 (1973).
(53) A. A. Forist and D. J. Webber, *ibid.*, **62,** 318 (1973).
(54) N. Mizumo, H. Takagi, and A. Kamada, *Vitamins*, **49,** 387 (1975); through *Chem. Abstr.*, **84,** 22039f (1976).
(55) N. Mizuno, M. Fujimoto, and A. Kamada, *ibid.*, **49,** 395 (1975); through *Chem. Abstr.*, **84,** 22040z (1976).
(56) M. Takacs, P. Kertesz, A. Vegh, and I. Simonyi, *Acta Pharm. Hung.*, **42,** 177 (1972); through *Chem. Abstr.*, **77,** 92787c (1972).
(57) L. W. Brown and A. A. Forist, *J. Pharm. Sci.*, **61,** 858 (1972).
(58) R. E. Huetterman and A. P. Shroff, *ibid.*, **63,** 74 (1974).
(59) T. Yamana, A. Tsuji, and Y. Mizukami, *Chem. Pharm. Bull.*, **22,** 1186 (1974).
(60) K. D. Dudley, T. C. Butler, and D. Johnson, *J. Pharmacol. Exp. Ther.*, **188,** 491 (1974).
(61) J. M. Blaha, A. M. Knevel, D. P. Kessler, J. W. Miney, and S. L. Hem, *J. Pharm. Sci.*, **65,** 1165 (1976).
(62) T. Yamana, A. Tsuji, K. Kanayama, and O. Nakano, *J. Antibiot.*, **27,** 1000 (1974).
(63) H. Bundgard, *Arch. Pharm. Chemi., Sci. Ed.*, **4,** 25 (1976); through *Chem. Abstr.*, **85,** 37161j (1976).
(64) T. O. Oesterling, *J. Pharm. Sci.*, **59,** 63 (1970).
(65) H. V. Maulding, D. Brusco, J. Polesuk, J. Nazareno, and A. F. Michaelis, *ibid.*, **61,** 1197 (1972).
(66) R. E. Notari, M. L. Chin, and R. Wittebort, *ibid.*, **61,** 1189 (1972).
(67) E. R. Garrett and J. Tsau, *ibid.*, **61,** 1052 (1972).
(68) R. E. Notari and J. DeYoung, *ibid.*, **64,** 1148 (1975).
(69) W. W. Han, G. J. Yakatan, and D. D. Maness, *ibid.*, **65,** 1198 (1976).
(70) A. Hussain, T. Higuchi, A. Hurwitz, and I. H. Pitman, *ibid.*, **61,** 371 (1972).
(71) N. Bodor, J. J. Kaminski, S. D. Worley, R. J. Colton, T. H. Lee, and J. W. Rabalais, *ibid.*, **63,** 1387 (1974).
(72) E. R. Garrett, T. W. Hermann, and H.-K. Lee, *ibid.*, **63,** 899 (1974).
(73) E. R. Garrett and J. Tsau, *ibid.*, **63,** 1563 (1974).
(74) A. Hussain, *ibid.*, **58,** 316 (1969).
(75) L. W. Brown and A. A. Forist, *ibid.*, **62,** 1365 (1973).
(76) J. A. Mollica, C. R. Rehm, and J. B. Smith, *ibid.*, **58,** 635 (1969).
(77) J. A. Mollica, C. R. Rehm, J. B. Smith, and H. K. Govan, *ibid.*, **60,** 1380 (1971).
(78) H. V. Maulding, P. Turi, D. Grossman, and J. P. Nazareno, *ibid.*, **64,** 1833 (1975).
(79) J. J. Zalipsky, D. M. Patel, and N. H. Reavey-Cantwell, *ibid.*, **63,** 1784 (1974).
(80) E. R. Garrett, B. C. Lippold, and J. B. Mielck, *ibid.*, **60,** 396 (1971).
(81) E. R. Garrett and C. M. Won, *ibid.*, **60,** 1801 (1971).
(82) D. E. Guttman and P. D. Meister, *J. Am. Pharm. Assoc., Sci. Ed.*, **47,** 773 (1958).
(83) E. Pawelczyk, R. Wachowski, and A. Romanowski, *Diss. Pharm. Pharmacol.*, **19,** 567 (1967).
(84) H. D. Beckstead, K. K. Kaistha, and S. J. Smith, *J. Pharm. Sci.*, **57,** 1952 (1968).
(85) E. Pawelczyk and R. Wachowiak, *Diss. Pharm. Pharmacol.*, **21,** 491 (1969).
(86) R. W. Schmid, *Helv. Chim. Acta*, **53,** 2239 (1970).
(87) J. Slingsby and D. A. Zuck, *Can. J. Pharm. Sci.*, **7,** 115 (1972).
(88) W. Weglowska and E. Szyszko, *Farm. Pol.*, **29,** 309 (1973).
(89) D. V. C. Awang, A. Vincent, and F. Matsui, *J. Pharm. Sci.*, **62,** 1673 (1973).
(90) A. J. Forlano, C. I. Jarowski, H. F. Hammer, and E. G. Merritt, *ibid.*, **59,** 121 (1970).
(91) R. P. Enever, A. L. W. Po, B. J. Millard, and E. Shotton, *ibid.*, **64,** 1497 (1975).
(92) I. H. Pitman, T. Higuchi, M. Alton, and R. Wiley, *ibid.*, **61,** 918 (1972).
(93) D. D. Dubash and W. R. Moore, *ibid.*, **61,** 386 (1972).
(94) C. A. Zittle, *Arch. Biochem. Biophys.*, **17,** 195 (1948); through *Chem. Abstr.*, **83,** 15580b (1975).
(95) R. J. Sasseti and H. Hugh Fundenberg, *Biochem. Pharmacol.*, **20,** 57 (1971).
(96) S. M. Blaug and B. Hajratwala, *J. Pharm. Sci.*, **61,** 556 (1972).
(97) T. Fukuda and T. Miyagi, *Vitamins*, **47,** 441 (1973); through *Chem. Abstr.*, **80,** 19485k (1974).
(98) M. I. Amin and J. T. Bryan, *J. Pharm. Sci.*, **62,** 1768 (1973).
(99) H. Roseboom and J. A. Fresen, *Pharm. Acta Helv.*, **50,** 55 (1975); through *Chem. Abstr.*, **83,** 15580b (1975).
(100) I. K. Shih, *J. Pharm. Sci.*, **60,** 786 (1971).
(101) B. R. Hajratwala, *ibid.*, **64,** 45 (1975).
(102) W. A. Cressman, E. T. Sugita, J. T. Doluisio, and P. J. Niebergall, *ibid.*, **58,** 1471 (1969).
(103) R. J. Harwood, P. J. Niebergall, E. T. Sugita, and R. L. Schnaare, *ibid.*, **61,** 82 (1972).
(104) R. E. Lindsay and S. L. Heni, *ibid.*, **61,** 202 (1972).
(105) M. J. Haddadin, T. Higuchi, and V. Stella, *ibid.*, **64,** 1759 (1975).

(106) E. Pawelczyk, Z. Plotkowakowa, and E. Ponitka, *Diss. Pharm. Pharmacol.*, **22,** 449 (1970).
(107) V. H. Mihranian, *Diss. Abst. Int.*, **36,** 2822B (1975).
(108) R. P. Dzhorbenadze, V. S. Bostoganshvili, R. M. Pinyazhko, and E. K. Kyantaliani, *Soobshch. Akad. Nauk Gruz. SSR,* **81,** 625 (1976); through *Chem. Abstr.*, **85,** 37140b (1976).
(109) H. Auterhoff and A. Walter, *Dtsch. Apoth.-Ztg.*, **115,** 1931 (1975); through *Chem. Abstr.*, **84,** 140653z (1976).
(110) E. Pawelczyk and M. Opielewicz, *Acta Pol. Pharm.*, **32,** 577 (1975); through *Chem. Abstr.*, **85,** 51663f (1976).
(111) H. Okada, V. Stella, J. Halsam, and N. Yata, *J. Pharm. Sci.*, **64,** 1665 (1975).
(112) S. Y. Yeh and J. L. Lach, *ibid.*, **60,** 793 (1971).
(113) G. B. Smith, L. M. Weinstock, F. E. Roberts, Jr., G. S. Brenner, A. M. Hoinowski, B. H. Arison, and A. W. Douglas, *ibid.*, **61,** 708 (1972).
(114) G. S. Rork and I. H. Pitman, *ibid.*, **64,** 216 (1975).
(115) L. V. Hopkins, J. P. Vacik, and W. Shelver, *ibid.*, **61,** 114 (1972).
(116) E. Shami, J. Dudzinski, L. Lachman, and J. Tingstad, *ibid.*, **62,** 1283 (1973).
(117) L. Roller, *Aust. J. Pharm. Sci.*, **2,** 20 (1973).
(118) H. W. Jun, C. W. Whitworth, and L. A. Luzzi, *J. Pharm. Sci.*, **61,** 1160 (1972).
(119) C. W. Whitworth, H. W. Jun, and L. A. Luzzi, *ibid.*, **62,** 1184 (1973).
(120) Y. Otagiri, K. Uekama, and K. Ikeda, *Chem. Pharm. Bull.*, **23,** 13 (1975).
(121) G. I. Loseva and N. I. Shukailo, *Antibiotiki (Moscow)*, **17,** 895 (1972); through *Chem. Abstr.*, **78,** 7786e (1973).
(122) B. Krielgard, *Arch. Pharm. Chemi,* **80,** 1083 (1973); through *Chem. Abstr.*, **80,** 124622a (1974).
(123) A. B. A. Jansen and R. Robinson, *Montash. Chem.*, **98,** 1017 (1967).
(124) H. Bundgaard, *J. Pharm. Sci.*, **60,** 1273 (1971).
(125) T. O. Oesterling, *Carbohydr. Res.*, **15,** 285 (1970).
(126) T. O. Oesterling and C. M. Metzler, *J. Pharm. Sci.*, **61,** 287 (1972).
(127) K. D. Schlecht and C. W. Frank, *ibid.*, **62,** 258 (1973).
(128) M. A. Nunes and E. Brochmann-Hanssen, *ibid.*, **63,** 716 (1974).
(129) D. C. Monkhouse, L. Van Campen, and A. J. Aguiar, *ibid.*, **62,** 576 (1973).
(130) H. Bundgaard, *Acta Pharm. Suec.*, **13,** 9 (1976); through *Chem. Abstr.*, **84,** 155597h (1976).
(131) M. A. Schwartz and W. L. Hayton, *J. Pharm. Sci.*, **61,** 906 (1972).
(132) G. N. Levy, J. V. Ioia, and E. J. Kuchinskas, *ibid.*, **63,** 1197 (1974).
(133) J. C. Dearden, *ibid.*, **61,** 1661 (1972).
(134) W. O. Foye and J.-R. Lo, *ibid.*, **61,** 1209 (1972).
(135) M. J. Akers, *Can. J. Pharm. Sci.*, **11,** 1 (1976); through *Chem. Abstr.*, **84,** 126659z (1976).
(136) E. Nuernberg, *Dtsch. Apoth.-Ztg.*, **114,** 411, 1715 (1974); through *Chem. Abstr.*, **82,** 34973c (1975).
(137) Y. Datt, *Pharmacos,* **17,** 41 (1972); through *Chem. Abstr.*, **79,** 35051a (1973).
(138) V. Parrak, *Farmatsiya (Moscow)*, **21,** 14 (1972); through *Chem. Abstr.*, **76,** 158234h (1972).
(139) J. Tingstad and J. Dudzinski, *J. Pharm. Sci.*, **62,** 1856 (1973).
(140) F. Ebel and O. Mastilovic, *Hem. Ind.*, **29,** 587 (1975); through *Chem. Abstr.*, **84,** 126704k (1976).
(141) D. G. Pope and J. L. Lach, *Pharm. Acta Helv.*, **50,** 165 (1975); through *Chem. Abstr.*, **83,** 103184f (1975).
(142) H. Stricku, *Pharm. Ind.*, **37,** 446 (1975) through *Chem. Abstr.*, **83,** 168340y (1975).
(143) S. L. Mills, V. L. Allen, R. S. Levinson, and W. F. Stansszek, *IRCS Med. Sci. Libr. Compend.*, **3,** 592 (1975); through *Chem. Abstr.*, **84,** 111560m (1976).
(144) R. Adamski and J. Sawicka, *Herba Pol.*, **20,** 57 (1974); through *Chem. Abstr.*, **82,** 64392e (1975).
(145) O. Valls, J. M. Lopez, M. Castillo, and V. Vilas, *Circ. Farm.*, **30,** 67 (1972); through *Chem. Abstr.*, **77,** 52266a (1972).
(146) Z. M. Akopyan, *Biol. Zh. Arm.*, **26,** 84 (1973); through *Chem. Abstr.*, **79,** 118266a (1973).
(147) V. K. Prasad, A. P. Granatek, and M. M. Mihotic, *Curr. Ther. Res., Clin. Exp.*, **16,** 505 (1974); through *Chem. Abstr.*, **81,** 82310k (1974).
(148) V. Naggar, N. A. Daabis, and M. M. Motawi, *Pharmazie,* **29,** 126 (1974); through *Chem. Abstr.*, **81,** 82304m (1974).
(149) K. Howorka, B. Howorka, and R. Meyer, *ibid.*, **28,** 136 (1973); through *Chem. Abstr.*, **78,** 128395k (1973).
(150) D. Monciu and M. Boteanu, *Farmacia (Bucharest)*, **22,** 467 (1974); through *Chem. Abstr.*, **84,** 111558s (1976).
(151) V. Springer, M. Struhar, M. Heliova, J. Majer, and M. Chalabala, *Cesk. Farm.*, **23,** 356 (1974); through *Chem. Abstr.*, **82,** 175202n (1975).
(152) R. F. Nite, U.S. pat. 3,966,905, June 29, 1976; through *Chem. Abstr.*, **85,** 83246p (1976).
(153) H. Auterhoff and C. I. Einberger, *Dsch. Apoth.-Ztg.*, **113,** 1817 (1973); through *Chem. Abstr.*, **80,** 52329k (1974).
(154) H. Seydel and R. Voigt, *Pharmazie,* **27,** 303 (1972); through *Chem. Abstr.*, **77,** 66162a (1972).
(155) G. Branchi and E. Mecarelli, *Farmaco Ed. Prat.*, **30,** 605 (1975); through *Chem. Abstr.*, **84,** 49810n (1976).
(156) J. J. V. DeSouza and B. K. Gupta, *Indian J. Pharm.*, **34,** 12 (1972); through *Chem. Abstr.*, **76,** 131454t (1972).
(157) G. N. Takacsi and V. Farkas, *Gyogyzereszet,* **16,** 288 (1972); through *Chem. Abstr.*, **77,** 130569t (1972).
(158) A. Puech, C. Duru, M. Jacob, and M. Esperandieu, *Trav. Soc. Pharm. Montpellier,* **36,** 101 (1976); through *Chem. Abstr.*, **85,** 99121e (1976).
(159) N. I. Laricheva, A. B. Marulin, Z. P. Fedorova, N. I. Andrievskii, L. F. Klimenko, and Z. M. Boltanova, *Gematol. Pereliv. Krovi,* **1972,** 107; through *Chem. Abstr.*, **78,** 7788g (1973).
(160) Z. I. Bul'varova, *Sb. Nauch. Tr. Tsent. Aptech. Nauch.-Issled Inst.*, **1971,** 75; through *Chem. Abstr.*, **77,** 118179h (1972).
(161) N. G. Seleznev and B. V. Nazarov, *Farmatsiya (Moscow)*, **24,** 65 (1975); through *Chem. Abstr.*, **84,** 35249z (1976).
(162) A. Karig, G. E. Peck, and G. J. Sperandio, *J. Pharm. Sci.*, **62,** 396 (1973).
(163) E. Ullmann and F. Sommer, *Pharm. Ind.*, **34,** 351 (1972); through *Chem. Abstr.*, **78,** 164069r (1973).
(164) T. Beyrich, W. Zywica, D. Kottke, B. Kemma, and W. Thiele, *Pharmazie,* **29,** 517 (1974); through *Chem. Abstr.*, **82,** 7608f (1975).
(165) S. Adamski and E. Pawlak, *Acta Pol. Pharm.*, **29,** 409 (1972); through *Chem. Abstr.*, **78,** 47713k (1973).
(166) A. F. Asker, M. A. Helal, and M. M. Motawi, *Pharmazie,* **26,** 90 (1971); through *Chem. Abstr.*, **74,** 115846a (1971).
(167) A. A. Kassem and A. Abd El-Bary, *Bull. Fac. Pharm., Cairo Univ.*, **11,** 161 (1972); through *Chem. Abstr.*, **81,** 140821r (1974).
(168) S. Shimizu, K. Yana, K. Furukawa, T. Takeda, Y. Mizuuchi, K. Narita, and T. Sato, *Iryo,* **27,** 742 (1973); through *Chem. Abstr.*, **82,** 175190g (1975).
(169) A. R. Ebian, M. A. Moustafa, S. A. Khalil, and M. M. Motawi, *J. Pharm. Sci.*, **64,** 1481 (1975).
(170) W. Erni and K. Leupin, *Pharm. Acta Helv.*, **50,** 275 (1975).
(171) A. Popovici and M. Rogosca, *Rev. Med.*, **21,** 24 (1975); through *Chem. Abstr.*, **84,** 35280c (1976).
(172) A. Popovici, *Farmacia (Bucharest)*, **21,** 109 (1973); through *Chem. Abstr.*, **79,** 70159p (1973).
(173) I. M. Pertsev, A. I. Goncharov, D. P. Salo, T. E. Sidorova, I. Y. Kholupyak, E. M. Dikaya, and V. M. Turchaneko, *Farm. Zh. Kiev,* **4,** 46 (1976); through *Chem. Abstr.*, **85,** 130460r (1976).
(174) M. Ponec-Waelsch and H. J. Hulsebosch, *Arch. Dermatol. Forsch.*, **249,** 141 (1974); through *Chem. Abstr.*, **81,** 29490t (1974).
(175) T. Cieszynski, *Acta Pol. Pharm.*, **32,** 371 (1975); through *Chem. Abstr.*, **84,** 79658m (1976).
(176) *Ibid.*, **31,** 99 (1974); through *Chem. Abstr.*, **81,** 111428n (1974).
(177) A. Nakamura and R. Okada, *Colloid Polym. Sci.*, **254,** 718 (1976); through *Chem. Abstr.*, **85,** 112718b (1976).
(178) M. J. Akers and J. L. Lach, *J. Pharm. Sci.*, **65,** 216 (1976).
(179) S. L. Nail, J. L. White, and S. L. Hem, *ibid.*, **65,** 1255 (1976).
(180) *Ibid.*, **65,** 1195 (1976).
(181) K. Thoma and E. Vasters, *Pharm. Ztg.*, **119,** 1591 (1974); through *Chem. Abstr.*, **82,** 77038u (1974).
(182) J. T. H. Ong and H. B. Kostenbauder, *J. Pharm. Sci.*, **65,** 1713 (1976).
(183) J. T. Carstensen and P. Pothisiri, *ibid.*, **64,** 37 (1975).
(184) P. Pothisiri and J. T. Carstensen, *ibid.*, **64,** 1931 (1975).
(185) E. Nelson, D. Eppich, and J. T. Carstensen, *ibid.*, **63,** 755 (1974).
(186) A. H. Kibbe, *Diss. Abst. Int.*, **34,** 5048-B (1974).

(187) R. E. Davis, *J. Phys. Chem.*, **63,** 307 (1959).
(188) A. R. Rogers, *J. Pharm. Pharmacol.*, **15,** 101T (1963).
(189) S. P. Ericksen and H. J. Stelmach, *J. Pharm. Sci.*, **54,** 1029 (1965).
(190) M. A. Zoglio, J. J. Windheuser, R. Vatti, H. V. Maulding, S. S. Kornblum, A. Jacobs, and H. Hamot, *ibid.*, **57,** 2080 (1968).
(191) H. V. Maulding and M. A. Zoglio, *ibid.*, **59,** 333 (1970).
(192) A. I. Kay and T. H. Simon, *ibid.*, **60,** 205 (1971).
(193) R. A. Anderson and M. Campbell, *Aust. J. Pharm.*, **52,** S81 (1971).
(194) B. W. Madsen, R. A. Anderson, D. Herbison-Evans, and W. Sneddon, *J. Pharm. Sci.*, **63,** 777 (1974).
(195) H. J. Borchardt and F. Daniels, *J. Am. Chem. Soc.*, **79,** 41 (1957).
(196) M. A. Zoglio, H. V. Maulding, W. H. Streng, and W. C. Vincek, *J. Pharm. Sci.*, **64,** 1381 (1975).
(197) I. Matsuura and M. Kawamata, *Yakugaku Zasshi*, **95,** 1255 (1975); through *Chem. Abstr.*, **84,** 49784g (1976).
(198) N. Okusa, *Chem. Pharm. Bull.*, **23,** 794 (1975).
(199) S. Szabo and B. Kovacs, *Gyogyszereszet*, **14,** 464 (1970); through *Chem. Abstr.*, **75,** 25039u (1971).
(200) A. Otuska, T. Wakimoto, and A. Takeda, *Yakugaku Zasshi*, **96,** 351 (1976).
(201) Y. Hammouda and S. A. Salakawy, *Pharmazie*, **26,** 636 (1971); through *Chem. Abstr.*, **75,** 154944w (1971).
(202) V. F. Naggar, A. S. Khalil, and N. A. Daabis, *ibid.*, **31,** 461 (1976); through *Chem. Abstr.*, **85,** 130471v (1976).
(203) M. J. Pikal, A. L. Lukes, and L. F. Ellis, *J. Pharm. Sci.*, **65,** 1278 (1976).
(204) Y. Matsuda and Y. Minamida, *Yakugaku Zasshi*, **96,** 425 (1976); through *Chem. Abstr.*, **85,** 10387a (1976).
(205) B. R. Hajratwala, *J. Pharm. Sci.*, **63,** 129 (1974).
(206) *Ibid.*, **63,** 1927 (1974).
(207) S. R. Dasgupta, S. Sikdar, and N. M. Ray, *Bull. Univ. Coll. Med., Calcutta Univ.*, **1969,** 7–8, 19–21; through *Chem. Abstr.*, **80,** 100148z (1974).
(208) A. S. Alam and E. L. Parrott, *J. Pharm. Sci.*, **60,** 263 (1971).
(209) E. Kristofferson and K. Keto, *Farm. Aikak*, **82,** 45 (1973); through Ref. 211.
(210) G. L. Mattok, I. J. McGilveray, and C. A. Mainville, *J. Pharm. Sci.*, **60,** 561 (1971).
(211) D. Barrett and J. T. Fell, *ibid.*, **64,** 335 (1975).
(212) L. Chafetz, *ibid.*, **60,** 335 (1971).
(213) S. Siggia, "Instrumental Methods of Organic Functional Group Analysis," Wiley-Interscience, New York, N.Y., 1972.
(214) S. Siggia, "Quantitative Organic Analysis via Functional Groups," Wiley, New York, N.Y., 1963.
(215) J. A. Mollica and K. S. Lin, *Bull. Parenter. Drug Assoc.*, **25,** 140 (1971).
(216) "The United States Pharmacopeia," 19th rev., Mack Publishing Co., Easton, Pa., 1975.
(217) "The National Formulary," 14th ed., Mack Publishing Co., Easton, Pa., 1975.
(218) D. C. Monkhouse and J. L. Lach, *Can. J. Pharm. Sci.*, **7,** 29 (1972).
(219) K. Syre, *Acta Pharm. Technol.*, **21,** 199 (1975); through *Chem. Abstr.*, **83,** 209340u (1975).
(220) S. H. Rubin, E. DeRitter, and J. B. Johnson, *J. Pharm. Sci.*, **65,** 963 (1976).
(221) G. S. D. Gupta and V. K. M. Rao, *Res. Ind.*, **15,** 111 (1970); through *Chem. Abstr.*, **75,** 25320r (1971).
(222) A. H. Thomas, *Analyst*, **101,** 321 (1976).
(223) S. L. Ali, *Pharm. Ztg.*, **121,** 201 (1976).
(224) T. O. Oesterling, W. Morozowich, and T. J. Roseman, *J. Pharm. Sci.*, **61,** 1873 (1972).
(225) B. Dorsch and R. Shangraw, *Am. J. Hosp. Pharm.*, **32,** 795 (1975).
(226) J. Lindquist and S. M. Farroha, *Analyst*, **100,** 377 (1975).
(227) E. M. Cohen, *J. Pharm. Sci.*, **60,** 1702 (1971).
(228) D. A. Hall, *ibid.*, **62,** 980 (1973).
(229) F. Feigl, V. Auger, and O. Frehder, *Mikrochemie*, **15,** 18 (1934); through Ref. 232.
(230) S. Soloway and A. Lipschitz, *Anal. Chem.*, **24,** 898 (1952).
(231) E. Schleider, D. M. Eno, J. A. Feldman, and A. M. Galinsky, *J. Pharm. Sci.*, **58,** 1258 (1969).
(232) J. A. Feldman and V. U. Patel, *ibid.*, **60,** 1696 (1971).
(233) "Code of Federal Regulations," Title 21, 436.205 (1975).
(234) F. Le Pedriel, C. Hanegraff, N. Chastagner, and E. LeMontety, *Ann. Farm. Fr.*, **26,** 227 (1968); through Ref. 236.
(235) M. C. Inamdar and N. N. Kaji, *Indian J. Pharm.*, **31,** 79 (1969).
(236) L. Chafetz, R. E. Daly, H. Schriftman, and J. J. Lomner, *J. Pharm. Sci.*, **60,** 463 (1971).
(237) S. Ahuja, D. Spiegel, and F. R. Brofazi, *ibid.*, **59,** 417 (1970).
(238) D. Spiegel, S. Ahuja, and F. R. Brofazi, *ibid.*, **61,** 1630 (1972).
(239) N. Wahba, D. A. Yassa, and R. S. Labib, *Analyst*, **99,** 397 (1974).
(240) R. B. Salama and H. A. El-Obeid, *ibid.*, **101,** 136 (1976).
(241) E. Fahmy, D. A. Yassa, and N. Wahba, *ibid.*, **101,** 616 (1976).
(242) L. Chafetz, *J. Pharm. Sci.*, **60,** 291 (1971).
(243) C. W. Whitworth, H. W. Jun, and L. A. Luzzi, *ibid.*, **62,** 1184 (1973).
(244) J. W. Munson and K. A. Connors, *ibid.*, **61,** 211 (1972).
(245) P. M. Monteleone, M. K. Vasiljev, and J. Bomstein, *ibid.*, **62,** 1830 (1973).
(246) B. M. Frantz, *ibid.*, **65,** 887 (1976).
(247) R. F. Miller, T. D. Sokoloski, L. A. Mitscher, A. C. Bonacci, and B. A. Hoener, *ibid.*, **62,** 1143 (1973).
(248) V. K. Prasad, R. A. Ricci, B. C. Nunning, and A. P. Granatek, *ibid.*, **62,** 1130 (1973).
(249) *Ibid.*, **62,** 1135 (1973).
(250) D. M. Rackham, *Talanta*, **23,** 269 (1976); through *Chem. Abstr.*, **85,** 51787z (1976).
(251) R. E. Schirmer, R. E. Zemer, and G. G. Cooke, *J. Pharm. Sci.*, **61,** 428 (1972).
(252) J. W. Turczan and T. Medwick, *ibid.*, **65,** 235 (1976).
(253) O. F. Nielson, E. J. Pedersen, L. S. Nielsen, and V. Faurby, *Arch. Pharm. Chemi, Sci. Ed.*, **3,** 84 (1975); through *Chem. Abstr.*, **84,** 22137m (1976).
(254) R. C. Sharma and S. K. Gupta, *J. Sci. Ind. Res.*, **34,** 641 (1975); through *Chem. Abstr.*, **85,** 51790v (1976).
(255) N. Trius and A. P. Arzamastev, *Farm. Zh. (Kiev)*, **31,** 27 (1976); through *Chem. Abstr.*, **85,** 51792x (1976).
(256) D. J. Berry, *Scan*, **5,** 14 (1974); through *Chem. Abstr.*, **84,** 184949e (1976).
(257) T. Inoue, *Iyakuhin Seiza No Buneski*, **1975,** 123; through *Chem. Abstr.*, **84,** 111709s (1976).
(258) *Ibid.*, **1975,** 132; through *Chem. Abstr.*, **84,** 111710k (1976).
(259) A. Ejiima, *Iyakukin Seiza No Buneski*, **1975,** 151; through *Chem. Abstr.*, **84,** 111711m (1976).
(260) S. Ahuja, *J. Pharm. Sci.*, **65,** 163 (1976).
(261) D. R. Baker, *Am. Lab.*, **8,** 93 (1976).
(262) A. P. Shroff, *ibid.*, **8,** 13 (1976).
(263) F. Bailey, *J. Chromatogr.*, **122,** 73 (1976).
(264) M. Ichinose, *Med. Pharm.*, **10,** 64 (1976); through *Chem. Abstr.*, **85,** 25431j (1976).
(265) K. Macek, in "Chromatography," E. Heftman, Ed., Van Nostrand Reinhold Co., New York, N.Y., 1975, p. 139.
(266) M. K. Youssef, E. A. Ibrahim, and I. A. Attia, *J. Pharm. Sci.*, **62,** 1998 (1973).
(267) N. G. Selezenev and B. V. Nazarov, *Sb. Nauchn. Tr., Ryazan Med Inst.*, **50,** 151 (1975); through *Chem. Abstr.*, **84,** 126687g (1976).
(268) S. Ahuja, "Quantitative Thin-layer Chromatography in Pharmaceutical Analysis," presented at FACSS Second National Meeting, Indianapolis, Ind., Oct. 7, 1975.
(269) J. C. Touchstone, "Quantitative Thin-layer Chromatography," Wiley, New York, N.Y., 1973.
(270) V. Massa, P. Susplugas, and G. Balansard, *Trav. Soc. Pharm. Montpellier*, **35,** 373 (1975); through *Chem. Abstr.*, **84,** 140791t (1976).
(271) A. Domingues-Gil, R. Cadorniga, and A. Valls, *Cienc. Ind. Farm.*, **7,** 163 (1975); through *Chem. Abstr.*, **83,** 168387u (1975).
(272) T. Stanciu, *Farmacia (Bucharest)*, **24,** 37 (1976); through *Chem. Abstr.*, **85,** 68340w (1976).
(273) M. I. Blake, K. Makris, and J. Hunt, *J. Pharm. Sci.*, **60,** 1694 (1971).
(274) G. H. Kronberg and B. H. Takman, *ibid.*, **62,** 823 (1973).
(275) E. Shotton and D. J. Priaulx, *J. Pharm. Pharmacol.*, **26,** 197 (1974).
(276) F. F. Cantwell, M. Domjan, and C. F. Hiskey, *J. Pharm. Sci.*, **63,** 599 (1974).
(277) W. W. Fike and N. W. Brake, *ibid.*, **61,** 615 (1972).
(278) J. R. Watson, P. Crescuolo, and F. Matsui, *ibid.*, **60,** 454 (1971).

(279) J. R. Watson, F. Matsui, P. M. J. McConnell, and R. C. Lawrence, *ibid.*, **61,** 929 (1972).
(280) G. Settinj, L. DiSimone, and M. R. DelGiudice, *J. Chromatogr.*, **116,** 263 (1976).
(281) L. A. Svensson, *Acta Pharm. Suec.*, **9,** 141 (1972); through *Chem. Abstr.*, **77,** 52261v (1972).
(282) M. P. Gruber, R. W. Klein, M. E. Foxx, and J. Campisi, *J. Pharm. Sci.*, **61,** 1147 (1972).
(283) J. J. Windheuser, J. L. Sutter, and A. Sarrif, *ibid.*, **61,** 1311 (1972).
(284) S. Patel, J. H. Perrin, and J. J. Windheuser, *ibid.*, **61,** 1794 (1972).
(285) B. L. Chang, B. F. Grabowski, and W. G. Haney, Jr., *ibid.*, **62,** 1337 (1973).
(286) D. L. Sondack, F. E. Gainer, and H. J. Wesselman, *ibid.*, **62,** 1344 (1973).
(287) B. J. Millard, D. J. Priaulx, and E. Shotton, *J. Pharm. Pharmacol., Suppl.*, **25,** 24P (1973).
(288) N. D. Greenwood and I. D. Guppy, *Analyst*, **99,** 313 (1974).
(289) R. W. Souter and A. Dinner, *J. Pharm. Sci.*, **65,** 457 (1976).
(290) B. S. Rutherford and R. H. Bishara, *ibid.*, **65,** 1322 (1976).
(291) B. J. Meakin, D. J. G. Davis, N. Cox, and J. Stevens, *Analyst*, **101,** 720 (1976).
(292) M. P. Rabinowtiz, P. Reisberg, and J. I. Bodin, *J. Pharm. Sci.*, **61,** 1974 (1972).
(293) O. D. Boughton, R. D. Brown, R. Bryant, F. J. Burger, and C. M. Combs, *ibid.*, **61,** 97 (1972).
(294) T. Kaneko, Y. Tsuji, and K. Suzuki, *Igaku No Ayumi*, **95,** 226 (1975); through *Chem. Abstr.*, **84,** 79651d (1976).
(295) A. DeLeenheer, J. E. Sinsheimer, and J. A. Burckhalter, *J. Pharm. Sci.*, **61,** 1659 (1972).
(296) *Analyst*, **100,** 136 (1975).
(297) F. H. Lincoln, U. Alexen, K. Green, H. Ohlsson, and B. Samuelsson, *Anal. Lett.*, **9,** 187 (1976).
(298) A. F. Michaelis, D. W. Cornish, and R. Vivilecchia, *J. Pharm. Sci.*, **62,** 1399 (1973).
(299) F. Bailey and P. N. Brittain, *J. Chromatogr.*, **83,** 431 (1973).
(300) F. Bailey, *Biochem. Soc. Trans.*, **3,** 861 (1975); through *Chem. Abstr.*, **84,** 140776s (1976).
(301) W. Morozowich, *J. Pharm. Sci.*, **63,** 800 (1974).
(302) R. W. Roos, *ibid.*, **61,** 1979 (1972).
(303) J. M. Blaha, A. M. Knevel, and S. L. Hem, *ibid.*, **64,** 1384 (1975).
(304) K. Tsuji and J. H. Robertson, *ibid.*, **64,** 1542 (1975).
(305) A. G. Butterfield, D. W. Hughes, W. L. Wilson, and N. J. Pound, *ibid.*, **64,** 316 (1975).
(306) E. Murgia, P. Richards, and H. F. Walton, *J. Chromatogr.*, **87,** 523 (1973).
(307) R. B. Poet and H. H. Pu, *J. Pharm. Sci.*, **62,** 809 (1973).
(308) T. C. Kram, *ibid.*, **61,** 254 (1972).
(309) J. A. Mollica, G. R. Padmanabhan, and R. Strusz, *Anal. Chem.*, **45,** 1859 (1973).
(310) D. J. Webber, *J. Pharm. Sci.*, **61,** 1797 (1972).
(311) D. Wittmer and W. G. Haney, Jr., *ibid.*, **63,** 588 (1974).
(312) M. H. Penner, *ibid.*, **64,** 1017 (1975).
(313) K. A. Tartivita, J. P. Sciarello, and B. C. Ruddy, *ibid.*, **65,** 1024 (1976).
(314) D. E. Williamson, *ibid.*, **65,** 138 (1976).
(315) K. S. Lundy and B. Salvesen, *Med. Norsk Farm. Selsk.*, **37,** 64 (1975).
(316) J. E. Evans, *Anal. Chem.*, **45,** 2428 (1973).
(317) P. P. Ascione and G. P. Chrekian, *J. Pharm. Sci.*, **64,** 1029 (1975).
(318) J. A. Mollica and R. F. Strusz, *ibid.*, **61,** 444 (1972).
(319) F. A. Fitzpatrick and S. Siggia, *Anal. Chem.*, **45,** 2310 (1973).
(320) L. D. Bighley and J. P. McDonnell, *J. Pharm. Sci.*, **64,** 1549 (1975).
(321) S. K. W. Khalil and W. H. Shelver, *ibid.*, **65,** 606 (1976).
(322) K. Tsuja and J. H. Robertson, *ibid.*, **65,** 400 (1976).
(323) R. W. Roos, *ibid.*, **63,** 594 (1974).
(324) K. Bhatia, *Anal. Chem.*, **45,** 1344 (1973).
(325) H. Bethke, B. Delz, and K. Stich, *J. Chromatogr.*, **123,** 193 (1976).
(326) J. R. Salmon and P. R. Wood, *Analyst*, **101,** 611 (1976).
(327) R. A. Henry, J. A. Schmit, and J. F. Diechman, *J. Chromatogr. Sci.*, **9,** 513 (1971).
(328) R. C. Williams, D. R. Baker, and J. A. Schmit, *ibid.*, **11,** 618 (1973).
(329) P. Larson, E. Murgia, T.-J. Hsu, and H. F. Walton, *Anal. Chem.*, **45,** 2306 (1973).
(330) "The Merck Index," 9th ed., M. Windholz, Ed., Merck & Co., Rahway, N.J., 1976.
(331) "Analytical Profiles of Drug Substances," K. Florey, Ed., Academic, New York, N.Y.
(332) M. Steczko, *Farm. Pol.*, **27,** 579 (1971); through *Chem. Abstr.*, **76,** 6680n (1972).
(333) M. A. El-Egakey, F. El-Khawas, A. G. Iskander, and M. M. Abd El-Khalek, *Pharmazie*, **29,** 466 (1974); through *Chem. Abstr.*, **82,** 21788w (1975).
(334) A. Stamm and C. Mathis, *J. Pharm. Belg.*, **28,** 328 (1937); through *Chem. Abstr.*, **79,** 70178u (1973).
(335) A. A. Kassem and W. Darwish, *Bull. Fac. Pharm., Cairo Univ.*, **11,** 129 (1972); through *Chem. Abstr.*, **82,** 7596a (1975).
(336) J. H. Wood, *Drug Dev. Commun.*, **2,** 33 (1976).
(337) "Code of Federal Regulations," Title 21, 250.300 (1976).
(338) H. L. M. Cox, *Pharm. Weekbl.*, **108,** 605 (1973); through *Chem. Abstr.*, **79,** 108032g (1973).
(339) K. Thoma and R. Groening, *Pharm. Ind.*, **36,** 876 (1974); through *Chem. Abstr.*, **82,** 129236d (1975).
(340) W. Kross and H. J. Roth, *Pharm. Ztg.*, **120,** 1490 (1975); through *Chem. Abstr.*, **84,** 22035b (1976).
(341) D. Banes, *J. Pharm. Sci.*, **57,** 893 (1968).
(342) "The United States Pharmacopeia," 19th rev., Mack Publishing Co., Easton, Pa., 1975, p. 7.
(343) "The National Formulary," 14th ed., Mack Publishing Co., Easton, Pa., 1975, p. 15.
(344) "The United States Pharmacopeia, 19th rev., Mack Publishing Co., Easton, Pa., 1975, p. 647.
(345) "The National Formulary," 14th ed., Mack Publishing Co., Easton, Pa., 1975, p. 888.
(346) "The United States Pharmacopeia," 19th rev., Second Interim Revision Announcement, Pertaining to USP XIX and NF XIV, July 1, 1976.
(347) E. O. Krueger, in "Control Procedures in Drug Production," W. L. Blockstein, Ed., University of Wisconsin, Madison, Wis., 1966, p. 39.
(348) D. A. Dean, *Drug Dev. Commun.*, **2,** 109 (1976).
(349) G. Huebner, *Pharm. Ind.*, **37,** 930 (1975); through *Chem. Abstr.*, **84,** 111522a (1976).
(350) C. F. Ross, "Packaging of Pharmaceuticals," Butterworth, London, England, 1975; through *Chem. Abstr.*, **84,** 65250k (1976).
(351) E. Spingler, *Pharm. Ind.*, **33,** 831 (1971); through *Chem. Abstr.*, **76,** 131459y (1972).
(352) V. E. Krogerus, E. Nieminen, and U. M. Savolainen, *Farm. Aikak*, 79, 101 (1970); through *Chem. Abstr.*, **74,** 34608x (1971).
(353) J. Surowiecki and L. Krowczynski, *Acta Pol. Pharm.*, **29,** 285 (1972); through *Chem. Abstr.*, **77,** 130564n (1972).
(354) A. Stawowczyk, L. Krowezynski, and D. Klose, *Farm. Pol.*, **32,** 201 (1976); through *Chem. Abstr.*, **85,** 68212f (1976).
(355) L. V. Sevenko, L. S. Tellerman, and G. S. Bashura, *Khim.-Farm. Zh.*, **10,** 94 (1976); through *Chem. Abstr.*, **85,** 99151q (1976).
(356) A. B. Reed, *Am. Perfum. Cosmet.*, **86** (1971).
(357) *Soc. Fr. Sci. Tech. Pharm., Sci. Tech. Pharm.*, **4,** 291, 315 (1975); through *Chem. Abstr.*, **83,** 197777b (1975).
(358) J. R. Cloche, *Labo-Pharma-Probl. Tech.*, **22,** 119, 123 (1974); through *Chem. Abstr.*, **81,** 140802k (1974).
(359) B. Arbona and B. Douchairie, *ibid.*, **22,** 135 (1974); through *Chem. Abstr.*, **81,** 140805p (1974).
(360) J. J. Farley and J. N. Drummond, *Bull. Parenter. Drug Assoc.*, **30,** 187 (1976).
(361) F. Jaumain-Denis, A. M. Guyot-Hermann, and M. Traisnel, *Bull. Soc. Pharm. Lille*, No. 2, 119 (1970); through *Chem. Abstr.*, **74,** 34607w (1971).
(362) S. Hombrowski and W. Zalewski, *Polim. Med.*, 1, 85 (1971); through *Chem. Abstr.*, **76,** 117441e (1972).
(363) J. H. DeWilde, *Pharm. Weekbl.*, **107,** 724 (1972); through *Chem. Abstr.*, **78,** 33818m (1973).
(364) E. Spingler, *ibid.*, **107,** 813 (1972); through *Chem. Abstr.*, **78,** 101901k (1973).
(365) B. Eric, *Am. Perfum. Cosmet.*, **87,** 27 (1972).
(366) A. I. Artem'ev, *Farmatsiya (Moscow)*, **19,** 29 (1970); through *Chem. Abstr.*, **74,** 15716q (1971).
(367) M. Traisnel, *Prod. Probl. Pharm.*, **26,** 126 (1971); through *Chem. Abstr.*, **75,** 25265b (1971).

(368) B. Skaletzki and H. Wollman, *Pharmazie*, **28**, 1 (1973); through *Chem. Abstr.*, **78**, 140385q (1973).
(369) V. Leoni, *Farmaco, Ed. Prat.*, **30**, 3 (1975); through *Chem. Abstr.*, **82**, 116009g (1975).
(370) J. Cooper, "Plastic Containers for Pharmaceuticals—Testing & Control," WHO Offset Publication No. 4, 1974.
(371) T. Beyrich and A. Mehr, *Pharmazie*, **30**, 715 (1975); through *Chem. Abstr.*, **84**, 126747b (1976).
(372) H. J. Senf and H. Wollmann, *ibid.*, **31**, 290 (1976); through *Chem. Abstr.*, **85**, 51723a (1976).
(373) M. Traisnel, *Prod. Probl. Pharm.*, **26**, 37 (1971); through *Chem. Abstr.*, **74**, 130292k (1971).
(374) "The United States Pharmacopeia," 19th rev., Mack Publishing Co., Easton, Pa., 1975, p. 707.
(375) R. F. Shangraw and A. M. Contractor, *J. Am. Pharm Assoc.*, **NS 512**, 633 (1972).
(376) "Code of Federal Regulations," Title 21, 250.300 (1976).
(377) V. A. Russell, W. Lund, and M. Lynch, *Pharm. J.*, **211**, 466 (1973); through *Chem. Abstr.*, **80**, 52339p (1974).
(378) R. Adamski and A. Socha, *Farm. Pol.*, **29**, 421 (1973); through *Chem. Abstr.*, **80**, 19464c (1974).
(379) E. R. Block and J. E. Bennett, *Antimicrob. Agents Chemother.*, **4**, 648 (1973); through *Chem. Abstr.*, **80**, 52328j (1974).
(380) A. Hiort, K. Karlsson, U. Meresaan, and S. O. Nilsson, *Sv. Farm. Tidskr.*, **78** (19), 896 (1974); through *Chem. Abstr.*, **82**, 160210q (1975).
(381) R. F. Bergstrom, A. L. Fites, and J. W. Lamb, *Am. J. Hosp. Pharm.*, **32**, 887 (1975); through *Chem. Abstr.*, **83**, 209364e (1975).
(382) C. I. Hicks, J. P. B. Gallardo, and J. K. Guillory, *ibid.*, **29**, 210 (1972).
(383) R. S. Levi and T. L. Benney, in "The Dating of Pharmaceuticals," J. J. Windheuser, Ed., University of Wisconsin, Madison, Wis., 1970, p. 58.
(384) J. D. Haynes, *J. Pharm. Sci.*, **60**, 927 (1971).
(385) S. Wahlgren, *Acta Pharm. Technol.*, **21**, 3 (1975); through J. E. Fairbrother, "Current Aspects of Pharmaceutical Analysis," *Pharm. J.*, **217**, 210 (1976).
(386) W. Grimm, *ibid.*, **21**, 73 (1975); through *ibid.*
(387) E. Spingler, *ibid.*, **21**, 89 (1975); through *ibid.*
(388) M. Feinberg, in "The Dating of Pharmaceuticals," J. J. Windheuser, Ed., University of Wisconsin, Madison, Wis., 1970, p. 143.
(389) J. L. Kiger, *Rev. Port. Farm.*, **23**, 271 (1973); through *Chem. Abstr.*, **80**, 100121k (1974).
(390) J. L. Kiger, *Rev. Int. Serv. Sante Armees Terre, Mer Air*, **47**, 707 (1974); through *Chem. Abstr.*, **82**, 160144w (1975).
(391) P. Schumacher, *Pharm. Ztg.*, **119**, 321 (1974); through *Chem. Abstr.*, **81**, 96343k (1974).
(392) C. J. Lintner, in "Remington's Pharmaceutical Sciences," 15th ed., 1975, p. 1419.
(393) J. T. Carstensen, "Methods of Stability Prediction," presented at the Manufacturing Controls Seminar, Proprietary Association/FDA, Cherry Hill, N.J., Oct. 21, 22, 1971.
(394) J. H. Graham, "Some Aspects of the Problem of Drug Stability," presented at FDA Drug Industry Workshop, Austin, Tex., Feb. 23, 1971.
(395) N. G. Lordi and M. W. Scott, *J. Pharm. Sci.*, **54**, 531 (1965).
(396) J. Bolos, M. Castillo, and V. Vilas. *Farmaco, Ed. Prat.*, **27**, 258 (1972); through *Chem. Abstr.*, **77**, 39129p (1972).
(397) W. Grimm, *Acta Pharm. Technol.*, **21**, 223 (1975); through *Chem. Abstr.*, **84**, 95580k (1976).
(398) J. T. Carstensen and K. S. E. Su, *Bull. Parenter. Drug Assoc.*, **25**, 287 (1971); through *Chem. Abstr.*, **76**, 63138r (1972).
(399) A. J. Woolfe and H. E. C. Worthington, *Drug Dev. Commun.*, **1**, 185 (1974–5).
(400) E. R. Garrett and R. F. Carper, *J. Am. Pharm. Assoc., Sci. Ed.*, **44**, 515 (1955).
(401) P. Turi, D. Brusco, H. V. Maulding, R. A. Tausendfreund, and A. F. Michaelis, *J. Pharm. Sci.*, **61**, 1811 (1972).
(402) G. W. Holyner, *Riechst. Aromen., Koerperpflegem.*, **25**, 66 (1975); through *Chem. Abstr.*, **83**, 168325x (1975).
(403) N. Yanishlieva and A. Popov, *Seifen, Oele, Fette, Wachse*, **101**, 185 (1975); through *Chem. Abstr.*, **83**, 120653a (1975).
(404) M. Traisnel and H. Robert, *Labo-Pharma-Probl. Tech.*, **21**, 63 (1973); through *Chem. Abstr.*, **79**, 70116x (1973).
(405) W. Grimm, *Pharm. Ind.*, **37**, 815 (1975); through *Chem. Abstr.*, **84**, 35226q (1976).
(406) N. F. H. Ho, *Perspect. Clin. Pharm.*, **421** (1972); through *Chem. Abstr.*, **82**, 47650v (1975).
(407) S. Vianello, N. Chemello, and O. Cuccuni, *Farmaco, Ed. Prat.*, **28**, 65 (1973); through *Chem. Abstr.*, **78**, 101940x (1973).
(408) B. M. Colombo, P. Causa, P. Primavera, and V. Villano, *ibid.*, **27**, 327 (1972); through *Chem. Abstr.*, **77**, 92777z (1972).
(409) J. Huang, *T'ai-Wan Yao Hsueh Tsa Chih*, **23**, 49 (1971); through *Chem. Abstr.*, **80**, 124673t (1974).
(410) "The United States Pharmacopeia," 19th rev., Mack Publishing Co., Easton, Pa., 1975, p. 9.
(411) "The National Formulary," 14th ed., Mack Publishing Co., Easton, Pa., 1975, p. 17.
(412) *Fed. Regist.*, **41** (31), 6878 (Feb. 13, 1976).
(413) J. T. Carstensen and E. Nelson, *J. Pharm. Sci.*, **65**, 311 (1976).
(414) "The United States Pharmacopeia," 19th rev., Mack Publishing Co., Easton, Pa., 1975, p. 708.
(415) "Code of Federal Regulations," Title 21, 312.1 (1976).
(416) *Ibid.*, 314.1 (1976).
(417) *Ibid.*, 432.5 (1976).
(418) "Guidelines: Manufacturing & Controls for IND's & NDA's, FDA Papers," June 1971.
(419) R. S. Silk, "Analytical Requirements for NDA's & IND's," presented at the First Eastern Regional Meeting, The Academy of Pharmaceutical Sciences, New Brunswick, N.J., Sept. 30, 1975.
(420) *Fed. Regist.*, **34**, 13553 (1969).
(421) *Ibid.*, **36**, 601 (1971).
(422) *Ibid.*, **41**, 6878 (1976).
(423) "Code of Federal Regulations," Title 21, 314.8 (1976).
(424) *Fed. Regist.*, **41**, 5283 (1976).
(425) *Ibid.*, **41**, 26842 (1976).
(426) *Ibid.*, **41**, 41857 (1976).
(427) "Current GLP in Drug Safety Evaluation in Lab Animals March 1976 Guidelines," Pharmaceutical Manufacturer's Assoc.
(428) *Fed. Regist.*, **41**, 51206 (1976).
(429) M. Blanco, S. Eriksen, and M. Boghosian, *D&CI*, **1970**, 44.
(430) C. H. Newman, presented at the Meeting of the Parenteral Drug Association in New York, Feb. 2, 1968.
(431) E. Dudar and A. David, *Proc. Conf. Appl. Phys. Chem.*, **1**, 265 (1971); through *Chem. Abstr.*, **76**, 103703e (1972).
(432) G. Neri, G. Guadagnini, and R. Mannucci, *Farmaco, Ed. Prat.*, **29**, 289 (1974); through *Chem. Abstr.*, **82**, 77046v (1975).

Griseofulvin–Phenobarbital Interaction: A Formulation-Dependent Phenomenon

F. JAMALI * and J. E. AXELSON ˣ

Received December 27, 1976, from the *Faculty of Pharmaceutical Sciences, University of British Columbia, Vancouver, British Columbia, Canada.* Accepted for publication July 13, 1977. *Present address: Faculty of Pharmacy, University of Tehran, Tehran 14, Iran.

Abstract □ The reported interaction of griseofulvin with phenobarbital was studied in the rat following oral administration of different dosage forms. A single oral dose of 15 mg of phenobarbital/kg 24 hr prior to the oral administration of a suspension of 100 mg of griseofulvin/kg in 0.5% polysorbate 80 significantly reduced plasma griseofulvin levels. An increase in the concentration of polysorbate 80 to 2% reduced the extent of the interaction from 50 to 32%. Phenobarbital did not influence plasma griseofulvin levels when griseofulvin was given in either 70% polyethylene glycol 300 (suspensions of 20 or 100 mg/kg) or 100% polyethylene glycol 600 (solution of 50 mg/kg). It is concluded that the observed interaction is formulation dependent and is a result of diminished dissolution and, consequently, reduced absorption of griseofulvin.

Keyphrases □ Griseofulvin—interaction with phenobarbital, effect of different dosage forms in rats □ Phenobarbital—interaction with griseofulvin, effect of different dosage forms in rats □ Dosage forms, various—griseofulvin, effect on interaction with phenobarbital in rats □ Interactions—griseofulvin with phenobarbital, effect of different dosage forms in rats □ Antifungal agents—griseofulvin, interaction with phenobarbital, effect of different dosage forms in rats □ Anticonvulsant–sedatives—phenobarbital, interaction with griseofulvin, effect of different dosage forms in rats

Griseofulvin is an orally administered antifungal agent whose erratic and incomplete absorption has been shown to be dissolution rate limited (1). Low aqueous solubility (15 mg/liter at 37°) and extensive metabolism make griseofulvin a potential candidate for drug interactions when agents capable of altering absorption and/or metabolism are coadministered. Phenobarbital induces the metabolism of several compounds (2–4). The systemic availability of some drugs is affected by agents capable of influencing GI motility (5–8). Existing evidence suggests that griseofulvin availability is reduced by an interaction with phenobarbital (9–12).

It was suggested that phenobarbital increases griseofulvin metabolism in humans (9) and rats (12) by enzyme induction. Riegelman *et al.* (11) observed a similar interaction when griseofulvin tablets were administered to humans. However, following intravenous administration of the drug in the presence and absence of phenobarbital, there was no perceptible effect on the plasma griseofulvin concentration *versus* time curves in test *versus* control animals. Riegelman *et al.* (11) suggested that the observed griseofulvin–phenobarbital interaction was a result of reduced absorption mediated by a complex mechanism involving enhanced bile flow and GI motility.

This proposal was based on the recognized ability of phenobarbital to enhance bile flow (13). Alternatively, if griseofulvin elimination was rate limited by its access to the liver *per se*, then enzyme induction would have no effect on the slope of the postdistribution phase of the plasma drug concentration–time curve. However, enzyme induction might significantly increase the fraction of dose metabolized on the first pass through the liver after oral administration. In the presence of such a complex mechanism, the metabolic alterations induced by phenobarbital would not be expected to alter the terminal elimination half-life of griseofulvin.

In view of the varied mechanisms postulated, it was of interest to examine the griseofulvin–phenobarbital interaction more closely. The present investigation determined and compared the oral absorption of griseofulvin from various polyethylene glycol solutions and polysorbate 80 suspension dosage forms in control and test animals receiving phenobarbital. The main interests were to evaluate the formulation dependency of the griseofulvin–phenobarbital interaction and to delineate the mechanisms involved.

EXPERIMENTAL

Animals and Treatments—Adult male Wistar rats, with an average weight of 250 g, were fasted for 24 hr prior to and during the experiments. Water was available *ad libitum*. All animals were maintained in metabolism cages in a controlled environment for at least 3 weeks prior to the experiments.

Micronized griseofulvin[1] (specific surface area of 1.32 m^2/g) was used in the preparation of five different dosage forms: (*a*) 100 mg/kg in 0.5% polysorbate 80, (*b*) 100 mg/kg in 2% polysorbate 80, (*c*) 20 mg/kg in 70% polyethylene glycol 300, (*d*) 100 mg/kg in 70% polyethylene glycol 300, and (*e*) 50 mg/kg in 100% polyethylene glycol 600. The first four preparations were suspensions, and the fifth was a solution. The dosage forms were administered *via* gastric intubations at a constant volume of 1 ml. Suspensions in 70% polyethylene glycol 300 were stirred at room temperature for 24 hr prior to administration to achieve equilibrium solubility.

Control rats received griseofulvin only. Test rats were treated orally with a single dose of a freshly prepared aqueous solution of 15 mg of phenobarbital sodium[2]/kg 24 hr prior to the griseofulvin administration.

Plasma Level Studies—Serial blood samples (100–250 μl) were taken from the tail artery of ether-anesthetized rats in heparinized caraway tubes at appropriate time intervals (Figs. 1–5).

All blood samples were immediately centrifuged for 15 min in a clinical centrifuge[3], and the plasma was assayed for intact drug.

Equilibrium Solubility of Griseofulvin in Presence of Polyethylene Glycol 300 and Polysorbate 80—Equilibrium solubility of griseofulvin in solutions containing different concentrations (percent weight per weight) of polyethylene glycol 300 (Fig. 6) and polysorbate 80 was measured. An excess amount of griseofulvin (25 mg/ml) was added to the aqueous solutions containing 0, 20, 50, 60, 70, and 100% polyethylene glycol 300 or 0.5, 2, and 5% polysorbate 80 in 25-ml flasks at room temperature and 37°. The contents of the flask were stirred using magnetic stirrers.

[1] Supplied by Dr. Milo Gibaldi, State University of New York at Buffalo, Amherst, N.Y.

[2] Lot 33150, supplied by British Drug Houses (Canada) Ltd., Toronto, Canada.

[3] IEC, Needham Heights, Mass.

Table I—Area under Plasma Concentration–Time Curves, *AUC*, Peak Plasma Concentrations, C_{max}, and Their Time of Occurrence, T_{max}, of Griseofulvin following Oral Administration of Single Doses of 100 mg/kg in 0.5% Polysorbate 80 to Control and Phenobarbital-Pretreated Rats

	Control Rats			Phenobarbital-Pretreated Rats		
	AUC, μg hr/ml	C_{max}, μg/ml	T_{max}, hr	*AUC*, μg hr/ml	C_{max}, μg/ml	T_{max}, hr
	37.5	7.35	6	26.9	4.82	5
	53.0	7.68	5	25.8	4.10	6
	37.3	6.92	6	19.3	3.64	6
	37.8	7.02	6	19.6	3.30	5
	40.8	6.02	6	19.2	2.72	5
	52.9	6.05	6	22.2	3.20	6
Mean	43.2	6.84	5.8	22.1	3.63	5.5
SE	3.1	0.28	0.2	1.4	0.30	0.2
CV, %	17.8	9.9	7.0	15.5	20.4	10.0
Statistical difference[a]				S	S	NS

[a] Determined by the Student *t* test (two tailed); $\alpha = 0.05$; S = significant; and NS = not significant.

After 24 and 48 hr, 1 ml of the contents was transferred into 15-ml centrifuge tubes and centrifuged for 20 min in a clinical centrifuge[3]. Aliquots of 20 μl of each supernate were transferred into 10-ml volumetric flasks and assayed for griseofulvin.

Assay Procedure—The electron-capture GLC method of Shah *et al.* (14) was employed with some modification to determine griseofulvin levels in plasma and various dosage forms (15). The following conditions were found to be satisfactory: glass column, 1.83 m long × 2 mm i.d. packed with 3% OV-25 on 80–100-mesh Chromosorb W; column oven temperature, 285°; injection port temperature, 250°; detector temperature, 350°; and carrier gas (95% argon–5% methane) flow, 40 ml/min. The injection port configuration permitted on-column injection. The peak height ratio (griseofulvin to diazepam) method was used to construct a standard curve and to quantitate griseofulvin.

This assay was specific for griseofulvin. The major metabolite of griseofulvin in the rat, 4-desmethylgriseofulvin, had a retention time of 7.5 min, nearly 2.5 min prior to griseofulvin. Under no circumstances was 4-desmethylgriseofulvin observed in the plasma samples analyzed.

Treatment of Data—Mean plasma griseofulvin levels and the deviation from the mean were calculated for each experiment. Plasma levels were plotted as a function of time, and the areas under the curves (*AUC*) were measured using a planimeter. The Student *t* test was used to measure statistically the significance of the differences at $\alpha = 0.05$[4].

RESULTS AND DISCUSSION

Griseofulvin Suspensions in Polysorbate 80—Mean plasma griseofulvin levels following oral administration of a single dose containing 100 mg of griseofulvin/kg in 0.5% polysorbate 80 to control rats and those pretreated orally with single doses of phenobarbital sodium

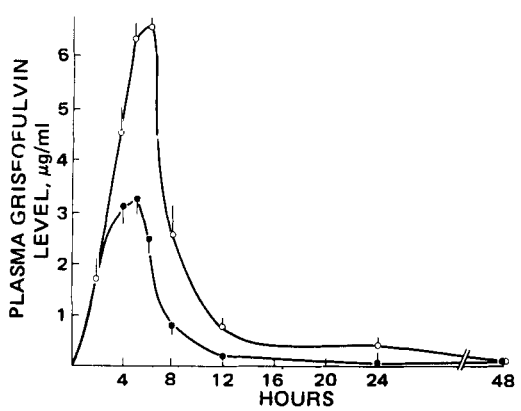

Figure 1—*Mean plasma griseofulvin levels* versus *time following oral administration of single doses of 100 mg/kg in 0.5% polysorbate 80 to control* (○, n = 6) *and phenobarbital-pretreated* (●, n = 6) *rats. Error bars represent the standard error of the mean.*

[4] Unless otherwise stated.

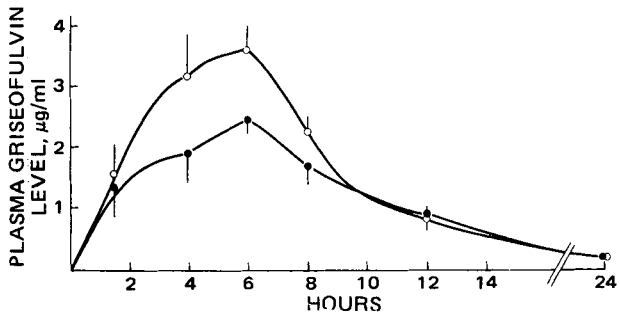

Figure 2—*Mean plasma griseofulvin levels* versus *time following oral administration of single doses of 100 mg/kg in 2% polysorbate 80 to control* (○, n = 4) *and phenobarbital-pretreated* (●, n = 5) *rats. Error bars represent the standard error of the mean.*

are shown in Fig. 1. Phenobarbital pretreatment reduced both the peak plasma griseofulvin levels and the area under the plasma griseofulvin concentration–time curve (*AUC*). The plasma levels were significantly different at all times except at 2 and 12 hr (Fig. 1).

The observed mean *AUC* in the test group was approximately 50% lower than that of the controls (Table I). The mean maximum plasma level, C_{max}, also was reduced by 47% in the test group (Table I). Phenobarbital treatment did not shorten the time of attainment of C_{max}, T_{max} (Table I). Since T_{max} is an indication of the absorption rate and since griseofulvin absorption has been shown to be dependent upon gastric emptying (5, 6), it is suggested that phenobarbital does not significantly influence gastric emptying in the rat.

The presence of surfactants has been shown to influence effectively the dissolution and, hence, the absorption of griseofulvin (16, 17). Thus, an increase in the surfactant concentration in the griseofulvin suspension dosage form was anticipated to optimize the dissolution process and indirectly to diminish the effect of phenobarbital. Therefore, a suspension containing 2% polysorbate 80 was prepared and administered to the rat in the presence and absence of phenobarbital.

Figure 2 depicts the plasma levels *versus* time of griseofulvin following administration of a single dose of a suspension of griseofulvin in 2% polysorbate 80 in the presence and absence of phenobarbital. Although phenobarbital pretreatment reduced the plasma griseofulvin levels, its effect was significant only at C_{max} ($\alpha = 0.1$) (Table II). The treatment also failed to influence significantly the *AUC* and T_{max} values (Table II). These observations indicate that a fourfold increase in the concentration of polysorbate 80 significantly reduced the extent of the interaction. Phenobarbital pretreatment, followed by the administration of a suspension of griseofulvin in 0.5% polysorbate 80, reduced the mean C_{max} by 50%. Under identical conditions when griseofulvin was formulated in 2% polysorbate 80, the barbiturate lowered the mean C_{max} by only 31%. Therefore, it is reasonable to suggest that a decreased dissolution rate may be mainly responsible for the griseofulvin–phenobarbital interaction. Since an increase in the surfactant concentration is expected to improve dissolution, the phenobarbital influence would be expected to diminish, as observed.

Comparison of control *AUC* values in Tables I and II suggests that

Table II—Area under Plasma Concentration–Time Curves, *AUC*, Peak Plasma Concentrations, C_{max}, and Their Time of Occurrence, T_{max}, of Griseofulvin following Oral Administration of Single Doses of 100 mg/kg in 2% Polysorbate 80 to Control and Phenobarbital-Pretreated Rats

	Control Rats			Phenobarbital-Pretreated Rats		
	AUC, μg hr/ml	C_{max}, μg/ml	T_{max}, hr	*AUC*, μg hr/ml	C_{max}, μg/ml	T_{max}, hr
	19.6	2.72	6	17.1	2.62	6
	35.2	4.60	6	15.7	2.42	6
	27.4	3.50	4	32.6	3.45	6
	37.6	4.22	4	22.1	2.32	4
				21.8	3.15	4
Mean	30.0	3.76	5.0	21.9	2.79	5.5
SE	4.0	0.41	0.5	1.6	0.22	0.3
CV, %	27.3	22.0	23.1	16.8	17.5	15.7
Statistical difference[a]				NS	$p <$ 0.1	NS

[a] Determined by the Student *t* test (two tailed); NS = not significant.

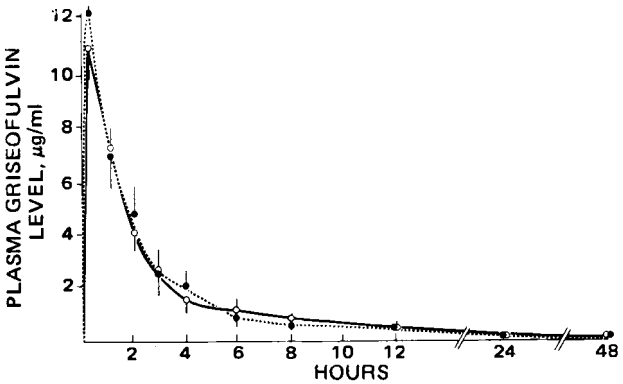

Figure 3—*Mean plasma griseofulvin levels* versus *time following oral administration of single doses of 50 mg/kg in 100% polyethylene glycol 600 to control* (○, n = 8) *and phenobarbital-pretreated* (●, n = 6) *rats. Error bars represent the standard error of the mean.*

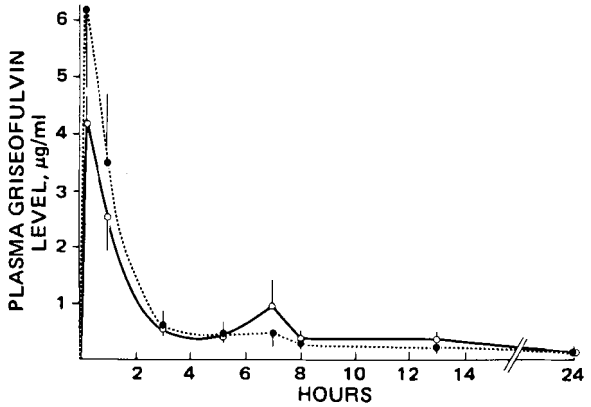

Figure 4—*Mean plasma griseofulvin levels* versus *time following oral administration of single doses of 20 mg/kg in 70% polyethylene glycol to control* (○, n = 4) *and phenobarbital-pretreated* (●, n = 4) *rats. Error bars represent the standard error of the mean.*

formation of a complex phase after an increase in the polysorbate 80 concentration decreased the relative bioavailability of griseofulvin approximately 31%. A complex opaque phase could be seen upon examination of the polysorbate 80 preparations *in vitro*. The solubility experiment revealed that the griseofulvin concentration in the clear phase of 0.5, 2, or 5% polysorbate 80 formulations was the same as in water (approximately 14 mg/liter). This result may indicate that griseofulvin is tightly bound to the complex phase and that drug availability may be limited by its release rate from this complex phase. Therefore, a shorter residence time in the region of the absorptive site should decrease the availability of the preparations with higher polysorbate 80 concentrations still further. Thus, the griseofulvin–phenobarbital interaction is unlikely to result from an increase in motility.

Addition of 2% polysorbate 80 to the griseofulvin suspension perhaps reduced relative drug bioavailability to such an extent that phenobarbital treatment could not reduce it further. Phenobarbital treatment and an increased concentration of polysorbate 80 may influence griseofulvin absorption by the same mechanism. Since the addition of extra surfactant to the preparation did not eliminate completely the effect of phenobarbital on the plasma griseofulvin levels, other mechanisms could also be involved in the interaction; preparations containing polyethylene glycol provided more information.

Griseofulvin in Polyethylene Glycol—The mean plasma levels following a single oral dose of 50 mg of griseofulvin/kg in polyethylene glycol 600 (solution) in control and phenobarbital-pretreated animals are plotted as a function of time in Fig. 3.

Phenobarbital predosing failed to affect the plasma griseofulvin levels when the drug was administered in solution (Fig. 3 and Table III). This observation clearly suggests that the griseofulvin–phenobarbital interaction is a formulation-dependent phenomenon and a result of reduced absorption. A drug–drug interaction mediated by enzyme induction or a change in the blood flow would be expected to be formulation independent for drugs with a high extraction ratio.

Griseofulvin formulation in a 100% polyethylene glycol 600 preparation noticeably changed the gut appearance. Therefore, polyethylene glycol 600 itself might have affected peristalsis and membrane permeability. The absorption properties of griseofulvin possibly might have been altered by the vehicle in both control and test rats. To clarify this point, two different griseofulvin dosage forms containing 100 mg of drug/kg in either 70% polyethylene glycol 600 or 70% polyethylene glycol 300 in distilled water were prepared and their effects on the gut were tested.

Single doses of 100 mg of griseofulvin/kg in either 70% polyethylene glycol 300 or 70% polyethylene glycol 600 (1 ml) were administered to two separate groups of five rats. One rat from each group was sacrificed at 1, 3, 5, 8, or 12 hr postdosing; after an abdominal incision, the gut was examined for any abnormalities.

While the 70% polyethylene glycol 600 preparation showed a noticeable increase in the volume of gut fluid, the 70% polyethylene glycol 300 preparation exerted no effect on the gross appearance of the gut. Therefore, 70% polyethylene glycol 300 was chosen as a vehicle to administer griseofulvin orally at two different concentrations (20 and 100 mg/kg). In addition, the effect of phenobarbital pretreatment on the plasma griseofulvin levels was studied. The mean plasma griseofulvin levels following administration of 20 and 100 mg of griseofulvin/kg in 70% polyethylene glycol 300 are plotted as a function of time in Figs. 4 and 5, respectively. Pretreatment with phenobarbital did not reduce the plasma griseofulvin concentrations of either of the 70% polyethylene glycol 300 preparations (Tables IV and V). This result was due, perhaps, to the wetting and solvent properties of polyethylene glycol.

Administration of 20 and 100 mg of griseofulvin/kg in 70% polyethylene glycol 300 yielded a rapid rise in the plasma concentration similar to that observed after griseofulvin in 100% polyethylene glycol 600. This observation is consistent with the rapid absorption of the dissolved fraction of drug in the suspension dosage forms. Attainment of approximately the same C_{max} following administration of both preparations to control rats (4.2–6.3 and 3.1–5.3 μg/ml for 20- and 100-mg/kg doses, respectively) supports this suggestion (Tables IV and V). The remaining fraction of the drug (undissolved fraction), however, was absorbed slowly and incompletely. As shown in Fig. 6, at equilibrium, 3.2 mg of griseofulvin was

Table III—Area under Plasma Concentration–Time Curves, *AUC*, and Peak Plasma Concentrations, C_{max}, following Oral Administration of 50 mg of Griseofulvin/kg in Polyethylene Glycol 600 (Solution) to Control and Phenobarbital-Pretreated Rats

	Control Rats		Phenobarbital-Pretreated Rats	
	AUC, μg hr/ml	C_{max}, μg/ml	*AUC*, μg hr/ml	C_{max}, μg/ml
	37.6	15.32	43.8	15.30
	55.5	12.01	24.4	8.53
	30.1	6.09	35.7	18.25
	41.3	12.33	35.3	7.68
	28.9	8.12	41.4	14.46
	32.6	9.23	35.2	9.36
Mean	37.7	10.52	36.0	12.26
SE	4.0	1.36	2.7	1.76
CV, %	26.3	31.7	18.7	35.2
Statistical difference[a]			NS	NS

[a] Determined by the Student *t* test (two tailed); $\alpha = 0.05$; NS = not significant.

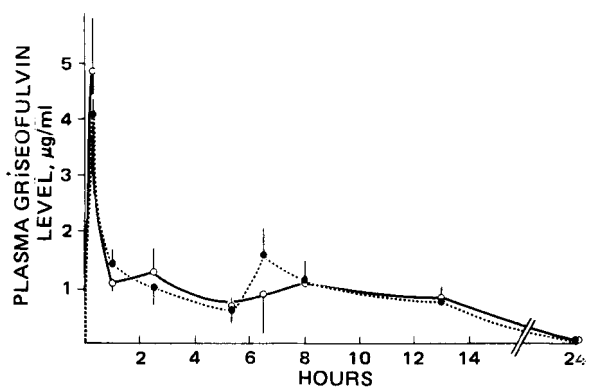

Figure 5—*Mean plasma griseofulvin levels* versus *time following administration of single doses of 100 mg/kg in 70% polyethylene glycol 300 to control* (○, n = 4) *and phenobarbital-pretreated* (●, n = 4) *rats. Error bars represent the standard error of the mean.*

Table IV—Area under Plasma Concentration–Time Curves, *AUC*, and Peak Plasma Concentrations, C_{max}, following Oral Administration of 20 mg of Griseofulvin/kg in 70% Polyethylene Glycol 300 to Control and Phenobarbital-Pretreated Rats

	Control Rats		Phenobarbital-Pretreated Rats	
	AUC, μg hr/ml	C_{max}, μg/ml	*AUC*, μg hr/ml	C_{max}, μg/ml
	9.3	3.77	16.8	9.95
	13.1	4.47	8.6	6.76
	12.3	5.32	11.4	4.63
	10.3	3.30	10.4	3.72
Mean	11.2	4.21	11.8	6.27
SE	0.8	0.44	1.7	1.38
CV, %,	15.7	20.8	29.8	44.2
Statistical difference[a]			NS	NS

[a] Determined by the Student *t* test (two tailed); $\alpha = 0.05$; NS = not significant.

dissolved in 1 ml of 70% polyethylene glycol 300 at 37°. Therefore, both suspensions had the same drug concentration in the supernate (3.2 mg/ml) but were different in their total griseofulvin concentration (5 or 25 mg/ml). Thus, the increase in the *AUC* from 11 to 17–18 μg hr/ml following administration of the higher dose, although small, may be related to the absorption of the undissolved fraction in the dosage form following dissolution.

The appearance of a second plasma concentration peak after 6–8 hr (Figs. 4 and 5) may also result from absorption of drug from the undissolved fraction of griseofulvin in the dosage form. Phenobarbital apparently did not reduce the absorption of either the dissolved or the undissolved fraction of griseofulvin when given in 70% polyethylene glycol 300. These observations further suggest that the observed griseofulvin–phenobarbital interaction may result from reduced dissolution rather than increased gut motility. If the gut motility had increased following phenobarbital pretreatment, it should have affected the absorption of the undissolved fraction of the dose. Because of the large fraction of undissolved drug in the preparation containing 100 mg of griseofulvin/kg in 70% polyethylene glycol 300, this effect should have been most profound. The undissolved fraction of the dose, due to the very slow dissolution rate, requires a longer residence time in the absorptive site to be dissolved and subsequently absorbed. Therefore, a reduced residence time is likely to reduce the total griseofulvin absorption (*i.e.*, as reflected by the *AUC*).

Absorption studies in this investigation revealed that griseofulvin availability in polyethylene glycol, unlike that of griseofulvin in polysorbate 80, is high. Once the drug was dissolved in polyethylene glycol, it was absorbed very rapidly (T_{max} = 20 min), while the griseofulvin absorption from polysorbate 80 was relatively slow. Bloedow and Hayton (18) reported a T_{max} of 8 hr following administration of griseofulvin in pure polysorbate 80 (solution). In this investigation, T_{max} values after administration of a suspension of griseofulvin in 0.5 or 2% polysorbate 80 were about 6 hr. A delayed T_{max}, coupled with the observed reduced *AUC* on increasing the concentration of polysorbate 80, indicates that the griseofulvin absorption rate decreases with an increasing polysorbate 80 concentration.

Phenobarbital pretreatment reduced the plasma griseofulvin levels when the drug was administered in tablet (in humans) (9, 11) or suspension forms containing polysorbate 80 (in the rat) (12). These dosage forms, unlike polyethylene glycol preparations, share the property of being very slowly absorbed. *In vivo*, bile salts probably accelerate the griseofulvin dissolution or release rate from these solid preparations. Preparations containing polyethylene glycol, however, may not, due to the solvent effect of the vehicle, be affected by this change.

Table V—Area under Plasma Concentration–Time Curves, *AUC*, and Peak Plasma Concentrations, C_{max}, following Oral Administration of 100 mg of Griseofulvin/kg in 70% Polyethylene Glycol 300 to Control and Phenobarbital-Pretreated Rats

	Control Rats		Phenobarbital-Pretreated Rats	
	AUC, μg hr/ml	C_{max}, μg/ml	*AUC*, μg hr/ml	C_{max}, μg/ml
	15.8	4.99	12.2	3.44
	17.8	3.73	25.6	4.37
	26.4	7.54	11.7	3.14
	14.2	3.11	18.3	5.32
Mean	18.5	4.84	16.9	4.07
SE	2.7	0.98	3.2	0.49
CV, %,	29.5	40.4	38.5	24.3
Statistical difference[a]			NS	NS

[a] Determined by the Student *t* test (two tailed); $\alpha = 0.05$; NS = not significant.

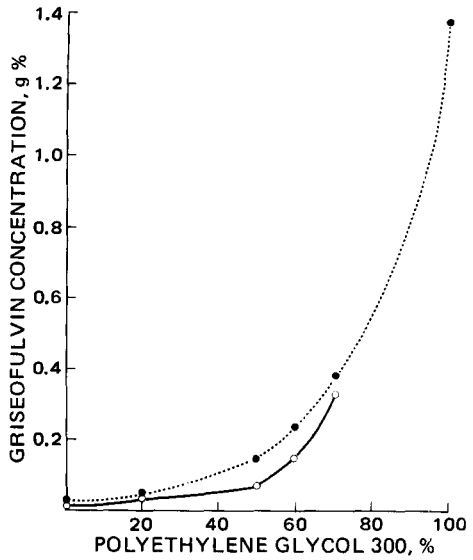

Figure 6—*Equilibrium solubility of griseofulvin in aqueous solutions containing different concentrations of polyethylene glycol 300 at room temperature (○) and 37° (●). Each point represents the average of two measurements.*

Griseofulvin solubility in an aqueous solution sharply increased after an increase in the concentration of the simulated intestinal bile salt mixture above the critical micelle concentration (17). This result is attributed to a micellar solubilization phenomenon. Klaassen (13) reported an increase in the bile flow accompanied with a decrease in the concentration of the bile salts following treatment with phenobarbital in the rat. Therefore, the observed reduction in the concentration of the bile salts (13) resulting from phenobarbital treatment may have reduced the solubility and, hence, the absorption of griseofulvin.

Recently, Lin and Symchowicz (10) observed that, *in vitro*, phenobarbital treatment was capable of increasing the maximum velocity, V_{max}, for griseofulvin metabolism in the rat and mouse. The treatment, however, did not alter the enzyme–substrate dissociation constant, K_m, for the reaction. The failure of phenobarbital to reduce the griseofulvin level after administration in polyethylene glycol contradicts the suggestion by Lin and Symchowicz (10) that the barbiturate may also induce griseofulvin metabolism *in vivo*.

Griseofulvin is eliminated almost exclusively *via* metabolism. The observed griseofulvin biological half-life in the rat is approximately 2 hr (15), an indication of very rapid elimination and rapid metabolism. This rate is, perhaps, due to a large capacity of the liver enzymes to metabolize this drug. In *in vitro* experiments, a given quantity of the drug is directly exposed to the enzymes. Therefore, an increase in the metabolizing capacity of the liver mediated by phenobarbital would yield a higher extent of metabolism *in vitro* (10, 12).

However, the mechanism may be different *in vivo*. The metabolism rate of griseofulvin may be limited by its access to the liver rather than by its metabolism *per se*. Therefore, *in vivo*, the inducing effect of phenobarbital on the liver enzyme, however profound, might exert no effect on the griseofulvin metabolism rate. This evidence supports the statement that *in vitro* observations may not necessarily be extrapolated to *in vivo* conditions. Therefore, it is suggested that the griseofulvin–phenobarbital interaction results from reduced availability and/or diminished dissolution caused by a reduction in the bile salt concentration rather than by induced metabolism or a decreased transit time in the absorption region.

Phenobarbital has been observed to reduce plasma concentrations of many other drugs, such as phenytoin, dicumarol (3), and digoxin (4). All these drugs, like griseofulvin, show low solubility in aqueous media but, unlike the latter, lack highly lipophilic properties. The shorter biological half-life observed in phenobarbital-pretreated subjects suggests that induced metabolism is responsible for the reduced plasma dicumarol

levels. However, the reduced plasma dicumarol level may also be partly due to reduced absorption. Considering the low dicumarol solubility, it is possible that a more complex mechanism consisting of simultaneous increased metabolism and reduced absorption may be involved in this interaction. Aggeler and O'Reilly (19) noted that heptabarbital appears to induce dicumarol metabolism while simultaneously reducing anticoagulant absorption.

Barbiturates interact with many drugs. This effect is usually attributed to the acknowledged ability of these compounds to induce the metabolism of other drugs. Less importance, however, has been given to another possible mechanism by which barbiturate administration may alter drug disposition, *e.g.*, an increase in bile flow with a simultaneous decrease in bile salt concentration. In this work, the influence of these changes was not directly studied. However, the evidence suggests that these mechanisms could be involved in the interactions between phenobarbital and poorly soluble drugs.

REFERENCES

(1) S. Symchowicz and B. Katchen, *J. Pharm. Sci.*, **57**, 1383 (1968).

(2) A. H. Conney, C. Davison, R. Gastel, and J. J. Burns, *J. Pharmacol. Exp. Ther.*, **130**, 1 (1960).

(3) S. A. Cucinell, A. H. Conney, M. Sansur, and J. J. Burns, *Clin. Pharmacol. Ther.*, **6**, 420 (1965).

(4) A. Kaldor, G. Somogyi, L. A. Debreczeni, and B. Gachalyi, *Int. J. Clin. Pharmacol.*, **12**, 403 (1975).

(5) J. E. Axelson and F. Jamali, presented at the Research Symposium and Research Conference of the Association of Faculties of Pharmacy of Canada, Ottawa, Canada, May 1974.

(6) F. Jamali and J. E. Axelson, presented at the Pharmaceutics Section, APhA Academy of Pharmaceutical Sciences, San Francisco meeting, Apr. 1975.

(7) J. Nimmo, R. C. Heading, P. Tothill, and L. F. Prescott, *Br. Med. J.*, **1**, 587 (1973).

(8) G. Levy, M. Gibaldi, and J. A. Procknal, *J. Pharm. Sci.*, **61**, 798 (1972).

(9) D. Busfield, K. J. Child, R. M. Atkinson, and E. G. Tomich, *Lancet*, **2**, 1042 (1963).

(10) C. Lin and S. Symchowicz, *Drug Metab. Rev.*, **4**, 75 (1975).

(11) S. Riegelman, M. Rowland, and W. L. Epstein, *J. Am. Med. Assoc.*, **213**, 426 (1970).

(12) D. Busfield, K. J. Child, and E. G. Tomich, *Br. J. Pharmacol.*, **22**, 137 (1964).

(13) C. D. Klaassen, *J. Pharmacol. Exp. Ther.*, **176**, 743 (1971).

(14) V. P. Shah, S. Riegelman, and W. L. Epstein, *J. Pharm. Sci.*, **61**, 634 (1972).

(15) F. Jamali, Ph.D. dissertation, University of British Columbia, Vancouver, British Columbia, Canada, 1976.

(16) W. A. Duncan, G. MacDonald, and M. J. Thornton, *J. Pharm. Pharmacol.*, **14**, 217 (1962).

(17) T. R. Bates, M. Gibaldi, and J. L. Kanig, *J. Pharm. Sci.*, **55**, 191 (1966).

(18) D. C. Bloedow and W. L. Hayton, *ibid.*, **65**, 328 (1976).

(19) P. Aggeler and R. O'Reilly, *J. Lab. Clin. Med.*, **74**, 229 (1969).

ACKNOWLEDGMENTS

Presented in part at the Research Symposium and Research Conference of the Association of Faculties of Pharmacy of Canada, Ottawa, Canada, May 20, 1974, and at the Pharmaceutics Section, APhA Academy of Pharmaceutical Sciences, San Francisco meeting, April 1975.

Supported by M.R.C. Grant MA-5358.

The analytical support of Mr. W. Campbell, Jr., of Hewlett-Packard, Ltd., is gratefully acknowledged.

Micro and Macro GLC Determination of Ethambutol in Biological Fluids

CHING S. LEE * and LESLIE Z. BENET ˣ

Received December 13, 1976, from the *Department of Pharmacy, School of Pharmacy, University of California, San Francisco, CA 94143.* Accepted for publication July 5, 1977. *Present address: College of Pharmacy, University of Florida, Gainesville, FL 32610.

Abstract □ Previously available GLC methods for ethambutol may only be used to measure quantities of drugs much greater than those found in biological fluids such as plasma and dialysate. A previously published GLC method for plasma samples is extended to measure ethambutol in dialysate. A second GLC method, involving derivatization with bis(trimethylsilyl)trifluoroacetamide and subsequent quantitation using a flame-ionization detector, is described for urine samples. With a dual-column and dual-detector gas–liquid chromatograph, simultaneous micro (plasma and dialysate) and macro (urine) determinations of ethambutol are possible.

Keyphrases □ Ethambutol—GLC analysis in biological fluids □ GLC—*analysis*, ethambutol in biological fluids □ Tuberculostatic antibacterials—ethambutol, GLC analysis in biological fluids

A previous publication (1) indicated that the available GLC methods may only be used to measure quantities of ethambutol[1] (I) much greater than those found in patient samples of blood, plasma, and dialysate. Pharmacokinetic study of I requires a sensitive and specific method of measuring the unchanged compound.

In this work, the GLC method previously used for plasma is extended to the measurement of I in dialysate. Ethambutol is largely excreted unchanged into the urine (2). To avoid the tedious and possibly erroneous serial dilution of the urine necessary for the GLC assay using an electron-capture detector, another GLC method for I, involving derivatization with bis(trimethylsilyl)trifluoroacetamide and subsequent quantitation using a flame-ionization detector, is described. Decanediol[2] (II) and *d*-2,2′-(ethylenediimino)-di-1-propanol[3] (III) are used as internal standards for the urine and the dialysate assay,

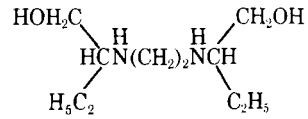

I

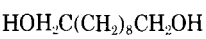

II

[1] Myambutol, Lederle Laboratories, Pearl River, N.Y.

[2] Aldrich Chemical Co., Milwaukee, Wis.

[3] Provided by Dr. Raymond Wilkinson, Lederle Laboratories, Pearl River, N.Y.

levels. However, the reduced plasma dicumarol level may also be partly due to reduced absorption. Considering the low dicumarol solubility, it is possible that a more complex mechanism consisting of simultaneous increased metabolism and reduced absorption may be involved in this interaction. Aggeler and O'Reilly (19) noted that heptabarbital appears to induce dicumarol metabolism while simultaneously reducing anticoagulant absorption.

Barbiturates interact with many drugs. This effect is usually attributed to the acknowledged ability of these compounds to induce the metabolism of other drugs. Less importance, however, has been given to another possible mechanism by which barbiturate administration may alter drug disposition, *e.g.*, an increase in bile flow with a simultaneous decrease in bile salt concentration. In this work, the influence of these changes was not directly studied. However, the evidence suggests that these mechanisms could be involved in the interactions between phenobarbital and poorly soluble drugs.

REFERENCES

(1) S. Symchowicz and B. Katchen, *J. Pharm. Sci.*, **57**, 1383 (1968).

(2) A. H. Conney, C. Davison, R. Gastel, and J. J. Burns, *J. Pharmacol. Exp. Ther.*, **130**, 1 (1960).

(3) S. A. Cucinell, A. H. Conney, M. Sansur, and J. J. Burns, *Clin. Pharmacol. Ther.*, **6**, 420 (1965).

(4) A. Kaldor, G. Somogyi, L. A. Debreczeni, and B. Gachalyi, *Int. J. Clin. Pharmacol.*, **12**, 403 (1975).

(5) J. E. Axelson and F. Jamali, presented at the Research Symposium and Research Conference of the Association of Faculties of Pharmacy of Canada, Ottawa, Canada, May 1974.

(6) F. Jamali and J. E. Axelson, presented at the Pharmaceutics Section, APhA Academy of Pharmaceutical Sciences, San Francisco meeting, Apr. 1975.

(7) J. Nimmo, R. C. Heading, P. Tothill, and L. F. Prescott, *Br. Med. J.*, **1**, 587 (1973).

(8) G. Levy, M. Gibaldi, and J. A. Procknal, *J. Pharm. Sci.*, **61**, 798 (1972).

(9) D. Busfield, K. J. Child, R. M. Atkinson, and E. G. Tomich, *Lancet*, **2**, 1042 (1963).

(10) C. Lin and S. Symchowicz, *Drug Metab. Rev.*, **4**, 75 (1975).

(11) S. Riegelman, M. Rowland, and W. L. Epstein, *J. Am. Med. Assoc.*, **213**, 426 (1970).

(12) D. Busfield, K. J. Child, and E. G. Tomich, *Br. J. Pharmacol.*, **22**, 137 (1964).

(13) C. D. Klaassen, *J. Pharmacol. Exp. Ther.*, **176**, 743 (1971).

(14) V. P. Shah, S. Riegelman, and W. L. Epstein, *J. Pharm. Sci.*, **61**, 634 (1972).

(15) F. Jamali, Ph.D. dissertation, University of British Columbia, Vancouver, British Columbia, Canada, 1976.

(16) W. A. Duncan, G. MacDonald, and M. J. Thornton, *J. Pharm. Pharmacol.*, **14**, 217 (1962).

(17) T. R. Bates, M. Gibaldi, and J. L. Kanig, *J. Pharm. Sci.*, **55**, 191 (1966).

(18) D. C. Bloedow and W. L. Hayton, *ibid.*, **65**, 328 (1976).

(19) P. Aggeler and R. O'Reilly, *J. Lab. Clin. Med.*, **74**, 229 (1969).

ACKNOWLEDGMENTS

Presented in part at the Research Symposium and Research Conference of the Association of Faculties of Pharmacy of Canada, Ottawa, Canada, May 20, 1974, and at the Pharmaceutics Section, APhA Academy of Pharmaceutical Sciences, San Francisco meeting, April 1975.

Supported by M.R.C. Grant MA-5358.

The analytical support of Mr. W. Campbell, Jr., of Hewlett-Packard, Ltd., is gratefully acknowledged.

Micro and Macro GLC Determination of Ethambutol in Biological Fluids

CHING S. LEE * and LESLIE Z. BENET ˣ

Received December 13, 1976, from the *Department of Pharmacy, School of Pharmacy, University of California, San Francisco, CA 94143.* Accepted for publication July 5, 1977. *Present address: College of Pharmacy, University of Florida, Gainesville, FL 32610.

Abstract □ Previously available GLC methods for ethambutol may only be used to measure quantities of drugs much greater than those found in biological fluids such as plasma and dialysate. A previously published GLC method for plasma samples is extended to measure ethambutol in dialysate. A second GLC method, involving derivatization with bis(trimethylsilyl)trifluoroacetamide and subsequent quantitation using a flame-ionization detector, is described for urine samples. With a dual-column and dual-detector gas–liquid chromatograph, simultaneous micro (plasma and dialysate) and macro (urine) determinations of ethambutol are possible.

Keyphrases □ Ethambutol—GLC analysis in biological fluids □ GLC—*analysis*, ethambutol in biological fluids □ Tuberculostatic antibacterials—ethambutol, GLC analysis in biological fluids

A previous publication (1) indicated that the available GLC methods may only be used to measure quantities of ethambutol[1] (I) much greater than those found in patient samples of blood, plasma, and dialysate. Pharmacokinetic study of I requires a sensitive and specific method of measuring the unchanged compound.

In this work, the GLC method previously used for plasma is extended to the measurement of I in dialysate. Ethambutol is largely excreted unchanged into the urine (2). To avoid the tedious and possibly erroneous serial dilution of the urine necessary for the GLC assay using an electron-capture detector, another GLC method for I, involving derivatization with bis(trimethylsilyl)trifluoroacetamide and subsequent quantitation using a flame-ionization detector, is described. Decanediol[2] (II) and *d*-2,2′-(ethylenediimino)-di-1-propanol[3] (III) are used as internal standards for the urine and the dialysate assay,

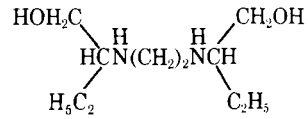

I

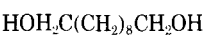

II

[1] Myambutol, Lederle Laboratories, Pearl River, N.Y.

[2] Aldrich Chemical Co., Milwaukee, Wis.

[3] Provided by Dr. Raymond Wilkinson, Lederle Laboratories, Pearl River, N.Y.

Table I—Recovery of Ethambutol (I) from Urine Using Flame-Ionization Detection Method (n = 7)

I Added, μg	I Found[a], μg	Recovery[a], %
10	9.9 ± 0.79	99.0 ± 7.9
20	19.7 ± 1.50	98.5 ± 7.5
30	29.8 ± 1.64	99.3 ± 5.5
50	49.8 ± 2.16	99.7 ± 4.3
70	69.9 ± 2.83	99.9 ± 4.0
100	100.3 ± 3.60	100.3 ± 3.6
10–100[b]	—	99.4 ± 5.5

[a] Expressed as mean ± *SD*. [b] n = 42.

respectively. With 3% OV-17, the trifluoroacyl and trimethylsilyl derivatives can be chromatographed under the same temperature conditions. Thus, with a dual-column and dual-detector gas–liquid chromatograph, the simultaneous micro (plasma and dialysate) and macro (urine) determinations of I become possible.

EXPERIMENTAL

Reagents—Bis(trimethylsilyl)trifluoroacetamide[4], trifluoroacetic anhydride[5], potassium hydroxide[6], and chloroform[6] were analytical reagent grade. Pyridine[5], benzene[6], and methylene chloride[6] were nanograde quality. Spectroquality chloroform[7] was used as a solvent in the derivatization of ethambutol by bis(trimethylsilyl)trifluoroacetamide.

Instrumentation—GLC analyses were carried out on a dual-column instrument[8] equipped with a flame-ionization detector and a scandium tritide electron-capture detector[9]. The columns were coiled, 1.8 m × 3 mm i.d., silanized glass, packed with 3% OV-17 on 100–120-mesh Chrom W A/W DMCS[10] (leading to the flame-ionization detector) and with 3% OV-17 on 100–120-mesh Gas Chrom Q[11] (leading to the electron-capture detector).

Nitrogen was used as the carrier gas at flow rates of 66.6 and 20 ml/min, measured at the flame-ionization detector base and the electron-capture detector base, respectively. The air flow rate was 300 ml/min, and the hydrogen flow rate was 27 ml/min. The temperature settings were: oven, 157°; injection ports, 210°; and detectors, 230°.

Mass Spectrometry—Chemical-ionization mass spectra were obtained using a quadrupole mass spectrometer[12]. Source pressures were maintained at 0.5 torr (isobutane). The source temperature was 150–170°. Samples (1 ± 0.5 μg) were placed into a glass capillary by a direct insertion probe, which was then gradually heated above 200° to effect volatilization.

Preparation of Standard Solutions—Ten milligrams of the hydrochloride salt of I was dissolved in distilled water to yield a stock solution of 1 mg/ml. Working standard solutions of 2, 4, 6, 10, 14, and 20 μg of I/ml were prepared and used to establish a GLC calibration curve and for addition to dialysate and urine for the determination of percent recovery. A stock solution of III containing 1 mg of its hydrochloride salt/ml was diluted 10-fold to give the working standard solution. Because of the sparing solubility of II in water, 1 mg of II was first dissolved in 250 μl of 1-propanol and then diluted with distilled water to a concentration of 100 μg/ml.

Measurement of Ethambutol in Biological Samples—Appropriate aliquots of urine, to which 10 μg of II had been added, were extracted with 8 ml of chloroform for 10 min under alkaline conditions. Portions of the chloroform extract were transferred to another tube and evaporated to

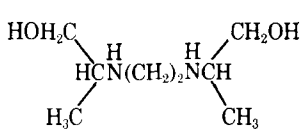

III

[4] Regis, Chicago, Ill.
[5] Pierce, Rockford, Ill.
[6] Mallinckrodt, St. Louis, Mo.
[7] MCB, Norwood, Ohio.
[8] Varian Aerograph model 2700.
[9] Tritium content: 1 Ci adsorbed on scandium.
[10] Varian Aerograph, Walnut Creek, Calif.
[11] Applied Science Laboratories, State College, Pa.
[12] Model 3200, Finnigan Corp., Sunnyvale, Calif.

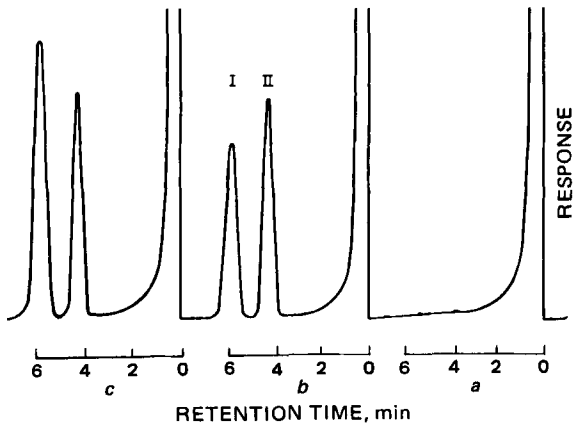

Figure 1—*Gas chromatograms of control human urine* (a), *control to which I (50 μg) and II (10 μg) were added* (b), *and human urine obtained 1 hr after dosing* (c).

dryness under nitrogen. Residues were dissolved in 0.1 ml of spectroquality chloroform. Derivatization was initiated by adding 10 μl of bis-(trimethylsilyl)trifluoroacetamide and was complete in 30 min.

For the dialysate assay, the same extraction procedures were followed as previously described, except that 2 ml of dialysate and 12.5 μg of III were used. Derivatization was initiated by adding 20 μl of trifluoroacetic anhydride and was completed in 2 hr. Aliquots of the reaction mixtures were injected into the gas chromatograph.

Standard urine and dialysate curves were constructed by plotting the peak height ratios (I to II and I to III) *versus* weight content of I. The peak height ratio of an unknown sample was then used to determine the amount of I present. The standard samples were run concurrently with the unknown samples as previously described.

Biological Studies—Six healthy adult volunteers received I intravenously and orally (tablet and solution) at a dose of 15 mg/kg within 6 months. Urine specimens were collected at the following intervals: 0–1, 1–2, 2–3, 3–4, 4–6, 6–8, 8–12, 12–24, 24–48, and 48–72 hr after drug administration.

One hemodialysis patient, regularly on 400 mg of I, was studied. Dialysates were collected at hourly intervals over a 4-hr dialysis period.

RESULTS AND DISCUSSION

Figure 1 presents gas chromatograms of the following samples using the flame-ionization detector: control human urine, control to which I and II were added, and human urine obtained 1 hr after dosing. Figure 2 presents gas chromatograms (electron-capture detection) of control dialysate, I and III added to control dialysate, and dialysate collected 1 hr after initiation of hemodialysis.

The reversed-time axis in Fig. 1 reflects the use of a dual-pen recorder where urine and dialysate samples were measured simultaneously. As indicated in Figs. 1*a* and 2*a*, no interfering peaks were found in the control urine or dialysate specimens. The trimethylsilyl derivative of I exhibited a retention time of 6 min, and the corresponding internal standard had a retention time of 4 min. The trifluoroacyl derivative of I exhibited a retention time of 4 min, and the corresponding internal standard had a retention time of 2.5 min.

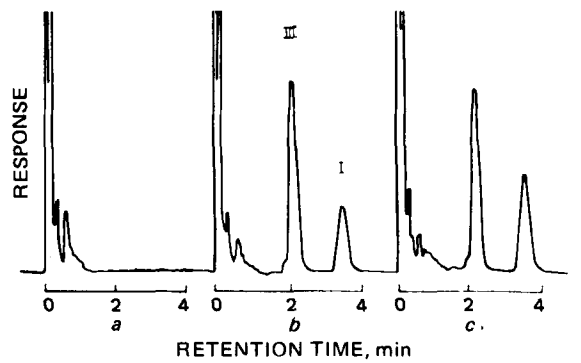

Figure 2—*Gas chromatograms of control dialysate* (a), *control to which I (0.3 μg) and III (12.5 μg) were added* (b), *and dialysate collected 1 hr after initiation of hemodialysis* (c).

Table II—Recovery of Ethambutol (I) from Dialysate Using Electron-Capture Detection Method (n = 6)

I Added, ng	I Found, ng	Recovery[a], %
100	102.2 ± 12.3	102.2 ± 12.3
200	200.3 ± 18.9	100.2 ± 9.5
300	297.1 ± 16.5	99.0 ± 5.5
500	491.6 ± 22.9	98.3 ± 4.6
700	692.8 ± 33.0	99.0 ± 4.7
1000	991.6 ± 37.6	99.2 ± 3.8
100–1000[b]	—	99.7 ± 6.7

[a] Expressed as mean ± *SD*. [b] n = 36.

Table III—Removal Rate of Ethambutol from a Hemodialysis Patient during a 4-hr Period

Hours	Dialysate Volume, liters	Concentration, μg/ml	Removal Rate, mg/hr
1	30.2	0.25	7.55
2	30.6	0.25	7.51
3	29.6	0.21	6.08
4	31.0	0.17	5.28

The results obtained following analysis of various amounts of I in control human urine are summarized in Table I. In the 10–100-μg range, the mean recovery of I from control urine was 99.4 ± 5.5% (n = 42). An excretion rate *versus* time plot in one subject following intravenous and oral dosing of ethambutol is shown in Fig. 3. Seventy-two-hour urinary excretion of unchanged drug in the six subjects accounted for 79.2 ± 3.3 (mean percent of dose ± *SD*), 63.4 ± 2.6, and 61.1 ± 3.8 for the intravenous, oral solution, and oral tablet doses, respectively. This result indicates that the availability of ethambutol from oral solution and tablet forms averaged 80 and 77%, respectively. The availability of the drug from the tablet was not significantly different from that for the solution.

Table II summarizes the results obtained following electron-capture analysis of various amount of I (10–1000 ng) added to dialysate. The mean recovery of I from control dialysate in the 10–1000-ng range was 99.7 ± 6.7% (n = 36). Removal of I by hemodialysis in one patient during 4 hr is seen in Table III.

When comparing the flame-ionization response and the electron-capture response (Figs. 1 and 2), an approximate 100-fold difference in detector sensitivity is evident. The electron-capture method of detection is required for samples such as blood, plasma, and, in particular, dialysate in which low levels of I are anticipated.

Drug removal by dialysis is sometimes hard to determine because of the large dialysate volume collected from the patient during the dialytic process (20–30-liters/hr interval). Concentration procedures (*e.g.*, rotary evaporation or extraction of the large dialysate volume with an organic solvent and subsequent evaporation of this solvent) are almost always required to bring the dialysate sample within the assay detection limits. With the highly sensitive electron-capture GLC method described here, only 2 ml of dialysate is needed for extraction.

The flame-ionization method is suitable for urine samples or for dosage form analysis in which high levels of I are anticipated. The flame-ionization method avoids the tedious and possibly erroneous dilution of the samples necessary for the electron-capture GLC assay.

Decanediol (II) was chosen as the internal standard for the urine assay because of its commercial availability at low cost. Since high concentrations of drug are measured in this assay, relatively large amounts of internal standard are required. However, II is not a good internal standard in the dialysate assay when trifluoroacetic anhydride is used as the derivatizing agent because of peak overlap.

Richard *et al.* (3) pointed out that only trimethylsilylimidazole derivatized I immediately and completely and that other trimethylsilylating agents required mild heating at 50° to complete the derivatization. In the present study, bis(trimethylsilyl)trifluoroacetamide with 1% trimethylchlorosilane satisfactorily derivatized I at room temperature, and less solvent interference was obtained than when trimethylsilylimidazole was used. The use of an internal standard presents an improvement over the other published techniques (3, 4).

The isobutane chemical-ionization mass spectra of I, the trimethylsilyl derivative of I, and the trifluoroacyl derivative of I can be seen in Figs. 4, 5, and 6, respectively. The major molecular ion at m/e 349 in Fig. 5 corresponds to the ditrimethylsilylated derivative of I. No peaks were

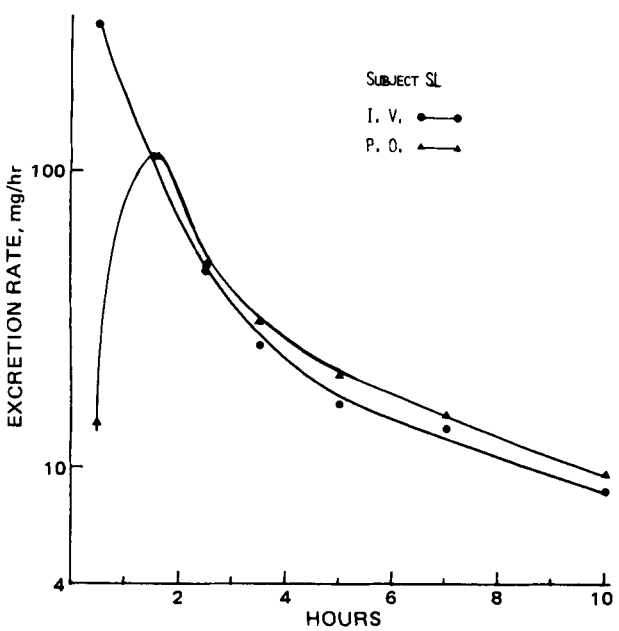

Figure 3—*Excretion rate* versus *time plot following intravenous and oral administrations of ethambutol in one subject.*

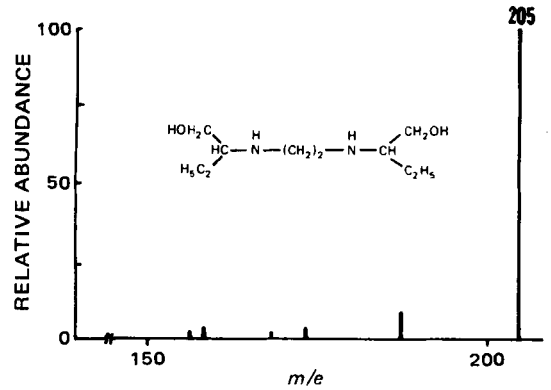

Figure 4—*Chemical-ionization mass spectrum of ethambutol using isobutane as the reagent gas.*

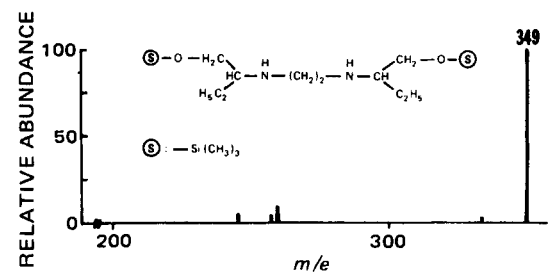

Figure 5—*Chemical-ionization mass spectrum of trimethylsilylated ethambutol using isobutane as the reagent gas.*

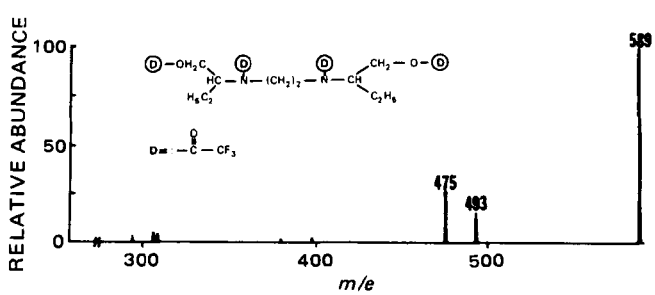

Figure 6—*Chemical-ionization mass spectrum of trifluoroacylated ethambutol using isobutane as the reagent gas.*

found beyond *m/e* 349, indicating that trimethylsilylation occurred at only two of the four possible reacting sites (*i.e.*, the two hydroxyl groups and the two secondary amines in I). The major molecular ions at *m/e* 589 and 493 in Fig. 6 correspond to the tetra- and tritrifluoroacylated derivatives of I, respectively, with relative abundance of approximately 100:15. The peak at *m/e* 475 (M^+) represents a breakdown product of the protonated molecular ion (MH^+) at *m/e* 589.

About 20% of ethambutol is metabolized to the carboxylic acid derivative and excreted in the urine (5). This highly polar compound is very poorly extracted into the organic phase in the procedure described here and, therefore, does not interfere with the assay of unchanged drug.

REFERENCES

(1) C. S. Lee and L. Z. Benet, *J. Chromatogr.*, **128**, 188 (1976).

(2) V. A. Place, E. A. Peets, D. A. Buyske, and R. R. Little, *Ann. N.Y. Acad. Sci.*, **135**, 775 (1966).

(3) B. M. Richard, J. E. Manno, and B. R. Manno, *J. Chromatogr.*, **89**, 80 (1974).

(4) A. Calo, C. Cardini, and V. Quercia, *ibid.*, **37**, 194 (1968).

(5) E. A. Peets, W. M. Sweeney, V. A. Place, and D. A. Buyske, *Am. Rev. Resp. Dis.*, **91**, 51 (1965).

ACKNOWLEDGMENTS

Presented at the APhA Academy of Pharmaceutical Sciences, New York meeting, May 1977.

Supported in part by Program Project Grant GM 16496 from the Institute of General Medical Sciences, National Institutes of Health, and by the Patent Fund from the Graduate Division, University of California, San Francisco. During this work, Dr. Lee received support as a National Institutes of Health Predoctoral Fellow through Training Grant GM 00728.

Hofmann Elimination with Diazomethane on Curare Bases and Selected Quaternary Tetrahydroisoquinoline Alkaloids

JANETTE A. NAGHAWAY and T. O. SOINE ˣ

Received June 17, 1977, from the *Department of Medicinal Chemistry, College of Pharmacy, University of Minnesota, Minneapolis, MN 55455.* Accepted for publication July 11, 1977.

Abstract □ Use of a large excess of alkali-free diazomethane resulted in a Hofmann elimination with selected curare bases and some other quaternary tetrahydroisoquinoline alkaloids. (+)-Tubocurarine chloride provided a monostilbene methine, *O,O*-dimethyltubocurinemethine, and a monostilbene–monostyrene compound, *O,O*-dimethyltubocurinedimethine. The major elimination products of (+)-isotubocurarine chloride and (+)-carnegine methiodide were monostyrene methines, *O,O*-dimethyltubocurineisomethine and carneginemethine, respectively. Treatment of (+)-laudanosine methiodide with potassium hydroxide, under the conditions of Hofmann degradation, or alkali-free diazomethane solution provided the same stilbene compound, laudanosinemethine. The structures of the elimination compounds were further confirmed by catalytic reduction and quaternization with methyl iodide.

Keyphrases □ Curare bases, various—Hofmann elimination reaction with diazomethane □ Tetrahydroisoquinoline alkaloids, various—Hofmann elimination reaction with diazomethane □ Elimination reactions, Hofmann—various curare bases and tetrahydroisoquinoline alkaloids with diazomethane □ Alkaloids, various quaternary—Hofmann elimination reaction with diazomethane

(+)-Tubocurarine chloride (I) has been the traditional standard against which the neuromuscular junction blocking potency of many compounds has been compared. Numerous studies have dealt with the structural requirements for neuromuscular junction blockers (1–3). Methylation of the phenolic groups in I is regarded as one means of enhancing its blocking activity. Hence, the potency of *O,O*-dimethyl-(+)-tubocurarine chloride (II) was reported to be four to nine times that of I (4–6). However, the II utilized in these pharmacological evaluations was obtained through the methylation of I under alkaline conditions using methyl iodide. These conditions would undoubtedly result in the quaternization of the tertiary amino group of I.

Using NMR spectroscopy and electrometric titration, Bick and Mcleod (7) revealed the diquaternary nature of a commercial sample of II. Therefore, the reported activity probably represents that of the diquaternary species, *O,O*-dimethyl-(+)-chondocurarine iodide (V), rather than the monoquaternary–monotertiary II. In fact, following the disclosure that I is actually a monoquaternary–monotertiary compound (8), there has not yet been any report on the actual activity of true II.

The stereochemical requirements for nondepolarizing neuromuscular junction blockers have been studied in these laboratories (9–12). The conclusion that moderately enhanced activity is associated with monoquaternary neuromuscular junction blockers with an *S*-configuration

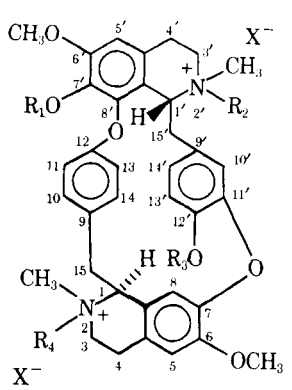

I: $R_1 = R_3 = R_4 = H$, $R_2 = CH_3$, X = Cl
II: $R_1 = R_2 = R_3 = CH_3$, $R_4 = H$, X = Cl
III: $R_1 = R_2 = R_3 = H$, $R_4 = CH_3$, X = Cl
IV: $R_1 = R_3 = H$, $R_2 = R_4 = CH_3$, X = Cl
V: $R_1 = R_2 = R_3 = R_4 = CH_3$, X = I

found beyond *m/e* 349, indicating that trimethylsilylation occurred at only two of the four possible reacting sites (*i.e.*, the two hydroxyl groups and the two secondary amines in I). The major molecular ions at *m/e* 589 and 493 in Fig. 6 correspond to the tetra- and tritrifluoroacylated derivatives of I, respectively, with relative abundance of approximately 100:15. The peak at *m/e* 475 (M^+) represents a breakdown product of the protonated molecular ion (MH^+) at *m/e* 589.

About 20% of ethambutol is metabolized to the carboxylic acid derivative and excreted in the urine (5). This highly polar compound is very poorly extracted into the organic phase in the procedure described here and, therefore, does not interfere with the assay of unchanged drug.

REFERENCES

(1) C. S. Lee and L. Z. Benet, *J. Chromatogr.*, **128**, 188 (1976).

(2) V. A. Place, E. A. Peets, D. A. Buyske, and R. R. Little, *Ann. N.Y. Acad. Sci.*, **135**, 775 (1966).

(3) B. M. Richard, J. E. Manno, and B. R. Manno, *J. Chromatogr.*, **89**, 80 (1974).

(4) A. Calo, C. Cardini, and V. Quercia, *ibid.*, **37**, 194 (1968).

(5) E. A. Peets, W. M. Sweeney, V. A. Place, and D. A. Buyske, *Am. Rev. Resp. Dis.*, **91**, 51 (1965).

ACKNOWLEDGMENTS

Presented at the APhA Academy of Pharmaceutical Sciences, New York meeting, May 1977.

Supported in part by Program Project Grant GM 16496 from the Institute of General Medical Sciences, National Institutes of Health, and by the Patent Fund from the Graduate Division, University of California, San Francisco. During this work, Dr. Lee received support as a National Institutes of Health Predoctoral Fellow through Training Grant GM 00728.

Hofmann Elimination with Diazomethane on Curare Bases and Selected Quaternary Tetrahydroisoquinoline Alkaloids

JANETTE A. NAGHAWAY and T. O. SOINE ˣ

Received June 17, 1977, from the *Department of Medicinal Chemistry, College of Pharmacy, University of Minnesota, Minneapolis, MN 55455.* Accepted for publication July 11, 1977.

Abstract □ Use of a large excess of alkali-free diazomethane resulted in a Hofmann elimination with selected curare bases and some other quaternary tetrahydroisoquinoline alkaloids. (+)-Tubocurarine chloride provided a monostilbene methine, *O,O*-dimethyltubocurinemethine, and a monostilbene–monostyrene compound, *O,O*-dimethyltubocurinedimethine. The major elimination products of (+)-isotubocurarine chloride and (+)-carnegine methiodide were monostyrene methines, *O,O*-dimethyltubocurineisomethine and carneginemethine, respectively. Treatment of (+)-laudanosine methiodide with potassium hydroxide, under the conditions of Hofmann degradation, or alkali-free diazomethane solution provided the same stilbene compound, laudanosinemethine. The structures of the elimination compounds were further confirmed by catalytic reduction and quaternization with methyl iodide.

Keyphrases □ Curare bases, various—Hofmann elimination reaction with diazomethane □ Tetrahydroisoquinoline alkaloids, various—Hofmann elimination reaction with diazomethane □ Elimination reactions, Hofmann—various curare bases and tetrahydroisoquinoline alkaloids with diazomethane □ Alkaloids, various quaternary—Hofmann elimination reaction with diazomethane

(+)-Tubocurarine chloride (I) has been the traditional standard against which the neuromuscular junction blocking potency of many compounds has been compared. Numerous studies have dealt with the structural requirements for neuromuscular junction blockers (1–3). Methylation of the phenolic groups in I is regarded as one means of enhancing its blocking activity. Hence, the potency of *O,O*-dimethyl-(+)-tubocurarine chloride (II) was reported to be four to nine times that of I (4–6). However, the II utilized in these pharmacological evaluations was obtained through the methylation of I under alkaline conditions using methyl iodide. These conditions would undoubtedly result in the quaternization of the tertiary amino group of I.

Using NMR spectroscopy and electrometric titration, Bick and Mcleod (7) revealed the diquaternary nature of a commercial sample of II. Therefore, the reported activity probably represents that of the diquaternary species, *O,O*-dimethyl-(+)-chondocurarine iodide (V), rather than the monoquaternary–monotertiary II. In fact, following the disclosure that I is actually a monoquaternary–monotertiary compound (8), there has not yet been any report on the actual activity of true II.

The stereochemical requirements for nondepolarizing neuromuscular junction blockers have been studied in these laboratories (9–12). The conclusion that moderately enhanced activity is associated with monoquaternary neuromuscular junction blockers with an *S*-configuration

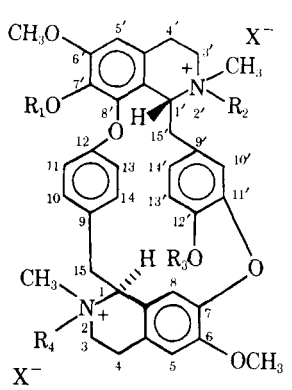

I: $R_1 = R_3 = R_4 = H$, $R_2 = CH_3$, X = Cl
II: $R_1 = R_2 = R_3 = CH_3$, $R_4 = H$, X = Cl
III: $R_1 = R_2 = R_3 = H$, $R_4 = CH_3$, X = Cl
IV: $R_1 = R_3 = H$, $R_2 = R_4 = CH_3$, X = Cl
V: $R_1 = R_2 = R_3 = R_4 = CH_3$, X = I

at the asymmetric carbon atom adjacent to the quaternary moiety (9) was given further credence by the results correlating the doubly enhanced curarimimetic activity of (+)-isotubocurarine chloride (III) over that of I (12). As an extension of the study of the neuromuscular junction blocking potencies of these diphenolic precursors and their *O*-methylated analogs, it seemed desirable to relate the activity of *O,O*-dimethyl-(+)-isotubocurarine with its isomer, *O,O*-dimethyl-(+)-tubocurarine.

The use of diazomethane for synthesizing the two dimethyl ethers was an obvious approach because diazomethane was employed successfully (8) for the synthesis of the dimethyl ether of (+)-tubocurarine acetate, although no experimental details have been reported. However, diazomethane has been found to participate in the Hofmann elimination reaction (13). Consequently, the present study was initiated to investigate the reaction of quaternary alkaloids with diazomethane and to give the experimental data omitted previously (13).

The investigation is of general interest because, in the past, unsuspecting workers, hoping only to *O*-methylate phenolic quaternary amines, could have generated unwanted methine bases with resultant confusion and loss of valuable compounds. Although Hofmann elimination can be carried out with considerably safer reagents, this reaction offers the possibility of an alternative route for the elimination of quaternary compounds if mild conditions are needed.

DISCUSSION

For the attempted preparation of *O,O*-dimethyl-(+)-tubocurarine from I, the method of Bick and Clezy (14) was followed utilizing an ethereal solution of diazomethane. Because the intent was to enhance the yield of the dimethyl ether, a fairly large excess of an alkali-free diazomethane solution was employed. However, even though the reagent was devoid of alkalinity, TLC examination of the crude reaction product revealed a multicomponent mixture, with the movement of the major spots appearing to correspond to free amines rather than to quaternary compounds. Consequently, it became of interest to isolate them and to determine their character.

Isolation of the major reaction components shown in Scheme I was achieved through combined column and preparative TLC. *O,O*-Dimethyltubocurinemethine (VI), the major fraction obtained, was characterized by UV and NMR spectroscopy. The NMR spectrum of VI revealed a singlet $N(CH_3)_2$ resonance (six protons), whose δ 2.28-ppm chemical shift can be ascribed to a tertiary rather than a quaternary amine, and a singlet NCH_3 resonance (three protons) at δ 2.46 ppm. The aromatic area integrated for 12 protons that could well account for 10 aromatic protons and two stilbene protons. Compound VI, which represents the fusion of two fragments similar to a mixture of laudanosine and laudanosinemethine, exhibited UV maxima at 225 (shoulder) and 284 nm, in good agreement with the values reported for laudanosine (15), and a shoulder at 303 nm, which can be assigned to a stilbene (*cis*) derivative. Although the formation of a *trans*-stilbene derivative is favored over the *cis*-isomer, the IR spectrum of VI did not show a strong band at 960 cm^{-1}, which is characteristic of *trans*-stilbene. The assigned methine structure was further supported by microanalysis and high-resolution mass spectrometry.

Catalytic reduction of VI (Scheme I) provided *O,O*-dimethyldihydrotubocurinemethine (VII), which exhibited UV maxima only at 225 (shoulder) and 280 nm and an NMR spectrum with only 10 protons in the aromatic region. Treatment of VII with methyl iodide resulted in an amorphous methiodide (VIII) whose UV maxima were similar to those of VII. In spite of attempts to crystallize VIII from several solvents and solvent mixtures, a crystalline compound could not be obtained.

The second fraction was recovered in small yield and was identified as *O,O*-dimethyltubocurinedimethine (IX) on the basis of spectroscopic data. Examination of the IR spectrum of IX indicated an olefinic styrene absorption at 885 cm^{-1}. The styrene UV maxima were detected at 265 and 293 (shoulder) nm. The NMR spectral data provided evidence for

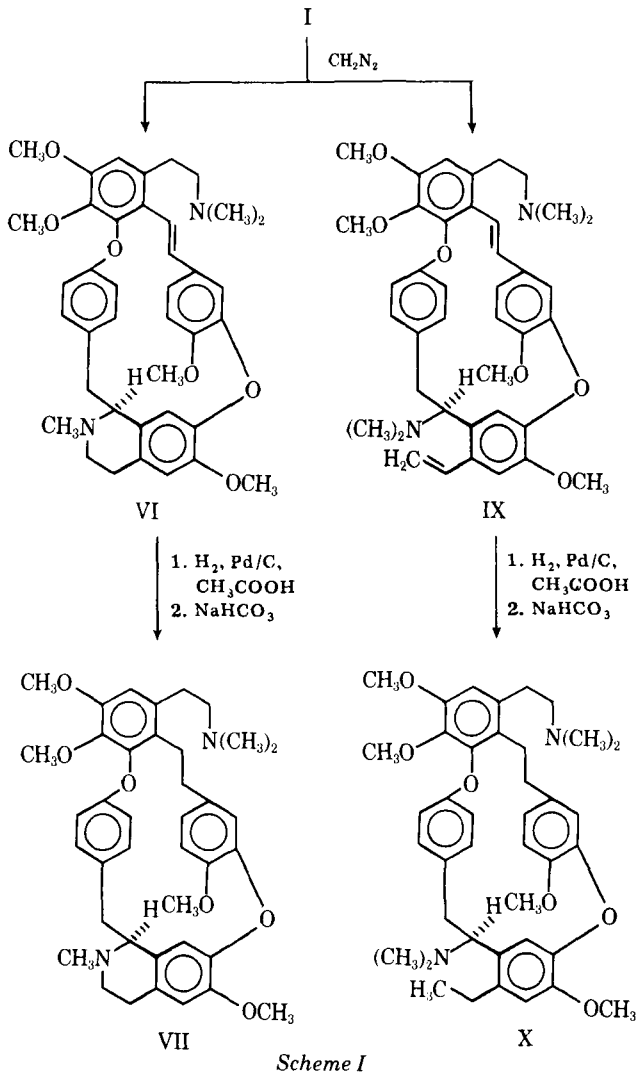

Scheme I

a monostyrene–monostilbene structure. It was apparent by the finding of two singlets at δ 2.23 and 2.25 ppm for two tertiary $N(CH_3)_2$ resonances (each integrated for six protons) that IX is most likely represented by a dimethine structure. This viewpoint was substantiated by the finding of 13 protons in the δ 5.75–7.05-ppm region, which can be assigned to 10 aromatic protons, two stilbene protons, and the X proton of the styrene moiety (Structure A), as well as the detection of the *AB* styrene protons in the region δ 5.11–5.50 ppm.

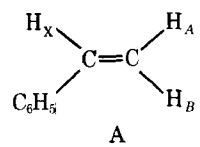

A

The formation of IX suggests the involvement of a diquaternary species, similar to *O,O*-dimethyl-(+)-chondocurarine iodide (V), in the elimination reaction. Therefore, the etherification of the phenolic hydroxyls in I by diazomethane was possibly accompanied by the interaction of the reagent with the hydrochloride portion to provide methyl chloride, resulting in the quaternization of the tertiary amino group of I to provide a diquaternary derivative. Reduction of the two olefinic bonds in IX produced *O,O*-dimethyltetrahydrotubocurinedimethine (X) (Scheme I), whose structural identity was substantiated by UV (maxima at 225 and 280 nm) and NMR (the appearance of 10 protons rather than 13 in the δ 5.71–6.92-ppm region and the loss of the *AB* styrene protons from the δ 5.11–5.50-ppm region) data.

To pursue the unexpected eliminations resulting from the employment of diazomethane, reactions of other quaternary tetrahydroisoquinoline systems were investigated. The exclusive formation of stilbene at the 2′-quaternary nitrogen of I was reinforced by the results of the elimination of (+)-chondocurarine chloride (IV) at the respective quaternary site (13).

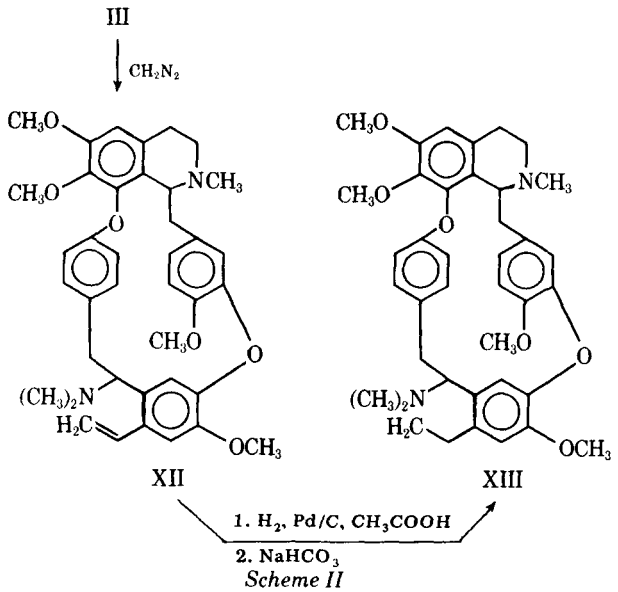

Scheme II

Since styrene was shown to be the product of elimination at the 2-quaternary nitrogen of IV (13), it seemed that it would be possible to obtain additional insight into the direction of elimination at the 2-quaternary site by subjecting III, which has the reverse order of quaternization to that of I, to the diazomethane reaction. (±)-Laudanosine methiodide (XV) and (+)-carnegine methiodide (XX) were the other candidates of choice because these compounds lack phenolic hydroxyls that can be alkylated by diazomethane and provide two alternative elimination routes.

The reaction of III with diazomethane was carried out in the same manner as for I. Preparative TLC was used for the isolation of the major component, identified as *O,O*-dimethyltubocurineisomethine (XII) (Scheme II). The IR spectrum of XII indicated a typical styrene absorption band at 885 cm^{-1}, which was deduced from the NMR spectrum which showed characteristic NCH_3 and $N(CH_3)_2$ singlets at δ 2.10 and 2.25 ppm, the former singlet being identical to that found for neutralized III at δ 2.10 ppm. Moreover, the *AB* styrene protons were detected between δ 5.10 and 5.56 ppm, and the δ 5.80–6.95-ppm area integrated for 11 protons, which can be assigned to 10 aromatic protons and the X proton of the styrene moiety. The UV spectrum of XII exhibited a confirmatory styrene band at 264 nm and a subsidiary styrene band at 303 (shoulder) nm.

Because of the broad melting-point range of XII and the lack of optical activity, coupled with very small amounts, it was decided to reduce it to the dihydro base (XIII) in the hope that more definitive evidence could be obtained for the structural argument. As outlined in Scheme II, catalytic reduction of XII provided *O,O*-dimethyldihydrotubocurineisomethine (XIII). The UV maxima of XIII were obtained at 225 (shoulder) and 280 nm, and the aromatic region of its NMR spectrum integrated for only 10 aromatic protons. Quaternization of XIII with methyl iodide produced an amorphous methiodide (XIV) with UV maxima similar to those of XIII.

A direct comparison between the product of the reaction of XV with diazomethane and laudanosinemethine (XVI), obtained under the conditions of Hofmann degradation, promised to provide additional information concerning the role of diazomethane. Thus, following the treatment of XV with a large excess of an alkali-free ethereal diazomethane solution (Scheme III), the major fraction was isolated successfully by preparative TLC. It was identified as *trans*-laudanosinemethine by spectral comparisons (IR and NMR) with spectra of XVI, obtained by Hofmann degradation of XV according to Battersby and Harper (16), and by high-resolution mass spectrometry.

A *trans*-stilbene structure was assigned by Battersby and Harper (16) to the major product of the usual Hofmann degradation of XV. That this structure was correct is reflected in a UV maximum at 330 nm and a minimum at 261 nm, which are very similar to those reported for *trans*-3,4,3′,4′-tetramethoxystilbene (17). In addition, the IR spectrum of XVI showed a *trans*-stilbene absorption band at 965 cm^{-1}. *trans*-Laudanosinemethine methiodide (XVII), obtained by treating XVI with methyl iodide, was also characterized by its UV spectral data and by its melting point. Furthermore, the melting point of *trans*-laudanosinemethine hydrochloride was not significantly different from the literature value

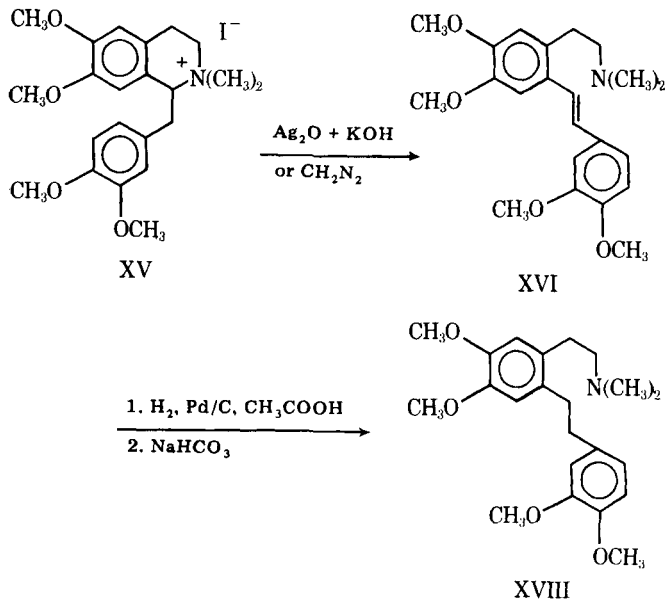

Scheme III

(16). The same methine was also obtained in smaller yield (23%) when (±)-laudanosine hydrochloride was treated with diazomethane under similar conditions.

Additional evidence substantiating the formation of XVI under the conditions of the diazomethane reaction was revealed by the susceptibility of the olefinic bond to reduction. As shown in Scheme III, catalytic hydrogenation of XVI produced dihydrolaudanosinemethine (XVIII). Formation of XVIII was apparent from the UV spectrum because of the disappearance of the *trans*-stilbene maximum and the appearance of new maxima at 225 and 280 nm. This result was also supported by high-resolution mass spectrometry and NMR data, which indicated the presence of five aromatic protons, as contrasted to XVI, which showed seven protons in the aromatic region (five aromatic and two olefinic protons). Upon quaternization of XVIII with methyl iodide, the resultant crystalline methiodide (XIX) exhibited a melting point in close agreement with the reported value (16).

The primary product of the reaction of (+)-carnegine methiodide (XX) with a large excess of alkali-free diazomethane was separated by preparative TLC and characterized as carneginemethine (XXI) (Scheme IV). The structural identity of XXI was ascertained by high-resolution mass spectrometry and NMR spectral data, which revealed a doublet at δ 1.34 ppm (three protons) for a methyl substituent and a singlet for $N(CH_3)_2$ resonance (six protons) at δ 2.25 ppm. Also, the *AB* styrene protons were detected between δ 5.07 and 5.56 ppm, and the aromatic area accounted for three protons which can be attributed to two aromatic protons and the X proton of the styrene segment. When XXI was treated with methyl iodide, the IR spectrum of the resultant crystalline methiodide (XXII) furnished the characteristic styrene absorption at 870 cm^{-1}. In addition, XXII exhibited UV maxima at 222, 265, and 292 (shoulder) nm, which could be ascribed to a styrene derivative.

Carneginemethine has never been reported previously, probably because of its fairly simple structure and the fact that Späth (18) did not carry out the usual degradative studies but relied on deductive reasoning followed by synthesis to prove the structure. Apparently, carneginemethine was not synthesized until the present study. Although no elemental analyses are presented, the structural substantiation seems secure on the basis of the NMR and mass spectral results without further analytical data.

Apparently, a Hofmann elimination reaction is initiated in the cited compounds by the action of diazomethane. Because the elimination reaction usually requires a strong base, possible alkaline contamination

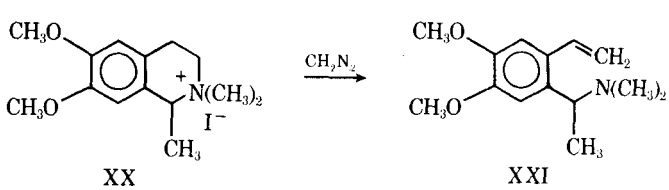

Scheme IV

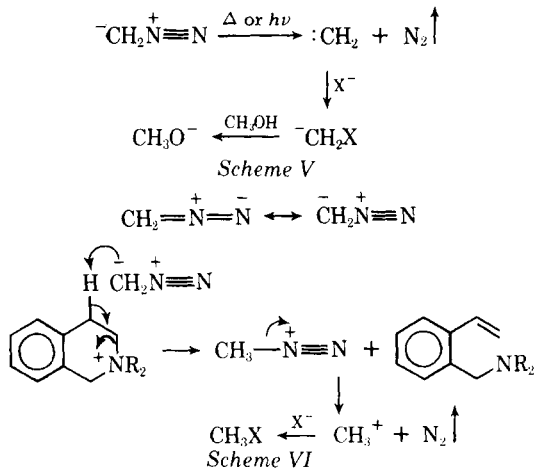

Scheme V

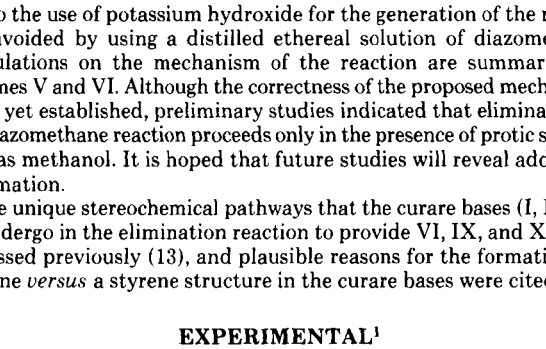

Scheme VI

due to the use of potassium hydroxide for the generation of the reagent was avoided by using a distilled ethereal solution of diazomethane. Speculations on the mechanism of the reaction are summarized in Schemes V and VI. Although the correctness of the proposed mechanisms is not yet established, preliminary studies indicated that elimination by the diazomethane reaction proceeds only in the presence of protic solvents such as methanol. It is hoped that future studies will reveal additional information.

The unique stereochemical pathways that the curare bases (I, III, and V) undergo in the elimination reaction to provide VI, IX, and XII were discussed previously (13), and plausible reasons for the formation of a stilbene *versus* a styrene structure in the curare bases were cited.

EXPERIMENTAL[1]

(+)-Tubocurarine Chloride (I) Reaction with Diazomethane[2]—An ice-cold ethereal solution of diazomethane (121 mmoles), generated from 12.5 g of *N*-nitrosomethylurea, was added incrementally over 4 days to a solution of I (0.50 g, 0.65 mmole) in methanol (300 ml). The reaction mixture was kept at room temperature; several hours after the last addition, the solvent was evaporated on a steam bath. The residue was dissolved in methanol and adsorbed on a small amount of neutral alumina (grade V).

This material was dried to give a powder, which was placed at the top of a neutral alumina column (30 g, 25 × 1.5 cm) and eluted with ethyl acetate (200 ml). Solvent evaporation under reduced pressure yielded a residue (0.30 g), which was then chromatographed on 1-mm silica gel HF-254 plates using 2.5% aqueous ammonia–ethyl acetate–2-propanol–methanol (0.7:3:3:4). Four bands were detected, with the two slower moving bands appearing to be the major components. The bands representing the major components were removed and extracted with mixtures of methanol–ethyl acetate as follows.

O,O-Dimethyltubocurinemethine (VI)—Extraction of the slowest moving band with methanol–ethyl acetate (3:2) afforded 0.065 g of VI, mp 90–92.5°, $[\alpha]_D^{25}$ + 187° (c 0.50, methanol); UV λ_{max} (log ϵ): 225 (4.66) and 284 (4.34) nm with an additional absorption in the 300–360-nm region which gave a shoulder at 303 nm (log ϵ 4.24); NMR ($CDCl_3$): δ 2.28 [s, 6H, $N(CH_3)_2$], 2.46 (s, 3H, NCH_3), 3.73 (s, 3H, OCH_3), 3.77 (s, 3H, OCH_3), 3.85 (s, 3H, OCH_3), 3.88 (s, 3H, OCH_3), and 5.82–7.08 (12H, aromatic and olefinic) ppm; high-resolution mass spectrum—M^+: calc. for $C_{39}H_{44}N_2O_6$: 636.3198, found: 636.3102.

Anal.—Calc. for $C_{39}H_{44}N_2O_6 \cdot H_2O$: C, 71.53; H, 7.08; N, 4.27. Found: C, 71.63; H, 7.13; N, 4.15.

O,O-Dimethyldihydrotubocurinemethine (VII)—A solution of VI (0.060 g, 0.094 mmole) in acetic acid (13 ml) was shaken with hydrogen and 10% palladium-on-carbon catalyst (0.049 g) at 46.5 psi for 62.5 hr. After filtration, the catalyst was washed with acetic acid; the combined filtrate and washings were evaporated under reduced pressure. The residue was dissolved in water (5 ml), neutralized with sodium bicarbonate, and extracted with chloroform (20 × 5 ml). Evaporation of the chloroform layer provided 0.035 g of the free base (58.3%), mp 77–78.5°, $[\alpha]_D^{25}$ + 262.8° (c 0.43, methanol); UV λ_{max} (log ϵ): 225 (4.70) and 280 (3.95) nm; NMR ($CDCl_3$): δ 2.33 [s, 6H, $N(CH_3)_2$], 2.46 (s, 3H, NCH_3), 3.68 (s, 3H, OCH_3), 3.70 (s, 3H, OCH_3), 3.81 (s, 3H, OCH_3), 3.83 (s, 3H, OCH_3), and 5.71–7.15 (10H, aromatic) ppm.

Anal.—Calc. for $C_{39}H_{46}N_2O_6$: C, 73.33; H, 7.26; N, 4.39. Found: C, 73.13; H, 7.26; N, 4.19.

Treatment of VII with methyl iodide provided the methiodide (VIII) as an amorphous compound, mp 236° (shrinkage at 229°), $[\alpha]_D^{25}$ + 187.1° (c 0.60, methanol).

O,O-Dimethyltubocurinedimethine (IX)—The second slow moving band obtained from the preparative silica plates was extracted with methanol–ethyl acetate (1:1). Evaporation of the solvent under reduced pressure gave 0.016 g of a solid (IX), mp 96° (collapsed at 92°), $[\alpha]_D^{25}$ + 60° (c 0.42, methanol); UV λ_{max} (log ϵ): 205 (4.67) and 265 (4.20) nm with an additional absorption between 290 and 360 nm which formed a shoulder at 293 nm (log ϵ 4.11); IR (KBr): 885 (styrene) cm^{-1}; NMR ($CDCl_3$): δ 2.23 [s, 6H, $N(CH_3)_2$], 2.25 [s, 6H, $N(CH_3)_2$], 3.68 (s, 3H, OCH_3), 3.72 (s, 3H, OCH_3), 3.80 (s, 3H, OCH_3), 3.86 (s, 3H, OCH_3), 5.11–5.50 (2H, *AB* styrene protons), and 5.75–7.05 (m, 13H, 10 aromatic, two stilbene, and one styrene protons) ppm.

Anal.—Calc. for $(C_{40}H_{46}N_2O_6)_2 \cdot 3H_2O$: C, 70.00; H, 7.17; N, 4.19. Found: C, 70.06; H, 7.33; N, 4.03.

Hydrogenation of IX in acetic acid with 10% palladium-on-carbon catalyst at 47 psi for 119 hr yielded the tetrahydro base (X) as a gum with the following properties: $[\alpha]_D^{25}$ + 20° (c 0.30, methanol); UV λ_{max} (log ϵ): 225 (4.79) and 280 (4.02) nm; NMR ($CDCl_3$): δ 2.22 [s, 6H, $N(CH_3)_2$], 2.30 [s, 6H, $N(CH_3)_2$], 3.65 (s, 3H, OCH_3), 3.70 (s, 3H, OCH_3), 3.82 (s, 6H, 2 OCH_3), and 5.71–6.92 (10H, aromatic) ppm.

A methiodide (XI), prepared from X with excess methyl iodide, provided an amorphous powder, mp 178.5° (shrinkage at 175°); $[\alpha]_D^{25}$ −10° (c 0.40, methanol).

(+)-Isotubocurarine Chloride Reaction with Diazomethane—(+)-Isotubocurarine chloride (III) (0.11 g, 0.15 mmole) was treated with diazomethane (24.30 mmoles) generated from 2.5 g of *N*-nitrosomethylurea in the same manner as described for I. The residue obtained after solvent removal was dissolved in ethyl acetate and filtered. The filtrate was evaporated under reduced pressure to give 0.060 g of a solid residue, which showed one major band on TLC. Separation by the same preparative TLC technique as that used for obtaining VI and IX provided XIII as the major component.

O,O-Dimethyldihydrotubocurineisomethine (XIII)—The band containing the major component was extracted with methanol–ethyl acetate (1:1). Evaporation of the solvent gave 0.014 g of a solid product, presumably XII, mp 98–104°. Further purification failed to improve the melting point, although the product appeared to be homogeneous on a silica TLC plate using 2.5% aqueous ammonia–ethyl acetate–2-propanol–methanol (0.7:3:3:4). The following data were noted for XII: $[\alpha]_D^{25}$ 00.00° (c 0.73, methanol); UV λ_{max} (log ϵ): 225 (4.80) and 264 (4.48) nm with an additional absorption in the 300–360-nm region which formed a shoulder at 303 nm (log ϵ 4.27); IR (KBr): 885 (styrene) cm^{-1}; NMR ($CDCl_3$): δ 2.10 (s, 3H, NCH_3), 2.25 [s, 6H, $N(CH_3)_2$], 3.66 (s, 3H, OCH_3), 3.68 (s, 3H, OCH_3), 3.81 (s, 3H, OCH_3), 3.83 (s, 3H, OCH_3), 5.10–5.56 (2H, *AB* styrene protons), and 5.80–6.95 (11H, 10 aromatic and one styrene protons) ppm.

Without further purification, XII (0.014 g, 0.022 mmole) in acetic acid (10 ml) was shaken with hydrogen and 0.012 g of palladium-on-carbon (10%) at 49 psi for 62 hr. The catalyst was filtered and washed with acetic acid; the filtrate, combined with the washings, was evaporated to dryness.

---

[1] Melting points were determined on a Mel-Temp melting-point apparatus and are uncorrected. Optical rotations were measured on a Perkin-Elmer 141 polarimeter. Analyses were performed by M-H-W Laboratories, Garden City, Mich. UV spectra were taken in methanol solutions with a Cary 14 recording spectrophotometer. IR spectra were obtained in potassium bromide pellets with a Perkin-Elmer 237 grating IR spectrophotometer. NMR spectra were measured with a Varian Associates model A-60D NMR spectrometer using tetramethylsilane as the internal standard. Mass spectral determinations were performed by the Mass Spectroscopy Laboratory Service, Department of Chemistry, University of Minnesota, Minneapolis, Minn., using a Hitachi Perkin-Elmer RMU-6D mass spectrometer or an AEI-MS 30 high-resolution mass spectrometer.

TLC was conducted on Brinkmann silica gel HF-254 plates of 0.25-mm thickness using 2.5% aqueous ammonia–ethyl acetate–2-propanol–methanol (0.7:3:3:4), Analtech silica gel GF-254 plates of 0.25-mm thickness with 2-butanone–water–88% formic acid (8:1:1), or Eastman Chromagram sheet 6063 alumina with a fluorescent indicator and acetone as a developing solvent. Visualization was done with both a UV lamp and iodine vapor. Brinkmann silica gel HF-254 powder was utilized in preparative TLC, and visualization was with the UV lamp. Woelm neutral alumina (activity grade V) was employed in column chromatography. (+)-Tubocurarine chloride was obtained from Sigma Chemical Co., St. Louis, MO 63118; Abbott Laboratories, North Chicago, IL 60064; and Organon Inc., West Orange, NJ 07052.

[2] Diazomethane was prepared from *N*-nitrosomethylurea according to the procedure of Arndt (19) and was dried over potassium hydroxide pellets for 2 days. No trace of alkali was detected when a large volume of the dried ethereal diazomethane solution was evaporated and tested for alkalinity by adding 5 ml of water to the residue and testing with pH sensitive paper. To ensure the absence of alkali, the ethereal diazomethane solution was distilled before use. No observable differences in subsequent reactivity from the potassium hydroxide pellet-dried ethereal diazomethane were noted.

The residue was dissolved in water (3 ml), neutralized with sodium bicarbonate, and extracted with chloroform (20 × 4 ml). Evaporation of the chloroform extract provided 0.012 g of the free base, which was subsequently purified on silica HF-254 plates using 2.5% aqueous ammonia–ethyl acetate–2-propanol–methanol (0.7:3:3:4).

The major band was extracted with methanol–ethyl acetate (1:1). Evaporation of the solvent under reduced pressure provided 0.0085 g (58.9%) of an amorphous compound (XIII), mp 94–97.5°, $[\alpha]_D^{25}$ −19.5° (c 0.80, methanol); UV λ_{max} (log ϵ): 225 (4.53) and 280 (3.77) nm; NMR ($CDCl_3$): δ 2.10 (s, 3H, NCH_3), 2.23 [s, 6H, $N(CH_3)_2$], 3.62 (s, 3H, OCH_3), 3.65 (s, 3H, OCH_3), 3.80 (s, 6H, 2 OCH_3), and 5.74–6.83 (10H, aromatic) ppm.

Anal.—Calc. for $(C_{39}H_{46}N_2O_6)_2 \cdot 5H_2O$: C, 68.49; H, 7.51; N, 4.09. Found: C, 68.50; H, 7.42; N, 3.59.

Treatment of XIII with methyl iodide provided an amorphous solid (XIV), mp 183° dec., $[\alpha]_D^{25}$ + 40° (c 0.70, methanol).

Laudanosinemethine (XVI)—(±)-Laudanosine methiodide (XV) (0.30 g, 0.60 mmole), prepared from papaverine methiodide according to the method of Mirza (20), was dissolved in methanol (350 ml) and treated with an ethereal solution of diazomethane (135.9 mmoles) generated from 14 g of *N*-nitrosomethylurea, which was added in three portions over 3 days. Evaporation of the solvent on a steam bath provided 0.28 g of a crude product, which was dissolved in 3 ml of chloroform and chromatographed on preparative silica HF-254 plates using 2.5% aqueous ammonia–ethyl acetate–2-propanol–methanol (0.7:3:3:4). The major band was removed and extracted with methanol–ethyl acetate (1:1). Evaporation of the solvent under reduced pressure yielded 0.11 g (49.5%) of a gummy material, which hardened to an amorphous powder, mp 74–77°; UV λ_{max} (log ϵ): 215 (4.42) and 330 (4.26) nm, λ_{min} (log ϵ): 261 (3.93) nm; IR (KBr): 965 (*trans*-stilbene) cm^{-1}; high-resolution mass spectrum—M^+: calc. for $C_{22}H_{29}NO_4$: 371.2095, found: 371.2117.

The hydrochloride salt, prepared in an 81.9% yield of white crystals, gave mp 217–219° [lit. (16) mp 220–221°]. The product was identical to one prepared by the classical method of Battersby and Harper (16). Their method involved treatment of XVI with excess silver oxide, followed by addition of excess potassium hydroxide to the filtrate, which was then refluxed to release the methine base. The Battersby and Harper process yielded 90.3% of the desired product in the present study.

Methiodides of XVI obtained by either of the two methods gave identical white crystalline products (XVII), mp 228–232° [lit. (16) mp 236–237°]; UV λ_{max} (log ϵ): 223 (4.32) and 331 (4.26) nm, λ_{min} (log ϵ): 262 (3.64) nm.

Dihydrolaudanosinemethine (XVIII)—An acetic acid solution of XVI (0.031 g, 0.084 mmole in 10 ml) was reduced by shaking with hydrogen and 10% palladium-on-carbon (0.025 g) at 48 psi for 68 hr. The catalyst was filtered and washed with acetic acid; the filtrate, combined with the washings, was evaporated. The residue was dissolved in water (2 ml), neutralized with sodium bicarbonate, and extracted with chloroform (15 × 4 ml). The chloroform layer was evaporated to provide 0.023 g (74%) of a gum; UV λ_{max} (log ϵ): 225 (4.27) and 280 (3.73) nm; NMR ($CDCl_3$): δ 2.27 [s, 6H, $N(CH_3)_2$], 3.76 (s, 3H, OCH_3), 3.78 (s, 3H, OCH_3), 3.82 (s, 6H, 2 OCH_3), and 6.59–6.72 (s, 5H, aromatic) ppm; high-resolution mass spectrum—M^+: calc. for $C_{22}H_{31}NO_4$: 373.2252, found: 373.2277.

The methiodide (XIX) of XVIII gave a melting point of 200–201° [lit. (16) mp 197°].

(+)-Carneginemethine (XXI)—A solution of (+)-carnegine methiodide[3] (XX) (0.10 g, 0.28 mmole) in methanol (200 ml) was treated over 3.5 days with an ice-cold ethereal solution of diazomethane (97 mmoles) generated from 10 g of *N*-nitrosomethylurea. After removal of the solvent by distillation, the crude reaction product was chromatographed on silica gel, and the major band was removed and extracted with methanol–ethyl acetate (1:1). Evaporation of the solvent under reduced pressure afforded 0.016 g (24.7%) of a gummy compound (XXI); NMR ($CDCl_3$): δ 1.34 (d, 3H, CH_3), 2.25 [s, 6H, $N(CH_3)_2$], 3.85 (s, 6H, 2 OCH_3), 5.07–5.56 (2H, styrene protons), and 6.79–7.25 (3H, two aromatic and one styrene protons) ppm; high-resolution mass spectrum—M^+: calc. for $C_{14}H_{21}NO_4$: 235.1572, found: 235.1573.

The methiodide (XXII) of XXI (0.014 g, 0.059 mmole) in ethyl acetate (5 ml) was obtained using excess methyl iodide. Recrystallization from methanol–ethyl acetate provided 0.019 g (84.6%) of white crystals, mp 179–181°, $[\alpha]_D^{25}$ −25.7° (c 0.4, methanol); UV λ_{max} (log ϵ): 222 (4.45) and 265 (3.98) nm with an additional absorption between 290 and 320 nm which gave a shoulder at 292 nm (log ϵ 3.39), λ_{min} (log ϵ): 246 (3.78) nm; IR (KBr): 870 (styrene) cm^{-1}.

REFERENCES

(1) "Neuromuscular Blocking and Stimulating Agents," vol. I, J. Cheymol, Ed., Pergamon, New York, N.Y., 1972.

(2) "The Pharmacological Basis of Therapeutics," 3rd ed., L. S. Goodman and A. Gilman, Eds., Macmillan, New York, N.Y., 1965, p. 601.

(3) C. M. Smith, E. W. Pelikan, L. R. Maramba, and K. R. Unna, *J. Pharmacol. Exp. Ther.*, **108**, 317 (1953).

(4) O. Wintersteiner and J. D. Dutcher, *Science*, **97**, 467 (1943).

(5) J. D. Dutcher, *J. Am. Chem. Soc.*, **68**, 419 (1946).

(6) H. O. J. Collier, S. K. Paris, and L. I. Woolfe, *Nature*, **161**, 817 (1948).

(7) I. R. C. Bick and L. J. Mcleod, *J. Pharm. Pharmacol.*, **26**, 985 (1974).

(8) A. J. Everett, L. A. Lowe, and S. Wilkinson, *Chem. Commun.*, **1970**, 1020.

(9) P. W. Erhardt and T. O. Soine, *J. Pharm. Sci.*, **64**, 53 (1975).

(10) A. A. Genenah, T. O. Soine, and N. A. Shaath, *ibid.*, **64**, 62 (1975).

(11) T. O. Soine, W. S. Hanley, N. A. Shaath, and A. A. Genenah, *ibid.*, **64**, 67 (1975).

(12) T. O. Soine and J. Naghaway, *ibid.*, **63**, 1643 (1974).

(13) J. Naghaway, N. Shaath, and T. O. Soine, *J. Org. Chem.*, **40**, 539 (1975).

(14) I. R. C. Bick and P. S. Clezy, *J. Chem. Soc.*, **1953**, 3893.

(15) A. W. Sangster and K. L. Stuart, *Chem. Rev.*, **65**, 69 (1965).

(16) A. R. Battersby and B. J. T. Harper, *J. Chem. Soc.*, **1962**, 3526.

(17) A. R. Battersby and I. A. Greenock, *ibid.*, **1961**, 2592.

(18) E. Späth, *Ber. Dtsch. Chem. Ges.*, **62**, 1021 (1929).

(19) F. Arndt, "Organic Syntheses," coll. vol. 2, Wiley, New York, N.Y., 1943, p. 165.

(20) R. Mirza, *J. Chem. Soc.*, **1957**, 4400.

[3] Prepared in these laboratories in another study by P. W. Erhardt and T. O. Soine [*J. Pharm. Sci.*, **64**, 53 (1975)].

Determination of Urinary Indolic Metabolites

ALVIN J. GREENBERG *x and ROGER KETCHAM

Received March 30, 1976, from the *Department of Pharmaceutical Chemistry, School of Pharmacy, University of California, San Francisco, CA 94143.* Accepted for publication July 7, 1977. *Present address: Department of Pharmacology, School of Medicine, University of California, San Francisco, CA 94143.

Abstract □ A rapid mass spectral assay for tryptophol, 5-hydroxytryptophol, and 3-indoleacetic acid, employing stable-isotope labeled internal standards, is described. The compounds were extracted from urine or buffer with ethyl acetate and quantitatively measured by chemical-ionization mass spectrometry. The calibration curves were linear over a range of 0.06–2.8 μg/ml. The technique was applied to the analysis of urine from patients with carcinoid tumors. In addition, the first synthesis of 5-methoxy-3-indoleacrylic acid is reported.

Keyphrases □ Indole derivatives, various—mass spectrometric analyses in human urine □ Mass spectrometry—analyses, various indole derivatives in human urine □ Tryptophan metabolites—various indole derivatives, mass spectrometric analyses in human urine □ Metabolites, tryptophan—various indole derivatives, mass spectrometric analyses in human urine

The metabolism of tryptophan by carcinoid tumors to indole and 5-hydroxyindole metabolites has been under investigation in this laboratory. Carcinoid tumors are usually malignant carcinomas arising from the argentaffin cells throughout the lung and GI tract (1). Associated with this tumor are large amounts of 5-hydroxytryptamine (I) present in the circulation and excessive urinary excretion of 5-hydroxy-3-indoleacetic acid (II), which constitute the biochemical hallmark of this disease (2–6).

BACKGROUND

Recent investigations (7) showed that some patients with carcinoid tumors exhibit low urinary II levels and/or elevated levels of other indolic metabolites. Determination of other excreted indolic metabolites may aid disease diagnosis and treatment. A mass spectral assay for three indolic metabolites, 3-indoleacetic acid (III), tryptophol (3-indoleethanol) (IV), and 5-hydroxytryptophol (V), is presented here.

3-Indoleacetic acid is a normal urinary metabolite and is present in the urine of patients with carcinoid tumors (7–9). A previously reported (8) assay for III was considered unsatisfactory because of the high probability of interference from other indolic compounds.

5-Hydroxytryptophol and its conjugates have been identified as normal metabolites in human urine and human and rat brain homogenates (10, 11). Ethanol consumption shifts tryptophan metabolism away from the oxidation metabolite, II, toward the reduced metabolite, V, as a result of the increased ratio of reduced to unreduced nucleotide cofactors effected by ethanol metabolism (12, 13). This alternation has been demonstrated in normal humans and in patients with carcinoid tumors (14). Thus, it was necessary to assay for V and the nonhydroxylated metabolite, IV, to account for tryptophan metabolites further. Previously reported assays for IV (15) and V (16) have detection limits of 1–5 μg.

In addition, 5-methoxy-3-indoleacrylic acid (VI) was synthesized to serve as an authentic standard to establish the presence of this compound as an excreted tryptophan metabolite. 3-Indoleacrylic acid was detected in the urine of a patient with carcinoid tumor (7). Moreover, 3-indoleacrylic acid and its glycine conjugate were found as urinary metabolites in normal humans (17, 18), in those with a chromosomal abnormality (19), in patients with Hartnup disease (20, 21), in a group of East Africans who had a high intake of bananas in their diet (22), and in six children with phenylketonuria (23). Therefore, it is established that 3-indoleacrylic acid and its conjugate are urinary metabolites in normal humans and in patients with certain diseases. It is thus possible that 5-hydroxy-3-indoleacrylic acid or 5-methoxy-3-indoleacrylic acid may also be excreted as a urinary metabolite, particularly in patients with carcinoid tumors where large amounts of 5-hydroxylated indole metabolites are excreted.

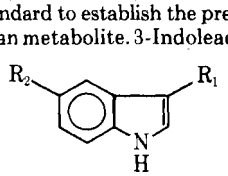

I: $R_1 = CH_2CH_2NH_2$, $R_2 = OH$
II: $R_1 = CH_2COOH$, $R_2 = OH$
III: $R_1 = CH_2COOH$, $R_2 = H$
IV: $R_1 = CH_2CH_2OH$, $R_2 = H$
V: $R_1 = CH_2CH_2OH$, $R_2 = OH$
VI: $R_1 = CH{=}CHCOOH$, $R_2 = OCH_3$

EXPERIMENTAL[1]

Chemistry—*Ethyl 3-Indolylglyoxylate*—To a stirred solution of indole (3.7 g, 32 mmoles) in 50 ml of ether at 0–5° was added oxalyl chloride (4.6 g, 36 mmoles) over 20 min. After 1 hr, 60 ml of absolute ethanol and 5 ml of triethylamine were added, and the reaction mixture was refluxed for 30 min. After cooling, the precipitate was collected and recrystallized from ethanol–water to give fine white needles, 5.45 g (80%), mp 183–185° [lit. (24) mp 186°].

Tryptophol-d_4—A suspension of ethyl 3-indolylglyoxylate (5.0 g, 23 mmoles) and lithium aluminum deuteride (3.36 g, 80 mmoles) in 100 ml of tetrahydrofuran was heated under reflux for 2 hr under nitrogen. Excess hydride was decomposed by addition of 10 ml of water. The resulting precipitate was filtered and washed with tetrahydrofuran, the combined filtrates were dried over anhydrous sodium sulfate, and the solvent was removed *in vacuo* to give an oil. Upon cooling, white crystals formed. These crystals were recrystallized from benzene–petroleum ether (bp 65–110°) to give white platelets, mp 57.5–58.5° [lit. (24) 58–59°]; chemical-ionization mass spectrum (isobutane): *m/e* 166 (MH^+).

Anal.—Calc. for $C_{10}H_7D_4NO$: C, 72.7; H, 9.1; N, 8.5. Found: C, 72.93; H, 8.88; N, 8.64.

5-Benzyloxytryptophol-d_4—To a solution of 5-benzyloxyindole (5.0 g, 22.4 mmoles) in 50 ml of ether at 0–5° was added, dropwise over 15 min, oxalyl chloride (3.3 g, 26 mmoles). The reaction mixture was stirred for 1 hr and filtered to give a red powder, which was collected and dried *in vacuo* to give 2.6 g (38%). The crude 5-benzyloxyindolylglyoxalyl chloride was added to a suspension of lithium aluminum deuteride (1.43 g, 34.1 mmoles) in 40 ml of dry tetrahydrofuran and refluxed for 2 hr under nitrogen.

The reaction mixture was decomposed with 10 ml of water, the precipitate was filtered and washed with tetrahydrofuran, and the combined tetrahydrofuran fractions were dried over anhydrous sodium sulfate and concentrated to an oil *in vacuo*. Upon standing at 5°, the oil solidified; three recrystallizations from benzene–petroleum ether (bp 65–110°) gave 875 mg (38%), mp 92–95° [lit. (25) mp 93–95°]; chemical-ionization mass spectrum (isobutane): *m/e* 272 (MH^+).

5-Hydroxytryptophol-d_4—A solution of 5-benzyloxytryptophol-d_4 (850 mg, 3.1 mmoles) in 25 ml of methanol was treated with 10% Pd/$BaSO_4$ (500 mg) under 1 atm of hydrogen. After 3 hr, the hydrogenolysis was complete; the reaction mixture was filtered, and the solvent was removed *in vacuo*. The residue was dissolved in ethyl acetate, treated with charcoal, and cooled to 5°. Petroleum ether (bp 65–110°) was added until the solution turned cloudy. The solution was allowed to stand at 5°, and fine white crystals were collected to give 110 mg (20%), mp 107–109.5° [lit. (25) mp 105–107°]; chemical-ionization mass spectrum (isobutane): *m/e* 182 (MH^+).

[1] Chemical-ionization mass spectrometry was performed on an AEI MS-9 spectrometer modified for chemical ionization and conducted under the following conditions: source pressure, 0.7 torr; and source temperature, 180°. NMR spectra were recorded on a Varian A-60 spectrometer. Melting points are uncorrected. Elemental analyses were performed by the Microanalytical Laboratory, Berkeley, Calif.

Anal.—Calc. for $C_{10}H_7D_4NO_2$: C, 66.3; H, 8.3; N, 7.7. Found: C, 66.43; H, 8.06; N, 7.52.

3-Indoleacetic Acid-d_7—A solution of 3-indoleacetic acid[2] (1.0 g, 5.7 mmoles) and 20 ml of 4.0 *N* DCl (99% atom)[3] in deuterium oxide (99.7% atom)[3] was stirred under reflux under nitrogen for 1 hr. The solvent was then removed *in vacuo*, fresh solvent was added, and the procedure was repeated nine times. The resulting residue was treated with ethereal diazomethane. Chemical-ionization mass spectrometry (isobutane) of the methyl ester showed molecular ions at *m/e* 194 (MH + 5), 195 (MH + 6), and 196 (MH + 7).

5-Methoxy-3-indoleacrylic Acid—A solution of 5-methoxyindole (2.94 g, 20 mmoles) in 20 ml of ether was added dropwise over 15 min to a solution of methyl magnesium bromide[4] (2.77 g, 25 mmoles) in 10 ml of ether under nitrogen and cooled to −5–0° in an ice bath. After stirring for 15 min, 3-chloroacrylic acid (2.13 g, 20 mmoles) in 20 ml of ether was added dropwise over 15 min. The reaction mixture was allowed to warm to room temperature, ammonium chloride (2.8 g) in 30 ml of water was added dropwise, and the precipitate was removed by filtration.

The filtrate was separated, and the aqueous phase, at pH 7.8, was extracted with ether. The pH of the aqueous phase was adjusted to 1.6 with 6 *N* HCl. The solution was cooled, and the white precipitate was collected. Recrystallization first from ethyl acetate–hexane (1:1) with charcoal treatment and then from ethanol–water gave 5-methoxy-3-indoleacrylic acid as white platelets, 259 mg (6%), mp 197–200°; NMR (dimethyl sulfoxide): δ 6.4, 7.9 (2d, 2H, CH=CH, J = 15 Hz), 6.8–8.0 (m, 5H, N-H, 2-H, 4-H, 6-H, and 7-H), 11.85 (s, CO_2H), and 3.8 (s, 3H, OCH_3) ppm; UV (absolute ethanol): 279 and 324 nm; chemical-ionization mass spectrum (isobutane) of methyl ester: *m/e* 232 (MH^+).

Anal.—Calc. for $C_{12}H_{11}NO_3$: C, 66.3; H, 5.1; N, 6.4. Found: C, 66.18; H, 4.97; N, 6.53.

Standards—Standard solutions of tryptophol, 5-hydroxytryptophol, 3-indoleacetic acid, and their deuterium-labeled analogs consisted of known amounts weighed to 0.01 ± 0.005 mg dissolved in 0.2 *M* phosphate buffer, pH 7.4, and had the following concentrations: tryptophol, 0.87 μg/μl; tryptophol-d_4, 0.51 μg/μl; 5-hydroxytryptophol, 0.79 μg/μl; 5-hydroxytryptophol-d_4, 0.71 μg/μl; 3-indoleacetic acid, 0.70 μg/μl; and 3-indoleacetic acid-d_7, 0.99 μg/μl.

Assay Standardization—Standard curves for quantitative measurement of tryptophol, 5-hydroxytryptophol, and 3-indoleacetic acid were obtained by adding known amounts of standard solutions of these compounds and their deuterium-labeled analogs to aqueous buffer or urine and extracting with ethyl acetate after adjusting the pH to 7.0 or 1.8. Microliter quantities of the standard solutions were obtained using an adjustable microliter pipet accurate to ±0.1%. These data were reproducible and gave essentially the same results for samples prepared in urine (pH adjusted) as for those in buffer alone.

Assay—A patient's 24-hr urine was collected and stored frozen without preservative until assayed. The frozen urines were thawed, the total volume and pH were recorded, and a 100-ml aliquot was removed for assay. Known amounts of deuterium-labeled standards were added to this aliquot in amounts equivalent to 500–1000 μg/24-hr urine. The urinary pH was adjusted to 7.0 by aqueous base and extracted with three 35-ml portions of ethyl acetate; these extracts were combined, dried over anhydrous sodium sulfate, and concentrated to dryness in a nitrogen stream. This fraction, containing neutral compounds, phenols, and weak bases, was then subjected to chemical-ionization mass spectral analysis.

The remaining urine fraction was brought to pH 1.8 by addition of 6.0 *N* HCl, saturated with sodium chloride, and extracted with three 35-ml portions of ethyl acetate. The extracts were combined, dried over anhydrous sodium sulfate, and concentrated to dryness. This fraction, containing organic acids, was then subjected to chemical-ionization mass spectral analysis after treatment with ethereal diazomethane.

RESULTS AND DISCUSSION

Tryptophol-d_4 and 5-Hydroxytryptophol-d_4—These compounds were prepared according to the procedures reported for tryptophol (24) and 5-hydroxytryptophol (25) with the modification that the ester or acid chloride was reduced with lithium aluminum deuteride to give the tetradeuteroethanol side chain.

3-Indoleacetic Acid-d_7—This compound was prepared by treating 3-indoleacetic acid and 4.0 *N* DCl in deuterium oxide under reflux. Exchange of the five aromatic protons of tryptophan when treated with trifluoroacetic acid-d_1 (26, 27) and of the four aromatic protons on 5-hydroxytryptophan when treated with 4.0 *N* DCl (28) has been reported. The methylene protons of 3-indoleacetic acid, being doubly activated, were also expected to be exchanged. Isobutane chemical-ionization mass spectral analysis of the methyl ester showed the mixture composition to be 65% d_7, 29% d_6, and 6% d_5, which was sufficient deuteration for use as an internal standard.

5-Methoxy-3-indoleacrylic Acid—3-Indoleacrylic acid has been synthesized (29) in 50% yield by the Doebner modification of the Knoevenagel reaction (30), a procedure found to be unsatisfactory for preparation of 5-methoxy- or 5-hydroxy-3-indoleacrylic acid[5]. Therefore, following the model of Woodward *et al.* (32), the Grignard salt of 5-methoxyindole was reacted with 3-chloroacrylic acid to give 5-methoxy-3-indoleacrylic acid. Extensive TLC, GLC[6], and mass spectral analysis of several urines from carcinoid patients failed to produce any evidence for the presence of 5-hydroxy- or 5-methoxy-3-indoleacrylic acid.

Assay—Chemical-ionization mass spectral analysis of the ethyl acetate extracts permitted quantitative measurement from the ratio of peak heights of MH^+ 162/166 for tryptophol, MH^+ 178/182 for 5-hydroxytryptophol, and MH^+ 190/197 for 3-indoleacetic acid. Interfering peaks from other neutral, phenolic, or basic compounds were nonexistent for masses 162/166 and 178/182. Interference from acidic compounds of mass 190/197 was negligible. The ratio times the amount of deuterium-labeled compound added gave the amount of unlabeled metabolite found. Standard curves were obtained by plotting micrograms found *versus* micrograms added. The assay gave a linear correlation over the following ranges: tryptophol, 0.4–2.8 μg/ml; 5-hydroxytryptophol, 0.06–2.4 μg/ml; and 3-indoleacetic acid, 0.1–2.5 μg/ml.

A common method of obtaining a standard curve utilizes a constant amount of internal standard while varying the known amount of compound under assay (33–35). This approach was unsatisfactory because a large error is involved in measurement and ratio determination when peak heights are vastly different. Accuracy is greatest when the ratios are less than 3:1. Thus, when analyzing an unknown sample, an approximate value was obtained and the sample was assayed again with an amount of deuterium standard added to approximate a 2:1 ratio.

Patient Assay—Only two 24-hr urines from patients with carcinoid tumor were available. Patient A had the following urinary levels: 3-indoleacetic acid, 0.25 mg/24 hr; tryptophol, <17 μg/24 hr; and 5-hydroxytryptophol, <123 μg/24 hr. Patient B had the following urinary levels: 3-indoleacetic acid, 0.17 mg/24 hr; tryptophol, <12 μg/24 hr; and 5-hydroxytryptophol, <55 μg/24 hr.

REFERENCES

(1) A. J. Simpson, *N.C. Med. J.*, **30,** 399 (1969).

(2) J. Waldenstrom, *Gastroenterology*, **35,** 565 (1958).

(3) K. L. Melmon and A. Sjoerdsma, *ibid.*, **47,** 104 (1964).

(4) J. A. Oates, K. L. Melmon, L. Gillespie, A. Sjoerdsma, and D. T. Mason, *Lancet*, **1,** 514 (1964).

(5) K. L. Melmon, A. Sjoerdsma, and D. T. Mason, *Am. J. Med.*, **39,** 568 (1965).

(6) R. M. Cohen, *Calif. Med.*, **114,** 1 (1971).

(7) H. E. Williams, K. M. Wilson, W. Trager, and K. L. Melmon, *Clin. Res.*, **19,** 406 (1971).

(8) H. Weissbach, W. King, A. Sjoerdsma, and S. Udenfriend, *J. Biol. Chem.*, **234,** 81 (1959).

(9) B. J. Haverback, B. Dyce, and H. V. Thomas, *N. Engl. J. Med.*, **262,** 754 (1960).

(10) V. E. Davis, J. L. Cashaw, J. A. Huff, and H. Brown, *Proc. Soc. Exp. Biol. Med.*, **122,** 890 (1967).

(11) D. Eccleston, A. T. B. Moir, H. W. Reading, and I. M. Ritchie, *Br. J. Pharmacol. Chemother.*, **28,** 367 (1966).

(12) A. Feldstein, H. Hoagland, K. Wong, and H. Freeman, *Q. J. Stud. Alcohol*, **25,** 218 (1964).

(13) V. E. Davis, H. Brown, J. A. Huff, and J. L. Cashaw, *J. Lab. Clin.*

[2] Sigma Chemical Co.

[3] Aldrich Chemical Co.

[4] Alfa-Ventron Corp.

[5] The starting material for this synthesis, 5-benzyloxy-3-indolecarboxaldehyde, is refractory to an aldol-type reaction because of the decreased electrophilicity of the carbonyl carbon. Extensive UV and IR analyses of this compound support this hypothesis. Similar difficulties with the same reaction involving 5-benzyloxy- or 5-hydroxy-substituted benzothiophene derivatives were reported (31).

[6] GLC was performed on a Varian 2100 gas chromatograph using a 0.9-m (3-ft) column packed with 2% OV-1 on 100–200-mesh Chromosorb GHP. The column oven temperature was programmed from 100 to 250° at 2°/min.

Med., **69**, 132 (1967).
(14) V. E. Davis, *Adv. Pharmacol.*, **6-B**, 143 (1968).
(15) O. Hutzinger, *J. Chromatogr.*, **40**, 117 (1969).
(16) S. Iskric, L. Stancic, and S. Kveder, *Clin. Chim. Acta*, **25**, 435 (1969).
(17) M. D. Armstrong, K. N. F. Shaw, M. J. Gortatowski, and H. Singer, *J. Biol. Chem.*, **232**, 17 (1958).
(18) A. J. Mandell and R. T. Rubin, *Life Sci.*, **4**, 1657 (1965).
(19) W. J. Mellman, L. A. Barness, T. A. Tedesco, and D. Besselman, *Clin. Chim. Acta*, **8**, 843 (1963).
(20) J. B. Jepson and M. J. Spiro, "The Metabolic Basis of Inherited Disease," McGraw-Hill, New York, N.Y., 1960, p. 1338.
(21) J. B. Jepson, *Adv. Pharmacol.*, **6-B**, 171 (1968).
(22) I. L. Hansen and M. A. Crawford, *J. Chromatogr.*, **22**, 330 (1966).
(23) G. Strohmeyer, *Arch. Exp. Klin. Dermatol.*, **219**, 743 (1964).
(24) T. Nogrady and T. W. Doyle, *Can. J. Chem.*, **42**, 485 (1964).
(25) S. Kveder, S. Iskric, and D. Keglevic, *Biochem. J.*, **85**, 447 (1962).
(26) B. Bak, C. Dambmann, and F. Nicolaisen, *Acta Chem. Scand.*, **21**, 1674 (1967).
(27) B. Bak, J. J. Led, and E. J. Pedersen, *ibid.*, **23**, 3051 (1969).
(28) G. W. Kirby, S. W. Shah, and M. Sandler, *Chem. Commun.*, **1967**, 819.
(29) K. N. F. Shaw, A. McMillan, A. G. Gudmundson, and M. D. Armstrong, *J. Org. Chem.*, **23**, 1171 (1958).
(30) G. Jones, *Org. React.*, **15**, 204 (1969).
(31) A. Dinner and E. Campaigne, *J. Med. Chem.*, **13**, 1205 (1970).
(32) R. B. Woodward, F. E. Bader, H. Bickel, A. Frey, and R. W. Kierstead, *J. Am. Chem. Soc.*, **78**, 2023 (1956).
(33) S. H. Koslow and A. R. Green, *Adv. Biochem. Psychopharmacol.*, **7**, 33 (1973).
(34) L. Bertillson and L. Palmer, *Science*, **177**, 74 (1972).
(35) F. Cattabeni, S. H. Koslow, and E. Costa, *ibid.*, **178**, 166 (1972).

ACKNOWLEDGMENTS

Supported in part by Cancer Research Funds of the University of California and the University of California Patent Fund.

The authors thank Dr. Hibbard E. Williams for clinical assistance and Dr. Robert Weinkam for technical assistance.

Inhibition of Rat Liver Mitochondrial Monoamine Oxidase by Chloramphenicol and 2-Amino-1-*p*-nitrophenylpropane-1,3-diol

SACHCHIDANANDA BANERJEE ˣ, PRANAB SANKAR BASU, and CHANDAN MITRA

Received August 30, 1976, from the *Research and Development Division, Dey's Medical Stores (Manufacturing) Limited, Calcutta-700019, India.* *Accepted for publication March 1, 1977.*

Abstract □ Inhibition of rat liver mitochondrial monoamine oxidase by chloramphenicol and its hydrolytic product, 2-amino-1-*p*-nitrophenylpropane-1,3-diol, was studied. The enzyme activity and its inhibition by these two compounds were optimum at pH 7.0 after preincubation for 60 min, the time needed for maximum enzyme–inhibitor complex formation. Enzyme activity could be restored after prolonged dialysis. Monoamine oxidase inhibition by chloramphenicol and its hydrolytic product was noncompetitive and reversible. Deamination of various monoamines was not to the same degree by these compounds. Of the different antimicrobials studied, only chloramphenicol and its hydrolytic product had a strong inhibitory effect on monoamine oxidase.

Keyphrases □ Chloramphenicol—effect on *in vitro* activity of rat liver mitochondrial monoamine oxidase □ Monoamine oxidase, rat liver mitochondrial—activity *in vitro*, effect of chloramphenicol and 2-amino-1-*p*-nitrophenylpropane-1,3-diol □ Enzyme activity—rat liver mitochondrial monoamine oxidase, effect of chloramphenicol and 2-amino-1-*p*-nitrophenylpropane-1,3-diol *in vitro* □ Antimicrobials—chloramphenicol and others, effect on *in vitro* activity of rat liver mitochondrial monoamine oxidase

Chloramphenicol and its hydrolytic product, 2-amino-1-*p*-nitrophenylpropane-1,3-diol, when administered intravenously to cats, produced vasodepression followed by an overshooting rise in blood pressure (1). Monoamine oxidase inhibitor drugs also produce hypotension followed by hypertension (2, 3). Therefore, it is possible that chloramphenicol and 2-amino-1-*p*-nitrophenylpropane-1,3-diol act as monoamine oxidase inhibitors, the subject of the present investigation.

Table I—Effect of Different Antimicrobials on Rat Liver Mitochondrial Monoamine Oxidase [a]

System	Monoamine Oxidase Activity[b]	Inhibition, %
Control	46	—
Plus streptomycin sulfate	46	Nil
Plus penicillin G sodium	46	Nil
Plus tetracycline hydrochloride	36	21.7
Plus chloramphenicol	16	65
Plus 2-amino-1-*p*-nitrophenylpropane-1,3-diol	17	63

[a] Results are means of five observations. Variations in individual observations were minimal. [b] Activity was defined as aldehyde formed, micromoles per 2.5 mg of protein per 30 min of incubation at 37°.

EXPERIMENTAL

Preparation of Monoamine Oxidase—Adult male albino rats, 200 g (average weight), were killed by stunning and decapitation after an overnight fast. The livers were pooled, homogenized in ice-cold 0.25 *M* sucrose to obtain a 10% (w/v) homogenate (4), washed with 0.25 *M* sucrose at 27,000×*g* for 20 min, and suspended in 0.001 *M* phosphate buffer (pH 7.0). A 1-ml aliquot of this suspension was equivalent to 1 g of tissue, and it was used as the source of monoamine oxidase.

Assay of Monoamine Oxidase Activity—The reaction mixture for the monoamine oxidase assay contained 0.025 *M* phosphate buffer (pH 7.0), 0.0125 *M* semicarbazide hydrochloride adjusted to pH 7.0, 0.01 *M* tyramine, and 0.1 ml of mitochondrial suspension as the enzyme source in a final volume of 2 ml. The optimum concentration of tyramine for measuring monoamine oxidase activity is 0.01 *M* (5–7). A higher concentration inhibits monoamine oxidase activity (8). Monoamine oxidase activity was measured at 420 nm (9).

Med., **69**, 132 (1967).
(14) V. E. Davis, *Adv. Pharmacol.*, **6-B**, 143 (1968).
(15) O. Hutzinger, *J. Chromatogr.*, **40**, 117 (1969).
(16) S. Iskric, L. Stancic, and S. Kveder, *Clin. Chim. Acta*, **25**, 435 (1969).
(17) M. D. Armstrong, K. N. F. Shaw, M. J. Gortatowski, and H. Singer, *J. Biol. Chem.*, **232**, 17 (1958).
(18) A. J. Mandell and R. T. Rubin, *Life Sci.*, **4**, 1657 (1965).
(19) W. J. Mellman, L. A. Barness, T. A. Tedesco, and D. Besselman, *Clin. Chim. Acta*, **8**, 843 (1963).
(20) J. B. Jepson and M. J. Spiro, "The Metabolic Basis of Inherited Disease," McGraw-Hill, New York, N.Y., 1960, p. 1338.
(21) J. B. Jepson, *Adv. Pharmacol.*, **6-B**, 171 (1968).
(22) I. L. Hansen and M. A. Crawford, *J. Chromatogr.*, **22**, 330 (1966).
(23) G. Strohmeyer, *Arch. Exp. Klin. Dermatol.*, **219**, 743 (1964).
(24) T. Nogrady and T. W. Doyle, *Can. J. Chem.*, **42**, 485 (1964).
(25) S. Kveder, S. Iskric, and D. Keglevic, *Biochem. J.*, **85**, 447 (1962).
(26) B. Bak, C. Dambmann, and F. Nicolaisen, *Acta Chem. Scand.*, **21**, 1674 (1967).
(27) B. Bak, J. J. Led, and E. J. Pedersen, *ibid.*, **23**, 3051 (1969).
(28) G. W. Kirby, S. W. Shah, and M. Sandler, *Chem. Commun.*, **1967**, 819.
(29) K. N. F. Shaw, A. McMillan, A. G. Gudmundson, and M. D. Armstrong, *J. Org. Chem.*, **23**, 1171 (1958).
(30) G. Jones, *Org. React.*, **15**, 204 (1969).
(31) A. Dinner and E. Campaigne, *J. Med. Chem.*, **13**, 1205 (1970).
(32) R. B. Woodward, F. E. Bader, H. Bickel, A. Frey, and R. W. Kierstead, *J. Am. Chem. Soc.*, **78**, 2023 (1956).
(33) S. H. Koslow and A. R. Green, *Adv. Biochem. Psychopharmacol.*, **7**, 33 (1973).
(34) L. Bertillson and L. Palmer, *Science*, **177**, 74 (1972).
(35) F. Cattabeni, S. H. Koslow, and E. Costa, *ibid.*, **178**, 166 (1972).

ACKNOWLEDGMENTS

Supported in part by Cancer Research Funds of the University of California and the University of California Patent Fund.

The authors thank Dr. Hibbard E. Williams for clinical assistance and Dr. Robert Weinkam for technical assistance.

Inhibition of Rat Liver Mitochondrial Monoamine Oxidase by Chloramphenicol and 2-Amino-1-*p*-nitrophenylpropane-1,3-diol

SACHCHIDANANDA BANERJEE ˣ, PRANAB SANKAR BASU, and CHANDAN MITRA

Received August 30, 1976, from the *Research and Development Division, Dey's Medical Stores (Manufacturing) Limited, Calcutta-700019, India.* *Accepted for publication March 1, 1977.*

Abstract □ Inhibition of rat liver mitochondrial monoamine oxidase by chloramphenicol and its hydrolytic product, 2-amino-1-*p*-nitrophenylpropane-1,3-diol, was studied. The enzyme activity and its inhibition by these two compounds were optimum at pH 7.0 after preincubation for 60 min, the time needed for maximum enzyme–inhibitor complex formation. Enzyme activity could be restored after prolonged dialysis. Monoamine oxidase inhibition by chloramphenicol and its hydrolytic product was noncompetitive and reversible. Deamination of various monoamines was not to the same degree by these compounds. Of the different antimicrobials studied, only chloramphenicol and its hydrolytic product had a strong inhibitory effect on monoamine oxidase.

Keyphrases □ Chloramphenicol—effect on *in vitro* activity of rat liver mitochondrial monoamine oxidase □ Monoamine oxidase, rat liver mitochondrial—activity *in vitro*, effect of chloramphenicol and 2-amino-1-*p*-nitrophenylpropane-1,3-diol □ Enzyme activity—rat liver mitochondrial monoamine oxidase, effect of chloramphenicol and 2-amino-1-*p*-nitrophenylpropane-1,3-diol *in vitro* □ Antimicrobials—chloramphenicol and others, effect on *in vitro* activity of rat liver mitochondrial monoamine oxidase

Chloramphenicol and its hydrolytic product, 2-amino-1-*p*-nitrophenylpropane-1,3-diol, when administered intravenously to cats, produced vasodepression followed by an overshooting rise in blood pressure (1). Monoamine oxidase inhibitor drugs also produce hypotension followed by hypertension (2, 3). Therefore, it is possible that chloramphenicol and 2-amino-1-*p*-nitrophenylpropane-1,3-diol act as monoamine oxidase inhibitors, the subject of the present investigation.

Table I—Effect of Different Antimicrobials on Rat Liver Mitochondrial Monoamine Oxidase [a]

System	Monoamine Oxidase Activity[b]	Inhibition, %
Control	46	—
Plus streptomycin sulfate	46	Nil
Plus penicillin G sodium	46	Nil
Plus tetracycline hydrochloride	36	21.7
Plus chloramphenicol	16	65
Plus 2-amino-1-*p*-nitrophenylpropane-1,3-diol	17	63

[a] Results are means of five observations. Variations in individual observations were minimal. [b] Activity was defined as aldehyde formed, micromoles per 2.5 mg of protein per 30 min of incubation at 37°.

EXPERIMENTAL

Preparation of Monoamine Oxidase—Adult male albino rats, 200 g (average weight), were killed by stunning and decapitation after an overnight fast. The livers were pooled, homogenized in ice-cold 0.25 *M* sucrose to obtain a 10% (w/v) homogenate (4), washed with 0.25 *M* sucrose at 27,000×*g* for 20 min, and suspended in 0.001 *M* phosphate buffer (pH 7.0). A 1-ml aliquot of this suspension was equivalent to 1 g of tissue, and it was used as the source of monoamine oxidase.

Assay of Monoamine Oxidase Activity—The reaction mixture for the monoamine oxidase assay contained 0.025 *M* phosphate buffer (pH 7.0), 0.0125 *M* semicarbazide hydrochloride adjusted to pH 7.0, 0.01 *M* tyramine, and 0.1 ml of mitochondrial suspension as the enzyme source in a final volume of 2 ml. The optimum concentration of tyramine for measuring monoamine oxidase activity is 0.01 *M* (5–7). A higher concentration inhibits monoamine oxidase activity (8). Monoamine oxidase activity was measured at 420 nm (9).

Table II—Variation of Preincubation Time on Rat Liver Mitochondrial Monoamine Oxidase Inhibition by Chloramphenicol and 2-Amino-1-*p*-nitrophenylpropane-1,3-diol [a]

System	Time of Preincubation, min 30	60	90
Control	32	46	28
Plus chloramphenicol, 12 mg	22 (31)	13 (72)	10 (62.5)
Plus 2-amino-1-*p*-nitrophenylpropane-1,3-diol, 12 mg	15 (40)	6 (86)	14 (50)

[a] The results are given as monoamine oxidase activity (aldehyde formed, micromoles per 2.5 mg of protein per 30 min of incubation at 37°) and are means of five observations. Variations in observations in each group were minimal. Figures in parentheses indicate percent inhibition.

Table III—Reversibility of Rat Liver Mitochondrial Monoamine Oxidase Inhibition by Chloramphenicol and 2-Amino-1-*p*-nitrophenylpropane-1,3-diol [a]

System	Monoamine Oxidase Activity[b] Before Dialysis	After Dialysis for 24 hr
Control	40	40
Plus chloramphenicol, 12 mg	11 (72.5)	38
Plus 2-amino-1-*p*-nitrophenylpropane-1,3-diol, 12 mg	5 (87.5)	41

[a] Results are means of five observations. Variations in observations in each group were minimal. An aliquot of the enzyme preparation was mixed with the inhibitor and dialyzed with 0.001 *M* cold phosphate buffer at 4–5°. In the control, the enzyme was dialyzed without any inhibitor. The time of preincubation was 60 min at 37°. Figures in parenthesis indicate percent inhibition. [b] Activity was defined as aldehyde formed, micromoles per 2.5 mg of protein per 30 min of incubation at 37°.

The *p*-hydroxyphenylacetaldehyde semicarbazone formed in the assay was converted to the corresponding 2,4-dinitrophenylhydrazone, the value of which was calculated from a calibration curve obtained with 2,4-dinitrophenylhydrazone derivative crystallized three times (10). When amines other than tyramine, *e.g.*, 5-hydroxytryptamine, norepinephrine, or epinephrine, were used, actual absorbance values also were recorded since the extinction of various 2,4-dinitrophenylhydrazone derivatives differs from that of *p*-hydroxyphenylacetaldehyde dinitrophenylhydrazone.

All incubations prior to the addition of the substrate were carried out at 37° for 1 hr. Later incubations were carried out at 37° for 30 min (maximum linearity) with air as the gas phase. Protein of the mitochondrial enzyme preparations was determined by the biuret method (11).

Effect of Different Antimicrobials on Rat Liver Mitochondrial Monoamine Oxidase—The effects of the addition of streptomycin sulfate, penicillin G sodium, tetracycline hydrochloride, chloramphenicol, and 2-amino-1-*p*-nitrophenylpropane-1,3-diol on liver monoamine oxidase activity were studied. All compounds were dissolved in water. Chloramphenicol and 2-amino-1-*p*-nitrophenylpropane-1,3-diol were dissolved in boiling water, an aliquot of which, when added to the incubation medium, did not show any precipitation. The same quantity of boiling water was added to the control system. The final concentration of each compound in the experimental system was 13×10^{-3} *M*.

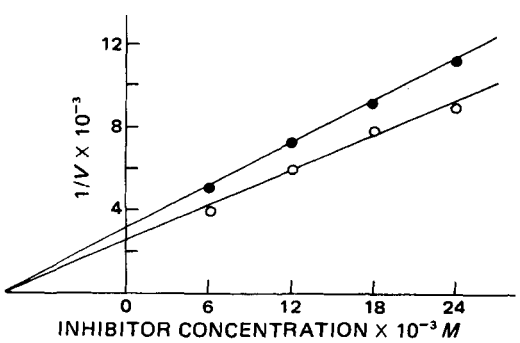

Figure 1—*Inhibition of rat liver mitochondrial monoamine oxidase by chloramphenicol. The enzyme preparation and the drug were mixed and added to the medium. After 60 min of preincubation, the substrate was added; the enzyme activity was determined after 30 min of incubation at 37°. Key:* ●, *0.005* M *tyramine; and* ○, *0.01* M *tyramine.*

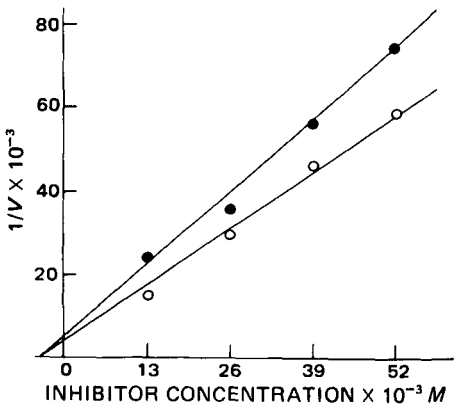

Figure 2—*Inhibition of rat liver mitochondrial monoamine oxidase by 2-amino-1-*p*-nitrophenylpropane-1,3-diol. Conditions of experiments were the same as described in Fig. 1. Key:* ●, *0.005* M *tyramine; and* ○, *0.01* M *tyramine.*

Reversibility of Rat Liver Monoamine Oxidase Inhibition by Chloramphenicol and 2-Amino-1-*p*-nitrophenylpropane-1,3-diol—To study the reversibility of monoamine oxidase inhibition, the enzyme and compound mixture was preincubated for 60 min at 37° for the formation of enzyme–inhibitor complex. It was then dialyzed in a dialysis sac with 0.001 *M* cold phosphate buffer (pH 7.0) for 24 hr. A portion of the same enzyme preparation was also dialyzed without the compounds in a similar manner. After 24 hr, the enzyme inside the sac was incubated with the substrate to determine monoamine oxidase activity.

Effect of Treatment of Rats with Chloramphenicol and 2-Amino-1-*p*-nitrophenylpropane-1,3-diol on Monoamine Oxidase Activities of Liver and Cardiac Muscle—Each of eight rats was given two daily intramuscular injections of 10 mg of chloramphenicol or 2-amino-1-*p*-nitrophenylpropane-1,3-diol dissolved in 0.5 ml of isotonic saline for 8 days. Control rats received only injections of isotonic saline. On the 9th day, after an overnight fast, the animals were sacrificed. The liver and heart were removed, the mitochondrial enzymes were isolated, and monoamine oxidase activity was determined.

RESULTS AND DISCUSSION

Inhibition of liver mitochondrial monoamine oxidase activity was maximum with chloramphenicol and 2-amino-1-*p*-nitrophenylpropane-1,3-diol, minimal with tetracycline, and absent with streptomycin and penicillin G (Table I). Therefore, liver monoamine oxidase inhibition was not a generalized effect of antimicrobials.

Enzyme–inhibitor complex formation started at 30 min, reached a maximum at 60 min, and diminished at 90 min (Table II). During the preincubation period of 60 min, concentrations of chloramphenicol assayed microbiologically (12) and of 2-amino-1-*p*-nitrophenylpropane-

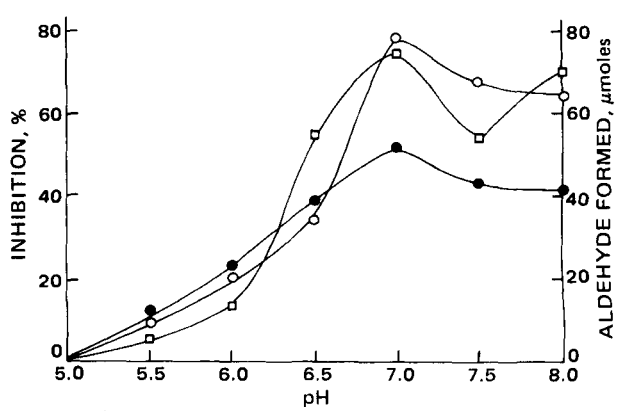

Figure 3—*Influence of pH on rat liver mitochondrial monoamine oxidase inhibition by chloramphenicol (○) or 2-amino-1-*p*-nitrophenylpropane-1,3-diol (□). The system without (●) or with the compounds (1.3×10^{-2} M) was first incubated for 60 min at 37° followed by the addition of tyramine (0.01* M*). The activity was determined after incubation for another 30 min. Phosphate buffer was used.*

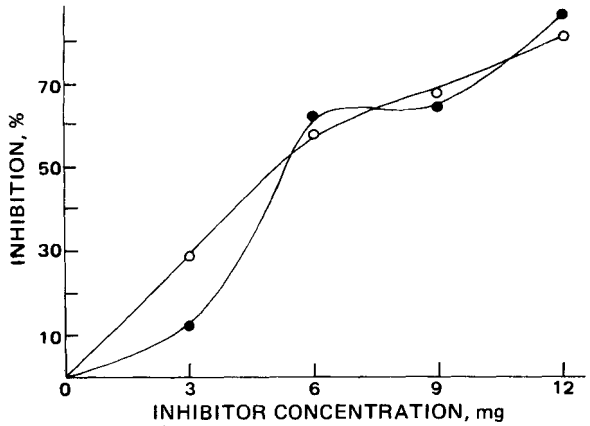

Figure 4—*Effect of different concentrations of chloramphenicol (○) or 2-amino-1-p-nitrophenylpropane-1,3-diol (●) on rat liver mitochondrial monoamine oxidase activity. Conditions of experiments were the same as described in Fig. 3.*

1,3-diol determined spectrophotometrically (13) in the incubation medium did not change. Therefore, the inhibition of monoamine oxidase activity by these compounds was the effect of these compounds *per se* and not a result of their degradation in the incubation medium. The diminution of monoamine oxidase inhibition after preincubation for 90 min might be due to the dissociation of the enzyme–inhibitor complex by the backward reaction.

The inhibition of rat liver monoamine oxidase by chloramphenicol and 2-amino-1-*p*-nitrophenylpropane-1,3-diol was reversible since the enzyme activity could be restored after dialysis for 24 hr (Table III). The inhibition was noncompetitive, with K_i values of 9×10^{-3} *M* for chloramphenicol (Fig. 1) and 3.9×10^{-3} *M* for 2-amino-1-*p*-nitrophenylpropane-1,3-diol (Fig. 2). Reversible noncompetitive inhibition with these compounds, however, is rarely seen.

Liver monoamine oxidase activity and its inhibition by chloramphenicol were optimum at pH 7.0, while the inhibition by 2-amino-1-*p*-nitrophenylpropane-1,3-diol exhibited a peak at pH 7.0 followed by a second peak at pH 8.0 (Fig. 3). With the addition of 12 mg of these compounds in the experimental system, inhibition of monoamine oxidase activity was 78% with chloramphenicol and 86% with 2-amino-1-*p*-nitrophenylpropane-1,3-diol (Fig. 4). These two compounds did not affect

Table IV—Effect of Chloramphenicol and 2-Amino-1-*p*-nitrophenylpropane-1,3-diol on the Oxidative Deamination of Different Monoamines by Rat Liver Mitochondrial Monoamine Oxidase [a]

	Monoamine Oxidase Activity[b]		
Monoamine	Control	With Chloramphenicol	With 2-Amino-1-*p*-nitrophenylpropane-1,3-diol
Tyramine	46 (0.28)	15 (0.09)	6 (0.04)
5-Hydroxytryptamine	29 (0.17)	14 (0.08)	19 (0.12)
Norepinephrine	5 (0.03)	4 (0.02)	3 (0.018)
Epinephrine	5 (0.03)	1 (0.006)	3 (0.018)

[a] Results are means of five observations. Variations in observations in each group were minimal. Figures in parentheses denote absorbance. The time of preincubation was 60 min. [b] Activity was defined as aldehyde formed, micromoles per 2.5 mg of protein per 30 min of incubation at 37°.

Table V—Tissue Mitochondrial Monoamine Oxidase Activities of Rats Injected with Chloramphenicol or 2-Amino-1-*p*-nitrophenylpropane-1,3-diol, 20 mg/Animal/Day for 8 Days [a]

	Monoamine Oxidase Activity[b]	
	Liver (per 2.5 mg of protein)	Cardiac Muscle (per 15 mg of protein)
Control	37 ± 0.05	25 ± 0.25
Chloramphenicol	25 ± 0.03	3 ± 0.14
2-Amino-1-*p*-nitrophenylpropane-1,3-diol	10 ± 0.008	3 ± 0.15

[a] Values are means of eight observations ± *SE*. [b] Activity was defined as aldehyde formed, micromoles per 30 min of incubation.

deamination of various monoamines to the same degree (Table IV), perhaps because of the unequal affinity of the substrate for the enzyme to form an enzyme–inhibitor complex. Tranylcypromine, a potent monoamine oxidase inhibitor, also showed similar variations with different biogenic monoamines (5). The monoamine oxidase inhibition by these compounds could be observed *in vivo*. Mitochondrial monoamine oxidase activities of liver and cardiac muscle of rats injected with these compounds were diminished (Table V).

Unlike tranylcypromine, pheniprazine, or iproniazid, which are potent monoamine oxidase inhibitors, chloramphenicol and 2-amino-1-*p*-nitrophenylpropane-1,3-diol were weak monoamine oxidase inhibitors; fairly high concentrations of these compounds had to be used.

When hydrolyzed, chloramphenicol loses dichloroacetic acid and is converted to 2-amino-1-*p*-nitrophenylpropane-1,3-diol, which has no antibacterial properties (14). Since both compounds inhibit liver mitochondrial monoamine oxidase activity, the inhibitory effect of chloramphenicol has no relation to its antimicrobial activity.

REFERENCES

(1) S. Banerjee, C. Mitra, and A. K. Mukherjee, *J. Pharm. Sci.*, **66**, 1239 (1977).

(2) "The Pharmacological Basis of Therapeutics," L. S. Goodman and A. Gilman, Eds., Macmillan, London, England, 1970, p. 733.

(3) A. Pletscher, *Proc. Int. Pharmacol. Meeting, 3rd*, **10**, 55 (1966).

(4) G. H. Hogeboom and N. C. Schneider, *J. Biol. Chem.*, **197**, 611 (1952).

(5) S. R. Guha, *Biochem. Pharmacol.*, **15**, 161 (1966).

(6) S. R. Guha and S. K. Ghosh, *ibid.*, **19**, 2929 (1970).

(7) S. S. Parmar, *ibid.*, **15**, 1497 (1966).

(8) S. R. Guha, P. S. Basu, and K. K. SenGupta, *Acta Biol. Med. Germ.*, **28**, 417 (1972).

(9) A. L. Green and T. M. Haughton, *Biochem. J.*, **78**, 173 (1961).

(10) D. Richter, *ibid.*, **31**, 2022 (1937).

(11) A. G. Gornall, C. J. Bardawill, and M. M. David, *J. Biol. Chem.*, **177**, 751 (1949).

(12) "Code of Federal Regulations," Title 21, parts 130–146e, U. S. Government Printing Office, Washington D.C., 1969, p. 252.

(13) "British Pharmaceutical Codex," Pharmaceutical Press, London, England, 1973, p. 689.

(14) A. J. Glazko, W. A. Dill, and M. C. Robstock, *J. Biol. Chem.*, **183**, 679 (1950).

ACKNOWLEDGMENTS

The authors thank Sri Bhupendra Nath Dey for use of laboratory facilities.

New GLC Analysis of Urushiol Congeners in Different Plant Parts of Poison Ivy, *Toxicodendron radicans*

JOHN C. CRAIG *, COY W. WALLER, STEPHEN BILLETS, and MAHMOUD A. ELSOHLY ˣ

Received April 25, 1977, from the *Research Institute of Pharmaceutical Sciences, School of Pharmacy, University of Mississippi, University, MS 38677.* Accepted for publication July 7, 1977. *Present address: Department of Chemistry, Western Kentucky University, Bowling Green, KY 42101.

Abstract □ Methods are presented for the direct GLC analysis of the catechol C_{15} alkenyl side-chain congeners contained in the urushiol fraction of poison ivy (*Toxicodendron radicans*) and the C_{17} homologs of poison oak (*Toxicodendron diversilobum*). A number of liquid phases were investigated and demonstrated varying degrees of separation. The methods developed were applied to the analysis of the urushiol fractions obtained from different plant parts of poison ivy. The effects of extraction before and after drying demonstrated that a larger percentage of urushiol was obtained when the fresh plant material was extracted with ethanol.

Keyphrases □ Urushiol fractions—obtained from different plant parts of *Toxicodendron radicans*, GLC analysis □ GLC—analysis, urushiol fractions obtained from different plant parts of *Toxicodendron radicans* □ *Toxicodendron radicans*—urushiol fractions obtained from different plant parts, GLC analysis

Contact with certain members of the plant family Anacardiaceae causes irritation, inflammation, and blistering of the skin. In the United States, the most widely encountered members of the genus *Toxicodendron*, which produce these symptoms in sensitive individuals, are poison ivy (*T. radicans*), western poison oak (*T. diversilobum*), eastern poison oak (*T. quercifolium*), and poison sumac (*T. vernix*). The systematics and growth patterns of these plants were studied thoroughly (1).

Poison ivy urushiol is a mixture of 3-*n*-pentadec(en)ylcatechols containing zero, one, two, or three double bonds in the side chain (2–5). Recent work (6) showed the urushiol of poison oak (*T. diversilobum*) to be a mixture of heptadec(en)ylcatechols. Furthermore, small quantities of the C_{15} and C_{17} homologs were found in poison oak urushiol and poison ivy extracts, respectively (7). Structure–activity relationships relating the length of the side chain and the number of double bonds to the dermatological properties of urushiol were determined (8, 9). Poison ivy and poison oak extracts have been used in the detection and prophylactic treatment of sensitivity (10–12).

In spite of all these studies, there has been no published methodology designed to quantitate the individual congeners of the urushiol, and no analysis has been reported of the urushiol content of the various plant components of any member of this family. In light of several studies (9, 13), current analytical methods should be expanded to monitor formulation procedures that will enhance the production of reliable dosage forms. This report describes methods to analyze the total urushiol content and/or congener ratios of the C_{15} urushiol of poison ivy and the C_{17} urushiol of poison oak.

Table I—Column Study of Trimethylsilyl Derivatized C_{15} Urushiols of Poison Ivy

Liquid Phase	Column Temperature[a]	Type of Separation
8% OV-1	215°	No separation of congeners
2% OV-17	215°	Baseline separation of saturated congener, shoulder separation of monoene
5% OV-17	215°	Baseline separation of saturated congener, shoulder separation of monoene
5% OV-25	205°	Monoene from diene and triene
5% OV-225	210°	Complete congener separation

[a] Isothermal values for maximum resolution and minimum retention time.

EXPERIMENTAL[1]

Plant Material—Poison ivy[2] (*T. radicans*) was collected in October 1975 in Oxford, Miss., and used immediately after collection. Samples of the young leaves and stems were dried at room temperature to determine the effects of drying on the urushiol content. Poison oak was obtained as an extract[3].

Extraction and Partitioning—The different plant parts of poison ivy including young and old leaves, young and large stems, berries, and bark of large stems (10 g) were extracted separately with 95% ethanol at room temperature in small percolators until exhaustion. In each case, the ethanol extract was evaporated *in vacuo* (40°) to give a syrupy residue. The residue was partitioned between water (15 ml) and chloroform (3 × 30 ml). The chloroform extract was dried over anhydrous sodium sulfate and evaporated, and the residue was transferred quantitatively to a 10-ml volumetric flask with chloroform and diluted to volume.

Internal Standard—As reported previously[4], 4-androstene-3,17-dione was a satisfactory internal standard when the liquid phase was OV-1, OV-17, or OV-25. However, when a more polar liquid phase was used, *i.e.*, OV-225, elution of the internal standard presented a serious problem. Thus, for the OV-225 liquid phase, dotriacontane[5] was used. A stock solution of dotriacontane was prepared in *n*-heptane (5 mg/ml). The response factors were linear over a 10:1 concentration range, and the urushiols were calculated as pentadecylcatechol.

Preparation of Samples for GLC Analysis—Aliquots of 1 ml of the extract were transferred to 1.5-ml sealable vials and dried under a nitrogen stream. To each vial were added 0.50 ml of internal standard stock solution, 0.25 ml of pyridine, and 0.5 ml of bis(trimethylsilyl)trifluoroacetamide[6]. The vials were capped, slightly heated with an air gun, and allowed to stand 30 min prior to injection.

RESULTS AND DISCUSSION

GLC methods for the identification of urushiol have been reported (14, 15), and the use of GLC–mass spectrometry for the quantitation of the

[1] A Beckman GC-45 gas chromatograph equipped with dual hydrogen flame-ionization detectors and interfaced to a digital computer (PDP-8) was used. Glass columns, 0.64 cm o.d. and 2 mm i.d. × 2.43 m, were packed with 80–100-mesh Gas Chrom Q, coated with the desired liquid phase. The operating conditions for the OV-225 column were: column, 210°; detector, 260°; and injection port, 230°. Nitrogen was the carrier gas with a flow rate of 15 ml/min. For GLC–mass spectrometry, a Varian 2740 instrument was used with the same column packing material and helical 2-mm i.d. × 1.2-m glass columns. This unit was interfaced to a DuPont 21-492 mass spectrometer.

[2] The plant material was authenticated by Professor Maynard W. Quimby, and herbarium specimens are stored in the drug plant herbarium, Department of Pharmacognosy, School of Pharmacy, University of Mississippi.

[3] Supplied by Hollister-Stier Laboratories, Spokane, Wash.

[4] Final Report to Food and Drug Administration, "Poison Oak (*Rhus toxicodendron*) and Poison Ivy (*Rhus radicans*) Preparation and Analysis of Dosage Forms," Contract FDA 73-155 (223-73-1155), Mar. 1, 1973, to Nov. 30, 1974 (submitted Mar. 1975).

[5] Aldrich Chemical Co., Milwaukee, Wis.

[6] Pierce Chemical Co., Rockford, Ill.

Table II—Total Urushiol and Congener Analysis of Poison Ivy Plant Parts[a]

Plant Part	Total Urushiol, %	Composition of Total Urushiol, % Saturated	Monoene	Diene	Triene
Fresh young leaves	0.38	7.2	17.8	9.1	65.9
Dry young leaves[b]	0.08	23.2	23.2	11.7	41.9
Large leaves	0.03	t[c]	19.0	12.2	68.0
Large stems	0.17	4.6	7.8	35.0	52.6
Dry young stems[b]	0.20	6.4	15.2	28.0	50.4
Fresh young stems	0.39	3.8	13.1	27.0	56.1
Bark	0.47	t[c]	8.1	31.3	59.9
Fruits	0.37	5.8	7.6	13.1	73.5

[a] Analysis performed on 5% OV-225, which separated all four congeners found in C_{15} urushiol. [b] Calculated as percent wet material. [c] Trace amount (<1% of total urushiol).

different congeners was discussed previously (16). The described techniques offer significant improvement over previous methods. Derivatization *via* silylation of the catechol nucleus is quantitative and rapid and does not require any workup when compared to the preparation of acetates. Separation of the saturated, mono-, di-, and triolefinic components is sufficient for the quantification of each. Furthermore, the necessity of a mass spectrometric analysis and such techniques as mass fragmentography are avoided.

The GLC analysis of the urushiol fraction is straightforward when trimethylsilyl derivatives are used. These derivatives were stable for at least 2 days and had good GLC characteristics. The degree of silylation and stability of these derivatives were confirmed using GLC–mass spectrometric techniques.

The choice of column used in the analysis is determined by the degree of separation and type of information desired. For example, with an OV-1 column, no separation of the congeners in the urushiol fraction is observed. Thus, if the object is to determine the total urushiol content under a single GLC peak, a nonpolar liquid phase should be used. But if it is desired to quantitate each congener in the urushiol fraction, a more polar liquid phase is needed. The best success was achieved with an OV-225 column (Fig. 1). As might be expected, liquid phases of intermediate polarity, such as OV-25, produced partial separation of these congeners.

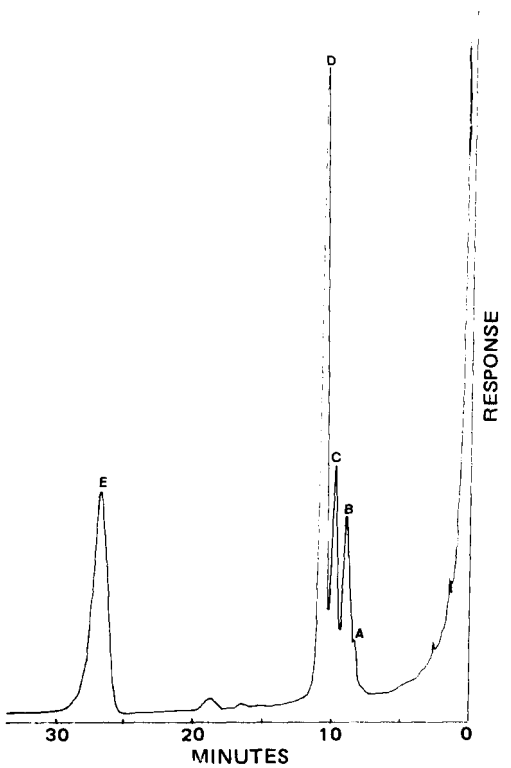

Figure 1—*Gas chromatogram of the trimethylsilyl derivatives of poison ivy urushiol (C_{15}) using OV-225 column. Key: A, saturated congener (relative retention time 0.31); B, monoene (relative retention time 0.33); C, diene (relative retention time 0.37); D, triene (relative retention time 0.40); and E, dotriacontane.*

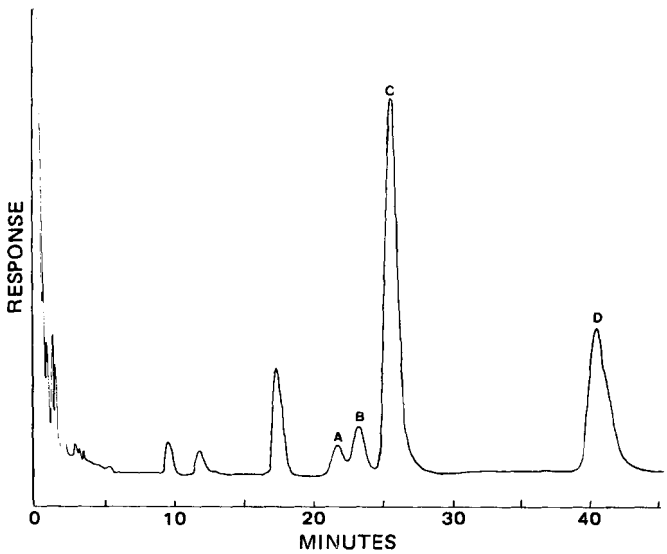

Figure 2—*Gas chromatogram of the trimethylsilyl derivatives of poison oak urushiol (C_{17}) using OV-25 column. Key: A, monoene; B, diene; C, triene; and D, androst-4-ene-3,17-dione.*

However, the OV-25 column, like the OV-225 column, provided complete separation of the C_{17} components of poison oak urushiol (Fig. 2).

Table I summarizes the GLC column analysis; this survey is not meant to be exhaustive but does represent the full range of separation required in any analysis of poison ivy urushiol by this technique. Application of this method to the analysis of poison ivy plant parts provides information on the distribution of urushiol throughout the plant.

Table II shows the total urushiol content and also provides a breakdown of the congeners found in the different plant parts. The highest concentration of total urushiol (0.47%) was found in the bark. This material was obtained by scraping the bark from the larger stems (2–4 cm in diameter). The fresh young leaves, fresh young stems, and fruits contained ~0.40% urushiol. In all cases, the large plant parts contained significantly less urushiol than those from younger plants. In all plant parts, the triene was the predominant congener, comprising more than 50% of the total urushiol when the plants were wet extracted; the fruits contained the highest triene concentration (73.5%). The leaves were the only plant parts to contain more monoene than diene. The highest diene concentration (35.0%) of the total urushiol was observed in the large stems.

Air drying of the stems and leaves reduced the total urushiol content. However, the most dramatic effect occurred with the young leaves, where a significant change in the congener ratios as well as in the total urushiol content was observed.

Chloroform, hexane, and ethanol were evaluated to determine the best solvent for extraction. Hexane was selected for the extraction of urushiol from dried material since the extracts were comparatively clean. However, if, as with the leaves, a significant amount of urushiol is lost upon drying, ethanol becomes the solvent of choice for wet extraction.

REFERENCES

(1) W. T. Gillis, *Rhodora*, **73**, 72, 161, 370, 465 (1971).

(2) G. A. Hill, V. Mattacotti, and W. D. Grahan, *J. Am. Chem. Soc.*, **56**, 3736 (1934).

(3) W. F. Symes and C. R. Dawson, *ibid.*, **76**, 2959 (1954).

(4) S. V. Sunthankar and C. R. Dawson, *ibid.*, **76**, 5070 (1954).

(5) K. H. Markiewitz and C. R. Dawson, *J. Org. Chem.*, **30**, 1610 (1965).

(6) M. D. Corbett and S. Billets, *J. Pharm. Sci.*, **64**, 1715 (1975).

(7) S. Billets, J. C. Craig, M. D. Corbett, and J. F. Vickery, *Phytochemistry*, **15**, 533 (1976).

(8) A. P. Kurtz and C. R. Dawson, *J. Med. Chem.*, **14**, 729 (1971).

(9) R. A. Johnson, H. Baer, C. H. Kirkpatrick, C. R. Dawson, and R. G. Khurana, *J. Allergy Clin. Immunol.*, **49**, 27 (1972).

(10) H. S. Mason and A. Lada, *J. Invest. Dermatol.*, **22**, 457 (1975).

(11) C. H. Ducan, *N.Y. Med. J.*, **104**, 901 (1916).

(12) G. A. Gellin, C. R. Wolf, and H. Milby, *Arch. Environ. Health*, **2**, 280 (1971).

(13) W. L. Epstein, H. Baer, C. R. Dawson, and R. G. Khurana, *Arch. Dermatol.*, **109**, 356 (1974).

(14) H. Baer, S. Srinivasan, R. T. Bowser, and A. Karmen, *J. Allergy*, **34**, 221 (1963).

(15) S. Srinivasan, H. Baer, R. Bowser, and A. Karmen, *Anal. Biochem.*, **6**, 234 (1963).

(16) M. Gross, H. Baer, and H. M. Fales, *Phytochemistry*, **14**, 2263 (1975).

ACKNOWLEDGMENTS

The authors thank Julia B. Hoelzeman and Kathy B. Hadley for their contributions.

GLC–Mass Spectral Analysis of Fungal Metabolites

DAVID B. REPKE *x, DALE THOMAS LESLIE ‡, and NICHOLAS G. KISH §

Received July 23, 1976, from **P.O. Box 899, Los Altos, CA 94022*, ‡*104 Whitney Avenue, Los Gatos, CA 95030*, and §*Ultrachem Corporation, Walnut Creek, CA 94596.* Accepted for publication July 11, 1977.

Abstract □ Four metabolites, hispidin, bisnoryangonin, muscimole, and ibotenic acid, from potentially psychoactive mushrooms were analyzed by GLC–mass spectrometry as their trimethylsilyl derivatives. This method was applied to the first two compounds in *Gymnopilus punctifolius* (Peck) Singer and to the last two compounds in *Amanita pantherina* (Fr.) Secr.

Keyphrases □ Hispidin—GLC–mass spectral analysis in mushrooms □ Bisnoryangonin—GLC–mass spectral analysis in mushrooms □ Muscimole—GLC–mass spectral analysis in mushrooms □ Ibotenic acid—GLC–mass spectral analysis in mushrooms □ GLC–mass spectrometry—analyses, hispidin, bisnoryangonin, muscimole, and ibotenic acid in mushrooms □ *Gymnopilus punctifolius*—GLC–mass spectral analysis of various components □ *Amanita pantherina*—GLC–mass spectral analysis of various components

A previous report described the GLC–mass spectral analysis of the trimethylsilyl derivatives of psilocin and psilocybin (1). As part of continuing studies of the chemical constituents of higher fungi, this report describes the GLC analysis of the trimethylsilyl derivatives of four such compounds and their mass spectral features. Bisnoryangonin (Ia), hispidin (IIa), muscimole (IIIa), and ibotenic acid (IVa) occur in various genera of the Hymenomycetes.

BACKGROUND

The styrylpyrone derivatives Ia and IIa were analyzed by TLC and IR, UV, and mass spectrometry (2, 3). Compound IIa was first reported (4–6) in certain species of Polyporaceous fungi. One or both of these compounds have been detected in various species of *Gymnopilus* Karsten (Cortinariaceae), *Pholiota* (Fr.) Kummer [including *Flammula* (Fr.) Kummer] (Strophariaceae or Cortinariaceae), and *Naematoloma* Karsten [= *Hypholoma* (Fr.) Kummer] (Strophariaceae) (2, 7–10). These and related compounds may be of considerable use in biochemical systematics (10–13).

The historical literature of Japan suggests the ethnomycological importance of *G. spectabilis* (Fr.) Smith[1] [= *Pholiota spectabilis* (Fr.) Quel.] (15, 16), but only occasional incidents of intoxication due to this species have been reported recently (17, 18). The presence of the related styrylpyrone yangonin (V) in the rhizomes of kava-kava (*Piper methysticum* Forst.) (19), the narcotic pepper used in the South Pacific, lends support to the possibility that this class of compounds might be psychoactive. However, limited pharmacological studies of the pure kava pyrones have not accounted for the activity of the whole plant (20).

Compounds IIIa and IVa were analyzed previously by paper chromatography (21–23) and paper electrophoresis (21, 24). Instrumental analysis of the pure compounds was performed by IR (21) and mass spectrometry (25). These compounds appear to be confined to a few species of the genus *Amanita* Pers. ex Hook., principally *A. muscaria* (L. ex Fr.) Hooker (21–23, 26), *A. pantherina* (Fr.) Secr. (23, 26), and *A. cothurnata* Atk. (26). The ethnobotanical importance of *A. muscaria* has been established (27). Although these mushrooms are the cause of numerous intoxications, both accidental and intentional (28), pure compounds IIIa and IVa have received limited pharmacological study (29–31).

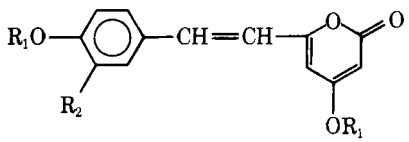

Ia: $R_1 = R_2 = H$
Ib: $R_1 = (CH_3)_3Si$, $R_2 = H$
IIa: $R_1 = H$, $R_2 = OH$
IIb: $R_1 = (CH_3)_3Si$, $R_2 = (CH_3)_3SiO$
V: $R_1 = CH_3$, $R_2 = H$

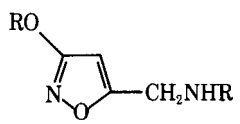

IIIa: R = H
IIIb: R = $(CH_3)_3Si$

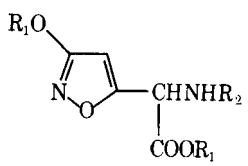

IVa: $R_1 = R_2 = H$
IVb: $R_1 = R_2$ $(CH_3)_3Si$
IVc: $R_1 = (CH_3)_3Si$, $R_2 = H$

The previously described methods have been adequate for the qualitative analysis of these compounds. However, quantitative analysis by these methods suffers from several disadvantages, especially for the highly polar, zwitterionic IIIa and IVa.

The facile decarboxylation of IVa to IIIa during extraction, analytical, and isolation procedures (23, 26) leads to an inaccurate estimation of individual components present in the mushroom. Occasionally, enrichment of fungal extracts by ion-exchange chromatography is necessary before analysis can proceed (26). Use of colorimetric reagents to visualize spots on a chromatogram can often be misleading, especially in quanti-

Table I—Chromatography Conditions, Retention Times [a], and Percent of Trimethylsilyl Derivatives

	Ib	IIb	IIIb	IVb	IVc
SE-30	250°, R_t 8.5 min	250°, R_t 15 min	150–250°, R_t 2.1 min	150–250°, R_t 5.4 min	150–250°, R_t 3.7 min
OV-101	—	—	100–200°, R_t 6.0 min	100–200°, R_t 13.1 min	100–200°, R_t 10.8 min
Percent [b] present in fungal extracts	0.44 (0.42) [c]	0.25 (0.21) [c]	0.046	0.002	—

[a] Relative to the solvent front. [b] Based on dry weight. [c] By isolation.

[1] This species might be identical with *G. junonious* (Fr.) Orton (14).

(13) W. L. Epstein, H. Baer, C. R. Dawson, and R. G. Khurana, *Arch. Dermatol.*, **109**, 356 (1974).

(14) H. Baer, S. Srinivasan, R. T. Bowser, and A. Karmen, *J. Allergy*, **34**, 221 (1963).

(15) S. Srinivasan, H. Baer, R. Bowser, and A. Karmen, *Anal. Biochem.*, **6**, 234 (1963).

(16) M. Gross, H. Baer, and H. M. Fales, *Phytochemistry*, **14**, 2263 (1975).

ACKNOWLEDGMENTS

The authors thank Julia B. Hoelzeman and Kathy B. Hadley for their contributions.

GLC–Mass Spectral Analysis of Fungal Metabolites

DAVID B. REPKE *x, DALE THOMAS LESLIE ‡, and NICHOLAS G. KISH §

Received July 23, 1976, from **P.O. Box 899, Los Altos, CA 94022*, ‡*104 Whitney Avenue, Los Gatos, CA 95030*, and §*Ultrachem Corporation, Walnut Creek, CA 94596.* Accepted for publication July 11, 1977.

Abstract □ Four metabolites, hispidin, bisnoryangonin, muscimole, and ibotenic acid, from potentially psychoactive mushrooms were analyzed by GLC–mass spectrometry as their trimethylsilyl derivatives. This method was applied to the first two compounds in *Gymnopilus punctifolius* (Peck) Singer and to the last two compounds in *Amanita pantherina* (Fr.) Secr.

Keyphrases □ Hispidin—GLC–mass spectral analysis in mushrooms □ Bisnoryangonin—GLC–mass spectral analysis in mushrooms □ Muscimole—GLC–mass spectral analysis in mushrooms □ Ibotenic acid—GLC–mass spectral analysis in mushrooms □ GLC–mass spectrometry—analyses, hispidin, bisnoryangonin, muscimole, and ibotenic acid in mushrooms □ *Gymnopilus punctifolius*—GLC–mass spectral analysis of various components □ *Amanita pantherina*—GLC–mass spectral analysis of various components

A previous report described the GLC–mass spectral analysis of the trimethylsilyl derivatives of psilocin and psilocybin (1). As part of continuing studies of the chemical constituents of higher fungi, this report describes the GLC analysis of the trimethylsilyl derivatives of four such compounds and their mass spectral features. Bisnoryangonin (Ia), hispidin (IIa), muscimole (IIIa), and ibotenic acid (IVa) occur in various genera of the Hymenomycetes.

BACKGROUND

The styrylpyrone derivatives Ia and IIa were analyzed by TLC and IR, UV, and mass spectrometry (2, 3). Compound IIa was first reported (4–6) in certain species of Polyporaceous fungi. One or both of these compounds have been detected in various species of *Gymnopilus* Karsten (Cortinariaceae), *Pholiota* (Fr.) Kummer [including *Flammula* (Fr.) Kummer] (Strophariaceae or Cortinariaceae), and *Naematoloma* Karsten [= *Hypholoma* (Fr.) Kummer] (Strophariaceae) (2, 7–10). These and related compounds may be of considerable use in biochemical systematics (10–13).

The historical literature of Japan suggests the ethnomycological importance of *G. spectabilis* (Fr.) Smith[1] [= *Pholiota spectabilis* (Fr.) Quel.] (15, 16), but only occasional incidents of intoxication due to this species have been reported recently (17, 18). The presence of the related styrylpyrone yangonin (V) in the rhizomes of kava-kava (*Piper methysticum* Forst.) (19), the narcotic pepper used in the South Pacific, lends support to the possibility that this class of compounds might be psychoactive. However, limited pharmacological studies of the pure kava pyrones have not accounted for the activity of the whole plant (20).

Compounds IIIa and IVa were analyzed previously by paper chromatography (21–23) and paper electrophoresis (21, 24). Instrumental analysis of the pure compounds was performed by IR (21) and mass spectrometry (25). These compounds appear to be confined to a few species of the genus *Amanita* Pers. ex Hook., principally *A. muscaria* (L. ex Fr.) Hooker (21–23, 26), *A. pantherina* (Fr.) Secr. (23, 26), and *A. cothurnata* Atk. (26). The ethnobotanical importance of *A. muscaria* has been established (27). Although these mushrooms are the cause of numerous intoxications, both accidental and intentional (28), pure compounds IIIa and IVa have received limited pharmacological study (29–31).

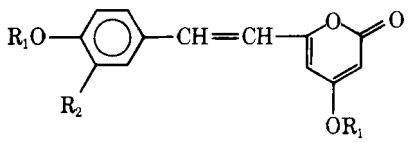

Ia: $R_1 = R_2 = H$
Ib: $R_1 = (CH_3)_3Si$, $R_2 = H$
IIa: $R_1 = H$, $R_2 = OH$
IIb: $R_1 = (CH_3)_3Si$, $R_2 = (CH_3)_3SiO$
V: $R_1 = CH_3$, $R_2 = H$

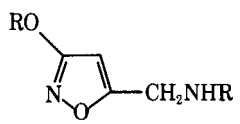

IIIa: R = H
IIIb: R = $(CH_3)_3Si$

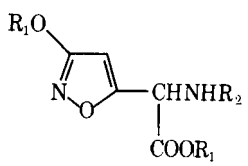

IVa: $R_1 = R_2 = H$
IVb: $R_1 = R_2$ $(CH_3)_3Si$
IVc: $R_1 = (CH_3)_3Si$, $R_2 = H$

The previously described methods have been adequate for the qualitative analysis of these compounds. However, quantitative analysis by these methods suffers from several disadvantages, especially for the highly polar, zwitterionic IIIa and IVa.

The facile decarboxylation of IVa to IIIa during extraction, analytical, and isolation procedures (23, 26) leads to an inaccurate estimation of individual components present in the mushroom. Occasionally, enrichment of fungal extracts by ion-exchange chromatography is necessary before analysis can proceed (26). Use of colorimetric reagents to visualize spots on a chromatogram can often be misleading, especially in quanti-

Table I—Chromatography Conditions, Retention Times [a], and Percent of Trimethylsilyl Derivatives

	Ib	IIb	IIIb	IVb	IVc
SE-30	250°, R_t 8.5 min	250°, R_t 15 min	150–250°, R_t 2.1 min	150–250°, R_t 5.4 min	150–250°, R_t 3.7 min
OV-101	—	—	100–200°, R_t 6.0 min	100–200°, R_t 13.1 min	100–200°, R_t 10.8 min
Percent [b] present in fungal extracts	0.44 (0.42) [c]	0.25 (0.21) [c]	0.046	0.002	—

[a] Relative to the solvent front. [b] Based on dry weight. [c] By isolation.

[1] This species might be identical with *G. junonious* (Fr.) Orton (14).

tative estimation. Most of these difficulties can be overcome utilizing GLC of the neutral, stable, and easily prepared derivatives I*b*, II*b*, III*b*, and IV*b*.

EXPERIMENTAL[2]

Muscimole monohydrate was prepared according to published procedures (32, 33). The melting point and IR and mass spectra were in agreement with those reported (21, 25).

Pileus tissue of air-dried *G. punctifolius* (Peck) Singer[3] (2) (89 mg) was ground to a powder with sand and transferred to a screw-capped tube. Methanol (5 ml) was added, and the tube was shaken at room temperature for 20 hr. The contents were filtered, and the collected solids were washed with two 5-ml portions of methanol. Then the combined filtrate and washings were concentrated to 5.0 ml, and 0.5 ml of this solution was transferred to a 1.0-ml vial[4].

The solvent was removed by evaporation in a nitrogen stream, and the residue was dried *in vacuo*. Bis(trimethylsilyl)trifluoroacetamide[5] (25 μl) was added, and the vial was closed with a septum-lined seal[6] and heated for 30 min at 140°. Aliquots of 1 μl were used for subsequent analyses.

Pileus tissue of freeze-dried *A. pantherina* (Fr.) Secr.[7] (1.56 g) was ground as already described and extracted with 30 ml of 10% aqueous methanol at 4° for 8 hr. The mixture was filtered, and the volume of the filtrate was adjusted to 30.0 ml. An aliquot of this solution (0.5 ml) was transferred to a reaction vial and treated as already described.

Quantitation was carried out based on the external standard technique used previously (1). Weighed samples of each of the four pure standards were mixed with bis(trimethylsilyl)trifluoroacetamide in reaction vials so that the final concentrations were 0.25% (w/v). The sealed vials were heated at 140°. Aliquots were removed every 15 min and analyzed by GLC for a total of 2 hr.

In each case, the reaction solutions attained homogeneity within 15–30 min; analyses of aliquots removed after 30 min showed no further increase in peak areas. When injection of equal volumes of each sample was repeated, reproducibility of detector response (as measured by peak areas) was within ±2%. Linearity of detector response was verified by injecting successively diluted volumes of each standard solution and comparing the peak areas obtained with the known concentrations of solutes.

Carpophores of *G. punctifolius*[3] (1.911 g) were ground and extracted by stirring with methanol (100 ml) for 20 hr. The solids were collected by filtration, and the filtrate was concentrated *in vacuo* to 10.0 ml. A second 100-ml extract of the filtered solids was shown to be devoid of I*a* and II*a* by TLC. Compounds I*a* and II*a* were isolated from the extract by preparative TLC, using 25% methanol in chloroform as the developing solvent. The separated bands (I*a*, R_f 0.58; and II*a*, R_f 0.44) were removed from the plates, and the compounds were eluted with 40% methanol in ethyl acetate.

The residue of I*a*, obtained by concentration of the eluate, was crystallized from methanol–ether to afford 8.0 mg (0.42%), mp 242–244° dec. [lit. (2) mp 244–246° dec.]. The residue of II*a* was precipitated from ethanol by addition of ethyl acetate, and the precipitate was isolated by centrifugation. After drying *in vacuo*, II*a* weighed 4.0 mg (0.21%), mp 228° [lit. (4) mp 256°]. The compounds were chromatographically homogeneous and indistinguishable from reference standards.

Table II—Mass Spectral Parameters[a] for Trimethylsilyl Derivatives

I*b*	II*b*	III*b*	IV*b*	IV*c*
372 (7%) (M + 2)	464 (12%) (M + 2)	244 (2%)	360 (2%)	272 (1%)
375 (18%) (M + 1)	463 (22%) (M + 1)	243 (8%) (M − 15)	359 (6%) (M − 15)	259 (2%)
374 (51%) (M +)	462 (50%) (M +)	169 (5%)	332 (2%)	258 (4%)
361 (2%)	449 (7%)	156 (2%)	331 (6%) (M − 43)	257 (20%)
360 (6%)	448 (13%)	147 (2%)	259 (7%)	156 (2%)
359 (19%) (M − 15)	447 (24%) (M − 15)	146 (3%)	258 (9%)	147 (3%)
347 (6%)	434 (7%) (M − 28)	144 (2%)	257 (45%) (M − 117)	121 (5%)
346 (19%) (M − 28)	419 (5%)	128 (4%)	218 (3%)	116 (3%)
319 (5%)	407 (3%) (M − 56)	114 (3%)	169 (2%)	100 (4%)
318 (18%) (M − 56)	406 (8%)	102 (10%)	148 (3%)	99 (3%)
317 (2%)	359 (4%)	100 (3%)	147 (15%)	89 (5%)
219 (3%)	346 (7%)	99 (2%)	133 (2%)	75 (15%)
99 (4%)	245 (3%)	89 (1%)	130 (4%)	74 (11%)
75 (13%)	229 (4%)	75 (10%)	103 (2%)	73 (100%)
74 (9%)	219 (4%)	74 (11%)	100 (5%)	45 (17%)
73 (100%)	191 (9%)	73 (100%)	99 (2%)	
69 (4%)	183 (5%)	59 (8%)	75 (11%)	
45 (15%)	147 (10%)	45 (18%)	74 (9%)	
	143 (5%)	44 (3%)	73 (100%)	
	99 (6%)	43 (6%)	59 (3%)	
	75 (33%)		45 (10%)	
	74 (35%)			
	73 (100%)			
	69 (5%)			
	45 (48%)			

[a] *m/e* (relative intensity).

RESULTS AND DISCUSSION

The derivatives I*b* and II*b* were widely separated under the isothermal conditions described. While II*b* was completely resolved from other components in the natural extract, some overlap with an adjacent peak was noted for I*b*. However, a mass spectrum comparable to that of the standard was obtained. The resolution of I*b* was not improved by changes in chromatographic conditions or stationary phases. The isoxazoles III*b* and IV*b* were well resolved under either set of conditions.

The concentrations of I*a* and II*a* in the collection of *G. punctifolius* used in this study were lower than those reported for this species previously (2). The quantities of III*a* and IV*a* in *A. pantherina* also appeared to be low compared to earlier findings (23). Both previous investigations were based on analysis by spot-intensity techniques on paper and thin-layer chromatograms. However, these methods are only semiquantitative (34). The isolated yields of IV*a* recently reported (26) from *A. pantherina* and of I*a* and II*a* from *G. punctifolius* reported here are compatible with data obtained by GLC (Table I).

Several factors could affect the quantities of I*a*, II*a*, III*a*, and IV*a* found in these organisms, including intraspecies variation based on season, year, and environment of collections and differences in handling and storage of specimens. With respect to the former, marked variation in isoxazole content was reported in collections of *A. muscaria* (35). The quantity of hispidin in *Polyporus hispidus* (Bull.) Fr. decreased with the increasing age of the carpophore (5). It was suggested that this decrease was due to the elaboration of hispidin into polymeric lignans; recently, polymeric hispidin derivatives were detected in several species containing I*a* and II*a* (10–13).

The mass spectra of the styrylpyrone trimethylsilyl derivatives (Table II) were characterized by intense molecular ion signals (*m/e* 462 and 374 for II*b* and I*b*, respectively). This result is rather unusual since trimethylsilyl ethers undergo facile loss of a methyl group (36). These M − 15 peaks were also present in the spectra of I*b* and II*b*. The base peak in each spectrum at *m/e* 73 due to the trimethylsilyl ion is a common occurrence in these derivatives (36).

[2] GLC was carried out with a Hewlett-Packard model 402 instrument with flame-ionization detectors. The columns used were: (*a*) a 0.75-m × 2.8-mm i.d. glass U-tube with 3% OV-101 on 100–120-mesh Gas Chrom Q with temperature programmed from 100 to 200° at 7.5°/min, and (*b*) a 1.2-m × 2.8-mm i.d. glass U-tube with 1.5% SE-30 on 100–120-mesh Gas Chrom W with temperature programmed from 150 to 250° at 7.5°/min or isothermally at 250°. The injector block temperature was 250°, the detector was at 280°, and the chart speed was 0.64 cm/min with helium carrier gas at 50 ml/min.

GLC–mass spectrometry was performed with a Finnigan 9500 gas chromatograph coupled to a Finnigan 3100 D quadrupole mass spectrometer through a single-stage glass jet separator. Data were acquired *via* a System/250 digital computer system. The mass spectrometer conditions were: interface temperature, 225°; transfer line, 175°; manifold temperature, 100°; and ion source potential, 70 ev. Chromatography conditions were the same as those used for GLC, except that the helium flow rate was 20 ml/min.

Analytical TLC was carried out on 0.25-mm layers of silica gel GF on glass plates. Preparative TLC was performed with 1-m × 20-cm glass plates coated with 0.75-mm layers of silica gel GF. The solvent system in both cases was 25% methanol in chloroform.

Standards of hispidin and bisnoryangonin were obtained from Dr. Lynn R. Brady, Department of Pharmaceutical Sciences, School of Pharmacy, University of Washington, Seattle, Wash. Natural ibotenic acid was obtained from Dr. William Scott Chilton, Department of Chemistry, University of Washington.

[3] *G. punctifolius* (Peck) Singer was collected in Grays Harbor County, Wash., in October 1975. This material is on deposit at the University of Washington Herbarium, Seattle, Wash., as LESLIE 2663.

[4] Hewlett-Packard 5080-8712.

[5] Regisil, Regis Chemical Co.

[6] Hewlett-Packard 5080-8713.

[7] *A. pantherina* (Fr.) Secr. was collected in Thurston County, Wash., in October 1975 and is on deposit at the University of Washington Herbarium, Seattle, Wash., as LESLIE 2629.

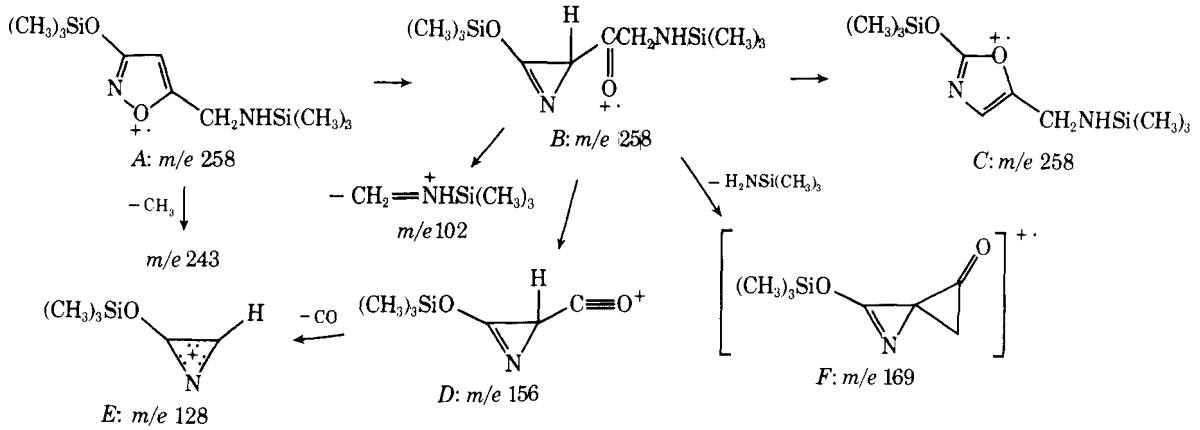

Scheme I

The fragmentation processes and rearrangements in the mass spectra of isoxazoles are complex (37–39). Scheme I shows several pathways proposed for the mass spectrum of III*b*. The rearrangement isoxazole → azirine → oxazole (*A* → *B* → *C*) (37) can lead to parallel fragmentation processes. Loss of methyl from a silyl group from any of the rearranged parent ions accounts for the *m/e* 243 signal. This process occurs so readily that the parent ion (*m/e* 258) is not evident. Production of trimethylsilylmethylimminium ion (*m/e* 102) followed by loss of carbon monoxide can lead to ions *D* (*m/e* 156) and *E* (*m/e* 128). Also, loss of trimethylsilylamine can lead to ions such as *F* (*m/e* 169), which can undergo further rearrangement. Similar fragmentations of ion *C* could also account for the signals at *m/e* 156 and 169.

The mass spectrum of IV*b* exhibited all typical fragmentations of trimethylsilylated α-amino acids (40), including M − 15 (*m/e* 359), M − 43 (331), M − 117 (257) due to loss of carbonyltrimethylsilyloxy, and *m/e* 218 due to loss of the amino acid side chain (36). The parent peak (*m/e* 374) was not present. Shorter reaction times or lower reaction temperatures resulted in the presence of variable amounts of a partially derivatized product, presumably IV*c*. The production of more than one trimethylsilyl derivative when various silylating reagents are used is not an uncommon occurrence with α-amino acids (40). However, quantitative derivatization giving only IV*b* occurred under the described conditions (see *Experimental*). Loss of carbon dioxide and a proton from IV*c* with retention of the trimethylsilyl group would account for the *m/e* 257 signal. This compound also exhibited fragments similar to those discussed for III*b*.

The decarboxylation of IV*a* to III*a* (41) did not occur during silylation of IV*a* since III*b* was not present in gas chromatograms of the reaction solutions. GLC offers accurate quantitative analysis of I*a*, II*a*, III*a*, and IV*a* directly from initial extracts. Sensitivity is in the 10^{-8}–10^{-7}-g range with analyses routinely run on 10–20 mg of dried fungal tissue. The strong signals for the parent ions of I*b* and II*b* and the combination of characteristic fragmentations for III*b* and IV*b* allow positive identification of these substances.

REFERENCES

(1) D. B. Repke, D. T. Leslie, D. M. Mandell, and N. G. Kish, *J. Pharm. Sci.*, **66,** 743 (1977).

(2) G. M. Hatfield and L. R. Brady, *Lloydia*, **34,** 260 (1971).

(3) *Ibid.*, **31,** 225 (1968).

(4) R. L. Edwards, D. G. Lewis, and D. V. Wilson, *J. Chem. Soc.*, **1961,** 4995.

(5) J. D. Bu'Lock, P. R. Leeming, and H. G. Smith, *ibid.*, **1962,** 2085.

(6) A. S. Ueno, S. Fukushima, T. Saika, and T. Harada, *Chem. Pharm. Bull.*, **12,** 376 (1964).

(7) G. M. Hatfield, Ph.D. dissertation, University of Washington, Seattle, Wash., 1968.

(8) G. M. Hatfield and L. R. Brady, *J. Pharm. Sci.*, **58,** 1298 (1969).

(9) L. R. Brady and R. G. Benedict, *ibid.*, **61,** 318 (1972).

(10) K. Gluchoff-Fiasson and R. Kühner, *C. R. Acad. Sci. Paris*, **284,** 1667 (1977).

(11) J.-L. Fiasson, K. Gluchoff-Fiasson, and W. Steglich, *Chem. Ber.*, **110,** 1047 (1977).

(12) M. Klaar and W. Steglich, *ibid.*, **110,** 1058 (1977).

(13) *Ibid.*, **110,** 1063 (1977).

(14) L. R. Hesler, "North American Species of Gymnopilus," Hafner, New York, N.Y., 1969, p. 23.

(15) R. G. Wasson, *Trans. Asiat. Soc. Jpn.*, **11,** 5 (1973).

(16) R. Imazeki, *ibid.*, **11,** 41 (1973).

(17) R. W. Buck, *N. Engl. J. Med.*, **276,** 391 (1967).

(18) R. G. Benedict, in "Microbial Toxins," S. Kadis, A. Ciegler, and S. J. Ajl, Eds., Academic, New York, N.Y., 1972, chap. 11.

(19) A. T. Shulgin, *Bull. Narcot.*, **25,** 59 (1973).

(20) M. W. Klohs, in "Ethnopharmacologic Search for Psychoactive Drugs," D. H. Efron, B. Holmstedt, and N. S. Kline, Eds., U.S. Government Printing Office, Washington, D.C., 1967, pp. 126–132.

(21) G. F. R. Müller and C. H. Eugster, *Helv. Chim. Acta*, **48,** 910 (1965).

(22) R. Good, G. F. R. Müller, and C. H. Eugster, *ibid.*, **48,** 927 (1965).

(23) R. G. Benedict, V. E. Tyler, Jr., and L. R. Brady, *Lloydia*, **29,** 333 (1966).

(24) J. Ott, P. S. Wheaton, and W. S. Chilton, *Physiol. Chem. Phys.*, **7,** 381 (1975).

(25) T. Yokobe and T. Takemoto, *Yakugaku Zasshi*, **89,** 1236 (1969).

(26) W. S. Chilton and J. Ott, *Lloydia*, **39,** 150 (1976).

(27) R. G. Wasson, "Soma, Divine Mushroom of Immortality," Harcourt Brace Jovanovich, New York, N.Y., 1971.

(28) J. Ott, *J. Psychedelic Drugs*, **8,** 27 (1976).

(29) W. Theobald, O. Büch, H. A. Kunz, P. Krupp, E. G. Stenger, and H. Heimann, *Arzneim.-Forsch.*, **18,** 311 (1968).

(30) P. G. Waser, in "Ethnopharmacologic Search for Psychoactive Drugs," D. H. Efron, B. Holmstedt, and N. S. Kline, Eds., U.S. Government Printing Office, Washington, D.C., 1967, p. 419.

(31) P. G. Waser and P. Bersin, in "Psychotomimetic Drugs," D. H. Efron, Ed., Raven, New York, N.Y., 1970, pp. 155–161.

(32) K. Tomita, M. Nagano, and N. Nakamura, Japanese pat. 68 16,136 (1968); through *Chem. Abstr.*, **70,** 57817w.

(33) A. R. Gagneux and F. Hafliger, U.S. pat. 3,397,209 (1968).

(34) H. Gänshirt, in "Thin-Layer Chromatography, A Laboratory Handbook," E. Stahl, Ed., Academic, New York, N.Y., 1965, pp. 44–51.

(35) C. H. Eugster, *Naturwissenschaften*, **55,** 305 (1968).

(36) A. E. Pierce, "Silylation of Organic Compounds," Pierce Chemical Co., Rockford, Ill., 1968.

(37) J. H. Bowie, R. K. M. R. Kallury, and R. G. Cooks, *Aust. J. Chem.*, **22,** 563 (1969).

(38) M. Ohashi, H. Kamachi, H. Kakisawa, A. Tatematsu, H. Yoshizume, and H. Nakata, *Tetrahedron Lett.*, **1968,** 379.

(39) M. Ohashi, H. Kamachi, H. Kakisawa, A. Tatematsu, H. Yoshizumi, H. Kano, and H. Nakata, *Org. Mass Spectrom.*, **2,** 195 (1969).

(40) W. J. A. VandenHeuvel and J. L. Smith, *J. Chromatogr. Sci.*, **8,** 567 (1970).

(41) P. Catalfomo and C. H. Eugster, *Bull. Narcot.*, **22,** 33 (1970).

ACKNOWLEDGMENTS

The authors thank Dr. Lynn R. Brady and Dr. William Scott Chilton for supplying three standards. They also thank Dr. László Tökés of the mass spectrometry laboratory, Syntex Research, Palo Alto, Calif., for discussions concerning the mass spectra. The assistance of Marcella Pearsall in the collecting of *A. pantherina* is gratefully acknowledged.

Thermodynamics of Mercaptopurine Dehydration

SARFARAZ NIAZI

Received May 11, 1977, from the *Department of Pharmacy, College of Pharmacy, University of Illinois at the Medical Center, Chicago, IL 60612.* Accepted for publication July 18, 1977.

Abstract □ The hydrate form of mercaptopurine was shown to undergo peritectic decomposition of its water molecule, localized dissolution, and dehydration around 125°. The anhydrate form was prepared by a thermal method, whose effectiveness was confirmed by X-ray diffraction, NMR spectroscopy, and differential scanning calorimetry. The activation energy for mercaptopurine dehydration calculated by various methods ranged from 45.74 to 63.04 kcal/mole. The dehydration enthalpy was calculated to be 8.27 kcal/mole by differential scanning calorimetry. The solution enthalpy for the hydrate was calculated to be 4.85 kcal/mole from its saturation solubility and differential scanning calorimetry. Anhydrate solubility in water was calculated based on initial dissolution rate data since the anhydrate converts to hydrate in aqueous media. The high degree of stability against interconversion of the hydrate and anhydrate forms and the higher solubility of the anhydrate suggest that use of the anhydrate might improve mercaptopurine bioavailability.

Keyphrases □ Mercaptopurine—thermodynamics of dehydration, stability of hydrate and anhydrate forms under various thermal conditions □ Thermodynamics—mercaptopurine dehydration, stability of hydrate and anhydrate forms under various thermal conditions □ Dehydration—thermodynamics, mercaptopurine, stability of hydrate and anhydrate under various thermal conditions □ Stability—mercaptopurine, hydrate and anhydrate forms, various thermal conditions □ Antineoplastic agents—mercaptopurine, thermodynamics of dehydration, stability of hydrate and anhydrate forms under various thermal conditions

Mercaptopurine, a potent purine inhibitor (1), is an effective anticancer drug. The monohydrate form generally gives erratic and low bioavailability (2). Mercaptopurine dehydration, resulting in a complete change in its polymorphic form, was recently reported (3). The anhydrate form also shows a higher dissolution rate, and its use has been recommended to improve bioavailability (3).

In this investigation, the thermodynamic parameters related to mercaptopurine dehydration were calculated and the relative stability of each form under various thermal conditions was estimated.

EXPERIMENTAL

Identification of Crystal Structure Modification and Dehydration—The purity of mercaptopurine[1] was confirmed by differential thermal analysis[2]. Repeat thermograms on mercaptopurine suggested an endothermic response and elevation of the thermodynamic energy at around 125°. This high energy compound was prepared by incubating mercaptopurine in an aluminum foil sack at 200° for 20 min. This treatment resulted in the complete transformation of mercaptopurine to the high energy form without decomposition, as evidenced by differential scanning calorimetry (3).

X-ray diffraction studies were performed on the two forms of mercaptopurine by smearing identical amounts (5 mg) on a double-stick tape fixed on a glass slide. The X-ray diffractometer[3] was run at 1.27 cm/min and 1°/2.54 cm with scanning from 10 to 35° (2θ) under the following conditions: Cu radiation, filtration through a nickel filter, 40 kv, 13 mamp, time constant 3, range 300, and scale expansion 21.

The loss of the water molecule upon heat treatment was also confirmed by NMR[4] studies. An excess of the anhydrate form was shaken in dimethyl sulfoxide[5] in the sample tube, and 100 scans were accumulated at 10-sec intervals with dimethyl sulfoxide set at 151.2 Hz. The aromatic peaks at 503.03 and 491.77 Hz were set equal to 2.0. Similar conditions were used for the hydrate, except for a higher sensitivity to pick up the water molecules in the organic phase released from mercaptopurine upon dissolution. In all instances, the amount of mercaptopurine dissolved was very small because of its solubility characteristics.

Conversion of Hydrate to Anhydrate as a Function of Heating Rate—Estimation of activation energies for the transition of the hydrate to the anhydrate form requires calculation of the amount of the hydrate remaining at various temperatures as a function of heating rates. Accurately weighed amounts (~8–9 mg) of mercaptopurine were transferred to differential scanning calorimetry pans, which were heated at 20, 5, or 2°/min. The sides of the cover were not crimped so that water could evaporate freely. The percent of the hydrate form remaining was calculated from the relative areas under the transition peaks obtained by using a planimeter[6].

Enthalpies of Dehydration and Fusion—Enthalpies were calculated by comparing the areas under the peaks with benzoic acid as the standard. All calculations were performed using a programmable desk-top computer[7].

RESULTS AND DISCUSSION

Purity of Mercaptopurine Forms—The drug supplied by the manufacturer was the monohydrate and showed the loss of the water molecule around 125° (Fig. 1). The purity of the compound was ascertained from the sharpness of the final melting point, since the reported melting points vary from 300 to 315° (4–10). Thermogram reruns showed a high degree of reproducibility, suggesting a lack of significant decomposition upon fusion. However, heating the compound a few degrees above its fusion resulted in decomposition.

Based on these thermal stability considerations, an incubation method was developed (3) for the preparation of the anhydrate. As expected, the

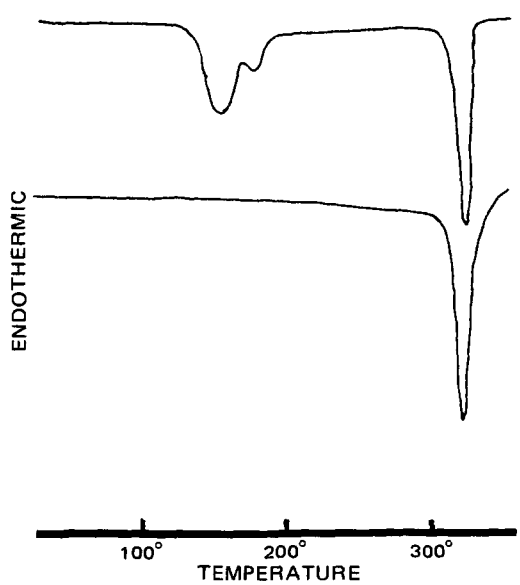

Figure 1—*Differential scanning calorimetry thermograms of mercaptopurine. Key: top, original drug; and bottom, heat-treated sample or rerun of sample in the top thermogram.*

[1] Supplied by Burroughs Wellcome Co., Research Triangle Park, N.C.
[2] A 990 thermal analyzer, E. I. du Pont de Nemours & Co., Wilmington, Del.
[3] Picker X-ray powder diffractometer.
[4] Varian T60A NMR spectrometer, Varian Instruments, Palo Alto, Calif.
[5] Dimethyl sulfoxide-d_6, Aldrich Chemicals, Milwaukee, Wis.
[6] Hruden, Germany.
[7] HP-97 calculator, Hewlett-Packard, Cupertino, Calif.

Table I—Main X-Ray Diffraction Peaks of Mercaptopurine Hydrates and Anhydrates

Original Compound (Hydrate)		Heat-Treated Compound (Anhydrate)	
Peak, $2\theta°$	Peak Height, cm	Peak, $2\theta°$	Peak Height, cm
11.8	3.4	10.7	6.9
12.8	1.2	14.3	3.9
14.8	17.7	15.9	5.0
15.4	1.5	20.0	3.4
23.6	2.3	20.3	2.0
25.3	4.6	21.5	1.8
26.0	6.9	24.8	5.1
27.7	9.1	28.5	8.4
29.6	12.3		
30.5	3.7		
34.2	2.7		

anhydrate showed an identical melting point and no endothermic response around 125°, suggesting complete conversion to the high energy form. The purity of the two forms was further established by X-ray diffraction studies, which showed a complete transition of the lattice structure upon dehydration. Table I reports the characteristic X-ray diffraction peaks for identification purposes.

The NMR studies proved exceedingly fruitful in detecting even traces of water in dimethyl sulfoxide from the hydrate. Both forms showed the characteristic aromatic peaks (Fig. 2) along with NH peaks around 819.74 Hz, equal to 1.74 and 1.95 for the anhydrate and hydrate, respectively. The aromatic peaks were set equal to 2.0. The dimethyl sulfoxide peak at 151.2 Hz was accompanied by the water peak at 1.5 from the hydrate, confirming the complete loss of water molecules upon the heat treatment described.

Dehydration Mechanism—The mechanism of mercaptopurine dehydration can be ascertained partly by differential scanning calorimetry (Fig. 1). The endothermic response occurring around 125° was composed of two peaks, attributed to the release and evaporation of water molecules since the sample pans were open to the atmosphere (*i.e.*, not crimped). The mechanism suggested here involved peritectic decomposition of the water molecule and formation of a solution, followed by the evaporation of the water molecule. This mechanism was suggested for various other compounds (10).

Support for this argument comes from the observation that, upon dehydration, mercaptopurine attains an entirely different lattice structure, which is more feasible if local dissolution is involved in the transition of structure. The reaction order for the transition process is most likely to be first order since higher order reactions occur only with difficulty in the solid state. As discussed later, this hypothesis was confirmed by thermodynamic measurements.

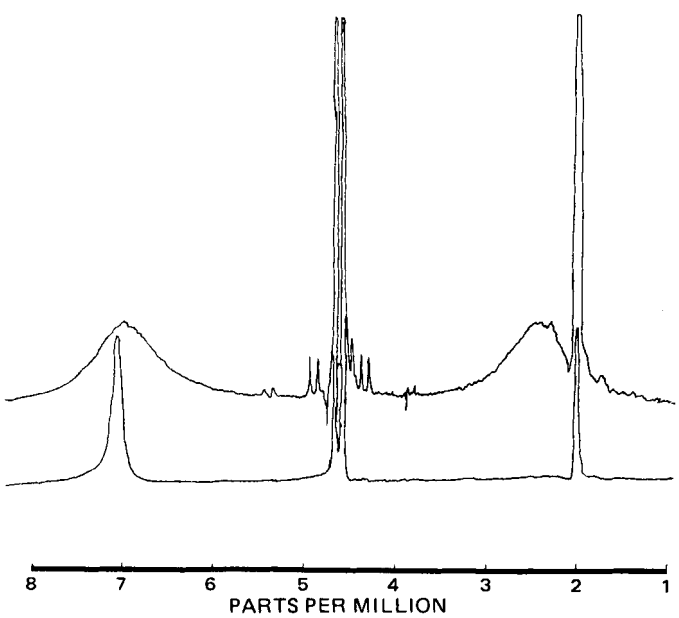

Figure 2—*NMR spectra of mercaptopurine hydrate (top) and anhydrate (bottom) in dimethyl sulfoxide.*

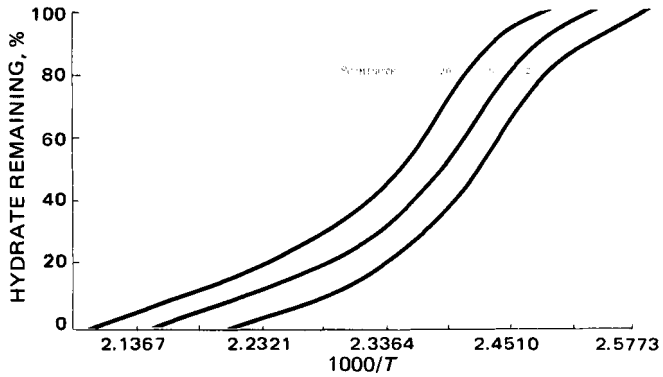

Figure 3—*Ozawa method for the calculation of temperature for a percent dehydration as a function of heating rates.*

Activation Energy of Dehydration—Although some work has been reported regarding the heat of solution of mercaptopurine (11), no study has reported the thermodynamic constants for the transition of mercaptopurine hydrate to the anhydrate.

The activation energy for mercaptopurine transition can be calculated by several methods (12–14). According to Ozawa (12), the kinetic equation for the nth-order reaction can be expressed as:

$$-\frac{dW}{dt} = W^n A e^{(-\Delta E)/RT} \qquad \text{(Eq. 1)}$$

where W is the fractional residual amount of solvate, T is the absolute temperature, R is the gas constant, t is time, ΔE is the activation energy, A is the frequency factor, and n is the order of reaction. A function, P, introduced by Doyle (15), is:

$$\left(\frac{\Delta E}{R}\right) P\left(\frac{\Delta E}{RT}\right) = \int_0^T e^{-(\Delta E)/RT}\, dt \qquad \text{(Eq. 2)}$$

If $\Delta E/RT$ is larger than 20, an approximation (16) can be made:

$$\log P\left(\frac{\Delta E}{RT}\right) \simeq -2.315 - 0.4567\frac{\Delta E}{RT} \qquad \text{(Eq. 3)}$$

Thus, if the weight of the solvate decreases to a given fraction at temperature T_i for the heating rate a_i:

$$\frac{A}{a_i R}\frac{\Delta E}{P}\frac{(\Delta E)}{RT_1} = \frac{A}{a_2 R}\frac{\Delta E}{P}\frac{(\Delta E)}{RT_2} = \ldots \qquad \text{(Eq. 4)}$$

By using Eq. 3, the following linear relations can be easily derived (12):

$$-\log a_1 - 0.4567\frac{\Delta E}{RT_1} = -\log a_2 - 0.4567\frac{\Delta E}{RT_2} = \ldots \qquad \text{(Eq. 5)}$$

Thus, the plots of log a *versus* the reciprocal absolute temperature for a given value of W must give a straight line, the slope of which gives the activation energy:

$$\Delta E = \frac{\text{slope} \times R}{0.4567} \qquad \text{(Eq. 6)}$$

The fraction of the hydrate form converted to the anhydrous form as a function of temperature can be calculated from the corresponding areas under the transition endothermic peak at different heating rates and plotted (Fig. 3). Similar profiles have been reported for the dehydration of other compounds (10). From Fig. 3, a constant fraction remaining for different heating rates can be determined as a function of temperature (Fig. 4). An excellent linear relationship ($r^2 > 0.99$) between the log of the heating rate and the reciprocal temperature suggests good application of Eq. 5 for this system. The activation energy calculated from the slopes ranged from 50.53 to 63.04 kcal/mole.

Another method for the calculation of activation energy, suggested by Kofstad (13), involves approximations of the orders of reaction:

$$(n+1)\ln(ANH) + \ln\frac{d\ln(ANH)}{dt} = \ln A - \frac{\Delta E}{RT} \qquad \text{(Eq. 7)}$$

Calculations using Eq. 7 for zero-, first-, and second-order reactions are plotted in Fig. 5. The calculated activation energies were 24.85–26.60 kcal/mole (zero order), 49.69–52.01 (first order), and 74.54–78.01 (second order). Although the energies calculated from this method for the first-order reaction were somewhat lower than the previous method if the reaction order is assumed to be the same, such approximations can be re-

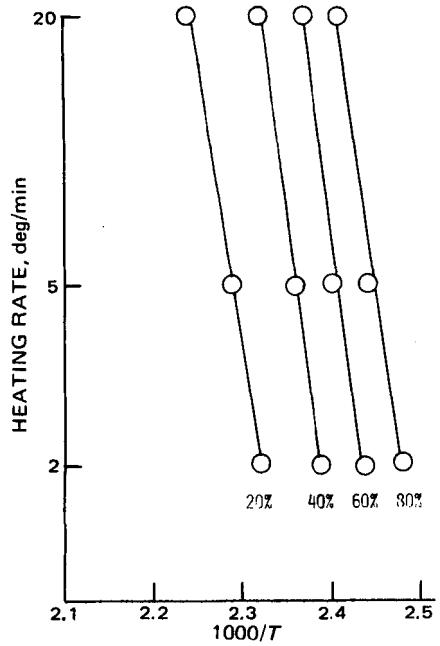

Figure 4—*Calculation of activation energy using Ozawa method. (See text for details.)*

garded as good correlation in view of the larger numbers of parameters and assumptions involved and the possibility of mixed orders of reactions. The order of reactions other than first yielded very low or high energies, excluding them as possible mechanisms.

A simpler method for the calculation of the activation energy, proposed by Kissinger (14), takes into account only the peak of temperature, Tp_1, of the endothermic response as a function of the heating rate:

$$\frac{\Delta Ea}{RTp^2} = \left[A + A(n-1)\frac{2RTp}{\Delta E}\right] e^{-\Delta E, RTp} \qquad \text{(Eq. 8)}$$

$$\frac{d \ln (a/Tp^2)}{d(1/T)} = -\frac{\Delta E}{R} \qquad \text{(Eq. 9)}$$

Figure 6 shows the Kissinger plot; the activation energy calculated from the slope was 45.74 kcal/mole. However, it was suggested (17) that slight measurement errors in this method result in significantly large errors in the activation energy. This method gave lower values for the activation energies than were calculated by the other two methods.

Discounting any significant errors inherent in the Kissinger method (14), the low activation energy can be explained mechanistically as suggested for mercaptopurine dehydration. As shown in Fig. 1, the peritectic decomposition of the water molecule is followed by energy absorption to evaporate it. Whereas the Ozawa (12) and Kofstad (13) methods

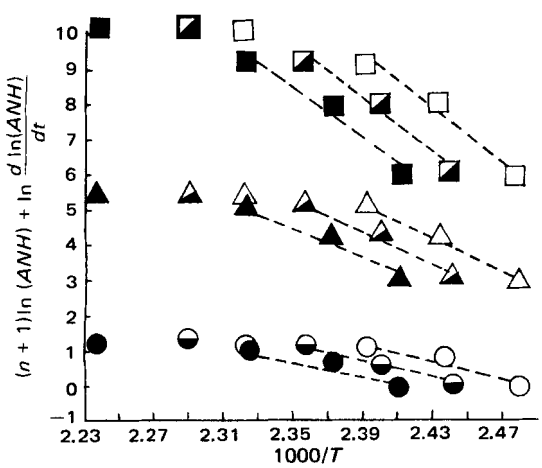

Figure 5—*Kofstad's method for the calculation of activation energies assuming second (squares), first (triangles), and zero (circles) orders for the reaction. Key: open symbols, 2°/min; half-closed symbols, 5°/min; and closed symbols, 20°/min.*

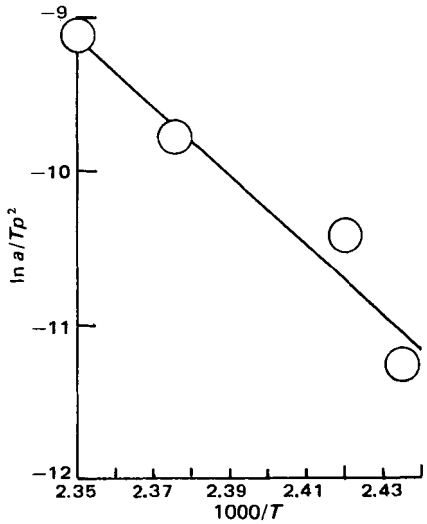

Figure 6—*Kissinger plot for the calculation of activation energy of mercaptopurine dehydration.*

consider the total process of dehydration, the Kissinger method (14) does not; the peak temperature (Eq. 8) represents the time at which the water molecule has not evaporated and thus refers only to peritectic decomposition.

The activation energies calculated for the transition of mercaptopurine by the three methods appear to be relatively high compared with reactions of a similar nature. The high activation energy would, therefore, mean a higher stability of both forms of mercaptopurine (18).

Enthalpy and Stability of Transition—The enthalpy of transition was calculated by comparing the areas under the endothermic peaks of mercaptopurine and the standard, benzoic acid, and was calculated to be 8.27 kcal/mole. This value is comparable to literature reports for glutethimide, theophylline, and succinylsulfathiazole (18). Since the transition enthalpy is much smaller compared to the activation energy, reasonable stability of the anhydrous form can be assumed.

This premise was confirmed by storing the anhydrate at room temperature for over 6 months without any significant conversion to the hydrate. Further support can be drawn from the calculation of the frequency factor for this reaction. With the data already given, a plot of the percent of the hydrate remaining against log $[(\Delta E/aR)P(\Delta E/RT)]$ (12) will give the plot whose lateral shift will be equal to the logarithm of the frequency factor (Fig. 7).

The lateral shift can be easily calculated since the reaction order is confirmed to be first. Thus (12):

$$\log A = \ln W - \log\left(\frac{\Delta E}{aR} P \frac{\Delta E}{RT}\right) \qquad \text{(Eq. 10)}$$

Table II reports the calculation of A using activation energies obtained from Kofstad's method for illustration. In a first-order reaction, the re-

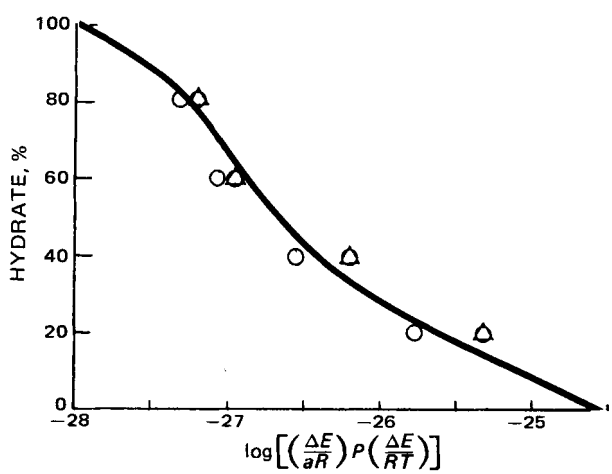

Figure 7—*Lateral shift for the calculation of frequency factor (Table II).*

Table II—Calculation of Frequency Factor for Mercaptopurine Dehydration

Heating Rate, deg/min	W	ΔE, cal	T, °K	$P\frac{\Delta E_a}{RT}$	log A[b]
20	0.8	49,690	415	1.168×10^{-30}	26.61
20	0.6	49,690	422	3.353×10^{-30}	25.87
20	0.4	49,690	420.5	1.1527×10^{-29}	24.92
20	0.2	49,690	447	1.1078×10^{-28}	23.25
5	0.8	52,010	409.5	2.453×10^{-32}	27.67
5	0.6	52,010	416.5	7.621×10^{-32}	26.89
5	0.4	52,010	424	2.462×10^{-31}	25.97
5	0.2	52,010	436.5	1.591×10^{-30}	24.47
2	0.8	50,520	403.5	6.394×10^{-32}	26.87
2	0.6	50,520	410.5	1.987×10^{-31}	26.08
2	0.4	50,520	418	6.420×10^{-31}	25.17
2	0.2	50,520	430.5	4.140×10^{-30}	23.66

[a] $P(\Delta E/RT)$ = antilog $[-2.315 - 0.4567(\Delta E/RT)]$. [b] Equation 9.

action rate constant can be expressed as:

$$K = Ae^{-\Delta E/RT} \quad \text{(Eq. 11)}$$

Table III reports the half-lives of mercaptopurine dehydration as a function of temperature. The high activation energy for dehydration makes this reaction highly susceptible to temperature changes; although it can be considered absolutely stable at room temperature, the half-life decreased to 3.4 min at 150°.

Heat of Solution and Solubilities—The heat of solution of mercaptopurine in water was recently reported to be 9.3 kcal/mole (11). However, when using the solubility determination developed in this laboratory, the heat of solution was determined by the following equation with the assumption of an ideal solution:

$$\Delta H(\text{kcal/mole}) = \ln \frac{Cs(\mu\text{g/ml})}{152.19} \frac{RT_{mp}T}{T_{mp} - T} \quad \text{(Eq. 12)}$$

The values of solution enthalpy thus calculated based on the melting-point range of 298–319° range from 4.75 to 4.95 kcal/mole. A direct measurement of fusion enthalpy made by comparing the areas under the curve to a standard compound gave a value of 5.5 kcal/mole, which is slightly higher than the calculated value since the ideality of solution may not be applicable here. Disagreement between the present values and those reported (11) may be due to the solubility determination used in the present study being more sensitive and relatively error free.

A direct determination of the solubility of the anhydrate cannot be made since it converts to the hydrate in an aqueous medium (3). However, based on the initial dissolution rates (3) of the anhydrate and the hydrate, the solubility can be correlated:

$$\frac{dC_h}{dt} \alpha\, Cs_h \quad \text{(Eq. 13)}$$

$$\frac{dC_{anh}}{dt} \alpha\, Cs_{anh} \quad \text{(Eq. 14)}$$

$$\frac{Cs_h}{Cs_{anh}} = \frac{dC_h/dt}{dC_{anh}/dt} \quad \text{(Eq. 15)}$$

where Cs_h is the solubility of the hydrate, and Cs_{anh} is the solubility of the anhydrate.

Based on the reported (3) dissolution rate constants of 0.25 and 0.16 min^{-1} from similar surface area particles, the anhydrate solubility is 404.68 μg/ml.

The presented data show that the mercaptopurine anhydrate is highly stable at room temperature and will dissolve faster in an aqueous medium in spite of its conversion to the hydrate. It is suggested that the anhydrate can result in improved bioavailability, and these studies will be reported.

Table III—Half-Lives of Mercaptopurine Dehydration as a Function of Temperature

Temperature	Half-Life, min
25°	3.69×10^{11}
50°	4.75×10^{8}
75°	1.59×10^{6}
100°	1.14×10^{4}
125°	1.53×10^{2}
150°	3.4×10^{0}
200°	5.62×10^{-3}

REFERENCES

(1) J. H. Burchenal, M. L. Murphy, R. R. Ellison, M. P. Sykes, T. C. Tan, L. A. Leone, D. A. Karnofsky, L. F. Craver, H. W. Drageon, and C. P. Rhoads, *Blood*, **8**, 965 (1953).

(2) T. L. Loo, J. K. Luce, M. P. Sullivan, and E. Frei, III, *Clin. Pharmacol. Ther.*, **9**, 180 (1968).

(3) M. L. Huang and S. Niazi, *J. Pharm. Sci.*, **66**, 608 (1977).

(4) "Pharmacopea Francaise VIII," Pharmacopia Gallica, Paris, France, 1965.

(5) "The Merck Index," 8th ed., Merck & Co., Rahway, N.J., 1968.

(6) "Dictionary of Organic Compounds," 4th ed., Oxford University Press, New York, N.Y., 1965.

(7) "The United States Pharmacopeia," 19th rev., Mack Publishing Co., Easton, Pa., 1975.

(8) "British Pharmacopoeia," Her Majesty's Stationery Office, University Printing House, Cambridge, England, 1973.

(9) "Hackh's Chemical Dictionary," 4th ed., McGraw-Hill, New York, N.Y., 1969.

(10) K. Sekiguchi, I. Horikoshi, and I. Himuro, *Chem. Pharm. Bull.*, **16**, 2495 (1968).

(11) Y. Arakawa, M. Nakano, K. Juni, and T. Arita, *ibid.*, **24**, 1654 (1976).

(12) T. Ozawa, *Bull. Chem. Soc. Jpn.*, **38**, 1881 (1965).

(13) P. Kofstad, *Nature*, **179**, 1362 (1957).

(14) H. E. Kissinger, *Anal. Chem.*, **29**, 1702 (1957).

(15) C. D. Doyle, *J. Appl. Polym. Sci.*, **5**, 285 (1961).

(16) *Ibid.*, **6**, 639 (1962).

(17) F. W. Wilburn, J. R. Hesford, and J. R. Flower, *Anal. Chem.*, **40**, 777 (1968).

(18) E. Shefter and T. Higuchi, *J. Pharm. Sci.*, **52**, 781 (1963).

ACKNOWLEDGMENTS

The author thanks Dr. W. Dunn and Dr. D. Venton, Department of Medicinal Chemistry, for their assistance in NMR studies.

Ultrasonic Method for Direct and Simultaneous Determination of Alcohol and Soluble Solids Content of Mouthwash

W. C. WINDER *, F. H. LOHMAN ‡x, R. F. TORDE *, and R. J. WAGNER *

Received May 20, 1977, from the *Department of Food Science, University of Wisconsin, Madison, WI 53706, and the ‡Toilet Goods Division, Procter and Gamble Co., Cincinnati, OH 45224. Accepted for publication July 29, 1977.

Abstract □ A technique for the determination of certain soluble species in solution by the changes they produce in the speed of propagation of ultrasonic waves in the solution was applied to measure the alcohol and soluble solids levels of mouthwashes. The simultaneous determination of these two quantities is made possible by measuring the wave velocity at two different temperatures. The method gives accurate, precise results for the general range of mouthwash compositions in use with appropriate calibration. The advantages of this method over other current methods are precision, speed, and convenience. It is not a suitable regulatory method, however, because calibration must be done with known variations of the particular mouthwash composition to be analyzed.

Keyphrases □ Alcohol—ultrasonic analysis in pharmaceutical formulations □ Solids, soluble—ultrasonic analysis in pharmaceutical formulations □ Ultrasonic analyses—alcohol and soluble solids in pharmaceutical formulations □ Mouthwashes—ultrasonic analysis of alcohol and soluble solids

Rapid, yet accurate, methods of analysis for the alcohol and soluble solids content of mouthwashes are essential in the toilet goods industry. Whether they are classified as "old drugs," "new drugs," or cosmetic products, mouthwashes, like wines, are subject to strict composition control for quality under some code of good manufacturing practice. The alcohol content is of primary interest for its germicidal activity and because of the legal requirements for strict accounting of its use. Determination of the soluble solids content may serve as an indicator of proper formulation for individual batches of mouthwash.

Currently, there are no officially validated methods for the determination of the alcohol and soluble solids content in mouthwashes. There are two methods in the USP (1) for determining alcohol in extracts and tinctures: a distillation method like the AOAC method and a GLC method. The individual manufacturers have, rather successfully, adapted or modified these methods used in the pharmaceutical industry and by the AOAC for determination of alcohol in wine and alcoholic beverages (2, 3). However, certain constituents of mouthwash such as glycerin and flavoring and foaming agents may interfere with the standard wine methods, and correction factors may have to be applied.

The GLC method and the AOAC distillation/specific gravity method have been adapted for the determination of alcohol. Both methods necessitate the attention of relatively skilled technicians; the GLC technique requires expensive equipment and does not consistently give the precision required, while the AOAC method is slow and tedious and requires a correction for glycerin when it is present.

Winder *et al.* (4) demonstrated that an instrument[1] that precisely measures the velocity of ultrasonic waves in a homogeneous liquid (solution) could be utilized to determine simultaneously the alcohol and extract content of finished wines rapidly and accurately. The ultrasonic wave velocity method depends on a correlation of the acoustic properties of a solution with its gross composition. In preliminary studies, it was demonstrated that if the soluble solids content of a mouthwash were held constant, an ultrasonic solution analyzer operating at 20° could be used to determine the alcoholic content. The standard deviation of differences between formulation values and the ultrasonic solution analyzer results was ±0.07% alcohol for six samples of specially prepared mouthwash. These initial values were well within the accuracy limits desired.

Since the soluble solids content as well as the alcohol content affects the acoustic properties of liquids, studies were made to determine whether the ultrasonic analyzer technique could be utilized for quality control analyses of mouthwash.

EXPERIMENTAL

Instrumentation for Acoustic Measurements—Figure 1 shows a diagram of the test cell and associated circuitry in the ultrasonic solution analyzer.

Built into the sample cell is a stainless steel reflector facing two ultrasonic ceramic transducers enclosed in stainless steel. The transducers are positioned at an approximately 20° angle from the reflector. Coaxial cables connect the transducers to the oscillator circuit of the electronic system. The electronic blocking oscillator produces a pulse of alternating voltage of short duration, which travels through the cable to the transmitting transducer.

By piezoelectric action, the electrical pulse alternately deforms and relaxes the ceramic element, causing it to vibrate at a high frequency. As a result, a short pulse of compressional energy is produced; it travels through the liquid, is reflected, and is received by the second transducer. The pressure variations of the sound pulse being received are changed to voltage variations, which indicate the useful output of the pulse. This output is sent through an automatic gain control device, which amplifies and shapes the signal. The signal is then returned to the oscillator, which triggers a second (or new) electrical pulse to be propagated through the circuit again.

The process keeps repeating itself as one pulse triggers the next. The

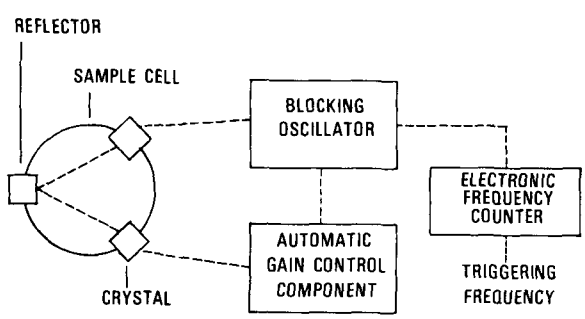

Figure 1—*Functional diagram of the ultrasonic solution analyzer.*

[1] Solution analyzer, Gould, Inc., Chesapeake Instrument Division, Shadyside, Md.

Table I—Effect of Soluble Solids Level on Solution Analyzer Triggering Frequency at Various Temperatures with Three Prepared Samples of Mouthwash

Soluble Solids, %	Δf_{10}		Δf_{20}		Δf_{30}		Δf_{41}		Δf_{65}	
11.0	2624	2	2074	14	1651	24	1220	32	500	51
10.0	2622	83	2060	63	1627	46	1188	31	449	1
9.0	2539		1997		1581		1157		448	

triggering rate is measured with a digital frequency counter, which displays the count on the face of the instrument. The rate of pulse initiation or triggering is a function of several constant factors: the temperature of the liquid medium, the path length in the sample cell, and the time delay of the electronic circuit. As a result, the only variable in the triggering rate or triggering frequency is the effect of the composition of the liquid sample. Thus, the triggering frequency is related directly to the sound velocity through the test medium.

For the study reported in this paper, knowledge of actual sound velocity through the sample was academic. Instead, all data were reported in terms of triggering frequency, an indirect measure of sound velocity. Since water is the continuous medium (primary solvent) in mouthwash, the triggering frequency value in distilled water at each test temperature was determined first. This value was subtracted from the triggering frequency observed with each sample to obtain the change caused by the constituents, other than water, in that sample. A change in triggering frequency from that in water was reported as Δf. All correlations of data were made in terms of Δf.

General Procedure—To operate the instrument, it is turned on and the water baths are allowed to equilibrate to precisely controlled temperatures (±0.01°). When the triggering frequency in water in the 35-ml test cell does not change during a 1-min interval, the sample and the water bath are at temperature equilibrium. The triggering frequency from the distilled water is programmed into the instrument as the reference point for direct readout of Δf values.

The water is then drained from the cell in about 5 sec by opening a solenoid valve connected to a vacuum system. The valve is closed, and about 20 ml of the new sample is introduced to flush the cell. After flushing, the test sample is then poured into the cell. A vacuum-operated outlet at the top of the test cell drains away any excess, thus eliminating the need for accurate measurement of the quantity of sample.

When the sample is in the test cell, the space above the cell is closed with a 5.1-cm (2-in.) cartridge of solid insulation to ensure precise temperature stability. The test sample is then allowed to temperature equilibrate, after which its triggering frequency is measured. The triggering frequency of the water is automatically subtracted from the triggering frequency of the test sample, and a Δf value is obtained for that temperature.

Choice of Test Temperatures—To determine both solids and alcohol in mouthwash systems with the ultrasonic solution analyzer, their respective effects on sound velocity must be dissimilar at two test temperatures. A graphical presentation of the data of Nozdrev (5) presented previously (4) illustrates the profound temperature effect on sound velocity in alcohol–water solutions. In the present study, each sample of several series of standard mouthwash samples was tested in ultrasonic solution analyzers operated at several temperatures until the best two temperatures for simultaneous determination of alcohol and soluble solids were chosen. Each standard mouthwash sample was prepared to a specific composition.

Table II—Summary of Solution Analyzer Δf Values for Five Levels of Alcohol and Soluble Solids at Three Different Temperatures

Sample	Normal Soluble Solids, %	Alcohol, % (w/v) 16.5	17.5	18.5	19.5	20.5
		Test Temperature = 20°				
E	90	2026	2074	2118	2154	2185
D	95	2046	2095	2136	2169	2195
A	100 (normal)	2082	2117	2159	2186	2210
B	105	2091	2138	2177	2208	2230
C	110	2120	2164	2201	2228	2246
		Test Temperature = 41°				
E	90	1162	1168	1170	1164	1149
D	95	1174	1178	1179	1172	1158
A	100 (normal)	1189	1193	1190	1186	1173
B	105	1206	1208	1203	1194	1178
C	110	1225	1225	1220	1207	1193
		Test Temperature = 65°				
E	90	443	417	377	338	284
D	95	450	418	380	342	291
A	100 (normal)	457	429	387	355	313
B	105	469	436	396	352	303
C	110	479	442	401	335	314

Table III—Standard Deviations of Differences, Ranges, and Mean Differences between As-Made Values and Solution Analyzer Values Obtained from Paired Data Taken at 20, 41, and 65° with 25 Samples of Moderate Soluble Solids Mouthwash

Temperature Combinations	Standard Deviations: Alcohol, % (w/v)	Standard Deviations: Soluble Solids[a]	Ranges: Alcohol, % (w/v)	Ranges: Soluble Solids[a]	Mean Differences: Alcohol, % (w/v)	Mean Differences: Soluble Solids[a]
20 and 65°	±0.09	±1.15	−0.14–+0.23	−2.53–+1.94	0	−0.010
20 and 41°	±0.10	±1.86	−0.32–+0.16	−3.54–+1.71	−0.012	−0.014
41 and 65°	±0.09	±1.38	−0.15–+0.26	−3.25–+1.76	0	−0.011

[a] Values are expressed as a percentage of normal soluble solids content.

RESULTS

Relationships among Parameters—To determine the effect of variations in the soluble solids content on sound velocity as a function of temperature, three specially prepared samples of mouthwash with a moderate (10%) soluble solids content were analyzed. The alcohol content of each sample was 18.5% (v/v), while the soluble solids content was 9, 10, and 11%. Each sample was tested in ultrasonic solution analyzers operating at 10, 20, 30, 41, and 65°. This temperature range covered the practical operating limits of the instruments. Below 20°, temperature control to within 0.01° was difficult to maintain; above 65°, vaporization of the alcohol and water occurred.

From the Δf values obtained and the incremental changes with temperature (Table I), it is apparent that the effect of the soluble solids content on Δf values is markedly different at different temperatures. These results indicate that a two-temperature method for the simultaneous determination of the alcohol and soluble solids content might be feasible.

To determine the soluble solids *versus* Δf relationships at different alcohol levels and the alcohol *versus* Δf relationships at different levels of soluble solids, 25 samples of a moderate soluble solids type of mouthwash were specially prepared in a 5 × 5 matrix. The alcohol content ranged from 18.9 to 23.7% (v/v) (17.0–20.0% w/v), and the soluble solids level ranged from 9.0 to 11.0%, representing 90–110% of the normal 10% level. All samples were tested in ultrasonic solution analyzers operating at 20, 41, and 65° (Table II).

These data were subjected to multiple regression analyses, and correlations were calculated to determine the best relationships among Δf values, alcohol content, and percentage of normal soluble solids.

The equations derived, expressing the appropriate relationships for data from determinations at 20, 41, and 65°, were of the following general type:

$$\Delta f_t = b_1 a + b_2 a^2 + b_3 s + c \qquad \text{(Eq. 1)}$$

where:

Δf_t = change in triggering frequency from that of water at 20, 41, or 65°
b_1 = regression coefficient for the alcohol content at 20, 41, or 65°
a = percentage of alcohol

Table IV—Standard Deviations of Differences, Ranges, and Mean Differences between the Actual Values and Solution Analyzer Values Obtained with Data Taken at 20 and 65° with 37 Samples of a Mouthwash of Moderate Soluble Solids Level

	Alcohol, % (v/v)	Soluble Solids, % of Normal
Standard deviation	±0.11	±1.08
Range of differences	−0.20–+0.30	−2.85–+1.46
Mean difference	+0.002	+0.002

Table V—Summary of Δf Values Obtained with Solution Analyzers Operated at 20 and 65° and Comparison of Formulated and Determined Values for Alcohol and Soluble Solids for 27 "Unknown" Standard Samples of Mouthwash of the Moderate Soluble Solids Class

Sample	Δf (20°)	Δf (65°)	Alcohol, % (v/v) Added	Found	Difference (Added − Found)	Percentage of Normal Soluble Solids Added	Found	Difference (Added − Found)
A'5	2034	482	18.25	18.10	+0.15	100	100.90	−0.90
A1	2071	457	18.99	19.01	−0.02	100	99.18	+0.82
A'6	2101	435	19.73	19.78	−0.05	100	98.52	+1.48
A2	2119	427	20.1	20.12	−0.02	100	99.76	+0.24
B'1	2037	492	17.89	17.89	0.00	105	104.38	+0.62
B'2	2069	477	18.48	18.53	−0.05	105	104.35	+0.65
B1	2095	467	18.9	19.00	−0.10	105	105.46	−0.46
B2	2140	434	20.1	20.14	−0.04	105	104.86	+0.14
B3	2178	395	21.3	21.34	−0.04	105	104.33	+0.67
C1	2123	478	18.9	18.99	−0.09	110	112.62	−2.62
C2	2166	443	20.1	20.17	−0.07	110	111.24	−1.24
C3	2199	405	21.3	21.30	0.00	110	109.98	+0.02
C4	2223	366	22.43	22.32	+0.11	110	109.31	+0.69
D'1	2032	457	18.59	18.66	−0.07	95	93.36	+1.64
D1	2046	449	18.9	18.97	−0.07	95	93.27	+1.73
D'2	2072	433	19.52	19.57	−0.05	95	93.31	+1.69
D2	2095	418	20.1	20.11	−0.01	95	93.72	+1.28
D3	2137	380	21.3	21.32	−0.02	95	94.04	+0.96
E'1	1858	495	16.05	16.18	−0.13	86	84.35	+1.65
E'2	1919	479	16.92	17.13	−0.21	86	85.20	+0.80
E'3	1972	458	18.0	18.09	−0.09	86	85.16	+0.84
E1	2026	443	18.9	18.93	−0.03	90	88.65	+1.35
E'4	2023	434	19.01	19.10	−0.09	86	85.83	+0.17
E2	2028	440	19.04	19.01	+0.03	90	88.16	+1.84
E3	2118	375	21.3	21.27	+0.03	90	89.60	+0.40
E4	2168	307	22.75	23.18	−0.43	90	90.93	−0.93
E5	2182	289	23.7	23.68	+0.02	90	92.53	−2.53
				Mean difference = −0.049			Mean difference = +0.41	
				Standard deviation of differences = ±0.13			Standard deviation of differences = ±1.25	

b_2 = regression coefficient for the percentage of alcohol squared at 20, 41, or 65°
a^2 = percentage of alcohol squared
b_3 = regression coefficient for the percentage of normal soluble solids at 20, 41, or 65°
s = percentage of normal soluble solids (normal = 100%)
c = ordinate at 20, 41, or 65°

The equations derived with data obtained at 20, 41, and 65° with the 25 samples were paired to produce three pairs of simultaneous equations (20 and 41, 20 and 65, and 41 and 65°). From these pairs, the alcohol and percentage variation from normal soluble solids contents of each sample were calculated by inserting the observed Δf values and solving the paired equations simultaneously. Comparisons of known values with ultrasonic solution analyzer values were made from standard deviations, means, and ranges of differences (Table III).

The best pair of test temperature equations was obtained with data taken at 20 and 65°. These superior results were attributed to the fact that a plot of Δf values against alcohol concentration exhibited a moderately steep positive slope for data at 20° whereas the slope was negative to about the same degree at 65°. Thus, the equations expressing the relationships for those temperatures were markedly different, lending accuracy to the results. At 41°, the plot was relatively horizontal; therefore, changes in Δf values with changes in alcohol concentration were relatively small and could not be expected to yield sensitive results. The slopes (changes in Δf/change in percent of alcohol) at constant soluble solids can be compared for the three test temperatures by reading across the horizontal lines of Δf values in Table II. Conversely, the slope (change in Δf/change in percent of normal soluble solids) at a constant percent of alcohol can be compared for the three test temperatures by reading down the vertical lines of Δf values.

The standard deviations of differences between the solution analyzer method and the theoretical values were ±0.09% alcohol and ±1.15 percentage of normal soluble solids. These results were considered to be excellent. Correlation coefficients for the 20 and 65° equations were 0.993 and 0.994, respectively.

Having established optimum temperatures for the simultaneous determination of alcohol and soluble solids, 12 additional samples in a 4 × 3 matrix were prepared to extend the alcohol range of samples studied. The alcohol content was varied in four steps from 16.0 to 19.0% (v/v) (from 14.1 to 16.6% w/v), and the soluble solids portion was prepared as 9.0, 10.0 (normal), and 11.0%. All samples were analyzed in ultrasonic solution analyzers operating at 20 and 65°. Data obtained with these 12 samples were combined with the data from the 5 × 5 matrix series to extend the alcohol range to 16.0–23.7% (v/v). New coefficients for the equations were derived from regression analysis, since the combined data were compatible.

With these equations, the alcohol and soluble solids content of each sample in the combined series was recalculated, and the results were compared with the nominal values of the standard formulations. A summary of the statistical analysis of these comparisons is presented in Table IV. Agreement between actual and determined values was excellent and not significantly different from that obtained with the previous 5 × 5 matrix series alone, indicating that accurate results could be obtained for both alcohol and soluble solids throughout the concentration ranges by these equations.

Validation of Method for Mouthwash with Moderate Soluble Solids Content—To confirm the accuracy and reproducibility of the procedures developed for mouthwash with moderate levels of soluble solids, 27 additional samples of known composition were prepared in which both alcohol and soluble solids contents were varied. In addition,

Table VI—Summary of Δf Values, Percentage of Normal Soluble Solids, and Percent Alcohol for Four Production Samples of a Moderate Soluble Solids Mouthwash

Sample	Δf_{20}	Δf_{65}	Alcohol, % (v/v) AOAC Method	Solution Analyzer (SA)	Difference (AOAC − SA)	Percentage of Normal Soluble Solids Standard Formulation	Solution Analyzer (SA)	Difference (Formulated − SA)
748	2072	453	19.20	19.11	+0.09	100.0	98.63	+1.37
749	2074	450	19.12	19.20	−0.08	100.0	98.23	+1.77
750	2084	448	19.29	19.33	−0.04	100.0	99.16	+0.84
751	2072	454	19.09	19.09	0.00	100.0	98.86	+1.14
					Average = −0.008			Average = +1.28

Table VII—Comparison of Formulated Values and Solution Analyzer Values Obtained from Analysis of 19 High Soluble Solids Type Mouthwashes

Sample Code	Alcohol, % (v/v)			Percentage of Normal Soluble Solids		
	Added	Solution Analyzer (SA)	Difference (Added − SA)	Added	Solution Analyzer (SA)	Difference (Added − SA)
31F082 A	15.78	15.83	−0.05	95	92.80	+2.20
31F082 B	15.86	16.01	−0.15	105	106.13	−1.13
31F082 C	15.92	15.94	−0.02	110	112.55	−2.55
31F082 D	18.10	18.39	−0.29	90	87.64	+2.36
31F082 E	18.24	18.38	−0.14	105	105.34	−0.34
31F082 F	18.29	18.43	−0.14	110	110.46	−0.46
31F082 G	20.51	20.76	−0.25	95	95.49	−0.49
31F082 H	20.45	20.63	−0.18	90	90.61	−0.61
31F082 I	20.62	20.80	−0.18	105	105.11	−0.11
31F082 J	22.83	22.98	−0.15	95	96.24	−1.24
31F082 K	22.79	22.82	−0.03	90	91.91	−1.91
31F082 L	23.01	23.32	−0.31	110	106.64	+3.36
30F129 B[a]	19.78	19.28	+0.50	100	100.09	−0.09
30F146 B	15.83	15.61	+0.22	100	99.63	+0.37
30F146 C	17.04	16.82	+0.22	100	100.00	0.00
30F146 D	18.22	18.09	+0.13	100	99.44	+0.56
30F146 E	20.56	20.44	+0.12	100	99.91	+0.09
30F146 F[a]	21.74	21.39	+0.35	100	99.91	+0.09
30F146 G[a]	22.92	22.56	+0.36	100	100.33	−0.33
		Mean difference = +0.0005			Mean difference = −0.012	
		Range of differences = +0.50–−0.31			Range of differences = +3.36–−2.55	
		Standard deviation of differences = ±0.239			Standard deviation of differences = ±1.42	

[a] Sample bottles with loose or cracked caps as received for ultrasonic solution analysis (likely alcohol loss).

four production samples of this type of mouthwash of "unknown" composition were selected. Each sample was analyzed, without prior knowledge of its composition, in ultrasonic solution analyzers operating at 20 and 65°.

The simultaneous equations using measured Δf values were solved with a digital computer. All calculations and references to soluble solids were expressed as a percentage of normal. Normal soluble solids was considered to be 100%. Thus, ±5% of normal was expressed as 105 and 95%, respectively. A detailed summary of Δf values and the percentage of alcohol and percentage of soluble solids calculated from the previously derived equations is presented in Table V.

Although results were slightly less accurate than those obtained on the 37 standard samples actually used for the derivation of the regression equations, they were still very good. An error in preparation probably accounts for the larger deviation in alcohol content of Sample E4.

Results of the four "unknown" production samples are presented in Table VI. The composition of these four samples was determined only after analysis by the solution analyzer was completed. The average differences were 0.05% alcohol and 1.28 percentage of normal soluble solids. These results represented good confirmation of the equations and the procedure.

Applicability of Method to Other Types of Mouthwash—To determine whether the methods and principles developed for mouthwash of a moderate soluble solids level could be applied more generally, samples simulating high and low soluble solids types were prepared and analyzed in the latest model of the ultrasonic solution analyzer[2]. Nineteen samples of high soluble solids types covering the ranges of 15.78–23.01% (v/v) (13.0–19.0% w/v) alcohol and 19.37, 21.52, and 23.67% soluble solids and seven samples of low soluble solids type covering the ranges of 27.27–33.87% (v/v) (24–30% w/v) alcohol and 2.62% soluble solids were analyzed at 20 and 65°. The newer model ultrasonic solution analyzer contains a computer module that is programmed to give a direct readout of the percentage of alcohol and soluble solids on the display panel.

Regression equations were developed for the percent of alcohol and percentage of normal soluble solids from the data at 20 and 65° for the high soluble solids type and for the percent of alcohol only with the low soluble solids type since the soluble solids content of this type had not been varied. Results are presented in Tables VII and VIII.

The standard deviation of differences for alcohol content between formulated values and ultrasonic solution analyzer values was slightly larger than that found with the larger population of moderate soluble solids mouthwash samples but was well within acceptable limits. Larger deviations might be expected, because the composition of samples in these series may have varied more widely from theoretical formulation values since much smaller samples were prepared. Also, some sample bottles exhibited cracked or loose caps after shipment for ultrasonic solution analysis. Again, specific gravity determinations to convert alcohol content from weight per volume to volume per volume were made several months later. Ultrasonic solution analysis offered an opportunity for alcohol evaporation in some samples.

[2] Model 2200, Gould, Inc., Chesapeake Instrument Division, Shadyside, Md.

DISCUSSION

Across the entire group from low to high soluble solids types of mouthwash, there was an overall range of 18% (v/v) alcohol and about 21% soluble solids absolute. Despite these wide ranges in composition and the very different constituents comprising the soluble solids portion in each type, it was possible to determine gross composition of any sample with acceptable accuracy.

When the soluble solids content was expressed as a percentage of normal, of course, each of the three types of mouthwash had to be treated separately since each had a different normal content. Within each type, accuracy was good; greater confidence with the general method could be achieved through an enlarged testing program in the high and low soluble solids types. Apparently, all three types can be tested utilizing a separate pair of simultaneous equations for each type. The possibility exists that other types of mouthwash may not conform to the acoustic properties

Table VIII—Comparison of Formulated Values and Solution Analyzer Values for Alcohol Content Obtained from Analysis of Seven Low Soluble Solids Mouthwash Samples at 20 and 65°

Sample Code	Alcohol, % (v/v)		
	Added	Solution Analyzer (SA)	Difference (Added − SA)
		20°	
31F144 A	30.70	30.62	+0.08
31F144 B	27.37	27.51	−0.14
31F144 C	28.53	28.13	+0.40
31F144 D	29.63	30.11	−0.48
31F144 E	31.73	31.40	+0.33
31F144 F	32.77	32.90	−0.13
31F144 G	33.87	33.88	−0.01
		Mean difference = +0.0071	
		Range of differences, = +0.40–−0.48	
		Standard deviation of differences = s = ±0.30%	
		65°	
31F144 A	30.70	30.65	+0.05
31F144 B	27.37	27.59	−0.22
31F144 C	28.53	28.08	+0.45
31F144 D	29.63	29.87	−0.24
31F144 E	31.73	31.71	+0.02
31F144 F	32.77	32.86	−0.09
31F144 G	33.87	33.82	+0.05
		Mean difference = +0.0029	
		Range of differences = +0.45–−0.24	
		Standard deviation of differences = s = ±0.23%	

found here. Nonetheless, the ultrasonic solution analyzer method offers great promise as a single, rapid, and accurate control procedure for determining the alcohol and soluble solids content of mouthwashes.

A distinct advantage over conventional methods of analysis is the test's simplicity. No alcohol distillation is necessary; in a one-step procedure, with the latest models of the instrument, values for two parameters are available within 5 min on a direct readout display.

REFERENCES

(1) "The United States Pharmacopeia," 19th rev., Mack Publishing Co., Easton, Pa., 1975, pp. 633, 634.

(2) "Methods of Analysis of the Association of Official Analytical Chemists," 12th ed., Association of Official Analytical Chemists, Washington, D.C., 1975, p. 194, Method 11.003.

(3) *Ibid.*, p. 194, Methods 11.006–11.009.

(4) W. C. Winder, D. J. Aulik, and A. C. Rice, *Am. J. Enol. Vitic.*, **21** (1970).

(5) V. F. Nozdrev, "Application of Ultrasonics in Molecular Physics," Gordon & Breach, New York, N.Y., 1963, pp. 475–477.

ACKNOWLEDGMENTS

Published with the approval of the Wisconsin Agricultural Experiment Station.

Supported in part by grants from Chesapeake Instrument Corp., Shadyside, Md., and Procter & Gamble Co., Cincinnati, Ohio.

The authors acknowledge the efforts of Dr. J. J. Benedict of Procter & Gamble Co. in getting Professor Winder and Dr. Lohman together on this development and for his encouragement and interest.

In Vitro Evaluation of Three Commercial Sustained-Release Papaverine Hydrochloride Products

ROBERT J. TIMKO and NICHOLAS G. LORDI ×

Received June 2, 1977, from the *College of Pharmacy, Rutgers—The State University, Busch Campus, Piscataway, NJ 08854.* Accepted for publication July 26, 1977.

Abstract □ Three commercial sustained-release papaverine hydrochloride products in the form of microencapsulated pellets were evaluated. Three different dissolution apparatuses were used: a continuous flow apparatus, the USP rotating basket apparatus, and a modified reciprocating basket apparatus. The frequency rate of the reciprocating basket apparatus could be varied from 0 to 32 strokes/min. Salicylic acid compacts were used as a standard to characterize each apparatus. A linear log–log correlation between dissolution rate and apparatus speed or flow rate was obtained. Release of papaverine hydrochloride from the commercial preparations was affected significantly by the pH of the dissolution media but not by the agitation intensity.

Keyphrases □ Papaverine hydrochloride—dissolution, three commercial sustained-release products, three different apparatuses compared □ Dissolution—papaverine hydrochloride, three commercial sustained-release products, three different apparatuses compared □ Apparatus, dissolution—three types compared, papaverine hydrochloride, three commercial sustained-release products □ Relaxants, smooth muscle—papaverine hydrochloride, dissolution, three commercial sustained-release products, three different apparatuses compared

In recent years, the study of dissolution of drugs from solid dosage forms has become increasingly important. The rate and extent of dissolution from tablets, capsules, and pellets affect both the absorption and therapeutic effect of a drug. Different formulations of the same drug may exhibit different absorption characteristics and, subsequently, different therapeutic activity (1).

Although it is agreed that dissolution testing is important, there is disagreement as to the apparatus and method that should be used as a standard. A simple inexpensive apparatus and method that could be used for most products would be ideal. Such a development is a difficult task, however, because of the numerous factors influencing dissolution testing. Some of these factors are related to the product, such as the physical–chemical properties of the drug and variations in formulation; others, such as the amount and type of solvent and the geometry of the container, are unrelated to the product.

The objective of this study was to evaluate the *in vitro* release characteristics of sustained-release papaverine hydrochloride pellets, produced by various manufacturers, under a variety of conditions. This evaluation was made in three different dissolution apparatuses using a nondisintegrating compact as a standard.

EXPERIMENTAL

Materials—Standard nondisintegrating disks have been used (2, 3) as a means of comparing different dissolution apparatuses. In this study, salicylic acid compacts were chosen as the standard and were used to characterize each apparatus under varying experimental conditions.

About 350 mg of salicylic acid powder[1] was compressed at 1860 kg, using a hydraulic press[2] with a motorized attachment operated at 1.0 cm/sec. Standard 0.95-cm concave punches were employed, and the die was held in place with an acrylic[3] mold. The compacts had an initial average weight of 345 mg with an average thickness and diameter of 0.465 and 0.961 cm, respectively.

The sustained-release papaverine products, A–C[4], were encapsulated pellets containing 150 mg of papaverine hydrochloride/capsule.

Test Fluids—Gastric fluid was prepared according to the method described in USP XIX without the addition of enzyme.

The other test fluids, pH 4.50, 6.00, and 7.00, contained 6.8 g of monobasic potassium phosphate/liter. The monobasic potassium phosphate was dissolved in about 950 ml of water, the pH was adjusted to the desired value with 36.5% (w/w) HCl or 5% (w/v) NaOH, and the volume was brought to 1 liter.

Assay Method—Beer's law curves were constructed for papaverine hydrochloride and salicylic acid. The maximum wavelengths for the two test materials are: salicylic acid in gastric fluid, λ = 302 nm; papaverine hydrochloride in gastric fluid, λ = 309 nm; papaverine hydrochloride in pH 4.50 fluid, λ = 309 nm; papaverine hydrochloride in pH 6.00 fluid, λ = 310 nm; and papaverine hydrochloride in pH 7.00 fluid, λ = 325 nm.

In most cases, these wavelengths allowed direct absorbance readings under experimental conditions. Linearity was followed in the concentration ranges used.

Dissolution Methods—Each of the three dissolution methods affected

[1] Reagent grade, J. T. Baker Chemical Co., Clifton, N.J.

[2] Model C, Fred S. Carver, Menomonee Falls, Wis.

[3] Lucite.

[4] Product A was lot 3H518, Vitarine Co.; Product B was Pavabid lot 12023, Marion Laboratories; and Product C was Cerespan lot 55282, USV Pharmaceutical Corp.

found here. Nonetheless, the ultrasonic solution analyzer method offers great promise as a single, rapid, and accurate control procedure for determining the alcohol and soluble solids content of mouthwashes.

A distinct advantage over conventional methods of analysis is the test's simplicity. No alcohol distillation is necessary; in a one-step procedure, with the latest models of the instrument, values for two parameters are available within 5 min on a direct readout display.

REFERENCES

(1) "The United States Pharmacopeia," 19th rev., Mack Publishing Co., Easton, Pa., 1975, pp. 633, 634.

(2) "Methods of Analysis of the Association of Official Analytical Chemists," 12th ed., Association of Official Analytical Chemists, Washington, D.C., 1975, p. 194, Method 11.003.

(3) *Ibid.*, p. 194, Methods 11.006–11.009.

(4) W. C. Winder, D. J. Aulik, and A. C. Rice, *Am. J. Enol. Vitic.*, **21** (1970).

(5) V. F. Nozdrev, "Application of Ultrasonics in Molecular Physics," Gordon & Breach, New York, N.Y., 1963, pp. 475–477.

ACKNOWLEDGMENTS

Published with the approval of the Wisconsin Agricultural Experiment Station.

Supported in part by grants from Chesapeake Instrument Corp., Shadyside, Md., and Procter & Gamble Co., Cincinnati, Ohio.

The authors acknowledge the efforts of Dr. J. J. Benedict of Procter & Gamble Co. in getting Professor Winder and Dr. Lohman together on this development and for his encouragement and interest.

In Vitro Evaluation of Three Commercial Sustained-Release Papaverine Hydrochloride Products

ROBERT J. TIMKO and NICHOLAS G. LORDI ×

Received June 2, 1977, from the *College of Pharmacy, Rutgers—The State University, Busch Campus, Piscataway, NJ 08854.* Accepted for publication July 26, 1977.

Abstract □ Three commercial sustained-release papaverine hydrochloride products in the form of microencapsulated pellets were evaluated. Three different dissolution apparatuses were used: a continuous flow apparatus, the USP rotating basket apparatus, and a modified reciprocating basket apparatus. The frequency rate of the reciprocating basket apparatus could be varied from 0 to 32 strokes/min. Salicylic acid compacts were used as a standard to characterize each apparatus. A linear log–log correlation between dissolution rate and apparatus speed or flow rate was obtained. Release of papaverine hydrochloride from the commercial preparations was affected significantly by the pH of the dissolution media but not by the agitation intensity.

Keyphrases □ Papaverine hydrochloride—dissolution, three commercial sustained-release products, three different apparatuses compared □ Dissolution—papaverine hydrochloride, three commercial sustained-release products, three different apparatuses compared □ Apparatus, dissolution—three types compared, papaverine hydrochloride, three commercial sustained-release products □ Relaxants, smooth muscle—papaverine hydrochloride, dissolution, three commercial sustained-release products, three different apparatuses compared

In recent years, the study of dissolution of drugs from solid dosage forms has become increasingly important. The rate and extent of dissolution from tablets, capsules, and pellets affect both the absorption and therapeutic effect of a drug. Different formulations of the same drug may exhibit different absorption characteristics and, subsequently, different therapeutic activity (1).

Although it is agreed that dissolution testing is important, there is disagreement as to the apparatus and method that should be used as a standard. A simple inexpensive apparatus and method that could be used for most products would be ideal. Such a development is a difficult task, however, because of the numerous factors influencing dissolution testing. Some of these factors are related to the product, such as the physical–chemical properties of the drug and variations in formulation; others, such as the amount and type of solvent and the geometry of the container, are unrelated to the product.

The objective of this study was to evaluate the *in vitro* release characteristics of sustained-release papaverine hydrochloride pellets, produced by various manufacturers, under a variety of conditions. This evaluation was made in three different dissolution apparatuses using a nondisintegrating compact as a standard.

EXPERIMENTAL

Materials—Standard nondisintegrating disks have been used (2, 3) as a means of comparing different dissolution apparatuses. In this study, salicylic acid compacts were chosen as the standard and were used to characterize each apparatus under varying experimental conditions.

About 350 mg of salicylic acid powder[1] was compressed at 1860 kg, using a hydraulic press[2] with a motorized attachment operated at 1.0 cm/sec. Standard 0.95-cm concave punches were employed, and the die was held in place with an acrylic[3] mold. The compacts had an initial average weight of 345 mg with an average thickness and diameter of 0.465 and 0.961 cm, respectively.

The sustained-release papaverine products, A–C[4], were encapsulated pellets containing 150 mg of papaverine hydrochloride/capsule.

Test Fluids—Gastric fluid was prepared according to the method described in USP XIX without the addition of enzyme.

The other test fluids, pH 4.50, 6.00, and 7.00, contained 6.8 g of monobasic potassium phosphate/liter. The monobasic potassium phosphate was dissolved in about 950 ml of water, the pH was adjusted to the desired value with 36.5% (w/w) HCl or 5% (w/v) NaOH, and the volume was brought to 1 liter.

Assay Method—Beer's law curves were constructed for papaverine hydrochloride and salicylic acid. The maximum wavelengths for the two test materials are: salicylic acid in gastric fluid, λ = 302 nm; papaverine hydrochloride in gastric fluid, λ = 309 nm; papaverine hydrochloride in pH 4.50 fluid, λ = 309 nm; papaverine hydrochloride in pH 6.00 fluid, λ = 310 nm; and papaverine hydrochloride in pH 7.00 fluid, λ = 325 nm.

In most cases, these wavelengths allowed direct absorbance readings under experimental conditions. Linearity was followed in the concentration ranges used.

Dissolution Methods—Each of the three dissolution methods affected

[1] Reagent grade, J. T. Baker Chemical Co., Clifton, N.J.

[2] Model C, Fred S. Carver, Menomonee Falls, Wis.

[3] Lucite.

[4] Product A was lot 3H518, Vitarine Co.; Product B was Pavabid lot 12023, Marion Laboratories; and Product C was Cerespan lot 55282, USV Pharmaceutical Corp.

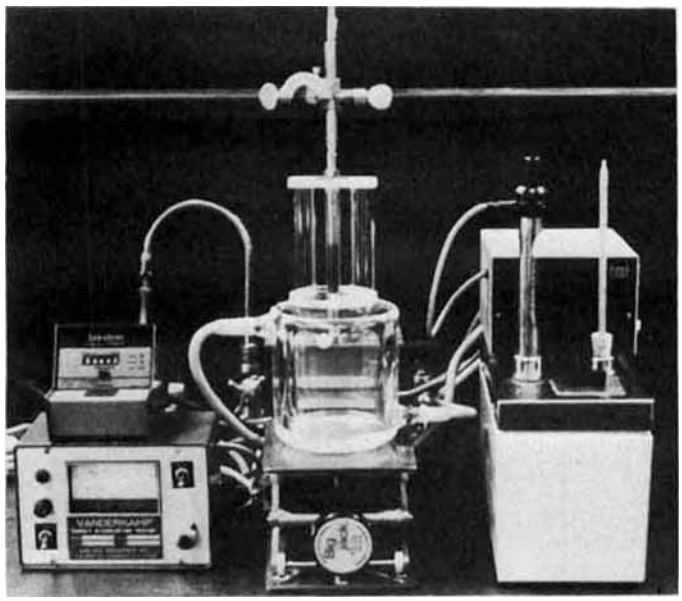

Figure 1—*Reciprocating basket apparatus.*

dissolution by a different mode of agitation. The continuous flow system utilized a flowing stream of liquid, which bathed the dosage form and caused the dissolved drug to be carried away in the effluent. The rotating basket apparatus caused agitation by the rotation of the basket containing the test material. Agitation in a vertical reciprocating apparatus was accomplished by the up and down movement of the basket rack assembly. Liquid moved into the tubes past the dosage form resting on the screen during the down stroke and then back into the bulk solution on the up stroke.

The continuous flow system was similar in design to the apparatus described by Tingstad *et al.* (2). The dissolution medium reservoir consisted of a 1-liter jacketed beaker maintained at 37.5 ± 0.5° by a constant-temperature regulator. The solid-state, variable-speed, peristaltic tubing pump[5] had a pump head[6] capable of delivering a maximum of 125 ml/min.

Effluent from the dissolution chamber was either routed with the aid of flexible tubing[7] through a spectrophotometer[8] adapted with a flow cell or collected as fractions. In some experiments, the recorder output of the spectrophotometer, which represents the derivative of the cumulative dissolution curve, was input into an analog computer[9]. The computer integrated the signal and, with a recorder[10], printed cumulative amount *versus* time.

A constant voltage source[11] was used to input an electrical signal of opposite sign and sufficient magnitude into the analog computer to reduce the electrical noise of the system's components to minimal levels. This step reduced the maximum error that might have resulted from the integration of an extraneous signal with the spectrophotometer output to about 1% over 100 min.

When the continuous flow system was operated with the analog attachment, the voltage output of the spectrophotometer was related to the cumulative amount of drug released in milligrams, C, from the dosage form as follows:

$$C = \frac{F}{KS}\int_0^t M\,dt = \frac{F}{KS}Mt \qquad \text{(Eq. 1)}$$

where F is the flow rate (milliliters per second), K is the absorptivity (milliliters per milligram), M is the millivolt output of the system, t is the time (seconds), and S is the millivolts per absorbance unit for the system. For this system, S = 33.33 mv/absorbance unit. The integrator time constant was 100 sec.

When the analog attachment was not used, effluent from the dissolution cell was collected as fractions and assayed individually because high absorbance values prevented direct readings. Fractions were collected at 2-min intervals for the first 10 min and at 5-min intervals for the next 20 min. Thereafter, effluent was collected in a large cumulating reservoir. A 2-ml aliquot was removed every 15 min for assay for the remainder of the test. As required, either a 1:5 or a 1:10 dilution was made to obtain absorbance readings.

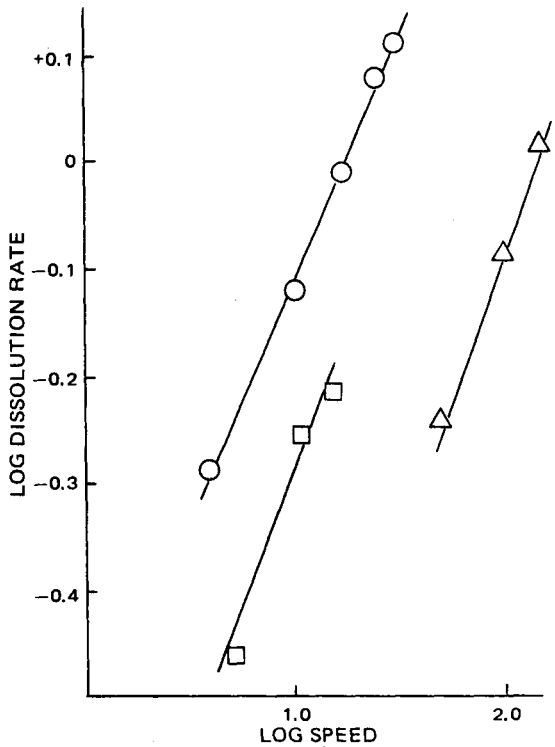

Figure 2—*Correlation of the dissolution rate of the salicylic acid compacts in gastric fluid with apparatus speed or flow rate. Key:* □, *continuous flow system;* ○, *reciprocating basket apparatus; and* △, *rotating basket apparatus.*

A variation in the general apparatus was made while studying the effect of varying pH on a single dosage form. A second jacketed beaker was placed in series with the first and also was maintained at 37.5°; this arrangement allowed for the switching of pH fluids (using additional tubing and a valve) without interrupting solvent flow. This experiment employed three test fluids in the following order: gastric fluid for 60 min, pH 4.50 fluid for 30 min, and pH 7.00 fluid for 60 min. Fractions were collected at 10-min intervals when the pH 4.50 and 7.00 fluids were used.

In the operation of the continuous flow system, the spectrophotometer was set at the desired wavelength, and the pump speed was adjusted to provide the fluid flow rate required. The system was allowed to equilibrate for at least 15 min before use. The recorder was adjusted to zero, and the spectrophotometer was nulled. The electrical noise of the system input to the analog integrator was adjusted with the aid of a constant voltage source to a minimal level so that it would not interfere with the spectrophotometer signal. The pump was then stopped.

The dissolution cell was then removed from the system, disassembled, and dried. The dosage form was placed on the lower support screen, and the cell was reassembled and put back in place. At time zero, the pump was restarted, and the amount of drug released was measured. Effluent was collected in a cumulating reservoir. The final volume of liquid was measured to obtain the average flow rate during the experiment.

The reciprocating basket apparatus (Fig. 1) consisted of a basket rack assembly, a 1-liter jacketed beaker attached to a temperature-regulating device maintained at 37.5 ± 0.5°, and a device[12] for raising and lowering the basket in the dissolution fluid at a constant frequency rate through a stroke distance of 5.5 ± 0.5 cm. The frequency rate of this device could be varied from 0 to 32 strokes/min, depending on the conditions desired.

The specially designed basket rack assembly consisted of two open-end glass tubes, 12 cm long × 21.5 mm i.d., with a wall 2 mm thick. The tubes

[5] Model 7555, Cole-Parmer Instrument Co., Chicago, Ill.
[6] Model 7014-20, Cole-Parmer Instrument Co., Chicago, Ill.
[7] Catalog No. 13-9110-5, Ace Scientific Supply Co., Linden, N.J.
[8] Model 222, Gilford Instrument Laboratories, Oberlin, Ohio.
[9] Model TR-20, Electronic Associates, West Long Branch, N.J.
[10] Mosley model H01-680, Hewlett-Packard, Downers Grove, Ill.
[11] Model EU-80A, Heathkit Corp., Fair Lawn, N.J.
[12] Model 74D-442-6, Van-Kel Industries, Inc., Chatham, N.J.

Table I—Values of a and b in $R = aS^b$ for the Various Dissolution Apparatuses

Method	a	b
Continuous flow system	0.15	0.54
Reciprocating basket apparatus	0.26	0.48
Rotating basket apparatus	0.067	0.55

were held in the vertical position by two plastic plates. The lower plate was 9 cm in diameter and 8 mm thick with two holes 24 mm in diameter equidistant from the center plate and equally spaced from each other. The upper plate was rectangular with convex sides. It measured 9 cm in length at its widest point and 7.2 cm at the edges, and it was 4.8 cm wide and 8 mm thick with two holes equidistant from the center identical in size to those in the bottom plate. It was held in place by a collar and set screw, which could be easily loosened to remove the glass tubes or screens when necessary.

The central shaft was 14.2 cm in length and 9 mm in diameter. It was attached to the bottom plate with a screw. The upper end could easily be attached to a shank if an extension was required. Two individual screens fit into the bottom plate below the tubes. Forty-mesh stainless steel screens were used.

When the vertical reciprocating apparatus was used, exactly 900.0 ml of test fluid was placed in the dissolution vessel and allowed to equilibrate at 37.5 ± 0.5°. One dosage form was placed in each of the two tubes of the basket. The basket assembly was immersed in the test medium so that it descended to 1 ± 0.1 cm from the bottom of the vessel on the downward stroke. The stroke rate was adjusted to the desired speed, and the test was begun.

Three milliliters of fluid was removed for assay at 15-min intervals for the length of the test. The removed fluid was immediately replaced with fresh liquid to maintain a constant volume. The aliquots were assayed spectrophotometrically at the wavelength required for the test fluid and compound. When necessary, dilutions were prepared. All aliquots were filtered through membrane filters[13] before assay.

The rotating basket apparatus met the requirements described in the official compendia (4, 5). The basket rotation rate was maintained at the desired revolutions per minute by a motor fitted with a speed-regulating device[5]. The entire assembly was immersed in a suitable water bath maintained at 37.5 ± 0.5°. The method of operation was as described in USP XIX. Three milliliters of fluid was removed from the dissolution vessel at 15-min intervals for assay. The removed fluid was immediately replaced with fresh fluid. The samples were assayed in the same manner as described for the reciprocating basket apparatus.

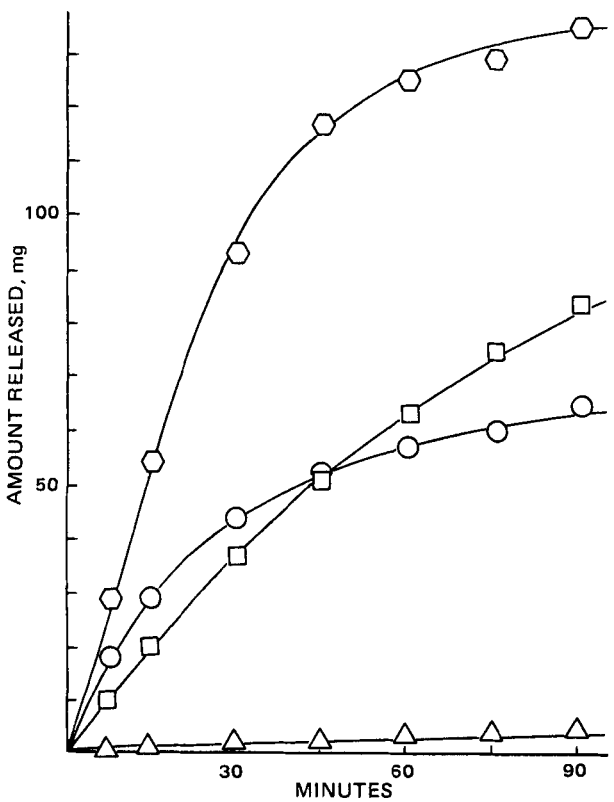

Figure 3—*Release curves for papaverine hydrochloride from Product A in the continuous flow system. Key: □, gastric fluid, flow rate = 10.1 ml/min; ○, pH 4.50 fluid, flow rate = 10.1 ml/min; ○, pH 6.00 fluid, flow rate = 10.3 ml/min; and △, pH 7.00 fluid, flow rate = 10.1 ml/min.*

[13] Catalog No. HAWP01300, Millipore Corp., Bedford, Mass.

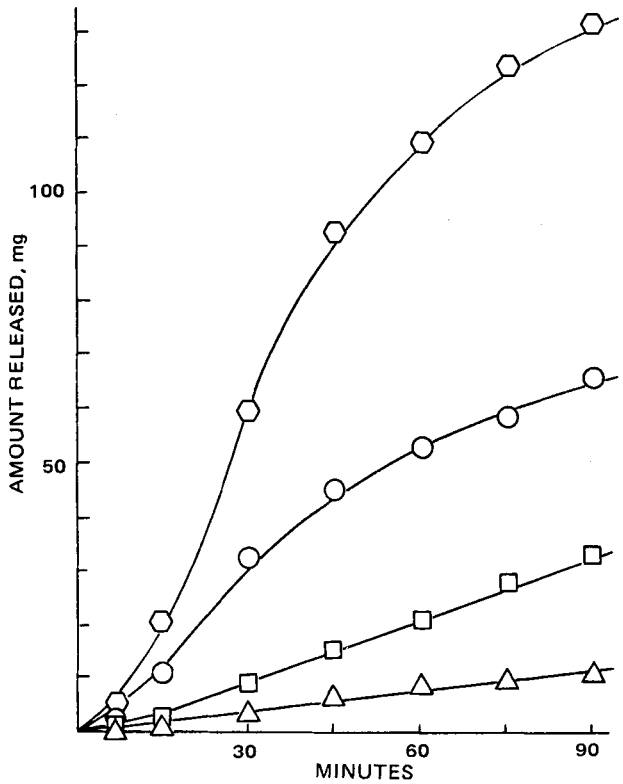

Figure 4—*Release curves for papaverine hydrochloride from Product B in the continuous flow system. Key: □, gastric fluid, flow rate = 10.0 ml/min; ○, pH 4.50 fluid, flow rate = 10.0 ml/min; ○, pH 6.00 fluid, flow rate = 10.4 ml/min; and △, pH 7.00 fluid, flow rate = 10.2 ml/min.*

The sustained-release papaverine hydrochloride pellets were removed from the capsule before placement in the various dissolution apparatuses. The emphasis was on the characterization of the drug release rate from the pellets. Any effect the gelatin capsules might have on the release rate was not considered.

Determinations involving salicylic acid were made in duplicate. Those involving the papaverine hydrochloride preparations were done in triplicate.

Solubility Determinations—The solubility of papaverine hydrochloride was determined in 0.1–1.0 N HCl, the test fluids, and fluids of varying pH obtained by mixing different proportions of gastric fluid USP and intestinal fluid USP, both without enzyme. Excess papaverine hydrochloride was placed in a 50-ml glass-stoppered flask together with 25.0 ml of fluid. The sample was shaken mechanically in a water bath maintained at 25.0 ± 0.5° and allowed to equilibrate. After equilibrium, an aliquot was removed and filtered. It was diluted as required with 0.2 N HCl; the concentration was determined spectrophotometrically at λ 309 nm.

RESULTS AND DISCUSSION

Characterization of Dissolution Methods—Dissolution is affected by many variables such as the degree of agitation, which becomes extremely important when comparing different apparatuses. Some investigations (6, 7) involving agitation led to the empirical relationship:

$$R = aS^b \qquad \text{(Eq. 2)}$$

where R is the dissolution rate (milligrams per minute), S is the apparatus speed (strokes per minute or revolutions per minute) or flow rate (milliliters per minute), and a and b are constants.

The salicylic acid compacts exhibited zero-order dissolution rates in gastric fluid in the different apparatuses. As the flow rate or apparatus speed was increased, the dissolution rate of the compacts increased.

Table II—Comparison of Sustained-Release Pellets in the Different Apparatuses

Product	Amount Released after 60 min in Gastric Fluid, mg		
	Continuous Flow System[a]	Reciprocating Basket[b]	Rotating Basket[c]
A	63.5 ± 4.8[d]	90.8 ± 7.8	76.2 ± 6.0
B	20.6 ± 0.8	43.0 ± 1.1	41.9 ± 2.1
C	32.8 ± 2.5	55.7 ± 0.7	53.2 ± 2.9

[a] Average flow rate = 10.0 ml/min. [b] Four strokes per minute. [c] At 50 rpm. [d] Mean ± *SD*.

When the dissolution rates of the compacts were plotted *versus* the flow rate or apparatus speed for the methods, using the logarithmic transformation of Eq. 2, a linear correlation was obtained (Fig. 2). The values of a and b, determined from the intercept and slope, respectively, are shown in Table I.

The constant a in Eq. 2 appears to be related to the velocity of the fluid flowing past the compact. For the continuous flow system, it has the dimensions of $mg/min^{(b-1)}ml^b$. In the reciprocating basket apparatus and the rotating basket apparatus, the solvent flow rate past the compact is determined by the basket stroke rate and basket rotation rate, respectively. Thus, in these instances, the value determined for a is proportional to that observed for the continuous flow system.

The value of the constant b depends on a number of factors including the processes controlling dissolution, the type of agitation, and the substance being studied. Cooper and Kingery (6) calculated a value for b of 0.5 in a diffusion-controlled process. The values determined for b in the different apparatuses are in good agreement with this theoretical value. They are also similar to the value of $b = 0.49$ reported for salicylic acid at pH 1.0 (7) and to the value of $b = 0.537$ reported for salicylic acid in various pH fluids (8).

Measurement of the dimensions of the salicylic acid compacts before and after each experimental run indicated that dissolution in the reciprocating basket and rotating basket apparatuses occurred over the whole compact surface since both its diameter and thickness decreased to the same extent. Fluid was constantly moved across all compact surfaces as a result of the varied solvent flow in both apparatuses. Dissolution in the continuous flow system, however, occurred predominantly from the side of the compact. The diameter of the compact decreased while the thickness remained essentially unchanged. Fluid flowed past the compact in a continuous stream, mainly in contact with only one surface.

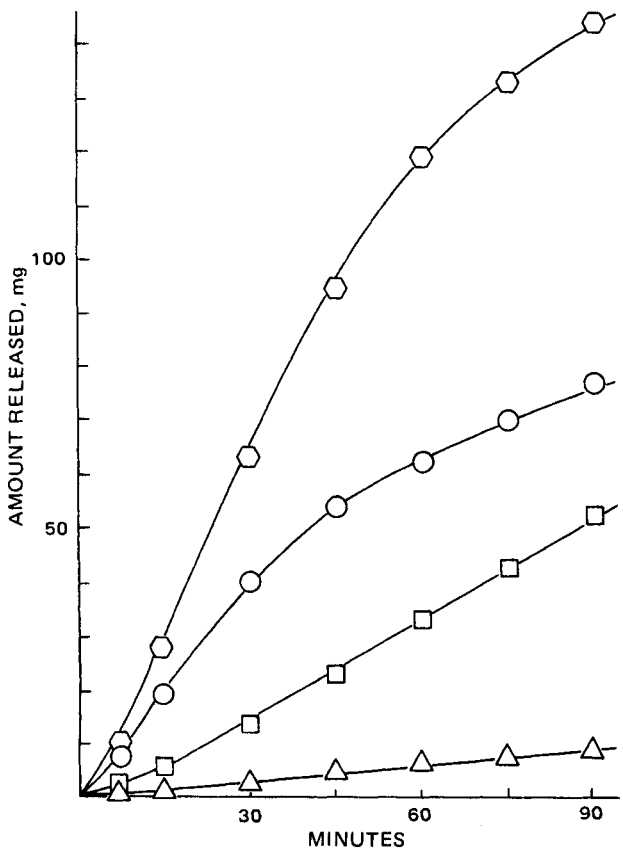

Figure 5—*Release curves for papaverine hydrochloride from Product C in the continuous flow system. Key: □, gastric fluid, flow rate = 10.0 ml/min; ○, pH 4.50 fluid, flow rate = 10.0 ml/min; ○, pH 6.00 fluid, flow rate = 10.2 ml/min; and △, pH 7.00 fluid, flow rate = 10.2 ml/min.*

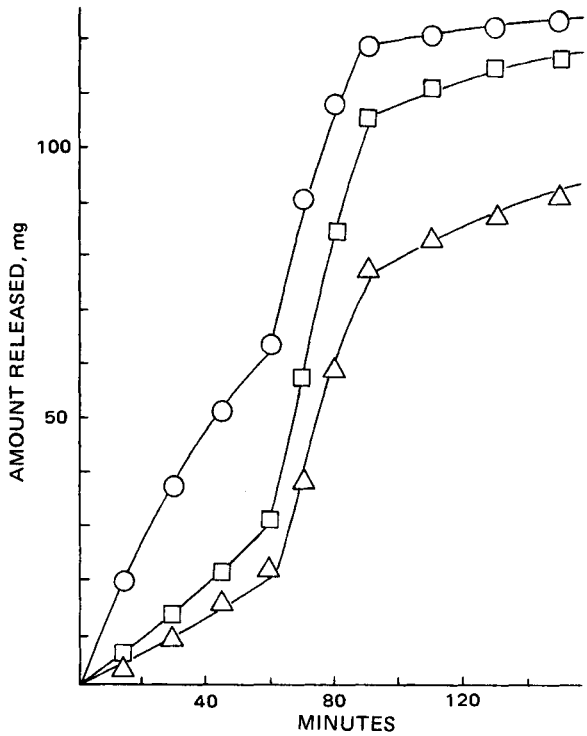

Figure 6—*Release curves for papaverine hydrochloride from the commercial sustained-release products in gastric fluid (60 min), pH 4.50 fluid (30 min), and pH 7.00 fluid (60 min) in the continuous flow system. Key: ○, Product A, flow rate = 10.3 ml/min; △, Product B, flow rate = 10.2 ml/min; and □, Product C, flow rate = 10.1 ml/min.*

Evaluation of Sustained-Release Papaverine Hydrochloride Products—Product A was used to study the effect of variations in agitation intensity on the *in vitro* drug release rate from the pellets. Experiments were conducted in the various dissolution apparatuses with gastric fluid as the test medium. No significant differences in the release rates from the pellets were seen when the apparatus speed or flow rate was varied. However, there was a slight upward trend with increasing agitation in the rotating basket apparatus and the continuous flow system. Preliminary investigations with Products B and C showed similar results.

The amount of papaverine released from the pellets varied among the apparatuses, but the rank order of the products remained unchanged (Table II). Gastric fluid was used as the test medium. An agitation intensity equivalent to a dissolution rate of salicylic acid of about 0.5 mg/min was used in each apparatus.

The effect of the pH of the test medium on the release rate of papaverine hydrochloride from the pellets was studied using the continuous flow system. The flow rate was maintained at 10.2 ● 0.2 ml/min. The effect of a single pH on the release rate was evaluated first (Figs. 3–5).

The sustained-release pellets had varied release rates in gastric fluid. Product A showed a release rate that was linear when the total amount released was plotted *versus* the square root of time. It appeared to follow the theoretical relationship proposed for solid drugs dispersed in solid matrixes (9). Products B and C, after an initial lag period, exhibited pseudo-zero-order release rates since the total amount of papaverine hydrochloride released increased linearly with time.

Release of papaverine hydrochloride from the pellets was greatest in pH 4.50 fluid and least in pH 7.00 fluid. The greatest difference among the products was in gastric fluid. The difference in the amount of papaverine released from the products in the various fluids was a result of both the pH-dependent solubility characteristics of the drug in the test media and the release characteristics of the pellets.

The effect of varying the pH of the test media on a single dosage form was also evaluated (Fig. 6). The release rate for each product showed pH

Table III—Solubility of Papaverine Hydrochloride at 25°

Fluid	Concentration, mg/ml
1.0 *N* HCl	1.5
0.50 *N* HCl	2.7
0.25 *N* HCl	4.6
0.10 *N* HCl	12.4
Gastric	10.6
pH 2.45[a]	22.8
pH 3.10[a]	23.1
pH 4.50[b]	30.0
pH 6.70[a]	<0.1
Intestinal	<0.1

[a] Mixture of gastric and intestinal fluids. [b] Test fluid.

dependency and apparently confirms the results of the first part of the experiment. The difference in the total amount of papaverine released between Products A and B was largely a result of the difference in the amount released in gastric fluid. Product C showed a greater release in pH 4.50 fluid.

The pKa of papaverine is 6.4 (10). However, the solubility of papaverine reaches a maximum about pH 4.5 and then decreases (Table III). The data indicate a significant common ion effect owing to the addition of excess chloride, which significantly reduces the dissociation of the hydrochloride salt, reducing its solubility.

CONCLUSIONS

The reciprocating basket apparatus with variable speed control has a wide range of usefulness. The stroke rate can be varied to obtain agitation intensities equivalent to those observed in both the continuous flow system and the rotating basket apparatus. Based on the results of this study, this apparatus appears to be suitable for evaluating the dissolution of nondisintegrating dosage forms. It fulfills the requirements recognized as necessary for an *in vitro* test. There is a controlled fluid flow rate past the dosage form. The agitation intensity can be varied as required, and the apparatus can be easily automated. The basket rack assembly has a modified top plate to provide sufficient room for sampling and replacement tubing.

The commercial sustained-release papaverine products had varied release rates in the test methods and pH fluids. Although no correlations with *in vivo* data were made, a general statement concerning these preparations is possible. It appears that the residence time of the pellets in the stomach and in the transition pH between the stomach and the intestines determines the amount of papaverine available for absorption. Little additional papaverine would be released from the pellets in the intestines because of its low solubility in this basic environment. Therefore, it may be possible to obtain an equivalent therapeutic effect from a standard dosage form of papaverine hydrochloride. Data reported (11) in a recent monograph on sustained-release papaverine hydrochloride are in agreement.

REFERENCES

(1) L. J. Leeson and J. T. Carstensen, "Dissolution Technology," Industrial Pharmaceutical Technology Section, APhA Academy of Pharmaceutical Sciences, Washington, D.C., 1974.

(2) J. E. Tingstad, E. Gropper, L. Lachman, and E. Shami, *J. Pharm. Sci.*, **62**, 293 (1973).

(3) R. J. Withey, *J. Pharm. Pharmacol.*, **23**, 573 (1971).

(4) "The United States Pharmacopeia," 19th rev., Mack Publishing Co., Easton, Pa., 1975, p. 651.

(5) "The National Formulary," 14th ed., Mack Publishing Co., Easton, Pa., 1975, pp. 892–894.

(6) A. R. Cooper and W. D. Kingery, *J. Phys. Chem.*, **66**, 665 (1962).

(7) G. Levy, *J. Pharm. Sci.*, **52**, 1039 (1963).

(8) J. H. Collett, J. A. Rees, and N. A. Dickinson, *J. Pharm. Pharmacol.*, **24**, 724 (1972).

(9) T. Higuchi, *J. Pharm. Sci.*, **52**, 1145 (1963).

(10) A. I. Briggs, *Trans. Faraday Soc.*, **50**, 80 (1954).

(11) H. B. Kostenbauder, *J. Am. Pharm. Assoc.*, **NS17**, 303 (1977).

ACKNOWLEDGMENTS

Presented at the Basic Pharmaceutics Section, APhA Academy of Pharmaceutical Sciences, New York meeting, May 1977.

Abstracted in part from a thesis submitted by R. J. Timko to the Graduate School, Rutgers University, in partial fulfillment of the Master of Science degree requirements.

The authors thank Van-Kel Industries, Chatham, N.J., for equipment.

Influence of Wax Coatings on Release Rate of Anions from Ion-Exchange Resin Beads

S. MOTYCKA and J. G. NAIRN ˣ

Received May 4, 1977, from the *Faculty of Pharmacy, University of Toronto, Toronto, Ontario, Canada M5S 1A1.* Accepted for publication July 26, 1977.

Abstract □ Ion-exchange resin beads were coated with various waxes to improve and control their release. The *in vitro* release rates of benzoate ions from the coated resin beads were then investigated using a rotating sieve basket technique. The dramatic differences in release rates observed with the different waxes can be discussed in terms of the wax to resin ratio and the solubility characteristics of the waxes. The initial release rates can be expressed in terms of a mathematical expression previously reported for the diffusion of ions in ion-exchange resins, thereby aiding in the elucidation of the effect of the waxes on release.

Keyphrases □ Waxes, various—coated on ion-exchange resin beads, effect on release of benzoate anions □ Resin beads, ion exchange—coated with various waxes, effect on release of benzoate anions □ Benzoate anions—release from ion-exchange resin beads, effect of coating with various waxes □ Release rates—benzoate anions from ion-exchange resin beads, effect of coating with various waxes

Ion-exchange resins are currently used as vehicles for preparing prolonged-release medication. Saunders and coworkers (1–3) investigated the effect of binding of drugs to ion-exchange resins and employed drug–resin complexes to prolong drug release, thereby increasing its duration of action. Abrahams and Linnell (4) indicated that drug release from the resin depends on the availability of ions within the GI tract. Subsequent papers indicated the value of employing ion-exchange resins to prolong the release of ephedrine (5) and amphetamine (6).

Table III—Solubility of Papaverine Hydrochloride at 25°

Fluid	Concentration, mg/ml
1.0 *N* HCl	1.5
0.50 *N* HCl	2.7
0.25 *N* HCl	4.6
0.10 *N* HCl	12.4
Gastric	10.6
pH 2.45[a]	22.8
pH 3.10[a]	23.1
pH 4.50[b]	30.0
pH 6.70[a]	<0.1
Intestinal	<0.1

[a] Mixture of gastric and intestinal fluids. [b] Test fluid.

dependency and apparently confirms the results of the first part of the experiment. The difference in the total amount of papaverine released between Products A and B was largely a result of the difference in the amount released in gastric fluid. Product C showed a greater release in pH 4.50 fluid.

The pKa of papaverine is 6.4 (10). However, the solubility of papaverine reaches a maximum about pH 4.5 and then decreases (Table III). The data indicate a significant common ion effect owing to the addition of excess chloride, which significantly reduces the dissociation of the hydrochloride salt, reducing its solubility.

CONCLUSIONS

The reciprocating basket apparatus with variable speed control has a wide range of usefulness. The stroke rate can be varied to obtain agitation intensities equivalent to those observed in both the continuous flow system and the rotating basket apparatus. Based on the results of this study, this apparatus appears to be suitable for evaluating the dissolution of nondisintegrating dosage forms. It fulfills the requirements recognized as necessary for an *in vitro* test. There is a controlled fluid flow rate past the dosage form. The agitation intensity can be varied as required, and the apparatus can be easily automated. The basket rack assembly has a modified top plate to provide sufficient room for sampling and replacement tubing.

The commercial sustained-release papaverine products had varied release rates in the test methods and pH fluids. Although no correlations with *in vivo* data were made, a general statement concerning these preparations is possible. It appears that the residence time of the pellets in the stomach and in the transition pH between the stomach and the intestines determines the amount of papaverine available for absorption. Little additional papaverine would be released from the pellets in the intestines because of its low solubility in this basic environment. Therefore, it may be possible to obtain an equivalent therapeutic effect from a standard dosage form of papaverine hydrochloride. Data reported (11) in a recent monograph on sustained-release papaverine hydrochloride are in agreement.

REFERENCES

(1) L. J. Leeson and J. T. Carstensen, "Dissolution Technology," Industrial Pharmaceutical Technology Section, APhA Academy of Pharmaceutical Sciences, Washington, D.C., 1974.

(2) J. E. Tingstad, E. Gropper, L. Lachman, and E. Shami, *J. Pharm. Sci.*, **62**, 293 (1973).

(3) R. J. Withey, *J. Pharm. Pharmacol.*, **23**, 573 (1971).

(4) "The United States Pharmacopeia," 19th rev., Mack Publishing Co., Easton, Pa., 1975, p. 651.

(5) "The National Formulary," 14th ed., Mack Publishing Co., Easton, Pa., 1975, pp. 892–894.

(6) A. R. Cooper and W. D. Kingery, *J. Phys. Chem.*, **66**, 665 (1962).

(7) G. Levy, *J. Pharm. Sci.*, **52**, 1039 (1963).

(8) J. H. Collett, J. A. Rees, and N. A. Dickinson, *J. Pharm. Pharmacol.*, **24**, 724 (1972).

(9) T. Higuchi, *J. Pharm. Sci.*, **52**, 1145 (1963).

(10) A. I. Briggs, *Trans. Faraday Soc.*, **50**, 80 (1954).

(11) H. B. Kostenbauder, *J. Am. Pharm. Assoc.*, **NS17**, 303 (1977).

ACKNOWLEDGMENTS

Presented at the Basic Pharmaceutics Section, APhA Academy of Pharmaceutical Sciences, New York meeting, May 1977.

Abstracted in part from a thesis submitted by R. J. Timko to the Graduate School, Rutgers University, in partial fulfillment of the Master of Science degree requirements.

The authors thank Van-Kel Industries, Chatham, N.J., for equipment.

Influence of Wax Coatings on Release Rate of Anions from Ion-Exchange Resin Beads

S. MOTYCKA and J. G. NAIRN ˣ

Received May 4, 1977, from the *Faculty of Pharmacy, University of Toronto, Toronto, Ontario, Canada M5S 1A1.* Accepted for publication July 26, 1977.

Abstract □ Ion-exchange resin beads were coated with various waxes to improve and control their release. The *in vitro* release rates of benzoate ions from the coated resin beads were then investigated using a rotating sieve basket technique. The dramatic differences in release rates observed with the different waxes can be discussed in terms of the wax to resin ratio and the solubility characteristics of the waxes. The initial release rates can be expressed in terms of a mathematical expression previously reported for the diffusion of ions in ion-exchange resins, thereby aiding in the elucidation of the effect of the waxes on release.

Keyphrases □ Waxes, various—coated on ion-exchange resin beads, effect on release of benzoate anions □ Resin beads, ion exchange—coated with various waxes, effect on release of benzoate anions □ Benzoate anions—release from ion-exchange resin beads, effect of coating with various waxes □ Release rates—benzoate anions from ion-exchange resin beads, effect of coating with various waxes

Ion-exchange resins are currently used as vehicles for preparing prolonged-release medication. Saunders and coworkers (1–3) investigated the effect of binding of drugs to ion-exchange resins and employed drug–resin complexes to prolong drug release, thereby increasing its duration of action. Abrahams and Linnell (4) indicated that drug release from the resin depends on the availability of ions within the GI tract. Subsequent papers indicated the value of employing ion-exchange resins to prolong the release of ephedrine (5) and amphetamine (6).

Table I—Characteristics of the Wax-Coated Resin Complex

Wax	Wax, g / Resin Complex, g[a]	Benzoate Released[b], mg/g of Resin Complex
No wax	0.0000	366.4
Beeswax	0.2460	363.9
Polyethylene glycol 6000	0.3630	353.9
Carnauba wax	0.1850	354.5
Hard paraffin	0.0813	359.8
Stearic acid	0.5920	369.9
Stearyl alcohol	0.0664	355.1

[a] Average values of triplicate determinations on three different preparations. [b] Expressed as milligrams of sodium benzoate per gram of resin complex exclusive of wax. These are average values of triplicate determinations on three different preparations.

BACKGROUND

An alternative approach to prolonged-release medication is drug dispersal within inert matrixes such as polyvinyl chloride, polyethylene (7, 8), and wax consisting of propylene glycol monostearate and hydrogenated castor oil (9). Various factors influence drug release such as the matrix, the drug, the drug concentration in the tablet, drug solubility, matrix additives, and solvents.

Spray-congealing procedures also were used to prepare sustained-release powders and tablets. The effect of selected formulations and production variables on the physical characteristics and dissolution behavior of the spray-congealed particles was investigated. The effect of various waxes, *e.g.*, white wax, carnauba wax, and cetyl alcohol, on a particular formulation was dependent upon the physical properties of the wax and drug–wax particles, the wax composition, and the dissolution medium (10). Modifiers in the spray-congealed wax formulations such as surfactant and hydrogenated castor oil altered the release rate significantly (11, 12).

Another method employed to obtain prolonged-release coated particles is simply to incorporate the drug particles with the melted wax. The coated drug particles are then obtained either by granulation (13) or dispersion (14).

The coating of ion-exchange resins has received considerably less attention and has generally been regarded as an example of a solid being coated by coacervation (15, 16). Coatings of ion-exchange resins also were employed to alter the taste characteristics of the drug product (17).

The purposes of this research were to investigate the coating of an ion-exchange resin–anion complex with different materials by a simple procedure and to determine the effect of the different coating materials on the release rate of the organic anion from the anion–resin complex. It was expected that by employing different materials, the release rate of the model drug, benzoate anion, already affected by the ion-exchange resin, would be further altered to an appreciable extent, depending on the properties of the coating material. This preparation method of sustained-release pharmaceuticals would permit control of drug release by both the ion-exchange resin and the external coating.

EXPERIMENTAL

Materials—The strongly basic, 20–50-mesh, ion-exchange resin[1] was screened wet, and the beads that passed through a 35-mesh but were retained on a 40-mesh screen were used. The resin was washed thoroughly several times with distilled water, and the floating beads were rejected. The resin was then dried in a vacuum desiccator over sodium hydroxide for about 5 days. The resin was purified by washing with absolute ethanol, ethanol–water mixtures, and eventually with water over 1 week.

The resin was conditioned in a column by conversion to the hydroxide form with 2 *N* NaOH and to the chloride form with 2 *N* HCl. This procedure was repeated once, and then the resin was thoroughly washed with water. The resin was then converted to the benzoate form by adding 0.05 *N* sodium benzoate USP solution until the effluent concentration was the same as the eluant concentration. The resin complex was washed thoroughly with distilled water, dried, washed with methanol, and dried. The average particle size, as determined by microscopic measurement of 30 resin beads, was 0.402 mm for wet beads and 0.363 mm for dry beads.

The coating waxes or materials, beeswax (white), polyethylene glycol 6000[2], carnauba wax, hard paraffin, stearic acid, and stearyl alcohol of USP standard or commercial quality, were used without further purification. The coated resin beads were prepared by adding 4 g of melted wax to 1.5 g of resin complex in a funnel fitted with a coarse-porosity fritted disk. The mixture was maintained in the liquid state by the use of a heating jacket and was stirred for 30 min. The excess wax was removed by suction, and the coating on the beads was allowed to harden. The mixture then was stirred with a glass rod to separate the beads after cooling or gently ground with mortar and pestle to separate beads when carnauba wax was used to produce a coarse powder.

The amount of wax covering on the beads was determined by extracting the coated beads (0.25 g) with about 500 ml of warm chloroform in a heated fritted funnel over 2 hr. The extracted beads were then dried to constant weight in a vacuum desiccator. The extraction of each preparation was carried out in triplicate.

Kinetic Studies—The release rate of the benzoate anion from the coated resin complex was determined by placing a known quantity (0.25 g) of the resin into a metal basket apparatus made with an 80-mesh screen similar to that described by Kressman and Kitchener (18). The basket, placed into a 500-ml round-bottom flask containing 200 ml of phosphate buffer maintained at 30° with a constant-temperature bath, was rotated at 1240 rpm. The phosphate buffer contained 12.095 g of dibasic potassium phosphate/liter of aqueous solution. The elution procedure was carried out in triplicate on a single wax preparation.

Spectrophotometric analysis of the eluted benzoate was carried out by removing 5-ml samples from the flask at suitable intervals. The samples were appropriately diluted with the phosphate buffer, and the absorbance was measured[3] at 224.5 nm, the wavelength of maximum absorption for benzoate anion (19, 20). The concentration of the solution was determined from a Beer–Lambert plot of sodium benzoate in phosphate buffer.

The concentration of the benzoate at 24 hr was taken to be the equilibrium concentration since this period was suitable from an experimental point of view and also relevant to prolonged-release medication. The amount of benzoate released from the resin complex during a kinetic run was determined by taking into account both the concentration of benzoate in the eluting solution and the amount of benzoate periodically removed for analysis.

RESULTS AND DISCUSSION

The ratios of wax to resin complexes are given in Table I. In general, the amount of wax bound per gram of resin was reasonably consistent; all except two values were within 20% of the average. In these two cases, however, the deviation was considerably greater. One sample of resin complex coated with stearyl alcohol was 35% greater than the average, and one sample of carnauba wax was 57% greater than the average. There were large differences among the wax to resin ratios for different waxes, even though the same coating procedure was employed.

The amount of wax covering the surface appeared to depend on the polar character of the wax. The most polar compounds, such as stearic acid and polyethylene glycol, were bound to a much greater extent than the less polar compounds, such as hard paraffin and stearyl alcohol. The other waxes, carnauba and beeswax, were bound to an intermediate extent. The wax to resin ratio was used to calculate the amount of resin complex, exclusive of wax, that was added to the basket for the kinetic studies during elution. Under microscopic examination, the coated resin complex beads had the following characteristics: paraffin, a smooth consistent surface; beeswax and stearic acid, a coherent slightly irregular layer; polyethylene glycol, irregular surface and agglomerated particles; and stearyl alcohol and carnauba wax, sharp edges and agglomerated particles. After elution with the buffer solution, the beads coated with carnauba wax, hard paraffin, and beeswax had a few particles of wax still adhering to the surface; in the other cases, all of the coating had been removed from the resin beads.

The total amount of benzoate, expressed as the amount of sodium salt, released per gram of resin complex after 24 hr of extraction is given in Table I. All values were within 7% of the average value. These results indicate that the amount of benzoate released after 24 hr is essentially independent of the kind or the amount of wax covering the resin complex since the total amounts released were all close to the value for the uncoated resin complex. The amount of benzoate released after 120 min was very close (>99%) to the amount released after 24 hr for the uncoated

[1] Dowex 1-X8, Dow Chemical Co., Midland, Mich.

[2] Carbowax.

[3] Beckman DU-2 spectrophotometer.

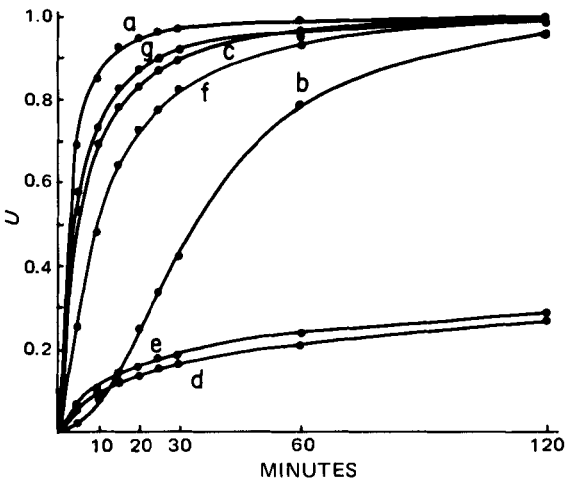

Figure 1—*Effect of a wax coating on the fractional attainment of equilibrium. Each point is the average of three kinetic experiments at the time indicated. Key: a, uncoated resin; b, beeswax; c, polyethylene glycol 6000; d, carnauba wax; e, hard paraffin; f, stearic acid; and g, stearyl alcohol.*

resin. Therefore, 24-hr values can be taken as appropriate equilibrium values for extraction of the coated resin complex as well as the uncoated resin complex under the conditions of the experiment.

To compare the effect of the wax coating on the release of benzoate from the resin complexes during the elution procedure as a function of time, the fractional attainment of equilibrium, U, is calculated from:

$$U = \frac{R}{R_\infty} \qquad \text{(Eq. 1)}$$

where R is the amount of anion released in time t and R_∞ is the amount released in 24 hr. This information is provided in Fig. 1. Since ion-exchange resins have been used to delay the release of drugs from the resin complex (3), the effect of waxes on further delaying the process is clearly indicated. It can be seen from these data that the order of delay of release of the benzoate was as follows: no wax < stearyl alcohol ~ polyethylene glycol < stearic acid < beeswax < hard paraffin ~ carnauba wax.

A number of physical properties of the waxes such as aqueous solubility, thickness of the wax layer, uniformity of coating, fracturing of the coat due to friction and impact in the elution apparatus, and fracture of the beads during hydration probably influence the release rate of the benzoate anion from the resin complex. The rapid release of the anion by polyethylene glycol can be explained by its high solubility in water (21), which allows the coating to dissolve rapidly and permits ion exchange to take place at only a slightly slower rate than the uncoated resin complex. The polyethylene glycol does, however, decrease the release rate in the early stages of the elution, indicating that even this highly soluble wax exerts some influence on the release rate and a certain amount of time is necessary to dissolve the wax so that the maximum rate can be obtained; overall, the rate was not decreased appreciably.

The relatively high elution rate of the resin complex covered with stearic acid may be attributed to its higher solubility in water [very slightly soluble (21)] compared to the remaining compounds. Another factor is the increase in the dispersibility of stearic acid in the slightly alkaline (pH 9.1) solution used as the elution medium as a result of ionization of this fatty acid.

Beeswax, carnauba wax, stearyl alcohol, and hard paraffin are classified as either practically insoluble or insoluble in water (21, 22). Accordingly, when used as coating materials on the resin complex, all of these compounds delay the release significantly. A comparison can be made among the three waxes that have acid values (21, 23): stearic acid, 206–209; beeswax, 17–24; and carnauba wax, 2.9–9.7. Thus, beeswax occupies an intermediate place both in the release rate and the ease of dispersibility in the medium as indicated by the acid value.

The very low release rate afforded by carnauba wax and hard paraffin can be attributed to their insolubility in water and/or lack of dispersibility in the slightly alkaline medium.

The rapid release by the stearyl alcohol covered beads, in spite of its insoluble nature, may be attributed to its ability to be hydrated to a slight degree and to the comparatively thin coat of stearyl alcohol on the resin complex as indicated by the low wax to resin value.

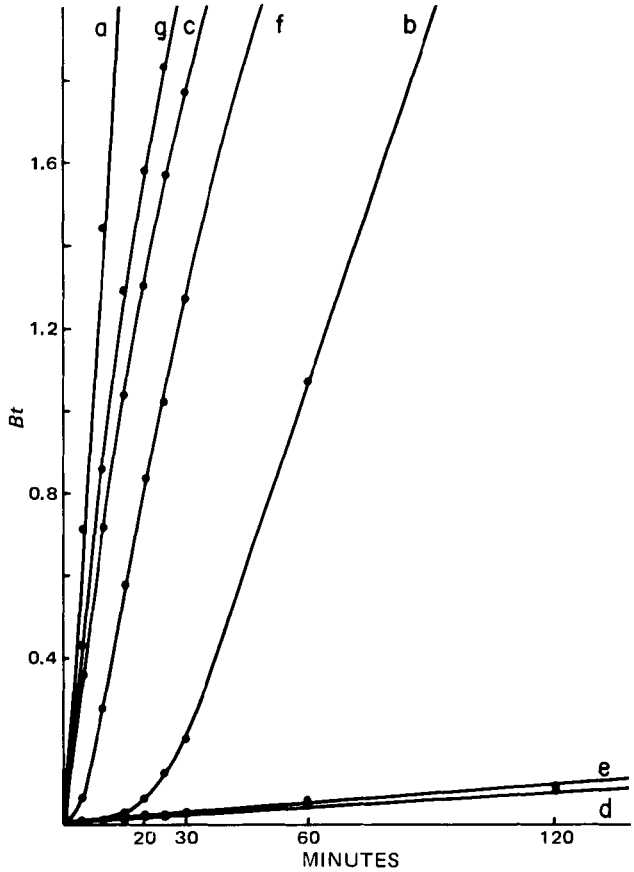

Figure 2—*The* Bt–t *plots for the elution of benzoate anion from coated and uncoated resin beads. Each point is the* Bt *value taken from the* U *values in Fig. 1. Key: a, uncoated resin; b, beeswax; c, polyethylene glycol 6000; d, carnauba wax; e, hard paraffin; f, stearic acid; and g, stearyl alcohol.*

A comparison of the wax to resin ratio suggests that, except for stearyl alcohol, there appears to be very little relationship between the fraction of attainment of equilibrium at 30 min, for example, and the wax to resin ratio. Hard paraffin and stearyl alcohol have similar ratios and solubilities in water, but the fraction of attainment of equilibrium is considerably different. A similar comparison can be made between beeswax and carnauba wax.

In view of the insolubility of waxes like hard paraffin and the fact that approximately 5% of equilibrium is attained even within a very short period after beginning elution, factors affecting the release rate other than solubility and dispersibility must be considered. After the wax-covered beads were prepared, microscopic examination indicated that the coating was rough in many cases; parts of some beads probably were not completely coated with wax. After elution, beads coated with the least soluble or the least dispersible of the waxes, namely, carnauba wax, hard paraffin, and beeswax, showed evidence of some wax adhering to the beads. Thus, with these harder waxes, fracture of the coating probably takes place during the elution procedure, giving rise to immediate release of the benzoate anion. Another factor to be considered is the cracking or rupture of some resin beads when they are hydrated rapidly or mechanically damaged during elution, thus exposing noncoated surface to the elution medium for immediate extraction.

The theoretical treatment of the kinetics of ion exchange was elucidated (24) and reviewed (25), and the rate equations appropriate to sustained release from ion-exchange resins were developed (3). The mathematical equation deals with the control of ion exchange within resin beads of spherical shape and uniform diameter in a solution of infinite volume. A number of experimental conditions did not meet these criteria; for example, the concentration of benzoate ion increased appreciably during the kinetic study, negating the requirement of infinite solution volume. The beads can be regarded as spherical, but diffusion would only likely take place where the coating had been removed. It is useful, however, to treat the release rate in this theoretical manner to aid in the interpretation of the effect of waxes.

The method of calculation is fully explained in the references (3, 25). The values of the fractional attainment of equilibrium are related to the rate constant B by a summation equation. The rate constant B is defined as $B = \pi^2 D/r^2$, where D is the effective diffusion coefficient and r is the mean particle radius of the resin beads. To calculate the rate constant, values of Bt corresponding to values of fractional attainment of equilibrium (26) are plotted against t and the slope of the line yields the rate constant B. These data are plotted in Fig. 2. If the line is straight, it can be assumed that ionic diffusion within the resin bead is the rate-controlling step in the diffusion process (26). It can be seen from Fig. 2 that the release rate from the uncoated resin beads yields a linear Bt–t relationship over a major portion of the graph, indicating that the diffusion of ions is controlled by particle diffusion.

While this theory cannot be applied strictly to the coated resin beads since interionic diffusion can hardly be expected to take place through the wax coating and the surface area of the beads exposed to the aqueous electrolyte solution will increase as the wax is dissolved or broken from the bead, it is useful to examine the Bt–t plots to assess diffusion characteristics.

Since the beads are not perfectly coated, it would be expected that release would begin immediately from any exposed surfaces. If the wax is rapidly removed, the maximal release rate should follow shortly thereafter. If the wax is removed at an intermediate rate, then the release rate would be expected to increase with time as the surface area is increased. Finally, if the wax is very slowly or incompletely removed, then the release rate should decrease with time due to the longer path length of diffusion within the resin bead.

The curves of the release from the beads coated with stearyl alcohol and polyethylene glycol 6000 are both similar in that the lines are slightly curved with a slightly smaller slope, indicating that the highly soluble polyethylene glycol 6000 and the thin coat of the stearyl alcohol have a small, but measurable, effect on the release of the benzoate ion compared to the uncoated resin. The curves of stearic acid and, especially, beeswax have very low slopes initially, but the slopes increase as time proceeds, indicating that the diffusion rate increases considerably within the first 10 min for stearic acid and within the first 30 min for beeswax and that some coating material is rapidly removed, thus exposing a greater surface area and allowing the maximum rate to be achieved.

The Bt–t plots of release from beads of resin coated with hard paraffin and carnauba wax are similar in that the release rate is very slow throughout the kinetic process. While the Bt–t plot appears to be linear, on an expanded vertical scale (10×) the curve has a decreasing slope, indicating a decrease in the rate with time due to much slower or incomplete removal of the wax coat from the bead's surface.

REFERENCES

(1) L. Saunders and R. Srivastava, *J. Chem. Soc.*, **1950**, 2915.

(2) *Ibid.*, **1952**, 2111.

(3) N. C. Chaudhry and L. Saunders, *J. Pharm. Pharmacol.*, **8**, 975 (1956).

(4) A. Abrahams and W. H. Linnell, *Lancet*, **2**, 1317 (1957).

(5) H. S. Bajpai, J. P. Gupta, and R. C. Gupta, *Clin. Med.*, **76**, 29 (1969).

(6) O. N. Hinsvark, A. P. Truant, D. J. Jenden, and J. A. Steinborn, *J. Pharmacokinet. Biopharm.*, **1**, 319 (1973).

(7) S. J. Desai, P. Singh, A. P. Simonelli, and W. I. Higuchi, *J. Pharm. Sci.*, **55**, 1235 (1966).

(8) *Ibid.*, **55**, 1224 (1966).

(9) J. B. Schwartz, A. P. Simonelli, and W. I. Higuchi, *J. Pharm. Sci.*, **57**, 278 (1968).

(10) A. G. Cusimano and C. H. Becker, *ibid.*, **57**, 1104 (1968).

(11) I. S. Hamind and C. H. Becker, *ibid.*, **59**, 511 (1970).

(12) P. M. John and C. H. Becker, *ibid.*, **57**, 584 (1968).

(13) J. B. Schwartz, A. P. Simonelli, and W. I. Higuchi, *ibid.*, **57**, 274 (1968).

(14) I. C. Robinson and C. H. Becker, *ibid.*, **57**, 49 (1968).

(15) R. E. Phares and G. J. Sperandio, *ibid.*, **53**, 515 (1964).

(16) A. M. Hussein, A. A. Kassem, A. Sina, and A. A. Badawy, *J. Pharm. Sci. UAR*, **11**, 1 (1970).

(17) S. Borodkin and D. P. Sundberg, *J. Pharm. Sci.*, **60**, 1523 (1971).

(18) T. R. E. Kressman and J. A. Kitchener, *Discuss. Faraday Soc.*, **7**, 90 (1949).

(19) J. L. Johnson, W. A. Struck, E. J. Scott, and J. E. Stafford, *Anal. Chem.*, **25**, 1490 (1953).

(20) L. Doub and J. M. Vandenbelt, *J. Am. Chem. Soc.*, **69**, 2714 (1947).

(21) "The Merck Index," 8th ed., Merck & Co., Rahway, N.J., 1968, pp. 123, 210, 782, 980.

(22) "Martindale, The Extra Pharmacopoeia," 26th ed., Pharmaceutical Press, London, England, 1972, pp. 1286, 2005.

(23) "The Handbook of Chemistry and Physics," 53rd ed., Chemical Rubber Co., Cleveland, Ohio, 1972, p. C753.

(24) G. E. Boyd, A. W. Adamson, and L. S. Myers, *J. Am. Chem. Soc.*, **69**, 2836 (1947).

(25) F. Helfferich, "Ion Exchange," McGraw-Hill, New York, N.Y., 1962, p. 250.

(26) D. Reichenberg, *J. Am. Chem. Soc.*, **75**, 589 (1953).

Distribution of Radiolabeled Subvisible Microspheres after Intravenous Administration to Beagle Dogs

H. G. SCHROEDER *, GUY H. SIMMONS, and PATRICK P. DeLUCA ˣ

Received May 9, 1977, from the *College of Pharmacy, University of Kentucky, Lexington, KY 40506.* Accepted for publication July 29, 1977. *Present address: The Upjohn Co., Kalamazoo, MI 49001.

Abstract □ The distribution and fate of intravenously administered microspheres in four size ranges were studied using Beagle dogs as an animal model. Administration of a dosage labeled with 200 μCi of cerium-141 permitted γ-camera observation. Animals were scanned upon dosing and again after 2 and 24 hr and 1, 2, and 4 weeks. The dogs were sacrificed after the 4-week scan to quantitate the final distribution. Whole organs were excised and homogenized, and the total radioactivity was determined by analyzing representative samples in a well counter. Image analysis revealed no distribution differences between bolus administration and 30-min infusion of doses of equal particle size and count. Spheres in the 25-, 15-, and 8-μm ranges lodged by the time necessary to secure the first image (approximately 20 min) and did not undergo any observable relocation; the 3-μm spheres appeared to be delayed in the lung. Well counting revealed that essentially all of the 25- and 15-μm doses and the major part of the 8-μm spheres were accounted for in the lungs after 4 weeks. Traces of the 8-μm spheres also were found in the liver, spleen, heart, and kidneys. Of the 3-μm spheres, over 75% were recovered in the liver, 17% in the spleen, 3% in the lung, and trace amounts in the kidneys and heart. Radioactivity in other organs and blood was negligible.

Keyphrases □ Microspheres, radiolabeled—tissue distribution after intravenous administration to dogs, bolus and infusion compared □ Distribution, tissue—radiolabeled microspheres, after intravenous administration to dogs, bolus and infusion compared □ Radiolabeled microspheres—tissue distribution after intravenous administration to dogs, bolus and infusion compared

For a quarter of a century, there has been a continual effort toward understanding the problems caused by particulate matter in injectables (1–9). Such efforts have been directed to determine the amounts as well as the origin and nature of contaminants in commonly used intravenous fluids (10–14). Removal of these contaminants with final filters significantly reduced the complications associated with intravenous fluid administration (15–19). Although a number of these reports implicated particulate matter in injectables as a major hazard, relatively little is known about distribution, relocation, elimination, modes of action, and possible acute effects. Much available information has been arrived at largely by conjecture.

The purpose of the present study was to gain further knowledge about the distribution of spheres of known size after intravenous injection. Such knowledge should permit a more rational assessment of the clinical significance of foreign particulate matter introduced into the bloodstream.

Radiolabeled microspheres have been used to study regional blood flow of the peripheral circulation (20, 21) as well as internal organs such as the kidneys (22) and the heart (23); to study cardiac output (24, 25); to study arteriovenous shunting, particularly in disease cases (26–28); to diagnose emboli (29); and to image or scan internal organs (30, 31). One review (32) traced the development and introduction of biodegradable spheres for circulation studies. The recognized advantages of these spheres, prepared by aggregation of human serum albumin, were that they could be metabolized rapidly and presented less chance of producing physiological alterations than did the inert spheres used earlier. Although the studies reported did not address the clinical consequences of particulate matter injected intravenously, they suggested an excellent means for assessing the distribution and fate of particulate matter that reaches the bloodstream.

EXPERIMENTAL

Preparation of Doses—The ^{141}Ce-labeled microspheres[1] were obtained as a suspension in physiological saline packaged in multiple-dose vials. A 20-ml dose contained the desired number of spheres as well as sufficient activity of 200 μCi found suitable for the experiment. Prior to withdrawing the precalculated dose, the vial of spheres was placed in an ultrasonic bath for 10 min to assure proper dispersion. Table I summarizes the properties of the spheres, the actual volume of suspension, and the number of spheres administered.

The actual sizes listed in Table I were obtained by a microscopic technique, and the size distribution and particle counts were verified by using an automatic electronic particle counter[2]. The radioactive dose intended was 200 μCi, but measurement of the specific activity of the actual dose administered revealed slight discrepancies which were corrected in all calculations. The measurement was performed by spiking nonradioactive homogenized tissue samples with a known volume of the suspension using an Eppendorf pipet. This approach was also employed to assess the efficiency of the γ-counter used in evaluating the radioactive contents of tissue samples of the dogs dosed.

Preparation of Experimental Animals—Small beagle dogs, 9.1–11.3 kg, were randomly assigned to four groups corresponding to the four particle-size ranges. Initially, three dogs were selected for each group. Prior to administering a dose, the dogs were anesthetized with 20 mg of pentobarbital sodium/kg iv. An indwelling catheter equipped with a three-way stopcock was inserted in the right radial vein, and 5% dextrose in 0.2 *N* saline was administered through an intravenous administration set with a medication chamber at a rate of 0.1 ml/min to maintain access to the vein until it was no longer needed. It was felt that this approach would reduce the chance of accidentally administering the dose in the muscle or under the skin.

Two dogs in each group were given the dose directly through the stopcock over 1 min. For comparison, the dose for the third dog was diluted to 60 ml in the medication chamber and administered as a constant intravenous infusion over 30 min. For rescans on subsequent days, the dogs were again anesthetized with pentobarbital sodium by direct venipuncture.

Scanning of Dogs—After drug administration, the dog was positioned securely under the PHO-γ-camera[3], with the chest facing the collimator plates (Fig. 1). To be sure no accumulation of radioactivity went undetected, several dogs were scanned twice (dotted circles in Fig. 1), but this practice proved to be unnecessary since no radiation could be detected outside of the central view.

Each dog was scanned until the camera had accumulated 200,000 emissions. Upon completion of the scan, the scanning time was recorded and a Polaroid picture of the distribution was obtained. The dogs were scanned immediately following administration and at 2 and 24 hr and 1, 2, and 4 weeks.

Preparation of Tissue Samples for Quantitative Determination of Distribution—On the day following the 4-week scan, selected dogs were anesthetized and sacrificed by administration of an overdose of saturated potassium chloride solution by direct cardiac puncture. In

[1] Nuclear Products Division, 3M Co., St. Paul, Minn.
[2] Model PC-305SSTA (D-2-60 sensor), High Accuracy Products Corp., Montclair, Calif.
[3] Searle model HP scintillation camera.

Table I—Properties of Radiolabeled Microspheres Used and Doses Administered

Size, μm		Dog	Specific	Total Dose Administered		
Nominal	Actual	Number	Activity, μCi/ml	Volume, ml	Radioactivity, μCi	Spheres (Millions)
3	3.3 ± 0.6	892	9.53	21.0 Infusion	200	817
3		1001	9.53	21.0 Infusion	200	817
3		888	9.53	21.0 Infusion	200	817
3		982	9.53	21.0 Bolus	200	817
3		885	0.465	21.5 Bolus	10	83.0
3		995	0.465	21.5 Bolus	10	83.0
8	8.9 ± 0.6	991	7.67	27.0 Infusion	207	34.0
8		983	7.67	27.0 Bolus	207	34.0
8		997	7.67	27.0 Bolus	207	34.0
15	16.1 ± 1.7	1004	9.56	22.7 Infusion	217	9.4
15		897	9.56	22.7 Bolus	217	9.4
15		898	9.56	22.7 Bolus	217	9.4
25	25.9 ± 0.9	829	9.06	20.5 Infusion	186	1.51
25		837	9.06	20.5 Bolus	186	1.51
25		830	9.06	20.5 Bolus	186	1.51

addition to blood samples, the following whole organs were removed: lung, heart, liver, spleen, kidneys, brain, gallbladder, and neck lymph nodes.

The organs were weighed and cut into cubes of about 1 cm. Distilled water was added to double the weight to facilitate homogenization, which was accomplished with a tissue homogenizer[4]. Aliquots between 5 and 10 g were weighed to within 50 mg using a top loading balance. The samples thus prepared were analyzed using an automatic γ-scintillation deepwell counter[5].

RESULTS AND DISCUSSION

Choice of Experimental Model—Polystyrene divinylbenzene microspheres were chosen as a model for particulate matter to maximize control and reproducibility. These microspheres are commercially available in the size ranges of interest and can be manufactured with a choice of several radioactive labels without further chemical treatment. Cerium-141 was selected because it possesses a strong γ-emission that can be detected with imaging equipment used with technetium Tc 99m. In addition, the cerium-141 half-life of about 33 days made it feasible to rescan the same experimental animal for up to 4 weeks, the duration of the study.

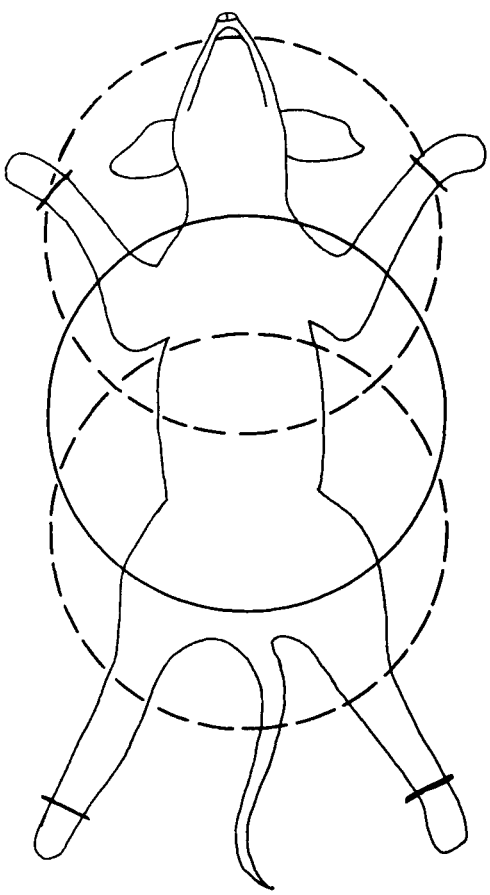

Figure 1—*Schematic representation of the field of view of the PHO-γ-camera.*

The choice of experimental animal was made on the basis of several considerations. The relatively limited resolution of about 10 mm for the camera available required the use of a large animal for imaging purposes. However, since the field of view was limited to a circle of about 30 cm in diameter, the animal could not be too large if imaging was to be accomplished in one exposure. Small dogs weighing 9.1–11.3 kg appeared to satisfy the geometric requirements. To minimize intraspecies variations, beagle dogs in that size range were chosen.

Qualitative Distribution Studies of 3-μm Spheres—Attempts to dose the full 200 μCi in the 3-μm range resulted in death by respiratory failure of three experimental animals. Although the amount of barbiturate was reduced for subsequent dogs after the first death and the dogs were placed on a respirator before starting the infusion, two additional dogs died of respiratory failure during the first scan. In an attempt to gather at least a minimum of information, a fourth dog was given the same dose of spheres. This dog survived the bolus of spheres and was scanned upon administration and 2 and 24 hr later.

Since the 3-μm spheres were the most likely to distribute over a wider area, the head and chest were scanned first, followed by a scan of the lower thorax and abdomen (Fig. 2). From the initial and 2-hr scans, it can be observed that initially a large portion of the spheres was retained in the lung. The initial scan of the lower body, which actually was started about 20 min after dosing because of the duration of the scan of the upper body, already shows a much heavier accumulation of particles in the area of the liver; the 2-hr scan reveals that the lung is rather clear of particles at this time.

Although the dog appeared to be in relatively good condition after the 2-hr scan, its condition deteriorated the following day. The 24-hr scan had to be done in a lateral position since the dog was unable to breathe in the supine position. This scan again shows that the spheres had almost entirely cleared the lungs after 24 hr. Since the dog's condition had deteriorated, it was sacrificed at this time.

Because of the death of the animals in the 3-μm group, two additional

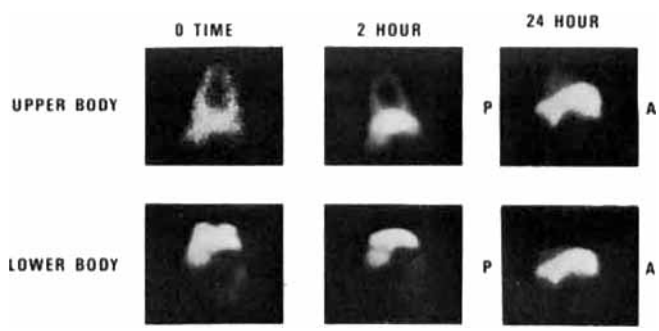

Figure 2—*Distribution of 3-μm spheres after intravenous administration. The 24-hr scan was done with the dog (No. 982) in a lateral position.*

[4] Tissumizer, model SDT, Tekmar Co., Cincinnati, Ohio.
[5] Bio-gamma, model 310, Beckman Instruments, Fullerton, Calif.

Table II—Comparison of Expected and Actual Scanning Times in Seconds [a]

Nominal Size, μm	Dog Number	Initial Scan (Actual)	2-Week Scan		4-Week Scan	
			Expected [b]	Actual	Expected [b]	Actual
8	991	919	1200	1278	1650	—
	983	1124	1500	1438	2010	1964
	997	951	1260	1183	1680	1756
15	1004	1024	1350	1309	1830	1810
	897	961	1260	1150	1710	1596
	898	979	1170	1066	1740	1674
25	829	2321	3060	2861	4140	4151
	837	1671	2190	1802	2970	2736
	830	1935	2250	2369	3450	3250

[a] Time for camera to observe 200,000 counts. [b] Calculated to the nearest 30 sec.

dogs were dosed using a 10-fold decrease in the number of spheres. Since the experiment was performed at a later date, the specific activity and, thus, the total radioactive dose had decreased to the level indicated in Table I. Although the two dogs given the lower doses in this size range could not be scanned, quantitative evaluation was obtained by analyzing the tissue samples.

Qualitative Distribution of Spheres in 8-, 15-, and 25-μm Size Ranges—The dogs assigned to these size groups did not suffer any major consequences, with one exception. One dog died of barbiturate overdose prior to the 2-week rescan. The fact that the dog belonged to the 8-μm group, *i.e.*, the second highest dose, may be coincidental since there appeared to be nothing wrong with the animal otherwise.

Analysis of the scans of the dogs dosed with spheres in the 8-, 15-, and 25-μm ranges revealed that the vast majority of these spheres were filtered out and retained in the lung. Figures 3–5 show the scans obtained from dogs that had received a bolus dose of 200 μCi in the size range of 8, 15, and 25 μm, respectively. From the rescans at 2 and 24 hr and 1, 2, and 4 weeks, it also appears evident that no major relocation of the spheres occurred following the initial distribution.

Figure 6 shows a comparison of the initial scans obtained by a bolus dose to the initial scans obtained by infusing the spheres over 30 min. Qualitatively, the distributions were the same, indicating that no major physiological changes took place over the short period selected for infusion.

Table II lists the actual scanning times of selected dogs in each size range. The expected scanning times are based on the initial scanning times, taking into account isotope decay. Since exact relocation of the dogs under the camera in successive scans is practically impossible, variations in the scan times can be expected; but the absence of major discrepancies between actual and predicted scan time appears to be a good indication that no elimination of spheres had taken place throughout the experiment.

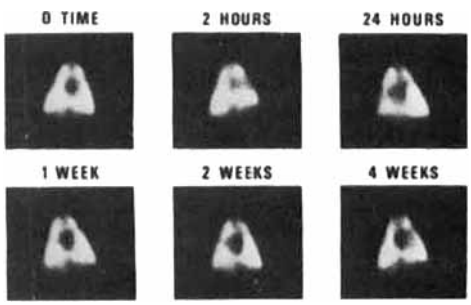

Figure 3—*Distribution of 8-μm spheres up to 4 weeks after bolus intravenous administration in Dog 997.*

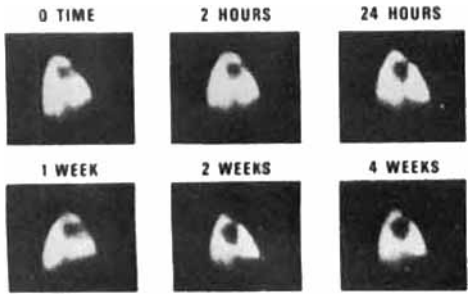

Figure 4—*Distribution of 15-μm spheres up to 4 weeks after bolus intravenous administration in Dog 897.*

The scanning time for the 25-μm treated dog was substantially longer than for the 8- and 15-μm treated dogs. Upon inspection of the quantitative results that follow, it can be noticed that the recovery of the 25-μm spheres was also very low. In the complete absence of radioactive counts in any of the other organs and with no evidence for relocation or elimination, underdosing due to faulty redispersion or other problems in drawing up the dose appears to be the only reasonable explanation. This conclusion is supported by the discrepancies observed in the scanning times.

Quantitative Recovery of Radioactive Spheres from Tissue Samples—The radioactive spheres that remained in the organs were quantitated. Blank tissue homogenates were used for dilution when count rates of undiluted homogenates were too high. Sample tubes were filled to about the same weight. Under these conditions, the efficiency of the counter was constant over the count rates observed.

From the qualitative distribution observed by means of the scanning, it appeared evident that there was no major variation between dogs in the same group. It was felt that sacrificing only one dog per group would be sufficient to obtain the results for the recovery and distribution of radioactive spheres in the 8-, 15-, and 25-μm size ranges. In the 3-μm range, both of the dogs were sacrificed to obtain an estimate of the variations in the distribution between these two animals. Although small samples of tissue were removed from one dog for a histological evaluation, the results presented in Table III are in good agreement, thus adding confidence to the results obtained from the single determination of the other size ranges.

CONCLUSION

The results of both qualitative and quantitative evaluations of the distribution indicate that most particles above 8 μm are filtered out by

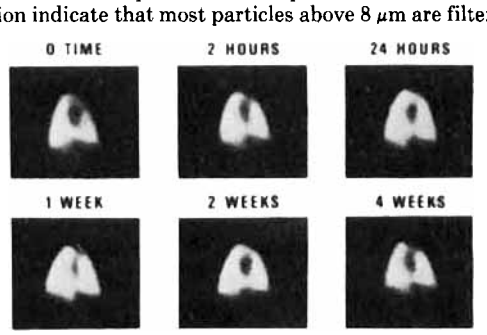

Figure 5—*Distribution of 25-μm spheres up to 4 weeks after bolus intravenous administration in Dog 837.*

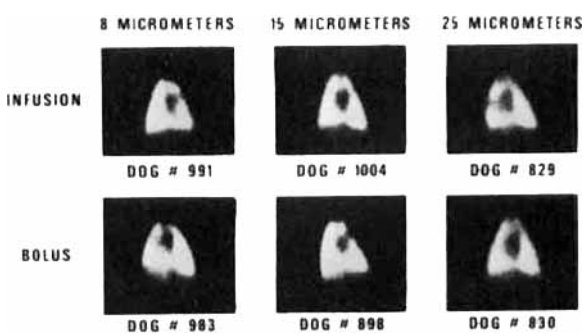

Figure 6—*Comparison of distribution after infusion and bolus administrations of radioactive microspheres (initial scan).*

Table III—Quantitative Recovery of Radioactivity in Organs Expressed as Percent of Dose

Organ	3 μm, Dog 885	3 μm, Dog 995	8 μm, Dog 997	15 μm, Dog 897	25 μm, Dog 937
Lung	3.2	2.7	91.2	94.8	62.72
Heart	—[a]	—[a]	0.1	—[a]	—[a]
Liver	76.2	78.7	0.6	—[a]	—[a]
Spleen	18.3	16.4	0.1	—[a]	—[a]
Kidneys	0.4	0.1	—[a]	—[a]	—[a]
Brain	—[a]	—	—	—	—
Gallbladder	—[a]	—	—[a]	—[a]	—[a]
Lymph node	—[a]	—	—[a]	—[a]	—[a]
Blood	—[a]	—	—[a]	—[a]	—[a]
Total recovery	98%	98%	92%	95%	63%

[a] Less than 0.05% of initial dose.

the lung and appear to localize there indefinitely.

The information obtained using the 3-μm spheres indicates an initial, presumably mechanical retention by the lungs with subsequent relocation by phagocytosis in the liver and the spleen for indefinite periods (33). More detailed studies of this phenomenon are warranted; by using spheres of higher specific activity or more sensitive scanning equipment, it would be possible to obtain more precise data on the relocation characteristics observed for these smaller spheres.

Although the administration of large doses of microspheres can be regarded as a major factor contributing to the death of several experimental animals, other possibilities must be taken into account. The relatively high maintenance doses of barbiturates needed to maintain the dogs absolutely still during scanning may have been responsible in part. Moreover, since the suspensions used were prepared elsewhere, there is no guarantee as to the purity of the vehicle. These points are raised since acute effect experiments at much higher levels of spheres did not result in death to any experimental animal (33).

REFERENCES

(1) B. E. Konwaler, *Am. J. Clin. Pathol.*, **20,** 385 (1950).

(2) E. J. Bruning, *Virchows Arch.*, **327,** 460 (1955).

(3) S. Sarrut and C. Nezelof, *Presse Med.*, **68,** 375 (1960).

(4) J. M. Garvan and B. W. Gunner, *Med. J. Aust.*, **2,** 140 (July 22, 1963).

(5) *Ibid.*, **2,** 1 (July 4, 1964).

(6) W. C. Walter, Food and Drug Administration Symposium on Safety of Large Volume Parenteral Solutions, Washington, D.C., July 1966.

(7) M. J. Groves, *J. Hosp. Pharm.*, **25,** 17 (1968).

(8) N. M. Davis, S. Turco, and E. Sivelly, *Am. J. Hosp. Pharm.*, **27,** 822 (1970).

(9) S. Turco and N. M. Davis, *Hosp. Pharm.*, **8,** 137 (1973).

(10) M. Sokol and J. Boyd, *Bull. Parenteral Drug Assoc.*, **22,** 9 (1968).

(11) B. Trasen, *ibid.*, **22,** 1 (1968).

(12) M. J. Groves and J. F. Major, *Pharm. J.*, **193,** 227 (1964).

(13) Y. S. Lim, S. Turco, and N. M. Davis, *Am. J. Hosp. Pharm.*, **30,** 518 (1973).

(14) J. Y. Masuda and J. H. Beckerman, *ibid.*, **30,** 72 (1973).

(15) D. W. Wilmore and S. J. Dudrick, *Arch. Surg.*, **99,** 462 (1969).

(16) P. B. Ryan, R. P. Rapp, P. P. DeLuca, W. O. Griffen, J. D. Clark, and D. Cloys, *Bull. Parenteral Drug Assoc.*, **27,** 1 (1973).

(17) P. P. DeLuca, R. P. Rapp, B. Bivins, H. E. McKean, and W. O. Griffen, *Am. J. Hosp. Pharm.*, **32,** 1001 (1975).

(18) H. G. Schroeder and P. P. DeLuca, *ibid.*, **33,** 543 (1976).

(19) S. Rusmin, P. P. DeLuca, R. Rapp, and B. Bivins, *Bull. Parenteral Drug Assoc.*, **31,** 1 (1977).

(20) H. N. Wagner, E. Jones, D. E. Tow, and J. K. Langen, *J. Nucl. Med.*, **6,** 150 (1965).

(21) P. A. Bradfeld, V. Lopez-Majano, and H. N. Wagner, *ibid.*, **8,** 542 (1967).

(22) M. A. Katz, R. C. Blantz, F. C. Rector, Jr., and D. W. Seldin, *Am. J. Physiol.*, **220,** 1903 (1971).

(23) M. Veda, S. Kaihara, K. Veda, Y. Sugislita, Y. Sasaki, and I. Masaliero, *Jpn. Heart J.*, **6,** 534 (1965).

(24) J. M. Neutze, F. Wyler, and M. R. Abraham, *Am. J. Physiol.*, **215,** 857 (1968).

(25) J. P. Archie, D. E. Fixler, J. R. Utley, and E. L. Carlson, *J. Appl. Physiol.*, **35,** 148 (July 1973).

(26) H. Veda, K. Kitani, H. Kameda, H. Yamada, and M. Jio, *Jpn. Heart J.*, **6,** 115 (1965).

(27) C. Dal Palu, G. Donnagio, J. Dal Zoho, and A. C. Pessina, *Scand. J. Gastroenterol.*, **3,** 425 (1968).

(28) H. W. Strauss, P. K. Hurley, B. A. Rhodes, and H. N. Wagner, *J. Lab. Clin.*, **74,** 597 (1969).

(29) H. N. Wagner, D. C. Sabiston, J. G. McAfee, D. Tow, and H. S. Stern, *N. Engl. J. Med.*, **271,** 377 (1964).

(30) R. Hofer, E. Orgris, and G. Pfeiffer, *J. Nucl. Med.*, **9,** 624 (1968).

(31) B. A. Rhodes and H. N. Wagner, *ibid.*, **10,** 432 (1969).

(32) H. N. Wagner, B. A. Rhodes, Y. Sasaki, and J. P. Ryan, *Invest. Radiol.*, **4,** 373 (1969).

(33) H. G. Schroeder, B. Bivins, G. Sherman, and P. P. DeLuca, *J. Pharm. Sci.*, **67,** 508 (1978).

ACKNOWLEDGMENTS

Presented at the Basic Pharmaceutics Section, APhA Academy of Pharmaceutical Sciences, New Orleans meeting, April 1976.

The work on which this report is based was supported by the Public Health Service, Food and Drug Administration, Department of Health, Education, and Welfare, Contract 223-77-3018.

The authors thank Ralph Mullins, Mary Standford, and James Wallace for assistance in the scanning, well counting, and animal handling, respectively.

Physiological Effects of Subvisible Microspheres Administered Intravenously to Beagle Dogs

H. G. SCHROEDER *, BRACK A. BIVINS, GERALD P. SHERMAN, and PATRICK P. DeLUCA ˣ

Received May 9, 1977, from the *College of Pharmacy, University of Kentucky, Lexington, KY 40506.* Accepted for publication July 29, 1977. *Present address: The Upjohn Co., Kalamazoo, MI 49001.

Abstract □ Experiments were performed to determine the acute effects of polystyrene microspheres in four size ranges (3, 8, 15, and 25 μm) upon intravenous administration to dogs. The parameters monitored were arterial pressure, arterial blood pH, blood gases (pO_2 and pCO_2), white blood cell count, heart rate, and single lead ECG. A filtered (particle-free) control volume was administered after establishing background readings for each dog for 30 min, and the monitoring was continued for an additional 30 min before dosing with the suspension of spheres. The animals were followed for up to 3 hr after dosing. Initial experiments with 15-μm spheres at bolus dose levels of 0.1, 1, 5, and 10 million spheres revealed no drastic changes in the clinical parameters monitored; therefore, an incremental dosing regimen was followed in which 0.5, 1, 5, and 40 million spheres/min were administered at sizes of 25, 15, 8, and 3 μm, respectively, for 1 hr (total of 30, 50, 300, and 2400 million spheres). Even at these exaggerated doses, the only appreciable change observed was a slight increase in white cell count. The dogs were further observed for 4 weeks after the experiment and appeared to remain normal. Histological evaluation of representative tissue samples showed no evidence of damage that could be attributed to the presence of microspheres in the organs.

Keyphrases □ Microspheres—intravenous administration to dogs, physiological effects evaluated □ Physiological effects—intravenous administration of microspheres to dogs

Many literature reports described the long-range effects on tissues caused by foreign insoluble materials contained in intravenous fluids (1). Most accounts reported adverse effects caused by particulate matter injected intravenously by accident or through limitations of the technique. One exception is a study (2) that evaluated the long-term biological effects of polystyrene spheres administered intravenously to rats.

In spite of the abundance of reports on long-range effects of foreign particulates on tissues, a sparsity of information exists on the acute effects of particulate matter injected intravenously. For obvious reasons, the acute effects have not been studied directly in humans. The few accounts are a direct consequence of accidental administration of air that resulted in massive embolism (3, 4) and accidental intravenous administration of suspensions not intended for such use (5, 6). One report (7) presents the results of this type of mistake: dizziness, shortness of breath, cyanosis, tachycardia, increased blood pressure, and death. Similar reactions were reported in drug abuse when tranquilizer tablets dispersed in water were injected intravenously (8–10).

Surprisingly, the acute effects of particulate matter injected in experimental animals have not been studied systematically. The only observation recorded in several reports is death, as was the case in early experiments dealing with the "toxicity" of ground glass, silica, and cotton fibers (11–14) and the one study (2) that attributed the death of several rats to unreasonably high levels of particulate matter. A recent study (15) of the distribution of radiolabeled microspheres also implicated the spheres as a major factor in the death of several experimental animals, and the resulting speculations emphasized the need for a systematic study to determine the acute effects of particulate matter injected intravenously.

The present study investigated the acute effects of particulate matter as a function of size and concentration and evaluated the histological damage induced by inert particulate matter of known size 4 weeks after administration.

EXPERIMENTAL

Preparation of Doses—Polystyrene divinylbenzene microspheres[1] were obtained in four nominal size ranges, 3, 8, 15, and 25 μm, as dry powder. The actual size distribution was verified microscopically. Although normal saline solution was a suitable vehicle for suspending the spheres at low doses, low molecular weight dextran was superior at the higher doses. Therefore, dextran was chosen as the suspending vehicle for some studies. Tables I and II summarize the properties of the suspensions used in the actual dosing.

A master suspension of spheres at the maximum possible concentration was prepared; from this suspension, the desired concentrations of spheres were prepared using particle-free diluent. Once the desired count per unit volume was obtained, the suspensions were filled into 50-ml multiple-dose vials, labeled, stoppered, and autoclaved for 20 min at 121°. Following sterilization, the suspensions were again monitored to assure that there were no changes in the size and count of the doses prepared.

All glassware and vials were washed thoroughly and dry heat sterilized at 180° for 4 hr before use. The stoppers were boiled for 30 min in 0.1% sodium pyrophosphate and thoroughly rinsed with filtered water for injection. The vehicles were filtered through a 0.22-μm membrane filter, and all operations were performed under laminar air flow conditions.

Preparation of Dogs—Small beagle dogs, 9.1–11.3 kg (20–25 lb), were randomly assigned to groups corresponding to each particle-size range. Following induction of anesthesia with 20 mg of pentobarbital sodium/kg iv, the dog was secured in a supine position to an operating table. With aseptic techniques, the right femoral vein and artery were catheterized, and 5% dextrose in 0.2 *N* saline[2] was administered through a 0.45-μm membrane filter at a rate of 0.1 ml/min. The artery was connected to a pressure transducer using tubing filled with heparinized saline. Stopcocks were placed in the line to allow removal of blood samples and subsequent flushing of the lines, and ECG electrodes were glued to the dog's limbs.

After the instrumentation was connected, the dog was allowed to stabilize for 30 min. Background samples and readings were obtained during this period. Blood pressure and ECG were recorded simultaneously on a two-channel polygraph recorder[3]; the pH and partial pressures of oxygen and carbon dioxide were obtained using a blood gas analyzer[4], and the cell counts were performed on an automatic counter[5].

Before the doses were administered, each dog was given a series of volume control doses of filtered vehicle and allowed to stabilize for an additional 30 min. Thus, each dog served as its own control. In addition, one dog was carried through a 4-hr experiment as a sham, and a second dog was evaluated extensively over 2 hr before receiving the microspheres. Multiple or repetitive bolus administration of microspheres was performed at 5-min intervals, starting after collection of data corresponding to background or volume control doses.

[1] Particle Information Services, Grants Pass, Ore.
[2] Travenol Laboratories, Morton Grove, Ill.
[3] Model 296, Sandborn, Waltham, Mass.
[4] Model 113, Instrumentation Labs, Lexington, Mass.
[5] Coulter counter model S, Coulter Electronics, Hialeah, Fla.

Table I—Characterization of Suspensions Used to Determine Acute Effects

Size, μm			Sphere Counts, 10^6/ml	Administration (Volume and Mode)	Nominal Dose, millions	Dog Number
Nominal	Actual	Vehicle				
Sham	—	Saline	0.000	25-ml single bolus	0.0	833
3	3.7 ± 0.8	Saline	1.120	10-ml single bolus	10.0	676
15	15.9 ± 1.0	Saline	0.014	10-ml single bolus	0.1	696
15	15.9 ± 1.0	Saline	0.097	10-ml single bolus	1.0	832
15	15.9 ± 1.0	Saline	0.405	25-ml single bolus	10.0	831
8	8.4 ± 0.6	Saline	0.987	12 × 10-ml repetitive bolus	120.0	1050
15	15.9 ± 1.0	Saline	0.405	10 × 5-ml repetitive bolus	20.0	847
25	24.7 ± 1.1	Saline	0.0051	12 × 20-ml repetitive bolus	12.0	1046
3	3.7 ± 0.8	Dextran	41.80	12 × 5-ml repetitive bolus	2400.0	1095
8	8.4 ± 0.6	Dextran	4.87	12 × 5-ml repetitive bolus	300.0	1057
15	15.9 ± 1.0	Dextran	1.03	12 × 5-ml repetitive bolus	60.0	1042
25	24.7 ± 1.1	Dextran	0.53	12 × 5-ml repetitive bolus	30.0	1080

Since no other procedures were performed on the dogs selected for the histological evaluation, the doses were administered intravenously *via* a right forelimb vein in unanesthetized animals. In an attempt to correlate information from this study with the findings of the previously reported distribution study (15), corresponding doses were prepared. Since matching of sizes for the 3-μm nominal spheres was expected to be critical due to their wider distribution over the body of the experimental animal, the tissue samples used for this pathological examination were taken from a dog that had received the reduced dose of 3-μm radioactive spheres (15). Four weeks after the administration, these dogs were anesthetized with 20 mg of pentobarbital sodium/kg iv and sacrificed by administering a saturated solution of potassium chloride by cardiac puncture.

The autopsy procedures were performed in the presence of a physician who observed the internal organs for gross changes such as color and size. Representative samples of organs were taken, placed in a 5% formaldehyde solution, and submitted to the pathology laboratory for preparation and evaluation of damage. Tissues selected for submission were based on findings of the previous distribution study (15). For the 25-μm treated dog, only a lung sample was submitted; in all other size ranges, samples included lung, heart, liver, spleen, and kidney. All samples were taken from corresponding locations within the organs; the lung samples were taken from the inferior segment of the lingula, heart samples were taken from the apex of the left ventricle, liver samples originated from the anterior edge of the right lobe, and the spleen and the left kidney specimens were wedged from the superior poles. All tissues were prepared by standard embedding techniques and sliced to a thickness of 10 μm with a microtome.

RESULTS

Acute Effects—The clinical data collected from the dogs that received a single dose of spheres are summarized in Table III. There was essentially no change in the blood pressure or pulse after single bolus dosing of microspheres. There was a slight difference between the sham and experimental animals in terms of oxygenation over the data collection period. As can be seen from Table III, the pO_2 of the sham animal increased 59% during the period of observation while the pO_2 of the dosed animals increased only slightly. There was minimal variation in the pH and pCO_2. The white cell counts in the experimental animals rose steadily, as much as 50–60%, after bolus injection of microspheres while the white cell count of the sham animal remained stable near the background value.

Table IV summarizes the clinical data obtained from the dogs that were given repetitive doses at the intermediate sphere count level. Once again, there were no appreciable changes in the heart rate and blood pressure readings; in two dogs, pH and pCO_2 values remained stable. The pO_2 rise noted in Dog 847 was accompanied by a decline in pCO_2, consistent with a change in ventilation over time. The white cell counts per cubic centimeter doubled for the 15- and 25-μm doses, while a substantially smaller increase of about 20% was observed for the 8-μm dose. The ECG's corresponding to the dogs in this group are reproduced in Fig. 1. Slight changes in the PR and QT intervals can be detected. There were also some

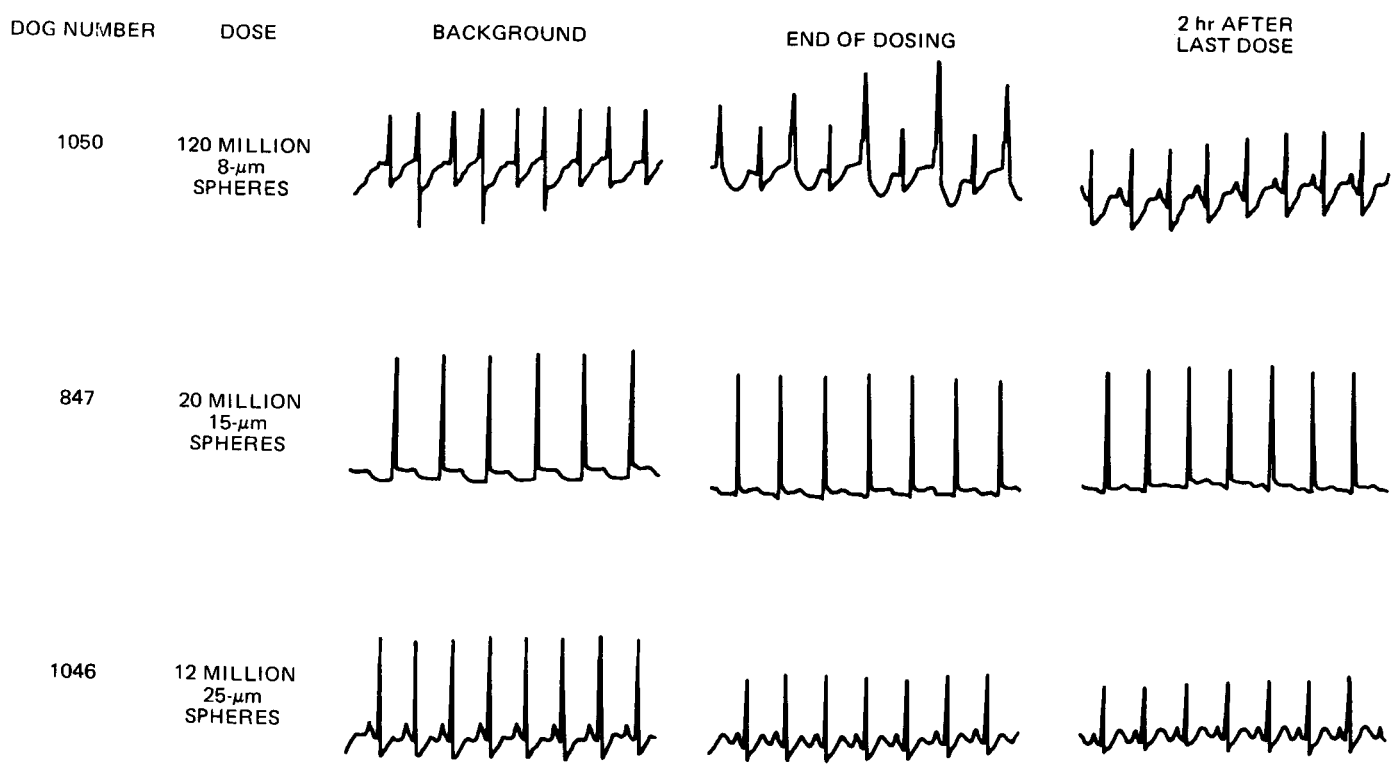

Figure 1—*ECG's of dogs that received repetitive doses of 8-, 15-, and 25-μm microspheres.*

Table II—Doses Administered for Histological Evaluation

Size, μm	Total Dose, millions	Dog Number
3.3 ± 0.6	83.0	995
8.4 ± 0.6	34.0	894
15.9 ± 1.0	9.40	984
24.7 ± 1.1	1.51	985

changes in the configuration of the QRS and ST segments, which can be attributed to the ventricular strain.

Because of the relatively small changes observed in the clinical parameters (except the white cell counts) and the ECG, the doses of spheres were increased substantially as indicated in Table I. The clinical data reported in Table V correspond to the dogs that received repetitive bolus injections at these high sphere concentrations in dextran. Even at these high concentrations, the heart rate, blood pressure, blood pH, and gases remained close to the background values. The highest increase in white blood cell count was observed for the 8-μm dose, from 7000 to 12,000 cells/cm^3. For the remaining size ranges, the changes were smaller than would be anticipated considering the increases observed at the intermediate dose level. The ECG's for the dogs that received spheres at the high levels are reproduced in Figs. 2–6. Although the changes observed were somewhat more pronounced, they were consistent with the changes observed at the intermediate dose levels.

Following the collection of clinical data, the dog's vein and artery were tied off and the animals were kept under observation for 4 weeks. None of the animals showed any abnormality in overall health, appearance, and behavior.

Histological Evaluation—The autopsies of the animals selected for this part of the study revealed no gross abnormalities in appearance, color, and size of the internal organs. Histological examination of the tissues of the dog that received the 3-μm spheres was relatively difficult because of the small size of the microspheres and the lack of a fluorescent label. The samples originating from the liver and the spleen showed a high concentration of spheres because of phagocytosis into an intracellular position. Similar observations were made on samples originating from the lungs, but no spheres could be found in the heart or kidney samples. Although spheres were found in several organs, there was no evidence of tissue damage in the form of inflammation, necrosis, or infarction associated with the lodgment of the microspheres.

The 8- and 15-μm spheres were found without difficulty in the tissue samples since the larger size and the fluorescent label made localization and observation easier. However, spheres were found only in the alveolar septal vessels of the pulmonary sections and, as observed for 3-μm spheres, no damage could be associated with the lodging of the 8- and 15-μm microspheres in the lung. The heart, liver, spleen, and kidney samples showed neither traces of spheres nor tissue damage.

The lung sample corresponding to the 25-μm particles revealed no evidence of spheres because the slices taken for evaluation were 10 μm thick and the microtome blade evidently dislodged the spheres from their sites rather than slicing them. Although a large number of the 15-μm spheres were observed in the corresponding sample, it is suspected that some spheres in that size range also were dislodged. An attempt to prepare thicker slices was not practical since the inherent tissue fluorescence of these thicker slices produced a diffuse bright fluorescent field in which individual spheres could not be distinguished. Since there was no evidence of tissue damage, the search for the spheres was not pursued further.

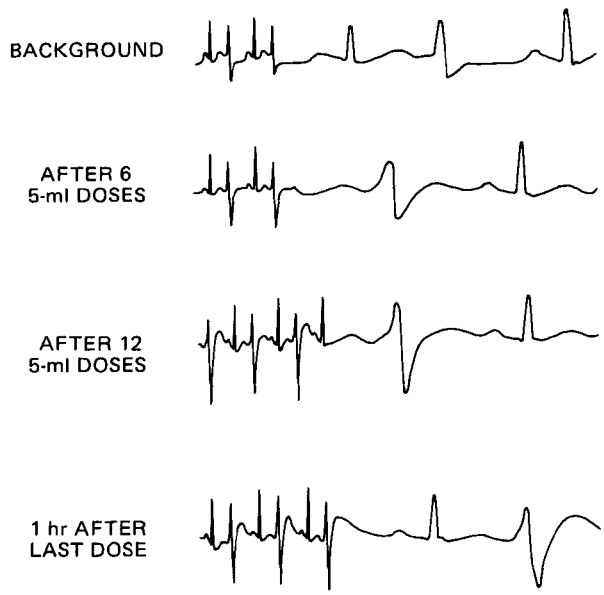

Figure 2—*ECG's of Dog 1095 that received 12 repetitive doses of filtered dextran solution.*

DISCUSSION

Choice of Model—Criteria for the selection of the beagle dog and polystyrene divinylbenzene microspheres were discussed previously (15). Additionally, in the manufacturing process for the microspheres, a fluorescent dye with an excitation wavelength of 485 nm and an emission maximum of 515 nm was incorporated into the spheres. The advantage of such spheres is that, in microscopy, the light can be admitted through a filter corresponding to the excitation wavelength (blue) while the observations are performed by placing a filter in the ocular corresponding to the emission wavelength (yellow). Thus, objects that possess these fluorescing properties are detected without interference from other materials present in the preparation. The risk of overlooking spheres is thus reduced, and spheres in a given preparation can be detected more

Table III—Clinical Data Obtained after Single Bolus Administration of Dose

Dog Number	Size, μm	Dose, 10^6	Event of Data Collection	Heart Rate per Minute	Blood Pressure, mm Hg	pH	pO_2	pCO_2	White Blood Cells, 10^3/ml
676	3	10	Background	88	205/110	7.52	99	18	20.0
			15 min after dose	86	200/110	7.50	105	16	26.5
			120 min after dose	86	200/110	7.50	100	21	27.7
696	15	0.1	Background	81	190/115	7.37	92	24	15.2
			75 min after dose	80	185/115	7.45	96	20	22.4
832	15	1	Background	88	205/100	7.33	88	38	11.6
			Volume control	84	200/105	7.31	89	40	12.2
			30 min after dose	86	205/105	7.27	81	44	13.0
			60 min after dose	84	205/100	7.28	87	40	13.6
			90 min after dose	84	210/105	7.30	92	36	14.4
			120 min after dose	84	190/100	7.30	92	38	14.3
831	15	10	Background	96	220/130	7.19	68	58	11.6
			Volume control	96	225/135	7.21	82	50	13.6
			30 min after dose	96	215/135	7.23	85	49	16.3
			75 min after dose	92	220/135	7.25	87	44	17.6
833	Sham		Background	76	210/125	7.26	63	52	14.7
			Volume control	74	205/130	7.23	72	57	14.4
			30 min after blank dose	76	205/125	7.22	74	59	12.8
			60 min after blank dose	72	205/130	7.24	72	56	12.6
			90 min after blank dose	74	205/130	7.23	70	59	13.7
			120 min after blank dose	74	205/130	7.22	79	55	14.2
			180 min after blank dose	74	200/125	7.26	100	54	15.9

Table IV—Clinical Data Obtained after Repetitive Bolus Administration

Dog Number	Size, μm	Dose, 10^6	Event at Data Collection	Heart Rate per Minute	Blood Pressure, mm Hg	pH	pO_2	pCO_2	White Blood Cells, 10^3/ml
1050	8	120	Background	125	200/120	7.36	96	45	11.8
			60 million	121	200/110	7.38	91	42	10.5
			120 million	116	195/115	7.38	86	44	10.2
			1 hr after last dose	116	205/115	7.40	89	36	12.5
			2 hr after last dose	108	200/125	7.38	87	41	13.6
847	15	20	Background	94	180/115	7.21	66	39	7.1
			10 million	95	180/115	7.22	70	42	8.9
			20 million	96	180/115	7.27	85	39	13.9
			1 hr after last dose	100	185/115	7.32	91	29	14.8
			2 hr after last dose	97	180/115				
1046	25	12	Background	114	200/130	7.34	91	36	8.1
			6 million	106	210/125	7.35	92	34	10.8
			12 million	104	205/130	7.34	96	35	12.1
			1 hr after last dose	104	195/125	7.37	83	38	15.0
			2 hr after last dose	100	200/115	7.37	81	37	15.7

rapidly. Once the spheres are located, the selective filters are removed for a more detailed analysis of that particular field of view in the preparation.

Choice of Clinical Parameters Monitored—Since pulmonary function should be compromised by the lodging of particles in the lung, possible effects were evaluated by monitoring the pH and the partial pressures of oxygen and carbon dioxide in the arterial blood. Since the heart would be pumping against an obstructed capillary bed, one could expect changes in the heart rate, blood pressure, and ECG. The potential inflammatory response due to microsphere embolization was monitored by determination of the white blood cell count.

The results of short-term histological evaluation appear to indicate that most particles above 8 μm were filtered out by the lung and localized there indefinitely. The information obtained using the 3-μm spheres seems to indicate retention by the lungs and that the major mechanism of removal from the bloodstream occurred by phagocytosis in the liver and the spleen, where these spheres appeared to locate. Gross examination upon autopsy and the histological evaluation indicated no evidence of tissue damage, in agreement with a similar study in which rats were used as the model (2). Although these observations apparently conflict with numerous accounts of tissue damage, it should be emphasized that samples were taken only 4 weeks after administration, a time that may be too short for permanent damage to be present or discernible. In addition, the microspheres used were relatively inert (compared to residues from antibiotics for example).

The clinical data obtained from this series of animals show minimal clinical changes due to the intravenous administration of microspheres. Two of three animals subjected to the high repetitive dosing with microspheres showed a drop in pO_2 over time. The one animal showing a rise in pO_2 had a concomitant decline in pCO_2, consistent with changes in ventilation outside the experimental conditions, and should thus be ignored. The fact that the decline in pO_2 can be discerned suggests that major intrapulmonary capillary obstruction is occurring. Additionally, the lack of change seen with the dextran-suspended microspheres in Table V may be related to the dextran vehicle, which is known to influence blood viscosity and platelet aggregation and thereby may have minimized the physiological impact of embolization due to the microspheres.

A consistent finding in all animals subjected to microsphere dosing is a steady rise in white blood cell count, presumably due to an inflammatory response secondary to pulmonary embolization with microspheres. This result correlates well with a previous observation in humans that there was a statistically significant difference in white blood counts in patients who received unfiltered intravenous fluids (particulate containing) compared to those who received filtered intravenous fluids (particulate free) (16). In the present study, there was no apparent correlation between the increase in white cell count and the size or dose level of the microspheres.

The ECG's obtained in this experiment leave no doubt that changes take place during and after intravenous administration of suspensions of microspheres. Although the response appears to increase with increasing dose, the fact that some changes occur during the administration of filtered control volumes points out the need for further investigation. The ventricular strain observed can be attributed to the doses of spheres, but the necessary procedures and experimental steps in the study cannot be overlooked as possible contributors to the changes observed.

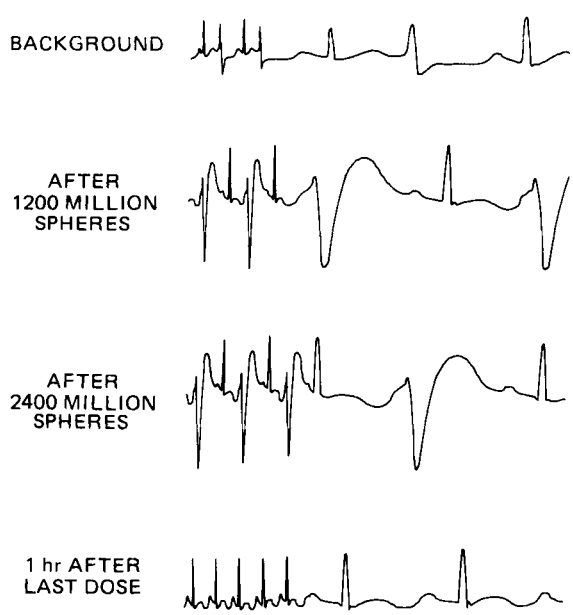

Figure 3—*ECG's of Dog 1095 that received repetitive doses of 3-μm spheres suspended in dextran solution.*

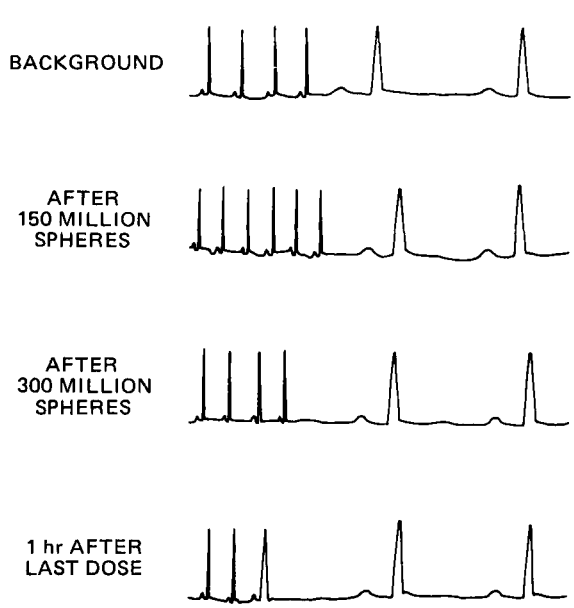

Figure 4—*ECG's of Dog 1057 that received repetitive doses of 8-μm spheres suspended in dextran solution.*

Table V—Clinical Data Obtained after Repetitive Bolus Administration of High Doses of Microspheres in Dextran Solution

Dog Number	Size, μm	Dose, 10^6	Event at Data Collection	Heart Rate per Minute	Blood Pressure, mm Hg	pH	pO_2	pCO_2	White Blood Cells, 10^3/ml
1095	3	2400	Background	110	210/105	7.30	96	35	15.4
			Volume control (six doses)	100	215/100	7.24	89	40	15.9
			Volume control (12 doses)	102	215/105	7.27	93	37	15.2
			1 hr after volume control	96	195/95	7.25	75	43	17.4
			1200 spheres administered	94	195/95	7.32	86	36	16.7
			2400 spheres administered	94	200/95	7.35	86	38	16.2
			1 hr after last dose	96	185/105	7.39	89	33	19.2
1057	8	300	Background	84	185/110	7.36	96	42	7.1
			150 spheres administered	100	210/105	7.37	71	42	7.9
			300 spheres administered	94	190/105	7.39	97	40	9.7
			1 hr after last dose	92	190/110	7.38	92	38	12.5
1042	15	60	Background	118	220/120	7.29	108	41	5.1
			30 spheres administered	110	220/115	7.31	107	34	5.5
			60 spheres administered	108	215/110	7.26	109	39	6.1
			1 hr after last dose	108	210/105	7.26	109	39	7.1
1080	25	30	Background	106	220/125	7.31	99	42	10.0
			15 spheres administered	98	215/100	7.27	94	57	9.6
			30 spheres administered	96	195/110	7.28	105	49	11.3
			1 hr after last dose	92	200/115	7.27	101	48	11.4

Although not observed in the present study, the deaths of experimental animals reported in other studies cannot be overlooked as acute effects; the particulate matter injected could have contributed. The literature over the past 15 years has cited the many negative aspects of particulate matter in parenterals, and it can be expected that there is a great potential for some long-term damage when particulate matter is introduced into the bloodstream. However, results of this study indicate that rather large numbers[6] of intravenously administered particles can be tolerated without any major immediate physiological or short-term histological effects. The risk of the damage must be evaluated against the recognized and proven benefit of intravenous therapy. In spite of the death of several experimental animals in other studies, the ability to compensate for the particulate load as seen in these animals is an important observation.

Although the main objectives of the study were accomplished in gathering information regarding acute physiological and short-term histological effects, much work lies ahead before the behavior and effects of injected particulate matter can be understood thoroughly. Extrapolation of the results of an animal study to humans can be misleading, but further experiments may be planned to approach the ultimate goal in a more meaningful manner. Repeating the present experiments using primates would be a step in that direction. As pointed out previously, more thorough monitoring in the form of intracardiac pressures, pulmonary artery and wedge pressures, lung compliance, more sophisticated ECG, *etc.*, will have to be performed using a sufficient number of experimental animals.

The results of this study lead to some interesting speculations regarding the use of particulate matter in the form of carefully prepared and controlled suspensions for intravenous and intraarterial therapy. The feasibility of such an approach has been documented to a certain extent by both the successful application of biodegradable spheres in diagnosis (17–19) and indications that poorly water-soluble drugs administered in nonaqueous solvents may precipitate in the bloodstream upon intravenous administration (20, 21). The present study suggests that the administration of suspensions into the bloodstream should be further evaluated.

Very potent insoluble drugs that require low doses (or deliberately prepared, poorly soluble prodrugs of soluble therapeutic agents) could be formulated in the appropriate size to lodge in the target organ, from which they could slowly release locally. One could speculate on achieving a sustained-release effect in addition to enhancing, by virtue of higher localized concentrations, the therapeutic effects while possibly minimizing undesirable side effects. It is hoped that this report will stimulate

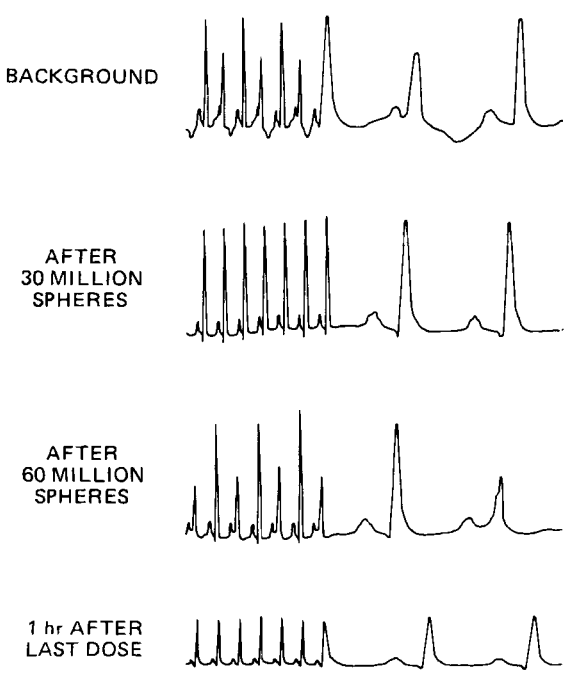

Figure 5—*ECG's of Dog 1042 that received repetitive doses of 15-μm spheres suspended in dextran solution.*

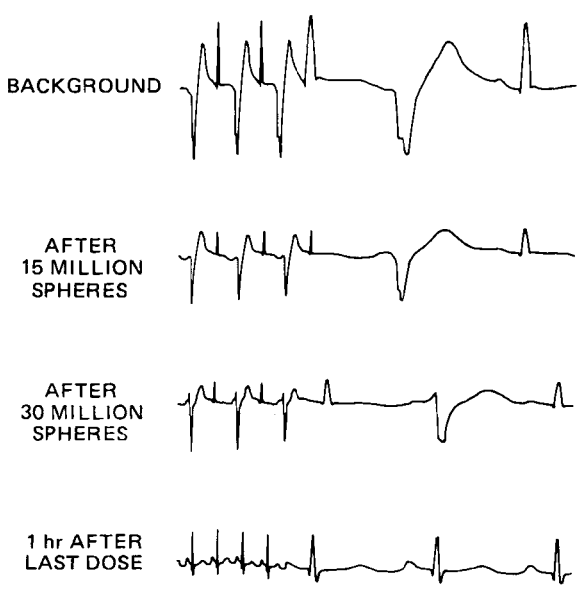

Figure 6—*ECG's of Dog 1080 that received repetitive doses of 25-μm spheres suspended in dextran solution.*

[6] The number of spheres administered in this experiment would be contained in several thousand liters of large-volume parenterals that meet the current USP standards.

further investigations of the behavior of particulate matter administered into the bloodstream.

REFERENCES

(1) S. Turco and N. M. Davis, *Hosp. Pharm.*, **8**, 137 (1973).

(2) R. M. Gesler, P. G. Garvin, B. Klamer, R. V. Robinson, C. R. Thompson, W. R. Gibson, F. C. Wheeler, and R. G. Carlson, *Bull. Parenteral Drug Assoc.*, **27**, 101 (1973).

(3) A. E. Yeakel, *J. Am. Med. Assoc.*, **204**, 175 (Apr. 1968).

(4) E. P. Holt, W. R. Webb, W. A. Cook, and M. O. Unal, *Ann. Thorac. Surg.*, **2**, 551 (1966).

(5) T. F. Downham and D. P. Ramos, *Mich. Med.*, **72**, 223 (1973).

(6) R. C. Bell, *Lancet*, **1**, 13 (1954).

(7) J. E. Galpin, A. W. Chow, T. T. Yoshikawa, and L. D. Guze, *Ann. Intern. Med.*, **81**, 358 (1974).

(8) W. H. Johnston and J. Waisman, *Arch. Pathol.*, **92**, 196 (1971).

(9) W. E. Atlee, *J. Am. Med. Assoc.*, **219**, 49 (Jan. 3, 1972).

(10) S. Richman and R. D. Harris, *Radiology*, **103**, 57 (Apr. 1972).

(11) L. V. Gardner and D. E. Cummings, *Am. J. Pathol.*, **9**, 751 (1933).

(12) E. J. King, H. Stantial, and M. Dolan, *Biochem. J.*, **27**, 1007 (1933).

(13) J. H. Brewer and J. H. Dunning, *J. Am. Pharm. Assoc., Sci. Ed.*, **36**, 287 (1947).

(14) W. Von Glahn and J. W. Hall, *Am. J. Pathol.*, **25**, 575 (1949).

(15) H. G. Schroeder, G. H. Simmons, and P. P. DeLuca, *J. Pharm. Sci.*, **67**, 504 (1978).

(16) P. P. DeLuca, R. P. Rapp, B. Bivins, H. E. McKean, and W. O. Griffen, *Am. J. Hosp. Pharm.*, **32**, 1001 (1975).

(17) R. Hofer, E. Orgis, and G. Pfeiffer, *J. Nucl. Med.*, **9**, 624 (1968).

(18) B. A. Rhodes and H. N. Wagner, *ibid.*, **10**, 432 (1969).

(19) H. N. Wagner, B. A. Rhodes, Y. Sasaki, and J. P. Ryan, *Invest. Radiol.*, **4**, 373 (1969).

(20) H. G. Schroeder and P. P. DeLuca, *Bull. Parenteral Drug Assoc.*, **28**, 1 (1974).

(21) K. Archie, L. Tz-Hong, J. F. Lamb, and H. S. Winchell, *J. Med. Chem.*, **19**, 279 (1976).

ACKNOWLEDGMENTS

Presented at the Basic Pharmaceutics Section, APhA Academy of Pharmaceutical Sciences, New Orleans meeting, April 1976.

The work on which this report is based was supported by the Public Health Service, Food and Drug Administration, Department of Health, Education, and Welfare, Contract 223-77-3018.

The authors thank Dr. Daniel A. Weiss, Professor of Pathology, for his guidance and consultation in the histological evaluations.

Correlation of Log *P* with Molecular Connectivity in Hydroxyureas: Influence of Conformational System on Log *P*

GEORGE R. PARKER

Received May 5, 1977, from the *Department of Medicinal Chemistry and Pharmacognosy, College of Pharmacy, University of Houston, Houston, TX 77004.* Accepted for publication August 1, 1977. Present address: College of Pharmacy, University of Oklahoma, Oklahoma City, OK 73190.

Abstract □ The correlation of log *P* (in octanol–water) with the nonempirical, topologically dependent, calculated molecular connectivity index ($^1\chi^v$) delineates substituted hydroxyureas into two families of linearly related groups of compounds. The first group, composed of the 3-substituted ethyl, *n*-propyl, and *n*-butyl analogs, is more hydrophilic than the 1-substituted methyl and ethyl and the 3-substituted isopropyl and *tert*-butyl analogs. The unsubstituted model compound hydroxyurea appears between the two groups in equal volumes of octanol. In octanol–water ratios of 5:1, log *P* approaches the range of the more hydrophilic group in high concentrations and becomes more lipophilic (similar to the other group) in lower concentrations. The differences in the relative hydrophilicities–lipophilicities of the two groups are rationalized in terms of the equilibria of internally hydrogen-bonded conformers to those that allow optimal interactions with solvent, water, or other hydroxyurea molecules. The concentration dependency observed with hydroxyurea appears to be due to the ease of interconversion of intermolecularly bonded conformers to those interacting with water, whereas the involvement of internally bonded conformers, which are apparently present to a greater degree in lower concentrations, increases the relative lipophilicity.

Keyphrases □ Hydroxyureas, various—log *P* in octanol–water correlated with molecular connectivity indexes □ Log *P*—various hydroxyureas in octanol–water, correlated with molecular connectivity indexes □ Molecular connectivity indexes—various hydroxyureas, correlated with log *P* in octanol–water □ Topological indexes—molecular connectivity, various hydroxyureas, correlated with log *P* in octanol–water

Many physicochemical properties are presently used in relating molecular structure to biological activities (structure–activity relationships) (1). The term physicochemical activity relationships has been suggested (2) to differentiate these methods from strictly structural approaches, *e.g.*, the Free–Wilson method, or from approaches that derive parameters from theoretical calculations on molecular structures, *e.g.*, quantum mechanical methods. The most extensively applied techniques are those that relate biological activity to free energy changes associated with drug transport through different environmental phases. Of the various methods of physicochemical or quantitative structure–activity relationships developed, Hansch analysis (3) has made significant contributions in the realm of quantitative structure–activity relationships and drug design, primarily because of the important role of transport and absorption in drug activity.

BACKGROUND

One primary function of Hansch analysis and other physicochemical and structure–activity methods is to predict optimal molecular or structural characteristics for the design of chemical agents to improve or optimize biological activity. Another utility of these methods might be to study the dynamics of drugs that have been synthesized, biologically tested, and evaluated for medicinal activity but for which there is not an accepted explanation for the activity or lack of biological activity of members of the class.

further investigations of the behavior of particulate matter administered into the bloodstream.

REFERENCES

(1) S. Turco and N. M. Davis, *Hosp. Pharm.*, **8**, 137 (1973).

(2) R. M. Gesler, P. G. Garvin, B. Klamer, R. V. Robinson, C. R. Thompson, W. R. Gibson, F. C. Wheeler, and R. G. Carlson, *Bull. Parenteral Drug Assoc.*, **27**, 101 (1973).

(3) A. E. Yeakel, *J. Am. Med. Assoc.*, **204**, 175 (Apr. 1968).

(4) E. P. Holt, W. R. Webb, W. A. Cook, and M. O. Unal, *Ann. Thorac. Surg.*, **2**, 551 (1966).

(5) T. F. Downham and D. P. Ramos, *Mich. Med.*, **72**, 223 (1973).

(6) R. C. Bell, *Lancet*, **1**, 13 (1954).

(7) J. E. Galpin, A. W. Chow, T. T. Yoshikawa, and L. D. Guze, *Ann. Intern. Med.*, **81**, 358 (1974).

(8) W. H. Johnston and J. Waisman, *Arch. Pathol.*, **92**, 196 (1971).

(9) W. E. Atlee, *J. Am. Med. Assoc.*, **219**, 49 (Jan. 3, 1972).

(10) S. Richman and R. D. Harris, *Radiology*, **103**, 57 (Apr. 1972).

(11) L. V. Gardner and D. E. Cummings, *Am. J. Pathol.*, **9**, 751 (1933).

(12) E. J. King, H. Stantial, and M. Dolan, *Biochem. J.*, **27**, 1007 (1933).

(13) J. H. Brewer and J. H. Dunning, *J. Am. Pharm. Assoc., Sci. Ed.*, **36**, 287 (1947).

(14) W. Von Glahn and J. W. Hall, *Am. J. Pathol.*, **25**, 575 (1949).

(15) H. G. Schroeder, G. H. Simmons, and P. P. DeLuca, *J. Pharm. Sci.*, **67**, 504 (1978).

(16) P. P. DeLuca, R. P. Rapp, B. Bivins, H. E. McKean, and W. O. Griffen, *Am. J. Hosp. Pharm.*, **32**, 1001 (1975).

(17) R. Hofer, E. Orgis, and G. Pfeiffer, *J. Nucl. Med.*, **9**, 624 (1968).

(18) B. A. Rhodes and H. N. Wagner, *ibid.*, **10**, 432 (1969).

(19) H. N. Wagner, B. A. Rhodes, Y. Sasaki, and J. P. Ryan, *Invest. Radiol.*, **4**, 373 (1969).

(20) H. G. Schroeder and P. P. DeLuca, *Bull. Parenteral Drug Assoc.*, **28**, 1 (1974).

(21) K. Archie, L. Tz-Hong, J. F. Lamb, and H. S. Winchell, *J. Med. Chem.*, **19**, 279 (1976).

ACKNOWLEDGMENTS

Presented at the Basic Pharmaceutics Section, APhA Academy of Pharmaceutical Sciences, New Orleans meeting, April 1976.

The work on which this report is based was supported by the Public Health Service, Food and Drug Administration, Department of Health, Education, and Welfare, Contract 223-77-3018.

The authors thank Dr. Daniel A. Weiss, Professor of Pathology, for his guidance and consultation in the histological evaluations.

Correlation of Log *P* with Molecular Connectivity in Hydroxyureas: Influence of Conformational System on Log *P*

GEORGE R. PARKER

Received May 5, 1977, from the *Department of Medicinal Chemistry and Pharmacognosy, College of Pharmacy, University of Houston, Houston, TX 77004.* Accepted for publication August 1, 1977. Present address: College of Pharmacy, University of Oklahoma, Oklahoma City, OK 73190.

Abstract □ The correlation of log *P* (in octanol–water) with the nonempirical, topologically dependent, calculated molecular connectivity index ($^1\chi^v$) delineates substituted hydroxyureas into two families of linearly related groups of compounds. The first group, composed of the 3-substituted ethyl, *n*-propyl, and *n*-butyl analogs, is more hydrophilic than the 1-substituted methyl and ethyl and the 3-substituted isopropyl and *tert*-butyl analogs. The unsubstituted model compound hydroxyurea appears between the two groups in equal volumes of octanol. In octanol–water ratios of 5:1, log *P* approaches the range of the more hydrophilic group in high concentrations and becomes more lipophilic (similar to the other group) in lower concentrations. The differences in the relative hydrophilicities–lipophilicities of the two groups are rationalized in terms of the equilibria of internally hydrogen-bonded conformers to those that allow optimal interactions with solvent, water, or other hydroxyurea molecules. The concentration dependency observed with hydroxyurea appears to be due to the ease of interconversion of intermolecularly bonded conformers to those interacting with water, whereas the involvement of internally bonded conformers, which are apparently present to a greater degree in lower concentrations, increases the relative lipophilicity.

Keyphrases □ Hydroxyureas, various—log *P* in octanol–water correlated with molecular connectivity indexes □ Log *P*—various hydroxyureas in octanol–water, correlated with molecular connectivity indexes □ Molecular connectivity indexes—various hydroxyureas, correlated with log *P* in octanol–water □ Topological indexes—molecular connectivity, various hydroxyureas, correlated with log *P* in octanol–water

Many physicochemical properties are presently used in relating molecular structure to biological activities (structure–activity relationships) (1). The term physicochemical activity relationships has been suggested (2) to differentiate these methods from strictly structural approaches, *e.g.*, the Free–Wilson method, or from approaches that derive parameters from theoretical calculations on molecular structures, *e.g.*, quantum mechanical methods. The most extensively applied techniques are those that relate biological activity to free energy changes associated with drug transport through different environmental phases. Of the various methods of physicochemical or quantitative structure–activity relationships developed, Hansch analysis (3) has made significant contributions in the realm of quantitative structure–activity relationships and drug design, primarily because of the important role of transport and absorption in drug activity.

BACKGROUND

One primary function of Hansch analysis and other physicochemical and structure–activity methods is to predict optimal molecular or structural characteristics for the design of chemical agents to improve or optimize biological activity. Another utility of these methods might be to study the dynamics of drugs that have been synthesized, biologically tested, and evaluated for medicinal activity but for which there is not an accepted explanation for the activity or lack of biological activity of members of the class.

Table I—Observed Log *P* and Calculated Molecular Connectivity ($^1\chi^v$) of Selected Hydroxyureas of Various Tautomeric Forms which Represent Conformers Possessing Various Localizations of π-Bond Character

Compound	R_1	R_2	Log *P*	Calculated $^1\chi^v$ of Hydroxyurea Species R_1NCNOH (=O)	$R_1NC{=}NOH$ (–OH)	$R_1N{=}CNOH$ (–OH)
Hydroxyurea	H	H	−1.27	0.966	0.959	0.947
1-Methylhydroxyurea	H	CH_3	−0.46	1.364	—	1.344
1-Ethylhydroxyurea	H	C_2H_5	−0.10	1.940	—	1.921
3-Ethylhydroxyurea	C_2H_5	H	−0.76	1.988	1.958	1.944
3-*n*-Propylhydroxyurea	*n*-C_3H_7	H	−0.22	2.488	2.458	2.444
3-Isopropylhydroxyurea	iso-C_3H_7	H	0.20	2.371	2.458	2.334
3-*n*-Butylhydroxyurea	*n*-C_4H_9	H	0.32	2.988	2.958	2.944
3-*tert*-Butylhydroxyurea	*tert*-C_4H_9	H	0.50	2.678	2.647	2.644

A drug class that fits this description is the hydroxyurea class of antileukemia, anticancer agents of which the simplest member, hydroxyurea, is the most active (4). Molecular modification has not resulted in an analog of superior biological action (5), and no accepted explanation has come forth as to why minor substitutions on the hydroxyurea nucleus diminish biological action. Since the molecular mechanism of action of hydroxyurea remains unknown, the relative contributions of drug absorption, transport, concentration, and dynamics at the site of action have not been established. The method of Hansch has been applied to hydroxyureas (6) to evaluate the relative importance of drug transportability by comparison of the predicted partition coefficients (log *P*) (*via* the summing of fragment values) *versus* the observed log *P* values determined in octanol–water. Most log *P* values for the substituted hydroxyureas were more hydrophilic than predicted, with the greatest differences (Δ log *P*) in predicted *versus* observed values being in the 3-substituted straight chain analogs, *e.g.*, ethyl, *n*-propyl, and *n*-butyl (all Δ log *P* of 0.70). The differences in predicted *versus* observed log *P* for the 1-substituted and bulky 3-substituted analogs were much less, and the observed log *P* for hydroxyurea was much more lipophilic than predicted utilizing the Hansch method.

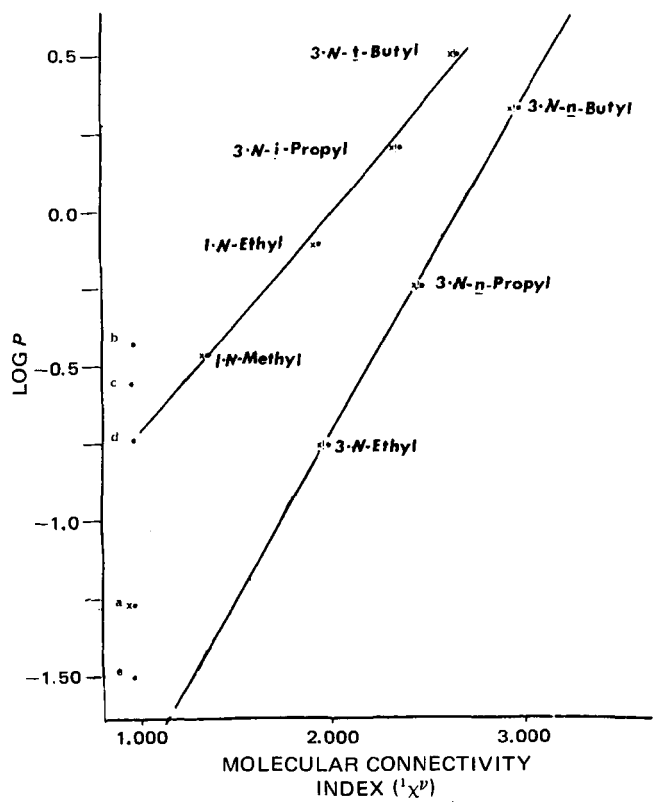

Figure 1—*Plot of log* P versus *valence molecular connectivity for selected hydroxyureas. Valence molecular connectivity is calculated for the* π*-bond at* C=O (*), C=N[1] (!), *and* C=N[3] (×). *Log* P *of hydroxyurea is shown at concentrations in octanol–water (1:1) (a) and in octanol–water (5:1) containing 0.1 (b), 0.5 (c), 1.0 (d), and 2.0 (e) g of solute.*

Log *P* was found recently to be related to the topological structure of a molecule, *e.g.*, the number and manner that atoms are arranged in a molecule (known as molecular connectivity) (7). The molecular connectivity index, χ, developed and utilized by Kier and coworkers (8, 9) and based on an earlier branching index by Randic (10), is a nonempirical, easily calculated value which seemingly encodes the shape and architecture of a molecule *via* the interatomic connections. The method of Kier and Hall, modified for the application to heteroatoms (valence connectivities) (8, 11, 12), was applied to the hydroxyurea series to determine if there was a correlation between log *P* and molecular structure as described by $^1\chi^v$.

EXPERIMENTAL

Hydroxyureas—Hydroxyurea[1], 1-methylhydroxyurea[1], and ethylhydroxyurea[1] were used as received. The 3-substituted analogs were synthesized according to the original procedure of Dresler and Stein (13) as modified (14, 15).

Log *P* Determinations—Log *P* values for the hydroxyureas were obtained as previously reported (6) by direct determination of the aqueous phase after equilibration for a minimum of 24 hr between octanol and water (pH 7). Log *P* was initially determined in equal volumes of water and octanol (50 ml of each) at concentrations containing 0.1, 0.5, and 1.0 g of hydroxyurea, with three determinations at each concentration. Determinations also were performed with five volumes of octanol to one volume of water, and only with unsubstituted hydroxyurea did the log *P* values vary appreciably.

Molecular Connectivity Index Calculation—The molecular connectivity was calculated according to the method of Kier and Hall as modified for molecules containing heteroatoms (8, 11, 12). The molecular skeleton was drawn, and each carbon atom in the skeleton was assigned a number, 1, 2, 3, or 4 (δ_i, δ_j), corresponding to the number of nonhydrogen atoms connected to the carbon atom. A number (δ_i^v, δ_j^v) was assigned to each heteroatom equivalent to the valence number minus the number of hydrogens connected to each heteroatom. A number was derived for each bond in calculating the product of the numbers associated with the two atoms of the bond. The reciprocal of the square root of this number was then computed and became the bond value. Finally, the bond values were summed to give a number, called the valence connectivity index ($^1\chi^v$) for the molecule; $^1\chi^v = \Sigma(\delta_i^v, \delta_j^v)^{-1/2}$.

For each hydroxyurea, three calculations were made: (*a*) for the molecule with a C=O bond at carbonyl carbon, (*b*) for a molecule with a C=N between the 1-nitrogen and carbonyl carbon, and (*c*) for a molecule with a N=C between the 3-nitrogen and carbonyl carbon.

The calculated connectivities ($^1\chi^v$) for each of these molecular species and the observed log *P* values for each of the hydroxyureas evaluated are listed in Table I. The plot of log *P versus* the connectivity index is shown in Fig. 1. The log *P versus* the connectivity index for unsubstituted hydroxyureas at various concentrations of compound and different ratios of octanol to water is also shown in Fig. 1.

DISCUSSION

Drug action is known to be dependent on many events that take place after a drug is placed in a biological system, regardless of whether it is

[1] Courtesy of Miss B. Stearns, Squibb Institute of Medical Research.

Table II—Log *P* of Hydroxyurea at Different Concentrations in Octanol–Water

Dissolved Solute, g	Octanol–Water (1:1)	Octanol–Water (5:1)
0.1	−1.19	−0.42
0.5	−1.20	−0.57
1.0	−1.27	−0.74
2.0	−1.41	−1.52

an *in vitro* or *in vivo* system or whether the system is a human patient or an enzyme. Most of these events, such as membrane passage, adsorption or desorption to macromolecules, and attachment to the biochemical site of action with the resultant biological response, are dependent on the structure of the drug. Any interactions between or with the biological systems are, therefore, dependent on the atomic and molecular composition of the drug.

Because of this fundamental principle of structure dependence in biological action, many investigators attempted to correlate drug action with various basic properties of drugs such as their physical properties (polarization, log *P*, solubilities, *etc.*) or their absolute or potential molecular structure (quantum mechanical structural analysis, solvent dependent conformational analysis, *etc.*). While the utility of these methods may not be established, it is evident that the fundamental structure of a drug molecule is the basis for its action, although the processes may be so complex that facile study may be difficult. If these basic concepts are applied to a relatively simple drug entity such as the antileukemia agent hydroxyurea, some processes taking place in a biological system eventually leading to drug action (or inaction as the case may be) may be made clearer.

By applying some concepts developed by Hansch for the hydroxyurea series, it could have been postulated, after the original discovery of hydroxyurea activity (16), that molecular modification should produce a better anticancer agent. This hypothesis assumes that more lipophilic analogs should show more optimal drug action, since absorption can take place more readily and allow more drug to be available at the site of action through better drug distribution (17). The more lipophilic homologs usually pass through membranes with greater ease and often have greater biological action as long as solubility, bulk tolerance, or some other parameter does not diminish drug action (18). Since molecular modification has not succeeded in improving the antineoplastic properties of unsubstituted hydroxyurea (simple methyl substitution at the 1- or 3-nitrogen reduces action considerably), it becomes an academic question as to the reason for the dramatic change in activity with relatively minimal structural change.

Application of Hansch analysis for the prediction of log *P* values by the summing of fragments (*f* values) indicates that the predicted log *P* values are all more lipophilic than found experimentally except for hydroxyurea and the 1-methyl and the 3-*p*-chlorophenyl analogs (6). The greatest differences in predicted *versus* observed log *P* values in this series were with the 3-substituted straight chain analogs (ethyl, propyl, and butyl), all of which had Δ log *P* values of 0.70, while the bulky 3-substituted analogs (isopropyl and *tert*-butyl) had Δ log *P* values of 0.15 and 0.26, respectively. The hydroxyureas with log *P* values closest to those predicted were the 1-methyl, 1-ethyl, and 3-*p*-chlorophenyl analogs (Δ log *P* values of −0.14, 0.04, and −0.04, respectively). The predicted log *P* value for the parent hydroxyurea also was calculated to be appreciably different than that found experimentally (Δ log *P* of −0.91) (Table II), indicating that the hydroxyurea series did not behave as expected in the octanol–water partitioning system or that Hansch's method did not apply to a system such as the hydroxyureas except for certain analogs.

Since log *P* and most properties related to the physical characteristics of drugs are dependent on the molecular architecture of the molecule in question, it seems fitting to include those parameters that take into consideration the topological aspects of drug molecules. The method of molecular connectivity lends itself to the quantification of molecular architecture among the hydroxyureas. The molecular index of connectivity appears to be a quantification of structure that permits correlation with additive and constitutive properties of molecules. The connectivity index $^1\chi$ or $^1\chi^v$ of any molecule is the summed total of the reciprocal square root of the product of each bond in the molecule (excluding bonds to hydrogen), and the value obtained has been linearly correlated with polarizability, cavity surface area, local anesthetic action (9), water solubility and boiling points (19), the partition coefficient (7), and biological action (20) and parabolically related in certain drug classes to biological action (21).

When the molecular connectivity is calculated by the established

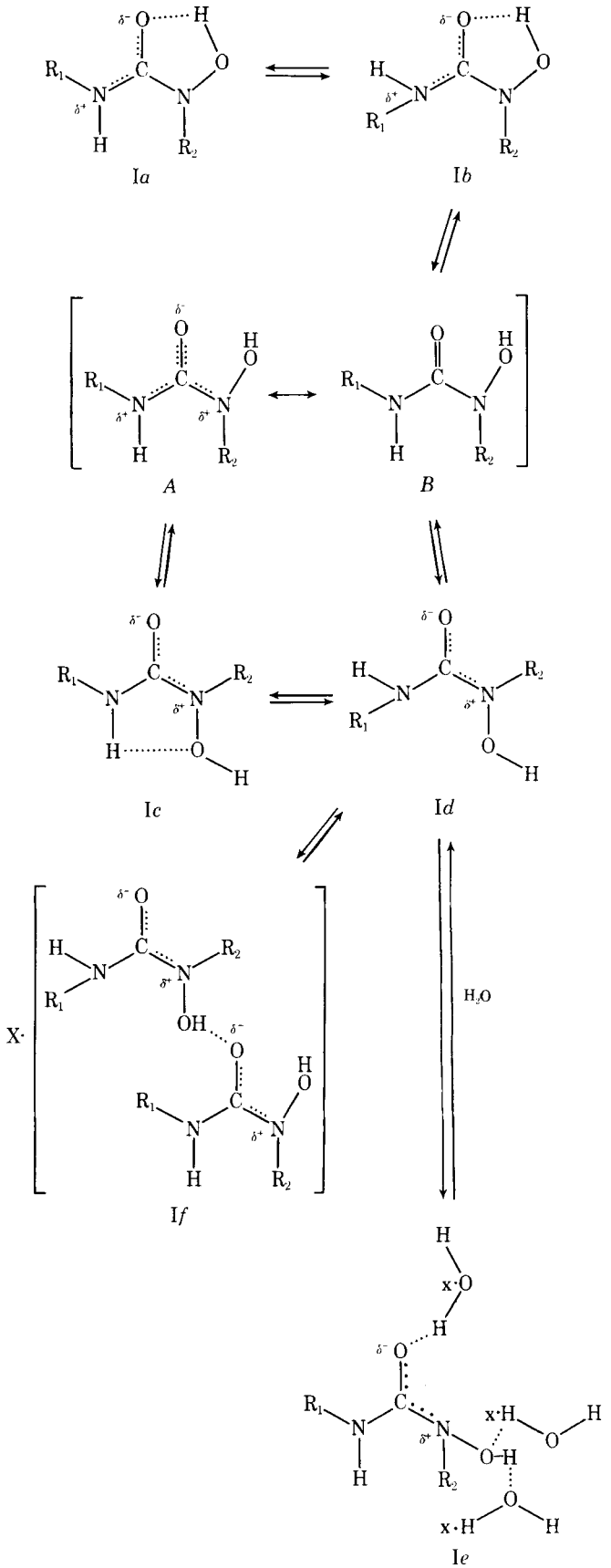

Scheme I—Conformational system of hydroxyureas depicted by canonical forms A and B, which allow interconversion to conformers Ia, Ib, and Ic, which possess internal hydrogen bonds, and to Id, which can interact with water (or solvent) to form solvate Ie or interact intermolecularly to form If.

procedure for the hydroxyureas under study and plotted against log P, two families of linearly related compounds are observed (Fig. 1) with hydroxyurea appearing between the two families (when hydroxyurea log P is determined in equal volumes of octanol–water). Compounds in the first group, composed of the 3-ethyl, 3-*n*-propyl, and 3-*n*-butyl analogs, are more hydrophilic than their counterparts in the second group, composed of the 1-ethyl, 3-isopropyl, and *tert*-butyl analogs, and include 1-methylhydroxyurea. Fundamental differences in the conformational equilibrium system of these hydroxyureas were identified previously by NMR (22) and IR (23) spectroscopy, and this behavior depended on the solvent.

Of the conformers possible in the hydroxyurea series (Scheme I), those stabilized by internal hydrogen bonding (Ia–Ic) are preferred by the members of the more lipophilic group (the 1-substituted and the 3-substituted bulky analogs). The more hydrophilic group appears to prefer the conformer that is not internally hydrogen bonded (Id) and thus can easily interact with solvent, water, or other hydroxyurea molecules (Ie and If). The partitioning characteristics of the hydroxyureas apparently depend on the ratio of the more lipophilic conformers (those internally hydrogen bonded) to those that can hydrogen bond to other species and thus are more hydrophilic. A compound of the first group would be expected to behave differently in a biophase in comparison to a compound of the second group because of the conformational preference. Although this behavior was apparent previously, it was not as markedly evident as when correlated with log P and molecular connectivity for the two classes of hydroxyureas.

In the plot of log P *versus* molecular connectivity, the parent drug hydroxyurea appears between the two other families of analogs when it is partitioned between equal volumes of octanol and water. This result most likely indicates that the conformational preference is not similar to that found in the other families of analogs but is probably a more equal distribution of possible conformers because of fast interconversions *via* rotations around nitrogen–carbonyl bonds. The conformational equilibria present in solution appear to differ for hydroxyurea and the 3-ethyl analog in the octanol phase when analyzed *via* the IR–X-ray crystal method of comparing solid and solution conformations (24), indicating that the conformational equilibria ratio for these two compounds is indeed different.

When log P for hydroxyurea is determined in a partitioning system of five volumes of octanol to one volume of water, the log P varies from −0.42 in a low concentration to −1.52 in a high concentration. This finding indicates that hydroxyurea behaves like a member of the more lipophilic class in low concentrations and approaches the behavior of the more hydrophilic class in high concentrations. This behavior can be rationalized according to Scheme I if it is considered that hydroxyurea can interact with: (*a*) itself (such as in conformers Ia–Ic), (*b*) lipophilic solvent when in all possible conformations, (*c*) water, or (*d*) other hydroxyurea molecules, as in conformer Id (to form solvate Ie and/or intermolecular bonded species If).

When the hydroxyurea concentration is low, the contribution of the conformer involved in intermolecular interactions is decreased, since this process is less likely to occur in lower hydroxyurea concentrations. The relative contribution of the internally bonded conformers increases, and the result is a greater partitioning into the more lipophilic octanol phase. At higher hydroxyurea concentrations, the likelihood of intermolecular interactions increases through the involvement of Id, increasing the overall contribution of this conformer in the equilibrium scheme. Interconversions through Id to species involving water or other hydroxyurea molecules may be favored rather than interconversion to conformers such as Ia–Ic, thus increasing the relative hydrophilicity of the molecular species involved. With the substituted hydroxyureas, concentration does not appear to play as significant a role in the equilibrium conformational scheme, possibly because the bulky substituents do not facilitate intermolecular interactions as easily as unsubstituted hydroxyurea.

In conclusion, the correlation of log P with valence molecular connectivity apparently delineates substituted hydroxyureas into two classes of compounds which differ in their conformational equilibria and relative lipophilicity–hydrophilicity. Unsubstituted hydroxyurea, on the other hand, can exist in different ratios of conformational equilibria, depending on the concentration in solution, but is not similar to either group of substituted analogs in equal volumes of octanol and water. In low concentrations, hydroxyurea appears more lipophilic in character and resembles the group of substituted analogs comprised of the 1- and 3-substituted bulky compounds. In higher concentrations, hydroxyurea becomes more hydrophilic and approaches the range of the other group of substituted analogs comprised of the 3-substituted straight chain compounds.

The unique behavior of hydroxyurea compared to the substituted analogs in regard to the different conformational equilibria present in an *in vitro* or *in vivo* biophase might be a factor in the low biological action of substituted hydroxyureas compared to the model compound. The concentration dependency observed in the partitioning of hydroxyurea between octanol and water may be clinically significant since a difference in an apparent log P of 1 unit or greater would appreciably change the absorption, membrane transport, and relative distribution potential (possibly to normal *versus* neoplastic tissue if more lipophilic) of the agent administered. This dependency on concentration in hydroxyurea warrants further study to determine if this property influences *in vitro* or *in vivo* antitumor activity by modifying the biodynamics involved in biological action.

REFERENCES

(1) R. D. Cramer, III, *Annu. Rep. Med. Chem.*, **11**, 301 (1976).

(2) F. E. Norrington, R. M. Hyde, S. G. Williams, and R. Wooten, *J. Med. Chem.*, **18**, 604 (1975).

(3) M. S. Tute, *Adv. Drug Res.*, **6**, 1 (1971).

(4) R. Hilf, C. Bell, I. Michel, J. J. Freeman, and A. Borman, *Cancer Res.*, **26**, 2286 (1966).

(5) G. R. Gale, *Biochem. Pharmacol.*, **17**, 235 (1968).

(6) G. R. Parker, T. L. Lemke, and E. C. Moore, *J. Med. Chem.*, **20**, 1221 (1977).

(7) W. A. Murray, L. H. Hall, and L. B. Kier, *J. Pharm. Sci.*, **64**, 1978 (1975).

(8) L. B. Kier and L. H. Hall, "Molecular Connectivity in Chemistry and Drug Research," Academic, New York, N.Y., 1976.

(9) L. B. Kier, L. H. Hall, W. J. Murray, and M. Randic, *J. Pharm. Sci.*, **64**, 1971 (1975).

(10) M. Randic, *J. Am. Chem. Soc.*, **97**, 6609 (1975).

(11) L. B. Kier and L. H. Hall, *J. Pharm. Sci.*, **65**, 1806 (1976).

(12) L. H. Hall and L. B. Kier, *ibid.*, **66**, 642 (1977).

(13) W. Dresler and R. Stein, *Justus Liebigs Ann. Chem.*, **150**, 242 (1869).

(14) R. E. Harmon, J. C. Dabrowiak, D. J. Brown, S. K. Gupta, M. Herbert, and D. Chitharanjan, *J. Med. Chem.*, **13**, 577 (1970).

(15) G. Clifton, S. R. Bryant, and C. G. Skinner, *ibid.*, **13**, 377 (1970).

(16) B. Stearns, K. A. Losee, and J. Bernstein, *ibid.*, **6**, 201 (1963). R. H. Adamson, M. Ben, and D. P. Rall, *Pharmacologist*, **5**, 271 (1963).

(17) A. A. Sinkula and S. H. Yalkowsky, *J. Pharm. Sci.*, **64**, 183 (1975).

(18) C. Hansch and J. M. Clayton, *ibid.*, **62**, 1 (1973).

(19) L. H. Hall, L. B. Kier, and W. J. Murray, *ibid.*, **64**, 1974 (1975).

(20) L. B. Kier, W. J. Murray, and L. H. Hall, *J. Med. Chem.*, **18**, 1272 (1975).

(21) W. J. Murray, L. B. Kier, and L. H. Hall, *ibid.*, **19**, 573 (1975).

(22) G. R. Parker, N. K. Hilgendorf, and J. G. Lindberg, *J. Pharm. Sci.*, **65**, 585 (1976).

(23) G. R. Parker and E. C. Moore, *ibid.*, **66**, 1040 (1977).

(24) G. R. Parker and J. D. Korp, *ibid.*, **67**, 239 (1978).

ACKNOWLEDGMENTS

Presented in part at the Fourth Annual Southcentral Medicinal Chemistry Meeting in Miniature (MALTO), Houston, Tex., May 1977, sponsored by Texas Southern College of Pharmacy.

The author thanks Miss Barbara Stearns of the Squibb Institute of Medical Research for the hydroxyurea, 1-methylhydroxyurea, and 1-ethylhydroxyurea.

Benzocaine Diffusion from Polyethylene Glycol through Human Stratum Corneum

ALBERT A. BELMONTE ˣ and WENDY TSAI

Received June 9, 1977, from the *School of Pharmacy, Auburn University, Auburn, AL 36830.* Accepted for publication July 26, 1977.

Abstract □ The diffusion, penetration, and surface effects of benzocaine incorporated in various polyethylene glycol ointment bases through human stratum corneum were studied. Benzocaine diffusion was measured by following the benzocaine concentration in the receiving compartment of a diffusion cell. The ointment was placed in the other cell compartment and was separated from the receiving compartment by sheets of human stratum corneum. Surface effects were monitored by scanning electron micrographs of the stratum corneum. Results showed a decrease in drug diffusion in the presence of relatively high amounts of the lower molecular weight portions of polyethylene glycol. Scanning electron microscope studies showed that both benzocaine and polyethylene glycol affect the surface structure of the stratum corneum. Thermal analysis indicated that benzocaine dissolves in polyethylene glycol.

Keyphrases □ Benzocaine—diffusion from various polyethylene glycol ointment bases through human stratum corneum □ Diffusion—benzocaine from various polyethylene glycol ointment bases through human stratum corneum □ Surface effects—benzocaine diffusion from various polyethylene glycol ointment bases through human stratum corneum □ Ointment bases—various polyethylene glycols, benzocaine diffusion through human stratum corneum □ Anesthetics, topical—benzocaine, diffusion from various polyethylene glycol ointment bases through human stratum corneum

Benzocaine (ethyl *p*-aminobenzoate) is used extensively as a local anesthetic. Its relatively slow absorption renders it especially useful in treating skin ulcers, wounds, and mucous surfaces. The anesthesia is usually not as complete as that induced by the soluble anesthetics but is longer lasting.

BACKGROUND

The rate of benzocaine release is greater from water-soluble bases than from other bases (1, 2). Physical and chemical relationships between the ointment base and the medicament are important (3–7). While many studies have been directed toward traditional ointment bases, only a limited amount of work has been done using water-soluble ointment bases including polyethylene glycols.

Water-soluble bases are anhydrous but are capable of absorbing small amounts of water, are soluble in water, and are water removable. Although some water-dispersible ointment bases are often classified as water soluble, polyethylene glycols are the only widely used water-soluble ointment bases. The polyethylene glycols range from liquids to waxy solids, depending on molecular weight; by blending various molecular weight fractions, different base consistencies are possible.

Polyethylene glycols are important in pharmaceuticals as anhydrous, stable, bland bases for external preparations. They demonstrate low oral and dermal toxicity and low irritating properties (8). The ability of polyethylene glycols to form inert, emollient bases has enhanced their use as washable vehicles (9).

Penetration of drug through the skin and subsequent systemic absorption have been of particular interest recently. A primary consideration of transepidermal penetration is the stratum corneum, since the impermeability of skin largely resides in the stratum corneum, which is mechanically strong and capable of resisting chemical attack (10). The main barriers of the stratum corneum are the dead cells that restrict the inward and outward movement of chemical substances (11). Analysis of penetration and electron microscope studies support the concept that the penetration barrier consists of a keratin–phospholipid complex in the dead and relatively dry cells (12, 13). The thickness of the stratum corneum varies between subjects and depends on body location.

EXPERIMENTAL

Reagents and Equipment—The chemicals used included benzocaine[1]; polyethylene glycols 200, 600, 4000, 6000, and 20,000[2]; sodium bicarbonate[3]; monobasic sodium phosphate[3]; dibasic sodium phosphate[3]; sodium hydroxide USP[4]; lyophilized trypsin[5]; formaldehyde USP[6]; amyl acetate (mixed isomers)[2]; and alcohol USP[7]. The purity of benzocaine and polyethylene glycols 4000, 6000, and 20,000 was checked using differential thermal analysis[8]. Unless otherwise noted, reagents were analytical grade, except the lyophilized trypsin, and were used as received.

Solutions were prepared from the reagents listed and included 6.6×10^{-2} *M* monobasic sodium phosphate, 6.6×10^{-2} *M* dibasic sodium phosphate, 0.1 *N* NaOH, 10% formaldehyde, 0.5% sodium bicarbonate, and 0.0001% trypsin. Two buffers, pH 5.9 and 4.9, were prepared from the phosphate solutions.

The equipment included a spectrophotometer[9] for the benzocaine assay, a constant-temperature shaker bath[10], and custom-made polymethacrylate diffusion cells[11] similar to those described by Patel and Foss (14). The scanning electron microscope studies were carried out on a laboratory scope[12] utilizing a critical point drying apparatus[13] and vacuum evaporator[14].

Ointment Formulation—Ointment bases were prepared using varying amounts of different molecular weight polyethylene glycols. Ointments were prepared by the use of heat and mechanical incorporation. The polyethylene glycols were placed in a vessel and heated on a steam bath until liquefied. The ointment was removed from the heat and stirred until congealed. Powdered benzocaine was incorporated by spatulation.

Approximately 25 ointment base formulations composed of combinations of polyethylene glycol 200, 600, 4000, 6000, and 20,000 were prepared. Four formulations were especially suitable pharmaceutically: 50% polyethylene glycol 4000 plus 50% polyethylene glycol 600 (I), 25% polyethylene glycol 4000 plus 75% polyethylene glycol 600 (II), 50% polyethylene glycol 6000 plus 50% polyethylene glycol 600 (III), and 25% polyethylene glycol 6000 plus 75% polyethylene glycol 600 (IV). Ointments were prepared by incorporation of 5% (w/w) benzocaine in each base.

Stratum Corneum Preparation—Human stratum corneum was obtained by treating human cadaver skin taken at autopsy. Full thickness samples of adult abdominal skin proximal to the umbilicus were taken at autopsy and separated by scalpel from underlying subcutaneous fat. The epidermal sheet was removed from the dermis after immersion of the whole skin in 60° water for 30 sec (15).

Epidermal sheets were placed dermal side down on several sheets of filter paper saturated with 0.0001% trypsin containing 0.5% sodium bicarbonate; the pH was adjusted to between 8.0 and 8.6. The filter paper was covered with proteolytic solution in a small petri dish, which was incubated overnight at 37°. After incubation, the tissue was placed on a flat surface. Any remaining epidermis was removed by gentle massage with a moistened cotton-tipped applicator.

[1] Eastman Kodak, Rochester, NY 14650.
[2] J. T. Baker, Phillipsburg, NJ 08865.
[3] Fisher Scientific, Fair Lawn, NJ 07410.
[4] Mallinckrodt, St. Louis, MO 63160.
[5] Worthington Biochemicals, Freehold, NJ 07728.
[6] Amend Drug & Chemical, Irvington, NJ 07111.
[7] U.S. Industrial Chemicals, New York, NY 10001.
[8] DuPont 990 thermal analyzer, DuPont Instruments, Wilmington, DE 19898.
[9] Beckman DB-G with recorder, Beckman Instruments, Fullerton, CA 92634.
[10] Model 50, Precision Scientific, Chicago, IL 60647.
[11] Davis Machine, Opelika, AL 36801.
[12] Advanced Metals Research model 1000, Burlington, MA 01803.
[13] Denton, Cherry Hill, NJ 08003.
[14] Denton model DV-502, Cherry Hill, NJ 08003.

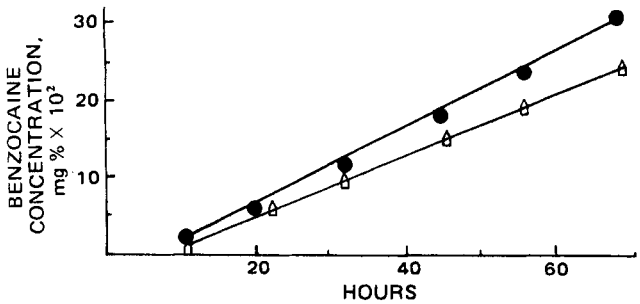

Figure 1—*Benzocaine diffusion through human stratum corneum at pH 5.9 from Ointments I (●) and II (△).*

The resultant stratum corneum was a smooth, transparent, resilient sheet. It was stored by floating on water and placed on aluminum foil. The resultant product has been shown to be stable even at ambient conditions for extended periods (16). Sample intactness was checked by optical microscopic examination prior to use.

Diffusion Study—Diffusion measurements were carried out by packing one-half of the cell with ointment, attaching the stratum corneum between the two half-cells, and then securing both sides tightly together. After assembly, the other cell compartment was filled with 20 ml of buffer through an opening that was subsequently stoppered. The entire assembly was immersed in the constant-temperature shaker bath, which was held to 37 ± 1°. The shaker bath was agitated at 100 oscillations/min.

At specified time intervals, 1-ml samples of buffer were withdrawn from the receptacle side of the cell. All sampling was done with replacement, and all experiments were done in duplicate with fresh stratum corneum. Blank ointments (no medicament) were also run for comparison.

Benzocaine appearance in the buffer compartment was measured by treating the 1-ml sample with 0.1 *N* NaOH and measuring the hydrolyzed benzocaine spectrophotometrically at its maximum absorbance, 267 nm. A standard curve was previously prepared similarly such that a direct correlation was shown between concentration and absorbance.

Thermal Analysis—All polyethylene glycols, benzocaine, ointment bases, and ointments containing benzocaine were studied by thermal analysis techniques. Differential scanning calorimetry was performed by hermetically sealing samples in cups. An empty cup was sealed in a similar manner and used as a reference. Samples were run from 11 to 200°, and results were recorded using an *x–y* recorder.

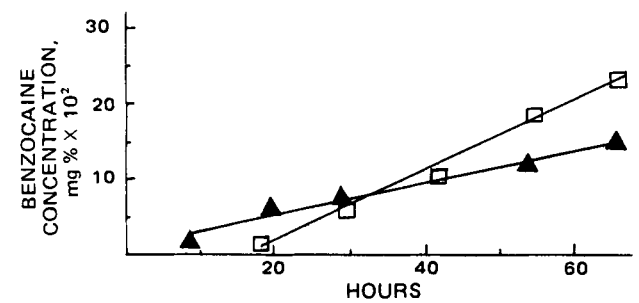

Figure 2—*Benzocaine diffusion through human stratum corneum at pH 5.9 from Ointments III (□) and IV (▲).*

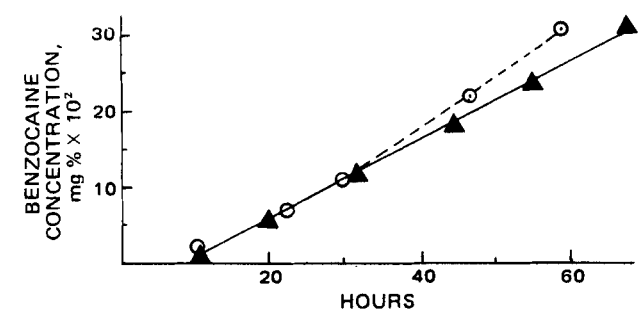

Figure 3—*Benzocaine diffusion through human stratum corneum from Ointment I at pH 4.9 (⊙) and 5.9 (▲).*

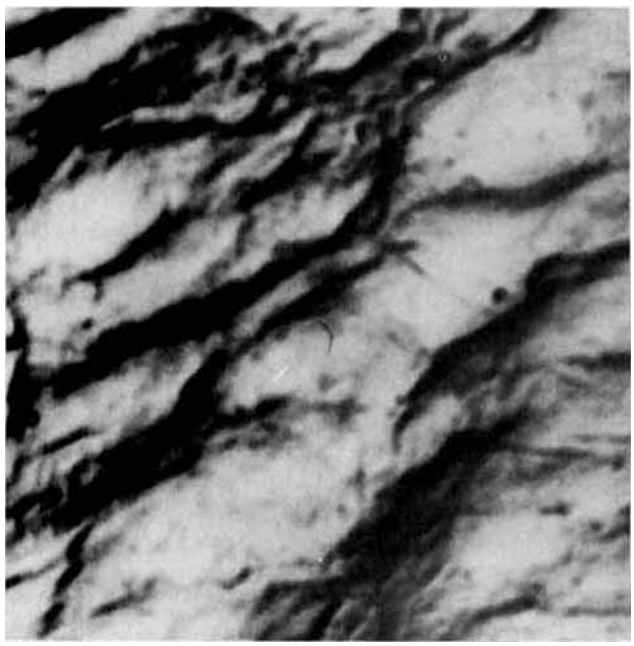

Figure 4—*Scanning electron micrograph of normal human stratum corneum (1000× magnification).*

Scanning Electron Microscopy—Stratum corneum samples before and after treatment were studied for surface structure changes. Samples were taken after exposure to blank ointment bases for comparison.

Specimens were washed with water after exposure to ointments and then soaked in 10% formaldehyde solution. Subsequently, they were dehydrated by exposure to increasing concentrations of ethanol and then exposed to amyl acetate for 5 min. Specimens were mounted on stubs and subjected to liquid carbon dioxide in the drying apparatus. After dehydration, sample coating was achieved using a 60% gold–40% palladium alloy in the vacuum evaporator.

RESULTS AND DISCUSSION

Figure 1 illustrates benzocaine diffusion from Ointments I and II through the stratum corneum into pH 5.9 buffer. Greater penetration

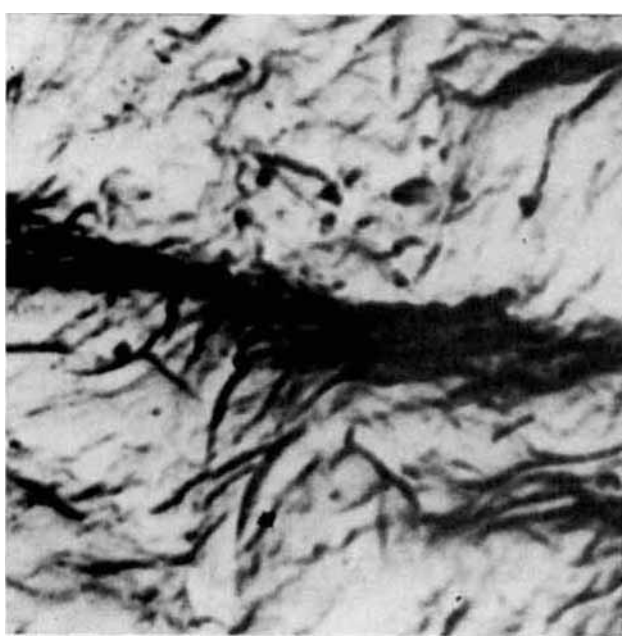

Figure 5—*Scanning electron micrograph of human stratum corneum after treatment with 5% benzocaine in Ointment I (1000× magnification).*

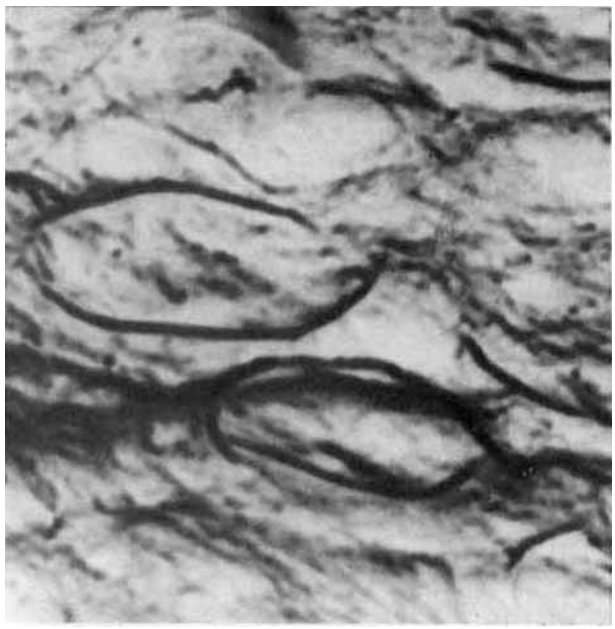

Figure 6—*Scanning electron micrograph of human stratum corneum after treatment with 5% benzocaine in Ointment II (1000× magnification).*

of benzocaine from the ointment containing 50% polyethylene glycol 600 (I) than from the 75% polyethylene glycol 600 ointment (II) is shown by the upward displacement and increases in slope for the Ointment I line. In Fig. 2, penetration again appears greater with the 50% polyethylene glycol 600 ointment (III) compared to the ointment containing 75% polyethylene glycol 600 (IV).

Figure 3 illustrates benzocaine transfer from Ointment I through the stratum corneum into pH 4.9 buffer solution. Similar results were obtained with Ointments II–IV. Alteration of pH in the receiving compartment did not significantly alter benzocaine diffusion in this system.

Figures 4–7 are scanning electron micrographs of human stratum corneum normally (Fig. 4) and after various treatments (Figs. 5–7). As shown in Fig. 5, there were noticeable changes in the surface structure of the stratum corneum after treatment with 5% benzocaine in 50% polyethylene glycol 4000 plus 50% polyethylene glycol 600 base (Ointment

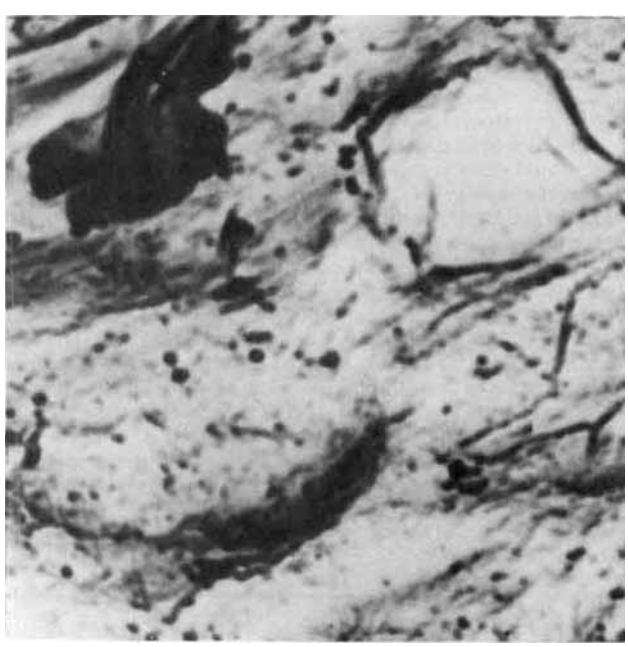

Figure 7—*Scanning electron micrograph of human stratum corneum after treatment with Ointment II (1000× magnification).*

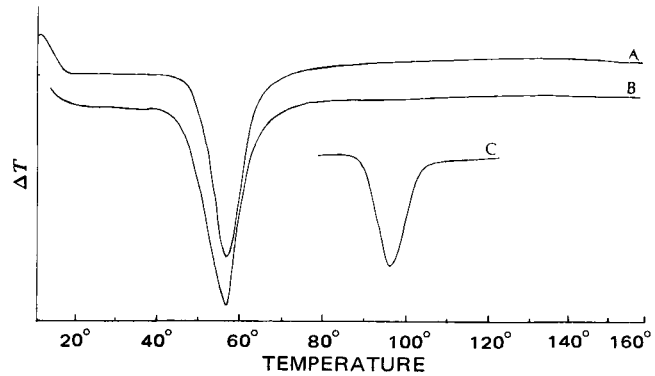

Figure 8—*Thermograms of Ointment III (A), 5% benzocaine in Ointment III (B), and pure benzocaine (C).*

I). A considerable increase in surface roughness was seen along with an increase in surface ridge sharpness.

Figure 6 shows a more prominent change in the physical structure from treatment with 5% benzocaine in 25% polyethylene glycol 4000 and 75% polyethylene glycol 600 (Ointment II). Considerable changes in physical structure appeared in the form of circumscribed hexagonal- and pentagonal-shaped areas. These circumscribed areas also appeared in blank (no benzocaine) ointments (Fig. 7). These results indicate that the ointment base affects the physical surface structure of human stratum corneum. In addition, ointments containing benzocaine have a similar but somewhat less pronounced effect. The principal effect appears to be a function of the polyethylene glycol 600 content.

Thermal analysis studies showed benzocaine dissolved in the polyethylene glycol ointment bases. Figure 8 shows thermograms of Ointment III with 5% benzocaine (curve B). Pure benzocaine exhibited an endotherm at 90–100° (curve C). The blank ointment (III without benzocaine) is shown as curve A. Similar curves were obtained with all other ointments.

CONCLUSIONS

Benzocaine release from various polyethylene glycol ointments appeared to depend on the polyethylene glycol composition. While various molecular weight fractions of polyethylene glycol could be blended for the desired consistency, ointments containing relatively large portions of lower molecular weight polyethylene glycols may retard benzocaine release. This finding may have implication for ointment formulations containing water-soluble ointment bases since polyethylene glycols are major constituents of many water-soluble bases currently used.

Alteration of pH in the receiving compartment of the diffusion cell did not influence drug release. However, considering the narrow pH range used, perhaps a greater pH differential should be chosen.

Thermal analysis showed that benzocaine dissolved in all polyethylene glycol ointment bases used. The solubility is, of course, dependent on the drug–polyethylene glycol interaction and does not occur with all drugs incorporated in polyethylene glycol bases. However, if a drug dissolves in polyethylene glycol, it may suggest release alteration if the polyethylene glycol composition is altered.

Scanning electron microscope results indicate that polyethylene glycol has a significant effect on the surface structure of the stratum corneum. Benzocaine may, in addition, have a surface effect; however, it appears to be a lesser effect compared to the polyethylene glycol ointment bases.

REFERENCES

(1) J. W. Ayers and P. A. Laskar, *J. Pharm. Sci.*, **63**, 1402 (1974).

(2) J. W. Ayers, D. Lorskulsint, and A. Lock, *ibid.*, **64**, 1958 (1975).

(3) N. F. H. Ho, J. S. Turi, C. Shipman, Jr., and W. I. Higuchi, *J. Theoret. Biol.*, **34**, 451 (1972).

(4) J. S. Turi, W. I. Higuchi, C. Shipman, Jr., and N. F. H. Ho, *J. Pharm. Sci.*, **61**, 1618 (1972).

(5) J. S. Turi, N. F. H. Ho, W. I. Higuchi, and C. Shipman, Jr., *ibid.*, **64**, 622 (1975).

(6) T. Higuchi, *J. Soc. Cosmet. Chem.*, **11**, 85 (1960).

(7) J. G. Wagner, *J. Pharm. Sci.*, **50**, 379 (1961).

(8) H. F. Smyth, C. P. Carpenter, and C. S. Weil, *J. Am. Pharm. Assoc., Sci. Ed.*, **39**, 349 (1950).

(9) *Ibid.*, **44**, 27 (1955).
(10) W. Montagna and W. C. Lobitz, Jr., "The Epidermis," Academic, New York, N.Y., 1964, p. 387.
(11) R. T. Tregear, "Physical Functions of the Skin," Academic, New York, N.Y., 1966.
(12) I. Brody, *J. Invest. Dermatol.*, **39**, 519 (1963).
(13) B. Idson, *J. Pharm. Sci.*, **64**, 901 (1975).
(14) N. K. Patel and N. E. Foss, *ibid.*, **53**, 94 (1964).
(15) R. J. Scheuplein, *J. Invest. Dermatol.*, **45**, 334 (1965).
(16) G. L. Wilkes, A. Nguyen, and R. Wildnauer, *Biochim. Biophys. Acta*, **304**, 267 (1973).

ACKNOWLEDGMENTS

Presented in part at the APhA Academy of Pharmaceutical Sciences, New Orleans meeting, April 1976.

The authors thank E. C. Mora for helpful discussions and J. H. Blalock for skin samples.

Effect of Acylated Amino Acids and Acylated Amino Acid Analogs on Microbial Antitumor Screen

THEODORE T. OTANI ˣ and MARY R. BRILEY

Received March 10, 1977, from the *Nucleic Acids Section, Laboratory of Pathophysiology, National Cancer Institute, National Institutes of Health, Bethesda, MD 20014.* Accepted for publication July 26, 1977.

Abstract □ A series of *N*-acetyl, *N*-propionyl, and *N*-chloroacetyl derivatives of amino acids and amino acid analogs was tested for growth-inhibitory activity using a *Lactobacillus casei* system as a prescreen for possible antitumor activity. While none of the acetyl or propionyl derivatives of these amino acids and amino acid analogs caused any remarkable inhibition, certain chloroacetyl derivatives exhibited significant activity. The chloroacetyl derivatives, especially those of essential amino acids and of analogs of essential amino acids, showed modest, but pharmacologically significant, inhibition; those of nonessential amino acids exhibited no activity. When two such inhibitory acyl derivatives were combined in a single assay, the extent of inhibition was neither additive nor synergistic but was that of the more active of the two test components.

Keyphrases □ Amino acids, various acylated—evaluated in microbial antitumor screen □ Acylated amino acids, various—evaluated in microbial antitumor screen □ Antitumor activity—various acylated amino acids evaluated in microbial screen □ Structure–activity relationships—various acylated amino acids evaluated in microbial antitumor screen

In a search for antineoplastic activities among a series of β-hydroxy-α-amino acids, some unsubstituted acids exhibited no growth-inhibitory action in a *Lactobacillus casei* test system, but their chloroacetyl derivatives showed pharmacologically significant activity in this system (1, 2). As a result of that observation, an investigation was initiated to note whether the behavior of other analogs of natural amino acids known to be antimetabolites might not be affected similarly by acylation.

The *N*-acetyl, *N*-chloroacetyl, and *N*-propionyl derivatives of a series of amino acids and amino acid analogs were prepared. These compounds were tested against an *L. casei* system (3) to determine the presence of growth-inhibitory capacity. This microbial system was selected as a prescreen for antitumor activity because of its capability of detecting, very quickly, a high percentage of compounds known to be active against tumors, using very small quantities of test compound (3). A study was also made to determine the existence of additive or synergistic properties when two inhibitory compounds were used simultaneously.

The present paper reports the results of these studies.

EXPERIMENTAL

The free amino acids, except for the isomers of β-hydroxymethoxinine and β-hydroxyhomomethionine which were prepared in this laboratory (4), were obtained commercially. The sources and purity data for the acyl derivatives are shown in Tables I–III. The commercially obtained free amino acids and acyl compounds were recrystallized, and all compounds were checked for purity by elemental analysis, melting-point determination, optical rotation determination, and Van Slyke nitrous acid determination of primary amino nitrogen (5) before use (Tables I–III). In addition, the free amino acids were checked by paper chromatography in at least four different solvent systems (*cf.*, 2).

The chloroacetyl and propionyl derivatives were prepared in this laboratory by acylation of the precursors by the conventional Schotten–Baumann procedure (*cf.*, 6). The chloroacetyl chloride[1] and propionyl chloride[1] used for the acylation and the propionic acid[1] and monochloroacetic acid[2] were freshly redistilled before use. The optically pure amino acids were prepared by asymmetric enzymatic hydrolysis of the racemic chloroacetyl derivatives and subsequent acid hydrolysis of the unsusceptible chloroacetyl-D-amino acid. The optically pure chloroacetyl-L-amino acids were prepared by acylation of the pure L-isomer, and the chloroacetyl-D-isomers were isolated from the resolution mixture as described (11). Hog renal acylase[3] was used for the hydrolysis of the acyl aliphatic amino acids, and pancreatic carboxypeptidase[4] was used for the hydrolysis of the acyl aromatic amino acid (11).

For the microbiological assay, the test compounds were dissolved in a small volume of water and the pH was adjusted to 6 by the addition of an appropriate volume of 0.1 *N* NaOH. L-Tyrosine required equimolar amounts of the base for solution, resulting in a basic solution. In some cases, gentle warming was required for complete solution. The test solutions were sterilized by filtration using an all-glass bacterial filter (ultrafine porosity).

The concentration of the test solution as prepared was 2 mg/ml and was equivalent to a concentration of 1 mg/ml in the assay system. For the experiments comparing the relative activities of the "active" compounds, the concentration of the test solution was 89.4 μmoles/10 ml as prepared and was equivalent to a concentration of 4.47 μmoles of the test compound/ml in the assay system. This concentration is equivalent to 1 mg of *N*-chloroacetyl-β-hydroxy-D-norleucine B/ml, the compound found previously to be the most active isomer of chloroacetyl-β-hydroxynorleucine (2).

All glassware used in the microbiological assay was cleaned in a metal ion-free cleaning agent[5].

[1] Eastman Organic Chemicals, Rochester, N.Y.
[2] Fisher Scientific Co., Silver Spring, Md.
[3] Nutritional Biochemicals, Cleveland, Ohio.
[4] Calbiochem, La Jolla, Calif.
[5] No-chromix, Godax Laboratories, New York, N.Y.

(9) *Ibid.*, **44**, 27 (1955).
(10) W. Montagna and W. C. Lobitz, Jr., "The Epidermis," Academic, New York, N.Y., 1964, p. 387.
(11) R. T. Tregear, "Physical Functions of the Skin," Academic, New York, N.Y., 1966.
(12) I. Brody, *J. Invest. Dermatol.*, **39**, 519 (1963).
(13) B. Idson, *J. Pharm. Sci.*, **64**, 901 (1975).
(14) N. K. Patel and N. E. Foss, *ibid.*, **53**, 94 (1964).
(15) R. J. Scheuplein, *J. Invest. Dermatol.*, **45**, 334 (1965).
(16) G. L. Wilkes, A. Nguyen, and R. Wildnauer, *Biochim. Biophys. Acta*, **304**, 267 (1973).

ACKNOWLEDGMENTS

Presented in part at the APhA Academy of Pharmaceutical Sciences, New Orleans meeting, April 1976.

The authors thank E. C. Mora for helpful discussions and J. H. Blalock for skin samples.

Effect of Acylated Amino Acids and Acylated Amino Acid Analogs on Microbial Antitumor Screen

THEODORE T. OTANI ˣ and MARY R. BRILEY

Received March 10, 1977, from the *Nucleic Acids Section, Laboratory of Pathophysiology, National Cancer Institute, National Institutes of Health, Bethesda, MD 20014.* Accepted for publication July 26, 1977.

Abstract □ A series of *N*-acetyl, *N*-propionyl, and *N*-chloroacetyl derivatives of amino acids and amino acid analogs was tested for growth-inhibitory activity using a *Lactobacillus casei* system as a prescreen for possible antitumor activity. While none of the acetyl or propionyl derivatives of these amino acids and amino acid analogs caused any remarkable inhibition, certain chloroacetyl derivatives exhibited significant activity. The chloroacetyl derivatives, especially those of essential amino acids and of analogs of essential amino acids, showed modest, but pharmacologically significant, inhibition; those of nonessential amino acids exhibited no activity. When two such inhibitory acyl derivatives were combined in a single assay, the extent of inhibition was neither additive nor synergistic but was that of the more active of the two test components.

Keyphrases □ Amino acids, various acylated—evaluated in microbial antitumor screen □ Acylated amino acids, various—evaluated in microbial antitumor screen □ Antitumor activity—various acylated amino acids evaluated in microbial screen □ Structure–activity relationships—various acylated amino acids evaluated in microbial antitumor screen

In a search for antineoplastic activities among a series of β-hydroxy-α-amino acids, some unsubstituted acids exhibited no growth-inhibitory action in a *Lactobacillus casei* test system, but their chloroacetyl derivatives showed pharmacologically significant activity in this system (1, 2). As a result of that observation, an investigation was initiated to note whether the behavior of other analogs of natural amino acids known to be antimetabolites might not be affected similarly by acylation.

The *N*-acetyl, *N*-chloroacetyl, and *N*-propionyl derivatives of a series of amino acids and amino acid analogs were prepared. These compounds were tested against an *L. casei* system (3) to determine the presence of growth-inhibitory capacity. This microbial system was selected as a prescreen for antitumor activity because of its capability of detecting, very quickly, a high percentage of compounds known to be active against tumors, using very small quantities of test compound (3). A study was also made to determine the existence of additive or synergistic properties when two inhibitory compounds were used simultaneously.

The present paper reports the results of these studies.

EXPERIMENTAL

The free amino acids, except for the isomers of β-hydroxymethoxinine and β-hydroxyhomomethionine which were prepared in this laboratory (4), were obtained commercially. The sources and purity data for the acyl derivatives are shown in Tables I–III. The commercially obtained free amino acids and acyl compounds were recrystallized, and all compounds were checked for purity by elemental analysis, melting-point determination, optical rotation determination, and Van Slyke nitrous acid determination of primary amino nitrogen (5) before use (Tables I–III). In addition, the free amino acids were checked by paper chromatography in at least four different solvent systems (*cf.*, 2).

The chloroacetyl and propionyl derivatives were prepared in this laboratory by acylation of the precursors by the conventional Schotten–Baumann procedure (*cf.*, 6). The chloroacetyl chloride[1] and propionyl chloride[1] used for the acylation and the propionic acid[1] and monochloroacetic acid[2] were freshly redistilled before use. The optically pure amino acids were prepared by asymmetric enzymatic hydrolysis of the racemic chloroacetyl derivatives and subsequent acid hydrolysis of the unsusceptible chloroacetyl-D-amino acid. The optically pure chloroacetyl-L-amino acids were prepared by acylation of the pure L-isomer, and the chloroacetyl-D-isomers were isolated from the resolution mixture as described (11). Hog renal acylase[3] was used for the hydrolysis of the acyl aliphatic amino acids, and pancreatic carboxypeptidase[4] was used for the hydrolysis of the acyl aromatic amino acid (11).

For the microbiological assay, the test compounds were dissolved in a small volume of water and the pH was adjusted to 6 by the addition of an appropriate volume of 0.1 *N* NaOH. L-Tyrosine required equimolar amounts of the base for solution, resulting in a basic solution. In some cases, gentle warming was required for complete solution. The test solutions were sterilized by filtration using an all-glass bacterial filter (ultrafine porosity).

The concentration of the test solution as prepared was 2 mg/ml and was equivalent to a concentration of 1 mg/ml in the assay system. For the experiments comparing the relative activities of the "active" compounds, the concentration of the test solution was 89.4 μmoles/10 ml as prepared and was equivalent to a concentration of 4.47 μmoles of the test compound/ml in the assay system. This concentration is equivalent to 1 mg of *N*-chloroacetyl-β-hydroxy-D-norleucine B/ml, the compound found previously to be the most active isomer of chloroacetyl-β-hydroxynorleucine (2).

All glassware used in the microbiological assay was cleaned in a metal ion-free cleaning agent[5].

[1] Eastman Organic Chemicals, Rochester, N.Y.
[2] Fisher Scientific Co., Silver Spring, Md.
[3] Nutritional Biochemicals, Cleveland, Ohio.
[4] Calbiochem, La Jolla, Calif.
[5] No-chromix, Godax Laboratories, New York, N.Y.

Table I—Purity Data of *N*-Acetyl Derivatives [a]

N-Acetyl Derivative	Source[b]	Melting Point, Reported	Melting Point, Observed[c]	Optical Rotation[d], $[\alpha]_D$ 21–24°, Reported	Optical Rotation[d], $[\alpha]_D$ 21–24°, Observed	Empirical Formula	Analysis[e], % Calc.	Analysis[e], % Obs.
DL-Allylglycine	1	114°[f]	116°	—	0° (A)	$C_7H_{11}NO_3$	C 53.49	53.76
							H 7.06	7.35
							N 8.91	8.98
DL-Leucine	2	159°[f]	163°	—	0° (A)	$C_8H_{15}NO_3$	C 55.47	55.76
							H 8.73	8.80
							N 8.09	8.33
L-Leucine[g]	2	185°[f]	193°	−21.3°[f] (A)	−23.0° (A)	$C_8H_{15}NO_3$	C 55.47	55.27
							H 8.73	8.95
							N 8.09	8.27
D-Leucine[g]	3	185°[f]	193°	+21.3°[f] (A)	+23.3° (A)	$C_8H_{15}NO_3$	C 55.47	55.76
							H 8.73	8.82
							N 8.09	8.15
DL-Norleucine[g]	4	105°[f]	99°	—	0° (W)	$C_8H_{15}NO_3$	C 55.47	55.67
							H 8.73	8.98
							N 8.09	8.15
D-Norleucine	2	112°[f]	113°	+20.0°[f] (W)	+20.5° (W)	$C_8H_{15}NO_3$	C 55.47	55.50
							H 8.73	8.92
							N 8.09	8.28
o-Fluoro-DL-phenylalanine	3	151–153°[h]	151–153°	—	0° (A)	$C_{11}H_{12}FNO_3$	C 58.66	58.54
							H 5.37	5.53
							N 6.22	6.12
m-Fluoro-DL-phenylalanine	2	156–158°[h]	153–154°	—	0° (A)	$C_{11}H_{12}FNO_3$	C 58.66	58.37
							H 5.37	5.42
							N 6.22	6.33
p-Fluoro-DL-phenylalanine	3	150–153°[h]	150–153°	—	0° (A)	$C_{11}H_{12}FNO_3$	C 58.66	58.60
							H 5.37	5.49
							N 6.22	6.40
β-2-Thienyl-DL-alanine	1	130°[i]	131–133°	—	0° (A)	$C_9H_{11}NO_3S$	C 50.69	50.67
							H 5.20	5.14
							N 6.57	6.50
β-3-Thienyl-DL-alanine hemihydrate	1	—	125–126°	—	0° (A)	$C_9H_{12}NO_{3\frac{1}{2}}S$	C 48.63	48.17
							H 5.14	5.22
							N 6.30	6.29

[a] Van Slyke nitrous acid determination of primary amino nitrogen (5) made on a 1-ml sample containing an equivalent of 0.3 mg of amino nitrogen (when hydrolyzed) yielded no detectable quantity of nitrogen. [b] Source of compounds: 1, prepared in this laboratory; 2, ICN Pharmaceuticals, Cleveland, Ohio; 3, Sigma Chemical Co., St. Louis, Mo.; and 4, Vega-Fox Biochemicals, Tucson, Ariz. Data on commercial products were obtained from recrystallized materials. [c] Melting points (uncorrected) were determined on a Fisher-Johns melting-point block. [d] Optical rotation was determined on a Rudolph polarimeter (Rudolph Research, Fairfield, N.J.), model 80, sodium lamp, using 100-mm tubes (bore size of 3 mm) and a sample capacity of 0.7 ml. (W) = water, (A) = absolute ethanol, c = 2. [e] Elemental analyses were performed by the Microanalytical Laboratory, National Institute of Arthritis, Metabolism, and Digestive Diseases, National Institutes of Health, Bethesda, Md. [f] *Cf.*, Ref. 6. [g] Used as obtained commercially. [h] The Aldrich Catalog-Handbook of Organic and Biochemicals, 1975–1976, p. 10. [i] *Cf.*, Ref. 7.

Table II—Purity Data of *N*-Propionyl Derivatives [a,b]

N-Propionyl Derivative	Observed Melting Point[c]	Observed Optical Rotation[d], $[\alpha]_D$ 22–24°	Empirical Formula	Analysis[e], % Calc.	Analysis[e], % Obs.
L-Alanine	87–88°	−35.4°	$C_6H_{11}NO_3$	C 49.64	49.71
				H 7.64	7.86
				N 9.65	9.55
DL-Allylglycine	85–86°	0°	$C_8H_{13}NO_3$	C 56.12	55.99
				H 7.65	7.44
				N 8.18	8.16
o-Fluoro-DL-phenylalanine	137–138°	0°	$C_{12}H_{14}FNO_3$	C 60.24	60.09
				H 5.90	5.96
				N 5.86	5.82
m-Fluoro-DL-phenylalanine	106–108°	0°	$C_{12}H_{14}FNO_3$	C 60.24	60.50
				H 5.90	6.04
				N 5.86	5.80
p-Fluoro-DL-phenylalanine	117–120°	0°	$C_{12}H_{14}FNO_3$	C 60.24	60.41
				H 5.90	5.96
				N 5.86	5.89
L-Leucine	142–144°	−22.0°	$C_9H_{17}NO_3$	C 57.73	57.80
				H 9.15	9.24
				N 7.48	7.33
DL-Norleucine	84–85°	0°	$C_9H_{17}NO_3$	C 57.73	57.98
				H 9.15	9.14
				N 7.48	7.29
β-2-Thienyl-DL-alanine	115–117°	0°	$C_{10}H_{13}NO_3S$	C 52.85	52.83
				H 5.76	5.58
				N 6.16	6.12
β-2-Thienyl-DL-β-alanine	186–187°	0°	$C_{10}H_{13}NO_3S$	C 52.85	52.92
				H 5.76	5.96
				N 6.16	6.28
β-3-Thienyl-DL-alanine hemihydrate	103–107°	0°	$C_{10}H_{14}NO_{3\frac{1}{2}}S$	C 50.83	50.95
				H 5.97	5.53
				N 5.93	5.86

[a] These compounds were prepared in this laboratory. [b] Van Slyke nitrous acid determination of primary amino nitrogen (5) made on a 1-ml sample containing an equivalent of 0.3 mg of amino nitrogen (when hydrolyzed) yielded no detectable quantity of nitrogen. [c] Melting points (uncorrected) were determined on a Fisher-Johns melting-point block. [d] Optical rotation was determined on a Rudolph polarimeter, model 80, sodium lamp, using 100-mm tubes (bore size of 3 mm) and a sample capacity of 0.7 ml in absolute ethanol, c = 2. [e] Elemental analyses were performed by the Microanalytical Laboratory, National Institute of Arthritis, Metabolism, and Digestive Diseases, National Institutes of Health, Bethesda, Md.

Table III—Purity Data of *N*-Chloroacetyl Derivatives [a]

N-Chloroacetyl Derivative	Source[b]	Melting Point, Reported	Melting Point, Observed[c]	Optical Rotation[d], $[\alpha]_D$ 22–24°, Reported	Optical Rotation[d], $[\alpha]_D$ 22–24°, Observed	Empirical Formula	Analysis[e], % Calc.	Analysis[e], % Obs.
L-Alanine	1	93°[f]	91–93°	−45.4° (W)[f]	−45.1° (W)	$C_5H_8ClNO_3$	C 36.27 H 4.86 N 8.46	35.97 4.93 8.25
D-Alanine	1	93°[f]	91–94°	+45.4° (W)[f]	+45.8° (W)	$C_5H_8ClNO_3$	C 36.27 H 4.86 N 8.46	36.15 4.95 8.18
L-Aspartic acid	2	144°[f]	140–144°	+4.0° (W)[f]	+3.5° (W)	$C_6H_8ClNO_5$	C 34.38 H 3.84 N 6.68	34.11 3.95 6.69
D-Aspartic acid	2	144°[f]	142–143°	−4.0° (W)[f]	−3.0° (W)	$C_6H_8ClNO_5$	C 34.38 H 3.84 N 6.68	34.09 3.95 6.67
DL-Allylglycine	2	—	87°	—	0° (A)	$C_7H_{10}ClNO_3$	C 43.88 H 5.26 N 7.26	44.15 5.07 7.31
L-Allylglycine	2	—	96–97°	—	+7.5° (W)	$C_7H_{10}ClNO_3$	C 43.88 H 5.26 N 7.26	43.78 5.18 7.38
D-Allylglycine	2	—	95–96°	—	−9.1° (W)	$C_7H_{10}ClNO_3$	C 43.88 H 5.26 N 7.26	43.58 5.32 7.31
o-Fluoro-DL-phenylalanine	2	—	134–136[c]	—	0° (A)	$C_{11}H_{11}ClFNO_3$	C 50.88 H 4.27 N 5.39	50.57 4.33 5.43
m-Fluoro-DL-phenylalanine	2	—	122–123°	—	0° (A)	$C_{11}H_{11}ClFNO_3$	C 50.88 H 4.27 N 5.39	50.77 4.25 5.47
p-Fluoro-DL-phenylalanine	2	—	140–143°	—	0° (A)	$C_{11}H_{11}ClFNO_3$	C 50.88 H 4.27 N 5.39	50.67 4.22 5.38
p-Fluoro-L-phenylalanine	2	—	116–117°	—	+42.3° (A)	$C_{11}H_{11}ClFNO_3$	C 50.88 H 4.27 N 5.39	50.63 4.33 5.32
p-Fluoro-D-phenylalanine	2	—	115–117°	—	−40.8° (A)	$C_{11}H_{11}ClFNO_3$	C 50.88 H 4.27 N 5.39	50.59 4.34 5.22
Glycine	3	100°[f]	99–100°	—	—	$C_4H_6ClNO_3$	C 31.70 H 3.99 N 9.24	31.40 3.84 9.24
β-Hydroxy-DL-homomethionine A	2	—	139–140°	—	0° (W)	$C_8H_{14}ClNO_4S$	C 37.58 H 5.52 N 5.48	37.54 5.61 5.56
β-Hydroxy-DL-homomethionine B	2	—	138–141°[k]	—	0° (W)	$C_8H_{14}ClNO_4S$	C — H — N 5.48	— — 5.11
β-Hydroxy-DL-methoxinine A	2	—	122–124°	—	0° (W)	$C_7H_{12}ClNO_5$	C 37.26 H 5.36 N 6.20	37.11 5.43 6.27
β-Hydroxy-DL-methoxinine B	2	—	152°	—	0° (W)	$C_7H_{12}ClNO_5$	C 37.26 H 5.36 N 6.20	37.46 5.45 6.37
DL-Isoleucine[g]	4	117°[h]	97–103°	—	0° (A)	$C_8H_{14}ClNO_3$	C 46.27 H 6.80 N 6.75	46.24 6.83 6.86
L-Isoleucine	4	74–75°[f]	82°	+25.0° (A)[f]	+25.3° (A)	$C_8H_{14}ClNO_3$	C 46.27 H 6.80 N 6.75	46.20 6.88 6.68
DL-Leucine	1	142°[f]	139–141°	—	0° (A)	$C_8H_{14}ClNO_3$	C 46.27 H 6.80 N 6.75	46.57 7.04 6.66
L-Leucine	2	133°[f]	133–134°	−15.8° (A)[f]	−14.9° (A)	$C_8H_{14}ClNO_3$	C 46.27 H 6.80 N 6.75	46.33 6.63 6.69
D-Leucine	1	134°[f]	133–134°	+16.2° (A)[f]	+15.1° (A)	$C_8H_{14}ClNO_3$	C 46.27 H 6.80 N 6.75	46.51 7.04 6.92
DL-Norleucine	2	116°[f]	112–113°	—	0° (A)	$C_8H_{14}ClNO_3$	C 46.27 H 6.80 N 6.75	46.41 7.03 6.67
L-Norleucine	2	76°[i]	76°	−17.0° (W)[i]	−17.2° (W)	$C_8H_{14}ClNO_3$	C 46.27 H 6.80 N 6.75	46.55 7.04 6.55
D-Norleucine	2	76°[f]	75°	+17.0° (W)[f]	+16.2° (W)	$C_8H_{14}ClNO_3$	C 46.27 H 6.80 N 6.75	45.98 6.97 6.63
DL-Norvaline	3	101°[f]	103°	—	0° (W)	$C_7H_{12}ClNO_3$	C 43.42 H 6.25 N 7.24	42.95 6.46 7.50

Table III—*(Continued)*

N-Chloroacetyl Derivative	Source[b]	Melting Point, Reported	Melting Point, Observed[c]	Optical Rotation[d], $[\alpha]_D$ 22–24°, Reported	Optical Rotation[d], $[\alpha]_D$ 22–24°, Observed	Empirical Formula	Analysis[e], % Calc.	Analysis[e], % Obs.
DL-Phenylalanine	5	130°[f]	127–130°	—	0° (A)	$C_{11}H_{12}ClNO_3$	C 54.67	54.42
							H 5.01	4.81
							N 5.80	6.03
L-Phenylalanine	3	125°[f]	125°	+50.4° (A)[f]	+48.0° (A)	$C_{11}H_{12}ClNO_3$	C 54.67	55.11
							H 5.01	5.06
							N 5.80	6.01
DL-Serine	2	123°[f]	124–126°	—	0° (A)	$C_5H_8ClNO_4$	C 33.07	33.17
							H 4.44	4.41
							N 7.72	7.90
β-2-Thienyl-DL-alanine	2	128°[f]	126–128°	—	0° (A)	$C_9H_{10}ClNO_3S$	C 43.72	43.51
							H 4.07	4.14
							N 5.66	5.79
β-2-Thienyl-L-alanine	2	120°[f]	120–122°	+46.5° (A)[f]	+47.2° (A)	$C_9H_{10}ClNO_3S$	C 43.72	44.00
							H 4.07	4.17
							N 5.66	5.70
β-2-Thienyl-D-alanine	2	120°[f]	119–120°	−47.2° (A)[f]	−44.0° (A)	$C_9H_{10}ClNO_3S$	C 43.72	43.60
							H 4.07	4.10
							N 5.66	5.67
β-2-Thienyl-DL-β-alanine	2	—	163–166°	—	0° (A)	$C_9H_{10}ClNO_3S$	C 43.72	43.74
							H 4.07	4.17
							N 5.66	5.60
β-3-Thienyl-DL-alanine	2	105–106°[j]	99–103°	—	0° (A)	$C_9H_{10}ClNO_3S$	C 43.72	43.44
							H 4.07	4.13
							N 5.66	5.50
L-Tryptophan	3	158°[f]	158–160°	+32.0° (A)[f]	+29.9° (A)	$C_{13}H_{13}ClN_2O_3$	C 55.63	55.63
							H 4.67	4.68
							N 9.98	10.07
L-Tyrosine	3	155°[f]	150–155°	+59.0° (A)[f]	+60.0° (A)	$C_{11}H_{12}ClNO_4$	C 51.27	151.19
							H 4.70	4.63
							N 5.44	5.57
DL-Valine	4	132°[f]	130°	—	0° (A)	$C_7H_{12}ClNO_3$	C 43.42	43.35
							H 6.25	5.98
							N 7.24	7.32
L-Valine	3	114°[f]	114°	+15.0° (A)[f]	+12.7° (A)	$C_{17}H_{12}ClNO_3$	C 43.42	43.62
							H 6.25	6.17
							N 7.24	7.24

[a] Van Slyke nitrous acid determinations of primary amino nitrogen (5) yielded no detectable quantity of nitrogen (*cf.*, Table I for details). [b] Source of compounds: 1, Cyclo Chemical Corp., Los Angeles, Calif.; 2, prepared in this laboratory; 3, Sigma Chemical Co., St. Louis, Mo.; 4, ICN Pharmaceuticals, Cleveland, Ohio; and 5, Nutritional Biochemicals Corp., Cleveland, Ohio. Data on commercial products were obtained from recrystallized materials. [c] Melting points (uncorrected) were determined on a Fisher-Johns melting-point block. Chloroacetyl-DL-homomethionine B bubbled at 112°. [d] Optical rotation was determined on a Rudolph polarimeter, model 80, sodium lamp (*cf.*, Table I). (W) = water, and (A) = absolute ethanol. For chloroacetyl-L- and chloroacetyl-D-aspartic acid, c = 5. [e] Elemental analyses were performed by the Microanalytical Laboratory, National Institute of Arthritis, Metabolism, and Digestive Diseases (*cf.*, Table I). [f] *Cf.*, Ref. 6. [g] Used as commercially obtained. [h] *Cf.*, Ref. 8. [i] *Cf.*, Ref. 9. [j] *Cf.*, Ref. 10. [k] Crude, melting point not sharp.

Lactobacillus casei 7469[6] was carried on agar[7] and subcultured in a broth[7] for the preparation of the inoculum. The inoculum was a 1:20 dilution in normal saline of the washed bacteria. The assay medium was a riboflavin assay medium[7] supplemented with a minimal amount of riboflavin[4] required to give optimal growth of the organism as determined by construction of a standard curve, plotting concentration of riboflavin in the medium against extent of growth, as measured by turbidity. The minimal riboflavin concentration that supported maximal growth, determined by assay, was 0.03 μg of riboflavin/ml of the final assay system. The pH of the assay system containing the highest level of the test compound was within 0.02 pH unit of a control tube, which contained water in place of the test solution, except that of L-tyrosine, for which the pH of the final assay system was 0.49 pH unit higher than that of the control. The details of the assay procedure were described previously (1).

The extent of growth was measured by determination of turbidity in Klett units on a Klett–Summerson photoelectric colorimeter equipped with a red filter (660 nm). The instrument was set to zero against a tube containing the medium in a concentration equivalent to that of the test system and refrigerated during the incubation of the experimental tubes (reagent blank).

RESULTS

No significant inhibition was observed with either the acetyl (Table IV) or the propionyl (Table V) derivatives of the amino acids and amino acid analogs.

With the exception of *p*-fluoro-DL-phenylalanine and β-3-thienyl-DL-alanine, which showed 48 and 36% inhibition, respectively, at 1 mg/ml, the free amino acids were inactive (Table VI). L-Tyrosine gave strong inhibition at that concentration, but this result was due to the fact that it had to be dissolved in an alkaline system. L-Isoleucine, an inactive compound in the assay system, showed inhibition under similar conditions (Table VII).

As in the studies of β-hydroxyamino acids (1, 2), the chloroacetyl derivatives of certain of these amino acids and amino acid analogs exhibited some growth-inhibitory capacity, but no such activity was noted with the corresponding unacylated mother compound (Tables VI and VIII).

Where an increased inhibition was observed, the degree varied (Table

Table IV—Effect of *N*-Acetyl Derivatives of Amino Acids and Amino Acid Analogs on Growth of *L. casei* 7469

N-Acetyl Derivative	Concentration, m*M*	Inhibition[a], %
DL-Allylglycine	6.36	3
DL-Leucine	5.77	+1[b]
L-Leucine	5.77	0
D-Leucine	5.77	0
DL-Norleucine	5.77	0
D-Norleucine	5.77	1
o-Fluoro-DL-phenylalanine	4.44	2
m-Fluoro-DL-phenylalanine	4.44	3
p-Fluoro-DL-phenylalanine	4.44	2
β-2-Thienyl-DL-alanine	4.69	4
β-3-Thienyl-DL-alanine	4.69	4

[a] Growth in inoculated controls (water *in lieu* of test solution), measured turbidimetrically, was 190–210 Klett units for different series of determinations. At least three duplicate determinations were made for each compound. The duplicate values in each determination agreed within ±5 Klett units. The standard deviation of a compound showing a mean value of 20% inhibition, for example, was 2.7, and the standard error was 0.95. Concentration of test compounds was 1.0 mg/ml; the value given is the final concentration in the assay system. For assay conditions, see text. [b] The + indicates stimulation of growth.

[6] American Type Culture Collection, Rockville, Md.

[7] Micro assay culture agar (Difco B319), micro inoculum broth (Difco B320), and riboflavin assay medium (Difco B325), Difco Laboratories, Detroit, Mich.

VIII). The most active chloroacetylated β-hydroxynorleucine isomer, *i.e.*, *N*-chloroacetyl-D-β-hydroxynorleucine B[8], as shown previously (2), exhibited about 50% inhibition at 1.0 mg/ml.

Most of the active chloroacetyl derivatives, when compared on an equimolar basis, showed activity of about 14–30% inhibition (Table IX). Although the extent of inhibition by these compounds was modest, it was dependent on concentration (Table VIII). When the optically pure isomers were tested, little difference in activity was noted, with the L-isomer showing a slightly, if any, greater activity than the D-antipode. With the exception of chloroacetyl-L-alanine, the active compounds generally were the chloroacetyl derivatives of "essential" amino acids or of analogs of essential amino acids. However, the *N*-chloroacetyl-β-hydroxyhomomethionines and the *N*-chloroacetyl-β-hydroxymethoxinines were inactive. When compared on an equimolar basis with other active chloroacetyl amino acids at a concentration equivalent to that of 1 mg of *N*-chloroacetyl-D-β-hydroxynorleucine B/ml or 4.47 μmoles/ml, the activity of chloroacetyl-L-alanine was negligible (Table IX).

When *N*-chloroacetyl-D-β-hydroxynorleucine B and chloroacetyl-β-2-thienyl-DL-alanine were present in equimolar quantities, each at the concentration of 4.47 μmoles/ml, the inhibition observed was that of the more active of the two compounds, *i.e.*, *N*-chloroacetyl-D-β-hydroxynorleucine B (Table X). Similarly, when combinations of chloroacetyl-DL-allylglycine and chloroacetyl-β-2-thienyl-DL-alanine and of chloroacetyl-DL-norleucine and chloroacetyl-β-2-thienyl-DL-alanine were tested, the effect was equivalent to that of the more active compound, namely, chloroacetyl-β-2-thienyl-DL-alanine in both cases (30% for the former combination and 30% for the latter). No additive nor synergistic action was observed.

That the inhibition was not caused by a nonenzymatic hydrolytic release of the constituent chloroacetic acid, which itself has been shown to be active (Table VIII), during preparation of the test solution or during incubation was excluded since no detectable quantity of primary amino nitrogen was observed when a determination of free amino nitrogen was made on the test solution or on the control solution using the Van Slyke nitrous acid method (4) (Table XI).

DISCUSSION

Although more acyl groups should be studied before a generalization is made, the observation that only compounds having one of the three acyl groups tested were active suggested that it was not the acylated configuration in general that caused the activation but, rather, the peculiarity of the chloroacetyl group. Indeed, while acetic acid and propionic acid, the hydrolytic products of two of these acyl compounds, were inactive in the test system, chloroacetic acid, the hydrolytic product of the third, showed remarkable activity (Table VIII). Neither acetyl nor propionyl groups, even when attached to known active antimetabolites such as *p*-fluorophenylalanine, showed any effect. In this connection, Fukushima and Toyoshima (12) observed tumor-inhibitory effects with certain propionyl amino acids.

Apparently, it is not the chloroacetyl moiety alone that contributes to the activity since not all chloroacetyl amino acids exhibit growth-inhibitory action (Table VIII). The nature of the amino acid moiety appears of some importance in the activation, because the chloroacetyl derivatives of only certain amino acids and amino acid analogs showed growth-inhibitory activity. Examination of Tables VIII and IX shows that, in general, the chloroacetyl derivatives of the amino acids considered essential or of the analogs of these essential amino acids were growth inhibitory[9]. Although chloroacetyl-L-alanine showed some activity, its activity appears to be questionable when compared on an equimolar basis with other active chloroacetyl amino acids (Table IX). However, the chloroacetyl derivatives of more amino acids, both of the essential and nonessential categories, should be studied before a more definite statement in this regard is made.

It appears that the activity is not related to an enzymatic hydrolytic release of chloroacetic acid, itself a remarkably active compound in this test system, since in some compounds showing activity the D-isomers were active to a degree. However, a racemase possibly could be present and be contributing to the activity of the D-isomers. But, to the knowledge of the authors, no such enzyme has been described in this test organism. The possibility of a nonenzymatic breakdown of the test compounds during preparation of the test solution or during incubation, causing a release of chloroacetic acid and the mother amino acid, was excluded in view of the observation that there was no increase of moieties containing free amino nitrogen in the test solution and in the control solution (Table XI), as determined by the Van Slyke nitrous acid determination.

It is possible that the inhibitory effect noted could be due to a small quantity of chloroacetic acid, or of amino acid moiety released, not detectable within the sensitivity of the nitrous acid method. However, this possibility is unlikely; the accuracy of the procedure, even with 0.05 mg of amino nitrogen present, was 1% (5). Moreover, even if the chloroacetyl compound is completely hydrolyzed, the degree of inhibition would be equivalent to the inhibition range noted for the test compound (Table IX).

The fact that both optical isomers were active as inhibitors in many of the active chloroacetyl compounds also suggests that, perhaps, a nonspecific physical property of the test compounds, such as solubility and permeability across the cell membrane, could partly be involved in the mechanism. However, this property could not be the sole mechanism since, although all four isomers of *N*-chloroacetyl-β-hydroxynorleucine were active, their activities were not equal, isomer D-B being appreciably more active than the other three isomers (2).

Although some amino acid analogs, *i.e.*, *p*-fluorophenylalanine and β-3-thienylalanine, showed about equal or somewhat higher activity than their corresponding chloroacetyl derivatives on a molar basis (calculated from Tables VI and VIII), mammalian studies using *p*-fluorophenylalanine (13) and β-3-thienylalanine (14–16) showed these compounds to be highly toxic. Although the chloroacetyl derivative in these cases

Table V—Effect of *N*-Propionyl Derivatives of Amino Acids and Amino Acid Analogs on Growth of *L. casei* 7469

N-Propionyl Derivative	Concentration, m*M*	Inhibition[a], %
L-Alanine	6.89	0
DL-Allylglycine	5.84	0
o-Fluoro-DL-phenylalanine	4.18	3
m-Fluoro-DL-phenylalanine	4.18	4
p-Fluoro-DL-phenylalanine	4.18	5
L-Leucine	5.34	0
DL-Norleucine	5.34	3
β-2-Thienyl-DL-alanine	4.40	3
β-2-Thienyl-DL-β-alanine	4.40	3
β-3-Thienyl-DL-alanine	4.40	9

[a] Growth in inoculated controls (water *in lieu* of test solution), measured turbidimetrically, was 190–210 Klett units. Concentration of test compounds was 1.0 mg/ml; the value given is the final concentration in the test system. For assay conditions, see text. For explanation of extent of variation of values, see footnote of Table IV.

Table VI—Effect of Amino Acids on Growth of *L. casei* 7469

Amino Acid	Concentration, m*M*	Inhibition[a], %
DL-Alanine	11.22	0
L-Aspartic acid	7.51	6
DL-Allylglycine	8.68	4
o-Fluoro-DL-phenylalanine	5.46	3
m-Fluoro-DL-phenylalanine	5.46	0
p-Fluoro-DL-phenylalanine	5.46	48
β-Hydroxy-DL-homomethionine A[b]	5.58	7
β-Hydroxy-DL-homomethionine B[b]	5.58	+3[c]
β-Hydroxy-DL-methoxinine A[b]	6.70	+1[c]
β-Hydroxy-DL-methoxinine B[b]	6.70	+1[c]
L-Isoleucine	7.62	0
DL-Leucine	7.62	+1
L-Leucine	7.62	−5
DL-Norleucine	7.62	+1[c]
DL-Norvaline	8.54	1
DL-Phenylalanine	6.05	+3
β-2-Thienyl-DL-alanine	5.84	8
β-2-Thienyl-DL-β-alanine	5.84	0
β-3-Thienyl-DL-alanine	5.84	36
L-Tryptophan	4.90	5
L-Valine	8.54	0

[a] Concentration of test compounds in the final assay system was 1.0 mg/ml. Growth of the inoculated control (water *in lieu* of test solution), measured turbidimetrically, was 190–210 Klett units. For assay conditions, see text. For explanation of extent of variation of values, see footnote of Table IV. [b] See text footnote 8 for explanation of diastereomeric designations. [c] The + indicates stimulation of growth.

[8] The diastereomeric forms are arbitrarily referred to as Isomers A and B, the former moving faster and the latter slower when chromatographed on paper using methyl ethyl ketone–1-butanol–ammonia–water (3:5:1:1) (*cf.*, 2).

[9] *N*-Chloroacetyl-L-threonine previously (1) showed no appreciable inhibition. The compound used for that experiment since then has become syrupy and could not be used for comparison under the present conditions.

Table VII—Effect of pH on Growth of *L. casei* 7469

Assay System[a]	pH	Inhibition[b], % 0.55 μmole/ml[c]	2.76 μmoles/ml[c]	5.52 μmoles/ml[c]
Water (inoculated control)	6.55	—	—	—
Test solution 1	7.01	0	18	64
Test solution 2	6.85	2	12	55
Test solution 3	6.52	0	0	0

[a] The assay system consisted of 2.5 ml of the test solution plus 2.5 ml of the medium. The inoculated control consisted of 2.5 ml of water *in lieu* of the test solution. The test solutions were as follows: 1, L-tyrosine, 20.0 mg, plus 1.10 ml of 0.1 *N* NaOH in a total volume of 10.0 ml; 2, L-isoleucine, 14.4 mg, plus 1.10 ml of 0.1 *N* NaOH in a total volume of 10.0 ml; and 3, L-isoleucine, 14.4 mg, plus 0.05 ml of 0.1 *N* NaOH in a total volume of 10.0 ml. [b] Growth of inoculated control, measured turbidimetrically, was 201 Klett units. [c] Final concentration of test solution in the assay system.

showed somewhat less activity than the corresponding nonacylated mother compounds, the administration of these antimetabolites as the chloroacetyl derivatives possibly may circumvent this undesirable property.

Table VIII—Effect of *N*-Chloroacetyl Derivatives of Amino Acids and Amino Acid Analogs on Growth of *L. casei* 7469[a]

N-Chloroacetyl Derivative	Concentration at 1 mg/ml, m*M*	Inhibition[b], % 0.1 mg/ml[c]	0.5 mg/ml[c]	1.0 mg/ml[c]
L-Alanine	6.04	2	5	14
D-Alanine	6.04	0	3	9
L-Aspartic acid	4.77	0	0	0
D-Aspartic acid	4.77	1	4	3
DL-Allylglycine	5.22	3	9	14
L-Allylglycine	5.22	2	8	16
D-Allylglycine	5.22	1	3	8
o-Fluoro-DL-phenylalanine	3.85	1	10	18
m-Fluoro-DL-phenylalanine	3.85	2	8	15
p-Fluoro-DL-phenylalanine	3.85	6	14	20
p-Fluoro-L-phenylalanine	3.85	6	14	25
p-Fluoro-D-phenylalanine	3.85	4	13	17
Glycine	6.60	4	6	10
β-Hydroxy-DL-homomethionine A	3.91	1	5	8
β-Hydroxy-DL-homomethionine B	3.91	+2[d]	+2[d]	3
β-Hydroxy-DL-methoxinine A	4.43	3	4	7
β-Hydroxy-DL-methoxinine B	4.43	+2[d]	2	11
DL-Isoleucine	4.82	3	14	20
L-Isoleucine	4.82	6	13	20
DL-Leucine	4.82	3	9	13
L-Leucine	4.82	3	11	15
D-Leucine	4.82	2	5	11
DL-Norleucine	4.82	3	12	20
L-Norleucine	4.82	6	14	22
D-Norleucine	4.82	1	7	14
DL-Norvaline	5.16	4	15	18
DL-Phenylalanine	4.14	0	10	20
L-Phenylalanine	4.14	5	10	19
DL-Serine	5.51	3	3	8
β-2-Thienyl-DL-alanine	4.04	10	16	25
β-2-Thienyl-L-alanine	4.04	9	19	34
β-2-Thienyl-D-alanine	4.04	1	13	23
β-2-Thienyl-DL-β-alanine	4.04	3	6	13
β-3-Thienyl-DL-alanine	4.04	3	10	24
L-Tryptophan	3.56	5	15	26
L-Tyrosine	3.88	+1	3	6
DL-Valine	5.16	6	12	18
L-Valine	5.16	6	10	18
Acetic acid[e]	16.65	1	1	4
Monochloroacetic acid[e]	10.58	11	34	54
Propionic acid[e]	13.50	1	2	3

[a] For details of assay procedure, see text. [b] Turbidity readings of the inoculated control tubes (containing no test compound) were 190–210 Klett units. For explanation of extent of variations of values, see footnote of Table IV. [c] Final concentration in assay system. [d] The + indicates stimulation of growth. [e] Free acids.

Table IX—Comparison of Effect of Equimolar Concentrations of *N*-Chloroacetyl Amino Acids and Amino Acid Derivatives on Growth of *L. casei* 7469[a]

N-Chloroacetyl Derivative	Inhibition[b], %
L-Alanine	9
DL-Allylglycine	16
L-Allylglycine	21
D-Allylglycine	9
o-Fluoro-DL-phenylalanine	21
m-Fluoro-DL-phenylalanine	19
p-Fluoro-DL-phenylalanine	16
p-Fluoro-L-phenylalanine	25
p-Fluoro-D-phenylalanine	14
β-Hydroxy-D-norleucine B	51
DL-Isoleucine	18
DL-Leucine	13
L-Leucine	18
D-Leucine	9
DL-Norleucine	20
L-Norleucine	22
D-Norleucine	9
DL-Norvaline	18
DL-Phenylalanine	20
β-2-Thienyl-DL-alanine	27
β-2-Thienyl-L-alanine	26
β-2-Thienyl-D-alanine	18
β-2-Thienyl-DL-β-alanine	15
L-Tryptophan	30
L-Valine	14
Monochloroacetic acid[c]	24
p-Fluoro-DL-phenylalanine[c]	35
β-3-Thienyl-DL-alanine[c]	20

[a] Maximum growth in inoculated control tube containing no test compound, measured turbidimetrically, was 198–205 Klett units. For explanation of extent of variation of values, see footnote of Table IV. [b] Concentration was 4.47 μmoles/ml and was the final concentration in the assay system. For details of assay procedure, see text. [c] Free acids.

The amino acid analogs selected in these experiments are known antimetabolites of the corresponding natural amino acids in certain selected systems (*cf.*, 17). For example, allylglycine is believed to be a metabolic antagonist of cysteine, norleucine of methionine, and the fluorophenylalanines of phenylalanine. The chloroacetyl derivatives of analogs that were believed to be antimetabolites of two different classes of antagonists were combined in a single assay system to note if additive or synergistic effects could be observed (Table X). The observation that there was no such effect, coupled with the observation that the activity of the inhibitory compounds (with the exception of *N*-chloroacetyl-D-β-hydroxynorleucine B) fell within a relatively narrow range (14–30%), suggests a common mode of inhibition among these compounds. It may be, for example, that because of sufficient structural similarity of the analogs to the natural amino acid, the difficulty of their metabolism lies not in the activation step of the protein synthetic pathway but in the subsequent utilization step of such activated amino acid analogs. The mode of inhibition by *N*-chloroacetyl-D-β-hydroxynorleucine B is probably different

Table X—Effect of Combination of Active Chloroacetyl Derivatives of Amino Acid Analogs on Growth of *L. casei* 7469

Compound	Inhibition[a], %
N-Chloroacetyl-β-hydroxy-D-norleucine B[b]	50
N-Chloroacetyl-*p*-fluoro-DL-phenylalanine	17
N-Chloroacetyl-β-hydroxy-D-norleucine B plus *N*-chloroacetyl-*p*-fluoro-DL-phenylalanine	53
N-Chloroacetyl-β-2-thienyl-DL-alanine	27
N-Chloroacetyl-β-hydroxy-D-norleucine B plus *N*-chloroacetyl-β-2-thienyl-DL-alanine	49
N-Chloroacetyl-DL-allylglycine	16
N-Chloroacetyl-β-hydroxy-D-norleucine plus *N*-chloroacetyl-DL-allylglycine	54
N-Chloroacetyl-DL-allylglycine plus *N*-chloroacetyl-β-2-thienyl-DL-alanine	30
N-Chloroacetyl-DL-norleucine	19
N-Chloroacetyl-DL-norleucine plus *N*-chloroacetyl-β-2-thienyl-DL-alanine	33

[a] Maximum growth of inoculated control tube, containing no test compound, measured turbidimetrically was 198 Klett units. [b] Concentration of each test compound in assay system was 4.47 μmoles/ml. For details of assay procedure, see text.

Table XI—Determination of Extent of Hydrolysis of *N*-Chloroacetyl-L-isoleucine during Incubation

System	Primary Amino Nitrogen[a], mg
1. Test solution[b], refrigerated 19 hr	0.002
2. Test solution, incubated at 37°, 19 hr	0.002
3. 2.5 ml of uninoculated medium plus 2.5 ml of water, refrigerated 19 hr[c]	0.298
4. 2.5 ml of uninoculated medium plus 2.5 ml of water, incubated at 37°, 19 hr	0.294
5. 2.5 ml of uninoculated medium plus 2.5 ml of test solution, refrigerated 19 hr	0.302
6. 2.5 ml of uninoculated medium plus 2.5 ml of test solution, incubated at 37°, 19 hr	0.305

[a] Determined by Van Slyke nitrous acid method (5). The volumes of solution taken for the analysis were 1.5 ml for Systems 1 and 2 and 1.0 ml for Systems 3–6. For the volumes taken, Systems 1 and 2 should yield 0.201 mg and Systems 3–6 should yield 0.368 mg of primary amino nitrogen when the test compound is completely hydrolyzed. For comments on sensitivity to method, see text. [b] Test solution was chloroacetyl-L-isoleucine, 20.0 mg, plus 0.96 ml of 0.1 *N* NaOH with the volume made to 10.0 ml with water; pH of the test solution was 6. [c] The pH of the assay system (2.5 ml of medium plus 2.5 ml of test solution) was 6.52.

from that of the other chloroacetyl derivatives that showed inhibition in the 15–30% range. In the former, for example, the isomer of chloroacetyl-β-hydroxynorleucine showing the greatest activity was of the D-configuration. However, it is difficult to deduce the mechanism of inhibition in experiments of this type since the system is too complex.

In view of the differences in metabolic behavior between the free amino acids and the *N*-chloroacetylated derivatives, it might prove useful to test these derivatives in suitable mammalian tumor systems; this testing is now being done.

REFERENCES

(1) T. T. Otani, *Cancer Chemother. Rep.*, **38**, 25 (1964).

(2) T. T. Otani and M. R. Briley, *J. Pharm. Sci.*, **65**, 534 (1976).

(3) G. E. Foley, R. E. McCarthy, V. M. Binns, E. E. Snell, B. M. Guirard, G. W. Kidder, V. C. Dewey, and P. S. Thayer, *Ann. N.Y. Acad. Sci.*, **76**, 413 (1958).

(4) T. T. Otani and M. R. Briley, *J. Pharm. Sci.*, **63**, 1253 (1974).

(5) D. D. Van Slyke, *J. Biol. Chem.*, **83**, 425 (1929).

(6) J. P. Greenstein and M. Winitz, in "Chemistry of the Amino Acids," Wiley, New York, N.Y., 1961.

(7) K. Dittmer, R. P. Martin, W. Herz, and S. J. Cristol, *J. Am. Chem. Soc.*, **71**, 1201 (1949).

(8) V. E. Price, J. B. Gilbert, and J. P. Greenstein, *J. Biol. Chem.*, **179**, 1169 (1949).

(9) K. R. Rao, S. M. Birnbaum, R. B. Kingsley, and J. P. Greenstein, *ibid.*, **198**, 507 (1952).

(10) F. W. Dunn and K. Dittmer, *ibid.*, **188**, 263 (1951).

(11) J. P. Greenstein, in "Methods in Enzymology," vol. III, S. P. Colowick and N. O. Kaplan, Eds., Academic, New York, N.Y., 1957, p. 554.

(12) K. Fukushima and S. Toyoshima, *Cancer Chemother. Rep., Part I*, **59**, 309 (1975).

(13) M. D. Armstrong and J. D. Lewis, *J. Biol. Chem.*, **188**, 91 (1951).

(14) V. du Vigneaud, H. Mckennish, Jr., S. Simmonds, K. Dittmer, and G. B. Brown, *ibid.*, **159**, 385 (1945).

(15) R. G. Garst, E. Campaigne, and H. G. Day, *ibid.*, **180**, 1013 (1949).

(16) M. F. Ferger and V. du Vigneaud, *ibid.*, **179**, 61 (1949).

(17) A. Meister, in "Biochemistry of the Amino Acids," 2nd ed., Academic, New York, N.Y., 1965, p. 233.

Thermal and Photolytic Decomposition of Methotrexate in Aqueous Solutions

DULAL C. CHATTERJI and JOSEPH F. GALLELLI ˣ

Received March 10, 1977, from the *Pharmacy Department, The Clinical Center, National Institutes of Health, Bethesda, MD 20014.* Accepted for publication August 4, 1977.

Abstract □ The chemical kinetics of thermal and photolytic degradation of methotrexate in aqueous solutions were studied. At above pH 7 and 85°, methotrexate hydrolyzed to yield mainly N^{10}-methylpteroylglutamic acid. The hydrolysis rate followed first-order kinetics with respect to methotrexate concentration and increased rapidly above pH 9. When methotrexate solutions were kept under laboratory fluorescent light, the major degradation products were 2,4-diamino-6-pteridinecarbaldehyde, 2,4-diamino-6-pteridinecarboxylic acid, and *p*-aminobenzoylglutamic acid. The photolytic reaction followed zero-order kinetics with respect to methotrexate concentration and was catalyzed by bicarbonate ion. Evidence is presented for a proposed sequential cleavage of methotrexate by a free radical mechanism for the photolysis. Commercial parenteral methotrexate was found to be quite stable as marketed when stored in the original vial at room temperature.

Keyphrases □ Methotrexate—thermal and photolytic decomposition in aqueous solutions □ Thermal decomposition—methotrexate in aqueous solutions □ Photolytic decomposition—methotrexate in aqueous solutions □ Decomposition—thermal and photolytic, methotrexate in aqueous solutions □ Stability—methotrexate in aqueous solutions □ Antineoplastic agents—methotrexate, thermal and photolytic decomposition in aqueous solutions

Methotrexate (4-amino-N^{10}-methylpteroylglutamic acid), a widely used antileukemic agent, is often administered in the form of an aqueous parenteral solution. Although it is recognized that methotrexate decomposes in light and alkaline solutions, the chemical kinetics of methotrexate decomposition have not been reported.

Since commercially available methotrexate is only about 86% pure (1) and contains several impurities (2, 3), it is important to know whether methotrexate degradation accounts for some of the impurities. Furthermore, it is important to ascertain the stability of commercial methotrexate when it is diluted in large-volume intravenous solutions. The present study was undertaken to elucidate the decomposition rate of aqueous solutions of methotrexate under fluorescent light and at high temperatures and to identify the degradation products. Chemical kinetic

Table XI—Determination of Extent of Hydrolysis of *N*-Chloroacetyl-L-isoleucine during Incubation

System	Primary Amino Nitrogen[a], mg
1. Test solution[b], refrigerated 19 hr	0.002
2. Test solution, incubated at 37°, 19 hr	0.002
3. 2.5 ml of uninoculated medium plus 2.5 ml of water, refrigerated 19 hr[c]	0.298
4. 2.5 ml of uninoculated medium plus 2.5 ml of water, incubated at 37°, 19 hr	0.294
5. 2.5 ml of uninoculated medium plus 2.5 ml of test solution, refrigerated 19 hr	0.302
6. 2.5 ml of uninoculated medium plus 2.5 ml of test solution, incubated at 37°, 19 hr	0.305

[a] Determined by Van Slyke nitrous acid method (5). The volumes of solution taken for the analysis were 1.5 ml for Systems 1 and 2 and 1.0 ml for Systems 3–6. For the volumes taken, Systems 1 and 2 should yield 0.201 mg and Systems 3–6 should yield 0.368 mg of primary amino nitrogen when the test compound is completely hydrolyzed. For comments on sensitivity to method, see text. [b] Test solution was chloroacetyl-L-isoleucine, 20.0 mg, plus 0.96 ml of 0.1 *N* NaOH with the volume made to 10.0 ml with water; pH of the test solution was 6. [c] The pH of the assay system (2.5 ml of medium plus 2.5 ml of test solution) was 6.52.

from that of the other chloroacetyl derivatives that showed inhibition in the 15–30% range. In the former, for example, the isomer of chloroacetyl-β-hydroxynorleucine showing the greatest activity was of the D-configuration. However, it is difficult to deduce the mechanism of inhibition in experiments of this type since the system is too complex.

In view of the differences in metabolic behavior between the free amino acids and the *N*-chloroacetylated derivatives, it might prove useful to test these derivatives in suitable mammalian tumor systems; this testing is now being done.

REFERENCES

(1) T. T. Otani, *Cancer Chemother. Rep.*, **38**, 25 (1964).

(2) T. T. Otani and M. R. Briley, *J. Pharm. Sci.*, **65**, 534 (1976).

(3) G. E. Foley, R. E. McCarthy, V. M. Binns, E. E. Snell, B. M. Guirard, G. W. Kidder, V. C. Dewey, and P. S. Thayer, *Ann. N.Y. Acad. Sci.*, **76**, 413 (1958).

(4) T. T. Otani and M. R. Briley, *J. Pharm. Sci.*, **63**, 1253 (1974).

(5) D. D. Van Slyke, *J. Biol. Chem.*, **83**, 425 (1929).

(6) J. P. Greenstein and M. Winitz, in "Chemistry of the Amino Acids," Wiley, New York, N.Y., 1961.

(7) K. Dittmer, R. P. Martin, W. Herz, and S. J. Cristol, *J. Am. Chem. Soc.*, **71**, 1201 (1949).

(8) V. E. Price, J. B. Gilbert, and J. P. Greenstein, *J. Biol. Chem.*, **179**, 1169 (1949).

(9) K. R. Rao, S. M. Birnbaum, R. B. Kingsley, and J. P. Greenstein, *ibid.*, **198**, 507 (1952).

(10) F. W. Dunn and K. Dittmer, *ibid.*, **188**, 263 (1951).

(11) J. P. Greenstein, in "Methods in Enzymology," vol. III, S. P. Colowick and N. O. Kaplan, Eds., Academic, New York, N.Y., 1957, p. 554.

(12) K. Fukushima and S. Toyoshima, *Cancer Chemother. Rep., Part I*, **59**, 309 (1975).

(13) M. D. Armstrong and J. D. Lewis, *J. Biol. Chem.*, **188**, 91 (1951).

(14) V. du Vigneaud, H. Mckennish, Jr., S. Simmonds, K. Dittmer, and G. B. Brown, *ibid.*, **159**, 385 (1945).

(15) R. G. Garst, E. Campaigne, and H. G. Day, *ibid.*, **180**, 1013 (1949).

(16) M. F. Ferger and V. du Vigneaud, *ibid.*, **179**, 61 (1949).

(17) A. Meister, in "Biochemistry of the Amino Acids," 2nd ed., Academic, New York, N.Y., 1965, p. 233.

Thermal and Photolytic Decomposition of Methotrexate in Aqueous Solutions

DULAL C. CHATTERJI and JOSEPH F. GALLELLI ˣ

Received March 10, 1977, from the *Pharmacy Department, The Clinical Center, National Institutes of Health, Bethesda, MD 20014.* Accepted for publication August 4, 1977.

Abstract □ The chemical kinetics of thermal and photolytic degradation of methotrexate in aqueous solutions were studied. At above pH 7 and 85°, methotrexate hydrolyzed to yield mainly N^{10}-methylpteroylglutamic acid. The hydrolysis rate followed first-order kinetics with respect to methotrexate concentration and increased rapidly above pH 9. When methotrexate solutions were kept under laboratory fluorescent light, the major degradation products were 2,4-diamino-6-pteridinecarbaldehyde, 2,4-diamino-6-pteridinecarboxylic acid, and *p*-aminobenzoylglutamic acid. The photolytic reaction followed zero-order kinetics with respect to methotrexate concentration and was catalyzed by bicarbonate ion. Evidence is presented for a proposed sequential cleavage of methotrexate by a free radical mechanism for the photolysis. Commercial parenteral methotrexate was found to be quite stable as marketed when stored in the original vial at room temperature.

Keyphrases □ Methotrexate—thermal and photolytic decomposition in aqueous solutions □ Thermal decomposition—methotrexate in aqueous solutions □ Photolytic decomposition—methotrexate in aqueous solutions □ Decomposition—thermal and photolytic, methotrexate in aqueous solutions □ Stability—methotrexate in aqueous solutions □ Antineoplastic agents—methotrexate, thermal and photolytic decomposition in aqueous solutions

Methotrexate (4-amino-N^{10}-methylpteroylglutamic acid), a widely used antileukemic agent, is often administered in the form of an aqueous parenteral solution. Although it is recognized that methotrexate decomposes in light and alkaline solutions, the chemical kinetics of methotrexate decomposition have not been reported.

Since commercially available methotrexate is only about 86% pure (1) and contains several impurities (2, 3), it is important to know whether methotrexate degradation accounts for some of the impurities. Furthermore, it is important to ascertain the stability of commercial methotrexate when it is diluted in large-volume intravenous solutions. The present study was undertaken to elucidate the decomposition rate of aqueous solutions of methotrexate under fluorescent light and at high temperatures and to identify the degradation products. Chemical kinetic

studies also were conducted to determine the order of the reactions and the influence of variables such as pH, ionic strength, and buffer species on the reaction rates.

EXPERIMENTAL

Reagents and Apparatus—Methotrexate USP reference substance[1], pure methotrexate prepared by purifying methotrexate USP by column chromatography on diethylaminoethylcellulose (1, 3), and commercial methotrexate preparations[2,3] were used. The four decomposition products from methotrexate were compared with authentic samples of N^{10}-methylpteroylglutamic acid[4], 2,4-diamino-6-pteridinecarbaldehyde[5], *p*-aminobenzoylglutamic acid[6], and 2-amino-4-hydroxy-6-pteridinecarboxylic acid[7].

The buffer generally employed was ammonium bicarbonate, although some studies were conducted with carbonate buffer, tris(hydroxymethyl)aminomethane buffer, or hydroxide ion provided by sodium hydroxide or ammonium hydroxide. The ionic strength of each buffered solution was adjusted with potassium chloride to 0.25.

All other chemicals were reagent grade.

All spectrophotometric analyses were carried out on a recording spectrophotometer[8]. The apparatus for high-pressure liquid chromatography (HPLC) (4) and column chromatography on diethylaminoethylcellulose (1, 3) were reported previously. All pH measurements were taken at room temperature with a pH meter[9].

Thermal Degradation Studies—Methotrexate samples were diluted with appropriate buffers to a concentration of 0.1 mg of methotrexate/ml unless otherwise specified. Concentrations of up to 1 mg of methotrexate/ml were used only to confirm the reaction order. For studies between pH 8.5 and 9.5, the buffered methotrexate samples were sealed in clear glass ampuls, wrapped in aluminum foil, and immersed in a constant-temperature oil bath maintained at 85 ± 0.1°. For studies between pH 10 and 12, where reactions were considerably faster, buffered methotrexate samples were kept in amber glass volumetric flasks, tightly stoppered, and immersed in the constant-temperature oil bath. At appropriate time intervals, a sample (either an individual ampul or an aliquot from a volumetric flask) was taken out, cooled to room temperature, and analyzed for intact methotrexate and degradation products by procedures described under *Method of Analysis*.

Photolytic Degradation Studies—The buffered methotrexate samples, as described for thermal degradation studies, were transferred to 25-ml clear glass volumetric flasks and placed in a specially constructed light box. The box, 60.96 × 30.48 × 43.18 cm (height), was equipped with two fluorescent bulbs[10], 10.16 cm apart near the center of the top lid. The floor of the box was covered with white paper to give a uniformly illuminated background. The intensity of the light near the floor of the box was checked with a photometer and was uniform. At appropriate time intervals, 0.5-ml portions of the sample solutions were withdrawn and analyzed for intact methotrexate and photodecomposition products as described under *Method of Analysis*.

Methotrexate Dosage Forms—Diluted and undiluted solutions of commercial methotrexate injection were studied. In studies of diluted solution, methotrexate injection was diluted to a concentration of about 0.1 mg of methotrexate/ml with distilled water, adjusted to an initial pH of 8.3, and not readjusted thereafter during the runs. The diluted solution was then sealed in ampuls for thermal degradation studies and in 25-ml volumetric flasks for photolytic studies as previously described.

Photolytic degradation studies on the undiluted injection were made in the original vial. For thermal degradation studies, the contents of several undiluted injection vials were pooled and transferred to 2-ml ampuls as previously described. Methotrexate tablets were assayed initially, crushed, triturated into fine powder, spread on a petri dish, and then kept in the light box for 1 month. All samples were analyzed at appropriate time intervals for methotrexate and its decomposition products as described under *Method of Analysis*.

[1] Lot 1260x8105, Lederle Laboratories.
[2] Lot 467-164, 50-mg/2-ml vials, Lederle Laboratories.
[3] Lot 422-109, 5-mg tablets, Lederle Laboratories.
[4] Drug Research and Development Program, Division of Cancer Treatment, National Cancer Institute.
[5] Obtained from R. L. Dion, Laboratory of Medicinal Chemistry and Biology, Developmental Therapeutics Program, National Cancer Institute.
[6] Pfaltz and Bauer, Stamford, Conn.
[7] Sigma Chemical Co., St. Louis, Mo.
[8] Cary 17, Varian Instrument Division, Palo Alto, Calif.
[9] Beckman Expandometic SS-2.
[10] Sylvania F15T8-CW, 45.72 cm long.

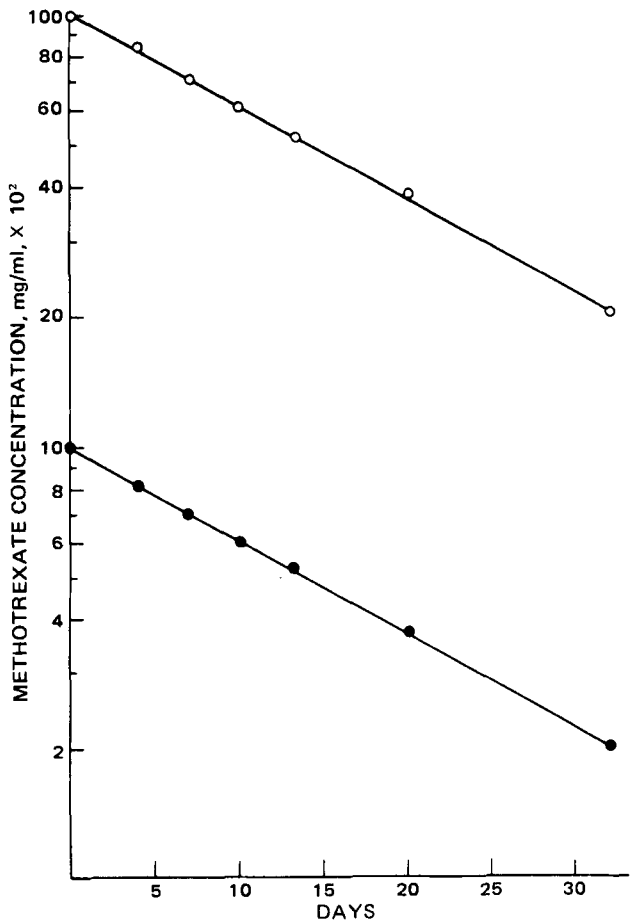

Figure 1—*Apparent first-order plots for the degradation of chromatographically pure methotrexate in the absence of light, pH 8.3, 0.1 M ammonium bicarbonate, 85°, and μ = 0.25. Key: ○, 1.0 mg of methotrexate/ml; and ●, 0.1 mg of methotrexate/ml.*

Investigational Methotrexate Injection—One gram of investigational methotrexate injection[11] was dissolved in 10 ml of distilled water; this solution was further diluted in an intravenous infusion bottle containing 500 ml of 0.05 *M* $NaHCO_3$ solution for injection and assayed. The infusion bottle was then kept on the laboratory counter and exposed to ordinary fluorescent light in the room for 24 hr. The intravenous solution was then analyzed for intact methotrexate and its decomposition products.

Method of Analysis—Intact methotrexate in the presence of its degradation products was assayed by HPLC using an anion-exchange resin column and eluting with a 0.6 *M* buffer (Mobile Phase 1) containing sodium phosphate and sodium perchlorate. The details of the column, solvent, sampling, and calculations were reported previously (4). Samples also were assayed on a diethylaminoethylcellulose column by gradient elution as reported in the literature (1, 4).

Determination and Identification of Degradation Products—The degradation products were initially separated by chromatography on a diethylaminoethylcellulose column (1, 3). The separated peaks were then identified by their UV spectra and retention times when compared with authentic samples. The degradation products were also monitored and measured by HPLC (4). For thermal decomposition products, the HPLC assay described under *Method of Analysis* was used. HPLC was also used for separation of photolytic products; however, a 0.005 *M* buffer[12] containing 3% acetonitrile (Mobile Phase 2) was used as the eluant.

RESULTS AND DISCUSSION

Methotrexate injection, as available commercially, is usually adjusted to pH 8.3. Therefore, most studies were conducted at pH 8.3 using am-

[11] Preservative-free methotrexate (Lot BC-76-221), 1-g vial manufactured for National Cancer Institute by BenVenue Laboratories, Bedford, Ohio.
[12] Buffer contained 0.0025 *M* sodium phosphates and 0.0025 *M* sodium perchlorate, pH 7.0.

Table I—Experimental Rate Constants for the Alkaline Hydrolysis of Methotrexate (0.1 mg/ml) at 85° in the Absence of Light and μ = 0.25

Sample	pH	Buffer	Half-Life, days	Rate, day^{-1}
Methotrexate USP	8.5	0.01 *M* NH_4HCO_3	13.0	0.0533
Methotrexate USP	8.5	0.1 *M* NH_4HCO_3	13.0	0.0533
Methotrexate USP	8.7	0.1 *M* NH_4HCO_3	13.8	0.0502
Methotrexate USP	9.0	0.1 *M* NH_4HCO_3	11.3	0.0613
Methotrexate USP	10.4	0.1 *M* NH_4HCO_3	0.416	1.666
Methotrexate USP	11.2	0.1 *M* NH_4HCO_3	0.158	4.378
Methotrexate USP	12.0	0.1 *M* NH_4HCO_3	0.038	18.14
Methotrexate USP	8.5	0.1 *M* tris(hydroxymethyl)aminomethane	9.1	0.076
Chromatographically pure methotrexate	8.5	0.1 *M* NH_4HCO_3	13.0	0.0533
Chromatographically pure methotrexate	8.5	0.1 *M* NH_4HCO_3	12.7	0.0546
Chromatographically pure methotrexate	8.5	0.1 *M* tris(hydroxymethyl)aminomethane	8.8	0.0787
Methotrexate injection[a] (undiluted)	8.3	—	17.0	0.0408

[a] Concentration of 25 mg/ml, initial pH 8.3, unbuffered.

monium bicarbonate buffer. The choice of the buffer was partially dictated by the purification method in which methotrexate in analytical quantities was purified by chromatographing on a diethylaminoethylcellulose column and eluting with a gradient of pH 8.3 ammonium bicarbonate buffer (1, 3).

Thermal Degradation—Figure 1 shows methotrexate degradation in 0.1 *M* ammonium bicarbonate at an initial pH of 8.3[13] and 85°. The linearity of the semilogarithmic plots with the same slope at two different methotrexate concentrations indicated that the reaction was first order with respect to intact drug. Table I shows the experimental rate constants and half-lives for methotrexate degradation in the absence of light at various pH values and buffers, 85°, and μ = 0.25. The hydrolysis rate increased with hydroxide ion (pH) and was independent of ammonium bicarbonate concentration at constant ionic strength. However, in the presence of pH 8.3 tris(hydroxymethyl)aminomethane, samples degraded 50% faster than those in ammonium bicarbonate.

Furthermore, as shown in Table I, there were no significant differences between the hydrolysis rate of chromatographically pure methotrexate and methotrexate USP. The hydrolysis rate of methotrexate USP and commercial methotrexate is also the same because methotrexate USP is used in the preparation of commercial methotrexate. However, this fact is not evident from the data in Table I, because the undiluted commercial methotrexate sample was unbuffered and its pH had changed during the run. In all linear first-order plots from which the rate constant was calculated in Table I, the correlation coefficient was 0.998 or better.

Identification of Thermal Decomposition Product—In alkaline conditions above pH 8 and 85°, the major degradation product was N^{10}-methylpteroylglutamic acid (II, Scheme I). The acid product was confirmed by chromatographing a degraded solution of methotrexate on a cellulose column, collecting the major degradation peak, and identifying it by its UV spectrum and retention time in the system compared to an authentic sample. The acid product was further identified by comparing the UV spectra and retention times of an authentic sample of N^{10}-methylpteroylglutamic acid and the degradation peak in the HPLC method.

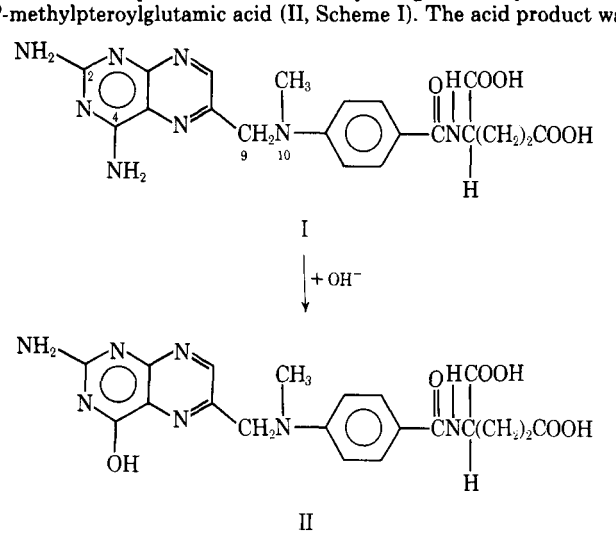

Scheme I

The product N^{10}-methylpteroylglutamic acid could be predicted because of the ease of alkaline hydrolysis of the 4-amino group as part of an amidine system. In comparison, the 2-amino group, as part of a quinidine system, is quite stable even under strongly alkaline conditions (5). The sequence of hydrolysis of methotrexate (I) at pH 8.3 and 85° is shown in Scheme I.

Photolytic Degradation of Methotrexate—Figure 2 shows methotrexate photolysis at room temperature in different concentrations of pH 8.3 ammonium bicarbonate. In all plots, the initial lag periods were followed by a zero-order loss of methotrexate with time. Identical samples, when stored in the absence of light at room temperature, did not undergo photolysis during the same period.

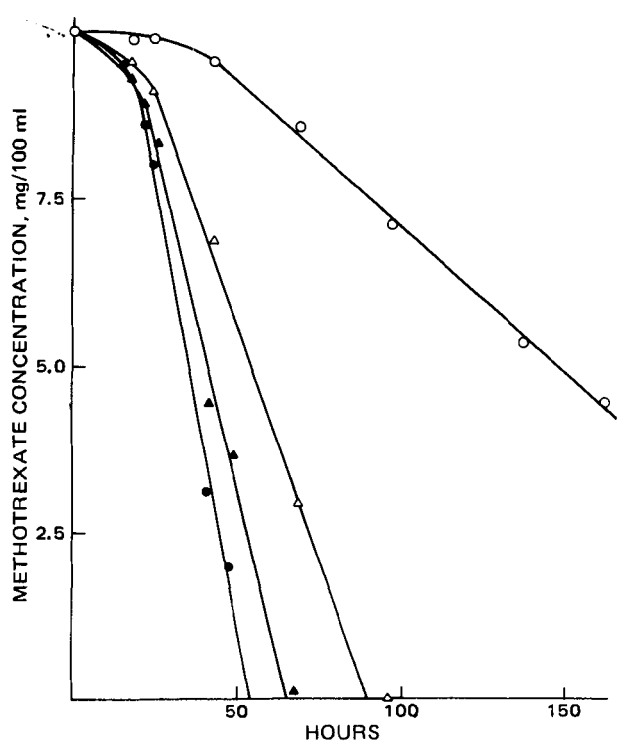

Figure 2—*Apparent zero-order plots for the photolytic degradation of chromatographically pure methotrexate at pH 8.3, 23 ± 2°, and μ = 0.25. Key (ammonium bicarbonate buffer): ○, 0.01 M; △, 0.05 M; ▲, 0.1 M; and ●, 0.15 M.*

[13] The pH value of 8.30 changes to 8.54 with time because of the volatility of the buffer (ammonia and carbon dioxide).

Table II—Photolytic Rate Constants and Lag Periods of Methotrexate Samples under Various Conditions in 25-ml Volumetric Flasks, pH 8.3, μ = 0.25, and Room Temperature

Run	Sample	Concentration, mg/ml	Buffer	Additives	Lag Period, hr	Rate, mg/ml × 10^4
1	Chromatographically pure methotrexate	0.1	None	None	72	1.6
2	Chromatographically pure methotrexate	0.1	0.01 *M* NH_4HCO_3	None	40	4.0
3	Chromatographically pure methotrexate	0.1	0.03 *M* NH_4HCO_3	None	30	10.0
4	Chromatographically pure methotrexate	0.1	0.05 *M* NH_4HCO_3	None	25	15.4
5	Chromatographically pure methotrexate	0.1	0.10 *M* NH_4HCO_3	None	23	20.0
6	Chromatographically pure methotrexate	0.1	0.10 *M* NH_4HCO_3	None	21	29.2
7	Chromatographically pure methotrexate	0.1	0.15 *M* NH_4HCO_3	None	20	26.0
8	Chromatographically pure methotrexate	0.1	0.25 *M* NH_4HCO_3	None	17	46.0
9	Chromatographically pure methotrexate	0.1	0.25 *M* NH_4HCO_3	0.1% edetate disodium	40	25.6
10	Chromatographically pure methotrexate	0.1	0.25 *M* NH_4HCO_3	2% 2-nitropropane	90	43.0
11	Chromatographically pure methotrexate	0.5	0.25 *M* NH_4HCO_3	None	17	52.0
12	Methotrexate USP	0.1	None	None	67	1.8
13	Methotrexate USP	0.1	0.10 *M* NH_4HCO_3	None	21	22.6
14	Methotrexate USP	0.1	0.25 *M* NH_4HCO_3	None	16	46.3
15	Methotrexate USP	0.1	0.1 *M* $NaHCO_3$	None	19	24.2
16	Methotrexate USP	0.1	0.1 *M* NH_4Cl	None	69	1.7
17	Methotrexate USP	0.1	0.1 *M* $NaHCO_3$ + 0.1 *M* NH_4Cl	None	22	21.6
18	Commercial injection	—	None	None	70	1.1

[a] Sample kept in 2-ml clear glass ampul.

Table II reports the photolytic rate constants and lag periods of methotrexate under various conditions. In Runs 8 and 11, different methotrexate concentrations degraded at approximately the same absolute rate (milligrams per hour) when other conditions such as light, vessel size, buffer concentration, and ionic strength were constant, and this result provides further support for a zero-order reaction.

Figure 2 and Table II show that photolyses of methotrexate solutions are strongly catalyzed by increasing ammonium bicarbonate concentration and that the same solution without ammonium bicarbonate is more stable to photodegradation. Additional studies in which either ammonium or bicarbonate was selectively excluded from the reaction mixture revealed that bicarbonate was the catalytic species (Table II, Runs 15 and 16).

Although no values are reported in the paper, the photodecomposition rate of methotrexate decreased when the light intensity was reduced. The rate also was influenced by the vessel size, which is predictable in photolytic reactions. As seen in Table II, Runs 5 and 6, a methotrexate solution sealed in a 2-ml clear glass ampul degraded about 1.5 times faster than the same sample kept in a 25-ml volumetric flask. This result can be explained by the larger surface area per milliliter of solution in the ampul. Finally, studies with the addition of edetate disodium slowed down the photolytic degradation rate, suggesting that trace metal-ion catalysis also may occur in the reaction.

Mechanism for Methotrexate Photolysis—Zero-order kinetics and the presence of a lag period (possibly explained by the buildup of the concentration of free radicals) strongly suggest a free radical mechanism for methotrexate photolysis. To support the proposed mechanism, a study was carried out in the presence of a free radical scavenger, 2-nitropropane. The lag period increased considerably in the presence of 2-nitropropane (Table II, Runs 8 and 10), which might have trapped the reactive free radical and thus delayed the onset of the reaction.

Identification of Photodegradation Products—Initial separation of degradation products was carried out in a cellulose column (1, 3). Figure 3 shows a chromatogram of a methotrexate solution approximately 60% photodegraded with three degradation peaks. The UV spectrum of peak 1 changed significantly with pH (Fig. 4) and provided a basis for its identification when compared with an authentic sample of 2,4-diamino-6-pteridinecarbaldehyde (6). Peak 2 exhibited a UV spectrum identical to that of 2,4-diamino-6-pteridinecarboxylic acid (7). Peak 3 was identified as *p*-aminobenzoylglutamic acid by its UV spectrum when compared to an authentic sample.

The HPLC method with a very dilute buffered eluant (Mobile Phase 2) was used for a more rapid identification of the photodegradation products. Figure 5*a* shows a chromatogram of methotrexate solution approximately 60% photodegraded; peak 1 (r_t = 7 min) was identified as 2,4-diamino-6-pteridinecarbaldehyde, peak 2 (r_t = 13 min) was

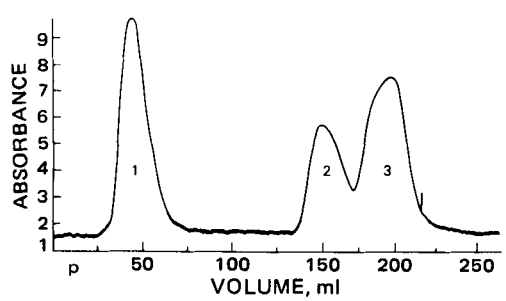

Figure 3—*Chromatogram of a partially photodegraded sample of methotrexate in 0.1* M *ammonium bicarbonate, pH 8.3, and 23 ± 2° from a cellulose ion-exchange column on linear gradient elution from 0.01 to 0.4* M *ammonium bicarbonate, pH 8.3. Key: peak 1, 2,4-diamino-6-pteridinecarbaldehyde; peak 2, 2,4-diamino-6-pteridinecarboxylic acid; and peak 3,* p*-aminobenzoylglutamic acid.*

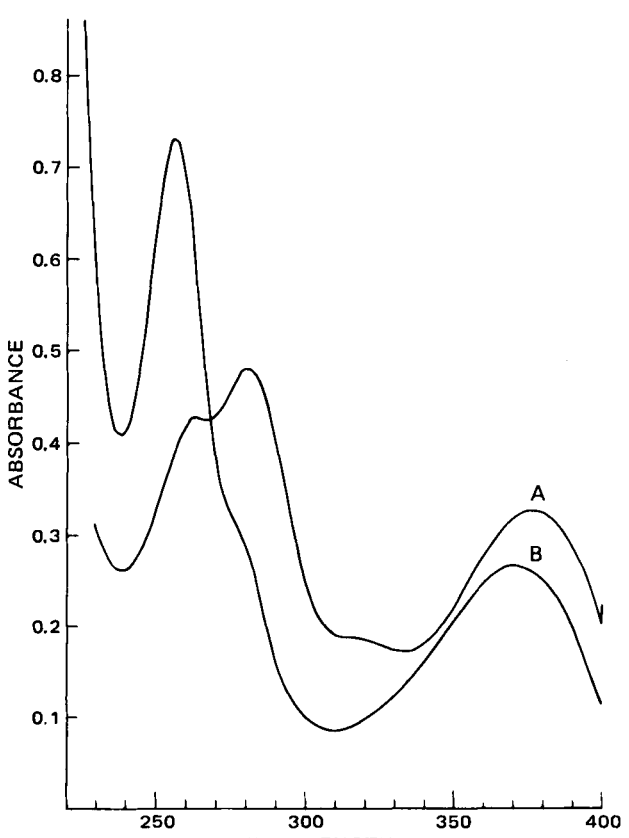

Figure 4—*UV spectra of peak 1 from Fig. 3 at two different pH values. Key: A, pH 8.3, 0.1* M *ammonium bicarbonate; and B, pH 13, 0.1* N *NaOH.*

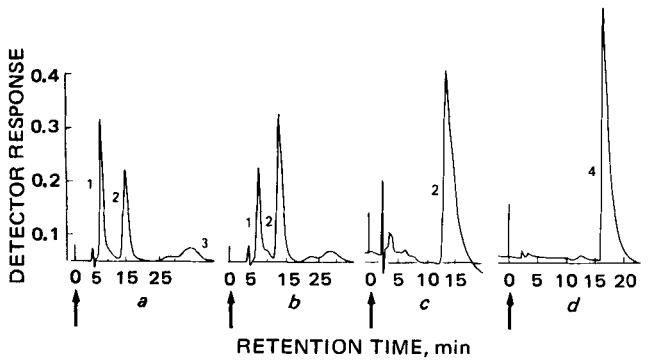

Figure 5—*HPLC changes for methotrexate photodegradation in 0.1 M ammonium bicarbonate (pH 8.3) at 23 ± 2° and μ = 0.25 with time. Key:* a, *2 days;* b, *6 days;* c, *20 days;* d, *fraction* c *boiled with 0.1* N *NaOH for 1 hr; peak 1, 2,4-diamino-6-pteridinecarbaldehyde; peak 2, 2,4-diamino-6-pteridinecarboxylic acid; peak 3,* p*-aminobenzoylglutamic acid; and peak 4, 4-amino-4-hydroxy-6-pteridinecarboxylic acid.*

identified as 2,4-diamino-6-pteridinecarboxylic acid, and peak 3 (r_t = 35 min) was identified as *p*-aminobenzoylglutamic acid when their UV spectra were compared to authentic samples. Figure 5*b* shows an increase in the acid peak 2 with a simultaneous decrease in the aldehyde peak 1 when the sample in Fig. 5*a* was exposed to additional light for 4 days.

When the sample in Fig. 5*b* was further exposed to light for 2 weeks, loss of peak 1 resulted in an increase in the formation of peak 2 (r_t = 13.5 min) (Fig. 5*c*). When the sample seen in Fig. 5*c* was boiled with 0.1 *N* NaOH for 1 hr, peak 2 shifted upfield and became peak 4 with a retention time (r_t = 18 min) (Fig. 5*d*) identical to that of an authentic sample of 2-amino-4-hydroxy-6-pteridinecarboxylic acid. Formation of peak 4 could be explained by the ease of hydrolysis of the 4-amino group of 2,4-diamino-6-pteridinecarboxylic acid in alkaline solution.

Identification of peak 3 warrants further discussion. To determine whether N–CH_3 cleavage occurs under the experimental conditions described for methotrexate photolysis, *p-N*-methylaminobenzoic acid (0.10 mg/ml) was dissolved in 0.25 *M* $NaHCO_3$ (pH 8.3) and kept under light. After about 10 days, 60% of the initial reactant, *p-N*-methylaminobenzoic acid, was converted to *p*-aminobenzoic acid. In a similar study in which sodium bicarbonate was omitted but the pH was maintained at 8.3, about 10% degradation occurred. It appears, therefore, that the bicarbonate ion has a photocatalytic effect in breaking the N–CH_3 bond when nitrogen is attached to an aromatic group. Considering the abundance of such groups in medicinal agents and the common use of bicarbonate buffers, this observation warrants further systematic investigation.

Scheme II presents the proposed sequence for photolytic reaction of methotrexate in the presence of bicarbonate buffer. As described earlier, 2-nitropropane trapping suggested the presence of bicarbonate free radicals. These radicals probably act as the catalyst in the initial breaking of N^{10}-alkyl linkages. In Scheme II, both alkyl linkages, CH_2–N and the N^{10}–CH_3, are shown to be cleaved in one step. However, this may not necessarily be true, and either of the alkyl groups could be cleaved first.

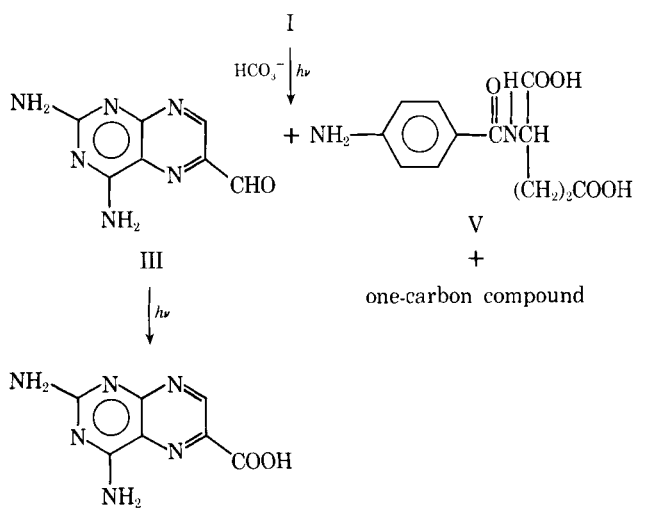

Scheme II

The relatively slow rate of cleavage of the methyl group from *p-N*-methylaminobenzoic acid compared to the rate of appearance of *p*-aminobenzoylglutamic acid suggests that *p-N*-methylaminobenzoylglutamic acid is not the precursor of *p*-aminobenzoylglutamic acid during methotrexate photolysis. Therefore, the methyl group must cleave away before or simultaneously with the CH_2–N group. Formation of 4-aminopteroylglutamic acid (aminopterin) as an intermediate is a possibility, but it has not been identified in the reaction mixture.

The formation of the aldehyde that oxidizes to the corresponding acid in alkaline pH also occurred in folic acid photolysis (8). In Scheme II, the conversion of 2,4-diamino-6-pteridinecarbaldehyde to 2,4-diamino-6-pteridinecarboxylic acid also was photocatalyzed; when the sample in Fig. 5*a* was kept in the dark for 4 days, there was no significant increase in the acid peak even though it was kept in moderate alkaline pH. The influence of the buffer species on the degradation products in the reaction has not been investigated, nor has the fate of the one-carbon compound coming from the methyl group attached to the N^{10}-portion of methotrexate. However, formaldehyde and formic acid may be the products formed that are similar to formation of 2,4-diamino-6-pteridinecarbaldehyde and 2,4-diamino-6-pteridinecarboxylic acid from the other substituent (2,4-diaminopteridylmethyl) on N^{10}.

Studies with Commercial Preparations—The results of a thermal study with commercial methotrexate injection at 85° are presented in Table I. The degradation rate of the injection was similar to that of methotrexate USP in 0.1 *M* ammonium bicarbonate at an initial pH of 8.3. Since methotrexate USP in 0.1 *M* ammonium bicarbonate kept in the dark at room temperature for 1 year showed about 3% degradation, one can assume that commercial methotrexate injection is at least as stable. Therefore, it was concluded that the injection should be stable (less than 10% degradation) for about 3 years at room temperature.

No photodegradation products previously described were found in recently manufactured commercial methotrexate injections stored in the original package for about 1 year. When methotrexate injection was diluted to 0.1 mg of methotrexate/ml with water and kept under light, there was only 5% degradation after 10 days and 11% degradation after 20 days. However, solutions of methotrexate USP without benzyl alcohol but otherwise identical to commercial methotrexate degraded 8% in 10 days and 17% in 20 days. Benzyl alcohol in the commercial injection apparently has some stabilizing effect against methotrexate photodegradation. However, methotrexate stability in undiluted concentrated solution is much different. Undiluted vials of 25 mg of methotrexate/ml in the original container, when kept under light for more than 1 month, showed negligible photodegradation. This result may be explained by the fact that the more concentrated the solution undergoing zero-order degradation, the smaller the percent degradation.

In high dose (10–25 g) methotrexate therapy, bicarbonate solutions are often administered along with methotrexate to alkalinize the urine and increase methotrexate excretion. Methotrexate mixed with bicarbonate in the infusion bottle may often be exposed to room light over 12–24 hr. Considering the catalytic effect of the bicarbonate ion on methotrexate photolysis, a study was carried out in light using a low concentration of methotrexate, 2 mg/ml (for a maximum percent degradation), and a high concentration of the bicarbonate ion (0.05 *M* $NaHCO_3$) in an infusion bottle. No photodegradation products were observed in 12 hr. This result may be explained by the fact that the solution was more concentrated (than solutions in the study) and that the lag period must be considerably longer in room light than in the light box used in the photolytic studies. Thus, mixing methotrexate in bicarbonate solution was acceptable if the solution was used within 12 hr. However, the bicarbonate ion catalyzes the photolysis of methotrexate and should be avoided if possible.

Methotrexate tablets, when powdered, spread over a large surface area, and kept under light, showed no photodegradation products over 2 months.

It can be concluded from the results of this study that, except for N^{10}-methylpteroylglutamic acid, the impurities in commercial methotrexate injection (2, 3, 9) did not result from the degradation of methotrexate but appear to have resulted during the synthesis of the drug.

REFERENCES

(1) J. F. Gallelli and G. Yokoyama, *J. Pharm. Sci.*, **56**, 387 (1967).

(2) W. P. Tong, J. Rosenburg, and D. B. Ludlum, *Lancet*, **2**, 19 (Oct. 1975).

(3) V. T. Oliverio, *Anal. Chem.*, **33**, 263 (1961).
(4) D. C. Chatterji and J. F. Gallelli, *J. Pharm. Sci.*, **66**, 1219 (1977).
(5) D. R. Seeger, D. G. Cosulich, J. M. Smith, and M. E. Hultquist, *J. Am. Chem. Soc.*, **72**, 4630 (1950).
(6) T. L. Loo, R. L. Dion, and R. H. Adamson, *J. Med. Chem.*, **8**, 713 (1965).
(7) R. L. Dion and T. L. Loo, *J. Org. Chem.*, **26**, 1857 (1961).
(8) O. H. Lowry, O. A. Bessey, and E. J. Crawford, *J. Biol. Chem.*, **180**, 389 (1949).
(9) D. C. Chatterji, A. G. Frazier, and J. F. Gallelli, *J. Pharm. Sci.*, in press.

ACKNOWLEDGMENTS

The authors thank Mrs. Altice G. Frazier for technical assistance.

Pharmacological Studies on *N*-Demethylated Carbachol

J. TRZECIAKOWSKI and C. Y. CHIOU ˣ

Received March 17, 1977, from the *Department of Pharmacology and Therapeutics, College of Medicine, University of Florida, Gainesville, FL 32610.* Accepted for publication August 2, 1977.

Abstract □ In attempts to find a drug more active than pilocarpine, the tertiary nitrogen derivative of carbachol, *N*-demethylated carbachol, was synthesized and tested on several autonomic nervous system preparations. *N*-Demethylated carbachol was active at muscarinic and nicotinic sites *in vivo* and *in vitro*. In superfusion studies, *N*-demethylated carbachol contracted the smooth muscle of the guinea pig ileum as well as skeletal muscles of frog rectus abdominis and chick biventer cervicis. *N*-Demethylated carbachol decreased blood pressure in the rat, with an ED_{50} (±*SEM*) of 4.82 ± 0.78 mg/kg. After close arterial injection to the cat superior cervical ganglion, *N*-demethylated carbachol elicited contractions of the nictitating membrane (ED_{50} of 1.68 ± 0.24 mg/kg) that were not significantly affected by atropine. *N*-Demethylated carbachol stimulated salivation in dog Wharton duct preparations with an ED_{50} of 2.55 ± 0.81 mg/kg. In contrast, pilocarpine had no effects on skeletal muscles *in vitro*, produced ganglionic effects blocked by atropine, had a prominent effect on salivation, and tended to elevate blood pressure.

Keyphrases □ *N*-Demethylated carbachol—synthesized, cholinergic activity evaluated *in vivo* and *in vitro* □ Carbachol, *N*-demethylated—synthesized, cholinergic activity evaluated *in vivo* and *in vitro* □ Cholinergic activity—*N*-demethylated carbachol evaluated *in vivo* and *in vitro*

It is desirable at times to produce effects that mimic the stimulation of autonomic pathways. One of the simplest ways of achieving this condition, at least in theory, would be administration of the appropriate neurotransmitter to the target organ. Acetylcholine, the transmitter at parasympathetic neuroeffector sites, is virtually useless as a therapeutic agent, largely because of its rapid hydrolysis by both acetylcholinesterase and butyrylcholinesterase. Studies on carbachol, the carbamic acid ester of choline, were reported in 1932 (1). Substitution of the carbamyl moiety in place of the acetyl group of acetylcholine increased resistance to hydrolysis by cholinesterases. At the same time, the essential pharmacological properties of acetylcholine were retained in the new ester.

Clinical use of carbachol has been hindered by the inability of the permanently charged molecule to penetrate biological membranes. Its effectiveness, *e.g.*, as an ophthalmic agent, was maintained only with high concentrations and the addition of wetting agents such as benzalkonium chloride to increase corneal penetration (2). Side effects and toxicity resulting from these procedures have reduced carbachol use in ophthalmology.

Drugs containing a tertiary nitrogen rather than a quaternary nitrogen moiety in their structures have the advantage of higher lipid solubility and can thus penetrate membranes. This ability accounts for the extensive topical use of pilocarpine in glaucoma treatment. This naturally occurring cholinomimetic alkaloid bears little structural resemblance to acetylcholine, however, and certain aspects of its action, mechanism, and inactivation are ambiguous (3).

Considerations of stability, penetrability, and structure suggest that a tertiary nitrogen derivative of carbachol might be an alternative to pilocarpine in ocular therapy.

At least two groups in the past have reported the synthesis of this tertiary nitrogen compound, 2-(dimethylamino)ethyl carbamate (*N*-demethylated carbachol) (I) (4, 5). Despite the therapeutic potential of such a derivative, little work has been done on its pharmacology. Therefore, studies were initiated to investigate its properties.

EXPERIMENTAL

Drugs—Compound I hydrochloride was prepared using a procedure described by Hazard *et al.* (5). Its identity was confirmed by melting point, elemental analysis, and mass and NMR spectral analysis. Acetylcholine iodide[1], atropine sulfate[1], pilocarpine nitrate[1], tubocurarine chloride[1], and carbachol[2] were used as received.

Superfused Guinea Pig Ileum Preparation—Guinea pigs, 300–500 g, were stunned; the terminal portion of the ileum was removed, cleaned, cut into 2-cm long segments, and suspended on a superfusion assembly with an isometric force transducer[3] under an initial tension of 1 g. Tyrode solution (137 m*M* NaCl, 2.7 m*M* KCl, 1.35 m*M* $CaCl_2$, 1.0 m*M* $MgCl_2$, 11.9 m*M* $NaHCO_3$, 0.36 m*M* NaH_2PO_4, and 11.1 m*M* dextrose), oxygenated with 95% O_2–5% CO_2, was pumped over the preparation at a rate of 3–4 ml/min with a peristaltic pump[4]. The superfusion fluid was maintained at room temperature since the ileum displayed less spontaneous activity at 25 than at 37°.

Drugs to be tested were dissolved in saline (0.9% NaCl) and injected directly into the stream of superfusion fluid. Doses were increased in a logarithmic fashion while drug concentrations were adjusted to keep the volume of each dose less than 0.1 ml. The tension developed by the muscle during contraction was recorded on a polygraph[5]. The maximum response of each muscle was taken as 100%, and all smaller responses were ex-

[1] Nutritional Biochemicals Corp., Cleveland, Ohio.
[2] City Chemical Corp., New York, N.Y.
[3] Myograph B, Narco Bio-Systems, Houston, TX 77017.
[4] Polystaltic pump, Buchler Instruments Co., Fort Lee, NJ 07024.
[5] Physiograph model Four-A, Narco Bio-Systems, Houston, TX 77017.

(3) V. T. Oliverio, *Anal. Chem.*, **33**, 263 (1961).
(4) D. C. Chatterji and J. F. Gallelli, *J. Pharm. Sci.*, **66**, 1219 (1977).
(5) D. R. Seeger, D. G. Cosulich, J. M. Smith, and M. E. Hultquist, *J. Am. Chem. Soc.*, **72**, 4630 (1950).
(6) T. L. Loo, R. L. Dion, and R. H. Adamson, *J. Med. Chem.*, **8**, 713 (1965).
(7) R. L. Dion and T. L. Loo, *J. Org. Chem.*, **26**, 1857 (1961).
(8) O. H. Lowry, O. A. Bessey, and E. J. Crawford, *J. Biol. Chem.*, **180**, 389 (1949).
(9) D. C. Chatterji, A. G. Frazier, and J. F. Gallelli, *J. Pharm. Sci.*, in press.

ACKNOWLEDGMENTS

The authors thank Mrs. Altice G. Frazier for technical assistance.

Pharmacological Studies on *N*-Demethylated Carbachol

J. TRZECIAKOWSKI and C. Y. CHIOU ˣ

Received March 17, 1977, from the *Department of Pharmacology and Therapeutics, College of Medicine, University of Florida, Gainesville, FL 32610.* Accepted for publication August 2, 1977.

Abstract □ In attempts to find a drug more active than pilocarpine, the tertiary nitrogen derivative of carbachol, *N*-demethylated carbachol, was synthesized and tested on several autonomic nervous system preparations. *N*-Demethylated carbachol was active at muscarinic and nicotinic sites *in vivo* and *in vitro*. In superfusion studies, *N*-demethylated carbachol contracted the smooth muscle of the guinea pig ileum as well as skeletal muscles of frog rectus abdominis and chick biventer cervicis. *N*-Demethylated carbachol decreased blood pressure in the rat, with an ED_{50} (±*SEM*) of 4.82 ± 0.78 mg/kg. After close arterial injection to the cat superior cervical ganglion, *N*-demethylated carbachol elicited contractions of the nictitating membrane (ED_{50} of 1.68 ± 0.24 mg/kg) that were not significantly affected by atropine. *N*-Demethylated carbachol stimulated salivation in dog Wharton duct preparations with an ED_{50} of 2.55 ± 0.81 mg/kg. In contrast, pilocarpine had no effects on skeletal muscles *in vitro*, produced ganglionic effects blocked by atropine, had a prominent effect on salivation, and tended to elevate blood pressure.

Keyphrases □ *N*-Demethylated carbachol—synthesized, cholinergic activity evaluated *in vivo* and *in vitro* □ Carbachol, *N*-demethylated—synthesized, cholinergic activity evaluated *in vivo* and *in vitro* □ Cholinergic activity—*N*-demethylated carbachol evaluated *in vivo* and *in vitro*

It is desirable at times to produce effects that mimic the stimulation of autonomic pathways. One of the simplest ways of achieving this condition, at least in theory, would be administration of the appropriate neurotransmitter to the target organ. Acetylcholine, the transmitter at parasympathetic neuroeffector sites, is virtually useless as a therapeutic agent, largely because of its rapid hydrolysis by both acetylcholinesterase and butyrylcholinesterase. Studies on carbachol, the carbamic acid ester of choline, were reported in 1932 (1). Substitution of the carbamyl moiety in place of the acetyl group of acetylcholine increased resistance to hydrolysis by cholinesterases. At the same time, the essential pharmacological properties of acetylcholine were retained in the new ester.

Clinical use of carbachol has been hindered by the inability of the permanently charged molecule to penetrate biological membranes. Its effectiveness, *e.g.*, as an ophthalmic agent, was maintained only with high concentrations and the addition of wetting agents such as benzalkonium chloride to increase corneal penetration (2). Side effects and toxicity resulting from these procedures have reduced carbachol use in ophthalmology.

Drugs containing a tertiary nitrogen rather than a quaternary nitrogen moiety in their structures have the advantage of higher lipid solubility and can thus penetrate membranes. This ability accounts for the extensive topical use of pilocarpine in glaucoma treatment. This naturally occurring cholinomimetic alkaloid bears little structural resemblance to acetylcholine, however, and certain aspects of its action, mechanism, and inactivation are ambiguous (3).

Considerations of stability, penetrability, and structure suggest that a tertiary nitrogen derivative of carbachol might be an alternative to pilocarpine in ocular therapy.

At least two groups in the past have reported the synthesis of this tertiary nitrogen compound, 2-(dimethylamino)ethyl carbamate (*N*-demethylated carbachol) (I) (4, 5). Despite the therapeutic potential of such a derivative, little work has been done on its pharmacology. Therefore, studies were initiated to investigate its properties.

EXPERIMENTAL

Drugs—Compound I hydrochloride was prepared using a procedure described by Hazard *et al.* (5). Its identity was confirmed by melting point, elemental analysis, and mass and NMR spectral analysis. Acetylcholine iodide[1], atropine sulfate[1], pilocarpine nitrate[1], tubocurarine chloride[1], and carbachol[2] were used as received.

Superfused Guinea Pig Ileum Preparation—Guinea pigs, 300–500 g, were stunned; the terminal portion of the ileum was removed, cleaned, cut into 2-cm long segments, and suspended on a superfusion assembly with an isometric force transducer[3] under an initial tension of 1 g. Tyrode solution (137 m*M* NaCl, 2.7 m*M* KCl, 1.35 m*M* $CaCl_2$, 1.0 m*M* $MgCl_2$, 11.9 m*M* $NaHCO_3$, 0.36 m*M* NaH_2PO_4, and 11.1 m*M* dextrose), oxygenated with 95% O_2–5% CO_2, was pumped over the preparation at a rate of 3–4 ml/min with a peristaltic pump[4]. The superfusion fluid was maintained at room temperature since the ileum displayed less spontaneous activity at 25 than at 37°.

Drugs to be tested were dissolved in saline (0.9% NaCl) and injected directly into the stream of superfusion fluid. Doses were increased in a logarithmic fashion while drug concentrations were adjusted to keep the volume of each dose less than 0.1 ml. The tension developed by the muscle during contraction was recorded on a polygraph[5]. The maximum response of each muscle was taken as 100%, and all smaller responses were ex-

[1] Nutritional Biochemicals Corp., Cleveland, Ohio.
[2] City Chemical Corp., New York, N.Y.
[3] Myograph B, Narco Bio-Systems, Houston, TX 77017.
[4] Polystaltic pump, Buchler Instruments Co., Fort Lee, NJ 07024.
[5] Physiograph model Four-A, Narco Bio-Systems, Houston, TX 77017.

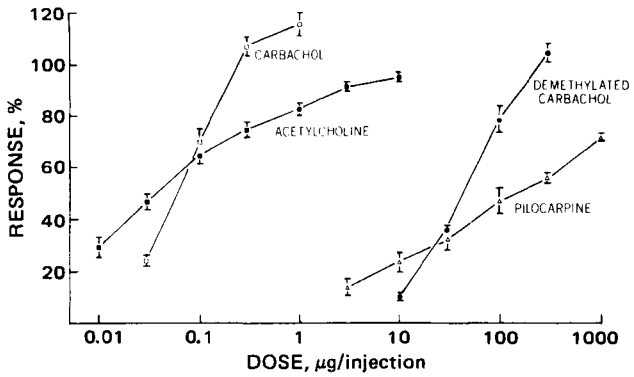

Figure 1—*Dose–response curves of acetylcholine, carbachol, N-demethylated carbachol, and pilocarpine in producing contracture of the smooth muscle of the guinea pig ileum using the superfusion technique. Each point is the mean of five values, and bars represent standard errors.*

pressed as percentages of this maximum response. Dose–response curves were constructed in this manner for acetylcholine, carbachol, pilocarpine, and *N*-demethylated carbachol. In a second set of experiments, dose–response curves for *N*-demethylated carbachol were constructed without and with atropine (1×10^{-8} *M*) in the superfusion fluid.

Superfused Frog Rectus Abdominis Muscle—*Rana pipiens*, 20–25 g, were stunned by a blow to the head, decapitated, and pithed. The rectus abdominis muscle was isolated and mounted for superfusion as described. Frog Ringer solution (110 m*M* NaCl, 2.01 m*M* KCl, 0.77 m*M* $CaCl_2$, 4.25 m*M* $NaHCO_3$, and 11.1 m*M* dextrose), oxygenated with 95% O_2–5% CO_2 at 25°, was used as the superfusion fluid.

Dose–response curves for acetylcholine, carbachol, *N*-demethylated carbachol, and pilocarpine were constructed before and during the treatment with tubocurarine (1×10^{-6} *M*).

Superfused Chick Biventer Cervicis Muscle—Baby chicks, 5–7 days old, were sacrificed with chloroform, and biventer cervicis muscles were dissected away from the body and mounted on superfusion assemblies under 1 g of initial tension. Tyrode solution, oxygenated with 95% O_2–5% CO_2 at 37°, was used for the superfusion fluid.

Experimental details for the construction of dose–response curves were the same as for the superfused guinea pig ileum preparation.

LD_{50} Study in Mice—ICR Charles River mice, 20–30 g, were given *N*-demethylated carbachol intraperitoneally with a microsyringe. The LD_{50} value was calculated according to the method of Litchfield and Wilcoxon (6).

Rat Blood Pressure—Holtzman rats, 300–400 g, were anesthetized with 1.6 g of urethan/kg. The carotid artery was cannulated with a polyethylene tubing attached to a pressure transducer. Drugs were injected through a cannula into the jugular vein, and any resulting changes in blood pressure were recorded on a polygraph[6]. Depressor responses were expressed as the percent change in the mean arterial pressure. Pressor effects were tabulated and analyzed as described later.

Dose–response data for each drug were plotted on log probit paper, and

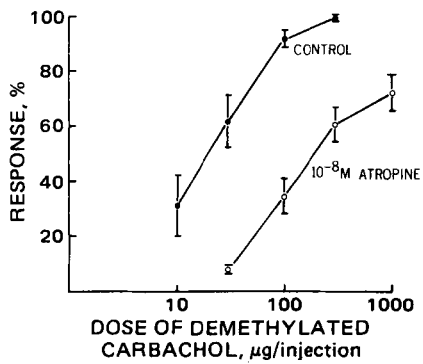

Figure 2—*Effects of atropine on the dose–response curves of N-demethylated carbachol in the superfused guinea pig ileum preparation. Each point is the mean of six values, and bars represent standard errors.*

[6] Model P-1000 A, Narco Bio-Systems, Houston, TX 77017.

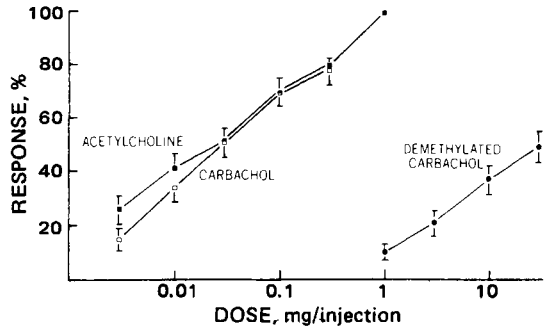

Figure 3—*Dose–response curves of acetylcholine, carbachol, and N-demethylated carbachol in producing transient contracture of the frog rectus abdominis muscle using the superfusion technique. Each point is the mean of six values, and bars represent standard errors.*

regression lines were fitted through the points. The ED_{50} value in each animal was calculated from the parameters of the lines, and values for all animals were then averaged to obtain a mean ED_{50} in this preparation.

Cat Superior Cervical Ganglion Nictitating Membrane—Cats of either sex, 2–3 kg, were anesthetized with 35 mg of pentobarbital sodium/kg intrahepatically. The femoral artery and vein were cannulated for monitoring blood pressure and drug injection. A pair of platinum electrodes was placed around the preganglionic sympathetic nerve fiber. A silk suture was sewn to the nictitating membrane and attached to an isometric force transducer under an initial tension of 1 g. After the lingual and external carotid arteries were tied and divided, a cannula was inserted into the common carotid artery; the ganglion was then perfused at a rate of 0.3–0.4 ml/min with an oxygenated Ringer solution (154 m*M* NaCl, 5.63 m*M* KCl, 1.63 m*M* $CaCl_2$, 5.95 m*M* $NaHCO_3$, and 5.55 m*M* dextrose). Acetylcholine, *N*-demethylated carbachol, and pilocarpine were injected into the same cannula, which was used to perfuse the ganglion.

Injections were given slowly over 1 min and in volumes not exceeding 0.4 ml. The increase in tension of the nictitating membrane following ganglionic stimulation by these agents was recorded on a polygraph. Responses to drugs were expressed as a percentage of the tension developed when the preganglionic trunk was stimulated electrically with monophasic square wave pulses of 10 v, 6 msec, and 20 Hz. Electrical stimulation was also used to test the viability of the preparation throughout the experiment. The methods for handling dose–response data and those of calculating ED_{50} values were identical to those described for rat blood pressure.

Dog Chorda Tympani–Wharton Duct—Mongrel dogs, 13–17 kg, were anesthetized with 40 mg of pentobarbital sodium/kg iv. The femoral artery and vein were cannulated for blood pressure measurements and drug injections. The Wharton duct was cannulated with polyethylene tubing (No. 90), which led to a 100-ml reservoir containing physiological saline. The outflow of the reservoir was positioned over a drop counter for recording on a polygraph.

Platinum electrodes were placed on the chorda tympani nerve, which was stimulated supramaximally for 1 sec every 10 sec with monophasic square wave pulses of 15 v, 2 msec, and 20 Hz. This stimulation produced a mean salivary flow rate of 20 drops/min. The dose producing the

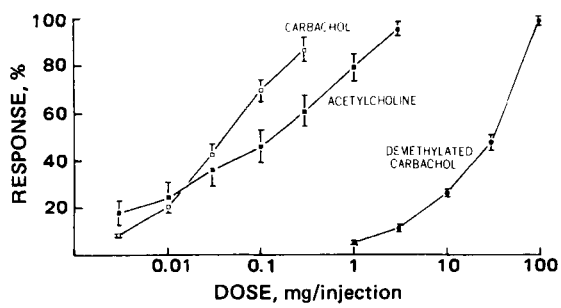

Figure 4—*Dose–response curves of acetylcholine, carbachol, and N-demethylated carbachol in producing transient contracture of the chick biventer cervicis muscle. Each point is the mean of five values, and bars represent standard errors.*

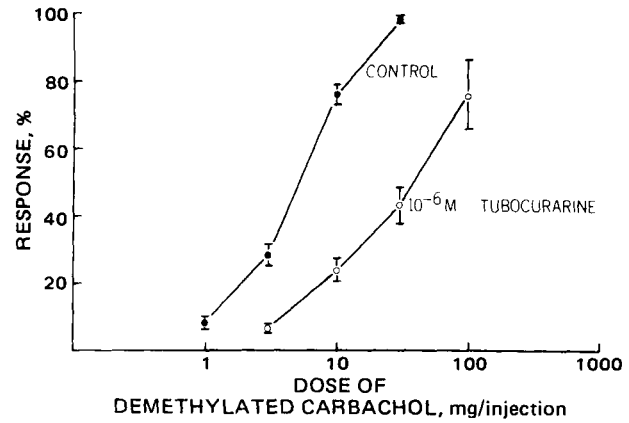

Figure 5—*Effect of tubocurarine on the dose–response curves of* N-*demethylated carbachol in the superfused chick biventer cervicis preparation. Each point is the mean of six values, and bars represent standard errors.*

greatest increase in salivary flow was taken as 100%, and all smaller responses were expressed as percentages of this maximum.

Isotonic saline was infused at a rate of 2 ml/min during the experiment to replace fluid lost through salivation.

Statistical Methods—The significance of differences between two values was tested with the Student *t* test (7).

The significance of differences in *N*-demethylated carbachol and pilocarpine effects on blood pressure in the rat preparation was tested with the following procedure. A 2 × 2 contingency table was constructed for each dose level at which *N*-demethylated carbachol and pilocarpine effects were compared. The number of times each drug dose was administered was recorded; the outcome was classed as a response if an increase in systolic pressure was observed and as a nonresponse if only a depressor effect was noted. The χ^2 procedure of Mantel and Haenzel was used to test the significance of differences between *N*-demethylated carbachol and pilocarpine actions over the entire dose range (8).

RESULTS

***In Vitro* Studies**—*N*-Demethylated carbachol contracted the superfused guinea pig ileum in doses ranging from 10 to 300 μg/injection (Fig. 1). Acetylcholine and carbachol were about 1000-fold more potent than this agent in causing contraction, presumably because of a greater affinity of the cholinergic receptor for quaternary nitrogen-containing compounds (9, 10). The dose–response curves of *N*-demethylated carbachol and carbachol had slopes that were parallel and much steeper than those of acetylcholine and pilocarpine curves. This result suggests that the mechanism of *N*-demethylated carbachol may be similar to that of carbachol but different from that of pilocarpine. This difference in slope of the dose–response curves also necessitates specification of the response level when one compares the potency of *N*-demethylated carbachol and pilocarpine. As can be seen from Fig. 1, *N*-demethylated carbachol is less potent than pilocarpine at low doses but becomes more potent at doses of 100 μg/injection and greater.

Atropine was added to the superfusion fluid to test whether the actions of *N*-demethylated carbachol were produced *via* stimulation of the muscarinic receptor. The dose–response curve obtained with low concentrations of *N*-demethylated carbachol was shifted to the right in a parallel fashion by 10^{-8} *M* atropine (Fig. 2). Higher doses of *N*-demethylated carbachol, however, did not completely reverse the blockade by atropine. Thus, *N*-demethylated carbachol and atropine do not appear to be strictly competitive at the muscarinic site.

Table I—ED_{50} Values of *N*-Demethylated Carbachol and Pilocarpine on *In Vivo* Preparations

Preparation	*N*-Demethylated Carbachol		Pilocarpine	
	n	mg/kg ± *SEM*	*n*	mg/kg ± *SEM*
Cat nictitating membrane	8	1.68 ± 0.84	9	3.10 ± 1.20
Dog Wharton duct	4	2.55 ± 0.81[a]	5	0.08 ± 0.02
Rat depressor response	7	4.82 ± 0.78[a]	7	38.07 ± 4.36

[a] Significantly different from pilocarpine at $p < 0.01$.

Figures 3 and 4 show the effects of *N*-demethylated carbachol on skeletal muscle preparations (frog rectus abdominis and chick biventer cervicis, respectively). The dose–response curves of *N*-demethylated carbachol in both preparations were nearly identical, with 50% maximum contraction evoked by 30 mg/injection. *N*-Demethylated carbachol was about 1000-fold less potent than acetylcholine and carbachol but was more potent than pilocarpine because no stimulation of the somatic fibers was seen with doses of pilocarpine as great as 10 mg/injection. The low solubility of this drug in concentrations greater than 10 mg/100 μl prevented the assay of higher doses. The dose–response curves of *N*-demethylated carbachol and carbachol were parallel, indicating similar mechanisms of action.

Figure 5 illustrates the competitive antagonism of *N*-demethylated carbachol effects at the neuromuscular junction (chick biventer cervicis nerve–muscle preparation) by the nondepolarizing blocker tubocurarine in a concentration of 10^{-6} *M*.

***In Vivo* Studies**—Injection of *N*-demethylated carbachol into the fluid perfusing the superior cervical ganglion resulted in dose-dependent contractions of the nictitating membrane that were immediate in onset and of short duration (Fig. 6). The ED_{50} value for *N*-demethylated carbachol in this preparation was 1.68 ± 0.84 mg/kg and did not differ significantly from the value calculated for pilocarpine (Table I). However, the responses to *N*-demethylated carbachol and pilocarpine differed in a qualitative sense; pilocarpine-induced contractions were delayed in onset, slow to reach a maximum, and of a relatively long duration (Fig. 6).

To determine whether the qualitative differences in *N*-demethylated carbachol and pilocarpine effects might be due to different sites of action in the ganglion, the drugs were readministered after an injection of 1 mg of atropine/kg iv, which is known to block muscarinic, but not nicotinic, receptors. Atropine had a slight effect on responses to 1 or 3 mg of *N*-demethylated carbachol/kg, but the responses to 1 mg of pilocarpine/kg were significantly reduced (Table II). Thus, the main site of pilocarpine action at the ganglion may be at muscarinic receptors whereas that of *N*-demethylated carbachol is not. The responses of the nictitating membrane to *N*-demethylated carbachol were reduced somewhat after atropine, but so were responses elicited by preganglionic electrical stimulation. These results indicate that only a small portion of the effects of *N*-demethylated carbachol as well as presynaptically released acetylcholine is mediated through atropine-sensitive sites that facilitate ganglionic transmission (11).

Figure 7 illustrates the ability of *N*-demethylated carbachol to increase

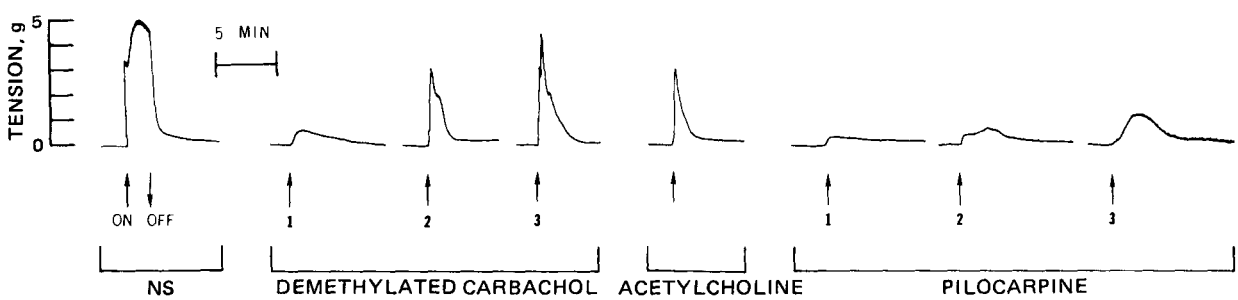

Figure 6—*Contraction of cat nictitating membrane by drugs. Electrical stimulation was applied to the preganglionic sympathic fibers (NS) with parameters mentioned under* Experimental. N-*Demethylated carbachol was administered at 0.1 (1), 0.3 (2), and 1.0 (3) mg/kg; pilocarpine was administered at 0.1 (1), 0.3 (2), and 1.0 (3) mg/kg.*

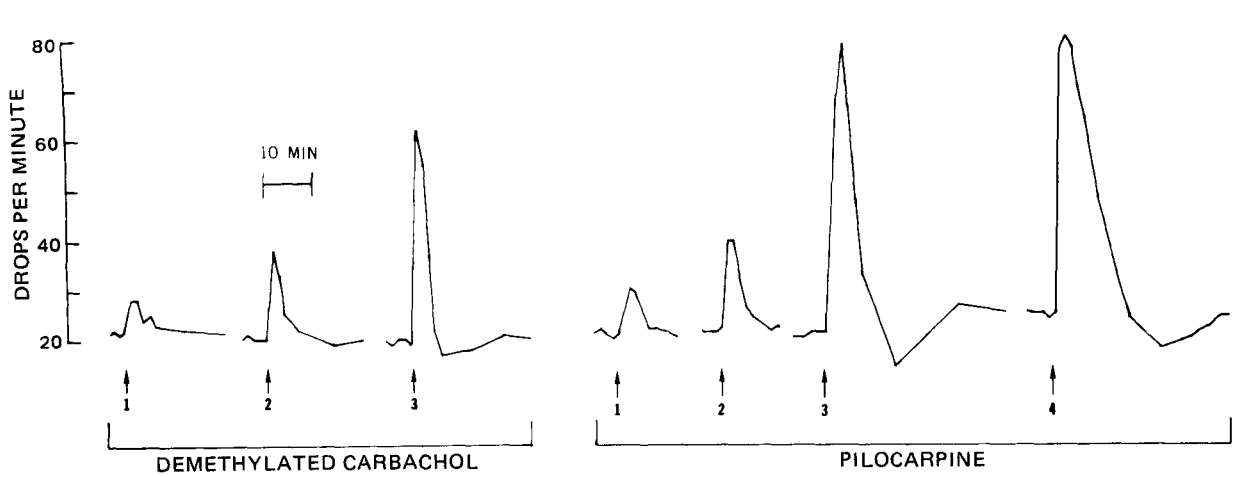

Figure 7—*Effect of drugs on the salivation rate in dog chorda tympani–Wharton duct preparations.* N-*Demethylated carbachol was administered at 0.3 (1), 1.0 (2), and 3.0 (3) mg/kg; pilocarpine was administered at 0.01 (1), 0.03 (2), 0.1 (3), and 0.3 (4) mg/kg.*

the salivation rate in the dog. The compound produced marked decreases in blood pressure in the same range of doses in which it increased salivation (Table I). It was not possible, therefore, to assay doses of *N*-demethylated carbachol that would produce the maximum salivary flow rate without risking the death of the animal. Pilocarpine, however, increased salivation at doses much lower than would have been predicted on the basis of its effects on blood pressure (Table I). The ED_{50} value of pilocarpine was statistically different from that of *N*-demethylated carbachol in the Wharton duct preparation. These results are in accord with the characteristic prominent action reported for pilocarpine on lacrimal, salivary, and sweat glands.

N-Demethylated carbachol was about 10 times more potent than pilocarpine in lowering the mean arterial blood pressure in the rat (Table I). In general, pilocarpine increased the pulse pressure to a greater extent than did *N*-demethylated carbachol. Furthermore, pressor effects were often observed either alone or following the depressor component. These pressor effects were observed following 80% (20 out of 25) of the pilocarpine administrations but were seen in only seven of the 28 instances in which *N*-demethylated carbachol was given. Statistical analysis of these results following the method of Mantel and Haenzel yielded a χ^2 value of 12.31, lending strong support to the notion that the two compounds have different modes of action (8).

The LD_{50} value of *N*-demethylated carbachol in mice was 501 mg/kg with a 95% confidence interval of 434–576 mg/kg. This result may be compared with the LD_{50} value of 500 mg/kg reported for pilocarpine given intraperitoneally to mice (12).

DISCUSSION

The most noticeable consequence of the *n*-demethylation of carbachol is the reduction of drug potency. With the dimethylamino derivative of acetylcholine, 40–300-fold greater concentrations of the tertiary nitrogen compound were required to achieve effects equal to acetylcholine (9, 10). The most encouraging finding of the present study, however, is that the potency of *N*-demethylated carbachol was higher than that of pilocarpine in all preparations tested except the Wharton duct salivation test in which pilocarpine was more potent than *N*-demethylated carbachol.

Table II—Effects of Atropine on Nictitating Membrane Responses

	Control		After 1 mg/kg Atropine	
Treatment	*n*	% Response	*n*	% Response
Electrical stimulation	6	100	6	62 ± 5
N-Demethylated carbachol, 1 mg/kg	6	30 ± 16	5	21 ± 13
N-Demethylated carbachol, 3 mg/kg	6	31 ± 15	6	26 ± 15
Pilocarpine, 1 mg/kg	6	27 ± 5	6	4 ± 2[a]

[a] Significantly different from control at $p < 0.01$, two-tailed test. Drug responses are expressed as percent of preatropine electrical stimulation response ± *SEM*. The absolute reading of the control electrical stimulation response was 45.9 ± 2.4 mm.

The antagonism of *N*-demethylated carbachol effects in the skeletal and smooth muscle preparations by low concentrations of tubocurarine and atropine indicates that the action mechanism of *N*-demethylated carbachol involves the cholinergic receptor. It does not reveal, however, whether the muscle stimulation is produced entirely by direct combination of drug with receptor or whether indirect mechanisms, such as the release of acetylcholine from the presynaptic nerve terminal or cholinesterase inhibition, are also involved. Further studies are planned to elucidate the action mechanism of *N*-demethylated carbachol.

Results from *in vitro* experiments indicate that *N*-demethylated carbachol, like carbachol and acetylcholine, stimulates both muscarinic and nicotinic sites. A characteristic feature of nicotinic receptors is that they generally require higher quantities of drug for stimulation than muscarinic receptors. This quality is illustrated in superfusion studies where doses of agonist 1000 times higher than those acting on guinea pig ilea were necessary to achieve contraction of the rectus abdominis and biventer cervicis muscles. Pilocarpine, on the other hand, seems to be devoid of any nicotinic activity.

In *in vivo* studies, *N*-demethylated carbachol again exerted both muscarinic and nicotinic actions. Doses of atropine that completely abolished the salivation and depressor effects of *N*-demethylated carbachol had little effect on the *N*-demethylated carbachol response on the nictitating membrane preparation, indicating that *N*-demethylated carbachol was acting at nicotinic receptors in the superior cervical ganglion. The ED_{50} of *N*-demethylated carbachol in this preparation, however, was not significantly different from the value in Wharton duct or blood pressure preparations in which *N*-demethylated carbachol effects were mediated through muscarinic receptors. The lower sensitivity expected for nicotinic sites in the sympathetic ganglion may have been offset by higher local concentrations of agonist resulting from close arterial drug injection.

In these studies, atropine blocked the effects of pilocarpine at the ganglion, as has been shown in the past (13, 14). Trendelenburg (15) demonstrated that pilocarpine's actions were unaffected by hexamethonium in doses that abolished membrane responses to preganglionic stimulation and intraarterial acetylcholine. Pilocarpine thus appears to be acting at ganglionic muscarinic receptors to produce nictitating membrane contraction.

While both *N*-demethylated carbachol and pilocarpine produced dose-dependent decreases in arterial pressure, over half of the intravenous injections of pilocarpine were followed by a secondary rise in blood pressure. This pressor response was abolished by atropine and α-adrenergic antagonists (16), ganglion depolarizing agents (17, 18), catecholamine depletion, and prevention of norepinephrine release from sympathetic terminals (18) but was unaffected by adrenalectomy (16, 17). Therefore, this secondary rise in pressure may result from stimulation of muscarinic receptors in sympathetic ganglia. Sympathetic activation may be responsible, at least in part, for the higher ED_{50} value of pilocarpine compared with that of *N*-demethylated carbachol in the rat blood pressure preparation, since this action would produce effects on the heart and blood vessels in opposition to those of direct vascular muscarinic depressor action.

The dog Wharton duct salivation preparation was the only instance in which pilocarpine was more potent than *N*-demethylated carbachol.

However, this prominent action of pilocarpine on salivary and other exocrine glands constitutes an undesirable effect in most cases (19). Stimulation of lacrimal glands following instillation of pilocarpine into the conjunctival sac would conceivably enhance its removal by tears into the nasolacrimal duct, thereby reducing its ocular penetration and increasing systemic absorption. These effects should be less evident with *N*-demethylated carbachol.

The use of the LD_{50}/ED_{50} ratio to compare the margin of safety of two drugs is not valid in instances where the slopes of the dose–response curves for toxicity and/or effect of the drugs are not parallel. For this reason, the observation of equal LD_{50} values for pilocarpine and *N*-demethylated carbachol does not necessarily imply that they have equal margins of safety. In addition, determinations of lethality may give no indication of the tendency of a drug to produce side effects. In this regard, preliminary studies showed marked irritation of the canine eye following topical application of a 1% pilocarpine solution while no irritation was observed after similar applications of *N*-demethylated carbachol in concentrations as high as 4%[7].

In summary, the tertiary nitrogen-containing analog of carbachol was tested and found to be an effective cholinergic stimulant active at both muscarinic and nicotinic sites. Unlike pilocarpine, *N*-demethylated carbachol shows less tendency to produce exocrine gland and sympathetic effects, properties that should make it a useful alternative to pilocarpine. Both compounds are currently being evaluated in a canine model of glaucoma.

REFERENCES

(1) H. Kreitmair, *Arch. Exp. Pathol. Pharmakol.*, **164**, 346 (1932).

(2) W. H. Havener, "Ocular Pharmacology," 3rd ed., Mosby, St. Louis, Mo., 1974, pp. 260–262.

(3) D. A. Newsome and I. E. Loewenfeld, *Surv. Ophthalmol.*, **18**, 399 (1974).

(4) R. D. Haworth, A. H. Lamberton, and D. Woodcock, *J. Chem. Soc. London*, **1947**, 176.

(5) R. Hazard, J. Cheymol, P. Chabrier, A. Sekera, and R. Eche-Fialaire, *Bull. Soc. Chim. Fr.*, **1961**, 2087.

(6) J. T. Litchfield and F. Wilcoxon, *J. Pharmacol. Exp. Ther.*, **96**, 99 (1949).

(7) A. Goldstein, "Biostatistics, An Introductory Text," Macmillan, New York, N.Y., 1964, pp. 45–55.

(8) C. W. Dunnet, in "Selected Pharmacological Testing Methods," A. Burger, Ed., vol. 3 of Medicinal Research Series, Dekker, New York, N.Y., 1968, pp. 28, 29.

(9) H. R. Ing, *Science*, **109**, 264 (1949).

(10) J. M. Van Rossum, *Arch. Int. Pharmacodyn. Ther.*, **140**, 592 (1962).

(11) R. L. Volle, *Pharmacol. Rev.*, **18**, 839 (1966).

(12) C. D. Barnes and L. G. Eltherington, "Drug Dosage in Laboratory Animals," rev. ed., University of California Press, Berkeley, Calif., 1973, p. 206.

(13) N. Ambache, *J. Physiol. (London)*, **110**, 164 (1949).

(14) L. C. Iorio and R. J. McIsaac, *J. Pharmacol. Exp. Ther.*, **151**, 430 (1966).

(15) U. Trendelenburg, *Br. J. Pharmacol.*, **9**, 481 (1954).

(16) M. A. Root, *J. Pharmacol. Exp. Ther.*, **101**, 125 (1951).

(17) U. Trendelenburg, *J. Physiol. (London)*, **129**, 337 (1955).

(18) U. Trendelenburg, *J. Pharmacol. Exp. Ther.*, **131**, 65 (1961).

(19) R. Rengstorff and M. Royston, *Am. J. Optom. Physiol. Opt.*, **53**, 70 (1976).

[7] Unpublished observations.

ACKNOWLEDGMENTS

Supported in part by National Eye Institute, National Institutes of Health, Grant EY-01624.

J. Trzeciakowski was supported in part by National Institutes of Health Training Grant GM-00760.

Effects of Compression Force, Particle Size, and Lubricants on Dissolution Rate

TITUS A. IRANLOYE * and EUGENE L. PARROTT ˣ

Received April 4, 1977, from the *College of Pharmacy, University of Iowa, Iowa City, IA 52242.* Accepted for publication July 26, 1977. *Present address: Igbaju-Ilorin, Nigeria.

Abstract □ The effects of compression force, particle size, and lubricant concentration on the dissolution rates of compressed disks of salicylic acid, aspirin, and an equimolar mixture of aspirin and salicylic acid were investigated. Compression forces from 450 to 9100 kg had no effect on dissolution rates. With 5% starch incorporated into an equimolar mixture of aspirin and salicylic acid, the dissolution rates were independent of compression forces from 910 to 9100 kg. A 10-fold change of particle size of the materials being compressed did not affect the dissolution rates. An increase in the concentration from 0.1 to 5% of calcium stearate, glyceryl monostearate, magnesium stearate, and stearic acid progressively slowed the dissolution rate. An increase in the concentration from 0.1 to 5% talc and polyethylene glycol 4000 did not affect the dissolution rates. An increase in the concentration of starch from 0.1 to 5% progressively increased the dissolution rates.

Keyphrases □ Dissolution rate—compressed disks of salicylic acid, aspirin, and equimolar mixture, effects of compression force, particle size, and lubricants □ Compression force—effect on dissolution rate of compressed disks of salicylic acid, aspirin, and equimolar mixture □ Particle size—effect on dissolution rate of compressed disks of salicylic acid, aspirin, and equimolar mixture □ Lubricants, various—effect on dissolution rate of compressed disks of salicylic acid, aspirin, and equimolar mixture □ Salicylic acid—compressed disks alone and equimolar mixture with aspirin, dissolution rate, effects of compression force, particle size, and lubricants □ Aspirin—compressed disks alone and equimolar mixture with salicylic acid, dissolution rate, effects of compression force, particle size, and lubricants

The kinetics of dissolution for pure materials and for two-component solids have been published (1–5). Various relationships between dissolution rate and compression force have been reported (6–11). As Knoechel *et al.* (12) suggested, although compression force may influence the dissolution rate, the formulation and the particular medicinal compound have a greater effect.

Finholt and Solvang (13) studied the effect of particle size of granules used to prepare phenacetin tablets on the dissolution rate. The rate was increased in diluted gastric

However, this prominent action of pilocarpine on salivary and other exocrine glands constitutes an undesirable effect in most cases (19). Stimulation of lacrimal glands following instillation of pilocarpine into the conjunctival sac would conceivably enhance its removal by tears into the nasolacrimal duct, thereby reducing its ocular penetration and increasing systemic absorption. These effects should be less evident with *N*-demethylated carbachol.

The use of the LD_{50}/ED_{50} ratio to compare the margin of safety of two drugs is not valid in instances where the slopes of the dose–response curves for toxicity and/or effect of the drugs are not parallel. For this reason, the observation of equal LD_{50} values for pilocarpine and *N*-demethylated carbachol does not necessarily imply that they have equal margins of safety. In addition, determinations of lethality may give no indication of the tendency of a drug to produce side effects. In this regard, preliminary studies showed marked irritation of the canine eye following topical application of a 1% pilocarpine solution while no irritation was observed after similar applications of *N*-demethylated carbachol in concentrations as high as 4%[7].

In summary, the tertiary nitrogen-containing analog of carbachol was tested and found to be an effective cholinergic stimulant active at both muscarinic and nicotinic sites. Unlike pilocarpine, *N*-demethylated carbachol shows less tendency to produce exocrine gland and sympathetic effects, properties that should make it a useful alternative to pilocarpine. Both compounds are currently being evaluated in a canine model of glaucoma.

REFERENCES

(1) H. Kreitmair, *Arch. Exp. Pathol. Pharmakol.*, **164**, 346 (1932).

(2) W. H. Havener, "Ocular Pharmacology," 3rd ed., Mosby, St. Louis, Mo., 1974, pp. 260–262.

(3) D. A. Newsome and I. E. Loewenfeld, *Surv. Ophthalmol.*, **18**, 399 (1974).

(4) R. D. Haworth, A. H. Lamberton, and D. Woodcock, *J. Chem. Soc. London*, **1947**, 176.

(5) R. Hazard, J. Cheymol, P. Chabrier, A. Sekera, and R. Eche-Fialaire, *Bull. Soc. Chim. Fr.*, **1961**, 2087.

(6) J. T. Litchfield and F. Wilcoxon, *J. Pharmacol. Exp. Ther.*, **96**, 99 (1949).

(7) A. Goldstein, "Biostatistics, An Introductory Text," Macmillan, New York, N.Y., 1964, pp. 45–55.

(8) C. W. Dunnet, in "Selected Pharmacological Testing Methods," A. Burger, Ed., vol. 3 of Medicinal Research Series, Dekker, New York, N.Y., 1968, pp. 28, 29.

(9) H. R. Ing, *Science*, **109**, 264 (1949).

(10) J. M. Van Rossum, *Arch. Int. Pharmacodyn. Ther.*, **140**, 592 (1962).

(11) R. L. Volle, *Pharmacol. Rev.*, **18**, 839 (1966).

(12) C. D. Barnes and L. G. Eltherington, "Drug Dosage in Laboratory Animals," rev. ed., University of California Press, Berkeley, Calif., 1973, p. 206.

(13) N. Ambache, *J. Physiol. (London)*, **110**, 164 (1949).

(14) L. C. Iorio and R. J. McIsaac, *J. Pharmacol. Exp. Ther.*, **151**, 430 (1966).

(15) U. Trendelenburg, *Br. J. Pharmacol.*, **9**, 481 (1954).

(16) M. A. Root, *J. Pharmacol. Exp. Ther.*, **101**, 125 (1951).

(17) U. Trendelenburg, *J. Physiol. (London)*, **129**, 337 (1955).

(18) U. Trendelenburg, *J. Pharmacol. Exp. Ther.*, **131**, 65 (1961).

(19) R. Rengstorff and M. Royston, *Am. J. Optom. Physiol. Opt.*, **53**, 70 (1976).

[7] Unpublished observations.

ACKNOWLEDGMENTS

Supported in part by National Eye Institute, National Institutes of Health, Grant EY-01624.

J. Trzeciakowski was supported in part by National Institutes of Health Training Grant GM-00760.

Effects of Compression Force, Particle Size, and Lubricants on Dissolution Rate

TITUS A. IRANLOYE * and EUGENE L. PARROTT ˣ

Received April 4, 1977, from the *College of Pharmacy, University of Iowa, Iowa City, IA 52242.* Accepted for publication July 26, 1977. *Present address: Igbaju-Ilorin, Nigeria.

Abstract □ The effects of compression force, particle size, and lubricant concentration on the dissolution rates of compressed disks of salicylic acid, aspirin, and an equimolar mixture of aspirin and salicylic acid were investigated. Compression forces from 450 to 9100 kg had no effect on dissolution rates. With 5% starch incorporated into an equimolar mixture of aspirin and salicylic acid, the dissolution rates were independent of compression forces from 910 to 9100 kg. A 10-fold change of particle size of the materials being compressed did not affect the dissolution rates. An increase in the concentration from 0.1 to 5% of calcium stearate, glyceryl monostearate, magnesium stearate, and stearic acid progressively slowed the dissolution rate. An increase in the concentration from 0.1 to 5% talc and polyethylene glycol 4000 did not affect the dissolution rates. An increase in the concentration of starch from 0.1 to 5% progressively increased the dissolution rates.

Keyphrases □ Dissolution rate—compressed disks of salicylic acid, aspirin, and equimolar mixture, effects of compression force, particle size, and lubricants □ Compression force—effect on dissolution rate of compressed disks of salicylic acid, aspirin, and equimolar mixture □ Particle size—effect on dissolution rate of compressed disks of salicylic acid, aspirin, and equimolar mixture □ Lubricants, various—effect on dissolution rate of compressed disks of salicylic acid, aspirin, and equimolar mixture □ Salicylic acid—compressed disks alone and equimolar mixture with aspirin, dissolution rate, effects of compression force, particle size, and lubricants □ Aspirin—compressed disks alone and equimolar mixture with salicylic acid, dissolution rate, effects of compression force, particle size, and lubricants

The kinetics of dissolution for pure materials and for two-component solids have been published (1–5). Various relationships between dissolution rate and compression force have been reported (6–11). As Knoechel *et al.* (12) suggested, although compression force may influence the dissolution rate, the formulation and the particular medicinal compound have a greater effect.

Finholt and Solvang (13) studied the effect of particle size of granules used to prepare phenacetin tablets on the dissolution rate. The rate was increased in diluted gastric

Table I—Effect of Compression Force on Dissolution Rate of 80/100-Mesh Material Compressed into a 1.27-cm Disk

Compression Force, kg	Rate of Mass Loss[a], g/hr		Dissolution Rate, g/hr/cm²	
	Aspirin	Salicylic Acid	Aspirin	Salicylic Acid
		Salicylic Acid		
450		0.047		0.037
1135		0.047		0.037
2270		0.047		0.037
3400		0.047		0.037
4550		0.045		0.036
5680		0.048		0.038
6820		0.045		0.036
7950		0.045		0.036
9100		0.048		0.038
	Aspirin			
450	0.076		0.060	
1135	0.080		0.063	
2270	0.074		0.059	
3400	0.079		0.062	
4550	0.078		0.062	
5680	0.077		0.060	
6820	0.079		0.062	
7950	0.077		0.061	
9100	0.078		0.062	
	Equimolar Aspirin and Salicylic Acid			
450	0.037	0.038	0.029	0.030
1135	0.042	0.040	0.033	0.032
2270	0.039	0.039	0.031	0.031
3400	0.038	0.037	0.030	0.029
4550	0.041	0.039	0.032	0.031
5680	0.038	0.039	0.032	0.031
6820	0.038	0.037	0.030	0.029
7950	0.036	0.037	0.028	0.029
9100	0.037	0.038	0.029	0.030

[a] Average of two determinations.

juice as the particle size was decreased; however, the opposite effect occurred when 0.1 *N* HCl was used as the dissolution medium. In another study, no difference was detected in dissolution of phenobarbital and phenacetin tablets containing starch and gelatin if the tablets were prepared from different sizes of granulation (14).

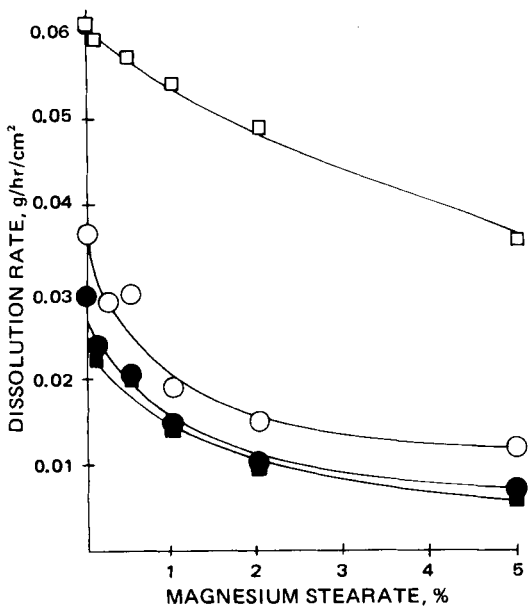

Figure 1—*Effect of concentration of magnesium stearate on dissolution rate of 80/100-mesh materials compressed at 1135 kg. Key: ○, salicylic acid; □, aspirin; ●, salicylic acid from equimolar mixture of aspirin and salicylic acid; and ■, aspirin from equimolar mixture of aspirin and salicylic acid.*

Table II—Effect of Particle Size of Materials Compressed at 1135 kg on Dissolution Rate of 1.27-cm Disks

Mesh Size Fraction	Rate of Mass Loss[a], g/hr		Dissolution Rate, g/hr/cm²	
	Aspirin	Salicylic Acid	Aspirin	Salicylic Acid
		Salicylic Acid		
40/60		0.050		0.039
60/80		0.050		0.039
80/100		0.051		0.040
100/140		0.050		0.039
140/200		0.051		0.040
	Aspirin			
40/60	0.076		0.060	
60/80	0.074		0.059	
80/100	0.080		0.063	
100/140	0.077		0.061	
140/200	0.080		0.063	
	Equimolar Aspirin and Salicylic Acid			
40/60	0.035	0.035	0.028	0.026
60/80	0.034	0.035	0.027	0.027
80/100	0.033	0.035	0.026	0.027
100/140	0.033	0.034	0.026	0.027
140/200	0.035	0.033	0.028	0.026

[a] Average of two determinations.

With triamterene tablets prepared from granules of different sizes, when terra alba or glycine was used as the excipient, the dissolution rate was increased as the particle size was decreased; however, when starch was the excipient, size had no effect on the dissolution rate (15). With salicylic acid tablets, the dissolution rate was increased as the granule size was decreased (16).

Although satisfactory in performing their function as lubricants, lubricants may possess the disadvantage of slowing dissolution. Increasing magnesium stearate to 1.5% caused a slowing of dissolution of phenobarbital tablets (17, 18), and 3% magnesium stearate slowed the dissolution of salicylic acid tablets (19). With triamterene tablets, an increase of lubricant greater than 2.5% caused a decrease in the dissolution rate (15). However, Finholt *et al.* (20) concluded that lubricants have very little effect on the dissolution rate of phenobarbital tablets.

The purpose of this investigation was to determine for the materials used the influence on the dissolution rate of compression force, particle size of the material being compressed, and concentration of lubricants with various particle sizes of materials being compressed.

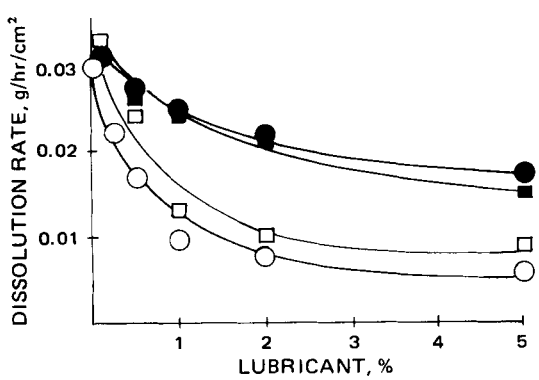

Figure 2—*Effect of concentration of calcium stearate and glyceryl monostearate on dissolution rate of 80/100-mesh equimolar mixture of aspirin and salicylic acid compressed at 1135 kg. Key: ○, salicylic acid with calcium stearate; □, aspirin with calcium stearate; ●, salicylic acid with glyceryl monostearate; and ■, aspirin with glyceryl monostearate.*

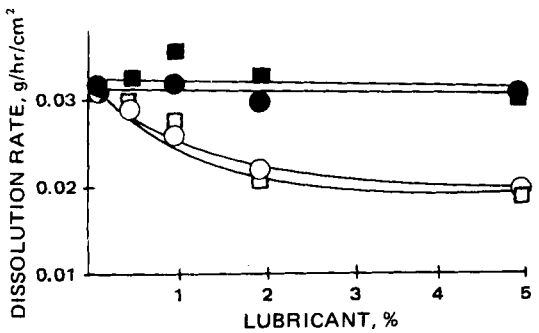

Figure 3—*Effect of concentration of stearic acid and polyethylene glycol 4000 on dissolution rate of 80/100-mesh materials compressed at 1135 kg. Key: ○, salicylic acid with stearic acid; □, aspirin with stearic acid; ●, salicylic acid with polyethylene glycol 4000; and ■, aspirin with polyethylene glycol 4000.*

EXPERIMENTAL

Preparation of Compressed Disks—Crystals of salicylic acid[1] and aspirin[2] were triturated with a mortar and pestle. The powdered drugs were separated by sieves into 40/60-, 60/80-, 80/100-, and 140/200-mesh size fractions. The materials were compressed by a hydraulic press[3] into flat-faced disks having diameters of 1.270 ± 0.005 cm. Compression forces ranged from 450 to 9100 kg.

Dissolution Rate—Disks were embedded in paraffin and mounted in a holder so that only a flat surface of the disk would be exposed to the dissolution medium. The dissolution rate was determined in 2 liters of distilled water at 25 ± 0.1° under conditions where the concentration did not exceed 5% of the solubility. The dissolution apparatus consisted of a 2-liter beaker in which a 3.0 × 1.5-cm stainless steel paddle, operating at 324 rpm, was positioned 1 cm above the exposed surface of a disk centered in the beaker bottom.

Samples were withdrawn by a pipet fitted with a filter and were analyzed spectrophotometrically according to a previously described method (5). The dissolution rate was defined as the grams of a compound dissolved from 1 cm^2 of surface of a disk/hr.

RESULTS AND DISCUSSION

Influence of Compression Force and Particle Size on Dissolution Rate—The data in Table I for compressed disks of salicylic acid, aspirin, and an equimolar mixture of aspirin and salicylic acid show that, under essentially sink conditions, the dissolution rate of nondisintegrating solids was independent of compression force from 450 to 9100 kg.

As shown in Table II for a size range of approximately 90 to 335 μm, the particle size of salicylic acid, aspirin, and an equimolar mixture of aspirin and salicylic acid compressed into a disk by a force of 1135 kg did not affect the dissolution rate of the nondisintegrating solid.

Kanke and Sekiguchi (6) found that, for benzoic acid, the compression force exerted no influence on the dissolution rate and that the size of sulfathiazole particles being compressed had no effect on the dissolution rate. The observed independence of dissolution rate from compression force and size of the material being compressed is in agreement with previous reports (4, 5, 20–23).

Influence of Concentration of Lubricants on Dissolution Rate—The general impression is that an increase in concentration of an insoluble lubricant in a compressed mass will slow the dissolution of the mass by decreasing the effective solid–solvent interface (19), by making the mass hydrophobic (23), and/or by physically coating the particles prior to compression (24). Hydrophobic lubricants investigated were calcium stearate[4], glyceryl monostearate[5], magnesium stearate[6], stearic acid[7], and talc[8]. The dissolution rates were determined using disks, containing from 0.1 to 5% lubricants of a 140/200-mesh size fraction, compressed at 1135 kg from an 80/100-mesh size of the materials.

As shown in Fig. 1, an increase in concentration of magnesium stearate

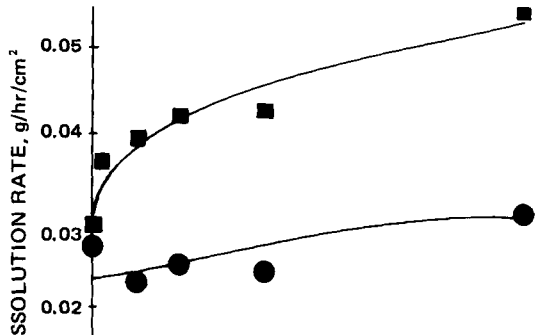

Figure 5—*Effect of concentration of starch on dissolution rate of 80/100-mesh equimolar mixture of aspirin and salicylic acid compressed at 1135 kg. Key: ●, salicylic acid; and ■, aspirin.*

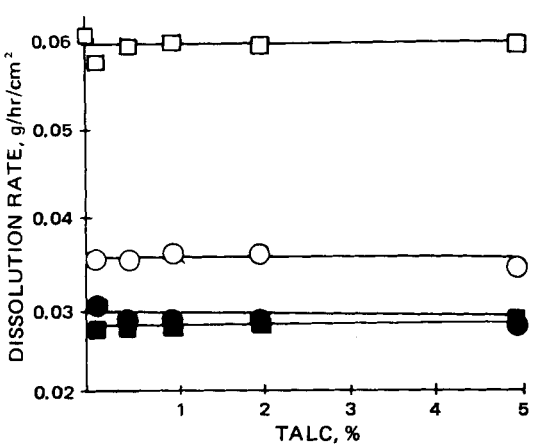

Figure 4—*Effect of concentration of talc on dissolution rate of 80/100-mesh materials compressed at 1135 kg. Key: ○, salicylic acid; □, aspirin; ●, salicylic acid from equimolar mixture of aspirin and salicylic acid; and ■, aspirin from equimolar mixture of aspirin and salicylic acid.*

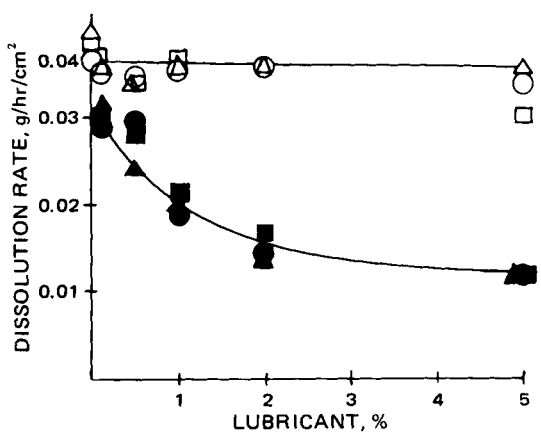

Figure 6—*Effect of particle size at various concentrations of lubricants on dissolution rate of salicylic acid compressed at 1135 kg. Key: □, 40/60-mesh size with talc; ○, 80/100-mesh size with talc; △, 140/200-mesh size with talc; ■, 40/60-mesh size with magnesium stearate; ●, 80/100-mesh size with magnesium stearate; and ▲, 140/200-mesh size with magnesium stearate.*

[1] Lot 733828, certified, Fisher Scientific Co.
[2] Lot 43904, USP, fine crystals, J.T. Baker Chemical Co.
[3] Carver press, model C.
[4] Lot A22, Matheson, Coleman and Bell.
[5] Purified, Fisher Scientific Co.
[6] Lot ENB, USP, Mallinckrodt.
[7] Lot WRHN, Mallinckrodt.
[8] Lot 3204560, J. T. Baker Chemical Co.

Table III—Effect of Compression Force on Dissolution Rate of 80/100-Mesh Equimolar Mixture of Aspirin and Salicylic Acid Containing 5% Starch Compressed into a 1.27-cm Disk

Compression Force, kg	Rate of Mass Loss[a], g/hr		Dissolution Rate, g/hr/cm²	
	Aspirin	Salicylic Acid	Aspirin	Salicylic Acid
910	0.059	0.035	0.047	0.028
1820	0.058	0.035	0.046	0.028
2730	0.060	0.034	0.048	0.028
3640	0.060	0.035	0.047	0.028
4550	0.060	0.034	0.040	0.026
5450	0.057	0.033	0.045	0.026
6360	0.063	0.036	0.049	0.028
7270	0.057	0.034	0.047	0.027
8190	0.060	0.036	0.048	0.029
9100	0.055	0.034	0.044	0.027

[a] Average of two determinations.

produced a slower dissolution rate of disks compressed of salicylic acid, aspirin, and an equimolar mixture of aspirin and salicylic acid. Similarly, an increase in concentration of calcium stearate, glyceryl monostearate, and stearic acid decreased the dissolution rates of disks of an equimolar mixture of aspirin and salicylic acid (Figs. 2 and 3).

These data seem to confirm the axiom that a sufficient quantity of a lubricant should be used to optimize tablet manufacture but that its concentration in a compressed tablet should be as low as practical to prevent a marked slowing of dissolution. With magnesium stearate, a concentration of 0.5% decreased the dissolution rates of salicylic acid and aspirin from compressed disks by approximately 20 and 7%, respectively, and decreased the dissolution rates of aspirin and salicylic acid from disks compressed of an equimolar mixture of aspirin and salicylic acid by approximately 33 and 27%, respectively.

Stearic acid, 1.0%, decreased the dissolution rates of aspirin and salicylic acid from compressed disks of an equimolar mixture of aspirin and salicylic acid by approximately 7 and 10%, respectively. Glyceryl monostearate, 0.5%, decreased the dissolution rates of aspirin and salicylic acid from compressed disks of an equimolar mixture of aspirin and salicylic acid by approximately 32 and 10%, respectively. Calcium stearate, 0.5%, decreased the dissolution rates of aspirin and salicylic acid from compressed disks of an equimolar mixture of aspirin and salicylic acid by approximately 20 and 40%, respectively.

Talc behaved differently from other hydrophobic lubricants. As shown in Fig. 4, the dissolution rates of disks compressed from salicylic acid, aspirin, and an equimolar mixture of aspirin and salicylic acid were essentially independent of concentrations of talc as great as 5%. It could be postulated that the stearates soften and spread under compression to provide a more coherent coverage of the matrix than talc.

If many hydrophobic lubricants slow dissolution, highly water-soluble lubricants, such as the polyethylene glycols, conversely could enhance

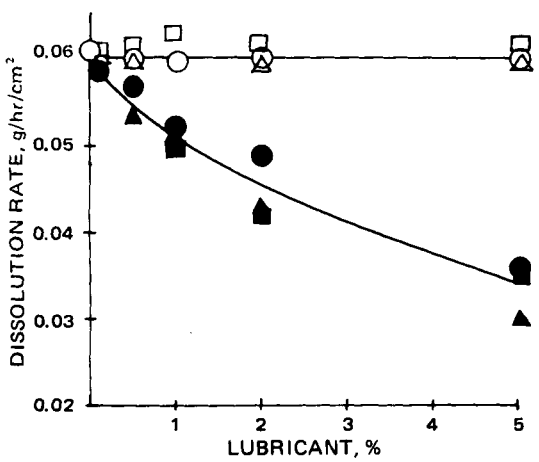

Figure 7—*Effect of particle size at various concentrations of lubricants on dissolution rate of aspirin compressed at 1135 kg. Key: □, 40/60-mesh size with talc; ○, 80/100-mesh size with talc; △, 140/200-mesh size with talc; ■, 40/60-mesh size with magnesium stearate; ●, 80/100-mesh size with magnesium stearate; and ▲, 140/200-mesh size with magnesium stearate.*

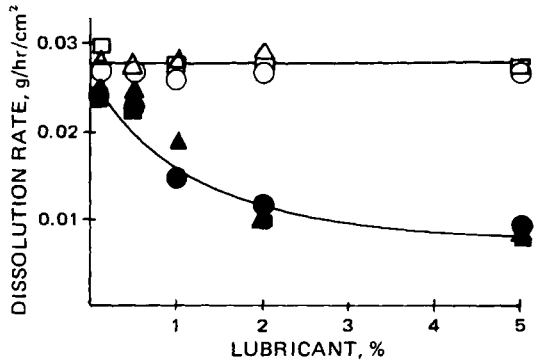

Figure 8—*Effect of particle size at various concentrations of lubricant on dissolution rate of salicylic acid from equimolar mixture of aspirin and salicylic acid compressed at 1135 kg. Key: ○, 40/60-mesh size with talc; □, 80/100-mesh size with talc; △, 140/200-mesh size with talc; ●, 40/60-mesh size with magnesium stearate; ■, 80/100-mesh size with magnesium stearate; and ▲, 140/200-mesh size with magnesium stearate.*

dissolution by increased wetting of, and better solvent penetration into, the mass (19). This enhancement did not occur with polyethylene glycol 4000. As shown in Fig. 3, the dissolution rates of disks compressed of an equimolar mixture of aspirin and salicylic acid were not affected by concentrations of polyethylene glycol 4000 as great as 5%. It may be that, to enhance dissolution, a lubricant must be simultaneously a water-soluble and surface-active substance.

Starch is a multipurpose excipient in commercial tablets; it is a good glidant and antiadhesive material, an excellent disintegrating agent, and an excellent binding agent (25). The dissolution rates from disks compressed at 1135 kg from an equimolar mixture of aspirin and salicylic acid were increased as the concentration of starch was increased (Fig. 5). It is difficult to apply the methodology used to determine intrinsic dissolution rates of nondisintegrating masses to compressed masses containing starch because the swelling of the starch causes flaking. As flaking occurs with a progressive roughening of the surface, the total surface of the solid exposed to the dissolution medium is increased. However, in the early period before gross flaking, the dissolution rates were more rapid as the concentration of starch was increased. Although the methodology is not absolute, it permits a comparison of the influence of various excipients on dissolution rate from compressed multicomponent masses.

Since starch has more than a single function in a tablet and swells mechanically when wet (26), the effect of compression force might influence characteristics of a tablet containing starch (27). The dissolution rates from disks compressed of an equimolar mixture of aspirin and salicylic acid containing 5% starch were determined at compression forces from 900 to 9100 kg. The dissolution rates were independent of the compression force (Table III).

Influence of Lubricants on Dissolution Rate of Disks Compressed from Different Sized Particles—The influence of the concentration

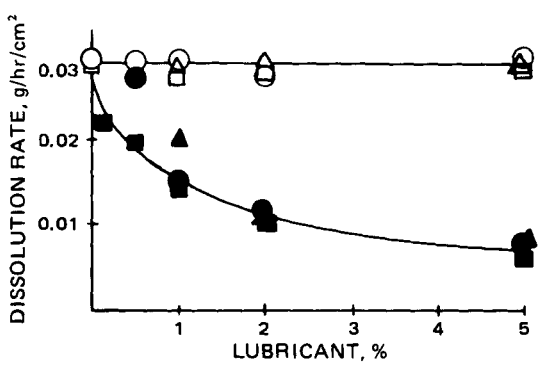

Figure 9—*Effect of particle size at various concentrations of lubricant on dissolution rate of aspirin from equimolar mixture of aspirin and salicylic acid compressed at 1135 kg. Key: ○, 40/60-mesh size with talc; □, 80/100-mesh size with talc; △, 140/200-mesh size with talc; ●, 40/60-mesh size with magnesium stearate; ■, 80/100-mesh size with magnesium stearate; and ▲, 140/200-mesh size with magnesium stearate.*

of a lubricant on the dissolution rate of a mass compressed at a given force was demonstrated for particles of 80/100-mesh size fraction. It is conceivable that a given weight of a lubricant may be distributed differently when blended with particles of different sizes and that different distributions may influence the dissolution of the compressed mass.

The dissolution rates of disks compressed at 1135 kg of 40/60-, 80/100-, and 140/200-mesh size fractions of salicylic acid containing 0.1–5% talc are shown in Fig. 6. The presence of talc in a concentration as great as 5% and the use of three size fractions of salicylic acid did not significantly alter the dissolution rates of the compressed disks. Similar results with talc were obtained from disks composed of aspirin (Fig. 7) and of an equimolar mixture of aspirin and salicylic acid (Figs. 8 and 9). The use of three size fractions of aspirin and an equimolar mixture of aspirin and salicylic acid with concentrations of talc from 0.1 to 5% did not alter the dissolution rates.

The dissolution rates of disks compressed at 1135 kg of 40/60-, 80/100-, and 140/200-mesh size fractions of salicylic acid, aspirin, and an equimolar mixture of aspirin and salicylic acid containing 0.1–5% magnesium stearate are shown in Figs. 6–9. As observed with talc, the dissolution rate, when using magnesium stearate, was independent of the size of the particles used to prepare the compressed disks.

REFERENCES

(1) E. Nelson, *J. Am. Pharm. Assoc., Sci. Ed.*, **46**, 607 (1957).

(2) M. Gibaldi and H. Weintraub, *J. Pharm. Sci.*, **57**, 832 (1968).

(3) W. I. Higuchi, N. A. Mir, and S. J. Desai, *ibid.*, **54**, 1405 (1965).

(4) E. L. Parrott, D. E. Wurster, and T. Higuchi, *J. Am. Pharm. Assoc., Sci. Ed.*, **44**, 269 (1955).

(5) S. A. Shah and E. L. Parrott, *J. Pharm. Sci.*, **65**, 1784 (1976).

(6) M. Kanke and K. Sekiguchi, *Chem. Pharm. Bull.*, **21**, 87 (1973).

(7) K. A. Khan and C. T. Rhodes, *Pharm. Acta Helv.*, **47**, 116 (1967).

(8) E. Cid and F. Jaminet, *ibid.*, **46**, 167 (1971).

(9) H. L. Smith, C. A. Baker, and J. H. Wood, *J. Pharm. Pharmacol.*, **23**, 536 (1971).

(10) D. Ganderton, J. W. Hadgraft, W. T. Respin, and A. G. Thompson, *Pharm. Acta Helv.*, **42**, 152 (1963).

(11) C. H. de Blaey, A. B. Weekers-Andersen, and J. Polderman, *Pharm. Weekbl.*, **106**, 893 (1971).

(12) E. L. Knoechel, C. C. Sperry, and C. J. Lintner, *J. Pharm. Sci.*, **56**, 116 (1967).

(13) P. Finholt and S. Solvang, *ibid.*, **57**, 1968 (1968).

(14) P. Finholt, H. Kristiansen, O. C. Schmidt, and K. Wold, *Medd. Nor. Farm. Selsk.*, **28**, 17 (1966).

(15) J. Yen, *Can. Pharm. J.*, **97**, 25 (1964).

(16) G. Levy, J. M. Antkowiak, J. A. Procknal, and D. C. White, *J. Pharm. Sci.*, **52**, 1047 (1963).

(17) G. Suren, *Dan. Tidsskr. Farm.*, **26**, 53 (1971).

(18) F. Jaminet, L. Delatre, and J. P. Delporte, *Pharm. Acta Helv.*, **44**, 418 (1969).

(19) G. Levy and R. H. Gumtow, *J. Pharm. Sci.*, **52**, 1139 (1963).

(20) P. Finholt, R. H. Pedersen, S. Solvang, and K. Wold, *Medd. Nor. Farm. Selsk.*, **28**, 238 (1966).

(21) G. Milosovich, *J. Pharm. Sci.*, **53**, 485 (1964).

(22) A. G. Mitchell and D. J. Savile, *J. Pharm. Pharmacol.*, **19**, 729 (1967).

(23) E. Shutton and K. Ridgway, "Physical Pharmaceutics," Clarendon Press, Oxford, England, 1971, p. 250.

(24) L. A. Bergman and F. J. Bandelin, *J. Pharm. Sci.*, **54**, 445 (1965).

(25) L. Lachman, H. A. Lieberman, and J. L. Kanig, "The Theory and Practice of Industrial Pharmacy," 2nd ed., Lea & Febiger, Philadelphia, Pa., 1976, pp. 327–329.

(26) N. R. Patel and R. E. Hoppenson, *J. Pharm. Sci.*, **55**, 1065 (1966).

(27) T. Higuchi, L. N. Elowe, and L. W. Busse, *J. Am. Pharm. Assoc., Sci. Ed.*, **43**, 685 (1954).

ACKNOWLEDGMENTS

Abstracted in part from a dissertation submitted by T. A. Iranloye to the Graduate College, University of Iowa, in partial fulfillment of the Master of Science degree requirements.

Recommendations to Eliminate Subjective Olfactory Methods from Compendial Identification Tests

GEORGE SCHWARTZMAN

Received May 24, 1977, from *Pharmaceutical Research and Testing, Food and Drug Administration, Washington, DC 20204.* Accepted for publication July 14, 1977.

Abstract □ Substitution of IR and UV absorption spectroscopy and use of the various test papers listed in the compendia provide satisfactory means of identifying drugs and other substances that presently require subjective odor identification.

Keyphrases □ Compendial odor identification tests—substitution of IR and UV spectroscopic methods recommended □ IR spectroscopy—recommended as substitute for compendial odor identification tests □ UV spectroscopy—recommended as substitute for compendial odor identification tests

Many identification tests in USP XIX (1) and NF XIV (2) monographs rely on detection of odors produced either by the test substance itself or by its reaction products. Olfactory methods are inherently undesirable, both because of the possible toxic nature of the inhaled substances and because all such tests are markedly and unpredictably influenced by such subjective and idiosyncratic factors as the experience and discriminatory powers of the analyst, sensory fatigue, and the presence of masking odors.

Compounding the subjective nature of such olfactory testing, a varied terminology is used to describe the odors actually produced. Tables I and II list the various terms used in USP XIX and NF XIV, respectively.

For many drug substances, the IR spectrum is distinctive and can be compared to a curve in the literature. Final identification is made by comparing the unknown spectrum with a curve obtained from a reference standard prepared similarly and run under the same conditions and, preferably, on the same instrument. One advantage of the IR spectrophotometer is the ease with which it handles samples in the solid, liquid, or gaseous state. Commercial test papers or those described in the compendia (USP XIX, p. 760) are also useful for confirming the identity of several gases evolved in monograph identity tests.

of a lubricant on the dissolution rate of a mass compressed at a given force was demonstrated for particles of 80/100-mesh size fraction. It is conceivable that a given weight of a lubricant may be distributed differently when blended with particles of different sizes and that different distributions may influence the dissolution of the compressed mass.

The dissolution rates of disks compressed at 1135 kg of 40/60-, 80/100-, and 140/200-mesh size fractions of salicylic acid containing 0.1–5% talc are shown in Fig. 6. The presence of talc in a concentration as great as 5% and the use of three size fractions of salicylic acid did not significantly alter the dissolution rates of the compressed disks. Similar results with talc were obtained from disks composed of aspirin (Fig. 7) and of an equimolar mixture of aspirin and salicylic acid (Figs. 8 and 9). The use of three size fractions of aspirin and an equimolar mixture of aspirin and salicylic acid with concentrations of talc from 0.1 to 5% did not alter the dissolution rates.

The dissolution rates of disks compressed at 1135 kg of 40/60-, 80/100-, and 140/200-mesh size fractions of salicylic acid, aspirin, and an equimolar mixture of aspirin and salicylic acid containing 0.1–5% magnesium stearate are shown in Figs. 6–9. As observed with talc, the dissolution rate, when using magnesium stearate, was independent of the size of the particles used to prepare the compressed disks.

REFERENCES

(1) E. Nelson, *J. Am. Pharm. Assoc., Sci. Ed.*, **46**, 607 (1957).

(2) M. Gibaldi and H. Weintraub, *J. Pharm. Sci.*, **57**, 832 (1968).

(3) W. I. Higuchi, N. A. Mir, and S. J. Desai, *ibid.*, **54**, 1405 (1965).

(4) E. L. Parrott, D. E. Wurster, and T. Higuchi, *J. Am. Pharm. Assoc., Sci. Ed.*, **44**, 269 (1955).

(5) S. A. Shah and E. L. Parrott, *J. Pharm. Sci.*, **65**, 1784 (1976).

(6) M. Kanke and K. Sekiguchi, *Chem. Pharm. Bull.*, **21**, 87 (1973).

(7) K. A. Khan and C. T. Rhodes, *Pharm. Acta Helv.*, **47**, 116 (1967).

(8) E. Cid and F. Jaminet, *ibid.*, **46**, 167 (1971).

(9) H. L. Smith, C. A. Baker, and J. H. Wood, *J. Pharm. Pharmacol.*, **23**, 536 (1971).

(10) D. Ganderton, J. W. Hadgraft, W. T. Respin, and A. G. Thompson, *Pharm. Acta Helv.*, **42**, 152 (1963).

(11) C. H. de Blaey, A. B. Weekers-Andersen, and J. Polderman, *Pharm. Weekbl.*, **106**, 893 (1971).

(12) E. L. Knoechel, C. C. Sperry, and C. J. Lintner, *J. Pharm. Sci.*, **56**, 116 (1967).

(13) P. Finholt and S. Solvang, *ibid.*, **57**, 1968 (1968).

(14) P. Finholt, H. Kristiansen, O. C. Schmidt, and K. Wold, *Medd. Nor. Farm. Selsk.*, **28**, 17 (1966).

(15) J. Yen, *Can. Pharm. J.*, **97**, 25 (1964).

(16) G. Levy, J. M. Antkowiak, J. A. Procknal, and D. C. White, *J. Pharm. Sci.*, **52**, 1047 (1963).

(17) G. Suren, *Dan. Tidsskr. Farm.*, **26**, 53 (1971).

(18) F. Jaminet, L. Delatre, and J. P. Delporte, *Pharm. Acta Helv.*, **44**, 418 (1969).

(19) G. Levy and R. H. Gumtow, *J. Pharm. Sci.*, **52**, 1139 (1963).

(20) P. Finholt, R. H. Pedersen, S. Solvang, and K. Wold, *Medd. Nor. Farm. Selsk.*, **28**, 238 (1966).

(21) G. Milosovich, *J. Pharm. Sci.*, **53**, 485 (1964).

(22) A. G. Mitchell and D. J. Savile, *J. Pharm. Pharmacol.*, **19**, 729 (1967).

(23) E. Shutton and K. Ridgway, "Physical Pharmaceutics," Clarendon Press, Oxford, England, 1971, p. 250.

(24) L. A. Bergman and F. J. Bandelin, *J. Pharm. Sci.*, **54**, 445 (1965).

(25) L. Lachman, H. A. Lieberman, and J. L. Kanig, "The Theory and Practice of Industrial Pharmacy," 2nd ed., Lea & Febiger, Philadelphia, Pa., 1976, pp. 327–329.

(26) N. R. Patel and R. E. Hoppenson, *J. Pharm. Sci.*, **55**, 1065 (1966).

(27) T. Higuchi, L. N. Elowe, and L. W. Busse, *J. Am. Pharm. Assoc., Sci. Ed.*, **43**, 685 (1954).

ACKNOWLEDGMENTS

Abstracted in part from a dissertation submitted by T. A. Iranloye to the Graduate College, University of Iowa, in partial fulfillment of the Master of Science degree requirements.

Recommendations to Eliminate Subjective Olfactory Methods from Compendial Identification Tests

GEORGE SCHWARTZMAN

Received May 24, 1977, from *Pharmaceutical Research and Testing, Food and Drug Administration, Washington, DC 20204.* Accepted for publication July 14, 1977.

Abstract □ Substitution of IR and UV absorption spectroscopy and use of the various test papers listed in the compendia provide satisfactory means of identifying drugs and other substances that presently require subjective odor identification.

Keyphrases □ Compendial odor identification tests—substitution of IR and UV spectroscopic methods recommended □ IR spectroscopy—recommended as substitute for compendial odor identification tests □ UV spectroscopy—recommended as substitute for compendial odor identification tests

Many identification tests in USP XIX (1) and NF XIV (2) monographs rely on detection of odors produced either by the test substance itself or by its reaction products. Olfactory methods are inherently undesirable, both because of the possible toxic nature of the inhaled substances and because all such tests are markedly and unpredictably influenced by such subjective and idiosyncratic factors as the experience and discriminatory powers of the analyst, sensory fatigue, and the presence of masking odors.

Compounding the subjective nature of such olfactory testing, a varied terminology is used to describe the odors actually produced. Tables I and II list the various terms used in USP XIX and NF XIV, respectively.

For many drug substances, the IR spectrum is distinctive and can be compared to a curve in the literature. Final identification is made by comparing the unknown spectrum with a curve obtained from a reference standard prepared similarly and run under the same conditions and, preferably, on the same instrument. One advantage of the IR spectrophotometer is the ease with which it handles samples in the solid, liquid, or gaseous state. Commercial test papers or those described in the compendia (USP XIX, p. 760) are also useful for confirming the identity of several gases evolved in monograph identity tests.

Table I—USP XIX Odor Identification Tests

Compound	Odor Description	Identification Test Odor
	Drugs	
Acetic acid	Recognizable	Ethyl acetate
Aluminum acetate solution	Recognizable	Ethyl acetate
Aluminum sulfate[a]	Not perceptible	Ammonia
Aspirin	Perceptible	Acetic acid, ethyl acetate
Busulfan	Perceptible	Methanesulfonic acid
Carbachol	Perceptible	Amine odor
Chloral hydrate	Recognizable	Chloroform
	Disagreeable	Phenyl isocyanide (poisonous)
Cocaine hydrochloride	Aromatic	Methyl benzoate
Cortisone acetate	Perceptible	Ethyl acetate
Ether[b,c]	Not perceptible	Foreign odor
Gelatin[c,d]	Disagreeable	Free from any
Glycerin[d]	Pungent vapor	Acrolein
Helium[c,e]	Discernible	No appreciable odor
Isoniazid	Perceptible	Pyridine
Methenamine mandelate	Liberated or evolved	Ammonia, almond odor of benzaldehyde
Methylprednisolone acetate	Perceptible	Ethyl acetate
Oxygen[c,e]	Discernible	No appreciable odor
Paraldehyde	Pungent	Acetaldehyde
Phentolamine mesylate	Recognizable	Sulfur dioxide
Potassium acetate	Recognizable	Ethyl acetate
Potassium chloride	Recognizable	Chlorine
Primidone	Evolved	Ammonia
Pyrazinamide	Perceptible	Ammonia
Sodium aminosalicylates[c,f]	Not perceptible	Hydrogen sulfide or sulfur dioxide
	Perceptible	Amyl alcohol
Sodium chloride	Recognizable	Chlorine
Sulfacetamide sodium	Perceptible	Acetamide
Precipitated sulfur	Recognizable	Sulfur dioxide
Thiopentyl sodium	Evolved and recognizable	Hydrogen sulfide
Trichloroacetic acid	Formation	Chloroform
	Disagreeable	Phenyl isocyanide (poisonous)
Zinc acetate	Recognizable	Ethyl acetate
Zinc chloride[a]	Recognizable and perceptible	Chlorine
	Pharmaceutical Ingredients	
Amaranth	Perceptible	Sulfur dioxide
Cellulose acetate phthalate	Perceptible	Ethyl acetate
Chlorobutanol	Disagreeable	Phenyl isocyanide (toxic)
Nitrogen[c,e]	Discernible	No appreciable odor
Propylene glycol	Evolved	Fruity odor, no sharp acrid odor of acrolein
Sodium acetate	Recognizable	Ethyl acetate
Sodium bisulfite	Recognizable Pungent	Sulfur dioxide

[a] Listed in monograph under Ammonium Salts. [b] Listed in monograph under Foreign Odor. [c] No recommendations for testing this compound. [d] Listed in monograph under Odor and Water-Insoluble Substances. [e] Listed in monograph under Odor. [f] Listed in monograph under Hydrogen Sulfide and Sulfur Dioxide.

By a combination of simple test reactions and UV and IR spectrophotometric identification, many olfactory tests in the compendial monographs can be eliminated. Judicious use of one or several such techniques is generally adequate for confirming the presence of all major functional groups to demonstrate that the molecule is intact and to provide specific "fingerprint" identification of the substance.

This paper reports the results of a survey of compendial monographs that specify olfactory tests. In every case, IR spectroscopy, alone or in combination with UV spectroscopy or one or more simple chemical tests, provided a superior, more specific method of identification. Typical spectra are shown in Figs. 1–7.

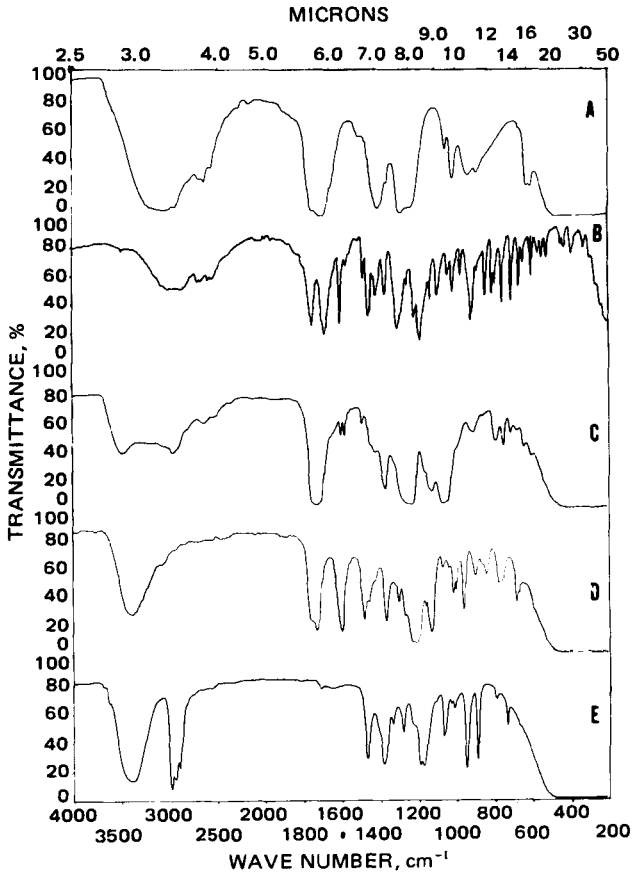

Figure 1—*IR spectra of acetic acid (A), aspirin (B), cellulose acetate phthalate (C), resorcinol monoacetate (D), and amylene hydrate (E).*

EXPERIMENTAL

IR absorption spectra were obtained as potassium bromide disks, as mineral oil[1] USP mulls, as melts on a sodium chloride plate, neat between polished sodium chloride crystals, or in a 10-cm gas cell by the following procedures.

For the potassium bromide disk preparation, usually 1–2 mg of sample was mixed thoroughly with 200 mg of potassium bromide in a 65-mm o.d. agate mortar with a pestle for 2 min. The mixture was placed in a potassium bromide die (13 mm), the plunger was inserted, and the assembly was placed in a press. The die was connected to a vacuum pump and evacuated. Then the assembly was pressed for 2 min at 9080 kg (20,000 lb). The vacuum was disconnected, the pressure was released, the disk was removed, and the IR spectrum was obtained.

For a melt, the sample was placed on a sodium chloride crystal, heated to the temperature required to melt the compound, and then cooled to room temperature. The crystal was placed in a demountable IR cell, and the IR spectrum was obtained.

For neat samples, a few drops of sample were placed on a sodium chloride crystal, a second sodium chloride crystal was placed on top of the sample, and the sample was gently squeezed to a uniform layer. The crystals were placed in a demountable IR cell, and the IR spectrum was obtained.

For mulls, about 10–15 mg of the sample was placed in a 65-mm agate mortar, a few drops of mineral oil USP were added, and a portion of the mixture was ground for 2 min. The mixture was then removed to a sodium chloride crystal, a second sodium chloride crystal was placed on top of the mull, and the crystals were squeezed gently to distribute the material evenly between them. The crystals were placed in a demountable IR cell, and the IR spectrum was obtained.

For gases, the materials needed to generate vapor were placed in a 10-ml glass-stoppered erlenmeyer flask, the stopper was inserted, and the flask was shaken for several minutes. Then the stopper was removed,

[1] Nujol.

Table II—NF XIV Odor Identification Tests

Compound	Odor Description	Identification Test Odor
	Drugs	
Alum, ammonium	Evolved	Ammonia
Alum, potassium	Evolved	No ammonia
Aminosalicylic acid[a,b]	Perceptible	Amyl alcohol
	Not percepitble	Hydrogen sulfide or sulfur dioxide
Ammonium chloride	Recognizable	Ammonia, chlorine
Amobarbital	Evolved	Ammonia
Amyl nitrite	Perceptible	Amyl valerate
Aspirin capsules	Perceptible	Acetic acid, ethyl acetate
Benzocaine	Recognizable	Alcohol
Betamethasone acetate	Perceptible	Ethyl acetate
Calcium aminosalicylate[a,b]	Perceptible	Amyl alcohol
	Not perceptible	Hydrogen sulfide or sulfur dioxide
Cetylpyridinium chloride	Perceptible	Pyridine
Chloral betaine	Recognizable	Chloroform
Chlorothiazide sodium for injection	Recognizable	Sulfur dioxide
	Pungent	
Cocaine	Aromatic	Methyl benzoate
Dehydrocholic acid[b,c]	—	Odorless
Digitalis[b]	—	Odor slight when dry, peculiar and characteristic when moistened
Ethamivan	—	Typical amine odor develops
Ethyl chloride[b,d]	Not perceptible	Foreign odor, acetaldehyde
Fluroxene[b,e]	Not perceptible	Foreign odor
Ichthammol[e]	Evolved	Ammonia
Sulfurated lime solution	Evolved	Hydrogen sulfide
Menadione sodium bisulfite	Recognizable	Sulfur dioxide
Methacholine chloride[b]	Perceptible	Ethyl acetate
		Trimethylamine
Methenamine	Recognizable	Formaldehyde
	Evolved	Ammonia
Methoxyflurane	Evolved	Hydrofluoric acid
Methylprednisolone acetate suspension	Perceptible	Ethyl acetate
Plantago seed[b,f]	—	Nearly odorless
Potassium aminosalicylate[a,b]	Perceptible	Amyl alcohol
	Not perceptible	Hydrogen sulfide or sulfur dioxide
Rauwolfia serpentina[b,g]	—	Odor indistinct, reminiscent of stored white potatoes
Resorcinol monoacetate	Recognizable	Ethyl acetate
Senna[b,h]	—	Odor is characteristic
Sodium hypochlorite solution	Evolved	Chlorine
Sublimed sulfur	Recognizable	Sulfur dioxide
Terpin hydrate	Aromatic	Strong aromatic
Vinyl ether[b]	Perceptible	Alcohol
	Not perceptible	No foreign odor
	Pharmaceutical Ingredients	
Amylene hydrate	Recognizable	Ethyl acetate
Benzyl alcohol	Noticeable	Benzaldehyde
Cardamon seed[b,i]	Aromatic	Aromatic
	Not perceptible	No foreign odor
Chloroform[b,j]	Evolved	Faint vinous or ether odor
Cinnamon[b,k]	Aromatic	Characteristically aromatic
Eriodictyon[b,l]	Aromatic	Aromatic
Ethyl acetate[m]	—	Acetous odor produced; does not resemble that of pineapple or banana
Paraffin	Evolved	Hydrogen sulfide
Peppermint[b]	Aromatic	Aromatic characteristic odor
Phenylmercuric acetate	Evolved	Nitrobenzene, ethyl acetate
Phenylmercuric nitrate	Evolved	Nitrobenzene
Sodium metabisulfite	Recognizable	Pungent odor
Sodium propionate	Recognizable	Propionic acid
Sulfurated potash	Evolved	Hydrogen sulfide
Spearmint[b]	Aromatic	Aromatic and characteristic
Tartaric acid	—	Resembling burning sugar
Vanilla[b]	Aromatic	Characteristic, agreeably fragrant and aromatic

[a] Listed in monograph under Hydrogen Sulfide and Sulfur Dioxide, *etc.* [b] No recommendations for testing this compound. [c] Listed in monograph under Odor on Boiling. [d] Listed in monograph under Nonvolatile Residue and Odor and under Alcohol. [e] Listed in monograph under Foreign Odor. [f] Listed in monograph under Odor and Taste. [g] Listed in monograph under Unground Rauwolfia serpentina Root. [h] Listed in monograph under Unground Alexandria Senna. [i] Listed in monograph under Unground Cardamon Seed. [j] Listed in monograph under Odorous and Chlorinated Decomposition Products and under Foreign Odor. [k] Listed in monograph under Unground Cinnamon. [l] Listed in monograph under Unground Eriodictyon. [m] Listed in monograph under Butyl or Amyl Derivatives.

and the vapors were quickly withdrawn into a 50-ml hypodermic syringe (without an attached needle). Care was taken not to touch the materials in the flask. The vapors were injected into an evacuated 10-ml gas cell[2], modified by inserting 20-gauge needles fitted with removable polytef plugs into the rubber septums in the entrance ports. This technique permitted easy injection with a syringe into the gas cell.

RESULTS AND DISCUSSION

Fifteen analysts in this laboratory were requested to identify nine different odors listed in identification tests of the compendial monographs. These odors, with the possible exception of amyl valerate, were those of compounds to which analysts are normally exposed in their training or laboratory experience. As shown in Table III, in four of the nine identification tests, fewer than half of the analysts identified the correct compound.

Tables I and II list some drugs for which the compendia require olfactory testing. Because of possible toxicity or irritation to many chemists, as well as their unfamiliarity with the odors of these compounds, the staff was not subjected to additional tests of these materials.

Examples are listed below to demonstrate the ease with which drugs can be identified without the possible exposure to dangerous malodorous compounds involved in subjective testing.

Tests Involving the Odor of Ethyl Acetate—In at least 15 monographs of the USP and NF, production of the odor of ethyl acetate is specified as an identification test (Tables I and II). In some cases, the intent of the test is to confirm the presence of the acetate anion of an inorganic salt, *e.g.*, aluminum acetate solution and sodium, potassium, and zinc acetates.

In other monographs, confirmation of the presence of an acetyl group in an organic substance is sought, *e.g.*, acetic acid, aspirin, resorcinol monoacetate, cellulose acetate phthalate, and various steroidal acetates. In both categories, the IR spectrum of the compendial substance provides a more suitable test; the acetate anion or acetyl group is readily confirmed by characteristic carbonyl absorption. The spectrum as a whole is uniquely characteristic for each substance. Figure 1A shows the IR spectrum of acetic acid, taken neat; it is distinct from that of other carboxylic acids.

Aspirin—Figure 1B shows the characteristic IR spectrum of aspirin. At present, there is no indication that aspirin exists in polymorphic states (3). In identifying the steroidal acetates, however, great care must be taken in preparing the potassium bromide disks since polymorphism for this class of compounds is well documented (4). Both sample and standard must be treated with identical solvents, heating conditions, halide matrix, pressure, and time.

A satisfactory test for aspirin capsules involves extracting the contents with chloroform, removing the solvent, and obtaining the IR spectrum of a potassium bromide disk of the dried extract.

If a separate test for acetate in organic salts is desired, the test described in USP XIX (p. 615) should be used. Ferric chloride TS is added to a solution of the salt, producing a deep-red color which is destroyed by addition of a mineral acid.

[2] Barnes-Econo-Gas-Cell part 0026-006, Barnes Engineering Co., Stamford, Conn.

Table III—Attempted Olfactory Identification of Various Odors by 15 Analysts

Compound (Odor)	Correct Identification	
	Number	%
Dilute acetic acid	10/15	67
Amyl alcohol	11/15	73
Amyl valerate	1/15	7
Ethyl acetate	7/15	47
Ethyl alcohol	12/15	80
Hydrogen sulfide	15/15	100
Methyl benzoate	4/15	26
Sulfur dioxide	6/15	40
No perceptible odor (water)	14/15	93

Cellulose Acetate Phthalate—USP XIX identification test A for cellulose acetate phthalate requires the generation of ethyl acetate, which is recognizable by its characteristic odor. A satisfactory characteristic identification of this product involves dissolving about 0.1 g of sample in 3 ml of acetone and pouring the solution onto a clean sodium chloride crystal; a glossy clear film is deposited as the acetone evaporates. An IR spectrum (Fig. 1C) of this film is satisfactory and characteristic for this material. This test eliminates the need for identification test B and satisfies the requirement of a glossy clear film in identification test C.

Resorcinol Monoacetate—The IR spectrum (Fig. 1D) of a neat solution of resorcinol monoacetate between sodium chloride crystals is a satisfactory and characteristic identity test for this drug. Likewise, the IR spectrum (Fig. 1E) of amylene hydrate neat between sodium chloride crystals is a satisfactory and characteristic identification for this alcohol.

Phenylmercuric Acetate—NF XIV identification tests A and B for phenylmercuric acetate require the evolution of nitrobenzene and ethyl acetate, both of which have characteristic odors. The UV spectrum (Fig. 2) of phenylmercuric acetate (approximately 0.75 mg/ml of 95% ethanol) is a characteristic curve of the phenyl moiety of the molecule and satisfies the identification requirement of test A.

To 100 mg of phenylmercuric acetate in a 10-ml erlenmeyer flask with a glass stopper, 500 ml of sulfuric acid and 1 ml of alcohol are added. The flask is then warmed with the stopper in place. The headspace vapors are removed with a 50-ml syringe and injected into a gas cell. The IR spectrum (Fig. 3C), which is characteristic of ethyl acetate vapor, is obtained.

Phenylmercuric Nitrate—NF XIV identification test A for phenylmercuric nitrate requires heating the compound with sulfuric acid; a vapor with the characteristic odor of nitrobenzene is evolved.

The IR spectrum (Fig. 4A) of a potassium bromide disk of phenylmercuric nitrate is a satisfactory and characteristic identification test.

Ethyl Acetate—Paradoxically, in the NF XIV monograph for ethyl acetate, its odor is not utilized; instead, it is burned and an "acetous" odor is produced. The IR spectrum of ethyl acetate itself (Fig. 4B, obtained neat) is, of course, characteristic and satisfactory for identification.

Tests Involving Ammonia—Numerous monographs rely on the generation of the odor of ammonia as an identification test; in other monographs, the *absence* of the odor of ammonia is a requirement. In all such cases, the red-to-blue transformation of moistened litmus paper (or the absence of this change) is a more sensitive and less subjective criterion for the evolution of ammonia.

Several of these monographs already specify that the IR and UV spectra be obtained, *e.g.*, primidone and pyrazinamide in USP XIX and benzocaine in NF XIV. Since these tests are satisfactory and unambiguous, the test for ammonia may be considered superfluous.

Methenamine—The NF XIV identification test for methenamine requires the identification of the odors of formaldehyde and ammonia. Although the test also confirms the presence of formaldehyde by stating that it darkens paper moistened with silver ammonium nitrate TS, the test does not confirm the presence of ammonia by moistened red litmus paper.

The IR spectrum of a potassium bromide disk of methenamine, described under IR absorption in the monograph, is a satisfactory identity test and eliminates the need for the present identification test.

Methenamine Mandelate—A similar case is methenamine mandelate in USP XIX. Identification test A requires dissolving about 0.5 g of methenamine mandelate in water, adding diluted sulfuric acid, and heating the solution. The evolved formaldehyde vapor turns silver-ammonia-nitrate TS paper brown and has a characteristic odor. An excess of sodium hydroxide added to the warm mixture liberates ammonia, which turns moistened red litmus paper blue.

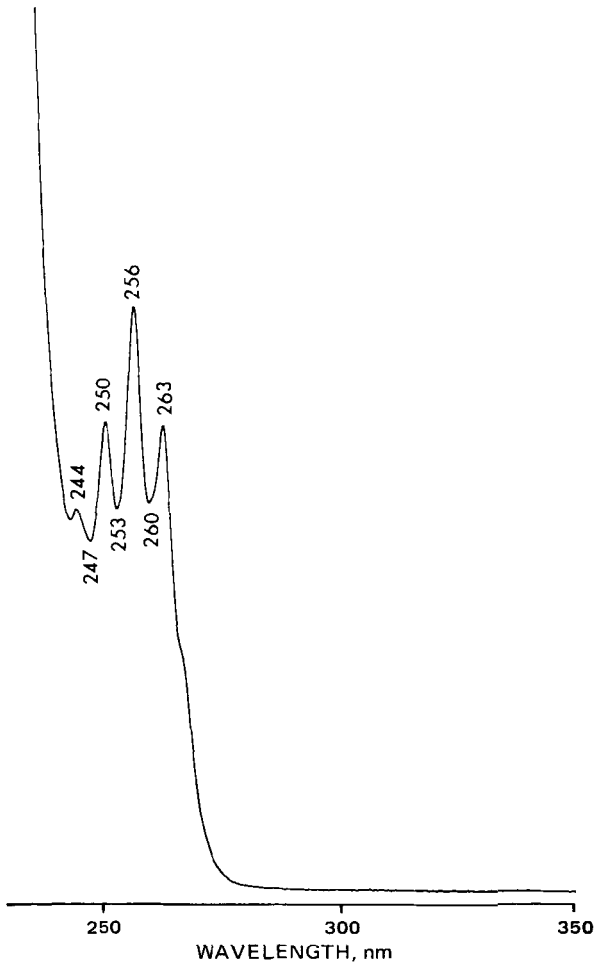

Figure 2—*UV spectrum of phenylmercuric acetate.*

In identification test B, 0.1 g of methenamine mandelate is dissolved in water, and potassium dichromate TS is added; the almond odor of benzaldehyde is evolved. An IR spectrum of a potassium bromide disk of methenamine mandelate (Fig. 4C) gives a satisfactory and characteristic identification curve.

Tests Involving Sulfur Dioxide—Seven monographs in USP XIX and NF XIV contain identity tests that depend on the detection of the odor of evolved sulfur dioxide; in two other monographs, the *absence* of sulfur dioxide is a requirement. Moistened starch iodate paper, which turns blue in the presence of sulfur dioxide, is used as a supplementary test in some cases.

It is suggested that the use of this indicator paper alone is sufficient to test for sulfur dioxide; for some of these monographs (*e.g.*, phentolamine mesylate, chlorothiazide sodium for injection, and menadione sodium bisulfite), a combination of IR and UV spectrophotometry, after suitable sample preparation, provides a much more specific means of identification.

Tests Involving Hydrogen Sulfide—The odor of hydrogen sulfide, although perhaps universally recognizable, is disagreeable and toxic. The detection of either its presence or absence is a requirement in several monographs. The darkening of moistened lead acetate paper is given as an additional test in most of these monographs; it is suggested that the olfactory test be eliminated.

Tests Involving Chlorine—For identification methods requiring the detection of the odor of chlorine (*e.g.*, potassium chloride USP, sodium chloride USP, zinc chloride USP, ammonium chloride NF, and sodium hypochlorite NF), it is recommended that only the test with starch iodide paper (which turns blue) and silver nitrate TS (which forms a white precipitate, insoluble in nitric acid but soluble in excess ammonia TS) be used.

Busulfan—The busulfan identification test in USP XIX involves dissolving busulfan in water, adding sodium hydroxide, and heating; a characteristic odor of methanesulfonic acid is perceptible. Preparation of a potassium bromide disk of busulfan and IR examination produce a

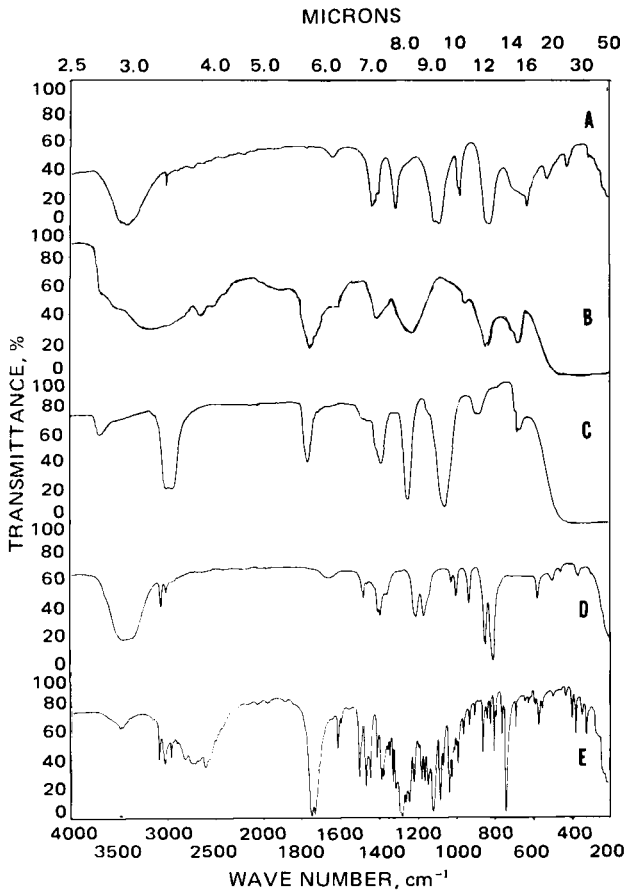

Figure 3—*IR spectra of chloral hydrate (A), trichloroacetic acid (B), ethyl acetate vapor (C), chlorobutanol (D), and cocaine hydrochloride (E).*

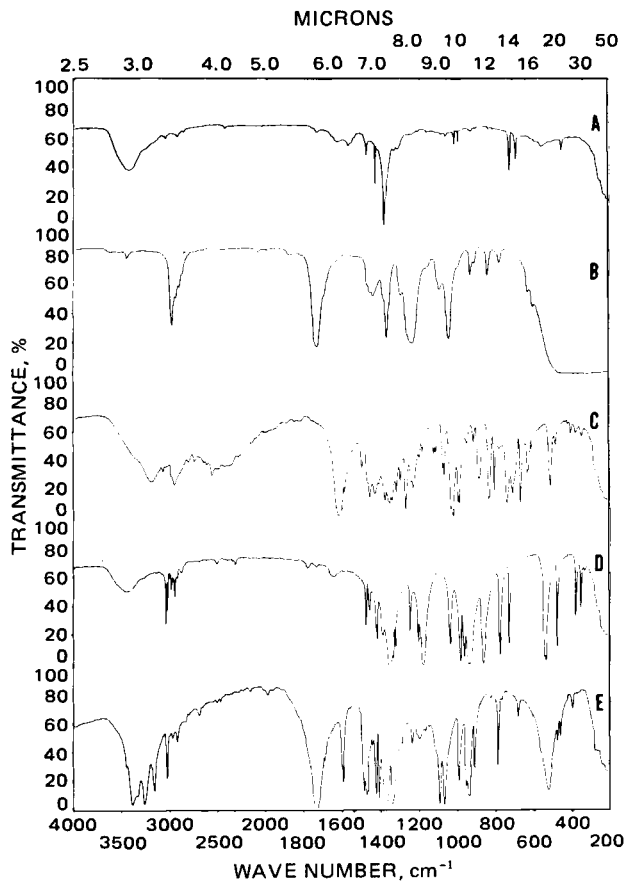

Figure 4—*IR spectra of phenylmercuric nitrate (A), ethyl acetate (B), methenamine mandelate (C), busulfan (D), and carbachol (E).*

characteristic spectrum (Fig. 4D). (Busulfan is an antineoplastic and should be handled with caution.)

Carbachol—In USP XIX identification test B for carbachol, 0.5 g of carbachol is boiled with alcoholic potassium hydroxide. A white precipitate is formed, and an amine odor is perceptible when the mixture cools. The IR spectrum of a potassium bromide disk of carbachol (Fig. 4E) gives a characteristic spectral curve and also eliminates the need for identification test A listed in the monograph.

Chloral Hydrate—USP XIX identification tests A and B for chloral hydrate require treating the drug with a sodium hydroxide solution to produce chloroform, which is recognizable by its odor. When chloral hydrate is warmed with a few drops of aniline and sodium hydroxide solution, the mixture has the intensely disagreeable odor of phenyl isocyanide (caution: poisonous).

The IR spectrum of a potassium bromide disk (Fig. 3A) gives a characteristic spectrum of chloral hydrate, thus eliminating the need for the two subjective olfactory tests. Although no chloral hydrate polymorphs have been detected in this laboratory, Kuhnert *et al.* (5) reported the presence of two polymorphic forms.

Trichloroacetic Acid—The USP XIX identification test for trichloroacetic acid requires heating the solution with an alkali hydroxide to form an alkali carbonate and chloroform. Addition of a few drops of aniline to the heated mixture also produces the disagreeable odor of phenyl isocyanide. The IR spectrum of a few crystals of trichloroacetic acid melted between sodium chloride crystals (Fig. 3B) is uniquely different from other aliphatic organic acids, giving a characteristic and satisfactory curve for identification of trichloroacetic acid.

Chlorobutanol—USP XIX identification test B for chlorobutanol requires heating the chemical with sodium hydroxide TS, mixing, and adding a few drops of aniline. Again, the disagreeable odor of phenyl isocyanide is produced.

An IR spectrum of a potassium bromide disk of chlorobutanol (Fig. 3D) gives a satisfactory and characteristic identity test.

Cocaine Hydrochloride—USP XIX identification test A for cocaine hydrochloride requires heating the drug with sulfuric acid at 100° and then cautiously mixing with a small volume of water. The mixture has the odor of methyl benzoate and, on cooling, yields crystals of benzoic acid.

An IR spectrum of a potassium bromide disk of cocaine hydrochloride (Fig. 3E) is very characteristic of this compound and also eliminates the need for identification tests A, B, and C of the monograph.

Glycerin—In the USP XIX identification test for glycerin, a few drops are heated with about 0.5 g of potassium bisulfate; pungent odors of acrolein are evolved.

Examination of a few drops of glycerin neat between two sodium chloride crystals in an IR spectrophotometer gives a characteristic IR spectrum (Fig. 5A).

Isoniazid—In USP XIX identification test A for isoniazid, a small amount of sample is mixed with about 0.5 g of anhydrous sodium carbonate. The mixture is then heated in a test tube over a small flame to produce an odor of pyridine.

An isoniazid mineral oil mull between sodium chloride plates gives a characteristic IR spectrum which can be used to identify isoniazid (Fig. 5B).

Cetylpyridinium Chloride—NF XIV identification test A for cetylpyridinium chloride involves a pyridine odor generated when the substance is heated to melting and browning. In the pyridine test, about 1 g of cetylpyridinium chloride is dissolved in sodium hydroxide solution without heating, and the odor of pyridine is *not* immediately perceptible. The IR and UV absorption tests in the monograph for cetylpyridinium chloride satisfy the identification requirement; the odor test is not needed.

Paraldehyde—In the USP XIX identification test, paraldehyde is heated with a small quantity of dilute sulfuric acid; the pungent odor of acetaldehyde is produced. A few drops of paraldehyde between potassium bromide crystals examined in an IR spectrophotometer produce a characteristic spectrum adequate for identification (Fig. 5C).

Sulfacetamide Sodium—USP XIX identification test B for sulfacetamide sodium requires converting the drug to sulfacetamide and heating until it boils, producing an oily liquid which has a characteristic odor. An IR spectrum obtained from a potassium bromide disk of either

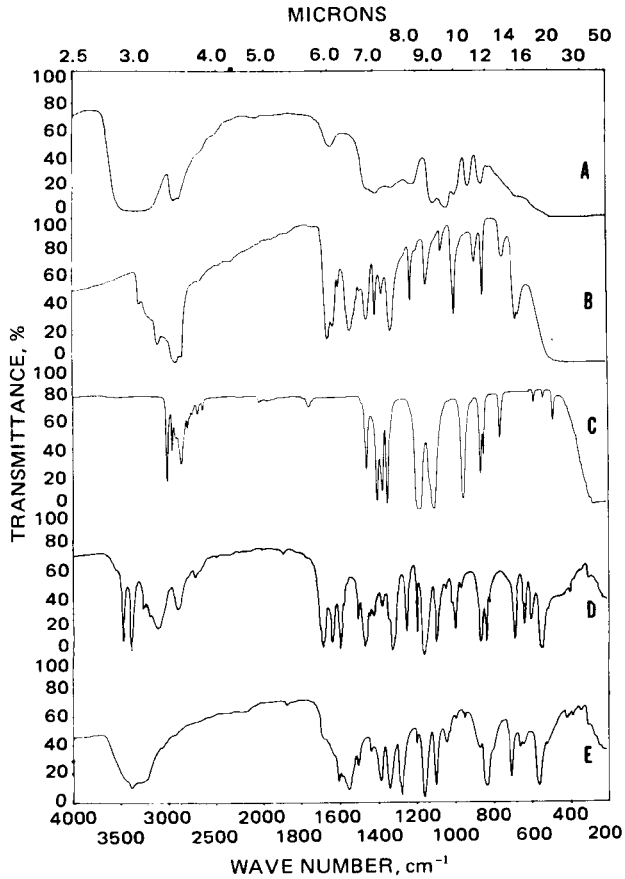

Figure 5—*IR spectra of glycerin (A), isoniazid (B), paraldehyde (C), sulfacetamide (D), and sulfacetamide sodium (E).*

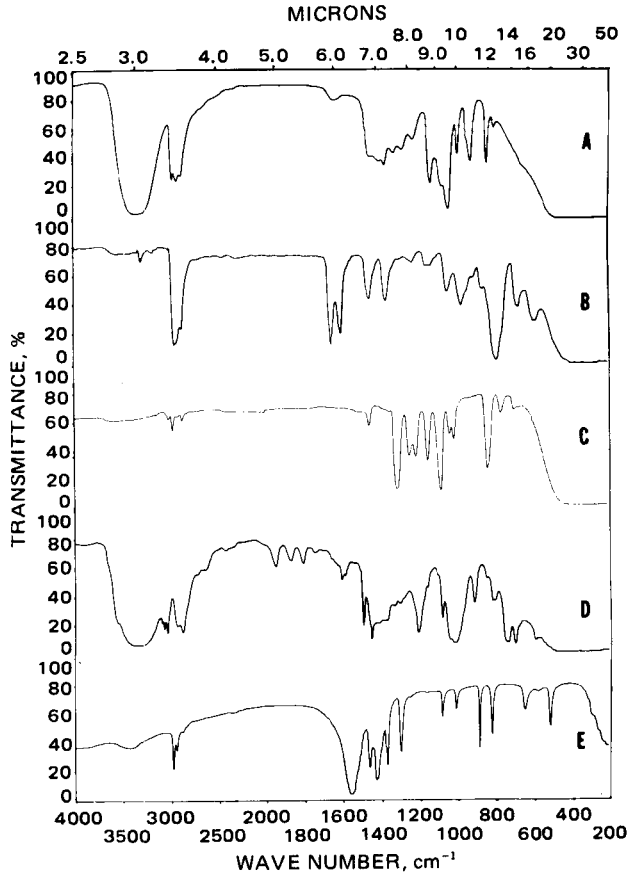

Figure 6—*IR spectra of propylene glycol (A), amyl nitrite mixture (B), methoxyflurane (C), benzyl alcohol (D), and sodium propionate (E).*

sulfacetamide produced in identification test A (Fig. 5D) or sulfacetamide sodium itself (Fig. 5E) is characteristic and satisfactory as an identification test. In a study by Yang and Guillory (6) on polymorphism in sulfonamides using various solvents, polymorphism was not detected for sulfacetamide.

Propylene Glycol—In the USP XIX identification test for propylene glycol, the viscous liquid is heated with 1 g of potassium bisulfate, producing a fruity odor. When propylene glycol is heated to dryness, no odor of acrolein is perceptible. The IR spectrum of propylene glycol (Fig. 6A) run neat between sodium chloride crystals is a satisfactory and characteristic identification for propylene glycol.

Amyl Nitrite—In the NF XIV identification test for amyl nitrite, a few drops of water and sulfuric acid are added to amyl nitrite and the product is diluted with water; the odor of amyl valerate is perceptible.

The following procedure is recommended to replace the odor identification. An amyl nitrite braided cover ampul is placed in a 10-ml glass-stoppered erlenmeyer flask and crushed with a glass rod; the flask is stoppered and shaken. The vapors are removed with a 50-ml syringe (no needle) and injected into a 10-cm IR gas cell fitted with sodium chloride windows. The vapors give a very specific and characteristic IR spectrum of amyl nitrite mixture (Fig. 6B). IR spectra of samples of this product from two different manufacturers were identical.

Chloral Betaine—In the NF XIV identification test for chloral betaine, a few milliliters of sodium hydroxide TS is added to the drug; chloroform, recognizable by its odor, is formed. The IR absorption test described in the monograph is satisfactory for characterizing chloral betaine; the odor test is not needed.

Cocaine—NF XIV identification test A for cocaine requires heating about 0.1 g of the alkaloid with 1 ml of sulfuric acid at 100° for approximately 5 min and then cautiously mixing with a few milliliters of water; the aromatic odor of methyl benzoate is produced. Identification test D (IR) in the monograph is satisfactory for characterizing cocaine, and identification test A is not needed.

Ethamivan—NF XIV identification test B for ethamivan requires the evolution of vapors that have a typical amine odor and turn red litmus blue. However, both the IR and UV absorption tests in the monograph are satisfactory for characterizing ethamivan. Therefore, identification test B should be eliminated.

Methoxyflurane—In NF XIV identification test B for methoxyflurane, the drug is heated with sulfuric acid and hydrofluoric acid is evolved. A 10-cm gas cell can be filled with methoxyflurane vapor, and an IR spectrum (Fig. 6C) is obtained that is distinctive from the spectra of chloroform, trichloroethylene, and halothane. This IR spectrum can be used to identify methoxyflurane when compared to the spectrum of NF methoxyflurane reference standard similarly measured.

Terpin Hydrate—The NF XIV identification test for terpin hydrate requires addition of a few drops of sulfuric acid to a hot solution of terpin hydrate; the liquid develops a strong aromatic odor. The IR absorption procedure described in the monograph for terpin hydrate is a satisfactory and characteristic test.

Benzyl Alcohol—The NF XIV identification test for benzyl alcohol requires treating a few drops of the alcohol with a solution of potassium permanganate; the odor of benzaldehyde is noticeable. The IR spectrum of benzyl alcohol (Fig. 6D) neat between two sodium chloride plates provides a satisfactory and characteristic identification.

Sodium Propionate—In NF XIV identification test C for sodium propionate, the salt is warmed with sulfuric acid to evolve propionic acid,

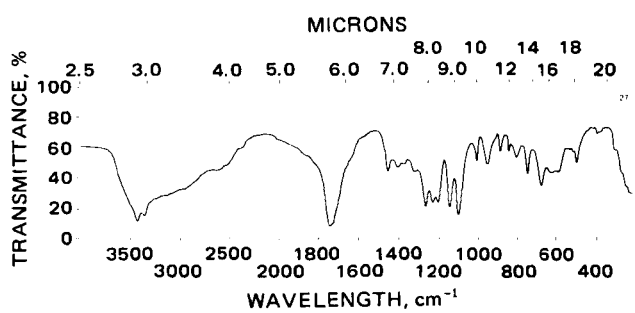

Figure 7—*IR spectrum of tartaric acid.*

recognizable by its odor. The IR spectrum (Fig. 6E) of a potassium bromide disk of sodium propionate is a satisfactory and characteristic test for this salt. It is suggested that identification test A for sodium remain in the monograph.

Tartaric Acid—In NF XIV identification test B for tartaric acid, the acid is ignited, emitting an odor resembling that of burnt sugar. The IR spectrum (Fig. 7) of a potassium bromide disk of tartaric acid is a satisfactory and characteristic test for this acid.

REFERENCES

(1) "The United States Pharmacopeia," 19th rev., Mack Publishing Co., Easton, Pa., 1975.

(2) "The National Formulary," 14th ed., Mack Publishing Co., Easton, Pa., 1975.

(3) G. Schwartzman, *J. Pharm. Pharmacol.*, **24**, 169 (1972).

(4) R. J. Mesley and C. A. Johnson, *ibid.*, **17**, 329 (1965).

(5) M. Kuhnert, O. R. Brandstaetter, and R. Ulmer, *Sci. Pharm.*, **41**, 97 (1973).

(6) S. S. Yang and J. K. Guillory, *J. Pharm. Sci.*, **61**, 26 (1972).

ACKNOWLEDGMENTS

Presented at the APhA Academy of Pharmaceutical Sciences, New York meeting, May 1977.

The modification of the gas cell was recommended by W. L. Brannon, Division of Drug Chemistry, Food and Drug Administration.

The author thanks Thomas D. Doyle, Division of Drug Chemistry, Food and Drug Administration, for critical review of the manuscript.

NOTES

Prodrug Approaches to Enhancement of Physicochemical Properties of Drugs IX: Acetaminophen Prodrug

ANWAR HUSSAIN ˣ, PRAKASH KULKARNI, and DONALD PERRIER

Received July 19, 1976, from the *Division of Drug Information and Technology, College of Pharmacy, University of Kentucky, Lexington, KY 40506* and *INTERx Research Corporation, Lawrence, Kans.* Accepted for publication June 29, 1977.

Abstract □ The synthesis, hydrolysis rate, and bioavailability of 1-(*p*-acetaminophenoxy)-1-ethoxyethane, an acetaminophen prodrug, are described. The prodrug is less soluble than acetaminophen and stable at neutral pH. However, in an acidic environment, the compound cleaves rapidly, generating acetaminophen. When both the prodrug and acetaminophen were administered to dogs in equivalent amounts, the blood acetaminophen levels were comparable.

Keyphrases □ Prodrugs—of acetaminophen, synthesis, hydrolysis rate, and bioavailability studied, dogs □ Acetaminophen prodrug—1-(*p*-acetaminophenoxy)-1-ethoxyethane synthesized, hydrolysis rate and bioavailability studied, dogs □ 1-(*p*-Acetaminophenoxy)-1-ethoxyethane—acetaminophen prodrug synthesized, hydrolysis rate and bioavailability studied, dogs □ Hydrolysis rate—acetaminophen prodrug studied, dogs □ Bioavailability—acetaminophen prodrug studied, dogs □ Analgesics—acetaminophen, prodrug synthesized, hydrolysis rate and bioavailability studied, dogs

Acetaminophen, a well-known analgesic–antipyretic drug, is widely used in oral dosage forms. The drug, however, is unpleasantly bitter, and attempts made to formulate it in an acceptable chewable dosage form intended especially for pediatric use have apparently not been very successful.

Repta and Hack (1) were successful in masking the bitterness of acetaminophen *via* derivation of the hydroxy group to form 2-(*p*-acetaminophenoxy)tetrahydropyran (I). Prodrug I was stable at neutral pH (pH of the saliva) but hydrolyzed in the gastric juice. This paper reports the synthesis, hydrolysis rate, and absorption of another acetaminophen prodrug where the hydroxy group was transiently blocked using ethyl vinyl ether. This prodrug, 1-(*p*-acetaminophenoxy)-1-ethoxyethane (II), has an advantage over the corresponding tetrahydropyran derivative (I) in that it reverts to acetaminophen 10 times faster. Therefore, the possibility that the prodrug might be absorbed as such is greatly minimized.

EXPERIMENTAL

Synthesis of II (2)—To a suspension containing 4 g of acetaminophen (0.26 mole) in freshly distilled ethyl acetate were added 30 ml (~0.4 mole) of freshly distilled ethyl vinyl ether and 0.2 ml of 0.4% *p*-toluenesulfonic acid in benzene. The suspension was stirred magnetically at room temperature until all suspended material was dissolved and a clear colorless solution was obtained, usually within 2–4 hr.

At the completion of the reaction, 0.2 ml of 0.4% pyridine in benzene was added. The solution obtained was transferred to a rotary evaporator,

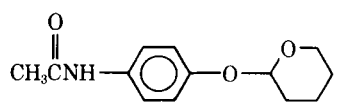

I

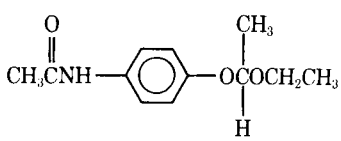

II

recognizable by its odor. The IR spectrum (Fig. 6E) of a potassium bromide disk of sodium propionate is a satisfactory and characteristic test for this salt. It is suggested that identification test A for sodium remain in the monograph.

Tartaric Acid—In NF XIV identification test B for tartaric acid, the acid is ignited, emitting an odor resembling that of burnt sugar. The IR spectrum (Fig. 7) of a potassium bromide disk of tartaric acid is a satisfactory and characteristic test for this acid.

REFERENCES

(1) "The United States Pharmacopeia," 19th rev., Mack Publishing Co., Easton, Pa., 1975.

(2) "The National Formulary," 14th ed., Mack Publishing Co., Easton, Pa., 1975.

(3) G. Schwartzman, *J. Pharm. Pharmacol.*, **24**, 169 (1972).

(4) R. J. Mesley and C. A. Johnson, *ibid.*, **17**, 329 (1965).

(5) M. Kuhnert, O. R. Brandstaetter, and R. Ulmer, *Sci. Pharm.*, **41**, 97 (1973).

(6) S. S. Yang and J. K. Guillory, *J. Pharm. Sci.*, **61**, 26 (1972).

ACKNOWLEDGMENTS

Presented at the APhA Academy of Pharmaceutical Sciences, New York meeting, May 1977.

The modification of the gas cell was recommended by W. L. Brannon, Division of Drug Chemistry, Food and Drug Administration.

The author thanks Thomas D. Doyle, Division of Drug Chemistry, Food and Drug Administration, for critical review of the manuscript.

NOTES

Prodrug Approaches to Enhancement of Physicochemical Properties of Drugs IX: Acetaminophen Prodrug

ANWAR HUSSAIN ˣ, PRAKASH KULKARNI, and DONALD PERRIER

Received July 19, 1976, from the *Division of Drug Information and Technology, College of Pharmacy, University of Kentucky, Lexington, KY 40506* and *INTERx Research Corporation, Lawrence, Kans.* Accepted for publication June 29, 1977.

Abstract □ The synthesis, hydrolysis rate, and bioavailability of 1-(*p*-acetaminophenoxy)-1-ethoxyethane, an acetaminophen prodrug, are described. The prodrug is less soluble than acetaminophen and stable at neutral pH. However, in an acidic environment, the compound cleaves rapidly, generating acetaminophen. When both the prodrug and acetaminophen were administered to dogs in equivalent amounts, the blood acetaminophen levels were comparable.

Keyphrases □ Prodrugs—of acetaminophen, synthesis, hydrolysis rate, and bioavailability studied, dogs □ Acetaminophen prodrug—1-(*p*-acetaminophenoxy)-1-ethoxyethane synthesized, hydrolysis rate and bioavailability studied, dogs □ 1-(*p*-Acetaminophenoxy)-1-ethoxyethane—acetaminophen prodrug synthesized, hydrolysis rate and bioavailability studied, dogs □ Hydrolysis rate—acetaminophen prodrug studied, dogs □ Bioavailability—acetaminophen prodrug studied, dogs □ Analgesics—acetaminophen, prodrug synthesized, hydrolysis rate and bioavailability studied, dogs

Acetaminophen, a well-known analgesic–antipyretic drug, is widely used in oral dosage forms. The drug, however, is unpleasantly bitter, and attempts made to formulate it in an acceptable chewable dosage form intended especially for pediatric use have apparently not been very successful.

Repta and Hack (1) were successful in masking the bitterness of acetaminophen *via* derivation of the hydroxy group to form 2-(*p*-acetaminophenoxy)tetrahydropyran (I). Prodrug I was stable at neutral pH (pH of the saliva) but hydrolyzed in the gastric juice. This paper reports the synthesis, hydrolysis rate, and absorption of another acetaminophen prodrug where the hydroxy group was transiently blocked using ethyl vinyl ether. This prodrug, 1-(*p*-acetaminophenoxy)-1-ethoxyethane (II), has an advantage over the corresponding tetrahydropyran derivative (I) in that it reverts to acetaminophen 10 times faster. Therefore, the possibility that the prodrug might be absorbed as such is greatly minimized.

EXPERIMENTAL

Synthesis of II (2)—To a suspension containing 4 g of acetaminophen (0.26 mole) in freshly distilled ethyl acetate were added 30 ml (~0.4 mole) of freshly distilled ethyl vinyl ether and 0.2 ml of 0.4% *p*-toluenesulfonic acid in benzene. The suspension was stirred magnetically at room temperature until all suspended material was dissolved and a clear colorless solution was obtained, usually within 2–4 hr.

At the completion of the reaction, 0.2 ml of 0.4% pyridine in benzene was added. The solution obtained was transferred to a rotary evaporator,

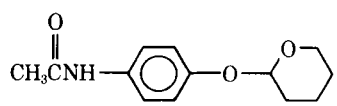

I

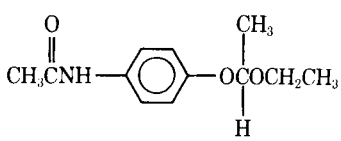

II

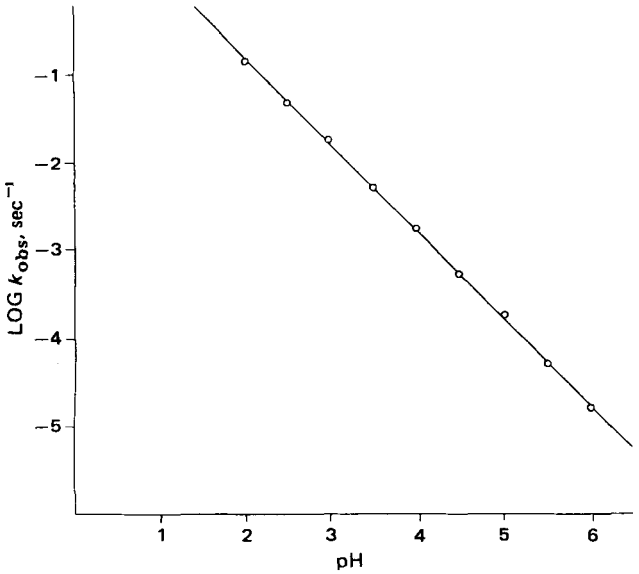

Figure 1—*The pH–rate profile for the hydrolysis of II at 25°.*

and some of the solvent and other volatile materials were removed at room temperature. Petroleum ether was added to the remaining viscous liquid, which was kept in the freezer for a few hours. The white precipitate which formed was filtered, washed with petroleum ether, and dried under vacuum at room temperature, yielding 5.6 g (88%), mp 60–61°. TLC of the solution of the prodrug in ethyl acetate showed only one spot.

The NMR spectra were consistent with the structure of II; NMR ($CDCl_3$): δ 8.36–8.66 (s, 1H, CNA_R), 6.86–7.63 (m, 4H, ArH), 5.18–5.53 [q, 1H, $OCH(CH_3)$], 3.36–3.99 (m, 2H, OCH_2CH_3), 2.03–2.30 (s, 3H, $COCH_3$), 1.39–1.61 [d, 3H, $OCH(CH_3)$], and 1.00–1.39 (t, 3H, CH_2CH_3) ppm.

Anal.—Calc. for $C_{12}H_{17}NO_3$: C, 64.55; H, 7.68. Found: C, 64.54; H, 7.73.

Kinetic Studies—A 0.03 *M* solution of the prodrug in spectral grade dioxane was freshly prepared. Approximately 150 μl was placed in a 2-cm UV cell, and approximately 6.5 ml of the buffer at the desired pH was added. The appearance of acetaminophen was followed spectrophotometrically at 290 nm. The aqueous solutions were prepared to contain 0.05 *M* total phosphate buffer, and the ionic strength was adjusted to 0.1 with potassium chloride. All solutions were equilibrated at 25 ± 0.1° before use.

Animal Studies—Two healthy male beagle dogs, 12 and 14 kg, were

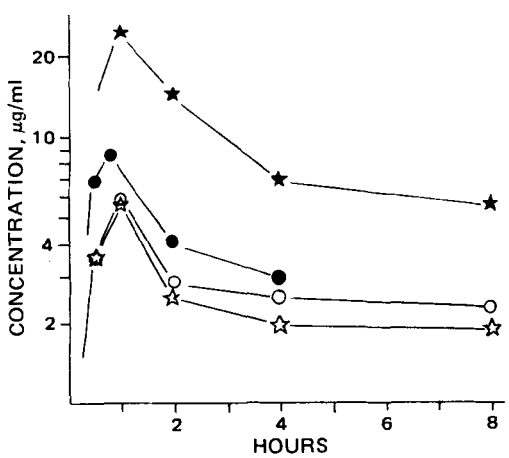

Figure 2—*Plasma acetaminophen concentration following the oral administration of acetaminophen and II. Dog 1 received 10-mg/kg doses of acetaminophen (○) and II (☆). Dog 2 received 25-mg/kg doses of acetaminophen (●) and II (★). The 0.5-hr prodrug and 8-hr acetaminophen samples for Dog 2 could not be obtained.*

Table I—Half-Lives and Observed First-Order Rate Constants of Hydrolysis of the Prodrug at Various pH Values at 25°

pH	Half-Life, sec	k_{obs}, sec^{-1}
2.0	4.24	1.62×10^{-1}
2.5	13	5.3×10^{-2}
3.0	42.7	1.62×10^{-2}
3.5	131	5.3×10^{-3}
4.0	421	1.62×10^{-3}
4.5	1,320	5.3×10^{-4}
5.0	4,218	1.62×10^{-4}
5.5	11,100	6.2×10^{-5}
6.0	43,780	1.59×10^{-5}

employed. Following a 24-hr fast, single doses of acetaminophen and the prodrug were administered with lactose in hard gelatin capsules 1 week apart. Water was available to the dogs during the experiment. Food was withheld for at least 6 hr postadministration. Dog 1 (12 kg) received 10 mg/kg, and Dog 2 (14 kg) received 25 mg/kg of acetaminophen and prodrug (as acetaminophen equivalents).

Blood samples, 5 ml, were withdrawn at 0.5, 1, 2, 4, and 8 hr postadministration. The blood was centrifuged, and the plasma was removed and stored at −20° until analyzed. The plasma acetaminophen levels were determined by GLC according to the procedure employed by Kostenbauder[1].

RESULTS AND DISCUSSION

To determine whether II does indeed cleave in an acidic environment, its hydrolysis rate was studied over the pH 2–6 range. As can be seen from the data in Table I and Fig. 1, the hydrolysis of the prodrug is acid catalyzed. The mechanism of hydrolysis of acetals was discussed thoroughly (3–5). In the pH 5–6 range, the prodrug remains intact for at least 1 hr. However, once in contact with an acidic environment such as that of the stomach, it cleaves rapidly, generating acetaminophen. The advantage of this prodrug over the corresponding tetrahydropyran prodrug (1) is that II cleaves 10 times faster. Therefore, the possibility that the prodrug is absorbed as such or passed to the more alkaline pH of the intestine is greatly minimized.

To compare the availability of II to that of acetaminophen, both compounds were given to dogs in capsule form. As can be seen from the data in Fig. 2, the plasma concentrations of the two compounds are comparable. Consequently, acetaminophen availability is not compromised *via* this approach.

It is not known at this time whether the prodrug is indeed less bitter than acetaminophen; human study is needed to obtain this information. However, based on the similarity of this prodrug to the corresponding tetrahydropyran derivative, the fact that II has equivalent aqueous solubility as the corresponding tetrahydropyran (solubility of II is 0.003 mole/liter; solubility of I is 0.003 mole/liter), and the fact that I is less bitter than acetaminophen, II also may possibly be less bitter than acetaminophen.

In view of the rapid hydrolysis rate of II to acetaminophen, the formulation parameters required to manufacture II in a conventional stable dosage form may be very stringent.

REFERENCES

(1) A. J. Repta and J. Hack, *J. Pharm. Sci.*, **62**, 1892 (1973).

(2) A. Hussain (to INTERx Research Corp., Lawrence, Kans.), U.S. pat. 3,786,090 (1974.)

(3) T. H. Fife and K. Jao, *J. Am. Chem. Soc.*, **90**, 408 (1968).

(4) T. H. Fife and L. H. Brod, *ibid.*, **92**, 1681 (1970).

(5) D. Piszkiewicz and T. Bruice, *ibid.*, **89**, 6237 (1967).

ACKNOWLEDGMENTS

Presented in part at the Industrial Pharmaceutical Technology Section, APhA Academy of Pharmaceutical Sciences, New Orleans meeting, April 1976.

[1] Dr. H. B. Kostenbauder, College of Pharmacy, University of Kentucky, Lexington, KY 40506, personal communication.

Quantitative Determination of Nalbuphine in Plasma Using Electron-Capture Detection

STEPHEN H. WEINSTEIN ˣ, MIRYAM ALTERAS, and JANET GAYLORD

Received May 9, 1977, from the *Pharmaceuticals Division, Biochemicals Department, E. I. du Pont de Nemours & Co., Wilmington, DE 19898.* Accepted for publication June 29, 1977.

Abstract □ A procedure for the determination of nalbuphine in plasma is presented. The compound and an internal standard are extracted into benzene–2-propanol from plasma at pH 10.4, followed by back-extraction into 0.1 *N* HCl. After the acid phase is washed with benzene and the compound is reextracted into benzene–2-propanol, the heptafluorobutyryl derivatives are formed and determined using electron-capture GLC. The lower limit of sensitivity is approximately 0.5 ng/ml, and the upper limit of the linear dynamic range is greater than 50 ng/ml. Peak plasma levels of 50 and 150 ng were observed in two dogs 10 and 20 min, respectively, after subcutaneous administration of 1 mg of nalbuphine/kg. Nalbuphine was detectable in plasma 5 hr after administration.

Keyphrases □ Nalbuphine—electron-capture GLC analysis in plasma □ GLC, electron capture—analysis, nalbuphine in plasma □ Analgesics—nalbuphine, electron-capture GLC analysis in plasma

Nalbuphine, (−)-17-(cyclobutylmethyl)-4,5α-epoxymorphinan-3,6α,14-triol[1], is a potent analgesic with narcotic antagonist activity in rodents (1) and humans (2). Clinical studies showed that the compound has low abuse potential (2), has analgesic potency similar to morphine, and may have a longer duration of action than morphine (3).

There have been no reports on the disposition and plasma levels of nalbuphine in animals or humans because of the insufficient sensitivity of currently used analytical methods. However, sensitive electron-capture GLC assays for the structurally similar compounds naltrexone (4, 5) and naloxone (4, 6) were reported.

The development of a sensitive electron-capture GLC method for nalbuphine in plasma is the subject of this report.

EXPERIMENTAL

Analytical Methodology—Up to 3 ml of plasma, containing 200 ng of naloxone as the internal standard, was placed in a 25-ml screw-capped centrifuge tube[2] (if less was used, the volume was made up to 3 ml with water), and the pH was adjusted to 10 with 2.5% NaOH. Then 1.5 ml of pH 10.4 phosphate buffer[3] was added, followed by 1.5 g of sodium chloride. This mixture was extracted with 12 ml of benzene[4] containing 1% 2-propanol by shaking on a wrist-action shaker for 30 min.

After centrifuging for 30 min at 2200×*g*, 10 ml of the upper organic layer was removed and placed in a 15-ml glass-stoppered centrifuge tube containing 1 ml of 0.1 *N* HCl. The tube was agitated on a mixer[5] for 1 min and then centrifuged for 10 min at 1240×*g*. The upper organic phase was discarded, and the remaining aqueous layer was washed with 6 ml of benzene. After discarding the benzene, the aqueous phase was adjusted to pH 10 with 0.01 *N* NaOH, and 1.5 ml of pH 10.4 phosphate buffer was added.

The alkaline aqueous phase was extracted into 6 ml of benzene containing 1% 2-propanol by shaking for 30 min on a wrist-action shaker. After centrifuging at 1240×*g* for 10 min, 5 ml of the upper benzene phase was evaporated to dryness in a 5-ml glass-stoppered centrifuge tube[6]. The samples were then dried overnight in a desiccator.

Anhydrous ether, 50 μl, was added to the dried sample by allowing it to wash down the sides of the tube; then 25 μl of heptafluorobutyric anhydride[7] was added. The tube was stoppered, and the mixture was agi-

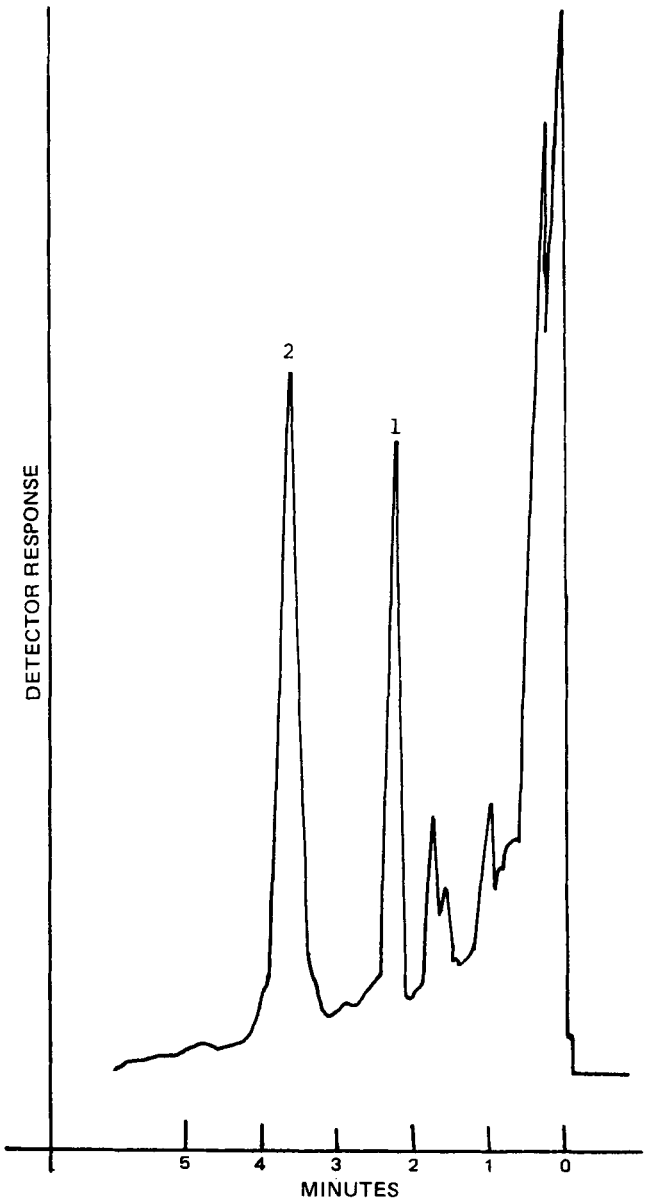

Figure 1—*Gas chromatogram of nalbuphine and internal standard (naloxone) extracted from dog plasma. Key: 1, naloxone heptafluorobutyrate; and 2, nalbuphine heptafluorobutyrate. Other peaks were due to the solvent and endogenous substances.*

[1] Nubain, Endo Laboratories.
[2] Corex.
[3] Potassium phosphate buffer was prepared by adding 5% (w/v) aqueous $K_3PO_4 \cdot x H_2O$ to 35% (w/v) aqueous K_2HPO_4 until pH 10.4 was attained.
[4] All organic solvents were Burdick and Jackson distilled in glass grade.
[5] Vortex.
[6] Evaporation was performed with a Buchler Evapo-Mix attached to a water aspirator.
[7] Pierce Chemicals, Rockford, Ill.

Table I—Plasma Nalbuphine Levels in Dogs after Subcutaneous Administration of 1 mg/kg

Hours	Plasma Nalbuphine Level, ng/ml	
	Dog 1	Dog 2
0.083	99	14
0.17	123	48
0.33	72	50
0.5	65	42
0.75	42	38
1.0	38	40
1.25	33	27
1.5	57	32
2.0	46	28
2.5	36	33
3.0	49	28
5.0	25	21

tated on a mixer for 5–10 sec, followed by incubation in a heating block[8] at 60° for 10 min. The incubated reaction mixture was then evaporated to dryness for 2 hr[9].

The dried product was dissolved in 25 μl of hexane, and 2–4-μl aliquots were injected into the gas chromatograph[10] equipped with a 2-mCi ^{63}Ni-electron-capture detector. The column was 3.8% methyl vinyl silicone gum rubber[11] (1.2 m long and 4 mm i.d.). Helium carrier gas, 75 ml/min, and 10% methane in argon (purge gas), 88 ml/min, were used. The oven, detector, and injection port temperatures were 235, 250, and 250°, respectively. The pulse interval setting was 50.

The peak heights of nalbuphine and naloxone heptafluorobutyrates were measured, and the ratio was calculated.

Dog Study—Nalbuphine hydrochloride in normal saline solution (5 mg/ml) was administered subcutaneously to two 10-kg beagle dogs, one male and one female, at a dose of 1 mg/kg. Blood was collected from the cephalic vein[12] in heparinized tubes at specified times after dosing. Plasma obtained after centrifugation was extracted and analyzed for nalbuphine by the described electron-capture GLC method.

[8] Temp-Blok, Lab-Line Instruments, Melrose Park, Ill.

[9] The Buchler Evapo-Mix was attached to a vacuum pump for this procedure. The derivatization procedure requires dry conditions and works well only when the relative humidity is 50% or less.

[10] F & M 402, Hewlett-Packard.

[11] UCC-W-982 on High Performance Chromosorb W, Hewlett-Packard.

[12] Butterfly-19 (Abbott) with a siliconized needle was placed in the vein.

RESULTS

The retention times of the heptafluorobutyryl derivatives of nalbuphine and naloxone were 3.7 and 2.2 min, respectively. Figure 1 is a typical chromatogram of nalbuphine extracted from dog plasma. Extracts of human plasma gave identical results. Human and dog plasma blanks extracted and treated with heptafluorobutyric acid showed no interfering peaks at the retention times of nalbuphine or naloxone heptafluorobutyryl derivatives.

The reproducibility of peak height ratios for quadruplicate samples of plasma made 10.0 and 1.0 ng/ml in nalbuphine hydrochloride was 5 and 14% (percent standard deviation), respectively. The recovery of nalbuphine added to plasma was 70% after correcting for aliquot losses during extraction. There was a linear relationship between the peak height ratio and the plasma concentration of naltrexone. The lower limit of sensitivity was approximately 0.5 ng/ml, and the upper limit of the linear dynamic range was greater than 50 ng/ml.

Table I presents the concentrations of nalbuphine found in the plasma of two dogs after subcutaneous administration of 1 mg of nalbuphine hydrochloride/kg. The peak concentrations were 123 and 50 ng/ml in Dogs 1 and 2, respectively. The peak times in the two dogs were 10 and 20 min (0.17 and 0.33 hr), respectively. Nalbuphine was still detectable in plasma 5 hr after administration.

REFERENCES

(1) H. Blumberg, H. B. Dayton, and P. S. Wolf, *Pharmacologist*, **10**, 198 (1968).

(2) D. R. Jasinski and P. A. Mansky, *Clin. Pharmacol. Ther.*, **13**, 78 (1971).

(3) W. T. Beaver and G. Feise, *ibid.*, **19**, 103 (1976).

(4) R. A. Sams, Ph.D. thesis, Ohio State University, Columbus, Ohio, 1975.

(5) V. K. Batra, R. A. Sams, R. H. Reuning, and L. Malspeis, "Abstracts, 17th National Meeting, APhA Academy of Pharmaceutical Sciences," vol. 4, 1975, p. 122.

(6) R. A. Sams, L. Malspeis, V. Batra, and R. H. Reuning, *ibid.*, p. 163.

Anti-Inflammatory 1-Substituted 2-Imidazolidinones

THOMAS J. SCHWAN ˣ, MARVIN M. GOLDENBERG, and NELSON J. MILES

Received February 7, 1977, from the *Research and Development Department, Norwich-Eaton Pharmaceuticals Division of Morton-Norwich Products, Inc., Norwich, NY 13815.* Accepted for publication June 22, 1977.

Abstract □ The synthesis and anti-inflammatory activity of a series of 1-substituted 2-imidazolidinones are reported. These compounds exerted marked anti-inflammatory activity in the carrageenan-induced hindpaw edema assay in the rat in doses that failed to elicit side effects. Their ED_{50} values were near the value of aspirin but markedly higher than the value of indomethacin.

Keyphrases □ 2-Imidazolidinones, 1-substituted—synthesized, anti-inflammatory activity evaluated □ Anti-inflammatory activity—various 1-substituted 2-imidazolidinones evaluated □ Structure-activity relationships—various 1-substituted 2-imidazolidinones evaluated for anti-inflammatory activity

A series of 1-(arylmethyl)-2-imidazolidinones was evaluated as anti-inflammatory agents. The target compounds, III–VI (Table I), were prepared by reaction of 2-imidazolidinone (I) with the appropriate arylmethyl chloride (II) (Scheme I).

DISCUSSION

The compounds were tested for anti-inflammatory activity according to a reported method (1). Each compound was suspended in 0.5% methylcellulose, and 300 mg/kg po was administered to three male Wistar

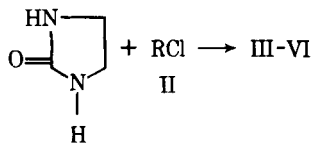

I

Scheme I

Table I—Plasma Nalbuphine Levels in Dogs after Subcutaneous Administration of 1 mg/kg

Hours	Plasma Nalbuphine Level, ng/ml	
	Dog 1	Dog 2
0.083	99	14
0.17	123	48
0.33	72	50
0.5	65	42
0.75	42	38
1.0	38	40
1.25	33	27
1.5	57	32
2.0	46	28
2.5	36	33
3.0	49	28
5.0	25	21

tated on a mixer for 5–10 sec, followed by incubation in a heating block[8] at 60° for 10 min. The incubated reaction mixture was then evaporated to dryness for 2 hr[9].

The dried product was dissolved in 25 μl of hexane, and 2–4-μl aliquots were injected into the gas chromatograph[10] equipped with a 2-mCi ^{63}Ni-electron-capture detector. The column was 3.8% methyl vinyl silicone gum rubber[11] (1.2 m long and 4 mm i.d.). Helium carrier gas, 75 ml/min, and 10% methane in argon (purge gas), 88 ml/min, were used. The oven, detector, and injection port temperatures were 235, 250, and 250°, respectively. The pulse interval setting was 50.

The peak heights of nalbuphine and naloxone heptafluorobutyrates were measured, and the ratio was calculated.

Dog Study—Nalbuphine hydrochloride in normal saline solution (5 mg/ml) was administered subcutaneously to two 10-kg beagle dogs, one male and one female, at a dose of 1 mg/kg. Blood was collected from the cephalic vein[12] in heparinized tubes at specified times after dosing. Plasma obtained after centrifugation was extracted and analyzed for nalbuphine by the described electron-capture GLC method.

[8] Temp-Blok, Lab-Line Instruments, Melrose Park, Ill.

[9] The Buchler Evapo-Mix was attached to a vacuum pump for this procedure. The derivatization procedure requires dry conditions and works well only when the relative humidity is 50% or less.

[10] F & M 402, Hewlett-Packard.

[11] UCC-W-982 on High Performance Chromosorb W, Hewlett-Packard.

[12] Butterfly-19 (Abbott) with a siliconized needle was placed in the vein.

RESULTS

The retention times of the heptafluorobutyryl derivatives of nalbuphine and naloxone were 3.7 and 2.2 min, respectively. Figure 1 is a typical chromatogram of nalbuphine extracted from dog plasma. Extracts of human plasma gave identical results. Human and dog plasma blanks extracted and treated with heptafluorobutyric acid showed no interfering peaks at the retention times of nalbuphine or naloxone heptafluorobutyryl derivatives.

The reproducibility of peak height ratios for quadruplicate samples of plasma made 10.0 and 1.0 ng/ml in nalbuphine hydrochloride was 5 and 14% (percent standard deviation), respectively. The recovery of nalbuphine added to plasma was 70% after correcting for aliquot losses during extraction. There was a linear relationship between the peak height ratio and the plasma concentration of naltrexone. The lower limit of sensitivity was approximately 0.5 ng/ml, and the upper limit of the linear dynamic range was greater than 50 ng/ml.

Table I presents the concentrations of nalbuphine found in the plasma of two dogs after subcutaneous administration of 1 mg of nalbuphine hydrochloride/kg. The peak concentrations were 123 and 50 ng/ml in Dogs 1 and 2, respectively. The peak times in the two dogs were 10 and 20 min (0.17 and 0.33 hr), respectively. Nalbuphine was still detectable in plasma 5 hr after administration.

REFERENCES

(1) H. Blumberg, H. B. Dayton, and P. S. Wolf, *Pharmacologist*, **10**, 198 (1968).

(2) D. R. Jasinski and P. A. Mansky, *Clin. Pharmacol. Ther.*, **13**, 78 (1971).

(3) W. T. Beaver and G. Feise, *ibid.*, **19**, 103 (1976).

(4) R. A. Sams, Ph.D. thesis, Ohio State University, Columbus, Ohio, 1975.

(5) V. K. Batra, R. A. Sams, R. H. Reuning, and L. Malspeis, "Abstracts, 17th National Meeting, APhA Academy of Pharmaceutical Sciences," vol. 4, 1975, p. 122.

(6) R. A. Sams, L. Malspeis, V. Batra, and R. H. Reuning, *ibid.*, p. 163.

Anti-Inflammatory 1-Substituted 2-Imidazolidinones

THOMAS J. SCHWAN ˣ, MARVIN M. GOLDENBERG, and NELSON J. MILES

Received February 7, 1977, from the *Research and Development Department, Norwich-Eaton Pharmaceuticals Division of Morton-Norwich Products, Inc., Norwich, NY 13815.* Accepted for publication June 22, 1977.

Abstract □ The synthesis and anti-inflammatory activity of a series of 1-substituted 2-imidazolidinones are reported. These compounds exerted marked anti-inflammatory activity in the carrageenan-induced hindpaw edema assay in the rat in doses that failed to elicit side effects. Their ED_{50} values were near the value of aspirin but markedly higher than the value of indomethacin.

Keyphrases □ 2-Imidazolidinones, 1-substituted—synthesized, anti-inflammatory activity evaluated □ Anti-inflammatory activity—various 1-substituted 2-imidazolidinones evaluated □ Structure-activity relationships—various 1-substituted 2-imidazolidinones evaluated for anti-inflammatory activity

A series of 1-(arylmethyl)-2-imidazolidinones was evaluated as anti-inflammatory agents. The target compounds, III–VI (Table I), were prepared by reaction of 2-imidazolidinone (I) with the appropriate arylmethyl chloride (II) (Scheme I).

DISCUSSION

The compounds were tested for anti-inflammatory activity according to a reported method (1). Each compound was suspended in 0.5% methylcellulose, and 300 mg/kg po was administered to three male Wistar

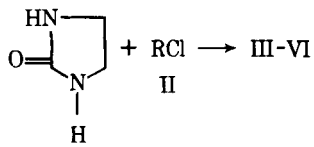

I

Scheme I

Table I—Physical and Analytical Data for 1-(Arylmethyl)-2-imidazolidinones (III-VI)

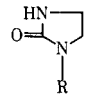

Compound	R	Melting Point	Yield, %	Recrystallization Solvent	Formula	Analyses, % Calc.	Analyses, % Found
III	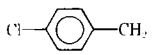	164-166°	19	Acetonitrile	$C_{10}H_{11}ClN_2O$	C 57.01 H 5.26 N 13.30	56.73 5.25 13.22
IV	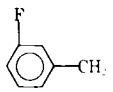	103-105°	28	Ether[a]	$C_{10}H_{11}FN_2O$	C 61.84 H 5.71 N 14.43	61.98 5.72 14.62
V	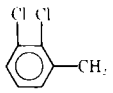	110-113°	12	Benzene	$C_{10}H_{10}Cl_2N_2O$	C 49.00 H 4.11 N 11.43	49.08 4.24 11.54
VI		153-155°	23	Methanol	$C_{14}H_{14}N_2O$	C 74.31 H 6.24 N 12.38	74.32 6.25 12.15

[a] Trituration of the crude product with ether gave analytically pure IV.

Table II—Anti-Inflammatory Evaluation

Compound	Dose, mg/kg po	Number of Rats	Percent Inhibition of Edema Formation[a] 4 hr	6 hr	ED_{50}[b], mg/kg
III	300	3	59.4	56.1	190
IV	300	3	55.9	76.6	155
V	300	3	68.9	69.2	103
VI	300	3	52.4	31.9	180
Aspirin	300	3	58.5	57.6	167
Indomethacin	10	10	63.0	49.0	10

[a] Compared to control (untreated) hindpaw 4 and 6 hr after carrageenan administration. [b] Calculated by the Litchfield and Wilcoxon method [J. T. Litchfield, Jr., and F. Wilcoxon, *J. Pharmacol. Exp. Ther.*, **96**, 99 (1949)] and based on inhibition of edema formation at the 4-hr interval.

rats, 1 hr prior to subplantar injection of 0.05 ml of a 1% solution of carrageenan[1] into the left hindfoot. The percentage reduction of edema formation (as compared to a nondrug-treated control) in the rat hindpaw was recorded 4 and 6 hr after carrageenan administration. For comparison, the reference anti-inflammatory drugs aspirin and indomethacin were tested (Table II). The ED_{50} value of each compound was also obtained by conducting antiedema studies in the presence of three to four lower doses of drug.

Compounds III–VI exhibited marked anti-inflammatory activity 4 hr after carrageenan injection. Compound V appeared to have a somewhat stronger antiedema effect than the other three compounds at 4 hr. The anti-inflammatory activity of three of the four compounds was maintained for 6 hr after carrageenan injection, the antiedema action of IV becoming even greater. A decrease in action was observed at 6 hr with VI. The activities of the four compounds compared favorably with the activity of aspirin but were less than the activity of indomethacin.

No side effects were noted with any compound based on this limited evaluation. When ED_{50} values of these compounds were obtained, V appeared to have the lowest value. Its effectiveness was greater than that of aspirin but less than that of indomethacin. Compounds III, IV, and VI appeared to be either slightly less or slightly more effective than aspirin.

EXPERIMENTAL[2]

The general procedure for the preparation of 1-(arylmethyl)-2-imidazolidinones (III–VI) (Table I) is as follows.

A mixture of 21.5 g (0.25 mole) of 2-imidazolidinone (I), 34.5 g (0.25 mole) of potassium carbonate, 10 g (0.06 mole) of potassium iodide, and 0.25 mole of the arylmethyl chloride (II) in 300 ml of dimethyl sulfoxide was stirred and heated at 100–105° for 3 hr; it was then cooled and poured into 1.3 liters of cold water. The mixture was extracted with 1.3 liters of chloroform, and the chloroform solution was washed with 150 ml of water, dried (magnesium sulfate), and concentrated to dryness *in vacuo* to give the crude product. Recrystallization from the appropriate solvent (Table I) gave the analytical sample.

The IR spectrum for 1-(4-chlorophenylmethyl)-2-imidazolidinone (III) showed 3.10 (NH) and 5.91 (C=O) μm. The NMR spectrum for III (dimethyl sulfoxide-d_6) showed δ 3.25 (s, 4H, imidazole 4-CH_2 and 5-CH_2), 4.22 (s, 2H, $C_6H_5CH_2$), 6.38 (t, 1H, exchangeable, NH), 7.26, and 7.43 (2 d, 4H, J = 9 Hz, phenyl CH) ppm.

The IR and NMR spectra of IV–VI were consistent with the assigned structures, and the physical and analytical data for III–VI are included in Table I.

REFERENCE

(1) C. A. Winter, E. A. Risley, and G. V. Nuss, *Proc. Soc. Exp. Biol. Med.*, **111**, 544 (1962).

ACKNOWLEDGMENTS

The authors are indebted to Mr. Warren Smith, Ms. Cora Jeffrey, and Ms. Donna George for the microanalyses and Ms. Connie Lloyd and Ms. Patricia Curtis for the NMR spectra. Mr. Jon Carpenter carried out the pharmacological testing.

[1] Viscarin, Algin Corporation of America.

[2] Melting points were determined on a Mel-Temp apparatus and are uncorrected. IR spectra were determined as mineral oil mulls using a Perkin-Elmer 137B spectrophotometer. NMR spectra were obtained on a Varian A-60A instrument and were compared with tetramethylsilane as an internal standard.

Potential Source of Error in Official Diazepam Assays

DAVID W. NEWTON

Received February 24, 1977, from the *Department of Pharmaceutics, Massachusetts College of Pharmacy, Boston, MA 02115.* Accepted for publication June 30, 1977.

Abstract □ A possible source of interference by a benzophenone hydrolysis product with the USP XIX spectrophotometric determination of diazepam in dosage forms is reported. A minor adaptation of the official assay procedures is briefly proposed as one method to correct this error.

Keyphrases □ Diazepam—spectrophotometric analysis in dosage forms, official method adapted to correct for potential interference by hydrolysis product □ Spectrophotometry—analysis, diazepam in dosage forms, official method adapted to correct for potential interference by hydrolysis product □ Hydrolysis product—diazepam, official spectrophotometric analysis in dosage forms adapted to correct for potential interference □ Sedatives—diazepam, spectrophotometric analysis in dosage forms, official method adapted to correct for potential interference by hydrolysis product

Recently, possible mechanisms for the hydrolysis of the 1,4-benzodiazepines oxazepam and diazepam (1) and chlordiazepoxide (2) to benzophenone final products were reported. 2-Methylamino-5-chlorobenzophenone and glycine were confirmed (1) as the previously reported final products of diazepam (3), but the sole, scant hydrolysis intermediate was not isolated. Depending on conditions, other medicinally useful 1,4-benzodiazepines, *e.g.*, flurazepam and clorazepate, yield benzophenone, acridone, and unspecified hydrolysis products (4, 5).

The estimation of a benzophenone degradation product in the presence of an intact 1,4-benzodiazepine derivative might be useful in the evaluation of both commercial and extemporaneous dosage forms of these drugs. A recent investigation (6), which included the estimation of diazepam and its benzophenone hydrolysis product in extemporaneous oral liquid products prepared from diazepam tablets, was the impetus for this report. An earlier clinical study using noncommercial diazepam suspensions cited no attempt to determine the stability or dispersion uniformity of the drug (7).

EXPERIMENTAL

Analytical standard quality diazepam[1] (I), mol. wt. 284.74, and 2-methylamino-5-chlorobenzophenone[2] (II), mol. wt. 245.71, were used without further purification. Diazepam injection[3] (III), 5 mg/ml, was obtained commercially. Spectra and absorbance values were determined with a recording spectrophotometer[4], and analytical grade reagents were used throughout.

Spectra of I and II were determined in alcohol USP and in acidic alcohol[5]. Beer's law plots for I and II in both solvents were linear over the 0.5–50.0-μg/ml concentration range. Concentrations of II and III were quantitatively adjusted in certain samples by adding an appropriate volume of an alcohol solution of II, 1.0 mg/ml, to the required volume of III. Otherwise, the official assay for diazepam injection (8) or the proposed method was followed.

[1] RO 5-2807, lot 545055, Hoffmann-La Roche, Nutley, N.J.
[2] RO 5-4365, lot PP-4, Hoffmann-La Roche, Nutley, N.J.
[3] Valium injection, 5 mg/ml, lot 0676-04066 (expires Apr. 1, 1978), Hoffmann-La Roche, Nutley, N.J.
[4] Beckman DB-GT grating spectrophotometer, Beckman Instruments, Fullerton, Calif.
[5] Sulfuric acid–alcohol (1:350), USP XIX (8).

DISCUSSION

From Fig. 1, it is evident that II in alcohol may be determined at approximately 405 nm without interference from I; I absorbs below 350 nm, reaching a maximum at approximately 315 nm. However, the absorbances of I and II in acidic alcohol overlap at the official wavelengths of 285 ± 2 and 368 ± 2 nm specified for diazepam tablets and injection, respectively (8).

Samples 6–8 (Table I) consisted of adequate II and III to simulate samples of diazepam injection in which approximately 5, 12.5, and 25%, respectively, of the diazepam had previously degraded to II. From the last column of Table II, it may be concluded that, according to the official method, Samples 6–8 conformed to official content standards by containing 90–110% of the labeled amounts of diazepam (8). However, the theoretical assay error values in Table II show that only Sample 6 meets the 90–110% diazepam content limits.

The pH-dependent separation of I and II by extraction of aqueous samples with chloroform was not effective. The pKa of diazepam was reported as 3.4 (9) and 3.5[6]. The pKa of II is probably very near this point because 1-methylamino-4-chlorobenzene has a pKa of about 4.3 (10), which would be lowered by the addition of an electron-withdrawing benzoyl radical *ortho* to the methylamino group.

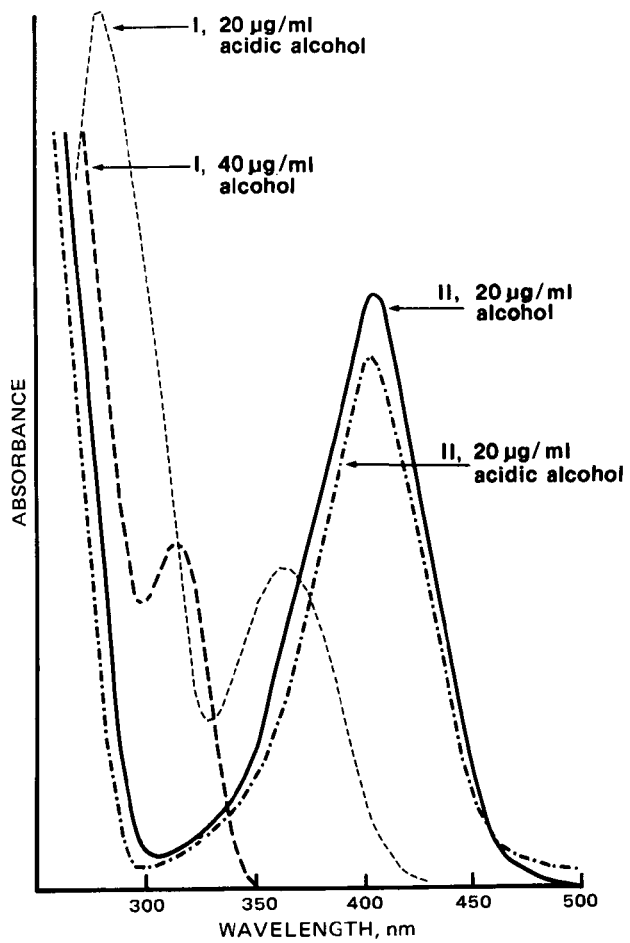

Figure 1—*Spectra of I and II in alcohol and acidic alcohol.*

[6] Dr. W. E. Scott, Hoffmann-La Roche, Nutley, N.J., Aug. 1975, personal communication.

Table I—Assay Data for Samples of I–III Determined Spectrophotometrically According to the USP XIX Procedure for III

Assay Sample[a]	Known or Labeled Quantity in Samples, mg			Absorbance, nm	
	I	II	III[b]	283	370
1	10.0	—	—	0.40	0.14
2	—	—	10.0	0.43	0.14
3	40.0	—	—	—[c]	0.56
4	—	—	40.0	—[c]	0.58
5	—	10.0	—	0.10	0.11
6	—	0.4	9.5	—[c]	0.57
7	—	1.1	8.8	—[c]	0.54
8	—	2.2	7.5	—[c]	0.51

[a] Average of three trials. [b] Volume of III expressed as diazepam content in milligrams. [c] Value exceeded scale denominations of instrument in settings used.

Table II—Assay Data for Simulated Degraded Samples of Diazepam Obtained by USP XIX Procedures

Sample	Diazepam Content, μg/ml		Error in Diazepam Content, %	
	Actual[a]	Found	Actual[b]	Found[b]
6	38.0	40.7	−5	1.8
7	35.0	38.6	−12.5	−3.5
8	30.0	36.4	−25	−9.0

[a] Based on values reported in Table I. [b] [(Content found − 40)/40] × 100.

The official assay procedures for diazepam dosage forms do not seem capable of adequately differentiating intact diazepam (I) from its final aromatic hydrolysis product (II). This is not surprising since many spectrophotometric procedures are somewhat nonspecific, being based on functional group analysis. However, the present ambiguity may be alleviated by the proposed method involving the simultaneous determination of two separate samples of diazepam dosage forms.

The first sample is processed according to official specifications (8), which permit greater sensitivity in determining diazepam spectrophotometrically. The second sample is treated accordingly, except that the chloroform extract residue is reconstituted with alcohol and the absorbance is read at 405 nm. This absorbance value multiplied by the value[7] 9.667 or 19.314 yields a quantitative estimate, in milligrams, of the amount of diazepam present as II in the original injection or tablet samples, respectively.

Neither glycine nor the yellow coloring material present in the only source of 5-mg diazepam tablets[8] marketed in the United States interferes with the determination of II. Interference by intermediate hydrolysis products other than II was not investigated.

[7] Calculated from Beer's law data for II in alcohol determined at 405 nm, dilution factors in the USP XIX procedures (8), and the formula weight ratio, 284.74 to 245.71, of I to II.

[8] Valium tablets, 5 mg, lot 6373-12225 (expires Jan. 1, 1981), Hoffmann–La Roche, Nutley, N.J.

Table III—Assay Data for Simulated Degraded Samples of Diazepam Determined According to the Proposed Method

Sample	Diazepam Content, μg/ml		Error in Diazepam Content, %	
	Actual[a]	Found[b]	Average	Range
6	38.0	39.1	2.9	2.3–3.1
7	35.0	35.6	1.7	1.2–2.5
8	30.0	30.9	3.0	2.6–3.3

[a] Based on values reported in Table I. [b] Average diazepam content corrected for interference of II with the USP XIX determination of III.

The assay results reported in Table II substantiate that significant error in the diazepam content of specimens also containing its major hydrolysis product, II, may not be detected by USP XIX assay procedures. In contrast, the data in Table III support the capability of the proposed method to quantitate diazepam accurately under these conditions.

REFERENCES

(1) W. W. Han, G. J. Yakatan, and D. D. Maness, *J. Pharm. Sci.*, **66,** 573 (1977).

(2) *Ibid.*, **65,** 1198 (1976).

(3) J. A. F. de Silva, M. A. Schwartz, V. Stefanovic, J. Kaplan, and L. D'Arconte, *Anal. Chem.*, **36,** 2099 (1964).

(4) B. C. Rudy and B. Z. Senkowski, in "Analytical Profiles of Drug Substances," vol. 3, K. Florey, Ed., Academic, New York, N.Y., 1974, pp. 321–323.

(5) J. A. Raihle and V. E. Papendick, in *ibid.*, vol. 4, 1975, pp. 108, 109.

(6) D. W. Newton, S. G. Schulman, and C. H. Becker, *Am. J. Hosp. Pharm.*, **33,** 450 (1976).

(7) G. P. DeLemos, W. R. Clement, and E. Nickels, *J. Am. Geriatr. Soc.*, **13,** 355 (1965).

(8) "The United States Pharmacopeia," 19th rev., Mack Publishing Co., Easton, Pa., 1975, pp. 135, 136.

(9) A. MacDonald, H. F. Michaelis, and B. Z. Senkowski, in "Analytical Profiles of Drug Substances," vol. 1, K. Florey, Ed., Academic, New York, N.Y., 1972, p. 90.

(10) A. Albert and E. P. Serjeant, "The Determination of Ionization Constants," 2nd ed., Chapman and Hall, London, England, 1971, p. 94.

ACKNOWLEDGMENTS

The author thanks Dr. W. E. Scott, Hoffmann–La Roche, Nutley, N.J., for donating samples of I and II. Appreciation is also expressed to Ms. Deborah K. Delano for the preparation of this manuscript.

Antitumor Agents XXVII: Effects of Helenalin on Anaerobic and Aerobic Metabolism of Ehrlich Ascites Cells

I. H. HALL ˣ, K. H. LEE, and S. A. ElGEBALY

Received March 10, 1977, from the *Division of Medicinal Chemistry, School of Pharmacy, University of North Carolina at Chapel Hill, Chapel Hill, NC 27514.* Accepted for publication July 15, 1977.

Abstract □ Evidence is presented that the antitumor agent helenalin, a sesquiterpene lactone, suppresses anaerobic glycolytic enzymes of tumor cells at a number of sites and not exclusively at glycogen synthetase and phosphofructokinase, previously proposed sites for inhibition by α-methylene-γ-lactones. Of the enzymes tested, the sulfhydryl-containing enzyme hexokinase was inhibited the maximum, *i.e.*, 83%, by helenalin treatment, whereas phosphofructokinase and glycogen synthetase were suppressed approximately 45%. Another sulfhydryl-bearing enzyme, aldolase, was decreased approximately 43%. Phosphorylase *a* was inhibited 65%, glucose-6-phosphatase was inhibited 46%, and succinic dehydrogenase was inhibited 59% by helenalin treatment. Mitochondrial oxidative phosphorylation processes were also significantly depressed in the presence of helenalin *in vitro* with either succinate or α-ketoglutarate as substrates. Thus, a number of enzymes of anaerobic and aerobic carbohydrate metabolism of Ehrlich ascites cells appear to be inhibited by helenalin, which supposedly can alkylate functional groups, *e.g.*, sulfhydryl groups of these enzymes, by a rapid Michael-type addition.

Keyphrases □ Helenalin—effects on anaerobic and aerobic metabolism of Ehrlich ascites cells □ Metabolism, anaerobic and aerobic—Ehrlich ascites cells, effects of helenalin □ Enzyme activity—effects of helenalin on anaerobic and aerobic metabolism of Ehrlich ascites cells □ Antitumor agents—helenalin, effects on anaerobic and aerobic metabolism of Ehrlich ascites cells

Helenalin (1), a sesquiterpene lactone, recently was shown to possess significant antitumor activity against Walker 256 ascites carcinosarcoma (Sprague–Dawley rats at 2.5 mg/kg/day, T/C = 316%) and Ehrlich ascites (CF_1 mice at 33.3 mg/kg/day, 99% inhibition) and to be marginally active against P-388 lymphocytic leukemia (DBA/2 mice at 25 mg/kg/day, T/C = 127%) (1) and Lewis lung carcinoma (C57BL 6 mice at 25 mg/kg/day, T/C = 142%)[1]. Further studies demonstrated that helenalin inhibited deoxyribonucleic acid (1) and protein synthesis but had little effect on ribonucleic acid synthesis of Ehrlich tumor cells (2). Deoxyribonucleic acid polymerase activity and phosphorylation of nuclear histones and nonhistone proteins were inhibited, whereas the level of 3′,5′-cyclic adenosine monophosphate was tripled by drug treatment of CF_1 male Ehrlich ascites tumor-bearing mice (1).

Kupchan and coworkers (3–5) demonstrated that the α-methylene-γ-lactone system can act as the alkylating center for cytotoxic antitumor lactone, *e.g.*, elephantopin, vernolepin, and euparotin acetate. A Michael-like reaction between biological nucleophiles, such as L-cysteine (3), or the sulfhydryl-containing enzymes, *e.g.*, phosphofructokinase (4) and glycogen synthetase (5), was proposed as the mechanism of these agents. *In vitro* helenalin, which contains both the α-methylene-γ-lactone and cyclopentenone moieties, alkylates sulfhydryl groups of cysteine and reduced glutathione (2). The effects of helenalin on the aerobic and anaerobic respiration of Ehrlich ascites tumor-bearing mice are now reported.

[1] Unpublished results. Lewis lung screening was carried out by the procedure outlined by R. I. Geran, N. H. Greenberg, M. M. MacDonald, A. M. Schumacher, and B. J. Abbott, *Cancer Chemother. Rep.*, **3**, 13 (1972), and references cited therein.

EXPERIMENTAL

Male CF_1 mice (~30 g) were implanted intraperitoneally on Day 0 with 10^6 Ehrlich ascites tumor cells. On Days 5, 6, and 7, animals were treated with 0.125 mg ip of helenalin suspended by homogenization in 0.05% polysorbate 80–water. Animals were sacrificed on Day 8, and the ascites fluid was collected from the peritoneal cavity and homogenized.

The following enzymatic activities were determined for both control and treated cells: glucose-6-phosphate dehydrogenase (6), glucose-6-phosphatase (7), hexokinase (8), glycogen synthetase (9), phosphofructokinase (10), aldolase (11), glyceraldehyde-3-phosphate dehydrogenase (12), lactic dehydrogenase (13), malic dehydrogenase (14), succinic dehydrogenase (15), total cellular adenosine triphosphatase (16), mitochondrial adenosine triphosphatase (17), and monoamine oxidase (18).

Phosphorylase *a* activity was determined as the disappearance of inorganic phosphate from the medium used for the phosphorylation of glucose when released from glycogen. The reaction medium contained 1 μmole of sodium phosphate, 2% glycogen, 0.3 μmole of 3′,5′-cyclic adenosine monophosphate, 2.0 μmoles of sodium fluoride, and 10 μmoles of tris(hydroxymethyl)aminomethane at pH 6.1 in a total volume of 0.1 ml. After incubation for 60 min at 37°, the inorganic phosphate was determined.

Fructose-1,6-diphosphatase was determined utilizing a reaction medium containing 60 μmoles of pH 9.4 glycine buffer, 1 μmole of fructose-1,6-diphosphate, and 1 μmole of manganese chloride (19). After incubation at 37° for 15 min, the inorganic phosphate was determined by the method of Chen *et al.* (20). The protein content for all assays was determined by the method of Lowry *et al.* (21).

In vitro effects of helenalin on Ehrlich ascites tumor oxidative phosphorylation in the presence and absence of adenosine diphosphate, utilizing succinate (flavin adenine dinucleotide-linked dehydrogenase) or α-ketoglutarate (nicotinamide adenine dinucleotide phosphate-linked dehydrogenase) as substrates, were measured. Oxygen consumption was measured with a Clark oxygen electrode connected to a Gilson oxygraph.

The reaction vessel contained 55 μmoles of sucrose, 22 μmoles of potassium chloride, 22 μmoles of dibasic potassium phosphate, 90 μmoles of succinate or 60 μmoles of α-ketoglutarate, 2 μmoles of adenosine triphosphate, and helenalin (0.2 mg in 0.05% polysorbate 80–water) in a total volume of 1.8 ml. After the basal metabolic (state 4) level was obtained, 0.257 μmole of adenosine diphosphate was added to obtain the adenosine diphosphate-stimulated respiration rate (state 3) (22).

RESULTS

Helenalin significantly reduced the enzymatic activity of glycolytic and Krebs cycle enzymes (Table I). Glucose-6-phosphate dehydrogenase activity for 8-day Ehrlich ascites cells was 0.5158 O.D. (optical density) unit/min/mg of protein based on the presence of 0.0056 μmole of nicotinamide adenine dinucleotide phosphate. Helenalin caused a 30% reduction in the activity of this enzyme. Glucose-6-phosphatase activity for the control was 7.594 μg of inorganic phosphate/mg of protein released in 15 min. Helenalin caused a 46% reduction in enzymatic activity. Hexokinase activity for the control was 0.169 O.D. unit/min/mg of protein based on the presence of 500 μmoles of nicotinamide adenine dinucleotide phosphate. Helenalin reduced the activity by 83%.

Glycogen synthetase activity for the control was 5036 dpm/mg of

Table I—Effects of Helenalin on Ehrlich Ascites Metabolism of 8-day CF_1 Male Mice (n = 6)

Compound	Control, 0.05% Polysorbate 80, $\bar{x} \pm SD$[a]	Helenalin, 0.125 mg/day, $\bar{x} \pm SD$[a]
In Vivo Enzymatic Assay		
Glucose-6-phosphate dehydrogenase	100 ± 27	70 ± 26
Glucose-6-phosphatase	100 ± 23	54 ± 25[b]
Hexokinase	100 ± 32	17 ± 2[b]
Glycogen synthetase	100 ± 24	56 ± 24[b]
Phosphorylase *a*	100 ± 19	35 ± 12[b]
Phosphofructokinase	100 ± 39	55 ± 15[b]
Fructose-1,6-diphosphatase	100 ± 26	70 ± 14
Aldolase	100 ± 22	57 ± 15[b]
Glyceraldehyde-3-phosphate dehydrogenase	100 ± 20	115 ± 8
Lactic dehydrogenase	100 ± 15	100 ± 22
Malic dehydrogenase	100 ± 18	92 ± 14
Succinic dehydrogenase	100 ± 22	41 ± 22[b]
Total cellular adenosine triphosphatase	100 ± 18	93 ± 29
Mitochondrial adenosine triphosphatase	100 ± 24	74 ± 20
Monoamine oxidase	100 ± 2	111 ± 4
In Vitro Oxidative Phosphorylation (0.2 mg of Helenalin)		
Succinate		
State 3	100 ± 4	60 ± 8[b]
State 4	100 ± 3	72 ± 8[b]
α-Ketogluturate		
State 3	100 ± 11	67 ± 10[b]
State 4	100 ± 5	48 ± 15[b]

[a] Mean of the percent of the control value and the standard deviation. The probable significance level (p) was determined by the Student t test. [b] p = 0.001.

protein; helenalin reduced the activity by 44%. Phosphorylase *a* activity for the control was 4.43 μg of inorganic phosphate taken up from the medium/hr/mg of protein; helenalin reduced this activity by 65%. Phosphofructokinase activity for the control was 0.252 O.D. unit/min/mg of protein based on 1.125 μmoles of reduced nicotinamide adenine dinucleotide; helenalin treatment reduced the activity by 45%. Fructose-1,6-diphosphatase activity of the control was 10.12 μg of inorganic phosphate released/mg of protein in 15 min; helenalin reduced the activity by 30%.

Aldolase activity for the control was 282 mU/mg of protein, which was reduced 43% by helenalin treatment. Glyceraldehyde-3-phosphate dehydrogenase activity for the control was 2.405 O.D. units/min/mg of protein based on 20.3 μmoles of nicotinamide adenine dinucleotide; helenalin treatment had no effect on this enzyme. Lactic dehydrogenase activity for the control was 5.696 O.D. units/min/mg of protein based on 0.12 μmole of reduced nicotinamide adenine dinucleotide and was not affected by helenalin treatment.

Malic dehydrogenase activity for the control was 0.7975 O.D. unit/min/mg of protein based on 15 μmoles of reduced nicotinamide adenine dinucleotide; helenalin had very little effect on this enzyme. Succinic dehydrogenase activity for the control was 0.0669 O.D. unit/min/mg of protein based on 15 μmoles of potassium ferricyanide; helenalin treatment caused a 59% suppression of enzymatic activity. Total cellular adenosine triphosphatase for the control was 9.873 μg of phosphate hydrolyzed/10 min/mg of protein. Helenalin treatment resulted in no change in activity.

Mitochondrial adenosine triphosphatase activity for the control was 1.139 μg of phosphate released/10 min/mg of protein. Helenalin treatment caused a 26% suppression of enzymatic activity, but this amount was not significant. The enzyme monoamine oxidase was very low in activity in Ehrlich ascites cells; no alteration was observed with helenalin treatment.

The respiration of Ehrlich ascites tumor cells in the presence of sodium succinate as a substrate in the absence of adenosine diphosphate (basal state 4 respiration) was 5.506 μl of oxygen/hr/mg of protein; in the presence of adenosine diphosphate-coupled oxidative phosphorylation (state 3), it was 6.487 μl of oxygen/hr/mg of protein. Sodium α-ketoglutarate resulted in a state 4 respiration of 2.525 μl of oxygen/hr/mg of protein, and state 3 respiration was 4.049 μl of oxygen/hr/mg of protein. Helenalin treatment caused a 40% reduction in state 3 and a 28% reduction in state 4 with succinate (flavin adenine dinucleotide-linked enzyme) and a 33% reduction in state 3 and a 52% reduction in state 4 with α-ketoglutarate (a nicotinamide adenine dinucleotide-linked enzyme). The vehicle polysorbate 80–water itself did not alter enzymatic activities of Ehrlich ascites cells, with the exception of state 3 respiration, which was depressed 12% in the presence of this vehicle.

DISCUSSION

Several studies have indicated that cancer cells are dependent on energy from the anaerobic glycolytic cycle and that the mitochondria of these cells are altered; *i.e.*, the mitochondria are tightly coupled (23), vary in number and morphology, and have modified swelling properties (24–26), depending on the type of cells and stage of differentiation, generally with a reduction in number and a more heterogeneous size and distribution (27). Reduction of adenosine diphosphate stimulated respiration; *i.e.*, coupled oxidative phosphorylation (state 3), as well as accelerated uncoupled electron transport respiration (state 4), has been observed with mitochondria from cancer cells (24). Supposedly, the tumor cell is dependent on the Embden–Meyerhof cycle as an energy source (25), which is critical for the cell's survival in view of the energy required for rapid nucleic and protein synthesis in proliferating cells.

Since the observation had previously been made that compounds containing the α-methylene-γ-lactone moiety inhibited sulfhydryl-bearing enzymes, a number of enzymes of the Embden–Meyerhof and Krebs cycle were examined as possible sites of inhibition by helenalin in Ehrlich ascites cells. Enzymes that regulate the availability of glucose for glycolysis, *e.g.*, hexokinase and phosphorylase *a*, were drastically inhibited by helenalin treatment. Other sulfhydryl-containing enzymes, such as the regulatory enzyme phosphofructokinase and aldolase, were also inhibited but to a lesser degree by helenalin. Enzymes later in the cycle, *e.g.*, glyceraldehyde-3-phosphate dehydrogenase and lactic dehydrogenase, were unaffected by helenalin treatment. Enzymes required for the reversal of glycolysis, *e.g.*, glucose-6-phosphatase, fructose-1,6-diphosphatase, as well as glycogen synthetase, were inhibited significantly by helenalin treatment.

The regulatory enzyme of the hexose monophosphate shunt, glucose-6-phosphate dehydrogenase, was reduced, but not significantly, by helenalin treatment. The mitochondrial enzyme succinic dehydrogenase was significantly reduced by helenalin treatment. This enzyme is reported to contain an iron–sulfur protein as an integral component. Malic dehydrogenase and monoamine oxidase activities were not affected by helenalin treatment.

Gosálvez *et al.* (28) attempted to correlate antitumor activity of compounds with the suppression of tumor respiration, *e.g.*, 4,6-diaminotriazine derivatives, naphthoquinone analogs, tritylthioalanine, carminomycin, piperazinedione, and methotrexate. Helenalin *in vitro* reduced basal oxygen consumption (electron transport) with both nicotinamide adenine dinucleotide and flavin adenine dinucleotide-linked enzymes of Ehrlich ascites cells. Oxidative phosphorylation (coupled respiration) also was inhibited in the presence of helenalin. The reduction in these processes did not appear to be due to the suppression of mitochondrial adenosine triphosphatase activity since the activity of this enzyme was not significantly different from the control activity, as was the total cellular adenosine triphosphatase activity. Helenalin had little effect on normal mouse liver oxidative phosphorylation processes.

CONCLUSION

Helenalin has the ability to inhibit both aerobic and anaerobic energy processes of tumor cells. The thesis that the α-methylene-γ-lactone component or the cyclopentenone ring (1) of the molecule has the ability to alkylate functional groups of these enzymes by a Michael-type addition is attractive. Whereas the inhibition of glycolytic metabolism is probably not the major mechanism of action of helenalin as an antitumor agent (*i.e.*, the mechanism is most likely inhibition of nucleic acid and protein synthesis), the fact that the energy available to cells for synthetic processes is seriously hampered and rate limiting in the presence of helenalin has an additive effect on the drug's actions on cellular metabolism and tumor inhibition.

REFERENCES

(1) I. H. Hall, K. H. Lee, E. C. Mar, and C. O. Starnes, *J. Med. Chem.*, **20**, 333 (1977).

(2) K. H. Lee, I. H. Hall, E. C. Mar, C. O. Starnes, S. A. ElGebaly, T.

G. Waddell, R. I. Hadgnaft, E. C. Ruffner, and I. Weidner, *Science*, **196**, 533 (1977).
(3) S. M. Kupchan, D. C. Fessler, M. A. Eakin, and T. J. Giacobbe, *ibid.*, **168**, 376 (1970).
(4) R. L. Hanson, H. A. Lardy, and S. M. Kupchan, *ibid.*, **168**, 378 (1970).
(5) C. H. Smith, J. Larner, A. M. Thomas, and S. M. Kupchan, *Biochim. Biophys. Acta*, **276**, 94 (1972).
(6) P. Cohen and M. A. Rosemeyer, *Eur. J. Biochem.*, **8**, 1 (1969).
(7) M. A. Swanson, *J. Biol. Chem.*, **184**, 647 (1950).
(8) D. G. Walker and J. J. Parry, in "Methods in Enzymology," vol. 9, W. A. Wood, Ed., Academic, New York, N.Y., 1967, p. 381.
(9) J. A. Thomas, K. K. Schlinder, and J. Larner, *Anal. Biochem.*, **25**, 486 (1968).
(10) T. E. Mansour, in "Methods in Enzymology," vol. 9, W. A. Wood, Ed., Academic, New York, N.Y., 1967, p. 430.
(11) P. V. C. Pinto, A. Kaplan, and P. A. VanDreal, *Clin. Chem.*, **15**, 349 (1969).
(12) W. S. Allison, in "Methods in Enzymology," vol. 9, W. A. Wood, Ed., Academic, New York, N.Y., 1967, p. 210.
(13) M. K. Schwartz and O. Bodansky, in *ibid.*, p. 294.
(14) S. Ochoa, A. H. Mehler, and A. Kornberg, *J. Biol. Chem.*, **174**, 979 (1948).
(15) D. V. DerVartanian and C. Veerger, *Biochim. Biophys. Acta*, **92**, 233 (1964).
(16) E. M. Suolinna, R. N. Buchsbaum, and E. Racker, *Cancer Res.*, **35**, 1865 (1975).
(17) A. E. Senior, S. E. McGowan, and R. Hilf, *ibid.*, **35**, 2061 (1975).
(18) P. S. Basu, *Biochem. Pharmacol.*, **24**, 2269 (1975).
(19) Modified from S. Pontremoli, in "Methods in Enzymology," vol. 9, W. A. Wood, Ed., Academic, New York, N.Y., 1967, p. 625.
(20) P. S. Chen, T. Y. Toribara, and H. Warner, *Anal. Chem.*, **28**, 1756 (1956).
(21) O. H. Lowry, N. J. Rosebrough, A. L. Farr, and R. J. Randall, *J. Biol. Chem.*, **193**, 265 (1951).
(22) I. H. Hall and G. L. Carlson, *J. Med. Chem.*, **19**, 1257 (1976).
(23) F. Rupert, W. Thorne, and F. L. Bygnave, *Cancer Res.*, **33**, 2562 (1973).
(24) H. D. Haberman, *ibid.*, **35**, 3332 (1975).
(25) K. W. McKern, "Hormones and Cancer," Academic, New York, N.Y., 1974, pp. 261–307.
(26) R. F. W. Thorne and F. L. Bygnove, *Cancer Res.*, **33**, 2562 (1973).
(27) D. F. H. Wallach, "Membrane Molecular Biology of Neoplastic Cells," Elsevier, New York, N.Y., 1975, p. 257.
(28) M. Gosálvez, R. Garcia-Canero, M. Blauco, and C. Gurucharri-Lloyd, *Cancer Treatment Rep.*, **60**, 1 (1976).

ACKNOWLEDGMENTS

Supported by Grants CH-19 and IN15-P from the American Cancer Society to K. H. Lee and I. H. Hall, respectively, and in part by the National Cancer Institute (CA-17625).

Intrapatient Variability of Serial Steady-State Plasma Tricyclic Antidepressant Concentrations

V. E. ZIEGLER, L. T. WYLIE, and JOHN T. BIGGS ˣ

Received May 18, 1977, from the *Department of Psychiatry, School of Medicine, Washington University, St. Louis, MO 63110.* Accepted for publication July 5, 1977.

Abstract □ Nine or 10 serial steady-state plasma measurements of amitriptyline, desipramine, desmethyldoxepin, doxepin, imipramine, nortriptyline, or protriptyline were made in 23 depressed patients. Each patient was monitored for compliance by pill counts, and sampling time was controlled carefully to determine intrapatient variability of steady-state tricyclic levels on a day-to-day basis. The coefficients of variation during serial sampling of the various ingested drugs were: amitriptyline, 21%; desipramine, 26%; doxepin, 21%; imipramine, 14%; nortriptyline, 13%; and protriptyline, 17%. The therapeutic ranges for the tricyclic antidepressants are relatively wide, so coefficients of variation of these magnitudes indicate that the position of an individual patient in relation to the optimal therapeutic range can be reliably determined on a clinical basis.

Keyphrases □ Plasma drug levels—various tricyclic antidepressants, intrapatient variability at steady state □ Antidepressants, various—plasma drug levels, intrapatient variability at steady state

Although it has been over 10 years since Hammer *et al.* (1) first demonstrated a 36-fold difference between the lowest and highest steady-state levels of desipramine in patients ingesting equal amounts of the same drug, the use of plasma tricyclic antidepressant levels as a practical way to improve patient management is only slowly being accepted. Since the evidence that plasma drug levels more closely correspond to therapeutic response than oral dosage, there has been marked interest in the routine determination of plasma tricyclic antidepressant levels as a method of improving clinical response (2–8) and predicting toxicity (9).

Although therapeutic ranges have been suggested for most of the marketed tricyclic antidepressants, the interpretation of the results of plasma tricyclic determinations is often difficult. Differences in optimal plasma therapeutic ranges have been caused by varying purity of the standard drugs used, assay and blood collection methods, and the patient populations studied. In addition, day-to-day variation occurs in the steady-state level in individual patients. This variation is influenced not only by the reliability of the drug assay techniques but by biological variation within the individual.

The purpose of this study was to determine the variation for the entire procedure, controlling for such factors as is practical in a clinical setting.

EXPERIMENTAL

Plasma tricyclic antidepressant levels were assayed by GLC–mass fragmentography by a method described previously (10). This method is specific for each drug monitored and does not assay undescribed metabolites. Differences between duplicate samples are less than 10%.

To examine the biological and laboratory variability of steady-state plasma levels, outpatients undergoing treatment for depression on level doses of drug for at least 2 weeks were subjected to nine or 10 serial samplings over 3 weeks. Patient compliance was monitored by pill counts.

G. Waddell, R. I. Hadgnaft, E. C. Ruffner, and I. Weidner, *Science*, **196**, 533 (1977).
(3) S. M. Kupchan, D. C. Fessler, M. A. Eakin, and T. J. Giacobbe, *ibid.*, **168**, 376 (1970).
(4) R. L. Hanson, H. A. Lardy, and S. M. Kupchan, *ibid.*, **168**, 378 (1970).
(5) C. H. Smith, J. Larner, A. M. Thomas, and S. M. Kupchan, *Biochim. Biophys. Acta*, **276**, 94 (1972).
(6) P. Cohen and M. A. Rosemeyer, *Eur. J. Biochem.*, **8**, 1 (1969).
(7) M. A. Swanson, *J. Biol. Chem.*, **184**, 647 (1950).
(8) D. G. Walker and J. J. Parry, in "Methods in Enzymology," vol. 9, W. A. Wood, Ed., Academic, New York, N.Y., 1967, p. 381.
(9) J. A. Thomas, K. K. Schlinder, and J. Larner, *Anal. Biochem.*, **25**, 486 (1968).
(10) T. E. Mansour, in "Methods in Enzymology," vol. 9, W. A. Wood, Ed., Academic, New York, N.Y., 1967, p. 430.
(11) P. V. C. Pinto, A. Kaplan, and P. A. VanDreal, *Clin. Chem.*, **15**, 349 (1969).
(12) W. S. Allison, in "Methods in Enzymology," vol. 9, W. A. Wood, Ed., Academic, New York, N.Y., 1967, p. 210.
(13) M. K. Schwartz and O. Bodansky, in *ibid.*, p. 294.
(14) S. Ochoa, A. H. Mehler, and A. Kornberg, *J. Biol. Chem.*, **174**, 979 (1948).
(15) D. V. DerVartanian and C. Veerger, *Biochim. Biophys. Acta*, **92**, 233 (1964).
(16) E. M. Suolinna, R. N. Buchsbaum, and E. Racker, *Cancer Res.*, **35**, 1865 (1975).
(17) A. E. Senior, S. E. McGowan, and R. Hilf, *ibid.*, **35**, 2061 (1975).
(18) P. S. Basu, *Biochem. Pharmacol.*, **24**, 2269 (1975).
(19) Modified from S. Pontremoli, in "Methods in Enzymology," vol. 9, W. A. Wood, Ed., Academic, New York, N.Y., 1967, p. 625.
(20) P. S. Chen, T. Y. Toribara, and H. Warner, *Anal. Chem.*, **28**, 1756 (1956).
(21) O. H. Lowry, N. J. Rosebrough, A. L. Farr, and R. J. Randall, *J. Biol. Chem.*, **193**, 265 (1951).
(22) I. H. Hall and G. L. Carlson, *J. Med. Chem.*, **19**, 1257 (1976).
(23) F. Rupert, W. Thorne, and F. L. Bygnave, *Cancer Res.*, **33**, 2562 (1973).
(24) H. D. Haberman, *ibid.*, **35**, 3332 (1975).
(25) K. W. McKern, "Hormones and Cancer," Academic, New York, N.Y., 1974, pp. 261–307.
(26) R. F. W. Thorne and F. L. Bygnove, *Cancer Res.*, **33**, 2562 (1973).
(27) D. F. H. Wallach, "Membrane Molecular Biology of Neoplastic Cells," Elsevier, New York, N.Y., 1975, p. 257.
(28) M. Gosálvez, R. Garcia-Canero, M. Blauco, and C. Gurucharri-Lloyd, *Cancer Treatment Rep.*, **60**, 1 (1976).

ACKNOWLEDGMENTS

Supported by Grants CH-19 and IN15-P from the American Cancer Society to K. H. Lee and I. H. Hall, respectively, and in part by the National Cancer Institute (CA-17625).

Intrapatient Variability of Serial Steady-State Plasma Tricyclic Antidepressant Concentrations

V. E. ZIEGLER, L. T. WYLIE, and JOHN T. BIGGS ˣ

Received May 18, 1977, from the *Department of Psychiatry, School of Medicine, Washington University, St. Louis, MO 63110.* Accepted for publication July 5, 1977.

Abstract □ Nine or 10 serial steady-state plasma measurements of amitriptyline, desipramine, desmethyldoxepin, doxepin, imipramine, nortriptyline, or protriptyline were made in 23 depressed patients. Each patient was monitored for compliance by pill counts, and sampling time was controlled carefully to determine intrapatient variability of steady-state tricyclic levels on a day-to-day basis. The coefficients of variation during serial sampling of the various ingested drugs were: amitriptyline, 21%; desipramine, 26%; doxepin, 21%; imipramine, 14%; nortriptyline, 13%; and protriptyline, 17%. The therapeutic ranges for the tricyclic antidepressants are relatively wide, so coefficients of variation of these magnitudes indicate that the position of an individual patient in relation to the optimal therapeutic range can be reliably determined on a clinical basis.

Keyphrases □ Plasma drug levels—various tricyclic antidepressants, intrapatient variability at steady state □ Antidepressants, various—plasma drug levels, intrapatient variability at steady state

Although it has been over 10 years since Hammer *et al.* (1) first demonstrated a 36-fold difference between the lowest and highest steady-state levels of desipramine in patients ingesting equal amounts of the same drug, the use of plasma tricyclic antidepressant levels as a practical way to improve patient management is only slowly being accepted. Since the evidence that plasma drug levels more closely correspond to therapeutic response than oral dosage, there has been marked interest in the routine determination of plasma tricyclic antidepressant levels as a method of improving clinical response (2–8) and predicting toxicity (9).

Although therapeutic ranges have been suggested for most of the marketed tricyclic antidepressants, the interpretation of the results of plasma tricyclic determinations is often difficult. Differences in optimal plasma therapeutic ranges have been caused by varying purity of the standard drugs used, assay and blood collection methods, and the patient populations studied. In addition, day-to-day variation occurs in the steady-state level in individual patients. This variation is influenced not only by the reliability of the drug assay techniques but by biological variation within the individual.

The purpose of this study was to determine the variation for the entire procedure, controlling for such factors as is practical in a clinical setting.

EXPERIMENTAL

Plasma tricyclic antidepressant levels were assayed by GLC–mass fragmentography by a method described previously (10). This method is specific for each drug monitored and does not assay undescribed metabolites. Differences between duplicate samples are less than 10%.

To examine the biological and laboratory variability of steady-state plasma levels, outpatients undergoing treatment for depression on level doses of drug for at least 2 weeks were subjected to nine or 10 serial samplings over 3 weeks. Patient compliance was monitored by pill counts.

Table I—Tertiary and Secondary Amine Tricyclic Antidepressant Plasma Levels in Depressed Outpatients following Serial Plasma Sampling ($\bar{x} \pm SD$)

Patient	Daily Dosage, mg	Number of Samples	Tertiary Amine, ng/ml	Secondary Amine, ng/ml	Total Tricyclic, ng/ml
			Amitriptyline[a]		
1	100	9	58.6 ± 12.6	128.4 ± 36.1	187.0 ± 37.5
2	100	10	53.6 ± 8.3	24.4 ± 3.1	80.0 ± 8.1
3	100	9	37.8 ± 8.1	56.7 ± 2.2	94.4 ± 17.6
4	150	10	62.2 ± 17.7	91.8 ± 20.7	154.0 ± 22.4
			Doxepin[a]		
1	100	10	13.7 ± 3.1	15.7 ± 3.4	29.4 ± 5.3
2	100	10	9.2 ± 2.7	21.2 ± 1.2	30.2 ± 2.6
3	100	10	15.3 ± 6.2	23.1 ± 6.8	38.4 ± 12.6
4	100	9	145.8 ± 15.9	93.7 ± 14.6	239.4 ± 26.0
			Imipramine[a]		
1	150	10	79.7 ± 11.4	54.2 ± 8.4	133.9 ± 17.2
2	150	10	227.8 ± 25.7	162.9 ± 27.4	390.7 ± 43.9
3	200	10	78.3 ± 13.3	112.0 ± 17.5	190.3 ± 27.4
4	200	10	110.3 ± 10.4	111.4 ± 16.0	221.7 ± 18.2

[a] Compound ingested.

In all cases, samples were drawn at the same hour of the day, thus controlling for sampling time and dosage schedule on an individual basis. The samples were assayed in duplicate to determine the coefficient of variation for the entire procedure.

RESULTS AND DISCUSSION

Table I shows the number of patients ingesting each tertiary amine tricyclic antidepressant, the individual dosage, the number of samplings, the tertiary amine plasma level and its active secondary amine metabolite plasma level, and the total plasma tricyclic level. The mean plasma level ± *SD* is expressed in nanograms per milliliter.

For the tertiary amines, amitriptyline, doxepin, or imipramine, both the parent drug and the corresponding secondary amine desmethyl metabolites, nortriptyline, desmethyldoxepin, and desipramine, were measured. As expected, the plasma levels on similar dosages varied markedly from individual to individual. The coefficient of variation for total tricyclic was 21% for patients ingesting amitriptyline, 21% for doxepin, and 14% for imipramine. This variation includes both laboratory and biological variations, including drug compliance in the individual patient. Drug compliance by pill count was above 95% in all patients.

Table II presents data in the same manner for patients ingesting the secondary amine tricyclic antidepressants, desipramine, nortriptyline, and protriptyline. Plasma levels of patients on similar dosages again varied markedly. The coefficient of variation for desipramine was 26%; for nortriptyline, it was 13%; and for protriptyline, it was 17%. The optimal therapeutic ranges for the tricyclic antidepressants are relatively wide, 50–150 ng/ml for nortriptyline (2, 4, 6), which is the drug with the narrowest optimal therapeutic range. Therefore, a 13–26% coefficient of variation indicates that the position of an individual patient in relationship to the optimal therapeutic range can be determined reliably. This is also true for overdose patients who are toxic (9). Evidence from a study (9) of acute overdose patients indicates serious medical complications are more frequent when maximum total plasma tricyclic antidepressant levels are above 1000 ng/ml, with death occurring at considerably higher levels, yielding a therapeutic index of greater than 10.

Table II—Plasma Tricyclic Antidepressant Levels in Depressed Outpatients following Serial Plasma Sampling ($\bar{x} \pm SD$)

Patient	Daily Dosage, mg	Number of Samples	Level, ng/ml
		Desipramine[a]	
1	100	9	55.9 ± 15.5
2	100	10	62.4 ± 25.3
3	150	10	105.2 ± 21.9
4	200	10	217.7 ± 33.3
		Nortriptyline[a]	
1	100	10	125.6 ± 12.5
2	100	9	74.3 ± 12.5
3	100	10	65.1 ± 9.3
4	150	10	150.7 ± 19.2
		Protriptyline[a]	
1	20	9	111.6 ± 15.2
2	30	10	144.3 ± 29.4
3	40	10	164.2 ± 31.1

[a] Compound ingested.

In conclusion, the large interpatient variability of steady-state plasma tricyclic levels has been of interest to pharmacologists since its discovery. The clinician has now become aware of the usefulness of plasma tricyclic antidepressant levels. It is necessary to consider the assay methods employed and individual variations in steady-state plasma levels based on intraindividual biological variation for the practical interpretation of routine plasma tricyclic measurements. The coefficient of variation during steady state must be considered carefully when patients are at extremes of the optimal therapeutic range before dosage is adjusted; however, this variation is small enough to allow for control of patients within the optimal therapeutic ranges for the various tricyclic antidepressants.

REFERENCES

(1) W. Hammer, C. M. Idelström, and F. Sjöqvist, *Excerpta Med. Ser. 122*, **1967**, 301.

(2) M. Åsberg, B. Crönholm, F. Sjöqvist, and D. Tuck, *Br. Med. J.*, **3**, 331 (1971).

(3) R. A. Braithwaite, R. Goulding, G. Theano, J. Bailey, and A. Coppen, *Lancet*, **2**, 1297 (1972).

(4) P. Kragh-Sørensen, M. Åsberg, and C. Eggert-Hansen, *ibid.*, **1**, 113 (1973).

(5) S. F. Whyte, A. J. MacDonald, G. J. Naylor, and J. P. Moody, *Br. J. Psychiatry*, **128**, 384 (1976).

(6) V. E. Ziegler, B. T. Co, J. R. Taylor, P. J. Clayton, and J. T. Biggs, *Clin. Pharmacol. Ther.*, **19**, 735 (1976).

(7) V. E. Ziegler, P. J. Clayton, J. R. Taylor, B. T. Co, and J. T. Biggs, *ibid.*, **20**, 458 (1976).

(8) A. H. Glassman, J. M. Perel, M. Shostak, S. J. Kantor, and J. L. Fleiss, *Arch. Gen. Psychiatry*, **34**, 197 (1977).

(9) J. M. Petit, D. G. Spiker, J. F. Ruwitch, V. E. Ziegler, A. N. Weiss, and J. T. Biggs, *Clin. Pharmacol. Ther.*, **21**, 47 (1977).

(10) J. T. Biggs, W. Holland, S. S. Chang, P. P. Hipps, and W. R. Sherman, *J. Pharm. Sci.*, **65**, 261 (1976).

ACKNOWLEDGMENTS

Supported in part by Public Health Service Grants MH-25571 and RR-00954.

Paper Chromatographic Determination of Chlortetracycline

M. K. YOUSSEF *[x], I. A. ATTIA, and S. SAFWAT

Received September 16, 1976, from the *Department of Pharmaceutics, Faculty of Pharmacy, Assiut University, Assiut, Egypt.* Accepted for publication July 8, 1977. *Present address: Faculty of Pharmacy, Tanta University, Tanta, Egypt.

Abstract □ Chlortetracycline was successfully separated from its degradation products and from other tetracyclines on a paper chromatogram previously impregnated with a mixture of edetate disodium and urea solution in pH 5.0 McIlvaine buffer. Chlortetracycline separation from its degradation products and from both tetracycline and oxytetracycline was attributed primarily to the complexation of these antibiotics with urea and edetate on the chromatogram. The separated spots were located under UV light, and their R_f values were calculated. Chlortetracycline recovery from the paper chromatogram was satisfactory (98.3 ± 0.002%). The developed method was successfully applied to the determination of chlortetracycline in various dosage forms. In addition, the method was adequate for monitoring chlortetracycline hydrochloride stability in aqueous solutions.

Keyphrases □ Chlortetracycline—paper chromatographic analysis in pharmaceutical preparations □ Chromatography, paper—analysis, chlortetracycline in pharmaceutical preparations □ Antibacterials—chlortetracycline, paper chromatographic analysis in pharmaceutical preparations

Previously (1, 2), paper chromatographic methods were developed for the quantitative determination of oxytetracycline and tetracycline.

Urea was reported to increase the water solubility of chlortetracycline through complex formation (3, 4). The use of a mixture of urea and edetate disodium aqueous solutions as an immobile phase was successfully applied to the paper chromatographic determination of tetracycline in pharmaceutical formulations (2). The objective of the present investigation was to establish a precise quantitative paper chromatographic determination of chlortetracycline in various dosage forms and in the presence of its degradation products.

EXPERIMENTAL

Preparation of Degradation Products—Degradation products of chlortetracycline such as isochlortetracycline, α-aureomycinic acid, β-aureomycinic acid, anhydrochlortetracycline, and dedimethylaminoaureomycinic acid were prepared from chlortetracycline hydrochloride[1] according to reported methods (5). They were separated by partial neutralization of the reaction medium and then filtered through a sintered-glass funnel. The collected precipitate was washed with distilled water until chloride ions disappeared. The products were then dried at 60° over phosphorus pentoxide under vacuum. Melting points, absorption spectra, and paper chromatography data proved their identities.

Impregnating Solution—A 100-ml quantity was prepared by dissolving 5 g of urea and 2 g of edetate disodium in pH 5.0 McIlvaine buffer (6).

Running Solvent—A 90-ml quantity was prepared by mixing 60 ml of chloroform with 30 ml of acetone. The mixture was saturated with solid urea and edetate *disodium*.

Chromatographic Separation of Chlortetracycline—Two series of chromatographic papers[2] were impregnated with the impregnating solution and blotted between sheets of absorbent papers. Then 10 μl of fresh methanolic solutions (1 mg/ml) of each chlortetracycline (international standard)[1], isochlortetracycline, anhydrochlortetracycline, dedimethylaminoaureomycinic acid, α-aureomycinic acid, and β-aureomycinic acid was separately spotted on each chromatogram of the first series while still damp. The second series was separately spotted with 10 μl of the standard fresh methanolic solutions (1 mg/ml) of each chlortetracycline hydrochloride, tetracycline hydrochloride[3], oxytetracycline base[3], and their mixture. The previously published chromatographic procedure (1, 2) was then adopted. The R_f values of the separated spots were calculated (Table I).

Table I—R_f Values and Fluorescence Colors under UV Light of Separated Antibiotics

Product	Fluorescence under UV light	R_f Value
Chlortetracycline	Yellow	0.60
Tetracycline	Yellow	0.24
Oxytetracycline	Yellow	0.10
Isochlortetracycline	Blue	0.34
α-Aureomycinic acid	Violet	0.33
β-Aureomycinic acid	Pale violet	0.13
Anhydrochlortetracycline	Orange	0.99
Dedimethylaminoaureomycinic acid	Pale violet	0.39
Epichlortetracycline	Yellow	0.27 or 0.07

Quantitative Determination of Chlortetracycline—The previously reported horizontal-line technique (1, 2) was applied for the estimation of chlortetracycline in tablets, injections, drops, ointments, suspensions, and solutions. Aliquots of 200 μl of the antibiotic methanolic solution (200 μg) were spotted on the impregnated chromatographic papers. The separated antibiotic zone was eluted by 20 ml of dilute hydrochloric acid (pH 1.8). Chlortetracycline in the acid eluate was determined spectrophotometrically[4] at 368 nm (7).

The procedure previously adopted for preparing samples of oxytetracycline before application to the chromatographic papers (1) was successfully applied for chlortetracycline preparations (Table II).

RESULTS AND DISCUSSION

Paper chromatographic separation of chlortetracycline from its degradation products was found to be most efficient when using papers previously impregnated with a mixture of urea and edetate disodium solution in pH 5.0 McIlvaine buffer. Low R_f values or diffuse spots were observed by separate use of either urea or edetate disodium solutions, respectively. These results were consistent with those previously observed for tetracycline (2).

Table I presents the observed colors of the separated spots under UV light and their R_f values.

This procedure was successfully applied to chlortetracycline separation from either tetracycline or oxytetracycline (Table I). Chlortetracycline was characterized by the highest R_f value, followed in decreasing order by tetracycline and oxytetracycline. Complex formation between tetracycline or oxytetracycline and the components of the impregnating solution was previously proved (1, 2). When chlortetracycline was eluted from the chromatogram using pH 5.0 McIlvaine buffer, it showed a shift of τ_{max} toward the shorter wavelength, thus confirming antibiotic complexation on the chromatogram. The formed complexes of tetracycline and oxytetracycline on the chromatogram were more water soluble than the chlortetracycline complex (Table I). This result was confirmed by the observed relatively higher tendency of the chlortetracycline spot to move with the mobile phase on the chromatogram (high R_f value).

Sharp and complete separation of chlortetracycline from its decomposition products was achieved by applying not more than 20 μg of the antibiotic/spot on the chromatogram. This procedure necessitated the application of 200 μg of the antibiotic as a horizontal line on the chromatographic paper, providing a final concentration of 10 μg/ml in the eluate.

[1] Provided by Lederle Laboratories.
[2] Whatman No. 1.
[3] Provided by the World Health Organization.
[4] Carl Zeiss, Jena.

Table II—Stated and Found Potencies of Chlortetracycline Hydrochloride (I) and Chlortetracycline Base (II) in Different Pharmaceutical Formulations

Dosage Form[a]	Composition	Stated Potency	Found Potency[b], (% *SD*)
Tablets	Collected from market	250 mg/tablet	98.9 (±0.001)
Ointment 1	Collected from market	1% (w/w)	98.0 (±0.010)
Ointment 2	Collected from market	3% (w/w)	99.7 (±0.001)
Ointment 3	I + polyoxyethylene 20 sorbitan (1% w/w) + petrolatum	3% (w/w)	99.3 (±0.002)
Ointment 4	I + absorption ointment base[c]	3% (w/w)	99.3 (±0.002)
Ointment 5	I + wool alcohol ointment[d]	3% (w/w)	99.3 (±0.001)
Injection	Collected from market	500 mg/ampul	95.0 (±0.005)
Drops	Collected from market	5.0 mg/ml	96.0 (±0.005)
Solution 1	I	5.0 mg/ml	100 (±0.001)
Solution 2	I + sodium metabisulfite (0.2% w/v)	5.0 mg/ml	98.0 (±0.002)
Solution 3	I + magnesium chloride hexahydrate (1:1 molar ratio)	5.0 mg/ml	98.0 (±0.001)
Solution 4	I + calcium chloride (1:1 molar ratio)	5.0 mg/ml	100 (±0.006)
Solution 5	I + edetate disodium (1:1 molar ratio)	5.0 mg/ml	98.0 (±0.001)
Solution 6	I + propylene glycol (10% w/w)	5.0 mg/ml	100 (±0.001)
Solution 7	I + polyethylene glycol 400 (10% w/w)	5.0 mg/ml	100 (±0.001)
Solution 8	I + saccharin sodium (10% w/w)	5.0 mg/ml	100 (±0.002)
Solution 9	I + *p*-hydroxybenzoic acid (0.2% w/v)	5.0 mg/ml	98.0 (±0.006)
Solution 10	I + propylparaben (0.2% w/v)	5.0 mg/ml	98.0 (±0.005)
Solution 11	I + sorbic acid (0.5% w/v)	5.0 mg/ml	100 (±0.010)
Suspension 1	II + tragacanth (1.5% w/v)	125 mg/5 ml	100 (±0.002)
Suspension 2	II + tragacanth (0.5% w/v) + sodium alginate (1.5% w/v)	125 mg/5 ml	98.7 (±0.00)
Suspension 3	II + tragacanth (0.5% w/v) + aluminum magnesium silicate[d] (1.2% w/v)	125 mg/5 ml	99.2 (±0.003)
Suspension 4	II + tragacanth (0.5% w/v) + povidone (2% w/v)	125 mg/5 ml	98.7 (±0.001)
Suspension 5	II + tragacanth (0.5% w/v) + carboxymethylcellulose sodium (2% w/v)	125 mg/5 ml	100 (±0.003)
Suspension 6	II + tragacanth (0.5% w/v) + syrup (1% w/v)	125 mg/5 ml	99.2 (±0.001)
Suspension 7	II + tragacanth (0.5% w/v) + glycerin (1% w/v)	125 mg/5 ml	100 (±0.003)
Suspension 8	II + tragacanth (0.5% w/v) + sorbitol (10% w/v)	125 mg/5 ml	98.0 (±0.002)
Suspension 9	II + tragacanth (0.5% w/v) + glycerin (1% w/v) + carmine (1% w/v)	125 mg/5 ml	99.0 (±0.002)
Suspension 10	II + tragacanth (0.5% w/v) + syrup (1% w/v) + carmine (1% w/v) + vitamin B compound[e] (0.2% w/v)	125 mg/5 ml	98.0 (±0.004)

[a] The vehicle used in all solutions and suspensions was purified water. [b] Average of five determinations. [c] USP XVIII, 1970, p. 809. [d] Veegum HV. [e] The British Pharmaceutical Codex, 1973, p. 819.

The recovery of the antibiotic from the chromatogram was found to be satisfactory when using dilute hydrochloric acid (pH 1.8). Chlortetracycline hydrochloride (international standard) was chromatographed to calculate the percent recovery. Nine determinations gave an average recovery of 98.3 ± 0.002%. The slight loss of the antibiotic during elution was greatly compensated for by chromatographing a reference standard for each determination. The absence of degradation spots on rechromatographing the international chlortetracycline standard proved the high stability of this antibiotic during chromatography. The formation of only one defined spot on rechromatographing the acid eluate of international chlortetracycline standard indicated that the antibiotic was not decomposed in this solution for at least 1 hr.

Table II lists the composition and analysis of various chlortetracycline preparations. The found potencies of the tested dosage forms were close to their stated potencies. The additives in the tested formulations did not interfere with the chromatographic determinations of the antibiotic by the presented method. The use of 0.1 *N* HCl to extract the antibiotic from the ointments before application on the chromatogram was unsatisfactory since it interfered with the complexation of chlortetracycline on the chromatogram. The use of distilled water instead of 0.1 *N* HCl as an extracting medium for chlortetracycline hydrochloride ointments overcame this difficulty.

Table III—Stability of Chlortetracycline Hydrochloride Solution (5 mg/ml) in Distilled Water Containing 10% (w/v) Dimethylformamide

Days	Potency, % Microbiological Method	Potency, % Chromatographic[a] Method (%*SD*)
0	100	100 (0.004)
2	95	74.4 (0.001)
3	88	68 (0.04)
4	54.5	50.3 (0.01)
5	51.0	27.3 (0.01)
6	56.0	24.5 (0.01)

[a] Average of five determinations.

Table III shows the potency of chlortetracycline hydrochloride solution (5 mg/ml) in water containing 10% (w/v) dimethylformamide at various time intervals when stored at 40°. The antibiotic contents of the stored solutions were determined by both the prescribed method and the official microbiological procedure (8). Results of the present chromatographic procedure agreed well with the microbiological method for the undecomposed preparation (initial determination). The higher results obtained with the microbiological technique, compared to those obtained with the chromatographic method (Table III), might be attributed to the antimicrobial activity of the decomposition products of chlortetracycline. Table III also indicates that the established chromatographic method is satisfactory for monitoring chlortetracycline stability.

In conclusion, the described method is adequate as either a control assay or a stability-indicating assay for the selective determination of chlortetracycline in dosage forms.

REFERENCES

(1) A. Sina, M. K. Youssef, A. A. Kassem, and I. A. Attia, *J. Pharm. Sci.*, **60**, 1544 (1971).

(2) M. K. Youssef, El A. Ibrahim, and I. A. Attia, *ibid.*, **62**, 1998 (1973).

(3) S. B. Greenbaum, G. Richard, and H. C. Klein, U.S. pat. 3,632,647; through *Chem. Abstr.*, **76**, 72317 (1972).

(4) C. Kawarski, Israeli pat. 12,701 (May 25, 1960); through *Chem. Abstr.*, **54**, 14589 (1960).

(5) T. Korzybski, Z. K. Gindifer, and W. Kurylowicz, "Antibiotics, Origin, Nature and Properties," vol. 1, Pergamon Press, London, England, 1967, pp. 466–471, 480.

(6) "Documenta Geigy, Scientific Tables," 6th ed., Basle, Switzerland, 1962, p. 314.

(7) V. G. Makauvich and T. N. Laznikova, *Med. Prom. SSSR*, **19**, 51 (1965); through *Chem. Abstr.*, **63**, 9746h (1965).

(8) "The British Pharmacopoeia," The Pharmaceutical Press, London, England, 1968, pp. 1313–1317.

tert-Butoxycarbonyl as a Convenient Protecting Group in Synthesis of Potential Centrally Active Dopamine Derivatives

RICHARD B. WALKER, JAMES W. AYRES ˣ, JOHN H. BLOCK, and ALBERT LOCK

Received February 21, 1977, from the *Departments of Pharmaceutical Science and Pharmaceutical Chemistry, School of Pharmacy, Oregon State University, Corvallis, OR 97331.* Accepted for publication July 8, 1977.

Abstract □ Several pivaloyl and pivaloyloxy esters and amides of dopamine were synthesized for possible antiparkinson activity. The compounds were synthesized by select *O*- and *N*-acylation and *N*-methylation procedures. The *tert*-butoxycarbonyl function is an effective and easily removed nitrogen-protecting group for dopamine. Preliminary biological testing results showed that all compounds tested elicited a hypothermic response in mice, while only *O,O*-dipivaloyl-*N,N*-dimethyldopamine reversed reserpine-induced motor depression in mice. However, it is difficult to conclude from the preliminary data that the observed biological effects were due to central dopaminergic receptor stimulation.

Keyphrases □ Dopamine derivatives, various—synthesized with *tert*-butoxycarbonyl as protecting group, CNS activity evaluated in mice □ CNS activity—various dopamine derivatives synthesized with *tert*-butoxycarbonyl as protecting group, evaluated in mice □ Structure–activity relationships—various dopamine derivatives synthesized with *tert*-butoxycarbonyl as protecting group, CNS activity evaluated in mice

Various 3,4-diesters of dopamine have been proposed as agents capable of crossing the blood–brain barrier and activating central dopamine receptors by hydrolytic release of dopamine in the brain (1–4). *N,N*-Dimethyl-*O,O*-diacetyldopamine effectively induced hypothermia (5, 6) and partially reversed oxotremorine-induced tremor in mice (2). Casagrande and Ferrari (3) synthesized 4-pivaloyl- and 3,4-dipivaloyldopamine plus several other dopamine esters containing more bulky acyloxy groups and suggested, without providing pharmacological data, that these compounds would provide sufficient lipophilicity and resistance to hydrolysis for entry into the central nervous system (CNS) before releasing the parent phenethylamine.

BACKGROUND

Various peptides of levodopa (L-3,4-dihydroxyphenylalanine) (7) and dopamine (8, 9) have both peripheral and central dopaminergic activity. In mice, various carbamates of amphetamine readily entered the CNS and released free amphetamine in the brain (10). Several other carbamate-latentiated drugs, such as normeperidine (11) and chlorphentermine (12), also were reported to have similar activity to the parent drug.

These reports suggest that certain amides as well as esters of dopamine should be capable of crossing the blood–brain barrier, and subsequent hydrolysis would release dopamine at the desired site of action. Such compounds may be potentially useful as antiparkinson agents, eliminating the high doses and subsequent peripheral side effects associated with levodopa.

Esters (II–IV) and amides (V and VI) of dopamine (I) containing either the pivaloyl or pivaloyloxy function were, therefore, synthesized and examined in mice for hypothermic activity and the ability to reverse reserpine-induced motor depression.

RESULTS AND DISCUSSION

Chemistry—The search for labile, lipophilic, centrally active dopamine analogs has been somewhat hindered by lack of a good protective group for the amino function. The benzyloxycarbonyl function has been used most often (1, 3). However, upon *O*-acylation, *N*-benzyloxycarbonyldopamine often gives oily products that resist crystallization. Difficulties in removal of the benzyloxycarbonyl moiety and N→O acyl migration also have been reported (13). In light of these reports, a protecting group was sought that is easily introduced, readily gives crystalline derivatives upon *O*-acylation, and is easily removed to yield *O*-acyldopamines in good yield. The *tert*-butoxycarbonyl function was found to meet these requirements (14).

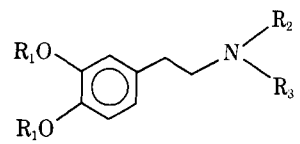

I: $R_1 = R_2 = R_3 = H$, hydrochloride
II: $R_1 = (CH_3)_3CCO$, $R_2 = R_3 = H$, hydrochloride
III: $R_1 = (CH_3)_3CCO$, $R_2 = R_3 = CH_3$, hydrochloride
IV: $R_1 = R_2 = (CH_3)_3CCO$, $R_3 = H$
V: $R_1 = (CH_3)_3CCO$, $R_2 = (CH_3)_3COCO$, $R_3 = H$
VI: $R_1 = R_3 = H$, $R_2 = (CH_3)_3COCO$

N-tert-Butoxycarbonyldopamine (VI) was synthesized from dopamine and *tert*-butoxyazidoformate in excellent yield. Best results were obtained by using a slight excess of reagent in the presence of triethylamine, with aqueous dioxane as the solvent. When a large excess of reagent was used, partial *O*-acylation occurred. The nitrogen-protecting group could be removed readily by treatment of VI with hydrogen chloride in ether.

Acylation of VI with pivaloyl chloride gave *N-tert*-butoxycarbonyl-*O,O*-dipivaloyldopamine (V); upon removal of the protecting group, V provided *O,O*-dipivaloyldopamine hydrochloride (II) in good yield. *N,N*-Dimethyl-*O,O*-dipivaloyldopamine (III) was synthesized from II by an adaption of the method of Schellenberg (13). The amine hydrochloride was dissolved in methanol and treated with formaldehyde and excess sodium borohydride. Treatment with hydrogen chloride in ether gave the hydrochloride. *O,O,N*-Tripivaloyldopamine (IV) was readily prepared from dopamine and excess pivaloyl chloride in high yield.

Biological Activity—Preliminary tests of five analogs of pivaloyl and pivaloyloxy esters and amides of dopamine were examined for potential antiparkinson activity. The two models used to estimate the agent's ability to stimulate dopaminergic receptors were the production of hypothermia (5, 6) and the antagonism of reserpine-induced motor depression in mice (15).

Barnett *et al.* (5) demonstrated that stimulation of dopaminergic receptors in the CNS produces hypothermia in mice. Horst *et al.* (15) demonstrated that reserpine-induced catatonia was reversed by levodopa and that this effect was directly correlated with brain dopamine levels. They suggested that the reversal of reserpine-induced catatonia is a good model to use in a search for antiparkinson drugs.

All compounds tested elicited hypothermic responses in mice 90 min after intraperitoneal injection. However, it is not possible to conclude from these preliminary results that the hypothermia elicited in mice following the administration of the test compounds was due to central dopaminergic stimulation, except perhaps for III, which also elicited a positive reserpine-induced motor depression reversal response.

EXPERIMENTAL

Chemistry—Melting points were determined in open glass capillaries and are uncorrected[1]. All compounds appeared as a single spot by TLC

[1] Thomas-Hoover Unimelt.

in two different solvent systems [petroleum ether–ether–chloroform (2:1:1) or butyl alcohol–chloroform (9:1)]. All compounds were characterized by elemental analyses[2], NMR spectroscopy[3], and IR spectroscopy[4].

N-tert-*Butoxycarbonyldopamine* (*VI*)—Dopamine hydrochloride (18 g, 0.1 mole) was dissolved in 70 ml of 70% aqueous triethylamine. The mixture was stirred in an ice bath under nitrogen, and a solution of 15 ml (0.015 mole) of *tert*-butoxycarbonyl azide in 50 ml of dioxane was added through a dropping funnel. The ice bath was removed, and the mixture was stirred 5 hr at room temperature under nitrogen. Water, 100 ml, was added, and the mixture was adjusted to pH 2 with 1 *N* HCl and then extracted with 2 × 75 ml of ether, which, in turn, was extracted with 100 ml of saturated aqueous sodium bicarbonate.

The ether layer was dried over anhydrous sodium sulfate, and the solvent was removed *in vacuo*, leaving a clear oil. This oil crystallized upon addition of petroleum ether, yielding 23.8 g (94%) of product. Recrystallization from benzene gave white crystals, mp 137–138°; IR: 1720 (ester, C=O), 1690 (amide, C=O), and 1520 (CN) cm^{-1}.

Anal.—Calc. for $C_{13}H_{19}NO_4$: C, 61.67; H, 7.51; N, 5.53. Found: C, 61.92; H, 7.53; N, 5.43.

N-tert-*Butoxycarbonyl*-O,O-*dipivaloyldopamine* (*V*)—Compound VI (2.41 g, 0.009 mole) was dissolved in 10 ml of triethylamine stirring in an ice bath under nitrogen. A solution of 3.6 ml (0.03 mole) of pivaloyl chloride in 10 ml of dioxane was added dropwise, and the mixture was stirred 2 hr at room temperature. Then water (50 ml) was added, and the pH was lowered to 4 with 1 *N* HCl. The mixture was extracted with 2 × 30 ml of ether, which, in turn, was extracted with 2 × 20 ml of saturated aqueous sodium bicarbonate.

The ether layer was dried over anhydrous sodium sulfate and removed *in vacuo*, yielding 4.7 g of clear oil. This oil crystallized upon standing overnight in a refrigerator; the yield was 3.3 g (87%). Petroleum ether crystallization gave 2.8 g of white crystals, mp 94–95°; IR: 1720 (ester, C=O) and 1690 (amide, C=O) cm^{-1}.

Anal.—Calc. for $C_{23}H_{35}NO_5$: C, 68.15; H, 9.64; N, 3.46. Found: C, 67.92; H, 8.68; N, 3.57.

O,O-*Dipivaloyldopamine Hydrochloride* (*II*)—Compound V (4.24 g, 0.01 mole) was dissolved in 25 ml of dry ether through which was passed a stream of hydrogen chloride gas for 10 min. The flask was stoppered and refrigerated for 1 hr. Then the ether was removed *in vacuo*, leaving a glassy solid. This solid solidified on standing in petroleum ether; the yield was 2.8 g (80%). Recrystallization from benzene–petroleum ether gave the pure product, mp 175–176°; IR: 1720 (ester, C=O) cm^{-1}.

Anal.—Calc. for $C_{18}H_{28}ClNO_4$: C, 60.42; H, 7.83; Cl, 9.93; N, 3.92. Found: C, 60.15; H, 7.81; Cl, 9.83; N, 3.94.

N,N-*Dimethyl*-O,O-*dipivaloyldopamine Hydrochloride* (*III*)—Compound II (1.8 g, 0.005 mole) was dissolved in 15 ml of absolute methyl alcohol, and 1.0 ml of 37% formaldehyde was added. Sodium borohydride, 1.0 g (0.025 mole), was added over 15 min. The mixture was then cooled to room temperature. Another 1.0 ml of formaldehyde was added, and the mixture was stirred 30 min. Then 20 ml of water was added, and the mixture was extracted with 3 × 20 ml of ether.

The ether layers were dried over anhydrous sodium sulfate and removed *in vacuo*, leaving a clear oil. This oil was dissolved in benzene saturated with hydrogen chloride gas. Removal of solvents gave 0.6 g (31%) of white crystals, mp 196–198°. Recrystallization from benzene–petroleum ether gave the pure product; IR: 1720 (ester, C=O) cm^{-1}.

Anal.—Calc. for $C_{20}H_{32}ClNO_4$: C, 62.23; H, 8.30; Cl, 9.21; N, 3.63. Found: C, 61.21; H, 8.20; Cl, 9.29; N, 3.78.

O,O,N-*Tripivaloyldopamine* (*IV*)—Dopamine hydrochloride (1.89 g, 0.01 mole) was placed in 20 ml of triethylamine–dioxane (1:1). Pivaloyl chloride (4.8 ml, 0.04 mole) was added dropwise under nitrogen, and the mixture was stirred for 2 hr at room temperature. Water (50 ml) was added, and the mixture was extracted with 3 × 25 ml of ether, which, in turn, was extracted with 2 × 25 ml of 0.1 *N* HCl.

The ether layer was dried over anhydrous sodium sulfate, filtered over charcoal, and removed *in vacuo*, leaving a golden oil. This oil crystallized upon addition of petroleum ether; the yield was 3.5 g (86%) of white crystals. Recrystallization from petroleum ether–benzene gave the pure product, mp 100–101°; IR: 1720 (ester, C=O) and 1680 (amide, C=O) cm^{-1}.

Anal.—Calc. for $C_{23}H_{35}NO_5$: C, 68.15; H, 8.64; N, 3.46. Found: C, 68.07; H, 8.68; N, 3.64.

Biology—Male albino mice[5], 20–30 g, were used in groups of three for each test compound in all experiments. Arbitrary doses of 250 mg/kg ip were used for the hypothermia testing; 125 mg/kg ip was used for the reserpine-induced motor depression reversal test. Rectal temperatures were measured by an electronic thermometer[6]. Motor activities were recorded on an activity counter[7].

Compounds I–III were dissolved in normal saline. Compounds IV–VI were dissolved in an ethanol–propylene glycol (1:3) solution. Reserpine[8] (5 mg/kg ip) was administered 24 hr prior to testing. All solutions were prepared immediately prior to use.

REFERENCES

(1) R. Borgman, J. J. McPhilips, R. E. Stitzel, and I. J. Goodman, *J. Med. Chem.*, **16**, 630 (1973).

(2) R. J. Borgman, M. R. Baylor, J. J. McPhilips, and R. E. Stitzel, *ibid.*, **17**, 427 (1974).

(3) C. Casagrande and G. Ferrari, *Farmaco, Ed. Sci.*, **28**, 143 (1973).

(4) R. M. Pinder, *Nature (London)*, **228**, 358 (1970).

(5) A. Barnett, J. Goldstein, and R. I. Taber, *Arch. Int. Pharmacodyn. Ther.*, **198**, 242 (1972).

(6) K. Fuxe and F. Sjoqvist, *J. Pharm. Pharmacol.*, **24**, 702 (1972).

(7) J. H. Biel, P. Somani, F. N. Minard, and L. J. Goldberg, "Frontiers in Catecholamine Research," Pergamon Press, London, England, 1973, pp. 901–903.

(8) A. M. Felix, D. P. Winter, S. S. Wang, I. D. Kulesha, W. R. Pool, D. L. Hane, and H. Sheppard, *J. Med. Chem.*, **17**, 422 (1974).

(9) A. M. Felix, *Chem. Abstr.*, **77**, 62317g (1972).

(10) A. J. Verbiscar and L. G. Abood, *J. Med. Chem.*, **13**, 1176 (1970).

(11) S. M. Kupchan and A. C. Isenberg, *ibid.*, **10**, 960 (1967).

(12) P. Bjurulf, S. Carlstrom, and G. Rorsman, *Acta Med. Scand. Soc.*, **182**, 273 (1967).

(13) K. A. Schellenberg, *J. Org. Chem.*, **28**, 3259 (1963).

(14) L. A. Carpino, C. A. Giza, and B. A. Carpino, *J. Am. Chem. Soc.*, **81**, 955 (1959).

(15) W. D. Horst, W. R. Pool, and H. E. Spiegel, *Eur. J. Pharmacol.*, **21**, 337 (1973).

ACKNOWLEDGMENTS

Presented at the Medicinal Chemistry Section, APhA Academy of Pharmaceutical Sciences, Orlando meeting, November 1976.

The authors express their appreciation to Abayomi Obadeyi for assistance in the synthesis and biological evaluation of the compounds.

[2] Chemical Analytical Service, Berkeley, Calif.

[3] Varian Associates model EM-360 with tetramethylsilane as the internal standard.

[4] Perkin-Elmer model 727.

[5] Carworth Farms No. 1.

[6] TRI Instruments.

[7] Lehigh Valley Electronics.

[8] Ciba Pharmaceutical Co.

Drug Absorption VIII: Kinetics of GI Absorption of Methotrexate

VINOD S. CHUNGI, DAVID W. A. BOURNE, and LEWIS W. DITTERT ˣ

Received March 12, 1977, from the *College of Pharmacy, University of Kentucky, Lexington, KY 40506.* Accepted for publication July 15, 1977.

Abstract □ The absorption of methotrexate from the lumen of the rat small intestine, *in situ*, was found to obey Michaelis–Menten kinetics. The values of V_{max} and K_m for the absorption process were 4.78×10^{-7} M/min and 1.49×10^{-5} M, respectively.

Keyphrases □ GI absorption—methotrexate from rat small intestine *in situ* □ Absorption, GI—methotrexate from rat small intestine *in situ* □ Methotrexate—GI absorption from rat small intestine *in situ* □ Antineoplastic agents—methotrexate, GI absorption from rat small intestine *in situ*

Previous papers in this series dealt with passive drug absorption from the rat GI lumen *in situ*. In some cases, the unionized drug form was the only species absorbed (1); in other cases, significant absorption of drug ions was observed (2). The blood perfusion rate of the GI membrane affected the passive absorption rate (3), but other physiological factors and the active pumping of a drug across the membrane have not been studied.

Methotrexate uptake by L-1210 mouse leukemia cells (4) and by other *in vivo* tissue and organ systems (5) was described in terms of Michaelis–Menten enzyme kinetics. It also was suggested that the GI absorption of methotrexate in mice is a saturable process (6), but the absorption kinetics have not been studied directly.

This study determined if methotrexate uptake from the lumen of the rat small intestine *in situ* obeys Michaelis–Menten enzyme kinetics and evaluated the kinetic uptake parameters.

EXPERIMENTAL

Male Sprague–Dawley rats[1], 200–250 g, were kept under observation for 7–10 days. Food was withdrawn 16–20 hr prior to the experiments, but water was allowed *ad libitum*. The rats were weighed and anesthetized with injections of ketamine hydrochloride[2], 60 mg/kg im, and pentobarbital sodium[3], 21 mg/kg ip. When additional doses of anesthetic were needed during an experiment, one-third of the initial doses of both agents were administered by the same routes.

Isolation and cannulation of the small intestine were carried out as previously described (1). The intestine was washed with normal saline. The drug solution was instilled, and 0.1-ml samples were collected every 5 min for 30 min.

Methotrexate[4] was prepared as a 10^{-4} M stock solution in 0.2% sodium bicarbonate and stored at 4° in a flask wrapped in aluminum foil. Although such solutions are stable for over 1 month (7), fresh stock solutions were prepared weekly. A stock solution of 3′,5′,9(*n*)-^{3}H-methotrexate sodium salt[5] in water was prepared such that 100 μl contained 0.1 μCi of radioactivity (2×10^{-11} mole of methotrexate). The stock solution containing radioactive methotrexate was frozen and stored in an amber multidose container under nitrogen.

Solutions for instillation into the intestine were prepared by diluting the stock solution of methotrexate to the desired concentration with normal saline and adding 100 μl of the radiolabeled stock solution. Thus, the radiolabeled methotrexate did not add significantly to the total concentrations of the solutions.

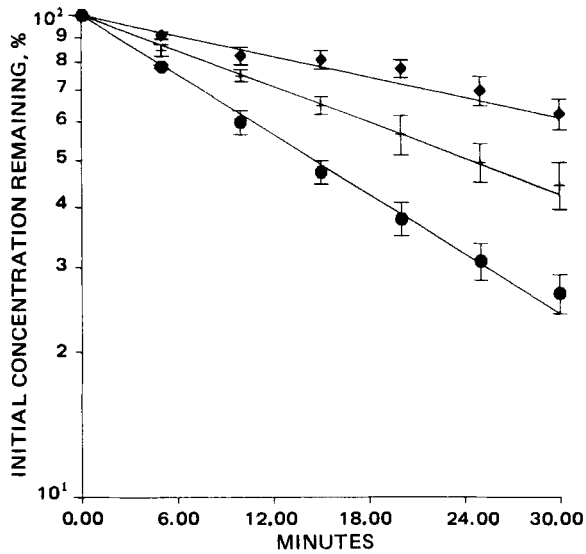

Figure 1—*Semilog plot of percent of initial concentration of methotrexate remaining* versus *time in the lumen of the* in situ *rat small intestine. The points are observed values (±SD). Initial concentrations of methotrexate were 1×10^{-5} M (◆), 1×10^{-6} M (+), and 1×10^{-8} M (●).*

The disappearance of methotrexate from the gut lumen was followed by removing 0.1-ml samples at 5-min intervals, diluting the samples in 15 ml of a scintillation cocktail [2,5-diphenyloxazole[6] (4 g), 1,4-bis[2-(5-phenyloxazolyl)]benzene[6] (0.1 g), octoxynol[6] (360 g), and toluene[6] (*q.s.* to 1000 ml)], and counting on a scintillation counter[7]. The counting efficiency was 26%. To confirm that the scintillation counting reflected only absorption of unchanged methotrexate, several samples at several concentrations from different animals were subjected to TLC analysis. Samples removed at 5, 15, and 30 min were spotted on TLC plates[8] and developed with acetic acid–acetone–methanol–benzene (5:5:20:70). After development, the chromatogram was scanned with a radiochromatogram scanner[9]. Each chromatogram contained only one spot. This spot had an R_f value identical to that of unchanged methotrexate.

RESULTS AND DISCUSSION

Semilogarithmic plots of percent of initial concentration of methotrexate remaining unabsorbed *versus* time are shown in Fig. 1. The apparent half-life of the absorption process increased from 15 min with an initial methotrexate concentration of 10^{-8} M to 45 min with an initial methotrexate concentration of 10^{-5} M. This decreasing absorption rate with increasing initial concentration of methotrexate indicated that absorption was nonlinear.

Figure 2 shows a plot of the fraction of administered dose absorbed from the gut lumen after 30 min *versus* the initial methotrexate concentration for a wide range of initial methotrexate concentrations. The

[1] Charles Rivers, Wilmington, MA 01887.
[2] Ketaject, Bristol Laboratories, Syracuse, NY 13201.
[3] Nembutal Sodium solution, Abbott Laboratories, North Chicago, IL 60064.
[4] Lederle Laboratories, Division of American Cyanamid Co., Pearl River, NY 10965.
[5] Amersham/Searle Corp., Arlington Heights, IL 60005.
[6] Scintillation grade, Research Products International Corp., Elk Grove Village, IL 60007.
[7] Packard Tri-Carb model 3375, Packard Instrument Co., Downers Grove, Ill.
[8] Silica gel G, EM Reagents Division, Brinkmann Instruments, Westbury, NY 11590.
[9] Model 7201, Packard Instrument Co., Downers Grove, Ill.

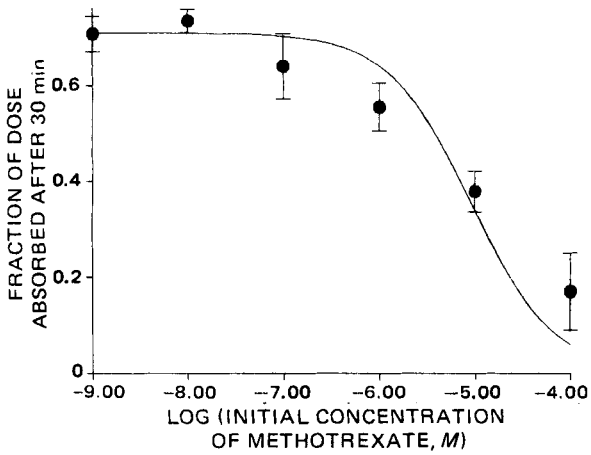

Figure 2—*Plot of fraction of dose absorbed after 30 min* versus *log (initial methotrexate concentration). The points were experimentally observed* (±SD), *and the line was calculated using Eq. 1 with* $K_m = 1.07 \times 10^{-5}$ M *and* $F_{max} = 0.71$.

value of F_{max} was used because the initial velocity could not be measured accurately at higher concentrations; therefore, this type of plot, obtained over a wide range of concentrations, gave an initial estimate of K_m for further investigations. At initial methotrexate concentrations greater than 10^{-7} M, there was a marked reduction in the fraction of the dose absorbed in 30 min, suggesting that the absorption process became saturated above this initial concentration.

The data shown in Fig. 2 were fitted, using the NONLIN program (8), to the following Michaelis–Menten equation (9):

$$F = (F_{max}K_m)/(K_m + X) \qquad \text{(Eq. 1)}$$

where F is the fraction of the administered dose absorbed after 30 min, F_{max} is the maximum fraction absorbed in 30 min, K_m is the Michaelis constant, and X is the initial concentration of methotrexate instilled in the gut lumen. The NONLIN calculated value of K_m was $1.07 \pm 0.35 \times 10^{-5}$ M, and the calculated value of F_{max} was 0.71 ± 0.03. These values and Eq. 1 were used to generate the lines in Fig. 2.

To obtain more accurate estimates of the Michaelis–Menten parameters, the absorption kinetics were further investigated using a narrow range of initial methotrexate concentrations near the calculated K_m value

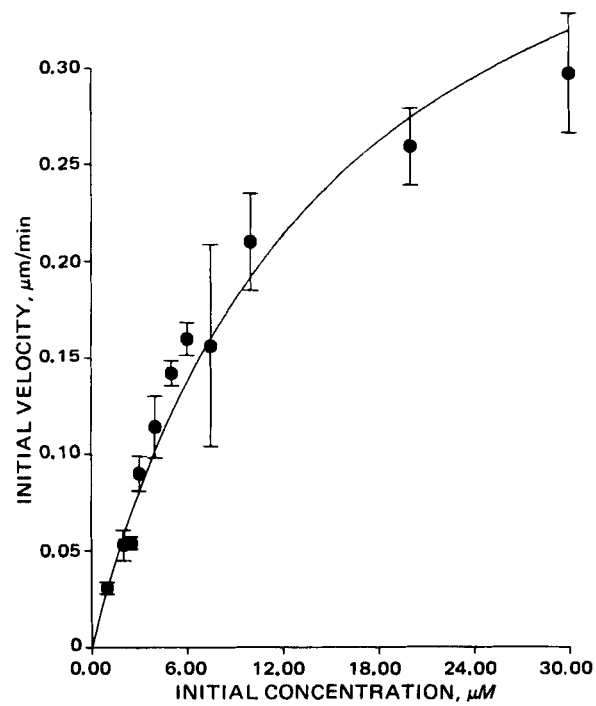

Figure 3—*Plot of initial velocity* versus *initial concentration. The points were experimentally observed* (±SD), *and the line was calculated using Eq. 2 with* $K_m = 1.49 \times 10^{-5}$ M *and* $V_{max} = 4.78 \times 10^{-7}$ M.

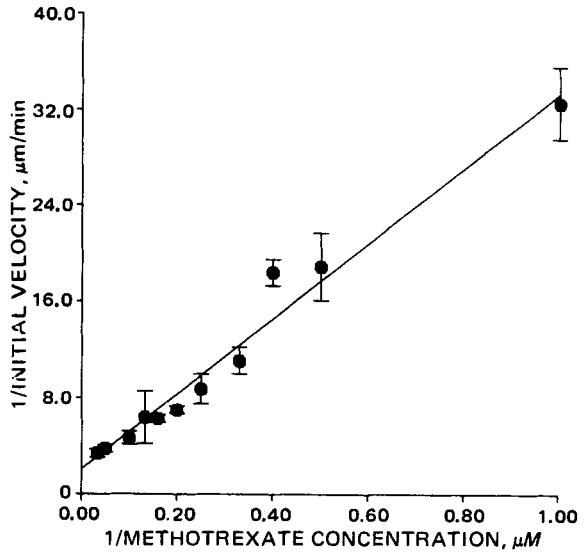

Figure 4—*Lineweaver–Burk-type plot of the data shown in Fig. 3. The points* (±SD) *were experimentally determined.*

of 1.07×10^{-5} M. Figure 3 shows a plot of the initial velocity of absorption *versus* the initial methotrexate concentration from 1×10^{-6} to 3×10^{-5} M. These data were fitted, using the NONLIN program, to the following Michaelis–Menten equation (9):

$$V = (V_{max}X)/(K_m + X) \qquad \text{(Eq. 2)}$$

where V is the observed initial velocity, V_{max} is the maximum initial velocity, and K_m and X are as defined in Eq. 1. During the fitting procedure, the data were weighted by the reciprocal of the variance. The variance of each point was calculated following linear regression of log (observed standard deviation)^2 *versus* log V (10). The calculated values of V_{max} and K_m were $4.78 \pm 0.75 \times 10^{-7}$ M/min and $1.49 \pm 0.32 \times 10^{-5}$ M. Figure 4 is a Lineweaver–Burk-type plot (11) of the data shown in Fig. 3. The solid lines in Figs. 3 and 4 were generated using Eq. 2 with $V_{max} = 4.78 \times 10^{-7}$ M/min and $K_m = 1.49 \times 10^{-5}$ M.

Absorption was saturable at a relatively low methotrexate concentration, suggesting that saturation could occur following therapeutic administration of methotrexate. This result is consistent with reports that higher methotrexate doses are incompletely absorbed in humans (12).

This study also demonstrates the utility of the *in situ* rat small intestine preparation for investigating active absorption processes.

REFERENCES

(1) J. T. Doluisio, N. F. Billups, L. W. Dittert, E. T. Sugita, and J. V. Swintosky, *J. Pharm. Sci.*, **58,** 1196 (1969).

(2) W. G. Crouthamel, G. H. Tan, L. W. Dittert, and J. T. Doluisio, *ibid.*, **60,** 1160 (1971).

(3) W. G. Crouthamel, L. Diamond, L. W. Dittert, and J. T. Doluisio, *ibid.*, **64,** 664 (1975).

(4) D. Goldman, N. S. Lichtenstein, and V. T. Oliverio, *J. Biol. Chem.*, **243,** 5007 (1968).

(5) R. L. Dedrick, D. S. Zaharko, and R. J. Lutz, *J. Pharm. Sci.*, **62,** 882 (1973).

(6) K. B. Bischoff, R. L. Dedrick, D. S. Zaharko, and J. A. Longstreth, *ibid.*, **60,** 1128 (1971).

(7) J. M. Kinkade, W. R. Vogler, and P. G. Dayton. *Biochem. Med.*, **10,** 337 (1974).

(8) C. M. Metzler, G. L. Elfing, and A. J. McEwen, "A User's Manual for NONLIN and Associated Programs," Research Biostatistics, Upjohn Co., Kalamazoo, Mich., Apr. 1974.

(9) L. Michaelis and M. L. Menten, *Biochem. Z.*, **49,** 333 (1913).

(10) J. G. Wagner, "Fundamentals of Clinical Pharmacokinetics," Drug Intelligence Publications, Hamilton, Ill., p. 289.

(11) H. Lineweaver and D. Burk, *J. Am. Chem. Soc.*, **56,** 658 (1934).

(12) "The Pharmacological Basis of Therapeutics," 5th ed., L. S. Goodman and A. Gilman, Eds., Macmillan, New York, N.Y., 1975, p. 1271.

Effects of Quinone Derivatives on an Experimental Tumor

M. M. de OLIVEIRA ˣ, M. C. F. LINARDI, and M. R. P. SAMPAIO

Received December 14, 1976, from the *Department of Pharmacology, Instituto Biológico de São Paulo, São Paulo, Brazil.* Accepted for publication July 11, 1977.

Abstract □ In continuation of studies on the activity of known solid tumor inhibitors, four acetylated glycosyl derivatives of 1,4-quinones were prepared and tested against Ehrlich ascitic tumor. All four compounds significantly inhibited growth of this neoplasm. UV, IR, and mass spectra are given for the three new synthetic quinone derivatives.

Keyphrases □ Quinone derivatives, acetylglycosyl—synthesized, evaluated for antitumor activity in mice □ Antitumor activity—various acetylglycosyl quinone derivatives evaluated for antitumor activity in mice □ Structure-activity relationships—various acetylglycosyl quinone derivatives evaluated for antitumor activity in mice

In the search for broader spectrum antitumor activity similar to that previously found with a lapachol derivative against leukemia P-388 (1), acetylated glycosides of natural quinones were prepared and tested against Ehrlich carcinoma.

Acetylated glucosides or galactosides of lawsone (2-hydroxy-1,4-naphthoquinone) (I), juglone (5-hydroxy-1,4-naphthoquinone) (II), and lapachol [2-hydroxy-3-(3-methyl-2-butenyl)-1,4-naphthoquinone] (III) were synthesized as derivatives. Juglone, found in *Juglans regia* L. (walnut), has been used as a fungicide in dermatosis (2); lawsone, from *Lawsonia alba* Lam. (Lythraceae) (henna), was known in ancient Egypt (2) as a component of cosmetics; several species of *Biognoneaceae* produce lapachol, a drug that has been studied for anticancer activity in its natural form or as derivatives (1, 3).

Normalization of glucose metabolism in tumor brain sections by natural glycosides differs according to the sugar moiety (4); for this reason, both galactose and glucose derivatives of lawsone were synthesized. Previous work (3, 5, 6) showed that both juglone and lapachol inhibit solid tumors (Walker carcinosarcoma 256 and Ehrlich solid carcinoma), while juglone and lawsone are effective against sarcoma 180. The purpose of this study was to investigate the action of derivatives of these quinones on the Ehrlich ascitic tumor.

EXPERIMENTAL[1]

2-(Tetraacetyl-β-D-galactopyranosyloxy)-1,4-naphthoquinone (IV)—To a solution of lawsone (870 mg, 5 mmoles) and 2,3,4,6-tetra-acetyl-α-galactopyranosyl bromide (2.877 g, 7 mmoles) in dry pyridine (20 ml) was added freshly prepared silver carbonate (966 mg, 3.5 mmoles). The mixture was stirred for 3 hr, the silver salts were filtered and washed with methanol, and the combined filtrates were treated with 5% aqueous acetic acid (200 ml). The resulting brown precipitate was washed with distilled water and dissolved in acetone; the residual salts were filtered, and the solution was then evaporated under vacuum.

The obtained solid was dissolved in chloroform and purified by silica gel column chromatography with elution using ethyl acetate. Compound IV was crystallized from ethyl acetate–methanol in a 756-mg yield (1.5 mmoles, 30%), mp 212–213°; IR (ν_{max}): 1740 (acetate), 1660 and 1680 (quinone), and 1240 (CO) cm^{-1}; UV (λ_{max}): 330 (log ϵ 3.83), 273 (4.31), 249 (4.36), and 243 (4.37) nm; mass spectrum: *m/e* 504 (0.1, M^+) and 331 (39, tetraacetylgalactose fragment).

Anal.—Calc. for $C_{24}H_{24}O_{12}$: C, 57.14; H, 4.76. Found: C, 57.11; H, 4.69.

2-(Tetraacetyl-β-D-glucopyranosyloxy)-1,4-naphthoquinone (V)—This compound was prepared by the same procedure as IV, using

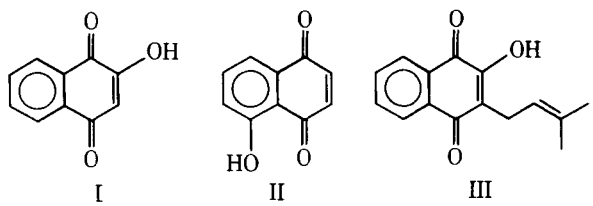

I II III

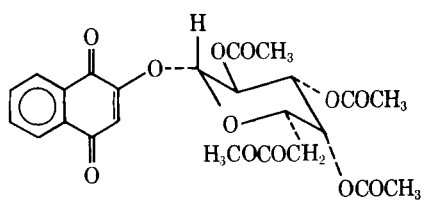

IV

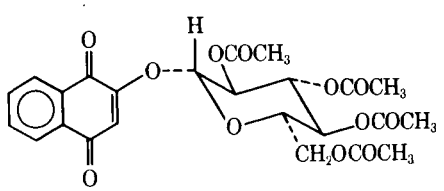

V

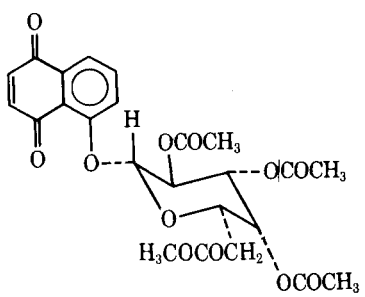

VI

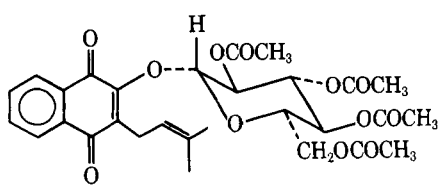

VII

[1] Melting points were measured on a modified Köfler block and are uncorrected. Elemental analyses were performed on a Hitachi 026 apparatus at the Instituto de Pesquisas Technológicas, São Paulo, Brazil. IR spectra were recorded in potassium bromide pellets on a Perkin-Elmer 124 spectrophotometer. UV spectra were recorded in methanol solution on a Perkin-Elmer 521 spectrophotometer. Mass spectra (70 ev) were run on a Hitachi RMU-7MG spectrometer at the Instituto de Pesquisas Technológicas. Lawsone and juglone were purchased from Kock-Light (England).

Table I—Activity of 1,4-Naphthoquinones and Their Glycosyl Derivatives against Ehrlich Ascites Carcinoma

Compound	Dose, mg/kg	Tumor Inhibition, %	Number of Survivors at Day 12	Weight Difference at Day 5
II	2.0	100.0	5/6	−2.5
	2.0	100.0	5/6	−2.7
	1.5	76.5	6/6	−1.1
	1.5	57.0	6/6	−1.7
VI	6.5	100.0	6/6	−1.4
	6.5	98.0	6/6	−2.5
	4.0	99.5	6/6	−2.1
	4.0	80.4	6/6	−2.2
I	10.0	0.0	6/6	−0.8
	10.0	0.0	5/6	−0.8
	8.0	0.0	6/6	−0.8
	8.0	0.0	6/6	+1.0
V	14.0	99.0	6/6	−1.6
	14.0	100.0	6/6	−2.3
	9.0	98.8	6/6	−1.6
	9.0	69.7	5/6	−1.7
IV	18.0	100.0	4/6	−6.0
	18.0	100.0	6/6	−3.2
	14.0	100.0	6/6	−2.9
	14.0	100.0	5/6	−3.9
	9.0	86.0	5/6	−3.5
	9.0	99.7	6/6	−2.5
III	150.0	12.0	6/6	−1.3
	150.0	0.0	4/6	−1.4
VII	150.0	95.4	6/6	−0.4
	150.0[a]	99.6	6/6	−5.6

[a] Not injected on 7th day.

lawsone (870 mg, 5 mmoles), 2,3,4,6-tetraacetyl-α-D-glucopyranosyl bromide (2.877 g, 7 mmoles), and active silver carbonate (966 mg, 3.5 mmoles) in dry pyridine (20 ml). The yield of glucosyl derivative was 697 mg (1.38 mmoles, 27.6%), mp 136–138° (ethyl acetate–methanol); IR (ν_{max}): 1740 (acetate), 1660 and 1680 (quinone), and 1230 (CO) cm^{-1}; UV (λ_{max}): 330 (log ϵ 3.80), 270 (4.31), 248 (4.35), and 243 (4.36) nm; mass spectrum: *m/e* 504 (0.2, M^+) and 331 (44, tetraacetylglucose fragment).

Anal.—Calc. for $C_{24}H_{24}O_{12}\cdot 0.25H_2O$: C, 56.64; H, 4.81. Found: C, 56.70; H, 4.75.

5-(Tetraacetyl-β-D-galactopyranosyloxy)-1,4-naphthoquinone (VI)—This compound was prepared by the same procedure as IV, using juglone (435 mg, 2.5 mmoles), 2,3,4,6-tetraacetyl-α-D-galactopyranosyl bromide (1.562 g, 3.8 mmoles), and active silver carbonate (469 mg, 1.7 mmoles) in dry pyridine (10 ml). The yield of galactosyl derivative was 302 mg (0.6 mmole, 24%), mp 80–82° (ethyl acetate–methanol); IR (ν_{max}): 1740 (acetate), 1650 and 1670 (quinone), and 1230 (CO) cm^{-1}; UV (λ_{max}) 250 nm (sh); mass spectrum: *m/e* 504 (0.1, M^+).

Anal.—Calc. for $C_{24}H_{24}O_{12}\cdot 0.25H_2O$: C, 56.64; H, 4.81. Found: C, 56.50; H, 5.06.

Lapachol (III)—Lapachol was extracted from *Tabebuia avellanedae* as described previously (1), mp 140°. The IR spectrum was superimposable on that of an authentic sample.

2-(3-Methyl-2-butenyl)-3-(tetraacetyl-β-D-glucopyranosyloxy)-1,4-naphthoquinone (VII)—The derivative was obtained from a solution of lapachol (1.210 g, 5 mmoles) and 2,3,4,6-tetraacetyl-α-D-glucopyranosyl bromide (2.877 g, 7 mmoles) by the same methods as the other derivatives. The yield was 458 mg (0.8 mmole, 18%), mp 62–65° dec.; the IR spectrum was superimposable on that of the previously prepared sample (1).

Biological Tests—The procedure of the National Cancer Institute was used (7). Swiss mice were inoculated with 5×10^6 viable cells of Ehrlich ascitic tumor from a donor 7 days after the cell passage. The drug was homogenized in a mortar with acetone (2%) and polysorbate 80 detergent (two drops). Controls received water, detergent, and acetone in the same proportion as used in the drug homogenate.

Drug treatment was given from the 1st to the 7th day. The animals were sacrificed on the 12th day, and the ascitic liquid was withdrawn and weighed. An experiment, to be valid, had to show more than 65% survivors on the day of evaluation.

Inhibition values equal to or higher than 58% were considered demonstrative of drug activity.

RESULTS AND DISCUSSION

All synthesized compounds showed activity on Ehrlich ascitic tumor (Table I). Of the parent quinones, only juglone inhibited tumor development; lapachol and lawsone were inactive. There seemed to be no modification in the anticancer effect when glucose or galactose derivatives were used; the activities of the two lawsone derivatives were very similar (Table I).

Improper homogenization probably accounted for the weight variations observed in experiments with the lapachol derivative (Table I). No better results could be obtained, however, in experiments with most of the other permitted vehicles (7).

In some experiments, 100% inhibition was obtained, and a pronounced reduction of ascites was found with all doses used. Although the growth of Ehrlich ascites cell tumor is fairly sensitive to many foreign materials, the protective effect of the glycosyl derivatives and the inactivity of the parent dihydroxyquinones (excepting juglone) point to a striking improvement over the capacity of the original compounds for being absorbed by the tumor cell.

REFERENCES

(1) M. C. F. Linardi, M. M. de Oliveira, and M. R. P. Sampaio, *J. Med. Chem.*, **18**, 1159 (1975).

(2) R. H. Thompson, "Naturally Occurring Quinones," 2nd ed., Academic, London, England, 1971, pp. 221, 222.

(3) J. L. Hartwell and B. J. Abbott, *Adv. Pharmacol. Chemother.*, **7**, 170 (1969).

(4) J. Dittmann, H. D. Hermann, and H. Palleske, *Arzneim.-Forsch.*, **21**, 1999 (1971).

(5) O. Gonçalves de Lima, G. M. Maciel, L. L. de Oliveira, A. L. Lacerda, L. C. Moreira, and D. G. Martins, *Rev. Inst. Antibiot.*, **12**, 3 (1972).

(6) O. Gonçalves de Lima, J. S. B. Coelho, I. L. D'Albuquerque, J. F. de Mello, D. G. Martins, A. L. Lacerda, and M. A. Moraes e Souza, *ibid.*, **11**, 21 (1971).

(7) R. I. Geran, N. H. Greenberg, M. M. Macdonald, A. M. Schumacher, and B. J. Abbott, *Cancer Chemother. Rep.*, **3**, 1 (1972).

ACKNOWLEDGMENTS

Supported in part by the Fundação de Amparo à Pesquisa do Estado de São Paulo (FAPESP) and CNPq (Rio de Janeiro).

The authors thank Professor Keith Brown of Campinas University, São Paulo, Brazil, for helpful discussions.

Structure–Activity Relationships of Anesthetic Ethers Using Molecular Connectivity

THÉRÈSE Di PAOLO

Received February 1, 1977, from the *Massachusetts College of Pharmacy, Boston, MA 02115.* Accepted for publication June 8, 1977. Present address: Department of National Defence, DMFR-4, Ottawa, Ontario, K1A OK2, Canada.

Abstract □ The structure–activity relationships in the anesthetic and toxic actions of 28 aliphatic ethers were simple functions of molecular connectivity indexes. These quantitative relationships are discussed briefly in the light of theories of the mechanism of action of general anesthetics.

Keyphrases □ Structure–activity relationships—various aliphatic ethers, anesthetic activity and toxicity related to molecular connectivity indexes □ Molecular connectivity indexes—various aliphatic ethers, related to anesthetic activity and toxicity □ Ethers, various aliphatic—anesthetic activity and toxicity related to molecular connectivity indexes □ Anesthetics—various aliphatic ethers, activity related to molecular connectivity indexes □ Toxicity—various aliphatic ethers, related to molecular connectivity indexes □ Topological indexes—molecular connectivity, various aliphatic ethers, related to anesthetic activity and toxicity

In theories of the mode of action (1, 2) and structure–activity relationships (3, 4) of general anesthetics, their solubility in lipophilic media and their oil–water partition coefficients have been emphasized as important factors governing their activity (1, 4). These properties are related to molecule size, and these studies also emphasized the importance of the volume of these anesthetics (1).

In support of this latter aspect, an excellent correlation was obtained between the anesthetic potency of a mixed group of anesthetics and a molecular connectivity term plus a term for the charge on the polar hydrogens (5). To test the validity of these findings further and to gain more information, a structure–activity study of 28 aliphatic ethers was undertaken. In this group, the polarity of the hydrogens does not vary significantly; hence, this factor is approximately constant. The anesthetic AD_{50} and LD_{50} toxicity data used are from Marsh and Leake (6).

EXPERIMENTAL

Molecular connectivity indexes were calculated in the usual manner (7). A short description of the calculation of $^1\chi$ and $^1\chi^v$ is given here.

The molecular skeleton is drawn, and each nonhydrogen atom is assigned a number, δ, corresponding to the number of nonhydrogen atoms connected to it; thus, $\delta = 1, 2, 3,$ or 4. A value for each molecule bond, c_k, is computed from each pair of bonded atoms by $c_k = (\delta_i\delta_j)_k^{-1/2}$, where k is the bond between atoms i and j. Finally, $^1\chi$ is the sum of the c_k values of all bonded atoms, $^1\chi = \Sigma_k c_k$.

The valence χ term, $^1\chi^v$, is calculated similarly, except that valence δ^v values are used. They are assigned on the basis of the expression $\delta^v = Z^v - h_i$, where Z^v is the number of valence electrons and h_i is the number of attached hydrogen atoms.

The complete set of connectivity indexes was calculated for the molecules in Tables I and II and statistically analyzed with a computer program[1] to find the best set of variables. All possible linear, inverse, and quadratic equations with one and two variables were calculated. The best equations obtained for one and two variables are reported.

RESULTS AND DISCUSSION

The statistical analysis showed that $^1\chi$ is the best connectivity term to correlate with anesthetic activity. The following equations were formulated from the data in Table I:

$$\log 1/c = 4.376\ (\pm 0.05) - \frac{3.729\ (\pm 0.15)}{^1\chi} \qquad \text{(Eq. 1)}$$

$$r = 0.979 \quad s = 0.076 \quad n = 28$$

$$F_{1,26} = 606.1,\ p < 0.001$$

$$\log 1/c = -0.365\ (\pm 0.18) + 1.865\ (\pm 0.13)^1\chi - 0.230\ (\pm 0.02)(^1\chi)^2 \qquad \text{(Eq. 2)}$$

$$r = 0.986 \quad s = 0.063 \quad n = 28$$

$$F_{2,25} = 449.1,\ p < 0.001$$

where c is the AD_{50} molar concentration of anesthetic. The 95% confidence intervals of the coefficients are shown in parentheses. Equations 1 and 2 account for 96% (r^2) and 97% (r^2), respectively, of the variance in $\log 1/c$, and the standard deviations are within experimental error.

Marsh and Leake (6) observed that, in general, as the molecular weight or molecular size increases, the activity increases and that within a group of compounds with the same total number of carbon atoms or the same molecular weight, the isomers with the longest straight chain or highest boiling point are the most active. Both Eqs. 1 and 2 account very well for these observations (Table I). Table I shows that $^1\chi$ increases as the molecules become larger, reflecting their size; for molecules with the same number of carbons, $^1\chi$ is smaller for the more branched isomers (*e.g.*, Compounds 3–8, 9–15, 16–23, 24–26, and 27–28 in Table I).

For anesthetic activity, two equations were formulated with comparable correlation statistics. In Eq. 1, the activity is inversely proportional to $^1\chi$; Eq. 2 is a parabolic relationship in $^1\chi$. These equations were derived from a limited group of molecules in a homologous series. The apex of the parabola defined by Eq. 2 is for $^1\chi = 4.05$, $\log 1/c = 3.42$. Table I shows that only two molecules are past the maximum and, in fact, are very close to it ($^1\chi = 4.26$, $\log 1/c = 3.30$, and $^1\chi = 4.20$, $\log 1/c = 3.45$). This result explains why Eqs. 1 and 2 describe equally well the variation in activity. More data points past the maximum would be required for an adequate structure–activity study.

The toxicity (LD_{50}) of these ethers also was analyzed using molecular connectivity. The statistical analysis showed that the number of edges (NEDG) is the best single variable to correlate with activity and that the best set of two variables is NEDG and $^1\chi^v$. The following equations were formulated from the data in Table II:

$$\log 1/c' = 0.311\ (\pm 0.02)\text{NEDG} + 1.034\ (\pm 0.12) \qquad \text{(Eq. 3)}$$

$$r = 0.945 \quad s = 0.132 \quad n = 25$$

$$F_{1,23} = 191.9,\ p < 0.001$$

$$\log 1/c' = 0.538\ (\pm 0.05)\text{NEDG} - 0.099\ (\pm 0.02)(^1\chi^v)^2 + 0.466\ (\pm 0.13) \qquad \text{(Eq. 4)}$$

$$r = 0.976 \quad s = 0.090 \quad n = 25$$

$$F_{2,22} = 222.2,\ p < 0.001$$

where c' is the LD_{50} molar concentration of the anesthetic. Equations 3 and 4 account for 89% (r^2) and 95% (r^2), respectively, of the variance in $\log 1/c'$, and the standard deviations are close to the experimental error. The topological designation "edge" corresponds in chemistry to a σ-bond. Thus, the NEDG variable is the number of σ-bonds in the hydrogen-suppressed molecule.

Marsh and Leake (6) reported that, in general, the toxicity increased as the molecular weight of the compounds increased, although the relationships were not exactly parallel to those of anesthetic activity. The difference in toxicity between the isomers of the same molecular weight does not show a clear pattern, although usually the asymmetric and branched chain compounds are more toxic. The very simple Eq. 3 ac-

[1] IBM REGR.

Table I—AD_{50} Values for Anesthesia of Mice by Aliphatic Ethers

Compound	$^1\chi$	log $1/c'$ Obs.[a]	log $1/c'$ Calc.[b]	$\lvert\Delta \log 1/c\rvert$	log $1/c$ Calc.[c]	$\lvert\Delta \log 1/c\rvert$	V, cm^3/mole
1 Dimethyl	1.414	1.85	1.74	0.11	1.81	0.04	31.04
2 Methyl ethyl	1.914	2.22	2.43	0.21	2.36	0.14	41.27
3 Methyl isopropyl	2.270	2.70	2.73	0.03	2.68	0.02	51.49
4 Diethyl	2.414	2.75	2.83	0.08	2.80	0.05	51.50
5 Divinyl	2.414	2.82	2.83	0.01	2.80	0.02	44.52
6 Ethyl vinyl	2.414	2.82	2.83	0.01	2.80	0.02	48.01
7 Methyl cyclopropyl	2.432	2.85	2.84	0.01	2.81	0.04	48.06
8 Methyl propyl	2.414	2.90	2.83	0.07	2.80	0.10	51.50
9 Methyl *tert*-butyl	2.561	3.00	2.92	0.08	2.90	0.10	61.71
10 Methyl isobutyl	2.770	3.00	3.03	0.03	3.04	0.04	61.72
11 Ethyl isopropyl	2.770	3.00	3.03	0.03	3.04	0.04	61.72
12 Methyl *sec*-butyl	2.808	3.04	3.04	0.00	3.06	0.02	61.72
13 Ethyl propyl	2.914	3.10	3.10	0.00	3.12	0.02	61.73
14 Ethyl cyclopropyl	2.932	3.10	3.11	0.01	3.13	0.03	58.29
15 Methyl butyl	2.914	3.15	3.10	0.05	3.12	0.03	61.73
16 Ethyl *tert*-butyl	3.061	3.15	3.16	0.01	3.19	0.04	71.94
17 Diisopropyl	3.126	3.15	3.18	0.03	3.22	0.07	71.94
18 Ethyl isobutyl	3.270	3.22	3.24	0.02	3.27	0.05	71.95
19 Ethyl *sec*-butyl	3.308	3.22	3.25	0.03	3.29	0.07	71.95
20 Propyl isopropyl	3.270	3.26	3.24	0.02	3.27	0.01	71.95
21 Ethyl butyl	3.414	3.30	3.28	0.02	3.32	0.02	71.96
22 Methyl pentyl	3.414	3.40	3.28	0.12	3.32	0.08	71.96
23 Dipropyl	3.414	3.40	3.28	0.12	3.32	0.08	71.96
24 Ethyl *tert*-pentyl	3.561	3.40	3.33	0.07	3.36	0.04	82.17
25 Ethyl isopentyl	3.846	3.45	3.41	0.04	3.41	0.04	82.18
26 Ethyl pentyl	3.914	3.45	3.43	0.02	3.41	0.04	82.19
27 Diisobutyl	4.260	3.30	3.47	0.17	3.41	0.11	92.40
28 Di-*sec*-butyl	4.202	3.45	3.49	0.04	3.41	0.04	92.40

[a] From Ref. 6. [b] Calculated using Eq. 1. [c] Calculated using Eq. 2.

counts well for the size effect on toxicity, and Eq. 4 refines the correlation, $^1\chi^v$ distinguishing the asymmetric and branching variations.

Equation 4 also refines Eq. 3 in that it accounts for the nonlinear variation in activity. In this respect, an inverse relationship with NEDG fits slightly better the toxicity activity variations than the linear form of Eq. 3: $\log 1/c' = 3.69 - 5.04/\text{NEDG}$ ($r = 0.952$, $s = 0.124$, $n = 25$, $F_{1,23} = 220.6$, $p < 0.001$), but Eq. 4 still gives the best results.

For the same molecules, the parabolic relationship between anesthetic activity and the octanol–water partition coefficient gave the following correlation statistics: $r = 0.966$, $s = 0.101$, and $n = 26$ (4); the two unsaturated ethers were omitted. Similarly, for the toxic activity, the following correlation statistics were obtained with $\log P$ and $(\log P)^2$: $r = 0.864$, $s = 0.208$, and $n = 25$ (8). The correlations reported here with molecular connectivity are clearly superior to those obtained with the octanol–water partition coefficients.

Bondi's (9) van der Waals volumes (V) of the ethers were calculated. The volumes of the ethers and their $^1\chi$ values are highly correlated ($V = -1.54 + 22.13\ ^1\chi$; $r = 0.977$, $s = 3.22$, $n = 28$). Therefore, for these ethers, $^1\chi$ is a very simply derived size variable. In comparing computed Bondi's van der Waals volumes with the $^1\chi$ values (Table I), it is clear that $^1\chi$ differentiates better the isomers (compare Compounds 3, 4, and 8; 10–13 and 15; 17–23; 24–26; and 27–28 in Table I).

The correlation between the anesthetic activity and Bondi's van der Waals volumes (V) is very good ($\log 1/c = 4.30 - 75.82/V$; $r = 0.959$, $s = 0.107$, $n = 28$), although inferior to Eq. 1. This result could be explained by the fact that Bondi's volume values have to be corrected for small rings and that they do not differentiate the isomeric variations as well as $^1\chi$. The correlation between the toxic activity and the volumes of the ethers gives the following statistics: $\log 1/c' = 4.00 - 80.31/V$ ($r = 0.916$, $s = 0.159$, $n = 25$). These results are superior to the quadratic $\log P$ equation but inferior to the molecular connectivity correlations.

The excellent correlations obtained for the anesthetic activity and the obvious relationship between $^1\chi$ and the molecular size for these ethers are in line with the Mullins critical volume hypothesis (1). This hypothesis

Table II—Toxicity (LD_{50}) of Ethers to Mice

Compound	NEDG	$^1\chi V$	log $1/c$ Obs.[a]	log $1/c$ Calc.[b]	$\lvert\Delta \log 1/c'\rvert$	log $1/c'$ Calc.[c]	$\lvert\Delta \log 1/c'\rvert$
1 Dimethyl	2	0.816	1.43	1.66	0.23	1.48	0.05
2 Methyl ethyl	3	1.404	1.74	1.97	0.23	1.89	0.15
3 Diethyl	4	1.992	2.22	2.28	0.06	2.23	0.01
4 Methyl isopropyl	4	1.799	2.26	2.28	0.02	2.30	0.04
5 Divinyl	4	1.288	2.33	2.28	0.05	2.45	0.12
6 Ethyl vinyl	4	1.640	2.34	2.28	0.06	2.35	0.01
7 Methyl propyl	4	1.904	2.45	2.28	0.17	2.26	0.19
8 Methyl cyclopropyl	5	1.960	2.75	2.59	0.16	2.78	0.03
9 Ethyl propyl	5	2.492	2.60	2.59	0.01	2.54	0.06
10 Ethyl isopropyl	5	2.386	2.60	2.59	0.01	2.59	0.01
11 Methyl butyl	5	2.404	2.70	2.59	0.11	2.58	0.12
12 Methyl isobutyl	5	2.260	2.79	2.59	0.20	2.65	0.14
13 Methyl *sec*-butyl	5	2.337	2.79	2.59	0.20	2.62	0.17
14 Methyl *tert*-butyl	5	2.112	2.79	2.59	0.20	2.72	0.07
15 Ethyl cyclopropyl	6	2.548	3.00	2.90	0.10	3.05	0.05
16 Dipropyl	6	2.992	2.79	2.90	0.11	2.81	0.02
17 Propyl isopropyl	6	2.886	2.82	2.90	0.08	2.87	0.05
18 Diisopropyl	6	2.781	2.82	2.90	0.08	2.93	0.11
19 Ethyl butyl	6	2.992	2.82	2.90	0.08	2.81	0.13
20 Ethyl isobutyl	6	2.847	2.82	2.90	0.08	2.89	0.07
21 Ethyl *sec*-butyl	6	2.924	2.85	2.90	0.08	2.85	0.00
22 Methyl pentyl	6	2.904	2.88	2.90	0.08	2.86	0.02
23 Ethyl *tert*-butyl	6	2.700	2.92	2.90	0.02	2.97	0.05
24 Ethyl pentyl	7	3.492	3.00	3.21	0.21	3.02	0.02
25 Ethyl *tert*-pentyl	7	3.138	3.15	3.21	0.06	3.18	0.03

[a] From Ref. 6. [b] Calculated using Eq. 3. [c] Calculated using Eq. 4.

states that anesthesia occurs when the volume of a hydrophobic region is caused to expand beyond a certain critical amount by the absorption of molecules of an inert substance. These results also are in agreement with a previous study of a mixed group of anesthetics (5) for which a size effect interpretation was proposed. More structure–activity studies of anesthetics are being completed to generalize these findings.

REFERENCES

(1) J. C. Miller and K. W. Miller, in "MTP International Review of Science, Biochemistry Series One," vol. 12, H. K. F. Blaschko, Ed., Butterworths, University Park Press, Baltimore, Md., 1975, p. 33.

(2) K. W. Miller, W. D. M. Paton, E. B. Smith, and R. A. Smith, *Anesthesiology*, **36**, 339 (1972).

(3) C. Hansch, A. Vittoria, C. Silipo, and P. Y. C. Jow, *J. Med. Chem.*, **18**, 546 (1975).

(4) W. R. Glave and C. Hansch, *J. Pharm. Sci.*, **61**, 589 (1972).

(5) T. Di Paolo, L. B. Kier, and L. H. Hall, *Mol. Pharmacol.*, **13**, 31 (1977).

(6) D. F. Marsh and C. D. Leake, *Anesthesiology*, **11**, 455 (1950).

(7) L. B. Kier and L. H. Hall, "Molecular Connectivity in Chemistry and Drug Research," Academic, New York, N.Y., 1976.

(8) C. Hansch and J. M. Dayton, *J. Pharm. Sci.*, **62**, 1 (1973).

(9) A. Bondi, *J. Phys. Chem.*, **68**, 441 (1964).

Molecular Connectivity in Quantitative Structure–Activity Relationship Study of Anesthetic and Toxic Activity of Aliphatic Hydrocarbons, Ethers, and Ketones

THÉRÈSE Di PAOLO

Received April 11, 1977, from the *Massachusetts College of Pharmacy, Boston, MA 02115.* Accepted for publication June 10, 1977. Present address: Department of National Defence, DMFR-4, Ottawa, Ontario, K1A 0K2, Canada.

Abstract □ The nonempirical molecular connectivity indexes of 27 aliphatic hydrocarbons, ethers, and ketones were calculated. Very good correlations were obtained between anesthetic (AD_{100}) and toxic (LD_{100} and LD_{50}) activities of these compounds and their molecular connectivity indexes. These quantitative structure–activity relationships are discussed briefly in the light of general anesthesia theories.

Keyphrases □ Molecular connectivity indexes—various aliphatic hydrocarbons, ethers, and ketones, related to anesthetic activity and toxicity □ Structure–activity relationships—various aliphatic hydrocarbons, ethers, and ketones, anesthetic activity and toxicity related to molecular connectivity indexes □ Anesthetics—various aliphatic hydrocarbons, ethers, and ketones, activity related to molecular connectivity indexes □ Toxicity—various aliphatic hydrocarbons, ethers, and ketones, related to molecular connectivity indexes □ Topological indexes—mclecular connectivity, various aliphatic hydrocarbons, ethers, and ketones, related to anesthetic activity and toxicity

Molecular connectivity is a method of quantitating the topological structure of organic molecules. This method derives numerical descriptors encoded with information about the number and kind of atoms and their bonding relationships to each other. It has been used successfully to arrive at structure–activity relationships with many classes of biological agents (1).

In a previous study with a mixed group of anesthetics, an excellent correlation was obtained between the relative anesthetic potency and a molecular connectivity term in addition to a term for the charge on the polar hydrogens (2).

To test further the validity of these findings and to gain more information for the interpretation of these results, structure–activity relationships of 27 anesthetic aliphatic hydrocarbons, ethers, and ketones were studied. Anesthetic and toxicity data for this group of molecules had been measured previously (2), and confidence limits of the experimental values are given. In this group, the polarity of the hydrogens does not vary much, so the effect of this factor on activity is fairly constant. In going to higher congeners of each alkane, ether, and ketone, the anesthetic and toxic activity increases, reaches a maximum, and then decreases. A parabolic relationship was found between the activity and the logarithm of the octanol–water partition coefficient or the molecular weight (3).

This group of compounds is a good example of nonlinear structure–activity relationships and will broaden the study of anesthetic activity. Since there are many measurements beyond the maximum, it can be determined accurately whether the structure–activity relationship is parabolic. Previous work on a series of ethers could not confirm this hypothesis (4).

EXPERIMENTAL

Molecular connectivity indexes were calculated, in the usual manner (1), for the molecules in Tables I and II and statistically analyzed with a system of programs developed to find the best set of variables.

The anesthetic (AD_{100}) and toxic (LD_{50} and LD_{100}) activities of the compounds studied are those of Jeppsson (3). The alkanes, ethers, and ketones were dissolved in an emulsion and administered intravenously to mice. The confidence limits given at $p = 0.05$ for the experimental data were used to compute the experimental standard error. Expressed as log $1/c$, these are values 0.17 for the AD_{100} activity and 0.13 and 0.06 for LD_{100} and LD_{50} activities, respectively.

RESULTS

The statistical analysis shows that ${}^1\chi$ and ${}^4\chi_p{}^v$ are the best connectivity terms to correlate with the AD_{100} anesthetic activity. The following equation was formulated from the data in Table I:

$$\log {}^1/c' = +2.895\ (\pm 0.324) - \frac{8.539\ (\pm 0.875)}{{}^1\chi} - 1.487\ (\pm 0.114){}^4\chi_p{}^v \quad \text{(Eq. 1)}$$

$$r = 0.943 \quad s = 0.170 \quad n = 27$$

$$F = 96.5,\ p < 0.001$$

states that anesthesia occurs when the volume of a hydrophobic region is caused to expand beyond a certain critical amount by the absorption of molecules of an inert substance. These results also are in agreement with a previous study of a mixed group of anesthetics (5) for which a size effect interpretation was proposed. More structure–activity studies of anesthetics are being completed to generalize these findings.

REFERENCES

(1) J. C. Miller and K. W. Miller, in "MTP International Review of Science, Biochemistry Series One," vol. 12, H. K. F. Blaschko, Ed., Butterworths, University Park Press, Baltimore, Md., 1975, p. 33.

(2) K. W. Miller, W. D. M. Paton, E. B. Smith, and R. A. Smith, *Anesthesiology*, **36**, 339 (1972).

(3) C. Hansch, A. Vittoria, C. Silipo, and P. Y. C. Jow, *J. Med. Chem.*, **18**, 546 (1975).

(4) W. R. Glave and C. Hansch, *J. Pharm. Sci.*, **61**, 589 (1972).

(5) T. Di Paolo, L. B. Kier, and L. H. Hall, *Mol. Pharmacol.*, **13**, 31 (1977).

(6) D. F. Marsh and C. D. Leake, *Anesthesiology*, **11**, 455 (1950).

(7) L. B. Kier and L. H. Hall, "Molecular Connectivity in Chemistry and Drug Research," Academic, New York, N.Y., 1976.

(8) C. Hansch and J. M. Dayton, *J. Pharm. Sci.*, **62**, 1 (1973).

(9) A. Bondi, *J. Phys. Chem.*, **68**, 441 (1964).

Molecular Connectivity in Quantitative Structure–Activity Relationship Study of Anesthetic and Toxic Activity of Aliphatic Hydrocarbons, Ethers, and Ketones

THÉRÈSE Di PAOLO

Received April 11, 1977, from the *Massachusetts College of Pharmacy, Boston, MA 02115.* Accepted for publication June 10, 1977. Present address: Department of National Defence, DMFR-4, Ottawa, Ontario, K1A 0K2, Canada.

Abstract □ The nonempirical molecular connectivity indexes of 27 aliphatic hydrocarbons, ethers, and ketones were calculated. Very good correlations were obtained between anesthetic (AD_{100}) and toxic (LD_{100} and LD_{50}) activities of these compounds and their molecular connectivity indexes. These quantitative structure–activity relationships are discussed briefly in the light of general anesthesia theories.

Keyphrases □ Molecular connectivity indexes—various aliphatic hydrocarbons, ethers, and ketones, related to anesthetic activity and toxicity □ Structure–activity relationships—various aliphatic hydrocarbons, ethers, and ketones, anesthetic activity and toxicity related to molecular connectivity indexes □ Anesthetics—various aliphatic hydrocarbons, ethers, and ketones, activity related to molecular connectivity indexes □ Toxicity—various aliphatic hydrocarbons, ethers, and ketones, related to molecular connectivity indexes □ Topological indexes—mclecular connectivity, various aliphatic hydrocarbons, ethers, and ketones, related to anesthetic activity and toxicity

Molecular connectivity is a method of quantitating the topological structure of organic molecules. This method derives numerical descriptors encoded with information about the number and kind of atoms and their bonding relationships to each other. It has been used successfully to arrive at structure–activity relationships with many classes of biological agents (1).

In a previous study with a mixed group of anesthetics, an excellent correlation was obtained between the relative anesthetic potency and a molecular connectivity term in addition to a term for the charge on the polar hydrogens (2).

To test further the validity of these findings and to gain more information for the interpretation of these results, structure–activity relationships of 27 anesthetic aliphatic hydrocarbons, ethers, and ketones were studied. Anesthetic and toxicity data for this group of molecules had been measured previously (2), and confidence limits of the experimental values are given. In this group, the polarity of the hydrogens does not vary much, so the effect of this factor on activity is fairly constant. In going to higher congeners of each alkane, ether, and ketone, the anesthetic and toxic activity increases, reaches a maximum, and then decreases. A parabolic relationship was found between the activity and the logarithm of the octanol–water partition coefficient or the molecular weight (3).

This group of compounds is a good example of nonlinear structure–activity relationships and will broaden the study of anesthetic activity. Since there are many measurements beyond the maximum, it can be determined accurately whether the structure–activity relationship is parabolic. Previous work on a series of ethers could not confirm this hypothesis (4).

EXPERIMENTAL

Molecular connectivity indexes were calculated, in the usual manner (1), for the molecules in Tables I and II and statistically analyzed with a system of programs developed to find the best set of variables.

The anesthetic (AD_{100}) and toxic (LD_{50} and LD_{100}) activities of the compounds studied are those of Jeppsson (3). The alkanes, ethers, and ketones were dissolved in an emulsion and administered intravenously to mice. The confidence limits given at $p = 0.05$ for the experimental data were used to compute the experimental standard error. Expressed as log $1/c$, these are values 0.17 for the AD_{100} activity and 0.13 and 0.06 for LD_{100} and LD_{50} activities, respectively.

RESULTS

The statistical analysis shows that ${}^1\chi$ and ${}^4\chi_p{}^v$ are the best connectivity terms to correlate with the AD_{100} anesthetic activity. The following equation was formulated from the data in Table I:

$$\log {}^1/c' = +2.895\ (\pm 0.324) - \frac{8.539\ (\pm 0.875)}{{}^1\chi} - 1.487\ (\pm 0.114){}^4\chi_p{}^v \quad \text{(Eq. 1)}$$

$$r = 0.943 \quad s = 0.170 \quad n = 27$$

$$F = 96.5,\ p < 0.001$$

Table I—AD_{100} Values for Loss of Righting Reflex of Mice by Aliphatic Hydrocarbons, Ethers, and Ketones

Compound	$^1\chi$	$^4\chi_p^v$	$-\log 1/c'$ Obs.[a]	$-\log 1/c'$ Calc.[b]	$\lvert\Delta \log 1/c'\rvert$
Pentane	2.414	0.354	1.052	1.167	0.115
Hexane	2.914	0.500	0.941	0.777	0.164
Heptane	3.414	0.677	0.458	0.614	0.156
Octane	3.914	0.854	0.391	0.552	0.161
Nonane	4.414	1.030	0.428	0.575	0.147
Decane	4.914	1.207	0.613	0.633	0.020
Undecane	5.414	1.384	0.810	0.743	0.067
Dodecane	5.914	1.561	1.124	0.869	0.255
Tridecane	6.414	1.737	1.119	1.020	0.099
Tetradecane	6.914	1.914	1.294	1.189	0.105
Pentadecane	7.414	2.091	1.516	1.367	0.149
Hexadecane	7.914	2.268	1.566	1.554	0.012
Heptadecane	8.414	2.444	1.538	1.755	0.217
Ethyl ether	2.414	0.204	1.036	0.944	0.092
Propyl ether	3.414	0.391	0.305	0.188	0.117
Butyl ether	4.414	0.595	0.104	−0.072	0.176
Pentyl ether	5.414	1.010	0.297	0.187	0.110
Hexyl ether	6.414	1.364	0.535	0.465	0.070
Heptyl ether	7.414	1.717	0.869	0.811	0.058
Octyl ether	8.414	2.071	1.188	1.201	0.013
3-Pentanone	2.808	0.250	0.657	0.517	0.140
4-Heptanone	3.808	0.683	0.121	0.366	0.245
5-Nonanone	4.808	0.873	−0.081	0.179	0.260
6-Undecanone	5.808	1.269	0.076	0.461	0.385
7-Tridecanone	6.808	1.623	0.978	0.774	0.204
8-Pentadecanone	7.808	1.976	1.127	1.136	0.009
9-Heptadecanone	8.808	2.330	1.455	1.543	0.088

[a] From Ref. 3; drug dose in millimoles per kilogram. [b] Calculated using Eq. 1.

where c' is the AD_{100} millimolar concentration of the anesthetic. This equation accounts for 89% (r^2) of the variance in $\log 1/c'$, and the standard deviation is at the level of experimental error.

The analysis for the toxic doses LD_{100} (c'') and LD_{50} (c''') of Table II led to the following equations:

$$\log 1/c'' = +3.903\ (\pm 0.442) - 1.195\ (\pm 0.097)^3\chi_p^v - \frac{17.77\ (\pm 1.81)}{^0\chi^v} \quad \text{(Eq. 2)}$$

$$r = 0.938 \quad s = 0.173 \quad n = 27$$

$$F = 87.3,\ p < 0.001$$

$$\log 1/c''' = +3.188\ (\pm 0.385) - 3.246\ (\pm 0.345)^6\chi_p^v - \frac{16.57\ (\pm 1.74)}{^0\chi^v} \quad \text{(Eq. 3)}$$

$$r = 0.941 \quad s = 0.149 \quad n = 15$$

$$F = 46.6,\ p < 0.001$$

For the LD_{100} toxicity, Eq. 2 accounts for 88% (r^2) of the variance in $\log 1/c''$, and the standard deviation is close to the experimental error. For the LD_{50} toxicity, Eq. 3 accounts for 89% (r^2) of the variance, and the standard deviation is larger than that experimentally calculated.

Nonlinear relationships were obtained in these three cases with different connectivity terms.

DISCUSSION

Equation 1, correlating the AD_{100} activity, contains $^1\chi$ and $^4\chi_p^v$. As shown in Table I, both these terms increase as the molecules become larger. When comparing the connectivity term values in Eq. 1, it is seen that $^1\chi$ is the important factor for the smaller congeners of these molecules up to a maximum and then $^4\chi_p^v$ becomes the main factor for the larger congeners. No parabolic relationship with connectivity terms gave as good results as these two terms.

Jeppsson (3) fitted parabolic relationships with log P and the molecular weights with these anesthetic activities. He did not group each class of molecules for his correlations but studied them in separate classes. To compare the present results with those of Jeppsson, the parabolic relationship with log P was calculated for the whole set to give $r = 0.814$, $s = 0.296$, $n = 27$, and $F = 23.6$; with the molecular weights, the values were $r = 0.762$, $s = 0.331$, $n = 27$, and $F = 16.6$. Clearly, the correlation with the connectivity terms is superior.

These results are also consistent with previous findings for a group of ethers (4) where the scarcity of points past the maximum did not permit a choice between an inverse or a parabolic relationship with $^1\chi$.

The equations correlating the LD_{100} and LD_{50} activities show similar dependence as functions of connectivity terms compared to Eq. 1 for AD_{100}. For smaller congeners, $^0\chi^v$ is the important factor up to a maximum; then $^3\chi_p^v$ for LD_{100} and $^6\chi_p^v$ for LD_{50} become the main factors for the larger congeners. Similarly, for these two cases, no parabolic relationships with connectivity terms gave as good results as these different connectivity terms. Again, the parabolic relationships with log P or the molecular weights calculated from Jeppsson's work are less satisfactory. For the parabolic LD_{100} correlation with log P, the following statistical values were obtained: $r = 0.761$, $s = 0.324$, $n = 27$, and $F = 16.5$; similarly, the molecular weight gave $r = 0.763$, $s = 0.323$, $n = 27$, and $F = 16.7$. The

Table II—Toxic Doses (LD_{50} and LD_{100}) of Some Alkanes, Ethers, and Ketones after Intravenous Administration to Mice

Compound	$^0\chi^v$	$^3\chi_p^v$	$-\log 1/c''$ Obs.[a]	$-\log 1/c''$ Calc.[b]	$\lvert\Delta \log 1/c''\rvert$	$^6\chi_p^v$	$-\log 1/c'''$ Obs.[a]	$-\log 1/c'''$ Calc.[c]	$\lvert\Delta \log 1/c'''\rvert$
Pentane	4.121	0.707	1.287	1.261	0.026	0.000	0.792	0.840	0.048
Hexane	4.828	0.957	0.984	0.920	0.064				
Heptane	5.535	1.207	0.660	0.757	0.097	0.177	0.346	0.387	0.041
Octane	6.243	1.456	0.574	0.683	0.109				
Nonane	6.950	1.707	0.672	0.697	0.025	0.338	0.233	0.296	0.063
Decane	7.657	1.957	0.807	0.765	0.042				
Undecane	8.364	2.207	1.020	0.869	0.151	0.515	0.520	0.473	0.047
Dodecane	9.071	2.457	1.195	0.990	0.205				
Tridecane	9.778	2.707	1.332	1.146	0.186	0.692	0.800	0.749	0.051
Tetradecane	10.485	2.956	1.466	1.321	0.145				
Pentadecane	11.192	3.207	1.660	1.513	0.147	0.869	1.217	1.109	0.108
Hexadecane	11.899	3.457	1.637	1.723	0.086				
Heptadecane	12.607	3.707	1.611	1.933	0.322				
Ethyl ether	3.822	0.408	1.329	1.241	0.088	0.000	1.129	1.155	0.026
Propyl ether	5.237	0.697	0.322	0.325	0.003	0.102	0.301	0.309	0.008
Butyl ether	6.651	1.284	0.297	0.298	0.001				
Pentyl ether	8.065	1.784	0.508	0.434	0.074	0.297	0.017	−0.168	0.185
Hexyl ether	9.479	2.284	0.677	0.694	0.017				
Heptyl ether	10.891	2.784	1.068	1.061	0.007	0.607	0.342	0.308	0.034
Octyl ether	12.308	3.284	1.386	1.463	0.077	0.784	0.689	0.700	0.011
3-Pentanone	4.322	0.789	1.125	1.146	0.021	0.000	0.776	0.641	0.135
4-Heptanone	5.737	1.058	0.375	0.455	0.080				
5-Nonanone	7.151	1.618	0.262	0.520	0.258	0.239	−0.013	−0.091	0.078
6-Undecanone	8.565	2.118	0.328	0.709	0.381	0.466	−0.161	0.264	0.425
7-Tridecanone	9.979	2.618	1.248	1.005	0.243				
8-Pentadecanone	11.394	3.118	1.702	1.389	0.313	0.760	0.723	0.738	0.015
9-Heptadecanone	12.808	3.618	1.596	1.809	0.213				

[a] From Ref. 3; drug dose in millimoles per kilogram. [b] Calculated using Eq. 2. [c] Calculated using Eq. 3.

parabolic LD_{50} correlation with log P or the molecular weight also gave poorer results as compared to the molecular connectivity correlations. The parabolic relationship between LD_{50} and log P gave $r = 0.826$, $s = 0.249$, $n = 15$, and $F = 12.9$; with the molecular weight, the values were $r = 0.653$, $s = 0.334$, $n = 15$, and $F = 4.5$.

The very good correlations for the anesthetic and toxic activities were obtained with nonempirically based molecular connectivity terms. The equations describing the activity variations were not parabolic but contained two different connectivity terms. It is questionable whether the same structural features quantitatively affect the activity uniformly in a homologous series. The same features probably govern activity for smaller congeners up to the maximum activity; but beyond it, these factors may be somewhat different. In this respect, nonlinear correlations bring to light the flexibility and discriminating power of molecular connectivity as compared to the usual quadratic form of log P.

Many mechanistic explanations for parabolic relationships have been given (5–7). The usual explanation is based on a partitioning model. Alternative mechanistic explanations include the principle of bulk tolerance, limited solubility of the higher members of a congeneric series, conformational distortion of the active site, and metabolic transformation. These explanations imply that molecular size is the governing influence. The molecular connectivity indexes that mirror molecular connectedness are most readily identified with the size and shape of molecules. Murray *et al.* (8) obtained excellent parabolic relationships between molecular connectivity and biological activity. They discussed and endorsed the molecular size explanation, as modeled by molecular connectivity.

That the molecular connectivity indexes reflect the size and shape of molecules also can be seen when going through the congeneric series of Tables I and II. Thus, the correlations obtained would also support the mechanistic explanation for parabolic relationships implying molecular size. More specifically for the anesthetic activity, this molecular size explanation is in line with the Mullins critical volume hypothesis (9). This hypothesis states that anesthesia occurs when the volume of a hydrophobic region is caused to expand beyond a certain critical amount by the absorption of molecules of an inert substance. The results obtained here are also in agreement with previous studies of a mixed group of anesthetics (2) and a group of ethers (4) for which a molecular size explanation of the correlations with molecular connectivity indexes was proposed.

REFERENCES

(1) L. B. Kier and L. H. Hall, "Molecular Connectivity in Chemistry and Drug Research," Academic, New York, N.Y., 1976.

(2) T. Di Paolo, L. B. Kier, and L. H. Hall, *Mol. Pharmacol.*, **13,** 31 (1977).

(3) R. Jeppsson, *Acta Pharmacol. Toxicol.*, **37,** 56 (1975).

(4) T. Di Paolo, *J. Pharm. Sci.*, **67,** 564 (1978).

(5) C. Hansch and J. M. Clayton, *ibid.*, **62,** 1 (1973).

(6) E. J. Lien, in "Medicinal Chemistry," vol. IV, J. Mass, Ed., Elsevier, Amsterdam, The Netherlands, 1974.

(7) T. Higuchi and S. S. Davis, *J. Pharm. Sci.*, **59,** 1376 (1970).

(8) W. J. Murray, L. B. Kier, and L. H. Hall, *J. Med. Chem.*, **19,** 573 (1976).

(9) J. C. Miller and K. W. Miller, in "MTP International Review of Science, Biochemistry Series One," vol. 12, H. K. F. Blaschko, Ed., Butterworths, University Park Press, Baltimore, Md., 1975, p. 33.

Correlation of Quinidine Absorption with Disintegration and Dissolution Rates

JEFFREY D. STRUM, JOHN W. EBERSOLE, JAMES M. JAFFE, JOHN L. COLAIZZI, and ROLLAND I. POUST ˣ

Received April 25, 1977, from the *Department of Pharmaceutics, School of Pharmacy, University of Pittsburgh, Pittsburgh, PA 15261.* Accepted for publication July 13, 1977.

Abstract □ The dissolution profiles of four commercial quinidine sulfate tablets were determined using the USP rotating-basket dissolution apparatus. Substantial differences in dissolution half-times were noted and compared to previously reported disintegration times, absorption rate constants, and times of appearance of peak serum concentrations. Rank-order correlations were observed among all combinations of *in vivo* and *in vitro* parameters, indicating that the absorption rates of these tablets are controlled by both disintegration and dissolution.

Keyphrases □ Quinidine sulfate—four commercial tablets, dissolution profiles determined and related to disintegration and absorption □ Dissolution—quinidine sulfate, four commercial tablets, profiles determined and related to disintegration and absorption □ Disintegration—quinidine sulfate, four commercial tablets, related to dissolution profiles □ Absorption—quinidine sulfate, four commercial tablets, related to dissolution profiles □ Cardiac depressants—quinidine sulfate, four commercial tablets, dissolution profiles determined and related to disintegration and absorption

A recent report (1) presented the results of a comparative bioavailability study of four commercially available, chemically equivalent brands of quinidine sulfate. No statistically significant differences in the extent of absorption from the four brands were observed. However, significant differences in the times of peak serum concentration and absorption rate constants were found, indicating differences in the absorption rate among certain pairs of products. A rank-order correlation was observed when mean disintegration times for the four tablet formulations were compared with values for peak time and the absorption rate constant. It seemed appropriate, therefore, to determine the dissolution profiles of these four brands of quinidine sulfate tablets and to investigate the relationships among disintegration, dissolution, and absorption rate.

EXPERIMENTAL

The dissolution properties of six tablets of each of the four brands[1] of quinidine sulfate tablets employed in the study of Strum *et al.* (1) were determined in 900 ml of 0.1 *N* HCl at 37° using the USP rotating-basket dissolution apparatus[2] at 25 rpm. Following preliminary trials, sampling

[1] Treatment A: quinidine sulfate tablets USP, lot 76F83A, Eli Lilly & Co., Indianapolis, Ind.; Treatment B: quinidine sulfate tablets USP, lot 7088A, Philips Roxane Laboratories, Columbus, Ohio; Treatment C: Quinora tablets, lot 72755, Lakeside Laboratories, Milwaukee, Wis.; Treatment D: quinidine sulfate tablets USP, lot 15840, Stanlabs, Portland, Ore. These lots are the same as those used by Strum *et al.* (1).

[2] Hanson Research Corp., Northridge, Calif.

parabolic LD_{50} correlation with log P or the molecular weight also gave poorer results as compared to the molecular connectivity correlations. The parabolic relationship between LD_{50} and log P gave $r = 0.826$, $s = 0.249$, $n = 15$, and $F = 12.9$; with the molecular weight, the values were $r = 0.653$, $s = 0.334$, $n = 15$, and $F = 4.5$.

The very good correlations for the anesthetic and toxic activities were obtained with nonempirically based molecular connectivity terms. The equations describing the activity variations were not parabolic but contained two different connectivity terms. It is questionable whether the same structural features quantitatively affect the activity uniformly in a homologous series. The same features probably govern activity for smaller congeners up to the maximum activity; but beyond it, these factors may be somewhat different. In this respect, nonlinear correlations bring to light the flexibility and discriminating power of molecular connectivity as compared to the usual quadratic form of log P.

Many mechanistic explanations for parabolic relationships have been given (5–7). The usual explanation is based on a partitioning model. Alternative mechanistic explanations include the principle of bulk tolerance, limited solubility of the higher members of a congeneric series, conformational distortion of the active site, and metabolic transformation. These explanations imply that molecular size is the governing influence. The molecular connectivity indexes that mirror molecular connectedness are most readily identified with the size and shape of molecules. Murray *et al.* (8) obtained excellent parabolic relationships between molecular connectivity and biological activity. They discussed and endorsed the molecular size explanation, as modeled by molecular connectivity.

That the molecular connectivity indexes reflect the size and shape of molecules also can be seen when going through the congeneric series of Tables I and II. Thus, the correlations obtained would also support the mechanistic explanation for parabolic relationships implying molecular size. More specifically for the anesthetic activity, this molecular size explanation is in line with the Mullins critical volume hypothesis (9). This hypothesis states that anesthesia occurs when the volume of a hydrophobic region is caused to expand beyond a certain critical amount by the absorption of molecules of an inert substance. The results obtained here are also in agreement with previous studies of a mixed group of anesthetics (2) and a group of ethers (4) for which a molecular size explanation of the correlations with molecular connectivity indexes was proposed.

REFERENCES

(1) L. B. Kier and L. H. Hall, "Molecular Connectivity in Chemistry and Drug Research," Academic, New York, N.Y., 1976.

(2) T. Di Paolo, L. B. Kier, and L. H. Hall, *Mol. Pharmacol.*, **13,** 31 (1977).

(3) R. Jeppsson, *Acta Pharmacol. Toxicol.*, **37,** 56 (1975).

(4) T. Di Paolo, *J. Pharm. Sci.*, **67,** 564 (1978).

(5) C. Hansch and J. M. Clayton, *ibid.*, **62,** 1 (1973).

(6) E. J. Lien, in "Medicinal Chemistry," vol. IV, J. Mass, Ed., Elsevier, Amsterdam, The Netherlands, 1974.

(7) T. Higuchi and S. S. Davis, *J. Pharm. Sci.*, **59,** 1376 (1970).

(8) W. J. Murray, L. B. Kier, and L. H. Hall, *J. Med. Chem.*, **19,** 573 (1976).

(9) J. C. Miller and K. W. Miller, in "MTP International Review of Science, Biochemistry Series One," vol. 12, H. K. F. Blaschko, Ed., Butterworths, University Park Press, Baltimore, Md., 1975, p. 33.

Correlation of Quinidine Absorption with Disintegration and Dissolution Rates

JEFFREY D. STRUM, JOHN W. EBERSOLE, JAMES M. JAFFE, JOHN L. COLAIZZI, and ROLLAND I. POUST ˣ

Received April 25, 1977, from the *Department of Pharmaceutics, School of Pharmacy, University of Pittsburgh, Pittsburgh, PA 15261.* Accepted for publication July 13, 1977.

Abstract □ The dissolution profiles of four commercial quinidine sulfate tablets were determined using the USP rotating-basket dissolution apparatus. Substantial differences in dissolution half-times were noted and compared to previously reported disintegration times, absorption rate constants, and times of appearance of peak serum concentrations. Rank-order correlations were observed among all combinations of *in vivo* and *in vitro* parameters, indicating that the absorption rates of these tablets are controlled by both disintegration and dissolution.

Keyphrases □ Quinidine sulfate—four commercial tablets, dissolution profiles determined and related to disintegration and absorption □ Dissolution—quinidine sulfate, four commercial tablets, profiles determined and related to disintegration and absorption □ Disintegration—quinidine sulfate, four commercial tablets, related to dissolution profiles □ Absorption—quinidine sulfate, four commercial tablets, related to dissolution profiles □ Cardiac depressants—quinidine sulfate, four commercial tablets, dissolution profiles determined and related to disintegration and absorption

A recent report (1) presented the results of a comparative bioavailability study of four commercially available, chemically equivalent brands of quinidine sulfate. No statistically significant differences in the extent of absorption from the four brands were observed. However, significant differences in the times of peak serum concentration and absorption rate constants were found, indicating differences in the absorption rate among certain pairs of products. A rank-order correlation was observed when mean disintegration times for the four tablet formulations were compared with values for peak time and the absorption rate constant. It seemed appropriate, therefore, to determine the dissolution profiles of these four brands of quinidine sulfate tablets and to investigate the relationships among disintegration, dissolution, and absorption rate.

EXPERIMENTAL

The dissolution properties of six tablets of each of the four brands[1] of quinidine sulfate tablets employed in the study of Strum *et al.* (1) were determined in 900 ml of 0.1 *N* HCl at 37° using the USP rotating-basket dissolution apparatus[2] at 25 rpm. Following preliminary trials, sampling

[1] Treatment A: quinidine sulfate tablets USP, lot 76F83A, Eli Lilly & Co., Indianapolis, Ind.; Treatment B: quinidine sulfate tablets USP, lot 7088A, Philips Roxane Laboratories, Columbus, Ohio; Treatment C: Quinora tablets, lot 72755, Lakeside Laboratories, Milwaukee, Wis.; Treatment D: quinidine sulfate tablets USP, lot 15840, Stanlabs, Portland, Ore. These lots are the same as those used by Strum *et al.* (1).

[2] Hanson Research Corp., Northridge, Calif.

times were adjusted so that at least four data points were obtained above and below the apparent $t_{50\%}$ value.

Samples of dissolution media, 5 ml, were withdrawn (and replaced with an equal volume of drug-free fluid) in a plastic disposable syringe[3] through an attached 3.81-cm, 22-gauge needle, the top of which was 5 cm beneath the surface of the fluid. These samples were immediately filtered through a 0.45-μm membrane[4] filter. The samples were then assayed spectrophotometrically[5] at 343 nm. It was determined that there was no interference in the readings due to tablet excipients. The observed concentrations were converted to amounts dissolved and, in turn, to percent dissolved by using the data from the content uniformity determinations reported by Strum *et al.* (1).

RESULTS AND DISCUSSION

The resulting percent dissolved *versus* time data for each tablet were then plotted on log probability graph paper according to the method of Wagner (2). A line of best fit was obtained by applying least-squares regression analysis to the transformed values of percent dissolved [transformed to z values as suggested by Lippmann (3)] *versus* logarithms of time. Linear plots were obtained in all cases with correlation coefficients ranging from 0.947 to 0.992. Values for $t_{50\%}$ were then calculated from the slopes and intercepts of the lines of best fit.

Means and standard deviations were calculated for each of the four products and are listed in Table I along with previously reported (1) mean disintegration times, t_{max} values, and k_a values. As can be seen from these results, rank-order correlations occur when both dissolution half-time and disintegration time are compared with the two *in vivo* parameters. Specifically, as the dissolution rate decreases, the absorption rate also decreases, as evidenced by decreasing k_a values and increasing t_{max} values. Similarly, increasing disintegration times (slower disintegration) also coincide with decreasing absorption rates. Because of the limited range of values and the lack of statistically significant differences between certain treatment pairs in the *in vivo* data, it was felt that it would be inappropriate to express these findings as linear relationships.

Based on the k_a values, it appears that dissolution $t_{50\%}$ values greater than 27 min and disintegration times greater than 7 min result in substantially decreased absorption rates. Thus, the absorption rates of these four brands of quinidine sulfate tablets apparently are controlled by both disintegration and dissolution.

Table I—Means and Standard Deviations of Dissolution Half-Time, Disintegration Time, Absorption Rate Constant, and Time of Peak Serum Concentration for Each of Four Commercially Available Brands of Quinidine Sulfate Tablets

Treatment	$t_{50\%}$, min	Disintegration Time, min[a]	k_a, hr^{-1}[a]	t_{max}, hr[a]
C	7.08 ± 0.76	1.00 ± 0.0	2.91 ± 2.17	1.63 ± 0.59
A	14.49 ± 1.20	4.08 ± 0.20	2.88 ± 2.47	1.84 ± 0.74
B	27.41 ± 1.63	7.16 ± 1.94	2.08 ± 2.21	2.27 ± 0.71
D	34.94 ± 3.98	17.83 ± 2.22	1.12 ± 0.46	2.54 ± 0.33

[a] Data from Ref. 1.

REFERENCES

(1) J. D. Strum, J. L. Colaizzi, J. M. Jaffe, P. C. Martineau, and R. I. Poust, *J. Pharm. Sci.*, **66**, 539 (1977).

(2) J. G. Wagner, *ibid.*, **58**, 1253 (1969).

(3) I. Lippmann, in "Dissolution Technology," L. J. Leeson and J. T. Carstensen, Eds., APhA Academy of Pharmaceutical Sciences, Washington, D.C., 1974, p. 194.

[3] Becton-Dickinson and Co., Rutherford, N.J.
[4] Millipore Corp., Bedford, Mass.
[5] Model DB-G spectrophotometer, Beckman Instruments, Fullerton, Calif.

Synthesis and Biological Activity of N^6-(n-Alkylureido)purine Ribonucleosides and Their 5′-Phosphates

CHUNG IL HONG *, A. MITTELMAN, and GIRISH B. CHHEDA ˣ

Received February 25, 1977, from the *Center for Developmental Oncology, Department of General Surgery, Roswell Park Memorial Institute, Buffalo, NY 14263.* Accepted for publication July 11, 1977. *Present address: Department of Neurosurgery, Roswell Park Memorial Institute, Buffalo, NY 14263.

Abstract □ Syntheses and biological activities of 12 N^6-(n-alkylureido)purine ribonucleosides (alkyl chain length of 1–10, 16, and 18 carbons) and three N^6-(n-alkylureido)purine ribonucleoside 5′-phosphates (chain length of 4, 9, and 10 carbons) are described. The N^6-(n-alkylureido)purine ribonucleosides were prepared by a reaction of (2′,3′,5′-tri-*O*-acetyl-β-D-ribofuranosyl)-9*H*-purine-6-carbamate and n-alkylamine in refluxing pyridine. The 5′-nucleotides were prepared by direct phosphorylation of the corresponding ribonucleoside with phosphorus oxychloride and triethyl phosphate. Some N^6-(n-alkylureido)purine ribonucleosides (n-octyl, n-nonyl, and n-decyl) and their nucleotides showed a marked antiproliferative activity against L-1210 cells in culture.

Keyphrases □ Purine ribonucleosides, substituted—synthesized, evaluated for cytotoxic activity *in vitro* □ Cytotoxic activity—various substituted purine ribonucleosides and 5′-phosphates evaluated *in vitro* □ Structure–activity relationships—various substituted purine ribonucleosides and 5′-phosphates evaluated for cytotoxic activity *in vitro*

In view of the growth-inhibitory activities by analogs of the anticodon-adjacent modified ribonucleoside *N*-(purin-6-ylcarbamoyl)-L-threonine ribonucleoside (I) against cells of leukemic origin grown in culture (1, 2), a series of N^6-(n-alkylureido)purine ribonucleosides of varying chain length (1–10, 16, and 18 carbons) were prepared for determination of structure–activity relationships.

Since the 5′-nucleotides had shown greater water solubility (3), as well as the ability to cross cell membranes (4), and acted as sustained-release forms for the nucleosides

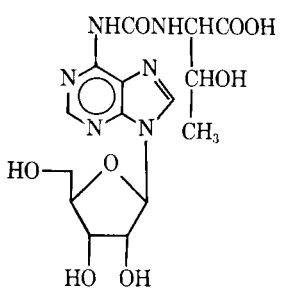

I

times were adjusted so that at least four data points were obtained above and below the apparent $t_{50\%}$ value.

Samples of dissolution media, 5 ml, were withdrawn (and replaced with an equal volume of drug-free fluid) in a plastic disposable syringe[3] through an attached 3.81-cm, 22-gauge needle, the top of which was 5 cm beneath the surface of the fluid. These samples were immediately filtered through a 0.45-μm membrane[4] filter. The samples were then assayed spectrophotometrically[5] at 343 nm. It was determined that there was no interference in the readings due to tablet excipients. The observed concentrations were converted to amounts dissolved and, in turn, to percent dissolved by using the data from the content uniformity determinations reported by Strum *et al.* (1).

RESULTS AND DISCUSSION

The resulting percent dissolved *versus* time data for each tablet were then plotted on log probability graph paper according to the method of Wagner (2). A line of best fit was obtained by applying least-squares regression analysis to the transformed values of percent dissolved [transformed to z values as suggested by Lippmann (3)] *versus* logarithms of time. Linear plots were obtained in all cases with correlation coefficients ranging from 0.947 to 0.992. Values for $t_{50\%}$ were then calculated from the slopes and intercepts of the lines of best fit.

Means and standard deviations were calculated for each of the four products and are listed in Table I along with previously reported (1) mean disintegration times, t_{max} values, and k_a values. As can be seen from these results, rank-order correlations occur when both dissolution half-time and disintegration time are compared with the two *in vivo* parameters. Specifically, as the dissolution rate decreases, the absorption rate also decreases, as evidenced by decreasing k_a values and increasing t_{max} values. Similarly, increasing disintegration times (slower disintegration) also coincide with decreasing absorption rates. Because of the limited range of values and the lack of statistically significant differences between certain treatment pairs in the *in vivo* data, it was felt that it would be inappropriate to express these findings as linear relationships.

Based on the k_a values, it appears that dissolution $t_{50\%}$ values greater than 27 min and disintegration times greater than 7 min result in substantially decreased absorption rates. Thus, the absorption rates of these four brands of quinidine sulfate tablets apparently are controlled by both disintegration and dissolution.

Table I—Means and Standard Deviations of Dissolution Half-Time, Disintegration Time, Absorption Rate Constant, and Time of Peak Serum Concentration for Each of Four Commercially Available Brands of Quinidine Sulfate Tablets

Treatment	$t_{50\%}$, min	Disintegration Time, min[a]	k_a, hr^{-1}[a]	t_{max}, hr[a]
C	7.08 ± 0.76	1.00 ± 0.0	2.91 ± 2.17	1.63 ± 0.59
A	14.49 ± 1.20	4.08 ± 0.20	2.88 ± 2.47	1.84 ± 0.74
B	27.41 ± 1.63	7.16 ± 1.94	2.08 ± 2.21	2.27 ± 0.71
D	34.94 ± 3.98	17.83 ± 2.22	1.12 ± 0.46	2.54 ± 0.33

[a] Data from Ref. 1.

REFERENCES

(1) J. D. Strum, J. L. Colaizzi, J. M. Jaffe, P. C. Martineau, and R. I. Poust, *J. Pharm. Sci.*, **66**, 539 (1977).

(2) J. G. Wagner, *ibid.*, **58**, 1253 (1969).

(3) I. Lippmann, in "Dissolution Technology," L. J. Leeson and J. T. Carstensen, Eds., APhA Academy of Pharmaceutical Sciences, Washington, D.C., 1974, p. 194.

[3] Becton-Dickinson and Co., Rutherford, N.J.
[4] Millipore Corp., Bedford, Mass.
[5] Model DB-G spectrophotometer, Beckman Instruments, Fullerton, Calif.

Synthesis and Biological Activity of N^6-(n-Alkylureido)purine Ribonucleosides and Their 5′-Phosphates

CHUNG IL HONG *, A. MITTELMAN, and GIRISH B. CHHEDA ˣ

Received February 25, 1977, from the *Center for Developmental Oncology, Department of General Surgery, Roswell Park Memorial Institute, Buffalo, NY 14263.* Accepted for publication July 11, 1977. *Present address: Department of Neurosurgery, Roswell Park Memorial Institute, Buffalo, NY 14263.

Abstract □ Syntheses and biological activities of 12 N^6-(n-alkylureido)purine ribonucleosides (alkyl chain length of 1–10, 16, and 18 carbons) and three N^6-(n-alkylureido)purine ribonucleoside 5′-phosphates (chain length of 4, 9, and 10 carbons) are described. The N^6-(n-alkylureido)purine ribonucleosides were prepared by a reaction of (2′,3′,5′-tri-*O*-acetyl-β-D-ribofuranosyl)-9*H*-purine-6-carbamate and n-alkylamine in refluxing pyridine. The 5′-nucleotides were prepared by direct phosphorylation of the corresponding ribonucleoside with phosphorus oxychloride and triethyl phosphate. Some N^6-(n-alkylureido)purine ribonucleosides (n-octyl, n-nonyl, and n-decyl) and their nucleotides showed a marked antiproliferative activity against L-1210 cells in culture.

Keyphrases □ Purine ribonucleosides, substituted—synthesized, evaluated for cytotoxic activity *in vitro* □ Cytotoxic activity—various substituted purine ribonucleosides and 5′-phosphates evaluated *in vitro* □ Structure–activity relationships—various substituted purine ribonucleosides and 5′-phosphates evaluated for cytotoxic activity *in vitro*

In view of the growth-inhibitory activities by analogs of the anticodon-adjacent modified ribonucleoside *N*-(purin-6-ylcarbamoyl)-L-threonine ribonucleoside (I) against cells of leukemic origin grown in culture (1, 2), a series of N^6-(n-alkylureido)purine ribonucleosides of varying chain length (1–10, 16, and 18 carbons) were prepared for determination of structure–activity relationships.

Since the 5′-nucleotides had shown greater water solubility (3), as well as the ability to cross cell membranes (4), and acted as sustained-release forms for the nucleosides

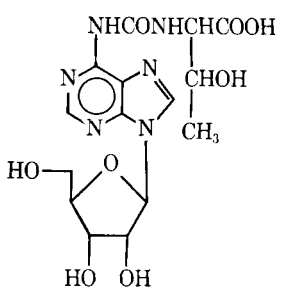

I

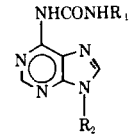

Table I—N^6-(*n*-Alkylureido)purine Ribonucleosides and 5′-Phosphates

Compound	R_1	R_2	Method	Yield, %	Melting Point[a]	Formula	Analysis, %	
							Calc.	Found
II[b]	CH_3	Ribosyl	A	92	199–200°	$C_{12}H_{16}N_6O_5 \cdot 0.5H_2O$	C 43.24	43.41
							H 5.13	5.15
							N 25.21	25.00
III	CH_2CH_3	Ribosyl	A	97.5	198°	$C_{13}H_{18}N_6O_5$	C 46.14	45.92
							H 5.36	5.53
							N 24.84	24.62
IV	$CH_2CH_2CH_3$	Ribosyl	A	98	184–185°	$C_{14}H_{20}N_6O_5$	C 47.71	47.74
							H 5.72	5.92
							N 23.85	23.63
V	$CH_2CH_2CH_2CH_3$	Ribosyl	A	54.5	127–129° s 174–175°	$C_{15}H_{22}N_6O_5$	C 49.17	49.22
							H 6.05	6.28
							N 22.94	23.05
VI	$CH_2(CH_2)_3CH_3$	Ribosyl	B	49	113–115° s 142–144°	$C_{16}H_{24}N_6O_5 \cdot 0.5H_2O$	C 49.34	49.38
							H 6.46	6.61
							N 21.58	21.64
VII	$CH_2(CH_2)_4CH_3$	Ribosyl	A	36	115–117° s 37–139°	$C_{17}H_{26}N_6O_5 \cdot 0.5H_2O$	C 50.60	50.38
							H 6.74	6.74
							N 20.83	20.78
VIII	$CH_2(CH_2)_5CH_3$	Ribosyl	B	70	81–83°	$C_{18}H_{28}N_6O_5$	C 52.93	52.76
							H 6.91	7.04
							N 20.58	20.82
IX[c]	$CH_2(CH_2)_6CH_3$	Ribosyl	B	84	96–98°	$C_{19}H_{30}N_6O_5 \cdot H_2O$	C 51.80	51.51
							H 7.31	7.20
							N 19.08	19.13
X	$CH_2(CH_2)_7CH_3$	Ribosyl	B	59.5	92–94° s 110–112°	$C_{20}H_{32}N_6O_5$	C 55.03	55.19
							H 7.39	7.57
							N 19.25	19.45
XI	$CH_2(CH_2)_8CH_3$	Ribosyl	B	46	127–128°	$C_{21}H_{34}N_6O_5$	C 55.98	55.95
							H 7.61	7.82
							N 18.65	18.88
XII	$CH_2(CH_2)_{14}CH_3$	Ribosyl	B	89	105–107°	$C_{27}H_{46}N_6O_5$	C 60.64	60.58
							H 8.67	8.71
							N 15.71	15.88
XIII	$CH_2(CH_2)_{16}CH_3$	Ribosyl	B	85	115–120° s 135–137°	$C_{29}H_{50}N_6O_5$	C 61.89	61.61
							H 8.95	9.05
							N 14.93	14.80
XIV	$CH_2CH_2CH_2CH_3$	Ribose 5′-phosphate	C	70	—	$C_{15}H_{21}BaN_6O_8P$	C 30.97	30.88
							H 3.64	3.82
							N 14.45	14.47
							P 5.33	5.39
XV	$CH_2(CH_2)_7CH_3$	Ribose 5′-phosphate	C	69	—	$C_{20}H_{31}BaN_6O_8P$	C 36.85	38.24
							H 4.79	5.21
							N 12.89	13.29
							P 4.75	5.02
XVI	$CH_2(CH_2)_8CH_3$	Ribose 5′-phosphate	C	87.5	—	$C_{21}H_{33}BaN_6O_8P$	C 37.88	37.77
							H 5.00	5.19
							N 12.62	12.78
							P 4.65	4.74

[a] s = soften. [b] This compound was prepared by the urethane method (1). [c] This compound was prepared by the isocyanate method (2).

(5), some potent ribosides were converted into their 5′-phosphates.

RESULTS AND DISCUSSION

The N^6-(*n*-alkylureido)purine ribonucleosides (II–V and VII) (Table I) were prepared in good yields by a reaction of 2′,3′,5′-tri-*O*-acetyladenosine and excess *n*-alkyl isocyanates in pyridine at 85–90° overnight, followed by deblocking of the acetyl groups in 4 *N* methanolic ammonia at room temperature (1). When the isocyanates were not available, the ureidopurine ribonucleosides (VI and VIII–XIII) were prepared by displacement of the ethoxy group of the urethane, ethyl 9-(2,3,5-tri-*O*-acetyl-β-D-ribofuranosyl)-9*H*-purine-6-carbamate (6), by 2 equivalents of *n*-alkylamines in pyridine at 120° overnight, followed by removal of the acetyl groups in methanolic ammonia.

N^6-(*n*-Alkylureido)purine riboside 5′-phosphates (XIV–XVI) were prepared by direct phosphorylation of the corresponding ribonucleosides with phosphorus oxychloride and triethyl phosphate at 0° in 50–90% yields (3, 7). Nonyl and decyl compounds (XV and XVI) precipitated out when the reaction mixtures were diluted with ice water. Indeed, the nucleotides improved the solubility in water (2 mg/ml, 10 times more soluble) as compared to that of the ribosides. The UV spectra of the alkylureido compounds were similar to those of I (Table II).

The compounds were tested for growth-inhibitory activity toward mammalian cells in axenic culture derived from mouse L-1210 leukemic cells (Table II). To relate the magnitude of the antiproliferative activity, compounds were assigned as >++, ++, +, ±, and NA at 1×10^{-4} and 1×10^{-5} *M* as indicated in Table II. Compounds with an alkyl chain 2–5 carbons long (III–VI) were marginally active against L-1210, while II (methyl) showed good activity. In VII–XI, the growth-inhibitory activity increased as the alkyl chain increased from 6 to 10 carbons; IX (*n*-octyl) (2), X (*n*-nonyl), and XI (*n*-decyl) were quite potent.

Compound XII (*n*-hexadecyl) was as active as IX–XI, and XIII was somewhat less active compared to the activity of IX–XI in the culture medium[1], which remained as a suspension during the assay. The 5′-nucleotides XV (*n*-nonyl) and XVI (*n*-decyl) were more water soluble and showed stronger antiproliferative activity than the corresponding nucleosides. The nucleotide XIV (*n*-butyl), like its nucleoside (V), was inactive. Evaluation of the octyl (IX), nonyl (X), and decyl (XI) compounds in mice bearing L-1210 leukemia is in progress.

[1] Dimethyl sulfoxide (0.5%) in Roswell Park Memorial Institute Medium 1640 plus 10% fetal calf serum.

Table II—UV Data and Biological Activity

Compound	UV_{max}, nm ($\epsilon \times 10^{-3}$) 0.1 N HCl[a]	70% Ethanol	0.1 N NaOH	Biological Activity (L-1210)[b] 1×10^{-4} M	1×10^{-5} M
II	277 (25.2)	269 (24.0) 276	278 (18.3) 298 (18.5)	++	
III	277 (24.2)	269 (23.5) 276 (19.3)	270 (13.9) 278 (14.5) 298 (16.1)	+	
IV	277 (24.0)	269 (22.2) 276 (18.3)	269 (20.9) 276 (18.1) 298 (15.7)	NA	
V	277 (24.9)	269 (24.1) 276 (20.1)	269 (22.0) 277 (19.4) 298 (16.5)	NA	
VI	277 (25.1)	269 (23.6) 276 (19.7)	270 (21.0) 277 (18.6) 298 (15.4)	+	
VII	277 (23.5)	270 (22.3) 276 (18.6)	269 (20.5) 277 (17.9) 299 (14.1)	++	
VIII	277 (23.9)	269 (22.6) 276 (18.9)	269 (19.7) 277 (17.5) 298 (14.0)	>++	
IX	270 (23.5) 277 (21.9)	269 (24.1) 277 (20.2)	271 (16.3) 278 (16.4) 298 (14.5)	>++	+
X	270 (22.4) 277 (21.1)	269 (23.9) 276 (19.9)	271 (15.2) 278 (15.5)	>++	+
XI	270 (23.3) 277 (21.9)	270 (24.3) 276 (20.3)	269 (13.1) 277 (13.3) 298 (11.5)	>++	++
XII	270 (21.9) 276 (20.5)	269 (22.6) 275 (19.0)	261 (15.1) 282 sh[c] (7.6)	>++	
XIII	268 (11.4)	270 (19.8) 276 (16.6)	261 (15.7) 283 sh[c] (7.1)	+	
XIV	270 (20.3) 277 (19.4)	269 (20.8) 277 (17.4)	280 (16.7) 278 (16.1) 298 (9.9)	NA	
XV	270 (21.6) 277 (20.9)	269 (23.2) 277 (19.3)	270 (17.4) 277 (16.5) 298 (9.4)		>++
XVI	270 (21.9) 277 (21.2)	269 (22.8) 277 (19.1)	270 (17.6) 277 (16.5) 198 (8.9)		>++

[a] Spectra for II–VIII were determined in aqueous 0.1 N HCl; spectra for IX–XVI were determined in 0.1 N HCl in 70% ethanol. [b] The notation represents the viable cell number relative to the controls at 1×10^{-4} and 1×10^{-5} M after 72 hr of incubation: >++, 0–30%; ++, 30–60%; +, 60–80%; ±, 80–90%; and NA, 90–110%. [c] sh = shoulder.

EXPERIMENTAL[2]

N^6-[(Ethylamino)carbonyl]adenosine (III): Method A—A stirred mixture of 2.76 g (7 mmoles) of 2′,3′,5′-tri-*O*-acetyladenosine and 2 ml of ethyl isocyanate in 50 ml of anhydrous pyridine was heated in a glass bomb at 85–90° overnight. After evaporating to dryness, the residue was azeotroped with toluene (20 ml) and stirred in 200 ml of 4 *N* methanolic ammonia at room temperature for 5 hr. The solvent was then evaporated to dryness, and the residue was dissolved in 100 ml of hot ethanol.

After cooling at 0° overnight, the product was collected on a filter and washed with cold ethanol and ether; the yield was 2.3 g (97%). The analytical sample was recrystallized from ethanol, mp 198°; IR: 1680 (ureido C=O) and 1620 and 1550 (C=C, C=N) cm^{-1}.

[2] Melting points were determined in capillary tubes on a Mel-Temp apparatus and are uncorrected. IR spectra were measured using Perkin-Elmer 457 and 137B spectrophotometers. UV spectra were recorded on Cary model 14 and Beckman Acta V spectrophotometers. Elemental analyses were carried out by Galbraith Laboratories, Knoxville, TN 37921, and by Heterocyclic Chemical Corp., Harrisonville, MO 64701.

N^6-[(*n*-Nonylamino)carbonyl]adenosine (X): Method B—A mixture of 3.26 g (7 mmoles) of ethyl 9-(2,3,5-tri-*O*-acetyl-β-D-ribofuranosyl)-9*H*-purine-6-carbamate (6), 2 g (14 mmoles) of *n*-nonylamine, and 200 ml of anhydrous pyridine was refluxed with stirring for 20 hr. After evaporating to dryness, the residue was azeotroped with toluene (20 ml) and then stirred in 200 ml of 4 *N* methanolic ammonia at room temperature for 5 hr. The solvent was evaporated to dryness, and the residue was dissolved into 100 ml of hot ethanol.

After cooling at room temperature for 1 hr, the white crystals were filtered and washed with cold ethanol and ether; the yield was 861 mg. Additional product was obtained from the filtrate in a yield of 950 mg; the total yield was 1.811 g (59.5%). The analytical sample was recrystallized from ethanol, mp 92–94° soften, 110–112° melted; IR: 3000 (CH), 1730, 1700 (ureido C=O), and 1625 (C=C, C=N) cm^{-1}.

N^6-[(*n*-Nonylamino)carbonyl]adenosine 5′-Phosphate (XV): Method C—To a cooled mixture of 2 ml (~14 mmoles) of phosphorus oxychloride and 80 ml of triethyl phosphate was added 3.05 g (7 mmoles) of X at 0°. The mixture was stirred at 0° for 18 hr and diluted with ice water (350 ml). The white solid, formed within a few minutes, was filtered and washed with cold water. The product was dried at room temperature, and the yield was 2.49 g (69%).

The product was then converted to the ammonium salt by passing the solution of the product in 2-propanol–concentrated ammonia–water (7:1:2) through a cellulose column (2). The analytical sample was obtained as the barium salt after equimolar amounts of the aqueous ammonium salt and barium iodide were mixed, followed by precipitating with acetone; IR: 2950 (CH), 1700 (ureido C=O), 1625, 1560 (C=C, C=N), 1260 (P=O), and 1070 (POC) cm^{-1}.

Growth-Inhibition Assays—The compounds were dissolved in dimethyl sulfoxide and allowed to remain at 37° overnight; this step achieved sterilization. Sterile growth medium was then added to bring the concentration of dimethyl sulfoxide to 0.5% and that of a compound to 10^{-4} and 10^{-5} *M*. At this dimethyl sulfoxide concentration, growth of control cultures was unaffected.

The assays were performed in test tubes without agitation. The tubes were inoculated with mouse leukemia cells (L-1210) from stock cultures in logarithmic growth to a starting density previously determined to be near the minimum required for initiation of logarithmic growth of control cultures (between 2 and 5×10^5 cells/ml). At 24-hr intervals, 0.2 ml was removed and mixed with trypan blue to a final concentration of 0.05%. Then the total and viable cells were counted in a hemocytometer. Cells able to exclude the dye were scored as viable. The compounds were rated as shown in Table II to indicate the following viable cell densities relative to controls after 72 hr of incubation: >++, 0–30%; ++, 30–60%; +, 60–80%; ±, 80–90%; and NA (not active), 90–110%.

REFERENCES

(1) C. I. Hong, G. B. Chheda, S. P. Dutta, E. O. Curtis, and G. L. Tritsch, *J. Med. Chem.*, **16**, 139 (1973).

(2) C. I. Hong, G. L. Tritsch, A. Mittelman, P. Hebborn, and G. B. Chheda, *ibid.*, **18**, 465 (1975).

(3) C. I. Hong and G. B. Chheda, *ibid.*, **16**, 956 (1973).

(4) W. Plunkett, L. Lapi, P. J. Ortiz, and S. S. Cohen, *Proc. Natl. Acad. Sci. USA*, **71**, 73 (1974).

(5) G. A. LePage, Y.-T. Lin, R. E. Orth, and J. A. Gottlieb, *Cancer Res.*, **32**, 2441 (1972).

(6) G. B. Chheda and C. I. Hong, *J. Med. Chem.*, **14**, 748 (1971).

(7) M. Yoshikawa, T. Kato, and T. Tanenishi, *Tetrahedron Lett.*, **50**, 5065 (1967).

ACKNOWLEDGMENTS

Supported by U.S. Public Health Service Grant CA 14185.

The authors thank Dr. E. D. Holyoke for his interest and encouragement in this work and Dr. G. L. Tritsch for help in assaying these compounds.

Separation and Spectrophotometric Determination of Theophylline and Hydroxyethyltheophylline in a Pharmaceutical Syrup

FABRIZIO De FABRIZIO

Received April 11, 1977, from the *Control Pharmaceutical Laboratory, Saphar Laboratories (PTY) Ltd., P.O. Box 2368, Johannesburg 2000, South Africa.* Accepted for publication July 28, 1977.

Abstract □ A simple chromatographic procedure was developed for the separation and determination of theophylline and hydroxyethyltheophylline. An aliquot of diluted syrup was pipetted into a chromatographic column containing a strong anion-exchange resin, which retains theophylline and allows the hydroxyethyl derivative to pass through it. Theophylline was subsequently eluted with 1 *N* HCl and determined by difference spectrophotometry at 284 nm; its derivative was determined at 272 nm.

Keyphrases □ Theophylline—chromatographic separation from hydroxyethyl derivative in pharmaceutical syrup, spectrophotometric analyses □ Hydroxyethyltheophylline—chromatographic separation from theophylline in pharmaceutical syrup, spectrophotometric analyses □ Chromatography, ion exchange—separation of theophylline and hydroxyethyl derivative in pharmaceutical syrup □ Spectrophotometry—analyses, theophylline and hydroxyethyl derivative in pharmaceutical syrup

Theophylline (I) is widely used for the treatment of asthma. Because of its low solubility, oral dosage forms are sometimes formulated with a more soluble derivative to enhance theophylline availability for prompt therapeutic effect. Although several methods were reported for the determination of theophylline alone and in combination with other drugs (1–5), few reports concerned the assay of its mixture containing hydroxyethyltheophylline (etofylline) (II). Kaniewska and Zyzynoky (6) analyzed I in the presence of II using a spectrophotometric titration in which the absorbance of argentometrically determined theophylline was subtracted from the total absorbance of both compounds and the content of II was calculated.

A titrimetric procedure also was reported (7) in which the determination of II was carried out by precipitating theophylline with excess mercuric acetate. The excess was then determined in a portion of filtrate by titration with ammonium rhodanide; another portion of filtrate was treated with excess 0.1 *N* iodide to determine II. Stuchlik *et al.* (8) described an electrophoresis method for the purification of II and hydroxypropyltheophylline from the unchanged starting substances. These procedures, although giving the required separation and determination of the two active ingredients in other formulations, were unsuitable for the syrup, where the weight ratio of theophylline to II was 8:1. Consequently, a new analytical method was needed.

EXPERIMENTAL

Apparatus—A recording spectrophotometer[1] with matched UV 1-cm cells was used. The glass column was 35 × 1 cm with a fritted glass disk and polytef stopcock.

Reagents—The following were used: 100–200-mesh ion-exchange resin[2], 6 *N* HCl in 50% (v/v) ethanol, 1 *N* HCl in water, 4 *N* NaOH in water, and 1 *N* NaOH in water.

[1] Pye Unicam SP-1800.
[2] Amberlite CG-400 (OH), British Drug Houses.

Table I—Recovery of I and II Mixed Standard in 50% (v/v) Ethanol

Mixture	I Amount Taken, mg	I Recovery, %	II Amount Taken, mg	II Recovery, %
a	79.3	98.3	9.7	101.0
b	80.5	97.9	9.3	100.6
c	81.1	99.0	9.8	99.7
d	79.9	98.7	10.1	98.8
e	79.7	97.9	9.7	101.3
f	81.4	97.8	9.9	98.7
g	80.7	98.3	9.4	99.1
h	80.1	99.1	10.5	98.8
Average, %	—	98.4	—	99.8
SD, %		±0.51		±1.07

Standard Solutions—Theophylline USP (anhydrous powder), 0.064 mg/ml, is prepared by dissolving about 64 mg, accurately weighed, in 100 ml of 1 *N* HCl and diluting stepwise with the same solvent. Hydroxyethyltheophylline (Aust. Phar. grade), 0.008 mg/ml, is prepared by dissolving about 80 mg, accurately weighed, in 100 ml of distilled water and diluting stepwise with the same solvent.

Column Preparation—Slurry 3 g of resin with 20–35 ml of water. Decant off the floating materials until the supernate is clear. Wash once with ethanol and then with water. Transfer to a column with the stopcock closed and let the resin settle by gravity. Drain the water and wash the resin with five 10-ml portions of 6 *N* HCl. Stir gently after each addition and then rinse twice with 50-ml portions of water. Add 20 ml of 4 *N* NaOH to the column and stir gently for a few seconds. Wash with water until the eluate is pH 4–7. Finally, top with a small pledget of glass wool and drain to level.

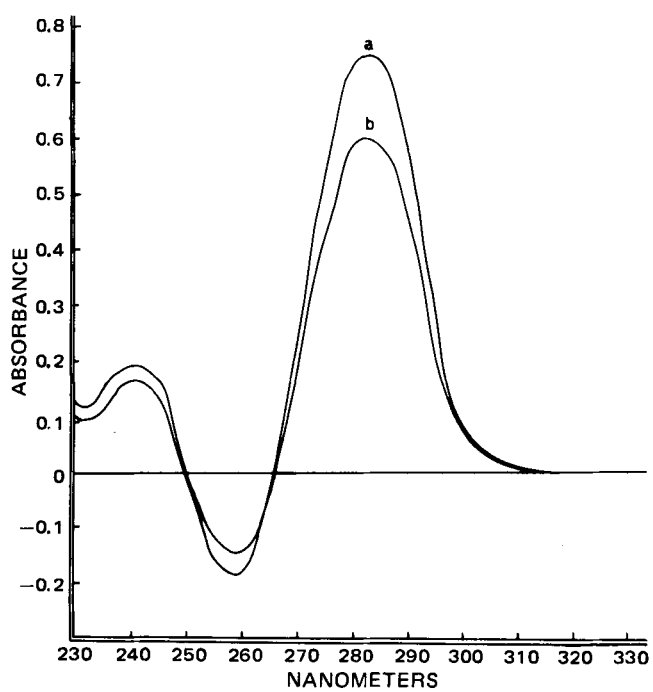

Figure 1—*Differential absorption spectra of 0.0190 mg of theophylline/ml (a) and 0.0152 mg of theophylline/ml plus saccharin sodium (b).*

Table II—Recoveries of I and II in the Two Laboratory Prepared Syrups

	Syrup 1				Syrup 2			
	I		II		I		II	
Test	Taken, mg	Found, %	Taken, mg	Found, %	Taken, mg	Found, %	Taken, mg	Found, %
1	81.0	98.5	10.5	97.9	80.0	101.3	9.5	100.6
2	80.9	97.9	11.6	100.5	79.9	100.0	9.3	98.8
3	80.1	99.8	12.0	100.9	75.6	98.8	10.4	97.8
4	79.8	99.9	9.5	98.5	77.6	97.8	9.1	99.3
5	81.2	100.3	9.7	97.9	81.3	99.1	9.6	98.8
6	82.0	98.1	10.5	99.3	82.0	98.6	11.4	101.5
7	75.0	99.4	10.3	101.6	79.9	98.3	12.0	100.7
8	79.9	100.7	11.6	100.3	79.8	99.3	9.1	98.6
Average, %	—	99.3	—	99.6	—	99.2	—	99.5
SD, %		±0.78		±1.42		±1.09		±1.27
CV		0.79		1.43		1.10		1.28

Repeat the treatment after each analysis.

Sample Treatment—Using a 10-ml pipet, draw the syrup[3] just to the meniscus and transfer to a 25-ml volumetric flask, allowing 5 min for drainage. Dilute to volume with distilled water and mix.

Determination—*Compound II*—Pipet 3 ml of diluted syrup into the prepared column and let the sample solution pass through at a rate of 1 ml/min. Collect the eluate in a 100-ml volumetric flask placed beneath the column. Add more water (80 ml) divided into portions, allowing each portion to sink into the resin. Remove the flask, dilute to volume with water, and mix. This solution contains II. Scan the sample and the standard solutions between 230 and 310 nm in 1-cm cells against water. Determine the absorbance at the maximum, about 272 nm, and calculate the concentration of II in the sample.

Theophylline—Drop the level of liquid in the column just above the glass wool pledget and then elute the column with 1 *N* HCl at a rate of 2 ml/min, collecting the eluate into a 100-ml volumetric flask to the mark. Pipet a 4-ml aliquot of this solution into each of two 50-ml volumetric flasks. To one flask, add water to volume (Solution A); to the other, add 4.1 ml of 1 *N* NaOH and then water to volume (Solution B). Measure the absorbance maximum of Solution B at 284 nm in 1-cm cells against Solution A. Compare the absorbance of the sample with that of the standard solution treated in a like manner (excluding the chromatographic step) and calculate the theophylline concentration in the syrup.

RESULTS AND DISCUSSION

Results for synthetic mixtures containing the two active ingredients alone are reported in Table I. The mixtures were dissolved in 50% (v/v) ethanol and then treated as the sample. The method was subjected to a test of the effect of excipients[4] by using excipient mixtures similar to the commercial product under study. The recoveries of two laboratory prepared syrups containing I, II, and excipients are shown in Table II. These simulated syrups were used for calculating the average, standard deviation, and coefficient of variation. Each syrup was assayed eight times.

The close agreement between the amount of each component taken and the determined value suggests that the procedure is unaffected by the excipients. Coloring material in this pharmaceutical preparation was held on the resin, and the other ingredients that passed through the column did not affect the direct spectrophotometric determination of II. A direct spectrophotometric determination of theophylline at about 271 nm would have been affected by the presence of saccharin sodium. This ingredient was held by the resin and eluted together with theophylline.

[3] The analysis was applied to a syrup containing 80 mg of I and 10 mg of II/15 ml.

[4] Excipients used were alcohol 95% BP, sucrose BP, saccharin sodium BP, amaranth BPC, and apricot flavor Naarden.

Table III—Analyses of Commercial Products

Sample	Component	Amount Declared, mg/5 ml	Amount Found, mg/5 ml	Percent of Declared Amount
A	I	80.0	81.5	101.9
	II	10.0	10.7	107.0
B	I	80.0	79.3	99.1
	II	10.0	9.6	96.0
C	I	80.0	82.3	102.9
	II	10.0	10.3	103.0
D	I	80.0	83.2	104.0
	II	10.0	10.5	105.0
E	I	80.0	76.8	96.0
	II	10.0	9.8	98.0

To cancel this interference, differential spectrophotometry was adopted for theophylline. Figure 1 shows the differential spectra of two prepared mixtures, one containing theophylline with all ingredients, including saccharin sodium, and the other without saccharin sodium. This technique was possible since theophylline, as a weak acid, can undergo a pH-induced shift. Although the conventional spectral change of solutions containing theophylline in acid and alkaline media are apparently minor (about 4 nm), useful difference spectra, with two maxima at about 240 and 284 nm and two isosbestic points, are produced, recording base against acid. An accurate adjustment of pH was not necessary to have theophylline, with a single ionizable group, directly conjugated to a chromophore. It was important to have the solutions of theophylline (acidic and alkaline) at least 2 pH units above and below the pK value to ensure that each species is in equilibrium at 99% spectral purity. Analyses of commercial products are shown in Table III.

This method is rapid and simple and allows the determination of the therapeutic ingredients from a single sample aliquot.

REFERENCES

(1) T. Higuchi and E. Brochmann-Hanssen, "Pharmaceutical Analysis," Interscience, New York, N.Y., 1961, p. 240.

(2) R. Foreman and M. I. Blake, *J. Pharm. Sci.*, **54**, 12 (1965).

(3) A. M. McEnirt, *J. Assoc. Offic. Agr. Chem.*, **40**, 926 (1957).

(4) D. C. Garrat, "The Quantitative Analysis of Drugs," Chapman & Hall, London, England, 1964, p. 143.

(5) D. J. Smith, *J. Assoc. Offic. Anal. Chem.*, **55**, 596 (1972).

(6) T. Kaniewska and W. Zyzynoky, *Zaklad Chemii Analitycznej Inst. Warzsawie, Poland;* through *J. Pharm. Pharmacol.*, **18**, 511 (1966).

(7) W. Poethke and J. Biederman, *Pharm. Zentralh.*, **104**, 225 (1965); through *Int. Pharm. Abstr.*, **16**, 1111 (1966).

(8) M. Stuchlik, I. Csiba, and L. Krasnek, *Cesk. Farm.*, **16**, 187 (1967); through *Int. Pharm. Abstr.*, **16**, 936 (1967).

Use of MULTDOS for Pharmacokinetic Analysis of Ethosuximide Data during Repetitive Administration of Single or Divided Daily Doses

WAYNE A. COLBURN and MILO GIBALDI ˣ

Received June 8, 1977, from the *Department of Pharmaceutics, School of Pharmacy, State University of New York at Buffalo, Amherst, NY 14260.* Accepted for publication July 26, 1977.

Abstract □ MULTDOS, a computer method to curve fit data obtained on multiple dosing, was used with either the 1969 or 1974 version of the NONLIN program to compare the pharmacokinetic parameters of ethosuximide during repetitive administration of single or divided daily doses. Elimination rate constants, excretion rate constants, and apparent volumes of distribution were similar between the two dosing regimens and essentially identical between the two nonlinear regression programs.

Keyphrases □ Computer analyses—MULTDOS and 1969 or 1974 NONLIN program, pharmacokinetic parameters of ethosuximide during single or divided daily doses compared □ Ethosuximide—pharmacokinetic parameters during single or divided daily doses compared using MULTDOS and 1969 or 1974 NONLIN computer program □ Pharmacokinetics—ethosuximide parameters during single or divided daily doses compared using MULTDOS and 1969 or 1974 NONLIN computer program □ Anticonvulsants—ethosuximide, pharmacokinetic parameters during single or divided daily doses compared using MULTDOS and 1969 or 1974 NONLIN computer program

Goulet *et al.* (1) compared once daily and three times daily ethosuximide administrations in healthy volunteers. Steady-state plasma ethosuximide concentrations and daily urinary excretion of unchanged drug and metabolite were comparable during either dosing regimen, supporting the use of a single daily dose for ethosuximide therapy.

Two recent articles concerned the pharmacokinetic analysis of data obtained during repetitive dosing (2, 3). The first report (2) considered the situation in which the pharmacokinetic parameters of the drug remain constant throughout, and the computer method employed is termed MULTDOS. The second report (3) concerned the development of a computer method, VARPARM, for those cases where there is dose-to-dose variation in one or more pharmacokinetic parameters. Both MULTDOS and VARPARM utilized the 1969 version of the nonlinear least-squares regression program NONLIN (4) as the main program. Inquiries as to the application of these methods with the 1974 version of NONLIN (5) led to the development of subroutines to be used with a modified version of the 1974 NONLIN.

The present report concerns the comparison of pharmacokinetic parameters obtained during repetitive dosing of ethosuximide as single or divided daily doses using the MULTDOS method with both the old and new versions of NONLIN.

EXPERIMENTAL

The basic MULTDOS method for fitting data was described previously (2). Utilization of the method with 1969 NONLIN has been modified since the original report so that the NONLIN package is self-sufficient; *i.e.*, the separate and independent DASCRU[1] subroutine need not be used. This modification was accomplished by having the multiple-dose routine call the numerical integration subroutine NUMINT in the NONLIN program. NUMINT subsequently calls a user-supplied subroutine F to solve the differential equations. Only a minor change is required in the NONLIN package to achieve this improvement[2].

Originally, we elected to input differential rather than integral equations (2, 3), and this approach is still favored. The use of differential equations is particularly convenient when fitting data to a complex, *e.g.*, nonlinear, pharmacokinetic model. On the other hand, if data are to be fit to a relatively simple pharmacokinetic model, the use of integral equations may be advantageous in that it requires less computer time and less modification of DFUNC.

The use of MULTDOS with 1974 NONLIN required modifications in the DASCRU, NONLIN, and SUMMARY subroutines, all of which are contained in the new NONLIN package, as well as in the user-supplied subroutine DFUNC[2]. The changes alter the logic so that the NONLIN program assumes the use of integrated functions even though differential equations are being used. The changes in DFUNC were required to follow the 1974 NONLIN logic.

The revised MULTDOS method with 1969 NONLIN and the newly developed MULTDOS method with 1974 NONLIN were tested successfully using ideal data before analyzing the ethosuximide data.

Plasma ethosuximide concentrations and urinary excretion rates during repetitive dosing were obtained from the study reported by Goulet *et al.* (1). Healthy subjects received 500 mg of ethosuximide, either as a single daily dose or as two 250-mg doses at 12-hr intervals for 14 days. The daily dose was then increased to 750 mg and administered either as a single daily dose or as three 250-mg doses at 6-, 6-, and 12-hr intervals each day for an additional 14 days. Blood and urine samples were collected for drug analysis at various times during the treatment and washout periods.

Average drug concentration data in plasma and urinary excretion rate data, weighted reciprocally, as well as initial parameter estimates for a one-compartment open model served as input for the programs. In each case, the plasma and urine data were fit simultaneously.

Table I—Comparison of Ethosuximide Pharmacokinetics Estimated by MULTDOS, Using 1969 NONLIN or 1974 NONLIN, from Simultaneous Curve Fits of Plasma Concentration and Urinary Excretion Data during Repetitive Administration of Single or Divided Daily Doses

Parameter[a]	Estimated with 1969 NONLIN[b]	Estimated with 1974 NONLIN[b]
	Single Daily Dose	
k_a	2.62 (545)	2.60 (675)
K	0.0132 (2)	0.0131 (2)
k_e	0.0026 (8)	0.0026 (12)
V/f	47.4 (4)	47.5 (4)
	Divided Daily Dose	
k_a	0.749 (29)	0.758 (29)
K	0.0138 (2)	0.0138 (2)
k_e	0.0029 (3)	0.0029 (7)
V/f	52.1 (2)	52.1 (2)

[a] k_a = absorption rate constant (hours^{-1}), K = elimination rate constant (hours^{-1}), k_e = urinary excretion rate constant, V = apparent volume of distribution (liters), and f = fraction of dose absorbed. [b] Mean estimate (*CV*, %).

RESULTS

The one-compartment model parameter estimates obtained by curve

[1] Available from IMSL, 6200 Hillcroft, Houston, TX 77036.

[2] Program information will be supplied on written request.

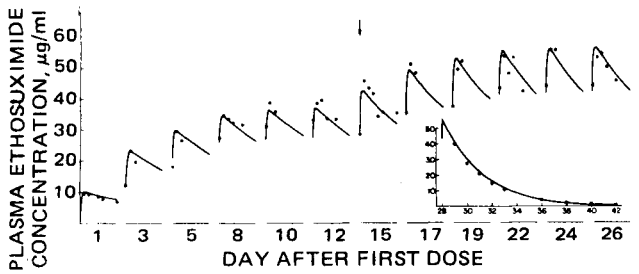

Figure 1—*MULTDOS curve fit to mean plasma ethosuximide concentrations during repetitive oral administration of single daily doses of 500 mg (Days 1–14) and 750 mg (Days 15–28). Inset shows plasma concentrations after the last dose.*

fitting the ethosuximide data using the MULTDOS method with either version of NONLIN are presented in Table I. The means and standard deviations for each parameter were, with one exception, quite similar between treatments (single daily doses *versus* divided daily doses) and were, in all cases, virtually identical between computer programs (1969 NONLIN *versus* 1974 NONLIN). The analysis suggests that there is more rapid absorption after the single compared to the divided daily doses. These differences, however, are of no significance in view of the large uncertainty associated with the absorption rate constant estimated from the single daily dose data. The reason for this uncertainty is that only one data point from the absorption phase was available each day for the pharmacokinetic analysis. When fitting the divided daily dose data, two or three such data points were available each day.

Plasma concentration–time data for the single and divided daily doses and the respective curve fits are shown in Figs. 1 and 2, respectively. Correlation coefficients of 0.991 and 0.996 were obtained between observed and predicted values for the respective treatments. As anticipated, differences between peak and trough levels of drug during a dosing interval at steady state were larger during the once-a-day dosing than during the divided daily dosing; but the mean steady-state plasma concentrations were quite similar, as previously reported (1).

The observed and predicted urinary excretion rates of ethosuximide

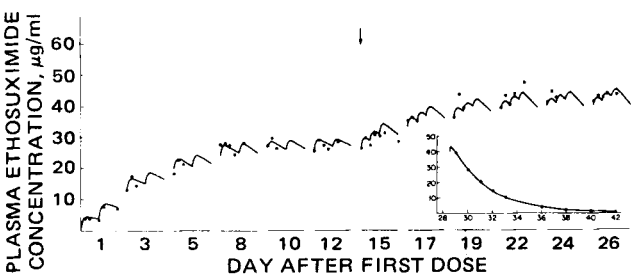

Figure 2—*MULTDOS curve fit to mean plasma ethosuximide concentrations during repetitive oral administration of divided daily doses of 500 mg (Days 1–14) and 750 mg (Days 15–28). Inset shows plasma concentrations after the last dose.*

Table II—Comparison of Observed and Predicted [a] Urinary Excretion Rates (Milligrams per Hour) of Ethosuximide during Multiple Dosing

Days	Single Daily Dose		Divided Daily Dose	
	Observed	Predicted	Observed	Predicted
0.5	1.3	1.1	1.0	0.6
7.5	3.7	3.8	3.3	3.7
11.5	4.4	4.1	4.6	4.0
13.5	4.8	4.1	4.4	4.0
14.5	5.2	4.7	4.8	4.7
21.5	5.8	6.1	6.3	6.2
25.5	5.3	6.2	5.4	6.4
27.5	6.6	6.3	6.5	6.4
29.5	3.5	3.3	3.8	3.7
31.5	1.4	1.8	1.8	1.9

[a] Predicted values were calculated by simultaneous curve fitting of plasma and urine data.

are presented in Table II. Correlation coefficients between observed and predicted data were 0.977 and 0.982 for the single and divided dose treatments, respectively. The correlation coefficients for the combined plasma and urine data were 0.994 and 0.997 for the respective treatments.

DISCUSSION

The present analysis of ethosuximide data obtained on multiple dosing indicates that the pharmacokinetic parameters are independent of the mode of administration. The elimination half-lives were 52.5 and 50.2 hr, and the apparent volumes of distribution (assuming complete absorption) were 47.4 and 52.1 liters for the single and divided daily doses, respectively. The results of this study also support the conclusion of Goulet *et al.* (1) that the use of single daily doses may be an effective regimen for ethosuximide therapy.

The data analysis further indicates that the MULTDOS method may be used with either version of NONLIN. Essentially identical parameter estimates, standard deviations, and correlation coefficients were obtained when using 1969 and 1974 NONLIN.

REFERENCES

(1) J. R. Goulet, A. W. Kinkel, and T. C. Smith, *Clin. Pharmacol. Ther.*, **20**, 213 (1976).

(2) W. A. Colburn, D. Shen, and M. Gibaldi, *J. Pharmacokinet. Biopharm.*, **4**, 469 (1976).

(3) W. A. Colburn and M. Gibaldi, *J. Pharm. Sci.*, **66**, 530 (1977).

(4) C. M. Metzler, Technical Report 7292/69/7292/005, Upjohn Co., Kalamazoo, Mich., 1969.

(5) C. M. Metzler, G. L. Elfring, and A. J. McEwen, "A Users Manual for NONLIN and Associated Programs," Upjohn Co., Kalamazoo, Mich., 1974.

ACKNOWLEDGMENTS

Supported in part by Grant GM-20852 from the National Institutes of Health.

Synthesis and Antimicrobial Activity of Ethyl *N*-Aryl-*S*-(triphenylstannyl)isothiocarbamates

EUGENE J. KUPCHIK *x, **MICHAEL A. PISANO** ‡, **HANS E. HANKE** *, and **WEN-CHANG R. TSENG** ‡

Received June 1, 1977, from the *Department of Chemistry and the ‡Department of Biological Sciences, St. John's University, New York, NY 11439. Accepted for publication July 26, 1977.

Abstract □ Five ethyl *N*-aryl-*S*-(triphenylstannyl)isothiocarbamates were synthesized by the reaction of triphenyltin iodide with the appropriate ethyl *N*-arylthiocarbamate in the presence of triethylamine. The IR spectrum of each compound was obtained over the 4000–200-cm^{-1} range, and some bands were assigned. These new compounds were found to be generally better antifungal agents than the previously tested *N*-substituted *N'*-cyano-*S*-(triphenylstannyl)isothioureas. The new compounds were also investigated for antibacterial activity and were especially inhibitory toward Gram-positive species. Except for their lower activity toward *Bacillus subtilis*, their antibacterial activity was identical to the previously tested *N*-phenyl-*N'*-cyano-*S*-(triphenylstannyl)isothiourea.

Keyphrases □ Isothiocarbamates, various—synthesized, evaluated for antibacterial and antifungal activity □ Antibacterial activity—various isothiocarbamates evaluated □ Antifungal activity—various isothiocarbamates evaluated □ Organotin compounds—various *N*-aryl-*S*-(triphenylstannyl)isothiocarbamates synthesized, evaluated for antibacterial and antifungal activity □ Structure–activity relationships—various isothiocarbamates evaluated for antibacterial and antifungal activity

Recently, the antifungal activity of five *N*-substituted *N'*-cyano-*S*-(triphenylstannyl)isothioureas (Series I) was described (1). The antifungal activity of one compound (I*a*, R = C_6H_5) was compared to that of its oxygen analog (II*a*, R = C_6H_5), and some differences were noted. Compound I*a* also was investigated for antibacterial activity and was

Table I—Ethyl *N*-Aryl-*S*-(triphenylstannyl)isothiocarbamates [a]

Compound	R	Yield, %[b]	Melting Point[c]	Formula	Analysis, %	Calc.	Found
III*a*	C_6H_5	84	113–114°	$C_{27}H_{25}NOSSn$	C	61.16	60.92
					H	4.75	4.80
					N	2.64	2.92
					S	6.05	6.24
					Sn	22.38	22.22
III*b*	*p*-FC_6H_4	91	79–82°	$C_{27}H_{24}FNOSSn$	C	59.15	59.17
					H	4.41	4.27
					F	3.47	3.64
					N	2.55	2.73
					S	5.85	5.80
					Sn	21.65	21.26
III*c*	*p*-$O_2NC_6H_4$	71	95–98°	$C_{27}H_{24}N_2O_3SSn$	C	56.37	56.52
					H	4.21	4.23
					N	4.87	5.07
					S	5.57	5.43
					Sn	20.63	20.92
III*d*	*p*-NCC_6H_4	97	82–85°	$C_{28}H_{24}N_2OSSn$	C	60.57	60.72
					H	4.36	4.57
					N	5.04	5.35
					S	5.77	6.06
					Sn	21.38	21.02
III*e*	2-Naphthyl	51	65–68°	$C_{31}H_{27}NOSSn$	C	64.16	64.18
					H	4.69	4.75
					N	2.41	2.70
					S	5.53	5.61
					Sn	20.45	20.30

[a] Triphenyltin iodide, ethyl *N*-arylthiocarbamate, and triethylamine (1:1:2 mole ratio) were allowed to react in ether at the reflux temperature for 40 hr (III*a*), 92 hr (III*b*), 17 hr (III*c*), 18 hr (III*d*), and 96 hr (III*e*). [b] Based on material melting within 5° of the analytical sample. [c] Refers to the analytical sample; recrystallization solvents were *n*-pentane (III*b*–III*d*), ether (III*a*), and ether–*n*-pentane (III*e*).

Table II—IR Spectra of Ethyl *N*-Aryl-*S*-(triphenylstannyl)isothiocarbamates [a]

Compound	C=N[b]	C_6H_5 Ring Vibration (2–4)	SnS (5)	Sn $(C_6H_5)_3$ (4, 6–10) ν_{as}	ν_s
III*a*	1623 s	453 s	320 s[c]	274 s	231[d]
III*b*	1621 s	442 s	359 s[e]	272 s	224 s[f]
III*c*	1621 s	452 s[g]	329 m[h]	269 s	224 s[i]
III*d*	1629 s	452 s[j]	314 m	266 s	242 s
III*e*	1613 s	452 s[k]	345 s	275 s	232 m[l]

[a] Values are expressed in centimeters^{-1}; s = strong, m = medium, and w = weak. The data for 4000–400 cm^{-1} were obtained using potassium bromide pellets. The data for 400–200 cm^{-1} were obtained using mineral oil. [b] This assignment is uncertain because of the presence of aromatic C=C bands in this region. [c] A band was present at 372 m cm^{-1}. [d] A band was present at 204 w cm^{-1}. [e] A band was present at 386 m cm^{-1}. [f] A band was present at 204 w cm^{-1}. [g] Bands were present at 444 s and 439 s cm^{-1}. [h] A band was present at 373 m cm^{-1}. [i] A band was present at 202 m cm^{-1}. [j] A band was present at 448 cm^{-1}. [k] A band was present at 445 s cm^{-1}. [l] Bands were present at 249 s and 260 s cm^{-1}.

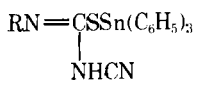

I

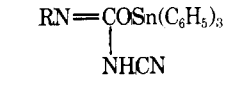

II

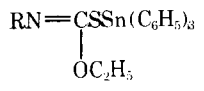

III

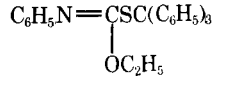

IV

especially inhibitory toward Gram-positive species; furthermore, its antibacterial activity was considerably greater than that of its oxygen analog.

The purpose of the present study was to evaluate the antimicrobial activity of another class of compounds having a tin–sulfur bond, namely, ethyl *N*-aryl-*S*-(triphenylstannyl)isothiocarbamates (Series III), and ethyl *N*-phenyl-*S*-tritylisothiocarbamate (IV), which is the carbon analog of III*a* (R = C_6H_5).

RESULTS AND DISCUSSION

Synthesis—Compounds III*a*–III*e* (Table I) are new compounds and were prepared by the reaction of triphenyltin iodide with the appropriate ethyl *N*-arylthiocarbamate in the presence of triethylamine (Scheme I). The compounds were identified by elemental analysis (Table I) and IR spectra (Table II). Compound IV was synthesized by allowing ethyl *N*-phenylisothiocarbamate to react with trityl chloride in the presence of triethylamine.

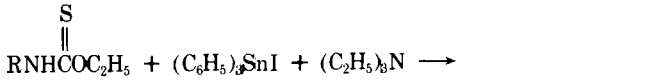

Scheme I

Biological Results—The data in Table III show that each organotin compound, except III*e*, behaved identically toward the test fungi. Compound III*e* differed from the other organotin compounds in that it did not completely inhibit the growth of *Cladosporium carpophilum* at 100 μg/ml. The organotin compounds showed the greatest activity toward *Trichophyton mentagrophytes*, completely inhibiting the growth of this fungus at 10 μg/ml. Compound IV exhibited considerably less antifungal activity than the organotin compounds, being completely inactive toward three fungi; it was most active against *C. carpophilum*, completely inhibiting the growth of this fungus at 100 μg/ml.

A comparison of the present data with those obtained previously for *N*-substituted *N'*-cyano-*S*-(triphenylstannyl)isothioureas (Series I) showed that III*a*–III*e* generally possess greater antifungal activity. For example, while most of the Series I compounds were completely inactive toward *C. carpophilum* and *Saccharomyces cerevisiae*, III*a*–III*d* completely inhibited the former at 100 μg/ml and partially inhibited the latter at 10 μg/ml. Furthermore, while many Series I compounds were inactive at 10 μg/ml, none of the Series III compounds failed to inhibit, at least partially, fungal growth at this concentration.

The data in Table IV show that each organotin compound behaved in an identical manner toward specific test bacteria. Both *Micrococcus agilis* and *Staphylococcus aureus* were inhibited completely at the lowest level (1 μg/ml) of organotin compound. Compound IV was considerably less active than the organotin compounds, being completely inactive against *Bacillus subtilis* and *Escherichia coli;* it did, however, completely inhibit *M. agilis* at 100 μg/ml. A comparison of the present data with those obtained previously for I*a* showed that III*a*–III*e* were considerably less active toward *B. subtilis* than I*a*.

EXPERIMENTAL[1]

Ethyl *N*-(*p*-Nitrophenyl)-*S*-(triphenylstannyl)isothiocarbamate (III*c*)—A mixture of triphenyltin iodide (9.54 g, 0.02 mole), ethyl *N*-(*p*-nitrophenyl)thiocarbamate (11) (4.53 g, 0.02 mole), triethylamine (4.05 g, 0.04 mole), and ether (250 ml) was refluxed for 17 hr. The solvent was evaporated below 35°, and the mixture was stirred with benzene (200 ml)

[1] Melting points were determined with a Mel-Temp capillary melting-point apparatus and are uncorrected. IR data were obtained with a Beckman IR 8 spectrophotometer. The far IR data were obtained with a Perkin-Elmer model FIS-3 IR spectrophotometer and with a Perkin-Elmer model 21 double-beam IR spectrophotometer fitted with a cesium bromide prism and purged with nitrogen. Elemental analyses were performed by Schwarzkopf Microanalytical Laboratory, Woodside, N.Y.

Table III—Antifungal Activity of Ethyl *N*-Aryl-*S*-(triphenylstannyl)isothiocarbamates and Ethyl *N*-Phenyl-*S*-tritylisothiocarbamate

Compound	*Aspergillus niger* (ATCC 12845)		*Chaetomium globosum* (ATCC 6205)		*Cladosporium carpophilum* (ATCC 12117)		*Fusarium moniliforme* (ATCC 10052)		*Myrothecium verrucaria* (ATCC 9095)		*Penicillium notatum* (ATCC 9179)		*Rhizopus stolonifer* (ATCC 10404)		*Saccharomyces cerevisiae* (ATCC 9896)		*Trichoderma viride* (ATCC 8678)		*Trichophyton mentagrophytes* (ATCC 9129)	
	1[a]	10	100	1	10	100	1	10	100	1	10	100	1	10	100	1	10	100	1	10	100
III*a*	+	+	+	+	+	+	2+	2+	2+	+	+	+	+	+	+	+	+	+	+	+	+
III*b*	+	+	+	+	+	+	2+	2+	2+	+	+	+	+	+	+	+	+	+	+	+	+
III*c*	+	+	+	+	+	+	2+	2+	2+	+	+	+	+	+	+	+	+	+	+	+	+
III*d*	+	+	+	+	+	+	2+	2+	2+	+	+	+	+	+	+	+	+	+	+	+	+
III*e*	+	+	−	+	−	−	+	−	−	+	+	−	+	+	−	−	−	−	+	+	+
IV	−	−	−	+	−	−	2+	−	−	−	−	−	−	−	−	−	−	−	−	−	−

[a] Indicates concentration of compounds employed in micrograms per milliliter; − indicates no inhibition of growth, + indicates partial inhibition of growth, and 2+ indicates complete inhibition of growth.

Table IV—Antibacterial Activity of Ethyl *N*-Aryl-*S*-(triphenylstannyl)isothiocarbamates and Ethyl *N*-Phenyl-*S*-tritylisothiocarbamate

Compound	*Bacillus subtillis*[a]			*Escherichia coli*			*Micrococcus agilis*			*Staphylococcus aureus*		
	1[b]	10	100	1	10	100	1	10	100	1	10	100
IIIa	−	+	+	−	−	+	2+	2+	2+	2+	2+	2+
IIIb	−	+	2+	−	−	+	2+	2+	2+	2+	2+	2+
IIIc	−	+	2+	−	−	+	2+	2+	2+	2+	2+	2+
IIId	−	+	2+	−	−	+	2+	2+	2+	2+	2+	2+
IIIe	−	+	2+	−	−	+	2+	2+	2+	2+	2+	2+
IV	−	−	−	−	−	−	−	+	2+	−	−	+

[a] Bacteria were obtained from the culture collection of the Department of Biological Sciences, St. John's University. [b] Indicates concentration of compounds employed in micrograms per milliliter; − indicates no inhibition of growth, + indicates partial inhibition of growth, and 2+ indicates complete inhibition of growth.

and filtered to give 2.98 g (65%) of triethylammonium iodide, mp 173–175° [lit. (12) mp 181°].

The benzene was evaporated from the filtrate below 35°, and the mixture was stirred with *n*-heptane and filtered to give 10.88 g (95%) of IIIc, mp 96–106°. Recrystallization from *n*-pentane gave 8.11 g (71%) of IIIc, mp 95–98°. Further recrystallization from *n*-pentane did not change the melting point.

The other compounds in Table I were prepared in a similar manner.

Ethyl *N*-Phenyl-*S*-tritylisothiocarbamate (IV)—A mixture of trityl chloride (5.58 g, 0.02 mole), ethyl *N*-phenylthiocarbamate (13) (3.63 g, 0.02 mole), triethylamine (4.05 g, 0.04 mole), and acetonitrile (200 ml) was stirred at 25° for 47 hr. The solvent was evaporated, the residue was stirred with benzene (200 ml), and the mixture was filtered to give 2.69 g (98%) of triethylammonium chloride, mp 255° [lit. (12) mp 253–254°].

The benzene was evaporated from the filtrate, the residue was stirred with *n*-heptane (100 ml), and the mixture was cooled and filtered to give 7.82 g (92%) of IV, mp 126–135°. Recrystallization from *n*-pentane gave 4.82 g (57%) of IV, mp 133–137°; IR: 1626 s (C=N) cm^{-1}.

Anal.—Calc. for $C_{28}H_{25}NOS$: C, 79.40; H, 5.95; N, 3.31; S, 7.57. Found: C, 79.47; H, 6.05; N, 3.48; S, 7.44.

Biological Methods—The compounds were individually dissolved in tetrahydrofuran except for IIId, which was solubilized in benzene. The preparation of sterile solutions of the compounds, the fungi employed, the antimicrobial testing procedures, and the determination of growth inhibition were reported previously (14).

The compounds also were investigated for antibacterial activity according to the procedure reported earlier (14).

REFERENCES

(1) E. J. Kupchik, M. A. Pisano, A. V. Raghunath, R. A. Cardona, N. Formaini, and C. Alleguez, *J. Pharm. Sci.*, **64**, 1259 (1975).

(2) C. J. Cattenach and E. F. Mooney, *Spectrochim. Acta A*, **24**, 407 (1968).

(3) L. Verdonck and G. P. van der Kelen, *J. Organomet. Chem.*, **40**, 135 (1972).

(4) R. C. Poller, *Spectrochim. Acta*, **22**, 935 (1966).

(5) H. Schumann, I. Schumann-Ruidisch, and M. Schmidt, in "Organotin Compounds," vol. 2, A. K. Sawyer, Ed., Dekker, New York, N.Y., chap. 6.

(6) J. R. May, W. R. McWhinnie, and R. C. Poller, *Spectrochim. Acta A*, **27**, 969 (1971).

(7) T. N. Srivastava and S. K. Tandon, *ibid.*, **27**, 593 (1971).

(8) T. N. Srivastava, *J. Organomet. Chem.*, **16**, P53 (1969).

(9) I. Wharf, J. Z. Lobos, and M. Onyszchuk, *Can. J. Chem.*, **48**, 2787 (1970).

(10) N. S. Dance, W. R. McWhinnie, and R. C. Poller, *J. Chem. Soc. Dalton Trans.*, **1976**, 2349.

(11) E. E. Reid, "Organic Chemistry of Bivalent Sulfur," vol. 4, Chemical Publishing Co., New York, N.Y., 1962, p. 274.

(12) I. Heilbron, "Dictionary of Organic Compounds," 4th ed., vol. 5, Oxford, London, England, 1965, p. 3126.

(13) E. E. Reid, "Organic Chemistry of Bivalent Sulfur," vol. 4, Chemical Publishing Co., New York, N.Y., 1962, p. 272.

(14) E. J. Kupchik, M. A. Pisano, D. K. Parikh, and M. A. D'Amico, *J. Pharm. Sci.*, **63**, 261 (1974).

Antifungal Properties of Halofumarate Esters

HERMAN GERSHON ˣ **and LARRY SHANKS**

Received May 31, 1977, from *Boyce Thompson Institute for Plant Research, Yonkers, NY 10701.* Accepted for publication July 26, 1977.

Abstract □ Alkyl esters (C_1–C_4) of the four halofumaric acids were tested for antifungal activity against *Candida albicans, Aspergillus niger, Mucor mucedo,* and *Trichophyton mentagrophytes* at pH 5.6 and 7.0 in the absence and presence of 10% beef serum in Sabouraud dextrose agar. The most toxic compound to each organism was: *C. albicans,* ethyl iodofumarate (0.054 mmole/liter); *A. niger,* methyl bromofumarate (0.090 mmole/liter); *M. mucedo,* methyl fluorofumarate (0.037 mmole/liter); and *T. mentagrophytes,* ethyl iodofumarate (0.020 mmole/liter). The order of overall activity of the six most toxic compounds was: ethyl iodofumarate > ethyl chlorofumarate > methyl iodofumarate = methyl bromofumarate > methyl chlorofumarate > ethyl bromofumarate.

Keyphrases □ Halofumarate alkyl esters, various—antifungal activity evaluated □ Antifungal activity—various halofumarate alkyl esters evaluated □ Structure–activity relationships—various halofumarate alkyl esters evaluated for antifungal activity

Interest in developing agents for activity against infections due to opportunistic fungi in debilitated and immunosuppressed patients led to a search for potentially useful classes of compounds (1–3). The fungi that are the most frequent invaders include species of *Candida, Aspergillus, Mucor,* and *Cryptococcus* (4).

DISCUSSION

A previous study of the fungitoxicity of 2-bromo-3-fluorosuccinate esters and related compounds indicated that a systematic examination of the halofumarate esters would be worthwhile (5). Fluorofumaric (6), chlorofumaric (7), bromofumaric (8), and iodofumaric (9) acids were esterified by heating under reflux with methanol, ethanol, 1-propanol,

Table IV—Antibacterial Activity of Ethyl *N*-Aryl-*S*-(triphenylstannyl)isothiocarbamates and Ethyl *N*-Phenyl-*S*-tritylisothiocarbamate

Compound	*Bacillus subtillis*[a]			*Escherichia coli*			*Micrococcus agilis*			*Staphylococcus aureus*		
	1[b]	10	100	1	10	100	1	10	100	1	10	100
IIIa	−	+	+	−	−	+	2+	2+	2+	2+	2+	2+
IIIb	−	+	2+	−	−	+	2+	2+	2+	2+	2+	2+
IIIc	−	+	2+	−	−	+	2+	2+	2+	2+	2+	2+
IIId	−	+	2+	−	−	+	2+	2+	2+	2+	2+	2+
IIIe	−	+	2+	−	−	+	2+	2+	2+	2+	2+	2+
IV	−	−	−	−	−	−	−	+	2+	−	−	+

[a] Bacteria were obtained from the culture collection of the Department of Biological Sciences, St. John's University. [b] Indicates concentration of compounds employed in micrograms per milliliter; − indicates no inhibition of growth, + indicates partial inhibition of growth, and 2+ indicates complete inhibition of growth.

and filtered to give 2.98 g (65%) of triethylammonium iodide, mp 173–175° [lit. (12) mp 181°].

The benzene was evaporated from the filtrate below 35°, and the mixture was stirred with *n*-heptane and filtered to give 10.88 g (95%) of IIIc, mp 96–106°. Recrystallization from *n*-pentane gave 8.11 g (71%) of IIIc, mp 95–98°. Further recrystallization from *n*-pentane did not change the melting point.

The other compounds in Table I were prepared in a similar manner.

Ethyl *N*-Phenyl-*S*-tritylisothiocarbamate (IV)—A mixture of trityl chloride (5.58 g, 0.02 mole), ethyl *N*-phenylthiocarbamate (13) (3.63 g, 0.02 mole), triethylamine (4.05 g, 0.04 mole), and acetonitrile (200 ml) was stirred at 25° for 47 hr. The solvent was evaporated, the residue was stirred with benzene (200 ml), and the mixture was filtered to give 2.69 g (98%) of triethylammonium chloride, mp 255° [lit. (12) mp 253–254°].

The benzene was evaporated from the filtrate, the residue was stirred with *n*-heptane (100 ml), and the mixture was cooled and filtered to give 7.82 g (92%) of IV, mp 126–135°. Recrystallization from *n*-pentane gave 4.82 g (57%) of IV, mp 133–137°; IR: 1626 s (C=N) cm^{-1}.

Anal.—Calc. for $C_{28}H_{25}NOS$: C, 79.40; H, 5.95; N, 3.31; S, 7.57. Found: C, 79.47; H, 6.05; N, 3.48; S, 7.44.

Biological Methods—The compounds were individually dissolved in tetrahydrofuran except for IIId, which was solubilized in benzene. The preparation of sterile solutions of the compounds, the fungi employed, the antimicrobial testing procedures, and the determination of growth inhibition were reported previously (14).

The compounds also were investigated for antibacterial activity according to the procedure reported earlier (14).

REFERENCES

(1) E. J. Kupchik, M. A. Pisano, A. V. Raghunath, R. A. Cardona, N. Formaini, and C. Alleguez, *J. Pharm. Sci.*, **64**, 1259 (1975).

(2) C. J. Cattenach and E. F. Mooney, *Spectrochim. Acta A*, **24**, 407 (1968).

(3) L. Verdonck and G. P. van der Kelen, *J. Organomet. Chem.*, **40**, 135 (1972).

(4) R. C. Poller, *Spectrochim. Acta*, **22**, 935 (1966).

(5) H. Schumann, I. Schumann-Ruidisch, and M. Schmidt, in "Organotin Compounds," vol. 2, A. K. Sawyer, Ed., Dekker, New York, N.Y., chap. 6.

(6) J. R. May, W. R. McWhinnie, and R. C. Poller, *Spectrochim. Acta A*, **27**, 969 (1971).

(7) T. N. Srivastava and S. K. Tandon, *ibid.*, **27**, 593 (1971).

(8) T. N. Srivastava, *J. Organomet. Chem.*, **16**, P53 (1969).

(9) I. Wharf, J. Z. Lobos, and M. Onyszchuk, *Can. J. Chem.*, **48**, 2787 (1970).

(10) N. S. Dance, W. R. McWhinnie, and R. C. Poller, *J. Chem. Soc. Dalton Trans.*, **1976**, 2349.

(11) E. E. Reid, "Organic Chemistry of Bivalent Sulfur," vol. 4, Chemical Publishing Co., New York, N.Y., 1962, p. 274.

(12) I. Heilbron, "Dictionary of Organic Compounds," 4th ed., vol. 5, Oxford, London, England, 1965, p. 3126.

(13) E. E. Reid, "Organic Chemistry of Bivalent Sulfur," vol. 4, Chemical Publishing Co., New York, N.Y., 1962, p. 272.

(14) E. J. Kupchik, M. A. Pisano, D. K. Parikh, and M. A. D'Amico, *J. Pharm. Sci.*, **63**, 261 (1974).

Antifungal Properties of Halofumarate Esters

HERMAN GERSHON ˣ **and LARRY SHANKS**

Received May 31, 1977, from *Boyce Thompson Institute for Plant Research, Yonkers, NY 10701.* Accepted for publication July 26, 1977.

Abstract □ Alkyl esters (C_1–C_4) of the four halofumaric acids were tested for antifungal activity against *Candida albicans, Aspergillus niger, Mucor mucedo,* and *Trichophyton mentagrophytes* at pH 5.6 and 7.0 in the absence and presence of 10% beef serum in Sabouraud dextrose agar. The most toxic compound to each organism was: *C. albicans,* ethyl iodofumarate (0.054 mmole/liter); *A. niger,* methyl bromofumarate (0.090 mmole/liter); *M. mucedo,* methyl fluorofumarate (0.037 mmole/liter); and *T. mentagrophytes,* ethyl iodofumarate (0.020 mmole/liter). The order of overall activity of the six most toxic compounds was: ethyl iodofumarate > ethyl chlorofumarate > methyl iodofumarate = methyl bromofumarate > methyl chlorofumarate > ethyl bromofumarate.

Keyphrases □ Halofumarate alkyl esters, various—antifungal activity evaluated □ Antifungal activity—various halofumarate alkyl esters evaluated □ Structure–activity relationships—various halofumarate alkyl esters evaluated for antifungal activity

Interest in developing agents for activity against infections due to opportunistic fungi in debilitated and immunosuppressed patients led to a search for potentially useful classes of compounds (1–3). The fungi that are the most frequent invaders include species of *Candida, Aspergillus, Mucor,* and *Cryptococcus* (4).

DISCUSSION

A previous study of the fungitoxicity of 2-bromo-3-fluorosuccinate esters and related compounds indicated that a systematic examination of the halofumarate esters would be worthwhile (5). Fluorofumaric (6), chlorofumaric (7), bromofumaric (8), and iodofumaric (9) acids were esterified by heating under reflux with methanol, ethanol, 1-propanol,

Table I—Halofumaric Acid Esters (ROOCCX=CHCOOR)

Compound	R	X	Yield, %	Boiling Point (mm) or Melting Point[a] Observed	Literature Value	$n_D^{25°}$	ν neat, cm^{-1} C=O	C=C	Formula		Analysis, % Calc.	Found
Ia	C_2H_5	F	52	62° (0.3)	—[b]	1.4309	1740	1675	$C_8H_{11}FO_4$	C	50.52	50.23
										H	5.83	5.95
										F	9.99	10.21
Ib	n-C_3H_7	F	63	79° (0.2)	—	1.4349	1740	1685	$C_{10}H_{15}FO_4$	C	55.04	54.76
										H	6.93	6.91
										F	8.71	8.65
Ic	n-C_4H_9	F	67	94.5–95.0° (0.1)	—	1.4379	1742	1690	$C_{12}H_{19}FO_4$	C	58.52	58.54
										H	7.78	7.46
										F	7.71	7.71
Id	CH_3	Cl	78	60° (0.2)	108° (15.0)[c]	1.4711	1742	1638	—	C	—	—
										H		
										Cl		
Ie	C_2H_5	Cl	75	110–112° (4.0)	119° (12.0)[c]	1.4600	1742	1638	—	C	—	—
										H		
										Cl		
If	n-C_3H_7	Cl	80	100° (0.3)	131–137° (7.0)[c]	1.4624	1740	1642	$C_{10}H_{15}ClO_4$	C	51.18	51.06
										H	6.44	6.40
										Cl	15.11	15.27
Ig	n-C_4H_9	Cl	59	130–131° (0.08)	166–210° (9.0)[d]	1.4625	1748	1640	$C_{12}H_{19}ClO_4$	C	54.86	54.97
										H	7.29	7.32
										Cl	13.44	13.40
Ih	CH_3	Br	45	30°	27.5–28.5°[c]	—	1750	1638	—	C	—	—
										H		
										Br		
Ii	C_2H_5	Br	72	91–92° (0.07)	145–155° (11.0)[e]	1.4801	1744	1632	—	C	—	—
										H		
										Br		
Ij	n-C_3H_7	Br	73	104° (0.07)	—	1.4770	1742	1632	$C_{10}H_{15}BrO_4$	C	43.03	43.32
										H	5.42	5.29
										Br	28.63	28.46
Ik	n-C_4H_9	Br	84	122–123° (0.1)	170–172° (8.0)[e]	1.4735	1750	1630	—	C	—	—
										H		
										Br		
Il	CH_3	I	85	51–52°	52–52.5°[f]	—	1736	1618	—	C	—	—
										H		
										I		
Im	C_2H_5	I	56	111–112° (1.0)	—	1.5139	1730	1610	$C_8H_{11}IO_4$	C	32.23	32.36
										H	3.72	3.70
										I	42.57	42.69
In	n-C_3H_7	I	80	118–119° (0.2)	—	1.5048	1730	1616	$C_{10}H_{15}IO_4$	C	36.83	37.06
										H	4.62	4.61
										I	38.91	39.02
Io	n-C_4H_9	I	76	140° (0.4)	—	1.4994	1740	1620	$C_{12}H_{19}IO_4$	C	40.69	41.04
										H	5.41	5.41
										I	35.83	35.53

[a] Analytical sample. [b] For ethyl fluoroethylenedicarboxylate, Ref. 10 reported bp 74° (1.5 mm) and $n_D^{20°}$ 1.4330. [c] Reference 8. [d] Reference 11. [e] Reference 12. [f] Reference 9.

and 1-butanol, respectively, using thionyl chloride as the catalyst. Of the 16 esters prepared, the following were reported previously: methyl fluorofumarate (5), ethyl fluoroethylenedicarboxylate (10), methyl chlorofumarate (8), ethyl chlorofumarate (8), *n*-propyl chlorofumarate (11), *n*-butyl chlorofumarate (11), methyl bromofumarate (8), ethyl bromofumarate (12), *n*-butyl bromofumarate (12), and methyl iodofumarate (9). Although *n*-propyl and *n*-butyl chlorofumarates appear in the literature (11), they were not adequately characterized, and the isomeric form of ethyl fluoroethylenedicarboxylate was not established.

The data characterizing the halofumarate esters are contained in Table I. The purity of the esters was verified by GLC.

The compounds were tested against *Candida albicans* (ATCC 10231), *Aspergillus niger* (ATCC 1004), *Mucor mucedo* (ATCC 7941), and *Trichophyton mentagrophytes* (ATCC 9129) in Sabouraud dextrose agar[1] at pH 5.6 and 7.0 in the absence and presence of 10% beef serum[2] according to published methods (1, 13) (Table II). Because these compounds are potential medicinal agents, the highest level tested was 100

[1] Difco.
[2] Miles Laboratories.

Table II—Antifungal Activity of Diesters of Halofumaric Acids at pH 5.6 and 7.0 in Sabouraud Dextrose Agar in the Presence and Absence of Beef Serum[a]

Compound	Level of Inhibition[b]															
	C. albicans				*A. niger*				*M. mucedo*				*T. mentagrophytes*			
	pH 5.6		pH 7.0		pH 5.6		pH 7.0		pH 5.6		pH 7.0		pH 5.6		pH 7.0	
	–[c]	+	–	+	–	+	–	+	–	+	–	+	–	+	–	+
Methyl fluorofumarate[d]	0.025	0.037	0.12	0.24	0.12	0.31	0.36	—[e]	<0.0062[f]	0.012	0.025	0.037	<0.0062	0.025	0.049	0.25
Ia	0.021	0.074	0.053	0.21	0.084	0.32	0.26	—	<0.0053	0.016	0.016	0.26	<0.0052	0.063	0.011	0.084
Ib	0.018	0.23	0.064	—	0.14	—	0.23	—	0.0091	0.14	0.023	0.28	<0.0049	0.23	<0.0049	—
Ic	0.012	0.24	0.065	—	0.24	—	—	—	0.028	—	0.041	—	<0.0041	0.20	0.012	—
Id	0.090	0.10	0.10	0.10	0.034	0.022	0.10	0.11	0.017	0.039	0.034	0.050	<0.0056	0.017	0.011	0.067
Ie	0.058	0.058	0.058	0.068	0.0096	0.015	0.058	0.097	0.0096	0.048	0.029	0.048	<0.0048	0.015	0.0096	0.058
If	0.026	0.077	0.068	0.21	0.051	0.051	0.21	—	0.017	0.17	0.051	0.34	0.013	0.013	0.017	0.17
Ig	0.053	0.19	0.11	0.19	—	—	—	—	0.011	0.15	0.023	—	0.011	0.11	0.015	0.19
Ih	0.054	0.063	0.081	0.090	0.063	0.072	0.081	0.090	0.013	0.018	0.022	0.063	<0.0045	0.013	0.013	0.040
Ii	0.020	0.056	0.028	0.12	0.020	0.048	0.080	0.16	0.016	0.016	0.032	0.12	<0.0040	<0.0040	<0.0040	0.024
Ij	0.011	0.018	0.032	0.14	0.057	0.036	0.072	—	0.014	0.029	0.043	0.18	<0.0036	0.050	0.011	0.072
Ik	0.029	0.16	0.033	0.23	—	—	—	—	0.026	0.13	0.039	—	0.0065	0.098	0.013	0.098
Il	0.026	0.026	0.052	0.067	0.059	0.059	0.11	0.11	<0.0037	0.0074	<0.0037	0.074	<0.0037	0.0074	0.0074	0.022
Im	0.017	0.020	0.047	0.054	0.054	0.040	0.10	0.10	0.030	0.040	0.040	0.060	<0.0034	0.010	0.0068	0.020
In	0.0092	0.028	0.021	0.12	0.092	0.092	0.15	—	<0.0031	0.028	0.0061	0.18	<0.0031	0.018	0.0091	0.061
Io	—	—	—	—	—	—	—	—	—	—	—	—	0.0056	0.11	0.017	0.11

[a] *C. albicans* and *M. mucedo* were incubated at 37° for 20 hr, and *T. mentagrophytes* and *A. niger* were incubated at 28° for 5 days. [b] Minimal concentrations of compound in millimoles per liter causing 100% inhibition of test organisms by recalculation of test data obtained in micrograms per milliliter. Activity to 10 μg/ml was obtained in increments of 1 μg/ml; activity from 10 to 20 μg/ml was obtained in increments of 2 μg/ml; and activity from 20 to 100 μg/ml, the highest level tested, was obtained in increments of 10 μg/ml. All tests were carried out in duplicate in "I" plate petri dishes. [c] – and + = absence and presence of 10% beef serum, respectively. [d] Data taken from Ref. 5. [e] — = not inhibitory below 100 μg/ml. [f] < = inhibitory at 1 μg/ml, the lowest level tested.

μg/ml; the results of greatest interest were those obtained at pH 7.0 in the presence of 10% beef serum.

Adjustment of the test medium from pH 5.6 to 7.0 and addition of 10% beef serum resulted in the reduction of antifungal activity in most cases. The methyl and ethyl esters of the halofumaric acids were more active than the *n*-propyl and *n*-butyl homologs. The most toxic compound to each organism was: *C. albicans*, ethyl iodofumarate (0.054 mmole/liter); *A. niger*, methyl bromofumarate (0.090 mmole/liter); *M. mucedo*, methyl fluorofumarate (0.037 mmole/liter); and *T. mentagrophytes*, ethyl iodofumarate (0.020 mmole/liter).

The first six most toxic compounds against each organism were ranked in order of activity. After averaging the ranks, the following order of overall antifungal activity was obtained: ethyl iodofumarate > ethyl chlorofumarate > methyl iodofumarate = methyl bromofumarate > methyl chlorofumarate > ethyl bromofumarate.

Methyl and ethyl chlorofumarates, methyl, ethyl, and *n*-butyl bromofumarates, and methyl iodofumarate were reported to possess antifungal properties (12–14). The mechanism of action was attributed to interference with the Krebs cycle (12). All four halofumaric acids are fumarase substrates (15).

EXPERIMENTAL[3]

To prepare *n*-propyl fluorofumarate, fluorofumaric acid (6) (1.5 g, 0.011 mole), 1-propanol (15 ml), and thionyl chloride (0.5 ml) were heated under reflux overnight. Sufficient water was added to cause the ester to come out of solution. The mixture was extracted (chloroform), the extract was washed (water) and dried (sodium sulfate), and the solvent was removed in a rotary still. Then the residue was fractionated under reduced pressure.

REFERENCES

(1) H. Gershon and L. Shanks, *Can. J. Microbiol.*, **21**, 1317 (1975).

(2) H. Gershon, L. Shanks, and D. Gawiak, *J. Med. Chem.*, **19**, 1069 (1976).

(3) H. Gershon and L. Shanks, *Can. J. Microbiol.*, **22**, 1198 (1976).

(4) A. S. Levine, R. G. Graw, Jr., and R. C. Young, *Semin. Hematol.*, **9**, 141 (1972).

(5) H. Gershon and L. Shanks, *J. Med. Chem.*, **20**, 606 (1977).

(6) M. S. Raasch, R. E. Miegel, and J. E. Castle, *J. Am. Chem. Soc.*, **81**, 2678 (1959).

(7) W. H. Perkin, *J. Chem. Soc.*, **53**, 695 (1888).

(8) K. v. Auwers and L. Harres, *Chem. Ber.*, **62**, 1678 (1929).

(9) J. Thiele and W. Peter, *Justus Liebigs Ann. Chem.*, **369**, 119 (1909).

(10) I. L. Knunyants, B. L. Dyatkin, and L. S. German, *Dok. Akad. Nauk SSSR*, **124**, 1065 (1959); through *Chem. Abstr.* **53**, 14920 (1959).

(11) M. Sumi, K. Konishi, and S. Kotera, Japanese pat. 68 29,571 (1968); through *Chem. Abstr.*, **70**, 67660d (1969).

(12) J. F. Grove, *Ann. Appl. Biol.*, **35**, 37 (1948).

(13) H. Gershon and R. Parmegiani, *J. Med. Chem.*, **10**, 186 (1967).

(14) I. Muirhead, *Ann. Appl. Biol.*, **36**, 250 (1949).

(15) R. L. Hill and J. W. Teipel, in "The Enzymes," vol. 5, P. D. Boyer, Ed., Academic, New York, N.Y., 1971, pp. 559–562.

ACKNOWLEDGMENTS

The authors thank A. T. Grefig for the IR spectra.

[3] Melting points were taken in a Thomas-Hoover melting-point apparatus and are uncorrected. GLC was performed on a Varian Aerograph model 1200 gas chromatograph with a flame-ionization detector to which was attached a Varian Aerograph model 20 recorder. The purity of the acids was established by GLC on a column of 3% Dexsil 400 on Anachrom A (90–100 mesh) purchased from Analabs, New Haven, Conn. All samples tested microbiologically were at least 95% pure. IR spectra were obtained with a Perkin-Elmer model 221 spectrophotometer, and refractive indexes were taken with an Abbe-3L B&L refractometer.

Quantitative Determination of Acetaminophen in Plasma

FOTIOS M. PLAKOGIANNIS ˣ **and AHMED M. SAAD**

Received February 14, 1977, from the *Department of Pharmaceutics, Arnold and Marie Schwartz College of Pharmacy and Health Sciences, Long Island University, Brooklyn, NY 11201.* Accepted for publication July 28, 1977.

Abstract □ A simple method is described for the rapid quantitative analysis of acetaminophen in plasma. The acetaminophen and its conjugates present in the plasma following drug administration are hydrolyzed with 4 *N* HCl to *p*-aminophenol. This compound is coupled with 5% vanillin reagent to form a stable yellow color whose concentration is determined spectrophotometrically at 395 nm. Application of this method to a study of three dogs treated with 650 mg of acetaminophen is described.

Keyphrases □ Acetaminophen—spectrophotometric analysis in plasma □ Spectrophotometry—analysis, acetaminophen in plasma □ Analgesics—acetaminophen, spectrophotometric analysis in plasma

The widespread use of acetaminophen as an antipyretic and mild analgesic has stimulated an interest in the development of a simple and rapid plasma determination. Several methods have been published for acetaminophen and its metabolites in blood and urine (1–8). A commonly used method (1, 2) involves acid hydrolysis of conjugated acetaminophen following extraction of the resulting *p*-aminophenol into ether and then its extraction from the organic solvent into dilute acid. The *p*-aminophenol is reacted with phenol in the presence of sodium hypobromite to form an indophenol dye whose concentration is determined spectrophotometrically. However, the sample must be allowed to stand for 40 min for maximum development of the blue color. In previously published papers (3, 4), the determination of acetaminophen in capsules by utilizing vanillin reagent was reported.

According to the method presented here for acetaminophen determination in plasma, the *p*-aminophenol is extracted from the ether extract by 1 *N* HCl. The acid extract, upon the addition of 5% vanillin reagent, immediately produces an intense yellow color, which can be measured at 395 nm.

EXPERIMENTAL

Reagents—All chemicals and reagents (analytical grade) were used without further purification, unless otherwise indicated.

Protocol—Three healthy adult beagle dogs were fasted overnight. Each received a 650-mg oral dose of acetaminophen consisting of two 325-mg capsules[1]. Venous blood specimens were withdrawn with evacuated tubes[2] containing ammonium heparinate as an anticoagulant. Specimens were taken prior to and at specified times after drug administration for 10 hr. Collected specimens were centrifuged immediately at 15,000 rpm and 4° using a refrigerated centrifuge[3] for 10 min. Plasma was separated and analyzed for total acetaminophen (1, 2, 5–7) by a modification of the method of Plakogiannis and Saad (4).

Analysis—To 2 ml of plasma in a polytef-lined screw-capped centrifuge tube (20 ml), 4 ml of 4 *N* HCl was added; the sample was then diluted with distilled water to 10 ml. The tube was centrifuged at 5000 rpm for 1 hr, and the clear supernate was placed in a boiling water bath for 1 hr. Each sample was treated two or three times with 4 ml of ether, and the *p*-aminophenol was then extracted from ether with 10 ml of 1 *N* HCl. To 2 ml of the acid extract, 5 ml of 5% vanillin in 2-propanol was added; the yellow color produced was measured[4] at 395 nm. Concentrations were determined from a previously constructed standard curve.

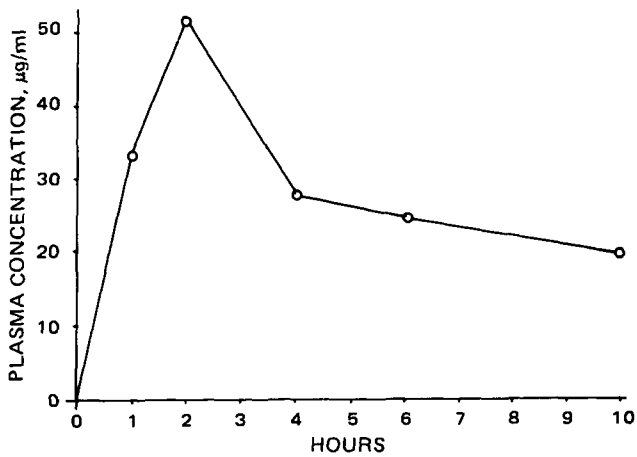

Figure 1—*Plot of plasma acetaminophen concentration* versus *time.*

RESULTS AND DISCUSSION

The biological disposition of acetaminophen in humans and animals has been extensively examined. It has been shown (9, 10) that 80% of the total dose is excreted in a conjugated form, which, upon acid hydrolysis, gives rise to *p*-aminophenol. In the present study, the plasma samples were analyzed for total, *i.e.*, free plus conjugated, acetaminophen. Plakogiannis and Saad (4, 11) showed that 4 *N* HCl and 1 hr of boiling are needed to obtain as complete hydrolysis as possible. The *p*-aminophenol then is reacted with 5% vanillin reagent in 2-propanol to produce immediately an intense yellow color, which is stable up to 24 hr.

The precision and accuracy of the method were determined by analysis of plasma samples spiked with 10, 20, 30, 40, and 50 µg of acetaminophen/ml. The recovered concentrations were equal to 98 ± 5% (mean ± *SD*).

Mean plasma concentrations observed at various sampling times from the three dogs are shown in Fig. 1. Maximum plasma concentrations of acetaminophen were observed within 2 hr, and easily measurable amounts were present at the end of the study (10 hr).

The present method appears to be accurate and precise and has the advantages over the procedure of Brodie and Axelrod (1, 2) of being less time consuming and more dependable due to color stability.

REFERENCES

(1) B. B. Brodie and J. Axelrod, *J. Pharmacol. Exp. Ther.*, **94**, 22 (1948).
(2) *Ibid.*, **97**, 58 (1949).
(3) J. B. Vaughan, *J. Pharm. Sci.*, **58**, 469 (1969).
(4) F. M. Plakogiannis and A. M. Saad, *ibid.*, **64**, 1547 (1975).
(5) G. Levy and H. Yamada, *ibid.*, **60**, 215 (1971).
(6) G. Levy and C.-G. Regårdh, *ibid.*, **60**, 608 (1971).
(7) A. A. Saouzas and K. C. Shenoy, *Can. J. Pharm. Sci.*, **3**, 90 (1968).
(8) J. E. Mrochek, S. Datz, W. H. Christie, and S. R. Dinsmore, *Clin. Chem.*, **20**, 1086 (1974).
(9) R. M. Welch, A. H. Conney, and J. J. Burns, *Biochem. Pharmacol.*, **15**, 522 (1966).
(10) R. M. Welch and A. H. Conney, *Clin. Chem.*, 11, 1065 (1969).
(11) F. Plakogiannis and A. Saad, *J. Pharm. Sci.*, **66**, 604 (1977).

[1] McNeil Laboratories.
[2] Vacutainer, Becton-Dickinson & Co.
[3] Sorvall, DuPont Co.
[4] Spectronic 200, Bausch & Lomb.

Improved GLC Determination of Plasma Nitroglycerin Concentrations

PETER S. K. YAP, EDWARD F. McNIFF, and HO-LEUNG FUNG ˣ

Received April 22, 1977, from the *Department of Pharmaceutics, School of Pharmacy, State University of New York at Buffalo, Amherst, NY 14214.* Accepted for publication August 3, 1977.

Abstract □ A specific and quantitative assay for determining nanogram levels of nitroglycerin in plasma was developed. The method involves stabilization of the drug in plasma with silver nitrate, followed by multiple extraction using purified hexane. Isosorbide dinitrate is added as the internal standard. The hexane extract is subsequently concentrated and injected into a glass column packed with 3% SP-2401 on 100–120-mesh Supelcoport at 140°. A ^{63}Ni-electron-capture detector gives a linear response over the range of 0.1–50 ng of nitroglycerin/ml of rat plasma. From spiked samples, the procedure gave a recovery of about 90%. There was little or no interference from the isomeric glyceryl dinitrates and endogenous compounds in rat or human plasma.

Keyphrases □ Nitroglycerin—GLC analysis in plasma □ GLC—analysis, nitroglycerin in plasma □ Vasodilators, coronary—nitroglycerin, GLC analysis in plasma

Rosseel and Bogaert (1, 2) recently reported a GLC procedure for the determination of nitroglycerin in human plasma with a claimed sensitivity of 0.5 ng/ml of plasma. That procedure represents a major advance in the analysis of trace levels of organic nitrates in biological fluids, but several problems are associated with it. First, to reach the claimed sensitivity, a volume of 5 ml of plasma/sample must be processed. This sample size severely limits the utilization of the assay in pharmacokinetic studies of nitroglycerin in small animals, *e.g.*, rats, from which serial withdrawal of large volumes of blood is impossible. Second, the chromatogram contains major interference peaks close to those of nitroglycerin and the internal standard, isosorbide dinitrate, making drug quantitation at lower concentrations much less reliable. Third, a total chromatogram time of 90 min is required because of the presence of some large peaks due to solvent impurities. This relatively long assay time impairs the efficiency of the procedure.

The present report describes attempts to develop a better assay for nitroglycerin in plasma. Modifications of the Rosseel and Bogaert assay were developed and appeared to remedy successfully the shortcomings mentioned.

EXPERIMENTAL

Standard Solutions—Nitroglycerin stock solutions in hexane[1] were prepared by extraction of a commercial 10% (w/w) nitroglycerin–lactose adsorbate[2] with the solvent and standardized by a modified USP method in which column elution was omitted and isooctane was substituted by hexane as the extraction solvent. Aqueous nitroglycerin stock solutions were prepared by dissolving the nitroglycerin–lactose in distilled water and standardized by a modified USP method in which the nitroglycerin was adsorbed onto siliceous earth in a beaker rather than on a column. The modified procedures gave the same results as the official method.

Isosorbide dinitrate, the internal standard, was provided[3] as a 25% (w/w) isosorbide dinitrate–lactose powder. To obtain the lactose-free internal standard, an aqueous solution of the powder was extracted with ether, which was then evaporated to dryness. The resultant solid was recrystallized from an aqueous alcoholic mixture, mp 70–71° (uncorr.) [lit. (3) mp 70°].

Purification of Hexane—About 600 ml of reagent grade hexane was washed twice with 300 ml of concentrated sulfuric acid, twice with 300 ml of distilled water, once with 300 ml of 1 *N* NaOH, and then twice with 300 ml of distilled water. The washed solvent was then passed through a column of silica gel[4] (about 50 g, packed as a slurry into a column 2 cm in diameter and 30 cm in height) and distilled in the presence of activated charcoal and lithium aluminum hydride. Each batch of solvent was tested by concentrating 2.4 ml of the purified solvent to about 20 μl (~120-fold), and a volume of 1–5 μl was injected onto the gas chromatograph. The organic solvent was approved for use in the assay when interfering impurity peaks were absent.

Extraction and GLC Assay—A volume of 0.2 ml of purified hexane was used for each extraction of an equal volume of plasma containing nitroglycerin. Rapid injection of the organic solvent into the plasma provided the required mixing, with minimal formation of an emulsion. The hexane layer (upper phase) was withdrawn, and the extraction was repeated for the specified number of times. In this manner, 12 extractions could be accomplished easily within 5 min. The hexane extracts were combined, and a known amount of isosorbide dinitrate in hexane was added.

The internal standard was added after extraction because preliminary experiments indicated that isosorbide dinitrate was not completely extracted by the present procedure. The amount of internal standard added depended on the nitroglycerin level to be determined. For samples containing about 0.1 ng of nitroglycerin/ml, about 0.1 ng of isosorbide dinitrate in 10 μl of hexane was added to each sample. Larger amounts of internal standard were added for samples containing higher drug levels to optimize GLC readings.

The combined hexane solution containing nitroglycerin and isosorbide dinitrate was then concentrated to approximately 20 μl, and 1–5 μl was injected into a glass column[5] packed with 3% SP-2401 on 100–120-mesh Supelcoport at a carrier gas (nitrogen) flow rate of about 60 ml/min. Inlet, column, and detector oven temperatures were set at 160, 140, and 180°, respectively. Quantification was effected *via* a ^{63}Ni-electron-capture detector[6].

RESULTS AND DISCUSSION

Use of Purified Hexane as Extracting Solvent—Rosseel and Bogaert (1, 2) showed that nitroglycerin in plasma can be extracted totally into ethyl acetate. From a recovery standpoint, ethyl acetate is a good extracting solvent because it has a superior solubility for nitroglycerin compared to other water-immiscible solvents. However, from the analytical point of view, ethyl acetate is a poor solvent because of its relative polarity and the difficulty in ridding it of contaminants. The polar plasma constituents it apparently extracts and the impurities it contains not only interfere with the quantitation of nitroglycerin and its major metabolites in the chromatogram but also limit the possible sensitivity of detection.

In this situation, a hydrocarbon solvent such as hexane has the opposite characteristics when compared to ethyl acetate. It is relatively easy to

[1] Fisher Scientific Co., Chemical Manufacturing Division, Fair Lawn, NJ 07410.

[2] Nitroglycerin 10% (w/w) in lactose, lot B17-H-1, ICI America, Atlas Chemical Division, Wilmington, DE 19899.

[3] Stuart Pharmaceuticals, Division of ICI United States, Wilmington, DE 19897.

[4] Silica gel Woelm for dry-column chromatography, Waters Associates, Framingham, MA 01701.

[5] Supelco, Bellefonte, PA 16823.

[6] Packard model 884 electron-capture detector at 40 v and Series 7500 gas chromatograph, Packard Instrument Co., Downers Grove, IL 60515.

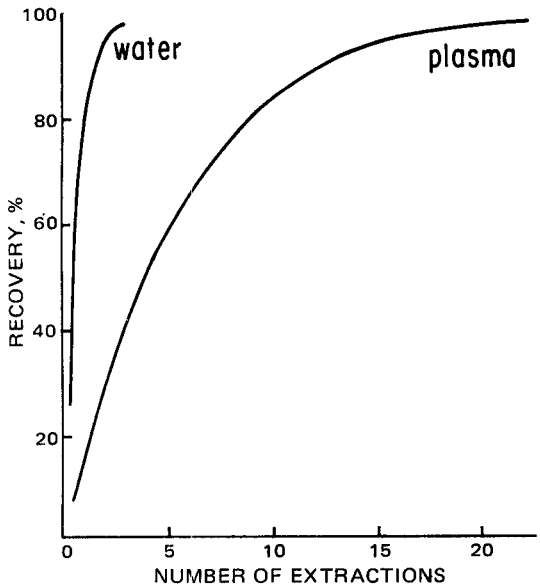

Figure 1—*Estimated percent nitroglycerin recovery from water and rat plasma* versus *number of extractions required. The curves are simulated using a phase volume ratio of 1 and partition coefficients of 4 and 0.2 for hexane–water and hexane–rat plasma, respectively.*

purify and does not extract as many polar plasma interfering substances. Its main disadvantage is, of course, its poor solubility for nitroglycerin. The partition coefficient of nitroglycerin between hexane and water was about 4 at room temperature. Between hexane and plasma, however, the partition coefficient was much lower, having a value of about 0.2. The much higher apparent solubility of nitroglycerin in plasma *versus* water may be attributed to plasma proteins and lipids that bind and/or solubilize the drug. Figure 1 shows the calculated (4) percent recovery of nitroglycerin as a function of the number of extractions from water and rat plasma, using an equal volume of hexane. For 90% recovery of nitroglycerin from rat plasma, 10 extractions would be required. Similarly, 21 extractions would enable a recovery of 99%.

Experimentally, a recovery of about 90% was achieved when nitroglycerin in spiked rat plasma was immediately extracted 12 times with equal volumes of hexane. When six extractions were performed, the recovery was 62%. These observed recovery percentages are consistent with the values predicted from the partition coefficient. The extraction efficiency of hexane from human plasma was similar to that from rat plasma. After 12 extractions, the nitroglycerin recovery was 92%.

In this assay, the combined hexane extract was concentrated to approximately 20 μl rather than to dryness followed by reconstitution as described in the procedure of Rosseel and Bogaert. This step prevented significant nitroglycerin losses (about 40%) when the hexane was totally evaporated. Loss of drug from total solvent evaporation was not prevented when ethyl acetate was added at 30% (v/v) to the combined hexane extracts. Complete recovery was obtained, however, when the hexane phase was concentrated to about 20 μl prior to injection onto the GLC column.

Stabilization of Nitroglycerin by Silver Nitrate—DiCarlo and Melgar (5) showed that nitroglycerin is rapidly degraded in rat serum; the half-life was approximately 20 min at 37°. Moreover, nitroglycerin degradation in rat serum can be inhibited significantly by iodoacetamide, silver nitrate, and *p*-chloromercuric benzoate (5). Silver nitrate was chosen for stabilization here because it is very poorly soluble in hexane and thus was not expected to cause additional problems during chromatography.

In fresh rat plasma, nitroglycerin degraded rapidly at ambient temperatures; approximately 25% of the original concentration was lost within 1 hr. Addition of silver nitrate to a final concentration of 0.05 *M* appeared to stabilize the drug for at least 1.5 hr, and only 20% of the nitroglycerin was destroyed after 12 hr. Addition of silver nitrate at the same final concentration to rat blood, however, resulted in extensive gelling of the sample, making plasma separation for drug analysis very difficult. Therefore, stability studies of nitroglycerin in whole blood spiked with silver nitrate were not conducted.

Adopted Procedure—Based on the previous findings, a final analytical procedure was adopted. For each 200-μl plasma sample, 10 μl of

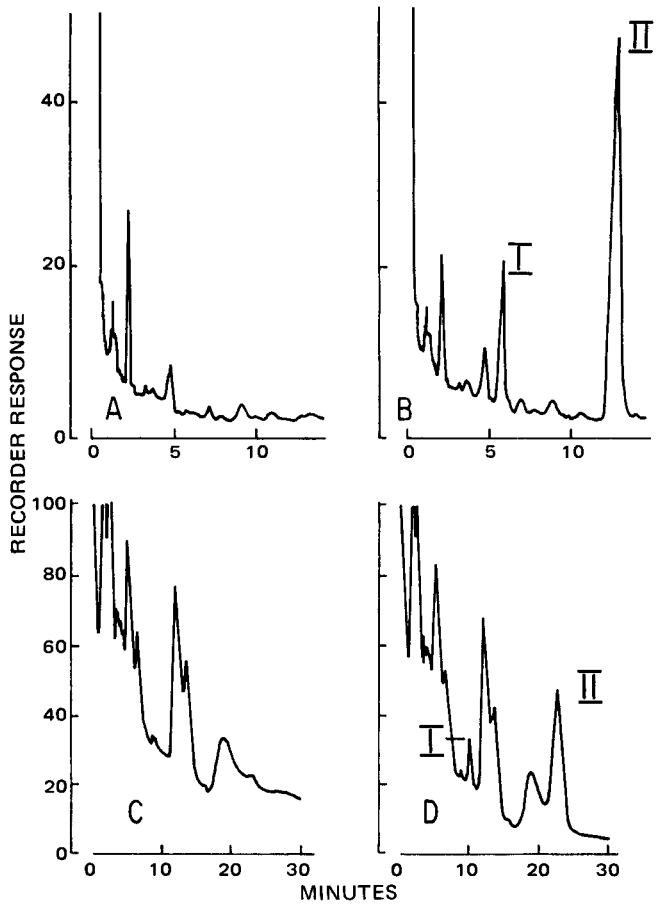

Figure 2—*Chromatograms of human plasma (A) and of human plasma with 4 ng of nitroglycerin/ml (B) as determined by the present procedure (electrometer setting of 8 × 10^{-10} amp), and chromatograms of human plasma (C) and of human plasma containing an estimated 3 ng of nitroglycerin/ml (D) as reported in Ref. 2 (electrometer setting of 1 × 10^{-9} amp). Key: I, nitroglycerin; and II, isosorbide dinitrate.*

1 *M* silver nitrate was first added; this sample was then extracted 12 times with equal volumes of purified hexane. After the internal standard was added to the combined extracts, the hexane solution was evaporated to approximately 20 μl under nitrogen; 1–5 μl of the concentrated solution was injected into the gas chromatographic column.

The present procedure offered a relatively "clean" chromatogram for rat and human plasma (Fig. 2A). Under the conditions used, the retention times of nitroglycerin and isosorbide dinitrate were 6 and 13 min, respectively. Occasionally, minor solvent impurity peaks were present, but they were broad and appeared between 25 and 35 min after injection. Figure 2B shows a chromatogram of human plasma spiked with 4 ng of nitroglycerin/ml. Chromatograms of human plasma (Fig. 2C) and human plasma estimated to contain about 3 ng of nitroglycerin/ml (Fig. 2D), as reported by Rosseel and Bogaert (2), are presented for comparison. The present procedure is superior when chromatogram clarity and assay time are considered.

The chromatographic peak of the isomeric dinitrates appeared at a retention time (about 3 min) at which there was no significant interference by other substances in the plasma and solvent. Although the extraction of dinitrates into hexane was poor (about 10–20%), the present nitroglycerin chromatogram offers a qualitative estimation of the dini-

Table I—Precision of GLC Assay of Nitroglycerin

Plasma Nitroglycerin Concentration, ng/ml		
Spiked	Observed (mean ± *SD*)	Range (*n*)[a]
0.095	0.099 ± 0.023	0.075–0.130 (7)
0.475	0.401 ± 0.095	0.291–0.504 (7)
2.00	1.95 ± 0.17	1.90–2.20 (6)
39.7	38.0 ± 1.6	35.1–40.0 (6)

[a] *n* = number of determinations.

trate level in the same plasma sample. This estimation apparently cannot be obtained directly from the Rosseel–Bogaert assay because of large interference peaks early in the chromatogram.

Linear calibration plots for nitroglycerin in rat and human plasma were obtained with the present procedure. The correlation coefficients of the lines were greater than 0.99. The precision and reproducibility of the present assay applied to plasma samples are shown in Table I. As expected, the relative standard deviations were higher (≃20%) for samples containing low concentrations of nitroglycerin (0.1 and 0.5 ng/ml) than for those with high concentrations. At 2 and about 40 ng/ml, the relative standard deviations were determined to be 8.6 and 4.2%, respectively. Saturation of the electron-capture detector occurred when the on-column amount of nitroglycerin exceeded about 0.5 ng.

Applications of the present technique in pharmacokinetic studies of nitroglycerin in a human subject (6) and in rats (7) are described elsewhere.

REFERENCES

(1) M. T. Rosseel and M. G. Bogaert, *J. Chromatogr.*, **64**, 364 (1972).

(2) M. T. Rosseel and M. G. Bogaert, *J. Pharm. Sci.*, **62**, 754 (1973).

(3) "The Merck Index," 9th ed., Merck & Co., Rahway, N.J., 1976.

(4) K. A. Connors, "A Textbook of Pharmaceutical Analysis," Wiley, New York, N.Y., 1967, p. 281.

(5) F. J. DiCarlo and M. D. Melgar, *Proc. Soc. Exp. Biol. Med.*, **131**, 406 (1969).

(6) H. P. Blumenthal, H.-L. Fung, E. F. McNiff, and S. K. Yap, *Br. J. Clin. Pharmacol.*, **4**, 241 (1977).

(7) P. S. K. Yap and H.-L. Fung, *J. Pharm. Sci.*, **67**, 584 (1978).

ACKNOWLEDGMENTS

Presented in part at the Pharmaceutical Analysis and Control Section, APhA Academy of Pharmaceutical Sciences, Orlando meeting, November 1976.

Abstracted in part from a dissertation submitted by P. S. K. Yap to the Graduate School, State University of New York at Buffalo, in partial fulfillment of the Doctor of Philosophy degree requirements.

Supported in part by General Research Support Grant 5S07RR0545414 from the National Institutes of Health.

Pharmacokinetics of Nitroglycerin in Rats

PETER S. K. YAP and HO-LEUNG FUNG ˣ

Received April 22, 1977, from the *Department of Pharmaceutics, School of Pharmacy, State University of New York at Buffalo, Amherst, NY 14214.* Accepted for publication August 3, 1977.

Abstract □ The plasma nitroglycerin levels obtained after intracardial (0.7 mg/kg), oral (7 mg/kg), and topical (7–14 mg/kg) doses of nitroglycerin in rats are reported. Nitroglycerin followed essentially one-compartment kinetics after intracardial administration, showing a mean half-life of about 4 min and a mean apparent volume of distribution of about 3 liters/kg. After oral drug administration, "flip-flop" kinetics were evident. The mean oral bioavailability was determined to be 1.6%, firmly supporting the contention that nitroglycerin is extensively metabolized during first passage through the liver. Under the experimental conditions studied, no detectable levels of nitroglycerin were observed after topical application.

Keyphrases □ Nitroglycerin—pharmacokinetics after intracardial, oral, and topical administrations in rats □ Pharmacokinetics—nitroglycerin after intracardial, oral, and topical administrations in rats □ Vasodilators, coronary—nitroglycerin, pharmacokinetics after intracardial, oral, and topical administrations in rats

Recent studies dealt with the analytical (1–3), stability (4–7), and formulation (6, 8–12) aspects of nitroglycerin. These studies showed definitively that nitroglycerin in sublingual tablets can be stabilized effectively against volatilization by the inclusion of macromolecules such as povidone (8–10), polyethylene glycol (6), and microcrystalline cellulose (8, 12).

BACKGROUND

Very little information is available, however, on the pharmacokinetics of nitroglycerin in animals and humans. The analytical difficulty associated with the determination of nanogram or subnanogram concentrations of the intact drug in biological fluids is a primary reason for the paucity of quantitative information regarding nitroglycerin absorption and disposition. Recently, a GLC assay (13) quantifying nitroglycerin in plasma at these low concentrations was developed. This assay offers a unique opportunity to initiate rigorous *in vivo* pharmacokinetic studies in animals and humans.

Nitroglycerin is used in oral sustained-release dosage forms for the prophylaxis of angina. The effectiveness of this mode of nitroglycerin administration was seriously questioned by Needleman *et al.* (14) who showed that the drug undergoes extensive first-pass metabolism after oral dosing. The intact nitroglycerin levels were much lower after oral administration than after the intravenous route. Their data, however, were not reported in sufficient detail to allow for the estimation of the bioavailability of an oral dose of nitroglycerin.

Recently, nitroglycerin was used in ointment form for the hemodynamic management of patients with chronic congestive heart failure (15). This administration route for nitroglycerin was reported to produce beneficial effects lasting for 3–6 hr after a single application. The therapeutic efficacy and duration of effect of nitroglycerin, therefore, appear to be highly dependent on the route of drug administration.

The present study deals with the effect of the administration route on nitroglycerin pharmacokinetics in the rat. A pilot, collateral study in humans after therapeutic sublingual, oral, and topical doses of nitroglycerin is reported elsewhere (16).

EXPERIMENTAL

Materials—A 1.16-mg/ml aqueous solution of nitroglycerin was prepared by dissolving the appropriate amount of 10% nitroglycerin–lactose adsorbate[1] in distilled water. Solution was effected by overnight mechanical agitation and confirmed by the kinetic assay (2). The internal standard, isosorbide dinitrate, was obtained by acetone extraction from a 25% (w/w) isosorbide dinitrate–lactose powder[2], followed by evaporation of the organic solvent. Male Sprague–Dawley rats, 270–340 g, were used.

Intracardial Experiments—Six rats were fasted overnight and given an intracardial dose of nitroglycerin (0.7 mg/kg) under ether anesthesia. The dosing volume was approximately 0.2 ml. Blood samples (0.5–0.8 ml) were obtained through orbital sinus puncture using heparinized capillary tubes. Half of the rats (A, B, and C) were anesthetized during blood

[1] Nitroglycerin 10% (w/w) in lactose, ICI America, Atlas Chemical Division, Wilmington, DE 19899.

[2] Stuart Pharmaceuticals, Division of ICI United States, Wilmington, DE 19897.

trate level in the same plasma sample. This estimation apparently cannot be obtained directly from the Rosseel–Bogaert assay because of large interference peaks early in the chromatogram.

Linear calibration plots for nitroglycerin in rat and human plasma were obtained with the present procedure. The correlation coefficients of the lines were greater than 0.99. The precision and reproducibility of the present assay applied to plasma samples are shown in Table I. As expected, the relative standard deviations were higher (≃20%) for samples containing low concentrations of nitroglycerin (0.1 and 0.5 ng/ml) than for those with high concentrations. At 2 and about 40 ng/ml, the relative standard deviations were determined to be 8.6 and 4.2%, respectively. Saturation of the electron-capture detector occurred when the on-column amount of nitroglycerin exceeded about 0.5 ng.

Applications of the present technique in pharmacokinetic studies of nitroglycerin in a human subject (6) and in rats (7) are described elsewhere.

REFERENCES

(1) M. T. Rosseel and M. G. Bogaert, *J. Chromatogr.*, **64**, 364 (1972).

(2) M. T. Rosseel and M. G. Bogaert, *J. Pharm. Sci.*, **62**, 754 (1973).

(3) "The Merck Index," 9th ed., Merck & Co., Rahway, N.J., 1976.

(4) K. A. Connors, "A Textbook of Pharmaceutical Analysis," Wiley, New York, N.Y., 1967, p. 281.

(5) F. J. DiCarlo and M. D. Melgar, *Proc. Soc. Exp. Biol. Med.*, **131**, 406 (1969).

(6) H. P. Blumenthal, H.-L. Fung, E. F. McNiff, and S. K. Yap, *Br. J. Clin. Pharmacol.*, **4**, 241 (1977).

(7) P. S. K. Yap and H.-L. Fung, *J. Pharm. Sci.*, **67**, 584 (1978).

ACKNOWLEDGMENTS

Presented in part at the Pharmaceutical Analysis and Control Section, APhA Academy of Pharmaceutical Sciences, Orlando meeting, November 1976.

Abstracted in part from a dissertation submitted by P. S. K. Yap to the Graduate School, State University of New York at Buffalo, in partial fulfillment of the Doctor of Philosophy degree requirements.

Supported in part by General Research Support Grant 5S07RR0545414 from the National Institutes of Health.

Pharmacokinetics of Nitroglycerin in Rats

PETER S. K. YAP and HO-LEUNG FUNG ˣ

Received April 22, 1977, from the *Department of Pharmaceutics, School of Pharmacy, State University of New York at Buffalo, Amherst, NY 14214.* Accepted for publication August 3, 1977.

Abstract □ The plasma nitroglycerin levels obtained after intracardial (0.7 mg/kg), oral (7 mg/kg), and topical (7–14 mg/kg) doses of nitroglycerin in rats are reported. Nitroglycerin followed essentially one-compartment kinetics after intracardial administration, showing a mean half-life of about 4 min and a mean apparent volume of distribution of about 3 liters/kg. After oral drug administration, "flip-flop" kinetics were evident. The mean oral bioavailability was determined to be 1.6%, firmly supporting the contention that nitroglycerin is extensively metabolized during first passage through the liver. Under the experimental conditions studied, no detectable levels of nitroglycerin were observed after topical application.

Keyphrases □ Nitroglycerin—pharmacokinetics after intracardial, oral, and topical administrations in rats □ Pharmacokinetics—nitroglycerin after intracardial, oral, and topical administrations in rats □ Vasodilators, coronary—nitroglycerin, pharmacokinetics after intracardial, oral, and topical administrations in rats

Recent studies dealt with the analytical (1–3), stability (4–7), and formulation (6, 8–12) aspects of nitroglycerin. These studies showed definitively that nitroglycerin in sublingual tablets can be stabilized effectively against volatilization by the inclusion of macromolecules such as povidone (8–10), polyethylene glycol (6), and microcrystalline cellulose (8, 12).

BACKGROUND

Very little information is available, however, on the pharmacokinetics of nitroglycerin in animals and humans. The analytical difficulty associated with the determination of nanogram or subnanogram concentrations of the intact drug in biological fluids is a primary reason for the paucity of quantitative information regarding nitroglycerin absorption and disposition. Recently, a GLC assay (13) quantifying nitroglycerin in plasma at these low concentrations was developed. This assay offers a unique opportunity to initiate rigorous *in vivo* pharmacokinetic studies in animals and humans.

Nitroglycerin is used in oral sustained-release dosage forms for the prophylaxis of angina. The effectiveness of this mode of nitroglycerin administration was seriously questioned by Needleman *et al.* (14) who showed that the drug undergoes extensive first-pass metabolism after oral dosing. The intact nitroglycerin levels were much lower after oral administration than after the intravenous route. Their data, however, were not reported in sufficient detail to allow for the estimation of the bioavailability of an oral dose of nitroglycerin.

Recently, nitroglycerin was used in ointment form for the hemodynamic management of patients with chronic congestive heart failure (15). This administration route for nitroglycerin was reported to produce beneficial effects lasting for 3–6 hr after a single application. The therapeutic efficacy and duration of effect of nitroglycerin, therefore, appear to be highly dependent on the route of drug administration.

The present study deals with the effect of the administration route on nitroglycerin pharmacokinetics in the rat. A pilot, collateral study in humans after therapeutic sublingual, oral, and topical doses of nitroglycerin is reported elsewhere (16).

EXPERIMENTAL

Materials—A 1.16-mg/ml aqueous solution of nitroglycerin was prepared by dissolving the appropriate amount of 10% nitroglycerin–lactose adsorbate[1] in distilled water. Solution was effected by overnight mechanical agitation and confirmed by the kinetic assay (2). The internal standard, isosorbide dinitrate, was obtained by acetone extraction from a 25% (w/w) isosorbide dinitrate–lactose powder[2], followed by evaporation of the organic solvent. Male Sprague–Dawley rats, 270–340 g, were used.

Intracardial Experiments—Six rats were fasted overnight and given an intracardial dose of nitroglycerin (0.7 mg/kg) under ether anesthesia. The dosing volume was approximately 0.2 ml. Blood samples (0.5–0.8 ml) were obtained through orbital sinus puncture using heparinized capillary tubes. Half of the rats (A, B, and C) were anesthetized during blood

[1] Nitroglycerin 10% (w/w) in lactose, ICI America, Atlas Chemical Division, Wilmington, DE 19899.

[2] Stuart Pharmaceuticals, Division of ICI United States, Wilmington, DE 19897.

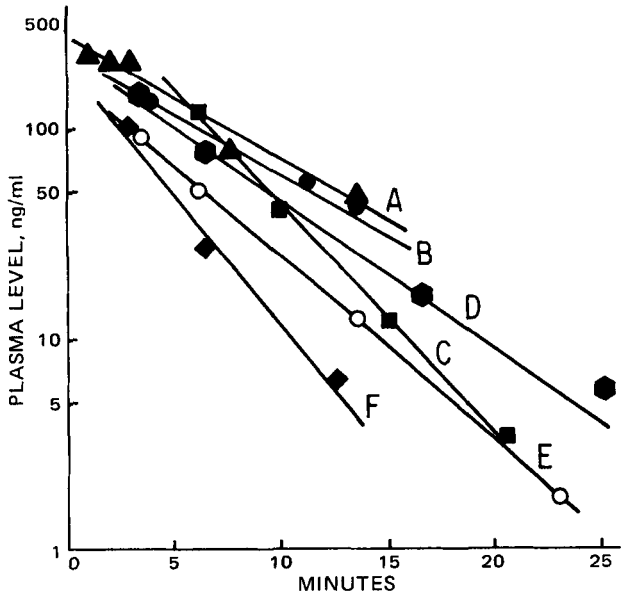

Figure 1—*Plasma nitroglycerin concentrations after intracardial administration of 0.7 mg of nitroglycerin/kg. The letters denote the different rats in the experiment.*

sampling while the others were not. The animals were not restrained except when blood samples were taken.

Oral and Topical Experiments—Five rats were each given a 7-mg/kg po dose of nitroglycerin in about 2 ml of aqueous solution by intubation under ether anesthesia. The animals were then placed in restraining cages. Topical doses of 7 and 14 mg of nitroglycerin/kg were administered to four and two animals, respectively, using a commercial nitroglycerin ointment[3]. The rats were placed in restraining cages after ether anesthesia, and the ointment (about 100–200 mg) was applied onto a 6.452-cm^2 area on the shaved back of the animals. Blood samples were obtained from the tail vein. All animals were fasted overnight with free access to water prior to drug administration.

Nitroglycerin Assay—Blood samples were centrifuged, and 0.2-ml plasma samples were removed. A 10-μl aliquot of 1 *M* silver nitrate immediately was added to the plasma to prevent enzyme degradation of the drug. Nitroglycerin was determined using the GLC assay recently developed (13).

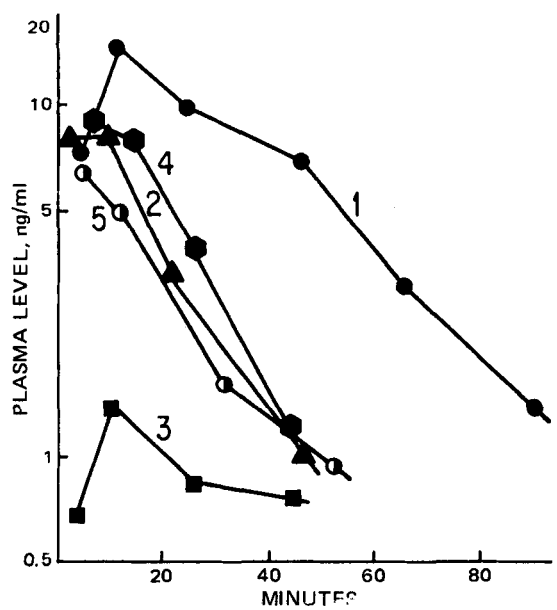

Figure 2—*Plasma nitroglycerin concentrations after oral administration (7 mg/kg) in rats. The numbers denote the different rats in the study.*

[3] Nitrobid ointment (2% nitroglycerin), Pharmaceutical Division, Marion Laboratories, Kansas City, MO 64137.

Table I—Pharmacokinetic Parameters[a] Obtained after Intracardial Administration of 0.7 mg of Nitroglycerin/kg

Rat	C_0, ng/ml	k_e, min^{-1}	$t_{1/2}$, min	V_d, liters/kg	$AUC_{0\to\infty}$
A	242	0.13	5.4	2.9	2024
B	200	0.11	6.1	3.5	1813
C	508	0.25	2.8	1.4	2421
D	198	0.14	4.9	3.5	1844
E	179	0.20	3.5	3.9	957
F	211	0.29	2.4	3.3	814
Mean	257	0.19	4.2	3.1	1646
SD	125	0.07	1.5	0.9	629

[a] Symbols are defined in the text.

RESULTS AND DISCUSSION

Kinetics following Intracardial Administration—The plasma nitroglycerin concentration–time curves obtained following intracardial injection of 0.7 mg of nitroglycerin/kg in Rats A–F are shown in Fig. 1. The disappearance of nitroglycerin in plasma followed first-order kinetics. Least-squares linear regression of the semilog plot of concentration *versus* time yielded a correlation coefficient greater than 0.99 for each animal. Using radioactive drug and cannulation techniques in rats, Needleman *et al.* (14) found that blood clearance of nitroglycerin was biphasic, with a distribution $t_{1/2}$ of less than 20 sec. Under the present experimental conditions, the distribution phase was not detected.

Table I lists the pharmacokinetic parameters calculated from the intracardial data. The plasma drug concentration at time zero, C_0, and the elimination rate constant, k_e, of the drug in each rat were obtained from the *y*-intercept and slope, respectively, of the least-squares fits of the respective log plasma nitroglycerin concentration–time curve. The biological half-life, $t_{1/2}$ (mean ± *SD*), was 4.2 ± 1.5 min. This value agrees with the values found using radioactive nitroglycerin (14, 17). An apparent volume of distribution, V_d, of 3.1 ± 0.9 liters/kg also was calculated. This rather high volume indicated that nitroglycerin is extensively distributed in the rat and is consistent with literature data (18, 19), which showed that, after administration of radioactive nitroglycerin, the radioactivity in blood constituted only a small fraction of the total radiolabeled dose.

Kinetics following Oral Administration—The plasma concentrations, C_p, as a function of time t after 7 mg of nitroglycerin/kg po are shown in Fig. 2. Biexponential plasma nitroglycerin concentration–time curves were observed in all animals after oral dosing. Peak plasma drug concentrations were generally detected within 12 min after drug administration. A one-compartment open model with an absorption step (absorption rate constant, k_a) was utilized in the kinetic analysis of these data. The integrated expression for the model is of the familiar form:

$$C_p = \frac{k_a FD}{V_d(k_e - k_a)}(e^{-k_a t} - e^{-k_e t}) \qquad \text{(Eq. 1)}$$

"Flip-flop" pharmacokinetics (20) appeared to be in operation upon oral nitroglycerin administration. This effect is to be expected for nitroglycerin because of its short biological half-life. Graphical calculation of pharmacokinetic parameters (using the mean value of k_e obtained previously) showed that the mean absorption rate constant was about 0.04 min^{-1}, about 20% of the magnitude of the elimination rate constant (0.19 min^{-1}) (Table II). These values were statistically different ($p < 0.02$) using the Student t test. Examination of the areas under the plasma concentration–time curve, $(AUC)_{0\to\infty}$, after oral administration revealed

Table II—Pharmacokinetic Parameters[a] Obtained after Oral Administration of 7 mg of Nitroglycerin/kg

Rat	k_a, min^{-1}	Absorption $t_{1/2}$, min	$AUC_{0\to\infty}$	F, %	V_d, liters/kg	t_{max} Obs.	t_{max} Calc.
1	0.030	23.0	622	3.78	2.3	13	12
2	0.058	12.0	204	1.24	3.0	5	6
3	0.016	43.4	100	0.61	2.7	11	10
4	0.058	12.0	234	1.42	2.7	7	8
5	0.042	16.5	167	1.01	2.7	5	5
Mean	0.041	21.4	265	1.61	2.7		
SD	0.018	13.1	205	1.25	0.3		

[a] Symbols are defined in the text.

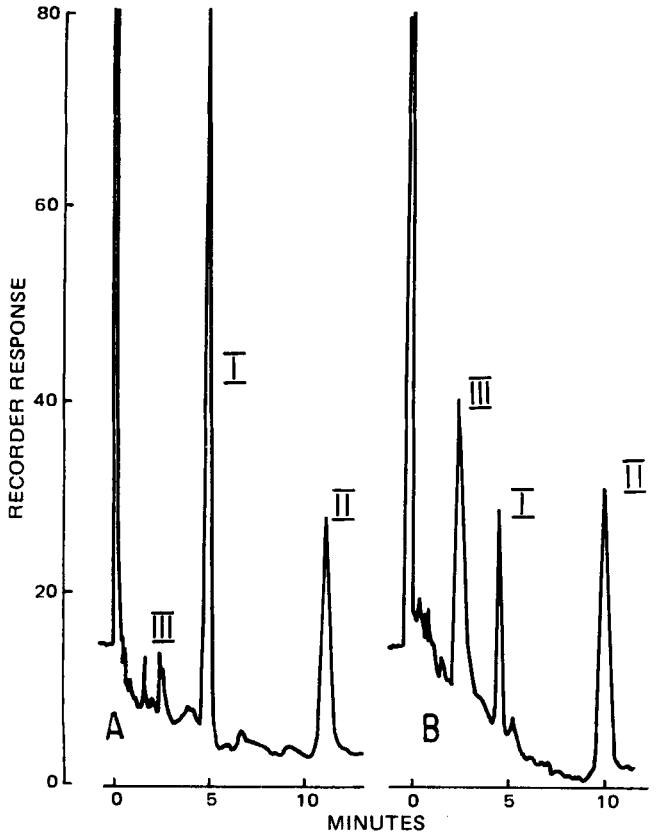

Figure 3—*Chromatograms of rat plasma 6.5 min after intracardial administration of 0.7 mg of nitroglycerin/kg (A) and 10 min after oral administration of 7 mg of nitroglycerin/kg (B) in rats. Key: I, nitroglycerin; II, isosorbide dinitrate; and III, isomeric glyceryl dinitrates.*

that they were only about 2% of those found after intracardial dosing. In the absence of dose-dependent elimination, the ratio $AUC_{oral}/AUC_{intracardial}$ after correction for dose could be equated to F, the fraction of the oral dose absorbed. The low magnitude of F and its considerable variability (Table II) support the general belief that nitroglycerin is extensively metabolized during its first passage through the liver (14).

The consistency of this pharmacokinetic treatment was examined *via* two parameters: the apparent volume of distribution and the time of peak plasma concentration, t_{max}. Equation 2 allows for the calculation of V_d from the oral data, using I, the extrapolated y-intercept, and other previously determined parameters:

$$V_d = \frac{k_a FD}{(k_e - k_a)I} \qquad \text{(Eq. 2)}$$

The V_d value calculated in this manner was 2.7 ± 0.3 liters/kg (mean ± *SD*). This value is not significantly different from that obtained after intracardial administration (3.1 ± 0.9 liters/kg). Equation 3 allows for the calculation of t_{max} after oral dosing:

$$t_{max} = \frac{2.303}{(k_a - k_e)} \log \frac{k_a}{k_e} \qquad \text{(Eq. 3)}$$

The calculated values were close to those observed (Table II).

Topical Nitroglycerin Administration in Rats—No detectable plasma nitroglycerin levels were observed after topical application of 7–14 mg of nitroglycerin/kg in the rat. This finding may be a result of very slow percutaneous absorption of the organic nitrate, leading to plasma drug concentrations beyond the assay detection limit. Since the nitroglycerin ointment used was petrolatum based, the release of the oil-soluble nitroglycerin was expected to be very slow. It is also possible that the rat skin (at the animal's back) is very impermeable to nitroglycerin penetration. The present animal model for skin absorption of nitroglycerin does not appear to reflect the situation with humans in whom topical nitroglycerin administration has been shown to be clinically effective (15).

Plasma Isomeric Glyceryl Dinitrate Levels—Figure 3 shows the typical chromatograms observed after intracardial (Fig. 3A) and oral (Fig. 3B) nitroglycerin administrations. Glyceryl dinitrates are the major metabolites of nitroglycerin in the rat and in other animals (14). Even though the recovery of isomeric glyceryl dinitrates from rat plasma is rather poor (~10–20%) in the assay of nitroglycerin, qualitative information regarding the metabolites may still be obtained from the chromatograms. In general, the peak height ratios of the dinitrates *versus* nitroglycerin were much higher at the early time points after oral administration, substantiating the conclusion of extensive first-pass metabolism after oral administration.

Very low levels of dinitrates were found after topical administration, suggesting again that the lack of nitroglycerin availability from this route of administration is due to poor absorption rather than extensive skin metabolism of the drug.

REFERENCES

(1) H.-L. Fung, P. Dalecki, E. Tse, and C. T. Rhodes, *J. Pharm. Sci.*, **62**, 696 (1973).

(2) S. K. Yap, C. T. Rhodes, and H.-L. Fung, *Am. J. Hosp. Pharm.*, **32**, 1039 (1975).

(3) S. K. Yap, C. T. Rhodes, and H.-L. Fung, *Anal. Chem.*, **47**, 1183 (1975).

(4) M. J. Pikal, A. L. Lukes, and L. F. Ellis, *J. Pharm. Sci.*, **65**, 1278 (1976).

(5) S. A. Fusari, *ibid.*, **62**, 122 (1973).

(6) *Ibid.*, **62**, 2012 (1973).

(7) B. Dorsch and R. Shangraw, *Am. J. Hosp. Pharm.*, **32**, 795 (1975).

(8) F. W. Goodhart, H. Gucluyildiz, R. E. Daly, L. Chafetz, and F. C. Ninger, *J. Pharm. Sci.*, **65**, 1466 (1976).

(9) H.-L. Fung, S. K. Yap, and C. T. Rhodes, *ibid.*, **63**, 1810 (1974).

(10) *Ibid.*, **65**, 558 (1976).

(11) S. K. Yap, A. Massumi, L. H. Golden, C. T. Rhodes, and H.-L. Fung, *Drug Dev. Commun.*, **2**, 193 (1976).

(12) M. D. Richman, C. D. Fox, and R. F. Shangraw, *J. Pharm. Sci.*, **54**, 447 (1965).

(13) P. S. K. Yap, E. F. McNiff, and H.-L. Fung, *ibid.*, **67**, 582 (1978).

(14) P. Needleman, S. Lang, and E. M. Johnson, Jr., *J. Pharmacol. Exp. Ther.*, **181**, 489 (1972).

(15) W. R. Taylor, J. S. Forrester, P. Magnusson, T. Takano, K. Chatterjee, and H. J. C. Swan, *Am. J. Cardiol.*, **38**, 469 (1976).

(16) H. P. Blumenthal, H.-L. Fung, E. F. McNiff, and S. K. Yap, *Br. J. Clin. Pharmacol.*, **4**, 241 (1977).

(17) S. Lang, E. M. Johnson, Jr., and P. Needleman, *Biochem. Pharmacol.*, **21**, 422 (1972).

(18) F. J. DiCarlo, M. C. Crew, L. J. Haynes, M. D. Melgar, and R. L. Gala, *ibid.*, **17**, 3179 (1968).

(19) J. R. Hodgson and C.-C. Lee, *Toxicol. Appl. Pharmacol.*, **34**, 449 (1975).

(20) M. Gibaldi and D. Perrier, "Pharmacokinetics," Dekker, New York, N.Y., 1975.

ACKNOWLEDGMENTS

Presented in part at the Pharmaceutical Analysis and Control Section, APhA Academy of Pharmaceutical Sciences, Orlando meeting, November 1976.

Abstracted in part from a dissertation submitted by P. S. K. Yap to the Graduate School, State University of New York at Buffalo, in partial fulfillment of the Doctor of Philosophy degree requirements.

Supported in part by General Research Support Grant 5S07RR0545414 from the National Institutes of Health.

Synthesis of 2-(Substituted Anilino) 4-(Substituted Phenyl)thiazoles

K. A. THAKAR ˣ, D. D. GOSWAMI, and S. R. CHOUDHARI

Received November 18, 1976, from the *Department of Chemistry, Marathwada University, Aurangabad-431002, India.* Accepted for publication July 28, 1977.

Abstract □ 2-(Substituted anilino) 4-(substituted phenyl)thiazoles were synthesized by condensing 2-haloketones with substituted thioureas. The biological screening of some compounds indicated hypoglycemic and hyperglycemic activity.

Keyphrases □ Thiazoles, various substituted—synthesized, evaluated for hypoglycemic and hyperglycemic activity □ Hypoglycemic activity—various substituted thiazoles evaluated □ Hyperglycemic activity—various substituted thiazoles evaluated □ Structure–activity relationships—various substituted thiazoles evaluated for hypoglycemic and hyperglycemic activity

Five-membered heterocyclic compounds with two or three similar or dissimilar hetero atoms are established hypoglycemic and hyperglycemic agents. A literature survey revealed that sulfur-containing compounds are relatively better hypo/hyperglycemic agents (1, 2), but no definite correlation was observed between the nature of sulfur-containing functional groups and hypo/hyperglycemic activity. Important hypoglycemic agents contain *N*-substituted urea and thiourea residues. Thiazoles contain a thiourea moiety, and 2-anilinothiazoles contain an *N*-substituted thiourea moiety. Therefore, it was thought that 2-anilinothiazoles might have hypo/hyperglycemic activity. Therefore, variously substituted 2-anilinothiazoles were synthesized, and some were tested for hypo/hyperglycemic activity.

EXPERIMENTAL

A mixture of a haloketone (0.01 mole), substituted thiourea (0.01 mole), and alcohol (10 ml) was refluxed on a water bath for 1.5 hr. The crystalline hydrochloride obtained was filtered and washed with ether to remove the unreacted ketone. It was then crystallized from aqueous alcohol. The hydrochloride was boiled with excess dilute ammonium hydroxide. The solid thus obtained was filtered, washed with water, and crystallized from 95% alcohol; the yield was 60–70%.

RESULTS AND DISCUSSION

Chemistry—Thiazole synthesis, as described by Hantzsch and Weber (3), was followed for the synthesis of Compounds 1–48 (Scheme I); it involved the condensation of 2-haloketones with thioureas. 2-Haloketones were readily available through the Friedel–Crafts reaction. All thioureas required were previously reported and were synthesized from commercially available substituted anilines by Kurzer's (4) procedure. The 2-haloketones and thioureas condensed smoothly in ethanol to form 2-(substituted anilino) 4-(substituted phenyl)thiazole hydrochlorides which, when made basic with ammonia, yielded Compounds 1–48.

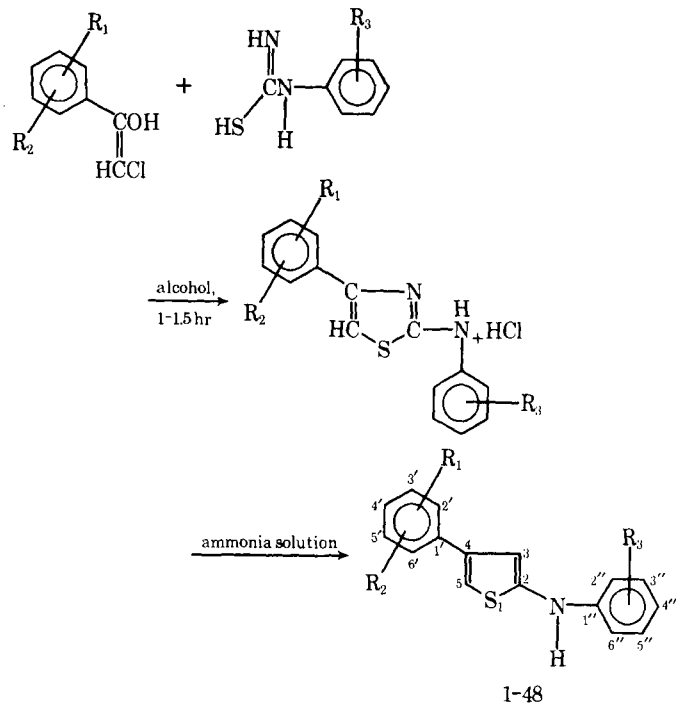

1-48

Scheme I

The formation of thiazole derivatives was determined by their sharp melting points, elemental analyses, and IR spectra (Table I).

Secondary amines show only a single NH-stretching band in the 3500–3200-cm^{-1} range (5). Russell and Thompson (6) extensively studied the IR spectra of secondary amines and examined both the intensity and frequency of the NH band in a wide range of compounds. They reported

Table I—Physical Constants, Elemental Analyses, and IR Spectral Data of 2-(Substituted Anilino) 4-(Substituted Phenyl)thiazoles

Compound	R_1 and R_2	R_3	Melting Point[a]	Carbon, % Calc.	Carbon, % Found	Hydrogen, % Calc.	Hydrogen, % Found	IR Frequencies, cm^{-1} Amino Group	IR Frequencies, cm^{-1} Thiazole Ring
1	3′,4′-Dichloro	H	158° (175°)	56.08	56.23	3.11	3.27	3590, 1620	1570, 1425, 1370, 1030, 820
2	3′,4′-Dichloro	2″-Chloro	115° (206°)	50.64	51.01	2.53	2.99	3230, 1590	1500, 1425, 1385, 1030, 830
3	3′,4′-Dichloro	3″-Chloro	105° (200°)	50.64	49.95	2.53	2.75	—	—
4	3′,4′-Dichloro	4″-Chloro	144° (203°)	50.64	50.80	2.53	2.35	3320, 1610	1560, 1440, 1400, 1026, 840
5	3′,4′-Dichloro	3″-Bromo	103° (198°)	45.00	44.85	2.25	2.52	—	—
6	3′,4′-Dichloro	4″-Bromo	150° (205°)	45.00	44.34	2.25	2.41	3380, 1590	1550, 1435, 1390, 1030, 800
7	3′,4′-Dichloro	2″-Hydroxy	219° (254°)	53.42	53.01	2.96	2.27	3320, 1620	1560, 1430, 1370, 1020, 820
8	3′,4′-Dichloro	3″-Hydroxy	185° (220°)	53.42	52.92	2.96	2.52	3200, 1600	1560, 1425, 1390, 1030, 800

(*continued*)

Table I—*Continued*

Compound	R_1 and R_2	R_3	Melting Point[a]	Carbon, %		Hydrogen, %		IR Frequencies, cm^{-1}	
				Calc.	Found	Calc.	Found	Amino Group	Thiazole Ring
9	3′,4′-Dichloro	4″-Hydroxy	114° (232°)	53.42	53.90	2.96	3.06	3500, 1610	1570, 1420, 1395, 1030, 820
10	3′,4′-Dichloro	2″-Methoxy	132° (180°)	54.70	54.51	3.47	3.85	3370, 1600	1540, 1440, 1380, 1020, 830
11	3′,4′-Dichloro	2″-Pyridyl	175° (243°)	52.57	52.85	2.79	2.32	3400, 1610	1540, 1470, 1380, 1020, 820
12	2′,5′-Dichloro	H	120° (190°)	56.08	56.15	3.11	3.58	3571, 1610	1567, 1430, 1370, 1040, 815
13	2′,5′-Dichloro	2″-Chloro	120° (206°)	50.64	50.82	2.53	3.11	1595	1555, 1464, 1380, 1045, 815
14	2′,5′-Dichloro	3″-Chloro	161° (202°)	50.64	50.99	2.53	2.82	3485, 1600	1560, 1430, 1370, 1006, 815
15	2′,5′-Dichloro	4″-Chloro	141° (195°)	50.64	50.41	2.53	3.06	3545, 1618	1580, 1450, 1370, 1042, 820
16	2′,5′-Dichloro	3″-Bromo	158° (205°)	45.00	44.94	2.25	2.52	1600	1560, 1455, 1380, 1045, 820
17	2′,5′-Dichloro	4″-Bromo	141° (188°)	45.00	45.26	2.25	3.02	1616	1576, 1450, 1370, 1040, 815
18	2′,5′-Dichloro	3″-Iodo	157° (210°)	40.27	40.71	2.01	2.24	1590	1540, 1450, 1370, 1040, 815
19	2′,5′-Dichloro	2″-Hydroxy	210° (236°)	53.42	53.54	2.96	3.34	3340, 1620	1570, 1450, 1370, 1040, 820
20	2′,5′-Dichloro	3″-Hydroxy	158° (230°)	53.42	53.58	2.96	2.84	3450, 1618	1570, 1425, 1370, 1035, 802
21	2′,5′-Dichloro	4″-Hydroxy	130° (225°)	53.42	52.57	2.96	2.96	3200, 1600	1570, 1420, 1370, 1030, 820
22	2′,5′-Dichloro	2″-Methoxy	96° (185°)	54.70	54.40	3.47	3.70	3260, 1600	1570, 1420, 1370, 1030, 820
23	2′,5′-Dichloro	3″-Methoxy	141° (144°)	54.70	54.33	3.47	4.14	3320, 1630	1570, 1420, 1370, 1040, 825
24	2′,5′-Dichloro	2″-Methyl	142° (208°)	59.07	59.01	3.69	3.72	3345, 1590	1560, 1430, 1375, 1040, 810
25	2′,5′-Dichloro	2″-Pyridyl	155° (258°)	52.57	52.25	2.79	4.56	3360, 1615	1550, 1460, 1380, 1040, 810
26	2′-Chloro-5′-methyl	H	194° (195°)	63.90	63.72	4.32	4.15	1590	1580, 1450, 1380, 1040, 800
27	2′-Chloro-5′-methyl	2″-Chloro	80° (198°)	57.32	57.52	3.58	3.28	—	—
28	2′-Chloro-5′-methyl	3″-Chloro	110° (205°)	57.32	57.01	3.58	3.72	3200, 1590	1550, 1415, 1370, 1040, 800
29	2′-Chloro-5′-methyl	4″-Chloro	176° (201°)	57.32	56.79	3.58	4.20	3200, 1590	1560, 1440, 1400, 1020, 820
30	2′-Chloro-5′-methyl	3″-Bromo	137° (206°)	48.98	48.57	3.26	3.03	—	—
31	2′-Chloro-5′-methyl	4″-Bromo	183° (202°)	48.98	48.70	3.26	2.80	3050, 1613	1570, 1445, 1340, 1100, 815
32	2′-Chloro-5′-methyl	2″-Hydroxy	168° (200°)	60.66	59.95	4.10	4.25	3350, 1625	1575, 1475, 1385, 1040, 815
33	2′-Chloro-5′-methyl	3″-Hydroxy	165° (210°)	60.66	60.43	4.10	3.89	3340, 1620	1565, 1440, 1380, 1030, 810
34	2′-Chloro-5′-methyl	4″-Hydroxy	135° (248°)	60.66	59.87	4.10	3.76	3500, 1650	1550, 1424, 1380, 1042, 815
35	2′-Chloro-5′-methyl	2″-Methoxy	70° (190°)	60.29	60.01	4.71	4.52	—	—
36	2′-Chloro-5′-methyl	4″-Methoxy	96° (163°)	60.29	59.95	4.71	5.03	—	—
37	2′-Chloro-5′-methyl	2″-Methyl	133° (198°)	64.86	64.92	4.77	4.23	3360, 1600	1560, 1440, 1380, 1030, 820
38	2′-Chloro-5′-methyl	4″-Methyl	187° (210°)	64.86	64.63	4.77	4.90	1590	1560, 1440, 1395, 1060, 815
39	2′-Chloro-5′-methyl	2″-Pyridyl	142° (220°)	59.70	59.93	3.98	4.23	—	—
40	2′-Bromo-5′-methyl	H	140° (195°)	55.65	55.46	3.75	4.50	3400, 1618	1570, 1450, 1380, 1060, 815
41	2′-Bromo-5′-methyl	2″-Chloro	142° (196°)	50.87	50.52	3.16	3.57	—	—
42	2′-Bromo-5′-methyl	4″-Chloro	189° (184°)	50.87	51.29	3.16	3.46	1600	1570, 1450, 1385, 1060
43	2′-Bromo-5′-methyl	3″-Bromo	137° (210°)	45.28	45.00	2.83	2.62	3540, 1580	1550, 1440, 1360, 1040, 810
44	2′-Bromo-5′-methyl	2″-Hydroxy	158° (185°)	53.19	53.47	3.60	3.32	3420, 1605	1570, 1465, 1380, 1065, 805
45	2′-Bromo-5′-methyl	4″-Hydroxy	205° (220°)	53.19	52.95	3.60	4.10	3500, 1640	1565, 1410, 1380, 1065, 810
46	2′-Bromo-5′-methyl	2″-Methoxy	80° (211°)	54.41	53.69	4.00	5.01	1590	1560, 1420, 1380, 1045, 820
47	2′-Bromo-5′-methyl	2″-Methyl	145° (192°)	56.82	57.55	4.17	3.87	3160, 1600	1550, 1420, 1380, 1030, 820
48	2′-Bromo-5′-methyl	2″-Pyridyl	143° (205°)	52.02	52.60	3.46	4.08	1615	1550, 1420, 1380, 810

[a] Figures in parentheses represent the melting points of the hydrochlorides.

Table II—Data of Hypo/Hyperglycemic Activity of 2-(Substituted Anilino) 4-(Substituted Phenyl)thiazoles

Compound	Increase (+) or Decrease (−) of Blood Glucose Affected by Compounds[a], %			Results
	1 hr	2 hr	4 hr	
2	−4	−4	+2	Inactive
3	−5	−17	−21	Hypoglycemic
4	+15	−4	−7	Inactive
6	−9	−14	−14	Hypoglycemic
7	−11	−9	−11	Inactive
9	+15	+5	+3	Hyperglycemic
12	+11	−3	−4	Hyperglycemic
14	+4	−7	−12	Hypoglycemic
15	+4	−16	−12	Hypoglycemic
17	+4	−12	−14	Hypoglycemic
19	−2	0	−5	Inactive
20	+11	+4	+2	Hyperglycemic
21	−3	−2	−2	Hypoglycemic
28	−10	−17	−12	Hypoglycemic
29	+2	−5	−2	Inactive
31	−2	+2	+2	Inactive
32	+5	−2	+3	Inactive
34	−13	−13	−9	Inactive
42	−3	−12	−9	Hypoglycemic

[a] Results are expressed as the percentage difference in milligrams between the mean change in control and treated groups after a drug dose of 150 mg/kg.

that the frequency falls in the 3350–3310-cm^{-1} range with low intensity in aliphatic secondary amines. In alkylaryl amines, the frequency rises to nearly 3450 cm^{-1} with a higher intensity. The absorption frequencies of diaryl secondary amines do not seem to have been studied in detail. Substituted 2-anilinothiazoles are secondary amines of this type. The NH-stretching frequencies in these compounds lie in the 3550–3320-cm^{-1} range.

The bands due to the NH deformation in secondary aromatic amines are confused to some extent because of C=C ring stretching absorption in the same region. The strong band in the 1640–1600-cm^{-1} region showed the characteristics of anilino structures in general.

The characteristic thiazole ring vibrations have been assigned as 1570-1540, 1470-1420, 1400-1370, and 1035-1025 cm^{-1} (7-9). The bands in the 800–700-cm^{-1} region at the low frequency region are associated with out-of-plane bending vibrations of the CH-stretching of the thiazole ring. The presence of these bands in the IR spectra of the compounds under study confirmed the presence of the thiazole ring.

Hypo/Hyperglycemic Activity—The activity was tested in normal rats (average weight of 200 g). They were divided into groups of seven and fed orally with test compounds (150 mg/kg) as solution in 5% gum tragacanth. Seven rats were kept as controls. Blood samples were drawn each hour from tail veins for glucose measurements. Changes in blood glucose content of the tested rats were compared with those of the controls at 1, 2, 4, and 48 hr in each case. The data of the *in vivo* activity tests are given in Table II.

A compound is considered hypoglycemically active if it produces a 30% decrease in blood glucose and hyperglycemically active if it produces a 10% increase in blood glucose:

$$\% \text{ change} = \frac{\Delta T - \Delta C}{\text{control glucose value at that hour}} \qquad \text{(Eq. 1)}$$

where ΔT is the change of blood glucose from zero time for treated groups and ΔC is the change of blood glucose from zero time for control groups.

REFERENCES

(1) M. Y. Mhasalkar, M. H. Shah, S. T. Nikam, K. G. Anantnarayan, and C. V. Deliwala, *J. Med. Chem.*, **14**, 260 (1971).

(2) J. C. Krantz and C. J. Carr, "Pharmacologic Principles of Medical Practice," 6th ed., Williams & Wilkins, Baltimore, Md., 1967, pp. 865–875.

(3) A. Hantzsch and J. H. Weber, *Chem. Ber.*, **20**, 3118, 3336 (1887); **21**, 938, 941 (1888).

(4) F. Kurzer, in "Organic Syntheses," coll. vol. IV, N. Rabjohn, Ed., Wiley, New York, N.Y., 1963, p. 180.

(5) L. J. Bellamy, "The Infrared Spectra of Complex Molecules" Wiley, New York, N.Y., 1959, p. 248.

(6) R. A. Russell and W. H. Thompson, *J. Chem. Soc.*, **1955**, 483.

(7) H. M. Randall, R. G. Fowler, N. Fusion, and J. R. Dangle, "Infrared Determination of Organic Structures," Van Nostrand, New York, N.Y., 1949.

(8) A. Taurins, J. G. E. Fenyes, and R. N. Jones, *Can. J. Chem.*, **35**, 423 (1957).

(9) A. R. Kartritzky, *Q. Rev.*, **13**, 353 (1959).

ACKNOWLEDGMENTS

The authors thank Dr. Charles E. Berkoff of Smith Kline and French Laboratories, Philadelphia, Pa., for extending screening facilities for the compounds and also the authorities of Marathwada University for awarding a Junior Research Fellowship to Mr. S. R. Choudhari.

Stereochemical Considerations in Structural Comparison of Enkephalins and Endorphins with Exogenous Opiate Agents

Keyphrases □ Stereochemistry—enkephalins and endorphins compared to endogenous opiates □ Methionine-enkephalin—stereochemistry compared to exogenous opiates □ Morphine—stereochemistry compared to enkephalins and endorphins □ Enkephalins—stereochemistry compared to exogenous opiates □ Opiates—stereochemistry compared to enkephalins and endorphins

To the Editor:

The existence in mammalian species of endogenous peptides, such as methionine-enkephalin (I), which act as ligands for opiate receptors, has generated considerable interest (1–3). The morphine-like properties of these peptide ligands lead to the question of their structural relationship with morphine (II) and congeneric opiates (4–9).

The resemblance between the primary structure of I and, for example, (−)-morphine (II), by virtue of their β-(4-hydroxyphenyl)ethylamine units, was discussed previously (6). (In Structures I and II, the * denotes the α-position of the tyramine unit. The absolute configurations for the asymmetric centers are all *S* for I and 5*R*, 6*S*, 9*R*, 13*S*, and 14*R* for II.) However, discrimination between enantiomeric ligands by the chiral macromolecular complex known as the opiate receptor is not addressed in an elementary tyramine relationship, which relies on the spatial arrangement of two interaction sites, the phenyl and amino functionalities, in an effectively achiral (10) tyramine unit. Comparison of I and II demonstrates that, in superimposing the amino and phenyl groups, α-substituents on the tyramine moieties are not congruent. (−)-L-Tyrosine has the *S*-configuration and (−)-morphine has the 9*R*-configuration (11–14), representing, in real terms, an opposite spatial distribution of functionality at this stereocenter.

Is the absolute stereochemistry of the 9*R* center in II and its congeners important for receptor binding and/or pharmacological activity? Among morphine-like structures, one enantiomer is commonly much more active than its counterpart (11, 12). Where the absolute stereochemistry is known or implied, the same configuration is found at the α-carbon of the tyramine unit (13–19), exemplified by a number of morphinan and 6,7-benzomorphan analgesic agonists and/or antagonists: II, (−)-3-hydroxy-*N*-methylisomorphinan (20), (−)-butorphanol (21), levorphanol, levallorphan, (−)-etorphine, (−)-nalorphine, and (−)-cyclazocine (22); as a series, these compounds have other portions of their structures, remote from the tyramine segment, grossly altered. The known correspondent enantiomers exhibit relatively little or no analgesic activity: *e.g.*, (+)-morphine, (+)-3-hydroxy-*N*-methylisomorphinan (20), (+)-cyclazocine (22), (+)-butorphanol (21), dextrophan, and (+)-3-hydroxy-*N*-allylmorphinan, and/or minimal binding (23) to receptor tissue (brain): *e.g.*, (+)-3-hydroxy-*N*-allylmorphinan and dextrophan. Thus, it seems that the stereochemistry at the α-tyramine carbon atom is specifically significant.

If a morphological comparison of II and I is deemed valid (4–9), then cognizance of the enantiomorphism of the tyramine segment becomes vital to arguments relating their structural characteristics. Thus, we were concerned that two groups of researchers (7–9) employed incorrect steric relationships to correlate the structures of I and II, improperly achieving coincidence of the phenyl, amino, and side chain [so-called three-point contact (8)] and simultaneously establishing an erroneous structure–activity pattern. One group of collaborators compared the structure of II with unnatural, all-D-I in one paper (7) and inactive (+)-morphine with natural I in another paper (8); Jones *et al.* (9) employed (+)-morphine in their comparison. Other investigators (4–6, 24) utilized correct stereostructures in their discussions[1]. In any case, the importance of chirality in relating the morphology of morphine-like opiates and of the enkephalins has never been explicitly enunciated.

Conformational factors for I are also important in the correlation of endogenous and exogenous opiate substances. For example, the absence of, or reduction in, activity for the enkephalin fragments tyr-gly-gly-phe (25) and tyr-gly-gly (26) and for the diastereomeric pentapeptide tyr-gly-gly-(D)-phe-met (9, 27) necessitates consideration of the nontyrosine amino acids of I and their conformational disposition (27, 28). At present, conflicting results exist with respect to the secondary structure (conformation) of I in solution, as determined spectroscopically (7, 9, 29, 30), so no definitive statement can be made on this point.

One can still acknowledge the first-order "tyramine"

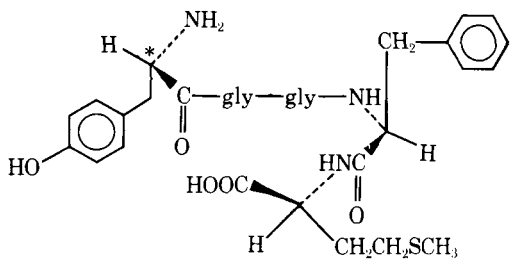

I

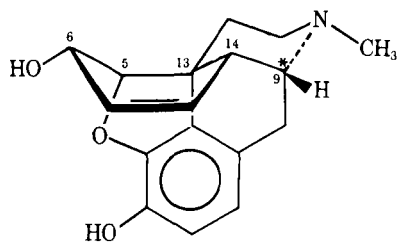

II

[1] To eliminate potential confusion, we wish to point out that the stereostructures given for (−)-morphine in "Principles of Drug Action," by A. Goldstein, L. Aronow, and S. M. Kalman (Wiley, New York, N.Y., 1st and 2nd eds., 1968 and 1974, pp. 53 and 34, respectively) are those of the analgesically inactive enantiomer (+)-morphine.

hypothesis (6) and the lack of correspondence of absolute stereochemistry at the α-carbon of the tyramine unit, the importance of which is reinforced by the virtual lack of activity (mouse vas deferens) of the D-tyr[1] derivative of I[2] (27, 31). The structure–activity relationship between I and II is thus marked by a reversal in stereospecificity. An analogous reversal (by enantiomorphism at the α-carbon stereocenter of a β-phenethylamine unit) occurs in the analgesics (−)-*N,N*-dimethyl-1,2-diphenylethylamine[3] (*R*-configuration) (32) and (+)-1-cyclohexyl-4-(1,2-diphenylethyl)piperazine[4] (*S*-configuration) (33).

Stereochemical inversions in structure–activity relationships are also exhibited in diphenylpropylamine (methadone-type) and certain anilide analgesics and may generally be interpreted in terms of differing substrate–receptor interactions (11, 34) and/or induced-fit theories (35). Recent suggestions (36) of opiate receptor heterogeneity (κ, μ, δ) are especially apropos to this latter stereochemical discussion and have relevance to a comparison of II and the enkephalins, given their stereochemical noncorrespondence.

Any model proposing to rationalize the structure–activity relationships of opiates must consider stereochemical inversion phenomena[5]. If the "tyramine" relationship mentioned is valid, then difficulties arise in defining a structure–activity relationship for II (and its analogs) and, *e.g.*, I.

(1) A. Goldstein, *Science*, **193**, 1081 (1976).
(2) J. L. Marx, *ibid.*, **193**, 1227 (1976).
(3) "Opiates and Endogenous Opioid Peptides," H. W. Kosterlitz, Ed., Elsevier/North Holland, Amsterdam, The Netherlands, 1976.
(4) A. F. Bradbury, D. G. Smyth, and C. R. Snell, *Nature*, **260**, 165 (1976).
(5) A. F. Bradbury, W. F. Feldberg, D. G. Smyth, and C. R. Snell, in "Opiates and Endogenous Opioid Peptides," Elsevier/North Holland, Amsterdam, The Netherlands, 1976, pp. 9–17.
(6) A. S. Horn and J. R. Rodgers, *J. Pharm. Pharmacol.*, **29**, 257 (1977).
(7) B. P. Roques, C. Garbay-Jaureguiberry, R. Oberlin, M. Anteunis, and A. K. Lala, *Nature*, **262**, 778 (1976).
(8) C. Garbay-Jaureguiberry, B. P. Roques, R. Oberlin, M. Anteunis, and A. K. Lala, *Biochem. Biophys. Res. Commun.*, **71**, 558 (1976).
(9) C. R. Jones, W. A. Gibbons, and V. Garsky, *Nature*, **262**, 779 (1976).
(10) W. L. Alworth, "Stereochemistry and Its Application in Biochemistry," Wiley–Interscience, New York, N.Y., 1972, pp. 30–38.
(11) P. S. Portoghese, *J. Pharm. Sci.*, **55**, 865 (1966).
(12) E. L. May and L. J. Sargent, in "Analgetics," G. deStevens, Ed., Academic, New York, N.Y., 1965, pp. 123–177.
(13) J. Kalvoda, P. Buchschacher, and O. Jeger, *Helv. Chim. Acta*, **38**, 1847 (1955).
(14) M. Corrodi and E. Hardegger, *ibid.*, **38**, 2038 (1955).
(15) J. H. van den Hende and N. R. Nelson, *J. Am. Chem. Soc.*, **89**, 2901 (1967).
(16) Y. K. Sawa and J. Irisawa, *Tetrahedron*, **21**, 1129 (1965).
(17) A. F. Casy and A. P. Parulkar, *J. Med. Chem.*, **12**, 178 (1969).
(18) A. F. Casy, *Prog. Med. Chem.*, **7**, 229 (1970).
(19) H. Merz, K. Stockhaus, and H. Wick, *J. Med. Chem.*, **18**, 996 (1975).
(20) M. Gates and W. G. Webb, *J. Am. Chem. Soc.*, **80**, 1186 (1958).
(21) I. Monković, H. Wong, A. W. Pircio, Y. G. Perron, I. J. Pachter, and B. Belleau, *Can. J. Chem.*, **53**, 3094 (1975).
(22) B. F. Tullar, L. S. Harris, R. L. Perry, A. K. Pierson, A. E. Soria, W. F. Wetterau, and N. F. Albertson, *J. Med. Chem.*, **10**, 383 (1967).
(23) C. B. Pert and S. H. Snyder, *Proc. Natl. Acad. Sci. USA*, **70**, 2243 (1973).
(24) A. Goldstein, J. S. Goldstein, and B. M. Cox, *Life Sci.*, **17**, 1643 (1975).
(25) N. Ling and R. Guillemin, *Proc. Natl. Acad. Sci. USA*, **73**, 3308 (1976).
(26) L. Terenius, A. Wahlström, G. Lindeberg, S. Karlsson, and U. Ragnarsson, *Biochem. Biophys. Res. Commun.*, **71**, 175 (1976).
(27) C. R. Beddell, R. B. Clark, G. W. Hardy, L. A. Lowe, F. B. Ubatuka, J. R. Vane, S. Wilkinson, K.-J. Chang, P. Cuatrecasas, and R. J. Miller, *Proc. Roy. Soc. London B*, **198**, 249 (1977).
(28) Y. Isogai, G. Némethy, and H. A. Scheraga, *Proc. Natl. Acad. Sci. USA*, **74**, 414 (1977), and references cited therein.
(29) S. Combrisson, B. P. Roques, and R. Oberlin, *Tetrahedron Lett.*, **1976**, 3455.
(30) H. E. Bleich, A. R. Day, R. J. Freer, and J. A. Glasel, *Biochem. Biophys. Res. Commun.*, **74**, 592 (1977).
(31) D. H. Coy, A. J. Kastin, A. V. Schally, O. Morin, N. G. Caron, F. Labrie, J. M. Walker, R. Fertel, G. G. Berntson, and C. A. Sandman, *ibid.*, **73**, 632 (1976).
(32) M. Nakazaki, I. Mita, and N. Toshioka, *Bull. Chem. Soc. Jpn.*, **36**, 161 (1963).
(33) H. Nakamura and M. Shimizu, *Arch. Int. Pharmacodyn. Ther.*, **221**, 105 (1976).
(34) P. S. Portoghese, *J. Med. Chem.*, **8**, 609 (1965).
(35) A. Korolkovas, "Essentials of Molecular Pharmacology," Wiley–Interscience, New York, N.Y., 1970, pp. 191, 273–286.
(36) J. A. H. Lord, A. A. Waterfield, J. Hughes, and H. W. Kosterlitz, in "Opiates and Endogenous Opioid Peptides," Elsevier/North Holland, Amsterdam, The Netherlands, 1976, pp. 275–280.

Bruce E. Maryanoff [x]
Michael J. Zelesko
Chemical Research Department
McNeil Laboratories, Inc.
Fort Washington, PA 19034

Received April 13, 1977.
Accepted for publication January 9, 1978.

[2] Also, D-tyr[1]-β_c-endorphin has minimal opiate activity (ileum assay) and analgesic potency compared to natural β_c-endorphin [see D. Yamashiro, L.-F. Tseng, B. A. Doneen, H. A. Loh, and C. H. Li, *Int. J. Peptide Protein Res.*, **10**, 159 (1977)].

[3] Spa.

[4] MT-45.

[5] A recent, simplistic model to explain structure–activity relationships of opiate agents unfortunately ignored absolute stereochemical factors [see A. P. Feinberg, I. Creese, and S. H. Snyder, *Proc. Natl. Acad. Sci. USA*, **73**, 4215 (1976)].

Absolute Drug Bioavailability II: Evaluation of Renal Clearance Perturbation Method Using Literature Data Assuring a Fraction Absorbed of Unity

Keyphrases □ Bioavailability, absolute—evaluation of renal clearance perturbation method using literature data assuring a fraction absorbed of unity □ Renal clearance—perturbation method evaluated using literature data assuring a fraction absorbed of unity

To the Editor:

Three years ago, a technique allowing an estimation of the absolute bioavailability of a drug without reference to a parenteral dose was reported (1). Since that time, two other reports (2, 3) suggested that this method is useful and reasonably accurate. However, the procedure has not been tested using data where the fraction absorbed is known. This communication reports the results of the application of the previously described technique to recently reported furosemide pharmacokinetic data obtained following intravenous administration.

hypothesis (6) and the lack of correspondence of absolute stereochemistry at the α-carbon of the tyramine unit, the importance of which is reinforced by the virtual lack of activity (mouse vas deferens) of the D-tyr[1] derivative of I[2] (27, 31). The structure–activity relationship between I and II is thus marked by a reversal in stereospecificity. An analogous reversal (by enantiomorphism at the α-carbon stereocenter of a β-phenethylamine unit) occurs in the analgesics (−)-*N,N*-dimethyl-1,2-diphenylethylamine[3] (*R*-configuration) (32) and (+)-1-cyclohexyl-4-(1,2-diphenylethyl)piperazine[4] (*S*-configuration) (33).

Stereochemical inversions in structure–activity relationships are also exhibited in diphenylpropylamine (methadone-type) and certain anilide analgesics and may generally be interpreted in terms of differing substrate–receptor interactions (11, 34) and/or induced-fit theories (35). Recent suggestions (36) of opiate receptor heterogeneity (κ, μ, δ) are especially apropos to this latter stereochemical discussion and have relevance to a comparison of II and the enkephalins, given their stereochemical noncorrespondence.

Any model proposing to rationalize the structure–activity relationships of opiates must consider stereochemical inversion phenomena[5]. If the "tyramine" relationship mentioned is valid, then difficulties arise in defining a structure–activity relationship for II (and its analogs) and, *e.g.*, I.

(1) A. Goldstein, *Science*, **193**, 1081 (1976).
(2) J. L. Marx, *ibid.*, **193**, 1227 (1976).
(3) "Opiates and Endogenous Opioid Peptides," H. W. Kosterlitz, Ed., Elsevier/North Holland, Amsterdam, The Netherlands, 1976.
(4) A. F. Bradbury, D. G. Smyth, and C. R. Snell, *Nature*, **260**, 165 (1976).
(5) A. F. Bradbury, W. F. Feldberg, D. G. Smyth, and C. R. Snell, in "Opiates and Endogenous Opioid Peptides," Elsevier/North Holland, Amsterdam, The Netherlands, 1976, pp. 9–17.
(6) A. S. Horn and J. R. Rodgers, *J. Pharm. Pharmacol.*, **29**, 257 (1977).
(7) B. P. Roques, C. Garbay-Jaureguiberry, R. Oberlin, M. Anteunis, and A. K. Lala, *Nature*, **262**, 778 (1976).
(8) C. Garbay-Jaureguiberry, B. P. Roques, R. Oberlin, M. Anteunis, and A. K. Lala, *Biochem. Biophys. Res. Commun.*, **71**, 558 (1976).
(9) C. R. Jones, W. A. Gibbons, and V. Garsky, *Nature*, **262**, 779 (1976).
(10) W. L. Alworth, "Stereochemistry and Its Application in Biochemistry," Wiley–Interscience, New York, N.Y., 1972, pp. 30–38.
(11) P. S. Portoghese, *J. Pharm. Sci.*, **55**, 865 (1966).
(12) E. L. May and L. J. Sargent, in "Analgetics," G. deStevens, Ed., Academic, New York, N.Y., 1965, pp. 123–177.
(13) J. Kalvoda, P. Buchschacher, and O. Jeger, *Helv. Chim. Acta*, **38**, 1847 (1955).
(14) M. Corrodi and E. Hardegger, *ibid.*, **38**, 2038 (1955).
(15) J. H. van den Hende and N. R. Nelson, *J. Am. Chem. Soc.*, **89**, 2901 (1967).
(16) Y. K. Sawa and J. Irisawa, *Tetrahedron*, **21**, 1129 (1965).
(17) A. F. Casy and A. P. Parulkar, *J. Med. Chem.*, **12**, 178 (1969).
(18) A. F. Casy, *Prog. Med. Chem.*, **7**, 229 (1970).
(19) H. Merz, K. Stockhaus, and H. Wick, *J. Med. Chem.*, **18**, 996 (1975).
(20) M. Gates and W. G. Webb, *J. Am. Chem. Soc.*, **80**, 1186 (1958).
(21) I. Monković, H. Wong, A. W. Pircio, Y. G. Perron, I. J. Pachter, and B. Belleau, *Can. J. Chem.*, **53**, 3094 (1975).
(22) B. F. Tullar, L. S. Harris, R. L. Perry, A. K. Pierson, A. E. Soria, W. F. Wetterau, and N. F. Albertson, *J. Med. Chem.*, **10**, 383 (1967).
(23) C. B. Pert and S. H. Snyder, *Proc. Natl. Acad. Sci. USA*, **70**, 2243 (1973).
(24) A. Goldstein, J. S. Goldstein, and B. M. Cox, *Life Sci.*, **17**, 1643 (1975).
(25) N. Ling and R. Guillemin, *Proc. Natl. Acad. Sci. USA*, **73**, 3308 (1976).
(26) L. Terenius, A. Wahlström, G. Lindeberg, S. Karlsson, and U. Ragnarsson, *Biochem. Biophys. Res. Commun.*, **71**, 175 (1976).
(27) C. R. Beddell, R. B. Clark, G. W. Hardy, L. A. Lowe, F. B. Ubatuka, J. R. Vane, S. Wilkinson, K.-J. Chang, P. Cuatrecasas, and R. J. Miller, *Proc. Roy. Soc. London B*, **198**, 249 (1977).
(28) Y. Isogai, G. Némethy, and H. A. Scheraga, *Proc. Natl. Acad. Sci. USA*, **74**, 414 (1977), and references cited therein.
(29) S. Combrisson, B. P. Roques, and R. Oberlin, *Tetrahedron Lett.*, **1976**, 3455.
(30) H. E. Bleich, A. R. Day, R. J. Freer, and J. A. Glasel, *Biochem. Biophys. Res. Commun.*, **74**, 592 (1977).
(31) D. H. Coy, A. J. Kastin, A. V. Schally, O. Morin, N. G. Caron, F. Labrie, J. M. Walker, R. Fertel, G. G. Berntson, and C. A. Sandman, *ibid.*, **73**, 632 (1976).
(32) M. Nakazaki, I. Mita, and N. Toshioka, *Bull. Chem. Soc. Jpn.*, **36**, 161 (1963).
(33) H. Nakamura and M. Shimizu, *Arch. Int. Pharmacodyn. Ther.*, **221**, 105 (1976).
(34) P. S. Portoghese, *J. Med. Chem.*, **8**, 609 (1965).
(35) A. Korolkovas, "Essentials of Molecular Pharmacology," Wiley–Interscience, New York, N.Y., 1970, pp. 191, 273–286.
(36) J. A. H. Lord, A. A. Waterfield, J. Hughes, and H. W. Kosterlitz, in "Opiates and Endogenous Opioid Peptides," Elsevier/North Holland, Amsterdam, The Netherlands, 1976, pp. 275–280.

Bruce E. Maryanoff [x]
Michael J. Zelesko
Chemical Research Department
McNeil Laboratories, Inc.
Fort Washington, PA 19034

Received April 13, 1977.
Accepted for publication January 9, 1978.

[2] Also, D-tyr[1]-β_c-endorphin has minimal opiate activity (ileum assay) and analgesic potency compared to natural β_c-endorphin [see D. Yamashiro, L.-F. Tseng, B. A. Doneen, H. A. Loh, and C. H. Li, *Int. J. Peptide Protein Res.*, **10**, 159 (1977)].

[3] Spa.

[4] MT-45.

[5] A recent, simplistic model to explain structure–activity relationships of opiate agents unfortunately ignored absolute stereochemical factors [see A. P. Feinberg, I. Creese, and S. H. Snyder, *Proc. Natl. Acad. Sci. USA*, **73**, 4215 (1976)].

Absolute Drug Bioavailability II: Evaluation of Renal Clearance Perturbation Method Using Literature Data Assuring a Fraction Absorbed of Unity

Keyphrases □ Bioavailability, absolute—evaluation of renal clearance perturbation method using literature data assuring a fraction absorbed of unity □ Renal clearance—perturbation method evaluated using literature data assuring a fraction absorbed of unity

To the Editor:

Three years ago, a technique allowing an estimation of the absolute bioavailability of a drug without reference to a parenteral dose was reported (1). Since that time, two other reports (2, 3) suggested that this method is useful and reasonably accurate. However, the procedure has not been tested using data where the fraction absorbed is known. This communication reports the results of the application of the previously described technique to recently reported furosemide pharmacokinetic data obtained following intravenous administration.

Pharmacokinetic theory predicts that:

$$F = \frac{\Delta Cl_R}{\text{dose}}\left[\frac{(AUC)(AUC')}{AUC' - AUC}\right] \qquad \text{(Eq. 1)}$$

where F is the fraction of the dose absorbed, AUC is the area under the plasma concentration–time curve, the prime notation indicates the AUC in the perturbed renal clearance state, and ΔCl_R is the difference in mean renal clearance between the two experiments (see Ref. 1 for details). Data from a furosemide–probenecid interaction study (4) were used exactly as reported in Table I of that article, and AUC and AUC' values for each individual were determined using the relationship AUC = dose/plasma clearance.

The fundamental mechanism used to perturb the renal clearance of furosemide in this interaction study with probenecid seems to be competition for the renal transport system, which actively secretes organic acids (4). In previous studies, it was observed that the improved reabsorption of weak bases from an alkaline tubular fluid was an appropriate perturbation technique (2) and that the reduction in lithium renal clearance caused by chlorothiazide yielded data (3) supporting the validity of Eq. 1. The principal virtues of the data from Ref. 4 are that the two doses were given parenterally (*i.e.*, F is known to be unity), the physiological status of the volunteers was well controlled, and the plasma and urine concentrations were confirmed by two independent analytical procedures, thus circumventing the assay difficulties that have hampered some furosemide disposition studies.

When Eq. 1 and the values of ΔCl_R, AUC, AUC', and the intravenous dose from Table I of Ref. 4 are used to estimate F, a value of 1.05 ± 0.11 (mean ± SEM) is obtained. This result appears to provide further support for the validity of Eq. 1.

(1) D. Lalka and H. Feldman, *J. Pharm. Sci.*, **63**, 1812 (1974).
(2) D. Lalka, M. B. Meyer, B. R. Duce, and A. T. Elvin, *Clin. Pharmacol. Ther.*, **19**, 757 (1976).
(3) R. I. Poust, A. G. Mallinger, J. Mallinger, J. M. Himmelhoch, J. F. Neil, and I. Hanin, *J. Pharm. Sci.*, **66**, 609 (1977).
(4) J. Honari, A. D. Blair, and R. E. Cutler, *Clin. Pharmacol. Ther.*, **22**, 395 (1977).

David Lalka ˣ
P. du Souich
A. J. McLean
Milo Gibaldi
Department of Pharmaceutics
School of Pharmacy
State University of New York
at Buffalo
Amherst, NY 14260

Received November 14, 1977.
Accepted for publication January 10, 1978.

BOOKS

REVIEWS

Microbiology—1977. Edited by DAVID SCHLESSINGER. American Society for Microbiology, 1913 I St., N.W., Washington, DC 20006. 1977. 593 pp. 17 × 26 cm. Price $22.00.

The book is divided into seven major and numerous minor sections, covering some of the more important and recent findings in microbiology.

Cell envelope and cell division in bacilli are represented by partial proceedings of the conference on bacilli (other material from the conference appeared in "Microbiology—1976"). Various topics concerning *Pseudomonas aeruginosa* and related components and their recognition by specific lymphocytes or other cell types are discussed. Modes of resistance to various antibiotics by the pseudomonads are covered. Endotoxins, cell wall antigens, and modulation of the immune response are presented in various manuscripts.

A historical review of pyrogen research by Otto Westphal *et al.*, and related articles on endotoxins and other cell wall components of Gram-negative bacteria and their biological activities proved to be very interesting and rewarding.

Viral infections are covered, including mechanisms involved in persistent viral infections, and the possible roles of defective virus in these infections. The roles of DNA in RNA viruses are also discussed. Animal and human models of persistent viral infections and live virus vaccines used in humans are topics also covered. Viruses and plasmids in fungi and protozoa are presented as an enlightening view of this little-known subject. Also in the field of virology is a series of studies of endogenous tumor viruses, including propagation, analysis, and regulation of various tumor viruses.

However, to me the most informative section dealt with novel aspects of penicillin action, including a short history written by Jack L. Strominger of the Department of Biochemistry and Molecular Biology, Harvard University, "How Penicillins Kill Bacteria."

"Microbiology—1977" continues the well-thought out series started in 1974 by David Schlessinger and fulfills the original aim of the series: to remedy part of the problem of keeping up with new developments in the field of microbiology.

Reviewed by Mary Ann Garth
Microbiological Assay Branch
National Center for Antibiotics Analysis
Food and Drug Administration
Washington, DC 20204

Fluorescence and Phosphorescence Spectroscopy: Physiochemical Principles and Practice. By STEPHEN G. SCHULMAN. Pergamon Press, Maxwell House, Fairview Park, Elmsford, NY 10523. 1977. 288 pp. 17 × 14.8 cm. Price $20.00.

The author states in his preface that this book "is written with the analytical chemist and biological scientist in mind and represents an attempt to make the instrumental, and especially the structural and environmental aspects of luminescence spectra intelligible to the reader with a general college background in chemistry and physics."

Chapter I, entitled "Photophysical Processes in Isolated Molecules," deals with a nonmathematic descriptive treatment of the subject. It serves to describe ideal systems and to define basic terms. Chapter II, "Photophysical Process in Molecules in Solution," surveys the effects of solvent–solute and solute–solute interactions on both the ground and excited states in electronic spectra. Chapter III is a brief description of the practical aspects of the instrumentation employed in the measurement

Pharmacokinetic theory predicts that:

$$F = \frac{\Delta Cl_R}{\text{dose}}\left[\frac{(AUC)(AUC')}{AUC' - AUC}\right] \qquad \text{(Eq. 1)}$$

where F is the fraction of the dose absorbed, AUC is the area under the plasma concentration–time curve, the prime notation indicates the AUC in the perturbed renal clearance state, and ΔCl_R is the difference in mean renal clearance between the two experiments (see Ref. 1 for details). Data from a furosemide–probenecid interaction study (4) were used exactly as reported in Table I of that article, and AUC and AUC' values for each individual were determined using the relationship AUC = dose/plasma clearance.

The fundamental mechanism used to perturb the renal clearance of furosemide in this interaction study with probenecid seems to be competition for the renal transport system, which actively secretes organic acids (4). In previous studies, it was observed that the improved reabsorption of weak bases from an alkaline tubular fluid was an appropriate perturbation technique (2) and that the reduction in lithium renal clearance caused by chlorothiazide yielded data (3) supporting the validity of Eq. 1. The principal virtues of the data from Ref. 4 are that the two doses were given parenterally (*i.e.*, F is known to be unity), the physiological status of the volunteers was well controlled, and the plasma and urine concentrations were confirmed by two independent analytical procedures, thus circumventing the assay difficulties that have hampered some furosemide disposition studies.

When Eq. 1 and the values of ΔCl_R, AUC, AUC', and the intravenous dose from Table I of Ref. 4 are used to estimate F, a value of 1.05 ± 0.11 (mean ± SEM) is obtained. This result appears to provide further support for the validity of Eq. 1.

(1) D. Lalka and H. Feldman, *J. Pharm. Sci.*, **63**, 1812 (1974).
(2) D. Lalka, M. B. Meyer, B. R. Duce, and A. T. Elvin, *Clin. Pharmacol. Ther.*, **19**, 757 (1976).
(3) R. I. Poust, A. G. Mallinger, J. Mallinger, J. M. Himmelhoch, J. F. Neil, and I. Hanin, *J. Pharm. Sci.*, **66**, 609 (1977).
(4) J. Honari, A. D. Blair, and R. E. Cutler, *Clin. Pharmacol. Ther.*, **22**, 395 (1977).

David Lalka ˣ
P. du Souich
A. J. McLean
Milo Gibaldi
Department of Pharmaceutics
School of Pharmacy
State University of New York
at Buffalo
Amherst, NY 14260

Received November 14, 1977.
Accepted for publication January 10, 1978.

BOOKS

REVIEWS

Microbiology—1977. Edited by DAVID SCHLESSINGER. American Society for Microbiology, 1913 I St., N.W., Washington, DC 20006. 1977. 593 pp. 17 × 26 cm. Price $22.00.

The book is divided into seven major and numerous minor sections, covering some of the more important and recent findings in microbiology.

Cell envelope and cell division in bacilli are represented by partial proceedings of the conference on bacilli (other material from the conference appeared in "Microbiology—1976"). Various topics concerning *Pseudomonas aeruginosa* and related components and their recognition by specific lymphocytes or other cell types are discussed. Modes of resistance to various antibiotics by the pseudomonads are covered. Endotoxins, cell wall antigens, and modulation of the immune response are presented in various manuscripts.

A historical review of pyrogen research by Otto Westphal *et al.*, and related articles on endotoxins and other cell wall components of Gram-negative bacteria and their biological activities proved to be very interesting and rewarding.

Viral infections are covered, including mechanisms involved in persistent viral infections, and the possible roles of defective virus in these infections. The roles of DNA in RNA viruses are also discussed. Animal and human models of persistent viral infections and live virus vaccines used in humans are topics also covered. Viruses and plasmids in fungi and protozoa are presented as an enlightening view of this little-known subject. Also in the field of virology is a series of studies of endogenous tumor viruses, including propagation, analysis, and regulation of various tumor viruses.

However, to me the most informative section dealt with novel aspects of penicillin action, including a short history written by Jack L. Strominger of the Department of Biochemistry and Molecular Biology, Harvard University, "How Penicillins Kill Bacteria."

"Microbiology—1977" continues the well-thought out series started in 1974 by David Schlessinger and fulfills the original aim of the series: to remedy part of the problem of keeping up with new developments in the field of microbiology.

Reviewed by Mary Ann Garth
Microbiological Assay Branch
National Center for Antibiotics Analysis
Food and Drug Administration
Washington, DC 20204

Fluorescence and Phosphorescence Spectroscopy: Physiochemical Principles and Practice. By STEPHEN G. SCHULMAN. Pergamon Press, Maxwell House, Fairview Park, Elmsford, NY 10523. 1977. 288 pp. 17 × 14.8 cm. Price $20.00.

The author states in his preface that this book "is written with the analytical chemist and biological scientist in mind and represents an attempt to make the instrumental, and especially the structural and environmental aspects of luminescence spectra intelligible to the reader with a general college background in chemistry and physics."

Chapter I, entitled "Photophysical Processes in Isolated Molecules," deals with a nonmathematic descriptive treatment of the subject. It serves to describe ideal systems and to define basic terms. Chapter II, "Photophysical Process in Molecules in Solution," surveys the effects of solvent–solute and solute–solute interactions on both the ground and excited states in electronic spectra. Chapter III is a brief description of the practical aspects of the instrumentation employed in the measurement

Pharmacokinetic theory predicts that:

$$F = \frac{\Delta Cl_R}{\text{dose}}\left[\frac{(AUC)(AUC')}{AUC' - AUC}\right] \qquad \text{(Eq. 1)}$$

where F is the fraction of the dose absorbed, AUC is the area under the plasma concentration–time curve, the prime notation indicates the AUC in the perturbed renal clearance state, and ΔCl_R is the difference in mean renal clearance between the two experiments (see Ref. 1 for details). Data from a furosemide–probenecid interaction study (4) were used exactly as reported in Table I of that article, and AUC and AUC' values for each individual were determined using the relationship AUC = dose/plasma clearance.

The fundamental mechanism used to perturb the renal clearance of furosemide in this interaction study with probenecid seems to be competition for the renal transport system, which actively secretes organic acids (4). In previous studies, it was observed that the improved reabsorption of weak bases from an alkaline tubular fluid was an appropriate perturbation technique (2) and that the reduction in lithium renal clearance caused by chlorothiazide yielded data (3) supporting the validity of Eq. 1. The principal virtues of the data from Ref. 4 are that the two doses were given parenterally (*i.e.*, F is known to be unity), the physiological status of the volunteers was well controlled, and the plasma and urine concentrations were confirmed by two independent analytical procedures, thus circumventing the assay difficulties that have hampered some furosemide disposition studies.

When Eq. 1 and the values of ΔCl_R, AUC, AUC', and the intravenous dose from Table I of Ref. 4 are used to estimate F, a value of 1.05 ± 0.11 (mean ± SEM) is obtained. This result appears to provide further support for the validity of Eq. 1.

(1) D. Lalka and H. Feldman, *J. Pharm. Sci.*, **63**, 1812 (1974).
(2) D. Lalka, M. B. Meyer, B. R. Duce, and A. T. Elvin, *Clin. Pharmacol. Ther.*, **19**, 757 (1976).
(3) R. I. Poust, A. G. Mallinger, J. Mallinger, J. M. Himmelhoch, J. F. Neil, and I. Hanin, *J. Pharm. Sci.*, **66**, 609 (1977).
(4) J. Honari, A. D. Blair, and R. E. Cutler, *Clin. Pharmacol. Ther.*, **22**, 395 (1977).

David Lalka ˣ
P. du Souich
A. J. McLean
Milo Gibaldi
Department of Pharmaceutics
School of Pharmacy
State University of New York
at Buffalo
Amherst, NY 14260

Received November 14, 1977.
Accepted for publication January 10, 1978.

BOOKS

REVIEWS

Microbiology—1977. Edited by DAVID SCHLESSINGER. American Society for Microbiology, 1913 I St., N.W., Washington, DC 20006. 1977. 593 pp. 17 × 26 cm. Price $22.00.

The book is divided into seven major and numerous minor sections, covering some of the more important and recent findings in microbiology.

Cell envelope and cell division in bacilli are represented by partial proceedings of the conference on bacilli (other material from the conference appeared in "Microbiology—1976"). Various topics concerning *Pseudomonas aeruginosa* and related components and their recognition by specific lymphocytes or other cell types are discussed. Modes of resistance to various antibiotics by the pseudomonads are covered. Endotoxins, cell wall antigens, and modulation of the immune response are presented in various manuscripts.

A historical review of pyrogen research by Otto Westphal *et al.*, and related articles on endotoxins and other cell wall components of Gram-negative bacteria and their biological activities proved to be very interesting and rewarding.

Viral infections are covered, including mechanisms involved in persistent viral infections, and the possible roles of defective virus in these infections. The roles of DNA in RNA viruses are also discussed. Animal and human models of persistent viral infections and live virus vaccines used in humans are topics also covered. Viruses and plasmids in fungi and protozoa are presented as an enlightening view of this little-known subject. Also in the field of virology is a series of studies of endogenous tumor viruses, including propagation, analysis, and regulation of various tumor viruses.

However, to me the most informative section dealt with novel aspects of penicillin action, including a short history written by Jack L. Strominger of the Department of Biochemistry and Molecular Biology, Harvard University, "How Penicillins Kill Bacteria."

"Microbiology—1977" continues the well-thought out series started in 1974 by David Schlessinger and fulfills the original aim of the series: to remedy part of the problem of keeping up with new developments in the field of microbiology.

Reviewed by Mary Ann Garth
Microbiological Assay Branch
National Center for Antibiotics Analysis
Food and Drug Administration
Washington, DC 20204

Fluorescence and Phosphorescence Spectroscopy: Physiochemical Principles and Practice. By STEPHEN G. SCHULMAN. Pergamon Press, Maxwell House, Fairview Park, Elmsford, NY 10523. 1977. 288 pp. 17 × 14.8 cm. Price $20.00.

The author states in his preface that this book "is written with the analytical chemist and biological scientist in mind and represents an attempt to make the instrumental, and especially the structural and environmental aspects of luminescence spectra intelligible to the reader with a general college background in chemistry and physics."

Chapter I, entitled "Photophysical Processes in Isolated Molecules," deals with a nonmathematic descriptive treatment of the subject. It serves to describe ideal systems and to define basic terms. Chapter II, "Photophysical Process in Molecules in Solution," surveys the effects of solvent–solute and solute–solute interactions on both the ground and excited states in electronic spectra. Chapter III is a brief description of the practical aspects of the instrumentation employed in the measurement

of fluorescence and phosphorescence. The final chapter is a general description of applications, followed by tables listing literature conditions for the fluorometric and phosphorimetric analyses of selected compounds of biological interest as well as a table summarizing literature fluorometric analyses of inorganic ions.

In the opinion of this reviewer, Chapters I and II best meet the needs of analytical chemists and biologists as described in the preface. They should serve the beginning investigator well and act as a bridge to the more advanced treatments of these subjects. To a lesser extent, this is also true for the chapter on instrumentation. However, this information is also readily available, with at least equal clairty, in the well-established texts on fluorometry as well as from the instrument manufacturers. The chapter on applications is very limited, and even the novice would be better served by using general texts on fluorescence assays.

Reviewed by Joseph E. Sinsheimer
College of Pharmacy
University of Michigan
Ann Arbor, MI 48109

Medical Botany: Plants Affecting Man's Health. By WALTER H. LEWIS and MEMORY P. F. ELVIN-LEWIS. Wiley, 605 Third Ave., New York, NY 10016. 1977. xii + 515 pp. 17 × 25 cm. Price $27.50.

Divided into three sections, this book covers injurious, remedial, and psychoactive plants. The authors use an effective style, arranging drugs by therapeutic use with descriptions of various diseases for which there are plant remedies. This style is suitable for a pharmacognosy textbook for beginning students who have not yet been introduced to disease states. The plant drugs are compared with drugs of synthetic origin. There is extensive use of charts and graphs.

The book is blighted by errors, only a sampling of which could be included here. Errors of grammar, spelling, or typesetting should have been prevented by proofreading, *e.g.*, an illustration of a beech tree is listed as *Sorbus aucuparia*. Some errors result from individuals writing on topics outside their expertise, *e.g.*, psyllium seed is listed under "Bulk Purgatives." Psyllium seed may fill up the large intestine so normal stools can be formed but has no purgative action. Some errors result from a lack of recognition of clinical significance, *e.g.*, purslane is included under "Internal Poisons." Although this information appears to be copied from Kingsbury, the evidence is based on a single report of sheep poisoning from Australia. Purslane is one of the safest of the wild edible plants.

Under "Mutagens," a list includes broccoli, brussel sprouts, cabbage, cauliflower, and kale. We are not told whether the other plants listed as mutagens are as safe as these vegetables or that the vegetables are dangerous mutagens. Errors also result from failure to distinguish between folk tales and modern medical practice. An unsuspecting reader may assume that the generous space devoted to garlic and bloodroot indicate that they are efficacious cancer remedies while, in reality, there is little justification for assuming that either is useful.

Errors of fact are also included, *e.g.*, ". . . methaqualone, a barbiturate addictive depressant . . . ." Methaqualone is not a barbiturate, nor does it induce addiction to barbiturates. "Separate in the female, the urethra . . . ." Whatever this means, the urethra is not separate in the female. "Symptoms of primary and secondary syphilis can resolve themselves naturally. . . ." These symptoms may go away, but the problem is not resolved. *Cannabis sativa* has only one name listed as a vernacular name, bhang. I have never heard that word used, but I have frequently heard of marijuana, grass, or joints.

Much of the information seems unrelated to the people for whom the book is written, undergraduate students as well as physicians. There are 21 pages of tables of "Chewing sticks for cleaning teeth" and "Plants used to relieve toothache." Few items listed are of significance in world medicine, and only one drug is important in the U.S. Most illustrations are stylized drawings from herbals published centuries ago. They are useful only as illustrations of old herbals.

This book is filled with fascinating information—the authors have undoubtedly done a lot of reading to come up with the amount of accurate information included. The name "Medical Botany" is not appropriate because a large percentage of the space is not occupied with botany and much of it is of little significance to medicine. The errors spoil the book. I can recommend it for professionals who are already knowledgeable about medicine or medical botany but who want historical and anthropological information, are interested in folklore, or who are doing research on plant remedies passed over (in many cases without having been adequately tested) by modern medicine.

Reviewed by C. Dwayne Ogzewalla
College of Pharmacy
University of Cincinnati
Cincinnati, OH 45267

Clofibrate and Related Analogs. A Comprehensive Review. Medicinal Research Series, Vol. 7. By DONALD T. WITIAK, HOWARD A. I. NEWMAN, and DENNIS R. FELLER. Dekker, 270 Madison Ave., New York, NY 10016. 1977. 287 pp. 15 × 23 cm. Price $27.50.

This monograph presents a concise and comprehensive review of the clinical and pharmacological studies of clofibrate and structurally related analogs. As a major prototype drug used in the treatment of hyperlipoproteinemia, a recognized risk factor associated with atherosclerotic lesions in coronary artery disease, clofibrate has captivated the imagination of many scientists working in this field. Sections of the book are devoted to clinical drug trials, clofibrate activity in various animal models of hyperlipidemia, structure–activity relationships of clofibrate-related analogs, proposed mechanisms of hypolipidemic action, drug-induced metabolic effects, and pharmacokinetic studies.

The clinical trials section reviews data concerning the efficacy of clofibrate in lowering serum lipid levels, reducing coronary artery damage, reversing cerebrovascular disease, eruptive xanthomas, hyperinsulinemia, diabetic retinopathy, Type I glycogen storage disease, and the symptoms of gout and diabetes insipidus. The pharmacological section summarizes the effects of clofibrate on the metabolism and distribution of free fatty acids, triglycerides, cholesterol, and lipoproteins, as well as effects on lipoprotein lipase activity and lipolysis in adipose tissue.

Other metabolic effects, not directly associated with the hypolipemic action of clofibrate, are also summarized. These topics include the effects of clofibrate on mitochondrial enzymes, liver peroxisomes, and hepatic enzyme induction. The book integrates the numerous findings from both human patients and experimental animal models and emphasizes the relationship between the hypolipidemic properties of these agents and their usefulness in the treatment of coronary artery disease.

This book also contains a useful Glossary of Selected Terms pertaining to coronary artery disease and its therapy. Containing 774 references, this well-written and comprehensive review is an excellent reference source and guide for clinicians and basic scientists in biochemistry, medicinal chemistry, pharmacology, physiology, and toxicology. It is of particular interest to scientists dedicated to the elucidation of the biological mechanisms of action and design of hypolipidemic agents.

Reviewed by William P. Heilman
Pharmaceutical Department
T. R. Evans Research Center
Diamond Shamrock Corporation
Painesville, OH 44077

Terpenoids and Steroids, Vol. 7. A Specialist Periodical Report. Edited by J. R. HANSON *et al.* The Chemical Society, Burlington House, London W1V 0BN, England. 1977. 359 pp. 15 × 22 cm. Price $50.00. Available from Special Issues Sales, American Chemical Society, 1155 Sixteenth Street, N.W., Washington, DC 20036.

This book is the seventh volume of terpenoids and steroids in a valuable series first published 6 years ago. Hanson has maintained the high standards set by K. H. Overton, editor of earlier volumes. The aim of each series of Specialist Periodical Reports is to provide a systematic comprehensive and critical review of progress in the major areas of chemical research. The various series, which now total 36, are being published annually or bienially on such topics as The Alkaloids; Amino-Acids, Peptides and Proteins; Biosynthesis; Carbohydrate Chemistry; Environmental Chemistry; Foreign Compound Metabolism in Mammals; and Photochemistry.

This volume does not contain a subject index but is organized in a systematic manner which facilitates finding any information being sought. The six pages in the Table of Contents outline this volume in detail. The chapters are divided into many sections, which are identified

of fluorescence and phosphorescence. The final chapter is a general description of applications, followed by tables listing literature conditions for the fluorometric and phosphorimetric analyses of selected compounds of biological interest as well as a table summarizing literature fluorometric analyses of inorganic ions.

In the opinion of this reviewer, Chapters I and II best meet the needs of analytical chemists and biologists as described in the preface. They should serve the beginning investigator well and act as a bridge to the more advanced treatments of these subjects. To a lesser extent, this is also true for the chapter on instrumentation. However, this information is also readily available, with at least equal clairty, in the well-established texts on fluorometry as well as from the instrument manufacturers. The chapter on applications is very limited, and even the novice would be better served by using general texts on fluorescence assays.

Reviewed by Joseph E. Sinsheimer
College of Pharmacy
University of Michigan
Ann Arbor, MI 48109

Medical Botany: Plants Affecting Man's Health. By WALTER H. LEWIS and MEMORY P. F. ELVIN-LEWIS. Wiley, 605 Third Ave., New York, NY 10016. 1977. xii + 515 pp. 17 × 25 cm. Price $27.50.

Divided into three sections, this book covers injurious, remedial, and psychoactive plants. The authors use an effective style, arranging drugs by therapeutic use with descriptions of various diseases for which there are plant remedies. This style is suitable for a pharmacognosy textbook for beginning students who have not yet been introduced to disease states. The plant drugs are compared with drugs of synthetic origin. There is extensive use of charts and graphs.

The book is blighted by errors, only a sampling of which could be included here. Errors of grammar, spelling, or typesetting should have been prevented by proofreading, *e.g.*, an illustration of a beech tree is listed as *Sorbus aucuparia*. Some errors result from individuals writing on topics outside their expertise, *e.g.*, psyllium seed is listed under "Bulk Purgatives." Psyllium seed may fill up the large intestine so normal stools can be formed but has no purgative action. Some errors result from a lack of recognition of clinical significance, *e.g.*, purslane is included under "Internal Poisons." Although this information appears to be copied from Kingsbury, the evidence is based on a single report of sheep poisoning from Australia. Purslane is one of the safest of the wild edible plants.

Under "Mutagens," a list includes broccoli, brussel sprouts, cabbage, cauliflower, and kale. We are not told whether the other plants listed as mutagens are as safe as these vegetables or that the vegetables are dangerous mutagens. Errors also result from failure to distinguish between folk tales and modern medical practice. An unsuspecting reader may assume that the generous space devoted to garlic and bloodroot indicate that they are efficacious cancer remedies while, in reality, there is little justification for assuming that either is useful.

Errors of fact are also included, *e.g.*, ". . . methaqualone, a barbiturate addictive depressant . . . ." Methaqualone is not a barbiturate, nor does it induce addiction to barbiturates. "Separate in the female, the urethra . . . ." Whatever this means, the urethra is not separate in the female. "Symptoms of primary and secondary syphilis can resolve themselves naturally. . . ." These symptoms may go away, but the problem is not resolved. *Cannabis sativa* has only one name listed as a vernacular name, bhang. I have never heard that word used, but I have frequently heard of marijuana, grass, or joints.

Much of the information seems unrelated to the people for whom the book is written, undergraduate students as well as physicians. There are 21 pages of tables of "Chewing sticks for cleaning teeth" and "Plants used to relieve toothache." Few items listed are of significance in world medicine, and only one drug is important in the U.S. Most illustrations are stylized drawings from herbals published centuries ago. They are useful only as illustrations of old herbals.

This book is filled with fascinating information—the authors have undoubtedly done a lot of reading to come up with the amount of accurate information included. The name "Medical Botany" is not appropriate because a large percentage of the space is not occupied with botany and much of it is of little significance to medicine. The errors spoil the book. I can recommend it for professionals who are already knowledgeable about medicine or medical botany but who want historical and anthropological information, are interested in folklore, or who are doing research on plant remedies passed over (in many cases without having been adequately tested) by modern medicine.

Reviewed by C. Dwayne Ogzewalla
College of Pharmacy
University of Cincinnati
Cincinnati, OH 45267

Clofibrate and Related Analogs. A Comprehensive Review. Medicinal Research Series, Vol. 7. By DONALD T. WITIAK, HOWARD A. I. NEWMAN, and DENNIS R. FELLER. Dekker, 270 Madison Ave., New York, NY 10016. 1977. 287 pp. 15 × 23 cm. Price $27.50.

This monograph presents a concise and comprehensive review of the clinical and pharmacological studies of clofibrate and structurally related analogs. As a major prototype drug used in the treatment of hyperlipoproteinemia, a recognized risk factor associated with atherosclerotic lesions in coronary artery disease, clofibrate has captivated the imagination of many scientists working in this field. Sections of the book are devoted to clinical drug trials, clofibrate activity in various animal models of hyperlipidemia, structure–activity relationships of clofibrate-related analogs, proposed mechanisms of hypolipidemic action, drug-induced metabolic effects, and pharmacokinetic studies.

The clinical trials section reviews data concerning the efficacy of clofibrate in lowering serum lipid levels, reducing coronary artery damage, reversing cerebrovascular disease, eruptive xanthomas, hyperinsulinemia, diabetic retinopathy, Type I glycogen storage disease, and the symptoms of gout and diabetes insipidus. The pharmacological section summarizes the effects of clofibrate on the metabolism and distribution of free fatty acids, triglycerides, cholesterol, and lipoproteins, as well as effects on lipoprotein lipase activity and lipolysis in adipose tissue.

Other metabolic effects, not directly associated with the hypolipemic action of clofibrate, are also summarized. These topics include the effects of clofibrate on mitochondrial enzymes, liver peroxisomes, and hepatic enzyme induction. The book integrates the numerous findings from both human patients and experimental animal models and emphasizes the relationship between the hypolipidemic properties of these agents and their usefulness in the treatment of coronary artery disease.

This book also contains a useful Glossary of Selected Terms pertaining to coronary artery disease and its therapy. Containing 774 references, this well-written and comprehensive review is an excellent reference source and guide for clinicians and basic scientists in biochemistry, medicinal chemistry, pharmacology, physiology, and toxicology. It is of particular interest to scientists dedicated to the elucidation of the biological mechanisms of action and design of hypolipidemic agents.

Reviewed by William P. Heilman
Pharmaceutical Department
T. R. Evans Research Center
Diamond Shamrock Corporation
Painesville, OH 44077

Terpenoids and Steroids, Vol. 7. A Specialist Periodical Report. Edited by J. R. HANSON *et al.* The Chemical Society, Burlington House, London W1V 0BN, England. 1977. 359 pp. 15 × 22 cm. Price $50.00. Available from Special Issues Sales, American Chemical Society, 1155 Sixteenth Street, N.W., Washington, DC 20036.

This book is the seventh volume of terpenoids and steroids in a valuable series first published 6 years ago. Hanson has maintained the high standards set by K. H. Overton, editor of earlier volumes. The aim of each series of Specialist Periodical Reports is to provide a systematic comprehensive and critical review of progress in the major areas of chemical research. The various series, which now total 36, are being published annually or bienially on such topics as The Alkaloids; Amino-Acids, Peptides and Proteins; Biosynthesis; Carbohydrate Chemistry; Environmental Chemistry; Foreign Compound Metabolism in Mammals; and Photochemistry.

This volume does not contain a subject index but is organized in a systematic manner which facilitates finding any information being sought. The six pages in the Table of Contents outline this volume in detail. The chapters are divided into many sections, which are identified

of fluorescence and phosphorescence. The final chapter is a general description of applications, followed by tables listing literature conditions for the fluorometric and phosphorimetric analyses of selected compounds of biological interest as well as a table summarizing literature fluorometric analyses of inorganic ions.

In the opinion of this reviewer, Chapters I and II best meet the needs of analytical chemists and biologists as described in the preface. They should serve the beginning investigator well and act as a bridge to the more advanced treatments of these subjects. To a lesser extent, this is also true for the chapter on instrumentation. However, this information is also readily available, with at least equal clairty, in the well-established texts on fluorometry as well as from the instrument manufacturers. The chapter on applications is very limited, and even the novice would be better served by using general texts on fluorescence assays.

Reviewed by Joseph E. Sinsheimer
College of Pharmacy
University of Michigan
Ann Arbor, MI 48109

Medical Botany: Plants Affecting Man's Health. By WALTER H. LEWIS and MEMORY P. F. ELVIN-LEWIS. Wiley, 605 Third Ave., New York, NY 10016. 1977. xii + 515 pp. 17 × 25 cm. Price $27.50.

Divided into three sections, this book covers injurious, remedial, and psychoactive plants. The authors use an effective style, arranging drugs by therapeutic use with descriptions of various diseases for which there are plant remedies. This style is suitable for a pharmacognosy textbook for beginning students who have not yet been introduced to disease states. The plant drugs are compared with drugs of synthetic origin. There is extensive use of charts and graphs.

The book is blighted by errors, only a sampling of which could be included here. Errors of grammar, spelling, or typesetting should have been prevented by proofreading, *e.g.*, an illustration of a beech tree is listed as *Sorbus aucuparia*. Some errors result from individuals writing on topics outside their expertise, *e.g.*, psyllium seed is listed under "Bulk Purgatives." Psyllium seed may fill up the large intestine so normal stools can be formed but has no purgative action. Some errors result from a lack of recognition of clinical significance, *e.g.*, purslane is included under "Internal Poisons." Although this information appears to be copied from Kingsbury, the evidence is based on a single report of sheep poisoning from Australia. Purslane is one of the safest of the wild edible plants.

Under "Mutagens," a list includes broccoli, brussel sprouts, cabbage, cauliflower, and kale. We are not told whether the other plants listed as mutagens are as safe as these vegetables or that the vegetables are dangerous mutagens. Errors also result from failure to distinguish between folk tales and modern medical practice. An unsuspecting reader may assume that the generous space devoted to garlic and bloodroot indicate that they are efficacious cancer remedies while, in reality, there is little justification for assuming that either is useful.

Errors of fact are also included, *e.g.*, ". . . methaqualone, a barbiturate addictive depressant . . . ." Methaqualone is not a barbiturate, nor does it induce addiction to barbiturates. "Separate in the female, the urethra . . . ." Whatever this means, the urethra is not separate in the female. "Symptoms of primary and secondary syphilis can resolve themselves naturally. . . ." These symptoms may go away, but the problem is not resolved. *Cannabis sativa* has only one name listed as a vernacular name, bhang. I have never heard that word used, but I have frequently heard of marijuana, grass, or joints.

Much of the information seems unrelated to the people for whom the book is written, undergraduate students as well as physicians. There are 21 pages of tables of "Chewing sticks for cleaning teeth" and "Plants used to relieve toothache." Few items listed are of significance in world medicine, and only one drug is important in the U.S. Most illustrations are stylized drawings from herbals published centuries ago. They are useful only as illustrations of old herbals.

This book is filled with fascinating information—the authors have undoubtedly done a lot of reading to come up with the amount of accurate information included. The name "Medical Botany" is not appropriate because a large percentage of the space is not occupied with botany and much of it is of little significance to medicine. The errors spoil the book. I can recommend it for professionals who are already knowledgeable about medicine or medical botany but who want historical and anthropological information, are interested in folklore, or who are doing research on plant remedies passed over (in many cases without having been adequately tested) by modern medicine.

Reviewed by C. Dwayne Ogzewalla
College of Pharmacy
University of Cincinnati
Cincinnati, OH 45267

Clofibrate and Related Analogs. A Comprehensive Review. Medicinal Research Series, Vol. 7. By DONALD T. WITIAK, HOWARD A. I. NEWMAN, and DENNIS R. FELLER. Dekker, 270 Madison Ave., New York, NY 10016. 1977. 287 pp. 15 × 23 cm. Price $27.50.

This monograph presents a concise and comprehensive review of the clinical and pharmacological studies of clofibrate and structurally related analogs. As a major prototype drug used in the treatment of hyperlipoproteinemia, a recognized risk factor associated with atherosclerotic lesions in coronary artery disease, clofibrate has captivated the imagination of many scientists working in this field. Sections of the book are devoted to clinical drug trials, clofibrate activity in various animal models of hyperlipidemia, structure–activity relationships of clofibrate-related analogs, proposed mechanisms of hypolipidemic action, drug-induced metabolic effects, and pharmacokinetic studies.

The clinical trials section reviews data concerning the efficacy of clofibrate in lowering serum lipid levels, reducing coronary artery damage, reversing cerebrovascular disease, eruptive xanthomas, hyperinsulinemia, diabetic retinopathy, Type I glycogen storage disease, and the symptoms of gout and diabetes insipidus. The pharmacological section summarizes the effects of clofibrate on the metabolism and distribution of free fatty acids, triglycerides, cholesterol, and lipoproteins, as well as effects on lipoprotein lipase activity and lipolysis in adipose tissue.

Other metabolic effects, not directly associated with the hypolipemic action of clofibrate, are also summarized. These topics include the effects of clofibrate on mitochondrial enzymes, liver peroxisomes, and hepatic enzyme induction. The book integrates the numerous findings from both human patients and experimental animal models and emphasizes the relationship between the hypolipidemic properties of these agents and their usefulness in the treatment of coronary artery disease.

This book also contains a useful Glossary of Selected Terms pertaining to coronary artery disease and its therapy. Containing 774 references, this well-written and comprehensive review is an excellent reference source and guide for clinicians and basic scientists in biochemistry, medicinal chemistry, pharmacology, physiology, and toxicology. It is of particular interest to scientists dedicated to the elucidation of the biological mechanisms of action and design of hypolipidemic agents.

Reviewed by William P. Heilman
Pharmaceutical Department
T. R. Evans Research Center
Diamond Shamrock Corporation
Painesville, OH 44077

Terpenoids and Steroids, Vol. 7. A Specialist Periodical Report. Edited by J. R. HANSON *et al.* The Chemical Society, Burlington House, London W1V 0BN, England. 1977. 359 pp. 15 × 22 cm. Price $50.00. Available from Special Issues Sales, American Chemical Society, 1155 Sixteenth Street, N.W., Washington, DC 20036.

This book is the seventh volume of terpenoids and steroids in a valuable series first published 6 years ago. Hanson has maintained the high standards set by K. H. Overton, editor of earlier volumes. The aim of each series of Specialist Periodical Reports is to provide a systematic comprehensive and critical review of progress in the major areas of chemical research. The various series, which now total 36, are being published annually or bienially on such topics as The Alkaloids; Amino-Acids, Peptides and Proteins; Biosynthesis; Carbohydrate Chemistry; Environmental Chemistry; Foreign Compound Metabolism in Mammals; and Photochemistry.

This volume does not contain a subject index but is organized in a systematic manner which facilitates finding any information being sought. The six pages in the Table of Contents outline this volume in detail. The chapters are divided into many sections, which are identified

of fluorescence and phosphorescence. The final chapter is a general description of applications, followed by tables listing literature conditions for the fluorometric and phosphorimetric analyses of selected compounds of biological interest as well as a table summarizing literature fluorometric analyses of inorganic ions.

In the opinion of this reviewer, Chapters I and II best meet the needs of analytical chemists and biologists as described in the preface. They should serve the beginning investigator well and act as a bridge to the more advanced treatments of these subjects. To a lesser extent, this is also true for the chapter on instrumentation. However, this information is also readily available, with at least equal clairty, in the well-established texts on fluorometry as well as from the instrument manufacturers. The chapter on applications is very limited, and even the novice would be better served by using general texts on fluorescence assays.

Reviewed by Joseph E. Sinsheimer
College of Pharmacy
University of Michigan
Ann Arbor, MI 48109

Medical Botany: Plants Affecting Man's Health. By WALTER H. LEWIS and MEMORY P. F. ELVIN-LEWIS. Wiley, 605 Third Ave., New York, NY 10016. 1977. xii + 515 pp. 17 × 25 cm. Price $27.50.

Divided into three sections, this book covers injurious, remedial, and psychoactive plants. The authors use an effective style, arranging drugs by therapeutic use with descriptions of various diseases for which there are plant remedies. This style is suitable for a pharmacognosy textbook for beginning students who have not yet been introduced to disease states. The plant drugs are compared with drugs of synthetic origin. There is extensive use of charts and graphs.

The book is blighted by errors, only a sampling of which could be included here. Errors of grammar, spelling, or typesetting should have been prevented by proofreading, *e.g.*, an illustration of a beech tree is listed as *Sorbus aucuparia*. Some errors result from individuals writing on topics outside their expertise, *e.g.*, psyllium seed is listed under "Bulk Purgatives." Psyllium seed may fill up the large intestine so normal stools can be formed but has no purgative action. Some errors result from a lack of recognition of clinical significance, *e.g.*, purslane is included under "Internal Poisons." Although this information appears to be copied from Kingsbury, the evidence is based on a single report of sheep poisoning from Australia. Purslane is one of the safest of the wild edible plants.

Under "Mutagens," a list includes broccoli, brussel sprouts, cabbage, cauliflower, and kale. We are not told whether the other plants listed as mutagens are as safe as these vegetables or that the vegetables are dangerous mutagens. Errors also result from failure to distinguish between folk tales and modern medical practice. An unsuspecting reader may assume that the generous space devoted to garlic and bloodroot indicate that they are efficacious cancer remedies while, in reality, there is little justification for assuming that either is useful.

Errors of fact are also included, *e.g.*, ". . . methaqualone, a barbiturate addictive depressant . . . ." Methaqualone is not a barbiturate, nor does it induce addiction to barbiturates. "Separate in the female, the urethra . . . ." Whatever this means, the urethra is not separate in the female. "Symptoms of primary and secondary syphilis can resolve themselves naturally. . . ." These symptoms may go away, but the problem is not resolved. *Cannabis sativa* has only one name listed as a vernacular name, bhang. I have never heard that word used, but I have frequently heard of marijuana, grass, or joints.

Much of the information seems unrelated to the people for whom the book is written, undergraduate students as well as physicians. There are 21 pages of tables of "Chewing sticks for cleaning teeth" and "Plants used to relieve toothache." Few items listed are of significance in world medicine, and only one drug is important in the U.S. Most illustrations are stylized drawings from herbals published centuries ago. They are useful only as illustrations of old herbals.

This book is filled with fascinating information—the authors have undoubtedly done a lot of reading to come up with the amount of accurate information included. The name "Medical Botany" is not appropriate because a large percentage of the space is not occupied with botany and much of it is of little significance to medicine. The errors spoil the book. I can recommend it for professionals who are already knowledgeable about medicine or medical botany but who want historical and anthropological information, are interested in folklore, or who are doing research on plant remedies passed over (in many cases without having been adequately tested) by modern medicine.

Reviewed by C. Dwayne Ogzewalla
College of Pharmacy
University of Cincinnati
Cincinnati, OH 45267

Clofibrate and Related Analogs. A Comprehensive Review. Medicinal Research Series, Vol. 7. By DONALD T. WITIAK, HOWARD A. I. NEWMAN, and DENNIS R. FELLER. Dekker, 270 Madison Ave., New York, NY 10016. 1977. 287 pp. 15 × 23 cm. Price $27.50.

This monograph presents a concise and comprehensive review of the clinical and pharmacological studies of clofibrate and structurally related analogs. As a major prototype drug used in the treatment of hyperlipoproteinemia, a recognized risk factor associated with atherosclerotic lesions in coronary artery disease, clofibrate has captivated the imagination of many scientists working in this field. Sections of the book are devoted to clinical drug trials, clofibrate activity in various animal models of hyperlipidemia, structure–activity relationships of clofibrate-related analogs, proposed mechanisms of hypolipidemic action, drug-induced metabolic effects, and pharmacokinetic studies.

The clinical trials section reviews data concerning the efficacy of clofibrate in lowering serum lipid levels, reducing coronary artery damage, reversing cerebrovascular disease, eruptive xanthomas, hyperinsulinemia, diabetic retinopathy, Type I glycogen storage disease, and the symptoms of gout and diabetes insipidus. The pharmacological section summarizes the effects of clofibrate on the metabolism and distribution of free fatty acids, triglycerides, cholesterol, and lipoproteins, as well as effects on lipoprotein lipase activity and lipolysis in adipose tissue.

Other metabolic effects, not directly associated with the hypolipemic action of clofibrate, are also summarized. These topics include the effects of clofibrate on mitochondrial enzymes, liver peroxisomes, and hepatic enzyme induction. The book integrates the numerous findings from both human patients and experimental animal models and emphasizes the relationship between the hypolipidemic properties of these agents and their usefulness in the treatment of coronary artery disease.

This book also contains a useful Glossary of Selected Terms pertaining to coronary artery disease and its therapy. Containing 774 references, this well-written and comprehensive review is an excellent reference source and guide for clinicians and basic scientists in biochemistry, medicinal chemistry, pharmacology, physiology, and toxicology. It is of particular interest to scientists dedicated to the elucidation of the biological mechanisms of action and design of hypolipidemic agents.

Reviewed by William P. Heilman
Pharmaceutical Department
T. R. Evans Research Center
Diamond Shamrock Corporation
Painesville, OH 44077

Terpenoids and Steroids, Vol. 7. A Specialist Periodical Report. Edited by J. R. HANSON *et al.* The Chemical Society, Burlington House, London W1V 0BN, England. 1977. 359 pp. 15 × 22 cm. Price $50.00. Available from Special Issues Sales, American Chemical Society, 1155 Sixteenth Street, N.W., Washington, DC 20036.

This book is the seventh volume of terpenoids and steroids in a valuable series first published 6 years ago. Hanson has maintained the high standards set by K. H. Overton, editor of earlier volumes. The aim of each series of Specialist Periodical Reports is to provide a systematic comprehensive and critical review of progress in the major areas of chemical research. The various series, which now total 36, are being published annually or bienially on such topics as The Alkaloids; Amino-Acids, Peptides and Proteins; Biosynthesis; Carbohydrate Chemistry; Environmental Chemistry; Foreign Compound Metabolism in Mammals; and Photochemistry.

This volume does not contain a subject index but is organized in a systematic manner which facilitates finding any information being sought. The six pages in the Table of Contents outline this volume in detail. The chapters are divided into many sections, which are identified

in boldface type in the text as well as in the Table of Contents. These sections are further divided into subsections. Chapter titles are found at the top of every second page of the text. The author index of 3500 names is helpful to those following the research of a given individual.

This review is illustrated with 2000 chemical structures. It is documented with 1900 references, most of which are listed at the bottom of the page of each chapter where first cited.

Part I, which covers the terpenoids, is divided into chapters including Monoterpenoids, Sesquiterpenoids, Diterpenoids, Triterpenoids, Carotenoids and Polyterpenoids, and Biosynthesis of Terpenoids and Steroids. Part II, which covers steroids, is divided into two large chapters entitled Steroid Properties, Reactions and Partial Synthesis and Steroid Total Synthesis. The omission of a compilation of references to review articles on subjects related to terpenoids or steroids is the only disappointment. Such compilations were included in most previous volumes of this series.

The biochemist will find the 50 pages on Biosynthesis and subsection on Steroid Radioimmunoassay and Labelled Steroids very useful.

This volume was prepared by nine reporters in addition to the editor. Chemists interested in terpenoids or steroids should have access to this volume and others in the series. They are valuable in reviewing any topic in these subject areas, in developing new ideas and in identifying references for consultation. I highly recommend this series.

Reviewed by Norman J. Doorenbos
College of Science
Southern Illinois University
Carbondale, IL 62901

Drug Design and Adverse Reactions. Edited by HANS BUNDGAARD, PER JUUL, and HELMER KOFOD. Academic, 111 Fifth Ave., New York, NY 10003. 1977. 382 pp. 16 × 24.5 cm.

This book contains a collection of 25 papers presented at the 10th Alfred Benzon Symposium held in Copenhagen on May 17–20, 1976, on drug design, with particular emphasis on the safety of pharmaceutical products and their ethical standards. These papers are grouped into four general areas: (*a*) damaging effects at tissue, cellular, and molecular levels, (*b*) allergic and immunological reactions, (*c*) molecular aspects of drug toxicity, and (*d*) status and perspectives.

In the first area, drug-induced lipidosis, ultrastructural evaluation of drug-induced cellular injury, neurocytochemistry of guanethidine, cytotoxicity of guanidines, lysosomotropic chemotherapy and applications to neoplastic and parasitic diseases, liver toxicity of isoniazid analogs, acetaminophen (paracetamol) hepatotoxicity, and prediction of local damage by intramuscular injection are discussed. The second general area includes discussions of assessment of the immune response to drugs, immunological aspects to drugs, antigenic determinants in drug allergy, allergic reactions to impurities and drug metabolites, penicillin antigenicity, hapten and immune response, and correlation of drug structure and toxicity mediated by both immune and nonimmune mechanisms.

The third general area, which shifts the attention from biology to chemistry, is composed of the following six topics: adverse reactions and chemical structure, structure–activity relationships of carcinogenic drugs, carcinogenicity of benzo[*a*]pyrene, metabolites of estrogens and gastagens, differential metabolism of enantiomers, and molecular structures with inherent toxicity. The remaining four presentations, chemical structure and toxic action, protein binding and adverse reactions, chemically reactive metabolites and toxicity, and drug delivery considerations, comprise the final general area of status and perspectives.

The ultimate goal of every medicinal chemist in drug design is to find useful drugs with specific action without uncontrollable toxicity. To achieve this goal, an understanding in many basic disciplines of science, including organic chemistry, analytical chemistry, physical chemistry, biochemistry, microbiology, molecular biology, pharmacology, toxicology, and immunology, is required. A correlation of the compounded knowledge to appreciate the chemical and biological mechanisms of drug action is also necessary. This book, which accumulates the presentations of "a mixed party attacking a complicated subject matter from different expert angles" (H. Kofod, opening remarks), is an attempt in this direction. Although, in general, many topics of discussion seem somewhat scattered and not closely interrelated, it is the consequence of a worthwhile attempt to study the problem of drug toxicity.

The participants, who are well established in their own field of study, tried their best to unveil the urgent problems, to point out the pitfalls, to align certain common factors and principles they observed, and to make suggestions. Here, a word of caution may be added. In this almost virgin field of drug design, suggestions and recommendations should only be made in the pretext of working hypotheses, and each should be treated with respect and used with caution. For example, if not the drug but one of its metabolites is responsible for the therapeutic action, the use of that metabolite or derivatives as a therapeutic agent was suggested. With due respect, this reviewer believes that the suggestion may not be adequate. Often a metabolite formed *in vivo* may be unstable or exist only with a short half-life. Even if the metabolite is stable and can be properly characterized and synthesized in the laboratory, one should also consider the problems of solubility, transport, absorption, *etc.*, which may be quite different from those of the original drug. Remember the story of the Trojan horse? The "metabolites" or "active species" are the soldiers inside; to eliminate the problem of transport, the entire Trojan horse, the original drug, may be needed.

At the end of this book, there is only an index of invited authors and discussants. This index may be useful for the meeting participants but is of little use to others. Perhaps the editors should consider installing a general subject index for the forthcoming meeting proceedings. This book is recommended as general reading to all scientists interested in the problem of drug design.

Reviewed by C. C. Cheng
Midwest Research Institute
Kansas City, MO 64110

NOTICES

Drug Dependence. Current Problems and Issues. Edited by M. M. GLATT. University Park Press, Chamber of Commerce Bldg., Baltimore, MD 21202. 1977. 332 pp. 14 × 22 cm. Price $28.50.

The Science and Technology of Gelatin. Edited by A. G. WARD and A. COURTS. Academic, 111 Fifth Ave., New York, NY 10003. 1977. 564 pp. 15 × 23 cm. Price $39.50.

Case Studies In Medical Physiology. By ROBERT S. ALEXANDER. Little Brown, 34 Beacon St., Boston. MA 02106. 1977. 170 pp. 13 × 22 cm. Price $6.95.

Health Organizations of the United States, Canada, and Internationally. 4th Ed. Edited by PAUL WASSERMAN and JANE K. BOSSART. Edwards Brothers, 2500 S. State St., Ann Arbor, MI 48104. 1977. 327 pp. 21 × 28 cm.

Haemostatic Drugs: A Critical Appraisal. By M. VERSTRAETE. Martinus Nijhoff, Lange Voorhout 9-11/P. O. Box 269, The Netherlands. 1977. 155 pp. 15 × 23 cm.

Molecular Biology, Biochemistry, and Biophysics 23: Secondary Metabolism and Cell Differentiation. By MARTIN LUCKNER, LUTZ NOVER, and HARTMUT BÖHM. Springer-Verlag, 175 Fifth Ave., New York, NY 10010. 1977. 130 pp. 19 × 24 cm. Price $21.20.

Medication Guide For Patient Counseling. 1st Ed. by DOROTHY L. SMITH. Lea & Febinger, 600 Washington Square, Philadelphia, PA 19106. 1977. 15 × 23 cm. Price $12.00.

Pharmacie. 5th Ed. Edited by YVAN TOUITOU. Masson, 14 E. 60th St., New York, NY 10022. 1977. 340 pp. 13 × 21 cm.

Chemotherapy of Solid Tumours. Report on a WHO Expert Committee. World Health Organization, 1211 Geneva 27, Switzerland. 1977. 106 pp. 14 × 20 cm. Price $4.00.

Drugs and Driving. NIDA Research Monograph 11. Edited by ROBERT E. WILLETTE. National Institute on Drug Abuse, 11400 Rockville Pike, Rockville, MD 20852. 1977. 15 × 23.5 cm. 137 pp. Price $1.70. Available from Superintendent of Documents, U. S. Government Printing Office, Washington, DC 20402.

Chemotherapy of Infection. By WILLIAM B. PRATT. Oxford University Press, 200 Madison Ave., New York, NY 10016. 1977. 462 pp. 15 × 23 cm. Price $9.95.

Topics in Antibiotic Chemistry, Vol. 1. Edited by P. G. SAMMES. Halsted, 605 Third Ave., New York, NY 10016. 1977. 217 pp. 16 × 24 cm. Price $28.50.

Herbicides and Fungicides—Factors Affecting Their Activity. Edited by N. R. McFARLANE. The Chemical Society, Burlington House, London, W1V OBN, England, 1977. 141 pp. 12 × 22 cm. Price $15.00.

in boldface type in the text as well as in the Table of Contents. These sections are further divided into subsections. Chapter titles are found at the top of every second page of the text. The author index of 3500 names is helpful to those following the research of a given individual.

This review is illustrated with 2000 chemical structures. It is documented with 1900 references, most of which are listed at the bottom of the page of each chapter where first cited.

Part I, which covers the terpenoids, is divided into chapters including Monoterpenoids, Sesquiterpenoids, Diterpenoids, Triterpenoids, Carotenoids and Polyterpenoids, and Biosynthesis of Terpenoids and Steroids. Part II, which covers steroids, is divided into two large chapters entitled Steroid Properties, Reactions and Partial Synthesis and Steroid Total Synthesis. The omission of a compilation of references to review articles on subjects related to terpenoids or steroids is the only disappointment. Such compilations were included in most previous volumes of this series.

The biochemist will find the 50 pages on Biosynthesis and subsection on Steroid Radioimmunoassay and Labelled Steroids very useful.

This volume was prepared by nine reporters in addition to the editor. Chemists interested in terpenoids or steroids should have access to this volume and others in the series. They are valuable in reviewing any topic in these subject areas, in developing new ideas and in identifying references for consultation. I highly recommend this series.

Reviewed by Norman J. Doorenbos
College of Science
Southern Illinois University
Carbondale, IL 62901

Drug Design and Adverse Reactions. Edited by HANS BUNDGAARD, PER JUUL, and HELMER KOFOD. Academic, 111 Fifth Ave., New York, NY 10003. 1977. 382 pp. 16 × 24.5 cm.

This book contains a collection of 25 papers presented at the 10th Alfred Benzon Symposium held in Copenhagen on May 17–20, 1976, on drug design, with particular emphasis on the safety of pharmaceutical products and their ethical standards. These papers are grouped into four general areas: (*a*) damaging effects at tissue, cellular, and molecular levels, (*b*) allergic and immunological reactions, (*c*) molecular aspects of drug toxicity, and (*d*) status and perspectives.

In the first area, drug-induced lipidosis, ultrastructural evaluation of drug-induced cellular injury, neurocytochemistry of guanethidine, cytotoxicity of guanidines, lysosomotropic chemotherapy and applications to neoplastic and parasitic diseases, liver toxicity of isoniazid analogs, acetaminophen (paracetamol) hepatotoxicity, and prediction of local damage by intramuscular injection are discussed. The second general area includes discussions of assessment of the immune response to drugs, immunological aspects to drugs, antigenic determinants in drug allergy, allergic reactions to impurities and drug metabolites, penicillin antigenicity, hapten and immune response, and correlation of drug structure and toxicity mediated by both immune and nonimmune mechanisms.

The third general area, which shifts the attention from biology to chemistry, is composed of the following six topics: adverse reactions and chemical structure, structure–activity relationships of carcinogenic drugs, carcinogenicity of benzo[*a*]pyrene, metabolites of estrogens and gastagens, differential metabolism of enantiomers, and molecular structures with inherent toxicity. The remaining four presentations, chemical structure and toxic action, protein binding and adverse reactions, chemically reactive metabolites and toxicity, and drug delivery considerations, comprise the final general area of status and perspectives.

The ultimate goal of every medicinal chemist in drug design is to find useful drugs with specific action without uncontrollable toxicity. To achieve this goal, an understanding in many basic disciplines of science, including organic chemistry, analytical chemistry, physical chemistry, biochemistry, microbiology, molecular biology, pharmacology, toxicology, and immunology, is required. A correlation of the compounded knowledge to appreciate the chemical and biological mechanisms of drug action is also necessary. This book, which accumulates the presentations of "a mixed party attacking a complicated subject matter from different expert angles" (H. Kofod, opening remarks), is an attempt in this direction. Although, in general, many topics of discussion seem somewhat scattered and not closely interrelated, it is the consequence of a worthwhile attempt to study the problem of drug toxicity.

The participants, who are well established in their own field of study, tried their best to unveil the urgent problems, to point out the pitfalls, to align certain common factors and principles they observed, and to make suggestions. Here, a word of caution may be added. In this almost virgin field of drug design, suggestions and recommendations should only be made in the pretext of working hypotheses, and each should be treated with respect and used with caution. For example, if not the drug but one of its metabolites is responsible for the therapeutic action, the use of that metabolite or derivatives as a therapeutic agent was suggested. With due respect, this reviewer believes that the suggestion may not be adequate. Often a metabolite formed *in vivo* may be unstable or exist only with a short half-life. Even if the metabolite is stable and can be properly characterized and synthesized in the laboratory, one should also consider the problems of solubility, transport, absorption, *etc.*, which may be quite different from those of the original drug. Remember the story of the Trojan horse? The "metabolites" or "active species" are the soldiers inside; to eliminate the problem of transport, the entire Trojan horse, the original drug, may be needed.

At the end of this book, there is only an index of invited authors and discussants. This index may be useful for the meeting participants but is of little use to others. Perhaps the editors should consider installing a general subject index for the forthcoming meeting proceedings. This book is recommended as general reading to all scientists interested in the problem of drug design.

Reviewed by C. C. Cheng
Midwest Research Institute
Kansas City, MO 64110

NOTICES

Drug Dependence. Current Problems and Issues. Edited by M. M. GLATT. University Park Press, Chamber of Commerce Bldg., Baltimore, MD 21202. 1977. 332 pp. 14 × 22 cm. Price $28.50.

The Science and Technology of Gelatin. Edited by A. G. WARD and A. COURTS. Academic, 111 Fifth Ave., New York, NY 10003. 1977. 564 pp. 15 × 23 cm. Price $39.50.

Case Studies In Medical Physiology. By ROBERT S. ALEXANDER. Little Brown, 34 Beacon St., Boston. MA 02106. 1977. 170 pp. 13 × 22 cm. Price $6.95.

Health Organizations of the United States, Canada, and Internationally. 4th Ed. Edited by PAUL WASSERMAN and JANE K. BOSSART. Edwards Brothers, 2500 S. State St., Ann Arbor, MI 48104. 1977. 327 pp. 21 × 28 cm.

Haemostatic Drugs: A Critical Appraisal. By M. VERSTRAETE. Martinus Nijhoff, Lange Voorhout 9-11/P. O. Box 269, The Netherlands. 1977. 155 pp. 15 × 23 cm.

Molecular Biology, Biochemistry, and Biophysics 23: Secondary Metabolism and Cell Differentiation. By MARTIN LUCKNER, LUTZ NOVER, and HARTMUT BÖHM. Springer-Verlag, 175 Fifth Ave., New York, NY 10010. 1977. 130 pp. 19 × 24 cm. Price $21.20.

Medication Guide For Patient Counseling. 1st Ed. by DOROTHY L. SMITH. Lea & Febinger, 600 Washington Square, Philadelphia, PA 19106. 1977. 15 × 23 cm. Price $12.00.

Pharmacie. 5th Ed. Edited by YVAN TOUITOU. Masson, 14 E. 60th St., New York, NY 10022. 1977. 340 pp. 13 × 21 cm.

Chemotherapy of Solid Tumours. Report on a WHO Expert Committee. World Health Organization, 1211 Geneva 27, Switzerland. 1977. 106 pp. 14 × 20 cm. Price $4.00.

Drugs and Driving. NIDA Research Monograph 11. Edited by ROBERT E. WILLETTE. National Institute on Drug Abuse, 11400 Rockville Pike, Rockville, MD 20852. 1977. 15 × 23.5 cm. 137 pp. Price $1.70. Available from Superintendent of Documents, U. S. Government Printing Office, Washington, DC 20402.

Chemotherapy of Infection. By WILLIAM B. PRATT. Oxford University Press, 200 Madison Ave., New York, NY 10016. 1977. 462 pp. 15 × 23 cm. Price $9.95.

Topics in Antibiotic Chemistry, Vol. 1. Edited by P. G. SAMMES. Halsted, 605 Third Ave., New York, NY 10016. 1977. 217 pp. 16 × 24 cm. Price $28.50.

Herbicides and Fungicides—Factors Affecting Their Activity. Edited by N. R. McFARLANE. The Chemical Society, Burlington House, London, W1V OBN, England, 1977. 141 pp. 12 × 22 cm. Price $15.00.

in boldface type in the text as well as in the Table of Contents. These sections are further divided into subsections. Chapter titles are found at the top of every second page of the text. The author index of 3500 names is helpful to those following the research of a given individual.

This review is illustrated with 2000 chemical structures. It is documented with 1900 references, most of which are listed at the bottom of the page of each chapter where first cited.

Part I, which covers the terpenoids, is divided into chapters including Monoterpenoids, Sesquiterpenoids, Diterpenoids, Triterpenoids, Carotenoids and Polyterpenoids, and Biosynthesis of Terpenoids and Steroids. Part II, which covers steroids, is divided into two large chapters entitled Steroid Properties, Reactions and Partial Synthesis and Steroid Total Synthesis. The omission of a compilation of references to review articles on subjects related to terpenoids or steroids is the only disappointment. Such compilations were included in most previous volumes of this series.

The biochemist will find the 50 pages on Biosynthesis and subsection on Steroid Radioimmunoassay and Labelled Steroids very useful.

This volume was prepared by nine reporters in addition to the editor. Chemists interested in terpenoids or steroids should have access to this volume and others in the series. They are valuable in reviewing any topic in these subject areas, in developing new ideas and in identifying references for consultation. I highly recommend this series.

Reviewed by Norman J. Doorenbos
College of Science
Southern Illinois University
Carbondale, IL 62901

Drug Design and Adverse Reactions. Edited by HANS BUNDGAARD, PER JUUL, and HELMER KOFOD. Academic, 111 Fifth Ave., New York, NY 10003. 1977. 382 pp. 16 × 24.5 cm.

This book contains a collection of 25 papers presented at the 10th Alfred Benzon Symposium held in Copenhagen on May 17–20, 1976, on drug design, with particular emphasis on the safety of pharmaceutical products and their ethical standards. These papers are grouped into four general areas: (*a*) damaging effects at tissue, cellular, and molecular levels, (*b*) allergic and immunological reactions, (*c*) molecular aspects of drug toxicity, and (*d*) status and perspectives.

In the first area, drug-induced lipidosis, ultrastructural evaluation of drug-induced cellular injury, neurocytochemistry of guanethidine, cytotoxicity of guanidines, lysosomotropic chemotherapy and applications to neoplastic and parasitic diseases, liver toxicity of isoniazid analogs, acetaminophen (paracetamol) hepatotoxicity, and prediction of local damage by intramuscular injection are discussed. The second general area includes discussions of assessment of the immune response to drugs, immunological aspects to drugs, antigenic determinants in drug allergy, allergic reactions to impurities and drug metabolites, penicillin antigenicity, hapten and immune response, and correlation of drug structure and toxicity mediated by both immune and nonimmune mechanisms.

The third general area, which shifts the attention from biology to chemistry, is composed of the following six topics: adverse reactions and chemical structure, structure–activity relationships of carcinogenic drugs, carcinogenicity of benzo[*a*]pyrene, metabolites of estrogens and gastagens, differential metabolism of enantiomers, and molecular structures with inherent toxicity. The remaining four presentations, chemical structure and toxic action, protein binding and adverse reactions, chemically reactive metabolites and toxicity, and drug delivery considerations, comprise the final general area of status and perspectives.

The ultimate goal of every medicinal chemist in drug design is to find useful drugs with specific action without uncontrollable toxicity. To achieve this goal, an understanding in many basic disciplines of science, including organic chemistry, analytical chemistry, physical chemistry, biochemistry, microbiology, molecular biology, pharmacology, toxicology, and immunology, is required. A correlation of the compounded knowledge to appreciate the chemical and biological mechanisms of drug action is also necessary. This book, which accumulates the presentations of "a mixed party attacking a complicated subject matter from different expert angles" (H. Kofod, opening remarks), is an attempt in this direction. Although, in general, many topics of discussion seem somewhat scattered and not closely interrelated, it is the consequence of a worthwhile attempt to study the problem of drug toxicity.

The participants, who are well established in their own field of study, tried their best to unveil the urgent problems, to point out the pitfalls, to align certain common factors and principles they observed, and to make suggestions. Here, a word of caution may be added. In this almost virgin field of drug design, suggestions and recommendations should only be made in the pretext of working hypotheses, and each should be treated with respect and used with caution. For example, if not the drug but one of its metabolites is responsible for the therapeutic action, the use of that metabolite or derivatives as a therapeutic agent was suggested. With due respect, this reviewer believes that the suggestion may not be adequate. Often a metabolite formed *in vivo* may be unstable or exist only with a short half-life. Even if the metabolite is stable and can be properly characterized and synthesized in the laboratory, one should also consider the problems of solubility, transport, absorption, *etc.*, which may be quite different from those of the original drug. Remember the story of the Trojan horse? The "metabolites" or "active species" are the soldiers inside; to eliminate the problem of transport, the entire Trojan horse, the original drug, may be needed.

At the end of this book, there is only an index of invited authors and discussants. This index may be useful for the meeting participants but is of little use to others. Perhaps the editors should consider installing a general subject index for the forthcoming meeting proceedings. This book is recommended as general reading to all scientists interested in the problem of drug design.

Reviewed by C. C. Cheng
Midwest Research Institute
Kansas City, MO 64110

NOTICES

Drug Dependence. Current Problems and Issues. Edited by M. M. GLATT. University Park Press, Chamber of Commerce Bldg., Baltimore, MD 21202. 1977. 332 pp. 14 × 22 cm. Price $28.50.

The Science and Technology of Gelatin. Edited by A. G. WARD and A. COURTS. Academic, 111 Fifth Ave., New York, NY 10003. 1977. 564 pp. 15 × 23 cm. Price $39.50.

Case Studies In Medical Physiology. By ROBERT S. ALEXANDER. Little Brown, 34 Beacon St., Boston. MA 02106. 1977. 170 pp. 13 × 22 cm. Price $6.95.

Health Organizations of the United States, Canada, and Internationally. 4th Ed. Edited by PAUL WASSERMAN and JANE K. BOSSART. Edwards Brothers, 2500 S. State St., Ann Arbor, MI 48104. 1977. 327 pp. 21 × 28 cm.

Haemostatic Drugs: A Critical Appraisal. By M. VERSTRAETE. Martinus Nijhoff, Lange Voorhout 9-11/P. O. Box 269, The Netherlands. 1977. 155 pp. 15 × 23 cm.

Molecular Biology, Biochemistry, and Biophysics 23: Secondary Metabolism and Cell Differentiation. By MARTIN LUCKNER, LUTZ NOVER, and HARTMUT BÖHM. Springer-Verlag, 175 Fifth Ave., New York, NY 10010. 1977. 130 pp. 19 × 24 cm. Price $21.20.

Medication Guide For Patient Counseling. 1st Ed. by DOROTHY L. SMITH. Lea & Febinger, 600 Washington Square, Philadelphia, PA 19106. 1977. 15 × 23 cm. Price $12.00.

Pharmacie. 5th Ed. Edited by YVAN TOUITOU. Masson, 14 E. 60th St., New York, NY 10022. 1977. 340 pp. 13 × 21 cm.

Chemotherapy of Solid Tumours. Report on a WHO Expert Committee. World Health Organization, 1211 Geneva 27, Switzerland. 1977. 106 pp. 14 × 20 cm. Price $4.00.

Drugs and Driving. NIDA Research Monograph 11. Edited by ROBERT E. WILLETTE. National Institute on Drug Abuse, 11400 Rockville Pike, Rockville, MD 20852. 1977. 15 × 23.5 cm. 137 pp. Price $1.70. Available from Superintendent of Documents, U. S. Government Printing Office, Washington, DC 20402.

Chemotherapy of Infection. By WILLIAM B. PRATT. Oxford University Press, 200 Madison Ave., New York, NY 10016. 1977. 462 pp. 15 × 23 cm. Price $9.95.

Topics in Antibiotic Chemistry, Vol. 1. Edited by P. G. SAMMES. Halsted, 605 Third Ave., New York, NY 10016. 1977. 217 pp. 16 × 24 cm. Price $28.50.

Herbicides and Fungicides—Factors Affecting Their Activity. Edited by N. R. McFARLANE. The Chemical Society, Burlington House, London, W1V OBN, England, 1977. 141 pp. 12 × 22 cm. Price $15.00.

MAY 1978
VOLUME 67 NUMBER 5

JOURNAL OF PHARMACEUTICAL SCIENCES

MARY H. FERGUSON
Editor

SHELLY ELLIOTT
Production Editor

JANET D. SHOFF
Copy Editor

EDWARD G. FELDMANN
Contributing Editor

SAMUEL W. GOLDSTEIN
Contributing Editor

BELLE R. BECK
Editorial Secretary

DAVID BOHARDT
Director of Publications

L. LUAN CORRIGAN
Assistant Director of Publications

EDITORIAL ADVISORY BOARD

JOHN AUTIAN	HERBERT A. LIEBERMAN
NORMAN R. FARNSWORTH	DAVID E. MANN, JR.
WILLIAM O. FOYE	GERALD J. PAPARIELLO
WILLIAM J. JUSKO	EDWARD G. RIPPIE

The *Journal of Pharmaceutical Sciences* is published monthly by the American Pharmaceutical Association at 2215 Constitution Ave., N.W., Washington, DC 20037. Second-class postage paid at Washington, D.C., and at additional mailing office.

All expressions of opinion and statements of supposed fact appearing in articles or editorials carried in this journal are published on the authority of the writer over whose name they appear and are not to be regarded as necessarily expressing the policies or views of the American Pharmaceutical Association.

Offices Editorial, Advertising, and Subscription Offices: 2215 Constitution Ave., N.W., Washington, DC 20037. Printing Offices: 20th & Northampton Streets, Easton, PA 18042.

Annual Subscriptions—United States and foreign, industrial and government institutions $50, educational institutions $50, individuals *for personal use only* $30; single copies $5. All foreign subscriptions add $5 for postage. Subscription rates are subject to change without notice. Members of the American Pharmaceutical Association may elect to receive the *Journal of Pharmaceutical Sciences* as a part of their annual $70 (foreign $75) APhA membership dues.

Claims Missing numbers will not be supplied if dues or subscriptions are in arrears for more than 60 days or if claims are received more than 60 days after the date of the issue, or if loss was due to failure to give notice of change of address. The Association cannot accept responsibility for foreign delivery when its records indicate shipment has been made.

Change of Address—Members and subscribers should notify at once both the Post Office and the American Pharmaceutical Association, 2215 Constitution Ave., N.W., Washington, DC 20037, of any change of address.

Microfilm Microfilm volumes are available from University Microfilms International, 300 N. Zeeb Road, Ann Arbor, MI 48106.

© Copyright 1978, American Pharmaceutical Association, 2215 Constitution Ave., N.W., Washington, DC 20037; all rights reserved.

DEVIOUS ROUTES TO GOVERNMENTAL REGULATION

So-called "Big Business" has long suffered from a public perception as being devious in many of its approaches and actions. It has been common to expect that business interests often will not be completely open and above board in their motives and objectives.

On the other hand, it is only in recent years that the public has come to view with comparable suspicion various proposals and actions involving government agencies, particularly at the federal level. Presumably, in a Democratic society, government is the people and honesty in government has been—or, more accurately, *had been*—taken for granted. However, the "Watergate affair," among other things, has done a good deal to change public attitudes rather drastically in this regard.

This may seem like a rather strange introduction to the subject of Food and Drug Administration regulations, but in our view there is a rather decided connection.

For example, on the surface, the concept of patient package inserts is very appealing. When one delves into the subject, a number of pragmatic considerations do arise, such as who will prepare them, who will distribute them, at what reader level will they be written, and so on. However, none of these questions would suggest that any ulterior motives may be involved on the part of the FDA in proposing that such inserts be provided with a given class of drugs.

Well, last fall the FDA published a notice with regard to amphetamines. The contemplated action would recognize the usefulness of these drugs in treating narcolepsy and minimal brain dysfunction but would eliminate the treatment of obesity as a recognized or approved use. Furthermore, it was also proposed that a patient package insert would be required and that such "patient labeling" would be given to the patient at the time the drug is dispensed.

What makes this proposal unusual is that the FDA would further mandate that the wording of the insert must include "warnings in layman's terms about using these drugs in weight reduction." But since weight reduction is not to be one of the approved uses, such a warning is academic and meaningless to any patient for whom the drug has been prescribed in accord with either of the approved uses. Obviously, therefore, this is a back-door approach on the part of FDA to exert a degree of control over the prescribing practices of physicians through subtle pressures brought to bear *via* the patient.

Inasmuch as the FDA has no jurisdiction over the practice of medicine—authority in this area residing with state government agencies—any FDA efforts to control physician prescribing for individual patients, albeit well intentioned, is improper. Consequently, it appears that this proposed wording requirement is nothing more than a devious effort to accomplish such control.

We have also heard similar concerns expressed by some research investigators.

Again, FDA has no direct authority, as such, to control drug research. However, when the agency does have the authority to monitor research subjects, to register clinical investigators, and to approve study protocols, it is a very short step indeed to cross over the line and to dictate how the research itself will be conducted.

Regulations, controls, and surveillance are recognized as very necessary safeguards for the public at large as well as for individual patients or test subjects. There can be little quarrel when the agency charged with responsibility in this area applies such rules properly and as they are intended. When, and if, that agency bends and distorts them in a manner to serve other purposes for which they were not intended, then there is legitimate cause for strong objection. Unfortunately, in resorting to such practices, the agency also damages whatever respect and credibility it may have previously enjoyed.

Edward G. Feldmann

MAY 1978
VOLUME 67 NUMBER 5

JOURNAL OF PHARMACEUTICAL SCIENCES

MARY H. FERGUSON
Editor

SHELLY ELLIOTT
Production Editor

JANET D. SHOFF
Copy Editor

EDWARD G. FELDMANN
Contributing Editor

SAMUEL W. GOLDSTEIN
Contributing Editor

BELLE R. BECK
Editorial Secretary

DAVID BOHARDT
Director of Publications

L. LUAN CORRIGAN
Assistant Director of Publications

EDITORIAL ADVISORY BOARD

JOHN AUTIAN	HERBERT A. LIEBERMAN
NORMAN R. FARNSWORTH	DAVID E. MANN, JR.
WILLIAM O. FOYE	GERALD J. PAPARIELLO
WILLIAM J. JUSKO	EDWARD G. RIPPIE

The *Journal of Pharmaceutical Sciences* is published monthly by the American Pharmaceutical Association at 2215 Constitution Ave., N.W., Washington, DC 20037. Second-class postage paid at Washington, D.C., and at additional mailing office.

All expressions of opinion and statements of supposed fact appearing in articles or editorials carried in this journal are published on the authority of the writer over whose name they appear and are not to be regarded as necessarily expressing the policies or views of the American Pharmaceutical Association.

Offices Editorial, Advertising, and Subscription Offices: 2215 Constitution Ave., N.W., Washington, DC 20037. Printing Offices: 20th & Northampton Streets, Easton, PA 18042.

Annual Subscriptions—United States and foreign, industrial and government institutions $50, educational institutions $50, individuals *for personal use only* $30; single copies $5. All foreign subscriptions add $5 for postage. Subscription rates are subject to change without notice. Members of the American Pharmaceutical Association may elect to receive the *Journal of Pharmaceutical Sciences* as a part of their annual $70 (foreign $75) APhA membership dues.

Claims Missing numbers will not be supplied if dues or subscriptions are in arrears for more than 60 days or if claims are received more than 60 days after the date of the issue, or if loss was due to failure to give notice of change of address. The Association cannot accept responsibility for foreign delivery when its records indicate shipment has been made.

Change of Address—Members and subscribers should notify at once both the Post Office and the American Pharmaceutical Association, 2215 Constitution Ave., N.W., Washington, DC 20037, of any change of address.

Microfilm Microfilm volumes are available from University Microfilms International, 300 N. Zeeb Road, Ann Arbor, MI 48106.

© Copyright 1978, American Pharmaceutical Association, 2215 Constitution Ave., N.W., Washington, DC 20037; all rights reserved.

DEVIOUS ROUTES TO GOVERNMENTAL REGULATION

So-called "Big Business" has long suffered from a public perception as being devious in many of its approaches and actions. It has been common to expect that business interests often will not be completely open and above board in their motives and objectives.

On the other hand, it is only in recent years that the public has come to view with comparable suspicion various proposals and actions involving government agencies, particularly at the federal level. Presumably, in a Democratic society, government is the people and honesty in government has been—or, more accurately, *had been*—taken for granted. However, the "Watergate affair," among other things, has done a good deal to change public attitudes rather drastically in this regard.

This may seem like a rather strange introduction to the subject of Food and Drug Administration regulations, but in our view there is a rather decided connection.

For example, on the surface, the concept of patient package inserts is very appealing. When one delves into the subject, a number of pragmatic considerations do arise, such as who will prepare them, who will distribute them, at what reader level will they be written, and so on. However, none of these questions would suggest that any ulterior motives may be involved on the part of the FDA in proposing that such inserts be provided with a given class of drugs.

Well, last fall the FDA published a notice with regard to amphetamines. The contemplated action would recognize the usefulness of these drugs in treating narcolepsy and minimal brain dysfunction but would eliminate the treatment of obesity as a recognized or approved use. Furthermore, it was also proposed that a patient package insert would be required and that such "patient labeling" would be given to the patient at the time the drug is dispensed.

What makes this proposal unusual is that the FDA would further mandate that the wording of the insert must include "warnings in layman's terms about using these drugs in weight reduction." But since weight reduction is not to be one of the approved uses, such a warning is academic and meaningless to any patient for whom the drug has been prescribed in accord with either of the approved uses. Obviously, therefore, this is a back-door approach on the part of FDA to exert a degree of control over the prescribing practices of physicians through subtle pressures brought to bear *via* the patient.

Inasmuch as the FDA has no jurisdiction over the practice of medicine—authority in this area residing with state government agencies—any FDA efforts to control physician prescribing for individual patients, albeit well intentioned, is improper. Consequently, it appears that this proposed wording requirement is nothing more than a devious effort to accomplish such control.

We have also heard similar concerns expressed by some research investigators.

Again, FDA has no direct authority, as such, to control drug research. However, when the agency does have the authority to monitor research subjects, to register clinical investigators, and to approve study protocols, it is a very short step indeed to cross over the line and to dictate how the research itself will be conducted.

Regulations, controls, and surveillance are recognized as very necessary safeguards for the public at large as well as for individual patients or test subjects. There can be little quarrel when the agency charged with responsibility in this area applies such rules properly and as they are intended. When, and if, that agency bends and distorts them in a manner to serve other purposes for which they were not intended, then there is legitimate cause for strong objection. Unfortunately, in resorting to such practices, the agency also damages whatever respect and credibility it may have previously enjoyed.

Edward G. Feldmann

Plaque Prevention: Suspension Theory and Ascorbic Acid and Urea

In 1966, Ecanow[1] suggested that plaque formation conformed to aspects of suspension–flocculation–coagulation theory. The process involving teeth commences with the adherence of a surfactant film on the tooth enamel. Surfactants can form a film even on clean teeth. Chemically, the surfactant may be a mucopolysaccharide, a glycoprotein, or other biosurfactant; or the surfactant may be supplied from exogenous sources.

Once the initial film of surfactant forms on the enamel surface, any insoluble particles present, such as viruses, carbohydrates, bacteria, and environmental pollutants (*e.g.*, smoke), will adhere to the film because of the surfactant's wetting action and the large specific surface area of the particles. These particles, in turn, act as loci for the adsorption of other surfactants from saliva and food, and thus the process continues. A large quantity of sorbed water molecules becomes intermixed with the developing matrix, and the result is the formation of a semisolid gel with micelles and coacervate systems present.

According to Bowen[2], the gel matrix is composed of proteins (40–45% dry weight) and carbohydrates (10–20% dry weight) and contains approximately 80% water. Unless these structured water systems are removed by brushing or dissolution, they tend to concentrate calcium phosphate and other calcium salts (which are bulk water insoluble), promoting the formation of a calculus state. This whole process is similar to that of caking in pharmacy[3].

We have found that a 40% solution of urea in water is effective in removing all but trace amounts of synthetic surfactants (dioctyl sodium sulfosuccinate[4] and benzalkonium chloride) and biosurfactant (lecithin) films from horse teeth. Clean teeth that are bathed with a solution of 40% urea will resist the initial adherence of the surfactant to the enamel surface. Even though the gel state plaque may have formed and increased in size, it has been our experience that both ascorbic acid (vitamin C) and urea are useful in plaque dissolution in the earlier stages of formation. But once the plaque has developed into a highly structured phase or once calculus has formed to a marked extent, the dissolution properties of ascorbic acid and urea fail to have the same pronounced effect.

The use of ascorbic acid in plaque prevention has been noted in the literature, but the results have been mixed. The explanation for the mechanism by which ascorbic acid acts in this role has, in general, been based on a biochemical approach. We believe that the mechanism of action can be explained on a physical–chemical basis. The observed results suggest that ascorbic acid behaves as a water structure breaker, which destroys the plaque matrix so the system becomes dispersible. Urea, which is known to be an even stronger structure breaker than ascorbic acid, should be even more effective in inhibiting plaque formation and, thus, a preventative in periodontal disease.

Urea has been used in the past for this purpose. Although the matrix breaking effects of urea have been previously reported[5], the mechanism of action as a prophylaxis for caries has been based on its ability to neutralize acids present in the plaque matrix. The similarity in dissolution processes between ascorbic acid and urea suggests that more than acid neutralization is involved[6]. This possibility is further indicated by the observation that the use of neutralizing agents is not appreciably effective. Using a model system (a horse tooth), we have found that plaque formation can be readily prevented; or once formed, it can be effectively dispersed by simple soaking in an aqueous solution containing 40% urea. Therefore, we suggest that urea be reconsidered for use (after appropriate safety tests) in concentrations up to 40% in mouthwashes as a preventative measure against plaque formation. We also recommend that insoluble colloids that are readily adsorbed on surfactant films be avoided in the formulation of oral products and that due consideration be given to the surfactant components in food, toothpastes, and mouthwashes since they may act as potential plaque formers.

Bernard Ecanow
Martin I. Blake
University of Illinois at the Medical Center
Chicago, IL 60612

Received March 3, 1978.

[1] B. Ecanow, U.S. Copyright A825763 (Ecanow, Skokie, Ill.), 1966.
[2] W. H. Bowen, *J. Am. Pharm. Assoc.*, **NS17**, 709 (1977).
[3] R. G. Wilson and B. Ecanow, *J. Pharm. Sci.*, **52**, 757 (1963).
[4] Aerosol OT.
[5] R. M. Stephan, *J. Dental Res.*, **22**, 63 (1943).
[6] S. Levin, "Vitamin C: Its Molecular Biology and Medical Potential," Academic, New York, N.Y., 1976, p. 61.

Carcinogenesis Hypothesis

My response to the letter entitled "Biological Foreign Particle Film Encapsulation," by Ecanow *et al.*[1] is: "Nonsense!" The authors' suggestion attributing "carcinogenesis" to the presence of inert "Class B" particle granules reminds me of the "spontaneous generation theory" for the origin of life. Here follows a more plausible and, ergo, less miraculous, albeit heuristic, hypothesis of my own to explain the observations reported[1].

The Class B particle complexes with the cellular material present and has the immunochemical characteristics of a Landsteiner hapteen[2]. The hapteen-like complex can initiate and provoke an autoimmune reaction. If the autoimmune reaction is massive, immunosuppression and immunological paralysis may ensue. If a virus or viral DNA, having appropriate affinity for the cellular matrix present, is available contemporaneously with a less-than-adequate immune response system, the viral triggering of a neoplasm may happen. Any chemical administered in doses large enough to be toxic will be immunosuppressive and can enable the viral initiation of a cancer.

In the studies establishing the identity of "carcinogens," the vast majority of the test animals die of infection. Only a small percentage survive long enough to develop cancers. Data accompanying official FDA reports on carcinogens never identify the infectious cause of death in the noncancerous test animals or rule out the coincidental presence of viruses. I am always amazed that prestigious journals like *J. Pharm. Sci.* fail to challenge the investigational adequacy of the mediocre research studies that important governmental policies use for rationalization. Before you accept any bureaucrat's allegations that sodium cyclamate or saccharin or Egyptian Henna are carcinogens, why don't you ask about the antibody titres of the test animals, if antibiotics were given to suppress infections, whether the presence of viruses or viral material was ruled out, and how competent and honest the investigators were?

I seem to be the only one who regularly raises these doubts. The APhA is cozy to the point where it does not exercise a virile and independent objectivity apropos federal government handouts. Beware, 1984 is only 6 years hence!

Sidney Silberberg
5725 Idlewild Avenue
Livermore, CA 94550

Received February 23, 1978.

[1] B. Ecanow, B. H. Gold, B. H. Moon, and R. S. Levinson, *J. Pharm. Sci.*, **67** (1), VIII (1978).
[2] K. Landsteiner, *Proc. Roy. Acad. Sci., Amsterdam*, **30**, 329 (1921).

Plaque Prevention: Suspension Theory and Ascorbic Acid and Urea

In 1966, Ecanow[1] suggested that plaque formation conformed to aspects of suspension–flocculation–coagulation theory. The process involving teeth commences with the adherence of a surfactant film on the tooth enamel. Surfactants can form a film even on clean teeth. Chemically, the surfactant may be a mucopolysaccharide, a glycoprotein, or other biosurfactant; or the surfactant may be supplied from exogenous sources.

Once the initial film of surfactant forms on the enamel surface, any insoluble particles present, such as viruses, carbohydrates, bacteria, and environmental pollutants (*e.g.*, smoke), will adhere to the film because of the surfactant's wetting action and the large specific surface area of the particles. These particles, in turn, act as loci for the adsorption of other surfactants from saliva and food, and thus the process continues. A large quantity of sorbed water molecules becomes intermixed with the developing matrix, and the result is the formation of a semisolid gel with micelles and coacervate systems present.

According to Bowen[2], the gel matrix is composed of proteins (40–45% dry weight) and carbohydrates (10–20% dry weight) and contains approximately 80% water. Unless these structured water systems are removed by brushing or dissolution, they tend to concentrate calcium phosphate and other calcium salts (which are bulk water insoluble), promoting the formation of a calculus state. This whole process is similar to that of caking in pharmacy[3].

We have found that a 40% solution of urea in water is effective in removing all but trace amounts of synthetic surfactants (dioctyl sodium sulfosuccinate[4] and benzalkonium chloride) and biosurfactant (lecithin) films from horse teeth. Clean teeth that are bathed with a solution of 40% urea will resist the initial adherence of the surfactant to the enamel surface. Even though the gel state plaque may have formed and increased in size, it has been our experience that both ascorbic acid (vitamin C) and urea are useful in plaque dissolution in the earlier stages of formation. But once the plaque has developed into a highly structured phase or once calculus has formed to a marked extent, the dissolution properties of ascorbic acid and urea fail to have the same pronounced effect.

The use of ascorbic acid in plaque prevention has been noted in the literature, but the results have been mixed. The explanation for the mechanism by which ascorbic acid acts in this role has, in general, been based on a biochemical approach. We believe that the mechanism of action can be explained on a physical–chemical basis. The observed results suggest that ascorbic acid behaves as a water structure breaker, which destroys the plaque matrix so the system becomes dispersible. Urea, which is known to be an even stronger structure breaker than ascorbic acid, should be even more effective in inhibiting plaque formation and, thus, a preventative in periodontal disease.

Urea has been used in the past for this purpose. Although the matrix breaking effects of urea have been previously reported[5], the mechanism of action as a prophylaxis for caries has been based on its ability to neutralize acids present in the plaque matrix. The similarity in dissolution processes between ascorbic acid and urea suggests that more than acid neutralization is involved[6]. This possibility is further indicated by the observation that the use of neutralizing agents is not appreciably effective. Using a model system (a horse tooth), we have found that plaque formation can be readily prevented; or once formed, it can be effectively dispersed by simple soaking in an aqueous solution containing 40% urea. Therefore, we suggest that urea be reconsidered for use (after appropriate safety tests) in concentrations up to 40% in mouthwashes as a preventative measure against plaque formation. We also recommend that insoluble colloids that are readily adsorbed on surfactant films be avoided in the formulation of oral products and that due consideration be given to the surfactant components in food, toothpastes, and mouthwashes since they may act as potential plaque formers.

Bernard Ecanow
Martin I. Blake
University of Illinois at the Medical Center
Chicago, IL 60612

Received March 3, 1978.

[1] B. Ecanow, U.S. Copyright A825763 (Ecanow, Skokie, Ill.), 1966.
[2] W. H. Bowen, *J. Am. Pharm. Assoc.*, **NS17**, 709 (1977).
[3] R. G. Wilson and B. Ecanow, *J. Pharm. Sci.*, **52**, 757 (1963).
[4] Aerosol OT.
[5] R. M. Stephan, *J. Dental Res.*, **22**, 63 (1943).
[6] S. Levin, "Vitamin C: Its Molecular Biology and Medical Potential," Academic, New York, N.Y., 1976, p. 61.

Carcinogenesis Hypothesis

My response to the letter entitled "Biological Foreign Particle Film Encapsulation," by Ecanow *et al.*[1] is: "Nonsense!" The authors' suggestion attributing "carcinogenesis" to the presence of inert "Class B" particle granules reminds me of the "spontaneous generation theory" for the origin of life. Here follows a more plausible and, ergo, less miraculous, albeit heuristic, hypothesis of my own to explain the observations reported[1].

The Class B particle complexes with the cellular material present and has the immunochemical characteristics of a Landsteiner hapteen[2]. The hapteen-like complex can initiate and provoke an autoimmune reaction. If the autoimmune reaction is massive, immunosuppression and immunological paralysis may ensue. If a virus or viral DNA, having appropriate affinity for the cellular matrix present, is available contemporaneously with a less-than-adequate immune response system, the viral triggering of a neoplasm may happen. Any chemical administered in doses large enough to be toxic will be immunosuppressive and can enable the viral initiation of a cancer.

In the studies establishing the identity of "carcinogens," the vast majority of the test animals die of infection. Only a small percentage survive long enough to develop cancers. Data accompanying official FDA reports on carcinogens never identify the infectious cause of death in the noncancerous test animals or rule out the coincidental presence of viruses. I am always amazed that prestigious journals like *J. Pharm. Sci.* fail to challenge the investigational adequacy of the mediocre research studies that important governmental policies use for rationalization. Before you accept any bureaucrat's allegations that sodium cyclamate or saccharin or Egyptian Henna are carcinogens, why don't you ask about the antibody titres of the test animals, if antibiotics were given to suppress infections, whether the presence of viruses or viral material was ruled out, and how competent and honest the investigators were?

I seem to be the only one who regularly raises these doubts. The APhA is cozy to the point where it does not exercise a virile and independent objectivity apropos federal government handouts. Beware, 1984 is only 6 years hence!

Sidney Silberberg
5725 Idlewild Avenue
Livermore, CA 94550

Received February 23, 1978.

[1] B. Ecanow, B. H. Gold, B. H. Moon, and R. S. Levinson, *J. Pharm. Sci.*, **67** (1), VIII (1978).
[2] K. Landsteiner, *Proc. Roy. Acad. Sci., Amsterdam*, **30**, 329 (1921).

JOURNAL OF PHARMACEUTICAL SCIENCES

MAY 1978
VOLUME 67 NUMBER 5

RESEARCH ARTICLES

Synthesis and Local Anesthetic Properties of Secondary Alkoxyalkylaminoacylanilides

GEORGE H. KRONBERG ˣ, RICHARD S. LEARD, ELIAS MEYMARIS, and BERTIL H. TAKMAN

Received May 31, 1977, from the *Research Laboratories, Astra Pharmaceutical Products, Inc., Framingham, MA 01701.* Accepted for publication August 24, 1977.

Abstract □ Nineteen secondary alkoxyalkylaminoacylanilides were prepared. They were weaker bases and were more hydrophilic than the corresponding analogs lacking the ether function. In 2% solution, these compounds blocked the rat sciatic nerve *in vivo* after relatively short onset times with good frequency of anesthesia. The duration of block was 0.4–1.5 times that of lidocaine. Their systemic toxicity was low, and their irritation liability in most instances was acceptable.

Keyphrases □ Alkoxyacylaminoacylanilides, various—synthesized, evaluated for local anesthetic activity in rats □ Anesthetic activity, local—various alkoxyacylaminoacylanilides evaluated in rats □ Structure-activity relationships—various alkoxyacylaminoacylanilides evaluated for local anesthetic activity in rats

A few alkoxyalkylaminoacetanilides related to lidocaine were described previously (1). This work has been extended, and 19 related secondary amines were prepared and studied as local anesthetics.

RESULTS AND DISCUSSION

Synthesis—The new compounds were synthesized using conventional methods according to the following two procedures.

1. Haloacylanilides (Table I) were refluxed with an alkoxyalkylamine in alcohol, benzene, or toluene, using excess amine as the proton acceptor.

2. Acrylanilides (Table II) were refluxed neat with an equimolar or excess amount of an alkoxyalkylamine.

The compounds obtained (Tables III and IV) were isolated and purified as described under *Experimental.*

The preparation of 3-haloacylanilides, using Löfgren's buffer method (2), was not always free of complications. Thus, the reaction between 2-ethylaniline and 3-bromobutyryl chloride resulted in a mixture of the expected compound, III (Table I), and the crotonyl compound, XI (Table II). Furthermore, the III yield was unacceptable. This tendency to eliminate also was observed in the reaction between 3-bromopropionyl chloride and 2-ethylaniline (3). In the latter case, only a small amount of 2′-ethylacrylanilide was formed, but the yield of the bromopropionanilide XLII was satisfactory.

When XIII was prepared from 2-ethylaniline and *trans*-2-methyl-2-butenoyl chloride (tiglyl chloride), experiments were performed using a molar excess of the aniline instead of sodium bicarbonate as a proton acceptor. This approach resulted in lower yields and inconvenient workup conditions and is, therefore, not recommended (*cf.*, Ref. 4). Attempts to distill the β-substituted amines XXII and XXIII resulted, as expected (5), in elimination of 2-methoxyethylamine and formation of the acryl (X) and crotonyl (XI) derivatives of 2-ethylaniline, respectively.

Significant amounts of 2-ethylaniline (39%) were formed in the preparation of the γ-substituted 4-(2-methoxyethylamino)-2′-ethylbutyranilide (XXV) from 4-chloro-2′-ethylbutyranilide (IV) and 2-methoxyethylamine by refluxing in anhydrous benzene for 4 hr. This phenomenon has never been observed in the synthesis of numerous α- and β-aminoacylanilides.

Two compounds could not be obtained with the aforementioned methods. Thus, 3-(2-methoxyethylamino)-2-methyl-2′-ethylbutyranilide could neither be prepared from the reaction between 2-methoxyethylamine and the bromo compound VIII nor obtained by addition of the alkoxyamine to the double bond of XIII. The 3-bromopivalyl derivative IX did not react with 2-methoxyethylamine to give 2,2-dimethyl-3-(2-methoxyethylamino)-2-ethylpropionanilide, which is not surprising in view of the similarity of Structure IX and neopentyl bromide.

Physicochemical Data—Determination of pKa values and partition coefficients (cod liver oil–water) (6) were made (Table IV). As expected, the introduction of an alkoxy group in the β-position to the amino nitrogen decreased the basicity. Löfgren (7) reported that the pKa values for 23 unsubstituted lidocaine homologs (α-aminoacylanilides) were in the 7.3–8.9 range, whereas the pKa values for the related α-alkoxyalkylaminoacylanilides, XIV–XXI and XXVI–XXXI, reported here ranged from 6.7 to 7.2. Compounds with a methyl on the amide nitrogen were the strongest bases in both series.

Lengthening of the acyl chain to β- and γ-substituted aminoacylanilides, XXII–XXV, increased the pKa values to 8.3–9.0, *i.e.*, to the higher part of the range for Löfgren's α-amines. Therefore, the influence of the β-alkoxy group was approximately compensated by the increased distance between the amine and amide groups.

The presence of the alkoxy group lowered the partition coefficient (decreased lipophilicity) and increased the water solubility of the bases considerably in comparison to unsubstituted analogs. Thus, the solubilities of the base form of the following compounds were: XV and XXIX, 6%; XXXI, 11%; and XVII, 39%.

Pharmacology—The following tests were performed according to methods described under *Experimental.*

1. Conduction anesthesia: Observations were made on the frequency of successful block of the sciatic nerve in the rat (8), the onset time, and the duration (Table V). In some cases, the effect of the addition of epinephrine to the local anesthetic solutions was studied.

Table I—Haloacylanilides

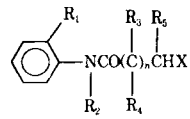

Compound	R_1	R_2	R_3	R_4	R_5	n	X	Yield, %	Recrystallization Solvent	Melting Point	Formula	Analysis, % Calc.	Found
I[a]	CH_3	CH_3	—	—	CH_3	0	Br	92	—	—	$C_{11}H_{14}BrNO$	C 51.6	51.6
												H 5.51	5.50
II	C_2H_5	H	—	—	C_2H_5	0	Br	84	95% ethanol	113.5–114.5°	$C_{12}H_{16}BrNO$	C 53.3	53.9
												H 5.97	6.03
III[b]	C_2H_5	H	H	H	CH_3	1	Br	92	Benzene–cyclohexane	113–114.5°	$C_{12}H_{16}BrNO$	C 53.3	53.7
												H 5.97	5.98
												Br 29.6	29.3
IV	C_2H_5	H	H	H	H	2	Cl	72	Benzene–petroleum ether	61.5–62°	$C_{12}H_{16}ClNO$	N 5.18	5.17
												C 63.9	63.9
												H 7.15	7.42
V[c]	$C(CH_3)=CH_2$	H	—	—	CH_3	0	Br	90	—	—	$C_{12}H_{14}BrNO$	C 53.7	53.5
												H 5.26	5.38
												Br 29.8	30.2
VI	$CH(CH_3)_2$	H	—	—	CH_3	0	Br	92	Cyclohexane	96–97°	$C_{12}H_{16}BrNO$	C 53.5	53.5
												H 5.97	5.96
												Br 29.6	29.7
VII	$C(CH_3)_3$	H	—	—	CH_3	0	Br	73	Cyclohexane	133.5–134°	$C_{13}H_{18}BrNO$	C 54.9	54.7
												H 6.38	6.34
												Br 28.1	28.1
VIII	C_2H_5	H	CH_3	H	CH_3	1	Br	43	2-Propanol	149–150°	$C_{13}H_{18}BrNO$	C 54.9	55.1
												H 6.38	6.45
												Br 28.1	28.0
IX	C_2H_5	H	CH_3	CH_3	H	1	Br	83	Acetone–petroleum ether	132–133°	$C_{13}H_{18}BrNO$	C 54.9	55.2
												H 6.38	6.63
												Br 28.1	28.3

[a] Boiling point 143–144°; n_D^{25} 1.5519. [b] Molecular weight: calc., 270; found, 267. [c] Analysis done on a small sample distilled under high vacuum.

2. Systemic toxicity (8): Estimates of the acute systemic toxicity (LD_{50}) were made following intraperitoneal and intravenous administrations in female albino mice (Table VI).

3. Irritation liability (9): The intradermal wheal technique in the rabbit back was used to compare the local irritation of most compounds (Table VI).

Local Anesthetic Properties (Table V)—The onset times of all new compounds were somewhat longer (generally 3–4 min) than that of lidocaine (1–2 min). Compound XXV was much slower in onset (8–11 min) than the others.

The frequency of anesthesia was good for all compounds except XXV, which only produced block in two-thirds of the injected animals, even in the experiments with 4% solutions. Compound XXV deviates structurally from the rest by being the only γ-aminoacylanilide.

Among the ester-type local anesthetics, *i.e.*, agents related to amylocaine (stovaine) and procaine, an increase in the distance between the aromatic ring and the (aliphatic) amino nitrogen from $COOCH_2CH_2$ (*e.g.*, procaine) to $COOCH_2CH_2CH_2$ does not influence the local anesthetic effects in a remarkably detrimental manner (10). Usually, the higher homolog is not too different from the lower one, and sometimes an advantageous change in the parameters is observed (*e.g.*, piperocaine) (11).

If, however, the similar change is made in aminoacylanilide local anesthetics, *i.e.*, a change from $NHCOCH_2CH_2$ to $NHCOCH_2CH_2CH_2$, a distinctly degenerative effect in local anesthetic properties can result.

The 1% solutions of the new compounds, except XXIII, produced a shorter duration of block than lidocaine; XXIII was about as effective as the reference compound. At the 2% level, XXIII blocked significantly longer than lidocaine ($p < 0.01$), whereas the other agents gave durations shorter or equal to that of the standard. However, XXII–XXV gave the most long-lasting blocks, and the distance between the amino nitrogen and the benzene ring is larger in these compounds than in the others.

The addition of epinephrine prolonged the duration of anesthesia of the new agents. Compound XVIII is a representative example of the series in this respect. The dose–duration curve (Fig. 1) for solutions containing epinephrine in a concentration of 1:100,000 (w/v) is significantly separated from the curve for plain anesthetic solutions. The prolongation of duration by epinephrine is further illustrated in Fig. 2, where the effects of increasing amounts of epinephrine on the duration are shown for three different concentration levels of XVIII.

Toxicity (Table VI)—None of the compounds was significantly more toxic systemically than lidocaine after intravenous and intraperitoneal administration.

The degree of irritation at the site of injection increased with increasing lipid partitioning (*cf.*, Table IV). This tendency is clear and in line with observations on many other series and depends obviously on the close relationship between compound solubility at tissue pH and lipophilicity. The good correlation between decreasing solubility at physiological pH and increasing irritation liability was convincingly demonstrated by Koelzer and Wehr (12).

The thioether analogs of XVIII and XXXI were reported previously (3). The significant biological difference observed between the oxygen

Table II—Acrylanilides

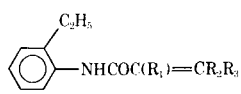

Compound	R_1	R_2	R_3	Yield, %	Melting Point	Recrystallization Solvent	Formula	Analysis, % Calc.	Found
X	H	H	H	66	107–108°	Aqueous ethanol	$C_{11}H_{13}NO$	C 75.4	75.5
								H 7.48	7.63
XI	H	H	CH_3	85	140.5–141°	Petroleum ether (bp 60–110°)	$C_{12}H_{15}NO$	C 76.2	76.3
								H 7.99	7.99
								N 7.40	7.37
XII	H	CH_3	CH_3	70	81.5–82.5°	2-Propanol–water	$C_{13}H_{17}NO$	C 76.8	77.1
								H 8.43	8.53
XIII[a]	CH_3	H	CH_3	71	71.5–72°	Petroleum ether (bp 30–60°)	$C_{13}H_{17}NO$	C 76.8	77.0
								H 8.43	8.37

[a] *trans*-Configuration.

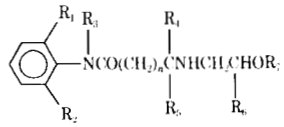

Table III—Alkoxyalkylaminoacylanilides

Compound	R_1	R_2	R_3	n	R_4	R_5	R_6	R_7	Form	Yield, %	Melting Point	Boiling Point (mm Hg)	n_D^{25}	Recrystallization Solvent
XIV	H	H	H	0	CH_3	H	H	CH_3	Base	76	61–62°	—	—	Petroleum ether (bp 60–110°)
XV	CH_3	H	H	0	CH_3	H	H	CH_3	Base	54	42.5–44°	135–137° (0.15)	—	Petroleum ether (bp 60–110°)
XVI	CH_3	H	H	0	CH_3	H	H	C_2H_5	Base	90	—	134–137° (0.11)	1.5224	—
XVII	CH_3	H	CH_3	0	CH_3	H	H	CH_3	Base	87	—	125°(0.08)	1.5159	—
XVIII	C_2H_5	H	H	0	CH_3	H	H	CH_3	Base	87	—	134–138° (0.11)	1.5260	—
XIX	C_2H_5	H	H	0	CH_3	H	H	C_2H_5	Base	89	—	145–147° (0.10)	1.5199	—
XX[a]	C_2H_5	H	H	0	CH_3	H	CH_3	CH_3	Hydrochloride	52	135–140°	—	—	2-Propanol–ether
XXI	C_2H_5	H	H	0	C_2H_5	H	H	CH_3	Base	85	—	133–135° (0.12)	1.5232	—
XXII	C_2H_5	H	H	1	H	H	H	CH_3	Hydrochloride	92	170.5–171°	—	—	2-Propanol
XXIII	C_2H_5	H	H	1	CH_3	H	H	CH_3	Hydrochloride	85	84–85°	—	—	Ethanol–ether
XXIV	C_2H_5	H	H	1	CH_3	CH_3	H	CH_3	Hexamate	63	112–112.5°	—	—	2-Propanol or acetone–ether
XXV	C_2H_5	H	H	2	H	H	H	CH_3	Hydrochloride	20	141–142°	—	—	Absolute ethanol
XXVI	CCH_3 ‖ CH_2	H	H	0	CH_3	H	H	CH_3	Oxalate	55	145–146°	—	—	Acetonitrile
XXVII	$CH(CH_3)_2$	H	H	0	CH_3	H	H	CH_3	Hydrochloride	95	138–140°	—	—	Ethanol–ether
XXVIII	$C(CH_3)_3$	H	H	0	CH_3	H	H	CH_3	Methanesulfonate	91	179–180°	—	—	Ethanol–ether
XXIX	CH_3	CH_3	H	0	H	H	H	C_2H_5	Base	58	50–51°	154–155° (0.15)	—	—
XXIX*a*									Hydrochloride		198.5–199°	—	—	Absolute ethanol–ether
XXX	CH_3	CH_3	H	0	H	H	CH_3	CH_3	Hydrochloride	53	136–140°	—	—	Ethanol–ether or ethyl acetate
XXXI	CH_3	CH_3	H	0	CH_3	H	H	CH_3	Base	71	56–57°	—	—	Cyclohexane–petroleum ether (bp 30–70°)
XXXII[a]	CH_3	CH_3	H	0	CH_3	H	CH_3	CH_3	Perchlorate	71	184–186°	—	—	2-Propanol

[a] Diastereomeric mixture.

and sulfur analogs is the much lower irritation liability of the oxygen ethers. This result is the expected consequence of the greater water solubility of the base form of the oxygen analogs.

EXPERIMENTAL[1]

Chemistry—2-Isopropenylaniline (XXXIII) (13) and 2-*tert*-butylaniline (XXXIV) (14) were prepared as described previously. 2-Isopropylaniline (XXXV) was prepared, following a literature method (15) for 3-bromoisopropylbenzene, by hydrogenation of 2-isopropenylaniline in ethyl acetate over 5% palladium-on-charcoal at the initial pressure of 3 atm; the yield was 95%.

Haloacylanilides—2-Chloro-2′,6′-acetoxylidide (XXXVI) (16), 2-bromo-2′,6′-acetoxylidide (XXXVII) (17), 2-bromopropionanilide (XXXVIII) (18), 2-bromo-2′-propionotoluidide (XXXIX) (18), 2-bromo-2′,6′-propionoxylidide (XL) (19), 2-bromo-2′-ethylpropionanilide (XLI) (3), and 3-bromo-2′-ethylpropionanilide (XLII) (3) were obtained by Löfgren's acetate buffer method (2) as described for II.

2-Bromo-*N*-methyl-2′-propionotoluidide (I)—A solution of 2-bromopropionyl bromide (91.5 g, 0.424 mole) in dry ether (50 ml) was added slowly, with stirring and cooling (5°), to a solution of *N*-methyl-2-toluidine (46.1 g, 0.380 mole) and dry pyridine (30.1 g, 0.380 mole) in anhydrous ether (200 ml). The mixture was left overnight, and the precipitated pyridinium bromide was filtered off and washed. The ether solution and washings were evaporated *in vacuo*, and the residual oil was distilled.

2-Bromo-2′-ethylbutyranilide (II)—2-Ethylaniline (46.1 g, 0.380 mole) was dissolved in 320 ml of acetic acid and cooled to 5–10°. 2-Bromobutyryl bromide (98.7 g, 0.429 mole) was added, and the solution was mixed; then, immediately, a cold solution of sodium acetate trihydrate (125 g, 0.922 mole) in 525 ml of water was added. After shaking for 30 min, the precipitate was filtered, washed with water, and recrystallized.

The following intermediates were prepared in the same manner as II: IV, from 4-chlorobutyryl chloride and 2-ethylaniline; VI, from 2-bromopropionyl bromide and XXXV; and VII, from 2-bromopropionyl bromide and XXXIV.

3-Bromo-2′-ethylbutyranilide (III)—To a solution of 2-ethylaniline (12.1 g, 0.0998 mole) in benzene (50 ml) was added, with stirring, 3-bromobutyryl chloride (20) (9.25 g, 0.0499 mole) dissolved in benzene (100 ml). Stirring was continued for 2 hr, and the resulting 2-ethylanilinium chloride was filtered and washed with benzene. From the evaporated benzene solution and washings was obtained a crystalline material, which was further purified by recrystallization.

2-Bromo-2′-isopropenylpropionanilide (V)—Compound V was prepared in the same way as III from 2-bromopropionyl bromide and XXXIII, using ether as a solvent. The nonsolidifying product could be used without further purification or be distilled *in vacuo*.

3-Bromo-2,2-dimethyl-2′-ethylpropionanilide (IX)—Hydroxypivaldehyde was converted into hydroxypivalic acid (21), from which bromopivalic acid (22) was obtained. This acid was transformed into bromopivalyl chloride (23), which was allowed to react with 2-ethylaniline

[1] Melting points (uncorrected) were obtained with a Thomas-Hoover capillary melting-point apparatus. IR spectra were recorded on a Perkin-Elmer Infracord 137 spectrophotometer and were as expected. The elemental analyses were provided by Schwarzkopf Microanalytical Laboratory, Woodside, N.Y.

Table IV—Alkoxyalkylaminoacylanilides: pKa, Partition Coefficients, and Analysis

Compound	pKa[a]	Partition[a,b] Coefficient	Formula	Analysis, % Calc.	Found
XIV	7.0	1.4	$C_{12}H_{18}N_2O_2$	C 64.8	64.6
				H 8.16	8.27
XV	6.9	1.0	$C_{13}H_{20}N_2O_2$	C 66.1	65.8
				H 8.53	8.58
XVI	6.8	4.5	$C_{14}H_{22}N_2O_2$	C 67.2	67.2
				H 8.86	8.88
XVII	7.2	1.0	$C_{14}H_{22}N_2O_2$	C 67.2	66.9
				H 8.86	8.91
XVIII	6.9	4.5	$C_{14}H_{22}N_2O_2$	C 67.2	66.8
				H 8.86	9.03
XIX	6.9	12	$C_{15}H_{24}N_2O_2$	C 68.1	67.8
				H 9.15	9.17
XX[c]	—	—	$C_{15}H_{25}ClN_2O_2$	C 59.9	59.8
				H 8.38	7.96
				Cl 11.8	11.7
XXI	6.7	13	$C_{15}H_{24}N_2O_2$	C 68.1	67.4
				H 9.15	9.09
XXII	8.3	—[d]	$C_{14}H_{23}ClN_2O_2$	C 58.6	58.1
				H 8.08	8.21
XXIII	8.3	1.9	$C_{15}H_{25}ClN_2O_2$	C 59.9	59.9
				H 8.38	8.58
				Cl 11.8	11.6
XXIV	8.8[e]	4.2	$C_{22}H_{39}N_3O_5S$	C 57.7	58.0
				H 8.59	8.62
XXV	>9.0[e]	0.84	$C_{15}H_{25}ClN_2O_2$	C 59.9	59.8
				H 8.38	8.12
				Cl 11.8	11.8
XXVI	6.8	24	$C_{17}H_{24}N_2O_6$	C 57.9	57.2
				H 6.87	6.92
XXVII	6.9	7.4	$C_{15}H_{25}ClN_2O_2$	C 59.9	59.4
				H 8.38	8.48
XXVIII	6.9	20	$C_{17}H_{30}N_2O_5S$	C 54.5	54.5
				H 8.07	8.39
				O 21.4	21.5
XXIX[f]	6.9	—[d]	$C_{14}H_{23}ClN_2O_2$	C 58.6	58.7
				H 8.08	8.08
XXX	7.1	0.9	$C_{14}H_{23}ClN_2O_2$	C 58.6	58.6
				H 8.08	8.31
XXXI	6.8	—[d]	$C_{14}H_{22}N_2O_2$	C 67.2	66.9
				H 8.86	9.06
XXXII[c]	—	—	$C_{15}H_{25}ClN_2O_6$	C 49.4	49.6
				H 6.91	6.57
				Cl 9.72	9.75
Lidocaine	7.9	36	—	—	

[a] A. Brändström, AB Hässle, Mölndal, Sweden, personal communication. [b] System: cod liver oil (Oleum Jecoris aselli, Pharmacop. Nord.)–water (6). [c] Diastereomeric mixture. [d] Partition coefficient low (0.6). [e] Approximate value. [f] Analysis performed on the hydrochloride.

in the same way as described for III, except that the reaction mixture was heated to 75° for 1 hr.

3-Bromo-2′-ethyl-2-methylbutyranilide (VIII)—At 0°, hydrobromic acid (30.4 g, 0.376 mole) was dissolved in ether (300 ml). Then XIII (16.5 g, 0.0812 mole) was added, and the homogeneous mixture was left for 2 weeks at room temperature. After several days at −20°, the separated solid material was filtered and recrystallized.

Acrylanilides (Table II)—These compounds were prepared by a literature method (24).

2′-Ethylacrylanilide (X)—Sodium hydroxide (97 ml, 1.25 *M*), 2-ethylaniline (12.1 g, 0.100 mole), and acryloyl chloride (10 g, 0.11 mole) were mixed and shaken vigorously for 5 min. After cooling, the precipitate was filtered, washed with water, and recrystallized.

2′-Ethylcrotonanilide (XI)—To a mixture of 2-ethylaniline (26.6 g, 0.220 mole), sodium bicarbonate (25.2 g, 0.300 mole), and dry acetone (250 ml) in a Morton flask equipped with a stirrer and reflux condenser was added a solution of crotonyl chloride (26.6 g, 0.254 mole) in dry acetone (100 ml) at such a rate that a moderate reflux was obtained. Refluxing was continued for 1 hr, and the reaction mixture was filtered hot. The separated inorganic salts were washed with acetone. The acetone solution was concentrated to 100 ml and diluted with 1 *M* HCl. The precipitated solid was filtered, washed with cold water, dried, and recrystallized.

2′-Ethyltiglanilide (XIII)—Compound XIII was prepared from 2-ethylaniline and tiglyl chloride (25) according to the procedure for XI; the mixture was refluxed for 2 hr.

2′-Ethylsenecioanilide (XII)—A solution of senecioyl chloride (25) (59.1 g, 0.498 mole) in toluene (150 ml) was added, with vigorous stirring,

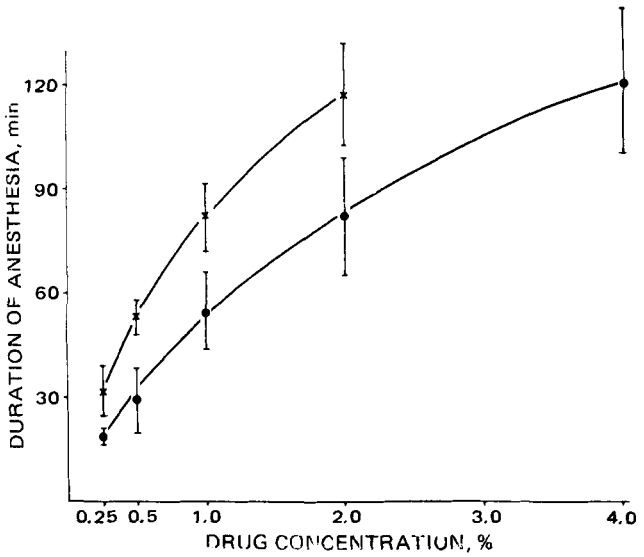

Figure 1—*Sciatic nerve block in the rat with XVIII. Key:* ●, *XVIII alone; and* ×, *XVIII with epinephrine, 1:100,000. Standard deviations are indicated by bars.*

to 2-ethylaniline (121 g, 0.999 mole) dissolved in toluene (1100 ml) over 15 min. Then the mixture was heated to 65° for 2 hr, the solvent was evaporated, and the oily residue was poured into 2 *M* HCl (400 ml). The solid was filtered, washed with dilute sodium bicarbonate solution and water, dried, and subsequently recrystallized.

Alkoxyalkylamines—2-Methoxyethylamine (XLIII) and 2-ethoxyethylamine (XLIV) were commercial products.

2-Methoxypropylamine (XLV) (26) and Bis(2-methoxypropyl)amine (XLVI)—Gaseous ammonia (51 g, 3.0 moles) was dissolved in cold methanol (300 ml) in an autoclave, and 1-bromo-2-methoxypropane (26) (45 g, 0.29 mole) was added. After heating at 50° for 48 hr, solvent and excess ammonia were evaporated. The residue was dissolved in 2 *M* HCl, washed with ether, made alkaline with 12.5 *M* NaOH, and extracted with ether. Then the extract was dried (sodium sulfate) and fractionated. The fraction boiling at 80–100° (XLV) was collected; the yield was 17 g (65%). Residues of several batches were distilled *in vacuo*, yielding XLVI, bp 84–90°/0.20–0.25 mm Hg. Equivalent weight ($C_8H_{19}NO_2$): calc., 161; found, 162.

Alkoxyalkylaminoacylanilides: 2-(2-Methoxyethylamino)propionanilide (XIV)—A solution of XXXVIII (1 mole) and XLIII (3.6 moles) in 700 ml of 95% ethanol was refluxed for 8 hr. The solvent and excess amine were evaporated under reduced pressure. The residue was dissolved in excess 6 *M* HCl, and the solution was washed with ether and made alkaline to pH 8–9 with 7 *M* NaOH. Then the base was taken up in ether. This solution was dried (sodium sulfate), the solvent was evaporated, and the solidifying residue was recrystallized.

The following compounds were prepared in a similar manner, except that the reaction product in certain instances was purified by distillation or by recrystallization of a suitable salt (Table III): XV, from XXXIX

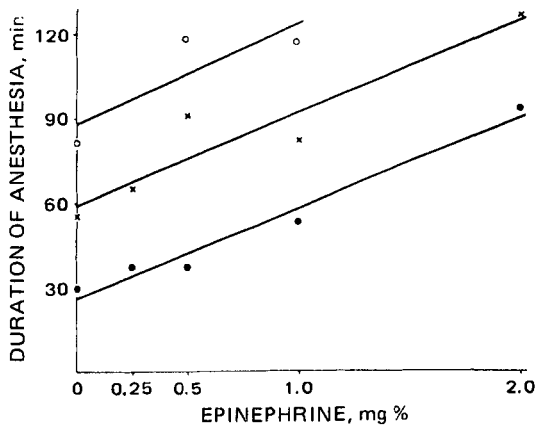

Figure 2—*Sciatic nerve block in the rat with XVIII. Key:* ●, *0.5% XVIII;* ×, *1% XVIII; and* ○, *2% XVIII.*

Table V—Local Anesthetic Activity: Sciatic Nerve Block in the Rat

Compound	pH of Solution	1% Onset, min	1% Duration[a], min	1% Frequency, %	2% Onset, min	2% Duration[a], min	2% Frequency, %	4% Onset, min	4% Duration[a], min	4% Frequency, %
XIV	6.7	—	—	—	3	41 ± 11	92	—	—	—
XV	6.4	3	28 ± 9	92	3	63 ± 13	89	3	67 ± 13	100
XVI	6.4	3	60 ± 42	67	3	84 ± 23	100	3	115 ± 8	100
XVII	6.8	—	—	—	3	50 ± 13	100	3	106 ± 17	100
XVIII	6.5	3	55 ± 11	92	3	82 ± 17	100	3	120 ± 22	100
XIX	6.2	—	—	—	3	67 ± 5	100	3	98 ± 8	100
XX	6–7	3–5	36 ± 6	92	3–5	56 ± 9	100	3	101 ± 10	100
XXI	6.3	3	66 ± 8	100	3	93 ± 7	100	3	>160[b]	100
XXII	6.3	4	69 ± 11	100	4	123 ± 19	83	—	—	—
XXIII	6.6	4	84 ± 15	100	4	151 ± 10	100	—	—	—
XXIV	6.0	3	58 ± 3	67	2	109 ± 16	100	—	—	—
XXV	6.7	—	0	0	8–11	118 ± 22	67	8–10	118 ± 26	67
XXVI	6.0	3	35 ± 5	100	3	72 ± 7	100	—	—	—
XXVII	6.0	3	29 ± 10	100	3	56 ± 8	100	—	—	—
XXVIII	6.0	—	—	—	3	58 ± 14	100	3	80 ± 17	100
XXIX	6.4	—	—	—	3	85 ± 18	100	—	—	—
XXX	6.0	—	—	—	3	55 ± 12	100	—	—	—
XXXI	6.3	3	51 ± 10	92	3	95 ± 18	96	—	—	—
XXXII	5.5–6.5	—	—	—	5	47 ± 12	100	—	—	—
Lidocaine	6.2	2	96 ± 10	100	1–2	115 ± 16	100	—	—	—

[a] Mean ± *SD*. [b] A third of the animals were still blocked after 12 hr.

and XLIII; XVI, from XXXIX and XLIV; XVII, from I and XLIII; XVIII, from XLI and XLIII; XIX, from XLI and XLIV; XXI, from II and XLIII; and XXII, from XLII and XLIII.

Compound XXII could not be distilled *in vacuo*. Elimination took place with the formation of X, identified by comparison to an authentic sample.

Compounds XX (from XLI and XLV), XXX (from XXXVII and XLV), and XXXII (from XL and XLV) were prepared as described for XIV, except that the reflux time was increased to 18–19 hr. The diastereomers of XX and XXXII were not separated.

Compounds XXVI (from V and XLIII), XVII (from VI and XLIII), and XXVIII (from VII and XLIII) were prepared by analogy to XIV with the following modification in procedure. After the ethanol had been evaporated from the reaction mixture, the residue was dissolved in chloroform. This solution was extracted exhaustively with 1 *M* HCl. The acid extract was washed with ether, whereafter the amine was liberated from the acid solution with 7 *M* NaOH and treated as described.

Compounds XXIX (from XXXVI and XLIV) and XXXI (from XL and XLIII) were prepared as described for XIV with the following difference. The treatment of the reaction residue with 6 *M* HCl left an undissolved solid (hydrochloride), which was filtered off and washed with ether. After an ether wash of the acid filtrate, the acid filtrate was again combined with the solid, and the mixture was made alkaline with 7 *M* NaOH and treated as described.

2′-Ethyl-4-(2-methoxyethyl)butyranilide (XXV)—Dry benzene (70 ml), IV (27.7 g, 0.123 mole), and dry XLIII (25.4 g, 0.338 mole) were refluxed for 4 hr. The volatiles were evaporated *in vacuo*. The residue was dissolved in 1 *M* HCl, and the solution was washed with ether, made alkaline to pH 10 with concentrated ammonia, and extracted with ether. After evaporation of the ether, the residue was subjected to a simplified countercurrent extraction in a four-funnel operation (27, 28) between phases of 400 ml of 0.067 *M* phosphate buffer (pH 7.0) and 200 ml of ether. From the ether fraction, an oil (5.8 g, 0.0479 mole, 39%), identified by its IR spectrum as 2-ethylaniline, was obtained. From the buffer fraction, a solid base (XXV) (6.4 g, 0.0242 mole, 20%) was obtained by extraction into ether at pH 10 and evaporation of the ether.

2′-Ethyl-3-(2-methoxyethylamino)butyranilide (XXIII)—*Method A*—A mixture of III (9.00 g, 0.0333 mole), dry XLIII (9.91 g, 0.132 mole), and anhydrous toluene (50 ml) was refluxed for 26.5 hr. The solvent was evaporated, and the residue was dissolved in 100 ml of 1 *M* HCl and washed with ether. The acid solution was made alkaline to pH 8.5 (7 *M* NaOH) and extracted with ether. After drying over anhydrous sodium sulfate, the solvent was evaporated, and the hydrochloride was prepared from the oily residue. The yield was 85%. On vacuum distillation of a part of the base residue, it decomposed into a solid neutral compound and a volatile amine. The solid was identical to XI (IR and mixed melting point).

Method B—A mixture of XI (3.40 g, 0.0180 mole) and XLIII (22.5 g, 0.299 mole) was refluxed for 8.5 hr. After evaporation *in vacuo* of excess aminoether, the residue was worked up as in Method A. The yield was 59%. Prolonged reaction times reduced the yield to 52% (17 hr) and 35% (20 hr).

2′ - Ethyl - 3 - (2-methoxyethylamino) - 3 - methylbutyranilide (XXIV)—A mixture of XII (14.0 g, 0.0689 mole) and XLIII (51.6 g, 0.687 mole) was refluxed for 40 hr. The unreacted aminoether was evaporated *in vacuo*, and the residue was taken up in 2 *M* HCl and extracted with ether to separate 4.50 g (32%) of unreacted XII. The acid solution was made alkaline (7 *M* NaOH) and extracted with ether. After drying over anhydrous sodium sulfate and evaporation of the ether, the residue was dissolved in absolute alcohol and an alcoholic solution of hexamic acid was added. The salt precipitated slowly and was filtered off after 2 hr.

Pharmacology and Toxicology—*Rat Sciatic Nerve Block* (*8*)—Solutions containing 10, 20, or 40 mg/ml of the hydrochlorides were prepared in isotonic saline; if another salt was used, an amount equivalent to the corresponding hydrochloride was employed. If epinephrine was desired as a constituent of the test solution, an appropriate amount of 0.1% stock solution of the vasoconstrictor was added before the solutions were brought to final volume. If necessary, the pH of the solution was adjusted with either dilute hydrochloric acid or sodium hydroxide. A volume of 0.20 ml was administered to female Wistar rats around the sciatic nerve at the midpoint of the femur (Table V).

Systemic Toxicity (*8*)—Isotonic saline solutions of the hydrochlorides, or other pharmaceutically acceptable salts in amounts equivalent to the

Table VI—Toxicity

Compound	LD_{50} (Mouse) iv, mg/kg	LD_{50} (Mouse) ip, mg/kg	Local Irritation[a] (Rabbit) 2% Solution	Local Irritation[a] (Rabbit) 4% Solution
XIV	70	275	—	—
XV	50	275	(+)	+
XVI	38	275	—	(+)
XVII	—	250	—	—
XVIII	38	250	—	0
XIX	36[b]	250	+++	+++
XX	45	300	(+)[c]	+[c]
XXI	26[b]	150	—	+++
XXII	65	250	(+)	+
XXIII	40	225	(+)	+
XXIV	22[b]	125	+	++
XXV	80[b]	400	(+)	+
XXVI	55[b]	350	++(+)	+++
XXVII	65[b]	450	(+)	(+)
XXVIII	115[d]	450	+	+
XXIX	35	130	(+)	(+)
XXX	35[b]	150	0	0
XXXI	40	120	0	0
XXXII	22	100	(+)	(+)
Lidocaine	25	130	—	—

[a] 0 = no irritation; + = some irritation; ++ = pronounced irritation; +++ = serious irritation, necrosis; parentheses indicate intermediate stages; and — = no determination. [b] One percent solution. [c] On addition of epinephrine (1:100,000), necrosis developed at both concentration levels. [d] Four percent solution.

corresponding hydrochloride, were prepared in concentrations of 10, 20, and 40 mg/ml. Acute intravenous or intraperitoneal toxicities were determined in female albino mice (Charles River CD random-bred). The results are estimates and should only be regarded as approximate LD_{50} values (Table VI).

Local Tissue Irritation (9)—Solutions were prepared containing 20 and 40 mg of the hydrochloride/ml (or equivalent amounts of other salts) in isotonic saline. Injections were made intradermally in female New Zealand White rabbits, and the effects were estimated from gross examination of the sites 24 hr after injection (Table VI).

REFERENCES

(1) B. H. Takman, G. Camougis, and N. M. Löfgren, *Acta Pharm. Suec.*, **6**, 373 (1969); *Chem. Abstr.*, **71**, 47999p (1969).

(2) N. Löfgren, "Studies on Local Anesthetics, Xylocaine®, A New Synthetic Drug," Haeggströms, Stockholm, Sweden, 1948, p. 25.

(3) G. H. Kronberg, R. S. Leard, and B. H. Takman, *J. Med. Chem.*, **16**, 739 (1973).

(4) L. I. Smith and W. W. Prichard, *J. Am. Chem. Soc.*, **62**, 778 (1940).

(5) B. Dofek and Č. Vrba, *Acta Fac. Pharm. Brun. Bratisl.*, **2**, 141 (1959).

(6) A. Brändström, *Acta Chem. Scand.*, **17**, 1218 (1963).

(7) N. Löfgren, "Studies on Local Anesthetics, Xylocaine®, A New Synthetic Drug," Haeggströms, Stockholm, Sweden, 1948, p. 95.

(8) G. Camougis and B. H. Takman, in "Methods in Pharmacology," vol. 1, A. Schwartz, Ed., Appleton-Century-Crofts, New York, N.Y., 1971, pp. 1–40.

(9) A. P. Truant, *Arch. Int. Pharmacodyn. Ther.*, **115**, 483 (1958).

(10) T. P. Carney, in "Medicinal Chemistry," vol. 1, C. M. Suter, Ed., Wiley, New York, N.Y., 1951, pp. 280–389.

(11) S. M. McElvain, *J. Am. Chem. Soc.*, **49**, 2835 (1927).

(12) P. P. Koelzer and K. H. Wehr, *Arzneim.-Forsch.*, **8**, 181 (1958).

(13) T. L. Jacobs, S. Winstein, R. B. Henderson, and E. C. Spaeth, *J. Am. Chem. Soc.*, **68**, 1310 (1946).

(14) J. B. Shoesmith and A. Mackie, *J. Chem. Soc.*, **1928**, 2334.

(15) W. E. Parham, E. L. Wheeler, R. M. Dodson, and S. W. Fenton, *J. Am. Chem. Soc.*, **76**, 5380 (1954).

(16) N. Löfgren, *Ark. Kemi Mineral. Geol.*, **22A** (18), 1 (1946).

(17) N. Löfgren and C. Tegnér, *Acta Chem. Scand.*, **9**, 493 (1955).

(18) A. Tigerstedt, *Chem. Ber.*, **25**, 2919 (1892).

(19) N. Löfgren and B. Lundqvist, *Sv. Kem. Tidskr.*, **58**, 206 (1946).

(20) D. M. Hall and E. E. Turner, *J. Chem. Soc.*, **1948**, 1909.

(21) L. Wessely, *Monatsh. Chem.*, **22**, 66 (1901).

(22) J. L. Green, Jr., and H. J. Hagemeyer, Jr., *J. Am. Chem. Soc.*, **77**, 3016 (1955).

(23) F. Nerdel, P. Weyerstahl, and U. Kretschmar, *Chem. Ber.*, **92**, 1329 (1959).

(24) E. Hofstetter and A. E. Wilder Smith, *Helv. Chim. Acta*, **36**, 1698 (1953).

(25) O. H. Wheeler, *J. Am. Chem. Soc.*, **78**, 3216 (1956).

(26) D. Gagnaire, *Bull. Soc. Chim. Fr.*, **1960**, 1813.

(27) E. Hultin, *Acta Chem. Scand.*, **15**, 879 (1961).

(28) *Ibid.*, **15**, 1130 (1961).

ACKNOWLEDGMENTS

The authors thank Dr. A. Brändström, AB Hässle, Mölndal, Sweden, for providing the physicochemical constants of Table IV and Mrs. Marie Hogan for performing the statistical analyses of the biological data.

Syntheses and Pharmacological Activity of *N*-Acyl-substituted Imidazolidinethiones and Thioimidazolines

JANICE H. ARCENEAUX *, HAROLD KOHN *x, MARIE LOUISE STEENBERG ‡, and JOSEPH P. BUCKLEY ‡x

Received May 26, 1977, from the **Department of Chemistry and the* ‡*College of Pharmacy, University of Houston, Houston, TX 77004.* Accepted for publication August 1, 1977.

Abstract □ A series of imidazolidinethiones and thioimidazolines was synthesized and tested for their effects on both forced and spontaneous motor activities as well as their ability to raise the convulsion threshold. The *N*-acyl-substituted 2-*p*-fluorobenzylthioimidazolines were the most active compounds, producing protection against maximal electroshock seizures and tonic convulsions induced by pentylenetetrazol. Both compounds had high LD_{50} values and safety indexes.

Keyphrases □ Imidazolidinethiones, substituted—synthesized, evaluated for CNS depressant and anticonvulsant activity □ Thioimidazolines, various—synthesized, evaluated for CNS depressant and anticonvulsant activity □ CNS depressant activity—evaluated in substituted imidazolidinethiones and various thioimidazolines □ Anticonvulsant activity—evaluated in substituted imidazolidinethiones and various thioimidazolines □ Structure–activity relationships—substituted imidazolidinethiones and various thioimidazolines evaluated for CNS depressant and anticonvulsant activity

An increasingly larger number of medicinal agents containing either the ureido (I) or the isoureido (II) moiety as part of their molecular framework have been developed recently (1–3). The syntheses and CNS depressant and anticonvulsant properties of a series of isomeric acyl-substituted imidazolidinethiones and thioimidazolines were described previously (4). Based on a limited number of compounds, the thioimidazolines examined all significantly prolonged the time for the onset of convulsions induced by maximal electroshock in male Swiss-Webster mice when compared to the isomeric imidazolidinethiones. To provide additional insight into the pharmacological properties of these two types of compounds, the thioimidazolines III–VI (5) and the imidazolidinethione VII were synthesized. In general, these compounds contain substituents that are more lipophilic in nature than those previously investigated (4).

The pharmacological data in the present report indicate

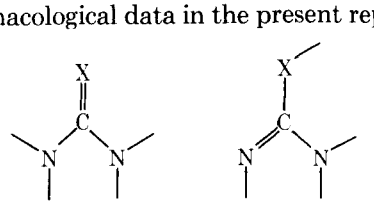

I II

corresponding hydrochloride, were prepared in concentrations of 10, 20, and 40 mg/ml. Acute intravenous or intraperitoneal toxicities were determined in female albino mice (Charles River CD random-bred). The results are estimates and should only be regarded as approximate LD_{50} values (Table VI).

Local Tissue Irritation (9)—Solutions were prepared containing 20 and 40 mg of the hydrochloride/ml (or equivalent amounts of other salts) in isotonic saline. Injections were made intradermally in female New Zealand White rabbits, and the effects were estimated from gross examination of the sites 24 hr after injection (Table VI).

REFERENCES

(1) B. H. Takman, G. Camougis, and N. M. Löfgren, *Acta Pharm. Suec.*, **6**, 373 (1969); *Chem. Abstr.*, **71**, 47999p (1969).

(2) N. Löfgren, "Studies on Local Anesthetics, Xylocaine®, A New Synthetic Drug," Haeggströms, Stockholm, Sweden, 1948, p. 25.

(3) G. H. Kronberg, R. S. Leard, and B. H. Takman, *J. Med. Chem.*, **16**, 739 (1973).

(4) L. I. Smith and W. W. Prichard, *J. Am. Chem. Soc.*, **62**, 778 (1940).

(5) B. Dofek and Č. Vrba, *Acta Fac. Pharm. Brun. Bratisl.*, **2**, 141 (1959).

(6) A. Brändström, *Acta Chem. Scand.*, **17**, 1218 (1963).

(7) N. Löfgren, "Studies on Local Anesthetics, Xylocaine®, A New Synthetic Drug," Haeggströms, Stockholm, Sweden, 1948, p. 95.

(8) G. Camougis and B. H. Takman, in "Methods in Pharmacology," vol. 1, A. Schwartz, Ed., Appleton-Century-Crofts, New York, N.Y., 1971, pp. 1–40.

(9) A. P. Truant, *Arch. Int. Pharmacodyn. Ther.*, **115**, 483 (1958).

(10) T. P. Carney, in "Medicinal Chemistry," vol. 1, C. M. Suter, Ed., Wiley, New York, N.Y., 1951, pp. 280–389.

(11) S. M. McElvain, *J. Am. Chem. Soc.*, **49**, 2835 (1927).

(12) P. P. Koelzer and K. H. Wehr, *Arzneim.-Forsch.*, **8**, 181 (1958).

(13) T. L. Jacobs, S. Winstein, R. B. Henderson, and E. C. Spaeth, *J. Am. Chem. Soc.*, **68**, 1310 (1946).

(14) J. B. Shoesmith and A. Mackie, *J. Chem. Soc.*, **1928**, 2334.

(15) W. E. Parham, E. L. Wheeler, R. M. Dodson, and S. W. Fenton, *J. Am. Chem. Soc.*, **76**, 5380 (1954).

(16) N. Löfgren, *Ark. Kemi Mineral. Geol.*, **22A** (18), 1 (1946).

(17) N. Löfgren and C. Tegnér, *Acta Chem. Scand.*, **9**, 493 (1955).

(18) A. Tigerstedt, *Chem. Ber.*, **25**, 2919 (1892).

(19) N. Löfgren and B. Lundqvist, *Sv. Kem. Tidskr.*, **58**, 206 (1946).

(20) D. M. Hall and E. E. Turner, *J. Chem. Soc.*, **1948**, 1909.

(21) L. Wessely, *Monatsh. Chem.*, **22**, 66 (1901).

(22) J. L. Green, Jr., and H. J. Hagemeyer, Jr., *J. Am. Chem. Soc.*, **77**, 3016 (1955).

(23) F. Nerdel, P. Weyerstahl, and U. Kretschmar, *Chem. Ber.*, **92**, 1329 (1959).

(24) E. Hofstetter and A. E. Wilder Smith, *Helv. Chim. Acta*, **36**, 1698 (1953).

(25) O. H. Wheeler, *J. Am. Chem. Soc.*, **78**, 3216 (1956).

(26) D. Gagnaire, *Bull. Soc. Chim. Fr.*, **1960**, 1813.

(27) E. Hultin, *Acta Chem. Scand.*, **15**, 879 (1961).

(28) *Ibid.*, **15**, 1130 (1961).

ACKNOWLEDGMENTS

The authors thank Dr. A. Brändström, AB Hässle, Mölndal, Sweden, for providing the physicochemical constants of Table IV and Mrs. Marie Hogan for performing the statistical analyses of the biological data.

Syntheses and Pharmacological Activity of *N*-Acyl-substituted Imidazolidinethiones and Thioimidazolines

JANICE H. ARCENEAUX *, HAROLD KOHN *x, MARIE LOUISE STEENBERG ‡, and JOSEPH P. BUCKLEY ‡x

Received May 26, 1977, from the **Department of Chemistry and the* ‡*College of Pharmacy, University of Houston, Houston, TX 77004.* Accepted for publication August 1, 1977.

Abstract □ A series of imidazolidinethiones and thioimidazolines was synthesized and tested for their effects on both forced and spontaneous motor activities as well as their ability to raise the convulsion threshold. The *N*-acyl-substituted 2-*p*-fluorobenzylthioimidazolines were the most active compounds, producing protection against maximal electroshock seizures and tonic convulsions induced by pentylenetetrazol. Both compounds had high LD_{50} values and safety indexes.

Keyphrases □ Imidazolidinethiones, substituted—synthesized, evaluated for CNS depressant and anticonvulsant activity □ Thioimidazolines, various—synthesized, evaluated for CNS depressant and anticonvulsant activity □ CNS depressant activity—evaluated in substituted imidazolidinethiones and various thioimidazolines □ Anticonvulsant activity—evaluated in substituted imidazolidinethiones and various thioimidazolines □ Structure–activity relationships—substituted imidazolidinethiones and various thioimidazolines evaluated for CNS depressant and anticonvulsant activity

An increasingly larger number of medicinal agents containing either the ureido (I) or the isoureido (II) moiety as part of their molecular framework have been developed recently (1–3). The syntheses and CNS depressant and anticonvulsant properties of a series of isomeric acyl-substituted imidazolidinethiones and thioimidazolines were described previously (4). Based on a limited number of compounds, the thioimidazolines examined all significantly prolonged the time for the onset of convulsions induced by maximal electroshock in male Swiss-Webster mice when compared to the isomeric imidazolidinethiones. To provide additional insight into the pharmacological properties of these two types of compounds, the thioimidazolines III–VI (5) and the imidazolidinethione VII were synthesized. In general, these compounds contain substituents that are more lipophilic in nature than those previously investigated (4).

The pharmacological data in the present report indicate

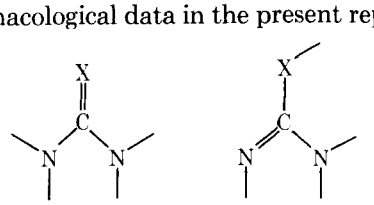

I II

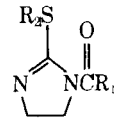

III: $R_1 = OCH_3$, $R_2 = CH_2CH{=}CH_2$
IV: $R_1 = CH_3$, $R_2 = CH_2CH{=}CH_2$
V: $R_1 = OCH_3$, $R_2 = CH_2C_6H_4$-*p*-F
VI: $R_1 = CH_3$, $R_2 = CH_2C_6H_4$-*p*-F

that V and VI afforded significant protection against maximal electroshock seizures and clonic convulsions induced by pentylenetetrazol in male Swiss-Webster mice.

EXPERIMENTAL

Melting points were determined with a melting-point apparatus[1] and are uncorrected. IR spectra[2] were calibrated against the 1601-cm^{-1} band of polystyrene. Proton NMR[3] spectra were taken in deuterochloroform, and values are reported in parts per million (δ) downfield from tetramethylsilane as the internal standard.

Preparation of *N*-Methoxycarbonyl-*N'*-phenylcarbamoylimidazolidinethione (VII)—To a stirred dimethoxyethane solution (50 ml) containing *N*-methoxycarbonylimidazolidinethione (VIII) (6) (1.00 g, 6 mmoles), 0.7 ml of phenyl isocyanate (6 mmoles) was slowly added (Scheme I). The solution was refluxed (120 hr) and then concentrated *in vacuo*. The white solid was reprecipitated from carbon tetrachloride–hexane in a yield of 1.60 g (96%), mp 164–165°; IR (KBr): 1740, 1690, and 1600 cm^{-1}; PMR: δ 3.94 (s, 3H), 3.95–4.20 (m, 4H), 7.05–7.66 (m, 5H), and 12.15–12.50 (broad s, 1H); mass spectrum[4]: *m/e* (relative intensity) 279 (22), 160 (98), 119 (100), 102 (26), and 72 (32).

Anal.[5]—Calc. for $C_{12}H_{13}N_2O_3S$: C, 51.60; H, 4.96; N, 15.04. Found: C, 51.45; H, 4.68; N, 15.00.

Pharmacology—Male rats[6], Wistar descendant, 150–200 g, were utilized for the gross observation studies. White male Swiss-Webster mice, 20–25 g, were used to investigate the effects of the compounds on forced and spontaneous motor activities and for anticonvulsant activity studies. The animals were initially acclimated to laboratory conditions for 3–4 days. The compounds were freshly prepared in a 5% polysorbate 80 suspension in 95% isotonic saline, and the volumes administered were 1 ml/kg ip for rats and 10 ml/kg ip for mice. The results that differed from control values at the $p < 0.05$ level (Student *t* test) were considered statistically significant.

The acute 24-hr intraperitoneal lethal dose was determined in mice using three dose levels, and the LD_{50} value was calculated using the method of Litchfield and Wilcoxon (7).

The effects of the compound on the gross behavior in rats were evaluated using a gross observation rating scale described by Watzman *et al.* (8) (Table I). The time course of drug effect was ascertained by checking items on the scale at 15 min prior to and 30, 60, 120, and 180 min following drug administration, with special emphasis on behavioral and autonomic effects. The effects of the compounds on forced and spontaneous motor activities were evaluated in mice utilizing a wooden rod (16-cm circumference), which was rotated at 4 rpm for the first 30 sec, at 6 rpm during the next 30 sec, and at progressively increasing speeds thereafter at 30-sec intervals (maximum 50 rpm) until the mouse fell off the rod.

Six animals were tested simultaneously and were given four trials, with two spaced 4–6 hr apart, on each of 2 consecutive days. The fourth trial was preceded by an interval of 50 min for the administration of the vehicle or one experimental compound. The drug or placebo effect for each animal was computed as a ratio of performance time on the fourth trial divided by performance time on the third trial.

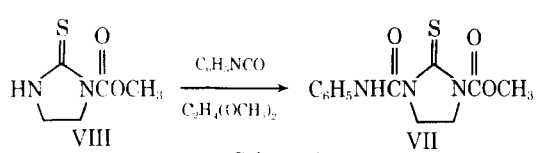

Scheme I

[1] Thomas-Hoover.
[2] Perkin-Elmer models 700 and 237B.
[3] Varian T-60.
[4] Hitachi Perkin-Elmer RMU-5H.
[5] Spang Microanalytical Laboratories.
[6] Texas Inbred, Houston, Tex.

Table I—Effect of Selected Imidazolidinethiones and Thioimidazolines on Gross Observation in Rats

Compound	Dose, mg/kg ip	Body Temperature	Pupil Size, mm	Respiration, breaths/min	Heart Rate, beats/min
III	Control	37.0°	5.0	120.0	440
	40	36.4°	5.8	90.8	345
IV	Control	38.5°	6.0	144.0	440
	40	37.0°	4.0	77.0	328
V	Control	39.0°	5.0	134.3	440
	400	37.8°	4.5	111.6	387
VI	Control	39.0°	5.0	171.4	512
	120	37.3°	3.4	92.7	350
VII	Control	39.0°	5.0	150.0	440
	400	38.9°	4.3	125.3	420

Table II—Effects of Selected Imidazolidinethiones and Thioimidazolines on Spontaneous and Forced Motor Activities in Mice

		Spontaneous Motor Activity		Forced Motor Activity	
Compound	Dose, mg/kg ip	Drug Treated, Mean ± *SE* (for 15 min)	Percent of Control	Drug Treated, Mean, sec ± *SE*	Percent of Control
III	5	277.3 ± 32.83	81	203.3 ± 13.84	121
	10	410.0 ± 89.03	69	152.8 ± 28.87	91
	20	204.3 ± 76.20	34[a]	143.1 ± 22.60	70
IV	5	687.0 ± 110.94	81	157.4 ± 18.27	93
	10	574.3 ± 53.00	68	132.4 ± 19.24	79
	20	387.3 ± 63.43	46[a]	117.4 ± 21.15	70
V	100	175.0 ± 26.46	50[a]	161.8 ± 13.41	90
	200	40.3 ± 12.39	12[a]	114.9 ± 18.73	64[a]
	400	29.0 ± 6.66	8[a]	49.2 ± 31.43	27[a]
VI	30	110.0 ± 53.36	57	117.2 ± 21.98	57[a]
	60	77.7 ± 21.67	40[a]	58.5 ± 13.13	28[a]
	120	28.0 ± 6.11	15[a]	23.9 ± 9.50	12[a]
VII	100	476.3 ± 119.27	92	129.8 ± 23.83	67[a]
	200	229.0 ± 62.07	44	84.4 ± 22.79	43[a]
	400	64.0 ± 19.66	12[a]	113.8 ± 28.54	58[a]
Phenytoin	5	679.0 ± 133.27	62	148.8 ± 11.62	68
	10	560.0 ± 32.58	51[a]	147.0 ± 6.84	67
	20	426.7 ± 57.51	39[a]	118.0 ± 21.87	54[a]

[a] $p < 0.05$.

The effects of the compounds on spontaneous motor activity in mice were determined using three photocell cages[7] (Table II). Two animals, treated with identical doses of the same compound, were placed in each of two photocell cages 50 min after drug administration; a 15-min count was initiated 5 min after the animals were placed in the cages. To negate the differences in sensitivity among units, each dose was tested in a factorial design in each of the three activity cages. Control animals were tested simultaneously at the same time intervals after administration of an equal volume of vehicle, and the ED_{50} value of each compound (defined as the dose that decreased the level of performance to 50% of the control scores) was calculated.

Anticonvulsant activity was investigated in mice. The effects of the compounds on convulsions and death produced by pentylenetetrazol (100 mg/kg sc) and strychnine sulfate (2 mg/kg ip) were investigated as described by Watzman *et al.* (8); the effects on maximal electroshock seizure were investigated as described by Swinyard *et al.* (9).

RESULTS AND DISCUSSION

Chemistry—The syntheses and spectral properties of the thioimidazolines III–VI were described previously (5). The molecular structure assigned to VII was the *N,N'*-disubstituted product rather than the isomeric *N,S*-disubstituted thioimidazoline. Support for this assignment is based on a satisfactory correlation of the spectral properties (NMR and IR) observed for VII with those absorptions previously identified as characteristic peaks for the imidazolidinethione ring system (5). In addition, a significant feature was noted in the mass spectral fragmentation pattern (ionization voltage = 70 ev) for VII. A discernible parent peak

[7] Woodard Research Corp.

Table III—LD_{50}, ED_{50}, and Safety Index Values for Selected Imidazolidinethiones and Thioimidazolines

Compound	LD_{50}^{24}, mg/kg ip	ED_{50}[a], mg/kg ip	Safety Index (LD_{50}/ED_{50})
III	88	14.8	5.9
IV	96	13.9	6.9
V	>1000	95.1	>10.5
VI	658	45.7	14.4
VII	>1000	190.1	>5.3
Phenytoin[b]	200	10.7	18.7

[a] Calculated from spontaneous motor activity, Table II. [b] Reference 4.

at *m/e* 279 was detected along with two characteristic fragments at P − 119 and P − 177. This pattern can be rationalized in terms of two successive McLafferty-type rearrangements of the starting molecular ion (5).

Pharmacological Evaluation—Male Wistar rats were utilized for the gross observation studies. White male Swiss-Webster mice were used to investigate the effects of III–VII on forced and spontaneous motor activities, as well as their ability to alter the threshold for convulsive seizures. The acute 24-hr intraperitoneal lethal dose effects were also determined in mice. The intraperitoneal doses used in the spontaneous and forced motor activity studies were: III and IV, 5, 10, and 20 mg/kg; V and VII, 100, 200, and 400 mg/kg; and VI, 30, 60, and 120 mg/kg. The doses used in the anticonvulsant studies were: V–VII, the same as in the activity studies; and III and IV, 10, 20, and 40 mg/kg. The highest doses indicated were used for the gross observation studies in rats.

All five compounds investigated in the gross observation studies did produce ptosis and decrease the startle response and grip strength. As Table I shows, the compounds also decreased body temperature, respiration, and heart rate. Compound VI was the most effective of the five compounds, producing a 78-breaths/min decrease in respiration, a 1.7° decrease in body temperature, a 162-beats/min decrease in heart rate, and a 1.6-mm decrease in pupil size. Compound VII was the least active of the five compounds.

The most toxic compounds examined were III and IV (Table III). Compounds V and VII had LD_{50} values greater than 1000 mg/kg ip, whereas III, IV, and VI had LD_{50} values of 88, 96, and 6.6 mg/kg ip, respectively (Table III). The ED_{50} value (calculated from spontaneous motor activity data) was highest for VII and lowest for IV (Table III). The safety indexes (LD_{50}/ED_{50}) determined were: III, 14.8; IV, 13.9; and VI, 14.4. Since V and VII had LD_{50} values greater than 1000 mg/kg, the precise safety index could not be determined.

All five compounds decreased both spontaneous and forced motor activities (Table II). The effects of III–VI were dose dependent in both tests; the effects of VII were dose dependent only in the spontaneous motor activity studies. Compounds III and IV, however, did have their maximum effect at 20 mg/kg; when the dose was increased to 40 mg/kg, the decrease in activity was less than the one produced by 20 mg/kg.

Table IV—Effects of Selected Thioimidazolines and Phenytoin on Convulsion Induced by Pentylenetetrazol (100 mg/kg sc)

Compound	Dose, mg/kg ip	Onset of Convulsion, sec ± *SE*	Percent Protected
V	0	747.2 ± 19.69[a]	0
	100	871.0 ± 88.98	0
	200	1390.3 ± 281.11[b]	0
	400	3710.0 ± 656.43[b]	70
VI	0	657.5 ± 36.11[a]	0
	30	750.1 ± 46.13[b]	0
	60	844.0 ± 28.35[b]	0
	120	969.0 ± 47.71[b]	0
	240	3565.0 ± 1820.00[b]	80
Phenytoin	0	475.09 ± 28.70[a]	0
	5	581.0 ± 46.33	0
	10	440.4 ± 24.24	0
	20	554.6 ± 13.90	0

[a] Timed for clonic convulsion, since drug-treated animals did not go into tonic convulsion. [b] $p < 0.05$.

Table V—Effects of Selected Thioimidazolines and Phenytoin on Convulsion Induced by Electroshock (60 mamp, 0.2 sec)

Compound	Dose, mg/kg ip	Onset of Convulsion, sec ± *SE*	Percent Protected
V	0	1.92 ± 0.17	0
	100	1.96 ± 0.17	0
	200	2.42 ± 0.14	0
	400	3.32 ± 0.20[a]	60
VI	0	1.18 ± 0.05	0
	30	2.01 ± 0.10	0
	60	2.10 ± 0.12[a]	0
	120	3.03 ± 0.19[a]	30
	240	4.53 ± 0.24[a]	70
Phenytoin	0	1.17 ± 0.06	0
	5	2.64 ± 0.17[a]	0
	10	5.00 ± 0.00[a]	80
	20	—	100

[a] $p < 0.05$.

The anticonvulsant studies showed that none of the compounds protected against strychnine convulsions. Table IV shows that at 400 mg/kg ip, V protected 70% of the mice from tonic convulsions and death induced by pentylenetetrazol; at 200 mg/kg ip, V did not protect the animals from death, but the onset of time of convulsion was significantly prolonged. Compound VI produced almost the same results as V; 120 mg/kg ip did not protect the animals, but the onset of time of convulsion was significantly prolonged; 240 mg/kg protected 80% of the animals from convulsion and death. Only V and VI produced protection against maximal electroshock seizures (Table V).

Phenytoin was tested for its effect on convulsions induced by strychnine, pentylenetetrazol, and maximal electroshock seizures to compare the effect of a known anticonvulsant with the five compounds investigated. Although a previous investigation (4) demonstrated that phenytoin decreased spontaneous motor activity without affecting forced motor activity, it decreased both spontaneous and forced motor activities by 61 and 46%, respectively, in the present study. The LD_{50}, ED_{50}, and safety index values are recorded in Table III.

Phenytoin (Table V) protected against maximal electroshock seizures at 10 and 20 mg/kg ip but did not show any protection against convulsions induced by strychnine or pentylenetetrazol (Table IV).

Compounds V and VI were the most active compounds with high LD_{50} and safety index values; both produced protection against maximal electroshock seizures and pentylenetetrazol. Both compounds are thioimidazolines with a *p*-fluorophenylmethylene substituent not found in any other compound, suggesting the importance of this link on a thioimidazoline for producing anticonvulsant activity.

REFERENCES

(1) W. T. Comer and A. W. Gomoll, in "Medicinal Chemistry," 3rd ed., part II, A. Burger, Ed., Wiley–Interscience, New York, N.Y., 1970, chap. 39, p. 1019.

(2) J. N. Delgado and E. I. Isaacson, in *ibid.*, chap. 52, p. 1386.

(3) A. Krentzberger, *Prog. Drug Res.*, **11**, 356 (1968).

(4) H. Kohn, B. A. Kohn, M. L. Steenberg, and J. P. Buckley, *J. Med. Chem.*, **20**, 158 (1977).

(5) H. Kohn, M. J. Cravey, J. H. Arceneaux, R. L. Cravey, and M. R. Willcott, III, *J. Org. Chem.*, **42**, 941 (1977).

(6) H. Kohn, *J. Am. Chem. Soc.*, **98**, 3690 (1976).

(7) J. T. Litchfield and F. J. Wilcoxon, *J. Pharmacol. Exp. Ther.*, **96**, 99 (1949).

(8) N. Watzman, A. A. Manian, H. Barry, III, and J. P. Buckley, *J. Pharm. Sci.*, **57**, 2089 (1968).

(9) E. Swinyard, W. Brown, and L. Goodman, *J. Pharmacol. Exp. Ther.*, **106**, 319 (1952).

ACKNOWLEDGMENTS

Supported by National Institutes of Health Grants GM 21790 and MH 25336.

Preliminary Pharmacokinetic Model of Pilocarpine Uptake and Distribution in the Eye

KENNETH J. HIMMELSTEIN *, IBRAHIM GUVENIR *, and THOMAS F. PATTON ‡x

Received April 5, 1977, from the *Department of Chemical and Petroleum Engineering and the ‡Department of Pharmaceutical Chemistry, University of Kansas, Lawrence, KS 66045. Accepted for publication August 3, 1977.

Abstract □ A pharmacokinetic model that permits prediction of aqueous humor pilocarpine levels following topical application to rabbit eyes was developed. The model is able to account for changes in both instilled solution volume and drug concentration. The model, although simplified, relies mainly on experimentally verifiable and independently measured parameters. Its utility lies in its ability to account quantitatively for the large drainage loss of instilled drug solutions and its predictive ability regardless of the instilled volume or concentration. The framework established by this model will allow further sophistication as more experimental data become available and should be adaptable to other ophthalmic drugs.

Keyphrases □ Pilocarpine—uptake and distribution in rabbit eye, preliminary pharmacokinetic model □ Pharmacokinetics—preliminary model of uptake and distribution of pilocarpine in rabbit eye □ Models, pharmacokinetic—developed for uptake and distribution of pilocarpine in rabbit eye □ Cholinergics, ophthalmic—pilocarpine, uptake and distribution in rabbit eye, preliminary pharmacokinetic model

The large drainage loss of instilled solutions can account for the relatively poor bioavailability of ophthalmic drugs (1), but other precorneal factors also are important in the disposition of topically applied ophthalmic drugs (2). The cornea, through which ophthalmic drugs must pass to reach the eye interior, is a complex membrane presenting several barriers to drug penetration (3–9). In spite of this knowledge, few systematic pharmacokinetic studies have been reported that permit a degree of predictability of the distribution of ophthalmic drugs under various dosing conditions.

BACKGROUND

Pilocarpine is an important ophthalmic drug and has been studied extensively (2, 9–23). Pilocarpine uptake into the rabbit eye is a complex combination of transport away from the cornea by an accentuated flow mechanism, uptake by various tissues, transport through the cornea, and distribution and elimination from the aqueous humor. Each component may be composed of, and/or supplemented by, other less important but still measurable phenomena such as diffusion away from the cornea and eye by transport through the conjunctiva, drug distribution to other tissues from the aqueous humor itself, and increased tear production and drainage rate of pilocarpine from the eye surface. Finally, protein binding in all compartments may affect free pilocarpine transport.

Data for these phenomena will be developed in the future; however, initially, the overall uptake of pilocarpine in the eye is examined to ascertain the major parameters contributing to the relatively small total uptake of topically applied pilocarpine. For that reason, a mathematical model described here, while simplifying somewhat the actual situation, will be a useful framework for future investigations of pilocarpine distribution, uptake, and elimination from the eye.

Although Makoid (24) recently considered a classical pharmacokinetic approach for pilocarpine distribution in the eye, his model did not consider the effects of instilled drop size on pilocarpine uptake. The uniqueness of the proposed model is that it is able to predict the effects of instilled drop size and concentration such that reasonable *a priori* predictions of aqueous humor pilocarpine levels can be made. It is hoped that this model will provide the framework for a more comprehensive model for pilocarpine as well as other drugs as more experimental data become available.

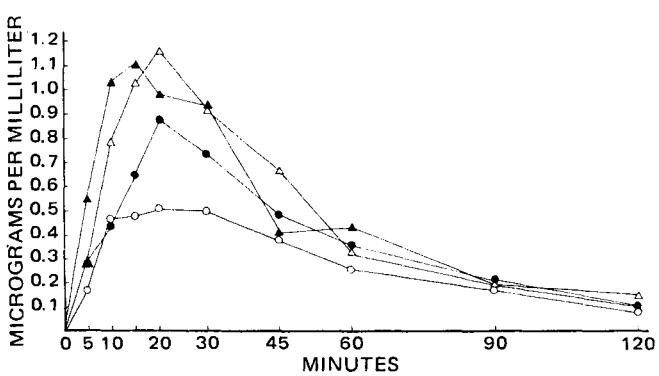

Figure 1—*Aqueous humor concentration–time profiles for pilocarpine nitrate following instillation of 5 (○), 10 (●), 15 (△), and 25 (▲) μl of a 1 × 10^{-2} M solution in rabbits.*

EXPERIMENTAL

Materials—Pilocarpine nitrate was obtained commercially[1] and used as received. Tritiated pilocarpine[2] (specific activity 4.1 Ci/mmole) in ethanol solution was evaporated several times prior to use as previously described (13) to remove any solvent that had become tritiated by exchange.

Male albino rabbits, 60–67 days old, were maintained in standard laboratory animal cages and allowed food and water *ad libitum*.

Computer calculations were performed on a digital computer[3].

Solution Preparation—Pilocarpine nitrate solutions were prepared in pH 6.24 isotonic Sorensen's phosphate buffer and were filtered but not sterile. Procedures for the preparation of tritiated solutions were described previously (13). Solutions were prepared fresh and kept for a maximum of 12 hr.

Aqueous Humor Pilocarpine Concentration–Time Profiles—During the experiments, test animals were kept in restraining boxes in the normal upright position. The head was unencumbered so that all normal eye movements were maintained. Rabbits were unanesthetized in all cases. Accurate volumes of solutions were instilled in rabbit eyes

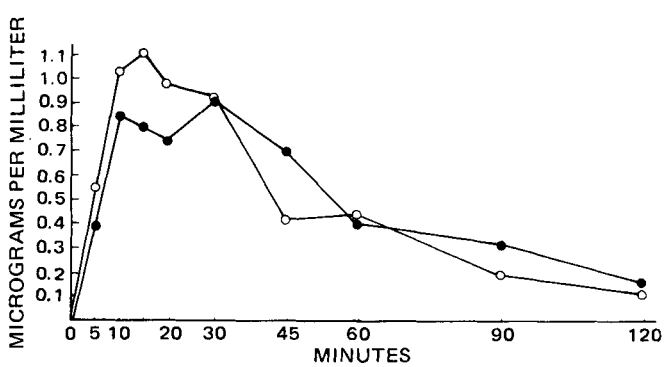

Figure 2—*Aqueous humor concentration–time profiles for pilocarpine nitrate following instillation of 25 μl of a 1 × 10^{-2} M solution (○) and 5 μl of a 1.61 × 10^{-2} M solution (●) in rabbits.*

[1] Sigma Chemical Co., St. Louis, Mo.
[2] New England Nuclear, Boston, Mass.
[3] Honeywell 66/60 at the University of Kansas Computation Center.

Table I—Calculated Areas under Aqueous Humor Concentration–Time Profiles for 25 μl of 1×10^{-2} *M* and for 5 μl of 1.61×10^{-2} *M* Pilocarpine Nitrate in 60-Day-Old Rabbits

Volume Instilled, ml	Concentration Instilled, *M*	Amount of Drug Instilled, μg	*AUC*, μg min/ml
0.025	1.00×10^{-2}	67.82	60.9
0.005	1.61×10^{-2}	21.87	67.2

using a microliter syringe[4]. During instillation, the lower eyelid was pulled slightly away from the globe but was returned to its normal position immediately after instillation.

At various times postinstillation (5, 10, 15, 20, 30, 45, 60, 90, and 120 min), rabbits were sacrificed with an overdose of pentobarbital sodium injected into a marginal ear vein. Eyes were immediately rinsed with distilled water and blotted with tissue, and aqueous humor was aspirated from the anterior chamber. At least 100 μl of aqueous humor was removed in each case. It is important that the elapsed time from animal sacrifice to removal of the aqueous humor sample be as short as possible. In these studies, the time period needed to sacrifice the animal and obtain aqueous humor from both eyes was less than 1 min.

Aqueous humor, 100 μl, was transferred[5] to a scintillation vial[6] containing 5 μl of prerefrigerated liquid scintillation cocktail[7]. After storage in the dark at room temperature for at least 24 hr, samples were counted[8]. Counts were then converted to micrograms of pilocarpine per milliliter of aqueous humor using suitable standard and blank corrections.

Aqueous humor concentration profiles for 5-, 10-, 15-, and 25-μl instilled volumes of 1×10^{-2} *M* pilocarpine were reported previously (25). Since these profiles were used to check the validity of the described pharmacokinetic model, they are reproduced in Fig. 1[9].

From the previous study (25), it was concluded that a considerable decrease in instilled volume coupled with a slight increase in instilled concentration should result in the same amount of drug reaching the eye interior as if much larger volumes were administered. By using a simple calculation, it was shown (25) that a 5-μl dose of 1.61×10^{-2} *M* pilocarpine nitrate should result in the same area under the curve as a 25-μl dose of 1.00×10^{-2} *M* pilocarpine nitrate. This experiment was performed, and the profiles are illustrated in Fig. 2. By using the trapezoidal rule with extrapolation to infinity, the areas under these two profiles were calculated (Table I).

MODEL

Development—The eye is viewed here as consisting of two major compartments. The first compartment represents the precorneal area. Its initial volume consists of the normal resident tear volume plus the volume of the instilled drop. There is a constant production and outflow

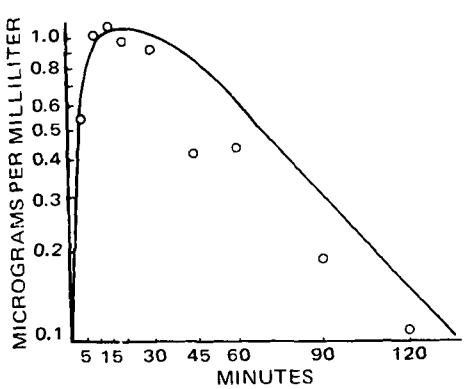

Figure 3—*Comparison of model-predicted (—) and experimental (○) aqueous humor concentrations following instillation of 25 μl of 1×10^{-2} M pilocarpine in rabbits.*

[4] Hamilton Co., Reno, Nev.
[5] Biopette, Schwarz/Mann, Orangeburg, N.Y.
[6] Mini vials, ICN, Isotope and Nuclear Division, Cleveland, Ohio.
[7] Aquasol, New England Nuclear, Boston, Mass.
[8] Beckman LS-150 liquid scintillation counter, Beckman Instruments, Fullerton, Calif.
[9] For clarity, standard error bars have been omitted. These values are reported in Ref. 25. Each point represents the mean of at least eight determinations.

Table II—Parameters Important to the Pharmacokinetic Model

Parameter	Value	Reference
V_0	7.5 μl	1
V_{AH}	311 μl	26
Q_T	0.66 μl/min	1
K	$(0.25 + 0.0113\ V_D)\ \text{min}^{-1}$	1
A	2 cm^2	26
L	0.035 cm	26
K_D	3.675×10^{-4} μl/cm min	
K_{el}	7.5 μl/min	

of tears from this compartment, and the drainage of instilled fluid is a function of drop size (1).

The second compartment represents the aqueous humor, which received pilocarpine by diffusion through the cornea. Various elimination mechanisms from the aqueous humor are lumped together into a single first-order elimination term. Although more mechanistic studies are in progress and some have been reported (9), this preliminary model views the cornea as a single homogeneous structure. In addition, no loss from the precorneal area by conjunctival absorption is included (2). A schematic representation of the model is shown in Scheme I.

The volume of fluid initially present in the precorneal area is a variable that depends on the size of the instilled pilocarpine drop. A flow balance (Eq. 1) is made where it is assumed that the densities of the tear fluid and drug solutions are those of water. It is also assumed that the amount of pilocarpine diffusing through the cornea does not significantly affect the tear fluid volume:

$$\begin{matrix}\text{rate of} \\ \text{change} \\ \text{in fluid} \\ \text{volume}\end{matrix} = \begin{matrix}\text{rate of} \\ \text{flow in}\end{matrix} - \begin{matrix}\text{rate of} \\ \text{flow out}\end{matrix} \qquad \text{(Eq. 1)}$$

Equation 2 shows the representation of the flow balance for pilocarpine in tear fluid:

$$\frac{dV_T}{dt} = Q_T - [Q_T + K(V_T - V_0)] \qquad \text{(Eq. 2)}$$

at $t = 0$ and $V_T = V_D + V_0$ and where V_T is the total volume in the precorneal area at any given time, T; Q_T is the normal tear production rate; K is a proportionality constant that is a function of the instilled drop size, V_D(1); and V_0 is the normal resident tear volume. The expression assumes that the tear production rate is not significantly altered by the instilled fluid. The drainage out of the eye is basically that which would normally occur plus a term that is proportional to the actual volume present less the amount normally there.

This differential equation can be solved directly and analytically, noting that at the instillation time the total drop volume is equal to the volume of tears normally there plus the instilled drop size. Solving the expression yields Eq. 3, which represents the total volume of the eye fluid as a function of time:

$$V_T = V_D e^{-Kt} + V_0 \qquad \text{(Eq. 3)}$$

This expression is identical to that derived previously (1).

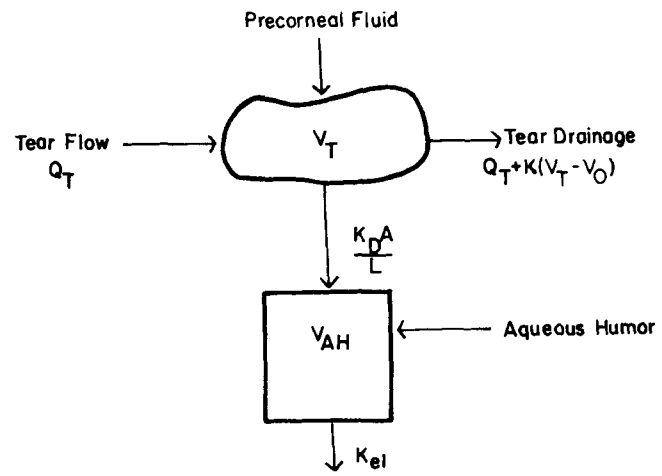

Scheme I

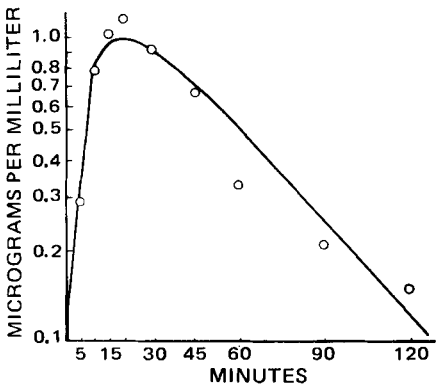

Figure 4—*Comparison of model-predicted (—) and experimental (O) aqueous humor concentrations following instillation of 15 μl of 1 × 10^{-2} M pilocarpine in rabbits.*

A mass balance is now written for pilocarpine in the tear fluid:

$$\begin{array}{l}\text{rate of}\\ \text{change in}\\ \text{mass in}\\ \text{tear fluid}\end{array} = \begin{array}{l}\text{rate of}\\ \text{transfer in}\\ \text{by flow}\end{array} - \begin{array}{l}\text{rate of}\\ \text{loss by}\\ \text{drainage}\end{array} - \begin{array}{l}\text{rate of}\\ \text{loss by}\\ \text{diffusion into}\\ \text{aqueous humor}\end{array} \quad \text{(Eq. 4)}$$

or, mathematically:

$$\frac{dV_TC_T}{dt} = 0 - [Q_T + K(V_T - V_0)]C_T - \frac{K_DA}{L}(C_T - C_{AH}) \quad \text{(Eq. 5)}$$

where C_T is the concentration in the tear fluid, K_D is the specific permeability rate, A is the cornea area, L is the cornea thickness, and C_{AH} is the concentration in the aqueous humor.

By taking the indicated derivative and substituting the value of V_T found into this expression, a simplified relationship results:

$$\frac{dC_T}{dt} = \frac{-Q_TC_t - \frac{K_DA}{L}(C_T - C_{AH})}{V_De^{-Kt} + V_0} \quad \text{(Eq. 6)}$$

This expression assumes that there is no appreciable loss into the conjunctiva and that the diffusion into the aqueous humor is linear. Finally, a similar mass balance is written for the aqueous humor compartment:

$$V_{AH}\frac{dC_{AH}}{dt} = \frac{K_DA}{L}(C_T - C_{AH}) - K_{el}C_{AH} \quad \text{(Eq. 7)}$$

where V_{AH} is the aqueous humor volume and K_{el} is the lumped first-order clearance parameter from the aqueous humor. Equations 6 and 7 can be solved numerically relatively easily, despite their involved nature, by the use of a digital computer.

To be able to evaluate the results of the model, certain parameters must be estimated. Table II lists the various parameters and the sources of these data. The instilled drop size of the pilocarpine solution is a variable quantity. Finally, the initial pilocarpine concentration is given by:

$$C_0 = \frac{V_DC_D}{V_D + V_0} \quad \text{(Eq. 8)}$$

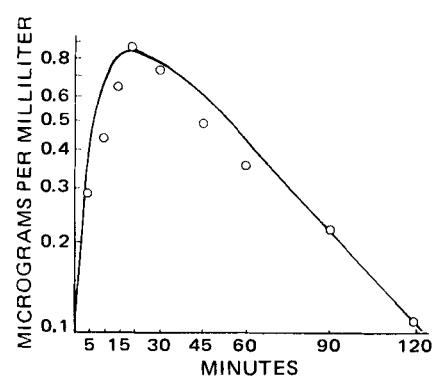

Figure 5—*Comparison of model-predicted (—) and experimental (O) aqueous humor concentrations following instillation of 10 μl of 1 × 10^{-2} M pilocarpine in rabbits.*

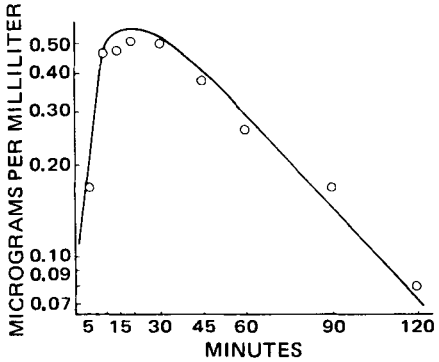

Figure 6—*Comparison of model-predicted (—) and experimental (O) aqueous humor concentrations following instillation of 5 μl of 1 × 10^{-2} M pilocarpine in rabbits.*

where C_D is the pilocarpine concentration in the instilled fluid. Thus, all parameters are measured, except the quantities K_D and K_{el}, which are estimated by applying the model to the data from an experiment where 15 μl of 1.00 × 10^{-2} M pilocarpine solution is instilled and then monitoring the aqueous humor concentration as a function of time. Thus, these two parameters are measured by experiment and evaluated in terms of the model. All of the other parameters are estimated from independent experiments.

Applications—Figures 3–6 show the results of the model applied to four different drop sizes of 1 × 10^{-2} M pilocarpine instilled into rabbit eyes. The model demonstrates that the aqueous humor pilocarpine concentration can be predicted reasonably well (r = 0.82 for the 15-μl instilled volume) over a range of instilled volumes. This result indicates that the drainage mechanism, which this model accounts for, is very important in explaining ultimate aqueous humor drug concentrations. The results are relatively poor at times greater than 1 hr, especially for a 25-μl drop, because of the lack of inclusion of a surrounding tissue of distribution (*i.e.*, the lens) in the model. This factor will be included as data become available. The present results certainly indicate the importance of precorneal considerations. The model is, however, deficient in its treatment of drug transport in the eye interior. Nevertheless, the results are good in terms of peak height and general trends for all drop sizes compared to the 15-μl base experiment, although the fit is not excellent in a least-squares sense.

In addition, as speculated previously (25), the model indicates that considerable reduction in drop size coupled with slight increases in drug concentration can permit dosage reduction without sacrifice of drug concentration in the eye interior. This situation is demonstrated in Fig. 7, which shows the results of an experiment where 25 μl of 1 × 10^{-2} M pilocarpine was instilled compared to an experiment where 5 μl of 1.61 × 10^{-2} M pilocarpine was instilled. The instilled volume was reduced by a factor of five and the overall dose of pilocarpine was reduced by about 70% without appreciable sacrifice of drug concentration in the aqueous humor. Figure 7 also shows that the model predicts these data reasonably well.

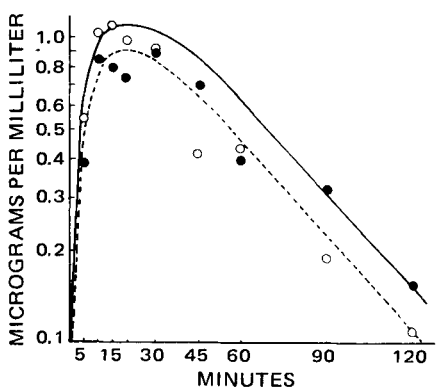

Figure 7—*Aqueous humor concentration–time profiles following instillation of 25 μl of 1 × 10^{-2} M pilocarpine (O, experimental data; and —, model prediction) and 5 μl of 1.61 × 10^{-2} M pilocarpine (●, experimental data; and - - -, model prediction).*

DISCUSSION

The data in Fig. 1 show that, for a constant instilled concentration, aqueous humor levels decrease as the instilled volume is decreased. However, aqueous humor drug levels do not decrease in proportion to dose size. For example, decreasing the instilled volume from 25 to 5 μl, a fivefold dosage reduction, results in only about a twofold reduction in the area under the curve of aqueous humor concentration *versus* time. Previous attempts at quantitation of pilocarpine uptake and distribution could not have predicted such an occurrence since available data on tear and instilled solution drainage were not quantitatively considered (1). The model developed here takes this factor into account and is, therefore, able to make reasonable predictions even when instilled volume and/or concentration are altered.

As has been mentioned, the data from Fig. 1 imply that a considerable decrease in instilled volume coupled with a slight increase in instilled concentration should result in the same amount of drug reaching the eye interior as if much larger volumes were administered. The data of Fig. 2 confirm this result, and Fig. 7 shows that the model also predicts it. It is confirmed that the model is sensitive to changes in both instilled volume and/or concentration. Such predictive capability has not previously been available.

Although the mathematics presented here are a simplification of the actual situation, the framework is now available that will allow refinement and addition of more sophisticated experimental data as they become available. Specifically, conjunctival absorption, protein binding, tissue distribution, and more mechanistic data on corneal absorption are needed. As such information becomes available, the treatment presented here can be refined to quantitate it. Furthermore, once all relevant parameters have been identified, the model should lend itself to quantitation of other ophthalmic drugs in addition to pilocarpine.

REFERENCES

(1) S. S. Chrai, T. F. Patton, A. Mehta, and J. R. Robinson, *J. Pharm. Sci.*, **62**, 1112 (1973).

(2) T. F. Patton and J. R. Robinson, *ibid.*, **65**, 1295 (1976).

(3) H. Benson, *Arch. Ophthalmol.*, **92**, 313 (1974).

(4) C. Dohlman, *Invest. Ophthalmol.*, **10**, 383 (1971).

(5) K. C. Swan and N. G. White, *Am. J. Ophthalmol.*, **25**, 1043 (1942).

(6) A. Kupferman, M. V. Pratt, K. SucKewer, and H. M. Leibowitz, *Arch. Ophthalmol.*, **91**, 373 (1974).

(7) A. Tonjum, *Acta Ophthalmol.*, **52**, 560 (1974).

(8) T. Iwata, M. Uyama, and K. Ohkawa, *Jpn. J. Ophthalmol.*, **19**, 139 (1975).

(9) J. Sieg and J. R. Robinson, *J. Pharm. Sci.*, **65**, 1816 (1976).

(10) D. H. Abramson, J. Coleman, M. Forbes, and L. A. Franzen, *Arch. Ophthalmol.*, **87**, 615 (1972).

(11) D. H. Abramson, S. Chang, and D. J. Coleman, *ibid.*, **94**, 914 (1976).

(12) P. C. Barsam, *Am. J. Ophthalmol.*, **73**, 742 (1972).

(13) S. S. Chrai and J. R. Robinson, *ibid.*, **77**, 735 (1974).

(14) P. P. Ellis, *Surv. Ophthalmol.*, **16**, 165 (1971).

(15) T. S. Friedman and T. F. Patton, *J. Pharm. Sci.*, **65**, 1095 (1976).

(16) K. Green and S. J. Downs, *Arch. Ophthalmol.*, **93**, 1165 (1975).

(17) L. S. Harris, T. W. Mittag, and M. A. Galin, *ibid.*, **86**, 1 (1971).

(18) D. L. Krohn and J. M. Breitfeller, *Invest. Ophthalmol.*, **13**, 312 (1974).

(19) R. Lazare and M. Horlington, *Exp. Eye Res.*, **21**, 281 (1975).

(20) F. J. Macri and J. J. Cevario, *Invest. Ophthalmol.*, **13**, 617 (1974).

(21) D. A. Newsome and R. Stern, *Am. J. Ophthalmol.*, **77**, 918 (1974).

(22) M. C. VanHoose and F. E. Leaders, *Invest. Ophthalmol.*, **13**, 377 (1974).

(23) T. F. Patton, Ph.D. thesis, University of Wisconsin, Madison, Wis., 1975.

(24) M. C. Makoid, Ph.D. thesis, University of Wisconsin, Madison, Wis., 1976.

(25) T. F. Patton, *J. Pharm. Sci.*, **66**, 1058 (1977).

(26) "The Rabbit in Eye Research," J. H. Prince, Ed., Charles C Thomas, Springfield, Ill., 1964.

ACKNOWLEDGMENTS

Supported by grants from the University of Kansas General Research Fund and the Children's Eye Care Foundation (CECF-RF-1976–77) and by University of Kansas Biomedical Sciences Support Grant RR-07037.

The authors are grateful to Mr. Ted S. Friedman for technical assistance.

Kinetics of Drug Transport and Concurrent Metabolism in Human Cell Cultures I: Theory

H. Y. ANDO *, N. F. H. HO, W. I. HIGUCHI ˣ, and C. SHIPMAN, Jr.

Received October 27, 1976, from the *College of Pharmacy, University of Michigan, Ann Arbor, MI 48104.* Accepted for publication April 28, 1977.

*Present address: Philadelphia College of Pharmacy and Science, Philadelphia, PA 19104.

Abstract □ A method for evaluating the passive permeability and single-step metabolism of drugs in suspension cultures of mammalian cells was formulated assuming linear kinetics. It was assumed that the metabolizing enzymes are driven by endogenous substrates present in steady-state quantities. The presence of the drug in radiolabeled tracer quantities was assumed to cause only a small perturbation from the endogenous steady-state operating point. The time course solutions for the drug and its metabolite are given in terms of macroscopic constants, and their physical interpretations are given in terms of metabolic and transport parameters.

Keyphrases □ Drug transport kinetics—evaluated in suspension cultures of mammalian cells, equations derived □ Metabolism, single step—evaluated for drugs in suspension cultures of mammalian cells, equations derived □ Kinetics—drug transport and concurrent metabolism in suspension cultures of mammalian cells, equations derived

The study of drug kinetics at the cellular level represents a microcosm of the traditional field of pharmacokinetics. Such a study, which includes cellular absorption, elimination, and metabolism *in vitro*, might be regarded as academic and possibly not as relevant as clinical studies *in vivo*. However, the ultimate resolution of the cancer problem and certain persistent viral infections may depend on knowledge of chemotherapy and kinetics at the cellular level. If the tumor problem is epigenetic and potentially reversible, as some investigators believe (1), then the ab-

DISCUSSION

The data in Fig. 1 show that, for a constant instilled concentration, aqueous humor levels decrease as the instilled volume is decreased. However, aqueous humor drug levels do not decrease in proportion to dose size. For example, decreasing the instilled volume from 25 to 5 μl, a fivefold dosage reduction, results in only about a twofold reduction in the area under the curve of aqueous humor concentration *versus* time. Previous attempts at quantitation of pilocarpine uptake and distribution could not have predicted such an occurrence since available data on tear and instilled solution drainage were not quantitatively considered (1). The model developed here takes this factor into account and is, therefore, able to make reasonable predictions even when instilled volume and/or concentration are altered.

As has been mentioned, the data from Fig. 1 imply that a considerable decrease in instilled volume coupled with a slight increase in instilled concentration should result in the same amount of drug reaching the eye interior as if much larger volumes were administered. The data of Fig. 2 confirm this result, and Fig. 7 shows that the model also predicts it. It is confirmed that the model is sensitive to changes in both instilled volume and/or concentration. Such predictive capability has not previously been available.

Although the mathematics presented here are a simplification of the actual situation, the framework is now available that will allow refinement and addition of more sophisticated experimental data as they become available. Specifically, conjunctival absorption, protein binding, tissue distribution, and more mechanistic data on corneal absorption are needed. As such information becomes available, the treatment presented here can be refined to quantitate it. Furthermore, once all relevant parameters have been identified, the model should lend itself to quantitation of other ophthalmic drugs in addition to pilocarpine.

REFERENCES

(1) S. S. Chrai, T. F. Patton, A. Mehta, and J. R. Robinson, *J. Pharm. Sci.*, **62**, 1112 (1973).

(2) T. F. Patton and J. R. Robinson, *ibid.*, **65**, 1295 (1976).

(3) H. Benson, *Arch. Ophthalmol.*, **92**, 313 (1974).

(4) C. Dohlman, *Invest. Ophthalmol.*, **10**, 383 (1971).

(5) K. C. Swan and N. G. White, *Am. J. Ophthalmol.*, **25**, 1043 (1942).

(6) A. Kupferman, M. V. Pratt, K. SucKewer, and H. M. Leibowitz, *Arch. Ophthalmol.*, **91**, 373 (1974).

(7) A. Tonjum, *Acta Ophthalmol.*, **52**, 560 (1974).

(8) T. Iwata, M. Uyama, and K. Ohkawa, *Jpn. J. Ophthalmol.*, **19**, 139 (1975).

(9) J. Sieg and J. R. Robinson, *J. Pharm. Sci.*, **65**, 1816 (1976).

(10) D. H. Abramson, J. Coleman, M. Forbes, and L. A. Franzen, *Arch. Ophthalmol.*, **87**, 615 (1972).

(11) D. H. Abramson, S. Chang, and D. J. Coleman, *ibid.*, **94**, 914 (1976).

(12) P. C. Barsam, *Am. J. Ophthalmol.*, **73**, 742 (1972).

(13) S. S. Chrai and J. R. Robinson, *ibid.*, **77**, 735 (1974).

(14) P. P. Ellis, *Surv. Ophthalmol.*, **16**, 165 (1971).

(15) T. S. Friedman and T. F. Patton, *J. Pharm. Sci.*, **65**, 1095 (1976).

(16) K. Green and S. J. Downs, *Arch. Ophthalmol.*, **93**, 1165 (1975).

(17) L. S. Harris, T. W. Mittag, and M. A. Galin, *ibid.*, **86**, 1 (1971).

(18) D. L. Krohn and J. M. Breitfeller, *Invest. Ophthalmol.*, **13**, 312 (1974).

(19) R. Lazare and M. Horlington, *Exp. Eye Res.*, **21**, 281 (1975).

(20) F. J. Macri and J. J. Cevario, *Invest. Ophthalmol.*, **13**, 617 (1974).

(21) D. A. Newsome and R. Stern, *Am. J. Ophthalmol.*, **77**, 918 (1974).

(22) M. C. VanHoose and F. E. Leaders, *Invest. Ophthalmol.*, **13**, 377 (1974).

(23) T. F. Patton, Ph.D. thesis, University of Wisconsin, Madison, Wis., 1975.

(24) M. C. Makoid, Ph.D. thesis, University of Wisconsin, Madison, Wis., 1976.

(25) T. F. Patton, *J. Pharm. Sci.*, **66**, 1058 (1977).

(26) "The Rabbit in Eye Research," J. H. Prince, Ed., Charles C Thomas, Springfield, Ill., 1964.

ACKNOWLEDGMENTS

Supported by grants from the University of Kansas General Research Fund and the Children's Eye Care Foundation (CECF-RF-1976–77) and by University of Kansas Biomedical Sciences Support Grant RR-07037.

The authors are grateful to Mr. Ted S. Friedman for technical assistance.

Kinetics of Drug Transport and Concurrent Metabolism in Human Cell Cultures I: Theory

H. Y. ANDO *, N. F. H. HO, W. I. HIGUCHI ˣ, and C. SHIPMAN, Jr.

Received October 27, 1976, from the *College of Pharmacy, University of Michigan, Ann Arbor, MI 48104.* Accepted for publication April 28, 1977.

*Present address: Philadelphia College of Pharmacy and Science, Philadelphia, PA 19104.

Abstract □ A method for evaluating the passive permeability and single-step metabolism of drugs in suspension cultures of mammalian cells was formulated assuming linear kinetics. It was assumed that the metabolizing enzymes are driven by endogenous substrates present in steady-state quantities. The presence of the drug in radiolabeled tracer quantities was assumed to cause only a small perturbation from the endogenous steady-state operating point. The time course solutions for the drug and its metabolite are given in terms of macroscopic constants, and their physical interpretations are given in terms of metabolic and transport parameters.

Keyphrases □ Drug transport kinetics—evaluated in suspension cultures of mammalian cells, equations derived □ Metabolism, single step—evaluated for drugs in suspension cultures of mammalian cells, equations derived □ Kinetics—drug transport and concurrent metabolism in suspension cultures of mammalian cells, equations derived

The study of drug kinetics at the cellular level represents a microcosm of the traditional field of pharmacokinetics. Such a study, which includes cellular absorption, elimination, and metabolism *in vitro*, might be regarded as academic and possibly not as relevant as clinical studies *in vivo*. However, the ultimate resolution of the cancer problem and certain persistent viral infections may depend on knowledge of chemotherapy and kinetics at the cellular level. If the tumor problem is epigenetic and potentially reversible, as some investigators believe (1), then the ab-

errant neoplastic state would not represent a mutation of genetic material but rather a persistent alteration in genetic expression that might be amenable to control by a new class of chemotherapeutic agents acting at the cellular level.

BACKGROUND

Although current understanding of the molecular biology of the tumor cell is insufficient to define the nature of the "persistent switches" that determine dedifferentiation and tumorigenesis, the interactions of the virus with the human host cell are understood to such a degree that modern antiviral therapy has "come of age" (2). It was only 17 years ago that many investigators believed that the viral and cellular processes were so similar that it would not be possible to design agents to distinguish between them. For these reasons, transport and metabolism at the cellular level must be evaluated.

The thymidine incorporation rate into DNA does not reflect accurately the DNA synthesis rate (3–5). One possible reason for this discrepancy is that the uptake rate of the precursor is rate limiting for its incorporation into the macromolecule in question (3, 6, 7). The simultaneous transport of precursors and the biosynthesis of macromolecules in isolated chloroplasts (8) and *Escherichia coli* B (9) were examined in suspension systems. No attempt was made to determine the limiting step in the incorporation of the precursors into the macromolecule.

Rashevsky (10) derived an expression for the total diffusional resistance of a spherical cell using an implicit assumption that the partition coefficient between the cell interior and the external medium is unity (11). Hearon (12) noted that Rashevsky's treatment assumed that the metabolism rate is the same at every point in the cell and that the average metabolism is different from zero. Since the cases considered by Rashevsky (10) and Hearon (13) were the zero- and first-order situations for the metabolism rate, Q, Best (11) stated that the actual Michaelis–Menten kinetics will be bound by these two cases.

Blum and Jenden (14) considered this same problem. To obtain the concentration profiles in an intermediate range, they expanded the metabolism rate factor, Q, by a first-order Taylor series and found an expression for the volume-averaged concentration inside of the cell. In their derivation, the value of C^*, the value of the substrate about which the expansion was taken, was arbitrary and was chosen to suit a particular situation.

Several expressions were derived to evaluate diffusional and biosynthetic parameters from experimental data. Best (15) derived an equation for a spherically symmetric metabolizing cell which accounts for transport and metabolism under the "quasisteady-state" assumption (when the metabolism rate and the transport rate are equal). The partition coefficient between the cell and the external medium was assumed to be unity, as in the treatment of Rashevsky (10). Best (16), using baker's yeast, evaluated the parameters for sucrose–invertase and glucose–hexokinase systems at different temperatures with nonlinear regression analysis. In the following discussion, the biosynthetic parameters and the transport parameters will be considered from temporal data.

THEORETICAL

Biosynthetic–Transport Model—Consider the one-step conversion of a drug, A, into a product, P, inside the spherically symmetric cell in a suspension culture. Scheme I depicts the model subsystem of an endogenous biosynthetic pathway that will be considered in this study. In this case, P_i is the terminal product of a biosynthetic pathway that may be sensitive to feedback inhibition. If A_o and P_o are the total amounts of drug and product, respectively, in the fluid compartment, if A_i and P_i are the total amounts of drug and product, respectively, inside the cell, and if X is the total amount of intermediate complex formed by enzyme E with drug A, then Scheme I may be represented by the reaction chain shown in Scheme II.

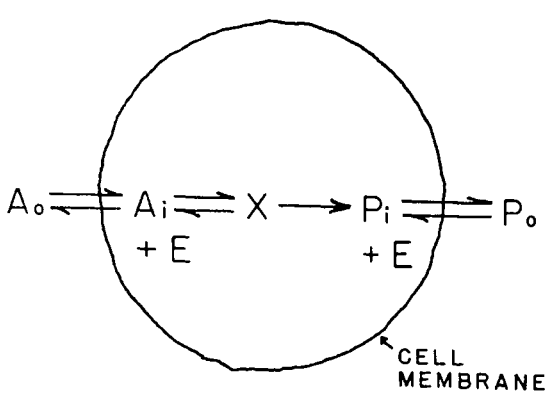

Scheme I

$$A_o \underset{k_2}{\overset{k_1}{\rightleftharpoons}} A_i + E \underset{k_4}{\overset{k_3}{\rightleftharpoons}} X \xrightarrow{k_5} E + P_i \underset{k_7}{\overset{k_6}{\rightleftharpoons}} P_o$$

Scheme II

This five-compartment system contains two physical and three chemical compartments. The physical compartments are due to the external fluid, denoted by the subscript o, and the cell interior, denoted by the subscript i, of the spherically symmetric cell in suspension; the chemical compartments are due to the three distinct chemical species A, X, and P. In this model, the formation of P_i is assumed to be irreversible, and the enzyme reactions are homogeneous in the cell.

The basic differential equations for this system are:

$$dA_o/dt = -k_1A_o + k_2A_i \quad \text{(Eq. 1)}$$

$$dA_i/dt = -k_2A_i - k_3EA_i + k_1A_o + k_4X \quad \text{(Eq. 2)}$$

$$dX/dt = -(k_4 + k_5)X + k_3EA_i \quad \text{(Eq. 3)}$$

$$dP_i/dt = -k_6P_i + k_5X + k_7P_o \quad \text{(Eq. 4)}$$

$$dP_o/dt = -k_7P_o + k_6P_i \quad \text{(Eq. 5)}$$

The transport parameters k_1, k_2, k_6, and k_7 are derivable from physical considerations, and they can be determined from independent experiments where biosynthesis is not a factor. This fact is important because once k_1, k_2, k_6, and k_7 are determined, the only rate constant that remains to be evaluated from the simultaneous biosynthetic–transport situation involves the biosynthetic process inside the cell. If it is assumed that the rate of change of X is much slower than that of A_i or P_i, Eq. 3 can be written after allowing for a brief, but negligible, induction period:

$$0 = -(k_4 + k_5)X + k_3EA_i \quad \text{(Eq. 6)}$$

or:

$$X = [k_3/(k_4 + k_5)]EA_i \quad \text{(Eq. 7)}$$

If K_m is defined as:

$$K_m = (k_4 + k_5)/k_3 \quad \text{(Eq. 8)}$$

then Eq. 7 becomes:

$$X = K_m^{-1}EA_i \quad \text{(Eq. 9)}$$

Substituting Eq. 9 into Eq. 2 yields:

$$dA_i/dt = -k_2A_i + k_1A_o - k_3EA_i + k_4K_m^{-1}EA_i \quad \text{(Eq. 10)}$$

or:

$$dA_i/dt = -k_2A_i + k_1A_o + (k_4K_m^{-1} - k_3)EA_i \quad \text{(Eq. 11)}$$

However, since $E = E_o - X$, then:

$$E = E_o - K_m^{-1}EA_i \quad \text{(Eq. 12)}$$

where E_o is the total amount of enzyme in the cell, and:

$$E = E_o/(1 + A_i/K_m) \quad \text{(Eq. 13)}$$

Using this expression for E in Eq. 11 yields:

$$dA_i/dt = -k_2A_i + k_1A_o + \frac{(k_4K_m^{-1} - k_3)}{(1 + K_m^{-1}A_i)}E_oA_i \quad \text{(Eq. 14)}$$

Since:

$$k_4K_m^{-1} - k_3 = k_3k_4/(k_4 + k_5) - k_3 = -k_5K_m^{-1} \quad \text{(Eq. 15)}$$

and:

$$V_m \equiv k_5E_o \quad \text{(Eq. 16)}$$

by definition, Eq. 14 becomes:

$$dA_i/dt = k_1A_o - k_2A_i - V_mA_i/(K_m + A_i) \quad \text{(Eq. 17)}$$

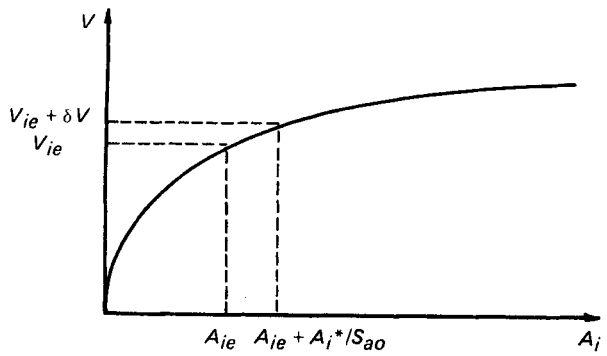

Figure 1—*Perturbation of an enzyme system from the operating point* (A_{ie}, V_{ie}).

Similar considerations applied to Eq. 4 give:

$$dP_i/dt = -k_6P_i + k_7P_o + V_mA_i/(K_m + A_i) \quad \text{(Eq. 18)}$$

Equations 1, 5, 17, and 18 completely describe the reaction chain of Scheme II when the steady state for the enzyme–substrate complex, X, is assumed.

Model Modified for Tracer Analysis—If it is assumed that the enzyme that metabolizes drug A is normally being driven by an endogenous substrate, A_{ie}, then the drug will add a substrate load on this enzyme which might be thought of as a perturbation on A_{ie}.

If A is the total amount of drug in the cell suspension system (the system considered here consists of the fluid and cells contained in an aliquot of volume V) and if A_i and A_o are the total amounts of drug inside of the cell and in the fluid milieu of the cell, then:

$$A = A_i + A_o \quad \text{(Eq. 19)}$$

Similarly, for the total amount of product in the system:

$$P = P_i + P_o \quad \text{(Eq. 20)}$$

Throughout this section, all definitions for A apply equally for P. The major chemical species are usually denoted with a capital letter, and the subscripting of this component is denoted with small letters. The one exception is the definition of specific activity. In this case, the chemical species is denoted with a small letter.

In the external medium, a radiolabeled drug has a specific activity:

$$S_{ao} = A_o^*/A_o \quad \text{(Eq. 21)}$$

where A_o^* is the total amount of labeled drug in the fluid compartment of the system. If it is assumed that the flux of cold drug and the flux of labeled drug are mutually independent, then as the tracer A_o^* enters the cell and becomes A_i^*, a total amount of drug A_i^*/S_{ao} has entered the cell from the external milieu of the cell at a time t. Thus:

$$A_i = A_{ie} + A_i^*/S_{ao} \quad \text{(Eq. 22)}$$

where A_{ie} is the total amount of cold endogenous drug inside the cell under stationary conditions.

Before the labeled drug entered the cell, the enzyme that catalyzed the reaction of A_i into P_i was being driven at a rate V_{ie} by A_{ie}. The increase in A_i by an amount A_i^*/S_{ao} caused the system to be perturbed from A_{ie}. This situation is shown in Fig. 1. Writing the perturbed rate as $V_{ie} + \delta V$ then gives:

$$V_{ie} + \delta V = \frac{V_mA_i}{K_m + A_i} \quad \text{(Eq. 23)}$$

$$V_{ie} + \delta V = \frac{V_m(A_{ie} + A_i^*/S_{ao})}{K_m + (A_{ie} + A_i^*/S_{ao})} \quad \text{(Eq. 24)}$$

$$V_{ie} + \delta V = \frac{V_mA_{ie}}{K_m + (A_{ie} + A_i^*/S_{ao})} + \frac{V_mA_i^*/S_{ao}}{K_m + (A_{ie} + A_i^*/S_{ao})} \quad \text{(Eq. 25)}$$

If it is assumed that the endogenous drug level is much larger than the amount A_i^*/S_{ao}, *i.e.*, $A_{ie} \gg A_i^*/S_{ao}$, then the equation becomes:

$$V_{ie} + \delta V \doteq V_mA_{ie}/(K_m + A_{ie}) + KA_i^*/S_{ao} \quad \text{(Eq. 26)}$$

where:

$$K \equiv V_m/(K_m + A_{ie}) \quad \text{(Eq. 27)}$$

But:

$$V_{ie} = V_mA_{ie}/(K_m + A_{ie}) \quad \text{(Eq. 28)}$$

Therefore:

$$\delta V = KA_i^*/S_{ao} \quad \text{(Eq. 29)}$$

Applying this result to Eq. 17 gives:

$$d(A_{ie} + A_i^*/S_{ao})/dt = k_1(A_{ox} + A_o^*/S_{ao}) - k_2(A_{ie} + A_i^*/S_{ao}) - V_{ie} - \delta V \quad \text{(Eq. 30)}$$

where A_{ox} is the total amount of cold precursor in the fluid milieu of the cells in the absence of A_o^*/S_{ao} under stationary conditions. Since:

$$dA_{ie}/dt = k_1A_{ox} - k_2A_{ie} - V_{ie} \quad \text{(Eq. 31)}$$

then:

$$dA_i^*/dt = k_1A_o^* - k_2A_i^* - S_{ao}\,\delta V \quad \text{(Eq. 32)}$$

and using Eq. 29 to eliminate δV yields:

$$dA_i^*/dt = k_1A_o^* - (k_2 + K)A_i^* \quad \text{(Eq. 33)}$$

Similarly, Eqs. 1, 18, and 5 become:

$$dA_o^*/dt = -k_1A_o^* + k_2A_i^* \quad \text{(Eq. 34)}$$

$$dP_i^*/dt = -k_6P_i^* + k_7P_o^* + KA_i^* \quad \text{(Eq. 35)}$$

$$dP_o^*/dt = -k_7P_o^* + k_6P_i^* \quad \text{(Eq. 36)}$$

respectively.

Closed System Requirement—For a closed system, it is necessary that:

$$T^* = A^* + P^* = \text{constant} \quad \text{(Eq. 37)}$$

where T^* is the total amount of label in the system and:

$$A^* = A_o^* + A_i^* \quad \text{(Eq. 38)}$$

$$P^* = P_o^* + P_i^* \quad \text{(Eq. 39)}$$

Adding Eqs. 33 and 34 yields:

$$dA^*/dt = -KA_i^* \quad \text{(Eq. 40)}$$

and adding Eqs. 35 and 36 gives:

$$dP^*/dt = KA_i^* \quad \text{(Eq. 41)}$$

But since:

$$dT^*/dt = dA^*/dt + dP^*/dt = 0 \quad \text{(Eq. 42)}$$

it can be seen that Eqs. 40 and 41 are redundant and really express the same condition. For a closed system, therefore, the following set of linear differential equations must be solved:

$$dA_i/dt = k_1A_o - (k_2 + K)A_i \quad \text{(Eq. 43)}$$

$$dP_i/dt = -k_6P_i + k_7P_o + KA_i \quad \text{(Eq. 44)}$$

$$dA/dt = -KA_i \quad \text{(Eq. 45)}$$

which are subject to the constraint that:

$$T = A + P \quad \text{(Eq. 46)}$$

In Eqs. 43–46, the label * has been omitted since all time-dependent variables refer to labeled quantities. In the remainder of this section and in those to follow, this will be understood. Since:

$$P = P_o + P_i \quad \text{(Eq. 47)}$$

$$A = A_o + A_i \quad \text{(Eq. 48)}$$

and with the constraint of Eq. 46 in Eqs. 47 and 48, it is found that:

$$P_o = T - A - P_i \quad \text{(Eq. 49)}$$

$$A_o = A - A_i \quad \text{(Eq. 50)}$$

Substituting Eqs. 49 and 50 into Eqs. 44 and 43, respectively, yields:

$$dA_i/dt = k_1A - (k_1 + k_2 + K)A_i \quad \text{(Eq. 51)}$$

$$dP_i/dt = k_7T - k_7A + KA_i - (k_6 + k_7)P_i \quad \text{(Eq. 52)}$$

Equations 45, 51, and 52 form a system of linear differential equations in three variables, A, A_i, and P_i.

In the next section, the solutions to this system of equations will be examined. One final remark, however, is in order with regard to the apparent enzyme rate constant K. Equation 27 can be rewritten as:

$$1/K = K_m/V_m + A_{ie}/V_m \qquad \text{(Eq. 53}a\text{)}$$

so that a plot of $1/K$ *versus* A_{ie} is linear; from such a plot, V_m and K_m can be determined. Since $V_m = k_5E_o$, Eq. 27 can be rewritten as:

$$K = \frac{k_5}{K_m + A_{ie}} E_o \qquad \text{(Eq. 53}b\text{)}$$

so k_5 can be determined from a linear plot of K *versus* E_o if A_{ie} is kept constant and K_m and A_{ie} are known. It remains to be seen if A_{ie} and E_o can be changed experimentally. If these parameters can be varied, then it is apparently possible to determine the fundamental rate parameters of the enzyme catalysis within the intact cell.

Solutions to Closed System Equations—The following assumptions were made to derive the differential equations, Eqs. 45, 51, and 52, for the closed system.

First, it was assumed that the rate of change of the enzyme–substrate complex, X, is much slower than the rate of change of either A_i or P_i within the cell; *i.e.*, transport of the substrate is much faster than the bioconversion of the substrate. This assumption was utilized to obtain an algebraic constraint on X (Eq. 9). In this model, the biosynthetic reaction is taken to be homogeneous within the cell.

Next, it was assumed that the endogenous levels of substrate within the cells, A_{ie}, did not change during the experiment. Thus, the cells must reach a steady state with respect to the synthesis of the endogenous product. In the light of feedback inhibition and other intracellular regulatory mechanisms, this assumption seems reasonable when the cells are not subject to sudden stress.

By using this constancy of A_{ie} as a steady-state operating point and assuming that the total amount of substrate that diffuses into the cells from the fluid media, A_i/S_{ao}, is much less than A_{ie}, the enzymatic rate of change of the substrate reduces to the linear expression (Eq. 26) with respect to its A_i* dependence. The effective linear rate constant for this enzyme reaction is given in Eq. 53*b*. In this derivation, it is implicit that only one substrate is involved that can limit the rate of the enzyme reaction. However, many biological reactions need a second and, sometimes, a third substrate.

Finally, it was assumed that the substrate and the product form a closed system such that the conversion of the ^{14}C-label can be assumed in the form described by Eqs. 37–39. If there are other routes of loss of the ^{14}C-label, then this conservation relationship cannot hold.

The initial and the final assumptions provided algebraic constraints that reduce the original five-compartment system to the three-compartment system expressed by Eqs. 45, 51, and 52. The solutions to this system of equations are derived in the *Appendix* and are:

$$A_i = A_{ib}e^{-\beta t} + A_{ia}e^{-\alpha t} \qquad \text{(Eq. 54)}$$

$$A = A_be^{-\beta t} + A_ae^{-\alpha t} \qquad \text{(Eq. 55)}$$

$$P_i = P_i(\infty) - P_{ib}e^{-\beta t} - P_{id}e^{-\delta t} - P_{ia}e^{-\alpha t} \qquad \text{(Eq. 56)}$$

where:

$$\alpha = \gamma/2 + \sqrt{(\gamma/2)^2 - Kk_1} \qquad \text{(Eq. 57)}$$

$$\beta = \gamma/2 - \sqrt{(\gamma/2)^2 - Kk_1} \qquad \text{(Eq. 58)}$$

$$\gamma = \alpha + \beta = k_1 + k_2 + K \qquad \text{(Eq. 59)}$$

$$\delta = k_6 + k_7 \qquad \text{(Eq. 60)}$$

$$A_{ib} = \frac{k_1A(0) - \beta A_i(0)}{\alpha - \beta} \qquad \text{(Eq. 61)}$$

$$A_{ia} = \frac{\alpha A_i(0) - k_1A(0)}{\alpha - \beta} \qquad \text{(Eq. 62)}$$

$$A_b = \frac{\alpha A(0) - KA_i(0)}{\alpha - \beta} \qquad \text{(Eq. 63)}$$

$$A_a = \frac{KA_i(0) - \beta A(0)}{\alpha - \beta} \qquad \text{(Eq. 64)}$$

$$P_b = \left(\frac{k_7 - \beta}{\delta - \beta}\right) A_b \qquad \text{(Eq. 65)}$$

$$P_a = \left(\frac{k_7 - \beta}{\alpha - \delta}\right) A_a \qquad \text{(Eq. 66)}$$

$$P_d = \frac{1}{(\delta - \beta)(\alpha - \delta)}\left\{1 - \frac{k_7}{k_6 + k_7}\alpha\beta T + (\gamma - \delta)(k_7 + \delta)P_i(0) - k_6KA_i(0)\right\} \qquad \text{(Eq. 67)}$$

$$P_i(\infty) = \frac{k_7T}{k_6 + k_7} \qquad \text{(Eq. 68)}$$

In these expressions, $A(0)$ and $A_i(0)$ are the values of A and A_i at time 0; $P_i(\infty)$ is the value of P_i at time ∞. The expression for A_o can be derived from Eqs. 38 and 54 and is given by:

$$A_o = (A_b - A_{ib})e^{-\beta t} + (A_a - A_{ia})e^{-\alpha t} \qquad \text{(Eq. 69)}$$

Similarly, P_o can be derived from Eqs. 37–39 and 54–56. This expression is not needed here.

In the described formulation, all quantities were computed in terms of the amount of the substance in a particular compartment for a sample of suspension, containing cells and fluid, of volume V. Volume V can be expressed as:

$$V = V_o + nV_i \qquad \text{(Eq. 70)}$$

where n is the number of cells in V, V_i is the volume of one cell, and V_o is the fluid volume. These equations can be converted to concentration units by dividing by the product of the volumes involved. For example, Eq. 61 would become, in concentration units:

$$[A_{ib}] = \frac{\left(\frac{V}{nV_i}\right)k_1[A(0)] - \beta[A_i(0)]}{\alpha - \beta} \qquad \text{(Eq. 71)}$$

where [ ] indicate the concentration of the quantity within the mass balance equations, Eqs. 47 and 48, become:

$$P = V_o[P_o] + nV_i[P_i] \qquad \text{(Eq. 72)}$$

$$A = V_o[A_o] + nV_i[A_i] \qquad \text{(Eq. 73)}$$

The solutions for A_i and A_o given by Eqs. 54 and 69, respectively, tend to zero as time tends to infinity. This behavior is expected for the substrate in the system when the reaction has been completed. The solutions for P_i and P_o, on the other hand, must tend to $P_i(\infty)$ and $P_o(\infty)$, respectively, as t tends to infinity. This means that:

$$T = P_i(\infty) + P_o(\infty) \qquad \text{(Eq. 74)}$$

from Eq. 37. Substituting Eq. 74 into Eq. 68 yields:

$$P_i(\infty) = \frac{k_7}{k_6 + k_7}[P_i(\infty) + P_o(\infty)] \qquad \text{(Eq. 75}a\text{)}$$

or:

$$\frac{P_i(\infty)}{P_o(\infty)} = \frac{k_7}{k_6} \qquad \text{(Eq. 75}b\text{)}$$

Expressing Eq. 75*b* in terms of concentration units gives:

$$\frac{[P_i(\infty)]}{[P_o(\infty)]} = \frac{V_ok_7}{nV_ik_6} \qquad \text{(Eq. 76)}$$

Turi (17) defined the intrinsic partition coefficient κ_p of a compound P between the cell fraction of n cells, each of volume V_i, and the fluid media of volume V_o as the ratio of the concentrations expressed in Eq. 76, *i.e.*:

$$\kappa_p = \frac{[P_i(\infty)]}{[P_o(\infty)]} \qquad \text{(Eq. 77)}$$

Since the relationship between the amounts and the concentrations of P_i and P_o at time ∞ are:

$$P_i(\infty) = nV_i[P_i(\infty)] \qquad \text{(Eq. 78)}$$

$$P_o(\infty) = V_o[P_o(\infty)] \qquad \text{(Eq. 79)}$$

and with Eqs. 74 and 77–79, it is found that:

$$P_i(\infty) = \frac{TnV_i\kappa_p}{(nV_i\kappa_p) + V_o} \qquad \text{(Eq. 80)}$$

$$P_o(\infty) = \frac{TV_o}{(nV_i\kappa_p) + V_o} \qquad \text{(Eq. 81)}$$

$$[P_i(\infty)] = \frac{\kappa_pT}{(nV_i\kappa_p) + V_o} \qquad \text{(Eq. 82)}$$

$$[P_o(\infty)] = \frac{T}{(nV_i\kappa_p) + V_o} \qquad \text{(Eq. 83)}$$

Equations 80–83 can be used to determine these asymptotic values of P_i and P_o from data independent of the biosynthetic or transport kinetics.

Determination of Transport Parameters—The transport parameters k_1, k_2, k_6, and k_7 can be derived in terms of physical constants. The expressions for these parameters are:

$$k_1 = \frac{3P_a}{a}\frac{nV_i}{V_o} \quad \text{(Eq. 84)}$$

$$k_2 = \frac{3P_a}{a\kappa_a} \quad \text{(Eq. 85)}$$

$$k_6 = \frac{3P_p}{a\kappa_p} \quad \text{(Eq. 86)}$$

$$k_7 = \frac{3P_p}{a}\frac{nV_i}{V_o} \quad \text{(Eq. 87)}$$

where a is the radius of the cell and P_a, P_p, and κ_p are the intrinsic permeability and partition coefficients of the drug and product, respectively. These parameters are very important because, by suitably arranging the experimental situation, they can be determined independently from the biosynthetic reaction. Thus, in the simultaneous biosynthetic–transport situation, the only parameters that remain to be determined are those associated with the enzymatic process. Turi (17) found that when fetal bovine serum was used in the medium of the uptake and release transport experiments, the binding of many drugs could be accounted for by assuming a linear binding model of the drug to the fetal bovine component of the medium. In this way, in the presence of fetal bovine serum, the effective permeability, P_{ce}, and the effective partition coefficient, κ_{ce}, of a drug C are the parameters that are measured experimentally. These are related to the intrinsic parameters P_c and κ_c by the expressions:

$$P_{ce} = \frac{P_c}{1 + \rho_b[S]} \quad \text{(Eq. 88)}$$

$$\kappa_{ce} = \frac{\kappa_c}{1 + \rho_b[S]} \quad \text{(Eq. 89)}$$

where ρ_b is the equilibrium serum–drug binding constant.

APPENDIX: SOLUTIONS TO BIOCONVERSION–TRANSPORT EQUATIONS

The equations to be solved are 45, 51, and 52. Substituting $\gamma = k_1 + k_2 + K$ in Eq. 51 yields:

$$dA_i/dt = -\gamma A_i + k_1 A \quad \text{(Eq. A1)}$$

Substituting $\delta = k_6 + k_7$ in Eq. 52 yields:

$$dP_i/dt = KA_i - k_7 A - \delta P_i + k_7 T \quad \text{(Eq. A2)}$$

Taking the Laplace transform of Eqs. A1, 45, and A2 yields, respectively:

$$(s + \gamma)a_i - k_1 a = A_i(0) \quad \text{(Eq. A3)}$$

$$Ka_i + sa = A(0) \quad \text{(Eq. A4)}$$

$$-Ka_i + k_7 a + (s + \delta)p_i = k_7 T/s + P_i(0) \quad \text{(Eq. A5)}$$

Since the determinant (det) of the matrix for a_i, a, and p_i is:

$$\det = (s + \beta)(s + \alpha)(s + \delta) \quad \text{(Eq. A6)}$$

where $\alpha = \gamma/2 + (\gamma/2)^2 - Kk_1$, $\beta = \gamma/2 - (\gamma/2)^2 - Kk_1$, $\alpha\beta = Kk_1$, $\gamma - \alpha = \beta$, and $\gamma - \beta = \alpha$. The solutions for a_i, a, and p_i can be found from Cramer's rule and are:

$$a_i = (s + \beta)^{-1}(s + \alpha)^{-1}k_1 A(0) + sA_i(0) \quad \text{(Eq. A7)}$$

$$a = (s + \beta)^{-1}(s + \alpha)^{-1}(s + \gamma)A(0) - KA_i(0) \quad \text{(Eq. A8)}$$

$$p_i = (s + \beta)^{-1}(s + \alpha)^{-1}(s + \delta)^{-1}A_i(0)\Delta_{13} - A(0)\Delta_{23} + P_i(0)\Delta_{33} + (s + \beta)^{-1}(s + \alpha)^{-1}(s + \delta)^{-1}s^{-1}k_7 T\Delta_{33} \quad \text{(Eq. A9)}$$

where the Δ_{ij} are the minors of the ijth element of the matrix formed from a_i, a, and p_i. Taking the inverse transforms yields:

$$A_i = A_{ib}e^{-\beta t} + A_{ia}e^{-\alpha t} \quad \text{(Eq. A10)}$$

$$A = A_b e^{-\beta t} + A_a e^{-\alpha t} \quad \text{(Eq. A11)}$$

$$P_i = P_i(\infty) - P_{ib}e^{-\beta t} - P_{id}e^{-\delta t} - P_{ia}e^{-\alpha t} \quad \text{(Eq. A12)}$$

$$\alpha = \gamma/2 + (\gamma/2)^2 - Kk_1 \quad \text{(Eq. A13)}$$

$$\beta = \gamma/2 - \sqrt{(\gamma/2)^2 - Kk_1} \quad \text{(Eq. A14)}$$

$$\gamma = \alpha + \beta = k_1 + k_2 + K \quad \text{(Eq. A15)}$$

$$\delta = k_6 + k_7 \quad \text{(Eq. A16)}$$

$$A_{ib} = \frac{k_1 A(0) - \beta A_i(0)}{\alpha - \beta} \quad \text{(Eq. A17)}$$

$$A_{ia} = \frac{\alpha A_i(0) - k_1 A(0)}{\alpha - \beta} \quad \text{(Eq. A18)}$$

$$A_b = \frac{\alpha A(0) - KA(0)}{\alpha - \beta} \quad \text{(Eq. A19)}$$

$$A_a = \frac{KA_i(0) - \beta A(0)}{\alpha - \beta} \quad \text{(Eq. A20)}$$

$$P_b = \left(\frac{k_7 - \beta}{\delta - \beta}\right) A_b \quad \text{(Eq. A21)}$$

$$P_a = \left(\frac{k_7 - \beta}{\alpha - \delta}\right) A_a \quad \text{(Eq. A22)}$$

$$B = \frac{1}{(\delta - \beta)(\alpha - \delta)}\left\{\left[1 - \frac{k_7}{k_6 + k_7}\right]\alpha\beta T + (\gamma - \delta)(k_7 + \delta)P_i(0) - k_6 K A_i(0)\right\} \quad \text{(Eq. A23)}$$

$$P_i(\infty) = \frac{k_7 T}{k_6 + k_7} \quad \text{(Eq. A24)}$$

REFERENCES

(1) A. C. Braun, in "Cancer," F. F. Becker, Ed., Plenum, New York, N.Y., 1975, pp. 3–20.

(2) T. H. Maugh, *Science*, **192**, 128 (1976).

(3) P. G. W. Plagemann and J. Erbe, *J. Cell Biol.*, **55**, 161 (1972).

(4) L. A. Smets, *J. Cell. Physiol.*, **74**, 63 (1969).

(5) P. Fuchs and A. Kohn, *J. Virol.*, **8**, 695 (1971).

(6) P. G. W. Plagemann and M. F. Roth, *Biochemistry*, **8**, 4782 (1969).

(7) P. G. W. Plagemann, *Biochim. Biophys. Acta*, **233**, 688 (1971).

(8) R. G. Jenden and J. A. Bassham, *ibid.*, **153**, 219 (1968).

(9) D. H. Duckworth, *Virology*, **40**, 673 (1970).

(10) N. Rashevsky, "Mathematical Biophysics," University of Chicago Press, New York, N.Y., 1948, pp. 9–25.

(11) J. B. Best, *Int. Rev. Cytol.*, **9**, 129 (1960).

(12) J. Z. Hearon, *Bull. Math. Biophys.*, **15**, 23 (1953).

(13) *Ibid.*, **15**, 111 (1953).

(14) J. J. Blum and D. J. Jenden, *Arch. Biochem. Biophys.*, **66**, 316 (1957).

(15) J. B. Best, *J. Cell. Comp. Physiol.*, **46**, 1 (1955).

(16) *Ibid.*, **46**, 29 (1955).

(17) J. S. Turi, Ph.D. thesis, University of Michigan, Ann Arbor, Mich., 1972, pp. 26–28.

Dissolution and Absorption of the Antineoplastic Agent Ellipticine

AQUILUR RAHMAN[x], **JAMES C. CRADOCK, and J. PAUL DAVIGNON**

Received April 4, 1977, from the *Pharmaceutical Resources Branch, National Cancer Institute, National Institutes of Health, Bethesda, MD 20014.* Accepted for publication August 2, 1977.

Abstract □ Ellipticine, a poorly water-soluble alkaloid, is active in several experimental tumor systems. Marked solubility increases were produced by polyvinylpyrrolidone of varying molecular weights (10,000–160,000) and were optimal (~13 mg/ml at 25°) with polyvinylpyrrolidone mol. wt. 10,000. Dissolution of ellipticine–polyvinylpyrrolidone (1:22 w/w) tablets in simulated gastric juice was superior to that of ellipticine hydrochloride. Release rates were controlled by combinations of polyvinylpyrrolidone polymers without affecting maximum dissolution at 37°. Physiological disposition of ellipticine–polyvinylpyrrolidone was compared with that of the hydrochloride salt and ellipticine in suspension following oral administration at 250 mg/kg in fasted mice. In comparison to the suspension, ellipticine tissue levels were about threefold higher with polyvinylpyrrolidone or hydrochloride preparations. Antitumor activity of the three preparations was evaluated intraperitoneally and orally *versus* L-1210 leukemia. The optimal dose of ellipticine–polyvinylpyrrolidone and ellipticine hydrochloride was lower than that of the suspension and suggested improved absorption.

Keyphrases □ Ellipticine—dissolution and GI absorption, effect of polyvinylpyrrolidone □ Dissolution—ellipticine, effect of polyvinylpyrrolidone □ Absorption, GI—ellipticine, effect of polyvinylpyrrolidone □ Polyvinylpyrrolidone—effect on dissolution and GI absorption of ellipticine □ Antineoplastic agents—ellipticine, dissolution and GI absorption, effect of polyvinylpyrrolidone

The plant alkaloid ellipticine (1) possesses marked antitumor activity *versus* transplantable murine tumors following intraperitoneal or oral administration. However, intravenous administration of ellipticine as the hydrochloride salt resulted in hemolysis, hypotension, and arrhythmias (2). Addition of citrate markedly reduced hemolysis but did not influence the cardiovascular side effects (3).

Since the intensity of the toxic effects was related to the administration rate, studies were directed toward an oral formulation. Ellipticine has a water solubility of about 1 mg/liter, which was markedly enhanced by polyvinylpyrrolidone. Solubility was affected by the molecular weight of the polymer and was optimal (about a 10^5-fold increase) at mol. wt. 10,000. This report concerns the development of an oral formulation and the influence of the preparation on physiological disposition and antitumor activity of ellipticine.

EXPERIMENTAL

Ellipticine[1] (NSC-71795) and polyvinylpyrrolidone mol. wt. 10,000[2], 40,000[2], and 160,000[3] were used. Other compounds were USP grade and were used without further purification.

Physiological Disposition—Male BDF-1 mice, 18–24 g, were fasted for 16 hr before and up to 12 hr after drug administration *via* oral intubation at 250 mg of ellipticine base/kg. Ellipticine, 12.5 mg/ml, was administered at 2% body weight in four formulations: a solution in 30% polyvinylpyrrolidone mol. wt. 10,000, a solution of the hydrochloride salt, a suspension in polyvinylpyrrolidone mol. wt. 10,000–160,000 (4:1), and a suspension in a 0.5% carboxymethylcellulose sodium vehicle.

Mice were killed by cervical dislocation in sets of two each at 2, 4, 8, 12, or 24 hr after oral administration. The liver, kidneys, heart, and spleen were rapidly excised, rinsed with 0.9% sodium chloride, and immediately frozen or homogenized. Frozen samples were stored at −20° and processed within 1 week. Blood was collected in a citrated syringe from a jugular vein.

The method of Hardesty *et al.* (4) was used with modification for tissue extraction and estimation of ellipticine equivalents. Liver and kidney samples were homogenized with four volumes of 0.05 *M* pH 7.4 phosphate buffer and extracted with two volumes of water-saturated ethyl acetate. After centrifugation at 6000 rpm for 20 min, the ethyl acetate layer was mixed with an equal volume of 0.01 *N* HCl. The acid layer was separated by centrifugation at 6000 rpm for 20 min, and the absorbance of this solution was determined[4] at 303 nm *versus* 0.01 *N* HCl. Estimation of ellipticine in 0.01 *N* HCl altered the λ_{max} of peak absorbance from 283 nm in ethyl acetate to 303 nm and improved sensitivity of the assay since the background absorbance at 303 nm was much less than at 283 nm. Spleen and heart samples were homogenized in about 10 volumes of 0.05 *M* phosphate buffer at pH 7.4.

Tissues from untreated mice were extracted as described and served as controls for hydrochloride- and suspension-treated animals. For the polyvinylpyrrolidone group, mice were injected with equivalent volumes of polyvinylpyrrolidone mol. wt. 10,000 and sacrificed 8 hr later; the tissues were extracted as described. Polyvinylpyrrolidone did not influence the background absorbance at 303 nm.

Before the disposition studies, recovery experiments were conducted. Ellipticine was added to ice-cold homogenates of all tissues to yield a 0.5-μg/ml mixture, and the tissues were extracted as described. Recovery ranged from 92 to 98%. Corrections for recovery were not applied, and each value represents the mean of three determinations. Total ellipticine equivalents were obtained after correction for background from a Beer-type plot ($E^{303}_{0.01\ N\ HCl}$ = 52,000) and expressed as micrograms of ellipticine equivalents per gram of tissue (wet weight).

Antitumor Evaluation—The effects of formulation variables on the antitumor activity of ellipticine were evaluated in the transplantable L-1210 tumor system according to National Cancer Institute protocols (5). Ellipticine was prepared as a suspension in 0.9% sodium chloride and in polyvinylpyrrolidone mol. wt. 10,000–160,000 (4:1) or as a solution of the hydrochloride salt and administered at 2% body weight daily for 9 days commencing 24 hr after intraperitoneal implant of 10^5 tumor cells. Each preparation was administered by intraperitoneal and oral routes. The data are expressed as the percent increase in lifespan (ILS) of drug-treated over vehicle-treated mice.

Formulation Studies—All tablet formulations were prepared to provide 25 mg of ellipticine base, 50 mg of microcrystalline cellulose, 1.2 mg of calcium stearate, and a total weight of 600 mg. Adjustments to formulas were made with polyvinylpyrrolidone or mannitol. All components were triturated thoroughly in a mortar. Tablets were prepared by direct compression on a single-punch tablet machine[5] equipped with a 1.43-cm die, and they exhibited a uniform yellow appearance. The ellipticine content was within 5% of the labeled amount.

The dissolution of ellipticine from these tablet mixtures was determined using essentially the rotating-basket method (6). A flask containing 500 ml of dissolution medium was immersed in a constant-temperature water bath at 37 ± 0.5°. After the tablet was inserted, the basket was rotated horizontally at 100 rpm. The geometry of the system was maintained by appropriate markings. At specified intervals, 5.0 ml was removed and filtered through a 0.22-μm membrane. The filtrate was analyzed spectrophotometrically at 293 nm after dilution with 0.05 *M* pH 7.4 phosphate buffer. The volume of the dissolution bath was maintained by replacement with an equal volume of medium.

[1] Drug Research and Development Program, National Cancer Institute.
[2] Aldrich Chemical Co., Milwaukee, Wis.
[3] GAF Corp., New York, N.Y.
[4] Cary 15 recording spectrophotometer, Cary Instruments, Monrovia, Calif.
[5] Stokes, Warminster, Pa.

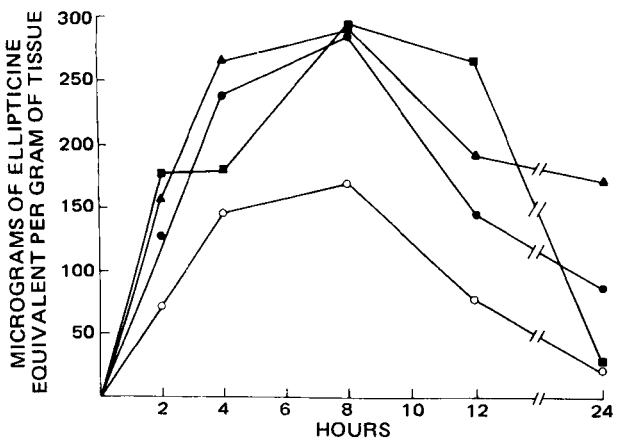

Figure 1—*Effect of formulation on the disposition of ellipticine in the liver. Ellipticine was administered to fasted mice at 250 mg/kg po by gavage in four formulations. Key: ●, ellipticine hydrochloride solution; ▲, ellipticine solution in 30% polyvinylpyrrolidone mol. wt. 10,000; ■, ellipticine suspension in 30% polyvinylpyrrolidone mol. wt. 10,000–160,000 (4:1); and ○, ellipticine suspension in 0.5% carboxymethylcellulose sodium.*

RESULTS

Ellipticine, a poorly water-soluble antineoplastic agent, is believed to exert its antitumor effect *via* intercalation with DNA (7). However, severe hemolysis and cardiovascular effects following intravenous administration have limited its utility. An oral formulation was sought that would provide excellent, but gradual, absorption of ellipticine. Marked improvement (about 10,000-fold) in ellipticine solubility could be achieved by salt formation or by complexation with polyvinylpyrrolidone mol. wt. 10,000 (8). The effect of these approaches on the pharmacological disposition and antitumor activity of oral ellipticine was evaluated in BDF-1 mice, the host for the L-1210 transplantable murine leukemia. The levels of ellipticine equivalents were obtained over 24 hr in the liver, kidneys, blood, spleen, and heart after administration of the drug as a solution or suspension.

Tissue levels in liver are temporally and qualitatively representative of the other tissues and are described in Fig. 1. Peak levels were observed at 8 hr after drug administration regardless of formulation. Ellipticine was rather rapidly absorbed and persisted for at least 12 hr in the liver. The drug levels following administration of the polyvinylpyrrolidone preparations were slightly higher or equivalent to the hydrochloride preparation, but both formulations provided tissue levels two- to threefold higher than the values observed in the suspension-treated mice.

Figure 2 presents the data for the kidneys. Although the tissue levels were lower, the relationship between the various formulations was the same. The drug levels in polyvinylpyrrolidone and hydrochloride groups

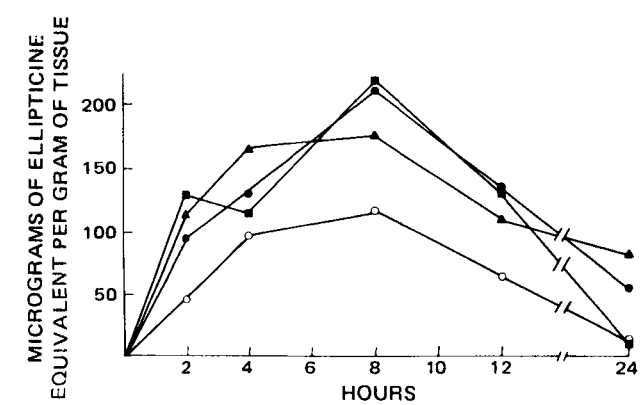

Figure 2—*Effect of formulation on the disposition of ellipticine in the kidneys. Ellipticine was administered to fasted mice at 250 mg/kg po by gavage in four formulations. Key: ●, ellipticine hydrochloride solution; ▲, ellipticine solution in 30% polyvinylpyrrolidone mol. wt. 10,000; ■, ellipticine suspension in 30% polyvinylpyrrolidone mol. wt. 10,000–160,000 (4:1); and ○, ellipticine suspension in 0.5% carboxymethylcellulose sodium.*

Table I—Effect of Formulation on the Physiological Disposition of Ellipticine [a]

Hours	Ellipticine Hydrochloride	Ellipticine–Polyvinylpyrrolidone Solution	Ellipticine–Polyvinylpyrrolidone Suspension	Ellipticine Suspension
		Spleen		
2	81	114	203	45
4	205	225	199	159
8	267	336	276	126
12	392	315	243	178
24	242	292	62	49
		Heart		
2	33	37	44	16
4	34	38	35	27
8	52	65	50	21
12	49	49	28	25
24	24	36	Not detectable	Not detectable
		Blood		
2	7.3	7.5	5.5	4.4
4	9.6	8.0	5.0	4.6
8	10.9	22.3	5.8	4.6
12	4.5	5.0	4.0	3.1
24	11.0	5.0	0.9	Not detectable

[a] Ellipticine was administered at 250 mg/kg po by gavage at 2% body weight to fasted mice. See text for description of formulation. Each value represents the mean of three determinations. Data are expressed as micrograms of ellipticine equivalents per gram of tissue (wet weight).

were very similar and about double the suspension-treated group. The results for spleen, heart, and blood samples are described in Table I. Drug levels in the spleen were intermediate between the liver and kidneys. In addition, the drug levels remained elevated at 12 hr and were the peak values in two instances. A similar observation was reported with daunorubicin, another intercalating agent (9). In contrast to the other tissues, the levels of ellipticine in the heart were low but similar with respect to the time of peak concentration and levels among the different formulations.

Blood ellipticine levels were uniformly low at all time periods and below detectable limits (0.25 μg/ml) at 24 hr in the suspension group. A high tissue to blood ratio was reported by other workers investigating the disposition of intercalating agents (10). The differences in tissue levels over the 4–12-hr period do not appear similarly reflected in blood levels.

The antitumor effects of three preparations *versus* the L-1210 murine leukemia were compared using several routes and administration schedules. The data are presented as the percent increase in median survival of the drug-treated animals over the vehicle-treated control group and are described for the daily 1–9 schedules by intraperitoneal and oral routes in Table II. The optimal doses of ellipticine by the intraperitoneal route for polyvinylpyrrolidone, hydrochloride, and suspension groups were 12.5, 12.5, and 25 mg/kg, respectively. Following oral

Table II—Effect of Ellipticine Formulation on Antitumor Activity [a] (Percent ILS)

Dose, mg/kg/day	Ellipticine Hydrochloride	Ellipticine–Polyvinylpyrrolidone Suspension	Ellipticine Suspension
	Intraperitoneal, Days 1–9		
25	4	27	137
12.5	116	114	95
6.2	57	69	59
3.1	24	40	52
	Oral, Days 1–9		
50	13	31	55
25	69	72	41
12.5	37	38	11
6.2	30	22	19

[a] Male mice were inoculated intraperitoneally with 10^5 L-1210 cells on Day 0. Drug formulations were administered intraperitoneally or orally on Days 1–9. Data are expressed as the percent increase in survival of drug-treated over vehicle-treated mice.

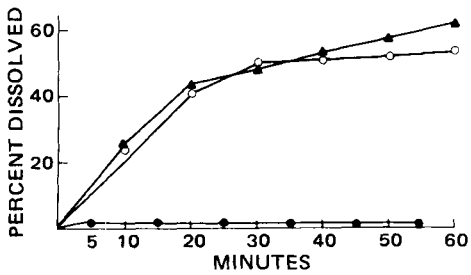

Figure 3—*Dissolution of ellipticine tablets at 37° in water. Key: ●, ellipticine–mannitol; ○, ellipticine–polyvinylpyrrolidone mol. wt. 10,000 (1:15.7); and ▲, ellipticine–polyvinylpyrrolidone mol. wt. 10,000 (1:22).*

administration, the optimal dose was one level higher in all cases. Within a particular route, the maximum ILS was quite similar among the preparations. Since a minimum ILS of 50% is required for activity (5), all preparations meet criteria in this tumor system.

Pharmacological disposition and antitumor studies indicated that polyvinylpyrrolidone and hydrochloride formulations of ellipticine were superior to ellipticine base. Therefore, tablet formulations incorporating these features were prepared and evaluated using *in vitro* dissolution at 37°. In Fig. 3, the dissolution rates of ellipticine tablets with polyvinylpyrrolidone mol. wt. 10,000 in ratios of 1:15.7 and 1:22 were plotted and compared to ellipticine tablets without polyvinylpyrrolidone. The inherent low solubility of ellipticine was evident from the dissolution data. The initial dissolution of the polyvinylpyrrolidone tablets was rapid and essentially the same at the two polyvinylpyrrolidone ratios. After 15 min, the rate slowed considerably, and dissolution of the 1:22 ratio was about 10% higher than the 1:15.7 preparation.

This experiment suggests a critical role of polyvinylpyrrolidone in the mixture. Presumably, polyvinylpyrrolidone initially is in high concentration at the liquid interface but dissolves rapidly. The dissolution rate of ellipticine thus subsides as the polyvinylpyrrolidone diffuses. An attempt was made to improve dissolution by decreasing the diffusion of the polymer *via* inclusion of a higher molecular weight, more viscous polyvinylpyrrolidone. In Fig. 4, the dissolution of ellipticine–polyvinylpyrrolidone mixtures in a 1:22 ratio is presented. Twenty percent of the polyvinylpyrrolidone portion was either mol. wt. 40,000 or 160,000. The dissolution plots for polyvinylpyrrolidone mol. wt. 10,000 alone and mol. wt. 10,000–40,000 (4:1) are essentially superimposable, and the amount dissolved was less than was observed with polyvinylpyrrolidone mol. wt. 10,000–160,000 (4:1). Although the plot is nonlinear with the last-mentioned preparation, the dissolution was more gradual than with polyvinylpyrrolidone mol. wt. 10,000 alone, suggesting that the increased viscosity of polyvinylpyrrolidone mol. wt. 160,000 decreases polymer diffusion from the tablet matrix.

In the diffusion layer model (11), the rate is influenced by the solubility of free drug and drug complex plus the diffusion coefficients of all polymeric species. In this case, the role of the free drug is negligible due to its low intrinsic solubility. The concentration of bound or solubilized drug

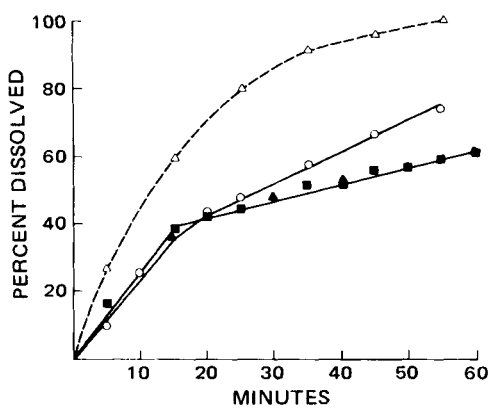

Figure 4—*Dissolution of ellipticine–polyvinylpyrrolidone (1:22) tablets at 37° in water. Key: ▲, polyvinylpyrrolidone mol. wt. 10,000; ■, polyvinylpyrrolidone mol. wt. 10,000–40,000 (4:1); ○, polyvinylpyrrolidone mol. wt. 10,000–160,000 (4:1); and △, polyvinylpyrrolidone mol. wt. 10,000–160,000 (4:1) using simulated gastric juice.*

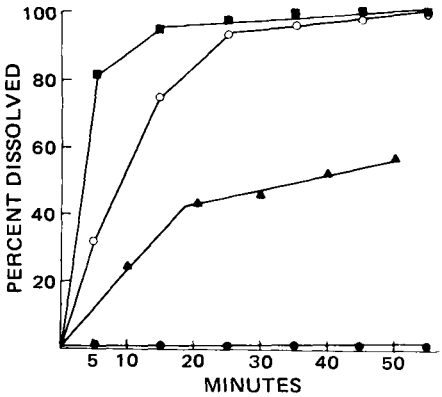

Figure 5—*Effect of media on the dissolution of ellipticine tablets at 37°. Key: ▲, ellipticine–polyvinylpyrrolidone mol. wt. 10,000 (1:22) in water; ○, ellipticine–polyvinylpyrrolidone mol. wt. 10,000 (1:22) in 2% polyvinylpyrrolidone; ●, ellipticine–mannitol in water; and ■, ellipticine–mannitol in 2.1% polyvinylpyrrolidone.*

at the interface depends on the solubility of unbound forms of drug in the diffusion layer and of polymers at the interface. Polyvinylpyrrolidone mol. wt. 160,000 molecules presumably render the diffusion layer more viscous and retard bulk flow of polyvinylpyrrolidone, thus enhancing the formation of drug–polymer complexes of high solubility.

To evaluate these assumptions, dissolution was carried out in polyvinylpyrrolidone 2.1 or 2% medium using tablets containing ellipticine base plus mannitol or ellipticine–polyvinylpyrrolidone mol. wt. 10,000 (1:22) ratio (Fig. 5). The final polyvinylpyrrolidone concentration in the medium was 2.1%. Dissolution data for the same tablets in water are presented for comparison. The ellipticine–mannitol tablet dissolved completely in polyvinylpyrrolidone in about 15 min. In contrast, the polyvinylpyrrolidone (1:22) tablet dissolved more slowly and reached an equivalent level in 25–35 min. With ellipticine–polyvinylpyrrolidone tablets, the presence of polyvinylpyrrolidone in the diffusion layer imparted a barrier to the boundary movement of ellipticine, thus impairing dissolution.

To approximate the *in vivo* environment more closely, dissolution studies were conducted on the ellipticine–polyvinylpyrrolidone mol. wt. 10,000–160,000 tablet and the ellipticine hydrochloride tablet in simulated gastric juice (12) at 37°. Complete dissolution of the polyvinylpyrrolidone preparation was achieved within 1 hr (Fig. 4). The enhanced dissolution was due in part to pH and formation of the protonated form of ellipticine. Surprisingly, the dissolution of ellipticine hydrochloride was markedly depressed (Fig. 6). Although dissolution was essentially complete in 5–10 min, only about 40% of the available ellipticine dissolved.

Since simulated gastric juice contains hydrochloric acid and sodium chloride at a chloride concentration of ~110 mEq/liter, the dissolution of ellipticine hydrochloride tablets was evaluated in 0.1 *N* HCl, 0.1 *N* H_2SO_4, and water. Hydrochloric acid also markedly depressed the dissolution of ellipticine. However, the dissolution of the same tablet in water or 0.1 *N* H_2SO_4 was rapid and plateaued at about 80% (Fig. 6). These data demonstrate that the chloride ion rather than pH depresses ellipticine hydrochloride dissolution; under conditions simulating the gastric en-

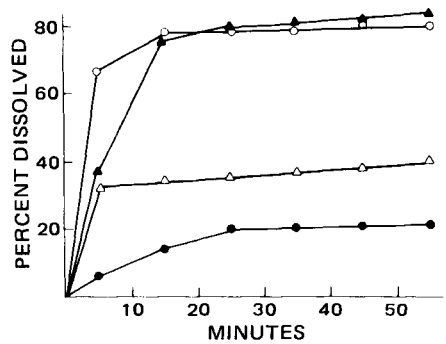

Figure 6—*Effect of media on the dissolution of ellipticine hydrochloride tablets at 37°. Key: ●, 0.1 N HCl; △, simulated gastric juice; ○, water; and ▲, 0.1 N H_2SO_4.*

vironment, dissolution of the ellipticine–polyvinylpyrrolidone preparation is essentially complete.

Similarly, Agharkar *et al.* (13) demonstrated that the dissolution of α-(2-piperidyl)-3,6-bis(trifluoromethyl)-9-phenanthrenemethanol, an antimalarial agent, was markedly depressed in 0.1 *N* HCl but not in an equivalent concentration of 0.1 *N* H_2SO_4. The solubility of this antimalarial was inversely related to the chloride-ion concentration, and the results were attributed to a common ion effect.

DISCUSSION

Several investigators described increases in solubility of various compounds by polyvinylpyrrolidone (14, 15), but the effect of this interaction on the dissolution rate has been varied. Polyvinylpyrrolidone reduced salicylic acid dissolution, and this effect was attributed to the increased viscosity or formation of a polyvinylpyrrolidone–salicylic acid complex (16). Dissolution rates of ephedrine hydrochloride, potassium chloride, and sodium chloride from compressed disks also were decreased by polyvinylpyrrolidone (17, 18). In contrast, Simonelli *et al.* (19) described enhanced solubility and dissolution of polyvinylpyrrolidone–sulfathiazole mixtures or coprecipitates. Solid dispersions of reserpine, a poorly water-soluble drug, with polyvinylpyrrolidone enhanced its *in vitro* dissolution and absorption. In addition, a polyvinylpyrrolidone–digitoxin coprecipitate exhibited enhanced dissolution and absorption as indicated by a decrease in the LD_{50} value (20, 21).

Polyvinylpyrrolidone also increased dissolution of hydroflumethiazide and hydrochlorothiazide (22, 23). Interestingly, the absorption of the drug in physical mixture with polyvinylpyrrolidone was superior to the coprecipitate or free drug (23). Simonelli (24) previously reported that ellipticine solubility was enhanced by preparation of a polyvinylpyrrolidone coprecipitate and used this technique to prepare a product for intravenous use. Toxicity inherent with intravenous ellipticine necessitated an alternative administration route.

The marked enhancement of ellipticine absorption by polyvinylpyrrolidone was investigated orally and was compared with salt formation. Absorption of ellipticine as a solution in polyvinylpyrrolidone mol. wt. 10,000 or as a mixture with mol. wt. 10,000–160,000 (4:1) was two- to threefold higher than that of the parent drug and equivalent to or slightly better than that of the hydrochloride salt. The polyvinylpyrrolidone mol. wt. 10,000–160,000 (4:1) mixture also exhibited antitumor activity by oral and intraperitoneal routes. When using the optimal dose level in milligrams per kilogram as an index of absorption, the optimal dose was one level less than that of the suspension of free drug and equivalent to that of the hydrochloride salt. The intraperitoneal data for polyvinylpyrrolidone and hydrochloride preparations indicate, however, that oral absorption is incomplete regardless of formulation. The optimal dose was one level lower than the oral one, and the response in terms of an increase in lifespan was higher. Similar comparisons of routes of administration were not carried out in the distribution studies. Mice receiving polyvinylpyrrolidone and hydrochloride preparations of ellipticine at 250 mg/kg ip died within 24 hr.

Since the biological experiments indicated comparability between polyvinylpyrrolidone and hydrochloride preparations, ellipticine dissolution from several tablet formulations was evaluated. As expected because of the marked effect of polyvinylpyrrolidone on the low intrinsic solubility of ellipticine (8), the dissolution was related to the polyvinylpyrrolidone concentration in the tablet. Dissolution data from polyvinylpyrrolidone mixtures were compatible with the diffusion layer model and demonstrated that drug release could be enhanced *in vitro* by inclusion of high and low molecular weight polymeric material.

Extrapolation of biological data described in this report to larger animals may be difficult since dissolution was avoided by administering two preparations in solution (polyvinylpyrrolidone mol. wt. 10,000 and hydrochloride salt). In contrast to the mouse, the dog or monkey would be administered ellipticine in a tablet. Marked differences in dissolution were observed *in vitro* in simulated gastric juice with tablet formulations similar to those evaluated *in vivo*. Studies are in progress to compare the absorption of ellipticine in polyvinylpyrrolidone mol. wt. 10,000–160,000 (4:1) with that of the hydrochloride preparation in dogs or monkeys.

REFERENCES

(1) M. Hayat, G. Mathe, E. Chenu, M. M. Janot, P. Potier, N. Dat-Xuong, A. Gave, T. Sevenet, J. Poisson, J. Miet, J. Le Men, F. Le Goffic, A. Gouyette, A. Ahond, L. K. Dalton, and T. A. Connors, *Biomedicine*, **21**, 101 (1974).

(2) E. Herman, J. Vick, and B. Burka, *Toxicol. Appl. Pharmacol.*, **18**, 743 (1971).

(3) M. A. Innis and I. P. Lee, *ibid.*, **22**, 304 (1976).

(4) C. T. Hardesty, N. A. Chaney, and J. A. R. Mead, *Cancer Res.*, **32**, 1884 (1972).

(5) R. I. Geran, N. H. Greenberg, M. M. McDonald, A. M. Schumacher, and B. J. Abbott, *Cancer Chemother. Rep., Part 3*, **3**, 1 (1972).

(6) "The United States Pharmacopeia," 19th rev., Mack Publishing Co., Easton, Pa., 1975, p. 651.

(7) K. W. Kohn, M. J. Waring, D. Glaubiger, and C. A. Friedman, *Cancer Res.*, **35**, 71 (1975).

(8) A. Rahman, J. P. Davignon, and J. C. Cradock, *Proc. Am. Assoc. Cancer Res.*, **17**, 119 (1976).

(9) N. R. Bachur, A. L. Moore, J. G. Bernstein, and A. Liu, *Cancer Chemother. Rep.*, **54**, 89 (1970).

(10) N. R. Bachur, R. C. Hildebrand, and R. S. Jaenke, *J. Pharmacol. Exp. Ther.*, **191**, 331 (1974).

(11) W. I. Higuchi, *J. Pharm. Sci.*, **56**, 315 (1967).

(12) "The United States Pharmacopeia," 19th rev., Mack Publishing Co., Easton, Pa., 1975, p. 765.

(13) S. Agharkar, S. Lindenbaum, and T. Higuchi, *J. Pharm. Sci.*, **65**, 747 (1976).

(14) T. Higuchi and R. J. Kuramoto, *J. Am. Pharm. Assoc., Sci. Ed.*, **43**, 393 (1954).

(15) D. Guttman and T. Higuchi, *ibid.*, **45**, 659 (1956).

(16) M. Gibaldi and H. Weintraub, *J. Pharm. Sci.*, **57**, 832 (1968).

(17) A. T. Florence and A. Rahman, *J. Pharm. Pharmacol., Suppl.*, **27**, 55 (1975).

(18) A. T. Florence, P. H. Elworthy, and A. Rahman, *ibid.*, **25**, 779 (1973).

(19) A. P. Simonelli, S. C. Mehta, and W. I. Higuchi, *J. Pharm. Sci.*, **58**, 538 (1969).

(20) E. I. Stupak and T. R. Bates, *ibid.*, **61**, 400 (1972).

(21) *Ibid.*, **62**, 1806 (1973).

(22) O. I. Corrigan and R. F. Timoney, *J. Pharm. Pharmacol.*, **27**, 759 (1975).

(23) O. I. Corrigan, R. F. Timoney, and M. J. Whelan, *ibid.*, **28**, 703 (1976).

(24) A. P. Simonelli, "Report to the National Cancer Institute," Contract PH 43-68-1284, 1969.

ACKNOWLEDGMENTS

Presented in part at the Basic Pharmaceutics Section, APhA Academy of Pharmaceutical Sciences, Orlando meeting, November 1976.

The authors thank Mrs. Dee Trageser and Mrs. Deloris Lewis for assistance in the preparation of this manuscript and Mr. Scott Hallgren for technical support. They also acknowledge the aid of Dr. William R. Cobb, Mason Research Institute, in obtaining antitumor evaluations.

Polyvinylpyrrolidone mol. wt. 160,000 was a specially dried powder and was generously provided by Dr. Louis Blecher of GAF Corp.

Thermodynamic Group Contributions for Hydroxyl, Amino, and Methylene Groups

J. HOWARD RYTTING ˣ, LARRY P. HUSTON, and TAKERU HIGUCHI

Received June 22, 1977, from the *Department of Pharmaceutical Chemistry, School of Pharmacy, University of Kansas, Lawrence, KS 66045.* Accepted for publication August 5, 1977.

Abstract □ The hydroxyl, amino, and methylene group contributions to the free energy of transfer from water to the organic phase, from water to the vapor phase, and from heptane to the vapor phase were determined from the Henry constants of aliphatic series of hydrocarbons, alcohols, and amines in dilute aqueous and heptane solutions. The Henry constant of each solution was measured using a vapor headspace GLC method with very dilute aqueous and organic solutions. Plotting the log of the Henry constant *versus* carbon number yielded a straight line from which the methylene group contribution was calculated. This value was −150 cal/mole for water to vapor, 760 cal/mole for heptane to vapor, and −910 cal/mole for water to the organic phase. The hydroxyl contribution was 6890 cal/mole for water to vapor, 1320 cal/mole for organic to vapor, and 5570 cal/mole for the transfer of a hydroxyl group from water to the organic phase. For the amino group, the free energy of transfer was 6470 cal/mole for water to vapor, 1490 cal/mole for heptane to vapor, and 4980 cal/mole for water to the organic phase. The values determined were in reasonable agreement with literature data. Such data can be used to predict the effects of various functional groups on the distribution and transport tendencies of drugs.

Keyphrases □ Thermodynamic group contributions—hydroxyl, amino, and methylene, free energy of transfer from one phase to another □ Hydrocarbons, aliphatic series—methylene group contribution to free energy of transfer from one phase to another □ Alcohols, aliphatic series—hydroxyl group contribution to free energy of transfer from one phase to another □ Amines, aliphatic series—amino group contribution to free energy of transfer from one phase to another

Over the years, considerable effort has been directed toward understanding the relationship between molecular structure and the distribution–transport characteristics of chemical and drug species. Although distribution is an equilibrium process and transport is a rate process, transport is subject to distribution for all passive diffusion processes and for most active transport phenomena in their presaturation phase. For example, a substantial portion of drug absorption involves partitioning into the rate-controlling membrane. The lipophilic–hydrophilic balance of ophthalmic drugs, for instance, largely determines their transcorneal absorption rate. Similarly, the GI absorption rate of passively absorbed drugs usually depends on their ability to partition into the rate-determining barrier membrane. This condition is also true for dermal agents.

BACKGROUND

Such basic considerations can be used to design and develop more effective drugs and form the rationale for the use of structure–activity relationships. Over the years, several *a priori* methods for predicting the thermodynamics of organic molecules in solution have been proposed. However, no single approach has been completely satisfactory. The thermodynamic parameters that define solution behavior provide a basis for predicting solubility and the distribution properties of molecules. A method that allows *a priori* estimation of solution behavior should have application in understanding the distribution and transport of drug molecules in the body.

Ideally, it is preferable to be able to predict how a particular solute will behave in a given solvent simply from the physical properties of the pure components (*e.g.*, molar volume, solubility parameter, dipole moment, and polarizability). However, rigorous methods based on this approach are limited almost entirely to mixtures of nonpolar species. The extension of statistical thermodynamics to binary systems has yet to provide good estimates of nonideal behavior, and often the derived equations are based on mathematically convenient approximations that have little physical significance. Consequently, a semiempirical group contribution approach appears to be an acceptable alternative.

In this approach, a molecule is considered to be composed of groups acting independently of the rest of the molecule and having certain associated thermodynamic properties. Therefore, the activity coefficient, free energy, or partition coefficient can be found from the sum of the values for the different groups comprising the molecule. In contrast to the more theoretical approaches, this method is derived solely from an analysis of empirical data. However, the results frequently assume a form similar to those mathematically derived from statistical mechanics. In cases where two polar groupings are close to each other on a solute molecule, some modification of the additive concept is necessary. However, there is no reason why such correction factors could not be calculated. This concept was originally introduced by Langmuir (1) as the "principle of independent surface action." It was refined and verified by Butler and coworkers in papers on the thermodynamics of hydration (2, 3).

The group contribution approach has been applied to the transfer of whole molecules from one phase to another (4). Its application to the transfer of various hydrocarbon groups from water to nonpolar solvents was reported (5). In this study, the group contribution approach is extended to polar groups. The hydroxyl, amino, and methylene group contributions to the free energy of transfer from water to the organic phase, from water to the vapor phase, and from heptane to the vapor phase were determined from the Henry constants of aliphatic series of hydrocarbons, alcohols, and amines in dilute aqueous and heptane solutions.

EXPERIMENTAL

Equipment and Reagents—All analyses were carried out on a gas chromatograph[1] with a dual hydrogen flame detector using helium as the carrier gas. For the alcohol studies, matched stainless steel dual columns[2] were used. For the amines, columns packed with acid-washed Chromosorb W[3] were used.

Gastight syringes[4] (2.5 or 10 ml) were used for injections. Serum vials[5], 30 ml, and rubber stoppers were used for solution equilibration. All amines and alcohols[6] had a purity of at least 99.5% as determined by GLC. These compounds were redistilled and stored over molecular sieves to remove possible traces of water.

Aqueous solutions were prepared with water distilled a second time from acid permanganate in an all-glass apparatus. Organic solutions were prepared with heptane[7] with a purity of at least 99.5% as ascertained by GLC.

To overcome the turbidity encountered during solution of the amines in distilled water and to reduce the proportion of ionized species present, 0.01 *N* NaOH was used as the aqueous phase for amines. To exclude carbon dioxide as much as possible, the distilled water was boiled before use.

Procedure—Dilute solutions (0.001–0.01 mole fraction) of either al-

[1] Beckman GC-45.
[2] Beckman 96670W, 1.830 m × 0.635 cm o.d., packed with C-22 Firebrick, 42–60 mesh, which had been coated with 30% (w/w) of a mixture consisting of (v/v): polyethylene glycol 600, three parts; diisodecyl phthalate, 10 parts; and Flexol 8N8, 15 parts.
[3] DMCS 80–100 mesh containing 5% (w/w) dc 550 as the liquid phase.
[4] Hamilton.
[5] Fisher.
[6] Polyscience Corp.
[7] Phillips Petroleum Co.

Table I—Henry Constants and γ_i^∞ Values in Water

Compound	Henry Constants: mm Hg/mole Fraction	Henry Constants: mm Hg/mole	P_i^{0a}, mm Hg	Measured γ_i^∞	Literature γ_i^∞
		Alcohols			
Methanol	187	3.37	122.2	1.53	4.51[b], 2.29[c], 1.51[d]
Ethanol	220	3.96	59.0	3.73	3.48[d], 3.69[e], 4.68[c]
1-Propanol	283	5.09	20.1	14.1	14.4[e], 12.5[b], 10.6[c]
2-Propanol	335	6.03	44.0	7.61	11.0[c], 6.54[d], 7.7[f]
1-Butanol	358	6.45	6.78	52.8	52.9[f]
2-Butanol	424	7.64	17.1	24.8	25.1[f], 24.7[d]
2-Methyl-1-propanol	516	9.29	11.6	44.5	43.2[f]
2-Methyl-2-propanol	547	9.85	42.4	12.9	11.8[f], 10.1[d]
1-Pentanol	461	8.30	2.17	212.5	214[f], 169[d]
1-Hexanol	600	10.8	0.72	834	903[f]
		Amines			
Butylamine	800	14.4	103.9	7.70	7.7[g]
Amylamine	1030	18.5	34.5	29.7	30.4[g]
Hexylamine	1310	23.6	11.4	114.5	109[g]
Heptylamine	1700	30.5	3.95	429	—
Octylamine	2170	39.1	1.34	1621	—
		Alkanes			
Pentane	5.33×10^7	9.61×10^5	513	1.04×10^5	—
Hexane	7.62×10^7	1.37×10^6	151	5.04×10^5	—
Heptane	8.63×10^7	1.56×10^6	45.7	1.89×10^6	—
Octane	1.35×10^8	2.42×10^6	14.0	9.61×10^6	—

[a] Vapor pressures for the alcohols are from Ref. 6, p. 384; those for the alkanes are from G. A. Riddick and W. G. Bunger, "Techniques of Chemistry, vol. II, Organic Solvents," A. Weissberger, Ed., Wiley-Interscience, New York, N.Y., 1970. [b] Reference 2. [c] Reference 11. [d] Reference 12. [e] Reference 13. [f] Reference 14. [g] Reference 15.

cohol or amine in water and heptane were prepared by weight in 25-ml glass-stoppered erlenmeyer flasks.

In the alcohol study, 2 ml of these solutions was then placed into 30-ml serum vials. The vials were tightly stoppered and placed in a constant-temperature water bath (25 ± 0.05°). The stoppers were punctured for approximately 15 sec to equalize vial pressure with atmospheric room pressure. The samples were allowed to equilibrate for a minimum of 15 min before analysis. Equilibration times of 5 min or more were satisfactory.

Samples of headspace gas ranging generally between 0.2 and 1.0 ml (dependent on the specific vapor pressure of the alcohol under study) were removed and injected into the gas chromatograph for analysis along with an equal amount of room air. An amount of air (equal to the total amount of sample removed) was replaced into the serum vial headspace between repeated injections. All data can be considered to be obtained under conditions of infinite dilution, so the concentrations of the species under investigation are equal to their activities.

For the amines in water and heptane, 4 ml of solution was placed into 30-ml serum vials. The vials were tightly stoppered with care to ensure that the amine solutions did not directly contact the rubber stoppers. The stoppers were punctured for approximately 30 sec to equalize vial pressure with atmospheric pressure. The vials were placed in a 25° water bath controlled to ±0.05°. The samples were allowed to equilibrate for 30 min before analysis. Less than 2-ml samples of headspace gas were removed and injected into the gas chromatograph for analysis along with an equal amount of room air.

RESULTS AND DISCUSSION

An ideal solution is defined as one that obeys Raoult's law and in which the activity of a component is equal to its mole fraction over the entire concentration range:

$$a_i = X_i \qquad \text{(Eq. 1)}$$

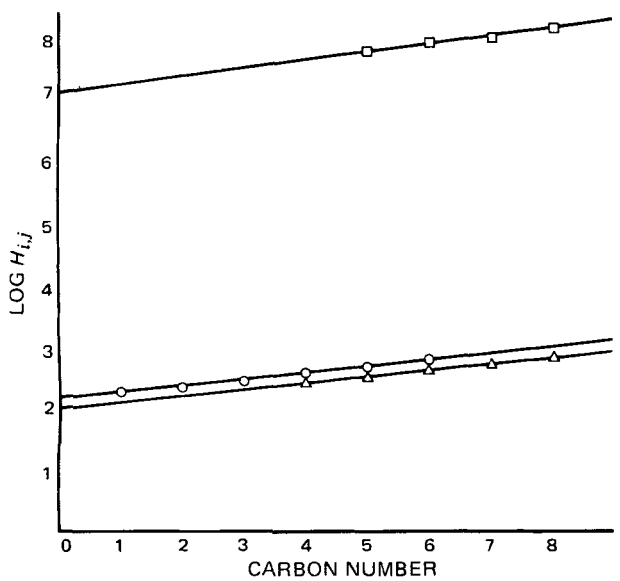

Figure 1—*Log Henry constants* versus *carbon number for homologous series of alkanes (□), alcohols (○), and amines (△) in water.*

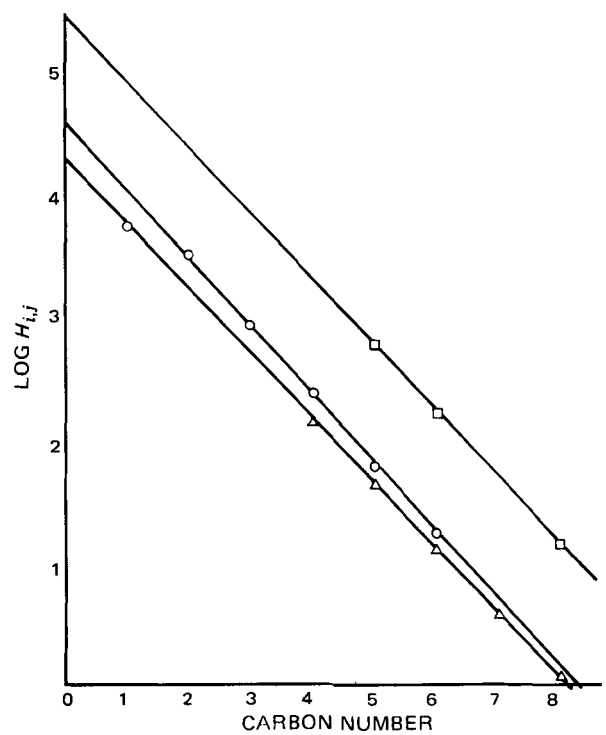

Figure 2—*Log Henry constants* versus *carbon number for homologous series of alkanes (□), alcohols (○), and amines (△) in heptane.*

Table II—Group Contribution to the Free Energy of Transfer, $\Delta(\Delta G)_x$, at 25°

Group	Process	System Studied	$\Delta(\Delta G)$, cal/mole: Measured	$\Delta(\Delta G)$, cal/mole: Literature
Methylene	Water to vapor phase	Alcohols and amines in water	−148	—
Methylene	Heptane to vapor phase	Alcohol in heptane	759	—
		Amines in heptane	703	—
		Alkanes in heptane	729	—
Methylene	Water to heptane phase	Alcohols	−907	−917[a], −877[b], −872[c], −850[d]
		Amines	−851	−849[e], −880[e]
Hydroxyl	Water to vapor phase	Alcohol in water	6880	—
Hydroxyl	Heptane to vapor phase	Alcohol in heptane	1320	—
Hydroxyl	Water to heptane phase	—	5570	5280[f], 5650[g]
Amino	Water to vapor phase	Amines in water	6470	—
Amino	Heptane to vapor phase	Amines in heptane	1490	—
Amino	Water to heptane phase	—	4980	5140[f]

[a] Reference 5. [b] Reference 17. [c] Reference 18. [d] Reference 19. [e] Reference 4, Table 21. [f] Reference 20. [g] Reference 21.

Deviations from ideal behavior are, therefore, reflected in the degree to which the value of the activity coefficient, γ_i, differs from unity, where:

$$\gamma_i = \frac{a_i}{X_i} \qquad \text{(Eq. 2)}$$

A disadvantage of a correlation based on γ_i values is that the standard state, the pure solute, is itself a complex environment. The choice of a pure solute as the standard state was criticized previously (6, 7). Rytting *et al.* (8) considered the choice of the standard state and concluded that the infinitely dilute solute in a reference hydrocarbon solvent is preferable for drug systems; *i.e.*, drug solution behavior should be examined on the basis of Henry's limiting law rather than Raoult's law, *i.e.*:

$$H_{i,j} = \frac{P_i}{X_i \gamma_i^*} \qquad \text{(Eq. 3)}$$

where $H_{i,j}$ is Henry's constant and γ_i^* is an activity coefficient that has a value of unity at infinite dilution.

Prausnitz (9) and Miller and Prausnitz (10) discussed the relationship between activity coefficients based on Raoult's law ($\gamma_i \rightarrow 1$ as $X_i \rightarrow 1$) and those based on Henry's law ($\gamma_i^* \rightarrow 1$ as $X_i \rightarrow 0$).

In the limit as $X_i \rightarrow 0$:

$$H_{i,j} = \gamma_i^\infty P_i^0 \qquad \text{(Eq. 4)}$$

where γ_i^∞ is the activity coefficient of the solute at infinite dilution in the solvent and the pure solute is taken as the standard state.

Table I shows the γ_i^∞ values and the Henry constants in both a mole fraction and molar scale for the alcohols and amines in water found in this study at 25° along with the P_i^0 values of the pure substances as recorded in the literature at 25°.

The values for the Henry constants of alkanes in water, also listed in Table I, were obtained by calculation from the solubility data of McAuliffe (16). He determined the solubilities in water at room temperature of various alkanes by direct injection of hydrocarbon-saturated water into a gas chromatograph and reported the solubilities in grams of hydrocarbon per 10^6 g of water.

The Henry constants for the alkanes in water were determined by converting the solubility data of McAuliffe into mole fraction, X_i, solubility. The following assumptions were made:

1. The activity of alkane must be the same in both phases that are in equilibrium with each other.
2. The miscibility of the two liquids being slight, the activity, a_i, of the alkane in the alkane-rich phase will be practically one, while the activity in the dilute aqueous phase will be equal to $X_s \gamma_i^\infty$, where X_s is the solubility expressed as a mole fraction. Thus, $X_s \gamma_i^\infty = 1$; and for a saturated solution of mole fraction X_s of pure alkane, one may write:

$$\gamma_i^\infty = \frac{1}{X_s} \qquad \text{(Eq. 5)}$$

Similarly, Henry constants are obtained as described earlier in Eq. 4. The calculated values for the γ_i^∞ and the Henry constants for the alkanes in water are listed in Table I. Although there is a lack of agreement among literature values, a relatively constant methylene group contribution is often observed within individual studies.

Figure 1 shows a plot of the log $H_{i,j}$ values *versus* carbon number for the alcohols and amines studied in water as well as for alkanes in water. The free energy of the methylene group is calculated from the slope of the line:

$$\Delta(\Delta G) = -RT \ln (\text{slope}) \qquad \text{(Eq. 6)}$$

The result was −148 cal/mole for the transfer of a methylene group from water to the vapor phase. Also, from Fig. 1, the hydroxyl and amine group contributions may be obtained by subtracting the alkane in water values from the alcohol in water and amine in water values for each corresponding carbon number:

$$\Delta(\Delta G)_X = -RT (\ln H_{i,jRX} - \ln H_{i,jRH}) \qquad \text{(Eq. 7)}$$

Table III—Henry Constants and γ_i^∞ Values in Heptane

Compound	Henry Constants: mm Hg/mole Fraction	Henry Constants: mm Hg/mole	P_i^{0a}, mm Hg	Measured γ_i^∞	Literature γ_i^∞
		Alcohols			
Methanol	4970	733	122.2	40.6	29.6[b], 92.6[c]
Ethanol	2800	414	59.0	47.5	16.5[b], 49[c]
1-Propanol	810	119.5	20.1	40.3	14.2[b]
2-Propanol	1550	229	44.0	35.3	32.4[c]
1-Butanol	226	33.4	6.78	33.4	13.6[b], 37.1[c]
2-Butanol	511	75.3	18.29	27.9	27.9[c]
2-Methyl-1-propanol	332	49.0	10.22	32.5	32.5[c]
2-Methyl-2-propanol	775	114	43.0	18.0	18.0[c]
1-Pentanol	59.0	8.71	2.17	27.2	—
1-Hexanol	17.1	2.52	0.72	23.8	—
		Amines			
Butylamine	132	19.5	104	1.27	—
Amylamine	41.8	6.16	34.5	1.21	—
Hexylamine	12.9	1.91	11.4	1.13	—
Heptylamine	3.79	0.56	3.95	0.96	—
Octylamine	1.17	0.17	1.34	0.87	—
		Alkanes			
Pentane	554	81.65	513.6	1.08	—
Hexane	156	23.0	151	1.03	—
Octane	13.9	2.04	14	0.99	—

[a] See footnote *a*, Table I. [b] Reference 22. [c] Reference 12.

The results are shown in Table II.

Figure 2 shows a plot of the log $H_{i,j}$ values (Table III) *versus* the carbon number for the alcohols, amines, and alkanes in heptane. The free energy of the methylene group was about 730 cal/mole for the transfer of a methylene group from organic to vapor phases. The hydroxyl and amino group contributions also may be obtained from Fig. 2 by subtracting the alkane in heptane values for each corresponding carbon number as in Eq. 7. These values were 1320 cal/mole for the hydroxyl group and 1490 cal/mole for the amino group from organic to vapor phases (Table II).

The group contribution to the free energy of transfer for the methylene group from water to organic phases was −851 cal/mole based on the data for the amines. The value found for the methylene group in the alcohol studies was −907 cal/mole. Both of these values agree with reported literature values for the methylene group (Table II).

The group contribution to the free energy of transfer for the amino group from water to the organic phase was 4980 cal/mole. Pescar and Martin (20) used GLC to study the thermodynamic solution properties of two-component volatile nonelectrolyte solutions at infinite dilution. Their method for the determination of γ_i^∞ was based on chromatographic retention volumes, and the value reported for the free energy contribution of transfer of the amino group from water to the organic phase was 5140 cal/mole.

The group contribution to the free energy change for the hydroxyl group from water to the organic phase was 5570 cal/mole, which is in reasonable agreement with the literature values shown in Table II.

REFERENCES

(1) I. Langmuir, *Colloid Symp. Monogr.*, **3**, 48 (1925).

(2) J. A. V. Butler, D. W. Thomson, and W. H. Maclennan, *J. Chem. Soc.*, **1933**, 674.

(3) J. A. V. Butler and P. Harrower, *Trans. Faraday Soc.*, **33**, 171 (1937).

(4) S. S. Davis, T. Higuchi, and J. H. Rytting, in "Advances in Pharmaceutical Sciences," vol. 4, H. S. Bean, A. H. Beckett, and J. E. Carless, Eds., Academic, London, England, 1974, pp. 73–261.

(5) M. J. Harris, T. Higuchi, and J. H. Rytting, *J. Phys. Chem.*, **77**, 2694 (1973).

(6) J. A. V. Butler, "Chemical Thermodynamics," 5th ed., Macmillan, London, England, 1962, p. 382.

(7) C. H. Deal and E. L. Derr, *Ind. Eng. Chem.*, **60**, 28 (1968).

(8) J. H. Rytting, T. Higuchi, and S. S. Davis, *J. Pharm. Sci.*, **61**, 816 (1972).

(9) J. M. Prausnitz, "Molecular Thermodynamics of Fluid Phase Equilibria," Prentice-Hall, Englewood Cliffs, N.J., 1969, pp. 190–192.

(10) R. C. Miller and J. M. Prausnitz, *Ind. Eng. Chem. Fundam.*, **8**, 449 (1969).

(11) "Chemical Engineering Handbook," 4th ed., R. H. Perry, C. H. Chilton, and S. D. Kirkpatrick, Eds., McGraw-Hill, New York, N.Y., 1963.

(12) G. J. Pierotti, C. H. Deal, and E. L. Derr, *Ind. Eng. Chem.*, **51**, 95 (1959).

(13) D. J. Crisp and H. A. Marr, *Proc. 2nd Conf. Surface Activ.*, **4**, 310 (1967).

(14) J. A. V. Butler, C. N. Ramchandani, and D. W. Thomson, *J. Chem. Soc.*, **1935**, 280.

(15) A. O. Christie and D. J. Crisp, *J. Appl. Chem.*, **17**, 11 (1967).

(16) C. McAuliffe, *J. Phys. Chem.*, **70**, 1267 (1966).

(17) B. Crugman, M.S. thesis, University of Kansas, Lawrence, Kans., 1971.

(18) R. S. Hansen, F. A. Miller, and S. D. Christian, *J. Phys. Chem.*, **59**, 391 (1955).

(19) T. Higuchi and S. S. Davis, *J. Pharm. Sci.*, **59**, 1376 (1970).

(20) R. E. Pescar and J. J. Martin, *Anal. Chem.*, **38**, 1661 (1966).

(21) D. E. Martire and P. Riedl, *J. Phys. Chem.*, **72**, 3478 (1968).

(22) D. C. Locke, *J. Gas Chromatogr.*, **5**, 202 (1967).

ACKNOWLEDGMENTS

Presented at the Basic Pharmaceutics Section, APhA Academy of Pharmaceutical Sciences, Orlando meeting, November 1976.

Abstracted in part from a dissertation submitted by L. P. Huston to the University of Kansas in partial fulfillment of the Doctor of Philosophy degree requirements.

Supported by the University of Kansas General Research Fund and Grant 1P01 GM 22357-01, National Institutes of Health. L. P. Huston was supported by Public Health Service Predoctoral Fellowship 5 F01 GM 38,977.

Spectrophotometric Determinations of 3-Dimethylaminomethylkhellin Hydrochloride and Khellin

HAMED ABU-SHADY * and E. H. GIRGIS ‡x

Received October 7, 1976, from the **Pharmaceutical Chemistry Department, Faculty of Pharmacy, Cairo University, Cairo, Egypt*, and the ‡*Stability Research Department, The Nile Company for Pharmaceuticals and Chemical Industries, El-Ameria, Cairo, A.R. Egypt.*
Accepted for publication August 9, 1977.

Abstract □ Spectrophotometric assays are proposed for the determination of 3-dimethylaminomethylkhellin hydrochloride and khellin in bulk chemical and dosage forms. The acid dye method, using methyl orange at pH 5, is applied to assay the amine in the form of an ion-pair extractable in chloroform with maximum absorbance at 420 nm. The perchloric acid method, depending on formation and extraction of the oxonium salts of both compounds, is used to assay the amine and khellin at 333 or 430 nm and at 325 or 410 nm, respectively. The reineckate method can be used to assay the amine as the reineckate derivative in acetone with maximum absorbance at 530 nm. However, small amounts of the amine (1.5–3 mg) can be determined as the reineckate in methanol with maximum absorbance at 245 nm. Stability determination of the two compounds can be done by the acid dye and perchloric acid methods. The three methods are sufficiently accurate, sensitive, and precise.

Keyphrases □ 3-Dimethylaminomethylkhellin—spectrophotometric analyses in bulk drug and dosage forms, various methods compared □ Khellin—spectrophotometric analyses in bulk drug and dosage forms, various methods compared □ Spectrophotometry—analyses, 3-dimethylaminomethylkhellin and khellin in bulk drug and dosage forms, various methods compared □ Spasmolytic agents—3-dimethylaminomethylkhellin and khellin, spectrophotometric analyses in bulk drug and dosage forms, various methods compared

3-Dimethylaminomethylkhellin hydrochloride (I) possesses approximately three times the spasmolytic activity of khellin and is only half as toxic (1). Clinical trials showed that I is well tolerated for the treatment of acute renal colics with negligible side effects (2).

For the quantitative determination of I, either the basic

The results are shown in Table II.

Figure 2 shows a plot of the log $H_{i,j}$ values (Table III) *versus* the carbon number for the alcohols, amines, and alkanes in heptane. The free energy of the methylene group was about 730 cal/mole for the transfer of a methylene group from organic to vapor phases. The hydroxyl and amino group contributions also may be obtained from Fig. 2 by subtracting the alkane in heptane values for each corresponding carbon number as in Eq. 7. These values were 1320 cal/mole for the hydroxyl group and 1490 cal/mole for the amino group from organic to vapor phases (Table II).

The group contribution to the free energy of transfer for the methylene group from water to organic phases was −851 cal/mole based on the data for the amines. The value found for the methylene group in the alcohol studies was −907 cal/mole. Both of these values agree with reported literature values for the methylene group (Table II).

The group contribution to the free energy of transfer for the amino group from water to the organic phase was 4980 cal/mole. Pescar and Martin (20) used GLC to study the thermodynamic solution properties of two-component volatile nonelectrolyte solutions at infinite dilution. Their method for the determination of γ_i^∞ was based on chromatographic retention volumes, and the value reported for the free energy contribution of transfer of the amino group from water to the organic phase was 5140 cal/mole.

The group contribution to the free energy change for the hydroxyl group from water to the organic phase was 5570 cal/mole, which is in reasonable agreement with the literature values shown in Table II.

REFERENCES

(1) I. Langmuir, *Colloid Symp. Monogr.*, **3**, 48 (1925).

(2) J. A. V. Butler, D. W. Thomson, and W. H. Maclennan, *J. Chem. Soc.*, **1933**, 674.

(3) J. A. V. Butler and P. Harrower, *Trans. Faraday Soc.*, **33**, 171 (1937).

(4) S. S. Davis, T. Higuchi, and J. H. Rytting, in "Advances in Pharmaceutical Sciences," vol. 4, H. S. Bean, A. H. Beckett, and J. E. Carless, Eds., Academic, London, England, 1974, pp. 73–261.

(5) M. J. Harris, T. Higuchi, and J. H. Rytting, *J. Phys. Chem.*, **77**, 2694 (1973).

(6) J. A. V. Butler, "Chemical Thermodynamics," 5th ed., Macmillan, London, England, 1962, p. 382.

(7) C. H. Deal and E. L. Derr, *Ind. Eng. Chem.*, **60**, 28 (1968).

(8) J. H. Rytting, T. Higuchi, and S. S. Davis, *J. Pharm. Sci.*, **61**, 816 (1972).

(9) J. M. Prausnitz, "Molecular Thermodynamics of Fluid Phase Equilibria," Prentice-Hall, Englewood Cliffs, N.J., 1969, pp. 190–192.

(10) R. C. Miller and J. M. Prausnitz, *Ind. Eng. Chem. Fundam.*, **8**, 449 (1969).

(11) "Chemical Engineering Handbook," 4th ed., R. H. Perry, C. H. Chilton, and S. D. Kirkpatrick, Eds., McGraw-Hill, New York, N.Y., 1963.

(12) G. J. Pierotti, C. H. Deal, and E. L. Derr, *Ind. Eng. Chem.*, **51**, 95 (1959).

(13) D. J. Crisp and H. A. Marr, *Proc. 2nd Conf. Surface Activ.*, **4**, 310 (1967).

(14) J. A. V. Butler, C. N. Ramchandani, and D. W. Thomson, *J. Chem. Soc.*, **1935**, 280.

(15) A. O. Christie and D. J. Crisp, *J. Appl. Chem.*, **17**, 11 (1967).

(16) C. McAuliffe, *J. Phys. Chem.*, **70**, 1267 (1966).

(17) B. Crugman, M.S. thesis, University of Kansas, Lawrence, Kans., 1971.

(18) R. S. Hansen, F. A. Miller, and S. D. Christian, *J. Phys. Chem.*, **59**, 391 (1955).

(19) T. Higuchi and S. S. Davis, *J. Pharm. Sci.*, **59**, 1376 (1970).

(20) R. E. Pescar and J. J. Martin, *Anal. Chem.*, **38**, 1661 (1966).

(21) D. E. Martire and P. Riedl, *J. Phys. Chem.*, **72**, 3478 (1968).

(22) D. C. Locke, *J. Gas Chromatogr.*, **5**, 202 (1967).

ACKNOWLEDGMENTS

Presented at the Basic Pharmaceutics Section, APhA Academy of Pharmaceutical Sciences, Orlando meeting, November 1976.

Abstracted in part from a dissertation submitted by L. P. Huston to the University of Kansas in partial fulfillment of the Doctor of Philosophy degree requirements.

Supported by the University of Kansas General Research Fund and Grant 1P01 GM 22357-01, National Institutes of Health. L. P. Huston was supported by Public Health Service Predoctoral Fellowship 5 F01 GM 38,977.

Spectrophotometric Determinations of 3-Dimethylaminomethylkhellin Hydrochloride and Khellin

HAMED ABU-SHADY * and E. H. GIRGIS ‡x

Received October 7, 1976, from the **Pharmaceutical Chemistry Department, Faculty of Pharmacy, Cairo University, Cairo, Egypt*, and the ‡*Stability Research Department, The Nile Company for Pharmaceuticals and Chemical Industries, El-Ameria, Cairo, A.R. Egypt.*
Accepted for publication August 9, 1977.

Abstract □ Spectrophotometric assays are proposed for the determination of 3-dimethylaminomethylkhellin hydrochloride and khellin in bulk chemical and dosage forms. The acid dye method, using methyl orange at pH 5, is applied to assay the amine in the form of an ion-pair extractable in chloroform with maximum absorbance at 420 nm. The perchloric acid method, depending on formation and extraction of the oxonium salts of both compounds, is used to assay the amine and khellin at 333 or 430 nm and at 325 or 410 nm, respectively. The reineckate method can be used to assay the amine as the reineckate derivative in acetone with maximum absorbance at 530 nm. However, small amounts of the amine (1.5–3 mg) can be determined as the reineckate in methanol with maximum absorbance at 245 nm. Stability determination of the two compounds can be done by the acid dye and perchloric acid methods. The three methods are sufficiently accurate, sensitive, and precise.

Keyphrases □ 3-Dimethylaminomethylkhellin—spectrophotometric analyses in bulk drug and dosage forms, various methods compared □ Khellin—spectrophotometric analyses in bulk drug and dosage forms, various methods compared □ Spectrophotometry—analyses, 3-dimethylaminomethylkhellin and khellin in bulk drug and dosage forms, various methods compared □ Spasmolytic agents—3-dimethylaminomethylkhellin and khellin, spectrophotometric analyses in bulk drug and dosage forms, various methods compared

3-Dimethylaminomethylkhellin hydrochloride (I) possesses approximately three times the spasmolytic activity of khellin and is only half as toxic (1). Clinical trials showed that I is well tolerated for the treatment of acute renal colics with negligible side effects (2).

For the quantitative determination of I, either the basic

Table I—Effect of pH on Extraction of I–Dye Complexes[a] in Chloroform

pH of Buffer Solution[b]	Absorbance (1 cm) of Complex Using Methyl Orange (1.28×10^{-3} M)	Bromthymol Blue (6.4×10^{-4} M)
3.0	0.340	0.465
4.0	0.470	0.485
4.6	0.535	—
5.0	0.590	0.545
5.5	0.580	—
6.0	0.360	0.555
7.0	0.100	0.555
7.5	—	0.525
8.0	—	0.290

[a] Obtained from 1.0 ml (200 μg) of I solution with 3.0 ml of the dye solution and 6 ml of the required buffer extracted with 20.0 ml of chloroform. [b] Phthalate buffers were pH 3–5.5, and phosphate buffers were pH 6–8.

tertiary amino group or the chromone moiety can be used. Methods generally applied for basic amino group determinations include titration in nonaqueous solvents or with anionic surfactants and precipitation with picric acid, silicotungstic acid, tetraphenylboron, reineckate, and acid dyes. The furanochromone moiety exhibits strong absorption bands in the UV region amenable to spectrophotometric determination (3, 4). Many color reactions were described for the qualitative identification of khellin (5–9), and some are applicable to its spectrophotometric assay (5, 9–11).

Previous methods for khellin require either relatively long procedures (10, 11), with low sensitivity in the color reactions (5, 9), or some preliminary separation to eliminate possible interferences with UV spectrophotometry (3).

This report describes some sensitive and rapid spectrophotometric methods for the determination of I and khellin. These methods can be adopted for their pharmaceutical formulations.

EXPERIMENTAL[1]

Materials and Reagents—The following were used: I[2]; khellin[3]; methyl orange[4] aqueous solutions ($0.642–6.4 \times 10^{-3}$ M); bromthymol blue[5] in pH 7 buffers ($2.4–12 \times 10^{-4}$ M); 0.05 M phthalate buffer (BP 1973), pH 3–5.5; 0.05 M phosphate buffer (BP 1973), pH 6–8; I standard solutions in pH 5 and 7 buffers (10 mg of I/250 ml of the required buffer); I standard aqueous solution (20 mg of I/100 ml of water); khellin standard aqueous solution (25 mg of khellin dissolved in 2.5 ml of acetic acid and diluted with water to 250 ml); I standard chloroform solution (20 mg of I/100 ml of chloroform); khellin standard chloroform solution (25 mg of khellin/250 ml of chloroform); perchloric acid solution (~60% w/w) (60 g of perchloric acid[6] diluted to 70 g with water); acetic acid[5]; chloroform[5]; ammonium reineckate solution (2 g of reineckate[7]/100 ml of methanol); methanol[4]; and acetone[4].

Sample Preparations—*Bulk Chemical and Dosage Forms of I*—Dissolve or dilute and filter, if necessary, a weighed quantity or measured volume of the sample in a suitable quantity of water. Make successive dilutions to reach approximately 40 or 200 μg or 3.3 mg of I/ml in the acid dye, perchloric acid, or reineckate methods, respectively. Perform dilutions with water, but use pH 5 buffer in the acid dye method.

Khellin Bulk Chemical and Dosage Forms—Dissolve a weighed quantity of the solid sample in the minimum amount of acetic acid, dilute with water, and filter, if necessary. Alternatively, dilute a measured volume of the liquid sample with water to obtain approximately 100 μg of khellin/ml.

[1] Spectrophotometric measurements were done on a Pye Unicam SP 500.
[2] Recrystallized.
[3] Memphis Chemical Co., Cairo, Egypt.
[4] El Nasr Co., Cairo, Egypt.
[5] E. Merck, Darmstadt, West Germany.
[6] Hopkin & Williams (71% w/w), Essex, England.
[7] Rhone Poulenc, Prolabo, France.

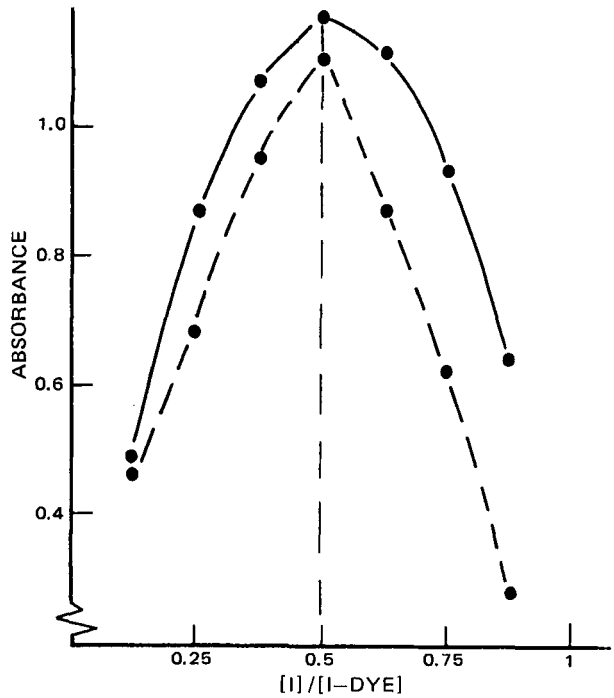

Figure 1—*Continuous variation curves obtained from 1.28×10^{-3} M solution of I with methyl orange (—) and from 8.4×10^{-4} M solution of I with bromthymol blue (– –).*

Acid Dye Assay—Pipet 3.0 ml of the I sample preparation into a 50-ml separator and dilute with 3.0 ml of the pH 5 buffer. Add 3.0 ml of methyl orange solution (3.2×10^{-3} M) and shake the mixture thoroughly for 2 min with 20.0 ml of chloroform. Separate and centrifuge the chloroform layer for 2 min at 2000 rpm and measure the absorbance at 420 nm against a chloroform blank made from the dye solution and the buffer.

Repeat the experiment three times and determine the exact amount of I from a calibration curve.

Perchloric Acid Assay—Pipet 2.0 ml of the I or khellin sample preparation into a 50-ml separator, saturate with sodium chloride, and shake the mixture thoroughly for 2 min with 15.0 ml of chloroform. Allow layers to separate. Transfer 10.0 ml of the chloroform layer into a dry 50-ml separator and add, with swirling, 2.0 ml of glacial acetic acid and 5.0 ml of perchloric acid solution. Shake gently and then separate and centrifuge the upper layer for 2 min at 2000 rpm.

Measure the absorbance of the separated layer at either 333 or 430 nm for I and at 325 or 410 nm for khellin against a blank of acetic acid. Determine the exact amount of I or khellin from constructed calibration curves at the specified wavelengths.

Reineckate Assay—Pipet 15.0 ml of the I sample preparation into a 100-ml beaker containing 10 ml of dilute hydrochloric acid (BP 1973). Precipitate I by adding, with continuous stirring, 25 ml of the ammonium reineckate methanolic solution and leave for 1 hr in the refrigerator.

Filter the I reineckate onto a sintered-glass crucible (porosity 4). Then wash with 2 × 5 ml of cold diluted ammonium reineckate solution (1 ml of the methanolic reineckate in 50 ml of water) and with 2 × 5 ml of ice cold water. Dissolve the I reineckate in 25.0 ml of acetone and measure the absorbance at 530 nm against an acetone blank. Determine the exact amount of I from a calibration curve.

RESULTS AND DISCUSSION

Compound I–Dye Complexes—Methyl orange and bromthymol blue formed complexes with I, with maximum absorbances in chloroform at 420 and 410 nm, respectively. Table I shows that optimum extraction of the dye complexes in chloroform occurred at about pH 5 with methyl orange and at pH 6–7 with bromthymol blue. Dye concentrations of 1.065×10^{-3} M methyl orange and 2.8×10^{-4} M bromthymol blue were required to reach maximum absorbance values at a fixed I concentration of 6.286×10^{-5} M in the aqueous phase. The color intensities of the yellow complexes in chloroform were stable for 2 hr at room temperature.

Stoichiometric Balance—Figure 1 illustrates a stoichiometric relationship of 1:1 between I and the acid dyes.

Adherence to Beer's Law—The yellow complexes of I (40–200 μg) with

Table II—Assay Results[a] of I in Pharmaceutical Preparations following the Acid Dye, Perchloric Acid, and Reineckate Spectrophotometric Methods

Dosage Form	Acid Dye Method	Perchloric Acid Method		Reineckate Method
		At 430 nm	At 333 nm	
Tablet (30 mg)	29.6	30.0	29.5	29.64
	29.6 29.73	29.5 29.66	29.5 29.50	29.64 29.45
	30.0 ± 0.2364	29.5 ± 0.2955	—	29.07 ± 0.3368
Tablet (50 mg)	53.83	54.75 54.40	53.44 53.72	—
	55.51 54.19	54.06 ± 0.6113	54.01 ± 0.499	—
	53.25 ± 1.335	—	—	—
Ampul, 2 ml im, A (50 mg)	48.00	47.95 48.16	—	48.0 48.0
	48.00 47.9	47.95	—	48.0
	47.71 ± 0.1714	48.60 ± 0.3841	—	—
B (50 mg)	51.63	51.25 51.25	50.88 51.06	53.50
	54.16 53.08	51.25	51.25 ± 0.3278	—
	53.37 ± 1.495	—	—	—
Ampul, 5 ml iv (30 mg)	29.16	29.12	30.0	29.00
	28.12 28.67	28.89 29.15	29.57 29.71	—
	28.75 ± 0.6146	29.45 ± 0.3309	29.57 ± 0.2541	—

[a] Shown in milligrams.

the acid dyes obeyed Beer's law. A 1.25 times increase in the sensitivity determination of I was obtained with methyl orange compared to bromthymol blue, as indicated by a more steep slope of color formation with the former.

Analysis of I in Pharmaceutical Preparations—Microamounts of I could be determined with methyl orange as a complex-forming agent. Table II shows good recovery and precision. Khellin, ω-acetylkhellinone, and dimethylamine, involved in the synthesis of I, did not interfere with the assay. However, when bromthymol blue was used, only dimethylamine interfered.

Effect of Decomposition Products—Aqueous acid solutions of I, autoclaved at 115° for 30 min, showed complete recovery of I by the acid dye method. Heating the material (50 mg) with 10% sodium hydroxide in 50% ethyl alcohol (6 ml) at the boiling point of the water bath for the same period resulted in a very low recovery (6.5%) of I by the same method. Accordingly, the acid dye method with methyl orange was considered valid for determining I in the presence of its decomposition products.

Perchloric Acid Oxonium Salt of I and Khellin—Khellin forms colored oxonium salts with concentrated sulfuric and phosphoric acids. The oxonium phosphate of khellin (7) readily hydrolyzes to khellin on addition of water. Likewise, khellin and I formed the corresponding oxonium salts with perchloric acid. On addition of water, however, I oxonium perchlorate underwent hydrolysis to I perchlorate (mp 202–203°), an amine.

Absorption of I and Khellin Oxonium Perchlorates in UV–Visible Region—The oxonium salts of I and khellin showed two maxima at 333 and 430 nm and at 325 and 410 nm, respectively. The absorption spectra of both compounds in the perchloric–acetic acid mixture as compared to those in methanol showed bathochromic shifts, attributed to the formation of new chromophoric entities (maxima at 430 and 410 nm) and hyperchromic shifts due to increases in absorption bands (maxima at 333 and 325 nm). Accordingly, the calculated $E^{1\%}_{1\,cm}$ values of I at 333 nm and of khellin at 325 nm in the acid mixture were ~143 and 252 instead of ~125 and 180 in methanol, respectively.

The absorption ratio for I oxonium salt at 333 nm compared to that at 430 nm was 2.026 ± 0.0208; for khellin oxonium salt, the absorption ratio at 325 nm compared to that at 410 nm is 2.021 ± 0.0513 (Table III).

Optimum Conditions for Extraction of Oxonium Salts—In the presence of small amounts of water, oxonium salts undergo hydrolysis. Accordingly, it was essential to extract I and khellin from water into chloroform before adding perchloric acid to form a stable oxonium salt. This extraction was completely accomplished by shaking sodium chloride-saturated I and khellin preparations (2.0–5.0 ml) with chloroform (15.0 ml). Complete recovery of I and khellin into chloroform was ascertained by the perchloric acid assay when different amounts of I and khellin standard aqueous solutions were extracted and compared with the standard chloroform solutions.

The optimum conditions for extraction of the oxonium salts were obtained by shaking I and khellin chloroform solutions (10.0 ml) with 60% (w/w) perchloric acid (5.0 ml) in the presence of acetic acid (2.0 ml). The presence of less than 2.0 ml of acetic acid did not allow good separation of perchloric acid from chloroform, and the use of higher concentrations of perchloric acid neither altered the color intensity nor contributed to the ease of separation of the two phases. Replacement of perchloric acid with syrupy phosphoric acid produced no change in the color intensity of the formed oxonium but caused difficulty in pipetting and withdrawal because of the high viscosity of the acid.

Stability of I and Khellin Oxonium Salts—The yellow colors of the oxonium salts in 60% (w/w) perchloric–acetic acid (5:2) remained stable for 2 hr at room temperature and tolerated the presence of trace amounts of moisture.

Adherence to Beer's Law—The oxonium salts in the acid mixture obeyed Beer's law for 120–400 μg of I at 333 nm, for up to 600 μg of I at 430 nm, for 50–200 μg of khellin at 325 nm, and for up to 300 μg of khellin at 410 nm.

Analysis of I and Khellin in Pharmaceutical Preparations—Tables II and IV include the assay results of I and khellin preparations through formation of the oxonium salt with perchloric acid. Absorbance was measured at either of their maximum peak wavelengths with sufficient accuracy and precision. The common solubilizers of khellin—*viz.*, urethan, sodium salicylate, sodium benzoate, glucose, and dihydroxypropyltheophylline, when added in 100 times the concentration of khellin, did not interfere with the assay.

Assay of I and Khellin Binary Mixtures—A total assay of I and khellin mixtures could be carried out by the perchloric acid assay at the predetermined isoabsorptive wavelength, 333.5 nm, of I and khellin. The method of location of the isoabsorptive point was practically determined on the separate materials as described previously (12). Compound I was then assayed by the acid dye method, and the amount of khellin could be obtained by difference. Alternatively, I and khellin could be individ-

Table III—Absorption Ratios of I and Khellin Oxonium Perchlorate Obtained from Absorbances at Maximum Peak Values

	I Oxonium Salt ($A_{333\ nm}/A_{430\ nm}$)	Khellin Oxonium Salt ($A_{325\ nm}/A_{410\ nm}$)
	2.023	2.071
	2.000	1.999
	2.060	2.055
	2.025	1.960
	2.014	
	2.036	
Mean	2.026 ± 0.0208	2.021 ± 0.0513

Table IV—Assay Results[a] of Khellin in Pharmaceutical Preparations following the Perchloric Acid Spectrophotometric Method

Dosage Form	410 nm	325 nm
Tablet (20 mg)	19.03	18.37
	18.92 18.96	18.37 18.41
	18.92 ± 0.650	18.50 ± 0.768
Ampul[b], 2 ml (100 mg)	103.1 103.9	103.10 102.79
	104.7 ± 1.417	102.48 ± 0.549
Ampul[c], 10 ml iv (30 mg)	29.40	29.25
	29.40 29.27	29.25 28.85
	28.95 ± 0.266	28.05 ± 0.709

[a] Shown in milligrams. [b] Lynamine, Memphis Chemical Co., Cairo, Egypt. [c] Glucolynamine, Memphis Chemical Co., Cairo, Egypt.

Table V—Recovery Results of I and Khellin in Synthetic Mixture Applying the Acid Dye and Perchloric Acid Methods

Mixture[a], mg	Acid Dye		Perchloric Acid			
			Total I and Khellin		% I	% Khellin
	Found, mg[b]	% Recovery	Found, mg[c]	% Recovery	Recovery[c]	Recovery[c]
I, 66.6, and khellin, 133.4	66.95	100.50	203.28	101.64	101.50	101.71
I, 133.4, and khellin, 66.6	135.56	101.62	197.72	98.36	98.3	98.46
I, 100, and khellin, 100	98.80	98.80	197.72	98.36	98.04	98.68
Mean		100.30 ± 1.42		99.45 ± 1.88		

[a] Dissolved in the minimum amount of acetic acid and appropriately diluted with the required solvent. [b] Mean of three results. [c] Mean of two results.

ually assayed by the same method, applying the absorbance ratio procedure for binary mixtures (13) at 325 and 333.5 nm. Table V presents the recovery results on synthetic mixtures and depicts sufficient accuracy and precision.

Effect of Decomposition Products—Results showed that the perchloric acid method could determine as low as 6.56 and 5.3% of I and khellin, respectively, in their alkaline hydrolysates, and the assay result of I agreed well with the result obtained by the acid dye method.

I Reineckate Derivative—A complete precipitation of I in an acid medium took place after 30 min with an aqueous solution of the reineckate reagent. However, with a 2% methanolic solution of the reineckate, an easily filtrable crystalline precipitate was quantitatively produced after 1 hr in the refrigerator. The reaction between I and reineckate proceeded in a stoichiometric relation of 1:1 (Table VI) and may be represented by Scheme I.

$$C_{16}H_{16}(CH_3)O_5N\cdot HCl + NH_4Cr(NH_3)_2(SCN)_4$$

I (0.5555 g)

$$\xrightarrow{H_2O} C_{16}H_{17}(CH_3)O_5NCr(NH_3)_2(SCN)_4 + NH_4Cl$$

I reineckate (1 g)

Scheme I

Compound I reineckate was slightly soluble in methanol and very soluble in acetone. It was not affected by heating at 105° for 1 hr.

In acetone solution, the reineckate derivative showed a maximum at 530 nm. In methanolic solution, it showed two maxima in the UV region at 245 and 310 nm.

Adherence to Beer's Law—Compound I reineckate obeyed Beer's law for I amounts of 20–70 mg/25 ml of acetone at 530 nm and for 200–500 μg/100 ml of methanol at 245 nm.

Quantitative Determination of I—Because a linear relation exists between I and amount of the precipitated reineckate, Table VI demonstrates assay results of I bulk chemical with good recovery and precision.

Spectrophotometric Analysis of I in Pharmaceutical Preparations—Results shown in Table II depict sufficient accuracy and precision.

CONCLUSION

Sensitive methods are described for the spectrophotometric determination of I and khellin in bulk chemical and pharmaceutical preparations. The applied techniques can differentiate and characterize I from khellin. Of these methods, the acid dye and perchloric acid techniques are stability indicating for I or both compounds.

Compound I, being a base, forms acid dye complexes with methyl orange at pH 5 and with bromthymol blue at pH 6–7. Accordingly, based on this ion-pair formation, optimum conditions were studied to assay I with methyl orange as a complex-forming agent between 40 and 200 μg of I at 420 nm.

Perchloric acid produced an oxonium salt with khellin, but with I it formed both the amine and oxonium salts. The UV–visible absorption spectra of I and khellin oxonium salts were compared and showed two maxima characterizing the chromone moiety of both I and khellin. The absorption ratios of the oxonium salts in the perchloric acid–acetic acid mixture at the maximum peak value in the UV region to the maximum peak value in the visible region represent fixed values.

For the spectrophotometric determination of I and khellin as the oxonium salts, optimum conditions for extraction and color development were chosen to permit the determination of 120–400 μg of I and 50–200 μg of khellin in the UV region and up to 600 μg of I and 300 μg of khellin in the visible region. Tablet excipients and solubilizers of khellin did not interfere.

Ammonium reineckate precipitated I in an acid medium in a stoichiometric relationship of 1:1. The precipitated reineckate is acetone soluble and forms the basis for a colorimetric determination of I (30–70 mg) at the maximum absorbance of 530 nm. A much more dilute solution of I reineckate in methanol (200–500 μg/100 ml) showed two maxima at 245 and 310 nm. Its high absorptivity at 245 nm was useful for determining 1.5–3 mg of I as the reineckate.

Table VI—Gravimetric Assay Results of I as the Reineckate Derivative

Sample, mg	Weight of Reineckate, mg	Found, mg	Recovery, %
52.25	96.0	53.34	102.1
	93.7 95.03	52.00 52.79	99.71 100.77
	95.4	53.03	101.50
56.0	100.9	56.04	100.07
58.5	105.9	58.82	100.55
	105.4	58.54	100.08
	105.0	58.32 58.56	99.69
	106.5 105.44	59.15	101.12 100.11
	104.4	58.00	99.13
60.0	109.0	60.66	101.10

REFERENCES

(1) S. A. Hafiz, H. Abu-Shady, and S. A. Tawab, *J. Egypt. Med. Assoc.*, Special No. **51**, 162 (1968).

(2) A. Maged, H. Abu-Shady, and H. El-Beially, *Kasr El-Aini J. Surg.*, **8**, 249 (1967).

(3) K. Samaan, A. M. Hossein, and M. S. El-Ridi, *Q. J.*, **20**, 502 (1947).

(4) F. G. Soloni and J. F. Marquez, *J. Am. Pharm. Assoc., Sci. Ed.*, **42**, 20 (1953).

(5) I. R. Fahmy, N. Badran, and F. Messeid, *J. Pharm. Pharmacol.*, **1**, 529 (1949).

(6) H. Laubie, *Bull. Soc. Pharm. Bordeaux*, **90**, 108 (1952).

(7) M. Z. Barakat and N. Badran, *J. Pharm. Pharmacol.*, **3**, 576 (1951).

(8) I. R. Fahmy and N. Badran, *ibid.*, **2**, 561 (1950).

(9) "Egyptian Pharmacopoeia" (Arabic text), Ministry of Public Health, Cairo, Egypt, 1972, p. 546.

(10) C. Horstmann, *Kulturpflanze*, **10**, 132 (1962); through *Chem. Abstr.*, **59**, 6708b (1963).

(11) M. S. Karawaya, M. El-Kiey, A. Sina, and G. Nour, *J. Pharm. Sci.*, **59**, 1025 (1970).

(12) M. Pernarowski, A. M. Knevel, and J. E. Christian, *ibid.*, **50**, 946 (1961).

(13) *Ibid.*, **50**, 943 (1961).

Identification and Quantitation of Impurities in Methotrexate

DULAL C. CHATTERJI, ALTICE G. FRAZIER, and JOSEPH F. GALLELLI ˣ

Received May 4, 1977, from the *Pharmacy Department, The Clinical Center, National Institutes of Health, Bethesda, MD 20014.* Accepted for publication August 15, 1977.

Abstract □ The impurities in bulk, commercial, and investigational methotrexate samples were chromatographically separated by gradient elution from a diethylaminoethylcellulose column. Besides the already known impurities in the bulk and commercial samples, two other impurities, 4-amino-N^{10}-methylpteroyl-*N*-methylglutamine and 2,4-diamino-N^{10}-methylpteramide, were identified. A new batch of methotrexate, synthesized for the National Cancer Institute for investigational use only, showed a different spectrum of impurities. The purity of all methotrexate samples studied was about 86% calculated on an anhydrous basis.

Keyphrases □ Methotrexate—chromatographic separation, UV, NMR, and mass spectral analyses of impurities in various formulations □ Impurities—in various formulations of methotrexate, chromatographic separation, UV, NMR, and mass spectral analyses □ Antineoplastic agents—methotrexate, chromatographic separation, UV, NMR, and mass spectral analyses of impurities in various formulations

Like many multisubstituted pteridines, pure methotrexate is difficult to prepare. Although methotrexate has been used as a folic acid antagonist for a long time and several reports discussed the detection of its impurities (1, 2), details of the quantitation and identification of impurities have not appeared. Recent use of 10–20-g quantities of methotrexate to treat certain neoplasias (3) renewed interest in this subject because significant amounts of impurities could be administered. Since some contaminants may have significant pharmacological activity, a systematic investigation to identify and quantitate these impurities was undertaken.

EXPERIMENTAL

Chromatographic Separation Procedure—Chromatography on a diethylaminoethylcellulose column as described previously (4, 5) was used as a separation technique. The procedures for preparing the column and buffer and for monitoring the peaks were as reported (4, 5), except that a linear gradient of 0.01–0.4 *M* ammonia–ammonium bicarbonate buffer (pH 8.3) was used as the eluant.

Identification and Quantitation of Impurities in Methotrexate—Between 10 and 25 mg of methotrexate USP reference substance was chromatographed in each batch. The peak tubes of different fractions, as indicated by the percent transmittance on the chromatogram, were then analyzed by UV spectrophotometry at various pH values. For further identification, similar fractions from several runs were pooled, quickly evaporated to a smaller volume in a flash evaporator, and then freeze dried. The freeze-dried samples were then analyzed by NMR and mass spectrometry.

NMR spectra[1] were obtained at 100 MHz using deuterium oxide as the solvent. Mass spectrometry was carried out on a computerized gas–liquid chromatograph–mass spectrometer[2] with a source temperature of 290°. The ionization potential for peak III was 70 ev, and the probe temperature was 190°. For peak II, the ionization potential was 9.2 ev and the probe temperature was 210°.

For quantitation, about 20 mg of methotrexate USP reference substance[3] was accurately weighed, loaded on the column, and chromatographed. The different fractions were then quantitatively collected, brought to a specific volume, and analyzed by UV spectrophotometry. Unless specified otherwise, all absorbance values reported were determined in pH 8.3 ammonia–ammonium bicarbonate buffer.

Similar studies to identify and quantitate impurities were conducted using commercially available methotrexate injection[4] and "for investigational use" methotrexate injection[5].

RESULTS AND DISCUSSION

The chromatographic separation of methotrexate USP reference substance is shown in Fig. 1; the percent transmittance was plotted against the volume of ammonia–ammonium bicarbonate buffer eluant. Besides the major peak (methotrexate), the transmittance of six other peaks is illustrated.

Identification of Impurities in Methotrexate USP—*Peak VII*—The UV spectrum of the major impurity, peak VII, was identical to that of an authentic sample of N^{10}-methylpteroylglutamic acid. The relative retention times of peak VII and of an authentic sample of N^{10}-methylpteroylglutamic acid also were found to be identical in a high-pressure liquid chromatographic system reported previously (6). The identity of the impurity was reported previously (1, 2).

Peak IV—Peak IV was identified as 2,4-diamino-N^{10}-methylpteroic acid by comparing its UV spectrum to that of an authentic sample. The identity of 2,4-diamino-N^{10}-methylpteroic acid as one impurity present in methotrexate also was reported by Tong *et al.* (1).

Peak III—The identity of peak III has not been reported. The UV spectrum of the compound was identical in all respects to that of methotrexate and suggested that the major chromophore, the 2,4-diamino-N^{10}-methylpteroyl moiety, was intact. Mass spectrometry of peak III indicated a molecular weight of 449 (methotrexate, 454) and showed peaks at *m/e* 449 (small), 308 (small), 275, 175 (base peak), 141, 134, and 84. The peak at 449 was attributed to the molecular ion peak. The peak at 175 was attributed to the 2,4-diamino-6-methylpteridine group, the peak at 134 was attributed to the *p*-*N*-methylaminobenzoyl group, and the peak at 308 was attributed to 2,4-diamino-N^{10}-methylpteroyl or the R group. Scheme I shows the possible structure and assignments for peak III. It appears that R (2,4-diamino-N^{10}-methylpteroyl, $C_{15}H_{14}N_7O$) has a substituent mass of 141.

Hydrolysis of peak III by boiling with sodium hydroxide yielded glutamic acid, which was identified on an amino acid analyzer by comparison with marker compounds. Results indicated the fragment (substituent on R) to be a glutamic acid derivative. Since the fragment mass was odd

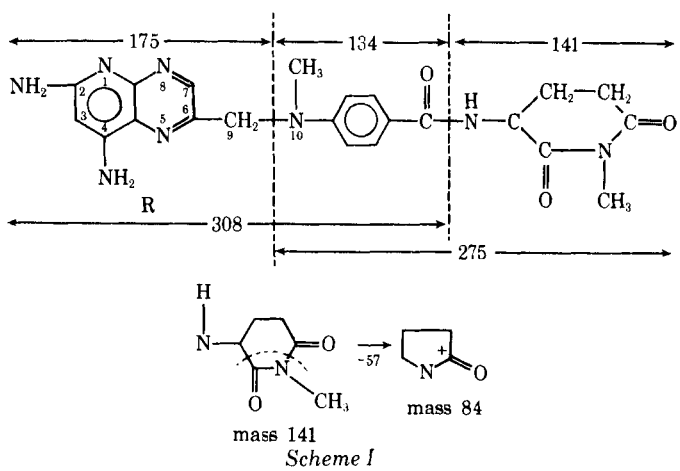

Scheme I

[1] Model XL-100-15 spectrometer, Varian Associates, Palo Alto, Calif.

[2] LKB 9000, LKB, Stockholm, Sweden.

[3] Lot 1260X8105, Lederle Laboratories, Division of American Cyanamid Co., Pearl River, N.Y.

[4] Lot 473-232, methotrexate sodium parenteral, 50 mg of methotrexate/vial, Lederle Laboratories, Division of American Cyanamid Co., Pearl River, N.Y.

[5] Lot BV-76-221, Ben Venue Laboratories, Bedford, Ohio, for National Cancer Institute as methotrexate for injection, preservative free, 1.0 g of methotrexate sodium/vial, for parenteral administration.

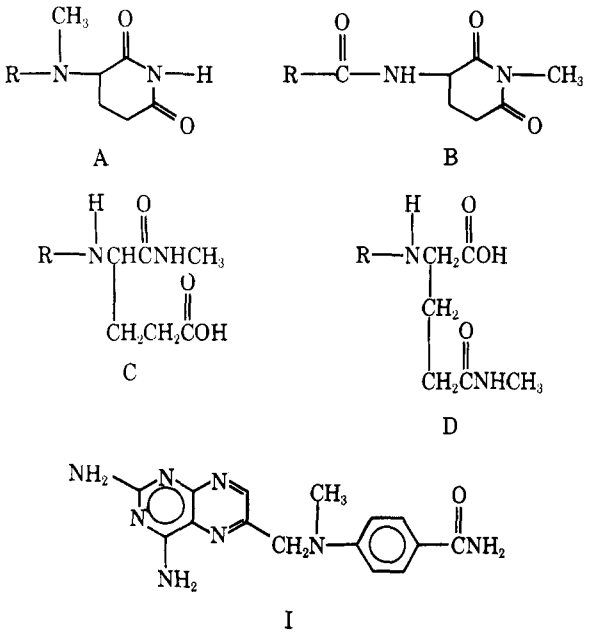

A B C D I

numbered, two nitrogens and the formula $C_8H_9N_2O_2$ (mass 141) were assigned to it.

Two structures were considered. Structure A, on hydrolysis, should yield *N*-methylglutamic acid and, therefore, was unlikely. Structure B should yield glutamic acid on hydrolysis and could account for the prominent peak at *m/e* 84 (Scheme I). Furthermore, to obtain a mass of 84 from Structure A, the route shown in Scheme II would have to be followed, which appears unlikely. This situation provided additional support for ruling out Structure A. Structure B could be the parent compound or could have resulted from dehydration and cyclization of the open chain amide, C or D, during mass spectrometry.

Cyclic Structure B was ruled out on the following basis.

1. The NMR spectrum of the compound did not show the expected peaks of an imide methyl as present in B; *i.e.*, there was no three-proton singlet at δ 4–5 ppm.
2. Cyclic Structure B would be nonionic in nature and should elute almost with the solvent front in the ion-exchange column.
3. The only difference between the NMR spectrum of peak III and that of methotrexate was a singlet at δ 2.6 ppm. This singlet integrated for three protons. The imide methyl (in B) would have a chemical shift much more downfield. However, the chemical shift is consistent with amide methyl structure of C or D.
4. The elution of the peak not with the solvent front, but still quite early, suggested a monocarboxylic acid structure.

Since the exact position of the methyl group (in C and D) was not confirmed, peak III was tentatively called a "glutamine derivative" and given Structure C or D.

Peak II—Peak II had a UV spectrum very close to methotrexate, indicating the presence of a 2,4-diamino-N^{10}-methylpteroyl group. Very early elution from the column also suggested the compound to be nonionic at pH 8.3 (pH of the eluting buffer). The mass spectrum of peak II (9.2 ev, probe temperature 210°) gave *m/e* 324 (molecular ion), 306, 175 (base peak), and 149. As for peak III, mass 175 was assigned to the 2,4-diamino-6-methylpteridine portion. Mass 149 was attributed to the *p*-*N*-methylaminobenzamide group. The peak at *m/e* 306 might have resulted from the dehydration of the amide to the corresponding nitrile at the high temperature of the probe. Therefore, peak II was assigned the structure 2,4-diamino-N^{10}-methylpteramide (I).

Peaks I and VI—Peak I was not identified. However, almost identical elution with the solvent front suggested that it is nonionic. The UV

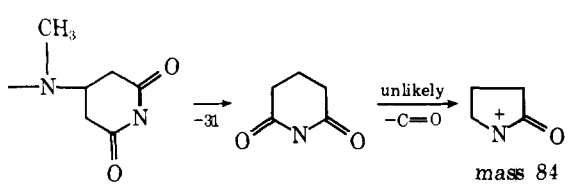

Scheme II

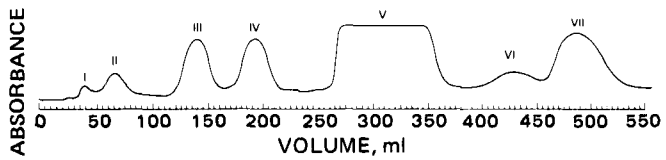

Figure 1—*Chromatogram of methotrexate USP reference substance from a cellulose column by linear gradient elution from 0.01 to 0.4* M *ammonia–ammonium bicarbonate buffer, pH 8.3.*

spectrum of the compound (pH 8.3) showed no peak around 300 nm, suggesting that the *p*-aminobenzoyl moiety was not present.

Peak VI also was not identified. However, delayed elution from a cellulose column suggested that the compound may have more than one anionic site at pH 8.3. Figure 2 shows UV spectra of peaks I and VI at pH 8.3.

Impurities in Methotrexate Injections—Commercial methotrexate injection[4], when chromatographed as described, appeared essentially similar to methotrexate USP regarding its impurities, except that the relative amounts were slightly different (Table I). The major impurities were the glutamine derivative (peak III), 2,4-diamino-N^{10}-methylpteroic acid (peak IV), and N^{10}-methylpteroylglutamic acid (peak VII). "For investigational use" methotrexate injection[3], however, had a different spectrum of impurities (Fig. 3). The only impurity common to both USP and investigational methotrexate appeared to be the glutamine derivative (peak III). All other impurities were new and have not been identified (Figs. 1 and 3).

Quantitation of Impurities in Methotrexate—The impurities in methotrexate were quantitated by determining their absorbance values at 257 nm for peak IV and at 302 nm for peaks II, III, and VII. The molar absorptivity, ϵ, of N^{10}-methylpteroylglutamic acid (peak VII) at 302 nm was the same as that of methotrexate at 302 nm (ϵ 24,500, based on anhydrous methotrexate) and was used to calculate the amount of peak VII in the samples. A molar absorptivity value of 21,700 at 257 nm for peak IV, as reported previously (7), was used to calculate the amount of peak IV in the samples.

The only other major impurity was peak III (glutamine derivative); for its calculation, its molar absorptivity at 302 nm was assumed to be the same as that of methotrexate at 302 nm and pH 8.3. The assumption was made because the UV spectrum at pH 8.3 of peak III and that of methotrexate are identical in every respect and the molar absorptivities of a wide range of substituted pteroyl groups (8, 9) are very similar (including that of N^{10}-methylpteroylglutamic acid, peak VII). However, because of the assumption, the percent impurity value reported for peak III, although correct for comparative purposes, may have some error on an absolute basis. Using similar arguments, the molar absorptivity of peak II was assumed to be the same as that of methotrexate at 302 nm (pH 8.3).

The percent purity of methotrexate in the three methotrexate preparations was determined by the previously reported method (4). Briefly, the percentage purity of methotrexate is calculated as a function of A_u/A_s, where A_s is the absorbance of the methotrexate solution before chromatographic separation and A_u is the absorbance of the pure metho-

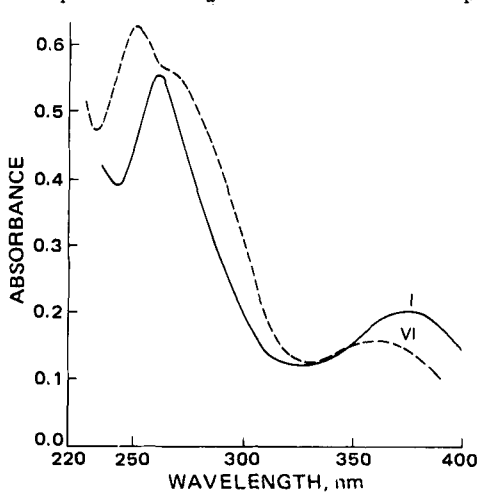

Figure 2—*UV spectra of peaks I (—) and VI (- - -), from chromatogram in Fig. 1, in ammonia–ammonium bicarbonate buffer, pH 8.3.*

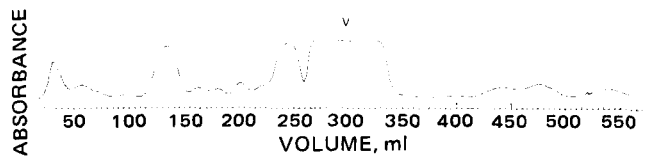

Figure 3—*Chromatogram of investigational methotrexate from a cellulose column by linear gradient elution from 0.01 to 0.4 M ammonia–ammonium bicarbonate buffer, pH 8.3.*

trexate solution after chromatographic separation. The procedure needs further explanation. The method implies that the absorptivities (on a weight basis rather than a molecular basis) of the impurities are identical to the absorptivity of methotrexate, which may not be absolutely true. However, as mentioned, the major impurities have similar UV spectra, extinction coefficients, and molecular weights. Therefore, the assumption is probably valid. Furthermore, even assuming a 25% error in the overall assumption, the absolute error in the determination of the purity of methotrexate would only be about 2% (total impurities are approximately 8%, and a 25% error would cause an absolute error of 8 × 0.25 = 2%). Therefore, this assumption, although not absolutely valid theoretically, is reasonable for practical calculations and correct for comparing various methotrexate samples if the impurities and their relative quantities are similar.

Table I—Comparative Percent Purity of Methotrexate and Quantitation of Its Impurities in Three Different Preparations

Compound	Concentration, % USP	Commercial Injection	Investigational Injection
Methotrexate (anhydrous basis)[a] (peak V)	86.0	86.2	86.7
N^{10}-Methylpteroylglutamic acid (peak VII)	4.0	5.2	—
2,4-Diamino-N^{10}-methylpteroic acid (peak IV)	1.5	2.6	—
4-Amino-N^{10}-methylpteroyl-N-methylglutamine (peak III)	1.6	1.2	—
2,4-Diamino-N^{10}-methylpteramide (peak II)	0.5	0.2	—
Unidentified impurities	1.0	0.5	—

[a] All methotrexate samples contained approximately 5% water.

Presented in Table I is the comparative percent purity of methotrexate and the identity and quantitation of its impurities in three different preparations. The percent purity of methotrexate in all three preparations was almost identical. In addition, methotrexate USP and commercial methotrexate injection had similar impurities. However, the investigational methotrexate preparation contained different impurities, which have not been identified (Figs. 1 and 3). These impurities warrant further investigation.

REFERENCES

(1) W. P. Tong, J. Rosenberg, and D. B. Ludlum, *Lancet*, **2**, 719 (1975).

(2) D. M. Valerino, *ibid.*, **2**, 1025 (1972).

(3) C. B. Pratt, D. Roberts, E. C. Shanks, and F. I. Warmath, *Cancer Res.*, **34**, 3326 (1974).

(4) J. F. Gallelli and G. Yokoyama, *J. Pharm. Sci.*, **56**, 387 (1967).

(5) V. T. Oliverio, *Anal. Chem.*, **33**, 263 (1961).

(6) D. C. Chatterji and J. F. Gallelli, *J. Pharm. Sci.*, **66**, 1219 (1977).

(7) C. C. Levy and P. Goldman, *J. Biol. Chem.*, **242**, 2933 (1967).

(8) D. B. Cosulich and J. M. Smith, *J. Am. Chem. Soc.*, **70**, 1924 (1948).

(9) D. R. Seeger, D. B. Cosulich, J. M. Smith, Jr., and M. D. Hultquist, *ibid.*, **71**, 1755 (1949).

ACKNOWLEDGMENTS

The authors are grateful to Dr. Henry Fales, Laboratory of Chemistry, National Heart, Lung, and Blood Institute, National Institutes of Health, for determining the mass and NMR spectra and for helpful comments.

Thermodynamics of Aqueous Solutions of Parabens

K. S. ALEXANDER, B. LAPRADE, J. W. MAUGER, and ANTHONY N. PARUTA ˣ

Received January 13, 1977, from the *College of Pharmacy, University of Rhode Island, Kingston, RI 02881.* Accepted for publication August 17, 1977.

Abstract □ The solubility of a related series of parabens was determined in water at four temperatures. The parabens chosen were the methyl through *n*-butyl *p*-hydroxybenzoates, and the temperature variations were 5° increments from 25 to 40°. These solutes are useful preservatives, especially combinations of the methyl and propyl ester derivatives. The chemical relationship of these compounds varied by successive linear methylene additions on the ester portion of the molecules. The thermodynamic values obtained for these aqueous systems could be related to these molecular variants since the remainder of the molecule was constant. For the overall thermodynamics, the free energy functions such as the ideal, actual, and excess were found to be smooth, nonlinear functions of the number of carbon atoms in the alkyl portion of the paraben esters. A linear relationship with the number of carbon atoms in the ester portion of these esters was found with the partial excess free energy of the solute.

Keyphrases □ Parabens, various—solubility in water at four temperatures, thermodynamic parameters related to number of carbon atoms □ Solubility—various parabens in water at four temperatures, thermodynamic parameters related to number of carbon atoms □ Thermodynamic parameters—related to solubility of various parabens in water at four temperatures □ Preservatives—various parabens, solubility in water at four temperatures, thermodynamic parameters related to number of carbon atoms

The thermodynamic parameters associated with solution phenomena were determined by studying the variation of solubility with temperature.

The well-known relationship of log mole fraction solubility *versus* reciprocal temperature allows for the determination of heats of solution, ΔH_s, and entropies of solutions, ΔS_s, from slopes and intercepts, respectively (1).

From heats of fusion, ideal mole fraction solubilities can be determined. From these basic derived quantities, mixing and excess functions also can be calculated.

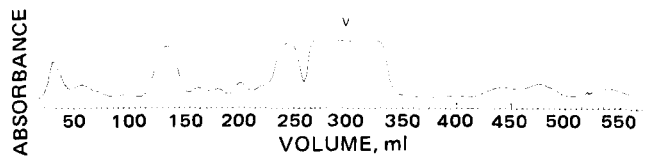

Figure 3—*Chromatogram of investigational methotrexate from a cellulose column by linear gradient elution from 0.01 to 0.4 M ammonia–ammonium bicarbonate buffer, pH 8.3.*

trexate solution after chromatographic separation. The procedure needs further explanation. The method implies that the absorptivities (on a weight basis rather than a molecular basis) of the impurities are identical to the absorptivity of methotrexate, which may not be absolutely true. However, as mentioned, the major impurities have similar UV spectra, extinction coefficients, and molecular weights. Therefore, the assumption is probably valid. Furthermore, even assuming a 25% error in the overall assumption, the absolute error in the determination of the purity of methotrexate would only be about 2% (total impurities are approximately 8%, and a 25% error would cause an absolute error of 8 × 0.25 = 2%). Therefore, this assumption, although not absolutely valid theoretically, is reasonable for practical calculations and correct for comparing various methotrexate samples if the impurities and their relative quantities are similar.

Table I—Comparative Percent Purity of Methotrexate and Quantitation of Its Impurities in Three Different Preparations

Compound	Concentration, % USP	Commercial Injection	Investigational Injection
Methotrexate (anhydrous basis)[a] (peak V)	86.0	86.2	86.7
N^{10}-Methylpteroylglutamic acid (peak VII)	4.0	5.2	—
2,4-Diamino-N^{10}-methylpteroic acid (peak IV)	1.5	2.6	—
4-Amino-N^{10}-methylpteroyl-N-methylglutamine (peak III)	1.6	1.2	—
2,4-Diamino-N^{10}-methylpteramide (peak II)	0.5	0.2	—
Unidentified impurities	1.0	0.5	—

[a] All methotrexate samples contained approximately 5% water.

Presented in Table I is the comparative percent purity of methotrexate and the identity and quantitation of its impurities in three different preparations. The percent purity of methotrexate in all three preparations was almost identical. In addition, methotrexate USP and commercial methotrexate injection had similar impurities. However, the investigational methotrexate preparation contained different impurities, which have not been identified (Figs. 1 and 3). These impurities warrant further investigation.

REFERENCES

(1) W. P. Tong, J. Rosenberg, and D. B. Ludlum, *Lancet*, **2**, 719 (1975).

(2) D. M. Valerino, *ibid.*, **2**, 1025 (1972).

(3) C. B. Pratt, D. Roberts, E. C. Shanks, and F. I. Warmath, *Cancer Res.*, **34**, 3326 (1974).

(4) J. F. Gallelli and G. Yokoyama, *J. Pharm. Sci.*, **56**, 387 (1967).

(5) V. T. Oliverio, *Anal. Chem.*, **33**, 263 (1961).

(6) D. C. Chatterji and J. F. Gallelli, *J. Pharm. Sci.*, **66**, 1219 (1977).

(7) C. C. Levy and P. Goldman, *J. Biol. Chem.*, **242**, 2933 (1967).

(8) D. B. Cosulich and J. M. Smith, *J. Am. Chem. Soc.*, **70**, 1924 (1948).

(9) D. R. Seeger, D. B. Cosulich, J. M. Smith, Jr., and M. D. Hultquist, *ibid.*, **71**, 1755 (1949).

ACKNOWLEDGMENTS

The authors are grateful to Dr. Henry Fales, Laboratory of Chemistry, National Heart, Lung, and Blood Institute, National Institutes of Health, for determining the mass and NMR spectra and for helpful comments.

Thermodynamics of Aqueous Solutions of Parabens

K. S. ALEXANDER, B. LAPRADE, J. W. MAUGER, and ANTHONY N. PARUTA ˣ

Received January 13, 1977, from the *College of Pharmacy, University of Rhode Island, Kingston, RI 02881.* Accepted for publication August 17, 1977.

Abstract □ The solubility of a related series of parabens was determined in water at four temperatures. The parabens chosen were the methyl through *n*-butyl *p*-hydroxybenzoates, and the temperature variations were 5° increments from 25 to 40°. These solutes are useful preservatives, especially combinations of the methyl and propyl ester derivatives. The chemical relationship of these compounds varied by successive linear methylene additions on the ester portion of the molecules. The thermodynamic values obtained for these aqueous systems could be related to these molecular variants since the remainder of the molecule was constant. For the overall thermodynamics, the free energy functions such as the ideal, actual, and excess were found to be smooth, nonlinear functions of the number of carbon atoms in the alkyl portion of the paraben esters. A linear relationship with the number of carbon atoms in the ester portion of these esters was found with the partial excess free energy of the solute.

Keyphrases □ Parabens, various—solubility in water at four temperatures, thermodynamic parameters related to number of carbon atoms □ Solubility—various parabens in water at four temperatures, thermodynamic parameters related to number of carbon atoms □ Thermodynamic parameters—related to solubility of various parabens in water at four temperatures □ Preservatives—various parabens, solubility in water at four temperatures, thermodynamic parameters related to number of carbon atoms

The thermodynamic parameters associated with solution phenomena were determined by studying the variation of solubility with temperature.

The well-known relationship of log mole fraction solubility *versus* reciprocal temperature allows for the determination of heats of solution, ΔH_s, and entropies of solutions, ΔS_s, from slopes and intercepts, respectively (1).

From heats of fusion, ideal mole fraction solubilities can be determined. From these basic derived quantities, mixing and excess functions also can be calculated.

Table I—Determined Mole Fraction Solubilities of the Parabens in Water

Solute	Mole Fraction Solubility $\times 10^5$			
	25°	30°	35°	40°
Methylparaben	26.0	33.0	41.1	46.1
Ethylparaben	9.6	12.2	14.9	17.2
Propylparaben	3.7	4.4	5.5	7.3
Butylparaben	2.3	3.2	4.0	4.7

Activity coefficients can be obtained from the ratio of ideal mole fraction solubility to the actual mole fraction solubility. Moreover, a partial excess free energy value can be determined that relates to an overall solution property.

The purposes of this study were to obtain information about the overall solution process in terms of ideal, actual, and excess free energies and to determine the relationship of the number of methylene groups in this normal alkyl series to these thermodynamic parameters. Because of the chemical relationship of these solutes, a relationship of thermodynamic values and chemical constitution might be observed.

With heats of fusion for these solutes available from the literature (2), the complete spectrum of thermodynamic elements could be obtained by calculation.

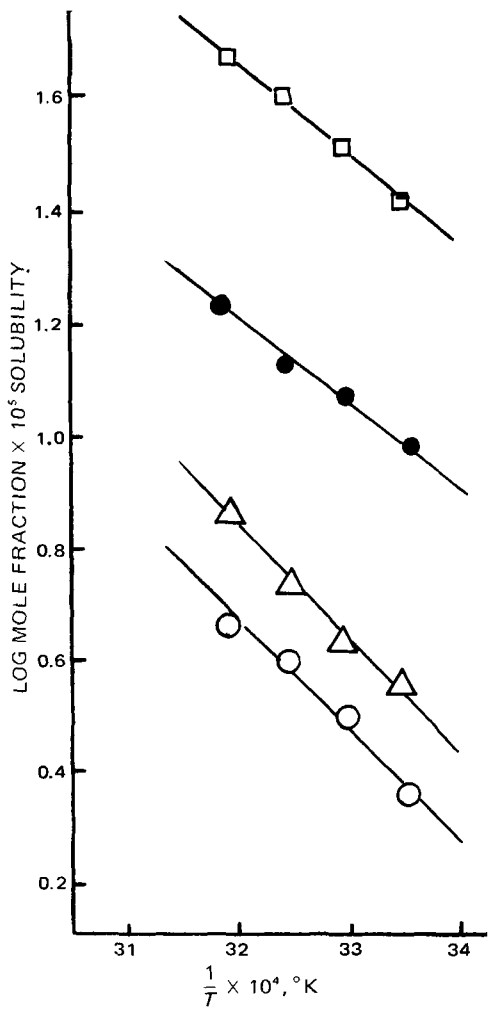

Figure 1—*Plot of the log mole fraction solubility as a function of reciprocal temperature for methylparaben (□), ethylparaben (●), propylparaben (△), and butylparaben (○).*

Table II—Ideal Mole Fraction Solubilities for the Parabens in Water

Solute	Ideal Mole Fraction Solubility			
	25°	30°	35°	40°
Methylparaben	0.157	0.178	0.200	0.224
Ethylparaben	0.189	0.213	0.239	0.267
Propylparaben	0.272	0.304	0.339	0.376
Butylparaben	0.450	0.500	0.553	0.610

EXPERIMENTAL

Equipment—A melting-point apparatus[1], a spectrophotometer[2], and a temperature-control unit[3] were used.

Materials—The chemicals were methyl *p*-hydroxybenzoate[4] (methylparaben), ethyl *p*-hydroxybenzoate[5] (ethylparaben), *n*-propyl *p*-hydroxybenzoate[6] (propylparaben), *n*-butyl *p*-hydroxybenzoate[7] (butylparaben), and distilled water. All solutes were within 1° of the literature melting-point value.

Method—Solubility was determined by a method previously described (3). The solubility of each solute was determined at least eight times at each temperature.

RESULTS AND DISCUSSION

The solubility of the parabens in water at the various temperatures is given in Table I in terms of mole fraction. The data were converted to log mole fraction solubility and plotted as a function of reciprocal temperature (Fig. 1). From these plots, the slopes and intercepts were obtained by least squares; they are related to the enthalpy of solution, ΔH_s, and the entropy of solution, ΔS_s, respectively.

The log mole fraction plots for these solutes are linear but not parallel to each other. This result implies that the enthalpy and entropy of solution vary for each solute.

Table II lists the calculated ideal mole fraction solubilities for these parabens at the four temperatures; the ideal mole fraction solubility equation was used. If the heats of fusion for the solutes are known, the ideal mole fraction solubility can be calculated. These values would hold for these solutes in any solvent system with which they form an ideal solution. These mole fractions are substantial in value and, no doubt, are far in excess of the determined or anticipated solubilities for these solutes in water. These mole fraction values vary from about 0.15 to 0.61, and one

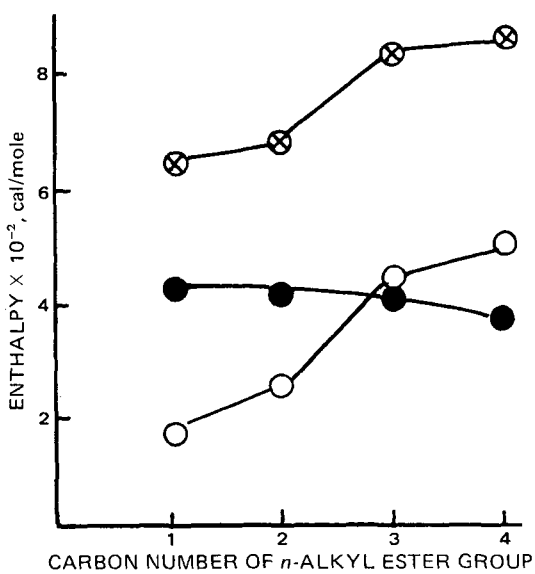

Figure 2—*Plot of the enthalpies of fusion (●), solution (⊗), and mixing (○), in calories per mole, as a function of the carbon number of the n-alkyl ester group of the parabens.*

[1] Hoover 6406, A. H. Thomas Co., Philadelphia, Pa.
[2] Cary model 16, Cary Instruments, Monrovia, Calif.
[3] Temptrol 150 Tempunit, Precision Scientific Co., Chicago, Ill.
[4] Lot 14, Matheson, Coleman and Bell.
[5] Lot EX665, Matheson, Coleman and Bell.
[6] Lot PX 1910, Matheson, Coleman and Bell.
[7] J. T. Baker Chemical Co.

Table III—Activity Coefficient for the Parabens in Water

Solute	Activity Coefficient of Solute, γ_2 25°	30°	35°	40°
Methylparaben	605	539	487	486
Ethylparaben	1,970	1,746	1,604	1,552
Propylparaben	7,352	6,909	6,164	5,151
Butylparaben	19,565	15,625	13,825	12,979

can consider a change in the "nature" of these binary mixtures at the higher values.

The solubilities in water varied in value from about 2.3×10^{-5} to 46.1×10^{-5} in terms of mole fraction. The activity coefficients calculated from the ratio of the ideal mole fraction solubilities to the actual mole fraction solubilities would be expected to be very large in magnitude. These "activity coefficients" were calculated (Table III). The magnitude of these values is illustrative of the fact that these systems of parabens in water are many orders of magnitude below the ideal solubilities and behave as highly nonideal solutions.

Table IV lists the thermodynamic elements for these solutes in water for the enthalpies of fusion, solution, and mixing, for the entropies of fusion, solution, and mixing, and for the ideal, actual, and excess free energies.

The heats of fusion for these compounds occur in a regular order, methylparaben possessing the highest heat of fusion and butylparaben possessing the lowest heat of fusion, with increasing differences as a function of carbon number.

The heat of solution and mixing both increase in magnitude with increasing nonpolarity, as evidenced by the increase in the alkyl portion of the ester group. These increases would be expected in aqueous systems as the molecular size increases.

The enthalpies of fusion, solution, and mixing were plotted as a function of the carbon number of the *n*-alkyl ester group on the molecule (Fig. 2). In this series of molecular variants, the differences in the determined properties between compounds are directly due to the incremental increase in the methylene groups since the remainder of the molecule remains constant. There is no pattern of the various enthalpies as a function of the carbon number of the alkyl ester portion of these molecules.

The entropies of fusion, solution, and mixing also were plotted as a function of the carbon number as previously described (Fig. 3). The entropies of fusion are quite similar in magnitude and are essentially invariant with increasing molecular size (Table IV). The entropies of solution and mixing also change with no apparent relationship to polarity or molecular size. Again, there seems to be no pattern of these individual

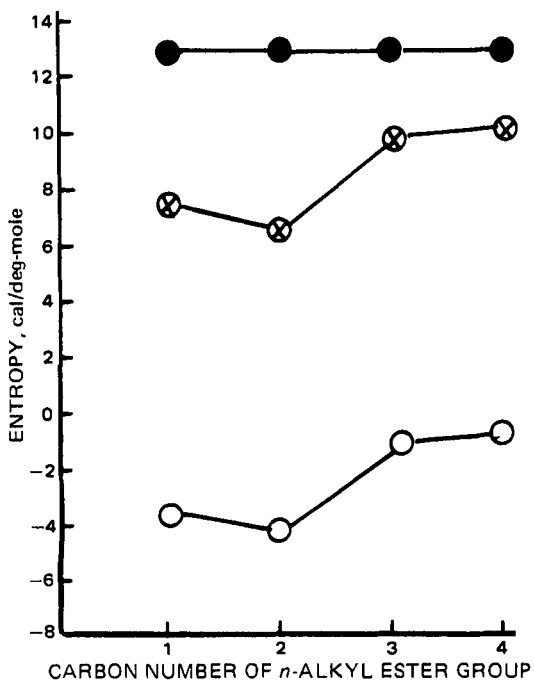

Figure 3—*Plot of the entropies of fusion (●), solution (⊗), and mixing (○), in calories per degree-mole, as a function of the carbon number of the* n*-alkyl ester group of the parabens.*

Table IV—Thermodynamic Values Obtained for the Parabens in Water

Solute	Enthalpy, cal/mole Fusion	Solution	Mixing	Entropy, cal/deg mole Fusion	Solution	Mixing	Free Energy, cal/mole Ideal	Actual	Excess
Methylparaben	4352	6516	1764	11.04	5.58	−5.46	985	4815	3830
Ethylparaben	4243	6906	2663	11.02	4.88	−6.14	882	5418	4536
Propylparaben	4026	8403	4387	10.90	7.72	−3.18	702	6093	5391
Butylparaben	3737	8778	5041	11.02	8.29	−2.73	376	6250	5874

Table V—Partial Excess Free Energy of the Solutes in Water

Solute	Partial Excess Free Energy of Solute, $\bar{F}_2^E$, cal/mole 25°	30°	35°	40°
Methylparaben	3915	3845	3783	3782
Ethylparaben	4637	4563	4512	4492
Propylparaben	5442	5404	5335	5225
Butylparaben	6040	5903	5828	5790

thermodynamic elements relative to carbon number or molecular size. However, these individual factors of enthalpy and entropy must be considered together to discern the overall effect, which would be the various free energy functions shown in Table IV. The ideal free energies follow a pattern of diminishing magnitude with carbon number; however, this pattern is not linear. The actual and excess free energies increase smoothly with the carbon number of the ester group in a nonlinear fashion.

The free energy function is a result of the combination of the appropriate values of enthalpy and entropy, where these factors act in opposition or in concert with one another depending on their signs and varying magnitudes.

In Fig. 4, the free energy functions calculated for these systems were plotted as a function of the carbon number of the ester group, and smooth nonlinear relationships were found. Specifically, the ideal free energy diminishes with the carbon number, whereas both the actual and excess

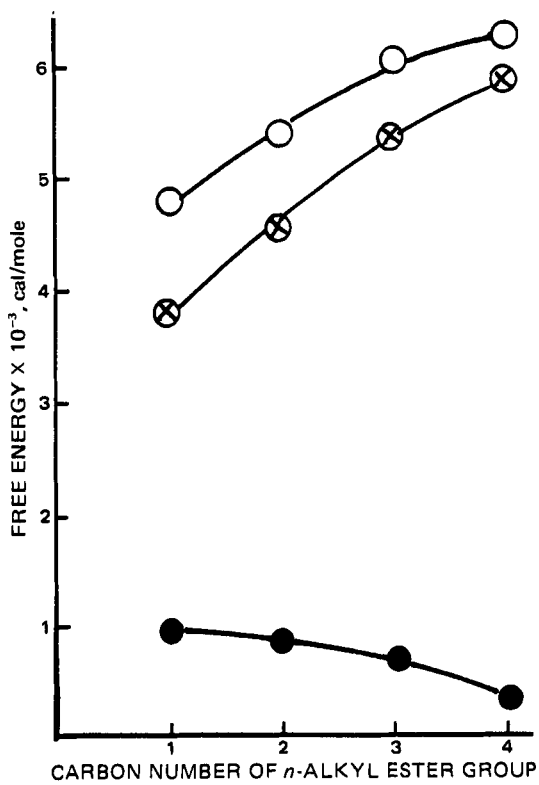

Figure 4—*Plot of the ideal (●), actual (○), and excess (⊗) free energies, in calories per mole, as a function of the carbon number of the* n*-alkyl ester group of the parabens.*

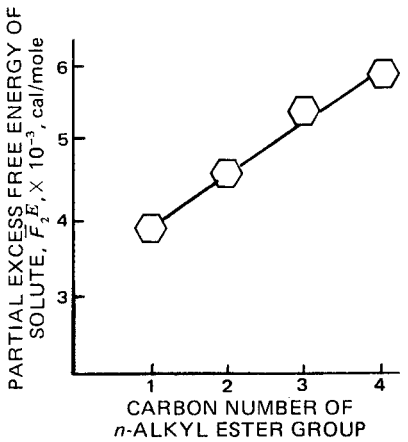

Figure 5—*Plot of the average partial excess free energy for the solute, in calories per mole, as a function of the carbon number of the* n*-alkyl ester group of the parabens.*

free energies increase with an increasing carbon number. The values obtained for these free energy functions, the actual and excess free energies, are substantial in magnitude and imply highly nonideal solution behavior for these parabens in water. This fact was also supported by the rather large activity coefficients determined for these solutes.

Thus, the free energy functions possess a nonlinear relationship with carbon number or molecular size.

An additional thermodynamic parameter, the partial excess free energy of the solute, was investigated. This parameter can be considered to be an overall property of the solution and can also be calculated from these results. The partial free energy, $\overline{F}_2^E$, can be written as:

$$\overline{F}_2^E = RT \ln \gamma_2 \qquad \text{(Eq. 1)}$$

where R is the gas constant, T is the absolute temperature, and γ_2 is the activity coefficient. Previously, it was stated that these activity coefficients were quite large in magnitude and implied highly nonideal behavior. However, when using these values and solving Eq. 1 for the partial free energy, entirely reasonable values of free energy were obtained (Table V). The calculated partial free energy values occurred in regular order with carbon number, and there were regular increases with increasing temperature. This result was expected as the solubility increased with temperature because the energy requirement of the overall system also increased.

Figure 5 shows plots of the partial excess free energy for these solutes as a function of the carbon number of the ester group. In this case, a linear relationship of partial excess free energy with carbon number is evidenced with an approximate slope of about 680 cal/mole/carbon atom.

The expression of the rate of change in partial excess free energy with carbon number allows for a definitive relationship of a thermodynamic parameter and molecular size.

Finally, a spectrum of thermodynamic elements can be easily obtained by studying solubilities at various temperatures once the heat of fusion values have been determined. Studies along these lines will be the subject of future reports.

REFERENCES

(1) B. H. Mahan, "Elementary Chemical Thermodynamics," Benjamin, New York, N.Y., 1963, chap. 4.

(2) F. A. Restaino and A. N. Martin, *J. Pharm. Sci.*, **53**, 636 (1964).

(3) P. A. Schwartz and A. N. Paruta, *ibid.*, **65**, 252 (1976).

Electron-Capture GLC Determination of Ibuprofen in Serum

DAVID G. KAISER ˣ **and ROBERT S. MARTIN**

Received April 25, 1977, from the *Research Laboratories, The Upjohn Company, Kalamazoo, MI 49001.* Accepted for publication August 22, 1977.

Abstract □ To evaluate drug–protein binding, a sensitive method for the determination of ibuprofen in submilliliter amounts of serum was required. A specific and highly sensitive procedure, based on benzene extraction of the acidified specimen, TLC of the benzene extract residue, formation of the pentafluorobenzyl esters of the materials eluted from the thin-layer chromatogram, and quantification of the pentafluorobenzyl esters by GLC, was developed. Utilizing electron-capture detection, the method is sensitive to 0.1 μg of ibuprofen/0.1 ml of serum. Statistical analyses indicated an average recovery of 97.7% with a standard deviation of ±7.3%. Mass spectrometric analysis, in conjunction with GLC, confirmed the specificity of the method for the intact drug. The procedure was applied successfully to drug absorption and drug–protein binding studies in humans.

Keyphrases □ Ibuprofen—electron-capture GLC analysis in serum, time course of protein binding in humans □ GLC, electron capture—analysis, ibuprofen in serum □ Protein binding—ibuprofen in humans, time course studied using electron-capture GLC analysis in serum □ Anti-inflammatory agents—ibuprofen, electron-capture GLC analysis in serum, time course of protein binding in humans

The pharmacology, toxicology, and biochemistry of ibuprofen[1] [(*RS*)-2-(4-isobutylphenyl)propionic acid] (I), a potent orally active anti-inflammatory agent in animals (1–6) and humans (7–9), have been reported.

In studies of the absorption, metabolism, and excretion of I, paper chromatographic (10) and GLC (5, 11–14) methods were utilized. All of these procedures required at least 1–5 ml of biological fluid for analysis of intact drug. This quantity constituted a serious limitation in studies where multiple blood specimens were needed for multiple analyses. The need for a sensitive analytical method to measure individual drugs in small amounts of biological fluids was apparent during drug interaction studies with I and aspirin (15).

To determine the time course of drug–protein binding in human volunteers participating in pharmacokinetic studies of I, a simple, specific, and highly sensitive method for the measurement of the intact drug in submilliliter amounts of serum was developed.

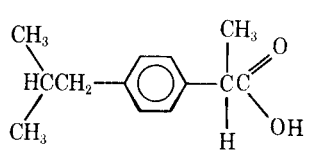

I

[1] Motrin, The Upjohn Co., and Brufen, Boots Co.

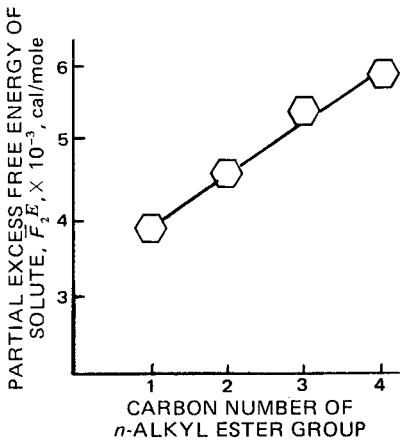

Figure 5—*Plot of the average partial excess free energy for the solute, in calories per mole, as a function of the carbon number of the* n*-alkyl ester group of the parabens.*

free energies increase with an increasing carbon number. The values obtained for these free energy functions, the actual and excess free energies, are substantial in magnitude and imply highly nonideal solution behavior for these parabens in water. This fact was also supported by the rather large activity coefficients determined for these solutes.

Thus, the free energy functions possess a nonlinear relationship with carbon number or molecular size.

An additional thermodynamic parameter, the partial excess free energy of the solute, was investigated. This parameter can be considered to be an overall property of the solution and can also be calculated from these results. The partial free energy, $\overline{F}_2^E$, can be written as:

$$\overline{F}_2^E = RT \ln \gamma_2 \qquad \text{(Eq. 1)}$$

where R is the gas constant, T is the absolute temperature, and γ_2 is the activity coefficient. Previously, it was stated that these activity coefficients were quite large in magnitude and implied highly nonideal behavior. However, when using these values and solving Eq. 1 for the partial free energy, entirely reasonable values of free energy were obtained (Table V). The calculated partial free energy values occurred in regular order with carbon number, and there were regular increases with increasing temperature. This result was expected as the solubility increased with temperature because the energy requirement of the overall system also increased.

Figure 5 shows plots of the partial excess free energy for these solutes as a function of the carbon number of the ester group. In this case, a linear relationship of partial excess free energy with carbon number is evidenced with an approximate slope of about 680 cal/mole/carbon atom.

The expression of the rate of change in partial excess free energy with carbon number allows for a definitive relationship of a thermodynamic parameter and molecular size.

Finally, a spectrum of thermodynamic elements can be easily obtained by studying solubilities at various temperatures once the heat of fusion values have been determined. Studies along these lines will be the subject of future reports.

REFERENCES

(1) B. H. Mahan, "Elementary Chemical Thermodynamics," Benjamin, New York, N.Y., 1963, chap. 4.

(2) F. A. Restaino and A. N. Martin, *J. Pharm. Sci.*, **53**, 636 (1964).

(3) P. A. Schwartz and A. N. Paruta, *ibid.*, **65**, 252 (1976).

Electron-Capture GLC Determination of Ibuprofen in Serum

DAVID G. KAISER ˣ **and ROBERT S. MARTIN**

Received April 25, 1977, from the *Research Laboratories, The Upjohn Company, Kalamazoo, MI 49001.* Accepted for publication August 22, 1977.

Abstract □ To evaluate drug–protein binding, a sensitive method for the determination of ibuprofen in submilliliter amounts of serum was required. A specific and highly sensitive procedure, based on benzene extraction of the acidified specimen, TLC of the benzene extract residue, formation of the pentafluorobenzyl esters of the materials eluted from the thin-layer chromatogram, and quantification of the pentafluorobenzyl esters by GLC, was developed. Utilizing electron-capture detection, the method is sensitive to 0.1 μg of ibuprofen/0.1 ml of serum. Statistical analyses indicated an average recovery of 97.7% with a standard deviation of ±7.3%. Mass spectrometric analysis, in conjunction with GLC, confirmed the specificity of the method for the intact drug. The procedure was applied successfully to drug absorption and drug–protein binding studies in humans.

Keyphrases □ Ibuprofen—electron-capture GLC analysis in serum, time course of protein binding in humans □ GLC, electron capture—analysis, ibuprofen in serum □ Protein binding—ibuprofen in humans, time course studied using electron-capture GLC analysis in serum □ Anti-inflammatory agents—ibuprofen, electron-capture GLC analysis in serum, time course of protein binding in humans

The pharmacology, toxicology, and biochemistry of ibuprofen[1] [(*RS*)-2-(4-isobutylphenyl)propionic acid] (I), a potent orally active anti-inflammatory agent in animals (1–6) and humans (7–9), have been reported.

In studies of the absorption, metabolism, and excretion of I, paper chromatographic (10) and GLC (5, 11–14) methods were utilized. All of these procedures required at least 1–5 ml of biological fluid for analysis of intact drug. This quantity constituted a serious limitation in studies where multiple blood specimens were needed for multiple analyses. The need for a sensitive analytical method to measure individual drugs in small amounts of biological fluids was apparent during drug interaction studies with I and aspirin (15).

To determine the time course of drug–protein binding in human volunteers participating in pharmacokinetic studies of I, a simple, specific, and highly sensitive method for the measurement of the intact drug in submilliliter amounts of serum was developed.

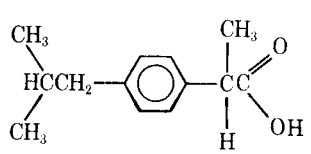

I

[1] Motrin, The Upjohn Co., and Brufen, Boots Co.

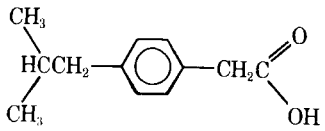

II

EXPERIMENTAL

Reagents and Materials—Compound I was synthesized[2], as was the internal standard ibufenac[3] (4-isobutylphenylacetic acid) (II). Acetone, benzene, cyclohexane, and methanol, distilled in glass, were used as supplied[4].

Stock solutions of I and II in methanol (60 μg/ml), pentafluorobenzyl bromide[5] in acetone (0.1 ml/100 ml), and aqueous 1 *N* HCl were stored in glass containers. All other chemicals were analytical reagent grade. 3-Cyanopropyl silicone[6] on 100–120-mesh Gas Chrom Q (10% w/w) was used as supplied.

Instrumentation—A two-speed reciprocating shaker[7] was used for shaking samples horizontally. A mixer[8] was used in eluting the zones removed from thin-layer chromatograms. GLC measurements were made with a chromatograph[9] equipped with a ^{63}Ni-electron-capture detector, a freestanding electron-capture linearizer[10], and a −0.1–1.0-mv dual-pen recorder[11]. All gas cylinders used for chromatography [*i.e.*, methane (5% v/v) in argon] were fitted with filters containing molecular sieve 4A.

TLC—All analytical chromatography was conducted on thin layers (250 μm) of silica gel 60 F_{254}[12], ascendingly developed in 10% (v/v) acetic acid in toluene. The separated materials were visualized by irradiation of the plates with a short wavelength (254-nm) UV lamp. Under these conditions, I and II as the free acids had approximately the same R_f values: 0.45 and 0.40, respectively.

GLC Conditions—All chromatography was conducted using U-shaped glass columns (1.83 m × 3 mm i.d.) packed with 10% (w/w) 3-cyanopropyl silicone on 100–120-mesh Gas Chrom Q. All newly prepared columns were preconditioned at 250° for 1 hr with no carrier gas flow and for 16 hr with a carrier gas flow of 10 ml/min. During analysis, the column, injection port, and electron-capture detector were maintained isothermally at 190, 260, and 325°, respectively. The flow rate of the methane (5% v/v) in argon, used as the carrier gas, was maintained at 55 ml/min. Under these conditions, the pentafluorobenzyl esters of I and II had retention times of 9.1 and 13.3 min, respectively (Fig. 1).

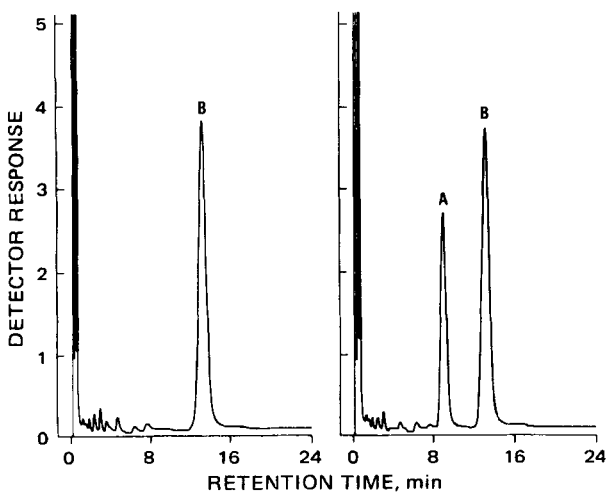

Figure 1—*Gas–liquid chromatograms of human serum extracts. Left: normal serum specimen. Right: serum specimen from subject 1 hr after single-dose oral administration of 400 mg of ibuprofen. Key: A, ibuprofen pentafluorobenzyl ester; and B, ibufenac pentafluorobenzyl ester.*

[2] Research Division, The Upjohn Co., Kalamazoo, Mich.
[3] Research Division, Boots Co., Nottingham, England.
[4] Burdick and Jackson Laboratories, Muskegon, Mich.
[5] Pierce Chemical Co., Rockford, Ill.
[6] Silar 10C, Applied Science Laboratories, State College, Pa.
[7] Eberbach and Sons, Ann Arbor, Mich.
[8] Vortex model K-500, Scientific Industries, Queens Village, N.Y.
[9] Model MT-220, Tracor Inc., Austin, Tex.
[10] Model 114556 B, Tracor Inc., Austin, Tex.
[11] Model MT-22, Westronics Inc., Fort Worth, Tex.
[12] EM Laboratories, Elmsford, N.Y.

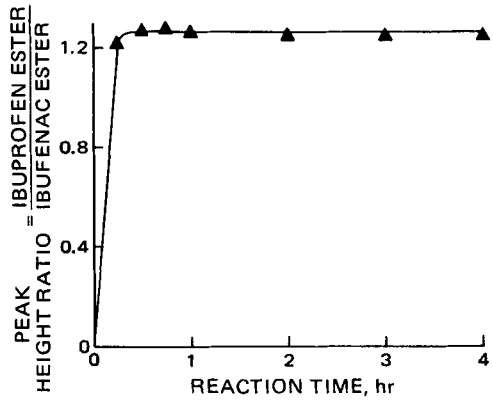

Figure 2—*Effect of reaction time on formation of ibuprofen pentafluorobenzyl ester.*

Protein Binding—For equilibrium dialysis studies, aliquots (0.8 ml) of serum from I-treated subjects were placed in a multicavity dialysis cell[13] on the side opposite to 0.8 ml of aqueous sodium phosphate buffer (0.01 *M*, pH 7.4) containing 0.09% (w/v) sodium chloride (5). The cells were agitated gently for 24 hr at 25°. The I concentration on each side of the dialysis membrane[14] was measured by GLC.

For ultrafiltration experiments, the apparatus (16) and procedure (17) reported previously were utilized. All specimens were centrifuged at 2000 rpm for 3 hr at 25°. The I concentration on each side of the membrane was measured by GLC.

Synthesis of Standard Materials—Place 500 mg of I in a suitable reaction flask. Add 20 ml of acetone, 1.5 ml of undiluted pentafluorobenzyl bromide, and 300 mg of anhydrous potassium carbonate and heat in a water bath at 60° for 5 hr. Evaporate to dryness with a gentle stream of nitrogen. Add 5 ml of water and 10 ml of cyclohexane. Shake for 10 min and allow the phases to separate. Transfer the cyclohexane to a fresh 15-ml centrifuge tube. Repeat the extraction with three additional 10-ml portions of cyclohexane and evaporate the pooled cyclohexane extracts to dryness with nitrogen. Recrystallize from methanol–ether and water.

Synthesize standard material for identification of the II pentafluorobenzyl ester, utilizing the same general reaction conditions as described for I.

Assay—*Preparation of Standards*—Pipet aliquots of the I stock solution, equivalent to 0.5, 1, 2, 3, 4, 5, and 6 μg, into polytef-lined screw-capped centrifuge tubes[15]. Add aliquots of the II stock solution, equivalent to 10 μg, to the same series of centrifuge tubes. Evaporate to dryness with a gentle stream of nitrogen. Add 0.1 ml of control serum to each centrifuge tube and mix well. Prepare an appropriate blank. Extract all standards in the same manner as described for the serum specimens. For analysis of submicrogram amounts of I in aqueous buffer, prepare appropriately diluted standards.

Preparation of Samples—Pipet aliquots of the II stock solution, equivalent to 10 μg, into a series of centrifuge tubes and evaporate to dryness with a gentle stream of nitrogen. Add 0.1 ml of the serum specimens and mix well. Add 0.25 ml of aqueous 1 *N* HCl and 5 ml of benzene and shake horizontally for 10 min. Centrifuge for 10 min at 2000 rpm and aspirate off the aqueous layer. Transfer a 4-ml aliquot of the benzene layer to a fresh 15-ml centrifuge tube and evaporate to dryness with a gentle stream of nitrogen. Wash down the walls of the centrifuge tube with 0.5 ml of chloroform and evaporate to dryness.

Reconstitute the benzene extract residues from the serum standards and samples in 50 μl of chloroform. Together with appropriate standards, spot all of each sample on thin layers of silica gel 60 F_{254} (*vide supra*). Ascendingly develop each plate for a distance of 165 mm, air dry all chromatograms thoroughly at room temperature (24°), and visualize the zones by irradiation with a 254-nm UV lamp. Then scrape the zones corresponding to I and II into screw-capped centrifuge tubes. Add 4 ml of methanol to each tube and gently agitate using the mixer. Centrifuge for 5 min at 2000 rpm. Transfer a 3-ml aliquot of the methanol layer to a fresh screw-capped centrifuge tube and evaporate to dryness with nitrogen.

[13] Chemical Rubber Co., Cleveland, Ohio.
[14] Visking cellophane, Union Carbide Corp., Food Product Division, Chicago, Ill.
[15] Bellco Glass, Vineland, N.J.

Table I—Recovery of Ibuprofen from Human Serum [a]

Added, μg/ml	Found, μg/ml	Recovery, %
0.10	0.083	83.0
0.20	0.215	107.5
0.50	0.549	109.8
5.0	4.75	95.0
10.0	9.54	95.4
20.0	19.21	96.1
30.0	29.21	97.4
40.0	39.62	99.1
50.0	48.50	97.0
60.0	58.18	97.0
	Mean ± *SD*	97.7 ± 7.3

[a] As compared to simple aqueous solution.

Add 25 mg of anhydrous potassium carbonate and a 1-ml aliquot of the pentafluorobenzyl bromide stock solution to each centrifuge tube. Cap tightly and heat in a water bath for 1 hr at 60°. Evaporate to dryness with nitrogen. Add 1 ml of water and 4 ml of cyclohexane. Shake for 10 min, and allow the phases to separate. Transfer 3 ml of the cyclohexane layer to a fresh centrifuge tube and evaporate to dryness. Reconstitute the residues in 0.2 ml of cyclohexane and inject a 2-μl aliquot for analysis into the chromatograph.

Calculations—The peak heights for I and II pentafluorobenzyl esters are measured. Peak height ratios are obtained by dividing the peak height of the I pentafluorobenzyl ester by the peak height of the II pentafluorobenzyl ester. Calibration curves for known concentrations of I in serum are prepared by plotting peak height ratios *versus* I concentrations, expressed as micrograms per milliliter. Values for unknown concentrations of I in serum specimens, obtained in the same manner, are then read directly from the graph or calculated from the slope of the standard curve.

Drug Administration to Humans—All subjects[16] were between 25 and 28 years; they ranged in body weight from 75.3 to 90.7 kg and in height from 1.70 to 1.83 m. All subjects were fasted for 16 hr prior to drug administration. Each then received a 400-mg dose of I in aqueous solution, and food was withheld for an additional 2 hr.

Blood specimens (10 ml) were withdrawn at predetermined time intervals from 0 to 16 hr after drug administration. The serum was harvested and stored at −18°.

RESULTS AND DISCUSSION

Synthesis and Identification of Pentafluorobenzyl Esters—Methods for the preparation of pentafluorobenzyl esters of carboxylic acids have been reported (18–20). The utility of pentafluorobenzyl derivatives for measuring microgram and submicrogram amounts of selected drugs in biological fluids has been described (21–23). A series of samples, containing known amounts of I and II, was prepared to determine optimal reaction times for formation of the pentafluorobenzyl esters. In studies with I, known amounts of II pentafluorobenzyl ester were added as the internal standard. Similarly, in studies with II, known amounts of I pentafluorobenzyl ester were added as the internal standard. The results indicated that ester formation for both compounds was completed within 30 min (Figs. 2 and 3). A reaction time of 1 hr was selected for convenience. In the presence of water and cyclohexane, the derivatives were stable for at least 96 hr.

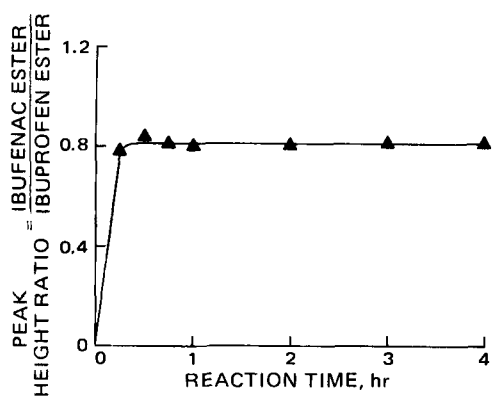

Figure 3—*Effect of reaction time on formation of ibufenac pentafluorobenzyl ester.*

[16] Informed written consent was obtained from each of the three normal human male volunteers prior to participation.

Table II—Recovery of Ibufenac from Human Serum [a]

Added, μg/ml	Found, μg/ml	Recovery, %
5.0	4.44	88.8
10.0	9.32	93.2
20.0	21.56	107.8
30.0	34.11	113.7
40.0	45.49	113.7
50.0	57.31	114.6
60.0	68.20	113.7
	Mean ± *SD*	106.5 ± 10.9

[a] As compared to simple aqueous solution.

Synthesis of standard material showed that the pentafluorobenzyl ester of I was a white crystalline material at room temperature, mp 32–34°; IR (mineral oil): 1745, 1655, 1525, 1510, 1165, 1125, 1055, and 940 cm^{-1}; NMR ($CDCl_3$): δ 0.95 (d, 6H), 1.50 (d, 3H), 1.90 (m, 1H), 2.45 (d, 2H), 3.70 (q, 1H), 5.2 (s, 2H), and 7.0–7.3 (m, 4H) ppm; mass spectrum: *m/e* 386 (M^+), 343 ($M^+ - 43$), 181, 162, 161, 119, 118, and 117.

Anal.—Calc. for $C_{20}H_{19}F_5O_2$: C, 62.17; H, 4.96; F, 25.36. Found: C, 62.44; H, 5.05; F, 24.38.

The pentafluorobenzyl ester of II was isolated as white crystals, mp 48–50°; IR (mineral oil): 1745, 1660, 1525, 1510, 1170, 1050, 935, and 925 cm^{-1}; NMR ($CDCl_3$): δ 0.90 (d, 6H), 1.85 (m, 1H), 2.4 (d, 2H), 3.6 (s, 2H), 5.2 (s, 2H), and 7.0–7.2 (m, 4H) ppm; mass spectrum: *m/e* 372 (M^+), 329 ($M^+ - 43$), 181, 147, 105, and 104.

Anal.—Calc. for $C_{19}H_{17}F_5O_2$: C, 61.29; H, 4.61; F, 25.51. Found: C, 61.35; H, 4.61; F, 26.04.

IR and mass spectrometric analyses, before and after GLC, supported the proposed structures and confirmed that the pentafluorobenzyl esters of I and II chromatographed as the intact molecules.

Assay Sensitivity and Specificity—At an attenuator setting of 32 on the electron-capture linearizer, 7.2 ng of I as its pentafluorobenzyl ester produced a full-scale response. However, under the assay conditions, the lower limit of detection sensitivity for I in extracts of human serum is 0.1

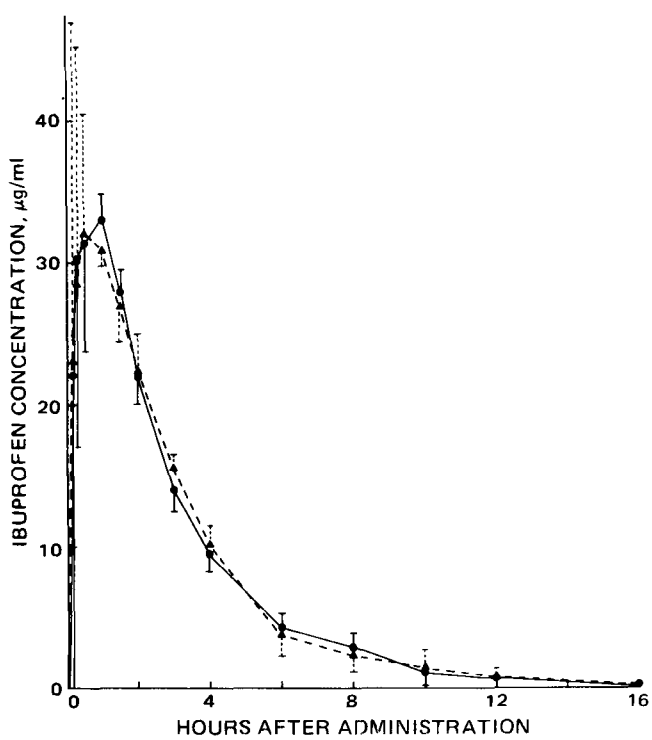

Figure 4—*Average* (±SD) *serum ibuprofen concentration* versus *time in humans* (n = 3) *after single-dose oral administration of 400 mg of drug in aqueous solution. Key:* ●—, *ibuprofen measured as methyl ester; and* ▲– –, *ibuprofen measured as pentafluorobenzyl ester.*

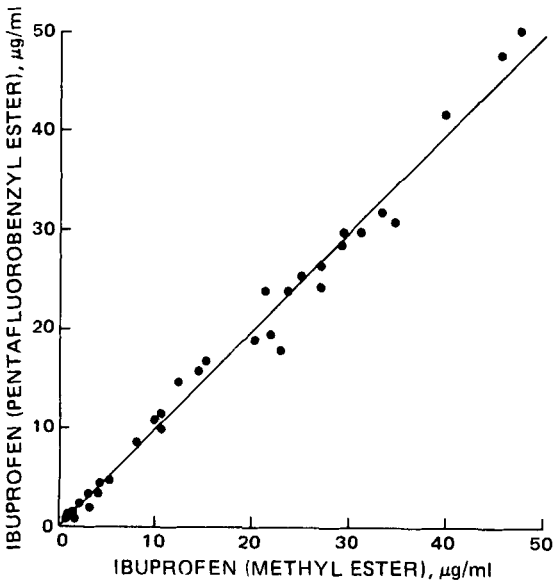

Figure 5—*Correlation of serum ibuprofen concentrations in drug-treated subjects when measured as the methyl ester (abscissa) and pentafluorobenzyl ester (ordinate). Least-squares regression analysis showed a slope of 0.999 and a correlation coefficient of 0.992.*

μg in 0.1–1.0 ml of the original sample aliquot. This value is based on a sample signal equivalent to 2% of full-scale response. Under the assay conditions described, a linear relationship between detector response and concentration is obtained for I over the range of 0–60 μg/ml. Quantification of serum specimens from drug-treated human subjects, using GLC in conjunction with mass spectrometry, showed that the material responding to the assay was identical to known I pentafluorobenzyl ester.

Recovery Experiments—Water or serum was added to known amounts of I and II in centrifuge tubes. The samples were mixed thoroughly and extracted with benzene. All extract residues were chromatographed on thin layers of silica gel 60 F_{254}, and the zones corresponding to I and II were eluted. The materials were esterified and analyzed *via* GLC. The results (Tables I and II) indicated that recoveries of I (97.7 ± 7.3%) and II (106.5 ± 10.9%) from serum were essentially quantitative as compared to simple aqueous samples.

Serum Levels of Ibuprofen in Humans—Results from the measurement of serum I concentrations in three normal human volunteers, after single-dose oral drug administration, demonstrated the utility of the method (Fig. 4). A peak mean (±*SD*) level of 31.9 ± 8.8 μg/ml was observed at 0.5 hr after drug administration, indicating rapid drug absorption from the aqueous solution. At 16 hr, serum drug concentrations were below the sensitivity level (*i.e.*, <0.1 μg/0.1 ml), indicating rapid drug disappearance from peripheral circulation. The serum drug disappearance half-life, as estimated from the average serum drug concentrations, was 1.94 hr. Analysis of the same samples, based on GLC of the I methyl ester (11), showed excellent agreement (Fig. 4) as evidenced by a slope of 0.999 and a correlation coefficient of 0.992 (Fig. 5).

In drug–protein binding studies, using equilibrium dialysis or ultrafiltration techniques, I concentrations on each side of the dialysis membrane were measured by GLC of the pentafluorobenzyl esters. The results, in excellent agreement with the *in vitro* studies of Mills *et al.* (5), showed that 99.7 ± 0.2% of the intact drug in peripheral circulation was bound to serum proteins during the 0–12-hr interval after drug administration. The combined results from these investigations showed that GLC of I, as the pentafluorobenzyl ester, could be used for evaluating drug–protein binding, pharmacokinetics, and drug availability from various dosage formulations with submilliliter amounts of human serum.

REFERENCES

(1) S. S. Adams, E. E. Cliffe, B. Lessel, and J. S. Nicholson, *J. Pharm. Sci.*, **56**, 1687 (1967).

(2) S. S. Adams, K. F. McCullough, and J. S. Nicholson, *Arch. Int. Pharmacodyn. Ther.*, **178**, 115 (1969).

(3) S. S. Adams, R. G. Bough, E. E. Cliffe, B. Lessel, and R. F. N. Mills, *Toxicol. Appl. Pharmacol.*, **15**, 310 (1969).

(4) S. S. Adams, R. G. Bough, E. E. Cliffe, W. Dickinson, B. Lessel, K. F. McCullough, R. F. N. Mills, J. S. Nicholson, and G. A. H. Williams, *Rheumatol. Phys. Med. Suppl.*, **1970**, 9.

(5) R. F. N. Mills, S. S. Adams, E. E. Cliffe, W. Dickinson, and J. S. Nicholson, *Xenobiotica*, **3**, 589 (1973).

(6) S. Masumoto, K. Takase, Y. Maruyama, and M. Okumura, *Pharmacometrics*, **6**, 77 (1972).

(7) C. D. Brooks, F. R. Schmid, J. Biundo, S. Blau, R. Gonzalez-Alcover, J. D. C. Gowans, E. Hurd, R. E. H. Partridge, and E. L. Tarpley, *Rheumatol. Phys. Med. Suppl.*, **1970**, 48.

(8) E. F. Davies and G. S. Avery, *Drugs*, **2**, 416 (1971).

(9) C. D. Brooks, C. A. Schlagel, N. C. Sekhar, and J. T. Sobota, *Curr. Ther. Res.*, **15**, 180 (1973).

(10) S. S. Adams and E. E. Cliffe, *J. Pharm. Pharmacol.*, **17**, 173 (1965).

(11) D. G. Kaiser and G. J. VanGiessen, *J. Pharm. Sci.*, **63**, 219 (1974).

(12) D. G. Kaiser and G. J. VanGiessen, *Pharmacologist*, **16**, 221 (1974).

(13) C. J. W. Brooks and M. T. Gilbert, *J. Chromatogr.*, **99**, 541 (1974).

(14) G. J. VanGiessen and D. G. Kaiser, *J. Pharm. Sci.*, **64**, 798 (1975).

(15) D. G. Kaiser and E. M. Glenn, *Res. Commun. Chem. Pathol. Pharmacol.*, **9**, 583 (1974).

(16) T. Y. Toribara, *Anal. Chem.*, **25**, 1286 (1953).

(17) T. Y. Toribara, A. R. Terepka, and P. A. Dewey, *J. Clin. Invest.*, **36**, 738 (1957).

(18) F. W. Kawahara, *Anal. Chem.*, **40**, 2073 (1968).

(19) H. Ehrsson, *Acta Pharm. Suec.*, **8**, 113 (1971).

(20) J. A. F. Wickramasinghe, W. Morozowich, W. E. Hamlin, and S. R. Shaw, *J. Pharm. Sci.*, **62**, 1428 (1973).

(21) D. G. Kaiser, S. R. Shaw, and G. J. VanGiessen, *ibid.*, **63**, 567 (1974).

(22) D. G. Kaiser and R. S. Martin, *ibid.*, **63**, 1579 (1974).

(23) J. A. F. Wickramasinghe and S. R. Shaw, *Biochem. J.*, **141**, 179 (1974).

ACKNOWLEDGMENTS

The authors thank Dr. S. S. Stubbs and Dr. K. A. DeSante for monitoring the clinical portion of the study.

Hydrolysis Kinetics of the Monophosphate Ester Triclofos Sodium

JOHN D. McRAE [x] **and LUCY M. TADROS**

Received December 15, 1976, from the *College of Pharmacy, University of Minnesota, Minneapolis, MN 55455.* Accepted for publication August 17, 1977.

Abstract □ The hydrolysis kinetics of the monophosphate ester triclofos sodium were studied in the pH 0.00–7.80 range, the 80.1–98.4° range, and ionic strengths of 0.02–1.50. The pK_1 and pK_2 values for triclofos were 1.00 ± 0.05 and 5.80 ± 0.05, respectively. The pH dependency observed was consistent with a theory in which the hydrolysis rates of the triclofos species follow the order: monoanion > unionized > dianion. The apparent first-order rate constants at 80.1° associated with each species were 6.4 ± 0.6 × 10^{-3}, 28.0 ± 0.5 × 10^{-3}, and 0.3 ± 0.1 hr^{-1}, respectively. Different Arrhenius activation energies were observed at pH 0.00, 3.50, and 7.80, at which values the unionized, monoanion, and dianion forms were the dominant species present, respectively. The reaction showed a modest positive kinetic salt effect at pH 3.50 and a modest negative effect at pH 7.80. Various mechanistic possibilities are discussed.

Keyphrases □ Triclofos sodium—hydrolysis kinetics, effect of pH, temperature, and ionic strength □ Hydrolysis kinetics—triclofos sodium, effect of pH, temperature, and ionic strength □ Kinetics—hydrolysis of triclofos sodium, effect of pH, temperature, and ionic strength □ Sedative-hypnotics—triclofos sodium, hydrolysis kinetics, effect of pH, temperature, and ionic strength

Triclofos sodium (2,2,2-trichloroethanol dihydrogen phosphate monosodium salt) (I) is marketed as a sedative–hypnotic whose pharmacological action is dependent on the *in vivo* liberation of trichloroethanol.

The only reported (1) *in vitro* hydrolysis of triclofos was conducted at 100° in 0.1 *N* HCl, 0.1 *N* NaOH, and 0.01 *M* formate buffer (pH 4.0); the hydrolysis was more rapid in the formate buffer than under the other two conditions studied. The pH dependencies of the hydrolysis rates of other phosphate monoesters were reported (2–13) to exhibit various patterns, and some pH–rate profiles indicated that the ester form most susceptible to hydrolysis was the monoanion. Since the one report (1) on triclofos hydrolysis did not establish any of the usual kinetic parameters, the purpose of this study was to determine such parameters to permit more precise stability predictions under various conditions.

EXPERIMENTAL

Materials—All chemicals were reagent grade except for pharmaceutical quality triclofos sodium[1]. Water was double distilled from a glass apparatus.

pKa Determinations—The pKa values of triclofos and maleic and acetic acids, used as part of the buffer systems, were determined by the Benet and Goyan (14) method as modified (15). For each acid, duplicate pK determinations were made at 80° in 0.75 *M* KCl in thermostated[2] vessels; pH measurements were made with glass and calomel electrodes, equilibrated and standardized at 80°, on the expanded scale of a pH meter[3]. The volumes of the solution being titrated and the titrant were measured at room temperature but corrected to 80° using literature values (16) for the volume dependency of pure water on temperature, with the assumption that these solutions would behave similarly. The titrant, a standardized sodium hydroxide solution, was 20-fold more concentrated than the titrated acid.

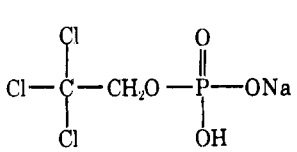

I

The following results were obtained: 0.1 *M* maleic acid, pK_1 = 1.56 ± 0.01 and pK_2 = 5.63 ± 0.03; 0.1 *M* acetic acid, pK = 4.55 ± 0.04; and 0.01 *M* triclofos sodium, pK_2 = 5.80 ± 0.05. In addition to yielding a pK value of the titrated acid, this procedure gives a value of the actual amount of acid present in the titrated system and, hence, permits a calculation of acid purity. The purity calculated for triclofos sodium was 96%.

Potentiometric titrations to determine the pK_1 for triclofos at 80° were performed with 4.053 *N* HCl on solutions that were 0.125, 0.2, 0.3, 0.4, and 0.5 *M* in triclofos sodium and 0.625, 0.55, 0.45, 0.35, and 0.25 *M*, respectively, in potassium chloride to produce an initial ionic strength of 0.75. The pK_1 for triclofos also was determined in 0.2 and 0.3 *M* triclofos sodium solutions with 1.3 and 1.2 *M* KCl added, respectively, to produce an initial ionic strength of 1.5. Since the present approach for the pK_1 determination differed from that used in the other pK determinations reported here, a discussion of the findings is given in the *Results and Discussion* section.

The pKa of tromethamine at 90° was determined by preparing three sets of solutions. Each was 0.1 *M* in tromethamine (primary standard grade base[4]) and 0.75 *M* in potassium chloride, and sufficient standardized hydrochloric acid was added to neutralize 0.25, 0.5, and 0.75 of the tromethamine base present. The pH values of these solutions were taken at 90°, and the pKa was calculated from the pH readings using the Henderson–Hasselbalch equation. The pKa of tromethamine obtained at 90° was 6.95 ± 0.01.

Mean Ionic Activity Coefficient of Hydrogen Ion—To determine the mean ionic activity coefficient for the hydrogen ion under the experimental conditions, solutions of 0.75, 0.875, 1.0, 1.125, 1.25, and 1.5 *M* KCl in carbon dioxide-free water were titrated at 80° with 4.053 *N* HCl. The pairs of volume *versus* pH data so obtained were converted to hydrogen-ion molarities and activities. Then the activity in each data pair was divided by its molarity to give a set of mean ionic activity coefficients for the hydrogen ion: 0.820 ± 0.006 in 0.75 *M* KCl, 0.840 ± 0.008 in 0.875 *M* KCl, 0.880 ± 0.01 in 1.0 *M* KCl, 0.900 ± 0.006 in 1.125 *M* KCl, 0.920 ± 0.006 in 1.25 *M* KCl, and 0.985 ± 0.024 in 1.5 *M* KCl. The increase in the activity coefficient with ionic strength in the potassium chloride concentration range used is consistent with a trend reported elsewhere for this type of system (17).

Triclofos Hydrolysis Studies—The hydrolysis of triclofos at 80.1° over the pH 0.00–6.89 range was studied by preparing triclofos sodium solutions in 0.001 *M* initial concentration in the following buffer systems: perchloric acid (pH 0.00–1.31), 0.1 *M* maleic acid–potassium hydrogen maleate (pH 1.81–3.04), 0.1 *M* acetic acid–sodium acetate (pH 3.50–5.05), and 0.1 *M* potassium hydrogen maleate–potassium maleate (pH 5.52–6.89). Potassium chloride was used to adjust the ionic strength to 0.75 in each buffer.

The solutions, in stoppered volumetric flasks, were brought to temperature equilibrium in a constant-temperature oil bath and then sampled by pipet in appropriate frequency and number to permit monitoring of the reaction from essentially zero time to attainment of equilibrium conditions. Reaction samples were quenched by chilling in an ice bath and then kept frozen in stoppered vials until all samples for a given kinetic run were assembled; they were then assayed for inorganic phosphate content. The pH of each reaction solution was measured at the end of the

[1] Lakeside Laboratories, Milwaukee, Wis.
[2] Haake model FK-10, Polyscience Corp., Evanston, Ill.
[3] Model 7415-EO, Leeds and Northrup Co., North Wales, Pa.
[4] Trizma Base, Sigma Chemical Co., St. Louis, Mo.

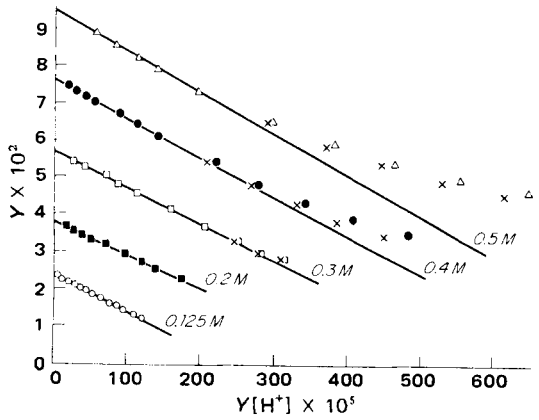

Figure 1—*Potentiometric titration data for 0.125–0.5* M *triclofos sodium plotted according to Eq. 1; ×'s are data points corrected for ionic strength changes during titration.*

run at room temperature, and no change from initial pH was observed greater than ±0.10.

The dependency of the 0.001 *M* triclofos hydrolysis rate on ionic strength at 80.1° was studied by preparing solutions in acetate buffers (0.05–0.10 *M*) at pH 3.50 and varying the ionic strength from 0.019 to 1.5 by adding potassium chloride. The ionic strength dependency of the reaction at 98.4° and pH 7.80 was studied in 0.1 *M* tromethamine buffers whose ionic strength was varied from 0.055 to 1.434 by adding potassium chloride.

The temperature dependency of the 0.001 *M* triclofos hydrolysis rate was followed at pH 0.00 at 80.1, 88.0, and 96.6° in perchloric acid buffers; at pH 3.50 at 80.1, 89.8, and 98.4° in 0.1 *M* acetate buffers; and at pH 7.80 at 90.0, 94.0, and 98.4° in 0.1 *M* tromethamine buffers. The tromethamine buffers were individually adjusted to pH 7.80 at each temperature because of the significant dependency of pH on temperature of basic buffers.

Separately prepared, duplicate runs were made of all kinetic experiments performed at each condition described.

Inorganic Phosphate Assay—Triclofos hydrolysis was followed by assaying for liberated inorganic phosphate by adaptation of the phosphomolybdenum blue assay (18). Aliquots of samples from the kinetic runs, representing an inorganic phosphate concentration of 0.1–0.6 μg/ml, were placed in 50-ml volumetric flasks. Then 2 ml of 2% (w/v) ammonium molybdate in 25% (v/v) sulfuric acid and 1 ml of 5% (w/v) stannous chloride in 6 *N* HCl were added. Each flask was brought to volume with water and allowed to stand 15 min.

The absorbance was measured at 720 nm in a 1-cm cell in a spectrophotometer[5] containing water in the reference cell. The absorbance of a blank, identical in composition to the sample cell except for the absence of the triclofos reaction mixture, was subtracted from sample readings. The net absorbance of each sample was converted to concentration using a standard curve prepared for each assay at the beginning of the assay. The standard curve was constructed using monobasic potassium phosphate in known concentrations of 0.2–0.6 μg/ml.

RESULTS AND DISCUSSION

Determination of pK_1 for Triclofos—Preliminary studies found that the pK_1 for triclofos was apparently less than 2.0, and efforts to determine its first dissociation constant in solutions of 0.01 *M* failed. This behavior agrees with results of Albert and Serjeant (19) who stated that ordinary potentiometric titration methods are unreliable for pK determinations on solutions where the negative logarithm of the concentration of the acid being titrated is greater than its pK value. It was, therefore, decided to determine the pK_1 for triclofos at several higher concentrations than those used in the kinetic runs and either to use such values or to extrapolate them to lower concentrations if the data seemed to justify this approach.

Since only the monosodium salt of triclofos was available rather than the free acid, this salt was used for pK_1 determinations. The method of Leeson and Brown (15) for pK determinations requires some modification

[5] Acta T. M. II UV–visible spectrophotometer, Beckman Instruments, Fullerton, Calif.

Table I—Values of pK_1 for Various Molarities of Triclofos Determined at Two Ionic Strengths at 80°

Molarity of Triclofos Sodium	Molarity of Potassium Chloride	Ionic Strength at Time Zero	pK_1
0.125	0.625	0.75	0.98
0.125	0.625	0.75	0.99
0.200	0.550	0.75	0.95
0.200	0.550	0.75	0.95
0.200	0.550	0.75	0.99
0.300	0.450	0.75	0.99
0.400	0.350	0.75	1.02
0.500	0.250	0.75	1.04
0.200	1.300	1.50	0.99
0.300	1.200	1.50	1.02

in the final equation when the conjugate base form (or salt) of the acid is titrated with strong acid. But by methods similar to those used earlier (14, 15), an equation of the following form can be developed:

$$Y = HA_o^- - \frac{1}{K_1} Y[H^+] \qquad \text{(Eq. 1)}$$

where:

$$Y = H^+ + Na_o^+ - Cl^- \qquad \text{(Eq. 2)}$$

and HA_o^- is the absolute number of moles of triclofos sodium added to the solution being titrated, H^+ is the absolute number of moles of the hydrogen ion present, Na_o^+ is the absolute number of moles of the sodium ion present due to the addition of triclofos sodium, Cl^- is the absolute number of moles of the chloride ion present due to the addition of hydrochloric acid titrant, $[H^+]$ is the molar concentration of the hydrogen ion present, and K_1 is the apparent first dissociation constant for triclofos.

To plot Y *versus* $Y[H^+]$ in accordance with Eq. 1 to obtain a linear relationship (the negative reciprocal of whose slope should give K_1), it is necessary to evaluate the terms in Y. Both H^+ and Cl^- can be obtained from calculations based on pH readings, titrant volume, normality data, and the experimentally determined mean ionic activity coefficient for the hydrogen ion. The value of Na_o^+ can be obtained by correcting the known amount of triclofos sodium added by its purity factor of 96% (obtained in the separate, independent determination of K_2 for triclofos as reported under *Experimental*).

Figure 1 gives five plots of titration data obtained at five different molarities of triclofos sodium as titrated with hydrochloric acid and plotted according to Eq. 1. The curves tend to be linear at values of $Y[H^+]$ less than 200×10^{-5} but show increasingly pronounced curvature for titrations of triclofos sodium of 0.3 *M* and higher where completion of the titration leads to values of $Y[H^+]$ greater than 200×10^{-5}. When the Y *versus* $Y[H^+]$ data for values of $Y[H^+]$ less than 200×10^{-5} are fitted by linear regression to a straight line, the straight lines shown in Fig. 1 result, permitting the calculation of pK_1 values (Table I). At ionic strengths of 0.75 and 1.5, the pK_1 can reasonably be assigned a value of 1.00 ± 0.05 under these limitations.

Since the actual kinetic runs were done with an initial triclofos sodium concentration of 0.001 *M*, the question of whether a pK_1 value of 1.0 is appropriate for application to the kinetic data must be considered. Even though the ionic strength in both the kinetic runs and the pK_1 determinations (at least at the beginning of the titrations used in the determinations) was either 0.75 or 1.5, the species contributing to this ionic strength were different in each case. The question of interest then becomes whether the first acid dissociation step of triclofos will be detectably different in an environment where the triclofos itself is contributing 0.125–0.5 of the total ionic strength of 0.75. Although a difference might be expected in the extent of acid dissociation occurring under such different environments, the data presented in Table I do not show any particular trend to higher or lower values of pK_1 as the triclofos sodium concentration drops from 0.5 to 0.125 *M*. Consequently, the use of a value of 1.00 ± 0.05 for pK_1 in the kinetic data seems justified.

The nonlinear behavior of parts of several curves in Fig. 1 could be due to several causes, including pH meter reading error due to faulty standardization (14). But this possibility seems unlikely here because careful attention was paid to this detail. Lack of constancy in the mean ionic activity coefficient of the hydrogen ion during the titration could also produce the observed curvatures. That this activity coefficient is a rather sensitive function of ionic strength was shown under *Experimental*. Assuming that triclofos has a pK_1 value of 1.0 permits one to approximate

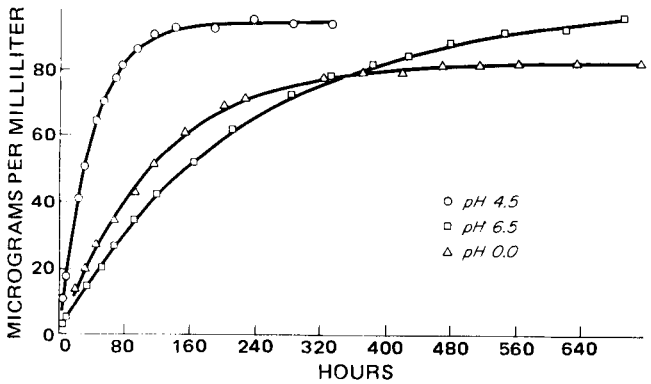

Figure 2—*Concentration of liberated inorganic phosphate* versus *time during hydrolysis of triclofos at 80.1° at three pH conditions.*

a more realistic ionic strength throughout the titration as it increases from its initial value of 0.75 because of the strong acid character of triclofos. Then, with the available data, estimates of the increasing mean ionic activity coefficient of the hydrogen ion at each pH during the titration were made, yielding finally the new points shown as ×'s in Fig. 1. While these points bring the data points closer to linearity, there is still significant curvature.

Since correction of hydrogen-ion activity coefficients does not fully eliminate the curvature in Fig. 1 plots, an additional cause of some or all of the nonlinearity may be that K_1 of Eq. 1 is an *apparent* dissociation constant rather than the thermodynamic dissociation constant. An apparent dissociation constant will vary with ionic strength to the extent that the activity coefficients (or their ratio) of the species involved in the equilibrium vary. In this case, where both ionic and nonionic species are involved in the equilibrium, one could probably expect a differing response to change in ionic strength by the charged and uncharged species. Whatever the exact cause of the nonlinearity, no further attempt was made to delineate this phenomenon because the main purpose of this part of the study—to obtain a value of pK_1 appropriately applicable to the treatment of the kinetic data—was satisfied adequately by using the limiting, linear parts of the curves since the conditions that yielded these data most closely duplicated the conditions of the kinetic experiments.

pH Dependency of Triclofos Hydrolysis—The simplest representation for the studied reaction would be as shown in Scheme I:

$$\text{triclofos} \underset{k_e}{\overset{k_h}{\rightleftharpoons}} \text{trichloroethanol} + \text{phosphoric acid}$$

Scheme I

where k_h is the observed hydrolysis rate constant and k_e is the observed esterification rate constant. Such a reaction would be first and second order in its hydrolysis and esterification steps, respectively. When the k_h/k_e ratio was expressed in terms of initial and equilibrium concentrations of triclofos (20), k_h was at least 300 times larger than k_e under all reaction conditions. Since $k_h \gg k_e$ and the reaction was always 65% or more complete at equilibrium, the data should conform reasonably well to a mathematical model for first-order hydrolysis.

When the concentration of inorganic phosphate, an expected hydrolysis product, is plotted *versus* time, the data exhibit the behavior shown in Fig. 2. The concentration *versus* time data for inorganic phosphate were processed by a computer program[6] designed to produce a nonlinear, least-squares fit to the following first-order equation for product appearance:

$$C = C_\infty(1 - e^{-k't}) \qquad \text{(Eq. 3)}$$

where C represents product concentration at time t and k' is the observed first-order rate constant for product appearance as it goes to a final concentration of C_∞. The computer program produces an estimate for both k' and C_∞. The solid lines in Fig. 2 are computer-drawn curves based on these computer estimates of k' and C.

In Fig. 3, the computer-generated values of k' are plotted as a function of pH, with the range of values from the duplicate runs at each pH indicated by the I-bars. The value of k' shown at pH 7.80 is an estimate of its value at 80.1° obtained by extrapolating values obtained at higher temperatures, using the Arrhenius equation. Examination of the pH dependency of k' reveals a pattern with the maximum rate between pH 1.8 and 4.0, suggesting, based on the values found for pK_1 and pK_2, a reaction rate largely dependent on the triclofos monoanion concentration with possible lesser contributions from the hydrolysis of the unionized and dianionic forms. If k_{H_2A}, k_{HA^-}, and $k_{A^{2-}}$ are the specific rate constants associated with hydrolysis of the unionized, monoanionic, and dianionic forms of triclofos, respectively, then the following relationship can be developed:

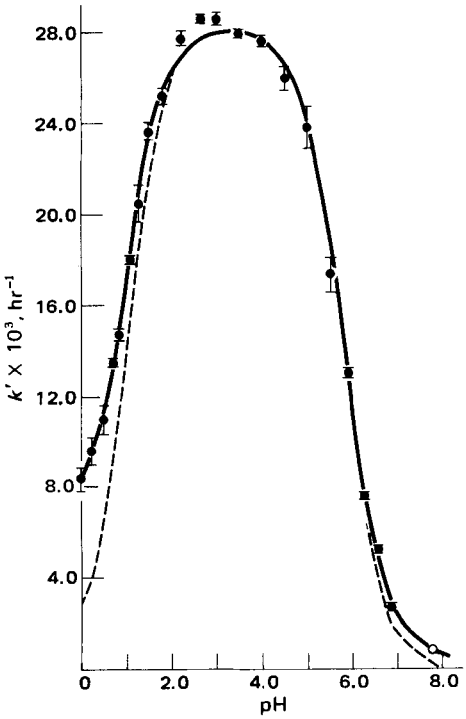

Figure 3—*Observed rate constant,* k', *for triclofos hydrolysis at 80.1° (●), or extrapolated to 80.1° (○),* versus *pH. Key (theoretical curves): – –, hydrolysis of triclofos monoanion form only; and —, combined hydrolysis of triclofos in unionized, monoanion, and dianion forms.*

$$k' = f_{H_2A}k_{H_2A} + f_{HA^-}k_{HA^-} + f_{A^{2-}}k_{A^{2-}} \qquad \text{(Eq. 4)}$$

where the terms f_{H_2A}, f_{HA^-}, and $f_{A^{2-}}$ represent the fraction of total triclofos in the system at any pH present in the forms indicated by the subscripts.

At pH 3.5, f_{H_2A} and $f_{A^{2-}}$ are approximately equal to zero and f_{HA^-} approaches 1.0 in value. At pH 7.80, $f_{H_2A} \cong 0.00$ while $f_{HA^-} \cong 0.01$ and $f_{A^{2-}} \cong 0.99$. If the average experimental value of k' at pH 3.50, *i.e.*, $28 \pm 0.5 \times 10^{-3}$ hr^{-1}, is equated to the specific rate constant, k_{HA^-}, then this value can be combined with experimental values of k' at pH 0.00 and 7.80 to calculate k_{H_2A} and $k_{A^{2-}}$. At pH 0.00:

$$k' \cong k_{H_2A}f_{H_2A} + k_{HA^-}f_{HA^-} \qquad \text{(Eq. 5}a\text{)}$$

At pH 7.80:

$$k' \cong k_{HA^-}f_{HA^-} + k_{A^{2-}}f_{A^{2-}} \qquad \text{(Eq. 5}b\text{)}$$

The values of f_{H_2A}, f_{HA^-}, and $f_{A^{2-}}$ needed for Eqs. 5*a* and 5*b* can be readily calculated from the separately determined values of K_1 and K_2 for triclofos. The results of this approach are: $k_{H_2A} = 6.4 \pm 0.6 \times 10^{-3}$ hr^{-1} and $k_{A^{2-}} = 0.3 \pm 0.1 \times 10^{-3}$ hr^{-1}.

When the calculated values for the specified rate constants are used to evaluate Eq. 4 over the pH 0.00–7.80 range, the data give the solid curve (hereafter designated as *k*th) shown in Fig. 3. The broken-line curve represents a theoretical curve based only on the product $k_{HA^-}f_{HA^-}$; this curve deviates significantly from the experimental results below pH 2.0 and to a more modest extent above pH 6.0. The solid curve defined by *k*th affords a reasonably good fit to the experimental data except that the experimental results all exceed the values predicted by *k*th at pH 2.25, 2.65, and 3.04. However, the difference between *k*th and the average value of the experimental data at these three pH values is ~3% or less.

[6] NONLIN program, The Upjohn Co., Kalamazoo, Mich., as adapted for use by Dr. Richard Hunt onto the CDC CYBER 74 system, University of Minnesota Computer Center.

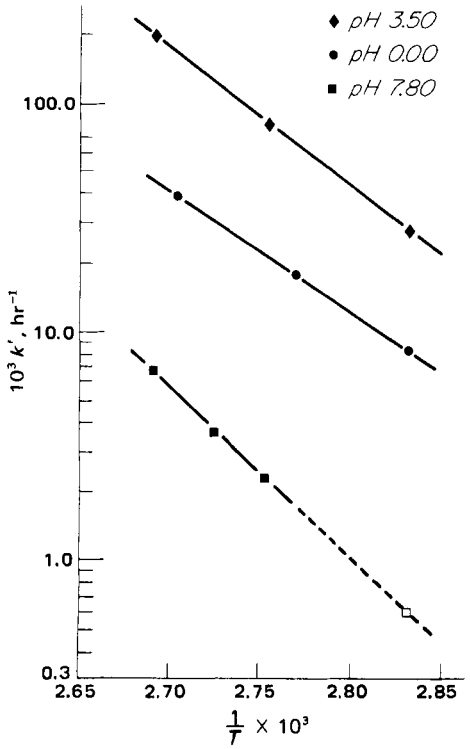

Figure 4—*Semilogarithmic plot of observed triclofos hydrolysis rate constant,* k′, *at three pH conditions* versus *reciprocal Kelvin temperature. Key:* □, *extrapolated value of* k′ *to 80.1° at pH 7.80.*

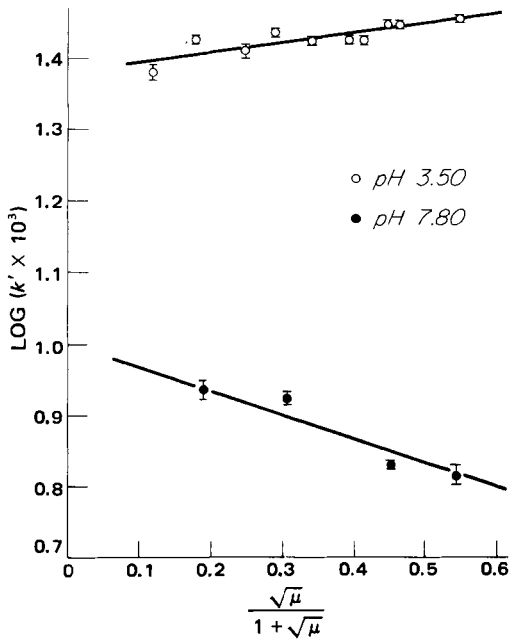

Figure 5—*Logarithm of* k′, *the observed triclofos hydrolysis rate constant,* versus $\mu^{1/2}/(1 + \mu^{1/2})$; μ *is ionic strength.*

The buffer system used at each of these three pH conditions (as well as at pH 1.81 where *k*th agrees well with the experimental data) depends upon the half-salt of maleic acid. Such half-salt species have been shown to exhibit strong catalytic effects upon hydrolysis of certain amides (21). Although general acid and base catalysis of esters is not common, it has been demonstrated (22, 23) in some cases, so the kinetic data in these particular maleate buffers may be exhibiting a buffer catalysis effect. The possibility that buffer catalysis might be the source of these deviations was not explored. To establish such apparently modest buffer effects would require use of significantly more concentrated buffers and, in the pH range involved, the maleate buffers were near the limits of their solubility as used.

Temperature Dependency of Triclofos Hydrolysis—Figure 4 gives the results of the temperature dependency studies at pH 0.00, 3.50, and 7.80 plotted as log *k′ versus* reciprocal temperature in accordance with the Arrhenius equation. Linear regression treatment of the data at each pH gives values for the activation energy, E_a, as follows: 24.1 kcal/mole at pH 0.00, 28.1 kcal/mole at pH 3.50, and 34.1 kcal/mole at pH 7.80.

At pH 3.50, about 100% of the total triclofos present is in the monoanion form, so that the activation energy at pH 3.50 probably can be properly identified as almost exclusively associated with monoanion hydrolysis. Evaluation of Eq. 5*a* at pH 0.00 leads to the conclusion that approximately 70% of the value of *k′* is due to unionized triclofos hydrolysis and the balance to monoanion hydrolysis. Consequently, the activation energy observed at pH 0.00 probably can be largely, but not exclusively, associated with the hydrolysis of undissociated triclofos. Finally, evaluation of Eq. 5*b* implies that about 50% of *k′* at pH 7.80 is associated with monoanion hydrolysis and 50% is associated with dianion hydrolysis. By this analysis, the activation energy observed at pH 7.80 is apparently a mixed function of the hydrolysis associated with the two dominant forms of triclofos present.

Ionic Strength Dependency of Triclofos Hydrolysis—Figure 5 gives the results of the kinetic runs at pH 3.50 and 80.1° in which ionic strength was varied; the results of similar runs at pH 7.80 and 98.4° also are shown in Fig. 5. The data in Fig. 5 are plotted as log *k′ versus* $\mu^{1/2}/(1 + \mu^{1/2})$, where μ is the ionic strength, based on an extended and modified form of the Debye–Huckel equation (24). Plots based on this equation should yield a linear relationship whose slope is proportional to the product of the charges carried by the reactive species forming the activated complex. Although this modified equation holds, in theory, only up to about an ionic strength of 0.1, it has been shown (25) to predict kinetic salt effects reliably in some pharmaceutical systems to as high as unity ionic strength.

The slope of the linear regression line in Fig. 5 fitted to the data at pH 3.50 is 0.14; the slope of the line fitted to the data at pH 7.80 is −0.37. Neither of these slopes fits exactly any theoretical model predicted by the equation used, but the relatively low values of the slopes are probably more consistent with the absence of ionic charge on at least one reactant rather than charges on all reactants (26).

CONCLUSIONS

The kinetic data reported here provide a basis for comparison with other studies on monophosphate ester hydrolysis (2–13). These studies all show little or no hydrolysis at pH conditions where the dianion species is dominant and usually show a maximum hydrolysis rate where the monoanion predominates. At lower pH conditions, the observed rate may show evidence of neutral species hydrolysis; in some cases, at a pH of about 0.5 and less, the rate may increase consistent with formation of a conjugate acid form of the ester that experiences hydrolysis.

Table II gives the hydrolysis rate of the neutral and monoanion forms of several phosphate esters relative to methyl phosphate as well as the values of the Arrhenius preexponential factor, *A*, and activation energy, E_a, for k_{HA^-}. The activation energy for monoanion hydrolysis is very similar for all esters so that any variation in rate is more a function of the preexponential or entropy term. For both k_{H_2A} and k_{HA^-}, but especially the former, the rate constant increases as the acid strength of the alcohol, ROH, of the ester increases (or, alternatively, the stability of the RO^- group increases).

A fully satisfactory mechanistic explanation for monophosphate ester hydrolysis has not been established. The comparatively ready monoanion

Table II—Comparative Kinetic Parameters[a] for Selected Monophosphate Esters at 100°

Compound	Relative Rates[b] k_{H_2A}	Relative Rates[b] k_{HA^-}	E_a[c], kcal/mole	10^{-14} A[c], min^{-1}
Methyl phosphate	1.0	1.00	30.6	3.88
Glycerol 1-phosphate	—	1.66	29.9	2.57
Triclofos	136.0	7.94	28.1	1.47
p-Tolyl phosphate	240.0	28.6	29.0	10.80
Phenyl phosphate	305.0	32.0	29.0	12.6
p-Nitrophenyl phosphate	3000.0	66.8	30.0	216.0

[a] Values listed for triclofos are based on data obtained in this study; values for other esters are from Ref. 13. [b] Hydrolysis rates for each ester relative to methyl phosphate for which $k_{HA^-} = 4.94 \times 10^{-4}$ min^{-1} and $k_{H_2A} = 0.06 \times 10^{-4}$ min^{-1}. [c] Both E_a and A are Arrhenius equation parameters for k_{HA^-}.

hydrolysis is not easy to explain, but the presence of both an OH^- group and an O^- group is evidently necessary since diphosphate esters monoanions do not hydrolyze with the same facility. Most proposed mechanisms for monoanion hydrolysis involve formation of a hydrogen-bonded complex with water as the reactive entity. In the current study on triclofos, the modest dependency of k_{HA^-} on ionic strength at pH 3.50 is not inconsistent with a bimolecular reaction between the monoanion and water since the activity coefficient of either species might vary with an ionic strength change of the range studied.

The neutral species rate constants, k_{H_2A} (Table II), are rather sensitive functions of the stability of RO^- as a departing species. A heterolytic reaction involving the phosphorus–oxygen bond, yielding protonated metaphosphoric acid that then undergoes rapid hydration, is consistent with these results (11) (Scheme II).

$$ROPO(OH)_2 \rightarrow RO^- + PO^+(OH)_2$$

Scheme II

An alternative mechanism involving direct attack by water on the phosphorus atom can be hypothesized and is also consistent with the experimental observations (11) (Scheme III).

$$ROPO(OH)_2 + OH_2 \rightarrow RO^- + H_2O^+PO(OH)_2$$

Scheme III

The activation energy determined at pH 0.00 for triclofos, which can be largely associated with the hydrolysis of the unionized form, is less in magnitude than that found at pH 3.50 where monoanion hydrolysis dominates. Neither this observed difference in activation energies nor data obtained by other investigators in phosphate ester hydrolysis studies permit selection between these two possible mechanisms.

Dianion hydrolysis of monophosphate esters has been reported to be minimal or unobserved in other systems studied (11). Although a reaction between the monoanion and hydroxide ion is kinetically equivalent to a reaction between the dianion and water, previous evidence and/or arguments (5, 6, 11) make the former possibility unlikely. In addition to these mechanistic possibilities, it has been argued (11) that, for hydrolytically reactive phosphate ester dianions, the results can be interpreted most simply in terms of dianion heterolysis (Scheme IV).

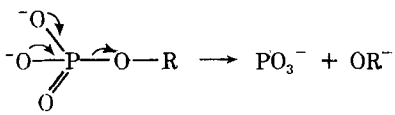

Scheme IV

This type of reaction would be expected to be aided by the two negative charges on the oxygen atoms, providing considerable driving force for the heterolysis. Even so, the activation energy of such a heterolytic breakdown would be expected to be fairly high; for 2,4-dinitrophenyl phosphate (11), the Arrhenius activation energy associated with dianion hydrolysis was greater than that for monoanion hydrolysis. For triclofos hydrolysis, a higher activation energy was observed at pH 7.80, where the dianion species dominated, than at pH 3.50, where the monoanion was the dominant species. Also, the dependence of the reaction rate constant at pH 7.80 on ionic strength was negative rather than positive as at pH 3.50. These differences in magnitude or character of reaction parameters at pH 7.80 *versus* 3.50 support the dependency of the reaction rate on pH and also indicate that some triclofos dianion hydrolysis occurs.

In summary, although this study does not permit definitive judgments on the mechanism(s) of triclofos hydrolysis throughout the pH range studied, it does provide sufficient information, particularly when compared with other such hydrolyses, to assign a hydrolysis role to the unionized, monoanion, and dianion ester forms.

REFERENCES

(1) Y. Hasegawa, O. Hoshino, and T. Ukita, *Yakugaku Zasshi*, **86**, 292 (1966).

(2) M. C. Bailly, *Bull. Soc. Chim. Fr.*, **9**, 421 (1942).

(3) A. Desjobert, *ibid.*, **14**, 809 (1947).

(4) W. W. Butcher and F. H. Westheimer, *J. Am. Chem. Soc.*, **77**, 2420 (1955).

(5) J. D. Chanley and E. Feasgeson, *ibid.*, **77**, 4002 (1955).

(6) P. W. Barnard, C. A. Bunton, D. R. Llewellyn, K. G. Oldham, B. L. Silver, and C. A. Vernon, *Chem. Ind.*, **1955**, 760.

(7) J. Kumamota and F. H. Westheimer, *J. Am. Chem. Soc.*, **77**, 2515 (1955).

(8) C. A. Bunton, D. R. Llewellyn, G. G. Oldham, and C. A. Vernon, *J. Chem. Soc.*, **1958**, 3574.

(9) *Ibid.*, **1958**, 3588.

(10) C. A. Vernon, *Chem. Soc., Spec. Publ.*, No. 8, 17 (1959).

(11) C. A. Bunton, E. J. Fendler, and J. H. Fendler, *J. Am. Chem. Soc.*, **89**, 1221 (1967).

(12) C. A. Bunton and E. Humeres, *J. Org. Chem.*, **34**, 572 (1969).

(13) P. W. C. Barnard, C. A. Bunton, D. Kellerman, M. M. Mhala, B. Silver, C. A. Vernon, and V. A. Welch, *J. Chem. Soc. B*, **1966**, 227.

(14) L. Z. Benet and J. E. Goyan, *J. Pharm. Sci.*, **54**, 983 (1965).

(15) L. J. Leeson and M. Brown, *ibid.*, **55**, 431 (1966).

(16) "Handbook of Physics and Chemistry," 46th ed., Chemical Rubber Co., Cleveland, Ohio, 1965–66, pp. F-4, F-5.

(17) H. S. Harned and B. B. Owen, "Physical Chemistry of Electrolytic Solutions," 3rd ed., Reinhold, New York, N.Y., 1958, p. 748.

(18) J. T. Woods and M. G. Mellon, *Ind. Eng. Chem. Anal. Ed.*, **13**, 760 (1941).

(19) A. Albert and E. P. Serjeant, "The Determination of Ionization Constants," 2nd ed., Chapman and Hall, London, England, 1971.

(20) A. A. Frost and R. C. Pearson, "Kinetics and Mechanisms," 2nd ed., Wiley, New York, N.Y., 1961, pp. 186, 187.

(21) P. Finholt and T. Higuchi, *J. Pharm. Sci.*, **51**, 655 (1962).

(22) E. R. Garrett, *J. Am. Chem. Soc.*, **79**, 5206 (1957).

(23) G. L. Schmir and T. C. Bruice, *ibid.*, **80**, 1173 (1958).

(24) G. Czapski and H. Schwarz, *J. Phys. Chem.*, **66**, 471 (1962).

(25) J. T. Carstensen, *J. Pharm. Sci.*, **59**, 1140 (1970).

(26) A. A. Frost and R. C. Pearson, "Kinetics and Mechanism," 2nd ed., Wiley, New York, N.Y., 1961, pp. 150–155.

ACKNOWLEDGMENTS

Abstracted in part from a dissertation submitted by L. M. Tadros to the University of Minnesota in partial fulfillment of the Master of Science degree requirements.

The authors thank Dr. Richard Hunt, Pennwalt Corp., Rochester, N.Y., and Mr. William Wargin, College of Pharmacy, University of Minnesota, for assistance in computer programming.

Effect of Enantiomeric Purity on Solubility Determination of Dexclamol Hydrochloride

SUNG-TSUEN LIU and ARTHUR HURWITZ ˣ

Received April 25, 1977, from *Pharmacy Research and Development, Ayerst Laboratories, Inc., Rouses Point, NY 12979.* Accepted for publication August 15, 1977.

Abstract □ The solubility of (±)-(4a,13b-*trans*)-[3(OH),13b(H)-*trans*]-3-isopropyl - 2,3,4,4a,8,9,13b,14- octahydro-1*H* - benzo-[6,7]cyclohepta[1,2,3-*de*]pyrido[2,1-*a*]isoquinolin-3-ol hydrochloride [(±)-I] was 3.3 mg/ml in pure water. Its resolved enantiomers exhibited about a fivefold increase in solubility. Dexclamol hydrochloride, the (+)-I enantiomer, is bioactive as a neuroleptic and is soluble to the extent of 16.4 mg/ml. However, raw material purity in relation to the amounts of (±)-I racemate present significantly influences solubility and optimum conditions for dissolution. The effect of trace amounts of (−)-I or (±)-I forms on the solubility of (+)-I enantiomer raw materials was explained through phase solubility studies. Conditions required for preparation of clear solutions using raw materials of varying purity can be determined with derived expressions. The application and limitations of using an enantiomer as a tool to improve solubility are discussed.

Keyphrases □ Dexclamol hydrochloride—solubility, effect of enantiomeric purity □ Enantiomeric purity—dexclamol hydrochloride, effect on solubility □ Solubility—dexclamol hydrochloride, effect of enantiomeric purity □ Sedatives—dexclamol hydrochloride, solubility, effect of enantiomeric purity

Pharmaceutical formulations of a wide variety of optically active compounds have been prepared. Usually, enantiomers exhibit differences in biological activity, and one enantiomer has a distinctive activity or advantage compared to the racemate (1, 2). Furthermore, racemic substances and their enantiomers often exhibit differences in physical properties such as melting point or solubility (3, 4). Recently, the application of a tertiary amine enantiomer to improve a pharmaceutical formulation was reported (5).

Dexclamol hydrochloride, (+)-I, is a potential neuroleptic agent (6–9). Its solubility is 16.4 mg/ml in pure water; that of (±)-I, (±)-(4a,13b-*trans*)-[3(OH),13b(H)-*trans*]-3- isopropyl-2,3,4,4a,8,9,13b,14-octahydro- 1*H*- benzo-[6,7]cyclohepta[1,2,3-*de*]pyrido[2,1-*a*]isoquinolin-3-ol hydrochloride, is only 3.3 mg/ml. Trace amounts of the bioinactive (−)-form or the (±)-form of I seriously interfere in the solubility determination of (+)-I.

The purpose of the present study was to investigate the interaction between (−)- and (+)-I. The effect of such interactions on solubility behavior was explained in terms of phase solubility. Effects of pH and common ion on the solubility of (+)-I also were investigated.

EXPERIMENTAL

Materials—Reagent grade chemicals and double-distilled water were used. Compounds (+)-I, (−)-I, and (±)-I were used as obtained[1].

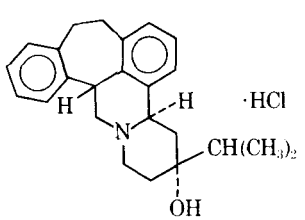

I

Solubility Determination—A jacketed 250-ml beaker was employed. Excess solid (+)-I, (−)-I, or (±)-I was introduced into 100 ml of water at 25 ± 1° in the beaker. The suspensions were stirred magnetically, and no significant differences in the solution concentration were observed after 4 hr of stirring. After equilibration, 10 ml of the suspension was sampled and filtered[2] for assay. A few experiments were carried out at 35°. The same experimental procedure was used to study the solubility of (+)-I and (±)-I in different concentrations of sodium chloride solutions.

Less than a 10% increase in solubility was observed for a 10° increase in temperature. Since solubility was relatively insensitive to small temperature changes, all phase solubility experiments were performed at room temperature (22 ± 2°). Physical mixtures containing 10% (−)-I–90% (+)-I, 30% (−)-I–70% (+)-I, and 50% (−)-I–50% (+)-I were used. Weighed amounts of these physical mixtures were introduced into 150-ml beakers containing a known volume of water. The suspended mixtures were stirred magnetically, and the solution concentrations were determined at intervals. To ensure equilibration, all reported phase solubility values were taken from samples after 24 hr of mixing. In most cases, equilibration was found in less than 10 hr.

Analytical Procedures—The (+)-I, (−)-I, and (±)-I all showed the same spectrum in the UV range. No significant differences in absorption intensity[3] were found at pH 2–9. Two absorption peaks were found at 263 and 270 nm. The molar absorptivity values, determined from Beer's law plots, were ϵ_{263} 610 M^{-1} cm^{-1} and ϵ_{270} 630 M^{-1} cm^{-1}.

In the solubility studies, the final saturated suspensions were filtered and the resulting precipitates were collected and then dissolved in the required amount of water. Both filtered saturated solutions and the solutions prepared by redissolving the precipitates were then checked by specific rotation measurement[4] at room temperature (22 ± 2°). The enantiomeric purity of these solutions was calculated from the measured specific rotation[4].

RESULTS AND DISCUSSION

Factors Influencing Solubility of Pure (+)-I, (−)-I, or (±)-I—At 25°, the aqueous solubilities of (+)-I and (±)-I were 16.4 and 3.3 mg/ml, respectively. The saturated solution pH values were 4.4 for (+)-I and 4.9 for (±)-I. The solubility of both materials decreased as the pH of the solution increased. For example, a nearly 100-fold reduction in solubility was found at pH 7 for (+)-I. The solubility–pH profile of (+)-I is shown in Fig. 1. Changes in solubility, S, with hydrogen-ion concentration can be expressed as:

$$S = [B] + [BH^+] = S_0\left(1 + \frac{[H^+]}{K_a}\right) \qquad \text{(Eq. 1)}$$

where S_0 is the intrinsic solubility and has a value of 1.45×10^{-4} M; B and BH^+ are the neutral and protonated species of I, respectively; and K_a is the ionization constant. For this compound, the pKa value obtained by a solubility method was 7.3.

Solubility products of the hydrochloride salt, defined as K_{sp} (hydrochloride salt) = $[BH^+][Cl^-] \times f_1^2$, were 1.28×10^{-3} and 6.1×10^{-5} mole^2/liter^2 for (+)-I and (±)-I, respectively (where $[BH^+]$ is the protonated amine concentration, $[Cl^-]$ is chloride-ion concentration, and f_1 is the activity coefficient of univalent ions). The activity coefficient of univalent ions, f_1, was calculated from the extended Debye–Huckel equation derived by Davies (10):

$$-\log f_1 = 0.509\left(\frac{\sqrt{U}}{1+\sqrt{U}} - 0.3U\right) \qquad \text{(Eq. 2)}$$

[1] Ayerst Research Laboratories, Montreal, Quebec, Canada.
[2] With 0.22-μm Millipore filter membrane.
[3] Perkin-Elmer model 402.
[4] Perkin-Elmer polarimeter model 40.

Table I—Phase Solubility of (+)-I and (−)-I at Room Temperature

System Composition, mg/ml	Solution Concentration mg/ml	Solution Concentration $M \times 10^3$	$[\alpha]_D^{R.T.}$ Solution	Optical Purity of (+)-I in Solution, %	$K_{sp} \times 10^5$, moles²/liter²
		30% (−)-I–70% (+)-I			
50.0	17.3	45.0	205°	92.3	—
33.3[a]	12.8	33.3	193°	87.0	—
25.0[a]	10.4	27.0	192°	86.5	—
16.6	7.31	19.2	188°	84.7	2.60
12.5	5.78	15.0	180°	81.1	1.93
8.33	4.63	12.0	150°	67.6	1.95
5.00	4.75	12.3	87°	39.2	3.20
3.33[b]	3.33	8.63	83°	37.4	—
2.86[b]	2.86	7.40	92°	41.0	—
		10% (−)-I–90% (+)-I			
30	16.7	43.3	209°	94.1	—
20	15.7	40.8	202°	91.0	—
15[a]	12.0	31.0	—	—	—
10	8.72	22.6	187°	84.2	3.71
5	5.01	13.0	174°	78.6	1.61
		50% (−)-I–50% (+)-I			
30	3.66	9.5	—	—	2.26
20	3.70	9.6	—	—	2.30
12.5	3.74	9.7	4°	~0	2.35
5	3.62	9.4	−2°	~0	2.21

[a] Precipitated solid was dissolved and analyzed for optical purity. [b] Clear solution with no solid excess.

where U is the ionic strength of the solution. In the sodium chloride-containing solution, solubilities of these hydrochloride salts decreased. For example, the solubility of (±)-I was 0.29 mg/ml in 0.14 M sodium chloride. For (+)-I, the solubility was decreased to 4.0 and 0.77 mg/ml in 0.2 and 1.0 M sodium chloride, respectively. The decrease in solubility of these hydrochloride salts in chloride-ion-containing solution was explained in terms of the common ion effect.

Interaction between (+)-I and (−)-I in Aqueous Solution—Typical results of the interaction between (+)-I and (−)-I are shown in Fig. 2. The physical mixture contained 30% (−)-I and 70% (+)-I. Curves A and B illustrate the change in solution concentration as a function of time upon introduction of 200 and 100 mg of a 30% (−)-I–70% (+)-I solid mixture into 10 ml of water. The added solid material readily dissolved initially. If no interaction occurs between (+)-I and (−)-I, dissolution should be complete and solution concentration should stay constant. However, the experimental results indicated that a strong interaction occurred between the dissolved (+)-I and (−)-I, which caused the precipitation of a new solid phase.

In 10 ml of water, the recrystallization process followed immediately after the dissolution when 200 mg of solid sample was used. In contrast, precipitation occurred 50 min after the introduction of a 100-mg sample. The interaction forming the racemate was time dependent. Several factors such as the composition of the physical mixture, the system composition, temperature, and the degree of supersaturation after dissolution as well as the fluid dynamics of the solution affect the precipitation rate of the racemate.

In general, the higher the degree of supersaturation, the faster was the precipitation rate. All precipitation solids collected showed optical behavior similar to that of (±)-I. These data gave strong evidence that the interaction between (+)-I and (−)-I resulted only in the precipitation of (±)-I. The final equilibrium concentration after complete precipitation was taken as the solubility or solution concentration in the phase solubility study.

Phase Solubility—Experimental results of phase solubility measurements and specific rotation of the equilibrated solution are summarized in Table I, where the system composition represents the total amounts of solid mixture added per unit volume of water. Plots of solution concentration *versus* system composition are shown in Fig. 3. Since only

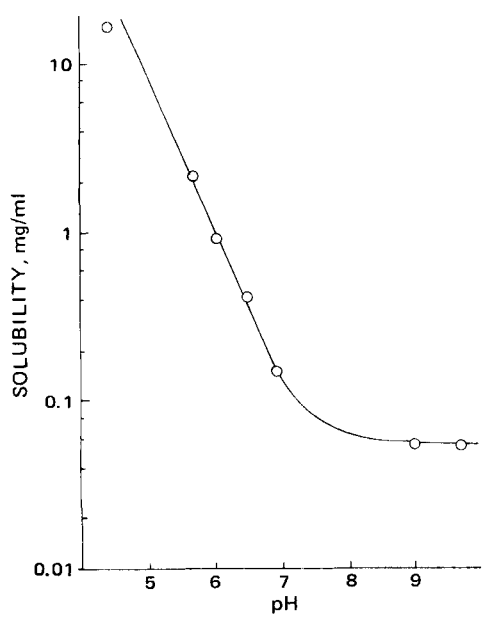

Figure 1—*The pH–solubility profile of (+)-I at 25°.*

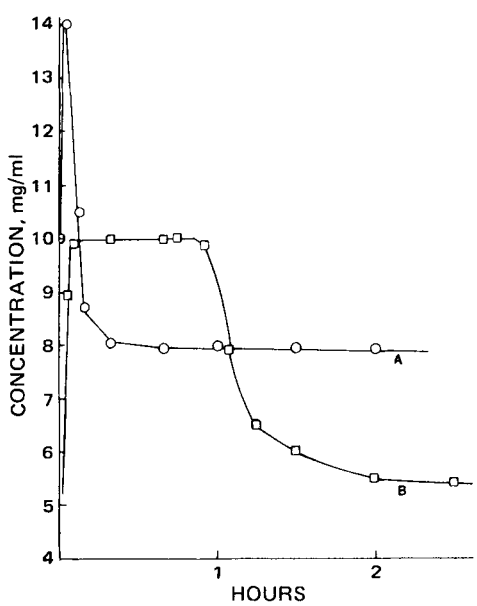

Figure 2—*Dissolution profile of 30% (−)-I–70% (+)-I physical mixture in water. Key: A, 200 mg of solid mixture in 10 ml of water; and B, 100 mg of solid mixture in 10 ml of water.*

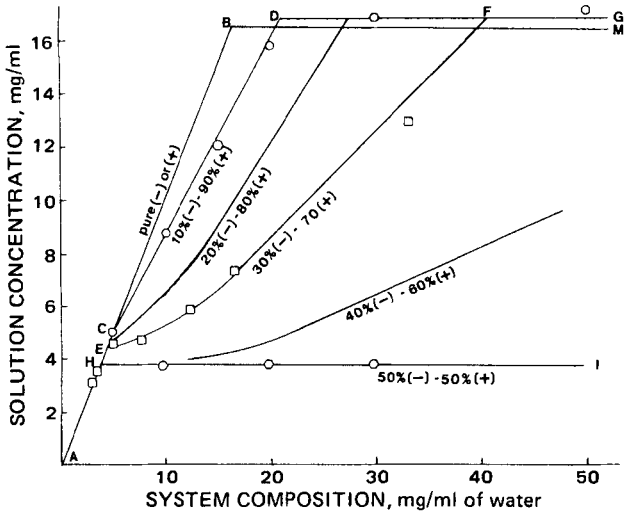

Figure 3—*Phase solubility of (+)-I and (−)-I mixture. Key: ○, □, and ○, experimental results; and —, calculated curves.*

(±)-I precipitated in all solution mixtures, these systems can be treated as simple systems containing (+)-I [or (−)-I] enantiomer, (±)-I racemate, and water (10).

In Fig. 3, line ABM is the solution–system composition curve of pure (+)-I or (−)-I enantiomer. Lines DG [10% (−)-I–90% (+)-I] and FG [30% (−)-I–70% (+)-I] represent systems saturated with both (+)-I and (±)-I forms. In this region, Eq. 3 and Schemes I and II should be satisfied and solution concentration should be constant:

$$K_{sp}[(\pm)\text{-I}] = [(+)\text{-I}_s] \times [(-)\text{-I}_s] \quad \text{(Eq. 3)}$$

$$(\pm)\text{-(solid)} \rightleftharpoons (+)\text{-I (solution)} + (-)\text{-I (solution)}$$
Scheme I

$$(+)\text{-I (solid)} \rightleftharpoons (+)\text{-I (solution)}$$
Scheme II

In a system saturated with (+)-I enantiomer:

$$[(+)\text{-I}_s] = \text{constant} \quad \text{(Eq. 4)}$$

and:

$$\text{solubility} = [(+)\text{-I}_s] + [(-)\text{-I}_s]$$

$$= [(+)\text{-I}_s] + \frac{K_{sp}[(\pm)\text{-I}]}{[(+)\text{-I}_s]} = \text{constant} \quad \text{(Eq. 5)}$$

where $[(+)\text{-I}_s]$ and $[(-)\text{-I}_s]$ are the solution concentrations of (+)-I and (−)-I, respectively, in a solution saturated with both (+)-I and (±)-I.

The regions where only (±)-I existed as the solid phase are shown by lines CD and EF in Fig. 3. From the phase rule (11), the solution concentration can be expected to change due to the existence of 1 degree of freedom. The solubility product for (±)-I, defined in Eq. 3, was calculated from the solubility data of a 50% (+)-I–50% (−)-I mixture. A value of 2.3 $\times 10^{-5}$ mole^2/liter^2 was thus obtained. Solubility products obtained from different composition mixtures in solutions saturated with only (±)-I are also shown in Table I. The values are in good agreement with those obtained from pure (±)-I. This finding is additional support for the conclusion that only solid (±)-I precipitated.

Theoretical calculations of solution concentration in (+)-I and (±)-I mixtures saturated only with (±)-I were made using the following equation:

$$\text{solution concentration (mg/ml)} = \left[[(+)\text{-I}] + \frac{K_{sp}[(\pm)\text{-I}]}{[(+)\text{-I}]}\right] \times \text{mol. wt.} \quad \text{(Eq. 6)}$$

where [(+)-I] is the concentration resulting from the amount of completely dissolved (+)-I together with the amount of dissolved (±)-I. Results of theoretical solubility curves are in excellent agreement with experimental data.

When unequal amounts of (+)-I and (−)-I are mixed, the solution concentration would be expected to increase gradually as the solid material added or system composition increases. Finally, the solution should become saturated with both (+)-I [or (−)-I] and (±)-I, and the solution concentration should remain constant. Solutions can be prepared at concentrations as high as the solubility of pure (+)-I or (−)-I by increasing the system composition of any unequal (+)-I and (−)-I mixture. However, the common undissolved solids visual test of the approach and achievement of solution saturation cannot be used in this system. In enantiomer racemate mixtures, undissolved solids can be detected well below the saturation of the enantiomer form. Therefore, it can be seen from the phase solubility curves that clear solution preparation is impossible without filtration in the regions where system composition is greater than solution concentration. For example, the highest clear solution concentration that can be achieved by dissolving a 10% (−)-I–90% (+)-I solid mixture in water without filtration is about 5 mg/ml.

The slope of the phase solubility curve for pure enantiomer should be close to 1. The difference between a slope of 1 and the slope for a raw material is equal to the percentage of the racemate in the raw material. Since the raw material purity was about 98%, the slope was very close to 1. Therefore, it would be very difficult to determine the amount of impurity in this range by this method. However, a trace amount of enantiomer contained in a racemate raw material could be determined using phase solubility analysis. In this case, the solubility line would be slightly higher than line HI (Fig. 3) for the racemate and have a positive slope. The percentage of enantiomer impurity could be determined easily.

Application and Limitations of Using Enantiomer Resolution to Improve Solubility—Enantiomer solubilities are often higher than those of their racemates. The degree of increase in solubility may range from a few percent to about fivefold. Therefore, resolution of racemates as a tool to improve solubility is not as effective as some other methods such as preparation of different polymorphs, solvates, or salt forms (12). However, the resolution of racemates may be the best available method with certain compounds.

In those cases, caution should be taken to determine the presence of trace amounts of racemate in the enantiomer raw materials. The clarity of prepared solutions and the apparent solubility could be influenced significantly. For example, the aqueous solubility of (+)-I is 16.4 mg/ml. Clear solutions at concentrations as high as 16 mg/ml can be prepared by dissolving extremely optically pure material in water. However, raw material containing 1.5% (−)-I dissolved incompletely when 11 mg of solid material was introduced into 1 ml of water.

REFERENCES

(1) A. F. Casy, in "Medicinal Chemistry," 3rd ed., vol. 1, A. Burger, Ed., Wiley–Interscience, New York, N.Y., 1970, pp. 81–87.

(2) T. C. Daniels and E. C. Jorgensen, in "Textbook of Organic, Medicinal and Pharmaceutical Chemistry," 6th ed., C. O. Wilson, O. Gisvold, and R. D. Doerge, Eds., Lippincott, Philadelphia, Pa., 1971.

(3) K. Mislow, "Introduction to Stereochemistry," Benjamin, New York, N.Y., 1966.

(4) "Handbook of Chemistry and Physics," 52nd ed., Chemical Rubber Co., Cleveland, Ohio, 1971–1972, p. C-743.

(5) A. J. Repta, M. J. Baltezor, and P. C. Bansal, *J. Pharm. Sci.*, **65**, 238 (1976).

(6) F. Bruderlein, L. Humber, and K. Voith, *J. Med. Chem.*, **18**, 185 (1975).

(7) P. H. Bird, F. T. Bruderlein, and L. G. Humber, *Can. J. Chem.*, **54**, 2715 (1976).

(8) T. A. Pugsley and W. Lippmann, *Naunyn-Schmiedebergs Arch. Pharmacol.*, **295**, 117 (1976).

(9) J. Jaramillo, *Can. J. Physiol. Pharmacol.*, **54**, 140 (1976).

(10) C. W. Davies, "Ion Association," Butterworths, London, England, 1962.

(11) W. J. Mader, in "Organic Analysis," vol. II, J. Mitchell, Jr., I. M. Kolthoff, E. S. Proskauer, and A. Weissberger, Eds., Interscience, New York, N.Y., 1954, pp. 253–276.

(12) S. Agharkar, S. Lindenbaum, and T. Higuchi, *J. Pharm. Sci.*, **65**, 747 (1976).

ACKNOWLEDGMENTS

Presented at the Basic Pharmaceutics Section, APhA Academy of Pharmaceutical Sciences, New York meeting, May 1977.

Quantitative Determination of Chlordiazepoxide and Its Metabolites in Serum by Fluorescence TLC–Densitometry

SY-RONG SUN

Received May 12, 1977, from the *Pharmaceutical Products Division, Abbott Laboratories, North Chicago, IL 60064.* Accepted for publication August 17, 1977.

Abstract □ A sensitive fluorescence TLC–densitometric procedure was developed for the specific determination of chlordiazepoxide (I) and its two metabolites, demoxepam (II) and desmethylchlordiazepoxide (III), in serum. After extraction from serum with ether, I, II, and III were separated by TLC and converted with a sulfuric acid spray to pale blue (R_f 0.63), green (R_f 0.54), and blue (R_f 0.45) fluorescence spots, respectively. Quantitation was accomplished by scanning the plate with a densitometer at 390 (I), 430 (II), and 390 (III) nm. The sensitivities were 0.05 (I), 0.01 (II), and 0.01 (III) μg/ml of serum. The procedure was successfully applied to measurement of I–III in human serum after oral administration of 20 mg of chlordiazepoxide hydrochloride.

Keyphrases □ Chlordiazepoxide—and metabolites, fluorescence TLC–densitometric analyses in serum □ Fluorescence TLC–densitometry—analyses, chlordiazepoxide and metabolites in serum □ Densitometry–fluorescence TLC—analyses, chlordiazepoxide and metabolites in serum □ Sedatives—chlordiazepoxide and metabolites, fluorescence TLC–densitometric analyses in serum

The determination of chlordiazepoxide (I) and its metabolite demoxepam (II) in plasma was reported previously (1). It was later modified (2) to include another metabolite, desmethylchlordiazepoxide (III). This determination is based on the quantitative conversion of I and III, by controlled hydrolytic conditions, to II. Compound II is converted, with light, to a compound exhibiting a characteristic fluorescence in alkaline solution, which is measured spectrofluorometrically.

The assay of I is the least accurate of the three since it involves the subtraction of one fluorescence (I and III) from another (III). The reported sensitivity is about 0.2–~0.3 μg/ml for each compound. Schwartz *et al.* (3) later increased the sensitivity to 0.1 μg/ml by using a spectrofluorometer containing a new xenon lamp. However, their procedure is not sensitive enough to measure demoxepam levels in any chlordiazepoxide-treated subject (3).

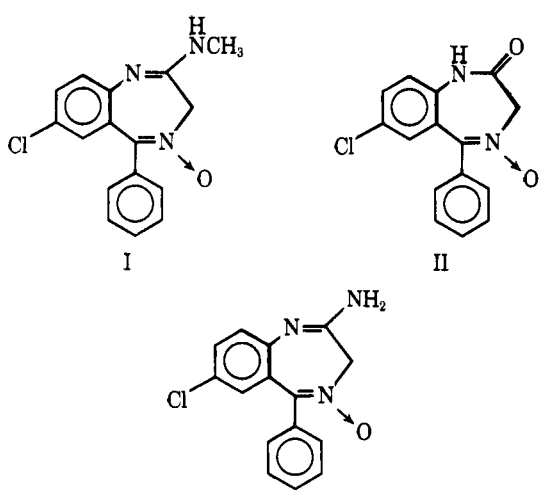

I

II

III

The present TLC–densitometric procedure is for the simultaneous specific determination of I–III in serum. The sensitivities for I, II, and III are 0.05, 0.01, and 0.01 μg/ml of serum, respectively, which are sufficient to monitor the blood levels of each compound in a chlordiazepoxide bioavailability study.

EXPERIMENTAL

Reagents and Materials—Chlordiazepoxide hydrochloride[1], demoxepam[2], and desmethylchlordiazepoxide[3] were used as supplied. Ether[4] was anesthetic grade, and the other chemicals were analytical reagent grade. TLC plates[5] (20 × 20 cm) were used as supplied.

Apparatus—A two-speed reciprocating shaker[6] and a refrigerated centrifuge[7] were used. Sample solutions in the test tubes were mixed[8] prior to analysis. Samples were spotted on TLC plates with an automatic TLC spotter[9] using polytef-tipped 50-μl syringes[10]. A TLC sprayer[11] was used to apply the sulfuric acid spray on the plates.

Preparation of Serum Standards—Five serum standards were extracted for each eight unknown samples. Serum standards contained I, II, and III at 1.5, 0.3, and 0.3 μg/ml, respectively, in the first standard; 1.0, 0.2, and 0.2 μg/ml, respectively, in the second standard; 0.5, 0.1, and 0.1 μg/ml, respectively, in the third standard; and 0.2, 0.04, and 0.04 μg/ml, respectively, in the fourth standard. The fifth standard was the serum blank[12].

The first serum standard was prepared by spiking the serum blank[12] with the following primary standard solutions: I hydrochloride, 100 μg/ml in water; II, 100 μg/ml in methanol; and III, 100 μg/ml in methanol.

Extraction Procedure—To 2 ml of serum sample or standard in a 20-ml screw-capped test tube were added 2 ml of 0.1 *M* K_2HPO_4 and 5 ml of ether. The tube was shaken reciprocally at 80 cpm for 5 min. After centrifugation at 3000 rpm for 5 min at 10°, 4 ml of the ether layer was immediately transferred to a 15-ml conical test tube and evaporated to dryness at 40° with filtered air. The residue was reconstituted with 1 ml of ether and dried again at 40° with filtered air. To the dry residue was added 50 μl of methanol, and the contents were mixed. The entire amount was taken up in a 50-μl syringe and spotted on a TLC plate using an automatic TLC spotter. The heating region of the automatic spotter was set at 35–40°.

Thirteen samples (eight unknowns and five standards) were spotted on each TLC plate. A horizontal line was scribed 2.5 cm from the top of the TLC plate, and the plate was developed to the line with chloroform–methanol–ammonium hydroxide (85:15:0.5). After the plate was dried overnight at room temperature, it was sprayed about six times with 7 *M* H_2SO_4. The spots were located with long wavelength UV light[13]. The compounds appeared as pale-blue (R_f 0.63, I), green (R_f 0.54, II), and blue (R_f 0.45, III) fluorescence spots on the TLC plate.

[1] 7-Chloro-2-methylamino-5-phenyl-3*H*-1,4-benzodiazepin-4-oxide hydrochloride, Abbott internal reference standard, A-21064, lot 351074, Abbott Laboratories, North Chicago, Ill.

[2] 7-Chloro-1,3-dihydro-5-phenyl-2*H*-1,4-benzodiazepin-2-one-4-oxide, NF reference standard, lot 69145.

[3] 7-Chloro-2-amino-5-phenyl-3*H*-1,4-benzodiazepin-4-oxide, Abbott internal reference standard, A-47203, Abbott Laboratories, North Chicago, Ill.

[4] Mallinckrodt Chemicals, St. Louis, Mo.

[5] Silica gel GF, 250 μm, Analtech, Inc., Newark, Del.

[6] Eberbach Corp., Ann Arbor, Mich.

[7] Sorvall Inc., Newtown, Conn.

[8] Vortex Genie, model K-550-GT, Scientific Industries, Springfield, Mass.

[9] Analytical Instrument Specialties, Libertyville, Ill.

[10] Scientific Products, McGaw Park, Ill.

[11] Sprayon power unit, Sprayon Products, Cleveland, Ohio.

[12] K-N Enterprises, Inc., Skokie, Ill.

[13] UV Viewbox, Ultra-Violet Products, San Gabriel, Calif.

Table I—Assay Reproducibility

Compound	Theoretical	Serum Concentration, μg/ml[a] Observed Run 1	Run 2	Run 3	Mean ± SD	Relative SD, %
I[b]	0.20	0.23	0.27	0.21	0.237 ± 0.031	13.1
	0.50	0.44	0.47	0.43	0.447 ± 0.021	4.7
	1.00	0.99	1.00	1.02	1.000 ± 0.015	1.5
	1.50	1.39	1.57	1.51	1.490 ± 0.092	6.2
II[c]	0.04	0.044	0.044	0.041	0.043 ± 0.0017	4.0
	0.10	0.098	0.106	0.091	0.098 ± 0.0075	7.7
	0.20	0.182	0.209	0.197	0.196 ± 0.0135	6.9
	0.30	0.284	0.308	0.316	0.303 ± 0.0167	5.5
III[d]	0.04	0.044	0.047	0.041	0.044 ± 0.0030	6.8
	0.10	0.096	0.099	0.099	0.098 ± 0.0017	1.8
	0.20	0.186	0.198	0.195	0.193 ± 0.0062	3.2
	0.30	0.291	0.308	0.314	0.304 ± 0.0119	3.9

[a] All 12 serum samples were on a single TLC plate. [b] R_f 0.63. [c] R_f 0.54. [d] R_f 0.45.

Densitometry—The TLC plate was scanned at 30 mm/min, in a direction perpendicular to the direction of development, with a densitometer[14] fitted with a suitable barrier filter in the compartment of the measuring head. The TLC plate was irradiated in the reflectance mode, using a xenon lamp as the light source, at the following maximum excitation wavelengths: I, barrier filter FL 43, λ_{max} 390 nm; II, barrier filter FL 46, λ_{max} 430 nm; and III, barrier filter FL 43, λ_{max} 390 nm.

The slit width was 0.5 × 12 mm. The chart speed of the recorder was 10 mm/min. The high voltage potential on the photomultiplier tube was set at 1, and the gain was set at 20 on the arbitrary scale of the instrument[15]. Each spot on the TLC plate was manually located to give maximum response.

RESULTS AND DISCUSSION

The excitation spectra for the fluorescence spots are shown in Fig. 1. These spectra were constructed by plotting the relative fluorescence intensity (as measured by the peak heights) at different excitation wavelengths.

The reproducibility of the assay is shown in Table I. Relative standard deviations in a triplicate study for I, II, and III ranged from 1.5 to 13.1%, from 5.5 to 7.7%, and from 1.8 to 6.8%, respectively, indicating good reproducibility.

Recoveries were 99.0 ± 1.2% (mean ± *SD*) for triplicate I serum samples at 1.5 μg/ml, 78.6 ± 4.5% for triplicate II serum samples at 0.3 μg/ml, and 83.6 ± 3.2% for triplicate III serum samples at 0.3 μg/ml. These values were calculated by comparing the peak height responses between the extracted serum samples and the theoretical amount of pure drug spotted on the TLC plate. TLC was used to achieve specificity (Fig. 2).

The sensitivity limits of the assay were about 0.05, 0.01, and 0.01 μg/ml of serum for I, II, and III, respectively (Table II). These values were calculated by fitting a regression line to the standard curve and taking the 95% confidence interval of the *y*-intercept (in peak height). The calculated sensitivity was the *x*-value (in concentration) corresponding to the upper part of this interval of the *y*-intercept. In calculating the sensitivity for I, the linear portion of the curve (the first four points only) was used.

The accuracy of the assay was tested by determining seven unknown spiked serum samples. The unknown serum concentrations were calculated from the standard curves obtained from the five serum standards

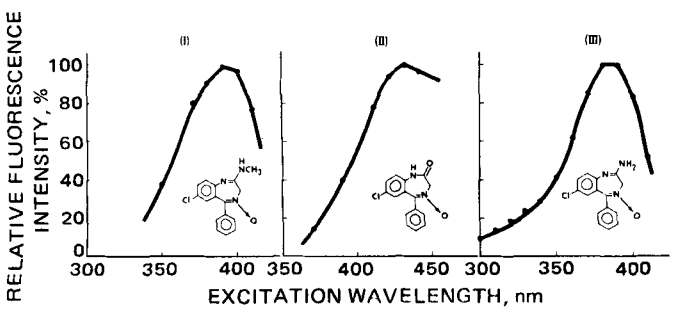

Figure 1—*Fluorescence excitation spectra of I–III.*

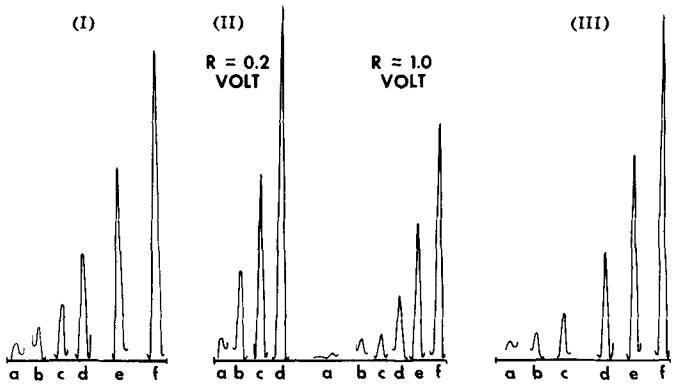

Figure 2—*TLC-densitometric tracings of serum extracts containing I–III. Key: a, serum blank; b, serum standard containing 0.05 μg of I/ml, 0.01 μg of II/ml, and 0.01 μg of III/ml; c, serum standard containing 0.10 μg of I/ml, 0.02 μg of II/ml, and 0.02 μg of III/ml; d, serum standard containing 0.20 μg of I/ml, 0.04 μg of II/ml, and 0.04 μg of III/ml; e, serum standard containing 0.50 μg of I/ml, 0.10 μg of II/ml, and 0.10 μg of III/ml; and f, serum standard containing 1.00 μg of I/ml, 0.20 μg of II/ml, and 0.20 μg of III/ml.*

extracted and spotted on the same TLC plate. The results (Table III) indicated good accuracy. This precision was due in part to the use of an automatic TLC spotter. This device allowed the simultaneous uniform spotting of all 13 samples within 15 min.

The developed method was used to measure serum concentrations of I–III in normal human subjects after oral administration of two 10-mg chlordiazepoxide hydrochloride capsules[16] in a single dose. The subjects were fasted for 12 hr prior to dosing. The drug was administered with 120 ml (4 oz) of water.

Typical serum concentration *versus* time curves for two human subjects are shown in Fig. 3. Peak serum chlordiazepoxide concentrations occurred at 40 min and were 1.16 and 1.10 μg/ml. Serum levels presisted to 32 hr (the final sampling time). The 0–32-hr *AUC*'s (areas under the curve) calculated by the trapezoidal rule were 5.73 and 8.59 μg × hr/ml. The serum chlordiazepoxide half-lives estimated from the terminal linear log concentration *versus* time plots were 10.3 and 9.5 hr. These values agreed with the ranges reported earlier (3–6). Serum II and III levels appeared soon after administration of the parent drug, and II levels slowly increased throughout the duration of blood sampling. The *AUC*'s for III for the two subjects were 3.78 and 6.35 μg × hr/ml, and the *AUC*'s for II were 1.49 and 1.34 μg × hr/ml.

The results indicate that the present method can be employed to quantitate serum I–III levels in a single-dose chlordiazepoxide bioavailability study. Differential spectrofluorometric methods (2, 3) generally used for chlordiazepoxide bioavailability studies (5–9) had a limit of sensitivity of about 0.1–0.2 μg/ml for I–III using 2-ml specimens. In all of these single-dose studies (3, 5, 6), plasma II levels were less than 0.2 μg/ml.

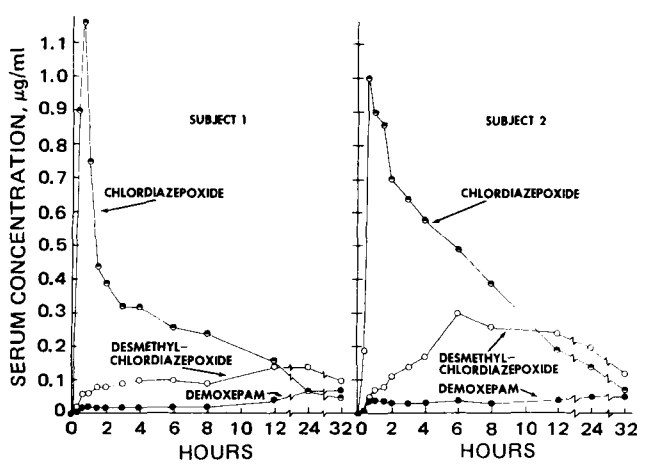

Figure 3—*Serum I–III levels of two individuals after 20 mg po of chlordiazepoxide hydrochloride capsules.*

[14] Zeiss PMQ II chromatogram spectrophotodensitometer, Carl Zeiss, Oberkochen, West Germany.

[15] Zeiss PMI indicator.

[16] Librium, Roche, lot 3672-02135.

Table II—Assay Sensitivity

Serum I Concentration, μg/ml	Peak Height, mm, R = 0.5 v[a]	Serum II Concentration, μg/ml	Peak Height, mm		Serum III Concentration, μg/ml	Peak Height, mm	
			R = 1 v	R = 0.2 v[a]		R = 1 v[a]	R = 0.2 v[a]
0	6	0	1.5	7	0	3	27
0.05[b]	11	0.01[b]	6	35	0.01[b]	8.5	64
0.10[b]	21	0.02[b]	11	75	0.02[b]	17.5	134
0.20	43	0.04	20	142	0.04	43	
0.50	77	0.10	55		0.10	81.5	
1.00	125	0.20	96		0.20	139	
1.50	156	0.30	139		0.30	196	
Least-Squares Linear Regression Calculation[c]							
Number of points	4 (first four samples)		7			7	
Slope	190.28		462.19			643.16	
y-Intercept ± 95% confidence limit	3.600 ± 9.026		2.690 ± 4.095			8.225 ± 9.664	
Correlation coefficient	0.991		0.999			0.996	
Calculated sensitivity, μg/ml[d]	0.0474		0.0089			0.0150	

[a] Recorder full-scale deflection. [b] Included here to determine the sensitivity. It was not included in the normal standards. [c] Reference 13. [d] The calculated sensitivity was the x-value (in concentration) corresponding to the upper part of the 95% confidence interval of the y-intercept (in response).

Table III—Accuracy of the Assay

Unknown Serum Sample Number	Serum Concentration, μg/ml								
	I			II			III		
	Theoretical	Calculated	% Difference	Theoretical	Calculated	% Difference	Theoretical	Calculated	% Difference
1	0.20	0.21	5.0	0.04	0.05	25.0	0.04	0.04	0
2	0.50	0.58	16.0	0.10	0.11	10.0	0.10	0.13	30.0
3	1.00	1.06	6.0	0.20	0.23	15.0	0.20	0.22	10.0
4	1.20	1.23	2.5	0.24	0.27	12.5	0.24	0.26	8.3
5	0.75	0.65	13.3	0.15	0.18	20.0	0.15	0.16	6.2
6	0.10	0.09	10.0	0.02	0.02	0	0.02	0.02	0
7	0.05	0.04	20.0	0.01	0.01	0	0.01	0.01	0
		Average	10.4		Average	11.8		Average	7.8

A specific spectrofluorometric determination of chlordiazepoxide in biological fluids with fluorescamine was reported previously (10). However, II and III could not be measured by this procedure. Zingales (11) reported the determination of chlordiazepoxide in plasma by an electron-capture GLC procedure that could not determine the metabolites. A thorough review of the determination of some 1,4-benzodiazepines and their metabolites in body fluids was described by Clifford and Smyth (12).

Strong fluorescence characteristics with a sulfuric acid spray on TLC plates are also observed for other 1,4-benzodiazepines such as diazepam, desmethyldiazepam, oxazepam, 4′-hydroxydesmethyldiazepam, and nitrazepam. A similar quantitative fluorescence–TLC method should be applicable for these compounds.

REFERENCES

(1) B. A. Koechlin and L. D'Arconte, *Anal. Biochem.*, **5**, 195 (1963).

(2) M. A. Schwartz and E. Postma, *J. Pharm. Sci.*, **55**, 1358 (1966).

(3) M. A. Schwartz, E. Postma, and Z. Gaut, *ibid.*, **60**, 1500 (1971).

(4) M. A. Schwartz, in "The Benzodiazepines," S. Garattini, E. Mussini, and L. D. Randall, Eds., Raven, New York, N.Y., 1973, pp. 53–74.

(5) D. J. Greenblatt, R. I. Shader, and J. Koch-Weser, *Am. J. Psychiat.*, **131**, 1395 (1974).

(6) H. G. Boxenbaum, K. A. Geitner, M. L. Jack, W. R. Dixon, H. E. Spiegel, J. Symington, R. Christian, J. D. Moore, L. Weissman, and S. A. Kaplan, *J. Pharmacokinet. Biopharm.*, **5**, 3 (1977).

(7) H. G. Boxenbaum, K. A. Geitner, M. L. Jack, W. R. Dixon, and S. A. Kaplan, *ibid.*, **5**, 25 (1977).

(8) T. C. Smith and C. E. Moyer, *Curr. Ther. Res.*, **20**, 204 (1976).

(9) L. A. Gottschalk, R. Biener, and E. C. Dinovo, *Res. Commun. Chem. Pathol. Pharmacol.*, **8**, 697 (1974).

(10) J. T. Stewart and J. L. Williamson, *Anal. Chem.*, **48**, 1182 (1976).

(11) I. A. Zingales, *J. Chromatogr.*, **61**, 237 (1971).

(12) J. M. Clifford and W. F. Smyth, *Analyst*, **99**, 241 (1974).

(13) A. Goldstein, "Biostatistics: An Introductory Text," Macmillan, New York, N.Y., 1967.

ACKNOWLEDGMENTS

Presented in part at the Pharmaceutical Analysis and Control Section, APhA Academy of Pharmaceutical Sciences, New York meeting, May 1977.

The author gratefully acknowledges the technical assistance of G. Thomas.

Alanine Derivatives with Reactive Groups

B. PAUL and W. KORYTNYK ×

Received December 27, 1976, from *Grace Cancer Drug Center, Department of Experimental Therapeutics, Roswell Park Memorial Institute, Buffalo, NY 14263.* Accepted for publication August 5, 1977.

Abstract □ The synthesis of diazoketone analogs of amino acids and associated problems were investigated with *N*-phthaloyl-DL-alanine serving as a model. The carboxyl was activated by conversion to the acid chloride or, under mild conditions, to the mixed anhydride obtained with ethyl chloroformate or dicyclohexylcarbodiimide; the product was reacted with diazomethane. Deblocking the phthaloyl group with hydrazine gave 3-amino-1-diazo-2-butanone as a well-characterized solid salt and as a less stable oil. Further reactions of the blocked diazoketone of DL-alanine, such as conversion to α-haloketones, Wolff rearrangement, and deuterium exchange on C-1 were investigated. 3-Amino-1-diazo-2-butanone had moderate inhibitory activity against mouse mammary adenocarcinoma in cell culture.

Keyphrases □ Alanine derivatives, various—synthesized, evaluated for cytotoxic activity □ Cytotoxic activity—various alanine derivatives evaluated □ Amino acids—various alanine derivatives synthesized, evaluated for cytotoxic activity □ Structure-activity relationships—various alanine derivatives evaluated for cytotoxic activity

Diazoketone or diazoester analogs of amino acids include well-known antibiotics such as 6-diazo-5-oxo-L-norleucine and azaserine, which were found to have antitumor activity. Both of these antibiotics owe their biological activity to their inhibitory activity on various enzymes in which glutamine is one of the substrates. Enzymes in the purine nucleotide biosynthetic pathway appear to be most sensitive to these agents (1–4). These enzymes include phosphoribosylformylglycinamidine synthetase (EC 6.3.5.3), carbamoyl-phosphate synthase (ammonia) (EC 2.7.2.5), and amidophosphoribosyltransferase (EC 2.4.2.14). In addition, 6-diazo-5-oxo-L-norleucine inhibited the synthesis of cytidine triphosphate from uridine triphosphate, of guanosine 5′-phosphate from xanthosine 5′-phosphate, and of D-glucosamine from fructose 6-phosphate (5). Azaserine alkylates, by its diazomethyl group, the thiol group of a cysteine residue in the active site of EC 6.3.5.3 (6–8) and was considered (9) to be the first example of a classical-type antimetabolite causing specific active-site-directed irreversible inhibition.

DISCUSSION

Analogs of other amino acids having either the diazoketone group or the chloroketone group are of interest as potentially antiproliferative agents. Certain cancer cells have an absolute requirement for cysteine (10, 11) and serine (12–15).

The synthesis of amino acid analogs with reactive groups presents challenges in terms of the choice of a blocking group suitable for introducing the reactive group and removable under mild conditions in the presence of such a group. Protection of the amino group with phthaloyl has been used extensively in peptide synthesis (16) and in the synthesis of certain amino acid homologs by the Wolff rearrangement. It offers the advantage of mild deblocking with hydrazine, protection of the two hydrogens of the amino group, and considerable stability. In this study, *N*-phthaloyl-DL-alanine (I, Scheme I) was used initially and various methods of introducing the diazoketone group, as well as various deblocking procedures, were investigated.

One target compound in this study was 3-amino-1-diazo-2-butanone, which has the potentiality of being an irreversible inhibitor of pyridoxal phosphate-containing enzymes such as L-alanine-glutamic acid transaminases. The analog has the required functionality for the initial

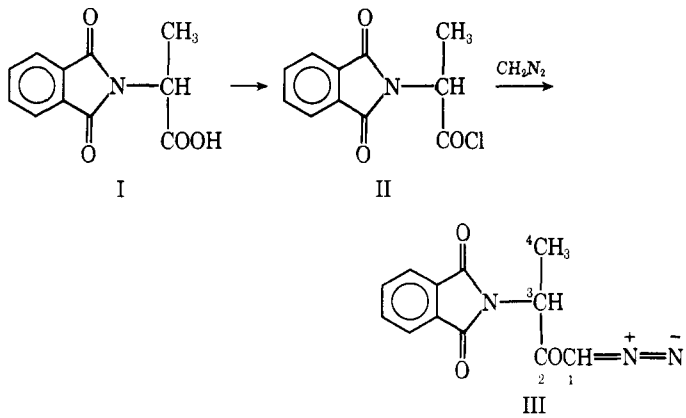

Scheme I

Schiff-base formation and the diazoketone group as a potential alkylating function. Some developed methods were applied to the synthesis of the corresponding cysteine derivatives (17). The diazoketone III was obtained either by interaction of diazomethane with the acid chloride II or directly from I by a mixed anhydride procedure with ethyl chloroformate or dicyclohexylcarbodiimide. The acid chloride II could be made either by the conventional method or by a milder method using thionyl chloride and dimethylformamide (18). These two procedures gave good yields of the diazoketone. The mixed anhydride method (19) gave good yields; but with the dicyclohexylcarbodiimide method, the yield was poor (27%), as might be expected (20), although this disadvantage is compensated for by the mildness of the method.

Some of the chemical properties and reactions of the blocked diazoketone were investigated before carrying out the deblocking experiments. Treatment of III with hydrochloric acid gave 1-chloro-3-phthalimido-2-butanone (IV, Scheme II). On treatment of III with hydrofluoric acid, however, 1-hydroxy-3-phthalimido-2-butanone (V) was isolated and not the expected fluoro compound. Reaction of III with hydrogen sulfide in the presence of ammonium sulfide gave 1-hydrazono-3-phthalimido-2-butanone (VI).

UV spectral studies on III led to the postulate that the most acidic hydrogen was in the 3-position, giving rise to the anion IX (21). To test this hypothesis, III was selectively deuterated with deuterium oxide in acetonitrile-d_3 in solution for 4 days at 55–60°. The ^{1}H-NMR spectrum of the product showed an exclusive incorporation of deuterium on C-1, as indicated in the structure shown for VII. This observation was confirmed by ^{13}C-NMR spectroscopy, which resulted in disappearance of the C-1 resonance in III on deuteration, permitting an unequivocal assignment of C-1 and C-3 resonances at 53.8 and 52.4 ppm, respectively. No deuterium exchange was observed in the related hydrazone derivative (VI) under similar conditions (see *Experimental*). Thus, the changes of UV absorption in III should be interpreted in terms of formation of the anion VIII, rather than the isomeric anion IX, which was assumed to be formed under these conditions (21).

Various methods for the preparation of homologs also were investigated. Application of silver oxide catalyzed the Wolff rearrangement of III in methanol, giving the higher homologous ester methyl 3-phthalimidobutyrate (X, Scheme III), which gave 3-aminobutyric acid (XI) on hydrolysis and 3-aminobutyrohydrazide (XII) on hydrazinolysis. Photochemical rearrangement of III in dry methanol also gave X, whereas pyrolysis in benzyl alcohol and γ-collidine at 175° in the absence of silver oxide gave the benzyl ester of the higher homologous acid (XIII).

Although cleavage of phthaloylalanine (I) with hydrazine gave rise to alanine and phthaloyl hydrazide exclusively, a similar reaction with III resulted in three products, which were separated by chromatography on a silica gel column (Scheme IV). In addition to the oily 3-amino-1-diazo-2-butanone (XIV), a solid phthaloyl hydrazide salt (XV) could also

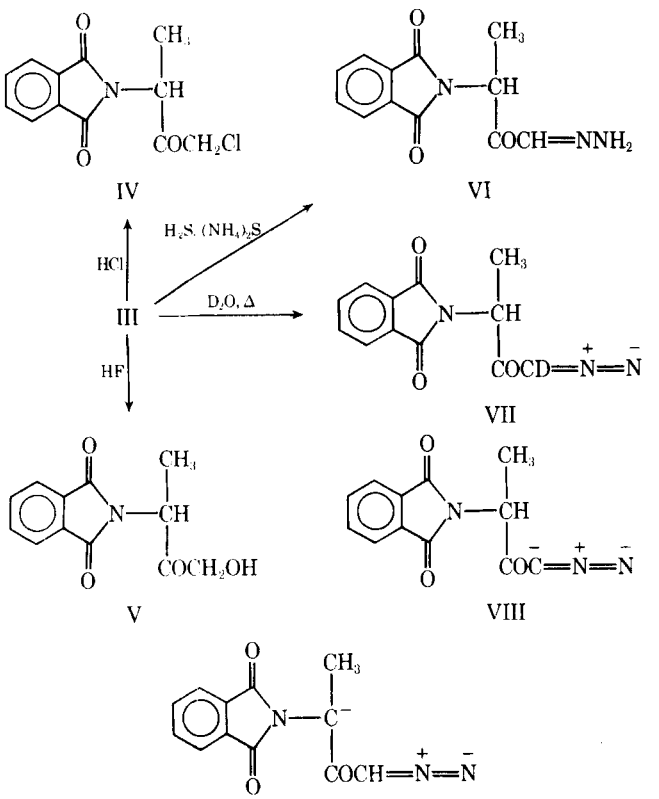

Scheme II

be isolated. Attempts to hydrazinolyze III with the unsymmetrical 1,1-dimethylhydrazine or the symmetrical 1,2-dimethylhydrazine at room temperature to avoid salt formation were not successful. The salt XV could not be dissociated by treating its ethyl acetate solution with aqueous sodium carbonate. The base XIV was unstable, probably because of self-condensation leading to a pyrazine derivative.

The compounds synthesized in this study were tested as inhibitors of the growth of mouse mammary adenocarcinoma (TA3) cells in culture[1]. Compound XIV at 1×10^{-4} *M* inhibited 20% of growth of these cells. The α-chloroacetyl derivative (IV), the substituted diazoketone derivative (III), and the phthaloylhydrazide salt (XV) were inactive at 10^{-4} *M*. The relative insolubility of VI precluded its being tested at a higher concentration than 3×10^{-5} *M*, at which it was inactive. In addition, higher homologous alanine derivatives such as XI and XII were inactive at 10^{-4} *M*.

EXPERIMENTAL[2]

1-Diazo-3-phthalimido-2-butanone (III)—*Method A: Acid Chloride Method*—A mixture of I (3.0 g, 13.7 mmoles) and excess thionyl chloride (10 ml, 0.14 mole) was heated at 60° with stirring for 1 hr, and a clear solution was obtained. The excess thionyl chloride was removed *in vacuo*. The residue was dissolved in dry benzene (3 × 25 ml), the solution was evaporated to remove traces of thionyl chloride, and the residue was dried *in vacuo* over potassium hydroxide.

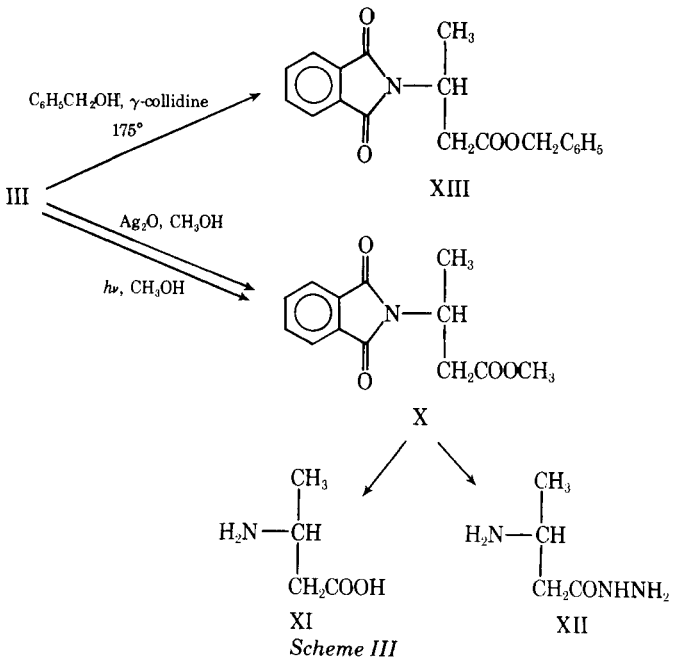

Scheme III

The crude product (3.25 g, 99%), mp 71–72°, was used for the next step without further purification. A solution of crude *N*-phthaloyl-DL-alanyl chloride (3.25 g, 13.6 mmoles) in dry benzene (25 ml) was added slowly, with stirring, to an ice-cold ethereal solution of diazomethane (3 g, 71.5 mmoles, from 21.5 g of *N*-methyl-*N*-nitroso-*p*-toluenesulfonamide[3]). The reaction mixture was left at room temperature overnight, and excess diazomethane and solvent were removed by passing nitrogen through the reaction mixture.

After the yellowish oily residue was dried *in vacuo*, crystalline material separated out. The solid material was filtered out and recrystallized from ethyl acetate. The yield was 2.6 g (78%), mp 107°; IR: ν_{max}^{KBr} 2119 (diazo), 1720, 1702, and 1691 (keto) cm^{-1}; ^{1}H-NMR ($CDCl_3$): δ 1.69 (d, CH_3, J = 7 Hz), 4.96 (q, 3-CH, J = 7 Hz), 5.51 (s, 1-CH), and 7.95 (aromatic H) ppm; ^{13}C-NMR ($CDCl_3$): 190.3 (2-C=O), 167.6 (phthaloyl C=O), 134.4, 131.9, 123.5 (aromatic C), 53.8 (1-CH), 52.4 (2-CH), and 14.6 (4-CH_3) ppm.

Anal.—Calc. for $C_{12}H_9N_3O_3$: C, 59.25; H, 3.73. Found: C, 59.13; H, 3.91.

Method B: Mixed Carboxylic-Carbonic Anhydride Method—A solution of I (2 g, 9.1 mmoles) in anhydrous tetrahydrofuran (25 ml) was cooled to −10° and treated with triethylamine (1.3 ml, 9.5 mmoles, dried over potassium hydroxide and distilled). Then freshly distilled ethyl chloroformate (0.9 ml, 9.3 mmoles) was added dropwise with stirring when a white precipitate of triethylamine hydrochloride separated out.

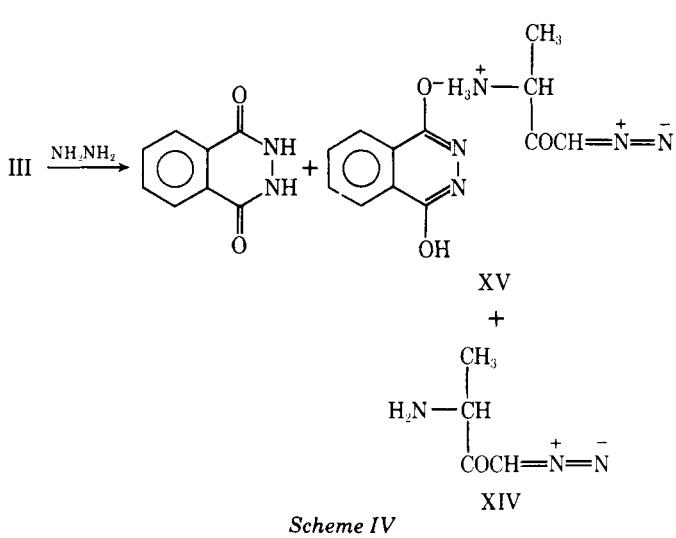

Scheme IV

[1] The mouse mammary adenocarcinoma cells (TA3) were grown in stationary tube cultures in RPMI 1640 medium containing 10% horse serum. An inoculum of 50,000 cells in 1 ml of medium was supplemented with 1 ml of medium containing the test compound. The tubes were incubated in an upright position for 3 days, and growth was estimated by protein assay. The growth in controls varied from six- to 10-fold. Every concentration (10^{-4}–10^{-6} *M*) was tested in five tubes each. For compounds found to be inhibitory, the tests were repeated at least twice. Variation between different tests was within ±10% for the 50% inhibitory concentration.

[2] Melting points (uncorrected) were determined by the capillary method. UV spectra were determined with a Cary model 14 spectrophotometer. IR spectra were determined with a Perkin-Elmer 457 spectrophotometer, ^{1}H-NMR spectra were obtained with a Varian A60A instrument, and ^{13}C-NMR spectra were obtained with a Varian XL-100A instrument. The positions of peaks are expressed in δ (parts per million) downfield from tetramethylsilane or sodium 2,2-dimethyl-2-silapentane-5-sulfonate for solutions in deuterium oxide. Thin-layer chromatograms were run on glass plates coated with Merck HF-254 silica gel; spots were detected by their UV absorption or by spraying with a ninhydrin reagent.

[3] Diazald, Aldrich Chemical Co., Milwaukee, Wis.

The reaction mixture was stirred at −10° for 0.5 hr and filtered, and the residue was washed with anhydrous ether (10 ml).

The filtrate and the washing were added slowly, with stirring, to an ice-cold ethereal solution of diazomethane (1.2 g, 28.6 mmoles, from 8.6 g of *N*-methyl-*N*-nitroso-*p*-toluenesulfonamide[3] in 80 ml of ether). The reaction mixture was left at room temperature overnight, and excess diazomethane and solvent were removed with a current of dry nitrogen. The oily residue was evaporated *in vacuo*, dissolved in ether (50 ml), and washed with water (20 ml), followed by 5% $NaHCO_3$ (20 ml) and again with water (20 ml). The ether extract was evaporated *in vacuo*, and crystalline material separated out. This material was filtered, washed with petroleum ether, and dried; the yield was 1.67 g (76%), mp 106–107°. The product was identical with that obtained by Method A on the basis of mixed melting-point, IR, NMR, and TLC data.

Method C: Dimethylformamide and Thionyl Chloride Method—Thionyl chloride (0.17 ml, 0.23 mmole) was added slowly with stirring to a solution of I (0.5 g, 2.2 mmoles) in dry dimethylformamide (5 ml), and the mixture was cooled to −10°. The stirring was continued at from −5 to −10° for 1 hr, and the reaction mixture was evaporated *in vacuo*. The residue was dissolved in dry benzene (5 ml), added to an ice-cooled ethereal solution of diazomethane (1.2 g, 28.6 mmoles, from 8.6 g of *N*-methyl-*N*-nitroso-*p*-toluenesulfonamide[3]), and left at room temperature overnight. Excess diazomethane and solvent were removed by passing dry nitrogen through the solution.

The residue was extracted with ether, and the ether was evaporated *in vacuo*. The residue was crystallized from a mixture of ether and petroleum ether; the yield was 0.33 g (60%), mp 106–107°. The compound was identical with the product obtained by Methods A and B.

Method D: Dicyclohexylcarbodiimide Method—Compound I (1 g, 4.56 mmoles) was added to a solution of dicyclohexylcarbodiimide (1 g, 4.8 mmoles) in dry tetrahydrofuran (15 ml); the solution turned turbid, and a white precipitate separated out. The suspension was stirred at room temperature for 4 hr, added slowly to an ice-cold ethereal solution of diazomethane (1.2 g, 28.6 mmoles, from 8.6 g of *N*-methyl-*N*-nitroso-*p*-toluenesulfonamide[3]), and left overnight at room temperature. Excess diazomethane and solvent were removed by passing nitrogen through the solution.

The residue was dried *in vacuo* and then taken up in ether. The white precipitate of dicyclohexylurea that separated out was removed by filtration. The filtrate was evaporated *in vacuo*, and the residue was crystallized from ether; the yield was 0.3 g (27%), mp 106–107°. The compound was identical with the product obtained by Methods A, B, and C.

1-Chloro-3-phthalimido-2-butanone (IV)—An ethereal solution of hydrochloric acid (5 ml, 24%) was added slowly to an ice-cold ethereal solution of 1-diazo-3-phthalimido-2-butanone (100 mg in 15 ml). The reaction mixture was stirred at room temperature overnight (18 hr) and was then evaporated *in vacuo*. The crystalline residue was taken up in petroleum ether, and the mixture was filtered.

The crystals were washed with petroleum ether and dried; the yield was 95 mg (92%), mp 119–120°. The compound gave a positive Baker's test (22); IR: ν_{max}^{KBr} 1771, 1741, and 1705 (keto) cm^{-1} but no diazo peak at 2119 cm^{-1}; ^{1}H-NMR ($CDCl_3$): δ 1.68 (d, CH_3, J = 7 Hz), 4.27 (s, 1-CH_2), 5.21 (q, 3-CH, J = 7 Hz), and 7.95 (aromatic protons) ppm.

Anal.—Calc. for $C_{12}H_{10}ClNO_3$: C, 57.26; H, 4.00; N, 5.56. Found: C, 57.22; H, 4.30; N, 5.81.

Attempted Synthesis of 1-Fluoro-3-phthalimido-2-butanone: Formation of 1-Hydroxy-3-phthalimido-2-butanone (V)—*Method A*—A solution of hydrofluoric acid (from 2 ml of aqueous 48% HF in 10 ml of anhydrous ether) was added dropwise to a stirring suspension of 1-diazo-3-phthalimido-2-butanone (100 mg) in anhydrous ether (25 ml) until a clear solution was obtained. The reaction mixture was stirred at room temperature for 1 hr and was then evaporated *in vacuo*; the resulting gum was dried *in vacuo*. TLC [benzene–ether (1:1)] of the product showed one major and two minor spots.

The product corresponding to the major spot was isolated by column chromatography on 200–325-mesh silica gel[4] with benzene–ether (1:1) as the eluent; the yield was 680 mg (71%), mp 81–82° (after crystallization from ether). IR, NMR, and elemental analyses indicated that the product was 1-hydroxy-3-phthalimido-2-butanone; IR: ν_{max}^{KBr} 3520, 3460 (OH), 1772, 1740, and 1705 (keto) cm^{-1}; ^{1}H-NMR ($CDCl_3$): δ 1.68 (d, CH_3, J = 7 Hz), 3.24 (b, OH), 4.42 (s, α-CH_2), 4.98 (q, 3-CH, J = 7 Hz), and 7.82 (aromatic protons) ppm.

Anal.—Calc. for $C_{12}H_{11}NO_4$: C, 61.79; H, 4.75; N, 6.00. Found: C, 62.14; H, 4.89; N, 5.88.

Method B—1-Diazo-3-phthalimido-2-butanone (500 mg) was suspended in anhydrous ether (30 ml), and the suspension was cooled in ice. Anhydrous hydrogen fluoride gas was passed through the suspension for 6 hr, and a clear solution was obtained. The solution was left overnight at room temperature and was then evaporated by a nitrogen stream. The residue, on TLC, showed the presence of the starting material and two spots of lower R_f, one corresponding to that of 1-hydroxy-3-phthalimido-2-butanone.

The residue was dissolved again in anhydrous ether (30 ml), and a slow stream of hydrogen fluoride gas was passed through this solution for 24 hr. Examination of the reaction product at 6-hr intervals indicated the presence of the starting material and a major spot due to 1-hydroxy-3-phthalimido-2-butanone. The major fraction was isolated by chromatography on silica gel and was identified as 1-hydroxy-3-phthalimido-2-butanone as described for Method A.

1-Hydrazono-3-phthalimido-2-butanone (VI)—Ammonium sulfide solution (4%, 4 drops) was added to an ice-cold solution of 1-diazo-3-phthalimido-2-butanone (100 mg in 10 ml of alcohol). Hydrogen sulfide gas was passed through the solution for 2.5 hr, and then nitrogen was passed through it for 1 hr. The yellowish solution was evaporated *in vacuo*, and the residue was crystallized from an alcohol–ether mixture. The suspension was filtered, and the crystals were washed and dried. The yield was 66 mg (66%), mp 182–183° (with frothing); IR: ν_{max}^{KBr} 3360, 3285, 3210 (NH_2), 1768, 1750, and 1720–1680 (C=O) cm^{-1}; ^{1}H-NMR (CD_3CN): δ 1.63 (d, CH_3, J = 7 Hz), 5.40 (q, 3-CH, J = 7 Hz), 7.20 (s, 1-CH), 7.95 (s, aromatic protons), 2.23, and 7.03 (b, NH_2) ppm; ^{13}C-NMR (CD_3CN): 194.4 (2-C=O), 168.8 (phthaloyl C=O), 135.2, 133.0, 123.9 (aromatic), 134.6 (1-CH), 51.6 (3-CH), and 15.2 (4-CH_3) ppm.

Anal.—Calc. for $C_{12}H_{11}N_3O_3$: C, 58.76; H, 4.52; N, 17.13. Found: C, 58.76; H, 4.80; N, 16.32.

Hydrazinolysis of III: Formation of 3-Amino-1-diazo-2-butanone (XIV) and Its Phthaloylhydrazide Salt (XV)—Triethylamine (1.8 ml, 13 mmoles) and a methanolic hydrazine solution (50%; 2 ml, 31.25 mmoles) were added slowly to a stirred solution of III (2 g, 4.23 mmoles, in 75 ml of methanol). The mixture was cooled in ice and stirred in a cold room for 16 hr. TLC [ethanol–water (7:3)] of the reaction mixture showed the absence of the starting material and the presence of two UV-absorbing and ninhydrin-positive spots.

The reaction mixture was evaporated *in vacuo* to remove triethylamine and unreacted hydrazine, the residue was taken up in ethyl acetate, and the white solid material that separated (phthaloylhydrazide) was removed by filtration. When the filtrate was evaporated *in vacuo*, a crystalline material separated out. This material was filtered off, washed with cold ether, and dried; the yield was 650 mg (29%), mp 120–121° dec. The presence of a diazo peak in the IR spectrum and of aromatic protons in the NMR spectrum indicated that the compound was a phthaloyl hydrazide salt of XIV; IR: ν_{max}^{KBr} 3220, 3208, 3050 ($^+NH_3$, OH phenolic), 2108 (diazo), 1630, 1595, 1575, and 1535 (keto) cm^{-1}; ^{1}H-NMR ($CDCl_3$): δ 1.66 (d, CH_3, J = 7 Hz), 4.86 (q, CH, J = 7 Hz), 5.63 (s, 2-CH), and 7.78 (aromatic protons) ppm.

Anal.—Calc. for $C_{12}H_{13}N_5O_3$: C, 52.35; H, 4.75; N, 25.44. Found: C, 52.40; H, 4.88; N, 25.67.

The mother liquor was concentrated, chromatographed on a column (55.8 × 1.9 cm) of 200–325-mesh silica gel, and eluted with methanol. The fraction corresponding to the lower R_f value was isolated as a brown gummy mass. It was dissolved in ethyl acetate, and the solution was filtered to remove traces of silica gel. After evaporation, the yield was 0.54 g (58%). The gum showed a diazo peak in its IR spectrum and the expected NMR spectrum. It decomposed slowly on standing, however, and the expected elemental analysis could not be obtained; ^{1}H-NMR ($CDCl_3$): 1.29 (d, CH_3, J = 7 Hz), 3.58 (q, 3-CH, J = 7 Hz), 5.67 (s, 1-CH), and 2.92 (NH_2) ppm; IR: ν_{max}^{KBr} 3340 (NH_2), 2108 (diazo), and 1630 (keto) cm^{-1}.

Methyl 3-Phthalimidobutyrate (X)—*Method A*—The DL-isomer was prepared by following the procedure described by Balenovic *et al.* (23) for the L-isomer, mp 60°; IR: ν_{max}^{KBr} 1771, 1773, 1706, and 1610 (C=O) cm^{-1}; ^{1}H-NMR ($CDCl_3$): δ 1.51 (d, CH_3, J = 7 Hz), 2.98 (m, 2-CH_2), 3.62 (s, ester CH_3), 4.82 (m, 3-CH), and 7.77 (m, aromatic protons) ppm.

Anal.—Calc. for $C_{13}H_{13}NO_4$: C, 63.14; H, 5.29; N, 5.66. Found: C, 63.24; H, 5.34; N, 5.59.

Method B (Photochemical Rearrangement)—A solution of III (0.5 g, 2.06 mmoles) in dry methanol (80 ml) was purged with dry nitrogen for 1 hr. Then it was cooled with circulating tap water and irradiated under nitrogen for 78 hr with a high-pressure mercury lamp[5] (100 w) in

[4] SilicAR CC7, Mallinckrodt, St. Louis, Mo.

[5] Hanovia Lamp Division, Newark, N.J.

an immersion well equipped with a Pyrex filter. The reaction mixture was evaporated *in vacuo*, and the residue was placed on a dry column (76 × 2.5 cm) containing 240 g of silica gel (activity grade III). Then the column was developed with ether–petroleum ether (1:1).

The fraction with R_f 0.40 was separated and extracted with ether. The ether solution was evaporated to dryness, and the residue was crystallized from petroleum ether; the yield was 148 mg (19%), mp 47–53°. The product was identical with that obtained by Method A on the basis of mixed melting-point, IR, NMR, and TLC data.

Benzyl 3-Phthalimidobutyrate (XIII)—Compound III (256 mg, 1.05 mmoles) was dissolved in benzyl alcohol [2 ml, purified as described by Wilds and Meader (24)] and redistilled γ-collidine (2 ml), and the solution was heated to 175° when vigorous nitrogen evolution started. The reaction was allowed to proceed until the evolution of nitrogen ceased (~15 min). After cooling, ether was added, and the resulting solution was extracted with dilute aqueous hydrochloric acid to remove γ-collidine. The ether layer was evaporated *in vacuo*.

The residue was placed on a dry column (102 × 2.5 cm) containing silica gel (activity grade III) and was developed with ether. The fraction with the highest R_f value was separated and extracted with chloroform. The chloroform extract was removed *in vacuo*, giving a yellow oil that could not be crystallized but gave the expected NMR spectrum; ^{1}H-NMR ($CDCl_3$): δ 1.52 (d, CH_3, J = 7 Hz), 3.07 (m, 2-CH_2), 4.58 (m, 3-CH), 5.05 (s, benzyl CH_2), 7.25 (s, benzyl aromatic protons), and 7.75 (m, phthaloyl aromatic protons) ppm.

3-Aminobutyric Acid (XI)—This compound was prepared by the method of Balenovic *et al.* (23) as described for the L-isomer. The yield was 141 mg (67%), mp 187–189°; IR: ν_{max}^{KBr} 3020, 2830, 2590 (NH_3), 1620, and 1580 (carboxylate C=O) cm^{-1}; ^{1}H-NMR (D_2O): δ 1.32 (d, CH_3, J = 7 Hz) and 3.58 (m, CH) ppm.

Anal.—Calc. for $C_4H_9NO_2$: C, 46.59; H, 8.80; N, 13.58. Found: C, 46.38; H, 8.64; N, 13.51.

Hydrazinolysis of X: Formation of 3-Aminobutyrohydrazide (XII)—Triethylamine (0.9 ml, 6.5 mmoles) and hydrazine (95%, 0.3 ml, 9.46 mmoles) were added to a solution of X (500 mg, 2.05 mmoles) in methanol (19 ml). The reaction mixture was stirred at room temperature for 67 hr, and a white precipitate of phthaloyl hydrazide separated out. This precipitate was filtered, and the filtrate was evaporated and dried completely *in vacuo*. TLC [methanol–chloroform (1:4)] showed two spots. The spot with the higher R_f was due to phthaloyl hydrazide (UV absorbing), and the one with the lower R_f was ninhydrin positive. By column chromatography, the fraction corresponding to the lower R_f was isolated and characterized as the hydrochloride. The yield was 80 mg (21%), mp 201–202°; IR: ν_{max}^{KBr} 2940 ($^+NH_3$) and 1689 (C=O) cm^{-1}; ^{1}H-NMR (D_2O): δ 1.32 (d, CH_3, J = 7 Hz), 2.70 (d, CH_2, J = 7 Hz), and 3.77 (q, CH, J = 7 Hz) ppm.

Anal.—Calc. for $C_4H_{11}N_3O{\cdot}2HCl$: C, 25.27; H, 6.89; N, 22.10. Found: C, 25.45; H, 6.67; N, 21.87.

REFERENCES

(1) E. C. Moore and G. A. LePage, *Cancer Res.*, **17**, 804 (1957).

(2) A. J. Tomisek, H. J. Kelly, and H. E. Skipper, *Arch. Biochem. Biophys.*, **64**, 437 (1956).

(3) D. A. Goldthwait, *J. Biol. Chem.*, **222**, 1051 (1956).

(4) J. F. Henderson and A. R. P. Paterson, "Nucleotide Metabolism," Academic, New York, N.Y., 1973.

(5) C. J. Bates and R. E. Handschumacher, in "Advances in Enzyme Regulation," vol. 7, G. Weber, Ed., Pergamon Press, Oxford, England, 1969, p. 183.

(6) T. C. French, I. B. David, R. A. Day, and J. M. Buchanan, *J. Biol. Chem.*, **238**, 2171 (1963).

(7) T. C. French, I. B. David, and J. M. Buchanan, *ibid.*, **238**, 2186 (1963).

(8) I. B. David, T. C. French, and J. M. Buchanan, *ibid.*, **238**, 2178 (1963).

(9) B. R. Baker, "Design of Active-Site-Directed Irreversible Enzyme Inhibitors," Wiley, New York, N.Y., 1967.

(10) G. E. Foley, E. F. Barell, R. A. Adams, and H. Lazarus, *Exp. Cell Res.*, **57**, 129 (1969).

(11) K. A. Harrap and D. E. M. Speed, *Br. J. Cancer Res.*, **18**, 809 (1964).

(12) T. Ohnuma, J. Waligunda, and J. F. Holland, *Cancer Res.*, **31**, 1640 (1971).

(13) J. A. Regan, H. Vodopick, S. Takeda, W. H. Lee, and F. M. Faulcon, *Science*, **163**, 1452 (1969).

(14) T. A. McCoy, M. Maxwell, and R. E. Neuman, *Cancer Res.*, **16**, 979 (1956).

(15) T. A. McCoy, M. Maxwell, and P. I. Kruse, Jr., *Proc. Soc. Exp. Biol. Med.*, **100**, 115 (1959).

(16) J. C. Sheehan and D. A. Johnson, *J. Am. Chem. Soc.*, **76**, 158 (1954).

(17) B. Paul and W. Korytnyk, *J. Med. Chem.*, **19**, 1002 (1976).

(18) G. A. Ivanovics, R. J. Rousseau, and R. K. Robins, *ibid.*, **14**, 1155 (1971).

(19) B. Penke, J. Czombos, L. Balaspiri, J. Petres, and K. Kovas, *Helv. Chim. Acta*, **53**, 1057 (1970).

(20) D. Hodson, G. Holt, and D. K. Wall, *J. Chem. Soc. C*, **1970**, 971.

(21) F. A. Miller and W. B. White, *J. Am. Chem. Soc.*, **79**, 5974 (1974).

(22) B. R. Baker, D. V. Santi, J. K. Coward, H. S. Shapiro, and J. H. Jordan, *J. Heterocycl. Chem.*, **3**, 434 (1966).

(23) K. Balenovic, D. Cerar, and Z. Fuks, *J. Chem. Soc.*, **1952**, 3316.

(24) A. L. Wilds and A. L. Meader, Jr., *J. Org. Chem.*, **13**, 763 (1948).

ACKNOWLEDGMENTS

Supported in part by research Grants CA-08793, CA-13038, and CA-16056 from the National Institutes of Health.

The authors are indebted to Dr. M. T. Hakala and Miss A. I. Mulhern for the biological evaluation of the reported compounds.

Stability Studies of Phenylbutazone and Phenylbutazone–Antacid Oral Formulations

F. MATSUI ˣ, D. L. ROBERTSON, P. LAFONTAINE, H. KOLASINSKI, and E. G. LOVERING

Received June 13, 1977, from the *Drug Research Laboratories, Health Protection Branch, Tunney's Pasture, Ottawa, Ontario, K1A 0L2, Canada.* Accepted for publication August 18, 1977.

Abstract □ Nineteen phenylbutazone and eight phenylbutazone–antacid solid oral formulations were stored in sealed bottles at room temperature and 37, 50, and 60° with ambient relative humidity and at 37° with 75% relative humidity. Samples were examined for intact drug content, decomposition profiles, and dissolution rates at selected time intervals up to 296 days. None of the phenylbutazone formulations showed any evidence of chemical instability when stored at ambient temperature, 37°, and 37° with 75% relative humidity. Measurable chemical degradation occurred only at 60°, with several formulations showing more than 50% degradation by the time the study was terminated. In some formulations, the extent of degradation varied greatly among tablets within the same bottle and between bottles of the same lot. Shelflife could not be predicted from the data. The results indicate that the temperatures used in accelerated studies should not exceed 50°. Dissolution rates tended to decrease with time at 60° and, to some extent, at 37° with 75% relative humidity and 50°. Chemical degradation occurred at 37° in some phenylbutazone–antacid formulations and was general at 50 and 60°. At 60°, the extent of degradation approached a maximum during the initial time periods, suggesting that a reactant involved in the degradation had been consumed. There were no significant changes in the dissolution time of antacid formulations.

Keyphrases □ Phenylbutazone—various solid oral formulations, stability, effect of temperature and humidity □ Stability—phenylbutazone, various solid oral formulations, effect of temperature and humidity □ Degradation—phenylbutazone, various solid oral formulations, effect of temperature and humidity □ Antirheumatic agents—phenylbutazone, various solid oral formulations, stability, effect of temperature and humidity

Phenylbutazone degradation was reported to occur in oxygen-free basic solutions (1), in oxygenated solutions (2), in acidic permanganate solutions (3), and in basic peroxide solutions (3). Degradation pathways in other solvents such as *N,N*-dimethylformamide, *N,N*-dimethylacetamide, diethyl carbonate, and propylene glycol–water were described (4). Injectable formulations of phenylbutazone degrade by hydrolysis and, to a lesser extent, by oxidation, yielding such products as 4-hydroxyphenylbutazone (I), α-carboxy-*N*-caproylhydrazobenzene (II), *cis*- and *trans*-azobenzene, and *n*-butylmalonic acid (5, 6). In suppository formulations, *N*-caproylhydrazobenzene (III), α-carboxy-α-hydroxy-*N*-caproylhydrazobenzene (IV), I, and II were identified after degradation by a process described as mainly oxidative (5, 7).

A study of tablet formulations of phenylbutazone stored at room temperature revealed some degradation in products formulated with antacids, but otherwise degradation was slight or not apparent (8). Mechanisms describing the degradation of injectable and suppository formulations (5) and accounting for the appearance of *N*-(α-ketocaproyl)-hydrazobenzene (V), II, and IV in tablets formulated with antacids (9) were proposed. Data to elucidate further the degradation mechanism were obtained by a study of the decomposition at elevated temperatures (10). Phenylbutazone tablets also are subject to physical instability, made manifest by a decrease in dissolution rate, probably due to polymorphism of phenylbutazone (11) or to a change in the properties of the gelatin and/or acacia subcoats of sugar-coated tablets (12).

This paper describes a study of the accelerated and ambient temperature aging of phenylbutazone and phenylbutazone–antacid solid oral formulations. The purpose of this work was to gain insight into the comparative behavior of formulations from different manufacturers.

EXPERIMENTAL

Materials—All formulations were obtained directly from the manufacturers. The following compounds were used as received: phenylbutazone[1], α-carboxy-*N*-caproylhydrazobenzene[2], *N*-caproylhydrazobenzene[2], *N*-(α-ketocaproyl)hydrazobenzene[2], α-hydroxy-*N*-caproylhydrazobenzene[2], and ethyl acetate[3] (glass distilled).

Diphenyl phthalate[4] was recrystallized from acetone–water. α-Carboxy-α-hydroxy-*N*-caproylhydrazobenzene was prepared by controlled alkaline hydrogen peroxide oxidation (10), and 4-hydroxyphenylbutazone was prepared by heating α-carboxy-α-hydroxy-*N*-caproylhydrazobenzene to a maximum temperature of 165° (10). Silica gel 60 F-254-precoated TLC plates[5] were used.

Protocol—Nineteen phenylbutazone and eight phenylbutazone–antacid formulations were stored[6] at ambient temperature (21–23° range), 37°, 37° with 75% relative humidity (13), 50°, and 60°. Time-zero analyses were carried out when the study began only on samples from bottles to be stored at ambient conditions. All original and rebottled samples stored under accelerated conditions were not opened until time-one analysis. The bottles were reclosed tightly by hand between sampling.

For all storage conditions except 60°, the entire study was performed on a single bottle of each formulation. For the 60° study, analysis at times one to five inclusive were done on one bottle, while a second bottle was used to duplicate the time-five study and to obtain time-six data.

Quantitation of undegraded phenylbutazone and estimation of I and the total of other degradates were accomplished by GLC. Compounds II and IV in the antacid formulations were estimated by TLC. GLC and TLC were employed to follow the degradation profile. Quantitative UV spectroscopy also was used to follow the degradation profile and to corroborate the GLC data, which indicated a major decrease in phenylbutazone content.

All chemical tests were carried out on composites of five tablets or the contents of five capsules. GLC analyses were performed on duplicate weighings. Dissolution rates were measured at selected time intervals.

GLC—The technique of Watson *et al.* (14), modified slightly, was utilized to determine undegraded phenylbutazone[7]. Accurately weighed sample aliquots equivalent to 100, 50, or 10 mg of phenylbutazone were treated with 2 ml of 10% hydrochloric acid (v/v) and 10.0 ml of 0.2% (w/v) diphenyl phthalate (internal standard) in ethyl acetate. The mixture was tumbled end-over-end at 100 rpm for 15 min and centrifuged, and 1.0 μl of the supernate was chromatographed on 5% OV-7 on Gas Chrom Q under isothermal conditions at 230°. All other conditions were as previously described (14).

[1] Mount Royal Chemicals, Montreal, Quebec, Canada.
[2] Geigy Pharmaceuticals, Basel, Switzerland.
[3] Caledon Laboratories, Georgetown, Ontario, Canada.
[4] Aldrich Chemical Co., Milwaukee, Wis.
[5] E. Merck, Darmstadt, Germany.
[6] Formulations A, B, C, E, F, G, H, J, K, M, N, O, AA, BB, CC, DD, FF, and GG were stored in their original containers. Formulations D, I, L, P, Q, R, S, EE, and HH were rebottled in amber prescription bottles (Wheaton Glass Co., Millville, N.J.) prior to storage.
[7] The coefficient of variation was 1.06%.

Table I—Chromatographic Characteristics of Phenylbutazone and Related Degradation Products

Compound	Relative[a] Retention Times	Relative[b] R_f	Color with Detection Agent A[c]	Color with Detection Agents A and B[d]
I	0.86	0.63[e]	No color	Yellow orange
II	0.48, 0.38, 0.11, 0.09, 0.58	0.53	Purple	Color intensified
III	0.48, 0.38, 0.58	0.82	Red purple	Color intensified
IV	0.09, 0.52, 0.48, 0.15	0.39	Purple	Color intensified
V	0.52, 0.38, 0.09	0.78	Red purple	Color intensified
VI	0.09, 0.52	0.69	Red purple	Color intensified
Hydrazobenzene	0.09, 0.15, 0.21	1.02	Yellow	Yellow orange
Azobenzene	0.09, 0.15	1.30, 1.15	Yellow	Yellow orange
Phenylbutazone	0.68		No color	Yellow orange

[a] Relative to the diphenyl phthalate internal standard in order of decreasing peak area. [b] Relative to phenylbutazone. [c] 0.5% potassium dichromate in 20% (v/v) H_2SO_4. [d] Concentrated sulfuric acid. [e] Merck GF 60 precoated.

All time-zero analyses were performed on sample aliquots containing 100 mg of drug. However, as degradation proceeded, the sample aliquots were reduced to contain 50 or 10 mg of the drug. This reduction was done to ensure that extraction of the intact drug was complete and that the quantities of I, II, and IV fell within the range for which the response factors were established and to avoid possible overestimation of phenylbutazone and I due to on-column cyclization of II and IV. Cyclization occurred when the amount of II and IV injected exceeded 1.0 μg. (The presence of 1.0 μg of II or IV would represent 100 and 20% degradation with respect to 1 and 5 μg of phenylbutazone.) When the amount of acid degradates approached 20% of the original drug content, the smallest sample equivalent was used.

Under the conditions of the GLC assay, phenylbutazone and I are stable but all other degradates exhibit on-column breakdown resulting in multiple peaks. Retention times of these peaks relative to diphenyl phthalate are given in Table I. Thus, in addition to the drug content, the GLC chromatograms provide an overall profile of the extent of decomposition with time. Reliable quantitation of the degradates by GLC was possible only when the decomposition pathway was simple and led just to the formation of II and/or IV, determined as total acid-type degradates in the phenylbutazone–antacid formulations, or in the formation of these acid derivatives and/or I in phenylbutazone formulations. As degradation became more complex, particularly with certain phenylbutazone formulations, quantitation of the degradates was less accurate.

TLC—A previously developed method (8) was used to estimate II and IV in antacid formulations and to obtain a qualitative profile of the degradation process for phenylbutazone tablets. This test was carried out on tablet or capsule extracts prepared for the GLC assay. The thin-layer chromatogram is qualitatively more informative than the gas chromatograms since comparison of the R_f characteristics and the color reactions of the extraneous spots with those of the degradates (Table I) permits identification of the individual degradates, particularly when degradation leads to the formation of numerous compounds.

UV Spectrophotometry—Tablet grinds or capsule contents were treated with 0.1 *N* NaOH and centrifuged; the absorbance ratio, 264/234 nm, of the supernate was determined.

Dissolution—A reciprocating apparatus similar to the USP disintegration apparatus was used, except that the official basket was replaced with a single-chamber basket with an 8.5-cm diameter bottom plate (15). The solvent was 900 ml of pH 7.2 phosphate buffer (16). The quantity of drug dissolved was measured by UV spectroscopy at 264 nm. Disintegration times were estimated visually as the time at which the capsule or tablet particles passed through the wire mesh covering the bottom of the chamber.

RESULTS AND DISCUSSION

Phenylbutazone Tablets—None of the phenylbutazone formulations studied showed any evidence of chemical instability when stored at ambient temperature, 37°, and 37° with 75% relative humidity. Formulations I and K showed a 10% loss after 269 days at 50°. The formulations were chemically labile at 60°, as shown by the continuing decrease in the intact drug content and the UV absorbancy ratio coupled with the progressive increase in the area of the extraneous peaks in the gas chromatograms or in the number of spots in the thin-layer chromatograms.

Table II—Degradation (Percent) of Phenylbutazone Tablets at 60°

Formulation	Bottle 1[a] 18 days	36 days	50 days	111 days	203 days	Bottle 2[b] 203 days	278 days
A	14	12	16	22	23	62	59
B			13	18	34	23	27
C			4	9	9	9	10
D			0	5	1	5	6
E	6		61	78	81	65	70
F	4	18	18	31	38	3	1
G	4	5	9	51	53	51	83
H			26	35	52	33	32
I			0	18	35	31	40
J	0	2	0	15	14	23	24
K			15	38	43	44	48
L			5	1	0	0	1
M			0	34	50	52	59
N	0	0	4	17	23	21	25
O			0	57	47	6	20
P			3	3	0	1	0
Q			4	5	8	2	6
R			3	2	1	2	0
S	0	3	5	25	31	17	9

[a] Bottle 1 was opened on the 1st day of sampling. [b] Bottle 2 was opened at Day 203.

The extent of degradation at 60° in 19 tablet formulations measured by GLC at selected intervals over 278 days is given in Table II. The extent of degradation among the formulations ranged from no degradation for Formulations D, L, P, and R to 83% loss in potency for Formulation G. Variations in the degree of degradation were present, in some cases, between bottles of the same formulation and within a single bottle. For example, Formulation F, after 203 days, exhibited 38 and 3% losses for Bottles 1 and 2, respectively, while Formulation H exhibited 52 and 5% losses for tablets from the same bottle after 203 days.

The variation in results between Bottles 1 and 2 (Formulation F) may be due to the fact that Bottle 1 was opened at Day 18 and reopened for subsequent sampling while Bottle 2 was not opened before Day 203. However, opened and unopened experimental conditions apparently did not affect Formulations C, G, I, K, M, and N. Greater stability was manifested by the unopened bottle for Formulations B, E, F, H, O, and S, but data for A and J indicate the reverse condition.

The different courses of the degradation reaction over the study period are illustrated by the chromatograms of Formulations K (Fig. 1) and E (Fig. 2). The degradative pathway of Formulation K became increasingly complex with time; that of Formulation E remained relatively simple throughout.

Phenylbutazone decomposition products present in the formulations after 203 days were identified by TLC (Table III). Compound I and the total of all other degradates were estimated by GLC (Table III). The latter estimates may be in error by 10% or more because the individual components exhibited different response factors and the composition of the mixture of degradates was variable. No quantitation was attempted with TLC. However, the most concentrated spots were noted, and the remaining spots were classified as intermediate or weak. Usually, the nature and relative amounts of the decomposition products in a specific formulation did not change during the study, although they varied considerably among formulations.

Examination of the TLC data (Table III) for 203 days of storage reveals that I was the main degradation product in 13 of the 19 formulations, indicating oxidation to be a prominent reaction pathway with most formulations. In Formulations C, E, and M, oxidation appeared to be the only significant degradative route since only the TLC spot and GLC peak corresponding to I were present to any appreciable extent. However, the plethora of decomposition products in Formulations B, G, K, N, and O suggests a complex degradation mechanism involving hydrolysis, oxidation, and decarboxylation. Apparently, the degradation mechanism and rate depend on the properties and composition of the individual formulations and not solely on the drug.

The nature of the decomposition products and the extent of degradation varied among individual tablets in Formulations G, I, K, M, and O. This result became apparent when tablet cores of two or more colors

Table III—TLC Profiles of Phenylbutazone Formulations after 203 Days at 60° [a]

Formulation	I GLC, %	I TLC	II	III	IV	V	VI	Azobenzene	Total Decomposition by GLC[b], %
A	20	S	W	W			W	W	
B[c]	9	S		W		W	W		7
C	10	S							
D			No degradation detected						
E	88	S			W		W		
F[c]	41	S		I			W		4
G	17	S	W		W	—[e]	W	W	19
H[c]	32	S	W	W	I	I			14
I[d]	20	S		W					3
J[d]	11	S		W					4
K[c]	15	I	W	S	W	W		W	40
K[d]	0		W	S	W	W			45
L			No degradation detected						
M[d]	43	S					W		
N	22	S	W	W					5
O	16	S				W	W	W	5
P			No degradation detected						
Q	0			W					5
R			No degradation detected						
S[c]	38	S		I					15

[a] Strong spots are indicated by S, intermediate spots by I, and weak spots by W. [b] Excluding I. [c] Brown cores. [d] Beige cores. [e] Identity of this extraneous spot has not been established.

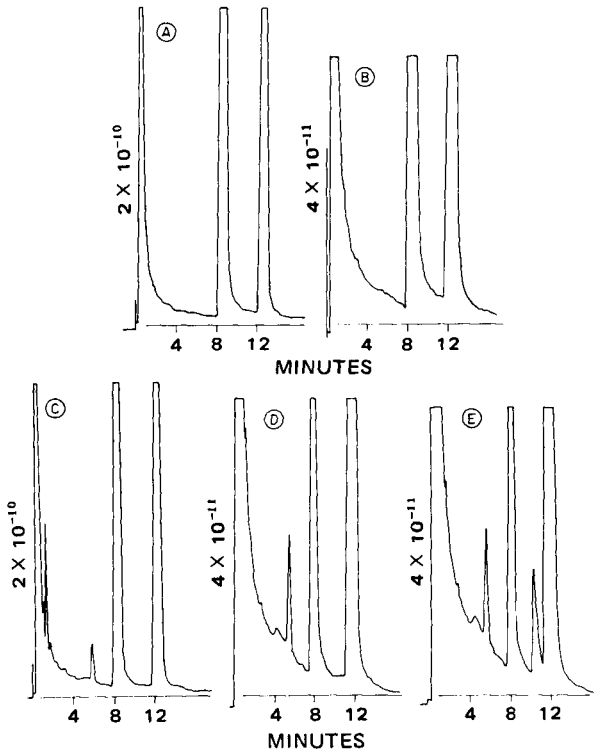

Figure 1—*Chromatograms of Formulation K. Key: A, ambient temperature, T_0 days, 10-μg injection; B, ambient temperature, T_{268} days, 5-μg injection; C, 60°, T_{50} days, 5-μg injection; D, 60°, T_{203} days, 1-μg injection (beige tablets); and E, 60°, T_{203} days, 1-μg injection (brown tablets). Retention times were: phenylbutazone, 8 min; diphenyl phthalate (internal standard), 12 min; and 4-hydroxyphenylbutazone, 10 min.*

were observed in the same bottle. Colors, not necessarily within a given bottle, ranged from yellow to beige to dark brown and black, the depth of color being indicative of the degree of degradation. Formulation K, which was typical, consisted of beige and the dark-brown tablets, both of which contained comparable amounts of several degradation products, except that the latter contained a much larger amount of I (Fig. 1). The tablet-to-tablet variability may reflect differences in the thickness of the tablet coating or in the permeability of the tablet cores, but there is no evidence to substantiate this hypothesis.

As decomposition proceeded, the absorbance at 264 nm decreased and the λ_{max} gradually shifted toward 234 nm (1, 6), resulting in a decrease in the absorbancy ratio A_{264}/A_{234}. Although there was no direct quantitative relationship between the loss in drug content as measured by GLC and the decrease in the absorbancy ratio, a gross increase in degradation was accompanied by a substantial decrease in the absorbancy ratio. For example, Formulation M yielded the following ratios: Bottle 1, 1.81 (0 day), 1.80 (50 days), and 0.91 (203 days); and Bottle 2, 0.90 (203 days) and 0.80 (278 days).

It was intended to calculate shelflives for the formulations, but this task proved impracticable since only formulations stored at 60° exhibited quantifiable degradation, although some degradation of Formulations I and K occurred at 50°. The large difference in degradation rates at 50 and 60° may indicate a threshold temperature at which the nature of the degradation mechanism changes. If so, accelerated aging studies of phenylbutazone tablets aimed at predicting shelflife are unreliable if they encompass rate measurements at temperatures over the threshold temperature.

The identification of the main degradation products of Formulations K and M, taken as representative of all formulations, was confirmed by isolation of the degradates from a TLC plate and comparison of the mass spectra, melting points, and GLC retention times with those of standard

Table IV—Dissolution (Percent) of Phenylbutazone Tablets at 60 min [a]

	60°								50°				37°, 75% Relative Humidity			
Formulation[b]	0 day	18 day	36 days	50 days	111 days	203 days, Bottle 1	203 days, Bottle 2	278 days	63 days	128 days	196 days	269 days	34 days	82 days	159 days	219 days
A (C)	95				100	71	21	20		82	79	82				
B (SC)	84	4		2	4	0	0	0	28	0	4	0			74	46
C (FC)	90				100	79	82	82								
D (FC)	98				100	90	83	84								
E (FC)	99			26	53	56										
F (FC)	0						No change detected									
G (SC)	95			93	100	0	0	0								
H (EC)	81			2	3		1	1	21	3		0	68	40		23
I (EC)	0						No change detected									
J (SC)	0						No change detected									
K (SC)	88			4	3		0	0	6	3	0	0	88	75	43	44
L (SC)	80			67	62	66	50	51	58	30	25	0		84	75	58
M (SC)	90			71	80	48	24	26								
N (SC)	93	78	65	16	16	0	0	0	84	47	39	29	92	86	98	
O (SC)	85	71		66	56	13	52	73								
P (SC)	98						No change detected									
Q (SC)	62			74	23	27	28	40	51	57	61	56	65	63	58	48
R (SC)							No change detected									
S (SC)	96	9		4	0	0	0	0	7	6	9	0	0	95	89	35

[a] At time 0, percent of label claim; at other times, percent of undegraded phenylbutazone. Mean of six tablets. [b] C = compressed, SC = sugar coated, FC = film coated, and EC = enteric coated.

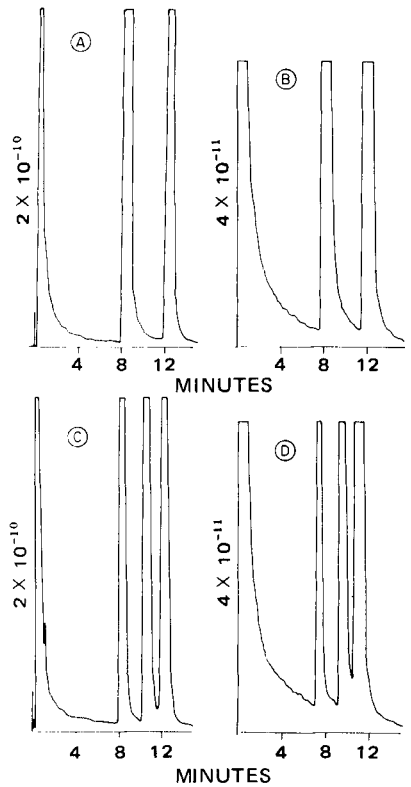

Figure 2—*Chromatograms of Formulation E. Key: A, ambient temperature, T_0 days, 10-μg injection; B, ambient temperature, T_{268} days, 5-μg injection; C, 60°, T_{50} days, 5-μg injection; and D, 60°, T_{203} days, 1-μg injection. Retention times were the same as for Fig. 1.*

compounds. The compounds identified were I (Formulation M) and III (Formulation K). Additional studies of Formulation G indicated the presence of one or more compounds not reported in previous phenylbutazone studies. One of these exhibited an R_f value similar to that of V, but the melting point was not the same. Work to identify this compound is in progress.

The amount of drug dissolved after 60 min was measured, and the results are expressed as a percentage of the amount of undegraded phenylbutazone present at the time of the measurement. Over 270 days, the amount dissolved did not change in any sample stored at room temperature. At 37°, Formulations K and Q became progressively less soluble, the amounts dissolved decreasing from 88 and 62% at zero time to 73 and 50% at 283 days, respectively.

Dissolution results for those formulations exhibiting a significant change with time at 37° with 75% relative humidity, 50°, and 60° are given in Table IV. Increases in the dissolution time of phenylbutazone tablets have been attributed to changes in the properties of the tablet coatings (12). All tablets included in this study were sugar, film, or enteric coated, but there appeared to be no relationship between the type of coating and the dissolution behavior.

Phenylbutazone–Antacid Formulations—Eight phenylbutazone–antacid formulations were subjected to accelerated aging for up to 190 days and temperatures up to 60°. Losses in drug content in samples stored at room temperature were not measurable. Degradation commenced in some formulations at 37° and 37° with 75% relative humidity and was evident in all formulations at 50 and 60° (Table V). As with the phenylbutazone tablets, the degradation rate varied among the formulations, but none of the formulations was completely stable at 60°. Gross differences among the individual dosage units in a given bottle were not evident, as was the case with the nonbuffered phenylbutazone tablets.

Under all storage conditions except ambient temperature, there was evidence of degradation during the first 60 days. The decomposition products formed during this period were II and IV, indicating that the main route of degradation was alkaline hydrolysis (1, 8). In samples stored at 37° and 37° with 75% relative humidity, the degradation appeared to cease after the initial 60 days. This result also occurred with samples stored at 50° except for Formulations CC and FF. Except for HH, all formulations at 60° continued to degrade over the entire study. At this temperature, after the initial 60 days, complex mixtures of degradates including II–VI and an unidentified compound were observed. These observations suggest that, after the initial period of hydrolysis, the stability characteristics of phenylbutazone–antacid formulations are similar to those of the phenylbutazone formulations. Cessation of hydrolysis may reflect exhaustion of available water in the formulations under examination.

The dissolution times of the phenylbutazone–antacid preparations did not change significantly under all time and temperature conditions of this study. Some tablet mottling was observed at 50 and 60°. At these temperatures, the capsule shells of Formulation HH softened and fused together so that the dissolution rate could not be measured.

Table V—Percent Losses in Drug Content of Phenylbutazone–Antacid Formulations with Time and Temperature [a]

	37°		37°, 75% Relative Humidity		50°		60°	
Formulation	*t*, days	Loss, %	*t*, days	Loss, %	*t*, days	Loss, %	*t*, days	Loss, %
AA, tablets	23	0	20	1	26	1	17	3
	41	1	41	0	43	3	43	5
	56	0	55	0	55	3	57	5
	89	1	85	0	89	4	87	5
	190	1	177	1	180	4	148	9
BB, capsules	22	4	20	2	26	8	16	6
	41	3	41	1	43	6	43	14
	56	3	55	2	55	9	57	16
	89	5	85	4	89	9	87	14
	190	7	177	4	180	10	148	20
CC, capsules	22	4	21	1	26	11	15	17
	41	9	41	2	43	12	43	28
	56	7	55	3	55	18	58	32
	89	6	85	5	89	21	88	36
	190	8	177	12	180	21	148	41
DD, capsules	21	0	21	0	26	3	15	4
	41	0	40	0	42	3	43	7
	56	0	54	0	55	4	57	6
	89	0	84	0	89	4	87	9
	190	0	177	1	180	6	148	16
EE, tablets	23		20		26	3	17	2
	42	2	41	1	43	3	43	7
	57	0	55	1	55	5	57	13
	90	4	85		89	4	87	9
	190	3	177		180	5	148	22
FF, tablets	22	4	20	2	26	10	17	9
	41	1	41	2	43	15	41	9
	56	3	55	2	55	8	55	20
	89	4	85	4	89	8	85	24
	190	5	177	4	180	20	148	33
GG, tablets	22	2	21	0	27	3	18	5
	41	4	41	2	43	6	41	16
	56	2	55	1	55	12	55	27
	89	0	85	1	89	12	85	25
	190	2	177	1	180	9	148	34
HH, capsules	21	4	20	3	10	0	10	7
	41	3	42	0	23	3	23	13
	56	6	55	6	37	6	43	8
	89	4	85	3	71	3	73	6
	190	4	177	6				

[a] Samples stored at 37° with 75% relative humidity presented difficulties in sampling.

CONCLUSIONS

The rate, extent, and mechanism of degradation in phenylbutazone tablets at 60° depend upon the tablet excipients and, possibly, the manufacturing process. The unformulated drug is stable at 60°. The degradation rate at 50° in tablets is much slower and may proceed by a different mechanism than that at 60°. Initially, at all temperatures except ambient, the mechanism by which the antacid formulations degrade appears to be mainly alkaline hydrolysis. After this initial period, the degradation process appears to change between 50 and 60°, becoming similar to that observed in phenylbutazone formulations. These observations suggest that accelerated studies aimed at predicting shelflife should not include temperatures much over 50°. Accelerated temperature testing is valid only if the degradation occurs by the same mechanism at all temperatures.

REFERENCES

(1) E. Pawelczyk and R. Wachowiak, *Diss. Pharm. Pharmacol.*, **21**, 491 (1969).

(2) *Ibid.*, **22**, 475 (1970).

(3) W. Awe and H. J. Kienert, *Pharm. Acta Helv.*, **38**, 805 (1963).

(4) J. Slingsby and D. A. Zuck, *Can. J. Pharm. Sci.*, **7**, 115 (1972).

(5) E. Pawelczyk and R. Wachowiak, *Acta Pol. Pharm.*, **26**, 425 (1969).

(6) E. Pawelczyk and R. Wachowiak, *Diss. Pharm. Pharmacol.*, **20**, 653 (1973).

(7) E. Pawelczyk and M. Zajac, *Acta Pol. Pharm.*, **27**, 104 (1970).

(8) H. D. Beckstead, K. K. Kaistha, and S. J. Smith, *J. Pharm. Sci.*, **57**, 1952 (1968).

(9) D. V. C. Awang, A. Vincent, and F. Matsui, *ibid.*, **62**, 1973 (1973).

(10) D. V. C. Awang and A. Vincent, *ibid.*, **65**, 68 (1976).

(11) H. G. Ibrahim, F. Pisano, and A. Bruno, *ibid.*, **66**, 669 (1977).

(12) D. Barrett and J. J. Fell, *ibid.*, **64**, 335 (1975).

(13) "Annual Book of ASTM Standards," Part 35, American Society for Testing and Materials, Philadelphia, Pa., 1975, p. 852.

(14) J. R. Watson, F. Matsui, R. C. Lawrence, and P. M. J. McConnell, *J. Chromatogr.*, **76**, 141 (1973).

(15) E. G. Lovering and C. A. Mainville, *Can. J. Pharm. Sci.*, in press.

(16) "The United States Pharmacopeia," 19th rev., Mack Publishing Co., Easton, Pa., 1975.

Simultaneous Determination of Reserpine and Hydrochlorothiazide in Two-Component Tablet Formulations by High-Performance Liquid Chromatography

A. G. BUTTERFIELD ˣ, E. G. LOVERING, and R. W. SEARS

Received March 7, 1977, from the *Drug Research Laboratories, Health Protection Branch, Ottawa, Ontario, K1A 0L2, Canada.* Accepted for publication August 22, 1977.

Abstract □ A high-performance liquid chromatographic procedure is presented for the simultaneous determination of reserpine and hydrochlorothiazide in two-component tablet formulations. An aliquot of a tetrahydrofuran extract of the tablet, containing polythiazide as an internal standard, is chromatographed on a microparticulate silica gel column using a mobile phase of 0.01% (v/v) diethylamine, 5% (v/v) chloroform, and 18% (v/v) 2-propanol in *n*-hexane. The relative standard deviations are 1.2 and 0.6% for the simultaneous determination of reserpine and hydrochlorothiazide, respectively. Seven commercial tablet formulations were found to contain 92.7–101.0% and 98.3–101.4% of the labeled amounts of reserpine and hydrochlorothiazide, respectively.

Keyphrases □ Reserpine—high-performance liquid chromatographic analysis, simultaneously with hydrochlorothiazide, in tablets □ Hydrochlorothiazide—high-performance liquid chromatographic analysis, simultaneously with reserpine, in tablets □ High-performance liquid chromatography—simultaneous analyses, hydrochlorothiazide and reserpine in tablets □ Diuretics—hydrochlorothiazide, high-performance liquid chromatographic analysis, simultaneously with reserpine, in tablets □ Antihypertensives—reserpine, high-performance liquid chromatographic analysis, simultaneously with hydrochlorothiazide, in tablets

Reserpine–hydrochlorothiazide formulations are marketed in Canada by several manufacturers. A rapid, accurate procedure, applicable to all formulations, was required for the simultaneous determination of both drugs in these preparations. Literature methods are based on many different techniques for the analysis of the individual compounds (1–5), but only an automated procedure (6) simultaneously determines both compounds. This automated procedure is useful for content uniformity purposes but is cumbersome for occasional use and is not specific for the determination of reserpine or hydrochlorothiazide since known impurities may interfere.

High-performance liquid chromatography (HPLC) has been used extensively for the analysis of mixtures (7–9) because of high specificity, speed, and sensitivity. The technique has been applied to the analysis of alkaloids (10–13) and thiazide diuretics (14–16), including the quantitative analysis of reserpine–chlorothiazide mixtures (16). This report describes an HPLC procedure for the simultaneous determination of reserpine and hydrochlorothiazide in two-component tablet formulations.

EXPERIMENTAL

Materials—Reserpine[1], hydrochlorothiazide[2], polythiazide[3], and 1-amino-3-chloro-4,6-benzenedisulfonamide[4] (I) were used as received. Both drug substances were essentially identical to the corresponding reference standards[5] when retention times, impurities, and response factors were compared by HPLC and when drug content was compared by the USP XIX assay procedure (5). Solvents and reagents were commercial analytical reagent grade, except for tetrahydrofuran[6] and *n*-hexane[6] which were UV grade. Tetrahydrofuran was stored under nitrogen.

Apparatus—A liquid chromatograph[7] fitted with a septumless injection port[7], a fixed-wavelength UV detector[8] (254 nm), and a computing integrator[9] was used. The detector was attenuated to 0.01 absorbance unit full scale (aufs).

Column—A 250 × 2.1-mm i.d. column[10] packed with 5-μm diameter silica gel[11], using a balanced density slurry technique similar to that described by Majórs (17), was used at ambient temperature and at a mobile phase flow rate of 90 ml/hr (210 bar).

Mobile Phase—A solution of 0.01% (v/v) diethylamine, 5% (v/v) chloroform, and 18% (v/v) 2-propanol in *n*-hexane was prepared as required. It was degassed (refluxed for 5 min) and stored in the solvent reservoir of the instrument.

Internal Standard Solution—A solution of polythiazide in tetrahydrofuran (0.1 mg/ml) was used.

Preparation of Standard Curves—Stock solutions of reserpine (0.10 mg/ml), hydrochlorothiazide (25 mg/ml), and polythiazide (0.5 mg/ml)

[1] Aldrich Chemical Co., Montreal, Canada.
[2] Merck Sharp and Dohme, Kirkland, Canada.
[3] Pfizer Co., Arnprior, Canada.
[4] Pfaltz and Bauer, Flushing, N.Y.
[5] United States Pharmacopeial Convention, Rockville, Md.
[6] Burdick and Jackson Laboratories, Muskegon, Mich.
[7] Model 4100, Varian Aerograph, Palo Alto, Calif.
[8] Model 440, Waters Associates, Milford, Mass.
[9] Autolab System I, Spectra-Physics, Santa Clara, Calif.
[10] Li-Chroma I.D., Alltech Associates, Arlington Heights, Ill.
[11] LiChrosorb SI 60, British Drug Houses, Toronto, Canada.

REFERENCES

(1) E. Pawelczyk and R. Wachowiak, *Diss. Pharm. Pharmacol.*, **21**, 491 (1969).

(2) *Ibid.*, **22**, 475 (1970).

(3) W. Awe and H. J. Kienert, *Pharm. Acta Helv.*, **38**, 805 (1963).

(4) J. Slingsby and D. A. Zuck, *Can. J. Pharm. Sci.*, **7**, 115 (1972).

(5) E. Pawelczyk and R. Wachowiak, *Acta Pol. Pharm.*, **26**, 425 (1969).

(6) E. Pawelczyk and R. Wachowiak, *Diss. Pharm. Pharmacol.*, **20**, 653 (1973).

(7) E. Pawelczyk and M. Zajac, *Acta Pol. Pharm.*, **27**, 104 (1970).

(8) H. D. Beckstead, K. K. Kaistha, and S. J. Smith, *J. Pharm. Sci.*, **57**, 1952 (1968).

(9) D. V. C. Awang, A. Vincent, and F. Matsui, *ibid.*, **62**, 1973 (1973).

(10) D. V. C. Awang and A. Vincent, *ibid.*, **65**, 68 (1976).

(11) H. G. Ibrahim, F. Pisano, and A. Bruno, *ibid.*, **66**, 669 (1977).

(12) D. Barrett and J. J. Fell, *ibid.*, **64**, 335 (1975).

(13) "Annual Book of ASTM Standards," Part 35, American Society for Testing and Materials, Philadelphia, Pa., 1975, p. 852.

(14) J. R. Watson, F. Matsui, R. C. Lawrence, and P. M. J. McConnell, *J. Chromatogr.*, **76**, 141 (1973).

(15) E. G. Lovering and C. A. Mainville, *Can. J. Pharm. Sci.*, in press.

(16) "The United States Pharmacopeia," 19th rev., Mack Publishing Co., Easton, Pa., 1975.

Simultaneous Determination of Reserpine and Hydrochlorothiazide in Two-Component Tablet Formulations by High-Performance Liquid Chromatography

A. G. BUTTERFIELD ˣ, E. G. LOVERING, and R. W. SEARS

Received March 7, 1977, from the *Drug Research Laboratories, Health Protection Branch, Ottawa, Ontario, K1A 0L2, Canada.* Accepted for publication August 22, 1977.

Abstract □ A high-performance liquid chromatographic procedure is presented for the simultaneous determination of reserpine and hydrochlorothiazide in two-component tablet formulations. An aliquot of a tetrahydrofuran extract of the tablet, containing polythiazide as an internal standard, is chromatographed on a microparticulate silica gel column using a mobile phase of 0.01% (v/v) diethylamine, 5% (v/v) chloroform, and 18% (v/v) 2-propanol in *n*-hexane. The relative standard deviations are 1.2 and 0.6% for the simultaneous determination of reserpine and hydrochlorothiazide, respectively. Seven commercial tablet formulations were found to contain 92.7–101.0% and 98.3–101.4% of the labeled amounts of reserpine and hydrochlorothiazide, respectively.

Keyphrases □ Reserpine—high-performance liquid chromatographic analysis, simultaneously with hydrochlorothiazide, in tablets □ Hydrochlorothiazide—high-performance liquid chromatographic analysis, simultaneously with reserpine, in tablets □ High-performance liquid chromatography—simultaneous analyses, hydrochlorothiazide and reserpine in tablets □ Diuretics—hydrochlorothiazide, high-performance liquid chromatographic analysis, simultaneously with reserpine, in tablets □ Antihypertensives—reserpine, high-performance liquid chromatographic analysis, simultaneously with hydrochlorothiazide, in tablets

Reserpine–hydrochlorothiazide formulations are marketed in Canada by several manufacturers. A rapid, accurate procedure, applicable to all formulations, was required for the simultaneous determination of both drugs in these preparations. Literature methods are based on many different techniques for the analysis of the individual compounds (1–5), but only an automated procedure (6) simultaneously determines both compounds. This automated procedure is useful for content uniformity purposes but is cumbersome for occasional use and is not specific for the determination of reserpine or hydrochlorothiazide since known impurities may interfere.

High-performance liquid chromatography (HPLC) has been used extensively for the analysis of mixtures (7–9) because of high specificity, speed, and sensitivity. The technique has been applied to the analysis of alkaloids (10–13) and thiazide diuretics (14–16), including the quantitative analysis of reserpine–chlorothiazide mixtures (16). This report describes an HPLC procedure for the simultaneous determination of reserpine and hydrochlorothiazide in two-component tablet formulations.

EXPERIMENTAL

Materials—Reserpine[1], hydrochlorothiazide[2], polythiazide[3], and 1-amino-3-chloro-4,6-benzenedisulfonamide[4] (I) were used as received. Both drug substances were essentially identical to the corresponding reference standards[5] when retention times, impurities, and response factors were compared by HPLC and when drug content was compared by the USP XIX assay procedure (5). Solvents and reagents were commercial analytical reagent grade, except for tetrahydrofuran[6] and *n*-hexane[6] which were UV grade. Tetrahydrofuran was stored under nitrogen.

Apparatus—A liquid chromatograph[7] fitted with a septumless injection port[7], a fixed-wavelength UV detector[8] (254 nm), and a computing integrator[9] was used. The detector was attenuated to 0.01 absorbance unit full scale (aufs).

Column—A 250 × 2.1-mm i.d. column[10] packed with 5-μm diameter silica gel[11], using a balanced density slurry technique similar to that described by Majórs (17), was used at ambient temperature and at a mobile phase flow rate of 90 ml/hr (210 bar).

Mobile Phase—A solution of 0.01% (v/v) diethylamine, 5% (v/v) chloroform, and 18% (v/v) 2-propanol in *n*-hexane was prepared as required. It was degassed (refluxed for 5 min) and stored in the solvent reservoir of the instrument.

Internal Standard Solution—A solution of polythiazide in tetrahydrofuran (0.1 mg/ml) was used.

Preparation of Standard Curves—Stock solutions of reserpine (0.10 mg/ml), hydrochlorothiazide (25 mg/ml), and polythiazide (0.5 mg/ml)

[1] Aldrich Chemical Co., Montreal, Canada.
[2] Merck Sharp and Dohme, Kirkland, Canada.
[3] Pfizer Co., Arnprior, Canada.
[4] Pfaltz and Bauer, Flushing, N.Y.
[5] United States Pharmacopeial Convention, Rockville, Md.
[6] Burdick and Jackson Laboratories, Muskegon, Mich.
[7] Model 4100, Varian Aerograph, Palo Alto, Calif.
[8] Model 440, Waters Associates, Milford, Mass.
[9] Autolab System I, Spectra-Physics, Santa Clara, Calif.
[10] Li-Chroma I.D., Alltech Associates, Arlington Heights, Ill.
[11] LiChrosorb SI 60, British Drug Houses, Toronto, Canada.

Table I—Retention Time and Capacity Factor of Reserpine, Hydrochlorothiazide, and Related Compounds

Compound	Retention Time[a], sec	Capacity Factor[b] (k')
Reserpine[c]	68	1.0
3-Isoreserpine[d]	50	0.5
3,4-Dehydroreserpine[e]	—[l]	—
3,4,5,6-Tetrahydroreserpine[e] (lumireserpine)	—[l]	—
Deserpidine[f]	61	0.8
Rescinnamine[g]	82	1.4
3,4,5-Trimethoxybenzoic acid[c]	—[l]	—
3,4,5-Trimethoxycinnamic acid[c]	—[l]	—
1-Amino-3-chloro-4,6-benzenedisulfonamide[h]	210	5.2
Hydrochlorothiazide[i]	320	8.5
Chlorothiazide	200	4.9
Methyclothiazide[f]	114	2.4
Bendroflumethiazide[j]	59	0.7
Polythiazide[k]	108	2.2

[a] Using 0.01% diethylamine, 5% chloroform, and 18% 2-propanol in n-hexane; 1.5 ml/min; and 250 × 2.1 mm LiChrosorb SI 60 (5 μm). [b] The $k' = (t_r - t_0)/t_0$, where t_r = retention time and t_0 = retention time of n-hexane. [c] Aldrich Chemical Co., Montreal, Canada. [d] Prepared by the method of MacPhillamy *et al.* (18). [e] Prepared by carrying out the "assay" for reserpine in USP XIX (5). [f] Abbott Laboratories, Montreal, Canada. [g] NF Reference Standard. [h] Pfaltz and Bauer, Flushing, N.Y. [i] Merck Sharp and Dohme, Kirkland, Canada. [j] Frank W. Horner, Ltd., Montreal, Canada. [k] Pfizer Co., Arnprior, Canada. [l] Retained peak.

in tetrahydrofuran were prepared. Standard solutions were prepared by pipetting 5 ml of the polythiazide stock solution into each of eight 25-ml volumetric flasks along with 1.0, 3.0, 5.0, 6.0, 7.0, 8.0, 9.0, or 10.0 ml of both the reserpine and hydrochlorothiazide stock solutions. Each solution was made up to volume with tetrahydrofuran, if necessary, and duplicate 7-μl aliquots of each standard solution were chromatographed. Samples were stored at 0° until they could be analyzed.

Preparation of Calibration Standard Solutions—Approximately 25 and 50 mg of reserpine were accurately weighed into separate 25-ml volumetric flasks, dissolved, and made up to volume with tetrahydrofuran. Each solution was diluted by pipetting 1.0 ml of the initial solution into a 10-ml flask and bringing to volume with tetrahydrofuran. Similarly, approximately 25 and 50 mg of hydrochlorothiazide were accurately weighed into separate 10-ml volumetric flasks. One milliliter of each diluted reserpine stock solution was pipetted into the flask containing the corresponding level of hydrochlorothiazide along with 2.0 ml of polythiazide internal standard solution (0.5 mg/ml). Each solution was made up to volume with tetrahydrofuran.

Duplicate 7-μl aliquots of the resulting solutions were chromatographed periodically to determine the slopes of the calibration curves. When not in use, the standards were stored in the dark at 0°. Calibration solutions were prepared daily.

Analysis of Pharmaceuticals—*Single-Tablet Assay*—A tablet was placed in a 16 × 125-mm screw-capped culture tube[12] and crushed to a fine powder with a glass rod. Then 10.0 ml of internal standard solution (0.1 mg/ml) was added to the tube, which was closed, tumbled on a rotator[13] at 30 rpm for 20 min, and centrifuged[14] at 2000 rpm for 5 min. Duplicate 7-μl aliquots of the supernate were chromatographed.

Tablet-Composite Assay—A tablet composite was prepared by grinding 20 tablets in a mechanical mill[15]. A quantity of powdered tablet material equivalent to one tablet was weighed into a 16 × 125-mm screw-capped culture tube. The sample was treated as previously described.

Calculations—*Calibration*—The slopes of the standard curves were calculated from the following equation, using data obtained by chromatographing the calibration solutions:

$$S = \frac{N_D C_I}{N_I C_D} \qquad \text{(Eq. 1)}$$

where S is the slope of the standard curve for the drug, either reserpine or hydrochlorothiazide; N_D is the peak height (millimeters) for reserpine or the peak area for hydrochlorothiazide; C_I is the concentration of the internal standard (milligrams per milliliter); N_I is the integrator counts

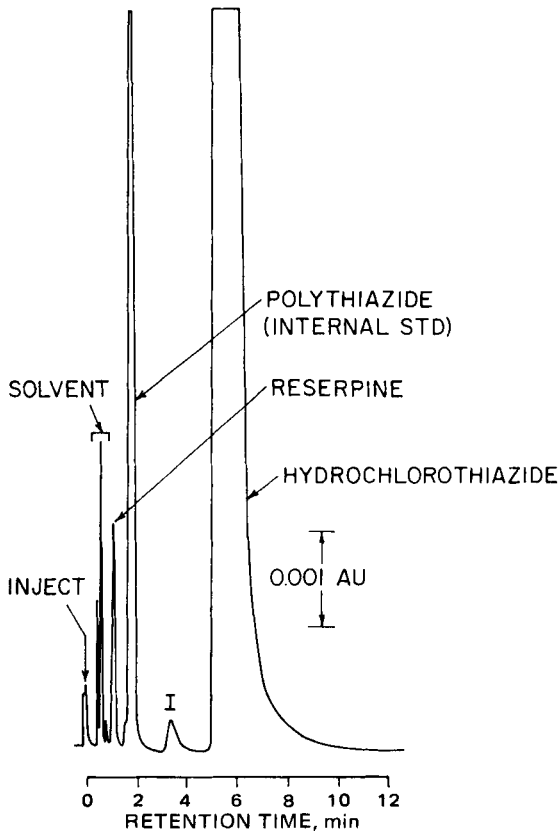

Figure 1—*High-performance liquid chromatogram of a tablet extract containing approximately 0.0125 mg of reserpine/ml, 0.1 mg of polythiazide/ml (internal standard), 2.5 mg of hydrochlorothiazide/ml, and a trace amount of I. Chromatographic conditions are given in the text.*

for the internal standard; and C_D is the concentration (milligrams per milliliter) of reserpine or hydrochlorothiazide.

Quantitation—The percent label claim for reserpine or hydrochlorothiazide was calculated from:

$$\%\ \text{label claim} = \frac{N_D C_I}{N_I \bar{S} W} \times 1000 \qquad \text{(Eq. 2)}$$

where W is the weight (milligrams) of reserpine or hydrochlorothiazide claimed to be present in the tablet or tablet composite analyzed and $\bar{S}$ is the mean slope of the appropriate standard curve.

RESULTS AND DISCUSSION

Chromatography—Previous reports on the HPLC analysis of reserpine–thiazide diuretic mixtures (14, 16) were based upon reversed-phase chromatography. Initial attempts to utilize this mode, employing a microparticulate reversed-phase column[16], were not pursued because the major component, hydrochlorothiazide, eluted ahead of the minor component, reserpine. Since peak shape and column efficiency were not satisfactory, no attempt was made to reverse this order of elution. Instead, a change was made to a forward-phase system with a microparticulate silica gel column. Mobile phase constituents were adjusted to elute reserpine immediately after the solvent front and to elute hydrochlorothiazide later. This system was desirable to maximize the response for reserpine.

The specificity of the procedure for reserpine was tested by chromatographing samples of several related compounds (Table I). Deserpidine[17] and rescinnamine[18], when present, appeared as shoulders on the reserpine peak. The presence of 3-isoreserpine and 3,4-dehydroreserpine in formulations has been reported (19). The former was well separated from reserpine, and the latter was retained on the column. If necessary, formulations can be tested for 3,4-dehydroreserpine by TLC (19).

[12] Canadian Laboratory Supplies, Montreal, Canada.
[13] Multi-Purpose rotator, Scientific Industries, Springfield, Mass.
[14] Model K, International Equipment Co., Needham Heights, Mass.
[15] Micro mill, Chemical Rubber Co., Cleveland, Ohio.
[16] μBondapak C_{18}, Waters Associates, Milford, Mass.
[17] Abbott Laboratories, Montreal, Canada.
[18] NF reference standard.

Table II—Analysis of Synthetic Solutions

Sample	Reserpine			Hydrochlorothiazide		
	Calculated, μg/Injection	Found, μg/Injection	Recovery, %	Calculated, μg/Injection	Found, μg/Injection	Recovery, %
1	0.151	0.152	100.7	15.48	15.69	101.3
2	0.045	0.045	99.7	30.08	30.08	100.0
3	0.090	0.091	100.9	26.64	26.12	98.0
4	0.045	0.044	98.4	25.27	24.89	98.5
5	0.090	0.089	98.9	24.88	25.41	102.1
Mean recovery, %			99.7			100.0
RSD, %			1.1			1.8

Table III—HPLC Analysis of Reserpine–Hydrochlorothiazide Tablet Formulations [a]

Formulation	Reserpine		Hydrochlorothiazide	
	Label, mg	Found [b], %	Label, mg	Found [b], %
A	0.2	96.1	50	101.4
B	0.125	100.1	25	97.8
C	0.125	98.0	25	100.1
D	0.125	101.0	50	98.3
E	0.10	92.7	25	99.2
F	0.20	99.3	50	98.5
G	0.125	100.6	25	98.6

[a] Tablet-composite assay. [b] Percent of label claim.

Trimethoxybenzoic acid[1] and trimethoxycinnamic acid[1], the hydrolysis products of reserpine and rescinnamine, respectively, either did not elute or eluted but were not detected. Samples of reserpic acid and methyl reserpate were not available, but, based on structural considerations, reserpic acid probably would be retained on the column and methyl reserpate would elute ahead of reserpine.

A common impurity in hydrochlorothiazide formulations, 1-amino-3-chloro-4,6-benzenedisulfonamide (I), was observed in several reserpine–hydrochlorothiazide tablet formulations. Comparison to authentic material showed that there was less than 0.5% I relative to the hydrochlorothiazide level in all cases. Figure 1 shows the separation of reserpine, polythiazide, I, and hydrochlorothiazide obtained when an aliquot of a tablet extract was chromatographed. The small shoulder on the front of the polythiazide peak was due to an impurity in the drug substance.

When commercial analytical reagent grade solvents capable of dissolving hydrochlorothiazide at the 5-mg/ml level, such as ethanol, methanol, and tetrahydrofuran, were used for extraction, the solvent front interfered with the reserpine peak. With tetrahydrofuran, this interference proved to be due either to the presence of butylated hydroxyanisole preservative or to tetrahydrofuran decomposition products. When preservative-free tetrahydrofuran[6] was used, satisfactory results were obtained if care was taken to store the solvent under nitrogen.

It may be necessary to adjust the proportion of mobile phase constituents slightly to obtain the desired separation with a particular column. The retention times of hydrochlorothiazide and polythiazide can be lengthened appreciably by increasing the proportion of diethylamine to 0.02–0.03%, or they can be shortened by increasing the proportion of 2-propanol, with only a marginal effect on reserpine retention. The reserpine retention time can be decreased by an increase in the proportion of chloroform, which only slightly affects the retention times of hydrochlorothiazide and polythiazide.

Linearity and Standard Curves—A plot of peak area *versus* the amount of polythiazide (internal standard) injected was linear up to about 1.4 μg/injection (0.2 mg/ml). A 0.1-mg/ml level was used in the analysis.

A standard curve for reserpine was constructed by plotting the ratio of the reserpine peak height to the internal standard peak area *versus* the ratio of the weight of reserpine to the weight of the internal standard. Similarly, a standard curve for hydrochlorothiazide was constructed by plotting the ratio of the hydrochlorothiazide peak area to the internal standard peak area *versus* the corresponding weight ratio.

The standard curve for reserpine, examined over the range of 28–280 ng/injection (4–40 μg/ml), was linear with a negligible intercept up to at least 280 ng/injection. The mean slope of the linear portion of the curve was 0.023 with a relative standard deviation of 1.2%. Similarly, the standard curve for hydrochlorothiazide, examined over the range of 7–70 μg/injection (1–10 mg/ml), was linear with a negligible intercept up to at least 50 μg/injection. The mean slope of the linear portion of the line was 1.08 with a relative standard deviation of 0.6%. Therefore, the standard curves were applicable to tablets containing from 0.04 to 0.40 mg of reserpine and from 10 to 100 mg of hydrochlorothiazide.

Duplicate injections of calibration standard solutions were chromatographed daily to determine the slopes of the standard curves. A check sample also was analyzed daily to confirm that the calibration of the system was accurate and to monitor system stability. This sample was drawn from a homogeneous tablet composite previously analyzed in quintuplicate. The slopes obtained from calibration standards varied over a range of approximately 2.5% during the assay. However, the working relative standard deviations obtained over the same period from check sample data were 1.2% for reserpine and 0.6% for hydrochlorothiazide.

Sample Preparation—The time required for constant extraction of reserpine and hydrochlorothiazide from the tablet mass was determined by tumbling crushed single tablets of a representative formulation for 5, 10, and 15 min in 10 ml of the internal standard solution. In each case, the sample was centrifuged briefly after the appropriate time interval and a 7-μl aliquot was chromatographed. The sample to internal standard peak height or area ratios were identical in all three cases, indicating constant extraction of both compounds in 5 min or less.

Extraction appeared to be complete based on response factor data and the label claim of the formulation examined. This result was proven using a geometric dilution procedure. Tablet-composite samples, equivalent to 0.25-, 0.5-, and 1.0-mg tablets, were prepared from a formulation containing 0.2 mg of reserpine and 50 mg of hydrochlorothiazide and analyzed using a 20-min tumbling time. The concentrations of both reserpine and hydrochlorothiazide in the three composite samples were in the ratio 1:2:4. These data showed that constant and complete extraction of the compounds of interest was effected in 20 min or less.

Repeated injection of an extracted sample showed that, at 22°, reserpine isomerized readily to 3-isoreserpine; cooling to 0° allowed samples to be stored for several hours with negligible isomerization. Accordingly, all samples were prepared only as required and were cooled to 0° as soon as possible after preparation. Because of the known sensitivity of reserpine to photooxidation, all work was performed in a darkened laboratory, and all samples were covered with aluminum foil.

Quantitation—Reproducibility of the chromatographic system was shown by chromatographing six 7-μl aliquots of an extract of a formulation labeled to contain 25 mg of hydrochlorothiazide and 0.125 mg of reserpine. The relative standard deviations of the sample to internal standard peak area ratios for hydrochlorothiazide and reserpine were ±0.64 and ±2.3%, respectively. However, since the relative standard deviation of the reserpine peak height to internal standard peak area ratios was only ±1.2%, this latter approach was used for quantitation of reserpine. The use of peak height for quantitation has the added advantage that accuracy can be maintained in the presence of the small, partially resolved, peaks (20), which occur if related alkaloids are present (*e.g.*, deserpidine and/or rescinnamine).

Five solutions of reserpine and hydrochlorothiazide, prepared in the same manner as the calibration standard solutions, were analyzed. The mean recoveries for the two compounds were 99.7 ± 1.1 and 100.0 ± 1.8%, respectively (Table II).

Five replicate samples of a composite, prepared from tablets labeled to contain 0.125 mg of reserpine and 25 mg of hydrochlorothiazide, were assayed. The relative standard deviations of the assay were ±0.64% for hydrochlorothiazide and ±0.70% for reserpine.

Seven commercial formulations of reserpine–hydrochlorothiazide tablets were analyzed in duplicate. Drug content, expressed as a percentage of the label claim, ranged from 92.7 to 101.0% for reserpine and from 98.3 to 101.4% for hydrochlorothiazide (Table III).

The minimum detectable level of I is approximately 25 ng/injection (2× noise). Therefore, as little as 0.05% of I could be detected in a formulation containing 50 mg of hydrochlorothiazide.

The described procedure is applicable to the determination of reserpine and hydrochlorothiazide in single tablets and in tablet composites. The procedure is unlikely to be suitable for the analysis of commercial reserpine–chlorothiazide formulations because of the poor solubility of chlorothiazide in tetrahydrofuran. However, the procedure should be suitable for the analysis of commercial polythiazide–reserpine formulations and deserpidine–methyclothiazide formulations. It may also be applicable to the analysis of single-component formulations of most of the drugs listed in Table I.

REFERENCES

(1) C. R. Szalkowski and W. J. Mader, *J. Am. Pharm. Assoc., Sci. Ed.*, **45**, 613 (1956).

(2) W. J. Mader, R. P. Haycock, P. B. Sheth, and R. J. Connelly, *J. Assoc. Offic. Agr. Chem.*, **43**, 291 (1960).

(3) T. Urbányi and H. Stober, *J. Pharm. Sci.*, **59**, 1824 (1970).

(4) A. I. Cohen, B. T. Keeler, N. H. Coy, and H. L. Yale, *Anal. Chem.*, **34**, 216 (1962).

(5) "The United States Pharmacopeia," 19th rev., Mack Publishing Co., Easton, Pa., 1975, pp. 235, 438.

(6) H. Kala, *Pharmazie*, **16**, 297 (1961).

(7) A. G. Butterfield and R. W. Sears, *J. Pharm. Sci.*, **66**, 1117 (1977).

(8) T. L. Sprieck, *ibid.*, **63**, 591 (1974).

(9) A. Menharth, F. P. Mahn, and J. E. Heveran, *ibid.*, **63**, 430 (1974).

(10) R. Verpoorte and A. B. Svendren, *J. Chromatogr.*, **100**, 227 (1974).

(11) R. A. Heacock, K. R. Langille, J. D. MacNeil, and R. W. Frei, *ibid.*, **77**, 425 (1973).

(12) M. H. Stutz and S. Sass, *Anal. Chem.*, **45**, 2134 (1973).

(13) G. H. Jolliffe and E. J. Shellard, *J. Chromatogr.*, **81**, 150 (1973).

(14) I. L. Honingberg, J. T. Stewart, A. P. Smith, and D. W. Hester, *J. Pharm. Sci.*, **64**, 1201 (1975).

(15) R. E. Moskalyk, R. A. Locock, L. G. Chatten, A. M. Veltman, and M. F. Bielech, *ibid.*, **64**, 1406 (1975).

(16) I. L. Honingberg, J. T. Stewart, A. P. Smith, R. D. Plunkett, and D. W. Hester, *ibid.*, **63**, 1762 (1974).

(17) R. E. Majors, *Anal. Chem.*, **44**, 1722 (1972).

(18) H. B. MacPhillamy, C. F. Huebner, E. Schlittler, A. F. St. André, and P. R. Ulshafer, *J. Am. Chem. Soc.*, **77**, 4355 (1955).

(19) G. E. Wright and T. Y. Tang, *J. Pharm. Sci.*, **61**, 299 (1972).

(20) L. R. Snyder, *J. Chromatogr. Sci.*, **10** (4), 200 (1972).

Determination of Serum Nadolol Levels by GLC–Selected Ion Monitoring Mass Spectrometry: Comparison with a Spectrofluorometric Method

PHILLIP T. FUNKE, MARY F. MALLEY, EUGENE IVASHKIV, and ALLEN I. COHEN ˣ

Received January 10, 1977, from the *Department of Analytical Research, Squibb Institute for Medical Research, Princeton, NJ 08540.* Accepted for publication August 24, 1977.

Abstract □ A method to determine the serum concentration of the β-adrenergic receptor blocking agent, nadolol, by GLC-selected ion monitoring mass spectrometry of the tri(trimethylsilyl) ether derivative is described. A basic solution of serum was extracted, known amounts of internal standard were added to the extract, and the extract was back-extracted into acidic media and lyophilized. The resulting solids were reacted with *N*-trimethylsilylimidazole. Coded serum samples of 12 subjects, given nadolol alone or in combination with a second drug, were analyzed. The ions at *m/e* 86 and 100 were monitored to establish the relative concentration ratio of nadolol and the internal reference *N*-methylnadolol. No interferences from blood components or other administered drugs were observed. A detection level of 6.95 ng/ml of serum was found.

Keyphrases □ Nadolol—GLC–mass spectrometric analysis in serum □ GLC–mass spectrometry—analysis, nadolol in serum □ Antiadrenergic agents—nadolol, GLC–mass spectrometric analysis in serum

Nadolol, 2,3-*cis*-1,2,3,4-tetrahydro-5-[2-hydroxy-3-(*tert*-butylamino)propoxy]-2,3-naphthalenediol (I), is a potent β-adrenergic receptor blocking agent (1, 2) that has no detectable metabolites (3, 4). With the assumption that no interfering metabolites were present, a fluorescence method previously was developed to determine serum nadolol concentrations (5). The GLC–mass spectrometric method was developed to monitor serum levels by selected ion monitoring, using a modification of the extraction procedure developed for the fluorescence method (5).

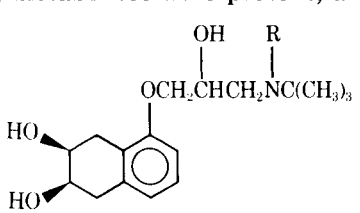

I: R = H

II: R = CH_3

EXPERIMENTAL

Reagents—Methanol, nitric acid, hydrochloric acid, and potassium chloride were reagent grade. Sodium hydroxide[1], *n*-butyl acetate[2], and petroleum ether (bp 30–60°) were used without further purification. Both nadolol[3] (I) and *N*-methylnadolol[3] (II) were used without further purification.

A solution of dimethyldichlorosilane[4] was used to condition the glassware used in the extraction and lyophilization procedures. The compounds were derivatized and the GLC column was conditioned with *N*-trimethylsilylimidazole in pyridine[5] (1.5 mEq/ml), obtained in 1-ml sealed glass ampuls.

Standard Solutions—Just prior to use, a solution of 40 ng of II/ml was prepared in *n*-butyl acetate. A stock solution of 4000 ng of I/ml in 0.1 *N* HCl was used to prepare the standard serum samples.

Glassware—All glassware used in the extraction procedure (150-mm screw-capped test tubes fitted with conical polypropylene liners[6] in plastic caps; 5- and 10-ml serological pipets[7]; 2- and 10-ml volumetric pipets[7]; and 10-, 25-, 50-, and 100-ml and 1- and 2-liter volumetric flasks[7])

[1] Aristar, BDH Chemicals Ltd., Poole, England.

[2] Gold Label-spectrophotometric grade, Aldrich Chemical Co., Milwaukee, Wis.

[3] E. R. Squibb & Sons, Princeton, N.J.

[4] Supelco, Inc., Bellefonte, Pa.; Sylon-CT is dimethyldichlorosilane in toluene (5%).

[5] Tri Sil Z, Pierce Chemical Co., Rockford, Ill.

[6] Catalog No. 24-420, Polyseal Corp., Jersey City, N.J.

[7] Fisher Scientific Co.

REFERENCES

(1) C. R. Szalkowski and W. J. Mader, *J. Am. Pharm. Assoc., Sci. Ed.*, **45**, 613 (1956).

(2) W. J. Mader, R. P. Haycock, P. B. Sheth, and R. J. Connelly, *J. Assoc. Offic. Agr. Chem.*, **43**, 291 (1960).

(3) T. Urbányi and H. Stober, *J. Pharm. Sci.*, **59**, 1824 (1970).

(4) A. I. Cohen, B. T. Keeler, N. H. Coy, and H. L. Yale, *Anal. Chem.*, **34**, 216 (1962).

(5) "The United States Pharmacopeia," 19th rev., Mack Publishing Co., Easton, Pa., 1975, pp. 235, 438.

(6) H. Kala, *Pharmazie*, **16**, 297 (1961).

(7) A. G. Butterfield and R. W. Sears, *J. Pharm. Sci.*, **66**, 1117 (1977).

(8) T. L. Sprieck, *ibid.*, **63**, 591 (1974).

(9) A. Menharth, F. P. Mahn, and J. E. Heveran, *ibid.*, **63**, 430 (1974).

(10) R. Verpoorte and A. B. Svendren, *J. Chromatogr.*, **100**, 227 (1974).

(11) R. A. Heacock, K. R. Langille, J. D. MacNeil, and R. W. Frei, *ibid.*, **77**, 425 (1973).

(12) M. H. Stutz and S. Sass, *Anal. Chem.*, **45**, 2134 (1973).

(13) G. H. Jolliffe and E. J. Shellard, *J. Chromatogr.*, **81**, 150 (1973).

(14) I. L. Honingberg, J. T. Stewart, A. P. Smith, and D. W. Hester, *J. Pharm. Sci.*, **64**, 1201 (1975).

(15) R. E. Moskalyk, R. A. Locock, L. G. Chatten, A. M. Veltman, and M. F. Bielech, *ibid.*, **64**, 1406 (1975).

(16) I. L. Honingberg, J. T. Stewart, A. P. Smith, R. D. Plunkett, and D. W. Hester, *ibid.*, **63**, 1762 (1974).

(17) R. E. Majors, *Anal. Chem.*, **44**, 1722 (1972).

(18) H. B. MacPhillamy, C. F. Huebner, E. Schlittler, A. F. St. André, and P. R. Ulshafer, *J. Am. Chem. Soc.*, **77**, 4355 (1955).

(19) G. E. Wright and T. Y. Tang, *J. Pharm. Sci.*, **61**, 299 (1972).

(20) L. R. Snyder, *J. Chromatogr. Sci.*, **10** (4), 200 (1972).

Determination of Serum Nadolol Levels by GLC–Selected Ion Monitoring Mass Spectrometry: Comparison with a Spectrofluorometric Method

PHILLIP T. FUNKE, MARY F. MALLEY, EUGENE IVASHKIV, and ALLEN I. COHEN ˣ

Received January 10, 1977, from the *Department of Analytical Research, Squibb Institute for Medical Research, Princeton, NJ 08540.* Accepted for publication August 24, 1977.

Abstract □ A method to determine the serum concentration of the β-adrenergic receptor blocking agent, nadolol, by GLC-selected ion monitoring mass spectrometry of the tri(trimethylsilyl) ether derivative is described. A basic solution of serum was extracted, known amounts of internal standard were added to the extract, and the extract was back-extracted into acidic media and lyophilized. The resulting solids were reacted with *N*-trimethylsilylimidazole. Coded serum samples of 12 subjects, given nadolol alone or in combination with a second drug, were analyzed. The ions at *m/e* 86 and 100 were monitored to establish the relative concentration ratio of nadolol and the internal reference *N*-methylnadolol. No interferences from blood components or other administered drugs were observed. A detection level of 6.95 ng/ml of serum was found.

Keyphrases □ Nadolol—GLC–mass spectrometric analysis in serum □ GLC–mass spectrometry—analysis, nadolol in serum □ Antiadrenergic agents—nadolol, GLC–mass spectrometric analysis in serum

Nadolol, 2,3-*cis*-1,2,3,4-tetrahydro-5-[2-hydroxy-3-(*tert*-butylamino)propoxy]-2,3-naphthalenediol (I), is a potent β-adrenergic receptor blocking agent (1, 2) that has no detectable metabolites (3, 4). With the assumption that no interfering metabolites were present, a fluorescence method previously was developed to determine serum nadolol concentrations (5). The GLC–mass spectrometric method was developed to monitor serum levels by selected ion monitoring, using a modification of the extraction procedure developed for the fluorescence method (5).

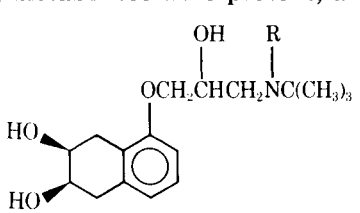

I: R = H

II: R = CH_3

EXPERIMENTAL

Reagents—Methanol, nitric acid, hydrochloric acid, and potassium chloride were reagent grade. Sodium hydroxide[1], *n*-butyl acetate[2], and petroleum ether (bp 30–60°) were used without further purification. Both nadolol[3] (I) and *N*-methylnadolol[3] (II) were used without further purification.

A solution of dimethyldichlorosilane[4] was used to condition the glassware used in the extraction and lyophilization procedures. The compounds were derivatized and the GLC column was conditioned with *N*-trimethylsilylimidazole in pyridine[5] (1.5 mEq/ml), obtained in 1-ml sealed glass ampuls.

Standard Solutions—Just prior to use, a solution of 40 ng of II/ml was prepared in *n*-butyl acetate. A stock solution of 4000 ng of I/ml in 0.1 *N* HCl was used to prepare the standard serum samples.

Glassware—All glassware used in the extraction procedure (150-mm screw-capped test tubes fitted with conical polypropylene liners[6] in plastic caps; 5- and 10-ml serological pipets[7]; 2- and 10-ml volumetric pipets[7]; and 10-, 25-, 50-, and 100-ml and 1- and 2-liter volumetric flasks[7])

[1] Aristar, BDH Chemicals Ltd., Poole, England.

[2] Gold Label-spectrophotometric grade, Aldrich Chemical Co., Milwaukee, Wis.

[3] E. R. Squibb & Sons, Princeton, N.J.

[4] Supelco, Inc., Bellefonte, Pa.; Sylon-CT is dimethyldichlorosilane in toluene (5%).

[5] Tri Sil Z, Pierce Chemical Co., Rockford, Ill.

[6] Catalog No. 24-420, Polyseal Corp., Jersey City, N.J.

[7] Fisher Scientific Co.

Table I—Precision of Peak Measurements

m/e	Average GLC[a] Peak Intensity, mv	Average GLC[b] Peak Area	SD of Area	CV, %
86	511	13,968	214.7	1.54
100	513	16,198	403.3	2.50
100	105	2,642	66.6	2.50
86	81	2,242	61.5	2.70
100	69	1,906	124.6	6.50
100	63	1,793	33.0	1.80

[a] Measurement within ±1 mv. [b] Average of three measurements.

was washed in detergent solution and thoroughly rinsed. After an overnight soak in 3 *N* HCl, the glassware was thoroughly rinsed with distilled water and dried.

Glassware used in the lyophilization and silylation procedures (13 × 100-mm culture tubes[8]; 250-μl conical reaction vials[9]; and 10-, 20-, 50-, and 100-μl micropipets[10]) was treated with hot concentrated nitric acid, thoroughly rinsed with distilled water and methanol, and dried under vacuum at 60°. The dried glassware was then treated with a solution of dimethyldichlorosilane in toluene[4], rinsed with toluene followed by methanol, dried in a vacuum oven at 60°, rinsed again with methanol, and redried under vacuum. The plastic screw caps with conical polypropylene liners[6] were soaked in detergent solution, rinsed thoroughly with distilled water, and air dried. The polytef-lined silicone rubber serum crimp-on caps[11] were soaked in methanol for 0.5 hr and vacuum dried at room temperature.

Extraction of Nadolol from Serum—Serum, 4 ml, was pipetted into a 150-mm screw-capped test tube. A total of 18 samples and six standards were processed at the same time. Three grams of potassium chloride and 2 ml of 5 *N* NaOH were added. The tubes were sealed with plastic screw caps with conical polypropylene liners[6] and shaken on a reciprocal action (300 strokes/min) shaker for 5 min. A 10-ml aliquot of II standard solution was added and the tubes were resealed, shaken for 5 min, and immediately centrifuged for 10 min[12] at 3000 rpm.

The phases were allowed to separate, and 8 ml of the butyl acetate layer (top) was transferred to a clean 150-mm test tube containing 2 ml of 0.1 *N* HCl and 20 ml of petroleum ether. After sealing, the tubes were shaken for 5 min and centrifuged at 3000 rpm for 5 min; then the top *n*-butyl acetate–petroleum ether layer was aspirated and discarded. The process was repeated after the addition of 10 ml of petroleum ether, sealing, shaking for 2 min, centrifuging for 2 more min, and removing the top petroleum ether layer by aspiration and discarding it[13].

Lyophilization of Aqueous Extract and Derivatization of Samples—The acidified solution was transferred with a silanized Pasteur pipet to a 13 × 100-mm silanized culture tube. The test tube walls were

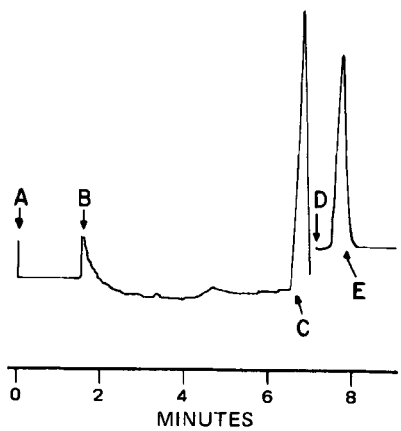

Figure 1—*Gas chromatogram of I and II monitored at* m/e *86 and 100, respectively. Key: A, point of injection; B,* m/e *86 monitored; C, peak of I monitored at* m/e *86; D,* m/e *100 monitored; and E, peak of II monitored at* m/e *100.*

[8] Catalog No. 9820, Corning Corp., Corning, N.Y.
[9] Catalog No. 4330-0540, Hewlett-Packard Corp.
[10] Wiretrol pipets, Drummond Scientific Co., Broomall, Pa.
[11] Catalog No. 5080-8713, Hewlett-Packard Corp.
[12] International centrifuge with horizontal head (IEC-266).
[13] A recovery of at least 60–70% of nadolol was obtained in the preliminary extraction procedure; however, 100% recoveries were observed in the fluorescence method (5) on which the extraction is based.

Table II—Limit of Detection of Nadolol in Serum[a]

Calibration	B_I	$\sigma_B \times 10^3$	$S \times 10^3$	N_L, ng	C_L, ng/ml of serum
1	0.0963	8.44	2.64	9.59	2.40
2	0.205	9.76	2.57	11.4	2.85
3	0.614	39.5	4.26	27.8	6.95
4	0.252	38.9	4.20	27.8[b]	6.95

[a] σ_B = standard deviation of blank values (B_I); B_I = average of intercept; S = slope of calibration curve determined by linear regression; $N_L = 3\sigma_B/S$, the minimum detection limit with a practical confidence level of 90%, in nanograms; $C_L = N_L/4$, the concentration detection limit in nanograms per milliliter of serum; and N = quantity of nadolol in nanograms. Area I/Area II = $B_L + S(N)$. [b] Only two measurements; other values are average of three measurements.

washed down with 0.5-ml aliquots of 0.1 *N* HCl, which were added to the culture tubes containing the acidified aqueous extract. The sample solutions were then frozen in dry ice for 30 min, and the solutions were lyophilized until all water had been removed. Then the tube walls were

Table III—Comparison of GLC–Mass Spectrometric Data with Fluorometric Data of Coded Human Serum after Administration of a Single Oral Dose of 80 mg of Nadolol

Patient	Leg	Drug	Sample Time, hr	GLC–Mass Spectrometric, ng/ml	Fluorometric, ng/ml
1	1	I	4	30.9	64.7
			12	22.1	35.2
	2	I + IV	1	66.1	74.7
			12	31.4	31.2
2	1	I + III	0	0.00	0.0
			2	38.3	37.2
			9	25.9	23.2
	2	I	9	25.4	22.9
3	1	I	6	39.4	36.9
			24	17.8	22.8
	2	I + III	2	99.5	96.0
			6	60.4	78.9
4	1	I + IV	1	18.5	11.4
			4	38.0	50.0
			12	16.3	24.0
	2	I	2	57.0	59.7
			12	29.6	37.3
5	1	I + IV	2	12.7	56.1
			24	33.9	38.0
	2	I	3	102.5	77.4
			6	49.1	52.5
			24	26.8	24.7
6	1	I + III	2	81.1	103.0
			9	19.5	32.8
			48	0.00	7.4
	2	I + IV	3	65.5	95.2
			12	17.4	29.4
			48	10.0	7.3
7	1	I + III	0	0.00	0.0
			3	87.1	67.8
			12	21.7	24.6
	2	I	1	10.4	17.1
			3	12.1	25.9
			12	12.0	14.7
8	1	I	0	0.00	1.5
			6	189.9	169.1
	2	I + III	6	60.2	77.4
			12	37.9	35.1
9	1	I + III	4	31.4	39.1
			9	33.9	46.3
			48	25.9	11.7
	2	I + III	0	0.00	3.3
			4	65.1	79.5
10	1	I	3	86.6	41.0
			6	30.9	33.7
			9	24.6	24.7
	2	I + IV	0	0.0	2.0
			6	28.6	24.3
			24	13.3	10.8
11	1	I + III	4	57.5	58.5
			6	30.7	36.9
			24	13.8	16.0
	2	I + IV	4	27.9	39.2
12	1	I + IV	0	3.3	2.0
			4	48.7	129.0
			9	23.1	35.0
	2	I + III	3	177.5	182.0
			6	48.9	75.1

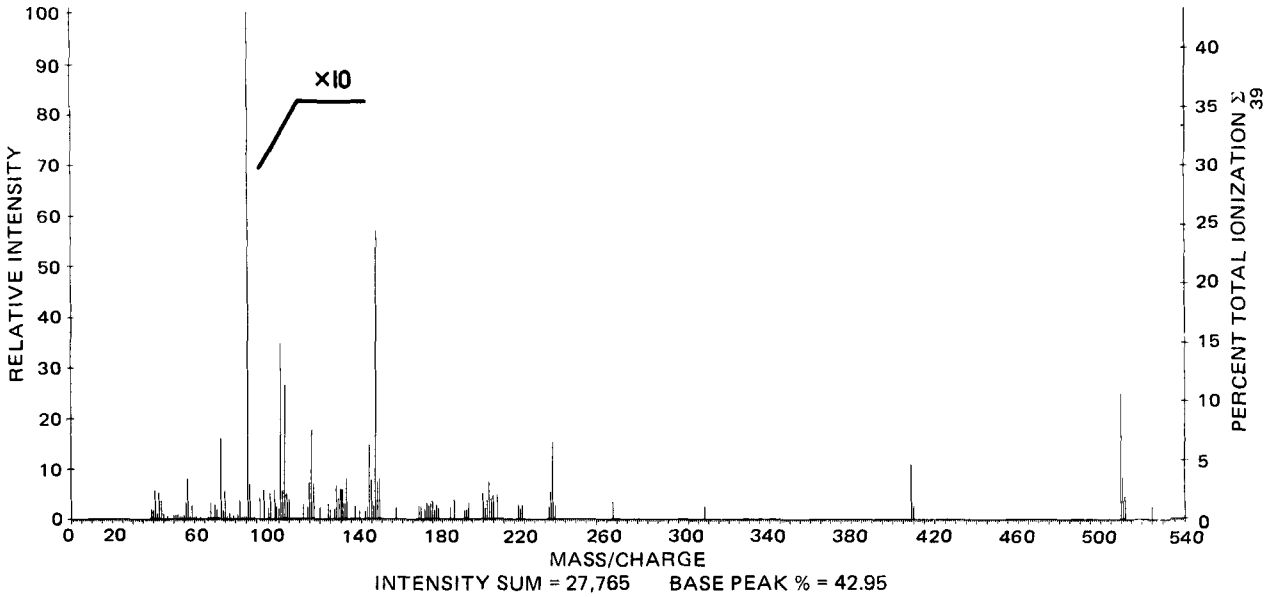

Figure 2—*Electron-impact mass spectrum of the tri(trimethylsilyl) ether of I.*

washed down with 0.5 ml of methanol, and the solvent was removed by evaporation under vacuum at room temperature.

Methanol was added again and evaporated to deposit the sample and internal reference in the bottom of the culture tube. The solids were dissolved in 100 μl of methanol, and this solution was transferred to a 250-μl conical reaction vial and evaporated to dryness under vacuum at room temperature. This process was performed six times to ensure a complete transfer. The extracted samples were reacted with 40 μl of *N*-trimethylsilylimidazole in pyridine in sealed vials for at least 10 hr at room temperature.

Calibration Curves—The standard curves were constructed with 4-ml serum samples containing 0, 80, 160, 240, 320, and 400 ng of I in 0.1 *N* HCl by the addition of the appropriate volume of stock solution. These serum samples were extracted by the recommended procedure already described. In one instance, 200 ng of internal reference was added to the 10 ml of extract. The average of the data generated from multiple injections of each standard solution was fitted to a straight line by linear regression analysis.

GLC—A temperature-programmed gas chromatograph[14] was equipped with a 1.8-m × 3-mm i.d. silanized glass column packed with 3% OV-1 on silanized 80–100-mesh support[15]. The column was connected directly to the inlet of the mass spectrometer by a 1.6-mm o.d. silanized glass-lined stainless steel[16] transfer line. Both the inlet line and the injector were maintained at 270°; the column temperature was programmed from 230 to 270° at 7.5°/min, commencing at the time of injection. The helium carrier gas[17] was dried[18] and regulated at 6.5 ml/min.

The syringe[19] was filled with 0.25 μl of *N*-trimethylsilylimidazole solution followed by 0.5–1.0 μl of sample. Samples were injected in random order, and at least two measurements were obtained for each reaction solution. No sample was injected consecutively. The retention time of I was approximately 6.7 min, and the relative retention index of II to I was 1.1 (Fig. 1).

Mass Spectrometry—The quadrupole mass spectrometer[20] was modified for differential pumping with 300- and 700-liters/min diffusion pumps on the source and analyzer, respectively. The gas chromatograph inlet was modified to enter axially to the electron-impact source and in-line-of-sight of the detector. The electron energy was maintained at 100 ev with an ion energy of 9 ev and a total emission of up to 1 mamp. The relative sensitivities of the *m/e* 86 and 100 ions were maintained constant by adjusting the ratio of the dc voltage to the Rf peak-to-peak voltages slightly, using a solution of 20 ng of each component, silanized, because some systematic drift occurred as a result of processing a number of samples over a period of time.

The computer[21] was interfaced to the mass spectrometer to control the selection of the ions and to measure the areas of GLC peaks generated by monitoring the *m/e* 86 and 100 ions of I and II, respectively (Fig. 1).

To maximize the signal-to-noise ratio (S/N), each selected ion was measured 512 times for 200 msec, producing a theoretical 22-fold enhancement. Approximately 50 points were taken for each GLC peak of I and the standard II.

RESULTS AND DISCUSSION

Initially, preparation of suitable derivatives of I and II for GLC posed some problems. Attempts to prepare the trifluoroacyl derivatives with anhydrides (6) yielded poorly defined mixtures of unknown composition. The recent report of Claeys *et al.* (7) indicated the difficulties in using these powerful acylating agents. Silylating agents containing chlorotrimethylsilane were rejected because the hydrogen chloride produced in the reaction forms salts with I and II and *N,O*-bis(trimethylsilyl)trifluoroacetamide[22] typically formed a mixture of di- and tri(trimethylsilyl) derivatives. Even with trimethylsilylimidazole, which consistently formed tri(trimethylsilylated) derivatives of I and II, care was exercised to eliminate water from the carrier gas, the column, and transfer lines to prevent partial hydrolysis, which would result in subsequent "ghosting." Because all samples were coded, it was extremely important that injection of prior samples, which may have had high levels of I, would not interfere with the measurement of low levels in subsequent samples. The GLC peaks (Fig. 1) indicate that little tailing occurred.

The electron-impact mass spectrum[23] of the tri(trimethylsilyl) ether derivative of I (Fig. 2) shows that the *m/e* 86 ion is 43% of the total ion current (summed from *m/e* 39 to 540) and that the corresponding *m/e* 100 ion of the silyl derivative of II (Fig. 3) is 37% of the total ion current (summed from *m/e* 39 to 540). While differences in relative intensities could be ascribed to instrument design, it was anticipated that the response of the base ions in the quadrupole mass spectrometer would be of the same order, if not identical.

No interferences were detected at the relatively low mass ions of *m/e* 86 and 100 from the extracts of fresh human serum obtained from a clinical study. However, significant interferences were observed with several commercial serum samples at these masses. These samples may have decomposed, but it is more likely that plastics or rubber components may have been inadvertently introduced during their preparation. As a precaution, polytef-lined caps were used with the silylation reaction vials and all caps used in the extraction procedure were lined with polypropylene. No changes were required in the methods of drawing human blood or in the preparation of serum, which was conducted under the supervision of the clinical monitor.

Errors that could be encountered in measurement of the areas of GLC

[14] Barber-Colman model 5170, G. D. Searle, Chicago, Ill.
[15] Supelco, Inc., Bellefonte, Pa.; Supelcoport is acid-washed silane-treated diatomite.
[16] Catalog No. 2-2378, 0.3-mm i.d., Supelco, Inc., Bellefonte, Pa.
[17] Ultrahigh purity, Union Carbide Inc.
[18] Gas purifier model 2-2316, Supelco, Inc., Bellefonte, Pa.
[19] Catalog No. 85-N, 5 μl, Hamilton.
[20] Electronic Associates, Long Branch, N.J.
[21] Model PDP 11/05, 16K core, Digital Equipment Corp., Maynard, Mass.
[22] BSTFA, Pierce Chemical Co., Rockford, Ill.
[23] AEI MS902.

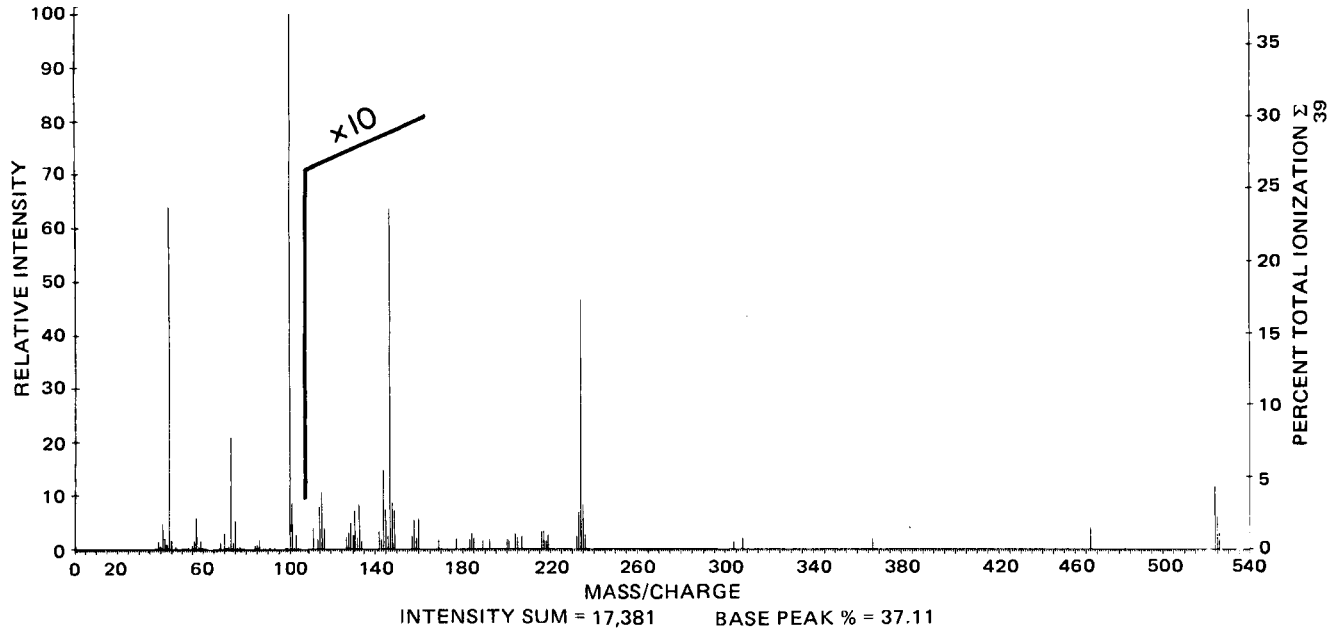

Figure 3—*Electron-impact mass spectrum of the tri(trimethylsilyl) ether of II.*

peaks are variation in peak shape, threshold detection, baseline corrections, and noise. The precision of measurement of several levels is summarized in Table I. With the exception of one 69-mv peak, the coefficient of variation ranged from 1.5 to 2.7% for peaks differing significantly in area. Thus, 0.5 ng of I injected on-column yields 2500 area units with a coefficient of variation of approximately 3% or less.

The calibration curves were made from serum samples to which both I and II were added prior to extraction or by the addition of I to serum and II to the *n*-butyl acetate extract, but no appreciable differences were observed. Therefore, II was added to the *n*-butyl acetate, permitting the convenient addition of known amounts from a stock solution to each sample. This procedure eliminated a source of error within the group of unknown and standard samples.

The standard deviation of the blank values, and the calculated detection limits (8), indicate the overall precision attainable (Table II). The overall detection limit, N_L, for four calibration curves varied from 9.6 to 27.8 ng of I or from 2.4 to 6.95 ng of I/ml of serum. In general, the detection level would be less than 7.0 ng/ml of serum[24] with a sensitivity equal to or less than the detection limit.

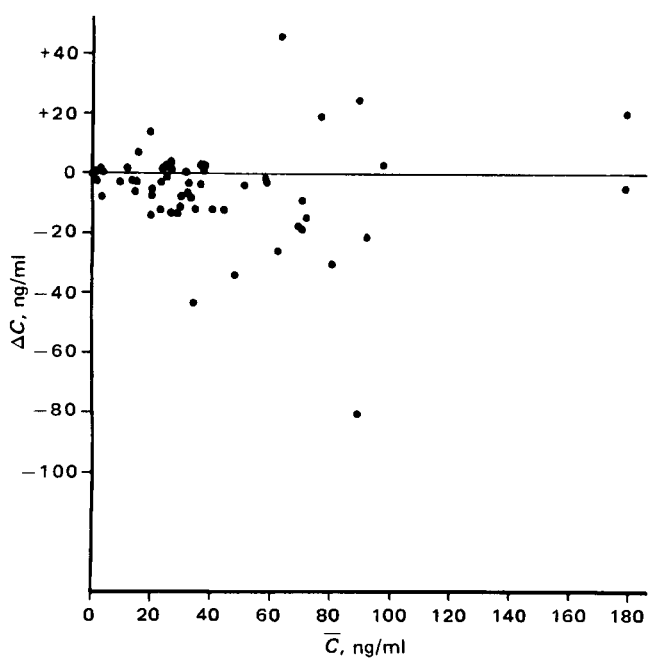

Figure 4—*Plot of difference between assays, ΔC (GLC–mass spectrometric − fluorometric)* versus *the average of the assays, C̄.*

Duplicate samples of blood were randomly sampled and coded for analysis by both the fluorescence method and the GLC–mass spectrometric method. In the study, subjects were given a single oral dose of 80 mg of I alone, in combination with hydrochlorothiazide (III), or in combination with furosemide (IV) (Table III). When a subject was given a second dose, a 2-week washout period intervened.

The data were correlated by linear regression analysis, which yielded a correlation coefficient of 0.9. Because there was a systematic trend indicating that the fluorometric results were greater than the GLC–mass spectrometric data, the difference between the two assays *versus* the average of the assays was plotted (9) (Fig. 4). Sixteen data sets fell above the $\Delta C = 0$ horizontal (GLC–mass spectrometric greater than fluorometric), four sets fell on the horizontal, and 37 sets fell below the horizontal (fluorometric greater than GLC–mass spectrometric).

The GLC–mass spectrometric data confirm the assumption that the fluorometric data represent a measure of the nadolol level in blood. The fluorometric method is more readily adaptable to processing a large number of samples, while the GLC–mass spectrometric method should be selected when specificity is required or when extremely low serum levels are to be measured.

REFERENCES

(1) D. B. Evans, M. T. Peschka, R. J. Lee, and R. J. Laffan, *Eur. J. Pharmacol.*, **35**, 17 (1976).

(2) R. A. Vukovich, S. Sanchez-Zambrano, A. Sasahara, L. J. Brannick, J. Belko, and P. Godin, presented at the 77th meeting of the American Society for Clinical Pharmacology and Therapeutics, Seattle, Wash., Mar. 1976.

(3) R. A. Vukovich, J. Dreyfuss, L. J. Brannick, J. Herrera, and D. A. Willard, presented at the 5th annual meeting of the American College of Clinical Pharmacology, Philadelphia, Pa., Apr. 30, 1976.

(4) K. K. Wong, J. Dreyfuss, J. M. Shaw, J. J. Ross, and E. C. Schreiber, *Pharmacologist*, **15**, 245 (1973) (Abstract 505).

(5) E. Ivashkiv, *J. Pharm. Sci.*, **66**, 1168 (1977).

(6) T. Walle, *ibid.*, **63**, 1885 (1974).

(7) M. Claeys, G. Muscettola, and S. P. Markey, *Biomed. Mass Spectrom.*, **3**, 110 (1976).

(8) J. D. Winefordner, in "Trace Analysis: Spectroscopic Methods for Elements," J. D. Winefordner, Ed., Wiley, New York, N.Y., 1976, chap. 1.

(9) P. G. Welling, K. P. Less, U. Khanna, and J. G. Wagner, *J. Pharm. Sci.*, **59**, 1621 (1970).

[24] The standard deviation of six patient blanks was 3.8 ng/ml of serum.

ACKNOWLEDGMENTS

Correlation and coding of serum samples were under the direction of Dr. D. Griffith, Clinical Pharmacology, who directed the human studies. The authors thank Mr. O. R. Kocy for the extraction of some early samples. The mass spectrometer conversion was greatly facilitated by Mr. C. Harter, Harter Tool and Die, Pennington, N.J., who fabricated the flanging for the vacuum system and new source components, under the direction of P. T. Funke. The contributions of Mr. T. Altman for the design and fabrication of the mass spectrometer–computer interface and of Mr. K. Schroeder for the computer program are also acknowledged.

Relationships between Chemical Structure and Inhibition of Human Placental Choline Acetyltransferase by Keto Analogs of Acetylcholine

ARVIND K. CHATURVEDI, PETER P. ROWELL, and B. V. RAMA SASTRY ˣ

Received May 13, 1977, from the *Department of Pharmacology, Vanderbilt University School of Medicine, Nashville, TN 37232.* Accepted for publication August 24, 1977.

Abstract □ Seven keto analogs of acetylcholine were synthesized and evaluated as inhibitors of human placental choline acetyltransferase. Their potencies for inhibition of horse serum cholinesterase and stimulation of cholinergic receptors in the longitudinal ileal muscle of the guinea pig were investigated. The most potent and selective inhibitor of choline acetyltransferase was (2-benzoylethyl)trimethylammonium chloride with an I_{50} of 3×10^{-6} *M*. It exhibited considerably low activities at muscarinic and nicotinic receptors and cholinesterases. Its high potency for inhibiting choline acetyltransferase was attributed to: (*a*) its cationic terminal, a site for an electron acceptor interaction; (*b*) an aryl moiety for hydrophobic and electron donor contributions; and (*c*) a positive charge on the carbon atom adjacent to the benzene ring due to the presence of the carbonyl group, which interacts with the nucleophilic residue on the enzyme.

Keyphrases □ Acetylcholine analogs, various—synthesized, evaluated as inhibitors of choline acetyltransferase □ Choline acetyltransferase activity—various acetylcholine analogs evaluated as inhibitors □ Enzyme activity—various acetylcholine analogs evaluated as inhibitors of choline acetyltransferase □ Structure–activity relationships—various acetylcholine analogs evaluated as inhibitors of choline acetyltransferase

Acetylcholine is synthesized *in vivo via* a coupled system involving an acetate-activating enzyme (acetyl coenzyme A synthetase) and an enzyme, choline acetyltransferase, that couples the activated acetate to choline. Therefore, an agent that inhibits the final step in the acetylcholine synthetic pathway is valuable for studying cholinergic mechanisms.

The lack of a suitable strong inhibitor has hampered study of cholinergic mechanisms related to this enzyme. Recently, 4-(1-naphthylvinyl)pyridine ($I_{50} = \sim 10^{-6}$ *M*) and related compounds were introduced (1–4) as inhibitors of choline acetyltransferase. These *trans*-isomers photoisomerize readily in solution to *cis*-isomers, which are poor inhibitors of choline acetyltransferase (4). During exposure to daylight, their use is limited for obtaining reliable data in *in situ* and *in vivo* pharmacological experiments.

Monohaloacetylcholines were synthesized, and their pharmacological activities were studied (5–10). Among haloacetylcholines, chloro-, bromo-, and iodoacetylcholines ($I_{50} = \sim 10^{-7}$–10^{-6} *M*) were strong specific inhibitors of choline acetyltransferase (11–15). However, they were hydrolyzed by cholinesterases (7, 8). The tertiary analogs of haloacetylcholines were less potent inhibitors of choline acetyltransferase than the corresponding quaternary ammonium compounds (15, 16). Persson (17, 18) prepared chloro-, bromo-, and iodoacetonyltrimethylammonium halides that inhibited choline acetyltransferase ($I_{50} = \sim 10^{-5}$–10^{-4} *M*). They were not chemically stable, and their specificity for inhibiting choline acetyltransferase is not known.

Haubrich and Wang (19) demonstrated that 5-hydroxy-1,4-naphthoquinone (juglone from the extract of walnut hulls) inhibits choline acetyltransferase. The selectivity of this inhibitor is not established. Several naphthoquinones were shown to inhibit acetylcholine formation in coupled acetylcholine synthesis using multienzyme systems (20). Recently, it was demonstrated (21, 22) that several thiol reagents inhibit choline acetyltransferase. However, these reagents inhibit all sulfhydryl-containing enzymes and are not specific for choline acetyltransferase.

All of these observations indicate that a highly potent, selective, and stable inhibitor has yet to be synthesized. Therefore, (2-benzoylethyl)trimethylammonium chloride and related compounds were synthesized and tested for their inhibition of choline acetyltransferase and their activities at various cholinergic sites (muscarinic receptors, nicotinic receptors, and cholinesterases).

EXPERIMENTAL

Materials—All compounds were keto analogs of acetylcholine and satisfied some requirements necessary for the inhibition of choline acetyltransferase. All were characterized by their sharp melting point, elemental analyses[1], and IR spectra[2]. Wherever necessary, they also were identified by UV absorption and NMR spectra. Their chemical structures and other characteristics are shown in Table I. Their interactions with various cholinergic sites are summarized in Table II.

4-Oxopentyltrimethylammonium Perchlorate (I)—Compound I was prepared by keeping an equimolar mixture (1.3 moles) of anhydrous trimethylamine and 5-chloro-2-pentanone in 150 ml of anhydrous ether in a pressure bottle at room temperature for 14 days. After this time, the separated solid (58.1 g, 24.8%) was filtered and dissolved in 100 ml of

[1] Performed by Galbraith Laboratories, Knoxville, TN 37921.

[2] Obtained with a Perkin-Elmer model 257 grating IR spectrophotometer equipped with sodium chloride optics in potassium bromide films in the range of 625–4000 cm^{-1}.

ACKNOWLEDGMENTS

Correlation and coding of serum samples were under the direction of Dr. D. Griffith, Clinical Pharmacology, who directed the human studies. The authors thank Mr. O. R. Kocy for the extraction of some early samples. The mass spectrometer conversion was greatly facilitated by Mr. C. Harter, Harter Tool and Die, Pennington, N.J., who fabricated the flanging for the vacuum system and new source components, under the direction of P. T. Funke. The contributions of Mr. T. Altman for the design and fabrication of the mass spectrometer–computer interface and of Mr. K. Schroeder for the computer program are also acknowledged.

Relationships between Chemical Structure and Inhibition of Human Placental Choline Acetyltransferase by Keto Analogs of Acetylcholine

ARVIND K. CHATURVEDI, PETER P. ROWELL, and B. V. RAMA SASTRY ˣ

Received May 13, 1977, from the *Department of Pharmacology, Vanderbilt University School of Medicine, Nashville, TN 37232.* Accepted for publication August 24, 1977.

Abstract □ Seven keto analogs of acetylcholine were synthesized and evaluated as inhibitors of human placental choline acetyltransferase. Their potencies for inhibition of horse serum cholinesterase and stimulation of cholinergic receptors in the longitudinal ileal muscle of the guinea pig were investigated. The most potent and selective inhibitor of choline acetyltransferase was (2-benzoylethyl)trimethylammonium chloride with an I_{50} of 3×10^{-6} *M*. It exhibited considerably low activities at muscarinic and nicotinic receptors and cholinesterases. Its high potency for inhibiting choline acetyltransferase was attributed to: (*a*) its cationic terminal, a site for an electron acceptor interaction; (*b*) an aryl moiety for hydrophobic and electron donor contributions; and (*c*) a positive charge on the carbon atom adjacent to the benzene ring due to the presence of the carbonyl group, which interacts with the nucleophilic residue on the enzyme.

Keyphrases □ Acetylcholine analogs, various—synthesized, evaluated as inhibitors of choline acetyltransferase □ Choline acetyltransferase activity—various acetylcholine analogs evaluated as inhibitors □ Enzyme activity—various acetylcholine analogs evaluated as inhibitors of choline acetyltransferase □ Structure–activity relationships—various acetylcholine analogs evaluated as inhibitors of choline acetyltransferase

Acetylcholine is synthesized *in vivo via* a coupled system involving an acetate-activating enzyme (acetyl coenzyme A synthetase) and an enzyme, choline acetyltransferase, that couples the activated acetate to choline. Therefore, an agent that inhibits the final step in the acetylcholine synthetic pathway is valuable for studying cholinergic mechanisms.

The lack of a suitable strong inhibitor has hampered study of cholinergic mechanisms related to this enzyme. Recently, 4-(1-naphthylvinyl)pyridine ($I_{50} = \sim 10^{-6}$ *M*) and related compounds were introduced (1–4) as inhibitors of choline acetyltransferase. These *trans*-isomers photoisomerize readily in solution to *cis*-isomers, which are poor inhibitors of choline acetyltransferase (4). During exposure to daylight, their use is limited for obtaining reliable data in *in situ* and *in vivo* pharmacological experiments.

Monohaloacetylcholines were synthesized, and their pharmacological activities were studied (5–10). Among haloacetylcholines, chloro-, bromo-, and iodoacetylcholines ($I_{50} = \sim 10^{-7}$–10^{-6} *M*) were strong specific inhibitors of choline acetyltransferase (11–15). However, they were hydrolyzed by cholinesterases (7, 8). The tertiary analogs of haloacetylcholines were less potent inhibitors of choline acetyltransferase than the corresponding quaternary ammonium compounds (15, 16). Persson (17, 18) prepared chloro-, bromo-, and iodoacetonyltrimethylammonium halides that inhibited choline acetyltransferase ($I_{50} = \sim 10^{-5}$–10^{-4} *M*). They were not chemically stable, and their specificity for inhibiting choline acetyltransferase is not known.

Haubrich and Wang (19) demonstrated that 5-hydroxy-1,4-naphthoquinone (juglone from the extract of walnut hulls) inhibits choline acetyltransferase. The selectivity of this inhibitor is not established. Several naphthoquinones were shown to inhibit acetylcholine formation in coupled acetylcholine synthesis using multienzyme systems (20). Recently, it was demonstrated (21, 22) that several thiol reagents inhibit choline acetyltransferase. However, these reagents inhibit all sulfhydryl-containing enzymes and are not specific for choline acetyltransferase.

All of these observations indicate that a highly potent, selective, and stable inhibitor has yet to be synthesized. Therefore, (2-benzoylethyl)trimethylammonium chloride and related compounds were synthesized and tested for their inhibition of choline acetyltransferase and their activities at various cholinergic sites (muscarinic receptors, nicotinic receptors, and cholinesterases).

EXPERIMENTAL

Materials—All compounds were keto analogs of acetylcholine and satisfied some requirements necessary for the inhibition of choline acetyltransferase. All were characterized by their sharp melting point, elemental analyses[1], and IR spectra[2]. Wherever necessary, they also were identified by UV absorption and NMR spectra. Their chemical structures and other characteristics are shown in Table I. Their interactions with various cholinergic sites are summarized in Table II.

4-Oxopentyltrimethylammonium Perchlorate (I)—Compound I was prepared by keeping an equimolar mixture (1.3 moles) of anhydrous trimethylamine and 5-chloro-2-pentanone in 150 ml of anhydrous ether in a pressure bottle at room temperature for 14 days. After this time, the separated solid (58.1 g, 24.8%) was filtered and dissolved in 100 ml of

[1] Performed by Galbraith Laboratories, Knoxville, TN 37921.

[2] Obtained with a Perkin-Elmer model 257 grating IR spectrophotometer equipped with sodium chloride optics in potassium bromide films in the range of 625–4000 cm^{-1}.

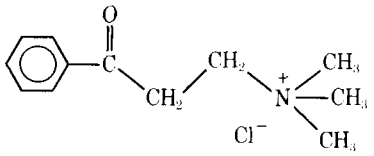

VII: (2-benzoylethyl)trimethylammonium chloride

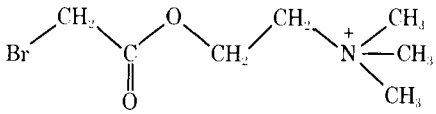

VIII: bromoacetylcholine

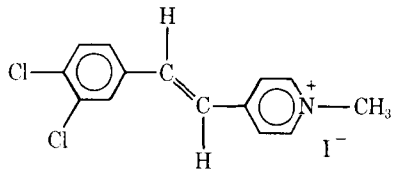

IX: 3',4'-dichloro-4-stilbazole methiodide

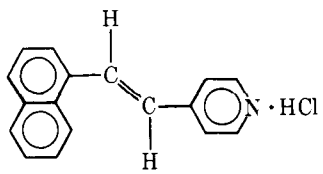

X: 4-(1-naphthylvinyl)pyridine

ice-cold absolute ethanol. To this solution, 32.5 g (46.4 ml) of 70% perchloric acid was added. A brown crystalline precipitate separated and was filtered and recrystallized from ethanol–ethyl acetate. The final product was obtained as colorless crystals.

4-[2-(1,3-Dioxolanyl)]pentyltrimethylammonium Chloride (II)—To an ice-cold solution of 50.0 g (0.304 mole) of 5-chloro-2-[2-(1,3-dioxolanyl)]pentane in 100 ml of dry toluene, 26.8 ml of anhydrous trimethylamine was added. The reaction mixture was kept in a pressure bottle for 7 days. The separated salt was filtered and recrystallized as a colorless product from acetonitrile–ethyl acetate.

1-Trimethylammonium-4-oxoheptyltrimethylammonium Diperchlorate (III)—An ice-cold solution of 1,7-dichloro-4-heptanone (40.0 g, 0.219 mole) in 100 ml of ether was treated with 38.5 ml of anhydrous trimethylamine. The reaction mixture thus obtained was kept in a pressure bottle at 40° for 7 days. The reaction product (43 g, 66%), a viscous mass, was dissolved in 75 ml of ice-cold absolute ethanol, and 20.7 ml of 70% perchloric acid was added. A brown crystalline precipitate (30 g) separated and was filtered and recrystallized from ethanol–water.

Ethyl 4-Trimethylammoniumbutyrate Chloride (IV)—Compound IV was prepared by keeping a mixture of ethyl 4-chlorobutyrate (50.0 g, 0.339 mole) and anhydrous trimethylamine (19.6 g, 0.339 mole) in 150 ml of dry toluene in a pressure bottle at room temperature for 15 days. The separated solid was filtered and recrystallized from acetonitrile as colorless crystals.

(3-Thenoylpropyl)trimethylammonium Chloride (V)—This compound was synthesized in the same manner as IV from 50.0 g (0.264 mole) of γ-chloro-2-butyrothienone and 23.3 ml of anhydrous trimethylamine. The product was recrystallized as light-brown prisms from isopropyl alcohol.

(3-Benzoylpropyl)trimethylammonium Chloride (VI)—Compound VI was prepared according to the procedure described for IV from 50 g (0.273 mole) of γ-chloro-2-butyrophenone and 24.1 ml of anhydrous trimethylamine. Upon recrystallization from ethanol–ethyl acetate, colorless needles were obtained.

(2-Benzoylethyl)trimethylammonium Chloride (VII)—This compound was synthesized by the procedures described for IV from 26.1 ml of anhydrous trimethylamine and 50 g (0.296 mole) of β-chloropropionophenone. The reaction product was recrystallized from isopropyl alcohol as colorless crystals.

Choline Acetyltransferase—Full-term human placentas were used as a source of enzyme. The enzyme was prepared and partially purified according to the methods described by Sastry and Henderson (23).

Inhibition of Choline Acetyltransferase—Modifications of previous methods (23, 24) were used for measuring choline acetyltransferase activity. The assay was performed in 75 × 10-mm test tubes, and the incubation medium consisted of 0.6 ml of potassium phosphate buffer (50 m*M*, pH 7.4) containing 300 m*M* NaCl, 0.2 m*M* physostigmine sulfate, 20 m*M* $MgSO_4$, 0.5 m*M* choline iodide, 3.36×10^{-5} *M* acetyl coenzyme A with 0.33 μCi of 1-^{14}C-acetyl coenzyme A, 1 mg of freeze-dried choline acetyltransferase/ml, 6.67 m*M* NaCN, 1.67 m*M* edetate disodium, and variable amounts of inhibitors.

After 10 min of incubation at 37°, 0.6 ml of ice-cold water was added to stop the reaction. The tubes were chilled in ice, and a 0.2-ml aliquot of the incubation mixture was placed immediately on a column (12 × 1 cm) of an anion-exchange resin[3]. The column was washed with 0.5 ml of deionized water four times. The effluent was collected in a scintillation vial, 15 ml of counting solution[4] was added, and the vial was cooled to 4° for 24 hr prior to being placed in a refrigerated liquid scintillation counter[5]. The radioactivity in the vial was proportional to the ^{14}C-acetylcholine formed.

Cholinesterase—This enzyme was prepared commercially[6] by a modified literature procedure (25) from horse serum and supplied as a stable lyophilized powder containing about 5 units/mg. One unit was equal to 1 μmole of acetylcholine hydrolyzed/min.

Inhibition of Cholinesterase—The ability of I–VII to inhibit cholinesterase activity was determined by the method of Ellman *et al.* (26). In this method, acetylthiocholine is hydrolyzed to thiocholine and acetic acid. Thiocholine reacts with 5,5-dithiobis-2-nitrobenzoate[7] to give the yellow 5-thio-2-nitrobenzoic anion. The reaction mixture consisted of 3 ml of sodium phosphate buffer (pH 8.0, 10 m*M*) containing 5,5-dithiobis-2-nitrobenzoate (0.32 m*M*), cholinesterase (0.01 mg/ml), acetylthiocholine (0.6 m*M*), and appropriate amounts of inhibitors. The absorbance was measured[8] every 2 min for 15 min at 412 nm, corresponding to the amount of acetylthiocholine hydrolyzed.

Stimulation of Cholinergic Receptors by I–VII—The effects of the new compounds were studied on the isolated longitudinal ileal muscle of the guinea pig by measuring their muscarinic and nicotinic activities according to the general methods previously described (10, 27). Longitudinal ileal muscles (2 cm in length) were obtained from male guinea pigs of common strain (200–400 g), which were sacrificed by blows on their heads. The muscles were suspended in organ baths containing 20 ml of pH 7.4 Tyrode solution, which was oxygenated with a mixture of 95% oxygen and 5% carbon dioxide. The Tyrode solution contained 124.9 m*M* NaCl, 2.68 m*M* KCl, 1.80 m*M* $CaCl_2$, 1.05 m*M* $MgCl_2$, 23.80 m*M* $NaHCO_3$, 0.41 m*M* NaH_2PO_4, and 11.10 m*M* dextrose. Compounds were added to the organ baths in 5–100-μl volumes. Contractions were measured by an isometric transducer[9], and rectilinear contraction heights were recorded using a physiograph[10].

The contractions by I–VII represent stimulation of both muscarinic receptors on the ileal smooth muscle and the nicotinic receptors in the Auerbach plexus. To separate the nicotinic receptor stimulation from the muscarinic receptor stimulation, contractions induced by I–VII also were measured in the Tyrode solution containing hexamethonium (37×10^{-6} *M*), which blocked the nicotinic receptors. The details of these methods were described previously (10, 27).

RESULTS

Inhibition of Choline Acetyltransferase by I–VII—All compounds inhibited the activity of choline acetyltransferase at 1×10^{-3} *M* (Table II). The I_{50} values of I, II, IV, and V were higher than 1×10^{-3} *M*. Compound I has a keto group attached to a quaternary nitrogen with an acyclic three-carbon chain. Replacement of the methyl group adjacent to carbonyl carbon of I by ethoxy or thiophene led to no increase in inhibitory potency. Similar results were also observed with II. However, the bis quaternary analog (III) increased inhibition.

Replacement of the methyl group of I by phenyl gave an active compound, VI ($I_{50} = 9.2 \times 10^{-5}$ *M*). Shortening the methylene chain linking the quaternary nitrogen and the carbonyl carbon in VI from three to two (as in VII) increased the inhibitory potency by a factor of 30. Compound

[3] Biorad AG-1-X8, chloride form, 200–400 mesh.
[4] Phase Combining System (PCS), Amersham/Searle Corp.
[5] Nuclear Chicago model III.
[6] Worthington Biochemicals, Freehold, N.J.
[7] Calbiochem, Los Angeles, Calif.
[8] Beckman model 25 automatic recording spectrophotometer.
[9] Model F-50 microdisplacement myograph transducer, Narco Biosystems.
[10] Desk model DMP-4A, Narco Biosystems.

Table I—Physical Constants of Keto Analogs of Acetylcholine

$(CH_3)_3\overset{+}{N}CH_2CH_2R$

Compound[a]	R	Melting Point	Yield, %	Molecular Formula		Analysis, % Calc.	Found
I	$CH_2\overset{O}{\overset{\|}{C}}CH_3$	127–129°	79	$C_8H_{18}ClNO_5$	C	39.42	39.44
					H	7.39	7.42
					Cl	14.57	14.65
					N	5.74	5.65
II		172–174°	44	$C_{10}H_{22}ClNO_2$	C	53.69	53.40
					H	9.84	9.66
					N	6.26	6.24
III	$CH_2\overset{O}{\overset{\|}{C}}CH_2CH_2CH_2\overset{+}{N}(CH_3)_3$	205–208°	49	$C_{13}H_{30}Cl_2N_2O_9$	C	36.36	36.51
					H	6.99	7.27
					Cl	16.55	16.51
					N	6.52	6.43
IV	$CH_2\overset{O}{\overset{\|}{C}}COCH_2CH_3$	95–97°	55	$C_9H_{20}ClNO_2 \cdot H_2O$	C	47.47	47.82
					H	9.67	9.65
					N	6.55	6.28
V	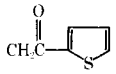	250–251°	31	$C_{11}H_{18}ClNOS$	C	53.33	53.41
					H	7.27	7.32
					N	5.65	5.78
					S	12.92	12.95
VI	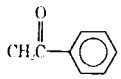	246–249°	36	$C_{13}H_{20}ClNO$	C	64.59	64.66
					H	8.28	8.42
					N	5.79	5.63
VII		180°	74	$C_{12}H_{18}ClNO$	C	63.29	63.09
					H	7.91	7.91
					N	6.15	6.15

[a] All compounds are chlorides except I and III which are perchlorates.

VII was the most potent inhibitor of choline acetyltransferase in the series.

Inhibition of Cholinesterase by I–VII—The I_{50} values (Table II) of all compounds were within the range of 2×10^{-3}–3×10^{-4} *M*. Various structural modifications of I did not result in significant changes in I_{50} values. Compounds I, II, and IV were equally active. Similarly, III and V–VII were equally active, and they were slightly more active than I, II, and IV in inhibiting cholinesterase.

Compound VII was about 50 times less active in inhibiting cholinesterase than in inhibiting choline acetyltransferase. Compound VI was only about three times more active in inhibiting choline acetyltransferase than in inhibiting cholinesterase.

Stimulation of Cholinergic Receptors by I–VII—The responses elicited by I–VII were contractions of the longitudinal muscle of the guinea pig ileum (Table II). All compounds exhibited higher ED_{50} and lower maximal effects than those of acetylcholine on the ileal muscle in the presence of hexamethonium, which blocked nicotinic receptors in this tissue (10, 27). Doses of atropine higher than 10^{-6} *M* blocked the contractions induced by all compounds. These observations indicate that all of these compounds were considerably less active than acetylcholine for stimulating muscarinic receptors. Of the two potent choline acetyltransferase inhibitors, the muscarinic activity of VI was not significant even at a dose of 2×10^{-2} *M*, and VII was about 160 times less active in stimulating muscarinic receptors than in inhibiting choline acetyltransferase.

In the absence of hexamethonium, the ED_{50} doses for all compounds were considerably lower than the corresponding doses in the presence of hexamethonium. But maximal effects of all compounds were significantly higher in the absence of hexamethonium than in the presence of hexamethonium. The effects of all compounds were blocked by atropine ($>10^{-6}$ *M*) on the ileal muscle even in the absence of hexamethonium. These observations indicate that these compounds stimulate nicotinic receptors in the Auerbach plexus and stimulate the ileal muscle through release of acetylcholine from postganglionic cholinergic nerve terminals.

Compound VI did not exhibit any activity on the ileum even in the absence of hexamethonium. Compound VII was about 15–20 times less active in stimulating ileal muscle than in inhibiting choline acetyltransferase. Compound VII produced a maximal effect at higher doses, which was about half of that of acetylcholine.

DISCUSSION

In the present series, VII was the most potent, stable, and selective inhibitor of choline acetyltransferase. The chemical structure of VII is similar to the structures of known potent inhibitors of choline acetyltransferase (VIII–X); it is somewhere between the structures of the two groups of strong inhibitors (styrylpyridine analogs and halogenated keto analogs of acetylcholine) of choline acetyltransferase.

Table II—Interactions of Keto Analogs of Acetylcholine at Various Cholinergic Sites

Compound	Inhibition, I_{50}, Mean ± *SE* (4)[a] Enzyme A[b]	Enzyme B[c]	Contraction of Ileal Muscle in Presence of Hexamethonium, Mean ± *SE* (6)[a] $(ED_{50}) \times 10^6$ *A*	Maximal Effect[d]	Contraction of Ileal Muscle in Absence of Hexamethonium, Mean ± *SE* (6)[a] $(ED_{50}) \times 10^6$ *B*	Maximal Effect[d]	Index of Discrimination (*A*/*B*)[e]
I	$>10^{-3}$	$(2.1 \pm 0.7)\ 10^{-3}$	42 ± 3	0.92	8.6 ± 0.7	1.14	4.9
II	$>10^{-3}$	$(2.4 \pm 1.0)\ 10^{-3}$	302 ± 3	0.80	73 ± 9	1.08	4.1
III	$(1.3 \pm 0.3)\ 10^{-4}$	$(2.8 \pm 1.0)\ 10^{-4}$	12333 ± 667	0.81	3125 ± 381	0.79	3.9
IV	$>10^{-3}$	$(2.7 \pm 1.0)\ 10^{-4}$	2.33 ± 0.04	1.0	1.4 ± 0.3	1.26	1.7
V	$>10^{-3}$	$(3.5 \pm 1.2)\ 10^{-4}$	NS[f]	NS[f]	134 ± 4	0.58	—
VI	$(9.2 \pm 1.5)\ 10^{-5}$	$(3.2 \pm 1.7)\ 10^{-4}$	NS[f]	NS[f]	NS[f]	NS[f]	—
VII	$(3.1 \pm 0.8)\ 10^{-6}$	$(1.6 \pm 0.2)\ 10^{-4}$	485 ± 49	0.27	54 ± 4	0.48	9.0
Acetylcholine	—	—	0.29 ± 0.02	1.0	0.14 ± 0.01	1.0	2.0

[a] The number in parentheses indicates the number of experiments. The I_{50} and ED_{50} values are given in moles per liter. [b] Partially purified choline acetyltransferase from human placenta. [c] Horse serum cholinesterase purified commercially by the Strelitz (25) procedure. [d] Relative intrinsic activity according to the nomenclature of Ariens (32). [e] Represents the ratio of ED_{50} doses in the presence of hexamethonium (C-6) and in the absence of hexamethonium. Contractions in the presence of hexamethonium indicate muscarinic activities, because hexamethonium blocks nicotinic receptors in this tissue. Contractions in the absence of hexamethonium indicate both combined muscarinic and nicotinic activities. The higher ratios (*A*/*B*) indicate higher nicotinic activities in relation to muscarinic activities. [f] No significant response at 2×10^{-2} *M*.

A structure–activity relationship study demonstrated three requirements for the inhibition of choline acetyltransferase by the alkylaminoethyl esters or their corresponding quaternary ammonium derivatives (15, 16): (*a*) a terminal cationic head on the amine end of the molecule, (*b*) the ability to delocalize (or stabilize) a partial negative charge on the acyl end, and (*c*) a leaving group on the α-carbon on the acyl end. Studies with other inhibitors indicated that only the first two requirements are essential for a strong inhibitor. For keto analogs of choline (17, 18), *e.g.*, 3-bromoacetonyltrimethylammonium bromide, a terminal cationic head and the ability to delocalize a partial negative charge are present.

Cavallito and collaborators (1, 3, 28) suggested that styrylpyridine analogs bind to the enzyme *via* hydrophobic and electron donor contributions of the aryl moiety and electron acceptor interaction of the pyridinium moiety. No specific binding contribution could be ascribed to the vinyl bridge other than transmission of electrons between the two rings and facilitation of coplanarity of the inhibitor. But Baker and Gibson (29–31) reported that the transmission of electrons from one ring to the other is of little consequence. They proposed that the double bond is polarized by a mesomeric interaction with the phenyl ring and the pyridyl ring, causing a partial positive charge on the carbon atom adjacent to the benzene ring and a partial negative charge on the carbon atom next to the pyridine ring. In this manner, a nucleophilic residue on the enzyme surface would have a strong interaction with the partial positive charge on the β-carbon to the pyridyl ring.

Compound VII has nearly all of the requirements necessary for the inhibition of choline acetyltransferase: (*a*) a cationic terminal, a site for an electron acceptor interaction; (*b*) an aryl moiety for hydrophobic and electron donor contributions; and (*c*) a positive carbon. There is no need for the C–C double bond which, with styrylpyridine analogs, helps to keep both the phenyl and pyridyl rings in one plane. Compound VII has only one phenyl ring attached to the quaternary nitrogen through single bonds. It can rotate with single bonds to acquire the necessary planarity to bind in a flat pocket of the enzyme. A partial positive charge on the carbon atom adjacent to the benzene ring due to the presence of keto oxygen interacts strongly with a nucleophilic residue on the enzyme.

REFERENCES

(1) C. J. Cavallito, H. S. Yan, J. C. Smith, and F. F. Foldes, *J. Med. Chem.*, **12,** 134 (1969).

(2) J. C. Smith, C. J. Cavallito, and F. F. Foldes, *Biochem. Pharmacol.*, **16,** 2438 (1967).

(3) C. J. Cavallito, H. S. Yan, T. Kapalau, J. C. Smith, and F. F. Foldes, *J. Med. Chem.*, **13,** 221 (1970).

(4) M. L. White and C. J. Cavallito, *Biochim. Biophys. Acta,* **206,** 242 (1970).

(5) C. Y. Chiou and B. V. R. Sastry, *Fed. Proc.*, **25,** 320 (1966).

(6) B. V. R. Sastry and C. Y. Chiou, *Chem. Ther.*, **2,** 164 (1967).

(7) C. Y. Chiou and B. V. R. Sastry, *Biochem. Pharmacol.*, **17,** 805 (1968).

(8) B. V. R. Sastry and C. Y. Chiou, *Biochim. Biophys. Acta,* **167,** 339 (1968).

(9) C. Y. Chiou and B. V. R. Sastry, *Arch. Int. Pharmacodyn. Ther.*, **181,** 94 (1969).

(10) C. Y. Chiou and B. V. R. Sastry, *J. Pharmacol. Exp. Ther.*, **172,** 351 (1970).

(11) D. Morris and D. S. Grewaal, *Life Sci.*, **8,** 511 (1969).

(12) G. I. Henderson and B. V. R. Sastry, *Fed. Proc.*, **31,** 561 (1972).

(13) B. V. R. Sastry and G. I. Henderson, *Toxicol. Appl. Pharmacol.*, **29,** 120 (1974).

(14) B. V. R. Sastry and G. I. Henderson, in "Drugs and Central Synaptic Transmission," P. B. Bradley and B. N. Dhawan, Eds., University Park Press, Baltimore, Md., 1976, pp. 89–98.

(15) P. P. Rowell and C. Y. Chiou, *Biochem. Pharmacol.*, **25,** 1093 (1976).

(16) P. P. Rowell and C. Y. Chiou, *Eur. J. Pharmacol.*, **40,** 83 (1976).

(17) B. O. Persson, *Acta Chem. Scand.*, **27,** 3307 (1973).

(18) B. O. Persson, *Acta Pharm. Suec.*, **11,** 77 (1974).

(19) D. R. Haubrich and P. F. L. Wang, *Biochem. Pharmacol.*, **25,** 669 (1976).

(20) D. Nachmansohn, *Handb. Exp. Pharmakol.*, **15,** 40 (1963).

(21) R. Roskoski, Jr., *J. Biol. Chem.*, **249,** 2156 (1974).

(22) R. Roskoski, Jr., C. T. Lim, and L. M. Roskoski, *Biochemistry,* **14,** 5105 (1975).

(23) B. V. R. Sastry and G. I. Henderson, *Biochem. Pharmacol.*, **21,** 787 (1972).

(24) B. K. Schrier and L. Schuster, *J. Neurochem.*, **14,** 977 (1967).

(25) F. Strelitz, *Biochem. J.*, **38,** 86 (1944).

(26) G. L. Ellman, D. Courtney, V. Andres, and R. M. Featherstone, *Biochem. Pharmacol.*, **7,** 75 (1961).

(27) B. V. R. Sastry and H. C. Cheng, *J. Pharmacol. Exp. Ther.*, **180,** 326 (1972).

(28) H. L. White and C. J. Cavallito, *Biochim. Biophys. Acta,* **206,** 343 (1970).

(29) B. R. Baker and R. E. Gibson, *J. Med. Chem.*, **14,** 315 (1971).

(30) *Ibid.*, **15,** 639 (1972).

(31) R. E. Gibson and B. R. Baker, *J. Med. Chem.*, **17,** 1290 (1974).

(32) E. J. Ariens, *Arch. Int. Pharmacodyn. Ther.*, **99,** 32 (1954).

ACKNOWLEDGMENTS

Supported in part by U.S. Public Health Service National Institutes of Health Grants NS-04699, HD-10607, HD-0861, GM-00058, and RR-05424 and by a grant from the Council for Tobacco Research, Inc.

A. K. Chaturvedi was supported by a postdoctoral research associateship from the U.S. Public Health Service, National Institutes of Health, Research Grant NS-04699, awarded by the National Institute of Neurological and Communicative Disorders and Stroke.

P. P. Rowell was supported by a postdoctoral research associateship from the U.S. Public Health Service, National Institutes of Health, Research Grant HD-0861, awarded by the National Institute of Child Health and Development.

Spectrophotometric Determination of Isoniazid in Presence of Its Hydrazones

M. B. DEVANI ˣ, C. J. SHISHOO, M. A. PATEL, and D. D. BHALARA

Received March 21, 1977, from the *Department of Pharmaceutical Chemistry, L.M. College of Pharmacy, Ahmedabad 380 009, India.* Accepted for publication August 24, 1977.

Abstract □ A spectrophotometric determination of isoniazid in the presence of its hydrazones was developed. The method involves the reaction between isoniazid and 2,3-dichloro-1,4-naphthoquinone in the presence of ammonia in an ethanolic medium. The colored product has an absorbance maximum at 640 nm. The Lambert–Beer law is obeyed in the 1–14-μg/ml range. The proposed method was applied to the analysis of isoniazid tablets. In commercial tablets, hydrazone formation due to the reaction between isoniazid and lactose was detected by TLC. The analysis of lactose-containing isoniazid tablets showed 10–22% lower recovery than that obtained by the official method. Hydrazone formation in tablets probably interferes with isoniazid bioavailability.

Keyphrases □ Isoniazid—spectrophotometric analysis in presence of its hydrazones in prepared mixtures and commercial tablets □ Spectrophotometry—analysis, isoniazid in presence of its hydrazones in prepared mixtures and commercial tablets □ Tuberculostatic antibacterials—isoniazid, spectrophotometric analysis in presence of its hydrazones in prepared mixtures and commercial tablets

The analysis of isoniazid in dosage forms has been the subject of extensive study. Bromometric (1), nonaqueous titrimetric (2), and spectrophotometric (3) methods have been proposed. Isoniazid reacts with carbonyl compounds to form hydrazones (4). Interaction of isoniazid with lactose was investigated in the solid state using diffuse reflectance spectrophotometry (5). According to this study, the reaction does not proceed to any appreciable degree under ambient conditions. However, the interaction can become significant in the presence of high humidity and at elevated temperatures.

BACKGROUND

The presence of glucose and lactose isonicotinoyl hydrazones has been detected in various dosage forms, *e.g.*, syrups and tablets (6, 7). The interaction of glucose and lactose with isoniazid probably interferes with the bioavailability of isoniazid from its dosage forms. Absorption of lactose isonicotinoyl hydrazone was almost negligible in animals (7, 8). Surprisingly, as much as 60–70% of isoniazid was converted to glucose hydrazone within 24 hr in syrups. Pharmacokinetic study in humans revealed that the bound isoniazid is neither absorbed nor converted to the free isoniazid in the first 6 hr.

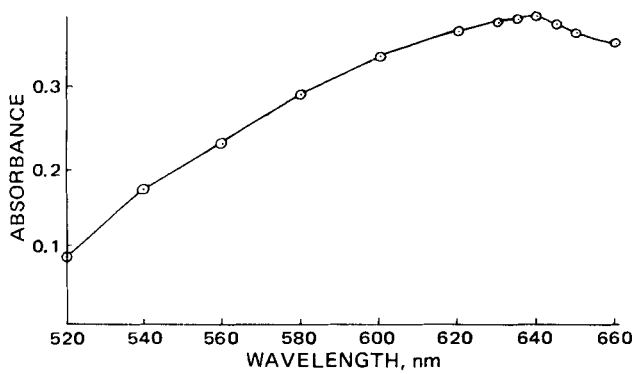

Figure 1—*Visible spectrum of the colored product obtained on reacting isoniazid with 2,3-dichloro-1,4-naphthoquinone.*

Recently, iodometric, nitrite, and bromometric methods, official in USP and BP, have been compared with the nonaqueous method (9). All official methods, as well as the nonaqueous titrimetric procedure, fail to make any distinction between isoniazid and its hydrazones. Therefore, it was of interest to develop a specific method for isoniazid in the presence of its hydrazones and to study the extent of hydrazone formation, if any, in tablets containing lactose as an adjuvant.

The proposed method is based on the reaction between isoniazid and 2,3-dichloro-1,4-naphthoquinone in ethanol. Reaction conditions such as the concentration of reagent and ammonia, time, and temperature have been standardized.

EXPERIMENTAL

Apparatus—All spectral measurements were carried out with a spectrophotometer[1] having four matched 10-ml cells of 1-cm light path.

Materials and Reagents—Ethanol BP, silica gel G[2], and isoniazid BP were employed. All other reagents were analytical grade.

2,3-Dichloro-1,4-naphthoquinone (10), glucose isonicotinoyl hydrazone (11), and lactose isonicotinoyl hydrazone (12) were synthesized as described previously.

Preparation of Ethanolic Ammonia (10% w/v)—Dry ammonia gas was passed through absolute ethanol at −5° until its weight had increased ~20%. The resulting solution was diluted with absolute ethanol to obtain a 10% (w/v) ammonia solution. The solution was stored at 5° in a refrigerator.

2,3-Dichloro-1,4-naphthoquinone Solution—This solution contained 0.034% (w/v) 2,3-dichloro-1,4-naphthoquinone in ethanol.

Standard Solutions—The following were used: 0.01% (w/v) isoniazid in ethanol (freshly prepared), 0.035% (w/v) lactose isonicotinoyl hydrazone in ethanol, and 0.022% (w/v) glucose isonicotinoyl hydrazone in ethanol.

Detection of Lactose Isonicotinoyl Hydrazone, Glucose Isonicotinoyl Hydrazone, Lactose, and Glucose—TLC, as described earlier (5, 13), was used to detect these compounds.

Determination of Wavelength of Maximum Absorbance—To the mixture of standard solution of isoniazid (2 ml) and ethanolic ammonia (6 ml), placed in a small flask and cooled in an ice bath, was added 2,3-dichloro-1,4-naphthoquinone solution (10 ml). The reaction mixture was kept in an ice bath for 25 min. The solution then was transferred quantitatively to a 25-ml volumetric flask with the aid of ice-cold ethanol, and the final volume was adjusted with cold ethanol. The reaction flask was placed in an ice bath. After 5 min, the absorbance was measured at 10-nm intervals from 520 to 660 nm against a blank. The blank contained 2,3-dichloro-1,4-naphthoquinone solution (10 ml) and ethanolic ammonia (6 ml) diluted to 25 ml with ethanol (Fig. 1).

Analysis of Isoniazid in Presence of Its Hydrazones in Synthetic Mixture—Aliquots of ethanolic isoniazid solution and its hydrazone solution were mixed with ammonia (6 ml) and cooled in an ice bath (Table I). 2,3-Dichloro-1,4-naphthoquinone solution (10 ml) was added to the mixture, which was analyzed as described. The amount of isoniazid was calculated by referring to the standard curve.

Analysis of Isoniazid Tablets—Twenty tablets were weighed and powdered, and the powder equivalent to 100 mg of isoniazid was weighed accurately. Four portions of 20 ml of ethanol were used to extract isoniazid from the tablet powder. Each extract was filtered[3], and the residue on the filter paper was washed with 10 ml of ethanol. The filtrate and

[1] Spectronic 20.
[2] E. Merck.
[3] Whatman No. 40 filter paper.

Table I—Analysis of Isoniazid and Its Hydrazones

Sample	Recovery, % USP Method[a]	Vanillin Method[b]	Proposed Method
Isoniazid	99.94 ± 0.52[c]	99.85 ± 0.62[c]	99.40 ± 0.76[c]
Glucose isonicotinoyl hydrazone	98.53 ± 0.59	—	—[d]
Lactose isonicotinoyl hydrazone	100.29 ± 0.68	—	—[d]
Isoniazid (50 mg) + glucose isonicotinoyl hydrazone (50 mg)	141.21 ± 0.85	—	99.45 ± 0.85
Isoniazid (100 mg) + glucose isonicotinoyl hydrazone (220 mg)	200.18 ± 0.86	105.80 ± 0.52	99.44 ± 0.87
Isoniazid (50 mg) + lactose isonicotinoyl hydrazone (100 mg)	159.40 ± 0.95	—	99.53 ± 0.76
Isoniazid (100 mg) + lactose isonicotinoyl hydrazone (350 mg)	205.61 ± 0.72	111.20 ± 0.81	99.62 ± 0.62

[a] Reference 16. [b] Reference 3. [c] Standard deviation was calculated from the results of 10 experiments. [d] Absorbance at 640 nm was insignificant.

Table II—Analysis of Isoniazid

Run	Recovery, % USP Method	Proposed Method
1	98.20	100.00
2	99.42	100.50
3	99.34	100.00
4	99.70	98.50
5	99.70	101.00
6	99.22	101.50
7	99.62	100.00
8	99.52	100.50
9	99.52	99.50
10	99.60	99.00
Mean	99.40	100.05
SD	±0.443	±0.91

washings were combined in a 100-ml volumetric flask and diluted to volume with ethanol.

The solution (10 ml) was diluted further with the same solvent to 100 ml and analyzed as described previously.

RESULTS

Concentration of 2,3-Dichloro-1,4-naphthoquinone—The absorbance at 640 nm of the colored product formed by the reaction of isoniazid (2 ml) and ammonia (6 ml) with 2,3-dichloro-1,4-naphthoquinone solution increased with an increase in the reagent concentration. The maximum absorbance was obtained in the presence of 10 ml of the reagent in 25 ml of the reaction mixture. On increasing the reagent quantity further, a slight decrease in intensity was observed (Fig. 2).

Concentration of Ammonia—A yellowish-green color was obtained on addition of 2,3-dichloro-1,4-naphthoquinone reagent (10 ml) to the mixture of isoniazid solution (2 ml) and ethanolic ammonia. Maximum color intensity was obtained in the presence of 6 ml of ammonia (10% w/v) in 25 ml of the reaction mixture (Fig. 3).

Temperature—The color intensity was maximum when the reaction mixture containing isoniazid solution (2 ml), alcoholic ammonia (6 ml),

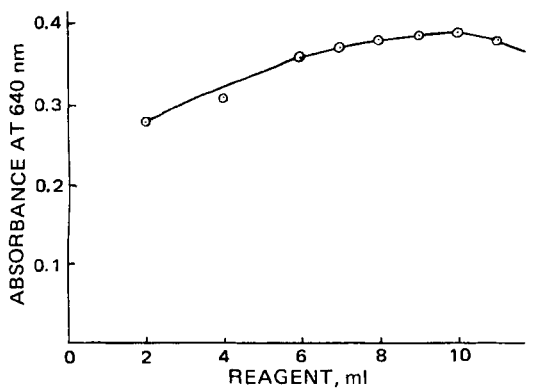

Figure 2—*Effect of reagent concentration on the absorbance at 640 nm.*

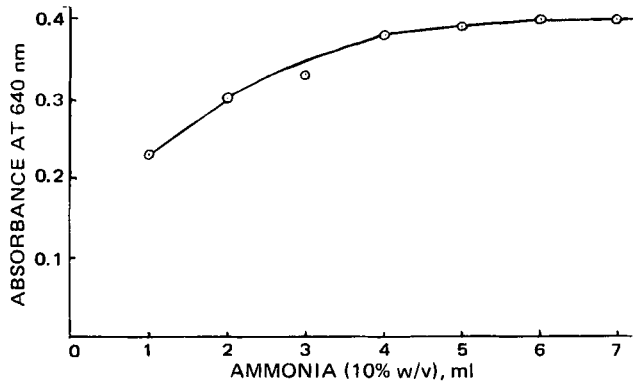

Figure 3—*Effect of ammonia concentration on the absorbance at 640 nm.*

and 2,3-dichloro-1,4-naphthoquinone reagent solution (10 ml) was kept in an ice bath for 25 min, and it remained constant on further standing. When the reaction was carried out at room temperature (25°), maximum color intensity was observed after 20 min; however, the color intensity obtained was low (Fig. 4).

Color Stability—Isoniazid solution (2 ml), ethanolic ammonia (6 ml), and 2,3-dichloro-1,4-naphthoquinone solution (10 ml) were reacted for 25 min in an ice bath. The reaction mixture was diluted to 25 ml with cold ethanol, and the flask was placed in an ice bath. After 5 min, the absorbance was measured at 640 nm. At ice bath temperature, the color intensity remained stable for more than 2 hr (Fig. 5).

Effect of Isoniazid Concentration—The absorbance at 640 nm was proportional to the amount of isoniazid in the concentration range of 1–14 μg/ml of the reaction mixture under experimental conditions.

DISCUSSION

The colored product obtained by reacting isoniazid with 2,3-dichloro-1,4-naphthoquinone in an aqueous basic medium was reported to be unstable (14). Therefore, the method was modified to increase the stability of the final colored product. Recently, a mechanism for the reaction between 2,3-dichloro-1,4-naphthoquinone and acid hydrazides was proposed (15). This method involves the reaction between isoniazid and 2,3-dichloro-1,4-naphthoquinone in an alcoholic medium containing ammonia. The colored product obtained has an absorbance maximum at 640 nm, and the color is stable for more than 2 hr.

Pure samples of isoniazid were analyzed by the USP (16) and the proposed methods. The results are in good agreement (Table II). Synthetic mixtures of isoniazid and its hydrazones were analyzed by the proposed procedure as well as the nitrite and vanillin methods (Table I). Both glucose isonicotinoyl hydrazone and lactose isonicotinoyl hydrazone were determined quantitatively by the official method (16) (Table I). No interference from hydrazones was observed in the proposed method, but the colorimetric procedure with vanillin gave higher recoveries for isoniazid in the presence of hydrazones (Table I). Although known to be imperfect, the vanillin method was employed in all earlier determinations of isoniazid in the presence of its hydrazones in biological fluids (6, 17). Because of the interference from hydrazones, a correction factor is used to compensate for the higher results obtained by this colorimetric method (17).

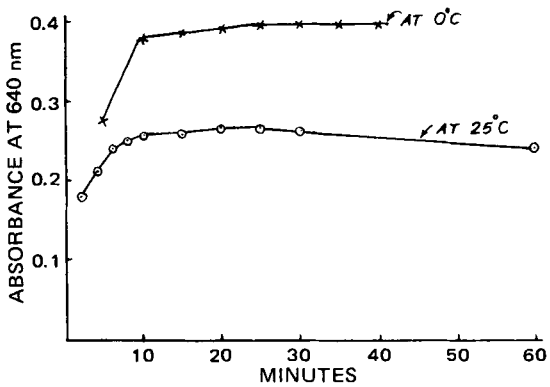

Figure 4—*Effect of time on absorbance at 640 nm.*

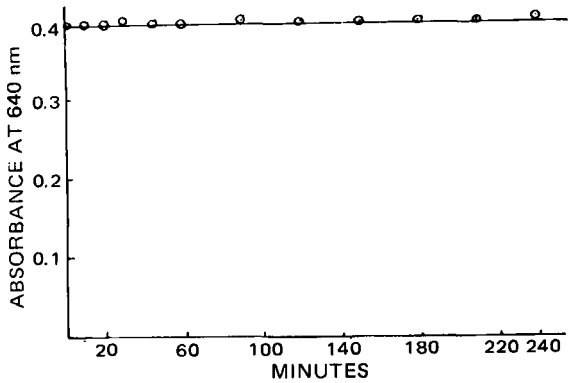

Figure 5—*Stability of colored product.*

For the present study, tablet samples were obtained from the local market. Five out of the eight samples were found by TLC to contain lactose and lactose isonicotinoyl hydrazone. Lactose-containing tablets (Table III, Samples A–D), when assayed by the proposed procedure, were found to contain between 78 and 90% of the labeled amount of free isoniazid. As much as 10–22% of isoniazid was present in the bound form with lactose and was probably not available for absorption. On the other hand, quantitative recoveries were obtained by the official method in the analysis of these tablets. Tablets that did not contain lactose gave comparable recoveries by both the official and the proposed methods.

When freshly prepared lactose-containing granules and the tablets prepared from them (Table III, Samples E and F) were analyzed by the proposed method, interaction between isoniazid and lactose was only 1–3%. Therefore, the significant interaction between isoniazid and lactose in the tablets apparently occurs only on standing over an extended period. The interaction seems to be negligible at the granulation stage.

The proposed method is specific for the estimation of isoniazid in the presence of its hydrazones. Significant interaction between isoniazid and lactose, resulting in the formation of lactose isonicotinoyl hydrazone, has been established. This interaction is likely to interfere with the bioavailability of isoniazid from its dosage forms.

Table III—Analysis of Isoniazid Tablets

Sample	Labeled Amount, mg/tablet	Recovery[a], mg/tablet: USP Method	Recovery[a], mg/tablet: Proposed Method	Presence of: Isoniazid Hydrazone	Presence of: Lactose
A	100	98.60	86.83	+	+
B	50	50.73	39.50	+	+
C	50	51.94	39.17	+	+
D	100	100.90	89.72	+	+
E[b]	300	305.21	301.20	+	+
F[c]	300	306.97	297.76	+	+
G	100	99.70	99.52	−	−
H	300	308.83	304.92	−	−
I	300	297.80	299.65	−	−

[a] Average result of three determinations. [b] Freshly prepared tablets. [c] Granules ready for the preparation of tablets.

REFERENCES

(1) "The British Pharmacopoeia," Pharmaceutical Press, London, England, 1968, p. 535.

(2) M. B. Devani and C. J. Shishoo, *J. Pharm. Sci.*, **59**, 90 (1970).

(3) H. N. Deeb, *Drug Stand.*, **22**, 198 (1954).

(4) "The Extra Pharmacopoeia," 26th ed., Pharmaceutical Press, London, England, 1972, p. 1872.

(5) W. H. Wu, T. F. Chin, and J. L. Lach, *J. Pharm. Sci.*, **59**, 1234 (1970).

(6) K. V. N. Rao, S. Kailasam, N. K. Menon, and S. Radhakrishna, *Indian J. Med. Res.*, **59**, 1343 (1971).

(7) K. Kakemi, T. Arita, H. Sezaki, and N. Takasugi, *Chem. Pharm. Bull.*, **13**, 551 (1965); through *Chem. Abstr.*, **63**, 7511 (1965).

(8) J. H. Peters and V. E. Hayes, *Arch. Int. Pharmacodyn. Ther.*, **159**, 328 (1966); through *Chem. Abstr.*, **64**, 13235e (1966).

(9) M. I. Blake, D. Bode, and H. J. Rhodes, *J. Pharm. Sci.*, **63**, 1303 (1974).

(10) F. Ullmann and M. Ettisch, *Ber. Dtsch. Chem. Ges.*, **54**, 259 (1921).

(11) H. H. Fox, *J. Org. Chem.*, **18**, 990 (1953).

(12) R. Yamamoto and H. Tanaka, *Yakuzaigaku*, **17**, 219 (1957); through *Chem. Abstr.*, **52**, 11849 (1958).

(13) P. G. Pifferi, *Anal. Chem.*, **37**, 925 (1965).

(14) S. C. Elliston and M. D. Hammond, *Analyst*, **90**, 298 (1965).

(15) J. A. Plaizier, J. G. Van Damme, and R. E. De Neve, *Anal. Chem.*, **48**, 1536 (1976).

(16) "The United States Pharmacopeia," 19th rev., Mack Publishing Co., Easton, Pa., 1975, p. 273.

(17) H. G. Boxenbaum and S. Riegelman, *J. Pharm. Sci.*, **63**, 1191 (1974).

ACKNOWLEDGMENTS

Presented at the Commonwealth Pharmaceutical Association, Bombay, India, January 1977.

The authors are grateful to Dr. N. H. Reavey-Cantwell, William H. Rorer Inc., Fort Washington, PA 19034, for financial assistance. They also thank Dr. C. S. Shah, Principal, L.M. College of Pharmacy, Ahmedabad, India.

Mathematical Basis of Point–Area Deconvolution Method for Determining *In Vivo* Input Functions

D. P. VAUGHAN ˣ and M. DENNIS

Received March 14, 1977, from the *School of Pharmacy, Sunderland Polytechnic, Sunderland, SR1 3SD, England.* Accepted for publication August 22, 1977.

Abstract □ The point–area method for deconvolution derives a "staircase" input function which, when convolved onto the characteristic function, gives an output function coincidental with the given output data points. The area–area method for deconvolution is shown to be erroneous.

Keyphrases □ Deconvolution—point–area and area–area methods for determining *in vivo* input functions compared □ Input functions, *in vivo*—deconvolution point–area and area–area methods of determination compared □ Pharmacokinetics—deconvolution point–area and area–area methods for determining *in vivo* input functions compared

The use of *in vitro* dissolution functions for predicting differences in the rate and extent of *in vivo* drug dissolution depends on a correspondence (isomorphism) between the two processes. Any rigorous investigation of such an isomorphism ultimately requires the derivation of the *in vivo* drug input function. This function can be derived for

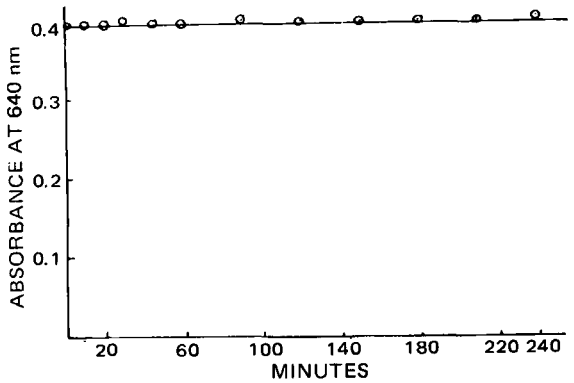

Figure 5—*Stability of colored product.*

For the present study, tablet samples were obtained from the local market. Five out of the eight samples were found by TLC to contain lactose and lactose isonicotinoyl hydrazone. Lactose-containing tablets (Table III, Samples A–D), when assayed by the proposed procedure, were found to contain between 78 and 90% of the labeled amount of free isoniazid. As much as 10–22% of isoniazid was present in the bound form with lactose and was probably not available for absorption. On the other hand, quantitative recoveries were obtained by the official method in the analysis of these tablets. Tablets that did not contain lactose gave comparable recoveries by both the official and the proposed methods.

When freshly prepared lactose-containing granules and the tablets prepared from them (Table III, Samples E and F) were analyzed by the proposed method, interaction between isoniazid and lactose was only 1–3%. Therefore, the significant interaction between isoniazid and lactose in the tablets apparently occurs only on standing over an extended period. The interaction seems to be negligible at the granulation stage.

The proposed method is specific for the estimation of isoniazid in the presence of its hydrazones. Significant interaction between isoniazid and lactose, resulting in the formation of lactose isonicotinoyl hydrazone, has been established. This interaction is likely to interfere with the bioavailability of isoniazid from its dosage forms.

Table III—Analysis of Isoniazid Tablets

Sample	Labeled Amount, mg/tablet	Recovery[a], mg/tablet: USP Method	Recovery[a], mg/tablet: Proposed Method	Presence of: Isoniazid Hydrazone	Presence of: Lactose
A	100	98.60	86.83	+	+
B	50	50.73	39.50	+	+
C	50	51.94	39.17	+	+
D	100	100.90	89.72	+	+
E[b]	300	305.21	301.20	+	+
F[c]	300	306.97	297.76	+	+
G	100	99.70	99.52	−	−
H	300	308.83	304.92	−	−
I	300	297.80	299.65	−	−

[a] Average result of three determinations. [b] Freshly prepared tablets. [c] Granules ready for the preparation of tablets.

REFERENCES

(1) "The British Pharmacopoeia," Pharmaceutical Press, London, England, 1968, p. 535.

(2) M. B. Devani and C. J. Shishoo, *J. Pharm. Sci.*, **59**, 90 (1970).

(3) H. N. Deeb, *Drug Stand.*, **22**, 198 (1954).

(4) "The Extra Pharmacopoeia," 26th ed., Pharmaceutical Press, London, England, 1972, p. 1872.

(5) W. H. Wu, T. F. Chin, and J. L. Lach, *J. Pharm. Sci.*, **59**, 1234 (1970).

(6) K. V. N. Rao, S. Kailasam, N. K. Menon, and S. Radhakrishna, *Indian J. Med. Res.*, **59**, 1343 (1971).

(7) K. Kakemi, T. Arita, H. Sezaki, and N. Takasugi, *Chem. Pharm. Bull.*, **13**, 551 (1965); through *Chem. Abstr.*, **63**, 7511 (1965).

(8) J. H. Peters and V. E. Hayes, *Arch. Int. Pharmacodyn. Ther.*, **159**, 328 (1966); through *Chem. Abstr.*, **64**, 13235e (1966).

(9) M. I. Blake, D. Bode, and H. J. Rhodes, *J. Pharm. Sci.*, **63**, 1303 (1974).

(10) F. Ullmann and M. Ettisch, *Ber. Dtsch. Chem. Ges.*, **54**, 259 (1921).

(11) H. H. Fox, *J. Org. Chem.*, **18**, 990 (1953).

(12) R. Yamamoto and H. Tanaka, *Yakuzaigaku*, **17**, 219 (1957); through *Chem. Abstr.*, **52**, 11849 (1958).

(13) P. G. Pifferi, *Anal. Chem.*, **37**, 925 (1965).

(14) S. C. Elliston and M. D. Hammond, *Analyst*, **90**, 298 (1965).

(15) J. A. Plaizier, J. G. Van Damme, and R. E. De Neve, *Anal. Chem.*, **48**, 1536 (1976).

(16) "The United States Pharmacopeia," 19th rev., Mack Publishing Co., Easton, Pa., 1975, p. 273.

(17) H. G. Boxenbaum and S. Riegelman, *J. Pharm. Sci.*, **63**, 1191 (1974).

ACKNOWLEDGMENTS

Presented at the Commonwealth Pharmaceutical Association, Bombay, India, January 1977.

The authors are grateful to Dr. N. H. Reavey-Cantwell, William H. Rorer Inc., Fort Washington, PA 19034, for financial assistance. They also thank Dr. C. S. Shah, Principal, L.M. College of Pharmacy, Ahmedabad, India.

Mathematical Basis of Point–Area Deconvolution Method for Determining *In Vivo* Input Functions

D. P. VAUGHAN ˣ and M. DENNIS

Received March 14, 1977, from the *School of Pharmacy, Sunderland Polytechnic, Sunderland, SR1 3SD, England.* Accepted for publication August 22, 1977.

Abstract □ The point–area method for deconvolution derives a "staircase" input function which, when convolved onto the characteristic function, gives an output function coincidental with the given output data points. The area–area method for deconvolution is shown to be erroneous.

Keyphrases □ Deconvolution—point–area and area–area methods for determining *in vivo* input functions compared □ Input functions, *in vivo*—deconvolution point–area and area–area methods of determination compared □ Pharmacokinetics—deconvolution point–area and area–area methods for determining *in vivo* input functions compared

The use of *in vitro* dissolution functions for predicting differences in the rate and extent of *in vivo* drug dissolution depends on a correspondence (isomorphism) between the two processes. Any rigorous investigation of such an isomorphism ultimately requires the derivation of the *in vivo* drug input function. This function can be derived for

linear systems by mathematical or numerical deconvolution of the response to some particular drug input and the characteristic response of the system (1–6).

A known method for numerical deconvolution is the so-called area–area method as detailed by Rescigno and Segre (7). However, this method is ambiguous, if not erroneous. Furthermore, there seems to be some confusion about its exact mathematical basis. For example, Benet and Chiang (8) implied that the method is only appropriate when the characteristic response is a single exponential function, and Wagner (9) shifted the derived data to recover a known input function, which would be inappropriate for an arbitrary input function.

For clarification, this deconvolution method is now derived, and it is shown how it relates an unknown input function to a "staircase" input.

THEORY AND DISCUSSION

If the body is regarded as a linear system, then the blood drug concentration–time curve, $Y(t)$, obtained with an arbitrary but finite drug input into the body can be described by the convolution integral:

$$Y(t) = \int_0^t \ln(\tau)G(t-\tau)\,d\tau = \ln(t)*G(t) \qquad \text{(Eq. 1)}$$

where $G(\tau)$ is the blood drug concentration–time function obtained with a unit drug impulse input (*i.e.*, the characteristic response) and $\ln(\tau)$ is the function that, when integrated between limits of $t = 0$ and t, yields the cumulative amount of drug delivered to the impulse input point [*i.e.*, $\ln(\tau)$ is the input function]. Throughout, it is assumed that both $G(t)$ and $\ln(t)$ are bounded nonnegative functions and Riemann integrable on $[0, \infty]$.

Even if $G(\tau)$ and $Y(\tau)$ are known analytically, the integral function defined by Eq. 1 cannot be solved, except in certain cases, for $\ln(\tau)$ by general formulas because the Laplace transform of Eq. 1:

$$y(s) = \ln(s)g(s) \qquad \text{(Eq. 2)}$$

with solution:

$$\ln(s) = \frac{y(s)}{g(s)} \qquad \text{(Eq. 3)}$$

cannot be transformed back into time space by the convolution theorem since $1/g(s)$ is not a Laplace transform (10). This fact indicates the need for general deconvolution methods. In general, numerical evaluation of $y(s)$ and $g(s)$, with subsequent numerical calculation of $\ln(s)$ and inversion, is unsuccessful because of instability (11, 12). Fourier transform methods have been used and are reasonably accurate (12). However, a simple numerical method would be advantageous.

Response to Staircase Input—A staircase input is defined as a finite set of rectangular pulses of duration $p_j - p_{j-1}$ and intensity I_j, each commencing at $t = p_{j-1}$ and ending at $t = p_j$ ($j \in 1, 2, 3 \ldots$), where $I_j \geq 0$, $t \geq 0$, and $p_0 = 0$. Then the response of a linear system to a staircase input at the time points p_j can be obtained by application of standard Laplace transformation methods (10):

$$Y(p_j) = \sum_{i=1}^{j} I_i \left[\int_0^{p_j - p_{i-1}} G(\tau)\,d\tau - \int_0^{p_j - p_i} G(\tau)\,d\tau \right] \qquad \text{(Eq. 4)}$$

where $j \in 1, 2, 3 \ldots$, $p_0 = 0$, and $Y(0) = 0$.

In particular, if the staircase pulse lengths are all equal, say $p_j - p_{j-1} = a$ for all j, then substitution of $p_j = ja$ and $p_i = ia$ into Eq. 4 gives:

$$Y(ja) = \sum_{i=1}^{j} I_i \int_{(j-i)a}^{(j-i+1)a} G(\tau)\,d\tau \qquad \text{(Eq. 5)}$$

where $j \in 1, 2, 3 \ldots$ and $Y(0) = 0$.

Given the exact output, $Y(p_j)$ at time points p_j or $Y(ja)$ at time points ja, and the function $G(\tau)$, a particular staircase input function can be recovered exactly by algebraic manipulation of Eq. 4 or 5. The details for an equal pulse length staircase input function are as follows.

By defining the pulse length as a and:

$$\int_{(n-1)a}^{na} G(\tau)\,d\tau \equiv A_n \qquad \text{(Eq. 6)}$$

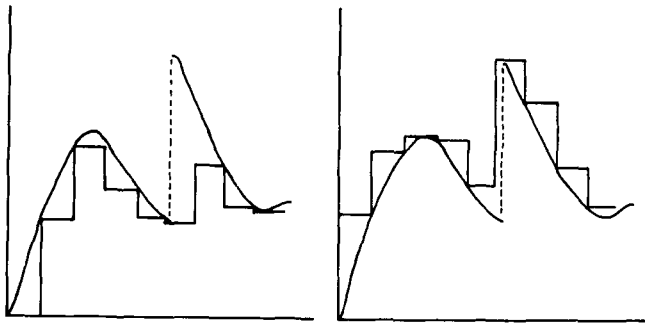

Figure 1—*Representation of an input function by a minimum (left) and maximum (right) staircase function.*

where $n \in 1, 2, 3 \ldots$, and then by applying Eq. 5 and rearranging, the I's are given by:

$$I_1 = \frac{Y(a)}{A_1} \qquad \text{(Eq. 7a)}$$

$$I_2 = \frac{Y(2a) - I_1A_2}{A_1} \qquad \text{(Eq. 7b)}$$

$$I_3 = \frac{Y(3a) - I_1A_3 - I_2A_2}{A_1} \qquad \text{(Eq. 7c)}$$

$$\vdots$$

$$I_n = \frac{Y(na) - I_1A_n - I_2A_{n-1} \ldots I_{n-1}A_2}{A_1} \qquad \text{(Eq. 7d)}$$

A similar set of equations can be constructed for unequal pulse lengths by applying Eq. 4.

Deconvolution Using Staircase Functions—Given the output of a linear system, $Y(p_j)$, at time points $t = p_j$ corresponding to some arbitrary input function, $\ln(t)$, and the appropriate $G(\tau)$, a staircase input function can always be derived from the data by applying Eq. 4 or 5. This derived staircase input function, $U_s(t)$, when convolved on $G(\tau)$, will yield a function exactly coincidental with the given output data points $Y(p_j)$ at $t = p_j$. Since $U_s(t)$ is derived using specific output data points and the integral of $G(\tau)$, it is appropriate to designate this deconvolution method as the point–area method.

That each step of the derived staircase function, $U_s(t)$, intersects the true input function, $\ln(t)$, can be shown as follows. For any nonnegative bounded and finite drug input, a staircase function, $U_1(t)$, exists such that the magnitude of each step is equivalent to the minimum value of $\ln(t)$ in each step period (Fig. 1, left), since:

$$\int_0^t U_1(\tau)\,d\tau < \int_0^t \ln(\tau)\,d\tau \qquad \text{(Eq. 8)}$$

the convolution of $U_1(t)$ on $G(\tau)$ is always less than the true output function in the time interval $(0, \infty)$. Similarly, there exists a staircase function, $U_2(t)$, such that the magnitude of each step is equivalent to the maximum value of $\ln(t)$ in each step period (Fig. 1, right), since:

$$\int_0^t U_2(\tau)\,d\tau > \int_0^t \ln(\tau)\,d\tau \qquad \text{(Eq. 9)}$$

the convolution of $U_2(t)$ on $G(\tau)$ is always greater than the true output function in the time interval $(0, \infty)$. Consequently, the staircase function, $U_s(t)$, which, when convolved on $G(\tau)$ is coincidental with the true output

Table I—Comparison of the Cumulative Drug Input and That Determined by Deconvolution [a]

Hours	Exact Cumulative Input, %	Estimated Cumulative Input, %	Error, %
1	49.99	49.15	−1.68
2	74.99	73.75	−1.65
3	87.49	86.07	−1.63
4	93.75	92.24	−1.61
5	96.87	95.33	−1.59
6	98.44	96.89	−1.57
7	99.22	97.67	−1.56

[a] Output data $Y(t)$ were generated at the times shown by application of Eq. 1, where $G(t) = 5e^{-0.4t} + 5e^{-0.2t}$ and $\ln(t) = 0.693e^{-0.693t}$. Cumulative drug input was estimated by application of Eqs. 7a–7d, and the exact input was determined by the integration of the input function.

Table II—Maximum Errors Associated with the Deconvolution for Various Input Functions [a]

Input Function α	Maximum Error, %
2	−4.56
1.5	−3.52
1.0	−2.40
0.693	−1.68
0.35	−0.86

[a] Output data $Y(t)$ were generated at $t = 1$ by Eq. 1 using the same $G(t)$ as in Table I and various input functions, $\ln(t) = \alpha e^{-\alpha t}$. Cumulative drug input was estimated by application of Eq. 7*a*, and the exact input was determined by the integration of the input function.

at the end of each step, intersects or is coincidental with the true input function in the period of each step.

The exact points of intersection for $U_s(t)$ and $\ln(t)$ cannot be specified since they depend on the exact form of the unknown input function. However, the cumulative *in vivo* drug input is the function most often required for comparison with *in vitro* dissolution data. The cumulative *in vivo* input is readily obtainable by multiplication of the derived I values by the period of each step and summation.

Since the derived staircase input function, $U_s(t)$, does not depend on the form of $G(\tau)$, the method is equally appropriate for any $G(\tau)$. Obviously, the accuracy of the derived cumulative input depends on the step length since, as all step lengths tend to zero, $U_s(t) \rightarrow \ln(t)$.

The cumulative input derived by the point–area method is an excellent approximation of the true cumulative input. Some results are presented in Table I. These data assume an exponential input function and a sampling period equal to the half-life of the input function; such an input function and sampling period are likely to represent extremes of those occurring in practice. The disposition function, $G(\tau)$, was arbitrarily chosen as a biexponential function.

As indicated by the data in Table I, the derived cumulative input slowly converges onto the true cumulative input and the maximum error occurs in the first period. The latter error is a function of the input function and the first output data point, as illustrated by the data in Table II. The 4.56% error corresponding to $\alpha = 2$ represents an extreme case since 86% of the input occurs in the first period.

Erroneous Area–Area Method of Deconvolution—Rescigno and Segre (7) described a perfectly valid method for the numerical convolution of two functions. Essentially, this method approximates one function to an equal pulse length staircase function such that the area of each step is identical to the area of the function itself during each step. The corresponding areas of the staircase function are then convolved on the other function. Analytically, this method corresponds to the multiplication of Eq. 5 by the pulse lengths, say a, and the output is given as $aY(ja)$, $j \in 1, 2, 3 \ldots$. Unfortunately, when inversing the procedure (*i.e.*, deconvolution), $aY(ja)$ is interpreted as the actual area of the output function:

$$\int_{(j-1)a}^{ja} Y(t)\,dt = aY(ja) \qquad \text{(Eq. 10)}$$

Obviously, the equality of Eq. 10 is erroneous for most output functions, $Y(t)$. Nevertheless, this method of deconvolution has been used and designated as the area–area method of deconvolution (8).

A comparison of the percentage errors of the area–area and point–area methods is given in Fig. 2. Output data $Y(t)$ were generated by Eq. 1 where $G(t) = 5e^{-0.2t}$ and $\ln(t) = 0.5e^{-0.5t}$. Exact cumulative input was determined by integration of the input function. The estimated cumulative input was determined by the method of Rescigno and Segre (7) for the area–area method and by Eqs. 7*a*–7*d* for the point–area method. As expected, the area–area method gave large and generally unpredictable errors.

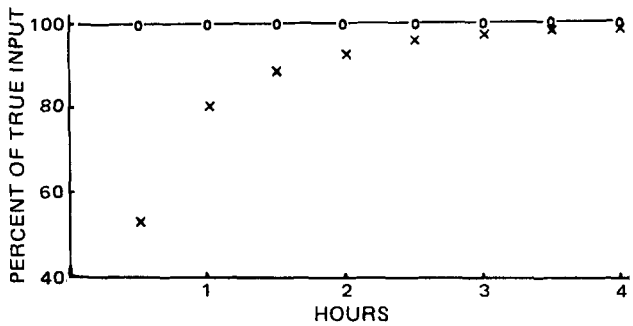

Figure 2—*Percentage errors in the cumulative drug input obtained by the point–area (O) and the area–area (×) methods of deconvolution. The solid line represents zero error.*

Input functions, as used in Eq. 1, define the drug input to the point at which an impulse input is applied to the body. The actual physical meaning of this function depends on how the characteristic response is defined. For example, if the characteristic response is defined as the resulting blood concentration–time function after an intravenous bolus dose and the data after an oral solution dose are deconvoluted, the resulting input function represents both drug absorption and transport through the liver. These concepts and definitions of input functions were discussed previously (13).

In conclusion, deconvolution using a staircase input function is a simple and accurate method for the assessment of cumulative *in vivo* drug input. The method does not require equally spaced output data points either during or after drug absorption as suggested by Wagner (9).

REFERENCES

(1) L. Z. Benet, *J. Pharm. Sci.*, **61**, 536 (1972).

(2) D. P. Vaughan and A. Trainor, *J. Pharmacokinet. Biopharm.*, **3**, 203 (1975).

(3) D. S. Riggs, "Control Theory and Physiological Feedback Mechanisms," Williams & Wilkins, Baltimore, Md., 1970, chap. 2.

(4) D. P. Vaughan and G. T. Tucker, *Eur. J. Clin. Pharmacol.*, **10**, 433 (1976).

(5) D. P. Vaughan, *J. Pharm. Pharmacol.*, **28**, 505 (1976).

(6) D. S. Riggs, "Control Theory and Physiological Feedback Mechanisms," Williams & Wilkins, Baltimore, Md., 1970, chap. 3.

(7) A. Rescigno and G. Segre, "Drug and Tracer Kinetics," Blaisdell, 1966, pp. 189–195.

(8) L. Z. Benet and C.-W. N. Chiang, in "Abstracts," 13th National Meeting, APhA Academy of Pharmaceutical Sciences, vol. 2, 1972, p. 169.

(9) J. G. Wagner, *J. Pharmacokinet. Biopharm.*, **3**, 457 (1975).

(10) G. Doetsch, "Guide to the Applications of Laplace Transforms," Van Nostrand, New York, N.Y., 1961, chap. 7.

(11) R. E. Bellman, B. E. Kalaba, and J. Lockett, "Numerical Inversion of the Laplace Transform," Elsevier, New York, N.Y., 1966.

(12) C. M. Coulam, H. R. Warner, H. W. Marshall, and J. B. Bassingthwaighte, *Comp. Biomed. Res.*, **1**, 124 (1967).

(13) D. P. Vaughan, *J. Pharmacokinet. Biopharm.*, **5**, 271 (1977).

Microionization Constants of Commercial Cephalosporins

WILLIAM H. STRENG

Received January 14, 1977, from *Merrell-National Laboratories, Division of Richardson-Merrell Inc., Cincinnati, OH 45215.* Accepted for publication August 23, 1977.

Abstract □ The equilibrium constants of five commercial cephalosporins were determined. Two are monoacidic and possess one K_a while three are amphoteric and have four microconstants. Although several assumptions were made in the calculations, good agreement was found between the compounds and with previously reported macroionization constants. By utilizing the microionization constants, the ratios of zwitterion to uncharged species were calculated to be in the 900–50,000 range and to have a maximum concentration between pH 3.5 and 5.

Keyphrases □ Cephalosporins, various—microionization equilibrium constants determined □ Microionization constants, equilibrium—determined for various cephalosporins □ Equilibrium constants, microionization—determined for various cephalosporins □ Antibacterials—various cephalosporins, microionization equilibrium constants determined

Recently, a method to determine the microionization constants of zwitterionic compounds was described (1). These amphoteric compounds, *i.e.*, those behaving as either proton acceptors or donors, undergo the equilibria given in Scheme I.

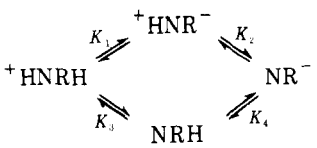

Scheme I

According to this scheme, loss of a proton from the doubly protonated molecule will form either the zwitterion, $^+HNR^-$, or the uncharged molecule, NRH. Following the loss of the first proton, a second proton can leave, with the equilibria given by the equilibrium constants K_2 and K_4. The relative amount of zwitterion and uncharged molecules is a constant given by:

$$\frac{[^+HNR^-]}{[NRH]} \approx \frac{K_1}{K_3} = \frac{K_4}{K_2} \qquad \text{(Eq. 1)}$$

The method described for elucidating all four constants is a complex procedure. To utilize the technique without modification, the compounds must possess a pH-dependent chromophore and be soluble enough to permit potentiometric titration. It will be shown that, as an alternative, the constants can be calculated if ionization constants of a structurally similar compound are known.

Five commercial cephalosporins were investigated: cephapirin[1] {3-[(acetyloxy)methyl]-8-oxo-7-[[(4-pyridinylthio)acetyl]amino]-5-thia-1-azabicyclo[4.2.0]oct-2-ene-2-carboxylic acid monosodium salt} (I), cephaloglycin[2] {[6*R*-[6α,7β(*R**)]]-3-[(acetyloxy)methyl]-7-[(aminophenylacetyl)amino]-8-oxo-5-thia-1-azabicyclo[4.2.0]-oct-2-ene-2-carboxylic acid} (II), cephalexin[2] {(+)-[6*R*-[6α,7β(*R**)]]-7-[(aminophenylacetyl)amino]-3-methyl-8-oxo-5-thia-1-azabicyclo[4.2.0]oct-2-ene-2-carboxylic acid} (III), cephalothin[2] {3-[(acetyloxy)methyl]-8-oxo-7-[(2-thienylacetyl)amino]-5-thia-1-azabicyclo[4.2.0]oct-2-ene-2-carboxylic acid sodium salt} (IV), and cefazolin[2] {(6*R-trans*)-3-[[(5-methyl-1,3,4-thiadiazol-2-yl)thio]-methyl]-8-oxo-7-[[(1*H*-tetrazol-1-yl)acetyl]amino]-5-thia-1-azabicyclo[4.2.0]-oct-2-ene-2-carboxylic acid monosodium salt} (V). Compounds I–III have two basic groups and, therefore, will have the equilibria expressed according to Scheme I; IV and V have one basic group and, therefore, have one pKa.

EXPERIMENTAL

Potentiometric Measurements—Potentiometric measurements were made at 25 ± 2° using the previously described equipment (1). The appropriate amount of compound (400–700 mg) was dissolved in water, and an excess of 0.15 *N* HCl was added to doubly protonate the diprotic compounds and singly protonate the monoprotic compounds. These solutions were then titrated with 0.15 *N* KOH, and the pH was measured with a meter[3] in the expanded scale mode.

Corrections for impurities based on microbiological potency values were made on III and V; a moisture content determination of II was made, and the appropriate correction was applied. The moisture content of I and III–V was assumed to be that given by the formula according to the manufacturer. At least two titrations were made for each compound.

Spectrophotometric Measurements—Spectrophotometric measurements[4] were made on I. Buffers were prepared at molar ionic strengths between 0.05 and 0.1 *M* over the pH 2–7.5 range. Aliquots of 1 ml of a stock solution of I were placed into 25-ml volumetric flasks and brought to volume with the appropriate buffers (final concentration was

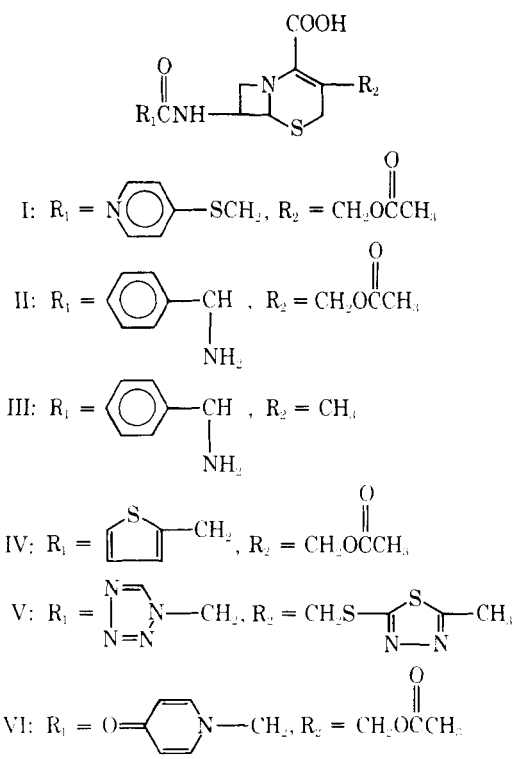

[1] Bristol Laboratories.
[2] Eli Lilly and Co.
[3] Beckman Century SS-1.
[4] Varian Cary 17.

Table I—pKa Values of Cephalosporins

Compound	pK_1	pK_2	pK_3	pK_4
I	1.83	5.48	4.78	2.53
II	1.78	7.22	6.46	2.53
III	2.48	7.59	6.46	3.60
IV	—	—	—	2.35
V	—	—	—	2.75
VI	1.70	2.80	1.97	2.53

11 μg/ml). Spectra were then obtained of these solutions. A maximum absorption at 290 nm was attributed to the protonated pyridine ring, and that at 258 nm was assigned to the nonprotonated ring.

THEORETICAL

In the following equations, { }, [ ], Y, and K represent activity, concentration, activity coefficient, and equilibrium constants, respectively, on a molar scale. The total concentrations of base added as titrant and of acid being titrated are given by [B] and [A].

Previously (1), an equation was derived having the form:

$$\alpha = K_1\frac{Y_{+HNRH}}{Y_{+HNR^-}}\beta + K_3\frac{Y_{+HNRH}}{Y_{NRH}}\beta + K_3K_4\frac{Y_{+HNRH}}{Y_{NR^-}}\gamma \quad \text{(Eq. 2)}$$

where:

$$\alpha = [B]\{H^+\}^3 + \frac{\{H^+\}^4}{Y_{H^+}} - \frac{K_\omega\{H^+\}^2}{Y_{OH^-}} \quad \text{(Eq. 3)}$$

$$\beta = [A]\{H^+\}^2 - [B]\{H^+\}^2 - \frac{\{H^+\}^3}{Y_{H^+}} + \frac{K_\omega\{H^+\}}{Y_{OH^-}} \quad \text{(Eq. 4)}$$

$$\gamma = 2[A]\{H^+\} - [B]\{H^+\} - \frac{\{H^+\}^2}{Y_{H^+}} + \frac{K_\omega}{Y_{OH^-}} \quad \text{(Eq. 5)}$$

By combining two sets of experimental data (potentiometric and spectrophotometric), the four equilibrium constants could be determined by using:

$$\{H^+\}^2\frac{Y_{NR^-}}{Y_{+HNRH}}\{[Z] - [A]\} = K_3\{H^+\}\frac{Y_{NR^-}}{Y_{NRH}}\left\{[B] + \frac{\{H^+\}}{Y_{H^+}} - \frac{K_\omega}{\{H^+\}Y_{OH^-}} - [A]\right\} + K_3K_4\left\{[B] + \frac{\{H^+\}}{Y_{H^+}} - \frac{K_\omega}{\{H^+\}Y_{OH^-}} - 2[A] + [Z]\right\} \quad \text{(Eq. 6)}$$

where [Z] is the total concentration of protonated nitrogen species obtained spectrophotometrically.

Equation 6 can be expressed in the simplified form given by:

$$\delta = K_3\epsilon + K_3K_4\xi \quad \text{(Eq. 7)}$$

from which it can be seen that values for K_3 and K_4 can be obtained by either graphical techniques or simultaneous equations.

The value of K_3 or K_4 obtained from Eq. 6 can be inserted into Eq. 2 to calculate the remaining constants. A plot of α/β *versus* γ/β should be linear with a slope of K_3K_4 and an intercept at $\alpha/\beta = 0$ equal to $K_1 + K_3$, while a plot of α/γ *versus* β/γ should be linear with a slope of $K_1 + K_3$ and an intercept at $\beta/\gamma = 0$ equal to K_3K_4. Because of the relationship between the four constants, it can be shown that $K_1K_2 = K_3K_4$. This approach to solving for the equilibrium constants leads to the conclusion that, with knowledge of one constant, the remaining constants can be determined using Eq. 2.

When acidic groups on a molecule are separated by large distances with no conjugation, there should be little interaction between the groups influencing the respective equilibria. Therefore, it should be possible to determine the microconstants for the diacidic cephalosporin compounds in Table I if a comparable equilibrium exists on a similar compound that is known. Combining the known value with either the calculated $K_1 + K_3$ or K_3K_4 will result in values for the unknown constants.

The selection of the best known value to use requires careful consideration because the sum $K_1 + K_3$ is obtained and it is better to select the

Table II—Comparison of Calculated pKa Values for I

Method[a]	pK_1	pK_2	pK_3	pK_4
A	1.83	5.48	4.78	2.53
B	1.85	5.44	4.47	2.81

[a] Method A used K_4 of VI; Method B combined spectrophotometric and potentiometric data.

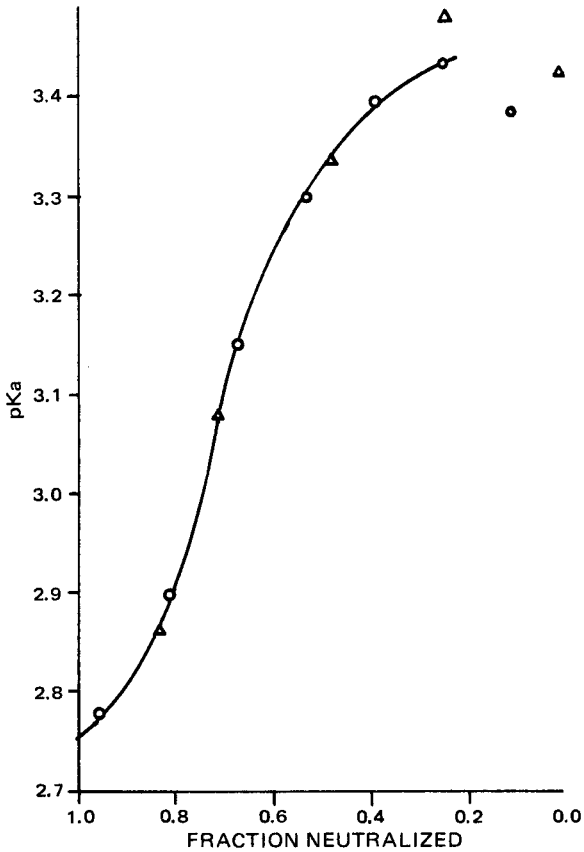

Figure 1—*Calculated pKa for V.*

smaller of these two constants as the known constant. That is, if K_3 is smaller than K_1, either K_3 or K_4 should be used as the known constant; if K_1 is smaller, then either K_1 or K_2 should be used.

The equilibrium constants for the monoprotic compounds were calculated using a standard equation in the form:

$$\eta = \theta K \quad \text{(Eq. 8)}$$

where:

$$\eta = \frac{Y_{A^-}}{Y_{HA}}\{H^+\}\left\{[B]\{H^+\} + \frac{\{H^+\}^2}{Y_{H^+}} - \frac{K_\omega}{Y_{OH^-}}\right\} \quad \text{(Eq. 9)}$$

$$\theta = [A]\{H^+\} - [B]\{H^+\} - \frac{\{H^+\}^2}{Y_{H^+}} + \frac{K_\omega}{Y_{OH^-}} \quad \text{(Eq. 10)}$$

RESULTS AND DISCUSSION

The equilibrium constants of I and II were determined using the value for pK_4 of 3-[(acetyloxy)methyl]-8-oxo-7-[[4-oxo-1(4*H*)-pyridinyl)acetyl]amino]-5-thia-1-azabicyclo[4.2.0]oct-2-ene-2-carboxylic acid (VI) previously reported (1). The equilibrium associated with pK_4 is the loss of the proton on the carboxylate group when the molecule is uncharged and satisfies the requirements for the selection of acceptable equilibria. On all three compounds, R_2 is the same and R_1 is different. Since R_1 is

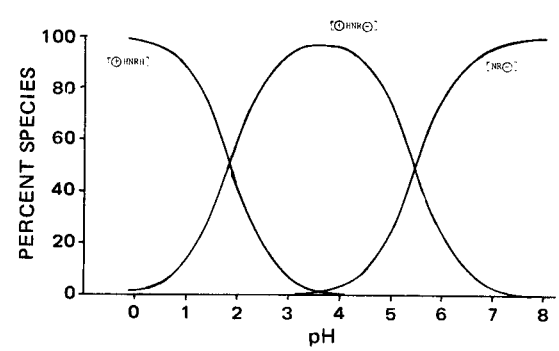

Figure 2—*Species profile for I.*

Table III—Correlation of Equilibrium Constants

Compound	—COOH pKa
Cephalosporin C[a]	3.1
D-Cephaloglycin[b]	4.4
L-Cephaloglycin[b]	4.6
7-Aminocephalosporanic acid[c]	1.75

[a] Reference 8. [b] Reference 3. [c] Reference 4.

separated from the carboxylic acid group by a large distance with no conjugation, K_4 would be expected to be the same. Table I lists the calculated pKa values for these compounds.

The equilibrium constant K_3 can be considered the same for II and III. Both compounds have the same R_1 group, with the NH_2 group acting as a proton acceptor. Since the NH_2 is separated by a large distance with no conjugation from the carboxylic acid group and R_1, K_3 should be the same. This equilibrium is the loss of a proton from the protonated NH_2 (NH_3^+) to form the uncharged molecule. The values thus obtained for III are given in Table I.

Also included in Table I are the values calculated for the monoprotic compounds IV and V. These constants were obtained from the experimental data using Eq. 8.

To check the validity of the assumption used to calculate the constants for I–III, the constants for I were determined by combining spectrophotometric with potentiometric data as explained previously (1). In Table II, the results of the calculations by both methods are given for comparison and show good correlation between the two methods for pK_1 and pK_2 and fair correlation for pK_3 and pK_4. The correlation between pK_3 and pK_4 is not unreasonable when considering the type of compound and the fact that different methods were used.

The pKa values for the carboxy group on cephalosporins having the R_2 group CH_2OCOCH_3 are listed in Table III. It would not be expected that these values should differ by more than ±0.5 unit, but a spread of 2.85 units exists. Of particular interest are the values for D- and L-cephaloglycins, which give an indication of the reliability to be expected in the pKa values for these compounds. The same investigators used the same method to obtain both values and show a difference of 0.2 pKa unit. Although they are optical isomers, the pKa values for the carboxy groups should be the same. Any effect on the pKa values due to the different isomers would manifest itself in the side-chain pKa's. On the contrary, the same values for the side-chain pKa's were found. From this result, it can be concluded that a spread of 0.2 pKa unit would not be unexpected when using the same method. When using different methods, the expected correlation would be less and a difference of 0.3 pKa unit would not be unreasonable. It was not possible to measure the microionization constants of II and III by this method since they do not possess pH-dependent chromophores.

The pKa values for I and II and compounds related to III were reported (2–4); only two K_a values (K_{13} and K_{24}) were given. It can be shown that the two K_a values are related to those reported here according to:

$$K_{13} = K_1 + K_3 \qquad \text{(Eq. 11)}$$

and:

$$\frac{1}{K_{24}} = \frac{1}{K_2} + \frac{1}{K_4} \qquad \text{(Eq. 12)}$$

The pKa values reported by Prasad *et al.* (2) for I are in reasonable agreement (2.03 and 5.35) with those given here (1.83 and 5.48). Spencer *et al.* (3) reported values for II of 4.4 and 7.22, the first of which is significantly different from that found here (1.78 and 7.22). The study by Spencer *et al.* (3), however, used a 66% dimethylformamide–water mixture for the solvent, which could cause this large a difference in the pKa values. Also, the value of 4.4 for pK_{13} is not consistent with the finding of Prasad *et al.* (2) or the value in Ref. 1, which indicate the carboxylic acid to have a pKa of about 2 with this R_2 group. Albert and Serjeant (5) discussed the effect of mixed solvents upon the pKa and indicated that it is extremely difficult to correlate equilibrium constants in mixed solvents with those in pure water.

Table IV—pH of Maximum Zwitterion Concentration and the Ratio $[^+HNR^-]/[NRH]$

Compound	pH	$[^+HNR^-]/[NRH]$
I	3.66	8.91×10^2
II	4.50	4.79×10^4
III	5.04	9.55×10^3
VI	2.25	1.86

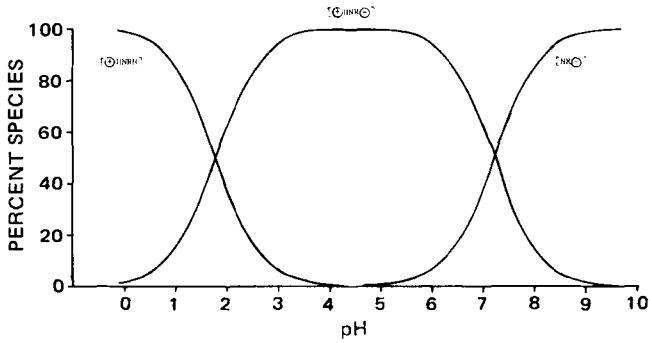

Figure 3—*Species profile for II.*

A direct comparison cannot be made with literature values for III. An estimate of the effect of the CH_3 group on carboxylic acid dissociation can be obtained from Stedman *et al.* (4). They found that the carboxy group has a pKa between 2.38 and 2.74 when the CH_3 group is present. This result is in good agreement with the 2.48 found here.

Neither pKa of the monoprotic compounds was reported. Stedman *et al.* (4) reported that changing the CH_3 group to $CH_2OC(=O)CH_3$ lowers the pKa of the carboxy group in compounds similar to IV. The pKa of V (2.75) appears reasonable when compared to IV.

The method used to determine the pKa values of I–III introduces a slight error since the assumption is made that the largest influence on the acidic groups is made by groups close to them. The fact that pK_1 for I, II, and VI and pK_2 for II and III are nearly the same indicates that there is little or no long-range influence in the uncharged molecules because the charged molecules have little effect on the equilibria. Any influence on the equilibria due to different groups would be expected to be greater when the groups are charged.

Compounds IV and V were not completely soluble in their acid forms at the concentrations required for the potentiometric titrations. Even though precipitation occurred, calculations were made using the data obtained. The pKa values calculated were not constant but did change in a systematic manner. A plot of the pKa values *versus* the fraction of acid neutralized could be extrapolated to a value of 1. Since the compounds were soluble when completely neutralized, the pKa value at this point should be correct. A plot of this type is given in Fig. 1.

In performing the calculations, an attempt was made to correct for activity effects by utilizing Davies equation (6) to approximate the single ion activities:

$$-\log Y_i = AZ_i^2 \left\{ \frac{\sqrt{I}}{1+\sqrt{I}} - 0.2I \right\} \qquad \text{(Eq. 13)}$$

where Y_i is the single ion activity coefficient, A is a parameter whose value at 25° is 0.5092 on a molar scale, Z_i is the charge of ion i, and I is the molar ionic strength. The advantage of this equation over the Debye–Hückel law is that it does not require the use of any ion size parameters.

An approximation was not made for the activity of the zwitterionic species because there is no expression comparable to Eq. 13. It was not expected that Y_{+-}[5] would deviate greatly from the ideal value of 1. It also was assumed that the uncharged species had an activity coefficient of 1, a reasonable assumption within the limits of the experiment.

In Figs. 2–5, the species profiles for I–III and VI, respectively, are

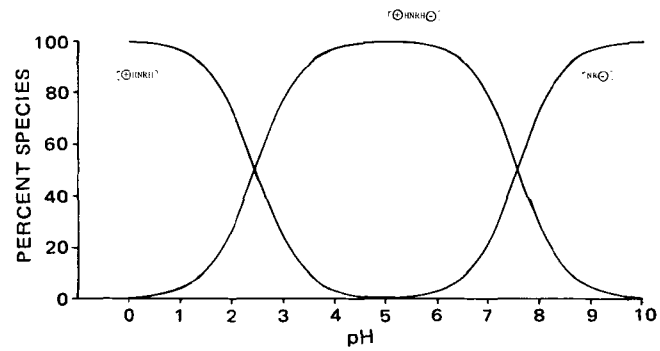

Figure 4—*Species profile for III.*

[5] The activity coefficient for the zwitterionic species.

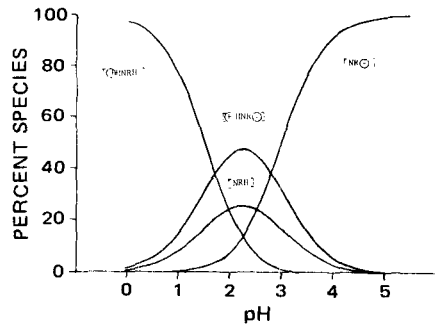

Figure 5—*Species profile for VI.*

shown. They were calculated using:

$$\%[^+HNRH] = 100 \Big/ \left\{1 + \frac{K_1}{[H^+]} + \frac{K_3}{[H^+]} + \frac{K_3K_4}{[H^+]^2}\right\} \quad \text{(Eq. 14)}$$

$$\%[NRH] = 100 \Big/ \left\{1 + \frac{[H^+]}{K_3} + \frac{K_4}{[H^+]} + \frac{K_1}{K_3}\right\} \quad \text{(Eq. 15)}$$

$$\%[^+HNR^-] = 100 \Big/ \left\{1 + \frac{[H^+]}{K_1} + \frac{K_2}{[H^+]} + \frac{K_3}{K_1}\right\} \quad \text{(Eq. 16)}$$

$$\%[NR^-] = 100 \Big/ \left\{1 + \frac{[H^+]}{K_2} + \frac{[H^+]}{K_4} + \frac{[H^+]^2}{K_3K_4}\right\} \quad \text{(Eq. 17)}$$

These equations are written in their most general forms. To simplify them, the percentages of one species can be expressed as percentage functions of the other species (7).

The maximum concentration of neutral molecules, either as zwitterions or uncharged molecules, occurs at the pH given by:

$$pH = \frac{pK_1 + pK_2}{2} = \frac{pK_3 + pK_4}{2} \quad \text{(Eq. 18)}$$

In Table IV, the pH at which the maximum zwitterion concentration occurs and the concentration ratio $[^+HNR^-]/[NRH]$ are given. Since K_1 is greater than K_3 for each compound, there are more zwitterions than uncharged molecules at any pH.

REFERENCES

(1) W. H. Streng, H. E. Huber, J. L. DeYoung, and M. A. Zoglio, *J. Pharm. Sci.*, **65**, 1034 (1976). W. H. Streng, *ibid.*, **66**, 1357 (1977).

(2) V. K. Prasad, W. H. Johns, M. W. Wingate, M. M. Mihotic, B. J. Southard, M. A. Kaplan, and A. P. Granatek, *Curr. Ther. Res.*, **16**, 1214 (1974).

(3) J. L. Spencer, E. H. Flynn, R. W. Roeske, F. Y. Siu, and R. R. Charwette, *J. Med. Chem.*, **9**, 746 (1966).

(4) R. J. Stedman, K. Swered, and J. R. E. Hoover, *ibid.*, **7**, 117 (1964).

(5) A. Albert and E. P. Serjeant, "Ionization Constants of Acids and Bases," Wiley, New York, N.Y., 1962, pp. 66–68.

(6) J. N. Butler, "Ionic Equilibrium. A Mathematical Approach," Addison-Wesley, Reading, Mass., 1964, p. 437.

(7) *Ibid.*, pp. 210–212.

(8) E. P. Abraham, *Q. Rev. Chem. Soc.*, **21**, 231 (1967).

High-Pressure Liquid Chromatographic Determination of Cycloheximide in Ointment and Suspension Formulations

LEO W. BROWN

Received June 27, 1977, from *The Upjohn Company, Kalamazoo, MI 49001.* Accepted for publication August 31, 1977.

Abstract □ A high-pressure liquid chromatographic procedure is described for the assay of the antibiotic cycloheximide in bulk drug and two experimental formulations. The method utilizes a reversed-phase C_{18} chromatographic column and refractive index detection. Possible impurities or degradation products, isocycloheximide, anhydrocycloheximide, and dimethylcyclohexanone, are well separated from cycloheximide by this procedure. Complete extraction of cycloheximide from the formulations was obtained. The assay has a relative standard deviation of approximately 1%.

Keyphrases □ Cycloheximide—high-pressure liquid chromatographic analysis in bulk drug and prepared formulations □ High-pressure liquid chromatography—analysis, cycloheximide in bulk drug and prepared formulations □ Antibiotics—cycloheximide, high-pressure liquid chromatographic analysis in bulk drug and prepared formulations

Cycloheximide[1] is used in several agricultural formulations. The compound is produced by fermentation from *Streptomyces griseus* and has been studied (1–6) for its fungicidal properties. It also has been used successfully as an abscission agent (7).

[1] Actidione, The Upjohn Co., Kalamazoo, Mich.

The chemical structure of cycloheximide (I) (mol. wt. 281; mp 120°; pK 11.2) has been characterized completely (8, 9). Degradation products of cycloheximide, 2,4-dimethylcyclohexanone, isocycloheximide (10), and anhydrocycloheximide, have been studied. Because of the β-hydroxy ketone moiety in cycloheximide, dehydration to anhydrocycloheximide is the predominant degradation pathway.

Cycloheximide has been determined microbiologically (11) and spectrophotometrically (12, 13). The latter procedures involve reactions to develop a color since cycloheximide has only end absorption in the UV. Both spectrophotometric procedures are relatively nonspecific. Even

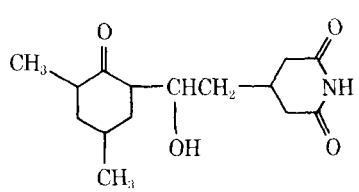

I

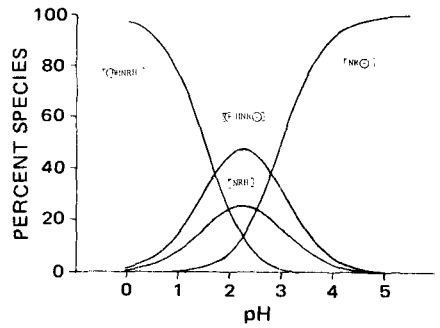

Figure 5—*Species profile for VI.*

shown. They were calculated using:

$$\%[^+HNRH] = 100 \Big/ \left\{1 + \frac{K_1}{[H^+]} + \frac{K_3}{[H^+]} + \frac{K_3K_4}{[H^+]^2}\right\} \quad \text{(Eq. 14)}$$

$$\%[NRH] = 100 \Big/ \left\{1 + \frac{[H^+]}{K_3} + \frac{K_4}{[H^+]} + \frac{K_1}{K_3}\right\} \quad \text{(Eq. 15)}$$

$$\%[^+HNR^-] = 100 \Big/ \left\{1 + \frac{[H^+]}{K_1} + \frac{K_2}{[H^+]} + \frac{K_3}{K_1}\right\} \quad \text{(Eq. 16)}$$

$$\%[NR^-] = 100 \Big/ \left\{1 + \frac{[H^+]}{K_2} + \frac{[H^+]}{K_4} + \frac{[H^+]^2}{K_3K_4}\right\} \quad \text{(Eq. 17)}$$

These equations are written in their most general forms. To simplify them, the percentages of one species can be expressed as percentage functions of the other species (7).

The maximum concentration of neutral molecules, either as zwitterions or uncharged molecules, occurs at the pH given by:

$$pH = \frac{pK_1 + pK_2}{2} = \frac{pK_3 + pK_4}{2} \quad \text{(Eq. 18)}$$

In Table IV, the pH at which the maximum zwitterion concentration occurs and the concentration ratio $[^+HNR^-]/[NRH]$ are given. Since K_1 is greater than K_3 for each compound, there are more zwitterions than uncharged molecules at any pH.

REFERENCES

(1) W. H. Streng, H. E. Huber, J. L. DeYoung, and M. A. Zoglio, *J. Pharm. Sci.*, **65**, 1034 (1976). W. H. Streng, *ibid.*, **66**, 1357 (1977).

(2) V. K. Prasad, W. H. Johns, M. W. Wingate, M. M. Mihotic, B. J. Southard, M. A. Kaplan, and A. P. Granatek, *Curr. Ther. Res.*, **16**, 1214 (1974).

(3) J. L. Spencer, E. H. Flynn, R. W. Roeske, F. Y. Siu, and R. R. Charwette, *J. Med. Chem.*, **9**, 746 (1966).

(4) R. J. Stedman, K. Swered, and J. R. E. Hoover, *ibid.*, **7**, 117 (1964).

(5) A. Albert and E. P. Serjeant, "Ionization Constants of Acids and Bases," Wiley, New York, N.Y., 1962, pp. 66–68.

(6) J. N. Butler, "Ionic Equilibrium. A Mathematical Approach," Addison-Wesley, Reading, Mass., 1964, p. 437.

(7) *Ibid.*, pp. 210–212.

(8) E. P. Abraham, *Q. Rev. Chem. Soc.*, **21**, 231 (1967).

High-Pressure Liquid Chromatographic Determination of Cycloheximide in Ointment and Suspension Formulations

LEO W. BROWN

Received June 27, 1977, from *The Upjohn Company, Kalamazoo, MI 49001.* Accepted for publication August 31, 1977.

Abstract □ A high-pressure liquid chromatographic procedure is described for the assay of the antibiotic cycloheximide in bulk drug and two experimental formulations. The method utilizes a reversed-phase C_{18} chromatographic column and refractive index detection. Possible impurities or degradation products, isocycloheximide, anhydrocycloheximide, and dimethylcyclohexanone, are well separated from cycloheximide by this procedure. Complete extraction of cycloheximide from the formulations was obtained. The assay has a relative standard deviation of approximately 1%.

Keyphrases □ Cycloheximide—high-pressure liquid chromatographic analysis in bulk drug and prepared formulations □ High-pressure liquid chromatography—analysis, cycloheximide in bulk drug and prepared formulations □ Antibiotics—cycloheximide, high-pressure liquid chromatographic analysis in bulk drug and prepared formulations

Cycloheximide[1] is used in several agricultural formulations. The compound is produced by fermentation from *Streptomyces griseus* and has been studied (1–6) for its fungicidal properties. It also has been used successfully as an abscission agent (7).

[1] Actidione, The Upjohn Co., Kalamazoo, Mich.

The chemical structure of cycloheximide (I) (mol. wt. 281; mp 120°; pK 11.2) has been characterized completely (8, 9). Degradation products of cycloheximide, 2,4-dimethylcyclohexanone, isocycloheximide (10), and anhydrocycloheximide, have been studied. Because of the β-hydroxy ketone moiety in cycloheximide, dehydration to anhydrocycloheximide is the predominant degradation pathway.

Cycloheximide has been determined microbiologically (11) and spectrophotometrically (12, 13). The latter procedures involve reactions to develop a color since cycloheximide has only end absorption in the UV. Both spectrophotometric procedures are relatively nonspecific. Even

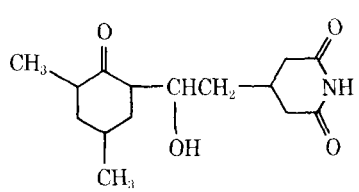

I

Table I—Assay Precision of Replicate Samples of Cycloheximide Bulk Drug

Sample Weight, mg	Peak Height Ratio		Ratio/Weight
5.601	0.6141		0.1096
7.955	0.8715		0.1096
6.714	0.7309		0.1089
7.553	0.8284		0.1097
8.866	0.9833		0.1109
8.682	0.9576		0.1103
		Average	0.1098
		RSD	0.62%

though the degradation products of cycloheximide are not microbiologically active (14), making the microbiological assay specific for cycloheximide, the assay gives no indication of the amount and nature of degradation products.

A GLC method was reported for the analysis of cycloheximide and its degradation products (14). This procedure involves silylation of cycloheximide followed by treatment with isopropyl alcohol to produce a monotrimethylsilyl derivative, which chromatographs as a single peak. Recently, two new experimental formulations of cycloheximide were developed in these laboratories. Since the GLC procedure was not successful with these formulations because of interference of excipients in derivatization, a high-pressure liquid chromatographic (HPLC) procedure was developed. The method utilizes a reversed-phase C_{18} chromatographic column and refractive index detection.

EXPERIMENTAL

HPLC Conditions—A liquid chromatograph[2] was used with a differential refractometer[3] detector. The column was reversed-phase C_{18} micro silica gel[4], 30 cm × 3.9 mm. Column pressure was maintained at 900 psi (0.8 ml/min), and a 25-μl injection volume was used with a 25-μl loop injector[5]. Chart speed was 2.54 cm/5 min, and attenuation on the refractive index detector was 9.6×10^{-5} refractive index unit full scale. The mobile phase was acetonitrile–methanol–water (125:20:355).

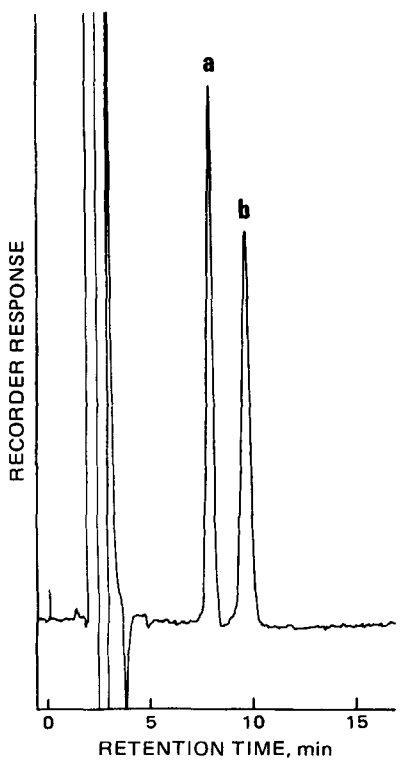

Figure 1—*Chromatogram of* p-*nitrobenzyl alcohol as internal standard (a) and cycloheximide (b).*

Table II—Assay Results of Recovery Study of Cycloheximide Added to 1.0 g of Suspension Formulation

Cycloheximide Added, mg	Peak Height Ratio		Cycloheximide Found, %
5.563	0.778		104.1
5.960	0.830		103.3
6.112	0.851		103.3
5.753	0.788		101.9
7.539	1.032		101.9
5.058	0.770		102.6
		Average	102.6
		RSD	0.9%

Internal Standard Solution—A methanol solution containing approximately 2.7 mg of *p*-nitrobenzyl alcohol/ml was prepared.

Reference Preparation—*For Cycloheximide in Ointment Formulation*—Approximately 7 mg of reference cycloheximide was accurately weighed and transferred to a 100-ml stoppered graduated cylinder. To this cylinder were added 0.7 g of ointment base, 2.0 ml of internal standard solution, 23 ml of methanol, and 75 ml of hexane. A stirring bar was added to the cylinder, which was then shaken to dissolve the ointment. After complete dissolution, the top hexane layer was removed by suction and the methanol layer was transferred to a 10-dram shell vial. The methanol was evaporated to approximately 2 ml with a nitrogen stream.

At the beginning of the evaporation, an immiscible top layer was formed and was removed by suction. Further evaporation produced a white precipitate. The mixture was transferred to a 15-ml centrifuge tube and centrifuged when approximately 2 ml of methanol remained in the

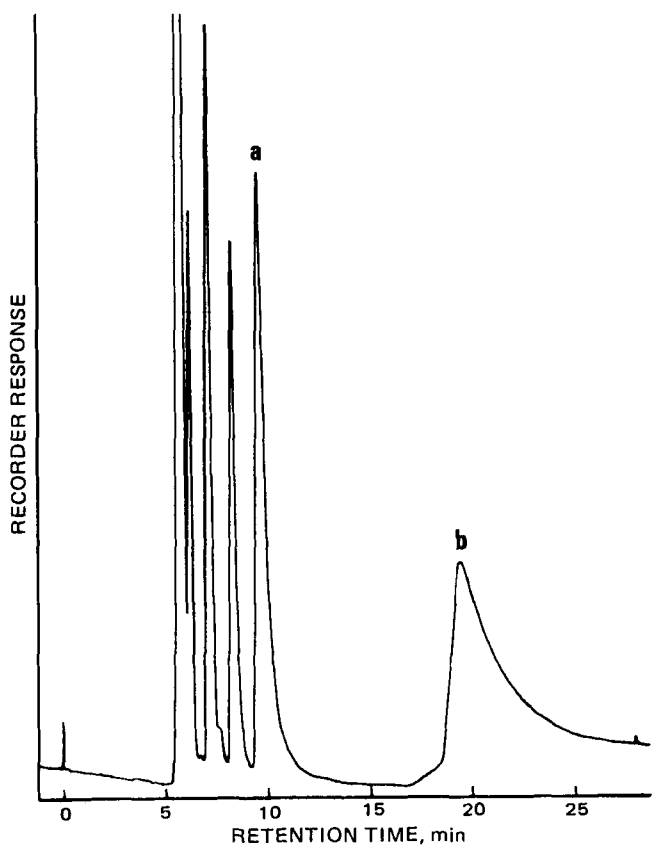

Figure 2—*Chromatogram of the suspension formulation on a silica gel column using ethyl acetate as the mobile phase. Peak a is cycloheximide, and b is propylene glycol in the formulation. All other peaks are ingredients in the formulation.*

[2] Model 830, DuPont Instrument Co., Wilmington, Del.
[3] Model R-401, Waters Associates.
[4] Bondapak, Waters Associates.
[5] Valco.

Table III—Recovery Results on Cycloheximide Added to Placebo Ointment

Weight of Cycloheximide, mg	Weight of Ointment, mg	Peak Height Ratio		Ratio/ Weight
7.019	6320	0.9231		0.1315
8.161	6530	1.0766		0.1318
7.551	7540	0.9904		0.1311
7.266	7190	0.9532		0.1311
6.717	6980	0.8815		0.1312
			Average	0.1313
			RSD	0.23%
6.657[a]	0	0.8454		0.1269
7.569[a]	0	0.9462		0.1250
			Average	0.1260
6.925[b]	0	0.8500		0.1227
6.958[b]	0	0.8564		0.1230
			Average	0.1229

[a] Carried through procedure without ointment. [b] Not extracted.

evaporation step. Approximately 1 ml of the clear supernate in the centrifuge tube was transferred to a 1-dram shell vial.

For Cycloheximide in Aqueous Suspension Formulation—Approximately 7 mg of reference cycloheximide was accurately weighed and transferred to a 3-dram shell vial. Internal standard solution, 2 ml, was added, and the vial was swirled to dissolve the cycloheximide.

Sample Preparation—*Cycloheximide in Ointment Formulation*—An ointment sample equivalent to approximately 7 mg of cycloheximide was accurately weighed and transferred to a 100-ml stoppered graduated cylinder. The sample was then treated in the same manner as the reference preparation, starting with the addition of 2.0 ml of internal standard solution.

Cycloheximide in Aqueous Suspension Formulation—The sample suspension was shaken vigorously to obtain a homogeneous mixture, and a sample equivalent to approximately 7 mg of cycloheximide was accurately weighed. The weighed sample was transferred to a 15-ml centrifuge tube. To this tube was added 10 ml of methanol and 2.0 ml of internal standard solution. Then the tube was shaken vigorously and centrifuged. Approximately 10 ml of the clear supernate was removed and evaporated with a nitrogen stream to less than 2 ml in a 3-dram shell vial. The volume was then adjusted to approximately 2 ml with methanol. The sample was mixed thoroughly and centrifuged or filtered to remove insoluble material.

Procedure—Sample and reference preparations were chromatographed using the chromatographic conditions described.

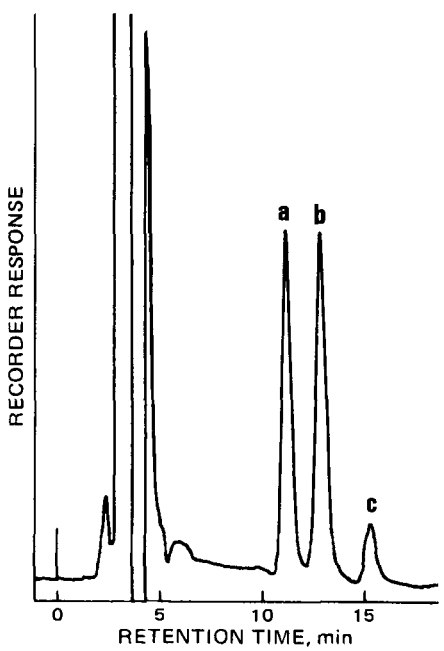

Figure 3—*Chromatogram of cycloheximide extracted from the suspension formulation. Peak a is* p*-nitrobenzyl alcohol used as the internal standard, b is cycloheximide, and c is a formulation ingredient.*

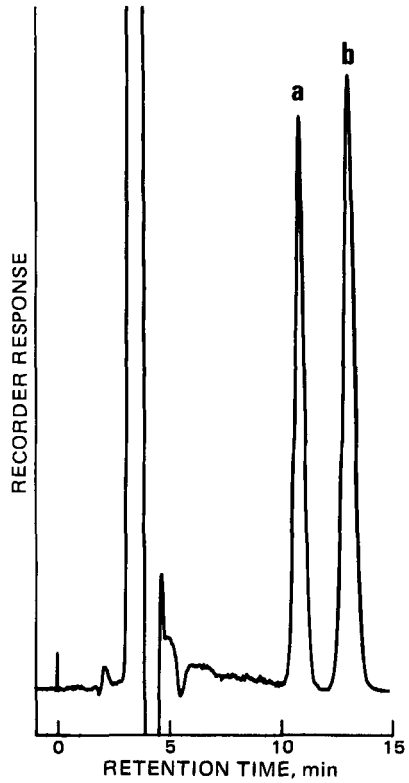

Figure 4—*Chromatogram of cycloheximide extracted from ointment. Peak a is* p*-nitrobenzyl alcohol used as an internal standard, and b is cycloheximide.*

Calculations—The following equation was used:

$$\% \text{ cycloheximide} = R_s/R_{ref} \times W_{ref}/W_s \times P \qquad \text{(Eq. 1)}$$

where R_s is the peak height ratio of the cycloheximide peak to the internal standard peak in the sample preparation; R_{ref} is the peak height ratio of the cycloheximide peak to the internal standard peak in the reference preparation; W_{ref} is the weight, in milligrams, of cycloheximide reference standard; W_s is the weight, in milligrams, of sample; and P is the purity of the cycloheximide reference expressed in percent.

RESULTS AND DISCUSSION

Samples of cycloheximide bulk drug were assayed by this HPLC procedure to check for linearity and precision (Table I). A relative standard deviation of less than 1% was obtained from six samples varying in weight from approximately 5 to 10 mg. A typical chromatogram is shown in Fig. 1.

To check recovery of cycloheximide from the aqueous suspension formulation, cycloheximide was added to a placebo formulation in varying amounts (Table II). Methanol was added to the sample preparation to increase the amount of clear supernate that could be removed after centrifugation. Addition of the internal standard solution eliminates the need to remove all of the supernate. Recovery was complete compared to a cycloheximide reference carried through the same extraction procedure. Addition of the placebo formulation to the reference preparation had no effect.

A GLC procedure (14) was tried for this aqueous suspension formulation, but the extraction procedures did not produce an extract that could be quantitatively derivatized. A silica gel column using HPLC was also tried for this formulation. A large tailing peak, identified as propylene glycol, eluted after cycloheximide, causing a longer assay time (Fig. 2). With the C_{18} reversed-phase column (Fig. 3), all formulation ingredients eluted before the cycloheximide peak except one, and it did not interfere. Only relatively polar formulation ingredients would be soluble in the methanolic solution used in the extraction. For this reason, a C_{18} column, which does not retain polar compounds, would be a better choice than a silica gel column, which retards their elution.

Development of an assay for cycloheximide in the ointment formulation was less difficult than that for the suspension formulation. A combination of hexane and methanol was used to extract the nonpolar oint-

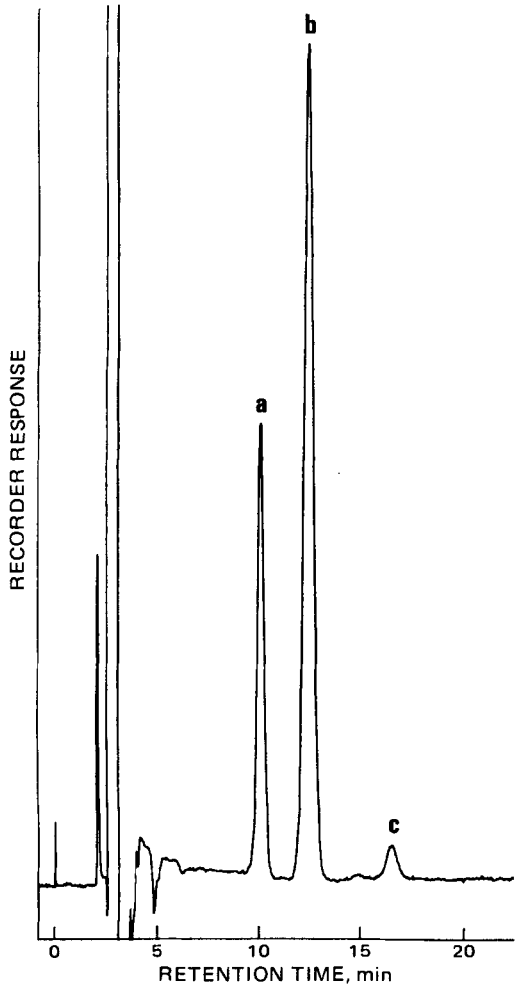

Figure 5—*Chromatogram of* p-*nitrobenzyl alcohol (a), cycloheximide (b), and isocycloheximide (c).*

ment ingredients into the upper hexane layer while the cycloheximide dissolved in the lower methanol layer. Assay results on cycloheximide added to placebo ointment, cycloheximide carried through the procedure but without placebo ointment, and cycloheximide not extracted are shown in Table III.

Results indicated only a slight difference between extracted and nonextracted cycloheximide. However, there was about a 7% difference in results comparing cycloheximide added to placebo ointment and carried through the extraction and results on nonextracted cycloheximide. This difference was due to the relative differences in solubilities of the internal standard and cycloheximide in the two solvent phases. The addition of ointment to a hexane–methanol system changes not only the relative volumes of the two layers but also their composition. For example, 50 ml each of hexane and methanol produced a system of about 14 ml in the upper layer and 84 ml in the lower layer. Addition of 1 g of ointment to the system produced an upper layer of about 20 ml and a lower layer of 79 ml.

To eliminate any bias, the reference preparation was treated in the same manner as the sample. Further work showed that the addition of 0.7 g of placebo ointment to the reference preparation was sufficient. Addition of 10 times that amount of ointment gave the same result. Complete extraction of 0.1% cycloheximide in ointment samples was obtained with a relative standard deviation of less than 0.5% by using the reference preparation with the small amount of placebo ointment added. A typical chromatogram of cycloheximide extracted from ointment is shown in Fig. 4. Placebo ointment carried through the procedure produced no interfering chromatographic peaks.

In quality control situations where many assays are performed over a short period, it is important that the chromatographic column retain its integrity. Since the column is stainless steel, it is difficult to determine whether there is buildup of formulation ingredients on the column. One way to determine this effect is to use a thin-layer plate of comparable support and to develop the plate with the mobile phase. Sample solutions of both cycloheximide formulations were applied to silica gel 60 F_{254} silanized (producing a reversed-phase plate) and developed with the mobile phase. All ointment formulation ingredients moved up the plate. However, a small amount of UV-absorbing material remained at the origin when the aqueous suspension formulation was developed on the plate. For this reason, the packing at the inlet of the HPLC column should be replaced after the assay of several suspension formulation samples.

The known impurities or degradation products, isocycloheximide, anhydrocycloheximide, and 2,4-dimethylcyclohexanone, were described previously (14) and were separated by GLC. Table IV shows the relative retention volumes for these impurities by this HPLC procedure. By GLC, the isocycloheximide peak was not baseline separated from the cycloheximide peak. By HPLC, the two peaks were well separated (Fig. 5).

Table IV—Relative Retention Volume of Possible Impurities or Degradation Products in Cycloheximide Samples

Compound	Relative Retention Volume[a]
Cycloheximide	1.00
Isocycloheximide	1.34
Anhydrocycloheximide	2.88
2,4-Dimethylcyclohexanone	0.49
Internal standard	0.77

[a] See *Experimental* for conditions.

REFERENCES

(1) I. M. Felber and D. L. Hammer, *Bot. Gaz. (Chicago)*, **110**, 324 (1948).

(2) D. L. Gill, *Phytopathology*, **40**, 333 (1950).

(3) C. D. Leaphart and E. F. Wicker, *Plant Dis. Rep.*, **52**, 6 (1968).

(4) D. Petersen and D. Cation, *ibid.*, **34**, 5 (1950).

(5) H. B. Tukey, *Science*, **108**, 664 (1948).

(6) J. R. Vaughn, *Phytopathology*, **41**, 36 (1951).

(7) W. C. Cooper and W. H. Henry, *J. Agr. Food Chem.*, **19**, 559 (1971).

(8) E. C. Kornfeld, R. G. Jones, and T. Parke, *J. Am. Chem. Soc.*, **71**, 150 (1949).

(9) B. C. Lawes, *ibid.*, **84**, 239 (1962).

(10) A. J. Lemin and J. H. Ford, *J. Org. Chem.*, **25**, 344 (1960).

(11) A. J. Whiffen, *J. Bacteriol.*, **56**, 283 (1948).

(12) A. A. Forist and S. Theal, *Anal. Chem.*, **31**, 1042 (1959).

(13) T. Okuda, M. Suzuki, Y. Egawa, and K. Ashino, *Chem. Pharm. Bull.*, **6**, 328 (1958).

(14) L. W. Brown, *Agr. Food Chem.*, **21**, 83 (1973).

Separation of Multisized Drug Suspensions into Narrow Distributions by Centrifugal Elutriation

STEPHEN A. HOWARD *x, JOHN W. MAUGER *, AURAWAN KHWANGSOPHA *, and PING LEE ‡

Received April 4, 1977, from the *School of Pharmacy and the ‡Department of Physiology and Biophysics, West Virginia University, Morgantown, WV 26506. Accepted for publication September 8, 1977.

Abstract □ A centrifugal elutriator rotor was used to separate suspensions of micronized hydrocortisone acetate and prednisolone acetate. Up to five distinct particle fractions could be isolated from a single parent suspension, and reasonable reproducibility was exhibited between various elutriator runs. Arithmetic means and associated standard deviations, based on volume, were calculated for each isolated fraction. These data demonstrate the narrowness and uniqueness of each fraction. The particle-size data show an apparent log-normal distribution for each isolate. The uniqueness of each fraction also was demonstrated by dissolution experiments where Fraction 1, the smallest fraction of prednisolone acetate, dissolved much more rapidly than Fraction 4, the largest fraction. The substantial difference in dissolution behavior of these two fractions of prednisolone acetate powder was biopharmaceutically significant.

Keyphrases □ Suspensions—separated into distinct particle-size fractions by centrifugal elutriation □ Particle-size fractions—suspensions separated by centrifugal elutriation □ Centrifugal elutriation—used to separate suspensions into distinct particle-size fractions □ Dosage forms—suspensions, separated into distinct particle-size fractions by centrifugal elutriation

Although it is well established that the particle size of suspended powders influences both the physical stability and dissolution rates of pharmaceutical suspensions, the monographs of only two official suspension products (insulin zinc suspension USP and sterile methylprednisolone acetate suspension NF) mention particle size. The lack of a simple method to obtain narrow populations of suspended material of varying sizes (in the micrometer range) is one major problem in establishing the optimum size requirements of a suspension product. With such a method, it would not be necessary to mill various lots of suspensions with differing particle-size distributions. Only one lot of suspension having a wide particle distribution would be required to separate out those size fractions needed for study. Thus, from a single suspension lot, samples could be obtained from which one could establish optimum product size requirements.

Critical study of dissolution kinetics is another investigational area where a separation technique such as described in this paper would prove invaluable. For example, the dissolution kinetics for multisized particle populations have been discussed (1–7). In some cases (8, 9), the experimental data were treated without calculation of the effect of particle-size distribution. Errors associated with this data treatment may be acceptable, except in cases of critical tests of dissolution rate theory (10). On the other hand, dissolution rate data for multisized methylprednisolone populations were compared with the theoretical expectation from a kinetic model that accounted for the distribution effects (2). The critical test of this dissolution model was influenced by the ability to measure and quantitate the true initial size distribution.

Another report (11) attempted to show that approximate cube root model equations, which incorporate distribution effects, were applicable to dissolution profiles of log-normal populations of oxalic acid particles. The log-normal populations were developed artificially from combined mesh fractions of oxalic acid particles grown under isothermal and nonisothermal conditions (11). An approach was evaluated to demonstrate the application of single-particle dissolution models to explain the dissolution kinetics of the 60–85-mesh fraction of tolbutamide particles (12). This approach permitted the calculation of the intrinsic dissolution profiles with a consideration of both size distribution and particle-size effects. All of these investigations point to the importance of controlling the particle-size distribution to study the dissolution model of interest critically. Therefore, a convenient and dependable method that allows control of particle-size distributions for critical dissolution tests for drug particles is necessary.

The purpose of the present study was to isolate narrow drug particle distributions from a drug suspension by centrifugal elutriation. The technique of centrifugal elutriation has been used in the biological sciences previously to separate cells from various tissues (13–17).

The general principle of elutriation is to counterbalance the sedimentation of particles under centrifugal force with a continuous flow of solution counter to the *g* force (18, 19). Suspended solids of varying sizes sediment at different rates under centrifugal force and may be separated by either varying the *g* force or the flow rate of the buffer, which is counter to the *g* force.

EXPERIMENTAL

Fraction Separation—An elutriation rotor[1] and centrifuge[2] were used. A 100-ml portion of suspension was infused into the elutriation chamber of the rotor in the centrifuge by a large peristaltic pump[3] in series with a smaller pump[4], which was used for fine adjustments of the flow rate. The loading flow rate was set at approximately 30 ml/min with the centrifuge running at approximately 2000 rpm.

After the drug particles were all loaded into the chamber, a volume of 0.9% NaCl was allowed to flow through the system. Collection of the first sample was then initiated simply by maintaining the same conditions described. After the first fraction appeared to be completely collected (determined by visual observation through the centrifuge window), the pump rate was increased to 53 ml/min and the second sample was collected. Once the second sample was collected, the centrifuge speed was reduced to approximately 1000 rpm and a third sample was removed.

The fourth sample was obtained at a pump rate of approximately 52 ml/min and a centrifuge speed of between 500 and 600 rpm. The fifth sample consisted of the residue left in the chamber after the pump and centrifuge were stopped. This fraction was removed by washing the chamber with 0.9% NaCl and collecting the residue. The exact pump centrifuge speeds used in each separation run are listed in Table I.

Particle-Size Measurement—An automated counter[5] was used for

[1] Model JE 6, Beckman Instrument Co., Fullerton, Calif.
[2] Model J-21B, Beckman Instrument Co., Fullerton, Calif.
[3] Model 1201 multispeed transmission, Harvard Apparatus Co., Millis, Mass.
[4] Model R-L175, Holter Co., Extracorporeal Medical Specialties Inc., King of Prussia, Pa.
[5] Model TA II, Coulter Electronics, Hialeah, Fla.

Table I—Centrifuge Conditions for Separation

Fraction	Pump Speed, ml/min	Centrifuge Speed, rpm			
		Run A[a]	Run B[b]	Run C[b]	Run D[c]
1	30	1830	2160	2030	2000
2	52	1830	2160	2030	2000
3	52	1140	1020	1070	1070
4	52	510	620	620	600
5	—	Residue	Residue	—	—

[a] Prednisolone acetate, 0.3%. [b] Prednisolone acetate, 0.6%. [c] Hydrocortisone acetate, 1%.

all particle-size measurements. This particular apparatus provides particle-size distributions based on equivalent sphere volume, which is converted to weight distribution if all material measured has the same density. The instrument has a 16-channel readout. Doublets and other multiple counts can be considered negligible by maintaining the dilution of the sample in the electrolyte. The instrument has a concentration meter which facilitates this process. Microscopic examination was also used to check for agglomerates.

The electrolyte solution[6] was presaturated with drug and double filtered through a 0.22-μm filter to avoid particle dissolution during measurement.

A population accessory was used to obtain a number count for each channel. Apertures of 200 and 50 μm were used in this study, and polystyrene beads[7] were used as standards to calibrate the channels.

Sample Preparation—The suspensions used were 0.3% prednisolone acetate[8] suspension in normal saline (Run A), 0.6% prednisolone acetate[8] in normal saline (Run B), 0.6% prednisolone acetate[8] in presaturated normal saline (Run C), and hydrocortisone acetate[9] in normal saline (Run D).

Each suspension was prepared using a mortar and pestle with gradual trituration. It was desirable to have as wide a distribution as possible for the initial trials.

Dissolution Determinations—During this study, all reported dissolution data were obtained using a device reported by Shah *et al.* (20) with the sample basket removed. The basic features of this apparatus are a large volume fluid container, a rotating filter assembly, and an external variable speed magnetic stirrer. The rotating filter assembly provides a variable intensity of mild laminar liquid agitation and also functions as an *in situ* nonclogging filter to permit efficient intermittent or continuous filtration of the dissolution fluid samples during dissolution.

One liter of distilled water was utilized as the dissolution medium. The temperature was maintained at 37°, and the stirring speed of the filter assembly was 300 rpm. A strobe lamp was employed to standardize the stirring speed.

Filtered fluid samples were continuously withdrawn at the rate of 100 ml/min and were circulated through a spectrophotometer[10] for assay and then back into the dissolution flask. The prednisolone acetate was assayed at 246 nm.

The dissolution experiments were initiated by injecting a predetermined amount of the desired fraction of prednisolone acetate suspension at a fixed position in the beaker, using a syringe fitted with an extra long needle. The final concentration was kept below 10% of saturation. The chart paper was marked at the exact time the suspension was introduced into the flask. The absorbance of dissolving prednisolone acetate was recorded at 5-sec intervals until 1500 sec from the digital display of the spectrophotometer and then periodically up until approximately 2 hr. A final 24-hr reading was taken to determine an equilibrium concentration.

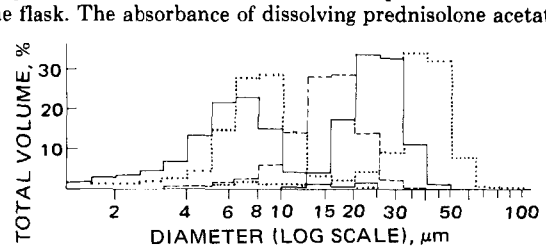

Figure 1—*Particle-size distributions of the five fractions of Run B using prednisolone acetate suspensions. Key (from left to right): —, Fraction 1; . . . , Fraction 2; – – –, Fraction 3; —, Fraction 4; and . . . . . , Fraction 5.*

[6] Isoton, Coulter Diagnostics Inc., Hialeah, Fla.
[7] Latex (2.02 mm diameter) and polystyrene (9.69 mm diameter), Coulter Electronics, Hialeah, Fla.
[8] Schering Laboratories, Bloomfield, N.J.
[9] Micronized, Pfizer Laboratories, Norwich, Conn.
[10] Cary 118, Varian Instrument, Palo Alto, Calif.

Table II—Mean Particle Diameter in Micrometers and Standard Deviation Based on Percent Volume Distribution

Fraction		Prednisolone Acetate			Hydrocortisone Acetate, D
		A	B	C	
1	Mean	5.9[a]	6.5[a]	5.5[a]	5.4[a]
	SD	2.7	3.4	2.4	1.8
2	Mean	7.2[a]	8.0[a]	6.6[a]	7.0[a]
	SD	2.5	2.7	2.4	3.3
3	Mean	11.9[a]	16.3[b]	13.4[b]	7.7[a]
	SD	2.8	5.9	4.8	2.9
4	Mean	25.4[b]	25.3[b]	21.3[b]	9.8[b]
	SD	6.1	6.2	5.6	3.5
5	Mean	33.4[b]	32.7[b]		
	SD	7.7	8.7		

[a] A 50-μm aperture tube was used. [b] A 200-μm aperture tube was used.

RESULTS AND DISCUSSION

As shown in Table I, three elutriation separation experiments were conducted with prednisolone acetate suspensions. In addition, a preliminary experiment was conducted utilizing a suspension of hydrocortisone acetate. A comparison of the means of percent volume particle distribution for these four separation runs can be seen in Table II.

Prednisolone acetate Runs A and B were conducted first, and both used the same lot of raw material. Run C utilized a new lot of prednisolone acetate and was conducted to check the previous two experiments.

The hydrocortisone acetate was the first material tested; although it yielded a good separation, the micronized sample did not contain a wide distribution of particles, especially large particles. Therefore, prednisolone acetate was utilized for most experiments. The result of the hydrocortisone acetate run is included to demonstrate the diversity and reproducibility of the process.

Fraction 1 contained most of the finest particles and was the first fraction collected. As shown in Table II, all mean particle sizes, including the hydrocortisone acetate run, yielded mean particle sizes within 1 μm of each other. The mean particle diameters were calculated from the discrete normalized data where the random variable is the average size per channel.

In the second fraction, the mean particle diameter for each run increased by slightly over 1 μm compared to the data shown for Fraction 1. Once again, the means were close, with no mean more than 1.5 μm apart and all means within 1 *SD* of one another.

Fraction 3 showed more diversification from run to run. The interpretation of these data is complex because the two runs conducted initially, Runs A and D (the hydrocortisone acetate run), were tested using a 50-μm aperture tube while the last two separations of prednisolone acetate were measured with a 200-μm aperture tube. This difference could possibly account for some diversity from run to run. An overlapping aperture tube technique might be more proper for these samples.

In each case, the mean diameter of the prednisolone acetate suspensions increased by approximately 5–8 μm from the next smaller fraction (Fraction 2), thus demonstrating successful separation. Since the micronized hydrocortisone acetate was lacking in larger particles, this fraction and the subsequent fraction (Fraction 4) had a smaller mean than the prednisolone acetate runs.

The prednisolone acetate Fraction 4 yielded mean particle sizes which were approximately 10 μm larger than the previous fraction. The mean particle diameters of each prednisolone acetate run were within 4 μm of one another, well within 1 *SD*.

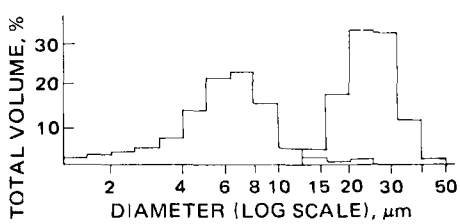

Figure 2—*Particle-size distributions of Fractions 1 (left) and 4 (right) of Run B, prednisolone acetate.*

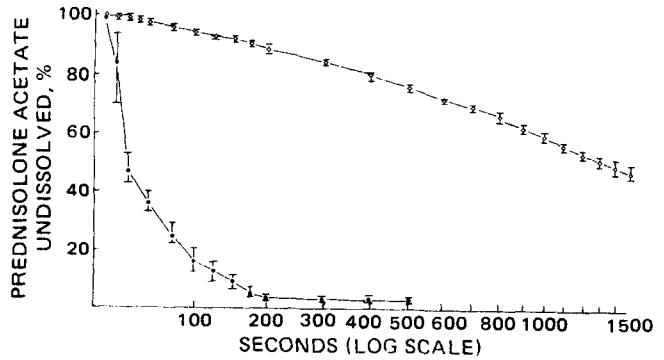

Figure 3—*Aqueous dissolution profiles of Fractions 1 (◇) and 4 (●) of prednisolone acetate suspensions from Run B. The points are the average of three experiments, and the bars are extremes of the three experiments.*

Fraction 5 consisted of washings from the elutriator chamber. Run C, which was conducted on a different lot of prednisolone acetate than Runs A and B, had insufficient washings to be collected. Hydrocortisone acetate, which was micronized and had few larger particles, also contained no particles within this fraction. All data for these two runs were extremely close, with a 7- or 8-μm increase in mean particle size from the previous fraction.

To demonstrate the nature of the shift of particle distribution from fraction to fraction, the particle distribution for Run B was plotted (Fig. 1). Five fractions were obtained, each with its own distinctive mean particle size. The only two fractions with heavy overlapping of particles were Fractions 1 and 2, which did show a shift of one channel. The other fractions all showed a shift of two or more channels.

Each fraction was distributed according to an apparent log-normal distribution. This fact is significant because of the widespread use of log-normal distributions in dissolution modeling (1–7, 11, 21, 22). Veng Pedersen (22), for example, assumed a log-normal distribution in successfully characterizing the dissolution of micronized glyburide using the cube root law.

To demonstrate the potential biological importance of the fraction differences, the aqueous dissolution rates of Fractions 1 and 4 of Run B were determined (Fig. 2). These two fractions provided two distinct particle-size distributions with essentially no overlapping of particle sizes.

The particle-size differences of these two fractions are dramatically demonstrated in the dissolution results (Fig. 3). These data indicate that 50% of Fraction 1 dissolved in less than 30 sec while 1400 sec elapsed before 50% of the large Fraction 4 dissolved.

The mixing of these fractions and the dissolution testing of other fractions would seem to be valuable tools in testing theories designed to predict dissolution kinetics from particle size. The design of sustained- or controlled-release suspensions from a mixing of fractions also may be another attractive possibility.

REFERENCES

(1) W. I. Higuchi and E. N. Hiestand, *J. Pharm. Sci.*, **52**, 67 (1963).

(2) W. I. Higuchi, E. L. Rowe, and E. N. Hiestand, *ibid.*, **52**, 162 (1963).

(3) J. Carstensen and M. Musa, *ibid.*, **61**, 223 (1972).

(4) D. Brooke, *ibid.*, **62**, 795 (1973).

(5) *Ibid.*, **63**, 344 (1974).

(6) J. Mauger and S. Howard, *J. Pharm. Sci.*, **65**, 1042 (1976).

(7) P. Veng Pedersen and K. F. Brown, *ibid.*, **64**, 1192 (1975).

(8) M. P. Short, P. Sharkey, and C. T. Rhodes, *ibid.*, **61**, 1732 (1972).

(9) J. Cobby, M. Mayersohn, and B. Farlinger, *Can. J. Pharm. Sci.*, **9**, 91 (1974).

(10) D. Brooke, *J. Pharm. Sci.*, **64**, 1409 (1975).

(11) J. T. Carstensen and M. Patel, *ibid.*, **64**, 1770 (1975).

(12) P. Veng Pedersen and K. F. Brown, *ibid.*, **65**, 1442 (1976).

(13) A. L. Flangas, *Prep. Biochem.*, **4**, 165 (1974).

(14) D. Glick, D. con Redlich, E. T. Juhos, and C. R. McEwen, *Exp. Cell Res.*, **65**, 23 (1974).

(15) R. J. Crabske, S. Lake, P. L. Gladhill, and M. L. Meistrich, *J. Cell Biol.*, **63**, 119a (1974).

(16) T. P. Stossel, R. J. Mason, T. D. Pollard, and M. Vaughan, *J. Clin. Invest.*, **51**, 604 (1972).

(17) R. J. Sanderson, N. E. Palmer, and K. E. Bird, *Biophys. J.*, **15**, 324 (1975).

(18) P. E. Lindahl, *Nature*, **161**, 648 (1948).

(19) C. R. McEwen, R. W. Stallard, and E. T. Juhos, *Anal. Biochem.*, **23**, 369 (1968).

(20) A. C. Shah, C. B. Peat, and J. F. Ochs, *J. Pharm. Sci.*, **62**, 671 (1973).

(21) P. Veng Pedersen and K. F. Brown, *ibid.*, **65**, 1981 (1976).

(22) P. Veng Pedersen, *ibid.*, **66**, 761 (1977).

Liquid Chromatography in Pharmaceutical Analysis IX: Determination of Muscle Relaxant–Analgesic Mixtures Using Normal Phase Chromatography

I. L. HONIGBERG ˣ, J. T. STEWART, and M. SMITH

Received June 1, 1977, from the *Department of Medicinal Chemistry, School of Pharmacy, University of Georgia, Athens, GA 30602.* Accepted for publication September 6, 1977.

Abstract □ High-pressure liquid chromatography was used to optimize the resolution of eight widely prescribed therapeutic agents commonly found in muscle relaxant–analgesic mixtures. The compounds were chromatographed on normal phase porous silica or cyanopropylsilane columns, using various solvent systems paired on the basis of Snyder's solvent selectivity scheme to give a polarity index for each system of 3.3. A carisoprodol, phenacetin, and caffeine mixture was selected to demonstrate the utility of the separation and quantification method. The mixture was chromatographed on a porous silica column, using tetrahydrofuran–toluene (50:50) at a flow rate of 2.0 ml/min. Each determination can be achieved in approximately 8 min with an accuracy of 3–5%.

Keyphrases □ Muscle relaxants, various—high-pressure liquid chromatographic analyses in mixtures with analgesics □ Analgesics, various—high-pressure liquid chromatographic analyses in mixtures with muscle relaxants □ High-pressure liquid chromatography—analyses, various muscle relaxants and analgesics in pharmaceutical mixtures

Muscle relaxant–analgesic mixtures are widely prescribed drugs. The continued interest in these laboratories in the use of high-pressure liquid chromatography (HPLC) for the separation and quantitation of multicomponent

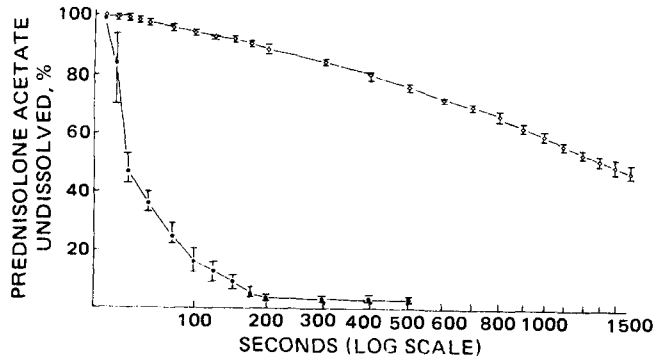

Figure 3—*Aqueous dissolution profiles of Fractions 1 (◇) and 4 (●) of prednisolone acetate suspensions from Run B. The points are the average of three experiments, and the bars are extremes of the three experiments.*

Fraction 5 consisted of washings from the elutriator chamber. Run C, which was conducted on a different lot of prednisolone acetate than Runs A and B, had insufficient washings to be collected. Hydrocortisone acetate, which was micronized and had few larger particles, also contained no particles within this fraction. All data for these two runs were extremely close, with a 7- or 8-μm increase in mean particle size from the previous fraction.

To demonstrate the nature of the shift of particle distribution from fraction to fraction, the particle distribution for Run B was plotted (Fig. 1). Five fractions were obtained, each with its own distinctive mean particle size. The only two fractions with heavy overlapping of particles were Fractions 1 and 2, which did show a shift of one channel. The other fractions all showed a shift of two or more channels.

Each fraction was distributed according to an apparent log-normal distribution. This fact is significant because of the widespread use of log-normal distributions in dissolution modeling (1–7, 11, 21, 22). Veng Pedersen (22), for example, assumed a log-normal distribution in successfully characterizing the dissolution of micronized glyburide using the cube root law.

To demonstrate the potential biological importance of the fraction differences, the aqueous dissolution rates of Fractions 1 and 4 of Run B were determined (Fig. 2). These two fractions provided two distinct particle-size distributions with essentially no overlapping of particle sizes.

The particle-size differences of these two fractions are dramatically demonstrated in the dissolution results (Fig. 3). These data indicate that 50% of Fraction 1 dissolved in less than 30 sec while 1400 sec elapsed before 50% of the large Fraction 4 dissolved.

The mixing of these fractions and the dissolution testing of other fractions would seem to be valuable tools in testing theories designed to predict dissolution kinetics from particle size. The design of sustained- or controlled-release suspensions from a mixing of fractions also may be another attractive possibility.

REFERENCES

(1) W. I. Higuchi and E. N. Hiestand, *J. Pharm. Sci.*, **52**, 67 (1963).

(2) W. I. Higuchi, E. L. Rowe, and E. N. Hiestand, *ibid.*, **52**, 162 (1963).

(3) J. Carstensen and M. Musa, *ibid.*, **61**, 223 (1972).

(4) D. Brooke, *ibid.*, **62**, 795 (1973).

(5) *Ibid.*, **63**, 344 (1974).

(6) J. Mauger and S. Howard, *J. Pharm. Sci.*, **65**, 1042 (1976).

(7) P. Veng Pedersen and K. F. Brown, *ibid.*, **64**, 1192 (1975).

(8) M. P. Short, P. Sharkey, and C. T. Rhodes, *ibid.*, **61**, 1732 (1972).

(9) J. Cobby, M. Mayersohn, and B. Farlinger, *Can. J. Pharm. Sci.*, **9**, 91 (1974).

(10) D. Brooke, *J. Pharm. Sci.*, **64**, 1409 (1975).

(11) J. T. Carstensen and M. Patel, *ibid.*, **64**, 1770 (1975).

(12) P. Veng Pedersen and K. F. Brown, *ibid.*, **65**, 1442 (1976).

(13) A. L. Flangas, *Prep. Biochem.*, **4**, 165 (1974).

(14) D. Glick, D. con Redlich, E. T. Juhos, and C. R. McEwen, *Exp. Cell Res.*, **65**, 23 (1974).

(15) R. J. Crabske, S. Lake, P. L. Gladhill, and M. L. Meistrich, *J. Cell Biol.*, **63**, 119a (1974).

(16) T. P. Stossel, R. J. Mason, T. D. Pollard, and M. Vaughan, *J. Clin. Invest.*, **51**, 604 (1972).

(17) R. J. Sanderson, N. E. Palmer, and K. E. Bird, *Biophys. J.*, **15**, 324 (1975).

(18) P. E. Lindahl, *Nature*, **161**, 648 (1948).

(19) C. R. McEwen, R. W. Stallard, and E. T. Juhos, *Anal. Biochem.*, **23**, 369 (1968).

(20) A. C. Shah, C. B. Peat, and J. F. Ochs, *J. Pharm. Sci.*, **62**, 671 (1973).

(21) P. Veng Pedersen and K. F. Brown, *ibid.*, **65**, 1981 (1976).

(22) P. Veng Pedersen, *ibid.*, **66**, 761 (1977).

Liquid Chromatography in Pharmaceutical Analysis IX: Determination of Muscle Relaxant–Analgesic Mixtures Using Normal Phase Chromatography

I. L. HONIGBERG ˣ, J. T. STEWART, and M. SMITH

Received June 1, 1977, from the *Department of Medicinal Chemistry, School of Pharmacy, University of Georgia, Athens, GA 30602.* Accepted for publication September 6, 1977.

Abstract □ High-pressure liquid chromatography was used to optimize the resolution of eight widely prescribed therapeutic agents commonly found in muscle relaxant–analgesic mixtures. The compounds were chromatographed on normal phase porous silica or cyanopropylsilane columns, using various solvent systems paired on the basis of Snyder's solvent selectivity scheme to give a polarity index for each system of 3.3. A carisoprodol, phenacetin, and caffeine mixture was selected to demonstrate the utility of the separation and quantification method. The mixture was chromatographed on a porous silica column, using tetrahydrofuran–toluene (50:50) at a flow rate of 2.0 ml/min. Each determination can be achieved in approximately 8 min with an accuracy of 3–5%.

Keyphrases □ Muscle relaxants, various—high-pressure liquid chromatographic analyses in mixtures with analgesics □ Analgesics, various—high-pressure liquid chromatographic analyses in mixtures with muscle relaxants □ High-pressure liquid chromatography—analyses, various muscle relaxants and analgesics in pharmaceutical mixtures

Muscle relaxant–analgesic mixtures are widely prescribed drugs. The continued interest in these laboratories in the use of high-pressure liquid chromatography (HPLC) for the separation and quantitation of multicomponent

Table I—Solvent Groups Adjusted to a Common Polarity Index [a]

	Hexane, Group 0	Butyl Ether, Group 1	Carbon Tetrachloride, Group 7
Tetrahydrofuran, Group 3	80:20[b] (Solvent A)	65:35 (Solvent B)	50:50[c] (Solvent C)
Methylene chloride, Group 5	100:0[d] (Solvent D)	100:0[d] (Solvent D)	95:5 (Solvent E)
Chloroform, Group 9	75:25 (Solvent F)	60:40 (Solvent G)	60:40 (Solvent H)

[a] See Ref. 15. [b] Solvent ratio = row/column. [c] Tetrahydrofuran–carbon tetrachloride forms an unstable mixture, so toluene was substituted for carbon tetrachloride in this mixture. [d] One hundred percent methylene chloride has a PI value of approximately 3.3.

dosage forms[1] led to an investigation of muscle relaxant–analgesic mixtures. Among the drugs in these mixtures are meprobamate, methocarbamol, carisoprodol, chlorzoxazone, acetaminophen, aspirin, phenacetin, and caffeine.

Existing methods for meprobamate in dosage forms include formol titrimetry (1) and colorimetry (2). Methocarbamol can be analyzed using a spectrophotometric method (3); carisoprodol is determined in mixtures containing phenacetin and caffeine by quantitation in the near IR range (4). GLC and TLC methods (5, 6) were reported for chlorzoxazone. Acetaminophen has been analyzed by UV and visible spectrophotometry (7, 8), and aspirin has been analyzed by aqueous (9) and nonaqueous (10) titrimetry, GLC (11), and liquid chromatography (12) in mixtures with phenacetin and caffeine. Spectrophotometry is a method of determination for phenacetin (13), and caffeine can be determined by nonaqueous titrimetry (14).

A recent paper (15) introduced the concept of solvent selectivity and the polarity index as two measurable parameters for the selection of proper solvent mixtures for HPLC. In the present study, the Snyder scheme (15) was applied to the separation of muscle relaxant–analgesic mixtures on porous silica and chemically bonded cyanopropylsilane columns. The suitability of each column for the separation problem was evaluated.

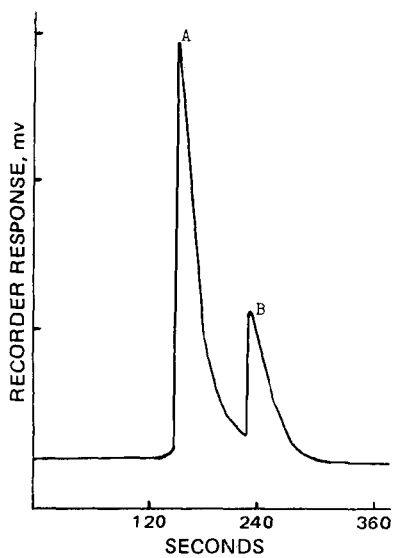

Figure 1—*Typical liquid chromatogram of a meprobamate–aspirin mixture in chloroform–carbon tetrachloride (60:40) on a cyanopropylsilane column at a flow rate of 2.0 ml/min. Key: A, aspirin; and B, meprobamate.*

[1] For other papers in this series, see S. J. Saxena, I. L. Honigberg, J. T. Stewart, and J. J. Vallner, *J. Pharm. Sci.*, **66**, 751 (1977).

Table II—Calibration Data for Standard Drug Solutions

Compound	Final Concentration, mg[a]	D/IS Ratio[b]	Slope	Intercept	$r \pm s_{y\cdot x}$
Carisoprodol	10.02	0.1667 ± 0.0605[c]			
	20.04	0.3572 ± 0.1291	0.0979	−0.0318	0.9999 ± 0.0024
	40.08	0.7539 ± 0.0732			
Phenacetin	7.97	0.5873 ± 0.0194			
	15.94	1.1714 ± 0.0542	0.3815	−0.0303	0.9999 ± 0.0103
	31.88	2.4067 ± 0.2444			
Caffeine	1.56	0.1186 ± 0.0201			
	3.12	0.2376 ± 0.0266	0.3706	0.0043	0.9999 ± 0.0013
	6.24	0.4662 ± 0.0414			

[a] Total milligrams per 5 ml of solution. [b] Data represent three replicate injections of standard solutions. D/IS is the ratio of the integrated area of the drug at some concentration divided by the integrated area of acetaminophen at a concentration of 55 mg/5 ml. [c] Confidence limits at $p = 0.05$.

EXPERIMENTAL[2]

Reagents and Chemicals—Powdered samples of meprobamate[3], methocarbamol[4], carisoprodol[3], chlorzoxazone[5], acetaminophen[6], aspirin[7], caffeine[6], and phenacetin[6] were used. All other chemicals and solvents were the highest quality commercially available.

Mobile Phases—The mobile phases consisted of varying proportions of chloroform mixed with carbon tetrachloride, hexane, or butyl ether; methylene chloride or methylene chloride mixed with carbon tetrachloride; and tetrahydrofuran mixed with toluene, hexane, or butyl ether such that the final composition of the mobile phase gave a polarity index (PI) value (15) of 3.3 (Table I). The solutions were prepared fresh daily.

Preparation of Drug Solutions—Solutions of each drug (5–10 mg/ml) were prepared by dissolving each powder in the appropriate mobile phase.

Internal Standard Solution—The stock internal standard solution (110 mg/10 ml) was prepared by dissolving acetaminophen[6] in tetrahydrofuran–toluene (50:50).

Standard Solutions for Calibration Curves—Separate stock solutions of carisoprodol (200.4 mg/10 ml), phenacetin (159.4 mg/10 ml), and caffeine (31.2 mg/10 ml) were prepared in tetrahydrofuran–toluene (50:50). Accurately pipetted volumes of 0.5, 1.0, and 2.0 ml of each stock solution were placed in 5-ml volumetric flasks. The internal standard stock solution, 1 ml, was added to each flask, followed by the addition of tetrahydrofuran–toluene (50:50) to volume.

The three concentrations of each drug were subjected to a linear regression analysis, and the slope and intercept were calculated (Table II).

Chromatographic Separation and Quantification—The degassed mobile phase was pumped through columns containing a small particle, fully porous silica packing material[8] or a monomolecular layer of a cyanopropylsilane chemically bonded to a small particle, fully porous support[9] at a flow rate of 2.0 ml/min at room temperature until a stable baseline was obtained. Replicate 40-μl injections of sample and standard solutions were made using a 100-μl syringe[10]. The chart recorder provided

[2] A Waters Associates liquid chromatograph (model ALC 202) equipped with an M-6000 pump, a differential RI detector, and an Infotronics integrator (model CRS-204) with digital printout, and Waters packed columns, 4 mm i.d. × 30 cm, were used.

[3] Wallace Laboratories, Cranbury, N.J.

[4] A. H. Robins, Richmond, Va.

[5] McNeil Laboratories, Fort Washington, Pa.

[6] Eastman Chemicals, Rochester, N.Y.

[7] Aldrich Chemicals, Milwaukee, Wis.

[8] μPorasil, ~10 μm, Waters Associates, Milford, Mass.

[9] μBondapak CN, ~10 μm, Waters Associates, Milford, Mass.

[10] Model B-110, Precision Sampling Corp., Baton Rouge, La.

Table III—Effect of Mobile Phase on Retention Times [a]

Mobile Phase Composition[b]	Meprobamate		Methocarbamol		Carisoprodol		Chlorzoxazone		Acetaminophen		Aspirin		Caffeine		Phenacetin	
	I	II	I	II	I	II	I	II	I	II	I	II	I	II	I	II
A	88	116	92	140	96	96	86	92	100	132	92	92	94	240	100	124
	(12)[c]	(12)	(8)	(20)	(8)	(8)	(8)	(8)	(4)	(16)	(10)	(8)	(8)	(16)	(4)	(12)
B	96	136	100	160	96	100	96	92	116	152	96	92	100	296	104	140
	(14)	(12)	(14)	(16)	(12)	(8)	(12)	(12)	(14)	(16)	(12)	(18)	(16)	(20)	(20)	(12)
C	96	172	92	208	96	108	96	96	96	170	92	94	106	300	116	146
	(8)	(16)	(12)	(19)	(8)	(8)	(16)	(6)	(12)	(12)	(6)	(8)	(16)	(32)	(12)	(10)
D	132	—[d]	120	—[d]	96	—[d]	129	—[d]	311	—[d]	112	—[d]	110	—[d]	108	—[d]
	(22)		(24)		(16)		(9)		(66)		(24)		(14)		(12)	
E	135	—[d]	125	—[d]	96	—[d]	141	—[d]	400	—[d]	123	—[d]	96	—[d]	117	—[d]
	(20)		(18)		(10)		(15)		(36)		(26)		(10)		(9)	
F	134	—[d]	126	—[d]	105	—[d]	162	700	111	—[d]	117	920	92	—[d]	120	1676
	(12)		(15)		(9)		(12)	(20)	(6)		(9)	(80)	(8)		(8)	(160)
G	129	—[d]	129	—[d]	112	—[d]	108	192	159	—[d]	88	200	104	—[d]	123	960
	(15)		(12)		(10)		(9)	(16)	(12)		(10)	(20)	(12)		(11)	(132)
H	236	—[d]	138	—[d]	107	—[d]	174	816	108	—[d]	168	1320	96	—[d]	129	700
	(18)		(15)		(9)		(20)	(52)	(6)		(18)	(108)	(8)		(9)	(200)

[a] Retention time is expressed as seconds measured as elapsed time between injection and attainment of the chromatographic peak maximum. The eluted peaks were monitored using refractive index detection. Column I is cyanopropylsilane; II is porous silica. [b] Letters refer to solvent compositions in Table I. [c] Base peak width expressed as seconds. [d] Retention time greater than 1800 sec.

a record of drug elution from the column as peaks on a chromatogram. In all cases, the quantification of solute was determined by digital integration of the peak area[2].

RESULTS AND DISCUSSION

This study determined the operating conditions for HPLC that would optimize the resolution of chemically unrelated therapeutic agents commonly found in muscle relaxant–analgesic mixtures. Two operating parameters were studied: (*a*) variations in solvent selectivity with constant polarity, and (*b*) variations in polarity of the stationary phase. The effects of these parameters on retention times and base peak widths of the drugs are shown in Table III. The eluted peaks were monitored using differential refractive index detection since many of the muscle relaxants are aliphatic compounds and do not possess satisfactory UV absorption.

Preliminary data revealed that the polarity index (PI) of the solvent mixture should be approximately 3.3 to obtain a k' between 3 and 10. According to the Snyder (15) approach, PI measures the solvent strength of a particular mixture. This solvent strength influences the retention time or k' for a particular solute mixture. In addition, the separability of a solute is affected by its proton donor, proton acceptor, and dipole interactions with the mobile phase. These latter parameters affect solvent selectivity. Pure solvents can be grouped into approximately nine categories based on the distribution of the constitutive properties mentioned. After a suitable PI value has been obtained for a particular solute mixture, other solvent categories are intermixed to give the same PI values (same k' value) so as to change solvent selectivity and to maximize resolution. The solvent systems used in this study are listed in Table I.

The stationary phases investigated were limited to a porous silica support and a cyanopropylsilane layer chemically bonded to a porous silica support. Generally, in the solvent systems studied, the porous silica column either had too great an affinity for the components investigated or the compounds were too rapidly eluted with a change in solvent selectivity. In contrast, the cyanopropylsilane column showed lower affinity for the drugs but allowed for better comparisons of solvent selectivity. Experience with the Snyder solvent selectivity scheme has shown it to be a valuable tool for limiting the intuitive aspects of solvent selection, especially in normal phase chromatography.

The following observations were noted for the drugs examined. Meprobamate was eluted on the cyanopropylsilane column with all solvent systems employed; but on the silica support, only the tetrahydrofuran mixtures successfully eluted the drug in less than 1800 sec. Resolution of the meprobamate–aspirin combination was observed in Solvents F–H (Table III) on the cyanopropylsilane column and in Solvents A and C on the silica column. In Solvents A, C, and G, aspirin traveled close to the solvent front and was difficult to distinguish from other components present at the front. Figure 1 illustrates a chromatogram of a meprobamate–aspirin mixture using Solvent H on the cyanopropylsilane column.

Methocarbamol eluted on the cyanopropylsilane column with all solvents investigated; on the silica column, only the tetrahydrofuran mixtures eluted the drug in less than 1800 sec. Resolution of the frequently prescribed methocarbamol–aspirin combination was observed in Solvents G and H on the cyanopropylsilane column and in Solvents A–C on the silica column. Only Solvent H on the cyanopropylsilane column gave satisfactory resolution in which both components showed adequate retention times. Although a mixture of methocarbamol, phenacetin, and aspirin was resolved using Solvents A–C on the silica column, aspirin traveled near the solvent front and was indistinguishable from interfering substances present at the front.

Elution of carisoprodol on the cyanopropylsilane column was achieved with all solvent systems. On the silica column, only Solvents A–C gave satisfactory retention times. The widely used mixture of carisoprodol,

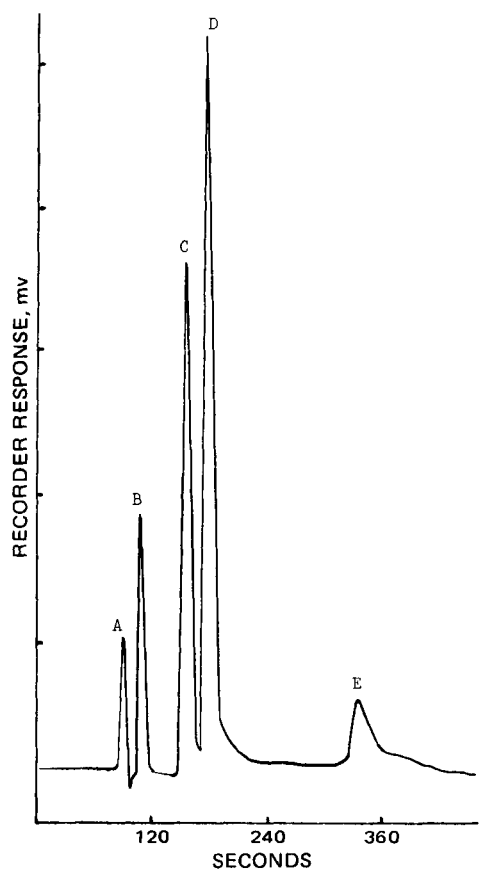

Figure 2—*Liquid chromatogram of a carisoprodol–phenacetin–caffeine mixture in tetrahydrofuran–toluene (50:50) on a porous silica column at a flow rate of 2.0 ml/min. Key: A, solvent front; B, carisoprodol; C, phenacetin; D, acetaminophen (internal standard); and E, caffeine.*

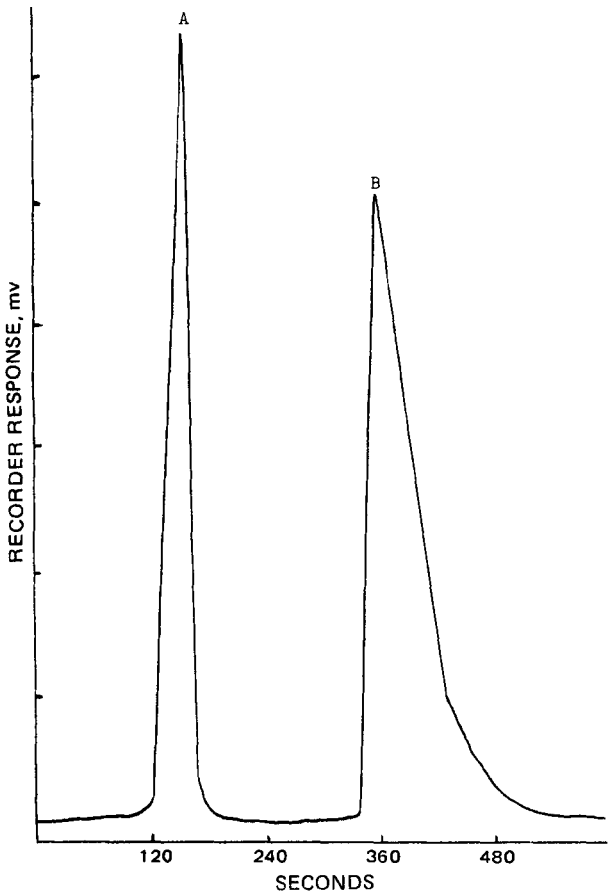

Figure 3—*Typical liquid chromatogram of a chlorzoxazone–acetaminophen mixture in methylene chloride–carbon tetrachloride (95:5) on a cyanopropylsilane column at a flow rate of 2.0 ml/min. Key: A, chlorzoxazone; and B, acetaminophen.*

phenacetin, and caffeine was separated using Solvent C on the silica column (Fig. 2). Other useful systems were Solvents C, F, and H on the cyanopropylsilane column and A and B on the silica column.

Chlorzoxazone was eluted by all solvent systems on the cyanopropylsilane column and by all solvents except D and E on the silica column. A chlorzoxazone–acetaminophen combination was satisfactorily separated on the cyanopropylsilane column with Solvent E (Fig. 3). Other useful systems were A and F–H on the cyanopropylsilane columns and A–C on the silica column. However, solvent systems in which one component is eluted in close proximity to the solvent front present problems in dosage form analysis because of the presence of inert ingredients that tend to elute at the front.

All of the solvent systems eluted acetaminophen on the cyanopropylsilane column. Solvents A–C were the only satisfactory solvents for the drug on the silica column.

Aspirin eluted from the cyanopropylsilane column with all of the solvents investigated. Solvents A–C and F–H eluted aspirin on the silica column in less than 1800 sec. Aspirin was eluted close to the solvent front

Table IV—Approximate Resolution [a] (R_s) Values for Carisoprodol–Phenacetin–Caffeine Mixture

Drug Mixture[b]	Cyanopropylsilane Column Mobile Phase[c]		Silica Column Mobile Phase		
	F	H	A	B	C
Caffeine and carisoprodol	1.5	1.3	—	—	—
Carisoprodol and phenacetin	1.8	2.4	2.8	4.0	4.2
Phenacetin and caffeine	—	—	8.3	9.8	7.3

[a] See Ref. 16. [b] On the cyano column, the drugs were eluted in the following order: caffeine, carisoprodol, and phenacetin. The order of elution from the silica column was carisoprodol, phenacetin, and caffeine. [c] Letters refer to solvent compositions in Table I.

Table V—Analysis of Carisoprodol, Phenacetin, and Caffeine in Known Mixture

Compound	Amount Added[a], mg	Amount Found[b], mg	Accuracy, %
Carisoprodol	20.04	20.77 ± 1.53[c]	3.64
Phenacetin	15.94	15.32 ± 0.92	3.89
Caffeine	3.12	2.98 ± 0.58	4.49

[a] Total milligrams per 5 ml of solution. [b] Based on six replicate determinations of known mixture. [c] Confidence limits at $p = 0.05$.

in approximately 50% of the solvents tested or had extremely long retention times in about 25% of the solvents.

All solvents were satisfactory for the elution of caffeine on the cyanopropylsilane column, and A–C were permissible to use with the silica column.

Phenacetin eluted on the cyanopropylsilane column using all solvents studied; on the silica column, Solvents A–C and F–H showed satisfactory elution.

Satisfactory quantitation of a multicomponent dosage form is dependent on adequate resolution of the components. The value R_s (16), a theoretical parameter, is a reasonable measurement of the separation of two species on a column. It can be approximated from any two drugs included in this investigation from information in Table III. A mixture of carisoprodol, phenacetin, and caffeine was selected to exemplify this situation. Table IV shows calculated R_s values for the drug combination in various solvent systems on both the cyanopropylsilane and silica columns. Solvent C was chosen for the quantitation since it represented the system in which good overall resolution was achieved and it allowed the use of acetaminophen as a convenient internal standard.

Figure 2 illustrates a chromatogram of the assayed drugs. Various concentrations of standard solutions of each drug dissolved in tetrahydrofuran–toluene (50:50) were chromatographed using the silica column. Acetaminophen was added to each solution as the internal standard. The area under the curve for each peak on the chromatograms was determined with a digital integrator. The ratio of each peak area to the area of the internal standard was calculated for each chromatogram. A linear regression line of these data for each drug gave the slope, intercept, and correlation coefficient for each calibration curve (Table II).

A known mixture containing a quantity of each drug present in the ratios found in a commercial dosage form[11] was chromatographed, and the ratios of drug peak areas/internal standard peak areas (D/IS) were calculated for each drug. The constants (slope and intercept) for the linear regression equation shown in Table II were used to solve for drug concentration [D/IS = slope (concentration) + intercept]. The calculations were performed on a programmable calculator. The data in Table V demonstrate the quantitative results obtained for the simulated dosage form. The utility of HPLC in the analysis of a carisoprodol–phenacetin–caffeine mixture is clearly demonstrated with an accuracy of 3–5%.

REFERENCES

(1) "The United States Pharmacopeia," 19th rev., Mack Publishing Co., Easton, Pa., 1975, p. 304.

(2) *Ibid.*, p. 305.

(3) "The National Formulary," 14th ed, Mack Publishing Co., Easton, Pa., 1975, p. 449.

(4) L. Allen, *J. Pharm. Sci.*, **63**, 912 (1974).

(5) K. D. Parker, C. R. Fontan, and P. L. Kirk, *Anal. Chem.*, **34**, 757 (1962).

(6) I. Ullah, D. E. Cadwallader, and I. L. Honigberg, *J. Chromatogr.*, **46**, 211 (1970).

(7) "The United States Pharmacopeia," 19th rev., Mack Publishing Co., Easton, Pa., 1975, p. 11.

(8) L. Chafetz, R. E. Daly, H. Schriftman, and J. J. Lomner, *J. Pharm. Sci.*, **60**, 463 (1971).

(9) "The United States Pharmacopeia," 19th rev., Mack Publishing Co., Easton, Pa., 1975, p. 38.

(10) S. Lin and M. I. Blake, *Anal. Chem.*, **38**, 549 (1966).

(11) R. C. Crippen and H. C. Freimuth, *ibid.*, **36**, 273 (1964).

(12) P. P. Ascione and G. P. Chrekian, *J. Pharm. Sci.*, **64**, 1029 (1975).

(13) J. E. Wallace, J. D. Biggs, H. E. Hamilton, L. L. Foster, and K.

[11] Soma Compound, Wallace Laboratories, Cranbury, N.J.

Blum, *ibid.*, **62**, 599 (1973).
(14) "The United States Pharmacopeia," 19th rev., Mack Publishing Co., Easton, Pa., 1975, p. 59.
(15) L. Snyder, *J. Chromatogr.*, **92**, 223 (1974).
(16) B. L. Karger, L. R. Snyder, and C. Horvath, "An Introduction to Separation Science," Wiley, New York, N.Y., 1973, pp. 146–150.

ACKNOWLEDGMENTS

Presented at the Pharmaceutical Analysis and Control Section, APhA Academy of Pharmaceutical Sciences, New York meeting, May 1977.

The authors acknowledge the technical assistance of W. Coldren and T. Bellnier.

High-Pressure Liquid Chromatographic Analysis of Melphalan in Plasma

S. Y. CHANG ˣ, D. S. ALBERTS, L. R. MELNICK, P. D. WALSON, and S. E. SALMON

Received April 22, 1977, from the *Section of Hematology and Oncology, Departments of Internal Medicine and Pharmacology, and the Cancer Center, College of Medicine, University of Arizona, Tucson, AZ 85724.* Accepted for publication September 1, 1977.

Abstract □ A new sensitive and rapid high-pressure liquid chromatographic determination of melphalan in plasma was developed. Recovery of 1 μg added to 1 ml of plasma at 23° was 94% but was greatly reduced at higher temperature. The method has been applied to plasma determinations of melphalan in rats and humans and is currently being utilized for human pharmacokinetic studies.

Keyphrases □ Melphalan—high-pressure liquid chromatographic analysis in plasma □ High-pressure liquid chromatography—analysis, melphalan in plasma □ Antineoplastic agents—melphalan, high-pressure liquid chromatographic analysis in plasma

Since melphalan [L-phenylalanine mustard, 4-bis(2-chloroethyl)amino-L-phenylalanine, NSC 8806] was synthesized (1), it has become an important drug for the treatment of various cancers, including multiple myeloma and ovarian and breast carcinoma (2–4). Little information is available concerning its pharmacokinetic properties in humans or animals because of its rapid hydrolytic degradation, which is common to alkylating agents (5–8).

The colorimetric assays utilizing nitrobenzylpyridine (7, 9–11) and the spectrofluorometric method (8) for the determination of melphalan (I) in biological fluids are not sensitive enough for the study of its pharmacokinetic properties. The fluorometric method for biological samples is not practical because of background interference and its lengthy nature (8). These methods are not specific; they measure the total concentration of alkylating agents including one hydrolysis product of I. A GLC method for I (12) has not been applied to biological samples. Recently, Furner *et al.* (13) reported a high-pressure liquid chromatographic (HPLC) method for the determination of I in animal serum.

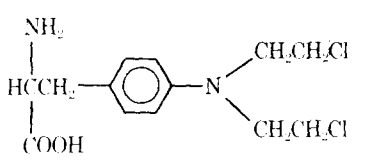

I

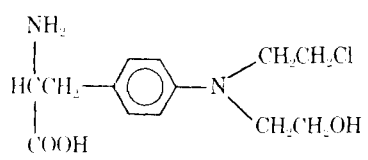

II

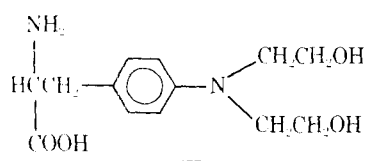

III

The present paper reports a sensitive and rapid HPLC method for the determination of I in biological fluids. Practical application of the developed method is demonstrated by *in vivo* determinations of the plasma I concentration in animals and humans. *In vitro* plasma recovery studies also are presented.

EXPERIMENTAL

Materials—Methanol[1] was used as received. Dansylproline[2] was used as an internal standard. The standard I[3] dissolved in methanol containing 2% acetic acid and the internal standard dissolved in methanol were stored at −20° at all times between usage. Aqueous solvents were filtered with a 0.45-μm cellulose acetate filter[4]. Methanol and other organic solvents were filtered with a fluoropore[4] prior to use.

Instrument Conditions—HPLC was performed with an apparatus consisting of two pumps[5], a solvent programmer[6], a detector[7], and a reversed-phase column[8]. An isocratic solvent system of water and methanol (1:1) with 1% acetic acid was delivered at the rate of 2 ml/min, and I was detected at 254 nm. The total analysis time per sample was approximately 20 min.

Extraction of I from Plasma—Five micrograms of internal standard was added to 1 ml of human plasma prior to extraction of I for *in vivo* studies. For *in vitro* studies, 2 μg of internal standard was added for every 1 μg of I. Two milliliters of methanol (0°) was added to 1 ml of plasma and mixed vigorously on a vortex mixer for 20 sec. The sample was then cooled at −60° (acetone and dry ice) for 3 min. The plasma–methanol mixture was centrifuged at 3000 rpm for 3 min on a clinical centrifuge. The clear methanolic solution, which contained the internal standard and I, was injected directly onto the column. Calculation of I was as follows:

[1] Burdick and Jackson Co., Muskegon, Mich.
[2] Pierce Chemical Co., Rockford, Ill.
[3] Obtained from the Division of Cancer Treatment, National Cancer Institute, Bethesda, Md.
[4] Millipore Corp., Bedford, Mass.
[5] Waters 6000, Waters Associates, Milford, Mass.
[6] Waters 600, Waters Associates, Milford, Mass.
[7] Waters 440, Waters Associates, Milford, Mass.
[8] Waters micro C_{18} column, Waters Associates, Milford, Mass.

Blum, *ibid.*, **62**, 599 (1973).
(14) "The United States Pharmacopeia," 19th rev., Mack Publishing Co., Easton, Pa., 1975, p. 59.
(15) L. Snyder, *J. Chromatogr.*, **92**, 223 (1974).
(16) B. L. Karger, L. R. Snyder, and C. Horvath, "An Introduction to Separation Science," Wiley, New York, N.Y., 1973, pp. 146–150.

ACKNOWLEDGMENTS

Presented at the Pharmaceutical Analysis and Control Section, APhA Academy of Pharmaceutical Sciences, New York meeting, May 1977.

The authors acknowledge the technical assistance of W. Coldren and T. Bellnier.

High-Pressure Liquid Chromatographic Analysis of Melphalan in Plasma

S. Y. CHANG ˣ, D. S. ALBERTS, L. R. MELNICK, P. D. WALSON, and S. E. SALMON

Received April 22, 1977, from the *Section of Hematology and Oncology, Departments of Internal Medicine and Pharmacology, and the Cancer Center, College of Medicine, University of Arizona, Tucson, AZ 85724.* Accepted for publication September 1, 1977.

Abstract □ A new sensitive and rapid high-pressure liquid chromatographic determination of melphalan in plasma was developed. Recovery of 1 μg added to 1 ml of plasma at 23° was 94% but was greatly reduced at higher temperature. The method has been applied to plasma determinations of melphalan in rats and humans and is currently being utilized for human pharmacokinetic studies.

Keyphrases □ Melphalan—high-pressure liquid chromatographic analysis in plasma □ High-pressure liquid chromatography—analysis, melphalan in plasma □ Antineoplastic agents—melphalan, high-pressure liquid chromatographic analysis in plasma

Since melphalan [L-phenylalanine mustard, 4-bis(2-chloroethyl)amino-L-phenylalanine, NSC 8806] was synthesized (1), it has become an important drug for the treatment of various cancers, including multiple myeloma and ovarian and breast carcinoma (2–4). Little information is available concerning its pharmacokinetic properties in humans or animals because of its rapid hydrolytic degradation, which is common to alkylating agents (5–8).

The colorimetric assays utilizing nitrobenzylpyridine (7, 9–11) and the spectrofluorometric method (8) for the determination of melphalan (I) in biological fluids are not sensitive enough for the study of its pharmacokinetic properties. The fluorometric method for biological samples is not practical because of background interference and its lengthy nature (8). These methods are not specific; they measure the total concentration of alkylating agents including one hydrolysis product of I. A GLC method for I (12) has not been applied to biological samples. Recently, Furner *et al.* (13) reported a high-pressure liquid chromatographic (HPLC) method for the determination of I in animal serum.

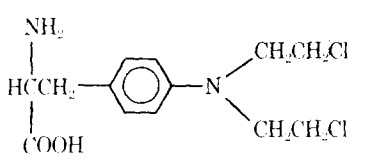

I

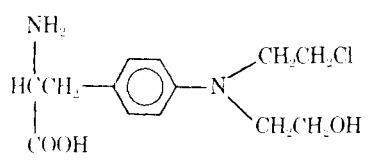

II

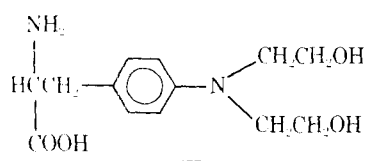

III

The present paper reports a sensitive and rapid HPLC method for the determination of I in biological fluids. Practical application of the developed method is demonstrated by *in vivo* determinations of the plasma I concentration in animals and humans. *In vitro* plasma recovery studies also are presented.

EXPERIMENTAL

Materials—Methanol[1] was used as received. Dansylproline[2] was used as an internal standard. The standard I[3] dissolved in methanol containing 2% acetic acid and the internal standard dissolved in methanol were stored at −20° at all times between usage. Aqueous solvents were filtered with a 0.45-μm cellulose acetate filter[4]. Methanol and other organic solvents were filtered with a fluoropore[4] prior to use.

Instrument Conditions—HPLC was performed with an apparatus consisting of two pumps[5], a solvent programmer[6], a detector[7], and a reversed-phase column[8]. An isocratic solvent system of water and methanol (1:1) with 1% acetic acid was delivered at the rate of 2 ml/min, and I was detected at 254 nm. The total analysis time per sample was approximately 20 min.

Extraction of I from Plasma—Five micrograms of internal standard was added to 1 ml of human plasma prior to extraction of I for *in vivo* studies. For *in vitro* studies, 2 μg of internal standard was added for every 1 μg of I. Two milliliters of methanol (0°) was added to 1 ml of plasma and mixed vigorously on a vortex mixer for 20 sec. The sample was then cooled at −60° (acetone and dry ice) for 3 min. The plasma–methanol mixture was centrifuged at 3000 rpm for 3 min on a clinical centrifuge. The clear methanolic solution, which contained the internal standard and I, was injected directly onto the column. Calculation of I was as follows:

[1] Burdick and Jackson Co., Muskegon, Mich.
[2] Pierce Chemical Co., Rockford, Ill.
[3] Obtained from the Division of Cancer Treatment, National Cancer Institute, Bethesda, Md.
[4] Millipore Corp., Bedford, Mass.
[5] Waters 6000, Waters Associates, Milford, Mass.
[6] Waters 600, Waters Associates, Milford, Mass.
[7] Waters 440, Waters Associates, Milford, Mass.
[8] Waters micro C_{18} column, Waters Associates, Milford, Mass.

Table I—Recovery of I from Plasma

Micrograms of I per Milliliter of Plasma	Recovery[a], % ± *SD*
1	93.5 ± 8.4
5	92.2 ± 3.5
10	89.9 ± 1.9
30	94.8 ± 2.6

[a] The immediate recovery of I at 23°.

$$\mu g \text{ of I} = \frac{\text{response of I sample}}{\text{response of internal standard sample}} \times \frac{\mu g \text{ of internal standard added}}{\text{relative weight response}} \quad \text{(Eq. 1)}$$

where:

$$\text{relative weight response} = \frac{\text{response of I}/\mu g}{\text{response of internal standard}/\mu g} \quad \text{(Eq. 2)}$$

Recovery—Various amounts of I (30, 10, 5, and 1 μg) and internal standard (twice the amount of I) were added to 1 ml of human plasma at 23°. The plasma was mixed well and then extracted for I as described. Experiments were run in quadruplicate.

Peak Identification—The I HPLC peak in plasma was identified as I by GLC–mass spectrometry[9]. Both trimethylsilyl and trifluoroacetyl *n*-butyl ester derivatives were used. Compound I in plasma was collected from the liquid chromatograph and then derivatized and introduced to a 3% OV-7 (0.5 m × 0.2 mm) column. The effluents were scanned for either an entire or a partial spectrum. The mass spectrometer was operated in the electron impact mode at 70 ev.

Stability of I in Plasma—The stability of I in plasma (30 μg/ml) was determined by the percent recovery of I after storing samples at −20° for 3 weeks or at −20° for 3 weeks followed by 3 weeks at 4°. All analyses were performed in triplicate. Stability also was determined at varying temperatures and incubation times, during which samples were taken at 1- or 2-hr intervals up to 12 hr. Plasma was maintained at 0, 23, and 37°. The 0° experiment was conducted over 24 hr.

Plasma I Concentration in Animals and Humans—Rats were given 6 mg/kg of I by intravenous injections over 1 min into a jugular venous catheter (14). Heparinized blood samples were taken at 5, 15, and 30 min and then hourly for 6 hr from a separate jugular catheter. Plasma levels of I were determined by HPLC.

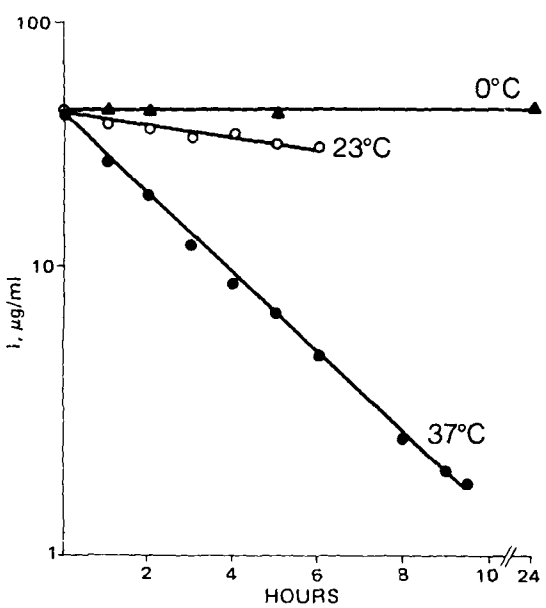

Figure 1—In vitro *recovery of I from human plasma as a function of temperature and incubation time. Compound I was added to human plasma in a concentration of 25 μg/ml and incubated at 0° (▲), 23° (○), and 37° (●). Aliquots were taken at designated time points and analyzed by HPLC.*

[9] Finnigan 3300-6100, Sunnyvale, Calif.

Table II—Stability of I

Age of Sample	Recovery, % ± *SD*	Remarks
0	94.8 ± 2.6	23°, immediate analysis
3 weeks	101.3 ± 5.2	−20° throughout
6 weeks	65.9 ± 3.5	3 weeks at −20° plus 3 weeks at 4°

Patients were given a 0.6-mg/kg dose of I by intravenous bolus injection or orally. Anticoagulated venous blood samples were drawn and quickly placed in ice. The plasma was separated by centrifugation and analyzed by HPLC as described.

RESULTS

Recovery—Recovery of 1, 5, 10, and 30 μg of I added to 1 ml of plasma at 23° is presented in Table I. The average recovery ranged from 90 to 95% and had greater standard deviation at lower concentrations.

Stability Studies—No change in the plasma I concentration was seen when 30 μg/ml was stored for 3 weeks at −20°. However, when the same sample was removed from −20° and placed at 4° for an additional 3 weeks, there was a 35% decrease in the plasma I concentration (Table II).

In contrast to the stability of I in plasma at low temperature, I was not stable in plasma at higher temperatures. The diminished recovery of I from human plasma at increasing temperature is shown in Fig. 1. Recovery of I was only 15% after 6 hr at 37°, as compared to 72% at 23° and over 95% at 4°. Similar diminution of recovery of I at higher temperature was observed in water. These results will be presented in detail elsewhere.

***In Vivo* Plasma Level Determination**—Figure 2 shows a standard chromatogram of 250 ng of I and 700 ng of internal standard. Figure 3 shows the human plasma background with added internal standard. A standard chromatogram of the HPLC assay of human plasma from a patient who had received an oral dose of I is shown in Fig. 4. The HPLC response indicates a human plasma concentration of 0.2 μg of I/ml. Serial concentrations of I in rat plasma after a dose of 6 mg/kg iv are shown in Fig. 5.

DISCUSSION

An accurate and sensitive determination of I in biological fluids is necessary for the study of its pharmacokinetics in animals and humans. An HPLC method (13) was reported that is far simpler and more sensitive than conventional colorimetric methods (7, 9–11). This HPLC method employs a solvent programming system requiring two pumps or a gradient generation system. The HPLC method in the present report utilizes an

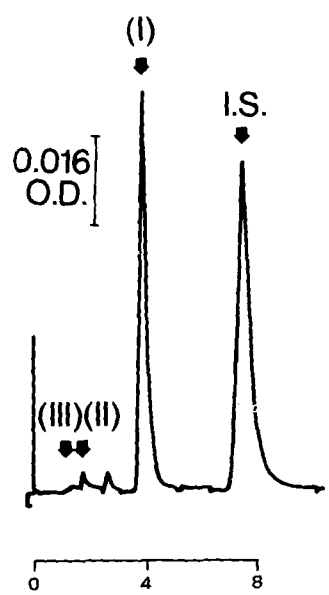

Figure 2—*Chromatogram of 250 μg of I and 700 μg of internal standard (I.S.) injected at 0.2 aufs.*

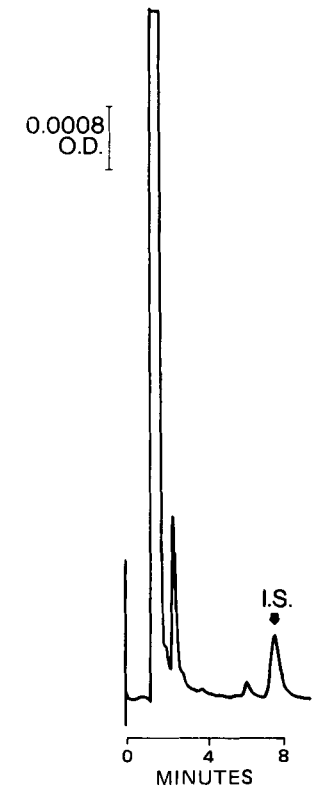

Figure 3—*Chromatogram of human plasma background. The equivalent to 10 μl of plasma and added internal standard (I.S.) were injected at 0.01 aufs.*

isocratic solvent system, and I is quantified using an internal standard. The internal standard, dansylproline, is added directly to plasma samples, after which I is extracted.

The statistics of recovery based on I *versus* the internal standard at 1, 5, 10, and 30 μg/ml indicate quantitative recovery of I. Furthermore, immediate extraction of I does not indicate any significant covalent binding to plasma proteins. When I was incubated in plasma at 37°, only 15% could be recovered after 6 hr. The diminished recovery at 37° may result from degradation or covalent plasma protein binding. The latter

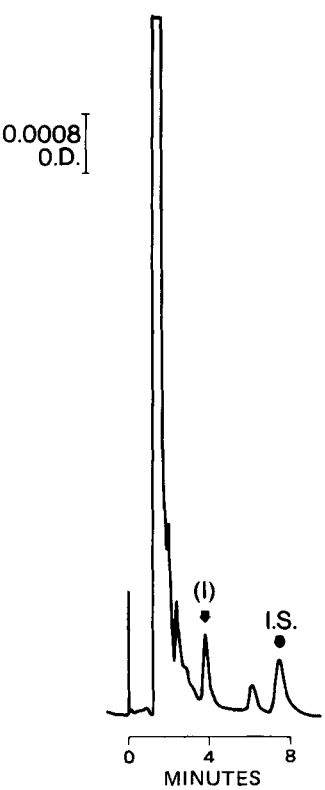

Figure 4—*Chromatogram of human plasma I concentration 4 hr after oral administration of 0.6 mg/kg. The final calculation indicates a concentration of 0.19 μg of I/ml of plasma.*

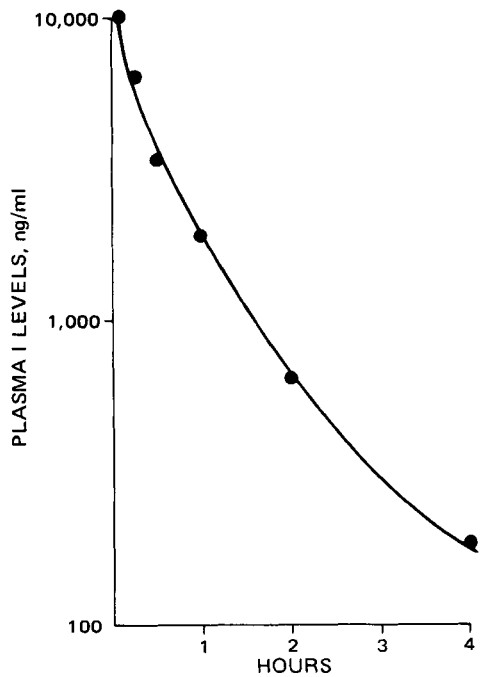

Figure 5—*Rat plasma I level. Compound I was administered to a rat at 6 mg/kg iv. Samples were drawn at the designated time points, and the plasma was analyzed with the HPLC method.*

is presumably not a major effect because similar degradation was observed in water (15).

The quantitative determination of II and III from biological samples is not possible because of background interference. Compounds II and III could be quantified in nonbiological fluids; however, to analyze these compounds in pharmacokinetic and biochemical pharmacology studies, a modification of the present method (*i.e.*, solvent programming) or other methods will be required.

The developed method is sensitive enough to measure the disappearance of I from human plasma after drug administration. Human pharmacokinetic studies are now underway. In preliminary studies, it was possible to measure plasma levels for as long as 13 hr after an intravenous dose of the drug. The minimum detectable level of I was 50 ng/ml of plasma. No important interfering peaks at the positions of I and the internal standard were observed.

The validity of the quantitative method has been confirmed by mass spectrometry. This HPLC method has been useful for the study of the degradation and protein binding properties of I (15).

REFERENCES

(1) F. Bergel and J. A. Stock, *J. Chem. Soc.*, **76**, 2409 (1954).

(2) R. B. Livingston and S. K. Carter, "Single Agents in Cancer Chemotherapy," Plenum, New York, N.Y., 1970, pp. 99–111.

(3) B. Clarkson, in "Antineoplastic and Immunosuppressive Agents 1," A. C. Sartorelli and D. G. Johns, Eds., Springer-Verlag, New York, N.Y., 1974, p. 172.

(4) R. Alexanenian, D. E. Bergsagel, P. J. Migliore, W. K. Vaughn, and C. D. Howe, *Blood*, **31**, 1 (1968).

(5) W. C. J. Ross, "Biological Alkylating Agents," Butterworths, London, England, 1962, pp. 19–31.

(6) J. H. Linford, *Biochem. Pharmacol.*, **8**, 343 (1961).

(7) O. M. Friedman and E. Boger, *Anal. Chem.*, **33**, 906 (1961).

(8) M. A. Chirigos and J. A. R. Mead, *Anal. Biochem.*, **7**, 259 (1964).

(9) O. Klatt, A. Griffin, and J. Stehlin, Jr., *Proc. Soc. Exp. Biol. Med.*, **104**, 629 (1960).

(10) J. Epstein, R. W. Rosenthal, and R. Ess, *Anal. Chem.*, **27**, 1435 (1955).

(11) H. Petering and G. Van Giessen, *J. Pharm. Sci.*, **52**, 1159 (1963).

(12) J. Goras, J. Knight, R. Iwamoto, and P. Liu, *ibid.*, **59**, 561 (1970).

(13) R. Furner, L. Mellett, R. Brown, and G. Duncan, *Drug. Metab.*

Dispos., **4**, 577 (1976).

(14) S. Nicolaidis, N. Rowland, M. Meile, P. Marfaing-Jallat, and A. Pesez, *Pharmacol. Biochem. Behav.*, **2**, 131 (1974).

(15) S. Y. Chang, D. S. Alberts, D. Farquhar, L. R. Melnick, P. D. Walson, and S. E. Salmon, *J. Pharm. Sci.*, **67**, 682 (1978).

ACKNOWLEDGMENTS

Supported in part by U.S. Public Health Service Grants CA-14102 and CA-17094 and research training Grant T22GM007103 from the National Institutes of Health, Bethesda, MD 20014.

Hydrolysis and Protein Binding of Melphalan

S. Y. CHANG ˣ, D. S. ALBERTS, D. FARQUHAR *, L. R. MELNICK, P. D. WALSON, and S. E. SALMON

Received April 22, 1977, from the *Section of Hematology and Oncology, Departments of Internal Medicine and Pharmacology, and the Cancer Center, College of Medicine, University of Arizona, Tucson, AZ 85724.* Accepted for publication September 1, 1977. *Department of Developmental Therapeutics, M. D. Anderson Hospital and Tumor Institute, Houston, TX 77025.

Abstract □ Melphalan (30 μg/ml) is completely hydrolyzed in water at 37° after 8 hr. At lower temperatures, hydrolysis proceeds at slower rates. The presence of bovine serum albumin retards hydrolysis of melphalan (30 μg/ml) in water. The melphalan hydrolysis rate is directly related to the bovine serum albumin concentration. At 37°, 8 g of bovine serum albumin/100 ml of water gives a recovery rate of melphalan similar to that of human plasma. *In vitro* alkylation of melphalan at 37° with human plasma containing 30 μg/ml, calculated by equilibrium dialysis, methanol extraction, and high-pressure liquid chromatographic analysis, is 30% after 8 hr.

Keyphrases □ Melphalan—hydrolysis, effect of bovine serum albumin, various temperatures □ Hydrolysis—melphalan, effect of bovine serum albumin, various temperatures □ Antineoplastic agents—melphalan, hydrolysis, effect of bovine serum albumin, various temperatures

The alkylation of nucleic acids and proteins by melphalan (I) has been studied using spectrophotometry, radiochemistry, and equilibrium dialysis (1, 2–4). Chirigos and Mead (2), using fluorometric detection and equilibrium dialysis, showed that 60% of I was covalently bound to plasma proteins at 26°. Other studies (1, 3, 4) also suggested covalent binding of I to proteins and nucleic acids.

It is necessary to understand the *in vitro* hydrolysis and alkylation of I to describe its pharmacokinetics in humans. This report documents the qualitative and quantitative aspects of adsorption, hydrolysis, and alkylation of I.

EXPERIMENTAL

Materials—^{14}C-Melphalan (^{14}C-ethyl labeled) was synthesized according to the method of Bergel and Stock (5) and purified by high-pressure liquid chromatography (HPLC) (6). Dansylproline[1] was used as an internal standard for HPLC.

Assay of I—Compound I was extracted and analyzed using a previously described HPLC method (6).

Recovery Studies—The hydrolysis rate of I to III and IV in water (Scheme I) at 0, 23, and 37° was studied. Thirty-five micrograms of I and 70 μg of internal standard were added to 1 ml of water, and samples were taken at various times for HPLC analysis as previously described (6). The rate constants, k, were calculated according to $k = 2.3 \log ([I]_0/[I]_t)/t$, where $[I]_0$ and $[I]_t$ are the concentrations of I at times zero and t.

To study the effect of protein on the I hydrolysis rate in water, 30 μg of I and 70 μg of internal standard were added to increasing concentrations of bovine serum albumin[2] in water (*e.g.*, 8, 13, and 25 g/100 ml at 37°). At designated intervals, samples were taken for HPLC analysis.

The extractability of I from, and degradation in, human plasma was studied *in vitro* at 37°. Three hundred micrograms of I (1.2 μCi of carbon-14) and 700 μg of internal standard were added to 10 ml of human plasma, and 1-ml aliquots were extracted with methanol at given intervals

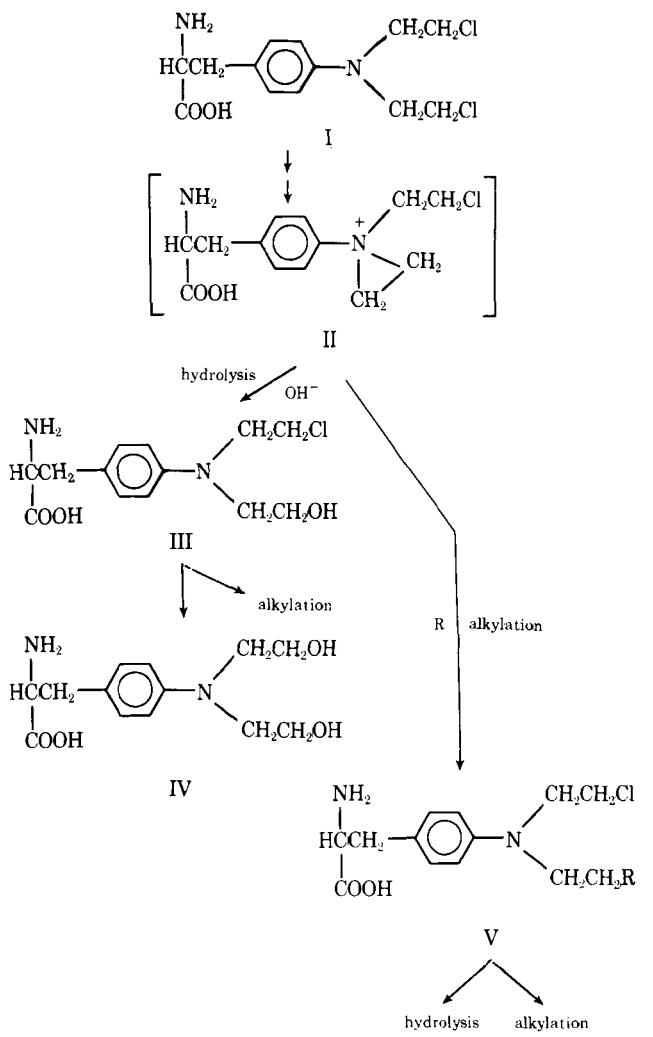

Scheme I

[1] Pierce Chemical Co., Rockford, Ill.

[2] Sigma Chemical Co., St. Louis, Mo.

Dispos., **4**, 577 (1976).

(14) S. Nicolaidis, N. Rowland, M. Meile, P. Marfaing-Jallat, and A. Pesez, *Pharmacol. Biochem. Behav.*, **2**, 131 (1974).

(15) S. Y. Chang, D. S. Alberts, D. Farquhar, L. R. Melnick, P. D. Walson, and S. E. Salmon, *J. Pharm. Sci.*, **67**, 682 (1978).

ACKNOWLEDGMENTS

Supported in part by U.S. Public Health Service Grants CA-14102 and CA-17094 and research training Grant T22GM007103 from the National Institutes of Health, Bethesda, MD 20014.

Hydrolysis and Protein Binding of Melphalan

S. Y. CHANG ˣ, D. S. ALBERTS, D. FARQUHAR *, L. R. MELNICK, P. D. WALSON, and S. E. SALMON

Received April 22, 1977, from the *Section of Hematology and Oncology, Departments of Internal Medicine and Pharmacology, and the Cancer Center, College of Medicine, University of Arizona, Tucson, AZ 85724.* Accepted for publication September 1, 1977. *Department of Developmental Therapeutics, M. D. Anderson Hospital and Tumor Institute, Houston, TX 77025.

Abstract □ Melphalan (30 μg/ml) is completely hydrolyzed in water at 37° after 8 hr. At lower temperatures, hydrolysis proceeds at slower rates. The presence of bovine serum albumin retards hydrolysis of melphalan (30 μg/ml) in water. The melphalan hydrolysis rate is directly related to the bovine serum albumin concentration. At 37°, 8 g of bovine serum albumin/100 ml of water gives a recovery rate of melphalan similar to that of human plasma. *In vitro* alkylation of melphalan at 37° with human plasma containing 30 μg/ml, calculated by equilibrium dialysis, methanol extraction, and high-pressure liquid chromatographic analysis, is 30% after 8 hr.

Keyphrases □ Melphalan—hydrolysis, effect of bovine serum albumin, various temperatures □ Hydrolysis—melphalan, effect of bovine serum albumin, various temperatures □ Antineoplastic agents—melphalan, hydrolysis, effect of bovine serum albumin, various temperatures

The alkylation of nucleic acids and proteins by melphalan (I) has been studied using spectrophotometry, radiochemistry, and equilibrium dialysis (1, 2–4). Chirigos and Mead (2), using fluorometric detection and equilibrium dialysis, showed that 60% of I was covalently bound to plasma proteins at 26°. Other studies (1, 3, 4) also suggested covalent binding of I to proteins and nucleic acids.

It is necessary to understand the *in vitro* hydrolysis and alkylation of I to describe its pharmacokinetics in humans. This report documents the qualitative and quantitative aspects of adsorption, hydrolysis, and alkylation of I.

EXPERIMENTAL

Materials—^{14}C-Melphalan (^{14}C-ethyl labeled) was synthesized according to the method of Bergel and Stock (5) and purified by high-pressure liquid chromatography (HPLC) (6). Dansylproline[1] was used as an internal standard for HPLC.

Assay of I—Compound I was extracted and analyzed using a previously described HPLC method (6).

Recovery Studies—The hydrolysis rate of I to III and IV in water (Scheme I) at 0, 23, and 37° was studied. Thirty-five micrograms of I and 70 μg of internal standard were added to 1 ml of water, and samples were taken at various times for HPLC analysis as previously described (6). The rate constants, k, were calculated according to $k = 2.3 \log ([I]_0/[I]_t)/t$, where $[I]_0$ and $[I]_t$ are the concentrations of I at times zero and t.

To study the effect of protein on the I hydrolysis rate in water, 30 μg of I and 70 μg of internal standard were added to increasing concentrations of bovine serum albumin[2] in water (*e.g.*, 8, 13, and 25 g/100 ml at 37°). At designated intervals, samples were taken for HPLC analysis.

The extractability of I from, and degradation in, human plasma was studied *in vitro* at 37°. Three hundred micrograms of I (1.2 μCi of carbon-14) and 700 μg of internal standard were added to 10 ml of human plasma, and 1-ml aliquots were extracted with methanol at given intervals

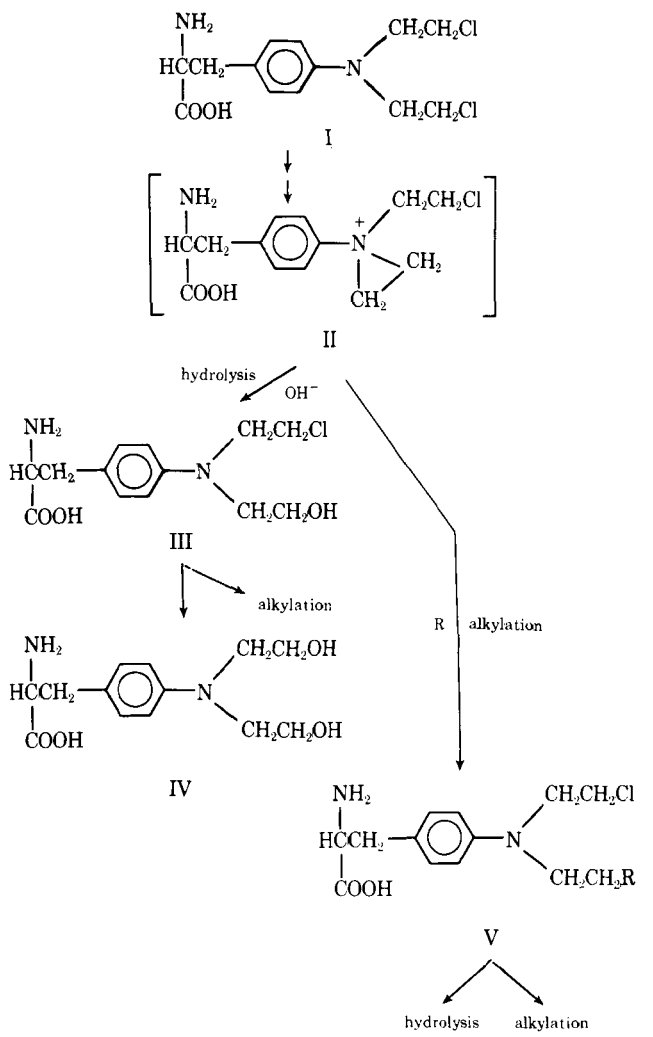

Scheme I

[1] Pierce Chemical Co., Rockford, Ill.

[2] Sigma Chemical Co., St. Louis, Mo.

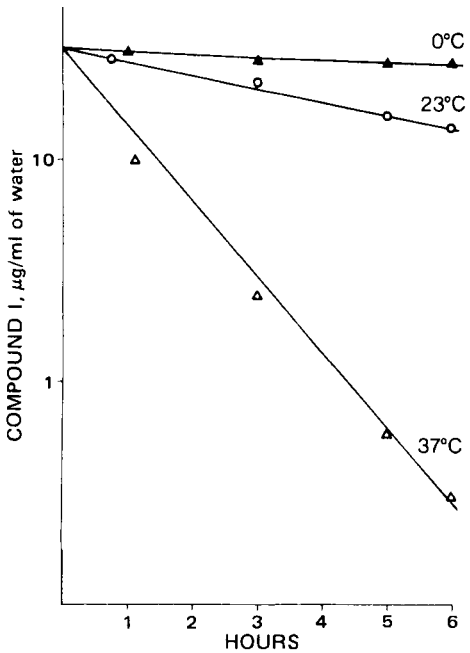

Figure 1—*Recovery of I from water. Compound I was added to distilled water (35 μg/ml) and incubated at 0° (▲), 23° (○), and 37° (△). Samples were taken at designated times and analyzed by HPLC.*

(6). The supernate of the methanol extracts, 0.1 ml, was assayed for total ^{14}C-content. These same samples were separated by HPLC into a 5-ml fraction of I and a 5-ml fraction of III plus IV. Each fraction was mixed with 20 ml of scintillation fluid[3] and assayed for carbon-14. The quenching effects of the HPLC solvent were corrected. At the same time, HPLC analysis of I was carried out, but quantification of III or IV by HPLC was not possible because of plasma background interference.

Equilibrium Dialysis—The dialysis apparatus[4] had a 2-ml capacity. A cellulose acetate membrane separated the system into symmetrical 1-ml chambers. One chamber contained ^{14}C-I (0.1 μCi of carbon-14) and 30 μg of I in 1 ml of human plasma, and the opposite chamber contained 1 ml of 0.05 *M* phosphate buffer (pH 7.4). After gentle shaking, 20 μl was removed from each chamber at intervals up to 25 hr and analyzed for ^{14}C-content. The dialyses were carried out at 4, 14, 23, and 37°.

Additional 4° experiments were performed and analyzed by HPLC. For these experiments, 100 μg of I was added to 1 ml of plasma. The internal standard was not used because of its high adsorption by the dialysis membrane. Compound I concentration was calculated using a standard response curve. Control dialysis experiments were also performed at 4, 14, and 37° in buffer.

RESULTS

Recovery—The hydrolysis of I in water as a function of temperature and incubation time is shown in Fig. 1. A rapid first-order kinetic degradation is shown with rate constants of 0.83/hr (37°), 0.13/hr (23°), and 0.04/hr (0°). The hydrolysis of I in water solutions of bovine serum albumin at 37° as a function of time and bovine serum albumin concentration is shown in Fig. 2. Hydrolysis rate constants of I in bovine serum albumin solution are 0.46/hr (8 g of bovine serum albumin/100 ml), 0.36/hr (13 g of bovine serum albumin/100 ml), and 0.24/hr (25 g of bovine serum albumin/100 ml). The *in vitro* hydrolysis rate constant of I from human plasma varied between 0.31 and ~0.45/hr at 37°.

Extraction of ^{14}C-I—Figure 3 shows the extractability of total carbon-14 from human plasma, the recovery rate of I and ^{14}C-I, and the hydrolysis of ^{14}C-I to ^{14}C-III and ^{14}C-IV at 37°. The recovery of total methanol-extractable carbon-14 at 37° slowly decreased to 70% of the initial concentration after 8 hr (Fig. 3). At any given time point, the sum of ^{14}C-I, ^{14}C-III, and ^{14}C-IV of the HPLC eluates was equivalent to the total methanol extraction of carbon-14 (Fig. 3).

The 75% recovery of ^{14}C-I (Fig. 3) at zero time was due to partial hydrolysis of ^{14}C-I to ^{14}C-III and ^{14}C-IV. The decrease in ^{14}C-I recovery can be accounted for by the increase in ^{14}C-III and ^{14}C-IV.

[3] Aquasol, New England Nuclear, Boston, Mass.
[4] Chemical Rubber Co., Cleveland, Ohio.

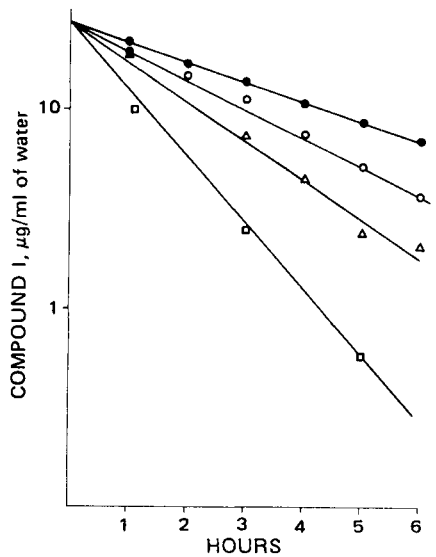

Figure 2—*Effect of bovine serum albumin on the recovery of I. Compound I (30 μg/ml) was added to various concentrations of bovine serum albumin and incubated at 37°. Samples were taken at designated time points and analyzed by HPLC. Key (concentration of bovine serum albumin): □, 0; △, 8 g/100 ml; ○, 13 g/100 ml; and ●, 25 g/100 ml.*

Dialysis Studies—The results of dialysis experiments at 4, 14, 23, and 37° are shown in Fig. 4. Equilibrium was reached in 8 hr at all temperatures. No adsorption of I to dialysis membranes was observed. At equilibrium, 33% of I remained bound to plasma proteins at 37°. At 23°, undialyzable I decreased to 15–20%. At 4°, 30% of I remained bound to plasma; however, this 30% was extractable with methanol (Table I).

***In Vitro* and *In Vivo* Studies**—Figure 5 shows the *in vitro* recovery of I (12 μg/ml) in plasma at 37° and an *in vivo* plasma decay curve for I (0.6-mg/kg iv bolus injection) in a patient with ovarian carcinoma.

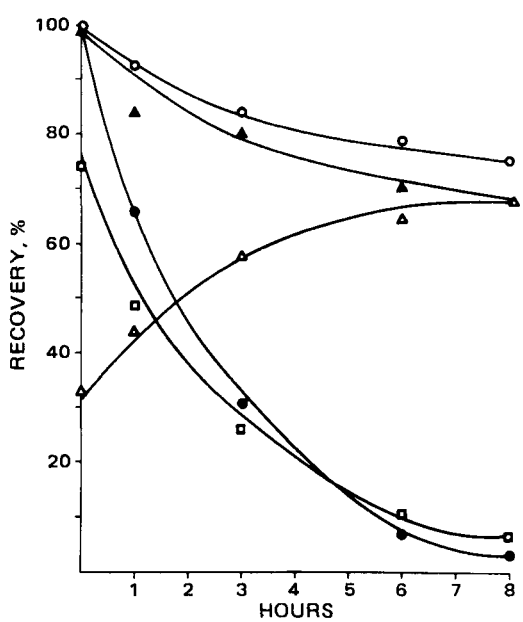

Figure 3—*Methanol extraction of ^{14}C-I and HPLC analyses. ^{14}C-Compound I (1.2 μCi/300 μg of I) was added to human plasma and incubated at 37°. At various times, aliquots were taken and extracted with methanol from which a portion was directly assayed for carbon-14 (▲) and a portion was assayed by HPLC for I (●). The eluate from the chromatograph was assayed for ^{14}C-I (□) and the mixture of ^{14}C-III and ^{14}C-IV (△); ○ denotes the sum total of ^{14}C-I, ^{14}C-III, and ^{14}C-IV of the HPLC eluate.*

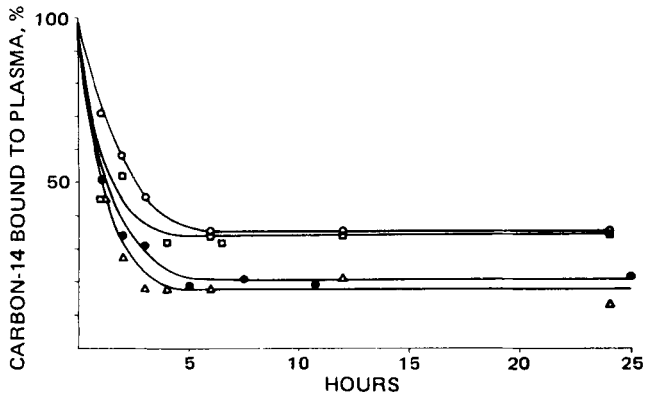

Figure 4—*Equilibrium dialysis of ^{14}C-I. ^{14}C-Compound I (0.1 μCi) and 30 μg of I were added to 1 ml of human plasma and dialyzed with 1 ml of a phosphate buffer (0.05 M, pH 7.4) at 4° (○), 14° (●), 23° (△), and 37° (□). Samples from both chambers were taken simultaneously at designated times and assayed for carbon-14.*

DISCUSSION

The hydrolysis of I to III and IV has been described (2, 6, 7). Compound I may form a reactive ammonium ion (II) and then be hydroxylated to III and IV (7–10). In such reactions, the hydrolysis of I would be expected to follow first-order kinetics (10–12). As shown in Figs. 1, 2, and 5, *in vitro* recoveries of I from water, bovine serum albumin, and human plasma followed first-order kinetics.

The present results show that bovine serum albumin or human plasma proteins retarded the hydrolysis rate of I *in vitro*. Linford (13) made a similar observation for chlorambucil. Because the quantification of III and IV by HPLC was not performed due to background interference, the chemical nature of unrecovered I remained undetermined. There is evidence that I undergoes extensive alkylation and physical adsorption to plasma proteins (1–4). Thirty percent of the initial carbon-14 was not extracted from plasma proteins at 37° after 8 hr (Fig. 3). This fact and the results of the dialysis experiments whereby 30% of carbon-14 remained undialyzable at 37° after 8 hr may indicate alkylation of I to plasma proteins.

Chirigos and Mead (2) terminated their dialysis experiments after 3 hr. The present results show that the equilibrium points at 4, 14, 25, and 37° were not reached until 8 hr (Fig. 4). The 30% undialyzable I seen at 4° may have been due to increased adsorption of I to plasma proteins at low temperature. As the temperature was increased, this physical adsorption was reversed (see 14 and 23° in Fig. 4). Also 30% undialyzable I at 4° was extractable with methanol (Table I).

There was a 10% difference at 8 hr between total methanol-extractable carbon-14 and the sum total ^{14}C-eluate of HPLC at times less than 8 hr because of an overcorrection of the quenching effect of the solvent.

The marked difference between the *in vitro* and *in vivo* recovery of I from human plasma is shown in Fig. 5. Clearly, pharmacokinetic studies of I will require careful analysis of spontaneous hydrolysis and protein adsorption as well as of physiological disposition and metabolism. The evidence for significant hydrolysis of I at room temperature in protein-free medium suggests that a parenteral solution of the drug should be prepared immediately prior to administration and should be kept cold or prepared with albumin in the diluent.

Table I—Equilibrium Dialysis of I in Human Plasma at 4° by HPLC Analysis

Time Elapsed	I, μg/ml
Zero time	100.0
1 hr, 10 min	79.9
4 hr, 15 min	52.9
8 hr, 50 min	39.6
21 hr, 30 min	35.0
22 hr	33.5

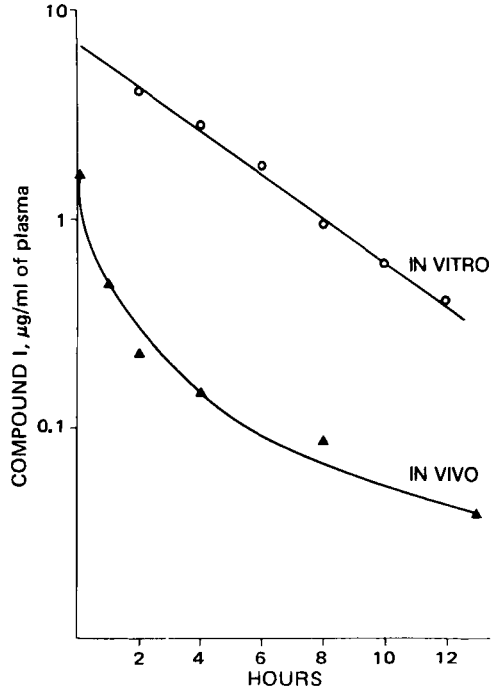

Figure 5—In vitro *and* in vivo *recovery of I from human plasma. Key:* ○, in vitro *recovery of I (12 μg/ml) at 37°; and* ▲, in vivo *recovery after patient received 0.6-mg/kg iv bolus injection.*

REFERENCES

(1) P. Cohn, *Br. J. Cancer*, **1**, 258 (1957).

(2) M. Chirigos and J. Mead, *Anal. Biochem.*, **7**, 259 (1964).

(3) A. Milner, O. Klatt, S. Young, and J. Stephlin, Jr., *Cancer Res.*, **25**, 259 (1965).

(4) R. P. Sanderson, J. M. McKenna, and W. S. Blackemore, *Nature*, **205**, 479 (1965).

(5) F. Bergel and J. Stock, *J. Chem. Soc.*, **76**, 2409 (1954).

(6) S. Y. Chang, D. S. Alberts, L. R. Melnick, P. D. Walson, and S. E. Salmon, *J. Pharm. Sci.*, **67**, 679 (1978).

(7) W. C. J. Ross, "Biological Alkylating Agents," Butterworths, London, England, 1962, pp. 19, 32, 60, 99.

(8) "Review of Medical Pharmacology," 5th ed., F. Meyers, E. Jawetz, and A. Goldfien, Eds., Lange Medical Publications, Los Altos, Calif., 1976, p. 470.

(9) R. B. Livingston and S. Carter, "Single Agents in Cancer Chemotherapy," Plenum, New York, N.Y., 1970, p. 100.

(10) W. C. J. Ross, in "Antineoplastic and Immunosuppressive Agents—I," A. Sartorelli and D. Johns, Eds., Springer-Verlag, New York, N.Y., 1974, p. 40.

(11) W. C. Gardiner, Jr., "Rates and Mechanisms of Chemical Reactions," Benjamin, New York, N.Y., 1969.

(12) E. S. Gould, "Mechanism and Structure in Organic Chemistry," Holt, Rinehart and Winston, New York, N.Y., 1959, pp. 159–192.

(13) J. H. Linford, *Biochem. Pharmacol.*, **8**, 343 (1961).

ACKNOWLEDGMENTS

Supported in part by U.S. Public Health Service Grants CA-14102 and CA-17094 and research training Grant T22GM007103 from the National Institutes of Health, Bethesda, MD 20014.

Elimination of a Quaternary Pyridinium Salt Delivered as Its Dihydropyridine Derivative from Brain of Mice

NICHOLAS BODOR ˣ, RICHARD G. ROLLER, and SALLY J. SELK

Received June 13, 1977, from *INTERx Research Corporation, Lawrence, KS 66044.* Accepted for publication September 1, 1977.

Abstract □ 1-Methylpyridine-2-carbaldehyde oxime, a quaternary pyridinium salt, can be delivered efficiently through the blood–brain barrier in its dihydropyridine prodrug form. This redox system was used to study the elimination rate from the brain of a small quaternary salt. It was found that the oxime is eliminated relatively fast from the brain, which supports a hypothesis for the existence of an active transport mechanism for eliminating organic ions from the brain. The possibilities of using the pyridinium salt ⇌ dihydropyridine redox system for specific delivery of drugs to the brain are discussed.

Keyphrases □ Pyridinium salt, substituted quaternary—and prodrug, elimination rate from brain, mice □ Prodrugs—dihydropyridine derivative of quaternary pyridinium salt, elimination rate from brain, mice □ Elimination rate—substituted quaternary pyridinium salt and prodrug from brain, mice

Many valuable chemotherapeutic agents are of limited use when the disease site lies within the central nervous system (CNS). The rates at which drugs or metabolic substrates penetrate the blood–brain barrier depend on their plasma concentration, cerebral blood flow, and barrier permeability. Although the blood–brain barrier is not a simple, anatomically well-defined unitary physical entity (1), it is generally accepted that lipid solubility, degree of ionic dissociation or protonation, and carrier-mediated or active transport govern the movement of molecules in and out of the brain, *i.e.*, the permeability of the blood–brain barrier.

Changes in permeability can be caused by several pathological and toxicological processes (2). A general increase in the barrier permeability, such as a nonspecific breakdown of the barrier has, however, severe consequences including cerebral edema. The passage of molecules into the brain also can be enhanced (3) by intrathecal injections and drug latentiation.

BACKGROUND

Since highly selective permeability changes are desired, drug latentiation, or the use of prodrugs, presents the most hopeful approach for delivery of molecules otherwise unable to penetrate the blood–brain barrier into the brain.

A dihydropyridine–pyridinium salt-type redox system recently was developed (4–6) to alter the delivery and distribution characteristics of quaternary pyridinium ring-containing drugs. The approach was used successfully to improve delivery of 1-methylpyridine-2-carbaldehyde oxime chloride (I) as its dihydropyridine derivative, 1-methyl-1,6-dihydropyridine-2-carbaldehyde oxime (II). Because of its lipophilic character, II distributes quickly into tissues and organs unaccessible for I and is then rapidly oxidized ($t_{1/2}$ = 1 min) to the active I form at the site(s) of action (7).

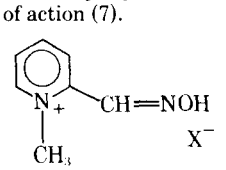

I

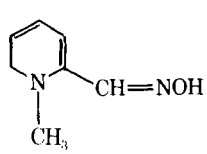

II

A highly successful delivery of a quaternary pyridinium salt, I, into the brain was achieved using the prodrug II (8). A dramatic increase in drug delivery to the brain and subsequent reactivation of blocked brain cholinesterase was realized. The importance of the reactivation of brain cholinesterase after exposure to organophosphates is well documented (9), from the point of view of both survival and psychiatric problems.

The treatment of neoplasms or infections in the CNS is hindered by the relative impermeability of the blood–brain barrier to most chemotherapeutic agents. To overcome this problem, the redox system could be used for specific delivery of a drug into the brain. Conceivably, a generalized version of the dihydropyridine ⇌ pyridinium salt approach can be extended to delivery into the brain of many drugs containing quaternary heteroaromatic structure or with the dihydropyridine–pyridinium part as a carrier system.

The hypothesis (4) is illustrated in Scheme I, where VII is an antitumor agent (AT), Z is the link between VII and the carrier pyridinium part, and R_1 is a substituent to control the release rate of VII from the quaternary derivative (III) delivered in this way to the brain. Examples for the link Z are: CH_2O, COO, COHNCRHO, and CH=NO.

It is important to note the possibility of a specific delivery to the brain. If the blood–brain barrier would hinder the efflux of the quaternary derivative formed in the brain after delivery, a slow infusion procedure would result in a specific higher concentration of the drug in the brain against the concentration gradient, since the quaternary salt formed in blood would be rapidly excreted, thus avoiding systemic toxicity.

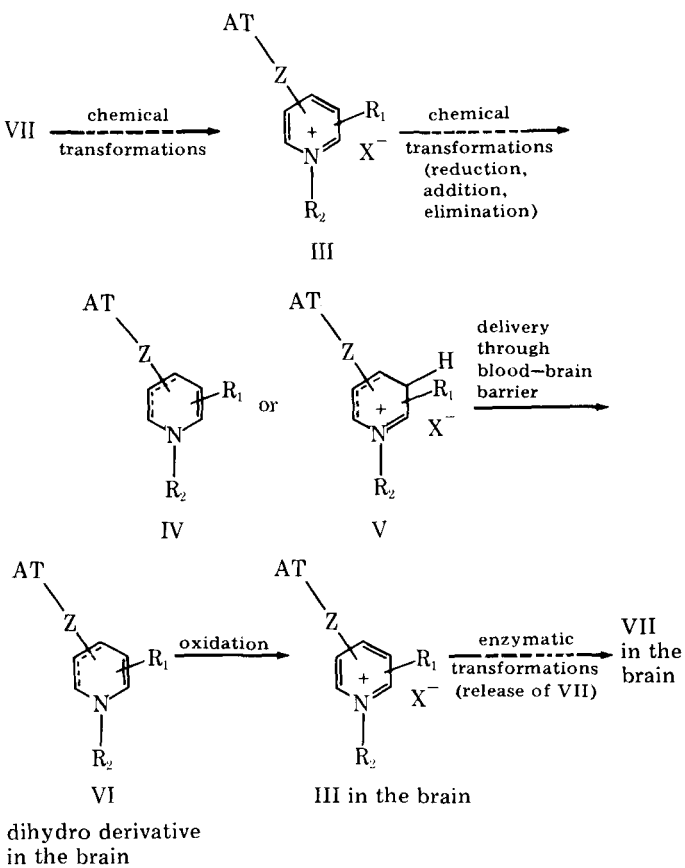

Scheme I

Table I—Distribution of I at Various Time Intervals after Intravenous Delivery as I and as II to White Mice [a]

Minutes	Concentration of I, % Dose/g of Tissue ± SE [b]					
	Blood [c]	Lungs	Kidney	Diaphragm	Heart	Brain
			I			
10	1.22 ± 0.22	1.88 ± 0.31	3.52 ± 0.47	0.79 ± 0.08	2.11 ± 0.13	0.35 ± 0.04
30	0.62 ± 0.16	1.49 ± 0.29	2.2 ± 0.13	0.67 ± 0.23	1.02 ± 0.15	0.38 ± 0.02
75	0.41 ± 0.06	0.97 ± 0.12	1.39 ± 0.16	0.17 ± 0.07	0.49 ± 0.08	0.35 ± 0.03
			II			
10	0.85 ± 0.1	3.55 ± 0.32	2.56 ± 0.28	3.77 ± 0.25	7.06 ± 1.01	2.65 ± 0.19
20	0.61 ± 0.08	1.89 ± 0.14	6.23 ± 0.68	2.70 ± 0.24	4.83 ± 0.64	1.47 ± 0.22
30	0.74 ± 0.05	1.85 ± 0.15	4.03 ± 1.07	2.85 ± 0.16	4.39 ± 0.23	1.40 ± 0.14
75	0.70 ± 0.07	0.50 ± 0.06	1.12 ± 0.08	1.08 ± 0.20	0.66 ± 0.08	0.54 ± 0.08
150	0.56 ± 0.10	0.40 ± 0.03	0.67 ± 0.03	0.61 ± 0.09	0.47 ± 0.05	0.24 ± 0.01
225	0.26 ± 0.03	0.24 ± 0.01	0.65 ± 0.09	0.28 ± 0.02	0.35 ± 0.06	0.21 ± 0.04

[a] Dose: 5 mg of ^{14}C-I or ^{14}C-II/kg. Specific activity: 1 mCi/mmole. [b] Each point is the average of six animals. [c] Expressed as percent of dose per milliliter.

The question then arises: Is the blood–brain barrier a one-way street?

It was suggested that restriction of intravascular materials from entry into the brain is not the only major role of the blood–brain barrier. More important, perhaps, is its capability of excreting detoxification and waste products into the blood (10). Although drugs pass from blood into cerebrospinal fluid at rates that apparently parallel their lipid solubility, they pass in the reverse direction at rates only partly dependent on this property. Although the rapid elimination of lipid-insoluble substances, such as mannitol, sucrose, and inulin, can occur through the arachnoid villi, an active transport system is also conceivable (11). Based on *in vitro* studies (3), it was concluded that an active transport system apparently pumps organic cations, such as hexamethonium, decamethonium, and *N'*-methylnicotinamide, from the cerebrospinal fluid to the blood.

Exactly the opposite conclusion was reached by Ross and Froden (12). They studied the elimination of a piperidinium quaternary salt, apparently formed *in situ* after delivery of a haloalkylamine, which undergoes cyclization to the quaternary salt, in the brain, as well. A significantly slower elimination from the brain of the formed piperidinium salt was observed. It was concluded that the outflow rate of the quaternary salt corresponded to the inflow rate. Similar results, however, were obtained for erythrocytes; the efflux of the quaternary salt was very slow (13).

Based on the success in direct delivery of I into the brain of mice, this model was chosen to verify the influx–efflux properties of I.

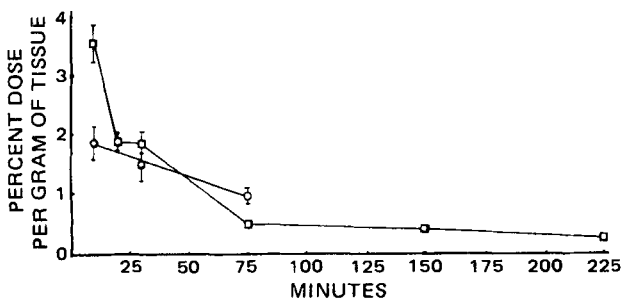

Figure 1—*Concentration of I in the lung tissues of mice as a function of time after administration of 5.0 mg/kg iv of I (○) and II (□).*

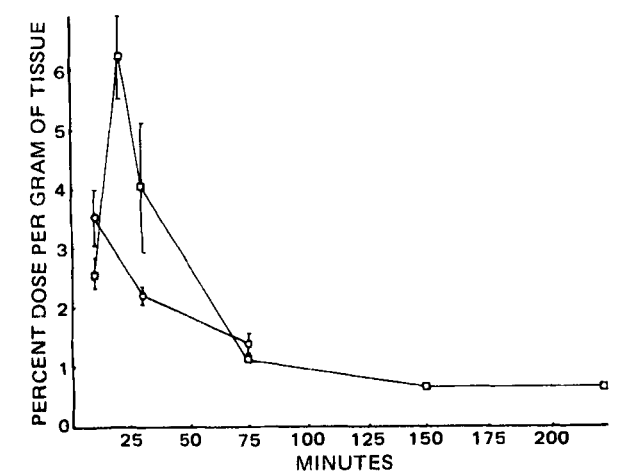

Figure 2—*Concentration of I in the kidney tissues of mice as a function of time after administration of 5.0 mg/kg iv of I (○) and II (□).*

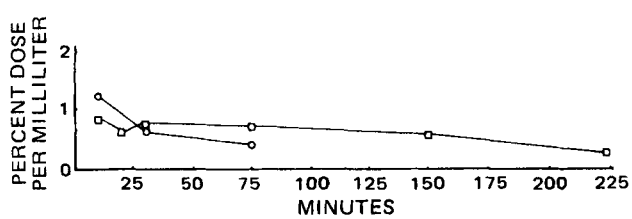

Figure 3—*Concentration of I in the blood of mice as a function of time after adminstration of 5.0 mg/kg iv of I (○) and II (□).*

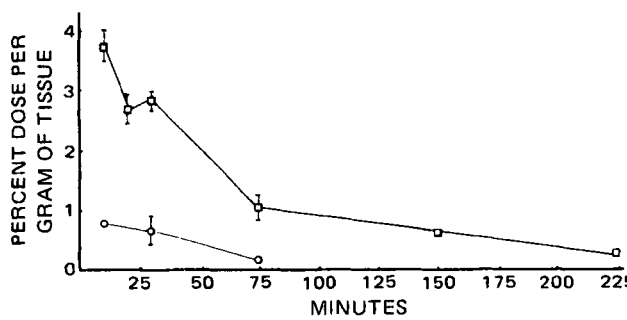

Figure 4—*Concentration of I in the diaphragm tissues of mice as a function of time after administration of 5.0 mg/kg iv of I (○) and II (□).*

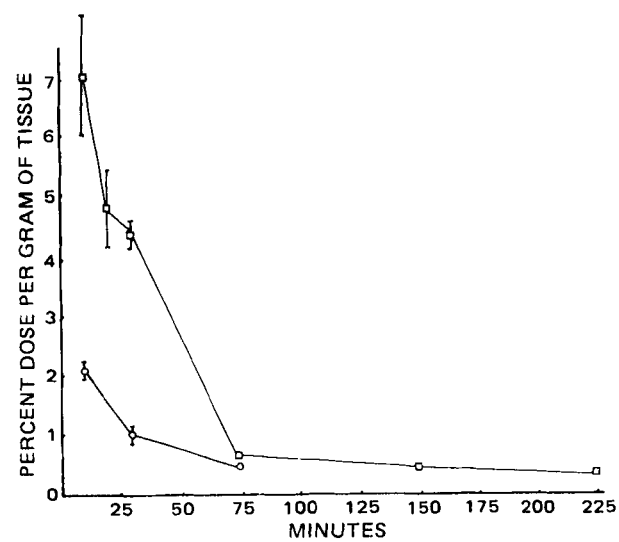

Figure 5—*Concentration of I in the heart tissues of mice as a function of time after administration of 5.0 mg/kg iv of I (○) and II (□).*

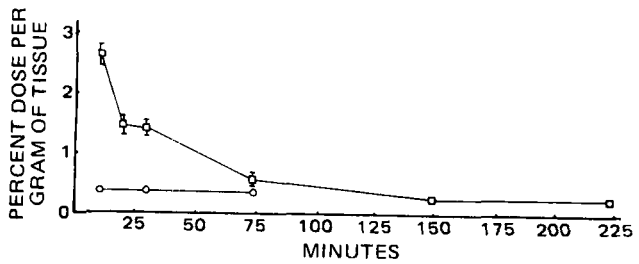

Figure 6—*Concentration of I in the brain tissues of mice as a function of time after administration of 5.0 mg/kg iv of I (○) and II (□).*

EXPERIMENTAL

Materials—^{14}C-Methyl iodide was used as received[1]. ^{14}C-Methyl-labeled I iodide and ^{14}C-II chloride were synthesized as previously described (6). Homogenization was carried out with a motor-driven glass homogenizer. Radioactive counting was performed in a liquid scintillation system[2].

Procedure—Radioactive I and II were dissolved separately in the appropriate amount of 0.9% sterile saline, and 0.2 ml was injected into the tail vein of two groups of white mice (ICR) weighing 28 ± 5 g. A group of 18 mice was given ^{14}C-I, and another group of 36 was given ^{14}C-II. Six animals from the ^{14}C-I group were decapitated after 10, 20, and 75 min; six from the ^{14}C-II group were decapitated at 10, 20, 30, 75, 150, and 225 min following administration.

The blood was collected after decapitation. Then the kidneys, brain, heart, lungs, and diaphragm were excised, washed with normal saline, and kept at −18° until prepared for counting. Samples of 0.1–0.4 ml of whole blood taken from the decapitated upper thorax were discolored with hydrogen peroxide and homogenized with 10 ml of distilled water. A 1-ml aliquot was added to 10 ml of the scintillation cocktail and counted for 10 min. Tissue samples were thawed, dried, and weighed; then they were discolored with 10 ml of 30% H_2O_2 and homogenized with 10 ml of distilled water. A 3-ml aliquot was added to 10 ml of the scintillation cocktail and counted for 10 min.

RESULTS AND DISCUSSION

As expected (8), radiochromatographic analyses showed that the radioactivity in the various organs was due to I, even after administration of II, since the *in vivo* II → I transformation is a fast process, $t_{1/2}$ = 1.04 min (7). Further metabolism of the I formed was a much slower process. The results are summarized in Table I.

The elimination of I from various organs, when administered as I and as II, is compared in Figs. 1–6. Except in the blood, I resulting from delivery by II achieved a significantly higher concentration than when administered as itself. This result could be expected based on the lipophilic character of II since its pKa = 6.32 (6); thus, it is essentially in the free base form in the plasma. The results confirmed again that a significant amount of I reaches the brain shortly after II administration while I is unable to penetrate the blood–brain barrier.

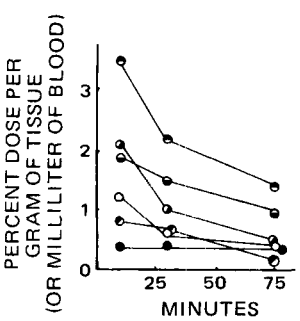

Figure 7—*Time dependence of relative distribution of I in various organs of mice after administration of 5 mg/kg iv of I, in blood (○), brain (●), heart (◕), diaphragm (◐), lungs (◒), and kidneys (◓).*

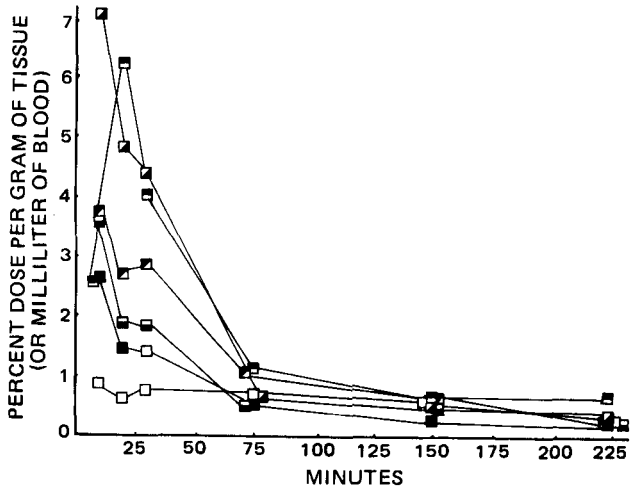

Figure 8—*Time dependence of relative distribution of I in various organs of mice, after administration of 5 mg/kg iv of II, in blood (□), brain (■), heart (◪), diaphragm (◧), lungs (◨), and kidneys (◩).*

The efflux of I from the various organs is compared in Figs. 7 and 8. The apparent elimination rate from the brain almost parallels the elimination rate from the other organs, except the blood.

In other words, the blood–brain barrier does not present any barrier properties for the efflux of I from the brain. The mechanism by which it is eliminated is unknown. It could be actively transported or eliminated through the arachnoid villi.

If it is accepted that larger, aliphatic quaternary salts are eliminated slowly (12) while, based on the present study, small pyridinium quaternary salts are excreted quickly from the brain, it seems possible that drugs could be delivered and concentrated specifically in the brain by using a carrier part. The carrier part would be eliminated quickly after its liberation from the quaternary derivative (III) formed as a result of the oxidative transformation of the dihydropyridine part.

REFERENCES

(1) E. C. Shuttleworth, Jr., *Prog. Exp. Tumor Res.*, **17**, 279 (1972).

(2) W. M. Pardridge, J. D. Connor, and I. L. Crawford, *CRC Crit. Rev. Toxicol.*, **1975**, 159.

(3) L. S. Schanker, *Antimicrob. Agents Chemother.*, **1966**, 1044.

(4) N. Bodor, in "Design of Biopharmaceutical Properties through Prodrugs and Analogs," E. B. Roche, Ed., American Pharmaceutical Association, Washington, D.C., 1977, p. 98.

(5) N. Bodor, E. Shek, and T. Higuchi, *Science*, **190**, 155 (1975).

(6) N. Bodor, E. Shek, and T. Higuchi, *J. Med. Chem.*, **19**, 102 (1976).

(7) E. Shek, T. Higuchi, and N. Bodor, *ibid.*, **19**, 108 (1976).

(8) *Ibid.*, **19**, 113 (1976).

(9) F. R. Sidell, *Clin. Toxicol.*, **7**, 1 (1974).

(10) O. Steinwall, *Acta Psychol. Neurol. Scand.*, **36**, 314 (1961).

(11) Y. Tochino and L. S. Schanker, *Am. J. Physiol.*, **208**, 666 (1965).

(12) S. B. Ross and O. Froden, *Eur. J. Pharmacol.*, **13**, 46 (1970).

(13) S. B. Ross, *J. Pharm. Pharmacol.*, **27**, 322 (1975).

ACKNOWLEDGMENTS

Presented in part at the APhA Academy of Pharmaceutical Sciences Symposium on Design of Biopharmaceutical Properties through Prodrugs and Analogs, Orlando, Fla., November 1976.

This paper is the fifth in the series: Improved Delivery through Biological Membranes. Previous paper: N. Bodor, K. B. Sloan, T. Higuchi, and K. Sasahara, *J. Med. Chem.*, **20**, 1435 (1977).

[1] New England Nuclear.

[2] An LS-150 Beckman liquid scintillation counter was used. Aquasol (New England Nuclear) was used as the scintillation cocktail.

Analysis of Binding of Daunorubicin and Doxorubicin to DNA Using Computerized Curve-Fitting Procedures

STEPHEN R. BYRN [x] **and GARY D. DOLCH** *

Received June 20, 1977, from the *Department of Medicinal Chemistry and Pharmacognosy, School of Pharmacy and Pharmacal Sciences, Purdue University, West Lafayette, IN 47907.* Accepted for publication September 6, 1977. *Present address: Analytical Research and Development Department, Ciba-Geigy Corp., Suffern, NY 10901.

Abstract □ The direct and difference spectroscopic methods of determining the binding constant of daunorubicin to DNA were compared. In addition, several other experimental parameters were varied, including the cell path length (1 or 10 cm), solution concentration, and analytical wavelength. The criterion used for judging the conditions and experimental methods was the attainment of a well-defined binding isotherm. Computerized least-squares curve fitting was used to determine the DNA binding constants from the binding isotherms and to compare the fit of a one-site and two-site model to the data. These studies showed that the best technique for determining the daunorubicin–DNA binding constants involved difference spectroscopic analysis of the absorbance change at 480 nm in long path length cells. In addition, overnight equilibration of daunorubicin–DNA complexes produced spectral changes, which indicated that methods involving prolonged equilibration would be inappropriate for daunorubicin–DNA binding studies. Computerized curve fitting of the data obtained from daunorubicin–DNA and doxorubicin–DNA solutions gave DNA binding constants of $1.27 \times 10^6\ M^{-1}$ for daunorubicin and $2.04 \times 10^6\ M^{-1}$ for doxorubicin and showed that a one-site model fit the data better than a two-site model. These binding constants are consistent with other physical and biological data and provide a very preliminary indication that DNA affinity and biological activity (*e.g.*, antitumor activity) may be related in the anthracyclines. In addition, the value of the number of binding sites obtained from the computerized curve-fitting program was 8/40 or 0.2, which is in agreement with the neighbor exclusion model. The methods and criterion used in this study describe a general approach for determining accurately the binding of drugs to DNA.

Keyphrases □ Daunorubicin—binding to DNA, direct and difference spectroscopic methods compared □ Doxorubicin—binding to DNA, direct and difference spectroscopic methods compared □ DNA—binding to daunorubicin and doxorubicin, direct and difference spectroscopic methods compared □ Spectroscopy—direct and difference methods of determining binding constants for daunorubicin and doxorubicin to DNA □ Binding constants—daunorubicin and doxorubicin to DNA, direct and difference spectroscopic methods compared □ Antineoplastic agents—daunorubicin and doxorubicin, binding to DNA, direct and difference spectroscopic methods compared

The binding of small molecules to nucleic acids is an important and widespread process in biochemistry (1–5), and improvements in the reliability of determining the binding constants of these interactions are needed. In addition, studies of drug–DNA interactions might improve knowledge of drug–receptor binding. Intercalation is a specific kind of DNA binding; it involves insertion of the agent between the base pairs of DNA or RNA (1, 6) and is associated with several simultaneously observed phenomena. These phenomena include UV or visible spectral changes and fluorescence spectral changes of the drug and changes in the hydrodynamic properties and X-ray fiber diffraction patterns of DNA. Individually, any one of these observations does not differentiate between intercalation and other types of nucleic acid binding. However, taken together, these observations provide strong evidence for intercalation.

BACKGROUND

Although several methods, including visible and fluorescence spectroscopy, circular dichroism, and equilibrium dialysis, are available for quantitatively determining the binding parameters of drugs to DNA, methods based on visible spectroscopy are the most widely used. The direct (7) and difference (8) spectroscopic methods are the most popular.

In the direct spectroscopic methods, the drug concentration is held constant and the changes in the drug spectrum are measured directly as the DNA concentration is varied. With the difference spectroscopic method, the DNA concentration is held constant and the changes in the drug spectrum are measured by subtracting the spectrum of the drug from the spectrum of the drug–DNA solution as the drug concentration is varied.

The data from these methods are usually interpreted using Eq. 1 (9, 10):

$$\frac{R}{C} = nK - KR \qquad \text{(Eq. 1)}$$

where R is the fraction of occupied sites, C is the concentration of free ligand, n is the total number of sites, and K is the intrinsic binding constant. According to Eq. 1, a plot of (R/C) *versus* R (Scatchard plot) gives a straight line with a slope of K and an intercept of n.

Comparisons of binding constants measured using spectroscopy and Scatchard plots (Table I) show a surprisingly large variation. This variation is too large to be entirely due to differences in the ionic strength of the solution since, for example, the binding constant of ethidium bromide to DNA is reported to be independent of ionic strength (Table I). An improved understanding of the reason for these variations and the relationship between binding constants measured by direct and difference spectroscopy is one aim of the research reported here.

In addition, the hazards of using reciprocal plots such as the Scatchard plot to derive the parameters K and n were noted previously (10, 11). For cases where the binding constant, K, is small and the data at saturation are incomplete, Klotz (10) showed that linear plots often could lead to an incorrect number of sites through bias or incorrect interpretation of the data. With intercalation, the binding constants are usually large and it is difficult to obtain complete and accurate data at low saturation. Under these circumstances, the bias and unequal weighting of the data inherent with the use of the Scatchard plot lead to errors in determining K. Large errors in the binding constant occur from data that are not measured over at least 75% of the adsorption isotherm (11).

A partial solution to the problems of bias and unequal weighting of the data utilizes computerized least-squares curve fitting of the data to the nonlinear form of Eq. 1:

$$R = \frac{nKC}{1 + KC} \qquad \text{(Eq. 2)}$$

using the programs of Fletcher and coworkers (12–14). These programs are versatile and enable the comparison of several models, including those containing single (Eq. 2) as well as multiple classes of sites:

$$R = \sum_{i=1}^{N} \frac{n_i K_i C}{1 + K_i C} \qquad \text{(Eq. 3)}$$

The anthracycline antibiotics daunorubicin (I) [(8*S*-*cis*)-8-acetyl-10-[(3-amino-2,3,6-trideoxy-α-L-*lyxo*-hexopyranosyl)oxy]-7,8,9,10-tetrahydro-6,8,11-trihydroxy-1-methoxy-5,12-naphthacenedione] and doxorubicin[1] (II) [(8*S*-*cis*)-10-[(3-amino-2,3,6-trideoxy-α-L-*lyxo*-hex-

[1] Adriamycin.

Table I—Binding Constants of Agents to Calf Thymus DNA Determined by Visible Spectroscopic Methods

Agent	Method	Solution	K, M^{-1}	n	Reference
Proflavine	Direct	0.1 M Phosphate–ethylenediaminetetraacetic acid, pH 6.8	1.66×10^6	0.14–0.16	39
Proflavine	Direct	Ionic strength 0.1, pH 6.2	8.97×10^5	0.14	—[a]
Ethidium bromide	Direct	0.04 M Tromethamine hydrochloride	1.43×10^6	0.19	4
Ethidium bromide	Direct	Independent of ionic strength	$\sim 6.6 \times 10^6$	—	40
Actinomycin	Direct	0.1 M Phosphate, pH 7	4.2×10^6	0.07	41
Actinomycin	Difference	0.1 M Phosphate, 0.18 M NaCl, pH 6.9	2.3×10^6	0.11	8
Actinomycin	Difference	0.001 M Phosphate, pH 7	8.9×10^6	0.08	42
Daunorubicin	Difference	0.1 M Tromethamine	3.3×10^6	0.18	15
Daunorubicin	Direct	0.15 M NaCl, pH 7.0	$7.2 (\pm 1.2) \times 10^6$	0.158 (0.003)	35

[a] Calculated from the data in Table I of Ref. 7.

opyranosyl)oxy] - 7,8,9,10-tetrahydro-6,8,11-trihydroxy - 8 - (hydroxyacetyl)-1-methoxy-5,12-naphthacenedione] comprise an excellent system for the application of computerized curve-fitting procedures to drug–DNA interactions. Numerous studies indicated that daunorubicin and doxorubicin bind to DNA by intercalation (15–20), and several lines of evidence suggest that DNA intercalation may be the basis of the biological (*e.g.*, anticancer) activity of these antibiotics (21–24).

In addition, many metabolites and derivatives of daunorubicin and doxorubicin are biologically active (25–29). Thus, a knowledge of the binding constants of these derivatives would allow a quantitative comparison of DNA binding and biological activity (29).

This paper reports a study of the binding of doxorubicin and daunorubicin to DNA, using both direct and difference spectroscopy. Computerized curve-fitting procedures were used to determine accurately the binding constant and number of binding sites.

EXPERIMENTAL

All spectra were recorded on a UV–visible spectrometer with either 1- or 10-cm quartz cells in 0.005 M potassium phosphate buffer, pH 7.4. All solutions were prepared using double-distilled, deionized water. Calf thymus DNA[2] was used for all experiments, and the concentration of the stock solution was determined using an absorptivity of $\epsilon_{260\ nm} = 6600\ M^{-1}\ cm^{-1}$. Doxorubicin hydrochloride, mp 189° [lit. (27) mp 188–190°], and doxorubicin hydrochloride, mp 201° [lit. (30, 31) mp 204–205°], were used as received[3].

Direct Spectral Method—A series of solutions was prepared in 10- or 100-ml volumetric flasks. The anthracycline concentration was constant, and the DNA concentration was varied to obtain the desired DNA to anthracycline concentration ratio. The spectra of the solutions were recorded from 400 to 600 nm with a blank containing the same DNA concentration as the sample. The resulting spectra were analyzed by the published procedure (7). In this analysis, the fraction bound, α_b, the concentration bound, C_b, and R were calculated as shown in Eqs. 4–6:

$$\alpha_b = \frac{A_{obs} - A_{free}}{A_{bound} - A_{free}} \quad \text{(Eq. 4)}$$

$$C_b = \alpha_b C_{total} \quad \text{(Eq. 5)}$$

$$R = \frac{C_b}{\text{total macromolecule concentration}} \quad \text{(Eq. 6)}$$

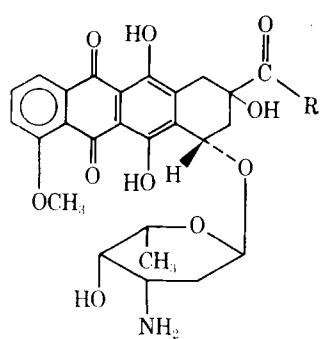

I: R = CH_3

II: R = CH_2OH

[2] Sigma Chemical.

[3] Courtesy of Dr. F. Arcamone, Farmitalia, Milan, Italy.

Adsorption isotherms, titration curves, and Scatchard plots were prepared using the R and $C_{free} = C_{total} - C_b$ calculated and the computer programs described.

Difference Spectral Method—A series of solutions in 100-ml volumetric flasks was prepared in which the concentration of DNA was held constant. The drug concentration was varied to obtain the desired DNA to drug concentration ratio. Each solution was recorded against a blank containing an equal concentration of the drug. Thus, the spectra recorded were the differences between the bound and free drug spectra. The absorbance differences at 480 nm, the total drug concentration, and the absorptivity difference, $\Delta\epsilon$, between the bound and free drug were used to calculate R and C_b:

$$C_b = \frac{\text{absorbance difference (observed)}}{\Delta\epsilon} \quad \text{(Eq. 7)}$$

Adsorption isotherms, titration curves, and Scatchard plots were prepared using the R and $C_{free} = C_{total} - C_b$ calculated and the computer programs described. These data were used to prepare Scatchard and binding plots, which were analyzed using the computer programs. The $\Delta\epsilon$ was taken as the difference between the absorptivities obtained by linear regression (least-squares) analysis of Beer's law plots for free drug and totally bound drug.

Determination of Analytical Wavelength and Effect of Overnight Equilibration—The binding of daunorubicin to DNA was studied by the direct spectral method, using a daunorubicin concentration of $3.72 \times 10^{-5}\ M$. The DNA concentration was varied to produce DNA phosphate to daunorubicin ratios between 10:1 and 0.2:1, and 1-cm cells were used. Based on the results of a preliminary study, two spectral regions were chosen for careful study: 450–500 and 530–540 nm. Adsorption isotherms (plots of R *versus* free daunorubicin) were prepared from the absorbances at 480 and 530 nm.

The effect of equilibration of DNA–daunorubicin solutions for extended times was investigated by preparing three solutions having a daunorubicin concentration of $3.72 \times 10^{-5}\ M$ and DNA phosphate to daunorubicin ratios of 0:1, 0.4:1, and 8:1. These solutions were stored in the dark at 3°. Samples were removed every other day for 2 weeks for analysis.

Determination of Optimum Concentration Ranges and DNA to Drug Ratios—Spectra of solutions containing DNA phosphate to daunorubicin ratios of 100:1 to 0.025:1 and a constant daunorubicin concentration of $3.72 \times 10^{-5}\ M$ were recorded in 1-cm cells. Based on these studies, ratios ranging from 10:1 to 0.2:1 were chosen for all further studies in 1-cm cells. Similar experiments showed that reproducible spectral changes could be obtained using DNA phosphate to daunorubicin ratios of 40:1 to 0.4:1 in 10-cm cells with a constant daunorubicin concentration of $3.76 \times 10^{-6}\ M$. These ratios were used in both the direct and difference spectroscopic studies in 10-cm cells.

Beer's Law Evaluations—Beer's law was evaluated for bound and free daunorubicin under various conditions in 1- and 10-cm cells. For 1-cm cells, seven absorbance readings were made over a range of 1.5×10^{-5}–$7.5 \times 10^{-5}\ M$; for 10-cm cells, the same number of measurements were made over a range of 1.5×10^{-6}–$7.5 \times 10^{-6}\ M$. Beer's law also was evaluated for DNA phosphate to daunorubicin ratios of 10:1 and 0.75:1 over a concentration range of 1.7×10^{-6}–$1 \times 10^{-5}\ M$ daunorubicin.

Computer Programs and Methods—Three programs were used; two were for the manipulation and display of binding data, and the third was the computerized least-squares curve-fitting program of Fletcher and Shrager (12).

The first program takes spectral data and converts it to binding data displayed in a convenient form. This program produces a table of C, log C, R, and R/C and Calcomp plots of R *versus* C, R *versus* log C, and (R/C) *versus* R. The second program, a modified version of Fletcher and Shrager's curve-fitting program, allows one to attempt to fit the data to

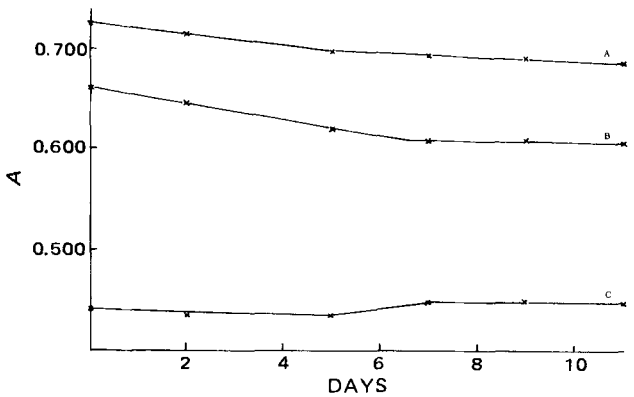

Figure 1—*Change in the absorbance of various daunorubicin solutions with respect to time. The DNA phosphate to daunorubicin ratios were: A, 0:1; B, 0.4:1; and C, 8:1.*

both the single-site (Scatchard) and multiple-site models. This program was modified to express n as a fraction and also as an integer. Arbitrarily, n was chosen to be an integer representing the number of molecules bound per 40 bases. This choice allowed qualitative gauging of the effect of allowing both n and K or just K to vary during the least-squares fitting procedure.

The other program plots the experimental R and C and R and log C values and draws the equation determined by the Fletcher and Shrager program through them. This plot provides a graphical display of how well the model actually fits the data. Details and listings of these programs were described previously (32).

RESULTS AND DISCUSSION

Studies of drug–DNA binding often have been carried out without adequate criteria for determining optimum experimental design. In this study, criteria allowing a systematic approach to the determination of the binding constants of drugs to DNA were used. A wide range of experimental conditions were tested, using the attainment of a well-defined adsorption isotherm (plot of R *versus* C) as a criterion for the selection of the best conditions. Scatchard plots were almost always made, but not extensively used, in these studies because of the work of Klotz (10) and Deranleau (11).

Studies of the effect of overnight equilibration on the visible absorbance of daunorubicin–DNA solutions were carried out to determine whether methods involving long equilibrations (*e.g.*, equilibrium dialysis) were feasible. Figure 1 shows that the absorbance of solutions containing DNA phosphate to daunorubicin ratios of 0:1 and 0.4:1 decreased and then leveled off. This result indicates that methods using overnight equilibration of daunorubicin–DNA solutions are not desirable.

Preliminary examination of the spectra of daunorubicin–DNA solutions (Fig. 2) indicated that several wavelengths could be used to determine the fractions of bound, R, and free, C, drug. The region beyond 550 nm was rejected because the absorbance was very wavelength dependent and a slight error in the wavelength would cause a large error in the absorbance. Two other wavelengths, 480 and 530 nm, were chosen as representative of the other most prominent regions of the spectrum.

The absorbance change from completely bound to free daunorubicin was only about 0.11 at 530 nm, but this change was 0.195 at 480 nm. In addition, the binding isotherms (Figs. 3 and 4) showed that the 480-nm isotherm plateaued but that the isotherm at 530 nm never reached a clear saturation plateau. These two factors indicated that absorbance changes at 480 nm should be used in all subsequent studies.

Having established the wavelength most suitable for analysis, the optimum concentration of daunorubicin and DNA was determined. Spectral studies of daunorubicin solutions and solutions containing DNA phosphate to daunomycin ratios of 8:1 in 1- and 10-cm cells showed that Beer's law was obeyed over the concentration range of 1.5×10^{-5}–7.5×10^{-6} M daunorubicin. This result is consistent with studies of daunorubicin dimerization, which showed a dimerization constant of 5.7×10^{2} M^{-1} (33). In contrast, acridine orange dimerizes even in 10^{-5} M solutions, and this dimerization interferes with studies of DNA binding (see, for example, Ref. 34).

Although Beer's law studies showed that both 1- and 10-cm cells were suitable for analysis, Figs. 3 and 4 show that binding plots of data obtained in 1-cm cells lack points in the region of low drug concentration

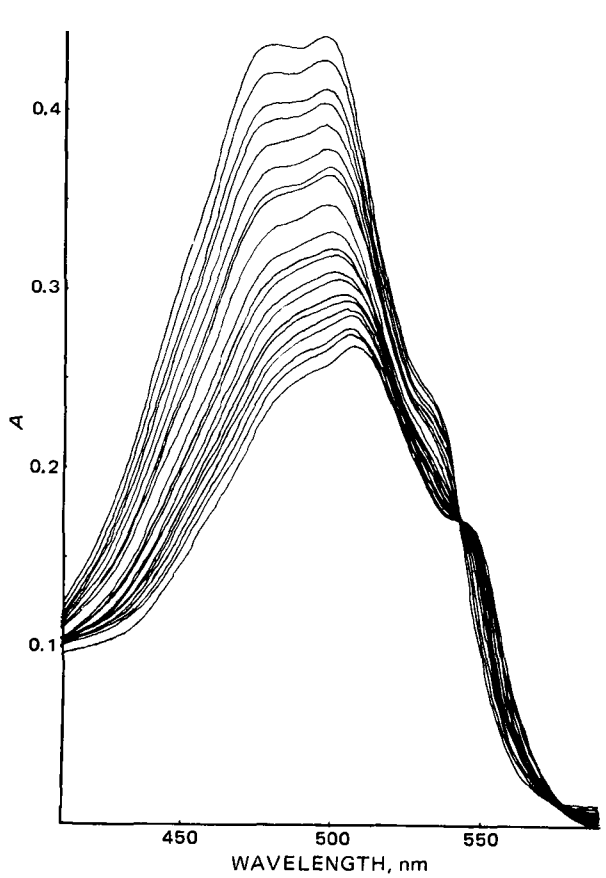

Figure 2—*Change in the absorption spectrum of daunorubicin in the presence of calf thymus DNA using 10-cm cells.*

C. This lack is a particularly serious problem since Deranleau (11) showed that these points were required for the accurate determination of binding constants. Figure 5 shows the adsorption isotherm obtained in 10-cm cells using daunorubicin and DNA concentrations one-tenth those used for the isotherm shown in Fig. 3. Obviously, the 10-cm cells are much more suitable for determining accurate binding constants. In addition, the error in the binding constants determined by computerized curve fitting of the data from the 10-cm cells was 10–15% while that for experiments in the 1-cm cells was 40–50%. The improved accuracy and ease of data analysis for the 10-cm cells were consistent with Waring's studies (4) of DNA–ethidium bromide binding in 4-cm cells.

The binding isotherms obtained from direct and difference spectroscopic studies of daunorubicin–DNA solutions in 10-cm cells were compared. Figure 6 shows the binding isotherm obtained using difference spectroscopy. A comparison of Figs. 5 and 6 clearly shows that difference spectroscopy gives more data points in the critical low C range. Therefore, difference spectroscopy is the method of choice for obtaining accurate binding constants since it gives the data points over a wider range of the binding isotherm (11). On the other hand, the direct spectroscopic method gives more points at the higher C values where the binding iso-

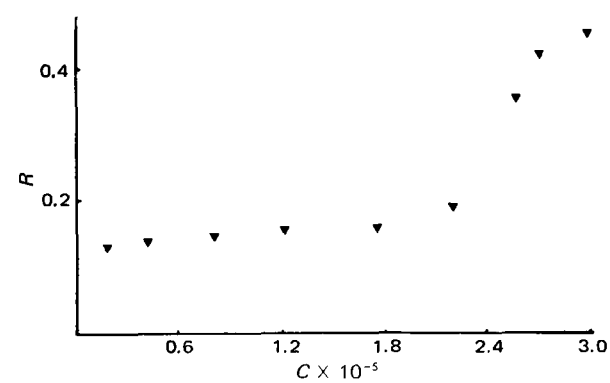

Figure 3—*Binding of daunorubicin to calf thymus DNA using the spectral change at 480 nm in 1-cm cells.*

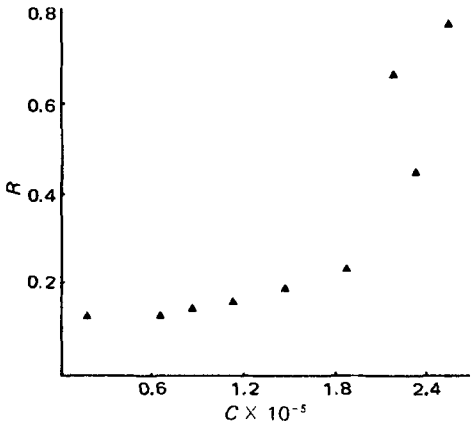

Figure 4—*Binding of daunorubicin to calf thymus DNA using the spectral change at 530 nm in 1-cm cells.*

therm plateaus and should provide a more accurate measure of the number of binding sites.

Studies using the direct spectral method gave a few points at low free drug concentration C because of the experimental procedure normally used (7). Data are measured at fixed drug and varying DNA concentrations; as the DNA concentration becomes large (and the free drug concentration becomes small), the spectra change very little when the binding constant K is large because essentially all drug in solution is completely bound. Thus, the steep changes in R occurring at low free drug concentrations (small C) where most drug is bound are associated with small spectral changes, and it is difficult to obtain data in this region. With difference spectroscopy, the DNA concentration is held constant and spectral changes are measured with increasing drug concentration as the difference between the spectrum of the free drug solution and the DNA–drug solution. Hence, small spectral changes start to occur only when further increases in the drug concentration produce very little additional change in the spectral difference between the free drug and the DNA–drug solution. This situation occurs when saturation and high drug concentrations are reached. Thus, in contrast to the direct spectral method, numerous points in the range of low free drug concentration can be obtained with the difference spectroscopic method.

The effect of the choice of limiting spectra on binding constants determined by difference and direct spectroscopic methods also was studied. The spectra of the bound and free drug were used to determine the $\Delta\epsilon$ in the difference spectroscopic method. Small random changes in $\Delta\epsilon$ had little effect on the binding constant. In contrast, in the direct spectral method, the spectrum taken as that of the completely bound drug had a substantial effect on the binding constant. For example, the spectra corresponding to DNA phosphate to daunorubicin ratios of 10:1, 20:1, 40:1, and 60:1 were chosen as those of totally bound daunorubicin and the data were analyzed by Scatchard plots. The binding constants varied from $3.7 \times 10^6\ M^{-1}$ for the 60:1 limit to $1.5 \times 10^7\ M^{-1}$ for the 10:1 limit.

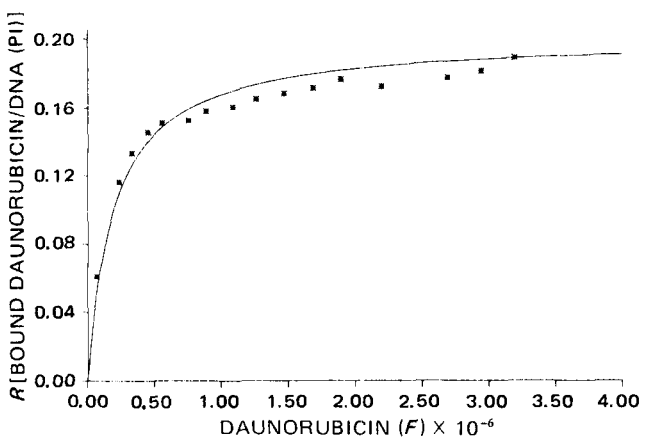

Figure 5—*Binding of daunorubicin to calf thymus DNA using direct spectroscopy [F refers to free daunorubicin and DNA (PI) refers to DNA phosphate]. Stars represent experimental data from the spectral change at 480 nm in 10-cm cells. The solid curve represents the adsorption isotherm generated from the computer-fitted model.*

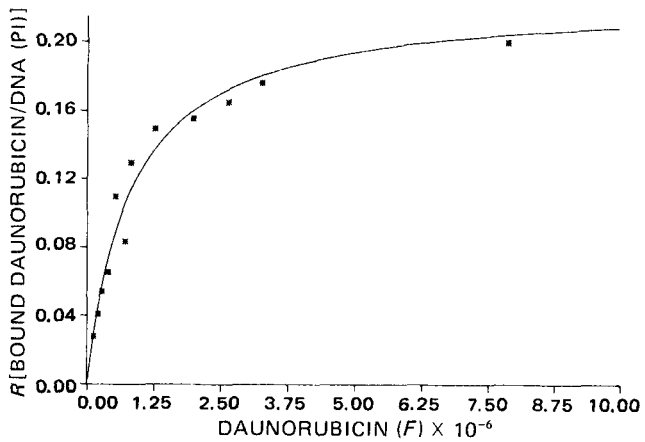

Figure 6—*Binding of daunorubicin to calf thymus DNA using difference spectroscopy. Stars represent experimental data from the difference spectra at 480 nm in 10-cm cells. The solid curve represents the adsorption isotherm generated from the computer-fitted model.*

This result is consistent with previous studies (11) since the choice of the limiting spectrum determines the number of points on the binding isotherm between saturation and zero and thus causes changes in the accuracy of the determination of K. In this example, the binding plot using the 10:1 ratio had only two points between saturation and zero, while the 60:1 limit gave a binding plot with five points in this region. The number of points between saturation and zero can thus have an important effect on the magnitude of the binding constant.

In this study, as the number of points between saturation and zero decreased, the binding constant increased. It is tempting to speculate that this trend explains the differences between daunorubicin–DNA binding constants determined by direct and difference spectroscopy, which are $7.2 \times 10^6\ M^{-1}$ (35) and $3.3 \times 10^6\ M^{-1}$ (21), respectively. In the present studies, the binding constants for both daunorubicin and doxorubicin to DNA were consistently higher when measured by direct spectroscopy. One study of actinomycin–DNA binding by difference spectroscopy gave a higher binding constant than that determined by direct spectroscopy (Table I), in disagreement with the trend noted previously.

In a typical linear Scatchard plot of (R/C) *versus* R, the number of points between saturation and zero is not apparent. For this reason and those discussed earlier, binding plots are preferred over Scatchard plots for the determination of binding constants.

In summary, the present studies show that, for the determination of daunorubicin–DNA and, presumably, anthracycline–DNA binding constants, the following conditions are best: 480 nm for absorbance measurements, 10-cm absorption cells, difference spectroscopic method, and binding plots instead of Scatchard plots.

Having determined the optimum experimental conditions and the best method of plotting the data, it was desirable to analyze these data by the least biased and most efficient method, computerized curve fitting. The computerized curve-fitting programs of Fletcher and Shrager (14) were modified for use with DNA–drug binding data. This modification allowed the determination of the binding constant that best fits the data with the number of sites free to vary as a fractional value per base. Comparison of two typical experiments, using data obtained from direct spectral studies of daunorubicin–DNA binding, gave the following parameters if n was allowed to vary: $K = 6.94 \times 10^6\ M^{-1} \pm 0.42$, $n = 0.188$, and $K = 5.26 \times 10^6\ M^{-1} \pm 0.40$, $n = 0.196$. However, the statistical data (14) indicated a dependence of one parameter on another because the condition codes were orders of magnitude larger than unity and had values of 78 and 98.

In an attempt to overcome this difficulty, n was also set at $[(n \times 40) - 1]/40 = 8/40$ and $[(n \times 40) + 1]/40 = 9/40$, and the data were refitted allowing only K to vary. Evaluation of the results for K fitted with each value of n revealed that the results obtained for n fixed at 8/40 provided the best model. An $n = 8/40 = 0.200$, as obtained using computerized curve-fitting procedures, is expected for the neighbor exclusion model (36). In addition, the values of K were in much better internal agreement with $K = 5.21 \times 10^6\ M^{-1} \pm 0.52$ and $4.75 \times 10^6\ M^{-1} \pm 0.33$ and condition codes = 2 and 3. The best qualitative explanation of these observations is that the program varies n and K to produce the best fit to the data; however, since n and K are interdependent, there is a series of values for n and K that gives nearly the same agreement with the data. Fixing n

Table II—Comparison of DNA Binding Ability and Biological Effects of Daunorubicin and Doxorubicin

Antibiotic	Binding Constant, $\times 10^6\ M^{-1}$	Increase in DNA Melting Temperature[a]	Inhibition of Cell Free Polymerase Reactions, ID_{50}[b], $\times 10^{-5}\ M$		Specific Inhibition of Cellular Nucleic[c] Acid Synthesis		Cell Killing Potential
			DNA	RNA	DNA[d]	RNA[e]	
Daunorubicin	1.27	13.4°	1.6	1.0	119	147	1×
Doxorubicin	2.04	14.8°	1.2	0.6	152	215	2×

[a] Reference 15. [b] Reference 43. [c] Specific inhibitory activity = percent inhibition/cellular concentration. [d] Reference 44. [e] Reference 45.

removes this interdependence and gives K values that are the best fit of the data with little increase in the error in K.

Attempts were also made to fit the direct spectral data to a two-site model (see Eq. 3). However, the error and condition code were much larger than for the one-site model, and it was concluded that a two-site model did not improve the fit to the data.

In addition to the computerized curve-fitting program, two other programs were written to assist in data analysis and display. The binding plots in this paper were produced using these programs and the Calcomp plotter.

Having established the optimum methods for the determination of the daunorubicin–DNA binding constants, identical methods were used to determine doxorubicin–DNA binding constants. Use of the identical methods was justified since the daunorubicin–DNA spectra were very similar to the doxorubicin–DNA spectra.

The binding constant for daunorubicin obtained using this procedure ($1.27 \times 10^6\ M^{-1}$) was significantly lower than that obtained by direct spectroscopy, which was $4.98 \times 10^6\ M^{-1}$ (the average of 5.21×10^6 and 4.75×10^6). This result agrees with a trend noted earlier that the small number of points between saturation and zero with binding plots obtained from the direct spectral method is associated with abnormally large binding constants.

Some reports (36, 37) showed that vagrant binding to a linear array of sites can cause exclusion of some sites, which leads to curved Scatchard plots and an overestimation of the binding constant. To circumvent this problem in studying binding to DNA, it was suggested (8, 36–38) that the y-intercept of the Scatchard plot should be used because $R/C = Kn$ at this point. The K obtained using the y-intercept of a Scatchard plot based on difference spectroscopic data was also $1.27 \times 10^6\ M^{-1}$, in exact agreement with the value determined by computerized curve fitting. Although exact agreement is probably fortuitous, the good agreement obtained substantiates the value of computerized curve fitting for DNA binding studies.

Doxorubicin has a significantly greater affinity for DNA than daunorubicin. The binding constants and n values were $1.27 \times 10^6\ M^{-1}$ (± 0.10) and $n = 8/40$ for daunorubicin and $2.04 \times 10^6\ M^{-1}$ (± 0.18) and $n = 8/40$ for doxorubicin. This result was true even if n was allowed to vary completely (32). This order of affinities is consistent with comparisons of several properties of doxorubicin and daunorubicin. Doxorubicin increased the melting temperature of DNA by 14.8° while daunorubicin only increased it by 13.4° (15). In addition, doxorubicin had a greater inhibitory effect on both cell free polymerase activity and cellular nucleic acid synthesis than daunorubicin (Table II).

One would expect that the melting-temperature increase and the binding constant would parallel each other regardless of the mechanism of action of the drug. If the mechanism involves DNA binding, then the inhibition of cell free polymerase activity and nucleic acid synthesis should also parallel DNA binding. Table II shows that this effect is indeed observed; these data, taken together, provide a preliminary indication that there may be a correlation between the DNA binding constant and biological activity in the anthracyclines. One recent report (29) also led to a similar suggestion that DNA binding and biological activity are related.

The binding constants determined in this study and the pains taken to ensure their accurate and unbiased determination suggest that the earlier order determined for the DNA binding constants of daunorubicin, $3.3 \times 10^6\ M^{-1}$, and doxorubicin, $2.3 \times 10^6\ M^{-1}$ (15), should be revised. Recent studies (29) using fluorescence spectroscopy gave DNA binding constants of $4.8 \times 10^6\ M^{-1}$ and $3.3 \times 10^6\ M^{-1}$ for doxorubicin and daunorubicin, respectively, in agreement with the order determined in this report.

REFERENCES

(1) V. A. Bloomfield, D. M. Crothers, and I. Tinoco, "Physical Chemistry of Nucleic Acids," Harper and Row, New York, N.Y., 1974.

(2) R. J. Douthart, J. P. Burnett, F. W. Beasley, and B. H. Frank, *Biochemistry*, **12**, 214 (1973).

(3) R. W. Armstrong and N. M. Panzer, *J. Am. Chem. Soc.*, **94**, 7650 (1972).

(4) M. J. Waring, *J. Mol. Biol.*, **13**, 269 (1965).

(5) E. J. Gabbay, K. Sanford, and S. Baxter, *J. Am. Chem. Soc.*, **94**, 2876 (1972).

(6) H. M. Sobell, S. C. Jain, T. D. Sakore, and C. E. Nordman, *Nature*, **231**, 200 (1971).

(7) A. R. Peacocke and J. N. H. Skerett, *Trans. Faraday Soc.*, **52**, 261 (1956).

(8) W. Muller and D. M. Crothers, *J. Mol. Biol.*, **35**, 251 (1968).

(9) G. Scatchard, *Ann. N.Y. Acad. Sci.*, **51**, 660 (1949).

(10) I. M. Klotz, *Acc. Chem. Res.*, **7**, 162 (1974).

(11) D. A. Deranleau, *J. Am. Chem. Soc.*, **91**, 4044 (1969).

(12) J. E. Fletcher and R. I. Shrager, "A Users Guide to Least Squares Model Fitting," DCRT Technical Report No. 1, 1968.

(13) J. E. Fletcher and A. A. Spector, *Comput. Biomed. Res.*, **2**, 164 (1968).

(14) J. E. Fletcher, A. A. Spector, and J. D. Ashbrook, *Biochemistry*, **9**, 4580 (1970).

(15) F. Zunio, R. Gambetta, A. DiMarco, and A. Zaccara, *Biochim. Biophys. Acta*, **277**, 489 (1972).

(16) E. Calendi, A. DiMarco, M. Reggiani, B. Scarpinato, and L. Valenti, *ibid.*, **103**, 25 (1965).

(17) M. M. Fishman and I. Schwartz, *Biochem. Pharmacol.*, **23**, 2147 (1973).

(18) F. Quadrifoglio and V. Crescenzi, *Biophys. Chem.*, **2**, 64 (1974).

(19) E. J. Gabbay, D. Grier, R. F. Fingerle, R. Reimer, R. Levy, S. W. Pearce, and W. D. Wilson, *Biochemistry*, **15**, 2062 (1976).

(20) W. J. Pigram, W. Fuller, and L. D. Hamilton, *Nature New Biol.*, **235**, 17 (1972).

(21) F. Zunio, A. DiMarco, A. Zaccara, and G. Luoni, *Chem.-Biol. Interact.*, **9**, 25 (1974).

(22) P. Chandra, A. DiMarco, F. Zunio, A. M. Casazza, D. Gericke, F. Guiliana, C. Soranzo, R. Thorbeck, A. Gotz, F. Arcamone, and M. Ghione, *Naturwissenschaften*, **59**, 448 (1972).

(23) V. Barthelemy-Clavey, G. Serros, and G. Aubel-Sadron, *Mol. Pharmacol.*, **11**, 640 (1975).

(24) S. Aktipis and N. Panayotatos, *Biochem. Biophys. Res. Commun.*, **68**, 465 (1976).

(25) S. Takanashi and N. R. Bachur, *Drug Metab. Disp.*, **4**, 79 (1976).

(26) D. W. Wilson, D. Grier, R. Reimer, J. D. Bauman, J. F. Preston, and E. J. Gabbay, *J. Med. Chem.*, **19**, 381 (1976).

(27) *Ibid.*, **19**, 381 (1976).

(28) L. Lenaz, A. Necco, T. Dasdia, and A. DiMarco, *Cancer Chemother. Rep., Part 1*, **58**, 769 (1974).

(29) A. DiMarco, A. M. Casazza, R. Gambetta, R. Supio, and F. Zunio, *Cancer Res.*, **36**, 1962 (1976).

(30) F. Arcamone, G. Francheschi, S. Penoco, and A. Selva, *Tetrahedron Lett.*, **1969**, 1003.

(31) A. DiMarco, M. Gaetani, and B. Scarpinato, *Cancer Chemother. Rep., Part 1*, **53**, 33 (1969).

(32) G. D. Dolch, Ph.D. thesis, Purdue University, 1976, Appendix I.

(33) V. Barthelemy-Clavey, J. C. Maurizot, J. L. Dimicoli, and P. Sicard, *FEBS Lett.*, **46**, 5 (1974).

(34) M. E. Lamm and D. M. Neville, Jr., *J. Phys. Chem.*, **69**, 3872 (1965).

(35) P. J. Gray and D. R. Phillips, *Eur. J. Cancer*, **12**, 237 (1976).

(36) D. M. Crothers, *Biopolymers*, **6**, 575 (1968).

(37) J. L. Bresloff and D. M. Crothers, *J. Mol. Biol.*, **95**, 103 (1975).

(38) D. E. V. Schmechel and D. M. Crothers, *Biopolymers*, **10**, 465 (1971).

(39) S. Das Gupta, D. N. Misra, and N. N. Das Gupta, *Biochim. Biophys. Acta*, **294**, 38 (1973).
(40) I. O. Walker, *ibid.*, **109**, 585 (1965).
(41) R. Bittman and L. Blau, *Biochemistry*, **14**, 2138 (1975).
(42) B. A. K. Chibber, A. Balasubramanian, and T. VisWanatha, *Can. J. Biochem.*, **51**, 204 (1973).
(43) M. F. Goodman, M. J. Bessman, and N. R. Bachur, *Proc. Natl. Acad. Sci., USA*, **71**, 11931 (1974).
(44) W. D. Meriwether and N. R. Bachur, *Cancer Res.*, **32**, 1137 (1972).
(45) N. R. Bachur, M. Steele, W. D. Meriwether, and R. C. Hildebrand, *J. Med. Chem.*, **19**, 651 (1976).

ACKNOWLEDGMENTS

Supported by an American Foundation of Pharmaceutical Education Predoctoral Fellowship to G. D. Dolch, by grants from the American Cancer Society and Indiana Elks Club, and in part by the National Institutes of Health.

Improved Stability of Proteins Immobilized in Microparticles Prepared by a Modified Emulsion Polymerization Technique

BO EKMAN and INGVAR SJÖHOLM ˣ

Received May 31, 1977, from the *Department of Pharmaceutical Biochemistry, Biomedical Center, Box 578, S-751 23 Uppsala, Sweden.* Accepted for publication September 6, 1977.

Abstract □ Proteins can be immobilized in spherical microparticles of polyacrylamide gel (having a diameter of about 1 μm) by an emulsion–polymerization technique. Highly cross-linked gels have a structure consisting of relatively large pores. This structure is advantageous when dealing with biologically active proteins acting on molecules dissolved in the surrounding medium. A rapid equilibrium is established between the interior of the particles and the medium, and rate-limiting diffusion is not observed. A suspension of carbonic anhydrase immobilized in microparticles will thus have kinetic properties very much like the free enzyme. In addition to the entrapment of the protein molecules in the three-dimensional network formed by the polyacrylamide threads, protein molecules are also fixed in the cross-linked threads of polyacrylamide. This fixation is probably responsible for the improved stability of the protein molecules against heat denaturation. Not even autoclaving at 110° for 30 min denatured the immobilized enzyme completely (more than 25% of the enzyme activity was left). The higher resistance of molecules in microparticles against proteolytic degradation also is documented.

Keyphrases □ Proteins—immobilized in polyacrylamide microparticles, effect on stability □ Microparticles, polyacrylamide—containing immobilized proteins, effect on stability □ Polyacrylamide microparticles—containing immobilized proteins, effect on stability □ Stability—proteins immobilized in polyacrylamide microparticles

The immobilization of proteins in polyacrylamide microparticles with a high degree of cross-linking (T-C = 8-25[1]) by emulsion polymerization was studied recently (2–4). The macromolecules apparently are immobilized by two mechanisms: fixation in the highly cross-linked threads of polyacrylamide and, if sufficiently large, entrapment in the network formed by the polyacrylamide threads (4). Consequently, the immobilized macromolecules will be localized partly on the microparticle surface, enabling them to react also with substrates or cells that cannot penetrate into the particles (2, 5). The highly cross-linked gels (C = 25%) also produce a network with relatively large pores, which is advantageous with biologically active proteins interacting with molecules dissolved in the surrounding medium because the macromolecules retain most of their activity when bound in the microparticles.

The present work was undertaken to investigate the consequences of the immobilization in highly cross-linked microparticles of polyacrylamide on the activity and stability of proteins, especially carbonic anhydrase. A fraction of the enzyme is remarkably stable, even against heat denaturation, while some enzymatic activity is lost in a normal way. A modified procedure is described for the large-scale microparticle preparation.

EXPERIMENTAL

Materials—Human serum albumin[2], immunoglobulin G[2], bovine β-lactoglobulin[3] (as a mixture of the A and B forms), protease[3] Type VI from *Streptomyces griseus*, and bovine carbonic anhydrase[3] (EC 4.2.1.1) were used without further purification. Acrylamide[3], *N,N'*-methylenebisacrylamide[3], *p*-nitrophenyl acetate[3], *N,N,N',N'*-tetramethylethylenediamine[3], tris(hydroxymethyl)aminomethane[3], and other chemicals were analytical grade.

Determination of Carbonic Anhydrase Activity—The esterase activity of carbonic anhydrase was determined with *p*-nitrophenyl acetate as the substrate (6). The enzyme (50 μg in free solution or in microparticles) was added to 5 ml of 0.05 *M* tris(hydroxymethyl)aminomethane hydrochloride buffer, pH 7.5. The formation of the hydrolysis products was followed spectrophotometrically at 400 nm. The velocity of the reaction is expressed as an increase in absorbance during 1 min.

Appropriate correction was made for the spontaneous hydrolysis of the substrate in samples not containing any enzyme. Microparticles of polyacrylamide not containing enzyme did not affect the reaction, as found in control experiments. The particles did not cause any light scattering at the wavelength used, and no sedimentation was detectable during the time of the measurement.

Protein Determination—The concentrations of human serum albumin, immunoglobulin G, and β-lactoglobulin were determined from the optical density at 280 nm. The $E^{1\%}_{1\,cm}$ values were 5.3 (7) for albumin, 13.6 for immunoglobulin, and 7.90 for lactoglobulin (8). The spectra were recorded with an automatic recording spectrophotometer at 400 nm to correct for the light-scattering effect (9). The amount of protein immobilized in the microparticles was determined after hydrolysis in 6 *M* HCl

[1] The nomenclature suggested by Hjertén (1) is used.

[2] KABI AB, Stockholm, Sweden.
[3] Sigma Chemical Co.

(39) S. Das Gupta, D. N. Misra, and N. N. Das Gupta, *Biochim. Biophys. Acta*, **294**, 38 (1973).
(40) I. O. Walker, *ibid.*, **109**, 585 (1965).
(41) R. Bittman and L. Blau, *Biochemistry*, **14**, 2138 (1975).
(42) B. A. K. Chibber, A. Balasubramanian, and T. VisWanatha, *Can. J. Biochem.*, **51**, 204 (1973).
(43) M. F. Goodman, M. J. Bessman, and N. R. Bachur, *Proc. Natl. Acad. Sci., USA*, **71**, 11931 (1974).
(44) W. D. Meriwether and N. R. Bachur, *Cancer Res.*, **32**, 1137 (1972).
(45) N. R. Bachur, M. Steele, W. D. Meriwether, and R. C. Hildebrand, *J. Med. Chem.*, **19**, 651 (1976).

ACKNOWLEDGMENTS

Supported by an American Foundation of Pharmaceutical Education Predoctoral Fellowship to G. D. Dolch, by grants from the American Cancer Society and Indiana Elks Club, and in part by the National Institutes of Health.

Improved Stability of Proteins Immobilized in Microparticles Prepared by a Modified Emulsion Polymerization Technique

BO EKMAN and INGVAR SJÖHOLM ˣ

Received May 31, 1977, from the *Department of Pharmaceutical Biochemistry, Biomedical Center, Box 578, S-751 23 Uppsala, Sweden.* Accepted for publication September 6, 1977.

Abstract □ Proteins can be immobilized in spherical microparticles of polyacrylamide gel (having a diameter of about 1 μm) by an emulsion–polymerization technique. Highly cross-linked gels have a structure consisting of relatively large pores. This structure is advantageous when dealing with biologically active proteins acting on molecules dissolved in the surrounding medium. A rapid equilibrium is established between the interior of the particles and the medium, and rate-limiting diffusion is not observed. A suspension of carbonic anhydrase immobilized in microparticles will thus have kinetic properties very much like the free enzyme. In addition to the entrapment of the protein molecules in the three-dimensional network formed by the polyacrylamide threads, protein molecules are also fixed in the cross-linked threads of polyacrylamide. This fixation is probably responsible for the improved stability of the protein molecules against heat denaturation. Not even autoclaving at 110° for 30 min denatured the immobilized enzyme completely (more than 25% of the enzyme activity was left). The higher resistance of molecules in microparticles against proteolytic degradation also is documented.

Keyphrases □ Proteins—immobilized in polyacrylamide microparticles, effect on stability □ Microparticles, polyacrylamide—containing immobilized proteins, effect on stability □ Polyacrylamide microparticles—containing immobilized proteins, effect on stability □ Stability—proteins immobilized in polyacrylamide microparticles

The immobilization of proteins in polyacrylamide microparticles with a high degree of cross-linking (T-C = 8-25[1]) by emulsion polymerization was studied recently (2–4). The macromolecules apparently are immobilized by two mechanisms: fixation in the highly cross-linked threads of polyacrylamide and, if sufficiently large, entrapment in the network formed by the polyacrylamide threads (4). Consequently, the immobilized macromolecules will be localized partly on the microparticle surface, enabling them to react also with substrates or cells that cannot penetrate into the particles (2, 5). The highly cross-linked gels (C = 25%) also produce a network with relatively large pores, which is advantageous with biologically active proteins interacting with molecules dissolved in the surrounding medium because the macromolecules retain most of their activity when bound in the microparticles.

The present work was undertaken to investigate the consequences of the immobilization in highly cross-linked microparticles of polyacrylamide on the activity and stability of proteins, especially carbonic anhydrase. A fraction of the enzyme is remarkably stable, even against heat denaturation, while some enzymatic activity is lost in a normal way. A modified procedure is described for the large-scale microparticle preparation.

EXPERIMENTAL

Materials—Human serum albumin[2], immunoglobulin G[2], bovine β-lactoglobulin[3] (as a mixture of the A and B forms), protease[3] Type VI from *Streptomyces griseus*, and bovine carbonic anhydrase[3] (EC 4.2.1.1) were used without further purification. Acrylamide[3], *N,N'*-methylenebisacrylamide[3], *p*-nitrophenyl acetate[3], *N,N,N',N'*-tetramethylethylenediamine[3], tris(hydroxymethyl)aminomethane[3], and other chemicals were analytical grade.

Determination of Carbonic Anhydrase Activity—The esterase activity of carbonic anhydrase was determined with *p*-nitrophenyl acetate as the substrate (6). The enzyme (50 μg in free solution or in microparticles) was added to 5 ml of 0.05 *M* tris(hydroxymethyl)aminomethane hydrochloride buffer, pH 7.5. The formation of the hydrolysis products was followed spectrophotometrically at 400 nm. The velocity of the reaction is expressed as an increase in absorbance during 1 min.

Appropriate correction was made for the spontaneous hydrolysis of the substrate in samples not containing any enzyme. Microparticles of polyacrylamide not containing enzyme did not affect the reaction, as found in control experiments. The particles did not cause any light scattering at the wavelength used, and no sedimentation was detectable during the time of the measurement.

Protein Determination—The concentrations of human serum albumin, immunoglobulin G, and β-lactoglobulin were determined from the optical density at 280 nm. The $E^{1\%}_{1\,cm}$ values were 5.3 (7) for albumin, 13.6 for immunoglobulin, and 7.90 for lactoglobulin (8). The spectra were recorded with an automatic recording spectrophotometer at 400 nm to correct for the light-scattering effect (9). The amount of protein immobilized in the microparticles was determined after hydrolysis in 6 *M* HCl

[1] The nomenclature suggested by Hjertén (1) is used.

[2] KABI AB, Stockholm, Sweden.
[3] Sigma Chemical Co.

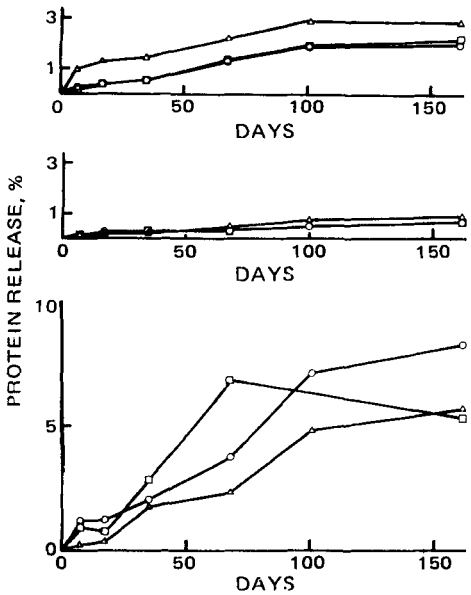

Figure 1—*Release of immobilized proteins during storage at room temperature from microparticles of polyacrylamide with T-C = 8-5 (○), T-C = 15-5 (△), and T-C = 8-25 (□). The immobilized proteins were β-lactoglobulin (top), human serum albumin (middle), and immunoglobulin G (bottom), and the particles were suspended in 0.1 M KCl and 0.005 M phosphate, pH 7.4 with 0.1% sodium azide.*

at 105° for 20 hr and subsequent amino acid analysis with an automatic amino acid analyzer.

Preparation of Microparticles—Microparticles with immobilized proteins were prepared using a modification of the method described by Ekman *et al.* (4). The protein was dissolved with acrylamide (1.5 g) and *N,N'*-methylenebisacrylamide (0.5 g) in 25 ml of 0.005 *M* sodium phosphate buffer, pH 7.4. After addition of the catalyst, ammonium peroxosulfate (100 μl of a solution of 0.5 g/ml), the solution was poured into a mixture consisting of 100 ml of toluene, 25 ml of chloroform, and 0.4 g of a detergent, poloxamer 188[4]. The mixture was homogenized to produce a water-in-oil emulsion[5]. The size of the water droplets was continuously measured in the microscope, and the emulsion was homogenized until a satisfactory size of the water droplets was obtained.

The homogenizer was then removed, and the emulsion was slowly stirred with a magnetic stirrer. The accelerator, *N,N,N',N'*-tetramethylethylenediamine (1 ml), was added to the emulsion, and polymerization started after a few minutes. During the whole procedure, oxygen was excluded from the system by bubbling nitrogen gas through the solution. After 30 min, the nitrogen stream was discontinued, and the phases were allowed to separate. The microparticles were washed with buffer by centrifugation until no more protein could be detected in the supernate.

Determination of Microparticle Density—The density of the microparticles was determined by density gradient centrifugation in a self-generating gradient of silica[6], according to Pertoft *et al.* (10), as previously described (4).

RESULTS

Leakage of Proteins from Microparticles—One early drawback observed in enzymes entrapped in polyacrylamide was loss of activity from the gel because of leakage. However, with highly cross-linked polyacrylamide (*e.g.*, with C = 25%), the immobilization is more stable (Fig. 1). Microparticles were prepared with lactoglobulin, albumin, and immunoglobulin, having Stokes radii of 2.67, 3.34, and 4.92 nm, respectively (4).

The microparticles were suspended in 0.1 *M* KCl with 0.005 *M* phosphate buffer, pH 7.4, so that the protein concentration was about 3, 7, and 20 mg/5-ml sample. The leakage was tested with three different gel types, T-C = 8-5, 8-25, and 15-5, respectively. Sodium azide (0.002%) was added as a preservative, and different samples were left at room temperature for the times stated in Fig. 1.

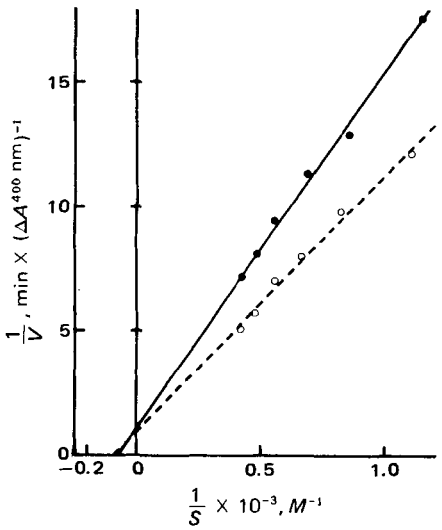

Figure 2—*Lineweaver-Burk plots for the hydrolysis of p-nitrophenyl acetate by bovine carbonic anhydrase. The enzyme was either used free in solution (○) or immobilized in microparticles (●).*

The protein released from the particles was determined (from the optical density) after centrifugation. As seen from Fig. 1, only small amounts of proteins were released. Thus, less than 1% albumin was lost from the particles after 5.5 months, while about 2% of lactoglobulin and 5–7% of immunoglobulin were lost.

Enzymatic Properties of Immobilized Carbonic Anhydrase—The kinetics of carbonic anhydrase in the free state and in microparticles are compared in Fig. 2. The hydrolysis rate of the chromogenic substrate *p*-nitrophenyl acetate was determined with the same total amount of enzyme in the two series. As expected, the velocity was somewhat lower with immobilized enzyme, and the maximal specific activity, as calculated from the *y*-axis intercept, was 12% lower. The Michaelis constant, K_m, was 13.0 m*M* for the immobilized enzyme compared to 10.5 m*M* for the soluble enzyme. The values are close to those found by Pocker and Stone (6).

Thermostability of Immobilized Carbonic Anhydrase—Figure 3 summarizes studies of the stability of carbonic anhydrase when exposed to higher temperatures for 5 and 30 min. After treatment at the temperatures shown, the samples were cooled with an ice bath. After 5 min, the samples were incubated at 25° for 30 min, and the enzymatic activity was then measured. The same amount of enzyme was used in all samples, and the initial velocity was used to calculate the residual enzymatic activity.

All of the free enzyme and a fraction of the immobilized enzyme were denatured at temperatures above 60°, with a "midpoint" at about 63°. However, a substantial fraction of the enzyme in the microparticles resisted the heat treatment; even after 30 min at 90°, more than 30% of the enzyme was still active. Not even autoclaving at 127° for 15 min dena-

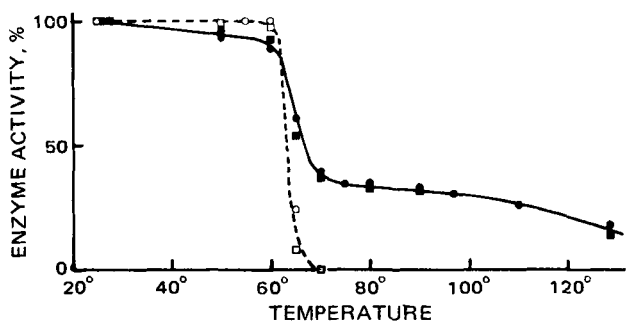

Figure 3—*Heat stability of carbonic anhydrase. The remaining enzymatic activity was measured after heating free enzyme for 5 (○) or 30 (□) min and immobilized enzyme for 5 (●) or 30 (■) min. Enzyme immobilized in microparticles was also kept in an autoclave for 5 and 30 min at 110 and 127°. Prior to the determination of the remaining activity, the samples were kept in an ice bath for 5 min and at room temperature for 15 min.*

[4] Pluronic F 68, Wyandotte Chemical Co., Wyandotte, Mich.
[5] An Ultraturrax TP 18-10 homogenizer was used.
[6] Ludox, E. F. du Pont de Nemours and Co., Wilmington, Del.

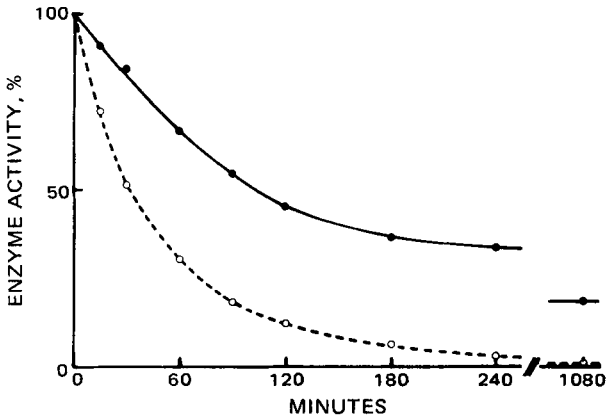

Figure 4—*Inactivation of bovine carbonic anhydrase (0.3 mg/ml) in 0.05 M tris(hydroxymethyl)aminomethane hydrochloride buffer, pH 7.5, by proteolytic digestion with protease VI (2.0 mg/ml). Carbonic anhydrase was either free in solution (○) or immobilized in microparticles (●), T-C = 8-25.*

tured the enzyme completely (about 15% was left), and autoclaving at 110° for 30 min left more than 25% of the enzyme intact.

Proteolytic Degradation of Carbonic Anhydrase—The increased thermal stability was paralleled by an increased stability against proteolytic enzymes (Fig. 4). In free solution, carbonic anhydrase was relatively rapidly inactivated by protease VI, an enzyme with broad specificity. In the microparticles, however, carbonic anhydrase was largely protected; the protease could only attack the protein molecules on the surface or situated close to the largest pores in the interior of the particles penetrable by it. Thus, about 65% of the enzyme activity in microparticles was retained after treatment for 1 hr; about 35% was retained in free solution.

Microparticle Density—In several applications, *e.g.*, in the isolation of specific cells in a cell population, the density of the microparticles is an essential factor (5). The modified procedure yields microparticles of a somewhat higher apparent density than the previously used procedure (Fig. 5). Thus, the density of particles with C = 25% increased from 1.08 to 1.13 g/cm^3. However, the general profile of the density curve was the same as found earlier, with a minimum value at C = 10% (4); particles with very low or very high concentrations of cross-linking agent had the same density as found earlier, about 1.15 g/cm^3, representing the value of the linear polyacrylamide. The reasons for these results are discussed later.

DISCUSSION

Immobilization of proteins in polyacrylamide gels was initially carried out as a block-polymerization procedure, subsequently followed by mechanical degradation of the gel to finer particles. The bead polymerization method constitutes a refinement of the technique, producing spherical particles by polymerizing a water solution of monomers and protein dispersed in an organic phase, as presented by Nilsson *et al.* (11). Enzymes immobilized in this manner show deviations from normal kinetics as exhibited in free solutions (decrease of V_{max} and increase of K_m), which may partly be due to the rate-limiting diffusion processes within the gel granules.

Small-size preparations with immobilized carbonic anhydrase were prepared previously by microencapsulation (12). Also, in this case, the K_m of carbonic anhydrase was increased, probably because of diffusion limitations through the membrane. By preparing particles with a small diameter, an enzyme preparation with kinetic properties very much like those of free enzyme was obtained. However, the small size is not the only explanation to the improved kinetics; the acrylic monomer composition contributes by ensuring a macroporous gel structure. In the microparticles, the K_m for carbonic anhydrase is virtually the same as in solution. However, the V_{max} is somewhat decreased. The results suggest that some enzymatic activity is lost in the microparticles, probably due to steric blockage of the active site by the gel structure or denaturation during preparation.

The increased stability of the immobilized compounds against heat denaturation and proteolytic enzyme degradation is dramatic. A large fraction of the immobilized carbonic anhydrase resisted treatment at 110° for 30 min. Possibly the imbedding of the enzyme within the polyacrylamide threads (4) stabilizes the conformation of the enzyme and protects the enzyme against proteolysis. Naturally, the fraction of the protein immobilized on the surface of the microparticles or close to the macropores in the gel structure has the same properties as soluble enzyme and will be lost during heat treatment and by proteolysis in a similar manner.

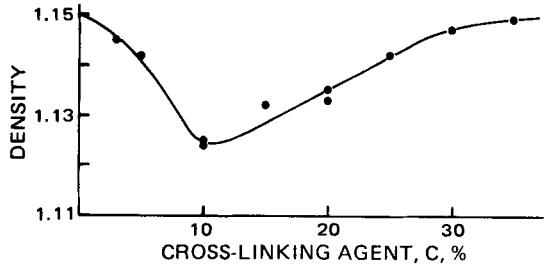

Figure 5—*Density of microparticles of polyacrylamide prepared from monomer solution containing different amounts of cross-linking agent (C). The total amount of monomer (T) was 8% in all cases.*

The modification of the method for the preparation of microparticles presented here eliminates some major difficulties of the previous method (4). In the earlier procedure, the catalyst–accelerator system is added immediately before homogenization of the water phase with the monomers in an organic phase. Since the polymerization proceeds very rapidly when once initiated, not even cooling of the mixture slows down polymerization markedly. Therefore, it is practically impossible to obtain a reproducible and narrow degree of dispersion, even with powerful homogenizers, before polymerization is completed. Moreover, the homogenizer easily ruptures the polymer spheres formed, resulting in a polymer preparation partly consisting of broken spheres of irregular size.

In the modified procedure, which can also be applied in large-scale preparation of microparticles, the accelerator is added to the mixture when a stable emulsion of desired dispersion degree is obtained. The size of the water droplets of the emulsion can be checked in the microscope to ensure that the particles formed have the wanted size within a narrow size distribution. In addition, the slow stirring during polymerization causes the particles to assume a spherical rather than an ellipsoidal form.

That the particles prepared by the modified procedure are more spherical and uniform is also apparent from the results of the density determinations. With C = 25%, the density found in the self-generating silica gradient is somewhat higher with the modified procedure. The higher density, *i.e.*, the smaller buoyancy effect during the centrifugation, is due to the "excluded volume effect" (10), which is smaller with a sphere than with an irregular particle of the same mass in the silica gel.

Earlier work in the field of immobilized enzymes has almost entirely been concerned with the use of enzymes as enzyme reactors in column chromatography. However, immobilized enzymes can also be conveniently used in batch procedures. The use of lactate dehydrogenase for the analysis in the picomole range of the pyruvate–lactate system has already been reported (3). The microparticles have a diameter of less than 1 μm and thus settle very slowly. They are easily pipettable in suspension. The immobilization also stabilizes the enzymes against heat denaturation and proteolytic degradation. Lactate dehydrogenase particles have been stored as a suspension at 4° for many months.

One drawback is the relatively small amount of protein immobilized in the microparticles during the preparation (about 3–10%). However, the protein is more effectively utilized in the small beads, where steric hindrance is minimized, and protein not immobilized can be regained from the washings of the microparticles after the preparation. The protein immobilized is very accessible to smaller molecules, *e.g.*, substrates. Moreover, the stability of the immobilized protein against proteolytic breakdown permits the use of microparticles in highly contaminated systems. Finally, the possibility to sterilize microparticles containing biologically active proteins by autoclaving may open up wide perspectives for the future use of immobilized proteins *in vivo*.

REFERENCES

(1) S. Hjertén, *Arch. Biochem. Biophys. Suppl.*, 1, 147 (1962).

(2) B. Ekman and I. Sjöholm, *Nature*, **257**, 825 (1975).

(3) S. E. Brolin, A. Ågren, B. Ekman, and I. Sjöholm, *Anal. Biochem.*, **78**, 577 (1977).

(4) B. Ekman, C. Lofter, and I. Sjöholm, *Biochemistry*, **15**, 5115 (1976).
(5) I. Ljungstedt, B. Ekman, and I. Sjöholm, *Biochem. J.*, **170**, 161 (1978).
(6) Y. Pocker and J. T. Stone, *Biochemistry*, **6**, 668 (1967).
(7) E. J. Cohn, W. L. Hughes, Jr., and J. H. Weare, *J. Am. Chem. Soc.* **69**, 1753 (1947).
(8) E. W. Davie, C. R. Newman, and P. E. Wilcox, *J. Biol. Chem.*, **234**, 2635 (1959).
(9) G. H. Beaven and F. R. Holiday, *Adv. Protein*, **7**, 319 (1952).
(10) H. Pertoft, L. Philipson, P. Oxelfelt, and S. Höglund, *Virology*, **33**, 185 (1967).
(11) H. Nilsson, R. Mosbach, and K. Mosbach, *Biochim. Biophys. Acta*, **268**, 253 (1972).
(12) R. C. Boguslaski and A. M. Janik, *ibid.*, **250**, 266 (1971).

ACKNOWLEDGMENTS

Supported by the Swedish Board for Technical Development (Project 75-4415), the Swedish Medical Research Council (Project 13X-3126), and the I.F. Foundation for Pharmaceutical Research, Stockholm.

The technical assistance of Mr. Börje Berg is gratefully acknowledged.

Permeability of Interstitial Space of Muscle (Rat Diaphragm) to Solutes of Different Molecular Weights

JEROME S. SCHULTZ ˣ and WILLIAM ARMSTRONG

Received April 7, 1977, from the *Department of Chemical Engineering, University of Michigan, Ann Arbor, MI 48109.* Accepted for publication September 21, 1977.

Abstract □ The transport characteristics of muscle interstitial space were determined using an isolated rat diaphragm preparation. Permeability of the interstitial space for extracellular solutes is one-thirtieth to one-fiftieth that of an equivalent thickness of water. However, most of this low permeability can be accounted for by correcting for the tortuosity and relative volume of interstitial space. The estimated diffusivity of solutes (mol. wt. 100–70,000) in the interstitial space of muscle is only about one-half to one-fifth less than in water alone.

Keyphrases □ Permeability—interstitial space of rat diaphragm muscle to solutes of different molecular weights □ Transport characteristics—interstitial space of rat diaphragm muscle, permeability to solutes of different molecular weights

The prediction of the transport rates at which solutes and drugs cross interstitial space—either from blood to tissue or from tissue to circulation—is dependent on a knowledge of the relative resistances of these regions to transport.

Although several studies focused on the capillary endothelium (1–3), less work has been done on defining the role of the interstitial space and how it affects the net transport rate between blood and tissues. In nonsteady-state experiments using tracers, a temporary interruption in blood flow affected solute transport in a manner attributed to diffusion resistance in the interstitial space (4). By treating muscle with hyaluronidase, the absorption rate of intramuscularly injected dextrans was accelerated (5). Other experiments (6, 7) involved measurement of permeation rates through polyglycon gels prepared to simulate the composition of interstitial polysaccharides; it was suggested that diffusion through muscle tissue might be highly restricted, especially with macromolecules.

The objective of this study was to find the relationship between solute size and solute mobility in the interstitial space of muscle. Tracer solutes were used which, except for tritiated water, are retained in the extracellular space of muscle tissue. And by imposing a dextran gradient across a muscle preparation, the influence of osmotic forces in interstitial transport was evaluated.

Because the diaphragm is constituted of striated muscle and because the flat, sheet-like configuration lends itself to measurements of transient and steady-state transport rates by conventional membrane-testing techniques, the diaphragm of the rat was used in these experiments. This muscle has been used extensively as an experimental preparation in transport studies (8), cellular uptake studies (9), and work on hormonal influences on transport and uptake (10).

EXPERIMENTAL

Rat Diaphragm Preparation—Sprague–Dawley male rats, mostly retired breeders[1], 250–500 g, were injected with 35 mg ip of pentobarbital.

After the abdominal cavity was opened with a midline incision, the vena cava was clamped about 1 cm caudal to the vena caval hiatus. A 1.0-mm longitudinal incision was made in the vessel, and a catheter[2] was introduced and secured with 3-0 silk suture. The thorax was opened just above the sternum, and the thoracic vena cava was tied. The catheter was connected to a syringe pump equipped with a glass 30- or 50-ml syringe, and retrograde perfusion of the diaphragm vascular bed with Krebs–Ringer bicarbonate buffer was begun (11).

The diaphragm was removed by cutting the abdominal wall with scissors just caudal to the costal border, girdling the animal. A similar girdling cut was made just cephalad to the costal rim, and the trunk of the rat was disconnected above and below the diaphragm with bone shears and scissors.

The excised diaphragm, still undergoing retrograde perfusion, was mounted on a rigid, flat, 1.6-mm polycarbonate ring, about 7 cm o.d. and 5 cm i.d., using straight pins at the costal margin which fit into predrilled 1-mm holes in the ring. Once mounted, the diaphragm was either suspended vertically above a specimen dish for the permeability experiments or submersed in a cocktail of buffer, radioactive tracer, and dye for the equilibration experiments.

[1] Spartan Research Animals, Inc., Haslett, Mich.
[2] Intramedic polyethylene tubing PE 160.

(4) B. Ekman, C. Lofter, and I. Sjöholm, *Biochemistry*, **15**, 5115 (1976).
(5) I. Ljungstedt, B. Ekman, and I. Sjöholm, *Biochem. J.*, **170**, 161 (1978).
(6) Y. Pocker and J. T. Stone, *Biochemistry*, **6**, 668 (1967).
(7) E. J. Cohn, W. L. Hughes, Jr., and J. H. Weare, *J. Am. Chem. Soc.* **69**, 1753 (1947).
(8) E. W. Davie, C. R. Newman, and P. E. Wilcox, *J. Biol. Chem.*, **234**, 2635 (1959).
(9) G. H. Beaven and F. R. Holiday, *Adv. Protein*, **7**, 319 (1952).
(10) H. Pertoft, L. Philipson, P. Oxelfelt, and S. Höglund, *Virology*, **33**, 185 (1967).
(11) H. Nilsson, R. Mosbach, and K. Mosbach, *Biochim. Biophys. Acta*, **268**, 253 (1972).
(12) R. C. Boguslaski and A. M. Janik, *ibid.*, **250**, 266 (1971).

ACKNOWLEDGMENTS

Supported by the Swedish Board for Technical Development (Project 75-4415), the Swedish Medical Research Council (Project 13X-3126), and the I.F. Foundation for Pharmaceutical Research, Stockholm.

The technical assistance of Mr. Börje Berg is gratefully acknowledged.

Permeability of Interstitial Space of Muscle (Rat Diaphragm) to Solutes of Different Molecular Weights

JEROME S. SCHULTZ ˣ and WILLIAM ARMSTRONG

Received April 7, 1977, from the *Department of Chemical Engineering, University of Michigan, Ann Arbor, MI 48109.* Accepted for publication September 21, 1977.

Abstract □ The transport characteristics of muscle interstitial space were determined using an isolated rat diaphragm preparation. Permeability of the interstitial space for extracellular solutes is one-thirtieth to one-fiftieth that of an equivalent thickness of water. However, most of this low permeability can be accounted for by correcting for the tortuosity and relative volume of interstitial space. The estimated diffusivity of solutes (mol. wt. 100–70,000) in the interstitial space of muscle is only about one-half to one-fifth less than in water alone.

Keyphrases □ Permeability—interstitial space of rat diaphragm muscle to solutes of different molecular weights □ Transport characteristics—interstitial space of rat diaphragm muscle, permeability to solutes of different molecular weights

The prediction of the transport rates at which solutes and drugs cross interstitial space—either from blood to tissue or from tissue to circulation—is dependent on a knowledge of the relative resistances of these regions to transport.

Although several studies focused on the capillary endothelium (1–3), less work has been done on defining the role of the interstitial space and how it affects the net transport rate between blood and tissues. In nonsteady-state experiments using tracers, a temporary interruption in blood flow affected solute transport in a manner attributed to diffusion resistance in the interstitial space (4). By treating muscle with hyaluronidase, the absorption rate of intramuscularly injected dextrans was accelerated (5). Other experiments (6, 7) involved measurement of permeation rates through polyglycon gels prepared to simulate the composition of interstitial polysaccharides; it was suggested that diffusion through muscle tissue might be highly restricted, especially with macromolecules.

The objective of this study was to find the relationship between solute size and solute mobility in the interstitial space of muscle. Tracer solutes were used which, except for tritiated water, are retained in the extracellular space of muscle tissue. And by imposing a dextran gradient across a muscle preparation, the influence of osmotic forces in interstitial transport was evaluated.

Because the diaphragm is constituted of striated muscle and because the flat, sheet-like configuration lends itself to measurements of transient and steady-state transport rates by conventional membrane-testing techniques, the diaphragm of the rat was used in these experiments. This muscle has been used extensively as an experimental preparation in transport studies (8), cellular uptake studies (9), and work on hormonal influences on transport and uptake (10).

EXPERIMENTAL

Rat Diaphragm Preparation—Sprague–Dawley male rats, mostly retired breeders[1], 250–500 g, were injected with 35 mg ip of pentobarbital.

After the abdominal cavity was opened with a midline incision, the vena cava was clamped about 1 cm caudal to the vena caval hiatus. A 1.0-mm longitudinal incision was made in the vessel, and a catheter[2] was introduced and secured with 3-0 silk suture. The thorax was opened just above the sternum, and the thoracic vena cava was tied. The catheter was connected to a syringe pump equipped with a glass 30- or 50-ml syringe, and retrograde perfusion of the diaphragm vascular bed with Krebs–Ringer bicarbonate buffer was begun (11).

The diaphragm was removed by cutting the abdominal wall with scissors just caudal to the costal border, girdling the animal. A similar girdling cut was made just cephalad to the costal rim, and the trunk of the rat was disconnected above and below the diaphragm with bone shears and scissors.

The excised diaphragm, still undergoing retrograde perfusion, was mounted on a rigid, flat, 1.6-mm polycarbonate ring, about 7 cm o.d. and 5 cm i.d., using straight pins at the costal margin which fit into predrilled 1-mm holes in the ring. Once mounted, the diaphragm was either suspended vertically above a specimen dish for the permeability experiments or submersed in a cocktail of buffer, radioactive tracer, and dye for the equilibration experiments.

[1] Spartan Research Animals, Inc., Haslett, Mich.
[2] Intramedic polyethylene tubing PE 160.

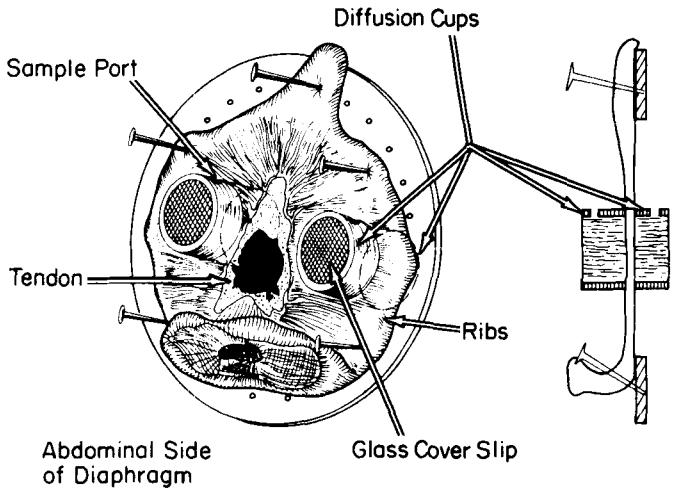

Figure 1—*Schematic diagram of the rat diaphragm preparation for the measurement of solute transport through the interstitial space of muscle. Diffusion cups were affixed to the muscle with a cyanoacrylate adhesive.*

Permeability Measurements—In the permeability experiments, two sets of matched cups were juxtaposed and secured on the diaphragm walls with adhesive (Fig. 1). The cups were fabricated from carefully sliced segments of polyvinyl chloride tubing[3] (12.7 mm i.d., 2.4 mm wall thickness); to one end of the sliced tube, a microscope slide coverglass was attached with a cyanoacrylate[4] adhesive. The open, cut surface of the cup was mounted directly on the diaphragm muscle with another cyanoacrylate[5] adhesive so that each pair of cups was in alignment, with the diaphragm constituting the partition between the chambers.

This method of attachment of the diffusion chambers precludes damage to muscle or vasculature due to clamping or other pressure-dependent attachments. The seal between the end of the plastic tubing and the tissue surface is remarkably strong and leakproof. When carefully applied, the adhesive does not invade onto the diaphragm surface within the chamber. The area of diaphragm available for diffusion may be confidently measured. In other published studies (8) where clamping arrangements were used, damage to tissue on the periphery of the chamber may have extended 1 mm beyond the cage; if so, and if the chamber was 1 cm in diameter, the damaged area may have included 20% of the experimental area.

Through 0.5-cm portals in the tops of the diffusion chambers, test solutions were introduced and monitored.

With the two sets of chambers, *i.e.*, one on the hepatic side and one on the splenic side, it was possible to run experiments either in duplicate or with a control and a variation on the same preparation.

Before test solutes were added to the chambers, the diaphragm preparation was allowed to come to equilibrium at room temperature (about 22°) with buffer solution in all cups for about 10 min. Tracer solutes were then added to the abdominal chambers, and the chambers on the pleural surface were monitored periodically for diffused materials.

Measurement of Interstitial Space—After the diaphragm was excised from the anesthetized rat and perfused 10 min with Krebs–Ringer bicarbonate buffer, it was ring mounted with pins and submersed in a solution containing the radioactive tracer of the solutes to be tested, 0.03% patent blue, and 1.5% bovine serum albumin in Krebs–Ringer bicarbonate buffer.

At intervals from 5 to 60 min, the mounted diaphragm was removed from the bath and placed on a rubber platform; a disk of muscle tissue, 0.95 cm in diameter, was excised with a tubular knife. Immediately after cutting out the tissue sample, the diaphragm was returned to the bath.

The tissue disk was rinsed 2 sec in 10 ml of 0.9% NaCl, blotted quickly on filter paper, and placed on a square of aluminum foil (1.5 × 1.5 cm) for weighing. It was then transferred to a screw-capped test tube (13 × 100 mm) containing 1.0 ml of 1.5% bovine serum albumin in Krebs–Ringer bicarbonate buffer and stored at 5° overnight to extract the patent blue.

[3] Tygon.
[4] Eastman 910.
[5] Formula 9, Johnson & Johnson.

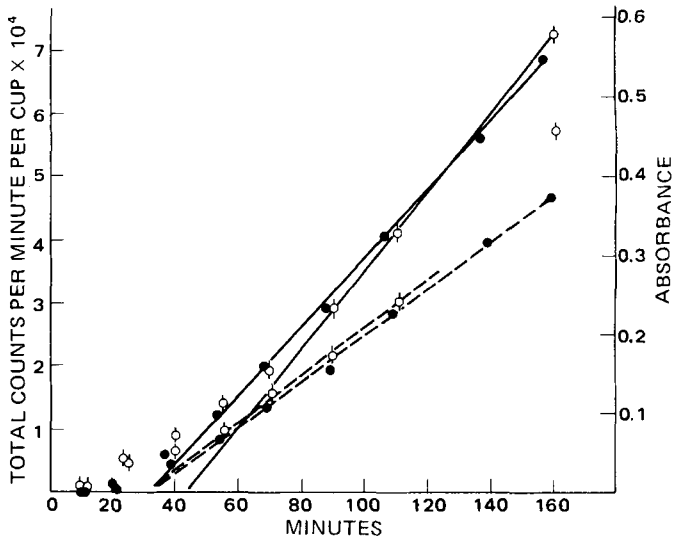

Figure 2—*Appearance of inulin and patent blue in the downstream chamber after the addition of tracers to the upstream chamber. Diffusion rates for two sections of the same diaphragm were slightly different, but relative transport rates for different solutes were about the same. Key: ○, ^3H-inulin; and ●, patent blue. Solid and dashed lines are for the individual sections of the diaphragm.*

On the following day, the tissue disk was transferred to a scintillation vial containing 1.0 ml of tissue solubilizer[6]. After digestion, 10 ml of toluene scintillant was added; the radioactive component in the tissue was measured by a scintillation counter.

The solution in which the disk had soaked was transferred to a spectrophotometric cell, and the absorbance of patent blue at 640 nm was recorded. An aliquot of this liquid component was removed and counted in the scintillant.

Internal standards were added when appropriate to compensate for the quenching effects of patent blue and solubilizer.

Analytical Methods—Absorbance measurements were obtained by transferring the contents of the diffusion chamber with a Pasteur pipet into a 1.0-ml spectrophotometer cell and reading the absorbance at 640 nm with a spectrophotometer. Radioactivities were measured by removal of aliquots, usually 10 μl, with disposable micropipets and counted in a liquid scintillation system.

Solutions and Materials—The Krebs–Ringer bicarbonate buffer had

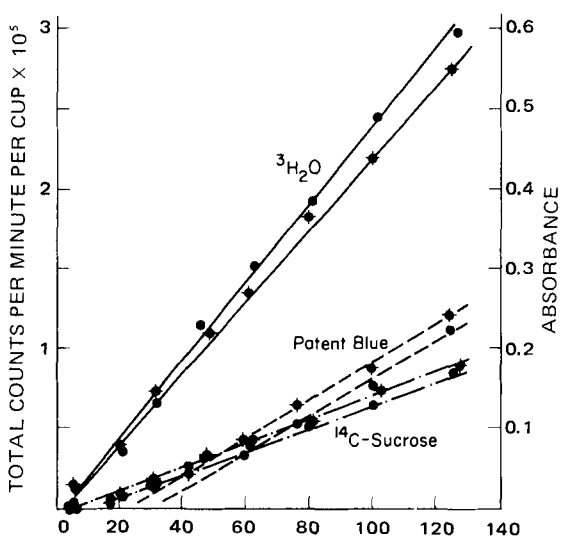

Figure 3—*Diffusion of ^3H-water, ^{14}C-sucrose, and patent blue across the rat diaphragm. One downstream chamber contained dextran T70 (●), and the other did not (-●-). The dextran osmotic pressure gradient does not augment transport rates.*

[6] Soluene 100, Packard.

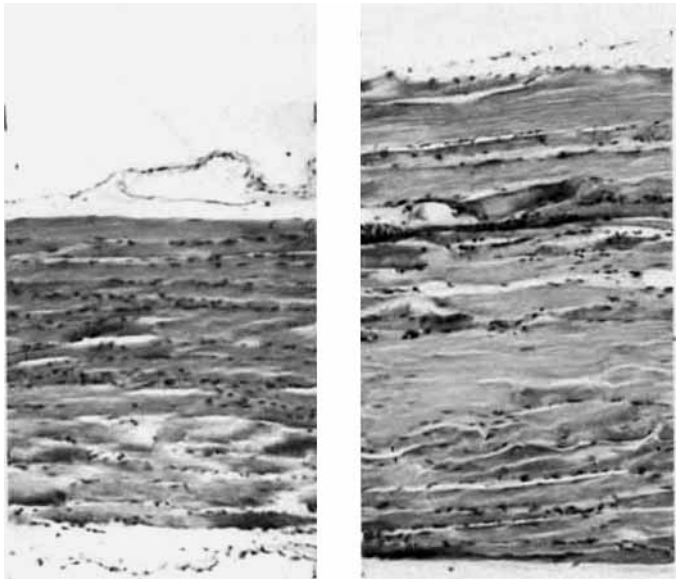

Figure 4—*Histological sections of rat diaphragm before (left) and after (right) a 3-hr diffusion experiment. Sections were made parallel to fiber length. Spacing between fibers was virtually unchanged by experimental procedure. (These sections were from two different animals.)*

the following composition: 0.7% NaCl, 0.035% KCl, 0.028% $CaCl_2$, 0.016% KH_2PO_4, 0.029% $MgSO_4 \cdot 7H_2O$, and 0.21% $NaHCO_3$.

^{131}I-Serum albumin[7] was dialyzed extensively to remove any free iodide. Patent blue violet[8], bovine serum albumin[9] (fraction V), ^{35}S-sodium sulfate[10], ^{14}C-D-sucrose[10], ^{3}H-methoxyinulin[10], ^{3}H-water[10], and dextrans[11] were used as received.

RESULTS

In Figs. 2 and 3, which show typical diffusion patterns, it is evident that before a steady-state gradient is established through the tissue, there is a lag period during which binding sites and dead-ended volumes are saturated. After this lag time, the flux through the tissue is essentially constant, indicating that the system has achieved a pseudosteady state under these experimental conditions. For slowly diffusing molecules such as albumin, the curve remains straight for several hours. For rapidly diffusing substances such as water, the permeation curve soon plateaus since both chambers equilibrate with tracer.

Generally, the lag time increases with the size of the solute species. This information can be used to estimate tortuosity and dead-end porosity (8, 12), but such calculations are thought to be very model dependent (13). For the analysis of the data presented here, only the constant slope portion of the permeation curve, or the pseudosteady-state portion, was used.

In all permeation experiments, patent blue was used as an extracellular reference marker. This dye does not bind to plasma proteins or tissue membranes (14). Besides providing an immediate indication of leaks within the diaphragm–chamber preparation, the dye also provided a convenient colorimetric control while other test solutes were measured by radiotracer techniques. In some experiments, two different isotopic tracers along with patent blue were used to obtain three relative diffusion rates from a single muscle preparation.

Figure 2 shows the diffusion results of duplicate experiments on the same diaphragm with patent blue and inulin as the tracer solutes. Whereas the average diffusion rates for the two chambers were slightly different, the inulin transport rate relative to patent blue transport was the same. Thus, by normalizing diffusion rates in relation to a reference molecule, the minor variations in tissue properties that may occur from one area of a tissue preparation to another or from animal to animal are effectively eliminated.

Diaphragm thickness measurements were made with an electronic contact micrometer before and after each experiment. The diffusion chambers were emptied and gently removed without damage to the diffusion surface area. The thickness of the diaphragm in this region increased by about 20% over 3 hr.

[7] Prepared by the Nuclear Pharmacy Department, University of Michigan.
[8] Color index 42045, Sigma Chemical Co.
[9] Sigma Chemical Co.
[10] New England Nuclear Corp.
[11] Pharmacia Fine Chemicals.

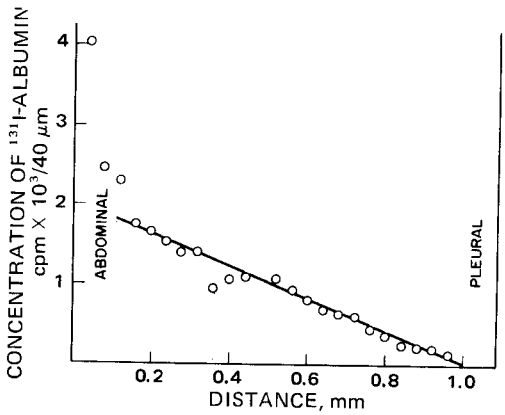

Figure 5—*Concentration profile of ^{131}I-albumin across a rat diaphragm after a steady-state permeation rate was attained. The tissue was quickly frozen and then sectioned parallel to the surface of the diaphragm.*

To determine whether the interstitial space underwent significant expansion during the experiments, tissue samples from control and experimental diaphragms were processed for histological comparison. The increase in tissue thickness during the experiment was caused by an apparent swelling of the muscle fibers rather than by the accumulation of liquid in the interstitial space. Photographs of histological samples are shown in Fig. 4.

The fact that the transmuscle flux remained constant for several hours suggests that the extracellular structure of the diaphragm remains stable at least during the experiment. If the interstitial space were to become edematous, solute mobility would increase, as reflected by an increase in the upward curvature of the lines in Figs. 2 and 3.

Portions of diaphragms used for the diffusion experiments were excised and analyzed for the distribution of tracer across the sheet of muscle. These sections were quickly frozen on a precooled slab and were sectioned longitudinally (parallel to the surface of the diaphragm) with a cryostatic microtome. Series of these sections were pooled in counting vials so that the profile of radioactivity across the thickness of the diaphragm was obtained.

A typical distribution is shown in Fig. 5. In this experiment, after achieving a steady-state flux, the distribution of ^{131}I-albumin was measured. The concentration of labeled albumin was generally linear from the abdominal to the plural surface; the amount of scatter found on the abdominal surface was attributed to technical problems in alignment of the microtome blade exactly with the diaphragm surface.

Linear concentration profiles are consistent with simple passive diffusion; other transport processes, such as bulk flow or carrier-mediated flow, are usually nonlinear. If the mesothelium that lines the pleural and abdominal surfaces of the diaphragm constituted a significant permeability barrier, discontinuities in the concentrations of radioactivity would have been found at both surfaces. But the tracer concentration at the pleural surface was essentially the same as in the downstream diffusion chamber, a value close to zero. At the abdominal surface, the radioactivity per unit volume of muscle was about 5% of the concentration in the upstream diffusion chamber. This finding is consistent with independent equilibrium measurements of albumin space in the diaphragm, which showed that about 8% of the muscle is available to albumin (Table I).

Boundary Layer Resistance—The fluid in the chambers affixed to the diaphragm in these experiments was not subjected to any mixing beyond that caused by density gradients. Therefore, the resistances at the tissue–fluid interface, *i.e.*, the unstirred boundary layer, would be expected to be large.

These diffusion resistances were measured by substituting a microporous filter for the diaphragm; this membrane was previously dipped in dilute agar, and then the diffusion cups were affixed by clamps. Agar coating was done to prevent bulk flow through the filter due to slight differences in liquid level. Transport rates of various solutes across the agar membrane were measured.

The fluxes of ^{3}H-water, ^{14}C-sucrose, and patent blue through the membrane were measured using the same procedures as in the diaphragm experiments. The permeability of the boundary layers, P_{layers} (one on each side of the membrane), for each solute was calculated from the series

Table I—Estimate of Solute Diffusivities in Rat Diaphragm

Solute	Permeability Rat Diaphragm, cm/sec × 10^6	Void Space, ψ	Estimated Tortuosity, τ	Diffusivity: Calculated in Diaphragm, cm^2/sec	Diffusivity: in Water, cm^2/sec	Ratio
Water	55.6	0.79 ± (3)[a]	1.5	6.8×10^{-6}	23.0×10^{-6}	0.30
Sodium sulfate	4.72	0.20 ± 0.008 (3)	2.5	3.6×10^{-6}	11.0×10^{-6}	0.33
Sucrose	2.79	0.31 ± 0.08 (4)	2.5	1.4×10^{-6}	5.1×10^{-6}	0.28
Patent blue violet	1.55	0.30 ± 0.08 (13)	2.5	0.82×10^{-6}	3.1×10^{-6}	0.27
Inulin	0.996	0.31 ± 0.09 (3)	2.5	0.51×10^{-6}	2.4×10^{-6}	0.21
Albumin	0.178	0.08 ± 0.04 (10)	2.5	0.36×10^{-6}	0.7×10^{-6}	0.52

[a] Numbers in parentheses indicate the number of observations.

resistant equation:

$$\frac{1}{P_{obs}} = \frac{1}{P_{layers}} + \frac{1}{P_{membrane}} \quad \text{(Eq. 1)}$$

where the individual permeability values were obtained from the experimental observations:

$$P_{obs} = \frac{(\Delta C/\Delta t)V_d}{A(C_u - C_d)} \quad \text{(Eq. 2)}$$

where $(\Delta C/\Delta t)$ is the slope of the lines shown in Figs. 2 and 3, V_d is the volume of the downstream chamber, A is the area available for diffusion, and $(C_u - C_d)$ is the concentration difference of solute between the upstream and downstream compartments.

The permeability of the microporous filter for each solute was estimated from the known properties of the filter (15): thickness = 0.0160, porosity = 0.8, tortuosity = 1.2, and $P_{membrane} = (D \times 0.8)/(0.016 \times 1.2)$, where D is the diffusion coefficient of the solute in water.

As shown in Fig. 6, the boundary layer permeability increases with solute diffusivity, as expected. The slope of the line is about 0.33, so $P_{layers} = \alpha D^{1/3}$ for this experimental apparatus. This 0.33-power dependency of boundary layer permeability differs from the value of 0.6 obtained in experiments where the solutions were mechanically stirred (16). Values of boundary layer permeability for each solute tested can be obtained by extrapolation (Fig. 6). For each solute except ^{3}H-water, the boundary layer permeability was considerably greater than the permeability of the diaphragm, so only very small corrections were necessary to make the permeability estimates for muscle.

Effect of Osmotic Gradient on Transport—A series of experiments was conducted to determine whether solute transport through muscle tissue was augmented by an osmotic gradient. An osmotic differential was achieved by preparing the downstream buffer to contain 4.5% dextran T70, a concentration that has an effective osmotic pressure of 52 cm H_2O. If the interstitial space of muscle consists of a very dense meshwork of carbohydrate polymers relatively impermeable to large molecules (6), one would expect the dextran to cause an osmotic water flow from upstream to downstream chambers. The apparent permeation rate would be higher because of the drag effect of the water flow on solute molecules.

Experiments did not support this expectation. Most of the comparative data on this point, about 35 experiments, were obtained with patent blue as the tracer substance. The mean permeability of patent blue across the diaphragm with a dextran gradient was $1.4 \pm 0.7 \times 10^{-6}$ cm/sec, which is not significantly different than the mean value of $1.3 \pm 0.4 \times 10^{-6}$ cm/sec obtained when no dextran was added to the downstream chamber. Similar results were obtained with the other solutes (Table II). For osmotic substances of the size of dextran T70, the matrix of polymers within the interstitial spece apparently is not tight enough to induce osmotic flow or, in other words, dextran T70 is not an oncotic agent for the rat diaphragm.

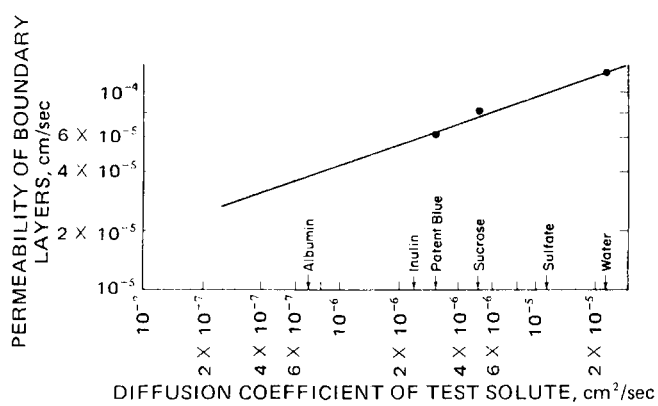

Figure 6—*Boundary layer resistances for various solutes. Measurements were made using ^{3}H-water, ^{14}C-sucrose, and patent blue. Other values were determined by interpolation.*

Permeability of Rat Diaphragm to Solutes—Since there was no statistical difference between permeation rates across the diaphragm with and without a dextran gradient, all data were pooled and used to obtain mean estimates of the permeability rates for each solute.

As mentioned, patent blue was a control solute in each experiment. Mean values for permeabilities were estimated by first relating the test solute permeability to its patent blue control and then averaging the data.

Based on the steady portion of the diffusion curves (Figs. 2 and 3), P_{obs} for each solute was calculated according to Eq. 2. For each solute, the $P_{solute}/P_{patent\ blue}$ ratio was calculated and averaged over all experiments for that solute; these mean values are given in the second column of Table III. The mean $P_{solute}/P_{patent\ blue}$ ratio was multiplied by the grand mean permeability for patent blue, 1.51×10^{-6} cm/sec, to obtain the estimate for the mean permeability of diaphragm muscle to each solute, $\overline{P}_s$. Mathematically:

$$\overline{P}_s = \left[\frac{\sum_1^i P_{si}/P_{PBi}}{i}\right]\left[\frac{\sum_1^n P_{PBn}}{n}\right] \quad \text{(Eq. 3)}$$

where i is the number of experiments with an individual solute (s), and n is the total number of observations of patent blue (PB) permeability. Each mean value for observed solute permeabilities was then corrected for the boundary layer permeability of each solute by Eq. 1 to obtain the permeability of the diaphragm for each solute given in the fourth column of Table III. The correction for boundary layer effects was less than 5% for all solutes except ^{3}H-water; therefore, the accuracy of the correction factors obtained from Fig. 6 is not critical to the results.

DISCUSSION

Of the solutes used, all except ^{3}H-water are confined to the extracellular space. Because of its facile transport across cell membranes, water penetrates muscle through both extracellular and intracellular paths. Therefore, the measured permeability of ^{3}H-water reflects some average resistance of the interstitial space and intracellular space.

The other five solutes are presumed to diffuse through the interstitial space alone, so their permeation rates can be compared meaningfully. In these experiments, the permeability of the interstitial space decreased with the increasing size of the probe solute by a factor of 26 (4.7/0.18),

Table II—Effect of Dextran T70 Gradient on the Permeability of Rat Diaphragm for Various Solutes (Paired Observations)

Solute	Permeability Control / Permeability with Dextran Gradient
^{3}H-Water	0.9 ± 0.4 (4)[a]
^{35}S-Sodium sulfate	1.0 ± 0.2 (4)
Patent blue violet	1.0 ± 0.3 (8)
^{131}I-Albumin	1.5 ± 0.4 (4)

[a] Numbers in parentheses indicate the number of observations.

Table III—Average Permeabilities of Diaphragm to Solutes

Solute	Permeability Relative to Patent Blue, P_s/P_{PB}	Mean Permeability, cm/sec × 10^6	Permeability (Corrected for Boundary Layers), cm/sec × 10^6	Permeability of Diaphragm Relative to Water Layer, $P_{diaphragm}/P_{water\ layer}$
Water	25.5 ± 9.7 (10)[a]	38.5	55.6	0.16
Sodium sulfate	2.99 ± 1.7 (5)	4.51	4.72	0.028
Sucrose	1.79 ± 0.55 (16)	2.70	2.79	0.036
Patent blue violet	(1.00)	1.51 ± 0.71 (56)	1.55	0.033
Inulin	0.65 ± 0.23 (13)	0.98	0.996	0.027
Albumin	0.117 ± 0.042 (17)	0.176	0.178	0.017

[a] Numbers in parentheses indicate the number of observations.

as expected, based on decreasing diffusion coefficients with increasing molecular diameter. The inherent effect of molecular mobility can be compensated for by comparing the measured muscle permeabilities to the permeability of a water layer of the same thickness as the rat diaphragm.

By using the equation $P_{water} = D_s/\delta$, where D_s is the diffusivity of the solute in water (Fig. 6) and δ is the equivalent water layer thickness, 0.065 cm, the $P_{diaphragm}/P_{water}$ ratio was calculated for each solute. The results are shown in the last column of Table III. The range of this ratio for the extracellular solutes is reduced to a factor of about 2, indicating that molecular mobility, *i.e.*, diffusivity, is one main parameter controlling transport in the interstitial space.

These data also show that, in the molecular weight range of 100–70,000, there is no major sieving effect with increases in molecular size within the interstitial space. This result is in contrast to the marked sieving effects attributed to the endothelial lining of capillaries (1).

However, the absolute values of the permeability ratios show that transport through the diaphragm is 30–50 times slower than an equivalent layer of water. As discussed below, the relatively slow transport through muscle may, to some extent, be imputed to the heterogeneous structure of muscle. Whatever the cause, the mean measured permeabilities should provide a sound basis for the estimation of steady-state rates at which extracellular solutes, drugs, hormones, and proteins transport across muscle tissue.

Muscle microanatomy has been studied in great detail. It is convenient to visualize a model of interstitial space as a complex network of voids intermingled with closely packed cylinders of muscle. The diffusional tortuosity of this space has not been determined accurately. Neither have accurate measurements been made of that fraction of the interstitial space which is dead ended, areas that, from the point of view of permeability, are cul-de-sacs. So, admittedly, to estimate diffusion coefficients of solutes in the interstitial space based only on flux measurements is hazardous. However, such estimates may be of value in revealing the relative influences on transport of tortuosity and void space.

The following model was assumed for permeability through a porous material:

$$P = \frac{D\psi}{L\tau} \qquad \text{(Eq. 4a)}$$

or:

$$D = \frac{PL\tau}{\psi} \qquad \text{(Eq. 4b)}$$

where D is the diffusion coefficient in the interstitial space, ψ is the void fraction, L is the geometric thickness of the tissue, and τ is the tortuosity of the extracellular path.

The calculations for the diffusion coefficient of each solute in muscle are summarized in Table I, with the fraction of total muscle volume accessible to each solute given in the third column. For water, the void volume was determined by drying; all other values were determined by equilibrium uptake experiments. The void volume for water is much higher than the others because it penetrates muscle cells as well as the extracellular fluid. Albumin, probably because of steric hindrance, appears to have a significantly smaller distribution space than the other extracellular solutes. Tortuosity estimates for muscle tissue ranging from 1.5 to 5.0 have been made based on the lag time to achieve pseudo-steady-state diffusion rates (8, 12, 13). Larger tortuosities are expressed for larger molecules because of steric interference in the transport of large particles (17).

Because it moves through parallel pathways, a low value of tortuosity was assigned to water; a moderate value of 2.5 was assigned to all other solutes. Estimates for the diffusion coefficients of the various probe solutes within interstitial space were calculated using Eq. 4*b* with a mean value of 0.065 cm for L. These values are listed in Table I, and the calculated diffusivities are compared to the diffusivities of these solutes in water. Overall, it appears that the mobility of solutes in interstitium is 0.2–0.5 of that in water and that the reduced mobility is not strongly correlated with molecular size.

If the use of Eq. 4*b* with the estimates of tortuosity and void fraction is appropriate, a major part of the low permeability values for whole muscle can be explained by these geometric factors. The remaining one-half to one-fifth reduction in mobility as compared to water may be due to a higher viscosity of the interstitial fluid and/or some diffusion hindrance due to the porous nature of the tissue (16).

Using fluorescence microscopy, Nakamura and Wayland (18) estimated the diffusion coefficient for albumin in rat mesentery and found it to be fairly close to its value in water. Their conclusion that substances move fairly freely within the interstitial space of tissues is corroborated by the present findings.

REFERENCES

(1) J. R., Pappenheimer, E. M. Renkin, and L. M. Borrero, *Am. J. Physiol.*, **167**, 13 (1951).

(2) D. Garlick and E. Renkin, *ibid.*, **219**, 1595 (1970).

(3) N. Simionescu, M. Simionescu, and G. Palade, *Thromb. Res. Suppl. 2*, **8**, 257 (1976).

(4) C. Crone and D. Garlick, *J. Physiol. (London)*, **210**, 387 (1970).

(5) R. Sund and J. Schou, *Acta Pharmacol. Toxicol.*, **23**, 194 (1965).

(6) T. C. Laurent, *Pfluegers Arch., Suppl.*, **336**, S21 (1972).

(7) B. N. Preston and J. M. Snowden, *Biopolymers*, **11**, 1627 (1972).

(8) N. Brookes and D. Mackay, *Br. J. Pharmacol.*, **41**, 367 (1971).

(9) D. M. Kipnis and C. F. Cori, *J. Biol. Chem.*, **224**, 681 (1957).

(10) T. Clausen, in "Current Topics in Membranes and Transport," vol. 6, F. Bronner and A. Kleinzeller, Eds., Academic, New York, N.Y., 1974, pp. 189–225.

(11) F. D. Hollanders, *Comp. Biochem. Physiol.*, **26**, 907 (1968).

(12) E. Page and R. S. Bernstein, *J. Gen. Phys.*, **47**, 1129 (1964).

(13) M. Suenson, D. R. Richmond, and J. B. Bassingthwaighte, *Am. J. Physiol.*, **227**, 1116 (1974).

(14) C. A. Wiederhelm, M. Show, T. Kehl, and J. Fox, *Microvasc. Res.*, **5**, 243 (1973).

(15) S. Suchdeo and J. S. Schultz, *Biochim. Biophys. Acta*, **352**, 412 (1974).

(16) R. E. Beck and J. S. Schultz, *ibid.*, **255**, 273 (1972).

(17) H. E. Schultze and J. Heremans, "Molecular Biology of Human Proteins," vol. 1, Elsevier, Amsterdam, The Netherlands, 1966.

(18) Y. Nakamura and H. Wayland, *Microvasc. Res.*, **9**, 1 (1975).

ACKNOWLEDGMENTS

Supported in part by National Institutes of Health Grant GM15152 and Research Career Development Award 1-K4-GM-8271 to J. S. Schultz.

Synthesis of Anticholinergic Agents: *N*-Methyl-4-piperidinyl α-Benzoyloxy-α-cyclopentylphenylacetate Salts

WILLIAM OROSHNIK * and GIANLUIGI SOLDATI ˣ

Received May 20, 1977, from *Carter Products Research, Division of Carter-Wallace, Inc., Cranbury, NJ 08512.* Accepted for publication August 1, 1977. *Present address: Chemo Dynamics Laboratory, Plainfield, NJ 08760.

Abstract □ The synthesis of a new anticholinergic agent, *N*-methyl-4-piperidinyl α-benzoyloxy-α-cyclopentylphenylacetate, obtained by reacting *N*-methyl-4-piperidinyl α-cyclopentylmandelate with benzoyl chloride in the presence of methyllithium, is reported. This material may be useful as an antiperspirant.

Keyphrases □ *N*-Methyl-4-piperidinyl α-benzoyloxy-α-cyclopentylphenylacetate—synthesized, anticholinergic and antiperspirant activity evaluated □ Anticholinergic activity—*N*-methyl-4-piperidinyl α-benzoyloxy-α-cyclopentylphenylacetate evaluated in rabbit eyes □ Antiperspirant activity—*N*-methyl-4-piperidinyl α-benzoyloxy-α-cyclopentylphenylacetate evaluated in humans

A synthetic substance with local antiperspirant activity that would be effective when applied topically, have low toxicity, and have no systemic effects would be highly desirable.

The effectiveness of anticholinergic drugs, for example, as antiperspirants is well documented (1–3). The benzoyl ester of scopolamine has been used repeatedly on skin at low concentration without measurable systemic effect (1), and 1-methyl-3-pyrrolidyl α-phenylcyclohexaneglycolate methobromide (4) has been found to be valuable for sweat inhibition.

DISCUSSION

N-Methyl-4-piperidinyl α-benzoyloxy-α-cyclopentylphenylacetate (II) was prepared by the reaction of *N*-methyl-4-piperidinyl α-cyclopentylmandelate (I) (5) with benzoyl chloride in the presence of methyllithium at −30°, according to Scheme I.

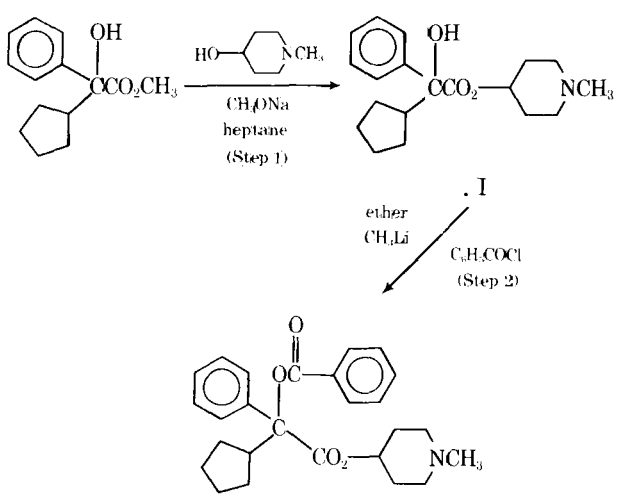

II

Scheme I

The sequence in Step 1 is not chemically unusual, but it is a convenient and economical route for the synthesis. Step 2, however, does represent a somewhat novel procedure. By the use of low temperature, it was possible to restrict the reaction to the hydroxyl group of the phenylacetate, with only minimum reactivity of the ester group even in the presence of excess methyllithium. Furthermore, when excess benzoyl chloride is added at this low temperature, it destroys the excess methyllithium before the latter can react with the ester group as the reaction temperature is again raised to room temperature. At room temperature, the only reactants remaining are the oxylithium group on the substrate and benzoyl chloride. A previously reported method for introducing an acyl group into a basic ester of similar structure concerned the synthesis of α-acyloxy derivatives of *N*-methyl-4-piperidinyl benzylates (6) and involved a multistep sequence.

The new drug, in the hydrochloride form, was investigated as an anticholinergic antiperspirant. The anticholinergic effect of this compound was determined in rabbit eyes, and its activity was established by measurements of pupil dilation.

The single-dose intraperitoneal LD_{50} in albino mice was 61 mg/kg. The single-dose oral LD_{50} in albino mice was 310 mg/kg.

The test compound was applied topically, up to 160 μg/kg, for 7 consecutive days to human skin without evidence of definite side effects. Further testing with 320- and 640-μg/kg doses also indicated freedom from side effects. ECG's taken before and after application of the two highest doses showed no detectable effects.

The standard antiperspirant back test was conducted on volunteers with concentrations of the test material of up to 4% in a 75% alcoholic solution. The substance was demonstrated to be significantly effective in reducing perspiration.

EXPERIMENTAL

***N*-Methyl-4-piperidinyl α-Benzoyloxy-α-cyclopentylphenylacetate Hydrochloride Hydrobromide (III)**—Methyl α-cyclopentylmandelate (233 g), *N*-methyl-4-piperidinol (115 g), heptane (bp 94–95°) (1540 ml), and sodium methoxide (9.1 g) were slowly distilled until the methanol–heptane azeotrope no longer passed over, as shown by the take-off temperature reaching and staying at 94° (3 hr). The mixture was then cooled, poured into 1 liter of water, and shaken vigorously. The heptane phase was separated and washed with successive portions of water until neutral and then dried over anhydrous magnesium sulfate, filtered, and concentrated under vacuum.

The concentrate was dissolved in 1 liter of dry methylene chloride, and hydrochloric acid was passed in at 0° with external cooling until the solution was saturated. The solution was then concentrated under vacuum to remove the excess acid, and the concentrate was redissolved in 1300 ml of warm methylene chloride. Approximately 2000 ml of acetone was then added, and the solvent was boiled off until crystals began to appear. The mixture was allowed to cool slowly to 25° and was then stored overnight at 3° to complete precipitation of the product. The precipitate was collected by filtration, washed with cold acetone (−10°; 3 × 200 ml), and dried under vacuum.

The combined filtrate and washings were concentrated to 500 ml under partial vacuum. The mixture was allowed to cool slowly and then was refrigerated overnight. On the next day, it was filtered, and the product was washed with cold acetone (−10°; 3 × 70 ml). The product was dried under vacuum, and 279 g was obtained (mp 221–223°). The entire yield was placed in a 3-liter flask containing 1 liter of 25% aqueous potassium carbonate and 1 liter of pentane.

This mixture was stirred mechanically at high speed until the suspended hydrochloride dissolved (4 hr). The pentane layer was separated, dried over potassium carbonate, filtered, and concentrated under vacuum. The concentrate was transferred to a 5-liter three-necked flask with benzene (250 ml), and then benzene was boiled off under vacuum, thus assuring anhydrous conditions. Anhydrous ether (3 liters) was then added, and the mixture was stirred until solution was complete.

The solution was then cooled to −35°, and 477 ml of methyllithium (1.8 *M* in ether) was added dropwise with rapid stirring. The temperature was maintained at −30° with a dry ice–acetone bath throughout the addition (2–3 hr). Benzoyl chloride (209 ml) was then added at −30°, and the mixture was stirred an additional 15 min at this temperature. The cooling bath was removed, and the mixture was stirred until it reached 25° and then was allowed to stand overnight.

The mixture was next cooled to 0°, and 800 ml of water was added slowly with rapid stirring. Then the ether was removed under vacuum, and 1 liter of methylene chloride was added. This phase was then separated, dried over magnesium sulfate, filtered, and concentrated again to 1 liter.

Hydrogen chloride gas was passed into the methylene chloride solution at 0° until the solution was saturated. The excess hydrogen chloride and the solvent were then removed under vacuum. One liter of anhydrous ether was then added to the syrup, and the mixture was stirred mechanically. Crystallization soon began. After 2 hr of stirring, the mixture was filtered; the product was washed with ether (3 × 300 ml) and dried under vacuum. The yield was 387.4 g, mp 180–184°. When recrystallized from methylene chloride–ether, the material melted at 185–187°.

Anal.—Calc. for $C_{26}H_{31}NO_4$·73% HBr·27% HCl: C, 63.63; H, 6.57; Br, 11.89; Cl, 1.95; N, 2.86; O, 13.05. Found: C, 63.48; H, 6.66; Br, 11.81; Cl, 1.86; N, 2.80; O, 12.88.

The mixed salt formation was probably due to the generation of bromide from lithium bromide present as a stabilizer in the methyllithium solution.

***N*-Methyl-4-piperidinyl α-Benzoyloxy-α-cyclopentylphenylacetate (II)**—Compound III (10 g) was slurried in 100 ml of ether and 100 ml of 10% aqueous sodium bicarbonate. As soon as two clear phases formed, the mixture was transferred to a separator; the ethereal phase was separated and dried over anhydrous magnesium sulfate. Evaporation of the ether gave an almost quantitative yield of a highly viscous oil. The material was eluted with chloroform–methanol (4:1) through a 22.2 × 2-cm silica gel column.

Anal.—Calc. for $C_{26}H_{31}NO_4$: C, 74.08; H, 7.41; N, 3.32; O, 15.18. Found: C, 73.83; H, 7.42; N, 3.40; O, 15.02.

***N*-Methyl-4-piperidinyl α-Benzoyloxy-α-cyclopentylphenylacetate Hydrochloride (IV)**—The free base (8.3 g), obtained as described, was dissolved in 200 ml of methylene chloride and 100 ml of ether. Gaseous hydrogen chloride was introduced at 0–10° until the solution was saturated. The solvent and the excess acid were removed under reduced pressure, and the viscous residue was covered with anhydrous ether. After a few hours, the ether was decanted, and the syrup was recovered with ether. After 24 hr, the crystallization was complete. The yield was 8 g. When recrystallized three times from methylene chloride–ether, the white crystalline material melted at 162.5–164°.

Anal.—Calc. for $C_{26}H_{32}ClNO_4$: C, 68.18; H, 7.04; Cl, 7.74; N, 3.05. Found: C, 67.87; H, 6.97; Cl, 7.53; N, 3.23.

***N*-Methyl-4-piperidinyl α-Benzoyloxy-α-cyclopentylphenylacetate Methiodide (V)**—Compound IV (5 g) was dissolved in 30 ml of water. Then 50 ml of ether was added, and the mixture was neutralized slowly with 10% aqueous potassium carbonate. The ethereal phase was then separated, dried over anhydrous magnesium sulfate, filtered, and evaporated. The residue was dissolved in 10 ml of anhydrous acetone, and 2 g of methyl iodide was added. The solution was refluxed for 4 hr. After cooling, ether was added to precipitate the product. Five grams of material was thus obtained. It was recrystallized from methanol–ether, mp 133–137°.

Anal.—Calc. for $C_{27}H_{34}INO_4$: C, 57.55; H, 6.08; N, 2.50. Found: C, 57.68; H, 6.27; N, 2.42.

***N*-Methyl-4-piperidinyl α-Benzoyloxy-α-cyclopentylphenylacetate Hydrobromide (VI)**—The free base obtained from 10 g of III was dissolved in 200 ml of methylene chloride–ether (1:1). Gaseous hydrogen bromide was passed through the solution until a strong acid reaction was obtained. The solvent was then evaporated under reduced pressure, and the viscous residue was covered with anhydrous ether for 2 days. The oil solidified upon standing after addition of some methylene chloride. The product was collected and crystallized with 30 ml of methylene chloride and 60 ml of ether. The 4.6 g of product was recrystallized twice from methylene chloride–ether, mp 185–186.5°.

Anal.—Calc. for $C_{26}H_{32}BrNO_4$: C, 62.15; H, 6.42; N, 2.78. Found: C, 61.56; H, 6.50; N, 2.87.

The IR spectra were determined from mineral oil mulls. Compounds III, IV, and VI exhibited a characteristic ammonium absorption at 2360–3640 cm^{-1}; in II–IV and VI, the carbonyl stretching vibration occurred at 1735–1750 cm^{-1} and the aromatic C=C absorption was observed at 1595–1600 cm^{-1}. None of the benzoylated materials showed absorption in the hydroxy region.

NMR spectra were obtained in a deuterated chloroform–tetramethylsiloxane system. Compounds III, IV, and VI exhibited peaks at δ 1.4–1.8, 2–2.2, 2.2–2.5, 3–3.4, 5–5.3, 7.2–7.8, and 8–8.4 ppm. The nine protons of the cyclopentyl ring occurred as a singlet at 1.6 ppm, the three *N*-methyl group protons were observed as a doublet at 2.4 ppm, and the aromatic protons occurred as a multiplet at 7.2–7.8 ppm. Compound II gave a similar spectrum with peaks in the same shift region as observed for the salts.

TLC, developed with a chloroform–methanol–acetic acid system, showed main spots at R_f 0.45, 0.44, 0.44, and 0.46 for II, III, IV, and VI, respectively. The mixed salt, III, was further identified by mass spectrometry. A parent peak at *m/e* 421.5 corresponding to the molecular weight of its base, II, was observed. The same retention time was noted for II–IV and VI by GLC. The methiodide salt, V, synthesized from II, was identified only by elemental analysis.

REFERENCES

(1) F. S. K. McMillan, H. H. Reller, and F. H. Snider, *J. Invest. Dermatol.*, **43**, 363 (1964).

(2) W. B. Shelly and P. N. Howarth, *J. Invest. Dermatol.*, **16**, 267 (1951).

(3) R. Brun and N. Hunziker, *Dermatologica*, **110**, 245 (1955).

(4) R. B. Stoughton, F. Chiu, W. Fritsch, and D. Nurse, *J. Invest. Dermatol.*, **42**, 151 (1964).

(5) A. Verweij, R. DeJong-Devos, and H. G. J. Teisman, *J. Chromatogr.*, **69**, 407 (1972).

(6) J. Klosa and G. Delmar, *J. Prakt. Chim.*, **16**, 71 (1962).

ACKNOWLEDGMENTS

The authors acknowledge the assistance of Mr. I. Alan Brenner, Mr. Fayez B. Ibrahim, and Mrs. Natalie J. Strez, Analytical Research, Carter-Wallace, Inc.

Theoretical Relationships between Area under the Curve and Route of Administration of Drugs and Their Precursors for Evaluating Sites and Pathways of Metabolism

K. SANDY PANG [x] **and JAMES R. GILLETTE**

Received April 25, 1977, from the *Laboratory of Chemical Pharmacology, National Heart, Lung, and Blood Institute, National Institutes of Health, Bethesda, MD 20014.* Accepted for publication August 2, 1977.

Abstract □ The bioavailability of a drug administered extrasystemically is a measure of the initial extraction of a compound by a series of eliminating events involving the intestinal mucosal enzymes, the gut bacterial microflora, the liver, and the lung. A theoretical analysis is presented to differentiate the processes of gut wall elimination and hepatic removal of a drug during this first-pass effect. The area under the blood concentration–time curve (*AUC*) for a drug and its metabolite is shown to be useful in determining the presence of these processes when a drug and its metabolite are administered concomitantly by different routes of administration. Furthermore, the fraction of a precursor transformed to its metabolite also can be determined by pharmacokinetic analysis of the *AUC* of a drug and its metabolite after administration of both substances.

Keyphrases □ Pharmacokinetics—theoretical analysis to differentiate gut wall elimination and hepatic removal, relationship between area under the curve and administration route □ Metabolism, drug—sites and pathways evaluated, theoretical analysis to differentiate gut wall elimination and hepatic removal, relationship between area under the curve and administration route

The effect of the route of administration on the bioavailability (defined as the fraction of drug reaching the site of sampling from the site of administration) of drugs has been the subject of several publications (1–6). An orally administered drug must be absorbed, survive the initial degradation by intestinal mucosal enzymes (7, 8) and bacterial flora (9–11), and escape hepatic elimination before it arrives at the site of sampling, usually a remote venous site. The lung, a potential organ of drug elimination (12), also interposes between the site of sampling and administration and can interact in this chain of eliminating events which constitutes the first-pass effect (3). The plasma also was reported to be an eliminating tissue (13).

DISCUSSION

The bioavailability on intravenous drug administration is usually taken as unity in the absence of removal of drug by either the plasma or the lung. Thus, the classical method of ascertaining the oral bioavailability is by the ratio of the area under the curve, *AUC* (14):

$$F = \frac{AUC_{po}}{AUC_{iv}} \frac{dose_{iv}}{dose_{po}} \quad \text{(Eq. 1)}$$

The overall availability, F, is furnished by a series of eliminating processes as described earlier and is the product of the fraction absorbed, f_{abs}, and the availabilities, f, of each eliminating organ in series:

$$F = f_{abs} f_{GW} f_L f_{lung} \quad \text{(Eq. 2)}$$

where the subscripts GW and L denote the gut wall and the liver, respectively. The lung does not often serve the role of a drug eliminating organ, although it reportedly eliminates many endogenous substances (12) and some drugs (15, 16). The general impact on the first-pass effect is thus usually attributable to gut wall and hepatic elimination. However, these two processes are often not differentiated.

The purpose of this paper is to present some theoretical considerations to enable identification of each process. This purpose can be achieved by coadministration of a drug, D, and its precursor, P, by various routes of administration. The situation is simplest when the kinetics of P and D are linear, and thus clearance is dose independent. The following discussion is restricted to those occasions in which the kinetics of P and D are linear, the conversion of the precursor to the drug takes place only in the liver, and the clearance of P by the liver is greater than that by other eliminating organs. Both P and D are also assumed to be completely absorbed unchanged through the portal venous blood during intraperitoneal administration.

Hepatic Extraction—When the precursor is converted to the drug solely in the liver, the fractional conversion of P to D will be f_m regardless of the administration route of P. The drug, generated *in situ* in hepatocytes after the administration of P, may undergo further metabolism in the liver before it enters the blood. The fraction of D extracted by the liver, $ER_{(D)}$, can be expressed in terms of the available fraction $f_{L(D)}$; *i.e.*, $ER_{(D)} = 1 - f_{L(D)}$. Moreover, the drug may be eliminated by extrahepatic tissues. Therefore, after the administration of the precursor and with the assumption that the precursor is completely absorbed from the various sites of administration, the area under the blood concentration–time curve of D is given by:

$$AUC_{(D)} \text{ from } P = \frac{f_m(1 - ER_{(D)})dose_{(P)}}{TBC_{(D)}} \quad \text{(Eq. 3)}$$

where the dose of P, $dose_{(P)}$, is expressed in moles, the blood concentration of P is expressed as molar concentration, and $TBC_{(D)}$ is the intravenous systemic or total body clearance of D. The intravenous total body clearance of D can be estimated on intravenous administration of D:

$$TBC_{(D)} = \frac{dose_{(D)iv}}{AUC_{(D)iv}} \quad \text{(Eq. 4)}$$

Substitution of Eq. 4 into Eq. 3 gives the extraction ratio of D:

$$ER_{(D)} = 1 - \frac{AUC_{(D) \text{ from } P}}{AUC_{(D)iv}} \frac{dose_{(D)iv}}{f_m dose_{(P)}} \quad \text{(Eq. 5)}$$

When the value of f_m is known, the extraction ratio of D is easily evaluated from Eq. 5. The value of f_m is normally estimated from the cumulative amount of the drug in the urine divided by the dose, but this value is underestimated when the drug is further metabolized by the liver once it is formed from its precursor and is almost impossible to estimate when the secondary and tertiary metabolites are formed by several pathways. It may be estimated from the $AUC_{(D)}$ value obtained after the intraperitoneal administration of D and that from P. When complete absorption of the drug occurs, the $AUC_{(D)}$ following an intraperitoneal administration of D is given by:

$$AUC_{(D)ip} = \frac{(1 - ER_{(D)})dose_{(D)ip}}{TBC_{(D)}} \quad \text{(Eq. 6)}$$

Dividing Eq. 3 by Eq. 6 and solving the resultant equation for f_m give:

$$f_m = \frac{AUC_{(D) \text{ from } P}}{AUC_{(D)ip}} \frac{dose_{(D)ip}}{dose_{(P)}} \quad \text{(Eq. 7)}$$

An alternative method of estimating the extraction ratio of D is by comparing the areas under the curve following intraperitoneal and intravenous administration of D:

$$ER_{(D)} = 1 - \frac{AUC_{(D)ip}}{AUC_{(D)iv}} \frac{dose_{(D)iv}}{dose_{(D)ip}} \quad \text{(Eq. 8)}$$

Other combinations of *AUC* measurements may be used to check the validity of the assumptions made in deriving the equations. The following treatment can be applied to ascertain if absorption is complete and if gut wall elimination occurs for the precursor. The area under the blood concentration–time curve of the precursor after a single oral dose is:

$$AUC_{(P)po} = \frac{f_{abs(P)} f_{GW(P)} f_{L(P)} dose_{(P)po}}{TBC_{(P)}} \quad \text{(Eq. 9)}$$

The equation of the area under the curve of the precursor following intraperitoneal administration upon complete absorption of the precursor is:

$$AUC_{(P)\text{ip}} = \frac{f_{L(P)}\text{dose}_{(P)\text{ip}}}{TBC_{(P)}} \quad \text{(Eq. 10)}$$

Substitution of Eq. 10 into Eq. 9 gives:

$$f_{\text{abs}(P)}f_{GW(P)} = \frac{AUC_{(P)\text{po}}}{AUC_{(P)\text{ip}}}\frac{\text{dose}_{(P)\text{ip}}}{\text{dose}_{(P)\text{po}}} \quad \text{(Eq. 11)}$$

Complete absorption and the absence of gut wall metabolism are indicated when the areas for oral and intraperitoneal administration are equal after correcting for the doses given.

Gut Wall Elimination—By a similar procedure, the overall available fraction after gut wall elimination may be obtained by administering the drug orally and intraperitoneally. Assuming the drug given intraperitoneally is completely absorbed, then:

$$f_{\text{abs}(D)}f_{GW(D)} = \frac{AUC_{(D)\text{po}}}{AUC_{(D)\text{ip}}}\frac{\text{dose}_{(D)\text{ip}}}{\text{dose}_{(D)\text{po}}} \quad \text{(Eq. 12)}$$

However, this estimate of availability also may be obtained by administering P intravenously and D orally. The drug D formed from P is subjected only to hepatic elimination before it is ultimately detected, and Eq. 3 is applied. A comparison of the area under the curve for D after its oral administration with that obtained after administration of its precursor (correcting for differences in doses) yields the fraction available subsequent to gut wall elimination and prior to hepatic elimination:

$$f_{\text{abs}(D)}f_{GW(D)} = \frac{AUC_{(D)\text{po}}}{AUC_{(D)\text{ from }P,\text{iv}}}\frac{f_m\text{dose}_{(P)\text{iv}}}{\text{dose}_{(D)\text{po}}} \quad \text{(Eq. 13)}$$

Multiple Doses—The single-dose method to evaluate the hepatic extraction ratio of the drug can be extrapolated to steady-state situations. After chronic drug administration of D by intravenous infusion (inf) and intraperitoneal injections (ip), the steady-state drug concentration in blood, $C_{ss(D)}$, is related to the drug administration rate, R, and the intravenous total body clearance as well as the extraction ratio in the following manner:

$$C_{ss(D)\text{inf}} = \frac{R_{(D)\text{inf}}}{TBC_{(D)}} \quad \text{(Eq. 14)}$$

$$\overline{C}_{ss(D)\text{ip}} = \frac{(1 - ER_{(D)})R_{(D)\text{ip}}}{TBC_{(D)}} \quad \text{(Eq. 15)}$$

Also, with chronic administration of the precursor, the steady-state concentration of D in blood can be expressed as:

$$\overline{C}_{ss(D)\text{ from }P} = \frac{f_m(1 - ER_{(D)})R_{(P)}}{TBC_{(D)}} \quad \text{(Eq. 16)}$$

where $R_{(P)}$ is the administration rate for P in moles per unit time. The hepatic extraction ratio under steady-state conditions is evaluated as:

$$ER_{(D)} = 1 - \frac{\overline{C}_{ss(D)\text{ from }P}}{C_{ss(D)\text{inf}}}\frac{R_{(D)\text{inf}}}{f_m R_{(P)}} \quad \text{(Eq. 17)}$$

$$ER_{(D)} = 1 - \frac{\overline{C}_{ss(D)\text{ip}}}{C_{ss(D)\text{inf}}}\frac{R_{(D)\text{inf}}}{R_{(D)\text{ip}}} \quad \text{(Eq. 18)}$$

Similar relationships are seen for chronic drug administrations as for single doses. The fractions available after gut wall elimination in these instances are:

$$f_{\text{abs}(D)}f_{GW(D)} = \frac{\overline{C}_{ss(D)\text{po}}}{\overline{C}_{ss(D)\text{ from }P}}\frac{f_m R_{(P)}}{R_{(D)\text{po}}} \quad \text{(Eq. 19)}$$

and:

$$f_{\text{abs}(D)}f_{GW(D)} = \frac{\overline{C}_{ss(D)\text{po}}}{\overline{C}_{ss(D)\text{ip}}}\frac{R_{(D)\text{ip}}}{R_{(D)\text{po}}} \quad \text{(Eq. 20)}$$

The coadministration of the precursor and the drug provides a distinct advantage over the administration of the drug on two different occasions, because the day-to-day variation even within the same subject can be avoided. However, an assay that can distinguish the drug as obtained from the administration of P from that obtained from the administration of D must be available. The problem can be overcome when the precursor and the drug are labeled with different isotopes, in which case it is possible to quantitate the area under the curve for D as generated from the precursor, or from the administration of D, within the same study.

REFERENCES

(1) S. Riegelman and M. Rowland, *J. Pharmacokinet. Biopharm.*, **1**, 419 (1973).

(2) M. Rowland, *J. Pharm. Sci.*, **61**, 70 (1972).

(3) M. Gibaldi, R. N. Boyes, and S. Feldman, *ibid.*, **60**, 1338 (1971).

(4) N. Senior, *Adv. Pharm. Sci.*, **4**, 363 (1974).

(5) P. A. Harris and S. Riegelman, *J. Pharm. Sci.*, **58**, 71 (1969).

(6) M. Gibaldi and S. Feldman, *ibid.*, **58**, 1477 (1969).

(7) E. J. Pantuck, K. C. Hsiao, S. A. Kaplan, R. Kuntzman, and A. H. Conney, *J. Pharmacol. Exp. Ther.*, **191**, 45 (1974).

(8) R. M. Welch, J. Cavallito, and A. Loh, *Toxicol. Appl. Pharmacol.*, **23**, 749 (1972).

(9) R. Gingell, J. W. Bridges, and R. T. Williams, *Xenobiotica*, **1**, 143 (1971).

(10) W. J. Jusko and G. P. Lewis, *J. Pharm. Sci.*, **62**, 69 (1973).

(11) B. G. Reddy, L. R. Pohl, and G. Krishna, *Biochem. Pharmacol.*, **25**, 1119 (1976).

(12) H. O. Heinemann and A. P. Fishman, *Physiol. Rev.*, **49**, 1 (1969).

(13) M. Rowland, S. Riegelman, P. A. Harris, and S. D. Sholkoff, *J. Pharm. Sci.*, **61**, 379 (1972).

(14) F. H. Dost, *Klin. Wochenschr.*, **36**, 655 (1958).

(15) A. G. E. Wilson, F. C. P. Law, and E. Eling, *J. Pharmacol. Exp. Ther.*, **199**, 360 (1976).

(16) Y. S. Bakhe and J. R. Vane, *Physiol. Rev.*, **54**, 1007 (1974).

Pharmacokinetic Studies on Ditazole, a Novel Inhibitor of Platelet Aggregation

F. MARCUCCI ˣ, R. RIVA, R. GOMENI, G. ZAVATTINI, P. SALVA LACOMBE *, and E. MUSSINI

Received June 13, 1977, from the *Istituto di Ricerche Farmacologiche 'Mario Negri,' Via Eritrea, 62, 20157 Milan, Italy.* Accepted for publication August 10, 1977. *Present address: Department of Farmacologia y Terapeutica, Universidad Autonoma, Barcelona, Spain.

Abstract □ The distribution of ditazole in blood and tissues of rats was determined by a simple GLC technique. Ditazole, after intravenous injection in rats (20 mg/kg), entered preferentially into the brain, the liver, and the heart in decreasing order. In the epididymal adipose tissue, the drug was present only in small amounts. Ditazole disappeared from the rat organs 4 hr after the treatment. The apparent ditazole half-life in rat blood was 41 min, the volume of distribution was 2.068 liters/kg, and the body clearance was 0.0345 liter/kg/min.

Keyphrases □ Ditazole—GLC analysis, pharmacokinetic study of blood and tissue distribution in rats □ GLC—analysis, ditazole in rat blood and tissues □ Pharmacokinetics—ditazole in rats, GLC analysis □ Distribution, tissue—ditazole in rats, GLC analysis □ Platelet aggregation inhibitors—ditazole, GLC analysis, pharmacokinetic study of blood and tissue distribution in rats

Ditazole (I) is a new nonsteroidal drug selected from a series of new oxazole derivatives (1). It possesses anti-inflammatory and antipyretic peripheral analgesia activities (2) and markedly inhibits platelet aggregation (3, 4).

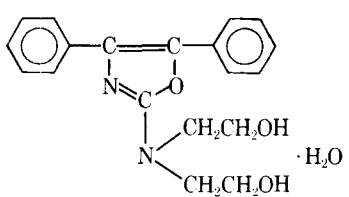

I

Some data illustrating ditazole metabolism in rats, rabbits, and humans after oral administration, using radioisotope techniques, were reported (5). Although these techniques are very sensitive, they cannot always detect whether the radioactivity found is wholly due to the administered labeled drug or to its metabolites. To overcome this limitation, a simpler and more rapid procedure for the analysis of blood and tissue ditazole levels was developed.

The GLC method described in this report was utilized for a pharmacokinetic investigation of ditazole in rats.

EXPERIMENTAL

Male Sprague–Dawley rats, 150 ± 5 g, were used.

Ditazole (20 mg/kg) in dimethyl sulfoxide–absolute ethanol–polysorbate 80[1]–water (0.2:1:2:7) was administered by intravenous injection.

Whole blood (1 ml), 1 *M* pH 7.4 phosphate buffer (2 ml), water (1 ml), and ether (10 ml) were placed in glass-stoppered centrifuge tubes. The tubes were shaken on a reciprocating shaker for 10 min and centrifuged at 4000×*g* for 10 min. The water phase was reextracted with 10 ml of ether; the combined organic phases were dried under vacuum and redissolved in a suitable volume of a solution containing the internal standard (diazepam) in acetonitrile (10 μg/ml). A 1-μl aliquot of the acetonitrile solution was mixed with 1 μl of *N,O*-bis(trimethylsilyl)trifluoroacetamide[2] in the same syringe and then injected into a chromatographic column.

The ditazole derivatization increased its GLC sensitivity by about 100-fold.

The animals were sacrificed by decapitation at various times after ditazole injection. The brain, heart, liver, and epididymal adipose tissue were rapidly removed and homogenized in ice-cold absolute ethanol (1:4 w/v). The homogenates were centrifuged at 4000×*g* for 20 min. The supernate was evaporated to dryness under vacuum, and the residue was dissolved in 5 ml of 6 *N* HCl and washed twice with 10 ml of ether. After shaking for 10 min, ethereal phases were discarded. The acidic phase was adjusted to neutral pH (7–7.5) and then reextracted twice with 10 ml of ether. The procedure with the ether extracts was identical with that described for blood extraction.

Recovery of ditazole from the tissues studied was around 80%, ranging from 75 ± 1 to 85 ± 3%.

The gas chromatograph[3] was equipped with a hydrogen flame-ionization detector. The stationary phase was 3% OV-17 on 100-120-mesh Gas Chrom Q packed into a 1-m glass column (internal diameter 4 mm, external diameter 6 mm).

The flow rates of hydrogen and air were 15 and 300 ml/min, respectively. The carrier gas, nitrogen, was used at a flow rate of 33 ml/min. The injection port temperature was 300°, the detector temperature was 300°, and the oven temperature was 270°.

Derivatization was performed on-column by mixing 1 μl of ditazole solution in acetonitrile with 1 μl of *N,O*-bis(trimethylsilyl)trifluoroacetamide in a syringe.

For ditazole identification and determination, the internal standard technique was used. Diazepam was employed as the internal standard because of its suitable retention time (1 min and 45 sec in comparison to 2 min for ditazole).

The peak area was determined by measuring, in convenient units, the height and the width of the peak at half-height. Ditazole can be quantitated by GLC when the relative peak area is used as a concentration index since a linear relationship exists between relative peak areas and drug concentration in the 10–40-μg range.

A typical gas chromatogram showing the separation of the ditazole derivative and the internal standard is shown in Fig. 1.

The chemical structure of the ditazole silyl derivative was confirmed by GLC–mass spectrometry. A mass spectrometer[4], fitted with a 2-m × 2-mm i.d. spiral glass column packed with 3% OV-17 on 100–120-mesh Gas Chrom Q, was employed. Helium was used as the carrier gas, and all mass spectra were obtained at 70 ev. Other parameters were: injection site temperature, 300°; molecular separator temperature, 260°; ion source temperature, 290°; accelerating voltage, 3 kv; and ionizing current, 20 μamp.

For the determination of the change of spectrum produced by the binding of ditazole to hepatic cytochrome P-450, the technique described by Omura and Sato (6, 7) was used.

RESULTS AND DISCUSSION

Table I shows the disposition pattern of ditazole in blood, brain, heart, liver, and adipose tissue of rats after intravenous administration of ditazole at 20 mg/kg. The ditazole concentration reached peak values at 5 min in all tissues except adipose tissue, for which peak values were attained at 30 min. The highest values of ditazole in the brain were reached 5 min after administration. The brain level of ditazole was reduced to an unmeasurable value by 4 hr after treatment.

[1] Tween 80.

[2] Pierce Chemical Co., Rockford, Ill.

[3] Model GI, Carlo Erba, Milan, Italy.

[4] LKB model 9000.

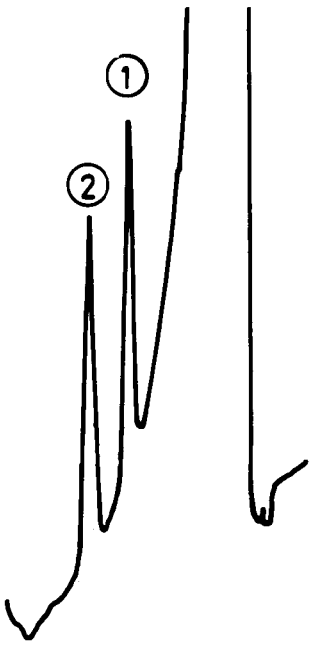

Figure 1—*Separation of the ditazole derivative (2) from the internal standard, diazepam (1).*

Ditazole also was found in high concentration in the liver 5 min after treatment; ditazole levels in the liver decreased with a slope similar to that seen in the brain. The heart levels, with a maximum at 5 min, decreased rapidly so that only small amounts were detected 1 hr after treatment.

Small amounts of ditazole were found in the adipose tissue, with a maximum of 5 μg at 30 min after administration. No measurable amounts were present after 1 hr.

The pharmacokinetic parameters of ditazole in rat blood following a 20-mg/kg iv administration were calculated using the NONLIN program (8) on a digital computer[5]. The apparent ditazole half-life in the rat blood was 41 min, its distribution volume was about 2 liters/kg, and its clearance was about 0.03 liter/kg/min. Areas under the blood ditazole concentration–time curves at time 0 and ∞ were 490 and 578 μg/ml × min, respectively.

[5] UNIVAC 1106.

Table I—Ditazole Levels[a] in the Blood, Brain, Liver, and Adipose Tissue of Rats after Administration of 20 mg/kg iv

Minutes after Ditazole Administration	Blood, μg/ml ± *SE*	Brain, μg/g ± *SE*	Heart, μg/g ± *SE*	Liver, μg/g ± *SE*	Adipose Tissue, μg/g ± *SE*
5	8.7 ± 1.0	79.7 ± 4.0	18 ± 0.2	29.6 ± 1.0	3.4 ± 0.1
30	4.9 ± 0.7	15.4 ± 1.0	10.2 ± 0.5	24.7 ± 0.7	5.0 ± 0.5
60	3.6 ± 0.7	7.6 ± 0.3	1.7 ± 0.2	7.0 ± 0.7	1.1 ± 0.1
120	1.5 ± 0.4	2.6 ± 0.1	<0.4	2.5 ± 0.3	<0.4
240	<0.4	<0.4	<0.4	<0.4	<0.4

[a] Each figure is the average of at least four determinations.

Studies on ditazole metabolism in rats after intravenous administration are lacking. Marchetti *et al.* (5) reported that ditazole elimination occurred slowly through urine and feces after oral administration; most of the drug was excreted unchanged. Among its metabolites, 4,5-diphenyl-4-oxazolin-2-one, 4,5-diphenyl-2-(2-oxyethyl)aminoxazole, and benzil were identified. Preliminary *in vitro* studies on ditazole metabolism by rat liver microsomal enzymes indicate that this drug is metabolized into two or three compounds not yet identified.

It is well known that drugs and other foreign compounds combine with hepatic cytochrome P-450 to produce difference spectra of two general types, I and II (9). With hepatic cytochrome P-450, ditazole gave a type II spectrum with λ_{max} and λ_{min} falling within the usual range.

REFERENCES

(1) E. Marchetti, G. Mattalia, and V. Rosnati, *J. Med. Chem.*, **11**, 1092 (1968).

(2) L. Caprino, F. Borrelli, and R. Falchetti, *Arzneim.-Forsch.*, **23**, 1972 (1973).

(3) *Ibid.*, **23**, 1277 (1973).

(4) G. de Gaetano, M. C. Tonolli, M. P. Bertoni, and M. C. Roncaglioni, *Haemostasis*, **6**, 127 (1977).

(5) E. Marchetti, G. Mattalia, and G. Bergesi, *Arzneim.-Forsch.*, **23**, 1291 (1973).

(6) T. Omura and R. Sato, *J. Biol. Chem.*, **239**, 2370 (1964).

(7) *Ibid.*, **239**, 2379 (1964).

(8) C. M. Metzler, "A User's Manual for NONLIN," Tech. Rep. 7292/69/7292/005, The Upjohn Co., Kalamazoo, Mich., Nov. 25, 1969.

(9) B. N. La Du, M. C. Mandel, and E. L. Way, "Fundamentals of Drug Metabolism and Drug Disposition," Williams & Wilkins, Baltimore, Md., 1971, p. 206.

Electronic Structure–Activity Relationships of Antibacterial Acridines

P. SINGH and S. P. GUPTA ˣ

Received June 9, 1977, from the *Department of Chemistry, Birla Institute of Technology and Science, Pilani 333031, India.* Accepted for publication August 3, 1977.

Abstract □ The antibacterial activity of a series of amino- and fluorinated acridines was studied in the framework of their electronic structures. To calculate the electronic structure, a simple Hückel molecular orbital theory was used. A statistical regression analysis revealed linear correlations between the activity and the electronic indexes, particularly the electron density at the ring nitrogen.

Keyphrases □ Acridines, various—antibacterial activity related to electronic structure □ Antibacterial activity—various acridines, related to electronic structure □ Electronic structure—various acridines, related to antibacterial activity □ Structure–activity relationships—various acridines, antibacterial activity related to electronic structure

The antibacterial activity of acridines has been found to be proportional to the fraction ionized as the cation (1–3). The simplest interpretation of the mode of action of acridine cations is that they compete with hydrogen ions for a vitally important anionic group on the bacterium (4). The vital activity of the vulnerable anionic group (A^-) of the bacterium is supposed to be reduced by the formation of a feebly dissociated complex (ABH) with the cation

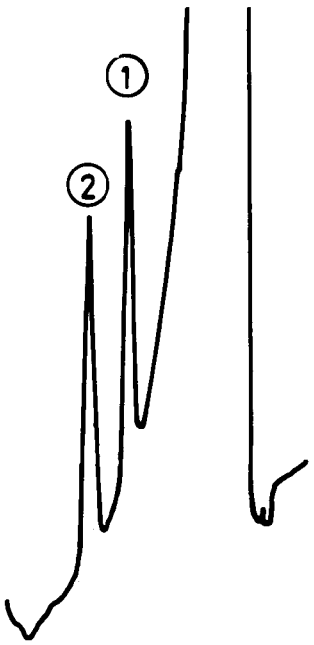

Figure 1—*Separation of the ditazole derivative (2) from the internal standard, diazepam (1).*

Ditazole also was found in high concentration in the liver 5 min after treatment; ditazole levels in the liver decreased with a slope similar to that seen in the brain. The heart levels, with a maximum at 5 min, decreased rapidly so that only small amounts were detected 1 hr after treatment.

Small amounts of ditazole were found in the adipose tissue, with a maximum of 5 μg at 30 min after administration. No measurable amounts were present after 1 hr.

The pharmacokinetic parameters of ditazole in rat blood following a 20-mg/kg iv administration were calculated using the NONLIN program (8) on a digital computer[5]. The apparent ditazole half-life in the rat blood was 41 min, its distribution volume was about 2 liters/kg, and its clearance was about 0.03 liter/kg/min. Areas under the blood ditazole concentration–time curves at time 0 and ∞ were 490 and 578 μg/ml × min, respectively.

[5] UNIVAC 1106.

Table I—Ditazole Levels[a] in the Blood, Brain, Liver, and Adipose Tissue of Rats after Administration of 20 mg/kg iv

Minutes after Ditazole Administration	Blood, μg/ml ± *SE*	Brain, μg/g ± *SE*	Heart, μg/g ± *SE*	Liver, μg/g ± *SE*	Adipose Tissue, μg/g ± *SE*
5	8.7 ± 1.0	79.7 ± 4.0	18 ± 0.2	29.6 ± 1.0	3.4 ± 0.1
30	4.9 ± 0.7	15.4 ± 1.0	10.2 ± 0.5	24.7 ± 0.7	5.0 ± 0.5
60	3.6 ± 0.7	7.6 ± 0.3	1.7 ± 0.2	7.0 ± 0.7	1.1 ± 0.1
120	1.5 ± 0.4	2.6 ± 0.1	<0.4	2.5 ± 0.3	<0.4
240	<0.4	<0.4	<0.4	<0.4	<0.4

[a] Each figure is the average of at least four determinations.

Studies on ditazole metabolism in rats after intravenous administration are lacking. Marchetti *et al.* (5) reported that ditazole elimination occurred slowly through urine and feces after oral administration; most of the drug was excreted unchanged. Among its metabolites, 4,5-diphenyl-4-oxazolin-2-one, 4,5-diphenyl-2-(2-oxyethyl)aminoxazole, and benzil were identified. Preliminary *in vitro* studies on ditazole metabolism by rat liver microsomal enzymes indicate that this drug is metabolized into two or three compounds not yet identified.

It is well known that drugs and other foreign compounds combine with hepatic cytochrome P-450 to produce difference spectra of two general types, I and II (9). With hepatic cytochrome P-450, ditazole gave a type II spectrum with λ_{max} and λ_{min} falling within the usual range.

REFERENCES

(1) E. Marchetti, G. Mattalia, and V. Rosnati, *J. Med. Chem.*, **11**, 1092 (1968).

(2) L. Caprino, F. Borrelli, and R. Falchetti, *Arzneim.-Forsch.*, **23**, 1972 (1973).

(3) *Ibid.*, **23**, 1277 (1973).

(4) G. de Gaetano, M. C. Tonolli, M. P. Bertoni, and M. C. Roncaglioni, *Haemostasis*, **6**, 127 (1977).

(5) E. Marchetti, G. Mattalia, and G. Bergesi, *Arzneim.-Forsch.*, **23**, 1291 (1973).

(6) T. Omura and R. Sato, *J. Biol. Chem.*, **239**, 2370 (1964).

(7) *Ibid.*, **239**, 2379 (1964).

(8) C. M. Metzler, "A User's Manual for NONLIN," Tech. Rep. 7292/69/7292/005, The Upjohn Co., Kalamazoo, Mich., Nov. 25, 1969.

(9) B. N. La Du, M. C. Mandel, and E. L. Way, "Fundamentals of Drug Metabolism and Drug Disposition," Williams & Wilkins, Baltimore, Md., 1971, p. 206.

Electronic Structure–Activity Relationships of Antibacterial Acridines

P. SINGH and S. P. GUPTA ˣ

Received June 9, 1977, from the *Department of Chemistry, Birla Institute of Technology and Science, Pilani 333031, India.* Accepted for publication August 3, 1977.

Abstract □ The antibacterial activity of a series of amino- and fluorinated acridines was studied in the framework of their electronic structures. To calculate the electronic structure, a simple Hückel molecular orbital theory was used. A statistical regression analysis revealed linear correlations between the activity and the electronic indexes, particularly the electron density at the ring nitrogen.

Keyphrases □ Acridines, various—antibacterial activity related to electronic structure □ Antibacterial activity—various acridines, related to electronic structure □ Electronic structure—various acridines, related to antibacterial activity □ Structure–activity relationships—various acridines, antibacterial activity related to electronic structure

The antibacterial activity of acridines has been found to be proportional to the fraction ionized as the cation (1–3). The simplest interpretation of the mode of action of acridine cations is that they compete with hydrogen ions for a vitally important anionic group on the bacterium (4). The vital activity of the vulnerable anionic group (A^-) of the bacterium is supposed to be reduced by the formation of a feebly dissociated complex (ABH) with the cation

Table I—Electronic Parameters for Regression Analysis and Observed and Calculated Antibacterial Activity of Aminoacridines

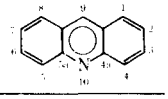

Substituent	q_N	q_{4a}	q_{5a}	log 1/C Obs. (3)	log 1/C Calc. (Eq. 7)	log 1/C Calc. (Eq. 4)	$\Delta E_{\pi b}$	log 1/C Calc. (Eq. 10)
4-Amino	1.234	0.966	0.961	3.699	3.884	4.012	2.537	3.968
2-Amino	1.239	0.964	0.961	4.000	4.047	4.119	2.543	4.089
3-Amino	1.256	0.957	0.958	4.903	4.490	4.485	2.562	4.475
9-Amino	1.294	0.959	0.959	5.204	5.216	5.301	2.604	5.328
4,5-Diamino	1.224	0.970	0.970	<3.699	3.913	3.797	2.531	3.846
2,7-Diamino	1.236	0.968	0.968	4.301	4.135	4.055	2.542	4.069
3,7-Diamino	1.253	0.961	0.965	5.204	4.578	4.420	2.560	4.435
3,6-Diamino	1.270	0.958	0.958	5.204	4.734	4.785	2.576	4.759
3,9-Diamino	1.305	0.960	0.960	5.204	5.441	5.537	2.615	5.551
4-Amino-5-methyl	1.232	0.967	0.963	<3.699	3.891	3.969	2.536	3.947
2-Amino-9-methyl	1.248	0.965	0.962	4.301	4.232	4.313	2.555	4.333
9-Amino-2-methyl	1.293	0.960	0.960	5.204	5.204	5.279	2.603	5.308
9-Amino-3-methyl	1.296	0.959	0.959	5.204	5.256	5.344	2.606	5.368
9-Amino-4-methyl	1.291	0.948	0.958	5.505	5.471	5.236	2.600	5.247
9-Amino-3-chloro	1.289	0.960	0.959	5.204	5.085	5.193	2.599	5.226
9-Amino-2-chloro	1.295	0.954	0.958	5.204	5.357	5.322	2.602	5.287
9-Amino-4-chloro	1.297	0.948	0.958	5.204	5.589	5.365	2.602	5.287
2-Amino-6-chloro	1.234	0.957	0.958	<3.699	4.055	4.012	2.538	3.988
3-Amino-9-chloro	1.234	0.964	0.963	<3.699	4.027	4.012	2.541	4.049
3-Amino-6-chloro	1.251	0.959	0.958	4.602	4.327	4.377	2.557	4.374

(BH^+) of the drug. The more feebly the complex is dissociated into A^- and BH^+ ions, the greater is the reduction in the vital activity of the anion. The dissociation of the complex is suppressed only when the cation (BH^+) is present in excess. Therefore, the activity of the drug (B) depends on its degree of cationization as BH^+.

BACKGROUND

Since the cationization of the acridines largely depends on the electron density of their ring nitrogen, q_N (the greater the q_N, the more the attraction for protons), it is expected that a correlation must exist between their antibacterial activity and q_N. The electron density is calculated by using a simple Hückel molecular orbital (HMO) method.

In the HMO method, the coulomb integral for a heteroatom x, α_x, is defined as:

$$\alpha_x = \alpha_0 + h_x\beta_0 \qquad \text{(Eq. 1)}$$

and the resonance integral for a bonded pair of carbon and heteroatom, β_{cx}, is defined as:

$$\beta_{cx} = k_{cx}\beta_0 \qquad \text{(Eq. 2)}$$

where α_0 and β_0 are the standard coulomb and resonance integrals for the carbon atom and the carbon–carbon bond, respectively; and h_x and k_{cx} are the semiempirical parameters under discussion. The values of these parameters for the present purpose have been taken from the literature (5).

If some heteroatoms were adjacent to a carbon atom, the coulomb integral for that carbon atom was taken as:

$$\alpha_c = \alpha_0 + 0.1 \sum_x^{adj} h_x\beta_0 \qquad \text{(Eq. 3)}$$

Equation 3 takes into account the inductive effect produced on the carbon atom by heteroatoms (6). The methyl group was treated as a hyperconjugation model.

The molecular orbital techniques have been successfully utilized in drug research (7). Like several physicochemical parameters, such as hydrophobicity, partition coefficients, and polarizability (8–13), many molecular orbital indexes (*e.g.*, charge density, free valence, delocalization energy, and energies of the highest occupied and lowest unoccupied molecular orbitals) have been found (7, 14–17) to be well correlated with biological responses of organic compounds. Recently, a new molecular parameter, known as molecular connectivity, was shown (18–23) to possess significant correlations with many physical properties and biological activities of compounds. The molecular connectivity index, χ (24), signifies the degree of branching or connectivity in a molecule.

RESULTS AND DISCUSSION

Table I gives the calculated electron densities at the ring nitrogen and the two neighboring carbon atoms (4a and 5a) of the bridges as well as the antibacterial activity for a series of aminoacridines. Similarly, Table II gives the same values for a series of fluorinated acridines. In Table I, log 1/C [C is the minimal bacteriostatic concentration (3) for *Streptococcus pyogenes* after 48 hr of incubation in 10% serum broth at 37° and pH 7.3], as expected, appears to be linearly correlated with q_N. Likewise, the mean K.D. time[1], t, in Table II appears to be proportional to q_N. A regression analysis (25) reveals the following three equations relating biological responses with q_N:

$$\log 1/C = 21.48q_N - 22.478$$
$$n = 20 \quad r = 0.896 \quad s = 0.309 \quad F^1_{18} = 73.30 \qquad \text{(Eq. 4)}$$

$$t_1 = 142.8q_N - 168.23$$
$$n = 33 \quad r = 0.605 \quad s = 1.419 \quad F^1_{31} = 17.91 \qquad \text{(Eq. 5)}$$

$$t_2 = 158.0q_N - 185.64$$
$$n = 33 \quad r = 0.551 \quad s = 1.806 \quad F^1_{31} = 13.55 \qquad \text{(Eq. 6)}$$

The statistical parameters, r, s, and F (F ratio between the variances of the calculated and observed activities) show that correlation between q_N and log 1/C is highly significant. In Eq. 4, F is highly significant at the 99% level [F^1_{18} (0.01) = 8.28]. In Eqs. 5 and 6, F also is significant at the 99% level [F^1_{31} (0.01) = 7.53] but not as highly as in Eq. 4. In the latter two equations, the correlation coefficient is also comparatively low (the correlation between log t and q_N was still less significant). The calculated values of activity from these equations are listed in the respective tables. There is good agreement between the calculated and observed values.

With acridines, q_N appears to be most important. The inclusion of q_{4a} and q_{5a}, the electron densities at the nearest neighbors of nitrogen that might affect the degree of cationization, in the regression analysis makes no significant improvement in the correlation in any case (compare the statistical parameters of Eqs. 7–9 with those of Eqs. 4–6, respectively, and the results obtained with them):

$$\log 1/C = 19.77q_N - 32.10q_{4a} + 39.42q_{5a} - 27.34$$
$$n = 20 \quad r = 0.910 \quad s = 0.305 \quad F^3_{16} = 24.34 \qquad \text{(Eq. 7)}$$

$$t_1 = 147.5q_N - 29.96q_{4a} + 14.25q_{5a} - 158.72$$
$$n = 33 \quad r = 0.638 \quad s = 1.42 \quad F^3_{29} = 6.11 \qquad \text{(Eq. 8)}$$

$$t_2 = 159.9q_N - 32.20q_{4a} + 9.66q_{5a} - 166.10$$
$$n = 33 \quad r = 0.585 \quad s = 1.82 \quad F^3_{29} = 4.69 \qquad \text{(Eq. 9)}$$

With aminoacridines, one more independent electronic index, delocalization energy, can be correlated with the activity. Since the amino-

[1] K.D. time stands for knockdown time of cockroaches after injecting the compound.

Table II—Electronic Parameters for Regression Analysis and Observed and Calculated Antibacterial Activity of Fluorinated Acridines

Substituent	q_N	q_{4a}	q_{5a}	Mean K.D. Time, t_1 (hr), 0.5% Concentration			Mean K.D. Time, t_2 (hr), 0.1% Concentration		
				Obs. (26)[a]	Calc. (Eq. 5)	Calc. (Eq. 8)	Obs. (26)	Calc. (Eq. 6)	Calc. (Eq. 9)
5-Chloro-3-fluoro	1.240	0.957	0.946	11.00	8.75	8.84	13.00	10.13	10.28
5-Chloro-8-fluoro	1.242	0.956	0.946	10.50	9.03	9.17	12.00	10.45	10.63
5-Chloro-6-fluoro	1.241	0.955	0.947	10.00	8.89	9.06	12.00	10.29	10.51
5-Chloro-3,6-difluoro	1.234	0.956	0.947	9.00	7.89	8.00	10.00	9.18	9.36
5-Chloro-3,8-difluoro	1.236	0.957	0.946	10.00	8.17	8.25	12.50	9.50	9.64
5-Amino-3-fluoro	1.227	0.963	0.966	9.50	6.89	7.03	10.75	8.08	8.20
5-Amino-8-fluoro	1.228	0.962	0.966	9.00	7.03	7.20	10.50	8.24	8.39
5-Amino-6-fluoro	1.227	0.961	0.966	8.50	6.89	7.09	9.50	8.08	8.26
5-Amino-3,6-difluoro	1.220	0.963	0.966	7.00	5.89	6.00	9.00	6.97	7.08
5-Amino-3,8-difluoro	1.222	0.963	0.965	7.50	6.18	6.28	9.50	7.29	7.39
3-Fluoro-5-phenoxy	1.232	0.960	0.958	8.00	7.60	7.74	9.00	8.87	9.02
8-Fluoro-5-phenoxy	1.234	0.960	0.958	8.00	7.89	8.04	9.50	9.18	9.34
6-Fluoro-5-phenoxy	1.232	0.959	0.959	7.00	7.60	7.79	8.00	8.87	9.06
3,6-Difluoro-5-phenoxy	1.226	0.959	0.958	7.00	6.75	6.89	8.50	7.92	8.09
3,8-Difluoro-5-phenoxy	1.227	0.961	0.958	6.50	6.89	6.97	8.00	8.08	8.19
3-Fluoro-5-*p*-fluorophenoxy	1.232	0.960	0.958	7.00	7.60	7.74	8.50	8.87	9.02
8-Fluoro-5-*p*-fluorophenoxy	1.230	1.050	1.031	6.50	7.32	5.79	7.50	8.55	6.51
6-Fluoro-5-*p*-fluorophenoxy	1.232	0.959	0.959	6.00	7.60	7.79	6.50	8.87	9.06
3,6-Difluoro-5-*p*-fluorophenoxy	1.226	0.960	0.959	6.50	6.75	6.87	8.50	7.92	8.07
3-Fluoro-5-phenylamino	1.228	0.963	0.963	5.75	7.03	7.13	6.50	8.24	8.33
8-Fluoro-5-phenylamino	1.229	0.962	0.964	5.50	7.17	7.32	6.50	8.39	8.53
6-Fluoro-5-phenylamino	1.227	0.975	0.953	5.50	6.89	6.48	7.00	8.08	7.69
3,6-Difluoro-5-phenylamino	1.222	0.977	0.952	5.50	6.18	5.67	5.75	7.29	6.81
3,8-Difluoro-5-phenylamino	1.223	0.963	0.963	6.00	6.32	6.40	6.25	7.45	7.53
3-Fluoro-5-*p*-fluorophenylamino	1.228	0.963	0.963	5.00	7.03	7.13	5.00	8.24	8.33
8-Fluoro-5-*p*-fluorophenylamino	1.229	0.962	0.963	4.50	7.17	7.31	5.50	8.39	8.52
6-Fluoro-5-*p*-fluorophenylamino	1.228	0.961	0.964	5.00	7.03	7.21	6.00	8.24	8.41
3,6-Difluoro-5-*p*-fluorophenylamino	1.221	0.963	0.964	5.50	6.03	6.11	5.75	7.13	7.22
3,8-Difluoro-5-*p*-fluorophenylamino	1.204	0.963	0.961	5.00	3.60	3.56	6.00	4.41	4.47
3-Fluoro-5-α-naphthylamino	1.228	0.963	0.963	8.00	7.03	7.13	9.00	8.24	8.33
8-Fluoro-5-α-naphthylamino	1.229	0.962	0.963	7.00	7.17	7.31	8.50	8.39	8.52
6-Fluoro-5-α-naphthylamino	1.245	0.976	0.943	8.00	9.46	8.97	8.50	10.92	10.44
3,6-Difluoro-5-α-naphthylamino	1.228	0.975	0.943	6.00	7.03	6.49	8.00	8.24	7.75

[a] The activity is against male and female cockroaches.

acridine cations exhibit the resonance phenomenon as shown in Scheme I, the degree of cationizations of aminoacridines depends (27) on the extra stabilization the cations gain by this resonance (delocalization). Hence, the difference in the delocalization energies of the ionized and unionized forms of aminoacridines, ΔDE, should be proportional to their activity. For the aminoacridines listed in Table I, ΔDE can be replaced by $\Delta E_{\pi b}$, the difference in the π-bond energies of their ionized and unionized forms, because all of these compounds have the same number of delocalized bonds of one kind in either form. A regression analysis reveals the following equation correlating log $1/C$ with $\Delta E_{\pi b}$:

$$\log 1/C = 20.52\ \Delta E_{\pi b} - 48.08$$
$$n = 20 \quad r = 0.897 \quad s = 0.307 \quad F_{18}^{1} = 74.42 \qquad \text{(Eq. 10)}$$

The statistical parameters of Eq. 10 are almost equal to those of Eq. 4, and the results obtained by the two equations nearly tally with each other. The reason is that a nearly perfect correlation exists between q_N and $\Delta E_{\pi b}$ (in Eq. 11, $r \cong 1$ and $s \cong 0.0$):

$$\Delta E_{\pi b} = 1.057 q_N + 1.235$$
$$n = 20 \quad r = 0.998 \quad s = 0.001 \quad F_{18}^{1} = 6299 \qquad \text{(Eq. 11)}$$

This result also shows that, from the antibacterial activity point of view, q_N is more important for acridines than the charge at any other atoms.

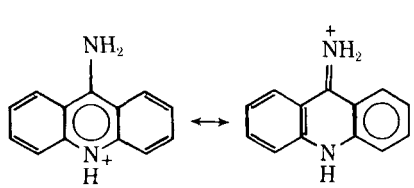

Scheme I

This electronic index can be successfully utilized to predict the antibacterial activity of any acridine before its synthesis.

REFERENCES

(1) A. Albert, S. Rubbo, and R. Goldacre, *Nature (London)*, **147**, 332 (1941).

(2) A. Albert, S. Rubbo, R. Goldacre, M. Davey, and J. Stone, *Br. J. Exp. Pathol.*, **26**, 160 (1945).

(3) A. Albert, in "Drug Design," vol. III, E. J. Ariëns, Ed., Academic, New York, N.Y., 1972.

(4) A. Albert "Selective Toxicity," Chapman and Hall, London, England, 1973.

(5) A. Streitwieser, Jr., "Molecular Orbital Theory for Organic Chemists," Wiley, New York, N.Y., 1961.

(6) K. Higasi, H. Baba, and A. Rembaum, "Quantum Organic Chemistry," Interscience, New York, N.Y., 1965, p. 148.

(7) L. B. Kier, "Molecular Orbital Theory in Drug Research," Academic, New York, N.Y., 1971.

(8) M. S. Tute, *Adv. Drug Res.*, **6**, 1 (1971).

(9) C. Hansch, in "Drug Design," vol. I, E. J. Ariëns, Ed., Academic, New York, N.Y., 1971, p. 271.

(10) L. B. Kier, *J. Pharm. Sci.*, **61**, 1394 (1972).

(11) H. D. Holtje and L. B. Kier, *J. Med. Chem.*, **17**, 814 (1974).

(12) H. D. Holtje and L. B. Kier, *J. Pharm. Sci.*, **63**, 1435 (1974).

(13) H. D. Holtje and L. B. Kier, *J. Theoret. Biol.*, **48**, 197 (1974).

(14) F. Peradejordi, A. N. Martin, and A. Cammarata, *J. Pharm. Sci.*, **60**, 577 (1971).

(15) T. K. Lin, Y. W. Chien, H. B. Desai, and P. K. Yonan, *Chem. Pharm. Bull.*, **24**, 2739 (1976).

(16) E. Mizuta, K. Nishikawa, K. Omura, and Y. Oka, *ibid.*, **24**, 2078 (1976).

(17) S. P. Gupta, S. S. Sharma, and P. Singh, *Indian J. Chem.*, **15B**, 731 (1977).
(18) L. B. Kier, L. H. Hall, W. J. Murray, and M. Randić, *J. Pharm. Sci.*, **64**, 1971 (1975).
(19) L. H. Hall, L. B. Kier, and W. J. Murray, *ibid.*, **64**, 1974 (1975).
(20) W. J. Murray, L. H. Hall, and L. B. Kier, *ibid.*, **64**, 1978 (1975).
(21) L. B. Kier, W. J. Murray, and L. H. Hall, *J. Med. Chem.*, **18**, 1272 (1975).
(22) L. B. Kier, W. J. Murray, M. Randić, and L. H. Hall, *J. Pharm. Sci.*, **65**, 1226 (1976).
(23) W. J. Murray, L. B. Kier, and L. H. Hall, *J. Med. Chem.*, **19**, 573 (1976).
(24) M. Randić, *J. Am. Chem. Soc.*, **97**, 6609 (1975).
(25) R. A. Fisher, "Statistical Methods for Research Workers," Oliver and Boyd, Edinburg, Scotland, 1970.
(26) K. C. Joshi and M. K. Tholia, *Agr. Biol. Chem.*, **38**, 1165 (1974).
(27) A. Pullman and B. Pullman, "Quantum Biochemistry," Interscience, New York, N.Y., 1963.

ACKNOWLEDGMENTS

The authors thank CSIR, New Delhi, India, for providing a Senior Research Fellowship to P. Singh.

Synthesis and Antitumor Evaluation of 4-Ethoxycarbonyl Cyclophosphamide Analogs

EMERSON L. FOSTER

Received January 7, 1977, from the *Veterans Administration Hospital, Indianapolis, IN 46202.* Accepted for publication March 31, 1977.

Abstract □ 4-Ethoxycarbonyl analogs of cyclophosphamide and its five-membered ring homolog were synthesized utilizing the cyclization method previously described. *N,N*-Bis(2-chloroethyl)-4-ethoxycarbonyl-1,3,2-oxazaphospholidin-2-amine 2-oxide demonstrated activity against L-1210 lymphoid leukemia whereas *N,N*-bis(2-chloroethyl)-4-(ethoxycarbonyl)tetrahydro-2*H*-1,3,2-oxazaphosphorin-2-amine 2-oxide did not. The oxazaphosphorin-2-amine was evaluated against human epidermoid carcinoma of the nasopharynx (cell culture). The results again were negative: $ED_{50} = 2.8 \times 10$.

Keyphrases □ Cyclophosphamide analogs—synthesized, antitumor activity evaluated □ Antitumor activity—evaluated in cyclophosphamide analogs □ Structure–activity relationships—4-ethoxycarbonyl cyclophosphamide analogs evaluated for antitumor activity

Previous studies demonstrated that cyclophosphamide is an active antitumor agent (1). The active principle responsible for significant inhibitory activity against Yashida sarcoma in rats and L-1210 leukemia in mice is 4-hydroxycyclophosphamide (1, 2). Compounds such as *N,N*-bis(2-chloroethyl) -4- ethoxycarbonyl -1,3,2- oxazaphospholidin-2-amine 2-oxide (I) and *N,N*-bis(2-chloroethyl)-4-(ethoxycarbonyl)tetrahydro -2*H*- 1,3,2-oxazaphosphorin-2-amine 2-oxide (II) were readily synthesized, as described previously (3), by reaction of *N,N*-bis(2-chloroethyl)phosphinamide dichloride (III) with DL-serine ethyl ester hydrochloride and DL-homoserine ethyl ester hydrochloride, respectively, in the presence of triethylamine (Scheme I). All products were isolated as oils. Elemental analysis data of I and II are shown in Table I. The antitumor activity of I and II was evaluated on the basis of survival[1] (Table II).

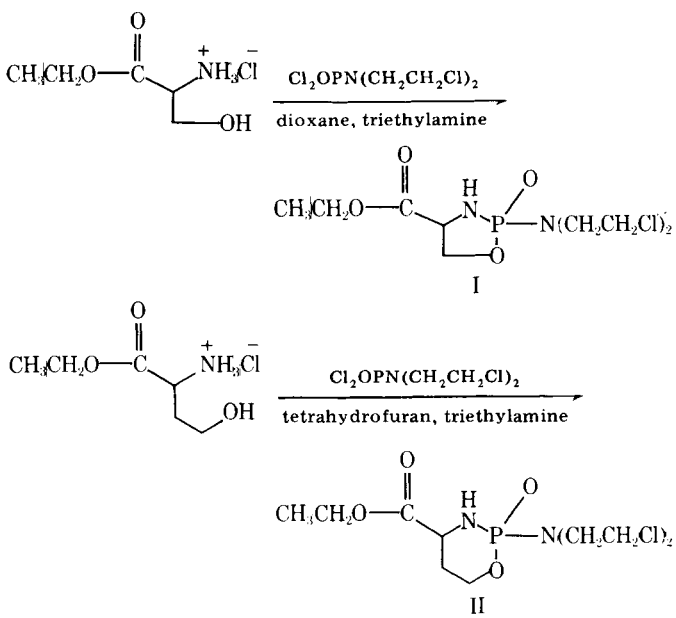

Scheme I

Table I—Physical Data for the 4-Ethoxycarbonyl Cyclophosphamide Analogs

Compound	Yield, %	Formula		Analysis, % Calc.	Found
I	35.4	$C_9H_{17}Cl_2N_2O_4P$	C	33.87	33.42
			H	5.37	5.43
			Cl	22.71	22.38
			N	8.77	8.41
			P	9.70	9.60
II	23.1	$C_{10}H_{19}Cl_2N_2O_4P$	C	36.05	36.04
			H	5.75	5.21
			Cl	21.28	21.13
			N	8.40	8.68
			P	9.29	9.45

EXPERIMENTAL[2]

Compound I—DL-Serine ethyl ester hydrochloride, 1.25 g (0.002 mole), was dissolved in warm dioxane and 4 ml (0.029 mole) of triethylamine and then added slowly to a solution of 2.43 g (0.009 mole) of III in dioxane while being stirred under a nitrogen atmosphere. The mixture was stirred overnight at room temperature.

The reaction mixture was then filtered, and the solvent was evaporated under reduced pressure. Separation on magnesium silicate[3] gave 1.5 g

[1] National Cancer Institute Drug Research and Development, National Institutes of Health, Bethesda, MD 20014.

[2] IR spectra were run on a Perkin-Elmer 247 spectrophotometer. Elemental analyses were performed by Galbraith Laboratories, Knoxville, Tenn.

[3] Florisil.

(17) S. P. Gupta, S. S. Sharma, and P. Singh, *Indian J. Chem.*, **15B**, 731 (1977).
(18) L. B. Kier, L. H. Hall, W. J. Murray, and M. Randić, *J. Pharm. Sci.*, **64**, 1971 (1975).
(19) L. H. Hall, L. B. Kier, and W. J. Murray, *ibid.*, **64**, 1974 (1975).
(20) W. J. Murray, L. H. Hall, and L. B. Kier, *ibid.*, **64**, 1978 (1975).
(21) L. B. Kier, W. J. Murray, and L. H. Hall, *J. Med. Chem.*, **18**, 1272 (1975).
(22) L. B. Kier, W. J. Murray, M. Randić, and L. H. Hall, *J. Pharm. Sci.*, **65**, 1226 (1976).
(23) W. J. Murray, L. B. Kier, and L. H. Hall, *J. Med. Chem.*, **19**, 573 (1976).
(24) M. Randić, *J. Am. Chem. Soc.*, **97**, 6609 (1975).
(25) R. A. Fisher, "Statistical Methods for Research Workers," Oliver and Boyd, Edinburg, Scotland, 1970.
(26) K. C. Joshi and M. K. Tholia, *Agr. Biol. Chem.*, **38**, 1165 (1974).
(27) A. Pullman and B. Pullman, "Quantum Biochemistry," Interscience, New York, N.Y., 1963.

ACKNOWLEDGMENTS

The authors thank CSIR, New Delhi, India, for providing a Senior Research Fellowship to P. Singh.

Synthesis and Antitumor Evaluation of 4-Ethoxycarbonyl Cyclophosphamide Analogs

EMERSON L. FOSTER

Received January 7, 1977, from the *Veterans Administration Hospital, Indianapolis, IN 46202.* Accepted for publication March 31, 1977.

Abstract □ 4-Ethoxycarbonyl analogs of cyclophosphamide and its five-membered ring homolog were synthesized utilizing the cyclization method previously described. *N,N*-Bis(2-chloroethyl)-4-ethoxycarbonyl-1,3,2-oxazaphospholidin-2-amine 2-oxide demonstrated activity against L-1210 lymphoid leukemia whereas *N,N*-bis(2-chloroethyl)-4-(ethoxycarbonyl)tetrahydro-2*H*-1,3,2-oxazaphosphorin-2-amine 2-oxide did not. The oxazaphosphorin-2-amine was evaluated against human epidermoid carcinoma of the nasopharynx (cell culture). The results again were negative: $ED_{50} = 2.8 \times 10$.

Keyphrases □ Cyclophosphamide analogs—synthesized, antitumor activity evaluated □ Antitumor activity—evaluated in cyclophosphamide analogs □ Structure–activity relationships—4-ethoxycarbonyl cyclophosphamide analogs evaluated for antitumor activity

Previous studies demonstrated that cyclophosphamide is an active antitumor agent (1). The active principle responsible for significant inhibitory activity against Yashida sarcoma in rats and L-1210 leukemia in mice is 4-hydroxycyclophosphamide (1, 2). Compounds such as *N,N*-bis(2-chloroethyl) -4- ethoxycarbonyl -1,3,2- oxazaphospholidin-2-amine 2-oxide (I) and *N,N*-bis(2-chloroethyl)-4-(ethoxycarbonyl)tetrahydro -2*H*- 1,3,2-oxazaphosphorin-2-amine 2-oxide (II) were readily synthesized, as described previously (3), by reaction of *N,N*-bis(2-chloroethyl)phosphinamide dichloride (III) with DL-serine ethyl ester hydrochloride and DL-homoserine ethyl ester hydrochloride, respectively, in the presence of triethylamine (Scheme I). All products were isolated as oils. Elemental analysis data of I and II are shown in Table I. The antitumor activity of I and II was evaluated on the basis of survival[1] (Table II).

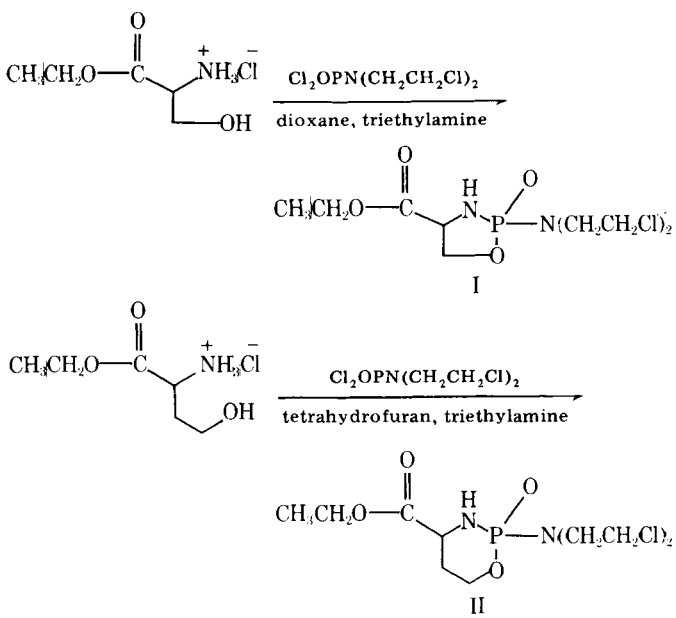

Scheme I

Table I—Physical Data for the 4-Ethoxycarbonyl Cyclophosphamide Analogs

Compound	Yield, %	Formula		Analysis, % Calc.	Found
I	35.4	$C_9H_{17}Cl_2N_2O_4P$	C	33.87	33.42
			H	5.37	5.43
			Cl	22.71	22.38
			N	8.77	8.41
			P	9.70	9.60
II	23.1	$C_{10}H_{19}Cl_2N_2O_4P$	C	36.05	36.04
			H	5.75	5.21
			Cl	21.28	21.13
			N	8.40	8.68
			P	9.29	9.45

EXPERIMENTAL[2]

Compound I—DL-Serine ethyl ester hydrochloride, 1.25 g (0.002 mole), was dissolved in warm dioxane and 4 ml (0.029 mole) of triethylamine and then added slowly to a solution of 2.43 g (0.009 mole) of III in dioxane while being stirred under a nitrogen atmosphere. The mixture was stirred overnight at room temperature.

The reaction mixture was then filtered, and the solvent was evaporated under reduced pressure. Separation on magnesium silicate[3] gave 1.5 g

[1] National Cancer Institute Drug Research and Development, National Institutes of Health, Bethesda, MD 20014.

[2] IR spectra were run on a Perkin-Elmer 247 spectrophotometer. Elemental analyses were performed by Galbraith Laboratories, Knoxville, Tenn.

[3] Florisil.

Table II—Screening Data Summary

Compound	Dose Number	Dosage, mg/kg	T/C[a], %	NSC Number
Cyclophosphamide	1	500	168	26271
	2	250	310	
	3	135	201	
	4	62.5	144	
I	1	750	129	252152
	2	500	124	
	3	330	123	
	4	250	106	
	5	220	105	
	6	62.5	99	
II	1	500	130[b]	266053
	2	500	118	
	3	500	110	
	4	333	106	
	5	333	111	
	6	250	114	
	7	222	108	
	8	222	111	
	9	62.5	108	

[a] Ratio of median survival time of tested animal to median survival time of control animals; expressed as percent. [b] Could not be confirmed.

(35.4%) of I as an oil. The product was eluted by benzene followed by methanol. It showed IR bands in mineral oil at 5.75, 7.75–8.30, 8.85–9.1, and 13.9 μm.

Compound II—Approximately 3.0 g (0.016 mole) of DL-homoserine ethyl ester hydrochloride and 4.14 g (0.016 mole) of III were suspended in tetrahydrofuran and heated. Triethylamine, 6.60 ml (0.047 mole), in tetrahydrofuran was added slowly. After addition was complete, the reaction mixture was kept overnight at room temperature.

The reaction was worked up as previously described to give 1.26 g (23.1%) of II as an oil. It showed IR bands in mineral oil at 5.75 and 13.9 μm. Other IR bands appeared but were broad and not well resolved.

RESULTS

Compounds I and II showed minimum activity relative to that demonstrated by cyclophosphamide. Generally speaking, an increase in survival of treated animals compared to control animals resulting in a test/control percent value of 125 or more is required to merit further investigation[1]. An attempt to increase the antitumor activity of cyclophosphamide by testing II against L-1210 lymphoid leukemia proved to be negative. The same can be said for I.

REFERENCES

(1) A. Takamizawa, S. Matsumato, T. Iwata, K. Katagiri, Y. Tachino, and K. Yamaguchi, *J. Am. Chem. Soc.*, **95**, 985 (1973).

(2) N. Camerman and A. Camerman, *ibid.*, **95**, 5038 (1973).

(3) E. L. Foster and R. T. Blickenstaff, *Steroids*, **24**, 737 (1974).

ACKNOWLEDGMENTS

The author thanks Dr. R. T. Blickenstaff for suggestions.

Simple and Rapid High-Pressure Liquid Chromatographic Simultaneous Determination of Aspirin, Salicylic Acid, and Salicyluric Acid in Plasma

GEOFFREY W. PENG, M. A. F. GADALLA, VICKY SMITH, ANNA PENG, and WIN L. CHIOU ˣ

Received April 14, 1977, from the *Department of Pharmacy and the Clinical Pharmacokinetics Laboratory, College of Pharmacy, University of Illinois at the Medical Center, Chicago, IL 60612.* Accepted for publication August 3, 1977.

Abstract □ A rapid and sensitive high-pressure liquid chromatographic assay was developed for aspirin, salicylic acid, and salicyluric acid in plasma. The procedure involves the solvent extraction of these compounds from plasma and separation using a reversed-phase column eluted by acidified aqueous acetonitrile. Small quantities of aspirin can be assayed directly in the presence of a large quantity of salicylic acid. The assay is also free from blank interference.

Keyphrases □ Aspirin—high-pressure liquid chromatographic analysis in plasma simultaneously with salicylic acid and salicyluric acid □ Salicylic acid—high-pressure liquid chromatographic analysis in plasma simultaneously with aspirin and salicyluric acid □ Salicyluric acid—high-pressure liquid chromatographic analysis in plasma simultaneously with aspirin and salicylic acid □ High-pressure liquid chromatography—analyses, aspirin, salicylic acid, and salicyluric acid simultaneously in plasma □ Analgesics—aspirin, salicylic acid, and salicyluric acid, simultaneous high-pressure liquid chromatographic analyses in plasma

Many procedures have been reported for quantifying salicylates in dosage forms and biological media because of the frequent and popular use of these drugs and their various pharmacological properties. The standard colorimetric (1) and fluorometric (2) determinations of aspirin and salicylic acid are not specific and measure aspirin only by difference after hydrolysis to salicylic acid. The differential spectrophotometric assay of the two salicylates based on the pH-dependent shift in their UV absorbances may require corrections because of overlap of their absorption spectra (3). Furthermore, when applied to biological samples, such as plasma, these procedures may yield high and variable blank values.

Several GLC determinations have been reported for aspirin and salicylic acid in dosage forms (4–6) and biological fluids (7–9). These methods are specific and sensitive and permit the assay of both compounds simultaneously without conversion of aspirin to salicylic acid. However, chemical derivatizations, such as silylations, are necessary to make these compounds suitable for GLC (7, 10). The chemical derivatizations are inherently time consuming (requiring up to 60 min) and can be complicated by hydrolysis of aspirin to salicylic acid (10) and multiple-product formation (ester and/or ether) for the latter (7).

TLC (11) and liquid chromatographic (12) methods for salicylates also were reported. Recently, an automated high-pressure liquid chromatographic (HPLC) analysis of aspirin, phenacetin, and caffeine in dosage forms was

Table II—Screening Data Summary

Compound	Dose Number	Dosage, mg/kg	T/C[a], %	NSC Number
Cyclophosphamide	1	500	168	26271
	2	250	310	
	3	135	201	
	4	62.5	144	
I	1	750	129	252152
	2	500	124	
	3	330	123	
	4	250	106	
	5	220	105	
	6	62.5	99	
II	1	500	130[b]	266053
	2	500	118	
	3	500	110	
	4	333	106	
	5	333	111	
	6	250	114	
	7	222	108	
	8	222	111	
	9	62.5	108	

[a] Ratio of median survival time of tested animal to median survival time of control animals; expressed as percent. [b] Could not be confirmed.

(35.4%) of I as an oil. The product was eluted by benzene followed by methanol. It showed IR bands in mineral oil at 5.75, 7.75–8.30, 8.85–9.1, and 13.9 μm.

Compound II—Approximately 3.0 g (0.016 mole) of DL-homoserine ethyl ester hydrochloride and 4.14 g (0.016 mole) of III were suspended in tetrahydrofuran and heated. Triethylamine, 6.60 ml (0.047 mole), in tetrahydrofuran was added slowly. After addition was complete, the reaction mixture was kept overnight at room temperature.

The reaction was worked up as previously described to give 1.26 g (23.1%) of II as an oil. It showed IR bands in mineral oil at 5.75 and 13.9 μm. Other IR bands appeared but were broad and not well resolved.

RESULTS

Compounds I and II showed minimum activity relative to that demonstrated by cyclophosphamide. Generally speaking, an increase in survival of treated animals compared to control animals resulting in a test/control percent value of 125 or more is required to merit further investigation[1]. An attempt to increase the antitumor activity of cyclophosphamide by testing II against L-1210 lymphoid leukemia proved to be negative. The same can be said for I.

REFERENCES

(1) A. Takamizawa, S. Matsumato, T. Iwata, K. Katagiri, Y. Tachino, and K. Yamaguchi, *J. Am. Chem. Soc.*, **95**, 985 (1973).

(2) N. Camerman and A. Camerman, *ibid.*, **95**, 5038 (1973).

(3) E. L. Foster and R. T. Blickenstaff, *Steroids*, **24**, 737 (1974).

ACKNOWLEDGMENTS

The author thanks Dr. R. T. Blickenstaff for suggestions.

Simple and Rapid High-Pressure Liquid Chromatographic Simultaneous Determination of Aspirin, Salicylic Acid, and Salicyluric Acid in Plasma

GEOFFREY W. PENG, M. A. F. GADALLA, VICKY SMITH, ANNA PENG, and WIN L. CHIOU ˣ

Received April 14, 1977, from the *Department of Pharmacy and the Clinical Pharmacokinetics Laboratory, College of Pharmacy, University of Illinois at the Medical Center, Chicago, IL 60612.* Accepted for publication August 3, 1977.

Abstract □ A rapid and sensitive high-pressure liquid chromatographic assay was developed for aspirin, salicylic acid, and salicyluric acid in plasma. The procedure involves the solvent extraction of these compounds from plasma and separation using a reversed-phase column eluted by acidified aqueous acetonitrile. Small quantities of aspirin can be assayed directly in the presence of a large quantity of salicylic acid. The assay is also free from blank interference.

Keyphrases □ Aspirin—high-pressure liquid chromatographic analysis in plasma simultaneously with salicylic acid and salicyluric acid □ Salicylic acid—high-pressure liquid chromatographic analysis in plasma simultaneously with aspirin and salicyluric acid □ Salicyluric acid—high-pressure liquid chromatographic analysis in plasma simultaneously with aspirin and salicylic acid □ High-pressure liquid chromatography—analyses, aspirin, salicylic acid, and salicyluric acid simultaneously in plasma □ Analgesics—aspirin, salicylic acid, and salicyluric acid, simultaneous high-pressure liquid chromatographic analyses in plasma

Many procedures have been reported for quantifying salicylates in dosage forms and biological media because of the frequent and popular use of these drugs and their various pharmacological properties. The standard colorimetric (1) and fluorometric (2) determinations of aspirin and salicylic acid are not specific and measure aspirin only by difference after hydrolysis to salicylic acid. The differential spectrophotometric assay of the two salicylates based on the pH-dependent shift in their UV absorbances may require corrections because of overlap of their absorption spectra (3). Furthermore, when applied to biological samples, such as plasma, these procedures may yield high and variable blank values.

Several GLC determinations have been reported for aspirin and salicylic acid in dosage forms (4–6) and biological fluids (7–9). These methods are specific and sensitive and permit the assay of both compounds simultaneously without conversion of aspirin to salicylic acid. However, chemical derivatizations, such as silylations, are necessary to make these compounds suitable for GLC (7, 10). The chemical derivatizations are inherently time consuming (requiring up to 60 min) and can be complicated by hydrolysis of aspirin to salicylic acid (10) and multiple-product formation (ester and/or ether) for the latter (7).

TLC (11) and liquid chromatographic (12) methods for salicylates also were reported. Recently, an automated high-pressure liquid chromatographic (HPLC) analysis of aspirin, phenacetin, and caffeine in dosage forms was

Table I—Linearity of Calibration Curves for Salicyluric Acid, Aspirin, and Salicylic Acid

Internal Standard in Plasma, μg/ml	Drug in Plasma, μg/ml	Peak Area Ratio[a]			Peak Area Ratio[a]/ Weight Ratio[b]		
		Salicyluric Acid[c,d]	Aspirin[d,e]	Salicylic Acid[d,f]	Salicyluric Acid	Aspirin	Salicylic Acid
5.0	0.5	0.156	0.119	0.186	1.56	1.19	1.86
5.0	2.0	0.614	0.412	0.668	1.54	1.03	1.72
5.0	5.0	1.56	1.065	1.721	1.56	1.07	1.72
5.0	10.0	3.03	2.16	3.53	1.52	1.08	1.77
160.0	50.0	0.495	0.355	0.611	1.58	1.14	1.96
160.0	100.0	0.971	0.689	1.11	1.55	1.10	1.78
160.0	200.0	2.00	1.42	2.31	1.60	1.14	1.85
160.0	300.0	3.00	2.15	3.68	1.60	1.15	1.96
				Average	1.56	1.11	1.83
				SD	0.041	0.074	0.097

[a] Area of drug/area of internal standard. [b] Weight of drug/weight of internal standard. [c] Linear regression line: $y = 0.320x - 0.144$, $r = 1.000$. [d] For linear regression analysis, the peak area ratios obtained using the 160-μg/ml internal standard were corrected to an internal standard concentration of 5 μg/ml by a factor of 32. [e] Linear regression line: $y = 0.229x - 0.141$, $r = 0.9999$. [f] Linear regression line: $y = 0.386x - 0.524$, $r = 0.9992$.

reported (13). This paper describes a simple and fast HPLC method for the simultaneous determination of salicylic acid, aspirin, and salicyluric acid in plasma, using only small quantities of samples.

EXPERIMENTAL

Reagents—Benzene[1], ethyl acetate[1], acetonitrile[2], phosphoric acid[1], phthalic acid[1], aspirin USP[3], salicylic acid USP[4], and salicyluric acid[5] were used.

Apparatus—A high-pressure liquid chromatograph, equipped with a column oven[6] and a valve injector[7], was employed. A microparticulate reversed-phase column[8] and a variable wavelength spectrophotometer[9] were used for separation and detection. A potentiometric recorder[10] and an integrator[11] were used for chromatogram recording and quantitation of the peak areas.

Procedures—An aliquot of 0.1 ml of plasma in a 13 × 100-mm conical tube was spiked with phthalic acid (160 or 5 μg/ml as the internal standard) and acidified with 1 drop of 85% phosphoric acid. The mixture was vortexed with 0.5 ml of benzene–ethyl acetate (1:1 v/v) for 30 sec and centrifuged for 1 min at about 2000 rpm. The organic layer was aspirated into another tube, and the solvent was evaporated under a stream of air or nitrogen while the tube was placed in an ice water bath.

The residue was dissolved in 50 μl of the mobile phase, consisting of 30% (v/v) acetonitrile in diluted phosphoric acid (0.05%, pH 2.5 ± 0.1), and 45 μl of the solution was injected into the column through the injector. The mobile phase flow rate was 1 ml/min. The quantitation was achieved by monitoring the UV absorbance of the column effluent at 237 nm. The column, used for all separations, was housed in an oven maintained at 50°. The ratios of the peak areas of the sample components to those of the internal standard were used to calculate concentrations of each component, based on calibration curves prepared from spiked plasma for the individual components.

To show the applicability of the proposed method to determine concentrations of aspirin and the two metabolites after dosing, a series of plasma samples from a 4-kg albino rabbit, treated intravenously with 200 mg of aspirin in 5 ml of polyethylene glycol 400 and saline solution, was analyzed similarly.

RESULTS AND DISCUSSION

It is difficult to measure accurately small concentrations of aspirin in the presence of large concentrations of salicylic acid in the same plasma sample (14). This difficulty can be overcome by the present HPLC method. Figure 1 shows the typical chromatograms of phthalic acid, salicyluric acid, aspirin, and salicylic acid from human and rabbit plasma samples. The retention times of these compounds were 3.7, 4.6, 5.3, and 7 min, respectively.

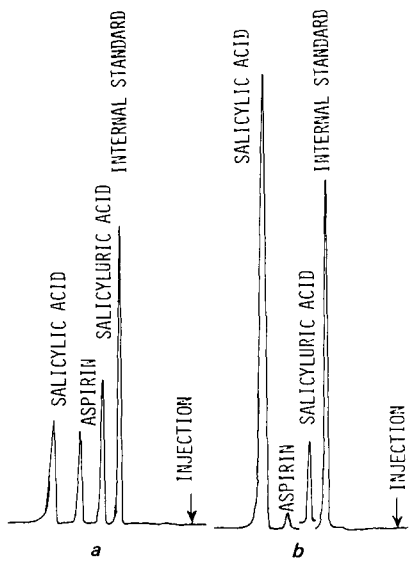

Figure 1—*Chromatograms of salicylates (5 mg %) in spiked human plasma (a) and in rabbit plasma samples at 30 min after administration of 50 mg of aspirin/kg iv (b). The salicyluric acid in* b *was recorded at 10 times greater sensitivity.*

The complete separation of the components in the chromatograms allows accurate measurements of a small quantity of aspirin or salicyluric acid in the presence of a large quantity of salicylic acid. The column separations were carried out at an elevated temperature to shorten the retention times and to increase the resolution. The chromatograms of human and rabbit plasma blanks showed no peaks that would interfere with the assay. The blank value was essentially zero by this method as compared to the high and variable blank values by spectrophotometric and fluorometric methods (7).

Table I illustrates the linearity of the calibration curves for aspirin, salicylic acid, and salicyluric acid in plasma in concentrations ranging from 0.5 to 300 μg/ml. The corrected response factors (peak area ratio/weight ratio) were fairly constant for the salicylates at all concentrations studied, indicating good linearity. Two concentrations of internal stan-

Table II—Assay Precision and Reproducibility

Compound	Concentration in Plasma, μg/ml	*n*	Concentration Found, μg/ml		*CV*, %
			Mean ± *SD*	Range	
Salicyluric acid	50.0	10	50.27 ± 0.93	49.02–51.96	1.85
	200.0	6	200.7 ± 6.69	196.08–203.73	3.33
Aspirin	50.0	10	49.98 ± 0.64	47.62–52.34	1.28
	200.0	6	201.36 ± 6.38	191.84–209.52	3.17
Salicylic acid	100.00	2	98.69 ± 1.86	97.37–100.00	1.88
	200.00	6	201.32 ± 7.70	190.35–210.52	3.82

[1] Fisher Scientific Co., Fair Lawn, N.J.
[2] Burdick & Jackson Laboratories, Muskegan, Mich.
[3] J.T. Baker Chemical Co., Phillipsburg, N.J.
[4] Merck & Co., West Point, Pa.
[5] Fox Chemical Co., Los Angeles, Calif.
[6] Model 601, Perkin-Elmer Corp., Norwalk, Conn.
[7] Glenco Scientific, Houston, Tex.
[8] μBondapak C_{18}, Waters Associates, Milford, Mass.
[9] Model LC-55, Perkin-Elmer Corp.
[10] Laboratory Data Control, Riviera Beach, Fla.
[11] Minigrator, Spectra-Physics, Santa Clara, Calif.

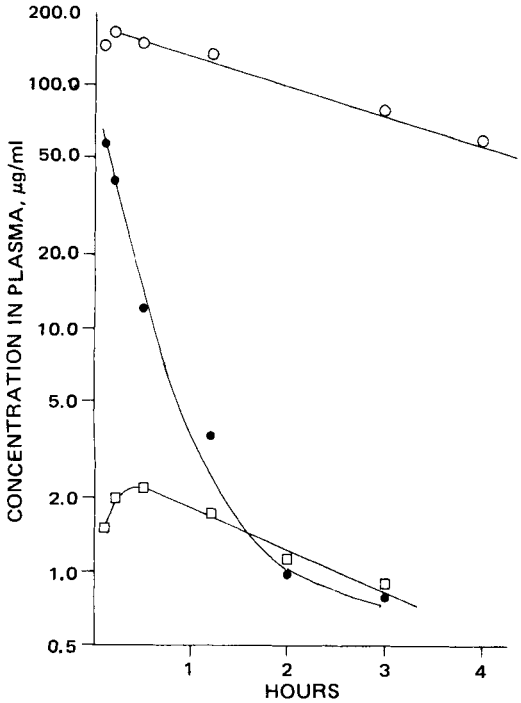

Figure 2—*Concentrations of aspirin (●), salicylic acid (○), and salicyluric acid (□) in rabbit plasma after administration of 50 mg of aspirin/kg iv.*

dard were used to improve accuracy. For least-squares linear regression analysis, the peak area ratios obtained using the 160-μg/ml internal standard were corrected to an internal standard concentration of 5 μg/ml by multiplying by a factor of 32. The assay precision and reproducibility are summarized in Table II. The coefficient of variation of these results was less than 4% in all concentrations investigated.

The time course of the concentrations of salicylic acid, aspirin, and salicyluric acid in plasma of the rabbit treated with 50 mg of aspirin/kg iv is shown in Fig. 2. The aspirin concentrations declined very rapidly in the first 2 hr. The salicylic acid concentrations were very high in the plasma shortly after drug administration and declined exponentially with a half-life of 2.42 hr. The salicyluric acid levels were relatively low, and the decay curve 0.5 hr after dosing appeared to be parallel to that of salicylic acid. No special effort was made to prevent aspirin hydrolysis, so the plasma concentration–time profiles might be different when such precautions are taken (7). These results indicate the feasibility of accurate assay of a small quantity of aspirin and salicyluric acid in the presence of a large quantity of salicylic acid.

The present method employed a mixture of ethyl acetate and benzene for extraction of the drug and internal standard from the acidified plasma samples. This solvent combination gave good recovery of these compounds (about 89–94%) while yielding essentially no interference from the plasma. The other solvent, such as ether, gave better recovery of these compounds but also extracted much material from the plasma that would interfere with the assay. The acidification of the plasma samples enhanced the recovery by solvent extraction because of the acidic nature of these compounds (13).

When the ethyl acetate–benzene extracts of the plasma samples were evaporated at ambient or higher temperature, erratic results, usually underestimations, were often obtained for salicylic acid. However, the results for salicylic acid became reproducible when the evaporation was carried out at lower temperatures by cooling the tubes in an ice water bath. Therefore, the erratic results were probably due to salicylic acid loss through sublimation. Although salicylic acid sublimes at 76° (15), salicylic acid sublimation during analysis manipulation has not been reported. Aspirin, salicyluric acid, and phthalic acid did not appear to sublime.

By simple solvent extraction on small samples, this method offers high sensitivity with essentially zero blank values. The capability to separate and measure salicyluric acid should make this method applicable also for salicyluric acid (a major metabolite) assay in urine samples. With 0.1-ml plasma samples, the present HPLC method can accurately and simultaneously measure salicyluric acid, salicylic acid, and aspirin in the same sample to concentrations as low as 0.5 μg/ml. The proposed method also can be used in pharmacokinetic and/or plasma level monitoring studies of aspirin or salicylates.

REFERENCES

(1) J. R. Leonards, *Clin. Pharmacol. Ther.*, **4**, 476 (1962).

(2) P. A. Harris and S. Riegelman, *J. Pharm. Sci.*, **56**, 713 (1967).

(3) J. I. Routh, N. A. Shane, E. G. Arrendondo, and W. D. Paul, *Clin. Chem.*, **13**, 734 (1967).

(4) J. G. Nikelly, *Anal. Chem.*, **36**, 2248 (1964).

(5) J. R. Watson, P. Crescuolo, and F. Matsui, *J. Pharm. Sci.*, **60**, 454 (1971).

(6) S. Patel, J. H. Perrin, and J. J. Windheuser, *ibid.*, **61**, 1794 (1972).

(7) L. J. Walter, D. F. Biggs, and R. T. Coutts, *ibid.*, **63**, 1754 (1974).

(8) M. J. Rance, B. J. Jordan, and J. D. Nichols, *J. Pharm. Pharmacol.*, **27**, 425 (1975).

(9) B. H. Thomas, G. Solomraj, and B. B. Coldwell, *ibid.*, **25**, 201 (1973).

(10) S. Ali, *Chromatographia*, **8**, 33 (1975).

(11) J. C. Morrison and J. M. Orr, *J. Pharm. Sci.*, **55**, 936 (1966).

(12) R. L. Stevenson and C. A. Burtis, *J. Chromatogr.*, **61**, 253 (1971).

(13) P. P. Ascione and G. P. Chrekian, *J. Pharm. Sci.*, **64**, 1029 (1975).

(14) K. O'dea, J. Putter, and F. Hoffmeister, *Arzneim.-Forsch.*, **25**, 801 (1975).

(15) "The Merck Index," 8th ed., Merck & Co., Rahway, N.J., 1974, p. 930.

ACKNOWLEDGMENTS

Supported in part by Special Projects Grant PHS-05D-619-02 from the Department of Health, Education, and Welfare.

Comparison of Stationary Phases in Reversed-Phase TLC for Correlation between Structure and Biological Response of Probiotics

AKIRA FUJII *§, KENNETH E. SHORES ‡¶, JAMES H. BUSH ‡‖, RICHARD J. GARASCIA ‡, and ELTON S. COOK *x

Received March 24, 1977, from the **Division of Chemistry and Biochemistry, St. Thomas Institute, Cincinnati, OH 45206,* and the ‡*Department of Chemistry, Xavier University, Cincinnati, OH 45207.* Accepted for publication August 8, 1977. §Present address: Department of Pharmacology, Nihon University School of Dentistry at Matsudo, 870-1, Sakaecho Nishi-2, Matsudo-shi, Chiba-ken 271, Japan. ¶Present address: Celanese Polymers and Specialties Co., Louisville, Ky. ‖Present address: Department of Chemistry, University of Wyoming, Laramie, Wyo.

Abstract □ A series of C_{16}, C_{18}, and C_{20} fatty acids and their ethyl esters and alcohols were investigated as possible stationary phases in reversed-phase TLC for the correlation between structure and biological response (antistaphylococcal activity). Ten probiotics (ω-amino acids and their L-histidine dipeptides) were used as the biologically active compounds. The mobile phase was 70% acetone in water. The best correlations were obtained with hexadecanoic acid (palmitic acid) or *cis*-9,*cis*-12,*cis*-15-octadecatrienoic acid, 1-hexadecanol or *cis*-9-octadecenol, and ethyl hexadecanoate for the fatty acids, their alcohols, and their ethyl esters, respectively. Among all compounds, the following relation was obtained: fatty acids = alcohols > ethyl esters > white paraffin oil.

Keyphrases □ Fatty acids and derivatives, various—evaluated as stationary phases in reversed-phase TLC for correlation between structure and biological response of probiotics □ TLC, reversed phase—various fatty acids and derivatives evaluated as stationary phases for correlation between structure and biological response of probiotics □ Probiotics, various—ω-amino acids and derivatives, reversed-phase TLC for correlation between structure and biological response, various fatty acids and derivatives evaluated as stationary phases □ ω-Amino acids and derivatives, various—reversed-phase TLC for correlation between structure and biological response, various fatty acids and derivatives evaluated as stationary phases □ Structure–activity relationships—various fatty acids and derivatives evaluated as stationary phases in reversed-phase TLC for correlation between structure and biological response of probiotics

In recent years, there has been increased interest in reversed-phase TLC for the correlation between structure and biological response of a series of probiotics (1, 2), *N*-*n*-alkyltritylamines (3), acridylmethanesulfonanilides (4), penicillin and cephalosporins (5), bis(dichloroacetamides) and vitamin K analogs (6), testosterone esters (7), sulfonamides (8), rifamycin derivatives (9), phenols (10), steroids (11), and benzenesulfonamide pyrimidines (12). An extensive review was prepared by Biagi *et al.* (5). Stationary phases were white paraffin oil (1–4, 12) and silicone[1] (5–11) on silica gel G thin-layer plates.

Since the correlation between structure and biological response depends greatly on the correlation between the physicochemical and biological behavior of the compounds and since the partition coefficient of the compounds is one of the most important physicochemical factors, further investigation of the stationary phase in reversed-phase TLC of probiotics was initiated.

The present investigation was undertaken to improve the correlation between structure and biological response of probiotics by studying a series of C_{16}, C_{18}, and C_{20} fatty acids and their esters and alcohols as stationary phases. These stationary phases were chosen to reproduce the fatty acid components of the cell membrane.

[1] Dow-Corning 200 fluid.

Table I—Stationary Phases

IUPAC Name	Common Name	Concentration, %
Eicosanoic acid	Arachidic acid[a]	0.5 (w/v)
Ethyl eicosanoate	Ethyl arachidate	0.5 (w/v)
cis-9,*cis*-12,*cis*-15-Octadecatrienoic acid	Linolenic acid	1.0 (v/v)
cis-9,*cis*-12-Octadecadienoic acid	Linoleic acid[a]	1.0 (v/v)
cis-9-Octadecenoic acid	Oleic acid	1.0 (v/v)
Octadecanoic acid	Stearic acid	0.5 (w/v)
Ethyl *cis*-9,*cis*-12-octadecadienoate	Ethyl linoleate	1.0 (w/v)
Ethyl *cis*-9-octadecenoate	Ethyl oleate	1.0 (v/v)
Ethyl octadecanoate	Ethyl stearate	0.5 (v/v)
cis-9-Octadecenol	Oleyl alcohol	1.0 (w/v)
1-Octadecanol	1-Octadecanol	0.5 (w/v)
cis-9-Hexadecenoic acid	Palmitoleic acid	1.0 (w/v)
Hexadecanoic acid	Palmitic acid	0.5 (w/v)
Ethyl hexadecanoate	Ethyl palmitate	1.0 (w/v)
1-Hexadecanol	Cetyl alcohol	0.5 (w/v)
—	White paraffin oil	5.0 (v/v)

[a] Eastman Organic Chemicals.

EXPERIMENTAL[2]

As in the previous study (2), the reversed-phase TLC R_m values were obtained by the method described by Boyce and Milborrow (3) using silica gel G TLC plates[3] (10 × 20 cm) coated with a 250-μm layer of silica gel G. After activation at 105° for 10 min, the plates were impregnated by allowing a reversed-phase compound solution in ether, except white paraffin oil which was dissolved in hexane, to cover the plate; the solvent was then evaporated at 40°. White paraffin oil, used previously (1, 2), served as the positive control. The other phases and the concentrations are summarized in Table I.

ω-Amino acids (glycine, β-alanine, γ-aminobutyric acid, δ-aminovaleric acid, and ε-aminohexanoic acid) and ω-aminoacyl-L-histidines (glycyl-L-histidine, β-alanyl-L-histidine, γ-aminobutyryl-L-histidine, δ-aminovaleryl-L-histidine, and ε-aminohexanoyl-L-histidine), which possess antistaphylococcal (probiotic) activity (13), were used as biologically active compounds. Biological response, defined as percent protection against mortality from staphylococcal infections in mice, was previously reported (13). L-Alanine was used as a control for reversed-phase TLC.

Solutions containing 1% of the compounds in 10% (v/v) 2-propanol were spotted and then developed[4] with 70% acetone in water (v/v), previously determined to be optimal (2). The spots were located by the ninhydrin reaction. The R_m values were calculated from:

$$R_m = \log(1/R_f - 1) \qquad \text{(Eq. 1)}$$

The R_m values were correlated with the biological response to the probiotics by computer[5] regression analysis. The program[6] was used to obtain least-squares fits for the data in first-, second-, and third-order

[2] Solvents and chemicals, except where indicated, were purchased from Fisher Scientific and Matheson, Coleman and Bell.
[3] Analtech, Inc.
[4] Polyethylene chamber, Analtech, Inc.
[5] IBM.
[6] Developed by the Statistics Department of Pennsylvania State University.

Table II—Regression Analysis (Antistaphylococcal Activity, Y) = $aX + b$ ($X = R_m$)

Compound	a	b	n	r	s
Hexadecanoic acid	77.6	30.0	10	0.944	9.19
cis-9-Hexadecenoic acid	83.5	11.3	10	0.909	11.60
Octadecanoic acid	67.9	40.7	10	0.854	14.50
cis-9-Octadecenoic acid	73.6	25.2	10	0.940	9.50
cis-9,*cis*-12-Octadecadienoic acid	70.6	38.2	10	0.929	10.30
cis-9,*cis*-12,*cis*-15-Octadecatrienoic acid	78.9	5.8	10	0.945	9.12
Eicosanoic acid	78.7	27.4	10	0.877	10.10
Ethyl hexadecanoate	107.0	19.7	10	0.929	10.30
Ethyl octadecanoate	109.0	10.2	10	0.921	10.90
Ethyl *cis*-9-octadecenoate	99.6	5.8	10	0.920	10.90
Ethyl *cis*-9,*cis*-12-octadecadienoate	98.0	−5.8	10	0.918	11.10
Ethyl eicosanoate	199.0	−11.8	10	0.880	13.20
1-Hexadecanol	109.0	14.7	10	0.933	10.00
1-Octadecanol	108.0	4.4	10	0.930	10.30
cis-9-Octadecenol	97.7	13.7	10	0.933	10.10
White paraffin oil	92.7	23.0	10	0.913	11.40

Table III—(Antistaphylococcal Activity, Y) = $aX^2 + bX + c$ ($X = R_m$)

Compound	a	b	c	n	r	s
Hexadecanoic acid	−18.6	87.4	30.4	10	0.845	9.70
cis-9-Hexadecenoic acid	8.1	76.6	12.2	10	0.893	12.40
Octadecanoic acid	−100.0	91.3	49.2	10	0.705	14.90
cis-9-Octadecenoic acid	−8.7	79.4	25.2	10	0.877	10.10
cis-9,*cis*-12-Octadecadienoic acid	8.1	68.9	37.4	10	0.624	11.00
cis-9,*cis*-12,*cis*-15-Octadecatrienoic acid	21.1	72.0	33.0	10	0.758	9.52
Eicosanoic acid	−17.3	88.4	27.5	10	0.861	10.70
Ethyl hexadecanoate	−4.2	109.0	19.6	10	0.885	11.00
Ethyl octadecanoate	−112.0	193.0	0.4	10	0.884	11.00
Ethyl *cis*-9-octadecenoate	41.8	65.9	10.3	10	0.911	11.40
Ethyl *cis*-9,*cis*-12-octadecadienoate	49.9	46.8	4.2	10	0.918	11.50
Ethyl eicosanoate	194.0	84.9	2.4	10	0.882	14.00
1-Hexadecanol	29.2	91.5	15.9	10	0.904	10.60
1-Octadecanol	30.2	84.0	7.7	10	0.917	10.90
cis-9-Octadecenol	14.0	88.3	14.5	10	0.900	10.70
White paraffin oil	12.9	86.4	23.0	10	0.838	12.20

Table IV—(Antistaphylococcal Activity, Y) = $aX^3 + bX^2 + cX + d$ ($X = R_m$)

Compound	a	b	c	d	n	r	s
Hexadecanoic acid	225.0	−159.0	81.7	33.8	10	0.866	9.59
cis-9-Hexadecenoic acid	599.0	−671.0	266.0	2.7	10	0.883	11.20
Octadecanoic acid	515.0	−194.0	34.7	47.8	10	0.851	14.70
cis-9-Octadecenoic acid	235.0	−212.0	99.5	99.5	10	0.871	9.44
cis-9,*cis*-12-Octadecadienoic acid	310.0	−56.4	19.1	40.2	10	0.926	10.30
cis-9,*cis*-12,*cis*-15-Octadecatrienoic acid	22.7	14.0	68.7	33.3	10	0.892	10.20
Eicosanoic acid	397.0	−290.0	96.6	32.6	10	0.869	9.76
Ethyl hexadecanoate	562.0	−382.0	148.0	22.1	10	0.871	11.30
Ethyl octadecanoate	973.0	−1080.0	450.0	−17.3	10	0.858	10.80
Ethyl *cis*-9-octadecenoate	195.0	−165.0	119.0	8.7	10	0.891	12.20
Ethyl *cis*-9-,*cis*-12-octadecadienate	91.7	−81.7	100.0	−1.1	10	0.900	12.40
Ethyl eicosanoate	0.0	194.0	84.9	2.4	10	0.882	14.00
1-Hexadecanol	340.0	−232.0	129.0	17.1	10	0.883	11.20
1-Octadecanol	292.0	−280.0	169.0	3.0	10	0.894	11.50
cis-9-Octadecenol	132.0	−102.0	108.0	15.0	10	0.874	11.50
White paraffin oil	−258.0	166.0	87.2	19.1	10	0.825	12.90

correlations in regression equations. The correlation coefficients and standard deviations of the regression equations also were determined.

RESULTS AND DISCUSSION

Tables II, III, and IV summarize the first-, second-, and third-order regression equations, respectively [where Y is biological response (antistaphylococcal activity), X is the R_m value, n is the number of points used (*i.e.*, number of compounds), r is the correlation coefficient, and s is the standard deviation of the regression equations]. First-order equations consistently resulted in the best correlations between R_m values and antistaphylococcal activity.

Comparison among the correlations obtained with saturated C_{18} fatty acids and C_{18} unsaturated acids indicated that improvement could be accomplished by using an unsaturated stationary phase, but no trend appeared evident between the amount of unsaturation and improvement.

The alcohols, ethyl eicosanoate, *cis*-9-octadecenol, 1-octadecanol, and 1-hexadecanol, gave essentially equivalent correlations, all being better than white paraffin oil. Comparison of the alcohols and their corresponding fatty acids, although limited, suggested slight superiority of the fatty acids.

Correlations of the esters, ethyl *cis*-9,*cis*-12-octadecadienoate, ethyl *cis*-9-octadecenoate, and ethyl hexadecanoate, were improved over white paraffin oil, but the correlation of ethyl eicosanoate was not. Among the esters, the best correlation was obtained with ethyl hexadecanoate. Comparison of the correlation of C_{18} esters with each other showed that all were approximately equal, although there was a slight decrease in correlation with increased unsaturation. The results also suggested that the esters did not give as great an improvement in the correlation between biological response and R_m values as did both the fatty acids and alcohols.

Of the 15 stationary phase materials investigated, 12 resulted in an improvement of the correlation between R_m and biological response over

that previously obtained with white paraffin oil. No definite relationships appeared evident when comparisons were made of chain length, amount of unsaturation, and functional group. The greatest improvement in the correlation between biological response and R_m for all stationary phases investigated was obtained with either *cis*-9,*cis*-12,*cis*-15-octadecatrienoic acid (linoleic acid) or hexadecanoic acid (palmitic acid).

Although no definite trend resulted from comparison between the stationary phase material and improvement of correlation, the following general relationship was found between functional group and improvement of correlation: fatty acids = alcohols > ethyl esters > white paraffin oil.

REFERENCES

(1) A. Fujii and E. S. Cook, *J. Med. Chem.*, **18**, 502 (1975).

(2) A. Fujii, J. H. Bush, K. E. Shores, R. G. Johnson, R. J. Garascia, and E. S. Cook, *J. Pharm. Sci.*, **66**, 844 (1977).

(3) C. B. C. Boyce and B. V. Milborrow, *Nature*, **208**, 537 (1965).

(4) B. F. Cain, R. N. Seelye, and G. J. Atwell, *J. Med. Chem.*, **17**, 922 (1974).

(5) G. L. Biagi, A. M. Barbaro, and M. C. Guerra, "Biological Correlations—The Hansch Approach," Advances in Chemistry Series, No. 114, American Chemical Society, Washington, D.C., 1972, chap. 5.

(6) J. D. Turnbull, G. L. Biagi, A. J. Merola, and D. G. Cornwell, *Biochem. Pharmacol.*, **20**, 1383 (1971).

(7) G. L. Biagi, A. M. Barbaro, O. Gandolfi, M. C. Guerra, and G. Cantelli-Forti, *J. Med. Chem.*, **18**, 873 (1975).

(8) G. L. Biagi, A. M. Barbaro, M. C. Guerra, G. Cantelli-Forti, and M. E. Francasso, *ibid.*, **17**, 28 (1974).

(9) A. N. Tischler, F. M. Thompson, L. J. Libertini, and M. Calvin, *ibid.*, **17**, 948 (1974).

(10) G. L. Biagi, O. Gandolfi, M. C. Guerra, A. M. Barbaro, and G. Cantelli-Forti, *ibid.*, **18**, 868 (1975).

(11) G. L. Biagi, M. C. Guerra, and A. M. Barbaro, *ibid.*, **13**, 944 (1970).

(12) J. K. Seydel, H. Ahrens, and W. Losert, *ibid.*, **18**, 234 (1975).

(13) A. Fujii, K. Tanaka, Y. Tsuchiya, and E. S. Cook, *ibid.*, **14**, 354 (1971).

ACKNOWLEDGMENTS

Presented in part at the Seventh Central Regional Meeting of the American Chemical Society, Morgantown, W.Va., May 1975, Abstract No. 60.

Abstracted in part from a dissertation submitted by K. E. Shores to the Graduate School, Xavier University, in partial fulfillment of the Master of Science degree requirements.

Supported in part by a grant from Stanley Drug Products, Inc., Division of Sperti Drug Products, Inc.

The authors thank Dr. Harvey A. Dube and Dr. Robert G. Johnson of the Chemistry Department, Xavier University, for their valuable suggestions.

Amino Acid Analogs IV: 4-Fluoroisoleucine

HERMAN GERSHON *x, LARRY SHANKS *, and DONALD D. CLARKE ‡

Received April 28, 1977, from the **Boyce Thompson Institute for Plant Research, Yonkers, NY 10701*, and the ‡*Department of Chemistry, Fordham University, Bronx, NY 10458.* Accepted for publication August 23, 1977.

Abstract □ 4-Fluoroisoleucine was produced by ammonolysis of 2-bromo-4-fluoro-3-methylpentanoic acid, which resulted from the bromofluorination of 4-methyl-2-pentenoic acid. It did not inhibit *Plasmodium berghei* in mice at 640 mg/kg and was not toxic to the animals. The fluoroamino acid inhibited *Aspergillus niger, Trichoderma viride, Myrothecium verrucaria, Trichophyton mentagrophytes,* and *Mucor mucedo* in Czapek solution agar at a concentration between 10^4 and 10^3 μg/ml. Growth of *Escherichia coli* was inhibited 25% at 900 μg/ml in a defined medium.

Keyphrases □ 4-Fluoroisoleucine—synthesized, evaluated for antimicrobial activity □ Antimicrobial activity—4-fluoroisoleucine evaluated □ Amino acid analogs—4-fluoroisoleucine synthesized and evaluated for antimicrobial activity

The preparation of straight chain 3-fluoroamino acids with three to seven carbon atoms as well as 3-fluorovaline was reported (1). The general approach employed started with the bromofluorination of the corresponding 2-alkenoic acid followed by ammonolysis.

DISCUSSION

In attempting to prepare 3-fluoroleucine, 4-methyl-2-pentenoic acid (2) was dissolved in liquid hydrofluoric acid with the subsequent addition of *N*-bromoacetamide. The expected product was not obtained. The resulting mixture was composed of two major products: 2-bromo-4-fluoro-3-methylpentanoic acid and 2-bromo-4,4-dimethyl-4-butyrolactone. The 2-bromo-4-fluoro-3-methylpentanoic acid was converted to 4-fluoroisoleucine by ammonlysis in liquid ammonia.

Identification of these compounds was made by elemental analysis and NMR spectroscopy (see *Experimental*). IR spectra of the three compounds were obtained (Fig. 1).

The neutral product obtained from the addition of the bromo and fluoro elements to 4-methyl-2-pentenoic acid contained no fluorine and showed two singlets in the NMR spectrum corresponding to three protons each at δ 1.48 and 1.63 ppm. This result indicated the fragment $(CH_3)_2C(-X)C$, in which X is an electronegative group that shifts the methyl groups from their original position near δ 1.10 ppm. The classic *ABX* spectrum located between δ 2.47–2.79 (*AB* portion) and 4.7 (*X* portion) ppm, with J_{AB} = 14.5 Hz, indicated geminal coupling of the protons on a saturated carbon atom. This result suggested the presence of the fragment CH_2CHBr. The IR spectrum of the compound (Fig. 1A) showed a strong peak at 1780 cm^{-1}. The spectral data were in agreement with the structure of the compound being 2-bromo-4,4-dimethylbutyrolactone.

The structures of the bromofluoro and fluoroamino acids were deduced from the NMR and IR spectra as follows. That fluorine was attached to a carbon atom bearing a proton was evident from the 49-Hz coupling to the proton centered at δ 5.2 ppm. This coupling was expected for the anticipated product, 2-bromo-3-fluoro-4-methylpentanoic acid. Instead of a doublet near δ 1.10 ppm (J = 7 Hz) of an area corresponding to six protons, characteristic of the isopropyl group as in the starting acid, the product of bromofluorination of 4-methyl-2-pentenoic acid showed a doublet at δ 1.12 ppm (J = 7 Hz) and a doublet of doublets centered at δ 1.37 ppm (J_{HH} = 6 Hz; J_{HF} = 29 Hz).

A comparison of the 60- and 100-MHz spectra indicated that the 29-Hz separation was a coupling constant rather than a chemical shift. The NMR spectrum showed that a rearrangement involving the isopropyl group of the starting acid had taken place. The doublet of doublets is indicative of the fragment CH_3CHF and was reported previously in the product of the addition of the bromo and fluoro elements to crotonic acid (1). Further confirmation that fluorine was present in the molecule and was coupled to the methyl group at δ 1.37 ppm and to the protons at C-3

that previously obtained with white paraffin oil. No definite relationships appeared evident when comparisons were made of chain length, amount of unsaturation, and functional group. The greatest improvement in the correlation between biological response and R_m for all stationary phases investigated was obtained with either *cis*-9,*cis*-12,*cis*-15-octadecatrienoic acid (linoleic acid) or hexadecanoic acid (palmitic acid).

Although no definite trend resulted from comparison between the stationary phase material and improvement of correlation, the following general relationship was found between functional group and improvement of correlation: fatty acids = alcohols > ethyl esters > white paraffin oil.

REFERENCES

(1) A. Fujii and E. S. Cook, *J. Med. Chem.*, **18**, 502 (1975).

(2) A. Fujii, J. H. Bush, K. E. Shores, R. G. Johnson, R. J. Garascia, and E. S. Cook, *J. Pharm. Sci.*, **66**, 844 (1977).

(3) C. B. C. Boyce and B. V. Milborrow, *Nature*, **208**, 537 (1965).

(4) B. F. Cain, R. N. Seelye, and G. J. Atwell, *J. Med. Chem.*, **17**, 922 (1974).

(5) G. L. Biagi, A. M. Barbaro, and M. C. Guerra, "Biological Correlations—The Hansch Approach," Advances in Chemistry Series, No. 114, American Chemical Society, Washington, D.C., 1972, chap. 5.

(6) J. D. Turnbull, G. L. Biagi, A. J. Merola, and D. G. Cornwell, *Biochem. Pharmacol.*, **20**, 1383 (1971).

(7) G. L. Biagi, A. M. Barbaro, O. Gandolfi, M. C. Guerra, and G. Cantelli-Forti, *J. Med. Chem.*, **18**, 873 (1975).

(8) G. L. Biagi, A. M. Barbaro, M. C. Guerra, G. Cantelli-Forti, and M. E. Francasso, *ibid.*, **17**, 28 (1974).

(9) A. N. Tischler, F. M. Thompson, L. J. Libertini, and M. Calvin, *ibid.*, **17**, 948 (1974).

(10) G. L. Biagi, O. Gandolfi, M. C. Guerra, A. M. Barbaro, and G. Cantelli-Forti, *ibid.*, **18**, 868 (1975).

(11) G. L. Biagi, M. C. Guerra, and A. M. Barbaro, *ibid.*, **13**, 944 (1970).

(12) J. K. Seydel, H. Ahrens, and W. Losert, *ibid.*, **18**, 234 (1975).

(13) A. Fujii, K. Tanaka, Y. Tsuchiya, and E. S. Cook, *ibid.*, **14**, 354 (1971).

ACKNOWLEDGMENTS

Presented in part at the Seventh Central Regional Meeting of the American Chemical Society, Morgantown, W.Va., May 1975, Abstract No. 60.

Abstracted in part from a dissertation submitted by K. E. Shores to the Graduate School, Xavier University, in partial fulfillment of the Master of Science degree requirements.

Supported in part by a grant from Stanley Drug Products, Inc., Division of Sperti Drug Products, Inc.

The authors thank Dr. Harvey A. Dube and Dr. Robert G. Johnson of the Chemistry Department, Xavier University, for their valuable suggestions.

Amino Acid Analogs IV: 4-Fluoroisoleucine

HERMAN GERSHON *x, LARRY SHANKS *, and DONALD D. CLARKE ‡

Received April 28, 1977, from the **Boyce Thompson Institute for Plant Research, Yonkers, NY 10701*, and the ‡*Department of Chemistry, Fordham University, Bronx, NY 10458.* Accepted for publication August 23, 1977.

Abstract □ 4-Fluoroisoleucine was produced by ammonolysis of 2-bromo-4-fluoro-3-methylpentanoic acid, which resulted from the bromofluorination of 4-methyl-2-pentenoic acid. It did not inhibit *Plasmodium berghei* in mice at 640 mg/kg and was not toxic to the animals. The fluoroamino acid inhibited *Aspergillus niger, Trichoderma viride, Myrothecium verrucaria, Trichophyton mentagrophytes,* and *Mucor mucedo* in Czapek solution agar at a concentration between 10^4 and 10^3 μg/ml. Growth of *Escherichia coli* was inhibited 25% at 900 μg/ml in a defined medium.

Keyphrases □ 4-Fluoroisoleucine—synthesized, evaluated for antimicrobial activity □ Antimicrobial activity—4-fluoroisoleucine evaluated □ Amino acid analogs—4-fluoroisoleucine synthesized and evaluated for antimicrobial activity

The preparation of straight chain 3-fluoroamino acids with three to seven carbon atoms as well as 3-fluorovaline was reported (1). The general approach employed started with the bromofluorination of the corresponding 2-alkenoic acid followed by ammonolysis.

DISCUSSION

In attempting to prepare 3-fluoroleucine, 4-methyl-2-pentenoic acid (2) was dissolved in liquid hydrofluoric acid with the subsequent addition of *N*-bromoacetamide. The expected product was not obtained. The resulting mixture was composed of two major products: 2-bromo-4-fluoro-3-methylpentanoic acid and 2-bromo-4,4-dimethyl-4-butyrolactone. The 2-bromo-4-fluoro-3-methylpentanoic acid was converted to 4-fluoroisoleucine by ammonlysis in liquid ammonia.

Identification of these compounds was made by elemental analysis and NMR spectroscopy (see *Experimental*). IR spectra of the three compounds were obtained (Fig. 1).

The neutral product obtained from the addition of the bromo and fluoro elements to 4-methyl-2-pentenoic acid contained no fluorine and showed two singlets in the NMR spectrum corresponding to three protons each at δ 1.48 and 1.63 ppm. This result indicated the fragment $(CH_3)_2C(-X)C$, in which X is an electronegative group that shifts the methyl groups from their original position near δ 1.10 ppm. The classic *ABX* spectrum located between δ 2.47–2.79 (*AB* portion) and 4.7 (*X* portion) ppm, with J_{AB} = 14.5 Hz, indicated geminal coupling of the protons on a saturated carbon atom. This result suggested the presence of the fragment CH_2CHBr. The IR spectrum of the compound (Fig. 1A) showed a strong peak at 1780 cm^{-1}. The spectral data were in agreement with the structure of the compound being 2-bromo-4,4-dimethylbutyrolactone.

The structures of the bromofluoro and fluoroamino acids were deduced from the NMR and IR spectra as follows. That fluorine was attached to a carbon atom bearing a proton was evident from the 49-Hz coupling to the proton centered at δ 5.2 ppm. This coupling was expected for the anticipated product, 2-bromo-3-fluoro-4-methylpentanoic acid. Instead of a doublet near δ 1.10 ppm (J = 7 Hz) of an area corresponding to six protons, characteristic of the isopropyl group as in the starting acid, the product of bromofluorination of 4-methyl-2-pentenoic acid showed a doublet at δ 1.12 ppm (J = 7 Hz) and a doublet of doublets centered at δ 1.37 ppm (J_{HH} = 6 Hz; J_{HF} = 29 Hz).

A comparison of the 60- and 100-MHz spectra indicated that the 29-Hz separation was a coupling constant rather than a chemical shift. The NMR spectrum showed that a rearrangement involving the isopropyl group of the starting acid had taken place. The doublet of doublets is indicative of the fragment CH_3CHF and was reported previously in the product of the addition of the bromo and fluoro elements to crotonic acid (1). Further confirmation that fluorine was present in the molecule and was coupled to the methyl group at δ 1.37 ppm and to the protons at C-3

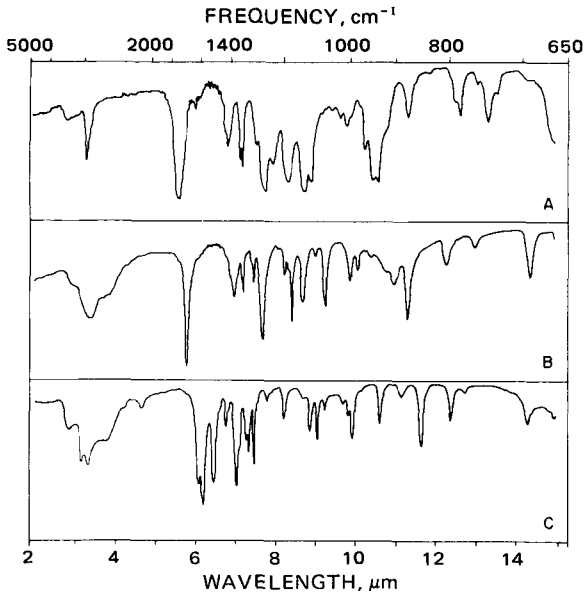

Figure 1—*IR spectra (neat) of: A, 2-bromo-4,4-dimethyl-4-butyrolactone; B, 2-bromo-4-fluoro-3-methylpentanoic acid (KBr); and C, 4-fluoroisoleucine.*

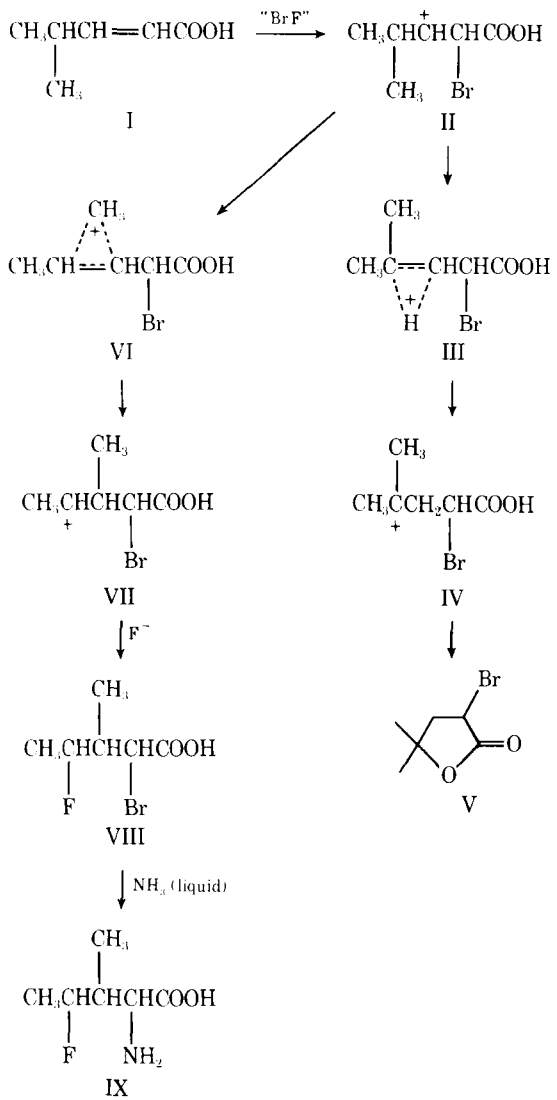

Scheme I

and C-4 was obtained from the ^{19}F-NMR spectrum of the product at 94 MHz. The IR spectrum (Fig. 1B) showed characteristic peaks at 1735 (C=O), 1128 (C—F), and 658 (C—Br) cm^{-1}. It was concluded from these spectra that the structure of the bromofluoro acid was 2-bromo-4-fluoro-3-methylpentanoic acid.

Replacement of the bromo substituent of 2-bromo-4-fluoro-3-methylpentanoic acid with amino yielded an amino acid with NMR characteristics similar to those of the bromofluoro acid. The fact that all NMR peaks could be assigned in a straightforward manner indicated that a single isomer of the amino acid had been obtained. The precise configuration could not be specified from the available data. The IR spectrum showed peaks at 1631 and 1597 (CO_2^-) and 1115 (CF) cm^{-1}. The spectral data were consistent with the structure 2-amino-4-fluoroisoleucine.

A synthetic sequence based on the nonclassical bridged carbonium ion (3), which could explain the formation of the identified compounds, is shown in Scheme I. 2-Bromo-4,4-dimethylbutyrolactone (V) would result from the hydride shift in the initial carbonium ion (II) to yield a tertiary carbonium ion (IV), which should be a lower energy intermediate. Thus, V is the major product isolated from the reaction mixture (60%). Carbonium ion II, which should yield 2-bromo-3-fluoro-4-methylpentanoic acid, would be expected to be of similar stability to the rearranged carbonium ion (VII) involving methyl migration. Why none of the expected product was obtained is not understood.

The methyl, ethyl, and *tert*-butyl esters of 4-fluoroisoleucine have been reported but not the free amino acid (4)[1].

The fluoroamino acid was tested against *Aspergillus niger* (ATCC 1004), *Trichoderma viride* (ATCC 8678), and *Myrothecium verrucaria* (ATCC 9095C) in Czapek solution agar[2] at pH 7.3 and against *Trichophyton mentagrophytes* (ATCC 9129) and *Mucor mucedo* (ATCC 7941) in the same medium in the presence of 10% beef serum[3] according to published methods (5). All fungi were completely inhibited at concentrations between 10^3 and 10^4 μg/ml. Growth of *Escherichia coli* (ATCC 9723) was inhibited 25% in a defined medium (6) at a level of 900 μg of fluoroamino acid/ml.

L-Isoleucine is essential for the growth of erythrocytic forms of *Plasmodium knowlesi* (7). Therefore, 4-fluoroisoleucine was tested against *Plasmodium berghei* in mice. Neither toxicity nor antiplasmodial activity was observed at 640 mg/kg, the highest level administered[4].

EXPERIMENTAL[5]

Bromofluorination of 4-Methyl-2-pentenoic Acid—4-Methyl-2-pentenoic acid (2) (89 g, 0.78 mole) was dissolved in 300 ml of liquid hydrogen fluoride kept at from −30 to −10° in a polyethylene bottle. To the mixture was added *N*-bromoacetamide (118 g, 0.85 mole) in small portions, with stirring, over 0.5 hr. Stirring was continued overnight, allowing the mixture to come to room temperature. Excess hydrogen fluoride was removed under a stream of air, and the residue was poured into a slurry of ice and water. The product was extracted with ether (3 × 150 ml).

2-Bromo-4-fluoro-3-methylpentanoic Acid (VIII)—The ether solution was extracted with 6 *N* NH_4OH (3 × 150 ml), and the aqueous phase was back-extracted with ether (2 × 100 ml). The ether extracts were combined for subsequent workup. The aqueous solution was acidified with hydrochloric acid and extracted with ether (3 × 100 ml). The ether solution, dried with sodium sulfate, was treated with cyclohexylamine dissolved in ether, with stirring, until a slightly basic reaction was detected.

After stirring for 2 hr, the mixture was refrigerated overnight. The cyclohexylamine salt was obtained by filtration (yield of 29.2 g, 12.8%). Then the salt was crystallized several times from an acetone–ether mixture, mp 132–133° (acetone).

Anal.—Calc. for $C_{12}H_{22}BrFNO_2$: C, 46.31; H, 7.13; Br, 25.68. Found: C, 46.44; H, 7.34; Br, 25.42.

[1] M. Hudlicky supplied an NMR spectrum of 4-fluoroisoleucine prepared in his laboratory. The details of his work will be published.

[2] Difco.

[3] Miles Laboratories.

[4] Testing was done by the Rane Laboratory, University of Miami, Miami, Fla.

[5] Melting points were taken in a Thomas-Hoover melting-point apparatus and are uncorrected. GLC was performed on a Varian Aerograph model 1200 gas chromatograph with a flame-ionization detector to which was attached a Varian Aerograph model 20 recorder. The purity of the acids was established by GLC of the trimethylsilyl esters on a column containing 1% Apiezon L on acid-washed Chromosorb W (80–100 mesh), previously treated with dimethyldichlorosilane. IR spectra were obtained with a Perkin-Elmer model 221 spectrophotometer. The 60-MHz NMR spectra were taken with a Varian A-60A spectrometer, and 100-MHz spectra were taken with a Varian XL-100 spectrometer.

Cyclohexylammonium 2-bromo-4-fluoro-3-methylpentanoate (29.0 g, 0.093 mole) was dissolved in 150 ml of 5% HCl with cooling. The mixture was extracted twice with 50-ml portions of chloroform. The solution was dried over sodium sulfate, and the solvent was evaporated under vacuum. The solid residue was crystallized from pentane (18.0 g, 10.9%), mp 72–74°. The analytical sample was crystallized from pentane, mp 74–76°; NMR (100 MHz, deuterochloroform, tetramethylsilane): δ 1.12 [d, C-3 CH_3, $J_{C\text{-}3}$ (H)—C-3 CH_3 = 7 Hz], 1.37 [dd, C-4 CH_3, $J_{C\text{-}4}$ (CH_3)—C-4 H = 6 Hz, $J_{C\text{-}4}$ (CH_3)—C-4 F = 29 Hz], 1.62–2.4 (m, C-3 H), 4.25 [d, C-2 H, $J_{C\text{-}2}$ (H)—C-3 H = 10 Hz], and 4.8–5.6 [m, C-4 H, $J_{C\text{-}4}$ (H)—C-4 F = 49 Hz, $J_{C\text{-}4}$ (H)—C-4 CH_3 = 7 Hz, $J_{C\text{-}4}$ (H)—C-3 H = 2 Hz] ppm.

Anal.—Calc. for $C_6H_{10}BrFO_2$: C, 33.82; H, 4.73; Br, 37.51; F, 8.92. Found: C, 33.59; H, 4.72; Br, 37.67; F, 8.92.

2-Bromo-4,4-dimethyl-4-butyrolactone (V)—The ether extract remaining after removal of 2-bromo-4-fluoro-3-methylpentanoic acid was dried over sodium sulfate and freed of solvent. The residue was distilled and yielded 90 g (60%) of product, bp 110–118°/5.0 mm. An analytical sample boiled at 88–90°/0.75 mm; NMR (60 MHz, deuterochloroform, tetramethylsilane): δ 1.48 [s, C-4 $(CH_3)_2$], 1.63 [s, C-4 $(CH_3)_2$], 2.47–2.79 (C-3 H_2, *AB* portions of *ABX* spectrum), and 4.7 (C-2 H, *X* portion of *ABX* spectrum, J_{AX} = 9 Hz, J_{BX} = 7 Hz, J_{AB} = 14.5 Hz) ppm.

Anal.—Calc. for $C_6H_9BrO_2$: C, 37.33; H, 4.70; Br, 41.40; O, 16.58. Found: C, 37.57; H, 4.72; Br, 41.48; O, 16.30.

4-Fluoroisoleucine (IX)—2-Bromo-4-fluoro-3-methylpentanoic acid (30 g, 0.14 mole) was dissolved in 175 ml of liquid ammonia and sealed in a stainless steel pressure vessel. After remaining at room temperature for 3 days, the excess ammonia was removed. The residue was dissolved in a small volume of water and adjusted to pH 5 with hydrobromic acid. The solution was evaporated under reduced pressure below 40°, and the residue was slurried repeatedly with methanol until a negative halogen test was obtained with silver nitrate.

The residue then was removed by filtration and dried under vacuum. The yield of product was 9.1 g (43.5%), mp 195.5–196° dec. An analytical sample was crystallized from a mixture of water and acetone, mp 202–202.5° dec.; NMR (100 MHz, deuterium oxide, sodium 2,2-dimethyl-2-silapentane-5-sulfonate): δ 1.13 [d, C-3 CH_3, $J_{C\text{-}3}$ (H)—C-3 CH_3 = 7 Hz], 1.36 [dd, C-4 CH_3, $J_{C\text{-}4}$ (CH_3)—C-4 H = 7 Hz, $J_{C\text{-}4}$ CH_3—C-4 F = 25 Hz], 1.9–2.4 (m, C-3 H), 3.78 [d, C-2 H, $J_{C\text{-}2}$ (H)—C-3 H = 4 Hz], and 4.4–5.2 [m, C-4 H, $J_{C\text{-}4}$ (H)—C-4 F = 50 Hz] ppm[6].

Anal.—Calc. for $C_6H_{12}FNO_2$: C, 48.31; H, 8.11; F, 12.74; N, 9.39. Found: C, 48.09; H, 8.10; F, 12.73; N, 9.30.

REFERENCES

(1) H. Gershon, M. W. McNeil, and E. D. Bergmann, *J. Med. Chem.*, **16**, 1407 (1973).

(2) B. J. Clarke and R. P. Hildebrand, *J. Inst. Brew.*, **73**, 60 (1967).

(3) S. Weinstein and B. K. Morse, *J. Am. Chem. Soc.*, **74**, 1133 (1952).

(4) D. Butina, *Diss. Abstr. Int.*, **36**, 5586B (1976).

(5) H. Gershon and R. Parmegiani, *J. Med. Chem.*, **10**, 186 (1967).

(6) B. D. Davis and E. S. Mingioli, *J. Bacteriol.*, **60**, 17 (1950).

(7) H. Polet and M. E. Conrad, *Proc. Soc. Exp. Biol. Med.*, **127**, 251 (1968).

ACKNOWLEDGMENTS

The authors thank E. A. Steck, Walter Reed Army Institute of Research, for the malarial test results on 4-fluoroisoleucine and A. T. Grefig for the IR spectra.

[6] The NMR spectrum of 3-fluorovaline as reported in Ref. 1 is now corrected to: δ 1.56 [d, C-3 CH_3, $J_{C\text{-}3}$ (CH_3)—F = 23 Hz] and 1.70 [d, C-3 $(CH_3)_2$, $J_{C\text{-}3}$ $(CH_3)_2$—F = 23 Hz] ppm. These results are based on a comparison of the 60- and 100-MHz spectra.

Modified NF Method for Quantitative Determination of Pentaerythritol Tetranitrate

V. DAS GUPTA

Received July 11, 1977, from the *College of Pharmacy, University of Houston, Houston, TX 77004.* Accepted for publication August 11, 1977.

Abstract □ A modified NF method for the quantitative determination of pentaerythritol tetranitrate is reported. A solution of powder is made directly from the dosage form in glacial acetic acid and is then reacted with phenoldisulfonic acid TS. The proposed method saves approximately 75% of the time required with the NF method. The results on six different commercial dosage forms with four different colors and three other active ingredients are reported.

Keyphrases □ Pentaerythritol tetranitrate—colorimetric analysis in dosage forms, NF method modified □ Colorimetry—analysis, pentaerythritol tetranitrate in dosage forms, NF method modified □ Vasodilators—pentaerythritol tetranitrate, colorimetric analysis in dosage forms, NF method modified

The NF method (1) for the quantitative determination of pentaerythritol tetranitrate (I) in dilutions and tablets is lengthy and tedious. The method requires boiling the powder in acetone at 60°, cooling it, centrifuging, and then evaporating the decanted solution at 35°. In the hands of inexperienced analysts, the recovery may not be quantitative. By eliminating these steps, 75% of the time required can be saved. This paper reports a modified NF method for the quantitative determination of I in dosage forms.

EXPERIMENTAL

Reagents and Chemicals—All chemicals and reagents were USP, NF, or ACS grade and were used without further purification.

Solutions—All solutions were prepared according to NF directions (1).

Assay—The dosage form was ground to a fine powder in a mortar. An appropriate quantity (accurately weighed), representing 0.5 mg of I, was transferred to a dry, clean, 150-ml beaker. Then 1 ml of glacial acetic acid was added, and the mixture was stirred for several minutes. A 2-ml quantity of phenoldisulfonic acid TS was added, and the mixture was allowed to stand for 5 min. Then 25 ml of water and 25 ml of ammonia TS were added, and the solution was allowed to cool.

The mixture was transferred to a 100-ml volumetric flask and brought to volume with water. The absorbance value of the clear solution was measured[1] at 409 nm against a reagent blank. For increased accuracy, the quantity of powder may be doubled. If so, all volumes should be doubled.

The modified method was tried on six commercial dosage forms containing four different colors; some contained another active ingredient. The results were calculated according to the NF formula (1) (Table I). The results obtained by the NF method (1) are also presented in Table I.

[1] Bausch & Lomb Spectronic 20.

Cyclohexylammonium 2-bromo-4-fluoro-3-methylpentanoate (29.0 g, 0.093 mole) was dissolved in 150 ml of 5% HCl with cooling. The mixture was extracted twice with 50-ml portions of chloroform. The solution was dried over sodium sulfate, and the solvent was evaporated under vacuum. The solid residue was crystallized from pentane (18.0 g, 10.9%), mp 72–74°. The analytical sample was crystallized from pentane, mp 74–76°; NMR (100 MHz, deuterochloroform, tetramethylsilane): δ 1.12 [d, C-3 CH_3, $J_{C\text{-}3}$ (H)—C-3 CH_3 = 7 Hz], 1.37 [dd, C-4 CH_3, $J_{C\text{-}4}$ (CH_3)—C-4 H = 6 Hz, $J_{C\text{-}4}$ (CH_3)—C-4 F = 29 Hz], 1.62–2.4 (m, C-3 H), 4.25 [d, C-2 H, $J_{C\text{-}2}$ (H)—C-3 H = 10 Hz], and 4.8–5.6 [m, C-4 H, $J_{C\text{-}4}$ (H)—C-4 F = 49 Hz, $J_{C\text{-}4}$ (H)—C-4 CH_3 = 7 Hz, $J_{C\text{-}4}$ (H)—C-3 H = 2 Hz] ppm.

Anal.—Calc. for $C_6H_{10}BrFO_2$: C, 33.82; H, 4.73; Br, 37.51; F, 8.92. Found: C, 33.59; H, 4.72; Br, 37.67; F, 8.92.

2-Bromo-4,4-dimethyl-4-butyrolactone (V)—The ether extract remaining after removal of 2-bromo-4-fluoro-3-methylpentanoic acid was dried over sodium sulfate and freed of solvent. The residue was distilled and yielded 90 g (60%) of product, bp 110–118°/5.0 mm. An analytical sample boiled at 88–90°/0.75 mm; NMR (60 MHz, deuterochloroform, tetramethylsilane): δ 1.48 [s, C-4 $(CH_3)_2$], 1.63 [s, C-4 $(CH_3)_2$], 2.47–2.79 (C-3 H_2, *AB* portions of *ABX* spectrum), and 4.7 (C-2 H, *X* portion of *ABX* spectrum, J_{AX} = 9 Hz, J_{BX} = 7 Hz, J_{AB} = 14.5 Hz) ppm.

Anal.—Calc. for $C_6H_9BrO_2$: C, 37.33; H, 4.70; Br, 41.40; O, 16.58. Found: C, 37.57; H, 4.72; Br, 41.48; O, 16.30.

4-Fluoroisoleucine (IX)—2-Bromo-4-fluoro-3-methylpentanoic acid (30 g, 0.14 mole) was dissolved in 175 ml of liquid ammonia and sealed in a stainless steel pressure vessel. After remaining at room temperature for 3 days, the excess ammonia was removed. The residue was dissolved in a small volume of water and adjusted to pH 5 with hydrobromic acid. The solution was evaporated under reduced pressure below 40°, and the residue was slurried repeatedly with methanol until a negative halogen test was obtained with silver nitrate.

The residue then was removed by filtration and dried under vacuum. The yield of product was 9.1 g (43.5%), mp 195.5–196° dec. An analytical sample was crystallized from a mixture of water and acetone, mp 202–202.5° dec.; NMR (100 MHz, deuterium oxide, sodium 2,2-dimethyl-2-silapentane-5-sulfonate): δ 1.13 [d, C-3 CH_3, $J_{C\text{-}3}$ (H)—C-3 CH_3 = 7 Hz], 1.36 [dd, C-4 CH_3, $J_{C\text{-}4}$ (CH_3)—C-4 H = 7 Hz, $J_{C\text{-}4}$ CH_3—C-4 F = 25 Hz], 1.9–2.4 (m, C-3 H), 3.78 [d, C-2 H, $J_{C\text{-}2}$ (H)—C-3 H = 4 Hz], and 4.4–5.2 [m, C-4 H, $J_{C\text{-}4}$ (H)—C-4 F = 50 Hz] ppm[6].

Anal.—Calc. for $C_6H_{12}FNO_2$: C, 48.31; H, 8.11; F, 12.74; N, 9.39. Found: C, 48.09; H, 8.10; F, 12.73; N, 9.30.

REFERENCES

(1) H. Gershon, M. W. McNeil, and E. D. Bergmann, *J. Med. Chem.*, **16**, 1407 (1973).

(2) B. J. Clarke and R. P. Hildebrand, *J. Inst. Brew.*, **73**, 60 (1967).

(3) S. Weinstein and B. K. Morse, *J. Am. Chem. Soc.*, **74**, 1133 (1952).

(4) D. Butina, *Diss. Abstr. Int.*, **36**, 5586B (1976).

(5) H. Gershon and R. Parmegiani, *J. Med. Chem.*, **10**, 186 (1967).

(6) B. D. Davis and E. S. Mingioli, *J. Bacteriol.*, **60**, 17 (1950).

(7) H. Polet and M. E. Conrad, *Proc. Soc. Exp. Biol. Med.*, **127**, 251 (1968).

ACKNOWLEDGMENTS

The authors thank E. A. Steck, Walter Reed Army Institute of Research, for the malarial test results on 4-fluoroisoleucine and A. T. Grefig for the IR spectra.

[6] The NMR spectrum of 3-fluorovaline as reported in Ref. 1 is now corrected to: δ 1.56 [d, C-3 CH_3, $J_{C\text{-}3}$ (CH_3)—F = 23 Hz] and 1.70 [d, C-3 $(CH_3)_2$, $J_{C\text{-}3}$ $(CH_3)_2$—F = 23 Hz] ppm. These results are based on a comparison of the 60- and 100-MHz spectra.

Modified NF Method for Quantitative Determination of Pentaerythritol Tetranitrate

V. DAS GUPTA

Received July 11, 1977, from the *College of Pharmacy, University of Houston, Houston, TX 77004.* Accepted for publication August 11, 1977.

Abstract □ A modified NF method for the quantitative determination of pentaerythritol tetranitrate is reported. A solution of powder is made directly from the dosage form in glacial acetic acid and is then reacted with phenoldisulfonic acid TS. The proposed method saves approximately 75% of the time required with the NF method. The results on six different commercial dosage forms with four different colors and three other active ingredients are reported.

Keyphrases □ Pentaerythritol tetranitrate—colorimetric analysis in dosage forms, NF method modified □ Colorimetry—analysis, pentaerythritol tetranitrate in dosage forms, NF method modified □ Vasodilators—pentaerythritol tetranitrate, colorimetric analysis in dosage forms, NF method modified

The NF method (1) for the quantitative determination of pentaerythritol tetranitrate (I) in dilutions and tablets is lengthy and tedious. The method requires boiling the powder in acetone at 60°, cooling it, centrifuging, and then evaporating the decanted solution at 35°. In the hands of inexperienced analysts, the recovery may not be quantitative. By eliminating these steps, 75% of the time required can be saved. This paper reports a modified NF method for the quantitative determination of I in dosage forms.

EXPERIMENTAL

Reagents and Chemicals—All chemicals and reagents were USP, NF, or ACS grade and were used without further purification.

Solutions—All solutions were prepared according to NF directions (1).

Assay—The dosage form was ground to a fine powder in a mortar. An appropriate quantity (accurately weighed), representing 0.5 mg of I, was transferred to a dry, clean, 150-ml beaker. Then 1 ml of glacial acetic acid was added, and the mixture was stirred for several minutes. A 2-ml quantity of phenoldisulfonic acid TS was added, and the mixture was allowed to stand for 5 min. Then 25 ml of water and 25 ml of ammonia TS were added, and the solution was allowed to cool.

The mixture was transferred to a 100-ml volumetric flask and brought to volume with water. The absorbance value of the clear solution was measured[1] at 409 nm against a reagent blank. For increased accuracy, the quantity of powder may be doubled. If so, all volumes should be doubled.

The modified method was tried on six commercial dosage forms containing four different colors; some contained another active ingredient. The results were calculated according to the NF formula (1) (Table I). The results obtained by the NF method (1) are also presented in Table I.

[1] Bausch & Lomb Spectronic 20.

Table I—Assay Results on Commercial Dosage Forms

Dosage Form	I per Dosage, mg	Other Active Ingredients, mg	Results on I, % Modified Method[a]	Results on I, % NF Method[a]
Green tablet	20	None	97.0	96.5
Yellow tablet	10	Phenobarbital, 15	98.4	98.0
White tablet	10	None	99.2	99.5
Orange tablet	20	Meprobamate, 200	99.2	98.9
Light-red tablet	20	Hydroxyzine hydrochloride, 10	99.2	99.5
Sustained-release capsule (white pellets)	30	None	105.9	105.2

[a] Average of two determinations.

DISCUSSION

The results (Table I) for various dosage forms indicate that the NF method (1) can be modified to save 75% of the time required for the analysis of I and to assure quantitative recoveries. The only precaution is that the powder must be finely ground, as required also by the NF method. It is recommended that this change be made in the NF procedure.

REFERENCE

(1) "The National Formulary," 14th ed., Mack Publishing Co., Easton, Pa., 1975, p. 540.

ACKNOWLEDGMENTS

Supported in part by Automated Prescription Systems, Pineville, La.

Synthesis of an Anti-Inflammatory 10,10a-Dihydro-1*H*,5*H*-imidazo[1,5-*b*]isoquinoline-1,3(2*H*)-dione

THOMAS J. SCHWAN ˣ, MARVIN M. GOLDENBERG, and ARTHUR C. ILSE

Received April 15, 1977, from the *Scientific Affairs Department, Norwich-Eaton Pharmaceuticals Division of Morton-Norwich Products, Inc., Norwich, NY 13815.* Accepted for publication August 10, 1977.

Abstract □ A new synthesis of imidazo[1,5-*b*]isoquinolines is reported. 2-[2-(Piperidino)ethyl]-10,10a-dihydro-1*H*,5*H*-imidazo[1,5-*b*]isoquinoline-1,3(2*H*)-dione hydrochloride was found to possess anti-inflammatory activity.

Keyphrases □ Imidazo[1,5-*b*]isoquinolines, substituted—synthesized, evaluated for anti-inflammatory activity □ Anti-inflammatory activity—evaluated in substituted imidazo[1,5-*b*]isoquinolines

The imidazo[1,5-*b*]isoquinoline ring system (I) has received little attention. Prior to work in this laboratory (1), all known members of this class of compounds were prepared by reaction of the appropriate 2,4-imidazolidinedione with a functionalized benzaldehyde (2–5). Since this sequence gives rise to compounds containing an oxo or thio group in the 5-position as well as a double bond at the 10–10a-position, it is not suitable for the synthesis of the projected compound, II, a derivative of III (Scheme I) containing the water-solubilizing piperidinoethyl function.

DISCUSSION

The target compound was readily prepared in a two-step sequence originating with the *d,l*-acid IV (6). Acid-catalyzed treatment of IV with potassium cyanate gave the unsubstituted III, and treatment of III with *N*-(2-chloroethyl)piperidine (V) afforded *d,l*-II.

Compound II was studied for anti-inflammatory activity in the conventional manner by determining its effectiveness in reducing the edematous inflammation induced by an injection of carrageenan (0.05 ml of a 1% solution) into the plantar surface of the rat hindpaw (7). At a dose of 300 mg/kg po, administered 1 hr before carrageenan, II caused moderate (44.2%) antagonism of edema formation 4 hr after the carrageenan injection; this antagonism decreased to 26.3% after 6 hr. Thus,

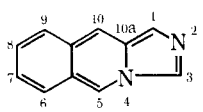

I

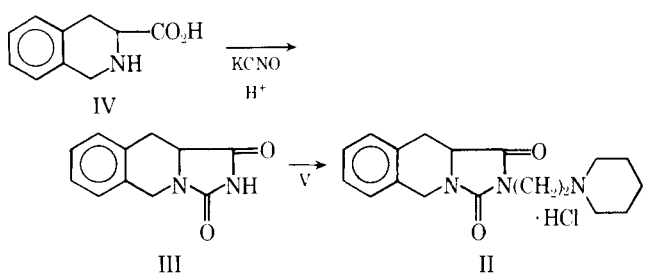

Scheme I

II possesses anti-inflammatory activity but with a shorter duration than that evoked by some standard anti-inflammatory drugs such as phenylbutazone (58% at 6 hr), indomethacin (49% at 6 hr), and ibuprofen (55% at 6 hr).

EXPERIMENTAL[1]

10,10a-Dihydro-1*H*,5*H*-imidazo[1,5-*b*]isoquinoline-1,3(2*H*)-dione (III)—To a suspension of 53.1 g (0.30 mole) of *d,l*-IV (6) in 1000 ml of acetic acid was added quickly a solution of 48.6 g (0.60 mole) of potassium cyanate in 150 ml of water. The mixture was stirred and heated on a steam bath at 90–95° for 90 min, and all solids were dissolved. Hydrochloric acid (3 *N*, 2400 ml) was added, and the resulting solution was stirred and refluxed for 20 hr. The solution was filtered while hot through a coarse sintered-glass funnel to remove mechanical impurities, and the filtrate was stored in the refrigerator for 18 hr; 44 g of the crude product was obtained.

Recrystallization from 1400 ml of alcohol gave 29.9 g (49%) of III, mp 225–231°. Further recrystallization from alcohol gave an analytical sample, mp 227–230°; IR: 3.14 (NH), 5.63, and 5.85 (C=O, imidazolidinedione) μm; NMR (dimethyl sulfoxide-d_6): δ 2.73–3.06 (m, 2, C-10 H_2), 4.05–4.96 (m, 3, C-5 H_2 and C-10a H), 7.25 (s, 4, aromatic CH), and 10.5–11.1 (broad s, 1, exchangeable, NH) ppm; mass spectrum M^+: *m/e* 202.

[1] Melting points were determined on a Mel-Temp apparatus, and those below 230° are corrected. IR spectra were determined as mineral oil mulls using a Perkin-Elmer 137B spectrophotometer. NMR spectra were obtained on a Varian A-60A instrument and were compared with tetramethylsilane as an internal standard. The mass spectrum was run on a Finnigan model 3300 mass spectrometer at the Mass Spectrometry Facility at Cornell University.

Table I—Assay Results on Commercial Dosage Forms

Dosage Form	I per Dosage, mg	Other Active Ingredients, mg	Results on I, % Modified Method[a]	Results on I, % NF Method[a]
Green tablet	20	None	97.0	96.5
Yellow tablet	10	Phenobarbital, 15	98.4	98.0
White tablet	10	None	99.2	99.5
Orange tablet	20	Meprobamate, 200	99.2	98.9
Light-red tablet	20	Hydroxyzine hydrochloride, 10	99.2	99.5
Sustained-release capsule (white pellets)	30	None	105.9	105.2

[a] Average of two determinations.

DISCUSSION

The results (Table I) for various dosage forms indicate that the NF method (1) can be modified to save 75% of the time required for the analysis of I and to assure quantitative recoveries. The only precaution is that the powder must be finely ground, as required also by the NF method. It is recommended that this change be made in the NF procedure.

REFERENCE

(1) "The National Formulary," 14th ed., Mack Publishing Co., Easton, Pa., 1975, p. 540.

ACKNOWLEDGMENTS

Supported in part by Automated Prescription Systems, Pineville, La.

Synthesis of an Anti-Inflammatory 10,10a-Dihydro-1*H*,5*H*-imidazo[1,5-*b*]isoquinoline-1,3(2*H*)-dione

THOMAS J. SCHWAN ˣ, MARVIN M. GOLDENBERG, and ARTHUR C. ILSE

Received April 15, 1977, from the *Scientific Affairs Department, Norwich-Eaton Pharmaceuticals Division of Morton-Norwich Products, Inc., Norwich, NY 13815.* Accepted for publication August 10, 1977.

Abstract □ A new synthesis of imidazo[1,5-*b*]isoquinolines is reported. 2-[2-(Piperidino)ethyl]-10,10a-dihydro-1*H*,5*H*-imidazo[1,5-*b*]isoquinoline-1,3(2*H*)-dione hydrochloride was found to possess anti-inflammatory activity.

Keyphrases □ Imidazo[1,5-*b*]isoquinolines, substituted—synthesized, evaluated for anti-inflammatory activity □ Anti-inflammatory activity—evaluated in substituted imidazo[1,5-*b*]isoquinolines

The imidazo[1,5-*b*]isoquinoline ring system (I) has received little attention. Prior to work in this laboratory (1), all known members of this class of compounds were prepared by reaction of the appropriate 2,4-imidazolidinedione with a functionalized benzaldehyde (2–5). Since this sequence gives rise to compounds containing an oxo or thio group in the 5-position as well as a double bond at the 10–10a-position, it is not suitable for the synthesis of the projected compound, II, a derivative of III (Scheme I) containing the water-solubilizing piperidinoethyl function.

DISCUSSION

The target compound was readily prepared in a two-step sequence originating with the *d,l*-acid IV (6). Acid-catalyzed treatment of IV with potassium cyanate gave the unsubstituted III, and treatment of III with *N*-(2-chloroethyl)piperidine (V) afforded *d,l*-II.

Compound II was studied for anti-inflammatory activity in the conventional manner by determining its effectiveness in reducing the edematous inflammation induced by an injection of carrageenan (0.05 ml of a 1% solution) into the plantar surface of the rat hindpaw (7). At a dose of 300 mg/kg po, administered 1 hr before carrageenan, II caused moderate (44.2%) antagonism of edema formation 4 hr after the carrageenan injection; this antagonism decreased to 26.3% after 6 hr. Thus,

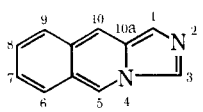

I

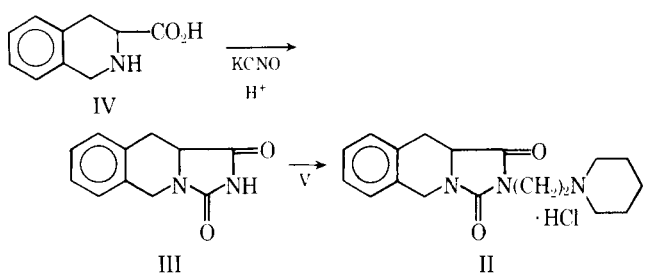

Scheme I

II possesses anti-inflammatory activity but with a shorter duration than that evoked by some standard anti-inflammatory drugs such as phenylbutazone (58% at 6 hr), indomethacin (49% at 6 hr), and ibuprofen (55% at 6 hr).

EXPERIMENTAL[1]

10,10a-Dihydro-1*H*,5*H*-imidazo[1,5-*b*]isoquinoline-1,3(2*H*)-dione (III)—To a suspension of 53.1 g (0.30 mole) of *d,l*-IV (6) in 1000 ml of acetic acid was added quickly a solution of 48.6 g (0.60 mole) of potassium cyanate in 150 ml of water. The mixture was stirred and heated on a steam bath at 90–95° for 90 min, and all solids were dissolved. Hydrochloric acid (3 *N*, 2400 ml) was added, and the resulting solution was stirred and refluxed for 20 hr. The solution was filtered while hot through a coarse sintered-glass funnel to remove mechanical impurities, and the filtrate was stored in the refrigerator for 18 hr; 44 g of the crude product was obtained.

Recrystallization from 1400 ml of alcohol gave 29.9 g (49%) of III, mp 225–231°. Further recrystallization from alcohol gave an analytical sample, mp 227–230°; IR: 3.14 (NH), 5.63, and 5.85 (C=O, imidazolidinedione) μm; NMR (dimethyl sulfoxide-d_6): δ 2.73–3.06 (m, 2, C-10 H_2), 4.05–4.96 (m, 3, C-5 H_2 and C-10a H), 7.25 (s, 4, aromatic CH), and 10.5–11.1 (broad s, 1, exchangeable, NH) ppm; mass spectrum M^+: *m/e* 202.

[1] Melting points were determined on a Mel-Temp apparatus, and those below 230° are corrected. IR spectra were determined as mineral oil mulls using a Perkin-Elmer 137B spectrophotometer. NMR spectra were obtained on a Varian A-60A instrument and were compared with tetramethylsilane as an internal standard. The mass spectrum was run on a Finnigan model 3300 mass spectrometer at the Mass Spectrometry Facility at Cornell University.

Anal.—Calc. for $C_{11}H_{10}N_2O_2$: C, 65.33; H, 4.98; N, 13.86. Found: C, 65.41; H, 4.80; N, 13.90.

2-[2-(Piperidino)ethyl]-10,10a-dihydro -1*H*,5*H*- imidazo[1,5-*b*]isoquinoline-1,3(2*H*)-dione Hydrochloride (II)—A mixture of 26.5 g (0.131 mole) of III, 48.2 g (0.262 mole) of V, 54.2 g (0.393 mole) of potassium carbonate, and 19.7 g (0.131 mole) of sodium iodide in 900 ml of dimethyl sulfoxide was stirred at 50–55° for 48 hr. An additional 24.1 g (0.131 mole) of V was added to the mixture, and stirring was continued at 50–55° for an additional 24 hr. Then the mixture was cooled, poured into 2.0 liters of cold water, and extracted with 4 × 400 ml of chloroform. The combined extracts were washed with 2 × 800 ml of water, dried (magnesium sulfate), and concentrated to dryness. The oil was boiled with 180 ml of ethanol, and the resulting suspension was stored in the refrigerator for 2 weeks. Filtration gave 9.0 g of unreacted III.

To the filtrate was added 40 ml of methanol saturated with hydrogen chloride. The resulting solid was recrystallized from 125 ml of ethanol to yield, after drying at 100° for 4 hr, 7.9 g (26% based on consumed III) of the product, mp 204–207°. An analytical sample, mp 237–239°, was obtained by recrystallization from ethanol; IR: 5.70 and 5.90 (C=O, imidazolidinedione) μm; NMR (dimethyl sulfoxide-d_6): δ 1.46–1.96 (broad m, 6, piperidine 3-CH_2, 4-CH_2, and 5-CH_2), 3.05–3.20 (m, 2, C-10 H_2), 3.16–3.50 (broad m, 4, piperidine 2-CH_2 and 6-CH_2), 3.73–5.00 (m, 7, C-5 H_2, C-10a H, and NCH_2CH_2N), 7.28 (s, 4, aromatic CH), and 10.9–11.4 (broad s, 1, exchangeable NH) ppm.

Anal.—Calc. for $C_{18}H_{23}N_3O_2$·HCl: C, 61.79; H, 6.91; N, 12.01. Found: C, 61.78; H, 7.02; N, 11.86.

REFERENCES

(1) T. J. Schwan, U.S. pat. 4,001,245 (Jan. 4, 1977).

(2) N. M. Turkevich and V. G. Zubenko, *Ukr. Khim. Zh.*, **26,** 222 (1960); through *Chem. Abstr.*, **54,** 24734b (1960).

(3) S. Nagase, *Nippon Kagaku Zasshi*, **81,** 940 (1960); through *Chem. Abstr.*, **56,** 1441a, 1442b (1962).

(4) *Ibid.*, **83,** 1284 (1962); through *Chem. Abstr.*, **60,** 5480f (1964).

(5) V. G. Zubenko and M. K. Mikhalevich, *Khim. Issled. Farm.*, **1970,** 26; through *Chem. Abstr.*, **76,** 46138y (1972).

(6) S. Archer, *J. Org. Chem.*, **16,** 430 (1951).

(7) C. A. Winter, E. A. Risley, and G. W. Nuss, *Proc. Soc. Exp. Biol. Med.*, **111,** 544 (1962).

ACKNOWLEDGMENTS

The authors are indebted to Mr. Nelson Miles for the synthesis of intermediates, Ms. Cora Jeffrey for the microanalyses, and Ms. Connie Lloyd for the NMR spectra.

dc Polarographic Determination of Hydroxylaminoeverninomicin D

PETER KABASAKALIAN, SAMI KALLINEY ˣ, and ANITA W. MAGATTI

Received June 24, 1977, from the *Development Division, Schering Corporation, Bloomfield, NJ 07003.* Accepted for publication August 18, 1977.

Abstract □ An analytical procedure for a tertiary alkylhydroxylamine, hydroxylaminoeverninomicin D, was developed. It involved the autoxidation of the compound in the presence of Cu(II) and subsequent polarographic reduction. Conditions are described for the quantitative determination of the possible impurities (everninomicin D and nitrosoeverninomicin D) in hydroxylaminoeverninomicin D.

Keyphrases □ Hydroxylaminoeverninomicin D—polarographic analysis, bulk drug □ Polarography—analysis, hydroxylaminoeverninomicin D, bulk drug □ Antibacterials—hydroxylaminoeverninomicin D, polarographic analysis, bulk drug

Everninomicins (1–3) produced by *Micromonospora carbonaceae* are highly active oligosaccharide antibiotics against Gram-positive bacteria including strains resistant to penicillins, tetracyclines, lincomycins, rifampin, macrolides, and chloramphenicol. The major component of the everninomicin complex (4) is everninomicin D (I). The chemical (5) or electrochemical (6) reduction of the tertiary nitro group in I yields hydroxylaminoeverninomicin D (II). Nitrosoeverninomicin D (III), undergoing similar reductions, also yields II. Compounds I–III possess equal *in vitro* activity against Gram-positive bacteria. However, II gives the highest blood level when administered intramuscularly to dogs.

A reported polarographic determination of alkylhydroxylamines was based on the formation of reproducible

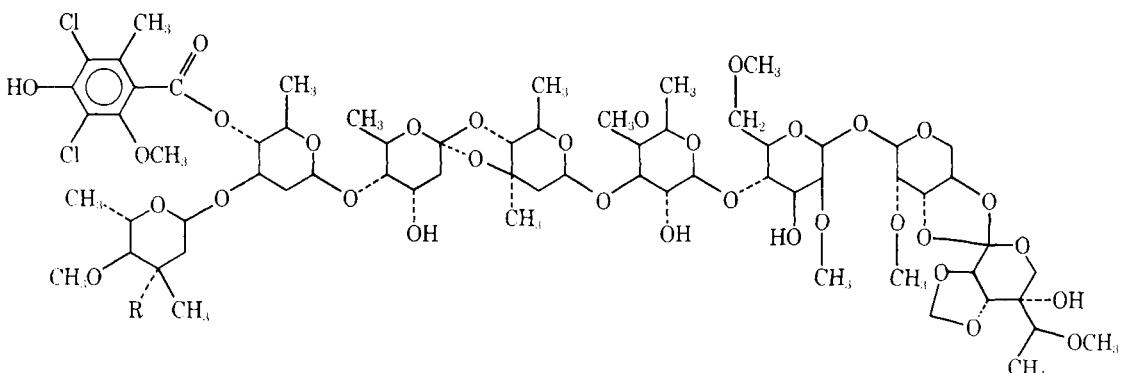

I: R = NO_2
II: R = NHOH
III: R = NO

Anal.—Calc. for $C_{11}H_{10}N_2O_2$: C, 65.33; H, 4.98; N, 13.86. Found: C, 65.41; H, 4.80; N, 13.90.

2-[2-(Piperidino)ethyl]-10,10a-dihydro -1*H*,5*H*- imidazo[1,5-*b*]isoquinoline-1,3(2*H*)-dione Hydrochloride (II)—A mixture of 26.5 g (0.131 mole) of III, 48.2 g (0.262 mole) of V, 54.2 g (0.393 mole) of potassium carbonate, and 19.7 g (0.131 mole) of sodium iodide in 900 ml of dimethyl sulfoxide was stirred at 50–55° for 48 hr. An additional 24.1 g (0.131 mole) of V was added to the mixture, and stirring was continued at 50–55° for an additional 24 hr. Then the mixture was cooled, poured into 2.0 liters of cold water, and extracted with 4 × 400 ml of chloroform. The combined extracts were washed with 2 × 800 ml of water, dried (magnesium sulfate), and concentrated to dryness. The oil was boiled with 180 ml of ethanol, and the resulting suspension was stored in the refrigerator for 2 weeks. Filtration gave 9.0 g of unreacted III.

To the filtrate was added 40 ml of methanol saturated with hydrogen chloride. The resulting solid was recrystallized from 125 ml of ethanol to yield, after drying at 100° for 4 hr, 7.9 g (26% based on consumed III) of the product, mp 204–207°. An analytical sample, mp 237–239°, was obtained by recrystallization from ethanol; IR: 5.70 and 5.90 (C=O, imidazolidinedione) μm; NMR (dimethyl sulfoxide-d_6): δ 1.46–1.96 (broad m, 6, piperidine 3-CH_2, 4-CH_2, and 5-CH_2), 3.05–3.20 (m, 2, C-10 H_2), 3.16–3.50 (broad m, 4, piperidine 2-CH_2 and 6-CH_2), 3.73–5.00 (m, 7, C-5 H_2, C-10a H, and NCH_2CH_2N), 7.28 (s, 4, aromatic CH), and 10.9–11.4 (broad s, 1, exchangeable NH) ppm.

Anal.—Calc. for $C_{18}H_{23}N_3O_2$·HCl: C, 61.79; H, 6.91; N, 12.01. Found: C, 61.78; H, 7.02; N, 11.86.

REFERENCES

(1) T. J. Schwan, U.S. pat. 4,001,245 (Jan. 4, 1977).

(2) N. M. Turkevich and V. G. Zubenko, *Ukr. Khim. Zh.*, **26,** 222 (1960); through *Chem. Abstr.*, **54,** 24734b (1960).

(3) S. Nagase, *Nippon Kagaku Zasshi*, **81,** 940 (1960); through *Chem. Abstr.*, **56,** 1441a, 1442b (1962).

(4) *Ibid.*, **83,** 1284 (1962); through *Chem. Abstr.*, **60,** 5480f (1964).

(5) V. G. Zubenko and M. K. Mikhalevich, *Khim. Issled. Farm.*, **1970,** 26; through *Chem. Abstr.*, **76,** 46138y (1972).

(6) S. Archer, *J. Org. Chem.*, **16,** 430 (1951).

(7) C. A. Winter, E. A. Risley, and G. W. Nuss, *Proc. Soc. Exp. Biol. Med.*, **111,** 544 (1962).

ACKNOWLEDGMENTS

The authors are indebted to Mr. Nelson Miles for the synthesis of intermediates, Ms. Cora Jeffrey for the microanalyses, and Ms. Connie Lloyd for the NMR spectra.

dc Polarographic Determination of Hydroxylaminoeverninomicin D

PETER KABASAKALIAN, SAMI KALLINEY ˣ, and ANITA W. MAGATTI

Received June 24, 1977, from the *Development Division, Schering Corporation, Bloomfield, NJ 07003.* Accepted for publication August 18, 1977.

Abstract □ An analytical procedure for a tertiary alkylhydroxylamine, hydroxylaminoeverninomicin D, was developed. It involved the autoxidation of the compound in the presence of Cu(II) and subsequent polarographic reduction. Conditions are described for the quantitative determination of the possible impurities (everninomicin D and nitrosoeverninomicin D) in hydroxylaminoeverninomicin D.

Keyphrases □ Hydroxylaminoeverninomicin D—polarographic analysis, bulk drug □ Polarography—analysis, hydroxylaminoeverninomicin D, bulk drug □ Antibacterials—hydroxylaminoeverninomicin D, polarographic analysis, bulk drug

Everninomicins (1–3) produced by *Micromonospora carbonaceae* are highly active oligosaccharide antibiotics against Gram-positive bacteria including strains resistant to penicillins, tetracyclines, lincomycins, rifampin, macrolides, and chloramphenicol. The major component of the everninomicin complex (4) is everninomicin D (I). The chemical (5) or electrochemical (6) reduction of the tertiary nitro group in I yields hydroxylaminoeverninomicin D (II). Nitrosoeverninomicin D (III), undergoing similar reductions, also yields II. Compounds I–III possess equal *in vitro* activity against Gram-positive bacteria. However, II gives the highest blood level when administered intramuscularly to dogs.

A reported polarographic determination of alkylhydroxylamines was based on the formation of reproducible

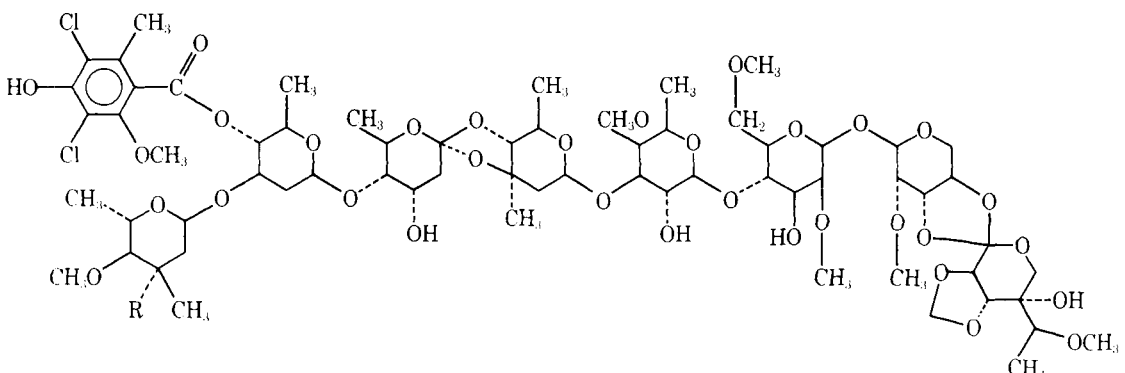

I: R = NO_2
II: R = NHOH
III: R = NO

Table I—Effect of pH on the Autoxidation of Hydroxylaminoeverninomicin D[a] in the Absence and Presence of Cu(II) in 50% Aqueous Methanol

pH[b]	$-E_{1/2}$ *versus* NCE, v	Cu(II)[c]	Aeration Time, min	Diffusion Current, μamp
9	0.40	Absent	15	0.20
		Absent	30	0.22
		Present	15	1.10
		Present	30	1.10
	1.24	Absent	15	0.52
		Absent	30	0.58
		Present	15	0.14
		Present	30	0.11
10	0.43	Absent	15	0.23
		Absent	30	0.25
		Present	15	1.15
		Present	30	1.17
	1.24	Absent	15	0.55
		Absent	30	0.65
		Present	15	0.00
		Present	30	0.00
11	0.47	Absent	15	0.24
		Absent	30	0.30
		Present	15	1.09
		Present	30	1.11
	1.23	Absent	15	0.56
		Absent	30	0.74
		Present	15	0.15
		Present	30	0.13
12	0.52	Absent	15	0.72
		Absent	30	0.85
		Present	15	0.94
		Present	30	0.93
	1.26	Absent	15	1.58
		Absent	30	1.98
		Present	15	0.11
		Present	30	0.13

[a] Concentration = 1 mg/ml. [b] Tertiary amine organic buffers. [c] Cu(II) = 10 ppm.

anodic waves in alkaline media (7). Since, in the presence of oxygen, alkylhydroxylamines yield irreproducible anodic waves which cannot be removed by nitrogen flushing, oxygen was removed using an alkaline sulfite solution.

Unfortunately, this procedure failed for II, since sulfite oxidation for the removal of oxygen is inhibited (8) in the presence of organic solvents (acetonitrile, dimethylformamide, and methanol) in which everninomicins must be prepared because of their poor solubility in water.

A polarographic analytical procedure was developed to assay II during synthesis and as a finished product. This method is based on the production of polarographically reducible functional groups in the autoxidation of II catalyzed by Cu(II) ions.

EXPERIMENTAL

Apparatus—All polarograms were recorded on a polarograph[1] equipped with a 3-ml H-type cell containing a normal calomel electrode (NCE) and a dropping mercury electrode. The cell compartments were separated by an agar plug and a fritted-glass diaphragm. The chloride ions in both the calomel cell and the agar plug were furnished by tetramethylammonium chloride.

Chemicals—All chemicals were the highest quality commercially available. Separate standard solutions of I–III were prepared from pure powder[2] in acetonitrile, dimethylformamide, or methanol.

Procedure—Separate stock solutions (>2 mg/ml) of I–III were prepared in acetonitrile, dimethylformamide, or methanol. Five milliliters of triethylamine (0.05 *M*)–hydrochloric acid (0.007 *M*) buffer and a volume of the stock solution containing 10 mg of I, II, or III were put into a 10-ml volumetric flask. The mixture was diluted to volume with the corresponding organic solvent. An aliquot was transferred to the polarographic cell and deaerated with prewashed (with a blank solution) argon for about 15 min.

The applied potential range was from 0.00 to −1.50 v (normal calomel electrode), and the current range was set at 2 μamp. Fifty microliters of 7 mg of Cu(II)/ml in 2 *N* ammonium hydroxide was added to the 10-ml volumetric flask and allowed to stand exposed to air at room temperature for 15 min. A second polarogram was obtained using an aliquot of the Cu(II)-containing mixture. The first polarogram served as a blank for the second one.

The mercury flow rate at an open circuit with mercury dropping into 0.1 *M* potassium chloride was 1.16 mg/sec, the drop time was 5.48 sec, and the mercury column height was 61.4 cm.

[1] Leeds and Northrup Electro-Chemograph Type E.
[2] Schering Corp., Bloomfield, N.J.

Table II—Effect of Cu(II) Concentration on the Autoxidation of Hydroxylaminoeverninomicin D[a] in 50% Aqueous Methanol at pH 10

Cu(II) Concentration, ppm	$-E_{1/2}$ *versus* NCE, v	Aeration Time, min	Diffusion Current, μamp
0	0.43	0	0.00
		15	0.16
		30	0.26
	1.24	0	0.00
		15	0.52
		30	0.76
5	0.43	0	0.48
		15	1.06
		30	1.06
	1.25	0	0.32
		15	0.00
		30	0.00
10	0.46	0	1.30
		15	1.14
		30	1.12
	1.24	0	0.07
		15	0.00
		30	0.00
25	0.44	0	1.44
		15	1.44
		30	1.53
50	0.46	0	1.01
		15	1.05
		30	1.04
100	0.44	0	1.38
		15	1.05
		30	1.02

[a] Concentration = 1 mg/ml.

RESULTS AND DISCUSSION

Compound II was not reduced polarographically over the potential range between 0.0 and −2.0 v (normal calomel electrode). However, buffered basic solutions (tertiary amine organic buffers) in 50% aqueous methanol, on standing in air, developed two polarographic reduction waves (Table I). The magnitude of these reduction currents depended on pH and time.

The presence of Cu(II) had a catalytic effect, increasing the first reduction wave ($E_{1/2} \sim -0.4$ v) while reducing the second wave ($E_{1/2} \sim -1.2$ v). At pH 10, the second wave was completely eliminated. With this optimum pH of 10, the effect of Cu(II) concentration on the reduction waves was determined (Table II). Between 0 and 30 min of aeration, the least amount of diffusion current variation occurred at 50 ppm of Cu(II). Consequently, pH 10 and 15 min aeration time were chosen as the optimum conditions for constructing a linear standard curve for II over a 0.1–1.6-mg/ml range. The slope of the diffusion current (measured at −0.6 v) *versus* the concentration curve of II was 0.80 μamp/mg/ml, while the detection limit was about 0.05 mg/ml.

Although I and III are not autoxidizable even in the presence of Cu(II), they yield polarographic reduction waves having nearly identical half-wave potentials ($E_{1/2}$) of about −1.2 v under the described conditions. When either one or both of these compounds are present as impurities in II, the total content of I and III can be determined from the first polarogram run in the absence of Cu(II).

Fifty percent aqueous acetonitrile or dimethylformamide solution can be used successfully in this procedure for following the electrochemical

synthesis of II. However 50% aqueous methanol is preferred for the analysis of pure II, since it yields a linear calibration line with a higher correlation coefficient.

REFERENCES

(1) M. J. Weinstein, G. M. Luedemann, E. Oden, and G. H. Wagman, *Antimicrob. Agents Chemother.*, **1964**, 24.

(2) G. H. Wagman, G. M. Luedemann, and M. J. Weinstein, *ibid.*, **1964**, 33.

(3) H. L. Herzog, E. Meseck, S. DeLorenzo, A. Murawski, W. Charney, and J. P. Rosselet, *Appl. Microbiol.*, **13**, 515 (1965).

(4) A. K. Ganguly, O. Z. Sarre, D. Greeves, and J. Morton, *J. Am. Chem. Soc.*, **97**, 1982 (1975).

(5) A. K. Ganguly, S. Szmulewicz, O. Z. Sarre, and V. M. Girijavallabhan, *J. Chem. Soc., Chem. Commun.*, **1976**, 609.

(6) P. Kabasakalian, S. Kalliney, A. K. Ganguly, and A. Westcott, U.S. pat. 3,998,708 (1976).

(7) P. E. Iversen and H. Lund, *Anal. Chem.*, **41**, 1322 (1969).

(8) L. C. Schroeter, *J. Pharm. Sci.*, **52**, 559 (1963).

Chemical Constituents of Gentianaceae XXIV: Anti-*Mycobacterium tuberculosis* Activity of Naturally Occurring Xanthones and Synthetic Analogs

S. GHOSAL ˣ, K. BISWAS, and R. K. CHAUDHURI *

Received May 17, 1977, from the *Pharmaceutical Chemistry Research Laboratory, Department of Pharmaceutics, Banaras Hindu University, Varanasi-5, India.* Accepted for publication August 24, 1977.

*Present address: Pharmazeutisches Institut der Universität, Bonn, West Germany.

Abstract □ Anti-*Mycobacterium tuberculosis* H37 RV data are presented for the individual xanthones of *Canscora decussata* Schult and *Swertia purpurascens* Wall (Gentianaceae); a few, from the former species, showed significant activity. Additionally, structure–activity relationships of these compounds are evaluated on the basis of the minimum inhibitory concentration data of 18 naturally occurring xanthones bearing 1,3,5-, 1,3,5,6-, 1,3,6,7-, 1,3,5,8-, 1,3,5,6,7-, and 1,3,6,7,8-oxygenated patterns and six synthetic analogs.

Keyphrases □ Xanthones, various—naturally occurring and synthetic, anti-*Mycobacterium tuberculosis* activity evaluated *in vitro* □ *Mycobacterium tuberculosis*—effect of various naturally occurring and synthetic xanthones *in vitro* □ Structure–activity relationships—various naturally occurring and synthetic xanthones evaluated for anti-*Mycobacterium tuberculosis* activity *in vitro*

A previous paper (1) described the significant anti-*Mycobacterium tuberculosis* activity of the total polyoxygenated xanthones of *Canscora decussata* Schult (Gentianaceae). This paper reports the identification of the potent anti-*M. tuberculosis* components of this plant. Additionally, the microbiological screening of synthetic analogs was conducted to evaluate the importance of the number and patterns of oxygenation of xanthones for this type of biological activity.

EXPERIMENTAL

Compounds—Xanthones I–IX, XII–XV, and XX–XXIV were available from previous investigations of *C. decussata* and *Swertia* species. Xanthone X was obtained by methylating IX with ethereal diazomethane. On permethylation with dimethyl sulfate and potassium carbonate in acetone under reflux (46 hr), IX gave XI. Xanthones XVI–XIX were prepared by using previously reported procedures (Table I).

References to the isolation or preparation of the compounds are given in the table.

Test—A description of the screening method of *M. tuberculosis* H37 RV growth inhibitor activity was given previously (1). The minimum inhibitory concentration (MIC) of the test compounds required for preventing the microorganism growth was recorded (Table I). The compounds that could not prevent growth of the microorganism up to a dose of 200 μg/ml were considered inactive.

RESULTS AND DISCUSSION

The MIC data (Table I) of the 24 xanthones suggest that, for a moderate to significant anti-*M. tuberculosis* activity, the xanthone nucleus should contain oxygen functions at 1,3- and 5,6- or 8-positions. Among the seven types of oxygenated xanthones tested for this activity, 1,3,5,6,7- and 1,3,6,7,8-pentaoxygenated xanthones (XII and XVIII, respectively) were the most potent. Furthermore, in these two types of oxygenated

Table I—Growth Inhibitor Activity of Polyoxygenated Xanthones against *M. tuberculosis* H37 RV

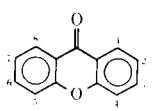

Number	Xanthone	Reference	MIC, mcg/ml
I	1,3,5-Trihydroxy	2	200
II	1-Methoxy-3,5-dihydroxy	2	Inactive
III	1,5-Dihydroxy-3-methoxy	3	Inactive
IV	1-Glucosyloxy-3-hydroxy-5-methoxy	4	Inactive
V	1-Hydroxy-3,5-dimethoxy	3	Inactive
VI	1,3,5,6-Tetrahydroxy	5	10
VII	1,3,5-Trihydroxy-6-methoxy	3	40
VIII	1,6-Dihydroxy-3,5-dimethoxy	6	100
IX	1,3,6,7-Tetrahydroxy	5	40
X	1-Hydroxy-3,6,7-trimethoxy	5	100
XI	1,3,6,7-Tetramethoxy	5	100
XII	1,3,6-Trihydroxy-5,7-dimethoxy	7	5
XIII	1,6,7-Trihydroxy-3,5-dimethoxy	7	40
XIV	1,5,6-Trihydroxy-3,7-dimethoxy	7	10
XV	7-Glucosyloxy-1,6-dihydroxy-3,5-dimethoxy	4	100
XVI	1,3,8-Trihydroxy	7, 8	10
XVII	1,8-Dihydroxy-3-methoxy	7, 8	40
XVIII	1,3,6,7,8-Pentahydroxy	7, 8	5
XIX	1,3,6-Trihydroxy-7,8-dimethoxy	7, 8	10
XX	1,3,5,8-Tetrahydroxy	9	100
XXI	1,5,8-Trihydroxy-3-methoxy	10	200
XXII	1,3,8-Trihydroxy-5-methoxy	10	200
XXIII	1-Glucosyloxy-3,5,8-trihydroxy	9	200
XXIV	1-Glucosyloxy-3-methoxy-5,8-dihydroxy	9	200
	Streptomycin sulfate[a]		0.5

[a] Standard antitubercular drug used for comparison of activity against this strain.

synthesis of II. However 50% aqueous methanol is preferred for the analysis of pure II, since it yields a linear calibration line with a higher correlation coefficient.

REFERENCES

(1) M. J. Weinstein, G. M. Luedemann, E. Oden, and G. H. Wagman, *Antimicrob. Agents Chemother.*, **1964**, 24.

(2) G. H. Wagman, G. M. Luedemann, and M. J. Weinstein, *ibid.*, **1964**, 33.

(3) H. L. Herzog, E. Meseck, S. DeLorenzo, A. Murawski, W. Charney, and J. P. Rosselet, *Appl. Microbiol.*, **13**, 515 (1965).

(4) A. K. Ganguly, O. Z. Sarre, D. Greeves, and J. Morton, *J. Am. Chem. Soc.*, **97**, 1982 (1975).

(5) A. K. Ganguly, S. Szmulewicz, O. Z. Sarre, and V. M. Girijavallabhan, *J. Chem. Soc., Chem. Commun.*, **1976**, 609.

(6) P. Kabasakalian, S. Kalliney, A. K. Ganguly, and A. Westcott, U.S. pat. 3,998,708 (1976).

(7) P. E. Iversen and H. Lund, *Anal. Chem.*, **41**, 1322 (1969).

(8) L. C. Schroeter, *J. Pharm. Sci.*, **52**, 559 (1963).

Chemical Constituents of Gentianaceae XXIV: Anti-*Mycobacterium tuberculosis* Activity of Naturally Occurring Xanthones and Synthetic Analogs

S. GHOSAL ˣ, K. BISWAS, and R. K. CHAUDHURI *

Received May 17, 1977, from the *Pharmaceutical Chemistry Research Laboratory, Department of Pharmaceutics, Banaras Hindu University, Varanasi-5, India.* Accepted for publication August 24, 1977.

*Present address: Pharmazeutisches Institut der Universität, Bonn, West Germany.

Abstract □ Anti-*Mycobacterium tuberculosis* H37 RV data are presented for the individual xanthones of *Canscora decussata* Schult and *Swertia purpurascens* Wall (Gentianaceae); a few, from the former species, showed significant activity. Additionally, structure–activity relationships of these compounds are evaluated on the basis of the minimum inhibitory concentration data of 18 naturally occurring xanthones bearing 1,3,5-, 1,3,5,6-, 1,3,6,7-, 1,3,5,8-, 1,3,5,6,7-, and 1,3,6,7,8-oxygenated patterns and six synthetic analogs.

Keyphrases □ Xanthones, various—naturally occurring and synthetic, anti-*Mycobacterium tuberculosis* activity evaluated *in vitro* □ *Mycobacterium tuberculosis*—effect of various naturally occurring and synthetic xanthones *in vitro* □ Structure–activity relationships—various naturally occurring and synthetic xanthones evaluated for anti-*Mycobacterium tuberculosis* activity *in vitro*

A previous paper (1) described the significant anti-*Mycobacterium tuberculosis* activity of the total polyoxygenated xanthones of *Canscora decussata* Schult (Gentianaceae). This paper reports the identification of the potent anti-*M. tuberculosis* components of this plant. Additionally, the microbiological screening of synthetic analogs was conducted to evaluate the importance of the number and patterns of oxygenation of xanthones for this type of biological activity.

EXPERIMENTAL

Compounds—Xanthones I–IX, XII–XV, and XX–XXIV were available from previous investigations of *C. decussata* and *Swertia* species. Xanthone X was obtained by methylating IX with ethereal diazomethane. On permethylation with dimethyl sulfate and potassium carbonate in acetone under reflux (46 hr), IX gave XI. Xanthones XVI–XIX were prepared by using previously reported procedures (Table I).

References to the isolation or preparation of the compounds are given in the table.

Test—A description of the screening method of *M. tuberculosis* H37 RV growth inhibitor activity was given previously (1). The minimum inhibitory concentration (MIC) of the test compounds required for preventing the microorganism growth was recorded (Table I). The compounds that could not prevent growth of the microorganism up to a dose of 200 μg/ml were considered inactive.

RESULTS AND DISCUSSION

The MIC data (Table I) of the 24 xanthones suggest that, for a moderate to significant anti-*M. tuberculosis* activity, the xanthone nucleus should contain oxygen functions at 1,3- and 5,6- or 8-positions. Among the seven types of oxygenated xanthones tested for this activity, 1,3,5,6,7- and 1,3,6,7,8-pentaoxygenated xanthones (XII and XVIII, respectively) were the most potent. Furthermore, in these two types of oxygenated

Table I—Growth Inhibitor Activity of Polyoxygenated Xanthones against *M. tuberculosis* H37 RV

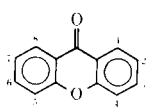

Number	Xanthone	Reference	MIC, mcg/ml
I	1,3,5-Trihydroxy	2	200
II	1-Methoxy-3,5-dihydroxy	2	Inactive
III	1,5-Dihydroxy-3-methoxy	3	Inactive
IV	1-Glucosyloxy-3-hydroxy-5-methoxy	4	Inactive
V	1-Hydroxy-3,5-dimethoxy	3	Inactive
VI	1,3,5,6-Tetrahydroxy	5	10
VII	1,3,5-Trihydroxy-6-methoxy	3	40
VIII	1,6-Dihydroxy-3,5-dimethoxy	6	100
IX	1,3,6,7-Tetrahydroxy	5	40
X	1-Hydroxy-3,6,7-trimethoxy	5	100
XI	1,3,6,7-Tetramethoxy	5	100
XII	1,3,6-Trihydroxy-5,7-dimethoxy	7	5
XIII	1,6,7-Trihydroxy-3,5-dimethoxy	7	40
XIV	1,5,6-Trihydroxy-3,7-dimethoxy	7	10
XV	7-Glucosyloxy-1,6-dihydroxy-3,5-dimethoxy	4	100
XVI	1,3,8-Trihydroxy	7, 8	10
XVII	1,8-Dihydroxy-3-methoxy	7, 8	40
XVIII	1,3,6,7,8-Pentahydroxy	7, 8	5
XIX	1,3,6-Trihydroxy-7,8-dimethoxy	7, 8	10
XX	1,3,5,8-Tetrahydroxy	9	100
XXI	1,5,8-Trihydroxy-3-methoxy	10	200
XXII	1,3,8-Trihydroxy-5-methoxy	10	200
XXIII	1-Glucosyloxy-3,5,8-trihydroxy	9	200
XXIV	1-Glucosyloxy-3-methoxy-5,8-dihydroxy	9	200
	Streptomycin sulfate[a]		0.5

[a] Standard antitubercular drug used for comparison of activity against this strain.

xanthones, those containing hydroxyl groups at 1,3- and 6- or 8-positions were more active than those containing other substituents (methoxy or glucosyloxy) at these positions.

Norswertianolin (1-glucosyloxy-3,5,8-trihydroxyxanthone) (XXIII) and swertianolin (1-glucosyloxy-3-methoxy-5,8-dihydroxyxanthone) (XXIV), which occur in a number of *Swertia* species (9–11), were previously reported to produce antitubercular activity, although their exact potency was not reported (11). In the present investigation, XXIII and XXIV exhibited only a weak anti-*M. tuberculosis* activity. The aglucone (XX) of XXIII appeared to be more active than the corresponding 1-*O*-glucosyl derivative, suggesting the importance of the free hydroxyl group at the 1-position for activity.

Hansch analysis (12) with the partition coefficients (π) and MIC values of I–XXIV was attempted but did not provide a good correlation. Electronic and steric factors also seemed to be responsible for the observed biological activity.

REFERENCES

(1) S. Ghosal and R. K. Chaudhuri, *J. Pharm. Sci.*, **64**, 888 (1975).

(2) S. Ghosal, K. Biswas, R. B. P. S. Chauhan, and R. K. Chaudhuri, *Phytochemistry*, **15**, 1041 (1976).

(3) R. K. Chaudhuri and S. Ghosal, *ibid.*, **10**, 2425 (1971).

(4) S. Ghosal, K. Biswas, and R. K. Chaudhuri, *J. Chem. Soc. Perkin Trans.*, **1**, 1597 (1977).

(5) S. Ghosal and R. K. Chaudhuri, *Phytochemistry*, **12**, 2035 (1973).

(6) S. Ghosal, R. K. Chaudhuri, and A. Nath, *J. Pharm. Sci.*, **62**, 137 (1973).

(7) S. Ghosal, R. K. Chaudhuri, and K. R. Markham, *J. Chem. Soc. Perkin Trans.*, **1**, 2538 (1974).

(8) R. K. Chaudhuri, Ph.D. thesis, Banaras Hindu University, Varanasi, India, 1973, p. 127.

(9) S. Ghosal, P. V. Sharma, and R. K. Chaudhuri, *J. Pharm. Sci.*, **63**, 1286 (1974).

(10) S. Ghosal, P. V. Sharma, R. K. Chaudhuri, and S. K. Bhattacharya, *ibid.*, **62**, 926 (1973).

(11) M. Komatsu and T. Tomimori, Japanese pat. 7,216,676 (1972); through *Chem. Abstr.*, **77**, 8578 (1972).

(12) C. Hansch, in "Drug Design," vol. 1, E. J. Ariens, Ed., Academic, New York, N.Y., 1971, p. 271.

ACKNOWLEDGMENTS

The authors thank Dr. M. H. Shah, Haffkine Institute, Bombay, India, for providing the microbiological screening data and Prof. Dr. F. Zymalkowski, Pharmazeutisches Institut der Universität, Bonn, West Germany, for providing counsel and laboratory facilities to R. K. Chaudhuri. K. Biswas thanks the Council of Scientific and Industrial Research, New Delhi, India, for a Research Fellowship.

Characterization of Products Derived from Aprindine Hydrochloride Photolysis

AARON D. KOSSOY ˣ **and GARY C. COOKE**

Received March 7, 1977, from the *Lilly Research Laboratories, Eli Lilly and Company, Indianapolis, IN 46206.* Accepted for publication August 29, 1977.

Abstract □ An investigation of the products resulting from the photolysis of aprindine hydrochloride is described. The compounds were characterized by GLC spiking experiments and combined GLC–mass spectrometry. In some cases, R_f values derived from TLC and/or preparative TLC and subsequent high-resolution mass spectral measurements also were employed for identification.

Keyphrases □ Aprindine hydrochloride—photolysis products identified by GLC and combined GLC–mass spectrometry □ GLC and combined GLC–mass spectrometry—identification of photolysis products of aprindine hydrochloride □ Photolysis—aprindine hydrochloride, products identified by GLC and GLC–mass spectrometry □ Cardiac depressants—aprindine hydrochloride, photolysis products identified by GLC and GLC–mass spectrometry

In a previous report (1), a GLC method was presented which effectively monitors the stability of the antiarrhythmic agent aprindine hydrochloride (2) [*N,N*-diethyl-*N'*-(2-indanyl)-*N'*-phenyl-1,3-propanediamine hydrochloride] (I). During this work, it was discovered that I is not stable to UV irradiation, as evidenced by extra peaks in the gas chromatograms obtained from GLC analysis of the photolysis solutions. Tentative identifications were suggested on the basis of GLC retention times, but detailed characterizations were not reported.

This report describes the characterization of the aprindine photoproducts *via* TLC, GLC, and combined GLC–mass spectrometry.

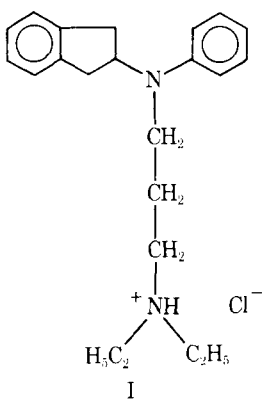

I

EXPERIMENTAL

GLC and combined GLC–mass spectrometric measurements were obtained using the instruments previously described (1). For this work, however, the combined gas chromatograph–mass spectrometer was interfaced to a data system[1] that provided a background subtraction routine as an option. Additionally, nonlinear temperature programming provided optimal resolution.

A typical run was carried out as follows: the oven was equilibrated at 120°, the sample was injected, and the chromatogram was recorded isothermally for 3.0 min. The oven temperature was then raised to 190°.

[1] The 150 data system, Systems Industries, Sunnyvale, Calif.

xanthones, those containing hydroxyl groups at 1,3- and 6- or 8-positions were more active than those containing other substituents (methoxy or glucosyloxy) at these positions.

Norswertianolin (1-glucosyloxy-3,5,8-trihydroxyxanthone) (XXIII) and swertianolin (1-glucosyloxy-3-methoxy-5,8-dihydroxyxanthone) (XXIV), which occur in a number of *Swertia* species (9–11), were previously reported to produce antitubercular activity, although their exact potency was not reported (11). In the present investigation, XXIII and XXIV exhibited only a weak anti-*M. tuberculosis* activity. The aglucone (XX) of XXIII appeared to be more active than the corresponding 1-*O*-glucosyl derivative, suggesting the importance of the free hydroxyl group at the 1-position for activity.

Hansch analysis (12) with the partition coefficients (π) and MIC values of I–XXIV was attempted but did not provide a good correlation. Electronic and steric factors also seemed to be responsible for the observed biological activity.

REFERENCES

(1) S. Ghosal and R. K. Chaudhuri, *J. Pharm. Sci.*, **64**, 888 (1975).

(2) S. Ghosal, K. Biswas, R. B. P. S. Chauhan, and R. K. Chaudhuri, *Phytochemistry*, **15**, 1041 (1976).

(3) R. K. Chaudhuri and S. Ghosal, *ibid.*, **10**, 2425 (1971).

(4) S. Ghosal, K. Biswas, and R. K. Chaudhuri, *J. Chem. Soc. Perkin Trans.*, **1**, 1597 (1977).

(5) S. Ghosal and R. K. Chaudhuri, *Phytochemistry*, **12**, 2035 (1973).

(6) S. Ghosal, R. K. Chaudhuri, and A. Nath, *J. Pharm. Sci.*, **62**, 137 (1973).

(7) S. Ghosal, R. K. Chaudhuri, and K. R. Markham, *J. Chem. Soc. Perkin Trans.*, **1**, 2538 (1974).

(8) R. K. Chaudhuri, Ph.D. thesis, Banaras Hindu University, Varanasi, India, 1973, p. 127.

(9) S. Ghosal, P. V. Sharma, and R. K. Chaudhuri, *J. Pharm. Sci.*, **63**, 1286 (1974).

(10) S. Ghosal, P. V. Sharma, R. K. Chaudhuri, and S. K. Bhattacharya, *ibid.*, **62**, 926 (1973).

(11) M. Komatsu and T. Tomimori, Japanese pat. 7,216,676 (1972); through *Chem. Abstr.*, **77**, 8578 (1972).

(12) C. Hansch, in "Drug Design," vol. 1, E. J. Ariens, Ed., Academic, New York, N.Y., 1971, p. 271.

ACKNOWLEDGMENTS

The authors thank Dr. M. H. Shah, Haffkine Institute, Bombay, India, for providing the microbiological screening data and Prof. Dr. F. Zymalkowski, Pharmazeutisches Institut der Universität, Bonn, West Germany, for providing counsel and laboratory facilities to R. K. Chaudhuri. K. Biswas thanks the Council of Scientific and Industrial Research, New Delhi, India, for a Research Fellowship.

Characterization of Products Derived from Aprindine Hydrochloride Photolysis

AARON D. KOSSOY ˣ **and GARY C. COOKE**

Received March 7, 1977, from the *Lilly Research Laboratories, Eli Lilly and Company, Indianapolis, IN 46206.* Accepted for publication August 29, 1977.

Abstract □ An investigation of the products resulting from the photolysis of aprindine hydrochloride is described. The compounds were characterized by GLC spiking experiments and combined GLC–mass spectrometry. In some cases, R_f values derived from TLC and/or preparative TLC and subsequent high-resolution mass spectral measurements also were employed for identification.

Keyphrases □ Aprindine hydrochloride—photolysis products identified by GLC and combined GLC–mass spectrometry □ GLC and combined GLC–mass spectrometry—identification of photolysis products of aprindine hydrochloride □ Photolysis—aprindine hydrochloride, products identified by GLC and GLC–mass spectrometry □ Cardiac depressants—aprindine hydrochloride, photolysis products identified by GLC and GLC–mass spectrometry

In a previous report (1), a GLC method was presented which effectively monitors the stability of the antiarrhythmic agent aprindine hydrochloride (2) [*N,N*-diethyl-*N'*-(2-indanyl)-*N'*-phenyl-1,3-propanediamine hydrochloride] (I). During this work, it was discovered that I is not stable to UV irradiation, as evidenced by extra peaks in the gas chromatograms obtained from GLC analysis of the photolysis solutions. Tentative identifications were suggested on the basis of GLC retention times, but detailed characterizations were not reported.

This report describes the characterization of the aprindine photoproducts *via* TLC, GLC, and combined GLC–mass spectrometry.

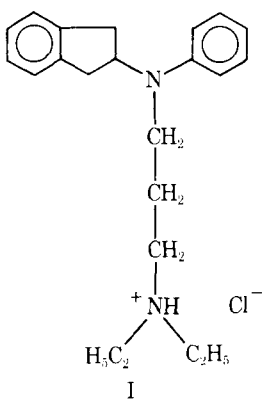

I

EXPERIMENTAL

GLC and combined GLC–mass spectrometric measurements were obtained using the instruments previously described (1). For this work, however, the combined gas chromatograph–mass spectrometer was interfaced to a data system[1] that provided a background subtraction routine as an option. Additionally, nonlinear temperature programming provided optimal resolution.

A typical run was carried out as follows: the oven was equilibrated at 120°, the sample was injected, and the chromatogram was recorded isothermally for 3.0 min. The oven temperature was then raised to 190°.

[1] The 150 data system, Systems Industries, Sunnyvale, Calif.

Table I—Chromatographic and Mass Spectral Data

GLC Component	Retention Time, min	Percent[a]	R_f[b]	Principal Ions (*m/e*)
1	0.3	0.5	—	—[c]
2	0.5	2.2	—	—[c]
3	1.3	3.7	—	91 ($C_7H_7^+$), 106 (M − HCN), 116 (M − NH_3), 133 (M^+)
4	2.2	—[d]	—	91 ($C_7H_7^+$), 105 (M − CH_2=NCH_3), 117 (M − CH_3NH·), 118 (M − CH_2=NH), 147 (M^+)
5	5.2	10.7	0.43	Series 1, 72, 86, 113; Series 2, 93, 106, 119, 120, 133, 134; 206 (M^+)
6	7.0	4.4	—	—[c]
7	7.5	5.8	0.12	Series 1, 73, 86, 100, 113; Series 2, 130, 158, 173; 246 (M^+)
8	7.9	6.0	0.84	77 ($C_6H_5^+$), 93 ($C_6H_5NH_2^{7+}$), 104 (133 − HCN), 106 (133 − CH_2=NH), 133 (M − C_6H_5·), 209 (M^+)
9	8.2	3.8	—	—[c]
10	14.6	9.6	0.67	Series 1, 58, 72, 86; Series 2, 208, 222, 236, 249; 116 ($C_9H_8^{7+}$), 178 (M − indan), 192 (M − C_8H_6), 294 (M^+)
11	17.5	53.3	0.51	—[c]
12	18.6	—[d]	—	—[c]

[a] Calculated from the chromatogram using peak area (height × width at half height). [b] Methanol–acetic acid (8:2) on silica gel. [c] See text. [d] Trace component.

After an additional 7.0 min, the temperature was raised again to 210°. The run was completed after 10 min at the latter setting. A similar procedure but a wider temperature range, 80–240°, provided the best resolution with the combined gas chromatograph–mass spectrometer.

The photolyses were run in methanol solution using a 250-ml photochemical reactor[2] equipped with a medium pressure 200-w mercury vapor immersion lamp[3], a nitrogen inlet, a cooling jacket, and a condenser. A filter sleeve[4] was fitted over the quartz jacket of the immersion unit to exclude all wavelengths below 220 nm. The solutions (typically 2.0 g in 200 ml) were purged with nitrogen for 30 min prior to irradiation and agitated during irradiation by a stream of nitrogen bubbles generated through a circular perforated glass tube placed on the bottom of the solution chamber.

At the conclusion of the photolyses (30.5 hr), the solution was concentrated on a rotary evaporator to one-tenth of its original volume. Aliquots of the concentrate were made alkaline with excess 10% sodium carbonate and extracted into chloroform. The chloroform extracts were employed in all subsequent work.

TLC was employed using 0.25-mm (for the determination of R_f values) and 0.50-mm (for preparative work) thick silica gel plates[5]. The analytical solvent system was methanol–acetic acid (8:2)[6], and the preparative system was ethyl acetate–triethylamine (95:5). The thin-layer plates were visualized by spraying with the Folin–Ciocalteu reagent (3) followed by 20% aqueous sodium carbonate. This procedure yields blue to blue-purple spots on a white background[6].

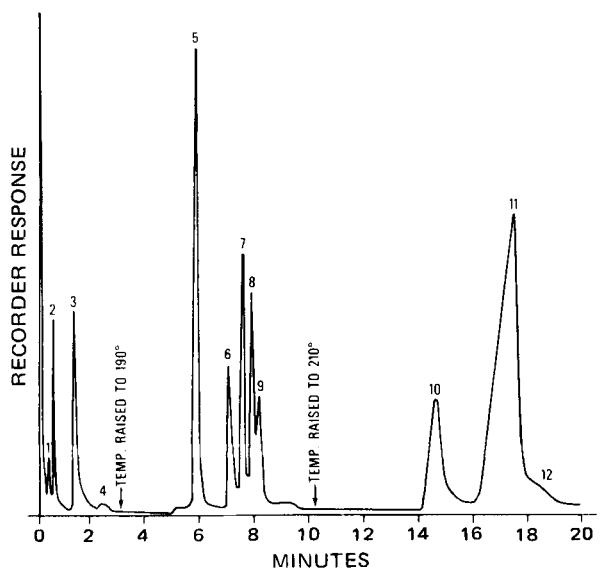

Figure 1—*Gas chromatogram obtained from the photolysis solution.*

[2] Catalog No. 6515-03, Ace Glass Inc., Vineland, N.J.
[3] Catalog No. 6515-32, Ace Glass Inc., Vineland, N.J.
[4] Catalog No. 6515-40, Vycor 7010 (Corning), Ace Glass Inc., Vineland, N.J.
[5] Silica gel 60 F_{254} plates, E. Merck, Darmstadt, West Germany.
[6] B. S. Rutherford and R. H. Bishara, Lilly Research Laboratories, Eli Lilly and Co., Indianapolis, IN 46206, unpublished work.

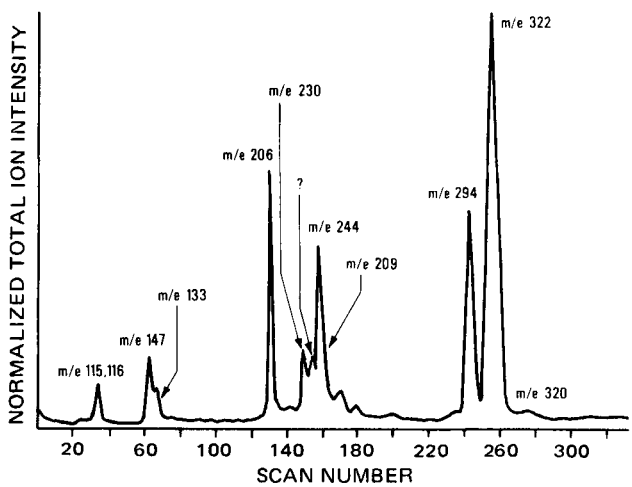

Figure 2—*Total ion intensity plot and molecular ions of the components derived from photolysis.*

Substances were isolated from the thin-layer plates by scraping off the appropriate zones, grinding them to a fine powder in a mortar, and adding the powder to spin thimbles[7] where the material was extracted by centrifugation using acetone–methanol (7:3). Accurate mass measurements[8] were obtained by peak matching at a resolution of 15,000.

All reagents were reagent or analytical grade and were used without further purification. Authentic samples of 2-anilinoindan[9], desethylaprindine[9], *N,N*-diethyl-*N'*-phenyl-1,3-propanediamine[9], and desphenylaprindine[10] were used.

RESULTS AND DISCUSSION

Figures 1 and 2 show the gas chromatogram and total ion plot (TII, normalized total ion intensity, *versus* mass spectral scan number) obtained at the conclusion of a typical photolysis. Some peak distortions occurred in the TII plot relative to the chromatogram. However, concentration–response studies with authentic materials allowed demonstration of the quantitative accuracy of the chromatogram.

The structures of the various components were determined by comparison with mass spectral literature data and with R_f values (TLC), retention times (GLC), and mass spectra of authentic materials.

Components 1 and 2—The mass spectral data for Components 1 and 2 were in excellent agreement with those previously published for *N,N*-diethylpropylamine (II) (4) and indene (III) (5).

Components 3, 4, and 8—The major ions observed in the mass spectra of Components 3 and 4 identified these substances as 2-aminoindan (IV) and 2-methylaminoindan (V), respectively. Mass spectral and chromatographic comparisons with authentic material showed Component 8 to be 2-anilinoindan (VI) (Table I).

[7] Terra-Marine Bioresearch, La Jolla, Calif.
[8] Varian MAT 731 mass spectrometer.
[9] Supplied by Dr. P. J. Murphy, Lilly Research Laboratories.
[10] Supplied by Dr. L. Dodion, A. Christiaens, S.A., Brussels, Belgium.

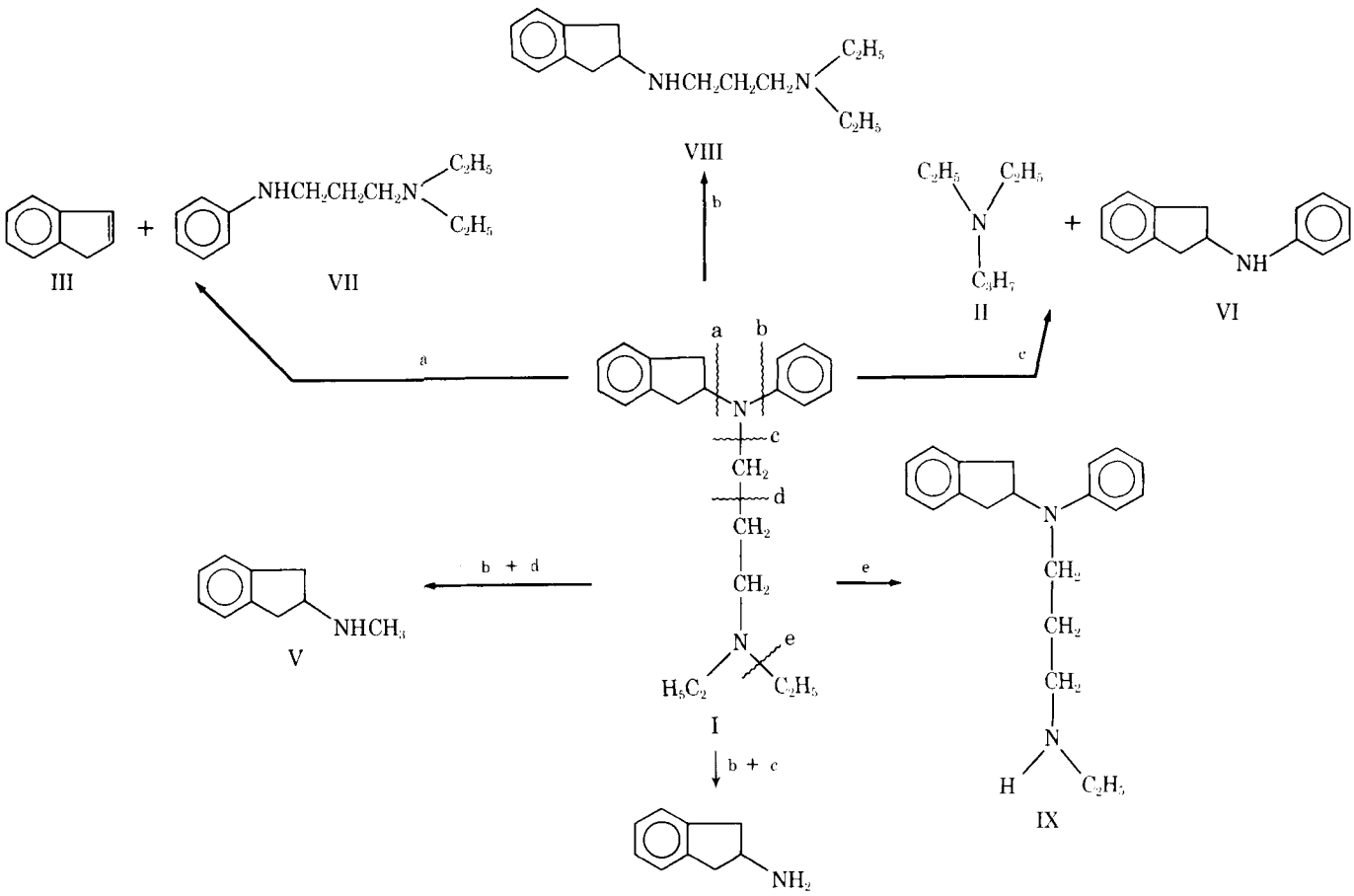

Scheme I

Components 5, 7, 10, and 11—The mass spectra of aprindine hydrochloride and a number of photoproducts showed analogous fragmentation patterns, which served as sensitive structural probes. Typically, Component 11 (aprindine, I) underwent fragmentation at positions α and β to the two nitrogens and the presence of two homologous series of ions (Series 1, *m/e* 72, 86, 100, and 114; and Series 2, *m/e* 222, 236, and 249) indicated these cleavages. In addition, the data suggested that each cleavage occurs in a dual mode such that the positive charge is found on both fragment ions.

Analogous ion series were observed for Components 5, 7, and 10 (Table I) and, together with the chromatographic comparisons with authentic materials and high-resolution mass spectrometry (*vide infra*) on Components 5 and 10, identified these substances as *N,N*-diethyl-*N'*-phenyl-1,3-propanediamine (VII), desphenylaprindine (VIII), and desethylaprindine (IX), respectively.

Components 6, 9, and 12—Components 6 and 12 were not positively identified, but the mass spectral data suggested that Component 6 was *N*-methyl-*N*-ethyl-*N'*-indanylpropanediamine (X) and Component 12 was a more highly oxidized analog of I, which is probably best represented by Structure XI.

Component 9 was so poorly resolved in the TII plot that definitive spectra could not be obtained in spite of extensive background subtraction.

Preparative TLC and High-Resolution Mass Spectrometry—Additional characterization data were obtained for Components 5 and 10 by preparative TLC followed by high-resolution mass spectrometry (see *Experimental* section). Measurements on the molecular ion of Component 5 yielded a value of 206.1780 (calc. for $C_{13}H_{22}N_2$: 206.1783). A similar determination for the molecular ion of Component 10 afforded a measured mass of 294.2088 (calc. for $C_{20}H_{26}N_2$: 294.2095).

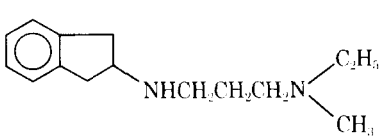

X

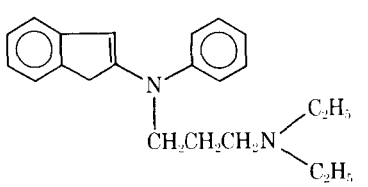

XI

CONCLUSIONS

The photolysis of aprindine resulted almost completely in products reflecting various combinations of C–N bond cleavages (Scheme I). The structural elucidations confirmed the suggestions made previously regarding the identities of two of the photoproducts (1) and showed that the photochemistry observed in this study is analogous to behavior suggested for other tertiary amines (6).

Compounds VI, VIII, and IX also have been shown to be metabolites of aprindine (2, 7, 8).

REFERENCES

(1) B. S. Rutherford and R. H. Bishara, *J. Pharm. Sci.*, **65**, 1322 (1976).

(2) H. Kesteloot, W. Van Mieghem, and H. De Geest, *Acta Cardiol.*, **28**, 145 (1973).

(3) E. Stahl, "Thin-Layer Chromatography," 2nd ed., Springer-Verlag, New York, N.Y., 1969, p. 878.

(4) "Eight Peak Index of Mass Spectra," 1st ed., vol. 1, Aldermaston,

Reading, United Kingdom, 1970, p. 54.
(5) *Ibid.*, p. 57.
(6) J. G. Calvert and J. N. Pitts, "Photochemistry," Wiley, New York, N.Y., 1966, p. 456.
(7) L. Dodion, J. M. DeSuray, M. Deblecker, and A. Georges, *Therapie*, **29**, 221 (1974).
(8) P. J. Murphy, *Acta Cardiol., Suppl. XVIII*, **29**, 131 (1974).

ACKNOWLEDGMENTS

The authors thank J. L. Occolowitz for the high-resolution mass spectral data and J. W. Gregory for assistance.

Structure–Activity Studies on Mutagenicity of Nitrosamines Using Molecular Connectivity

LEMONT B. KIER *x, RICHARD J. SIMONS ‡, and LOWELL H. HALL ‡

Received August 3, 1977, from the **Department of Pharmaceutical Chemistry, Medical College of Virginia, Virginia Commonwealth University and MCV/VCU Cancer Center, Richmond, VA 23298*, and the ‡*Department of Chemistry, Eastern Nazarene College, Quincy, MA 02170.* Accepted for publication September 1, 1977.

Abstract □ The structure–activity relationship of a series of nitrosamines was evaluated for mutagenic potency as measured in the Ames test. The structural description was made using molecular connectivity. A good correlation was found.

Keyphrases □ Nitrosamines, various—mutagenic potency related to molecular connectivity indexes □ Mutagenicity—various nitrosamines, related to molecular connectivity indexes □ Molecular connectivity indexes—various nitrosamines, related to mutagenic potency □ Structure–activity relationships—various nitrosamines, mutagenic potency related to molecular connectivity indexes

The mutagenicity of a molecule is important in assembling a profile of its toxicity and environmental effects. It was stated (1) that there is a correlation between mutagenicity and carcinogenicity, high enough to warrant the routine testing for this property. Such a test is currently used in some laboratories (2).

The compounds are tested on petri plates with mutants of *Salmonella typhimurium*. Homogenates of rat or human liver are added to the plates. The number of revertants per nanomole is determined from dose–response curves and is an indication of the compound's mutagenicity. McCann *et al.* (1), using the Ames test, recently evaluated 300 compounds of various types.

The nitrosamines, known to occur in cigarette smoke, nitrate pickled meat, and smoked fish (3), were studied (1). It was demonstrated (4) with experimental animals that nitrosamines are potent carcinogens.

In this study, previous data (1) on mutagenicity were used as a measure of potency to examine the structural influences on this activity. Fifteen nitrosamines (Table I), tested under identical conditions and having precisely reported data, were considered.

EXPERIMENTAL

To evaluate the structure–activity relationships in this series, a recently developed method, molecular connectivity (5), was used. This method for describing the structure of a molecule has its roots in topology. A series of indexes reflect a weighted count of subgraphs which, from simple calculations, lead to values encoding considerable structural information. The information makes possible the evaluation of structural features influencing physical property values (6) and biological activity (7–9). The use of extended terms (10) and the application of molecular connectivity to heteroatoms (11) make the method ideally suited for a study of the structure–activity relationships of biologically important molecules.

RESULTS

A systematic search of the connectivity indexes for the molecules in Table I revealed two relationships with nearly equal quality. By expressing the activity as the natural log number of revertants per nanomole, the following equations were found:

$$\ln R = 2.398\ (\pm 0.032)\ {}^{0}\chi - 4.095\ (\pm 0.132)\ {}^{1}\chi^{v} - 5.590\ (\pm 1.158) \quad \text{(Eq. 1)}$$

$$r = 0.964 \quad s = 1.09 \quad n = 15 \quad F = 78.8\ (p < 0.02)$$

$$\ln R = 2.946\ (\pm 0.066)\ {}^{2}\chi - 9.090\ (\pm 0.729)\ {}^{4}\chi_{p}{}^{v} - 4.662\ (\pm 1.052) \quad \text{(Eq. 2)}$$

$$r = 0.967 \quad s = 1.05 \quad n = 15 \quad F = 85.2\ (p < 0.02)$$

Both equations predict the ln R to less than 10% of the log range of experimental values in this set. The common structural feature in the set is the nitrosamine group and must be considered to be necessary, but not sufficient, for potency. Subsidiary structural features, quantified by

Table I—Mutagenicity/Carcinogenicity of Nitrosamines

	Compound	ln R[a]	Equation 1, Calc. ln R	Equation 2, Calc. ln R
1	Dipropyl-*N*-nitrosamine	−2.526	−2.573	−2.711
2	Dibutyl-*N*-nitrosamine	−1.897	−3.276	−2.128
3	Dipentyl-*N*-nitrosamine	−2.996	−3.979	−3.747
4	*N*-Nitrosopyrrolidine	−3.912	−3.626	−4.232
5	*N*-Nitrosomorpholine	−2.813	−2.247	−1.857
6	*N*-Nitrosopiperidine	−4.605	−3.977	−4.798
7	*N*-Methyl-*N*-nitroso-*N*′-nitroguanidine	7.226	5.176	5.287
8	*N*-Ethyl-*N*-nitroso-*N*′-nitroguanidine	5.858	4.513	4.020
9	*N*-Propyl-*N*-nitroso-*N*′-nitroguanidine	3.689	4.161	3.791
10	*N*-Butyl-*N*-nitroso-*N*′-nitroguanidine	3.892	3.811	3.959
11	*N*-Isobutyl-*N*-nitroso-*N*′-nitroguanidine	4.344	4.792	5.304
12	*N*-Pentyl-*N*-nitroso-*N*′-nitroguanidine	3.091	3.669	3.264
13	*N*-Hexyl-*N*-nitroso-*N*′-nitroguanidine	1.668	3.317	2.699
14	*N*-Nitrosomethylurea	1.482	1.716	2.676
15	*N*-Nitrosoethylurea	0.095	1.117	1.069

[a] Natural log of revertants per nanomole.

Reading, United Kingdom, 1970, p. 54.
(5) *Ibid.*, p. 57.
(6) J. G. Calvert and J. N. Pitts, "Photochemistry," Wiley, New York, N.Y., 1966, p. 456.
(7) L. Dodion, J. M. DeSuray, M. Deblecker, and A. Georges, *Therapie*, **29**, 221 (1974).
(8) P. J. Murphy, *Acta Cardiol., Suppl. XVIII*, **29**, 131 (1974).

ACKNOWLEDGMENTS

The authors thank J. L. Occolowitz for the high-resolution mass spectral data and J. W. Gregory for assistance.

Structure–Activity Studies on Mutagenicity of Nitrosamines Using Molecular Connectivity

LEMONT B. KIER *x, RICHARD J. SIMONS ‡, and LOWELL H. HALL ‡

Received August 3, 1977, from the **Department of Pharmaceutical Chemistry, Medical College of Virginia, Virginia Commonwealth University and MCV/VCU Cancer Center, Richmond, VA 23298*, and the ‡*Department of Chemistry, Eastern Nazarene College, Quincy, MA 02170.* Accepted for publication September 1, 1977.

Abstract □ The structure–activity relationship of a series of nitrosamines was evaluated for mutagenic potency as measured in the Ames test. The structural description was made using molecular connectivity. A good correlation was found.

Keyphrases □ Nitrosamines, various—mutagenic potency related to molecular connectivity indexes □ Mutagenicity—various nitrosamines, related to molecular connectivity indexes □ Molecular connectivity indexes—various nitrosamines, related to mutagenic potency □ Structure–activity relationships—various nitrosamines, mutagenic potency related to molecular connectivity indexes

The mutagenicity of a molecule is important in assembling a profile of its toxicity and environmental effects. It was stated (1) that there is a correlation between mutagenicity and carcinogenicity, high enough to warrant the routine testing for this property. Such a test is currently used in some laboratories (2).

The compounds are tested on petri plates with mutants of *Salmonella typhimurium*. Homogenates of rat or human liver are added to the plates. The number of revertants per nanomole is determined from dose–response curves and is an indication of the compound's mutagenicity. McCann *et al.* (1), using the Ames test, recently evaluated 300 compounds of various types.

The nitrosamines, known to occur in cigarette smoke, nitrate pickled meat, and smoked fish (3), were studied (1). It was demonstrated (4) with experimental animals that nitrosamines are potent carcinogens.

In this study, previous data (1) on mutagenicity were used as a measure of potency to examine the structural influences on this activity. Fifteen nitrosamines (Table I), tested under identical conditions and having precisely reported data, were considered.

EXPERIMENTAL

To evaluate the structure–activity relationships in this series, a recently developed method, molecular connectivity (5), was used. This method for describing the structure of a molecule has its roots in topology. A series of indexes reflect a weighted count of subgraphs which, from simple calculations, lead to values encoding considerable structural information. The information makes possible the evaluation of structural features influencing physical property values (6) and biological activity (7–9). The use of extended terms (10) and the application of molecular connectivity to heteroatoms (11) make the method ideally suited for a study of the structure–activity relationships of biologically important molecules.

RESULTS

A systematic search of the connectivity indexes for the molecules in Table I revealed two relationships with nearly equal quality. By expressing the activity as the natural log number of revertants per nanomole, the following equations were found:

$$\ln R = 2.398\ (\pm 0.032)\ {}^{0}\chi - 4.095\ (\pm 0.132)\ {}^{1}\chi^{v} - 5.590\ (\pm 1.158) \quad \text{(Eq. 1)}$$

$$r = 0.964 \quad s = 1.09 \quad n = 15 \quad F = 78.8\ (p < 0.02)$$

$$\ln R = 2.946\ (\pm 0.066)\ {}^{2}\chi - 9.090\ (\pm 0.729)\ {}^{4}\chi_{p}{}^{v} - 4.662\ (\pm 1.052) \quad \text{(Eq. 2)}$$

$$r = 0.967 \quad s = 1.05 \quad n = 15 \quad F = 85.2\ (p < 0.02)$$

Both equations predict the ln R to less than 10% of the log range of experimental values in this set. The common structural feature in the set is the nitrosamine group and must be considered to be necessary, but not sufficient, for potency. Subsidiary structural features, quantified by

Table I—Mutagenicity/Carcinogenicity of Nitrosamines

	Compound	ln R[a]	Equation 1, Calc. ln R	Equation 2, Calc. ln R
1	Dipropyl-*N*-nitrosamine	−2.526	−2.573	−2.711
2	Dibutyl-*N*-nitrosamine	−1.897	−3.276	−2.128
3	Dipentyl-*N*-nitrosamine	−2.996	−3.979	−3.747
4	*N*-Nitrosopyrrolidine	−3.912	−3.626	−4.232
5	*N*-Nitrosomorpholine	−2.813	−2.247	−1.857
6	*N*-Nitrosopiperidine	−4.605	−3.977	−4.798
7	*N*-Methyl-*N*-nitroso-*N*′-nitroguanidine	7.226	5.176	5.287
8	*N*-Ethyl-*N*-nitroso-*N*′-nitroguanidine	5.858	4.513	4.020
9	*N*-Propyl-*N*-nitroso-*N*′-nitroguanidine	3.689	4.161	3.791
10	*N*-Butyl-*N*-nitroso-*N*′-nitroguanidine	3.892	3.811	3.959
11	*N*-Isobutyl-*N*-nitroso-*N*′-nitroguanidine	4.344	4.792	5.304
12	*N*-Pentyl-*N*-nitroso-*N*′-nitroguanidine	3.091	3.669	3.264
13	*N*-Hexyl-*N*-nitroso-*N*′-nitroguanidine	1.668	3.317	2.699
14	*N*-Nitrosomethylurea	1.482	1.716	2.676
15	*N*-Nitrosoethylurea	0.095	1.117	1.069

[a] Natural log of revertants per nanomole.

the connectivity indexes, influence the degree of potency as manifested in this test.

DISCUSSION

The set contains three subclasses of nitrosamines: alkyl, guanidino, and ureido derivatives. Within the alkyl subset are three cyclic derivatives. The equations treat these subsets equally well for the correlation with potency.

The activities exhibited by the entire set range over five natural log units (nearly 12 orders of magnitude). The equations thus can discriminate between quite potent and virtually inactive molecules. On this basis, the structural analysis derived from this admittedly limited set of nitrosamines may have utility as a theoretical screen for other untested nitrosamines.

A negative test is a result less than 0.01 revertant/nmole ($\ln R < -4.61$) (1). Results greater than 1.0 revertant/nmole ($\ln R > 0.00$) are positive to the degree of the value. McCann *et al.* (1) claimed a 90% correspondence between carcinogenicity and mutagenicity.

An examination of the equations reveals certain structure–activity relationships. The ability of the equations to discriminate between the subclasses is illustrated by a comparison of Compounds 2 and 8. Both have the same number of nonhydrogen atoms but vastly different activities. Both equations account for this difference. The activity of Compound 5 is correctly predicted to be less than its isostere, Compound 6. In Eq. 1, the $^0\chi$ values are the same for both; however, the $^1\chi^v$ value is less for Compound 5 because the valence connectivity delta assignment for oxygen in the ring is greater than the ring methylene delta in Compound 6. The cyclic molecules generally have a larger $^1\chi^v$ value than the noncyclic molecules and, therefore, are correctly predicted to be less active than cyclic molecules of about the same size.

This limited set of data provided a good relationship between a molecular connectivity description of structure and mutagenic potency (1) in the Ames test. This result may be a useful beginning to the development of theoretical prediction of mutagenic potential in discrete chemical classes of molecules. Examination of additional nitrosamines, similarly tested, should afford a constructive challenge to this approach. The intention is to examine other classes of mutagenic molecules using molecular connectivity.

REFERENCES

(1) J. McCann, E. Choi, E. Yamasaki, and B. N. Ames, *Proc. Natl. Acad. Sci. USA*, **72**, 5135 (1975).

(2) B. N. Ames, F. D. Lee, and W. E. Durston, *ibid.*, **70**, 782 (1973).

(3) W. J. Serfontein and P. Hurter, *S. Afr. Cancer Bull.*, **110**, 62 (1966).

(4) H. Druckey, R. Pressman, S. Cluankovic, and D. Schmall, *Z. Krebsforsch.*, **69**, 103 (1967).

(5) L. B. Kier and L. H. Hall, "Molecular Connectivity in Chemistry and Drug Research," Academic, New York, N.Y., 1976.

(6) L. H. Hall, L. B. Kier, and W. J. Murray, *J. Pharm. Sci.*, **64**, 1974 (1975).

(7) T. DiPaolo, L. B. Kier, and L. H. Hall, *Mol. Pharmacol.*, **12**, 13 (1977).

(8) L. B. Kier, L. H. Hall, and W. J. Murray, *J. Med. Chem.*, **18**, 1272 (1975).

(9) L. H. Hall and L. B. Kier, *J. Pharm. Sci.*, **66**, 642 (1977).

(10) L. B. Kier, W. J. Murray, M. Randic, and L. H. Hall, *ibid.*, **65**, 1226 (1976).

(11) L. B. Kier and L. H. Hall, *ibid.*, **65**, 1806 (1976).

Determination of Plasma Hydrochlorothiazide Levels in Humans

E. REDALIEU ˣ, V. V. TIPNIS, and W. E. WAGNER, Jr.

Received July 8, 1977, from the *Research Department, Pharmaceuticals Division, Ciba-Geigy Corporation, Ardsley, NY 10502 and Summit, NJ 07901.* Accepted for publication August 30, 1977.

Abstract □ A method for determining plasma hydrochlorothiazide levels was developed with a sensitivity of 5 ng/ml. Accuracy and precision were demonstrated over the 5–648-ng/ml range by an overall recovery of 95 ± 8%. The detector response was linear for the 5–250-ng/ml range. The method was sufficiently sensitive for hydrochlorothiazide bioavailability studies and also was applicable for the determination of whole blood drug levels. Plasma levels in two subjects reached peak levels of 428 and 450 ng/ml at 2.5 and 2 hr, respectively, after a 50-mg dose. Whole blood levels at 3 hr after the same dose were 547 and 851 ng/ml and were approximately 2.5 times the 3-hr plasma levels.

Keyphrases □ Hydrochlorothiazide—GLC analysis in plasma □ GLC—analysis, hydrochlorothiazide in plasma □ Diuretics—hydrochlorothiazide, GLC analysis in plasma

The diuretic hydrochlorothiazide has been used clinically for a number of years. In spite of the availability of GLC (1, 2) and liquid chromatographic (3, 4) methods, only limited human plasma level data have been published. Plasma levels were reported (1) in four subjects, but levels past 4 hr (6 and 24 hr) were noted for only one subject. Plasma level–time curves were reported for a single subject (5), as was an average curve from eight subjects covering 9 hr following administration (6).

This paper reports individual plasma level data obtained in a study with two male volunteers. Plasma hydrochlorothiazide levels were determined using a modification of the GLC method reported previously (2).

EXPERIMENTAL

Procedure—Plasma (2 ml) was pipetted into a 12-ml polytef[1]-lined screw-capped centrifuge tube. The internal standard, the bromo analog of hydrochlorothiazide (6-bromo-3,4-dihydro-2*H*-1,2,4-benzothiadiazine-7-sulfonamide 1,1-dioxide), was added (200 μl of a 1-μg/ml solution in methanol), and the sample was mixed thoroughly on a vortex mixer[2]. Then methyl isobutyl ketone[3] (5 ml) was added, and the tightly closed tube was vigorously shaken horizontally on a platform shaker[4] for 20 min.

Following centrifugation for 20 min, 4 ml of the organic layer was transferred to a clean 12-ml centrifuge tube. Sodium hydroxide (2.5 ml, 0.1 *M*) was added, and the tightly closed tube was vigorously shaken for 20 min. Following centrifugation for 15 min, 2 ml of the aqueous layer was transferred to a clean 12-ml centrifuge tube. A solution of tetrahex-

[1] Teflon, E.I. du Pont de Nemours, Wilmington, Del.
[2] Scientific Industries Inc., Springfield, Mass.
[3] J. T. Baker, Phillipsburg, N.J.
[4] Eberbach Corp., Ann Arbor, Mich.

the connectivity indexes, influence the degree of potency as manifested in this test.

DISCUSSION

The set contains three subclasses of nitrosamines: alkyl, guanidino, and ureido derivatives. Within the alkyl subset are three cyclic derivatives. The equations treat these subsets equally well for the correlation with potency.

The activities exhibited by the entire set range over five natural log units (nearly 12 orders of magnitude). The equations thus can discriminate between quite potent and virtually inactive molecules. On this basis, the structural analysis derived from this admittedly limited set of nitrosamines may have utility as a theoretical screen for other untested nitrosamines.

A negative test is a result less than 0.01 revertant/nmole ($\ln R < -4.61$) (1). Results greater than 1.0 revertant/nmole ($\ln R > 0.00$) are positive to the degree of the value. McCann *et al.* (1) claimed a 90% correspondence between carcinogenicity and mutagenicity.

An examination of the equations reveals certain structure–activity relationships. The ability of the equations to discriminate between the subclasses is illustrated by a comparison of Compounds 2 and 8. Both have the same number of nonhydrogen atoms but vastly different activities. Both equations account for this difference. The activity of Compound 5 is correctly predicted to be less than its isostere, Compound 6. In Eq. 1, the $^0\chi$ values are the same for both; however, the $^1\chi^v$ value is less for Compound 5 because the valence connectivity delta assignment for oxygen in the ring is greater than the ring methylene delta in Compound 6. The cyclic molecules generally have a larger $^1\chi^v$ value than the noncyclic molecules and, therefore, are correctly predicted to be less active than cyclic molecules of about the same size.

This limited set of data provided a good relationship between a molecular connectivity description of structure and mutagenic potency (1) in the Ames test. This result may be a useful beginning to the development of theoretical prediction of mutagenic potential in discrete chemical classes of molecules. Examination of additional nitrosamines, similarly tested, should afford a constructive challenge to this approach. The intention is to examine other classes of mutagenic molecules using molecular connectivity.

REFERENCES

(1) J. McCann, E. Choi, E. Yamasaki, and B. N. Ames, *Proc. Natl. Acad. Sci. USA*, **72**, 5135 (1975).

(2) B. N. Ames, F. D. Lee, and W. E. Durston, *ibid.*, **70**, 782 (1973).

(3) W. J. Serfontein and P. Hurter, *S. Afr. Cancer Bull.*, **110**, 62 (1966).

(4) H. Druckey, R. Pressman, S. Cluankovic, and D. Schmall, *Z. Krebsforsch.*, **69**, 103 (1967).

(5) L. B. Kier and L. H. Hall, "Molecular Connectivity in Chemistry and Drug Research," Academic, New York, N.Y., 1976.

(6) L. H. Hall, L. B. Kier, and W. J. Murray, *J. Pharm. Sci.*, **64**, 1974 (1975).

(7) T. DiPaolo, L. B. Kier, and L. H. Hall, *Mol. Pharmacol.*, **12**, 13 (1977).

(8) L. B. Kier, L. H. Hall, and W. J. Murray, *J. Med. Chem.*, **18**, 1272 (1975).

(9) L. H. Hall and L. B. Kier, *J. Pharm. Sci.*, **66**, 642 (1977).

(10) L. B. Kier, W. J. Murray, M. Randic, and L. H. Hall, *ibid.*, **65**, 1226 (1976).

(11) L. B. Kier and L. H. Hall, *ibid.*, **65**, 1806 (1976).

Determination of Plasma Hydrochlorothiazide Levels in Humans

E. REDALIEU ˣ, V. V. TIPNIS, and W. E. WAGNER, Jr.

Received July 8, 1977, from the *Research Department, Pharmaceuticals Division, Ciba-Geigy Corporation, Ardsley, NY 10502 and Summit, NJ 07901.* Accepted for publication August 30, 1977.

Abstract □ A method for determining plasma hydrochlorothiazide levels was developed with a sensitivity of 5 ng/ml. Accuracy and precision were demonstrated over the 5–648-ng/ml range by an overall recovery of 95 ± 8%. The detector response was linear for the 5–250-ng/ml range. The method was sufficiently sensitive for hydrochlorothiazide bioavailability studies and also was applicable for the determination of whole blood drug levels. Plasma levels in two subjects reached peak levels of 428 and 450 ng/ml at 2.5 and 2 hr, respectively, after a 50-mg dose. Whole blood levels at 3 hr after the same dose were 547 and 851 ng/ml and were approximately 2.5 times the 3-hr plasma levels.

Keyphrases □ Hydrochlorothiazide—GLC analysis in plasma □ GLC—analysis, hydrochlorothiazide in plasma □ Diuretics—hydrochlorothiazide, GLC analysis in plasma

The diuretic hydrochlorothiazide has been used clinically for a number of years. In spite of the availability of GLC (1, 2) and liquid chromatographic (3, 4) methods, only limited human plasma level data have been published. Plasma levels were reported (1) in four subjects, but levels past 4 hr (6 and 24 hr) were noted for only one subject. Plasma level–time curves were reported for a single subject (5), as was an average curve from eight subjects covering 9 hr following administration (6).

This paper reports individual plasma level data obtained in a study with two male volunteers. Plasma hydrochlorothiazide levels were determined using a modification of the GLC method reported previously (2).

EXPERIMENTAL

Procedure—Plasma (2 ml) was pipetted into a 12-ml polytef[1]-lined screw-capped centrifuge tube. The internal standard, the bromo analog of hydrochlorothiazide (6-bromo-3,4-dihydro-2*H*-1,2,4-benzothiadiazine-7-sulfonamide 1,1-dioxide), was added (200 μl of a 1-μg/ml solution in methanol), and the sample was mixed thoroughly on a vortex mixer[2]. Then methyl isobutyl ketone[3] (5 ml) was added, and the tightly closed tube was vigorously shaken horizontally on a platform shaker[4] for 20 min.

Following centrifugation for 20 min, 4 ml of the organic layer was transferred to a clean 12-ml centrifuge tube. Sodium hydroxide (2.5 ml, 0.1 *M*) was added, and the tightly closed tube was vigorously shaken for 20 min. Following centrifugation for 15 min, 2 ml of the aqueous layer was transferred to a clean 12-ml centrifuge tube. A solution of tetrahex-

[1] Teflon, E.I. du Pont de Nemours, Wilmington, Del.
[2] Scientific Industries Inc., Springfield, Mass.
[3] J. T. Baker, Phillipsburg, N.J.
[4] Eberbach Corp., Ann Arbor, Mich.

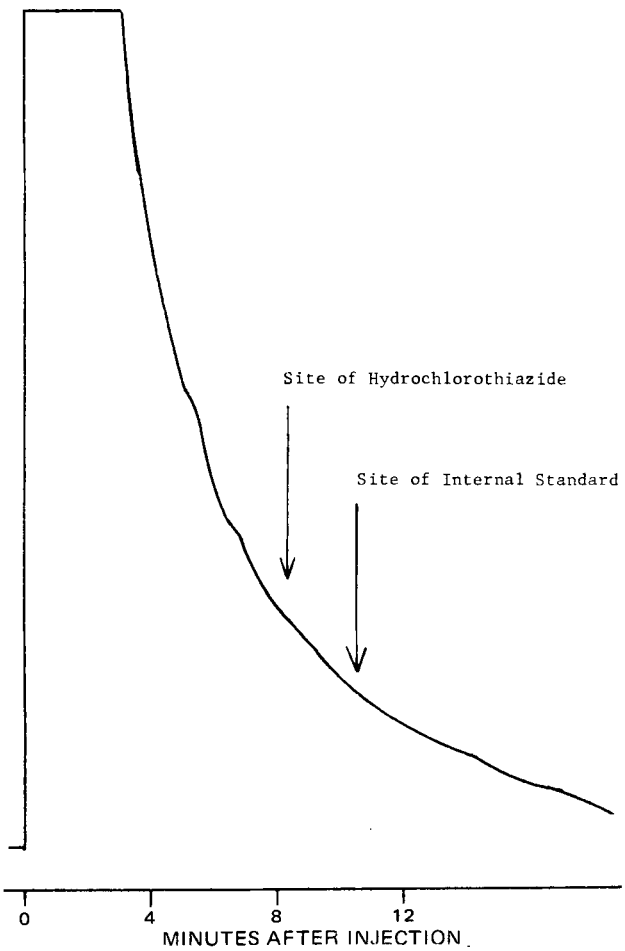

Figure 1—*Gas chromatogram of human plasma blank from a subject before hydrochlorothiazide administration.*

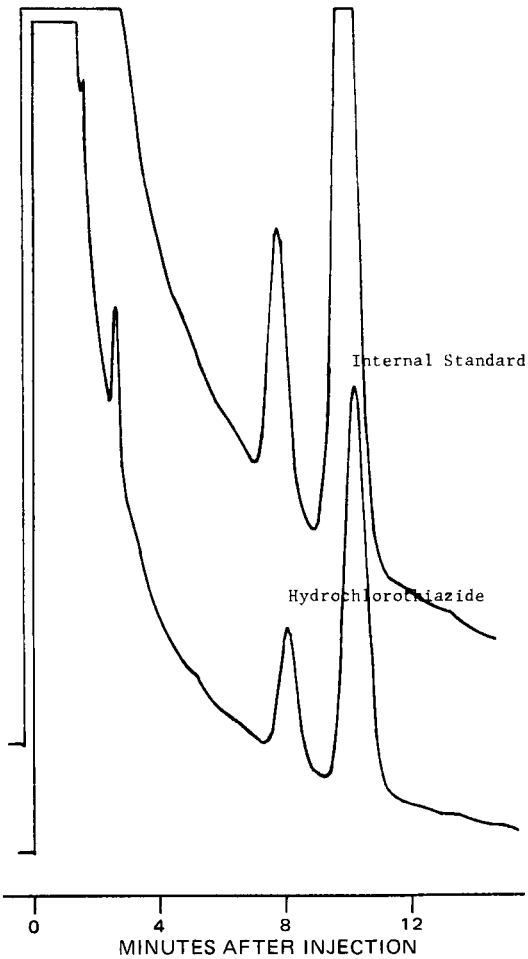

Figure 2—*Gas chromatogram of human plasma from a subject after hydrochlorothiazide administration (with internal standard added) using the dual-pen recorder technique.*

ylammonium hydrogen sulfate[5] (50 μl, 0.1 *M* in water, neutralized with sodium hydroxide) and 5 ml of 0.5 *M* methyl iodide in dichloromethane were added. The tightly closed tube was shaken horizontally for 30 min in a thermostatic heating block[6] (50°) mounted on a platform shaker.

Following centrifugation for 15 min, 4 ml of the organic layer was transferred to an 8-ml culture tube with a 6-mm o.d. × 10-mm long tip at the bottom; the solvent was then evaporated at room temperature under a nitrogen stream. A suitable volume of cyclohexane was added, and the closed tube was placed in an ultrasonic bath for 5 min. Following centrifugation for 15 min, 2 μl of the solution was injected into the gas chromatograph.

A gas chromatograph[7] with a linearized electron-capture detector[8] and a dual-pen recorder[9] were used. The recorder was run with both pens operating simultaneously: one with a 1-mv range, the second with a 2-mv range. A 0.9-m × 2-mm i.d. glass column was packed with 80–100-mesh 1% OV-225 on an acid-washed, dimethylchlorosilane-treated support[10] and was conditioned at 260° for 48 hr before use. The carrier gas was 95% argon–5% methane at a 50-ml/min flow rate. Oven, injection port, and detector temperatures were 260, 275, and 325°, respectively. The oven temperature was reduced to 200° overnight to increase the column life.

The hydrochlorothiazide concentration in a sample was determined by comparing the peak height ratio (hydrochlorothiazide derivative peak height/internal standard derivative peak height) to a standard curve of peak height ratio *versus* hydrochlorothiazide concentration. The standard curve was generated daily by carrying spiked plasma standards of several known concentrations through the procedure along with the samples.

Human Study—The subjects, two healthy white males, did not eat after dinner on the day prior to the study but were permitted to drink fluids without caffeine. Before leaving home on the day of the study, each subject drank at least 200 ml of water.

Control blood samples were obtained from each prior to the administration of one 50-mg hydrochlorothiazide tablet[11]. Subjects received 200 ml of water with their tablet and hourly thereafter for 8 hr. A light breakfast was served 2 hr after drug administration.

Blood samples (10 ml) were obtained at 30-min intervals for the first 3 hr and at 4, 6, 8, and 24 hr. All blood samples were collected in heparinized tubes. The 10-ml samples were centrifuged as soon as they were collected, and the separated plasma was frozen immediately. An additional 5-ml blood sample was obtained at 1, 2, and 3 hr. These samples were transferred to properly labeled containers and frozen.

RESULTS AND DISCUSSION

The method used for hydrochlorothiazide analysis in plasma differed from that of Lindstrom *et al.* (2) in three ways. First, the use of phosphate buffer was not necessary. Second, the use of the bromo analog of hydrochlorothiazide as the internal standard, instead of chlorthalidone, permitted the internal standard to be added directly to the whole blood sample before extraction. And, third, a more polar liquid phase (OV-225) was used in place of SE-30 for the chromatographic separation.

Typical gas chromatograms for human plasma from a male volunteer before and after oral administration of a 50-mg hydrochlorothiazide tablet are shown in Figs. 1 and 2, respectively. Derivatized hydrochlorothiazide, whether from blank plasma with authentic hydrochlorothiazide added or from plasma samples obtained following hydrochlorothiazide administration, afforded a well-defined peak with a retention time of ap-

[5] A. B. Hassle, Molndal, Sweden.
[6] Multi-Temp-Blok, Lab-Line Instruments, Melrose Park, Ill.
[7] Model 5710A, Hewlett-Packard, Avondale, Pa.
[8] Model 18713A, Hewlett-Packard, Avondale, Pa.
[9] Model A-25, Varian, Palo Alto, Calif.
[10] Supelcoport, Supelco, Inc., Bellefonte, Pa.

[11] Esidrix, Ciba-Geigy Corp.

Table I—Recovery of Hydrochlorothiazide from Plasma Samples [a]

Added Concentration, ng/ml	Found Individual Values, % of Added Concentration					
5	100	100	100	—	—	—
16	106	94	94	94	94	—
29	83	86	83	100	—	—
49	106	102	84	—	—	—
51	86	80	86	84	—	—
65	92	89	88	—	—	—
118	91	85	82	81	—	—
162	99	102	102	99	99	—
200	97	93	91	88	—	—
243	103	93	109	—	—	—
324	98	102	101	91	108	102
329	102	93	99	97	—	—
486	95	100	104	—	—	—
648	95	108	98	—	—	—
	Overall recovery ± *SD*			95 ± 8%		

[a] Prepared by adding known amounts of hydrochlorothiazide to control human plasma.

proximately 8 min. The derivatized internal standard also afforded a well-defined peak, its retention time being approximately 10.5 min.

Accuracy and Precision—Accuracy and precision were determined by calculating recovery as a percent of the added concentration for all samples over the range of hydrochlorothiazide levels from 5 to 648 ng/ml (Table I). The overall recovery of 95 ± 8% (*SD*) demonstrated good accuracy and precision.

Linearity—Standard curves, developed from plasma spiked with hydrochlorothiazide over the 5–250-ng/ml range, exhibited good linearity as demonstrated by a typical correlation coefficient of 0.998 for the linear regression line. The reliability of determining low concentrations of hydrochlorothiazide (25 ng/ml or less) can be increased by using a standard curve over the 5–75-ng/ml range.

Sensitivity—As seen in Table I, the method has good accuracy and precision at a plasma hydrochlorothiazide concentration as low as 5 ng/ml. Concentrations below this level have not been studied.

Stability—Samples were prepared by adding hydrochlorothiazide to control plasma to obtain concentrations of 15, 74, and 149 ng/ml. The samples were analyzed immediately and divided into aliquots which were then frozen. Analysis of duplicate samples of each concentration after 2 months of storage at −20° afforded average recoveries of 100, 99, and 98% for the three concentrations, respectively. These results demonstrate that hydrochlorothiazide is stable in plasma, under frozen storage conditions, for at least 2 months.

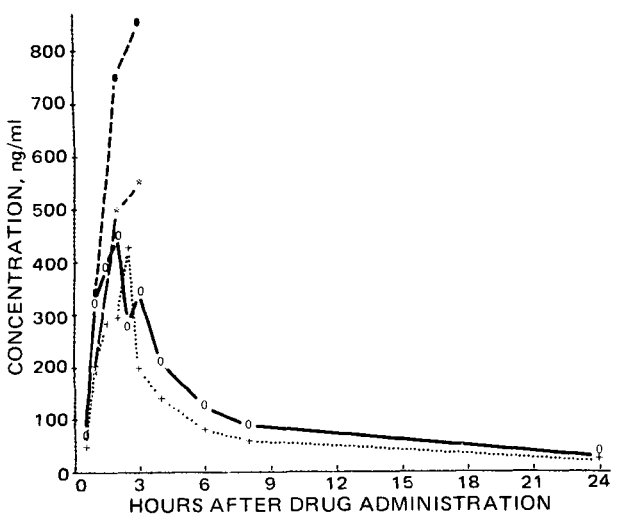

Figure 3—*Plasma (+ and O) and whole blood (* and ●) levels of hydrochlorothiazide following oral administration of one 50-mg commercial tablet to two volunteers.*

Table II—Plasma and Whole Blood Hydrochlorothiazide Levels following Oral Administration of 50 mg

Hours	Subject 1	Subject 2
	Plasma Levels, ng/ml	
0.5	46	69
1	201	320
1.5	282	387
2	294	450
2.5	428	276
3	199	342
4	140	205
6	80	120
8	58	83
24	18	24
	Blood Levels, ng/ml	
1	185	338
2	493	747
3	547	851

Clinical Study—Plasma and whole blood hydrochlorothiazide levels following oral administration of one 50-mg commercial hydrochlorothiazide tablet to two volunteers are summarized in Fig. 3 and Table II. Predose (zero-time) plasma specimens were devoid of any material at the hydrochlorothiazide retention time. Peak plasma levels were observed at 2.5 and 2 hr in Subjects 1 and 2, respectively. Plasma hydrochlorothiazide concentrations declined rapidly at first from peak values but slowed appreciably by 8 hr after administration. This latter decline was in agreement with the 13.1-hr half-life of the β-phase reported by Beermann *et al.* (5). Areas under these plasma level–time curves (0–24 hr) were 1811 and 2494 hr × ng/ml for Subjects 1 and 2, respectively.

Whole blood levels were monitored at 1, 2, and 3 hr after administration. These levels were highest at 3 hr. Blood and plasma levels were comparable at 1 hr after administration; but by 3 hr after administration, the blood levels were approximately 2.5 times the plasma levels. This phenomenon of markedly higher whole blood than plasma levels was reported by Beermann *et al.* (5), who found levels of radioactivity in red blood cells 3.5 times those observed in plasma. Similarly, whole blood levels of chlorthalidone and a carbonic anhydrase inhibitor, 2-amino-4-phenylsulfonylbenzenesulfonamide, were reported to be 6–35 times as high as the respective plasma levels in humans (7, 8). The mechanism underlying these findings has not been elucidated.

REFERENCES

(1) W. J. A. VandenHeuvel, V. F. Gruber, R. W. Walker, and F. J. Wolf, *J. Pharm. Sci.*, **64**, 1309 (1975).

(2) B. Lindstrom, M. Molander, and M. Groschinsky, *J. Chromatogr.*, **114**, 459 (1975).

(3) M. J. Cooper, A. R. Sinaiko, M. W. Anders, and B. L. Mirkin, *Anal. Chem.*, **48**, 1110 (1976).

(4) A. S. Christophersen, K. E. Rasmussen, and B. Salvesen, *J. Chromatogr.*, **132**, 91 (1977).

(5) B. Beermann, M. Groschinsky-Grind, and A. Rosen, *Clin. Pharmacol. Ther.*, **19**, 531 (1976).

(6) B. Beermann, M. Groschinsky-Grind, and B. Lindstrom, *Eur. J. Clin. Pharmacol.*, **11**, 203 (1977).

(7) P. Collste, M. Garle, M. D. Rawlins, and F. Sjoqvist, *ibid.*, **9**, 319 (1976).

(8) J. Lund, H. E. Pedersen, P. Z. Olsen, and E. F. Hvidberg, *Clin. Pharmacol. Ther.*, **12**, 902 (1971).

ACKNOWLEDGMENTS

The authors are indebted to Dr. L. H. Werner, Ciba-Geigy Corp., Summit, N.J., for a generous supply of 6-bromo-3,4-dihydro-2*H*-1,2,4-benzothiadiazine-7-sulfonamide 1,1-dioxide. The technical assistance of Mrs. A. Le Sher is gratefully acknowledged.

Differential Spectrophotometric Determination of Tyrosine and Tryptophan in Pharmaceutical Amino Acid Solutions

J. DEMEESTER *x, **M. BRACKE** *, **R. VOCHTEN** ‡, and **A. LAUWERS** *

Received June 27, 1977, from the *Laboratory of General Biochemistry and of Physical Pharmacy, State University of Gent, Wolterslaan 12, B-9000 Gent, Belgium, and the ‡Laboratory of Industrial Technology, University of Antwerp, Middelheimlaan 1, B-2020 Antwerpen, Belgium. Accepted for publication August 30, 1977.

Abstract □ A method is proposed for the simultaneous determination of tyrosine and tryptophan in solutions by differential spectrophotometry. The concentrations are calculated from the measurement of the absorbance of the amino acid mixture in an alkaline medium and from the differential absorbance of the alkaline solution against the acid solution at 294.4 nm. A comparison with three other well-known methods is discussed.

Keyphrases □ Tyrosine—spectrophotometric analysis simultaneously with tryptophan in solutions □ Tryptophan—spectrophotometric analysis simultaneously with tyrosine in solutions □ Spectrophotometry, differential—simultaneous analyses of tyrosine and tryptophan in solutions □ Amino acids—tyrosine and tryptophan, simultaneous spectrophotometric analyses in solutions

For the determination of tyrosine and tryptophan in solutions, various widely used spectrophotometric methods are based on the fact that the absorption spectra of both amino acids differ in acid and in alkaline media. These methods have been used frequently for the analysis of proteins and peptides where wavelength shifts occur. The most important spectrophotometric routine methods that can be performed without computer-assisted least-squares or linear programming techniques (1–3) have been considered using known amino acid mixtures. When extreme tyrosine to tryptophan ratios are to be determined, large errors are observed. Therefore, a simple method without these inconveniences is desired.

The proposed method uses the same principles but takes advantage of differential absorbance measurements and uses only one wavelength to improve simplicity and accuracy. The objectives of this study were to develop a practical procedure for routine applications, to define general formulas for individual adaptations to special problems, and to evaluate the statistical errors. Furthermore, the proposed procedure was compared with the mentioned methods.

EXPERIMENTAL

General—The absorption spectra of vacuum-dried tyrosine[1] and tryptophan[2] were recorded in an alkaline medium (0.1 *M* NaOH), and an isosbestic point was found at 294.4 nm (ϵ^{OH^-}) corresponding to the literature value (1). The measurements were performed on a calibrated spectrophotometer[3] with a resolution of 0.1 nm. Molar absorptivities (ϵ) of vacuum-dried tyrosine and tryptophan at 294.4 nm were calculated by linear regression analysis from series of dilutions in 0.1 *M* HCl and 0.1 *M* NaOH (correlation coefficients were greater than 0.9998) and are expressed in M^{-1} cm^{-1} with their standard errors.

For tyrosine in an acid medium, the value $\epsilon_{tyr}^{H^+}$ was 25.07 ± 0.008; for tryptophan, $\epsilon_{trp}^{H^+}$ was 1330 ± 9. In an alkaline medium for both tyrosine and tryptophan, ϵ^{OH^-} was 2465 ± 6.

[1] Product 8371, Merck, Darmstadt, West Germany.
[2] Product 8404, Merck, Darmstadt, West Germany.
[3] Cary 14, Varian Instruments.

Table I—Absorbance Values, Calculated Tyrosine and Tryptophan Molar Concentrations (c_{tyr} and c_{trp}, Respectively), and Their Relative Errors in Percent [a]

Tyrosine to Tryptophan	A^{OH^-}	ΔA	$10^5\, c_{tyr}$	$10^5\, c_{trp}$	Percent Error Tyrosine	Percent Error Tryptophan
10:0	0.4134	0.4068	16.59	0.19	−0.5	—
9:1	0.4080	0.3809	14.79	1.76	−1.4	+5.6
8:2	0.4066	0.3515	12.66	3.75	−5.0	+12.6
7:3	0.4104	0.3377	11.40	5.25	−2.3	+5.0
6:4	0.4132	0.3274	10.51	6.25	+5.1	−6.2
5:5	0.4103	0.2985	8.40	8.25	+0.8	−1.0
4:6	0.4132	0.2784	6.76	10.00	+1.3	+0.1
3:7	0.4115	0.2547	5.00	11.70	0.0	+0.2
2:8	0.4103	0.2340	3.45	13.19	+3.6	−1.1
1:9	0.4150	0.2127	1.66	15.18	−0.6	+1.2
0:10	0.4104	0.1856	−0.26	16.91	–	+1.4

[a] The total amino acid concentration was 166 μM.

The following simple equations can be set up when differential measurements of absorbance, ΔA, are made of the alkaline mixture against the acid mixture with molar concentrations of tyrosine and tryptophan, c_{tyr} and c_{trp}, respectively:

$$\Delta A = \Delta A_{tyr} + \Delta A_{trp} = c_{tyr}(\epsilon^{OH^-} - \epsilon_{tyr}^{H^+})l + c_{trp}(\epsilon^{OH^-} - \epsilon_{trp}^{H^+})l \quad \text{(Eq. 1)}$$

$$A^{OH^-} = (c_{tyr} + c_{trp})\epsilon^{OH^-}l \quad \text{(Eq. 2)}$$

From these equations follows:

$$c_{tyr} = \frac{\Delta A - A^{OH^-}\dfrac{\epsilon^{OH^-} - \epsilon_{trp}^{H^+}}{\epsilon^{OH^-}}}{l(\epsilon_{trp}^{H^+} - \epsilon_{tyr}^{H^+})} \quad \text{(Eq. 3)}$$

By substituting the calculated ϵ values into Eqs. 2 and 3, the formulas to calculate the molar concentrations of both amino acids are obtained:

$$c_{tyr} = \frac{\Delta A - 0.4605A^{OH^-}}{1305} \quad \text{(Eq. 4)}$$

$$c_{trp} = \frac{A^{OH^-}}{2465} - c_{tyr} \quad \text{(Eq. 5)}$$

The most probable errors on the molar concentrations were calculated using the classical partial differential formulas and yielded, for tyrosine:

$$s_{tyr}^2 = \frac{1.212s^2 + (0.00782)^2A^2}{(1305)^2} + \frac{(15)^2}{(1305)^4}(\Delta A - 0.460A^{OH^-})^2 \quad \text{(Eq. 6)}$$

and for tryptophan:

$$s_{trp}^2 = \frac{1.980s^2 + (0.00628)^2A^2}{(1305)^2} + \frac{(15)^2}{(1305)^4}(\Delta A - 0.990A^{OH^-})^2 \quad \text{(Eq. 7)}$$

where s is the standard error on the absorbance measurements.

Procedure—Dilute the amino acid mixture until a total concentration of tyrosine and tryptophan of about 200–800 μM is obtained; this is Solution U.

Measure (in triplicate) in 1-cm UV cells in a wavelength-calibrated dual-beam spectrophotometer at 294.4 nm and in absorbance scale:

Table II—Relative Errors in Percent on the Concentrations of Tyrosine and Tryptophan Determined with the Four Spectrophotometric Methods[a]

Tyrosine to Tryptophan Ratio	Reference 1		Reference 2		Reference 3		Present Method	
	Tyrosine	Tryptophan	Tyrosine	Tryptophan	Tyrosine	Tryptophan	Tyrosine	Tryptophan
1:9	+51	+0.7			+400	−39	+6.0	−0.7
2:8	−20	+11			+120	−33	+3.0	−1.5
3:7	−3	−2.2			+83	−36	−3.0	+0.4
4:6	+0.8	−1.5	+4.1	−1.3	+50	−34	+1.6	−1.0
5:5	−4.8	−1.2	+6.4	−7.1	+29	−35	+1.2	−1.8
6:4	0	−1.5	−13	−1.4	+23	−36	+0	−1.5
7:3	+3.9	−6.1			+15	−32	−5.6	+3.0
8:2	+1.5	−9.1			+6	−27	−1.5	+3.0
9:1	−0.7	−18			+1.3	−36	−1.3	+12.0

[a] The total amino acid concentration was 330 μM.

1. A mixture of 10 ml of Solution U with 10 ml of 0.2 *M* NaOH (sample beam) against a mixture of 10 ml of 0.2 *M* NaOH with 10 ml of clean water (reference beam); this gives the absorbance value A^{OH^-}.
2. A mixture of 10 ml of Solution U with 10 ml of 0.2 *M* NaOH (sample beam) against a mixture of 10 ml of Solution U with 10 ml of 0.2 *M* HCl (reference beam); this gives the absorbance value ΔA.

From Eqs. 4 and 5, the molar concentrations of tyrosine and tryptophan after dilution are obtained so that it is a simple procedure to obtain the original concentration by multiplying by 2 and by the dilution factor used. Other experimental procedures (*e.g.*, other cells) can be considered when using Eqs. 2 and 3.

RESULTS

The method was controlled experimentally using known amino acid mixtures with different concentration ratios. Table I gives the experimental values, and Fig. 1 shows the deviation of the experimentally found concentrations from the real concentrations. Figure 1 also shows the computed plots of the theoretical 2*s* most probable error limits, calculated from Eqs. 6 and 7; the value of *s* was taken as 0.003, corresponding to the spectrophotometer specifications.

All experimental values were means of three absorbance measurements.

This method was compared with the most important spectrophotometric methods previously described (1–3). Table II gives the relative errors in percent of the concentrations in the four methods.

DISCUSSION

Good results were found with the method of Goodwin and Morton (1) except at extreme ratios (Table II). Two wavelength settings are needed. The method of Bencze and Schmid (2) gives good results only with approximately equimolar solutions. With more extreme ratios, many difficulties are encountered. The method of Brown *et al.* (3) is less accurate in the whole range.

The proposed method, in general, gives less error than the other methods, especially at higher amino acid ratios. Moreover, the found errors are in good agreement with the expected values of the general error theory, so that when a determination is performed, the expected error in concentration can be calculated easily from Eqs. 6 and 7. Only one wavelength is needed for the assay, so no supplementary scatter in the results occurs from bad wavelength settings. The wavelength accuracy eventually can be checked with known amino acid solutions.

This proposed method is less accurate than some other methods when the tyrosine and tryptophan content of unhydrolyzed protein solutions is measured because of the wavelength shifts of the absorbance spectra

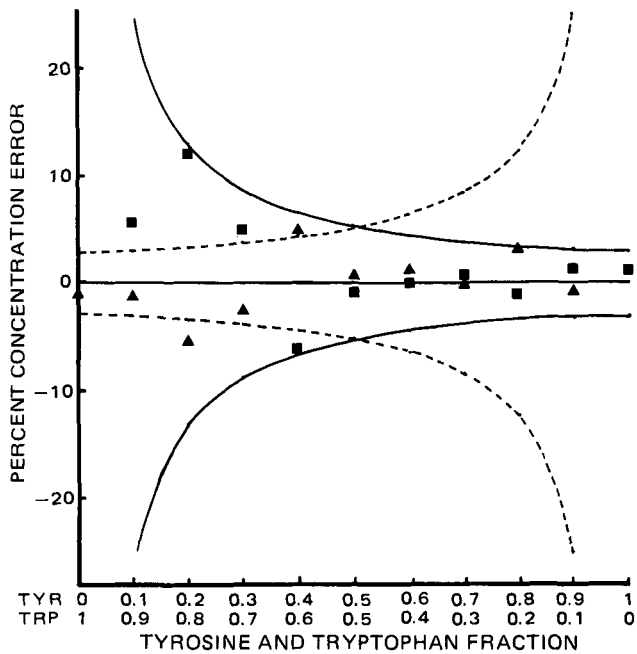

Figure 1—*Plot of the ratios of tyrosine to tryptophan (the total concentration equals 166* μM) versus *the deviations in percent of the concentrations of tyrosine* (▲) *and tryptophan* (■). *The* 2s *(95%) most probable error limits for tyrosine* (- - -) *and tryptophan* (—) *were calculated from Eqs. 6 and 7.*

of both amino acids in proteins. The only interfering amino acids are thyroxine and the thyronines, which do not occur in normal protein hydrolysates or amino acid mixtures. The present method can be very useful when it is important to control the amino acid composition of intravenous and other pharmaceutical preparations, because no interference exists from other amino acids at this high wavelength.

REFERENCES

(1) T. W. Goodwin and R. A. Morton, *Biochem. J.*, **40**, 628 (1946).
(2) W. L. Bencze and K. Schmid, *Anal. Chem.*, **29**, 1193 (1957).
(3) J. R. Brown, N. Greenshields, M. Yamasaki, and H. Neurath, *Biochemistry*, **2**, 867 (1963).

Determination of Clonazepam in Tablets by dc Polarography

C. T. VINH ˣ, J. BRAUN, and J. R. PLOURDE

Received May 17, 1977, from the *Faculty of Pharmacy, University of Montreal, Montreal, Quebec, Canada H3C 3J7.* Accepted for publication August 29, 1977.

Abstract □ A simple and convenient method for the routine determination of clonazepam in tablets by dc polarography is described. Clonazepam is extracted from the sample by ethanol and diluted with pH 4.15 acetate buffer in a volumetric flask. The filtered solution is then polarographed at the dropping mercury electrode *versus* the saturated calomel electrode. The polarographic wave is well developed; the determination is quantitative, precise, and accurate.

Keyphrases □ Clonazepam—dc polarographic analysis in tablets □ dc Polarography—analysis, clonazepam in tablets □ Anticonvulsants—clonazepam, dc polarographic analysis in tablets

Several methods, *e.g.*, electron-capture GLC (1–7) and radioimmunoassay (8), have been reported for the determination of clonazepam. These methods, although highly sensitive, are time consuming and require meticulous handling and skilled technical operations.

Polarographic reduction of the nitro group of clonazepam in whole blood has been reported (9). Differential pulse polarographic analysis of major urinary metabolites of clonazepam has been accomplished by reduction of the azomethine group (3).

This study was undertaken to develop a simple, rapid, and reliable dc polarographic analysis for clonazepam[1], 5-(2-chlorophenyl)-1,3-dihydro-7-nitro-2*H*-1,4-benzodiazepin-2-one, in tablets. Properly applied, the polarographic method is stoichiometrically valid and reproducible.

EXPERIMENTAL

Apparatus—A recording polarograph[2] equipped with a polarograph stand, which includes the dropping mercury electrode, a saturated calomel electrode, and a nitrogen bubbler placed in a standard cell, was used.

Reagents and Chemicals—A pH 4.15 acetate buffer was prepared by mixing 41.0 ml of 0.2 *M* acetic acid with 9.0 ml of 0.2 *M* sodium acetate.

For the stock standard solution, 60 mg of clonazepam standard was dissolved in 190 ml of 95% ethanol in a 200-ml volumetric flask and diluted to volume with the same solvent.

Sample Preparation—Twenty tablets were accurately weighed, and the average weight per tablet was determined. These tablets were finely ground, and the equivalent of tablet powder containing 2 mg of clonazepam was accurately weighed. The powder was transferred into a 100-ml volumetric flask, 10 ml of 95% ethanol was added, and the flask was shaken for about 10 min. Then 50 ml of acetate buffer was added; the flask was shaken for another 10 min and diluted to volume with the buffer. The solution was filtered through filter paper[3], discarding the first 20 ml of filtrate.

Polarography—The filtered solution (25 ml) was transferred into the polarographic cell, and oxygen-free nitrogen was bubbled through it for 10–15 min. The polarogram was recorded from 0.00 to −0.5 v (applied voltage on the dropping mercury electrode *versus* the saturated calomel electrode). The other conditions were: mercury height, 45 cm; drop time, 2.8 sec; and sensitivity, 1×10^{-8} amp/mm of the scale of the recorder. A suitable damping was applied. The height of diffusion current (i_D) was measured. The standard clonazepam solutions, 1, 1.5, 2, 2.5, and 3 mg/100 ml of pH 4.15 acetate buffer containing 10% of 95% ethanol, were polarographed under the same conditions, and the wave heights were measured. A calibration curve, diffusion current *versus* concentration, was then established.

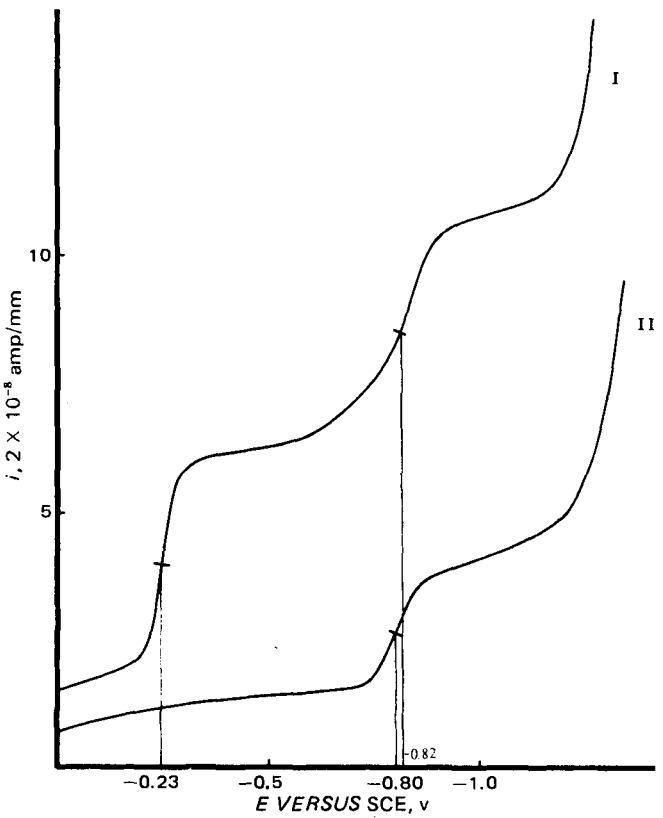

Figure 1—*Polarograms of clonazepam (I) and diazepam (II) in acetate buffer–ethanol.*

Calculations—By referring the diffusion current, i_D, measured for the sample to the calibration curve, the amount of clonazepam, C_x, in the weight of sample taken, W_s, can be found using:

$$\text{mg of clonazepam/tablet} = \frac{C_x \times W_t}{W_s} \qquad \text{(Eq. 1)}$$

where W_t is the average tablet weight.

RESULTS AND DISCUSSION

When clonazepam was polarographed in pH 4.15 acetate buffer, two reduction waves were observed. The half-wave potentials were −0.23 and −0.82 v (*versus* the saturated calomel electrode) (Fig. 1).

Table I—Diffusion Current at Different Concentrations of Clonazepam Standard

Clonazepam Concentration, mg/ml	i_D, 1×10^{-8} amp
0.030	118.5
0.025	97.0
0.020	76.5
0.015	56.5
0.010	37.0

[1] Rivotril, Hoffmann-La Roche, Vaudreuil, Quebec, Canada.
[2] Polarocord, type E 261 R, Methrohm AG, Herisau, Switzerland.
[3] S & S No. 595.

Table II—Analysis and Recovery of Clonazepam in Tablets

Assay before Addition of Standard				Assay after Addition of Standard			
Sample	Theoretical Concentration, mg/100 ml	Assay Value, mg/100 ml	% Theory	Sample	Theoretical Concentration, mg/100 ml	Amount Added, mg	Amount Found, mg
			2-mg Tablets				
A	2	1.91	95.5	F	1	1	1.96
B	2	1.90	95.2	G	1	1	1.96
C	2	1.92	96.0	H	1	1	1.96
D	2	1.93	96.5	I	1	2	2.93
E	2	1.89	94.5	J	1	2	2.93
Average		1.91		K	1	2	2.90
Range		1.89–1.93					
SD		1.58×10^{-2}					
			0.5-mg Tablets				
L	2.0	2.0	100.0	Q	1	1	2.0
M	2.0	2.01	100.6	R	1	1	1.99
N	2.0	2.01	100.7	S	1	1	1.98
O	2.0	2.01	100.7	T	1	2	2.97
P	2.0	2.01	100.7	U	1	2	2.96
Average		2.008		V	1	2	2.98
Range		2.0–2.01					
SD		1.08×10^{-2}					

Table III—Single-Tablet Assays of Clonazepam

2-mg Tablets				0.5-mg Tablets			
Sample	Theoretical Concentration, mg/100 ml	Assay Value, mg/100 ml	% Theory	Sample	Theoretical Concentration, mg/25 ml	Assay Value, mg/25 ml	% Theory
1	2	1.920	96.0	1	0.5	0.494	98.7
2	2	1.934	96.7	2	0.5	0.494	98.7
3	2	1.934	96.7	3	0.5	0.496	99.3
4	2	1.908	95.4	4	0.5	0.502	100.3
5	2	1.908	95.4	5	0.5	0.503	100.6
6	2	1.894	94.7	6	0.5	0.500	100.0
7	2	1.934	96.7	7	0.5	0.496	99.3
8	2	1.928	96.4	8	0.5	0.496	99.3
9	2	1.936	96.8	9	0.5	0.494	98.7
10	2	1.908	95.4	10	0.5	0.494	98.7
Average		1.920		Average		0.497	
Range		1.894–1.936		Range		0.494–0.503	
SD		1.50×10^{-2}		*SD*		3.48×10^{-3}	

The basic difference between clonazepam and diazepam is the presence of a nitro group on C-7 of the clonazepam structure while diazepam bears a chlorine atom at the same position. Both structures have a carbonyl group. When polarographed under the same conditions, diazepam gave only a single reduction wave with a half-wave potential of −0.80 v (Fig. 1). It may be assumed that both compounds undergo the same polarographic reduction of their respective carbonyl group. The first wave for clonazepam, absent with diazepam, may be attributed to the nitro group. This more positive wave (Fig. 2) was used for the quantitative determination of clonazepam. A plot of the diffusion current *versus* the concentration of clonazepam was linear in the range of 1–3 mg/100 ml (Table I). Maxima suppressors were not needed since no maximum was observed. Clonazepam is stable at pH 4.15. All operations were carried out at room temperature.

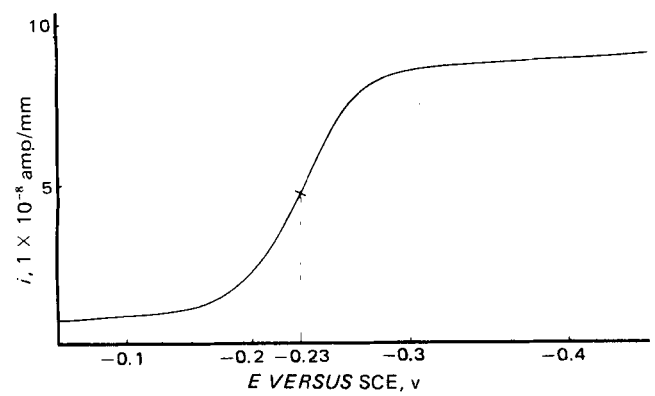

Figure 2—*Clonazepam reduction wave used for its assay.*

Each of the two dosage forms currently available was analyzed in two ways: analysis of clonazepam in the original unaltered dosage form and analysis of the sample after addition of a specific amount of clonazepam standard. This procedure was followed to ensure that the extraction was adequate and that all clonazepam had been dissolved and to test the accuracy of the polarographic method. The results are shown in Table II.

The wave obtained for clonazepam under the described conditions was well developed. As shown in Table II, clonazepam was quantitatively extracted and determined with excellent accuracy and precision without interference from any other component in the dosage form.

The method was also applied to a single-tablet assay (Table III).

This polarographic method is simple, rapid, and quite suitable for routine assay as well as for single-tablet assays.

REFERENCES

(1) J. Naestaft and N. E. Larkin, *J. Chromatogr.*, **93,** 113 (1974).

(2) J. A. F. de Silva and I. Bekersky, *ibid.*, **99,** 447 (1974).

(3) J. A. F. de Silva, C. V. Puglisi, and N. Munno, *J. Pharm. Sci.*, **63,** 520 (1974).

(4) H. J. Knop, E. Van der Kleijn, and L. C. Edmunds, *Pharm. Weekbl.*, **110,** 297 (1975).

(5) J. A. de Silva and I. Bekersky, *Anal. Chem.*, **48,** 10 (1976).

(6) G. J. G. Parry and D. G. Ferry, *J. Chromatogr.*, **128**, 166 (1976).
(7) J. P. Cano, J. Catalin, *et al.*, *Eur. J. Toxicol. Environ. Hyg.*, **9**, 213 (1976).
(8) W. R. Dixon, R. L. Young, R. Ning, and A. Liebman, *J. Pharm. Sci.*, **66**, 235 (1977).
(9) A. Kobiela-Krzyzanowska, *Pharmazie*, **31**, 649 (1976).

ACKNOWLEDGMENTS

Supported in part by University of Montreal CAFIR Grant 175-16-635.

The authors thank Hoffmann–La Roche Ltd. (Canada) for samples and acknowledge the technical assistance of Mr. Merceano Desousa.

Solubility of Calcium Oxalate in 1-Alkanols and Ethanol–Water Mixtures

JUSTINA A. MOLZON, JOAN M. LAUSIER, and ANTHONY N. PARUTA ˣ

Received November 8, 1976, from the *College of Pharmacy, University of Rhode Island, Kingston, RI 02881.* Accepted for publication August 15, 1977.

Abstract □ Solubility profiles for calcium oxalate were determined in pure 1-alkanols and ethanol–water mixtures at 20°. The magnitude of solubility in the aliphatic alcohols was highest in methanol and decreased in a nonlinear fashion as the dielectric constant decreased, going to *n*-decanol. In ethanol–water mixtures, the solubility increased nonlinearly with water content or increasing dielectric constants. The work factor for these systems was also calculated and, as expected, a "mirror image" to the solubility profiles was evidenced. In the mixed solvent system, a dramatic change in the magnitude of solubility occurred after a dielectric constant value of about 60, indicating ionic association or ion-pairs below this value. The Born relationship of solubility and ionic size was tested in the ethanol–water system, and the ionic size of the divalent species of about 2.27 Å agreed with the theoretical ionic size of about 2.4 Å. These results indicate that the water number of calcium is 8 or that a monolayer of dipoles surrounds this divalent cationic species.

Keyphrases □ Calcium oxalate—solubility in various 1-alkanols and ethanol–water mixtures □ Solubility—calcium oxalate in various 1-alkanols and ethanol–water mixtures

Calcium oxalate, a component of certain types of "body" stones, is a typical example of a metallo-organic substance whose solubility characteristics should be a major area of investigation. This study is an initial effort into determining these solubility profiles in a series of pure 1-alkanols and ethanol–water mixtures. Since calcium oxalate is highly insoluble, its solubility as a function of polarity would be determined by covering the range of polarity by various solvents and solvent mixtures. Additionally, the spectrum of polarity would be manifested by the dielectric constants of the solvent systems. Thus, the charge-separating ability of various solvents would be indicative of their effect on the ionization and subsequent dissociation of the solute measured by the solubility product of calcium oxalate.

BACKGROUND

Calcium oxalate is considered to be insoluble in both polar and nonpolar solvents (1). It may occur as a mono-, di-, or trihydrate, with the monohydrate being the most stable form as well as the least soluble (2, 3). The monohydrate has a solubility product of 2.57×10^{-9} mole/liter at 25° (4).

In 1929, Hammarsten (5) studied the solubility of calcium oxalate, applying the Debye–Huckel theory of ion activity in the presence of urinary electrolytes. A "salting-in" increase in solubility was found by the use of sodium chloride, monobasic sodium phosphate, potassium chloride, and magnesium chloride. Also, pH had no effect when varied over the usual physiological range.

Shehyn and Pall (6) studied the solubility of calcium oxalate as a function of the ionic strength of various salts. Other studies relating to solubility in salt solutions also were performed (7–9). Finlayson *et al.* (10) presented information on the complex set of equilibria of calcium oxalate in aqueous systems. An ionizable salt, sodium salicylate, was studied previously in mixed solvent systems of various types (11).

EXPERIMENTAL

Chemicals—Calcium oxalate[1], calcium chloride[2], methanol[3], ethanol[4], 1-propanol[5], 1-butanol[6], 1-pentanol[7], 1-hexanol[8], 1-octanol[9], 1-decanol[10], and distilled deionized water were used. The purity and anhydrous nature of the solvents were tested as previously described (11).

Equipment—A refractometer[11], a demineralizer[12], a centrifuge[13], and an oscillometer[14] were used.

The refractometer was used to check the purity of the solvents, and the oscillometer was used to determine dielectric constants.

Procedure—A rotating apparatus holding screw-capped glass vials was filled with the appropriate solvent or solvent mixture and rotated at 40 rpm in the presence of excess calcium oxalate. The temperature was maintained at 20° by a temperature control unit[15]. Samples were withdrawn with pipets through a glass wool wrap after equilibration for 24 hr. The samples were centrifuged at 1000 rpm for 10 min because of the fine nature of particles, and a clear supernate at 20° was drawn for analysis on an atomic absorption spectrophotometer[16].

The samples were analyzed from previously determined calibration curves with known concentrations of calcium as calcium chloride in the appropriate solvents or solvent mixtures. These measurements were made with a calcium vapor lamp at the 4227-Å absorption line for gaseous calcium atoms at a source current of 12 μamp using an acetylene–air mixture.

For the pure solvents and up to about 40% water in the mixed solvent system, 12 samples were analyzed. At higher water concentrations to pure water, eight samples were tested for calcium concentration. These results

[1] Lot 762198, certified powder, J. T. Baker Chemical Co.
[2] Lot XGZ, anhydrous, Mallinckrodt Chemical Works.
[3] Lot VMN, anhydrous, spectrophotometric grade, Mallinckrodt Chemical Works.
[4] Absolute, U.S. Industrial Chemical Co.
[5] Lot 35592, "Baker Analyzed," J. T. Baker Chemical Co.
[6] Lot TDY, analytical reagent, Mallinckrodt Chemical Works.
[7] Lot 776291, certified, U.S. Industrial Chemical Co.
[8] Lot H1330, Aldrich Chemical Co.
[9] Lot 22, Mallinckrodt Chemical Works.
[10] Lot 17, Matheson, Coleman and Bell.
[11] Abbe-3, Bausch & Lomb Optical Co.
[12] Bantam model BD-1, Barnstead Still and Sterilizer Co.
[13] Damon/IEC Division, Damon Corp.
[14] Chemical model V, E. H. Sargent and Co.
[15] Temptrol 150, Precision Scientific Co.
[16] Model 3D3, Perkin-Elmer Corp.

(6) G. J. G. Parry and D. G. Ferry, *J. Chromatogr.*, **128**, 166 (1976).
(7) J. P. Cano, J. Catalin, *et al.*, *Eur. J. Toxicol. Environ. Hyg.*, **9**, 213 (1976).
(8) W. R. Dixon, R. L. Young, R. Ning, and A. Liebman, *J. Pharm. Sci.*, **66**, 235 (1977).
(9) A. Kobiela-Krzyzanowska, *Pharmazie*, **31**, 649 (1976).

ACKNOWLEDGMENTS

Supported in part by University of Montreal CAFIR Grant 175-16-635.

The authors thank Hoffmann–La Roche Ltd. (Canada) for samples and acknowledge the technical assistance of Mr. Merceano Desousa.

Solubility of Calcium Oxalate in 1-Alkanols and Ethanol–Water Mixtures

JUSTINA A. MOLZON, JOAN M. LAUSIER, and ANTHONY N. PARUTA ˣ

Received November 8, 1976, from the *College of Pharmacy, University of Rhode Island, Kingston, RI 02881.* Accepted for publication August 15, 1977.

Abstract □ Solubility profiles for calcium oxalate were determined in pure 1-alkanols and ethanol–water mixtures at 20°. The magnitude of solubility in the aliphatic alcohols was highest in methanol and decreased in a nonlinear fashion as the dielectric constant decreased, going to *n*-decanol. In ethanol–water mixtures, the solubility increased nonlinearly with water content or increasing dielectric constants. The work factor for these systems was also calculated and, as expected, a "mirror image" to the solubility profiles was evidenced. In the mixed solvent system, a dramatic change in the magnitude of solubility occurred after a dielectric constant value of about 60, indicating ionic association or ion-pairs below this value. The Born relationship of solubility and ionic size was tested in the ethanol–water system, and the ionic size of the divalent species of about 2.27 Å agreed with the theoretical ionic size of about 2.4 Å. These results indicate that the water number of calcium is 8 or that a monolayer of dipoles surrounds this divalent cationic species.

Keyphrases □ Calcium oxalate—solubility in various 1-alkanols and ethanol–water mixtures □ Solubility—calcium oxalate in various 1-alkanols and ethanol–water mixtures

Calcium oxalate, a component of certain types of "body" stones, is a typical example of a metallo-organic substance whose solubility characteristics should be a major area of investigation. This study is an initial effort into determining these solubility profiles in a series of pure 1-alkanols and ethanol–water mixtures. Since calcium oxalate is highly insoluble, its solubility as a function of polarity would be determined by covering the range of polarity by various solvents and solvent mixtures. Additionally, the spectrum of polarity would be manifested by the dielectric constants of the solvent systems. Thus, the charge-separating ability of various solvents would be indicative of their effect on the ionization and subsequent dissociation of the solute measured by the solubility product of calcium oxalate.

BACKGROUND

Calcium oxalate is considered to be insoluble in both polar and nonpolar solvents (1). It may occur as a mono-, di-, or trihydrate, with the monohydrate being the most stable form as well as the least soluble (2, 3). The monohydrate has a solubility product of 2.57×10^{-9} mole/liter at 25° (4).

In 1929, Hammarsten (5) studied the solubility of calcium oxalate, applying the Debye–Huckel theory of ion activity in the presence of urinary electrolytes. A "salting-in" increase in solubility was found by the use of sodium chloride, monobasic sodium phosphate, potassium chloride, and magnesium chloride. Also, pH had no effect when varied over the usual physiological range.

Shehyn and Pall (6) studied the solubility of calcium oxalate as a function of the ionic strength of various salts. Other studies relating to solubility in salt solutions also were performed (7–9). Finlayson *et al.* (10) presented information on the complex set of equilibria of calcium oxalate in aqueous systems. An ionizable salt, sodium salicylate, was studied previously in mixed solvent systems of various types (11).

EXPERIMENTAL

Chemicals—Calcium oxalate[1], calcium chloride[2], methanol[3], ethanol[4], 1-propanol[5], 1-butanol[6], 1-pentanol[7], 1-hexanol[8], 1-octanol[9], 1-decanol[10], and distilled deionized water were used. The purity and anhydrous nature of the solvents were tested as previously described (11).

Equipment—A refractometer[11], a demineralizer[12], a centrifuge[13], and an oscillometer[14] were used.

The refractometer was used to check the purity of the solvents, and the oscillometer was used to determine dielectric constants.

Procedure—A rotating apparatus holding screw-capped glass vials was filled with the appropriate solvent or solvent mixture and rotated at 40 rpm in the presence of excess calcium oxalate. The temperature was maintained at 20° by a temperature control unit[15]. Samples were withdrawn with pipets through a glass wool wrap after equilibration for 24 hr. The samples were centrifuged at 1000 rpm for 10 min because of the fine nature of particles, and a clear supernate at 20° was drawn for analysis on an atomic absorption spectrophotometer[16].

The samples were analyzed from previously determined calibration curves with known concentrations of calcium as calcium chloride in the appropriate solvents or solvent mixtures. These measurements were made with a calcium vapor lamp at the 4227-Å absorption line for gaseous calcium atoms at a source current of 12 μamp using an acetylene–air mixture.

For the pure solvents and up to about 40% water in the mixed solvent system, 12 samples were analyzed. At higher water concentrations to pure water, eight samples were tested for calcium concentration. These results

[1] Lot 762198, certified powder, J. T. Baker Chemical Co.
[2] Lot XGZ, anhydrous, Mallinckrodt Chemical Works.
[3] Lot VMN, anhydrous, spectrophotometric grade, Mallinckrodt Chemical Works.
[4] Absolute, U.S. Industrial Chemical Co.
[5] Lot 35592, "Baker Analyzed," J. T. Baker Chemical Co.
[6] Lot TDY, analytical reagent, Mallinckrodt Chemical Works.
[7] Lot 776291, certified, U.S. Industrial Chemical Co.
[8] Lot H1330, Aldrich Chemical Co.
[9] Lot 22, Mallinckrodt Chemical Works.
[10] Lot 17, Matheson, Coleman and Bell.
[11] Abbe-3, Bausch & Lomb Optical Co.
[12] Bantam model BD-1, Barnstead Still and Sterilizer Co.
[13] Damon/IEC Division, Damon Corp.
[14] Chemical model V, E. H. Sargent and Co.
[15] Temptrol 150, Precision Scientific Co.
[16] Model 3D3, Perkin-Elmer Corp.

Table I—Solubility of Calcium Oxalate in Various Notations at 20° as a Function of the Dielectric Constants and Work Factors of the Aliphatic Alcohols Listed

Alcohol	Dielectric[a] Constant	Work[b], ergs × 10^{12}	Average Calcium Concentration, ppm	Calcium Concentration × 10^5, moles/liter	Solubility Product, K_{sp}, × 10^{10} moles/liter
Methanol	32.6	1.2	0.064	0.045	0.00203
Ethanol	24.4	1.6	0.052	0.037	0.00134
1-Propanol	20.2	1.9	0.040	0.028	0.00079
1-Butanol	17.2	2.2	0.033	0.023	0.00054
1-Pentanol	14.9	2.6	0.029	0.020	0.00042
1-Hexanol	13.4	3.1	0.025	0.018	0.00031
1-Octanol	9.9	3.9	0.023	0.016	0.00026
1-Decanol	8.0	4.8	0.017	0.012	0.00014

[a] Determined by oscillometric method. [b] Calculated from $W = 2e_1e_2/\epsilon r$.

Table II—Solubility of Calcium Oxalate in Various Notations at 20° as a Function of the Dielectric Constants and Work Factors of the Relative Concentration of Ethanol–Water Mixtures

Volume Percent of Water	Dielectric[a] Constant	Work[a], ergs × 10^{12}	Average Calcium Concentration, ppm	Calcium Concentration, × 10^5 moles/liter	Solubility Product, K_{sp}, × 10^{10} moles/liter
0	24.4	1.6	0.05	0.035	0.0012
10	29.3	1.3	0.06	0.042	0.0018
20	34.3	1.1	0.15	0.106	0.0110
30	39.7	0.97	0.24	0.169	0.028
40	46.0	0.83	0.43	0.303	0.092
50	52.3	0.73	0.65	0.458	0.209
60	58.3	0.66	0.87	0.613	0.375
70	64.0	0.60	1.40	0.986	0.972
80	69.3	0.55	2.43	1.71	2.93
90	74.1	0.52	3.90	2.75	7.54
100	78.5	0.49	5.33	3.75	14.08

[a] See Table 1.

were averaged for each solvent and solvent mixture, and the variation in replicate samples was about 0.001–0.005 ppm of calcium. The larger variations were found at low concentrations, leading to an error of about 10%. The smaller variations occurred for relatively higher concentrations, with errors of about 1–2 and <0.1% at calcium concentrations of about 0.1 and about 1 ppm or above, respectively.

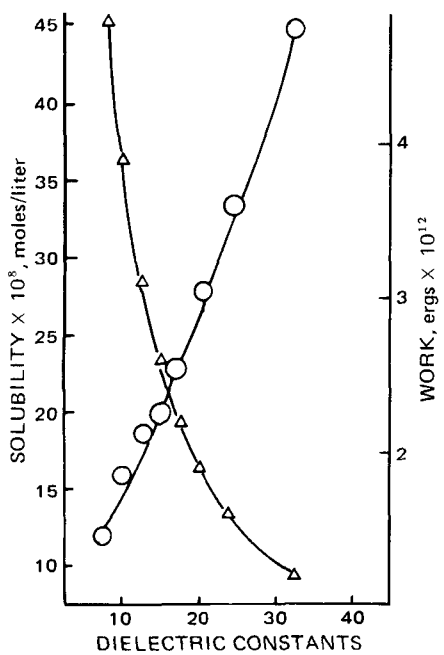

Figure 1—*Plot of the solubility at 20° of calcium oxalate, in moles per liter (○), and the work factor, in ergs (△), as a function of the dielectric constant of the 1-alkanols.*

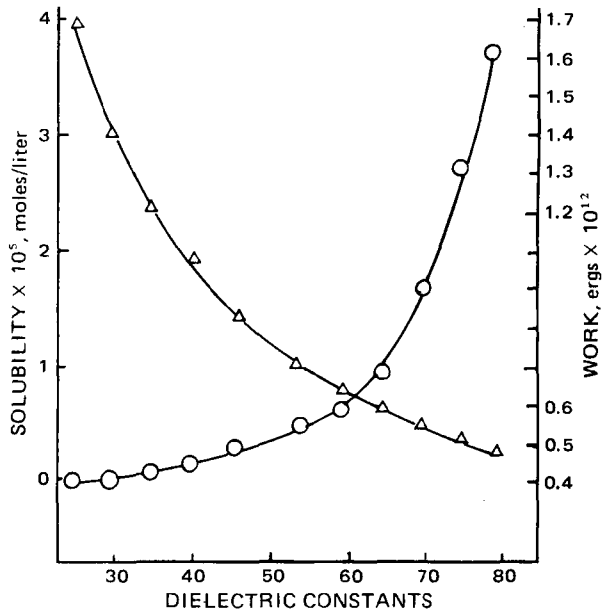

Figure 2—*Plot of the solubility at 20° of calcium oxalate, in moles per liter (○), and the work factor, in ergs (△), as a function of the dielectric constants of ethanol–water mixtures.*

RESULTS AND DISCUSSION

The experimentally determined solubilities of this solute, expressed in various concentration notations at 20° in the 1-alkanols and ethanol–water mixtures, are given in Tables I and II. The dielectric constants and work factors are also listed. The solubility in these cases increased with increasing dielectric constants and decreasing work factors. For the pure alcohols, the solubility increased in a nonlinear fashion from 1-decanol to methanol. Similarly, the solubility in ethanol–water mixtures also increased with increasing water content. This result indicates an enhancement of dissociation with increasing dielectric constants, as expected from Coulomb's law.

Figure 1 shows a plot of calcium solubility, expressed in moles per liter, *versus* the dielectric constants of the aliphatic alcohols. A nonlinear isothermal solubility profile is evidenced, which is the mirror image of the calculated work factors in these alcohols (also plotted in Fig. 1).

In Fig. 2, calcium solubility in moles per liter is plotted in the same manner for the ethanol–water mixtures; the same characteristics were observed. The solubility increased with increasing water content; at a dielectric constant of about 60, there was a dramatic increase in solubility disproportionate with water concentration.

This portion of the solubility isotherm was approximately linear and was supported by the work of Larson and Hunt (12), which states that

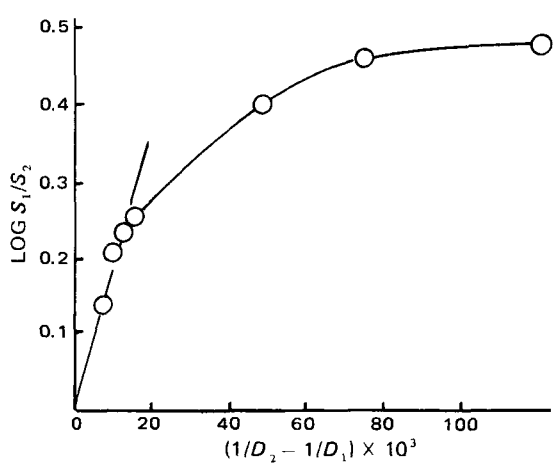

Figure 3—*Plot of the log of the solubility ratio for calcium oxalate at 20° as a function of the reciprocals of the dielectric constants of the ethanol–water mixtures.*

divalent ionic species are associated below this dielectric constant value. The decreasing solubility with increasing nonpolarity suggests increasing association of the calcium and oxalate moieties as a partially dissociated ion-pair. These ion-pairs would be strongly associated at lower dielectric constants, resulting in diminished solubility, with the association decreasing in strength as the dielectric constant of the medium increased.

Since the data were available, the Born theory (13) could be tested for validity in predicting the average ion radius once solubilities had been determined in two solvents of varying dielectric constants. These calculations were given previously (11) and are summarized here. In Fig. 3, $\log S_1/S_2$ for calcium oxalate is plotted *versus* the reciprocal of the difference in dielectric constants in the ethanol–water mixtures.

A straight-line relationship is observed at water concentrations of 60% (v/v) to pure water. The slope of this line has a value of 53. From this slope, an average ion radius of 2.27 Å was calculated.

The theoretical ionic radius for calcium and oxalate could be obtained from ionic radii and water numbers. The calcium ion possesses a water number of 8–12, and the oxalate ion has a water number of 2. The radius for the oxalate anion was about 2.4 Å. For calcium with a water number of 8, indicating a monolayer of water dipoles, the average ion radius was also 2.4 Å. With a water number of 12, a bimolecular layer of water dipoles is present and the radius was 3.6 Å.

The good agreement of the average ion radius from theoretical consideration of 2.4 Å and the experimentally determined value of 2.27 Å supports the use of the Born expression and suggests that the calcium ion in these binary systems possesses a water number of 8.

REFERENCES

(1) "The Merck Index," 7th ed., Merck & Co., Rahway, N.J., 1960, p. 196.

(2) E. L. Prien and E. L. Prien, Jr., *Am. J. Med.*, **45**, 659 (1968).

(3) G. Hammarsten, in "Etiologic Factors in Renal Lithiasis," A. J. Butt, Ed., Charles C Thomas, Springfield, Ill., 1956, pp. 89–94.

(4) "Handbook of Chemistry and Physics," 49th ed., Chemical Rubber Co., Cleveland, Ohio, 1968, p. B-307.

(5) G. Hammarsten, *C. R. Trav. Lab. Carlsberg*, **17**, 1 (1929).

(6) H. Shehyn and D. B. Pall, *J. Phys. Colloid Chem.*, **44**, 166 (1940).

(7) G. H. Miller, C. W. Vermeulen, and J. D. Moore, *J. Urol.*, **79**, 607 (1958).

(8) J. S. Elliot and E. Eusebio, *Invest. Urol.*, **3**, 72 (1965).

(9) *Ibid.*, **2**, 428 (1965).

(10) B. Finlayson, R. Roth, and L. DuBois, in "Urinary Calculi," International Symposium on Renal Stone Research, Madrid, Spain, 1972, pp. 1–7.

(11) A. N. Paruta and J. W. Mauger, *J. Pharm. Sci.*, **60**, 432 (1971).

(12) R. C. Larson and H. Hunt, *J. Phys. Chem.*, **43**, 417 (1939).

(13) M. Born, *Z. Phys.*, **1**, 45 (1920).

ACKNOWLEDGMENTS

Abstracted in part from a thesis submitted by J. A. Molzon to the University of Rhode Island in partial fulfillment of the Master of Science degree requirements.

Pyrrole, Furan, and Thiophene Oxamates as Potential Antiallergy Agents

FREDDA H. BRIGGS, WILLIAM T. PELLETIER, and C. DeWITT BLANTON, Jr. ˣ

Received July 28, 1977, from the *Department of Medicinal Chemistry, School of Pharmacy, University of Georgia, Athens, GA 30602.* Accepted for publication September 8, 1977.

Abstract □ Nine heterocyclic oxamic acid derivatives were synthesized and tested in the rat passive cutaneous anaphylactic assay as potential antiallergy agents. Some compounds also were tested for their effects on cholesterol–lipoprotein levels and for diuretic, antidiabetic, and antifertility activities in rats.

Keyphrases □ Heterocyclic oxamates, various—synthesized, evaluated as antiallergy agents □ Oxamates, various heterocyclic—synthesized, evaluated as antiallergy agents □ Antiallergy agents, potential—various heterocyclic oxamates evaluated □ Structure–activity relationships—various heterocyclic oxamates evaluated as antiallergy agents

Some years ago, several heterocyclic oxamates (II*a*–II*i*, Table I) were synthesized (Scheme I) as possible precursors for various indole isosteres. Although these efforts proved unsuccessful, routine screening[1] of these new compounds in the rat passive cutaneous anaphylaxis (PCA) assay as potential antiallergy agents (1–3) showed some significant activity (*viz.*, II*a*, Table II) (4). Subsequently, the activity (parenterally) was shown to reside in the free acid (5). Antiallergic activity associated with novel oxamic acids was noted recently (6–13), and Sellstedt *et al.* (14) described structure–activity relationships between the oxamates and cromolyn sodium, "the only compound on the market that prophylactically inhibits the liberation of the mediators of allergic reactions initiated by antibody-antigen interactions" (14).

In addition to the evaluation for antiallergic activity, pharmacological test data were obtained for diuretic activity in fasted rats (II*a*–II*c*, II*e*–II*i*, and III) (15) and antidiabetic activity in rats (II*b*, II*c*, II*e*, II*h*, and III) (16). No significant activity was observed. In an antifertility test (17), II*h* administered subcutaneously to three female rats (10 mg/day) prevented conception in all animals, and the compound was considered active by the criteria of this test. In the modified procedure of Tinsho *et al.* (18) for effect on cholesterol–lipoprotein levels in rats, II*a* lowered both serum cholesterol (T/C = 0.67) and serum lipoprotein (T/C = 0.63) fractions significantly at 50 mg/kg po. However, II*a* was inactive in preventing experimental thrombosis.

EXPERIMENTAL[2]

The amino-substituted heterocycles, I*a*–I*f*, were prepared by the procedure of Gewald and coworkers (19–21). 2-Amino-5-ethoxycarbon-

[1] From The Upjohn Co.'s biological evaluation program.

[2] Melting points were determined on a Thomas-Hoover apparatus (capillary method) and are uncorrected. NMR spectra were determined on a Hitachi Perkin-Elmer R 20A high-resolution NMR spectrometer, using tetramethylsilane as the internal reference. IR spectra were determined on a Perkin-Elmer 237B grating spectrophotometer, using the potassium bromide technique. UV spectra were determined in methanol solution with a Perkin-Elmer 202 UV–visible spectrophotometer. Elemental analyses were determined by Atlantic Microlab, Atlanta, Ga. TLC was performed on Eastman chromatogram sheets, type 6060 (silica gel).

divalent ionic species are associated below this dielectric constant value. The decreasing solubility with increasing nonpolarity suggests increasing association of the calcium and oxalate moieties as a partially dissociated ion-pair. These ion-pairs would be strongly associated at lower dielectric constants, resulting in diminished solubility, with the association decreasing in strength as the dielectric constant of the medium increased.

Since the data were available, the Born theory (13) could be tested for validity in predicting the average ion radius once solubilities had been determined in two solvents of varying dielectric constants. These calculations were given previously (11) and are summarized here. In Fig. 3, $\log S_1/S_2$ for calcium oxalate is plotted *versus* the reciprocal of the difference in dielectric constants in the ethanol–water mixtures.

A straight-line relationship is observed at water concentrations of 60% (v/v) to pure water. The slope of this line has a value of 53. From this slope, an average ion radius of 2.27 Å was calculated.

The theoretical ionic radius for calcium and oxalate could be obtained from ionic radii and water numbers. The calcium ion possesses a water number of 8–12, and the oxalate ion has a water number of 2. The radius for the oxalate anion was about 2.4 Å. For calcium with a water number of 8, indicating a monolayer of water dipoles, the average ion radius was also 2.4 Å. With a water number of 12, a bimolecular layer of water dipoles is present and the radius was 3.6 Å.

The good agreement of the average ion radius from theoretical consideration of 2.4 Å and the experimentally determined value of 2.27 Å supports the use of the Born expression and suggests that the calcium ion in these binary systems possesses a water number of 8.

REFERENCES

(1) "The Merck Index," 7th ed., Merck & Co., Rahway, N.J., 1960, p. 196.

(2) E. L. Prien and E. L. Prien, Jr., *Am. J. Med.*, **45**, 659 (1968).

(3) G. Hammarsten, in "Etiologic Factors in Renal Lithiasis," A. J. Butt, Ed., Charles C Thomas, Springfield, Ill., 1956, pp. 89–94.

(4) "Handbook of Chemistry and Physics," 49th ed., Chemical Rubber Co., Cleveland, Ohio, 1968, p. B-307.

(5) G. Hammarsten, *C. R. Trav. Lab. Carlsberg*, **17**, 1 (1929).

(6) H. Shehyn and D. B. Pall, *J. Phys. Colloid Chem.*, **44**, 166 (1940).

(7) G. H. Miller, C. W. Vermeulen, and J. D. Moore, *J. Urol.*, **79**, 607 (1958).

(8) J. S. Elliot and E. Eusebio, *Invest. Urol.*, **3**, 72 (1965).

(9) *Ibid.*, **2**, 428 (1965).

(10) B. Finlayson, R. Roth, and L. DuBois, in "Urinary Calculi," International Symposium on Renal Stone Research, Madrid, Spain, 1972, pp. 1–7.

(11) A. N. Paruta and J. W. Mauger, *J. Pharm. Sci.*, **60**, 432 (1971).

(12) R. C. Larson and H. Hunt, *J. Phys. Chem.*, **43**, 417 (1939).

(13) M. Born, *Z. Phys.*, **1**, 45 (1920).

ACKNOWLEDGMENTS

Abstracted in part from a thesis submitted by J. A. Molzon to the University of Rhode Island in partial fulfillment of the Master of Science degree requirements.

Pyrrole, Furan, and Thiophene Oxamates as Potential Antiallergy Agents

FREDDA H. BRIGGS, WILLIAM T. PELLETIER, and C. DeWITT BLANTON, Jr. ˣ

Received July 28, 1977, from the *Department of Medicinal Chemistry, School of Pharmacy, University of Georgia, Athens, GA 30602.* Accepted for publication September 8, 1977.

Abstract □ Nine heterocyclic oxamic acid derivatives were synthesized and tested in the rat passive cutaneous anaphylactic assay as potential antiallergy agents. Some compounds also were tested for their effects on cholesterol–lipoprotein levels and for diuretic, antidiabetic, and antifertility activities in rats.

Keyphrases □ Heterocyclic oxamates, various—synthesized, evaluated as antiallergy agents □ Oxamates, various heterocyclic—synthesized, evaluated as antiallergy agents □ Antiallergy agents, potential—various heterocyclic oxamates evaluated □ Structure–activity relationships—various heterocyclic oxamates evaluated as antiallergy agents

Some years ago, several heterocyclic oxamates (II*a*–II*i*, Table I) were synthesized (Scheme I) as possible precursors for various indole isosteres. Although these efforts proved unsuccessful, routine screening[1] of these new compounds in the rat passive cutaneous anaphylaxis (PCA) assay as potential antiallergy agents (1–3) showed some significant activity (*viz.*, II*a*, Table II) (4). Subsequently, the activity (parenterally) was shown to reside in the free acid (5). Antiallergic activity associated with novel oxamic acids was noted recently (6–13), and Sellstedt *et al.* (14) described structure–activity relationships between the oxamates and cromolyn sodium, "the only compound on the market that prophylactically inhibits the liberation of the mediators of allergic reactions initiated by antibody-antigen interactions" (14).

In addition to the evaluation for antiallergic activity, pharmacological test data were obtained for diuretic activity in fasted rats (II*a*–II*c*, II*e*–II*i*, and III) (15) and antidiabetic activity in rats (II*b*, II*c*, II*e*, II*h*, and III) (16). No significant activity was observed. In an antifertility test (17), II*h* administered subcutaneously to three female rats (10 mg/day) prevented conception in all animals, and the compound was considered active by the criteria of this test. In the modified procedure of Tinsho *et al.* (18) for effect on cholesterol–lipoprotein levels in rats, II*a* lowered both serum cholesterol (T/C = 0.67) and serum lipoprotein (T/C = 0.63) fractions significantly at 50 mg/kg po. However, II*a* was inactive in preventing experimental thrombosis.

EXPERIMENTAL[2]

The amino-substituted heterocycles, I*a*–I*f*, were prepared by the procedure of Gewald and coworkers (19–21). 2-Amino-5-ethoxycarbon-

[1] From The Upjohn Co.'s biological evaluation program.

[2] Melting points were determined on a Thomas-Hoover apparatus (capillary method) and are uncorrected. NMR spectra were determined on a Hitachi Perkin-Elmer R 20A high-resolution NMR spectrometer, using tetramethylsilane as the internal reference. IR spectra were determined on a Perkin-Elmer 237B grating spectrophotometer, using the potassium bromide technique. UV spectra were determined in methanol solution with a Perkin-Elmer 202 UV–visible spectrophotometer. Elemental analyses were determined by Atlantic Microlab, Atlanta, Ga. TLC was performed on Eastman chromatogram sheets, type 6060 (silica gel).

Table I—Oxamic Acid Derivatives

Compound	X	R_1	R_2	R_3	R_4	Yield[a], %	Melting Point	Formula	Analysis, % Calc.	Found
II*a*	NH	CH_3	CH_3	CN	C_2H_5	66.1	132–133°	$C_{11}H_{13}N_3O_3$	C 56.17	56.27
									H 5.53	5.67
									N 17.87	17.74
II*b*	O	CH_3	CH_3	CN	H	22.5[b]	172–173°	$C_9H_8N_2O_4$	C 51.92	52.13
									H 3.85	4.09
									N 13.46	13.25
II*c*	O	CH_3	CH_3	CN	C_2H_5	50[c]	97–100°	$C_{11}H_{12}N_2O_4$	C 55.93	56.06
									H 5.08	5.18
									N 11.86	11.93
II*d*	S	CH_3	CH_3	CN	C_2H_5	71.4	85–87°	$C_{11}H_{12}N_2O_3S$	C 52.37	52.13
									H 4.79	4.77
									N 11.10	11.15
									S 12.71	12.93
II*e*	S	H	C_6H_5	$COOC_2H_5$	C_2H_5	70.6	102–105°	$C_{17}H_{17}NO_5S$	C 58.79	58.66
									H 4.90	5.04
									N 4.03	4.06
II*f*	S	CH_3	CH_3	$COOC_2H_5$	C_2H_5	81.6	87–89°	$C_{13}H_{17}NO_5S$	C 52.17	52.31
									H 5.69	5.85
									N 4.68	4.86
II*g*	S	$COOC_2H_5$	H	H	C_2H_5	44.1	140–142°	$C_{11}H_{13}NO_5S$	C 48.71	48.72
									H 4.80	4.99
									N 5.17	5.25
									S 11.81	11.86
II*h*	O	$COOC_2H_5$	H	H	C_2H_5	50.7	127–129°	$C_{11}H_{13}NO_6$	C 51.76	51.73
									H 5.09	5.17
									N 5.49	5.61
II*i*		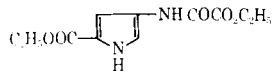				32.8	183–185°	$C_{11}H_{14}N_2O_5$	C 51.97	52.04
									H 5.51	5.73
									N 11.02	11.15

[a] All compounds were recrystallized from 95% ethanol, unless indicated otherwise. [b] Methanol. [c] Ethyl acetate–ligroin.

Table II—Inhibition of Rat Passive Cutaneous Anaphylactic Reaction[a]

Compound	Inhibition[b], % 50 mg/kg iv	10 mg/kg iv	1 mg/kg iv
II*a*	100	90	54
II*b*	63	63	25
II*c*	38	—	—
II*d*[c]	—	—	—
II*e*	0	—	—
II*f*	0	—	—
II*g*	0	—	—
II*i*	12	—	—
III	0	—	—

[a] Data were collected in the laboratory of Dr. H. G. Johnson, The Upjohn Co. [b] Ethyl 2-cyanophenyloxamate (14) exhibited 53% inhibition at 200 mg/kg ip. [c] See Ref. 6.

ylthiophene (I*g*) was prepared by the method of Sy and deMalleray (22). 2-Amino-5-ethoxycarbonylfuran (I*h*) (23) was prepared by Raney nickel reduction of ethyl 5-nitrofuroate (24). 2-Ethoxycarbonyl-4-aminopyrrole (I*i*) was prepared by Raney nickel reduction of 2-ethoxycarbonyl-4-nitropyrrole (25).

Ethyl (3-Cyano-4,5-dimethyl-2-pyrrolyl)oxamate (II*a*)—The procedure for the synthesis of II*a* is given as representative for II*c*–II*i*. To 10 g (0.074 mole) of 2-amino-3-cyano-4,5-dimethylpyrrole (I*a*), dissolved in 300 ml of ethyl acetate[3], 7.59 g of triethylamine was added. To this solution, at about 0°, 10.24 g of ethyl oxalyl chloride in 25 ml of ethyl acetate was added slowly with stirring. A yellow precipitate formed immediately, and the reaction mixture was stirred for about 2 hr in an ice bath and for 1 hr at room temperature. The triethylamine hydrochloride was removed by filtration, and the filtrate was stored for about 16 hr. Evaporation of the solvent *in vacuo* gave a reddish solid, mp 100–120°. Recrystallization from 95% ethanol gave 11.5 g of bright-yellow product, mp 132–133°.

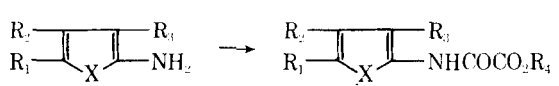

I*a*–I*i* II*a*–II*i*

Scheme I

[3] Ether or tetrahydrofuran also may be utilized.

3-Cyano-4,5-dimethylfuryloxamic Acid (II*b*)—2-Amino-4,5-dimethyl-3-cyanofuran (I*b*) (6.8 g, 0.05 mole) was dissolved in 100 ml of anhydrous ether and 6 ml of triethylamine. This solution was treated cautiously by the dropwise addition of 7.6 g (0.06 mole) of oxalyl chloride in 80 ml of ether. The reaction mixture was stirred for 2 hr and then allowed to stand overnight at room temperature. A yellowish solid was removed from the ether solution by filtration. This solid was suspended in water to remove triethylamine hydrochloride, and the insoluble residue was collected and dried. After recrystallization from dimethylformamide–water, this material (4.3 g) melted at 263–264° and proved to be the *N,N'*-bis(3-cyano-4,5-dimethyl-2-furyl)oximide (III).

Anal.—Calc. for $C_{16}H_{14}N_4O_4$: C, 58.90; H, 4.29; N, 17.18. Found: C, 59.13; H, 4.31; N, 17.34.

The ether filtrate from the above was removed *in vacuo*, and the residue was washed with water, collected, and air dried. After recrystallization from methanol, this material (2.3 g, 22.5%) melted at 172–173°; NMR (dimethyl sulfoxide-d_6): δ 2.0 (s, 3H, CH_3), 2.2 (s, 3H, CH_3), 6.45 (broad, 1H, NHCO), and 11.65 (broad, 1H, COOH) (see Table I for analyses).

REFERENCES

(1) H. G. Johnson and C. A. VanHout, *Proc. Soc. Exp. Biol. Med.*, **143**, 427 (1973).

(2) J. B. Wright and H. G. Johnson, *J. Med. Chem.*, **16**, 861 (1973).

(3) C. M. Hall, H. G. Johnson, and J. B. Wright, *ibid.*, **17**, 685 (1974).

(4) C. D. Blanton, Jr., and H. G. Johnson, U.S. pat. 3,838,166 (1974); through *Chem. Abstr.*, **81**, 151991x (1974).

(5) H. G. Johnson, J. B. Wright, C. M. Hall, and D. T. Warner, U.S. pat. 3,836,541 (1974); through *Chem. Abstr.*, **82**, 16700g (1975).

(6) W. J. Wechter and J. B. Wright, German Offen. 2,509,457 (1975); through *Chem. Abstr.*, **84**, 30865n (1976).

(7) J. B. Wright, A. A. Sinkula, and C. M. Hall, German Offen. 2,525,164 (1975); through *Chem. Abstr.*, **84**, 89846k (1976).

(8) J. B. Wright and A. A. Sinkula, German Offen. 2,525,250 (1975); through *Chem. Abstr.*, **84**, 89854m (1976).

(9) C. M. Hall and H. G. Johnson, German Offen. 2,445,002 (1975); through *Chem. Abstr.*, **83**, 79083z (1975).

(10) A. A. Sinkula, U.S. pat. 3,962,308 (1976); through *Chem. Abstr.*, **85**, 160060c (1976).

(11) J. B. Wright, C. M. Hall, and A. A. Sinkula, German Offen. 2,525,188 (1975); through *Chem. Abstr.*, **84**, 105408b (1976).

(12) C. M. Hall and H. G. Johnson, U.S. pat. 3,963,660 (1976); through *Chem. Abstr.*, **85**, 123776v (1976).
(13) J. B. Wright and H. G. Johnson, *J. Med. Chem.*, **20**, 166 (1977).
(14) J. H. Sellstedt, C. J. Guinosso, A. J. Begany, S. C. Bell, and M. Rosethale, *ibid.*, **18**, 926 (1975).
(15) L. L. Skaletzky, B. F. Graham, and J. Szmuszkovicz, *ibid.*, **12**, 977 (1969).
(16) G. C. Gerritsen and W. E. Dulin, *J. Pharmacol. Exp. Ther.*, **150**, 491 (1965).
(17) G. W. Duncan, S. C. Lyster, and J. B. Wright, *Proc. Soc. Exp. Biol. Med.*, **120**, 725 (1965).
(18) A. Tinsho, I. Shimizu, T. Takenawa, H. Hikuchi, and T. Rukjo, *J. Pharm. Soc. Jpn.*, **92**, 879 (1972).
(19) K. Gewald, *Z. Chem.*, **1**, 349 (1961).
(20) K. Gewald, *Chem. Ber.*, **99**, 1002 (1966).
(21) K. Gewald, E. Schinke, and H. Böttcher, *ibid.*, **99**, 94 (1966).
(22) M. Sy and B. deMalleray, *Bull. Soc. Chim. Fr.*, **1963**, 1276.
(23) M. R. Marquis, *C.R.*, **136**, 1454 (1903).
(24) B. T. Freure and J. R. Johnson, *J. Am. Chem. Soc.*, **53**, 1142 (1931).
(25) W. J. Hale and W. Hoyt, *ibid.*, **37**, 2551 (1915).

ACKNOWLEDGMENTS

All pharmacological test results were provided from the research laboratories of The Upjohn Co., Kalamazoo, Mich.

Synthesis of *as*-Triazines as Potential Antiviral Agents

MICHAEL W. DAVIDSON and DAVID W. BOYKIN, Jr. ˣ

Received July 7, 1977, from the *Department of Chemistry, Georgia State University, Atlanta, GA 30303.* Accepted for publication September 2, 1977.

Abstract □ Four acenaphtho[1,2-*e*]-*as*-triazines and 11 5,6-diaryl-*as*-triazines, all substituted with an aliphatic or aromatic amino function in the 3-position, were synthesized. Two acenaphthotriazines were active against vesicular stomatitis virus in tissue culture.

Keyphrases □ *as*-Triazines, various substituted—synthesized, antiviral activity evaluated □ Antiviral activity—various substituted *as*-triazines evaluated □ Structure–activity relationships—various substituted *as*-triazines evaluated for antiviral activity

The broad spectrum antiviral activity of the 5*H*-*as*-triazino[5,6-*b*]indoles (1–3), as well as reports of antiviral activity of other *as*-triazines (4–6), prompted preparation of a series of related analogs for evaluation as potential antiviral agents. This effort consisted of the synthesis of two series, one containing a coplanar ring system and the other containing a similar number of aromatic rings but not in a coplanar arrangement.

The first series, 9-substituted acenaphtho[1,2-*e*]-*as*-triazines (Table I), is modeled after the 5-alkyl-*as*-triazino[5,6-*b*]indoles in that a hydrophobic moiety (the acenaphtho ring) is substituted for the alkylindolo ring. The resulting compounds contain a planar aromatic surface, similar to that of the *as*-triazinoindoles, but lacking the steric factors contributed by the alkyl group, which can rotate above and below the plane of the fused rings.The second series of compounds, 3-substituted 5,6-diaryl-*as*-triazines (Table II), was prepared to determine the necessity of the planar fused rings in antiviral activity by building a system that could not attain a coplanar configuration. All compounds (Tables I and II) were substituted with alkyl or aryl amino side chains, which have been demonstrated to be efficacious in antiviral triazines (2, 3).

RESULTS AND DISCUSSION

The synthetic pathways utilized in the preparation of I–XX are similar and consist of the acid- or base-catalyzed condensation of either thiosemicarbazide or semicarbazide hydrochloride with acenaphthoquinone or the appropriately substituted benzil. Products of the thiosemicarbazide–quinone condensation could be treated directly with the desired alkyl or aryl amine to produce the corresponding derivatives, II–V. However, the 5,6-diaryl-*as*-triazin-3(2*H*)-ones do not react with the amines, necessitating their conversion to the corresponding 3-chloro derivatives by reaction with phosphoryl chloride. The enhanced reactivity of 3-chloro-5,6-diaryl-*as*-triazines allowed their facile conversion to X–XX.

Compounds III–V, X–XV, and XVII–XX were subjected to both *in vitro* and *in vivo* antiviral activity screens as described under *Experimental.* A tissue culture evaluation of III and IV indicated activity when the compounds were exposed to cells challenged with vesicular stomatitis virus, a single-stranded RNA rabies-like virus, as determined by the dye retention assay. The activity of IV against vesicular stomatitis virus (active at 25 μg/ml of culture medium) was greater than that of III (active at 50 μg/ml); however, IV also exhibited a greater toxicity (50 μg/ml) to cell cultures than did III (toxic at 250 μg/ml). Other compounds failed to demonstrate any significant *in vitro* activity against vesicular stomatitis virus.

All compounds were judged inactive when tested *in vitro* (under similar conditions) against the following viruses: respiratory syncytial, parainfluenza-3, herpes simplex, rhinovirus-14, shipping fever (bovine parainfluenza-3), and Newcastle disease.

The *in vivo* antiviral evaluation system consisted of an encephalomyocarditis virus-in-mouse screen in which activity is determined by a prolongation of survival time in the treated animals. None of the compounds demonstrated activity.

Because several related 3,5-diamino-*as*-triazines (7) have exhibited antimalarial activity, X–XX also were evaluated for *in vivo* antimalarial activity in mice infected with *Plasmodium berghei* by the method of Osdene *et al.* (8). None of the compounds showed any significant activity in the malaria screen.

EXPERIMENTAL[1]

All melting points were obtained using an oil bath melting-point apparatus and are uncorrected. Satisfactory IR spectra were obtained, and the expected PMR spectra were obtained in deuterochloroform (tetramethylsilane standard).

Acenaphtho[1,2-*e*]-*as*-triazine-9(8*H*)-thione (I)—Attempts to prepare this compound by the method reported for the corresponding

[1] Elemental analyses were determined by Atlantic Microlab, Atlanta, Ga.

(12) C. M. Hall and H. G. Johnson, U.S. pat. 3,963,660 (1976); through *Chem. Abstr.*, **85**, 123776v (1976).
(13) J. B. Wright and H. G. Johnson, *J. Med. Chem.*, **20**, 166 (1977).
(14) J. H. Sellstedt, C. J. Guinosso, A. J. Begany, S. C. Bell, and M. Rosethale, *ibid.*, **18**, 926 (1975).
(15) L. L. Skaletzky, B. F. Graham, and J. Szmuszkovicz, *ibid.*, **12**, 977 (1969).
(16) G. C. Gerritsen and W. E. Dulin, *J. Pharmacol. Exp. Ther.*, **150**, 491 (1965).
(17) G. W. Duncan, S. C. Lyster, and J. B. Wright, *Proc. Soc. Exp. Biol. Med.*, **120**, 725 (1965).
(18) A. Tinsho, I. Shimizu, T. Takenawa, H. Hikuchi, and T. Rukjo, *J. Pharm. Soc. Jpn.*, **92**, 879 (1972).
(19) K. Gewald, *Z. Chem.*, **1**, 349 (1961).
(20) K. Gewald, *Chem. Ber.*, **99**, 1002 (1966).
(21) K. Gewald, E. Schinke, and H. Böttcher, *ibid.*, **99**, 94 (1966).
(22) M. Sy and B. deMalleray, *Bull. Soc. Chim. Fr.*, **1963**, 1276.
(23) M. R. Marquis, *C.R.*, **136**, 1454 (1903).
(24) B. T. Freure and J. R. Johnson, *J. Am. Chem. Soc.*, **53**, 1142 (1931).
(25) W. J. Hale and W. Hoyt, *ibid.*, **37**, 2551 (1915).

ACKNOWLEDGMENTS

All pharmacological test results were provided from the research laboratories of The Upjohn Co., Kalamazoo, Mich.

Synthesis of *as*-Triazines as Potential Antiviral Agents

MICHAEL W. DAVIDSON and DAVID W. BOYKIN, Jr. ˣ

Received July 7, 1977, from the *Department of Chemistry, Georgia State University, Atlanta, GA 30303.* Accepted for publication September 2, 1977.

Abstract □ Four acenaphtho[1,2-*e*]-*as*-triazines and 11 5,6-diaryl-*as*-triazines, all substituted with an aliphatic or aromatic amino function in the 3-position, were synthesized. Two acenaphthotriazines were active against vesicular stomatitis virus in tissue culture.

Keyphrases □ *as*-Triazines, various substituted—synthesized, antiviral activity evaluated □ Antiviral activity—various substituted *as*-triazines evaluated □ Structure–activity relationships—various substituted *as*-triazines evaluated for antiviral activity

The broad spectrum antiviral activity of the 5*H*-*as*-triazino[5,6-*b*]indoles (1–3), as well as reports of antiviral activity of other *as*-triazines (4–6), prompted preparation of a series of related analogs for evaluation as potential antiviral agents. This effort consisted of the synthesis of two series, one containing a coplanar ring system and the other containing a similar number of aromatic rings but not in a coplanar arrangement.

The first series, 9-substituted acenaphtho[1,2-*e*]-*as*-triazines (Table I), is modeled after the 5-alkyl-*as*-triazino[5,6-*b*]indoles in that a hydrophobic moiety (the acenaphtho ring) is substituted for the alkylindolo ring. The resulting compounds contain a planar aromatic surface, similar to that of the *as*-triazinoindoles, but lacking the steric factors contributed by the alkyl group, which can rotate above and below the plane of the fused rings.The second series of compounds, 3-substituted 5,6-diaryl-*as*-triazines (Table II), was prepared to determine the necessity of the planar fused rings in antiviral activity by building a system that could not attain a coplanar configuration. All compounds (Tables I and II) were substituted with alkyl or aryl amino side chains, which have been demonstrated to be efficacious in antiviral triazines (2, 3).

RESULTS AND DISCUSSION

The synthetic pathways utilized in the preparation of I–XX are similar and consist of the acid- or base-catalyzed condensation of either thiosemicarbazide or semicarbazide hydrochloride with acenaphthoquinone or the appropriately substituted benzil. Products of the thiosemicarbazide–quinone condensation could be treated directly with the desired alkyl or aryl amine to produce the corresponding derivatives, II–V. However, the 5,6-diaryl-*as*-triazin-3(2*H*)-ones do not react with the amines, necessitating their conversion to the corresponding 3-chloro derivatives by reaction with phosphoryl chloride. The enhanced reactivity of 3-chloro-5,6-diaryl-*as*-triazines allowed their facile conversion to X–XX.

Compounds III–V, X–XV, and XVII–XX were subjected to both *in vitro* and *in vivo* antiviral activity screens as described under *Experimental.* A tissue culture evaluation of III and IV indicated activity when the compounds were exposed to cells challenged with vesicular stomatitis virus, a single-stranded RNA rabies-like virus, as determined by the dye retention assay. The activity of IV against vesicular stomatitis virus (active at 25 μg/ml of culture medium) was greater than that of III (active at 50 μg/ml); however, IV also exhibited a greater toxicity (50 μg/ml) to cell cultures than did III (toxic at 250 μg/ml). Other compounds failed to demonstrate any significant *in vitro* activity against vesicular stomatitis virus.

All compounds were judged inactive when tested *in vitro* (under similar conditions) against the following viruses: respiratory syncytial, parainfluenza-3, herpes simplex, rhinovirus-14, shipping fever (bovine parainfluenza-3), and Newcastle disease.

The *in vivo* antiviral evaluation system consisted of an encephalomyocarditis virus-in-mouse screen in which activity is determined by a prolongation of survival time in the treated animals. None of the compounds demonstrated activity.

Because several related 3,5-diamino-*as*-triazines (7) have exhibited antimalarial activity, X–XX also were evaluated for *in vivo* antimalarial activity in mice infected with *Plasmodium berghei* by the method of Osdene *et al.* (8). None of the compounds showed any significant activity in the malaria screen.

EXPERIMENTAL[1]

All melting points were obtained using an oil bath melting-point apparatus and are uncorrected. Satisfactory IR spectra were obtained, and the expected PMR spectra were obtained in deuterochloroform (tetramethylsilane standard).

Acenaphtho[1,2-*e*]-*as*-triazine-9(8*H*)-thione (I)—Attempts to prepare this compound by the method reported for the corresponding

[1] Elemental analyses were determined by Atlantic Microlab, Atlanta, Ga.

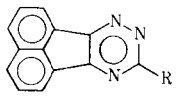

Table I—9-(3-Substituted Propylamino)acenaphtho[1,2-*e*]-*as*-triazines[a]

Number	R	Melting Point	Yield, %	Formula	Analysis, % Calc.	Found
II	$NH(CH_2)_3OH$	201–202°	46	$C_{16}H_{14}N_4O$	C 69.16	69.16
					H 5.04	5.25
III	$NH(CH_2)_3N(CH_3)_2$	173–174.5°	68	$C_{18}H_{19}N_5$	C 70.82	70.71
					H 6.23	6.39
IV	$NH(CH_2)_3N(C_2H_5)_2$	115–116°	62	$C_{20}H_{23}N_5$	C 72.07	71.91
					H 6.91	7.01
V	$NH(CH_2)_3N(C_2H_5)_2$	92–93°	56	$C_{24}H_{31}N_5$	C 74.07	74.14
					H 7.97	7.93

[a] All compounds were recrystallized from acetonitrile.

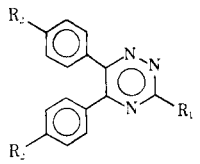

Table II—3-Substituted 5,6-Diaryl-*as*-triazines

Number	R_1	R_2	Melting Point	Yield, %	Formula	Analysis, % Calc.	Found
X[a]	$NH(CH_2)_3OH$	H	137–138°	92	$C_{18}H_{18}N_4O$	C 70.59	70.30
						H 5.88	6.09
						N 18.30	18.07
XI[a]	$NH(CH_2)_3N(C_2H_5)_2$	H	112–114°	64	$C_{22}H_{27}N_5$	C 73.13	73.08
						H 7.49	7.56
						N 19.39	19.23
XII[a]	$NH(CH_2)_3N(C_4H_9)_2$	H	69–70.5°	69	$C_{26}H_{35}N_5$	C 74.82	74.89
						H 8.39	8.42
						N 16.79	16.79
XIII[a]	$NH(CH_2)_3OH$	Cl	169–170°	87	$C_{18}H_{16}Cl_2N_4O$	C 57.60	57.46
						H 4.27	4.20
XIV[b]	$NH(CH_2)_3N(C_2H_5)_2$	Cl	127–128°	56	$C_{22}H_{25}Cl_2N_5$	C 61.40	61.30
						H 5.81	6.05
XV[b]	$NH(CH_2)_3N(C_4H_9)_2$	Cl	104–105.5°	62	$C_{26}H_{33}Cl_2N_5$	C 64.20	64.21
						H 6.79	6.85
XVI[b]	$NHCHCH_3$ | $(CH_2)_3N(C_2H_5)_2$	Cl	87–90°	56	$C_{24}H_{29}Cl_2N_5$	C 62.88	62.94
						H 6.33	6.48
						N 15.28	15.23
XVII[a]	3-Hydroxyanilino	H	253–254.5°	65	$C_{21}H_{16}N_4O$	C 74.12	74.16
						H 4.71	4.76
						N 16.47	16.53
XVIII[b]	3-Hydroxyanilino	Cl	274–275.5°	88	$C_{21}H_{14}Cl_2N_4O$	C 61.60	61.87
						H 3.42	3.34
XIX[c]	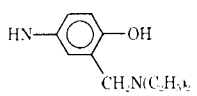	H	198–200°	52	$C_{26}H_{27}N_5O$	C 73.41	73.54
						H 6.35	6.37
						N 16.47	16.51
XX[b]	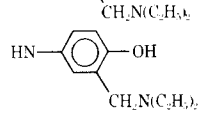	Cl	230–232°	22	$C_{26}H_{25}Cl_2N_5O$	C 63.16	63.22
						H 5.06	5.19

[a] Recrystallized from ethanol. [b] Recrystallized from acetonitrile. [c] Recrystallized from benzene.

phenanthro[5,6-*e*]-*as*-triazine (9) resulted in poor yields, but the procedure outlined by Gladych *et al.* (2) for the synthesis of the analogous indolo[2,3-*e*]-*as*-triazine afforded good yields. Thus, a mixture of thiosemicarbazide (1 g, 0.011 mole), acenaphthoquinone (1.7 g, 0.093 mole), and sodium carbonate (2.2 g, 0.02 mole) was refluxed for 9 hr in 50 ml of water, filtered hot, cooled, and then acidified with acetic acid. The precipitate was collected, recrystallized once from acetonitrile (85% yield, mp 272–273°), and used in subsequent synthesis without further purification. The analytical sample melted at 275–276°.

Anal.—Calc. for $C_{13}H_7N_3S$: C, 65.82; H, 2.95; N, 17.72. Found: C, 65.74; H, 2.95; N, 17.68.

9-(3-Substituted Propylamino)acenaphtho[1,2-*e*]-*as*-triazines (II–V, Table I)—In a typical reaction, a mixture of I (2 g, 0.0084 mole) in 10 ml of *N',N'*-diethylaminopropane-1,3-diamine was refluxed for 5 hr or until evolution of hydrogen sulfide gas had ceased (detected with lead acetate test paper). After cooling, the mixture was poured into 100 ml of cold water. The precipitate was collected and recrystallized from acetonitrile to yield 65% 9-(3-diethylaminopropylamino)acenaphtho[1,2-*e*]-*as*-triazine (IV).

5,6-Diaryl-*as*-triazin-3(2*H*)-ones (VI and VII)—Utilizing the method described by Blitz (10), these compounds were obtained by refluxing a mixture of the appropriate benzil [prepared by the benzoin condensation (11) followed by oxidation (12)] with an equimolar amount of semicarbazide hydrochloride in acetic acid for 3 hr, with subsequent precipitation of the product by addition of water. Recrystallization from ethanol gave a melting point of 223–225° (59% yield) for the 5,6-diphenyl derivative (VI) [lit. (11) mp 224–225°].

3-Chloro-5,6-diaryl-*as*-triazines (VIII and IX)—In a modification (13) of the reported procedure (9), the 3-chloro analogs of VI and VII were prepared by slowly adding phosphoryl chloride (5 ml) to the appropriate 3(2*H*)-one derivative (0.0031 mole) in 1–2 ml of *N,N*-dimethylaniline and refluxing the resulting combination for 1 hr or until hydrogen chloride gas evolution had ceased. After cooling, the mixture was cautiously poured onto 500 g of ice with vigorous stirring. The resulting precipitate was collected and triturated with 1 *M* NaOH before being recrystallized from methanol to yield 51% of VIII, mp 156–157° [lit. (9) mp 157°]. Similarly, starting with VII (mp 238–240°), which was used directly without further characterization, a yield of 30% of the 5,6-bis(4-chloro-

phenyl) derivative (IX), mp 165–167°, was obtained.

Anal.—Calc. for $C_{15}H_8Cl_3N_3$: C, 53.49; H, 2.38. Found: C, 53.57; H, 2.47.

3-(3-Substituted Alkylamino)-5,6-diaryl-*as*-triazines (X–XV, Table II)—The method for preparing these compounds was essentially identical to that employed for the analogous acenaphtho[1,2-*e*]-*as*-triazines II–V, except that reaction times were decreased to 30 min because of an enhanced ease of displacement of the 3-chloro moiety.

3-(5-Diethylamino-2-pentylamino)-5,6-bis(4-chlorophenyl)-*as*-triazine (XVI, Table II)—This compound was prepared in a manner analogous to that described for X–XV, except that the solvent was removed *in vacuo* after reflux and the resulting oil was triturated with dilute base (1 *M* NaOH), filtered, and recrystallized from acetonitrile, mp 87–90° (56% yield).

3-Substituted Arylamino-5,6-diaryl-*as*-triazines (XVII–XX, Table II)—The general procedure for the preparation of 3-arylamino analogs of VIII and IX was as follows. To a mixture of VIII in toluene (0.0075 mole in 10 ml) was added an excess of 3-hydroxyaniline, and the resulting slurry was refluxed for 3–6 hr and poured into cold water. The resulting precipitate was collected. Recrystallization from ethanol or acetonitrile afforded a 65% yield of XVII, mp 253–254.5°. The synthesis of 3-(α-diethylaminomethyl)-4-hydroxyaniline was conducted as described by Burckhalter *et al.* (14); the product, without isolation, was allowed to react directly with the desired triazine (VIII or IX) in aqueous solution to yield XIX (52% yield) and XX (22% yield).

Antiviral Evaluation Screens—*Method A: Plaque Reduction Assay*—This system was utilized in the antiviral evaluation of compounds *versus* herpes simplex, parainfluenza-3, and respiratory syncytial viruses. Compounds were suspended in a culture medium and applied to a representative population in a series of replicate human epidermoid larynx carcinoma cell cultures known to be susceptible to the challenge viruses. An appropriate number of cultures were maintained as inoculated, but untreated, controls; others were exposed to the compound alone (to ascertain toxicity); still others remained as untreated and uninfected control cultures.

All cell cultures were incubated at 35° for the duration of the experiments. Upon termination of the experiment, the cultures were stained with neutral red (a vital stain) and examined for compound toxicity. Cultures that, by visual inspection, stained less intensely than the untreated controls were considered to have received a toxic dose of the compound in question and were subsequently disregarded. The cell cultures were then fixed in formalin and stained with gentian violet, and the number of viral-produced plaques was determined. An active compound was defined as one in which at least two nontoxic concentrations resulted in a 50% or greater plaque reduction in treated cell cultures.

Method B: Dye Retention Assay—Viruses evaluated with this system were rhinovirus-14 (propagated in human epitheloid cervix carcinoma cells), shipping fever and vesicular stomatitis (propagated in canine kidney cells), and Newcastle disease (propagated in mouse connective tissue). This evaluation procedure was essentially the same as Method A, except that, instead of subsequent staining with gentian violet, the cultures were washed with buffered saline after being stained with neutral red and the retained dye was then extracted with buffered methanol–formalin.

By this procedure, the amount of retained dye can be quantitatively determined by spectrophotometric methods. Active, nontoxic compounds were those in which the treated cell cultures retained at least 75% of the dye (neutral red), as judged on a scale where uninfected controls demonstrated 100% dye retention and virus-infected controls showed 0% dye retention.

Method C: Encephalomyocarditis Virus/Mouse Assay—In this system, mice were injected subcutaneously with a controlled titer of encephalomyocarditis virus adjusted to produce death after 4–5 days in untreated control animals. Compounds to be screened were suspended in a 0.4% 2-methoxyethanol[2]–0.5% polysorbate 80[3] solution at 10 mg/ml. Test animals were inoculated either intraperitoneally or subcutaneously with this suspension 1 hr prior to virus administration. A compound was judged active when it produced a mean survival time of 12–14 days in treated animals. The mean survival time controls usually died at 4.5 days. The validity of the assay was demonstrated by production of a control group of mice pretreated with 10 μg of poly(I)·poly(C), an interferon inducer.

REFERENCES

(1) J. M. Gwaltney, *Proc. Soc. Exp. Biol. Med.*, **133**, 1149 (1970).

(2) J. M. Z. Gladych, R. Hornby, J. Hunt, D. Jack, J. J. Boyle, R. J. Ferlauto, R. Haff, C. Kormendy, F. Stanfield, and R. Stewart, *J. Med. Chem.*, **15**, 277 (1972).

(3) R. F. Haff, J. J. Boyle, R. Stewart, R. Ferlauto, J. M. Z. Gladych, J. Hunt, and D. Jack, *Nature (London)*, **221**, 286 (1969).

(4) I. Nakata and T. Ueda, *Yakugaku Zasshi*, **80**, 1068 (1960); through *Chem. Abstr.*, **55**, 561 (1961).

(5) T. Ueda and M. Furukawa, *Chem. Pharm. Bull.*, **12**, 100 (1964).

(6) F. Sorm, *Acta Virol.*, **6**, 364 (1962).

(7) L. C. March, G. Bajwa, J. Lee, K. Wasti, and M. M. Joullié, *J. Med. Chem.*, **19**, 845 (1976).

(8) T. S. Osdene, P. Russell, and L. Rane, *J. Med. Chem.*, **10**, 431 (1967).

(9) P. Laakso, R. Robinson, and H. Vandrewala, *Tetrahedron*, **1**, 103 (1957).

(10) H. Blitz, *Chem. Ber.*, **38**, 1417 (1905).

(11) H. Willgerodt and K. Ucke, *J. Prakt. Chem.*, **86**, 281 (1912).

(12) R. E. Lutz and R. Murphey, *J. Am. Chem. Soc.*, **71**, 478 (1949).

(13) B. F. Cain, R. Seelye, and G. Atwell, *J. Med. Chem.*, **17**, 922 (1974).

(14) J. H. Burckhalter, F. Tendick, E. Jones, P. Jones, W. Holcomb, and A. Rawlins, *J. Am. Chem. Soc.*, **70**, 1363 (1948).

ACKNOWLEDGMENTS

The authors are indebted to the A. H. Robins Co. for the antiviral screening results through the courtesy of Dr. R. W. Tankersley, Jr., Dr. H. Randall Munson, Jr., and Dr. William J. Welstead. The antimalarial testing was provided by the Walter Reed Army Institute of Research. Partial support for this research was generously provided by Dr. Robert S. Robinson, Dr. Roger Miles, and Dr. Clark Robinson. Discussions of this research with Dr. B. P. Das were helpful.

[2] Methocellosolve.
[3] Tween 80.

New Compounds: Isoquinoline Derivatives as Simple Emetine Models

R. M. PICCIRILLI, E. O. SNOKE, R. F. WATTS, and F. D. POPP ˣ

Received July 11, 1977, from the *University of Missouri–Kansas City, Kansas City, MO 64110.* (Work was done at the University of Missouri–Kansas City and Clarkson College of Technology.) Accepted for publication August 31, 1977.

Abstract □ Several new isoquinolines were prepared using Reissert compounds. A few compounds were screened, and they exhibited no antineoplastic activity.

Keyphrases □ Isoquinoline derivatives, various—synthesized, evaluated for antineoplastic activity □ Antineoplastic activity—various isoquinoline derivatives evaluated □ Structure–activity relationships—various isoquinoline derivatives evaluated for antineoplastic activity

In view of the antineoplastic activity of emetine (I), the preparation of simple models of this system was studied.

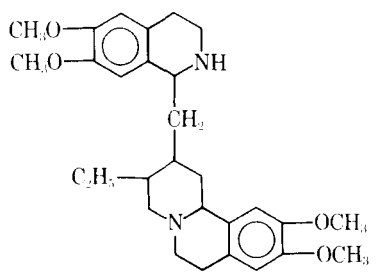

I

DISCUSSION

Reaction of the anion of the Reissert compounds derived from isoquinoline and 6,7-dimethoxyisoquinoline with 4-picolyl chloride gave, after hydrolysis, II and III. These compounds can be considered as models containing three of the five rings of emetine. During preliminary studies to extend this reaction, IV was prepared by reduction of the corresponding 4-methoxycarbonyl compound (1).

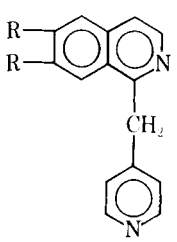

II: R = H
III: R = CH_3O

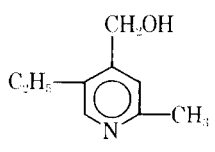

IV

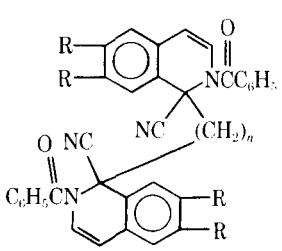

Va: R = H, n = 3
Vb: R = H, n = 4
Vc: R = H, n = 5
VI: R = OCH_3, n = 3

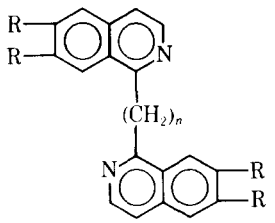

VIIa: R = H, n = 3
VIIb: R = H, n = 4
VIII: R = OCH_3, n = 3

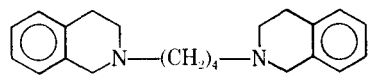

IX

In an attempt to prepare models with the two isoquinoline units separated by three carbons as in emetine, the Reissert adduct Va, formed by reaction of the anion of 1-cyano-2-benzoyl-1,2-dihydroisoquinoline with 1,3-dibromopropane (2), was hydrolyzed to VIIa. This compound was converted to its mono methiodide, which had a T/C value of 120% at 12.5 mg/kg against the P-388 lymphocytic leukemia and of 117% at 12.5 mg/kg against the L-1210 lymphoid leukemia. This same sequence was repeated to give, *via* VI, VIII as its hydrochloride. This compound had no activity (T/C = 104% at 100 mg/kg) against the P-388 lymphocytic leukemia. Compounds Vb, Vc, VIIb, and XIII were also prepared.

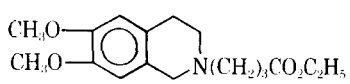

X

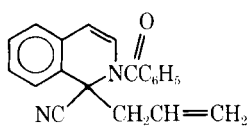

XI

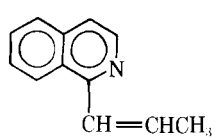

XII

Attempts to form a 4-bromobutylisoquinolinium salt from 1,4-dibromobutane and isoquinoline gave only the bis adduct, which was reduced by catalytic hydrogenation to IX as its dihydrobromide. This compound had no activity (T/C = 102% at 50 mg/kg) against the L-1210 lymphoid leukemia.

Compound X was prepared by reduction of the quaternary salt obtained from 6,7-dimethoxyisoquinoline and ethyl γ-bromobutyrate. Also, reaction of the anion of the isoquinoline Reissert compound with allyl chloride gave an adduct (XI), which, on base hydrolysis, underwent isomerization to yield XII rather than the expected 1-allylisoquinoline.

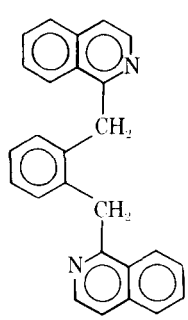

XIII

EXPERIMENTAL

Reaction of Isoquinoline Reissert Compound with 4-Picolyl Chloride Hydrochloride: Preparation of 1-(4-Picolyl)-1-cyano-2-benzoyl-1,2-dihydroisoquinoline—A stirred slurry of 1.64 g (0.01 mole) of 4-picolyl chloride hydrochloride in 30 ml of dimethylformamide and 0.50 g (0.01 mole) of 50% sodium hydride in oil was added to a solution of 0.50 g (0.01 mole) of 50% sodium hydride in oil and 2.6 g (0.01 mole) of isoquinoline Reissert compound in 30 ml of dimethylformamide. The mixture was stirred for 1 hr and then poured over 500 g of cracked ice. The insoluble material was chromatographed on alumina with chloroform to give a white solid (0.70 g), which was recrystallized from cyclohexane–benzene, mp 137–138°; IR (KBr): 1670 and 1610 cm^{-1}; NMR ($CDCl_3$): δ 8.32 (2H), 7.40–6.70 (11H), 6.40 (1H), and 3.60 (2H) ppm.

Anal.—Calc. for $C_{23}H_{17}N_3O$: C, 78.61; H, 4.87; N, 11.96. Found: C, 78.71; H, 4.99; N, 11.96.

Base Hydrolysis of 1-(4-Picolyl)-1-cyano-2-benzoyl-1,2-dihydroisoquinoline—The title compound (2.00 g, 0.0057 mole) was heated in a solution of 8 g (0.14 mole) of potassium hydroxide in 25 ml of water and 25 ml of ethanol for 30 min. The ethanol was removed, and the water solution was extracted with chloroform. The chloroform extracts were evaporated to dryness, and the residue (0.92 g of II) was recrystallized from cyclohexane, mp 86–87°; IR (KBr): 1600 cm^{-1}; NMR ($CDCl_3$): δ 8.50 (2H), 7.50 (5H), 4.60 (1H), and 2.10 (1H) ppm.

Anal.—Calc. for $C_{12}H_{15}N_2$: C, 81.78; H, 5.49; N, 12.71. Found: C, 81.89; H, 5.61; N, 12.79.

Reaction of 1-Cyano-2-benzoyl-1,2-dihydro-6,7-dimethoxyisoquinoline with 4-Picolyl Chloride Hydrochloride—To a slurry of 1.64 g (0.01 mole) of 4-picolyl chloride hydrochloride in 30 ml of dimethylformamide, cooled in an ice bath and under a nitrogen atmosphere, was added 0.60 g (0.012 mole) of 50% sodium hydride in oil; the reaction was then stirred for 10 min. To the solution of 4-picolyl chloride were added 3.22 g (0.01 mole) of the 6,7-dimethoxyisoquinoline Reissert compound and 0.60 g (0.012 mole) of 50% sodium hydride in oil, and the reaction was stirred for 2.5 hr. Then the reaction was poured over ice and filtered to give 3.45 g (83%). The crude material was recrystallized from ethanol–dioxane, mp 192–193°; IR (KBr): 1660 cm^{-1}.

Anal.—Calc. for $C_{25}H_{21}N_3O_3$: C, 72.97; H, 5.14. Found: C, 72.84; H, 5.12.

Hydrolysis of 1-(4-Picolyl)-1-cyano-2-benzoyl-1,2-dihydro-6,7-dimethoxyisoquinoline—A solution of 1.55 g (0.004 mole) of the title compound, 25 ml of water, 25 ml of ethanol, and 8.5 g (0.15 mole) of potassium hydroxide was refluxed for 4.5 hr. The ethanol was removed *in vacuo*, water was added, and the mixture was filtered to give 1.05 g (100%) of III. This material was recrystallized from ethyl acetate, mp 159–160°; IR (KBr): 2950 and 1610 cm^{-1}; NMR ($CDCl_3$): δ 8.50 (2H), 7.2 (6H), 4.6 (2H), and 4.0 (6H) ppm.

Anal.—Calc. for $C_{17}H_{16}N_2O_2$: C, 72.83; H, 5.75. Found: C, 72.73; H, 5.84.

Reduction of 4-Methoxycarbonyl-5-ethyl-2-methylpyridine—To a solution of 0.50 g of lithium aluminum hydride in 10 ml of ether was added a solution of 3.40 g (0.022 mole) of 4-hydroxymethyl-5-ethyl-2-methylpyridine in 10 ml of ether at a rate to maintain reflux. The solution was then heated at reflux for 1 hr. To the reaction mixture was then added 5 ml of ethyl acetate, and the solution was refluxed for 15 min. To the cooled solution was added 20 ml of 6 *N* HCl, and the solution was stirred for 10 min. The layers were separated, and the ether layer was washed with 5% HCl. The acid extracts were made basic by the addition of sodium carbonate, and the aqueous solution was extracted with chloroform. The chloroform extracts were dried (sodium carbonate) and evaporated to give 1.60 g (53%) of the alcohol IV, mp 89–90°, from ligroin.

Anal.—Calc. for $C_9H_{13}NO_3$: C, 71.48; H, 8.66. Found: C, 71.61; H, 8.58.

Preparation of 1,3-Bis(1-isoquinolyl)propane (VII*a*)—To 11 g (0.02 mole) of 1,3-bis(1-cyano-2-benzoyl-1,2-dihydroisoquinolinyl)propane were added 150 ml of 95% ethanol and 150 ml of a 16% KOH solution. The mixture was refluxed on a steam bath for 2 hr, the ethanol was distilled, and the resulting mixture was poured into ice. Salt was added, and 4.25 g of VII*a* precipitated and was recrystallized from ligroin, mp 96–97°.

Anal.—Calc. for $C_{21}H_{18}N_2$: C, 84.53; H, 6.08. Found: C, 84.58; H, 5.93.

Preparation of VII*a* Monomethiodide—A mixture of 2.25 g (0.0075 mole) of VII*a* and 30 ml of methyl iodide was heated on a steam bath for a few minutes. Ether was added to give 4.30 g (100%) of white solid, which was recrystallized from 95% ethanol, mp 233–235°.

Anal.—Calc. for $C_{22}H_{21}IN_2$: C, 60.00; H, 4.80; I, 28.82; N, 6.36. Found: C, 59.87; H, 4.85; I, 28.75; N, 6.47.

Reaction of 1-Cyano-1,2-benzoyl-6,7-dimethoxy-1,2-dihydroisoquinoline with 1,3-Dibromopropane—To a mixture of 6.4 g (0.02 mole) of the Reissert compound and 2.02 g (0.01 mole) of 1,3-dibromopropane in 40 ml of dimethylformamide, under nitrogen in an ice bath, was added 1.10 g (0.023 mole) of 50% sodium hydride in oil; the reaction was then stirred for 2 hr. The reaction mixture was poured onto ice and filtered to give a quantitative yield of 1,3-bis(2-benzoyl-6,7-dimethoxy-1-isoquinolyl)propane (VI), which could not be crystallized, mp 84–100°; IR (KBr): 1660 cm^{-1}.

Hydrolysis of VI—A mixture of 3.5 g (0.004 mole) of VI, 17% KOH, and some ethanol was heated on a steam bath for 3 hr and allowed to stand overnight. The ethanol was removed *in vacuo*, and the solution was filtered to give 1.00 g (46%) of VIII. The solid was suspended in acetone, and a few drops of concentrated hydrochloric acid were added. The mixture was heated on a steam bath for a few minutes, cooled, and filtered to give the dihydrochloride hydrate of VIII. The compound was recrystallized from 95% ethanol, mp 229–230°; IR (KBr): 1640 and 1620 cm^{-1}; NMR (dimethyl sulfoxide-d_6): 3.0–4.0 (18H), 8.0 (*AB* quartet, 4H), 7.2 (4H), and 5.0 (H_2O) ppm.

Anal.—Calc. for $C_{25}H_{26}N_2O_4 \cdot H_2O \cdot 2HCl$: C, 58.94; H, 5.93; Cl, 13.92; N, 5.49. Found: C, 59.03; H, 5.92; Cl, 13.89; N, 5.61.

Alkylation of Additional Reissert Compounds—In a procedure similar to that described for VI, 1,4-bromobutane gave V*b* (99%), mp 200–201° from 95% ethanol; IR (KBr): 1680 and 1650 cm^{-1}.

Anal.—Calc. for $C_{38}H_{30}N_4O_2$: C, 79.42; H, 5.26; N, 9.75. Found: C, 78.95; H, 5.66; N, 9.80.

The use of 1,5-dibromopentane permitted the isolation of V*c* in a 94% yield, mp 185–187° from 95% ethanol; IR (KBr): 1680 and 1650 cm^{-1}.

Anal.—Calc. for $C_{39}H_{32}N_4O_2$: C, 79.57; H, 5.48. Found: C, 79.43; H, 5.45.

Hydrolysis of Reissert Adducts—In a procedure similar to that described for VI, V*b* yielded VII*b*, mp 119–120°; IR (KBr): 1630, 1580, and 1650 cm^{-1}.

Anal.—Calc. for $C_{22}H_{20}N_2$: C, 84.58; H, 6.45; N, 8.97. Found: C, 84.20; H, 6.32; N, 8.75.

This compound forms a dihydrochloride salt, mp 262–265°.

Anal.—Calc. for $C_{22}H_{20}N_2 \cdot 2HCl$: C, 68.57; H, 5.76; Cl, 18.40; N, 7.27. Found: C, 68.57; H, 5.71; Cl, 18.33; N, 7.29.

Similarly, α,α′-*o*-xylyene(1-cyano-2-benzoyl-1,2-dihydroisoquinoline) (2) gave XIII, mp 146–147°.

Anal.—Calc. for $C_{26}H_{20}N_2$: C, 86.63; H, 5.59. Found: C, 86.66; H, 5.54.

Preparation of 1,4-Bis(*N*-1,2,3,4-tetrahydroisoquinolyl)butane (IX)—A mixture of 4.3 g of 1,4-dibromobutane and 2.6 g of isoquinoline was heated on a steam bath for 15 min, and acetone was then added. Filtration and recrystallization from ethanol gave 2.1 g of the diquaternary salt as the dihydrate, mp 262–263°.

Anal.—Calc. for $C_{22}H_{22}Br_2N_2 \cdot 2H_2O$: C, 51.78; H, 5.13; Br, 31.32; N, 5.49. Found: C, 51.83; H, 5.38; Br, 31.20; N, 5.54.

A mixture of 3.31 g of IX in 100 ml of ethanol with 50 mg of platinum oxide was hydrogenated. The mixture was made basic, filtered, and acidified with 47% hydrobromic acid. Partial concentration *in vacuo* gave, after recrystallization from ethanol–ether, 2.1 g of IX dihydrobromide, mp 242–245°.

Anal.—Calc. for $C_{22}H_{30}Br_2N_2$: C, 54.78; H, 6.27; Br, 33.14; N, 5.81. Found: C, 54.67; H, 6.41; Br, 33.23; N, 5.72.

2-(3-Ethoxycarbonylpropyl) - 6,7-dimethoxy-1,2,3,4-tetrahydroisoquinoline (X) Hydrobromide—A mixture of 3.78 g (0.02 mole) of 6,7-dimethoxyisoquinoline and 3.90 g (0.02 mole) of ethyl γ-bromobutyrate was heated on a steam bath for 15 min. The resultant tacky residue was heated with acetone to give 4.10 g (54%), mp 160–165°. The solid was converted to the picrate for analysis, mp 123–125° from ethanol; IR (KBr): 1725 cm^{-1}; NMR (dimethyl sulfoxide-d_6): 10.2 (1H), 8.90 (A_2B_2, 2H), 8.1 (2H), 5.0 (2H), 3.6–4.2 (12H), and 1.2 (3H) ppm.

Anal.—Calc. for $C_{23}H_{24}N_4O_{11}$: C, 51.87; H, 4.54; N, 10.52. Found: C, 52.06; H, 4.48; N, 10.41.

A solution of 3.00 g (0.0085 mole) of the salt, 50 ml of absolute ethanol, and 5 mg of platinum oxide was shaken under hydrogen for 6 hr. The solution was filtered and taken to dryness, and the residue was treated with ether to give 2.40 g (79%) of X hydrobromide. The product was recrystallized from acetone, mp 173–174°; IR (KBr): 1725 cm^{-1}.

Anal.—Calc. for $C_{17}H_{26}BrNO_4$: C, 52.58; H, 6.75; N, 3.60. Found: C, 52.57; H, 6.55; N, 3.59.

Hydrolysis of this ester gave the acid hydrobromide, mp 220–222°.

Anal.—Calc. for $C_{15}H_{22}BrNO_4$: C, 50.01; H, 6.16; N, 3.89. Found: C, 49.82; H, 6.34; N, 3.89.

Reaction of Reissert Anion with Allyl Chloride—To 10.4 g (0.04 mole) of 2-benzoyl-1-cyano-1,2-dihydroisoquinoline in 100 ml of dimethylformamide and 8.0 g of allyl chloride was added 2.00 g of 50% sodium hydride in oil, and the mixture was stirred for 1 hr. The reaction mixture was poured over ice and allowed to stand overnight. The solution was extracted with chloroform, and the chloroform extracts were washed with water. The dried (sodium sulfate) chloroform extracts were taken to dryness *in vacuo*, and the residue was recrystallized from 95% ethanol to give 6.7 g (55%) of 1-allyl-2-benzoyl-1-cyano-1,2-dihydroisoquinoline (XI), mp 98–100°; IR (KBr): 1680 cm^{-1}; NMR (CCl_4): δ 7.5 (9H), 6.4 (1H), 5.6 (1H), 5.4 (1H), 5.2 (2H), and 3.1 (2H) ppm.

Anal.—Calc. for $C_{20}H_{16}N_2O$: C, 79.97; H, 5.37; N, 9.33. Found: C, 80.08; H, 5.43; N, 9.37.

Hydrolysis of X—A solution containing 3.00 g (0.01 mole) of X, 35 ml of water, 5 ml of ethanol, and 12 g of potassium hydroxide was refluxed for 48 hr. The basic reaction mixture was poured into 200 ml of water, and the aqueous solution was extracted with chloroform. The chloroform extracts were extracted with 5% HCl, the acid extracts were made basic with sodium carbonate, and the basic solution was extracted with chloroform. The dried (sodium sulfate) extracts were distilled at 88°/0.1 mm to give 1.24 g (73%) of 1-isoquinolylpropene (XII). The compound was converted to the picrate for analysis, mp 180–182°; IR (NaCl): 3080 and 1650 cm^{-1}; NMR (CCl_4): δ 8.0 (8H) and 1.9 (3H) ppm.

Anal.—Calc. for $C_{18}H_{14}N_4O_7$: C, 54.27; H, 3.54; N, 14.06. Found: C, 53.51; H, 3.63; N, 13.92.

REFERENCES

(1) J. Berson and N. Cohen, *J. Org. Chem.*, **20**, 1461 (1955).

(2) F. D. Popp, C. W. Klinowski, R. Piccirilli, D. H. Purcell, Jr., and R. F. Watts, *J. Heterocycl. Chem.*, **8**, 313 (1971).

ACKNOWLEDGMENTS

Supported in part by Grant CA-10965 from the National Cancer Institute, National Institutes of Health.

COMMUNICATIONS

Unusual Reversible Attack by Sodium Bisulfite on Physostigmine

Keyphrases □ Sodium bisulfite—effect on physostigmine molecule in solution □ Physostigmine—effect of sodium bisulfite on molecule in solution □ Antioxidants—sodium bisulfite, effect on physostigmine molecule in solution □ Ophthalmic cholinergics—physostigmine, effect of sodium bisulfite on molecule in solution

To the Editor:

Sodium bisulfite is used as an antioxidant in ophthalmic preparations containing physostigmine. Although physostigmine was shown to be stable in the presence of sodium bisulfite (1), the previous study was mainly concerned with the catalytic effect of the antioxidant on the hydrolysis rate of the carbamate linkage of the drug.

We recently observed interesting reactions between physostigmine and bisulfite. When sodium bisulfite solutions ranging in concentration from 0.01 to 0.4 *M* were mixed with 1×10^{-4} *M* physostigmine at pH 5.5 directly into the spectrophotometric[1] cell, the absorbance at 330 nm rapidly increased. At this wavelength and concentration, physostigmine has no absorbance; sodium bisulfite was present in both the sample and the blank. A semilog plot of $(A_\infty - A_t)$ against time resulted in a first-order plot (Fig. 1). The observed first-order rate constants depended on the bisulfite concentration (Fig. 2). Furthermore, at a given physostigmine concentration and in the presence of varying bisulfite concentrations, the equilibrium absorbance at 330 nm changed as a function of the bisulfite concentration (Fig. 3), indicating that an equilibrium condition existed between the species involved.

The ^{13}C-NMR spectra of aqueous solutions of physostigmine and physostigmine containing excess sodium bisulfite (molar ratio 2:1) indicate that the reaction between the two species involved an attack by bisulfite on carbon-10a of physostigmine. As seen from the NMR spectra (Fig. 4), the signal from carbon-10a (δ 98.92 ppm) disappeared when bisulfite was added. Instead, two new signals were observed, δ 88.74 and 92.32 ppm, suggesting the formation of two new species.

Since carbon-10a is partly responsible for the optical activity of physostigmine, one would anticipate changes in the optical rotation of physostigmine upon the addition

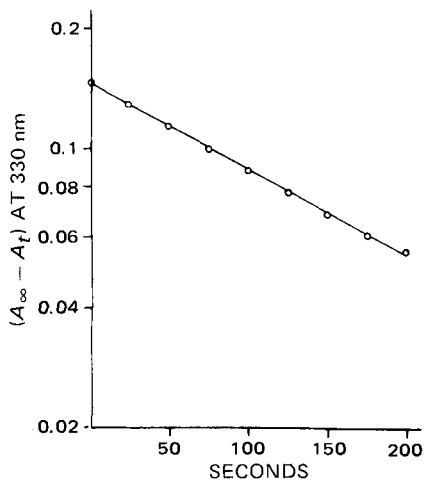

Figure 1—*Semilog plot of* $(A_\infty - A_t)$ *at 330 nm against time at pH 5.5 and 25°. Sodium bisulfite = 4.87* $\times 10^{-2}$ *M; physostigmine = 2.5* $\times 10^{-3}$ M.

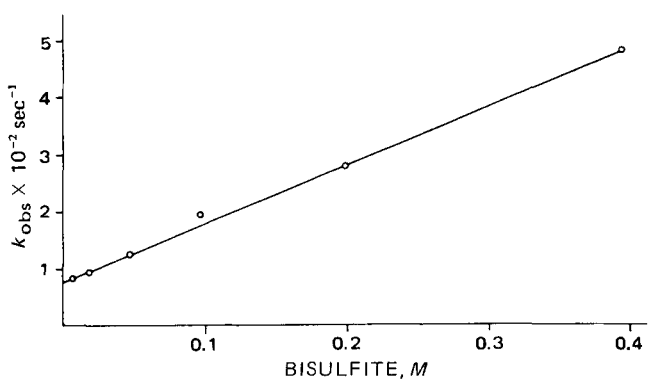

Figure 2—*Dependency of the observed first-order rate constant at pH 5.5 on bisulfite concentration.*

[1] Cary 15 recording spectrophotometer.

Reaction of Reissert Anion with Allyl Chloride—To 10.4 g (0.04 mole) of 2-benzoyl-1-cyano-1,2-dihydroisoquinoline in 100 ml of dimethylformamide and 8.0 g of allyl chloride was added 2.00 g of 50% sodium hydride in oil, and the mixture was stirred for 1 hr. The reaction mixture was poured over ice and allowed to stand overnight. The solution was extracted with chloroform, and the chloroform extracts were washed with water. The dried (sodium sulfate) chloroform extracts were taken to dryness *in vacuo*, and the residue was recrystallized from 95% ethanol to give 6.7 g (55%) of 1-allyl-2-benzoyl-1-cyano-1,2-dihydroisoquinoline (XI), mp 98–100°; IR (KBr): 1680 cm^{-1}; NMR (CCl_4): δ 7.5 (9H), 6.4 (1H), 5.6 (1H), 5.4 (1H), 5.2 (2H), and 3.1 (2H) ppm.

Anal.—Calc. for $C_{20}H_{16}N_2O$: C, 79.97; H, 5.37; N, 9.33. Found: C, 80.08; H, 5.43; N, 9.37.

Hydrolysis of X—A solution containing 3.00 g (0.01 mole) of X, 35 ml of water, 5 ml of ethanol, and 12 g of potassium hydroxide was refluxed for 48 hr. The basic reaction mixture was poured into 200 ml of water, and the aqueous solution was extracted with chloroform. The chloroform extracts were extracted with 5% HCl, the acid extracts were made basic with sodium carbonate, and the basic solution was extracted with chloroform. The dried (sodium sulfate) extracts were distilled at 88°/0.1 mm to give 1.24 g (73%) of 1-isoquinolylpropene (XII). The compound was converted to the picrate for analysis, mp 180–182°; IR (NaCl): 3080 and 1650 cm^{-1}; NMR (CCl_4): δ 8.0 (8H) and 1.9 (3H) ppm.

Anal.—Calc. for $C_{18}H_{14}N_4O_7$: C, 54.27; H, 3.54; N, 14.06. Found: C, 53.51; H, 3.63; N, 13.92.

REFERENCES

(1) J. Berson and N. Cohen, *J. Org. Chem.*, **20**, 1461 (1955).

(2) F. D. Popp, C. W. Klinowski, R. Piccirilli, D. H. Purcell, Jr., and R. F. Watts, *J. Heterocycl. Chem.*, **8**, 313 (1971).

ACKNOWLEDGMENTS

Supported in part by Grant CA-10965 from the National Cancer Institute, National Institutes of Health.

COMMUNICATIONS

Unusual Reversible Attack by Sodium Bisulfite on Physostigmine

Keyphrases □ Sodium bisulfite—effect on physostigmine molecule in solution □ Physostigmine—effect of sodium bisulfite on molecule in solution □ Antioxidants—sodium bisulfite, effect on physostigmine molecule in solution □ Ophthalmic cholinergics—physostigmine, effect of sodium bisulfite on molecule in solution

To the Editor:

Sodium bisulfite is used as an antioxidant in ophthalmic preparations containing physostigmine. Although physostigmine was shown to be stable in the presence of sodium bisulfite (1), the previous study was mainly concerned with the catalytic effect of the antioxidant on the hydrolysis rate of the carbamate linkage of the drug.

We recently observed interesting reactions between physostigmine and bisulfite. When sodium bisulfite solutions ranging in concentration from 0.01 to 0.4 *M* were mixed with 1×10^{-4} *M* physostigmine at pH 5.5 directly into the spectrophotometric[1] cell, the absorbance at 330 nm rapidly increased. At this wavelength and concentration, physostigmine has no absorbance; sodium bisulfite was present in both the sample and the blank. A semilog plot of $(A_\infty - A_t)$ against time resulted in a first-order plot (Fig. 1). The observed first-order rate constants depended on the bisulfite concentration (Fig. 2). Furthermore, at a given physostigmine concentration and in the presence of varying bisulfite concentrations, the equilibrium absorbance at 330 nm changed as a function of the bisulfite concentration (Fig. 3), indicating that an equilibrium condition existed between the species involved.

The ^{13}C-NMR spectra of aqueous solutions of physostigmine and physostigmine containing excess sodium bisulfite (molar ratio 2:1) indicate that the reaction between the two species involved an attack by bisulfite on carbon-10a of physostigmine. As seen from the NMR spectra (Fig. 4), the signal from carbon-10a (δ 98.92 ppm) disappeared when bisulfite was added. Instead, two new signals were observed, δ 88.74 and 92.32 ppm, suggesting the formation of two new species.

Since carbon-10a is partly responsible for the optical activity of physostigmine, one would anticipate changes in the optical rotation of physostigmine upon the addition

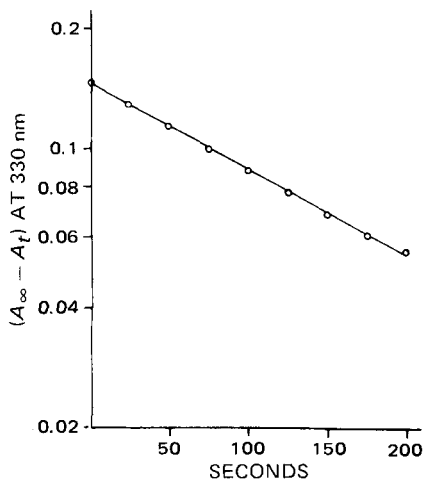

Figure 1—*Semilog plot of* $(A_\infty - A_t)$ *at 330 nm against time at pH 5.5 and 25°. Sodium bisulfite = 4.87* $\times 10^{-2}$ *M; physostigmine = 2.5* $\times 10^{-3}$ M.

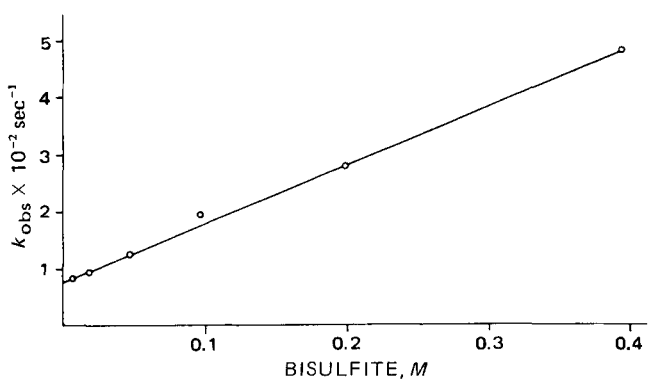

Figure 2—*Dependency of the observed first-order rate constant at pH 5.5 on bisulfite concentration.*

[1] Cary 15 recording spectrophotometer.

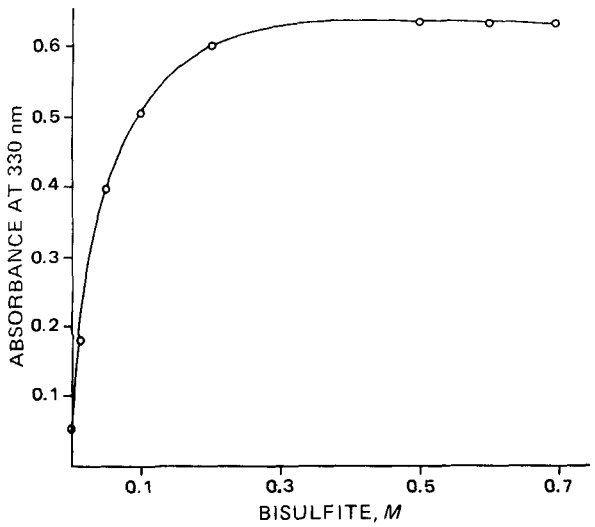

Figure 3—*Dependency of the physostigmine–bisulfite equilibrium absorbance at 330 nm on bisulfite concentration in the presence of a constant physostigmine concentration.*

of sodium bisulfite. Such changes did occur (Fig. 5). In the presence of excess bisulfite, the optical rotation was completely reversed. However, upon dilution of the physostigmine–bisulfite mixture at pH 5.5 with buffer (pH 9.5) and extraction of physostigmine with hexane, the optical rotation of the hexane solution corresponded to that of an equimolar solution of physostigmine. This result indicates that the reverse reaction resulted in the formation of physostigmine in its original configuration.

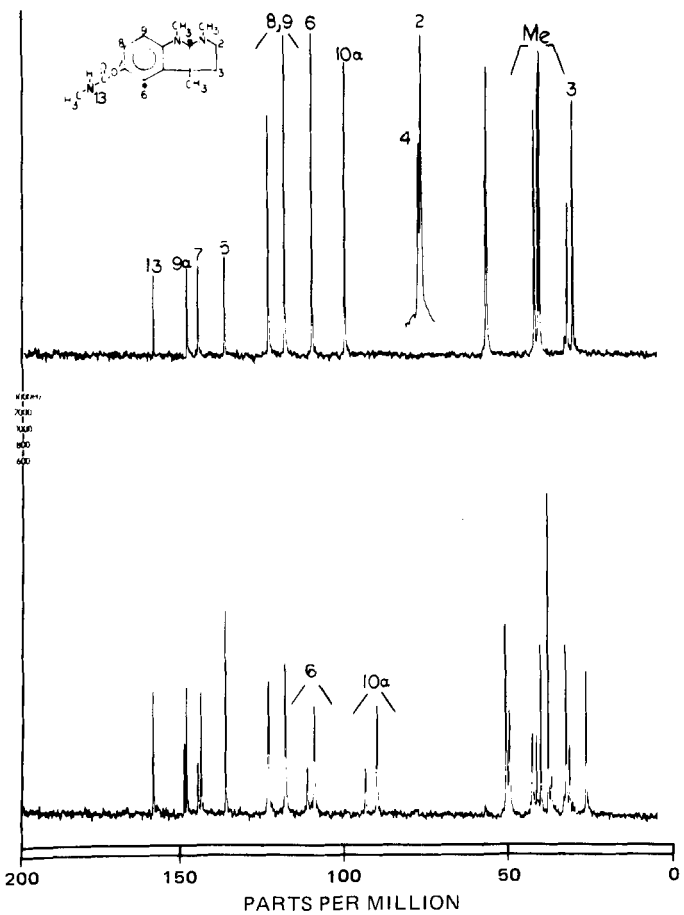

Figure 4—^{13}C-*NMR spectra of physostigmine and physostigmine–bisulfite solutions.*

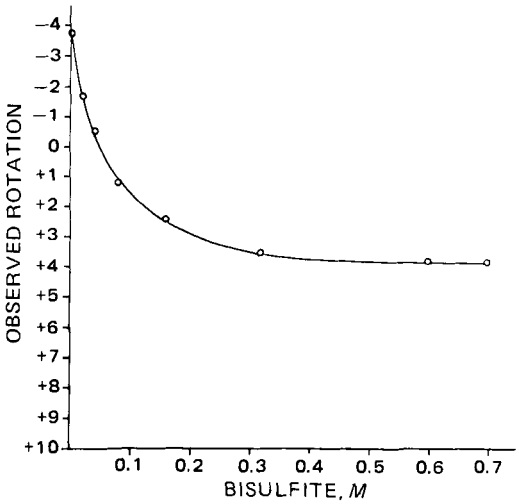

Figure 5—*Plot showing the change in the optical rotation of physostigmine in the presence of varying amounts of bisulfite at pH 5.5.*

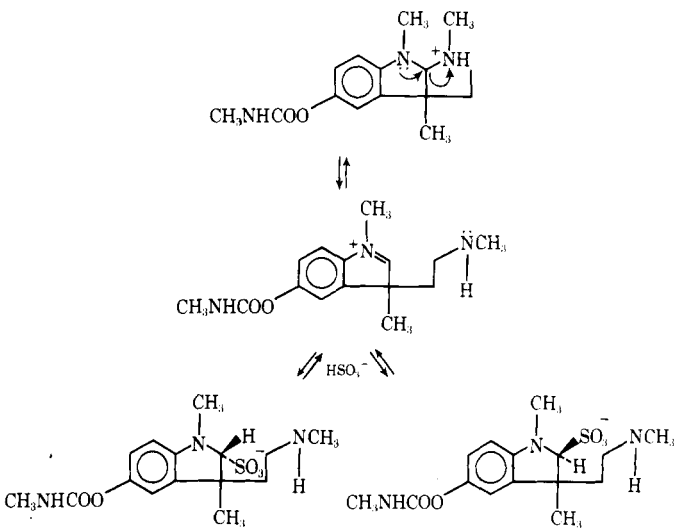

Scheme I

The equilibrium constant K = [phys − bisulf]$_{eq}$/[phys]$_{eq}$[bisulf]$_{eq}$ calculated from both the spectrophotometric and polarimetric data (Figs. 3 and 5) was 38 ± 2 M^{-1} at pH 5.5. The second-order rate constant for the reaction, calculated from the data of Fig. 2, was 0.103 M^{-1} sec^{-1} at pH 5.5. The reverse rate k_{-1} at pH 5.5, calculated from the intercept of Fig. 2, was 0.67 × 10^{-2}. The equilibrium constant calculated from the ratio of K_1[bisulfite]/k_{-1} was 30 M^{-1}, close to the value calculated from the direct measurements of the equilibrium constant.

Reaction Scheme I is consistent with these data. The significance of these findings in regard to the biological activity of physostigmine as well as the elucidation of the overall mechanism of these reactions is being investigated.

(1) G. Fletcher and D. J. G. Davies, *J. Pharm. Pharmacol.*, **20**, 108S (1968).

Anwar Hussain ˣ
H. Wahner
J. Triplett
College of Pharmacy
University of Kentucky
Lexington, KY 40506

Received October 31, 1977.
Accepted for publication February 10, 1978.

REVIEWS

Kinetics of Drug Action. Handbook of Experimental Pharmacology. Vol. 47. Edited by J. M. van ROSSUM. Springer-Verlag, 175 Fifth Ave., New York, NY 10010. 1977. 436 pp. 17 × 24.7 cm. Price $101.20.

The aim of this book, as stated by the Editor, is: "to present an integrated treatment of the kinetics of drug action, covering the principles of drug transport, kinetics of drug absorption, distribution, and elimination as well as the principles of drug–receptor interactions under steady-state conditions and the kinetics of the drug–receptor interaction." Since the action of a drug in the body is basically a kinetic event, a thorough appreciation of the fundamentals of kinetic concepts is essential to the understanding of the nature of drug action. This book is a comprehensive survey of the available knowledge (mostly through 1974) on many of the kinetic aspects of drug action.

Chapter 1, Physicochemical Fundamentals and Thermodynamics of the Membrane Transport of Drugs, covers several important topics of the membrane transport of drugs and biological substances, with a particular emphasis on kinetic and thermodynamic principles relevant to transport phenomena. The molecular structure and physicochemical models of biomembranes are critically evaluated. Although many books and review articles have exclusively dealt with the theories of membrane transport, this chapter serves as a useful review of the subject and assists the reader to understand better the role of biological membranes in drug action.

Chapter 2, Pharmacokinetics, prepared by the Editor from the work left by the late Professor E. Krüger-Thiemer, begins with the definitions of pharmacokinetic terms in common use and then presents an excellent outline of pharmacokinetics. This chapter will be of great value to anyone who requires a quick access to the basic principles of pharmacokinetics.

Chapter 3, Pharmacokinetics of Biotransformation, deals with kinetic aspects of drug metabolism. Many specific as well as stereotype examples of drug elimination by enzymatic reactions are succinctly described, with sufficient illustrations taken from the research data.

Chapters 4, 5, and 6 are on General Theory of Drug–Receptor Interaction, A Critical Survey of Receptor Theories of Drug Action, and Drug–Receptor Inactivation: A New Kinetic Model, respectively. These chapters cover the molecular concepts of drug–receptor interactions, historical development of receptor theories and their limitations, and mathematical equations relevant to the receptor models. The discussion also includes the general principles of drug action and receptor inactivation theories. Each chapter is written with ample background information and is well referenced.

The final chapter, entitled Kinetics of Drug–Receptor Interaction, presents a critical review of the kinetic concepts of drug–receptor interaction from the approach of the drug to the receptor to the formation of an active complex and the dissociation of the complex thereafter. The nature of the receptor site, conformational changes in the drug–receptor complex, and intermolecular forces responsible for the reactions are also discussed. In the Appendix, several mathematical equations for the development of the receptor kinetics are derived.

In summary, most of the information in this book can be found elsewhere, but the book justifies its value by covering in one volume several related subjects essential to the understanding of drug action. I recommend this book to beginners as well as to those who are well advanced in the areas of molecular pharmacology and pharmacokinetics. Regrettably, its excessively high price could prevent many from acquiring a personal copy.

Reviewed by H. Won Jun
School of Pharmacy
University of Georgia
Athens, GA 30602

Aromatic and Heteroaromatic Chemistry. Vol. 5. A Specialist Periodical Report. Edited by C. W. BIRD and G. W. H. CHEESEMAN. The Chemical Society, Burlington House, London W1V 0BN, England. 1977. 566 pp. 14.5 × 22.5 cm. Price $70.00. Available from Special Issues Sales, American Chemical Society, 1155 Sixteenth St., N.W., Washington, DC 20036.

This volume surveys the chemical literature abstracted between July 1975 and June 1976 and covered by Vols. 83 and 84 of *Chemical Abstracts*. The organization and high standard established by earlier volumes in this series are maintained in this fifth volume.

The report is comprised of 14 chapters. The 15 international contributing experts have condensed and organized an enormous volume of material into a very readable book. All sections are liberally illustrated with chemical structures and reaction sequences. A random turn of the pages quickly provides information on synthetic work, mechanism studies, stereochemistry, and a fascinating range of exciting and intriguing aromatic and heteroaromatic compounds.

The chapter titles include: Ring Systems of Topical Interest; Intermolecular and Intramolecular Cyclization Reactions in Ring Synthesis; Cycloaddition Reactions; Ring Transformations; Electrophilic Substitution on Carbon; Electrophilic Substitution on Heteroatoms; Nucleophilic Substitution; Aromatic Substitution by Free Radicals, Carbenes, and Nitrenes; Addition Reactions; Ring-cleavage Reactions; Reactions of Substituents; Porphyrins and Related Compounds; Naturally Occurring Oxygen-ring Compounds; and Other Naturally Occurring Compounds. Although a subject index is not present, the volume has a complete author index and includes some 3071 literature citations.

As a reference book, this report will be invaluable to a large number of chemists who wish to keep abreast of the varied research activities in aromatic and heteroaromatic chemistry.

This is the last report for which Professors Bird and Cheeseman will act as Senior Reporters. They are to be commended for their leadership and guidance in setting the standards of quality recognized for this series. The stated objective of providing a service to the active specialist chemist has been well served by these reports.

Reviewed by C. DeWitt Blanton, Jr.
School of Pharmacy
University of Georgia
Athens, GA 30602

NOTICES

Antifungal Compounds, Vol. 2: Interactions in Biological and Ecological Systems. Edited by MALCOLM R. SIEGEL and HUGH D. SISLER. Dekker, 270 Madison Ave., New York, NY 10016. 1977. 674 pp. 15 × 23 cm. Price $65.00.

The Chemistry of Pyrroles. By R. ALAN JONES and GERRITT P. BEAN. Academic (London), 24-28 Oval Road, London, NW1 7DX, England. 1977. 525 pp. 15 × 23 cm. Price $41.00.

Microemulsions: Theory and Practice. Edited by LEON M. PRINCE. Academic, 111 Fifth Ave., New York, NY 10003. 1977. 179 pp. 15 × 23 cm. Price $12.00.

Receptors and Recognition, Series A, Vol. 3. Edited by P. CUATRECASAS and M. F. GREAVES. Halsted, 605 Third Ave., New York, NY 10016. 1977. 166 pp. 15 × 24 cm. Price $24.50.

Water, Wastes and Health in Hot Climates. Edited by RICHARD FEACHEM, MICHAEL McGARRY, and DUNCAN MARA. Wiley, 605 Third Ave., New York, NY 10016. 1977. 399 pp. 15 × 23 cm.

Biological Bases of Psychiatric Disorders. Edited by ALAN FRAZER and ANDREW WINOKUR. Spectrum, 175-20 Wexford Terrace, Jamaica, NY 11432. 1977. 271 pp. 17 × 25 cm. Price $15.00.

The Lymphocyte: Structure and Function, Part II. Edited by JOHN J. MARCHALONIS. Dekker, 270 Madison Ave., New York, NY 10016. 1977. 704 pp. 15 × 23 cm. Price $37.50.

Radiotracer Techniques and Applications, Vol. 2. Edited by E. ANTHONY EVANS and MITSUO MURAMATSU. Dekker, 270 Madison Ave., New York, NY 10016. 1977. 1211 pp. 15 × 23 cm. Price $49.75.

Current Developments in Psychopharmacology, Vol. 4. Edited by WALTER B. ESSMAN and L. VALZELLI. Spectrum, 175-20 Wexford Terrace, Jamaica, NY 11432. 1977. 295 pp. 15 × 23 cm. Price $25.00.

REVIEWS

Kinetics of Drug Action. Handbook of Experimental Pharmacology. Vol. 47. Edited by J. M. van ROSSUM. Springer-Verlag, 175 Fifth Ave., New York, NY 10010. 1977. 436 pp. 17 × 24.7 cm. Price $101.20.

The aim of this book, as stated by the Editor, is: "to present an integrated treatment of the kinetics of drug action, covering the principles of drug transport, kinetics of drug absorption, distribution, and elimination as well as the principles of drug–receptor interactions under steady-state conditions and the kinetics of the drug–receptor interaction." Since the action of a drug in the body is basically a kinetic event, a thorough appreciation of the fundamentals of kinetic concepts is essential to the understanding of the nature of drug action. This book is a comprehensive survey of the available knowledge (mostly through 1974) on many of the kinetic aspects of drug action.

Chapter 1, Physicochemical Fundamentals and Thermodynamics of the Membrane Transport of Drugs, covers several important topics of the membrane transport of drugs and biological substances, with a particular emphasis on kinetic and thermodynamic principles relevant to transport phenomena. The molecular structure and physicochemical models of biomembranes are critically evaluated. Although many books and review articles have exclusively dealt with the theories of membrane transport, this chapter serves as a useful review of the subject and assists the reader to understand better the role of biological membranes in drug action.

Chapter 2, Pharmacokinetics, prepared by the Editor from the work left by the late Professor E. Krüger-Thiemer, begins with the definitions of pharmacokinetic terms in common use and then presents an excellent outline of pharmacokinetics. This chapter will be of great value to anyone who requires a quick access to the basic principles of pharmacokinetics.

Chapter 3, Pharmacokinetics of Biotransformation, deals with kinetic aspects of drug metabolism. Many specific as well as stereotype examples of drug elimination by enzymatic reactions are succinctly described, with sufficient illustrations taken from the research data.

Chapters 4, 5, and 6 are on General Theory of Drug–Receptor Interaction, A Critical Survey of Receptor Theories of Drug Action, and Drug–Receptor Inactivation: A New Kinetic Model, respectively. These chapters cover the molecular concepts of drug–receptor interactions, historical development of receptor theories and their limitations, and mathematical equations relevant to the receptor models. The discussion also includes the general principles of drug action and receptor inactivation theories. Each chapter is written with ample background information and is well referenced.

The final chapter, entitled Kinetics of Drug–Receptor Interaction, presents a critical review of the kinetic concepts of drug–receptor interaction from the approach of the drug to the receptor to the formation of an active complex and the dissociation of the complex thereafter. The nature of the receptor site, conformational changes in the drug–receptor complex, and intermolecular forces responsible for the reactions are also discussed. In the Appendix, several mathematical equations for the development of the receptor kinetics are derived.

In summary, most of the information in this book can be found elsewhere, but the book justifies its value by covering in one volume several related subjects essential to the understanding of drug action. I recommend this book to beginners as well as to those who are well advanced in the areas of molecular pharmacology and pharmacokinetics. Regrettably, its excessively high price could prevent many from acquiring a personal copy.

Reviewed by H. Won Jun
School of Pharmacy
University of Georgia
Athens, GA 30602

Aromatic and Heteroaromatic Chemistry. Vol. 5. A Specialist Periodical Report. Edited by C. W. BIRD and G. W. H. CHEESEMAN. The Chemical Society, Burlington House, London W1V 0BN, England. 1977. 566 pp. 14.5 × 22.5 cm. Price $70.00. Available from Special Issues Sales, American Chemical Society, 1155 Sixteenth St., N.W., Washington, DC 20036.

This volume surveys the chemical literature abstracted between July 1975 and June 1976 and covered by Vols. 83 and 84 of *Chemical Abstracts*. The organization and high standard established by earlier volumes in this series are maintained in this fifth volume.

The report is comprised of 14 chapters. The 15 international contributing experts have condensed and organized an enormous volume of material into a very readable book. All sections are liberally illustrated with chemical structures and reaction sequences. A random turn of the pages quickly provides information on synthetic work, mechanism studies, stereochemistry, and a fascinating range of exciting and intriguing aromatic and heteroaromatic compounds.

The chapter titles include: Ring Systems of Topical Interest; Intermolecular and Intramolecular Cyclization Reactions in Ring Synthesis; Cycloaddition Reactions; Ring Transformations; Electrophilic Substitution on Carbon; Electrophilic Substitution on Heteroatoms; Nucleophilic Substitution; Aromatic Substitution by Free Radicals, Carbenes, and Nitrenes; Addition Reactions; Ring-cleavage Reactions; Reactions of Substituents; Porphyrins and Related Compounds; Naturally Occurring Oxygen-ring Compounds; and Other Naturally Occurring Compounds. Although a subject index is not present, the volume has a complete author index and includes some 3071 literature citations.

As a reference book, this report will be invaluable to a large number of chemists who wish to keep abreast of the varied research activities in aromatic and heteroaromatic chemistry.

This is the last report for which Professors Bird and Cheeseman will act as Senior Reporters. They are to be commended for their leadership and guidance in setting the standards of quality recognized for this series. The stated objective of providing a service to the active specialist chemist has been well served by these reports.

Reviewed by C. DeWitt Blanton, Jr.
School of Pharmacy
University of Georgia
Athens, GA 30602

NOTICES

Antifungal Compounds, Vol. 2: Interactions in Biological and Ecological Systems. Edited by MALCOLM R. SIEGEL and HUGH D. SISLER. Dekker, 270 Madison Ave., New York, NY 10016. 1977. 674 pp. 15 × 23 cm. Price $65.00.

The Chemistry of Pyrroles. By R. ALAN JONES and GERRITT P. BEAN. Academic (London), 24-28 Oval Road, London, NW1 7DX, England. 1977. 525 pp. 15 × 23 cm. Price $41.00.

Microemulsions: Theory and Practice. Edited by LEON M. PRINCE. Academic, 111 Fifth Ave., New York, NY 10003. 1977. 179 pp. 15 × 23 cm. Price $12.00.

Receptors and Recognition, Series A, Vol. 3. Edited by P. CUATRECASAS and M. F. GREAVES. Halsted, 605 Third Ave., New York, NY 10016. 1977. 166 pp. 15 × 24 cm. Price $24.50.

Water, Wastes and Health in Hot Climates. Edited by RICHARD FEACHEM, MICHAEL McGARRY, and DUNCAN MARA. Wiley, 605 Third Ave., New York, NY 10016. 1977. 399 pp. 15 × 23 cm.

Biological Bases of Psychiatric Disorders. Edited by ALAN FRAZER and ANDREW WINOKUR. Spectrum, 175-20 Wexford Terrace, Jamaica, NY 11432. 1977. 271 pp. 17 × 25 cm. Price $15.00.

The Lymphocyte: Structure and Function, Part II. Edited by JOHN J. MARCHALONIS. Dekker, 270 Madison Ave., New York, NY 10016. 1977. 704 pp. 15 × 23 cm. Price $37.50.

Radiotracer Techniques and Applications, Vol. 2. Edited by E. ANTHONY EVANS and MITSUO MURAMATSU. Dekker, 270 Madison Ave., New York, NY 10016. 1977. 1211 pp. 15 × 23 cm. Price $49.75.

Current Developments in Psychopharmacology, Vol. 4. Edited by WALTER B. ESSMAN and L. VALZELLI. Spectrum, 175-20 Wexford Terrace, Jamaica, NY 11432. 1977. 295 pp. 15 × 23 cm. Price $25.00.

REVIEWS

Kinetics of Drug Action. Handbook of Experimental Pharmacology. Vol. 47. Edited by J. M. van ROSSUM. Springer-Verlag, 175 Fifth Ave., New York, NY 10010. 1977. 436 pp. 17 × 24.7 cm. Price $101.20.

The aim of this book, as stated by the Editor, is: "to present an integrated treatment of the kinetics of drug action, covering the principles of drug transport, kinetics of drug absorption, distribution, and elimination as well as the principles of drug–receptor interactions under steady-state conditions and the kinetics of the drug–receptor interaction." Since the action of a drug in the body is basically a kinetic event, a thorough appreciation of the fundamentals of kinetic concepts is essential to the understanding of the nature of drug action. This book is a comprehensive survey of the available knowledge (mostly through 1974) on many of the kinetic aspects of drug action.

Chapter 1, Physicochemical Fundamentals and Thermodynamics of the Membrane Transport of Drugs, covers several important topics of the membrane transport of drugs and biological substances, with a particular emphasis on kinetic and thermodynamic principles relevant to transport phenomena. The molecular structure and physicochemical models of biomembranes are critically evaluated. Although many books and review articles have exclusively dealt with the theories of membrane transport, this chapter serves as a useful review of the subject and assists the reader to understand better the role of biological membranes in drug action.

Chapter 2, Pharmacokinetics, prepared by the Editor from the work left by the late Professor E. Krüger-Thiemer, begins with the definitions of pharmacokinetic terms in common use and then presents an excellent outline of pharmacokinetics. This chapter will be of great value to anyone who requires a quick access to the basic principles of pharmacokinetics.

Chapter 3, Pharmacokinetics of Biotransformation, deals with kinetic aspects of drug metabolism. Many specific as well as stereotype examples of drug elimination by enzymatic reactions are succinctly described, with sufficient illustrations taken from the research data.

Chapters 4, 5, and 6 are on General Theory of Drug–Receptor Interaction, A Critical Survey of Receptor Theories of Drug Action, and Drug–Receptor Inactivation: A New Kinetic Model, respectively. These chapters cover the molecular concepts of drug–receptor interactions, historical development of receptor theories and their limitations, and mathematical equations relevant to the receptor models. The discussion also includes the general principles of drug action and receptor inactivation theories. Each chapter is written with ample background information and is well referenced.

The final chapter, entitled Kinetics of Drug–Receptor Interaction, presents a critical review of the kinetic concepts of drug–receptor interaction from the approach of the drug to the receptor to the formation of an active complex and the dissociation of the complex thereafter. The nature of the receptor site, conformational changes in the drug–receptor complex, and intermolecular forces responsible for the reactions are also discussed. In the Appendix, several mathematical equations for the development of the receptor kinetics are derived.

In summary, most of the information in this book can be found elsewhere, but the book justifies its value by covering in one volume several related subjects essential to the understanding of drug action. I recommend this book to beginners as well as to those who are well advanced in the areas of molecular pharmacology and pharmacokinetics. Regrettably, its excessively high price could prevent many from acquiring a personal copy.

Reviewed by H. Won Jun
School of Pharmacy
University of Georgia
Athens, GA 30602

Aromatic and Heteroaromatic Chemistry. Vol. 5. A Specialist Periodical Report. Edited by C. W. BIRD and G. W. H. CHEESEMAN. The Chemical Society, Burlington House, London W1V 0BN, England. 1977. 566 pp. 14.5 × 22.5 cm. Price $70.00. Available from Special Issues Sales, American Chemical Society, 1155 Sixteenth St., N.W., Washington, DC 20036.

This volume surveys the chemical literature abstracted between July 1975 and June 1976 and covered by Vols. 83 and 84 of *Chemical Abstracts*. The organization and high standard established by earlier volumes in this series are maintained in this fifth volume.

The report is comprised of 14 chapters. The 15 international contributing experts have condensed and organized an enormous volume of material into a very readable book. All sections are liberally illustrated with chemical structures and reaction sequences. A random turn of the pages quickly provides information on synthetic work, mechanism studies, stereochemistry, and a fascinating range of exciting and intriguing aromatic and heteroaromatic compounds.

The chapter titles include: Ring Systems of Topical Interest; Intermolecular and Intramolecular Cyclization Reactions in Ring Synthesis; Cycloaddition Reactions; Ring Transformations; Electrophilic Substitution on Carbon; Electrophilic Substitution on Heteroatoms; Nucleophilic Substitution; Aromatic Substitution by Free Radicals, Carbenes, and Nitrenes; Addition Reactions; Ring-cleavage Reactions; Reactions of Substituents; Porphyrins and Related Compounds; Naturally Occurring Oxygen-ring Compounds; and Other Naturally Occurring Compounds. Although a subject index is not present, the volume has a complete author index and includes some 3071 literature citations.

As a reference book, this report will be invaluable to a large number of chemists who wish to keep abreast of the varied research activities in aromatic and heteroaromatic chemistry.

This is the last report for which Professors Bird and Cheeseman will act as Senior Reporters. They are to be commended for their leadership and guidance in setting the standards of quality recognized for this series. The stated objective of providing a service to the active specialist chemist has been well served by these reports.

Reviewed by C. DeWitt Blanton, Jr.
School of Pharmacy
University of Georgia
Athens, GA 30602

NOTICES

Antifungal Compounds, Vol. 2: Interactions in Biological and Ecological Systems. Edited by MALCOLM R. SIEGEL and HUGH D. SISLER. Dekker, 270 Madison Ave., New York, NY 10016. 1977. 674 pp. 15 × 23 cm. Price $65.00.

The Chemistry of Pyrroles. By R. ALAN JONES and GERRITT P. BEAN. Academic (London), 24-28 Oval Road, London, NW1 7DX, England. 1977. 525 pp. 15 × 23 cm. Price $41.00.

Microemulsions: Theory and Practice. Edited by LEON M. PRINCE. Academic, 111 Fifth Ave., New York, NY 10003. 1977. 179 pp. 15 × 23 cm. Price $12.00.

Receptors and Recognition, Series A, Vol. 3. Edited by P. CUATRECASAS and M. F. GREAVES. Halsted, 605 Third Ave., New York, NY 10016. 1977. 166 pp. 15 × 24 cm. Price $24.50.

Water, Wastes and Health in Hot Climates. Edited by RICHARD FEACHEM, MICHAEL McGARRY, and DUNCAN MARA. Wiley, 605 Third Ave., New York, NY 10016. 1977. 399 pp. 15 × 23 cm.

Biological Bases of Psychiatric Disorders. Edited by ALAN FRAZER and ANDREW WINOKUR. Spectrum, 175-20 Wexford Terrace, Jamaica, NY 11432. 1977. 271 pp. 17 × 25 cm. Price $15.00.

The Lymphocyte: Structure and Function, Part II. Edited by JOHN J. MARCHALONIS. Dekker, 270 Madison Ave., New York, NY 10016. 1977. 704 pp. 15 × 23 cm. Price $37.50.

Radiotracer Techniques and Applications, Vol. 2. Edited by E. ANTHONY EVANS and MITSUO MURAMATSU. Dekker, 270 Madison Ave., New York, NY 10016. 1977. 1211 pp. 15 × 23 cm. Price $49.75.

Current Developments in Psychopharmacology, Vol. 4. Edited by WALTER B. ESSMAN and L. VALZELLI. Spectrum, 175-20 Wexford Terrace, Jamaica, NY 11432. 1977. 295 pp. 15 × 23 cm. Price $25.00.

JUNE 1978
VOLUME 67 NUMBER 6

JOURNAL OF PHARMACEUTICAL SCIENCES

MARY H. FERGUSON
Editor

SHELLY ELLIOTT
Production Editor

JANET D. SHOFF
Copy Editor

EDWARD G. FELDMANN
Contributing Editor

SAMUEL W. GOLDSTEIN
Contributing Editor

BELLE R. BECK
Editorial Secretary

DAVID BOHARDT
Director of Publications

L. LUAN CORRIGAN
Assistant Director of Publications

EDITORIAL ADVISORY BOARD

JOHN AUTIAN
NORMAN R. FARNSWORTH
WILLIAM O. FOYE
WILLIAM J. JUSKO
HERBERT A. LIEBERMAN
DAVID E. MANN, JR.
GERALD J. PAPARIELLO
EDWARD G. RIPPIE

The *Journal of Pharmaceutical Sciences* is published monthly by the American Pharmaceutical Association at 2215 Constitution Ave., N.W., Washington, DC 20037. Second-class postage paid at Washington, D.C., and at additional mailing office.

All expressions of opinion and statements of supposed fact appearing in articles or editorials carried in this journal are published on the authority of the writer over whose name they appear and are not to be regarded as necessarily expressing the policies or views of the American Pharmaceutical Association.

Offices—Editorial, Advertising, and Subscription Offices: 2215 Constitution Ave., N.W., Washington, DC 20037. Printing Offices: 20th & Northampton Streets, Easton, PA 18042.

Annual Subscriptions—United States and foreign, industrial and government institutions $50, educational institutions $50, individuals *for personal use only* $30; single copies $5. All foreign subscriptions add $5 for postage. Subscription rates are subject to change without notice. Members of the American Pharmaceutical Association may elect to receive the *Journal of Pharmaceutical Sciences* as a part of their annual $70 (foreign $75) APhA membership dues.

Claims—Missing numbers will not be supplied if dues or subscriptions are in arrears for more than 60 days or if claims are received more than 60 days after the date of the issue, or if loss was due to failure to give notice of change of address. The Association cannot accept responsibility for foreign delivery when its records indicate shipment has been made.

Change of Address—Members and subscribers should notify at once both the Post Office and the American Pharmaceutical Association, 2215 Constitution Ave., N.W., Washington, DC 20037, of any change of address.

Microfilm—Microfilm volumes are available from University Microfilms International, 300 N. Zeeb Road, Ann Arbor, MI 48106.

© Copyright 1978, American Pharmaceutical Association, 2215 Constitution Ave., N.W., Washington, DC 20037; all rights reserved.

A PROBLEM AND A SOLUTION

In the federal bureaucracy where the number of problems awaiting resolution seems almost limitless, we sometimes encounter the ironic situation of having solutions for problems that no longer exist. The difficulty in terminating pertinent government committees once such problems have been resolved is the genesis of the proposals for so-called "sunset legislation."

More often, however, rather than an overabundance of solutions, we in the health-care field are faced with problems ranging from runaway costs to mal-distribution of practitioners. Most of these problems are difficult at best and even appear to defy solution.

Hence, it is a welcome, if rare, relief when a solution appears on the horizon at the same time when one is grappling with a difficult problem. In our view, this situation appears to exist in one aspect of the blockbuster drug bill, S.2755, appropriately titled the "Drug Regulation Reform Act of 1978."

This omnibus bill has a host of features, many of which are good and some of which are bad, but in this column we are going to address only one aspect—a facet that has drawn relatively little attention from any other quarter.

Over the years, drugs have been approved for marketing under current federal law based on certain specified uses as spelled out in the pertinent drug's official labeling. Later on, certain drugs have accidently been found to be useful in treating some other condition not included among the uses listed in the approved labeling. Such discoveries are generally made by practitioners in the course of their daily routine. These practitioners often will pass along the information informally *via* corridor discussion with colleagues, or at most, *via* the letters column in some medical journal.

However, these testimonials clearly do not constitute the necessary scientific data sufficient to document the value of the drug for the particular alternative use. Consequently, the Food and Drug Administration cannot authorize expanding the indications for use stated in the labeling for the drug until data from suitable scientific studies have been made available that will support such claims. And, in our view, this stand is entirely proper.

On the other hand, the drug manufacturer usually has little incentive to undertake the costly studies to develop such documentation. After all, the drug is already approved for marketing, and the extra expense of developing these additional data will probably not be recouped through extra sales demand for the product.

But some of these so-called "unapproved uses of approved drugs" may represent important applications of considerable value in medical treatment. For example, years ago, the local anesthetic agent lidocaine was found to be useful in treatment of cardiac arrhythmia. Indeed, its use for this purpose was credited with saving any number of lives. But, for any number of reasons, if a drug does have a valid and justified ancillary use, that fact should be stated on the label; and, in turn, that means that someone has to see that those scientific studies are performed that were mentioned in the preceding paragraphs.

A tentative answer to this dilemma is advanced in Section 108 (h) (2) of S.2755. This subsection provides for inclusion in the drug entity monograph of a requirement that, in order to obtain a license to manufacture a drug product under that monograph, any person might be compelled to conduct scientific investigations relating to other uses of the drug—even uses that the manufacturer may not wish to endorse. On both moral and economic grounds, we find it difficult to agree with this approach.

Later on, however, under Section 201, the bill provides for the establishment of a National Center for Clinical Pharmacology. This new Center would fulfill a variety of research and training functions.

The language in the bill specifically states that either *"upon request or on its own initiative, the Center may conduct and support research in clinical pharmacology and clinical pharmacy, including investigations (1) of the safety and effectiveness of existing and new uses of drug products, ..."* The bill goes on to list several other meaningful roles that the Center would serve. But it is this first-stated purpose that is pertinent to this discussion. Note that its mandate specifically covers research on new uses for drugs to establish their safety and effectiveness for such purposes.

Expenditure of public funds to fulfill this need appears justified and in the best interest of all parties concerned: the government, the drug industry, the health care professions, and the general public. Not only is the problem evident, but so too is its solution.

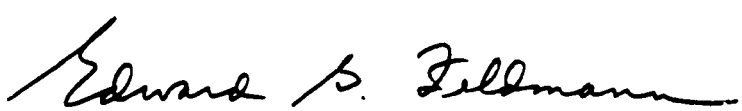

JUNE 1978
VOLUME 67 NUMBER 6

JOURNAL OF PHARMACEUTICAL SCIENCES

MARY H. FERGUSON
Editor

SHELLY ELLIOTT
Production Editor

JANET D. SHOFF
Copy Editor

EDWARD G. FELDMANN
Contributing Editor

SAMUEL W. GOLDSTEIN
Contributing Editor

BELLE R. BECK
Editorial Secretary

DAVID BOHARDT
Director of Publications

L. LUAN CORRIGAN
Assistant Director of Publications

EDITORIAL ADVISORY BOARD

JOHN AUTIAN
NORMAN R. FARNSWORTH
WILLIAM O. FOYE
WILLIAM J. JUSKO
HERBERT A. LIEBERMAN
DAVID E. MANN, JR.
GERALD J. PAPARIELLO
EDWARD G. RIPPIE

The *Journal of Pharmaceutical Sciences* is published monthly by the American Pharmaceutical Association at 2215 Constitution Ave., N.W., Washington, DC 20037. Second-class postage paid at Washington, D.C., and at additional mailing office.

All expressions of opinion and statements of supposed fact appearing in articles or editorials carried in this journal are published on the authority of the writer over whose name they appear and are not to be regarded as necessarily expressing the policies or views of the American Pharmaceutical Association.

Offices—Editorial, Advertising, and Subscription Offices: 2215 Constitution Ave., N.W., Washington, DC 20037. Printing Offices: 20th & Northampton Streets, Easton, PA 18042.

Annual Subscriptions—United States and foreign, industrial and government institutions $50, educational institutions $50, individuals *for personal use only* $30; single copies $5. All foreign subscriptions add $5 for postage. Subscription rates are subject to change without notice. Members of the American Pharmaceutical Association may elect to receive the *Journal of Pharmaceutical Sciences* as a part of their annual $70 (foreign $75) APhA membership dues.

Claims—Missing numbers will not be supplied if dues or subscriptions are in arrears for more than 60 days or if claims are received more than 60 days after the date of the issue, or if loss was due to failure to give notice of change of address. The Association cannot accept responsibility for foreign delivery when its records indicate shipment has been made.

Change of Address—Members and subscribers should notify at once both the Post Office and the American Pharmaceutical Association, 2215 Constitution Ave., N.W., Washington, DC 20037, of any change of address.

Microfilm—Microfilm volumes are available from University Microfilms International, 300 N. Zeeb Road, Ann Arbor, MI 48106.

© Copyright 1978, American Pharmaceutical Association, 2215 Constitution Ave., N.W., Washington, DC 20037; all rights reserved.

A PROBLEM AND A SOLUTION

In the federal bureaucracy where the number of problems awaiting resolution seems almost limitless, we sometimes encounter the ironic situation of having solutions for problems that no longer exist. The difficulty in terminating pertinent government committees once such problems have been resolved is the genesis of the proposals for so-called "sunset legislation."

More often, however, rather than an overabundance of solutions, we in the health-care field are faced with problems ranging from runaway costs to mal-distribution of practitioners. Most of these problems are difficult at best and even appear to defy solution.

Hence, it is a welcome, if rare, relief when a solution appears on the horizon at the same time when one is grappling with a difficult problem. In our view, this situation appears to exist in one aspect of the blockbuster drug bill, S.2755, appropriately titled the "Drug Regulation Reform Act of 1978."

This omnibus bill has a host of features, many of which are good and some of which are bad, but in this column we are going to address only one aspect—a facet that has drawn relatively little attention from any other quarter.

Over the years, drugs have been approved for marketing under current federal law based on certain specified uses as spelled out in the pertinent drug's official labeling. Later on, certain drugs have accidently been found to be useful in treating some other condition not included among the uses listed in the approved labeling. Such discoveries are generally made by practitioners in the course of their daily routine. These practitioners often will pass along the information informally *via* corridor discussion with colleagues, or at most, *via* the letters column in some medical journal.

However, these testimonials clearly do not constitute the necessary scientific data sufficient to document the value of the drug for the particular alternative use. Consequently, the Food and Drug Administration cannot authorize expanding the indications for use stated in the labeling for the drug until data from suitable scientific studies have been made available that will support such claims. And, in our view, this stand is entirely proper.

On the other hand, the drug manufacturer usually has little incentive to undertake the costly studies to develop such documentation. After all, the drug is already approved for marketing, and the extra expense of developing these additional data will probably not be recouped through extra sales demand for the product.

But some of these so-called "unapproved uses of approved drugs" may represent important applications of considerable value in medical treatment. For example, years ago, the local anesthetic agent lidocaine was found to be useful in treatment of cardiac arrhythmia. Indeed, its use for this purpose was credited with saving any number of lives. But, for any number of reasons, if a drug does have a valid and justified ancillary use, that fact should be stated on the label; and, in turn, that means that someone has to see that those scientific studies are performed that were mentioned in the preceding paragraphs.

A tentative answer to this dilemma is advanced in Section 108 (h) (2) of S.2755. This subsection provides for inclusion in the drug entity monograph of a requirement that, in order to obtain a license to manufacture a drug product under that monograph, any person might be compelled to conduct scientific investigations relating to other uses of the drug—even uses that the manufacturer may not wish to endorse. On both moral and economic grounds, we find it difficult to agree with this approach.

Later on, however, under Section 201, the bill provides for the establishment of a National Center for Clinical Pharmacology. This new Center would fulfill a variety of research and training functions.

The language in the bill specifically states that either *"upon request or on its own initiative, the Center may conduct and support research in clinical pharmacology and clinical pharmacy, including investigations (1) of the safety and effectiveness of existing and new uses of drug products, ..."* The bill goes on to list several other meaningful roles that the Center would serve. But it is this first-stated purpose that is pertinent to this discussion. Note that its mandate specifically covers research on new uses for drugs to establish their safety and effectiveness for such purposes.

Expenditure of public funds to fulfill this need appears justified and in the best interest of all parties concerned: the government, the drug industry, the health care professions, and the general public. Not only is the problem evident, but so too is its solution.

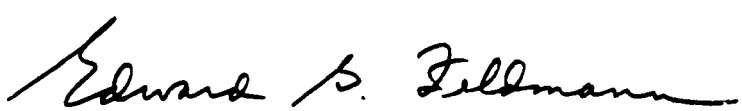

Bioequivalence and Interchangeability

The primary purpose of a bioequivalence study is to determine if two products containing the same active ingredient(s) in the same amount(s) can be used interchangeably. Contrary to prevailing opinion, we believe such studies are of doubtful value with regard to product substitution.

According to the current regulations, two drug products are deemed bioequivalent when their average bioavailabilities are similar. Appreciable individual differences in bioavailability are often tolerated as long as the overall means are similar. For example, in the proposed Bioequivalence Requirement for certain anticonvulsants[1] and tricyclic antidepressants[2], two products can be declared bioequivalent even though the relative bioavailability in half of the test subjects may differ by 25% or more. While intrasubject variation may contribute to the observed range in a given study, the possibility of a real difference among individuals cannot be denied.

In view of this fact, bioequivalence studies should be designed so that the mean subject response as a function of product performance can be assessed. In statistical terminology, this is called a subject-by-product interaction. The quantitative assessment of the significance of this effect requires a study design in which each product is replicated at least once in each subject. With this experimental design, differences in subject response due to product differences can be separated from those due simply to intrasubject variability. Unfortunately, this kind of design is rarely, if ever, used in bioequivalence studies[3]. Therefore, the frequency with which a subject-by-product interaction occurs among so-called bioequivalent products is not known.

Consider the implications of a situation where two products are deemed bioequivalent on average but a significant subject-by-product interaction exists. The substitution of one by the other would result in a loss of therapy or an increase in side effects in a significant fraction of the patient population. Thus, even though average bioequivalence may be an adequate guide to product selection on initiation of therapy, it is far from reassuring as the basis for product substitution.

Although the proposed change in experimental approach would represent an improvement in the state of the art, it is not without practical limitations. In particular, this approach only reduces the risk of inappropriate substitution for the population but fails to warrant the appropriateness of a particular substitution in a given patient. The only way to maintain adequate therapy with substitution is to retitrate the patient. This approach causes unnecessary burdens on both the patient and the physician. In our view, substitution, with proper assurances, is more costly than the difference in the price of a prescription.

In summary, if the intent of bioequivalent studies is to assure product interchangeability, the current criterion is necessary but insufficient. Additional studies with improved experimental designs would strengthen the scientific basis for substitution, but the continuation of proper therapy cannot be assured for all patients. The need for dose titration is understood on initiation of therapy and is similarly indicated upon product substitution. Common sense suggests that once titrated and maintained on a product, patients should remain on that product.

S. Hwang
P. B. Huber
M. Hesney
K. C. Kwan
Merck Sharp & Dohme
Research Laboratories
West Point, PA 19486

Received April 18, 1978.

[1] *Fed. Regist.*, 39677 (Aug. 6, 1977).
[2] *Fed. Regist.*, 6967 (Feb. 17, 1978).
[3] R. G. Stoll, R. A. Schwartz, G. C. Chao, A. Yacobi, D. J. Weidler, J. W. Ayres, E. Sakmar, M. R. Hallmark, and J. G. Wagner, *Clin. Pharmacol. Ther.*, **23**, 131 (1978).

JOURNAL OF PHARMACEUTICAL SCIENCES

JUNE 1978
VOLUME 67 NUMBER 6

RESEARCH ARTICLES

Structure–Activity Studies of Barbiturates Using Pattern Recognition Techniques

A. J. STUPER * **and P. C. JURS** ˣ

Received August 31, 1977, from the *Department of Chemistry, Pennsylvania State University, University Park, PA 16802.* Accepted for publication September 29, 1977. *Present address: Research Laboratories, Rohm and Haas Co., Spring House, PA 19477.

Abstract □ The relationship between molecular structure and duration of depressant effect for barbiturates was investigated. A data set of 160 5,5′-disubstituted barbiturates with various acyclic substituents was coded using 47 numerical descriptors including fragments, substructures, environmental descriptors, and molecular connectivity indexes. All descriptors were derived directly from the connection tables of the barbiturates. Using an interactive error-correction feedback algorithm, linear discriminant functions were developed that could dichotomize the data set with respect to several thresholds separating longer from shorter acting compounds. Feature selection was used to focus on the relatively few structural descriptors sufficient to support linear separability. For three specific thresholds, nine, 11, and nine descriptors were sufficient. The importance of these descriptors and the utility of the technique are discussed. Predictive abilities of approximately 94% were obtained for known barbiturates of the same general molecular types.

Keyphrases □ Structure–activity relationships—various barbiturates, prediction of duration of depressant effects using pattern recognition system based on structural descriptors □ Barbiturates, various—prediction of duration of depressant effects using pattern recognition system based on structural descriptors □ Pattern recognition system—based on structural descriptors, applied to prediction of duration of depressant effects of various barbiturates

The study of systematic alteration of molecular structure and its effect on biological activity has been of interest since the first drug was discovered. The pursuit of compounds with enhanced activity often requires choices between several possible alternatives made by reliance on the intuition and experience of the chemist. Although intuitive procedures have produced many new and useful compounds, they are not necessarily the optimal method of enhancing biological activity. Recently, there have been attempts to quantify this procedure through methods that predict a compound's action based on the results obtained for compounds of similar structure. The information provided by such methods can be used as an indication of whether a particular alteration holds promise. The best known of these procedures is Hansch analysis (1, 2).

Hansch analysis provides a means of relating the change in the level of biological activity with changes in the physical and chemical properties of a series of drug molecules. This analysis is accomplished by fitting the relative biological responses, A_i, to an equation of the form:

$$\log (A_i) = a(\log P)^2 + b \log P + \rho\sigma + cE_s + d \qquad \text{(Eq. 1)}$$

where P is the octanol–water partition coefficient, σ is the Hammett constant for the substituents under study, E_s is the Taft steric parameter, and a, b, c, d, and ρ are constants determined by multiple linear regression.

Recent reports indicated an alternative method of elucidating structure–activity relationships. Hansch *et al.* (3) discussed application of hierarchial clustering techniques to substituent selection. Ting *et al.* (4) reported correlations between the low-resolution mass spectra of 66 drugs and their activity as sedatives or tranquilizers.

Applications of pattern recognition to investigations of structure–activity relations have been reported by using substructural parameters as descriptors of biological action (5–7). Other examples of using structurally derived parameters in studies involving pattern recognition also exist (8, 9). Several methods of pattern recognition were applied to a set of compounds of accepted therapeutic utility, and the application of pattern recognition methods to structure–activity studies of pharmaceuticals was discussed (10, 11). While objections to some methods used to describe the data sets have arisen (12–14), there is almost universal agreement that a compound's activity is related to its structure.

The present study demonstrates the application of an interactive pattern recognition system to the development of rules that predict the duration time of barbiturate action on the basis of information provided solely from the molecular structure. The results of classification are used further to deduce which of the given parameters are most effective in the determination of these rules. Also, the potential of the method for augmentation of chemical intuition is discussed.

Table I—List of Compounds Forming the Data Set

Compound	R_2	Duration, min	Compound	R_2	Duration, min
		$R_1 = CH_3$			
1	$(CH_3)_3CCH$	580	2	$CH_3(CH_2)_5$	260
3	$CH_3(CH_2)_3CH(CH_3)$	227	4	$CH_3(CH_2)_3CH(CH_3CH_2)CH_2$	223
5	$H_2C{=}C(CH_3)$	60	6	$CH_3CH{=}C(CH_3)$	120
7	$CH_3CH_2HC{=}C(CH_3)$	60	8	$CH_3HC{=}C(CH_3CH_2)$	60
9	$CH_3(CH_2)_2HC{=}C(CH_3)$	60	10	$(CH_3)_2CHC{=}C(CH_3)$	36
11	$CH_3(CH_2)_3HC{=}C(CH_3)$	24	12	$CH_3CH_2SCH_2$	330
13	$CH_3(CH_2)_3SCH_2$	150			
		$R_1 = CH_3CH_2$			
14	CH_3CH_2	1400	15	$CH_3CH_2CH_2$	1140
16	$CH_3CH(CH_3)$	1520	17	$CH_3CH_2CH_2CH_2$	450
18	$CH_3CH(CH_3)CH_2$	540	19	$CH_3CH_2CH(CH_3)$	600
20	$CH_3CH_2CH_2CH_2CH_2$	220	21	$CH_3CH_2CH(CH_3)CH_2$	190
22	$(CH_3)_3CCH_2$	200	23	$CH_3CH_2CH(CH_3CH_2)$	300
24	$CH_3(CH_2)_5$	45	25	$CH_3(CH_2)_2CH(CH_3)CH_2$	210
26	$CH_3CH_2C(CH_3)_2CH_2$	60	27	$CH_3(CH_2)_3CH(CH_3)$	90
28	$CH_3CH_2CH(CH_3CH_2)CH$	300	29	$CH_3(CH_2)_6$	120
30	$(CH_3)_2CHCH_2CH(CH_3)CH_2$	54	31	$(CH_3)_2CH(CH_2)_2CH(CH_3)$	50
32	$CH_3CH_2CH(CH_3)CH_2CH(CH_3)$	74	33	$CH_3(CH_2)_2CH(CH_3CH_2CH_2)$	81
34	$CH_3(CH_2)_2CH(CH_3)CH_2CH_2CH_2$	60	35	$CH_3CH_2CH(CH_3)CH_2CH(CH_3)CH_2$	60
36	$CH_3(CH_2)_3CH(CH_3CH_2)CH_2$	75	37	$CH_3(CH_2)_4CH(CH_3CH_2)$	60
38	$CH_3(CH_2)_5CH(CH_3)$	150	39	$CH_3(CH_2)_2CH(CH_3)CH(CH_3CH_2)CH_2$	240
40	$(CH_3)_2CH(CH_2)_2CH(CH_3CH_2)CH_2$	120	41	$H_2C{=}CH$	288
42	$H_2C{=}C(CH_3)$	150	43	$CH_3CH_2HC{=}CH$	18
44	$CH_3HC{=}C(CH_3)$	180	45	$(CH_3)_2C{=}CH$	240
46	$CH_3(CH_2)_2HC{=}CH$	96	47	$CH_3CH_2HC{=}C(CH_3)$	24
48	$(CH_3)_2CHHC{=}CH$	12	49	$CH_3HC{=}C(CH_3CH_2)$	42
50	$CH_3(CH_2)_2HC{=}C(CH_3)$	72	51	$CH_3(CH_2)_3HC{=}C(CH_3)$	6
52	$CH_3CH_2HC{=}C(CH_3CH_2CH_2)$	6	53	$H_2C{=}CHCH(CH_3)$	720
54	$H_2C{=}C(CH_3)CH_2$	326	55	$CH_3HC{=}CHCH_2$	372
56	$CH_3CH_2OCH(CH_3)$	460	57	$CH_3(CH_2)_2OCH(CH_3)$	150
58	$CH_3(CH_2)_3OCH(CH_3)$	150	59	$(CH_3)_3CCH_2OCH(CH_3)$	75
60	$CH_3CH_2OC(H_2C)$	200	61	$(CH_3)_3COC(H_2C)$	63
62	$CH_3(CH_2)_2SCH_2$	59	63	$(CH_3)_2CHSCH_2$	139
64	$H_2C{=}CHCH_2SCH_2$	117	65	$CH_3(CH_2)_3SCH_2$	66
66	$CH_3(CH_2)_4SCH_2$	75	67	$(CH_3)_3CCH_2SCH_2$	37
68	$CH_3(CH_2)_2CH(CH_3)SCH_2$	62	69	$CH_3(CH_2)_5SCH_2$	15
70	$(CH_3CH_2)_2CHCH_2SCH_2$	22	71	$CH_3CH_2SCH(CH_3CHCH_3)$	12
72	$CH_3(CH_2)_3SCH(CH_3)$	34	73	$CH_3(CH_2)_3SCH(CH_3CH_2)$	52
74	$CH_3(CH_2)_4SCH(CH_3)$	28	75	$(CH_3)_3CCH_2SCH(CH_3)$	41
76	$CH_3(CH_2)_2CH(CH_3)$	180			
		$R_1 = CH_3CH_2CH_2$			
77	$CH_3CH_2CH_2CH_2CH_2$	4	78	$CH_3CH_2CH(CH_3)CH_2$	165
79	$CH_3(CH_2)_5$	1	80	$CH_3(CH_2)_6$	15
81	$CH_3HC{=}CH$	60	82	$CH_3CH_2HC{=}CH$	18
83	$(CH_3)_2CHHC{=}CH$	18	84	$H_2C{=}C(CH_3)$	168
85	$CH_3HC{=}C(CH_3)$	30	86	$CH_3CH_2HC{=}C(CH_3)$	18
87	$CH_3HC{=}C(CH_3CH_2)$	24	88	$H_2C{=}CHCH(CH_3)$	420
89	$H_2C{=}C(CH_3)CH_2$	300	90	$CH_3HC{=}CHCH_2$	120
91	$CH_3CH_2OCH(CH_3)$	162	92	$CH_3CH_2SCH_2$	150
93	$CH_3(CH_2)_3SCH_2$	76	94	$CH_3(CH_2)_3SCH(CH_3)$	35
95	$(CH_3)_2CHCH_2SCH(CH_3)$	45			
		$R_1 = (CH_3)_2CH$			
96	$(CH_3)_2CHCH_2$	25	97	$CH_3HC{=}CH$	36
98	$CH_3CH_2HC{=}CH$	36	99	$CH_3(CH_2)_2HC{=}CH$	18
100	$(CH_3)_2CHHC{=}CH$	12	101	$CH_3CH_2HC{=}C(CH_3)$	18
102	$CH_3C{=}C(CH_3CH_2)$	18	103	$H_2C{=}CHCH(CH_3)$	210
104	$CH_3HC{=}CHCH_2$	200	105	$CH_3CH_2SCH_2$	86
106	$CH_3(CH_2)_3SCH_2$	38			
		$R_1 = CH_3(CH_2)_3$			
107	$CH_3CH_2CH(CH_3)$	16	108	$(CH_3)_3C$	1
109	$CH_3HC{=}CH$	12	110	$CH_3CH_2HC{=}CH$	18
111	$H_2C{=}C(CH_3)$	90	112	$CH_2HC{=}C(CH_3)$	60
113	$H_2C{=}CHCH(CH_3)$	110	114	$CH_3HC{=}CHCH_2$	40
115	$(CH_3)_2C{=}CHCH_2$	30	116	$CH_3CH_2OCH(CH_3)$	120
		$R_1 = CH_3(CH_2)_3$			
117	$CH_3CH_2SCH_2$	74	118	$CH_3(CH_2)_3SCH_2$	95
		$R_1 = H_2C{=}CH$			
119	$CH_3CH_2CH_2CH_2$	288	120	$(CH_3)_3CCH$	192
		$R_1 = H_2C{=}CH(CH_3)$			
121	$H_2C{=}CHCH_2$	102	122	$(CH_3)_2CHCH_2$	90
123	$CH_3CH_2CH_2CH_2$	30	124	$(CH_3)_3CCH$	18
		$R_1 = CH_3HC{=}C(CH_3)$			
125	$H_2C{=}CHCH_2$	30			

Table I—(*Continued*)

Compound	R_2	Duration, min	Compound	R_2	Duration, min
		$R_1 = H_2C{=}CHCH_2$			
126	$CH_3(CH_2)_3CH(CH_3)$	108	127	$H_2CHCH(CH_3)$	456
128	$CH_3CH_2OCH(CH_3)$	300	129	$CH_3CH_2OC(CH_2)$	300
130	$CH_3(CH_2)_2OCH(CH_3)$	204	131	$(CH_3)_3CCH_2OCH_2$	900
132	$H_2C{=}C(CH_3)CH_2$	380	133	$CH_3CH_2SCH_2$	164
134	$CH_3(CH_2)_2SCH_2$	117	135	$CH_3(CH_2)_3SCH_2$	123
136	$CH_3(CH_2)_3SCH(CH_3)$	34	137	$(CH_3)_2CHCH_2$	162
138	$(CH_3)_3CCH_2$	96	139	$H_2C{=}CHCH_2$	880
140	$(CH_3)_2CH$	720	141	$CH_3(CH_2)_2CH(CH_3)$	150
		$R_1 = CH_3HC{=}CHCH_2$			
142	$(CH_3)_3CCH$	40	143	$CH_3(CH_2)_2CH(CH_3)$	66
144	$CH_3CH_2CH(CH_3)$	120	145	$(CH_3)_3CHCH_2$	45
		$R_1 = (CH_3)_2C{=}CHCH_2$			
146	$(CH_3)_2C{=}CHCH_2$	70	147	$CH_3CH_2CH(CH_3)$	120
		$R_1 = CH_3CH_2OCH(CH_3)$			
148	$(CH_3)_3CCH_2$	102	149	$CH_3(CH_2)_2CH(CH_3)$	108
		$R_1 = CH_3(CH_2)_2OCH(CH_3)$			
150	$CH_3CH_2CH_2CH(CH_3)$	300			
		$R_1 = CH_3SCH_2$			
151	$(CH_3)_2CHCH_2$	108			
		$R_1 = CH_3CH_2SCH_2$			
152	CH_3CH_2	143	153	$(CH_3)_2CHCH_2$	81
154	$CH_3CH_2CH(CH_3)$	61	155	$(CH_3)_3CCH_2$	8
156	$CH_3(CH_2)_2CH(CH_3)$	35			
		$R_1 = CH_3CH_2SCH(CH_3)$			
157	$CH_3(CH_2)_5$	12			
		$R_1 = H_2C{=}CHCH_2SCH(CH_3)$			
158	$(CH_3)_2CHCH_2$	28			
		$R_1 = CH_3(CH_2)_3SCH_2$			
159	$(CH_3)_2CHCH_2$	78	160	$CH_3CH_2CH(CH_3)$	69

METHOD OF APPROACH

The assumptions underlying the pattern recognition approach to structure–activity studies are similar to those of Hansch analysis. The factors that govern the activity of a compound are viewed as combinations of a molecule's electronic, steric, and lipophilic properties. It is felt, however, that the structure of the molecule is the overriding factor in the determination of a compound's physical properties and, therefore, its biological activity. Thus, it should be possible to decompose a structure into a set of descriptors that provide information correlating to biological activity.

This approach involves two problems: (*a*) how to develop parameters that relate structural modifications to changes in biological activity, and (*b*) what type of method to use in defining these relationships once sufficiently informative parameters are found.

Several types of descriptors that can be derived directly from the molecule structure are available. Methods for their development were reported previously (15).

In the present study, binary pattern classifiers were employed to develop a relationship between structure and biological action. Use of these classifiers in the form of a linear learning machine was described in detail elsewhere (16–18). Implementation involves representing the ith molecular structure as an n dimensional vector, $X_i = (x_1, x_2, x_3, \ldots, x_n)$, such that each component, x_j, is the value of one structural descriptor. Thus, each compound is represented as a point in n space whose position is determined by its structural descriptors. The assumption is that compounds of similar activity will cluster in the same general region of space. Earlier studies indicated that this clustering occurs for parameters described in Ref. 15, as well as those used in Hansch analysis (7, 8).

If two clusters can be separated from each other by a linear surface (hyperplane), they are said to be linearly separable. In practice, discrimination between clusters is made by calculating the dot products of the data vectors with a weight vector, W, normal to the surface of the hyperplane. All data vectors on one side of the plane will have a positive dot product; all those on the opposite side will have a negative dot product. A separating plane can be developed by choosing an initial weight vector and iteratively correcting it until all members of a cluster have the same dot product sign. Once such a surface is developed, it can be used to predict the cluster to which an unknown belongs.

Since any member of the data set not used to develop the discriminant surface is effectively an unknown, the data set itself can be used to estimate the predictive ability of the discriminant. This step is accomplished by dividing the data into two sets, one to develop the discriminant (training set) and one to test the ability of the discriminant to classify unknowns (prediction set) correctly.

The best measure of predictive ability is obtained by leaving out one compound and using the remaining compounds as the training set. The surface developed from the training set is used to predict the cluster into which the remaining (and, therefore, unknown) compound belongs. This procedure is continued until each member of the data set has been left out of the training set once. The predictive ability is the number of correct classifications divided by the total number of classifications. For a finite set, this method is considered the most unbiased estimator of predictive ability (19, 20). Approximations to this measurement can be made by repeating the process several times using a larger prediction set.

Since no assumptions regarding the distribution of the data are required, the use of a linear surface to discriminate between several classes (clusters) present in the data is a quite general approach. Such methods are termed nonparametric. Discussions of the capabilities and limitations of nonparametric methods of discriminant development can be found elsewhere (16–18).

The linear learning machine, as well as the descriptor development routines used in this study, is currently implemented in a general interactive pattern recognition package called ADAPT[1], coded in FORTRAN IV. A detailed discussion of the architecture of this system was given elsewhere (21).

DATA SET

The set of compounds consisted of 160 5,5′-disubstituted barbiturates (Table I) selected from a standard reference (22). These compounds range in molecular weight from 172 to 276 and have durations of action ranging from 10 to 1600 min. Administration was either intraperitoneal or subcutaneous, using mice, rats, or rabbits. The fact that this data set is heterogeneous in mode of administration and test species but can still be dealt with using pattern recognition methods illustrates one strength of the approach. The methods employed in pattern recognition will often allow study of incomplete, ill-defined, or otherwise imperfect sets of compounds, while many other more rigorous methods demand better quality data sets. The success enjoyed in analyzing this barbiturate data

[1] Executed on the Pennsylvania State University Department of Chemistry MODCOMP II/25 computer.

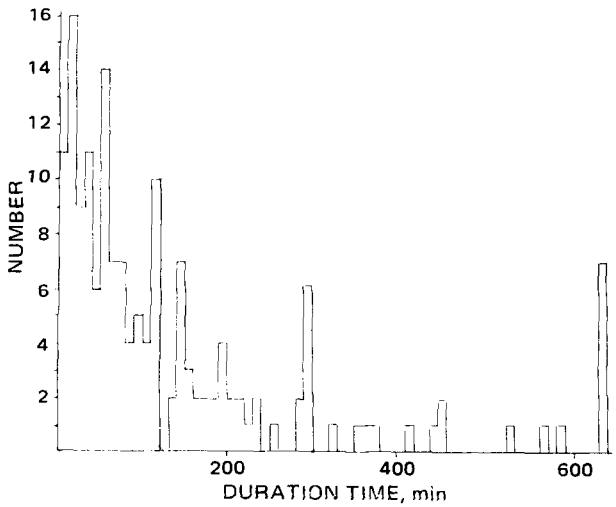

Figure 1—*Histogram of barbiturate duration times.*

set is meant to indicate how pattern recognition methods can be used; it is not meant to point out how to synthesize new barbiturates.

The compounds were grouped into classes according to the duration of depressant effect. These classes were formed by dividing the duration time, expressed in minutes, by 10. The resulting class designation was rounded up if the remainder was five or greater and down otherwise. Thus, a compound whose duration time was 227 min was placed in Class 23, whereas a compound having a duration time of 223 min was placed in Class 22. Compounds with a duration greater than 650 min were placed in Class 65. This approach resulted in a total of 65 different classes, distributed as shown in Fig. 1.

Four types of descriptors were employed for these studies; numeric fragment descriptors, substructural descriptors, environmental descriptors, and molecular connectivity descriptors (Table II). The descriptors were generated using the automated descriptor packages described previously.

While the nature of the atom, bond, and substructural descriptors is obvious, further comment is necessary regarding the environment and molecular connectivity descriptors. The environment descriptor takes into account how different parts of the molecule are connected by providing a measure of the local environment of a single atom fragment. This analysis is accomplished by combining the fragment's first and second nearest neighbors and their bonds into a single parameter that reflects the chemical environment around the fragment. Three types of environment descriptors are employed: the bond environment descriptor (BED), which uses only the number of bonds to calculate a descriptor value; the weighted environment descriptor (WED), which uses the type of bond in the calculation; and the augmented environmental descriptor (AED), which uses both the type of atom and type of bond in the calculation. Further discussion of these descriptors is given in Ref. 15.

The molecular connectivity descriptor provides a measure of the connectivity for the entire molecule. The concept was developed by Randic (23) and used in structure–activity studies (24, 25). A number of correlations between the molecular connectivity and several different physical parameters were described (23–29). The connectivity index is calculated directly from the connection table representation of the molecules as described in Ref. 25. In the present study, the simple index, the index corrected for rings, and the square of these indexes were used as descriptors. Ring correction was accomplished by subtracting from the simple index a value equal to the average of the contributions from all bonds contained in a ring. The descriptors were then multiplied by 10 and truncated to integer values.

Thus, the data set consists of 160 compounds, each coded with 47 descriptors. In no case does any one descriptor, or any binary combination of descriptors, contain sufficient information to classify the data successfully. Preprocessing of the raw data prior to classification consisted of autoscaling so that each descriptor had an average of zero and a standard deviation of 127. This method allowed the data to be truncated to integer values with a negligible loss of precision (recalculation after truncation yielded a standard deviation of 127 and a mean of 0 ± 0.17).

The learning machine requires that a constant-valued descriptor be added to the data set. A value of 250 was used because it provided for fast training and high predictive abilities. This parameter is discussed further in Ref. 30.

Table II—Molecular Structure Descriptors

Atom and Bond Descriptors			
1	Number of atoms	2	Number of bonds
3	Number of carbon atoms	4	Number of nitrogen atoms
5	Number of oxygen atoms	6	Number of single bonds
7	Number of double bonds	8	Length[a]

	Environment Descriptors		
	Atom Centered Fragment	**General[b]**	**Cyclic**
9–11	CH_3	A–C	—
12–14	CH_2	A–C	—
15–17	CH	A–C	—
18–23	C	A–C	A–C
24–26	O=	A–C	—
27–29	HC=	A–C	—
30–35	>C=	A–C	A–C

Substructural Descriptors					
36	CH_3CH_2	37	$CH(CH_3)CH_2$	38	CH_3
39	CH_2	40	CH_2CH_2	41	$CH_3CH_2CH_2$
42	CH	43	HC=		
Molecular Connectivity Descriptors[c]					
44	MC1	45	MC2	46	MC3
47	MC4				

[a] Length = 4* (number of single bonds) + 2* (number of double bonds). [b] A is the bond environment descriptor, B is the weighted environment descriptor, and C is the augmented environmental descriptor. [c] MC1 is the simple index, MC2 is the ring corrected index, MC3 is the square of the simple index, and MC4 is the square of the ring corrected index.

RESULTS

The duration of the barbiturate depressant effect is highly dependent on the conditions under which a compound is tested. The data compiled for this study represent a series of studies on different animals at different laboratories, so a large degree of variation within the data is expected. However, several series of compounds were tested as a group and, therefore, trends in the duration correlating to structural alterations may exist.

To account for these variations, any one classifier will develop a discriminant that answers the question: "Is the duration time less than x minutes?" Compounds within 30 min of this duration time are not used to develop the discriminant. With the class designations formed as noted previously, there are 61 possible ways of forming two clusters (longer or shorter than duration x) such that a gap of three classes lies between the clusters. Initial studies showed that it was possible to develop discriminants for each of these 61 cluster sets; however, only three such sets will be used to demonstrate the method.

Set I assigned all members in Classes 1–10 to the short duration cluster and 14–65 to the long duration cluster, Set II assigned classes 1–20 to the short duration cluster and 24–65 to the long duration cluster, and Set III assigned Classes 1–24 to the short duration cluster and 28–65 to the long duration cluster. With these three sets, discriminants can be developed to classify compounds as having a duration less than 100 min, less than 200 min, or less than 240 min. Compounds belonging to a class of longer duration would not be assigned to any of these duration regions.

One method of assessing the reliability of these discriminant functions is to subdivide each of the three sets such that each successive group contains more members in the prediction set and fewer members in the training set. These groups can be used to estimate the predictive ability and to determine which descriptors support the discriminant function's ability to separate the cluster of short duration barbiturates from those of long duration. If, within each set of clusters, the descriptors selected vary significantly and the predictive abilities are quite different, it would be clear that no clusters actually existed and that no relation between the structure and duration was found.

Results for the predictive ability tests and for feature selection using Descriptors 1–43 are shown in Table III. The portion of the data placed into the prediction set is indicated at the top of each column. Equal percentages of both the long and short duration clusters were taken to form these sets. The remaining members were placed into the training set. Ten such sets were formed for each percentage group. The highest predicting of these sets was used to select the features responsible for the discriminant's ability to classify the data.

Table III—Comparison of the Descriptors Retained for Each Cluster Set

	Set I				Set II				Set III			
Descriptor	Total	10%	15%	20%	Total	10%	15%	20%	Total	10%	15%	20%
1									×			
2												×
3	×											
5		×	×	×	×	×		×	×	×	×	×
6	×	×	×				×	×	×		×	
7	×	×	×	×	×	×	×	×		×	×	×
8					×				×			
9			×	×								
10		×	×				×					
11					×	×			×			
12	×											
14			×									
15	×	×	×	×	×	×	×	×	×			
16					×	×	×	×	×		×	
17								×				
19									×			
20					×							
21						×						
23					×		×		×			
27	×	×	×	×							×	
28		×	×							×		×
30								×	×		×	
32	×	×		×				×	×	×	×	×
33		×			×	×	×					
34			×	×	×		×		×	×	×	×
35	×			×		×	×	×	×	×	×	×
36	×	×	×	×								
37								×		×	×	×
38				×					×	×	×	×
39	×	×		×		×	×					
40					×			×	×	×	×	×
41			×									
42					×	×	×	×				
43	×		×		×	×	×	×				
Reference[a]												
Initial	—	100	95.5	96.6	—	100	100	96.8	—	100	95.4	96.9
Final	—	100	100	100	—	100	100	93.6	—	100	95.4	96.9
Total set[b]												
Initial	—	92.0	88.2	89.0	—	91.9	90.4	91.0	—	91.9	93.3	93.4
Final	—	92.7	91.8	92.4	—	94.4	93.0	92.9	—	95.0	95.4	95.3

[a] Predictive ability for feature selection reference set. [b] Average predictive ability for the 10 prediction sets within each percentage group.

Feature selection was accomplished using the variance feature selection method (30). The retained descriptors are indicated by an ×. The predictive ability is the average for all 10 sets before and after the feature selection process. Total refers to the results of feature selection using all members of each cluster. Reference refers to the results for the one prediction and training set used in feature selection. The members of this prediction set were never used to develop the discriminant function and, therefore, represent total unknowns.

The molecular connectivity descriptors (Descriptors 44–47) were not included in these initial studies to keep the ratio of compounds to descriptors above 3:1. This step is necessary to ensure that a nontrivial discriminant function is developed (31). To include Descriptors 44–47, a reduced set of the first 43 descriptors was chosen. This was accomplished for each set by pooling those descriptors from Table III that were selected three or more times. Using these as the initial descriptors, each set of clusters was feature selected using the variance method. The resulting descriptors represent a minimum set; that is, if any selected descriptors are excluded from the training process, a linear discriminant function that separates the data cannot be developed. Descriptors 44–47 were then added to these reduced sets, and each was once again subject to variance feature selection. The descriptors ultimately selected for each set of clusters is shown in Table IV. Predictive abilities were estimated using the leave-one-out procedure.

Table V lists the mean values, autoscale factors, and weight vectors for the Set I discriminant. To predict whether an unknown has an activity of less than 100 min, the descriptors from Table IV are generated and

Table IV—Descriptors Selected for Cluster Sets I–III

Set I		Set II		Set III	
Atom and Bond Descriptors		Atom and Bond Descriptors		Atom and Bond Descriptors	
Number of oxygen atoms Number of double bonds		Number of oxygen atoms Number of double bonds		Number of oxygen atoms	
Substructural Descriptors	Environment Descriptors[a]	Substructural Descriptors	Environment Descriptors[a]	Substructural Descriptors	Environment Descriptors[a]
CH_3CH_2	CH_3 (General B) HC (General A) >C= (General C) >C= (Cyclic A) HC= (General A)	CH_3CH_2 HC HC=	CH_3 (General C) HC (General B) >C= (Cyclic A) >C= (Cyclic C)	CH_3 CH_2CH_2 $CH(CH_3)CH_2$	HC (General A) HC = (General A) >C= (General C) >C= (Cyclic C)
Molecular Connectivity[b]		Molecular Connectivity[b]		Molecular Connectivity[b]	
MC2 Average 93.8% predictive ability		MC4 Average 92.9% predictive ability		MC4 Average 93.7% predictive ability	

[a] See footnote *b* of Table II. [b] See footnote *c* of Table II.

Table V—Weight Vector and Normalizing Factors for Cluster Set I

Descriptor	Mean Value	Mult/Sigma	Weight Vector
5	3.907	431.4560	−0.2197
7	3.527	220.8830	−0.4915
10	18.376	15.6835	0.0441
15	8.457	13.7709	−0.2994
27	5.527	16.4919	0.4415
32	112.648	11.4809	0.2787
33	45.994	104.7780	0.2545
36	1.333	158.7940	−0.1682
45	63.752	15.3582	0.5009
$n + 1$	250		0.0453

these values are scaled by subtracting the mean value for that descriptor, multiplying the result by the normalizing factor, and truncating the results to integers. The result is a nine-component vector. By using a value of 250 as the 10th component, the dot product between this vector and the weight vector is calculated. If the sign of the dot product is positive, the activity is less than 100 min.

The calculation for the barbiturate having R_1 = ethyl and R_2 = *sec*-pentyl is given as an example. This compound is not part of the original data set and, therefore, constitutes an unknown. The duration is reported to be 180 min (32). Calculation of the descriptors in Set I yields the vector X = (3, 3, 19, 17, 0, 106, 47, 2, 71). Normalizing this vector yields X_n = (−41, −116, 9, 117, −91, −76, 105, 105, −42). Adding the extra component and calculating the dot products yield −30.6. Since the sign of the dot product is negative, the duration is estimated as being greater than 100 min. Discriminant functions can be used to predict activities and unknowns, as done here, using a simple calculation performed with a desk calculator (if the descriptors can be hand calculated).

DISCUSSION

The fact that discriminants could be developed successfully for a data set as diverse and heterogeneous as this one indicates that information concerning the duration of depressant effect is contained in the structures of these compounds. While it is possible to develop discriminant functions that show chance correlations (31), the experiments performed indicate that such correlations were not responsible for the behavior of the discriminants.

The reliability of relations found using nonparametric discriminant analysis is a function of the discrimination ability of the classifier. Discrimination ability is a measure of the classifier's ability to find a separating discriminant function. In each set studied, the learning machine could find a discriminant that separated short duration members from long duration members. If chance correlations were responsible for this separation ability, the features selected for the members in the training set would not support a separating discriminant for members of the training and prediction set. For each different training set in Table III, the descriptors chosen were similar. Additional experiments showed that these descriptors would support a discriminant that separated all members of the training and prediction sets. Thus, the structural features intrinsic to the development of a discriminant for the training set are also intrinsic to the relations for the prediction set.

The predictive ability of a discriminant is dependent on how the discriminant was developed. The linear learning machine does not necessarily provide a discriminant that yields the best predictive ability. While a training set may be linearly separable, there is an infinite number of separating discriminants. Thus, even though it is possible to use the descriptors selected by the training set to develop a discriminant for the prediction set, that fact does not imply that such a function will perform well. The predictive ability is a gauge of how well a discriminant will classify the data not used in developing that function. When developed from several different training sets, a discriminant developing chance correlations would demonstrate low or variable predictive ability. The studies described in Table III show that decreasing the number of members used to develop the discriminant function does not substantially degrade its predictive performance.

The discriminants developed by the learning machine are quite general. Not only can they distinguish between different structures, but they also can describe differences in duration between congeners. Structures 17, 20, and 24 constitute a congeneric series of increasing alkyl chain length. The fact that discriminants could be developed for all 61 possible divisions of the data set indicates that these compounds can be distinguished. Similarly, a branched series such as Compounds 16, 19, and 27 is accounted for. The duration of structural isomers such as Compounds 24, 25, and 27 and between Compounds 53 and 54 is also described.

In this light, it is interesting to investigate some of the six compounds that could not be accounted for using these descriptors. Compound 29 is a member of the series of Compounds 14, 15, 17, 20, and 24 and its duration time might be expected to be less than that for Compound 24. Its duration, however, deviates from the order implied by these compounds since it is unexpectedly large. Most likely, the differences in its activity can be attributed to changes in lipophilic properties due to the sizable side chain. Similarly, Compound 38 belongs to the series of Compounds 16, 19, and 27. Its duration also deviates from that implied by the other members in the series. Similar arguments can be made for Compounds 5 and 44, which do not fit the pattern followed by the remainder of the data set.

The ability to identify quickly those compounds differing from the larger body of data is an advantage of this approach to structure–activity studies. Once these differences are identified, they can be used to gain further information concerning the action of these compounds.

The structural parameters used in these studies appear consistent with the observed properties of the barbiturates. The lack of any dominant structural feature indicates a lack of specificity for the receptor site with which the compounds interact. The descriptors chosen through feature selection indicate that properties of chain length and the extent of branching are the major influences on barbiturate duration. The amount of shielding of the 5-position may be responsible for many of the lipophilic properties (33). Descriptors 32, 33, and 35 were included in the final sets of features for the three thresholds. These environment descriptors would extend to the secondary position of R_1 and R_2 and could conceivably account for this shielding. Similarly, the molecular connectivity descriptors provide information on the degree of branching which, in turn, can be related to lipophilic properties.

While it was not the intent to develop a discriminant for all barbiturates, evidence of the utility of the discriminants developed was provided by prediction of the activity of the compound having R_1 = ethyl and R_2 = *sec*-pentyl. The duration time of this compound was correctly predicted to lie between 100 and 200 min by using the discriminant given in Table V in combination with those from Sets II and III. Clearly, once a discriminant has been developed and the descriptors generated, the actual prediction process is quite straightforward.

A question naturally arises concerning the possibility of using the parameters from pattern recognition analysis to produce structures of a specific activity. A direct path to this goal is not possible. Table VI can

Table VI—Statistics for Final Set of Descriptors Selected for Cluster Set I

	Mean		Standard Deviation			
Descriptor	Compounds below Threshold[a]	Compounds above Threshold[a]	Compounds below Threshold[a]	Compounds above Threshold[a]	Highest Value	Lowest Value
5	3.04	3.18	0.24	0.38	4	3
7	3.52	3.54	0.56	0.61	5	3
10	19.91	16.19	9.00	7.55	41	0
15	8.56	8.34	9.26	9.30	36	0
27	6.50	4.15	9.20	5.40	29	0
32	114.96	109.35	13.20	8.78	141	102
33	46.16	45.77	1.17	1.13	49	43
36	1.37	1.28	0.82	0.78	3	0
45	66.24	60.21	9.70	8.00	81	42

[a] Fifty-six compounds in long duration cluster, and 90 in low duration cluster.

be used to demonstrate this statement. The table gives pertinent statistics for each feature used to define the duration of the barbiturates with respect to Set I. Listed are the standard deviation of the descriptors and the numerical average of the descriptor values. The highest and lowest values give information concerning the range of descriptor values.

Although the average values for the two classes differ from each other, the standard deviation is larger than this difference. Therefore, the individual descriptors, while providing structural information, are not the sole indicators of activity. With atom, bond, and substructural descriptors, the average value can be related directly to the structural composition of the molecule. However, average values for the environment and molecular connectivity descriptors are difficult or impossible to interpret because they are related to the structure in a complex manner.

Average values indicate only the relative presence of a particular descriptor and cannot be construed as indicating the amount necessary for activity. A case in point is the number of oxygen atoms in the molecule. This number ranges between three and four. The barbiturate ring accounts for three of these atoms. A value greater than three accounts for the number in the side chains. The fact that, on the average, the class of longer acting molecules contains slightly more oxygen atoms does not imply that adding oxygen guarantees an increase in the activity. The number, placement, and chemical environment of an oxygen govern its effectiveness, not its mere presence. If the activity of a molecule is to be described by use of structural parameters, each must be viewed as a single contribution to, rather than the single indication of, that action.

Since structurally derived descriptors reflect the composition of the structure, they are interdependent. Changes in composition generally affect the value of several structural parameters simultaneously. Most notably affected are the environment and molecular connectivity descriptors. However, substructural content is also affected by slight alterations in the structure. Such alterations affect the placement of the molecule in the space formed by its descriptors and, therefore, affect the results of classification. This effect occurs because the biological activity expressed as a function of the molecular structure is a vector representation of the descriptors describing that structure.

The discriminant developed from pattern recognition analysis can be thought of as a transform, which maps a structure vector onto one of the two cluster regions. The reverse mapping cannot be accomplished directly. Alternatively, structural descriptors can be viewed as indicating the electronic, steric, and lipophilic properties of a molecule. No one descriptor is an effective gauge of all of these properties. Each is a component in their description. Knowing these properties does not allow the direct construction of active molecules.

Although the parameters used in the pattern recognition analysis cannot be used directly to construct active molecules, they can be used to predict the effectiveness of hypothetical structures. This prediction offers a pragmatic aid in the synthesis problem; *i.e.*, given a choice of molecules that appear to be equally likely candidates for synthesis, how does one optimize the chances of synthesizing the most active. If a data base exists that details past successes and failures, then a plausible solution is to use the data base to develop rules that estimate the activity of a candidate structure. Since pattern recognition develops rules that define "similarity," application of the methods as described in the preceding sections will aid in the synthesis decision.

Another manner in which these techniques could prove useful is for large-scale prescreening. The derivation of structural parameters is rapid enough to allow several thousand prospective structures to be described and tested using a discriminant developed from a set of compounds known to be active. Those compounds that the discriminant notes as being the highest acting can then be considered for further testing. Prediction results from the sets studied indicate that such classifiers can perform with a high degree of reliability.

The ultimate purpose in the study of effects of structural alterations on biological action is to produce new, more effective compounds. Useful tools are those that produce information pertinent to this problem. Historically, the chemist has used a structural diagram of the molecule as a gauge for altering the structure. The number and diversity of active compounds attest to the success of this approach. Since the effectiveness of this approach is dependent on the judgment of the chemist, use of mathematical techniques to augment these judgments may well increase the effectiveness of this procedure.

REFERENCES

(1) W. J. Dunn, *Ann. Rep. Med. Chem.*, **8**, 313 (1973).

(2) G. Redl, R. D. Cramer Tert., and C. E. Berkoff, *Chem. Soc. Rev.*, **3**, 273 (1974).

(3) C. Hansch, S. H. Unger, and A. B. Forsythe, *J. Med. Chem.*, **16**, 1217 (1973).

(4) K. L. Ting, R. C. T. Lee, G. W. A. Milne, M. Shapiro, and A. M. Guarino, *Science*, **180**, 417 (1973).

(5) B. R. Kowalski and C. F. Bender, *J. Am. Chem. Soc.*, **96**, 916 (1974).

(6) K. C. Chu, R. J. Feldman, M. B. Shapiro, G. F. Hazard, Jr., and R. I. Geran, *J. Med. Chem.*, **18**, 539 (1975).

(7) A. J. Stuper and P. C. Jurs, *J. Am. Chem. Soc.*, **97**, 182 (1975).

(8) F. Darvas, *J. Med. Chem.*, **17**, 799 (1974).

(9) K. C. Chu, D. E. Goldender, and A. B. Rosonblit, *Comp. Biomed. Res.*, **6**, 411 (1973).

(10) A. Cammarata and G. K. Menon, *J. Med. Chem.*, **19**, 739 (1976).

(11) G. K. Menon and A. Cammarata, *J. Pharm. Sci.*, **66**, 304 (1977).

(12) C. L. Perrin, *Science*, **183**, 551 (1974).

(13) J. T. Clerc, P. Naegeli, and J. Seibl, *Chimia*, **27**, 639 (1973).

(14) S. H. Unger, *Cancer Chem. Rep., Part 2*, **4**, 47 (1974).

(15) W. E. Brugger, A. J. Stuper, and P. C. Jurs, *J. Chem. Inf. Comp. Sci.*, **16**, 105 (1976).

(16) N. T. Nilsson, "Learning Machines," McGraw-Hill, New York, N.Y., 1965.

(17) J. T. Tou and R. C. Gonzalez, "Pattern Recognition Principles," Addison-Wesley, Reading, Mass., 1974.

(18) R. O. Duda and P. E. Hart, "Pattern Classification and Scene Analysis," Wiley–Interscience, New York, N.Y., 1973.

(19) L. Kanal, *IEEE Trans. Inf. Theory*, **IT-20**, 697 (1974).

(20) P. A. Lachenbruch and R. M. Micke, *Technometrics*, **10**, 1 (1968).

(21) A. J. Stuper and P. C. Jurs, *J. Chem. Inf. Comp. Sci.*, **16**, 99 (1976).

(22) F. F. Blicke and R. H. Cox, "Medical Chemistry," vol. IV, Wiley–Interscience, New York, N.Y., 1959.

(23) M. Randic, *J. Am. Chem. Soc.*, **97**, 6609 (1975).

(24) L. B. Kier, W. J. Murray, and L. H. Hall, *J. Med. Chem.*, **18**, 1272 (1975).

(25) L. B. Kier and L. H. Hall, "Molecular Connectivity in Chemistry and Drug Research," Academic, New York, N.Y., 1976.

(26) L. B. Kier, L. H. Hall, W. J. Murray, and M. Randic, *J. Pharm. Sci.*, **64**, 1971 (1975).

(27) L. H. Hall, L. B. Kier, and W. J. Murray, *ibid.*, **64**, 1975 (1975).

(28) W. J. Murray, L. H. Hall, and L. B. Kier, *ibid.*, **64**, 1979 (1975).

(29) W. J. Murray, L. B. Kier, and L. H. Hall, *J. Med. Chem.*, **19**, 573 (1976).

(30) G. S. Zander, A. J. Stuper, and P. C. Jurs, *Anal. Chem.*, **47**, 1085 (1975).

(31) A. J. Stuper and P. C. Jurs, *J. Chem. Inf. Comp. Sci.*, **16**, 238 (1976).

(32) E. E. Swanson and W. E. Fry, *J. Am. Pharm. Assoc., Sci. Ed.*, **29**, 509 (1940).

(33) C. Hansch and S. M. Anderson, *J. Med. Chem.*, **10**, 745 (1967).

Spectrofluorometric Determination of Alkoxy-Substituted Benzylimidazolidinones in Biological Fluids

J. ARTHUR F. de SILVA ˣ, NANCY MUNNO, LUCIUS D'ARCONTE †, and NORMAN STROJNY

Received April 1, 1977, from the *Department of Biochemistry and Drug Metabolism, Hoffmann-La Roche Inc., Nutley, NJ 07110.* Accepted for publication September 8, 1977. †Deceased.

Abstract □ Sensitive and specific spectrofluorometric assays were developed for the determination of *d,l*-4-(3,4-dimethoxybenzyl)-2-imidazolidinone and *d,l*-4-(3-butoxy-4-methoxybenzyl)-2-imidazolidinone in blood and urine. Each compound is selectively extracted from buffered blood or urine and oxidized with alkaline permanganate to its respective fluorescent benzoic acid derivative, which is quantitated in acetic acid in ethanol (1:99). The method was applied to the determination of blood levels and urinary excretion in the dog following the administration of single intravenous and oral doses of each compound.

Keyphrases □ Imidazolidinones, substituted—spectrofluorometric analyses in biological fluids □ Spectrofluorometry—analyses, substituted imidazolidinones in biological fluids

The alkoxy-substituted benzylimidazolidinones *d,l*-4-(3,4-dimethoxybenzyl)-2-imidazolidinone (I) and *d,l*-4-(3-butoxy-4-methoxybenzyl)-2-imidazolidinone (II) (Scheme I) were synthesized by Gruenman and Hoffer (1). Compound I is of clinical interest because of its cardiovascular inotropic effects as a vasodilator and for increased cardiac output (2, 3) and as a hypolipemic agent (4), while II has shown activity as a phosphodiesterase inhibitor (5–9).

Although both compounds are aromatic in nature, neither their UV absorption nor intrinsic fluorescence nor phosphorescence was sufficiently intense to enable their quantitation as the intact moiety. Investigation of possible derivatization reactions prompted the use of oxidation in alkaline permanganate, involving the cleavage of the methylene (CH_2) bridge in these compounds to form strongly fluorescent benzoic acid derivatives (III and IV, Scheme I). A similar reaction was reported in the analysis of the dihydrofolate reductase inhibitor trimethoprim (10) used as a potentiator in antibacterial combinations with sulfonamides. The chemistry of these reactions is also amenable to assay automation (11).

Both I and II were readily oxidized to yield their respective benzoic acids (III and IV), which were dissolved in acetic acid in ethanol (1:99) and quantitiated spectrofluorometrically at 345 nm with excitation at 295 nm. The sensitivity limit of the assay is 0.25 μg of I or 0.10 μg of II/ml of blood or urine using a 4-ml specimen/assay.

The method was applied to the determination of blood levels and urinary excretion in the dog following the administration of single doses of I or II by intravenous and oral routes.

EXPERIMENTAL

Standard Solutions—The analytical standards required were: I, $C_{12}H_{16}N_2O_3$, mol. wt. 236.3, mp 152–153°, and II, $C_{15}H_{22}N_2O_3$, mol. wt. 278.36, mp 126–127°, both of pharmaceutical grade purity (>99%). 3,4-Dimethoxybenzoic acid (III) (veratric acid[1]), $C_9H_{10}O_4$, mol. wt. 182.18, mp 180–181°; and 3-butoxy-4-methoxybenzoic acid (IV), $C_{12}H_{16}O_4$, mol. wt. 224, mp 143°, purity >99%.

Ten milligrams each of I–IV were accurately weighed and transferred into separate 10-ml volumetric flasks and dissolved in 10 ml of ethanol. These stock solutions (A-1, A-2, A-3, and A-4) contained 1 mg of the respective compounds/ml. Dilutions (1:10) of each were made in ethanol to prepare working solutions (B-1, B-2, B-3, and B-4) containing 100 μg/ml.

Separate serial dilutions of B-3 and B-4 were made with 1% acetic acid–ethanol (1:99 v/v) to yield standard solutions in the concentration range of 0.25–5.0 μg/ml. These solutions were used to obtain a calibration curve for the determination of the efficiency of the alkaline potassium permanganate oxidation of I and II to their respective benzoic acids.

Instruments—The spectrofluorometer[2] used was equipped with a 150-w zenon arc energy source[3] and photomultiplier[4]. It was used with the 10-nm slit arrangement in all four positions, with the instrument energy adjusted for maximum sensitivity using a standard solution of III and IV.

Reagents—All inorganic reagents were analytical reagent grade. They were used without further purification and were prepared in distilled deionized water. These reagents included 1 *M* KH_2PO_4–$K_2HPO_4 \cdot 3H_2O$ buffer, pH 7.0 (12); 1 *M* H_3BO_3–Na_2CO_3–KCl buffer, pH 9.0, prepared as described previously (13); alkaline potassium permanganate solution (0.1 *M* in 0.1 *N* NaOH); 0.1 *N* HCl; 0.5 *N* HCl; 1.0 *N* H_2SO_4; 0.1 *N* NaOH; and 0.5 *N* NaOH.

The Dragendorff reagent used was a modification[5] from a published procedure (14) and was prepared as follows. Solution A was 0.85 g of bismuth nitrate dissolved in 10 ml of acetic acid and diluted to 50 ml with distilled water. Solution B was 20 g of potassium iodide dissolved in 50 ml of water. Five milliliters each of Solutions A and B were mixed and diluted to 50 ml with 10% H_2SO_4, followed by the addition of 0.1 ml of 30% H_2O_2 to hasten the "aging" of the solution. The solution must be "aged" for at least 24 hr prior to use. This reagent is stable for 3–4 months but should be discarded when an appreciable precipitation of iodine becomes apparent.

The organic reagents used were ethyl acetate[6] (spectrograde), ether[6] (absolute) from a freshly opened can, formaldehyde[7] (37% solution), alcohol[8] (USP 200 proof), and acetic acid in ethanol (1:99 v/v).

Analysis of I in Blood—Whole blood, 1–4 ml, was pipetted into a 50-ml centrifuge tube for analysis. Along with the samples, a specimen of control blood and duplicate specimens of control blood containing internal standards of 2.5 and 5.0 μg of I, added by evaporation to dryness at 40° under nitrogen of 0.025 and 0.05 ml of Solution B-1, were processed. Six milliliters of 1.0 *M* phosphate buffer (pH 7) was added to all specimens, which were then extracted with 2 × 15 ml of ethyl acetate.

The samples were extracted by shaking for 10 min on a reciprocating shaker and centrifuging at 2000 rpm in a refrigerated centrifuge at 5° for 10 min. The supernatant ethyl acetate was transferred into another 50-ml tube, and the extracts were combined. The combined ethyl acetate extract was evaporated to dryness. The residue was dissolved in 3 ml of 0.5 *N* HCl and backwashed with 2 × 5-ml portions of ether by mixing vigorously for 1 min on a variable speed test tube mixer[9]. Then the samples were centrifuged, and the ether supernate was discarded.

All samples and standards were neutralized by the addition of 1.5 ml

[1] Aldrich Chemical Co.

[2] Model Mark I spectrofluorometer equipped with a specially selected high UV energy source and photomultiplier, Farrand Optical Co., Mount Vernon, N.Y.

[3] Hanovia lamp, Engelhardt Industries, Newark, N.J.

[4] RCA IP-28 (lumen output 10) photomultiplier.

[5] R. Colarusso, E. Heylweil, and B. Z. Senkowski, Hoffmann-La Roche Inc., 1970, unpublished data on file.

[6] Mallinckrodt Chemical Co.

[7] Allied Chemical Co.

[8] Pharmaco, Division of Publicker Industries.

[9] Vortex Supermixer, Lab-Line Instruments, Melrose Park, Ill.

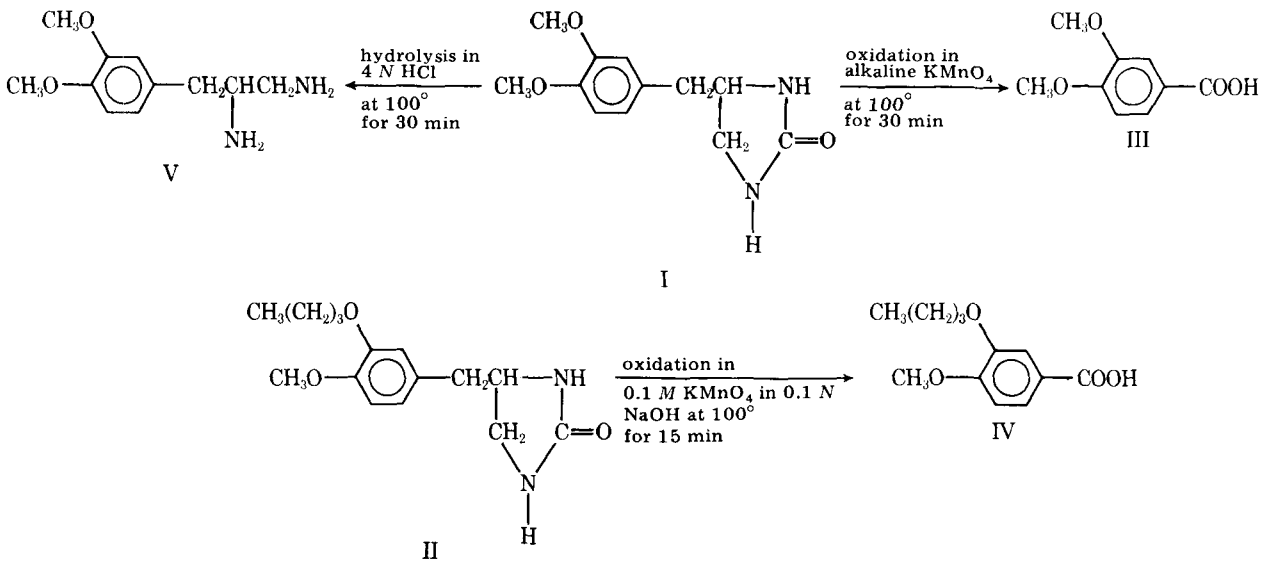

Scheme I

of 0.1 *N* NaOH, and all residual ether was expelled by placing tubes in a 90° water bath for approximately 10 min and shaking the tubes every few minutes. At this point, standard solutions of I may be included for the determination of the percent conversion to III.

One milliliter of 0.1 *M* alkaline $KMnO_4$ solution was added to each tube, and the tube was placed in a boiling water bath for 5 min. A second 1-ml aliquot of 0.1 *M* alkaline $KMnO_4$ solution was then added to all tubes, which were replaced in the water bath for 5 min until equilibrated and then stoppered. The tubes were allowed to remain in the boiling water bath for 30 min for completion of the oxidation reaction and then were removed and cooled in an ice bath.

A 0.2-ml aliquot of formaldehyde (37%) was then added to each tube to reduce the excess permanganate to manganous dioxide, forming a brown precipitate while decolorizing the pink solution. The tubes were mixed well and allowed to stand for 5 min, and then sufficient 1 *N* H_2SO_4 (~1–2 ml) was added to dissolve the manganous dioxide precipitate to manganous sulfate. The tubes were then extracted twice with 10 ml of ether by shaking for 10 min on a reciprocating shaker. The samples were centrifuged, and the ether extracts were combined in a 15-ml centrifuge tube by evaporating the extracts sequentially to dryness.

The residue was dissolved in 3 ml of acetic acid in ethanol (1:99 v/v), and the fluorescence of this solution was determined at 345 nm with excitation at 295 nm. The fluorescence readings were corrected for control (blank) fluorescence, and the concentration of the drug in the unknowns was determined by direct comparison of their fluorescence to that of the internal standards processed along with the unknowns.

Analysis of II in Blood—Whole blood, 1–4 ml, was pipetted into a 50-ml centrifuge tube for analysis. Along with the samples, a specimen of control blood and duplicate specimens of control blood containing 2.5 and 5 μg of II as internal standards (suitable aliquots of Solution B-2) were processed. Six milliliters of pH 9.0, 1 *M* borate KCl–Na_2CO_3 buffer was added to all specimens, which were then extracted with 2 × 15 ml of ether.

The samples were extracted by shaking for 10 min on a reciprocating shaker and centrifuging at 2000 rpm at 5° for 10 min. The supernatant ether was transferred into another 50-ml tube, and the extracts were combined. The combined ether extracts were evaporated to dryness, and the residues were dissolved in 2 ml of 0.1 *N* HCl. At this point, standard solutions of II may be included for the determination of the percent conversion to IV.

Each solution was made alkaline by the addition of 1.0 ml of 0.5 *N* NaOH, followed by the addition of 2.5 ml of 0.1 *M* alkaline $KMnO_4$ solution to each tube. The tubes were then placed in a 100° water bath for exactly 15 min to effect the oxidation of II to IV. The tubes were removed and cooled immediately in an ice bath. A 0.2-ml aliquot of formaldehyde (37%) was added to each tube, which was mixed well and allowed to stand for 5 min (as in the assay for I). The rest of the procedure for II was identical to that for I.

Procedure for Urine Samples—*Directly Extractable Unconjugated Fraction*—The extraction procedure for I from urine was identical to that for blood. The specimens for analysis were processed along with a control specimen and duplicate control specimens containing 2.5 and 5.0 μg of added authentic standards. For I, the residue of the ethyl acetate extract of urine was dissolved in 100 μl of ethanol and transferred quantitatively onto a 20 × 20-cm silica gel chromatoplate[10]; the centrifuge tube was rinsed with an additional 50 μl of ethanol to effect a quantitative transfer.

The chromatoplate was developed for 11–15 cm, ascending in chloroform–ethyl acetate–methanol (90:10:10). The sample areas corresponding to I were identified by reference to authentic standards (25 μg) of I run alongside the sample extracts ($R_f \simeq 0.50$), eluted into 5 ml of ethanol, and evaporated to dryness. The residues were dissolved in 3 ml of 0.5 *N* HCl, and the samples were processed as in the procedure for I, beginning with the neutralization step prior to the addition of alkaline permanganate.

The extraction of urine for II was carried out with ethyl acetate similarly to that for I. The residues were dissolved in 100 μl of ethanol and transferred to a silica gel chromatoplate as for I, and the plate was developed in benzene–methanol–acetic acid (90:10:10). After development, the sample areas for II were identified ($R_f \simeq 0.50$) and eluted with 3 ml of 0.1 *N* HCl, and a 2-ml aliquot was processed as described in the blood assay for II.

Conjugated Fraction—Following extraction of the unconjugated free fraction, the urine specimen was titrated to pH 5.3 and incubated at 37° for 2.5 hr with an enzyme preparation containing 150,000 units of glucuronidase and 50,000 units of sulfatase/ml[11] in a metabolic shaking incubator[12] to deconjugate any glucuronide–sulfate metabolites. The sample was extracted at pH 5.3 with the appropriate solvent and analyzed by TLC as described for I or II for acidic metabolites and then adjusted to pH 9.0, reextracted, and analyzed for basic metabolites.

An aliquot of the respective extracts was initially analyzed by TLC for the qualitative identification of metabolites using the procedure described below. A larger aliquot was then reanalyzed by TLC for the quantitation of metabolites (previously identified by R_f and their reaction to the Dragendorff treatment) by elution into methanol, followed by alkaline permanganate oxidation as previously described.

Qualitative Identification of I and II by TLC—Compounds I and II were difficult to detect on chromatoplates because of their poor UV absorption. For qualitative identification of I or II, the plate was sprayed with the modified Dragendorff reagent and heated in an oven at 100–104° for 30 min. The plate was then examined under short- and longwave UV light. Intact I and II and any metabolites containing the benzyl-2-imidazolidinone moiety were observed as bright blue-green to yellow fluorescent spots against a dark background. The visual sensitivity limit was about 0.5–1.0 μg of I or II.

This process is chemically destructive for II. However, when the addition product formed with I was eluted with ethanolic 0.5 *N* HCl (2:1) and examined fluorometrically, excitation and emission spectra similar

[10] E. Merck (F_{254}) silica gel G, 60-μm particle size, 250-μm bed thickness, Brinkmann Instruments, Westbury, N.Y.

[11] Glusulase, Endo Laboratories, Garden City, Long Island, N.Y.

[12] Dubnoff metabolic shaking incubator, GCA/Precision Scientific Instruments, Chicago, Ill.

Table I—Luminescence Properties of I and II and Their Benzoic Acid Derivatives

Compound	Solvent[a]	Fluorescence (25° C) Excitation/ Emission Maxima, nm	Fluorescence (25° C) Intensity, TM[b]/ μg/ml	Fluorescence (25° C) Sensitivity Limit, μg/ml	Phosphorescence (77° K) Excitation/ Emission Maxima, nm	Phosphorescence (77° K) Intensity, TM[b]/ μg/ml	Phosphorescence (77° K) Sensitivity Limit, μg/ml
I	1	280/315	80	1	285/455	1.2	20.0
	2	280/317	80	1	—	—	—
V	2	280/317	80	1	—	—	—
III	1	295/345	1500	0.1	290/435	550	0.050
II	1	280/315	80	1	285/440	3.3	10.0
	2	280/317	80	1	—	—	—
IV	1	295/345	1300	0.1	295/435	420	0.050

[a] Solvent 1 is acetic acid in ethanol (1:99), and Solvent 2 is ethanol–0.5 *N* HCl (2:1). [b] Fluorescence (TM) units = transmittance (T) × meter multiplier factor (M).

to those of authentic I were detected with about the same fluorescence quantum yield as I. Neither product was formed in solution with the Dragendorff reagent at either ambient or elevated temperature.

RESULTS AND DISCUSSION

The UV absorption spectra of I in 0.5 *N* HCl and 0.5 *N* NaOH showed a maximum of 228.5 nm ($A/\mu g/ml = 0.035$), a minimum at 253 nm, and a second maximum at 278.5 nm. The spectrum in ethanol showed a maximum at 231 nm ($A/\mu g/ml = 0.038$), a minimum at 253 nm, and a second maximum at 281 nm. The UV absorption spectra of II in ethanolic 0.5 *N* HCl and in 0.5 *N* NaOH showed a maximum at about 230 nm ($A/\mu g/ml = 0.026$ for ethanol) with a minimum at 250 nm and a second maximum at 280 nm. The weak UV absorption of these compounds, coupled with high blank values from biological samples, precluded its usefulness in an assay.

The luminescence properties of I and II and their respective benzoic acid derivatives were determined using the spectrofluorometer[2] modified to accommodate a Lewis–Kasha phosphoroscope as described previously (15) (Table I). Compounds I and II had weak intrinsic fluorescence and phosphorescence. The intrinsic fluorescence of I in ethanol–0.5 *N* HCl (2:1) (excitation 280/emission 317 nm) was linear with concentration in the range of 2.5–50.0 μg of I/ml of final solution. The sensitivity limit for blood or urine was 2.5–3.0 μg of I/ml using a 4-ml sample/assay and was not deemed sufficiently sensitive for pharmacokinetic studies. A similar direct assay of II was not feasible because the necessary "cleanup" by backwashing acid solutions of II results in losses of II and the unwashed samples have a high and variable background fluorescence.

Investigation of possible derivatives that could be used to measure therapeutic levels of I led to acid hydrolysis of I in 4 *N* HCl to 3-(3,4-dimethoxyphenyl)-2-aminopropylamine (V, Scheme I). This compound exhibited weak fluorescence properties similar to intact I and, therefore, was not investigated further. Alkaline hydrolysis did not yield any usable derivatives.

Oxidation of the methylene group of I with alkaline permanganate at 100° for 30 min, using a modification of a similar reaction in the assay of trimethoprim (10), produced >65% yield of III. The reaction product was characterized by two-dimensional thin-layer cochromatography with authentic III, using benzene–methanol–acetic acid (90:10:5) in the first dimension and ethyl acetate–methanol–concentrated ammonium hydroxide (90:10:5) in the second dimension. The alkaline permanganate oxidation reaction also was applicable to II.

The optimum yield of IV, about 65 ± 5.0%, was obtained by oxidation at 100° for exactly 15 min. Prolonged oxidation caused an apparent breakdown of IV and a decrease in the fluorescence. The reaction products were characterized by two-dimensional TLC, utilizing benzene–methanol–acetic acid (90:10:10) in the first dimension and ethyl acetate–ethanol–ammonium hydroxide (90:10:5) in the second dimension. One major product was detected with R_f values of 0.48 and 0.04 in the respective systems. This product ran as one spot when cochromatographed with authentic IV.

Two minor products were also seen on the chromatoplate[10]. Component 1, R_f 0.48 and 0.00, exhibited weak fluorescence with spectra similar to those of IV; Component 2, R_f 0.26 and 0.05, did not exhibit any significant fluorescence. Their chemical structures have not been elucidated. No residual unconverted parent compound was detectable on the plate at the R_f of II—*viz.*, 0.44 and 0.47 in the respective systems, indicating complete oxidation of the compound.

The benzoic acid derivatives III and IV exhibited strong fluorescence and phosphorescence in acetic acid in ethanol (1:99) (Table I). In each case, the fluorescence yield was linear with concentration in the range of 0.10–25 μg/3 ml of final solution. The intrinsic fluorescence was used as the basis for developing a sensitive assay in biological fluids.

Extraction of I from blood or urine at different pH values using different solvents yielded complete recovery at pH 7.0 in ethyl acetate but not in ether. When 0.5 *N* HCl was used to back-extract I into the acid as a cleanup step, I was completely recovered into the acid phase from ether but not from ethyl acetate. The overall recovery of 0.5–5.0 μg of I was about 92 ± 5% from 1 or 4 ml of blood when the blood was extracted into ethyl acetate at pH 7.0 and evaporated to a residue, the residue was dissolved in 0.5 *N* HCl, and the acid was backwashed with ether as a cleanup step; that from 1 or 4 ml of urine was about 86 ± 5%. However, the overall recovery of I taken through the entire assay, including oxidation in alkaline permanganate and measurement as III, was 60 ± 5% and reflects the limitation of the yield of this step. The complete evaporation of ether from the aqueous phase prior to oxidation was essential because the presence of ether or its peroxides reduced the permanganate with precipitation of manganous dioxide and resulted in incomplete and/or erratic

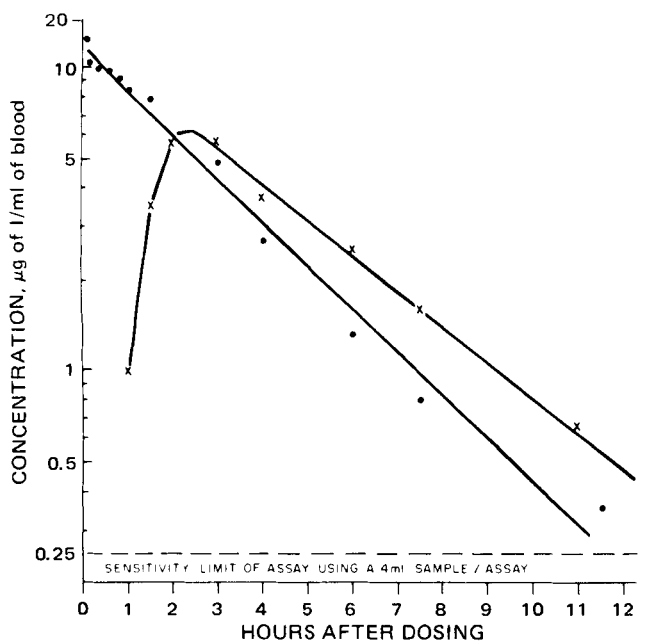

Figure 1—*Blood level fall-off curves of I in a dog following single intravenous (●) and oral (×) administration of a 100-mg dose.*

Table II—Urinary Excretion of I following the Administration of Single 100-mg Doses by Intravenous and Oral Routes

Route	Hours	Micrograms per Milliliter	Total, mg	Cumulative Percent of Dose Recovered
Intravenous	0–24	74.0	28.11	28.1
	24–26	16.0	2.62	30.7
	26–47	0.8	0.38	31.1
Oral	0–24	83.0	28.21	28.2
	24–48	1.1	0.42	28.6

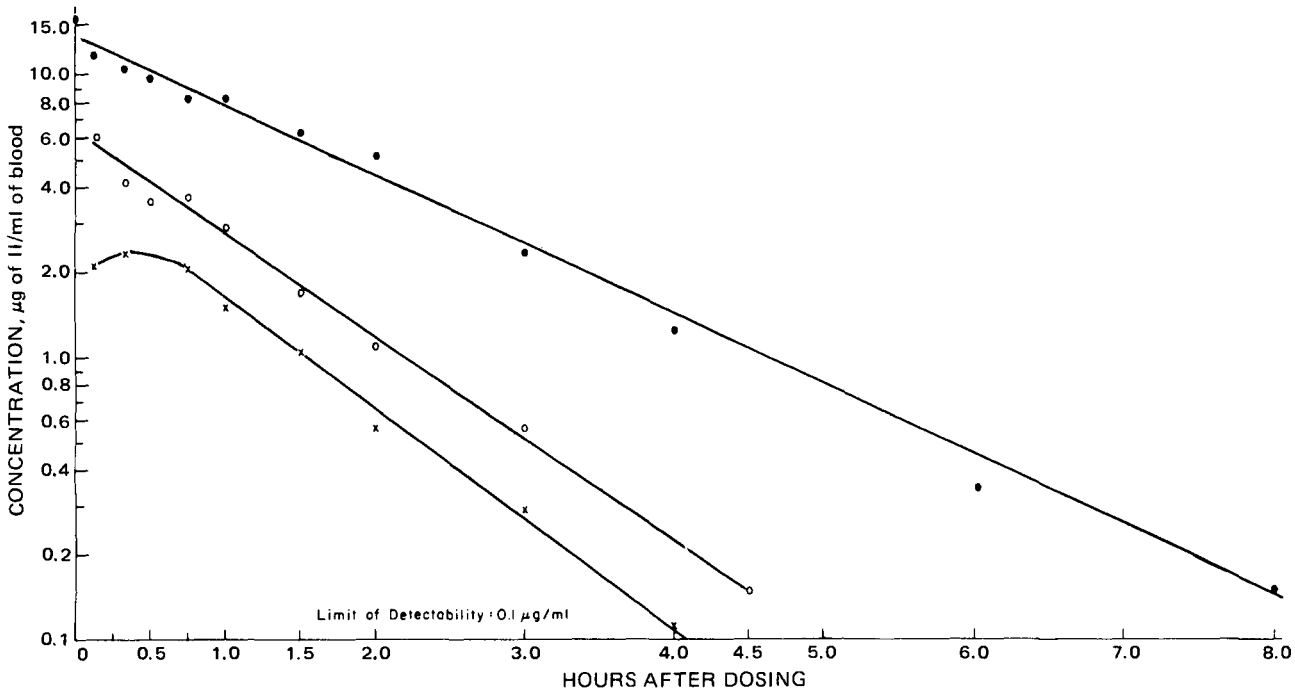

Figure 2—*Blood level fall-off curves of II in a dog following intravenous and oral administration. Key: ●, 10 mg/kg iv; O, 5 mg/kg iv; and ×, 5-mg/kg oral suspension in polysorbate 80.*

oxidation of I to III. The sensitivity limit of the assay was 0.25 μg of I/ml of blood or urine using a 4-ml specimen/assay and a sample to blank fluorescence ratio of 2:1 as the limit of detectability.

Compound II differed significantly from I in its partitioning behavior. Extraction of II from blood or urine at different pH values using different solvents indicated that II was completely recovered at pH 9.0 in ether or ethyl acetate. However, II could not be back-extracted into 0.1 *N* HCl as a cleanup step, nor could an acid solution be backwashed without loss of II. The ether extracts of blood at pH 9.0 were relatively free of impurities, and the oxidation step reduced blood blank values significantly. Thus, evaporation of ether extracts and dissolution of the residues in 0.1 *N* HCl, followed by alkaline permanganate oxidation, resulted in sufficiently low blanks for the analysis of up to 4 ml of blood. Extraction of urine was accomplished with ethyl acetate. Although the recovery of II in ether was 89 ± 6% from blood and 80 ± 5% from urine, the overall recovery of II, including the alkaline permanganate oxidation step and measurement as IV, was 60 ± 5%. The sensitivity limit of the assay was 0.10–0.20 μg of II/ml of blood or urine using a 4-ml specimen/assay.

Application of Assay for I in Biological Specimens—To demonstrate the utility of the assay, blood I concentrations and urinary excretion of I were determined following the intravenous and oral administration of single 100-mg doses given to the same dog 7 days apart. The intravenous dose was administered in propylene glycol solution, while the oral dose was the pure drug hand packed in a gelatin capsule.

Following both intravenous and oral dosing, blood levels were measurable for up to 11 hr and were below the sensitivity limit of the assay thereafter. The blood level data were plotted semilogarithmically with time in Fig. 1. Following the intravenous administration of I, the least-squares fit of a monoexponential equation to the blood concentration–time curve resulted in an estimated half-life of about 2 hr. The lag in the oral blood level curve probably reflects slow absorption. TLC examination of the extracts of the dog blood specimens showed the presence of only intact I.

The urinary excretion data following intravenous and oral administration of I are given in Table II. The amount of intact I recovered in the urine in 0–48 hr was 31% following intravenous administration and 28.6% following oral administration of I. TLC examination of the dog urine extracts showed small amounts of an unidentified metabolite in addition to I. This unconjugated metabolite yielded III upon oxidation in alkaline permanganate.

Small amounts of I and a metabolite were detected following enzymatic hydrolysis, two-dimensional TLC using ethyl acetate–acetone–methanol (85:15:15) in the first dimension and benzene–methanol (66:35) in the second dimension, and the Dragendorff visualization treatment previously described. The respective R_f values for I were 0.38 and 0.62; and for the metabolite, they were 0.08 and 0.27. This metabolite did not form a fluorescent derivative similar to III by alkaline permanganate oxidation. Its structure has not been elucidated.

Application of Assay for II in Biological Specimens—To demonstrate the utility of the assay for II, blood concentrations and urinary excretion of II were determined in a dog following intravenous and oral administration. Intravenous doses of 5 and 10 mg of II/kg were administered in propylene glycol solution to the same dog 7 days apart. A single 5-mg/kg suspension in polysorbate 80[13] was administered orally to a second dog. The blood level data were plotted semilogarithmically with time in Fig. 2.

Following intravenous administration of II, the least-squares fit of a monoexponential equation to the blood level–time curves resulted in estimated half-lives of approximately 1.2 hr for the 10-mg/kg dose and 0.9 hr for the 5-mg/kg dose. Following oral administration of a 5-mg/kg dose as a suspension in polysorbate 80[13], early blood levels indicated rapid absorption. TLC examination of the ether extracts of the dog blood specimens for II, using the solvent system described for the urine assay, showed the presence of only the intact drug.

The urinary excretion of II is listed in Table III. The intact drug accounted for about 1.9, 1.0, and 1.2% of the 10- and 5-mg/kg iv doses and the 5-mg/kg po dose, respectively, in the directly extractable unconjugated fraction. Chromatographic examination of the ethyl acetate extracts of the unconjugated fraction in a 0–24-hr dog urine specimen showed the presence of intact II and considerable amounts of UV-absorbing components. Dragendorff treatment did not produce any fluorescent area other than that for II.

Following extraction of the free fraction and enzymatic hydrolysis, the ethyl acetate extract (pH 5.3) of the deconjugated fraction was analyzed by one-dimensional TLC, using benzene–methanol–acetic acid (90:10:10),

Table III—Urinary Excretion of II in the Dog following the Intravenous and Oral Administration of the Drug

Dose, mg/kg	Route	Total Milligrams Excreted[a]	Dose Excreted as Intact II, %
10 (118 mg)	Intravenous	2.23	1.89
5 (53 mg)	Intravenous	0.499	0.95
5 (63 mg)	Oral	0.736	1.17

[a] The 0–24-hr postdosing urine pool.

[13] Tween 80, Sigma Chemical Co., St. Louis, Mo.

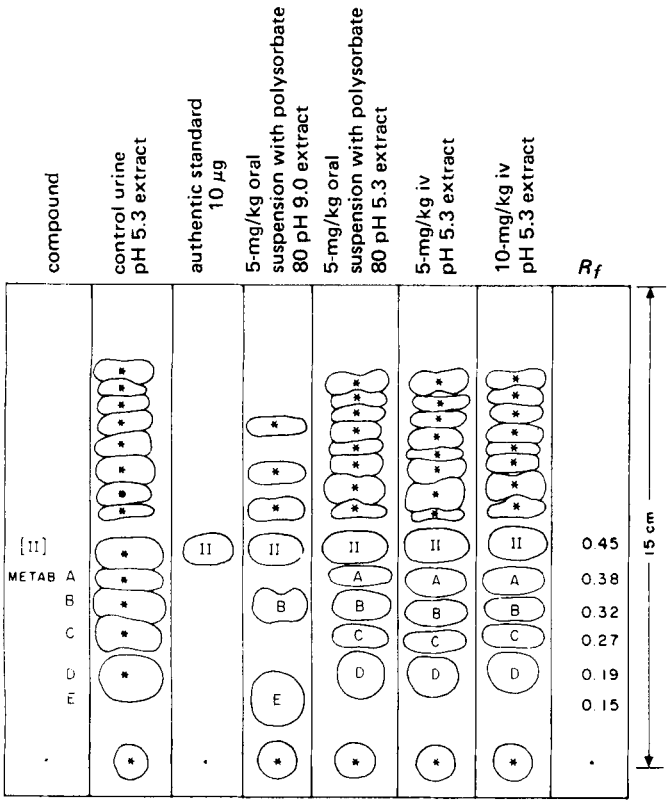

Figure 3—*Thin-layer chromatogram of ethyl acetate extracts of a 0–24-hr pool of urine (after enzyme incubation) from dogs treated with II by intravenous and oral routes of administration. (* = UV-absorbing components in the sample extract that do not fluoresce on either Dragendorff treatment or alkaline permanganate oxidation.)*

and showed the presence of intact II (R_f 0.45) and four metabolites (A–D) at R_f values of 0.38, 0.32, 0.27, and 0.19 (Fig. 3). These metabolites appeared as UV-absorbing bands and could be distinguished from coextracted endogenous urinary components by their intense yellow to blue-green fluorescence produced after Dragendorff treatment.

The urine was then titrated to pH 9.0 and extracted with two volumes (15 ml) of ethyl acetate. The residue of this extract, when analyzed by TLC, showed another metabolite (II-E) which migrated with R_f 0.15. This compound did not form a fluorescent product with the Dragendorff reagent and was detected as a pale-white area against a charred background after heating. The compound also did not form a fluorescent derivative upon alkaline permanganate oxidation.

Since urinary Metabolites A–D produced fluorescent products similar to IV by the alkaline permanganate oxidation reaction, it was assumed that the 3-butoxy-4-methoxybenzyl portion of the molecule was intact and that metabolic alteration was confined to the imidazolidinone portion of the molecule for these metabolites.

When Metabolites A–D were eluted, oxidized, and measured fluorometrically, their concentrations corresponded to 1.3, 1.4, and 0.7% of the doses, respectively, assuming that these compounds behaved identically to II in the assay procedure. The conjugated metabolite (II-E) appeared to be the major urinary metabolite by UV absorption on the TLC plate but it did not form a fluorescent benzoic acid and, therefore, could not be quantitated. It is conceivable that either the 3-butoxy and/or the 4-methoxy group was dealkylated to yield a phenolic metabolite and that the corresponding benzoic acid derivative formed did not fluoresce under the acidic solvent conditions used. The excretion data in the dog showed that the intact drug was not excreted in the urine in significant amounts. The analysis of feces was hampered by high blank values resulting from interfering materials in the extract. Nevertheless, the analysis of feces did show that fecal excretion of intact II accounted for less than 10% of the dose.

Assay Specificity—The assay for I or II in blood was deemed to be specific for the respective parent compounds by virtue of selective extraction and the absence of interfering metabolites. The analysis of urine for the free or directly extractable and the conjugated fractions required chromatographic separation to effect specificity prior to quantitation.

REFERENCES

(1) V Gruenman and M. Hoffer, U.S. pat. 3,636,039 (Jan. 18, 1972).

(2) M. W. Osborne, J. J. Wenger, and R. A. Moe, *J. Pharmacol. Exp. Ther.*, **176**, 174 (1971).

(3) M. W. Osborne, J. J. Wenger, M. T. Zanko, and R. J. Barrett, *Eur. J. Pharmacol.*, **28**, 1 (1974).

(4) C. Dalton, J. B. Quinn, C. R. Burghardt, and H. Sheppard, *J. Pharmacol. Exp. Ther.*, **173**, 270 (1970).

(5) H. Sheppard, G. Wiggan, and W. H. Tsien, in "Advances in Cyclic Nucleotide Research, Vol. 1, Physiology and Pharmacology of Cyclic AMP," P. Greengard, G. A. Robinson, and R. Paoletti, Eds., Raven, New York, N.Y., 1972, pp. 103–112.

(6) T. C. Hamilton, *Br. J. Pharmacol.*, **46**, 386 (1972).

(7) A. J. Blume, C. Dalton, and H. Sheppard, *Proc. Natl. Acad. Sci. USA*, **70**, 3099 (1973).

(8) H. Sheppard and W. H. Tsien, *Biochim. Biophys. Acta (E)*, **341**, 489 (1974).

(9) N. Prasad and R. Prasad, *Br. J. Cancer*, **34**, 249 (1976).

(10) D. E. Schwartz, B. A. Koechlin, and R. E. Weinfeld, *Chemotherapy (Basel), Suppl.*, **14**, 22 (1969).

(11) S. A. Kaplan, R. E. Weinfeld, and T. L. Lee, *J. Pharm. Sci.*, **62**, 1865 (1973).

(12) J. A. F. de Silva, M. A. Schwartz, V. Stefanovic, J. Kaplan, and L. D'Arconte, *Anal. Chem.*, **36**, 2099 (1964).

(13) J. A. F. de Silva and C. V. Puglisi, *ibid.*, **42**, 1725 (1970).

(14) R. Munier and M. Machebouef, *Bull. Soc. Chim. Biol.*, **33**, 846 (1951).

(15) J. A. F. de Silva, N. Strojny, and K. Stika, *Anal. Chem.*, **48**, 144 (1976).

ACKNOWLEDGMENTS

The authors thank Mr. K. McFaden and Mr. S. Cotler for conducting the animal experiments, Mr. Robert McGlynn for drawing the figures, and Mrs. A. Szilagyi, Mrs. D. Foster, and Mrs. W. Morley for manuscript preparation.

Studies on Drug Metabolism by Use of Isotopes XX: Ion Cluster Technique for Detection of Urinary Metabolites of 1-Butyryl-4-cinnamylpiperazine by Mass Chromatography

SHIN-ICHI MORISHITA, SHIGEO BABA ˣ, and YŪZŌ NAGASE

Received January 31, 1977, from the *Tokyo College of Pharmacy, 1432-1 Horinouchi, Hachioji, Tokyo 192-03, Japan.* Accepted for publication September 14, 1977.

Abstract □ An ion cluster technique and mass chromatography were used for the structural elucidation of several unidentified urinary metabolites of 1-butyryl-4-cinnamylpiperazine (I) in mice and guinea pigs. The urinary metabolites in guinea pigs and mice receiving a single 100-mg/kg dose of an equimolar mixture of 1-butyryl-4-[aromatic-d_5]-cinnamylpiperazine (I-d_5) hydrochloride and I hydrochloride (I:I-d_5) were purified and subjected to trimethylsilyl derivatization with bis(trimethylsilyl)acetamide, followed by GLC–mass spectrometry–computer analysis. Appropriate fragment and molecular ions of unidentified metabolites were selected based on the major mass fragment ions appearing in the mass spectra of the previously identified metabolites of I to provide the mass chromatograms. The presence of ion clusters as doublet peaks in the mass chromatograms indicated that the corresponding total ion peaks originated from the administered I:I-d_5. The mass spectra of selected scans from the total ion chromatogram were plotted, and the structures of unidentified metabolites were readily determined by the presence of ion clusters separated by 3–5 mass units and by the shift of the fragment ions. By using this technique, six previously unidentified metabolites were identified in the urine of guinea pigs and two were identified in the urine of mice.

Keyphrases □ 1-Butyryl-4-cinnamylpiperazine—ion cluster–mass chromatographic analyses of urinary metabolites in mice and guinea pigs □ Ion cluster–mass chromatography—analyses, urinary metabolites of 1-butyryl-4-cinnamylpiperazine in mice and guinea pigs □ Mass chromatography–ion cluster technique—analyses, urinary metabolites of 1-butyryl-4-cinnamylpiperazine in mice and guinea pigs □ Metabolites, urinary—of 1-butyryl-4-cinnamylpiperazine, ion cluster–mass chromatographic analyses in mice and guinea pigs □ Analgesics—1-butyryl-4-cinnamylpiperazine, ion cluster–mass chromatographic analyses of urinary metabolites in mice and guinea pigs

Metabolism of 1-butyryl-4-cinnamylpiperazine (I) hydrochloride, developed as an analgesic (1), was studied in the rat by GLC (2) and a radioactive isotope tracer technique (3). With the latter method, the following metabolites of I were identified and quantified in rat urine: 1-butyryl-4-(4-hydroxycinnamyl)piperazine (II), 1-cinnamylpiperazine (III), 1-(4-hydroxycinnamyl)piperazine (IV), benzoic acid, hippuric acid, 4-hydroxybenzoic acid, and 4-hydroxyhippuric acid. Furthermore, studies on the species differences in I metabolism among experimental animals such as mice, guinea pigs, and rabbits by inverse radioactive isotope dilution analysis suggested that there also were several unidentified metabolites in the urine of mice and guinea pigs (4).

Structures of drug metabolites commonly are elucidated by mass and GLC–mass spectrometry and NMR and IR spectroscopy. It is, however, difficult to decide whether the spectra obtained are from the drug itself or other biological impurities. In mass spectrometry, an ion cluster technique (5–9), using a drug labeled with a stable isotope, facilitates the differentiation of the drug metabolites from other impurities by the presence of doublet peaks and offers information about the structures of metabolites by the shift of ion cluster-forming fragment ions. The metabolites isolated by TLC from the urine of animals receiving an equimolar mixture of I and 1-butyryl-4-[aromatic-d_5]-cinnamylpiperazine (I:I-d_5) were analyzed previously (10) with a mass spectrometer equipped with a direct inlet system. In this experiment, ^{14}C-labeled I was used to locate the metabolites on TLC. However, as is often the case, isolation by TLC alone was not sufficient to obtain a clear mass spectrum.

In the present experiment, metabolites of I:I-d_5 were separated by GLC and the metabolites were readily recognizable from the presence of the doublet peaks on the mass chromatograms (11, 12) obtained by a GLC–mass spectrometer–computer system. The present paper describes a mass chromatographic procedure coupled with an ion cluster technique for the identification of the unidentified metabolites of I.

EXPERIMENTAL

Labeled Compound—1-Butyryl-4-[aromatic-d_5]-cinnamylpiperazine (I-d_5) was synthesized according to the method described previously (10).

Authentic Compounds—Compound II hydrochloride (2), III dihydrochloride (13), IV dihydrochloride monohydrate (2), and 1-butyryl-4-(3-methoxy-4-hydroxycinnamyl)piperazine (V) (10) were synthesized in this laboratory.

1-Butyryl-4-(3-phenyl-2,3-dihydroxypropyl)piperazine (VI) was synthesized as follows. An absolute ether (10 ml) solution of I (2.20 g) was added, dropwise, to osmium tetroxide (2.00 g) in 25 ml of absolute ether at room temperature. The brown cyclic osmate ester formed immediately. To complete the reaction, the reaction mixture was allowed to stand for

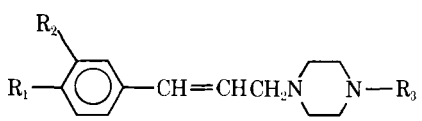

I: $R_1 = R_2 = H$, $R_3 = COC_3H_7$
II: $R_1 = OH$, $R_2 = H$, $R_3 = COC_3H_7$
II′: $R_1 = H$, $R_2 = (OH)$, $R_3 = COC_3H_7$
III: $R_1 = R_2 = R_3 = H$
IV: $R_1 = OH$, $R_2 = R_3 = H$
V: $R_1 = OH$, $R_2 = OCH_3$, $R_3 = COC_3H_7$
VII: $R_1 = R_2 = H$, $R_3 = COCH(OH)C_2H_5$
VIII: $R_1 = R_2 = H$, $R_3 = COCH_2CH(OH)CH_3$
IX: $R_1 = OH$, $R_2 = H$, $R_3 = COCH(OH)C_2H_5$
X: $R_1 = OH$, $R_2 = H$, $R_3 = COCH_2CH(OH)CH_3$
XII: $R_1 = R_2 = OH$, $R_3 = COC_3H_7$

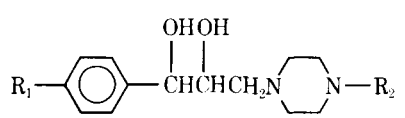

VI: $R_1 = H$, $R_2 = COC_3H_7$
XI: $R_1 = OH$, $R_2 = COC_3H_7$

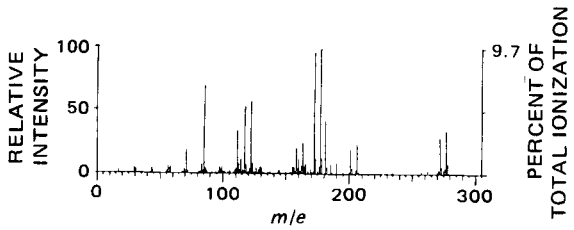

Figure 1—*Mass spectrum of an equimolar mixture of I and I-*d_5.

12 hr at room temperature. The product was separated, washed with absolute ether, and hydrolyzed with a solution of sodium sulfite (5 g) in ethanol–water (1:2 v/v, 200 ml) under reflux for 3 hr. After cooling, a dark-brown precipitate was filtered off, and the filtrate was evaporated under reduced pressure. The residue was dissolved in water and the solution was extracted with ether.

After evaporation of the ether, the oily residue was subjected to column chromatography [silica gel C-200[1], 100–200 mesh, 3.2 cm i.d. and 30 cm in height, eluting solvent of chloroform–methanol (95:5 v/v)]. Colorless oily liquids, VI (750 mg) and I (85 mg), were collected in the 228–288-ml and 144–216-ml fractions, respectively. TLC[2] (silica gel 60 F-254) of VI thus separated showed a single spot with two different solvent systems, butanol–acetic acid–water (4:1:2 v/v, R_f 0.27) and chloroform–methanol–28% ammonium hydroxide (90:9:1 v/v, R_f 0.59). The mass spectrum of VI exhibited ions at *m/e* 306 ($M^{+}\cdot$), 288 ($M^{+}\cdot - H_2O$), 169, and 99. The hydrochloride of VI recrystallized from ethanol–ether (1:3 v/v) gave a colorless hygroscopic powder.

Anal.—Calc. for $C_{17}H_{27}ClN_2O_3$: C, 59.55; H, 7.94; N, 8.17. Found: C, 59.28; H, 8.06; N, 7.66.

Preparation of Biological Samples—Three DDY strain[3] male mice, ~20 g, and Hartley male guinea pigs, ~400 g, were injected with a single 100-mg/kg sc dose of I:I-d_5 hydrochloride dissolved in water. Urine samples were then collected for 24 (mice) or 12 (guinea pig) hr and kept frozen until analysis. Aliquots of urine samples (half in volume) were adjusted to pH 8 with a saturated sodium carbonate solution and subjected to column chromatography on an ion-exchange resin[4] (glass column of 8 mm i.d., 5 cm in height for mouse urine and 30 cm in height for guinea pig urine).

The column was washed with water (100 ml for mice urine and 600 ml for guinea pig urine), and I and its metabolites were eluted with methanol. The methanol eluate was concentrated to dryness under reduced pressure. The residue was dissolved in dry pyridine (0.2 ml for mice and 0.5 ml for guinea pigs), and 60-μl portions of the urine samples were trimethylsilylated with 20 μl of bis(trimethylsilyl)acetamide at 60° for 10 min. These samples were concentrated to 40 μl under a stream of dry nitrogen, and aliquots (1–2 μl) were injected into the gas chromatograph.

Analysis—A GLC–mass spectrometer[5] and a data processing system[6] connected to a minicomputer[7] were used. The GLC conditions were: column, 1-m × 3-mm i.d. glass column packed with 1.5% SE-30 on 60–80-mesh Chromosorb W; column temperature, programmed at 5°/min from 100 to 270°; flash heater temperature, 250°; and helium flow rate, 20 ml/min. The mass spectrometer conditions were: separator temperature, 280°; ionization source temperature, 310°; and ionization energy, 20 ev. For peak e and the trimethylsilyl derivative of VI, mass spectra were scanned under the following conditions: separator temperature, 240°; ionization source temperature, 270°; and ionization energy, 17 ev.

Eight minutes following injection of the sample, automatic magnet scanning was initiated, covering an *m/e* range of 50–550 every 8 sec. All scanning data were stored in the data processing system. Mass chromatograms were obtained on a digital plotter for selected mass numbers. Background-subtracted mass spectra also were obtained on the digital plotter.

RESULTS AND DISCUSSION

When an equimolar mixture of labeled and unlabeled compounds is used, fragment ions give their respective peaks in doublet form at the same retention time on the mass chromatogram. However, if there is a marked isotope effect on the retention time, this type of doublet peak is not formed. Therefore, to detect the drug metabolites by an ion cluster technique coupled with mass chromatography, the isotope effect of the labeled compound on the GLC retention time must be negligible.

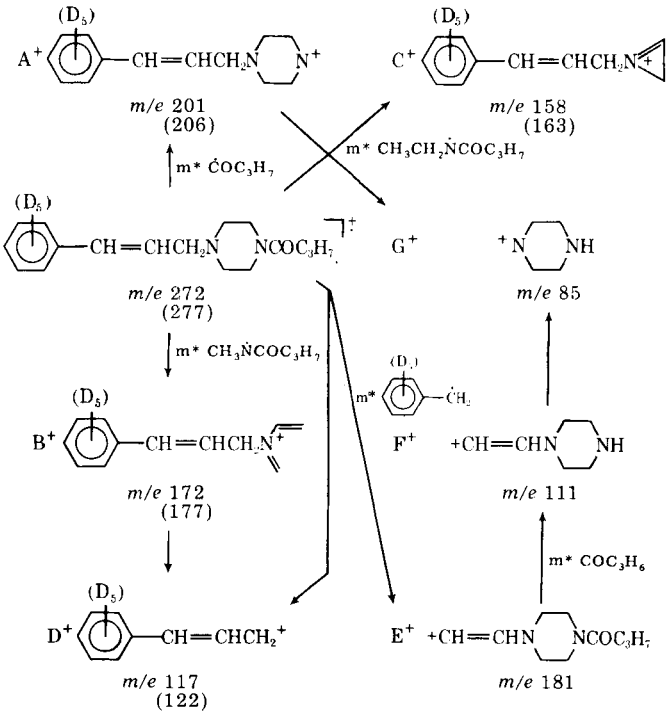

Scheme I—Fragmentation pathways of I and I-d_5. *Figures in parentheses indicate the* m/e *value of deuterium-labeled compound.*

The retention time of a deuterium-labeled compound is shorter than that of the unlabeled compound (14); this isotope effect is influenced by the number and position of deuterium atoms in the labeled molecule. For instance, compounds with deuterium-labeled benzene rings, such as *l*-[aromatic-d_5]-ephedrine (oxazolidone derivative), L-[aromatic-d_5]-phenylalanine (enamine methyl ester derivative), and I-d_5 showed 1–2-sec shorter retention times than the unlabeled compounds under the GLC conditions employed. However, in mass chromatography, the scanning interval is generally much longer than this isotope effect. In the present study on I metabolism by an ion cluster technique and mass chromatography, the doublet peaks observed on the mass chromatograms were derived from ion cluster-forming ions of I:I-d_5 and its metabolites.

The mass spectrum of I:I-d_5 and its fragmentation pathways are shown in Fig. 1 and Scheme I, respectively. Ions produced from I:I-d_5 were divided into two groups, an ion cluster-forming group retaining the benzene ring and a nonion cluster-forming group lacking the benzene ring. Rearrangement of deuterium attached to the benzene ring was not observed in the fragmentation of I:I-d_5 (Fig. 1). The fragment ions of the former and the latter groups were named as indicated in Scheme I.

Typical examples of mass chromatograms obtained from the urine of guinea pigs and mice administered I:I-d_5 are presented in Fig. 2. The following ions were selected to obtain these mass chromatograms: a fragment ion at *m/e* 85 (ion G), which appeared in all mass spectra of I and its metabolites identified by a radioactive isotope tracer technique (2); fragment ions at *m/e* 117:122 (ion C), corresponding to the cinnamyl moiety, and at *m/e* 205:209, corresponding to the 4-hydroxylated cinnamyl moiety; the molecular ions of monohydroxylated I:I-d_5 at *m/e* 360:364, 365 and of dihydroxylated I:I-d_5 at *m/e* 448:452; and other ions of possible metabolites of I:I-d_5.

Not all peaks appearing on the total ion chromatogram originated from I:I-d_5. A peak originating from I:I-d_5 was selected when the retention time of the total ion chromatogram peak coincided with the retention time of two or more ion chromatogram peaks and the mass spectrum of this peak showed ion clusters separated by 3–5 mass units. Introduction of hydroxyl groups into the benzene ring is indicated by reduction in the spacing of the ion cluster.

For example, the retention time of the total ion chromatogram peak c in Fig. 2A (scan number 79) coincided with that of *m/e* 85, 117, and 122 ion chromatogram peaks. The mass spectrum of this peak c showed ion

[1] Wako Pure Chemical Industries, Tokyo, Japan.
[2] Merck.
[3] National Institute of Health, Shinagawa-ku, Tokyo, Japan.
[4] Amberlite XAD-2.
[5] LKB-9000, Shimadzu Seisakusho Ltd., Kyoto, Japan.
[6] GCMSPAC-300, Shimadzu Seisakusho Ltd., Kyoto, Japan.
[7] OKITAC-4300, Oki Electric Industry Co., Tokyo, Japan.

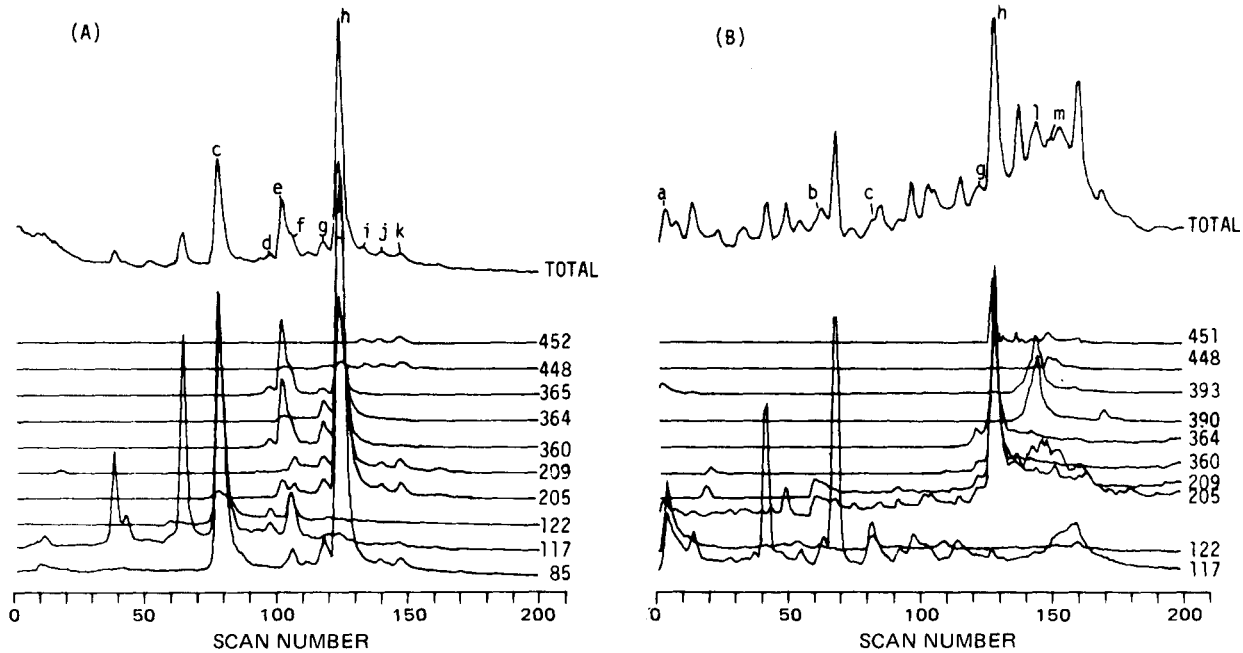

Figure 2—*Mass chromatograms of urinary metabolites of an equimolar mixture of I and I-*d_5 *in guinea pigs (A) and in mice (B).*

clusters separated by 5 mass units each and was the same as the mass spectrum of I:I-d_5 (Fig. 1). From these observations, it became apparent that the total ion chromatogram peak c originated from I:I-d_5. In a similar manner, eight other total ion chromatogram peaks (peaks d–k) shown in Fig. 2A and seven total ion chromatogram peaks (peaks a–c, g, h, l, and m) in Fig. 2B originated from I:I-d_5 or its metabolites. Total ion chromatogram peaks a, b, and h corresponded to Metabolites III, IV, and II, respectively, which had been identified by a radioactive isotope tracer technique. Their identity was confirmed by investigating the retention time on GLC and the mass spectrum of trimethylsilylated authentic compounds.

Mass spectra of total ion chromatogram peaks d, f, e, i, j, k, and l are shown in Figs. 3A, 3B, 4A, 4B, 5A, 5B, and 6, respectively. Whether or not singlet ions appearing in these mass spectra originated from the metabolites in question was determined as follows. Mass chromatograms were recorded by assigning the *m/e* values of the singlet ions (*e.g.*, ions at *m/e* 131, 180, and 269 of the mass spectrum of the total ion chromatogram peak j, Fig. 5A) and those of the ion cluster-forming ions (*e.g.*, *m/e* 205:209, 260:264, and 448:452, Fig. 7). When the scan number of the singlet ion peak coincided with that of the ion cluster-forming ion peak, the singlet ions in question were confirmed to have originated from the drug itself. Figure 7 shows that ions at *m/e* 131 and 269 belong to the metabolite of peak j, while an ion at *m/e* 180 does not belong to the peak. In Figs. 3B, 4B, and 5B, the star (*) indicates an ion peak not associated with the metabolites in question.

The structural elucidation of unidentified metabolites of I:I-d_5 (total ion chromatogram peaks d–g and i–m) was carried out as follows.

Total Ion Chromatogram Peaks d and f—In these mass spectra (Fig. 3), ion clusters separated by 5 mass units each were observed. The *m/e* values of the molecular ion (*m/e* 360:365) and the fragment ion (*m/e* 269) were 88 mass units higher than those of the molecular ion (*m/e* 272:277) and the fragment ion E (*m/e* 181) of I:I-d_5. These ions possessed a butyryl group. These facts indicated the introduction of a hydroxyl group into the butyryl group of I:I-d_5.

In the mass spectrum of peak d, a very intense peak at *m/e* 131 [$(CH_3)_3SiO^+{=}C_3H_6$], which would be formed from α-cleavage of the butyryl moiety, indicated that the hydroxylation occurred at the α-position of the butyryl group. On the other hand, in the mass spectrum of peak f, a fragment ion at *m/e* 117 was of higher intensity than a fragment ion at *m/e* 122, although these two ions (*m/e* 117:122) formed an ion cluster of equal intensity in the mass spectrum of peak d. This result is explained by the contribution of the fragment ion of *m/e* 117 [$(CH_3)_3SiO^+{=}C_2H_4$] resulting from the α-cleavage of the butyryl moiety. From these facts, the metabolites of peaks d and f were assigned as 1-(1-hydroxybutyryl)-4-cinnamylpiperazine (VII) and 1-(2-hydroxybutyryl)-4-cinnamylpiperazine (VIII), respectively.

Total Ion Chromatogram Peak e—The mass spectrum of peak e (Fig. 4A) gave dominant singlet peaks at *m/e* 169 and 271. Ion clusters at *m/e* 360:365 (I plus trimethylsilyloxy group minus one proton), 435:440 (I plus two trimethylsilyloxy groups minus 15), and 450:455 (I plus two trimethylsilyloxy groups) were of low intensity but were observed clearly. The presence of the molecular ion at *m/e* 450:455 and of the intensive singlet ion at *m/e* 169 and 271 suggested the possibility of the introduction of two hydroxyl groups into the double bond of the cinnamyl group to give rise to VI. This reaction was confirmed by investigating the retention time on GLC and the mass spectrum of trimethylsilylated authentic VI.

Total Ion Chromatogram Peak g—The mass spectrum of peak g showed the same molecular and fragment ions as that of peak h, although

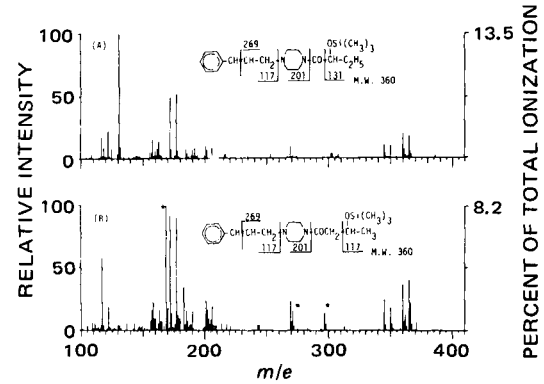

Figure 3—*Mass spectra of peak d (A) and peak f (B).*

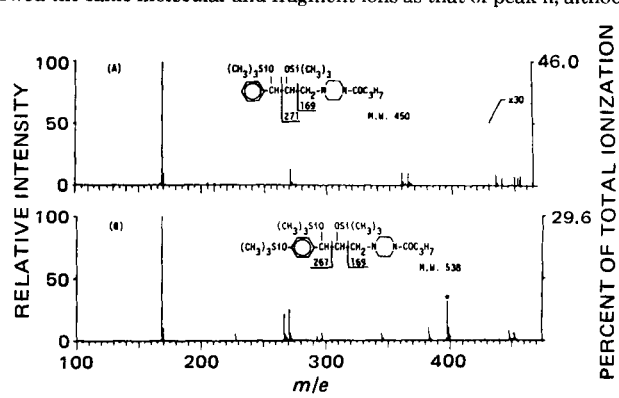

Figure 4—*Mass spectra of peak e (A) and peak i (B).*

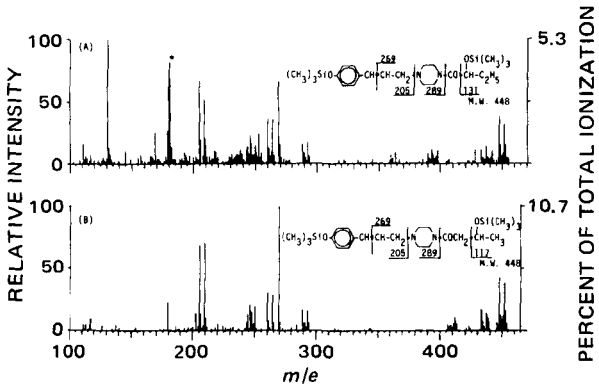

Figure 5—*Mass spectra of peak j (A) and peak k (B).*

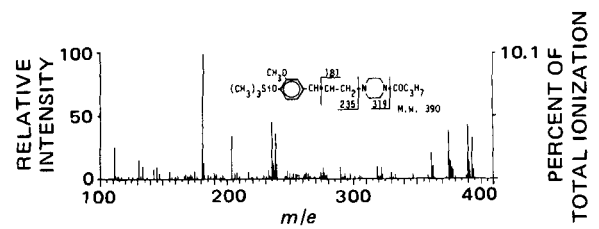

Figure 6—*Mass spectrum of peak l.*

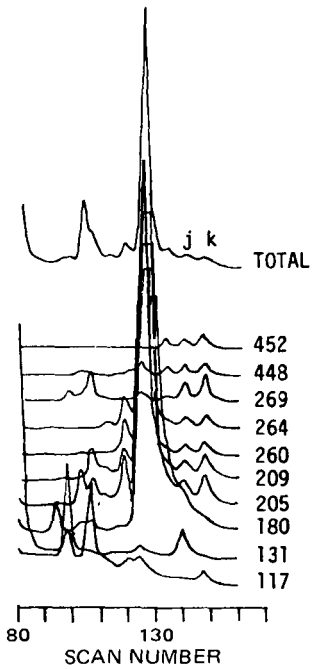

Figure 7—*Mass chromatogram of urinary metabolites of an equimolar mixture of I and I-d_5 in guinea pigs.*

the relative intensities were different. Each ion cluster was 4 mass units apart in both mass spectra. These observations indicated that the metabolite of peak g was an *ortho*- or a *meta*-isomer of II.

Total Ion Chromatogram Peak i—The mass spectrum of peak i (Fig. 4B) gave an intense singlet peak at *m/e* 169 as observed in the mass spectrum of peak e. In this mass spectrum, the ion cluster at *m/e* 360:365 of peak e shifted to *m/e* 448:452, suggesting the introduction of three hydroxyl groups into the molecule, one in the benzene ring and two in the double bond of the cinnamyl group. The occurrence of an ion cluster at *m/e* 267:271 (in the mass spectrum of peak i), which was not observed in the mass spectrum of peak e, can be reasonably explained by resonance stabilization of the fragment ion produced by an α-cleavage (Scheme II). The metabolite of peak i was then assigned as 1-butyryl-4-[3-(4-hydroxyphenyl)-2,3-dihydroxypropyl]piperazine (XI).

Total Ion Chromatogram Peaks j and k—The mass spectra of peaks j and k (Fig. 5) showed the same ion peaks, except for the ion at *m/e* 131 that was only in the former and the ion at *m/e* 117 that was only in the latter (Fig. 7). In these mass spectra, the molecular ion (*m/e* 448:452) was 176 mass units higher (two trimethylsilyloxy groups) than that of I:I-d_5, and the fragment ions possessing either a benzene ring or a butyryl group (ions A–E) were 88 mass units (trimethylsilyloxy group) higher than the corresponding fragment ions of I:I-d_5. In addition, ion clusters in the mass spectra of peaks j and k were 4 mass units apart, whereas ion clusters in the mass spectrum of I:I-d_5 were 5 mass units apart.

These facts suggested the introduction of two hydroxyl groups into the molecule, one in the butyryl group and the other in the benzene ring. Moreover, the presence of the fragment ion at *m/e* 131 in the mass spectrum of peak j and the fragment ion at *m/e* 117 in the mass spectrum of peak k indicated that peaks j and k were derived from 1-(1-hydroxybutyryl)-4-(4-hydroxycinnamyl)piperazine (IX) and 1-(2-hydroxybutyryl)-4-(4-hydroxycinnamyl)piperazine (X), respectively.

Total Ion Chromatogram Peak l—The mass spectrum of peak l (Fig. 6) showed ion clusters 3 mass units apart (*m/e* 235:238, 319:322, and 390:393). In this mass spectrum, ion clusters at *m/e* 272:277 ($M^{+\cdot}$), *m/e* 201:206 (ion A), and 117:122 (ion C) of I:I-d_5 shifted by 118 mass units

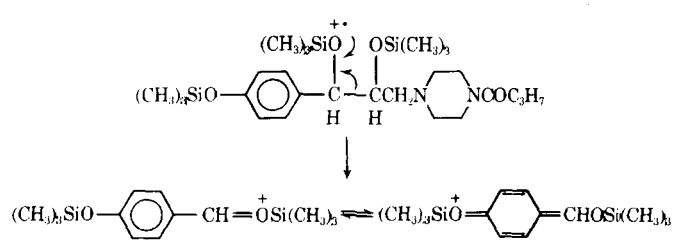

Scheme II

(trimethylsilyloxy plus methoxy group), giving rise to ion clusters at *m/e* 390:393, 319:322, and 235:238, respectively. These facts suggested that peak l originated from V. The GLC retention time and the mass spectrum of trimethylsilylated authentic V confirmed the structure of the metabolite of peak l as V.

Total Ion Chromatogram Peak m—High background resulting from biological materials obscured part of the mass spectrum of peak m. However, an ion cluster at *m/e* 448:451, separated by 3 mass units, was observed clearly, suggesting that the metabolite of peak m might be 1-butyryl-4-(3,4-dihydroxycinnamyl)piperazine (XII).

The I metabolites identified by the present method from guinea pigs and mice are summarized in Table I. Oxidation of the cinnamyl moiety to give VI and XI and hydroxylation of the butyryl group to give VII–X occurred in guinea pigs; in mice, 3,4-dihydroxylation of the benzene ring occurred and a hydroxyl group at the 3-position readily methylated, resulting in V. In a previous study (4), it was demonstrated that the metabolism of I in rabbits proceeded predominantly by 4-hydroxylation of the benzene ring and *N*-deacylation of the butyryl group.

There are, therefore, marked species differences in I metabolism among the experimental animals studied. Furthermore, in studies on the species differences in I metabolism (4), significant amounts of benzoic acid and hippuric acid originating from this compound were detected in the urine of guinea pigs, while these metabolites were found in negligible amounts in mice. These facts suggest that benzoic acid is formed through dihydroxylation of the olefinic moiety of I.

The present study applied mass chromatography combined with an ion cluster technique for the separation and differentiation of the unidentified metabolites in a complex mixture of biological materials. The

Table I—Sources of the Metabolites of I Elucidated by Mass Chromatography Coupled with an Ion Cluster Technique

Peak	Metabolite	Guinea Pigs	Mice
a	III		+
b	IV		+
c	I	+	+
d	VII[a]	+	
e	VI[a]	+	
f	VIII[a]	+	
g	II'[a]	+	+
h	II	+	+
i	XI[a]	+	
j	IX[a]	+	
k	X[a]	+	
l	V[a]		+
m	XII[a]		+

[a] New metabolites.

ion cluster technique was effective not only for the differentiation of the metabolites from other biological impurities but also for the structural elucidation. The metabolic transformation of the drug molecule was easily recognized by the shift of the fragment ions. Labeling the benzene ring of I with deuterium atoms readily clarified the metabolic transformations occurring in the benzene ring, since the elimination of each deuterium atom due to the biotransformation reduced the spacing of the ion clusters by 1 mass unit.

REFERENCES[8]

(1) T. Irikura, K. Nishino, N. Ito, M. Ito, and H. Ohkubo, *Jpn. J. Pharmacol.*, **20**, 287 (1970).

(2) H. Terayama, T. Narue, S. Kasai, M. Numata, H. Nakayama, T. Saito, and T. Irikura, *Chem. Pharm. Bull.*, **21**, 12 (1973).

(3) T. Irikura, Y. Nagatsu, S. Baba, and H. Sone, *Yakugaku Zasshi*, **94**, 802 (1974).

(4) S. Baba and S. Morishita, *Chem. Pharm. Bull.*, **23**, 1949 (1975).

(5) D. R. Knapp, T. E. Gaffney, and R. E. McMahon, *Biochem. Pharmacol.*, **21**, 425 (1972).

(6) R. E. McMahon, H. R. Sulivan, S. L. Due, and F. J. Marshall, *Life. Sci.*, **12**, 463 (1973).

(7) A. Zimmer, A. Prox, H. Pelzer, and R. Hankwitz, *Biochem. Pharmacol.*, **22**, 2213 (1973).

(8) W. E. Braselton, Jr., J. C. Orr, and L. L. Engel, *Anal. Biochem.*, **53**, 64 (1973).

(9) Y. Tanaka and M. Sano, *Chem. Pharm. Bull.*, **24**, 804 (1976).

(10) S. Baba, S. Morishita, and Y. Nagatsu, *Yakugaku Zasshi*, **96**, 1293 (1976).

(11) R. A. Hites and K. Biemann, *Anal. Chem.*, **42**, 855 (1970).

(12) H. Miyazaki, M. Ishibashi, M. Inoue, and M. Itoh, *J. Chromatogr.*, **99**, 553 (1974).

(13) T. Irikura, K. Musuzawa, K. Nishino, M. Kitagawa, H. Uchida, N. Ichinoseki, and M. Ito, *J. Med. Chem.*, **11**, 801 (1968).

(14) C. C. Sweeley, W. H. Elliott, I. Fries, and R. Ryhage, *Anal. Chem.*, **38**, 1549 (1966).

[8] For Part XIX, see M. Horie, S. Baba, Y. Kashida, and C. Hamada, *Yakugaku Zasshi*, **97**, 805 (1977).

Effect of Salicylamide and Acetaminophen on Dextromethorphan Hydrobromide Metabolism: Possible Pharmacological Implications

GOLLAMUDI RAMACHANDER *x, FLORENCE D. WILLIAMS, and JANE FRANCES EMELE

Received April 1, 1977, from the *Consumer Products Group, Warner Lambert Company, Morris Plains, NJ 07950.* Accepted for publication September 9, 1977.

*Present address: Department of Medicinal Chemistry, College of Pharmacy, University of Tennessee Center for the Health Sciences, Memphis, TN 38163.

Abstract □ The effect of salicylamide and acetaminophen on the metabolic fate of dextrorphan, the primary metabolite of dextromethorphan, was studied *in vivo* in the rat. Plasma dextrorphan levels were measured at 5-min intervals up to 20 min and at longer intervals up to 2 hr after dextromethorphan hydrobromide was administered orally either alone or in combination with salicylamide and acetaminophen. The combination gave rise to higher plasma dextrorphan levels than did dextromethorphan hydrobromide alone at most sampling times. Conjugation of dextrorphan was inhibited almost quantitatively by salicylamide and acetaminophen at the 5-min sampling time. Salicylamide alone increased the plasma dextrorphan levels when it was coadministered with dextromethorphan, but the differences were not statistically significant. The antitussive activity of dextromethorphan hydrobromide in the unanesthetized dog was faster in onset, greater in intensity, and longer in duration when it was coadministered with salicylamide and acetaminophen. It is suggested that salicylamide and acetaminophen may inhibit the metabolic inactivation of dextrorphan, thereby improving the cough-inhibiting potential of dextromethorphan hydrobromide.

Keyphrases □ Dextromethorphan hydrobromide—metabolism, effect of salicylamide and acetaminophen, rats □ Metabolism—dextromethorphan hydrobromide, effect of salicylamide and acetaminophen, rats □ Salicylamide—effect on metabolism of dextromethorphan hydrobromide in rats □ Acetaminophen—effect on metabolism of dextromethorphan hydrobromide in rats □ Antitussives—dextromethorphan hydrobromide, metabolism, effect of salicylamide and acetaminophen, rats □ Analgesics—acetaminophen and salicylamide, effect on metabolism of dextromethorphan hydrobromide in rats

Many drugs are eliminated from the body by biotransformation to glucuronide and sulfate conjugates that are pharmacologically inactive. The enzyme systems responsible for the formation of such metabolites are saturable at relatively low drug concentrations (1, 2). Concomitant administration of drugs that undergo conjugation *in vivo* was reported to result in a competitive inhibition of the respective enzymatic processes (3–5).

The main routes of metabolism of dextromethorphan, a widely used nonnarcotic antitussive agent, are *O*- and *N*-demethylation followed by subsequent conjugation of the desmethyl metabolites to glucuronides and sulfates, with *O*-demethylation being the predominant pathway (6–10). The *O*-demethylation product, dextrorphan (*d*-3-hydroxy-*N*-methylmorphinan), was reported to possess antitussive activity in the dog (11). Salicylamide, a weak analgesic and antipyretic agent, is metabolized primarily to the ether glucuronide and ester sulfate (2). The main metabolites of the analgesic drug acetaminophen are the glucuronide and sulfate conjugates (12, 13).

Self-administration of analgesic preparations along with antitussives is common. This investigation determined, in experimental animals, if the biotransformation of dextromethorphan is affected by concurrent administration of salicylamide or a combination of salicylamide and acetaminophen and if the antitussive activity of dextromethorphan is altered by such multidrug therapy.

EXPERIMENTAL

Materials—The drugs and chemicals used were: dextromethorphan

ion cluster technique was effective not only for the differentiation of the metabolites from other biological impurities but also for the structural elucidation. The metabolic transformation of the drug molecule was easily recognized by the shift of the fragment ions. Labeling the benzene ring of I with deuterium atoms readily clarified the metabolic transformations occurring in the benzene ring, since the elimination of each deuterium atom due to the biotransformation reduced the spacing of the ion clusters by 1 mass unit.

REFERENCES[8]

(1) T. Irikura, K. Nishino, N. Ito, M. Ito, and H. Ohkubo, *Jpn. J. Pharmacol.*, **20**, 287 (1970).

(2) H. Terayama, T. Narue, S. Kasai, M. Numata, H. Nakayama, T. Saito, and T. Irikura, *Chem. Pharm. Bull.*, **21**, 12 (1973).

(3) T. Irikura, Y. Nagatsu, S. Baba, and H. Sone, *Yakugaku Zasshi*, **94**, 802 (1974).

(4) S. Baba and S. Morishita, *Chem. Pharm. Bull.*, **23**, 1949 (1975).

(5) D. R. Knapp, T. E. Gaffney, and R. E. McMahon, *Biochem. Pharmacol.*, **21**, 425 (1972).

(6) R. E. McMahon, H. R. Sulivan, S. L. Due, and F. J. Marshall, *Life. Sci.*, **12**, 463 (1973).

(7) A. Zimmer, A. Prox, H. Pelzer, and R. Hankwitz, *Biochem. Pharmacol.*, **22**, 2213 (1973).

(8) W. E. Braselton, Jr., J. C. Orr, and L. L. Engel, *Anal. Biochem.*, **53**, 64 (1973).

(9) Y. Tanaka and M. Sano, *Chem. Pharm. Bull.*, **24**, 804 (1976).

(10) S. Baba, S. Morishita, and Y. Nagatsu, *Yakugaku Zasshi*, **96**, 1293 (1976).

(11) R. A. Hites and K. Biemann, *Anal. Chem.*, **42**, 855 (1970).

(12) H. Miyazaki, M. Ishibashi, M. Inoue, and M. Itoh, *J. Chromatogr.*, **99**, 553 (1974).

(13) T. Irikura, K. Musuzawa, K. Nishino, M. Kitagawa, H. Uchida, N. Ichinoseki, and M. Ito, *J. Med. Chem.*, **11**, 801 (1968).

(14) C. C. Sweeley, W. H. Elliott, I. Fries, and R. Ryhage, *Anal. Chem.*, **38**, 1549 (1966).

[8] For Part XIX, see M. Horie, S. Baba, Y. Kashida, and C. Hamada, *Yakugaku Zasshi*, **97**, 805 (1977).

Effect of Salicylamide and Acetaminophen on Dextromethorphan Hydrobromide Metabolism: Possible Pharmacological Implications

GOLLAMUDI RAMACHANDER *x, FLORENCE D. WILLIAMS, and JANE FRANCES EMELE

Received April 1, 1977, from the *Consumer Products Group, Warner Lambert Company, Morris Plains, NJ 07950.* Accepted for publication September 9, 1977.

*Present address: Department of Medicinal Chemistry, College of Pharmacy, University of Tennessee Center for the Health Sciences, Memphis, TN 38163.

Abstract □ The effect of salicylamide and acetaminophen on the metabolic fate of dextrorphan, the primary metabolite of dextromethorphan, was studied *in vivo* in the rat. Plasma dextrorphan levels were measured at 5-min intervals up to 20 min and at longer intervals up to 2 hr after dextromethorphan hydrobromide was administered orally either alone or in combination with salicylamide and acetaminophen. The combination gave rise to higher plasma dextrorphan levels than did dextromethorphan hydrobromide alone at most sampling times. Conjugation of dextrorphan was inhibited almost quantitatively by salicylamide and acetaminophen at the 5-min sampling time. Salicylamide alone increased the plasma dextrorphan levels when it was coadministered with dextromethorphan, but the differences were not statistically significant. The antitussive activity of dextromethorphan hydrobromide in the unanesthetized dog was faster in onset, greater in intensity, and longer in duration when it was coadministered with salicylamide and acetaminophen. It is suggested that salicylamide and acetaminophen may inhibit the metabolic inactivation of dextrorphan, thereby improving the cough-inhibiting potential of dextromethorphan hydrobromide.

Keyphrases □ Dextromethorphan hydrobromide—metabolism, effect of salicylamide and acetaminophen, rats □ Metabolism—dextromethorphan hydrobromide, effect of salicylamide and acetaminophen, rats □ Salicylamide—effect on metabolism of dextromethorphan hydrobromide in rats □ Acetaminophen—effect on metabolism of dextromethorphan hydrobromide in rats □ Antitussives—dextromethorphan hydrobromide, metabolism, effect of salicylamide and acetaminophen, rats □ Analgesics—acetaminophen and salicylamide, effect on metabolism of dextromethorphan hydrobromide in rats

Many drugs are eliminated from the body by biotransformation to glucuronide and sulfate conjugates that are pharmacologically inactive. The enzyme systems responsible for the formation of such metabolites are saturable at relatively low drug concentrations (1, 2). Concomitant administration of drugs that undergo conjugation *in vivo* was reported to result in a competitive inhibition of the respective enzymatic processes (3–5).

The main routes of metabolism of dextromethorphan, a widely used nonnarcotic antitussive agent, are *O*- and *N*-demethylation followed by subsequent conjugation of the desmethyl metabolites to glucuronides and sulfates, with *O*-demethylation being the predominant pathway (6–10). The *O*-demethylation product, dextrorphan (*d*-3-hydroxy-*N*-methylmorphinan), was reported to possess antitussive activity in the dog (11). Salicylamide, a weak analgesic and antipyretic agent, is metabolized primarily to the ether glucuronide and ester sulfate (2). The main metabolites of the analgesic drug acetaminophen are the glucuronide and sulfate conjugates (12, 13).

Self-administration of analgesic preparations along with antitussives is common. This investigation determined, in experimental animals, if the biotransformation of dextromethorphan is affected by concurrent administration of salicylamide or a combination of salicylamide and acetaminophen and if the antitussive activity of dextromethorphan is altered by such multidrug therapy.

EXPERIMENTAL

Materials—The drugs and chemicals used were: dextromethorphan

Table I—Effect of Coadministering Dextromethorphan Hydrobromide with Salicylamide on the Plasma Dextrorphan Levels in Rats

Minutes Postdrug	Plasma Dextrorphan Levels, ng/ml[a]: Dextromethorphan Hydrobromide, 10 mg/kg	Plasma Dextrorphan Levels, ng/ml[a]: Dextromethorphan Hydrobromide, 10 mg/kg, plus Salicylamide, 15 mg/kg
5	7 ± 2 (10)	44 ± 17 (9)
10	127 ± 17 (10)	170 ± 15 (10)
15	185 ± 22 (12)	214 ± 23 (12)
20	245 ± 23 (10)	239 ± 21 (11)
30	209 ± 15 (10)	218 ± 18 (10)
45	120 ± 16 (8)	133 ± 22 (8)
60	153 ± 21 (9)	110 ± 16 (10)

[a] Mean ± *SE*. Numbers in parentheses refer to number of animals. One determination was made on each rat.

hydrobromide[1]; dextrorphan[1]; ethyl acetate[2], spectroquality; and *n*-hexane[3], analytical reagent grade.

Methods—*Determination of Dextrorphan in Plasma*—Unconjugated dextrophan was determined by the procedure of Ramachander *et al.* (14). Plasma (3.0 ml) was adjusted to pH 9.5 by the addition of about 0.6 ml of a saturated solution of sodium carbonate and extracted with 15 ml of ethyl acetate. The mixture was centrifuged, and a 12-ml aliquot of the organic layer was shaken with 3.0 ml of 1.0 *N* HCl.

The acid layer was separated, and its fluorescence was measured[4]. The fluorescence and excitation wavelengths were 310 and 280 nm, respectively, and the slit dials were set to give a bandpass of 8 nm for excitation and 5 nm for fluorescence. The concentrations of dextrorphan in the samples were read from a calibration curve whose validity was determined by including three or four known concentrations of the drug added to rat plasma with each series of unknowns.

Varying concentrations of dextrorphan (5–500 ng/ml) were added to normal rat plasma in the presence of 20 μg of salicylamide or 20 μg of salicylamide plus 20 μg of acetaminophen. The plasma was then assayed for free and total dextrorphan. Salicylamide and acetaminophen did not interfere with the measurement of dextrorphan. Salicylamide, 15 mg/kg, or salicylamide, 15 mg/kg, plus acetaminophen, 10 mg/kg, was administered orally to rats, and blood was obtained at 15 and 30 min. Known amounts of dextrorphan were added to the separated plasma, which was analyzed according to the described procedure. The measurement and recoveries of dextrorphan were unaffected.

Determination of Total Dextrorphan (Free and Conjugated) in Plasma—Plasma samples obtained at 0 and 5 min after dextromethorphan hydrobromide (10 mg/kg) administration were analyzed for total dextrorphan by the method of Ramachander *et al.* (14). Plasma (3.0 ml) was adjusted to pH 5.5 with 3.0 *N* acetic acid and incubated at 37° for 2 hr with 0.16 ml of an enzyme solution[5] containing 100,000 units of β-glucuronidase and 50,000 units of sulfatase/ml. The conjugates of dextrorphan appeared to undergo quantitative hydrolysis by 2 hr because longer periods of incubation did not improve the recoveries of the free drug. The pH was then adjusted to 9.5 with a saturated solution of sodium carbonate, and the mixture was analyzed for dextrorphan.

A calibration curve was constructed by plotting fluorescence intensity against concentration of dextrorphan added to drug-free plasma. Regression analysis of the least-squares line fitting the data points provided an equation for the curve as $y = 0.2658x + 3.728$ with $r = 0.9956$, where y represents fluorescence units and x is nanograms of dextrorphan per milliliter of plasma. Recovery of added amounts of dextrorphan to plasma was 70%. To determine method precision, eight samples to which dextrorphan was added to plasma to yield a concentration of 400 ng/ml and four samples containing 600 ng/ml were analyzed in duplicate over 6 months. The coefficients of variation at these two concentrations were 8 and 4%, respectively.

The fluorescence spectrum of dextrorphan extracted from plasma was identical with that of dextrorphan in 1.0 *N* HCl but not with that of the unmetabolized drug. Extracts from plasma of rats administered dextromethorphan hydrobromide exhibited fluorescence spectra characteristic of dextrorphan but not of dextromethorphan.

[1] Hoffmann-La Roche Inc., Nutley, N.J.
[2] Matheson, Coleman and Bell, Norwood, Ohio.
[3] Mallinckrodt Chemical Works, St. Louis, Mo.
[4] Perkin-Elmer model MPF-3 fluorescence spectrophotometer.
[5] Glusulase, Endo Laboratories, Garden City, N.Y.

Table II—Effect of Coadministering Dextromethorphan Hydrobromide with Salicylamide and Acetaminophen on the Plasma Dextrorphan Levels in Rats

Minutes Postdrug	Plasma Dextrorphan Levels, ng/ml[a]: Dextromethorphan Hydrobromide, 10 mg/kg	Plasma Dextrorphan Levels, ng/ml[a]: Dextromethorphan Hydrobromide, 10 mg/kg, plus Salicylamide, 15 mg/kg, plus Acetaminophen, 10 mg/kg
0	0	0
5	7 ± 3[b]	60 ± 10[b]
10	127 ± 26	227 ± 59
15	180 ± 22[c]	314 ± 39[c]
20	243 ± 20	240 ± 35
30	230 ± 38	245 ± 63
45	135 ± 16	174 ± 23
60	145 ± 34	159 ± 23
90	69 ± 14	93 ± 28
120	48 ± 11	74 ± 16

[a] Mean of 10 rats ± *SE*. [b] Significance of the difference between the two treatment groups was <0.05 as determined by the two-tailed *t* test. [c] Significance of the difference between the two treatment groups was <0.01.

Treatment of Animals—Groups of 10 female Sprague–Dawley rats, 160–200 g, were fasted for 18 hr. They then received by stomach tube aqueous solutions of: (*a*) dextromethorphan hydrobromide, 10 mg/kg; (*b*) a combination of dextromethorphan hydrobromide, 10 mg/kg, and salicylamide, 15 mg/kg; or (*c*) a mixture of dextromethorphan hydrobromide, 10 mg/kg, salicylamide, 15 mg/kg, and acetaminophen, 10 mg/kg. Blood samples were withdrawn into heparinized tubes by cardiac puncture immediately prior to and at 5, 10, 15, 20, 30, 45, 60, 90, and 120 min after drug administration.

Plasma was separated by centrifugation and analyzed for free or total dextrorphan according to one of the described procedures. For the determination of total dextrorphan, only the samples obtained at 0 and 5 min were used. Ten rats were used per time period for the determination of either free or total dextrorphan. Plasma from one rat was employed to obtain one experimental value of either free or total dextrorphan.

Evaluation of Antitussive Activity in Unanesthetized Dogs—The antitussive activity was determined according to the method of Tedeschi *et al.* (15), which involves counting the number of coughs produced by an electrically induced vibration of a tracheal magnet. Three preparations were administered to four dogs in a crossover design. The dogs were fasted for 18 hr and were given by a stomach tube: (*a*) dextromethorphan hydrobromide, 5.0 mg/kg, as a 25-ml aqueous solution followed by two successive washes with 25 ml of water each; (*b*) dextromethorphan hydrobromide–salicylamide–acetaminophen (5:7.5:5), 17.5 mg/kg, as a 35-ml aqueous solution followed by two successive washings with 20 ml of water each; (*c*) dextromethorphan hydrobromide–salicylamide–acetaminophen (5:3.25:2.5), 10.75 mg/kg, as a 35-ml aqueous solution followed by two washings with 20 ml of water each; or (*d*) salicylamide–acetaminophen (7.5:5) 12.5 mg/kg, as a 35-ml aqueous solution followed by two washings with 20 ml of water each. All drugs were originally brought into solution by gentle warming in a water bath at 40° and then cooled to room temperature as clear solutions.

Control readings were taken for 3 hr before medication and at 5, 10, 15, and 20 min and 1, 2, 3, and 4 hr thereafter. Drug effects were calculated in terms of percent inhibition of the number of coughs.

RESULTS

Effect of Coadministering Dextromethorphan Hydrobromide with Salicylamide on Plasma Dextrorphan Levels—Upon oral administration of dextromethorphan hydrobromide, 10 mg/kg, to female rats, dextrorphan appeared in plasma at very low levels (7 ng/ml) by 5 min, reached peak levels (245 ng/ml) at 20 min, and declined thereafter. Coadministration of the same dose of dextromethorphan with salicylamide, 15 mg/kg, resulted in higher average concentrations of dextrorphan at 5, 10, 15, 30, and 45 min. The differences, however, were not statistically significant ($p > 0.05$). The results are summarized in Table I.

Effect of Coadministering Dextromethorphan Hydrobromide with Salicylamide and Acetaminophen on Plasma Dextrorphan Levels—The effects of coadministering dextromethorphan hydrobromide (10 mg/kg) with salicylamide (15 mg/kg) and acetaminophen (10 mg/kg) on the average plasma levels are shown in Table II. When the drug

Table III—Effect of Enzyme Hydrolysis on Plasma Dextrorphan Levels in Rats 5 min after the Oral Administration of Dextromethorphan Hydrobromide, Either Alone or in Combination with Salicylamide

Treatment	Plasma Dextrorphan Levels, ng/ml (Mean ± *SE*)[a]	
	Free	Total[b]
Dextromethorphan hydrobromide, 10 mg/kg	7 ± 3[c]	71 ± 10[c,d]
Dextromethorphan hydrobromide, 10 mg/kg, plus salicylamide, 15 mg/kg, and acetaminophen, 10 mg/kg	60 ± 10[d]	74 ± 14[d]

[a] Ten rats were used in each treatment group. [b] Free plus conjugated. Determined after hydrolysis with glucuronidase and arylsulfatase. [c] Significance of the difference between the two treatment groups was <0.01 as determined by the two-tailed *t* test. [d] The three treatment groups were not significantly different from each other.

was administered alone, dextrorphan appeared at very low levels in plasma by 5 min, reached peak levels (243 ng/ml) at 20 min, and declined thereafter. In the postabsorption phase of the curve, a plateau was noticed between 45 and 60 min. With the drug combination, a significantly higher average dextrorphan concentration (60 ng/ml) was noted at 5 min ($p < 0.05$). A mean peak concentration of 314 ng/ml was attained earlier and was significantly higher than the 15-min average concentration of 180 ng/ml obtained after administration of dextromethorphan alone.

Effect of Coadministration of Dextromethorphan Hydrobromide with Salicylamide and Acetaminophen on Relative Amounts of Free and Total Dextrorphan in Rat Plasma—Five minutes after the oral administration of dextromethorphan hydrobromide (10 mg/kg), the mean plasma dextrorphan level in a group of 10 rats was 7 ng/ml (Table III). Enzyme hydrolysis of the 5-min plasma samples from 10 similarly treated rats resulted in an average concentration of 71 ng/ml, which was significantly higher than the value of 7 ng/ml from the former group ($p < 0.01$). Five minutes after the oral administration of dextromethorphan hydrobromide (10 mg/kg) with salicylamide (15 mg/kg) and acetaminophen (10 mg/kg), the mean plasma dextrorphan concentration in a group of 10 rats was 60 ng/ml. Upon enzyme hydrolysis of the plasma samples from 10 similarly treated rats, the average concentration of the metabolite was 74 ng/ml. The latter three groups were not significantly different from each other.

Effect of Salicylamide and Acetaminophen on Antitussive Activity of Dextromethorphan Hydrobromide in Unanesthetized Dogs—The cough inhibition elicited by a 5.0-mg/kg dose of dextromethorphan hydrobromide administered alone or in combination with salicylamide and acetaminophen in unanesthetized dogs is illustrated in Fig. 1. When coadministered with salicylamide (3.25 mg/kg) and acetaminophen (2.50 mg/kg), the antitussive activity of dextromethorphan hydrobromide (5.00 mg/kg) at 20 min was significantly higher than when given alone ($p < 0.05$). The combination of the same dose of the latter with salicylamide (7.5 mg/kg) and acetaminophen (5.0 mg/kg) was even more potent with respect to:

1. Onset of activity. The combination was significantly more active than dextromethorphan hydrobromide at 5 min ($p < 0.02$).
2. Intensity of effect. The percent cough inhibition with the combination at 20 and 60 min was 48.3 and 38.0, respectively; that with the drug alone was 14.5 and 14.3, respectively. The levels of significance of these differences were $p < 0.05$ at 20 min and $p < 0.01$ at 60 min.
3. Duration of activity. Whereas dextromethorphan hydrobromide had marginal activity at 4 hr (percent cough inhibition, 1.5), the combination was significantly more active (percent cough inhibition, 12.5, $p < 0.02$).

Salicylamide and acetaminophen (7.5:5), 12.5 mg/kg, had a negligible antitussive effect. The cough inhibition at any time interval was less than 2%.

DISCUSSION

Kamm *et al.* (6) observed that the primary metabolic pathway of dextromethorphan in the rat is *O*-demethylation, leading to the formation of dextrorphan. Although 3-hydroxymorphinan was present in the urine and bile of rats treated with dextromethorphan, there was no evidence for the presence of 3-methoxymorphinan in these fluids. It was proposed that the formation of 3-hydroxymorphinan may be explained by very rapid *O*-dealkylation of 3-methoxymorphinan to the completely dealkylated 3-hydroxymorphinan.

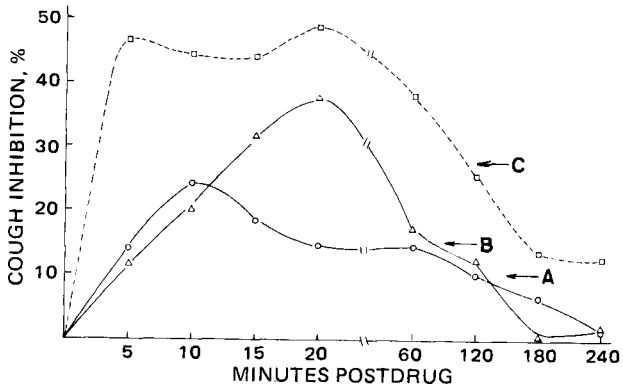

Figure 1—*Effect of salicylamide and acetaminophen on the antitussive activity of dextromethorphan hydrobromide in the unanesthetized dog. Key: A, dextromethorphan hydrobromide, 5 mg/kg; B, dextromethorphan hydrobromide, 5 mg/kg, plus salicylamide, 3.25 mg/kg, plus acetaminophen, 2.5 mg/kg; and C, dextromethorphan hydrobromide, 5 mg/kg, plus salicylamide, 7.5 mg/kg, plus acetaminophen, 5 mg/kg. Each point represents an average of values from four dogs.*

Competitive inhibition of glucuronide and sulfate formation by salicylamide and acetaminophen was reported in humans (16). The observed elevation in the plasma dextrorphan levels in the presence of salicylamide and acetaminophen may be due to similar phenomena, with the three drugs acting as competing substrates. This possibility finds rationale in the observation that all plasma dextrorphan was present in the free form 5 min after the administration of the combination to the rat whereas only 10% was unconjugated after treatment of the animals with dextromethorphan alone. Salicylamide alone had some effect in increasing the plasma dextrorphan levels when coadministered with dextromethorphan hydrobromide, but the observed differences were not statistically significant. The effect was more pronounced when salicylamide and acetaminophen were coadministered with dextromethorphan hydrobromide.

Upon oral administration to dogs, dextromethorphan was metabolized to dextrorphan, 3-methoxymorphinan, and 3-hydroxymorphinan (9). Of these metabolites, only dextrorphan was reported to possess antitussive activity in the dog (11). The present investigation demonstrates that salicylamide and acetaminophen potentiate the antitussive activity of dextromethorphan hydrobromide in the dog. On the basis of findings in the rat, this potentiation may be a result of an inhibition of the conjugation of dextrorphan, the *O*-demethylated metabolite of dextromethorphan, to pharmacologically inactive metabolites. It is possible that processes other than metabolic intervention are operative in the dog inasmuch as the combination had a more prolonged effect in this species than in the rat. More comprehensive studies appear necessary to delineate precisely the site of inhibition by salicylamide and acetaminophen in the metabolic pathway of dextromethorphan.

These findings are of importance in multiple drug therapy and its clinical implications.

REFERENCES

(1) W. Barr, *Drug Inf. Bull.*, **3**, 27 (1969).
(2) G. Levy and T. Matsuzawa, *J. Pharmacol. Exp. Ther.*, **156**, 285 (1967).
(3) G. Levy and J. H. Procknal, *J. Pharm. Sci.*, **57**, 1330 (1968).
(4) G. Ramachander, F. D. Williams, and J. F. Emele, *ibid.*, **62**, 1498 (1973).
(5) E. Dybing, *Biochem. Pharmacol.*, **25**, 1421 (1976).
(6) J. J. Kamm, A. B. Taddeo, and E. J. Van Loon, *J. Pharmacol. Exp. Ther.*, **158**, 437 (1967).
(7) K. Willner, *Arzneim.-Forsch.*, **12**, 26 (1963).
(8) C. Elison and H. Elliott, *J. Pharmacol. Exp. Ther.*, **144**, 265 (1964).
(9) A. Brossi, O. Hafliger, and O. Schneider, *Arzneim.-Forsch.*, **5**, 62 (1955).
(10) R. Versie, A. Noirsfalise, M. Neven, and R. Malchair, *Ann. Med. Leg.*, **42**, 561 (1962).
(11) W. M. Benson, P. F. Stefko, and L. O. Randall, *J. Pharmacol. Exp. Ther.*, **109**, 189 (1953).
(12) A. J. Cummings, M. L. King, and B. K. Martin, *Br. J. Pharmacol. Chemother.*, **29**, 150 (1967).

(13) G. L. Mattock, I. J. McGilveray, and D. Cook, *Can. J. Pharm. Sci.*, **6**, 35 (1971).
(14) G. Ramachander, F. D. Williams, and J. F. Emele, *J. Pharm. Sci.*, **66**, 1047 (1977).
(15) R. E. Tedeschi, D. H. Tedeschi, J. T. Hitchens, L. Cook, P. A. Mattis, and E. J. Fellows, *J. Pharmacol. Exp. Ther.*, **126**, 338 (1959).
(16) G. Levy and H. Yamada, *J. Pharm. Sci.*, **60**, 215 (1971).

ACKNOWLEDGMENTS

Part of the antitussive studies were conducted at Pharmakon Laboratories, Scranton, Pa., by Dr. Richard Matthews, to whom the authors express their appreciation. The authors also acknowledge the interest of Dr. Herbert A. Lieberman.

Bioavailability of Erythromycin Stearate: Influence of Food and Fluid Volume

P. G. WELLING *x, H. HUANG, P. F. HEWITT, and L. L. LYONS

Received June 20, 1977, from the *Center for Health Sciences, School of Pharmacy, University of Wisconsin, Madison, WI 53706.* Accepted for publication September 9, 1977. *Present address: School of Medicine, Department of Therapeutics and Clinical Pharmacology, Queen Elizabeth Hospital, Edgbaston, Birmingham B15 2TH, England.

Abstract □ The influence of various test meals and coadministered water volumes on erythromycin stearate bioavailability from orally dosed film-coated tablets was studied in healthy human subjects. Serum erythromycin levels were uniformly reduced by all test meals, with the reduction in mean peak serum levels varying from 47 to 60%. Serum erythromycin levels also were reduced significantly in fasted individuals when the accompanying water volume was reduced from 250 to 20 ml. The apparent drug absorption rate constant was not influenced by treatments. This result is probably due to rapid degradation of solubilized, unabsorbed drug in the GI tract. Higher and more uniform serum erythromycin levels are obtained when erythromycin stearate tablets are given on an empty stomach together with an adequate water volume.

Keyphrases □ Erythromycin stearate—bioavailability, effect of food and fluid volume, humans □ Bioavailability—erythromycin stearate, effect of food and fluid volume, humans □ Absorption, GI—erythromycin stearate, effect of food and fluid volume, humans □ Antibacterials—erythromycin stearate, bioavailability, effect of food and fluid volume, humans

Since the introduction of erythromycin in 1952 (1) and subsequent observations that the drug may be irregularly absorbed from the GI tract (2), a large number of derivatives and formulations have been prepared to optimize its stability and absorption.

The bioavailability of one such derivative, erythromycin stearate, has been examined from an oral suspension (3, 4) and film-coated tablets (4–6). One study (4) suggested that erythromycin stearate in film-coated tablets may be absorbed into the circulation at a faster rate than erythromycin base from coated tablets. However, the overall absorption efficiency of antibiotic from the two dosage forms was similar.

Reports on the influence of food on erythromycin stearate absorption are conflicting. Absorption from the suspension appears not to be influenced by food (3), while absorption from film-coated tablets is reduced (5, 6). However, the reported studies have several shortcomings in that the types and sizes of meals and the time intervals between eating and dosing were generally not specified. Furthermore, the volumes of fluid ingested with the drug were not described. The only mention of fluid volume occurred in one study (6) where subjects took the drug with as much fluid as desired.

In view of the marked influence that different meals, varying time intervals between food and drug ingestion, and volumes of fluid taken with a drug may have on drug absorption (7), this study examined erythromycin stearate bioavailability in human volunteers with these factors carefully controlled.

EXPERIMENTAL

The overall design was similar to that described previously (8). Subjects were two female and four male healthy volunteers. The females were 22 and 24 years old and weighed 64 and 50 kg. The males were 22–33 years old (mean 27) and weighed 66–82 kg (mean 73). All subjects were shown to be in good physical condition by medical examination.

Protocol—Verbal assurance was obtained from all subjects that they had taken no known enzyme-inducing agents for 1 month, and no other drugs for 1 week, preceding the study. Subjects were instructed to take no drugs other than the required doses of erythromycin stearate during the study.

Subjects were fasted overnight before each treatment and were permitted to eat no food, apart from test meals, until 4 hr after dosing. On the morning of a treatment, each subject drank 250 ml of water on arising, at least 1 hr before dosing. Medication was administered at 8:00 am; blood samples (~5 ml) were collected from a forearm vein for serum in vacuum tubes[1] immediately before and at 0.5, 1, 2, 4, 6, 8, and 12 hr after dosing. Serum was deep frozen (−18°) until assayed. Assays were routinely carried out within 1 week of sampling.

Treatments—Erythromycin stearate was administered as single 500-mg doses consisting of two 250-mg film-coated tablets[2]. High carbohydrate, high protein, and high fat meals were prepared and standardized as described previously (9). The following treatments were administered:

Treatment 1—Two tablets with 250 ml of water immediately following a standard high carbohydrate meal.

Treatment 2—Two tablets with 250 ml of water immediately following a standard high fat meal.

Treatment 3—Two tablets with 250 ml of water immediately following a standard high protein meal.

Treatment 4—Two tablets with 20 ml of water on a fasted stomach.

Treatment 5—Two tablets with 250 ml of water on a fasted stomach.

[1] Vacutainers.
[2] Bristamycin, Bristol Laboratories.

(13) G. L. Mattock, I. J. McGilveray, and D. Cook, *Can. J. Pharm. Sci.*, **6**, 35 (1971).
(14) G. Ramachander, F. D. Williams, and J. F. Emele, *J. Pharm. Sci.*, **66**, 1047 (1977).
(15) R. E. Tedeschi, D. H. Tedeschi, J. T. Hitchens, L. Cook, P. A. Mattis, and E. J. Fellows, *J. Pharmacol. Exp. Ther.*, **126**, 338 (1959).
(16) G. Levy and H. Yamada, *J. Pharm. Sci.*, **60**, 215 (1971).

ACKNOWLEDGMENTS

Part of the antitussive studies were conducted at Pharmakon Laboratories, Scranton, Pa., by Dr. Richard Matthews, to whom the authors express their appreciation. The authors also acknowledge the interest of Dr. Herbert A. Lieberman.

Bioavailability of Erythromycin Stearate: Influence of Food and Fluid Volume

P. G. WELLING *x, H. HUANG, P. F. HEWITT, and L. L. LYONS

Received June 20, 1977, from the *Center for Health Sciences, School of Pharmacy, University of Wisconsin, Madison, WI 53706.* Accepted for publication September 9, 1977. *Present address: School of Medicine, Department of Therapeutics and Clinical Pharmacology, Queen Elizabeth Hospital, Edgbaston, Birmingham B15 2TH, England.

Abstract □ The influence of various test meals and coadministered water volumes on erythromycin stearate bioavailability from orally dosed film-coated tablets was studied in healthy human subjects. Serum erythromycin levels were uniformly reduced by all test meals, with the reduction in mean peak serum levels varying from 47 to 60%. Serum erythromycin levels also were reduced significantly in fasted individuals when the accompanying water volume was reduced from 250 to 20 ml. The apparent drug absorption rate constant was not influenced by treatments. This result is probably due to rapid degradation of solubilized, unabsorbed drug in the GI tract. Higher and more uniform serum erythromycin levels are obtained when erythromycin stearate tablets are given on an empty stomach together with an adequate water volume.

Keyphrases □ Erythromycin stearate—bioavailability, effect of food and fluid volume, humans □ Bioavailability—erythromycin stearate, effect of food and fluid volume, humans □ Absorption, GI—erythromycin stearate, effect of food and fluid volume, humans □ Antibacterials—erythromycin stearate, bioavailability, effect of food and fluid volume, humans

Since the introduction of erythromycin in 1952 (1) and subsequent observations that the drug may be irregularly absorbed from the GI tract (2), a large number of derivatives and formulations have been prepared to optimize its stability and absorption.

The bioavailability of one such derivative, erythromycin stearate, has been examined from an oral suspension (3, 4) and film-coated tablets (4–6). One study (4) suggested that erythromycin stearate in film-coated tablets may be absorbed into the circulation at a faster rate than erythromycin base from coated tablets. However, the overall absorption efficiency of antibiotic from the two dosage forms was similar.

Reports on the influence of food on erythromycin stearate absorption are conflicting. Absorption from the suspension appears not to be influenced by food (3), while absorption from film-coated tablets is reduced (5, 6). However, the reported studies have several shortcomings in that the types and sizes of meals and the time intervals between eating and dosing were generally not specified. Furthermore, the volumes of fluid ingested with the drug were not described. The only mention of fluid volume occurred in one study (6) where subjects took the drug with as much fluid as desired.

In view of the marked influence that different meals, varying time intervals between food and drug ingestion, and volumes of fluid taken with a drug may have on drug absorption (7), this study examined erythromycin stearate bioavailability in human volunteers with these factors carefully controlled.

EXPERIMENTAL

The overall design was similar to that described previously (8). Subjects were two female and four male healthy volunteers. The females were 22 and 24 years old and weighed 64 and 50 kg. The males were 22–33 years old (mean 27) and weighed 66–82 kg (mean 73). All subjects were shown to be in good physical condition by medical examination.

Protocol—Verbal assurance was obtained from all subjects that they had taken no known enzyme-inducing agents for 1 month, and no other drugs for 1 week, preceding the study. Subjects were instructed to take no drugs other than the required doses of erythromycin stearate during the study.

Subjects were fasted overnight before each treatment and were permitted to eat no food, apart from test meals, until 4 hr after dosing. On the morning of a treatment, each subject drank 250 ml of water on arising, at least 1 hr before dosing. Medication was administered at 8:00 am; blood samples (~5 ml) were collected from a forearm vein for serum in vacuum tubes[1] immediately before and at 0.5, 1, 2, 4, 6, 8, and 12 hr after dosing. Serum was deep frozen (−18°) until assayed. Assays were routinely carried out within 1 week of sampling.

Treatments—Erythromycin stearate was administered as single 500-mg doses consisting of two 250-mg film-coated tablets[2]. High carbohydrate, high protein, and high fat meals were prepared and standardized as described previously (9). The following treatments were administered:

Treatment 1—Two tablets with 250 ml of water immediately following a standard high carbohydrate meal.

Treatment 2—Two tablets with 250 ml of water immediately following a standard high fat meal.

Treatment 3—Two tablets with 250 ml of water immediately following a standard high protein meal.

Treatment 4—Two tablets with 20 ml of water on a fasted stomach.

Treatment 5—Two tablets with 250 ml of water on a fasted stomach.

[1] Vacutainers.
[2] Bristamycin, Bristol Laboratories.

Table I—Average Serum Erythromycin Concentrations (±1 *SD*) from All Treatments

Treatment	Serum Erythromycin Level, μg/ml							
	0.0 hr	0.5 hr	1 hr	2 hr	4 hr	6 hr	8 hr	12 hr
1 Carbohydrate	0	0.01 ± 0.02	0.17 ± 0.41	1.16 ± 1.40	0.59 ± 0.47	0.29 ± 0.21	0.13 ± 0.01	0.04 ± 0.03
2 Fat	0	0.11 ± 0.17	0.41 ± 0.24	1.43 ± 0.85	0.66 ± 0.22	0.24 ± 0.10	0.11 ± 0.05	0.03 ± 0.02
3 Protein	0	0.05 ± 0.06	0.36 ± 0.49	1.03 ± 0.89	0.49 ± 0.18	0.19 ± 0.09	0.10 ± 0.05	0.03 ± 0.02
4 Fasting 20 ml	0	0.05 ± 0.10	0.59 ± 0.42	1.43 ± 0.55	1.30 ± 0.49	0.69 ± 0.27	0.40 ± 0.18	0.14 ± 0.08
5 Fasting 250 ml	0	0.36 ± 0.43	1.33 ± 1.08	2.65 ± 1.14	1.73 ± 0.51	0.83 ± 0.27	0.41 ± 0.16	0.13 ± 0.09
Paired *t*-test[a]	0	NSD[b]	5 > 1	5 > 3,4	4 > 1–3; 5 > 1–4	4,5 > 1–3	4,5 > 1–3	4,5 > 1–3

[a] Differences significant at $p < 0.05$. [b] No significant differences.

Tablets were swallowed whole. Problems associated with test meal preparation made treatment randomization impractical, and all subjects received the same treatment at the same time. Treatments were administered at least 1 week apart.

Assay—Serum erythromycin levels were determined using a microbiological cup plate diffusion method with *Sarcina lutea* (ATCC 9341) as the test organism and neomycin assay agar[3] as the growth medium.

Data Analysis—Individual serum erythromycin levels were fitted to a one-compartment open model with first-order absorption and elimination, using the program NREG on a digital computer[4] as described previously (8). Attempts to use more complex models to fit the individual data sets produced only slight increases in coefficients of determination and caused considerable increases in variances of pharmacokinetic constants.

Serum erythromycin levels at each sampling time and also pharmacokinetic constants were compared among and between treatments by analysis of variance and by paired *t*-test (8).

RESULTS

Mean serum erythromycin levels, together with the results of statistical analysis, are given in Table I; the data are summarized in Fig. 1. Circulating levels of erythromycin were reduced significantly by the test meals throughout the entire sampling period. Although peak erythromycin levels occurred at approximately the same time from all treatments, antibiotic concentrations were generally reduced to one-half the fasted values by the high fat meal and to somewhat less than one-half the fasted values by the high carbohydrate and high protein meals.

Serum erythromycin levels also were reduced when the accompanying water volume was changed from 250 to 20 ml in fasted individuals. The resulting serum erythromycin profiles were intermediate between those obtained from the other fasting treatment and those from postprandial doses. The 2- and 4-hr erythromycin levels were significantly reduced by the low water volume in fasted subjects. Serum erythromycin levels tended to be more consistent among subjects from Treatment 5 than from all other treatments. Although the high fat meal tended to produce somewhat higher serum erythromycin levels than the other meals at 2 and 4 hr, differences in erythromycin levels among nonfasted treatments were not significant.

The similar times of peak erythromycin levels in all treatments (Table II) suggest that the lower levels observed after nonfasted treatments and, to a lesser extent, after the low water volume treatment are caused by a reduction in the overall extent of drug absorption rather than the rate.

Mean values of all pharmacokinetic constants, obtained from individual data sets, are given in Table II.

The rather low coefficients of determination observed with all treatments were due to the considerable variance in the data, both among individuals and in the same individual. Considerable scatter in circulating levels of erythromycin following oral doses of various erythromycin formulations was reported previously (3–6).

Despite the considerable differences in serum erythromycin profiles from fasted and nonfasted treatments, there were no significant differences between the absorption rate constants or their associated absorption half-times. The lag time for appearance of drug in serum was higher following the high fat treatment than all other treatments. However, there was considerable individual variation in this value.

The rate constant for elimination of erythromycin from serum was also essentially treatment independent, although this parameter was significantly higher after the high protein meal compared to the low water volume treatment.

Differences in the extent of erythromycin stearate absorption from the different treatments are indicated by the *FD/V* values and by the areas under serum erythromycin level *versus* time curves. The *FD/V* value, which provides a rate-independent estimate of relative drug absorption, shows that erythromycin stearate absorption was impaired by about 43% in fasted individuals when the accompanying water volume was reduced from 250 to 20 ml. The test meals reduced absorption by 53–64%.

Similar reductions due to low water volume and test meals were obtained in truncated areas under serum level curves to 2 and 12 hr after dosing and also in total areas from zero to infinite time. However, differences in the 0–12-hr and total areas between the two fasted treatments were somewhat less than the differences in *FD/V* values because of the somewhat larger elimination rate constants after Treatment 5 compared to those after Treatment 4. Considerable individual variation was observed in some area values. However, unlike the situation with lag times, the variation in area values tended to be less with the fasted treatments than with the nonfasted treatments.

DISCUSSION

The observed reduction in the overall absorption efficiency of erythromycin stearate due to food and also to low fluid volumes, and yet the relative constancy of the absorption rate constant between treatments, may readily be rationalized in terms of the various factors contributing to the magnitude of k_a. Perrier and Gibaldi (10) showed that the apparent absorption rate constant, obtained from standard blood level curve-stripping techniques, reflects the overall rate of drug loss from the absorption site by all processes rather than the intrinsic absorption rate constant.

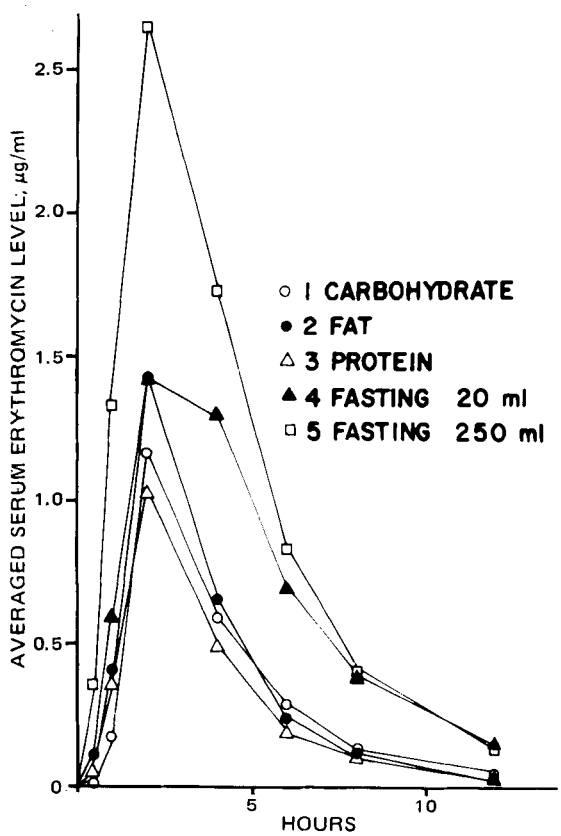

Figure 1—*Mean serum erythromycin levels.*

[3] Bacto antibiotic medium 11, Difco Laboratories.
[4] Univac model 1110.

Table II—Values of Pharmacokinetic Constants (±1 *SD*)

Constant	Treatment 1	2	3	4	5	Paired *t*-Test
k_a[a], hr^{-1}	0.59 ± 0.26	0.68 ± 0.28	0.66 ± 0.34	0.57 ± 0.20	0.61 ± 0.25	NSD
$t_{1/2\ (abs)}$[b], hr	1.5 ± 0.9	1.2 ± 0.6	1.3 ± 0.6	1.3 ± 0.4	1.3 ± 0.5	NSD
k_{el}[c], hr^{-1}	0.36 ± 0.03	0.42 ± 0.06	0.42 ± 0.15	0.30 ± 0.08	0.36 ± 0.07	3 > 4
$t_{1/2\ (elim)}$[d], hr	1.9 ± 0.1	1.7 ± 0.3	1.8 ± 0.5	2.5 ± 0.8	2.0 ± 0.4	NSD
FD/V[e], μg/ml	1.8 ± 1.6	2.2 ± 1.1	1.7 ± 0.9	2.7 ± 0.9	4.7 ± 1.2	5 > 1–4
t_0[f], hr	0.83 ± 0.68	0.17 ± 0.26	0.25 ± 0.42	0.25 ± 0.27	0.08 ± 0.20	1 > 2–5
r^2[g]	0.80 ± 0.01	0.85 ± 0.10	0.73 ± 0.10	0.92 ± 0.06	0.88 ± 0.07	4 > 1,3
Area[h] 0 → 2, μg hr/ml	0.5 ± 0.7	1.1 ± 0.5	0.8 ± 0.6	1.2 ± 0.6	2.5 ± 1.0	5 > 1–4
Area[h] 0 → 12, μg hr/ml	4.1 ± 3.5	4.7 ± 1.8	3.6 ± 2.0	8.2 ± 2.7	11.9 ± 2.1	4 > 1–3; 5 > 1–4
Area[i] 0 → ∞, μg hr/ml	4.8 ± 3.9	5.2 ± 2.0	4.0 ± 2.1	9.3 ± 3.0	13.2 ± 2.6	4 > 1–3; 5 > 1–4
Peak height, μg/ml	1.3 ± 1.3	1.4 ± 0.8	1.2 ± 0.7	1.7 ± 0.5	3.0 ± 0.9	5 > 1–4
Time of peak height, hr	3.3 ± 1.6	2.3 ± 0.8	2.2 ± 1.0	3.0 ± 1.1	2.7 ± 1.0	NSD

[a] First-order rate constant for appearance of erythromycin in serum. [b] Absorption half-time. [c] First-order rate constant for loss of erythromycin from serum. [d] Elimination half-life. [e] Fraction (F) of administered dose (D) absorbed, expressed as a concentration in its distribution volume (V) in the body. [f] Lag time between dosing and the appearance of erythromycin in serum. [g] Coefficient of determination ($\Sigma\ obs^2 - \Sigma\ dev^2)/\Sigma\ obs^2$. [h] Obtained by trapezoidal rule. [i] Obtained from the relationship FD/Vk_{el} = Area 0 → ∞.

Erythromycin stearate is acid labile. Once the film coating of the tablet has been penetrated during prolonged residence in the stomach due to food, the presence of which tends to neutralize the gastric acidity, the drug is lost from this site because of absorption into the bloodstream, stomach emptying with subsequent absorption from the small intestine, and acid-catalyzed degradation. Although these various factors must contribute differently to the observed values of k_a in the different treatments, the data in this study indicate that the sum of their different contributions is similar.

These results show that the efficiency of erythromycin stearate absorption from film-coated tablets is markedly reduced by three test meals. Therefore, these observations are consistent with previous studies in which mean peak serum erythromycin levels were reduced by food by about 40% (5) and about 60% (6). Both studies reported greater individual variation in circulating erythromycin levels than presently obtained. This result may be due to insufficient control of diets and fluid volumes in the earlier studies.

In addition, the results show that reduction in accompanying fluid volume can depress serum erythromycin levels significantly. This result is probably related to the low aqueous solubility of erythromycin stearate. Reduction of the water volume might be expected to inhibit considerably the dissolution of erythromycin stearate and, hence, its bioavailability. However, solubility cannot be the only contributing factor. Because the drug also must be in solution to be chemically degraded, one would expect the absorption rate constant to be similarly reduced. Although the k_a value for Treatment 4 tended to be low, differences in the value of this constant between treatments were not significant.

A probable explanation for this phenomenon may be that, with the smaller administered water volume, stomach emptying is delayed relative to that with the larger volume (11) and there is less dilution of gastric acidic secretions. These effects would result in delayed transit of drug to the optimal absorption sites in the small intestine with increased chance of acid-catalyzed degradation. Reduction in accompanying fluid volume reduced the rate or extent of absorption of other fat-soluble drugs (8, 9). This property appears to be common to this type of compound.

During a recent study, serum erythromycin levels were measured following intravenous doses[5]. Data from this dosage form were analyzed in terms of the two-compartment model; the overall distribution volume, V_{dss}, based on circulating levels of combined free and bound erythromycin, was calculated to be approximately 70% of body weight in normal individuals.

Substitution of this value into individual FD/V values obtained in the present study permits the value of FD, the fraction of the administered dose that is ultimately absorbed, to be calculated. Expressing this value as a percentage of the 500-mg dose yields the following values for the different treatments: carbohydrate, 18.3 ± 18.4%; fat, 21.5 ± 12.3%; protein, 16.1 ± 8.5%; fasting with 20 ml of water, 26.3 ± 10.9%; and fasting with 250 ml of water, 44.5 ± 13.8%.

Although these percentages are only approximations, they indicate the efficiency of erythromycin stearate absorption from this dosage form and may explain the considerable individual variations in circulating levels of this antibiotic after oral doses.

The results obtained show that test meals may markedly inhibit the bioavailability of erythromycin stearate from orally dosed tablets, giving rise to depressed circulating levels of antibiotic. Additionally, they show that absorption is inhibited if an inadequate volume of fluid is ingested with the drug. It is, therefore, recommended that erythromycin stearate tablets be administered, wherever possible, on an empty stomach and accompanied by an adequate volume of water.

These results and recommendations are based on a single-dose study. The influence of food and fluid volumes on the absorption of various erythromycin products following both single and repeated doses is currently being investigated.

[5] P. G. Welling and W. A. Craig, unpublished data.

REFERENCES

(1) J. M. McGuire, R. L. Bunch, R. C. Anderson, H. E. Boaz, H. E. Flynn, H. M. Powell, and J. W. Smith, *Antibiot. Chemother.*, **2**, 281 (1952).

(2) L. E. Josselyn and J. C. Sylvester, *ibid.*, **3**, 63 (1952).

(3) J. C. Sylvester and L. E. Josselyn, *ibid.*, **3**, 930 (1953).

(4) L. E. Josselyn, C. Endicott, and J. C. Sylvester, *Antibiot. Annu.*, **1954–1955**, 279.

(5) H. A. Hirsch and M. Finland, *Am. J. Med. Sci.*, **237**, 55 (1959).

(6) W. E. Clapper, M. Mostyn, and G. H. Meade, *Antibiot. Med. Clin. Ther.*, **7**, 91 (1960).

(7) P. G. Welling, *J. Pharmacokinet. Biopharm.*, **5**, 291 (1977).

(8) P. G. Welling, H. Huang, P. A. Koch, W. A. Craig, and P. O. Madsen, *J. Pharm. Sci.*, **66**, 549 (1977).

(9) P. G. Welling, L. L. Lyons, W. A. Craig, and G. A. Trochta, *Clin. Pharmacol. Ther.*, **17**, 475 (1975).

(10) D. Perrier and M. Gibaldi, *J. Pharm. Sci.*, **62**, 225 (1973).

(11) J. N. Hunt and I. MacDonald, *J. Physiol. (London)*, **126**, 459 (1954).

ACKNOWLEDGMENTS

Supported by Grant GM 20327 from the National Institutes of Health.

Quantitative Crystallinity Determinations for β-Lactam Antibiotics by Solution Calorimetry: Correlations with Stability

M. J. PIKAL ˣ, A. L. LUKES, JOHN E. LANG, and K. GAINES

Received November 24, 1976, from the *Lilly Research Laboratories, Eli Lilly and Co., Indianapolis, IN 46206.* Accepted for publication September 19, 1977.

Abstract □ The solution calorimetry method is based on the observation that amorphous forms are normally significantly higher in energy than are crystalline forms. The utility and validity of the calorimetric method were investigated for cephalothin sodium, cefazolin sodium, cefamandole nafate, and cefamandole sodium. Amorphous, partially crystalline, and crystalline forms were prepared and characterized by X-ray diffraction (powder), by solution calorimetry, and, for cephalothin sodium, by the thermal decomposition rate at 50°. Qualitatively, there was a good correlation between calorimetric crystallinity and the (less precise) crystallinity derived from X-ray data. The energy and structure of the amorphous state depend on the history of the sample; even samples of the same crystalline polymorph, containing no amorphous phase, may differ in energy. Thus, the *absolute* value of the crystallinity (X-ray or calorimetric) depends on the choice of amorphous and crystalline standards. The heat of solution is a precise (±1%) and unambiguous measure of the *relative* crystallinity; and provided amorphous and crystalline standards are appropriately chosen, the calorimetric crystallinity correlates well with chemical stability.

Keyphrases □ Crystallinity—determination by solution calorimetry, β-lactam antibiotics, correlated with chemical stability □ Antibiotics, β-lactam—crystallinity determined by solution calorimetry, correlated with chemical stability □ Calorimetry, solution—determinations of crystallinity of β-lactam antibiotics, correlated with chemical stability □ Stability, chemical—β-lactam antibiotics, correlated with crystallinity determined by solution calorimetry

The importance of polymorphism to an understanding of pharmaceutical systems is well recognized (1–6). Partial crystallinity is a special class of polymorphism and may have significant effects on dissolution rates (5, 6) and chemical stability (7). The magnitude of the observed difference in the dissolution rate (5, 6) or stability (7) between amorphous and crystalline phases suggests that even a small amount of amorphous phase in an otherwise crystalline sample is sufficient to alter measurably physical and chemical properties.

Methodology for determining precise degrees of crystallinity is needed to characterize fully the solid phase. Such methodology, specifically applied to β-lactam antibiotics, is the subject of this report. In principle, any extensive property that varies smoothly with the fraction of the crystalline phase in crystalline/amorphous mixtures may be used to measure crystallinity.

BACKGROUND

X-ray diffraction is the traditional method for crystallinity measurements (8–13). Although essential for qualitative identification of the crystalline phase present, X-ray powder patterns are not well suited for quantitative crystallinity measurements on β-lactam antibiotics. Precision is lacking, orientation effects[1] may result in systematic errors, and, because of pattern complexity, the separation of amorphous scattering from the total diffraction pattern is somewhat ambiguous. These problems are not unique to β-lactam antibiotics. Crystallinity measurements on polymers are subject to the same artifacts and ambiguities (10–13).

Quantitative degrees of crystallinity may be evaluated from heat of solution measurements (17). This method is based on the observation (14, 17–21) that, for many solids, the energy of the amorphous form is significantly higher than the energy of the crystalline form. The heat of solution, or calorimetric, percent crystallinity, P_c, is defined by:

$$P_c = 100\left[\frac{\Delta\bar{H}^\circ_s - \Delta\bar{H}^\circ_a}{\Delta\bar{H}^\circ_c - \Delta\bar{H}^\circ_a}\right] \qquad \text{(Eq. 1)}$$

where $\Delta\bar{H}^\circ_s$, $\Delta\bar{H}^\circ_c$, and $\Delta\bar{H}^\circ_a$ are the heats of solution to infinite dilution (in any fixed solvent) of the sample, the 100% crystalline standard, and the 100% amorphous standard, respectively. Thus, as with the usual relative X-ray and density methods (8–12), the partially crystalline sample is assumed to be a mixture of the two standard states (two-state model). Since the energy of a mixture of two solid phases is rigorously given by the sum of the energies of each phase, Eq. 1 is exact for mixtures of amorphous and crystalline standards. Provided the energy difference between crystalline and amorphous states is large, calorimetric crystallinities are potentially more precise, less subject to artifacts, and less ambiguous than crystallinity data derived from X-ray diffraction.

The objective of this research was to investigate the heat of solution as a measure of the crystallinity of β-lactam antibiotics, with specific consideration given to: (*a*) interference from contaminants (*e.g.*, water), (*b*) the magnitude of the energy difference between crystalline and amorphous forms, (*c*) the uniqueness of the amorphous and crystalline standards, (*d*) correlation of calorimetric and X-ray diffraction data, and (*e*) correlation of chemical stability with calorimetric crystallinity for partially crystalline samples.

The compounds and polymorphs studied are summarized in Table I. A sample was classified as amorphous when the X-ray diffraction pattern (powder) showed no distinct peaks and the sample was nonbirefringent (microscopic examination under polarized light).

EXPERIMENTAL

Sample Preparation—*Cefazolin Sodium*—The crystalline α-form (pentahydrate) was prepared by recrystallization from aqueous ethanol (22). The monohydrate was prepared by suspending the α-form in anhydrous ethanol. The identity of each crystal form was verified by X-ray diffraction.

The precipitated forms (Samples 4 and 5, Table I) were prepared by rapidly pouring 20 ml of a 50% solution of cefazolin sodium in water–acetonitrile (1:1) into 300 ml of anhydrous ethanol. A gel first formed, which then was transformed into nonbirefringent beads about 80 μm in diameter. The system was allowed to age for several hours and then was filtered. The solid was air dried overnight and then was vacuum dried. The solid product exhibited birefringence. The X-ray diffraction patterns were qualitatively similar to the monohydrate pattern. However, the samples were very poorly crystallized, and a positive identification of the crystal form could not be made.

Sample 7 (Table I) was spray dried[2] from a 25% aqueous solution with an inlet temperature of 150° and an outlet temperature of 100°, yielding glassy amorphous beads 10–20 μm in diameter. The amorphous freeze-dried sample (Sample 8, Table I) was prepared by freeze drying an aqueous solution at low temperature as previously described (7).

[1] Orientation effects may be eliminated by reducing the sample to a fine powder by grinding. However, since grinding reduces the crystallinity of many materials (6, 14, 15), it cannot be employed in crystallinity determinations. Sample rotation may be used to minimize orientation effects if the diffractometer is modified suitably (16). These specialized modifications were not available for the research described in this report.

[2] Komline-Sanderson, 91-cm (36-in.) diameter, or equivalent laboratory model spray drier.

Table I—Effect of Physical Form on Energy of Solids: Heats of Solution at Infinite Dilution in Water at 25°

Sample	Compound	Physical Form[a]	Water Content, % (w/w)	Heat of Solution[b], $\Delta H°_s$, kcal/mole
1	Cefazolin sodium	Crystalline, pentahydrate (α-form)	15.9	+7.8
2	Cefazolin sodium	Crystalline, monohydrate	4.0	+4.4
3	Cefazolin sodium	Weak crystalline, vacuum-dehydrated monohydrate	0.2	−1.4
4	Cefazolin sodium	Weak crystalline, precipitated[c]	0.3	−2.0
5	Cefazolin sodium	Weak crystalline, precipitated[c]	0.3	−3.5
5a	Cefazolin sodium	Weak crystalline, precipitated[c]	4.0	+0.8
6	Cefazolin sodium	Weak crystalline, vacuum-dehydrated α-form	0.0	−3.2
7	Cefazolin sodium	Amorphous, spray dried	0.3	−4.5
8	Cefazolin sodium	Amorphous, freeze dried	0.1	−5.4
9	Cefamandole nafate[d]	Crystalline, γ-form	0.0	1.92 ± 0.05
10	Cefamandole nafate[d]	Crystalline, γ-form[e]	0.1	1.48 ± 0.05
11	Cefamandole nafate[d]	Weak crystalline, vacuum-desolvated α-form	0.1	−1.0
12	Cefamandole nafate[d]	Amorphous, spray dried	0.3	−3.4 ± 0.1
13	Cefamandole nafate[d]	Amorphous, freeze dried	0.1	−4.4 ± 0.1
14	Cefamandole sodium[d]	Crystalline, monohydrate	4.0	0.26 ± 0.05
15	Cefamandole sodium[d]	Crystalline, vacuum-dehydrated monohydrate	0.2	−1.84 ± 0.05
16	Cefamandole sodium[d]	Amorphous, spray dried	0.1	−3.1
17	Cefamandole sodium[d]	Amorphous, freeze dried	0.4	−5.3
18	Cephalothin sodium	Crystalline	0.1	1.9 ± 0.1
19	Cephalothin sodium	Crystalline	0.0	1.67 ± 0.02
20	Cephalothin sodium	Crystalline	0.0	1.47 ± 0.05
21	Cephalothin sodium	Crystalline, mortar ground Sample 20	0.1	1.20 ± 0.08
22	Cephalothin sodium	Amorphous, freeze dried	0.1	−4.1 ± 0.1
23	Penicillin G potassium	Crystalline	0.1	−0.32 ± 0.05
24	Penicillin G potassium	Amorphous, freeze dried	0.5	−5.4

[a] Crystalline = 100% birefringent particles, sharp X-ray pattern with low diffuse scattering; weak crystalline ≈ 100% birefringent particles, weak and diffuse X-ray pattern; amorphous = nonbirefringent, no distinct peaks in the X-ray pattern. [b] Uncertainty, ~ ±0.2 kcal/mole for the sample studied except when specifically indicated otherwise. The uncertainty corresponds roughly to the 90% confidence level. [c] Weakly crystalline even with 5% water. Appears to be poorly crystallized monohydrate. [d] The chemical structure of this compound may be found in Table I of Ref. 7. [e] Probably has an amorphous layer coating the crystals (see *Experimental*).

Cefamandole Nafate—Samples 9 and 10 (Table I) were crystallized as one lot from a methanol solution by the addition of 2-propanol, yielding nonsolvated crystalline material. One portion of the filter cake was first air dried overnight and then vacuum dried (25°/24 hr; 40°/24 hr) to yield Sample 9. The remaining portion was placed directly into a 50° oven and vacuum dried overnight to yield Sample 10. This procedure presumably caused an amorphous coating on the crystal surface because of partial dissolution at high temperature and subsequent evaporation of solvents (methanol, 2-propanol, and atmospheric moisture contamination).

Crystalline α-form cefamandole nafate (Sample 11) was prepared by adding an acetone solution of sodium 2-ethylhexanoate to an acetone solution of the acid form of cefamandole nafate. The resulting crystals (probably an acetone–water mixed solvate) were vacuum dried to remove all traces of solvent.

Amorphous freeze-dried cefamandole nafate was prepared as previously described (7). Sample 12 was spray dried from a 25% aqueous solution with inlet and outlet temperatures of 107 and 75°, respectively.

Cefamandole Sodium—The monohydrate (Sample 14) was prepared by passing nitrogen at 50% relative humidity through a fluidized bed of crystalline methanol solvate at 25°. The conversion of methanolate to monohydrate was complete within 24 hr. The methanolate crystals were obtained by addition of sodium acetate to a methanol solution of purified cefamandole acid. The freeze-dried amorphous sample was prepared as previously described (7). The spray-dried amorphous sample was prepared by spray drying a 20% aqueous solution with inlet and outlet temperatures of 90 and 70°, respectively.

Cephalothin Sodium—Sample 20 (Table I) was commercial[3] cephalothin sodium used as received except for vacuum drying. Samples 18 and 19 were commercial samples that were recrystallized four times by salting out cephalothin sodium from a 20% aqueous solution with sodium chloride and sodium lactate, respectively. Sample 21 was prepared by vigorous mortar grinding of Sample 20.

Amorphous freeze-dried cephalothin sodium (Sample 22) was prepared by freeze drying a 20% aqueous solution at low temperatures (7). The partially crystalline freeze-dried samples (Samples 26–28, Table II) were prepared using essentially the same procedure, except that the frozen solutions were allowed to anneal at −5° for 3–18 hr. A sample of the freeze-dried material in each vial was examined microscopically under polarized light, and the vials were separated into three classes. The contents of all vials of a given class were combined to yield three samples: Sample 26, essentially all particles showing birefringence; Sample 27, mostly birefringent material[4]; and Sample 28, roughly one-half birefringent material.

Sample 25 (Table II) was spray dried from a 20% aqueous solution, using an inlet air temperature of 150° and an outlet temperature of 70°. The sample was initially poorly crystallized (heat of solution, −0.06 kcal/mole) and was allowed to anneal at ambient temperature for 2 months to yield essentially crystalline material (heat of solution, +1.39 kcal/mole; essentially 100% birefringent beads ~30 μm in diameter). Although some discoloration of the powder occurred during the annealing process, the extent of decomposition was too small to detect by iodometric assay or TLC (7). Sample 29 was spray dried from a solution composed of 18% cephalothin sodium, 2% diethylcarbonate, and 80% water to yield a mixture of birefringent and glassy nonbirefringent beads 10–20 μm in diameter. The air temperatures were as indicated for Sample 25.

Penicillin G Potassium and Cephaloridine—Penicillin G potassium samples were prepared as previously described (7). Cephaloridine was δ-form (3) crystalline material of commercial origin[2].

Assay Methods and Sample Purity—Cefazolin sodium, cefamandole nafate, and cefamandole sodium were assayed by polarographic techniques (24, 25); an automated iodometric procedure (26) was used for the other β-lactams. Assay for the free 3′-side chain of cefamandole, 1-methyl-5-mercapto-1,2,3,4-tetrazole, a decomposition product, was performed by polarography (24, 25). TLC (7) was used as a qualitative check on purity.

The crystalline and partially crystalline samples were 98+% pure as determined by assay and were one-spot materials on TLC. The amorphous samples were 96+% pure (assay results), and some showed trace quantities (~1%) of decomposition products by TLC.

[3] Eli Lilly and Co., Indianapolis, Ind.

[4] The fraction of birefringent material was estimated by microscopic examination under polarized light as the stage was rotated. The resulting visual estimation was highly approximate.

Table II—Comparison of Degrees of Crystallinity for Cephalothin Sodium Evaluated from X-ray Diffraction, Calorimetry, and Chemical Stability

Sample	Sample Origin	$\Delta H°_s$, kcal/mole (≤0.1% H_2O)	Percent Crystalline				
			X-Ray[a]			50° Stability	
			External Method	Internal Method	Calorimetry[b]	Dry	31% R.H.
18	Laboratory crystallized	1.9	100	100	100	100	100
19	Laboratory crystallized	1.67	77	70	96	—	—
20	Commercial lots	1.47	72	67	93	101(3)	100 (0.5)
25	Spray dried[c]	1.39	69	55	92	102 (1)	97 (6)
26	Freeze dried[d]	1.15	62	51	88	101 (2)	100 (0)
27	Freeze dried[e]	0.32	57	48	74	86 (11)	—
28	Freeze dried[e]	−0.84	47	40	54	77 (2)	85 (1)
29	Spray dried[f]	−1.30	37	34	47	54 (1)	44 (10)

[a] With fixed data for amorphous and crystalline standards, the reproducibility (standard deviation) of crystallinity for a given sample is about ±3% for both methods when all data are taken on the same day, as with the data in Table II. From the reproducibility of the data for a given sample and the reproducibility of the data for crystalline and amorphous standards, and standard error in an X-ray crystallinity was estimated to be about ±5%. The internal X-ray method may be subject to an additional (systematic) error because of orientation effects. [b] The reproducibility of the calorimetric crystallinity was about ±0.6% (*SD*). Considering also uncertainty in the calorimetric data for the amorphous and crystalline standards, the standard error in a calorimetric crystallinity was estimated to be about ±1%. [c] Heat of solution did not change upon aging at 50° for 2 months. [d] During 24 months at 25°, the heat of solution increased from 1.15 to 1.46 kcal/mole. [e] Partial crystallization occurred during the stability determination (microscopic examination). [f] No crystallization was detected during the stability determination (microscopic examination).

Water contents were determined by Karl Fischer titrations. Residual solvents, other than water, were determined to be less than ~0.1% by GLC, NMR spectroscopy, or the difference between thermal gravimetric analysis mass loss and the water content.

Calorimetry—Heats of solution were determined with a commercial isothermal calorimeter system[5] similar in design to the calorimeter developed by Arnett *et al.* (27). The sample container used in this research (Fig. 1) was essentially a stainless steel tube sealed at both ends with removable plastic plugs. The plugs were fitted with rubber O-rings coated with silicone stopcock grease to ensure a good seal between the contents of the tube (*e.g.*, the sample) and the calorimeter solvent (*e.g.*, water).

The sample container was placed in the calorimeter cell through an opening in the cell head. The sample was exposed to the solvent by pulling up on disk A (Fig. 1) to remove the top plug and then pushing down on disk B to remove the bottom plug. The heat of opening was zero within the sensitivity of the calorimeter (0.04 cal). For most samples, complete dissolution was achieved within 30–60 sec.

Standard calorimetric procedures were followed (27, 28). The final solution concentrations were normally less than 0.02 *M*. Heats of solution for sodium and potassium salts were corrected to infinite dilution, assuming that, as a first approximation, the heats of dilution were the same as for potassium chloride (29) at the equivalent molar concentration. The accuracy of this approximation, within ±0.03 kcal/mole, was verified for cephalothin sodium at concentrations up to 0.1 *M*.

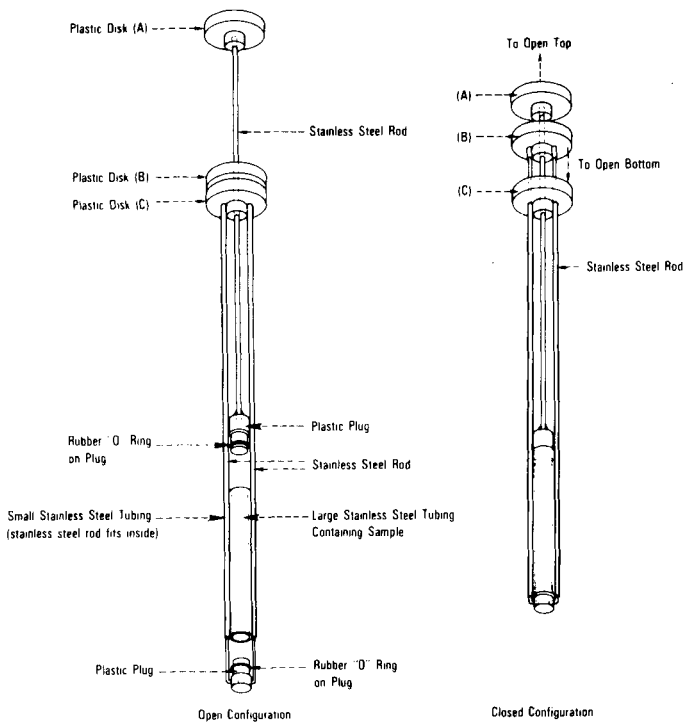

Figure 1—*Diagram of calorimeter sample container.*

[5] Guild Electronics, 400-115, SKC Inc., Pittsburgh, PA 15200.

The calorimetric accuracy was periodically checked by measuring the heat of solution of potassium chloride[6] in water and by measuring the heat of dissolving 2-amino-2-(hydroxymethyl)-1,3-propanediol[7] in an excess of 0.1 *N* HCl. Results were within 1% of the accepted literature values (30, 31).

All sample transfers of anhydrous material were carried out at near zero relative humidity[8].

X-Ray, Stability, and Water Absorption Measurements—X-ray scattering data were obtained using commercial X-ray diffractometers[9] with CuKα radiation and a nickel filter.

Stability data were generated as described previously for cephalothin sodium (7). The extent of decomposition at 50° was determined at a single predetermined aging time (3 weeks to 6 months, depending on crystallinity and water content). The decomposition rate was calculated assuming first-order decomposition.

For Samples 22 (Table I) and 27–29 (Table II), water absorption was determined at 25° and 31% relative humidity by placing 2–5 g of dried sample in a desiccator containing solid calcium chloride hexahydrate in equilibrium with its saturated aqueous solution. The desiccator was evacuated, and the water absorbed at equilibrium was determined gravimetrically. The uncertainty in water content was estimated to be less than ±0.1% H_2O. Water absorption for samples of high crystallinity and low water absorption was determined by a more sensitive procedure. Nitrogen at 31% relative humidity was passed over a sample suspended from one arm of an electromagnetic microbalance. The increase in mass was monitored, and the water sorbed was calculated from the equilibrium mass. The uncertainty in water content measured by this method was about ±0.01% H_2O.

RESULTS AND DISCUSSION

Effects of Solvation (Table I and Figs. 3 and 5)—Dehydration of a cephalosporin in either amorphous or solvated crystalline form results in a strong exothermic shift in the heat of solution. With the exception

[6] Mallinckrodt reagent grade, recrystallized from water.

[7] Baker Ultrex grade.

[8] Glove bag, Instruments for Research and Industry, Cheltenham, Pa. The glove bag was continuously purged with air equilibrated with anhydrous calcium sulfate.

[9] Norelco, Mt. Vernon, N.Y. The data reported in Fig. 2 were obtained from a recently acquired instrument, model XRG-3000 (scintillation counter detector). All other data were obtained from another (older) instrument, type 12045B/3 (Geiger counter detector). The settings on model XRG-3000 were chosen to give peak intensities (for a given crystalline sample) comparable to the corresponding intensities measured with instrument 12045B/3. With each instrument, all data were taken with the same instrument settings using the same procedures. The detector of the XRG-3000 was less sensitive to diffraction of the continuous spectrum; therefore, the apparent background scattering was slightly lower with the XRG-3000 model, particularly at low angles. Thus, the data in Fig. 2 may not be compared quantitatively with the scattering data reported in Figs. 3 and 4.

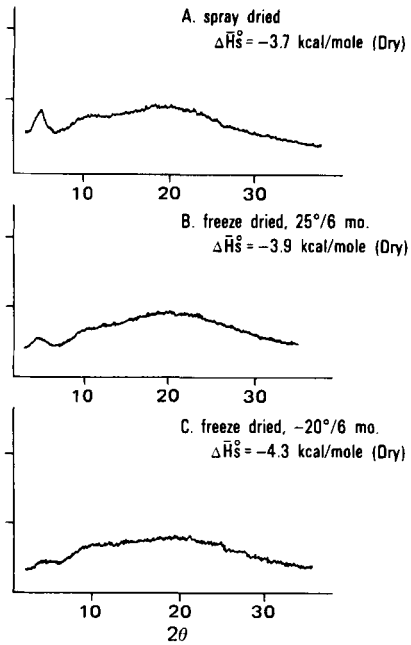

Figure 2—*X-ray diffraction and heats of solution for amorphous forms of cefamandole nafate. Experimental heats of solution (Tables I and III) were corrected to zero water content using 1 kcal/mole/1% H_2O (w/w) as the correction factor.*

of cefamandole sodium monohydrate, desolvated crystals exhibited a weak and diffuse X-ray pattern (Fig. 3), indicating some loss of crystallinity upon desolvation. However, at least for cefazolin sodium pentahydrate, the structural changes occurring on dehydration were completely reversible. Rehydration restored the strong X-ray pattern, and the heat of solution returned to the value characteristic of the pentahydrate (+7.8 kcal/mole).

The exothermic shift of the heat of solution on dehydration is probably due to two effects: (*a*) the crystallinity decreases on dehydration; and (*b*) since a wet solid is already partially hydrated, the (exothermic) hydration energy upon solution is less in magnitude, and the heat of solution is more

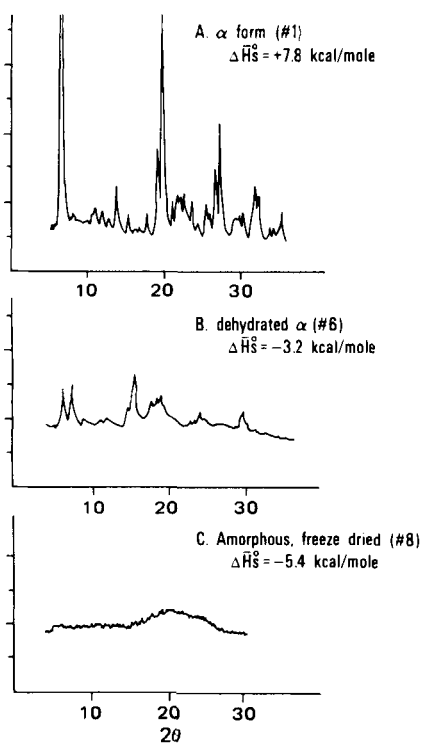

Figure 3—*X-ray diffraction and heats of solution for crystalline, weakly crystalline, and amorphous forms of cefazolin sodium.*

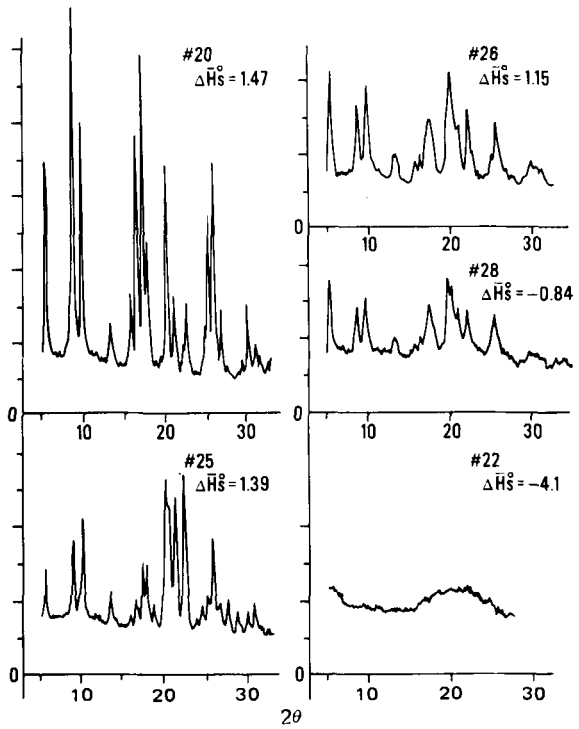

Figure 4—*X-ray diffraction and heats of solution for cephalothin sodium samples of differing degrees of crystallinity.*

endothermic. The magnitude of the exothermic shift for amorphous cephalothin sodium (Fig. 5) was comparable to that observed for crystalline solvates (Fig. 5 and Table I), suggesting that the second effect was the greatest.

Protection of calorimetry samples from atmospheric moisture is essential. Amorphous and desolvated crystalline cephalosporins are extremely hygroscopic, absorbing 3–5% (w/w) water at 30% relative humidity. In view of the sensitivity of the heat of solution to water content, water contamination could result in serious errors.

Excess Energy of Amorphous Forms—As expected, amorphous forms of a compound were energy rich and had more exothermic heats of solution than corresponding crystalline forms (Table I). In general, the energy difference was large, ~6 kcal/mole. However, the magnitude of the energy difference between crystalline and amorphous forms for a given compound (excess energy) was not unique.

The differences in heats of solution between spray-dried and freeze-dried amorphous samples of the same compound (Table I) were real and could not be attributed to residual impurities. Moreover, at least for cefamandole nafate and cefamandole sodium, freeze-dried amorphous samples appeared to anneal slightly upon aging (Table III).

Although the heat of solution clearly becomes more endothermic upon aging (Table III), interpretation of the results in terms of a change in structure is obscured by the increase in decomposition that occurs on aging. As a measure of decomposition upon aging, the mole percent of the free 3′-side chain (1-methyl-5-mercapto-1,2,3,4-tetrazole) is given for each sample (Table III). One might argue that the observed endo-

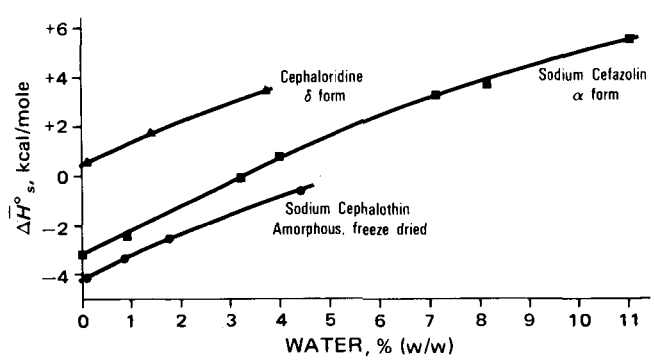

Figure 5—*Effect of water content on the heat of solution of cephalosporins in water at 25°.*

Table III—Changes in Heats of Solution on Aging for Amorphous Freeze-Dried Cefamandole Sodium and Cefamandole Nafate

Aging Condition	Cefamandole Nafate (0.1% H_2O) $\Delta H°_s$, kcal/mole[a]	Cefamandole Nafate (0.1% H_2O) Free 3′-Side Chain, mole %	Cefamandole Sodium (0.4% H_2O) $\Delta H°_s$, kcal/mole[a]	Cefamandole Sodium (0.4% H_2O) Free 3′-Side Chain, mole %
Initial	−4.4	1.2	−5.3	1.7
6 months/−20°	−4.2	1.4	−5.2	2.0
3 months/−5°	−3.9	1.3	−5.2	1.1
1 month/25°	−4.0	2.1	−5.3	2.4
3 months/25°	—	—	−4.9	2.9
6 months/25°	−3.8	2.7	−4.8	3.5
3 weeks/40°	−3.8	3.6	−4.9	3.9
24 hr/60°	−3.6	4.0[b]	−4.6	5.9[c]

[a] $\Delta H°_s$ is heat of solution to infinite dilution in water at 25°. Estimated uncertainty = ±0.1 kcal/mole. [b] Extent of decomposition by polarographic assay for cefamandole nafate, 3%. [c] Extent of decomposition by polarographic assay for cefamandole sodium, 7%.

thermic shift in the heat of solution upon aging reflects contamination of the sample by decomposition products. If the endothermic shift is attributed to decomposition, the heat of solution of the decomposition products would have to be ~ +210 cal/g, which seems much too high. (The heat of solution of crystalline 1-methyl-5-mercapto-1,2,3,4-tetrazole was only +46 cal/g.) Therefore, some type of annealing phenomenon apparently occurred.

Slight differences in the X-ray diffraction patterns of amorphous samples were also evident, as demonstrated in Fig. 2 for cefamandole nafate. Differences were particularly evident at $2\theta = 5°$. The annealed freeze-dried sample (Fig. 2B), aged at 25° for 6 months, was intermediate between the spray-dried sample (Fig. 2A) and the freeze-dried sample stored at −20° for 6 months (Fig. 2C). The latter sample (Fig. 2C) was typical of freshly prepared freeze-dried material.

Although subtle, the differences shown in Fig. 2 are reproducible. Two additional lots of both spray-dried and freeze-dried cefamandole nafate were examined by X-ray diffraction and calorimetry with essentially the same results. To facilitate a quantitative comparison independent of systematic intensity errors, an order parameter, X, is defined by:

$$X = \frac{h_p}{h_D} \qquad \text{(Eq. 2)}$$

where h_p is the height of the broad peak at $2\theta = 5°$ and h_D represents the corrected diffuse (background) scattering at 5°. The parameters h_p and h_D are calculated as follows. A straight line is drawn connecting the point on the diffraction curve at $2\theta = 3.5°$ with the minimum at $2\theta = 7°$; h_p is the vertical distance between this line and the peak at 5°. The distance between the straight line and the zero intensity axis represents the sum of h_D and various extraneous background effects such as incoherent scattering, air scattering, and diffraction of the continuous spectrum. Then a straight line is constructed as described for a 100% crystalline standard (Sample 9). The vertical distance between zero intensity and this line at 5° is taken as the intensity of the extraneous background (incoherent scattering, air scattering, and diffraction of the continuous spectrum).

The mean order parameters (for the three samples studied) and their corresponding error limits (90% confidence) were: spray dried, $X = 1.34 \pm 0.09$; aged freeze dried (6 months/25°), $X = 0.92 \pm 0.15$; and fresh freeze dried (or 6 months/−20°), $X = 0.62 \pm 0.15$. While the difference between aged and fresh freeze-dried material was significant at the 90% confidence level, more data are needed to verify the difference. However, the difference between spray-dried and fresh freeze-dried materials was clearly significant. Thus, spray-dried amorphous material appears to be an annealed form of amorphous material. While there is little experimental precedent for this observation, differences in structure between amorphous samples of the same compound have ample theoretical support (15, 32–34).

Samples 18–20 (Table I) were crystalline cephalothin sodium samples (same polymorph) with slightly different heats of solution. The X-ray patterns were qualitatively alike (see Sample 20, Fig. 4) but differed slightly in the magnitude of background scattering. All samples were crystallized from aqueous solution by salting out with either sodium lactate (Samples 19 and 20) or sodium chloride (Sample 18). Sample 20 was a representative commercial sample[3], while Samples 18 and 19 were laboratory samples prepared by four recrystallizations of the commercial sample. No difference in sample purity was detected (see *Experimental*), and none of the samples appeared to be a mixture of amorphous and crystalline phases[10].

For lack of a plausible alternative interpretation, the energy differences among Samples 18–20 were attributed to differences in crystal perfection, *e.g.*, point defects or dislocations. While similar observations were noted for potassium chloride (30), the energy differences observed for cephalothin sodium were much greater.

The ambiguity in the definition of crystalline and amorphous causes uncertainty in the choice of standards for use in crystallinity measurements. While this uncertainty does not affect a precise comparison between samples, the numerical value of the crystallinity is obviously not unique. In this study, the lowest energy crystalline preparation (most endothermic heat of solution) was selected as the crystalline standard and the highest energy amorphous preparation (most exothermic heat of solution) was the amorphous standard. In some applications, it may be desirable to use a crystalline standard similar in perfection to the crystalline phase in the partially crystalline samples investigated.

Correlation of Calorimetric and X-Ray Data—Qualitatively, there was a good correlation between X-ray crystallinity and calorimetric data for partially crystalline samples.

1. Heats of solution of cephalothin sodium became more exothermic as the X-ray patterns became weaker and more diffuse[11] (Fig. 4).
2. Cefazolin sodium Samples 4 and 5 (Table I), which appeared to be poorly crystallized monohydrate, had weak X-ray patterns even at the monohydrate composition and also had heats of solution more exothermic than well-crystallized material (Samples 2 and 3).
3. The sample of the crystalline γ-form of cefamandole nafate, believed to have an amorphous layer coating the crystals (Sample 10, Table I), had a slightly more exothermic heat of solution than the "standard" 100% crystalline Sample 9.
4. The more exothermic heat of solution for mortar-ground cephalothin sodium (Sample 21, Table I) was consistent with the observed loss of crystallinity on grinding (6, 10, 14).

A quantitative comparison of X-ray and calorimetric crystallinities is given in Table II for a series of cephalothin sodium samples. Percent crystallinity by calorimetry was evaluated from Eq. 1, using Samples 18 and 22 as the crystalline and amorphous standards, respectively. With the same standards, X-ray crystallinities were evaluated[12] by an external

[10] Since microscopic examination indicated that all particles were birefringent, the only plausible postulate involving an amorphous phase is that the crystals are coated with a thin layer of amorphous phase, presumably formed during vacuum drying. However, cephalothin sodium readily crystallizes when an aqueous solution is vacuum dried. Moreover, even under relatively mild conditions, amorphous cephalothin sodium degrades to yield small amounts of highly colored product, which gives the amorphous powder an amber color. Therefore, the presence of a surface amorphous phase in Sample 20 of the proportions indicated by the calorimetric data (~7%) would cause the solid to develop an amber color upon aging in much the same manner as an amorphous solid. However, Sample 20 did not develop significant color upon aging.

[11] The peak broadening observed in Samples 26 and 28 may be a result of small crystal size and/or strain. Differences between Samples 20 and 25 were probably due mainly to orientation effects. The crystals in Sample 20 were large (~100 μm longest dimension) bladed and prismatic particles, likely to exhibit preferred orientation when compacted into the sample holder. Preferred orientation should be minimal for the other samples in Fig. 4. Scanning electron microscope studies showed that each birefringent bead in Sample 25 had a very irregular rock-like surface with no single bladed or prismatic crystals in evidence. Sample 26 was composed of bundles of small (~20 μm longest dimension) bladed and needle-like crystals which appeared to be fused together and, in many cases, bent. Specific surface areas for Samples 20, 26, and 22 were 0.59, 7.5, and ≤0.2 m^2/g [Brunauer, Emmett, and Teller (BET) N_2 adsorption], respectively.

[12] Crystalline and background scattering were separated by a smooth background curve drawn through the minima between Bragg reflections (11), maintaining a contour similar to that shown by the amorphous standard (Sample 22). The intensity between this curve and the zero intensity axis (the background) is due to the coherent amorphous scattering of interest and various extraneous background effects (incoherent scattering, air scattering, and diffraction of the continuous spectrum). It was assumed that the background scattering for the crystalline standard (Sample 18) was due only to the extraneous background. Thus, the desired amorphous scattering for a given sample was obtained by subtracting the crystalline standard background from the sample background.

The external method defines the crystallinity P_x as $P_x = 100\,(1 - I_a/I°_a)$, where I_a and $I°_a$ are the amorphous scattering intensities at $2\theta = 21°$ for the sample of interest and the amorphous standard, respectively. For the internal method, crystalline and background intensities are integrated (with a planimeter) between 2θ values of 5 and 28.8°. The integrated crystalline and amorphous intensities, A_c and A_a, respectively, are assumed to be proportional to the weight fraction of the respective phase, f_i ($i = c, a$); $A_c = k_c f_c$ and $A_a = k_a f_a$, where k_c and k_a are constants evaluated by calibration with the crystalline and amorphous standards, respectively. The percent crystallinity is then given by $P_x = 10^2 f_c = [100\,K(A_c/A_a)]/[1 + K(A_c/A_a)]$, where $K = k_a/k_p = 0.83$. The external method described here is probably more accurate since it is free of systematic errors due to orientation effects. The only advantage of the internal method is that some systematic intensity errors tend to cancel since both intensities in the ratio refer to the same diffraction pattern.

method based on the reduction in intensity of the background scattering at $2\theta = 21°$ (the amorphous halo peak) resulting from an increase in crystallinity (12, 17) and by an internal method (17) based on the ratio of integrated amorphous and crystalline intensities.

If a partially crystalline sample were simply a mixture of the amorphous and crystalline standards (two-state model), all valid measures of crystallinity would give identical results. The lack of quantitative agreement between X-ray and calorimetric crystallinities (Table II) is due mostly to the failure of the two-state model. Since the two-state model recognizes neither variations in defect structure of crystals nor variations in the structure of amorphous materials, quantitative agreement between different measures of crystallinity cannot be expected. A similar lack of agreement between different measures of crystallinity was noted for polymers (10–13). However, the order of decreasing crystallinities (Table II) was the same for both X-ray and calorimetric data.

Crystallinity and Chemical Stability—Since amorphous cephalothin sodium is much less stable than the crystalline form, one would expect a correlation between calorimetric crystallinity and chemical stability. To facilitate comparison of calorimetric crystallinity and stability, the percent crystallinity *via* stability, P_s, is defined by:

$$P_s = 100(1 - k_s/k_a) \qquad \text{(Eq. 3)}$$

where k_s and k_a are the apparent first-order decomposition rates for the sample and amorphous standard, respectively. The crystalline standard is stable under the test conditions (7), so its decomposition rate is essentially zero and does not appear in Eq. 3. Stability at 50° was determined for both dry samples ($\leq 0.1\%$ H_2O) and samples exposed to a relative humidity of 31% (at 25°). The P_s values are compared with calorimetric crystallinities in Table II. The number in parentheses after the stability crystallinity figure is the difference in crystallinity measured between duplicate samples. If the sample crystallinity remained constant during the stability test and if the two-state model was rigorous, quantitative agreement of calorimetric and stability crystallinities would be observed. However, the two-state model is not rigorous, and annealing during the stability test probably slightly increased the crystallinity measured *via* stability for Samples 26–28 (footnotes *c–f*, Table II). Calorimetric crystallinity in excess of 93% ($\Delta\overline{H}°_s = 1.47$ kcal/mole) does not appear to be obtainable by annealing (footnotes *c–f*, Table II).

With Sample 18 as the crystalline standard, agreement between stability and calorimetric crystallinities (Table II) was only approximate. The chemical stability data for Samples 20, 25, and 26 were not consistent with a sample containing more than 1–2% of amorphous phase. The 7–12% loss in calorimetric crystallinity (28–38% by the external X-ray method) for Samples 20, 25, and 26 cannot be attributed to the presence of an amorphous phase. This apparent anomaly may be resolved if one accepts the proposal of significant differences in crystal perfection between crystalline samples and further postulates that differences in crystal perfection have little effect on chemical stability.

Both Samples 18 and 19 were highly purified, carefully crystallized samples and may not be representative of the crystal perfection obtainable by routine crystallization, freeze drying, or spray drying. Thus, if the objective of crystallinity measurements on cephalothin sodium is to predict stability of samples prepared by routine processes, Sample 20 would be a more reasonable choice for the 100% crystalline standard.

Crystallinity and Water Absorption—Amorphous cephalothin sodium absorbs far more water than the crystalline form, and the amount of water absorbed at 25° and a relative humidity of 31% can serve as a reasonably good measure of the degree of crystallinity[13] (Fig. 6). However, the correlation between crystallinity and water absorption was poor at calorimetric crystallinities above 88%. For samples of 88, 92, 93, 96, and 100% crystallinity, the corresponding water absorption data were 0.23, 0.28, 0.18, 0.24, and 0.04% (w/w). The lack of a good correlation was not due to experimental error in either calorimetric crystallinities (footnote *b*, Table II) or water contents (see *Experimental*). Perhaps factors other than crystallinity (*i.e.*, surface area or trace surface impurities) affect water absorption.

For highly crystalline samples, one might expect that water absorption would be directly proportional to surface area. However, from the limited data available, this reasonable speculation does not appear valid. Samples 20 and 26 had specific surface areas of 0.59 and 7.5 m^2/g (BET nitrogen adsorption), respectively. However, the water absorption was nearly the same for both samples: 0.18% (Sample 20) and 0.23% (Sample 26).

[13] It appears that water absorption accelerates crystallization of the amorphous phase. Thus, to avoid changes in crystallinity during the measurement process, high humidity should be avoided and the absorption experiment should be done quickly (within 24 hr).

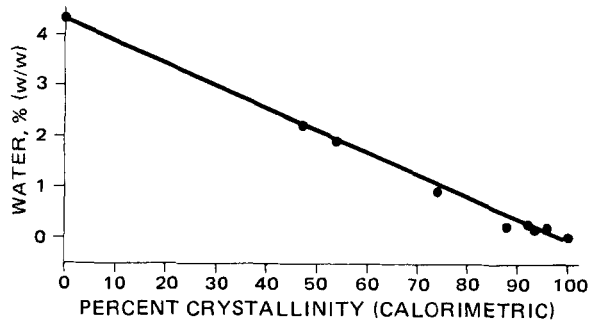

Figure 6—*Water absorption at 31% relative humidity at 25°; correlation with calorimetric crystallinity data from Table II.*

CONCLUSIONS

The heat of solution is a precise unambiguous measure of the relative crystallinity of a sample containing only one crystal form. The energy of the amorphous state depends, to some extent, on the method of preparation, and even crystalline samples of the same polymorphic form containing no amorphous phase may differ in energy. Thus, the absolute value of the percent crystallinity depends on the choice of amorphous and crystalline standards. Provided the standards are appropriately chosen, the calorimetric crystallinity can provide a useful indicator for the chemical stability of a β-lactam antibiotic.

REFERENCES

(1) J. Haleblian and W. McCrone, *J. Pharm. Sci.*, **58**, 911 (1969).

(2) M. A. Moustafa, A. R. Ebian, S. A. Khalil, and M. M. Motawi, *J. Pharm. Pharmacol.*, **23**, 868 (1971).

(3) J. Haleblian, R. Koda, and J. Biles, *J. Pharm. Sci.*, **60**, 1485 (1971).

(4) R. Pfeiffer, K. Yang, and M. Tucker, *ibid.*, **59**, 1809 (1970).

(5) Y. Kawashima, M. Saito, and H. Takenaka, *J. Pharm. Pharmacol.*, **27**, 1 (1975).

(6) A. T. Florence, E. G. Salole, and J. B. Stenlake, *ibid.*, **26**, 479 (1974).

(7) M. J. Pikal, A. L. Lukes, and J. E. Lang, *J. Pharm. Sci.*, **66**, 1312 (1977).

(8) A. Wlochowicz and A. Jeziorny, *J. Polym. Sci., Polym. Chem. Ed.*, **12**, 793 (1974).

(9) L. G. Roldan, F. Rahl, and A. R. Paterson, *J. Polym. Sci. C*, **1965**, 145.

(10) W. O. Statton, *ibid.*, **1967**, 33.

(11) M. L. Miller, "The Structure of Polymers," Reinhold, New York, N.Y., 1966, chap. 10.

(12) R. L. Miller, in "Encyclopedia of Polymer Science and Technology," vol. 4, Interscience, New York, N.Y., 1966, p. 449.

(13) V. D. Gupta and R. B. Beevers, *Chem. Rev.*, **62**, 665 (1962).

(14) I. Motooka, G. Hashizume, and M. Kobayashi, *J. Phys. Chem.*, **73**, 3012 (1969).

(15) R. Roy, *J. Non-Cryst. Solids*, **3**, 33 (1970).

(16) Z. W. Wilchinsky, *Rev. Sci. Instrum.*, **40**, 5921 (1969).

(17) M. P. Temple and M. J. Zarzycki, *C. R. Acad. Sci. Paris (Ser. C)*, **280**, 1443 (1975).

(18) K. Kishimoto, H. Suga, and S. Seki, *Bull. Chem. Soc. Jpn.*, **46**, 3020 (1973).

(19) D. K. Hunt and A. C. T. Hsu, *J. Colloid Interface Sci.*, **48**, 105 (1974).

(20) F. E. Filisko and R. S. Raghava, *J. Appl. Phys.*, **45**, 4151 (1974).

(21) A. G. Mathews, C. J. Schram, and D. Minty, *Nature*, **211**, 959 (1966).

(22) K. Kariyone, H. Harada, M. Kurita, and T. Takano, *J. Antibiot.*, **23**, 131 (1970).

(23) J. H. Chapman, J. E. Page, A. C. Parker, D. Rogers, C. J. Sharp, and S. E. Staniforth, *J. Pharm. Pharmacol.*, **20**, 418 (1968).

(24) E. C. Richard and G. G. Cooke, *J. Pharm. Sci.*, **66**, 379 (1977).

(25) D. A. Hall, *ibid.*, **62**, 980 (1973).

(26) L. P. Marrelli, in "Cephalosporins and Penicillins," E. H. Flynn, Ed., Academic, New York, N.Y., 1972, chap. 14.

(27) E. M. Arnett, W. G. Bentrude, J. J. Burke, and P. Duggleby, *J. Am. Chem. Soc.*, **87**, 1541 (1965).

(28) I. Wadsö, *Sci. Tools*, **13**, 33 (1966).
(29) G. N. Lewis and M. Randall, "Thermodynamics," 2nd ed., K. S. Pitzer and L. Brewer, Eds., McGraw-Hill, New York, N.Y., 1961.
(30) S. R. Gunn, *J. Phys. Chem.*, **69**, 2902 (1965).
(31) R. J. Irving and I. Wadsö, *Acta Chem. Scand.*, **18**, 195 (1964).
(32) M. R. Anseau, *Phys. Lett.*, **43A**, 57 (1973).
(33) J. E. Hiller, *Naturwiss. Rundsch.*, **6**, 49 (1953).
(34) W. A. Weyl and E. C. Morboe, *J. Soc. Glass Technol.*, **43** (1959).

ACKNOWLEDGMENTS

The authors thank the members of the Analytical Chemistry Groups at Eli Lilly for performing the required assay work. They also thank their Lilly associates, Mr. K. S. Yang, Dr. S. Schildcrout, and Dr. L. Tensmeyer, for providing samples of some cephalosporins and Mr. H. W. Smith and Mr. D. A. Spurgeon for performing the X-ray diffractometer measurements.

Interaction of Doxorubicin with Phospholipid Monolayers

FEDERICO A. VILALLONGA ˣ and EDWARD W. PHILLIPS

Received June 13, 1977, from the *College of Pharmacy, University of Florida, Gainesville, FL 32610.* Accepted for publication September 14, 1977.

Abstract □ The energies of interaction of doxorubicin hydrochloride and sodium 1,2,4-trihydroxy-9,10-dioxo-3-anthracenesulfonate with dipalmitoylphosphatidylethanolamine and dipalmitoyllecithin monolayers spread at the air–water interface were estimated from the increase in surface pressure with increasing concentrations of the subphase-injected compound. Their orders of magnitude were consistent with those of the energies of interaction of doxorubicin and acridines with double-stranded DNA, which suggests that the same type of van der Waals forces are operative.

Keyphrases □ Doxorubicin—energy of interaction with phospholipid monolayers at air–water interface □ Phospholipid monolayers—energy of interaction with doxorubicin and substituted anthracenesulfonate at air–water interface □ Monolayers, phospholipid—energy of interaction with doxorubicin and substituted anthracenesulfonate at air–water interface □ Antineoplastic agents—doxorubicin, energy of interaction with phospholipid monolayers at air–water interface

Doxorubicin is an anthracycline glycoside antibiotic formed by the tetracyclic quinoid aglycone doxorubicinone and the amino sugar daunosamine (1–3). Its cationic form shows antitumor activity (4). The anthracyclines are representative of a class of drugs whose pharmacological activity depends on their binding with nucleic acids and the subsequent inhibition of nucleic acid synthesis (5).

The energies of interaction of alkanols with dipalmitoyllecithin and dipalmitoylphosphatidylethanolamine monolayers spread at the air–water interface were recently correlated with their permeabilities across biomembranes and with the partition coefficients between (*a*) red cell membranes and water and (*b*) phospholipid liposomes and water (6). The present study examines the surface activity of doxorubicin and its energy of interaction with phospholipid monolayers spread at the air–water interface.

EXPERIMENTAL

Reagents—Doxorubicin (I) hydrochloride[1] and sodium 1,2,4-trihydroxy-9,10-dioxo-3-anthracenesulfonate[2] (II) were used without further purification. Dipalmitoyllecithin[3] (III), dipalmitoylphosphatidylethanolamine[4] (IV), the hexane[5] used for the preparation of the spreading solutions, and the distilled water used as subphase and for the preparation of the aqueous solutions fulfilled the requirements previously specified (7, 8).

Instruments and Methods—A 9-cm diameter polytef dish, provided with two identical microburets[6] and a polytef-coated stirring bar, was used as a trough. Surface tension was measured with a Wilhelmy platinum plate attached to an electrobalance[7] whose output was fed into a dual-pen recorder[8]. The methods for the measurement of the surface tension of aqueous solutions and of the change of the surface pressure of the phospholipid monolayer as a function of time after the injection of the drug in the subphase already were described (6–8). The criterion of equilibrium was the constancy, ± 0.1 dyne/cm, of the surface pressure increment, $\Delta\pi$, over 30 min. In all injection experiments, the initial surface pressure, π, of the phospholipid monolayer was 5 ± 0.1 dynes/cm and the temperature was 20 ± 1°.

RESULTS

The surface tensions of aqueous solutions (10^{-4}, 10^{-5}, 10^{-6}, and 10^{-7} *M*) I hydrochloride and II were equal to the surface tension of the pure distilled water used to prepare the solutions (72.80 dynes/cm) within the limits of experimental error (±0.1 dyne/cm). The pH values of the I hydrochloride solutions were 5.3, 5.5, 5.4, and 5.6, respectively, and those of the II solutions were 4.1, 4.3, 4.8, and 5.0, respectively.

Typical plots of the increment of the surface pressure, $\Delta\pi$ (dynes per centimeter), as a function of time, *t* (minutes), after the injection of I hydrochloride and II beneath III and IV monolayers are given in Fig. 1 for the same final concentration (4.28×10^{16} molecules/cm^3) of the drug injected in the subphase. The kinetics of the processes are similar, but the highest value of the equilibrium surface pressure was found for the injection of I beneath the IV monolayer (Table I). The energies of interaction were estimated from the slopes of the reciprocals of the equilibrium surface pressures, $\Delta\pi_{eq}$ (dynes per centimeter), after the injection against the reciprocals of increasing final concentrations, *n* (molecules per cubic centimeter), of the subphase-injected drug (7, 8). Such energies are given in Table I.

DISCUSSION

In accordance with the Gibbs adsorption equation, the fact that the surface tension of water is not affected by the presence of 10^{-4}–10^{-7} *M* concentrations of I hydrochloride or II indicates that the concentrations of these solutes at the interfacial region are identical with the concentrations of the bulk aqueous solutions in both cases; *i.e.*, no spontaneous adsorption of those molecules takes place at the air–aqueous solution interface between these concentrations.

[1] Adriamycin, Adria Laboratories, Wilmington, Del.
[2] Pfaltz & Bauer, Flushing, N.Y.
[3] Applied Science Laboratories, State College, Pa.
[4] Schwarz-Mann Research Laboratories, Orangeburg, N.Y.
[5] J. H. Baker Chemical Co., Phillipsburg, N.J.
[6] Manostat, New York, N.Y.
[7] Cahn Division, Ventron Instruments Corp., Paramount, Calif.
[8] Leeds Northrup, North Wales, Pa.

(28) I. Wadsö, *Sci. Tools*, **13**, 33 (1966).
(29) G. N. Lewis and M. Randall, "Thermodynamics," 2nd ed., K. S. Pitzer and L. Brewer, Eds., McGraw-Hill, New York, N.Y., 1961.
(30) S. R. Gunn, *J. Phys. Chem.*, **69**, 2902 (1965).
(31) R. J. Irving and I. Wadsö, *Acta Chem. Scand.*, **18**, 195 (1964).
(32) M. R. Anseau, *Phys. Lett.*, **43A**, 57 (1973).
(33) J. E. Hiller, *Naturwiss. Rundsch.*, **6**, 49 (1953).
(34) W. A. Weyl and E. C. Morboe, *J. Soc. Glass Technol.*, **43** (1959).

ACKNOWLEDGMENTS

The authors thank the members of the Analytical Chemistry Groups at Eli Lilly for performing the required assay work. They also thank their Lilly associates, Mr. K. S. Yang, Dr. S. Schildcrout, and Dr. L. Tensmeyer, for providing samples of some cephalosporins and Mr. H. W. Smith and Mr. D. A. Spurgeon for performing the X-ray diffractometer measurements.

Interaction of Doxorubicin with Phospholipid Monolayers

FEDERICO A. VILALLONGA ˣ and EDWARD W. PHILLIPS

Received June 13, 1977, from the *College of Pharmacy, University of Florida, Gainesville, FL 32610.* Accepted for publication September 14, 1977.

Abstract □ The energies of interaction of doxorubicin hydrochloride and sodium 1,2,4-trihydroxy-9,10-dioxo-3-anthracenesulfonate with dipalmitoylphosphatidylethanolamine and dipalmitoyllecithin monolayers spread at the air–water interface were estimated from the increase in surface pressure with increasing concentrations of the subphase-injected compound. Their orders of magnitude were consistent with those of the energies of interaction of doxorubicin and acridines with double-stranded DNA, which suggests that the same type of van der Waals forces are operative.

Keyphrases □ Doxorubicin—energy of interaction with phospholipid monolayers at air–water interface □ Phospholipid monolayers—energy of interaction with doxorubicin and substituted anthracenesulfonate at air–water interface □ Monolayers, phospholipid—energy of interaction with doxorubicin and substituted anthracenesulfonate at air–water interface □ Antineoplastic agents—doxorubicin, energy of interaction with phospholipid monolayers at air–water interface

Doxorubicin is an anthracycline glycoside antibiotic formed by the tetracyclic quinoid aglycone doxorubicinone and the amino sugar daunosamine (1–3). Its cationic form shows antitumor activity (4). The anthracyclines are representative of a class of drugs whose pharmacological activity depends on their binding with nucleic acids and the subsequent inhibition of nucleic acid synthesis (5).

The energies of interaction of alkanols with dipalmitoyllecithin and dipalmitoylphosphatidylethanolamine monolayers spread at the air–water interface were recently correlated with their permeabilities across biomembranes and with the partition coefficients between (*a*) red cell membranes and water and (*b*) phospholipid liposomes and water (6). The present study examines the surface activity of doxorubicin and its energy of interaction with phospholipid monolayers spread at the air–water interface.

EXPERIMENTAL

Reagents—Doxorubicin (I) hydrochloride[1] and sodium 1,2,4-trihydroxy-9,10-dioxo-3-anthracenesulfonate[2] (II) were used without further purification. Dipalmitoyllecithin[3] (III), dipalmitoylphosphatidylethanolamine[4] (IV), the hexane[5] used for the preparation of the spreading solutions, and the distilled water used as subphase and for the preparation of the aqueous solutions fulfilled the requirements previously specified (7, 8).

Instruments and Methods—A 9-cm diameter polytef dish, provided with two identical microburets[6] and a polytef-coated stirring bar, was used as a trough. Surface tension was measured with a Wilhelmy platinum plate attached to an electrobalance[7] whose output was fed into a dual-pen recorder[8]. The methods for the measurement of the surface tension of aqueous solutions and of the change of the surface pressure of the phospholipid monolayer as a function of time after the injection of the drug in the subphase already were described (6–8). The criterion of equilibrium was the constancy, ± 0.1 dyne/cm, of the surface pressure increment, $\Delta\pi$, over 30 min. In all injection experiments, the initial surface pressure, π, of the phospholipid monolayer was 5 ± 0.1 dynes/cm and the temperature was 20 ± 1°.

RESULTS

The surface tensions of aqueous solutions (10^{-4}, 10^{-5}, 10^{-6}, and 10^{-7} *M*) I hydrochloride and II were equal to the surface tension of the pure distilled water used to prepare the solutions (72.80 dynes/cm) within the limits of experimental error (±0.1 dyne/cm). The pH values of the I hydrochloride solutions were 5.3, 5.5, 5.4, and 5.6, respectively, and those of the II solutions were 4.1, 4.3, 4.8, and 5.0, respectively.

Typical plots of the increment of the surface pressure, $\Delta\pi$ (dynes per centimeter), as a function of time, *t* (minutes), after the injection of I hydrochloride and II beneath III and IV monolayers are given in Fig. 1 for the same final concentration (4.28×10^{16} molecules/cm^3) of the drug injected in the subphase. The kinetics of the processes are similar, but the highest value of the equilibrium surface pressure was found for the injection of I beneath the IV monolayer (Table I). The energies of interaction were estimated from the slopes of the reciprocals of the equilibrium surface pressures, $\Delta\pi_{eq}$ (dynes per centimeter), after the injection against the reciprocals of increasing final concentrations, *n* (molecules per cubic centimeter), of the subphase-injected drug (7, 8). Such energies are given in Table I.

DISCUSSION

In accordance with the Gibbs adsorption equation, the fact that the surface tension of water is not affected by the presence of 10^{-4}–10^{-7} *M* concentrations of I hydrochloride or II indicates that the concentrations of these solutes at the interfacial region are identical with the concentrations of the bulk aqueous solutions in both cases; *i.e.*, no spontaneous adsorption of those molecules takes place at the air–aqueous solution interface between these concentrations.

[1] Adriamycin, Adria Laboratories, Wilmington, Del.
[2] Pfaltz & Bauer, Flushing, N.Y.
[3] Applied Science Laboratories, State College, Pa.
[4] Schwarz-Mann Research Laboratories, Orangeburg, N.Y.
[5] J. H. Baker Chemical Co., Phillipsburg, N.J.
[6] Manostat, New York, N.Y.
[7] Cahn Division, Ventron Instruments Corp., Paramount, Calif.
[8] Leeds Northrup, North Wales, Pa.

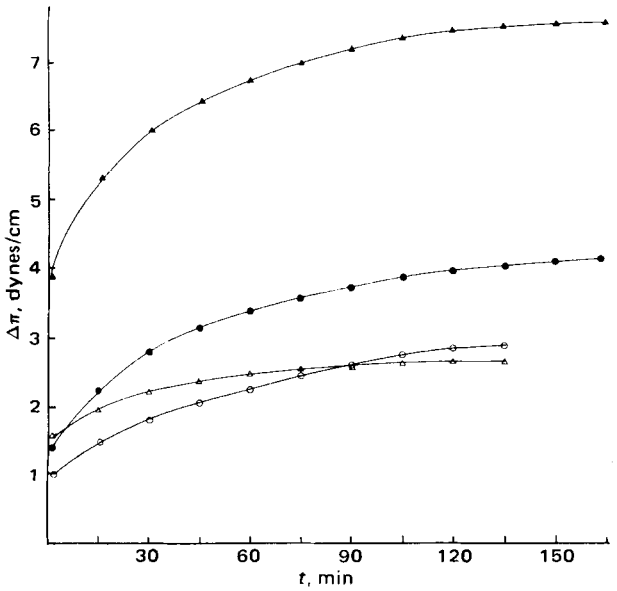

Figure 1—*Typical plots of the change of the surface pressure, $\Delta\pi$, against time, t, after the injection of a final concentration of 4.28 × 10^{16} molecules/cm^3 of I hydrochloride beneath IV (▲), I hydrochloride beneath III (●), II beneath IV (△), and II beneath III (○).*

The protolytic equilibria of I recently were studied by electronic absorption spectroscopy (9). The only species significantly present in the region below pH 7.0 is the singly charged species, with the positive charge located at the amino sugar group. Accordingly, under the experimental conditions (pH 5.3–~5.6), I is positively charged in these aqueous solutions. From the reported (10) pK values of cyclic sulfonic acids, it can be reasonably assumed that II under the experimental conditions (pH 4.1–~5.0) exists in aqueous solutions primarily as the negatively charged form.

Compound IV forms a condensed liquid monolayer. The strong P^-–N^+ electrostatic interaction of the zwitterionic hydrophilic polar groups jointly with the attractive forces between the hydrocarbon chains of neighboring molecules should produce a rigid structuring of the monolayer where any net electrical charge is essentially negligible. The surface area that corresponds to each molecule that forms the monolayer was 40 ± 2 Å^2 at 5 ± 0.1 dynes/cm and 20 ± 1° (8). From the cross-section area of a straight saturated hydrocarbon chain (18–19 Å), the average total number of molecules necessary to form the monolayer under the experimental conditions (10.7 × 10^{15} molecules) (8), and the total surface area of the air–water interface (42.56 cm^2), it can be estimated that the phospholipid molecules occupy between 95.5 and 90.5% of the total surface area, leaving only 4.5–9.5% of free or accessible area of the air–water interface.

Compound III forms a relatively less condensed monolayer at the air–water interface because the shielding effect of the positively charged amino group by the three methyl groups decreases the attractive potential between neighboring molecules (8). The surface area that corresponds to each molecule of the monolayer was 55 ± 2 Å^2 at 20 ± 1° and 5 ± 0.1 dynes/cm, and the average total number of molecules necessary to form the monolayer was 7.7 × 10^{15} molecules (8). In this case, the estimation of the percentage of the total surface area of the air–water interface occupied by the III molecules gives between 65.1 and 68.8%, leaving 34.9–31.2% of free or accessible area.

From literature data on IV (11) and III (12) monolayers, it can be reasonably assumed that the change of the ionic strength (~10^{-4}) resulting from the different final concentrations of the subphase-injected substance will have a negligible effect, if any, on the surface pressure of the phospholipid monolayers.

Theoretical treatments based on the "osmotic approach" and on the concept of "accessible area" have been proposed to explain the penetration of insoluble monolayers by molecules injected in the aqueous subphase (13–15). The accessible area, a, of an insoluble monolayer is defined by (14):

$$a = A - NA_m \qquad \text{(Eq. 1)}$$

where A is the total surface area of the air–water interface, N is the total number of monolayer molecules, and A_m is the area actually occupied by each molecule of the monolayer.

Table I—Surface Pressures of Phospholipid Monolayers and Energies of Interaction after the Injection of I Hydrochloride and II so that the Final Subphase Concentration is *n*

Phospholipid Monolayer	I Hydrochloride			II		
	n, molecules/cm^3	$\Delta\pi_{eq}$, dynes/cm	ψ, kcal/mole	n, molecules/cm^3	$\Delta\pi$, dynes/cm	ψ, kcal/mole
IV	4.28 × 10^{16}	7.7		4.28 × 10^{16}	2.7	
	8.26 × 10^{16}	8.9	7.9	8.26 × 10^{16}	3.6	6.9
	11.96 × 10^{16}	9.7		11.96 × 10^{16}	4.1	
III	4.28 × 10^{16}	4.2		4.28 × 10^{16}	3.0	
	8.26 × 10^{16}	5.4	7.1	8.26 × 10^{16}	4.7	6.4
	11.96 × 10^{16}	6.2		11.96 × 10^{16}	5.8	

The equilibrium penetration is considered as the equilibrium adsorption of the injected molecules at the air–water interface covered with the monolayer, and the adsorption is assumed to occur at the aqueous spaces between monolayer molecules, obeying the equation (12):

$$\Gamma_f = \Gamma_w - A_m\Gamma_w(1/\hat{A}) \qquad \text{(Eq. 2)}$$

where Γ_f and Γ_w are the equilibrium surface concentrations of the injected molecules on a monolayer-covered surface and on a monolayer-free air–water interface, respectively, and $\hat{A} = A/N$ is the area that corresponds to each monolayer molecule.

The increase in the surface pressure, $\Delta\pi$, observed in all cases after the injection of I hydrochloride and II beneath the phospholipid monolayers is in accordance with the osmotic approach and can be considered to be produced by an increased number of molecules at the interface because of the incorporation of the molecules of the injected substance at this surface tension-determining region (13).

The average accessible area of the IV monolayer in the experiments presented here was 7%, and that of the III monolayer was 33%. The results (Table I) indicate that the increase in surface pressure of a IV monolayer produced by the injection of equimolecular amounts of I hydrochloride is, on the average, 64% higher than that produced on a III monolayer. If the increase of the surface pressure of the phospholipid monolayer is reasonably taken as an indication of the extent of adsorption, these results contradict the idea that adsorption at the aqueous spaces between the monolayer molecules is wholly responsible for that increase.

The increase of the surface pressure produced on a IV monolayer by the injection of equimolecular amounts of II is, on the average, 27% lower (Table I) than that produced on a III monolayer. In this case, the results seem to be in accordance with the higher accessible area or aqueous space of the III monolayer. However, the estimated energies of interaction (Table I) are higher in the case of the IV monolayer, which is the more condensed monolayer, *i.e.*, that contains more phospholipid molecules per unit surface area at the same initial surface pressure.

The adsorption of I hydrochloride and II at the aqueous spaces between the monolayer phospholipid molecules is difficult to reconcile, in any case, with the absence of spontaneous adsorption at a monolayer free air–water interface as shown by the independence of the surface tension of the aqueous solutions of both substances with respect to their bulk molar concentrations. Without spontaneous adsorption at the air–water interface, the average statistical distribution of the injected molecules ought to be uniform throughout the whole system. The fact that the surface pressure of the phospholipid monolayer increases steadily after the injection to attain an equilibrium value, $\Delta\pi_{eq}$, seems to indicate an uneven distribution, with part of the injected molecules incorporated at, and restricted to, the surface tension-determining region, possibly through interactions with the phospholipid monolayer molecules.

It was suggested (7, 8) that in the interaction of alkyl sulfates and alkyltrimethylammonium ions with dipalmitoylglycerol, III, and IV monolayers, the first step was the orientation of the polar charged head of the injected surfactant ion toward the attractive centers of the hydrophilic moiety of the molecules that form the monolayer and that the subsequent increase of the surface pressure reflected the subsequent interaction of the hydrocarbon chains with the hydrophobic moiety, mainly through van der Waals forces. When the C_1–C_{14} alkanols interacted with III and IV monolayers, the phospholipid monolayers behaved similarly to ultrathin oil phases (6).

The interaction of I hydrochloride and II with the phospholipid monolayers seems to obey a similar pattern (Fig. 1). The smaller values of the equilibrium surface pressure, $\Delta\pi_{eq}$ (Table I), obtained with equimolecular amounts of II for both monolayers may be related to its smaller

tricyclic hydrophobic moiety as compared with the tetracyclic hydrophobic moiety of I that, in turn, may account for the higher energies of interaction found for I.

Based on the intercalation model to describe the binding of acridines to DNA by insertion between adjacent base pairs (16–18), it recently was proposed (19) that, in the interaction of I with nucleic acids, the positive charge of the amino sugar associates through electrostatic forces with negatively charged phosphate groups of the DNA chain while the tetracyclic hydrophobic moiety, through van der Waals interactions, inserts itself between adjacent base pairs. The binding energy of the acridines to double-stranded DNA is about 6–10 kcal/mole (20). The binding energy of I to double-stranded DNA, recently estimated by using the values of the association constants measured with spectroscopic methods (19), is about 7–12 kcal/mole.

The results presented here seem to indicate that the same type and order of magnitude of van der Waals forces are in effect in the interaction of I and II with phospholipid monolayers.

REFERENCES

(1) F. Arcannone, G. Cassinelli, A. DiMarco, and M. Gaetani, British pat. 1,101,278 (Dec. 10, 1969); Dom. Berv. Ital. 1506 A/67 (Apr. 18, 1967).

(2) T. H. Smith, A. N. Fujiwara, D. W. Henry, and W. W. Lee, *J. Am. Chem. Soc.*, **98,** 1969 (1976).

(3) E. M. Acton, A. N. Fujiwara, and D. W. Henry, *J. Med. Chem.*, **17,** 659 (1974).

(4) H. Berg and K. Edkardt, *Z. Naturforsch.*, **256,** 362 (1970).

(5) A. DiMarco, in "Antibiotics," vol. 1, D. Gottlieb and P. D. Shaw, Eds., Springer-Verlag, Berlin, Germany, 1967, p. 190.

(6) F. A. Vilallonga, E. R. Garrett, and J. S. Hunt, *J. Pharm. Sci.*, **66,** 1229 (1977).

(7) F. A. Vilallonga, E. R. Garrett, and M. Cereijido, *ibid.*, **61,** 1720 (1972).

(8) F. A. Vilallonga and E. R. Garrett, *ibid.*, **62,** 1605 (1973).

(9) R. J. Sturgeon and S. G. Schulman, *ibid.*, **66,** 958 (1977).

(10) R. A. Robinson and R. H. Stokes, "Electrolyte Solutions," Butterworths Scientific Publications, London, England, 1959, p. 534.

(11) M. M. Standish and B. A. Pethica, *Trans. Faraday Soc.*, **64,** 1113 (1968).

(12) F. A. Vilallonga, M. Fernandez, C. Rotunno, and M. Cereijido, *Biochim. Biophys. Acta,* **183,** 98 (1969).

(13) F. M. Fowkes, *J. Phys. Chem.*, **65,** 355 (1961).

(14) M. A. McGregor and F. T. Barnes, *J. Colloid Interface Sci.*, **49,** 362 (1974).

(15) *Ibid.*, **54,** 439 (1976).

(16) L. S. Lerman, *J. Biol.*, **3,** 18 (1961).

(17) L. S. Lerman, *Proc. Natl. Acad. Sci. USA*, **49,** 94 (1963).

(18) L. S. Lerman, *J. Cell. Comp. Physiol. Suppl.*, **1,** 64 (1964).

(19) R. J. Sturgeon, Ph.D. dissertation, University of Florida, Gainesville, Fla., 1977.

(20) A. R. Peacocke, in "Acridines," 2nd ed., R. M. Acheson, Ed., Interscience, New York, N.Y., 1973, chap. 14.

ACKNOWLEDGMENTS

The authors are grateful to Dr. S. G. Schulman for the doxorubicin hydrochloride sample, which was a gift from Adria Laboratories.

^{13}C-NMR Spectroscopy of Tropane Alkaloids

ALY M. TAHA *x and G. RÜCKER

Received June 28, 1977, from the *Institut für Pharmazeutische Chemie der Westfälischen Wilhelms-Universität, 58-62 Hittorfstr., D-4400 Münster (Westf), West Germany.* Accepted for publication September 14, 1977. *Present address: Faculty of Pharmacy, University of Assiut, Assiut, Egypt.

Abstract □ The natural abundance ^{13}C-NMR spectra of tropine, atropine, scopolamine, cocaine, atropine methonitrate, and *dl*-tropic acid were determined at 22.63 MHz. With the aid of proton decoupling techniques and by comparison with analogous simpler compounds, it was possible to make self-consistent and unambiguous assignments of all carbon resonances for these alkaloids. Some important chemical shift trends were observed and should be useful in the identification of similar systems.

Keyphrases □ Tropane alkaloids, various—^{13}C-NMR spectra determined, carbon resonances assigned □ Alkaloids, various tropane—^{13}C-NMR spectra determined, carbon resonances assigned □ ^{13}C-NMR spectroscopy—various tropane alkaloids, spectra determined, carbon resonances assigned

The proton magnetic resonance (PMR) spectra of alkaloids often are too complex to be useful in the structure elucidation of this large class of naturally occurring compounds. The complexity results from extensive spin–spin coupling among protons, overlap of numerous resonance patterns, line broadening arising from intermolecular association and/or ^{14}N-quadrupolar relaxation effects. Natural abundance ^{13}C-NMR spectroscopy has been especially useful in such cases (1).

The tropane alkaloids have been well characterized by structural and stereochemical investigations (2). However, only one limited ^{13}C-NMR study, concentrating on the nonaromatic part of atropine, has been reported (3). The undertaking of a more detailed study was stimulated during the examination of the stability of tropane alkaloids in organic solvents when, consequently, need arose as to the structure elucidation of closely similar compounds. In addition, the broad acceptance of ^{13}C-NMR spectroscopy as a new powerful tool of structural analysis awaits only the accumulation of chemical shift data on compounds representative of all types of natural products.

This report concerns the application of pulse and Fourier transform ^{13}C-NMR techniques to structure assignments of tropane alkaloids.

EXPERIMENTAL

^{13}C-NMR Spectra—^{13}C-NMR spectra were determined at 22.63 MHz in the Fourier transform mode using a spectrometer[1] interfaced with a computer system[2]. The spectrometer features field stabilization *via* internal deuterium lock. Alkaloidal bases were dissolved in chloroform-*d*, and tropic acid was dissolved in methanol-d_4; either a dimethyl sulfoxide-d_6 or deuterated methanol–deuterium oxide mixture (6:4) was used

[1] Brucker W-90 pulse.
[2] Brucker-Nicolet B-NC-12.

tricyclic hydrophobic moiety as compared with the tetracyclic hydrophobic moiety of I that, in turn, may account for the higher energies of interaction found for I.

Based on the intercalation model to describe the binding of acridines to DNA by insertion between adjacent base pairs (16–18), it recently was proposed (19) that, in the interaction of I with nucleic acids, the positive charge of the amino sugar associates through electrostatic forces with negatively charged phosphate groups of the DNA chain while the tetracyclic hydrophobic moiety, through van der Waals interactions, inserts itself between adjacent base pairs. The binding energy of the acridines to double-stranded DNA is about 6–10 kcal/mole (20). The binding energy of I to double-stranded DNA, recently estimated by using the values of the association constants measured with spectroscopic methods (19), is about 7–12 kcal/mole.

The results presented here seem to indicate that the same type and order of magnitude of van der Waals forces are in effect in the interaction of I and II with phospholipid monolayers.

REFERENCES

(1) F. Arcannone, G. Cassinelli, A. DiMarco, and M. Gaetani, British pat. 1,101,278 (Dec. 10, 1969); Dom. Berv. Ital. 1506 A/67 (Apr. 18, 1967).

(2) T. H. Smith, A. N. Fujiwara, D. W. Henry, and W. W. Lee, *J. Am. Chem. Soc.*, **98,** 1969 (1976).

(3) E. M. Acton, A. N. Fujiwara, and D. W. Henry, *J. Med. Chem.*, **17,** 659 (1974).

(4) H. Berg and K. Edkardt, *Z. Naturforsch.*, **256,** 362 (1970).

(5) A. DiMarco, in "Antibiotics," vol. 1, D. Gottlieb and P. D. Shaw, Eds., Springer-Verlag, Berlin, Germany, 1967, p. 190.

(6) F. A. Vilallonga, E. R. Garrett, and J. S. Hunt, *J. Pharm. Sci.*, **66,** 1229 (1977).

(7) F. A. Vilallonga, E. R. Garrett, and M. Cereijido, *ibid.*, **61,** 1720 (1972).

(8) F. A. Vilallonga and E. R. Garrett, *ibid.*, **62,** 1605 (1973).

(9) R. J. Sturgeon and S. G. Schulman, *ibid.*, **66,** 958 (1977).

(10) R. A. Robinson and R. H. Stokes, "Electrolyte Solutions," Butterworths Scientific Publications, London, England, 1959, p. 534.

(11) M. M. Standish and B. A. Pethica, *Trans. Faraday Soc.*, **64,** 1113 (1968).

(12) F. A. Vilallonga, M. Fernandez, C. Rotunno, and M. Cereijido, *Biochim. Biophys. Acta,* **183,** 98 (1969).

(13) F. M. Fowkes, *J. Phys. Chem.*, **65,** 355 (1961).

(14) M. A. McGregor and F. T. Barnes, *J. Colloid Interface Sci.*, **49,** 362 (1974).

(15) *Ibid.*, **54,** 439 (1976).

(16) L. S. Lerman, *J. Biol.*, **3,** 18 (1961).

(17) L. S. Lerman, *Proc. Natl. Acad. Sci. USA*, **49,** 94 (1963).

(18) L. S. Lerman, *J. Cell. Comp. Physiol. Suppl.*, **1,** 64 (1964).

(19) R. J. Sturgeon, Ph.D. dissertation, University of Florida, Gainesville, Fla., 1977.

(20) A. R. Peacocke, in "Acridines," 2nd ed., R. M. Acheson, Ed., Interscience, New York, N.Y., 1973, chap. 14.

ACKNOWLEDGMENTS

The authors are grateful to Dr. S. G. Schulman for the doxorubicin hydrochloride sample, which was a gift from Adria Laboratories.

^{13}C-NMR Spectroscopy of Tropane Alkaloids

ALY M. TAHA *x and G. RÜCKER

Received June 28, 1977, from the *Institut für Pharmazeutische Chemie der Westfälischen Wilhelms-Universität, 58-62 Hittorfstr., D-4400 Münster (Westf), West Germany.* Accepted for publication September 14, 1977. *Present address: Faculty of Pharmacy, University of Assiut, Assiut, Egypt.

Abstract □ The natural abundance ^{13}C-NMR spectra of tropine, atropine, scopolamine, cocaine, atropine methonitrate, and *dl*-tropic acid were determined at 22.63 MHz. With the aid of proton decoupling techniques and by comparison with analogous simpler compounds, it was possible to make self-consistent and unambiguous assignments of all carbon resonances for these alkaloids. Some important chemical shift trends were observed and should be useful in the identification of similar systems.

Keyphrases □ Tropane alkaloids, various—^{13}C-NMR spectra determined, carbon resonances assigned □ Alkaloids, various tropane—^{13}C-NMR spectra determined, carbon resonances assigned □ ^{13}C-NMR spectroscopy—various tropane alkaloids, spectra determined, carbon resonances assigned

The proton magnetic resonance (PMR) spectra of alkaloids often are too complex to be useful in the structure elucidation of this large class of naturally occurring compounds. The complexity results from extensive spin–spin coupling among protons, overlap of numerous resonance patterns, line broadening arising from intermolecular association and/or ^{14}N-quadrupolar relaxation effects. Natural abundance ^{13}C-NMR spectroscopy has been especially useful in such cases (1).

The tropane alkaloids have been well characterized by structural and stereochemical investigations (2). However, only one limited ^{13}C-NMR study, concentrating on the nonaromatic part of atropine, has been reported (3). The undertaking of a more detailed study was stimulated during the examination of the stability of tropane alkaloids in organic solvents when, consequently, need arose as to the structure elucidation of closely similar compounds. In addition, the broad acceptance of ^{13}C-NMR spectroscopy as a new powerful tool of structural analysis awaits only the accumulation of chemical shift data on compounds representative of all types of natural products.

This report concerns the application of pulse and Fourier transform ^{13}C-NMR techniques to structure assignments of tropane alkaloids.

EXPERIMENTAL

^{13}C-NMR Spectra—^{13}C-NMR spectra were determined at 22.63 MHz in the Fourier transform mode using a spectrometer[1] interfaced with a computer system[2]. The spectrometer features field stabilization *via* internal deuterium lock. Alkaloidal bases were dissolved in chloroform-*d*, and tropic acid was dissolved in methanol-d_4; either a dimethyl sulfoxide-d_6 or deuterated methanol–deuterium oxide mixture (6:4) was used

[1] Brucker W-90 pulse.
[2] Brucker-Nicolet B-NC-12.

Table I—^{13}C-Chemical Shifts for Tropane Alkaloids in Deuterochloroform [a] (Nonaromatic Moiety)

Carbon Identification	Multiplicity [b]	Tropine	Atropine	Scopolamine	Atropine Methonitrate [b]	Cocaine
1	d	59.7	59.2	57.3	64.5	64.5
2	t	38.8	35.8*	30.2	32.1	49.9 (d)
3	d	63.3	67.4	66.3	67.9	66.6
4	t	38.8	35.6*	30.4	32.1	35.2
5	d	59.7	59.2	57.3	64.5	61.3
6	t	25.5	24.7*	55.4* (d)	24.6*	25.0
7	t	25.5	25.05*	55.8* (d)	24.7*	25.0
NCH_3 (9)	q	39.8	39.7	41.6	44.4 (a)	40.7
NCH_3 (10)	q	—	—	—	51.2 (e)	—
OCH_3	q	—	—	—	—	50.8
C=O	s	—	—	—	—	170.2

[a] Chemical shifts are in parts per million downfield from tetramethylsilane. Starred (*) values may be interchanged for the same compound. [b] Signal multiplicity obtained from SFORD spectra: s = singlet, d = doublet, t = triplet, and q = quartet; (a) = axial orientation, (e) = equatorial orientation.

as the solvent for atropine methonitrate. All samples were contained in precision-ground 10-mm o.d. tubes.

The spectra were obtained at ambient temperature by using the deuterium resonance of the solvent as the lock signal. The carbon signal of solvents provided the internal reference for chemical shift measurements, taking the frequency of the central peaks of the deuterated chloroform triplet as 1742.51 Hz (*i.e.*, 77.00 ppm downfield relative to tetramethylsilane), of the deuterated methanol septet as 1065.873 Hz (47.10 ppm), and of the dimethyl sulfoxide-d_6 septet as 895.672 Hz (39.58 ppm). In some runs, 5% tetramethylsilane was also added as an additional reference for control of the solvent signal. The chemical shifts reported are accurate to within 0.03 ppm.

For each compound, two spectra were determined. In one, all proton lines were decoupled by a broad band (~2.5 kHz) irradiation from an incoherent 90-MHz source (noise-modulated total proton decoupling). In the other run, a single-frequency off-resonance decoupling (SFORD) spectrum was made. Interferograms were stored in 8K (8000 channels) of computer memory with 8K output data points in the transformed-phase corrected real spectrum, and the chemical shifts were determined on 6000-Hz sweepwidth spectra. The typical pulse width was 2.5 μsec and the delay time between pulses was 1.2 sec, with a phase-alternating pulse sequence to eliminate residual noncoherent system noise echo effects.

Acquisition times averaged 1–2 over 8K data points for 0.5–0.8 *M* concentrations. Double this time was required for SFORD spectra.

Chemicals—Atropine and tropine bases, as well as *dl*-tropic acid and atropine methonitrate, were obtained commercially in analytical grade[3] and required no further purification. Cocaine and scopolamine bases were prepared from the salts obtained in pharmaceutical grade[3] by employing standard procedures (4). The melting points and $[\alpha]_D$ values of these prepared bases agreed with literature values.

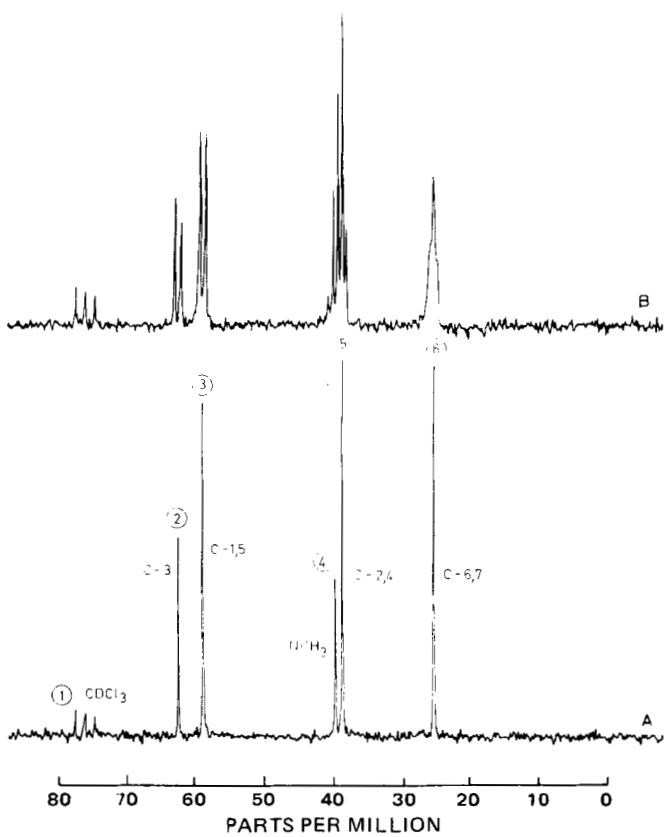

Figure 1—^{13}C-NMR spectra of tropine in deuterated chloroform. Key: A, broad band decoupled spectrum; and B, off-resonance decoupled spectrum.

RESULTS AND DISCUSSION

Most of the ^{13}C-NMR chemical shift assignments for the tropane alkaloids (Tables I and II) were based on empirical correlations and the principle of additivity of substituent effects, which have been summarized in reported equations (5, 6). Although these equations were based on simple paraffins, the qualitative trends found for the ^{13}C-shifts in paraffins have been extended to predict the relative order of ^{13}C-chemical shifts in other compounds (7–9). The most important of these trends are: (*a*) that substitution of a carbon (or a more electronegative atom or group) for a directly attached hydrogen produces a downfield shift [*i.e.*, the more carbons alpha to the carbon in question, the more downfield the ^{13}C-shift (α-effect)]; (*b*) that substitution of a carbon or other atom for a hydrogen attached to a carbon alpha to the carbon in question also produces a downfield shift [*i.e.*, the more substitution at the carbon alpha to the carbon in question, the more downfield the ^{13}C-shift (β-effect)]; and (*c*) that hydrogens or other groups attached to carbons gamma to the carbon in question produce an upfield shift (γ-effect). The α- and β-effects are presumably through bond effects while the γ-effect is a steric compression effect (10).

The numbering system for tropane alkaloids is shown in Structure I.

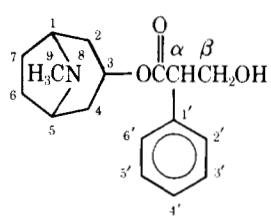

I

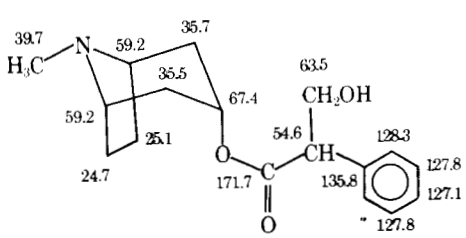

II

[3] Merck, Darmstadt, German Federal Republic.

Table II—^{13}C-Chemical Shifts for Tropane Alkaloids [a] (Aromatic Moiety)

Carbon Identification	Multiplicity	Atropine	Scopolamine	Atropine Methonitrate	Tropic Acid	Cocaine
1′	s	135.9	135.4	136.0	136.7	130.2
2′	d	128.3	128.3	129.7	128.1	127.9
3′	d	127.8	127.6	128.9	128.6	129.3
4′	d	127.1	127.3	128.9	127.1	132.5
5′	d	127.8	127.6	128.9	128.6	129.3
6′	d	128.3	128.3	129.7	128.1	127.9
C=O	s	171.6	171.2	173.4	175.2	165.5
α-CH	d	54.6	54.0	54.3	54.7	—
β-CH_2OH	t	63.4	63.4	64.5	64.0	—

[a] See footnote of Table I.

The ^{13}C-chemical shifts for the alkaloids are shown in Tables I and II. Some spectra are illustrated in Figs. 1–5, while the chemical shifts for atropine are indicated on its formula in Structure II. In each case, noise-decoupled and SFORD spectra were obtained. The former (broad band decoupling) yielded a single line signal for each carbon atom type with peak intensity roughly proportional to the number of carbons; the multiplicities generated in the SFORD spectra enabled the distinction between methyl (quartet), methylene (triplet), methine (doublet), and quaternary (including carbonyl) (singlet) carbon resonances.

The ^{13}C-resonances of the tropane alkaloids can be grouped into two main regions corresponding to the tropane ring and the aromatic acid moiety of the molecules (Tables I and II).

Tropane Ring—In tropine, there are five separate signals in the 20–65-ppm ^{13}C-chemical shift region relative to tetramethylsilane (Table I and Fig. 1). The symmetry-induced structural simplicity of tropine rendered it an easy object for assignment and facilitated later assignments of more complex molecules. The farthest downfield signal corresponds to C-3 carrying the hydroxyl group, while the *N*-methyl carbon is easily assigned the 39.8-ppm peak on the basis of SFORD multiplicity as well as peak intensity. The overlapping triplet at 38.8 ppm is due to C-2 and C-4, while the poorly resolved triplet farthest upfield is assigned to C-6 and C-7. The remaining methine signals at 59.7 ppm obviously belong to the C-1 and C-5 identical carbons. Evaluation of these signals was based on the additivity of substituents previously mentioned as well as comparison with β-methylene shift values of piperidine, pyrrolidine, and their *N*- and *C*-methyl derivatives (11–13) and the expected α-alkyl substituent effects (7, 8, 14, 15).

The weak shielding of C-2 and C-4 and the strong upfield shift of C-6 and C-7 indicate that the *N*-methyl group in tropine is oriented equatorially relative to the piperidine ring. The spectrum of atropine methonitrate (Table I) shows two distinct *N*-methyl signals, the upfield one corresponding to axial orientation and the lower field signal corresponding to equatorial orientation. The spectrum of this quaternary salt also exhibits a general downfield shift of most signals, amounting to 5 ppm for the α-carbon and 10 ppm for the equatorial methylene signal.

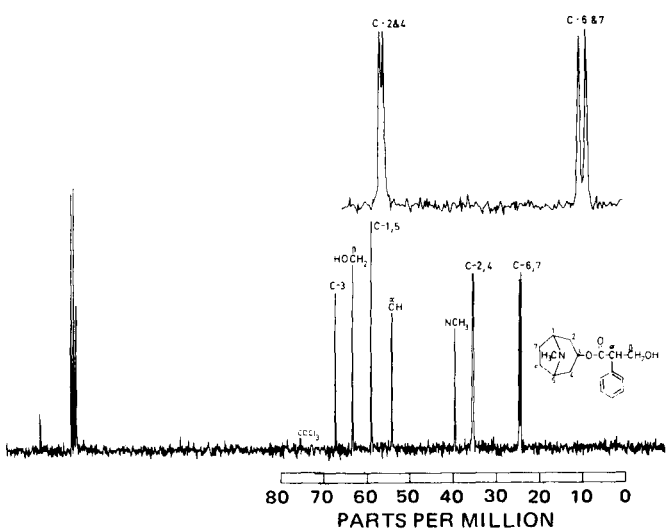

Figure 2—^{13}*C-NMR broad band decoupled spectrum of atropine in deuterated chloroform. The upper curve is a scale expansion of the signals of C-2, C-4 and C-6, C-7.*

Therefore, the quaternized salts should be useful as diagnostic derivatives for ^{13}C-NMR analysis similar to the *N*-oxides (3) in view of the strong chemical shift changes. Unfortunately, however, different solvents are usually required for the free alkaloid and the salt so solvent effects are superimposed upon the derivative effects.

That ^{13}C-NMR spectroscopy is a more powerful and useful tool than PMR spectroscopy, especially in revealing subtle structural details, is illustrated by the splitting of the signals for C-6 and C-7 as well as for C-2 and C-4 in atropine into fine doublets in comparison with the singlets observed in the unesterified tropine (Fig. 2). This observation suggests unsymmetrical orientation of the tropic acid moiety, probably due to hydrogen bond formation between the hydroxyl group of this acid and its carbonyl function and the general inclination of the ester group at C-3 to the lower plane of the azabicyclo ring. The same trend is also found in the spectrum of scopolamine (Fig. 3) but not in the signal of C-6 and C-7 in cocaine in which the aromatic moiety lacks the hydroxyl group. The obvious future application of this revealing of fine structural details would be in the possible greater understanding of the bioeffects of these

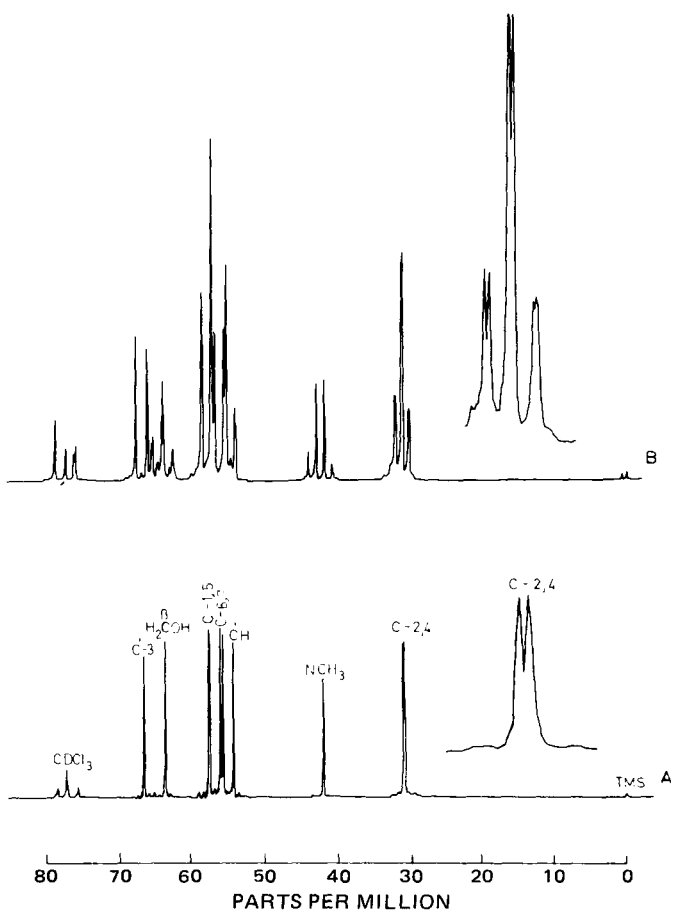

Figure 3—^{13}*C-NMR spectra of scopolamine (nonaromatic region) in deuterated chloroform. Key: A, broad band decoupled spectrum; and B, off-resonance decoupled spectrum. The signals for C-2 and C-4 are shown expanded on the right-hand side of both spectra.*

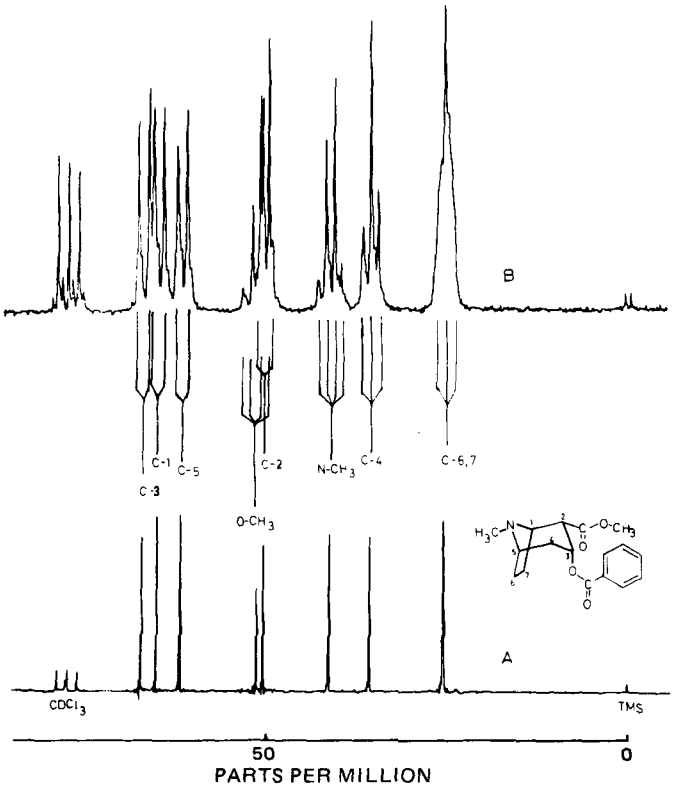

Figure 4—^{13}C-*NMR spectra of cocaine (nonaromatic region) in deuterated chloroform. Key: A, broad band decoupled spectrum; and B, off-resonance decoupled spectrum.*

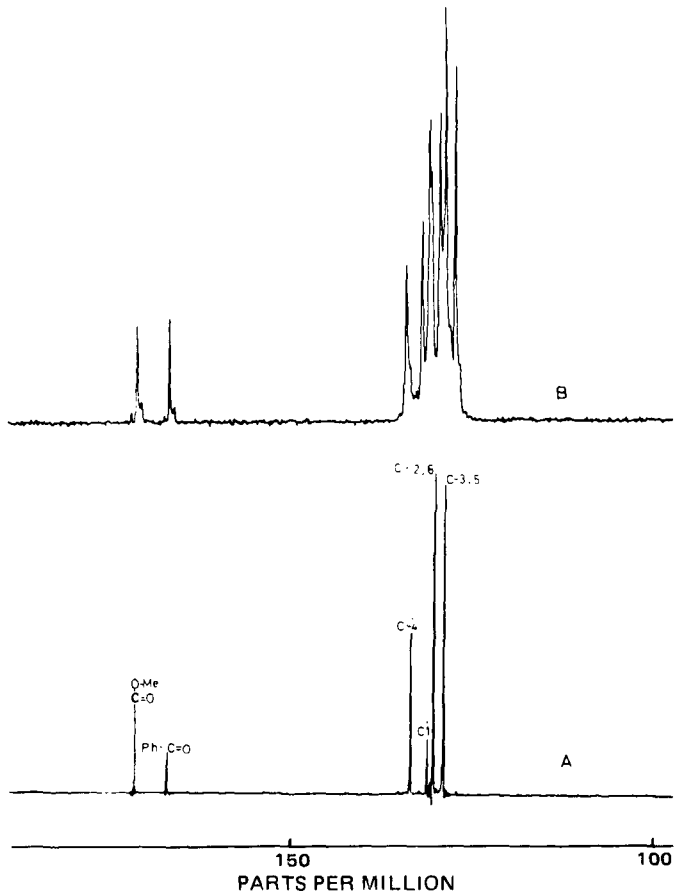

Figure 5—^{13}C-*NMR spectra of cocaine (aromatic region) in deuterated chloroform. Key: A, broad band decoupled spectrum; and B, off-resonance decoupled spectrum.*

compounds based on a closer knowledge of molecular orientation at receptors and in body fluids. The assignment of the α-CH and β-CH_2OH carbons of atropine, scopolamine, and atropine methonitrate was based on SFORD multiplicity as well as inspection of the spectra of the separate moieties: tropine and tropic acid (Tables I and II).

The lack of symmetry of the ecgonine moiety of cocaine makes its ^{13}C-NMR analysis more difficult. However, the simpler aryl moiety, as well as the ^{13}C-NMR effects observed among *N*- and *C*-methyl piperidines and piperidones (11–13), aided in the shift assignments. Substitution of the ester group at C-2 for hydrogen brings about a considerable downfield shift of the ^{13}C-signal of this carbon (Table I and Fig. 4), amounting to a 14-ppm lower field than the corresponding carbon in atropine, and the SFORD multiplicity is now the expected doublet.

The assignment of signals for C-6, C-7, and C-4 was straightforward based on comparison with other alkaloids and SFORD spectra. The differentiation between the two quartets due to *O*- and *N*-methyl groups was based on reported observations on analogous systems (1–8), where the lower field peaks were assigned to carbons bonded to oxygen. Generally, a carbon bonded to nitrogen resonates about 10-ppm higher field than a similarly substituted carbon bonded to oxygen (1, 8, 14). Consideration of α- and β-effects, as well as comparison with other tropanes, aided in the assignment of the most downfield signal of ecgonine to C-3 and the second and third signals higher field to C-1 and C-5, respectively (Fig. 4 and Table I). All three carbons, however, have the same SFORD multiplicity.

Aromatic Moiety—The aromatic region of the spectra of tropyl and benzoyl esters could be assigned without difficulty from the carbon-to-hydrogen coupling patterns (SFORD multiplicity) and intensities of peaks, as well as the alternating shielding and deshielding effect of the substituent at C-1′ (Table II). Thus, the carbon with the substituent (C-1′) did not show the 160-Hz directly bonded carbon–hydrogen coupling. The *para*-carbon peaks had only half the intensity of either *ortho*- or *meta*-carbons. The latter could be distinguished from each other by the difference in the spectral pattern arising from long range CH coupling (16). The electron-donating CH_2OH substituent in tropic acid showed the expected alternating shielding and deshielding effect on the even- and odd-numbered carbons, respectively. This result aided in assigning the farthest upfield signal in the aromatic region of tropic acid (Table II) to C-4′, the next downfield peak to C-2′ and C-6′, and the remaining methine signals to C-3′ and C-5′. The single carbonyl carbon of tropic acid was easily assigned the farthest downfield signal. It is shifted some 4 ppm upfield in the esterified alkaloids relative to the unsubstituted acid, following the general trend found among carboxylic acid and esters (7–9, 16).

This order of aromatic carbon signals is reversed in the benzoyl moiety of cocaine (Fig. 5) because of the reverse in the shielding parameters of aromatic carbons induced by the directly attached electron-abstracting carbonyl group. Thus, the even-numbered carbons are deshielded more than the odd-numbered ones. This result aided in assignment of the half-intense methine signal at 132.5 in the cocaine spectrum to C-4′ and the singlet at 130.2 to C-1′. The next upfield twice-intense signals were assigned to C-2′, C-6′, and C-3′, C-5′, respectively. The differentiation of the two carbonyl carbons of cocaine (Tables I and II and Fig. 5) was based on substitution parameters (8) and comparison with similar systems (17).

CONCLUSION

Because of the recent advances in instrumentation, ^{13}C-NMR spectroscopy is becoming an increasingly useful tool in structural investigation and compound identification. The substituent additivity parameters utilized in this work proved again that empirical schemes are most important in the prediction of structure from ^{13}C-NMR spectra and encourage the expansion of the data bank to include all possible structural variations. Many subtle and important structural features could be revealed by simple inspection of spectra. In comparison, the PMR spectrum of simple methyl benzoate required complete computer simulation (18). This evaluation of ^{13}C-NMR shifts of a limited group of alkaloids should be a useful contribution to this expanding field of structural elucidation.

REFERENCES

(1) W. O. Crain, Jr., W. C. Wildman, and T. D. Roberts, *J. Am. Chem. Soc.*, **93**, 990 (1971).

(2) R. H. F. Manske, "The Alkaloids," vol. 13, Academic, New York, N.Y., 1971, pp. 269–304.
(3) E. Wenkert, J. S. Bindra, C. J. Chang, D. W. Cochran, and F. M. Schell, *Acc. Chem. Res.*, **7**, 47 (1974).
(4) T. Higuchi and E. Brochmann-Hanssen, "Pharmaceutical Analysis," Interscience, New York, N.Y., 1961, pp. 313–543.
(5) L. P. Lindeman and J. Q. Adams, *Anal. Chem.*, **43**, 1245 (1971).
(6) D. M. Grant and E. G. Paul, *J. Am. Chem. Soc.*, **86**, 2984 (1964).
(7) G. C. Levy and G. L. Nelson, "Carbon-13 NMR for Organic Chemists," Wiley–Interscience, New York, N.Y., 1977, chap. 3.
(8) E. Breitmaier and W. Voelter, "13 C-NMR Spectroscopy," Verlag Chemie, Weinheim, West Germany, 1974, and references cited therein.
(9) E. Pretsch, T. Clerc, J. Seibel, and W. Simon, "Tabellen zur Strukturaufklärung Organischer Verbindungen," Springer-Verlag, Berlin, Germany, 1976, pp. C5-C265.
(10) D. K. Dalling and D. M. Grant, *J. Am. Chem. Soc.*, **94**, 5318 (1972).
(11) G. Ellis and R. G. Jones, *J. Chem. Soc. Perkin II*, **1972**, 437.
(12) A. J. Jones and M. M. Hassan, *J. Org. Chem.*, **37**, 2332 (1972).
(13) J. B. Lambert, D. A. Netzel, H. Sun, and K. K. Lilianstron, *J. Am. Chem. Soc.*, **98**, 3778 (1976).
(14) J. B. Sothers, "Carbon-13 NMR Spectroscopy," Academic, New York, N.Y., 1972.
(15) L. F. Johnson and W. C. Jankowski, "Carbon-13 NMR Spectra," Wiley–Interscience, New York, N.Y., 1972.
(16) K. N. Scott, *J. Am. Chem. Soc.*, **94**, 8564 (1972).
(17) S. W. Pelletier and Z. Djarmati, *ibid.*, **98**, 2626 (1976).
(18) K. N. Scott, *J. Magn. Reson.*, **2**, 361 (1970).

ACKNOWLEDGMENTS

Supported by a grant from the Alexander von Humboldt Foundation.

Colorimetric Determination of Catecholamines by 2,3,5-Triphenyltetrazolium Chloride

NAWAL A. EL-RABBAT and NABIL M. OMAR ˣ

Received May 16, 1977, from the *Department of Pharmaceutical Chemistry, Faculty of Pharmacy, University of Assiut, Assiut, Egypt.* Accepted for publication September 22, 1977.

Abstract □ A convenient spectrophotometric method was developed for the determination of epinephrine, levarterenol, isoproterenol, and methyldopa by reduction of 2,3,5-triphenyltetrazolium chloride and subsequent measurement of the formazan at 485 nm. With absolute alcohol as the solvent, maximum color absorption was attained in 30 min at 25° in the presence of 0.1 *N* KOH. Evidence is provided to account for the reduction of the tetrazolium salt at the expense of the epinephrine catechol moiety. In addition to the considerably high values of the molar absorptivities of the chromogen formed, ideal adherence of the color absorption to the Beer–Lambert law permitted a sensitive microdetermination of these catecholamines in both pure forms and pharmaceutical formulations. The tetrazolium interaction was selective. No interference was encountered from common catecholamine antioxidants, adjuvants, or noncatechol degradation products.

Keyphrases □ Epinephrine—colorimetric analysis in bulk drug and dosage forms □ Levarterenol—colorimetric analysis in bulk drug and dosage forms □ Isoproterenol—colorimetric analysis in bulk drug and dosage forms □ Methyldopa—colorimetric analysis in bulk drug and dosage forms □ Colorimetry—analyses, epinephrine, levarterenol, isoproterenol, and methyldopa in bulk drug and dosage forms □ Catecholamines, various—colorimetric analyses in bulk drug and dosage forms □ Adrenergic agents—epinephrine, levarterenol, and isoproterenol, colorimetric analyses in bulk drug and dosage forms □ Antihypertensives—methyldopa, colorimetric analysis in bulk drug and dosage forms

The presence of various catecholamine congeners in many pharmaceutical formulations necessitates a rapid, economical, and sensitive analytical method. Most of these derivatives are officially assayed by chemical, titrimetric, and spectrophotometric procedures (1, 2). Because of their phenolic and basic functions, catecholamines interact with many chromogenic reagents such as potassium ferricyanide–ferric chloride (3), alkali ferrocyanates (4), *p*-nitrophenyldiazonium chloride (5), nitrosomercurials (6), and alkali molybdates (7). Other earlier reported chromogens include iodine, ferric ion, nitrous acid, and 1,2-naphthoquinone 4-sodium sulfonate (8). However, accurate colorimetric determinations of pharmaceutical catecholamines using their reducing potential have not been developed.

The present study investigated 2,3,5-triphenyltetrazolium chloride as a convenient reagent for the colorimetric determination of epinephrine, levarterenol, isoproterenol, and methyldopa, both in pure forms and dosage formulations. The fact that tetrazolium salts can be reduced selectively into highly colored formazan dyes constituted the basis of the current work (9).

EXPERIMENTAL

Instrumentation—A double-beam spectrophotometer[1], a pH meter[2] fitted with a sealed calomel electrode, a shielded glass electrode, and a suitable thermostated[3] water bath were used.

Catecholamines—Pharmaceutical grade epinephrine hydrochloride, levarterenol bitartrate, isoproterenol hydrochloride, and methyldopa were utilized as the working standards.

Catecholamine Dosage Forms—The following commercial formulations were analyzed: methyldopa tablets[4], epinephrine injection[5], procaine–epinephrine injection[6], levarterenol injection[7], and isoproterenol solution[8].

Reagents—*Tetrazolium Solution*—Dissolve 0.5 g of pure 2,3,5-tri-

[1] Spektromom-203, MOM, Budapest, Hungary.
[2] Radelkis OP-401/2, Budapest, Hungary.
[3] T-606 MTA, Budapest, Hungary.
[4] Contains 250 mg of methyldopa/tablet; El-Kahira-MSD, Cairo, Egypt.
[5] Contains 1.0 mg of epinephrine/1-ml ampul; Misr Co. for Pharmaceuticals, Cairo, Egypt.
[6] Contains 10.0 μg of epinephrine and 10.0 mg of procaine hydrochloride/1-ml ampul; El-Nile Co. for Pharmaceuticals, Cairo, Egypt.
[7] Contains 1.0 mg of levarterenol/1-ml ampul; El-Nile Co. for Pharmaceuticals, Cairo, Egypt.
[8] Isoprenaline, contains 10.0 mg of isoproterenol hydrochloride/1 ml of solution; El-Nile Co. for Pharmaceuticals, Cairo, Egypt.

(2) R. H. F. Manske, "The Alkaloids," vol. 13, Academic, New York, N.Y., 1971, pp. 269–304.
(3) E. Wenkert, J. S. Bindra, C. J. Chang, D. W. Cochran, and F. M. Schell, *Acc. Chem. Res.*, **7**, 47 (1974).
(4) T. Higuchi and E. Brochmann-Hanssen, "Pharmaceutical Analysis," Interscience, New York, N.Y., 1961, pp. 313–543.
(5) L. P. Lindeman and J. Q. Adams, *Anal. Chem.*, **43**, 1245 (1971).
(6) D. M. Grant and E. G. Paul, *J. Am. Chem. Soc.*, **86**, 2984 (1964).
(7) G. C. Levy and G. L. Nelson, "Carbon-13 NMR for Organic Chemists," Wiley–Interscience, New York, N.Y., 1977, chap. 3.
(8) E. Breitmaier and W. Voelter, "13 C-NMR Spectroscopy," Verlag Chemie, Weinheim, West Germany, 1974, and references cited therein.
(9) E. Pretsch, T. Clerc, J. Seibel, and W. Simon, "Tabellen zur Strukturaufklärung Organischer Verbindungen," Springer-Verlag, Berlin, Germany, 1976, pp. C5-C265.
(10) D. K. Dalling and D. M. Grant, *J. Am. Chem. Soc.*, **94**, 5318 (1972).
(11) G. Ellis and R. G. Jones, *J. Chem. Soc. Perkin II*, **1972**, 437.
(12) A. J. Jones and M. M. Hassan, *J. Org. Chem.*, **37**, 2332 (1972).
(13) J. B. Lambert, D. A. Netzel, H. Sun, and K. K. Lilianstron, *J. Am. Chem. Soc.*, **98**, 3778 (1976).
(14) J. B. Sothers, "Carbon-13 NMR Spectroscopy," Academic, New York, N.Y., 1972.
(15) L. F. Johnson and W. C. Jankowski, "Carbon-13 NMR Spectra," Wiley–Interscience, New York, N.Y., 1972.
(16) K. N. Scott, *J. Am. Chem. Soc.*, **94**, 8564 (1972).
(17) S. W. Pelletier and Z. Djarmati, *ibid.*, **98**, 2626 (1976).
(18) K. N. Scott, *J. Magn. Reson.*, **2**, 361 (1970).

ACKNOWLEDGMENTS

Supported by a grant from the Alexander von Humboldt Foundation.

Colorimetric Determination of Catecholamines by 2,3,5-Triphenyltetrazolium Chloride

NAWAL A. EL-RABBAT and NABIL M. OMAR ˣ

Received May 16, 1977, from the *Department of Pharmaceutical Chemistry, Faculty of Pharmacy, University of Assiut, Assiut, Egypt.* Accepted for publication September 22, 1977.

Abstract □ A convenient spectrophotometric method was developed for the determination of epinephrine, levarterenol, isoproterenol, and methyldopa by reduction of 2,3,5-triphenyltetrazolium chloride and subsequent measurement of the formazan at 485 nm. With absolute alcohol as the solvent, maximum color absorption was attained in 30 min at 25° in the presence of 0.1 *N* KOH. Evidence is provided to account for the reduction of the tetrazolium salt at the expense of the epinephrine catechol moiety. In addition to the considerably high values of the molar absorptivities of the chromogen formed, ideal adherence of the color absorption to the Beer–Lambert law permitted a sensitive microdetermination of these catecholamines in both pure forms and pharmaceutical formulations. The tetrazolium interaction was selective. No interference was encountered from common catecholamine antioxidants, adjuvants, or noncatechol degradation products.

Keyphrases □ Epinephrine—colorimetric analysis in bulk drug and dosage forms □ Levarterenol—colorimetric analysis in bulk drug and dosage forms □ Isoproterenol—colorimetric analysis in bulk drug and dosage forms □ Methyldopa—colorimetric analysis in bulk drug and dosage forms □ Colorimetry—analyses, epinephrine, levarterenol, isoproterenol, and methyldopa in bulk drug and dosage forms □ Catecholamines, various—colorimetric analyses in bulk drug and dosage forms □ Adrenergic agents—epinephrine, levarterenol, and isoproterenol, colorimetric analyses in bulk drug and dosage forms □ Antihypertensives—methyldopa, colorimetric analysis in bulk drug and dosage forms

The presence of various catecholamine congeners in many pharmaceutical formulations necessitates a rapid, economical, and sensitive analytical method. Most of these derivatives are officially assayed by chemical, titrimetric, and spectrophotometric procedures (1, 2). Because of their phenolic and basic functions, catecholamines interact with many chromogenic reagents such as potassium ferricyanide–ferric chloride (3), alkali ferrocyanates (4), *p*-nitrophenyldiazonium chloride (5), nitrosomercurials (6), and alkali molybdates (7). Other earlier reported chromogens include iodine, ferric ion, nitrous acid, and 1,2-naphthoquinone 4-sodium sulfonate (8). However, accurate colorimetric determinations of pharmaceutical catecholamines using their reducing potential have not been developed.

The present study investigated 2,3,5-triphenyltetrazolium chloride as a convenient reagent for the colorimetric determination of epinephrine, levarterenol, isoproterenol, and methyldopa, both in pure forms and dosage formulations. The fact that tetrazolium salts can be reduced selectively into highly colored formazan dyes constituted the basis of the current work (9).

EXPERIMENTAL

Instrumentation—A double-beam spectrophotometer[1], a pH meter[2] fitted with a sealed calomel electrode, a shielded glass electrode, and a suitable thermostated[3] water bath were used.

Catecholamines—Pharmaceutical grade epinephrine hydrochloride, levarterenol bitartrate, isoproterenol hydrochloride, and methyldopa were utilized as the working standards.

Catecholamine Dosage Forms—The following commercial formulations were analyzed: methyldopa tablets[4], epinephrine injection[5], procaine–epinephrine injection[6], levarterenol injection[7], and isoproterenol solution[8].

Reagents—*Tetrazolium Solution*—Dissolve 0.5 g of pure 2,3,5-tri-

[1] Spektromom-203, MOM, Budapest, Hungary.
[2] Radelkis OP-401/2, Budapest, Hungary.
[3] T-606 MTA, Budapest, Hungary.
[4] Contains 250 mg of methyldopa/tablet; El-Kahira-MSD, Cairo, Egypt.
[5] Contains 1.0 mg of epinephrine/1-ml ampul; Misr Co. for Pharmaceuticals, Cairo, Egypt.
[6] Contains 10.0 μg of epinephrine and 10.0 mg of procaine hydrochloride/1-ml ampul; El-Nile Co. for Pharmaceuticals, Cairo, Egypt.
[7] Contains 1.0 mg of levarterenol/1-ml ampul; El-Nile Co. for Pharmaceuticals, Cairo, Egypt.
[8] Isoprenaline, contains 10.0 mg of isoproterenol hydrochloride/1 ml of solution; El-Nile Co. for Pharmaceuticals, Cairo, Egypt.

Table I—Effect of Potassium Hydroxide on Epinephrine–Tetrazolium Interaction

Milliliters Added per 10 ml of Assay Solution[a]		
0.1% KOH	0.5% Tetrazolium Chloride	Absorbance, 485 nm
0.50	3.0	0.050
0.50	5.0	0.080
0.50	7.0	0.120
1.00	3.0	0.290
1.00	4.0	0.310
1.00	5.0	0.370
1.00	6.0	0.370
2.00	3.0	0.080
2.00	5.0	0.080
2.00	7.0	0.105

[a] *Containing* 1.0 μg of epinephrine base/ml.

phenyltetrazolium chloride[9] in 100 ml of absolute ethanol[10]. This reagent should be freshly prepared, although it may be kept for longer periods if stored in a dark, cool place.

Potassium Hydroxide Solution—Prepare 0.1% (w/v) carbonate-free[9] solution in absolute ethanol.

Standard Solutions—Dissolve an accurately weighed amount of the appropriate working standard in absolute ethanol and dilute the solution quantitatively and stepwise with absolute ethanol to obtain a final concentration of 10.0 μg of catecholamine base/ml.

Assay Samples—*Injections and Solutions*—Pipet 1.0 ml, or the measured contents of a single-dose container of the injection, into a suitable volumetric flask and dilute with absolute ethanol to obtain ~10 μg of the claimed amine content/ml of the prepared solution.

Tablets—Place a single powdered tablet, or its equivalent from a composite of 20 tablets, in a 100-ml volumetric flask and add 5 ml of 1% (w/v) HCl and 20 ml of absolute ethanol. Allow the mixture to stand for 30 min with frequent shaking, bring to volume with absolute ethanol, mix well, and filter through a dry filter into a dry flask. Discard the first portions of the filtrate. Dilute an aliquot of this sample with absolute ethanol to afford a concentration of ~10 μg of the claimed amine content/ml of the prepared solution.

Procedure—Pipet 1.0 ml of the standard (or of the appropriately prepared sample) solution into a 10-ml volumetric flask. Add, in order, 5.0 ml of tetrazolium solution and 1.0 ml of potassium hydroxide solution; then dilute to volume with absolute ethanol, mixing well after each addition. Allow the solution to stand in the dark in a 25.0 ± 0.1° water bath for 30 min. Transfer the solution into a 1-cm glass cell and determine its absorbance at 485 nm *versus* a blank prepared from 1.0 ml of absolute ethanol and treated similarly.

RESULTS AND DISCUSSION

Tetrazolium–Epinephrine Interaction—The utility of 2,3,5-triphenyltetrazolium chloride as an efficient reagent for both detection and colorimetric determination of α-ketolic steroids (10, 11), reducing sugars (12, 13), and ascorbic acid (13, 14) is well documented. For ascorbic acid, use is made of the reducing potential of the α,β-diol groups for the transformation of the tetrazolium salt into a highly colored formazan derivative.

Catecholamines constitute an important class of pharmaceutical compounds that contain such dihydroxy groups within a phenolic structure and, therefore, may make the reduction of tetrazolium salts possible. Since this reduction is generally enhanced by the use of strong bases (9), considerable care was taken to guard against the instability of catecholamines in an alkaline medium.

Preliminary trials to induce the reduction of 2,3,5-triphenyltetrazolium chloride by ethanolic solutions of epinephrine hydrochloride in the presence of such weakly basic buffers as 1.0% (w/v) aqueous solutions of sodium acetate or sodium metaborate (pH ~8.0–8.5) were almost futile. However, an intense red-colored product, with maximum absorption at 485 nm, was readily formed when the interaction was carried out in the presence of ~0.05–0.25% (w/v) alcoholic potassium hydroxide solutions. At higher alkali concentrations, another weak absorption interfered at 395 nm and was more prominent when the interaction was effected in the presence of 0.30% (w/v) alcoholic tetraethylammonium hydroxide. The latter is usually used in much higher concentrations (~1.0%) as the conventional basic medium prescribed for the reduction of 2,3,5-triphenyltetrazolium chloride (8).

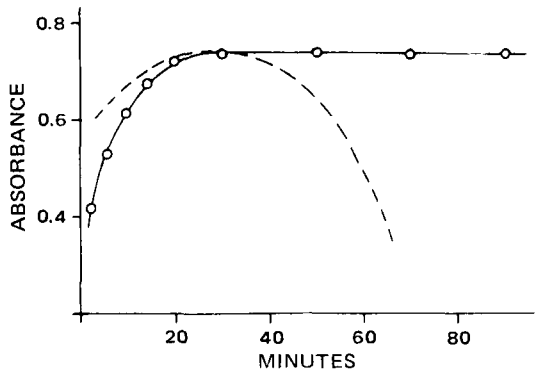

Figure 1—*Effect of time and temperature on color development at 25° (—) and at boiling water bath temperature (- - -).*

No interference with formazan color absorption at 485 nm could be traced when 1.0 ml of ~0.20–0.30% (w/v) ethanolic potassium hydroxide was added to 1.0 ml of the standard epinephrine hydrochloride solution that was already mixed with different volumes of the tetrazolium salt solution. Obviously, this order of addition reduced side reactions between epinephrine and the alkali.

A further rigorous investigation was carried out to assess the least alkali concentration that would induce maximum interaction between fixed aliquots of the tetrazolium reagent and standard epinephrine solutions. An appreciable increase of the 485-nm color absorption was achieved by use of 0.10 mg of potassium hydroxide and 2.50 mg of tetrazolium chloride/ml of the final catecholamine solution for assay (Table I). A concurrent investigation of the color–time curve (Fig. 1) indicated a 30-min interaction period to bring color development to a constant at 25°. The formazan remained stable for at least 24 hr.

Reduction of the tetrazolium reagent was accelerated by carrying out the interaction with epinephrine at the temperature of a boiling water bath. However, a gradual destruction of the intense red color followed, with a distinct drop in the absorptivity after ~40 min (Fig. 1). Moreover, no reproducible measurements of the color absorption could be attained. This result might be a consequence of competitive side oxidation reactions of the catecholamine at such elevated temperature. Potential interference with the tetrazolium–epinephrine interaction because of fluctuations in the reaction temperature was eliminated by carrying out the process at 25°.

Reaction Mechanism—A strong reducing group is a decisive criterion for an efficient interaction with 2,3,5-triphenyltetrazolium chloride, whose oxidation–reduction potential approximates −0.2 v (9). Such a condition can be fulfilled by the amine and/or catechol moieties of epinephrine, each of which is known to be oxidized selectively (15). Clarification of this point was achieved by an investigation of 2,3,5-triphenyltetrazolium chloride interactions with catechol, ephedrine sulfate, and phenylephrine hydrochloride.

Neither ephedrine nor phenylephrine could induce the formation of formazan under various experimental conditions, while a direct red color response was manifested by catechol, with a molar absorptivity of 4.14×10^4 at 485 nm. This finding indicated a key effect for the catechol

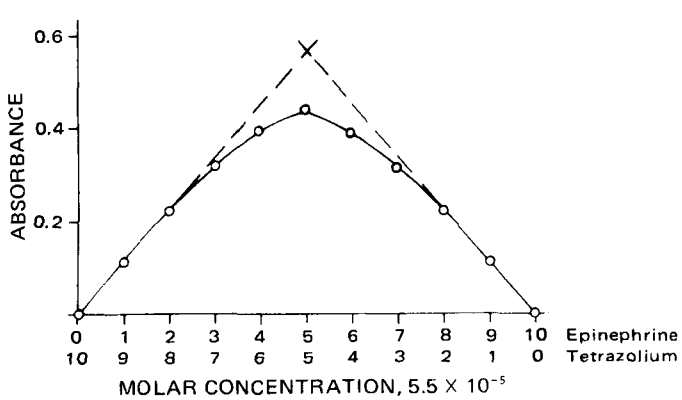

Figure 2—*Molar variation curve of the epinephrine–tetrazolium interaction at 25° in the presence of 1.0 ml of 0.1% KOH solution.*

[9] BDH, England.
[10] Aldehyde-free spectrograde, Merck, Germany.

Table II—Analysis of Epinephrine Standard Solutions

Replication	Epinephrine, Added, μg/ml	Found, %[a]	SD
1	0.25	100.37	0.66
2	0.50	99.59	0.75
3	0.75	99.68	0.57
4	1.00	100.50	0.61
5	1.50	100.28	0.58
6	2.00	99.70	0.45
7	2.50	100.27	0.56
8	3.00	99.65	0.62
	Mean recovery, % = 100.00		
	Pooled SD, $\pm S_p$, % = 0.38		

[a] Average of five determinations.

function in bringing about the oxidation of epinephrine by the tetrazolium salt. In fact, this reaction can be considered as an extension of the reduction of epinephrine by aliphatic diols (12–14) into the aromatic series.

As assessed by the continuous molar variation method (Fig. 2), epinephrine interacts with 2,3,5-tetrazolium chloride on a unimolar basis. Only limited suggestions can be made concerning the nature of the oxidation product(s) of the catecholamine. Mainly, formation of *o*-quinone derivatives would be expected since similar products are quite common for catechol and epinephrine (15, 16). Supporting this possibility is the nature of tetrazolium salts as efficient hydride-ion acceptors (17–19). Since the catechol-derived phenolate anion has hydride-ion donor properties (20), an interpretation of the entire tetrazolium–epinephrine interaction in terms of an intermolecular hydride-ion transfer reaction (Scheme I) seems plausible.

Quantitative Analysis—At fixed experimental conditions, the quantity of the formazan depended on the amount of epinephrine added to reduce the tetrazolium salt. A linear regression analysis of the Beer's plot at 485 nm revealed excellent adherence (r = 0.9996) up to a concentration of 3.0 μg (A = ~1.1) of the catecholamine/ml of the assayed solution. This result permitted the development of the interaction into a sensitive spectrophotometric analysis of epinephrine on account of the high value of the molar absorptivity observed, $\epsilon_a = 6.78 \times 10^4$.

Other catecholamines that behaved similarly with 2,3,5-tetrazolium chloride included working standards of levarterenol, isoproterenol, and methyldopa, with ϵ_a values corresponding to 3.38×10^4, 5.48×10^4, and 6.61×10^4, respectively (calculated with respect to the molar concentration of the free anhydrous bases). Replicate analysis of epinephrine working standards (Table II) revealed both high accuracy and sensitivity of the investigated colorimetric determination.

Assay of Dosage Forms—2,3,5-Triphenyltetrazolium chloride was not reduced by chlorobutanol, sodium metabisulfite, procaine hydrochloride, acacia, or starch. These ingredients constitute the major antioxidants, common adjuvants, and tablet excipients encountered in many catecholamine dosage forms. Potential interference by reducing sugars could be eliminated by alcohol extraction prior to analysis. As revealed by the data given in Table III, the tetrazolium method proved applicable to the analysis of different dosage forms of the studied catecholamine derivatives with remarkable accuracy.

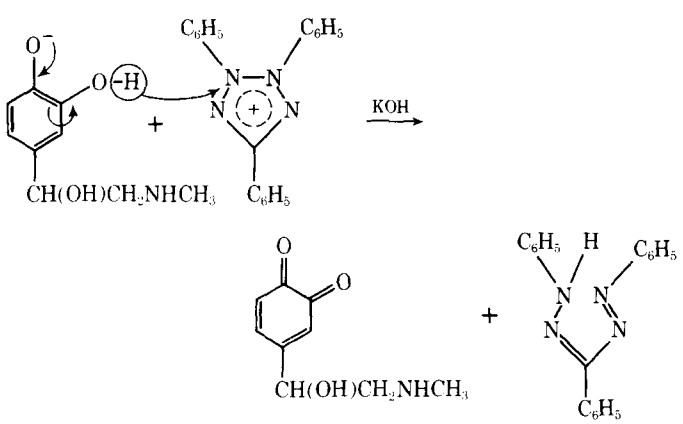

Scheme I

Table III—Analysis of Dosage Forms of Epinephrine, Levarterenol, Isoproterenol, and Methyldopa

Preparation[a]	Catecholamine Content, mg/Unit Label Claim	Found[b]	Added	Recovered
Epinephrine injection	1.0	0.98	1.0	1.97
Procaine–epinephrine injection	0.010	0.011	0.020	0.031
Levarterenol injection	1.0	0.97	0.50	1.45
Isoproterenol solution	10.0	9.86	5.0	14.90
Methyldopa tablets	250	247.3	100	346.6

[a] See *Experimental* for additional details. [b] Average of three determinations.

Interference with catecholamine analysis by noncatechol degradation products such as adrenochrome and adrenoquinone was not observed. Since these products are the major degradation derivatives of most catecholamines and are usually encountered in cases of autoxidation and metal-catalyzed and aerobic oxidations (21), this result indicates that the presented method is stability indicating in cases where the decomposition products do not have intact catechol moieties. Apart from its general validity for the analysis of catecholamines, the proposed procedure offers several advantages over current methods in terms of time, sensitivity, and convenience. It should also have utility in automated assays.

REFERENCES

(1) "The United States Pharmacopeia," 19th rev., Mack Publishing Co., Easton, Pa., 1975, pp. 274, 320.

(2) "British Pharmacopoeia 1973," University Printing House, Cambridge, England, 1973, pp. 257, 304.

(3) O. B. Genius, *Arzneim-Forsch.*, **24**, 119 (1974).

(4) J. I. Routh and R. E. Bannow, *Clin. Chem.*, **17**, 872 (1971).

(5) T. K. Pomażańska, *Acta Pol. Pharm.*, **26**, 519 (1969); through *Chem. Abstr.*, **72**, 103792 (1970).

(6) H. Jensen, J. P. Gillet, and E. Nenzil, *Ann. Biol. Clin.*, **26**, 73 (1968); through *Chem. Abstr.*, **68**, 102195 (1968).

(7) T. Halmekoski and A. Kivinen, *Farm. Aikak*, **75**, 223 (1966); through *Chem. Abstr.*, **66**, 5796 (1967).

(8) "Pharmaceutical Analysis," T. Higuchi and E. Brochmann-Hanssen, Eds., Interscience, New York, N.Y., 1961, pp. 42, 493.

(9) R. Kuhn and D. Jerchel, *Chem. Ber.*, **74**, 949 (1941).

(10) W. J. Mader and R. R. Buck, *Anal. Chem.*, **24**, 666 (1952).

(11) D. Banes, *J. Am. Pharm. Assoc., Sci. Ed.*, **42**, 669 (1953).

(12) A. M. Mattson and C. O. Jensen, *Anal. Chem.*, **22**, 182 (1950).

(13) "Spot Tests in Organic Analysis," F. Feigel, Ed., Elsevier, Amsterdam, The Netherlands, 1960, p. 477.

(14) M. H. Hashmi, A. Abdul Subhan, A. Viegas, and A. Ahmad, *Mikrochim. Acta*, **3**, 457 (1970).

(15) J. Pirwitz and O. Sherer, *Arch. Exp. Pathol. Pharmakol.*, **210**, 209 (1950).

(16) E. Adler, I. Falkehag, and P. Smith, *Acta Chem. Scand.*, **16**, 529 (1962).

(17) A. V. Eltsov, *Zh. Org. Khim.*, **1**, 1112 (1965).

(18) A. V. Eltsov and N. M. Omar, *ibid.*, **4**, 711 (1968).

(19) N. M. Omar and A. V. Eltsov, *ibid.*, **4**, 1294 (1968).

(20) D. N. Kursanov and Z. N. Parnes, *Russ. Chem. Rev.*, **30**, 598 (1961).

(21) "Progress in Medicinal Chemistry," G. Ellis and G. West, Eds., Elsevier, Amsterdam, The Netherlands, 1973, pp. 275–291.

Extraction of Daunorubicin and Doxorubicin and Their Hydroxyl Metabolites: Self-Association in Aqueous Solution

STAFFAN EKSBORG

Received May 5, 1977, from *Karolinska Pharmacy, Fack, S-104 01 Stockholm 60, Sweden.* Accepted for publication September 21, 1977.

Abstract □ The extraction of daunorubicin and doxorubicin and their hydroxyl metabolites daunorubicinol and doxorubicinol was studied using chloroform–1-pentanol (9:1) as the organic phase. Because of differences in acid dissociation constants, the pH for optimum extraction varied from 8.0 to 8.6 for the different compounds. Self-association in the aqueous phase significantly influenced the distribution ratio. Constants for the formation of dimers and tetramers in aqueous solutions were about $10^{4.5}$ and 10^{12}, respectively.

Keyphrases □ Daunorubicin—organic-aqueous distribution, self-association in aqueous phase □ Doxorubicin—organic-aqueous distribution, self-association in aqueous phase □ Distribution, organic-aqueous—daunorubicin and doxorubicin and hydroxyl metabolites □ Antineoplastic agents—daunorubicin, doxorubicin, and hydroxyl metabolites, organic-aqueous distribution, self-association in aqueous phase

Daunorubicin (I) and doxorubicin (II) are cytotoxic antibiotics used for the treatment of leukemia and solid tumors (1–3). Their cytotoxic effect has been attributed to complex formation with DNA resulting in an inhibition of RNA and DNA syntheses (4–8). The main metabolites of daunorubicin and doxorubicin, daunorubicinol (III) and doxorubicinol (IV), respectively, also have cytotoxic activity (8–10).

Self-association in aqueous solutions has been reported for planar aromatic ring systems (11–14). Dimerization of I in aqueous solutions has been studied by various physicochemical methods (photometry, circular dichroism, and NMR spectroscopy) (15). The self-association of I and II was investigated by studying its effect on the absorption spectrum and the distribution ratio to an organic phase.

The optimum conditions for extraction of I and II and their metabolites can be calculated from the constants presented.

EXPERIMENTAL

All experiments were carried out at 25.0 ± 0.1°.

Chemicals—Doxorubicin[1], doxorubicinol[1], daunorubicin[2], and daunorubicinol[2] were used as obtained. Chloroform was extracted with water to remove ethanol.

Aqueous and organic phases were equilibrated carefully before use. All other chemicals and solvents were analytical grade.

Photometric Measurements—The photometric determinations[3] of acid dissociation constants were based on the following measurements.

Stock solutions of I and II in distilled water were diluted with pH 9.1–10.5 carbonate buffers, 10^{-1} *M* phosphoric acid, or 10^{-2} *M* sodium hydroxide. The absorbance at 480 nm was measured within 60 sec after dilution to avoid decomposition of the components. The slit width of the photometer was kept constant within each series. The absorbance of at least two dilutions was measured at each pH value[4].

Partition Experiments—The partition experiments were performed in centrifuge tubes using equal phase volumes (10–20 ml) and mechanical shaking for 30 min in a thermostated bath. After centrifugation, the phases were separated by a capillary siphon.

The concentrations of the components were determined fluorometrically[5] (436 nm/555 nm) or photometrically (253 nm) in both phases: in the aqueous phase by direct measurement[6] and in the organic phase after reextraction to 0.1 *M* H_3PO_4. The spectrophotofluorometer was standardized against a solution of daunorubicin in 0.1 *M* H_3PO_4 before each measurement.

RESULTS AND DISCUSSION[7]

Photometric Determination of Acid Dissociation Constants—Compounds I and II have identical absorption spectra, which change drastically from acidic to basic media because of the protolysis of the two phenolic groups (Fig. 1). Studies of absorption spectra revealed that the acid dissociation constant of the second phenolic group was $<10^{-12}$. The exact value of the constant could not be established because of the low stability of the compounds in strongly alkaline media.

In the pH range where the dissociation of the second phenolic group is negligible (pH <11), the protolysis of the compounds can be illustrated by Scheme I.

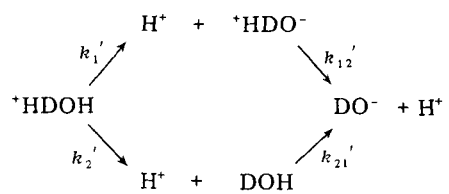

Scheme I

Four forms of the compounds occur: the ammonium ($^+$HDOH), the phenolate (DO^-), the uncharged (DOH), and the zwitterion ($^+HDO^-$).

The microscopic constants (16), k_1', k_2', k_{12}', and k_{21}', are defined by:

$$k_1' = \frac{a_h[^+HDO^-]}{[^+HDOH]} \quad \text{(Eq. 1)}$$

$$k_2' = \frac{a_h[DOH]}{[^+HDOH]} \quad \text{(Eq. 2)}$$

$$k_{12}' = \frac{a_h[DO^-]}{[^+HDO^-]} \quad \text{(Eq. 3)}$$

$$k_{21}' = \frac{a_h[DO^-]}{[DOH]} \quad \text{(Eq. 4)}$$

Photometric determination of the microscopic constants with graphic computation according to Edsall *et al.* (16), based on determined concentrations of species with protolyzed and unprotolyzed phenolic groups[8], is illustrated in Fig. 2. Plots of α_{OH} as a function of pM_{OH}^*, where:

$$\alpha_{OH} = \frac{C_{DO^-}}{C_D} \quad \text{(Eq. 5)}$$

[1] Supplied by Farmitalia, Milan, Italy.

[2] Supplied by Pharma Rhodia, Stockholm, Sweden.

[3] The photometers used were a Zeiss PMQ III with 10.0- and 50.0-mm cells and a Pye Unicam model 1800 with 10.0-mm cells.

[4] Orion Research model 701 digital pH meter equipped with an Ingold combined electrode type 401.

[5] Aminco-Bowman 4-8202 B spectrophotofluorometer.

[6] Molar absorptivity at 253 nm was 2.1×10^4 (pH 1.0–7.5).

[7] The following symbols, not defined in the text, are used: [ ] and [ ]$_{org}$ are the concentrations of molecules and ions in aqueous and organic phases, respectively; C_{DO^-} is the total concentration of the species in the aqueous phase containing a protolyzed phenolic group; C_{DOH} is the total concentration of the species in the aqueous phase containing unprotolyzed phenolic groups; $C_D = C_{DO^-} + C_{DOH}$ is the total concentration in the aqueous phase; and $C_{D_{org}}$ is the total concentration in the organic phase.

[8] $C_{DOH}/C_{DO^-} = (A_B - A)/(A - A_A)$, where A, A_A, and A_B are the absorbances at 480 nm in buffer, 0.1 *M* H_3PO_4, and 10^{-2} *M* NaOH, respectively (16).

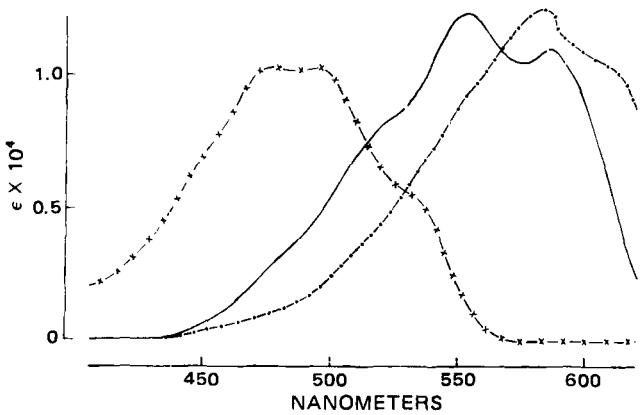

Figure 1—*Absorption spectra of I. Key: ×, pH 2.0 and 7.5; —, pH 10.9; and ●, pH 14 (1 M NaOH). The total concentration was 10^{-5} M.*

and:

$$M_{OH}^{*} = \frac{a_h C_{DO^-}}{C_{DOH}} \qquad \text{(Eq. 6)}$$

showed a variation of pM_{OH}^{*} not only with α_{OH} but also with C_D at constant values of α_{OH}. Hence, the protolysis of the phenolic groups is not only affected by the pH of the aqueous solutions but also by equilibrium processes dependent on the concentration of the drugs, *e.g.*, formation of aggregates. Therefore, the results presented in Fig. 2 cannot be used directly for the determination of the microscopic constants.

At constant pH, the ratio C_{DOH}/C_{DO^-} increased with increasing total concentration, which will be the case when $^{+}HDOH$ and DOH are involved in association processes (*e.g.*, dimerization and tetramerization) to a greater extent than $^{+}HDO^{-}$ and DO^{-}. Experiments were carried out in the pH range where the $^{+}HDOH$ form is unlikely. Under the assumptions that C_{DO^-} includes only monomeric forms:

$$C_{DO^-} = [^{+}HDO^{-}] + [DO^{-}] \qquad \text{(Eq. 7)}$$

and that C_{DOH} includes the monomer and dimer of the noncharged form:

$$C_{DOH} = [DOH] + 2[(DOH)_2] \qquad \text{(Eq. 8)}$$

the following equation is valid:

$$\frac{C_{DOH}}{C_{DO^-}} = \frac{[DOH]}{C_{DO^-}} + \frac{2[(DOH)_2]}{C_{DO^-}} \qquad \text{(Eq. 9)}$$

which, by substitution of the dimerization constant $K_{2(DOH)}$ defined by:

$$K_{2(DOH)} = \frac{[(DOH)_2]}{[DOH]^2} \qquad \text{(Eq. 10)}$$

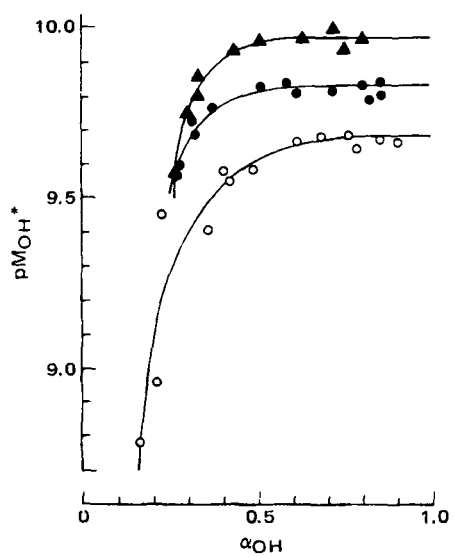

Figure 2—*Photometric determination of microscopic constants for I. Key (total concentration): ▲, 2.125 × 10^{-4} M; ●, 1.063 × 10^{-4} M; and ○, 2.503 × 10^{-5} M.*

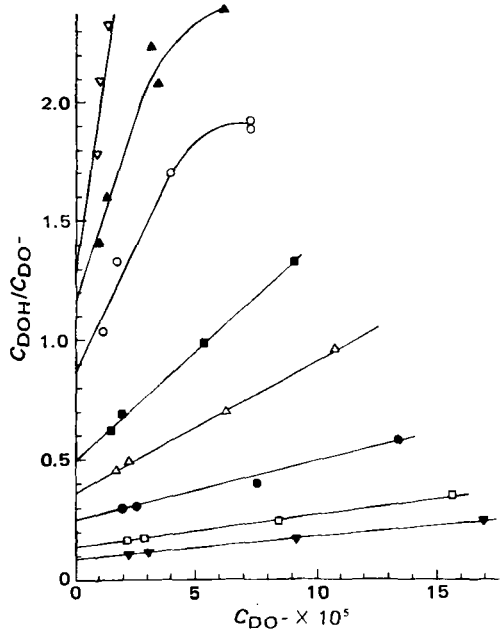

Figure 3—*Photometric determination of acid dissociation constants and dimerization constant of I. The total concentration was (0.250–2.125) × 10^{-4} M in carbonate buffer, μ = 0.1. Key (pH): ▼, 10.56; □, 10.42; ●, 10.18; △, 9.99; ■, 9.83; ○, 9.54; ▲, 9.38; and ▽, 9.14.*

and:

$$M_{OH} = \frac{a_h([^{+}HDO^{-}] + [DO^{-}])}{[DOH]} = \frac{a_h C_{DO^-}}{[DOH]} \qquad \text{(Eq. 11)}$$

gives:

$$\frac{C_{DOH}}{C_{DO^-}} = \frac{a_h}{M_{OH}} + \frac{2K_{2(DOH)}a_h^{2}C_{DO^-}}{M_{OH}^{2}} \qquad \text{(Eq. 12)}$$

In the pH 9.8–10.5 range, plots of C_{DOH}/C_{DO^-} *versus* C_{DO^-} at constant pH gave straight lines (Fig. 3), supporting the validity of Eq. 12. Deviations from linearity were obtained at lower pH (9.1–9.5) values, with the increase of C_{DOH}/C_{DO^-} declining at higher C_{DO^-}. This decline may be the result of an association process involving $^{+}HDO^{-}$ (*e.g.*, dimerization of $^{+}HDO^{-}$), while formation of higher aggregates than dimers of DOH, *e.g.*, tetramers, results in a deviation from linearity with a steepening of the curve with increasing C_{DO^-}.

Calculations from intercepts of plots in the pH 9.4–10.5 range according to Eq. 12 showed that pM_{OH} did not vary with α_{OH} (range of 0.4–0.95). Therefore, it can be concluded that formation of the zwitterion in the monomeric form is negligible; hence, $k_2' \gg k_1'$ (16).

For both I and II, $pM_{OH} = pk_{21}' = 9.54 \pm 0.03$, *i.e.*, the acid dissociation constant of the first phenolic group is not affected by the addition of an alcoholic group in the side chain. The obtained value of pk_{21}' also probably is valid for III and IV. For I and II, log $K_{2(DOH)}$ = 4.2 and 4.3, respectively, was obtained in the pH 9.8–10.5 range from slopes of plots according to Eq. 12.

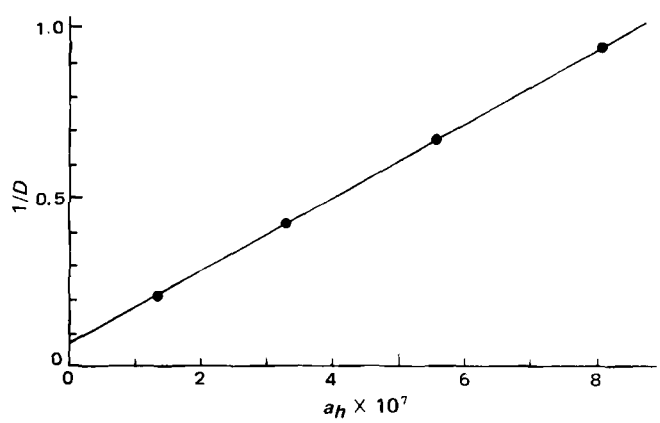

Figure 4—*Evaluation of k_d and k_2' for II. (Conditions were as given in Table I.)*

Table I—Partition Coefficients

Compound	pH	$C_{aq} \times 10^7$ [a]	$C_{org} \times 10^7$ [b]	$-\log k_d k_2' \pm SEM$	$\log k_d \pm SEM$	$pk_2' \pm SEM$
I	4.34–5.78	0.35–7.5	0.57–22.9	4.90 ± 0.01	1.5 ± 0.1	6.4 ± 0.1
III	5.85–6.69	0.37–1.36	1.66–17.4	5.65 ± 0.01	0.99 ± 0.07	6.64 ± 0.08
II	5.55–6.86	0.34–16.5	0.53–13.8	6.03 ± 0.01	1.17 ± 0.05	7.20 ± 0.05
IV	6.47–7.22	9.44–12.5	1.11–4.22	7.48 ± 0.01	0.21 ± 0.09	7.69 ± 0.09

[a] Aqueous phase: pH > 5.0, phosphate buffer, $\mu = 0.1$; and pH < 5.0, citrate buffer, $\mu = 0.1$. [b] Organic phase was chloroform–1-pentanol (9:1).

Table II—Dimerization and Tetramerization Constants

Compound	pH	$C_{aq} \times 10^4$ [a]	$C_{org} \times 10^5$ [b]	$\log K_{(2)} \pm SE$	$\log K_{(4)} \pm SE$	$\log K_{2(DOH)} \pm SE$ [c]
I	4.34–4.88	0.43–5.49	0.65–5.71	4.48 ± 0.06	12.0 ± 0.1	4.2 ± 0.1
II	5.78–6.20	0.18–3.26	0.80–9.55	4.49 ± 0.02	12.3 ± 0.2	4.3 ± 0.1

[a] Aqueous phase: pH > 6.0, phosphate buffer, $\mu = 0.1$; and pH < 6.0, citrate buffer, $\mu = 0.1$. [b] Organic phase was chloroform–1-pentanol (9:1). [c] Determined photometrically (aqueous solution system) at pH 9.8–10.5 (carbonate buffer, $\mu = 0.1$), $C_D = (0.25–2.1) \times 10^{-4}$ M.

Distribution Coefficients—Fluorescence and absorption spectra of I extracted into chloroform–1-pentanol (9:1) from a pH 7 buffer and an aqueous solution of I at pH 2 showed good agreement in location and intensity of maxima. Therefore, it can be assumed that this type of drug is extracted in the uncharged form, *i.e.*, DOH (17). Under the assumption that only monomeric forms are present, the distribution ratio, D, can be written as:

$$D = \frac{C_{D_{org}}}{C_D} = \frac{k_d}{a_h/k_2' + k_1'/k_2' + k_{21}'/a_h + 1} \quad \text{(Eq. 13)}$$

where the distribution coefficient, k_d, is defined by:

$$k_d = \frac{[DOH]_{org}}{[DOH]} \quad \text{(Eq. 14)}$$

Optimal extraction is obtained when $pH = (pk_2' + pk_{21}')/2$.

When $pH \leq pk_{21}' - 1$, Eq. 13 can be transformed to:

$$\frac{1}{D} = \frac{1}{k_d}\left(1 + \frac{k_1'}{k_2'}\right) + \frac{a_h}{k_d k_2'} \quad \text{(Eq. 15)}$$

From the photometric determination of acid dissociation constants, it can be concluded that $k_1'/k_2' \ll 1$. Therefore, a plot of $1/D$ *versus* a_h gives $1/k_d$ as the intercept and $1/k_d \times k_2'$ as the slope (Fig. 4).

Results obtained in partition experiments with I–IV, using chloroform–1-pentanol (9:1) and buffers as the organic and aqueous phases, respectively, are given in Table I. The dissociation constant of the amino group was strongly dependent on the substitution in the side chain. Inspection of molecular models revealed that hydrogen bond formation between the amino group at the sugar moiety and the keto and/or hydroxyl groups at the side chain was most likely to occur. It can also be concluded that the metabolites are more hydrophilic than the parent drugs, the difference being most pronounced for II and IV (*cf.*, 18).

From Eq. 13, it follows that the distribution ratio is strongly dependent on the pH of the aqueous phase, as illustrated in Fig. 5, which shows log D as a function of pH. The calculation of log D is based on determined values of k_d, pk_2', and pk_{21}' and is valid under the assumption that only monomeric forms occur. The pH for optimal extraction varies for the different compounds, *e.g.*, $pH_{opt} = 8.0$ for I and 8.6 for IV, and is independent of the organic solvent used for the extraction. This fact must be taken into account in the extraction of the unchanged drugs and their metabolites from biological samples (19–24).

In the pH 4.3–6.2 range, the distribution ratio of I and II decreases with increasing concentration at constant pH ($C_{aq} > 10^{-5}$ M). Generally, this will be the case when association formation (*e.g.*, dimerization and tetramerization) occurs to a higher extent in the aqueous than in the organic phase.

In this pH range, however, monomers of I and II can be assumed to be present mainly in the forms of $^+$HDOH and DOH. Dimers and tetramers probably will have the compositions $(^+HDOH)_n \cdot (DOH)_{2-n}$ and $(^+HDOH)_m \cdot (DOH)_{4-m}$, respectively, where n and m are the numbers of positively charged species in the dimers and tetramers formed. The negatively charged species are present in too a low concentration to form dimers and tetramers. Under the assumption that only the monomer, DOH_{org}, is present in the organic phase, the following equation is valid:

$$D = \frac{[DOH]_{org}}{[^+HDOH] + [DOH] + 2[(^+HDOH)_n(DOH)_{2-n}] + 4[(^+HDOH)_m(DOH)_{4-m}]} \quad \text{(Eq. 16)}$$

Equation 16 can be given the form:

$$\frac{1}{D} = a_0 + a_1 C_{D_{org}} + a_2 C_{D_{org}}^3 \quad \text{(Eq. 17)}$$

where:

$$a_0 = \frac{1}{k_d} + \frac{a_h}{k_d k_2'} \quad \text{(Eq. 18)}$$

$$a_1 = \frac{2K_{(2)} a_h^n}{k_d^2 k_2'^n} \quad \text{(Eq. 19)}$$

$$a_2 = \frac{4K_{(4)} a_h^m}{k_d^4 k_2'^m} \quad \text{(Eq. 20)}$$

The dimerization and tetramerization constants, $K_{(2)}$ and $K_{(4)}$, respectively, are defined by:

$$K_{(2)} = \frac{[(^+HDOH)_n(DOH)_{2-n}]}{[^+HDOH]^n[DOH]^{2-n}} \quad \text{(Eq. 21)}$$

$$K_{(4)} = \frac{[(^+HDOH)_m(DOH)_{4-m}]}{[^+HDOH]^m[DOH]^{4-m}} \quad \text{(Eq. 22)}$$

and a_0, a_1, and a_2 were estimated from $1/D$ and $C_{D_{org}}$ at constant pH by multiple linear regression.

The relative amounts of monomer, dimer, and tetramer were approximately 13–44, 55–67, and 1–20%, respectively, for I and 22–59, 40–56, and 1–22%, respectively, for II, calculated from the estimates of a_0, a_1, and a_2 and the total concentration in the aqueous phase. Under these experimental conditions, high accuracy can be expected for the estimates (25). Due to the few experimental points at each pH (N = 9–10), the precision of the estimates was rather low.

The values of $k_d k_2'$ calculated from plots of a_0 *versus* a_h were in agreement with values presented in Table I, but the precision was considerably lower (±0.2 log unit, *SE*).

Plots of a_1 *versus* a_h^2 and a_2 *versus* a_h^4 gave straight lines for both I and II, indicating that the dimers and tetramers formed were composed

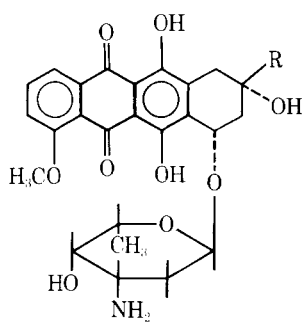

I: R = C(=O)CH_3
II: R = C(=O)CH_2OH
III: R = CH(OH)CH_3
IV: R = CH(OH)CH_2OH

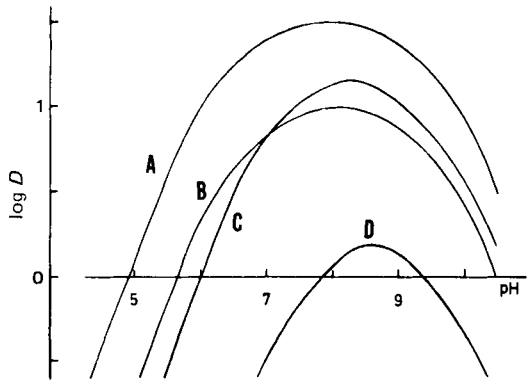

Figure 5—*Variation of the distribution ratio with pH of the aqueous phase. Calculations were based on constants given in Table I and* $pk_{21}' = 9.54$. *Key: A, I; B, III; C, II; and D, IV.*

of positively charged species (Fig. 6). The values of $K_{(2)}$ and $K_{(4)}$, calculated from the slopes and the values of k_d and k_2' from Table I, are presented in Table II. Table II also includes dimerization constants determined photometrically in aqueous solution.

The constants for dimerization of $^+$HDOH and DOH showed fairly good agreement, indicating that interaction between the molecules is due to their ring systems (26). This result is further supported by the fact that no dimerization of the phenolate form (DO^-) was found; *i.e.*, dimerization was prevented by the negative charge in the ring system.

The constants for dimerization of I given in Table II differ considerably from those presented elsewhere (15), which were determined at such high concentration ranges that I probably was mainly present as higher aggregates.

A test of an extraction model including formation of the dimer and trimer gave about the same residual variance as the model including formation of the dimer and tetramer but was unreliable because of the fact that the estimates $a_1 < 0$ and $a_0 > 1/D_{min}$ (25).

The constants for dimerization and tetramerization of I and II presented are of such a high magnitude that they have to be taken into account not only for calculations of distribution ratios at $C_D > 10^{-6}$ *M* but also for the determination of binding constants, *e.g.*, in DNA complex (27–29).

Disturbing association processes are probably responsible for the great difference between published data on acid dissociation constants of the amino group (pk = 8.2–8.99) determined by potentiometric titration of approximately 10^{-3} *M* solutions (30–32) and those presented in this paper.

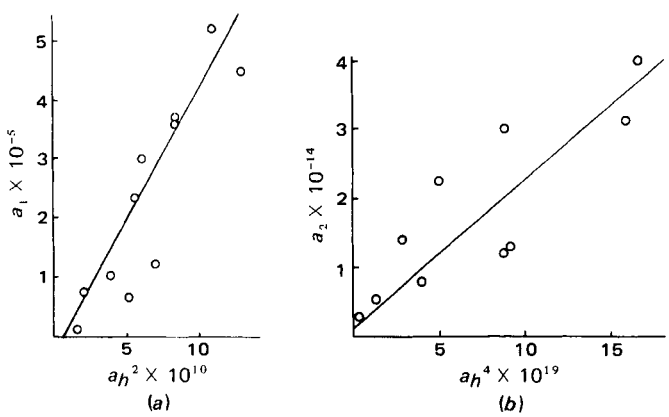

Figure 6—*Evaluation of constants for dimerization (a) and tetramerization (b) of I. (Conditions were as given in Table II.)*

REFERENCES

(1) "Rubidomycin. Recent Results in Cancer Research," J. Bernard, R. Paul, M. Boiron, C. Jacquillat, and R. Maral, Eds., Springer-Verlag, New York, N.Y., 1969.

(2) R. H. Blum and S. K. Carter, *Ann. Intern. Med.*, **80**, 249 (1974).

(3) S. K. Carter, *J. Natl. Cancer Inst.*, **55**, 1265 (1975).

(4) W. J. Pigram, W. Fuller, and L. D. Hamilton, *Nature New Biol.*, **235**, 17 (1972).

(5) F. Zunino, R. Gambetta, A. DiMarcj, and A. Zaccara, *Biochim. Biophys. Acta*, **277**, 489 (1972).

(6) A. DiMarco, F. Zunino, R. Silvestrini, C. Gambarucci, and R. A. Gambetta, *Biochem. Pharmacol.*, **20**, 1323 (1971).

(7) E. Calendi, A. DiMarco, M. Reggiani, B. Scarpinato, and L. Valentini, *Biochim. Biophys. Acta*, **103**, 25 (1965).

(8) M. A. Asbell, E. Schwartzbach, I. Wodinsky, and D. W. Yesair, *Cancer Chemother. Rep., Part 1*, **56**, 315 (1972).

(9) N. R. Bachur, *Biochem. Pharmacol. Suppl. 2*, 207 (1974).

(10) N. R. Bachur, *Cancer Chemother. Rep., Part 3*, **6**, 153 (1975).

(11) N. S. Angerman, T. A. Victor, C. L. Bell, and S. S. Danyluk, *Biochemistry*, **11**, 2402 (1972).

(12) J.-L. Dimicoli and C. Hélène, *J. Am. Chem. Soc.*, **95**, 1036 (1973).

(13) M. Schröder-Nielsen, *Acta Pharm. Suec.*, **11**, 541 (1974).

(14) P.-O. Lagerström, *ibid.*, **12**, 215 (1975).

(15) V. Barthelemy-Clavey, J. C. Maurizot, J.-L. Dimicoli, and P. Sicard, *FEBS Lett.*, **46**, 5 (1974).

(16) J. T. Edsall, R. B. Martin, and B. R. Hollingworth, *Proc. Natl. Acad. Sci. USA*, **44**, 505 (1958).

(17) G. Schill and K. Gustavii, *Acta Pharm. Suec.*, **1**, 24 (1964).

(18) E. Arena, N. d'Alessandro, L. Dusonchet, N. Gebbia, F. Gerbasi, M. Palazzoadriona, A. Raineri, L. Rausa, and E. Tubaro, *Arzneim.-Forsch.*, **21**, 1258 (1971).

(19) D. H. Huffman, R. S. Benjamin, and N. R. Bachur, *Clin. Pharmacol. Ther.*, **13**, 895 (1972).

(20) W. A. Creasey, L. S. McIntosh, T. Brescia, O. Odujinrin, G. T. Aspnes, E. Murray, and J. C. Marsh, *Cancer Res.*, **36**, 216 (1976).

(21) N. R. Bachur and M. Gee, *J. Pharmacol. Exp. Ther.*, **177**, 567 (1971).

(22) R. Rosso, C. Ravazzoni, M. Esposito, R. Sala, and L. Santi, *Eur. J. Cancer*, **8**, 455 (1972).

(23) R. Huloven and J. P. Desager, *J. Chromatogr.*, **125**, 369 (1976).

(24) R. S. Benjamin, C. E. Riggs, Jr., and N. R. Bachur, *Clin. Pharmacol. Ther.*, **14**, 592 (1973).

(25) M. Schröder-Nielsen, *Acta Pharm. Suec.*, **13**, 439 (1976).

(26) P. O. P. Ts'o and S. I. Chan, *J. Am. Chem. Soc.*, **86**, 4176 (1964).

(27) F. Zunino, R. Gambetta, A. DiMarco, G. Luoni, and A. Zaccara, *Biochem. Biophys. Res. Commun.*, **69**, 744 (1976).

(28) T. A. Marks and J. M. Venditti, *Cancer Res.*, **36**, 496 (1976).

(29) P. J. Gray and D. R. Phillips, *Eur. J. Cancer*, **12**, 237 (1976).

(30) F. Arcamone, G. Cassinelli, G. Franceschi, S. Pencho, C. Pol, S. Redaelli, and A. Selva, in "International Symposium on Adriamycin," S. K. Carter, A. DiMarco, M. Ghione, I. H. Krakoff, and G. Mathé, Eds., Springer-Verlag, New York, N.Y., 1972, pp. 9–22.

(31) D. W. Wilson, D. Grier, R. Reimer, J. D. Bauman, J. F. Preston, and E. J. Gabbay, *J. Med. Chem.*, **19**, 381 (1976).

(32) R. Skovsgaard and N. I. Nissen, *Dan. Med. Bull.*, **22**, 62 (1975).

ACKNOWLEDGMENTS

The author thanks Professor Göran Schill, Dr. Hans Ehrsson, Dr. Sten-Ove Nilsson, and Dr. J. Lars G. Nilsson for valuable discussions.

The excellent technical assistance of Miss Ulla Lönroth and Mrs. Birgit Dittmer is gratefully acknowledged.

Relationship between Steroid Permeability across Excised Rabbit Cornea and Octanol–Water Partition Coefficients

RONALD D. SCHOENWALD ˣ **and RICHARD L. WARD**

Received July 13, 1977, from the *Ophthalmic Biopharmaceutics Group, Alcon Laboratories, Fort Worth, TX 76101.* Accepted for publication September 22, 1977.

Abstract □ Permeability rates were determined across excised rabbit corneas for 11 steroids. Permeability coefficients for each steroid were calculated, and their logarithms were plotted against their respective log octanol–water partition coefficients. A parabolic relationship resulted, with an optimum log permeability and coefficient observed at a log P_0 of 2.9. From these experimental results, an improvement in ophthalmic bioavailability of dexamethasone acetate as compared to dexamethasone is predicted and correlates with literature results.

Keyphrases □ Permeability—of various steroids across excised rabbit corneas, related to octanol–water partition coefficients □ Partition coefficients, octanol–water—related to permeability of various steroids across excised rabbit corneas □ Steroids, various—permeability across excised rabbit corneas related to octanol–water partition coefficients

The amount of drug that ultimately penetrates the cornea is often largely determined by physiological factors such as the extent of drainage, blinking, and/or tearing during the first 4–6 min after topical dosing (1). The time-honored approach to resisting drainage has been through the use of viscous solutions. Water-soluble polymers such as methylcellulose, hydroxypropyl methylcellulose, and polyvinyl alcohol impart a slight lowering of surface tension and an increase in viscosity to ophthalmic solutions. The increase in viscosity prolongs contact of the drug in the eye, thereby resisting drainage (2, 3); a lowering of the surface tension improves mixing with the precorneal tear film (4). In rabbits, a two- to threefold improvement in pilocarpine bioavailability has been found for viscous aqueous solutions (2, 3).

Another approach to improving ophthalmic bioavailability has been to increase drug absorption into the eye. For example, it was reasoned (5) that the enhancement of the lipophilicity of epinephrine through the use of a dipivalyl ester would facilitate penetration through the lipoidal layers of the cornea. Prodrug concentrations of 0.1%, administered twice daily for 1 month, significantly reduced intraocular pressure in hypotensive patients (6). The prodrug is reported to be about 100 times more effective than epinephrine in the management of glaucoma and about 100–400 times weaker than epinephrine in affecting the cardiovascular system of dogs and cats (7).

In terms of improved efficacy, the final evaluation of an analog or prodrug must come from *in vivo* studies. However, optimization of permeability based on molecular modification can be assessed more reliably from a model devoid of extraneous physiological factors (8, 9). Such a model should focus primarily on enhanced permeability as a function of molecular modification.

The purpose of this study was to determine the relationship between the permeability of various structurally related steroids across an excised rabbit cornea and their octanol–water partition coefficients.

EXPERIMENTAL

Materials—Ten tritium-labeled steroids and one ^{14}C-labeled steroid were purchased[1]. Identification of each steroid was confirmed by TLC using two solvent systems[2]. This step was accomplished by dissolving unlabeled steroids[3] in methanol along with the labeled steroid and determining R_f values for each by scintillation[4] and UV[5] spectroscopic methods. Purification consisted of removing volatile, labile tritium, using low temperature vacuum evaporation of alcoholic and then aqueous solvents (11). Monitoring the aqueous distillate for radioactivity indicated that removal of labile tritium by solvent evaporation was complete after three distillations[6]. All other chemicals were reagent grade.

Excised Corneal Preparation Procedure—A 1–1.5-kg young albino rabbit was sacrificed by injecting 20–30 ml of air into the marginal ear vein. The intact eye along with the lids and conjunctival sac was then enucleated. According to a published procedure (12, 13), the exposed cornea of the enucleated eye was placed carefully on a specially designed corneal holder, which maintained the cornea curvature and held the eye in place. Various tissues of the eye were dissected away, leaving the cornea, a small ring of scleral tissue, and palpebral conjunctiva, which was tied to the corneal holder.

The conjunctiva and scleral tissue served as a gasket and permitted the cornea to be suspended within the block system without inducing significant trauma or curvature distortion to the corneal endothelium or epithelium (12, 14). The block system[7] consisted of two cylindrical compartments separated by the cornea. The compartment adjacent to the endothelial surface of the cornea was designated the internal side, whereas the compartment adjacent to the epithelial side was referred to as the external side.

Study Procedure—Within 20 min of death, the cornea was mounted within the preheated block system and clamped into place; 6.0 ml of preheated (37°) glutathione Ringers solution[8] was added to the internal side. Then 6.0 ml of preheated glutathione Ringers solution, containing labeled and unlabeled steroids, was added to the external compartment. These solutions were prepared about 1 hr prior to the start of the experiment.

[1] From New England Nuclear, Boston, Mass.: 6,7-^3H-prednisolone, lot 747-276; 1,2-^3H-hydrocortisone, lot 853-184; 7-^3H-testosterone, lot 772-277; 1,2-^3H-desoxycorticosterone, lot 853-169; 1,2-^3H-cortexolone, lot 951-024; 6,7-^3H-triamcinolone acetonide, lot 635-258; 6,7-^3H-dexamethasone, lot 998-003; and 6,7-^3H-dexamethasone acetate, lot 690-1348. From Amersham/Searle, Arlington Heights, Ill.: 4-^{14}C-progesterone, lot CFA.148, batch 42; 1,2-^3H-fluorometholone, lot TRQ.974, batch 21474; and 6,7-^3H-prednisolone 21-acetate, lot TRQ.915, batch 20806.

[2] Solvent systems specific for each steroid and suggested by the manufacturer were used; methylene chloride–acetone (4:1) was suggested by Stahl (10) for general steroid use and also was used.

[3] Progesterone (Aldrich, lot 021957), hydrocortisone (Sigma, lot 25C-0319), prednisolone (Sigma, lot 23C-1900), desoxycorticosterone (Aldrich, lot 031847), testosterone (Aldrich, lot 112457), cortexolone (Aldrich, lot 06181), triamcinolone acetonide (Sigma, lot 26C-0211), dexamethasone (Alcon RPA 5399), dexamethasone acetate (Sigma, lot 83C-1700), fluorometholone (Farmila, lot 56/015), and prednisolone acetate (Organon, lot 92305).

[4] The silica gel was scraped from the origin to the solvent front (Quanata/Gram, Fairfield, N.J. LQDT prescored 20 × 20-cm TLC plates) in 1-cm increments. Every centimeter of silica gel was placed in a separate vial, scintillation fluid was added, and the vials were counted.

[5] Visual location of spot with the short wavelength of a UV lamp (Ultra-Violet Products, San Gabriel, Calif.).

[6] Less than 1.5% total radioactivity was recovered in distillate.

[7] The block system and corneal holder were purchased from Mr. Harold Eick through the cooperation of Dr. H. F. Edelhauser, Department of Physiology, Medical College of Wisconsin, Milwaukee, Wis.

[8] This solution differed from the glutathione bicarbonate Ringers solution used in Ref. 12 in that sodium bicarbonate was replaced with 0.77 g of sodium biphosphate/liter to maintain the pH at 7.2 ± 0.2 during the experiment.

The concentration of steroid[9] used in each experiment was significantly lower than the drug's reported solubility in water at 25 or 37° (15). The specific activities of each steroid test solution[10] were adjusted so that nanogram levels could be detected on the internal side. This condition required relatively high specific activities for practically insoluble steroids. The block system containing the excised cornea was placed on a hot plate[11] preadjusted to maintain the solution temperature within 35–37°. The temperature was periodically measured to assure that the solution temperature remained within the specified range. The block system and the hot plate were surrounded by Styrofoam for insulation against temperature fluctuations.

As soon as the solutions were added to each side, circulation of fluids was induced by slowly bubbling air at a rate of approximately two or three bubbles per second. Samples of 0.1 ml were taken[12] from the internal side. The first sample was withdrawn within 1 min of adding the solution to the external side. This sample represented the zero-time sample and also served as a control. If the conjunctiva was accidently perforated during the surgical procedure, then fluid would be exchanged rapidly between compartments within this 1st min. Under these conditions, the zero-time sample would yield a counting rate well above background and indicate that the kinetic data were invalid. Subsequent samples were taken every 0.5 hr for 4 hr.

All samples were immediately placed into a scintillation vial[13] containing 10 ml of scintillation solution[14]. A like volume of solution was removed and discarded from the external side at each time increment. Thus, the cornea remained in hydrostatic equilibrium on both sides of the system. All vials containing tracer and scintillation solution were dark adapted for 18 hr or more and counted[15]. The external standardization method (16) was used to determine counting efficiencies and, therefore, permitted the quantity of steroid present in each sample to be calculated.

Partition Coefficient—All partition coefficients are expressed as averaged log octanol–water and were taken from Leo *et al.* (17). For dexamethasone acetate, no value was listed; however, the acetate ester could be estimated readily from the parent molecule, dexamethasone (17, 18). An octanol–water system was chosen because of the large volume of data that has been generated for correlation studies (17, 18).

RESULTS

All corneas were judged clear at the end of each 4-hr experiment[16]. Figure 1 represents a typical plot of data for the penetration of dexamethasone acetate and dexamethasone across an excised cornea. A short lag time was observed, representing the time required for drug to reach steady state in the cornea. Following the lag time, the data followed a linear relationship. The individual experiments yielded highly linear correlations as judged by the Pearson r (>0.975). In addition, no trends in nonlinearity were observed with time. This result indicated that the steady-state permeability rate was constant with time as required by Eqs. 1–3.

The transfer of substances across membranes by simple diffusion has been described (20) as a simplification of Fick's law according to:

$$\frac{dq}{dt} = \frac{DA(PC)}{T}(C_E - C_I) \qquad \text{(Eq. 1)}$$

where dq/dt is the permeability rate or the rate of drug quantity penetrating the cornea at time t, D is the diffusion coefficient of steroid through the excised cornea (square centimeters per second), A is the area of the absorbing surface of the cornea, T is the thickness of the cornea, (PC) is the partition coefficient (ratio of the drug concentration in the barrier membrane to the *in vitro* testing solution), C_E is the drug concentration on the external side, and C_I is the drug concentration on the internal side.

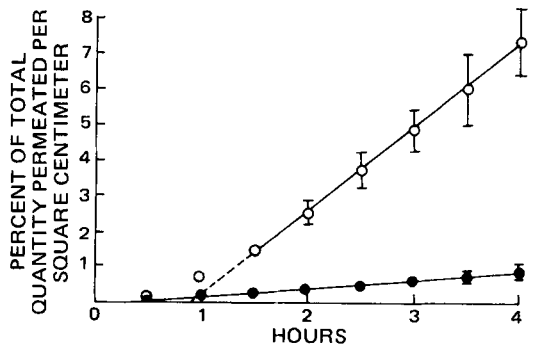

Figure 1—*Permeability of dexamethasone acetate* (○) *and dexamethasone* (●) *across an excised rabbit cornea. Each point represents a mean of four determinations. The vertical bars indicate 1* SD; *bars that are absent were smaller than the circle. The slope of the line represents the steady-state permeability rate.*

For these experiments, samples taken from the internal side were considered negligible in drug concentration when compared to the external side[17]. Therefore, C_I was eliminated from the equation, and C_E was considered a constant through the time course of the experiments. Therefore, Eq. 1 can be rewritten as:

$$\frac{dq}{dt} = \frac{DA(PC)}{T} C_E \qquad \text{(Eq. 2)}$$

When q is plotted *versus* t, the linear portion of the plot represents the steady-state permeability rate. The least-squares slope of each individual experiment was determined and averaged. Each averaged slope value was divided by an averaged value[18] of A, 1.089 cm^2. To compare the results from each steroid experiment, each averaged slope value was also divided by the C_E value used for each steroid. Consequently, the final value represented a permeability coefficient $[D(PC)/T]$ with units of square centimeters per second. When expressed in logarithmic form, this relationship becomes:

$$\log (P_{\text{perm}}) = \log \frac{D}{T} + \log (PC) \qquad \text{(Eq. 3)}$$

Figure 2 illustrates the parabolic nature of the data when the logarithms of permeability and partition coefficients are plotted against one another. The data could be best represented by a second-order power series[19]:

$$\log (P_{\text{perm}}) = -0.28 (\log P)^2 + 1.7 \log P - 7.0 \qquad \text{(Eq. 4)}$$

where $\log (P_{\text{perm}})$ is the logarithm of the permeability coefficient (centimeters per second), and $\log P$ is the logarithm of the octanol–water partition coefficient.

An optimum $\log P_0$ value of 2.9 was found by setting $d \log (P_{\text{perm}})/d \log P$ equal to zero and solving for $\log P_0$ (21). Figure 2 predicts a decrease in permeability once a partition coefficient of 2.9 is reached. According to Flynn and Yalkowsky (22), limited solubility is often responsible for the parabolic shape of many structure–activity curves. As a consequence, the solubility of progesterone was determined carefully under the exact test conditions of the permeability experiments (same solution, temperature, *etc.*). A solubility of 14.1 ± 1.46 μg/ml (n = 3) was obtained for progesterone. Therefore, to be certain that solubility would not influence the results, a concentration of 0.90 μg/ml, which was greater than 1 log unit below the drug's solubility, was chosen for study.

If the progesterone results are excluded from consideration, the remaining 10 steroids approach a plateau, as predicted by the kinetic model

[9] The concentration (micrograms per milliliter) of each steroid placed into the external compartment was: prednisolone, 16.7; hydrocortisone, 267; testosterone, 25; progesterone, 0.90; desoxycorticosterone, 133; dexamethasone, 83.3; dexamethasone acetate, 1.33; triamcinolone acetonide, 8.33; prednisolone acetate, 8.33; cortexolone, 267; and fluorometholone, 1.17.

[10] The specific activity (microcuries per milligram) of each radioactive steroid tracer was: prednisolone, 236; hydrocortisone, 15.4; testosterone, 119; progesterone, 151.1; desoxycorticosterone, 26.5; dexamethasone, 41.2; dexamethasone acetate, 2554; triamcinolone acetonide, 353; prednisolone acetate, 603; cortexolone, 12.1; and fluorometholone, 931.

[11] Model 4812, 15 × 15 cm, Cole Parmer, Chicago, Ill.

[12] Eppendorf pipettor, Brinkmann Instruments, Westbury, N.Y.

[13] With Polyseal core liners, Kimble, Toledo, Ohio.

[14] Handifluor Scintillar, Mallinckrodt, St. Louis, Mo.

[15] LS-230 liquid scintillation counter, Beckman Instruments, Fullerton, Calif.

[16] Each cornea was judged clear if typewritten print could be identified through the cornea at the end of each experiment. The clarity of the cornea is related to its hydration level; a normal cornea measures 78% (19). As the hydration level increases, the thickness of the cornea also increases; however, linear steady-state plots of drug penetrating the cornea generally result as long as the hydration level is below 85%. These latter corneas are cloudy and typewritten print cannot be read through them. Measurements were carried out for fluorometholone, prednisolone acetate, and progesterone and were 82.2 ± 0.6% (n = 4), 82.6% (n = 1), and 82.6 ± 0.8% (n = 4), respectively.

[17] After 4 hr, samples taken from the internal side were 3% or less of the concentration on the external side, with the exception of dexamethasone acetate which was 7.4%.

[18] Dr. H. Edelhauser, Department of Physiology, Medical College of Wisconsin, Milwaukee, Wis., personal communication.

[19] Nonlinear regression was performed using the BMDX85 program on a CDC6400 computer.

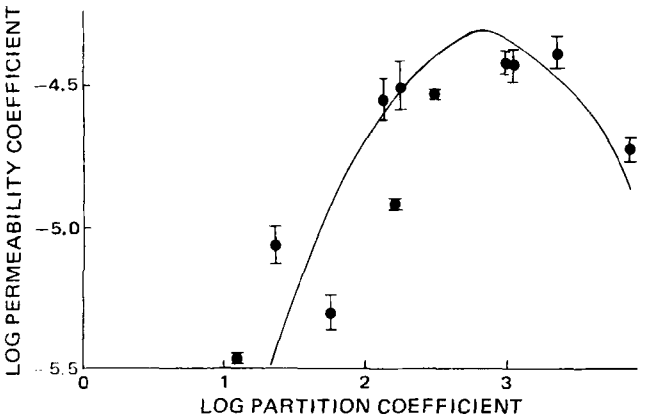

Figure 2—*Computer-generated curvilinear relationship between the log permeability coefficient of 11 labeled steroids and their respective log octanol–water partition coefficients. From left to right, the steroids are prednisolone, hydrocortisone, dexamethasone, fluorometholone, triamcinolone acetonide, prednisolone acetate, cortexolone, desoxycorticosterone, dexamethasone acetate, testosterone, and progesterone. The vertical bars represent 1* SD.

of Yalkowsky and Flynn (23). However, the value obtained for progesterone is statistically different ($p < 0.05$) from desoxycorticosterone, dexamethasone acetate, and testosterone, all of which are associated with maximum permeability. To determine if the carbon-14 label resided with progesterone during the experiment, an aliquot was taken from the external side following each experiment and chromatographed on silica gel thin-layer plates. Results showed that 95% of the label was associated with the progesterone molecule.

DISCUSSION

Equation 3 requires that the data follow a linear relationship with respect to the logarithms of permeability and partitioning coefficients. However, Fig. 2 shows a linear increase in log (P_{perm}) but begins to level off with log PC for cortexolone, desoxycorticosterone, and dexamethasone acetate. As discussed by Sinkula and Yalkowsky (24), the increase in permeability cannot go on indefinitely with an increase in the hydrophobicity of the homolog series; several reasons were given for the decline. Strictly speaking, progesterone and testosterone do not belong to the corticosteroid class of compounds; they lack a 17α-hydroxyl group. Therefore, if they are deleted from Fig. 2, the kinetic model best describes the remaining data.

The parabola in Fig. 2 identifies a specific optimal partition coefficient for steroids, expressed as log P_0, and predicts that a decreased intrinsic corneal penetration results if the optimal partitioning behavior is either decreased or increased. The kinetic model (23), which suggests that a plateau is a more precise relationship, identifies only a lower limit above which an intrinsic optimal penetration is theoretically predicted. Regardless of whether the parabola or the kinetic interpretation best describes the results, the data can be useful in the design of optimally permeable ophthalmic drugs. For practical purposes, optimal penetration can be considered to occur when $d \log (P_{perm})/d \log P$ begins to approach zero, which in Fig. 2 is represented by a log P of about 2.5–3.0.

Optimal penetration is desirable because a more rapid penetration rate leads to higher peak concentrations and lower quantities lost to nasolacrimal drainage. This condition permits a lower dose to be administered without sacrificing drug activity and promotes a lowered potential for systemic side effects. Even though the kinetic model predicts a plateau, ophthalmic bioavailability would not always be expected to follow the same relationship with an increase in log P. According to Eq. 2, the penetration rate is a function of the drug concentration as well as the partition coefficient. However, as molecular modification produces a more hydrophobic analog, aqueous solubility decreases. Also, the residence time of nondissolved drug particles in the eye is limited; therefore, expulsion of the particles by the eye may take place before solubilization may occur.

Under these conditions, the partition coefficient and solubility would tend to cancel one another in terms of increased penetration. Consequently, improved ophthalmic bioavailability would reach an upper limit or perhaps decrease if a low enough tear solubility is produced. If the parent drug is very soluble, however, then molecular modification may reduce solubility as partitioning is improved. But because the administered therapeutic dose never approaches its tear solubility, bioavailability is enhanced. Dipivalylepinephrine represents an example of this type.

The data generated in this study showed that the addition of an acetate functional group to the 21-hydroxy position of prednisolone and dexamethasone improved the log partitioning by 2 and 1.7 times over each parent drug. Based on permeability calculations, prednisolone and dexamethasone esters penetrated the excised cornea 7.4 and 8.2 times faster than the respective parent drugs. The observed improvement in *in vitro* permeability may not necessarily extrapolate to a significant improvement in ophthalmic bioavailability. However, when tested *in vivo*, a large difference in ophthalmic bioavailability was observed for dexamethasone acetate in comparison to dexamethasone.

In a study by Kupferman *et al.* (25), 0.1% petrolatum base ointments of ^{14}C-dexamethasone and ^{14}C-dexamethasone acetate were dosed in volumes of 50 μl to normal rabbits. After sacrificing animals at fixed times, the drug was assayed in aqueous and corneal tissue samples. The area under the corneal dose–time curve was 4.5 times greater for the acetate. Aqueous humor levels were detected for the ester but not for the parent drug. This latter study established, to a limited extent, a correlation between the *in vitro* corneal permeability model and an improvement in *in vivo* ophthalmic bioavailability.

REFERENCES

(1) S. S. Chrai, T. F. Patton, A. Mehta, and J. R. Robinson, *J. Pharm. Sci.*, **62**, 1112 (1973).

(2) S. S. Chrai and J. R. Robinson, *ibid.*, **63**, 1218 (1974).

(3) T. F. Patton and J. R. Robinson, *ibid.*, **64**, 1312 (1975).

(4) D. A. Benedetta, D. O. Shah, and H. E. Kaufman, *Invest. Ophthalmol.*, **14**, 887 (1975).

(5) A. Hussain and J. E. Truelove, *J. Pharm. Sci.*, **65**, 1510 (1976).

(6) M. B. Kaback, S. M. Podos, T. S. Harbin, A. Mandell, and B. Becker, *Am. J. Ophthalmol.*, **81**, 768 (1976).

(7) D. A. McClure, in "Prodrugs as Novel Drug Delivery Systems," T. Higuchi and V. Stella, Eds., American Chemical Society, Washington, D.C., 1975, pp. 224–235.

(8) M. Katz and Z. J. Shaikh, *J. Pharm. Sci.*, **54**, 591 (1965).

(9) B. J. Poulsen, E. Young, V. Coquilla, and M. Katz, *ibid.*, **57**, 928 (1968).

(10) E. Stahl, "Thin-layer Chromatography," Springer-Verlag, New York, N.Y., 1965, p. 262.

(11) S. S. Chrai and J. R. Robinson, *Am. J. Ophthalmol.*, **77**, 735 (1974).

(12) D. S. Hull, J. E. Hine, H. F. Edelhauser, and R. A. Hyndiuk, *Invest. Ophthalmol.*, **13**, 457 (1974).

(13) H. F. Edelhauser, J. R. Hoffert, and P. O. Fromm, *ibid.*, **4**, 290 (1965).

(14) B. E. McCarey, H. F. Edelhauser, and D. L. Van Horn, *ibid.*, **12**, 410 (1973).

(15) P. Kabasakalian, E. Britt, and M. D. Yudis, *J. Pharm. Sci.*, **55**, 642 (1966).

(16) C. H. Wang and D. C. Willis, "Radiotracer Methodology in Biological Science," Prentice Hall, Englewood Cliffs, N.J., 1965, pp. 134, 135.

(17) A. Leo, C. Hansch, and D. Elkins, *Chem. Rev.*, **71**, 525 (1971).

(18) C. Hansch, in "Drug Design," E. J. Ariens, Ed., Academic, New York, N.Y., 1975, pp. 284–290.

(19) B. O. Hedbys and S. Mishima, *Exp. Eye Res.*, **5**, 221 (1966).

(20) D. S. Riggs, "The Mathematical Approach to Physiological Problems," Williams & Wilkins, Baltimore, Md., 1963, p. 185.

(21) C. Hansch and J. M. Clayton, *J. Pharm. Sci.*, **62**, 1 (1973).

(22) G. L. Flynn and S. H. Yalkowsky, *ibid.*, **61**, 838 (1972).

(23) S. H. Yalkowsky and G. L. Flynn, *ibid.*, **62**, 210 (1973).

(24) A. A. Sinkula and S. H. Yalkowsky, *ibid.*, **64**, 181 (1975).

(25) A. Kupferman, M. V. Pratt, K. Suckewer, and H. Leibowitz, *Arch. Ophthalmol.*, **91**, 373 (1972).

Effect of Formulation Factors on Penetration of Hydrocortisone through Mouse Skin

VIJAY SHAHI and JOEL L. ZATZ ˣ

Received July 25, 1977, from the *College of Pharmacy, Rutgers—The State University, Piscataway, NJ 08854.* Accepted for publication September 23, 1977.

Abstract □ The effect of formulation factors on the steady-state flux of hydrocortisone through mouse skin was evaluated. The flux of hydrocortisone from solutions containing propylene glycol as a cosolvent varied inversely with the propylene glycol concentration. Solutions containing 2-propanol gave flux values higher than those obtained from propylene glycol solutions and independent of the 2-propanol concentration. Addition of polysorbate 80 to 2-propanol–water solutions produced an increase in flux at low surfactant concentrations that reached an apparent limiting value at higher concentrations. The penetration flux was the same from solutions and gels. The role of vehicle–skin interactions in penetration is emphasized.

Keyphrases □ Hydrocortisone—penetration through mouse skin, effect of formulation factors □ Penetration—hydrocortisone through mouse skin, effect of formulation factors □ Glucocorticoids—hydrocortisone, penetration through mouse skin, effect of formulation factors

The effect of formulation additives on drug permeation through skin has been investigated (1–3). The penetration rate of a topical agent may be influenced by drug–vehicle, drug–skin, and vehicle–skin interactions. In the clinical assessment of a topical agent, the vehicle may significantly affect drug release and skin penetration, thereby altering biological activity (4–7). If drug–skin and vehicle–skin interactions can be ignored, optimal penetration takes place when the drug concentration in the vehicle is equal to its solubility (6).

The release characteristics of a topical vehicle have been studied by determining the partition coefficient of the drug between the vehicle and a suitable organic solvent (4, 6). However, to study the effect of vehicles on the barrier function of the stratum corneum, permeation experiments using skin as a membrane are more meaningful. The use of *in vitro* diffusion models to screen topical vehicles to optimize drug penetration is convenient. Furthermore, there is evidence that results obtained with excised human skin in a diffusion cell correlate with those obtained *in vivo* (8).

This study investigated the effect of vehicle composition on percutaneous absorption of hydrocortisone, using excised mouse skin as a model membrane. Mouse skin was chosen for permeation studies for two reasons: the rank order of permeation of several drugs through skin of various animals and human skin was the same, and the permeation rates were always slowest in the human. Hydrocortisone penetrates human skin very slowly (10), requiring about 2 weeks to approach a steady state.

EXPERIMENTAL

Materials—Hydrocortisone[1] was used as received. 2-Propanol[2] and chloroform[2] were spectral grade. Propylene glycol[3], 1-octanol[2], sodium chloride[2], and chlorobutanol[4] were reagent grade. The surfactant used in some formulations was polysorbate 80[5]. Hydroxyethylcellulose[6] was employed as a gelling agent. All materials were used as supplied. Water was double distilled in an all-glass still.

Preparation of Solutions—Accurately weighed amounts of hydrocortisone were dissolved in the desired volume of propylene glycol or 2-propanol, and distilled water was added to volume. Solutions containing surfactant were prepared by adding an aliquot of an aqueous solution of the surfactant to the previously dissolved hydrocortisone. The solutions were stored in a refrigerator for about 36 hr and assayed for hydrocortisone before use.

Preparation of Gels—An aliquot of the hydrocortisone solution was transferred to a glass-stoppered conical flask and allowed to cool in the refrigerator. An appropriate amount of hydroxyethylcellulose was sprinkled on the surface of the cooled solutions, and the polymer was dissolved by intermittent shaking of the flask. The clear gels were stored in the refrigerator for 48 hr before use.

Preparation of Membranes—Excised abdominal skin of 15–20-week-old male albino mice, 20–25 g, was used. The skin was shaved on the epidermal side. Tissues on the dermal side up to and including the blood vessels were removed. The skin was washed with distilled water and mounted in the diffusion cell.

Apparatus—An *in vitro* cell similar to the one described by Weiss and Sciarrone (11) was used. The cell was fitted with an air condenser to minimize evaporation of the hydrocortisone solution or gel. The temperature of the water flowing in the closed circulatory system was kept at 24.5 ± 0.1°. The receptor phase consisted of normal saline solution containing 0.25% chlorobutanol.

Donor samples, 1 ml, were placed on the epidermal side of the membrane. Samples of the receptor phase, 25 ml, were removed at intervals and assayed for hydrocortisone. Saline containing chlorobutanol was immediately added to the receptor phase to maintain a constant volume. The donor phase was not stirred, but a magnetic stirrer was used in the receptor phase. The stirring rate was 60 rpm.

Assay—An extraction procedure was used. A 10-ml aliquot of a sample containing hydrocortisone was pipetted into a 15-ml centrifuge tube. Chloroform–octanol (3:1), 5 ml, was added, and the tube was shaken mechanically for 15 min and then centrifuged. The aqueous phase constituted the top layer in the tube. Any organic phase floating on the top was removed by aspiration.

The aqueous phase absorbance was read[7] at 242 nm with water as the blank. The difference in absorbance, ΔA, of the aqueous layer before, A_b, and after, A_e, extraction was proportional to the hydrocortisone concentration. A ΔA *versus* concentration plot was linear, passing through the origin. Chlorobutanol and sodium chloride did not interfere. Compounds that entered the receptor phase from the skin membranes had no effect on the accuracy of the assay.

Solubility Studies—An excess of hydrocortisone was weighed and transferred to a 25-ml volumetric flask, and the cosolvent was pipetted into the flask. Where surfactant was included, the required amount was then added as an aqueous solution. The system was then diluted to volume with distilled water. The flasks were allowed to stand in a water bath thermostatically controlled at 24.5 ± 0.1°. The solutions were hand shaken at intervals, filtered, and analyzed daily for several days.

A second technique was used as a check. Aliquots of 25 ml of the preconstituted solvents were pipetted into 50-ml volumetric flasks containing 0.3 g of hydrocortisone. The flasks were then placed in a shaker thermostatically controlled at 24.5 ± 0.1°. The solutions were analyzed at 48 and 96 hr after filtration. Both methods gave essentially equivalent results.

[1] Merck Sharp and Dohme, West Point, Pa.
[2] Fisher Scientific Co., Fair Lawn, N.J.
[3] Ruger Chemical Co., Irvington, N.J.
[4] City Chemical Co., New York, N.Y.
[5] Atlas Chemical Industries, Wilmington, Del.
[6] Natrosol 250M, Hercules Inc., Wilmington, Del.
[7] Beckman spectrophotometer.

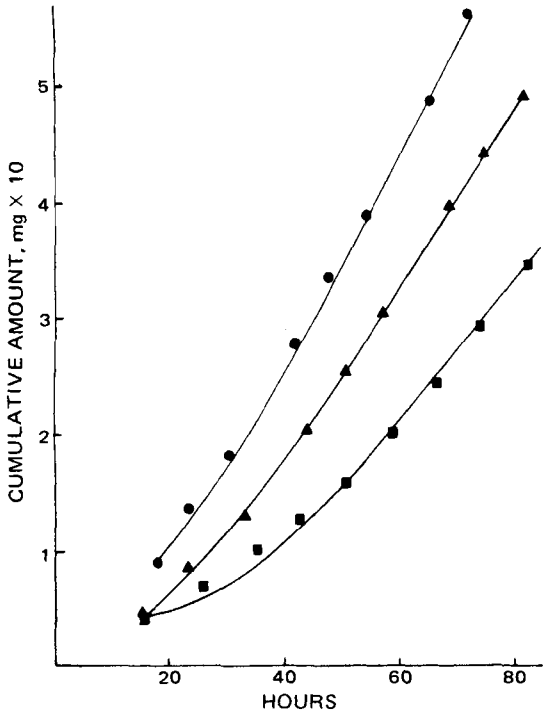

Figure 1—*Hydrocortisone penetration through mouse skin from a 0.2% solution in 40% (v/v) 2-propanol and water. Each curve represents skin from a different animal.*

Surface Tension—Surface tension values were determined by the Wilhelmy plate method (12).

RESULTS AND DISCUSSION

Figure 1 shows typical penetration curves obtained using different skin membranes with the same hydrocortisone formulation. The volume of the donor solution remained constant during the experiments. The penetration rate was slow at first but gradually increased until it became constant; it remained constant until about 50% of the hydrocortisone was transferred to the receptor phase. If the volume of the donor phase was changed from 1.0 to 0.5 ml, there was no significant change in the steady-state penetration rates.

To evaluate the effect of formulation on hydrocortisone penetration, the steady-state rate for each experiment was determined and divided by the exposed area of the membrane to yield the penetration flux. Each experiment was performed at least in triplicate. The values of penetration flux were averaged, and the mean was utilized as an index of percutaneous absorption for that formulation.

During the steady-state phase, the transdermal route is believed to represent the major pathway for permeation through skin (13). Other routes involving penetration through hair follicles, sweat ducts, and sebaceous glands also may contribute, but these routes are most important before steady state is reached. Unless there is restricted diffusion through the living epidermal and dermal cells because of poor water solubility, the stratum corneum represents the most important barrier to penetration among the skin layers. Passage of drug across the stratum corneum is, therefore, the rate-limiting step in permeation through the skin at steady state. Two equations were suggested (4) to describe the steady-state penetration flux, J, under these circumstances:

$$J = \frac{K_m C_v D}{L} \qquad \text{(Eq. 1)}$$

where K_m is the partition coefficient between the stratum corneum and the vehicle, C_v is the drug concentration in the vehicle, D is the diffusion coefficient of the drug through the stratum corneum, and L is the effective barrier thickness. An equivalent expression is:

$$J = \frac{a_v D}{\gamma_s L} \qquad \text{(Eq. 2)}$$

where a_v is the activity of the drug in the vehicle and γ_s is the activity coefficient of the drug in the skin barrier. The value of γ_s is usually taken to be constant, so changes in penetration are attributed to alterations in the activity of the drug in the vehicle.

Table I—Penetration Flux of Hydrocortisone from 0.2% Aqueous Solutions Containing Propylene Glycol

Propylene Glycol, % (v/v)	Mean Flux ± *SD*, μg/hr/cm²	Hydrocortisone Solubility, mg/ml
25	0.119 ± 0.007	1.79
40	0.089 ± 0.006	2.20
60	0.078 ± 0.003	3.08

The influence of propylene glycol concentration on hydrocortisone penetration from aqueous solutions is summarized in Table I. The hydrocortisone concentration was kept constant at 0.2%. When the donor solution contained 60% propylene glycol, the penetration rate of hydrocortisone progressively increased after about 70 hr. This change in penetration rate from the constant values observed up to 70 hr was probably due to membrane deterioration (7). The mean flux from 60% propylene glycol solutions (Table I) was calculated from data obtained prior to this upturn in penetration. The solution containing 25% propylene glycol was slightly supersaturated but showed no visible evidence of precipitation after storage for several months.

The values in Table I indicate that hydrocortisone flux decreased with increasing concentrations of propylene glycol. Raising the propylene glycol concentration in the vehicle increased hydrocortisone solubility, implying an enhanced affinity of the drug for the vehicle. This solubility increase resulted in a reduction in K_m, the partition coefficient (Eq. 1), and thereby reduced the penetration flux. The pattern of behavior obtained with hydrocortisone in propylene glycol–water mixtures through mouse skin was similar to that observed (6) for fluocinonide through human skin.

Table II shows the effect of increasing 2-propanol concentrations on the flux of hydrocortisone penetration from aqueous solutions. The values were higher than those obtained from any propylene glycol solution. There was no evidence of membrane damage. Hydrocortisone solubility in the solutions was increased considerably at the higher 2-propanol concentrations. In fact, 2-propanol was a more effective cosolvent than propylene glycol. Nevertheless, in contrast to the propylene glycol solutions, increasing the 2-propanol concentration did not reduce the penetration flux of hydrocortisone significantly.

According to Eq. 2, the penetration flux is proportional to drug activity in the donor solution. At saturation, hydrocortisone activity is considered to be unity; at other concentrations, activity cannot be calculated exactly from the available data, but the ratio of hydrocortisone concentration to its solubility in the vehicle has been suggested as a useful approximation (5). The data from Tables I and II are plotted in Fig. 2 to show the relationship between the penetration flux of hydrocortisone and the ratio of concentration to solubility in aqueous vehicles containing propylene glycol and 2-propanol. Hydrocortisone penetration from propylene glycol–water solutions behaved in accordance with Eq. 2. As the ratio of concentration to solubility decreased, so did the flux.

On the other hand, Eq. 2 does not seem to fit the data for the 2-propanol–water mixtures. The penetration flux was practically independent of the concentration–solubility ratio over a wide range of values. Moreover, the flux at an activity of unity was quite different, depending on the solvent system. However, if γ_s can be considered constant, Eq. 2 states that the flux should be independent of the solvent composition at the same thermodynamic activity.

This difference in flux can only be explained by considering interactions between the 2-propanol solutions and the membrane. The stratum corneum is not an inert structure. Solvent migration from the vehicle into the stratum corneum may alter the effective resistance of the barrier to penetration of other substances. This effect is not necessarily due to damage to the stratum corneum but may be caused by partial solvation of the stratum corneum by the penetrating solvent. As an example, Scheuplein and Ross (14) found that octanol increased the butanol penetration rate through excised human epidermis. When the octanol was washed out of the membrane, it regained its previous resistance to butanol.

Although the penetration rates for propylene glycol and 2-propanol

Table II—Penetration Flux of Hydrocortisone from 0.2% Aqueous Solutions Containing 2-Propanol

2-Propanol, % (v/v)	Mean Flux ± *SD*, μg/hr/cm²	Hydrocortisone Solubility, mg/ml
20	0.217 ± 0.007	1.79
40	0.214 ± 0.037	9.10
60	0.196 ± 0.036	18.2

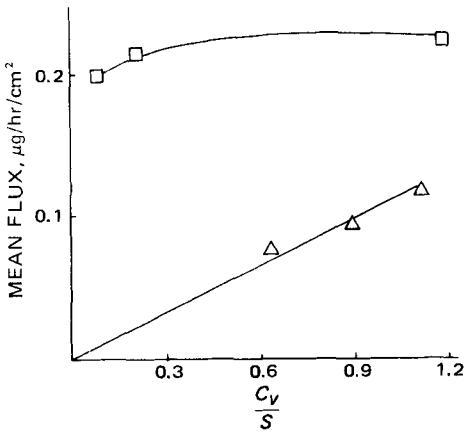

Figure 2—*Mean steady-state flux of hydrocortisone as a function of the ratio of concentration to solubility in the vehicle. Key: □, 2-propanol–water vehicle; and △, propylene glycol–water vehicle.*

through mouse skin were not measured, there is evidence that 2-propanol is likely to be a much better penetrant. Equivalent concentrations of 1-butanol penetrated human stratum corneum about 60 times faster than did 2,3-butanediol (13). Apparently, the addition of a second hydroxyl moiety slows penetration markedly. 2-Propanol probably penetrates into the stratum corneum of the mouse skin membranes and alters the barrier characteristics. It is possible that the presence of 2-propanol in the stratum corneum increases hydrocortisone partitioning from the vehicle.

Solutions containing varying concentrations of hydrocortisone in 40% 2-propanol were studied (Fig. 3). The penetration flux of hydrocortisone was proportional to the drug concentration. In other words, at a constant 2-propanol concentration, the product of K_m and D is a constant. This result shows that a linear relationship between flux and drug concentration does not necessarily rule out vehicle–skin interactions.

Addition of polysorbate 80 to aqueous solutions containing 40% 2-propanol and 0.2% hydrocortisone gave penetration rates that were higher than those for hydrocortisone solutions without surfactant. Figure 4 shows the effect of increasing polysorbate 80 concentrations on the penetration flux of hydrocortisone. The penetration rate of hydrocortisone increased rapidly at low surfactant concentrations and approached a limiting value at higher concentrations. There was no significant difference in the steady-state flux obtained at 0.51 and 1.0% polysorbate 80.

Alteration of the penetration flux from solution by nonionic surfactants may be due to: (*a*) changes in the thermodynamic activity of the drug in the vehicle; (*b*) better wetting, *i.e.*, promotion of contact between the

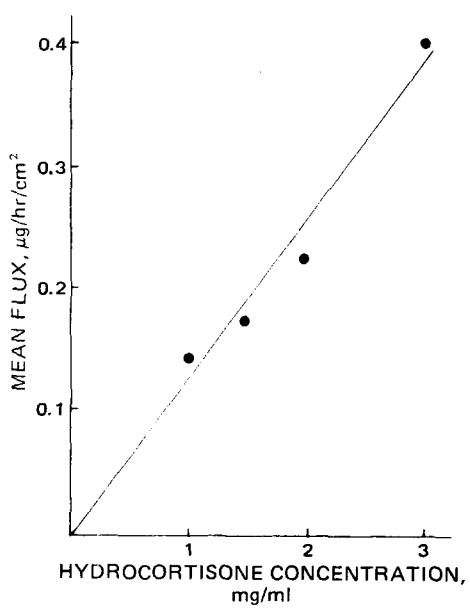

Figure 3—*Mean steady-state flux of hydrocortisone from aqueous solutions containing 40% 2-propanol.*

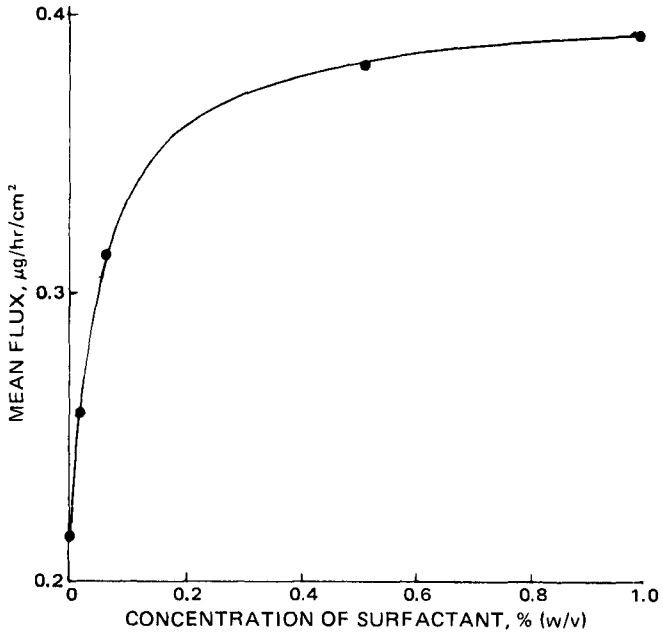

Figure 4—*Mean steady-state flux of 0.2% hydrocortisone from aqueous solutions containing 40% 2-propanol and polysorbate 80.*

solution and skin surface; and/or (*c*) surfactant–membrane interactions.

The enhanced penetration rate of hydrocortisone from solutions containing polysorbate 80 does not seem to be due to an effect of the surfactant in the thermodynamic activity of hydrocortisone in the donor system. Surfactants often form micelles in aqueous systems. Incorporation of a drug into micelles should lower its thermodynamic activity in the vehicle. However, micelle formation was suppressed at the 2-propanol concentration used in this study. Moreover, the surfactant had only a slight effect on hydrocortisone solubility, so that the ratio of hydrocortisone concentration to solubility was not markedly different in the surfactant solutions and in the solution containing no surfactant.

Wetting may be a factor in percutaneous absorption because skin is a low energy surface (15). However, in these experiments, the surface tension of the hydrocortisone solution was unchanged by the addition of increasing surfactant concentrations. All solutions had a surface tension of 26.5–26.9 dynes/cm. The critical surface tension of mouse skin has not been reported. The value for human skin is 27.5 dynes/cm (15). The relatively low values of the solution surface tensions and the lack of effect of the surfactant on surface tension rule out wetting as a significant factor in the influence of polysorbate 80 on hydrocortisone penetration from 2-propanol–water systems.

These considerations lead to the conclusion that the enhancement of hydrocortisone penetration by polysorbate 80 is due to a surfactant–membrane interaction.

Experimentally, polysorbate 80 did not appear to have any deleterious effect on the mouse skin membranes. The penetration plots for systems with polysorbate 80 were quite similar in shape to those obtained without surfactant. There were no changes in slope after steady state was attained, which would signal membrane deterioration. The fact that a limiting value of hydrocortisone penetration was reached is further evidence against membrane damage since such an effect would be expected to be most pronounced at higher surfactant concentrations.

Although the results of the penetration studies do not point to the exact mechanism by which polysorbate 80 exerts its effect, the limiting value of the steady-state flux at higher surfactant concentrations suggests a saturation phenomenon. The shape of Fig. 4 is similar to that of an adsorption isotherm.

Enhanced drug penetration in the presence of nonionic surfactants was reported previously (16–18). Various explanations for the effect of the surfactants were offered, but solubility or some other measure of drug activity in the donor systems was not determined and surface tensions were not measured. For these reasons, it is difficult to compare the conclusions of this study regarding surfactant effects with previous work.

Both Eqs. 1 and 2 assume that drug movement through the vehicle to the epidermal surface is a fast process relative to the transport rate across intact skin. The same assumption was used in interpreting the data

Table III—Steady-State Flux of Hydrocortisone from Solutions and Gels Containing 0.2% Hydrocortisone and 40% 2-Propanol

Polysorbate 80, % (w/v)	Formulation	Mean Flux ± SD, μg/hr/cm²
0	Solution	0.214 ± 0.037
0	Gel	0.239 ± 0.038
0.51	Solution	0.377 ± 0.008
0.51	Gel	0.367 ± 0.024

presented in this paper. From the intercept of the linear portion of the penetration plots with the abscissa, the hydrocortisone diffusion coefficient in the membrane was calculated (10) to be about 10^{-12} cm²/sec. The hydrocortisone diffusion coefficient in water is about 4.6×10^{-6} cm²/sec (19). Although the diffusion coefficient in the donor solutions was probably somewhat larger or smaller than this figure, it is clear that the hydrocortisone diffusion rate across the skin was much slower than that of the drug in the unstirred donor phase.

In some experiments, gels of practically the same composition were used in place of the hydrocortisone solutions. The gels differed from the solutions only in that they contained 1% hydroxyethylcellulose as a gelling agent. There was no significant difference in the penetration rate between the gels and the solutions (Table III). This result was true whether polysorbate 80 was included or not. The increased viscosity of the solution on the addition of the gelling agent did not influence penetration significantly. This finding might be anticipated since changes in macroscopic viscosity in a gel system usually do not lead to marked changes in the diffusion coefficient of a drug dissolved in the gel (20). Therefore, with the gels as with the solutions, hydrocortisone transport through the skin was rate limiting and the relatively minor changes in the hydrocortisone diffusion coefficient in the donor did not affect the flux.

An interesting application of this phenomenon is that preliminary formulation work involving percutaneous absorption can be conducted using simple solutions of the drug in a device similar to the cell used in this study. If the finished dosage form is to be a gel, the preliminary results should be useful indicators of how the gel will perform.

REFERENCES

(1) M. Katz and B. Poulsen, in "Handbook of Experimental Pharmacology," vol. 28, Concepts in Biochemical Pharmacology Part I, B. B. Brodie and J. R. Gillette, Eds., Springer, New York, N.Y., 1971, pp. 107–174.

(2) J. W. Hadgcraft, *Br. J. Dermatol.*, **81**, 386 (1972).

(3) B. J. Poulsen, in "Drug Design," vol. IV, E. J. Ariens, Ed., Academic, New York, N.Y., 1973, pp. 149–192.

(4) B. J. Poulsen, E. Young, V. Coquilla, and M. Katz, *J. Pharm. Sci.*, **57**, 928 (1968).

(5) M. R. Coldman, B. J. Poulsen, and T. Higuchi, *ibid.*, **58**, 1098 (1969).

(6) J. Ostrenga, C. Steinmetz, and B. J. Poulsen, *ibid.*, **60**, 1175 (1971).

(7) J. Ostrenga, J. Haleblian, B. J. Poulsen, B. Ferrell, N. Mueller, and S. Shastri, *J. Invest. Dermatol.*, **56**, 392 (1971).

(8) T. J. Franz, *ibid.*, **64**, 194 (1975).

(9) M. J. Bartek and J. A. LaBuddle, in "Animal Models in Dermatology," H. I. Maibach, Ed., Churchill Livingston, New York, N.Y., 1975, pp. 103–120.

(10) R. J. Scheuplein, I. H. Blank, G. J. Brunner, and D. J. Macfarlane, *J. Invest. Dermatol.*, **52**, 63 (1969).

(11) A. L. Weiss and B. J. Sciarrone, *J. Pharm. Sci.*, **58**, 980 (1969).

(12) A. W. Adamson, in "Physical Chemistry of Surfaces," 2nd ed., Interscience, New York, N.Y., 1967, p. 26.

(13) R. J. Scheuplein and I. H. Blank, *Physiol. Rev.*, **51**, 702 (1971).

(14) R. J. Scheuplein and L. Ross, *J. Soc. Cosmet. Chem.*, **21**, 853 (1970).

(15) A. Rosenberg, R. Williams, and G. Cohen, *J. Pharm. Sci.*, **62**, 920 (1973).

(16) A. J. Aguiar and M. A. Weiner, *ibid.*, **58**, 210 (1969).

(17) T. Fredriksson, *Acta Dermato-Venereol.*, **49**, 55 (1969).

(18) W. W. Shen, A. G. Danti, and F. N. Bruscato, *J. Pharm. Sci.*, **65**, 1781 (1976).

(19) J. T. Carstensen, in "Dissolution Technology," L. J. Leeson and J. T. Carstensen, Eds., APhA Academy of Pharmaceutical Sciences, Washington, D.C., 1974, p. 11.

(20) W. I. Higuchi, *Proc. Am. Assoc. Colleges Pharm. Teachers Seminar*, **1961**, p. 13.

ACKNOWLEDGMENTS

Presented in part at the Basic Pharmaceutics Section, APhA Academy of Pharmaceutical Sciences, New York meeting, May 1977.

Rapid Blue Tetrazolium Procedure for Analysis of Corticosteroids in Pharmaceutical Preparations

R. E. GRAHAM *x, E. R. BIEHL ‡, and C. T. KENNER ‡

Received August 22, 1977, from the **Dallas District, Food and Drug Administration, Dallas, TX 75204,* and the ‡*Department of Chemistry, Southern Methodist University, Dallas, TX 75275.* Accepted for publication September 23, 1977.

Abstract □ A rapid quantitative analysis of nine selected corticosteroids and corticosteroid esters at room temperature is described. The procedure is similar to the official blue tetrazolium reaction for corticosteroids, except that methylene chloride instead of alcohol USP is used as a solvent and the reagents are dissolved in or diluted with nonaqueous solvents. These two modifications reduce the medium polarity, which increases the reaction rate. The reactions are complete in 7–18 min, and the formazans are stable for at least 90 min. The results from 15 different pharmaceutical formulations, 12 containing hydrocortisone and three containing prednisolone acetate, show that the proposed method gives results that compare favorably with those obtained by the official blue tetrazolium, isoniazid, and phenylhydrazine procedures.

Keyphrases □ Corticosteroids, various—blue tetrazolium spectrophotometric analyses in pharmaceutical preparations □ Blue tetrazolium—reaction with various corticosteroids, spectrophotometric analyses in pharmaceutical preparations □ Spectrophotometry—analyses using blue tetrazolium reaction, various corticosteroids in pharmaceutical preparations

The blue tetrazolium reaction is widely used for the analysis of corticosteroids. USP XIX (1) and NF XIV (2) use a slightly modified procedure of Mader and Buck (3) for corticosteroid analysis. Blue tetrazolium (I), 3,3′-(3,3′-dimethoxy-4,4′-biphenylylene)bis(2,5-diphenyl-2*H*-tetrazolium chloride), oxidizes the α-keto moiety of the C_{17} side chain of corticosteroids in strongly alkaline solution (4) and is reduced quantitatively to a highly colored formazan whose concentration is measured spectrophotometrically.

Table III—Steady-State Flux of Hydrocortisone from Solutions and Gels Containing 0.2% Hydrocortisone and 40% 2-Propanol

Polysorbate 80, % (w/v)	Formulation	Mean Flux ± SD, μg/hr/cm²
0	Solution	0.214 ± 0.037
0	Gel	0.239 ± 0.038
0.51	Solution	0.377 ± 0.008
0.51	Gel	0.367 ± 0.024

presented in this paper. From the intercept of the linear portion of the penetration plots with the abscissa, the hydrocortisone diffusion coefficient in the membrane was calculated (10) to be about 10^{-12} cm²/sec. The hydrocortisone diffusion coefficient in water is about 4.6×10^{-6} cm²/sec (19). Although the diffusion coefficient in the donor solutions was probably somewhat larger or smaller than this figure, it is clear that the hydrocortisone diffusion rate across the skin was much slower than that of the drug in the unstirred donor phase.

In some experiments, gels of practically the same composition were used in place of the hydrocortisone solutions. The gels differed from the solutions only in that they contained 1% hydroxyethylcellulose as a gelling agent. There was no significant difference in the penetration rate between the gels and the solutions (Table III). This result was true whether polysorbate 80 was included or not. The increased viscosity of the solution on the addition of the gelling agent did not influence penetration significantly. This finding might be anticipated since changes in macroscopic viscosity in a gel system usually do not lead to marked changes in the diffusion coefficient of a drug dissolved in the gel (20). Therefore, with the gels as with the solutions, hydrocortisone transport through the skin was rate limiting and the relatively minor changes in the hydrocortisone diffusion coefficient in the donor did not affect the flux.

An interesting application of this phenomenon is that preliminary formulation work involving percutaneous absorption can be conducted using simple solutions of the drug in a device similar to the cell used in this study. If the finished dosage form is to be a gel, the preliminary results should be useful indicators of how the gel will perform.

REFERENCES

(1) M. Katz and B. Poulsen, in "Handbook of Experimental Pharmacology," vol. 28, Concepts in Biochemical Pharmacology Part I, B. B. Brodie and J. R. Gillette, Eds., Springer, New York, N.Y., 1971, pp. 107–174.

(2) J. W. Hadgcraft, *Br. J. Dermatol.*, **81**, 386 (1972).

(3) B. J. Poulsen, in "Drug Design," vol. IV, E. J. Ariens, Ed., Academic, New York, N.Y., 1973, pp. 149–192.

(4) B. J. Poulsen, E. Young, V. Coquilla, and M. Katz, *J. Pharm. Sci.*, **57**, 928 (1968).

(5) M. R. Coldman, B. J. Poulsen, and T. Higuchi, *ibid.*, **58**, 1098 (1969).

(6) J. Ostrenga, C. Steinmetz, and B. J. Poulsen, *ibid.*, **60**, 1175 (1971).

(7) J. Ostrenga, J. Haleblian, B. J. Poulsen, B. Ferrell, N. Mueller, and S. Shastri, *J. Invest. Dermatol.*, **56**, 392 (1971).

(8) T. J. Franz, *ibid.*, **64**, 194 (1975).

(9) M. J. Bartek and J. A. LaBuddle, in "Animal Models in Dermatology," H. I. Maibach, Ed., Churchill Livingston, New York, N.Y., 1975, pp. 103–120.

(10) R. J. Scheuplein, I. H. Blank, G. J. Brunner, and D. J. Macfarlane, *J. Invest. Dermatol.*, **52**, 63 (1969).

(11) A. L. Weiss and B. J. Sciarrone, *J. Pharm. Sci.*, **58**, 980 (1969).

(12) A. W. Adamson, in "Physical Chemistry of Surfaces," 2nd ed., Interscience, New York, N.Y., 1967, p. 26.

(13) R. J. Scheuplein and I. H. Blank, *Physiol. Rev.*, **51**, 702 (1971).

(14) R. J. Scheuplein and L. Ross, *J. Soc. Cosmet. Chem.*, **21**, 853 (1970).

(15) A. Rosenberg, R. Williams, and G. Cohen, *J. Pharm. Sci.*, **62**, 920 (1973).

(16) A. J. Aguiar and M. A. Weiner, *ibid.*, **58**, 210 (1969).

(17) T. Fredriksson, *Acta Dermato-Venereol.*, **49**, 55 (1969).

(18) W. W. Shen, A. G. Danti, and F. N. Bruscato, *J. Pharm. Sci.*, **65**, 1781 (1976).

(19) J. T. Carstensen, in "Dissolution Technology," L. J. Leeson and J. T. Carstensen, Eds., APhA Academy of Pharmaceutical Sciences, Washington, D.C., 1974, p. 11.

(20) W. I. Higuchi, *Proc. Am. Assoc. Colleges Pharm. Teachers Seminar*, **1961**, p. 13.

ACKNOWLEDGMENTS

Presented in part at the Basic Pharmaceutics Section, APhA Academy of Pharmaceutical Sciences, New York meeting, May 1977.

Rapid Blue Tetrazolium Procedure for Analysis of Corticosteroids in Pharmaceutical Preparations

R. E. GRAHAM *x, E. R. BIEHL ‡, and C. T. KENNER ‡

Received August 22, 1977, from the **Dallas District, Food and Drug Administration, Dallas, TX 75204,* and the ‡*Department of Chemistry, Southern Methodist University, Dallas, TX 75275.* Accepted for publication September 23, 1977.

Abstract □ A rapid quantitative analysis of nine selected corticosteroids and corticosteroid esters at room temperature is described. The procedure is similar to the official blue tetrazolium reaction for corticosteroids, except that methylene chloride instead of alcohol USP is used as a solvent and the reagents are dissolved in or diluted with nonaqueous solvents. These two modifications reduce the medium polarity, which increases the reaction rate. The reactions are complete in 7–18 min, and the formazans are stable for at least 90 min. The results from 15 different pharmaceutical formulations, 12 containing hydrocortisone and three containing prednisolone acetate, show that the proposed method gives results that compare favorably with those obtained by the official blue tetrazolium, isoniazid, and phenylhydrazine procedures.

Keyphrases □ Corticosteroids, various—blue tetrazolium spectrophotometric analyses in pharmaceutical preparations □ Blue tetrazolium—reaction with various corticosteroids, spectrophotometric analyses in pharmaceutical preparations □ Spectrophotometry—analyses using blue tetrazolium reaction, various corticosteroids in pharmaceutical preparations

The blue tetrazolium reaction is widely used for the analysis of corticosteroids. USP XIX (1) and NF XIV (2) use a slightly modified procedure of Mader and Buck (3) for corticosteroid analysis. Blue tetrazolium (I), 3,3′-(3,3′-dimethoxy-4,4′-biphenylylene)bis(2,5-diphenyl-2*H*-tetrazolium chloride), oxidizes the α-keto moiety of the C_{17} side chain of corticosteroids in strongly alkaline solution (4) and is reduced quantitatively to a highly colored formazan whose concentration is measured spectrophotometrically.

A recent paper (5) showed that the reaction rate of I with corticosteroids was inversely proportional to the dielectric constant and directly proportional to the hydrogen bonding ability of the solvent. Furthermore, the substitution of 20.0 ml of methylene chloride for alcohol USP in the I assay for steroids greatly speeds the reaction while the quantitative nature and specificity of the compendial procedure (1, 2) are retained. The monographs for various corticosteroids utilizing I as the official procedure require a 45–90-min color development time along with various special techniques such as that for flurandrenolide (6) which requires a water bath maintained at 40 ± 1°, accurately timed intervals, and subsequent quenching of the reaction with glacial acetic acid.

The data presented in this paper show that the reaction of I with nine selected steroids in methylene chloride is quantitative, up to six times as rapid as in alcohol USP, essentially complete in 15 min, and requires no special handling. Analysis of 15 different commercial formulations shows that the results obtained with the proposed procedure compare favorably with the results obtained by the official I procedure (1) as well as the Umberger isoniazid (7) and the Silber–Porter (8) reactions.

EXPERIMENTAL

Apparatus—The following were used: UV–visible recording spectrophotometers[1] with 1-cm stoppered quartz cells, glass chromatographic columns for partition chromatography (2.2 × 25 cm constricted at one end to 0.4 × 5 cm), an aluminum tamping rod, an electrobalance[2], and TLC equipment[3].

Materials—Alcohol USP, analytical reagent grade absolute ethanol, and distilled-in-glass grade acetonitrile, chloroform, *n*-heptane, absolute methanol, and methylene chloride were used along with blue tetrazolium[4], 10% aqueous tetramethylammonium hydroxide[5], and acid-washed diatomaceous earth[6]. Also used were USP reference standard cortisone acetate, hydrocortisone, hydrocortisone acetate, prednisolone acetate, and prednisone; NF reference standard dexamethasone, fluprednisolone, and flurandrenolide; cortisone[7]; and dihydrocortisone[8].

Reagents—A 1% solution of tetramethylammonium hydroxide was prepared by diluting 5.00 ml of the 10% aqueous solution to 50.0 ml with absolute ethanol. Blue tetrazolium, 5 mg/ml, was prepared by dissolving 50.0 mg in 10.0 ml of absolute methanol. Standard corticosteroid solutions were prepared to contain 0.010 mg of steroid/ml in methylene chloride, unless otherwise indicated.

Mutually saturated acetonitrile–*n*-heptane was prepared as follows. Acetonitrile, 25 ml, was mixed with 300 ml of *n*-heptane (sufficient for two determinations) in a separator, agitated vigorously for 2 min, and allowed to stand until both layers were clear. These mutually saturated solutions were used whenever acetonitrile or *n*-heptane is indicated in these directions.

Sample Preparation—*Suspensions*—After the suspension was mixed well, duplicate samples were taken immediately with 5-ml pipets (T.C.) and drained into separate 100-ml beakers. The pipets were washed twice with 0.5-ml portions each of acetonitrile, methanol, and *n*-heptane into the same beakers, and the procedure was continued as directed under *Column Preparation.*

Creams and Ointments—A composite of several containers was prepared, and a sample of about 5 g was weighed accurately into a beaker. Methanol, 30 ml, was added, and the mixture was heated on the steam bath with periodic agitation to incipient boiling to dissolve the sample. It was then cooled in an ice bath until the residue solidified, and the liquid was decanted into a 100-ml volumetric flask. The extraction was repeated three times with 20-ml portions of methanol.

The combined sample extracts were adjusted to room temperature and diluted to volume with methanol. An accurately measured aliquot containing about 1 mg of corticosteroid was evaporated to dryness carefully. The sample residue was dissolved in 1.5 ml each of acetonitrile and *n*-heptane for cleanup as directed under *Column Preparation.*

Lotions—The contents of several containers were mixed well and centrifuged at 400 rpm for 20 min. From 1.0 to 5.0 ml of sample, depending on the concentration, was transferred to a 100-ml flask by pipet (T.C.). The pipet was washed with methanol, and the sample was diluted to volume with methanol. An accurately measured aliquot, equivalent to about 1 mg of corticosteroid, was evaporated carefully just to dryness on the steam bath. The sample residue was dissolved in 1.5 ml of acetonitrile and 1.5 ml of *n*-heptane for cleanup as directed under *Column Preparation.*

Gels—A composite of several containers was mixed well, and a sample of about 2.5 g, accurately weighed, was made up to 100.0 ml with alcohol USP. An accurately measured aliquot, equivalent to about 1 mg of corticosteroid, was evaporated carefully just to dryness on the steam bath. The sample residue was dissolved in 1.5 ml of acetonitrile and 1.5 ml of *n*-heptane for cleanup as directed under *Column Preparation.*

Column Preparation—*Acetonitrile Layer*—A glass wool plug was inserted in the bottom of a chromatographic column. Then a 4-g portion of diatomaceous earth was thoroughly mixed with 4.0 ml of acetonitrile, transferred to the column, and packed firmly with a tamping rod.

Sample Layer—The sample solution, prepared as directed under *Sample Preparation,* was mixed thoroughly with 3 g of diatomaceous earth to yield a light fluffy mixture. It was then transferred to the column above the acetonitrile layer and packed firmly. The sample beaker, tamping rod, spatula, and funnel were dry washed with about 1 g of diatomaceous earth, which was added to the column. The same equipment was dry washed with glass wool, which was placed on top of the sample layer plus washings and packed firmly. The beaker was retained and washed with the *n*-heptane and chloroform used during column elution.

The sample beaker was washed with 150 ml of *n*-heptane in small portions and transferred to the column to maintain a liquid head approximately 12 cm above the column bed. The last wash was allowed to drain completely from the column, the tip was rinsed with alcohol USP, and the entire effluent was discarded. A new beaker was placed under the column, and the sample beaker was washed with 125 ml of chloroform in small portions, which were added to the column to maintain the liquid level close to the top of the column.

The last portion was allowed to drain completely, and the tip was rinsed with alcohol USP. The effluent was evaporated carefully just to dryness on a steam bath under a hood to ensure complete removal of the acetonitrile. The residue was dissolved and diluted accurately to volume with methylene chloride, which contained approximately 0.010 mg of corticosteroid/ml.

Isoniazid Method—The procedure of Umberger (7) was used, except that the hydrochloric acid concentration was doubled to increase the sensitivity.

Phenylhydrazine Method—The procedure of Silber and Porter (8) was followed.

Blue Tetrazolium Method—The procedure given in USP XIX (1) was followed.

Proposed Method—Aliquots of 20 ml were run by the I procedure given in USP XIX (1), except that the tetramethylammonium hydroxide reagent was diluted with absolute ethanol instead of alcohol USP, the blue tetrazolium reagent was prepared with absolute methanol in place of alcohol USP, the spectrophotometric scans from 720 to 490 nm were made against methylene chloride as reference instead of the reagent blank, and the scans were started 15 min after tetramethylammonium hydroxide addition. The scans were always made in the order of reagent blank, standard, sample, and reagent blank, and the reagent blank was kept in the dark between the original and final scans. The absorbance was read from the absorbance maximum at about 525 nm.

Each measured absorbance value had to be corrected for the continuously increasing reagent blank absorbance. The correction for each reading was obtained by dividing the increase in absorbance of the reagent blank by the number of scans (omitting the original reagent blank scan) to obtain an average increase per scan. This average was then multiplied by the scan number and added to the original reagent blank absorbance. The net absorbance was then calculated by subtracting the corrected reagent blank absorbance from the measured absorbance for that scan.

Replication Studies of Absorbances Produced by Proposed Blue Tetrazolium Method—Accurately weighed portions of each of the 10

[1] Cary models 15 and 17.
[2] Cahn model G-2.
[3] Eastman 6060 silica gel.
[4] Dajac Laboratories.
[5] Eastman Organic Chemicals.
[6] Celite 545, Johns-Manville Product Corp.
[7] K and K Laboratories.
[8] Mann Research Laboratories.

Table I—Absorbance Replication of Proposed Procedure

Run	Cortisone	Cortisone Acetate	Dexamethasone	Dihydrocortisone Acetate	Fluprednisolone	Flurandrenolide	Hydrocortisone	Hydrocortisone Acetate	Prednisolone Acetate	Prednisone
1[a]	0.629	0.569	0.575	0.535	0.580	0.521	0.584	0.544	0.512	0.568
2	0.628	0.574	0.578	0.535	0.592	0.516	0.584	0.531	0.511	0.571
3	0.630	0.575	0.586	0.535	0.580	0.518	0.586	0.534	0.511	0.577
4	0.630	0.572	0.585	0.534	0.591	0.521	0.587	0.539	0.511	0.574
5	0.631	0.573	0.584	0.536	0.587	0.528	0.586	0.536	0.516	0.573
6	0.623	0.574	0.579	0.536	0.581	0.530	0.584	0.538	0.519	0.576
7	0.627	0.571	0.579	0.538	0.592	0.534	0.582	0.542	0.516	0.580
8	0.627	0.573	0.579	0.540	0.585	0.538	0.586	0.549	0.509	0.580
9	0.617	0.571	0.587	0.536	0.581	0.532	0.587	0.542	0.514	0.581
10	0.617	0.572	0.581	0.543	0.582	0.539	0.587	0.543	0.515	0.579
11	0.627	0.572	0.586	0.526	0.581	0.536	ND[b]	0.538	ND[b]	0.578
12	ND[b]	0.569	0.587	0.541	0.583	ND[b]	ND[b]	0.541	ND[b]	0.581
Average	0.626	0.572	0.582	0.536	0.585	0.528	0.585	0.540	0.513	0.576
SD[c]	0.0046	0.0020	0.0040	0.0056	0.0040	0.0076	0.0016	0.0059	0.0033	0.0043
RSD, %	0.73	0.35	0.69	1.0	0.68	1.4	0.27	1.1	0.64	0.75

[a] Standards were run consecutively in the order 1–12. [b] ND = not determined. [c] Calculated from the range by the method of Dean and Dixon (9).

corticosteroid standards were dissolved in and diluted to 250.0 ml with methylene chloride to yield solutions containing approximately 0.010 mg/ml. Ten to 12 20.0-ml aliquots of each were analyzed by the proposed method, and the absorbances were determined (Table I). All solutions were kept in the dark during color development. The relative standard deviation, calculated from the range (9), varied from 0.35 to 1.4% with an overall average of 0.76%.

Beer's Law Study—More concentrated solutions, up to 3.5 mg/100 ml, were prepared for each of the 10 standards in methylene chloride. Aliquots of 2.00 or 3.00, 5.00, 10.0, 15.0, and 20.0 ml of each solution were taken, diluted to 20.0 ml with methylene chloride, and put through the proposed method. Absorbances ranged from 0.090 to 1.867, and correlation coefficients of 0.9993 or better were obtained for each steroid using a least-squares fitting program.

Color Development Time and Formazan Stability—A 20.0-ml aliquot of each of the 10 standards was tested according to the proposed method, except that the solution was transferred to a cell immediately after tetramethylammonium hydroxide addition. Readings were taken every minute *versus* a reagent blank for 90 min, and the time necessary to reach maximum absorption was noted for each steroid. The results (Table II) show that completion of the reaction, except for flurandrenolide, requires 7–18 min and that the formazan is stable for at least 90 min after reagent addition.

RESULTS AND DISCUSSION

The results of the analyses of 15 different pharmaceutical preparations containing corticosteroid and corticosteroid esters by the proposed procedure are shown in Table III. Duplicate analyses were run for each sample by four different methods. The results obtained by the proposed method compare favorably with those achieved by the official I procedure (1). Results of analyses obtained by the isoniazid and phenylhydrazine methods also are in agreement with those of the two I procedures, with the exception of Sample 8. The higher values obtained by the isoniazid method, which measures the amount of conjugated ketone in ring A of corticosteroid molecules, indicates possible decomposition of the C_{17} side chain in this sample. Interference to the I reaction by both methods in Sample 5 was confirmed by the method of variation of absorbance with time previously reported (10). Averages for all determinations of all samples by the four methods (Table III) show excellent agreement.

Table II—Reaction Time and Stability of Formazan in Methylene Chloride

Steroid	Time to Maximum Absorbance, min	Absorbance			Absorbance per Micromole[b]
		Original Maximum[a]	60 min	90 min	
Cortisone	10	0.670	0.682	0.685	1.045
Cortisone acetate	11	0.549	0.549	0.543	1.000
Dexamethasone	11	0.530	0.548	0.548	1.028
Dihydrocortisone acetate	13	0.570	0.578	0.577	1.043
Flupredniso lone	12	0.610	0.622	0.622	1.031
Flurandrenolide[c]	—	—	0.548	0.570	—
Hydrocortisone	18	0.579	0.590	0.596	1.039
Hydrocortisone acetate	13	0.620	0.629	0.627	1.056
Prednisolone acetate	16	0.509	0.510	0.509	1.020
Prednisone	7	0.583	0.571	0.563	1.019

[a] The absorbance noted at the time specified in the preceding column. [b] See Ref. 11 for definition. The average was 1.031. [c] The absorption maximum was not reached in 90 min.

Because of the low solubility of water in methylene chloride, it is necessary to substitute water-free solvents for alcohol USP for the dilutions of tetramethylammonium hydroxide and for the preparation of the I reagent for use in the proposed procedure to prevent the formation of liquid emulsions. Furthermore, the presence of small amounts of dissolved water increases the polarity of the solvent medium and increases the time required for the reaction to reach completion. A recent paper (5) showed that an increase in water content from 0.9 to 1.2% increased the time required for the hydrocortisone reaction with I to reach maximum absorbance from 13 to 90 min.

Beer's law was obeyed between 0.5 and 0.50 mg/24 ml for all 10 corticosteroids.

Reaction of I with flurandrenolide for 15 min produced an absorbance of 0.486, which is equivalent to 1.034 absorbance units/μmole or one reduction unit (11). This result indicates that the oxidation of the α-keto group was complete in 15 min, even though the absorbance continued to rise for 90 min. The increase is similar to the reaction of triamcinolone (11) and indicates the release of a second reduction unit through the slow hydrolysis of the cyclic diacetal with the acetone group of flurandrenolide. Apparently, the hydrolysis rate of the cyclic diacetal is the rate-limiting step in this reaction, and the absorbance increase could be expected to continue until hydrolysis is complete. The proposed method can be used for flurandrenolide and similar molecules by quenching the reaction by the addition of acetic acid to the blank, standard, and sample in rapid succession 15 min after the addition of tetramethylammonium hydroxide, at which time oxidation of the $C_{20,21}$ α-keto group is complete.

The rate studies (Table II) show that the reaction of I with nine selected corticosteroids and corticosteroid esters in methylene chloride was complete at room temperature in relatively short periods—from 7 to 18 min. Once the reaction was complete, the formazan was stable for at least 90 min from the time of tetramethylammonium hydroxide addition. The average value calculated in absorbance units per micromole produced from the reaction of I with the nine corticosteroids (Table II) was 1.031 in methylene chloride, identical to the average value of 1.031 previously reported (11) for 21 corticosteroid reactions with I in alcohol USP. Agreement of these values indicates that the reaction of these corticosteroids with I in methylene chloride is quantitative and is as sensitive as the comparable reaction in alcohol USP.

While the I reaction with steroids is complete in the specified time and the formazan produced is stable, the absorption of the blank continues to increase with time. The rate of absorbance increase in the light-protected blank is slower than the rate of absorbance increase of the blank in the reference cell when a long series of scans is necessary. As a consequence, the procedure described in USP XIX (1), which requires that the samples be scanned *versus* a reagent blank, will cause an error of approximately 0.001 absorbance unit/min when a long series of scans is made. The correct net absorbance for the samples can be obtained only

Table III—Analysis of Typical Pharmaceutical Formulations

Sample	Type of Sample[a]	Amount Declared, %	Found, % of Declared: Blue Tetrazolium, Proposed Method	Blue Tetrazolium, USP XIX Method	Isoniazid	Phenylhydrazine
1	Cream	0.25	95.0, 97.8	91.2, 91.7	96.0, 95.6	91.5, 90.8
2	Cream	0.5	96.7, 101.4	96.6, 100.0	94.1, 97.7	93.8, 98.5
3	Cream	1	97.1, 97.6	99.2, 98.6	98.6, 99.6	96.1, 100.3
4	Gel	1	97.5, 99.9	97.5, 97.4	99.9, 97.9	99.5, 97.9
5	Lotion	0.25	97.1, 96.9	96.2, 97.2	92.8, 88.1	ND[b]
6	Lotion	0.5	100.0, 95.9	99.5, 96.3	ND[b]	101.2, 98.8
7	Lotion	0.5	99.8, 99.2	99.6, 99.2	100.9, 101.3	99.2, 100.4
8	Lotion	0.125	90.5, 89.0	92.4, 92.8	102.2, 99.3	97.9, 95.8
9	Lotion	0.25	95.4, 96.6	96.3, 98.0	98.5, 97.8	95.2, 96.9
10	Lotion	0.5	98.7, 99.0	102.4, 102.6	101.9, 101.2	102.9, 102.3
11	Lotion	1.0	103.2, 104.4	106.4, 106.6	101.1, 101.3	103.2, 103.2
12	Lotion	1.0	94.3, 92.6	94.4, 91.2	92.5, 91.0	93.5, 94.6
13	Ointment[c]	0.25	98.6, 97.3	94.9, 94.7	98.8, 98.0	97.5, 98.5
14	Suspension[c]	0.25	89.3, 91.2	87.9, 89.8	88.4, 87.8	86.9, 92.7
15	Suspension[c]	0.25	71.6, 73.6	73.3, 74.8	74.0, 72.3	72.3, 73.5
	Average		95.2	95.3	95.3	95.6

[a] The steroids were hydrocortisone in Samples 1–12 and prednisolone acetate in Samples 13–15. [b] ND = not determined. [c] Product also contained 10% sodium sulfacetamide.

by scanning against the solvent and calculating the corrected net absorbance as shown under *Experimental*.

Methylene chloride solutions undergo evaporative concentration from glass-stoppered volumetric flasks at a daily average rate of approximately 0.1%[9] (v/v). This result indicates that the same standard could be used for several days without significant change. In this study, however, the standards were used only on the day of preparation.

In some cases, the corticosteroid was so slowly soluble in methylene chloride that it was necessary to let it stand for 1 hr with periodic agitation or place it in an ultrasonic instrument for not more than 30 sec to ensure complete solution.

The proposed procedure for the analysis of corticosteroids with I is rapid and quantitative. In most cases, the reaction is complete within 15 min after addition of the tetramethylammonium hydroxide reagent and the formazans produced are stable for at least 90 min. Analysis of 15 different pharmaceutical products for corticosteroids by the proposed I procedure gave results that compared favorably with those obtained by three different analytical methods.

[9] Unpublished work.

REFERENCES

(1) "The United States Pharmacopeia," 19th rev., Mack Publishing Co., Easton, Pa., 1975, p. 622.

(2) "The National Formulary," 14th ed., Mack Publishing Co., Easton, Pa., 1975, p. 976.

(3) W. J. Mader and R. R. Buck, *Anal. Chem.*, **24**, 666 (1952).

(4) R. E. Graham and C. T. Kenner, *J. Pharm. Sci.*, **62**, 103 (1973).

(5) R. E. Graham, E. R. Biehl, and C. T. Kenner, *ibid.*, **65**, 1048 (1976).

(6) "The United States Pharmacopeia," 19th rev., Mack Publishing Co., Easton, Pa., 1975, p. 210.

(7) E. J. Umberger, *Anal. Chem.*, **27**, 768 (1955).

(8) R. H. Silber and C. C. Porter, *J. Biol. Chem.*, **210**, 923 (1954).

(9) R. B. Dean and W. J. Dixon, *Anal. Chem.*, **23**, 636 (1951).

(10) R. E. Graham, P. A. Williams, and C. T. Kenner, *J. Pharm. Sci.*, **59**, 1472 (1970).

(11) R. E. Graham, E. R. Biehl, C. T. Kenner, G. H. Luttrell, and D. L. Middleton, *ibid.*, **64**, 226 (1975).

Preferential Localization of Radiolabeled Liposomes in Liver

GEORGE H. HINKLE *x, GORDON S. BORN, WAYNE V. KESSLER, and STANLEY M. SHAW

Received May 23, 1977, from the *Bionucleonics Department, School of Pharmacy and Pharmacal Sciences, West Lafayette, IN 47907.* Accepted for publication September 28, 1977.

*Present address: University of Oklahoma, Tulsa Medical College, Tulsa, OK 74114.

Abstract □ Liposome formulations were studied to achieve an efficient entrapment procedure for the production of liposomes of ^{99m}Tc-pentetic acid. The entrapment efficiency was studied by separation of the product using column chromatography. The particle-size range of the prepared liposomes was evaluated using electron microscopy. Entrapment techniques and separation procedures led to a liposome preparation with particles in the colloidal size range (0.001–0.5 μm). Dramatic differences in the organ distribution of the liposome preparation in mice were produced when different particle-size ranges were injected. Liposomes eluted in the first fraction after the void volume led to a maximum uptake by the liver and spleen 10 min after intravenous injection. Liposomes from pooled fractions provided less than half of the activity in the liver, as did the narrow size range liposome preparation.

Keyphrases □ Liposomes, radiolabeled—^{99m}Tc-pentetic acid, organ distribution in mice, effect of particle size □ Radiolabeled liposomes—^{99m}Tc-pentetic acid, organ distribution in mice, effect of particle size □ ^{99m}Tc-Pentetic acid liposomes—organ distribution in mice, effect of particle size □ Distribution, organ—^{99m}Tc-pentetic acid liposomes in mice, effect of particle size □ Particle size—^{99m}Tc-pentetic acid liposomes, effect on organ distribution in mice

Liposomes have been described as minute vesicles composed of lipid bilayers (1). Spontaneous formation of liposomes occurs when a combination of certain lipids is dispersed throughout an aqueous solution (2). Materials dissolved in the aqueous solution become trapped in the enclosed aqueous compartments, which form in an alter-

Table III—Analysis of Typical Pharmaceutical Formulations

Sample	Type of Sample[a]	Amount Declared, %	Found, % of Declared: Blue Tetrazolium, Proposed Method	Blue Tetrazolium, USP XIX Method	Isoniazid	Phenylhydrazine
1	Cream	0.25	95.0, 97.8	91.2, 91.7	96.0, 95.6	91.5, 90.8
2	Cream	0.5	96.7, 101.4	96.6, 100.0	94.1, 97.7	93.8, 98.5
3	Cream	1	97.1, 97.6	99.2, 98.6	98.6, 99.6	96.1, 100.3
4	Gel	1	97.5, 99.9	97.5, 97.4	99.9, 97.9	99.5, 97.9
5	Lotion	0.25	97.1, 96.9	96.2, 97.2	92.8, 88.1	ND[b]
6	Lotion	0.5	100.0, 95.9	99.5, 96.3	ND[b]	101.2, 98.8
7	Lotion	0.5	99.8, 99.2	99.6, 99.2	100.9, 101.3	99.2, 100.4
8	Lotion	0.125	90.5, 89.0	92.4, 92.8	102.2, 99.3	97.9, 95.8
9	Lotion	0.25	95.4, 96.6	96.3, 98.0	98.5, 97.8	95.2, 96.9
10	Lotion	0.5	98.7, 99.0	102.4, 102.6	101.9, 101.2	102.9, 102.3
11	Lotion	1.0	103.2, 104.4	106.4, 106.6	101.1, 101.3	103.2, 103.2
12	Lotion	1.0	94.3, 92.6	94.4, 91.2	92.5, 91.0	93.5, 94.6
13	Ointment[c]	0.25	98.6, 97.3	94.9, 94.7	98.8, 98.0	97.5, 98.5
14	Suspension[c]	0.25	89.3, 91.2	87.9, 89.8	88.4, 87.8	86.9, 92.7
15	Suspension[c]	0.25	71.6, 73.6	73.3, 74.8	74.0, 72.3	72.3, 73.5
	Average		95.2	95.3	95.3	95.6

[a] The steroids were hydrocortisone in Samples 1–12 and prednisolone acetate in Samples 13–15. [b] ND = not determined. [c] Product also contained 10% sodium sulfacetamide.

by scanning against the solvent and calculating the corrected net absorbance as shown under *Experimental*.

Methylene chloride solutions undergo evaporative concentration from glass-stoppered volumetric flasks at a daily average rate of approximately 0.1%[9] (v/v). This result indicates that the same standard could be used for several days without significant change. In this study, however, the standards were used only on the day of preparation.

In some cases, the corticosteroid was so slowly soluble in methylene chloride that it was necessary to let it stand for 1 hr with periodic agitation or place it in an ultrasonic instrument for not more than 30 sec to ensure complete solution.

The proposed procedure for the analysis of corticosteroids with I is rapid and quantitative. In most cases, the reaction is complete within 15 min after addition of the tetramethylammonium hydroxide reagent and the formazans produced are stable for at least 90 min. Analysis of 15 different pharmaceutical products for corticosteroids by the proposed I procedure gave results that compared favorably with those obtained by three different analytical methods.

[9] Unpublished work.

REFERENCES

(1) "The United States Pharmacopeia," 19th rev., Mack Publishing Co., Easton, Pa., 1975, p. 622.

(2) "The National Formulary," 14th ed., Mack Publishing Co., Easton, Pa., 1975, p. 976.

(3) W. J. Mader and R. R. Buck, *Anal. Chem.*, **24**, 666 (1952).

(4) R. E. Graham and C. T. Kenner, *J. Pharm. Sci.*, **62**, 103 (1973).

(5) R. E. Graham, E. R. Biehl, and C. T. Kenner, *ibid.*, **65**, 1048 (1976).

(6) "The United States Pharmacopeia," 19th rev., Mack Publishing Co., Easton, Pa., 1975, p. 210.

(7) E. J. Umberger, *Anal. Chem.*, **27**, 768 (1955).

(8) R. H. Silber and C. C. Porter, *J. Biol. Chem.*, **210**, 923 (1954).

(9) R. B. Dean and W. J. Dixon, *Anal. Chem.*, **23**, 636 (1951).

(10) R. E. Graham, P. A. Williams, and C. T. Kenner, *J. Pharm. Sci.*, **59**, 1472 (1970).

(11) R. E. Graham, E. R. Biehl, C. T. Kenner, G. H. Luttrell, and D. L. Middleton, *ibid.*, **64**, 226 (1975).

Preferential Localization of Radiolabeled Liposomes in Liver

GEORGE H. HINKLE *x, GORDON S. BORN, WAYNE V. KESSLER, and STANLEY M. SHAW

Received May 23, 1977, from the *Bionucleonics Department, School of Pharmacy and Pharmacal Sciences, West Lafayette, IN 47907.* Accepted for publication September 28, 1977.

*Present address: University of Oklahoma, Tulsa Medical College, Tulsa, OK 74114.

Abstract □ Liposome formulations were studied to achieve an efficient entrapment procedure for the production of liposomes of ^{99m}Tc-pentetic acid. The entrapment efficiency was studied by separation of the product using column chromatography. The particle-size range of the prepared liposomes was evaluated using electron microscopy. Entrapment techniques and separation procedures led to a liposome preparation with particles in the colloidal size range (0.001–0.5 μm). Dramatic differences in the organ distribution of the liposome preparation in mice were produced when different particle-size ranges were injected. Liposomes eluted in the first fraction after the void volume led to a maximum uptake by the liver and spleen 10 min after intravenous injection. Liposomes from pooled fractions provided less than half of the activity in the liver, as did the narrow size range liposome preparation.

Keyphrases □ Liposomes, radiolabeled—^{99m}Tc-pentetic acid, organ distribution in mice, effect of particle size □ Radiolabeled liposomes—^{99m}Tc-pentetic acid, organ distribution in mice, effect of particle size □ ^{99m}Tc-Pentetic acid liposomes—organ distribution in mice, effect of particle size □ Distribution, organ—^{99m}Tc-pentetic acid liposomes in mice, effect of particle size □ Particle size—^{99m}Tc-pentetic acid liposomes, effect on organ distribution in mice

Liposomes have been described as minute vesicles composed of lipid bilayers (1). Spontaneous formation of liposomes occurs when a combination of certain lipids is dispersed throughout an aqueous solution (2). Materials dissolved in the aqueous solution become trapped in the enclosed aqueous compartments, which form in an alter-

Table I—Organ Distribution of Pooled Fractions of Liposomes in Mice at Various Time Intervals

Minutes after Injection	Blood (1 g)	Liver	Kidneys	Urinary Bladder and Urine	Spleen	Small Intestine	Lungs	Heart
1	23.5[a] ± 2.3	35.3 ± 3.1	2.6 ± 0.1	0.5 ± 0.3	2.8 ± 0.9	2.2 ± 0.8	1.7 ± 0.3	0.7 ± 0.2
3	19.8 ± 0.4	37.9 ± 1.7	3.5 ± 0.4	4.1 ± 0.6	2.7 ± 0.4	2.1 ± 0.5	1.0 ± 0.6	0.3 ± 0.3
5	17.6 ± 3.5	43.8 ± 7.4	3.2 ± 0.9	4.8 ± 2.6	2.4 ± 0.1	1.7 ± 0.2	0.7 ± 0.1	0.2 ± 0.02
10	11.0 ± 0.9	41.6 ± 0.9	1.9 ± 0.2	9.6 ± 0.9	3.0 ± 0.6	2.1 ± 0.3	0.8 ± 0.05	0.2 ± 0.03
15	10.1 ± 3.7	44.1 ± 5.3	1.9 ± 0.3	10.7 ± 7.9	3.2 ± 1.3	1.8 ± 0.4	0.6 ± 0.1	0.1 ± 0.05
30	4.9 ± 0.9	37.9 ± 3.7	2.9 ± 0.5	22.1 ± 3.6	2.0 ± 0.1	3.2 ± 0.3	0.4 ± 0.1	0.09 ± 0.01
60	1.7 ± 0.2	29.8 ± 1.3	1.4 ● 0.3	50.1 ± 11.5	2.1 ± 0.5	2.1 ± 0.3	0.2 ± 0.09	0.06 ± 0.03

[a] Percentage of injected dose per organ or per gram ± *SD*. Mean of four mice.

nating, concentric fashion with the lipid bilayers. In addition, lipid-soluble materials may be incorporated in the formed liposomes if added to the lipids forming the bilayer structures. These properties make liposomes ideal carriers of drugs, enzymes, and other biologically important compounds (3–11).

The components of the formed liposomes, the nature of the material entrapped in the aqueous compartment, and the size of the structures all contribute to the initial degree of entrapment of the aqueous material and the stability of the preparation (1–7, 12–14). The biological distribution of the entrapped materials follows that of the liposome carrier (2–11). The direction of liposomes to specific target cells *in vivo* by altering the surface or structure of the liposomes is being studied (15–17).

Phagocytosis of small diameter liposomes by the Kupffer cells of the liver occurs within minutes after intravenous injection (9–11, 16–18). The phagocytic removal of liposomes by the reticuloendothelial system hinders their use as drug carriers to afford specific delivery of medically important agents to sites of action other than the reticuloendothelial system. However, this property has been used to obtain diagnostic information about the liver and spleen and may lead to the use of liposomes as a delivery system for radiopharmaceuticals (19–23).

After a study of the preparation of radiolabeled liposomes [^{99m}Tc-pentetic acid[1] (^{99m}Tc-I)] and their uptake in mice was completed in this laboratory, a similar study was reported (23). The maximum uptake by the liver reported was less than 45%. The present study shows that greater than 90% uptake can be obtained by control of liposome size. Two different lipid combinations and different sonication times were evaluated. Although some results show little difference from those already reported (23), it is important to describe a procedure for the preparation of radiolabeled liposomes of the correct particle size that achieves maximum localization in the liver.

EXPERIMENTAL

Preparation of Liposomes of ^{99m}Tc-I—The effect of the inclusion of oppositely charged amphiphiles in the liquid composition on the entrapment of ^{99m}Tc-I into the liposomes was studied using two formulations. Negatively charged liposomes were prepared using 15.75 μmoles of dimyristoyllecithin[2], 4.5 μmoles of cholesterol[2], and 2.25 μmoles of dicetyl phosphate[2] (a 7:2:1 molar ratio). Positively charged liposomes contained 2.25 μmoles of stearylamine[3] in their formulation, replacing the dicetyl phosphate.

The procedure for the preparation of liposomes was identical for both negative and positive formulations. The lipids were weighed, dissolved in chloroform, and combined. The combined lipid solution was transferred to a 10-ml pear-shaped flask, and the chloroform was removed by rotary evaporation under reduced pressure. The open flask containing the thin layer of lipid on its walls was transferred to a desiccator and placed under vacuum for 1 hr to remove any remaining chloroform.

In-house kits, as described by Eckelman and Richards (24), for the rapid preparation of ^{99m}Tc-I were prepared. ^{99m}Tc-Labeling of I was carried out while the pear-shaped flask remained in the desiccator under vacuum.

One milliliter of the freshly prepared ^{99m}Tc-I solution was added to the pear-shaped flask, and the thin lipid film was dispersed by vortex mixing for 10 min at high speed. The flask was placed in a lead shield and allowed to stand at room temperature for 2 hr. This step allowed the formation and swelling of the liposomes, in which the aqueous ^{99m}Tc-I solution became entrapped between the lipid bilayers. The flask was then placed in a water bath sonicator[4], which generated frequencies of 50–55 kHz and sonicated for varying lengths of time depending on the experiment being performed.

To prevent oxidation and hydrolysis of the lipids due to heat generated by the sonication procedure, the temperature of the water was maintained below 20° by the addition of crushed ice to the sonication bath. A second 2-hr interval of standing at room temperature was used after sonication to allow swelling and continued liposome formation.

A sample of the liposome (^{99m}Tc-I) preparation was placed on a 1.5 × 30-cm column of a gel chromatography medium[5] equilibrated with isotonic sodium phosphate buffer (pH 7.05) eluant. Forty fractions were collected, each having a volume of 2 ml. To determine the degree of liposome entrapment of the ^{99m}Tc-I, a 10-μl aliquot of each fraction was counted in an automatic γ-counter. A second elution of the column after the addition of 0.1% hydrogen peroxide was performed to remove any hydrolyzed technetium. These counts were added to the counts of the free ^{99m}Tc-I species after decay corrections.

The degree of entrapment of ^{99m}Tc-I was expressed as the percentage of the total activity eluted from the column found in the liposome peak. The variability of entrapment due to lipid composition was determined using positive or negative liposome formulations and a sonication time of 45 min. The variability due to sonication time was determined using the positive liposome formulation and sonication times of 15, 30, 45, and 60 min.

Size Determinations Using Electron Microscopy—The preparation of liposomes for electron microscopy studies was identical to that discussed previously except for the addition of 1 ml of 3.3 *mM* potassium iodide solution to the pear-shaped flask prior to the entrapment of ^{99m}Tc-I. A negative staining technique was employed by diluting the liposome preparation with an equal volume of a 0.5% solution of phosphotungstic acid and allowing this mixture to stand for 1 hr. A small amount of this preparation was placed on a carbon-coated grid[6] and allowed to air dry. The grid was then examined on an electron microscope[7].

Animal Studies—*In vivo* distribution studies of positively charged liposomes were performed using male Swiss mice, 23–29 g. The positive liposome formulation was used because of the apparent increase entrapment of ^{99m}Tc-I over the negative liposome formulation. After vortex mixing of the injection preparation to obtain a homogeneous suspension, 0.2 ml was administered intravenously in the caudal vein; the mouse was sacrificed by cervical separation after the allotted distribution time. Organs of interest were weighed and counted along with blood samples and 0.2-ml samples of the injection preparation. Corrections were made

[1] Previously referred to as diethylenetriaminepentaacetic acid.
[2] *Sigma Chemical Co., St. Louis, Mo.*
[3] K & K Laboratories, Plainview, N.Y.
[4] Model B-12, Bransonic, Shelton, Conn.
[5] Sephadex G-50 (fine), Pharmacia Fine Chemicals, Piscataway, N.J.
[6] Formvar, Ernest F. Fullam, Inc., Schenectady, N.Y.
[7] Hitachi model HU-11A.

Table II—Localization of a Colloidal Particle-Size Range Sample of Liposomes in Mice at Various Time Intervals

Minutes after Injection	Run	Blood (1 g)	Liver	Kidneys	Spleen	Lungs
5	1	1.4[a] ± 0.7	91.7 ± 0.7	0.9 ± 0.1	5.1 ± 1.2	0.9 ± 0.1
	2	3.1 ± 0.1	87.8 ± 0.8	1.6 ± 0.1	2.6 ± 0.5	1.3 ± 0.2
10	1	1.2 ± 0.1	93.4 ± 3.1	0.9 ± 0.1	3.3 ± 1.1	0.8 ± 0.1
	2	2.3 ± 0.3	90.1 ± 1.8	1.6 ± 0.3	3.3 ± 1.6	1.0 ± 0.2
15	1	1.3 ± 0.7	92.1 ± 2.9	0.8 ± 0.1	4.5 ± 0.9	0.5 ± 0.1
	2	1.8 ± 0.2	91.6 ± 1.2	1.6 ± 0.1	2.6 ± 0.2	1.1 ± 0.2

[a] Percentage of injected dose per organ or per gram ± *SD*. Mean of three mice.

for the physical decay of technetium Tc 99m, and the results were expressed as percentage of injected dose per organ or per gram of tissue.

In one study, organ distribution of a wide particle-size range sample of liposomes was performed by combining the cloudy liposome fractions into one injection preparation. A 45-min sonication time was used to produce the wide particle-size distribution of liposomes. In a second study, liver localization of liposomes was accomplished using the fraction containing colloidal particle-size range liposomes for injection. The volume of the injection preparation was increased by the addition of eluant buffer.

The 45-min sonication time was used in the animal studies because it provided the greatest number of liposomes in the colloidal size range in comparison with 15-, 30-, and 60-min sonication periods. Preliminary studies involving light and electron microscopy techniques showed that colloidal size particles were being prepared with each sonication time period. Sonication for 15 min resulted in a large number of liposomes approaching 10 μm in diameter. Longer periods of sonication produced small diameter structures whose passage through the gel chromatography medium was retarded during separation attempts. The 45-min sonication time produced few liposomes greater than 0.5 μm, and separation of the labeled liposomes from the free ^{99m}Tc-I using gel chromatography provided the colloidal size structures in the first fraction following the void volume.

RESULTS

Preparation of Liposomes of ^{99m}Tc-I—Separation of the liposome preparation from the free ^{99m}Tc-I by column chromatography provided a determination of the degree of entrapment along with a liposome preparation for animal studies. Figure 1 shows the degree of entrapment of ^{99m}Tc-I in two preparations differing in lipid composition. The mean percentage of ^{99m}Tc-I activity in the liposome fractions of negatively charged liposomes, as calculated from a total of six entrapment studies, was 1.86 ± 0.34. The mean percentage of ^{99m}Tc-I activity in the liposome fractions of positively charged liposomes, as calculated from 12 entrapment studies, was 8.14 ± 1.66. A significant increase in the degree of entrapment was seen with positively charged liposomes.

Figure 2 summarizes the results of entrapment of ^{99m}Tc-I into positively charged liposomes produced with various sonication time intervals. The sonication time intervals were chosen because they produced liposomes in the colloidal size range. Application of the Newman–Keuls test to the data led to the conclusion that the 60-min sonication time produced significantly lower (p = 0.05) entrapment yields than did 15-, 30-, and 45-min times, which did not differ from each other significantly. The slight decrease in entrapment with a 60-min sonication time was expected since the larger liposomes produced at the other times can entrap more aqueous solution between their numerous lipid bilayers.

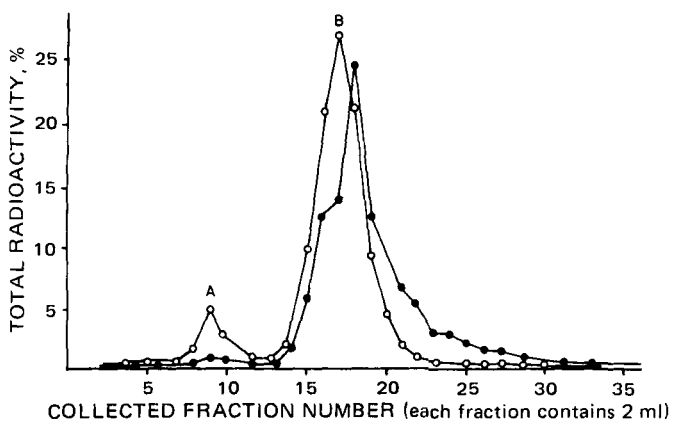

Figure 1—*Elution pattern of positively* (○) *and negatively* (●) *charged liposomes showing the liposome peak* (*A*) *and the ^{99m}Tc-I peak* (*B*).

Size Determination—Figure 3 shows the concentric lamellar structures enclosing aqueous channels of the liposome. The electron micrograph shows two liposomes from the injection preparation made from the first fraction obtained from gel filtration. Subsequent studies of the liposomes contained in the first fraction after the void volume showed the presence of liposomes ranging from 0.1 to 2 μm in diameter. Successive fractions contained small diameter liposomes, which remained in the circulation for extended periods.

Animal Studies—Table I illustrates the organ distribution of liposome from the pooled fractions of a chromatographed liposome preparation. Four animals were used for each time interval. A rapid initial decrease in circulating blood activity was seen within 3 min following the partial clearance of liposomes from the blood. The blood activity did remain somewhat elevated for at least 15 min, apparently because of the presence of small diameter liposomes that were not removed by the liver.

After 30 min, the liver activity decreased with an increase in the urinary bladder (urine) activity. Biodegradation of the liposomes allowed the release of free ^{99m}Tc-I into the circulation, which eventually was excreted in the urine. Hepatic activity decreased slowly, probably because of the biodegradation of liposomes competing with a continuous uptake of liposomes from the circulation. Distribution intervals of 5, 10, and 15 min provided optimum liver uptake of the formed liposomes and were used for successive animal studies.

The use of liposomes from the first fraction after the void volume as the injection suspension resulted in maximum uptake by the liver (Table II). The study was initially completed using three animals per time interval and then repeated in identical fashion. The ability of gel filtration to fractionate the prepared liposomes according to their size is evident when comparing these results with those of Table I. By using an injection suspension composed of the larger liposome structures, the blood activity was significantly reduced. In addition, preferential uptake by the liver

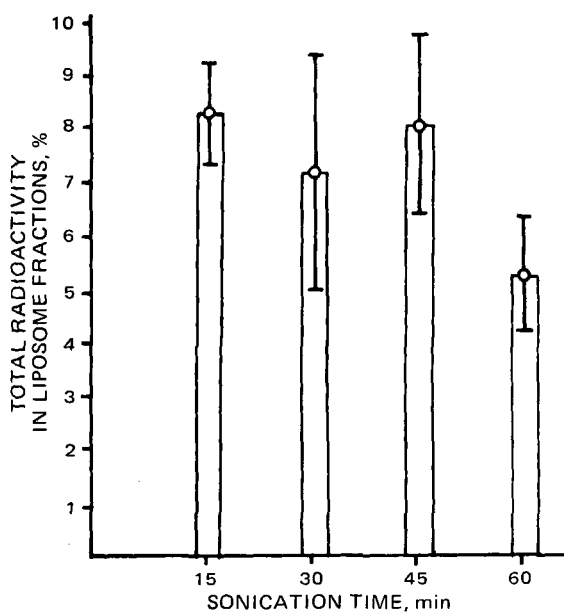

Figure 2—*Effect of sonication time on the entrapment of ^{99m}Tc-I into positively charged liposomes* (*mean* ± SD).

Figure 3—*Electron micrograph of liposomes (80,000×).*

occurred, providing 93.4% of the total dose in the liver at the maximum uptake level. In this particular situation, this localization of the liposomes yielded an organ to background ratio of uptake suitable for imaging.

DISCUSSION

The preparation of a liposome suspension that provided maximum localization in the organ of interest depended primarily upon the use of liposome structures of suitable particle size. Liposomes were distributed to other tissue sites when the particle size of the injection material was not restricted. An injection preparation of the desired particle-size range was prepared by the use of controlled sonication times and gel filtration column chromatography to separate the different particle-size ranges. Column chromatography also provided the means for determining the degree of entrapment of the labeled chelate in the liposomes. Fractionation of the resultant liposome particles provided an injection preparation that yielded a maximum uptake in the liver of over 93% of the total dose.

The ability of this radiopharmaceutical to provide hepatic blood flow data, γ-camera images of the liver, and liver function data appears promising. The fast blood clearance along with target organ accumulation of the activity would decrease the background activity around the liver, producing quality images.

An important advantage of this radiopharmaceutical over those currently used for liver imaging is its biodegradation property. The breakdown *in vivo* of the liposome preparation is quite rapid, with over 50% of the total dose appearing in the urine after 60 min. The first important result of this breakdown is a shorter biological half-life than that of technetium Tc 99m–sulfur colloid, which has an effective half-life dependent on the physical half-life of technetium Tc 99m. In addition to the reduced radiation dose to the patient, additional diagnostic procedures, if necessary, may be performed sooner when liposomes are used for liver studies.

Furthermore, the ability of liposomes to provide information on liver function may lead to additional use of this preparation. After localization in the liver, it appears the liver enzymes disrupt the liposomal membranes, allowing the entrapped aqueous material to be released. By monitoring the amount of radioactivity remaining in the liver with time, an indication of the functioning capacity of the liver may be obtained.

Investigations concerning improvement of the entrapment yield along with the production of a liposome product with an increased radioactive concentration are being planned. In addition, decreasing the labeling procedure time, which could lead to the development of a kit preparation suitable for human use, is being studied.

REFERENCES

(1) A. D. Bangham, M. M. Standish, and J. C. Watkins, *J. Mol. Biol.*, **13**, 238 (1965).

(2) G. Gregoriadis, *FEBS Lett.*, **36**, 292 (1973).

(3) A. D. Bangham, *Prog. Biophys. Mol. Biol.*, **18**, 29 (1968).

(4) G. Gregoriadis, P. D. Leathwood, and B. E. Ryman, *FEBS Lett.*, **14**, 95 (1971).

(5) G. Sessa and G. Weissman, *J. Biol. Chem.*, **245**, 3295 (1970).

(6) D. Papahadjopoulos, G. Poste, and E. Mayhew, *Biochim. Biophys. Acta*, **363**, 404 (1974).

(7) D. Papahadjopoulos, G. Poste, W. J. Vail, and J. L. Biedler, *Cancer Res.*, **36**, 2988 (1976).

(8) G. Gregoriadis, C. D. V. Black, and A. W. Segal, *Clin. Sci. Mol. Med.*, **49**, 99 (1975).

(9) G. Gregoriadis, D. Putnam, L. Louis, and D. Neerunjun, *Biochem. J.*, **140**, 323 (1974).

(10) G. Gregoriadis and B. E. Ryman, *ibid.*, **129**, 123 (1972).

(11) S. X. Straub, R. F. Garry, and W. E. Magee, *Infect. Immun.*, **10**, 783 (1974).

(12) M. K. Jain, *Curr. Top. Membr. Transp.*, **6**, 1 (1971).

(13) D. Papahadjopoulos and N. Miller, *Biochim. Biophys. Acta*, **135**, 624 (1967).

(14) J. H. Kaplan, *ibid.*, **290**, 399 (1972).

(15) U. E. Rahman and B. J. Wright, *J. Cell. Biol.*, **59**, 276a (1973).

(16) G. Gregoriadis and D. E. Neerunjun, *Eur. J. Biochem.*, **47**, 179 (1974).

(17) R. L. Juliano and D. Stamp, *Biochem. Biophys. Res. Comm.*, **63**, 651 (1975).

(18) A. W. Segal, E. J. Wills, J. E. Richmond, G. Slavin, C. D. V. Black, and G. Gregoriadis, *Br. J. Exp. Pathol.*, **55**, 320 (1974).

(19) I. R. McDougall, J. K. Dunnick, M. L. Goris, and J. P. Kriss, *J. Nucl. Med.*, **16**, 488 (1975).

(20) I. R. McDougall, J. K. Dunnick, M. G. McNamee, and J. P. Kriss, *Proc. Natl. Acad. Sci. USA*, **71**, 3487 (1974).

(21) J. K. Dunnick, I. R. McDougall, S. Aragon, M. L. Goris, and J. P. Kriss, *J. Nucl. Med.*, **16**, 483 (1975).

(22) G. Gregoriadis, E. J. Wills, C. P. Swain, and A. S. Tavill, *Lancet*, **1**, 1313 (1974).

(23) V. J. Caride, W. Taylor, J. A. Cramer, and A. Gottschalk, *J. Nucl. Med.*, **17**, 1067 (1976).

(24) W. Eckelman and P. Richards, *ibid.*, **11**, 761 (1970).

Cobaltous Chloride-Induced Hypothermia in Mice I: Effect of Pretreatment with Anticholinergic Drugs

DAVID H. BURKE

Received September 1, 1977, from the *Division of Pharmacology, School of Dentistry, Marquette University, Milwaukee, WI 53233.*
Accepted for publication September 26, 1977.

Abstract □ The hypothermic response following intraperitoneal doses (6.25, 12.5, and 25 mg/kg) of cobaltous chloride was investigated in Swiss albino mice. The magnitude and duration of rectal temperature depression were dose related. In each case, maximal hypothermia was evident within 30 min after injection. Body temperature depression was noted 30 min after oral, subcutaneous, intraperitoneal, intravenous, and intracerebral administration of cobaltous chloride. Cobalt was most active when administered intracerebrally, suggesting a central component to the thermolytic response. Rectal temperature depression following cobaltous chloride was dependent on the ambient temperature. The time course of the effect of cobaltous chloride on rectal and cutaneous tail temperature was noted. Cutaneous tail temperature depression occurred throughout the rectal temperature response, suggesting that cobalt may decrease heat production. Pretreatment with atropine sulfate, hexamethonium bromide, or nicotine failed to modify the temperature response to cobalt. Chlorpromazine hydrochloride pretreatment resulted in a partial antagonism of cobalt-induced hypothermia, presumably through a mechanism other than cholinergic blockade.

Keyphrases □ Cobaltous chloride—mechanism of hypothermic response in mice, effect of pretreatment with anticholinergics □ Hypothermia—induced by cobaltous chloride in mice, mechanism, effect of pretreatment with anticholinergics □ Anticholinergics—effect of pretreatment on hypothermic response to cobaltous chloride in mice

The complex system that maintains body temperature within narrow limits in homiotherms is highly susceptible to insult by drugs and chemicals. For example, the general anesthetics and peripheral vasodilators cause hypothermia through a nonspecific depression of the central nervous system (CNS) (1). Nitroprusside produces hypothermia indirectly through the influence of released cyanide on cellular respiration (2). Oxotremorine causes hypothermia through a central cholinergic mechanism (3, 4).

Pilot studies in this laboratory revealed that cobaltous chloride produces a pronounced fall in the body temperature of mice. This study investigated the temperature response to cobaltous chloride in mice. It was anticipated that the findings would provide insight into the mechanism by which this agent produces body temperature depression.

EXPERIMENTAL

Male Swiss albino mice, 20–25 g, were housed in groups of 20 with *ad libitum* access to laboratory food[1] and water for several days prior to the study. For 24 hr prior to and including the experiment time, the mice were kept in a draft-free room at a constant temperature.

Drug solutions were freshly prepared with distilled water in concentrations (calculated as the salt) such that a volume of 0.01 ml/g was delivered. Intracerebral injections, however, were administered in a fixed volume of 0.01 ml/mouse.

A thermistor thermometer[2] was used for obtaining rectal and cutaneous temperatures. Rectal temperatures were recorded with a thermistor probe inserted to a distance of 2.5 cm and held in position until constant readings were attained. Cutaneous temperatures were obtained by placement of a disk probe on the base of the tail. A small amount of electrode paste was applied to the surface of the disk probe.

Intracerebral injections were accomplished according to the method of Haley and McCormick (5). Cobaltous chloride or water (warmed to 38°) was administered at a point lateral to the midline joining the anterior bases of the ears. A 22-gauge needle attached to a microliter syringe[3] was inserted through the skull to a depth of 3 mm. The prior injection of several animals with a solution of methylene blue (0.5%) resulted in dye localization in the third and fourth ventricles.

At the start of each day's testing, the mice were placed singly in circular wire-mesh cages and individual weights were obtained with a triple-beam balance[4]. Immediately following weight determination, initial temperatures were recorded and treatment administration was accomplished. Temperatures were recorded again at various intervals. Unless otherwise stated, all treatments were given intraperitoneally. Controls received distilled water (0.01 ml/g). To study the influence of various anticholinergic agents on cobalt-induced hypothermia, pretreatment injections (water, atropine sulfate, chlorpromazine hydrochloride, hexamethonium bromide, or nicotine) were given 30 min prior to recording initial temperatures.

In comparison of mean temperature changes (*i.e.*, the difference between temperature immediately prior to and at the appropriate interval following treatment), statistical significance was determined by use of the Student *t* test. Temperature differences were considered significant at the probability level of 5% or less.

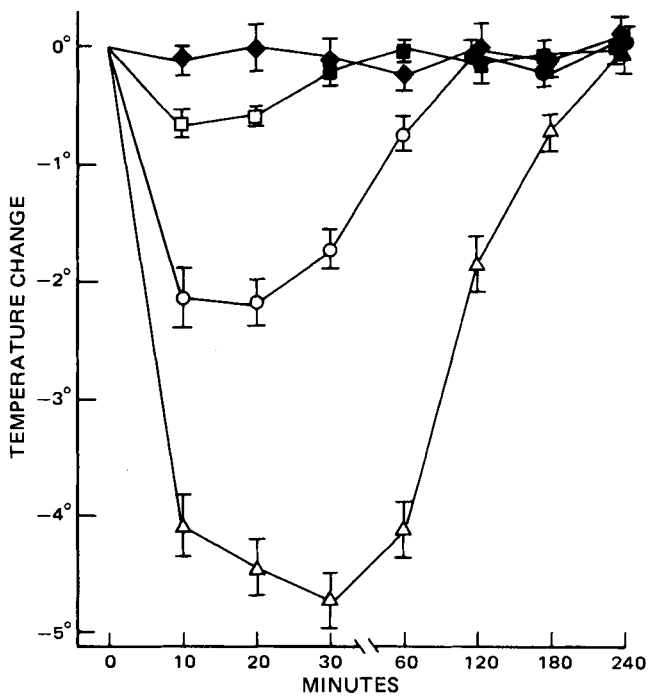

Figure 1—*Time course of the effect of a 0.01-ml/g ip dose of distilled water (◆) and 6.25- (■), 12.5- (●), and 25- (▲) mg/kg ip doses of cobaltous chloride on the rectal temperature in mice. Water and cobaltous chloride were administered at zero time. Open symbols denote significant difference ($p < 0.05$) from water treatment at the corresponding time interval. Each point represents the average of 12 determinations. Vertical bars represent standard errors.*

[1] Wayne Lab, Blox.
[2] Model 46 Tele-thermometer, Yellow Springs Instrument Co., Yellow Springs, Ohio.
[3] Hamilton.
[4] Ohaus.

Table I—Body Temperature Changes 30 min after Cobaltous Chloride Administration by Various Routes in Mice

Route	Water		Cobaltous Chloride (25 mg/kg)	
	Initial Temperature	Temperature Change (Mean ± *SE*)[a]	Initial Temperature	Temperature Change (Mean ± *SE*)[a,b]
Oral	37.94°	−0.03 ± 0.15°	38.06°	−2.18 ± 0.53°
Subcutaneous	37.53°	−0.34 ± 0.25°	37.68°	−2.72 ± 0.41°
Intraperitoneal	37.57°	−0.24 ± 0.16°	37.73°	−3.98 ± 0.17°
Intravenous	37.83°	+0.05 ± 0.19°	37.80°	−3.84 ± 0.29°
Intracerebral	37.93°	−0.68 ± 0.15°	38.03°	−4.38 ± 0.28[c]

[a] Temperature changes represent the difference between body temperature recorded initially and that obtained 30 min following water or cobaltous chloride treatment in groups of 12 mice. [b] Compared to water by the corresponding route, $p < 0.05$. [c] Each animal received 0.01 ml of a 0.25% cobaltous chloride solution.

Table II—Body Temperature Changes 30 min after Intraperitoneal Injection of Cobaltous Chloride to Mice at Various Ambient Temperatures

Ambient Temperature	Water		Cobaltous Chloride (25 mg/kg)	
	Initial Temperature	Temperature Change (Mean ± *SE*)[a]	Initial Temperature	Temperature Change (Mean ± *SE*)[a]
18°	36.49°	+0.25 ± 0.14°	36.32°	−6.33 ± 0.41°[b]
23°	37.33°	−0.04 ± 0.19°	37.93°	−4.11 ± 0.51°[b]
28°	37.68°	−0.21 ± 0.13°	38.07°	−1.07 ± 0.14°[b]
33°	38.47°	+0.16 ± 0.18°	38.93°	+0.28 ± 0.14°

[a] Temperature changes represent the difference between body temperature recorded initially and that obtained 30 min following water or cobaltous chloride treatment in groups of 12 mice. [b] Compared to water at the corresponding ambient temperature, $p < 0.05$.

RESULTS

The effect of cobaltous chloride (6.25, 12.5, and 25 mg/kg ip) on the rectal temperature of mice over 4 hr is shown in Fig. 1. At the dosage level of 6.25 mg/kg, cobalt produced body temperature depression lasting approximately 20 min. The magnitude and duration of the hypothermic response were increased with higher doses. Body temperature often fell by more than 6° within 30 min of injection of cobaltous chloride at the 25-mg/kg level. Hypothermia was always accompanied by depression of locomotor activity. Visible shivering and increased muscle tone were unapparent during and upon recovery from hypothermia.

Cobaltous chloride was administered to groups of 12 mice by several routes, and the effect on body temperature was noted 30 min later (Table I). Significant hypothermia occurred following administration of this agent (25 mg/kg) by the oral (−2.18°), subcutaneous (−2.72°), intraperitoneal (−3.98°), and intravenous (−3.84°) routes. Cobalt was most active when administered intracerebrally; fixed doses (0.01 ml of a 0.25% solution) caused an average temperature drop of 4.38°.

The influence of ambient temperature on the thermal response of mice to cobaltous chloride (25 mg/kg ip) is illustrated in Table II. Animals exposed to environmental temperatures of 18, 23, and 28° had respective drops of 6.33, 4.11, and 1.07°; mice exposed to 33° ambient temperature did not exhibit hypothermia.

Figure 2 depicts the time course of changes in rectal and cutaneous tail temperatures after the administration of cobaltous chloride (25 mg/kg ip). Immediately prior to drug injection, rectal and cutaneous temperatures averaged 37.67 and 25.41°, respectively. The rectal temperature response was similar to that presented in Fig. 1. Cutaneous temperature was depressed throughout the entire rectal temperature response.

The effect of pretreatment with various compounds on the hypothermic response to cobaltous chloride (25 mg/kg ip) is presented in Table III. Atropine (5.0 mg/kg), nicotine (0.25 mg/kg), and hexamethonium (10 mg/kg) were incapable of altering cobalt-induced body temperature depression. The combination of chlorpromazine (1.0 mg/kg) and cobaltous chloride resulted in hypothermia amounting to 2.36°. This value was significantly higher than the 4.33° drop obtained with cobalt in the presence of water.

DISCUSSION

A paucity of information exists concerning the influence of cobalt(II) on the mammalian body temperature. Hypothermia in rats was reported (6) following cobaltous chloride administration, 4 mg/kg. The results of the present investigation showed cobaltous chloride to be a potent hypothermic agent in mice. The intensity of this response was dependent on the dose, route of administration, and ambient temperature.

Evidence has been provided that cobalt elicits hypothermia through an action on the CNS. For example, in doses incapable of causing body temperature depression systemically, the intracerebral administration of this agent produced a marked hypothermic response.

Hypothermia results from either a decrease in heat production or an increase in heat dissipation. Cobaltous chloride appears to lower body temperature by decreasing heat production. For example, throughout the entire rectal temperature response, cutaneous tail temperature was reduced (Fig. 2).

Cobaltous chloride appears to produce a collapse of thermoregulation rather than a shift in the hypothalamic set point. Table II shows that mice exposed to an environmental temperature of 18° produced a mean fall in body temperature of 6.33°, as compared to a 1.07° drop following exposure to an ambient temperature of 28°. Exposure to a high environmental temperature (33°) prevented this hypothermic response. Such observations would not be anticipated if cobalt causes a lowering of the set point.

Tremorine (1,4-dipyrolidino-2-butyne) elicits profound hypothermia in mice (7). The temperature response to tremorine is dependent on the ambient temperature (8). Oxotremorine, the active metabolite of tremorine, produces marked hypothermia in mice through a cholinergic action on the CNS (9). The hypothermic response to oxotremorine in rats

Table III—Effect of Pretreatment with Various Anticholinergic Agents on the Hypothermic Response to Cobaltous Chloride in Mice

Pretreatment	Dose, mg/kg	Treatment[a]			
		Water		Cobaltous Chloride (25 mg/kg)	
		Initial Temperature	Temperature Change (Mean ± *SE*)[b]	Initial Temperature	Temperature Change (Mean ± *SE*)
Water	—	37.30°	+0.15 ± 0.10°	37.70°	−4.33 ± 0.19°
Atropine	5.0	37.26°	−0.13 ± 0.16°	37.68°	−4.01 ± 0.29°
Nicotine	0.25	37.61°	+0.15 ± 0.08°	37.67°	−4.17 ± 0.30°
Chlorpromazine	1.0	36.33°	−0.23 ± 0.10°	36.48°	−2.36 ± 0.22°[d]
Hexamethonium	10.0	37.73°	+0.07 ± 0.15°	37.61°	−4.34 ± 0.20°

[a] Pretreatments (intraperitoneal) were administered 30 min before intraperitoneal water and cobaltous chloride to groups of 12 mice. [b] Temperature changes represent the difference between body temperature recorded initially and that obtained 30 min after treatment. [c] Compared to water–water (pretreatment–treatment), $p < 0.05$. [d] Compared to water–cobaltous chloride (pretreatment–treatment), $p < 0.05$.

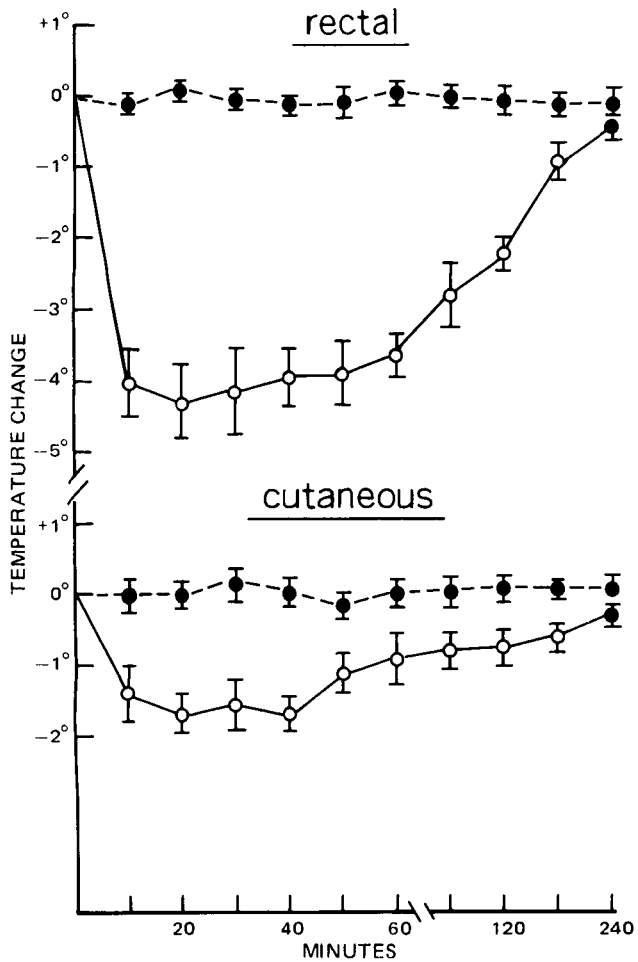

Figure 2—*Time course of the effect of distilled water (0.01 ml/g ip) (●- - -●) and cobaltous chloride (25 mg/kg ip) (●—●) on rectal and cutaneous tail temperature in mice. Water and cobaltous chloride were administered at zero time. Open symbols denote significant difference ($p < 0.05$) from water treatment at the corresponding time interval. Each point represents the average of 12 determinations. Vertical bars represent standard errors.*

was attributed to decreased heat production (10). Although not causing peripheral symptoms such as tremor, salivation, miosis, and diarrhea, cobaltous chloride exhibited similar thermoregulatory characteristics to those of oxotremorine, namely a central decrease in heat production that is dependent on the ambient temperature. On the basis of these similarities, it is possible that cobalt produces hypothermia through a central cholinergic mechanism.

Oxotremorine-induced hypothermia can be prevented in rodents by treatment with atropine (9, 11, 12). Pretreatment with atropine in the present study did not alter cobalt-induced hypothermia. Thus, it appears unlikely that cobalt produces body temperature depression through an action on central or peripheral muscarinic receptors. Likewise, the failure of nicotine and hexamethonium to prevent hypothermia precludes an influence of cobalt on central or peripheral nicotinic receptors.

Chlorpromazine was shown to partially antagonize oxotremorine-induced hypothermia in mice; this antagonism was attributed to a weak anticholinergic effect of the phenothiazine (12). Similarly, the present results showed a partial blockade of cobalt-induced hypothermia by chlorpromazine (Table III). It seems doubtful, however, that this antagonism was mediated through a central cholinolytic action, since atropine, as well as nicotine, was incapable of producing a similar blockade.

Local anesthetic and noncompetitive α-adrenergic blocking activities have been demonstrated for chlorpromazine (13). It is possible that one or both of these actions may be involved in the prevention of cobalt-induced hypothermia in mice.

REFERENCES

(1) P. Lomax and G. V. Knox, in "The Pharmacology of Thermoregulation," E. Schönbaum and P. Lomax, Eds., Karger, New York, N.Y., 1973, p. 147.

(2) D. H. Burke, *Toxicol. Appl. Pharmacol.*, in press.

(3) P. Spencer, *Life Sci.*, **5**, 1015 (1966).

(4) W. E. Kirkpatrick, *Proc. West. Pharmacol. Soc.*, **10**, 51 (1967).

(5) T. Haley and W. McCormick, *Br. J. Pharmacol.*, **12**, 12 (1957).

(6) W. Janaskovic and J. Davidovic, *Vojnosanit. Pregl.*, **14**, 530 (1957).

(7) G. M. Everett, L. E. Blockus, and I. M. Shepperd, *Science*, **124**, 79 (1956).

(8) L. E. Blockus and G. M. Everett, *Fed. Proc.*, **16**, 1209 (1957).

(9) P. S. J. Spencer, *Br. J. Pharmacol.*, **25**, 442 (1965).

(10) P. Lomax and D. J. Jenden, *Int. J. Neuropharmacol.*, **5**, 353 (1966).

(11) W. E. Kirkpatrick and P. Lomax, *Life Sci.*, **6**, 2273 (1967).

(12) D. H. Burke and D. E. Mann, Jr., *J. Pharm. Sci.*, **59**, 1814 (1970).

(13) P. Lomax and W. E. Kirkpatrick, "The Phenothiazines and Structurally Related Drugs," Raven, New York, N.Y., 1974, pp. 719–729.

ACKNOWLEDGMENTS

Presented at the Pharmacology and Toxicology Section, APhA Academy of Pharmaceutical Sciences, Phoenix meeting, November 1977.

Supported in part by a grant from the Marquette University Committee on Research.

The author is indebted to Julie Baron and Bobbi Stewart for assistance and to J. C. Brooks and G. P. O'Hara for helpful suggestions.

Quantitative GLC Determination of *cis*- and *trans*-Isomers of Doxepin and Desmethyldoxepin

M. T. ROSSEEL *x, **M. G. BOGAERT** *, and **M. CLAEYS** ‡

Received July 5, 1977, from the *J. F. & C. Heymans Institute of Pharmacology, University of Ghent, De Pintelaan 135, B-9000 Ghent, Belgium, and the ‡Laboratory for Mass Spectrometry, Department of Organic Chemistry, University of Ghent, Krijgslaan 271 (S4), B-9000 Ghent, Belgium, "Aangesteld Navorser" of the Belgian Nationaal Fonds voor Wetenschappelijk Onderzoek (N.F.W.O.). Accepted for publication September 28, 1977.

Abstract □ A GLC method for the simultaneous quantitative determination of the *cis*- and *trans*-isomers of doxepin and desmethyldoxepin in human plasma was developed. The method involves the use of a capillary column for efficient separation of the four compounds and the internal standards, amitriptyline and nortriptyline. A high sensitivity is obtained with a nitrogen detector, enabling quantitation of the compounds in plasma of humans treated chronically with doxepin. Confirmation of the identity of the *cis*- and *trans*-isomers of doxepin and desmethyldoxepin in biological samples was carried out by selected ion monitoring.

Keyphrases □ Doxepin, *cis* and *trans*—simultaneous GLC analyses in human plasma □ Desmethyldoxepin, *cis* and *trans*—simultaneous GLC analyses in human plasma □ GLC—simultaneous analyses, *cis*- and *trans*-doxepin and desmethyldoxepin in human plasma □ Antidepressants—*cis*- and *trans*-doxepin, simultaneous GLC analyses in human plasma

Doxepin, 11-(3-dimethylaminopropylidene)-6*H*-dibenz[*b*,*e*]oxepin, is structurally related to imipramine and amitriptyline. A 15:85% mixture of the *cis*- and *trans*-isomers of doxepin is used as an antidepressant agent.

The determination of the plasma levels of a drug such as doxepin would help optimize therapy, but only limited data are available (1). The problem is complicated by the fact that the *N*-demethylated metabolite, desmethyldoxepin, has pharmacological activity. Furthermore, for the metabolite and the unchanged product, *in vivo* conversion of the *cis*-isomer into the less active *trans*-isomer has been suggested (1).

Several GLC methods (2–4) and a GLC selected ion monitoring method (5) for simultaneous measurement of doxepin and desmethyldoxepin were published, but none permits differentiation between the isomeric forms for both products.

The present paper describes a method for the separate determination of nanogram amounts of the *cis*- and *trans*-isomers of both doxepin and desmethyldoxepin in plasma, using capillary GLC with nitrogen detection; in some instances, a packed column was used. The identity of the peaks on the chromatograms was confirmed by chemical-ionization mass spectrometry.

EXPERIMENTAL

Materials—Doxepin hydrochloride (specified as 83.2% *trans* and 16.8% *cis*) and desmethyldoxepin hydrochloride (no specifications) were available as powders[1]. By using capillary GLC and assuming equal detector responses for the *cis*- and *trans*-isomers, values of 82% *trans* and 18% *cis* were found for doxepin and values of 96.7% *trans* and 3.3% *cis* were calculated for desmethyldoxepin; these ratios were used for quantitation. The internal standards, amitriptyline[2] and nortriptyline[3], were purchased as 1% solutions. The derivatizing reagent was trifluoroacetic anhydride[4]. All other solvents and reagents were analytical grade.

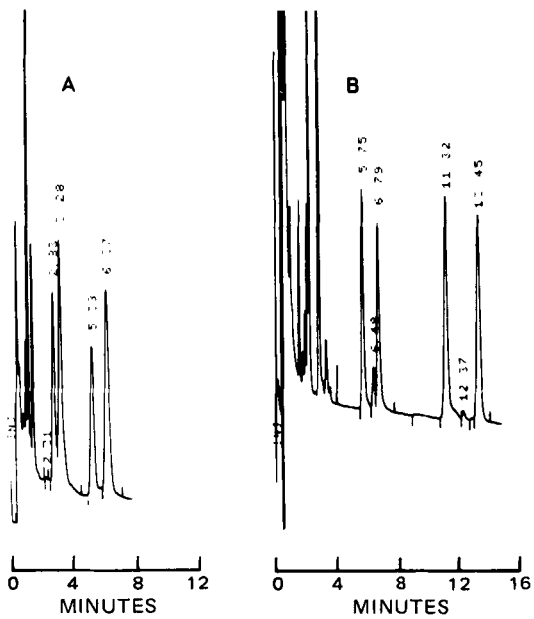

Figure 1—*Gas chromatograms of 1 ml of extracted human plasma. Retention time, R_t, data and the amounts of the drugs added to 1 ml of plasma are given. A (packed column): R_t 2.83, amitriptyline (100 ng); R_t 3.28, cis-doxepin (27 ng) and trans-doxepin (123 ng); R_t 5.38, N-trifluoroacetylnortriptyline (100 ng); and R_t 6.37, trans-(N-trifluoroacetyl)desmethyldoxepin (145 ng). B (capillary column): R_t 5.75, amitriptyline (100 ng); R_t 6.48, cis-doxepin (18 ng); R_t 6.79, trans-doxepin (82 ng); R_t 11.32, N-trifluoroacetylnortriptyline (100 ng); R_t 12.37, cis-(N-trifluoroacetyl)desmethyldoxepin (3.3 ng); and R_t 13.45, trans-(N-trifluoroacetyl)desmethyldoxepin (96.7 ng).*

Glassware—All glassware was silanized by soaking for 1 hr in a 5% solution of trimethylchlorosilane in benzene, rinsed with benzene and methanol, dried for 1 hr at 100°, and rinsed with ethyl acetate immediately before use.

Instrumental Conditions—A gas chromatograph[5], equipped with a dual nitrogen–phosphorus flame-ionization detector, was used. GLC was performed on a 20-m × 0.5-mm i.d. glass capillary column[6], coated with OV-17, with a hydrogen flow of 4 ml/min or on a 1.80-m × 2-mm i.d. glass column containing 3% OV-17[7] on 80–100-mesh Gas Chrom Q[8] with a helium flow of 30 ml/min. Temperatures were: injector, 300°; column, 230°; and detector, 300°. For capillary GLC, direct on-column injection of 0.2-μl samples without stream splitting was used. Detector conditions were set on the highest response. The peak areas were recorded on a recording integrator[9].

A chemical-ionization gas chromatograph–mass spectrometer[10], equipped with an all-glass chromatographic inlet system and interfaced

[1] Pfizer.
[2] Tryptizol, Merck Sharp & Dohme.
[3] Nortrilen, Lundbeck.
[4] Pierce Chemical Co.
[5] Hewlett-Packard 5730 A series.
[6] RSL (Research Specialties for Laboratories), Belgium.
[7] Applied Science Laboratories.
[8] Supelco.
[9] Hewlett-Packard 3380 A.
[10] Finnigan 3200.

Table I—Abundances for Ions in the Methane Chemical-Ionization Spectra of Doxepin, Amitriptyline, and the *N*-Trifluoroacetyl Derivatives of Desmethyldoxepin and Nortriptyline [a]

Compound	*m/e* (Relative Intensities)
cis-Doxepin	235 (6.9), 278 (30.4), 279 (5.2), 280 (100), 281 (28.4), 282 (2.8), 308 (16.1), 309 (6.3), 320 (2.9)
trans-Doxepin	235 (2.0), 278 (13.3), 279 (3.1), 280 (100), 281 (21.9), 308 (13.6), 309 (3.7), 320 (2.5)
Amitriptyline	91 (5.4), 233 (3.2), 276 (47.4), 277 (13.1), 278 (100), 279 (22.0), 280 (3.3), 306 (18.2), 307 (4.3), 318 (2.5)
cis-(*N*-Trifluoroacetyl)-desmethyldoxepin	107 (12.3), 135 (2.3), 140 (4.3), 168 (10.5), 195 (2.3), 234 (9.6), 235 (100), 236 (11.7), 263 (15.5), 264 (2.0), 268 (12.6), 269 (2.0), 275 (4.5), 342 (5.4), 361 (2.4), 362 (68.2), 363 (12.9), 390 (9.6), 402 (2.8)
trans-(*N*-Trifluoroacetyl)-desmethyldoxepin	91 (2.1), 107 (18.2), 128 (5.2), 135 (2.9), 140 (6.5), 154 (2.4), 168 (31.9), 195 (3.0), 213 (3.0), 221 (3.8), 234 (17.6), 235 (100), 236 (12.7), 237 (2.5), 263 (13.0), 264 (3.0), 268 (15.2), 269 (2.9), 275 (2.7), 342 (7.9), 360 (2.7), 361 (5.2), 362 (78.1), 363 (16.2), 390 (13.6), 391 (2.2), 402 (5.2)
N-Trifluoroacetyl-nortriptyline	130 (2.0), 211 (9.2), 212 (2.0), 231 (4.1), 232 (20.1), 233 (47.8), 234 (8.8), 261 (10.5), 262 (2.0), 273 (2.0), 359 (7.2), 360 (100), 361 (23.5), 362 (2.6), 388 (14.2), 389 (3.7), 400 (3.9), 401 (2.0)

[a] Due to the high abundance of reagent gas ions in the low mass region, the abundances, expressed as relative intensities, are presented only for ions above *m/e* 70; relative intensity values are only given for ions with a relative intensity ≥2%.

with a data system[11], was used[12]. GLC was carried out on a 50-m × 0.5-mm i.d. glass capillary column, coated with SE-30, with a helium flow of 10 ml/min; for the working conditions used, this flow gave the best results. Temperatures were: injector, 250°; column, 235°; and interface, 250°. The reagent gas, methane, was added as makeup gas until the source pressure reached 1 torr. The mass spectrometric conditions were: electron energy, 150 ev; emission current, 0.5 mamp; continuous dynode electron multiplier voltage, 2.2 kv; and preamp range, 10^{-8} amp/v for analysis of plasma samples and 10^{-7} amp/v for recording of reference spectra.

Extraction and Derivatization—A 100-μl aliquot of an internal standard solution containing 100 ng of amitriptyline and 100 ng of nortriptyline, 50 μl of 0.0005 *M* triethylamine, and 0.1 ml of 5 *N* NaOH were added to 1 ml of plasma in a 10-ml glass-stoppered centrifuge tube. The mixture was extracted with 4 ml of *n*-hexane by shaking for 20 min horizontally. After centrifugation for 10 min at 6000 rpm, the organic phase was transferred with a Pasteur pipet to a 6-ml glass-stoppered conical tube, and the organic phase was removed under a gentle stream of nitrogen at room temperature until about 100 μl was left.

Another 4 ml of *n*-hexane was added to the aqueous phase, which was shaken and centrifuged as before. This 4 ml was then transferred to the same conical tube, and the solvent was removed under nitrogen. Before evaporation was complete, the conical tube wall was washed down with 300 μl of *n*-hexane, and the hexane was evaporated to about 200 μl; 40 μl of trifluoroacetic anhydride was added.

After the tube was stoppered, the mixture was left to react for 10 min at 50°. The sample was taken to dryness under nitrogen. The residue was stored at −18° and used within 6 hr. For GLC analysis, the residues were dissolved in 10 μl of ethyl acetate; aliquots of 0.2 μl were injected on the capillary column, whereas aliquots of 2 μl were used on the packed column.

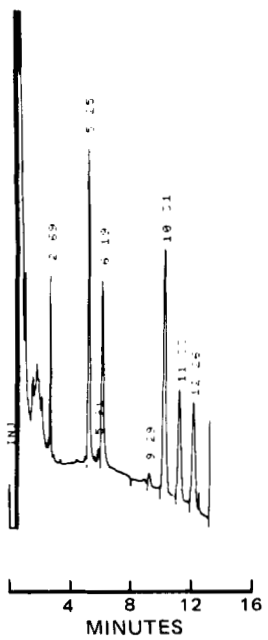

Figure 2—*Gas chromatogram of extracted human plasma. Aliquots of 100 ng of amitriptyline (R_t 5.25) and 100 ng of nortriptyline (R_t 10.31) were added to 1 ml of plasma of Subject WM receiving a daily dose of 200 mg of doxepin. Key:* R_t *5.91,* cis-*doxepin;* R_t *6.19,* trans-*doxepin;* R_t *11.33,* cis-*(N - trifluoroacetyl)desmethyldoxepin; and* R_t *12.26,* trans-*(N-trifluoroacetyl)desmethyldoxepin.*

Quantitation—Standard solutions (0.01%) of doxepin and desmethyldoxepin were prepared. From these solutions, 1:100 dilutions were made before use. Standards for the calibration curve were prepared by adding 10–200 ng of the doxepin isomeric mixture and 10–200 ng of the desmethyldoxepin isomeric mixture to drug-free 1-ml plasma samples and by carrying these samples through the extraction and derivatization procedures, including the addition of 100 ng of the internal standards. Amitriptyline and nortriptyline were selected as internal standards for doxepin and desmethyldoxepin, respectively, because of their close structural relationship.

Quantitation was based on GLC peak area ratios of the compounds *versus* their respective internal standards. Area ratios for the standard mixtures were plotted against the concentration of the product under study, and an unweighted least-squares linear regression analysis was performed. Unknown drug concentrations were estimated from the calibration curve.

Human Samples—Blood samples were taken from two female patients, 38 (WM) and 65 (SM) years old, taking 75 and 200 mg of doxepin/day, respectively, for 2 weeks. The last dose was administered at 8 pm; blood was drawn at 8 am. Plasma was obtained by centrifugation and was stored frozen (−20°) until analyzed.

RESULTS AND DISCUSSION

While doxepin and its internal standard amitriptyline gave rise to symmetrically shaped peaks, the more polar secondary amines, desmethyldoxepin and its internal standard nortriptyline, tailed when analyzed as such. To improve peak shape, volatile *N*-trifluoroacetyl derivatives were formed using trifluoroacetic anhydride. The identity of the GLC peaks was checked by chemical-ionization mass spectrometry. The abundances for ions in the methane chemical-ionization spectra of doxepin, amitriptyline, and the *N*-trifluoroacetyl derivatives of desmethyldoxepin and nortriptyline are summarized in Table I.

The methane chemical-ionization spectra of the tertiary amines I and III were characterized by an intense protonated molecular ion (MH^+). The spectra of the *N*-trifluoroacetyl derivatives of the secondary amines

Table II—Accuracy, Reproducibility, and Recovery of the Procedure for Extraction and GLC Determination on a Capillary Column of Doxepin (*cis*- and *trans*-Isomers) and Desmethyldoxepin Added to 1 ml of Blank Plasma [a]

Compound	Quantity Added to 1 ml of Plasma, ng	Mean Assay Results, % (± *RSD*)	Mean Recovery[b], % (± *RSD*)
Doxepin			
trans	41.0	97.8 (±7.1)	88.1 (±7.1)
cis	9.0	107.8 (±6.8)	93.6 (±8.2)
trans	82.0	99.3 (±3.8)	96.0 (±6.1)
cis	18.0	109.4 (±7.6)	97.5 (±7.9)
Desmethyldoxepin			
trans	48.3	96.7 (±2.9)	88.1 (±4.9)
trans	96.7	100.1 (±3.8)	82.0 (±3.8)
cis	3.3	106.1 (±6.1)	84.9 (±7.8)

[a] All determinations were done five times. [b] Recovery was calculated by comparing the area ratios obtained by adding the substances before and after extraction, while the internal standard was always added before extraction.

[11] Finnigan 6000.

[12] All selected ion monitoring was performed by using this data system and the revision H software.

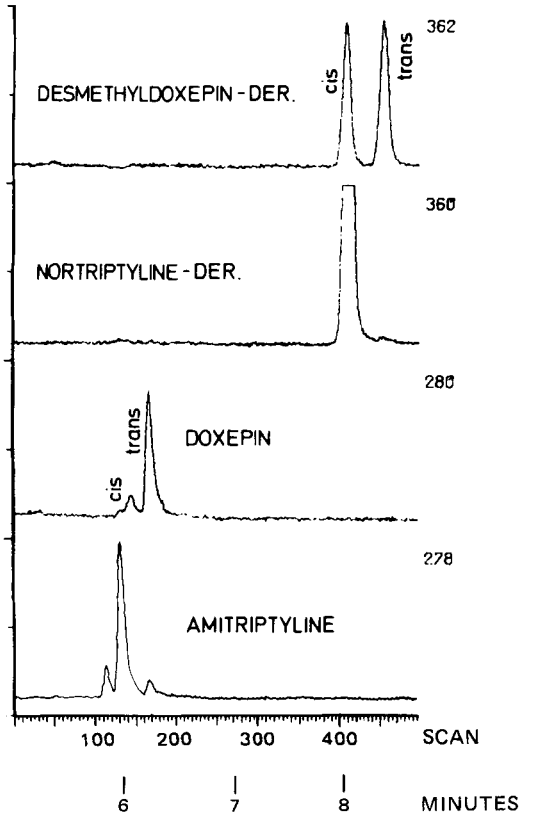

Figure 3—*Selected ion monitoring analysis of a plasma extract in which the [MH]$^+$ ions of doxepin, amitriptyline, and* N*-trifluoroacetyl derivatives of desmethyldoxepin and nortriptyline were monitored. The amitriptyline signal on the* m/e *278 trace is plotted as the 100% peak.*

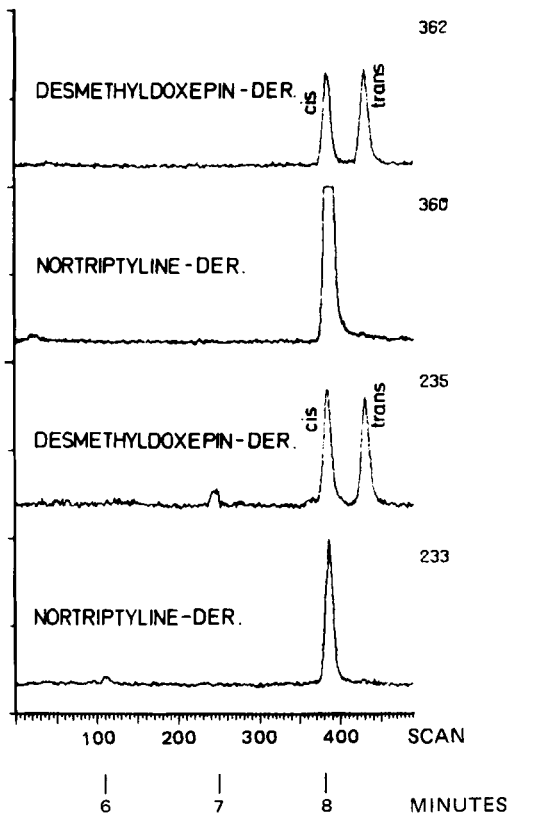

Figure 4—*Selected ion monitoring analysis of a plasma extract in which the [MH]$^+$ ion and [MH−$CF_3CONHCH_3$]$^+$ fragment ion of the* N*-trifluoroacetyl derivatives of desmethyldoxepin and nortriptyline were monitored. The* N*-trifluoroacetylnortriptyline signal on the* m/e *233 trace is plotted as the 100% peak.*

II and IV showed two prominent ions, the MH^+ ion and a fragment ion, corresponding with loss of a $CF_3CONHCH_3$ moiety from the side chain. These ions were selected for confirming the identity of the GLC peaks obtained for the tricyclic drugs in biological samples.

Representative gas chromatograms of extracted human plasma samples spiked with doxepin and desmethyldoxepin are shown in Fig. 1 for the capillary column; for comparison, the results on a packed column are also shown. The use of a short capillary column had the advantage of improved resolution (the peaks of *cis*- and *trans*-doxepin overlapped on the packed column), resulting in higher specificity. The capillary column also had the advantage that an interfering peak of unknown origin, occurring in some plasma samples, was separated from the doxepin peak whereas it completely coeluted on the packed column.

The use of a capillary column also resulted in greater absolute sensitivity compared to a packed column, but it had the disadvantage of decreased sample loading capacity (0.2 μl instead of 2 μl on the packed column). Therefore, the overall sensitivity was similar for both columns (2 ng/ml of plasma for doxepin and 1 ng/ml for desmethyldoxepin). The accuracy and reproducibility of the assay for doxepin and desmethyldoxepin, as well as the extraction recovery, are given in Table II. Calibration curves were made on 4 separate days over 2 weeks. The least-squares linear regression analysis of the calibration curve for *trans*-doxepin gave a slope of 0.0114 ± 0.0021 and a y-intercept of 0.0155 ± 0.0132 (r 0.995–0.998). The curve for *trans*-desmethyldoxepin had a slope 0.0099 ± 0.0006 and a y-intercept of −0.0300 ± 0.0064 (r 0.994–0.999). With each set of unknown samples, a four-point standard curve was made. The calibration curves for the *trans*-isomers were also used for estimation of the corresponding *cis*-isomers, extracted in a similar way as the *trans*-isomers, and can be expected to yield equal detector responses.

An example of a typical GLC analysis of a plasma sample from a patient receiving doxepin chronically is given in Fig. 2. Both doxepin and desmethyldoxepin were present in the two isomeric forms.

The identity of the GLC peaks was confirmed by selected ion monitoring of specific ions, formed upon chemical ionization with methane as a reagent gas. Figure 3 shows a representative analysis, in which the protonated molecular ions, $[MH]^+$, of doxepin, amitriptyline, N-triflu-

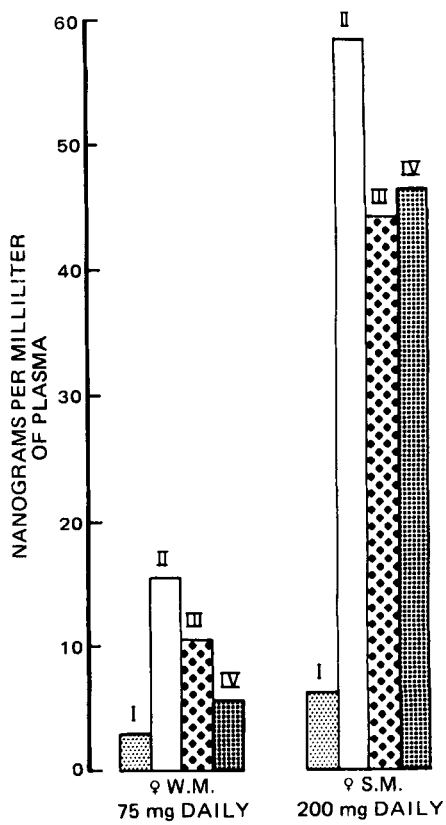

Figure 5—*Plasma levels of* cis*-doxepin (I),* trans*-doxepin (II),* cis*-desmethyldoxepin (III), and* trans*-desmethyldoxepin (IV) in two patients receiving doxepin for 2 weeks.*

oroacetyldesmethyldoxepin, and *N*-trifluoroacetylnortriptyline at *m/e* 280, 278, 362, and 360, respectively, were monitored.

Figure 4 shows the analysis in which the $[MH]^+$ ion and the $[MH - CF_3CONHCH_3]^+$ fragment ion of *N*-trifluoroacetyldesmethyldoxepin and *N*-trifluoroacetylnortriptyline at *m/e* 362, 360, 235, and 233 were monitored. The ratios of the $[MH]^+$ and $[MH - CF_3CONHCH_3]^+$ selected ion traces obtained from the analysis of a biological sample (Fig. 4) were 0.82 and 0.87 for the *N*-trifluoroacetyl derivatives of *cis*- and *trans*-desmethyldoxepin, respectively. These values are in close agreement with the theoretical values of 0.68 and 0.78 obtained from the mass spectra, which were recorded under the same experimental conditions (Table I), confirming as such the presence of the *N*-trifluoroacetyl derivatives of *cis*- and *trans*-desmethyldoxepin. Since *N*-trifluoroacetylnortriptyline overlapped with *cis*-(*N*-trifluoroacetyl)desmethyldoxepin on the SE-30 capillary column used in the selected ion monitoring experiments, the ^{13}C-isotope contributions of the nortriptyline signals were taken into account for calculating the true ratio of the $[MH]^+$ and $[MH - CF_3CONHCH_3]^+$ signals of *cis*-(*N*-trifluoroacetyl)desmethyldoxepin.

Preliminary results of the plasma levels obtained in two patients receiving chronic doxepin therapy are given in Fig. 5. The *trans*-isomer of doxepin was more prominent than its *cis*-form. For desmethyldoxepin, however, a considerable fraction occurred as the *cis*-form, although the product given to the patients contained only approximately 15% *cis*- *versus* 85% *trans*-isomer.

More patients are now being studied to evaluate if the levels of *cis*- and *trans*-doxepin and desmethyldoxepin can be correlated with clinical outcome.

REFERENCES

(1) R. M. Pinder, R. N. Brogden, T. M. Speight, and G. S. Avery, *Drugs*, **13**, 161 (1977).

(2) D. C. Hobbs, *Biochem. Pharmacol.*, **18**, 1941 (1969).

(3) J. E. O'Brien and O. N. Hinsvark, *J. Pharm. Sci.*, **65**, 1068 (1976).

(4) S. F. Reite, *Med. Norsk. Farm. Selskap.*, **37**, 141 (1975).

(5) A. Frigerio, C. Pantarotto, R. Franco, R. Gomeni, and P. L. Morselli, *J. Chromatogr.*, **130**, 354 (1977).

ACKNOWLEDGMENTS

The authors thank Dr. J. Gordts (Pfizer) for supplying doxepin and desmethyldoxepin and Dr. R. Deberdt and Dr. E. Suy for allowing them to study their patients.

Simple, Rapid, and Micro High-Pressure Liquid Chromatographic Determination of Plasma Griseofulvin Levels

ROGER L. NATION, GEOFFREY W. PENG, VICKY SMITH, and WIN L. CHIOU ˣ

Received July 25, 1977, from the *Clinical Pharmacokinetics Laboratory and the Department of Pharmacy, College of Pharmacy, University of Illinois at the Medical Center, Chicago, IL 60612.* Accepted for publication September 29, 1977.

Abstract □ A rapid high-pressure liquid chromatographic assay is described for the quantitative determination of griseofulvin in plasma. An aliquot (25–100 μl) of plasma was deproteinized by a simple procedure involving the addition of 2.5 volumes of acetonitrile, vortex mixing for a few seconds, and centrifugation for 1 min. The clear supernate, 50 μl, was injected into the high-pressure liquid chromatograph. A reversed-phase column was used with a mobile phase of distilled water–acetonitrile (1:1) at a flow rate of 2 ml/min and was operated at ambient temperature. A fluorescent detector with an excitation wavelength of 260 nm was employed to monitor the column effluent. Griseofulvin had a retention time of 3.8 min. This procedure yields reproducible results with high sensitivity; plasma concentrations as low as 50 ng/ml can be measured. Several commonly used drugs do not interfere. Analysis of plasma samples collected from a rabbit injected with griseofulvin indicated that the procedure is suitable for pharmacokinetic studies and clinical monitoring of plasma concentrations in patients. Assay turnaround time is less than 6 min. For clinical monitoring of plasma griseofulvin concentrations, a sample volume as small as 10 μl can be used.

Keyphrases □ Griseofulvin—high-pressure liquid chromatographic analysis in plasma □ High-pressure liquid chromatography—analysis, griseofulvin in plasma □ Antifungal agents—griseofulvin, high-pressure liquid chromatographic analysis in plasma

Griseofulvin is administered orally for treatment of fungal infections of the skin, hair, and nails in humans; this drug treatment is sometimes required for many months. The incidence of relatively minor untoward effects associated with the use of griseofulvin may be as high as 15%, but more serious reactions occur less frequently (1).

BACKGROUND

A number of factors could possibly influence the time course of blood griseofulvin concentrations following multiple oral doses. For example, a reduction of the extent of systemic biological availability was demonstrated in human subjects administered single doses of certain griseofulvin formulations (2, 3). Repeated single oral doses of the same batch of some griseofulvin products resulted in extremely variable extents of absorption in some subjects (2). Additionally, the concurrent administration of phenobarbital decreased blood levels of griseofulvin by impairing its absorption (4, 5). The metabolic clearance of griseofulvin is subject to wide interindividual variability (2), and this factor alone may result in pronounced differences (probably severalfold) in blood levels of the drug among individuals receiving the same dosage regimen. In view of the chronic nature of griseofulvin therapy and the factors influencing its pharmacokinetic profile, it may be beneficial to patient care to monitor plasma drug concentrations, particularly if toxicity or therapeutic failure is suspected (6).

Spectrofluorometric and GLC methods were described previously for the quantitative determination of griseofulvin in plasma. The spectrofluorometric assay (2) and modifications of it (7, 8) require 0.5–1 ml of plasma, time-consuming extraction and evaporation steps, and the reading of fluorescence intensity of the final aqueous solution both before and after the addition of sulfuric acid. Moreover, griseofulvin metabolites interfere with the method (8). The lower detection limit of the spectrofluorometric procedures is approximately 0.1 μg of griseofulvin/ml of plasma.

GLC with an electron-capture detector was used for the estimation of griseofulvin in plasma (8). The preparation of plasma samples for analysis involved extraction and evaporation, dissolution of the residue in benzene, and injection into the gas chromatograph. Because of the nonlinear response of the detector, the standard curve was nonlinear above about

oroacetyldesmethyldoxepin, and *N*-trifluoroacetylnortriptyline at *m/e* 280, 278, 362, and 360, respectively, were monitored.

Figure 4 shows the analysis in which the $[MH]^+$ ion and the $[MH - CF_3CONHCH_3]^+$ fragment ion of *N*-trifluoroacetyldesmethyldoxepin and *N*-trifluoroacetylnortriptyline at *m/e* 362, 360, 235, and 233 were monitored. The ratios of the $[MH]^+$ and $[MH - CF_3CONHCH_3]^+$ selected ion traces obtained from the analysis of a biological sample (Fig. 4) were 0.82 and 0.87 for the *N*-trifluoroacetyl derivatives of *cis*- and *trans*-desmethyldoxepin, respectively. These values are in close agreement with the theoretical values of 0.68 and 0.78 obtained from the mass spectra, which were recorded under the same experimental conditions (Table I), confirming as such the presence of the *N*-trifluoroacetyl derivatives of *cis*- and *trans*-desmethyldoxepin. Since *N*-trifluoroacetylnortriptyline overlapped with *cis*-(*N*-trifluoroacetyl)desmethyldoxepin on the SE-30 capillary column used in the selected ion monitoring experiments, the ^{13}C-isotope contributions of the nortriptyline signals were taken into account for calculating the true ratio of the $[MH]^+$ and $[MH - CF_3CONHCH_3]^+$ signals of *cis*-(*N*-trifluoroacetyl)desmethyldoxepin.

Preliminary results of the plasma levels obtained in two patients receiving chronic doxepin therapy are given in Fig. 5. The *trans*-isomer of doxepin was more prominent than its *cis*-form. For desmethyldoxepin, however, a considerable fraction occurred as the *cis*-form, although the product given to the patients contained only approximately 15% *cis*- *versus* 85% *trans*-isomer.

More patients are now being studied to evaluate if the levels of *cis*- and *trans*-doxepin and desmethyldoxepin can be correlated with clinical outcome.

REFERENCES

(1) R. M. Pinder, R. N. Brogden, T. M. Speight, and G. S. Avery, *Drugs*, **13**, 161 (1977).

(2) D. C. Hobbs, *Biochem. Pharmacol.*, **18**, 1941 (1969).

(3) J. E. O'Brien and O. N. Hinsvark, *J. Pharm. Sci.*, **65**, 1068 (1976).

(4) S. F. Reite, *Med. Norsk. Farm. Selskap.*, **37**, 141 (1975).

(5) A. Frigerio, C. Pantarotto, R. Franco, R. Gomeni, and P. L. Morselli, *J. Chromatogr.*, **130**, 354 (1977).

ACKNOWLEDGMENTS

The authors thank Dr. J. Gordts (Pfizer) for supplying doxepin and desmethyldoxepin and Dr. R. Deberdt and Dr. E. Suy for allowing them to study their patients.

Simple, Rapid, and Micro High-Pressure Liquid Chromatographic Determination of Plasma Griseofulvin Levels

ROGER L. NATION, GEOFFREY W. PENG, VICKY SMITH, and WIN L. CHIOU ˣ

Received July 25, 1977, from the *Clinical Pharmacokinetics Laboratory and the Department of Pharmacy, College of Pharmacy, University of Illinois at the Medical Center, Chicago, IL 60612.* Accepted for publication September 29, 1977.

Abstract □ A rapid high-pressure liquid chromatographic assay is described for the quantitative determination of griseofulvin in plasma. An aliquot (25–100 μl) of plasma was deproteinized by a simple procedure involving the addition of 2.5 volumes of acetonitrile, vortex mixing for a few seconds, and centrifugation for 1 min. The clear supernate, 50 μl, was injected into the high-pressure liquid chromatograph. A reversed-phase column was used with a mobile phase of distilled water–acetonitrile (1:1) at a flow rate of 2 ml/min and was operated at ambient temperature. A fluorescent detector with an excitation wavelength of 260 nm was employed to monitor the column effluent. Griseofulvin had a retention time of 3.8 min. This procedure yields reproducible results with high sensitivity; plasma concentrations as low as 50 ng/ml can be measured. Several commonly used drugs do not interfere. Analysis of plasma samples collected from a rabbit injected with griseofulvin indicated that the procedure is suitable for pharmacokinetic studies and clinical monitoring of plasma concentrations in patients. Assay turnaround time is less than 6 min. For clinical monitoring of plasma griseofulvin concentrations, a sample volume as small as 10 μl can be used.

Keyphrases □ Griseofulvin—high-pressure liquid chromatographic analysis in plasma □ High-pressure liquid chromatography—analysis, griseofulvin in plasma □ Antifungal agents—griseofulvin, high-pressure liquid chromatographic analysis in plasma

Griseofulvin is administered orally for treatment of fungal infections of the skin, hair, and nails in humans; this drug treatment is sometimes required for many months. The incidence of relatively minor untoward effects associated with the use of griseofulvin may be as high as 15%, but more serious reactions occur less frequently (1).

BACKGROUND

A number of factors could possibly influence the time course of blood griseofulvin concentrations following multiple oral doses. For example, a reduction of the extent of systemic biological availability was demonstrated in human subjects administered single doses of certain griseofulvin formulations (2, 3). Repeated single oral doses of the same batch of some griseofulvin products resulted in extremely variable extents of absorption in some subjects (2). Additionally, the concurrent administration of phenobarbital decreased blood levels of griseofulvin by impairing its absorption (4, 5). The metabolic clearance of griseofulvin is subject to wide interindividual variability (2), and this factor alone may result in pronounced differences (probably severalfold) in blood levels of the drug among individuals receiving the same dosage regimen. In view of the chronic nature of griseofulvin therapy and the factors influencing its pharmacokinetic profile, it may be beneficial to patient care to monitor plasma drug concentrations, particularly if toxicity or therapeutic failure is suspected (6).

Spectrofluorometric and GLC methods were described previously for the quantitative determination of griseofulvin in plasma. The spectrofluorometric assay (2) and modifications of it (7, 8) require 0.5–1 ml of plasma, time-consuming extraction and evaporation steps, and the reading of fluorescence intensity of the final aqueous solution both before and after the addition of sulfuric acid. Moreover, griseofulvin metabolites interfere with the method (8). The lower detection limit of the spectrofluorometric procedures is approximately 0.1 μg of griseofulvin/ml of plasma.

GLC with an electron-capture detector was used for the estimation of griseofulvin in plasma (8). The preparation of plasma samples for analysis involved extraction and evaporation, dissolution of the residue in benzene, and injection into the gas chromatograph. Because of the nonlinear response of the detector, the standard curve was nonlinear above about

Table I—Standard Curve for Griseofulvin in Plasma [a]

Plasma Griseofulvin Concentration, μg/ml	Griseofulvin Peak Height [b]	Response Factor [c]
0.05	1.3	26.0
0.1	2.3	23.0
0.5	12.4	24.8
1.0	25.3	25.3
2.0	49.7	24.9
3.0	75.6	25.2

[a] Linear regression equation: $y = 25.1493x - 0.1288$, $r = 0.9999$. [b] Peak height in centimeters at detector sensitivity of 0.1 μamp with a 10-mv recorder. [c] Peak height divided by griseofulvin concentration.

1.5 μg/ml; therefore, for measurement of higher concentrations of griseofulvin, a smaller volume of plasma or a larger volume of benzene to make up the assay solution was needed. Variation in the response of the electron-capture detector made it necessary to run standard curves daily when plasma samples were analyzed. The assay sensitivity was 0.05 μg/ml using 1-ml plasma samples.

The present paper reports a very simple, rapid, sensitive, and specific micro high-pressure liquid chromatographic (HPLC) method for the determination of griseofulvin in plasma.

EXPERIMENTAL

Materials—Griseofulvin[1], glass-distilled acetonitrile[2] and ethanol[2], and distilled water were used.

Spectrofluorometric Studies—Excitation and emission spectra[3] of griseofulvin fluorescence in the HPLC mobile phase were obtained.

HPLC System—Analyses were performed at ambient temperature with a system consisting of a mobile phase delivery pump[4], a sample injection apparatus[5], a 30-cm microparticulate reversed-phase HPLC column[6], a liquid chromatographic fluorescence detector[7], and a potentiometric 25.4-cm recorder[8]. The mobile phase was prepared by mixing equal volumes of acetonitrile and distilled water, and this solution was passed through the HPLC system at 2.0 ml/min. Unless otherwise specified, the fluorescence detector was operated with the excitation wavelength set at 260 nm, and an interference filter (KV 389) was used to select the fluorescence emission for detection. Recorder chart speed was 4 mm/min.

Preparation of Standard Curves—Plasma samples were spiked with griseofulvin by adding 5–7.5 μl of ethanolic griseofulvin stock solution to 500-μl plasma aliquots. The analysis of rabbit plasma samples containing griseofulvin gave the same results when the samples were analyzed with and without the addition of the equivalent proportion of ethanol used for spiking standards. Griseofulvin concentrations in the spiked plasma samples were 0.05, 0.1, 0.5, 1.0, 2.0, and 3.0 μg/ml.

Aliquots of 100 μl of spiked plasma samples were pipetted into 13 × 100-mm screw-capped culture tubes. After the addition of 250 μl of acetonitrile to each tube, the mixture was vortex mixed for a few seconds and centrifuged at 2000 rpm for approximately 1 min. Most of the clear supernate was poured into another culture tube, and 50 μl of this solution was then injected. A plasma sample, without the addition of griseofulvin, also was treated in the same way. Similarly, another batch of pooled human plasma and of plasma obtained from six patients receiving other drugs was analyzed without the addition of griseofulvin.

Reproducibility Studies—Two 3-ml aliquots of pooled plasma were spiked such that the plasma griseofulvin concentrations were 0.5 and 1.0 μg/ml. Each plasma sample was assayed for griseofulvin concentration in 20 replicates on the same day using 0.1-ml plasma aliquots and the procedure described under *Preparation of Standard Curves*. Additionally, the plasma sample spiked with 0.5 μg of griseofulvin/ml was assayed once a day on 4 days over 1 week.

Drug Interference Study—Thirteen drugs and drug metabolites were tested for potential interference of the griseofulvin assay by using ethanolic stock solutions of the compounds for direct chromatography or by spiking blank plasma with the compounds, adding 2.5 volumes of acetonitrile, vortexing, centrifuging, and injecting 50 μl of the supernate into the liquid chromatograph.

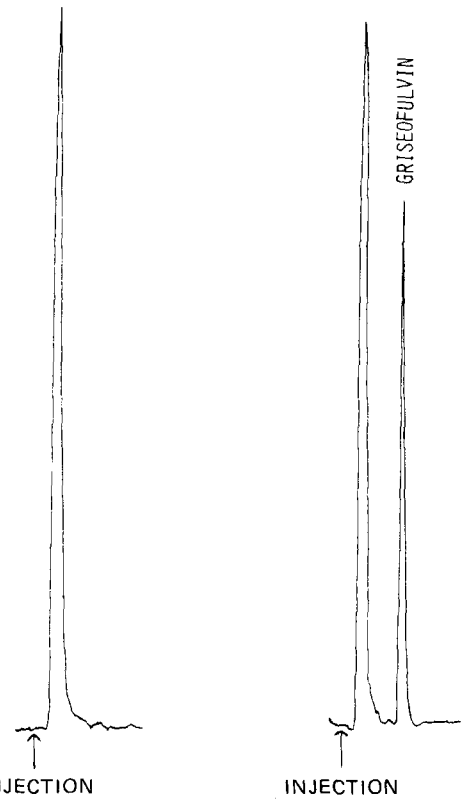

Figure 1—*Chromatograms of blank human plasma (left) and human plasma spiked with 0.5 μg of griseofulvin/ml (right).*

Preliminary Study in a Rabbit—Griseofulvin, 16 mg in 3.2 ml of polyethylene glycol 400, was infused over 1 min into the medial vein of one ear of a 4-kg albino rabbit. Blood samples (0.5 ml) were collected from the marginal vein of the contralateral ear prior to drug administration and at intervals for 6 hr. Blood samples were placed in heparinized tubes which were centrifuged immediately to obtain plasma. The separated plasma samples were stored at −20° until analysis.

RESULTS AND DISCUSSION

Chromatograms resulting from acetonitrile treatment and HPLC of blank human plasma, together with similarly treated plasma previously spiked with griseofulvin, are shown in Fig. 1. Griseofulvin eluted from the reversed-phase column as a symmetrical peak with a retention time of 3.8 min and was well resolved from the more polar endogenous fluorescing compounds of plasma.

Standard curves based on the peak height of griseofulvin from the HPLC of acetonitrile-treated human plasma samples spiked with various drug concentrations were linear over the range of plasma drug concentrations from 0.05 to 3.0 μg/ml and had an intercept close to the origin. Plasma concentrations in patients receiving griseofulvin orally in clinical practice would be expected to fall within the range of concentrations spanned by the standard curve (3). Data used to establish a typical standard curve are summarized in Table I. The correlation coefficient of 0.9999 and the constancy of response factors (peak height divided by concentration) both indicate good linearity.

The reproducibility of the method on a given day was very good. The coefficient of variation ($n = 20$) of the procedure at 0.5 and 1.0 μg of griseofulvin/ml in plasma was 0.82 and 1.9%, respectively. Additionally, the day-to-day reproducibility of the method was good; the coefficient of variation for the analysis of the same plasma sample on 4 days was 3.4%. However, since the analysis is carried out without the use of an internal standard, at least one standard sample should be assayed on those days when unknown plasma samples are analyzed.

The analysis of various batches of pooled human plasma and of plasma obtained from a number of individual patients, without the addition of griseofulvin, indicated the existence in some samples of a very small peak

[1] Sigma Chemical Co., St. Louis, Mo.
[2] Burdick and Jackson Laboratories, Muskegon, Mich.
[3] Aminco-Bowman spectrophotofluorometer, American Instrument Co., Silver Spring, Md.
[4] Model M-6000A, Waters Associates, Milford, Mass.
[5] Model U6K, Waters Associates, Milford, Mass.
[6] μBondapak C_{18}, Waters Associates, Milford, Mass.
[7] Model FS 970, Schoeffel Instrument Corp., Westwood, N.J.
[8] Laboratory Data Control, Riviera Beach, Fla.

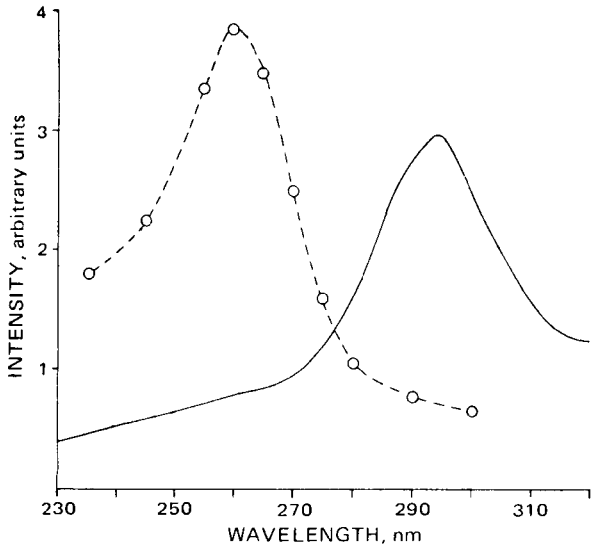

Figure 2—*Fluorescence excitation spectrum of griseofulvin recorded using a spectrophotofluorometer (—) and peak height of griseofulvin from HPLC analysis as a function of the excitation wavelength setting of the flowthrough fluorescence detector (- - -).*

with a similar retention time to griseofulvin. The peak was too small to estimate its contribution accurately, but it was probably only 5–15 ng/ml. Therefore, this factor should not reduce the usefulness of this analytical method for the clinical monitoring of plasma griseofulvin concentrations.

The apparent difference in the fluorescence excitation spectra of griseofulvin as recorded using a conventional spectrophotofluorometer compared to the flowthrough fluorescence detector, which was used to monitor the effluent from the HPLC column, is of interest. Using the spectrophotofluorometer and an emission wavelength of 425 nm, griseofulvin dissolved in the HPLC mobile phase had an excitation maximum of 295 nm; but upon repeated HPLC of a standard griseofulvin solution, the peak height was at a maximum at an excitation wavelength of 260 nm when the KV 389 filter was used to control fluorescence emission in the fluorescence detector (Fig. 2).

Difference in the relative spectral distribution of source intensity in the two instruments is the most likely explanation for the apparent difference in the excitation spectra. The deuterium source in the HPLC detector has peak radiant intensity at a considerably lower wavelength than the xenon source in the spectrophotofluorometer. This finding indicates that with griseofulvin, and probably other compounds, the excitation spectrum obtained with a spectrophotofluorometer may be of limited value for predicting the optimum excitation wavelength to be used in the fluorescent detection of the compound in the effluent from an HPLC column. This situation probably would not exist if both instruments contained the same type of source.

The deproteinization of plasma samples with acetonitrile proved to be a simple, rapid, and effective method of preparing samples for HPLC analysis. The addition of 2.5 volumes of acetonitrile to 1 volume of plasma, followed by brief vortexing and centrifugation, resulted in a clear supernate with the protein material forming a solid mass, which adhered to the base of the culture tube. Therefore, the supernate could be poured off to another tube, although this step is not necessary since an aliquot of the supernate can be injected directly into the liquid chromatograph.

This method of deproteinizing plasma samples with acetonitrile has been employed successfully in this laboratory for the HPLC analysis of several compounds including creatinine (9), aspirin, salicylic acid, salicyluric acid, theophylline, procainamide, and *N*-acetylprocainamide. Other ratios of acetonitrile to plasma may be satisfactory for preparation of plasma samples. Indeed, an acetonitrile to plasma ratio of 1:1 was reported for the denaturation of plasma protein prior to the HPLC determination of theophylline in plasma (10). However, the larger the ratio of acetonitrile to plasma, the more complete may be the deproteinization step, with the less likelihood of blockage of HPLC columns. Addition of trichloroacetic acid to the supernate of the mixture of 1 volume of plasma and 2.5 volumes of acetonitrile does not result in further precipitation, whereas this may not be the case at lower ratios of acetonitrile to plasma.

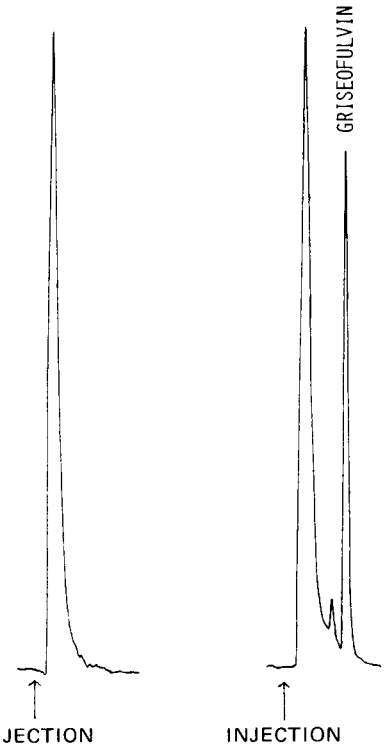

Figure 3—*Chromatograms of blank rabbit plasma (left) and plasma collected from a rabbit 125 min after intravenous administration (right). Griseofulvin concentration was 0.48 μg/ml.*

Other water-miscible organic solvents such as methanol or acetone also can be used to deproteinize plasma. When these solvents are employed, the resulting precipitate is very fine. The supernate may contain particulate matter, which would necessitate a filtration step. For example, an HPLC method for determination of amphotericin B in plasma involved the addition of methanol to plasma, followed by periods of vortexing (15 sec), standing (10 min), and centrifugation (10 min at 2000×*g*) (11). The supernate obtained after centrifugation was filtered, and an aliquot of the filtrate was injected into the liquid chromatograph (11).

For the setting up of standard curves, 100-μl aliquots of plasma were deproteinized with acetonitrile. Smaller volumes of plasma also may be used if there is a shortage. The treatment of 25- and 100-μl aliquots of two spiked plasma samples (griseofulvin concentration of 0.5 and 2.0 μg/ml) with 2.5 volumes of acetonitrile and injection of 50 μl yielded the same value for the griseofulvin concentration in the samples. For the analysis of small volumes of pediatric plasma samples, even smaller volumes of plasma can be used (*e.g.*, 10 μl) with a corresponding reduction in injection volume and sensitivity.

The injection volume of 50 μl was chosen as being adequate to achieve the sensitivity required for clinical monitoring and pharmacokinetic studies. Increasing the injection volume resulted in a less than proportional increase in griseofulvin peak height. For example, increasing the injection volume from 50 to 100 μl resulted in only a 78% increase in peak height. This effect was probably due mainly to a peak broadening resulting from a slower transfer of total sample from the injection loop onto the head of the column as the sample size increased.

None of the compounds tested for potential interference (acetaminophen, methotrexate, ampicillin, aspirin, caffeine, ephedrine, phenobarbital, phenytoin, salicylic acid, salicyluric acid, tetracycline, theobromine, and theophylline) interfered with the analysis. Additionally, no interference from drugs was observed when plasma from patients receiving multiple-drug therapy was assayed.

To investigate the suitability of the griseofulvin analysis for monitoring plasma drug levels, a rabbit was given griseofulvin intravenously and blood samples were collected. Figure 3 shows chromatograms resulting from acetonitrile treatment and HPLC of predose blank rabbit plasma and similarly treated plasma obtained from the rabbit after griseofulvin administration. In addition to the griseofulvin peak, a smaller peak with a retention time of 2.95 min was present in the samples collected after drug administration. This additional peak was not present when stock solutions of griseofulvin or acetonitrile-treated spiked plasma were in-

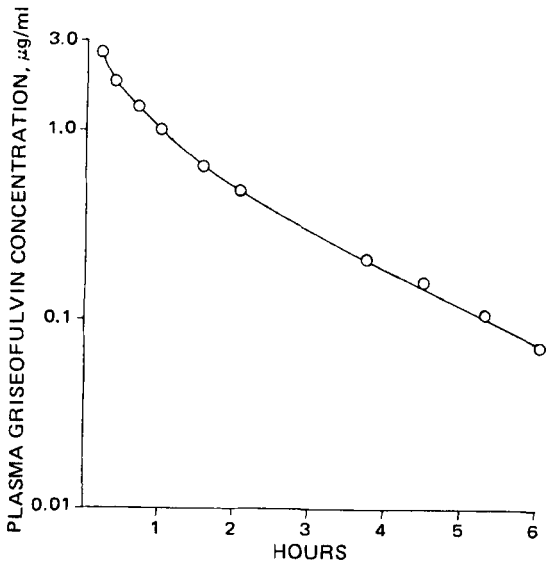

Figure 4—*Plasma griseofulvin concentration as a function of time in a 4-kg rabbit given 16 mg of griseofulvin intravenously over 1 min.*

jected into the liquid chromatograph, indicating that the peak was not due to another component or an impurity in the griseofulvin. It seems most likely that the peak was due to a metabolite of griseofulvin, although the structure of this compound is unknown. The time course of plasma griseofulvin concentrations in the rabbit is shown in Fig. 4.

The described method for quantitative determination of griseofulvin in plasma offers several advantages over the spectrofluorometric (2, 7, 8) and GLC (8) methods. The HPLC procedure is simple and rapid, with a turnaround time of 5–6 min required for each sample. The analysis uses only a small volume of plasma and is specific and reproducible; commonly used drugs do not interfere. The method is well suited for the clinical monitoring of plasma griseofulvin concentrations or for pharmacokinetic studies.

REFERENCES

(1) "The Pharmacological Basis of Therapeutics," L. S. Goodman and A. Gilman, Eds., Macmillan, New York, N.Y., 1975.

(2) M. Rowland, S. Riegelman, and W. L. Epstein, *J. Pharm. Sci.*, **57**, 984 (1968).

(3) W. L. Chiou and S. Riegelman, *ibid.*, **60**, 1376 (1971).

(4) S. Riegelman, M. Rowland, and W. L. Epstein, *J. Am. Med. Assoc.*, **213**, 426 (1970).

(5) D. Busfield, K. J. Child, R. M. Atkinson, and E. G. Tomich, *Lancet*, **2**, 1042 (1963).

(6) S. Riegelman and W. Sadee, "Clinical Pharmacokinetics: A Symposium," APhA Academy of Pharmaceutical Sciences, Washington, D.C., 1974, p. 169.

(7) V. P. Shah, S. Riegelman, and W. L. Epstein, *J. Pharm. Sci.*, **61**, 634 (1972).

(8) H. J. Schwarz, B. A. Waldman, and V. Madrid, *ibid.*, **65**, 370 (1976).

(9) W. L. Chiou, M. A. F. Gadalla, and G. W. Peng, *ibid.*, **67**, 182 (1978).

(10) J. W. Nelson, A. L. Cordry, C. G. Aron, and R. A. Bartell, *Clin. Chem.*, **23**, 124 (1977).

(11) I. Nilsson-Ehle, T. T. Yoshikawa, J. E. Edwards, M. C. Schotz, and L. B. Guze, *J. Infect. Dis.*, **135**, 414 (1977).

Stability of Furosemide in Aqueous Systems

A. G. GHANEKAR, V. DAS GUPTA ˣ, and CHARLES W. GIBBS, Jr. *

Received February 28, 1977, from the *College of Pharmacy, University of Houston, Houston, TX 77004.* Accepted for publication September 28, 1977. *Present address: Harris County Hospital District Pharmacy, Taub Loop, Houston, TX 77030.

Abstract □ A stability-indicating assay for furosemide based on high-pressure liquid chromatography was developed. The method is sensitive, accurate, and precise. The standard deviation based on six injections of the standard solution was ±1.37%. This method was used to study furosemide stability in various aqueous solutions and dosage forms. Stability tests were conducted at room temperature as well as at higher temperatures (45, 65, and 85°) at various pH values and with different vehicles. Some decomposition products were identified.

Keyphrases □ Furosemide—high-pressure liquid chromatographic analysis, stability in aqueous solutions and dosage forms □ High-pressure liquid chromatography—analysis, furosemide in aqueous solutions and dosage forms □ Stability—furosemide in aqueous solutions and dosage forms, high-pressure liquid chromatographic analysis □ Diuretics—furosemide, high-pressure liquid chromatographic analysis, stability in aqueous solutions and dosage forms

Furosemide is extensively used as a diuretic. Very little information is available concerning its stability, possibly because of the lack of a stability-indicating assay. The USP method (1) for furosemide in injections and tablets is based on UV absorption. A fluorometric method for furosemide in urine and serum also was reported (2), but any other fluorescent substances interfere with the assay. Furosemide was reported to be unstable in acidic media (3). The USP (1) indicates that the pH of the injection should be between 8.9 and 9.3.

The present investigations were undertaken to develop a stability-indicating assay for furosemide using high-pressure liquid chromatography (HPLC) and to study furosemide stability in aqueous systems.

EXPERIMENTAL

Chemicals and Reagents—All chemicals and reagents were ACS, NF, or USP quality and were used without further purification.

Preparation of Solutions and Dosage Forms—The solutions and dosage forms prepared are given in Table I.

Apparatus—A high-pressure liquid chromatograph[1] equipped with a UV detector (254 nm), a recorder[2], and an integrator[3] was used.

Column—A column[4] (30 cm × 4 mm i.d.) of a very nonpolar packing material, consisting of octadecyltrichlorosilane permanently bonded by silicon–carbon bonds, was used.

Chromatographic Conditions—The chromatographic mobile phase was 0.01 *M* $(NH_4)_2HPO_4$ in water containing 25% (v/v) methanol. The

[1] Model ALC 202, equipped with U6K universal chromatograph injector, Waters Associates, Milford, Mass.
[2] Omniscribe 5213-12, Houston Instruments, Austin, Tex.
[3] Autolab Minigrator, Spectra-Physics, Santa Clara, Calif.
[4] μBondapak C_{18}, Catalog No. 27324, Waters Associates, Milford, Mass.

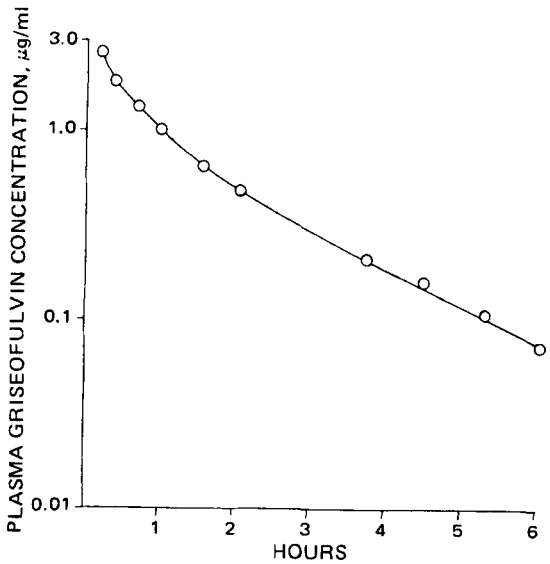

Figure 4—*Plasma griseofulvin concentration as a function of time in a 4-kg rabbit given 16 mg of griseofulvin intravenously over 1 min.*

jected into the liquid chromatograph, indicating that the peak was not due to another component or an impurity in the griseofulvin. It seems most likely that the peak was due to a metabolite of griseofulvin, although the structure of this compound is unknown. The time course of plasma griseofulvin concentrations in the rabbit is shown in Fig. 4.

The described method for quantitative determination of griseofulvin in plasma offers several advantages over the spectrofluorometric (2, 7, 8) and GLC (8) methods. The HPLC procedure is simple and rapid, with a turnaround time of 5–6 min required for each sample. The analysis uses only a small volume of plasma and is specific and reproducible; commonly used drugs do not interfere. The method is well suited for the clinical monitoring of plasma griseofulvin concentrations or for pharmacokinetic studies.

REFERENCES

(1) "The Pharmacological Basis of Therapeutics," L. S. Goodman and A. Gilman, Eds., Macmillan, New York, N.Y., 1975.

(2) M. Rowland, S. Riegelman, and W. L. Epstein, *J. Pharm. Sci.*, **57**, 984 (1968).

(3) W. L. Chiou and S. Riegelman, *ibid.*, **60**, 1376 (1971).

(4) S. Riegelman, M. Rowland, and W. L. Epstein, *J. Am. Med. Assoc.*, **213**, 426 (1970).

(5) D. Busfield, K. J. Child, R. M. Atkinson, and E. G. Tomich, *Lancet*, **2**, 1042 (1963).

(6) S. Riegelman and W. Sadee, "Clinical Pharmacokinetics: A Symposium," APhA Academy of Pharmaceutical Sciences, Washington, D.C., 1974, p. 169.

(7) V. P. Shah, S. Riegelman, and W. L. Epstein, *J. Pharm. Sci.*, **61**, 634 (1972).

(8) H. J. Schwarz, B. A. Waldman, and V. Madrid, *ibid.*, **65**, 370 (1976).

(9) W. L. Chiou, M. A. F. Gadalla, and G. W. Peng, *ibid.*, **67**, 182 (1978).

(10) J. W. Nelson, A. L. Cordry, C. G. Aron, and R. A. Bartell, *Clin. Chem.*, **23**, 124 (1977).

(11) I. Nilsson-Ehle, T. T. Yoshikawa, J. E. Edwards, M. C. Schotz, and L. B. Guze, *J. Infect. Dis.*, **135**, 414 (1977).

Stability of Furosemide in Aqueous Systems

A. G. GHANEKAR, V. DAS GUPTA ˣ, and CHARLES W. GIBBS, Jr. *

Received February 28, 1977, from the *College of Pharmacy, University of Houston, Houston, TX 77004.* Accepted for publication September 28, 1977. *Present address: Harris County Hospital District Pharmacy, Taub Loop, Houston, TX 77030.

Abstract □ A stability-indicating assay for furosemide based on high-pressure liquid chromatography was developed. The method is sensitive, accurate, and precise. The standard deviation based on six injections of the standard solution was ±1.37%. This method was used to study furosemide stability in various aqueous solutions and dosage forms. Stability tests were conducted at room temperature as well as at higher temperatures (45, 65, and 85°) at various pH values and with different vehicles. Some decomposition products were identified.

Keyphrases □ Furosemide—high-pressure liquid chromatographic analysis, stability in aqueous solutions and dosage forms □ High-pressure liquid chromatography—analysis, furosemide in aqueous solutions and dosage forms □ Stability—furosemide in aqueous solutions and dosage forms, high-pressure liquid chromatographic analysis □ Diuretics—furosemide, high-pressure liquid chromatographic analysis, stability in aqueous solutions and dosage forms

Furosemide is extensively used as a diuretic. Very little information is available concerning its stability, possibly because of the lack of a stability-indicating assay. The USP method (1) for furosemide in injections and tablets is based on UV absorption. A fluorometric method for furosemide in urine and serum also was reported (2), but any other fluorescent substances interfere with the assay. Furosemide was reported to be unstable in acidic media (3). The USP (1) indicates that the pH of the injection should be between 8.9 and 9.3.

The present investigations were undertaken to develop a stability-indicating assay for furosemide using high-pressure liquid chromatography (HPLC) and to study furosemide stability in aqueous systems.

EXPERIMENTAL

Chemicals and Reagents—All chemicals and reagents were ACS, NF, or USP quality and were used without further purification.

Preparation of Solutions and Dosage Forms—The solutions and dosage forms prepared are given in Table I.

Apparatus—A high-pressure liquid chromatograph[1] equipped with a UV detector (254 nm), a recorder[2], and an integrator[3] was used.

Column—A column[4] (30 cm × 4 mm i.d.) of a very nonpolar packing material, consisting of octadecyltrichlorosilane permanently bonded by silicon–carbon bonds, was used.

Chromatographic Conditions—The chromatographic mobile phase was 0.01 *M* $(NH_4)_2HPO_4$ in water containing 25% (v/v) methanol. The

[1] Model ALC 202, equipped with U6K universal chromatograph injector, Waters Associates, Milford, Mass.
[2] Omniscribe 5213-12, Houston Instruments, Austin, Tex.
[3] Autolab Minigrator, Spectra-Physics, Santa Clara, Calif.
[4] μBondapak C_{18}, Catalog No. 27324, Waters Associates, Milford, Mass.

Table I—Solutions and Dosage Forms Prepared

Solution	Vehicle	Furosemide Concentration, mg/ml	pH	Other Ingredients (If Any)
1	0.01 *N* NaOH	0.5[a]	—	—[b,c]
2	0.1 *N* NaOH	1.0	13	—[b,c]
3	0.1 *N* HCl	1.0	1.2	—[b,c]
4	0.04 *M* $(NH_4)_2HPO_4$	1.0	8	—[b,c]
5	Phosphate buffers (0.05 *M*)	0.5	See Table IV	—[b,c]
6	Water	0.5	4.2 (adjusted with acetic acid)	—[b,c]
7	Water	1.0[b]	See Table III	Various percentages of sugar
8	Commercial vehicle[c]	1.0 and 2.0	7.4[d] 7.5[d]	
9	50% (v/v) glycerin in water	1.0	5.6	Methylparaben, 0.005% Propylparaben, 0.002%
10	70% sorbitol in water	1.0	6.8	Methylparaben, 0.005% Propylparaben, 0.002%
11	50% sorbitol in water	1.0	8.5 (adjusted with 0.1 *N* NaOH)	Methylparaben, 0.005% Propylparaben, 0.002%
12	50% sorbitol in water with 20% (v/v) alcohol	1.0	8.5	Methylparaben, 0.005% Propylparaben, 0.002%
13	50% sorbitol in water with 10% (v/v) alcohol	1.0	8.5	Methylparaben, 0.005% Propylparaben, 0.002%
14	85% sugar in water	1.0[b]	8.2 (adjusted with 4% $NaHCO_3$)	—[b]

[a] For a standard solution, it was further diluted with water to a concentration of 50 μg/ml. [b] Prepared from furosemide injection. [c] Syrpalta syrup, Emerson Laboratories, Dallas, Tex. The syrup also contained dye(s), flavor(s), and sodium benzoate (as confirmed during these investigations). An 8.0-ml quantity of 4% $NaHCO_3$/50 ml of the syrup was added to raise the pH to keep furosemide in solution. [d] The pH values are of the recompounded samples; pH values of the original samples were not determined.

temperature was ambient, and the flow rate was 2.0 ml/min. The detector was set at a sensitivity of 0.16 absorbance unit for full-scale deflection, and the chart speed was 30.5 cm/hr.

Procedure for Furosemide—*In Solution and Liquid Dosage Forms*—An appropriate quantity of the solution or dosage form was diluted with water to a 50-μg/ml concentration, and 40 μl was injected. For purposes of comparison, an identical volume of the standard solution was injected after the assay solution was eluted.

In Tablets—One tablet was ground and mixed with 4 ml of methanol. Then enough 0.05 *M* sodium bicarbonate was added to bring the solution to 100.0 ml. The solution was filtered (if necessary), the clear filtrate was diluted with water to a concentration of 50 μg of furosemide/ml, and 40 μl was injected as already described.

Calculations—Since preliminary investigations indicated that the peak area of furosemide was directly related to the concentration, the results were calculated using the following equation:

$$\frac{A_a}{A_s} \times 100 = \% \text{ of label claim} \qquad \text{(Eq. 1)}$$

where A_a is the peak area of the assay sample and A_s is the peak area of the standard sample. The results on commercial tablets and injection were 101.8 and 99.6% of the label claim, respectively. The standard deviation based on six injections of the standard solution was ±1.37%.

A sample chromatogram is presented in Fig. 1A.

The investigations indicated (Fig. 1B) that the developed method was stability indicating *versus* the USP method (1), which was not. For example, a 42-month-old sample in an 85% solution of sugar in water whose pH was adjusted to 8.2 with sodium bicarbonate gave 26.1% by the developed method (Fig. 2C) *versus* 82.1% by the USP method. Therefore, stability studies on the dosage forms and solutions were conducted using the developed method.

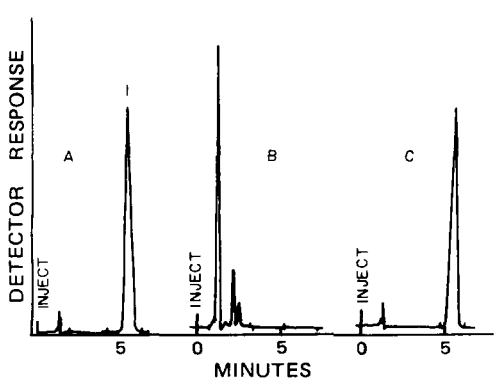

Figure 1—*Chromatograms of furosemide from solutions. Peak 1 is from furosemide. Key: A, from a standard solution; B, from a solution in 0.1 N HCl after 30 days of storage at 65°; and C, from a solution in 0.1 N NaOH after 30 days of storage at 65°.*

Stability Studies—*Solution in Commercial Vehicle Containing 2.0 mg of Furosemide/ml (Table I)*—This solution was divided into various portions and stored at 45, 65, and 85° as well as at room temperature. The portions were assayed frequently (Table II). A solution of furosemide in the commercial vehicle (1.0 mg/ml) when stored at room temperature showed more decomposition than the 2.0-mg/ml solution (Table II).

Solutions Containing Sugar—The solutions of furosemide (1.0 mg/ml) in water containing various percentages of sucrose were stored at 65° and assayed after 3 weeks (Table III).

Aqueous Solutions in Phosphate Buffers, Acetic Acid, Hydrochloric Acid, and Sodium Hydroxide—These solutions were stored at 65° for 30 days and assayed (Table III).

Dibasic Ammonium Phosphate—An aqueous solution in dibasic ammonium phosphate was stored for 24 hr at room temperature and

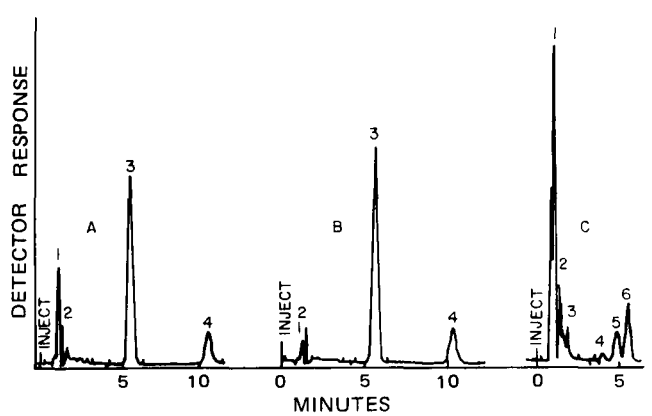

Figure 2—*Chromatograms of furosemide from dosage forms. A: in 50% aqueous solution of sorbitol after 3 weeks of storage at 65°. Peak 3 is from furosemide, peak 4 is from methylparaben, and peaks 1 and 2 are from the solvent and decomposition products of furosemide. B: same as A except that 20% (v/v) alcohol was substituted for 20% water. C: in simple syrup after 3.5 years of storage at room temperature. Peak 6 is from furosemide; peaks 1 and 2 are from sugar, solvent, levulinic acid, and 4-chloro-5-sulfamoylanthranilic acid; peaks 3 and 5 are similar to the peaks obtained from a solution of furfuryl alcohol in water after 3 weeks of storage at room temperature; and peak 4 is from furfuryl alcohol.*

Table II—Assay Results on Furosemide [a] (with 8.0 ml of 4% Sodium Bicarbonate) in Conmercial Vehicle at Various Temperatures

Storage Temperature (±1°)	Original Concentration, mg/ml	Percent of Furosemide Retained after 7 Days	14 Days	21 Days	28 Days	30 Days	42 Days	49 Days	56 Days	60 Days	87 Days	90 Days
45°	2	—	94.1[b]	—	92.9	—	91.2	—	—	—	84.9	—
65°	2	—	91.4[b]	—	91.7	—	—	87.1	84.7	—	70.9[b]	—
85°	2	92.5	87.5	81.9	68.9[b]	—	—	—	—	—	—	—
24°	2	—	—	—	—	93.8	—	—	—	88.0[c]	—	87.5[c]
24°	1	—	—	—	—	95.7	—	—	—	89.6	—	86.2

[a] Lasix injection was used to make these solutions. [b] These results may not be reliable due to minor mechanical problems in the integrator, but they do not affect the conclusions of this study. [c] These results may not be reliable due to the growth of fungus, but they do not affect the conclusions of this study.

Table III—Percentages of Furosemide Retained in Various Aqueous Solutions after 30 Days (21 Days for Sugar Solutions) of Storage at 65°

Solution Containing	Initial pH	Final pH	Percent Retained
10% sugar	8.5	4.9	82.3
20% sugar	8.1	4.3	60.5
30% sugar	8.2[b]	4.3	55.5
50% sugar	7.9	4.0	43.9
60% sugar	7.8	4.0	44.1
70% sugar	7.7	3.9	40.3
85%[b] sugar	7.6	3.9	40.3
Phosphate buffer	5.0	—	88.6
Phosphate buffer	4.8	—	76.8
Phosphate buffer	4.65	—	72.1
Phosphate buffer	4.55	—	67.1
Acetate	4.2	—	11.5
Hydrochloric acid	1.2	—	0.0
Sodium hydroxide	13	—	99.5

[a] Initial pH values were higher since the samples were made using furosemide injection whose pH was 8.9. [b] The pH of simple syrup was approximately 6.5.

stability. The pH is apparently indirectly responsible for furosemide decomposition in sugar solutions (Table III) since they changed considerably and were acidic (Table III). The pH changes in sorbitol solutions were not as wide as in sugar or glycerin (Tables III and IV), so sorbitol solutions were studied further. Alcohol appears to have a stabilizing effect (Table IV). Since more than 10% (v/v) alcohol is a reasonable upper limit in pediatric dosage forms, alcoholic concentrations were kept to a minimum. Only two concentrations (10 and 20% v/v) were studied.

The samples prepared in the commercial vehicle (2.0 mg/ml) that contained sodium benzoate as the preservative showed fungus growth after about 30 days. This growth was expected since sodium benzoate is not a good preservative in a basic medium. It is the undissociated benzoic acid that prevents fungus growth. No such problem was noticed with parabens as the preservatives (0.005% methylparaben and 0.002% propylparaben). These preservatives did not interfere with the assay (Figs. 2A and 2B).

The decomposition of furosemide (I) appears to follow Scheme I as reported by Kovar *et al.* (3). The presence of decomposition products in a 3.5-year-old sample (Fig. 2C) was confirmed by injecting solutions of furfuryl alcohol (II) (0.1 ml/250 ml of water), levulinic acid (III) (1 ml/250 ml of water), and 4-chloro-5-sulfamoylanthranilic acid (IV) (20 mg/100 ml of methanol). The solution of furfuryl alcohol in water decomposed quite fast, even at room temperature. The decomposition of furfuryl alcohol appears to be complex (Fig. 2C) and not a simple decomposition to levulinic acid as reported by Kovar *et al.* (3).

Table IV—Percentages of Furosemide Retained when Solution Contained Either Glycerin, Sorbitol, or Sorbitol with Alcohol

Solution in	pH	Stored at (±1°)	Percent Retained after 21 Days	30 Days	61 Days	120 Days	155 Days	182 Days
50% glycerin	5.7	65°	78.9 (4.6)[a]	—	—	—	—	—
70% sorbitol	6.8	65°	88.4 (5.7)	—	—	—	—	—
50% sorbitol	8.5[b]	65°	81.7 (4.9)	—	—	—	—	—
50% sorbitol with 20% alcohol	8.5[b]	65°	93.3 (4.7)	—	77.4 (4.7)	—	—	—
50% sorbitol with 20% alcohol	8.5[b]	24°	99.5 (7.1)	—	99.0 (6.7)	—	—	—
50% sorbitol with 10% alcohol	8.5[b]	65°	90.8	—	81.1 (4.8)	21.7 (4.0)	10.4 (3.9)	0 (3.9)
50% sorbitol with 10% alcohol	8.5[b]	24°	99.3	99.2 (6.1)	—	97.5[c] (5.8)	99.2 (5.6)	99.3 (5.5)

[a] Observed pH. [b] The pH was adjusted with 0.1 *N* NaOH solution in water. [c] It appears that there is an error in this reading.

assayed to determine if furosemide, like ethacrynic acid[5], undergoes fast decomposition in the presence of ammonium ions. No decomposition of furosemide was noted.

Aqueous Solutions in Glycerin and Sorbitol—These solutions were stored at 65° and at room temperature for varying periods and reassayed (Table IV). Since the investigations indicated that sorbitol was better than glycerin (from a stability point of view) and that alcohol had a stabilizing effect, dosage forms in sorbitol in which part of the water was replaced with alcohol were also investigated (Table IV).

DISCUSSION

The method developed for the quantitative determination of furosemide appears to be stability indicating (Figs. 1A, 1B, and 2A–2C). It is accurate, precise (standard deviation based on six injections of the standard solution was ±1.37%), and sensitive. The peak area was directly related to concentration (range tested was 0.5–3 μg of furosemide) with a correlation coefficient of 0.99996. The USP method (1), based on UV absorption, is not stability indicating since a 3.5-year-old sample in simple syrup gave 82.1% *versus* only 26.1% by the developed method. In the two commercial dosage forms (injection and tablets), no decomposition was noted in samples that were at least 3 years old. Furosemide was very unstable in acidic media and very stable in basic media (Table III).

Sugar appears to have an adverse effect (Table III) on furosemide

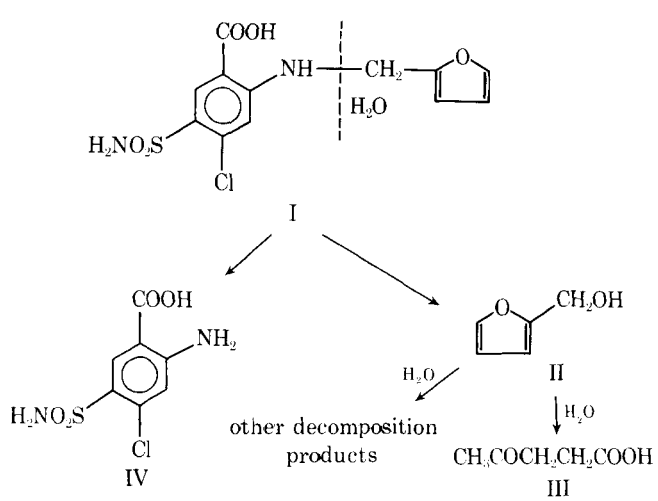

Scheme I

[5] The study on ethacrynic acid will be presented in a separate report.

Considering this discussion and the results, it is possible to formulate a liquid dosage form with limited stability containing sorbitol, alcohol (10–20% v/v), and preservatives (methylparaben and propylparaben). The pH should be adjusted to at least 8.5 with sodium hydroxide in water. The shelflife of the dosage form may be extended for more than 1 year by adding an overage of about 5% of furosemide.

The data were not treated mathematically because the pH values were not constant (Table III) because of the hydrolysis of sugar. The commercial vehicle also contained high concentration of sugar. No attempt was made to buffer the dosage forms heavily to prevent pH changes. If a biologically safe buffer can be used to maintain the pH value at around 8.5, it would certainly stabilize the dosage form further.

REFERENCES

(1) "The United States Pharmacopeia," 19th rev., Mack Publishing Co., Easton, Pa., 1975, pp. 213, 214.

(2) A. W. Forrey, B. Kimpel, A. D. Blair, and R. E. Cutler, *Clin. Chem.*, **20,** 152 (1974).

(3) K. A. Kovar, G. P. Wojtovicz, and H. Auterhoff, *Arch. Pharm.*, **307,** 657 (1974).

ACKNOWLEDGMENTS

The authors thank Hoechst-Roussel Pharmaceuticals Inc. for a generous supply of furosemide powder and injections.

Quantitation of Cocaine and Its Principal Metabolite, Benzoylecgonine, by GLC–Mass Spectrometry Using Stable Isotope Labeled Analogs as Internal Standards

SATYA P. JINDAL ˣ and PER VESTERGAARD

Received June 27, 1977, from the *Rockland Research Institute, Orangeburg, NY 10962.* Accepted for publication October 12, 1977.

Abstract □ A quantitative GLC–mass spectrometric assay was developed for the determination of cocaine and its principal metabolite, benzoylecgonine, in human urine. The assay utilizes selective ion focusing to monitor in a GLC effluent the molecular ions of cocaine and benzoylecgonine generated by electron-impact ionization. Cocaine-d_3 and benzoylecgonine-d_3 were the internal standards. The assay can measure 2 ng of cocaine/ml and 5 ng of benzoylecgonine/ml with about 5% precision. The curves relating the amounts of cocaine and benzoylecgonine added *versus* the amounts found over a large range of cocaine and benzoylecgonine concentrations were straight lines with nearly zero intercepts and slopes of 0.98 ± 0.01 and 0.97 ± 0.01, respectively. The method was used for the analysis of urinary cocaine and benzoylecgonine in cocaine addicts. Assay specificity was confirmed by complete identity of the mass spectra of cocaine and benzoylecgonine with those of authentic materials.

Keyphrases □ Cocaine—GLC–mass spectrometric analysis in human urine □ Benzoylecgonine—GLC–mass spectrometric analysis in human urine □ GLC–mass spectrometry—analyses, cocaine and benzoylecgonine in human urine □ Narcotics—cocaine and benzoylecgonine, GLC–mass spectrometric analyses in human urine

Cocaine abuse (1–5) has prompted considerable interest in methods for the detection and quantitation of the parent drug and its metabolites in biological fluids and tissues. TLC and the enzyme multiplied immunoassay technique (EMIT) are the most frequently employed screening methods for the detection of cocaine in human urine. However, these methods are inherently only semiquantitative at best. Although cocaine may be determined by GLC, the amount of unchanged cocaine excreted in human urine (2, 6) is generally below the method's limits of detection (7, 8).

BACKGROUND

A rather sensitive GLC procedure (9) for cocaine is based on the reduction of cocaine with lithium aluminum hydride, derivatization of the reduced product with pentafluoropropionic anhydride, and subsequent detection by electron capture. This method is sensitive but unspecific, and it is not applicable to cocaine in biological specimens. Besides cocaine, benzoylecgonine, ecgonine, and possibly other metabolites (10) of cocaine are converted by the procedure (9) to the same derivative. Therefore, the GLC-measured cocaine concentration cannot be the true concentration of cocaine alone.

Recently, a GLC procedure for cocaine and benzoylecgonine in the urine of cocaine users was reported (11). The method involves methylation of urinary benzoylecgonine to cocaine by treatment with diazomethane, thereby measuring combined benzoylecgonine and cocaine. Original cocaine was determined in a separate extract without the methylation step. Thus, benzoylecgonine could be determined by difference. Cocaine is metabolized in the human body rather rapidly (12), benzoylecgonine being the major metabolite (13, 14). Consequently, most urine samples of cocaine users contain trace amounts of unchanged drug and large concentrations of benzoylecgonine. Furthermore, cocaine and benzoylecgonine have rather widely different and variable extraction efficiencies, and one ends up dealing with differences of rather large and very small numbers. As a result, this assay is of limited usefulness.

This paper describes a GLC–mass spectrometric assay of cocaine and benzoylecgonine in human urine. Selective ion monitoring, the technique built on combined GLC–mass spectrometry with selective focusing on suitable fragments of the molecular ion (mass fragmentography) or the molecular ion itself, is a well-established technique, used widely in pharmacology (15, 16). This technique was used to develop a sensitive and specific assay for cocaine and benzoylecgonine in human urine with site-specific deuterium-labeled cocaine and benzoylecgonine as internal standards.

EXPERIMENTAL

Materials—Analytical grade cocaine hydrochloride[1], benzoylecgonine[2], norcocaine hydrochloride[3], methyl iodide-d_3[4], and *N*-ethyl-*N*-nitro-*N*-nitrosoguanidine[5] were used without further purification. All solvents were analytical grade[6]. Silanized tubes[7] (10 ml) with screw caps[8] were used for urine extraction; final solvent evaporation was performed in 5-ml glass-stoppered centrifuge tubes[9]. Pasteur pipets with hand-

[1] Mallinckrodt Chemical Works, New York, N.Y.
[2] Techman Inc., Park Forest South, Ill.
[3] Norcocaine hydrochloride was a gift from Dr. Sally, Chemistry Department, University of Wisconsin.
[4] International Chemical & Nuclear Corp., Irvine, Calif.
[5] Pfaltz & Bauer, Flushing, N.Y.
[6] Fisher Scientific Co., Pittsburgh, Pa.
[7] Kimble, Owens-Illinois, Toledo, Ohio.
[8] Lined with Teflon (DuPont).
[9] Pyrex 8084.

Considering this discussion and the results, it is possible to formulate a liquid dosage form with limited stability containing sorbitol, alcohol (10–20% v/v), and preservatives (methylparaben and propylparaben). The pH should be adjusted to at least 8.5 with sodium hydroxide in water. The shelflife of the dosage form may be extended for more than 1 year by adding an overage of about 5% of furosemide.

The data were not treated mathematically because the pH values were not constant (Table III) because of the hydrolysis of sugar. The commercial vehicle also contained high concentration of sugar. No attempt was made to buffer the dosage forms heavily to prevent pH changes. If a biologically safe buffer can be used to maintain the pH value at around 8.5, it would certainly stabilize the dosage form further.

REFERENCES

(1) "The United States Pharmacopeia," 19th rev., Mack Publishing Co., Easton, Pa., 1975, pp. 213, 214.

(2) A. W. Forrey, B. Kimpel, A. D. Blair, and R. E. Cutler, *Clin. Chem.*, **20,** 152 (1974).

(3) K. A. Kovar, G. P. Wojtovicz, and H. Auterhoff, *Arch. Pharm.*, **307,** 657 (1974).

ACKNOWLEDGMENTS

The authors thank Hoechst-Roussel Pharmaceuticals Inc. for a generous supply of furosemide powder and injections.

Quantitation of Cocaine and Its Principal Metabolite, Benzoylecgonine, by GLC–Mass Spectrometry Using Stable Isotope Labeled Analogs as Internal Standards

SATYA P. JINDAL ˣ and PER VESTERGAARD

Received June 27, 1977, from the *Rockland Research Institute, Orangeburg, NY 10962.* Accepted for publication October 12, 1977.

Abstract □ A quantitative GLC–mass spectrometric assay was developed for the determination of cocaine and its principal metabolite, benzoylecgonine, in human urine. The assay utilizes selective ion focusing to monitor in a GLC effluent the molecular ions of cocaine and benzoylecgonine generated by electron-impact ionization. Cocaine-d_3 and benzoylecgonine-d_3 were the internal standards. The assay can measure 2 ng of cocaine/ml and 5 ng of benzoylecgonine/ml with about 5% precision. The curves relating the amounts of cocaine and benzoylecgonine added *versus* the amounts found over a large range of cocaine and benzoylecgonine concentrations were straight lines with nearly zero intercepts and slopes of 0.98 ± 0.01 and 0.97 ± 0.01, respectively. The method was used for the analysis of urinary cocaine and benzoylecgonine in cocaine addicts. Assay specificity was confirmed by complete identity of the mass spectra of cocaine and benzoylecgonine with those of authentic materials.

Keyphrases □ Cocaine—GLC–mass spectrometric analysis in human urine □ Benzoylecgonine—GLC–mass spectrometric analysis in human urine □ GLC–mass spectrometry—analyses, cocaine and benzoylecgonine in human urine □ Narcotics—cocaine and benzoylecgonine, GLC–mass spectrometric analyses in human urine

Cocaine abuse (1–5) has prompted considerable interest in methods for the detection and quantitation of the parent drug and its metabolites in biological fluids and tissues. TLC and the enzyme multiplied immunoassay technique (EMIT) are the most frequently employed screening methods for the detection of cocaine in human urine. However, these methods are inherently only semiquantitative at best. Although cocaine may be determined by GLC, the amount of unchanged cocaine excreted in human urine (2, 6) is generally below the method's limits of detection (7, 8).

BACKGROUND

A rather sensitive GLC procedure (9) for cocaine is based on the reduction of cocaine with lithium aluminum hydride, derivatization of the reduced product with pentafluoropropionic anhydride, and subsequent detection by electron capture. This method is sensitive but unspecific, and it is not applicable to cocaine in biological specimens. Besides cocaine, benzoylecgonine, ecgonine, and possibly other metabolites (10) of cocaine are converted by the procedure (9) to the same derivative. Therefore, the GLC-measured cocaine concentration cannot be the true concentration of cocaine alone.

Recently, a GLC procedure for cocaine and benzoylecgonine in the urine of cocaine users was reported (11). The method involves methylation of urinary benzoylecgonine to cocaine by treatment with diazomethane, thereby measuring combined benzoylecgonine and cocaine. Original cocaine was determined in a separate extract without the methylation step. Thus, benzoylecgonine could be determined by difference. Cocaine is metabolized in the human body rather rapidly (12), benzoylecgonine being the major metabolite (13, 14). Consequently, most urine samples of cocaine users contain trace amounts of unchanged drug and large concentrations of benzoylecgonine. Furthermore, cocaine and benzoylecgonine have rather widely different and variable extraction efficiencies, and one ends up dealing with differences of rather large and very small numbers. As a result, this assay is of limited usefulness.

This paper describes a GLC–mass spectrometric assay of cocaine and benzoylecgonine in human urine. Selective ion monitoring, the technique built on combined GLC–mass spectrometry with selective focusing on suitable fragments of the molecular ion (mass fragmentography) or the molecular ion itself, is a well-established technique, used widely in pharmacology (15, 16). This technique was used to develop a sensitive and specific assay for cocaine and benzoylecgonine in human urine with site-specific deuterium-labeled cocaine and benzoylecgonine as internal standards.

EXPERIMENTAL

Materials—Analytical grade cocaine hydrochloride[1], benzoylecgonine[2], norcocaine hydrochloride[3], methyl iodide-d_3[4], and *N*-ethyl-*N*-nitro-*N*-nitrosoguanidine[5] were used without further purification. All solvents were analytical grade[6]. Silanized tubes[7] (10 ml) with screw caps[8] were used for urine extraction; final solvent evaporation was performed in 5-ml glass-stoppered centrifuge tubes[9]. Pasteur pipets with hand-

[1] Mallinckrodt Chemical Works, New York, N.Y.
[2] Techman Inc., Park Forest South, Ill.
[3] Norcocaine hydrochloride was a gift from Dr. Sally, Chemistry Department, University of Wisconsin.
[4] International Chemical & Nuclear Corp., Irvine, Calif.
[5] Pfaltz & Bauer, Flushing, N.Y.
[6] Fisher Scientific Co., Pittsburgh, Pa.
[7] Kimble, Owens-Illinois, Toledo, Ohio.
[8] Lined with Teflon (DuPont).
[9] Pyrex 8084.

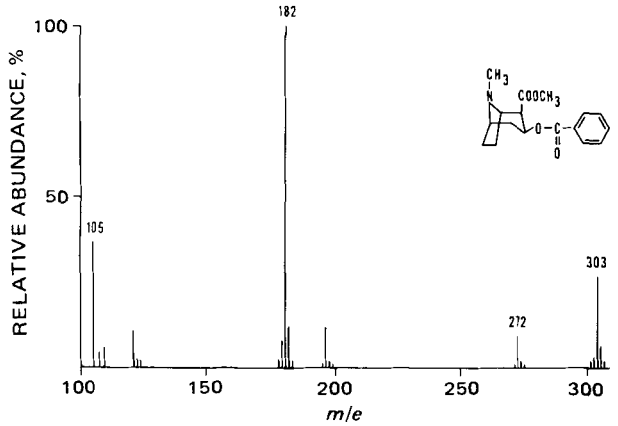

Figure 1—*Electron ionization (70 ev) mass spectrum of cocaine.*

drawn constricted tips were utilized for all solution transfers. Urine samples of cocaine addicts[10] were processed as soon as obtained.

Cocaine-d_3 (*N*-methyl-d_3) was synthesized by treatment of norcocaine with methyl iodide-d_3 using an established procedure for the alkylation of secondary amines (17). Benzoylecgonine-d_3 (*N*-methyl-d_3) was prepared from the labeled cocaine using a known procedure (18) for the synthesis of unlabeled benzoylecgonine from cocaine. Both labeled compounds showed satisfactory mass spectral (electron-impact ionization) characteristics. A selective ion detection analysis of cocaine-d_3 showed the presence of an ion equivalent to 97 ± 0.15% (n = 5) cocaine-d_3. A similar analysis of benzoylecgonine-d_3 showed the presence of an ion equivalent to 96 ± 0.16% (n = 5) benzoylecgonine-d_3.

Extraction of Cocaine and Benzoylecgonine from Urine—*Cocaine*—To 3 ml of urine was added an appropriate amount of cocaine-d_3 (typically 46.7 ng/ml) as an internal standard. The urine was adjusted to pH 9 with 1 *N* NH_4OH and extracted twice with 5 ml of chloroform. The organic fractions were combined, 1 ml of 0.1 *N* HCl was added, and the solution was shaken for 15 min. The organic layer was discarded, and the aqueous phase was adjusted to pH 9 with 1 *N* NH_4OH and extracted twice with 4 ml of chloroform. The organic fractions were combined and dried, and the solvent was evaporated at 40° under a gentle stream of nitrogen. Recovery of cocaine added to control human urine was studied at the 10-ng/ml level.

Benzoylecgonine—To 1 ml of urine was added an appropriate amount of benzoylecgonine-d_3 (typically 120 ng/ml) as an internal standard. The urine was adjusted to pH 9 with 0.1 *N* NH_4OH and extracted twice with 5 ml of chloroform–2-propanol (4:1 v/v). The organic fraction was dried with sodium sulfate and filtered, and the solvent was removed at 60° under a gentle stream of nitrogen. Recovery of benzoylecgonine added to control human urine was studied at the 50-ng/ml level.

Formation of Derivatives—Cocaine is thermally stable, has enough vapor pressure, and can be gas chromatographed as such. Consequently, the dried urinary extract was reconstituted in 50 μl of benzene, and approximately 1 μl was injected into the GLC–mass spectrometer for mass fragmentographic assay.

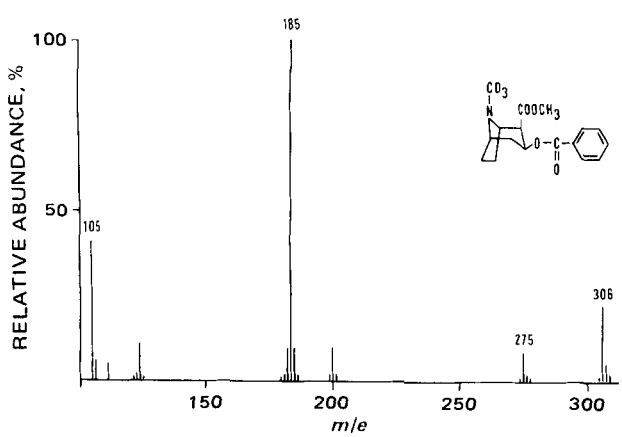

Figure 2—*Electron ionization (70 ev) mass spectrum of cocaine-*d_3.

[10] Aliquots (20 ml) of urine samples of cocaine addicts from metropolitan New York City were obtained from the New York State Narcotic Addiction Control Commission, Testing and Research Laboratory, Brooklyn, N.Y.

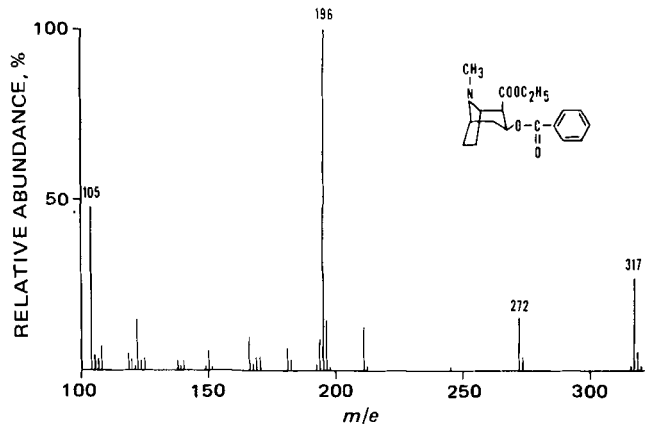

Figure 3—*Electron ionization (70 ev) mass spectrum of benzoylecgonine ethyl ester.*

Benzoylecgonine in the urinary extract was converted to the corresponding ethyl ester by treatment with diazoethane (19). In a typical experiment, potassium hydroxide (1 g) was dissolved in 2 ml of water and 5 ml of ether was added. The biphasic solution was stored in the freezer at −20° for 1 hr. Then *N*-ethyl-*N*-nitro-*N*-nitrosoguanidine (~2 mg) was added, and the reaction mixture was placed in the freezer. In a few minutes, the ether phase turned pale yellow.

Benzoylecgonine from the urinary extract was taken up in ethanol (200 μl) and cooled to −20°, and 250 μl of pale-yellow ether solution containing diazoethane was added. The solution was stored in the freezer for 15 min. The material was removed from the freezer and warmed to room temperature, and the solvents were removed under a gentle stream of nitrogen at 40°. The residue was taken up in 5 ml of chloroform, 1 ml of 0.1 *N* HCl was added, and the mixture was shaken for 15 min and centrifuged.

The organic phase was discarded, the aqueous layer was adjusted to pH 9 with 0.1 *N* NH_4OH, 5 ml of benzene was added, and the solution was shaken for 15 min and centrifuged. The benzene solution was dried with sodium sulfate and filtered, benzene was removed at 40° under a stream of nitrogen, and the residue was reconstituted in 50 μl of benzene. An aliquot (1 μl) of this solution was injected into the GLC–mass spectrometer for the mass fragmentographic assay.

Instrumentation—The magnetic sector, single-focusing mass spectrometer[11] was interfaced with a gas chromatograph and equipped with a multiple ion detector/peak matcher accessory (MID/PM) (15, 16). GLC was performed on a 1.8-m glass column (2 mm i.d.) silanized with 5% dimethyldichlorosilane in toluene and packed with 1.5% OV-1 on 100–200-mesh Gas Chrom Q. The column was conditioned for 24 hr at 280° with a flow rate of 20 ml of helium/min. The column temperature was 205°, the flash heater was at at 230°, the separator was at 235°, and the ion source was at 250°.

The accelerating voltage was 3.5 kv in the scan mode and 3.0 kv in the

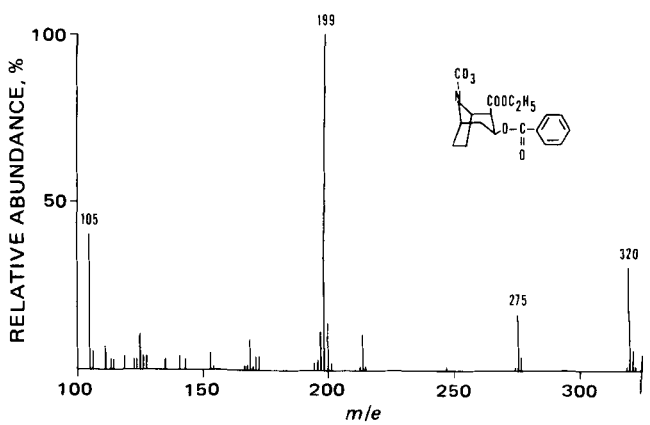

Figure 4—*Electron ionization (70 ev) mass spectrum of benzoylecgonine ethyl ester-*d_3.

[11] LKB 9000, LKB, Stockholm, Sweden.

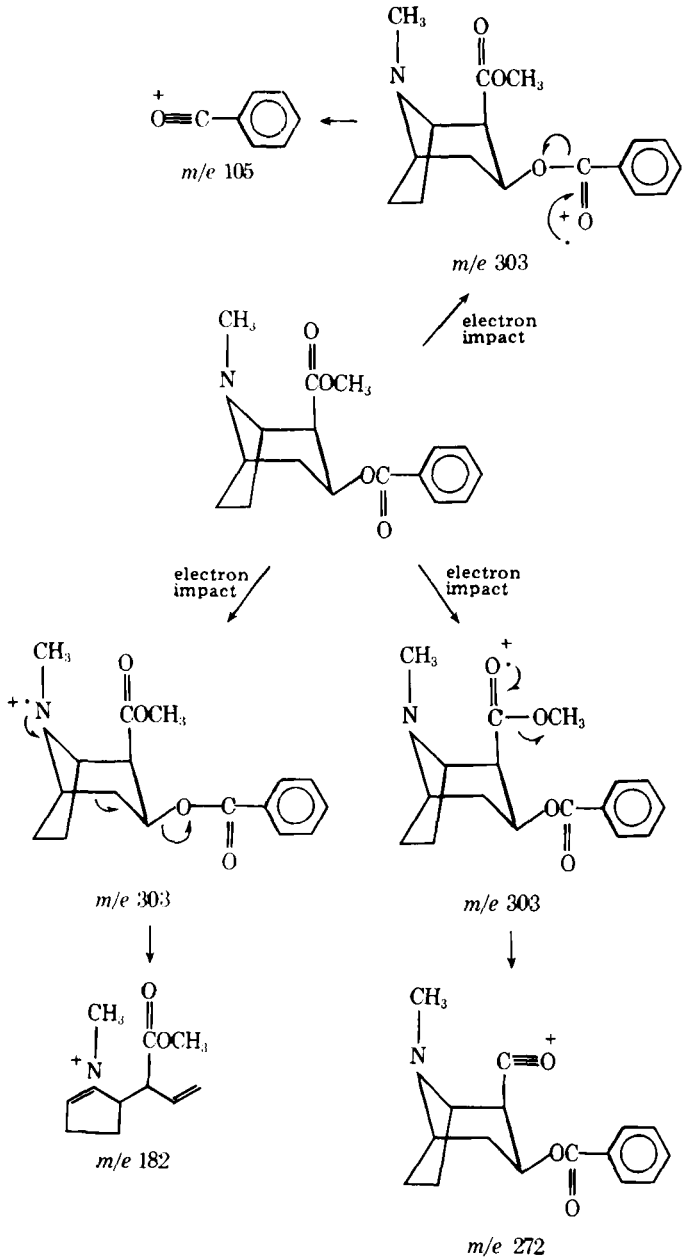

Scheme I

multiple ion detector mode, the ionization potential was 70 ev, and the trap current was set at 60 μamp. The magnetic field was kept constant by focusing the background ion (column bleed) at *m/e* 281, and the additional voltages were 245, 213, 102, and 73 v for measuring ion intensities at *m/e* 303, 306, 317, and 320, respectively. The retention times of cocaine and benzoylecgonine ethyl ester were 2.5 and 3.5 min, respectively.

RESULTS AND DISCUSSION

The mass spectrum of cocaine (Fig. 1) showed a molecular ion at *m/e* 303, a base peak at *m/e* 182 ($M - C_6H_5CO_2$), and another intense peak at *m/e* 105 (benzoyl cation). The fragmentation pattern depicted in Scheme I was readily discernible. The molecular ion formed either by loss of a lone-pair electron from a nitrogen atom or a lone-pair electron from an oxygen atom underwent energetically favorable fragmentation (20–22) to give the observed ions.

The mass spectrum of cocaine-d_3 (Fig. 2) showed an M^+ at *m/e* 306 and was similar to that of cocaine. Most ions were shifted to a higher mass by 3 amu, except the benzoyl cation, *m/e* 105, which was a common fragment ion from both cocaine and cocaine-d_3. The mass spectrum of benzoylecgonine ethyl ester (Fig. 3) showed an M^+ at *m/e* 317, and the fragmentation pattern was rather similar to that of cocaine. The spectrum of benzoylecgonine ethyl ester-d_3 (Fig. 4) was similar to that of the unlabeled isomer, the appropriate ions being shifted to a higher mass by 3 amu.

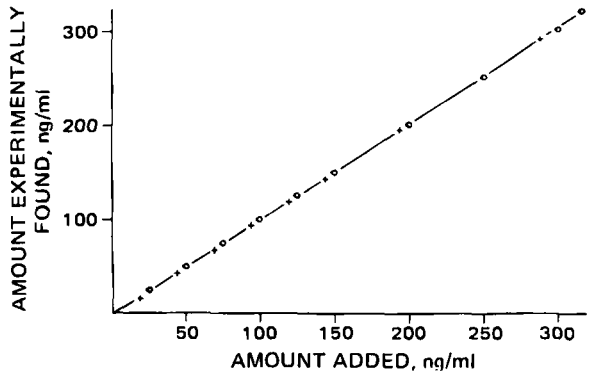

Figure 5—*Curve relating amounts of cocaine (0–255 ng) (+) and benzoylecgonine (0–321 ng) (O) added to control urine* versus *the amounts found using the method described. For these samples, 46.7 ng of cocaine-*d_3*/ml and 121 ng of benzoylecgonine-*d_3*/ml were added as internal standards.*

Control human urine samples subjected to the described procedure for cocaine and benzoylecgonine analysis showed no significant background ions at *m/e* 303, 306, 317, and 320. Known amounts of cocaine and benzoylecgonine, along with their isotopic analogs in fixed amounts, were added to control urine and processed as described. Cocaine and benzoylecgonine were quantitated from the ratios of ion intensities at *m/e* 303/306 and 317/320, respectively. Analysis of cocaine data (Fig. 5) gave a slope of 0.98 ± 0.01 and an intercept of 0.18 ± 0.2 ng. Similarly, benzoylecgonine data (Fig. 5) gave a slope of 0.97 ± 0.01 and an intercept of 0.3 ± 0.2 ng. These data affirm a simple linear relationship between the appropriate ion intensity ratios and concentrations of cocaine and benzoylecgonine and exclude any isotope exchange or any significant kinetic isotope effect in the fragmentation process.

Five samples containing 10 ng of cocaine/ml and 50 ng of benzoylecgonine/ml were analyzed using 7.5 ng of cocaine-d_3/ml and 19.5 ng of benzoylecgonine-d_3/ml as internal standards. The results for these samples were 9.7 ± 0.3 ng/ml for cocaine and 49.0 ± 3.0 ng/ml for benzoylecgonine. These samples were assayed in duplicate; in this set, exactly the same amounts were taken as before but the internal standards were added after the extraction. The recoveries for these samples, based on comparison of the ion intensity ratios of the two sets, were 80 ± 9% for cocaine (*m/e* 303/306) and 65 ± 12% for benzoylecgonine (*m/e* 317/320). The wide range of recoveries observed is expected in trace analysis and is attributed to variable glassware and GLC column adsorption.

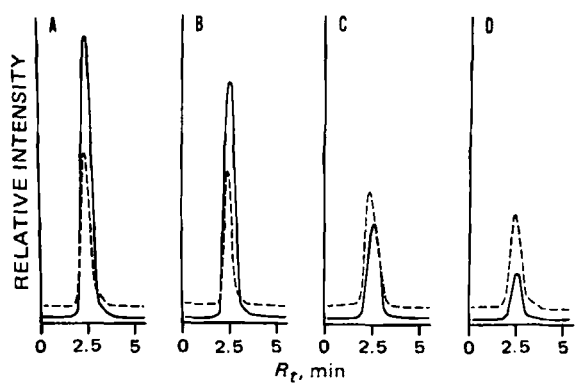

Figure 6—*Selective ion chromatograms for cocaine* (m/e *303*) (—) *along with cocaine-*d_3 (m/e *306*) (- - -). *A: Urine obtained from Subject 1. The internal standard cocaine-*d_3 (m/e *306*) *concentration was 46.7 ng/ml. The cocaine concentration was found to be 91 ng/ml. B: Urine obtained from Subject 2. The internal standard cocaine-*d_3 (m/e *306*) *concentration was 46.7 ng/ml, and the cocaine concentration was found to be 75 ng/ml. C: Urine obtained from Subject 3. The internal standard cocaine-*d_3 (m/e *306*) *concentration was 46.7 ng/ml, and the cocaine concentration was found to be 42 ng/ml. D: Urine obtained from Subject 4. The internal standard cocaine-*d_3 (m/e *306*) *concentration was 5.1 ng/ml, and the cocaine concentration was found to be 2.2 ng/ml.*

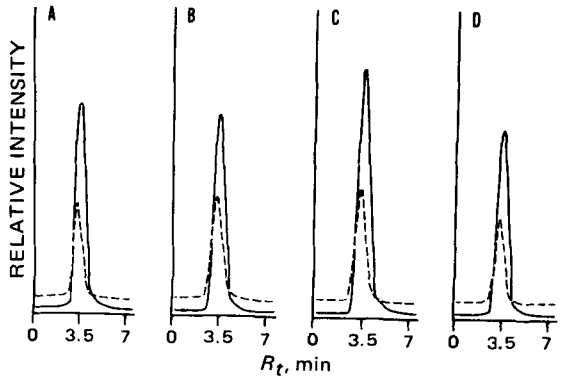

Figure 7—*Selective ion chromatograms for benzoylecgonine ethyl ester* (m/e *317*) (—) *along with benzoylecgonine ethyl ester-*d_3 (m/e *320*) (- - -). *In each sample, 750 ng of deuterated analog/ml was added. A: Urine obtained from Subject 1. Benzoylecgonine* (m/e *317*) *was found to be 1.60 μg/ml. B: Urine obtained from Subject 2. Benzoylecgonine* (m/e *317*) *was found to be 1.50 μg/ml. C: Urine obtained from Subject 3. Benzoylecgonine* (m/e *317*) *was found to be 1.80 μg/ml. D: Urine obtained from Subject 4. Benzoylecgonine* (m/e *317*) *was found to be 1.80 μg/ml.*

Several urine samples of cocaine addicts were assayed for cocaine and benzoylecgonine. Figures 6 and 7 illustrate the mass chromatograms at *m/e* 303–306 (cocaine–cocaine-d_3) and 317–320 (benzoylecgonine–benzoylecgonine-d_3), respectively. The urinary analyses of cocaine and benzoylecgonine of some cocaine addicts are presented in Table I.

The assay for cocaine and its principal metabolite presented here is sensitive, specific, and applicable to other body fluids and tissues. The sensitivity of the assay, being a function of extraction efficiencies, GLC column conditions, and the ion source, cannot be quoted in absolute terms. With near zero leak current in the ion source, clean and freshly silanized GLC columns and glassware, and better than 50% recoveries, an assay sensitivity of approximately 2 ng of cocaine/ml and 5 ng of benzoylecgonine/ml is possible.

The results from the control human urine show good specificity of the assay; however, the observed specificity from control human urine cannot be extrapolated to the urinary analysis of cocaine addicts. Recently, several illicit cocaine samples were found to contain significant amounts of lidocaine, procaine, heroin, and aspirin (23). These materials, if present in the urine, might interfere in current screening methods for cocaine analysis. None of these mentioned drugs shows significant response at *m/e* 303–320 on electron-impact ionization at the retention time of materials of interest (24); therefore, these contaminants can be safely ignored.

The mass chromatogram obtained from biological extracts (Figs. 6 and 7) showed clean and symmetrical peaks; furthermore, these biological extracts were pure enough so that the entire mass spectra of cocaine and

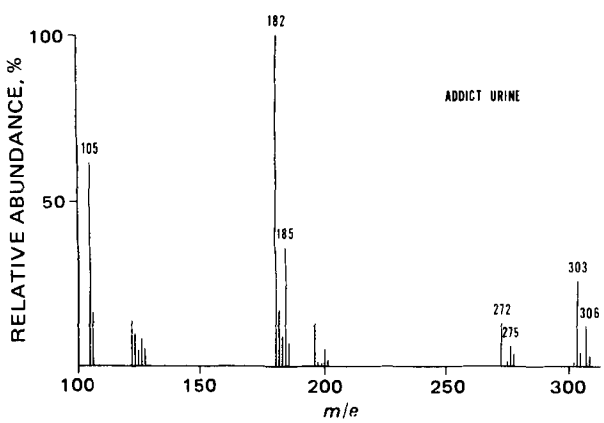

Figure 8—*Mass spectrum of cocaine along with the added internal standard cocaine-*d_3 *from the urine extract of Subject 1.*

Table I—Analyses of Cocaine and Benzoylecgonine in Urine of Cocaine Addicts [a]

Subject	Cocaine Found, ng/ml	Benzoylecgonine Found, μg/ml
1	91 ± 1	1.60 ± 0.02
2	76 ± 0.5	1.50 ± 0.02
3	42 ± 0.4	1.80 ± 0.03
4	2 ± 0.21	1.80 ± 0.022

[a] Analysis of duplicate runs, using 3 ml of urine for cocaine determination and 1 ml of urine for benzoylecgonine determination.

benzoylecgonine could be recorded. The mass spectrum of urinary cocaine with added cocaine-d_3 (Fig. 8) showed expected doublets at *m/e* 303–306 and 182–185. Also of some significance was a singlet of increased relative ion intensity at *m/e* 105, a common fragment ion from the two isomeric species. The mass spectrum of urinary benzoylecgonine was also identical to that of the authentic material.

REFERENCES

(1) K. K. Brown, R. H. Schingler, M. G. Chuabal, and M. H. Malone, *J. Chromatogr.*, **87**, 211 (1973).

(2) M. L. Basto and D. B. Hoffman, *J. Chromatogr. Sci.*, **12**, 269 (1974).

(3) G. Volsky, "Illicit Traffic of Cocaine Growing by Leaps and Bounds in Miami," *New York Times* (Feb. 1, 1970).

(4) "Cocaine Found on the Rise," *Washington Star News* (Apr. 10, 1974).

(5) T. Onis, "Cocoa Means Cocaine. It Is Also a Way of Life," *New York Times* (Feb. 9, 1973).

(6) D. J. Berry and J. Grove, *J. Chromatogr.*, **61**, 111 (1971).

(7) F. Fisch and W. D. C. Wilson, *ibid.*, **40**, 164 (1969).

(8) H. E. Sine, N. P. Kubasik, and J. Waytash, *Clin. Chem.*, **19**, 340 (1973).

(9) J. W. Blake, R. S. Ray, J. S. Noonan, and P. W. Murdick, *Anal. Chem.*, **46**, 288 (1974).

(10) P. K. Nyack, A. L. Misra, and S. J. Mulé, *J. Pharmacol. Exp. Ther.*, **196**, 556 (1976).

(11) J. E. Wallace, H. E. Hamilton, D. E. King, D. J. Bason, H. A. Schwertsner, and S. C. Harris, *Anal. Chem.*, **48**, 34 (1976).

(12) C. Van Dyke, P. G. Barash, P. Jatlow, and R. Byck, *Science*, **191**, 859 (1976).

(13) F. Fisch and W. D. C. Wilson, *J. Pharm. Pharmacol.*, **21**, 135 (1969).

(14) B. Testa and P. Tenner, "Drug Metabolism—Chemical and Biological Aspects," Dekker, New York, N.Y., 1976, p. 139.

(15) C. G. Hammar, B. Holmstedt, and R. Ryhage, *Anal. Biochem.*, **25**, 53e (1968).

(16) B. Holmstedt and L. Palmer, *Adv. Biochem. Psychopharmacol.*, **7**, 1 (1973).

(17) R. L. Hawks, I. J. Kopin, R. W. Colburn, and N. B. Thoa, *Life Sci.*, **15**, 2189 (1974).

(18) T. L. Bosin, F. C. Garbrecht, and M. G. Raymond, *Res. Commun. Chem. Pathol. Pharmacol.*, **11**, 405 (1975).

(19) L. Bertilsson and L. Palmer, *Science*, **177**, 74 (1972).

(20) H. Budzikiewicz, C. Djerrassi, and D. H. Williams, "Structure Elucidation of Natural Products by Mass Spectrometry," vol. I, Holden-Day, San Francisco, Calif., 1969, p. 219.

(21) C. A. Grob, *Bull. Soc. Chim. Fr.*, **1960**, 1360.

(22) C. A. Grob, "Theoretical Organic Chemistry" (Kekule Symposium), Butterworth, London, England, 1959, p. 114.

(23) *Drug Survival News*, **Sept.–Oct. 1976**, 5.

(24) J. K. Baker, *Anal. Chem.*, **49**, 906 (1977).

ACKNOWLEDGMENTS

Supported by Grant DA 00327 and by the Department of Mental Hygiene, State of New York, Office of Research.

Dr. S. J. Mule, Commissioner, New York State Drug Abuse Control Commission, is gratefully acknowledged for providing the urine samples of cocaine addicts. Mrs. Theresa Lutz and Sidney Bernstein are gratefully acknowledged for making the illustrations.

Methods for Storage of Antimicrobial Effectiveness Test Inoculum Suspensions below Freezing

THOMAS E. BOHANNON ˣ and LAN-FUN LI WEN

Received July 18, 1977, from the *Quality Control Department, Hoffmann-La Roche, Inc., Nutley, NJ 07110.* Accepted for publication October 5, 1977.

Abstract □ Studies were conducted to determine the suitability of storage below freezing of some antimicrobial effectiveness test inoculum organisms: *Staphylococcus aureus, Escherichia coli, Pseudomonas aeruginosa,* and *Candida albicans.* Several solutions used for protecting microorganisms subjected to storage below freezing were compared. Comparison of 10% dextrose with other solutions (distilled water; 0.07 *M* phosphate buffer, pH 7.0, with 15% glycerol; and 0.07 *M* phosphate buffer, pH 7.0, with 7.5% dimethyl sulfoxide) demonstrated that inoculum suspensions were most stable when prepared with 10% dextrose. After storage for 6 months at −50° in a freezer, inoculum suspensions prepared with 10% dextrose retained viability and demonstrated suitability for use in antimicrobial effectiveness tests of dosage forms containing preservatives.

Keyphrases □ Antimicrobial effectiveness test inoculum organisms, various—storage below freezing, effect of various solutions □ Microorganisms, various—in antimicrobial effectiveness test inoculum suspensions, storage below freezing, effect of various solutions

Inoculum suspensions for antimicrobial effectiveness tests are prepared from fresh stock cultures of *Staphylococcus aureus* (ATCC 6538), *Escherichia coli* (ATCC 8739), *Pseudomonas aeruginosa* (ATCC 9027), and *Candida albicans* (ATCC 10231). Frequent preparation of these fresh suspensions is time consuming. Since it was reported that vitamin (1, 2) and antibiotic (3) assay inoculum suspensions can be stored in a ready state below freezing without significant loss of viability or performance characteristics, the present investigation was initiated to determine the suitability of preparing antimicrobial effectiveness test inoculum suspensions for storage in a ready state below freezing.

Bulk inoculum suspensions were prepared and stored below freezing in aliquots subsequently tested for viability and performance in antimicrobial effectiveness tests. In determining the percentage viability, the viable counts of the antimicrobial effectiveness test inoculum suspensions after storage for a period below freezing were compared with the initial viable counts of the bulk suspensions before freezing. In testing for their suitability as antimicrobial effectiveness test inoculum suspensions, antimicrobial effectiveness tests were performed on a parenteral product using the inocula stored below freezing and nonfrozen inocula. This product contained benzyl alcohol as a preservative.

EXPERIMENTAL

Preparation of Bulk Inoculum Suspensions—The bacterial cultures, *S. aureus, E. coli,* and *P. aeruginosa,* were grown for 24 hr at 35° on soybean casein digest agar slants[1]. The yeast culture of *C. albicans* was grown for 48 hr at 35° on Sabouraud dextrose agar slants[2]. Four solutions were used to prepare the bulk inoculum suspensions: distilled water; 10% dextrose; 0.07 *M* phosphate buffer, pH 7.0, with 15% glycerol; and 0.07 *M* phosphate buffer, pH 7.0, with 7.5% dimethyl sulfoxide.

After autoclaving, quantities of these solutions were dispensed into sterile jars. For *P. aeruginosa* and *E. coli,* 200 ml of each of the four solutions was dispensed. For *S. aureus,* 100 ml of each of the four solutions was dispensed. And for *C. albicans,* 50 ml of each of the four solutions was dispensed.

The cultures were harvested from the agar slants and suspended in the various solutions as follows. A 1-ml aliquot of solution was placed aseptically onto each agar slant, and cultures were scraped free from the surface of the slants with a sterile loop and pooled back into the bulk suspensions. Enough cells were harvested until the percent transmittance of these suspensions corresponded to 10^8–10^9 cells/ml, as approximately determined from standard curves.

Preparation of Standard Curves of Percent Transmittance *versus* Viable Counts of Inoculum Suspensions—To determine the percent transmittance, 1.0 ml of bacterial suspension was mixed with 9.0 ml of pH 7.2 Butterfield phosphate buffer contained in a colorimeter tube. The percent transmittance of this 10-fold dilution was read on a colorimeter[3] at 420 nm following adjustment to zero with a buffer blank. For yeast suspensions, a 100-fold dilution was used to determine the percent transmittance.

For determination of the viable counts of microorganisms in inoculum suspensions and in the suspensions used for preparing the standard curves, the following procedure was used since it simulates the actual antimicrobial effectiveness test procedure. A 0.01-ml quantity of suspension was added aseptically with a glass serological pipet (1/10 in 1/100 ml) to 10 ml of sterile pH 7.2 Butterfield phosphate buffer. Subsequently, in duplicate, 0.01 ml of each 1000-fold dilution was placed aseptically with a glass serological pipet (1/10 in 1/100 ml) into a sterile petri dish (20 × 100 mm). Soybean casein digest agar was added to the plates containing bacteria, and Sabouraud dextrose agar was added to the plates containing yeast. All plates were incubated at 35° for 3 days and then counted.

The standard curves were constructed by plotting the percent transmittance at 420 nm *versus* the viable count per milliliter of suspension on semilog paper. The standard curves were subsequently used in preparing inoculum suspensions with counts of approximately 10^8–10^9 viable cells/ml.

Freezing and Storage of Antimicrobial Effectiveness Test Inocula below Freezing—Before freezing, the initial viable count of each bulk suspension was determined as already described. Then 5-ml quantities of the bulk suspensions were placed aseptically into sterile 10-ml flint glass vials[4]. The vials were capped with sterile 13-mm butyl stoppers[5] and 13-mm aluminum triple seals[5], which were crimped with a crimper[6]. Then the vials were placed into a low temperature freezer[7] and stored at −50°.

Determination of Percentage Viability of Inoculum Suspensions after Storage—At various intervals, vials containing each suspension were taken from the freezer and thawed by being placed into a water bath at 25°. Immediately after thawing, the viable counts of these suspensions were determined as previously described. The percentage viability of the suspensions was determined with the following formula:

$$\text{percentage viability of inoculum suspension after storage at } -50° = \frac{\text{viable count after storage at } -50° \times 100}{\text{initial viable count before freezing}} \quad \text{(Eq. 1)}$$

Antimicrobial Effectiveness Test Procedure—After storage of inoculum suspensions for 0, 2, 4, and 6 months at −50°, 10-ml quantities

[1] Bacto-tryptic soy agar, Difco Laboratories, Detroit, Mich.
[2] Bacto-Sabouraud dextrose agar, Difco Laboratories, Detroit, Mich.
[3] Spectronic 20 colorimeter, Bausch & Lomb, Rochester, N.Y.
[4] Kimble Glass Co., Montclair, N.J.
[5] West Co., Phoenixville, Pa.
[6] Fermpress, West Co., Phoenixville, Pa.
[7] Ultra-low freezer model ULT-1285-B-2, Revco Inc., West Columbia, S.C.

Table I—Viable Counts and Percentage Viability of Inoculum Suspensions of *S. aureus* (ATCC 6538) after Various Storage Times at −50°

Storage Time at −50°	Distilled Water		10% Dextrose		0.07 *M* Phosphate Buffer, pH 7.0, with 15% Glycerol		0.07 *M* Phosphate Buffer, pH 7.0, with 7.5% Dimethyl Sulfoxide	
	Counts/ml of Suspension, $\times 10^{-8}$	Viability, %	Counts/ml of Suspension, $\times 10^{-8}$	Viability, %	Counts/ml of Suspension, $\times 10^{-8}$	Viability, %	Counts/ml of Suspension, $\times 10^{-8}$	Viability, %
Zero time[a]	5.4	100	4.8	100	4.8	100	4.2	100
1 Day	6.0	111	4.8	100	4.8	100	4.2	100
2 Months	4.8	88	4.5	94	4.2	88	3.6	86
4 Months	4.5	83	3.3	69	3.6	75	3.3	79
6 Months	4.5	83	4.5	94	4.2	88	4.2	100

[a] The counts per milliliter of bulk suspension before freezing are used as zero time counts, which are considered as 100% viable as a basis for the percentage viability calculations.

Table II—Viable Counts and Percentage Viability of Inoculum Suspensions of *E. coli* (ATCC 8739) after Various Storage Times at −50°

Storage Time at −50°	Distilled Water		10% Dextrose		0.07 *M* Phosphate Buffer, pH 7.0, with 15% Glycerol		0.07 *M* Phosphate Buffer, pH 7.0, with 7.5% Dimethyl Sulfoxide	
	Counts/ml of Suspension, $\times 10^{-8}$	Viability, %	Counts/ml of Suspension, $\times 10^{-8}$	Viability, %	Counts/ml of Suspension, $\times 10^{-8}$	Viability, %	Counts/ml of Suspension, $\times 10^{-8}$	Viability, %
Zero time[a]	5.4	100	6.0	100	4.8	100	6.0	100
1 Day	2.1	39	5.4	90	5.4	113	5.4	90
2 Months	4.2	78	4.8	80	4.8	100	4.8	80
4 Months	3.0	55	3.0	50	3.6	75	3.3	55
6 Months	5.4	100	4.8	80	5.4	113	5.1	85

[a] The counts per milliliter of bulk suspension before freezing are used as zero time counts, which are considered as 100% viable as a basis for the percentage viability calculations.

of the product were transferred aseptically to sterile screw-capped test tubes (150 × 20 mm) to which 0.01 ml of each thawed inoculum suspension was added aseptically with a glass serological pipet (1/10 in 1/100 ml) and mixed. The product–inoculum mixtures were allowed to stand at room temperature. After 5 and 30 min (for the bacteria) and 1, 2, 4, 6, and 7 hr, and on a daily basis thereafter, loopfuls containing approximately 0.01 ml of each product–inoculum mixture were transferred to soybean casein digest agar slants and 13-ml quantities of fluid soybean casein digest medium[8] for the bacteria and to Sabouraud dextrose agar slants and 13-ml quantities of fluid Sabouraud medium[9] for the yeast.

The bacterial cultures were incubated at 35° and the yeast cultures were incubated at 23°. After 7 days, these cultures were examined visually for the presence or absence of growth as indicated by turbidity.

RESULTS

Determination of Viability of Inoculum Suspensions after Storage—Tables I–IV show the average counts per milliliter of two replicate determinations for all inoculum suspensions and their percentage viability after storage at −50° for up to 6 months. These data indicate that maintenance of viability differed according to culture and solution. The loss of viability was minimal in all suspensions of *S. aureus* and *E. coli* (Tables I and II). With suspensions of *C. albicans* and *P. aeruginosa*, however, there was a greater loss of viability after storage below freezing.

With *C. albicans*, the most severe loss of viability occurred in distilled water, where there was only 21% viability within 2 months and only 13% viability after 6 months (Table III). In the other solutions, even after 6 months, the percentage viability of this culture was 44% in buffered glycerol, 78% in buffered dimethyl sulfoxide, and 68% in 10% dextrose. However, with *C. albicans*, viability generally was best maintained in 10% dextrose.

With *P. aeruginosa*, a rapid decline in viability in all solutions occurred within 1 day (Table IV). Then the percentage viability in all solutions tended to decline much more slowly for the remainder of the 6-month storage. However, as with *C. albicans*, viability was best maintained in 10% dextrose. After 1 day, the percentage viability of *P. aeruginosa* in 10% dextrose was greater than in the other solutions.

After storage below freezing for 6 months, the percentage viability of *P. aeruginosa* ranged from 40% in 10% dextrose to only 19% in buffered glycerol.

Antimicrobial Effectiveness Test Results—Table V shows the last time at which each inoculum suspension prepared in distilled water and 10% dextrose survived contact with the product and the first time at which death of each inoculum suspensions was recorded. It is apparent from these data that this product, which contained benzyl alcohol as an antimicrobial agent, showed similar antimicrobial activity against both nonfrozen inocula and the corresponding inocula stored for 6 months at −50°.

Furthermore, this product showed similar antimicrobial activity against inocula prepared in distilled water and 10% dextrose and stored for 2 and 4 months at −50°. These data were not shown since they did not vary significantly from the data of Table V.

DISCUSSION

Effect of Solutions on Viability and Performance of Antimicrobial Effectivensss Test Inocula—It is best to prepare antimicrobial effectiveness test inoculum suspensions in 10% dextrose prior to storage below freezing since the viability of the cultures was best maintained in this solution. After storage for 6 months, the viable count of all inocula prepared in 10% dextrose was high enough for an initial concentration of 10^5–10^6-microorganisms/ml of product in the antimicrobial effectiveness test experiments. Moreover, in terms of qualitative response, the inocula prepared in this solution retained suitability for use in antimicrobial effectiveness tests.

Nonfrozen inocula and inocula stored for 2, 4, and 6 months at −50° showed similar susceptibility to the antimicrobial activity of the preservative in the product. For each culture, both nonfrozen inocula and corresponding inocula stored for 2, 4, and 6 months at −50° that were prepared in 10% dextrose showed similar survival times in contact with the product. These inocula were also killed by the preservative system of the product within similar time intervals.

Development of Procedures for Storage of Antimicrobial Effectiveness Test Inocula—These procedures were based on the factors associated with the preservation of vitamin assay cultures below freezing. As stated previously (4), the number of bacteria surviving subfreezing temperatures is influenced by the initial count of viable cells when frozen, the rate of the freezing and thawing process, the temperature of storage (0–−20° being more destructive than below −20°), the time or duration

[8] Bacto-tryptic soy broth, Difco Laboratories, Detroit, Mich.
[9] Bacto-fluid Sabouraud medium, Difco Laboratories, Detroit, Mich.

Table III—Viable Counts and Percentage Viability of Inoculum Suspensions of *C. albicans* (ATCC 10231) after Various Storage Times at −50°

Storage Time at −50°	Distilled Water		10% Dextrose		0.07 *M* Phosphate Buffer, pH 7.0, with 15% Glycerol		0.07 *M* Phosphate Buffer, pH 7.0, with 7.5% Dimethyl Sulfoxide	
	Counts/ml of Suspension, × 10^{-8}	Viability, %	Counts/ml of Suspension, × 10^{-8}	Viability, %	Counts/ml of Suspension, × 10^{-8}	Viability, %	Counts/ml of Suspension, × 10^{-8}	Viability, %
Zero time[a]	3.8	100	1.9	100	1.9	100	1.7	100
1 Hour	1.7	45	2.1	110	1.9	100	1.7	100
2 Months	0.8	21	1.5	80	1.3	70	1.7	100
4 Months	0.8	21	2.1	110	1.5	80	1.3	78
6 Months	0.5	13	1.3	68	0.8	44	1.3	78

[a] The counts per milliliter of bulk suspension before freezing are used as zero time counts, which are considered as 100% viable as a basis for the percentage viability calculations.

Table IV—Viable Counts and Percentage Viability of Inoculum Suspensions of *P. aeruginosa* (ATCC 9027) after Various Storage Times at −50°

Storage Time at −50°	Distilled Water		10% Dextrose		0.07 *M* Phosphate Buffer, pH 7.0, with 15% Glycerol		0.07 *M* Phosphate Buffer, pH 7.0, with 7.5% Dimethyl Sulfoxide	
	Counts/ml of Suspension, × 10^{-8}	Viability, %	Counts/ml of Suspension, × 10^{-8}	Viability, %	Counts/ml of Suspension, × 10^{-8}	Viability, %	Counts/ml of Suspension, × 10^{-8}	Viability, %
Zero time[a]	6.6	100	6.0	100	5.4	100	6.6	100
1 Day	4.2	70	4.8	80	4.2	78	4.8	72
2 Months	2.7	41	3.6	60	3.0	55	3.3	50
4 Months	1.8	27	3.3	55	1.5	27	2.1	36
6 Months	2.1	32	2.4	40	1.0	19	1.5	23

[a] The counts per milliliter of bulk suspension before freezing are used as zero time counts, which are considered as 100% viable as a basis for the percentage viability calculations.

Table V—Antimicrobial Effectiveness of Benzyl Alcohol in the Formulation of the Test Product against Inoculum Suspensions Stored at −50° for Various Intervals

Solution	Test Culture	Storage Interval: Nonfrozen Control Inocula[a] Survived[b]	Nonfrozen Control Inocula[a] Killed[c]	Inocula Stored 6 Months at −50° Survived[b]	Inocula Stored 6 Months at −50° Killed[c]
Distilled water	*S. aureus*	7 hr	1 day	7 hr	1 day
	E. coli	5 min	30 min	5 min	30 min
	P. aeruginosa	5 min	30 min	5 min	30 min
	C. albicans	1 day	2 days	1 day	2 days
10% dextrose solution	*S. aureus*	7 hr	1 day	6 hr	7 hr
	E. coli	5 min	30 min	5 min	30 min
	P. aeruginosa	5 min	30 min	5 min	30 min
	C. albicans	1 day	2 days	2 days	5 days

[a] These inocula had viable counts comparable to the inocula stored at −50°. [b] The last time at which each inoculum suspension survived contact with the formulation of the test product. [c] The first time at which death of each inoculum suspension was recorded.

of the storage period, and the physical protection offered by the solutions in which the microorganisms are frozen.

Accordingly, enough cells were harvested into the bulk solutions to provide 10^8–10^9 viable cells/ml in the antimicrobial effectiveness test inocula even after extended storage below freezing.

The inoculum suspensions were frozen slowly, because rapid freezing of microbial suspensions with dry ice and acetone previously was unsuccessful (1). Furthermore, preservation of vitamin assay inoculum suspensions by lyophilization was not feasible, because only 2–3% of the organisms subjected to this process survived (1).

Although vitamin assay inoculum suspensions have been stored successfully for 5 years at −40° after slow freezing (2), it was felt that storage of the antimicrobial effectiveness test inocula for 6 months below freezing would be sufficient for routine laboratory uses. This temperature for storage (−50°) was selected because better survival of microorganisms at lower storage temperatures has been demonstrated (5).

Distilled water, 10% dextrose, 0.07 *M* phosphate buffer, pH 7.0, with 15% glycerol, and 0.07 *M* phosphate buffer, pH 7.0, with 7.5% dimethyl sulfoxide were selected as test solutions since each confers physical protection to microorganisms subjected to freezing and storage below freezing. The 0.07 *M* phosphate buffer, pH 7.0, without additives gave protection to *E. coli* stored at −9° (4). The 0.07 *M* phosphate buffer, pH 7.0, with 15% glycerol is recommended for preservation of some vitamin assay inoculum suspensions below freezing, because the viability of these suspensions and their efficacy as vitamin assay inocula were maintained in this solution (1, 2).

Dimethyl sulfoxide (7.5%) afforded protection to strains of the alga *Euglena gracilis*, subjected to freezing in liquid nitrogen at −196° (6), and distilled water was recommended for the preservation of test organism suspensions for antibiotic assays. For instance, *S. aureus* was maintained at least 1 year in distilled water without any significant loss in viability and with acceptable dose response to various antibiotics (3).

Finally, dextrose was indicated as a protective agent for tissues (7). Furthermore, with suspension in 10% dextrose, the viability and dose response of antibiotic assay cultures as *Sarcina lutea* (ATCC 9341) were retained satisfactorily after storage below freezing[10].

REFERENCES

(1) A. E. Tanguay, *Appl. Microbiol.*, **7**, 84 (1959).

(2) A. E. Tanguay, J.C. Martin, and M. H. Blanchard, "Developments in Industrial Microbiology," vol. 6, American Institute of Biological Sciences, Washington, D.C., 1974, p. 175.

[10] The use of 10% dextrose for preparation of inocula for storage below freezing was recommended by Mrs. Celina Bernhart, Antibiotic Assay Laboratory, Quality Control Department, Hoffmann-La Roche, in a personal communication.

(3) D. T. Salt, B. Arret, and J. Wilner, *J. Pharm. Sci.*, **62**, 2040 (1973).
(4) R. W. Squires and S. E. Hartsell, *Appl. Microbiol.*, **3**, 40 (1955).
(5) D. H. Howard, *J. Bacteriol.*, **71**, 625 (1956).
(6) S. W. Hwang, "Freezing and Drying of Microorganisms," University Park Press, Baltimore, Md., 1969, p. 169.
(7) B. J. Luyet and J. F. Keane, Jr., *Biodynamica*, **139**, 119 (1952).

ACKNOWLEDGMENTS

The authors thank J. Felix, M. Emery, and F. Mamaril, Quality Control Department, Hoffmann–La Roche, for providing technical consultation and for reviewing this manuscript. In addition, they thank C. Bernhart for her technical consultation and R. Russomanno of the same Quality Control Department for his interest and encouragement.

Thiamine Whole Blood Pharmacokinetics in Rats Using Both a Specific ^{35}S-Thiamine Liquid Scintillation Assay and the Thiochrome Fluorescence Assay

J. D. PIPKIN and V. J. STELLA ˣ

Received June 16, 1977, from the *Department of Pharmaceutical Chemistry, University of Kansas, Lawrence, KS 66045.* Accepted for publication September 30, 1977.

Abstract □ The study of factors altering the CNS and GI absorption of thiamine in rats required the development of a specific assay for thiamine from 100-μl samples of blood and plasma and small quantities of tissue. The specific thiochrome fluorescence assay for thiamine was modified to handle microsamples and to use ^{35}S-thiamine. This sensitive and specific radioassay using ^{35}S-thiamine gave pharmacokinetic parameters for 4-mg/kg iv doses of thiamine in rats equivalent to those using the less sensitive thiochrome fluorescence assay. The new assay, because of its lower limit of detection, allowed the study of the time profile of thiamine after a 1-mg/kg iv dose in rats. Such a time profile could not have been followed using the standard thiochrome fluorescence assay.

Keyphrases □ Thiamine—radiochemical analysis in blood, compared to fluorometric analysis, pharmacokinetics in rats □ Radiochemistry—analysis, thiamine in blood, compared to fluorometric analysis □ Pharmacokinetics—thiamine in rats □ Vitamins—thiamine, radiochemical analysis in blood, compared to fluorometric analysis, pharmacokinetics in rat

The thiochrome (II, Scheme I) fluorescence assay for thiamine (I) in biological fluids was described previously (1–12). Specific assays for thiamine with either ^{14}C- or ^{35}S-thiamine utilized electrophoric separations (12) or the ion-exchange system as in the thiochrome fluorescence assay (1). The study (1) using ion exchange did not, however, determine assay specificity in an *in vivo* system.

The present paper reports the modification of the specific thiochrome fluorescence assay for thiamine in whole blood to its use with microsamples and ^{35}S-thiamine and demonstrates its use in following the pharmacokinetics of intravenously administered thiamine at low doses to rats.

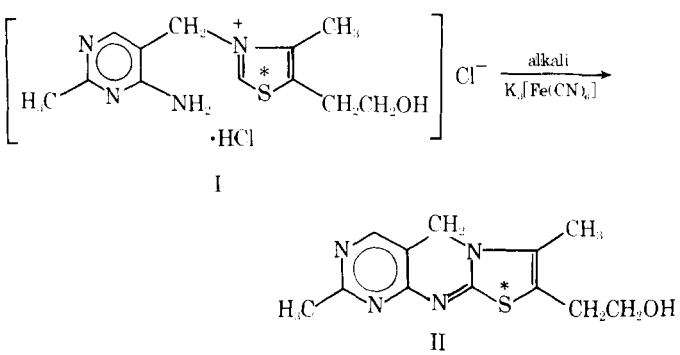

Scheme I

Quantitative studies of factors altering the central nervous system (CNS) and GI absorption of thiamine (vitamin B_1) have been limited. Thiamine, being a very water-soluble compound with a quaternary nitrogen, is poorly absorbed into the CNS (13) and poorly absorbed from the GI tract (14–17). Thiamine passes through those barriers because it is actively transported (13–17). However, as with other active transport systems, thiamine absorption is both saturable and/or easily inhibited (13–17). These absorption characteristics have been implicated in Wernicke's encephalopathy (14–18) in alcoholics, in the terminal children's disorder Leigh's disease (19–27), and in polioencephalomalacia in feedlot cattle (28, 29).

A study of thiamine pharmacokinetics in whole blood as a preliminary to the study of the effects of lipid-soluble thiamine prodrugs (30) in altering thiamine distribution required the development of a specific and sensitive assay for free thiamine (nonphosphorylated) and total thiamine (thiamine plus its mono-, di-, and triphosphate esters) in 100-μl samples of whole blood and plasma and small quantities of tissue, *e.g.*, brain tissue.

EXPERIMENTAL

Reagents and Materials—All reagents were analytical grade, and all aqueous solutions were prepared using glass-distilled deionized water. The primary source for reagent preparation and storage was the review of Mickelsen and Yamamoto (6). Reagent preparation and storage also were discussed elsewhere (1–12).

The ^{35}S-thiamine was obtained commercially[1] as two different lots of varying specific activity. Radiochemical purity was determined by paper chromatography and TLC, and chemical purity was checked by IR spectrophotometry. Thiamine hydrochloride was obtained commercially[2] with its purity confirmed by bioassay.

[1] Amersham/Searle Corp. Arlington Heights, Ill., lot A05006, specific activity 176 mCi/mmole and lot E06046, specific activity 233 mCi/mmole.
[2] Sigma Chemical Co., St. Louis, Mo.

(3) D. T. Salt, B. Arret, and J. Wilner, *J. Pharm. Sci.*, **62**, 2040 (1973).
(4) R. W. Squires and S. E. Hartsell, *Appl. Microbiol.*, **3**, 40 (1955).
(5) D. H. Howard, *J. Bacteriol.*, **71**, 625 (1956).
(6) S. W. Hwang, "Freezing and Drying of Microorganisms," University Park Press, Baltimore, Md., 1969, p. 169.
(7) B. J. Luyet and J. F. Keane, Jr., *Biodynamica*, **139**, 119 (1952).

ACKNOWLEDGMENTS

The authors thank J. Felix, M. Emery, and F. Mamaril, Quality Control Department, Hoffmann–La Roche, for providing technical consultation and for reviewing this manuscript. In addition, they thank C. Bernhart for her technical consultation and R. Russomanno of the same Quality Control Department for his interest and encouragement.

Thiamine Whole Blood Pharmacokinetics in Rats Using Both a Specific ^{35}S-Thiamine Liquid Scintillation Assay and the Thiochrome Fluorescence Assay

J. D. PIPKIN and V. J. STELLA ˣ

Received June 16, 1977, from the *Department of Pharmaceutical Chemistry, University of Kansas, Lawrence, KS 66045.* Accepted for publication September 30, 1977.

Abstract □ The study of factors altering the CNS and GI absorption of thiamine in rats required the development of a specific assay for thiamine from 100-μl samples of blood and plasma and small quantities of tissue. The specific thiochrome fluorescence assay for thiamine was modified to handle microsamples and to use ^{35}S-thiamine. This sensitive and specific radioassay using ^{35}S-thiamine gave pharmacokinetic parameters for 4-mg/kg iv doses of thiamine in rats equivalent to those using the less sensitive thiochrome fluorescence assay. The new assay, because of its lower limit of detection, allowed the study of the time profile of thiamine after a 1-mg/kg iv dose in rats. Such a time profile could not have been followed using the standard thiochrome fluorescence assay.

Keyphrases □ Thiamine—radiochemical analysis in blood, compared to fluorometric analysis, pharmacokinetics in rats □ Radiochemistry—analysis, thiamine in blood, compared to fluorometric analysis □ Pharmacokinetics—thiamine in rats □ Vitamins—thiamine, radiochemical analysis in blood, compared to fluorometric analysis, pharmacokinetics in rat

The thiochrome (II, Scheme I) fluorescence assay for thiamine (I) in biological fluids was described previously (1–12). Specific assays for thiamine with either ^{14}C- or ^{35}S-thiamine utilized electrophoric separations (12) or the ion-exchange system as in the thiochrome fluorescence assay (1). The study (1) using ion exchange did not, however, determine assay specificity in an *in vivo* system.

The present paper reports the modification of the specific thiochrome fluorescence assay for thiamine in whole blood to its use with microsamples and ^{35}S-thiamine and demonstrates its use in following the pharmacokinetics of intravenously administered thiamine at low doses to rats.

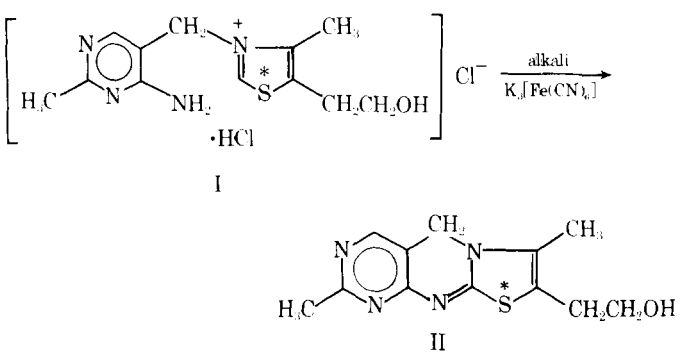

Scheme I

Quantitative studies of factors altering the central nervous system (CNS) and GI absorption of thiamine (vitamin B_1) have been limited. Thiamine, being a very water-soluble compound with a quaternary nitrogen, is poorly absorbed into the CNS (13) and poorly absorbed from the GI tract (14–17). Thiamine passes through those barriers because it is actively transported (13–17). However, as with other active transport systems, thiamine absorption is both saturable and/or easily inhibited (13–17). These absorption characteristics have been implicated in Wernicke's encephalopathy (14–18) in alcoholics, in the terminal children's disorder Leigh's disease (19–27), and in polioencephalomalacia in feedlot cattle (28, 29).

A study of thiamine pharmacokinetics in whole blood as a preliminary to the study of the effects of lipid-soluble thiamine prodrugs (30) in altering thiamine distribution required the development of a specific and sensitive assay for free thiamine (nonphosphorylated) and total thiamine (thiamine plus its mono-, di-, and triphosphate esters) in 100-μl samples of whole blood and plasma and small quantities of tissue, *e.g.*, brain tissue.

EXPERIMENTAL

Reagents and Materials—All reagents were analytical grade, and all aqueous solutions were prepared using glass-distilled deionized water. The primary source for reagent preparation and storage was the review of Mickelsen and Yamamoto (6). Reagent preparation and storage also were discussed elsewhere (1–12).

The ^{35}S-thiamine was obtained commercially[1] as two different lots of varying specific activity. Radiochemical purity was determined by paper chromatography and TLC, and chemical purity was checked by IR spectrophotometry. Thiamine hydrochloride was obtained commercially[2] with its purity confirmed by bioassay.

[1] Amersham/Searle Corp. Arlington Heights, Ill., lot A05006, specific activity 176 mCi/mmole and lot E06046, specific activity 233 mCi/mmole.
[2] Sigma Chemical Co., St. Louis, Mo.

Thiamine hydrochloride solution for injection was prepared in the following manner. ^{35}S-Thiamine hydrochloride, specific activity 176 or 233 mCi/mmole, and unlabeled thiamine hydrochloride were dissolved in an isotonic sodium chloride solution to final concentrations of 1 and 0.25 mg/100 μl, corresponding to 57 and 110 μCi/100 μl, respectively. These solutions were such that injection of 100 μl to 250-g rats resulted in thiamine dosing of 4 and 1 mg/kg, respectively.

***In Vivo* Animal Studies**—Four male Sprague–Dawley rats[3], 340–400 g, were used for the 4-mg/kg study; five rats, 200–250 g, were used for the 1-mg/kg study. The rats were maintained in stainless steel cages for 1–3 weeks prior to use and were fed standard rat food[4], with food and water allowed *ad libitum*.

For the pharmacokinetic study, the rats were anesthetized with urethan[2] (1 g/kg ip). The animals were then placed on an operating table maintained at 37°. Each animal then received the appropriate dose of thiamine hydrochloride administered intravenously *via* the dorsal vein of the penis. Serial blood sampling into 100-μl micropipets[5] (pretreated with an anticoagulant solution[6]) was from the severed tail vein at the appropriate times.

Sample Handling and Extraction—*Free and Total Whole Blood Assay*—Blood samples in the 100-μl micropipets were placed directly into 15-ml conical centrifuge tubes[7] containing 5 ml of 0.1 *N* HCl. The micropipets were then crushed to release the 100 μl of blood. After thorough vortex mixing[8], the centrifuge tubes were placed in a boiling water bath for 30 min to release membrane-bound free thiamine. The tubes and their contents were then cooled, 2 ml of 10% freshly prepared metaphosphoric acid[9] was added, and the contents were diluted to 10 ml in the calibrated tubes. The tubes were thoroughly mixed and allowed to stand for 10 min. They were then centrifuged[10], and 8 ml of the protein-free supernate was removed and placed in a 15-ml centrifuge tube containing 0.6 ml of 2.5 *M* sodium acetate[11]. The contents of the tubes were then diluted to 10 ml with water.

To prepare samples for the total thiamine (free thiamine plus its phosphorylated esters) assay, an aliquot of the above final solution was incubated overnight at 37° with 3 ml of a 2% amylase[12] suspension in a shaking water bath. If a plasma assay was desired, plasma, after separation from red blood cells, was treated in an identical manner to the whole blood.

Free and Total Thiamine Tissue Assay—Brain tissue was used as an example of tissue from which thiamine can be assayed. The excised brain of rats was maintained in refrigerated isotonic physiological buffer for 1–2 hr prior to assay. The brain was patted dry with tissue paper, and the wet weight was determined. The entire tissue was then placed in a calibrated homogenizing tube, heated on a boiling water bath for 30 min, homogenized in 10 ml of 0.1 *N* HCl, and then returned to the boiling water bath for another 15 min. A 5-ml aliquot of a 10% metaphosphoric acid solution was then added, and the suspension was diluted to 20 ml and allowed to stand for 10 min. The suspension was then centrifuged for 10 min, and 15 ml of the supernate was removed and placed in a 25-ml volumetric flask containing 1.1 ml of 2.5 *M* sodium acetate. The solution was diluted to 25 ml with water.

To prepare the sample for total thiamine determination, 8 ml of the 25-ml solution was added to 5 ml of a 2% amylase[12] suspension and incubated overnight at 37° in a shaking water bath. On the following day, this solution was diluted to 25 ml with pH 4.5 acetate buffer, and 8 ml of this solution was used for further analysis.

Standards Preparation—For the 4- and 1-mg/kg iv thiamine hydrochloride studies, three 100-μl blood samples were drawn prior to injecting thiamine hydrochloride. These samples were treated identically to postdosing samples, except that 100 μl of diluted stock thiamine hydrochloride solution was added to the centrifuge tubes containing the 5 ml of 0.1 *N* HCl to give concentrations of thiamine in the expected concentration range to be assayed. Similar procedures were used for preparing standard curves for tissue samples.

Thiamine Isolation and Oxidation Step—The blood and tissue extracts were applied to columns prepared with a cation-exchange resin[13]. (See Ref. 9 for a description of column preparation and elution techniques.) After eluting with acidified potassium chloride, 5 ml of the collected 25-ml eluate (8 ml for the 1-mg/kg study and for brain samples) was slowly released into a 50-ml conical centrifuge tube[3] containing 3 ml of an aqueous solution, which was 0.03% in potassium ferricyanide and 15% in sodium hydroxide. The solution was mixed continuously on a vortex mixer during the addition. Immediately after the addition was complete, 15 ml of isobutyl alcohol[14] was rapidly added *via* an automatic pipet[15]. The two-phase system was vigorously mixed on a vortex mixer for 90 sec and then centrifuged for 60 sec. The isobutyl alcohol fraction was removed immediately after the centrifugation step.

Detection Methods—*Fluorometric Analysis*—Approximately 9 ml of the isobutyl alcohol fraction was collected and dried over ~2 g of anhydrous sodium sulfate. The sample was clarified by centrifuging for 5 min at 1500 rpm. An aliquot of the dried isobutyl alcohol was analyzed fluorometrically[16] at 370 (excitation wavelength) and 420 (emission wavelength) nm. The excitation and emission slit widths were adjusted to 10 nm, and the instrument was used in the ratio record mode. Blanks for fluorometric analysis were of the same composition as the oxidized samples, but 3 ml of 15% NaOH was substituted for the 3 ml of potassium ferricyanide–sodium hydroxide solution.

The relative intensity of the sample due to thiochrome (and thiamine) was calculated by subtracting the blank intensity from the sample intensity. The relative intensity was then related to the concentration of endogenous and/or exogenous thiamine in micrograms per milliliter of blood or plasma or micrograms per gram of fresh brain *via* the standard curve, which was linear and was resolved by least-squares analysis[17].

Liquid Scintillation Detection—Five milliliters of the isobutyl alcohol extract was pipetted into a scintillation vial[18] containing 10 ml of an appropriate scintillation solvent[19]. The vial was stored in a dark cool place for 24–48 hr prior to counting. Radioactivity counting was performed in a liquid scintillation counting system[20] using the carbon-14 and tritium optimized window. External standard ratio was recorded to confirm counting efficiencies. Blanks as previously described also were used for the scintillation counting.

Relative counts per minute were calculated by subtracting the blank counts from the sample counts. The relative counts were related to the concentration of exogenous thiamine hydrochloride per milliliter of blood *via* the standard curve, which was linear and was resolved by least-squares analysis.

Procedure Modifications—The procedures described were used to determine free and total thiamine in whole blood, plasma, and brain tissue. The techniques for determining endogenous thiamine (free and total) were the same as described, except that the fluorometric assay obviously had to be used and 200-μl samples were needed for whole blood. Endogenous levels were estimated from standard curve plots of net relative fluorescence intensity[21] *versus* added exogenous thiamine using the standard addition technique. The fluorescence in the absence of added thiamine (corrected for solvent blank, *etc.*) was attributed to endogenous thiamine.

The procedures outlined were used for a study of thiamine pharmacokinetics after thiamine hydrochloride administration of 1–4 mg/kg. With doses greater than 4 mg/kg, a straight fluorometric assay could be used. The procedures were identical to those described, except that only cold thiamine hydrochloride was administered, standard curves were adjusted appropriately, and thiamine was determined fluorometrically.

Thiamine Pharmacokinetics Analysis—The pharmacokinetics of thiamine hydrochloride in rats were fit to a two-compartment model (4, 31, 32). This model predicts that the data for blood thiamine hydrochloride levels *versus* time in rats after rapid intravenous injection should show a biexponential decay. The decay curve should be described by:

$$C_B = Ae^{-\alpha t} + Be^{-\beta t} \qquad \text{(Eq. 1)}$$

[3] ARS/Sprague–Dawley, Madison, Wis.
[4] Wayne Lab-Blox, Allied Mills, Chicago, Ill.
[5] Corning microsampling glass disposable capillary pipets, Scientific Products, Kansas City, Mo.
[6] Edetate disodium, 10% aqueous solution, Fisher Scientific Co., Fair Lawn, N.J.
[7] Pyrex tubes, No. 8062.
[8] Vortex Genie, Scientific Products, McGaw Park, Ill.
[9] Mallinckrodt Chemical Works, St. Louis, Mo.
[10] Dynac II centrifuge, Clay-Adams, Parsippany, N.J.
[11] J. T. Baker Chemical Co., Phillipsburg, N.J.
[12] Diastase, a nonspecific enzyme mixture, also known as Clarase, used to cleave phosphorylated thiamine to thiamine, Fisher Scientific Co., Fair Lawn, N.J.
[13] Decalso, an artificial zeolite available through Fisher Scientific Co., Fair Lawn, N.J. Some lots showed low recoveries. New batches should be thoroughly tested.
[14] Certified 99 mole % pure. Fisher Scientific Co., Fair Lawn, N.J.
[15] Repipet, Labindustries, Berkeley, Calif.
[16] Hitachi Perkin-Elmer model MPF-2A spectrofluorometer, Perkin-Elmer Corp., Norwalk, Conn.
[17] Hewlett-Packard model 9810A.
[18] LSC vials, 20-ml capacity, Wheaton Scientific, Millville, N.J.
[19] Aquasol, New England Nuclear, Boston, Mass.
[20] LS-150, Beckman, Fullerton, Calif.
[21] Net relative fluorescence intensity (that due to added thiamine only) equals total relative fluorescence intensity minus (relative fluorescence intensity due to endogenous thiamine plus background).

Table I—Endogenous Free and Total Thiamine Levels in Fresh Excised Rat Brain Determined Fluorometrically

Parameter	Present Study (n), $\mu g/g \pm SEM$	Literature Values (References), $\mu g/g$
Free thiamine in fresh brain	0.186 ± 0.101 (7)	0.26–0.40 (35–37)
Total thiamine in fresh brain	3.30 ± 0.12 (5)	3.0–3.1 (37, 38)

where C_B is the blood level at any time, t, and A, α, B, and β are parameters that were adequately described elsewhere (31, 32). The data for each animal and each analytical method were fit to Eq. 1 utilizing the simplex optimization method[22] (33, 34) for nonlinear curve fitting. The mean values for these parameters using each analytical method were determined and statistically compared using the Student t test. The mean values for A, α, B, and β were used to generate the lines representing mean blood levels *versus* time decay curves for thiamine hydrochloride in rats.

RESULTS AND DISCUSSION

The thiochrome fluorometric technique measures the total fluorescence of a particular sample. This fluorescence has contributions from exogenous as well as endogenous thiamine. Endogenous and/or exogenous thiamine is determined by direct extrapolation from a plot of net relative fluorescence intensity[21] *versus* added thiamine. The liquid scintillation assay described, on the other hand, measures only exogenous thiamine.

Normal endogenous levels of free and total thiamine levels in excised rat brains were determined using the described fluorometric assay. The values found in the present study (Table I) compare favorably with previously reported values (35–38).

These procedures (fluorometric and liquid scintillation detection) required considerable time and effort. Numerous procedures that purport to shorten the assay time for thiamine were attempted. For example, a recently published procedure (11) was attempted but gave inconsistent as well as low fluorescence readings compared to the described procedure.

Variables (6, 39) affecting the sensitivity and reproducibility of the fluorometric procedure require attention to reagent purity, preparation, and storage. Of particular importance were the purity of the isobutyl alcohol and the mesh size of the cation-exchange resin.

The isobutyl alcohol used[14] was satisfactory because it gave low background fluorescence. Other sources of isobutyl alcohol obtained were not satisfactory. Attempts made to purify and recycle the isobutyl alcohol using the procedure described by Friedemann and Kmieciak (8) failed. The purification of the used isobutyl alcohol was not only time consuming but the isobutyl alcohol still gave high and unsatisfactory reagent fluorescence after purification. Similarly, some lots of the cation-exchange resin gave low recoveries of thiamine after elution. It was determined that the mesh size of the unsatisfactory lots was below the optimum required for efficient elution. New lots of the cation-exchange resin were tested for their exchange efficiency prior to routine use.

Timing was critical in the oxidation step. The time schedule must be strictly followed to obtain both consistent and reproducible results. Throughout the assay, reagents and working solutions must be protected from dust and other particulates.

Liquid scintillation samples counted immediately after the addition of isobutyl alcohol to the scintillation cocktail showed somewhat inconsistent results. This problem was traced to the presence of small amounts of aqueous sodium hydroxide carryover into the isobutyl alcohol, leading to the phenomenon of chemiluminescence. The increase in counts due to chemiluminescence was overcome by storing the samples for 1–2 days in a cool, dark environment prior to counting.

The pharmacokinetics of thiamine administered at 4 mg/kg iv to rats were previously fit to a two-compartment model (4). In the present experiment, administration of a 4-mg/kg iv thiamine hydrochloride dose was found to follow two-compartment model behavior over the limited time period studied. The two-compartment model predicts that the thiamine blood level *versus* time curve in rats after a rapid intravenous injection should show a biexponential decay and be described by Eq. 1.

[22] The program was developed by Dr. W. White and various graduate students in the Department of Pharmaceutical Chemistry, University of Kansas. The program was run on a Hewlett-Packard model 2100 computer. For copies of the program and further information, contact Dr. W. White.

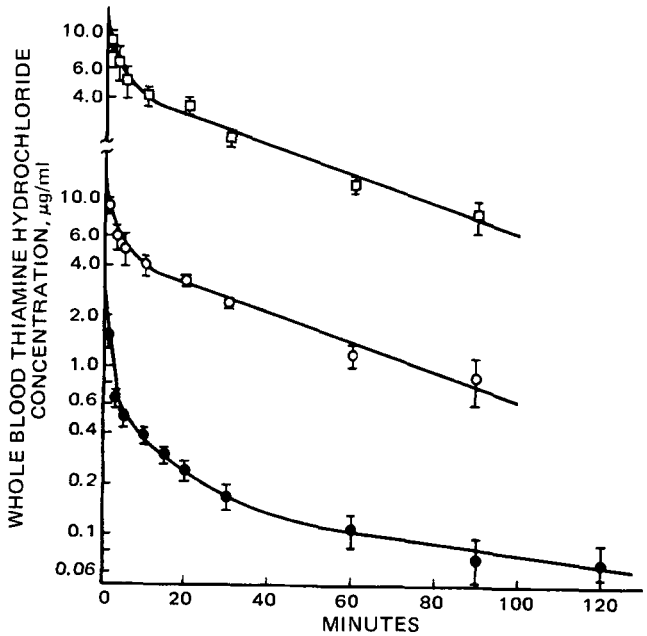

Figure 1—*Time course of whole blood concentration* ± SEM *of thiamine hydrochloride in rats administered 1- and 4-mg/kg iv doses of thiamine hydrochloride. Each point is the mean of four (4 mg/kg) or five (1 mg/kg) animals. The analytical procedures were the liquid scintillation assay (●, 1 mg/kg; and ○, 4 mg/kg) and the thiochrome fluorometric assay (□, 4 mg/kg). Lines for the 4-mg/kg dose were generated utilizing the pharmacokinetic parameters in Table II.*

Figure 1 shows the blood level *versus* time plots for exogenous thiamine decay in rats administered 4 mg/kg iv. Table II lists the pharmacokinetic parameters derived from the nonlinear curve fitting of the blood level–time plots for both the fluorometric and liquid scintillation procedures. The mean values were compared using the Student t test for the two detection methods. Table II also lists the calculated t values and the appropriate t values at the $2p = 0.05$ significance level and the indicated degrees of freedom.

The mean parameters for the fluorometric assay did not differ significantly from the mean parameters using the liquid scintillation procedure at the significance level indicated. The solid lines in Fig. 1 were drawn by a fit to Eq. 1, utilizing the mean values of A, α, B, and β determined for each detection method.

The liquid scintillation technique was used in following the whole blood

Table II—Pharmacokinetic Parameters for the Apparent Disappearance of Thiamine Hydrochloride from Whole Blood in Rats Administered a 4-mg/kg iv Dose of Thiamine Hydrochloride

Animal	A, μg/ml	α, min^{-1}	B, μg/ml	β, min^{-1}	$t_{1/2}$, min
	Fluorometric Assay				
1	6.90	0.258	6.44	0.0315	22
2	8.42	0.494	4.30	0.0192	36
3	6.72	0.666	3.83	0.0172	40
4	7.94	0.217	4.32	0.0164	42
Mean	7.50	0.41	4.72	0.0211	35
SEM	0.41	0.10	0.58	0.0035	
	Liquid Scintillation Assay				
1	7.22	0.369	6.83	0.0336	21
2	9.13	0.524	4.67	0.0226	31
3	7.90	0.710	3.53	0.0133	52
4	7.36	0.180	3.79	0.0138	50
Mean	7.90	0.45	4.70	0.0208	39
SEM	0.43	0.11	0.75	0.0048	
t statistic	0.683	0.240	0.018	0.042	
Degrees of freedom (df)	6	6	6	6	
$t_{0.05}$[a], $df = 6$	2.447	2.447	2.447	2.447	

[a] Two-tail criterion, significance level $2p = 0.05$.

time profile of exogenous thiamine after administration of a 1-mg/kg iv dose of ^{35}S-thiamine hydrochloride (Fig. 1). The fluorometric procedure could not have been used to follow the time profile of exogenous thiamine blood levels, because considerable data in the blood level–time profile would have been collected at levels that would have fallen below accurate detection by the fluorometric method. This result is a consequence of increasing reagent blank fluorescence intensity and increasing noise in the reagent blank and sample fluorescence intensity recorded signals. Of course, some of the profile could have been followed using the fluorometric method, and it could also have been used if larger blood samples were taken. However, the latter alternative would entail sacrificing individual animals at appropriate times. Consequently, much larger numbers of animals for each dose would have been required, as well as the loss of proper controls available with serial blood sampling over an extended period from single animals.

The lower level of detection for thiamine for 100-μl blood samples using the fluorometric assay is 0.3 μg/ml, while the lower level of detection using the liquid scintillation assay (using ^{35}S-thiamine of specific activity 233 mCi/mmole) is 0.05 μg/ml. It appears from Fig. 1 that thiamine whole blood pharmacokinetics is dose dependent. These differences will be discussed in a later paper where data for the time profile of thiamine hydrochloride in the dose range of 1–36 mg/kg will be presented.

In conclusion, the advantages of the liquid scintillation assay are its ability to determine exogenous thiamine in the presence of endogenous thiamine and the low level of detection it affords. This last point, of course, will be dependent on the specific activity of ^{35}S-thiamine that can be purchased or prepared.

Another important advantages of the liquid scintillation assay is that once the thiamine (free and/or total) has been isolated *via* oxidation to thiochrome and extracted into the isobutyl alcohol layer, the labeled samples can be counted at the investigator's convenience (keeping in mind the relatively short half-life of sulfur-35 of 87.2 days). In the fluorometric assay, fluorescence intensity from isobutyl alcohol-extracted thiochrome deteriorates with time. Chemical quenching and chemiluminescence with the liquid scintillation assay can be problems if unrecognized. Balanced against the advantages of the liquid scintillation are disadvantages of not being able to determine endogenous thiamine directly and the added expense of purchasing the ^{35}S-thiamine.

REFERENCES

(1) K. Ikeda, Y. Itokawa, and M. Fujiwara, *J. Vitaminol.*, **17,** 155 (1971).

(2) M. Fujiwara and K. Matsui, *Anal. Chem.*, **25,** 810 (1953).

(3) "Official Methods of Analysis of the Association of Official Analytical Chemists," 11th ed., Association of Official Analytical Chemists, Washington, D.C., 1970, p. 771.

(4) H. Nogami, H. Hanano, S. Awazu, and T. Fuwa, *Chem. Pharm. Bull.*, **18,** 1937 (1970).

(5) "Methods of Vitamin Assay," 3rd ed., Interscience, New York, N.Y., 1966, chap. 6.

(6) O. Mickelsen and R. S. Yamamoto, "Methods of Biochemical Analysis," vol. 6, Interscience, New York, N.Y., 1958, p. 191.

(7) R. Strohecker and H. M. Henning, "Vitamin Assay Tested Methods," CRC Press, Cleveland, Ohio, 1965, p. 65.

(8) T. E. Friedemann and T. C. Kmieciak, *J. Lab. Clin. Med.*, **28,** 1262 (1943).

(9) H. B. Burch, O. A. Bessey, R. H. Love, and O. H. Lowry, *J. Biol. Chem.*, **198,** 477 (1952).

(10) T. Myint and H. B. Houser, *Clin. Chem.*, **11,** 617 (1965).

(11) E. E. Edwin, R. Jackman, and N. Hebert, *Analyst*, **100,** 689 (1975).

(12) Y. Itokawa and J. R. Cooper, in "Methods in Enzymology," vol. 18, D. B. McCormick and L. D. Wright, Eds., Academic, New York, N.Y., 1970, p. 91.

(13) S. Cohen, A. Uzan, and G. Valette, *Biochem. Pharmacol.*, **11,** 721 (1962).

(14) A. D. Thomson, *Clin. Sci.*, **31,** 167 (1966).

(15) A. D. Thomson, H. Baker, and C. M. Leevy, *J. Lab. Clin. Med.*, **76,** 34 (1970).

(16) A. D. Thomson, H. Baker, and C. M. Leevy, *Am. J. Clin. Nutr.*, **21,** 537 (1968).

(17) P. A. Tomasulo and R. M. H. Kates, *ibid.*, **21,** 1341 (1968).

(18) A. D. Thomson, D. Frank, H. Baker, and C. M. Leevy, *Ann. Intern. Med.*, **74,** 529 (1971).

(19) D. Leigh, *J. Neurosurg. Psychiat.*, **14,** 216 (1951).

(20) B. E. Cleyron, R. H. Dobbs, and A. D. Patrick, *Arch. Dis. Child.*, **42,** 467 (1967).

(21) J. H. Pincus, *Dev. Med. Child Neurol.*, **14,** 87 (1972).

(22) J. H. Pincus, J. R. Cooper, Y. Itokawa, and M. Gumbinas, *Arch. Neurol.*, **24,** 511 (1971).

(23) J. H. Pincus, Y. Itokawa, and J. R. Cooper, *Neurology*, **19,** 841 (1969).

(24) J. H. Pincus, G. B. Solitare, Y. Itokawa, Y. Hashitani, and J. R. Cooper, *ibid.*, **21,** 444 (1971).

(25) M. L. Weil, J. H. Menkes, K. N. F. Shaw, and J. H. Pincus, *Clin. Res.*, **19,** 229 (1971).

(26) W. A. Sharemata, W. A. Cooper, and J. R. Joseph, *Neurology*, **21,** 456 (1971).

(27) V. J. A. Montpetit, F. Anderman, S. Carpenter, J. S. Fawcett, D. Zborowska-Sluis, and H. R. Eiberson, *Brain*, **94,** 1 (1971).

(28) F. M. Loew, J. M. Bettany, and C. E. Halifax, *Can. J. Comp. Med.*, **39,** 291 (1975).

(29) E. E. Edwin and G. Lewis, *J. Dairy Res.*, **38,** 79 (1971).

(30) V. Stella, *Aust. J. Pharm. Sci.*, **NS2,** 57 (1973).

(31) H. Nogami, M. Henano, and S. Awazu, *Chem. Pharm. Bull.*, **17,** 2097 (1969).

(32) J. G. Wagner, "Fundamentals of Clinical Pharmacokinetics," Drug Intelligence Publications, Hamilton, Ill., 1975, pp. 57–127.

(33) S. N. Deming and S. L. Morgan, *Anal. Chem.*, **45,** 278A (1973).

(34) S. N. Deming and P. B. King, *Res./Dev.*, **May 1974,** 22.

(35) P. M. Dreyfus, *J. Neurochem.*, **4,** 183 (1959).

(36) *Ibid.*, **8,** 139 (1961).

(37) A. Von Muralt, *Ann. N.Y. Acad. Sci.*, **92,** 499 (1961).

(38) K.-H. Kiessling, *Biochim. Biophys. Acta*, **46,** 603 (1961).

(39) H. N. Haugen, *Scand. J. Clin. Lab., Invest.* **12,** 253 (1960).

ACKNOWLEDGMENTS

Presented at the Basic Pharmaceutics Section, APhA Academy of Pharmaceutical Sciences, New York meeting, May 1977.

Supported by Grant NS 11998 from the National Institute of Neurological and Communicative Disorders and Stroke, National Institutes of Health, the University of Kansas General Research Fund, and a grant from Abbott Laboratories.

Simultaneous Multicomponent Drug Determinations with a Vidicon Spectrometer

ALAN E. McDOWELL and HARRY L. PARDUE ˣ

Received July 8, 1977, from the *Department of Chemistry, Purdue University, West Lafayette, IN 47907.* Accepted for publication October 6, 1977.

Abstract □ A vidicon spectrometer, useful for absorption spectrophotometry over the 210–800-nm spectral region and capable of scanning a portion of this region at repetition rates of 250 scans/sec, was applied for the simultaneous determination of multicomponent drug formulations without a separation. Results are reported for two drug preparations containing two and four active components. The average of ratios of determined to expected values for the six active components contained in both formulations was 99.2% based on the specified tablet contents. Relative standard errors for the analyses were less than 3%. Other potential applications of the vidicon spectrometer are discussed briefly.

Keyphrases □ Vidicon spectrometer—used in simultaneous determination of multicomponent drug formulations without prior separation □ Spectrophotometry—use of vidicon spectrometer in simultaneous determination of multicomponent drug formulations without prior separation

UV–visible spectrophotometry and spectrofluorometry are used extensively in the pharmaceutical sciences (1). Various applications were reported recently, including quantitative determinations of drugs, metabolites, and degradation products in several sample types; pharmacokinetic studies; determinations of equilibrium constants; determinations of enzyme activities; and separation methods such as extraction and chromatography. Thus, there is good reason to note instrumental developments that improve or extend the capabilities of the methods.

Instruments used currently either operate at a single wavelength or utilize relatively slow mechanical wavelength scanning systems. This report describes an alternative approach to spectrophotometric instrumentation, replacing the mechanical scanning systems with an all-electronic scanning system. The approach uses conventional dispersion optics and a vidicon or television camera tube detector. The detector is useful from about 210 nm to well above 800 nm and can be used to select one or a few wavelengths electronically or to scan segments of the UV–visible region with repetition rates as fast as 250 scans/sec. This paper discusses one type of application where this scanning capability is used to advantage and suggests others.

The analytical problem involves the simultaneous determination of two or more components in pharmaceutical preparations without a separation step. The method utilizes matrix equations to resolve multiwavelength data from the vidicon spectrometer into the concentrations of individual components in each sample. Of the two drug preparations used as illustrative examples, one[1] contained four active components and the other[2] contained two active components and one excipient that absorbed radiant energy in the spectral range of interest. Results are reported for both synthetic mixtures and processed dosage forms.

For the synthetic mixtures, the relative standard errors for individual components ranged from 0.8 to 3%; ratios of found *versus* expected values for the dosage forms ranged from 96 to 104% with an overall average of 99.2%.

INSTRUMENTATION

The word "vidicon" is a generic term that represents a group of devices used as television camera tubes and imaging detectors. The spectrometer developed in this laboratory utilizes a silicon target vidicon. Because the vidicon-based spectrometer is a relatively new development, the concepts and characteristics are discussed briefly so that potential advantages and limitations can be understood.

Figure 1 is a conceptual representation of the vidicon spectrometer, and Fig. 2A represents typical spectral data obtained with the instrument. These spectra were photographed from a display oscilloscope interfaced to a computer that records and processes the data. Each display represents the average of 1000 individual spectra recorded during 10 sec for each solution.

For absorption spectroscopy, polychromatic radiation from a suitable source is passed through the sample cell where different wavelengths, λ, are attenuated, depending on the spectral characteristics of the sample. The emerging radiation is then focused onto the entrance slit of a conventional monochromator. Suitable dispersion optics then separate the attenuated polychromatic radiation into a spectrum, which is focused in a plane usually occupied by the exit slit of the monochromator. In this application, the exit slit is removed and the active surface of the vidicon tube is located in the focal plane so that the different wavelengths illuminate different points along one axis of the active surface of the tube. Thus, a spectrum is displayed along the wavelength axis of the tube.

The circle at the right of the exit focal plane is intended to emphasize the fact that the active surface of the vidicon consists of a two-dimensional array of photodetectors. Although the silicon target vidicon may consist of up to 500,000 individual photodiodes, technical problems limit the number of independent electronic resolution elements to about 40,000, or about 200 along each axis. Therefore, the spectrum displayed across the active surface of the vidicon is resolved into some 200 spectral resolution elements.

The electronic scanning feature results from the fact that individual resolution elements are examined by an electron beam, which is scanned electronically across the surface in a manner analogous to a cathode ray tube. When the electron beam strikes a resolution element, it produces an electric charge proportional to the integrated light intensity on that element since it was last examined. Thus, as the beam moves across the surface, it produces an output signal profile representative of the intensity *versus* wavelength pattern, which is the intensity spectrum. Since the electron beam can be scanned very rapidly across the active surface, the scan rate is limited to the detector response rate; for the silicon target vidicon, this scan rate is limited to slower than 1000 scans/sec for the highest reliability.

While it is not clear from this diagram, an image of the entrance slit for each resolution element is developed along the vertical axis of the detector. Thus, many photodiodes along the vertical axis respond to the same wavelength. The scanning format is such that the signal for each wavelength resolution element represents an average of several hundred detectors along the vertical axis for that wavelength. This feature and the integrating character of the silicon photodiodes contribute signal averaging to each data point.

More complete details of the system were reported elsewhere (2, 3), and only the more salient features are summarized here. The silicon target vidicon has a useful spectral range from about 210 nm to beyond 800 nm; selected segments from this range can be scanned with repetition rates up to 250 scans/sec, with intensity data being recorded at up to 200

[1] Excedrin, Bristol-Myers Co., New York, N.Y.
[2] Fedahist, Dooner Laboratories, Haverhill, Mass.

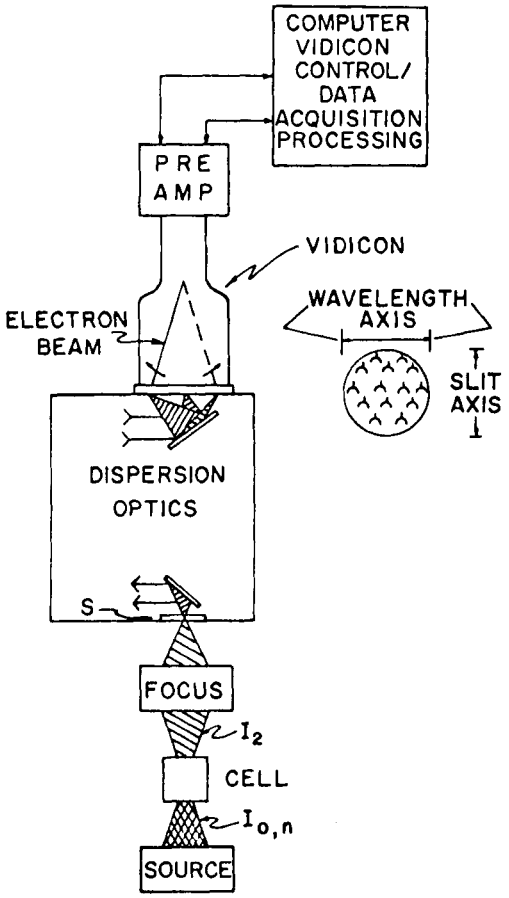

Figure 1—*Schematic representation of vidicon spectrometer.*

wavelengths during each scan. The spectrometer exhibits an uncertainty of about 0.001 absorbance unit throughout this range and has a linear dynamic range of at least four orders of magnitude of intensity (3). Because the spectral scans are performed electronically and involve no mechanical motion, wavelength resolution elements are selected very reproducibly. This latter feature is important for signal averaging applications and for the multiwavelength applications discussed.

The system has some potential limitations. Because there is only a finite number of resolution elements, the user must exercise a tradeoff between spectral resolution and spectral range. Furthermore, the silicon target vidicon is a unity gain detector and does not have the spectral sensitivity of a photomultiplier. Finally, because the sample is illuminated with polychromatic radiation, any tendency toward photodecomposition or fluorescence could represent more severe problems in this type of instrument than in conventional spectrophotometers where the sample is illuminated with monochromatic radiation attenuated by the monochromator.

All of these limitations are real, but none has proven serious. Photodecomposition has been a problem only in some preliminary work with a reaction involving sodium nitroprusside.

EXPERIMENTAL

Reagents and Standards—All solutions were prepared in distilled water that had been further purified by being passed through a cation–anion-exchange resin column.

Buffers—A pH 10, 0.1 *M* ammonia buffer was prepared by dissolving 4.08 g of ammonium chloride and 21.6 ml of concentrated ammonium hydroxide in water and diluting to 4 liters. A pH 4.7, 0.1 *M* acetate buffer was prepared by dissolving 16.4 g of sodium acetate and 11.4 ml of concentrated acetic acid in water and diluting to 4 liters.

Standards—A stock solution of each active ingredient in the four-component sample was prepared by dissolving 0.0408 g of salicylic acid[3], 0.0203 g of acetaminophen[4], 0.0208 g of caffeine[4], and 0.0402 g of salicylamide[4] in pH 10 ammonia buffer and diluting each solution to 100 ml with the same buffer. Standard solutions (4–40 mg of salicylic acid and salicylamide/liter and 2–20 mg of caffeine and acetaminophen/liter) were prepared by diluting appropriate amounts of stock solutions with ammonia buffer. The synthetic mixtures (M1–M7 in Table I) were prepared by diluting appropriate amounts of stock solutions to 100 ml with ammonia buffer.

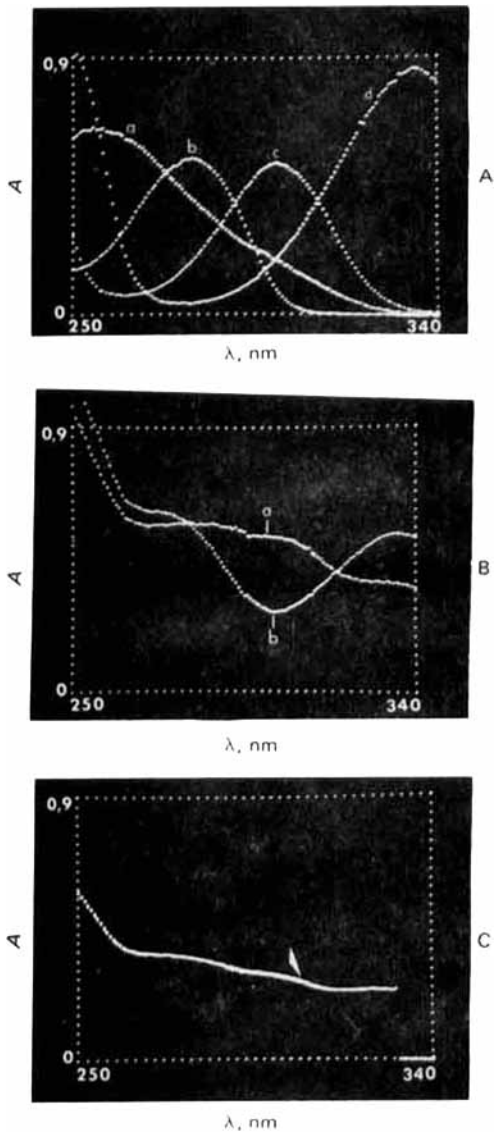

Figure 2—*Spectra for the four-component sample. A. Pure components: a, acetaminophen (10 mg/liter); b, caffeine (10 mg/liter); c, salicylic acid (20 mg/liter); and d, salicylamide (20 mg/liter). B. Synthetic mixtures containing 6, 4, 12, and 8 mg/liter (a) and 6, 6, 0, and 12 mg/liter (b), respectively, of the four components in A. C. Superimposed spectra of a tablet extract and a mixture of 4.0, 2.8, 6.1, and 5.3 mg/liter, respectively, of the four components in A.*

A stock solution of each active ingredient in the two-component sample was prepared by dissolving 0.0320 g of chlorpheniramine maleate[5] and 0.4813 g of pseudoephedrine hydrochloride[4] in pH 4.7 acetate buffer and diluting to 100 ml with the same buffer. Standard solutions containing 3–22 mg of chlorpheniramine maleate/liter and 48–340 mg of pseudoephedrine hydrochloride/liter were prepared by diluting appropriate amounts of each stock solution with acetate buffer. The synthetic mixtures (M8–M16 in Table I) were prepared by diluting appropriate amounts of stock solutions to 100 ml with acetate buffer.

Procedure—Each four-component tablet was crushed and equilibrated with ammonia buffer for 10–15 min, after which the supernate

[3] J. T. Baker Co., Phillipsburg, N.J.
[4] Sigma Chemical Co., St. Louis, Mo.
[5] Dow Chemical Co., Indianapolis, Ind.

Table I—Synthetic Mixtures of Pure Components Analyzed by the Matrix Method

Mixture	Concentration, mg/liter			
	Salicylic Acid	Caffeine	Salicylamide	Acetaminophen
M1	12	4	8	6
M2	12	6	12	0
M3	0	6	12	6
M4	16	6	12	2
M5	8	12	8	4
M6	14	3	8	6
M7	8	4	0	8
	Pseudoephedrine Hydrochloride		Chlorpheniramine Maleate	
M8	0		16.0	
M9	241		0.0	
M10	241		16.0	
M11	289		3.2	
M12	144		6.4	
M13	337		9.6	
M14	48.1		12.8	
M15	193		19.2	
M16	96.3		22.4	

was removed by filtration and diluted to 250 ml with ammonia buffer. Then 1.00 ml of the diluted solution was again diluted to 100 ml with ammonia buffer, and this latter solution was used in the measurement step.

Each two-component tablet was crushed and equilibrated for 10–15 min with acetate buffer, after which the supernate was removed by filtration and diluted to 250 ml with acetate buffer. This diluted solution was used in the measurement step.

Because the vidicon-based spectrometer is a single-beam instrument, each intensity measurement must be corrected for dark current. This step is done for each set of runs by storing a dark current reading for each resolution element in the computer memory and then subtracting that dark current value from the 100% T and sample intensities at each wavelength before computing percent T and/or absorbance.

A scan repetition rate of 100 scans/sec was used. For each standard, synthetic mixture, and real sample, 1000 spectral scans were averaged. The average absorbances at selected wavelengths were used to establish absorptivity matrixes from standards and to compute concentrations in synthetic mixtures and real samples. For the two-component sample, five standard solutions containing known amounts of each of the pure components were used, and absorbance data at 15 approximately equally spaced wavelengths between 250 and 280 nm were used to establish the absorptivity matrix. For the four-component sample, six standards and 16 approximately equally spaced wavelengths between 250 and 340 nm were used to establish the absorptivity matrix. Absorbance data for each synthetic mixture and sample at the same wavelengths for which absorptivity data were evaluated were used to compute sample composition.

Mathematical Formulation—The computational procedure was presented previously (4) and will be discussed only briefly. Beer's law is used in matrix form:

$$A = KC \qquad \text{(Eq. 1}a\text{)}$$

where A is a k by m matrix of absorbances of m mixtures at k analytical wavelengths, K is a k by n matrix of absorptivities of n components at k analytical wavelengths, and C is an n by m matrix of concentrations of n components in each m mixture. The absorptivity matrix is evaluated as:

$$K = AC^T(CC^T)^{-1} \qquad \text{(Eq. 1}b\text{)}$$

where C^T is the transpose matrix of C. When the absorptivity matrix has been determined, unknown concentrations are computed as:

$$C_u = QA_u \qquad \text{(Eq. 2)}$$

where C_u is a column matrix of concentrations of each n component, $Q = (K^TK)^{-1}K^T$ is an n by k matrix, A_u is a column matrix of absorbances of the unknown at the k analytical positions, and K^T represents the transpose of the absorptivity matrix.

This calculation gives the least-squares multiple regression fit of the component spectral curves to the data. The net result of the calculations is a set of concentrations of the n components in the sample mixture that gives the best fit to the spectral data.

RESULTS AND DISCUSSION

Results are reported for two pharmaceutical preparations. In each case, analyses were performed both on synthetic mixtures prepared from pure components and on tablets treated as described. The synthetic mixture data are included to give some indication of the dynamic range of the method and to provide statistical data against which results for real samples can be compared.

All uncertainties are reported at ±1 *SD*.

Four-Component Sample—The four active components were: acetaminophen, 97 mg; caffeine, 65 mg; aspirin, 195 mg; and salicylamide, 130 mg. Synthetic mixtures and tablets were processed as described and treated as four-component mixtures.

Pure Components and Synthetic Mixtures—At pH 10, aspirin is converted to salicylic acid and is treated as such in this discussion. Curves a–d in Fig. 2A represent the absorption spectra of acetaminophen (10 mg/liter), caffeine (10 mg/liter), salicylic acid (20 mg/liter), and salicylamide (20 mg/liter). All spectra overlapped, but there were significant differences among them.

Figure 2B represents spectra for two different mixtures of three or more of these components. The lower absorbance of curve a near 340 nm is a clear indication that there was less salicylamide in this solution than in that represented by curve b. On the other hand, the dip in curve b is a clear indication that there was less salicylic acid in the solution represented by curve b than in that represented by curve a. These differences in shape are utilized by the matrix equations to resolve mixture spectra into the compositions of individual components.

Figure 2C represents the overlapped spectra of a solution of the soluble components from a tablet and a standard mixture containing the nominal amount of each component in the tablet. As indicated earlier, the matrix program resolves the unknown spectrum into the amounts of the four components that give the best fit to the spectrum.

Six synthetic mixtures were analyzed by the proposed procedure. Regression equations (found *versus* added) were $y = 0.98x + 0.07$ mg/liter for acetaminophen, $y = 1.01x - 0.04$ mg/liter for caffeine, $y = 1.0x + 0.03$ mg/liter for salicylic acid, and $y = 1.01x - 0.03$ mg/liter for salicylamide. More complete statistical data are presented in Table II. The correlation coefficients suggest good linearity, and the slopes and intercepts suggest good agreement between computed and added values.

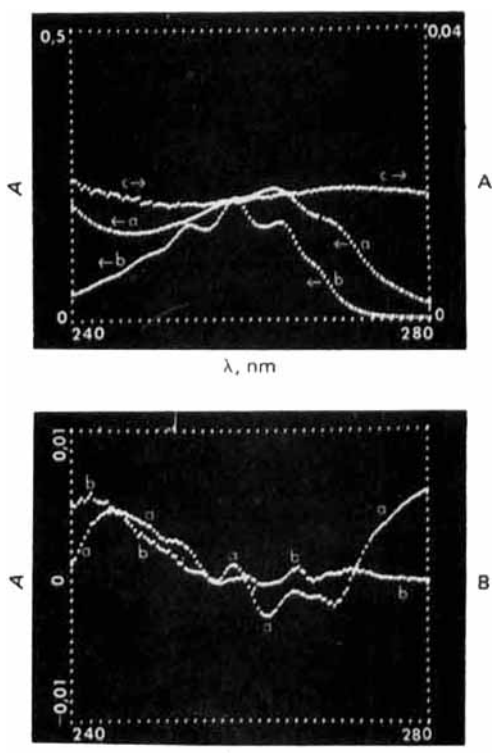

Figure 3—*Spectral data for the two-component sample. A. Spectra of pure components: a, chlorpheniramine maleate (16.0 mg/liter); b, pseudoephedrine hydrochloride (241 mg/liter); and c, lactose. B. Tablet regression residuals for two-component treatment (a) and three-component treatment (b).*

Table II—Statistics for the Regression of Found *versus* Added Concentrations of Drugs in Synthetic Mixtures

Drug	Slope ± *SD*	Intercept ± *SD*, mg/liter	*SE* of Estimate, mg/liter	Correlation Coefficient
Acetaminophen	0.980 ± 0.019	0.07 ± 0.05	0.106	0.9974
Caffeine	0.998 ± 0.008	−0.04 ± 0.03	0.076	0.9995
Salicylic acid	0.998 ± 0.010	0.03 ± 0.05	0.101	0.9994
Salicylamide	1.014 ± 0.004	−0.03 ± 0.02	0.003	0.9999
	Two-Component Treatment			
Chlorpheniramine maleate	1.014 ± 0.004	−0.10 ± 0.06	0.09	0.9999
Pseudoephedrine hydrochloride	0.990 ± 0.007	0.03 ± 1.54	2.39	0.9996
	Three-Component Treatment			
Chlorpheniramine maleate	1.005 ± 0.007	0.12 ± 0.09	0.14	0.9997
Pseudoephedrine hydrochloride	0.977 ± 0.007	1.35 ± 1.5	2.39	0.9996

Tablets—The dilution factor used for the tablets corresponds to nominal concentrations of 3.9, 2.6, 6.0, and 5.2 mg/liter for acetaminophen, caffeine, salicylic acid, and salicylamide, respectively. Nine individual tablets processed *via* the proposed procedure yielded average values of 3.8 ± 0.2, 2.5 ± 0.1, 6.1 ± 0.4, and 5.2 ± 0.3 mg/liter for the four components, respectively. The differences between expected and found results compared favorably with the standard estimates of error reported in Table II for the synthetic mixtures. Additional information related to these data are summarized in Table III.

Two-Component Sample—The two-component sample contained chlorpheniramine maleate, 4 mg, and pseudoephedrine hydrochloride, 60 mg. Results are reported for synthetic mixtures and processed tablets, treated as two- and three-component mixtures. The third component was a water-soluble excipient (lactose) having measurable absorbance.

Pure Components and Synthetic Mixtures—Curves a and b in Fig. 3A represent absorbance spectra of 16 mg of chlorpheniramine maleate/liter and 241 mg of pseudoephedrine hydrochloride/liter in pH 4.7 buffer. There is no wavelength at which both components can be determined independently of the other. The multiwavelength method was applied to eight mixtures containing known amounts of each component. Regression equations (found *versus* added) were $y = 1.014x - 0.10$ mg/liter for chlorpheniramine maleate and $y = 0.99x + 0.03$ mg/liter for pseudoephedrine hydrochloride. More complete statistical data are included in Table II. The correlation coefficients, slopes, and intercepts suggest good linearity and good agreement between expected and found values.

Tablets—When individual tablets are dissolved and diluted to 250 ml with buffer, they should yield nominal concentrations of 16 mg of chlorpheniramine maleate/liter and 240 mg of pseudoephedrine hydrochloride/liter. When eight tablets were prepared and treated as two-component samples, the average results obtained were 17.9 and 217 mg/liter, respectively, for the two components, corresponding to so-called recoveries of 112 and 90.5%. These results are not satisfactory for this determination.

The reason for the problem can be illustrated with curve a in Fig. 3B. This curve represents the residuals (or difference spectrum) between the average of the spectra for the tablets and the absorbance spectrum predicted by the matrix program. The wavelength range from 250 to 280 nm is the range fit by the matrix equation. The residual plot deviates from zero by as much as 0.005 absorbance unit near 280 nm, suggesting that the matrix program has not been able to fit the data to within the uncertainty limits of 0.001 absorbance unit imposed by the instrument.

These data suggested another absorbing species, which was not being accounted for. Subsequent inquiries identified an excipient in the sample as lactose. Curve c in Fig. 3A represents the absorption spectrum of lactose (note expanded scale). The important feature of this spectrum is the relatively high absorbance near 280 nm where absorbances for both active components are lowest. With this information, the tablets were then treated as three-component unknowns including lactose; values of 16.7 and 230 mg/liter were obtained and compared to expected values of 16 and 240 mg/liter, respectively. Curve b in Fig. 3B represents the residuals obtained from this fit of the data. Between 250 and 280 nm, the fit was close to the 0.001 absorbance unit uncertainty of the instrument.

Table III—Analyses of Tablet Preparations

Component	Concentration, mg/liter Expected	Found (*SD*)	Ratio × 100 (Found/Expected)
	Four-Component Tablets		
Acetaminophen	3.9	3.8 (0.2)	97.4
Caffeine	2.6	2.5 (0.1)	96.2
Salicylic acid	6.0	6.1 (0.4)	101.6
Salicylamide	5.2	5.2 (0.3)	100.0
		Average	98.8
	Two-Component Tablets		
Chlorpheniramine maleate	16	16.7 (0.8)	104
Pseudoephedrine hydrochloride	240	230 (1.7)	96
		Average	100

The data for the active components based on three-component treatment are summarized in Table III. When the data for the synthetic mixtures were treated by taking into consideration the possible interference, the regression equations of found *versus* added drugs were $y = 1.005x + 0.12$ mg/liter for chlorpheniramine maleate and $y = 0.98x + 1.35$ mg/liter for pseudoephedrine hydrochloride. More complete statistics are included in Table II.

Although the three-component treatment is necessary to account for the absorbing excipient in the two-component tablets, this treatment might be expected to degrade the results of synthetic mixtures because none of the excipient was added to these samples. That this does occur is apparent from the statistical data presented in Table II for the two- and three-component treatments.

Applications of a *t*-test with the standard deviations of slopes and intercepts for synthetic mixtures in Table II indicated that none of the slopes was statistically different from unity and that none of the intercepts was statistically different from zero at the 95% confidence level. The standard error of estimate is an important statistic because it indicates by how much the experimental values can be expected to deviate from the least-squares line for the data. The 95% confidence intervals were 0.27, 0.20, 0.26, and 0.085 mg/liter for acetaminophen, caffeine, salicylic acid, and salicylamide, respectively, and 0.33 and 5.6 mg/liter for chlorpheniramine maleate and pseudoephedrine hydrochloride, respectively, by the three-component treatment.

Applications of a *t*-test with standard deviations for tablets in Table III indicated that "found" results for all components except psuedoephedrine hydrochloride were within the 95% confidence limits. The 95% confidence limits for pseudoephedrine hydrochloride ($n = 8$) were ±4.0 mg/liter, and the difference between expected and found values exceeded this range. This apparent discrepancy cannot be explained at this time.

While comparison data for the components determined in this work are not available, the agreement between expected and found values for both the two- and four-component samples is comparable to results reported recently for other two-component mixtures analyzed with the aid of a liquid chromatographic separation prior to the measurement step (5). The uncertainties that range between 1 and 4% are consistent with those generally expected when more involved separation methods are applied to real samples.

Projections—This work demonstrated one type of application in which the rapid scanning capability of a vidicon detector can be used advantageously. This same instrument system has been used effectively as a multiwavelength detector for liquid chromatography (6), offering several advantages in comparison with single-wavelength or mechanically scanned detectors. Other workers performed multicomponent determinations with other array detectors used for derivative spectroscopy (7) and as fluorescence detectors (8). All of these and other possible applications exhibit real potential for pharmaceutical analyses.

REFERENCES

(1) C. A. Janicki, R. K. Gilpin, E. S. Moyer, R. H. Almond, Jr., and R. H. Erlich, *Anal. Chem.*, **49**, 110R (1977).

(2) M. J. Milano, H. L. Pardue, T. E. Cook, R. E. Santini, D. W. Margerum, and J. M. T. Raycheba, *ibid.*, **46**, 374 (1974).
(3) M. J. Milano and H. L. Pardue, *ibid.*, **47**, 25 (1975).
(4) J. Sustek, *ibid.*, **46**, 1676 (1974).
(5) R. M. Rocco, D. C. Abbott, R. W. Giese, and B. L. Karger, *Clin. Chem.*, **23**, 705 (1977).
(6) A. E. McDowell and H. L. Pardue, *Anal. Chem.*, **49**, 1171 (1977).
(7) M. J. Milano and K. Kim, *ibid.*, **49**, 555 (1977).
(8) I. M. Warner, J. B. Callis, E. R. Davidson, and G. D. Christian, *Clin. Chem.*, **22**, 1483 (1976).

ACKNOWLEDGMENTS

Supported in part by Research Grant GM 13326-11 from the National Institutes of Health.

The authors thank Mr. Jim Audibert, Dooner Laboratories, for supplying information about Fedahist tablets.

Fluorometric TLC Determination of Free and Conjugated Propranolol, Naphthoxylactic Acid, and *p*-Hydroxypropranolol in Human Plasma and Urine

Y. GARCEAU, I. DAVIS, and J. HASEGAWA ˣ

Received July 29, 1977, from the *Biopharmacy Laboratory, Pharmacy Research and Development Division, Ayerst Laboratories, Inc., Rouses Point, NY 12979.* Accepted for publication October 13, 1977.

Abstract □ Sensitive, specific, and reproducible TLC methods are described for the determination of propranolol and its major metabolites in humans, conjugated propranolol, free and conjugated naphthoxylactic acid, and free and conjugated *p*-hydroxypropranolol. The drug or metabolites are extracted from plasma or urine with ether and applied to TLC plates of silica gel or microcrystalline cellulose. After development, the plates are scanned in a spectrodensitometer equipped to measure fluorescence in the UV and blue regions of the light spectrum. Quantitation is achieved by comparing the areas under the peaks obtained from the unknowns to those obtained from standards applied to the same plate. Limits of quantitation in plasma are: free propranolol, 2 ng/ml; free *p*-hydroxypropranolol, 10 ng/ml; conjugated propranolol, 15 ng/ml; total (free and conjugated) naphthoxylactic acid, 25 ng/ml; and conjugated *p*-hydroxypropranolol, 50 ng/ml. These methods were used to obtain plasma level data in a volunteer after one single dose of propranolol and in patients under propranolol therapy. The R_f values of some known metabolites of propranolol obtained in various TLC developing systems are also presented.

Keyphrases □ Propranolol—and major metabolites, fluorometric TLC analyses in human plasma and urine □ Fluorometric TLC—analyses, propranolol and major metabolites in human plasma and urine □ TLC fluorometry—analyses, propranolol and major metabolites in human plasma and urine □ Cardiac depressants—propranolol and major metabolites, fluorometric TLC analyses in human plasma and urine

In addition to β-adrenergic blockade, propranolol (I) has been reported to have antihypertensive, antianxiety, anticonvulsant, and antianginal effects (1–5). Over 95% of an orally administered dose of propranolol is metabolized to several different substances in humans (6–11). The major metabolites in humans were identified as conjugated propranolol (II), *p*-hydroxypropranolol (III), and naphthoxylactic acid (IV) in their free and conjugated forms.

GLC methods were reported for propranolol and *p*-hydroxypropranolol in biological fluids (12–14). For the routine analysis of unchanged propranolol, wet fluorometric procedures are commonly used (15–18). Recently, a high-pressure liquid chromatographic (HPLC) method was reported (19). The present report describes simple, sensitive, and highly specific methods to assay I, II, and free and conjugated III and IV in human plasma and urine.

EXPERIMENTAL

Materials—All reagents and solvents were analytical reagent grade. TLC plates of silica gel or microcrystalline cellulose, 10 × 20 cm, were used. The plates were divided into 10 equal channels, 1 cm wide, with a scoring device[1]. Samples were applied to the plates with 25- or 50-μl microdispensers[2].

Acetate buffer, 0.1 *M*, pH 4.7, was prepared by dissolving 0.37 g of sodium acetate in 100 ml of distilled water and adjusting to pH 4.7 with acetic acid. Enzyme solutions[3] were prepared in distilled water. Standard solutions of I hydrochloride[4], III hydrochloride[4], and IV[4] were prepared in methanol. Ether[5], refluxed for 30 min in the presence of lithium aluminum hydride and distilled in an all-glass apparatus, was used for extracting III.

Determination of Free Propranolol—Human plasma or urine, 5 ml, was made basic with 1.0 ml of 1 *N* NaOH and shaken for 15 min with 40 ml of ether. After centrifugation, the organic phase was transferred and dried with 12 g of sodium sulfate. A 25-ml aliquot of the ether extract was transferred to a clean conical tube and evaporated under nitrogen[6] at 45°. The inside of the tube was washed with 1 ml of ethanol, and the solution was evaporated to dryness.

The dry residue was dissolved in 100 μl of ethanol, and aliquots of 25 μl were applied to a prescored TLC plate of silica gel 60[7]. Standard solutions of propranolol also were spotted on the same plate. The plate was

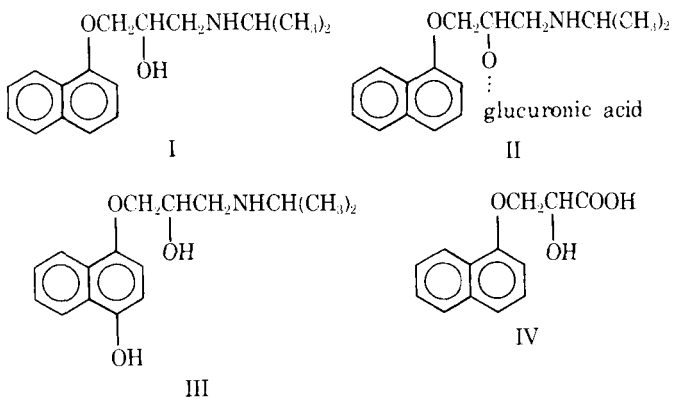

[1] SDA 320, Schoeffel Instrument Corp.
[2] Dialamatic, Drummond Scientific Co.
[3] Glusulase, Endo Laboratories.
[4] Imperial Chemical Industries, Great Britain.
[5] Mallinckrodt, Fisher, or Matheson, Coleman and Bell.
[6] N-Evap, Organomation Associates.
[7] E. Merck.

(2) M. J. Milano, H. L. Pardue, T. E. Cook, R. E. Santini, D. W. Margerum, and J. M. T. Raycheba, *ibid.*, **46**, 374 (1974).
(3) M. J. Milano and H. L. Pardue, *ibid.*, **47**, 25 (1975).
(4) J. Sustek, *ibid.*, **46**, 1676 (1974).
(5) R. M. Rocco, D. C. Abbott, R. W. Giese, and B. L. Karger, *Clin. Chem.*, **23**, 705 (1977).
(6) A. E. McDowell and H. L. Pardue, *Anal. Chem.*, **49**, 1171 (1977).
(7) M. J. Milano and K. Kim, *ibid.*, **49**, 555 (1977).
(8) I. M. Warner, J. B. Callis, E. R. Davidson, and G. D. Christian, *Clin. Chem.*, **22**, 1483 (1976).

ACKNOWLEDGMENTS

Supported in part by Research Grant GM 13326-11 from the National Institutes of Health.

The authors thank Mr. Jim Audibert, Dooner Laboratories, for supplying information about Fedahist tablets.

Fluorometric TLC Determination of Free and Conjugated Propranolol, Naphthoxylactic Acid, and *p*-Hydroxypropranolol in Human Plasma and Urine

Y. GARCEAU, I. DAVIS, and J. HASEGAWA ˣ

Received July 29, 1977, from the *Biopharmacy Laboratory, Pharmacy Research and Development Division, Ayerst Laboratories, Inc., Rouses Point, NY 12979.* Accepted for publication October 13, 1977.

Abstract □ Sensitive, specific, and reproducible TLC methods are described for the determination of propranolol and its major metabolites in humans, conjugated propranolol, free and conjugated naphthoxylactic acid, and free and conjugated *p*-hydroxypropranolol. The drug or metabolites are extracted from plasma or urine with ether and applied to TLC plates of silica gel or microcrystalline cellulose. After development, the plates are scanned in a spectrodensitometer equipped to measure fluorescence in the UV and blue regions of the light spectrum. Quantitation is achieved by comparing the areas under the peaks obtained from the unknowns to those obtained from standards applied to the same plate. Limits of quantitation in plasma are: free propranolol, 2 ng/ml; free *p*-hydroxypropranolol, 10 ng/ml; conjugated propranolol, 15 ng/ml; total (free and conjugated) naphthoxylactic acid, 25 ng/ml; and conjugated *p*-hydroxypropranolol, 50 ng/ml. These methods were used to obtain plasma level data in a volunteer after one single dose of propranolol and in patients under propranolol therapy. The R_f values of some known metabolites of propranolol obtained in various TLC developing systems are also presented.

Keyphrases □ Propranolol—and major metabolites, fluorometric TLC analyses in human plasma and urine □ Fluorometric TLC—analyses, propranolol and major metabolites in human plasma and urine □ TLC fluorometry—analyses, propranolol and major metabolites in human plasma and urine □ Cardiac depressants—propranolol and major metabolites, fluorometric TLC analyses in human plasma and urine

In addition to β-adrenergic blockade, propranolol (I) has been reported to have antihypertensive, antianxiety, anticonvulsant, and antianginal effects (1–5). Over 95% of an orally administered dose of propranolol is metabolized to several different substances in humans (6–11). The major metabolites in humans were identified as conjugated propranolol (II), *p*-hydroxypropranolol (III), and naphthoxylactic acid (IV) in their free and conjugated forms.

GLC methods were reported for propranolol and *p*-hydroxypropranolol in biological fluids (12–14). For the routine analysis of unchanged propranolol, wet fluorometric procedures are commonly used (15–18). Recently, a high-pressure liquid chromatographic (HPLC) method was reported (19). The present report describes simple, sensitive, and highly specific methods to assay I, II, and free and conjugated III and IV in human plasma and urine.

EXPERIMENTAL

Materials—All reagents and solvents were analytical reagent grade. TLC plates of silica gel or microcrystalline cellulose, 10 × 20 cm, were used. The plates were divided into 10 equal channels, 1 cm wide, with a scoring device[1]. Samples were applied to the plates with 25- or 50-μl microdispensers[2].

Acetate buffer, 0.1 *M*, pH 4.7, was prepared by dissolving 0.37 g of sodium acetate in 100 ml of distilled water and adjusting to pH 4.7 with acetic acid. Enzyme solutions[3] were prepared in distilled water. Standard solutions of I hydrochloride[4], III hydrochloride[4], and IV[4] were prepared in methanol. Ether[5], refluxed for 30 min in the presence of lithium aluminum hydride and distilled in an all-glass apparatus, was used for extracting III.

Determination of Free Propranolol—Human plasma or urine, 5 ml, was made basic with 1.0 ml of 1 *N* NaOH and shaken for 15 min with 40 ml of ether. After centrifugation, the organic phase was transferred and dried with 12 g of sodium sulfate. A 25-ml aliquot of the ether extract was transferred to a clean conical tube and evaporated under nitrogen[6] at 45°. The inside of the tube was washed with 1 ml of ethanol, and the solution was evaporated to dryness.

The dry residue was dissolved in 100 μl of ethanol, and aliquots of 25 μl were applied to a prescored TLC plate of silica gel 60[7]. Standard solutions of propranolol also were spotted on the same plate. The plate was

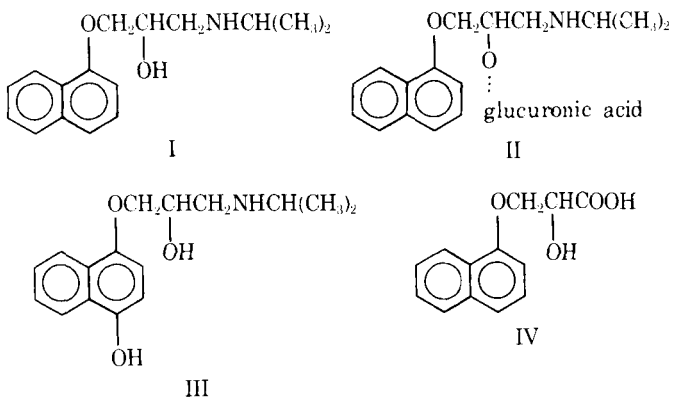

[1] SDA 320, Schoeffel Instrument Corp.
[2] Dialamatic, Drummond Scientific Co.
[3] Glusulase, Endo Laboratories.
[4] Imperial Chemical Industries, Great Britain.
[5] Mallinckrodt, Fisher, or Matheson, Coleman and Bell.
[6] N-Evap, Organomation Associates.
[7] E. Merck.

Table I—Recovery Experiments of Free Propranolol in Human Plasma and Urine

Plasma					Urine		
Amount Spiked, ng/ml	Amount Recovered, ng/ml				Amount Spiked, ng/ml	Amount Recovered, ng/ml	
	Run 1	Run 2	Run 3	Run 4		Run 1	Run 2
5	5	5	5	5	10	8	10
10	10	9	9	9	20	16	17
20	20	18	17	18	30	32	28
30	26	27	29	25	40	37	35
40	38	37	39	39	500	520	510
50	47	47	49	50	1000	940	890
	Mean	95.1%				Mean 92.4%	
	SD	6.5%				*SD* 8.7%	

developed in a saturated tank containing methanol (100 ml)–concentrated ammonium hydroxide (0.4 ml). After developing 12 cm, the plate was air dried and then sprayed with propylene glycol–water (50:50). It was then scanned in a spectrodensitometer[8] equipped with a density computer[9]. The light source was a xenon–mercury 200-w lamp[10].

The instrument was operated in the fluorescence mode with excitation set at 290 nm. Emission was filtered with a UV-transmitting, visible-absorbing filter[11] having a transmission band between 300 and 420 nm, with maximum transmission at 365 nm. A UV clear filter[12] also was used. Gain was set between 600 and 700 on the arbitrary scale of the spectrodensitometer. Scanning and chart speeds were 10.2 cm/min. Quantitation was achieved by comparing the areas under the peaks obtained from the unknowns to those obtained from the standards.

Determination of Conjugated Propranolol—Plasma or urine, 0.5 ml, was mixed with 2 ml of acetate buffer and 1 ml of an enzyme solution[3] containing 2000 units of β-glucuronidase and 500 units of sulfatase. The plasma mixture was incubated at 37° for 90 min, and the urine mixture was incubated at 37° for 17 hr. After incubation, 1.0 ml of 1 *N* NaOH was added, and the sample was shaken with 40 ml of ether for 15 min.

The ether phase was transferred and dried with 12 g of sodium sulfate. A 30-ml aliquot was transferred to a conical tube and evaporated under a nitrogen[6] stream at 45°. The inside of the tube was washed with 1 ml of ethanol, and this solution was evaporated to dryness. The dry residue was dissolved in 100 μl of ethanol, and aliquots of 25 μl of plasma extract or 10 μl of urine extract were applied to a prescored TLC plate of silica gel 60[7] along with standard solutions of propranolol. The plate was developed in a saturated tank containing 100 ml of benzene–isopropyl alcohol–dimethylformamide–acetic acid (70:10:10:10). The plate was sprayed and subjected to densitometry as described under *Determination of Free Propranolol.*

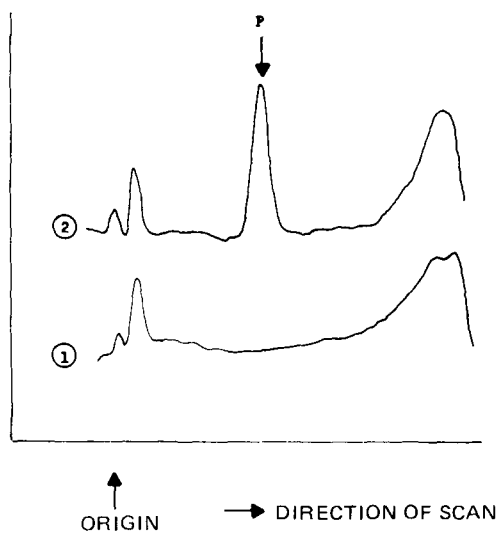

Figure 1—*Chromatograms of extracts of plasma obtained from a volunteer before (1) and 1 hr after (2) 40 mg po of propranolol hydrochloride. The* R_f *value of propranolol is indicated by the arrow.*

[8] Model SD 3000, Schoeffel Instrument Corp.
[9] Model SDC 300, Schoeffel Instrument Corp.
[10] Hanovia Lamp Division, Comrand Precision Ind.
[11] C.S. 7.51, Corning.
[12] C.S. 0.52, Corning.

The procedure outlined quantitates total propranolol. Conjugated propranolol is obtained by subtracting free from total drug.

Determination of Naphthoxylactic Acid—A 0.5-ml sample of plasma or urine was mixed with 2 ml of the acetate buffer and 1 ml of an enzyme solution[3] containing 2000 units of β-glucuronidase and 500 units of sulfatase. The mixture was incubated at 37° for the following time periods: plasma sample, 2 hr; and urine sample, 17 hr. After incubation, the sample was made alkaline with 1 ml of 1 *N* NaOH and extracted with 40 ml of ether. The ether extract was discarded, and the aqueous phase was acidified with 1.5 ml of 1 *N* HCl and extracted with 40 ml of ether for 15 min.

The ether extract was dried with 10 g of sodium sulfate, and a 25-ml aliquot was transferred to a clean conical tube and evaporated under nitrogen[6] at 45°. The inside of the tube was washed with 1 ml of ethanol, and the solution was evaporated to dryness. The dry residue was reconstituted with 100 μl of ethanol. Aliquots of 25 μl of the reconstituted plasma extracts and 5 μl of the urine extracts were applied to a prescored TLC plate of silica gel[13]. Standard solutions of IV were also applied to the same plate. The plate was developed in a saturated tank containing 100 ml of benzene–isopropyl alcohol–dimethylformamide–acetic acid (70:10:10:10). The plate was then sprayed and scanned in a spectrodensitometer as described under *Determination of Free Propranolol.*

This procedure measures total (conjugated and free) IV acid. Free acid can be determined by the same method, omitting the enzyme hydrolysis step.

Determination of *p*-Hydroxypropranolol—A 1.0-ml sample of plasma was mixed with 2 ml of acetate buffer and 0.5 ml of an enzyme solution[3] containing 10,000 units of β-glucuronidase and 2500 units of sulfatase. The mixture was incubated at 37° for 30 min. After incubation, 5 ml of pH 10 buffer[14] was added, and the sample was shaken with 40 ml of ether for 15 min.

For urine assay, a 0.1-ml sample was mixed with 0.5 ml of acetate buffer, 0.1 ml of 0.1 *N* ethylenediaminetetraacetic acid, and 0.1 ml of an enzyme solution containing 20,000 units of β-glucuronidase and 5000 units of sulfatase. The mixture was incubated at 37° for 20 min, after which 3 ml of pH 10 buffer[14] was added and the sample was extracted with 40 ml of ether.

The extract mixtures were centrifuged, and 30 ml of the ether phase was transferred to clean tubes and evaporated under nitrogen[6] at 45°. Remaining traces of water were removed by adding 4 ml of benzene–ethanol (5:2) to the tubes. The azeotropic mixture thus formed could be dried completely under nitrogen[6] at 45°. The dry residue was then dissolved in 100 μl of ethanol. The extraction and evaporation steps were carried out in 50-ml conical polypropylene tubes[15]. The reasons for using this type of tube are discussed later.

Aliquots of 25 μl of plasma extracts or 10 μl of urine extracts were applied to a TLC plate of microcrystalline cellulose[16]. Standard solutions of III were also applied to the same plate. The plate was developed in a saturated tank containing 100 ml of ethyl acetate–acetone–water (40:45:15). After development, the plate was air dried and scanned in a spectrodensitometer[8] operated in the fluorescence mode. Excitation wavelength was set at 300 nm, and emission was passed through a blue filter[17] with maximum transmission at 420–440 nm and a cutoff filter[18]. Quantitation was achieved by comparing the areas under the peaks obtained from the unknowns to those obtained from the standards.

[13] Macherey-Nagel. It is advisable to predevelop these plates to obtain a clean background.
[14] R-1280, Anachemia.
[15] Falcon 2070.
[16] Avicel, thickness 250 μm, Analtech.
[17] C.S. 5.60, Corning.
[18] C.S. 3.75, Corning.

Table II—Recovery Experiments of Propranolol in Human Plasma and Urine after Spiked Samples Were Submitted to Procedure to Assay Conjugated Propranolol

Plasma				Urine			
Amount Spiked, ng/ml	Amount Recovered, ng/ml			Amount Spiked, ng/ml	Amount Recovered, ng/ml		
	Run 1	Run 2	Run 3		Run 1	Run 2	Run 3
25	25	22	27	100	91	107	101
50	48	53	46	250	266	266	266
100	93	93	101	500	490	533	533
250	250	232	256	750	746	773	720
500	522	426	501				
	Mean 97.7%				Mean 101.9%		
	SD 6.3%				*SD* 5.2%		

This procedure measures total III. To assay free III, a 2-ml sample of plasma or urine was mixed with 4 ml of pH 10 buffer[14] and extraction was carried out as described. Conjugated III can be obtained by subtracting free from total metabolite.

Recovery Experiments—Samples of human plasma or urine were spiked with solutions of varying concentrations of I hydrochloride, IV, or III hydrochloride and subjected to the described analytical procedures.

Linearity of Response and Limit of Quantitation—Solutions of varying concentrations of I hydrochloride, IV, and III hydrochloride were spotted on TLC plates and subjected to chromatography to determine the linear ranges of instrument response. The limit of quantitation was set as an "area under the peak" of 10 units since the instrument could reliably integrate such areas under the conditions used.

***In Vivo* Experiment**—One healthy male volunteer was given 80 mg po of I hydrochloride[19]; blood samples were obtained at 0.5, 1, 2, 3, 4, 5, 6, 8, and 12 hr after dosing. A preadministration sample was also obtained. The blood was transferred to tubes containing ethylenediaminetetraacetic acid, mixed, and centrifuged. The plasma was transferred to clean tubes and frozen until assayed. Blood samples also were obtained from patients undergoing propranolol therapy and receiving the drug in 40-mg doses three or four times daily or in 160-mg doses four times daily. Blood specimens were treated as described.

RESULTS AND DISCUSSION

Free Propranolol—On a thin layer of silica gel, I has fluorescent properties similar to those observed in the wet state (15, 16). The emission filter[11] used transmits between 300 and 420 nm with maximum transmission at 365 nm. The clear filter[12] was used to filter off excitation radiation.

In the TLC system described, I had an R_f value of 0.34 and was separated from plasma and urine components. Figure 1 shows chromatograms obtained from the plasma of a human volunteer prior to and after administration of I hydrochloride. Propranolol was free of interference from its metabolites. Drug extraction was carried out at alkaline pH so that the acidic metabolites were not extracted. The basic metabolite, deisopropylpropranolol, and the neutral metabolite, 1-(α-naphthoxy)-2,3-propanediol, were separated from propranolol during chromatography, having R_f values of 0.15 and 0.84, respectively. Instrument response as determined by the area under the peak was linear over the range of 0–100 ng/spot, with a correlation coefficient of 0.999. The limit of quantitation was 2 ng/spot, equivalent to 2 ng/ml of plasma or urine.

Mean recovery from spiked plasma samples was 95.1 ± 6.5% *SD*, n = 24 (Table I). Mean recovery from spiked urine samples was 92.4 ± 8.7% *SD*, n = 12. All concentration units were calculated as nanograms of propranolol hydrochloride since it was the standard material used.

Spraying the TLC plates with propylene glycol–water is critical. Moisturizing the plate increases sensitivity 10-fold. Propylene glycol acts as a moisture-retaining agent and delays water evaporation from the plate. If a plate is sprayed properly, readings are stable for at least 10 min. This time is sufficient to scan a plate containing a minimum of six spotted channels. Since fluorescence intensity depends on moisture content, care must be taken to ensure even spraying of a plate.

The 10 × 20-cm plates are used because the width of the spray can be adjusted to cover the width of the plate completely. Uniform spraying is achieved by using an up and down motion. With the spray bottle 60 cm (24 in.) from the plate, 40 up and down passes are sufficient to provide adequate moisture, consuming about 30 ml of the spraying solution. Overspraying results in an erratic baseline, and underspraying causes a loss of sensitivity.

Conjugated Propranolol—The procedure described to assay this metabolite was also highly specific. In the TLC system used, the R_f values were: propranolol, 0.20; deisopropylpropranolol, 0.07; and 1-(α-naphthoxy)-2,3-propanediol, 0.67. There was no interference from the acidic metabolites due to the high extraction pH. Clean backgrounds were obtained from blank plasma and urine extracts.

Since the assay included an enzymatic hydrolysis step, it was essential

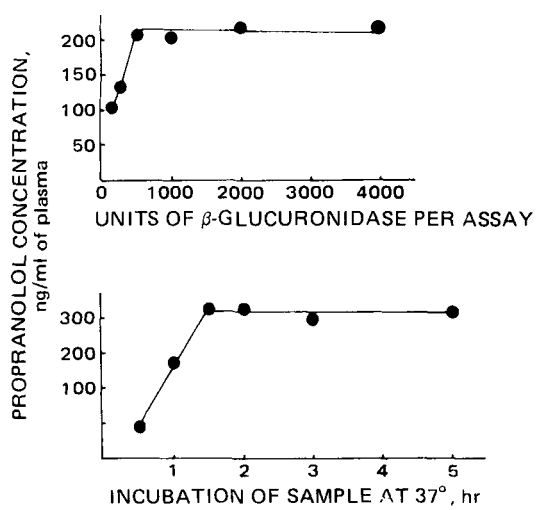

Figure 2—*Effects of enzyme concentration and time of incubation at 37° on the amount of propranolol released when a 0.5-ml plasma sample was subjected to hydrolysis in the presence of β-glucuronidase and sulfatase. Top: units of sulfatase were one-fourth those indicated for β-glucuronidase. Plasma sample was obtained from a patient receiving propranolol therapy (40 mg four times daily). Bottom: time of incubation of plasma sample at 37° in the presence of 2000 units of β-glucuronidase and 1000 units of sulfatase. Plasma sample was obtained from a patient receiving propranolol therapy (40 mg three times daily).*

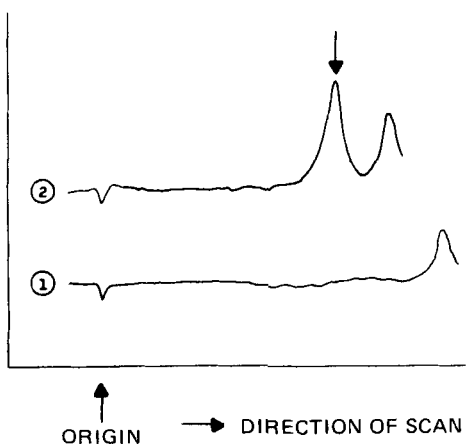

Figure 3—*Chromatograms of extracts of plasma obtained from a volunteer before (1) and 3 hr after (2) 40 mg po of propranolol hydrochloride. The R_f value of IV is indicated by the arrow.*

[19] Two 40-mg Inderal-40 tablets, Ayerst Laboratories.

Table III—Recovery Experiments of IV in Human Plasma and Urine

Plasma				Urine		
Amount Spiked, ng/ml	Amount Recovered, ng/ml			Amount Spiked, μg/ml	Amount Recovered, μg/ml	
	Run 1	Run 2	Run 3		Run 1	Run 2
250	254	231	246	2.5	2.6	2.5
500	546	473	440	5.0	4.7	5.3
750	763	695	675	7.5	6.4	6.6
1000	873	867	902	10.0	9.3	10.0
	Mean 94.4%				Mean 96.5%	
	SD 6.9%				*SD* 7.4%	

Table IV—Recovery Study of III in Human Plasma

Method for Free III				Method for Total III			
Amount Spiked, ng/ml	Amount Recovered, ng/ml			Amount Spiked, ng/ml	Amount Recovered, ng/ml		
	Run 1	Run 2	Run 3		Run 1	Run 2	Run 3
10	10	11	10	50	29	28	28
25	24	25	26	100	69	69	66
50	47	47	51	250	151	140	165
100	105	102	94	500	369	338	359
250	207	234	239	1000	688	646	688
500	390	440	480				
	Mean 96.4%				Mean 64.8%		
	SD 7.8%				*SD* 6.1%		

to determine if propranolol was stable under these conditions. Therefore, control plasma and urine samples were spiked with known amounts of propranolol and submitted to the procedure, including enzyme hydrolysis (Table II). Mean recovery of drug added to plasma was 97.7 ± 6.3% *SD*, n = 15. Mean recovery of drug added to urine was 101.9 ± 5.2% *SD*, n = 12. The limits of quantitation were 15 ng/ml of plasma and 50 ng/ml of urine.

Propranolol has been reported to be metabolized to a glucuronide conjugate in humans and animals (6, 9, 11, 20). The incubation periods and the enzyme concentrations used in enzyme hydrolysis were adequate to release the propranolol moiety maximally from the conjugate. Since no standard material of propranolol conjugate was available, plasma and urine samples were taken from patients receiving propranolol therapy and subjected to hydrolysis under varying conditions of enzyme concentrations and incubation times until a maximum amount of free propranolol was obtained (Fig. 2).

Compound IV—In the procedure described, IV was free of interference from propranolol and its known metabolites. The amine and neutral metabolites were removed during the alkaline extraction step. The acidic substances had the following R_f values: IV, 0.54; III, 0.06; *p*-hydroxy-1-(α-naphthoxy)-2,3-propanediol, 0.43; naphthoxyacetic acid, 0.71; α-naphthol, 0.74; and dihydroxynaphthalene, 0.61. Propranolol itself had an R_f value of 0.12. Compound IV was also free of interference from extractable plasma and urine components. Figure 3 shows a chromatogram of an extract of plasma containing the metabolite.

The areas under the peaks of IV were linear over the range of 0–250 ng/spot, with a correlation coefficient of 0.995. Mean recovery from spiked plasma was 94.4 ± 6.9% *SD*, n = 12 (Table III). Mean recovery from spiked urine was 96.5 ± 7.4% *SD*, n = 8. Since the spiked samples were submitted to enzyme hydrolysis before extraction, results of the recovery study indicated that IV was stable under the conditions used. The limits of quantitation were 25 ng/ml of plasma and 125 ng/ml of urine. The concentrations of enzymes and the incubation periods used were adequate to release the IV moiety maximally from the conjugates. Little is known about the conjugation of this metabolite. However, IV is present in plasma and urine in both free and conjugated forms. The question of the type of conjugate, glucuronide or sulfate, remains.

Compound III—This metabolite fluoresces strongly in the blue region of the light spectrum, with maximum emission between 400 and 450 nm.

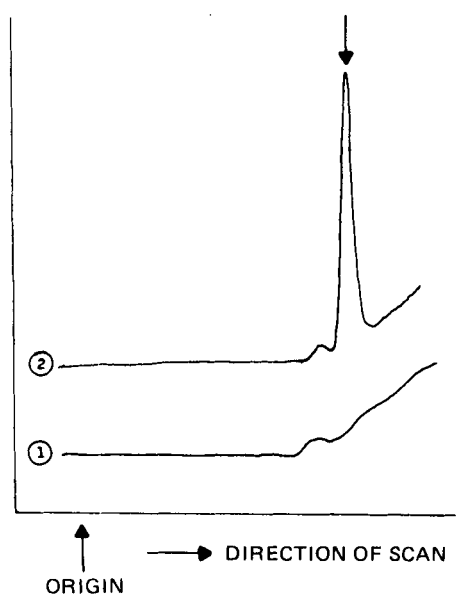

Figure 4—*Chromatograms of plasma extracts obtained from a volunteer before (1) and 0.5 hr after (2) 80 mg po of propranolol hydrochloride. The R_f value of III is indicated by the arrow.*

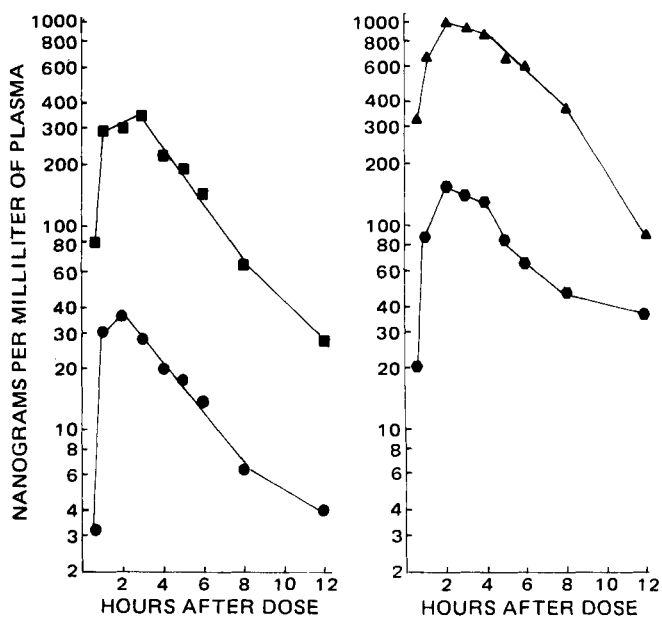

Figure 5—*Plasma levels of propranolol and metabolites following one single dose of 80 mg po of propranolol hydrochloride to a human volunteer. Key: ●, free propranolol; ■, conjugated propranolol; ●, total (free plus conjugated) III; and ▲, total (free plus conjugated) IV.*

Table V—Recovery Study of III in Human Urine

Method for Free III			Method for Total III		
Amount Spiked, ng/ml	Amount Recovered, ng/ml		Amount Spiked, mcg/ml	Amount Recovered, μg/ml	
	Run 1	Run 2		Run 1	Run 2
100	93	80	5.0	3.4	3.5
250	206	230	10.0	7.5	7.7
500	390	410	15.0	10.6	9.8
1000	790	830	25.0	20.3	20.3
	Mean 83.6%			Mean 73.5%	
	SD 5.7%			*SD* 5.9%	

Table VI—Plasma Levels (Nanograms per Milliliter) of Free Propranolol and Metabolites in Three Patients Receiving Propranolol Therapy

Patient	Dose, mg	Hours after Last Dose	Free Propranolol	Conjugated Propranolol	Total IV	Conjugated III
1	40 three times daily	4	25	348	684	377
2	40 four times daily	3	95	368	—[a]	478
3	160 four times daily	3	261	1630	1160	1233

[a] Not done.

In the system described, III had an R_f value of 0.57 and was separated from plasma and urine components. Chromatograms of plasma extracts are shown in Fig. 4. Compound III was also free of interference from the parent drug propranolol and its known metabolites. Compound IV and naphthoxyacetic acid were not extracted at pH 10.

Metabolites α-naphthol, dihydroxynaphthalene, 1-(α-naphthoxy)-2,3-propanediol, and its *p*-hydroxy derivative moved with the solvent front in the TLC system used (R_f 1.0). Propranolol and deisopropylpropranolol had R_f values of 0.59 and 0.53, respectively, and overlapped with the III peak. However, their maximum fluorescence emission (365 nm) was not transmitted through the blue filter[17] used and the compounds did not interfere with the assay. In fact, propranolol concentrations as high as 1.1 μg/ml of plasma and 13.3 μg/ml of urine did not interfere with the determination of III.

Data from recovery experiments done in plasma and urine are given in Tables IV and V, respectively. Mean recoveries of III from spiked plasma were 96.4% when the method for free III was used and 64.8% when the method for conjugated III was used. Similarly, mean recoveries from spiked urine were 83.6 and 73.5% when these respective methods were used. The lower recoveries obtained with the procedure used to assay the conjugate were due to the instability of III during enzyme hydrolysis. Compound III is itself metabolized to glucuronide and/or sulfate conjugates (9).

To determine if the III moiety was released completely from the conjugate during enzyme hydrolysis, plasma and urine samples from patients under propranolol therapy were incubated at 37° for different time periods and with different concentrations of enzyme solutions until maximum release of III was observed. Large concentrations of enzymes were used to keep the incubation time to a minimum since III degrades during incubation at 37°. Incubation of plasma or urine samples with the enzyme concentrations specified (see *Experimental*) was adequate to achieve maximum release after 30 min. Incubation for longer periods resulted in some loss of metabolite.

Limits of quantitation were: free III, 10 ng/ml of plasma or 100 ng/ml of urine; and conjugated III, 50 ng/ml of plasma or 2 μg/ml of urine.

Compound III is unstable and care must be exercised to prevent its degradation. Since it is sensitive to metal ions, blood specimens were always obtained in tubes containing ethylenediaminetetraacetic acid. It was extremely sensitive to peroxides present in the ether used for extraction. All traces of peroxides were removed by refluxing the solvent in the presence of lithium aluminum hydride followed by distillation in an all-glass apparatus immediately before use.

Compound III was heat labile and, therefore, enzyme hydrolysis could not be carried out at a temperature exceeding 37°. It was very labile when dried on a glass surface. When ether extracts of the metabolite were evaporated to dryness in glass tubes, complete loss of the metabolite was observed. Since this result could have been due to the presence of contaminating metal ions on the glass surface, evaporation was always carried out in polypropylene disposable tubes. Even with this type of material, however, it was essential that the tube be removed from the evaporation bath as soon as dried and that the residue be dissolved in ethanol immediately. Leaving the dry residue unattended even for a few minutes resulted in some loss of metabolite. Microcrystalline cellulose plates were used for TLC because silica gel, aluminum oxide, and polyamide plates caused degradation of the metabolite.

Compound III was not stable in refrigerated plasma. More than 80% of metabolite added to plasma samples was lost after 6 days of refrigeration at 4°. However, when kept frozen at −20°, the samples were stable for 1 month.

Levels of Propranolol and Metabolites in Human Plasma—To demonstrate the applicability of the methods, plasma level–time curves of propranolol and its three major metabolites obtained after administration of 80 mg po of propranolol hydrochloride to a human volunteer are shown in Fig. 5. In addition, plasma concentrations of the same substances in patients under propranolol therapy are given in Table VI. Free III could not be detected after a single dose of propranolol because its concentration was probably below the limit of detection of 10 ng/ml of plasma.

CONCLUSIONS

Sensitive, specific, and reproducible methods have been described for the determination of free propranolol and three of its metabolites in biological fluids. The methods are simple, relatively rapid, and especially useful when a large number of samples must be assayed. The methods offer several advantages over those already published.

The spectrofluorometric procedures (15–18), although convenient for analysis of a large number of samples, suffer from a lack of specificity since the metabolite deisopropylpropranolol is extractable under conditions specified in the assays. Similarly, the specificity of the HPLC method (19) with regard to the metabolites deisopropylpropanolol and 1-(α-naphthoxy)-2,3-propanediol has not been demonstrated. The GLC procedures (12–14) are specific and sensitive. However, in the authors' laboratory, they have proven time consuming and subject to complications because of a sensitive derivatization step.

The advantages of the TLC methods reside in their specificity and simplicity in so far as there is no need for derivatization, and the extraction, evaporation, and TLC spotting steps are quite straightforward. One person can easily analyze 20 samples in 1 working day.

REFERENCES

(1) B. Prichard and P. Gillam, *Br. Med. J.*, **1**, 7 (1969).

(2) K. Granville-Grossman and P. Turner, *Lancet*, **1**, 788 (1966).

(3) G. Leszkoozky and P. Tardos, *J. Pharm. Pharmacol.*, **17**, 518 (1965).

(4) P. Gillam and B. Prichard, *Br. Med. J.*, **2**, 337 (1965).

(5) J. Harner, T. Grandjean, L. Melendey, and G. Sowton, *ibid.*, **2**, 720 (1964).

(6) P. A. Bond, *Nature*, **213**, 721 (1967).

(7) J. W. Paterson, M. E. Conolly, and C. T. Dollery, *Pharmacol. Clin.*, **2**, 127 (1970).

(8) G. L. Tindell, T. Walle, and T. E. Gaffney, *Life Sci.*, **11**, 1029 (1972).

(9) T. Walle and T. E. Gaffney, *J. Pharmacol. Exp. Ther.*, **182**, 83 (1972).

(10) T. Walle, J. I. Morrison, and G. L. Tindell, *Res. Commun. Chem. Pathol. Pharmacol.*, **9**, 1 (1974).
(11) H. Ehrsson, "Abstracts of the 1975 Pittsburgh Conference on Analytical Chemistry and Applied Spectroscopy," Cleveland, Ohio, Mar. 1975, Paper 102.
(12) E. DiSalle, K. M. Baker, S. R. Bareggi, W. D. Watkins, C. A. Chidsey, A. Frigerio, and P. L. Morselli, *J. Chromatogr.*, **84**, 347 (1973).
(13) T. Walle, *J. Pharm. Sci.*, **63**, 1885 (1974).
(14) T. Walle, J. Morrison, K. Walle, and E. Conradi, *J. Chromatogr.*, **114**, 351 (1975).
(15) D. G. Shand, E. M. Nuckolls, and J. A. Oates, *Clin. Pharmacol. Ther.*, **11**, 112 (1970).
(16) J. W. Black, W. A. M. Duncan, and R. G. Shanks, *Br. J. Pharmacol.*, **25**, 577 (1965).
(17) P. K. Ambler, B. N. Singh, and M. Lever, *Clin. Chim. Acta*, **54**, 373 (1974).
(18) L. Offerhaus and J. R. Vander Vecht, *Br. J. Clin. Pharmacol.*, **3**, 1061 (1976).
(19) W. D. Mason, E. N. Amick, and O. H. Weddle, *Anal. Lett.*, **10**, 515 (1977).
(20) H. Ehrsson, *J. Pharm. Pharmacol.*, **27**, 971 (1975).

ACKNOWLEDGMENTS

The authors express their gratitude to Mr. M. Caron for help in designing the protocol for the *in vivo* experiments and to Dr. C. Orzech and Mr. F. Gemmill who synthesized some propranolol metabolites.

Determination of Indoprofen in Physiological Fluids by Reversed-Phase Liquid Chromatography

DUANE B. LAKINGS *x, WILLIAM J. HAGGERTY *, GAIL REHAGEN *, and HOWARD BARTH ‡

Received July 25, 1977, from the **Chemical Sciences Division, Midwest Research Institute, Kansas City, MO 64110,* and ‡*Hercules, Inc., Wilmington, DE 19899.* Accepted for publication October 5, 1977.

Abstract □ A rapid, sensitive, reversed-phase high-performance liquid chromatographic procedure was developed for the quantitative analysis of indoprofen in plasma and urine. Minimal sample preparation is required for the analysis of unconjugated urinary or plasma drug levels. The method provided quantitative results for indoprofen levels of 0.5–50 μg/ml of plasma and 0.5–200 μg/ml of urine and had a lower detection limit of 1 ng. Total urinary indoprofen levels required enzymatic hydrolysis of the conjugated drug prior to analysis. Results are presented for the plasma and urinary excretion levels of indoprofen for a patient receiving a single oral dose.

Keyphrases □ Indoprofen—high-performance liquid chromatographic analysis in biological fluids □ High-performance liquid chromatography—analysis, indoprofen in biological fluids □ Analgesics—indoprofen, high-performance liquid chromatographic analysis in biological fluids

Indoprofen, *dl*-2-[4-(1-oxo-2-isoindolinyl)phenyl]propanoic acid, has analgesic activity in animals and humans (1–4). In humans, indoprofen appears unchanged in plasma (5) and enantiomeric enrichment is not significant (6). Tosolini *et al.* (7) reported that indoprofen was excreted as the glucuronide conjugate and that enzymatic hydrolysis was required prior to determining urinary excretion levels.

GLC methods for the analysis of indoprofen in plasma and urine have been reported (6–8). While each method has analytical validity and sufficient sensitivity, they all require extraction of indoprofen from the biological fluid and derivatization to provide the necessary volatility for GLC analysis. These extraction and derivatization steps are time consuming and, consequently, expensive for extensive bioavailability studies.

To overcome these difficulties in sample preparation and to maintain the necessary selectivity and sensitivity for low level analysis, a method was developed using reversed-phase high-performance liquid chromatography (HPLC). The method is applicable to both urine and plasma samples containing indoprofen and has sensitivity at the nanogram level.

EXPERIMENTAL

Reagents—Acetonitrile[1] was used as received. The water was first deionized and then distilled to remove any contaminants. For enzymatic hydrolysis of conjugated drug, aryl sulfatase[2] containing β-glucuronidase was used.

Reference Compound and Internal Standard—A reference standard of indoprofen[3] (I) was used to develop the analytical method. The internal standard (II) selected for quantitation was the pentanoic acid homolog of indoprofen[3].

HPLC Conditions—To determine the optimal wavelength for UV detection of indoprofen, reference standard was dissolved in methanol and its UV spectrum was obtained. The standard has a λ_{max} at 282 nm with an absorptivity (ε 282) of 14,200 ($E^{1\%}_{1\,cm}$ = 505). The reported $E^{1\%}_{1\,cm}$ value for indoprofen is 500 ± 25 (λ_{max} 283)[4]. A 280-nm filter was used.

The liquid chromatograph was constructed from components and consisted of a high pressure pump[5], a loop injector[6], and a UV detector[7]. The initial HPLC conditions used for urinary analysis consisted of a Zorbox ODS[8] (250 × 2 mm i.d.) column and an eluent of 40% acetonitrile

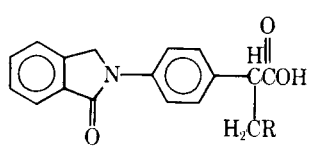

I: R = H
II: R = CH_2CH_3

[1] Nanograde, Mallinckrodt Chemical Works, St. Louis, Mo.
[2] Sigma Chemical Co., St. Louis, Mo. (31,000 units/g of solid; 1 unit will hydrolyze 1.0 μmole of nitrocatechol sulfate/hr at pH 5.0 at 37°).
[3] Adria Laboratories, Columbus, Ohio.
[4] Dr. Werner Hausmann, Adria Laboratories, Columbus, Ohio, personal communication.
[5] Model 6000A, Waters Associates, Milford, Mass.
[6] Model UK6, Waters Associates, Milford, Mass.
[7] Model 440, Waters Associates, Milford, Mass.
[8] DuPont Co., Wilmington, Del.

(10) T. Walle, J. I. Morrison, and G. L. Tindell, *Res. Commun. Chem. Pathol. Pharmacol.*, **9**, 1 (1974).
(11) H. Ehrsson, "Abstracts of the 1975 Pittsburgh Conference on Analytical Chemistry and Applied Spectroscopy," Cleveland, Ohio, Mar. 1975, Paper 102.
(12) E. DiSalle, K. M. Baker, S. R. Bareggi, W. D. Watkins, C. A. Chidsey, A. Frigerio, and P. L. Morselli, *J. Chromatogr.*, **84**, 347 (1973).
(13) T. Walle, *J. Pharm. Sci.*, **63**, 1885 (1974).
(14) T. Walle, J. Morrison, K. Walle, and E. Conradi, *J. Chromatogr.*, **114**, 351 (1975).
(15) D. G. Shand, E. M. Nuckolls, and J. A. Oates, *Clin. Pharmacol. Ther.*, **11**, 112 (1970).
(16) J. W. Black, W. A. M. Duncan, and R. G. Shanks, *Br. J. Pharmacol.*, **25**, 577 (1965).
(17) P. K. Ambler, B. N. Singh, and M. Lever, *Clin. Chim. Acta*, **54**, 373 (1974).
(18) L. Offerhaus and J. R. Vander Vecht, *Br. J. Clin. Pharmacol.*, **3**, 1061 (1976).
(19) W. D. Mason, E. N. Amick, and O. H. Weddle, *Anal. Lett.*, **10**, 515 (1977).
(20) H. Ehrsson, *J. Pharm. Pharmacol.*, **27**, 971 (1975).

ACKNOWLEDGMENTS

The authors express their gratitude to Mr. M. Caron for help in designing the protocol for the *in vivo* experiments and to Dr. C. Orzech and Mr. F. Gemmill who synthesized some propranolol metabolites.

Determination of Indoprofen in Physiological Fluids by Reversed-Phase Liquid Chromatography

DUANE B. LAKINGS *x, WILLIAM J. HAGGERTY *, GAIL REHAGEN *, and HOWARD BARTH ‡

Received July 25, 1977, from the **Chemical Sciences Division, Midwest Research Institute, Kansas City, MO 64110,* and ‡*Hercules, Inc., Wilmington, DE 19899.* Accepted for publication October 5, 1977.

Abstract □ A rapid, sensitive, reversed-phase high-performance liquid chromatographic procedure was developed for the quantitative analysis of indoprofen in plasma and urine. Minimal sample preparation is required for the analysis of unconjugated urinary or plasma drug levels. The method provided quantitative results for indoprofen levels of 0.5–50 μg/ml of plasma and 0.5–200 μg/ml of urine and had a lower detection limit of 1 ng. Total urinary indoprofen levels required enzymatic hydrolysis of the conjugated drug prior to analysis. Results are presented for the plasma and urinary excretion levels of indoprofen for a patient receiving a single oral dose.

Keyphrases □ Indoprofen—high-performance liquid chromatographic analysis in biological fluids □ High-performance liquid chromatography—analysis, indoprofen in biological fluids □ Analgesics—indoprofen, high-performance liquid chromatographic analysis in biological fluids

Indoprofen, *dl*-2-[4-(1-oxo-2-isoindolinyl)phenyl]propanoic acid, has analgesic activity in animals and humans (1–4). In humans, indoprofen appears unchanged in plasma (5) and enantiomeric enrichment is not significant (6). Tosolini *et al.* (7) reported that indoprofen was excreted as the glucuronide conjugate and that enzymatic hydrolysis was required prior to determining urinary excretion levels.

GLC methods for the analysis of indoprofen in plasma and urine have been reported (6–8). While each method has analytical validity and sufficient sensitivity, they all require extraction of indoprofen from the biological fluid and derivatization to provide the necessary volatility for GLC analysis. These extraction and derivatization steps are time consuming and, consequently, expensive for extensive bioavailability studies.

To overcome these difficulties in sample preparation and to maintain the necessary selectivity and sensitivity for low level analysis, a method was developed using reversed-phase high-performance liquid chromatography (HPLC). The method is applicable to both urine and plasma samples containing indoprofen and has sensitivity at the nanogram level.

EXPERIMENTAL

Reagents—Acetonitrile[1] was used as received. The water was first deionized and then distilled to remove any contaminants. For enzymatic hydrolysis of conjugated drug, aryl sulfatase[2] containing β-glucuronidase was used.

Reference Compound and Internal Standard—A reference standard of indoprofen[3] (I) was used to develop the analytical method. The internal standard (II) selected for quantitation was the pentanoic acid homolog of indoprofen[3].

HPLC Conditions—To determine the optimal wavelength for UV detection of indoprofen, reference standard was dissolved in methanol and its UV spectrum was obtained. The standard has a λ_{max} at 282 nm with an absorptivity (ε 282) of 14,200 ($E^{1\%}_{1\,cm}$ = 505). The reported $E^{1\%}_{1\,cm}$ value for indoprofen is 500 ± 25 (λ_{max} 283)[4]. A 280-nm filter was used.

The liquid chromatograph was constructed from components and consisted of a high pressure pump[5], a loop injector[6], and a UV detector[7]. The initial HPLC conditions used for urinary analysis consisted of a Zorbox ODS[8] (250 × 2 mm i.d.) column and an eluent of 40% acetonitrile

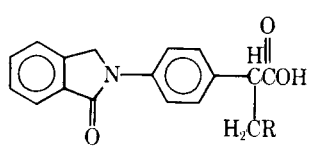

I: R = H
II: R = CH_2CH_3

[1] Nanograde, Mallinckrodt Chemical Works, St. Louis, Mo.
[2] Sigma Chemical Co., St. Louis, Mo. (31,000 units/g of solid; 1 unit will hydrolyze 1.0 μmole of nitrocatechol sulfate/hr at pH 5.0 at 37°).
[3] Adria Laboratories, Columbus, Ohio.
[4] Dr. Werner Hausmann, Adria Laboratories, Columbus, Ohio, personal communication.
[5] Model 6000A, Waters Associates, Milford, Mass.
[6] Model UK6, Waters Associates, Milford, Mass.
[7] Model 440, Waters Associates, Milford, Mass.
[8] DuPont Co., Wilmington, Del.

Table I—Linearity and Reproducibility of Indoprofen Analysis

Sample	Indoprofen per Milliliter	Relative Weight Response Sample A	Sample B	Sample C
1	25.0 ng	1.77	1.65	1.78
2	50.1 ng	1.78	1.76	1.79
3	100.2 ng	1.80	1.79	1.81
4	200.4 ng	1.80	1.75	1.80
5	501.0 ng	1.80	1.81	1.78
6	1.002 μg	1.78	1.77	1.81
7	2.004 μg	1.80	1.80	1.83
8	5.01 μg	1.79	1.81	1.82
9	10.02 μg	1.84	1.82	1.79
10	25.05 μg	1.79	1.80	1.85
11	50.10 μg	1.84	1.83	1.87
	Average = 1.797	*SD* = ±0.037	*RSD* = 2.1	

Table II—Stability of Indoprofen Analysis on Succeeding Days

Sample	Indoprofen, ng/ml	Relative Weight Response Day 1[a] A	Day 1[a] B	Day 2[a] A	Day 2[a] B	Average
1	25.0	1.77	1.65	1.67	1.73	1.71
2	50.1	1.78	1.76	1.69	1.82	1.76
3	100.2	1.80	1.79	1.77	1.80	1.79
4	200.4	1.80	1.75	1.77	1.79	1.78
5	501.0	1.80	1.81	1.81	1.78	1.80
6	1002	1.77	1.77	1.78	—	1.77

[a] Day of analysis for the same indoprofen standard solution.

in 0.175 *M* acetic acid. Later, for the plasma level determinations, a μBondapak C_{18}[9] (300 × 4 mm i.d.) column was used. The flow rate was maintained at 1.0 ml/min, and the temperature was ambient. Injection volumes varied between 20 and 50 μl depending on the drug concentration.

Method for Plasma Indoprofen Levels—A recently reported method (9) for the rapid and simple precipitation of serum proteins prior to HPLC analysis was adapted. Equal volumes of plasma and acetonitrile (containing 3.0 μg of internal standard) first were mixed thoroughly, and the sample was centrifuged at 2000 rpm to remove the precipitated protein. An aliquot of the resulting clear solution was then assayed by HPLC.

Method for Free Indoprofen Levels in Urine—A procedure similar to the plasma level method was employed to determine the urinary excretion level of free indoprofen. A 0.5-ml urine specimen was combined with 0.75 ml of acetonitrile (containing 22 μg of internal standard). An aliquot of this mixture was then analyzed directly by HPLC. Centrifugation to remove the precipitate was required for only a few samples.

Figure 1—*Chromatograms of indoprofen standards. Key: A, 10 μg of indoprofen/ml (peak 1) and 20 μg of internal standard/ml (peak 2); and B, 20 ng of indoprofen/ml (peak 1) and 200 ng of internal standard/ml (peak 2).*

[9] Waters Associates, Milford, Mass.

Table III—Recovery of Indoprofen from Plasma

Sample	Indoprofen Added, μg	Internal Standard, μg	Calculated, μg	Recovery, %
1	0.50	1.5	0.515	103
2	1.25	1.5	1.24	99
3	2.00	1.5	2.00	100
4	2.75	1.5	2.42	88
5	3.5	1.5	3.04	87
6	3.5	1.5	3.18	91
			Average	95
			SD	7

Method for Total Indoprofen Levels in Urine—To determine the total amount of indoprofen excreted in urine, the conjugated drug first must be hydrolyzed. The optimum conditions necessary for complete hydrolysis were evaluated; the conditions chosen consisted of incubating a 2-ml aliquot of urine with 2 ml of an enzyme solution at 37° for 16 hr. The enzyme solution contained 2 mg of aryl sulfatase-β-glucuronidase in 0.14 *M* sodium acetate, pH 5. After incubation, 1 ml of the hydrolyzed sample was added to 1 ml of acetonitrile containing the internal standard (22 μg/ml). An aliquot of this solution was analyzed by HPLC.

Calculations—The level of indoprofen (I) present in plasma and urine samples was calculated from the relative weight response (RWR) of

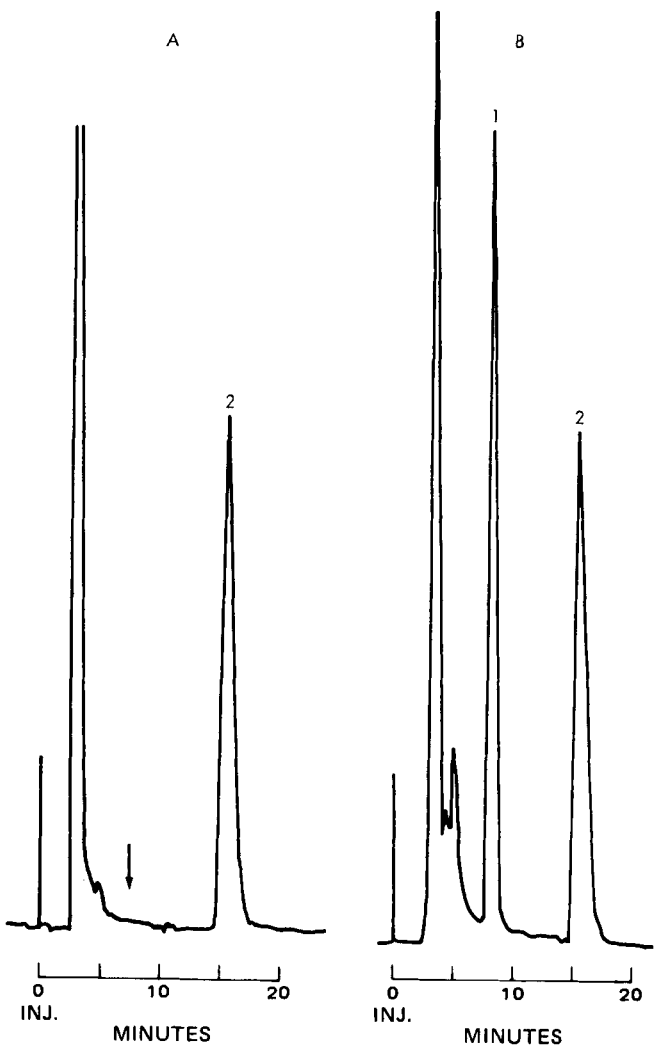

Figure 2—*Chromatograms of indoprofen in plasma. Key: A, blank plasma sample (arrow indicates indoprofen elution position); and B, plasma sample at 8 hr after dosing; indoprofen (peak 1) concentration = 4.2 μg/ml, internal standard (peak 2) concentration = 3.2 μg/ml.*

Table IV—Urinary Excretion of Indoprofen

Sample	Hours	Total Volume, ml	Free I[a], mg	Average	Total I[b], mg	Average
1A	0–2	44	0.43	0.47	26	30
1B			0.51		33	
2A	2–4	102	0.73	0.77	41	38
2B			0.82		34	
3A	4–6	472	0.75	0.75	55	45
3B			—		34	
4A	6–8	100	0.18	0.18	11	12
4B			0.18		12	
5A	8–12	364	0.12	0.12	33	33
5B			0.12		32	
6A	12–24	135	0.24	0.22	9	9
6B			0.19		8	
Total				2.56		163

[a] Free I: calculate level of unconjugated indoprofen in each collection period as described in text. [b] Total I: calculate level of total (free and conjugated) indoprofen in each collection period.

standard solutions. The equations used were:

$$\text{RWR I/II} = \frac{\text{PH std I}}{\text{PH II}} \times \frac{\text{wt II}}{\text{wt std I}} \quad \text{(Eq. 1)}$$

$$\mu\text{g of I/sample} = \frac{\text{PH I}}{\text{PH II}} \times \frac{\text{wt II}}{\text{RWR I/II}} \quad \text{(Eq. 2)}$$

$$\mu\text{g of I/ml} = \frac{\mu\text{g of I/sample}}{\text{ml/sample}} \quad \text{(Eq. 3)}$$

where PH is the peak height, wt is the weight of II in micrograms, μg of I/sample is the micrograms present in an aliquot of plasma or urine, and μg of I/ml is the micrograms present in a milliliter of plasma or urine.

RESULTS

The HPLC method was evaluated to determine the linearity, reproducibility, and minimum detectable limit. Table I presents the data for the single injection of triplicate samples of standards from 25 ng/ml to 50 μg/ml. Excellent precision and linearity were obtained with an average relative weight response of 1.80 and a standard deviation and relative standard deviation of 0.037 and 2.1, respectively. The minimum detectable limit of indoprofen by HPLC was 1 ng with a 5:1 signal to noise ratio.

Succeeding day reproducibility was determined by analyzing the samples from the precision study on the next day (Table II). No differences were detected in the relative weight response of the 25–1000-ng standards analyzed on succeeding days. Figure 1 shows typical HPLC chromatograms for indoprofen and the internal standard. The recovery of indoprofen added to normal plasma was determined at concentrations of 500 ng–3.5 μg/ml of plasma (Table III). Quantitative recovery at all levels was obtained with an average recovery of 95% and a standard deviation of ±7%.

The level of indoprofen present in the plasma of a subject given a single oral dose of 200 mg was determined. Blood samples obtained at various times after dosing were centrifuged to obtain the plasma. Typical chromatograms for plasma analysis are given in Fig. 2. Figure 3 illustrates the decay of indoprofen after the single oral dose.

The urinary excretion levels of free and conjugated drug were determined for the same subject. Urine was collected in six collection periods for 24 hr after the dose, and duplicate analyses were made for both free and conjugated drug (Table IV). A total of 2.51 mg of indoprofen (1.25% of the total dose) was excreted as free drug during 24 hr, and 167 mg of

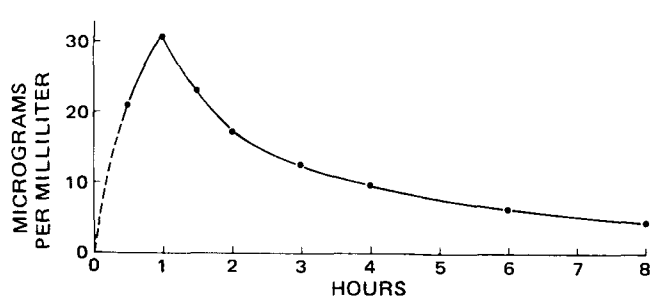

Figure 3—*Plasma decay for indoprofen after a single oral dose of 200 mg.*

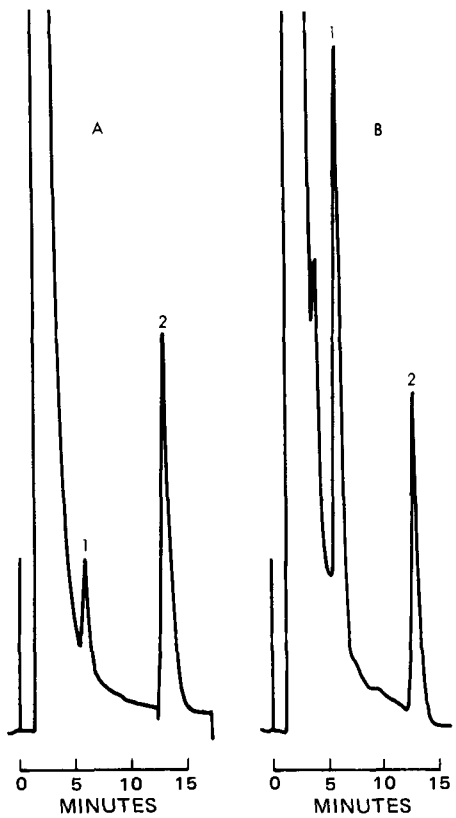

Figure 4—*Chromatograms of indoprofen in urine. Key: A, neat urine, 6–8-hr collection, indoprofen (peak 1) concentration = 1.8 μg/ml; and B, hydrolyzed urine, 12–24-hr collection, indoprofen concentration = 62 μg/ml.*

indoprofen (83.5% of the total dose) was excreted in 24 hr as the free and conjugated drug. Chromatograms obtained for free and total urinary indoprofen are presented in Fig. 4.

DISCUSSION

The developed method has the required selectivity and sensitivity for low level analysis and the precision and accuracy necessary for quantitation. Plasma and urinary excretion levels (free and total) of indoprofen were determined for a subject receiving a single oral dose. The plasma decay curve agrees closely with the data of an earlier report (8).

REFERENCES

(1) A. Buttinoni, A. Cuttica, J. Franceschini, V. Mandelli, G. Orsini, N. Passerini, C. Turba, and R. Tommosini, *Arzeneim.-Forsch.*, **23**, 1100 (1973).

(2) L. M. Fuccella, F. Conti, G. Corvi, V. Mandelli, M. Randelli, and G. Stefanelli, *Clin. Pharmacol. Ther.*, **17**, 277 (1975).

(3) S. Pedronetto, F. Gorini, V. Mandelli, and L. M. Fuccella, *J. Int. Med. Res.*, **3**, 16 (1975).

(4) V. Ventafridda, G. Martino, V. Mandelli, and A. Emanueli, *Clin. Pharmacol. Ther.*, **17**, 284 (1975).

(5) L. M. Fuccella, G. C. Coldaniga, E. Moro, V. Tamassia, G. P. Tosolini, and G. Valzelli, *Eur. J. Clin. Pharmacol.*, **6**, 256 (1973).

(6) G. P. Tosolini, A. Forgione, E. Moro, and V. Mandelli, *J. Chromatogr.*, **92**, 61 (1974).

(7) G. P. Tosolini, E. Moro, A. Forgione, M. Ranghieri, and V. Mandelli, *J. Pharm. Sci.*, **63**, 1072 (1974).

(8) R. V. Smith, D. W. Humphrey, and H. Escalona-Castillo, *ibid.*, **66**, 132 (1977).

(9) S. J. Soldin and J. G. Hill, *Clin. Chem.*, **22**, 856 (1976).

ACKNOWLEDGMENTS

Supported through a contract with Adria Laboratories, Columbus, OH 43215.

The authors thank Mr. Carlos Lizarrage, Midwest Research Institute, for technical assistance and Dr. W. Hausmann and Dr. M. J. Williamson, Adria Laboratories, for helpful discussions and recommendations.

Determination of Phytonadione in Elemental Diets by TLC–Spectrophotodensitometry

GEORGE B. HORN

Received July 8, 1976, from the *Pharmaceutical Research Division, Scientific Affairs Department, Norwich-Eaton Pharmaceuticals Division of Morton-Norwich Products, Inc., Norwich, NY 13815.* Accepted for publication October 12, 1977. Present address: Allied Chemical Corp., Frankford Plant, Philadelphia, PA 19137.

Abstract □ The quantitative analysis of phytonadione in several elemental diet formulations at levels ranging from 90 to 150 ppb is described. After extraction with petroleum ether, the sample is cleaned up by silica gel column chromatography and separated on a TLC plate; phytonadione is determined by reflectance densitometry. Recovery data show that the method is accurate ($\bar{X}$ = 97%) and has a precision (*RSD*) of ±6%.

Keyphrases □ Phytonadione—TLC–spectrophotodensitometric analysis in elemental diet formulations □ TLC–spectrophotodensitometry—analysis, phytonadione in elemental diet formulations □ Vitamins—phytonadione, TLC–spectrophotodensitometric analysis in elemental diet formulations

Phytonadione (vitamin K_1, 2-methyl-3-phytyl-1,4-naphthoquinone) is a naturally occurring K vitamin. Its principal use in dietary or medicinal preparations is as an antihemorrhagic agent (1). Although the vitamin is usually measured by a biological assay (2), the procedure is time consuming and otherwise unsuitable for multiple analyses.

Chemical assays have been reported which employ colorimetry (3, 4), TLC (5, 6), GLC (7–9), polarography (10, 11), and liquid chromatography (12). However, for application to elemental diet formulations containing ~100 ppb of phytonadione, most of these techniques are unsuitable because of high background interference. This paper describes a chromatographic system that separates and quantitates phytonadione in two elemental diet formulations[1] at dosage levels ranging from 0.09 to 0.15 μg/g.

EXPERIMENTAL

Equipment—All measurements were made on a spectrodensitometer[2] equipped with a 200-w xenon–mercury lamp[3], a density computer[4], a strip-chart recorder[5], and a digital integrator[6]. The instrument was operated in the reflectance mode using the dual-beam system. Samples were scanned at 270 nm using a slit width of 1 mm at a scanning speed of 2.54 cm/min. The recorder was operated at a chart speed of 5.1 cm/min. The digital integrator was operated at a slope sensitivity of 0.5, a threshold of 50, and a voltage of 0.1.

Reagents and Materials—Phytonadione[7] was used without further purification. All organic solvents and reagents were reagent grade or purer. The chlorinated hydrocarbon solvents used as column eluents were specially purified by separately percolating ~5 liters of spectroanalyzed grade 1,2-dichloroethane or reagent grade carbon tetrachloride through a dual-packed column of basic alumina[8] (30 × 50 cm) in the upper layer and acidic alumina[9] (30 × 50 cm) in the lower layer.

Precoated silica gel TLC plates[10] (20 × 20 cm) were developed in a glass chamber[11] (21.5 × 8 × 23 cm) completely lined with absorbent paper[12] using toluene. Samples were spotted with a microliter pipet[13].

Column chromatography was conducted in glass columns[14] (19 × 300 mm) using silica gel[15] and 1,2-dichloroethane–carbon tetrachloride (40:60 v/v) as the solvent.

All evaporations were conducted on a steam bath under a nitrogen stream to prevent oxidative losses of phytonadione. Either 125- or 250-ml erlenmeyer flasks were used with a custom-designed evaporation adapter attached (Fig. 1). A nitrogen stream at ~325 ml/min was introduced into the flask *via* a Pasteur pipet inserted into the evaporation adapter. Four simultaneous evaporations were made possible by directing the gas stream from a nitrogen cylinder[16] into a four-port manifold positioned over the bath. Separate nitrogen streams were then directed into each flask by rubber tubing connected to the Pasteur pipets.

Procedure—The system consists of four main parts: a liquid–solid extraction of the diet to isolate the lipid fraction containing phytonadione, column chromatography to separate phytonadione from most of the neutral and polar lipids, TLC to resolve phytonadione, and measurement by reflectance spectrophotodensitometry. Since phytonadione is extremely light sensitive (14), all analytical operations were conducted under subdued light.

Standard Solutions—Separate standard solutions were prepared for each elemental diet formulation (I and II).

Standard Solution A—Phytonadione, 30 mg, was dissolved in hexane and brought to 50 ml in a volumetric flask.

Standard Solution B (for Elemental Diet I)—A 250-μl aliquot of Standard Solution A was transferred to a 50-ml volumetric flask and diluted to volume with hexane.

Standard Solutions C_1 and C_2 (for Elemental Diet II)—A 3-ml aliquot of Standard Solution A was transferred to a 50-ml volumetric flask and diluted to volume with hexane (C_1). A 1-ml aliquot of Solution C_1 was transferred to a 10-ml volumetric flask and diluted to volume with hexane (C_2).

Column Standards—A 2-ml aliquot of Solution B (or C_2) was transferred onto a silica gel column and processed exactly as a sample.

Sample Extraction—Individual packets (80 g) of the elemental diet (I or II) were transferred to Büchner funnels[17] and extracted with one 75-ml portion and then two 60-ml portions of petroleum ether (bp 30–60°). The combined extracts were evaporated to dryness under nitrogen using the special assembly described. While still under nitrogen, the flask was placed in a beaker of cool water. The residue was immediately taken up in ~1 ml of hexane, which was introduced through the evaporation adapter *via* a syringe[18].

Column Chromatography—Silica gel[15] was reactivated by heating 500-g lots in a 110° oven for 4 hr, followed by cooling to room temperature in a desiccator. Columns (one for a standard plus one for each sample) were then prepared using a slurry technique with 14 g of the activated silica gel and 45 ml of column eluent. After the slurry was transferred into the column, the column was rinsed with 5–10 ml of column eluent and allowed to drain until the liquid level was ~1 mm above the adsorbent.

With the column flow stopped, the sample extract was quantitatively transferred onto the column using 1–2 ml of hexane to assist the transfer.

[1] Vivonex standard diet, unflavored (I), and Vivonex high nitrogen diet, unflavored (II), containing phytonadione at dosage levels of approximately 0.15 and 0.09 μg/g, respectively (Norwich Pharmacal Co., Norwich, N.Y.). The two products (13) are supplied as soluble powders in 80-g packets, which are dispersed in water shortly before administration.
[2] Model SD3000, Schoeffel Instrument Corp.
[3] Hanovia Lamp Division, Conrad Precision Industries.
[4] Model SDC300, Schoeffel Instrument Corp.
[5] Model Y196411-007-000-610-opt102-110, Honeywell.
[6] Model SDR304, Schoeffel Instrument Corp.
[7] USP quality, Hoffmann-La Roche.
[8] AG10, 100–200 mesh, Bio-Rad Laboratories.
[9] AG4, 100–200 mesh, Bio-Rad Laboratories.
[10] Silica gel 60, F-254, Brinkmann Instruments Co.
[11] Chromaflex developing tank, Kontes Glass Co.
[12] Saturation pads, Camag, Inc.
[13] A 100-μl Wiretrol, Drummond Scientific Co.
[14] K420530, Kontes Glass Co.
[15] Woelm 200, Waters Associates.
[16] Prepurified grade, Matheson Gas Products.
[17] Fritted glass, medium porosity, Corning Glass Co.
[18] A 10-ml glass Luer-tip syringe equipped with a 1.3-cm 27-gauge Luer-tip needle, Becton-Dickinson.

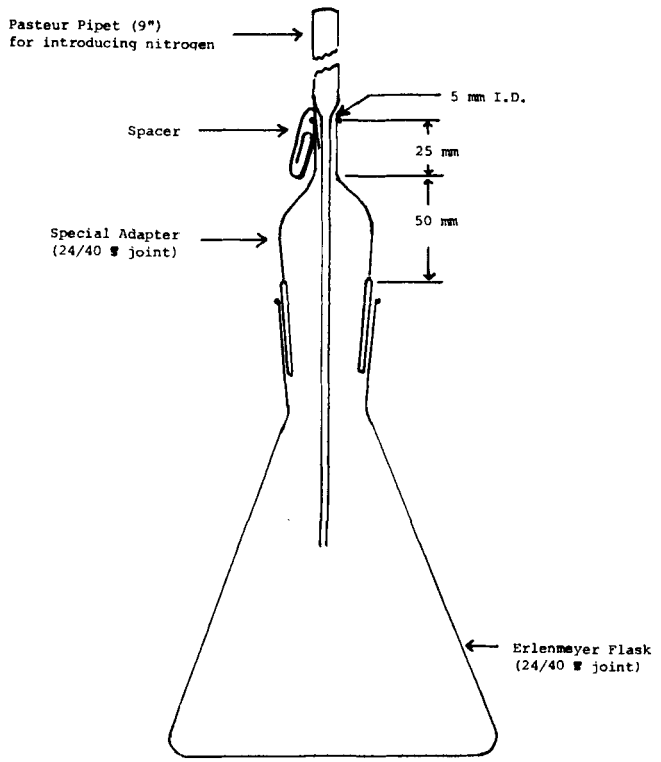

Figure 1—*Evaporation device.*

[*Note:* All quantitative transfers were performed by rinsing down the walls of the flask with a small stream of solvent (~0.5 ml) delivered from a syringe[18] and carefully transferring to the appropriate receiver. Three rinses were generally sufficient to ensure a quantitative transfer.]

The flow rate was adjusted to 1.5 ml/min, and the sample was consolidated onto the column head. The column was eluted with 120 ml of 1,2-dichloroethane–carbon tetrachloride (40:60 v/v). The eluate was collected in a 125-ml erlenmeyer flask containing 1 ml of a citric acid solution, prepared at 300 μg/ml by dissolving ~15 mg of citric acid monohydrate in ~5 ml of methanol and diluting to 50 ml with column eluent.

The column eluate was evaporated to dryness under nitrogen, the residue was taken up in ~1 ml of hexane (as described), and the solution was transferred quantitatively to a 2-ml volumetric flask using a small funnel.

TLC—TLC plates were divided into 20 1-cm tracks using a scoring device[19]. A score line was made perpendicular to the tracks exactly 13 cm above the origin. The plates were activated by heating in an oven at 105° for 2 hr and stored in a desiccator.

Aliquots (100 μl) of samples, column standards[20], and one plate standard[21], containing similar quantities of phytonadione (Elemental Diet I, 600 ng; Elemental Diet II, 360 ng), were spotted in duplicate in alternate tracks of a TLC plate under a stream of air. The plate was developed in toluene to a 13-cm score line and dried in a hot air stream[22]. A routine visual inspection of the plate under shortwave UV light was made to verify the position of the phytonadione (R_f ~0.40) and to evaluate the resolution.

Reflectance Spectrophotodensitometry—The spectrodensitometer[2] was adjusted for reflectance mode operation, as previously described, and the TLC plate was placed in the plate frame. The beam was then centered over the developed column standard spot (R_f ~0.40), and the pen was adjusted to ~90% of full-scale deflection using the range and vernier (gain) controls. Each phytonadione spot on the plate was then scanned in the direction of development. Area estimates were obtained for each peak from the digitized data. The results were then calculated from the average values obtained based on the column standard.

[19] Model SDA320, Schoeffel Instrument Co.

[20] A solution of phytonadione (in hexane) applied to the column and processed through the method.

[21] A solution of phytonadione (in hexane) spotted directly on the plate and processed through the method.

[22] Heat gun, model HG751, Master Appliance Corp., Racine, Wis.

Table I—Recovery of Phytonadione from Synthetic Samples of Elemental Diet I

Percent of Theory[a] (Approximation)	Phytonadione Added, μg/80 g[b]	Found, μg/80 g[c]	Recovery, %
80	9.82	9.86	100.4
	9.82	9.34	95.1
	9.82	10.02	102.0
	9.82	10.36	105.5
100	12.29	12.86	104.6
	12.29	11.31	92.0
	12.29	11.81	96.1
	12.29	11.92	97.0
120	14.76	12.92	87.5
	14.76	13.59	92.1
	14.76	13.34	90.4
	14.76	15.29	103.6
			$\bar{X}$ = 97.2
			SD = 6.0
			RSD = ±6.2

[a] The theoretical level of phytonadione in Elemental Diet I is about 0.15 μg/g or 12 μg/80 g. [b] Phytonadione was added to the diet by blending a dry Elemental Diet I concentrate into the remaining placebo (an Elemental Diet I blank) in a twin-shell blender. [c] Each determination was based on duplicate aliquots of samples and standards being spotted on the plate.

RESULTS AND DISCUSSION

The absorption maximum of phytonadione was 270 nm. A spectrophotodensitometric response study at this wavelength showed a linear relationship for plate loads ranging from 40 to 1000 ng of phytonadione. An area ratio technique was used to minimize day-to-day fluctuations.

Sample Extraction—Phytonadione was extracted efficiently from the (powdered) elemental diet with petroleum ether. Studies showed that the direct extraction of the dry diet gave less background interference than did a partitioning extraction of the diet from an aqueous solution.

Column Chromatography—Attempts were made to separate the vitamin from the diet excipients on both silica gel and alumina columns. While neither approach gave a complete separation, the silica gel column provided sufficient cleanup for use in conjunction with a final TLC separation.

Because of the relatively high lipid levels in the diet extract, 14 g of silica gel was required per column. A slurry-packing technique was pre-

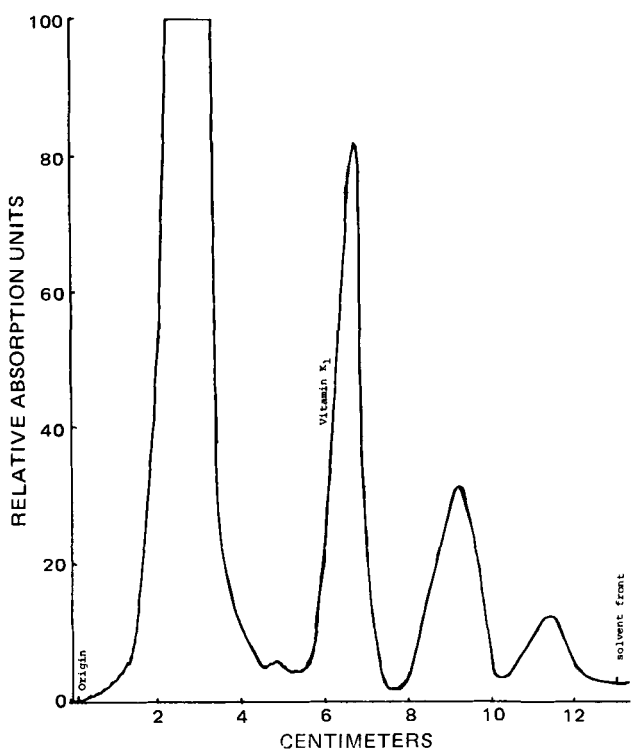

Figure 2—*Reflectance densitometric scan (270 mm) of Elemental Diet I.*

Table II—Assay of Elemental Diets I and II

Elemental Diet	Sample, g	Phytonadione, μg/g Found[b]	Theory, %
I[a]	79.1	0.128	83.5
	80.0	0.154	100.2
	79.9	0.135	87.7
	79.8	0.128	83.6
	80.7	0.136	88.3
	80.0	0.142	92.4
		$\bar{X}$ =	89.3
		SD =	6.3
		RSD =	±7.1
II[c]	80.9	0.094	102.2
	80.5	0.106	115.2
	82.0	0.090	97.8
	81.7	0.090	97.8
	82.7	0.098	106.3
		$\bar{X}$ =	103.9
		SD =	7.3
		RSD =	±7.0

[a] The phytonadione level in Elemental Diet I is about 0.15 μg/g. [b] Each determination was based on duplicate aliquots of samples and standards being spotted on the plate. [c] The phytonadione level in Elemental Diet II is about 0.09 μg/g.

ferred over a dry-packing procedure, since it gave more homogeneous packings and yielded more reproducible recoveries.

Several elution procedures were investigated during method development. A successive elution approach, using a relatively nonpolar eluent followed by a more polar eluent mixture, failed to give the desired separation. The chosen system employs an eluent of 1,2-dichloroethane–carbon tetrachloride (40:60 v/v), which elutes the vitamin prior to the main lipid fraction. All grades of chlorinated hydrocarbons should be purified, as indicated, to remove any interfering impurities.

Citric acid (300 μg) was added to each receiver prior to elution to protect phytonadione against oxidation during the subsequent evaporation step. This method was required to protect the standard, since the sample solution was amply protected by antioxidants in the formulation.

TLC–Spectrophotodensitometry—Phytonadione was separated effectively from diet excipients by the final TLC procedure. A typical scan of an Elemental Diet I sample is shown in Fig. 2. Peaks other than phytonadione have not been identified.

Separate standard solutions were required for each elemental diet formulation to provide equivalent phytonadione plate loads. The plate standard was run as a check on column standard loss. If column standard loss exceeded 20%, the entire run was arbitrarily rejected because of uncertainties in either the sample or standard.

Method Performance—Method accuracy was estimated by processing 12 synthetic samples of Elemental Diet I, prepared at 80, 100, and 120% of the theoretical level[1], by the final method. Recovery data (Table I) showed an ungrouped mean value of 97.2%. Elemental Diet I blanks (placebo) processed through the method showed no peak for phytonadione.

Method precision was estimated by assaying regular production samples of Elemental Diets I and II. These data (Table II) showed an average percent label of 89.3 and 103.9 for the respective diets, with an estimated precision (*RSD*) of ±7%.

Table III—Recovery Data: Comparison of Synthetic Samples of Elemental Diet I[a] Prepared before and after Aging the Placebo 1 Month at 50°

	Recovery, %	
	Before Aging	After Aging
Elemental Diet I placebo	0	0
Elemental Diet I samples	92.6	97.7
	105.7	98.2
	94.8	86.7
	100.7	96.0
	102.7	94.5
$\bar{X}$ =	99.3	94.6
SD =	5.5	4.7
RSD =	±5.5	±4.9

[a] All synthetic samples were prepared by spiking the Elemental Diet I placebo with phytonadione (in hexane) immediately before assaying.

Comparisons also were made by assaying synthetic samples prepared from both fresh and aged (1 month at 50°) placebos. These results (Table III) showed mean recovery values of 99.3 and 94.5% for the fresh and aged diets, respectively. Comparison of the means by a *t*-test showed no significant difference at the 95% confidence limits. Thus, there are no adverse effects emanating from placebo artifacts formed during storage.

REFERENCES

(1) D. L. Schneider, H. B. Fluckiger, and J. D. Manes, *Pediatrics*, **53**, 273 (1974).

(2) H. J. Almquist, *Biol. Symp.*, **12**, 508 (1947).

(3) K. Schilling and H. Dam, *Acta Chem. Scand.*, **12**, 348 (1958).

(4) J. V. Scudi and R. P. Buhs, *J. Biol. Chem.*, **141**, 451 (1941).

(5) K. Egger, *Planta*, **64**, 41 (1965).

(6) J. D. Manes, H. B. Fluckiger, and D. L. Schneider, *J. Agr. Food Chem.*, **20**, 1130 (1972).

(7) P. P. Nair and D. A. Turner, *J. Am. Oil Chem. Soc.*, **40**, 353 (1963).

(8) D. A. Libby, A. R. Presser, and A. J. Sheppard, *J. Assoc. Offic. Anal. Chem.*, **50**, 806 (1967).

(9) G. H. Dialameh and R. E. Olson, *Anal. Biochem.*, **32**, 263 (1969).

(10) E. B. Hershberg, J. K. Wolfe, and L. F. Fieser, *J. Am. Chem. Soc.*, **62**, 3516 (1940).

(11) J. J. Aaron and J. D. Winefordner, *Anal. Chem.*, **44**, 2122 (1972).

(12) R. C. Williams, J. A. Schmit, and R. A. Henry, *J. Chromatogr. Sci.*, **10**, 494 (1972).

(13) "Physician's Desk Reference," 29th ed., Medical Economics Co., Oradell, N.J., pp. 763–772.

(14) H. R. Rosenberg, "Chemistry and Physiology of the Vitamins," Interscience, New York, N.Y., 1942, pp. 481–509.

Difference Spectrophotometric Determination of *p*-Hydroxybenzoic Acid in Presence of Its Esters

D. W. FINK ˣ, H. C. FINK, J. W. TOLAN, and J. BLODINGER

Received June 6, 1977, from *Merck Sharp and Dohme Research Laboratories, Rahway, NJ 07065.* Accepted for publication October 12, 1977.

Abstract □ A difference spectrophotometric analytical method was developed for the selective determination of *p*-hydroxybenzoic acid in the presence of its alkyl esters without prior separation. Based on the spectral shift to a shorter wavelength accompanying carboxyl dissociation, the procedure measures as little as 2% of this acid in mixtures with the alkyl ester preservatives and has an accuracy of 2% mean relative error over the 0.16–12.0 μg of *p*-hydroxybenzoic acid/ml range.

Keyphrases □ *p*-Hydroxybenzoic acid—difference spectrophotometric analysis in presence of alkyl esters □ Spectrophotometry, difference—analysis, *p*-hydroxybenzoic acid in presence of alkyl esters

Previous studies (1, 2) reported that standard procedures for the determination of alkyl *p*-hydroxybenzoate preservatives (parabens) typically require sample isolation to separate *p*-hydroxybenzoic acid prior to measurement. Operations involving derivatization, liquid–liquid partitioning, or chromatographic separation using either thin-layer or column techniques have been used. For example, the interference of *p*-hydroxybenzoic acid in the direct spectrophotometric determination of its esters was eliminated by separation on diatomaceous earth (2); liquid–liquid partitioning also was used to accomplish this same end (3, 4). In addition, instrumental methods using GLC (5–8) and high-pressure liquid chromatography (HPLC) (1, 9) were developed.

This report describes a simple and rapid spectrophotometric method based on an application of the difference spectrophotometric technique (10) for the selective determination of *p*-hydroxybenzoic acid in the presence of its alkyl esters. A pH-induced shift in the spectrum of this acid is used over a range in which the spectra of the esters are pH independent, thus effectively canceling their interferences and obviating any preliminary separation. The primary application is for the stability-indicating measurement of these preservatives through determination of the acid as the hydrolytic degradate.

EXPERIMENTAL

Instrumentation—UV absorption spectra were recorded on a spectrophotometer[1] equipped with 0–0.1 and 0–1.0 absorbance unit full-scale slide wires. The pH measurements were made at 20° with a pH meter[2] and combination electrode[3], calibrated using standard buffers[4].

Materials—*p*-Hydroxybenzoic acid, its methyl ester (methylparaben), and propyl ester (propylparaben)[5] were used without further purification. Buffers, 0.1 *M*, were prepared using anhydrous dibasic sodium phosphate[6] and reagent grade hydrochloric acid[7]. Deionized water was used throughout.

UV Difference Spectrophotometry—Duplicate 5-ml aliquots of aqueous samples and analytical standard were transferred to 50-ml centrifuge tubes; 5 ml of 0.1 *N* HCl was added to one, and 5 ml of pH 5.9 buffer was added to the other. Difference spectra were recorded over the 220–330-nm range with the acidic solution in the sample cell and the pH 5.9-buffered solution in the reference cell after manually adjusting the baseline control to set the pen at $A = 0.4$ with $\lambda = 330$ nm. Absorption difference values, ΔA, were determined from the maxima and minima, $A_{260} - A_{235}$, after applying baseline corrections from the difference spectrum of blank solutions.

Analytical Procedure—Aqueous solutions of *p*-hydroxybenzoic acid and its methyl and propyl esters were prepared. (The propyl ester was first dissolved in a small amount of methyl alcohol.) Dilutions were made with water to obtain the desired concentration, and difference spectra were obtained as described. Values for $\Delta A = A_{260} - A_{235}$ were calculated from each spectrum, and the quantitative determination of the *p*-hydroxybenzoic acid concentration of each sample was obtained by comparison of ΔA to a previously prepared calibration line of ΔA against a known acid concentration.

RESULTS

Absorption Spectra—*Conventional Spectra*—The conventional UV absorption spectra of *p*-hydroxybenzoic acid (3.62×10^{-5} *M*) and of methylparaben (3.29×10^{-5} *M*) in pH 5.9 buffer, 0.1 *N* HCl, and 0.1 *N* NaOH were studied in detail (11) (Fig. 1). The spectrum of the neutral acid in 0.1 *N* HCl was nearly identical to the absorption spectrum of the ester in the same medium; both compounds in this environment exhibited an absorption band at λ_{max} 254 nm, with a molar absorptivity of 1.4×10^4 liters/mole cm at this wavelength and with a width at half-height of 34 nm.

In basic solution (pH > 9), this absorption band shifted to a longer wavelength accompanying the usual dissociation of the phenolic proton. For *p*-hydroxybenzoic acid alone, however, a spectral shift to a higher energy occurred in the pH 5–8 range, representing the monoanionic species. The absorption spectrum of the ester was pH independent in the pH 1–6 range.

Difference Spectrum—Figure 2 presents the difference absorption spectrum of *p*-hydroxybenzoic acid recorded as described at six concentrations in the 2.0–12.0-μg/ml range. This spectrum exhibited a maximum at 260 nm, a minimum at 235 nm, and isosbestic points at 221 and 246 nm.

Calibration Line—Eleven aqueous solutions of *p*-hydroxybenzoic acid were prepared in the 0.32–24.0-μg/ml range, and their difference spectra were recorded as described. After dilution, the concentrations of the analytical solutions were 0.16–12.0 μg/ml; some representative difference spectra are shown in Fig. 2.

A calibration line was obtained from the 11 difference spectra by plotting the difference between the maximum and minimum of each spectrum ($\Delta A = A_{260} - A_{235}$) against concentration after applying corrections for the blank solutions. The correlation coefficient of the resulting line was 1.000, and the standard error of estimate from a linear regression analysis was 0.024, demonstrating excellent linearity over this concentration range.

Analysis—Recovery experiments for *p*-hydroxybenzoic acid over the 0.20–10.0-μg/ml range in mixtures with its esters are summarized in Table I. These mixtures were prepared in the aqueous solution and analyzed by the described procedure. Different amounts of methylparaben and propylparaben were added to simulate their combination use.

The results demonstrate that the esters did not interfere with the determination of *p*-hydroxybenzoic acid over the concentration ranges examined (Table I). As little as 2% of the acid was detected accurately in the presence of its esters; excellent results were obtained as well for solutions in which the acid was the predominant species. These results had a mean relative error of 1.9% ($SD = 3.9\%$).

Similar results were obtained using the 0–0.1 absorbance unit full-scale slide wire for solutions containing up to about 1.2 μg of *p*-hydroxybenzoic

[1] Cary 15.
[2] Corning model 12.
[3] Corning 476050.
[4] Corning 477070.
[5] Eastman Kodak Co.
[6] Baker analyzed reagent.
[7] Reagent, Merck.

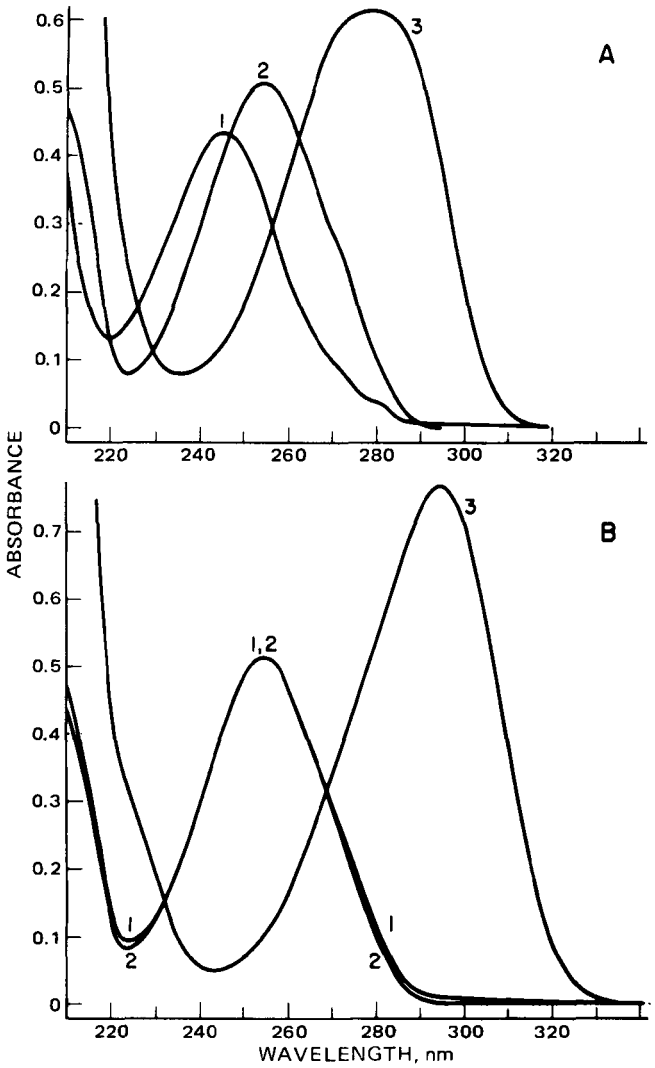

Figure 1—*Absorption spectra of 3.62 × 10^{-5} M p-hydroxybenzoic acid (A) and 3.29 × 10^{-5} M methylparaben (B) in pH 5.9 buffer (1), 0.1 N HCl (2), and 0.1 N NaOH (3).*

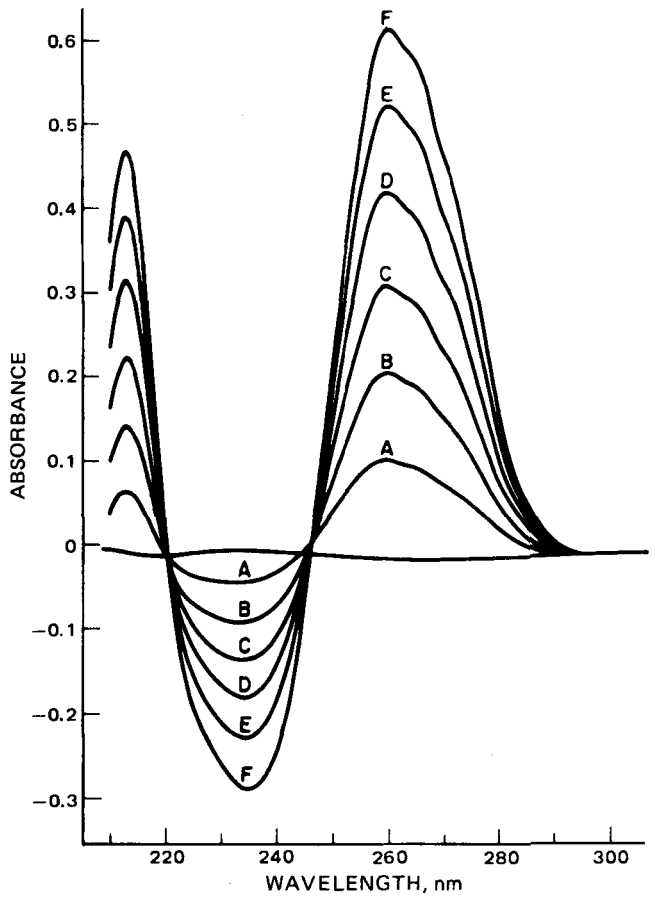

Figure 2—*Difference spectrum of p-hydroxybenzoic acid as a function of concentration. Sample solutions were prepared in 0.1 N HCl; reference solutions were prepared in pH 5.9 phosphate buffer. Concentrations are 2.0 (A), 4.0 (B), 6.0 (C), 8.0 (D), 10.0 (E), and 12.0 (F) μg of p-hydroxybenzoic acid/ml.*

acid/ml. For either slide wire, however, it was necessary to keep the total concentration of acid plus ester below about 30 μg/ml to allow sufficient light to pass to the detector on the instrument; above this concentration, the large slit width required precluded accurate measurements.

DISCUSSION

Difference spectroscopy was discussed previously (10). This technique is appropriate for analyses of formulations because other UV-absorbing species can be tolerated if they do not exhibit a spectral shift with the analate perturbation. This particular difference spectrophotometric application was indicated previously (12). It was suggested that two measurements at pH 1 and 7 could be used to determine *p*-hydroxybenzoic acid and its ester in the presence of each other.

The principles of this method are apparent from a consideration of the spectra. Unlike the esters, the acid can exist in three acid–base species. A red shift of the long wavelength band with dissociation is a property common to many *meta*- and *para*-substituted phenols (11, 13, 14). The absorption spectra of the neutral acid and the ester are nearly identical, demonstrating that the proton on the carboxyl group creates the same delocalized electronic structure as the alkyl group; these compounds are indistinguishable at pH < 4.

In neutral solution (pH 5–8), the absorption spectrum of the acid shifts to a shorter wavelength—from λ_{max} 254 to 244 nm. This blue shift accompanying dissociation of the carboxyl group (at pH 4.5) appears regularly for aromatic rings with this substituent. As discussed (11) and examined (15) previously, both of these spectral shifts reflect the electron donor and acceptor tendencies of the protonated species and their corresponding conjugate bases.

The spectral change occurring with the first ionization forms the basis for the determination of this acid by difference spectroscopy. In this technique, the reference cell contains the acid in the monoanionic form and the sample cell contains a solution with the same concentration of the analate in the neutral conjugate acid form. The recorded spectrum is the difference between the spectra of these two species. This difference spectrum exhibited a maximum at 260 nm, corresponding to net absorption by the sample, and a minimum at 235 nm, corresponding to net absorption by the reference. The difference in absorbance between the maximum and the minimum was directly proportional to the *p*-hydroxybenzoic acid concentration and obeyed Beer's law to at least 12 μg of *p*-hydroxybenzoic acid/ml, with an average absorptivity in this concentration range of 7.88 × 10^{-2} ml/cm μg for the 11 calibration measurements.

This technique is potentially useful for the analyses of formulations because it compensates for interferences in the sample by having the same interferences (*e.g.*, the esters) present at equal concentration in both the sample and reference cells. Because the absorption spectrum of the ester is pH independent in the pH 1–5.9 range, it does not interfere.

The pKa values of the phenolic and carboxylic groups of *p*-hydroxybenzoic acid are 9.5 and 4.5, respectively (16), establishing that the optimum sensitivity of the difference spectrophotometric technique will be realized with a pH 7.0 buffer, where the fraction of the acid existing as the monoanion (Fig. 1A, spectrum 1) is maximized (>99%). However, at this pH, the alkyl *p*-hydroxybenzoate esters interfere by contributing to the difference spectrum. Because the pKa values of the parabens are in the 8.4–8.5 range (17), approximately 3% of these esters are ionized at pH 7. Hence, pH 5.9, where only 0.3% of the esters are ionized, was selected to reduce this interference. At this pH, some sensitivity is sacrificed to achieve this selectivity; *i.e.*, 96% of the acid exists as the monoanionic species, causing a 4% reduction in sensitivity.

Each difference spectrum of *p*-hydroxybenzoic acid recorded in the presence of the esters intersected zero at 246 and 221 nm, the isosbestic

Table I—Determination of *p*-Hydroxybenzoic Acid in the Presence of Its Alkyl Esters

p-Hydroxybenzoic Acid Taken, μg/ml	Ester Added, μg/ml		ΔA	*p*-Hydroxybenzoic Acid Found, μg/ml
	Propylparaben	Methylparaben		
0.20	0	10.0	0.020	0.22
0.40	0	10.0	0.033	0.39
0.80	0	4.0	0.069	0.86
	0	8.0	0.070	0.88
	0	10.0	0.068	0.85
	0	12.0	0.062	0.77
1.20	0	10.0	0.096	1.22
1.60	0	10.0	0.122	1.56
			0.125	1.60
2.00	0	4.0	0.166	2.14
	0	8.0	0.162	2.09
	0	10.0	0.157	2.02
	4.0	4.0	0.165	2.13
	8.0	0	0.155	2.00
3.20	0	10.0	0.242	3.14
4.00	0	8.0	0.310	4.04
		10.0	0.305	3.97
	4.0	4.0	0.308	4.01
	8.0	0	0.310	4.04
6.00	0	8.0	0.458	5.99
	4.0	4.0	0.460	6.02
10.00	0	8.0	0.762	9.99
	4.0	4.0	0.766	10.0
	8.0	0	0.762	9.99

points between the two species. This result is additional confirmation, as described previously (10), that the esters do not interfere at these points. Moreover, in this example of difference spectroscopy, the interferences were not at low concentration levels but were present at up to 50 times the analate concentration. In addition, as Table I demonstrates, this method is applicable in the presence of mixtures of alkyl paraben esters, giving the total amount of hydrolysis. To determine the relative decomposition of individual esters in mixtures, further direct measurements would be required.

This method is convenient since it avoids the usual preliminary separations and is more rapid than the other methods previously reported. This procedure is especially useful in kinetic studies to monitor the paraben degradation under selected conditions. It possesses the usually sought analytical attributes of simplicity, short analysis time, selectivity, stability of the measurement, linearity, sensitivity, accuracy, and precision.

REFERENCES

(1) F. F. Cantwell, *Anal. Chem.*, **48**, 1854 (1976).

(2) M. Batchelder, H. I. Tarlin, and G. Williamson, *J. Pharm. Sci.*, **61**, 252 (1972).

(3) N. N. Raval and E. L. Parrott, *ibid.*, **56**, 274 (1967).

(4) D. Grant, Ph.D. dissertation, University of Iowa, Iowa City, Iowa, 1967 (University Microfilms, Ann Arbor, Mich., 67-16, 769).

(5) S. J. Donato, *J. Pharm. Sci.*, **54**, 917 (1965).

(6) P. Daenens and L. Laruelle, *J. Assoc. Offic. Anal. Chem.*, **56**, 1515 (1973).

(7) M. Wilcox, *J. Pharm. Sci.*, **56**, 642 (1967).

(8) J. L. Lach and J. S. Sawardeker, *ibid.*, **54**, 424 (1965).

(9) F. A. Fitzpatrick, A. F. Summa, and A. D. Cooper, *J. Soc. Cosmet. Chem.*, **26**, 377 (1975).

(10) T. D. Doyle and F. R. Fazarri, *J. Pharm. Sci.*, **63**, 1921 (1974).

(11) L. Doub and J. M. Vandenbelt, *J. Am. Chem. Soc.*, **69**, 2714 (1947).

(12) T. R. Aalto, M. C. Firman, and N. E. Rigler, *J. Am. Pharm. Assoc., Sci. Ed.*, **42**, 449 (1953).

(13) E. L. Wehry and L. B. Rogers, *J. Am. Chem. Soc.*, **87**, 4234 (1965).

(14) T. Higuchi, K. P. Patel, F. R. Bonow, and J. Landsman, *J. Am. Pharm. Assoc., Sci. Ed.*, **41**, 293 (1952).

(15) P. E. Stevenson, *J. Mol. Spectrom.*, **15**, 220 (1965).

(16) L. G. Sillen and A. E. Martell, "Stability Constants of Metal-Ion Complexes," Special Publication 17, The Chemical Society, London, England, 1964, p. 533.

(17) L. A. Cohen and W. M. Jones, *J. Am. Chem. Soc.*, **85**, 3397 (1963).

Simultaneous Determination of Procainamide and *N*-Acetylprocainamide in Plasma by High-Performance Liquid Chromatography

A. G. BUTTERFIELD ˣ, J. K. COOPER, and K. K. MIDHA

Received March 28, 1977, from the *Drug Research Laboratories, Health Protection Branch, Ottawa, Canada K1A OL2.* Accepted for publication October 12, 1977.

Abstract □ A sensitive, specific, high-performance liquid chromatographic procedure is described for the simultaneous determination of procainamide and its metabolite, *N*-acetylprocainamide, in plasma. Basic plasma (2.0 ml), containing pheniramine maleate as an internal standard, is partitioned with methylene dichloride. The organic extract is concentrated to between 0.3 and 0.5 ml, and 100-μl aliquots are chromatographed on a microparticulate silica gel column using 0.1% acetic acid–20% 0.1 *M* ammonium acetate in acetonitrile as the mobile phase. With a fixed-wavelength (254-nm) UV detector, both compounds can be quantitated in the 0.1–8.0-μg/ml of plasma range.

Keyphrases □ Procainamide—high-performance liquid chromatographic analysis simultaneously with *N*-acetylprocainamide in plasma □ *N*-Acetylprocainamide—high-performance liquid chromatographic analysis simultaneously with procainamide in plasma □ High-performance liquid chromatography—simultaneous analyses, procainamide and *N*-acetylprocainamide in plasma □ Cardiac depressants—procainamide, high-performance liquid chromatographic analysis simultaneously with *N*-acetylprocainamide in plasma

Several spectrofluorometric and colorimetric procedures were reported (1–5) for the determination of procainamide in plasma; however, these procedures lack specificity because of interference either from *N*-acetylprocainamide, the active metabolite of procainamide (6), or from endogenous materials. Several specific GLC procedures were reported (7–11) for procainamide, but not for *N*-acetylprocainamide, in plasma. One GLC procedure was re-

Table I—Determination of *p*-Hydroxybenzoic Acid in the Presence of Its Alkyl Esters

p-Hydroxybenzoic Acid Taken, μg/ml	Ester Added, μg/ml		ΔA	*p*-Hydroxybenzoic Acid Found, μg/ml
	Propylparaben	Methylparaben		
0.20	0	10.0	0.020	0.22
0.40	0	10.0	0.033	0.39
0.80	0	4.0	0.069	0.86
	0	8.0	0.070	0.88
	0	10.0	0.068	0.85
	0	12.0	0.062	0.77
1.20	0	10.0	0.096	1.22
1.60	0	10.0	0.122	1.56
			0.125	1.60
2.00	0	4.0	0.166	2.14
	0	8.0	0.162	2.09
	0	10.0	0.157	2.02
	4.0	4.0	0.165	2.13
	8.0	0	0.155	2.00
3.20	0	10.0	0.242	3.14
4.00	0	8.0	0.310	4.04
		10.0	0.305	3.97
	4.0	4.0	0.308	4.01
	8.0	0	0.310	4.04
6.00	0	8.0	0.458	5.99
	4.0	4.0	0.460	6.02
10.00	0	8.0	0.762	9.99
	4.0	4.0	0.766	10.0
	8.0	0	0.762	9.99

points between the two species. This result is additional confirmation, as described previously (10), that the esters do not interfere at these points. Moreover, in this example of difference spectroscopy, the interferences were not at low concentration levels but were present at up to 50 times the analate concentration. In addition, as Table I demonstrates, this method is applicable in the presence of mixtures of alkyl paraben esters, giving the total amount of hydrolysis. To determine the relative decomposition of individual esters in mixtures, further direct measurements would be required.

This method is convenient since it avoids the usual preliminary separations and is more rapid than the other methods previously reported. This procedure is especially useful in kinetic studies to monitor the paraben degradation under selected conditions. It possesses the usually sought analytical attributes of simplicity, short analysis time, selectivity, stability of the measurement, linearity, sensitivity, accuracy, and precision.

REFERENCES

(1) F. F. Cantwell, *Anal. Chem.*, **48**, 1854 (1976).

(2) M. Batchelder, H. I. Tarlin, and G. Williamson, *J. Pharm. Sci.*, **61**, 252 (1972).

(3) N. N. Raval and E. L. Parrott, *ibid.*, **56**, 274 (1967).

(4) D. Grant, Ph.D. dissertation, University of Iowa, Iowa City, Iowa, 1967 (University Microfilms, Ann Arbor, Mich., 67-16, 769).

(5) S. J. Donato, *J. Pharm. Sci.*, **54**, 917 (1965).

(6) P. Daenens and L. Laruelle, *J. Assoc. Offic. Anal. Chem.*, **56**, 1515 (1973).

(7) M. Wilcox, *J. Pharm. Sci.*, **56**, 642 (1967).

(8) J. L. Lach and J. S. Sawardeker, *ibid.*, **54**, 424 (1965).

(9) F. A. Fitzpatrick, A. F. Summa, and A. D. Cooper, *J. Soc. Cosmet. Chem.*, **26**, 377 (1975).

(10) T. D. Doyle and F. R. Fazarri, *J. Pharm. Sci.*, **63**, 1921 (1974).

(11) L. Doub and J. M. Vandenbelt, *J. Am. Chem. Soc.*, **69**, 2714 (1947).

(12) T. R. Aalto, M. C. Firman, and N. E. Rigler, *J. Am. Pharm. Assoc., Sci. Ed.*, **42**, 449 (1953).

(13) E. L. Wehry and L. B. Rogers, *J. Am. Chem. Soc.*, **87**, 4234 (1965).

(14) T. Higuchi, K. P. Patel, F. R. Bonow, and J. Landsman, *J. Am. Pharm. Assoc., Sci. Ed.*, **41**, 293 (1952).

(15) P. E. Stevenson, *J. Mol. Spectrom.*, **15**, 220 (1965).

(16) L. G. Sillen and A. E. Martell, "Stability Constants of Metal-Ion Complexes," Special Publication 17, The Chemical Society, London, England, 1964, p. 533.

(17) L. A. Cohen and W. M. Jones, *J. Am. Chem. Soc.*, **85**, 3397 (1963).

Simultaneous Determination of Procainamide and *N*-Acetylprocainamide in Plasma by High-Performance Liquid Chromatography

A. G. BUTTERFIELD ˣ, J. K. COOPER, and K. K. MIDHA

Received March 28, 1977, from the *Drug Research Laboratories, Health Protection Branch, Ottawa, Canada K1A OL2.* Accepted for publication October 12, 1977.

Abstract □ A sensitive, specific, high-performance liquid chromatographic procedure is described for the simultaneous determination of procainamide and its metabolite, *N*-acetylprocainamide, in plasma. Basic plasma (2.0 ml), containing pheniramine maleate as an internal standard, is partitioned with methylene dichloride. The organic extract is concentrated to between 0.3 and 0.5 ml, and 100-μl aliquots are chromatographed on a microparticulate silica gel column using 0.1% acetic acid–20% 0.1 *M* ammonium acetate in acetonitrile as the mobile phase. With a fixed-wavelength (254-nm) UV detector, both compounds can be quantitated in the 0.1–8.0-μg/ml of plasma range.

Keyphrases □ Procainamide—high-performance liquid chromatographic analysis simultaneously with *N*-acetylprocainamide in plasma □ *N*-Acetylprocainamide—high-performance liquid chromatographic analysis simultaneously with procainamide in plasma □ High-performance liquid chromatography—simultaneous analyses, procainamide and *N*-acetylprocainamide in plasma □ Cardiac depressants—procainamide, high-performance liquid chromatographic analysis simultaneously with *N*-acetylprocainamide in plasma

Several spectrofluorometric and colorimetric procedures were reported (1–5) for the determination of procainamide in plasma; however, these procedures lack specificity because of interference either from *N*-acetylprocainamide, the active metabolite of procainamide (6), or from endogenous materials. Several specific GLC procedures were reported (7–11) for procainamide, but not for *N*-acetylprocainamide, in plasma. One GLC procedure was re-

ported (12) for procainamide and *N*-acetylprocainamide in urine or for *N*-acetylprocainamide in plasma.

High-performance liquid chromatographic (HPLC) procedures were reported for procainamide and lidocaine (13) and for the simultaneous determination of procainamide and *N*-acetylprocainamide in plasma (14). The latter procedure has a reported quantitation as low as 1 μg/ml, adequate sensitivity for clinical work but not for single-dose studies.

None of the available procedures is sufficiently sensitive and/or specific to determine both procainamide and *N*-acetylprocainamide in plasma at the 0.1-μg/ml level. This report describes such a procedure and shows that it can be used to determine drug and metabolite levels following a single oral dose (375 mg) of procainamide hydrochloride.

EXPERIMENTAL

Materials—Procainamide hydrochloride[1] and pheniramine maleate[2] were used as received. *N*-Acetylprocainamide was synthesized from procainamide[2] (15). The proton magnetic resonance spectrum for the product was consistent with the structure of *N*-acetylprocainamide, and a single peak was obtained when the product was examined by HPLC. Solvents and reagents were commercial analytical reagent grade, except for *n*-hexane[3] which was UV grade.

Apparatus—A liquid chromatograph[4] fitted with a valve-loop injector[5] with a 100-μl loop, a fixed-wavelength UV detector[4] (254 nm), and a computing integrator[6] was used. The detector was attenuated to 0.02 absorbance unit full scale (aufs), and the integrator output was attenuated ×16 throughout.

Column—A 250 × 2.16-mm i.d. column packed with 5-μm silica gel[7], using a balanced density slurry technique similar to that described by Majors (16), was used at ambient temperature and a mobile phase flow rate of 60 ml/hr (135 bars).

Mobile Phase—A solution of 0.1% (v/v) acetic acid and 20% (v/v) 0.1 *M* aqueous ammonium acetate in acetonitrile was prepared as required, degassed (refluxed for 5 min), and transferred to the solvent reservoir of the instrument.

Internal Standard—A solution of pheniramine maleate in distilled water (8.9 μg/ml) was used.

Preparation of Standard Curves—Aqueous stock solutions of ammonium hydroxide (0.1 *N*), procainamide hydrochloride (23.1 mg/500 ml), and *N*-acetylprocainamide (20.0 mg/500 ml) were prepared. Standard solutions of procainamide and *N*-acetylprocainamide were prepared by pipetting 80, 60, 40, 20, 10, 5, 2, or 1 ml of both procainamide and *N*-acetylprocainamide stock solutions into each of eight 200-ml volumetric flasks. The resulting solutions were diluted to volume with distilled water.

Extracted standard solutions were prepared by pipetting 2.0 ml of blank plasma, 1.0 ml of procainamide–*N*-acetylprocainamide standard solution, 0.5 ml of 0.1 *N* ammonium hydroxide, 1.0 ml of internal standard, and 15.0 ml of methylene dichloride into a 50-ml screw-capped polypropylene tube[8]. The tube was tightly capped, shaken on a flat-bed shaker[9] at 180 cpm for 10 min, and centrifuged[10] at 3000 rpm for 10 min. A 10-ml aliquot of the organic layer was transferred to a 15-ml conical polypropylene tube[8] and concentrated[11] at 55° under a dry nitrogen stream to 0.3–0.5 ml. The sample was mixed[12] for 10 sec, and duplicate 100-μl aliquots were chromatographed.

Preparation of Calibration Standard Solutions—Two calibration solutions were prepared and chromatographed daily to check the slopes of the standard curves. The solutions were prepared in the same manner as those used for the construction of the standard curves, using procainamide–*N*-acetylprocainamide standard solutions at 0.4 and 4.0 μg/ml (equivalent to 0.2 and 2.0 μg/ml of plasma, respectively).

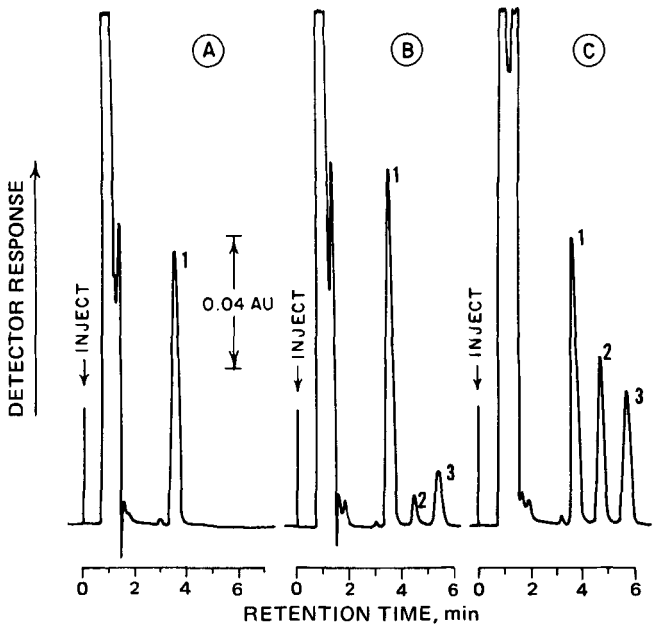

Figure 1—*Chromatograms of an extract of 2 ml of blank plasma containing 6 μg of pheniramine (1) internal standard (A); an extract of 2 ml of spiked plasma containing pheniramine (6 μg), procainamide (2, 0.2 μg/ml) and* N*-acetylprocainamide (3, 0.2 μg/ml) (B); and an extract of a 2-ml plasma sample taken 2 hr postdose (375 mg) estimated to contain 1.3 μg of procainamide/ml and 0.63 μg of* N*-acetylprocainamide/ml (C).*

Determination of Procainamide and *N*-Acetylprocainamide in Plasma—Plasma was treated as described under *Preparation of Standard Curves*, except that 1.0 ml of water was substituted for the procainamide–*N*-acetylprocainamide standard solution. Duplicate 100-μl aliquots of the final solution were chromatographed.

Plasma Level Study—Procainamide hydrochloride[13] (375 mg) was administered orally with 100 ml of water to a 65-kg human male who had fasted overnight. Blood samples, 10 ml, were withdrawn from the cubital vein with heparinized evacuated tubes[14] before dosing and at 10 different times up to 24 hr after dosing. Blood samples were centrifuged, and the plasma was transferred to clean glass tubes before storage at −10°.

Recovery Study—A solution of procainamide hydrochloride (1.155 μg/ml) and *N*-acetylprocainamide (1.0 μg/ml) and a solution of pheniramine maleate (8.9 μg/ml) in methylene dichloride were prepared. Aliquots (1.0 and 4.0 ml) of the procainamide–*N*-acetylprocainamide solution were pipetted into conical polypropylene tubes along with 1.0-ml aliquots of the pheniramine maleate solution. The solutions were mixed[12] briefly and concentrated[11] at 55° under a nitrogen stream to 0.3–0.5 ml. Duplicate 100-μl aliquots of each solution were chromatographed, and the mean sample to internal standard peak area ratios for each drug level were designated as the 100% values.

To determine recovery of procainamide and *N*-acetylprocainamide, 2.0 ml of blank plasma was spiked with 1.0 ml of an aqueous solution of procainamide hydrochloride (1.155 or 4.62 μg/ml) and *N*-acetylprocainamide (1.0 or 4.0 μg/ml). To each solution were added 1.0 ml of distilled water, 0.5 ml of 0.1 *N* ammonium hydroxide, and 15 ml of methylene dichloride. The samples were partitioned as previously described, and 10 ml of the organic layer was transferred to a polypropylene tube containing 1 ml of a methylene dichloride solution of pheniramine maleate (8.9 mg/ml). The resulting solution was concentrated and chromatographed as previously described. The mean sample to internal standard peak area ratios were compared to the 100% values, and the percent recovery was calculated for each level. The recovery of pheniramine maleate was determined similarly, using procainamide as an external standard.

Quantitation—Spiked plasma extracts were chromatographed, and

[1] E. R. Squibb & Sons, Montreal, Canada.
[2] Pfaltz and Bauer, Flushing, N.Y.
[3] Burdick and Jackson Laboratories, Muskegon, Mich.
[4] Model 4100, Varian Aerograph, Palo Alto, Calif.
[5] Model CV-6-UHPa, Valco Instruments Co., Houston, Tex.
[6] Autolab System I, Spectra-Physics, Santa Clara, Calif.
[7] LiChrosorb SI60, British Drug Houses, Toronto, Canada.
[8] Nalge Co., Rochester, N.Y.
[9] Eberbach Crop., Ann Arbor, Mich.
[10] Model HN-S, International Equipment Co., Needham Heights, Mass.
[11] Thermolyne Dri-Bath, Fisher Scientific Co., Ottawa, Canada.
[12] Vortex Genie, Fisher Scientific Co., Ottawa, Canada.
[13] A commercial capsule formulation.
[14] Vacutainers, Becton Dickinson & Co., Mississauga, Ontario, Canada.

Table I—Extractability of Procainamide, *N*-Acetylprocainamide, and Pheniramine from Plasma

Level, μg/ml	Procainamide, % Recovery[a] ± *RSD*	*N*-Acetylprocainamide, % Recovery[a] ± *RSD*	Pheniramine, % Recovery[a] ± *RSD*	*n*
0.5	97.8 ± 4.4	102.8 ± 2.7	—	9
2.0	96.6 ± 0.4	98.9 ± 1.5	—	6
6.0	—	—	98.1 ± 3.3	4

[a] Calculated from recovery values to allow for only 10 ml out of 15 ml of sample being carried through the procedure.

a standard curve was constructed by plotting the ratio of sample to internal standard peak area *versus* the concentration of drug or metabolite (micrograms per milliliter of plasma). Calibration standards were chromatographed periodically to monitor the slope of the standard curve. Unknown plasma samples were analyzed by comparison of peak area ratios to the standard curve.

RESULTS AND DISCUSSION

Procainamide, *N*-acetylprocainamide, and the internal standard (pheniramine) were completely separated and eluted in less than 7 min (Fig. 1B). No interference from endogenous plasma constituents was experienced (Fig. 1A). Mass spectral evidence showed that collected peaks from chromatographed plasma and extracts of spiked blank plasma were identical, indicating that no metabolites of procainamide or *N*-acetylprocainamide interfered.

Stopped-flow injection[4] was used early in the study, but a sample volume in excess of 15–20 μl resulted in excessive peak broadening. Valve-loop injection allowed a 100-μl sample to be chromatographed without affecting peak shape.

A 2.2-mm i.d. column was used to maximize peak height. The peak height obtained with this column was typically about three times that obtained with a 4.6-mm. i.d. column of the same length. Silica gel of 5-μm diameter provided a column that exhibited adequate efficiency and resolution and that can be easily prepared at low cost.

The use of aqueous mobile phases with silica gel columns is often avoided; in certain circumstances, however, this technique has proven to be very useful. Silica gel is somewhat soluble in water, particularly above pH 8, but in practice this solubility has not been a problem. After extended use under aqueous conditions, a silica gel column exhibits some settling of the packed bed (1–2 mm), but this condition is easily remedied by careful addition of moist silica gel to fill the void. The column employed was used over 5 months with only a slight loss of efficiency.

Detector response for *N*-acetylprocainamide (peak area/unit weight) was approximately double that of procainamide, a situation that allows low metabolite levels to be determined despite the longer retention time (5.7 *versus* 4.7 min).

Finding a suitable internal standard for this assay was somewhat difficult. Tetracaine, procaine, methoxyphenamine, and pyrilamine were tried and rejected. Tetracaine exhibited low detector response and presented solubility problems when an adequate quantity was used. Procaine hydrolyzed rapidly under the conditions of the assay. Methoxyphenamine gave a double peak after extraction from certain plasma samples. Pyrilamine also occasionally gave a double peak and, in addition, the shape of the peak varied. This latter observation was explained as being due to the early elution of the compound ($k' = 1.7$). Pheniramine ($k' = 4.3$), the internal standard eventually chosen, eluted just ahead of procainamide. Although occasional broadening of this peak was observed, peak area was unaffected.

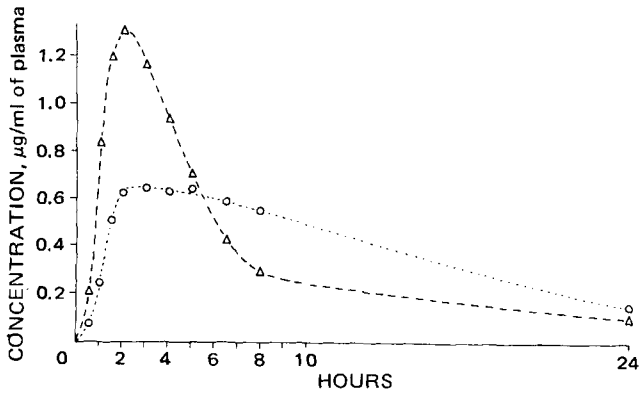

Figure 2—*Plasma profile of procainamide (△) and* N*-acetylprocainamide (○) after a single oral dose (375 mg) of procainamide hydrochloride.*

Aqueous standard solutions of procainamide and *N*-acetylprocainamide exhibited no apparent decomposition after storage for over 6 months at 23°. Solutions of pheniramine maleate appear to be stable for at least 2 weeks at 4°. Extracted procainamide samples gave similar results after storage for 16 hr at 4° as when freshly prepared, but samples generally were analyzed immediately after preparation.

Injection of standard solutions prepared to contain various concentrations of solute provided a linear detector response up to about 6 μg/injection of procainamide hydrochloride, 3.5 μg/injection of *N*-acetylprocainamide, and 4 μg/injection of pheniramine maleate. Standard curves were linear with negligible intercepts over the 0.1–0.8-μg/ml range, with slopes of 0.432 ml/μg for procainamide and 0.832 ml/μg for *N*-acetylprocainamide. Injection of calibration standards over 3 weeks showed that the slopes varied by less than 2% from the values reported.

Nonlinear calibration curves were obtained for both procainamide and *N*-acetylprocainamide if samples were extracted in glass or silanized glass tubes. This phenomenon was attributed to drug adsorption on the glass surface. Carr *et al.* (14) reported similar nonlinearities but overcame the problem by using polypropylene tubes for extraction. Similarly, when polypropylene tubes were used for extraction and concentration in the present study, linear calibration curves were obtained for levels of both drug and metabolite as low as 0.1 μg/ml of plasma.

The extractability of procainamide, *N*-acetylprocainamide, and pheniramine is reported in Table I. The accuracy and precision of the procedure are demonstrated in Table II. Standard solutions prepared over the 0.1–8.0-μg/ml of plasma range were analyzed as described under *Experimental.*

Application of the procedure to the determination of procainamide and *N*-acetylprocainamide in plasma following a single 375-mg oral dose of procainamide hydrochloride is demonstrated in Fig. 2. For plasma from three dosed volunteers, curves with similar shapes were obtained. A first-pass effect has been demonstrated for procainamide (17). This phenomenon was indicated in this study by the presence of *N*-acetylprocainamide approximately 30 min after dosing and by peak plasma levels for both procainamide and *N*-acetylprocainamide about 2 hr after dosing, followed by a slow decline in the metabolite level.

The described HPLC procedure is precise, accurate, and specific for the drug and its metabolite. Furthermore, it is of sufficient sensitivity to determine plasma levels following single doses (375 mg) of the drug

Table II—HPLC Estimation of Procainamide and *N*-Acetylprocainamide Added to Plasma

Concentration, μg/ml	*n*	Procainamide Mean Area Ratio	Procainamide Slope[a]	Procainamide *RSD*, %	*N*-Acetylprocainamide Mean Area Ratio	*N*-Acetylprocainamide Slope[a]	*N*-Acetylprocainamide *RSD*, %
0.1	3	0.043	0.43	5.7	0.081	0.81	5.3
0.2	6	—	—	—	0.169	0.84	4.8
0.5	8	0.225	0.45	3.9	0.417	0.83	1.9
0.8	6	0.352	0.44	1.7	—	—	—
1.0	3	0.455	0.46	0.3	0.834	0.83	1.3
2.0	3	0.902	0.46	1.2	1.670	0.84	1.3
8.0	3	3.460	0.43	0.9	6.53	0.82	1.4
		Mean	0.445	3.1		0.829	1.6

[a] Slope = mean area ratio/concentration.

and should be suitable for single- or multiple-dose pharmacokinetic or bioavailability studies.

REFERENCES

(1) L. C. Mark, H. J. Kayden, J. M. Steele, J. R. Cooper, I. Berlin, E. A. Rovenstein, and B. B. Brodie, *J. Pharmacol. Exp. Ther.*, **102**, 5 (1951).

(2) J. Koch-Weser and S. W. Klein, *J. Am. Med. Assoc.*, **215**, 1454 (1971).

(3) S. Bellet, S. E. Zeeman, and S. A. Hirsh, *Am. J. Med.*, **13**, 145 (1952).

(4) J. Koch-Weser, S. W. Klein, L. L. Foo-Canto, J. A. Kastor, and R. W. Desanatis, *N. Engl. J. Med.*, **281**, 1253 (1969).

(5) J. M. Sterling and W. G. Haney, *J. Pharm. Sci.*, **63**, 1448 (1974).

(6) J. Dreyfuss, J. T. H. Bigger, Jr., A. J. Cohen, and E. C. Schreiber, *Clin. Pharmacol. Ther.*, **13**, 366 (1972).

(7) A. J. Atkinson, Jr., M. Parker, and J. Strong, *Clin. Chem.*, **18**, 643 (1972).

(8) J. Sterling, S. Cox, and W. G. Haney, *J. Pharm. Sci.*, **63**, 1744 (1974).

(9) D. M. Ottonstein, *J. Chromatogr. Sci.*, **11**, 136 (1973).

(10) K. J. Simons and R. H. Levy, *J. Pharm. Sci.*, **64**, 1967 (1975).

(11) J. Meola and M. Vanko, *Clin. Chem.*, **18**, 579, 643 (1972).

(12) E. Karlsson, L. Molin, B. Norlander, and F. Sjoqvist, *Br. J. Clin. Pharmacol.*, **1**, 467 (1974).

(13) R. F. Adams, F. L. Vandmark, and G. Schmidt, *Clin. Chim. Acta*, **69**, 515 (1976).

(14) K. Carr, R. L. Woosley, and J. A. Oates, *J. Chromatogr.*, **129**, 363 (1976).

(15) J. Dreyfuss, J. J. Ross, Jr., and E. C. Schreiber, *Arzneim.-Forsch.*, **21**, 948 (1971).

(16) R. A. Majors, *Anal. Chem.*, **44**, 1722 (1972).

(17) C. Graffner, G. Johnsson, and J. Sjögren, *Clin. Pharmacol. Ther.*, **17**, 414 (1975).

Noninvasive Polarographic Measurement of Drug Dissolution

M. R. HACKMAN ˣ **and M. A. BROOKS**

Received July 18, 1977, from the *Department of Biochemistry and Drug Metabolism, Hoffmann-La Roche Inc., Nutley, NJ 07110.* Accepted for publication October 14, 1977.

Abstract □ Polarographic analysis was applied successfully to dissolution studies and content uniformity assessment of both capsules and tablets, using a dropping mercury electrode with the modified Levy beaker method. The described noninvasive technique places the polarographic sensor probe directly into the dissolution flask and thus simplifies dissolution measurement by eliminating transfer lines and pumps typically required with the invasive (sampling) mode of analysis. A continuous sampling flowcell with polarographic detection was also evaluated for invasive measurements. Continuous dissolution profiles and content uniformity were determined for chlordiazepoxide, trimethoprim, ornidazole, and isoniazid, using the invasive and noninvasive sampling modes. Results obtained for these drugs showed excellent precision with both sampling techniques. In addition, excellent correlation to UV spectrophotometric data was obtained.

Keyphrases □ Polarography, noninvasive—applied to drug dissolution and content uniformity assessment of various capsules and tablets □ Dissolution, drug—noninvasive polarographic study of various capsules and tablets □ Content uniformity—noninvasive polarographic assessment of various capsules and tablets

The dissolution rate of a drug is determined by measuring the amount dissolved per unit of time. These measurements are obtained conventionally by two invasive sampling techniques: (*a*) discrete sampling of the medium in the dissolution flask, followed by spectrophotometric analysis; and (*b*) continuous sampling and measurement by pumping of the dissolution medium through a UV spectrophotometer. A proposed means of obtaining dissolution data is *via* direct or noninvasive measurement by placement of an analyzing sensor directly into the dissolution flask. Spectrophotometric measurement using the noninvasive technique is not possible because of the lack of a spectrophotometric probe. Other limitations of a spectrophotometric method include disturbances caused by the stirring action, the presence of excipients, and a limited linear dynamic range.

Voltammetric analysis, which has been well documented for assays of drugs in dosage forms (1, 2) and biological fluids (3, 4), can be applied to both invasive and noninvasive dissolution measurements. The only prerequisite is that the drug undergo voltammetric reduction or oxidation in the dissolution medium. Voltammetric analysis is ideally suited for drug dissolution measurements since the technique has a wide linear dynamic range. In addition, these assays are specific for the compound of interest in the presence of excipients. The method also permits the analysis of content uniformity on the same sample after dissolution. Feher *et al.* (5) reported the use of voltammetry for the continuous invasive measurement of the dissolution of aminopyrine and promethazine by oxidation using a silicone rubber-based graphite electrode. Gaglia *et al.* (6) recently reported the noninvasive voltammetric analysis of the dissolution of nitroglycerin tablets by reduction of the nitro group at a rotating platinum electrode.

The use of a polarographic sensor, the dropping mercury electrode (DME), for drug dissolution measurement is being described for the first time. The dropping mercury electrode, when used either in a flowcell (continuous invasive measurement) or directly in the dissolution flask (noninvasive measurement), has the distinct advantage over other voltammetric sensors of presenting a constantly renewable surface for analysis. Therefore, it is not subject to a buildup of interferences during dissolution.

Polarography was used in this study to measure the dissolution rate of four drugs, chlordiazepoxide (I), or-

and should be suitable for single- or multiple-dose pharmacokinetic or bioavailability studies.

REFERENCES

(1) L. C. Mark, H. J. Kayden, J. M. Steele, J. R. Cooper, I. Berlin, E. A. Rovenstein, and B. B. Brodie, *J. Pharmacol. Exp. Ther.*, **102**, 5 (1951).

(2) J. Koch-Weser and S. W. Klein, *J. Am. Med. Assoc.*, **215**, 1454 (1971).

(3) S. Bellet, S. E. Zeeman, and S. A. Hirsh, *Am. J. Med.*, **13**, 145 (1952).

(4) J. Koch-Weser, S. W. Klein, L. L. Foo-Canto, J. A. Kastor, and R. W. Desanatis, *N. Engl. J. Med.*, **281**, 1253 (1969).

(5) J. M. Sterling and W. G. Haney, *J. Pharm. Sci.*, **63**, 1448 (1974).

(6) J. Dreyfuss, J. T. H. Bigger, Jr., A. J. Cohen, and E. C. Schreiber, *Clin. Pharmacol. Ther.*, **13**, 366 (1972).

(7) A. J. Atkinson, Jr., M. Parker, and J. Strong, *Clin. Chem.*, **18**, 643 (1972).

(8) J. Sterling, S. Cox, and W. G. Haney, *J. Pharm. Sci.*, **63**, 1744 (1974).

(9) D. M. Ottonstein, *J. Chromatogr. Sci.*, **11**, 136 (1973).

(10) K. J. Simons and R. H. Levy, *J. Pharm. Sci.*, **64**, 1967 (1975).

(11) J. Meola and M. Vanko, *Clin. Chem.*, **18**, 579, 643 (1972).

(12) E. Karlsson, L. Molin, B. Norlander, and F. Sjoqvist, *Br. J. Clin. Pharmacol.*, **1**, 467 (1974).

(13) R. F. Adams, F. L. Vandmark, and G. Schmidt, *Clin. Chim. Acta*, **69**, 515 (1976).

(14) K. Carr, R. L. Woosley, and J. A. Oates, *J. Chromatogr.*, **129**, 363 (1976).

(15) J. Dreyfuss, J. J. Ross, Jr., and E. C. Schreiber, *Arzneim.-Forsch.*, **21**, 948 (1971).

(16) R. A. Majors, *Anal. Chem.*, **44**, 1722 (1972).

(17) C. Graffner, G. Johnsson, and J. Sjögren, *Clin. Pharmacol. Ther.*, **17**, 414 (1975).

Noninvasive Polarographic Measurement of Drug Dissolution

M. R. HACKMAN ˣ **and M. A. BROOKS**

Received July 18, 1977, from the *Department of Biochemistry and Drug Metabolism, Hoffmann-La Roche Inc., Nutley, NJ 07110.* Accepted for publication October 14, 1977.

Abstract □ Polarographic analysis was applied successfully to dissolution studies and content uniformity assessment of both capsules and tablets, using a dropping mercury electrode with the modified Levy beaker method. The described noninvasive technique places the polarographic sensor probe directly into the dissolution flask and thus simplifies dissolution measurement by eliminating transfer lines and pumps typically required with the invasive (sampling) mode of analysis. A continuous sampling flowcell with polarographic detection was also evaluated for invasive measurements. Continuous dissolution profiles and content uniformity were determined for chlordiazepoxide, trimethoprim, ornidazole, and isoniazid, using the invasive and noninvasive sampling modes. Results obtained for these drugs showed excellent precision with both sampling techniques. In addition, excellent correlation to UV spectrophotometric data was obtained.

Keyphrases □ Polarography, noninvasive—applied to drug dissolution and content uniformity assessment of various capsules and tablets □ Dissolution, drug—noninvasive polarographic study of various capsules and tablets □ Content uniformity—noninvasive polarographic assessment of various capsules and tablets

The dissolution rate of a drug is determined by measuring the amount dissolved per unit of time. These measurements are obtained conventionally by two invasive sampling techniques: (*a*) discrete sampling of the medium in the dissolution flask, followed by spectrophotometric analysis; and (*b*) continuous sampling and measurement by pumping of the dissolution medium through a UV spectrophotometer. A proposed means of obtaining dissolution data is *via* direct or noninvasive measurement by placement of an analyzing sensor directly into the dissolution flask. Spectrophotometric measurement using the noninvasive technique is not possible because of the lack of a spectrophotometric probe. Other limitations of a spectrophotometric method include disturbances caused by the stirring action, the presence of excipients, and a limited linear dynamic range.

Voltammetric analysis, which has been well documented for assays of drugs in dosage forms (1, 2) and biological fluids (3, 4), can be applied to both invasive and noninvasive dissolution measurements. The only prerequisite is that the drug undergo voltammetric reduction or oxidation in the dissolution medium. Voltammetric analysis is ideally suited for drug dissolution measurements since the technique has a wide linear dynamic range. In addition, these assays are specific for the compound of interest in the presence of excipients. The method also permits the analysis of content uniformity on the same sample after dissolution. Feher *et al.* (5) reported the use of voltammetry for the continuous invasive measurement of the dissolution of aminopyrine and promethazine by oxidation using a silicone rubber-based graphite electrode. Gaglia *et al.* (6) recently reported the noninvasive voltammetric analysis of the dissolution of nitroglycerin tablets by reduction of the nitro group at a rotating platinum electrode.

The use of a polarographic sensor, the dropping mercury electrode (DME), for drug dissolution measurement is being described for the first time. The dropping mercury electrode, when used either in a flowcell (continuous invasive measurement) or directly in the dissolution flask (noninvasive measurement), has the distinct advantage over other voltammetric sensors of presenting a constantly renewable surface for analysis. Therefore, it is not subject to a buildup of interferences during dissolution.

Polarography was used in this study to measure the dissolution rate of four drugs, chlordiazepoxide (I), or-

Table I—Drug Dissolution and Formulation Content of Compounds Assayed by Polarographic Measurement

Compound	Chemical Name	Empirical Formula	Molecular Weight	Melting Point	Standard/ Sample Weight	Amount of Gelatin Required, mg
I[a]	7-Chloro-2-methylamino-5-phenyl-3*H*-1,4-benzodiazepine 4-oxide	$C_{16}H_{14}ClN_3O$	299.71	236–236.5°	8.92[b]	60.0[c]
II	2-Methyl-5-nitro-1*H*-imidazole-1-(3-methoxy-2-propanol)	$C_7H_{10}ClN_3O_3$	219.5	77–78°	500	25.0
III	2,4-Diamino-5-(3,4,5-trimethoxybenzyl)pyrimidine	$C_{14}H_{18}N_4O_3$	290.33	199°	100	0
IV	4-Pyridinecarboxylic acid hydrazide	$C_6H_4N_3O$	137.15	171–173°	100	0

[a] Formulated as the hydrochloride salt. [b] This weight is equivalent to the amount of chlordiazepoxide contained in 10 mg of chlordiazepoxide hydrochloride. [c] Capsule contained 40 mg of gelatin; 20 mg of additional gelatin was required.

nidazole (II), trimethoprim (III), and isoniazid (IV), by both noninvasive and invasive techniques. The reduction current was monitored at either the peak reduction potential (E_p) for differential pulse polarography or at the limiting current plateau for sampled dc polarography. Upon completion of the dissolution rate measurement, formulation content was measured by performing polarographic scans of applied potential *versus* current.

EXPERIMENTAL

Reagents—The dissolution medium was 0.1 *N* HCl prepared by mixing 16.7 ml of concentrated (12 *N*) HCl (ACS reagent grade) in 2000 ml of distilled deionized water.

The stock gelatin solution (50 mg/ml) was prepared by weighing 5.00 g of gelatin USP and dissolving it in 100 ml of boiling 0.1 *N* HCl by stirring. The hot solution was then cooled and stored in a glass-stoppered bottle.

Standards of I–IV are indicated in Table I.

Apparatus—The Levy–Hayes beaker dissolution apparatus (7) was modified by replacing the beaker with a specially constructed round-bottom flask. The flask was designed so that 350 ml of fluid would occupy 75% of the rounded area. It was 12.5 cm in overall height (4.5-cm neck and 8.0-cm rounded area) with a 9-cm diameter mouth and a diameter of 10.5 cm at the midpoint of the rounded area. Thermoregulation was achieved using a 0–100° contact thermometer[1] connected to a relay control box[2] using a 750-w flexible immersion heater[3]. The bath stirrer was a variable speed stirring motor[4] with a 25.4-cm three-blade polyethylene paddle.

The polarograph[5] was used in conjunction with a drop timer[6]. The display was achieved through the use of an *x–y* recorder mainframe[7] with a precision dc switching/time base module[8] for the *x*-axis and a precision dc switching module[9] for the *y*-axis.

Deaeration was accomplished by flowing prepurified nitrogen[10] through a coarse-porosity micro filter stick[11]. Special electrodes and flowcells were used with the two modes of polarographic drug dissolution.

Noninvasive Polarographic Equipment—A tapered dropping mercury electrode (indicator electrode) was prepared by drawing out a 30-cm length of dropping mercury electrode capillary (6–12 sec)[12] to approximately 50% of its outer diameter and cutting it into two pieces at the narrowest part. A 20-cm length of 22-gauge platinum wire[13] was used as the auxiliary electrode. The reference electrode was a saturated calomel electrode[14] (SCE). The correct placement of the three electrodes in the special dissolution flask for noninvasive measurements is shown in Fig. 1.

Invasive Polarographic Equipment—The reference electrode was identical to that used in the noninvasive mode. The electrode, along with the sample line probe[11] (coarse-porosity filter stick) and return lines to the flowcell, was placed in the upper portion of the dissolution flask. The flowcell (Fig. 2) was a 55-mm glass tube (4 mm i.d.) to which was attached a 15-mm glass side arm (8 mm i.d.) at an angle of 60° containing the dropping mercury electrode [10-cm length of capillary tubing (2–5 sec)][15]. A glass connector[16] was attached to the upper portion of the flowcell *via* a polyvinyl chloride tubing sleeve, which served as an inlet for the dissolution medium. This same connector allowed for venting of trapped

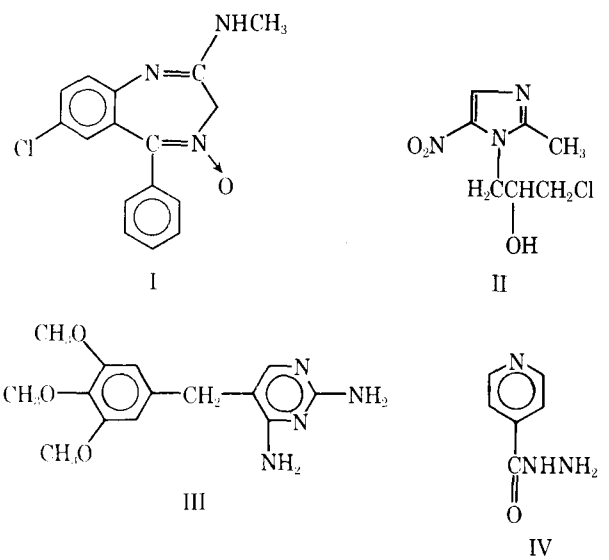

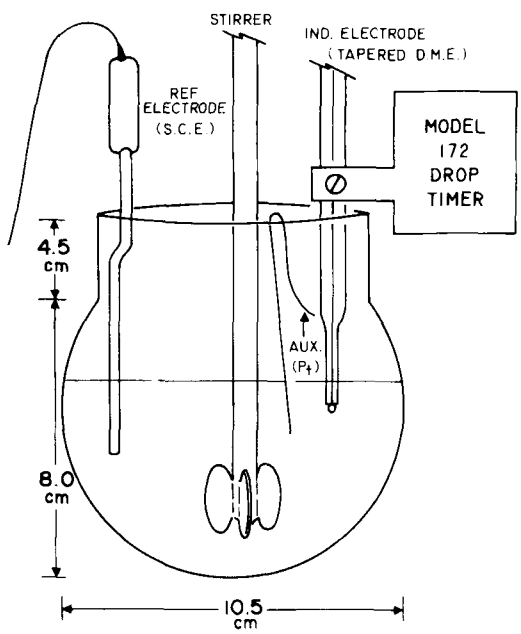

Figure 1—*Dissolution flask with electrode placement for noninvasive polarographic determination.*

[1] Catalog No. 22-3088/02, Ace Scientific, Linden, N.J.
[2] Catalog No. 22-3365/01, Ace Scientific, Linden, N.J.
[3] Catalog No. 18-6420/05, Ace Scientific, Linden, N.J.
[4] Catalog No. 22-1800/01, Ace Scientific, Linden, N.J.
[5] Model 174, Princeton Applied Research Corp., Princeton, N.J.
[6] Model 172, Princeton Applied Research Corp., Princeton, N.J.
[7] Houston-Omnigraphic model 2200, Houston Instruments, Bellaire, Tex.
[8] Houston-Omnigraphic model 6, Houston Instruments, Bellaire, Tex.
[9] Houston-Omnigraphic model 3, Houston Instruments, Bellaire, Tex.
[10] Matheson Gas Products, East Rutherford, N.J.
[11] Catalog No. JM-5385-S, SGA Scientific, Bloomfield, N.J.
[12] Catalog No. S-29417, Sargent-Welch, Springfield, N.J.
[13] B&S.
[14] Catalog No. 39178, Beckman Instruments, Mountainside, N.J.
[15] Catalog No. S-29419, Sargent-Welch, Springfield, N.J.
[16] Catalog No. 116-0202P03, Technicon Instruments, South Plainfield, N.J.

Table II—Instrument Parameters for Polarographic Measurement of Drug Dissolution and Formulation Content

Compound	Mode	Measuring Potential, v *versus* SCE	Time Base Rate, sec/in.	Scan Range, v	Current Range, μamp	
					Noninvasive	Invasive
I	Differential pulse	−0.600	100	−0.450 to −0.800	20	10
II	Differential pulse	−0.070	200	+0.075 to −0.300	500	500
IV	Differential pulse	−0.685	100	−0.300 to −0.850	200	500
III	Sampled dc	−1.300	200	−1.000 to −1.450	20	50

air bubbles in the flowcell through the capillary arm, which was fitted with a polyethylene nipple[17]. A 3-ml syringe, fitted with a length of 1.59-mm (0.0625-in.) polyvinyl chloride tubing, was placed over the nipple for removal of trapped air bubbles.

A mercury separator, which served as a collector for used mercury and as an outlet for the dissolution medium, was attached to the lower portion of the flowcell *via* another polyvinyl chloride sleeve. The separator was constructed from a 4.76-mm ($^3/_{16}$-in.) i.d. Y-tube, which was modified by removal of the three nipples and by sealing in a 22-gauge platinum wire[13] in the lower arm. Polyvinyl chloride tubing, 4.76 mm ($^3/_{16}$ in. i.d.), was attached to the lower arm of the mercury separator and closed off *via* a tubing clamp. This clamp allowed for removal of excess mercury from the flow system. The mercury level in the lower arm of the Y-tube was maintained slightly above the platinum wire electrode, producing a mercury pool as the auxiliary electrode.

A single-speed peristaltic pump[18] with a 2.79-mm (0.110-in.) (3.9 ml/min) polyvinyl chloride pump tube was used[19]. The connections from the dissolution flask to the flowcell and back to the flask are outlined in Fig. 3. All tubing to the flowcell was narrow bore polyethylene [0.58 mm (0.023 in. i.d.)]. The return line to the dissolution flask was polyethylene tubing [1.59 mm (0.0625 in. i.d.)].

Instrumental Parameters—The polarograph was operated in either the differential pulse or sampled dc mode (Table I), using a scan rate of 5 mv/sec with a 0.5-sec drop time. In the differential pulse mode, the pulse modulation amplitude was −50 mv. The measuring potential, current range, and time base were adjusted to the required setting (Table II), and the low pass filter was not used. The capillary characteristics were: the standard dropping mercury electrode at 22°, m = 2.39 mg/sec, $m^{2/3}\,t^{1/6}$ = 1.593; and the tapered dropping mercury electrode at 22°, m = 0.907 mg/sec, $m^{2/3}\,t^{1/6}$ = 0.8345, and at 37°, m = 1.25 mg/sec, $m^{2/3}\,t^{1/6}$ = 1.032.

Noninvasive Procedure—*Standard*—A 300-ml aliquot of 0.1 *N* HCl containing the required amount of gelatin was added to the dissolution flask and was thermally equilibrated to 37°. During this interval (approximately 5 min), the solution was deaerated with nitrogen by means of the micro filter stick. After deaeration, the required weight of standard was dissolved in the medium with the aid of the stirrer. The stirrer was adjusted to 50 rpm, and the appropriate polarographic measuring potential was set. Complete dissolution was noted by a current plateau lasting at least 5 or 10 min at a recorder rate of 100 or 200 sec/2.54 cm, respectively. After dissolution, the stirrer was turned off, the recorder was converted to the x–y mode, and a polarographic scan was made.

Formulation—The dissolution flask was drained using a water aspirator, and the flask was rinsed several times with distilled water. New dissolution medium was added to the flask, thermally equilibrated, and deaerated as already described. The recorder was reconverted to the time base mode, which was engaged simultaneously with the dropping of the tablet (or capsule) into the dissolution medium. (To ensure that total immersion of the capsule occurred, a paper clip was placed around the capsule as a weight.) The dissolution kinetic curve was monitored until a current plateau was measured. The initial potential was set, and the polarographic scan was recorded using the x–y mode.

Invasive Procedure—The procedure was identical to the noninvasive procedure except that after the dissolution medium was thermally equilibrated, the pump was turned on and the entire flow system was filled. In addition, any air bubbles present were removed by pulling air from the vent (Fig. 2) with a 3-ml syringe fitted with a length of 1.59-mm (0.0625-in.) polyvinyl chloride tubing. All measurements of both dissolution and formulation content in this mode were made with the stirrer operational.

After completion of the analysis of the standard and while the pump was running, the return line was removed from the dissolution flask and placed into a waste receptacle, such as a 125-ml erlenmeyer flask. The dissolution flask was then rinsed several times with distilled water, allowing enough time for the rinse to run through the entire flow system. Upon final rinsing, the lines and flowcell were dried by pumping with air. After the lines were dry, the return line was replaced in the dissolution flask, a new dissolution medium was added, and the analysis of the drug in the dosage form was carried out.

Calculation of Percent Dissolved at t_{25}, t_{50}, and t_{75}—The heights from the extrapolated baseline to the current plateau for the standard (I_{100}, standard) and sample (I_{100}) were measured. These two heights will be virtually equal if the drug in the dosage form is completely dissolved. Based on the value of I_{100}, the time at 25, 50, and 75% dissolution was determined by extrapolating to the x-axis. [In the invasive mode, the delay time, the time for the dissolved sample to traverse the distance from the flask to the detector (experimentally determined to be 72 sec) must be subtracted from the t_{25}, t_{50}, and t_{75} times of dissolution.] An example of this type of calculation is shown for the invasive determination of ornidazole in Fig. 4.

Calculation of Content Uniformity Using Differental Pulse Po-

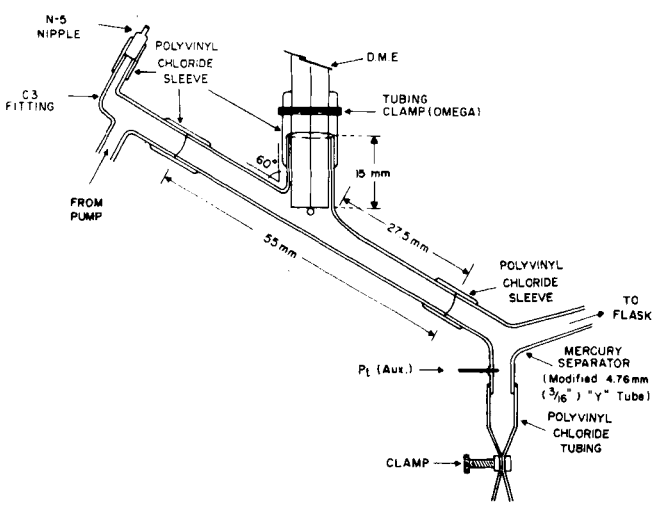

Figure 2—*Flowcell for invasive polarographic measurement.*

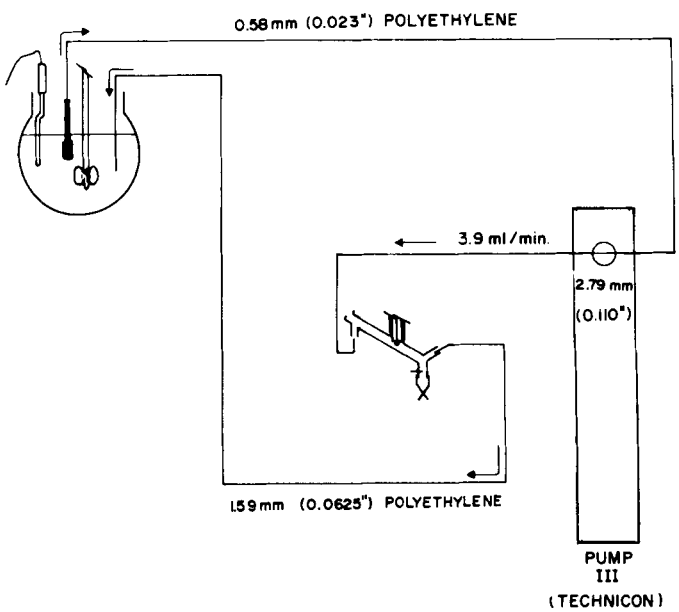

Figure 3—*Flow diagram for invasive measurement.*

[17] Catalog No. 116-0002PO1, Technicon Instruments, South Plainfield, N.J.
[18] Catalog No. 133-A014, Technicon Instruments, South Plainfield, N.J.
[19] Catalog No. 190-0427P16, Technicon Instruments, South Plainfield, N.J.

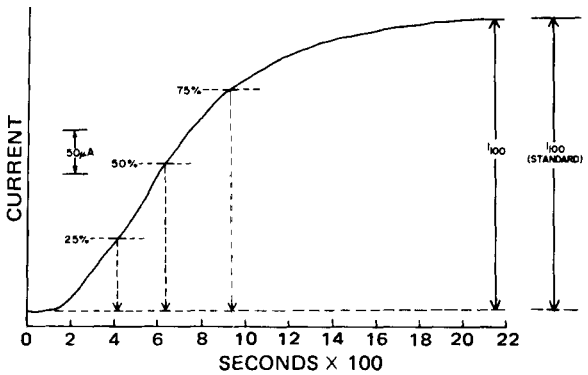

Figure 4—*Typical calculation for determination of dissolution times for ornidazole.*

larography—The measurement of the peak height, H, in centimeters was converted to a current, I, in microamperes, using the following relationship (Fig. 5A):

$$I = \frac{H}{25.4} \times \text{current range} \qquad \text{(Eq. 1)}$$

The currents of the standard, I_s, and the unknown, I_u, were determined, and the ratio of the currents to the known standard concentration, C_s, was used to determine the unknown concentration, C_u, by the following relationship:

$$C_u = \frac{C_s}{I_s} \times I_u \qquad \text{(Eq. 2)}$$

In a similar manner, the concentration was determined for the sampled dc curve. The plateau height was calculated as the difference from the measuring potential to the extrapolated baseline (Fig. 5B).

RESULTS AND DISCUSSION

Special equipment, except the tapered dropping mercury electrode, is not necessary for the noninvasive polarographic measurement of drug dissolution. The electrode modification was necessary to decrease the natural drop time to greater than 0.5 sec at 37°, as required for mechanical dislodgment.

In contrast, both the invasive polarographic method and the spectrophotometric method require special pumping equipment, flowcell (Fig. 2), and sample lines (Fig. 3) to measure drug dissolution. In this mode, it is critical that all three electrodes be immersed in the continuous stream of the dissolution medium to ensure electrical conductivity. Thus, it is essential that all air bubbles be removed from the lines at the vent in the upper end of the flowcell. If this condition is not met, a large potential, resulting from a break in the feedback loop of the potential generating circuitry, will be applied across the indicator and reference electrodes; the system will go into electrical overload, with possible damage to the electrodes.

Changes in conductivity also were experienced when mercury was permitted to leave the flowcell and enter the dissolution flask. To trap the mercury falling from the dropping mercury electrode, a mercury separator was incorporated into the lower end of the flowcell. This device

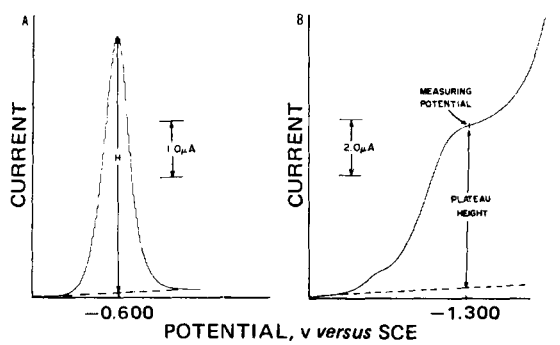

Figure 5—*Typical calculation for formulation content. Key: A, differential pulse polarogram of chlordiazepoxide; and B, sampled dc polarogram of trimethoprim.*

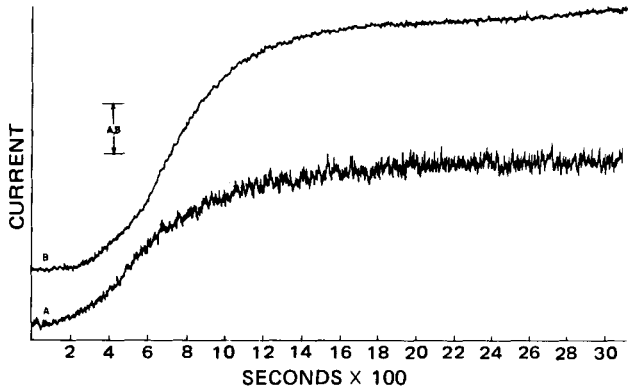

Figure 6—*Typical dissolution kinetic curve for a capsule containing 8.92 mg of chlordiazepoxide. Key: A, 20 μamp and noninvasive; and B, 10 μamp and invasive.*

collected all spent mercury and could be easily drained through the tubing attached to the lower arm of the separator. If long dissolution times are encountered (≃1 hr), this side arm may be drained during the assay.

The reduction of a species at the dropping mercury electrode takes place at the surface of the mercury drop. Therefore, anything that affects that surface, such as stirring, particles, or surface-active agents, will affect the resulting signal. In the noninvasive mode, the sensing electrode is in close proximity to the stirrer, so effects from stirring are significant. The currents measured during the process are a sum of currents due to migration resulting from the stirring as well as natural diffusion. The removal of the stirrer from the immediate vicinity of the electrode (Fig. 1) reduces irregular migration due to the vortex action of stirring and greatly diminishes noise on the drug dissolution curve.

A stirring rate of 50 rpm maintains this noise level at a minimum to allow for measurement of as little as 8.56 mg of chlordiazepoxide (Fig. 6A). A stirring rate of 100 rpm produces an unacceptably low signal to noise ratio, which prevents measurement of low concentrations (10–50 mg), but it can be used with formulations containing levels of active ingredients in excess of 100 mg. The collision of suspended particles with the dropping mercury electrode introduces only slight disturbances to the reduction signal. The determination of formulation content in the noninvasive mode is performed without stirring after completion of the dissolution of the drug. A more stable signal results without the stirring action, so a higher degree of precision and accuracy is obtained. This effect can be attributed to the elimination of the vortex action of the stirrer and/or sedimentation of the particulate matter.

The current measured in the invasive mode is controlled by a laminar type of flow of material past the electrode surface, which shows little turbulance and is virtually free of noise. Particles that might block the flowcell or disrupt the flow are excluded *via* the use of the filter stick. Thus, measurement of drug dissolution can be carried out at both 50 and 100 rpm and with formulations below 10 mg. The resultant dissolution curves obtained in the invasive mode (see Fig. 6B for the determination of chlordiazepoxide) are easier to interpret than from the noninvasive mode. In the invasive mode, formulation content measurement is performed with the stirrer operational and the dissolution medium contin-

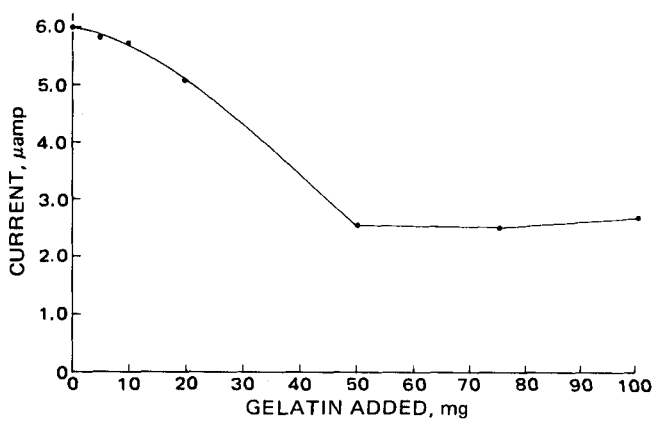

Figure 7—*Effect of gelatin on the polarographic reduction of chlordiazepoxide.*

Table III—Dissolution Characteristics: Mean Time (Minutes ± *SD*) for 25, 50, and 75% Dissolution (t_{25}, t_{50}, and t_{75}, Respectively)

Formulation	Noninvasive				Invasive			
	t_{25}	t_{50}	t_{75}	n[a]	t_{25}	t_{50}	t_{75}	n
I	8.56 ± 0.76	13.1 ± 1.7	18.5 ± 2.9	7	6.00 ± 0.61	9.17 ± 1.4	15.1 ± 2.8	4
II	6.83 ± 0.55	11.3 ± 1.8	19.4 ± 3.2	4	6.00 ± 1.0	10.6 ± 1.5	17.2 ± 2.4	4
III	6.20 ± 0.77	13.1 ± 1.6	24.4 ± 2.7	5	9.3 ± 2.3	17.5 ± 3.2	29.8 ± 6.0	6
IV	3.83 ± 0.50	6.46 ± 0.82	8.23 ± 1.0	6	5.23 ± 1.1	7.10 ± 1.0	9.98 ± 1.1	5

[a] Number of replicate samples assayed.

Table IV—Determination of Formulation Content

Compound	Invasive		Noninvasive	
	% of Claim ± *SD*	n[a]	% of Claim ± *SD*	n
I	97.7 ± 3.2	5	99.5 ± 3.3	7
II	96.6 ± 1.1	5	99.4 ± 3.0	8
III	98.2 ± 2.8	6	97.9 ± 0.74	5
IV	92.1 ± 2.0	5	90.9 ± 1.7	6

[a] Number of replicate samples assayed.

uously pumped through the flowcell to ensure electrical continuity.

Compounds I–IV were selected for this experiment because they contained different reducible functional groups, thus demonstrating the utility of the polarographic method over a wide range of concentrations (10–500 mg/sample), and because they were completely soluble in the dissolution medium.

Compound I was formulated as a 10-mg gelatin capsule[20]. Chlordiazepoxide has three electrochemically reducible functional groups—*viz.*, the 1,2- and 4,5-azomethine and N^4-oxide bonds (8). The reduction of the 4,5-azomethine bond, which is the most sensitive and easily measured, was used for drug dissolution studies. The gelatin in capsules is a natural surfactant and will affect the dropping mercury electrode. Small amounts of gelatin (approximately 0.003%) are widely used for suppression of surface effects on the mercury drop called maxima (9). Since these same surfactants can also suppress the polarographic reduction curve, their concentration in drug dissolution determinations must be held constant.

The effect of adding varying amounts of gelatin, from 5 to 100 mg, on the reduction current of 8.92 mg of chlordiazepoxide was determined (Fig. 7). The data indicated that the addition of gelatin resulted in a progressive decline in the reduction current until a total of 50 mg was added; a constant plateau was noted in the region of 50–75 mg of gelatin added. Since the No. 2 capsule used in the chlordiazepoxide formulation weighed about 40 mg, an additional 20 mg of gelatin was added to ensure constant suppression. Consequently, a total of 60 mg of gelatin was added to the dissolution medium for the measurement of standards of chlordiazepoxide.

Compound II was formulated as a 500-mg tablet. The compound demonstrates polarographic activity due to the reduction of the nitro functional group (10). At the high concentration encountered for the analysis of these tablets, a polarographic maximum was noted (9). This phenomenon was demonstrated in the form of exaggerated and distorted differential pulse polarographic peaks, which invalidated peak height measurement. The addition of 25 mg of gelatin eliminated peak distortion and simplified peak height measurement.

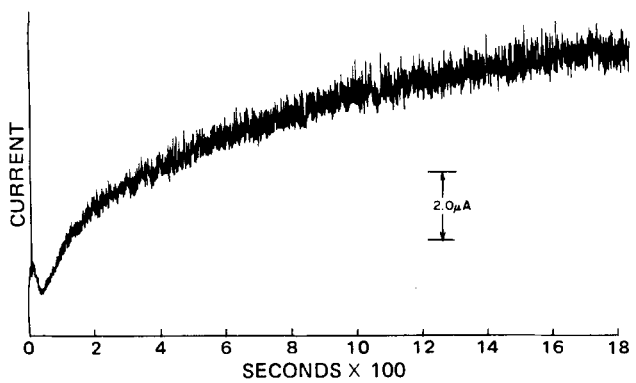

Figure 8—*Dissolution curve of trimethoprim.*

[20] Librium is the hydrochloride salt of chlordiazepoxide.

Compound III was formulated as a 100-mg tablet. The compound demonstrates polarographic activity due to the reduction of the azomethine groups in the pyrimidine ring (11). The use of differential pulse polarography for the assay of this compound is not feasible because the reduction is a two-step process in which the close proximity of the reduction potentials results in overlapping peaks. By using sampled dc polarography, a current is obtained that equals the summation of the two-step reduction process and yields a signal proportional to concentration.

The drug dissolution curve for trimethoprim employing both the invasive and noninvasive modes demonstrated a characteristic dip at the beginning of the dissolution curve (Fig. 8). The phenomenon was not noted with the assay of a placebo. Although no definite explanation for this phenomenon is known, it may be related to large changes in concentration that occur at the onset of the assay, with resultant surface effects at the dropping mercury electrode. The shape of the curve did not invalidate drug dissolution measurements made by extrapolating the baseline from the lowest portion of the dip.

Compound IV also was formulated as a 100-mg tablet. The polarographic reduction yields four peaks (Fig. 9). The first is due to the reduction of the hydrazide moiety, and the second and third are due to the stepwise reduction of the carbonyl group (12). The fourth peak is probably due to the reduction of the azomethine bond in the pyridine ring. The choice of the second peak (E_p = −0.685 v *versus* saturated calomel electrode) for analytical measurement was based upon the ease of measurement at that peak potential as well as its higher relative sensitivity.

Table III indicates that both the noninvasive and invasive method of polarographic drug dissolution yielded essentially the same values for the four drugs tested. The tablet to tablet variability (standard deviation) using either technique gave similar results.

All four formulations were tested for drug content. Comparisons were made with standard data on potency such as the content uniformity specifications outlined in the USP. All four formulations fell well within the content uniformity specifications as shown in Table IV. Formulation content measurements were also performed on the same samples of II and IV by polarography (noninvasive) and UV spectrophotometry (discrete sampling). The UV analysis of II and IV required dilution by factors of 1:100 and 1:25, respectively, to bring the absorbance values within the usable range of the spectrophotometer. This requirement further demonstrates the utility of the wide linear dynamic range of the polarographic method, which requires no dilutions to measure these concentrations. Table V indicates that essentially identical results are obtained using either technique.

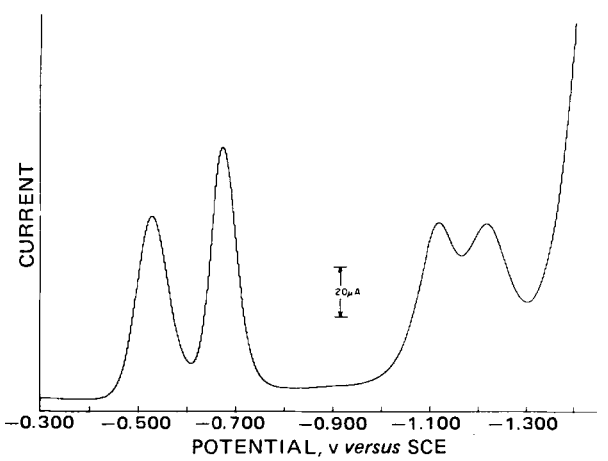

Figure 9—*Differential pulse polarogram of isoniazid (333 μg/ml in 0.1 N HCl).*

Table V—Formulation Content Determined by UV Spectrophotometry and Differential Pulse Polarography

Tablet	Concentration by UV, mg	Concentration by Differential Pulse Polarography, mg
Orindazole		
1	501.9	507.0
2	518.2	519.2
3	498.5	502.4
Mean ± *SD*	506.4 ± 11.3	509.5 ± 9.2
Isoniazid		
1	93.56	92.50
2	97.69	96.25
3	96.75	95.88
Mean ± *SD*	96.0 ± 1.77	94.9 ± 1.26

CONCLUSION

Polarographic measurement of drug dissolution and formulation content of four different drug formulations demonstrated the utility of polarography to provide such data with high accuracy and precision. The technique provides for measurement of compounds with varied chemical structures contained in formulations covering a wide range of concentrations and in the presence of excipients. The tapered dropping mercury electrode served as an excellent sensor for noninvasive measurements, thereby precluding the use of flowcells, transfer lines, and pumps as well as simplifying the calculation of data. Invasive measurements were also made by incorporating the dropping mercury electrode into a specially designed flowcell to obtain continuously sampled polarographic data.

REFERENCES

(1) P. Zuman and M. Brezina, in "Progress in Polarography," vol. II, P. Zuman and I. M. Kolthoff, Eds., Interscience, New York, N.Y., 1962.

(2) H. Hoffmann and J. Volke, in "Electroanalytical Chemistry," vol. 10 in the series "Advances in Analytical Chemistry and Instrumentation," H. W. Nurnberg, Ed., Wiley, London, England, 1974.

(3) J. A. F. de Silva and M. A. Brooks, in "Drug Fate and Metabolism," vol. 2, E. R. Garrett and J. L. Hirtz, Eds., Dekker, New York, N.Y., 1978.

(4) M. A. Brooks, J. A. F. de Silva, and M. R. Hackman, *Am. Lab.*, **5** (9), 23 (1973).

(5) Z. Feher, G. Nagy, K. Toth, and E. Pungor, *Analyst*, **99**, 699 (1974).

(6) C. A. Gaglia, Jr., J. J. Lomner, B. L. Leonard, and L. Chafetz, *J. Pharm. Sci.*, **65**, 1691 (1976).

(7) G. Levy and B. A. Hayes, *N. Engl. J. Med.*, **262**, 1053 (1960).

(8) M. R. Hackman, M. A. Brooks, J. A. F. de Silva, and T. S. Ma, *Anal. Chem.*, **46**, 1075 (1974).

(9) L. Meites, in "Polarographic Techniques," 2nd ed., Interscience, New York, N.Y., 1965.

(10) M. A. Brooks, L. D'Arconte, and J. A. F. de Silva, *J. Pharm. Sci.*, **65**, 112 (1976).

(11) M. A. Brooks, J. A. F. de Silva, and L. M. D'Arconte, *Anal. Chem.*, **45**, 263 (1973).

(12) Y. P. Kitaev and G. K. Budnikov, *Bull. Acad. Sci. USSR, Div. Chem. Sci.*, **1967**, 535.

Functional Group Contribution of Bile Salt Molecules to Partitioning of a Quaternary Ammonium *N*,*N*-Dimethyl Derivative of Propranolol

H. K. LEE ˣ, Y. W. CHIEN, T. K. LIN, and H. J. LAMBERT

Received July 28, 1977, from *Searle Laboratories, G. D. Searle & Co., Skokie, IL 60076.* Accepted for publication October 12, 1977.

Abstract □ A quaternary ammonium *N*,*N*-dimethyl derivative of propranolol was extracted from pH 7.4 phosphate buffer into 1-octanol as ion-pairs with 12 different bile salts. The binding number, n, and the extraction constant, K_e, were determined. To obtain group contribution values of the bile salt molecule from the ion-pair extraction data, multiple linear regression analysis by the Free–Wilson technique was applied. The results showed that the fundamental premise of the functional group's contribution to the ion-pair extraction is valid. The functional groups of counterions contribute to the partitioning of the ammonium compound independently and additively in this system.

Keyphrases □ Bile salt molecules—functional group contribution to ion-pair partitioning of quaternary ammonium derivative of propranolol □ Quaternary ammonium salts—*N*,*N*-dimethyl derivative of propranolol, ion-pair partitioning, functional group contribution of bile salt molecules □ Ion-pair partitioning—*N*,*N*-dimethyl derivative of propranolol, functional group contribution of bile salt molecules

The effect of the structure of the pairing ion on quaternary ammonium compounds has received considerable attention (1). Partitioning of organic salts or complexes was reported to be influenced by the molecular weight of the organic ions, the branching effect of the aliphatic amine cations, and the organic solvent (2, 3).

A comprehensive group contribution study based on partition coefficient measurement was presented (4). From the consistency of the thermodynamic data, it was concluded that ion-pair extraction equilibria provide a feasible method for determining group contribution. The use, with some limitations, of ion-pair extraction data to obtain group contribution values was demonstrated (5).

The *N*,*N*-dimethyl derivative of propranolol chloride, *N*,*N*-dimethyl-1-isopropylamino-3-(1-naphthyloxy)-2-propanol chloride (I), has antiarrhythmic activity without significant β-blocking and local anesthetic effects (6). In general, quaternary ammonium compounds are absorbed poorly from the GI tract because of their cationic nature (7). This poor absorption might be circumvented if the cationic nature of the onium head could be masked by ion-pair formation. The present investigation studied the interaction between I and bile salt molecules by the group

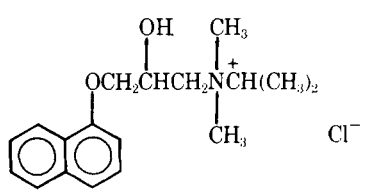

I

Table V—Formulation Content Determined by UV Spectrophotometry and Differential Pulse Polarography

Tablet	Concentration by UV, mg	Concentration by Differential Pulse Polarography, mg
Orindazole		
1	501.9	507.0
2	518.2	519.2
3	498.5	502.4
Mean ± *SD*	506.4 ± 11.3	509.5 ± 9.2
Isoniazid		
1	93.56	92.50
2	97.69	96.25
3	96.75	95.88
Mean ± *SD*	96.0 ± 1.77	94.9 ± 1.26

CONCLUSION

Polarographic measurement of drug dissolution and formulation content of four different drug formulations demonstrated the utility of polarography to provide such data with high accuracy and precision. The technique provides for measurement of compounds with varied chemical structures contained in formulations covering a wide range of concentrations and in the presence of excipients. The tapered dropping mercury electrode served as an excellent sensor for noninvasive measurements, thereby precluding the use of flowcells, transfer lines, and pumps as well as simplifying the calculation of data. Invasive measurements were also made by incorporating the dropping mercury electrode into a specially designed flowcell to obtain continuously sampled polarographic data.

REFERENCES

(1) P. Zuman and M. Brezina, in "Progress in Polarography," vol. II, P. Zuman and I. M. Kolthoff, Eds., Interscience, New York, N.Y., 1962.

(2) H. Hoffmann and J. Volke, in "Electroanalytical Chemistry," vol. 10 in the series "Advances in Analytical Chemistry and Instrumentation," H. W. Nurnberg, Ed., Wiley, London, England, 1974.

(3) J. A. F. de Silva and M. A. Brooks, in "Drug Fate and Metabolism," vol. 2, E. R. Garrett and J. L. Hirtz, Eds., Dekker, New York, N.Y., 1978.

(4) M. A. Brooks, J. A. F. de Silva, and M. R. Hackman, *Am. Lab.*, **5** (9), 23 (1973).

(5) Z. Feher, G. Nagy, K. Toth, and E. Pungor, *Analyst*, **99**, 699 (1974).

(6) C. A. Gaglia, Jr., J. J. Lomner, B. L. Leonard, and L. Chafetz, *J. Pharm. Sci.*, **65**, 1691 (1976).

(7) G. Levy and B. A. Hayes, *N. Engl. J. Med.*, **262**, 1053 (1960).

(8) M. R. Hackman, M. A. Brooks, J. A. F. de Silva, and T. S. Ma, *Anal. Chem.*, **46**, 1075 (1974).

(9) L. Meites, in "Polarographic Techniques," 2nd ed., Interscience, New York, N.Y., 1965.

(10) M. A. Brooks, L. D'Arconte, and J. A. F. de Silva, *J. Pharm. Sci.*, **65**, 112 (1976).

(11) M. A. Brooks, J. A. F. de Silva, and L. M. D'Arconte, *Anal. Chem.*, **45**, 263 (1973).

(12) Y. P. Kitaev and G. K. Budnikov, *Bull. Acad. Sci. USSR, Div. Chem. Sci.*, **1967**, 535.

Functional Group Contribution of Bile Salt Molecules to Partitioning of a Quaternary Ammonium *N*,*N*-Dimethyl Derivative of Propranolol

H. K. LEE ˣ, Y. W. CHIEN, T. K. LIN, and H. J. LAMBERT

Received July 28, 1977, from *Searle Laboratories, G. D. Searle & Co., Skokie, IL 60076.* Accepted for publication October 12, 1977.

Abstract □ A quaternary ammonium *N*,*N*-dimethyl derivative of propranolol was extracted from pH 7.4 phosphate buffer into 1-octanol as ion-pairs with 12 different bile salts. The binding number, n, and the extraction constant, K_e, were determined. To obtain group contribution values of the bile salt molecule from the ion-pair extraction data, multiple linear regression analysis by the Free–Wilson technique was applied. The results showed that the fundamental premise of the functional group's contribution to the ion-pair extraction is valid. The functional groups of counterions contribute to the partitioning of the ammonium compound independently and additively in this system.

Keyphrases □ Bile salt molecules—functional group contribution to ion-pair partitioning of quaternary ammonium derivative of propranolol □ Quaternary ammonium salts—*N*,*N*-dimethyl derivative of propranolol, ion-pair partitioning, functional group contribution of bile salt molecules □ Ion-pair partitioning—*N*,*N*-dimethyl derivative of propranolol, functional group contribution of bile salt molecules

The effect of the structure of the pairing ion on quaternary ammonium compounds has received considerable attention (1). Partitioning of organic salts or complexes was reported to be influenced by the molecular weight of the organic ions, the branching effect of the aliphatic amine cations, and the organic solvent (2, 3).

A comprehensive group contribution study based on partition coefficient measurement was presented (4). From the consistency of the thermodynamic data, it was concluded that ion-pair extraction equilibria provide a feasible method for determining group contribution. The use, with some limitations, of ion-pair extraction data to obtain group contribution values was demonstrated (5).

The *N*,*N*-dimethyl derivative of propranolol chloride, *N*,*N*-dimethyl-1-isopropylamino-3-(1-naphthyloxy)-2-propanol chloride (I), has antiarrhythmic activity without significant β-blocking and local anesthetic effects (6). In general, quaternary ammonium compounds are absorbed poorly from the GI tract because of their cationic nature (7). This poor absorption might be circumvented if the cationic nature of the onium head could be masked by ion-pair formation. The present investigation studied the interaction between I and bile salt molecules by the group

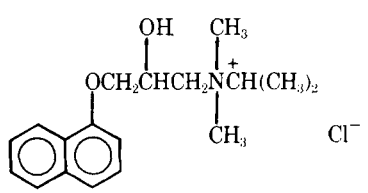

I

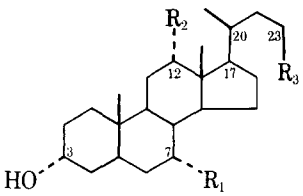

II–XIII: R_1 = R_2 = H or OH, R_3 = COONa, $CONHCH_2COONa$, or $CONHCH_2CH_2SO_3Na$

contribution approach, because group contribution data of the bile salt molecules (II) might be used to design a system to enhance the bioavailability of I.

EXPERIMENTAL

Material—Twelve different bile salts[1] and I[2] were used as received. Grade 1 (99% pure) 1-octanol[3] was the organic phase in the partitioning studies.

Partition Studies—Octanol saturated with pH 7.4 phosphate buffer and pH 7.4 phosphate buffer saturated with octanol were used. The bile salts and I were dissolved in pH 7.4 phosphate buffer (0.1 *M*). The I concentration was kept constant at 10^{-4} *M*, with only the bile salt concentration being varied between 10^{-4} and 10^{-3} *M*. A 10-ml aliquot of each aqueous buffer solution containing I, the bile salt, and octanol was placed in a screw-capped test tube and vigorously agitated for 2 min[4].

The aqueous layer was withdrawn by syringe and centrifuged at 1000 rpm for 20 min. The I concentration in the aqueous phase before and after partitioning was measured spectrophotometrically at λ_{max} 292 nm, and the apparent distribution constant of I was then calculated.

RESULTS AND DISCUSSION

Extraction Constant—The extraction constant was derived using the assumptions that the bile salt existed as the ion-pair with the quaternary ammonium ion in the organic phase, the cation and anion were completely dissociated in the aqueous phase (8, 9), and the concentration of the free anion of the bile salt in the organic phase was negligible compared with that of the free anion in the aqueous phase. The extraction of quaternary cation into the organic phase may be represented by Schemes I and II:

$$[A^+]_{aq} + n[B^-]_{aq} \overset{K_e}{\rightleftharpoons} [AB_n]_{org}$$

Scheme I

$$[A^+]_{aq} \overset{K_0}{\rightleftharpoons} [A^+]_{org}$$

Scheme II

where $[A^+]_{aq}$ represents the quaternary cation in the aqueous phase, $[A^+]_{org}$ is the quaternary cation in the organic phase, $[B^-]_{aq}$ is the anion in the aqueous phase, $[AB_n]_{org}$ is the ion-pair in the organic phase, n is the binding number of the anion against 1 mole of the quaternary cation, K_0 is the extraction constant for partitioning of the quaternary cation into the organic phase, and K_e is the extraction constant for partitioning of the ion-pair into the organic phase.

The apparent distribution constant of the quaternary ammonium compound, D_Q, measured experimentally, is defined as:

$$D_Q = \frac{[A_t]_{org}}{[A^+]_{aq}} = \frac{[AB_n]_{org} + [A^+]_{org}}{[A^+]_{aq}} \qquad \text{(Eq. 1)}$$

where the total concentration of A in the organic phase, $[A_t]_{org}$, is the sum of $[AB_n]_{org}$ and $[A^+]_{org}$.

The mathematical expression for the extraction constant, K_e, is:

$$K_e = \frac{[AB_n]_{org}}{[A^+]_{aq}[B^-]^n_{aq}} \qquad \text{(Eq. 2)}$$

[1] A grade, Calbiochem, San Diego, CA 92112.
[2] Provided by Chemical Development Group, Searle Laboratories.
[3] Aldrich Chemical Co., Milwaukee, WI 53233.
[4] Two minutes of vigorous agitation with a Vortex G mixer (Scientific Products, McGaw Park, Ill.) yielded better extraction of I than overnight shaking with a wrist-action mechanical shaker (model S-500, Kraft Apparatus, Mineola, N.Y.).

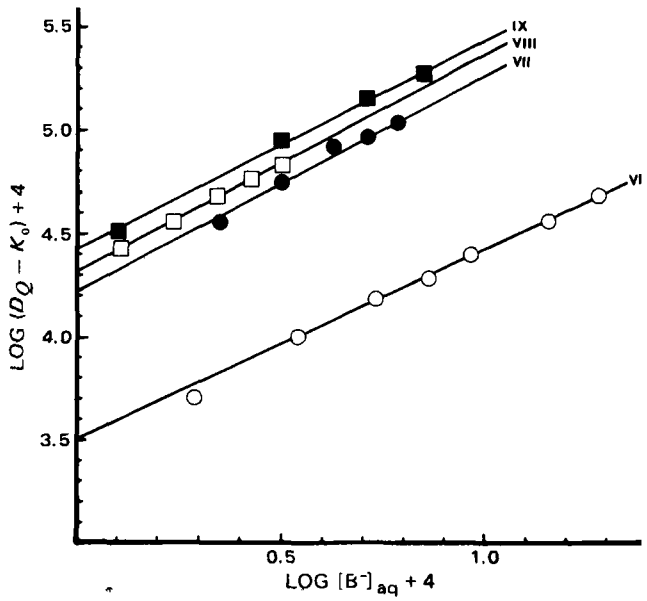

Figure 1—*Log-log plots of the distribtuion ratio of the ion-pair in the organic phase and of I in the aqueous phase, ($D_Q - K_0$), to the concentration of the glycocholic acid derivatives in the aqueous phase, $[B^-]_{aq}$. Key: VI, glycocholate; VII, glycochenodeoxycholate; VIII, glycodeoxycholate; and IX, glycolithocholate.*

Equation 2 may be expressed in the logarithmic form as:

$$\log K_e = \log \frac{[AB_n]_{org}}{[A^+]_{aq}} - n \log [B^-]_{aq} \qquad \text{(Eq. 3)}$$

Combining Eqs. 3 and 1 and rearranging give:

$$\log (D_Q - K_0) = \log K_e + n \log [B^-]_{aq} \qquad \text{(Eq. 4)}$$

The binding number, n, of the anion and the extraction constant, K_e, can be estimated from the slope of the line and antilog of the intercept value obtained by plotting $\log (D_Q - K_0)$ *versus* $\log [B^-]_{aq}$. The plots of some data are presented in Figs. 1 and 2, and n and K_e values are listed in Table I.

All systems followed a good linear relationship, as defined by Eq. 4,

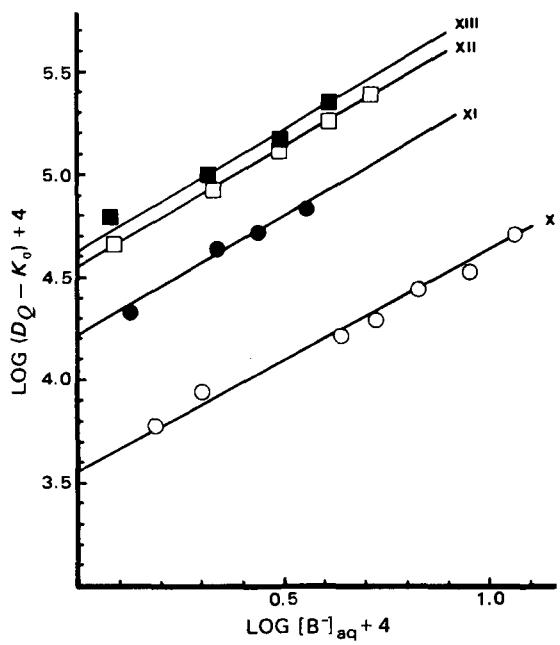

Figure 2—*Log-log plots of the distribution ratio of the ion-pair in the organic phase and of I in the aqueous phase, ($D_Q - K_0$), to the concentration of the taurocholic acid derivatives in the aqueous phase, $[B^-]_{aq}$. Key: X, taurocholate; XI, taurochenodeoxycholate; XII, taurodeoxycholate; and XIII, taurolithocholate.*

Table I—Structures of Bile Salts, Ion-Pair Extraction Constant, K_e, and Binding Number, n

Number	Bile Salt	R_1	R_2	R_3	K_e	n
II	Cholate	OH	OH	COO^-	1.375×10^3	0.97
III	Chenodeoxycholate	OH	H	COO^-	1.652×10^3	0.91
IV	Deoxycholate	H	OH	COO^-	1.862×10^3	0.98
V	Lithocholate	H	H	COO^-	1.742×10^3	0.94
VI	Glycocholate	OH	OH	$CONHCH_2COO^-$	2.716×10^3	0.98
VII	Glycochenodeoxycholate	OH	H	$CONHCH_2COO^-$	1.694×10^4	1.06
VIII	Glycodeoxycholate	H	OH	$CONHCH_2COO^-$	2.143×10^4	1.01
IX	Glycolithocholate	H	H	$CONHCH_2COO^-$	2.570×10^4	1.02
X	Taurocholate	OH	OH	$CONH(CH_2)_2SO_3^-$	3.972×10^3	0.98
XI	Taurochenodeoxycholate	OH	H	$CONH(CH_2)_2SO_3^-$	1.660×10^4	0.94
XII	Taurodeoxycholate	H	OH	$CONH(CH_2)_2SO_3^-$	3.672×10^4	1.13
XIII	Taurolithocholate	H	H	$CONH(CH_2)_2SO_3^-$	4.813×10^4	1.01

and these slopes, n, were close to unity. Therefore, the initial assumptions are valid. The interaction between I and bile salt is a 1:1 ion-pair formation, so any contribution from 1:2 or 1:3 binding in the aqueous or organic phase would be negligible. Since micellization of bile salts in an aqueous solution can occur (9), the bile salt concentration in this study was far below the critical micelle concentration to avoid micelle formation.

Functional Group Contribution—The mathematical model developed by Free and Wilson (10) to study structure–activity relationships is applicable to analogous series of compounds with corresponding activity data. The Free–Wilson model is based on the assumption that each substituent makes an additive and constant contribution to the activity and is expressed by:

$$\text{activity (linear or log values)} = \mu + \sum_{ij} G_{ij}X_{ij} \qquad \text{(Eq. 5)}$$

where μ is the overall average of activity of the parent skeleton and G_{ij} is the activity contribution of the substituent X_i in position j ($X_{ij} = 1$ if the substituent X_i is in position j; otherwise, $X_{ij} = 0$).

A procedure similar to the Free–Wilson method was used to determine the group contribution of all respective substituents of the bile salts by ion-pair formation with the quaternary ammonium compound. All activities were expressed as log K_e, and μ was assigned the value of the parent molecule. As a limiting condition, the group contribution for a hydrogen substituent at any position was assigned a value of zero.

Table II—Structural Matrix and Log Extraction Constant of the Ion-Pair for Observed and Calculated Values

Bile Salt[a]	R_1, OH	R_2, OH	R_3[b] A	B	C	Log K_e Observed	Calculated[c]
II	1	1	1	0	0	3.175	2.959
III	1	0	1	0	0	3.218	3.164
IV	0	1	1	0	0	3.270	3.289
V	0	0	1	0	0	3.241	3.493
VI	1	1	0	1	0	3.434	3.834
VII	1	0	0	1	0	4.229	4.039
VIII	0	1	0	1	0	4.331	4.163
IX	0	0	0	1	0	4.410	4.368
X	1	1	0	0	1	3.599	3.998
XI	1	0	0	0	1	4.220	4.202
XII	0	1	0	0	1	4.565	4.327
XIII	0	0	0	0	1	4.684	4.532

[a] Each bile salt number corresponds to those given in Table I. [b] A, B, and C at R_3 were COO^-, $CONHCH_2COO^-$, and $COHN(CH_2)_2SO_3^-$, respectively. [c] Calculated by multiple linear regression analysis.

Table III—Group Contribution of Substituents and Overall Average Activity of Parent Skeleton, μ, Calculated by Free–Wilson Technique

Substituent	Group Contribution
7α-OH	−0.329
12α-OH	−0.205
23-COO^-	0.117
23-$CONHCH_2COO^-$	0.992
23-$CONH(CH_2)SO_3^-$	1.156
μ	3.376

The hydrogens of the groups at the 7- (R_1) and 12- (R_2) positions were not included in the matrix. However, the hydrogens at the 23-position (R_3) were entered as log K_e = 0, 0, 0, and 0, and the sum of the group contribution for A, B, C, and H at R_3 was set at zero. In this way, the group contribution values of A, B, and C became positive contribution values because the formation of the ion-pair between the negatively charged R_3 and the positively charged quaternary ammonium head should enhance the partitioning of I into the organic phase.

It was necessary to calculate the contribution values for the five functional groups and the parent compound. The 17 simultaneous equations with seven unknowns were solved by multiple linear regression analysis. The 12 bile salts and their log K_e values are presented in Table II, and functional group contributions are shown in Table III. The results of statistical analysis showed that the multiple correlation coefficient of the regression was 0.994 and the standard deviation was 0.27. The F test proved significant at a 99% confidence level, and 98% of the variance was explained.

Comparison of the functional group contribution values (Table III) shows that the significant activity enhancement groups are conjugated glycine (B) and taurine (C) groups, which increase the activity by a factor of 10 over a single carboxylate ion (A). This result suggests that the terminal positive quaternary nitrogen of I is more effectively shielded by a conjugated glycine or conjugated taurine moiety to give a neutral species by electrostatic interaction than is a simple carboxylate ion.

The activity-lowering group seems to be the hydroxyl group at the 7α- and 12α-positions. When both 7α-OH and 12α-OH are present, the partitioning activity is substantially reduced, probably because of the steric hindrance effect of 7α-OH and 12α-OH on the hydrophobic interaction between the steroid skeleton of bile salts and the aromatic portion of I, in addition to the hydrogen bonding effect of the hydroxyl group.

These results show that the functional groups contribute to the total activity almost independently and additively in this system. This approach utilizes an extrathermodynamic property that has linear free energy relationships. Thus, the total free energy change of the process is the sum of the independent contributions from the functional groups in this system. These findings also suggest that ion-pair extraction varying with the functional groups of counterion molecules can be applicable to the group contribution approach to enhance the bioavailability of a quaternary ammonium compound.

REFERENCES

(1) S. S. Davis, T. Higuchi, and J. H. Rytting, in "Advances in Pharmaceutical Sciences," vol. 4, H. S. Bean, A. H. Beckett, and J. E. Carless, Eds., Academic, New York, N.Y., pp. 73–261.

(2) G. J. Divata and J. A. Biles, *J. Pharm. Sci.*, **50**, 916 (1961).

(3) R. L. Hull and J. A. Biles, *ibid.*, **53**, 869 (1964).

(4) M. J. Harris, T. Higuchi, and J. H. Rytting, *J. Phys. Chem.*, **77**, 2694 (1973).

(5) H. L. Fung and Y. H. Ow, *J. Pharm. Sci.*, **61**, 1967 (1972).

(6) D. P. Schuster, B. R. Lucches, N. L. Nobel, M. N. Mimnaugh, R. E. Counsell, and F. J. Rniffen, *J. Pharmacol. Exp. Ther.*, **184**, 213 (1973).

(7) R. R. Levine, M. R. Blair, and B. B. Clark, *ibid.*, **114**, 78 (1955); R. R. Levine and E. W. Pelikan, *ibid.*, **131**, 319 (1961); R. R. Levine and B. B. Clark, *ibid.*, **121**, 63 (1957); R. R. Levine, *ibid.*, **129**, 296 (1960).

(8) B. Fransson and G. Schill, *Acta Pharm. Suec.*, **12**, 107 (1975).

(9) D. M. Small, in "The Bile Acids," P. P. Nair and D. Kritchevsky, Eds., Plenum, New York, N.Y., 1971, p. 249.

(10) S. M. Free and J. W. Wilson, *J. Med. Chem.*, **7**, 395 (1964).

Hydrolysis and Subsequent Cyclization of Etazolate Hydrochloride and Related Compounds in Aqueous Solutions: Application of PMR and Mass Spectrometry in Accelerated Stability Studies

MOHINDAR S. PUAR, PHILLIP T. FUNKE, and ALLEN I. COHEN ˣ

Received May 23, 1977, from the *Squibb Institute for Medical Research, Princeton, NJ 08540.* Accepted for publication October 19, 1977.

Abstract □ The hydrolysis of etazolate hydrochloride, an inhibitor of cyclic nucleotide 3′,5′-monophosphate phosphodiesterase that degrades cyclic adenosine 3′,5′-monophosphate (cyclic AMP) to adenosine 5′-monophosphate, and related compounds was studied by PMR and mass spectrometry. The compounds underwent reversible acid-catalyzed hydrolysis in aqueous solutions at 60°, followed by cyclization to a major and a minor product formed by independent pathways. Under the experimental conditions, the minor product was stable. The formation rate of the major product, 6-ethyl-1,6-dihydrodipyrazolo[3,4-*b*:3′,4′-*d*]pyridin-3(2*H*)-one, was considerably greater than that of the minor component, 3-ethoxy-6-ethyl-1,6-dihydrodipyrazolo[3,4-*b*:3′,4′-*d*]pyridine. For the 6-methyl analog of etazolate, the rate of methyl deuteration was considerably slower than the rate of cyclization.

Keyphrases □ Etazolate hydrochloride—hydrolysis in aqueous solutions, PMR and mass spectral stability studies □ Hydrolysis—etazolate hydrochloride in aqueous solutions, PMR and mass spectral stability studies □ Stability—etazolate hydrochloride in aqueous solutions, PMR and mass spectral studies □ Tranquilizers—etazolate hydrochloride, hydrolysis in aqueous solutions, PMR and mass spectral stability studies

NMR and mass spectrometry have been employed extensively to monitor the aqueous stability of pharmacologically active compounds (1). The usual procedure involves monitoring the PMR spectra of acidic, basic, and neutral aqueous solutions kept at 60–65° over 4–5 days. Gross changes in the PMR spectra permit the identification of degradation products.

Information obtained under these drastic conditions is useful in designing bulk stability and preformulation studies. Indeed, many compounds are stable under these conditions and as well in the subsequent bulk and formulation stability studies. The aqueous stability of an inhibitor of cyclic nucleotide 3′,5′-monophosphate phosphodiesterase, etazolate[1] [ethyl 1-ethyl-4-(isopropylidenehydrazino)-1*H*-pyrazolo[3,4-*b*]pyridine-5-carboxylate] hydrochloride (I), and related 1*H*-pyrazolo[3,4-*b*]pyridines[2] (2) is reported to demonstrate the utility of the approach in establishing the degradation rate and identification of products formed during the aqueous hydrolysis of I.

EXPERIMENTAL

PMR spectra were obtained on a 100-MHz NMR spectrometer[3], which was internally locked to the ^{2}H-frequency of 15.4 MHz. PMR data in aqueous solutions and in dimethyl sulfoxide-d_6 are presented in Tables I and II, respectively. Low- and high-resolution mass spectra were taken on a double-focusing mass spectrometer[4] using a direct insertion probe. Data were acquired *via* frequency-modulated analog tape, which was subsequently processed with the aid of a computer[5] using published programs (6). The pH or pD values were measured with a pH meter[6] with combination pH electrodes.

The calculations were performed by measuring the areas under the respective resonances in the PMR spectra of solutions of known concentrations:

$$\%\ \text{hydrolysis} = \frac{\text{area under acetone resonance} \times 100}{\text{area under acetone resonance} + \text{area under N=C(CH}_3)_2\ \text{group}} \quad \text{(Eq. 1)}$$

or:

$$\%\ \text{hydrolysis} = \frac{\text{area under acetone resonance} \times 100}{\text{area under N=C(CH}_3)_2\ \text{resonance at time 0}} \quad \text{(Eq. 2)}$$

$$\%\ \text{cyclization}^7 = \frac{\text{area under CH}_3\ \text{resonance of C}_2\text{H}_5\text{OD} \times 100}{0.5 \times \text{area of CH}_3\ \text{resonances at time 0}} \quad \text{(Eq. 3)}$$

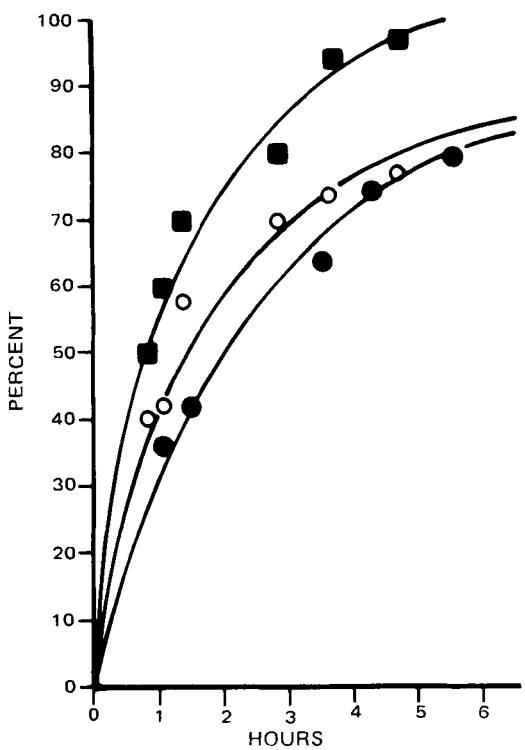

Figure 1—*Rates of hydrolysis [■, loss of N=C(CH$_3$)$_2$ group] and cyclization (○, formation of C$_2$H$_5$OD) of II compared to the rate of cyclization (●, formation of C$_2$H$_5$OD) of V at 65° in aqueous acidic (pH 1.5) solutions.*

[1] SQ20009, E. R. Squibb and Sons, Princeton, N.J.

[2] The compounds, prepared by Dr. H. Höhn, Dr. T. Denzel, and Dr. W. Janssen (3–5), were supplied through the Squibb chemical distribution center and represented typical batches used in clinical and formulation studies.

[3] Varian Associates model XL-100-15.

[4] Associated Electrical Industries model M-902.

[5] Digital Equipment Corp. model PDP-11.

[6] Orion Research model 701.

[7] Conceivably, the rates of ester hydrolysis and cyclization are similar. However, no XIV was found when IV was reacted (Scheme I). Perhaps the nucleophilic attack by the hydrazino group facilitates the cyclization, with a concurrent loss of the ester group. Additionally, the percentage cyclization calculated from the area of the aromatic proton resonances of X, although producing less accurate data because of the errors in measuring a single proton, was comparable to the data obtained from the area measurements of liberated ethanol.

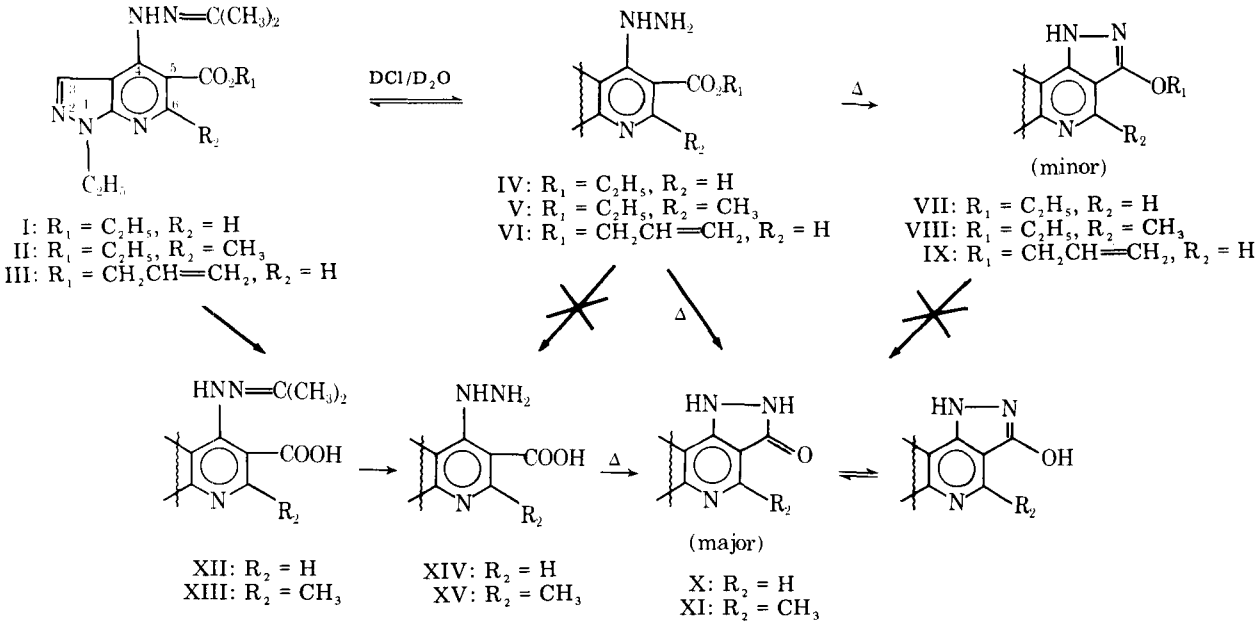

Scheme I

and:

$$\% \text{ deuteration} = \frac{\text{area under C-6 } CH_3 \text{ resonance} \times 100}{\text{area under C-6 } CH_3 \text{ resonance at time 0}} \qquad \text{(Eq. 4)}$$

The kinetic data (60°) are presented in Table III. The plots of log *c versus* time were linear and the slopes were calculated by the method of least squares with an error of ±25%. The pseudo-first-order rate constants for hydrolysis, k_H, cyclization, k_C, and deuteration, k_D, are presented in Table IV.

RESULTS AND DISCUSSION

Semicarbazones, oximes, and phenylhydrazones exist in equilibrium with their constituents in aqueous solutions (7). Similarly, isopropylidenes I–III (Scheme I) establish an acid-catalyzed equilibrium between I, II, or III and their respective hydrazides IV, V, or VI and acetone in deuterium oxide solutions.

The rate of liberation of acetone[8] from I–III was identical at similar concentrations and pH values[9]. Furthermore, the extent of hydrolysis of I–III or their formation from the corresponding hydrazides IV–VI and acetone was temperature dependent. Approximately 50% of I was converted to IV between 32 and 40°, but only 25% was hydrolyzed at 20°. Furthermore, I could be formed from IV and acetone[10]; *e.g.*, with acetone-d_6, 45% of I-d_6 was formed at 32° as determined by PMR and mass spectrometry. When nitrogen was bubbled through a solution of I for 7 hr, to remove liberated acetone from the solution, the PMR spectrum showed the formation of 50% IV.

At 65°, the PMR spectrum of a solution of I indicated the presence of secondary products. The structural elucidation of these products was initiated. The extent of the various products present was evaluated by measuring the relative areas under the various resonances. The formation of ethanol-d_1 C_2H_5OD was determined by measuring the areas of resonances at δ 3.58 (quartet) and 1.06 (triplet) ppm, comparing them to the ethyl proton resonances of I and IV occurring at the chemical shifts of δ 4.40 (quartet) and 1.45 (triplet) ppm. With the 6-methyl analog, II, the C-6 methyl proton resonance at δ 2.78 ppm was compared to the resonance at δ 2.7 ppm of a reaction product.

Although acetone generated from the hydrolysis of the isopropylidene group of I and II was present, neither of the respective hydrazides IV and V was observed. The cyclization rates of IV and V were subsequently shown to be reproducible, and IV and V form the same products that result from the heating of acidic solutions of I and II at 65°.

Scheme I represents the chemical transformations taking place at 65°. The pseudo-first-order rate constants are given in Table IV. The PMR spectra of the reaction products of I after drying indicated a major and a minor component. High-resolution mass spectrometry of the major component demonstrated the composition of a molecular ion (M^+) at *m/e* 203 to be C_9H_9NO. The structure of the major component was confirmed as X by comparison of its PMR and mass spectra with those of an authentic sample.

The diagnostic proton resonances in dimethyl sulfoxide-d_6 are δ 8.29 and 9.1 ppm for the heterocyclic protons, which are within the experimental error of authentic X (δ 8.24 and 9.03 ppm) (*cf.*, Table II). The mass spectrometric analysis of the products derived from IV show that X was the major product. A minor component (~10%) with an M^+ of *m/e* 231 was assigned Structure VII. In the acidic aqueous solution, this component had heterocyclic proton shifts of δ 8.04 and 8.63 ppm. The assignment of the fragmentation of the major product X and the minor product VII is shown in Scheme II.

The percent conversion of II to V and the subsequent cyclization of V to XI are shown as a function of time in Fig. 1. In deuterium oxide–deuterium chloride (pD 1), the isopropylidene group of a 5-mg/ml solution of II was completely hydrolyzed in 21.5 hr at 65°. Compound V subsequently formed two products. The PMR spectrum showed a shift of the heterocyclic proton from δ 8.53 to 8.0 ppm and of the pyridyl methyl from δ 2.84 to 2.62 ppm. The mass spectrum of the evaporated solution demonstrated that the major product was XI (the 6-methyl analog of X) and that the minor product was VIII (the 6-methyl analog of VII) along

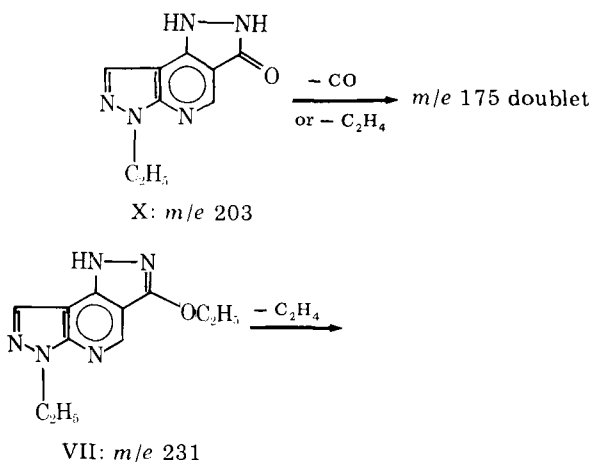

Scheme II

[8] The chemical shift of liberated acetone was indistinguishable from that of added acetone.

[9] Dr. D. A. Wadke, Squibb Institute for Medical Research, New Brunswick, N.J., personal communication.

[10] Acetone bound to IV does not exist in any substantial amount.

Table I—PMR Data in Aqueous Solutions [a]

Compound	Concentration, mg/ml	Solvent and pD	Chemical Shift of Proton, ppm					
			H_3	H_6	CH_2	CH_3	N=C-$(CH_3)_2$	CH_3 of Acetone
I	7	0.1 *N* DCl–D_2O, pD = 1.5	8.23	8.56	4.41 m	1.48 t 1.55 t	2.05 2.25	2.31
II	5	pD = 1	8.53	2.84	4.45 m	1.41 t 1.44 t	2.12 2.23	2.21
	10	pD = 1.9	8.39	2.77	4.40 m	1.43 t 1.46 t	2.05 2.22	2.20
III	8	pD = 1.3	8.24	8.58	4.36 q	1.45 t	1.99 2.17	2.20 (6.0, 5.4 CH=CH_2)
IV		0.01 *N* DCl–D_2O, pD = 1.5	8.67	8.73	4.38 q 4.40 q	1.44 t 1.49 t		
V	10	pD = 1.9	8.62	2.70	4.30 q 4.42 q	1.35 t 1.41 t		
VI		pD = 1.3	8.66	8.71	4.36 m	1.45 t		6.0, 5.4 CH=CH_2
VII		pD = 0.9	8.35	8.97	4.45 m	1.43 t 1.46 t		—[b]
X		pD = 2	8.15	8.72	4.43 q	1.45 t		—[c]
		0.1 *N* DCl–D_2O, pD = 2	8.01	8.59	4.48 q	1.45 t		—[b]
XI		pD = 1.9	7.98	2.62	4.36 q	1.45 t		—[d]
XII		0.1 *N* DCl–D_2O, pD = 2.0	8.57	8.75	4.42 q	1.55 t	2.15 2.25	2.31

[a] Parts per million from external 3-(trimethylsilyl)-1-propanesulfonic acid sodium salt. [b] Authentic sample. [c] Chemical shifts are the average of the chemical shifts of the products from I, III, IV, and XII. [d] Chemical shifts are the average of the product obtained from II and V.

Table II—PMR Data of 1*H*-Pyrazolo[3,4-*b*]pyridines in Dimethyl Sulfoxide-d_6 [a]

Compound	Chemical Shift, ppm					
	CH_2	CH_3	N=C$(CH_3)_2$	H_3	R_2	NH
I	4.35 q 4.49 q	1.37 t 1.42 t	2.04 2.19	8.46	8.65	11.58
II	4.38 q 4.57 q	1.36 t 1.40 t	2.07 2.19	8.53	2.83	11.56
IV	4.35 q 4.59 q	1.35 t 1.40 t		8.52	8.62	8.22
VII[b]	4.54 q	1.43 t		8.16	8.72	10.50
X[b]	4.60 q	1.44 t		8.24	9.03	9.07
X[c]	4.64 q	1.46 t		8.29	9.10	11.06
XI	4.47 q	1.43 t		8.03	2.79	11.52

[a] Parts per million from tetramethylsilane internal reference; q = quartet (J = 7 Hz) and t = triplet (J = 7 Hz). [b] Authentic sample prepared according to U.S. pat. 3,787,430 (Jan. 22, 1974), assigned to E. R. Squibb & Sons. [c] Sample obtained after heating an aqueous solution of I at 65° for 6 days and stripping off water. Traces of I were present.

with residual amounts of V. The fragmentation of VIII and XI (Scheme III) is analogous to the respective products VII and X.

The PMR spectra of a deuterium oxide–deuterium chloride (pD 1.3) solution of 9 mg of III/ml heated to 60° for 24 hr showed the complete loss of the isopropylidene group, at a rate six times slower than was observed for I and II. During the next 7 days, the resonances due to the allyl ester group slowly disappeared and the resonances of the major product appeared. The PMR and mass spectra of this degradation product were

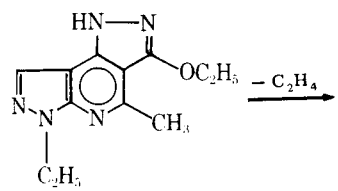

VIII: *m/e* 245

m/e 217 $\xrightarrow[\text{or} - C_2H_4]{-CO}$ *m/e* 189 doublet

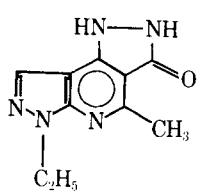

$\xrightarrow[\text{or} - C_2H_4]{-CO}$ *m/e* 189 doublet

XI: *m/e* 217

Scheme III

identical to those obtained from I and IV and the spectra of authentic X. The rate data indicate that the cyclization rate was somewhat slower for the allyl ester III than for the ethyl ester I, perhaps because the allyl group is somewhat more resistant to hydrolysis. In addition to X, the mass spectrum of the degradation product also indicated the presence of the minor product IX (M^+, *m/e* 243).

Mechanistic Pathways—While both the ester and isopropylidene groups were concurrently hydrolyzed in acidic media, the hydrolysis rate of the latter was much faster. On the other hand, when a large amount of I was hydrolyzed, small amounts of the isopropylidene acid XII (M^+, *m/e* 261) and the hydrazide acid XIV (M^+, *m/e* 221) were detected in the mass spectrum. No XIV was detected, however, when the hydrazide ester IV was reacted under the same conditions. Again, competitive cyclization rates precluded the formation of this compound in any appreciable amount.

To establish the pathway for the formation of X from XII, an authentic sample of XII, the free acid of I, was dissolved in deuterium oxide–deuterium chloride and heated for 2 weeks. The chemical shifts of the product of δ 8.23, 8.80, 4.40, and 1.51 ppm were comparable to those of authentic X. While **X** was the major reaction product, the mass spectra also indicated the presence of small amounts of XIV (M^+, *m/e* 221). The cyclized product, X, was formed after hydrolysis of the isopropylidene groups to XIV and subsequent cyclization according to Scheme I.

Attempts to Hydrolyze VII to X—To establish further the degradation pathway, an authentic sample of the enol ether, VII, was heated in the usual way: 3.3 mg/ml in deuterium oxide–deuterium chloride, pD 0.9, at 65° for 9 days. No change in chemical shifts was noted. Thus, VII is not the precursor of X and both are formed by different and independent pathways. In the hydrolysis of I or IV, X was formed at a faster rate than VII.

Deuteration Rate of C-6 Methyl Group—Prolonged heating of II or V in the deuterated solvent resulted in the loss of the 6-methyl proton

Table III—Kinetic Data [a]

Hydrolysis							
I[b]		I[c]		II[d]		III[d]	
Minutes	Concentration, moles, × 10^{-3}	Minutes	Concentration, moles, × 10^{-3}	Minutes	Concentration, moles, × 10^{-2}	Minutes	Concentration, moles, × 10^{-2}
0	3.46	0	3.46	0	3.4	0	2.2
7	3.39	42	3.29	50	1.7	20	2.0
20	3.32	55	3.36	65	1.4	58	2.0
35	3.04	76	3.22	80	1.0	128	1.6
52	2.66	96	3.01	215	0.2	188	1.5
74	2.35	135	2.70	275	0.1	248	1.2
107	2.21	175	2.67				
145	2.11	212	2.63				

Cyclization				Deuteration			
II[d]		V[d]		II		V	
Minutes	Concentration, moles, × 10^{-2}	Minutes	Concentration, moles, × 10^{-2}	Hours	Concentration, moles, × 10^{-2}	Hours	Concentration, moles, × 10^{-2}
50	2.0	0	4.0	0	2.48	0	2.85
65	2.0	65	2.6	22.4	1.71	22.5	1.91
85	1.5	93	2.3	67.7	1.14	67.7	1.45
170	1.0	213	1.4	115.1	0.99	115.1	1.17
215	0.9	258	1.0				
275	0.8	333	0.8				

[a] Concentrations are of the starting material. [b] At 40°. [c] At 20°. [d] At 60°.

Table IV—Pseudo-First-Order Rate Constants (Minutes^{-1}) at 60°

Compound	k_H	k_C	k_D
I	1.0×10^{-2} [a]	—	—
II	1.27×10^{-2}	4.33×10^{-3}	1.29×10^{-4}
III	2.28×10^{-3}	—	—
V	—	4.79×10^{-3}	1.20×10^{-4}

[a] Calculated from 20 and 40° data.

resonance, which is attributed to an acid-catalyzed deuterium–protonium exchange. Mass spectral analysis of the products obtained from the hydrolysis of the C-6 methyl compounds, II and V, in the deuterated aqueous medium indicated 33% monodeuteration and 7% dideuteration of the C-6 methyl group (30% overall deuteration by PMR) of II. The

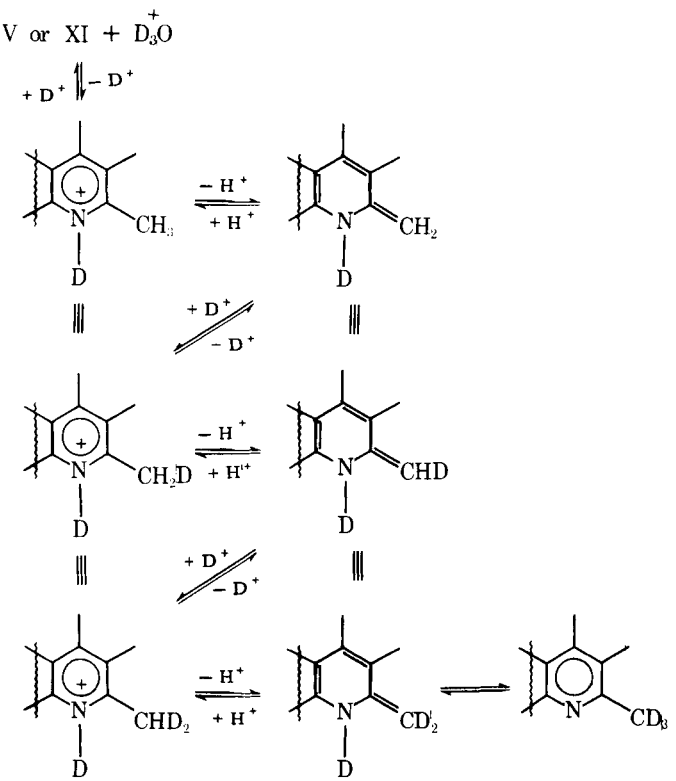

Scheme IV

Table V—Deuteration Rate of the Methyl Group of V and XI [a]

Hours	Percent CH_3 of V Present	Percent CH_3 of XI Present
0	100	100
22.4	67	69
67.7	51	46
115.1	41	40

[a] Measured by disappearance of methyl group, by integration. Concentration of 7.5 mg/ml (pD = 1.9).

extent of deuteration was essentially the same in V.

Whereas the α-methyl protons in 6,7,8-trimethyllumazine (8) and methylpyridine (9) exchange with deuterium, they do not exchange in the presence of mineral acids. A small amount of deuterium was incorporated into the methyl group of 2-picoline when refluxed in deuterium oxide for several days, however. The results of the deuteration[11] rate of the C-6 methyl group of V and XI (Scheme IV) are summarized in Table V. The data demonstrate that the C-6 methyl protons of both compounds exchanged with the deuterium of the solvent at substantially the same rate, which was significantly slower than the rates of hydrolysis (by a factor of 100) and cyclization (by a factor of 30) (Table IV). The mass spectra of the resulting samples confirmed the extent of deuteration determined from their PMR spectra.

REFERENCES

(1) A. I. Cohen, P. T. Funke, and M. S. Puar, *J. Pharm. Sci.*, **62**, 1559 (1973).

(2) B. Beer, M. Chasin, D. E. Clody, J. R. Vogel, and Z. P. Horovitz, *Science*, **176**, 428 (1972). Z. P. Horovitz, B. Beer, D. E. Clody, J. R. Vogel, and M. Chasin, *Psychosomatics*, **13**, 85 (1972).

(3) H. Höhn, T. Denzel, and W. Janssen, *J. Heterocycl. Chem.*, **9**, 235 (1972).

(4) H. Höhn, I. Polacek, and E. Schulze, *J. Med. Chem.*, **16**, 1340 (1973).

(5) H. Höhn and T. Denzel, U.S. pat. 3,787,430 (Jan. 22, 1974).

(6) P. J. Black and A. I. Cohen, paper presented at the Twentieth Annual Conference on Mass Spectrometry and Allied Topics, Dallas, Tex., June 4, 1972.

(7) E. S. Gould, "Mechanism and Structure in Organic Chemistry," Holt, Rinehart and Winston, New York, N.Y., 1957, p. 543.

(8) R. Stewart and J. M. McAndless, *J. Chem. Soc., Perkin II*, **1972**, 376.

(9) W. E. Parham and P. E. Olson, *Tetrahedron Lett.*, **1973**, 4783.

[11] To minimize the dilution of the deuterium content of the solution, the compounds were dissolved in methanol-d_1, which produced immediate exchange of the amine and/or hydroxyl protons. The solution was evaporated and the solid was treated successively twice more in the same manner.

Solubilization of Naphthalene by Sodium Cholate and Pattern of Self-Association of Sodium Cholate in 0.15 *M* Sodium Chloride

JOHN R. CARDINAL ˣ, YUNIK CHANG *, and DARRYL D. IVANSON

Received August 18, 1977, from the *Department of Pharmaceutics, College of Pharmacy, University of Utah, Salt Lake City, UT 84112.* Accepted for publication October 19, 1977. *Present address: College of Pharmacy, University of Kansas, Lawrence, KS 66044.

Abstract □ Naphthalene solubility was determined in aqueous 0.15 *M* NaCl containing sodium cholate in the 0–0.05 *M* concentration range at 25 ± 0.1°. Sodium cholate tends to self-associate in aqueous solutions. Most often, the association pattern has been described in terms of a monomer–micellar model in which it is assumed that no association occurs below the critical micelle concentration. By comparison of the experimental solubilization curve with curves calculated on the basis of the monomer–micellar model, it was shown that this model is inappropriate for the self-association pattern of sodium cholate. The solubility data were consistent with a model that assumes that sodium cholate associates to form dimers, trimers, and higher aggregates with an average aggregation number of 7.63. Model calculations suggest that naphthalene is solubilized by dimers and higher aggregates. Solubilization of naphthalene by trimers appears to be negligible.

Keyphrases □ Naphthalene—solubilization by sodium cholate in 0.15 *M* NaCl □ Solubilization—of naphthalene by sodium cholate in 0.15 *M* NaCl □ Sodium cholate—solubilization of naphthalene and self-association in 0.15 *M* NaCl □ Association, self—sodium cholate in 0.15 *M* NaCl, multiple aggregate model □ Bile salts—sodium cholate, solubilization of naphthalene and self-association in 0.15 *M* NaCl

Bile salts are physiological surfactants that play an important role in the solubilization of lipids such as cholesterol, fatty acids, and lecithin (1–3). In the presence of lecithin and/or fatty acids, complex mixed micelles are formed that have a high capacity for the solubilization of lipophilic species such as cholesterol (4–6). In the absence of lecithin and fatty acids, the bile salts also can solubilize lipophilic species such as cholesterol in water; however, the extent of solubilization is markedly decreased (5, 6). In spite of this decrease, it has been shown from *in vitro* studies that pure bile salt solutions are more effective in the dissolution of cholesterol gallstones than are the mixed micellar solutions (7). Pure bile salt solutions seem to be more effective clinically in cholesterol gallstone dissolution by T-tube infusion (8, 9).

The monomer–micellar model is often utilized to describe the solubilization of lipophilic solutes by the bile salts (1–3). This model is analogous to that used for flexible chain surfactants and assumes that the solute partitions into the micelle formed by the bile salts. Below the critical micellization concentration (CMC), this model assumes that surfactant association and, therefore, solubilization of lipophilic solutes do not occur. Above the CMC, it is assumed that solubilization is proportional to the concentration of micellized species. More complex models of the association of the bile salts also have been suggested. For example, Ekwell *et al.* (10) and Fontell (11–13) argued that discrete solubilization limits exist and that the average size of the bile salt aggregates undergoes discrete changes at these solubilization limits.

More recently, it was argued, using data on the solubilization of naphthalene by sodium cholate in the absence of added electrolytes, that both of the discussed models are inconsistent with the experimental data and that a complex association pattern exists (14). It was concluded that the solubilization data were consistent with a model that includes dimers and one or more higher oligomers. Support for this model was obtained from studies on the light scattering of the bile salts in the presence of added electrolytes (15). It was concluded that the trihydroxy bile salts associate to form dimers, trimers, and a higher aggregate containing approximately eight monomeric units. The association pattern was not strongly influenced by the concentration of added electrolytes or by the degree of conjugation of the bile salt.

In the present study, the solubilization of naphthalene by sodium cholate in aqueous 0.15 *M* NaCl was determined in the range from 0 to 0.05 *M* sodium cholate. The experimental solubilization curve was compared with curves calculated on the basis of various models for the self-association of sodium cholate. The solubilization data were consistent with the multiple aggregate model for the self-association of sodium cholate.

EXPERIMENTAL

Materials—Cholic acid[1] was purified as previously described (15). Sodium cholate was obtained from cholic acid by titration of aqueous solutions of the free acid to pH 10.0 with sodium hydroxide. The solid salts were obtained by flash evaporation of the solvent, followed by drying overnight in a vacuum oven at 45°. Naphthalene[2] was recrystallized four times from methanol and sublimed before use.

Apparatus—Absorbance measurements were made using silica cells of 1-cm pathlength in a spectrophotometer[3]. Samples for the solubilization studies were maintained at 25 ± 0.1° in a constant-temperature water bath[4].

Solubility Experiments—Stock solutions of sodium cholate in 0.15 *M* NaCl were adjusted to pH 10.0. The desired concentrations of sodium cholate were prepared by volumetric dilution of this stock solution. For the solubilization experiments, 5 ml of a sodium cholate solution was placed in a 2-dram vial to which an excess of naphthalene crystals had been added. The vial was sealed with parafilm and allowed to rotate in the water bath at 25 ± 0.1° for 3 days. An appropriate volume of solvent, usually 2 ml, was then withdrawn with a pipet whose tip had been covered with glass wool to filter excess naphthalene crystals from the samples.

This solution was quickly added to a volumetric flask containing a volume of water nearly sufficient to yield the desired final volume of solution. This step was required to prevent the precipitation and sublimation of naphthalene. The dilutions were made in such a fashion that the final concentrations in the diluted samples were far from saturation. Each reported naphthalene solubility value is an average of at least four samples.

The naphthalene concentrations were obtained by absorbance measurements at 276 nm. The extinction coefficient of naphthalene was 5.00 × 10^3 liters/mole cm, in good agreement with the values of 5.07 × 10^3 and 4.946 × 10^3 liters/mole cm reported previously (14, 16).

[1] J. T. Baker Chemical Co., Phillipsburg, N.J.
[2] Amersham/Searle Corp., Des Plaines, Ill.
[3] Model 240, Gilford Instrument Co., Oberlin, Ohio.
[4] Model 2095, Forma Scientific Marietta, Ohio.

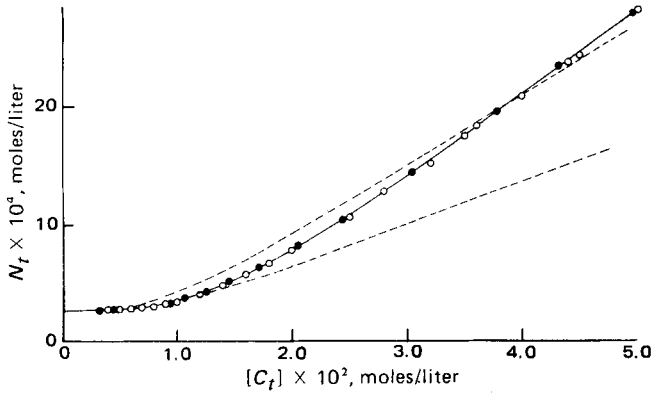

Figure 1—*Solubility of naphthalene,* N_t, *in aqueous 0.15* M *NaCl solutions of sodium cholate at 25°. Key: — and* O, *experimental values;* ●, *multiple aggregate model; lower dashed (– –) line, monomer–micellar model,* K = *150; and upper dashed (– –) line, monomer–micellar model,* K = *250.*

RESULTS AND DISCUSSION

The solubility of naphthalene, N_t, in sodium cholate solutions varying in concentration from 0 to 0.05 M is shown in Fig. 1. The solubility of naphthalene in 0.15 M NaCl, N_0, was 2.615×10^{-4} M. This value was higher than expected based on previously reported values of 2.55×10^{-4} M (14) and 2.62×10^{-4} M (16) for naphthalene solubility in water. For comparison, naphthalene solubility in water was found to be 2.79×10^{-4} M. When using this value for the water solubility and 0.22 for the salting coefficient in the Setschenow equation (16), naphthalene solubility in 0.15 M NaCl was calculated to be 2.59×10^{-4} M. Therefore, the results obtained for naphthalene solubility in water and 0.15 M NaCl in the present study appear to be internally consistent. The reasons for the discrepancy between the present values and those reported previously are not known. Presumably, a small amount of impurity exists in naphthalene; however, it could not be removed by the recrystallization and sublimation steps used in the purification of this sample.

The curve shown in Fig. 1 is similar to that reported previously (14) for naphthalene solubility in sodium cholate in the absence of added electrolytes. At low sodium cholate concentrations, naphthalene solubility increased slowly with increasing concentrations of sodium cholate. This increase was followed by a region of mild curvature. Then at high concentrations of sodium cholate, naphthalene solubility increased nearly linearly with increases in the sodium cholate concentration. This curve shows no distinct "kinks" or "breaks," which are required of both the monomer–micellar model (1–3) and the model of Ekwell *et al.* (10) and Fontell (11–13), and, therefore, appears to be inconsistent with this model (14).

To demonstrate this point more clearly, model calculations, according to the monomer–micellar model, of the variation of naphthalene solubility as a function of the sodium cholate concentration are presented in Fig. 1 as dashed lines. According to the monomer–micellar model, the variation in the total concentration, C_t, as a function of the monomer concentration, b_1, is given by:

$$C_t = [b_1] + n\beta_n[b_1]^n \qquad \text{(Eq. 1)}$$

where n is the aggregation number and β_n is the association constant for micelle formation. The association constant, β_n, is defined as:

$$\beta_n = \frac{[b_n]}{[b_1]^n} \qquad \text{(Eq. 2)}$$

where b_n represents the concentration of micellized species. Equations 1 and 2 are strictly valid only for uncharged species under the assumption that activity coefficients for monomers and micelles are constant. For ionic micelles, counterion binding becomes important (17). However, for the systems investigated here, the counterion concentration is large and effectively constant, so Eqs. 1 and 2 should be valid without correction (18).

Under saturation conditions and the assumption that the increase in the naphthalene concentration arises from solubilization by the cholate micelles, the amount of naphthalene solubilized, defined as $\Delta N = N_t - N_0$, where N_t is the total solubility and N_0 is the solubility in the absence of cholate, can be written as (14):

$$\Delta N = KN_0n\beta_n[b_1]^n \qquad \text{(Eq. 3)}$$

where K is a proportionality constant. In the presence of naphthalene, Eq. 1 must be rewritten to include a term that accounts for the aggregates containing naphthalene. Under these conditions, Eq. 1 becomes (14):

$$C_t = [b_1] + n\beta_n[b_1]^n + KN_0n\beta_n[b_1]^n \qquad \text{(Eq. 4)}$$

Equations 3 and 4 can be utilized to calculate the variation in the naphthalene solubility as a function of the cholate concentration provided that estimates of n and β_n are available. (The value of the proportionality constant, K, can be obtained by fitting the calculated curve to the experimental values.) Literature estimates of the aggregation number, n, for sodium cholate in 0.15 M NaCl are generally from about 4 to 6 (1–3). Recently, an indepth analysis of light-scattering data according to the monomer–micellar model found an aggregation number of 5.83 and an association constant of 8×10^8 liters/mole (19). Since these values were corrected for the nonideality effects in light scattering as discussed by Vrij and Overbeek (20), they were utilized for the present calculation.

In an attempt to fit the experimental solubility curve according to this model, two values of the proportionality constant, K, were used. The lower dashed curve in Fig. 1 was obtained with a value of 150 for K. This curve is in good agreement with the experimental curve at low cholate concentrations but in rather poor agreement at high concentrations. The upper dashed curve in Fig. 1 was calculated with a value of 250 for K. In this case, the agreement is improved at high concentrations but is poor at the lower concentrations.

These results suggest that the monomer–micellar model is inappropriate for describing the self-association pattern of sodium cholate. However, this lack of agreement possibly might arise from a poor choice of assumptions concerning the model rather than from the failure of the model itself. For example, the presence of a solubilized species can lead to an alteration in the micellar properties and to low estimates of the CMC. This lowering of the CMC is proportional to the mole fraction of the solubilized species (21). In the present case, even at the highest concentrations considered, the term $KN_0n\beta_n[b_1]^n$, *i.e.*, the concentration of aggregates containing naphthalene, represents only 5% of the total. Therefore, this small concentration of aggregates containing naphthalene should have relatively minor effects on the overall association pattern.

A second point is the validity of the estimates of the aggregation number and the association constants used in the model calculations. These estimates were obtained from a light-scattering study in which it was concluded that the monomer–micellar model gives a poor fit to the experimental light-scattering curves (19). In that study, a similar conclusion was reached about the necessary variation of the association constant required to fit the experimental curve in the low and high concentration regions. Finally, an independent study (22) using an ultrasonic absorption method also concluded that the monomer–micellar model does not describe adequately the overall self-association pattern of sodium cholate. Based on these studies, the conclusion that the monomer–micellar model does not describe adequately the overall self-association pattern of sodium cholate in 0.15 M NaCl seems justified.

Previous investigators (14, 15, 22) argued that the self-association pattern of the trihydroxy bile salts is complex and involves small aggregates together with higher oligomers. A specific model for sodium cholate self-association was proposed (15), and it was suggested that sodium cholate associates to form dimers, trimers, and larger aggregates with an average aggregation number of 7.63. This model yielded good agreement with the light-scattering curves for sodium cholate in various 0.15 M sodium halides. Since the association constants for the formation of the various aggregates are known from this study, it is possible to apply this model to the solubilization data obtained in the current study.

According to this multiple aggregate model, the total amount of naphthalene solubilized by cholate can be written as:

$$\Delta N = K_2'N_02K_2[b_1]^2 + K_3'N_03K_2K_3[b_1]^3 + K'_{7.63}N_07.63\beta_{7.63}[b_1]^{7.63} \qquad \text{(Eq. 5)}$$

where K_2, K_3, and $\beta_{7.63}$ are the association constants for the formation of the dimer, trimer, and large aggregate, respectively; and K_2', K_3', and $K'_{7.63}$ are the proportionality constants relating the amounts solubilized by the dimer, trimer, and large aggregate to the monomer equivalent concentration of these aggregates, respectively. The total concentration of cholate, C_t, at any given monomer concentration, b_1, can be defined as:

$$C_t = [b_1] + 2K_2[b_1]^2 + 3K_2K_3[b_1]^3 + 7.63\beta_{7.63}[b_1]^{7.63} + K_2'N_02K_2[b_1]^2 + K_3'N_03K_2K_3[b_1]^3 + K'_{7.63}N_07.63\beta_{7.63}[b_1]^{7.63} \qquad \text{(Eq. 6)}$$

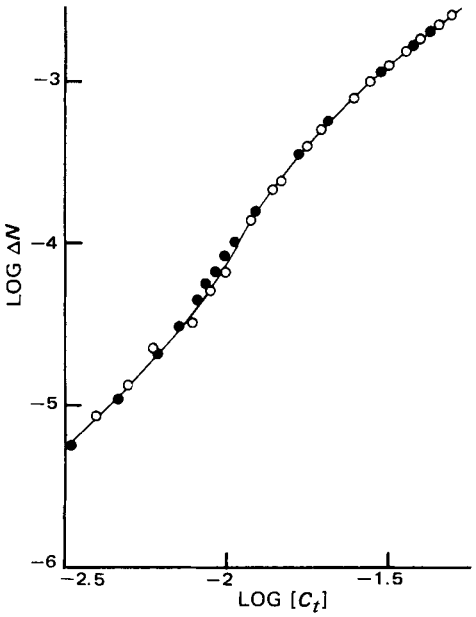

Figure 2—*Logarithm of the excess naphthalene solubility,* ΔN, *plotted against the logarithm of the cholate concentration,* C_t. *Key:* O, *experimental points; and* ●, *multiple aggregate model.*

Two assumptions are important in relating Eqs. 5 and 6 to the solubilization data: (*a*) that the presence of the solute (naphthalene) does not alter the average size of the aggregates formed, and (*b*) that the association constants K_2, K_3, and $\beta_{7.63}$ are not affected by the solute. If assumption *a* is not valid, there should be a poor fit of the calculated curves to the experimental values. If assumption *b* is not valid, the variation in the association constants should not be observable since any changes in the constants would be absorbed in the proportionality constants K_2', *etc.*, needed to fit the solubilization data. However, this assumption ought to be a reasonably good one since the solvent properties of water should not be affected by the small amount of solute present in these solutions.

To compare the experimental solubilization data with this model, log ΔN was plotted *versus* log $[C_t]$ in Fig. 2. By using this figure, K_2' can be obtained by fitting the experimental curve at very low total cholate concentrations. This calculation assumes that the contributions of the larger aggregates to the excess solubility of naphthalene is small in this region. This assumption is reasonable since the initial slope of the plot of log ΔN *versus* log $[C_t]$ is 2, which indicates that the dimer is responsible for solubilization in this region (14). With the value of K_2' already obtained, the value of $K_{7.63}'$ was obtained by fitting the experimental curve at high cholate concentrations. This procedure assumes that K_3' is small, which appears to be reasonable.

Given these values of K_2' and $K_{7.63}'$ and the values of $K_2 = 7.2$, $K_3 = 293$, and $\beta_{7.63} = 2.74 \times 10^{12}$ liters/mole from Ref. 15, the total solubility curve of naphthalene as a function of the total cholate concentration was calculated (Fig. 1). The excess solubility of naphthalene also was calculated and plotted (Fig. 2). From both plots, it can be seen that the calculated values are in good agreement with the experimental curve. The values of the proportionality constants used in fitting the curve are $K_2' = 165$ and $K_{7.63}' = 372$.

As mentioned previously, this calculated curve was obtained by setting $K_3' = 0$. Some attempts were made to improve the fits shown in Figs. 1 and 2 by inclusion of values for K_3', with suitable reductions in the values of K_2' and $K_{7.63}'$. In all cases, however, the fit of the calculated curve with the experimental curve was much worse, especially in the low concentration region. This result seems reasonable when considering molecular models of the cholic acid molecules. Although the arrangement of the monomeric species in the trimer is not known, it can be seen from molecular models that three cholate monomers can be arranged such that a compact cylinder is formed with very little void space. In this arrangement, the hydrophobic faces of the cholate molecules are in contact, and the hydrophilic faces are exposed to water. The inclusion of a naphthalene molecule in this structure would disrupt the compact nature of the aggregate and increase the net exposure of the hydrophobic portions of the cholate molecule to water.

It is concluded, therefore, that the solubilization data are inconsistent with any model of sodium cholate self-association that includes only the monomer and a higher aggregate. The solubilization data can be shown to be in agreement with the multiple aggregate model of Chang and Cardinal (19). It is hoped that the model described in this paper will apply to the solubilization of hydrophobic molecules in general by the trihydroxy bile salts. In addition, this model may be of value in understanding the mechanism by which the bile salts dissolve gallstones clinically.

REFERENCES

(1) A. F. Hofmann and D. M. Small, *Annu. Rev. Med.*, **18**, 333 (1967).

(2) M. C. Carey and D. M. Small, *Am. J. Med.*, **49**, 590 (1970).

(3) D. M. Small, in "The Bile Acids," P. P. Nair and D. Kritchevsky, Eds., Plenum, New York, N.Y., 1971, chap. 8.

(4) W. H. Admirand and D. M. Small, *J. Clin. Invest.*, **47**, 1043 (1968).

(5) D. H. Neiderhiser and H. P. Roth, *Proc. Soc. Exp. Biol. Med.*, **128**, 221 (1968).

(6) N. Tamesue, T. Inoue, and K. Juniper, Jr., *Am. J. Dig. Dis.*, **18**, 670 (1973).

(7) W. I. Higuchi, S. Prakongpan, V. Surpuriya, and F. Young, *Science*, **178**, 633 (1972).

(8) L. Way, W. Admirand, and J. E. Dunphy, *Ann. Surg.*, **176**, 347 (1972).

(9) L. Lansford, S. Mehta, and F. Kern, Jr., *Br. Soc. Gastroenterol.*, **15**, 48 (1974).

(10) P. Ekwell, K. Fontell, and A. Sten, *Proc. Int. Congr. Surf. Act., 2nd*, **1957**, 397.

(11) K. Fontell, *Kolloid Z.-Z. Polym.*, **244**, 246 (1971).

(12) *Ibid.*, **244**, 253 (1971).

(13) *Ibid.*, **250**, 333 (1972).

(14) P. Mukerjee and J. R. Cardinal, *J. Pharm. Sci.*, **65**, 882 (1976).

(15) Y. Chang and J. R. Cardinal, *ibid.*, **67**, 174 (1978).

(16) J. E. Gordon and R. L. Thorne, *J. Phys. Chem.*, **71**, 4390 (1967).

(17) P. Mukerjee, *Adv. Colloid Interface Sci.*, **1**, 241 (1967).

(18) P. Mukerjee, *J. Phys. Chem.*, **76**, 565 (1972).

(19) Y. Chang, Ph.D. thesis, University of Utah, Salt Lake City, Utah, 1977.

(20) A. Vrij and J. T. G. Overbeek, *J. Colloid Sci.*, **17**, 570 (1962).

(21) P. Mukerjee and K. J. Mysels, "Critical Micelle Concentrations of Aqueous Surfactant Systems," NSRDS-NBS 36, U.S. Government Printing Office, Washington, D.C., 1971.

(22) A. Djavanbakht, K. M. Kale, and R. Zana, *J. Colloid Interface Sci.*, **59**, 139 (1977).

ACKNOWLEDGMENTS

Presented in part at the APhA Academy of Pharmaceutical Sciences, Phoenix meeting, November 1977.

Abstracted in part from a dissertation submitted by Y. Chang to the University of Utah in partial fulfillment of the Doctor of Philosophy degree requirements.

Supported by the University of Utah Research Committee.

Secondary Disulfonamides and Secondary Tetrasulfondiamides as Proposed New Biological Alkylating Agents

RONALD E. MASTERS *x and WILLIAM J. ROST

Received June 13, 1977, from the *School of Pharmacy, University of Missouri–Kansas City, Kansas City, MO 64110.* Accepted for publication September 19, 1977. *Present address: School of Pharmacy, Samford University, Birmingham, AL 35209.

Abstract □ Secondary disulfonamides and secondary tetrasulfondiamides were prepared for antineoplastic activity testing. For the disulfonamides, one alkyl series (*n*-butyl), three aralkyl series (benzyl, phenethyl, and phenpropyl), and one diaralkyl series (diphenpropyl) were prepared. Two series of tetrasulfondiamides were made from diamines, one in which the central methylene chain was varied from four to six and another using the tetrasubstituted sulfonyl derivative of xylylenediamine. Thirteen final compounds were synthesized. Ten of these compounds and four intermediates have not been reported previously. Preliminary screening results for the final compounds are given.

Keyphrases □ Sulfonamides, secondary—synthesized, evaluated for antineoplastic activity □ Antineoplastic activity—various secondary disulfonamides and tetrasulfondiamides evaluated □ Structure–activity relationships—various secondary disulfonamides and tetrasulfondiamides evaluated for antineoplastic activity

Recently, the synthesis of a series of *N*-alkyl- and *N*-aralkyl-*N,N*-disulfonamides was reported (1) in a study involving the deamination of primary aliphatic amines. Compounds in which R_1 (Scheme I) was *n*-pentyl, isopentyl, *n*-hexyl, cyclohexyl, 1-methylhexyl, 1-methylheptyl, *n*-octyl, benzyl, and phenethyl and R_2 was phenyl, *p*-tolyl, *p*-bromophenyl, *p*-nitrophenyl, *m*-nitrophenyl, and trifluoromethyl were prepared (1). Only a few scattered reports of the intentional synthesis of this type of compound have appeared in the literature (1, 2). This class of compounds is known to undergo carbon–nitrogen bond cleavage in the presence of nucleophiles (3). [Typical nucleophiles are iodide, bromide, and aniline in dimethylformamide at about 100° for short periods (4).] In this way, a saturated carbon becomes bonded directly to the nucleophile. The leaving group is the disulfonamide anion, and the reaction has been reported to be near the S_N2 end of the spectrum for nucleophilic substitutions at a saturated carbon (3).

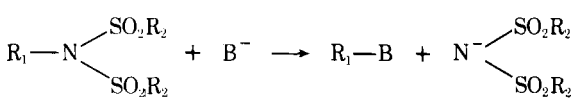

Scheme I

Secondary disulfonamides are potential biological alkylating agents. Furthermore, the corresponding compounds derived from diamines, *i.e.*, secondary tetrasulfondiamides[1]—previously unreported—have the potential to cross-link DNA by dialkylation. Thus, a new type of biological alkylating agent in which R_1 is the alkylating moiety is proposed. To explore this idea, representative disulfonamides and tetrasulfondiamides were synthesized for antineoplastic activity screening. In all cases, a primary amine or diamine was chosen so that the resulting disulfonamide or tetrasulfondiamide would be the least hindered to react most readily with cellular nucleophiles. The disulfonamides are monofunctional alkylating compounds. Many monofunctional agents have demonstrated significant anticancer activity; however, the most active agents are bifunctional (5).

In the disulfonamides, the alkylating moiety on the nitrogen is represented by alkyl, aralkyl, substituted aralkyl, and diaralkyl groups. The lengths of the methylene chains in the bifunctional compounds are varied slightly from that of busulfan.

This paper describes the synthesis and reports the preliminary antineoplastic activity of the 13 final compounds prepared.

RESULTS AND DISCUSSION

The intermediate primary sulfonamides and primary disulfonamides were prepared according to well-established procedures from the corresponding primary amines or diamines (6).

For the synthesis of the secondary disulfonamides and tetrasulfondiamides, the procedure of DeChristopher *et al.* (1) was used. This procedure involved the *in situ* generation of the sodium salt of the sulfonamide or disodium salt of the disulfonamide by sodium hydride. The sulfonamides or disulfonamides were dissolved in dry dimethylformamide, and a 50% oil dispersion of sodium hydride was added slowly with stirring. A 10% excess of the appropriate molar amount of the base was used. Stirring was continued for 30 min following addition of sodium hydride. A 10% excess of the appropriate molar amount of *p*-toluenesulfonyl chloride was then added; stirring was continued for another 30 min, except for the disulfonamide of hexamethylenediamine which required 1 hr of stirring because of the poor solubility of the disodium salt in dimethylformamide.

These reactions were run at room temperature in open beakers. The crude disulfonamides and tetrasulfondiamides were isolated by quenching the dimethylformamide reaction mixtures in water and filtering the crude products. The crude final products were washed with water and purified by recrystallization from the appropriate solvent(s). Tables I and II list the final compounds.

Table III shows the testing results obtained from the National Cancer Institute. Activity, host animal, tumor employed, vehicle used, and various dosage levels administered are shown for each compound. The intraperitoneal route was used. The parameter measured for antitumor activity in XI*b* and XII*b* was mean tumor weight; median survival time was used for all other compounds. Compound XI*b* showed presumptive activity in its initial test.

The tumors chosen for testing against the individual compounds were selected by the National Cancer Institute. Unfortunately, none of the compounds was tested against L-1210, which, according to protocol, should be employed in the current stage-one screen for synthetic compounds (7). Because of the limited number of compounds tested, conclusions regarding the antitumor activity of this new class of alkylating agents are premature.

EXPERIMENTAL

***N*-(3-Phenyl-1-propyl)-*p*-toluenesulfonamide (VIII*a*)**—Into a 250-ml round-bottom flask fitted with a mechanical stirrer were placed 6.75 g (0.05 mole) of 3-phenyl-1-propylamine, 5 ml of water, and 9.55 g (0.05 mole) of *p*-toluenesulfonyl chloride. To this mixture was added, with stirring, 20 ml of 10% NaOH in portions over 1 hr. The reaction was

[1] For the purpose of analogy, the difunctional compounds are referred to as secondary tetrasulfondiamides. However, in naming them chemically, they are probably better referred to as tetrasubstituted diamines.

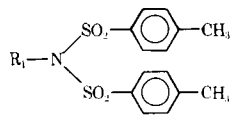

Table I—Physical Constants of Secondary Disulfonamides

Compound	R_1	Melting Point[a]	Yield, %	Empirical Formula	Analysis[b], % Calc.	Found
I*b*	n-C_4H_9	86–87°[c]	76.1	$C_{18}H_{23}NO_4S_2$	C 56.67 H 6.08 N 3.67	56.50 6.19 3.59
II*b*	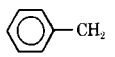	158.5–160°[d]	83.1	$C_{21}H_{21}NO_4S_2$	C 60.70 H 5.09 N 3.37	60.75 5.03 3.39
III*b*	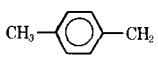	167–168°	65.7	$C_{22}H_{23}NO_4S_2$	C 61.52 H 5.40 N 3.26	61.49 5.42 3.20
IV*b*	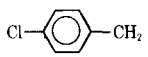	125–127°	76.7	$C_{21}H_{20}ClNO_4S_2$	C 56.06 H 4.48 N 3.11	56.00 4.70 3.32
V*b*	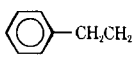	100–101°[f]	82.6	$C_{22}H_{23}NO_4S_2$	Not determined	
VI*b*[e]	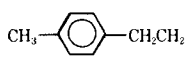	99–100.5°	78.7	$C_{23}H_{25}NO_4S_2$	C 62.28 H 5.68 N 3.16	62.45 5.81 3.35
VII*b*	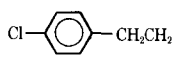	120–121°	87.1	$C_{22}H_{22}ClNO_4S_2$	C 56.95 H 4.78 N 3.02	57.09 4.68 3.39
VIII*b*	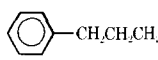	112–113°	90.9	$C_{23}H_{25}NO_4S_2$	C 62.28 H 5.68 N 3.16	62.45 5.75 3.28
IX*b*[e]	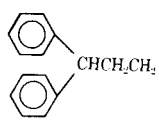	143–144°	90.4	$C_{29}H_{29}NO_4S_2$	C 67.03 H 5.62 N 2.70	66.89 5.80 2.74

[a] Melting points were taken on a Thomas-Hoover capillary melting-point apparatus and are uncorrected. [b] Determined by Het-Chem-Co of Harrisonville, Mo. [c] Reference 8. [d] Reference 9. [e] New intermediate. [f] Reference 6.

heated on a steam bath during the addition of sodium hydroxide and for 1 additional hr. After cooling, the crude product was filtered, washed with water, and recrystallized from methanol–water (3:1), giving 9 g (62.5%), mp 64–65° [lit. (6) mp 66–67°]; IR ($CHCl_3$): 3370, 1330, and 1160 cm^{-1}.

***N*-(3-Phenyl-1-propyl)-*N*,*N*-di-*p*-toluenesulfonamide (VIII*b*)**—To a solution of 7.2 g (0.025 mole) of VIII*a* in 100 ml of dry dimethylformamide in an open beaker was added 1.32 g (0.0275 mole) of 50% NaH. After stirring for 30 min at room temperature, 5.2 g (0.0275 mole) of *p*-toluenesulfonyl chloride was added. Stirring was continued for 30 min, and the mixture was then poured into water. After standing overnight, the crude product was filtered, washed with water, and recrystallized from equal parts of acetone and ethanol, yielding 10 g (90.9%), mp 112–113°; IR ($CHCl_3$): NH stretching region blank, 1370 and 1165 cm^{-1}. The NMR ($CDCl_3$) spectrum had a trio of coupled triplets at 2.00, 2.59, and 3.68 ppm (J = 8 Hz) (2H each); an aromatic methyl singlet at 2.41 ppm (on top of the middle set of triplets) (6H); and aromatic multiplets at 6.90–8.00 ppm (13H).

Anal.—Calc. for $C_{23}H_{25}NO_4S_2$: C, 62.28; H, 5.68; N, 3.16. Found: C, 62.45; H, 5.75; N, 3.28.

***N*,*N*′-Di-(*p*-toluenesulfonyl)pentamethylenediamine (XI*a*)**—Into a 250-ml round-bottom flask fitted with a mechanical stirrer were placed 5.1 g (0.05 mole) of 1,5-diaminopentane, 5 ml of water, 19.1 g (0.1 mole) of *p*-toluenesulfonyl chloride, and 40 ml of 10% NaOH. The mixture was

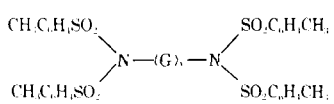

Table II—Physical Constants of Secondary Tetrasulfondiamides

Compound	G	x	Melting Point[a]	Yield, %	Empirical Formula	Analysis[b], % Calc.	Found
X*b*	CH_2	4	185–186°	76.2	$C_{32}H_{36}N_2O_8S_4$	C 54.53 H 5.15 N 3.97	54.51 5.49 4.06
XI*b*[c]	CH_2	5	129–130°	88.4	$C_{33}H_{38}N_2O_8S_4$	C 55.13 H 5.33 N 3.90	55.15 5.03 4.03
XII*b*	CH_2	6	214–215°	61.9	$C_{34}H_{40}N_2O_8S_4$	C 55.72 H 5.50 N 3.82	55.45 5.37 3.93
XIII*b*[c]		1	187–188°	80.2	$C_{36}H_{36}N_2O_8S_4$	C 57.43 H 4.82 N 3.72	57.28 4.72 3.79

[a,b] See Table I. [c] New intermediate.

Table III—Antitumor Testing Results

Compound	Activity[a]	Dose, mg/kg		PS[b]	B1[c]	WA[d]
I*b*	–	400		CDF_1 mouse		
		200				
		100		T[e]		
II*b*	×, –	400	100	CDF_1 mouse		
		200	50	T		
		100	25			
III*b*	–	400		CDF_1 mouse		
		200				
		100		T		
IV*b*	–	200		CDF_1 mouse		
		100				
		50		M[f]		
V*b*	–	200		CDF_1 mouse		
		100				
		50		M		
VI*b*	–	200		CDF_1 mouse		
		100				
		50		M		
VII*b*	–	200		CDF_1 mouse		
		100				
		50		M		
VIII*b*	–	200		CDF_1 mouse		
		100				
		50		M		
IX*b*	×, –	400	100	CDF_1 mouse		
		200	50			
		100	25	T		
X*b*	–	400		BDF_1 mouse		
		200				
		100		M		
XI*b*	+, –	150	400			Random bred albino rat
		75	200			
		37.5	100			
		18.7				
		9.4				0[g]
XII*b*	–, –	150	400			Random bred albino rat
		75	200			
		37.5	100			
		18.7				
		9.4				0
XIII*b*	–	400			BDF_1 mouse	
		200				
		100			M	

[a] Presumptive activity, +; no activity indicated, –; toxic doses, ×. [b] P-388 lymphocytic leukemia. [c] B16 melanocarcinoma. [d] Walker carcinosarcoma 256. [e] Saline with polysorbate 80. [f] Hydroxypropylcellulose. [g] Other.

heated on a steam bath with stirring for 2 hr. After cooling, the crude product was filtered, washed with water, and recrystallized from ethanol, yielding 15.4 g (75.2%) of tan crystals, mp 132–134°; IR ($CHCl_3$): 3320, 1330, and 1160 cm^{-1}.

***N,N,N′,N′*-Tetra-(*p*-toluenesulfonyl)pentamethylenediamine (XI*b*)**—To a solution of 6.15 g (0.015 mole) of XI*a* in 150 ml of dry dimethylformamide in an open beaker was added 1.584 g (0.033 mole) of 50% NaH. After stirring for 30 min at room temperature, 6.3 g (0.033 mole) of *p*-toluenesulfonyl chloride was added. Stirring was continued for 30 min, and the mixture was then poured into water. After standing overnight, the crude product was filtered, washed with water, and recrystallized from equal parts of acetone and ethanol, giving 9.6 g (88.4%), mp 129–130°; IR ($CHCl_3$): NH stretching region blank, 1370 and 1165 cm^{-1}. The NMR ($CDCl_3$) spectrum had an aliphatic region at 0.6–1.90 ppm (6H); an aromatic methyl singlet at 2.44 ppm (12H); an NCH_2 triplet centered at 3.60 ppm, J = 7 Hz (4H); and an aromatic *AA′BB′* quartet centered at 7.57 ppm, J_{ab} = 8 Hz (16H).

Anal.—Calc. for $C_{33}H_{38}N_2O_8S_4$: C, 55.13; H, 5.33; N, 3.90. Found: C, 55.15; H, 5.03; N, 4.03.

REFERENCES

(1) P. J. DeChristopher, J. P. Adamek, G. D. Lyon, S. A. Klein, and R. J. Baumgarten, *J. Org. Chem.*, **39**, 3525 (1974).

(2) H. Stetter and H. Hansmann, *Chem. Ber.*, **90**, 2728 (1957).

(3) P. J. DeChristopher, Ph.D. thesis, University of Illinois at Chicago Circle, Chicago, Ill., 1971.

(4) P. J. DeChristopher, J. P. Adamek, G. D. Lyon, J. J. Galante, H. E. Haffner, R. J. Boggio, and R. J. Baumgarten, *J. Am. Chem. Soc.*, **91**, 2384 (1969).

(5) A. Burger, "Medicinal Chemistry," 3rd ed., Wiley, New York, N.Y., 1970, p. 683.

(6) W. H. Carothers, C. F. Bickford, and G. J. Hurwitz, *J. Am. Chem. Soc.*, **49**, 2914 (1927).

(7) "Instruction 14, Screening Data Summary Interpretation and Outline of Current Screen," Drug Evaluation Branch, Drug Research and Development, Division of Cancer Treatment, National Cancer Institute, Bethesda, Md., rev. Nov. 1973.

(8) R. D'Arcy, C. A. Grob, T. Kaffenberger, and V. Krasnobajew, *Helv. Chim. Acta*, **49**, 202 (1965).

(9) S. J. Angyal and R. C. Rassack, *J. Chem. Soc.*, **1949**, 2703.

ACKNOWLEDGMENTS

Adapted in part from a dissertation submitted by R. E. Masters to the University of Missouri–Kansas City in partial fulfillment of the Doctor of Philosophy degree requirements.

Rearrangement of *N*-Benzyl-2-cyano-2-(hydroxyimino)acetamide

CHARLES M. DARLING ˣ **and C. P. CHEN**

Received August 3, 1977, from the *School of Pharmacy, Auburn University, Auburn, AL 36830.* Accepted for publication September 19, 1977.

Abstract □ The reduction of *N*-benzyl-2-cyano-2-(hydroxyimino)-acetamide resulted in the formation of *N*-benzyl-1,2-ethanediamine and *N*-benzyl-*N'*-methyl-1,2-ethanediamine in approximately an equimolar ratio. The formation of the two unexpected products is explained by the migration of a cyano group in a Beckmann-type rearrangement.

Keyphrases □ *N*-Benzyl -2- cyano-2-(hydroxyimino)acetamide—reduced, two diamines formed by Beckmann-type rearrangement □ Beckmann-type rearrangement—in reduction of *N*-benzyl-2-cyano-2-(hydroxyimino)acetamide, two diamines formed □ Diamines—formed by reduction of *N*-benzyl-2-cyano-2-(hydroxyimino)acetamide by Beckmann-type rearrangement

A Beckmann-type rearrangement of a compound (benzoyl cyanide oxime) containing a cyano group attached directly to the carbon atom of an oxime group was reported by Zimmermann (1). Hydrolysis of the product led to formation of *N*-phenyloxamide, indicating that the cyano group did not migrate. The authors were unable to find an example of a rearrangement in the literature in which a cyano group was the migrating group.

In a reduction of *N*-benzyl-2-cyano-2-(hydroxyimino)-acetamide (I) with sodium bis(2-methoxyethoxy)aluminum hydride[1], an equimolar ratio of *N*-benzyl-1,2-ethanediamine (II) and *N*-benzyl-*N'*-methyl-1,2-ethanediamine (III) was obtained (Scheme I) in less than 10% yield. The formation of the two unexpected products may be explained by the migration of a cyano group in a Beckmann-type arrangement.

EXPERIMENTAL[2]

Compound I—A mixture of *N*-benzyl-2-cyanoacetamide (2) (34.8 g, 0.20 mole) and sodium nitrite (20.7 g, 0.30 mole) in toluene (500 ml) was heated to reflux. Concentrated hydrochloric acid (26 ml, 0.26 mole) was added dropwise during 2 hr, and the resulting mixture was heated at reflux for 4 hr. The lower layer was separated and poured into a mixture of ice and water.

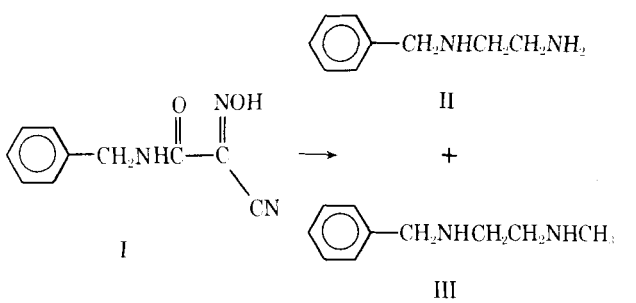

Scheme I

After filtering, the residue was washed with cold water and recrystallized from water, yielding 23.4 g (57.6%), mp 159.5–161°; IR (KBr): 3350 (oxime OH), 2230 (cyano), and 1645 (amide, C=O) cm^{-1}; NMR (acetone-d_6): δ 4.42 (m, 2H, CH_2), 7.27 (s, 5H, C_6H_5), 8.2 (broad, 1H, deuterium exchangeable), and 13.2 (broad, 1H, deuterium exchangeable) ppm.

Anal.—Calc. for $C_{10}H_9N_3O_2$: C, 59.11; H, 4.46; N, 20.68. Found: C, 59.11; H, 4.46; N, 20.73.

Reduction of I to II and III Dihydrochlorides—A solution of I (20.3 g, 0.10 mole) in dry tetrahydrofuran (150 ml) was added dropwise to a solution of sodium bis(2-methoxyethoxy)aluminum hydride in benzene (168 ml, 0.58 mole). The mixture was heated at reflux for 5 hr. Excess hydride was decomposed by successively adding absolute ethanol (25 ml), benzene (175 ml), and 10% sodium hydroxide solution (164 ml). The benzene layer was separated and washed with water (3 × 100 ml). The benzene solution was extracted with dilute hydrochloric acid (3 × 100 ml), and the combined acid extracts were neutralized with saturated sodium carbonate solution.

The basic solution was then extracted with chloroform (9 × 100 ml), and the dried chloroform extract was concentrated *in vacuo*. The oily residue (18 g) was distilled, 1.6 g, bp 32–67°/0.025 mm. The distillate was converted to a hydrochloride salt with concentrated hydrochloric acid in acetone. Fractional recrystallization from methanol–activated charcoal gave III, 0.92 g (3.9%), mp 273–274°. Mixed melting-point determination with an authentic sample (3, 4) showed no depression.

Anal.—Calc. for $C_{10}H_{16}N_2 \cdot 2HCl$: C, 50.64; H, 7.65; N, 11.81. Found: C, 50.69; H, 7.44; N, 11.91.

The filtrates were combined and concentrated *in vacuo*. The residue was fractionally recrystallized from absolute ethanol to obtain II, 0.84 g (3.8%), mp 243–248°. Mixed melting-point determination with an authentic sample showed no depression.

Anal.—Calc. for $C_9H_{14}N_2 \cdot 2HCl$: C, 48.44; H, 7.23; N, 12.55. Found: C, 48.81; H, 7.39; N, 12.50.

Authentic Sample of III Dihydrochloride—Following a modification of the method of Crochet and Blanton (5), a mixture of II (7.5 g, 0.05 mole) and triethyl orthoformate (40 ml) was heated at reflux for 5 hr. After concentrating *in vacuo*, absolute ethanol (40 ml) was added and cooled to ice bath temperature. Sodium borohydride (3.7 g, 0.10 mole) was added with stirring, and the mixture was heated at reflux temperature for 16 hr. The mixture was concentrated *in vacuo*, the residue was dissolved in water, and the mixture was extracted with ether (3 × 50 ml). The dried ether extract (anhydrous magnesium sulfate) was concentrated *in vacuo*, and the residue was distilled, bp 89–98°/0.25 mm [lit. (3) bp 79–80.5°/0.02 mm]. The hydrochloride salt, prepared from acetone and concentrated hydrochloric acid, was recrystallized from ethanol (95%) and activated charcoal, 1.6 g (13.6%), mp 274–277°.

Anal.—Calc. for $C_{10}H_{16}N_2 \cdot 2HCl$: C, 50.64; H, 7.65; N, 11.81. Found: C, 50.21; H, 7.47; N, 11.99.

***N*-Benzyl-*N'*-cyanooxamide (IV)**—Using a modification of the method of Kretov and Momsenko (6), a mixture of ethyl oxalyl chloride (9.45 g, 0.069 mole) in benzene (100 ml) was cooled to 5° and triethylamine (13.96 g, 0.138 mole) was added dropwise with stirring. Cyanamide (2.91 g, 0.069 mole) was added in small portions, and the mixture was stirred at ambient temperatures for 20 hr. Petroleum ether (200 ml, bp 30–60°) was added, and the lower layer was diluted with dioxane (100 ml) after decanting. The mixture was filtered and the residue was washed with dioxane (50 ml).

The combined filtrate and washing were added to petroleum ether (200

[1] Red-Al, a 70% solution in benzene, Aldrich Chemical Co., Milwaukee, Wis.

[2] Elemental analyses were performed by Atlantic Microlab, Atlanta, GA 30366. IR spectra were obtained using a Beckman Acculab 6 spectrophotometer. NMR spectra were obtained using a Varian T60A spectrometer, and values are in parts per million (δ) from tetramethylsilane as the internal standard. Melting points were taken in open capillary tubes and are uncorrected. GLC analyses were performed using a Carle 9500 gas chromatograph with a 3% SE-30 column at 150°.

ml), and the mixture was decanted. The lower layer was cooled to −12°, and benzylamine (12.2 g, 0.11 mole) was then added dropwise with stirring. The mixture was stirred at ambient temperature for 16 hr and filtered. The residue was dissolved in methanol and treated with activated charcoal, and the product was precipitated with isopropyl ether, 2.8 g (12.5% crude yield), mp 151–153°; IR (KBr): 2190 (cyano) and 1660 (amide) cm^{-1}.

Several attempts to isolate the product led to decomposition, as evidenced by the disappearance of IR absorption of the cyano group. Therefore, the product was used in the next step without further purification.

Reduction of IV—Crude IV (1.3 g, 0.005 mole) was suspended in anhydrous tetrahydrofuran (200 ml) and added dropwise to a solution of sodium bis(2-methoxyethoxy)aluminum hydride in benzene (10 ml, 0.034 mole). The mixture was heated at reflux temperature for 3.5 hr. After stirring at ambient temperature for 13 hr, excess hydride was decomposed by successively adding ethanol (95%, 4 ml) and water (6 ml). The supernate was separated and concentrated *in vacuo*.

The oily residue was dissolved in chloroform (20 ml) and washed with water (3 × 10 ml). The dried chloroform solution (anhydrous magnesium sulfate) was evaporated *in vacuo*, and the residue was converted to a hydrochloride salt with acetone and concentrated hydrochloric acid. The product was recrystallized from absolute ethanol, 0.1 g (0.6% overall), mp 272–276°. Mixed melting-point determination with an authentic sample of III dihydrochloride showed no depression.

RESULTS AND DISCUSSION

In several repeat experiments, different workup procedures did not improve the yields of II and III. The components of the black tar, which make up the bulk of the crude yield, were not resolved.

Products II and III were identified as hydrochloride salts by microanalyses and mixed melting-point determinations with authentic samples. GLC analyses of the free bases provided confirming evidence.

Migration of a cyano group in a Beckmann-type rearrangement of I would be expected to yield IV as an intermediate. However, only starting

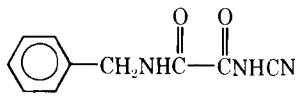

IV

material was recovered (90%) when I was treated under conditions known to cause a Beckmann rearrangement (7). When IV was treated under the same reducing conditions as I, only one product, III, was isolated. GLC analysis of the filtrate from the recrystallization of this reduction product failed to detect the presence of II.

Additional studies will be required to elucidate the rearrangement mechanism. However, sufficient evidence is presented to propose the migration of a cyano group.

REFERENCES

(1) M. R. Zimmermann, *J. Prakt. Chem.*, **66**, 353 (1902); through *Org. React.*, **11** (1960).

(2) O. C. Dermer and J. King, *J. Org. Chem.*, **8**, 168 (1943).

(3) E. Jucker and E. Rissi, *Helv. Chim. Acta*, **45**, 2383 (1962).

(4) S. C. Dickerman and A. J. Besozzi, *J. Org. Chem.*, **19**, 1855 (1954).

(5) R. A. Crochet, Jr., and C. D. Blanton, Jr., *Synthesis*, **1974**, 55.

(6) A. E. Kretov and A. P. Momsenko, *Zh. Org. Khim.*, **1**, 1734 (1965); through *Chem. Abstr.*, **64**, 3344 (1966).

(7) A. I. Vogel, "Practical Organic Chemistry," 3rd ed., Academic, New York, N.Y., 1956, p. 741.

ACKNOWLEDGMENTS

Abstracted in part from a thesis submitted by C. P. Chen to the School of Pharmacy, Auburn University, in partial fulfillment of the Master of Science degree requirements.

The technical assistance of Gloria Klase Ingram is gratefully acknowledged.

Interaction of Tricyclic Antipsychotic and Antidepressant Drugs with 1-Anilino-8-naphthalenesulfonic Acid

H. W. JUN ˣ and P. C. RUENITZ

Received November 15, 1976, from the *Department of Pharmacy, School of Pharmacy, University of Georgia, Athens, GA 30602.* Accepted for publication September 9, 1977.

Abstract □ The binding of 1-anilino-8-naphthalenesulfonic acid to selected tricyclic antipsychotic and antidepressant drugs was studied by fluorescence spectroscopy. The acid exhibited an increase in fluorescence intensity accompanied by a hypsochromic shift of the emission λ_{max} in the presence of these drugs. These fluorescence characteristics, in addition to those of acid–drug complexes after addition of potassium chloride or urea, suggested that binding was hydrophobic. The spectra also provided evidence regarding the importance of certain structural features of drugs in determining the nature of binding.

Keyphrases □ 1-Anilino-8-naphthalenesulfonic acid—binding to various antipsychotic and antidepressant drugs, fluorometric study □ Antipsychotics, various—binding to 1-anilino-8-naphthalenesulfonic acid, fluorometric study □ Antidepressants, various—binding to 1-anilino-8-naphthalenesulfonic acid, fluorometric study □ Binding—1-anilino-8-naphthalenesulfonic acid to various antipsychotics and antidepressants, fluorometric study □ Fluorometry—study of binding of 1-anilino-8-naphthalenesulfonic acid to various antipsychotics and antidepressants

Studies of molecular interactions in aqueous solution are important for elucidating the nature and mechanism of drug–protein binding in the body. Information pertaining to such interactions between small molecules can permit possible prediction of this drug–biomolecule binding. One technique commonly used is to measure spectral changes of drugs on binding to other molecules. Several reports (1, 2) concerned the use of absorption spectra for drug binding studies. Fluorescence spectroscopy (3) also was used to study molecular interactions.

Fluorescent probes, recently applied in drug–protein binding studies, are minimally fluorescent in their free form in aqueous solution. When these compounds are bound to other molecules, their spectral properties such as intensity and maximal emission wavelength change, reflecting their molecular environment. These spectral

ml), and the mixture was decanted. The lower layer was cooled to −12°, and benzylamine (12.2 g, 0.11 mole) was then added dropwise with stirring. The mixture was stirred at ambient temperature for 16 hr and filtered. The residue was dissolved in methanol and treated with activated charcoal, and the product was precipitated with isopropyl ether, 2.8 g (12.5% crude yield), mp 151–153°; IR (KBr): 2190 (cyano) and 1660 (amide) cm^{-1}.

Several attempts to isolate the product led to decomposition, as evidenced by the disappearance of IR absorption of the cyano group. Therefore, the product was used in the next step without further purification.

Reduction of IV—Crude IV (1.3 g, 0.005 mole) was suspended in anhydrous tetrahydrofuran (200 ml) and added dropwise to a solution of sodium bis(2-methoxyethoxy)aluminum hydride in benzene (10 ml, 0.034 mole). The mixture was heated at reflux temperature for 3.5 hr. After stirring at ambient temperature for 13 hr, excess hydride was decomposed by successively adding ethanol (95%, 4 ml) and water (6 ml). The supernate was separated and concentrated *in vacuo*.

The oily residue was dissolved in chloroform (20 ml) and washed with water (3 × 10 ml). The dried chloroform solution (anhydrous magnesium sulfate) was evaporated *in vacuo*, and the residue was converted to a hydrochloride salt with acetone and concentrated hydrochloric acid. The product was recrystallized from absolute ethanol, 0.1 g (0.6% overall), mp 272–276°. Mixed melting-point determination with an authentic sample of III dihydrochloride showed no depression.

RESULTS AND DISCUSSION

In several repeat experiments, different workup procedures did not improve the yields of II and III. The components of the black tar, which make up the bulk of the crude yield, were not resolved.

Products II and III were identified as hydrochloride salts by microanalyses and mixed melting-point determinations with authentic samples. GLC analyses of the free bases provided confirming evidence.

Migration of a cyano group in a Beckmann-type rearrangement of I would be expected to yield IV as an intermediate. However, only starting

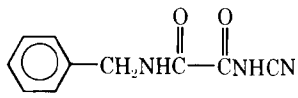

IV

material was recovered (90%) when I was treated under conditions known to cause a Beckmann rearrangement (7). When IV was treated under the same reducing conditions as I, only one product, III, was isolated. GLC analysis of the filtrate from the recrystallization of this reduction product failed to detect the presence of II.

Additional studies will be required to elucidate the rearrangement mechanism. However, sufficient evidence is presented to propose the migration of a cyano group.

REFERENCES

(1) M. R. Zimmermann, *J. Prakt. Chem.*, **66**, 353 (1902); through *Org. React.*, **11** (1960).

(2) O. C. Dermer and J. King, *J. Org. Chem.*, **8**, 168 (1943).

(3) E. Jucker and E. Rissi, *Helv. Chim. Acta*, **45**, 2383 (1962).

(4) S. C. Dickerman and A. J. Besozzi, *J. Org. Chem.*, **19**, 1855 (1954).

(5) R. A. Crochet, Jr., and C. D. Blanton, Jr., *Synthesis*, **1974**, 55.

(6) A. E. Kretov and A. P. Momsenko, *Zh. Org. Khim.*, **1**, 1734 (1965); through *Chem. Abstr.*, **64**, 3344 (1966).

(7) A. I. Vogel, "Practical Organic Chemistry," 3rd ed., Academic, New York, N.Y., 1956, p. 741.

ACKNOWLEDGMENTS

Abstracted in part from a thesis submitted by C. P. Chen to the School of Pharmacy, Auburn University, in partial fulfillment of the Master of Science degree requirements.

The technical assistance of Gloria Klase Ingram is gratefully acknowledged.

Interaction of Tricyclic Antipsychotic and Antidepressant Drugs with 1-Anilino-8-naphthalenesulfonic Acid

H. W. JUN ˣ and P. C. RUENITZ

Received November 15, 1976, from the *Department of Pharmacy, School of Pharmacy, University of Georgia, Athens, GA 30602.* Accepted for publication September 9, 1977.

Abstract □ The binding of 1-anilino-8-naphthalenesulfonic acid to selected tricyclic antipsychotic and antidepressant drugs was studied by fluorescence spectroscopy. The acid exhibited an increase in fluorescence intensity accompanied by a hypsochromic shift of the emission λ_{max} in the presence of these drugs. These fluorescence characteristics, in addition to those of acid–drug complexes after addition of potassium chloride or urea, suggested that binding was hydrophobic. The spectra also provided evidence regarding the importance of certain structural features of drugs in determining the nature of binding.

Keyphrases □ 1-Anilino-8-naphthalenesulfonic acid—binding to various antipsychotic and antidepressant drugs, fluorometric study □ Antipsychotics, various—binding to 1-anilino-8-naphthalenesulfonic acid, fluorometric study □ Antidepressants, various—binding to 1-anilino-8-naphthalenesulfonic acid, fluorometric study □ Binding—1-anilino-8-naphthalenesulfonic acid to various antipsychotics and antidepressants, fluorometric study □ Fluorometry—study of binding of 1-anilino-8-naphthalenesulfonic acid to various antipsychotics and antidepressants

Studies of molecular interactions in aqueous solution are important for elucidating the nature and mechanism of drug–protein binding in the body. Information pertaining to such interactions between small molecules can permit possible prediction of this drug–biomolecule binding. One technique commonly used is to measure spectral changes of drugs on binding to other molecules. Several reports (1, 2) concerned the use of absorption spectra for drug binding studies. Fluorescence spectroscopy (3) also was used to study molecular interactions.

Fluorescent probes, recently applied in drug–protein binding studies, are minimally fluorescent in their free form in aqueous solution. When these compounds are bound to other molecules, their spectral properties such as intensity and maximal emission wavelength change, reflecting their molecular environment. These spectral

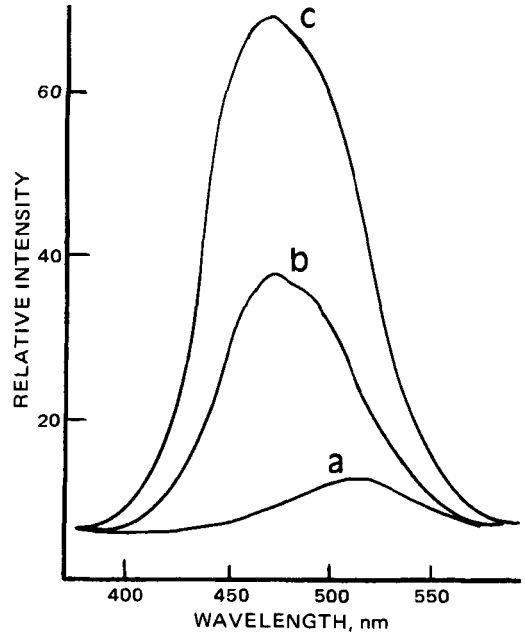

Figure 1—*Fluorescence emission spectra of the probe in pH 5.8 phosphate buffer (curve a) and on addition of trimeprazine (curve b) or chlorpromazine (curve c). The excitation maximum was set at 387 nm.*

changes have been measured to study their binding characteristics to enzymes (4), blood proteins (5), hormones (6), and blood cells (7). In particular, 1-anilino-8-naphthalenesulfonic acid (I) has often been used as a tool to study the site and nature of hydrophobic binding.

This paper reports a study of fluorescence spectral characteristics of I in the presence of several relatively small molecules, representing the dibenzazepine and phenothiazine classes of central nervous system active drugs.

EXPERIMENTAL

Materials—1-Anilino-8-naphthalenesulfonic acid[1] (I), chlorpromazine hydrochloride[2], trimeprazine tartrate[2], imipramine[3], and desipramine[3] were used. Spectroscopic grade methanol[4] was the solvent for the probe. All other chemicals were reagent grade. Water was double distilled from glass containers.

Apparatus—All fluorescence measurements were made on a spectrophotofluorometer[5] equipped with a 150-w xenon lamp and lp21 photomultiplier tube. Spectra were recorded with an x–y recorder[6].

Methods—Measurements were made in a fluorescence cell using 2-ml aliquots of aqueous solutions of imipramine, desipramine, chlorpromazine, and trimeprazine (all 2 mM). To each aliquot was added 5 μl of a 10 mM methanolic solution of I, and the fluorescence emission spectra were taken at 25 ± 1° at an excitation wavelength of 387 nm. Solutions of the drugs in the absence of added I exhibited negligible fluorescence spectra under the same experimental conditions.

RESULTS

Interaction of Chlorpromazine and Trimeprazine with I—Figure 1 shows emission spectra of I in water and in the presence of trimeprazine and chlorpromazine. Chlorpromazine caused a spectral shift in its emission maxima from 520 to 485 nm, accompanied by a large increase in fluorescence intensity (curve c). When chlorpromazine was present in large excess, the enhancement in fluorescence intensity as a function of I concentration was approximately linear (Fig. 2), suggesting a proportional increase in the fraction of the bound form of I in the system.

Table I—Influence of Potassium Chloride and Urea on the Relative Fluorescence of I–Chlorpromazine and I–Imipramine Complexes

Compounds Dissolved in Water	Emission Maxima, nm[a]	Relative Fluorescence
0.01 mM I	520	1
2 mM chlorpromazine	485	2
2 mM chlorpromazine, 0.01 mM I	485	30
2 mM chlorpromazine, 0.01 mM I, 3% KCl	485	100
2 mM chlorpromazine, 0.01 mM I, 2 M urea	485	6
2 mM imipramine	487	2
2 mM imipramine, 0.01 mM I	487	20
2 mM imipramine, 0.01 mM I, 3% KCl	487	70
2 mM imipramine, 0.01 mM I, 2 M urea	487	10

[a] The excitation maximum was 387 nm.

The presence of potassium chloride in the I–chlorpromazine system further increased fluorescence intensity. In contrast, addition of urea decreased fluorescence (Table I). The effects of potassium chloride and urea concentration on fluorescence intensity appeared concentration dependent.

A solution of I in the presence of trimeprazine exhibited less fluorescence increase compared to chlorpromazine (Fig. 1).

Interaction of Imipramine and Desipramine with I—Fluorescence spectra of I in water and in the presence of imipramine or desipramine are recorded in Fig. 3. Similar spectral changes were observed in the presence of each compound. When the concentration of free imipramine was high, the fluorescence intensity of the I–imipramine complex increased as a function of the I concentration (curve b, Fig. 2). The effects of urea and potassium chloride on fluorescence intensity of the I–imipramine complex were similar to those of the probe–chlorpromazine interaction (Table I).

DISCUSSION

Compound I and other fluorescent compounds interact with large biomolecules such as plasma proteins and enzymes and thus have served as probes in studies of small molecule–protein binding (4, 5, 8). Less attention, however, has been directed toward interactions of I with relatively small organic drug molecules. In this study, fluorescence spectral changes of I were found to be due to its hydrophobic interaction with the drug molecules in an aqueous solution.

A hypsochromic shift accompanied by an increased emission intensity was seen in the spectra of I in the presence of chlorpromazine, trimeprazine, imipramine, and desipramine. These spectral characteristics are indicative of interactions involving hydrophobic binding. Similar changes in the spectra of I due to hydrophobic interactions with biological macromolecules were established. When I was dissolved in nonpolar

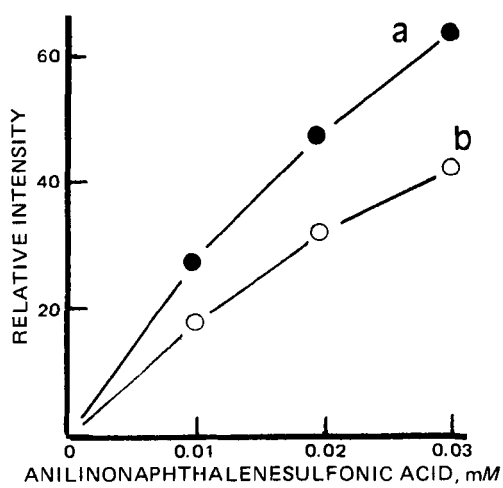

Figure 2—*Relative fluorescence intensity of I–chlorpromazine (curve a) and I–imipramine (curve b) interactions as a function of I concentration. The drug concentration was 2 × 10^{-3} M in water.*

[1] Aldrich Chemical Co., Milwaukee, Wis.
[2] Smith Kline & French Laboratories, Philadelphia, Pa.
[3] Geigy Pharmaceuticals, Ardsley, N.Y.
[4] Matheson, Coleman & Bell, Norwood, Ohio.
[5] Aminco-Bowman, American Instrument Co., Silver Spring, Md.
[6] Omnigraphic, Houston Instruments, Bellaire, Tex.

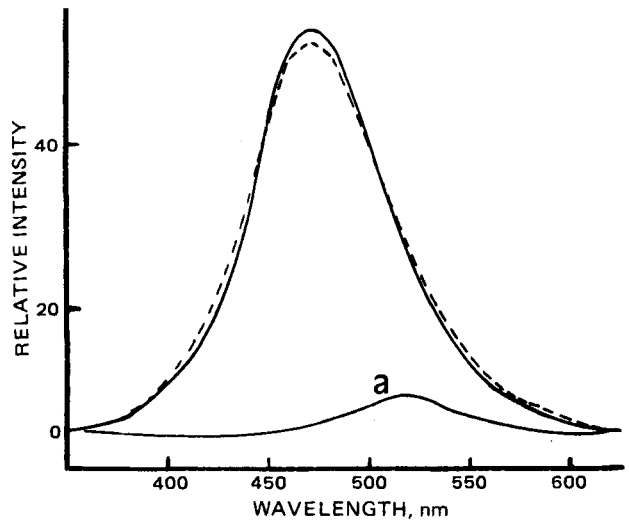

Figure 3—*Fluorescence emission spectra of the probe in pH 7.0 phosphate buffer (curve a) and when bound to imipramine (—) and to desipramine (- - -). The excitation maximum was set at 387 nm.*

solvents, it exhibited a large hypsochromic shift and increased fluorescence intensity (9–12). A direct correlation between the hydrophobicity of the solvent and the degree of spectral changes was found. It was suggested that hypsochromic shifts and enhanced fluorescence intensity were due to the conservation of excited energy in environments of decreasing polarity. The effects of potassium chloride and urea, which are known to bring about salting-out and salting-in effects, respectively, on the fluorescence properties of the I–chlorpromazine and I–imipramine complexes (Table I) provided additional evidence of the hydrophobic nature of the interaction.

Comparison of curves b and c in Fig. 1 suggested that chlorpromazine forms a stronger complex with I than does trimeprazine. The 2-chloro substituent in one aromatic ring of chlorpromazine appears to increase hydrophobic binding over the latter compound, which contains no chlorine substituents in its phenothiazine ring system. The greater ability of chlorpromazine to lower surface tension in aqueous solution relative to trimeprazine also was attributed to the greater hydrophobic effect of the 2-chlorophenothiazine ring of chlorpromazine (13). It was suggested that hydrophobic binding of these and related drugs to bovine serum albumin involved principally the phenothiazine moiety, with substituents attached to its nitrogen atom being of little significance in this regard (14). In accordance with this theory, the phenothiazine ring of chlorpromazine and, to a somewhat lesser extent, that of trimeprazine interact hydrophobically with the anilinonaphthalene ring of I, which causes the spectral changes.

The spectra of solutions of I in the presence of imipramine and desipramine exhibited similar emission spectra (Fig. 3). These compounds are structurally dissimilar only in the lack of a one side-chain methyl group in desipramine. Each contains a dibenzazepine ring system, which is presumably involved principally in hydrophobic binding with I, as in the case of the drugs containing a phenothiazine ring. This finding supports the suggestion (14) that side-chain substitution does not contribute to hydrophobic binding, since its participation in these otherwise structurally identical compounds would be expected to cause spectral differences.

REFERENCES

(1) J. L. Irvin and E. M. Irvin, *J. Biol. Chem.*, **196**, 651 (1952).

(2) C. F. Chignell, *Mol. Pharmacol.*, **5**, 244 (1969).

(3) D. A. Labianca, G. N. Taylor, and G. S. Hammond, *J. Am. Chem. Soc.*, **94**, 3679 (1972).

(4) L. Brand, J. R. Gohke, and D. S. Rao, *Biochemistry*, **6**, 3510 (1967).

(5) C. F. Chignell, *Mol. Pharmacol.*, **6**, 1 (1970).

(6) S. M. Aloj, K. C. Ingham, and H. Edelhoch, *Arch. Biochem. Biophys.*, **155**, 478 (1973).

(7) B. Rubalcava, D. M. Muñoz, and C. Gitler, *Biochemistry*, **8**, 2742 (1969).

(8) R. F. Chen and J. C. Kernohan, *J. Biol. Chem.*, **242**, 5813 (1967).

(9) L. Stryer, *J. Mol. Biol.*, **13**, 482 (1965).

(10) G. M. Edelman and W. O. McClure, *Acc. Chem. Res.*, **1**, 65 (1968).

(11) A. Hamabata, S. Chang, and P. H. von Hippel, *Biochemistry*, **12**, 1278 (1973).

(12) P. Mukerjee and K. J. Mysels, *Natl. Stand. Ref. Data Ser., Natl. Bur. Stand.*, No. 36 (1971).

(13) G. Zografi and M. V. Munshi, *J. Pharm. Sci.*, **59**, 819 (1970).

(14) J. Krieglstein, W. Meiler, and J. Stoob, *Biochem. Pharmacol.*, **21**, 985 (1972).

Synthesis of Antifungal 2-Substituted Phthalimidines

THOMAS J. SCHWAN ˣ **and JOSEPH E. GRAY**

Received August 19, 1977, from the *Research and Development Department, Norwich-Eaton Pharmaceuticals Division of Morton-Norwich Products, Inc., Norwich, NY 13815.* Accepted for publication September 16, 1977.

Abstract □ An improved synthesis of phthalimidine is reported. Two *N*-substituted phthalimidines were synthesized by alkylation of the parent compound, and they showed complete inhibition of *Microsporum* and *Trichophyton* species at 10–100 μg/ml in an agar dilution test. Both compounds were inactive against *Candida albicans* at 100 μg/ml or *Aspergillus niger* at 250 μg/ml.

Keyphrases □ Phthalimidines, substituted—synthesized, evaluated for antifungal activity □ Antifungal activity—various substituted phthalimidines evaluated □ Structure–activity relationships—various substituted phthalimidines evaluated for antifungal activity

Several *N*-substituted phthalimidines were desired for antifungal screening, so a convenient route to the parent compound I (Scheme I) was sought.

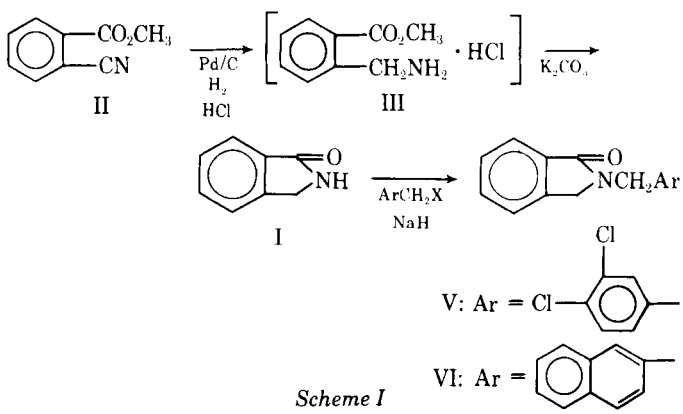

Scheme I

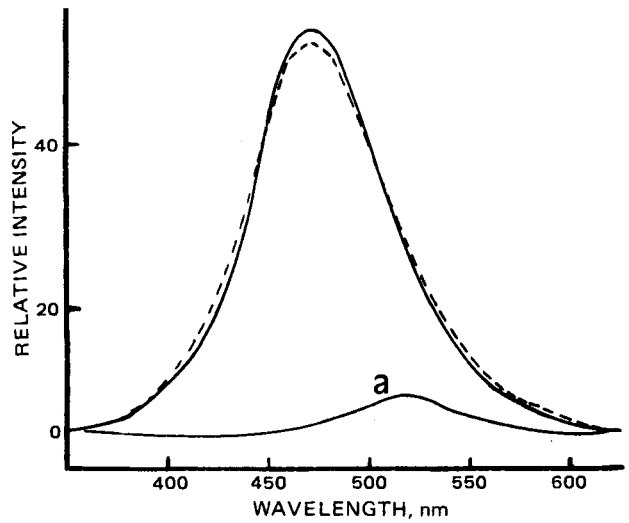

Figure 3—*Fluorescence emission spectra of the probe in pH 7.0 phosphate buffer (curve a) and when bound to imipramine (—) and to desipramine (- - -). The excitation maximum was set at 387 nm.*

solvents, it exhibited a large hypsochromic shift and increased fluorescence intensity (9–12). A direct correlation between the hydrophobicity of the solvent and the degree of spectral changes was found. It was suggested that hypsochromic shifts and enhanced fluorescence intensity were due to the conservation of excited energy in environments of decreasing polarity. The effects of potassium chloride and urea, which are known to bring about salting-out and salting-in effects, respectively, on the fluorescence properties of the I–chlorpromazine and I–imipramine complexes (Table I) provided additional evidence of the hydrophobic nature of the interaction.

Comparison of curves b and c in Fig. 1 suggested that chlorpromazine forms a stronger complex with I than does trimeprazine. The 2-chloro substituent in one aromatic ring of chlorpromazine appears to increase hydrophobic binding over the latter compound, which contains no chlorine substituents in its phenothiazine ring system. The greater ability of chlorpromazine to lower surface tension in aqueous solution relative to trimeprazine also was attributed to the greater hydrophobic effect of the 2-chlorophenothiazine ring of chlorpromazine (13). It was suggested that hydrophobic binding of these and related drugs to bovine serum albumin involved principally the phenothiazine moiety, with substituents attached to its nitrogen atom being of little significance in this regard (14). In accordance with this theory, the phenothiazine ring of chlorpromazine and, to a somewhat lesser extent, that of trimeprazine interact hydrophobically with the anilinonaphthalene ring of I, which causes the spectral changes.

The spectra of solutions of I in the presence of imipramine and desipramine exhibited similar emission spectra (Fig. 3). These compounds are structurally dissimilar only in the lack of a one side-chain methyl group in desipramine. Each contains a dibenzazepine ring system, which is presumably involved principally in hydrophobic binding with I, as in the case of the drugs containing a phenothiazine ring. This finding supports the suggestion (14) that side-chain substitution does not contribute to hydrophobic binding, since its participation in these otherwise structurally identical compounds would be expected to cause spectral differences.

REFERENCES

(1) J. L. Irvin and E. M. Irvin, *J. Biol. Chem.*, **196**, 651 (1952).

(2) C. F. Chignell, *Mol. Pharmacol.*, **5**, 244 (1969).

(3) D. A. Labianca, G. N. Taylor, and G. S. Hammond, *J. Am. Chem. Soc.*, **94**, 3679 (1972).

(4) L. Brand, J. R. Gohke, and D. S. Rao, *Biochemistry*, **6**, 3510 (1967).

(5) C. F. Chignell, *Mol. Pharmacol.*, **6**, 1 (1970).

(6) S. M. Aloj, K. C. Ingham, and H. Edelhoch, *Arch. Biochem. Biophys.*, **155**, 478 (1973).

(7) B. Rubalcava, D. M. Muñoz, and C. Gitler, *Biochemistry*, **8**, 2742 (1969).

(8) R. F. Chen and J. C. Kernohan, *J. Biol. Chem.*, **242**, 5813 (1967).

(9) L. Stryer, *J. Mol. Biol.*, **13**, 482 (1965).

(10) G. M. Edelman and W. O. McClure, *Acc. Chem. Res.*, **1**, 65 (1968).

(11) A. Hamabata, S. Chang, and P. H. von Hippel, *Biochemistry*, **12**, 1278 (1973).

(12) P. Mukerjee and K. J. Mysels, *Natl. Stand. Ref. Data Ser., Natl. Bur. Stand.*, No. 36 (1971).

(13) G. Zografi and M. V. Munshi, *J. Pharm. Sci.*, **59**, 819 (1970).

(14) J. Krieglstein, W. Meiler, and J. Stoob, *Biochem. Pharmacol.*, **21**, 985 (1972).

Synthesis of Antifungal 2-Substituted Phthalimidines

THOMAS J. SCHWAN ˣ **and JOSEPH E. GRAY**

Received August 19, 1977, from the *Research and Development Department, Norwich-Eaton Pharmaceuticals Division of Morton-Norwich Products, Inc., Norwich, NY 13815.* Accepted for publication September 16, 1977.

Abstract □ An improved synthesis of phthalimidine is reported. Two *N*-substituted phthalimidines were synthesized by alkylation of the parent compound, and they showed complete inhibition of *Microsporum* and *Trichophyton* species at 10–100 μg/ml in an agar dilution test. Both compounds were inactive against *Candida albicans* at 100 μg/ml or *Aspergillus niger* at 250 μg/ml.

Keyphrases □ Phthalimidines, substituted—synthesized, evaluated for antifungal activity □ Antifungal activity—various substituted phthalimidines evaluated □ Structure–activity relationships—various substituted phthalimidines evaluated for antifungal activity

Several *N*-substituted phthalimidines were desired for antifungal screening, so a convenient route to the parent compound I (Scheme I) was sought.

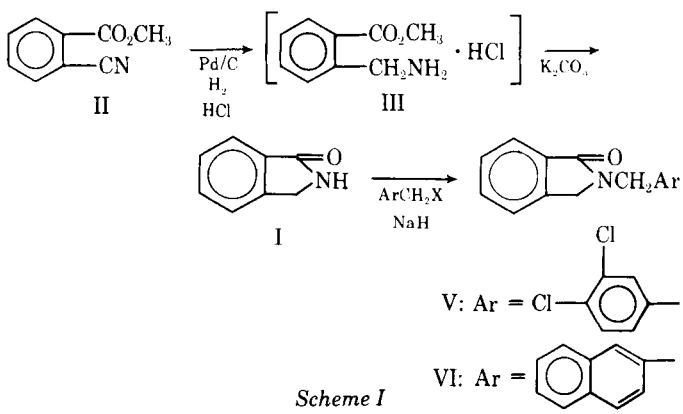

Scheme I

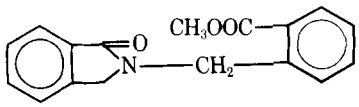

IV

Target compound I was prepared in a yield of 88% by the palladium-on-carbon hydrogenation of methyl 2-cyanobenzoate (II) and subsequent cyclization of the resultant amine (III). This method is a variation of that originally reported by Velluz and Amiard (1), who obtained 46–67% yields of I contaminated with *N*-(2-methoxycarbonylbenzyl)phthalimidine (IV) when Raney nickel was employed in the hydrogenation. No trace of IV was evident in the present work.

Alkylation of I with the appropriate halo compound gave the 3,4-dichlorobenzyl compound V and the 2-naphthylmethyl compound VI. That alkylation occurred on nitrogen rather than oxygen was ascertained by carbonyl absorption in the IR spectra of V and VI.

Compound VI was slightly more active than V when challenged by six dermatophytic organisms in an agar dilution test (Table I). Neither compound was active against *Candida albicans* at 100 μg/ml or *Aspergillus niger* at 250 μg/ml.

EXPERIMENTAL[1]

Chemistry—*Phthalimidine (I)*—A mixture of 48.6 g (0.302 mole) of II, 2.0 g of 5% palladium-on-carbon (50% moisture), 500 ml of methanol, and 500 ml of ethanol saturated with hydrogen chloride was shaken with hydrogen on a Parr apparatus until the theoretical quantity of hydrogen was consumed (24 hr).

The catalyst was filtered and washed with 2 × 100 ml of methanol. To the filtrate and combined washings was added 40 g of potassium carbonate. The mixture was stirred and refluxed for 20 hr and concentrated to dryness *in vacuo*, and the solid residue was stirred with 150 ml of water for 2.0 hr.

The solid was filtered, and the filtrate was extracted with 2 × 150 ml of chloroform. The extracts were combined, dried (magnesium sulfate), and concentrated to dryness. The residue was combined with the original solid.

Recrystallization from 235 ml of acetonitrile gave, in two crops, 35.4 g (88%) of the product, mp 151–152.5°. Further recrystallization from water gave an analytical sample, mp 148–151° [lit. (1) mp 149°]; IR: 3.11 (NH), 5.88–5.97 (C=O), and 6.25 (C=C) μm.

Anal.—Calc. for C_8H_7NO: C, 72.16; H, 5.30; N, 10.52. Found: C, 72.42; H, 5.23; N, 10.61.

N-(3,4-Dichlorobenzyl)phthalimidine (V)—A mixture of 13.3 g (0.100 mole) of I, 8.0 g of sodium hydride 60% in mineral oil (4.80 g, 0.200 mole), and 19.5 g (0.100 mole) of 3,4-dichlorobenzyl chloride in 175 ml of toluene was stirred and refluxed for 18 hr. Methanol (25 ml) was added to destroy excess sodium hydride, and the mixture was concentrated to dryness *in vacuo*. The residue was partitioned between 200 ml of water and 200 ml of chloroform. The chloroform layer was separated, and the aqueous layer was extracted with 2 × 100 ml of chloroform. The combined extracts were washed with 200 ml of water, dried (magnesium sulfate), and concentrated to dryness *in vacuo* to give 33.5 g of an oil; this oil was washed with 75 ml of cold hexane.

Crystallization from 125 ml of toluene gave 13.1 g of material, which was boiled with 325 ml of heptane. The heptane solution was combined with the toluene filtrate, and the mixture was concentrated to dryness. Crystallization of the residue from 30 ml of toluene gave 5.1 g (17%) of the product, mp 92–105°. Further recrystallization from heptane gave an analytical sample, mp 105–106°; IR: 5.97 (C=O), 6.29, and 6.40 (C=C) μm; NMR (deuterochloroform): δ 4.30 (s, 2, phthalimidine CH_2), 4.76 (s, 2, NCH_2Ar), and 7.05–8.00 (m, 7, phenyl CH) ppm.

Anal.—Calc. for $C_{15}H_{11}Cl_2NO$: C, 61.66; H, 3.80; N, 4.80. Found: C, 61.71; H, 3.92; N, 4.70.

N-(2-Naphthylmethyl)phthalimidine (VI)—A mixture of I (16.1 g, 0.121 mole), 30.94 g (0.140 mole) of 2-(bromomethyl)naphthalene, and 8.0 g of sodium hydride 60% in mineral oil (4.80 g, 0.20 mole) in 150 ml of toluene was stirred and refluxed for 16 hr and cooled. Then 3.0 ml of methanol was added. After dilution with 250 ml of water, the mixture was stirred for 1 hr. The toluene layer was separated, and the aqueous layer was extracted with 100 ml of toluene. The combined organic extracts were washed with 150 ml of water, dried (magnesium sulfate), and concentrated to dryness *in vacuo*. Crystallization from 40 ml of toluene gave 12.6 g (46%) of the product, mp 97–102°. Further recrystallization from toluene gave an analytical sample, mp 103–106°; IR: 5.92 (C=O) and 6.20 (C=C) μm; NMR (deuterochloroform): δ 4.23 (s, 2, phthalimidine CH_2), 4.93 (s, 2, NCH_2Ar), and 7.00–8.00 (m, 11, aryl CH) ppm.

Anal.—Calc. for $C_{19}H_{15}NO$: C, 83.49; H, 5.53; N, 5.13. Found: C, 83.76; H, 5.67; N, 4.94.

Mycology—The antifungal activity of the compounds was determined by a minimum inhibitory concentration procedure (2) for *C. albicans* and by an agar dilution procedure (3) for *Aspergillus, Trichophyton,* and *Microsporum* species. In the latter procedure, with incubation at 25°, complete inhibition of growth for 10 days is the criterion for an active compound.

Table I—MIC [a] by Agar Dilution Method in Sabouraud's Dextrose Agar

Test Organism [b]	V	VI
Microsporum canis (M-4)	100	100
Microsporum audouini (M-17)	100	10
Microsporum gypseum (M-108)	100	100
Trichophyton mentagrophytes (M-93)	100	100
Trichophyton tonsurans (M-76)	100	100
Trichophyton rubrum (M-107)	10	10

[a] Minimum inhibitory concentration, micrograms per milliliter of medium. Compounds were dissolved in dimethylformamide (2). [b] The numbers in parentheses are Norwich-Eaton Pharmaceuticals culture numbers.

REFERENCES

(1) L. Velluz and G. Amiard, *Bull. Soc. Chim.*, **1946,** 690; through *Chem. Abstr.*, **41,** 3445 (1947).

(2) D. C. Grove and W. A. Randall, "Assay Methods of Antibiotics: A Laboratory Manual," Medical Encyclopedia, New York, N.Y., 1955.

(3) G. F. Reddish, "Antiseptics, Fungicides and Chemical and Physical Sterilization," 1st ed., Lea & Febiger, New York, N.Y., 1954, pp. 135, 136.

ACKNOWLEDGMENTS

The authors are indebted to Ms. Cora Jeffrey for the microanalyses, Ms. Connie Lloyd for the NMR spectra, and Mr. Ralph Bush and Mr. Larry Wood for assistance in the antifungal studies.

[1] Melting points were determined on a Mel-Temp apparatus, and those below 230° are corrected. IR spectra were determined as mineral oil mulls using a Perkin-Elmer 137B spectrophotometer. NMR spectra were obtained on a Varian A-60A instrument and were compared with tetramethylsilane as an internal standard.

Structure–Activity Relationships among *In Vivo* Active Germacranolides

S. MORRIS KUPCHAN †, J. W. ASHMORE *, and A. T. SNEDEN ‡x

Received August 9, 1977, from the *Department of Chemistry, University of Virginia, Charlottesville, VA 22901.* Accepted for publication September 22, 1977. *Present address: Department of Chemistry, University of California at Berkeley, Berkeley, CA 94720. ‡Present address: Department of Chemistry, Virginia Commonwealth University, Richmond, VA 23284. †Deceased.

Abstract □ Nine structurally related germacranolides from *Eupatorium semiserratum* and *Eriophyllum confertiflorum* were assayed in two standard tumor systems (PS and KB) to determine the structural features required for *in vivo* antileukemic activity. The moieties necessary for *in vivo* activity were found to be an α,β-unsaturated ester side chain adjacent to the γ-lactone and either a primary or secondary allylic alcohol or both.

Keyphrases □ Germacranolides—isolated from *Eupatorium semiserratum* and *Eriophyllum confertiflorum*, antineoplastic activity evaluated □ *Eupatorium semiserratum*—germacranolides isolated, antineoplastic activity evaluated □ *Eriophyllum confertiflorum*—germacranolides isolated, antineoplastic activity evaluated □ Antineoplastic activity—germacranolides isolated from *Eupatorium semiserratum* and *Eriophyllum confertiflorum* evaluated □ Structure–activity relationships—germacranolides isolated from *Eupatorium semiserratum* and *Eriophyllum confertiflorum* evaluated for antineoplastic activity

The discovery of antineoplastic activity in various sesquiterpene lactones derived from plant sources has stimulated considerable synthetic and biological interest in these compounds, and several studies relating structural features to cytotoxicity were reported recently (1–5). However, with the exception of the pseudoguianolide helenalin (I) (6, 7), few reports correlated structural requirements with *in vivo* activity.

The relatively large amounts of material necessary for *in vivo* testing (because of the high doses required to show activity) has imposed serious limitations on structure–activity studies of many compounds, especially natural products, which are available only in small quantities. Comparisons of compounds with diverse structural differences and functionalities that have potentially different modes of action can also complicate the interpretation of test results. Therefore, the study reported here concentrated on eriofertin (II), eriofertopin (V), and deacetyleupaserrin (VIII), germacranolides that are structurally similar and that have shown significant *in vivo* activity[1] against P-388 lymphocytic leukemia in the mouse (Table I).

The compounds are multifunctional. They contain an α-methylene butyrolactone ring, a functionality that has been shown to be necessary for cytotoxicity (1), and an unsaturated ester moiety adjacent to the lactone ring. Oxygenation in the form of either an OH or *O*-acyl group adjacent to the α-methylene butyrolactone moiety has been shown to increase the rate of cysteine addition to the butyrolactone ring (1) and may account, in part, for the significant *in vivo* activity. These compounds also contain primary and secondary allylic alcohols, which may serve as potential alkylation sites for a nucleophile on a biological macromolecule.

EXPERIMENTAL[2]

Deacetyleupaserrin (VIII), eupaserrin (IX), and acetyleupaserrin (X) were available from *Eupatorium semiserratum* DC (Asteraceae) as described previously (9).

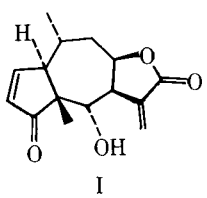

I

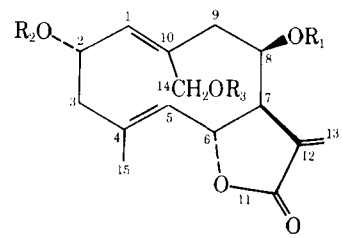

II: R_1 = 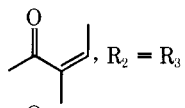 , $R_2 = R_3 = H$

III: R_1 = 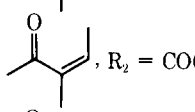 , $R_2 = COCH_3$, $R_3 = H$

IV: R_1 = 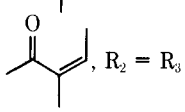 , $R_2 = R_3 = COCH_3$

V: R_1 = 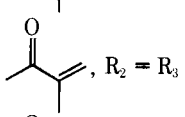 , $R_2 = R_3 = H$

VI: R_1 = 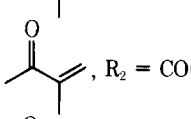 , $R_2 = COCH_3$, $R_3 = H$

VII: R_1 = 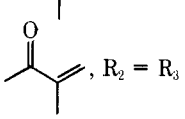 , $R_2 = R_3 = COCH_3$

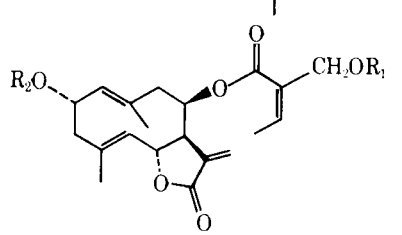

VIII: $R_1 = R_2 = H$
IX: $R_1 = COCH_3$, $R_2 = H$
X: $R_1 = R_2 = COCH_3$

[1] Cytotoxicity and *in vivo* activity were assayed under the auspices of the National Cancer Institute according to standard protocols (8). Compounds II–X show cytotoxic activity against KB cell culture in the range of $ED_{50} = 10–10^{-1}$ μg/ml.

[2] Melting points were determined on a Mettler FP2 melting-point apparatus and are uncorrected. UV absorption spectra were determined on a Beckman model DK-2A recording spectrophotometer. IR spectra were determined on a Perkin-Elmer model 257 recording spectrophotometer. NMR spectra were determined on a JEOL PS-100 p FT NMR spectrometer interfaced to a Texas Instruments JEOL 980A computer, with tetramethylsilane as the internal standard. Mass spectra were determined on Hitachi Perkin-Elmer model RMU-6E and AEI model MS902 spectrometers at the University of Virginia. Values of $[\alpha]_D$ were determined on a Perkin-Elmer model 141 polarimeter.

Table I—Activity of II–X against P-388 Lymphocytic Leukemia in the Mouse

Compound	Dose, mg/kg	Weight Difference[a]	T/C, %[b]
II	40	−2.4	130
	20	−2.2	148
	10	−2.0	121
III	30	0.7	86
	15	1.2	93
	7.5	0.7	98
IV	40	1.7	126
	20	−1.1	109
	10	0.9	95
V	40	−3.6	Toxic
	20	−2.0	167
	10	−1.4	159
VI	30	−0.8	130
	15	0.2	120
	7.5	1.3	115
VII	30	−0.2	106
	15	−0.7	100
	7.5	−1.9	101
VIII	18	−2.1	150
	12	−0.2	155
	8.0	−0.4	160
IX	44	−2.4	150
	30	−2.3	145
	20	−2.1	122
X	30	−2.0	123
	15	−1.7	123
	7.5	−0.6	101

[a] The difference, in grams, between the weights of test and control animals. [b] The ratio (expressed as a percent) of the median survival time of the treated group of mice to the median survival time of the control group. A T/C ≥ 125% indicates activity in the National Institutes of Health protocol (8).

Eriofertopin (V) and 2-*O*-acetyleriofertopin (VI) were isolated from *Eriophyllum confertiflorum* Gray (Asteraceae)[3], and eriofertopin diacetate (VII) was prepared from eriofertopin as described previously (10). Eriofertin (II), 2-*O*-acetyleriofertin (III), and eriofertin diacetate (IV) were isolated from *E. confertiflorum* or prepared as described below. Compounds II–IV had all been reported previously (11), but complete spectral data for II and III were not given.

Isolation Procedure—Fractionation of a 95% ethanol (soxhlet) extract of *E. confertiflorum* (1 kg), guided by assays against human carcinoma of the nasopharynx cell culture (KB) and P-388 lymphocytic leukemia in the mouse (PS), showed the activity to be successively concentrated in the chloroform phase of a chloroform–water partition, the 10% aqueous methanol phase of a 10% aqueous methanol–*n*-hexane[4] partition, the 20% aqueous methanol phase of a 20% aqueous methanol–carbon tetrachloride partition, and the chloroform phase of a chloroform–40% aqueous methanol partition. Column chromatography of the final chloroform partition on silica gel 60[5] yielded two active fractions.

Eriofertin (II)—Extensive preparative TLC of the more polar fraction on silica gel 60 gave a more polar compound, eriofertopin (V), as described previously (10), and a less polar compound, eriofertin (II), as a brittle white foam, $[\alpha]_D^{21}$ +70° (c, 1.0 in $CHCl_3$); IR ($CHCl_3$): 3430, 1765, and 1725 cm^{-1}; NMR ($CDCl_3$): δ 1.70 (3H, s, 4-CH_3), 1.87 (3H, d, J = 1.2 Hz, 2′-CH_3), 1.97 (3H, d, J = 8 Hz, 3′-CH_3), 2.99 (1H, m, 7-H), 3.37 (2H, dd, J = 5.4, 14.4 Hz, 9-H_2), 3.76, 4.26 (2H, 2d, J = 12.7 Hz, 14-H_2), 4.83 (1H, dt, J = 5.8, 10 Hz, 2-H), 5.05 (3H, m, 1-H, 5-H, 6-H), 5.64, 6.33 (2H, 2d, J = 3.4 Hz, 13-H_2), 5.82 (1H, m, 8-H), and 6.13 (1H, dq, J = 1.2, 8 Hz, 3′-H) ppm; mass spectrum: *m/e* 363.1793 (M^+ + H, calc. for $C_{20}H_{27}O_6$, 363.1808).

2-*O*-Acetyleriofertin (III)—Extensive preparative TLC of the less polar column fraction on silica gel 60 gave a more polar compound, 2-*O*-acetyleriofertopin (VI), as described previously (10), and a less polar compound, 2-*O*-acetyleriofertin (III), as an oil, $[\alpha]_D^{21}$ +45.4° (c, 1.0 in $CHCl_3$); IR ($CHCl_3$): 3500, 1765, 1733, and 1725 cm^{-1}; NMR ($CDCl_3$): δ 1.77 (3H, s, 4-CH_3), 1.86 (3H, d, J = 1.2 Hz, 2′-CH_3), 1.97 (3H, d, J = 8 Hz, 3′-CH_3), 2.08 (3H, s, 2-$OCOCH_3$), 2.97 (1H, m, 7-H), 3.19 (2H, dd, J = 5.6, 14.0 Hz, 9-H_2), 3.75, 4.40 (2H, 2d, J = 13.7 Hz, 14-H_2), 5.10 (3H, m, 1-H, 5-H, 6-H), 5.66, 6.33 (2H, 2d, J = 3.4 Hz, 13-H_2), 5.75 (1H, m, 2-H), 5.82 (1H, m, 8-H), and 6.13 (1H, dq, J = 1.2, 8 Hz, 3′-H) ppm; mass spectrum: *m/e* 405 (M^+ + H).

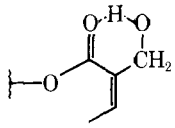

A

Eriofertin Diacetate (IV)—Eriofertin (5.0 mg) was treated with 0.25 ml of acetic anhydride and 0.5 ml of pyridine in 1.0 ml of benzene for 20 hr at room temperature, affording IV (2.2 mg) [identical with reported melting point, IR, NMR, and mass spectral data (11)].

RESULTS AND DISCUSSION

As can be seen in Table I, acetylation had a pronounced effect on the antileukemic activities of eriofertin (II), eriofertopin (V), and deacetyleupaserrin (VIII). Eupaserrin (IX), in which the primary allylic alcohol of the sarracinate moiety had been acetylated, was approximately as active as the diol but at a much higher dose. This activity could be a result of the more efficient transport of VIII compared to IX to the active site. When both alcohols of VIII were acetylated, the antileukemic activity was lost. This same effect was noted with both II and V.

2-*O*-Acetyleriofertin (III) and 2-*O*-acetyleriofertopin (VI), compounds in which the secondary allylic alcohol was acetylated, showed either a lack of or greatly diminished antileukemic activity. Acetylation of both alcohols in II and V, affording eriofertin diacetate (IV) and eriofertopin diacetate (VII), respectively, also resulted in greatly diminished *in vivo* activity. These results suggest that the primary allylic alcohol and, particularly, the secondary allylic alcohol contribute to the high *in vivo* activity of these compounds.

The ester moieties also exhibit some effect on the antileukemic activity, with the compounds containing methacrylate (V) and sarracinate (VIII) esters being somewhat more active than those with angelate (II) and acetylsarracinate (IX) esters. The reduced activity of II as compared to V may be a result of steric hindrance to the addition of a biological nucleophile by the larger β-methyl group of the angelate in II as compared to the smaller β-hydrogen of the methacrylate moiety in V. In the acetylsarracinate moiety of IX, the possibility of intramolecular hydrogen bonding such as Structure A in the sarracinate moiety of VIII, which might facilitate conjugate addition, has been eliminated, decreasing the rate of addition of a biological nucleophile to the acetylsarracinate group.

It is apparent that an α-methylene butyrolactone ring alone is not sufficient for *in vivo* antileukemic activity among the germacranolides discussed. An α,β-unsaturated ester side chain adjacent to the γ-lactone and a primary or secondary allylic alcohol appear to be vital for high *in vivo* activity. These and analogous functional groups can be found in most of the germacranolides and many of the other sesquiterpene lactones that have demonstrated significant *in vivo* activity.

REFERENCES

(1) S. M. Kupchan, M. A. Eakin, and A. M. Thomas, *J. Med. Chem.*, **14**, 1147 (1971).

(2) K.-H. Lee, E.-S. Huang, C. Piantadosi, J. S. Pagano, and T. A. Geissman, *Cancer Res.*, **31**, 1649 (1971).

(3) P. A. Grieco, J. A. Naguez, Y. Masaki, K. Hiroi, M. Nishizawa, A. Rosowsky, S. Oppenheim, and H. Lazarus, *J. Med. Chem.*, **20**, 71 (1977).

(4) A. Rosowsky, N. Papathanasopoulas, H. Lazarus, G. E. Foley, and E. J. Modest, *ibid.*, **17**, 672 (1974).

(5) G. A. Howie, P. E. Manni, and J. M. Cassady, *ibid.*, **17**, 840 (1974).

(6) K.-H. Lee, R. Meck, C. Piantadosi, and E.-S. Huang, *ibid.*, **16**, 299 (1973).

(7) K.-H. Lee, I. H. Hall, E.-C. Mar, C. O. Starnes, S. A. El Gebaly, T. G. Waddell, R. I. Hadgraft, C. G. Ruffner, and I. Weidner, *Science*, **196**, 533 (1977).

(8) R. I. Geran, N. H. Greenberg, M. M. MacDonald, A. M. Schumacher, and B. J. Abbott, *Cancer Chemother. Rep., Part 3*, **3**, 1 (1972).

(9) G. R. Pettit and G. M. Cragg, *Experientia*, **29**, 781 (1973).

(10) S. M. Kupchan, J. W. Ashmore, and A. T. Sneden, *Phytochem-*

[3] Stems, leaves, and flowers were collected in California in April 1973. Dr. Robert E. Perdue, Jr., U.S. Department of Agriculture, Beltsville, Md., supplied the dried plant material in accordance with the program developed by the National Cancer Institute. Voucher specimen SPJ-3303 is on deposit at the Beltsville Agricultural Research Center of the U.S. Department of Agriculture, Beltsville, Md.

[4] Skelly-B.

[5] E. Merck.

istry, in press.
(11) T. Saitoh, T. A. Geissman, T. G. Waddell, W. Herz, and S. V. Bhat, *Rev. Latinoamer. Quim.*, **2**, 69 (1971).

ACKNOWLEDGMENTS

Supported by grants from the National Cancer Institute (CA-11718) and the American Cancer Society (CH-42M) and by a contract with the Division of Cancer Treatment, National Cancer Institute (N01-CM-67002).

The authors thank Dr. T. A. Waddell, Department of Chemistry, University of Tennessee at Chattanooga, for authentic IR spectra of II and IV, and Dr. Waddell and Dr. W. Herz, Department of Chemistry, Florida State University, for copies of Ref. 10.

J. W. Ashmore was a National Institute of Health Postdoctoral Fellow (Grant 1-F32-CA-05673-01).

Comparative Pharmacokinetics of Coumarin Anticoagulants XXXV: Examination of Possible Pharmacokinetic Interaction between (*R*)-(+)- and (*S*)-(−)-Warfarin in Humans

GERHARD LEVY *x, **ROBERT A. O'REILLY** ‡, and **LEMUEL B. WINGARD, Jr.** §

Received August 22, 1977, from the *Department of Pharmaceutics, State University of New York at Buffalo, Amherst, NY 14260, the ‡Department of Medicine, Santa Clara Medical Center, San Jose, CA 95128, and the §Department of Pharmacology, University of Pittsburgh, Pittsburgh, PA 15261. Accepted for publication September 20, 1977.

Abstract □ The elimination kinetics and anticoagulant effect produced by single 1.5-mg/kg doses of (*R*)-(+)-, (*S*)-(−)-, and racemic warfarin were determined in 10 healthy men. The results obtained in experiments with the individual enantiomers were used to predict the elimination kinetics and anticoagulant effect of racemic warfarin, assuming that there is no interaction between the two enantiomers. These predictions were compared to experimental results, and no significant differences were observed. This finding suggests that there are no pronounced pharmacokinetic or pharmacodynamic interactions between single large doses of (*R*)-(+)- and (*S*)-(−)-warfarin in humans.

Keyphrases □ Warfarin—(*R*)-(+)- and (*S*)-(−)-forms, elimination kinetics and anticoagulant effect compared, humans □ Elimination kinetics—(*R*)-(+)- and (*S*)-(−)-warfarin compared, humans □ Anticoagulant effect—(*R*)-(+)- and (*S*)-(−)-warfarin compared, humans □ Pharmacokinetics—(*R*)-(+)- and (*S*)-(−)-warfarin compared, humans □ Enantiomers—(*R*)-(+)- and (*S*)-(−)-warfarin, elimination kinetics and anticoagulant effect compared, humans

The anticoagulant warfarin is used therapeutically in the racemic form. The constituents of the racemic mixture, (*R*)-(+)- and (*S*)-(−)-warfarin, differ in pharmacokinetic characteristics, anticoagulant potency, and metabolic fate (1–9). The plasma warfarin concentrations of rats after intravenous administration of a dose of racemic warfarin are essentially equal to the sum of the concentrations observed after separate administration of half of the dose of each individual enantiomer, suggesting that one enantiomer does not measurably affect the pharmacokinetics of the other (8). On the other hand, Chan *et al.* (3) observed that the metabolic pattern of single doses of racemic warfarin in humans is not equivalent to the sum of the patterns obtained from administration of the individual enantiomers, suggesting an interaction between the two enantiomers (3).

To examine the possible pharmacokinetic and pharmacodynamic implications of the apparent metabolic interaction in humans, the kinetics of elimination and anticoagulant effect of a single dose of racemic warfarin were compared with the kinetics predicted on the basis of results obtained by separate administration of the individual enantiomers.

EXPERIMENTAL

Ten healthy men, 21–51 years old, received single oral doses of (*R*)-(+)-, (*S*)(−)-, and racemic warfarin, 1.5 mg/kg, at intervals of at least 1 month. Daily blood samples were obtained for 9 days, and the warfarin concentration and the prothrombin complex activity were determined in plasma. Details of these procedures were described previously (9).

The apparent volume of distribution, V_d, the elimination rate constant, k_{el}, and the total body clearance, *TC*, were determined (10), and the synthesis rate of prothrombin complex activity, R_{syn}, was calculated (11). The pharmacokinetic and pharmacodynamic data obtained following separate administration of the two enantiomers were used to make quantitative predictions of pharmacokinetic and pharmacodynamic patterns of single doses of racemic warfarin (6, 8).

RESULTS AND DISCUSSION

The total body clearances of (*R*)-(+)- and (*S*)-(−)-warfarin were 1.30 ± 0.47 and 2.08 ± 0.70 ml/hr/kg (mean ± *SD*), respectively. The individual data are reported elsewhere (10). The experimentally determined and predicted individual values of k_{el}, V_d, and *TC* for racemic warfarin are presented in Table I. There were no statistically significant differences between the experimental and predicted values; the correlation between

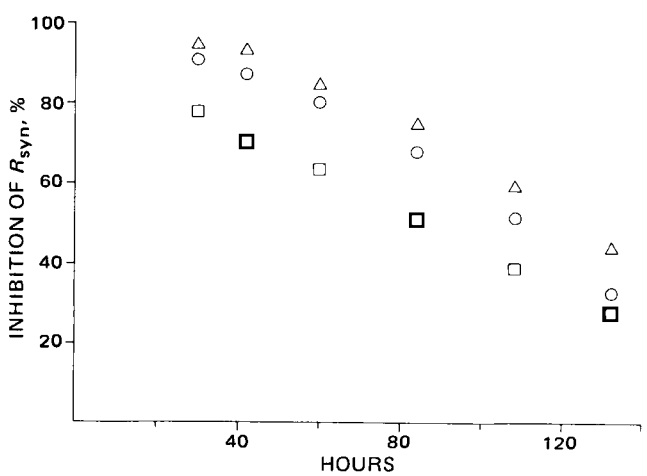

Figure 1—*Time course of inhibition of prothrombin complex activity synthesis rate, R_{syn}, produced by a single oral 1.5-mg/kg dose of* (S)-(−)-*warfarin* (△), *racemic warfarin* (○), *and* (R)-(+)-*warfarin* (□). *Average of data from 10 subjects.*

istry, in press.
(11) T. Saitoh, T. A. Geissman, T. G. Waddell, W. Herz, and S. V. Bhat, *Rev. Latinoamer. Quim.*, **2**, 69 (1971).

ACKNOWLEDGMENTS

Supported by grants from the National Cancer Institute (CA-11718) and the American Cancer Society (CH-42M) and by a contract with the Division of Cancer Treatment, National Cancer Institute (N01-CM-67002).

The authors thank Dr. T. A. Waddell, Department of Chemistry, University of Tennessee at Chattanooga, for authentic IR spectra of II and IV, and Dr. Waddell and Dr. W. Herz, Department of Chemistry, Florida State University, for copies of Ref. 10.

J. W. Ashmore was a National Institute of Health Postdoctoral Fellow (Grant 1-F32-CA-05673-01).

Comparative Pharmacokinetics of Coumarin Anticoagulants XXXV: Examination of Possible Pharmacokinetic Interaction between (*R*)-(+)- and (*S*)-(−)-Warfarin in Humans

GERHARD LEVY *x, **ROBERT A. O'REILLY** ‡, and **LEMUEL B. WINGARD, Jr.** §

Received August 22, 1977, from the *Department of Pharmaceutics, State University of New York at Buffalo, Amherst, NY 14260, the ‡Department of Medicine, Santa Clara Medical Center, San Jose, CA 95128, and the §Department of Pharmacology, University of Pittsburgh, Pittsburgh, PA 15261. Accepted for publication September 20, 1977.

Abstract □ The elimination kinetics and anticoagulant effect produced by single 1.5-mg/kg doses of (*R*)-(+)-, (*S*)-(−)-, and racemic warfarin were determined in 10 healthy men. The results obtained in experiments with the individual enantiomers were used to predict the elimination kinetics and anticoagulant effect of racemic warfarin, assuming that there is no interaction between the two enantiomers. These predictions were compared to experimental results, and no significant differences were observed. This finding suggests that there are no pronounced pharmacokinetic or pharmacodynamic interactions between single large doses of (*R*)-(+)- and (*S*)-(−)-warfarin in humans.

Keyphrases □ Warfarin—(*R*)-(+)- and (*S*)-(−)-forms, elimination kinetics and anticoagulant effect compared, humans □ Elimination kinetics—(*R*)-(+)- and (*S*)-(−)-warfarin compared, humans □ Anticoagulant effect—(*R*)-(+)- and (*S*)-(−)-warfarin compared, humans □ Pharmacokinetics—(*R*)-(+)- and (*S*)-(−)-warfarin compared, humans □ Enantiomers—(*R*)-(+)- and (*S*)-(−)-warfarin, elimination kinetics and anticoagulant effect compared, humans

The anticoagulant warfarin is used therapeutically in the racemic form. The constituents of the racemic mixture, (*R*)-(+)- and (*S*)-(−)-warfarin, differ in pharmacokinetic characteristics, anticoagulant potency, and metabolic fate (1–9). The plasma warfarin concentrations of rats after intravenous administration of a dose of racemic warfarin are essentially equal to the sum of the concentrations observed after separate administration of half of the dose of each individual enantiomer, suggesting that one enantiomer does not measurably affect the pharmacokinetics of the other (8). On the other hand, Chan *et al.* (3) observed that the metabolic pattern of single doses of racemic warfarin in humans is not equivalent to the sum of the patterns obtained from administration of the individual enantiomers, suggesting an interaction between the two enantiomers (3).

To examine the possible pharmacokinetic and pharmacodynamic implications of the apparent metabolic interaction in humans, the kinetics of elimination and anticoagulant effect of a single dose of racemic warfarin were compared with the kinetics predicted on the basis of results obtained by separate administration of the individual enantiomers.

EXPERIMENTAL

Ten healthy men, 21–51 years old, received single oral doses of (*R*)-(+)-, (*S*)(−)-, and racemic warfarin, 1.5 mg/kg, at intervals of at least 1 month. Daily blood samples were obtained for 9 days, and the warfarin concentration and the prothrombin complex activity were determined in plasma. Details of these procedures were described previously (9).

The apparent volume of distribution, V_d, the elimination rate constant, k_{el}, and the total body clearance, *TC*, were determined (10), and the synthesis rate of prothrombin complex activity, R_{syn}, was calculated (11). The pharmacokinetic and pharmacodynamic data obtained following separate administration of the two enantiomers were used to make quantitative predictions of pharmacokinetic and pharmacodynamic patterns of single doses of racemic warfarin (6, 8).

RESULTS AND DISCUSSION

The total body clearances of (*R*)-(+)- and (*S*)-(−)-warfarin were 1.30 ± 0.47 and 2.08 ± 0.70 ml/hr/kg (mean ± *SD*), respectively. The individual data are reported elsewhere (10). The experimentally determined and predicted individual values of k_{el}, V_d, and *TC* for racemic warfarin are presented in Table I. There were no statistically significant differences between the experimental and predicted values; the correlation between

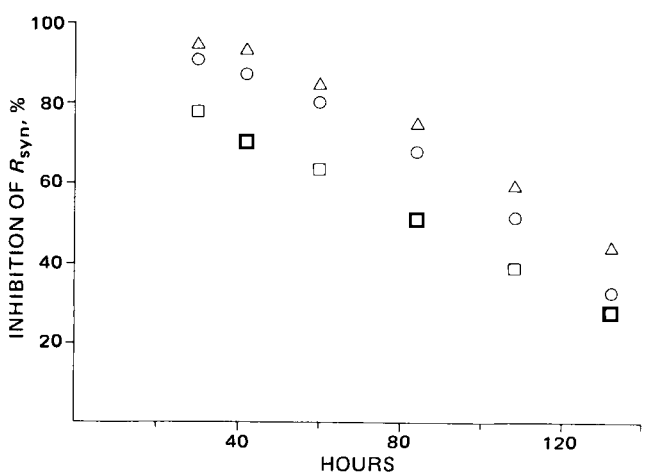

Figure 1—*Time course of inhibition of prothrombin complex activity synthesis rate, R_{syn}, produced by a single oral 1.5-mg/kg dose of* (S)-(−)-*warfarin* (△), *racemic warfarin* (○), *and* (R)-(+)-*warfarin* (□). *Average of data from 10 subjects.*

Table I—Experimentally Determined and Predicted Pharmacokinetic Constants for the Elimination of a Single Dose of Racemic Warfarin, 1.5 mg/kg, by Healthy Men

Subject	Elimination Rate Constant, hr^{-1}		Volume of Distribution, ml/kg		Total Body Clearance, ml/hr/kg	
	Experimental[a]	Predicted[b]	Experimental[a]	Predicted[b]	Experimental[a]	Predicted[b]
N-30	0.0162	0.0144	112	111	1.81	1.60
N-31	0.0138	0.0135	122	106	1.68	1.43
N-33	0.0157	0.0160	117	87	1.84	1.39
N-39	0.0172	0.0191	124	105	2.13	2.01
N-40	0.0186	0.0146	114	114	2.12	1.66
N-41	0.0136	0.0158	144	69	1.96	1.09
N-44	0.0171	0.0161	104	116	1.78	1.87
N-46	0.0144	0.0123	113	125	1.63	1.54
N-48	0.0146	0.0105	87	81	1.26	0.85
N-50	0.0193	0.0187	115	114	2.22	2.13
Mean	0.0161	0.0151	115	103	1.84	1.56
SD	0.0020	0.0027	51	18	0.29	0.40

[a] For a 1.5-mg/kg dose of racemic warfarin. [b] Simulated on the basis of a combined dose of (*R*)-(+)- and (*S*)-(−)-warfarin, 0.75 mg/kg each.

experimental and predicted *TC* values was significant ($r = 0.73$, $p < 0.02$).

The experimental and predicted values for percent inhibition of R_{syn} by racemic warfarin from 30 to 132 hr are listed in Table II. As reported previously, the predicted values differ somewhat depending on whether the calculations are made by first estimating the contribution of (*S*)-(−)-warfarin and then that of (*R*)-(+)-warfarin, or in reverse order, unless the slope of the R_{syn} *versus* log plasma concentration regression line of the two enantiomers is identical (6). Since these slopes are not identical in humans (10), the initial predictions were made by averaging the results of the two methods of calculation (Procedure A). As shown in Table II, these predictions yielded slightly higher values than were found experimentally, the differences being statistically significant at 30, 42, and 60 hr. On the other hand, excellent agreement was obtained between experimental and predicted values when the predicted values were calculated just by first estimating the contribution of the (*R*)-(+)-enantiomer and then estimating the contribution of the (*S*)-(−)-enantiomer (Procedure B).

The average time courses of inhibition of R_{syn} following administration of (*R*)-(+)-, (*S*)-(−)-, or racemic warfarin in single doses of 1.5 mg/kg are shown in Fig. 1. These data reflect the greater potency of (*S*)-(−)-warfarin despite its more rapid elimination than (*R*)-(+)-warfarin.

Table II—Experimentally Determined and Predicted Inhibition of Prothrombin Complex Activity Synthesis Rate, R_{syn}, after Oral Administration of a Single Dose of Racemic Warfarin, 1.5 mg/kg, to 10 Healthy Men

Hours	Inhibition of R_{syn}, % (mean ± *SD*)		
	Experimental	Predicted by Procedure A[a]	Predicted by Procedure B[a]
30	91 ± 6	98 ± 5[b]	97 ± 6
42	87 ± 4	96 ± 6[b]	92 ± 7
60	80 ± 5	86 ± 6[b]	81 ± 6
84	68 ± 15	71 ± 8	67 ± 9
108	52 ± 21	57 ± 12	53 ± 13
132	33 ± 19	43 ± 16	38 ± 17

[a] See *Results and Discussion* for difference between Procedures A and B. [b] Statistically significantly different from experimental mean value ($p < 0.05$).

The results of this investigation indicate that there are no pronounced pharmacokinetic or pharmacodynamic interactions between single doses of (*R*)-(+)- and (*S*)-(−)-warfarin in humans. The highest plasma concentrations observed in individual subjects following administration of racemic warfarin ranged from 7.6 to 11.9 μg/ml, considerably above the usual therapeutic concentration range of 1–2 μg/ml (12). Thus, the conditions of this investigation were favorable for eliciting a drug interaction on acute dosing. However, the results do not preclude the occurrence of a significant interaction between the enantiomers of warfarin during chronic administration.

REFERENCES

(1) A. Breckenridge and M. L'E. Orme, *Life Sci.*, **11**, 337 (1972).

(2) A. Breckenridge, M. Orme, H. Wesseling, R. J. Lewis, and R. Gibbons, *Clin. Pharmacol. Ther.*, **15**, 424 (1974).

(3) K. K. Chan, R. J. Lewis, and W. F. Trager, *J. Med. Chem.*, **15**, 1265 (1972).

(4) D. S. Hewick, *J. Pharm. Pharmacol.*, **24**, 661 (1972).

(5) D. S. Hewick and J. McEwen, *ibid.*, **25**, 458 (1973).

(6) G. Levy, R. A. O'Reilly, and L. B. Wingard, Jr., *Res. Commun. Chem. Pathol. Pharmacol.*, **7**, 359 (1974).

(7) R. J. Lewis, W. F. Trager, K. K. Chan, A. Breckenridge, M. Orme, M. Rowland, and W. Schary, *J. Clin. Invest.*, **53**, 1607 (1974).

(8) A. Yacobi and G. Levy, *J. Pharmacokinet. Biopharm.*, **2**, 239 (1974).

(9) R. A. O'Reilly, *Clin. Pharmacol. Ther.*, **16**, 348 (1974).

(10) L. B. Wingard, Jr., R. A. O'Reilly, and G. Levy, *ibid.*, **23**, 212 (1978).

(11) R. Nagashima, R. A. O'Reilly, and G. Levy, *Clin. Pharmacol. Ther.*, **10**, 22 (1969).

(12) A. Yacobi, J. A. Udall, and G. Levy, *ibid.*, **19**, 552 (1976).

ACKNOWLEDGMENTS

Supported in part by Grants GM 20852, GM 22860, and HL 8058 and by use of the Prophet Computer System from the National Institutes of Health.

Rapid and Micro High-Pressure Liquid Chromatographic Method for Simultaneous Determination of Procainamide and *N*-Acetylprocainamide in Plasma

M. A. F. GADALLA, GEOFFREY W. PENG, and WIN L. CHIOU ˣ

Received April 25, 1977, from the *Clinical Pharmacokinetics Laboratory and the Department of Pharmacy, College of Pharmacy, University of Illinois at the Medical Center, Chicago, IL 60612.* Accepted for publication September 19, 1977.

Abstract □ A rapid and simple high-pressure liquid chromatographic method was developed for the simultaneous determination of plasma levels of procainamide and its major metabolite, *N*-acetylprocainamide. Plasma samples were deproteinized with acetonitrile, and the supernate was chromatographed on a cation-exchange column. The assay can be carried out on as little as 20 μl of plasma and requires only about 7 min for each sample. No interference was found in plasma samples from cardiac patients receiving procainamide. This method is simple, fast, and useful for routine therapeutic monitoring and for pharmacokinetic studies of procainamide and its metabolite.

Keyphrases □ Procainamide—high-pressure liquid chromatographic analysis simultaneously with *N*-acetylprocainamide in plasma □ *N*-Acetylprocainamide—high-pressure liquid chromatographic analysis simultaneously with procainamide in plasma □ High-pressure liquid chromatography—analyses, procainamide and *N*-acetylprocainamide simultaneously in plasma □ Cardiac depressants—procainamide, high-pressure liquid chromatographic analysis simultaneously with *N*-acetylprocainamide in plasma

The importance of monitoring plasma procainamide concentrations has been realized for more than 2 decades (1). As much as a sevenfold difference in plasma procainamide concentrations could result from the same daily dose regimen (1, 2). Large variations were found in the daily dose of procainamide necessary to suppress ventricular arrhythmias in different patients (3).

BACKGROUND

The individual disparity in drug absorption, metabolism, and excretion was postulated as a plausible explanation for observed variations (4). These observations indicate that the plasma procainamide concentration correlates more closely than the dose regimen to the therapeutic and toxic responses in patients. The optimal antiarrhythmic activity of procainamide occurs in the 4–8-μg/ml plasma concentration range. Concentrations between 8 and 16 μg/ml are considered potentially toxic. Toxicity, such as arrhythmia and hypertension, often is associated with concentrations greater than 16 μg/ml (1).

N-Acetylprocainamide, the major metabolite of procainamide, also has antiarrhythmic activity comparable to that of the parent drug (5); its concentrations in plasma could range from 60 to 180% of procainamide (6). Therefore, it is highly desirable to monitor simultaneously plasma concentrations of procainamide and *N*-acetylprocainamide. Methods to measure one or both of these compounds in biological samples include spectrophotometry (1, 6), fluorometry (1), GLC (4, 7), mass fragmentography (8), TLC densitometry (6), and high-pressure liquid chromatography (HPLC) (9, 10).

The spectrophotometric (1, 6) and fluorometric (1) methods are less selective and cannot measure procainamide and *N*-acetylprocainamide simultaneously. The mass fragmentographic method (8) is probably not convenient for routine monitoring. The GLC (7) and TLC (6) methods can measure the two compounds simultaneously in biological fluids. The HPLC method has been used for procainamide and lidocaine in serum (9). More recently, an HPLC determination of procainamide and *N*-acetylprocainamide was described (10). All these reported methods require 1 or 2 ml of sample and use up to 6 ml of solvent for extraction.

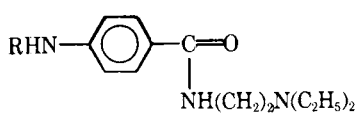

I: R = H
II: R = CH_3CO

This paper reports a simple and fast HPLC method for the simultaneous determination of procainamide and *N*-acetylprocainamide with as little as 20 μl of plasma.

EXPERIMENTAL

Reagents—Procainamide hydrochloride[1], *N*-acetylprocainamide hydrochloride[1], ammonium phosphate[2], phosphoric acid[2], and acetonitrile[3] were used.

Apparatus—The HPLC system consisted of solvent delivery pumps[4], a septumless sample injector[5], an ion-exchange column[6], and a spectrophotometric detector[7].

Procedure—Aliquots of 0.1 ml of plasma in 13 × 100-mm culture tubes were vortexed with 0.25 ml of acetonitrile for 10 sec and centrifuged for 1 min. The clear supernate was poured directly into another set of culture tubes (although this step is not necessary). Aliquots of 100 μl were injected into the column and chromatographed.

The mobile phase consisted of 80% (v/v) 0.1 *M* ammonium phosphate acidified with phosphoric acid (0.05%) to pH 2.5 ± 0.05 and 20% acetonitrile; the flow rate was 2 ml/min. The separated sample components from the column effluent were monitored by UV absorption at 274 nm, and the chromatograms were recorded on a potentiometric recorder at 0.02 absorbance unit full scale and a chart speed of 4 mm/min.

The calibration curves were prepared by analyzing 0.1-ml plasma samples spiked with procainamide and *N*-acetylprocainamide (0.88 mg/ml–21.22 μg/ml) from concentrated stock solutions in methanol and plotting the peak heights *versus* the concentrations. Peak height measurements were used for all quantitations. All separations were carried out at ambient temperature.

RESULTS AND DISCUSSION

The UV spectra of procainamide (I) and *N*-acetylprocainamide (II) are shown in Fig. 1. With the mobile phase as a solvent, procainamide showed absorption maxima at 282 and 204 nm while *N*-acetylprocainamide showed absorption maxima at 268 and 205 nm. These data suggest that the most sensitive detections can be obtained by monitoring absorbance at 205 nm. Although UV absorbance measurements at wavelengths as low as 199 nm have been used in liquid chromatography (9) to obtain very sensitive detection, attempts to monitor these compounds at 205 nm encountered some difficulty because of the interference of some endogenous plasma compounds. Therefore, the absorbance at 274 nm appears to be the optimal compromise between sensitivity and selectivity.

Since procainamide is a weak base [pKa 9.4 (11)] and is ionized at a low pH, a cation-exchange column was chosen. Although a reversed-phase column had been used successfully for the quantitation of procainamide (9), the ion-exchange column was preferred in that it separated both the parent drug and its metabolite. A good linear relationship between peak height measurements and concentrations was observed even when a large volume (up to 100 μl) of sample was injected. When a large volume of

[1] E. R. Squibb & Sons, Princeton, N.J.
[2] Fisher Scientific, Fair Lawn, N.J.
[3] Burdick & Jackson Laboratories, Muskegon, Mich.
[4] Model A-6000, Waters Associates, Milford, Mass.
[5] U6K, Waters Associates, Milford, Mass.
[6] Partisil PXS 10/25 SCX, Whatman, Clifton, N.J.
[7] Model LC 55, Perkin-Elmer Corp., Norwalk, Conn.

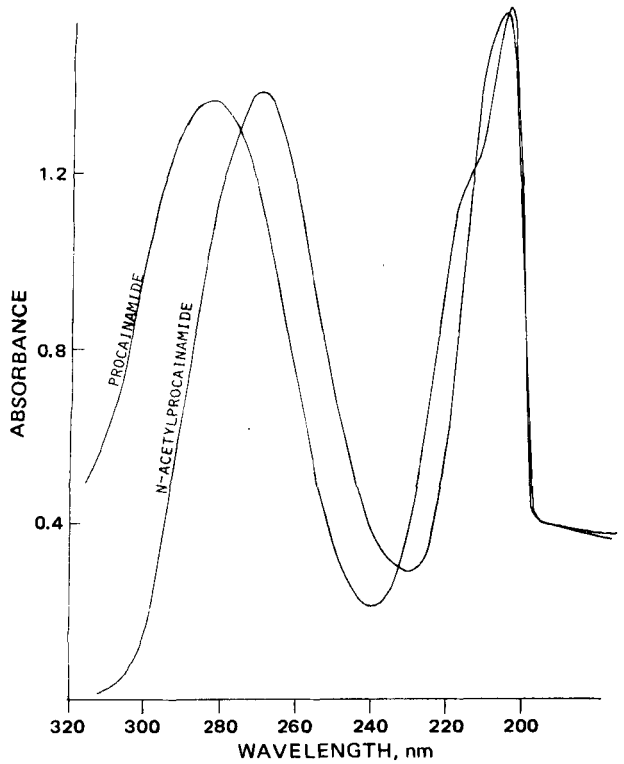

Figure 1—*UV spectra of procainamide hydrochloride (20 μg/ml) and N-acetylprocainamide hydrochloride (20 μg/ml) in the HPLC mobile phase.*

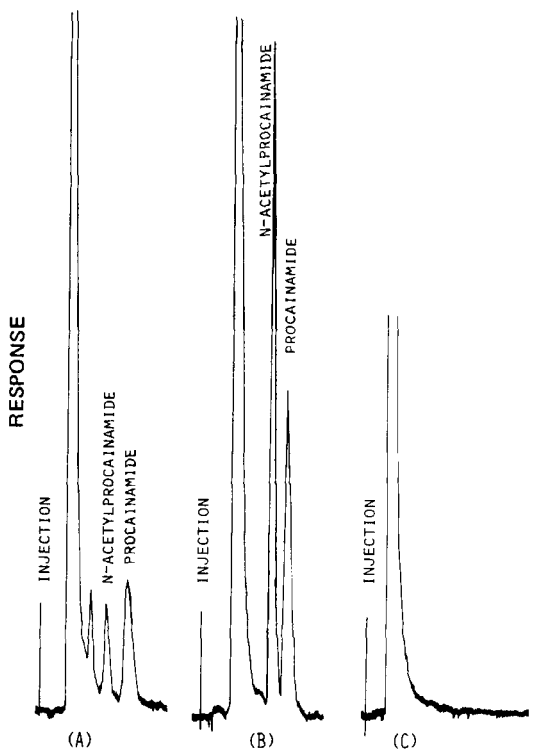

Figure 2—*Chromatograms of procainamide (2.8 μg/ml) and N-acetylprocainamide (1.1 μg/ml) from plasma of a patient on procainamide (A), from spiked (7.5 μg/ml) plasma (B), and plasma blank (C).*

sample was chromatographed on a reversed-phase column, peak broadening was generally observed, and accurate measurement of the peak height became more difficult.

Figure 2 shows a chromatogram of procainamide and *N*-acetylprocainamide from a plasma sample obtained immediately after administration of 750 mg of procainamide by intravenous infusion over 20 min to an adult patient. Chromatograms of a plasma blank with and without addition of procainamide and *N*-acetylprocainamide are also included. Plasma samples from both healthy subjects and renal patients showed no peak that would interfere with the assay. Under the conditions employed, procainamide and *N*-acetylprocainamide were eluted from the ion-exchange column at 5 and 4 min, respectively (Fig. 2).

The linearity of standard curves of procainamide and *N*-acetylprocainamide is shown in Table I. The peak heights were proportional to plasma concentrations for both compounds in all ranges studied (up to 21 μg/ml), as indicated by the fairly constant response factors (peak height/concentration). The coefficients of variation for the intraassay ($n = 4$) and interassay ($n = 6$) of procainamide (1.73 μg/ml) were 6.36 and 8.67%, respectively. The coefficients of variation for *N*-acetylprocainamide (1.77 μg/ml) were 1.72 and 2.25% for the intraassay ($n = 4$) and interassay ($n = 6$), respectively. By this method, the low limit of detection was 0.2 μg/ml for both compounds in plasma, which is better than the reported GLC assay (7).

Table I—Linearity of Standard Curves for Procainamide and *N*-Acetylprocainamide

Concentration[a] Spiked in Plasma, μg/ml	Peak Height, cm		Response Factor[b]	
	Procainamide	*N*-Acetylprocainamide	Procainamide	*N*-Acetylprocainamide
0.88	1.0	2.3	1.14	2.61
1.77	2.0	4.5	1.13	2.54
2.65	3.0	6.85	1.13	2.58
3.54	4.1	9.0	1.16	2.54
7.07	8.1	17.9	1.15	2.53
10.61	11.9	26.8	1.12	2.53
14.14	16.0	36.1	1.13	2.55
21.22	23.8	54.0	1.12	2.54
		Average	1.135	2.553
		SD	0.013	0.028

[a] As free base of drugs. [b] Peak height/concentration.

This procedure was employed successfully to monitor the plasma procainamide and *N*-acetylprocainamide levels of patients receiving procainamide and other drugs such as phenobarbital. In all patient samples analyzed, no interference was encountered. In samples showing excessive hemolysis of red blood cells, successful assays also could be performed. Analysis of plasma supplemented with phenytoin, salicylic acid, sulfisoxazole, chloramphenicol, and acetaminophen showed that these drugs did not interfere with the assay.

By using the simple deproteinization method for sample preparation, no solvent extraction, transfer, or evaporation steps were needed. The simplicity of the procedure can help in reducing experimental errors.

Acetonitrile precipitated plasma proteins as a solid mass, adhering to walls of the culture tube after mild centrifugation (2000 rpm), to give a clear supernate which was easy to pour out, almost quantitatively. Other water-miscible organic solvents, such as methanol, ethanol, and acetone, were less satisfactory in that a clear supernate could not be obtained with mild centrifugation. Although procainamide and its metabolite are partially bound to proteins in plasma (6), the recovery from plasma by acetonitrile deproteinization was essentially 100%, based on the peak area analysis, as compared to the addition of acetonitrile to the aqueous solutions of both compounds in the ratio of 2.5:1 (v/v). However, the peak heights from the procainamide-spiked plasma were 20% shorter from equal concentrations spiked in water. This result may be due to the peak widening effect. However, this effect was not found with *N*-acetylprocainamide.

Since, at higher concentrations (>1 μg/ml), chromatograms from the injection of 50 μl of supernates of the acetonitrile–plasma mixture gave peak heights sufficient for accurate quantitation, the assay can be carried out on as little as 20 μl of plasma deproteinized with 50 μl of acetonitrile. This method should be useful when only a small amount of sample is available. The results can be obtained in about 7 min for a single sample. In terms of speed, sensitivity, and simplicity, this method is superior to most methods reported for monitoring plasma levels of procainamide and *N*-acetylprocainamide.

REFERENCES

(1) J. Koch-Weser and S. W. Klein, *J. Am. Med. Assoc.*, **215**, 1454 (1971).

(2) J. Koch-Weser, *Ann. N.Y. Acad. Sci.*, **179**, 370 (1971).

(3) R. D. Patton, E. Patten, E. Stein, and A. D. Damato, *J. Am. Med. Assoc.*, **209**, 1221 (1969).

(4) A. J. Atkinson, Jr., M. Parker, and J. M. Strong, *Clin. Chem.*, **18**, 643 (1972).

(5) J. Elson, J. M. Strong, W. K. Lee, and A. J. Atkinson, Jr., *Clin. Pharmacol. Ther.*, **17**, 134 (1975).

(6) M. M. Reidenberg, D. E. Dayer, M. Levy, and H. Warner, *ibid.*, **17**, 722 (1975).

(7) T. P. Gibson, J. Matusik, H. A. Nelson, J. Wilkinson, and W. A. Brigg, *ibid.*, **17**, 395 (1975).

(8) J. M. Strong, J. S. Dutcher, W. K. Lee, and A. J. Atkinson, Jr., *ibid.*, **18**, 613 (1975).

(9) R. F. Adams, F. L. Vandermark, and G. Schmidt., *Clin. Chim. Acta*, **69**, 515 (1976).

(10) J. S. Dutcher and J. M. Strong, *Clin. Chem.*, **23**, 1318 (1977).

(11) J. R. Koup, W. J. Jusko, and A. L. Goldfarb, *J. Pharm. Sci.*, **64**, 2008 (1975).

ACKNOWLEDGMENTS

Supported in part by Special Projects Grant PHS-05D-619-02 from the Department of Health, Education, and Welfare.

Synthesis of Potential Antineoplastic Agents XXVI: 1,3,4,6,7,11b-Hexahydro-9,10-dimethoxy-2*H*-benzo[*a*]2-quinolizinone Derivatives

F. D. POPP *x **and R. F. WATTS** ‡

Received May 23, 1977, from the **Department of Chemistry, University of Missouri–Kansas City, Kansas City, MO 64110,* and the ‡*Department of Chemistry, Clarkson College of Technology, Potsdam, NY 13676.* Accepted for publication September 22, 1977.

Abstract □ A number of 3-alkyl-1,3,4,6,7,11b-hexahydro-9,10-dimethoxy-2*H*-benzo[*a*]2-quinolizinones and 2-substituted 3-ethyl-1,3,4,6,7,11b-hexahydro-9,10-dimethoxy-2*H*-benzo[*a*]quinolizines were prepared and submitted for antineoplastic and anticonvulsant screening.

Keyphrases □ Benzo[*a*]quinolizines, various substituted—synthesized, evaluated for antineoplastic and anticonvulsant activity □ Antineoplastic activity—evaluated in various substituted benzo[*a*]quinolizines □ Anticonvulsant activity—evaluated in various substituted benzo[*a*]quinolizines □ Structure–activity relationships—various substituted benzo[*a*]quinolizines evaluated for antineoplastic and anticonvulsant activity

During work directed toward the synthesis of analogs of emetine (I), 1,3,4,6,7,11b-hexahydro-9,10-dimethoxy-3-ethyl-2*H*-benzo[*a*]2-quinolizinone (II) was synthesized (1). The hydrochloride salt of II was active in the L-1210 lymphoid leukemia system.

DISCUSSION

To determine the effect of structure on the antineoplastic activity of II hydrochloride, a series of related compounds was prepared. The compounds investigated fall into two categories: analogs in which the ethyl group of II has been replaced by a series of other alkyl groups (III*a*–III*i* and V, Table I) and analogs in which the carbonyl group of II has been replaced by other groups (IV*a*–IV*i*, VI, and VII, Table II).

The compounds in Table I were prepared by reaction of 3,4-dihydro-6,7-dimethoxyisoquinoline and the appropriate Mannich bases (1). New compounds, including the dimer V, are discussed under *Experimental*. All known compounds had melting points in agreement with reported values (2–4).

Compounds IV*a*–IV*c* were prepared by the method of Openshaw and Whittaker (5), as was the propyl analog VI. The oxime (IV*d*) (6) and IV*e* and IV*f* (7) were prepared by previously reported methods. The preparation of the remaining compounds in Table II is reported under *Experimental*.

The compounds in Tables I and II were screened through the Drug Evaluation Branch of the National Cancer Institute in the L-1210 lymphoid leukemia or P-388 lymphocytic leukemia systems. None of the compounds with groups in place of the 2-carbonyl possessed any significant antineoplastic activity (Table II). A number of the analogs in Table

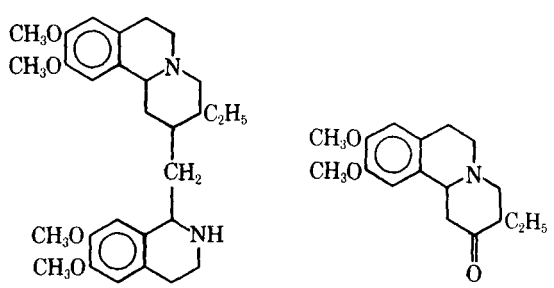

I

II

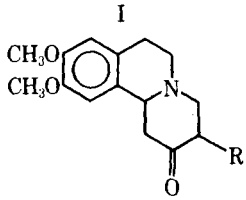

III*a*–III*i*

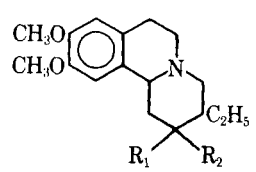

IV*a*–IV*i*

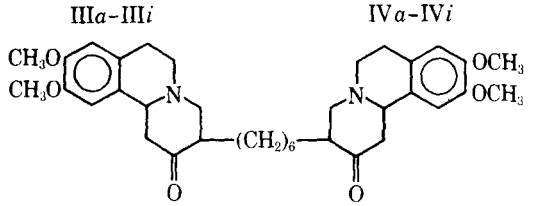

V

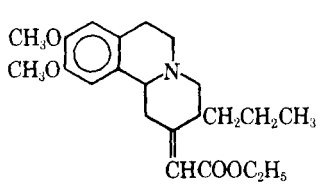

VI

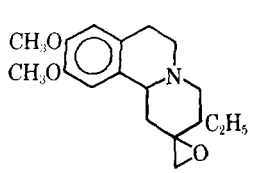

VII

(3) R. D. Patton, E. Patten, E. Stein, and A. D. Damato, *J. Am. Med. Assoc.*, **209**, 1221 (1969).

(4) A. J. Atkinson, Jr., M. Parker, and J. M. Strong, *Clin. Chem.*, **18**, 643 (1972).

(5) J. Elson, J. M. Strong, W. K. Lee, and A. J. Atkinson, Jr., *Clin. Pharmacol. Ther.*, **17**, 134 (1975).

(6) M. M. Reidenberg, D. E. Dayer, M. Levy, and H. Warner, *ibid.*, **17**, 722 (1975).

(7) T. P. Gibson, J. Matusik, H. A. Nelson, J. Wilkinson, and W. A. Brigg, *ibid.*, **17**, 395 (1975).

(8) J. M. Strong, J. S. Dutcher, W. K. Lee, and A. J. Atkinson, Jr., *ibid.*, **18**, 613 (1975).

(9) R. F. Adams, F. L. Vandermark, and G. Schmidt., *Clin. Chim. Acta*, **69**, 515 (1976).

(10) J. S. Dutcher and J. M. Strong, *Clin. Chem.*, **23**, 1318 (1977).

(11) J. R. Koup, W. J. Jusko, and A. L. Goldfarb, *J. Pharm. Sci.*, **64**, 2008 (1975).

ACKNOWLEDGMENTS

Supported in part by Special Projects Grant PHS-05D-619-02 from the Department of Health, Education, and Welfare.

Synthesis of Potential Antineoplastic Agents XXVI: 1,3,4,6,7,11b-Hexahydro-9,10-dimethoxy-2*H*-benzo[*a*]2-quinolizinone Derivatives

F. D. POPP *x **and R. F. WATTS** ‡

Received May 23, 1977, from the **Department of Chemistry, University of Missouri–Kansas City, Kansas City, MO 64110,* and the ‡*Department of Chemistry, Clarkson College of Technology, Potsdam, NY 13676.* Accepted for publication September 22, 1977.

Abstract □ A number of 3-alkyl-1,3,4,6,7,11b-hexahydro-9,10-dimethoxy-2*H*-benzo[*a*]2-quinolizinones and 2-substituted 3-ethyl-1,3,4,6,7,11b-hexahydro-9,10-dimethoxy-2*H*-benzo[*a*]quinolizines were prepared and submitted for antineoplastic and anticonvulsant screening.

Keyphrases □ Benzo[*a*]quinolizines, various substituted—synthesized, evaluated for antineoplastic and anticonvulsant activity □ Antineoplastic activity—evaluated in various substituted benzo[*a*]quinolizines □ Anticonvulsant activity—evaluated in various substituted benzo[*a*]quinolizines □ Structure–activity relationships—various substituted benzo[*a*]quinolizines evaluated for antineoplastic and anticonvulsant activity

During work directed toward the synthesis of analogs of emetine (I), 1,3,4,6,7,11b-hexahydro-9,10-dimethoxy-3-ethyl-2*H*-benzo[*a*]2-quinolizinone (II) was synthesized (1). The hydrochloride salt of II was active in the L-1210 lymphoid leukemia system.

DISCUSSION

To determine the effect of structure on the antineoplastic activity of II hydrochloride, a series of related compounds was prepared. The compounds investigated fall into two categories: analogs in which the ethyl group of II has been replaced by a series of other alkyl groups (III*a*–III*i* and V, Table I) and analogs in which the carbonyl group of II has been replaced by other groups (IV*a*–IV*i*, VI, and VII, Table II).

The compounds in Table I were prepared by reaction of 3,4-dihydro-6,7-dimethoxyisoquinoline and the appropriate Mannich bases (1). New compounds, including the dimer V, are discussed under *Experimental*. All known compounds had melting points in agreement with reported values (2–4).

Compounds IV*a*–IV*c* were prepared by the method of Openshaw and Whittaker (5), as was the propyl analog VI. The oxime (IV*d*) (6) and IV*e* and IV*f* (7) were prepared by previously reported methods. The preparation of the remaining compounds in Table II is reported under *Experimental*.

The compounds in Tables I and II were screened through the Drug Evaluation Branch of the National Cancer Institute in the L-1210 lymphoid leukemia or P-388 lymphocytic leukemia systems. None of the compounds with groups in place of the 2-carbonyl possessed any significant antineoplastic activity (Table II). A number of the analogs in Table

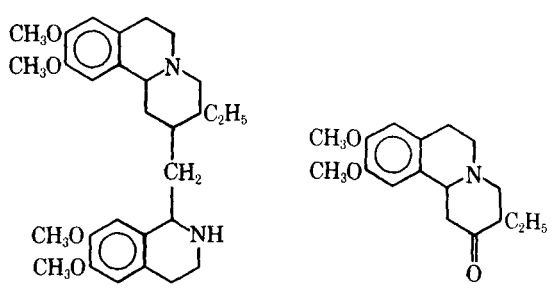

I

II

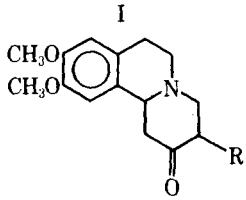

III*a*–III*i*

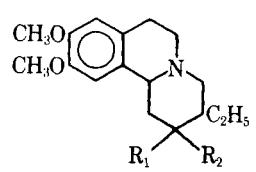

IV*a*–IV*i*

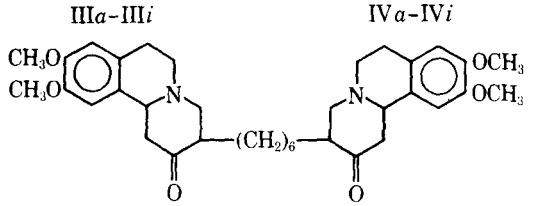

V

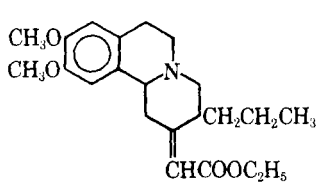

VI

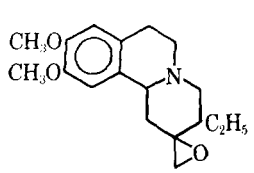

VII

Table I—Analogs of II in which the Ethyl Group Has Been Replaced

Compound	R	LE[a] Dose, mg/kg	LE[a] T/C[c], %	PS[b] Dose, mg/kg	PS[b] T/C[c], %
III*a*	H	50	130	12.5	111
III*b*	CH_3	200	127	—	—
III*c* hydrochloride	C_2H_5	400	134	300	128
III*c* methiodide	C_2H_5	—	—	50	106
III*d* hydrochloride	n-C_3H_7	—	—	200	128
III*e*	n-C_4H_9	400	97	—	—
III*e* hydrochloride	n-C_4H_9	100	103	—	—
III*f*	$CH_2CH(CH_3)_2$	400	123	50	103
III*g*	$CH_2CH_2CH{=}CH_2$	—	—	50	113
III*h*	$CH_2C(CH_3){=}CH_2$	—	—	200	131
III*i*	$CH_2C_6H_5$	—	—	50	101
III*i* hydrochloride	$CH_2C_6H_5$	—	—	200	104
V	—	—	—	200	99

[a] L-1210 lymphoid leukemia. [b] P-388 lymphocytic leukemia. [c] Ratio of test (T) evaluation to control (C) evaluation expressed as a percentage.

I possessed activity in the L-1210 or p-388 system, but the results were too scattered to draw any meaningful structure–activity correlations. While some compounds were active, the activity was not sufficient for further investigation.

A number of the compounds also were screened for anticonvulsant activity. A few compounds exhibited activity (Table III), but it was not sufficient for further investigation.

EXPERIMENTAL

Synthesis of III*a*–III*i* and V—These compounds were prepared by the method of Whittaker (1). A solution of 3,4-dihydro-6,7-dimethoxyisoquinoline (0.035 mole) in cold water (30 ml) was just neutralized with concentrated hydrochloric acid, treated with the appropriate Mannich base (0.038 mole), and set aside at room temperature for 3 days. The crystals were triturated under water and filtered.

Compound III*g*, mp 120–122° (methanol), was obtained in a 38% yield.

Anal.—Calc. for $C_{19}H_{23}NO_3$: C, 72.40; H, 7.93. Found: C, 72.59; H, 7.72.

Compound V, mp 207–209° (chloroform–acetone), was obtained in a 52% yield; IR: 1700 cm^{-1}.

Anal.—Calc. for $C_{36}H_{48}N_2O_6$: C, 71.54; H, 7.94; N, 4.63. Found: C, 71.51; H, 7.99; N, 4.67.

Compound II methiodide was formed from II in 85% yield in the usual manner, mp 196–197° (methanol).

Anal.—Calc. for $C_{18}H_{26}INO_3$: N, 3.25. Found: N, 3.24.

Synthesis of VI—A solution of triethylphosphonoacetate (52 ml) in dimethylformamide was added to solid potassium *tert*-butoxide (22.4 g), and III*d* in dimethylformamide (200 ml) was then added at 0°. The solution was allowed to warm to room temperature and stand overnight. It was diluted with water and extracted with ether. The dried ether extracts were evaporated to give a 52% yield of VI, mp 91–93° (ethanol); IR: 1690 and 1630 cm^{-1}.

Anal.—Calc. for $C_{22}H_{31}NO_4$: C, 70.80; H, 8.31; N, 3.75. Found: C, 70.82; H, 8.34; N, 3.81.

Synthesis of IV*g*—A solution of II (0.01 mole) in dimethoxyethane (250 ml), under nitrogen, was treated with potassium *tert*-butoxide (0.1 mole) in butanol (100 ml). A solution of tosylmethyl isocyanide (0.012 mole) in dimethoxyethane (25 ml) was then added over 1 hr. After stirring for 1 hr, the solution was poured into water (500 ml) and extracted with chloroform. The dried chloroform extracts were evaporated to give a 42% yield of IV*g*, mp 140–142° (hexane); IR: 2225 cm^{-1}.

Anal.—Calc. for $C_{18}H_{24}N_2O_2$: C, 72.02; H, 7.99; N, 9.33. Found: C, 71.98; H, 8.03; N, 9.38.

Synthesis of IV*h*—The ester IV*b* (5) (0.02 mole) was dissolved in tetrahydrofuran (100 ml), and lithium aluminum hydride (1 g) was added slowly. After refluxing for 24 hr, calcium hydroxide was added. After filtration, the mixture was concentrated to give a light-yellow oil (IR: 3350 cm^{-1}). The oil was dissolved in benzene (100 ml) and cooled to 0°, and freshly distilled thionyl chloride (10 ml) was added dropwise. The mixture was stirred in the cold for 1 hr and at room temperature for 5 hr. Concentration *in vacuo* gave 89% of the hydrochloride of IV*h*, mp 211–212° (butanol).

Anal.—Calc. for $C_{19}H_{29}Cl_2NO_2$: C, 61.00; H, 7.75; Cl, 18.95; N, 3.74. Found: C, 60.98; H, 7.84; Cl, 18.94; N, 3.77.

Synthesis of IV*i*—To an ice-cold solution of II hydrochloride (0.01 mole) in water (75 ml) was added slowly, with stirring, a solution of sodium cyanide (0.011 mole) in water (15 ml). After stirring for 3 hr at room temperature, the mixture was filtered to give a 51% yield of IV*i*, mp 118–120° (benzene–hexane). This compound can also be prepared by another route (8).

Anal.—Calc. for $C_{18}H_{24}N_2O_3$: C, 68.37; H, 7.59; N, 8.86. Found: C, 68.32; H, 7.57; N, 8.78.

This compound was also converted to its hydrochloride, mp 208–210°.

Anal.—Calc. for $C_{18}H_{25}ClN_2O_3$: C, 61.31; H, 7.09; N, 7.94. Found: C, 61.23; H, 6.95; N, 7.45.

Synthesis of Epoxide VII—This procedure is based on the work of Piccirilli (9). A mixture of sodium hydride (0.035 mole) and trimethylsulfoxonium iodide (0.022 mole) in dimethyl sulfoxide (40 ml) was stirred, under nitrogen, for 15 min; then II (0.02 mole) in dimethyl sulfoxide (50 ml) was added dropwise. After stirring for 1 hr at room temperature and for 1 hr at 50°, the solution was poured onto ice and extracted with chloroform. The dried extracts were evaporated to give a 67% yield of VII, mp 111–112° (ethanol).

Anal.—Calc. for $C_{18}H_{25}NO_3$: C, 71.26; H, 8.30; N, 4.62. Found: C, 71.35; H, 8.32; N, 4.57.

Table II—Analogs of II in which the Carbonyl Group Has Been Replaced

Compound	R_1	R_2	LE[a] Dose, mg/kg	LE[a] T/C[c], %	PS[b] Dose, mg/kg	PS[b] T/C[c], %
IV*a*		$=CHCO_2C_2H_5$	100	96	—	—
IV*b*	H	CH_2CO_2-C_2H_5	—	—	25	114
IV*c* hydrochloride	H	CH_2CO_2H	—	—	50	95
VI	—	—	—	—	50	96
IV*d*		=NOH	—	—	200	112
IV*e*	H	OH	110	200	—	—
IV*f* hydrochloride	H	Cl	—	—	50	101
IV*g*	H	CN	—	—	50	93
IV*h* hydrochloride	H	CH_2CH_2Cl	—	—	50	106
IV*i*	OH	CN	—	—	200	102
VII	—	—	—	—	12.5	114

[a] L-1210 lymphoid leukemia. [b] P-388 lymphocytic leukemia. [c] Ratio of test (T) evaluation to control (C) evaluation expressed as a percentage.

Table III—Anticonvulsant Screening

Compound	MES[a] Dose, mg/kg	MES[a] Protection[c]	MET[b] Dose, mg/kg	MET[b] Protection[c]
III*a*	300	0/1	300	0/1
III*b*	300	0/1	300	0/1
III*c* hydrochloride	300	1/1[d]	300	0/1
III*c*	300	0/1	300	1/1
			100	1/1[e]
III*e*	300	0/1	300	0/1
III*h*	300	0/1	300	1/1
III*i*	300	0/1	300	0/1
V	300	0/1	300	0/1
IV*a*	300	0/1	300	1/1[d]
IV*d*	300	0/1	300	0/1

[a] Maximal electroshock seizure test. [b] Subcutaneous pentylenetetrazol (Metrazol) seizure threshold test. [c] Number of animals protected per number of animals treated. Tests were carried out at 30 min and 4 hr after intraperitoneal administration. [d] Thirty minutes but not 4 hr. [e] Four hours but not 30 min.

REFERENCES

(1) N. Whittaker, *J. Chem. Soc. C*, **1969**, 85.

(2) H. T. Openshaw and N. Whittaker, *J. Chem. Soc.*, **1963**, 1449.

(3) A. Brossi, H. Lindlar, M. Walter, and O. Schneider, *Helv. Chim. Acta*, **41**, 119 (1958).

(4) K. Mizukami, *Chem. Pharm. Bull.*, **6**, 312 (1958).

(5) H. T. Openshaw and N. Whittaker, *J. Chem. Soc.*, **1963**, 1461.
(6) C. Szantay and D. Beke, *Chem. Ber.*, **95**, 2132 (1962).
(7) A. Brossi, L. Chopard-dit-Jean, and O. Schneider, *Helv. Chim. Acta*, **41**, 1793 (1958).
(8) R. F. Watts and F. D. Popp, *Heterocycles*, **6**, 47 (1977).
(9) R. Piccirilli, Ph.D. dissertation, Clarkson College of Technology, Potsdam, N.Y., 1974.

ACKNOWLEDGMENTS

Supported in part by Grant CA-10965 from the National Cancer Institute, National Institutes of Health.

The authors thank Dr. H. B. Wood, Jr., Dr. R. Krall, and Mr. A. W. Spang for aid in obtaining the antineoplastic testing, anticonvulsant testing, and microanalytical results, respectively.

Quantitative Determinations of Two Decongestants and an Antihistamine in Combination Using Paired Ion High-Pressure Liquid Chromatography

A. G. GHANEKAR and V. DAS GUPTA ˣ

Received July 14, 1977, from the *College of Pharmacy, University of Houston, Houston, TX 77004.* Accepted for publication September 23, 1977.

Abstract □ A single method for the quantitative determinations of three active ingredients, phenylephrine hydrochloride, phenylpropanolamine hydrochloride, and brompheniramine maleate, and one inactive ingredient (sodium benzoate) in a commercial product for colds is reported. The method is based on paired ion high-pressure liquid chromatography using 1-heptanesulfonic acid as the counterion. It is accurate and precise. The relative standard deviations based on six readings are reported. This method is sensitive; less than 1 μg of each ingredient can be assayed. The peak area of each ingredient is related to its concentration.

Keyphrases □ Phenylephrine hydrochloride—high-pressure liquid chromatographic analysis in dosage forms □ Phenylpropanolamine hydrochloride—high-pressure liquid chromatographic analysis in dosage forms □ Brompheniramine maleate—high-pressure liquid chromatographic analysis in dosage forms □ High-pressure liquid chromatography—analyses, phenylephrine hydrochloride, phenylpropanolamine hydrochloride, and brompheniramine maleate in dosage forms □ Adrenergics—phenylephrine hydrochloride and phenylpropanolamine hydrochloride, high-pressure liquid chromatographic analyses in dosage forms □ Antihistaminics—brompheniramine maleate, high-pressure liquid chromatographic analysis in dosage forms

One commercial product[1] for colds contains two decongestants, phenylephrine hydrochloride (I) and phenylpropanolamine hydrochloride (II), and an antihistamine, brompheniramine maleate (III). The dosage forms, sustained-release tablets and elixir, also contain excipients, some of which (especially colors and preservatives in the elixir) may interfere with the analysis of the active ingredients. No single method is available to determine the active ingredients quantitatively.

The USP method (1) for the quantitative determination of I is based on column chromatography. This method is quite tedious and time consuming. A GLC method was reported for the quantitative determination of I (2), but it requires derivatization and is quite lengthy. Other methods available for the analysis of I were reviewed (2). A quantitative colorimetric method for II in pharmaceutical dosage forms was reported (3), but other primary and secondary amines interfered. The only method available for the quantitative analysis of III in combination with other drugs apparently is that of Hudanick (4), which requires reaction with cyanogen bromide, a highly toxic and volatile reagent.

The paired ion extraction technique for the quantitative drug analysis is well documented. The theory and some possible uses of this method were reported (5) and reviewed (6). Numerous applications also were reported for thyroid hormones and sulfa drugs (7), dyes (8), niacin and niacinamide (9), and the simultaneous determinations of hydrocortisone and hydrocortisone phosphate (10).

This paper reports the simultaneous quantitative determinations of I–III in commercial dosage forms. The method is based on paired ion high-pressure liquid chromatography (HPLC), which identifies the compounds. Moreover, inactive ingredients also separate out and may be identified or determined quantitatively without additional work.

EXPERIMENTAL

Chemicals and Reagents—All chemicals and reagents were USP, NF, or ACS grade and were used without further purification. 1-Heptanesulfonic acid sodium salt[2] (IV) was used as received.

Apparatus—A high-pressure liquid chromatograph[3] capable of operating at an inlet pressure up to 6000 psig was used. A multiple wavelength detector[4] was used. For convenience, the wavelength was set at 254 nm (usually found in fixed wavelength detectors) for all ingredients. The detector was attached to a recorder[5] and an integrator[6]. The column[7] (30 cm × 4 mm i.d.) was purchased and used as received.

Chromatographic Solvents—A 13% (v/v) solution of acetonitrile in water containing 1.8% (v/v) acetic acid with or without 0.005 *M* IV was used. The pH of both solvents was 2.6 ± 0.05.

Chromatographic Conditions—The temperature was ambient. The flow rate was 0.6 ml/min (inlet pressure of approximately 300 psig) for the first 12 min and then was 3.6 ml/min (inlet pressure of approximately 3000 psig). The absorbance unit for full-scale deflection was 0.04, and the chart speed was 30.5 cm/hr.

Preparation of Stock Solutions—All stock solutions were prepared in water using a simple solution method. Heating to about 90° for approximately 5 min was required to dissolve III. The concentrations of the

[1] Dimetapp, A. H. Robins, Richmond, Va.

[2] Eastman Kodak Co., Rochester, N.Y.
[3] Waters ALC 202 equipped with a U6K Universal injector, Waters Associates, Milford, Mass.
[4] Spectroflow monitor 770, Schoeffel Instrument Corp., Westwood, N.J.
[5] Omniscribe 5213-12, Houston Instruments, Austin, Tex.
[6] Autolab Minigrator, Spectra-Physics, Santa Clara, Calif.
[7] μBondapak CN, Waters Associates, Milford, Mass.

(5) H. T. Openshaw and N. Whittaker, *J. Chem. Soc.*, **1963**, 1461.
(6) C. Szantay and D. Beke, *Chem. Ber.*, **95**, 2132 (1962).
(7) A. Brossi, L. Chopard-dit-Jean, and O. Schneider, *Helv. Chim. Acta*, **41**, 1793 (1958).
(8) R. F. Watts and F. D. Popp, *Heterocycles*, **6**, 47 (1977).
(9) R. Piccirilli, Ph.D. dissertation, Clarkson College of Technology, Potsdam, N.Y., 1974.

ACKNOWLEDGMENTS

Supported in part by Grant CA-10965 from the National Cancer Institute, National Institutes of Health.

The authors thank Dr. H. B. Wood, Jr., Dr. R. Krall, and Mr. A. W. Spang for aid in obtaining the antineoplastic testing, anticonvulsant testing, and microanalytical results, respectively.

Quantitative Determinations of Two Decongestants and an Antihistamine in Combination Using Paired Ion High-Pressure Liquid Chromatography

A. G. GHANEKAR and V. DAS GUPTA ˣ

Received July 14, 1977, from the *College of Pharmacy, University of Houston, Houston, TX 77004.* Accepted for publication September 23, 1977.

Abstract □ A single method for the quantitative determinations of three active ingredients, phenylephrine hydrochloride, phenylpropanolamine hydrochloride, and brompheniramine maleate, and one inactive ingredient (sodium benzoate) in a commercial product for colds is reported. The method is based on paired ion high-pressure liquid chromatography using 1-heptanesulfonic acid as the counterion. It is accurate and precise. The relative standard deviations based on six readings are reported. This method is sensitive; less than 1 μg of each ingredient can be assayed. The peak area of each ingredient is related to its concentration.

Keyphrases □ Phenylephrine hydrochloride—high-pressure liquid chromatographic analysis in dosage forms □ Phenylpropanolamine hydrochloride—high-pressure liquid chromatographic analysis in dosage forms □ Brompheniramine maleate—high-pressure liquid chromatographic analysis in dosage forms □ High-pressure liquid chromatography—analyses, phenylephrine hydrochloride, phenylpropanolamine hydrochloride, and brompheniramine maleate in dosage forms □ Adrenergics—phenylephrine hydrochloride and phenylpropanolamine hydrochloride, high-pressure liquid chromatographic analyses in dosage forms □ Antihistaminics—brompheniramine maleate, high-pressure liquid chromatographic analysis in dosage forms

One commercial product[1] for colds contains two decongestants, phenylephrine hydrochloride (I) and phenylpropanolamine hydrochloride (II), and an antihistamine, brompheniramine maleate (III). The dosage forms, sustained-release tablets and elixir, also contain excipients, some of which (especially colors and preservatives in the elixir) may interfere with the analysis of the active ingredients. No single method is available to determine the active ingredients quantitatively.

The USP method (1) for the quantitative determination of I is based on column chromatography. This method is quite tedious and time consuming. A GLC method was reported for the quantitative determination of I (2), but it requires derivatization and is quite lengthy. Other methods available for the analysis of I were reviewed (2). A quantitative colorimetric method for II in pharmaceutical dosage forms was reported (3), but other primary and secondary amines interfered. The only method available for the quantitative analysis of III in combination with other drugs apparently is that of Hudanick (4), which requires reaction with cyanogen bromide, a highly toxic and volatile reagent.

The paired ion extraction technique for the quantitative drug analysis is well documented. The theory and some possible uses of this method were reported (5) and reviewed (6). Numerous applications also were reported for thyroid hormones and sulfa drugs (7), dyes (8), niacin and niacinamide (9), and the simultaneous determinations of hydrocortisone and hydrocortisone phosphate (10).

This paper reports the simultaneous quantitative determinations of I–III in commercial dosage forms. The method is based on paired ion high-pressure liquid chromatography (HPLC), which identifies the compounds. Moreover, inactive ingredients also separate out and may be identified or determined quantitatively without additional work.

EXPERIMENTAL

Chemicals and Reagents—All chemicals and reagents were USP, NF, or ACS grade and were used without further purification. 1-Heptanesulfonic acid sodium salt[2] (IV) was used as received.

Apparatus—A high-pressure liquid chromatograph[3] capable of operating at an inlet pressure up to 6000 psig was used. A multiple wavelength detector[4] was used. For convenience, the wavelength was set at 254 nm (usually found in fixed wavelength detectors) for all ingredients. The detector was attached to a recorder[5] and an integrator[6]. The column[7] (30 cm × 4 mm i.d.) was purchased and used as received.

Chromatographic Solvents—A 13% (v/v) solution of acetonitrile in water containing 1.8% (v/v) acetic acid with or without 0.005 *M* IV was used. The pH of both solvents was 2.6 ± 0.05.

Chromatographic Conditions—The temperature was ambient. The flow rate was 0.6 ml/min (inlet pressure of approximately 300 psig) for the first 12 min and then was 3.6 ml/min (inlet pressure of approximately 3000 psig). The absorbance unit for full-scale deflection was 0.04, and the chart speed was 30.5 cm/hr.

Preparation of Stock Solutions—All stock solutions were prepared in water using a simple solution method. Heating to about 90° for approximately 5 min was required to dissolve III. The concentrations of the

[1] Dimetapp, A. H. Robins, Richmond, Va.

[2] Eastman Kodak Co., Rochester, N.Y.
[3] Waters ALC 202 equipped with a U6K Universal injector, Waters Associates, Milford, Mass.
[4] Spectroflow monitor 770, Schoeffel Instrument Corp., Westwood, N.J.
[5] Omniscribe 5213-12, Houston Instruments, Austin, Tex.
[6] Autolab Minigrator, Spectra-Physics, Santa Clara, Calif.
[7] μBondapak CN, Waters Associates, Milford, Mass.

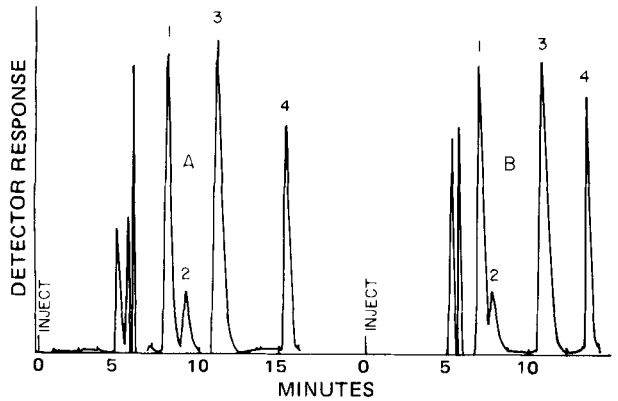

Figure 1—*Sample chromatograms from the standard mixture. Key: A, using mobile phase containing IV; and B, using mobile phase without IV. Peaks 1–4 are from I, II, sodium benzoate, and III, respectively.*

stock solutions were 0.1% each for I, II, and sodium benzoate and 0.08% for III.

Preparation of Standard Solutions—A 10.0-ml quantity of the stock solution was diluted to 100.0 ml with water. A standard mixture containing all active ingredients and sodium benzoate was prepared by mixing 10.0 ml of the stock solution and bringing it to volume (100.0 ml) with water.

Sample Preparation—*Commercial Elixir*—A 5.0-ml quantity of the elixir was diluted to 50.0 ml with water. Based on the label claim, this solution contained the same concentrations of ingredients as the standard mixture.

Sustained-Release Tablets—Ten or 20 tablets were accurately weighed and ground to a fine powder. Enough powder to represent one tablet was weighed accurately and transferred to a 150-ml beaker. Then 40 ml of water was added, and the mixture was heated to about 90° for approximately 5 min and then allowed to cool. The mixture was brought to volume (50.0 ml) with water and filtered. The first 15 ml of filtrate was discarded, and then a portion was collected and diluted 1:3 with water. Based on the label claim, this dilution contained the same concentration of the ingredients as the standard mixture.

All Active Ingredients and Sodium Benzoate—The assay sample (10.0 μl) was injected into the chromatograph using mobile phase with IV. For comparison purposes, an identical volume of the standard mixture was injected after the assay sample was eluted.

Calculations—Since preliminary investigations indicated that the peak area of each ingredient was directly related to concentration (range of 0.5–1.5 μg for I, II, and sodium benzoate and of 0.4–1.2 μg for III), the results were calculated by direct comparison of the peak areas:

$$\frac{A_a}{A_s} \times 100 = \% \text{ of label claim} \qquad \text{(Eq. 1)}$$

where A_a is the peak area of the ingredient in the assay sample and A_s is the peak area of the same ingredient in the standard mixture.

The results are presented in Table I, and sample chromatograms are presented in Figs. 1 and 2. A typical chromatogram using mobile phase without IV is also presented in Fig. 1. The relative standard deviations on all active ingredients and sodium benzoate based on six repeated injections are also presented in Table I.

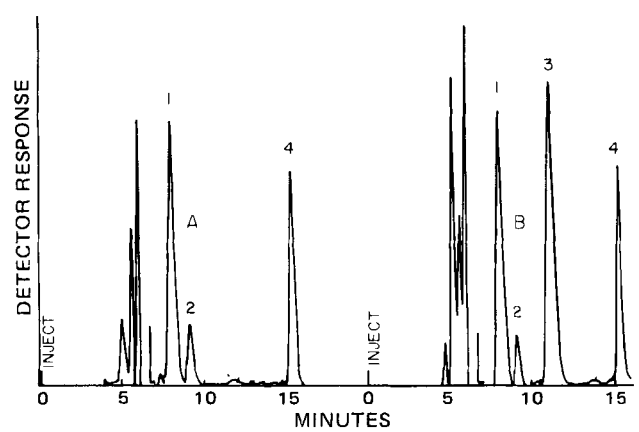

Figure 2—*Sample chromatograms from dosage forms. Key: A, from tablets using mobile phase containing IV; and B, from an elixir using mobile phase containing IV. Peaks 1–4 are from I, II, sodium benzoate, and III, respectively.*

Table I—Assay Results for Various Active Ingredients and Sodium Benzoate

Sample	Assay Results[a], % of Label Claim I	II	III	Sodium Benzoate
Sustained-release tablet	99.6	106.2	101.7	—[b]
Sustained-release tablet[c]	102.9	80.2	65.1	—[b]
Elixir	97.6	92.1	96.9	96.9[d]
Elixir[c]	100.3	118.2[e]	102.6	102.7[d]
RSD[f], %	1.15	1.59	1.78	0.93

[a] Average of three. [b] Tablets did not contain sodium benzoate. [c] Tablets and elixir were from a different manufacturer. [d] There was no label claim. The results are based on 0.1% in the elixir. [e] The manufacturer claimed that the product contained a substantial overage of III for extended shelflife. [f] Based on six injections of the standard mixture.

DISCUSSION

The results (Table I and Fig. 2) indicate that, using a single injection, it is possible to separate all three active ingredients and sodium benzoate present in commercial dosage forms. While assaying active ingredients, sodium benzoate (a preservative present in the elixir) can be assayed without additional time.

The method developed is accurate and precise (Table I). For each ingredient, the area of the peak was directly related to the concentration (range of 0.5–1.5 μg for I, II, and sodium benzoate and of 0.4–1.2 μg for III).

The method is sensitive; less than 1 μg of any ingredient can be assayed. The sensitivity can be improved by decreasing the absorbance units for full-scale deflection and by using the wavelength of maximum absorption instead of 254 nm. For example, the phenylephrine assay is six times more sensitive at 273 nm than at 254 nm. Since sensitivity was not a problem, 254 nm, which is usually found in most fixed wavelength detectors, was used.

The low results on II and III in one commercial dosage form (Table I) cannot be explained easily since these ingredients are supposed to be stable in solid dosage forms. It may be that the manufacturer used some alkaline excipients. The sustained-release tablets may have been made by incorporating part of the active ingredients in the coating, which could cause the problem. The type of excipients used or the processes involved in the manufacturing of these tablets could not be determined.

To use the developed method, it should be determined if the excipients (especially colors and preservatives in liquid dosage forms) interfere.

This report is another example of the application of paired ion HPLC. Without the addition of IV (a counterion), I and II could not be separated (Fig. 1).

REFERENCES

(1) "The United States Pharmacopeia," 19th rev., Mack Publishing Co., Easton, Pa., 1975, p. 378.

(2) L. J. Dombrowski, P. M. Comi, and E. L. Pratt, *J. Pharm. Sci.*, **62**, 1761 (1973).

(3) D. Burke, V. S. Venturella, and B. Z. Senkowski, *ibid.*, **63**, 269 (1974).

(4) H. Hudanick, *ibid.*, **53**, 332 (1964).

(5) B. A. Persson and B. L. Karger, *J. Chromatogr. Sci.*, **12**, 521 (1974).

(6) Bulletin No. D61, Waters Associates, Milford, Mass., May 1976.

(7) B. L. Karger, S. C. Su, S. Marchese, and B. A. Persson, *J. Chromatogr. Sci.*, **12**, 678 (1974).

(8) D. P. Wittmer, N. O. Nuessle, and W. G. Haney, Jr., *Anal. Chem.*, **47**, 1422 (1975).

(9) S. P. Sood, D. P. Wittmer, S. A. Ismaiel, and W. G. Haney, Jr., *J. Pharm. Sci.*, **66**, 40 (1977).

(10) J. Korpi, D. P. Wittmer, B. J. Sandmann, and W. G. Haney, Jr., *ibid.*, **65**, 1087 (1976).

ACKNOWLEDGMENTS

The authors thank A. H. Robins, Richmond, Va., for the brompheniramine maleate powder.

Constant Blood Withdrawal Method for Area under Plasma Concentration–Time Curve

C. R. KOWARSKI *x **and A. A. KOWARSKI** ‡

Received July 19, 1977, from the *School of Pharmacy, Temple University, Philadelphia, PA 19140, and the ‡Department of Pediatrics, Johns Hopkins University, Baltimore, MD 21205. Accepted for publication September 29, 1977.

Abstract □ The area under the plasma concentration–time curve (*AUC*) was measured after an intravenous injection of sodium salicylate and after intragastric administration of aspirin, using either an intermittent sampling and the trapezoid rule (*AUC*–trapezoid) or the recently introduced constant blood withdrawal method (*AUC*–integrated concentration). Six dogs were used in each study. The *AUC*–integrated concentration was significantly higher than the *AUC*–trapezoid. The difference between the two methods was more significant after the intravenous infusion than after the intragastric administration. The higher *AUC*–integrated concentration was attributed to the inclusion of the initial plasma levels, which is an inherent advantage of the constant blood withdrawal method.

Keyphrases □ Plasma concentration–time curves—*AUC* determined by constant blood withdrawal and intermittent sampling methods compared, sodium salicylate and aspirin in dogs □ *AUC*—determined by constant blood withdrawal and intermittent sampling methods compared, sodium salicylate and aspirin in dogs □ Pharmacokinetics—*AUC* determined by constant blood withdrawal and intermittent sampling methods compared, sodium salicylate and aspirin in dogs

Since the pharmacological effect of drugs can be related to their concentration in the plasma and to the duration of their presence in the plasma pool, the area under the plasma concentration peak has become an important parameter in the evaluation and quantitation of the bioavailability of various drugs (1–5). Most presently used methods for calculating the area under the plasma concentration–time curve (*AUC*) are based on a multiple sampling protocol. Each plasma sample is assayed separately. The plasma concentration–time curve is then constructed either by connecting the points with straight lines (the trapezoid method) or by fitting the function to the points and then calculating the integral of the curve.

Previously (6, 7), the constant blood withdrawal method for calculation of the *AUC* in pharmacokinetic studies was described. In this method, integration is achieved by the constant blood withdrawal apparatus. This method does not require prior knowledge of the shape of the concentration–time curve and greatly reduces the number of assays (1–5). This investigation compared the multiple sampling method with the constant blood withdrawal method.

EXPERIMENTAL

Determination of *AUC* after Intravenous Administration of Sodium Salicylate—Six adult female Beagle dogs were fasted for 24 hr prior to each experiment. Dogs 1–3 each received 800 mg of sodium salicylate in a sterile solution as a single intravenous pulse. Dogs 4–6 were injected with 400 mg of sodium salicylate. The catheter was left in place and flushed by a slow drip of saline. Constant withdrawal of blood from a vein in another limb was initiated just prior to the pulse injection, using a nonthrombogenic, presterilized, disposable set with a withdrawal pump as previously described (6). The withdrawal rate was set at 5 ml/hr and was continued for 4 hr.

In addition to the constant withdrawal, 5-ml blood samples were withdrawn from another vein every 2 min for the first 10 min and subsequently at 20, 40, 60, 80, 120, 140, 160, 180, 200, 22.0, and 240 min. The plasma salicylic acid level was measured by a previously described method (8). The salicylic acid concentration in the constant withdrawal pool was the integrated concentration (IC-4 hr). The *AUC* or $\int_0^4 c\,dt$ was then calculated as follows:

$$\int_0^4 c\,dt = \text{IC-4 hr} \times 4 \qquad \text{(Eq. 1)}$$

The *AUC* was also calculated from the intermittent samples by the trapezoid rule.

Table I—Intravenous Administration of Sodium Salicylate

Dog	*AUC*–Trapezoid	*AUC*–Integrated Concentration
1	627	745
2	615	700
3	610	688
Mean ± 1 *SD*	617 ± 8.7	711 ± 30.0
	$p < 0.01$	
4	376	400
5	374	410
6	373	384
Mean ± 1 *SD*	374 ± 1.5	398 ± 13.1
	$p < 0.05$	

Determination of *AUC* after Ingestion of Aspirin—Six dogs were used. A nonthrombogenic intravenous catheter was introduced as previously described. A lubricated gavage tube was inserted through the mouth of each dog into the stomach. Four 324-mg aspirin tablets were crushed, suspended in 80 ml of water, and administered through the gavage tube. The nonthrombogenic catheter was connected to the constant withdrawal pump, which was set to withdraw at a rate of 5 ml/hr. The blood was collected over 4 hr, spun, and separated. The salicylic acid concentration in the sample constituted the integrated concentration for the collection period (IC- 4 hr). The *AUC* was calculated as previously described.

Concurrently with the continuous withdrawal, blood samples were withdrawn every 15 min from another limb. The plasma salicylic acid concentration of these samples also was determined.

RESULTS AND DISCUSSION

The *AUC* of salicylic acid was determined in each dog by the trapezoid rule (*AUC*–trapezoid) and then by the constant blood withdrawal method (*AUC*–integrated concentration) (Table I). The *AUC* by the nonthrombogenic constant blood withdrawal method (*AUC*–integrated concentration) was significantly higher than the *AUC*–trapezoid. It was concluded that the initial plasma salicylic acid levels contributed significantly more to the *AUC* than was assumed by the trapezoid rule.

This observation is in agreement with previous conclusions (7) drawn from measurement of the sulfamethizole clearance rate using the constant infusion, the intermittent sampling, and the constant withdrawal methods. The constant blood withdrawal method yielded a clearance of sulfamethizole that was in good agreement with the clearance obtained by the constant infusion method, thereby confirming its accuracy.

Therefore, the constant blood withdrawal method yields results that are inherently more accurate than the intermittent sampling method. Even determination of the plasma level at 2-min intervals during the initial period could not fully compensate for the inaccuracy of the multiple intermittent sampling method. An additional advantage of the constant blood withdrawal method is the saving in the multiple determinations of the plasma drug concentrations. Instead of the 17 separate assays used in the intermittent method, only one determination of the plasma drug concentration was required by the constant withdrawal method.

Since the difference between the intermittent sampling method and

Table II—Intragastric Administration of 1296 mg of Aspirin

Dog	AUC after 4 hr, hr × mg/liter: AUC–Trapezoid Intermittent Sampling Method	AUC–Integrated Concentration Constant Withdrawal Method
1	555	568
2	492	492
3	491	590
4	425	513
5	717	856
6	522	590
Mean ± 1 *SD*	554 ± 100	601 ± 131
	$p < 0.05$	

the constant blood withdrawal method is mainly due to the peak plasma level observed during the initial period, the difference may become negligible when the plasma concentration–time curve does not contain a peak at the initial period. Table II contains the results of a comparison between the *AUC*–trapezoid determined by the intermittent sampling method and the *AUC*–integrated concentration determined by the nonthrombogenic constant blood withdrawal method after intragastric administration of aspirin. As expected, the difference was not as great as the difference observed in the previous experiment, but it was still significant ($p < 0.05$, paired t test). The plasma concentration–time curve of salicylic acid after intragastric administration of aspirin did not contain the sharp early peak seen after intravenous administration. Despite the gradual increase in the plasma salicylic acid level, the *AUC* was not adequately described by the multiple sampling method.

When the shape of the plasma concentration–time curve is of interest, the collection of blood for the constant blood withdrawal method can be interrupted at predetermined intervals. Therefore, a series of integrated concentrations can be obtained by determining the plasma concentration during each constant blood withdrawal interval. The use of an interruption method increases the number of determinations of the plasma drug concentration, thus reducing one advantage of uninterrupted continuous withdrawal. The advantages of this approach were discussed previously (9).

REFERENCES

(1) J. G. Wagner, *J. Pharm. Sci.*, **56,** 652 (1967).

(2) J. C. K. Loo and S. Riegelman, *ibid.*, **57,** 918 (1968).

(3) J. G. Wagner, J. I. Northam, C. D. Alway, and O. S. Carpenter, *Nature*, **207,** 1301 (1965).

(4) R. C. Batterman, *N. Engl. J. Med.*, **258,** 213 (1958).

(5) G. A. Cronk, *ibid.*, **258,** 219 (1958).

(6) A. Kowarski, R. G. Thompson, C. J. Migeon, and R. M. Blizzard, *J. Clin. Endocrinol. Metab.*, **32,** 356 (1971).

(7) C. R. Kowarski, C. Giancatarino, R. Kraemer, D. Brecht, and A. A. Kowarski, *J. Pharm. Sci.*, **65,** 450 (1976).

(8) B. B. Brodie, A. Udenfriend, and A. F. Coburn, *J. Pharmacol. Exp. Ther.*, **80,** 114 (1944).

(9) B. Vogelstein, A. A. Kowarski, and P. S. Lietman, *Clin. Pharmacol. Ther.*, **22,** 131 (1977).

ACKNOWLEDGMENTS

Supported in part by Grant R01-HD-06284-05 from the U.S. Public Health Service, Bethesda, Md.

The following students participated in the study as part of their undergraduate research program: A. A. Milicia, L. A. Mays, W. Tengood, R. Kuhl, G. Sloto, L. Jones, and S. Crane.

Constituents of *Cannabis sativa* L. XIII: Stability of Dosage Form Prepared by Impregnating Synthetic (−)-Δ^9-*trans*-Tetrahydrocannabinol on Placebo *Cannabis* Plant Material

GLENDA S. LEWIS and CARLTON E. TURNER ˣ

Received May 23, 1977, from the *Research Institute of Pharmaceutical Sciences, School of Pharmacy, University of Mississippi, University, MS 38677.* Accepted for publication October 6, 1977.

Abstract □ Synthetic (−)-Δ^9-*trans*-tetrahydrocannabinol impregnated on placebo *Cannabis* decomposed only 6.3% after being stored for 1 year at −18°. Storage at 5° and room temperature under various conditions led to severe decomposition. The amount of cannabinol observed when (−)-Δ^9-*trans*-tetrahydrocannabinol decomposed indicates that cannabinol is not the only decomposition product.

Keyphrases □ *Cannabis sativa* L.—stability of dosage form prepared by impregnating synthetic (−)-Δ^9-tetrahydrocannabinol on placebo *Cannabis* plant material □ Stability—dosage form prepared by impregnating synthetic (−)-Δ^9-tetrahydrocannabinol on placebo *Cannabis* plant material □ (−)-Δ^9-Tetrahydrocannabinol—impregnated on placebo *Cannabis* plant material, stability of dosage form □ Dosage forms—prepared by impregnating synthetic (−)-Δ^9-tetrahydrocannabinol on placebo *Cannabis* plant material, stability

The potency of *Cannabis* preparations varies significantly according to cannabinoid ratios (1). Recently, to overcome these variations, researchers have used placebo *Cannabis* plant material impregnated with synthetic (−)-Δ^9-*trans*-tetrahydrocannabinol (I). However, this procedure also has disadvantages: (*a*) several months are required for the simplest preclinical or clinical study, (*b*) storage conditions in laboratories are not standardized, (*c*) several solvent systems may be used in the impregnation procedure, and (*d*) synthetic I and I in natural *Cannabis* preparations decompose at different rates under different storage conditions (2, 3).

In view of the disadvantages and other considerations[1], this paper reports findings on the stability of a dosage form prepared by impregnating synthetic I on placebo *Cannabis* plant material.

[1] The authors are under contract from the National Institute on Drug Abuse to provide various *Cannabis* preparation to researchers.

Table II—Intragastric Administration of 1296 mg of Aspirin

Dog	AUC after 4 hr, hr × mg/liter: AUC–Trapezoid Intermittent Sampling Method	AUC–Integrated Concentration Constant Withdrawal Method
1	555	568
2	492	492
3	491	590
4	425	513
5	717	856
6	522	590
Mean ± 1 *SD*	554 ± 100	601 ± 131
	$p < 0.05$	

the constant blood withdrawal method is mainly due to the peak plasma level observed during the initial period, the difference may become negligible when the plasma concentration–time curve does not contain a peak at the initial period. Table II contains the results of a comparison between the *AUC*–trapezoid determined by the intermittent sampling method and the *AUC*–integrated concentration determined by the nonthrombogenic constant blood withdrawal method after intragastric administration of aspirin. As expected, the difference was not as great as the difference observed in the previous experiment, but it was still significant ($p < 0.05$, paired t test). The plasma concentration–time curve of salicylic acid after intragastric administration of aspirin did not contain the sharp early peak seen after intravenous administration. Despite the gradual increase in the plasma salicylic acid level, the *AUC* was not adequately described by the multiple sampling method.

When the shape of the plasma concentration–time curve is of interest, the collection of blood for the constant blood withdrawal method can be interrupted at predetermined intervals. Therefore, a series of integrated concentrations can be obtained by determining the plasma concentration during each constant blood withdrawal interval. The use of an interruption method increases the number of determinations of the plasma drug concentration, thus reducing one advantage of uninterrupted continuous withdrawal. The advantages of this approach were discussed previously (9).

REFERENCES

(1) J. G. Wagner, *J. Pharm. Sci.*, **56,** 652 (1967).

(2) J. C. K. Loo and S. Riegelman, *ibid.*, **57,** 918 (1968).

(3) J. G. Wagner, J. I. Northam, C. D. Alway, and O. S. Carpenter, *Nature*, **207,** 1301 (1965).

(4) R. C. Batterman, *N. Engl. J. Med.*, **258,** 213 (1958).

(5) G. A. Cronk, *ibid.*, **258,** 219 (1958).

(6) A. Kowarski, R. G. Thompson, C. J. Migeon, and R. M. Blizzard, *J. Clin. Endocrinol. Metab.*, **32,** 356 (1971).

(7) C. R. Kowarski, C. Giancatarino, R. Kraemer, D. Brecht, and A. A. Kowarski, *J. Pharm. Sci.*, **65,** 450 (1976).

(8) B. B. Brodie, A. Udenfriend, and A. F. Coburn, *J. Pharmacol. Exp. Ther.*, **80,** 114 (1944).

(9) B. Vogelstein, A. A. Kowarski, and P. S. Lietman, *Clin. Pharmacol. Ther.*, **22,** 131 (1977).

ACKNOWLEDGMENTS

Supported in part by Grant R01-HD-06284-05 from the U.S. Public Health Service, Bethesda, Md.

The following students participated in the study as part of their undergraduate research program: A. A. Milicia, L. A. Mays, W. Tengood, R. Kuhl, G. Sloto, L. Jones, and S. Crane.

Constituents of *Cannabis sativa* L. XIII: Stability of Dosage Form Prepared by Impregnating Synthetic (−)-Δ^9-*trans*-Tetrahydrocannabinol on Placebo *Cannabis* Plant Material

GLENDA S. LEWIS and CARLTON E. TURNER ˣ

Received May 23, 1977, from the *Research Institute of Pharmaceutical Sciences, School of Pharmacy, University of Mississippi, University, MS 38677.* Accepted for publication October 6, 1977.

Abstract □ Synthetic (−)-Δ^9-*trans*-tetrahydrocannabinol impregnated on placebo *Cannabis* decomposed only 6.3% after being stored for 1 year at −18°. Storage at 5° and room temperature under various conditions led to severe decomposition. The amount of cannabinol observed when (−)-Δ^9-*trans*-tetrahydrocannabinol decomposed indicates that cannabinol is not the only decomposition product.

Keyphrases □ *Cannabis sativa* L.—stability of dosage form prepared by impregnating synthetic (−)-Δ^9-tetrahydrocannabinol on placebo *Cannabis* plant material □ Stability—dosage form prepared by impregnating synthetic (−)-Δ^9-tetrahydrocannabinol on placebo *Cannabis* plant material □ (−)-Δ^9-Tetrahydrocannabinol—impregnated on placebo *Cannabis* plant material, stability of dosage form □ Dosage forms—prepared by impregnating synthetic (−)-Δ^9-tetrahydrocannabinol on placebo *Cannabis* plant material, stability

The potency of *Cannabis* preparations varies significantly according to cannabinoid ratios (1). Recently, to overcome these variations, researchers have used placebo *Cannabis* plant material impregnated with synthetic (−)-Δ^9-*trans*-tetrahydrocannabinol (I). However, this procedure also has disadvantages: (*a*) several months are required for the simplest preclinical or clinical study, (*b*) storage conditions in laboratories are not standardized, (*c*) several solvent systems may be used in the impregnation procedure, and (*d*) synthetic I and I in natural *Cannabis* preparations decompose at different rates under different storage conditions (2, 3).

In view of the disadvantages and other considerations[1], this paper reports findings on the stability of a dosage form prepared by impregnating synthetic I on placebo *Cannabis* plant material.

[1] The authors are under contract from the National Institute on Drug Abuse to provide various *Cannabis* preparation to researchers.

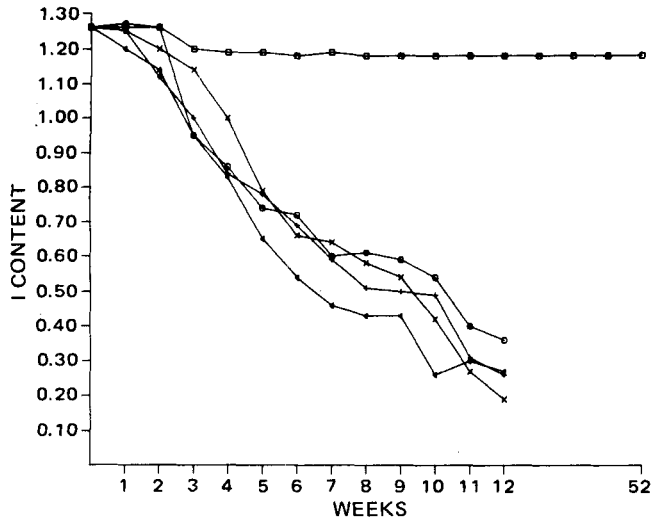

Figure 1—*Decomposition rate of (−)-Δ⁹-trans-tetrahydrocannabinol under different storage conditions. Key: □, freezer at −18°; ○, refrigerator at 5°; ▲, room temperature (25°) under nitrogen and exposed to laboratory light; +, room temperature (25°) uncapped and exposed to air and laboratory light; and ×, room temperature (25°) in the dark and exposed to air.*

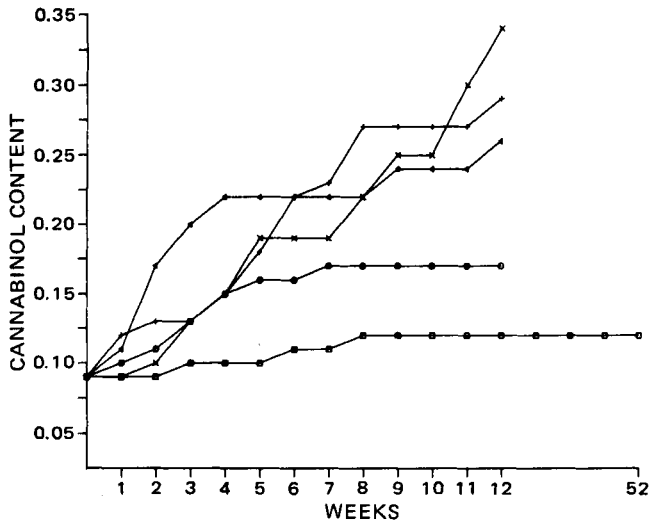

Figure 2—*Cannabinol content resulting from the decomposition of (−)-Δ⁹-trans-tetrahydrocannabinol. Storage conditions were the same as those reported in Fig. 1.*

EXPERIMENTAL

Preparation of Placebo—Manicured[2] *Cannabis sativa* L. (300 g) from an Indian variant[3] grown in Mississippi was extracted with hexane (8 × 1.5 liters) to provide a placebo containing trace amounts of cannabinoids.

Impregnation of Placebo with I—To 300 g of placebo *Cannabis* in an indented 3-liter, round-bottom flask was added 6 g of synthetic I in 500 ml of petroleum ether (bp 60–80°). The flask was attached to a rotary evaporator[4] and rotated vigorously *in vacuo* under mild heat until the solvent was removed. Rotation continued until the placebo material no longer lumped and/or adhered to the walls of the flask. The impregnated material was then analyzed in triplicate and was shown to be coated homogeneously with 1.26% (w/w) of I[5].

The coated material was then bottled in wide-mouth amber glass bottles sealed with plastic caps with a paper lining and stored under the following conditions: (*a*) in the freezer at −18°, (*b*) in the refrigerator at 5°, (*c*) at room temperature (25°) under nitrogen and exposed to laboratory light, (*d*) at room temperature (25°) uncapped and exposed to air and laboratory light, and (*e*) at room temperature (25°) in the dark and exposed to air. Ethanol, ether, methylene chloride, and chloroform were unsatisfactory in impregnating I on placebo material. Analytical data obtained by GLC were so inconsistent that no dosage forms could be prepared.

RESULTS AND DISCUSSION

Turk *et al.* (4) reported that a sample of 100% synthetic I at 0° decomposed to cannabinol (II) in the ratio of 97.1:2.9% over 5 months. Razdan *et al.* (5) reported that synthetic I oxidized to II at the rate of 10%/month at 25°. These data suggest II as the only decomposition product of synthetic I, but Turner *et al.* (2) reported that the amount of II plus I in stored plant material does not account for the original amount of I present. This report suggested the possibility of unidentified cannabinoids being intermediates in the decomposition of I to II and/or that naturally occurring I, when stored in plant material, may decompose by a different pathway. Thus, it seemed imperative to observe the ratios of I, II, and other cannabinoids in this study.

The placebo *Cannabis* prepared contained trace amounts of cannabidiol (III) and cannabichromene (IV), 0.02% I, and 0.02% II. After impregnating the placebo material with synthetic I, the cannabinoid content was: I, 1.26%; II, 0.09%; and III plus IV, trace (<0.01%) amounts.

Samples from each storage condition were anlayzed every week for 12 weeks; after that time, the lowest value for I observed (Fig. 1) was 0.19% in samples stored in the dark at room temperature. Uncapped samples at room temperature exposed to air and light and samples stored at room temperature under nitrogen and exposed to laboratory light contained 0.26 and 0.27%, respectively. The samples stored in the refrigerator contained 0.36% of I. Thus, the decomposition rate for these storage conditions varied from 85 to 71%. No available data explain why samples stored at room temperature in the dark and exposed to air decompose at a faster rate than samples stored under nitrogen and exposed to light at the same temperature. This unexpected observation occurred in a replication.

Samples stored in the freezer at −18° decomposed 6.3% at the end of 12 weeks. Due to the excessive decomposition of all other samples, only the samples at −18° were observed further. These samples proved stable with no additional decomposition up to 52 weeks. In natural *Cannabis* plant material, I stored at −18° decomposed at a rate of 3.83%/year (2).

The data indicate that placebo material, impregnated as described and stored at −18°, is stable for at least 1 year and can be used in experimental designs. Impregnated *Cannabis* plant material not stored under freezer conditions should not be used, and any data published on *Cannabis* impregnated with I where storage under freezer conditions was not specified are suspect at best. Moreover, temperature seems to be the most critical factor in initiating the decomposition of I.

Data on the ratios of I and II are presented in Figs. 1 and 2, respectively. When observing these ratios in samples stored at −18°, it is impossible to state that II is not the only decomposition product of I. However, in all other samples, I decomposed drastically with no corresponding increase in II. For example, in samples stored under nitrogen and light at room temperature, I decreased from 1.26 to 0.27% and II increased from 0.11 to 0.26%. This result strongly indicates that additional products are formed in the decomposition mechanism of I to II and does not support previous reports (4, 5). This point was supported recently when two new cannabinoids were isolated and characterized from an extract of *Cannabis:* (+)-cannabitriol and (−)-10-ethoxy-9-dihydroxy-$\Delta^{6a(10a)}$-tetrahydrocannabinol (6). Neither cannabinoid was detectable by routine GLC; however, by using the silylation method described by Turner *et al.* (7), both compounds were detectable by GLC.

Furthermore, new unidentified cannabinoids of the cannabitriol type are currently being investigated as possible products formed when synthetic or naturally stored I decomposes. Since confusion exists as to the mechanistic pathway from I to II and since most active metabolites of I are hydroxylated, the cannabitriol-type molecules may be present in natural *Cannabis* and placebo *Cannabis* impregnated with I and may be responsible for much of the unexplained pharmacological data on *Cannabis* products (8).

[2] Manicured material is devoid of seeds and large stems; manicuring is accomplished by passing the material through a 10-mesh sieve.

[3] Seed Code IN-B, original seed obtained from Dr. C. K. Atal, Regional Research Laboratory, Jammutawi, India.

[4] Buchi/Brinkmann Rotavapor-R.

[5] Analyses were performed as reported by C. E. Turner, K. W. Hadley, J. H. Holley, S. Billets, and M. L. Mole, Jr., *J. Pharm. Sci.*, **64**, 810 (1975).

REFERENCES

(1) C. E. Turner and K. W. Hadley, *Arch. Invest. Med.*, **5**, 141 (1974).

(2) C. E. Turner, K. W. Hadley, P. S. Fetterman, N. J. Doorenbos, M. W. Quimby, and C. Waller, *J. Pharm. Sci.*, **62**, 1601 (1973).

(3) C. E. Turner and J. T. Henry, *ibid.*, **64**, 357 (1975).

(4) R. E. Turk, J. E. Manno, N. C. Jain, and R. B. Forney, *J. Pharm. Pharmacol.*, **23**, 190 (1971).

(5) R. K. Razdan, A. J. Puttick, B. A. Zikto, and G. R. Handrick, *Experientia*, **28**, 122 (1972).

(6) M. A. Elsohly, F. S. El-Feraly, and C. E. Turner, *Lloydia*, **40**, 275 (1977).

(7) C. E. Turner, K. W. Hadley, J. Henry, and M. L. Mole, *J. Pharm. Sci.*, **63**, 1872 (1974).

(8) C. W. Waller, J. Johnson, J. Buelke, and C. E. Turner, "Marihuana, An Annotated Bibliography," Macmillan Information, New York, N.Y., 1976.

ACKNOWLEDGMENTS

Supported by Contract HSM-42-70-109 from the National Institute on Drug Abuse and the Research Institute of Pharmaceutical Sciences, School of Pharmacy, University of Mississippi.

The authors are grateful to Dr. Mahmoud Elsohly for assistance.

Metabolism and Excretion of Normorphine in Dogs

S. Y. YEH ˣ, R. L. McQUINN *, H. A. KREBS, and C. W. GORODETZKY

Received August 19, 1977, from the *National Institute on Drug Abuse, Division of Research, Addiction Research Center, Lexington, KY 40511.* Accepted for publication October 3, 1977. *Present address: College of Pharmacy, University of Kentucky, Lexington, KY 40506.

Abstract □ Normorphine metabolism was studied in dogs given 20 mg of normorphine hydrochloride/kg sc. Free and conjugated normorphine excreted in the urine over 144 hr represented 32 and 32%, respectively, of the administered dose. Eighty percent of the urinary excretion of the drug occurred within 9 hr. One percent of the administered dose was excreted as free normorphine in the feces. The urine was chromatographed on a column. Evaporation of the washing and methanolic effluent yielded a residue, which was purified by crystallization from aqueous methanol. Results of UV and IR studies, elemental analysis, and determination of normorphine and glucuronic acid content established the identity of this metabolite as normorphine 3-glucuronide. Dihydronormorphine and dehydronormorphine were detected with GLC–mass spectrometry as minor metabolites.

Keyphrases □ Normorphine—metabolism and excretion in dogs □ Metabolism—normorphine in dogs □ Excretion—normorphine in dogs □ Narcotic analgesics—normorphine, metabolism and excretion in dogs

A normorphine conjugate was observed in the urine of humans and laboratory animals after administration of normorphine, morphine, and codeine (1–6), but its nature has not been characterized. The excretion of normorphine in the dog, the isolation and characterization of the normorphine conjugate as normorphine 3-glucuronide, and the detection of dihydronormorphine and dehydronormorphine as minor metabolites are discussed in this report.

EXPERIMENTAL

Materials and Methods—Normorphine hydrochloride[1], 20 mg/kg sc, was injected into two female dogs deprived of food for 24 hr and hydrated by intubation with about 500 ml of water. The dogs were housed in individual metabolic cages, and urine and feces were collected for 144 hr.

Normorphine was determined by GLC in the urine and feces, with and without hydrolysis, as described (4). Specimens were hydrolyzed with acid or β-glucuronidase[2] (4). Free and total normorphine were estimated from unhydrolyzed and hydrolyzed specimens, respectively. Conjugated normorphine was calculated as the difference between the total and the free drug.

GLC–Mass Spectrometry—Chemical-ionization mass spectral data were obtained on a gas chromatograph–mass spectrometer[3] as described (7). The mass fragment pattern of obvious GLC peaks was analyzed. In addition, the whole chromatogram was scanned for possible normorphine metabolite ions such as morphine, norcodeine, *N*-hydroxynormorphine, dihydronormorphine, and monohydroxynormorphine.

Isolation of Normorphine Metabolites—An aliquot of the first 24-hr urine was centrifuged and passed through a resin[4] column (2.1 × 40 cm). The column was washed with 150 ml of distilled water and eluted with 300 ml of 2.5% NH_4OH in methanol. The water washing and the methanol eluate were separately evaporated to syrupy residues under reduced pressure in a water bath at 50°. The residues were suspended in 20 ml of 2% NH_4OH and extracted three times with 1,2-dichloroethane containing 30% 2-propanol. The extracts were concentrated for identification of free normorphine metabolites. The aqueous phase was used to isolate conjugated normorphine as described below.

An aliquot of the free base fraction along with authentic normorphine was chromatographed on instant TLC sheets impregnated with silica gel[5], with ethyl acetate–methanol–ammonium hydroxide (17:2:1) as the developing solvent. After a portion of the chromatogram was sprayed with iodoplatinate, three spots appeared with R_f values of 0.6 (pinkish), 0.73, which corresponds to authentic normorphine (bluish purple), and 0.95 (bluish purple). The chromatogram was sectioned horizontally according to the zones 0–75 (R_f 0.3), 76–110 (R_f 0.6), 111–140 (R_f 0.73), and 141–155 (R_f 0.95) mm and eluted with methanol. The eluates were concentrated and analyzed by GLC.

The aqueous phase was evaporated to a syrupy residue. The residue was triturated with methanol to yield methanol-soluble and methanol-insoluble fractions. The methanol-insoluble fraction was recrystallized from aqueous methanol and dried under vacuum, and it yielded 50 mg of snow-white crystalline material. Approximately 60% of the conjugate was isolated from the water washing fractions.

The methanol-soluble fraction was chromatographed on instant TLC sheets impregnated with silica gel[5], with 1-butanol–acetic acid–water (35:3:10) (Solvent A) as the developing solvent. A section of the chromatogram was sprayed with iodoplatinate solution and showed four spots at R_f 0.0, 0.33, 0.6, and 0.9. The chromatogram was sectioned horizontally according to zones 0–50 (R_f 0.33), 51–120 (R_f 0.6), and 121–150 (R_f 0.9) mm and eluted with water. The eluate was concentrated, hydrolyzed with

[1] Merck Sharp & Dohme, Philadelphia, Pa.
[2] Sigma Chemical Co., St. Louis, Mo.
[3] Finnigan model 3300.
[4] Amberlite XAD-2 resin, Rohm & Haas Co., Philadelphia, Pa.
[5] Gelman Instrument Co., Ann Arbor, Mich.

REFERENCES

(1) C. E. Turner and K. W. Hadley, *Arch. Invest. Med.*, **5**, 141 (1974).

(2) C. E. Turner, K. W. Hadley, P. S. Fetterman, N. J. Doorenbos, M. W. Quimby, and C. Waller, *J. Pharm. Sci.*, **62**, 1601 (1973).

(3) C. E. Turner and J. T. Henry, *ibid.*, **64**, 357 (1975).

(4) R. E. Turk, J. E. Manno, N. C. Jain, and R. B. Forney, *J. Pharm. Pharmacol.*, **23**, 190 (1971).

(5) R. K. Razdan, A. J. Puttick, B. A. Zikto, and G. R. Handrick, *Experientia*, **28**, 122 (1972).

(6) M. A. Elsohly, F. S. El-Feraly, and C. E. Turner, *Lloydia*, **40**, 275 (1977).

(7) C. E. Turner, K. W. Hadley, J. Henry, and M. L. Mole, *J. Pharm. Sci.*, **63**, 1872 (1974).

(8) C. W. Waller, J. Johnson, J. Buelke, and C. E. Turner, "Marihuana, An Annotated Bibliography," Macmillan Information, New York, N.Y., 1976.

ACKNOWLEDGMENTS

Supported by Contract HSM-42-70-109 from the National Institute on Drug Abuse and the Research Institute of Pharmaceutical Sciences, School of Pharmacy, University of Mississippi.

The authors are grateful to Dr. Mahmoud Elsohly for assistance.

Metabolism and Excretion of Normorphine in Dogs

S. Y. YEH ˣ, R. L. McQUINN *, H. A. KREBS, and C. W. GORODETZKY

Received August 19, 1977, from the *National Institute on Drug Abuse, Division of Research, Addiction Research Center, Lexington, KY 40511.* Accepted for publication October 3, 1977. *Present address: College of Pharmacy, University of Kentucky, Lexington, KY 40506.

Abstract □ Normorphine metabolism was studied in dogs given 20 mg of normorphine hydrochloride/kg sc. Free and conjugated normorphine excreted in the urine over 144 hr represented 32 and 32%, respectively, of the administered dose. Eighty percent of the urinary excretion of the drug occurred within 9 hr. One percent of the administered dose was excreted as free normorphine in the feces. The urine was chromatographed on a column. Evaporation of the washing and methanolic effluent yielded a residue, which was purified by crystallization from aqueous methanol. Results of UV and IR studies, elemental analysis, and determination of normorphine and glucuronic acid content established the identity of this metabolite as normorphine 3-glucuronide. Dihydronormorphine and dehydronormorphine were detected with GLC–mass spectrometry as minor metabolites.

Keyphrases □ Normorphine—metabolism and excretion in dogs □ Metabolism—normorphine in dogs □ Excretion—normorphine in dogs □ Narcotic analgesics—normorphine, metabolism and excretion in dogs

A normorphine conjugate was observed in the urine of humans and laboratory animals after administration of normorphine, morphine, and codeine (1–6), but its nature has not been characterized. The excretion of normorphine in the dog, the isolation and characterization of the normorphine conjugate as normorphine 3-glucuronide, and the detection of dihydronormorphine and dehydronormorphine as minor metabolites are discussed in this report.

EXPERIMENTAL

Materials and Methods—Normorphine hydrochloride[1], 20 mg/kg sc, was injected into two female dogs deprived of food for 24 hr and hydrated by intubation with about 500 ml of water. The dogs were housed in individual metabolic cages, and urine and feces were collected for 144 hr.

Normorphine was determined by GLC in the urine and feces, with and without hydrolysis, as described (4). Specimens were hydrolyzed with acid or β-glucuronidase[2] (4). Free and total normorphine were estimated from unhydrolyzed and hydrolyzed specimens, respectively. Conjugated normorphine was calculated as the difference between the total and the free drug.

GLC–Mass Spectrometry—Chemical-ionization mass spectral data were obtained on a gas chromatograph–mass spectrometer[3] as described (7). The mass fragment pattern of obvious GLC peaks was analyzed. In addition, the whole chromatogram was scanned for possible normorphine metabolite ions such as morphine, norcodeine, *N*-hydroxynormorphine, dihydronormorphine, and monohydroxynormorphine.

Isolation of Normorphine Metabolites—An aliquot of the first 24-hr urine was centrifuged and passed through a resin[4] column (2.1 × 40 cm). The column was washed with 150 ml of distilled water and eluted with 300 ml of 2.5% NH_4OH in methanol. The water washing and the methanol eluate were separately evaporated to syrupy residues under reduced pressure in a water bath at 50°. The residues were suspended in 20 ml of 2% NH_4OH and extracted three times with 1,2-dichloroethane containing 30% 2-propanol. The extracts were concentrated for identification of free normorphine metabolites. The aqueous phase was used to isolate conjugated normorphine as described below.

An aliquot of the free base fraction along with authentic normorphine was chromatographed on instant TLC sheets impregnated with silica gel[5], with ethyl acetate–methanol–ammonium hydroxide (17:2:1) as the developing solvent. After a portion of the chromatogram was sprayed with iodoplatinate, three spots appeared with R_f values of 0.6 (pinkish), 0.73, which corresponds to authentic normorphine (bluish purple), and 0.95 (bluish purple). The chromatogram was sectioned horizontally according to the zones 0–75 (R_f 0.3), 76–110 (R_f 0.6), 111–140 (R_f 0.73), and 141–155 (R_f 0.95) mm and eluted with methanol. The eluates were concentrated and analyzed by GLC.

The aqueous phase was evaporated to a syrupy residue. The residue was triturated with methanol to yield methanol-soluble and methanol-insoluble fractions. The methanol-insoluble fraction was recrystallized from aqueous methanol and dried under vacuum, and it yielded 50 mg of snow-white crystalline material. Approximately 60% of the conjugate was isolated from the water washing fractions.

The methanol-soluble fraction was chromatographed on instant TLC sheets impregnated with silica gel[5], with 1-butanol–acetic acid–water (35:3:10) (Solvent A) as the developing solvent. A section of the chromatogram was sprayed with iodoplatinate solution and showed four spots at R_f 0.0, 0.33, 0.6, and 0.9. The chromatogram was sectioned horizontally according to zones 0–50 (R_f 0.33), 51–120 (R_f 0.6), and 121–150 (R_f 0.9) mm and eluted with water. The eluate was concentrated, hydrolyzed with

[1] Merck Sharp & Dohme, Philadelphia, Pa.
[2] Sigma Chemical Co., St. Louis, Mo.
[3] Finnigan model 3300.
[4] Amberlite XAD-2 resin, Rohm & Haas Co., Philadelphia, Pa.
[5] Gelman Instrument Co., Ann Arbor, Mich.

Table I—Urinary and Fecal Excretion (Percent of Administered Dose) of Normorphine and Normorphine Conjugate in the Dog

	Urine				Fecal[a]
	Free Normorphine		Conjugated Normorphine		Free Normorphine
Hours	Dog 1[b]	Dog 2	Dog 1	Dog 2	Dog 1
0–3	13.35		4.92		
3–6	4.52		16.29		
6–9	7.65		5.86		
9–12	1.98		0.09		
12–24	3.24		1.73		
0–24	30.74	29.66	24.37	24.95	1.00
24–48	0.56	2.00	5.68	5.19	0.05
48–72	0.23	1.15	1.26	0.95	0.0
72–96	0.03	0.44	0.53	0.24	0.0
96–120	0.04	0.48	0.10	0.36	0.0
120–144	0.0	0.47	0.0	0.32	0.0
Total	31.60	32.33	31.94	32.08	1.05

[a] Conjugated normorphine was not found in the feces. [b] The urinary bladder of Dog 1 was catheterized.

hydrochloric acid or with β-glucuronidase, extracted, and derivatized for analysis by GLC.

RESULTS AND DISCUSSION

Urinary and Fecal Excretion of Normorphine—Free and conjugated normorphine excreted in the urine over 144 hr represented 32 and 32%, respectively, of the administered dose (Table I). Eighty percent of the urinary excretion of free and conjugated drug occurred within 9 hr in one catheterized dog. One percent of the administered drug was excreted in the feces in one dog. The low recovery of normorphine in the feces was probably due to hydrolysis of the normorphine conjugate in the gut and reabsorption[6].

The extent of conjugation of normorphine appears different from that of morphine. More than 50% of excreted normorphine found in the urine of dogs, monkeys, and humans was in the free form (1, 2), whereas only about 10% of excreted morphine found in the urine of the same species was in the free form and 90% was in the conjugated form (4, 8, 11).

Characterization of Normorphine Metabolites—*Normorphine Conjugate*—Acid hydrolysis of the conjugate gave a product identical with normorphine on TLC, GLC, and GLC–mass spectrometry. The conjugate was soluble in acid, slightly soluble in water, and insoluble in methanol and other organic solvents. It was positive with the glucuronide test (12) and negative with the phenolic test (13). It did not melt or decompose below 300°.

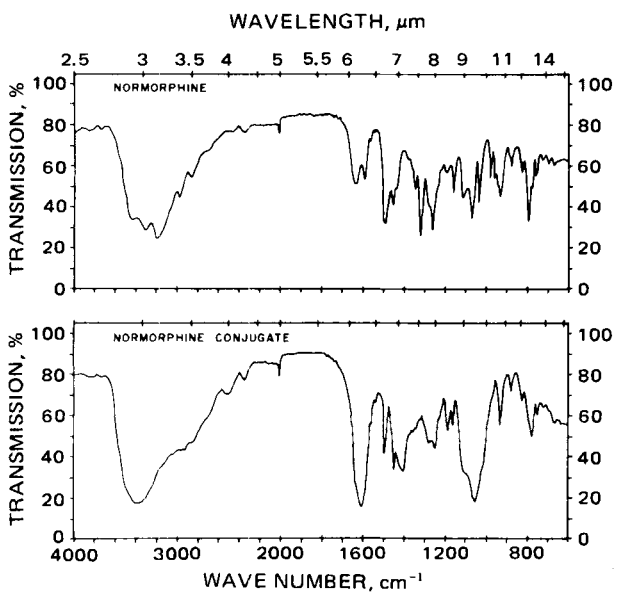

Figure 1—*IR spectrum of authentic normorphine and normorphine 3-glucuronide isolated from dog urine.*

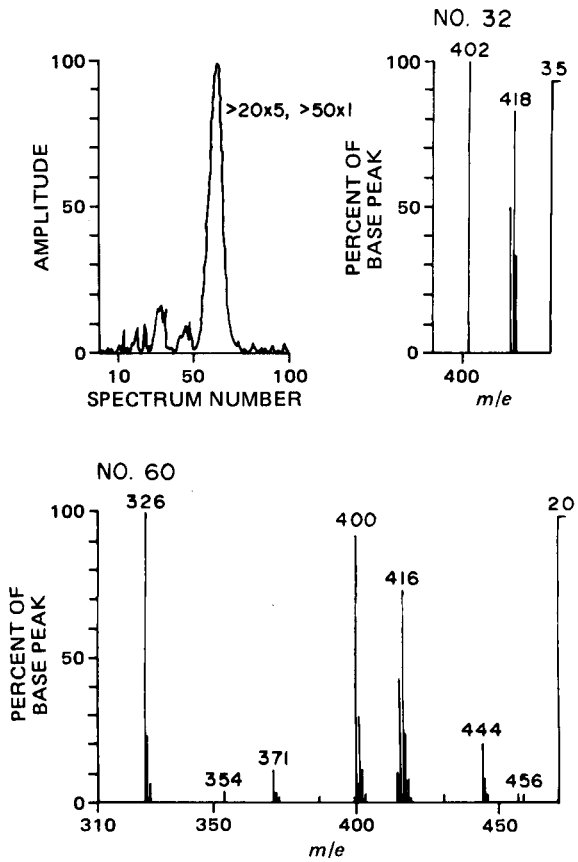

Figure 2—*Integrated total ion current chromatogram of an extract of the hydrolyzed methanol-soluble fraction as the trimethylsilyl derivative. Mass spectrum No. 32 showed characteristics of dihydronormorphine, and No. 60 showed characteristics of normorphine.*

The purified conjugate showed a single spot at R_f 0–0.1 on instant TLC sheets impregnated with silica gel[4] and developed with Solvent A. The R_f value of the conjugate in the methanol eluate was 0.3–0.4; the R_f value appeared to change in the process of purification. The R_f value of the conjugate on paper[7] chromatography, developed with 1-butanol–acetic acid–water (4:1:2), was 0.2.

The IR spectrum of the conjugate as a potassium bromide pellet showed strong absorption bands at 3400, 1610, 1400, and 1070 cm^{-1}, indicating the presence of polyhydroxyl, carbonyl, carboxyl, and ether groups (Fig. 1). The UV spectra of the conjugate in hydrochloric acid medium showed a maximum at 283 nm and a minimum of 256 nm. The $E^{1\%}_{1\,cm}$ was 220. The conjugate in an alkaline medium did not show a bathochromic shift, indicating that the phenolic group was masked. After acid hydrolysis, it did show a bathochromic shift.

Anal.—Calc. for $C_{22}H_{26}NO_9$ (normorphine 3-glucuronide): C, 58.43; H, 5.86; N, 3.13. Found: C, 59.02; H, 5.59; N, 2.79.

The normorphine content of the conjugate was 60.94% as determined by UV and 60.70% by GLC after hydrolysis, extraction, and derivatization. The content of glucuronic acid was 45.5%. The theoretical values for normorphine 3-glucuronide are 60.64% normorphine and 43.39% glucuronic acid.

Detection of Dihydronormorphine—A small peak at *m/e* 418, corresponding to dihydronormorphine as the trimethylsilyl derivative (the amine group was not silylated under the conditions described), was detected in the hydrolyzed eluate of the 0–50-mm zone (R_f 0.3) of the chromatogram of the methanol-soluble portion of the triturated syrupy residue (Fig. 2). Normorphine, like morphine, was expected to be biotransformed to dihydronormorphine since dihydromorphine was found as a minor metabolite of morphine (14).

Detection of Dehydronormorphine—A small peak at *m/e* 558, corre-

[6] Although no data are available on the biliary excretion of normorphine and its conjugate(s), normorphine, like morphine, probably is excreted largely in the bile (8–10).

[7] Waterman No. 1.

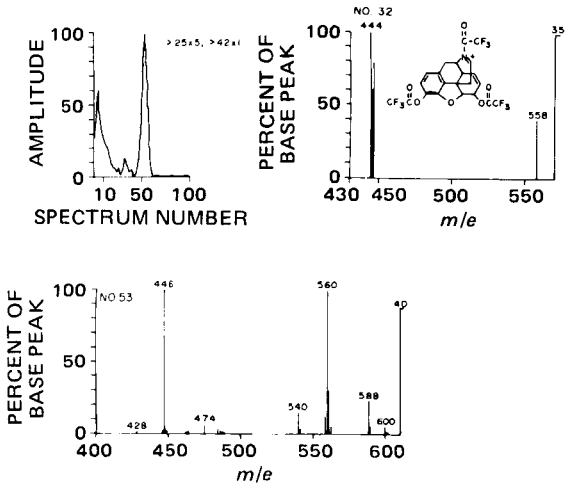

Figure 3—*Integrated total ion current chromatogram of an extract of the free base drug fraction as the trifluoroacetyl derivative. Mass spectrum No. 32 showed characteristics of dehydronormorphine, and No. 53 showed characteristics of normorphine.*

sponding to dehydronormorphine as the trifluoroacetyl derivative, was observed in the eluate of the 140–155-mm zone (R_f 0.9) of the thin-layer chromatogram of the free base drug fraction (Fig. 3). Although there is no direct evidence for the presence of *N*-hydroxynormorphine, dehydronormorphine may have resulted from dehydration of *N*-hydroxynormorphine during purification, derivatization, and GLC analysis. Meperidine *N*-oxide has been shown to undergo dehydration during GLC analysis (15, 16).

Morphine, norcodeine, and codeine were not detected in the free or the conjugated form. This result confirms the reports that the methylation of normorphine does not play a significant role in the metabolism of normorphine (17–20).

REFERENCES

(1) J. Sloan, A. Eisenman, H. F. Fraser, and H. Isbell, in "Abstracts of Fall Meeting of the American Society of Pharmacologists," Ann Arbor, Mich., 1958, p. 31.

(2) A. L. Misra, H. I. Jacoby, and L. A. Woods, *J. Pharmacol. Exp. Ther.*, **132,** 311 (1961).

(3) A. L. Misra, S. J. Mulé, and L. A. Woods, *Nature (London)*, **190,** 82 (1961).

(4) S. Y. Yeh, *J. Pharmacol. Exp. Ther.*, **192,** 201 (1975).

(5) S. Y. Yeh and L. A. Woods, *Arch. Int. Pharmacodyn. Ther.*, **191,** 231 (1971).

(6) W. O. R. Ebbinghausen, J. Mowat, and P. Vestergaard, *J. Pharm. Sci.*, **62,** 146 (1973).

(7) S. Y. Yeh, C. W. Gorodetzky, and H. A. Krebs, *ibid.*, **66,** 1288 (1977).

(8) L. A. Woods, *J. Pharmacol. Exp. Ther.*, **112,** 158 (1954).

(9) C. T. Walsh and R. Levine, *ibid.*, **195,** 303 (1975).

(10) S. Y. Yeh and L. A. Woods, *ibid.*, **166,** 86 (1969).

(11) L. B. Mellett and L. A. Woods, *ibid.*, **116,** 77 (1956).

(12) Z. Dische, *J. Biol. Chem.*, **167,** 189 (1947).

(13) M. Volterra, *Am. J. Clin. Pathol.*, **12,** 525, 580 (1942); in "Practical Physiological Chemistry," 13th ed., P. B. Hawk, B. L. Oser, and W. H. Summerson, Eds., Blakiston, New York, N.Y., 1954, p. 939.

(14) S. Y. Yeh, *Pharmacologist*, **18,** 178 (1976).

(15) C. Lindberg and C. Bogentoft, *Acta Pharm. Suec.*, **12,** 507 (1975).

(16) W. G. Stillwell, C. S. Myran, and J. T. Stewart, *Res. Commun. Chem. Pathol. Pharmacol.*, **14,** 605 (1976).

(17) D. H. Clouet, *Life Sci.*, **1,** 31 (1962).

(18) D. H. Clouet, *Biochem. Pharmacol.*, **12,** 967 (1963).

(19) S. J. Mulé and G. J. Mannering, *Bull. Narc.*, **17,** 27 (1965).

(20) R. J. Miller, C. Jolles, and H. Rapoport, *Phytochemistry*, **12,** 597 (1973).

ACKNOWLEDGMENTS

The preliminary report of the study appeared in *Fed. Proc.*, **34,** 814 (1975).

Local Anesthetic Activity and Acute Toxicity of *N*-Substituted 1,2,3,4-Tetrahydro-1- and 2-naphthylamines

ANTHONY T. DREN ˣ, BARBARA A. BOPP, DONN M. EBERT, ADOLPH O. GEISZLER, JAMES B. HOLLAND, BRUCE W. HORROM, and D. A. DUNNIGAN

Received August 16, 1976, from the *Department of Pharmacology and Medicinal Chemistry and the Department of Organic Research, Abbott Laboratories, North Chicago, IL 60064.* Accepted for publication September 29, 1977.

Abstract □ Seven *N*-substituted 1,2,3,4-tetrahydro-1- and three 2-naphthylamines were prepared and tested for local anesthetic activity in the rabbit corneal reflex test and the mouse sciatic nerve block test. At 0.1 and 1%, three 1-alkylamino compounds had durations of action comparable to that of tetracaine in the rabbit corneal reflex test and were considerably more potent than lidocaine. The other four 1-alkylamino derivatives were inactive or at best minimally active. The durations of action of 1% concentrations of the three 2-alkylamino compounds were equivalent to that of 1% lidocaine in the corneal reflex test. In the mouse sciatic nerve block test, the three active 1-alkylamino compounds were considerably longer acting than either tetracaine or lidocaine. Three 1-alkylamino and the three 2-alkylamino compounds showed toxicity equal to or greater than lidocaine, while two 1-alkylamino and two 2-alkylamino compounds showed toxicity equal to or greater than tetracaine by the intraperitoneal route in mice. *N*-Heptyl-1,2,3,4-tetrahydro-6-methoxy-1-naphthylamine methanesulfonate was the most promising local anesthetic in these series.

Keyphrases □ 1,2,3,4-Tetrahydro-1- and 2-naphthylamines, *N*-substituted—synthesized, local anesthetic activity and toxicity evaluated □ Local anesthetic activity—various *N*-substituted 1,2,3,4-tetrahydro-1- and 2-naphthylamines evaluated □ Toxicity—various *N*-substituted 1,2,3,4-tetrahydro-1- and 2-naphthylamines evaluated □ Structure-activity relationships—various *N*-substituted 1,2,3,4-tetrahydro-1- and 2-naphthylamines evaluated for local anesthetic activity and toxicity

A series of methoxy-1- and 2-aminoindans and naphthylamines previously was synthesized as potential antiparkinsonian agents (1). When these compounds were tested for dopaminergic activity, some were inhibitors of monoamine oxidase. Subsequently, additional compounds were prepared in which the substituent on the amine was

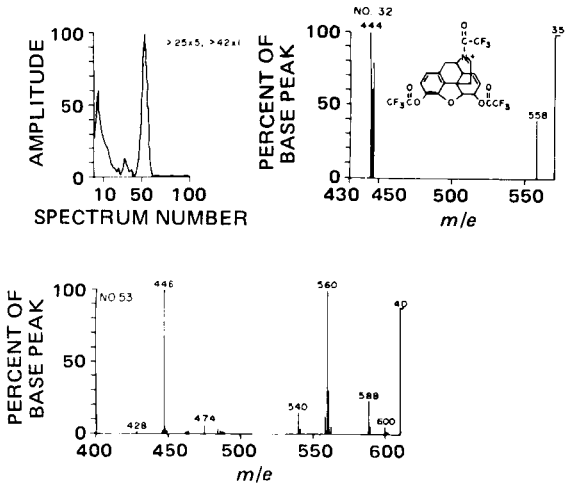

Figure 3—*Integrated total ion current chromatogram of an extract of the free base drug fraction as the trifluoroacetyl derivative. Mass spectrum No. 32 showed characteristics of dehydronormorphine, and No. 53 showed characteristics of normorphine.*

sponding to dehydronormorphine as the trifluoroacetyl derivative, was observed in the eluate of the 140–155-mm zone (R_f 0.9) of the thin-layer chromatogram of the free base drug fraction (Fig. 3). Although there is no direct evidence for the presence of *N*-hydroxynormorphine, dehydronormorphine may have resulted from dehydration of *N*-hydroxynormorphine during purification, derivatization, and GLC analysis. Meperidine *N*-oxide has been shown to undergo dehydration during GLC analysis (15, 16).

Morphine, norcodeine, and codeine were not detected in the free or the conjugated form. This result confirms the reports that the methylation of normorphine does not play a significant role in the metabolism of normorphine (17–20).

REFERENCES

(1) J. Sloan, A. Eisenman, H. F. Fraser, and H. Isbell, in "Abstracts of Fall Meeting of the American Society of Pharmacologists," Ann Arbor, Mich., 1958, p. 31.

(2) A. L. Misra, H. I. Jacoby, and L. A. Woods, *J. Pharmacol. Exp. Ther.*, **132,** 311 (1961).

(3) A. L. Misra, S. J. Mulé, and L. A. Woods, *Nature (London)*, **190,** 82 (1961).

(4) S. Y. Yeh, *J. Pharmacol. Exp. Ther.*, **192,** 201 (1975).

(5) S. Y. Yeh and L. A. Woods, *Arch. Int. Pharmacodyn. Ther.*, **191,** 231 (1971).

(6) W. O. R. Ebbinghausen, J. Mowat, and P. Vestergaard, *J. Pharm. Sci.*, **62,** 146 (1973).

(7) S. Y. Yeh, C. W. Gorodetzky, and H. A. Krebs, *ibid.*, **66,** 1288 (1977).

(8) L. A. Woods, *J. Pharmacol. Exp. Ther.*, **112,** 158 (1954).

(9) C. T. Walsh and R. Levine, *ibid.*, **195,** 303 (1975).

(10) S. Y. Yeh and L. A. Woods, *ibid.*, **166,** 86 (1969).

(11) L. B. Mellett and L. A. Woods, *ibid.*, **116,** 77 (1956).

(12) Z. Dische, *J. Biol. Chem.*, **167,** 189 (1947).

(13) M. Volterra, *Am. J. Clin. Pathol.*, **12,** 525, 580 (1942); in "Practical Physiological Chemistry," 13th ed., P. B. Hawk, B. L. Oser, and W. H. Summerson, Eds., Blakiston, New York, N.Y., 1954, p. 939.

(14) S. Y. Yeh, *Pharmacologist*, **18,** 178 (1976).

(15) C. Lindberg and C. Bogentoft, *Acta Pharm. Suec.*, **12,** 507 (1975).

(16) W. G. Stillwell, C. S. Myran, and J. T. Stewart, *Res. Commun. Chem. Pathol. Pharmacol.*, **14,** 605 (1976).

(17) D. H. Clouet, *Life Sci.*, **1,** 31 (1962).

(18) D. H. Clouet, *Biochem. Pharmacol.*, **12,** 967 (1963).

(19) S. J. Mulé and G. J. Mannering, *Bull. Narc.*, **17,** 27 (1965).

(20) R. J. Miller, C. Jolles, and H. Rapoport, *Phytochemistry*, **12,** 597 (1973).

ACKNOWLEDGMENTS

The preliminary report of the study appeared in *Fed. Proc.*, **34,** 814 (1975).

Local Anesthetic Activity and Acute Toxicity of *N*-Substituted 1,2,3,4-Tetrahydro-1- and 2-naphthylamines

ANTHONY T. DREN ˣ, BARBARA A. BOPP, DONN M. EBERT, ADOLPH O. GEISZLER, JAMES B. HOLLAND, BRUCE W. HORROM, and D. A. DUNNIGAN

Received August 16, 1976, from the *Department of Pharmacology and Medicinal Chemistry and the Department of Organic Research, Abbott Laboratories, North Chicago, IL 60064.* Accepted for publication September 29, 1977.

Abstract □ Seven *N*-substituted 1,2,3,4-tetrahydro-1- and three 2-naphthylamines were prepared and tested for local anesthetic activity in the rabbit corneal reflex test and the mouse sciatic nerve block test. At 0.1 and 1%, three 1-alkylamino compounds had durations of action comparable to that of tetracaine in the rabbit corneal reflex test and were considerably more potent than lidocaine. The other four 1-alkylamino derivatives were inactive or at best minimally active. The durations of action of 1% concentrations of the three 2-alkylamino compounds were equivalent to that of 1% lidocaine in the corneal reflex test. In the mouse sciatic nerve block test, the three active 1-alkylamino compounds were considerably longer acting than either tetracaine or lidocaine. Three 1-alkylamino and the three 2-alkylamino compounds showed toxicity equal to or greater than lidocaine, while two 1-alkylamino and two 2-alkylamino compounds showed toxicity equal to or greater than tetracaine by the intraperitoneal route in mice. *N*-Heptyl-1,2,3,4-tetrahydro-6-methoxy-1-naphthylamine methanesulfonate was the most promising local anesthetic in these series.

Keyphrases □ 1,2,3,4-Tetrahydro-1- and 2-naphthylamines, *N*-substituted—synthesized, local anesthetic activity and toxicity evaluated □ Local anesthetic activity—various *N*-substituted 1,2,3,4-tetrahydro-1- and 2-naphthylamines evaluated □ Toxicity—various *N*-substituted 1,2,3,4-tetrahydro-1- and 2-naphthylamines evaluated □ Structure-activity relationships—various *N*-substituted 1,2,3,4-tetrahydro-1- and 2-naphthylamines evaluated for local anesthetic activity and toxicity

A series of methoxy-1- and 2-aminoindans and naphthylamines previously was synthesized as potential antiparkinsonian agents (1). When these compounds were tested for dopaminergic activity, some were inhibitors of monoamine oxidase. Subsequently, additional compounds were prepared in which the substituent on the amine was

Table I—Physical and Chemical Data for *N*-Substituted 1,2,3,4-Tetrahydro-1-naphthylamines

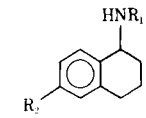

Compound	R_1	R_2	Formula	Salt	Melting Point
I	$(CH_2)_6CH_3$	6-OCH_3	$C_{18}H_{29}NO$	Methanesulfonate	88–90.5°
II	$(CH_2)_6CH_3$	5-OCH_3	$C_{18}H_{29}NO$	Hydrochloride	126–128.5°
III	$(CH_2)_7CH_3$	6-OCH_3	$C_{19}H_{31}NO$	Hydrochloride	118–120°
IV	$(CH_2)_8CH_3$	6-OCH_3	$C_{20}H_{33}NO$	Hydrochloride	125–127°
V	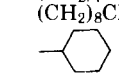	6-OCH_3	$C_{17}H_{25}NO$	Hydrochloride	216°
VI	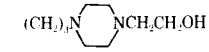	6-OCH_3	$C_{20}H_{33}N_3O_2$	3-Hydrochloride	225°
VII	$CH_2CH_2CONH_2$	6-OCH_3	$C_{14}H_{20}N_2O_2$	Hydrochloride	205–206°

varied to examine the relationship between physical properties and the potency of monoamine oxidase inhibition (2). In a broad pharmacological screening program, it was observed that one of the naphthylamines had local anesthetic activity. This paper describes the synthesis of *N*-substituted 1,2,3,4-tetrahydro-1- and 2-naphthylamines (Tables I and II) and testing for local anesthetic activity.

EXPERIMENTAL

Chemistry—N-*Substituted 1,2,3,4-Tetrahydro-1-naphthylamines (I–VII)*—To prepare I–VII, 5- or 6-methoxy-3,4-dihydro-1(2*H*)-naphthalenone was reacted with the appropriate alkyl- or cycloalkylamines to produce substituted ketamines, which, in turn, were hydrogenated to give the final amine products. A benzene solution of the appropriate naphthalenone and amine was refluxed for approximately 72 hr until 1 molar equivalent of water was collected in a water separator. *p*-Toluenesulfonic acid was employed as a catalyst. The ketamines were isolated by removal of the solvent and then reduced with Raney nickel catalyst in ethanol until no additional uptake of hydrogen was noted. The reaction mixture was filtered, the solvent was removed, and the product was purified by distillation. The free bases could be converted to the salt form by reaction with a pharmaceutically acceptable acid, *e.g.*, hydrochloric, methanesulfonic, or acetic.

N-*Substituted 1,2,3,4-Tetrahydro-2-naphthylamines (VIII–X)*—To prepare VIII and IX, 5-methoxy-1-methyl-3,4-dihydro-2(1*H*)-naphthalenone and 6-methoxy-2(1*H*)-naphthalenone were reacted with cyclopropylamine and cyclopropylcarbinylamine, respectively, as already described. The ketamines were reduced with sodium borohydride in methanol solution. The crude product was made basic and extracted in ether, and the ethereal solution was then washed with hydrochloric acid; this process was repeated as necessary. The product was purified by distillation, treated with ethereal hydrochloric acid, and crystallized.

A second method was used in the preparation of X. *N*-Hydroxypropyl-1,2,3,4-tetrahydro-6-methoxy-2-naphthylamine and thionyl chloride were allowed to react overnight in chloroform solution at room temperature. The crude hydrochloride was precipitated, filtered, washed with ether, and recrystallized from methanol–ether solution.

Table II—Physical and Chemical Data for *N*-Substituted 1,2,3,4-Tetrahydro-2-naphthylamines

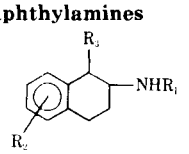

Compound[a]	R_1	R_2	R_3	Formula	Melting Point
VIII		6-OCH_3	H	$C_{15}H_{21}NO$	231–232°
IX		5-OCH_3	CH_3	$C_{15}H_{19}NO$	187–189°
X	$(CH_2)_3Cl$	6-OCH_3	H	$C_{14}H_{20}ClNO$	207–208.5°

[a] All were hydrochlorides.

Pharmacology and Toxicology—*Rabbit Corneal Reflex Test*—Topical anesthetic activity was evaluated in the rabbit corneal reflex test originally described by Sollmann (3). A volume of 0.1 ml of the local anesthetic solution (0.1 or 1%) was instilled into the conjunctival sac of each eye; the cornea was not rinsed following drug application. The presence or absence of the corneal reflex (blinking) was determined by touching the cornea with a stiff hair at 5-min intervals. Tetracaine hydrochloride (0.1%) and lidocaine hydrochloride (1%) were used as reference standards. Each concentration was tested in three to six rabbit eyes.

Mouse Sciatic Nerve Block Test—Conduction anesthesia was evaluated using the mouse sciatic nerve block test, a modification of the method in rats originally described by Camougis and Takman (4). A volume of 0.05 ml of a 1% solution was injected into the midthigh region of female ICR mice so that the drug was localized around the sciatic nerve. Following injection, the mice were observed to determine the frequency and duration of the motor nerve blocks as well as any systemic effects. Tetracaine hydrochloride (1%) and lidocaine hydrochloride (1%) were used as reference standards. Each compound was tested in 10 mice. The results are expressed as the mean duration of anesthesia ± *SEM*.

Acute Toxicity—The compounds were administered intraperitoneally to groups of three female ICR mice in doses ranging from 30 to 1000 mg/kg. The LD_{50} values were estimated graphically.

RESULTS

The results of testing derivatives I–VII in the rabbit corneal reflex test are presented in Table III. Compounds I–III were active at a concentration of 0.1% and were comparable in potency to tetracaine. Neither changing the position of the methoxy group (I and II) nor increasing the length of the alkyl chain on the nitrogen by one carbon (I and III) appreciably affected activity. Compound I also was tested as the acetate salt. The durations of action of both the methanesulfonate and acetate salts of I were similar, but the acetate appeared to be less irritating to tissue.

Table III—Activity of *N*-Substituted 1,2,3,4-Tetrahydro-1-naphthylamines

Compound	Rabbit Corneal Reflex Test: Concentration, %	Rabbit Corneal Reflex Test: Mean Duration (Range) of Anesthesia, min	Mouse Sciatic Nerve Block Test[a], Duration of Action, min, Mean ± *SE*
I	1.0	140.0 (120–150)	96.8 ± 17.4
	0.1	43.3 (35–52)	
II	1.0	130.0 (120–135)	40.0 ± 5.1
	0.1	30.0 (20–40)	
III	1.0	140.0 (135–150)	96.3 ± 23.3
	0.1	38.0 (25–55)	
IV	1.0	3.3 (0–10)	—
V	1.0	17.5 (0–45)	—
VI	1.0	No effect	—
VII	1.0	No effect	—
Tetracaine hydrochloride	1.0	55.0 (45–60)	13.6 ± 5.8
	0.1	32.5 (22–42)	
Lidocaine hydrochloride	—	—	5.7 ± 1.9

[a] All compounds were tested at 1%.

Table IV—Activity of *N*-Substituted 1,2,3,4-Tetrahydro-2-naphthylamines in Rabbit Corneal Reflex Test[a]

Compound	Mean Duration (Range) of Anesthesia, min
VIII	21.8 (15–27)
IX	9.4 (5–15)
X	20.5 (15–27)
Lidocaine hydrochloride	13.3 (10–15)

[a] All compounds were tested at 1%.

In contrast to these highly active derivatives, IV, which has a nine-carbon chain on the nitrogen, was active in only one of three eyes but was relatively insoluble. The compound with a cyclohexyl ring (V) rather than the straight alkyl chain was active at 1% but had a relatively short duration of action; it also was only partially soluble at 1%. The introduction of hetero chains on the alkylamino group resulted in two compounds, VI and VII, which were inactive in the rabbit corneal reflex test.

Derivatives VIII–X were tested at a concentration of 1% and were all active in this test (Table IV). The potency and duration of anesthesia with these compounds were less than those observed with I–III but were generally comparable to those of lidocaine.

Derivatives I–III, which were active in the rabbit corneal reflex test, also were tested in the mouse sciatic nerve block test (Table III). Changing the position of the methoxy group from six to five (I and II) appeared to decrease the duration of action; increasing the length of the alkylamino group by one carbon (I and III) had no effect on the local anesthetic activity in this test.

The estimated intraperitoneal LD_{50} values are presented in Table V. The LD_{50} values of I and III, which exhibited the best local anesthetic activity in the rabbit corneal reflex and mouse sciatic nerve block tests, were similar. These LD_{50} values were lower than the value of lidocaine but comparable to that of tetracaine.

These preliminary pharmacological evaluations suggested that the potency, duration of action, and relative safety of I and III were as great or greater than those of tetracaine. Compound I, *N*-heptyl-1,2,3,4-tetrahydro-6-methoxy-1-naphthylamine methanesulfonate, was identified as the most promising local anesthetic compound in these series and has been examined in more detail (5).

Table V—Estimated LD_{50} Values of *N*-Substituted 1,2,3,4-Tetrahydro-1- and 2-naphthylamines, Tetracaine, and Lidocaine in Mice

Compound	Estimated LD_{50}, mg/kg ip
I	50
II	100
III	50
IV	200
V	200
VI	500
VII	300
VIII	80
IX	175
X	40
Tetracaine hydrochloride	75
Lidocaine hydrochloride	175

REFERENCES

(1) Y. C. Martin, C. H. Jarboe, R. A. Krause, K. R. Lynn, D. Dunnigan, and J. B. Holland, *J. Med. Chem.*, **16**, 147 (1973).

(2) Y. C. Martin, J. B. Holland, C. H. Jarboe, and N. Plotnikoff, *ibid.*, **17**, 409 (1974).

(3) T. Sollmann, *J. Pharmacol. Exp. Ther.*, **11**, 17 (1918).

(4) G. Camougis and B. H. Takman, in "Methods in Pharmacology," A. Schwartz, Ed., Appleton-Century-Crofts, New York, N.Y., 1971, pp. 1–40.

(5) B. A. Bopp, A. T. Dren, D. M. Ebert, and A. O. Geiszler, *J. Pharm. Sci.*, **67**, 882 (1978).

Local Anesthetic Activity and Acute Toxicity of *N*-Heptyl-1,2,3,4-tetrahydro-6-methoxy-1-naphthylamine Methanesulfonate

BARBARA A. BOPP, ANTHONY T. DREN ˣ, DONN M. EBERT, and ADOLPH O. GEISZLER

Received August 16, 1976, from the *Department of Pharmacology and Medicinal Chemistry, Abbott Laboratories, North Chicago, IL 60064.* Accepted for publication September 29, 1977.

Abstract □ *N*-Heptyl -1,2,3,4- tetrahydro-6-methoxy-1-naphthylamine methanesulfonate (I) is a potent, long lasting local anesthetic. It was as potent as tetracaine and at least 10 times more potent than lidocaine in the rabbit corneal reflex, guinea pig wheal, and mouse sciatic nerve block tests. The threshold anesthetic concentration (TAC), defined as the concentration required to produce anesthesia lasting 5 min, was calculated from each linear regression line fitted to the log dose–duration data, and these values were used to compare the potencies of the local anesthetics. In the rabbit corneal reflex test, the TAC values were 0.04% for I, 0.04% for tetracaine, and 0.66% for lidocaine. In the guinea pig wheal test, I had a TAC of 0.02%, which was equipotent to tetracaine and 11 times more potent than lidocaine; epinephrine (1:100,000) prolonged the duration of action of all three local anesthetics but had the least effect with I. In the mouse sciatic nerve block test, the TAC values were 0.06% for I, 0.10% for tetracaine, and 0.86% for lidocaine. The acute LD_{50} values of I in mice were 138 mg/kg sc and 26 mg/kg iv. By either route, I was less toxic than tetracaine and more toxic than lidocaine. Comparison of the LD_{50} and TAC values in the mouse sciatic nerve block test indicated that I had a greater therapeutic index than either reference standard.

Keyphrases □ *N*-Heptyl -1,2,3,4- tetrahydro-6-methoxy-1-naphthylamine methanesulfonate—local anesthetic activity and acute toxicity evaluated □ Local anesthetic activity—*N*-heptyl-1,2,3,4-tetrahydro-6-methoxy-1-naphthylamine methanesulfonate evaluated □ Toxicity—*N*-heptyl-1,2,3,4-tetrahydro-6-methoxy-1-naphthylamine methanesulfonate evaluated

Several *N*-substituted 1,2,3,4-tetrahydro-1-naphthylamines, originally synthesized as antiparkinsonian agents (1) and monoamine oxidase inhibitors (2), showed potent local anesthetic activity in the rabbit corneal reflex test. Consequently, other 1- and 2-alkylamino derivatives were prepared and tested for local anesthetic activity (3). This

Table IV—Activity of *N*-Substituted 1,2,3,4-Tetrahydro-2-naphthylamines in Rabbit Corneal Reflex Test[a]

Compound	Mean Duration (Range) of Anesthesia, min
VIII	21.8 (15–27)
IX	9.4 (5–15)
X	20.5 (15–27)
Lidocaine hydrochloride	13.3 (10–15)

[a] All compounds were tested at 1%.

In contrast to these highly active derivatives, IV, which has a nine-carbon chain on the nitrogen, was active in only one of three eyes but was relatively insoluble. The compound with a cyclohexyl ring (V) rather than the straight alkyl chain was active at 1% but had a relatively short duration of action; it also was only partially soluble at 1%. The introduction of hetero chains on the alkylamino group resulted in two compounds, VI and VII, which were inactive in the rabbit corneal reflex test.

Derivatives VIII–X were tested at a concentration of 1% and were all active in this test (Table IV). The potency and duration of anesthesia with these compounds were less than those observed with I–III but were generally comparable to those of lidocaine.

Derivatives I–III, which were active in the rabbit corneal reflex test, also were tested in the mouse sciatic nerve block test (Table III). Changing the position of the methoxy group from six to five (I and II) appeared to decrease the duration of action; increasing the length of the alkylamino group by one carbon (I and III) had no effect on the local anesthetic activity in this test.

The estimated intraperitoneal LD_{50} values are presented in Table V. The LD_{50} values of I and III, which exhibited the best local anesthetic activity in the rabbit corneal reflex and mouse sciatic nerve block tests, were similar. These LD_{50} values were lower than the value of lidocaine but comparable to that of tetracaine.

These preliminary pharmacological evaluations suggested that the potency, duration of action, and relative safety of I and III were as great or greater than those of tetracaine. Compound I, *N*-heptyl-1,2,3,4-tetrahydro-6-methoxy-1-naphthylamine methanesulfonate, was identified as the most promising local anesthetic compound in these series and has been examined in more detail (5).

Table V—Estimated LD_{50} Values of *N*-Substituted 1,2,3,4-Tetrahydro-1- and 2-naphthylamines, Tetracaine, and Lidocaine in Mice

Compound	Estimated LD_{50}, mg/kg ip
I	50
II	100
III	50
IV	200
V	200
VI	500
VII	300
VIII	80
IX	175
X	40
Tetracaine hydrochloride	75
Lidocaine hydrochloride	175

REFERENCES

(1) Y. C. Martin, C. H. Jarboe, R. A. Krause, K. R. Lynn, D. Dunnigan, and J. B. Holland, *J. Med. Chem.*, **16**, 147 (1973).

(2) Y. C. Martin, J. B. Holland, C. H. Jarboe, and N. Plotnikoff, *ibid.*, **17**, 409 (1974).

(3) T. Sollmann, *J. Pharmacol. Exp. Ther.*, **11**, 17 (1918).

(4) G. Camougis and B. H. Takman, in "Methods in Pharmacology," A. Schwartz, Ed., Appleton-Century-Crofts, New York, N.Y., 1971, pp. 1–40.

(5) B. A. Bopp, A. T. Dren, D. M. Ebert, and A. O. Geiszler, *J. Pharm. Sci.*, **67**, 882 (1978).

Local Anesthetic Activity and Acute Toxicity of *N*-Heptyl-1,2,3,4-tetrahydro-6-methoxy-1-naphthylamine Methanesulfonate

BARBARA A. BOPP, ANTHONY T. DREN ˣ, DONN M. EBERT, and ADOLPH O. GEISZLER

Received August 16, 1976, from the *Department of Pharmacology and Medicinal Chemistry, Abbott Laboratories, North Chicago, IL 60064.* Accepted for publication September 29, 1977.

Abstract □ *N*-Heptyl -1,2,3,4- tetrahydro-6-methoxy-1-naphthylamine methanesulfonate (I) is a potent, long lasting local anesthetic. It was as potent as tetracaine and at least 10 times more potent than lidocaine in the rabbit corneal reflex, guinea pig wheal, and mouse sciatic nerve block tests. The threshold anesthetic concentration (TAC), defined as the concentration required to produce anesthesia lasting 5 min, was calculated from each linear regression line fitted to the log dose–duration data, and these values were used to compare the potencies of the local anesthetics. In the rabbit corneal reflex test, the TAC values were 0.04% for I, 0.04% for tetracaine, and 0.66% for lidocaine. In the guinea pig wheal test, I had a TAC of 0.02%, which was equipotent to tetracaine and 11 times more potent than lidocaine; epinephrine (1:100,000) prolonged the duration of action of all three local anesthetics but had the least effect with I. In the mouse sciatic nerve block test, the TAC values were 0.06% for I, 0.10% for tetracaine, and 0.86% for lidocaine. The acute LD_{50} values of I in mice were 138 mg/kg sc and 26 mg/kg iv. By either route, I was less toxic than tetracaine and more toxic than lidocaine. Comparison of the LD_{50} and TAC values in the mouse sciatic nerve block test indicated that I had a greater therapeutic index than either reference standard.

Keyphrases □ *N*-Heptyl -1,2,3,4- tetrahydro-6-methoxy-1-naphthylamine methanesulfonate—local anesthetic activity and acute toxicity evaluated □ Local anesthetic activity—*N*-heptyl-1,2,3,4-tetrahydro-6-methoxy-1-naphthylamine methanesulfonate evaluated □ Toxicity—*N*-heptyl-1,2,3,4-tetrahydro-6-methoxy-1-naphthylamine methanesulfonate evaluated

Several *N*-substituted 1,2,3,4-tetrahydro-1-naphthylamines, originally synthesized as antiparkinsonian agents (1) and monoamine oxidase inhibitors (2), showed potent local anesthetic activity in the rabbit corneal reflex test. Consequently, other 1- and 2-alkylamino derivatives were prepared and tested for local anesthetic activity (3). This

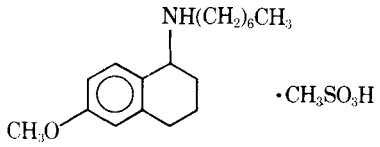

I

paper describes the pharmacological studies on the local anesthetic activity and acute toxicity of the most potent member of these series, *N*-heptyl-1,2,3,4-tetrahydro-6-methoxy-1-naphthylamine methanesulfonate (I).

EXPERIMENTAL

Local Anesthetic Activity—Three test procedures, the rabbit corneal reflex test, the guinea pig wheal test, and the mouse sciatic nerve block test, were used to evaluate the local anesthetic activity of I. For comparison, lidocaine hydrochloride and tetracaine hydrochloride were tested concurrently; all concentrations are expressed as salts.

Simultaneous linear regression analysis was used to fit the best line to the log dose–duration data in each test. The threshold anesthetic concentration (TAC), defined as the concentration required to produce anesthesia lasting 5 min, was calculated from each regression line. This parameter has frequently been used to compare the potencies of local anesthetics (4).

Rabbit Corneal Reflex Test—Topical anesthetic activity was evaluated in the rabbit corneal reflex test originally described by Sollmann (5). A volume of 0.1 ml of the local anesthetic solution was instilled into the conjunctival sac of each eye; the cornea was not rinsed following drug application. The presence or absence of the corneal reflex (blinking) was determined by touching the cornea with a stiff hair at 5-min intervals. Each concentration (three or four per compound) was tested in six rabbit eyes.

Guinea Pig Wheal Test—Infiltration anesthetic activity was evaluated in the guinea pig wheal test using a modification of the method of Bulbring and Wajda (6). Each wheal was made by injecting 0.1 ml of the local anesthetic solution intradermally on the shaved back of a male albino guinea pig. The presence or absence of anesthesia was evaluated at 5-min intervals by the skin twitch response to pricking of the wheal area with a hypodermic needle. Six to eight wheals were made with each of the three concentrations tested for each drug. The wheals were examined 24 hr later to evaluate any tissue irritation. This test was also used to determine the effects of the addition of epinephrine (1:100,000) to the local anesthetic solutions.

Mouse Sciatic Nerve Block Test—Conduction anesthesia was evaluated using the mouse sciatic nerve block test, a modification of the method originally developed in rats (7). A volume of 0.05 ml of the local anesthetic solution was injected into the midthigh region of female ICR mice so that the drug was localized around the sciatic nerve. Following injection, the mice were observed to determine the frequency and duration of the motor nerve blocks as well as any systemic effects. For each drug, 10 mice were tested at each concentration (four or five per compound).

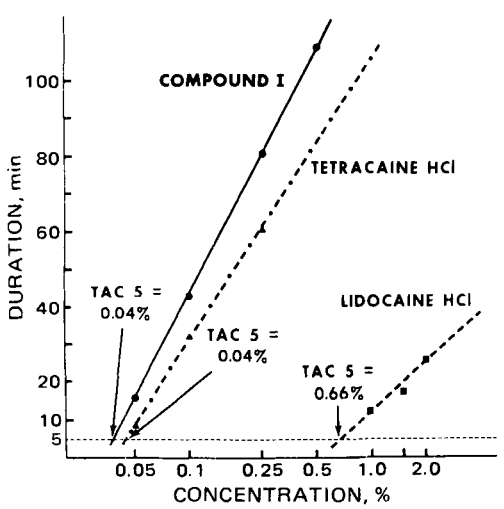

Figure 1—*Activities of local anesthetics in the rabbit corneal reflex test.*

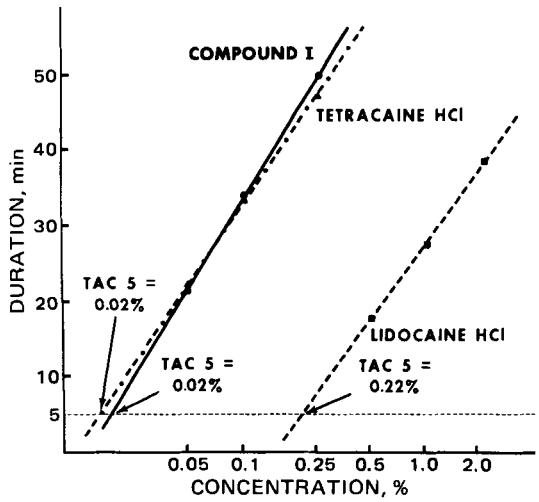

Figure 2—*Activities of local anesthetics in the guinea pig wheal test.*

Acute Toxicity—Acute toxicity was determined in female ICR mice following either intravenous or subcutaneous administration. Ten mice were tested at each dose level, and five or six doses were used for each LD_{50} determination. The survivors were observed for 1 week. The LD_{50} values were calculated by the method of Litchfield and Wilcoxon (8).

RESULTS

Rabbit Corneal Reflex Test—The dose–response curves in the rabbit corneal reflex test are presented in Fig. 1. Compound I and tetracaine were active in the same concentration range, but lidocaine was at least 10 times less potent. The TAC values were 0.04% for I, 0.04% for tetracaine, and 0.66% for lidocaine. The slopes of the three lines were significantly different, with I having the steepest dose–response line.

Guinea Pig Wheal Test—The dose–duration curves in the guinea pig wheal test are shown in Fig. 2. The slopes of the three lines were not significantly different. The potencies of I and tetracaine did not differ significantly, and both compounds were approximately 11 times as potent as lidocaine. Examination of the wheals 24 hr after injection indicated that I caused more tissue irritation than either tetracaine or lidocaine.

The addition of the vasoconstrictor epinephrine increased the duration of the anesthesia produced by I approximately twofold while that of tetracaine was increased 2.5 times (Fig. 3). Epinephrine exerted the most pronounced effect when added to the lidocaine solutions. The duration of anesthesia was increased 2.8 times with the 0.5% solution and 5.3 times with the 2% solution. The addition of epinephrine also increased the amount of tissue irritation caused by all three local anesthetics. A similar incidence of irritation was seen with I and tetracaine when epinephrine was present in the test solutions.

Mouse Sciatic Nerve Block Test—The results of the sciatic nerve block test are shown in Fig. 4. At the lowest concentration tested, 0.05%, I was effective in 80% of the mice and tetracaine was effective in 90% of the mice. Lidocaine was ineffective at 0.05 and 0.1% concentrations and

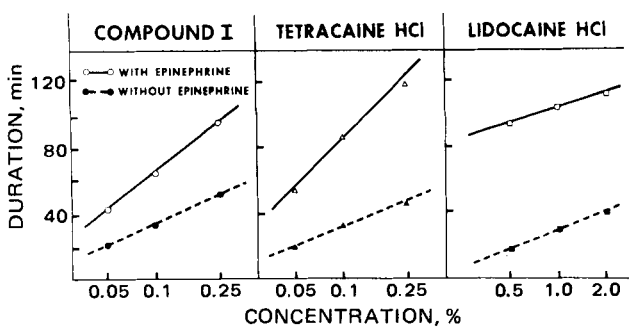

Figure 3—*Epinephrine (1:100,000) potentiation of local anesthetic activity using guinea pig wheal test.*

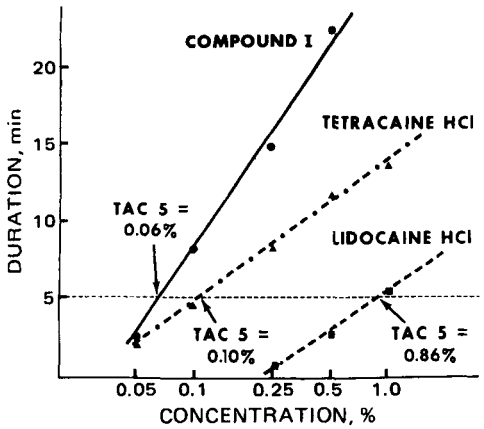

Figure 4—*Activities of local anesthetics in the mouse sciatic nerve block test.*

effective in 50% of the mice at the 0.25% concentration. The TAC values calculated from the regression lines were 0.06% for I, 0.10% for tetracaine, and 0.86% for lidocaine. For an average body weight of 20 g, the TAC values were 1.7, 2.5, and 21.4 mg/kg for I, tetracaine and lidocaine, respectively.

The slopes of the three lines were significantly different. As indicated by the slopes, the duration of anesthesia caused by the higher concentrations of I (0.25 and 0.5%) was longer than that produced by the same concentration of tetracaine. No overt symptoms were observed in the mice receiving I or lidocaine. However, at the 0.5 and 1.0% concentrations of tetracaine, representing approximately 12.5 and 25 mg/kg, jerks, tremors, and mild clonic convulsions were noted.

Therapeutic ratios were calculated for the three local anesthetics based on the TAC values, expressed in milligrams per kilogram, from the mouse sciatic nerve block test and the intravenous or subcutaneous LD_{50} values (Table I). The intravenous therapeutic ratio of I was three times higher than tetracaine and 15 times higher than lidocaine. The subcutaneous therapeutic ratio of I was 5.5 times higher than tetracaine and 9.5 times higher than lidocaine.

Table I—Comparison of I, Tetracaine, and Lidocaine

Parameter	I	Tetracaine Hydrochloride	Lidocaine Hydrochloride
Local anesthetic activity (TAC values)			
Rabbit corneal reflex, %	0.04	0.04	0.66
Guinea pig wheal, %	0.02	0.02	0.22
Mouse sciatic nerve, %	0.06	0.10	0.86
	1.7[a]	2.5[a]	21.4[a]
Acute toxicity in mice			
Intravenous LD_{50}, mg/kg	26	13	36
Subcutaneous LD_{50}, mg/kg	138	35	190
Therapeutic ratios in mice			
Intravenous LD_{50}/sciatic nerve TAC	15.3	5.0	1.7
Subcutaneous LD_{50}/sciatic nerve TAC	81.2	14.0	8.9

[a] Mouse sciatic nerve TAC percentages converted to milligrams per kilogram assuming an average body weight of 20 g. Values were used in therapeutic ratio calculations.

Table II—Acute Intravenous and Subcutaneous Toxicity in Mice

Compound	Subcutaneous LD_{50}, mg/kg	Intravenous LD_{50}, mg/kg
I	138 (118–162)[a]	26 (23.4–28.8)
Tetracaine hydrochloride	35 (28.7–42.7)	13 (11.6–13.7)
Lidocaine hydrochloride	190 (169.5–213)	36 (31.8–40.7)

[a] The 95% confidence limits.

Acute Toxicity—The LD_{50} values for the three local anesthetics are found in Table II. The LD_{50} values of I were 138 mg/kg sc and 26 mg/kg iv. Tetracaine was four times more toxic than I when administered subcutaneously and twice as toxic intravenously. By either route of administration, I was 1.4 times as toxic as lidocaine. Overt effects observed in the mice receiving I included decreased activity, jerks, tremors, opisthotonus, and clonic convulsions; similar effects were seen in the mice receiving either tetracaine or lidocaine.

DISCUSSION

These studies have indicated that I is a potent local anesthetic with a long duration of action and relatively low acute toxicity. As shown by the threshold anesthetic concentrations summarized in Table I, the potency of I in the rabbit corneal reflex, guinea pig wheal, and mouse sciatic nerve block tests was comparable to that of tetracaine and at least 10 times greater than that of lidocaine. By either the subcutaneous or intravenous route of administration, I was less toxic than tetracaine but more toxic than lidocaine in mice.

Compound I represents a chemically novel type of local anesthetic since most currently marketed agents are either *p*-aminobenzoic acid derivatives such as tetracaine or amide derivatives related to lidocaine. This difference in structure might lessen the likelihood of allergic reactions among individuals known to be sensitive to the existing classes of local anesthetics.

REFERENCES

(1) Y. C. Martin, C. H. Jarboe, R. A. Krause, K. R. Lynn, D. Dunnigan, and J. B. Holland, *J. Med. Chem.*, **16**, 147 (1973).

(2) Y. C. Martin, J. B. Holland, C. H. Jarboe, and N. Plotnikoff, *ibid.*, **17**, 409 (1974).

(3) A. T. Dren, B. A. Bopp, D. M. Ebert, A. O. Geiszler, J. B. Holland, B. W. Horrom, and D. A. Dunnigan, *J. Pharm. Sci.*, **67**, 880 (1978).

(4) F. P. Luduena, *Ann. Rev. Pharmacol.*, **9**, 503 (1963).

(5) T. Sollmann, *J. Pharmacol. Exp. Ther.*, **11**, 17 (1918).

(6) W. Bulbring and I. Wajda, *ibid.*, **85**, 78 (1945).

(7) G. Camougis and B. H. Takman, in "Methods of Pharmacology," A. Schwartz, Ed., Appleton-Century-Crofts, New York, N.Y., 1971, pp. 1–40.

(8) J. T. Litchfield and W. F. Wilcoxon, *J. Pharmacol. Exp. Ther.*, **96**, 99 (1949).

ACKNOWLEDGMENTS

Presented in part at the Federation of American Societies of Experimental Biologists, Atlantic City meeting, April 1975.

Identification of a Street Drug as *N*-Ethyl-1-phenylcyclohexylamine, a Phencyclidine Analog

KEITH BAILEY

Received March 17, 1977, from *Drug Research Laboratories, Health Protection Branch, Tunney's Pasture, Ottawa, Ontario, K1A OL2, Canada.* Accepted for publication October 19, 1977.

Abstract □ The identification of *N*-ethyl-1-phenylcyclohexylamine in a street drug sample is described. Spectroscopic data suitable for the identification of the substance are presented.

Keyphrases □ *N*-Ethyl-1-phenylcyclohexylamine—identified in street sample by NMR, IR, and mass spectral data □ Abuse drugs—*N*-ethyl-1-phenylcyclohexylamine identified in street sample by NMR, IR, and mass spectral data □ Phencyclidine analogs—*N*-ethyl-1-phenylcyclohexylamine identified in street sample by NMR, IR, and mass spectral data

Phencyclidine (I) is a commonly encountered illicit synthetic drug on the street (1–3). Details of the synthesis of I and its analogs and homologs have been published (4–6). Because I is controlled under Schedule III of the Controlled Substances Act in the United States and under the Narcotic Control Act in Canada, it is to be expected that analogs having a similar pharmacological profile will be prepared and distributed on the illicit market (7, 8). The thiophene analog (known as thio-PCP) (II) and the pyrrolidine analog (III) have been positively identified in street samples (8), and the former is controlled under Schedule I of the Controlled Substances Act.

Methods for the unequivocal identification of I–III and three closely related tertiary amines have been published (9). The ethyl homolog, *N*-ethyl-1-phenylcyclohexylamine (IV), also known as cyclohexamine, PCE, CL-45, and CI-400, is said to have been available in California since about 1969 (8), but information and descriptions suitable for identification have not been published.

Psychic disturbances were seen with I and IV when their potential as anesthetics was explored (10), and investigations in humans were rapidly abandoned. This paper reports the identification of IV in a street sample. Spectroscopic and chromatographic properties of authentic material useful for its identification are described.

EXPERIMENTAL

Apparatus—A gas chromatograph equipped with a flame-ionization detector[1] and fitted with a 6-mm × 1.8-m glass column packed with 5% OV-7 on 80–100-mesh Chromosorb W (HP)[2] was used. The operating temperatures were 150, 250, and 275° for the oven, injector, and detector, respectively.

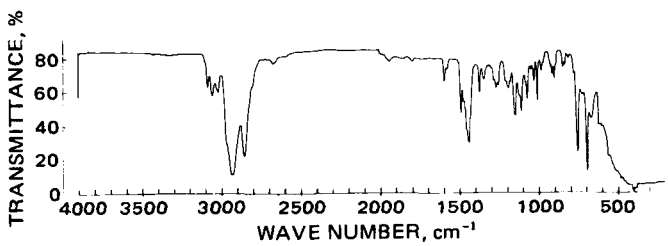

Figure 1—*IR spectrum of IV base as film on sodium chloride plates.*

TLC was carried out with 0.25-mm silica gel[3] precoated on glass[4]. The compounds were detected with iodoplatinate spray reagent, with which they produced magenta spots.

NMR spectra were recorded[5] at 40°, using tetramethylsilane as the reference standard. IR spectra were recorded[6] using natural films between sodium chloride plates for the free bases and potassium bromide disks for the salts. UV spectra were recorded[7] in ethanol solutions. Mass spectra were obtained by direct probe insertion on a spectrometer[8] operated with the probe at 160° and an ionization energy of 70 ev.

Spot Tests—The original sample was examined with Marquis, Mecke, and Froehde reagents (11); in each case, there was effervescence without color development. A flakey blue precipitate, insoluble in stannous chloride, was obtained with the cobalt thiocyanate test (12).

Isolation of IV (13)—The sample (about 25 mg of colorless crystals) was dissolved in 1% tartaric acid solution (0.5 ml) and triturated with a mixture of chloroform (1 ml), sodium bicarbonate (1 g), and acid-washed diatomaceous earth[9] (1 g). The mixture was transferred to a short glass

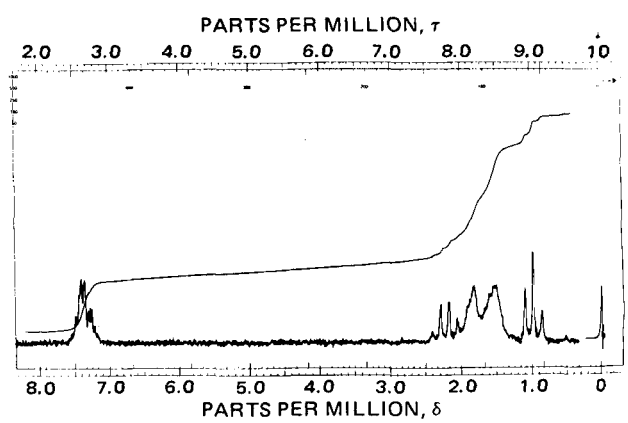

Figure 2—*NMR spectrum of IV base in deuterochloroform with deuterium oxide added.*

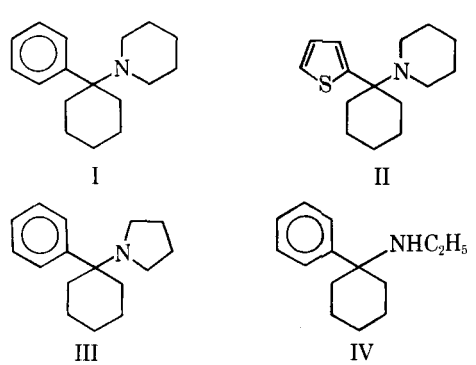

I II III IV

[1] Series 3000, Hydroflow Co., Toronto, Ontario, Canada.
[2] Chromatographic Specialties, Brockville, Ontario, Canada.
[3] Merck.
[4] EM Laboratories, Elmsford, N.Y.
[5] Model A-60A spectrometer, Varian Instruments, Palo Alto, Calif.
[6] Model 625 spectrophotometer, Perkin-Elmer Corp., Norwalk, Conn.
[7] Model DBGT spectrophotometer, Beckman Instruments, Fullerton, Calif.
[8] Hitachi Perkin-Elmer RMU-6L, Perkin-Elmer Corp., Norwalk, Conn.
[9] Celite 545, Chromatographic Specialties.

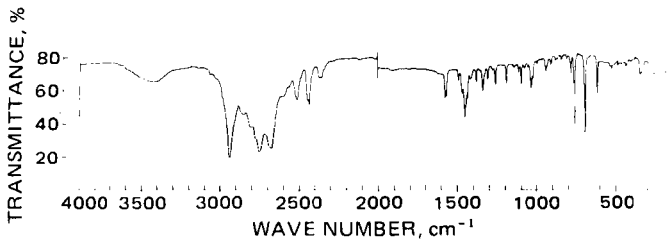

Figure 3—*IR spectrum of IV hydrochloride in potassium bromide disk.*

column, and the liberated components were eluted with chloroform (15 ml). The base was then extracted into 0.1 *N* H_2SO_4 (2 × 1 ml), which, in turn, was made alkaline with concentrated ammonia and finally extracted with chloroform (0.5 ml). Evaporation of the solvent gave IV as a colorless oil.

This procedure successfully isolated IV from excipients present in samples in the form of "decks" and "microdots" submitted for analysis on subsequent occasions.

Synthesis of IV—Authentic IV was synthesized in two ways: (*a*) by acetylation of 1-phenylcyclohexylamine (14) with acetic anhydride in acetic acid, followed by reduction of the resulting acetamide with lithium aluminum hydride (4); and (*b*) by the reaction of phenyllithium with *N*-ethylcyclohexanecarbonitrile (5). The product was converted into the hydrochloride salt, which was purified by recrystallization from a mixture of 2-propanol with ether (~3:1), mp 232–234° (with sublimation) [lit. (5) mp 240–242° and 236–238°].

Anal.—Calc. for $C_{14}H_{21}N$·HCl: C, 70.12; H, 9.25; N, 5.84. Found: C, 70.08; H, 9.27; N, 5.80.

The base was regenerated from the salt by addition of potassium carbonate solution and extracted into ether. IR, NMR, and mass spectra of the substance isolated from the sample and of authentic IV were compared. (The spectral data presented in this paper were obtained with authentic IV.)

RESULTS AND DISCUSSION

The results of the spot tests resembled those observed in these laboratories for samples containing cocaine or phencyclidine (I). The IR spectrum of the isolated base (Fig. 1) resembled spectra of I and its phenyl analogs (9) but notably lacked absorption bands at 2800 and 960 cm^{-1}. The bands at about 760 and 700 cm^{-1} suggested that a monosubstituted benzene ring was present, and a phencyclidine-like structure was inferred. The integrated proton NMR spectrum (Fig. 2) indicated that the compound had both cyclohexyl (δ 1.2–2.0 ppm) and ethylamino (δ 0.98-ppm triplet and 2.20-ppm quartet) moieties present with a mono-substituted benzene ring (δ 7.15–7.55 ppm), and it was surmised that the isolated material was IV.

Authentic IV was compared by IR, proton NMR, and mass spectral data with the isolated unknown, and the samples were found to be identical. The salt form of the original sample was not known, but a similar sample received at a later date was shown (mass spectrometry) to be the hydrochloride. IR, proton NMR, and mass spectral data from IV and its hydrochloride, suitable for identification purposes, are presented in Figs. 1–5. The IR spectrum of IV hydrochloride (Fig. 3) was quite different from those of tertiary amine analogs (9), especially in

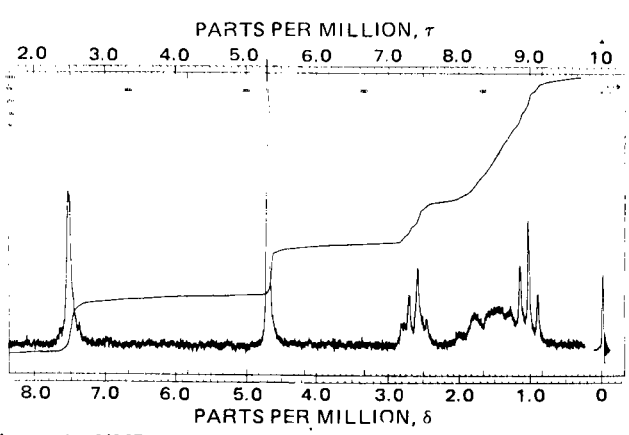

Figure 4—*NMR spectrum of IV hydrochloride in deuterium oxide.*

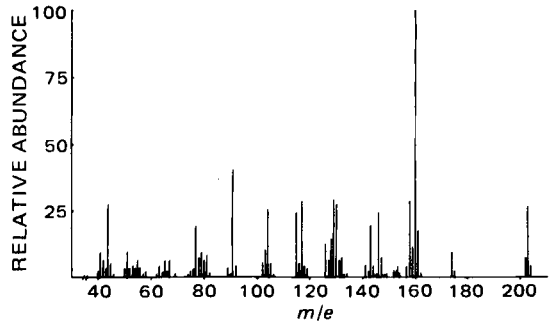

Figure 5—*Normalized mass spectrum of IV.*

showing strong absorption from 2660 to 2800 cm^{-1}, associated with the NH stretching of a secondary ammonium ion.

The mass spectrum of IV (Fig. 5) resembled spectra of the phenyl analogs reported (9) in having a moderately intense molecular ion M^+ (at 203), the base peak at M − 43 (160), and intense ions at 158, 143, 130, 129, 117, 115, 104, and 91 amu, all of which are of very minor intensity in the thienyl series. The UV spectrum of IV hydrochloride in ethanol was exactly like spectra of I and III hydrochlorides, having λ_{max} 252, 257, 261, and 268 nm. Compound II hydrochloride is distinguished by having λ_{max} 232 nm (9).

Phencyclidine (I) and analogs II and III were easily distinguished from IV by TLC on silica gel, using acetone–12 *N* ammonia (99:1), because they had R_f values of 0.66, 0.68, 0.55, and 0.49, respectively. It was difficult to distinguish III and IV with ethanol–5 *N* ammonia (9:1) (9), however, which gave R_f values of 0.70, 0.72, 0.63, and 0.65 for I–IV, respectively.

GLC of I–IV on 5% OV-7 at 150° gave peaks at 24.7, 24.6 (decomposition product at 3.8), 17.8, and 5.1 min, respectively, and the emergent material from IV was identified by mass spectrometry as the unchanged amine. Raising the column temperature resulted in their increasing decomposition to materials of shorter retention times, which have not been investigated.

It is possible that a cursory examination of IV by spot tests might lead to its reported (8) confusion with the commonly found phencyclidine. The IR spectra of the two bases are also quite similar in the fingerprint region, 1500–400 cm^{-1}. Therefore, the complete IR spectrum should be examined, and particular attention should be paid to the behavior at 2800 and 960 cm^{-1} where phencyclidine, but not IV, exhibits absorption bands. Proton NMR and mass spectrometry appear to be suitable for the unequivocal identification of these compounds (9).

REFERENCES

(1) J. K. Brown and M. H. Malone, *Clin. Toxicol.*, **9**, 145 (1976).

(2) R. S. Burns and S. E. Lerner, *ibid.*, **9**, 473 (1976).

(3) J. A. Marshman, M. P. Ramsay, and E. M. Sellers, *Toxicol. Appl. Pharmacol.*, **35**, 129 (1976).

(4) V. H. Maddox, E. F. Godefroi, and R. F. Parcell, *J. Med. Chem.*, **8**, 230 (1965).

(5) A. Kalir, H. Edery, Z. Pelah, D. Balderman, and G. Porath, *ibid.*, **12**, 473 (1969).

(6) E. F. Godefroi, V. H. Maddox, and R. F. Parcell, U.S. pat. 3,097,136 (1963); through *Chem. Abstr.*, **59**, 13881 (1963).

(7) A. T. Shulgin, *Clin. Toxicol.*, **8**, 405 (1975).

(8) A. T. Shulgin and D. E. MacLean, *ibid.*, **9**, 553 (1976).

(9) K. Bailey, D. R. Gagné, and R. K. Pike, *J. Assoc. Off. Anal. Chem.*, **59**, 81 (1976).

(10) E. F. Domino, in "International Review of Neurobiology," vol. 6, C. C. Pfeiffer and J. R. Smythies, Eds., Academic, New York, N.Y., 1964, pp. 303–347.

(11) T. A. Gonzales, M. Vance, M. Helpern, and C. J. Umberger, "Legal Medicine, Pathology and Toxicology," 2nd ed., Appleton-Century-Crofts, New York, N.Y., 1954, pp. 1211, 1213, 1234.

(12) A. N. Masoud, *J. Pharm. Sci.*, **64**, 841 (1975).

(13) H. D. Beckstead and W. N. French, "Some Analytical Methods for Drugs Subject to Abuse," Department of National Health and Welfare, Ottawa, Canada, 1971.

(14) A. Kalir and Z. Pelah, *Isr. J. Chem.*, **5**, 223 (1967).

ACKNOWLEDGMENTS

The author thanks Mrs. D. Gagné and Mr. D. Legault for technical assistance.

Simplified GLC Assay for Lidocaine in Plasma

B. J. KLINE [x] **and M. F. MARTIN**

Received July 25, 1977, from the *Department of Pharmacy and Pharmaceutics, School of Pharmacy, Medical College of Virginia, Virginia Commonwealth University, Richmond, VA 23298.* Accepted for publication October 13, 1977.

Abstract □ A simple, rapid GLC method for the determination of lidocaine in plasma is described. After addition of mepivacaine as an internal standard, the plasma sample is deproteinated and centrifuged. The supernate is alkalinized, and the lidocaine and internal standard are extracted into a microvolume of carbon disulfide. By using GLC with a flame-ionization detector, linear concentration–response curves were obtained in the 1–6-μg/ml range. The method can easily determine plasma concentrations at the 250-ng/ml level when a 1-ml plasma sample is analyzed.

Keyphrases □ Lidocaine—GLC analysis in plasma □ GLC—analysis, lidocaine in plasma □ Anesthetics, topical—lidocaine, GLC analysis in plasma

Interest in the analysis of lidocaine in biological media has persisted for over 25 years. The acid–dye methods were subject to interference by metabolites and other endogenous alkaline substances (1, 2) and, therefore, did not give reliable estimates of lidocaine concentrations. Other than for metabolism, disposition, and excretion studies, there has not been a critical need for plasma lidocaine level determinations until its recent application in the control of ventricular arrhythmias by intravenous infusion (3).

GLC has been the analytical method of choice (4–13), but none of the literature procedures met all of this laboratory's requirements. A simple, rapid GLC method using a flame-ionization detector is presented here.

EXPERIMENTAL

Reagents—Lidocaine hydrochloride monohydrate[1], mepivacaine hydrochloride[2], reagent grade carbon disulfide[3], trichloroacetic acid[3], and sodium hydroxide[3] were used as received. Drug concentrations were determined as the free base.

Apparatus—A gas chromatograph[4] fitted with a 1.8-m (6-ft) × 2-mm (i.d.) glass column, packed with 3% OV-17 on 100–120-mesh Gas Chrom Q, and a flame-ionization detector was used. The column oven was operated at 210° with an optional (see *Results and Discussion*) program involving a 5.0-min initial hold, a 40°/min program to 270°, and a final temperature hold of 2.5 min. The injector temperature was 240°, and the flame-ionization detector temperature was 280°. The carrier gas was nitrogen at a flow rate of 30 ml/min. A 10-mv recorder was used, and the electrometer range was set at 10^{-11} ampere full scale.

Procedure—To a 12-ml glass-stoppered centrifuge tube were added 1 ml of plasma, 2 ml of mepivacaine hydrochloride solution (2 μg/ml in water) as the internal standard, and 1 ml of 1.8 *N* trichloroacetic acid aqueous solution, in that order. The tube was mixed gently for 5–10 sec on a vortex mixer and centrifuged at 2200 rpm. The supernate was transferred to a clean 12-ml centrifuge tube, and 1 ml of 5 *N* NaOH and 100 μl of carbon disulfide were added.

Then the tube was vigorously mixed on a vortex mixer for 45 sec and centrifuged at 2000 rpm, and 3 μl of the carbon disulfide layer was injected into the GLC column. The lidocaine concentration in the plasma sample was determined from a calibration curve of lidocaine/mepivacaine peak height ratio *versus* lidocaine concentration from drug-free plasma or aqueous standard solutions.

[1] Gift from Astra Pharmaceutical Products, Worcester, Mass.
[2] Gift from Sterling-Winthrop Research Institute, Rensselaer, N.Y.
[3] Fisher Scientific Co., Pittsburgh, Pa.
[4] Model 90885, Packard Instrument Co., Downers Grove, Ill.

RESULTS AND DISCUSSION

Evaluation of Published Procedures—Most published GLC procedures initially extracted lidocaine into an organic solvent from alkalinized plasma. At that point, some investigators evaporated the organic solvent and dissolved the residue in a microvolume of injection solvent (5–7). Others performed multiple extractions between organic and aqueous media, presumably to eliminate interferences (8–12). Several methods utilized an alkaline flame-ionization detector to achieve selectivity and sensitivity (7, 11–13).

Initially, the method of Benowitz and Rowland (6) was investigated because of its claimed sensitivity (0.01 μg/ml) but was abandoned because the extraction of lidocaine into ether from an alkaline aqueous medium appeared to be incomplete and, during extraction, ether dissolved enough water to interfere in the GLC determination. Freezing the aqueous layer (9) or drying the ether extract with a desiccant did not eliminate the latter problem. Because of the need for a rapid assay, a procedure involving multiple extractions or an evaporation step should be avoided. After the development of this method, a high-pressure liquid chromatographic (HPLC) procedure for lidocaine (and procainamide) in serum was published (14). It also involved extraction and evaporation and, because of the low UV absorptivity of lidocaine, required a 205-nm UV detector.

Selection of Extraction and Injection Solvent—The use of benzene for direct extraction and injection (13) was abandoned because of its large solvent peak with the flame-ionization detector. Methylene chloride similarly gave a large solvent peak and yielded intractable emulsions during the extraction step. Carbon disulfide is an injection solvent that gives minimal response with the flame-ionization detector and extracts lidocaine from alkaline solution (6). However, initial attempts at extracting alkalinized plasma with carbon disulfide produced emulsions that could not be broken by centrifuging.

Deproteination of the plasma with trichloroacetic acid provided a medium from which the lidocaine could be extracted after alkalinization. It was determined that the lidocaine and mepivacaine were stable in the carbon disulfide-alkalinized plasma mixture at least overnight under refrigeration. Benowitz and Rowland (6) stated that similar samples were stable for 7 days in the carbon disulfide layer.

Development of GLC Conditions—OV-17 was selected as the liquid phase because it already had been used in the GLC analysis of lidocaine (6). After screening numerous compounds, mepivacaine was selected as the internal standard because of its structural similarity to lidocaine (both anilides) and its desirable extraction and chromatographic properties in this procedure.

Figure 1A is a chromatogram of an actual plasma sample containing 500 ng of lidocaine/ml, and Fig. 1B is a chromatogram of drug-free plasma analyzed by this procedure. Under the described conditions, the retention time of lidocaine was 1–2 min and that of mepivacaine was 3–4 min. No interference was observed in the blank plasma scan at these retention times.

The optional column oven temperature program was required in the analysis of some patient samples to prevent a large peak that eluted after the mepivacaine from interfering with subsequent injections. Since this interference was not consistently observed, it was presumed to be another drug and not the plasticizer from the blood collection tube stopper. This substance has been reported to interfere in other plasma GLC analyses (15, 16). No attempt was made to identify this interference since it was readily eliminated by the brief temperature program.

Calibration Curve—Calibration curves were initially constructed by spiking blank plasma with 1, 2, 4, and 6 μg of lidocaine/ml and analyzing these standards by the described procedure. A calibration curve of peak height ratio *versus* lidocaine concentration was linear with a correlation coefficient of 1.000, a slope of 0.778, and a *y*-intercept of 0.004. Calibration curves prepared with water (but eliminating the initial centrifugation since no protein was present) were essentially identical to those prepared with blank plasma. Further confirmation of this result comes from the fact that the mean value for a 2-μg/ml spiked plasma control repetitively analyzed by three different technicians using aqueous

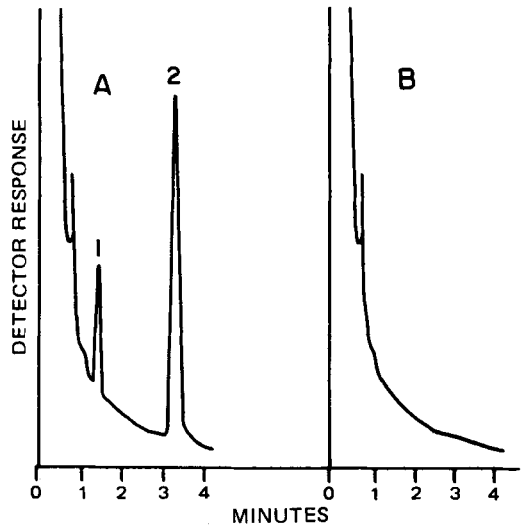

Figure 1—*Gas–liquid chromatograms. Key: A, human plasma sample containing 500 ng of lidocaine/ml (1) and mepivacaine (internal standard) (2); and B, blank plasma.*

calibration curves was 2.0 μg/ml. Since the method is linear, calibration curves were replaced by single-point calibrations. Linearity was confirmed down to 500 ng/ml.

Precision—A synthetic sample was prepared by spiking blank plasma with lidocaine at the 2-μg/ml level. This sample was then analyzed 10 times. The coefficient of variation for the peak height ratio was 5.7%.

Sensitivity—As can be seen from Fig. 1A, 500 ng/ml was easily measurable while 250 ng/ml was readily detectable. By increasing instrumental sensitivity or sample volume, it may be possible to detect even lower levels, but such levels are considerably subtherapeutic (17).

Interferences—Although authentic metabolites of lidocaine were never tested in this procedure, the lidocaine GLC peaks from several patient samples were examined on a gas chromatograph–mass spectrometer. The mass spectra corresponded to that of lidocaine, indicating that no interfering compounds (metabolites or other drugs) were eluting with the lidocaine. During pharmacokinetic profiles of 18 patients, the peak height of mepivacaine remained essentially constant within each run, suggesting that other medications or lidocaine metabolites were not eluting with the internal standard peak. Therefore, it is concluded that the method is specific for lidocaine in the presence of its metabolites.

Extraction Recovery—An aqueous solution of lidocaine hydrochloride containing the lidocaine base equivalent of 2 μg/ml was analyzed in this procedure. The chromatographic peak was compared to that obtained by direct injection of a carbon disulfide solution containing the equivalent concentration of lidocaine base. With the assumption of equal injection volumes, the peak height comparison indicated that at least 94% of the lidocaine was extracted from the alkaline aqueous solution by the microvolume of carbon disulfide.

Conclusions—A method has been described for the GLC analysis of plasma lidocaine levels. It is simple and rapid because it avoids multiple extractions and solvent evaporations and utilizes a flame-ionization detector. The method is linear, precise, accurate, and sensitive. It has been in use for over 1 year in this pharmacokinetics laboratory where it has been applied to the generation of pharmacokinetic profiles on patients who have been administered lidocaine as an endotracheal spray.

REFERENCES

(1) C.-Y. Sung and A. P. Truant, *J. Pharmacol. Exp. Ther.*, **112,** 432 (1954).

(2) L. A. Woods, J. Cochin, E. G. Fornefeld, F. G. McMahon, and W. H. Seevers, *ibid.*, **101,** 188 (1951).

(3) D. C. Harrison and E. L. Alderman, *Mod. Treat.*, **9,** 139 (1972).

(4) G. Svinhufvud, B. Ortengren, and S.-E. Jacobsson, *J. Clin. Lab. Invest.*, **17,** 162 (1965).

(5) G. T. Tucker, *Anesthesiology*, **32,** 255 (1970).

(6) N. Benowitz and M. Rowland, *ibid.*, **39,** 639 (1973).

(7) J. D. Cameron, *Clin. Chim. Acta*, **56,** 307 (1974).

(8) J. B. Keenaghan, *Anesthesiology*, **29,** 110 (1968).

(9) G. A. Edhorn, *Can. Anaesth. Soc. J.*, **18,** 189 (1971).

(10) J. B. Keenaghan and R. N. Boyes, *J. Pharmacol. Exp. Ther.*, **180,** 454 (1972).

(11) K. K. Adjepon-Yamoak and L. F. Prescott, *J. Pharm. Pharmacol.*, **26,** 889 (1974).

(12) T. R. Irgens, W. M. Henderson, and W. H. Shelver, *J. Pharm. Sci.*, **65,** 608 (1976).

(13) H. B. Hucker and S. C. Stauffer, *ibid.*, **65,** 926 (1976).

(14) R. F. Adams, F. L. Vandemark, and G. J. Schmidt, *Clin. Chim. Acta*, **69,** 515 (1976).

(15) A. W. Missen and S. J. Dickson, *Clin. Chem.*, **20,** 1247 (1974).

(16) L. J. Dusci and L. P. Hackett, *ibid.*, **22,** 1236 (1976).

(17) C. L. Winek, *ibid.*, **22,** 832 (1976).

ACKNOWLEDGMENTS

Presented at the Pharmaceutical Analysis and Control Section, APhA Academy of Pharmaceutical Sciences, Orlando meeting, November 1976.

Stability-Indicating Methods for Quantitative Determination of Spironolactone Using High-Pressure Liquid Chromatography and Blue Tetrazolium Reaction

V. DAS GUPTA ˣ and A. G. GHANEKAR

Received March 17, 1977, from the *College of Pharmacy, University of Houston, Houston, TX 77004.* Accepted for publication October 17, 1977.

Abstract □ Stability-indicating methods for the quantitative determination of spironolactone were developed. The methods are based on high-pressure liquid chromatography and a reaction with blue tetrazolium. Both methods are accurate, precise, and sensitive and gave excellent results with commercial tablets, including those containing hydrochlorothiazide in addition to spironolactone. The blue tetrazolium method cannot be used in the presence of high concentrations of either polyethylene glycols or water. Spironolactone decomposition in water or polyethylene glycol appears to follow pseudo-first-order kinetics. The decomposition constant at 65° was 0.0253/day in water *versus* 0.115/day in polyethylene glycol ointment base USP.

Keyphrases □ Spironolactone—high-pressure liquid chromatographic and colorimetric analyses in tablets □ High-pressure liquid chromatography—analysis, spironolactone in tablets □ Colorimetry—analysis based on blue tetrazolium reaction, spironolactone in tablets □ Diuretics—spironolactone, high-pressure liquid chromatographic and colorimetric analyses in tablets

Spironolactone (I) is extensively used as a diuretic. The USP procedure (1) for the quantitative determination of spironolactone in tablets, based on UV absorption, is not a stability-indicating method since the decomposition products of spironolactone absorb at the same wavelength. A fluorometric procedure was reported for the quantitative determination of spironolactone in biological fluids (2), but this method is tedious and time consuming. Some steroids were separated using acetonitrile–diatomaceous earth (3). *n*-Heptane was used for elution, and spironolactone in the eluate was assayed using the isoniazid reaction.

This article reports stability-indicating methods for the quantitative determination of spironolactone. The methods investigated are based on high-pressure liquid chromatography (HPLC) and a reaction with blue tetrazolium similar to that of corticosteroids.

EXPERIMENTAL

Chemicals and Reagents—All chemicals and reagents were ACS, USP, or NF grade and were used without further purification.

Apparatus—A high-pressure liquid chromatograph[1] equipped with a UV detector (254 nm), a recorder[2], and an integrator[3] was used.

Column—A column[4] (30 cm × 4 mm i.d.) of a semipolar packing material, consisting of a monomolecular layer of cyanopropylsilane permanently bonded to silica, was used.

Chromatographic Conditions—The chromatographic solvent was 0.02 *M* KH_2PO_4 in water containing 40% (v/v) ethanol. The temperature was ambient, and the flow rate was 2.4 ml/min. The detector was set at a sensitivity of 0.08 absorbance unit full scale, and the chart speed was 30.5 cm/hr.

[1] ALC 202, equipped with U6K universal chromatograph injector, Waters Associates, Milford, Mass.
[2] Omniscribe 5213-12, Houston Instruments, Austin, Tex.
[3] Autolab Minigrator, Spectra-Physics, Santa Clara, Calif.
[4] μBondapak CN, Catalog No. 84042, Waters Associates, Milford, Mass.

Table I—Data on Concentrations of Spironolactone *versus* Areas or Absorbance Values

Quantity of Spironolactone, μg	Method	Areas or Absorbance Values
0.25	HPLC	14,147
0.5	HPLC	28,160
1.0	HPLC	56,218
125	Blue tetrazolium	0.262
250	Blue tetrazolium	0.521
375	Blue tetrazolium	0.785

Preparation of Solutions—A stock solution of spironolactone was prepared by dissolving 25.0 mg of I in enough alcohol to make 100.0 ml.

Standard Solution in Alcohol—A standard solution of I in alcohol was prepared by diluting 10.0 ml of the stock solution to 100.0 ml with alcohol.

Standard Solution in Water—A standard solution in water was prepared by diluting 10.0 ml of the stock solution to 100.0 ml with water.

HPLC Assay of Tablets—Grind one tablet or transfer powder equivalent to one tablet or 25 mg of I (if a synthetic mixture) in a mortar and mix with 40 ml of alcohol with a pestle. Transfer the powder to a 100-ml volumetric flask with the aid of more alcohol to bring to volume. Filter and reject the first 20 ml of the filtrate and then dilute 10.0 ml of the clear filtrate to 100.0 ml with either water or alcohol, depending on the standard solution to be used for comparison purposes. Inject 20 μl into the chromatograph. As a control, inject 20 μl of the standard solution after the assay sample is eluted.

Since preliminary investigations indicated (Table I) that the spironolactone peak area was related directly to the concentration, the results were calculated using:

$$\frac{A_a}{A_s} \times 100 = \% \text{ of label claim} \qquad \text{(Eq. 1)}$$

where A_a is the peak area of the assay sample and A_s is the peak area of the standard sample. The results on commercial dosage forms are presented in Table II, and sample chromatograms are presented in Fig. 1.

Blue Tetrazolium Assay—The same procedure is used as reported

Table II—Assay Results on Commercial Tablets

Number	Commercial Sample (Claim)	Synthetic Mixture (Composition)	Percent[a] of Claim Found HPLC[b]	Percent[a] of Claim Found Blue Tetrazolium
1	25 mg of I	—	99.8	99.4
2	25 mg of I	—	97.8	97.2
3	25 mg each of I and II	—	101.7	101.8
4	—	25 mg of I and 50 mg of II	100.2	99.4
5	—	25 mg each of I and II	99.6	99.8
6	—	25 mg of I and 10 mg of II	99.8	101.2

[a] Average of two results. Maximum variation between two readings was 1.2%. [b] Based on five injections of the same solution. Standard deviation was ±0.98%. Results on different lots of solutions on different days showed similar deviations.

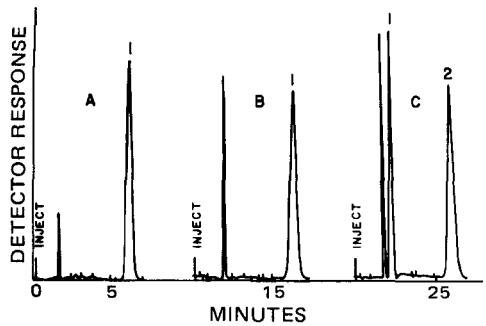

Figure 1—*Sample chromatograms. Key: A, from a standard solution in water; B, from a standard solution in alcohol; C, from a tablet containing 25 mg each of I and II; Peak 1, from II; and Peak 2, from I.*

for HPLC for the preparation of assay sample, except that the last dilution is made with alcohol only. Pipet 10.0 ml each of the standard solution in alcohol and the assay sample into separate glass-stoppered 50-ml conical flasks. Dilute each solution to 20.0 ml with alcohol. In a third flask, pipet 20.0 ml of alcohol to serve as the blank and follow the USP procedure (4) for steroids, starting with " . . . add 2.0 ml of a solution . . . ," except that it should be allowed to stand for 150 instead of 90 min (150 min is required for the reaction to go to completion).

If the dosage form or the synthetic mixture contained hydrochlorothiazide (II), an equivalent amount (based on the label claim) was added to the reagent blank also. An appropriate quantity of the alcoholic solution of II was transferred to the flask and then brought to 20.0 ml with alcohol.

Effect of Water on Blue Tetrazolium Reaction—To determine the effect of water on the blue tetrazolium method, the method described was followed using the standard solution. Before diluting the standard to 20.0 ml with alcohol, an appropriate quantity of water (2.0, 4.0, and 6.0 ml) was added. Water was also added to the reagent blank. The results, based on the standard with no water, were 12.3, 0.41, and 0% for 2.0, 4.0, and 6.0 ml of water added, respectively.

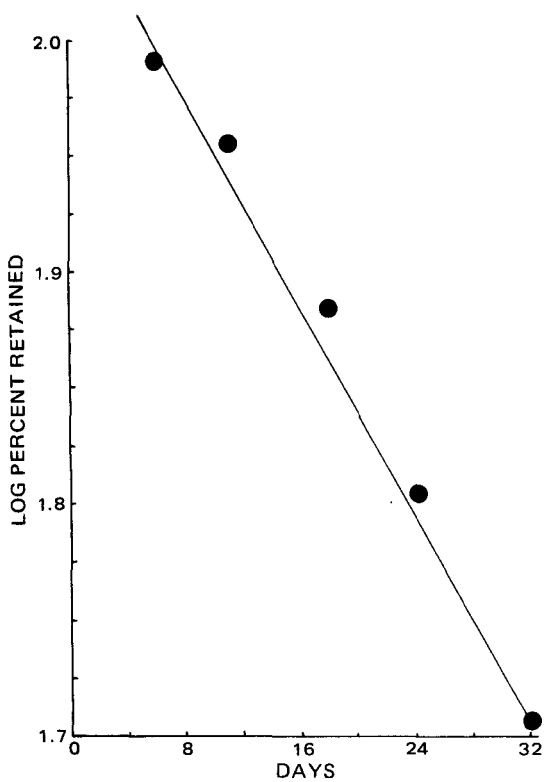

Figure 2—*Pseudo first-order plot of log percent retained* versus *time when spironolactone in water (initial concentration of 0.0025%) was stored at 65°.*

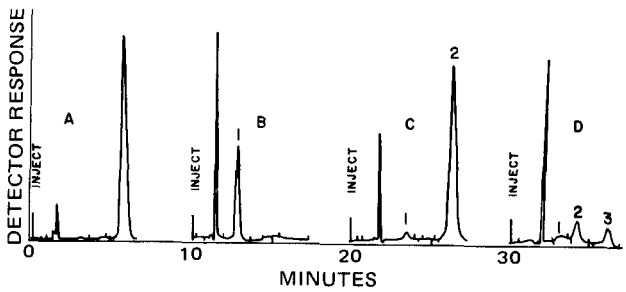

Figure 3—*Sample chromatograms from decomposed solutions. Key: A, from a solution decomposed with 0.1 N HCl (no decomposition was noticed); B, from a solution decomposed with 0.1 N NaOH (all was decomposed); C, from a standard solution in water decomposed for 14 days at 65°; Peak 1, from the decomposition product; Peak 2, from spironolactone; D, from a standard solution (0.0025%) in polyethylene glycol ointment base decomposed for 20 days at 65°; Peak 3, from spironolactone; and all other peaks, from the decomposition products.*

Since preliminary investigations indicated (Table I) that Beer's law was followed, the results were calculated by direct comparison of readings[5] of the assay and standard solution (Table II).

Stability Tests—A standard solution in water was stored at 65° and assayed frequently using the HPLC method (Figs. 2 and 3C).

A 10.0-ml quantity of the stock solution was mixed with 10 g of polyethylene glycol ointment base USP (5), stored at 65°, and assayed frequently using HPLC (Figs. 3D and 4).

A 25.0-ml quantity of the standard solution in alcohol was mixed with 5.0 ml of 0.1 *N* H_2SO_4 and boiled until the volume was reduced to approximately 10 ml. The mixture was cooled, neutralized with 0.1 *N* NaOH, brought to volume (25.0 ml) with alcohol, and assayed using HPLC (Fig. 3A). No I decomposition was noticed.

A 25.0-ml quantity of the standard solution in alcohol was mixed with 5.0 ml of 0.1 *N* NaOH and boiled until the volume was reduced to approximately 10 ml. The mixture was cooled, neutralized with 1 *N* HCl, brought to volume (25.0 ml) with alcohol, and assayed using all three methods. The results were 0, 4, and 33.4% by the HPLC, blue tetrazolium, and UV absorption methods, respectively. The maximum was at about 239 nm. The chromatogram is presented in Fig. 3B.

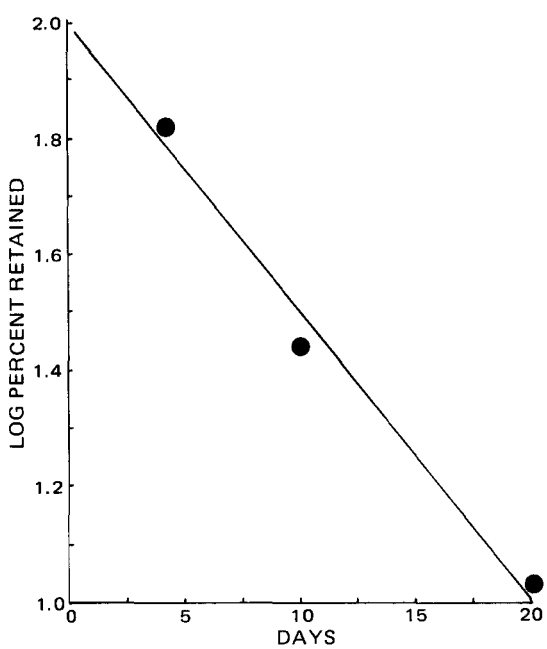

Figure 4—*Pseudo-first-order plot of log percent retained* versus *time when spironolactone in polyethylene glycol ointment base (initial concentration of 0.0025%) was stored at 65°.*

[5] Bausch & Lomb Spectronic 20.

DISCUSSION

The USP method (1) for the quantitative determination of spironolactone in tablets does not appear to be stability indicating since an almost completely decomposed sample indicated that 33.4% of the drug was still intact. The HPLC method showed a potency of 0% (Fig. 3B). The blue tetrazolium method, which indicated a potency of 4%, cannot be reliable because of the presence of a small amount of water in this system; water interferes with this reaction (see *Experimental* and Ref. 6). At lower concentrations (less than 5% of I), clearly identifiable peaks were obtained by the HPLC method. The quantitation of the results was not very accurate.

A high concentration of polyethylene glycol ointment base (above 100 mg in the reaction flask) strongly interfered with a blue tetrazolium assay. In the presence of polyethylene glycols and/or water, the HPLC method should be preferred. The HPLC method is also more sensitive (Table I). There was no interference from hydrochlorothiazide in the HPLC method (Table II and Fig. 1C). In the blue tetrazolium method, an equivalent amount of hydrochlorothiazide must be added to the reagent blank for more accurate results.

The HPLC method is sensitive, accurate, and precise (the standard deviation based on five readings was ±0.98%). The area of the peak was directly related to the concentration range tested (0.25–1.0 μg of I). In water, the peak was sharper than in alcohol (Figs. 1A and 1B). With the UV absorption technique, the standard solution in alcohol absorbed no light at 288 nm (maximum was at 239 nm) while the completely decomposed sample (with 0.1 *N* NaOH) showed maximum absorption at 288 nm. It may be possible to develop a stability-indicating assay based on two readings at two different wavelengths. The study was not pursued further.

Spironolactone decomposition, both in water and polyethylene glycol ointment base USP (5), appears to follow pseudo-first-order reaction kinetics (Figs. 2 and 4). The *K* values at 65° were estimated to be 0.0253/day in water *versus* 0.115/day in polyethylene glycol ointment base.

Whenever new prepacked HPLC columns are purchased, the flow rate or the percentage of alcohol may have to be changed to obtain the same retention time.

REFERENCES

(1) "The United States Pharmacopeia," 19th rev., Mack Publishing Co., Easton, Pa., 1975, p. 470.

(2) W. Sadee, M. Dagcioglu, and S. Riegelman, *J. Pharm. Sci.*, **61**, 1126 (1972).

(3) R. E. Graham and C. T. Kenner, *ibid.*, **62**, 1845 (1973).

(4) "The United States Pharmacopeia," 19th rev., Mack Publishing Co., Easton, Pa., 1975, p. 624.

(5) *Ibid.*, p. 566.

(6) R. E. Graham, E. R. Biehl, and C. T. Kenner, *J. Pharm. Sci.*, **65**, 1048 (1976).

ACKNOWLEDGMENTS

The authors thank Searle Laboratories, Chicago, Ill., for the generous supply of spironolactone powder.

COMMUNICATIONS

Plasma Protein Binding of Diazepam after a Single Dose of Sodium Oleate

Keyphrases □ Diazepam—plasma protein binding, effect of sodium oleate in rats □ Binding, plasma protein—diazepam, effect of sodium oleate in rats □ Sodium oleate—effect on plasma protein binding of diazepam in rats □ Sedatives—diazepam, plasma protein binding, effect of sodium oleate in rats

To the Editor:

Competitive displacement of drugs from plasma protein binding sites is well known, but most information has been derived from *in vitro* studies. Accordingly, little is known regarding the time course of such drug interactions. Specifically, we have been studying whether the decreased plasma protein binding of drugs after the administration of a displacing agent can be accounted for by the concentration of the displacing agent in the plasma. The unusually prolonged impairment of the plasma protein binding of diazepam after a single intravenous dose of sodium oleate is the subject of this communication.

In the first experiment, six male Sprague–Dawley rats were infused (0.6 ml/hr iv) for 1 hr with a buffered (phosphate) aqueous solution (pH 7.2) of sodium ^{3}H-oleate (7 mEq/liter). Blood samples were obtained during and for 14 days after intravenous infusion. The rats were randomly paired into three groups, and the blood was pooled for each pair to ensure adequate amounts of plasma. Three control rats were infused with saline (0.6 ml) for 1 hr, and blood was drawn periodically for 14 days.

Plasma oleate concentrations in treated rats were determined using the modified Dole extraction method (1, 2) in conjunction with liquid scintillation counting. Plasma binding of ^{14}C-diazepam (initial concentration of 400 ng/ml) was determined by equilibrium dialysis against an equal volume of phosphate buffer (0.1 *M*, pH 7.2) at 37° for 18 hr, followed by liquid scintillation counting of buffer and plasma.

The second experiment consisted of administering a bolus dose of sodium oleate (0.6 ml, 7 mEq/liter, premixed with 1 ml of blood) to two rats or of saline (0.6 ml) to two rats. Blood samples were taken immediately before, 5–10 min after, and 24 hr after the intravenous dose. Diazepam binding in plasma was determined by equilibrium dialysis as described.

Plasma binding of diazepam in saline-treated rats was essentially constant over 14 days (Fig. 1). In contrast, the free fraction of diazepam was elevated significantly in

Table I—Free Fraction of Diazepam in Rat Plasma Obtained before and after Intravenous Administration of Sodium Oleate or Saline

	Saline		Sodium Oleate	
Sample	Rat 1	Rat 2	Rat 1	Rat 2
Before dosing	0.100	0.112	0.106	0.121
5–10 min after dosing	0.099	0.112	0.176	0.194
24 hr after dosing	0.096	0.114	0.157	0.146

DISCUSSION

The USP method (1) for the quantitative determination of spironolactone in tablets does not appear to be stability indicating since an almost completely decomposed sample indicated that 33.4% of the drug was still intact. The HPLC method showed a potency of 0% (Fig. 3B). The blue tetrazolium method, which indicated a potency of 4%, cannot be reliable because of the presence of a small amount of water in this system; water interferes with this reaction (see *Experimental* and Ref. 6). At lower concentrations (less than 5% of I), clearly identifiable peaks were obtained by the HPLC method. The quantitation of the results was not very accurate.

A high concentration of polyethylene glycol ointment base (above 100 mg in the reaction flask) strongly interfered with a blue tetrazolium assay. In the presence of polyethylene glycols and/or water, the HPLC method should be preferred. The HPLC method is also more sensitive (Table I). There was no interference from hydrochlorothiazide in the HPLC method (Table II and Fig. 1C). In the blue tetrazolium method, an equivalent amount of hydrochlorothiazide must be added to the reagent blank for more accurate results.

The HPLC method is sensitive, accurate, and precise (the standard deviation based on five readings was ±0.98%). The area of the peak was directly related to the concentration range tested (0.25–1.0 μg of I). In water, the peak was sharper than in alcohol (Figs. 1A and 1B). With the UV absorption technique, the standard solution in alcohol absorbed no light at 288 nm (maximum was at 239 nm) while the completely decomposed sample (with 0.1 *N* NaOH) showed maximum absorption at 288 nm. It may be possible to develop a stability-indicating assay based on two readings at two different wavelengths. The study was not pursued further.

Spironolactone decomposition, both in water and polyethylene glycol ointment base USP (5), appears to follow pseudo-first-order reaction kinetics (Figs. 2 and 4). The *K* values at 65° were estimated to be 0.0253/day in water *versus* 0.115/day in polyethylene glycol ointment base.

Whenever new prepacked HPLC columns are purchased, the flow rate or the percentage of alcohol may have to be changed to obtain the same retention time.

REFERENCES

(1) "The United States Pharmacopeia," 19th rev., Mack Publishing Co., Easton, Pa., 1975, p. 470.

(2) W. Sadee, M. Dagcioglu, and S. Riegelman, *J. Pharm. Sci.*, **61**, 1126 (1972).

(3) R. E. Graham and C. T. Kenner, *ibid.*, **62**, 1845 (1973).

(4) "The United States Pharmacopeia," 19th rev., Mack Publishing Co., Easton, Pa., 1975, p. 624.

(5) *Ibid.*, p. 566.

(6) R. E. Graham, E. R. Biehl, and C. T. Kenner, *J. Pharm. Sci.*, **65**, 1048 (1976).

ACKNOWLEDGMENTS

The authors thank Searle Laboratories, Chicago, Ill., for the generous supply of spironolactone powder.

COMMUNICATIONS

Plasma Protein Binding of Diazepam after a Single Dose of Sodium Oleate

Keyphrases □ Diazepam—plasma protein binding, effect of sodium oleate in rats □ Binding, plasma protein—diazepam, effect of sodium oleate in rats □ Sodium oleate—effect on plasma protein binding of diazepam in rats □ Sedatives—diazepam, plasma protein binding, effect of sodium oleate in rats

To the Editor:

Competitive displacement of drugs from plasma protein binding sites is well known, but most information has been derived from *in vitro* studies. Accordingly, little is known regarding the time course of such drug interactions. Specifically, we have been studying whether the decreased plasma protein binding of drugs after the administration of a displacing agent can be accounted for by the concentration of the displacing agent in the plasma. The unusually prolonged impairment of the plasma protein binding of diazepam after a single intravenous dose of sodium oleate is the subject of this communication.

In the first experiment, six male Sprague–Dawley rats were infused (0.6 ml/hr iv) for 1 hr with a buffered (phosphate) aqueous solution (pH 7.2) of sodium ^{3}H-oleate (7 mEq/liter). Blood samples were obtained during and for 14 days after intravenous infusion. The rats were randomly paired into three groups, and the blood was pooled for each pair to ensure adequate amounts of plasma. Three control rats were infused with saline (0.6 ml) for 1 hr, and blood was drawn periodically for 14 days.

Plasma oleate concentrations in treated rats were determined using the modified Dole extraction method (1, 2) in conjunction with liquid scintillation counting. Plasma binding of ^{14}C-diazepam (initial concentration of 400 ng/ml) was determined by equilibrium dialysis against an equal volume of phosphate buffer (0.1 *M*, pH 7.2) at 37° for 18 hr, followed by liquid scintillation counting of buffer and plasma.

The second experiment consisted of administering a bolus dose of sodium oleate (0.6 ml, 7 mEq/liter, premixed with 1 ml of blood) to two rats or of saline (0.6 ml) to two rats. Blood samples were taken immediately before, 5–10 min after, and 24 hr after the intravenous dose. Diazepam binding in plasma was determined by equilibrium dialysis as described.

Plasma binding of diazepam in saline-treated rats was essentially constant over 14 days (Fig. 1). In contrast, the free fraction of diazepam was elevated significantly in

Table I—Free Fraction of Diazepam in Rat Plasma Obtained before and after Intravenous Administration of Sodium Oleate or Saline

	Saline		Sodium Oleate	
Sample	Rat 1	Rat 2	Rat 1	Rat 2
Before dosing	0.100	0.112	0.106	0.121
5–10 min after dosing	0.099	0.112	0.176	0.194
24 hr after dosing	0.096	0.114	0.157	0.146

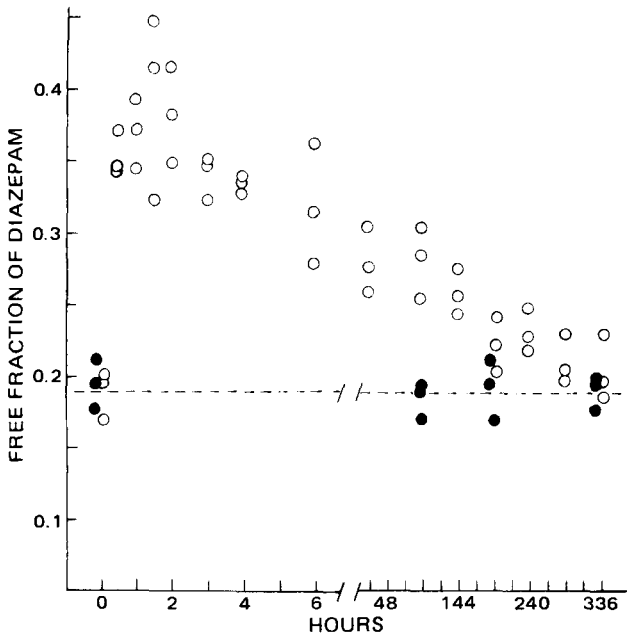

Figure 1—*Plasma protein binding of diazepam in rats after a 1-hr intravenous infusion of sodium oleate* (○) *or saline* (●).

oleate-treated rats. A maximum free fraction was observed 30–60 min after infusion. The unbound fraction of diazepam decreased continuously thereafter, but it was still higher than that observed in saline-treated rats after 7 days.

The maximum concentration of oleate in plasma (about 75 μmoles/liter) was observed at the termination of infusion. Thereafter, plasma concentrations of this fatty acid declined rapidly. Within 3 hr after administration, the plasma oleate concentration was less than 10 μmoles/liter. The reduction in plasma binding of diazepam appears to be unrelated to *in vivo* plasma oleate concentrations since *in vitro* addition of sodium oleate to plasma to produce concentrations comparable to those found 3 hr after *in vivo* administration had virtually no effect on diazepam binding. The same conclusions apply when sodium oleate is given as an intravenous bolus (Table I).

The prolonged impaired ability of plasma to bind diazepam after sodium oleate administration may be related to a slowly reversible change in the plasma proteins induced by the initially high concentrations of oleate or to the persistence of biotransformation products that can displace diazepam from binding sites. A more detailed report concerning the effects of sodium oleate on the plasma protein binding of phenytoin is in preparation.

(1) V. P. Dole, *J. Clin. Invest.*, **35**, 150 (1956).
(2) V. P. Dole and H. Meinertz, *J. Biol. Chem.*, **235**, 2595 (1960).

Wayne A. Colburn
Milo Gibaldi ˣ
Department of Pharmaceutics
School of Pharmacy
State University of New York at Buffalo
Amherst, NY 14260

Received February 10, 1978.
Accepted for publication March 24, 1978.
Supported in part by Grant GM-20852 from the National Institutes of Health.

BOOKS

REVIEWS

The Alkaloids. Vol. 7. A Specialist Periodical Report. Edited by M. F. GRUNDON. The Chemical Society, Burlington House, London W1V OBN, England. 1977. x + 332 pp. 13.5 × 21.5 cm. Price $50.00. Available from Special Issues Sales, American Chemical Society, 1155 16th St., N.W., Washington, DC 20036.

M. F. Grundon is the senior reporter for the seventh volume of "The Alkaloids," which reviews the alkaloids literature published between July 1975 and June 1976. The reviews of Amaryllidaceae, *Erythrina*, imidazole, purine, and peptide alkaloids, which were not covered in Vol. 6, cover the period 1974–1976.

Each chapter effectively summarizes the important aspects of recent progress made on the particular types of alkaloids reviewed. Ample use of structures and schematics facilitates the clear presentations.

R. B. Herbert has again written an excellent chapter on biosynthesis, which includes recent work on secondary microbial metabolites as well as the various classes of alkaloids. It is of interest to note the increasing frequency of reporting the use of doubly-labeled precursors for biosynthetic work.

The major types of alkaloids are covered in the next 14 chapters, with the indole and isoquinoline alkaloids again representing the areas of most activity. The fast-growing use of ^{13}C-NMR spectroscopy for structure determination is becoming more evident. The final chapter (16) on miscellaneous alkaloids includes a section on unclassified alkaloids, which are presented in alphabetical order of plant or microbial source. The last section is noted to indicate the thorough reviewing characteristic of this series.

Volume 7 of this series continues the same concise format and style of the previous volumes. This reviewer especially likes the continued practice of placing the references on the page cited. For those who wish to keep abreast of the developments in the field of alkaloid chemistry, this volume is highly recommended despite the rather high cost.

Reviewed by Susan Tafur
Lilly Research Laboratories
Eli Lilly and Company
Indianapolis, IN 46226

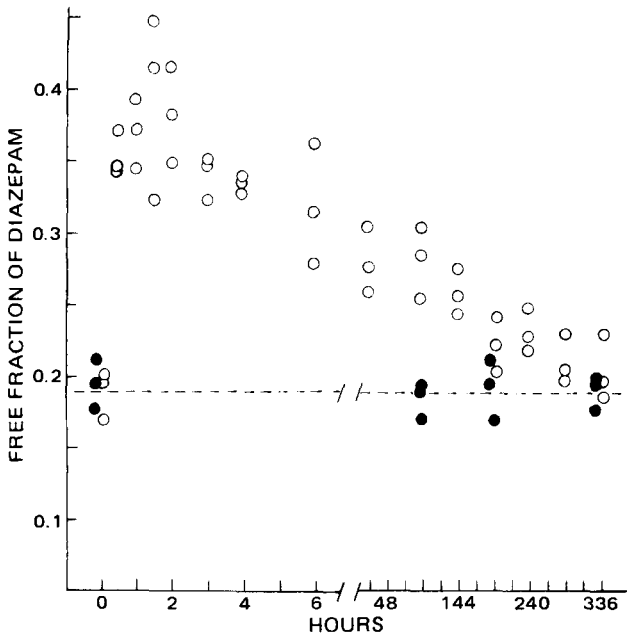

Figure 1—*Plasma protein binding of diazepam in rats after a 1-hr intravenous infusion of sodium oleate* (○) *or saline* (●).

oleate-treated rats. A maximum free fraction was observed 30–60 min after infusion. The unbound fraction of diazepam decreased continuously thereafter, but it was still higher than that observed in saline-treated rats after 7 days.

The maximum concentration of oleate in plasma (about 75 μmoles/liter) was observed at the termination of infusion. Thereafter, plasma concentrations of this fatty acid declined rapidly. Within 3 hr after administration, the plasma oleate concentration was less than 10 μmoles/liter. The reduction in plasma binding of diazepam appears to be unrelated to *in vivo* plasma oleate concentrations since *in vitro* addition of sodium oleate to plasma to produce concentrations comparable to those found 3 hr after *in vivo* administration had virtually no effect on diazepam binding. The same conclusions apply when sodium oleate is given as an intravenous bolus (Table I).

The prolonged impaired ability of plasma to bind diazepam after sodium oleate administration may be related to a slowly reversible change in the plasma proteins induced by the initially high concentrations of oleate or to the persistence of biotransformation products that can displace diazepam from binding sites. A more detailed report concerning the effects of sodium oleate on the plasma protein binding of phenytoin is in preparation.

(1) V. P. Dole, *J. Clin. Invest.*, **35**, 150 (1956).
(2) V. P. Dole and H. Meinertz, *J. Biol. Chem.*, **235**, 2595 (1960).

Wayne A. Colburn
Milo Gibaldi ˣ
Department of Pharmaceutics
School of Pharmacy
State University of New York at Buffalo
Amherst, NY 14260

Received February 10, 1978.
Accepted for publication March 24, 1978.
Supported in part by Grant GM-20852 from the National Institutes of Health.

BOOKS

REVIEWS

The Alkaloids. Vol. 7. A Specialist Periodical Report. Edited by M. F. GRUNDON. The Chemical Society, Burlington House, London W1V OBN, England. 1977. x + 332 pp. 13.5 × 21.5 cm. Price $50.00. Available from Special Issues Sales, American Chemical Society, 1155 16th St., N.W., Washington, DC 20036.

M. F. Grundon is the senior reporter for the seventh volume of "The Alkaloids," which reviews the alkaloids literature published between July 1975 and June 1976. The reviews of Amaryllidaceae, *Erythrina*, imidazole, purine, and peptide alkaloids, which were not covered in Vol. 6, cover the period 1974–1976.

Each chapter effectively summarizes the important aspects of recent progress made on the particular types of alkaloids reviewed. Ample use of structures and schematics facilitates the clear presentations.

R. B. Herbert has again written an excellent chapter on biosynthesis, which includes recent work on secondary microbial metabolites as well as the various classes of alkaloids. It is of interest to note the increasing frequency of reporting the use of doubly-labeled precursors for biosynthetic work.

The major types of alkaloids are covered in the next 14 chapters, with the indole and isoquinoline alkaloids again representing the areas of most activity. The fast-growing use of ^{13}C-NMR spectroscopy for structure determination is becoming more evident. The final chapter (16) on miscellaneous alkaloids includes a section on unclassified alkaloids, which are presented in alphabetical order of plant or microbial source. The last section is noted to indicate the thorough reviewing characteristic of this series.

Volume 7 of this series continues the same concise format and style of the previous volumes. This reviewer especially likes the continued practice of placing the references on the page cited. For those who wish to keep abreast of the developments in the field of alkaloid chemistry, this volume is highly recommended despite the rather high cost.

Reviewed by Susan Tafur
Lilly Research Laboratories
Eli Lilly and Company
Indianapolis, IN 46226

Mass Spectrometry in Drug Metabolism. Edited by ALBERTO FRIGERIO and EMILIO L. GHISALBERTI. Plenum, 227 W. 17th St., New York, NY 10011. 1977. 532 pp. 16 × 25 cm. Price $42.50.

This book is a compilation of 32 individual papers and invited reviews covering selected areas of techniques and applications of mass spectrometry in the field of drug metabolism. The papers assembled were presented at the International Symposium on Mass Spectrometry in Drug Metabolism, Mario Negri Institute for Pharmacologic Research, Milan, Italy.

Many different authors of varying backgrounds and expertise from all parts of the world contributed to this collection. As a result of this diversity of background and interest, the volume is truly representative of the state of the art of the study of drug metabolism, using mass spectrometry as the analytical tool.

The material was grouped into three major areas: Drug Metabolism, Development in Methodology, and Drug Abuse. Included under the heading Drug Metabolism are the categories: Identification of Drugs and Drug Metabolites, Quantification of Drugs and Drug Metabolites, and Intermediates in the Metabolism of Drugs. The Developments in Methodology section was divided into Developments in Methodology and Stable Isotope Labeling. This systematic arrangement of the papers in the Table of Contents allows simple location of topic. There is also a chemical compound and technique index, which is excellent for quick location of desired information.

Titles range from Blood Concentrations of Monoacylcadaverines in Schizophrenia to Field Desorption Mass Spectrometry of Pharmacologically Active Salts. There is a topical entry on the role of mass spectrometry on trends in drug abuse.

The highlight of the book is the presence of excellent review articles on such topics as selective ion monitoring in drug research and chemical-ionization mass spectrometry in the identification of drug metabolites. Of particular interest was a presentation on the role of computers in GLC–mass spectrometry, which dealt with the computer's role in the control of operation, detection, confirmation of identity, and quantification of metabolites. Each review is complete with a thorough bibliography which would facilitate further readings on these topics. The typical chapter is complete with illustrations such as normalized mass spectra, gas chromatographs, and metabolic schemes.

The papers contained in this book represent a wide variety of interests. The quality, quite naturally, varies with each author. For this reason, a single all encompassing review of the book cannot be done. It can be stated that the form of the manuscript with the ideal table of contents and complete index, clear illustrations, and bibliography makes it an enjoyable learning tool.

This compilation has true scientific merit, and I feel that it would be a definite asset to any scientific library. Metabolic chemists and other pharmaceutical scientists will find the book extremely useful. Mass spectrometrists certainly will be interested in this volume from many aspects, and they will find it useful in keeping abreast with the many faceted advances in mass spectral technology.

Reviewed by Charles F. Kuhlman
Research Division
Wyeth Laboratories, Inc.
Radnor, PA 19087

Venoms: Chemistry and Molecular Biology. By ANTHONY T. TU. Wiley, 605 Third Ave., New York, NY 10016. 1977. 560 pp. 17 × 25 cm. Price $34.50.

This book consists of four parts: General Background and Compositions of Snake Venoms, Enzymes in Snake Venoms, Properties and Actions of Snake Venoms, and Other Venoms.

For the first time, information concerning the molecular weight, structure (amino acid sequence), and biochemical, toxicological, and pharmacological properties of snake venoms throughout the world has been put together in one book. This book will be useful not only to students but also to researchers in this field. The book deals mostly with the chemical and biochemical aspects of snake venoms, with major emphasis on enzymatic properties of venoms, amino acid sequence, and structural configurations of venoms, which are the recent advances in analytical biochemistry.

Enzymes found in snake venoms include phospholipase A_2, phosphomonoesterase, phosphodiesterase, 1-amino acid oxidase, acetylcholinesterase, proteases, and esterases. Enzyme inhibitors also are discussed, and properties and actions of venoms of sea snakes, elapidae, viperidae, crotalidae, and colubridae are described. Tissue distribution of venoms in animals, binding site of neurotoxins to acetylcholine receptors, chemistry and structures of neurotoxins, and pharmacology of snake venoms, including hemolysis, blood coagulation, hemorrhage, and myonecrosis, are discussed with illustrations. Autonomic pharmacological substances (histamine, bradykinin and its potentiator, and angiotensinase inhibitor) and teratogenic and immunologic aspects of cobra venom in conjunction with its toxic properties are discussed.

Descriptions of various chemical agents effective in neutralizing the toxic factors of snake venoms are particularly useful. The chemical agents include steroids, carbohydrates (mucopolysaccharides and heparin), sulfur-containing compounds (thioglycolate, cysteine, glutathione, and thiourea), chelating agents, antihistamines, and procaine. Physical agents such as UV, cobalt-60, and X-rays are also included.

In addition to snake venoms, the nature of venoms from other land animals (scorpion, spider, bee, wasp, ant, and gila monster) is described and their chemical structures, biochemical properties, immunology, and pharmacology are discussed.

Many electron micrographs of actions of snake venoms on synaptic vesicles, muscles, glomerulus, collagen fibers, *etc.*, supplied by the author's laboratory are particularly interesting and informative. The book contains 101 figures, 67 tables, 31 schemes, and numerous illustrations.

Reviewed by C. L. Huang
College of Pharmacy and Allied Health Professions
Wayne State University
Detroit, MI 48201

Pharmaceutical Microbiology. Edited by W. B. HUGO and A. D. RUSSELL. Blackwell Scientific Publications, 8 John St., London, WC 1N 2ES, England. 1977. 352 pp. 15 × 24 cm.

This handsomely printed and illustrated soft cover, multi-authored textbook meets the needs of its intended audience of undergraduate pharmacy students. The first part is a 65-page concise statement of the biology of microbes. Also, a 15-page chapter devoted to an outline of immunology serves as an introduction to a following chapter on the manufacture and quality control of immunological products. A one-page concluding chapter is the prognostication of the editors of future developments in microbiology.

The remainder of the book is divided into two parts. The first deals with the nature and manufacture of antimicrobial agents. The second is a presentation of microbiological aspects of pharmaceutical processing. These parts are the great strength of the book as a textbook for pharmacy students. These chapters deal specifically with those aspects of microbiology of direct significance for the pharmacist and the pharmaceutical industry. Included are subjects such as the manufacture and assay of antibiotics, the nature of disinfection, the sterilization process, and requirements for good manufacturing practice.

The authors deserve praise for their success in outlining in a concise manner the microbiological aspects of the pharmaceutical industry. The pharmacist who stands at the interface between the pharmaceutical industry and the consumer will find this textbook suitable to his or her needs. The book is well written and stylistically acceptable in spite of its multi-authored origin. In sum, the book can be recommended as an authoritative, though elementary, introduction to pharmaceutical microbiology.

Reviewed by Carl Lamanna
Pharmaceutical Research and Testing
Bureau of Drugs
Washington, DC 20204

Mass Spectrometry in Drug Metabolism. Edited by ALBERTO FRIGERIO and EMILIO L. GHISALBERTI. Plenum, 227 W. 17th St., New York, NY 10011. 1977. 532 pp. 16 × 25 cm. Price $42.50.

This book is a compilation of 32 individual papers and invited reviews covering selected areas of techniques and applications of mass spectrometry in the field of drug metabolism. The papers assembled were presented at the International Symposium on Mass Spectrometry in Drug Metabolism, Mario Negri Institute for Pharmacologic Research, Milan, Italy.

Many different authors of varying backgrounds and expertise from all parts of the world contributed to this collection. As a result of this diversity of background and interest, the volume is truly representative of the state of the art of the study of drug metabolism, using mass spectrometry as the analytical tool.

The material was grouped into three major areas: Drug Metabolism, Development in Methodology, and Drug Abuse. Included under the heading Drug Metabolism are the categories: Identification of Drugs and Drug Metabolites, Quantification of Drugs and Drug Metabolites, and Intermediates in the Metabolism of Drugs. The Developments in Methodology section was divided into Developments in Methodology and Stable Isotope Labeling. This systematic arrangement of the papers in the Table of Contents allows simple location of topic. There is also a chemical compound and technique index, which is excellent for quick location of desired information.

Titles range from Blood Concentrations of Monoacylcadaverines in Schizophrenia to Field Desorption Mass Spectrometry of Pharmacologically Active Salts. There is a topical entry on the role of mass spectrometry on trends in drug abuse.

The highlight of the book is the presence of excellent review articles on such topics as selective ion monitoring in drug research and chemical-ionization mass spectrometry in the identification of drug metabolites. Of particular interest was a presentation on the role of computers in GLC–mass spectrometry, which dealt with the computer's role in the control of operation, detection, confirmation of identity, and quantification of metabolites. Each review is complete with a thorough bibliography which would facilitate further readings on these topics. The typical chapter is complete with illustrations such as normalized mass spectra, gas chromatographs, and metabolic schemes.

The papers contained in this book represent a wide variety of interests. The quality, quite naturally, varies with each author. For this reason, a single all encompassing review of the book cannot be done. It can be stated that the form of the manuscript with the ideal table of contents and complete index, clear illustrations, and bibliography makes it an enjoyable learning tool.

This compilation has true scientific merit, and I feel that it would be a definite asset to any scientific library. Metabolic chemists and other pharmaceutical scientists will find the book extremely useful. Mass spectrometrists certainly will be interested in this volume from many aspects, and they will find it useful in keeping abreast with the many faceted advances in mass spectral technology.

Reviewed by Charles F. Kuhlman
Research Division
Wyeth Laboratories, Inc.
Radnor, PA 19087

Venoms: Chemistry and Molecular Biology. By ANTHONY T. TU. Wiley, 605 Third Ave., New York, NY 10016. 1977. 560 pp. 17 × 25 cm. Price $34.50.

This book consists of four parts: General Background and Compositions of Snake Venoms, Enzymes in Snake Venoms, Properties and Actions of Snake Venoms, and Other Venoms.

For the first time, information concerning the molecular weight, structure (amino acid sequence), and biochemical, toxicological, and pharmacological properties of snake venoms throughout the world has been put together in one book. This book will be useful not only to students but also to researchers in this field. The book deals mostly with the chemical and biochemical aspects of snake venoms, with major emphasis on enzymatic properties of venoms, amino acid sequence, and structural configurations of venoms, which are the recent advances in analytical biochemistry.

Enzymes found in snake venoms include phospholipase A_2, phosphomonoesterase, phosphodiesterase, 1-amino acid oxidase, acetylcholinesterase, proteases, and esterases. Enzyme inhibitors also are discussed, and properties and actions of venoms of sea snakes, elapidae, viperidae, crotalidae, and colubridae are described. Tissue distribution of venoms in animals, binding site of neurotoxins to acetylcholine receptors, chemistry and structures of neurotoxins, and pharmacology of snake venoms, including hemolysis, blood coagulation, hemorrhage, and myonecrosis, are discussed with illustrations. Autonomic pharmacological substances (histamine, bradykinin and its potentiator, and angiotensinase inhibitor) and teratogenic and immunologic aspects of cobra venom in conjunction with its toxic properties are discussed.

Descriptions of various chemical agents effective in neutralizing the toxic factors of snake venoms are particularly useful. The chemical agents include steroids, carbohydrates (mucopolysaccharides and heparin), sulfur-containing compounds (thioglycolate, cysteine, glutathione, and thiourea), chelating agents, antihistamines, and procaine. Physical agents such as UV, cobalt-60, and X-rays are also included.

In addition to snake venoms, the nature of venoms from other land animals (scorpion, spider, bee, wasp, ant, and gila monster) is described and their chemical structures, biochemical properties, immunology, and pharmacology are discussed.

Many electron micrographs of actions of snake venoms on synaptic vesicles, muscles, glomerulus, collagen fibers, *etc.*, supplied by the author's laboratory are particularly interesting and informative. The book contains 101 figures, 67 tables, 31 schemes, and numerous illustrations.

Reviewed by C. L. Huang
College of Pharmacy and Allied Health Professions
Wayne State University
Detroit, MI 48201

Pharmaceutical Microbiology. Edited by W. B. HUGO and A. D. RUSSELL. Blackwell Scientific Publications, 8 John St., London, WC 1N 2ES, England. 1977. 352 pp. 15 × 24 cm.

This handsomely printed and illustrated soft cover, multi-authored textbook meets the needs of its intended audience of undergraduate pharmacy students. The first part is a 65-page concise statement of the biology of microbes. Also, a 15-page chapter devoted to an outline of immunology serves as an introduction to a following chapter on the manufacture and quality control of immunological products. A one-page concluding chapter is the prognostication of the editors of future developments in microbiology.

The remainder of the book is divided into two parts. The first deals with the nature and manufacture of antimicrobial agents. The second is a presentation of microbiological aspects of pharmaceutical processing. These parts are the great strength of the book as a textbook for pharmacy students. These chapters deal specifically with those aspects of microbiology of direct significance for the pharmacist and the pharmaceutical industry. Included are subjects such as the manufacture and assay of antibiotics, the nature of disinfection, the sterilization process, and requirements for good manufacturing practice.

The authors deserve praise for their success in outlining in a concise manner the microbiological aspects of the pharmaceutical industry. The pharmacist who stands at the interface between the pharmaceutical industry and the consumer will find this textbook suitable to his or her needs. The book is well written and stylistically acceptable in spite of its multi-authored origin. In sum, the book can be recommended as an authoritative, though elementary, introduction to pharmaceutical microbiology.

Reviewed by Carl Lamanna
Pharmaceutical Research and Testing
Bureau of Drugs
Washington, DC 20204

Mass Spectrometry in Drug Metabolism. Edited by ALBERTO FRIGERIO and EMILIO L. GHISALBERTI. Plenum, 227 W. 17th St., New York, NY 10011. 1977. 532 pp. 16 × 25 cm. Price $42.50.

This book is a compilation of 32 individual papers and invited reviews covering selected areas of techniques and applications of mass spectrometry in the field of drug metabolism. The papers assembled were presented at the International Symposium on Mass Spectrometry in Drug Metabolism, Mario Negri Institute for Pharmacologic Research, Milan, Italy.

Many different authors of varying backgrounds and expertise from all parts of the world contributed to this collection. As a result of this diversity of background and interest, the volume is truly representative of the state of the art of the study of drug metabolism, using mass spectrometry as the analytical tool.

The material was grouped into three major areas: Drug Metabolism, Development in Methodology, and Drug Abuse. Included under the heading Drug Metabolism are the categories: Identification of Drugs and Drug Metabolites, Quantification of Drugs and Drug Metabolites, and Intermediates in the Metabolism of Drugs. The Developments in Methodology section was divided into Developments in Methodology and Stable Isotope Labeling. This systematic arrangement of the papers in the Table of Contents allows simple location of topic. There is also a chemical compound and technique index, which is excellent for quick location of desired information.

Titles range from Blood Concentrations of Monoacylcadaverines in Schizophrenia to Field Desorption Mass Spectrometry of Pharmacologically Active Salts. There is a topical entry on the role of mass spectrometry on trends in drug abuse.

The highlight of the book is the presence of excellent review articles on such topics as selective ion monitoring in drug research and chemical-ionization mass spectrometry in the identification of drug metabolites. Of particular interest was a presentation on the role of computers in GLC–mass spectrometry, which dealt with the computer's role in the control of operation, detection, confirmation of identity, and quantification of metabolites. Each review is complete with a thorough bibliography which would facilitate further readings on these topics. The typical chapter is complete with illustrations such as normalized mass spectra, gas chromatographs, and metabolic schemes.

The papers contained in this book represent a wide variety of interests. The quality, quite naturally, varies with each author. For this reason, a single all encompassing review of the book cannot be done. It can be stated that the form of the manuscript with the ideal table of contents and complete index, clear illustrations, and bibliography makes it an enjoyable learning tool.

This compilation has true scientific merit, and I feel that it would be a definite asset to any scientific library. Metabolic chemists and other pharmaceutical scientists will find the book extremely useful. Mass spectrometrists certainly will be interested in this volume from many aspects, and they will find it useful in keeping abreast with the many faceted advances in mass spectral technology.

Reviewed by Charles F. Kuhlman
Research Division
Wyeth Laboratories, Inc.
Radnor, PA 19087

Venoms: Chemistry and Molecular Biology. By ANTHONY T. TU. Wiley, 605 Third Ave., New York, NY 10016. 1977. 560 pp. 17 × 25 cm. Price $34.50.

This book consists of four parts: General Background and Compositions of Snake Venoms, Enzymes in Snake Venoms, Properties and Actions of Snake Venoms, and Other Venoms.

For the first time, information concerning the molecular weight, structure (amino acid sequence), and biochemical, toxicological, and pharmacological properties of snake venoms throughout the world has been put together in one book. This book will be useful not only to students but also to researchers in this field. The book deals mostly with the chemical and biochemical aspects of snake venoms, with major emphasis on enzymatic properties of venoms, amino acid sequence, and structural configurations of venoms, which are the recent advances in analytical biochemistry.

Enzymes found in snake venoms include phospholipase A_2, phosphomonoesterase, phosphodiesterase, 1-amino acid oxidase, acetylcholinesterase, proteases, and esterases. Enzyme inhibitors also are discussed, and properties and actions of venoms of sea snakes, elapidae, viperidae, crotalidae, and colubridae are described. Tissue distribution of venoms in animals, binding site of neurotoxins to acetylcholine receptors, chemistry and structures of neurotoxins, and pharmacology of snake venoms, including hemolysis, blood coagulation, hemorrhage, and myonecrosis, are discussed with illustrations. Autonomic pharmacological substances (histamine, bradykinin and its potentiator, and angiotensinase inhibitor) and teratogenic and immunologic aspects of cobra venom in conjunction with its toxic properties are discussed.

Descriptions of various chemical agents effective in neutralizing the toxic factors of snake venoms are particularly useful. The chemical agents include steroids, carbohydrates (mucopolysaccharides and heparin), sulfur-containing compounds (thioglycolate, cysteine, glutathione, and thiourea), chelating agents, antihistamines, and procaine. Physical agents such as UV, cobalt-60, and X-rays are also included.

In addition to snake venoms, the nature of venoms from other land animals (scorpion, spider, bee, wasp, ant, and gila monster) is described and their chemical structures, biochemical properties, immunology, and pharmacology are discussed.

Many electron micrographs of actions of snake venoms on synaptic vesicles, muscles, glomerulus, collagen fibers, *etc.*, supplied by the author's laboratory are particularly interesting and informative. The book contains 101 figures, 67 tables, 31 schemes, and numerous illustrations.

Reviewed by C. L. Huang
College of Pharmacy and Allied Health Professions
Wayne State University
Detroit, MI 48201

Pharmaceutical Microbiology. Edited by W. B. HUGO and A. D. RUSSELL. Blackwell Scientific Publications, 8 John St., London, WC 1N 2ES, England. 1977. 352 pp. 15 × 24 cm.

This handsomely printed and illustrated soft cover, multi-authored textbook meets the needs of its intended audience of undergraduate pharmacy students. The first part is a 65-page concise statement of the biology of microbes. Also, a 15-page chapter devoted to an outline of immunology serves as an introduction to a following chapter on the manufacture and quality control of immunological products. A one-page concluding chapter is the prognostication of the editors of future developments in microbiology.

The remainder of the book is divided into two parts. The first deals with the nature and manufacture of antimicrobial agents. The second is a presentation of microbiological aspects of pharmaceutical processing. These parts are the great strength of the book as a textbook for pharmacy students. These chapters deal specifically with those aspects of microbiology of direct significance for the pharmacist and the pharmaceutical industry. Included are subjects such as the manufacture and assay of antibiotics, the nature of disinfection, the sterilization process, and requirements for good manufacturing practice.

The authors deserve praise for their success in outlining in a concise manner the microbiological aspects of the pharmaceutical industry. The pharmacist who stands at the interface between the pharmaceutical industry and the consumer will find this textbook suitable to his or her needs. The book is well written and stylistically acceptable in spite of its multi-authored origin. In sum, the book can be recommended as an authoritative, though elementary, introduction to pharmaceutical microbiology.

Reviewed by Carl Lamanna
Pharmaceutical Research and Testing
Bureau of Drugs
Washington, DC 20204

NOTICES

Predicting Dependence Liability of Stimulant and Depressant Drugs. Edited by TRAVIS THOMPSON and KLAUS R. UNNA. University Park Press, Chamber of Commerce Bldg., Baltimore, MD 21202. 1977. 328 pp. 15 × 23 cm. Price $19.50.

Infection Control in Health Care Facilities: Microbiological Surveillance. Edited by KENNETH R. CUNDY and WILLIAM BALL. University Park Press, Chamber of Commerce Bldg., Baltimore, MD 21202. 1977. 217 pp. 14 × 23 cm. Price $16.50.

Quality Control in Toxicology. Edited by G. E. PAGET. University Park Press, Chamber of Commerce Bldg., Baltimore, MD 21202. 1977. 128 pp. 14 × 22 cm. Price $19.75.

Quality Control in the Clinical Laboratory: A Procedural Text. By PAUL J. OTTAVIANO and ARTHUR F. DISALVO. University Park Press, Chamber of Commerce Bldg., Baltimore, MD 21202. 1977. 223 pp. 15 × 23 cm. Price $14.95.

The Ethical Pharmaceutical Industry and Some of Its Economic Aspects. An Annotated Bibliography. Compiled by DAVID C. SEVIGNY. Addiction Research Foundation, 33 Russell St., Toronto, Ontario, Canada. 1977. 521 pp. 15 × 23 cm. Price $10.00.

Recent Developments in the Pharmacology of Inflammatory Mediators. Edited by I. L. BONTA. Birkhauser Verlag, P.O. Box 34, CH-4010 Basel, Switzerland. 1977. 177 pp. 16 × 24 cm.

Fluorescent Antibody Techniques and Their Applications. 2nd Ed. Edited by AKIYOSHI KAWAMURA, JR. University Park Press, Chamber of Commerce Bldg., Baltimore, MD 21202. 1977. 292 pp. 17 × 25 cm.

How to Form Your Own Professional Corporation. By TED NICHOLAS. Enterprise Publishing Co., Suite 501, Beneficial Bldg., Market St., Wilmington, DE 19801. 1977. 160 pp. 21 × 28 cm.

An Introduction to Organic Chemistry. By WILLIAM H. REUSCH. Holden-Day, 500 Sansome St., San Francisco, CA 94111. 1977. 817 pp. 18 × 26 cm. Price $19.95.

Membranous Elements and Movement of Molecules. Methodological Surveys Vol. 6. Edited by ERIC REID. Wiley, 605 Third Ave., New York, NY 10016. 1977. 412 pp. 15 × 23 cm. Price $45.00.

Blood Policy: Issues and Alternatives. Edited by DAVID B. JOHNSON. American Enterprise Institute for Public Policy Research, Washington, DC. 1977. 212 pp. 15 × 24 cm. Price $4.75.

Chemical Process Industries. 4th Ed. By R. NORRIS SHREVE and JOSEPH A. BRINK, JR. McGraw-Hill Book Co., 1221 Avenue of the Americas, New York, NY 10020. 1977. 814 pp. 17 × 24 cm. Price $23.75.

Prevention and Detection of Cancer. Part I. Prevention. Vol. 1. Etiology. Edited by HERBERT E. NIEBURGS. Dekker, 270 Madison Ave., New York, NY 10016. 1977. 1191 pp. 18 × 26 cm. Price $62.50.

Biomedical Applications of Immobilized Enzymes and Proteins. Vol. 2. Edited by THOMAS MING SWI CHANG. Plenum, 227 W. 17th St., New York, NY 10011. 1977. 359 pp. 16 × 25 cm. Price $39.50.

Alcoholism. New Knowledge and New Responses. Edited by GRIFFITH EDWARDS and MARCUS GRANT. University Park Press, Chamber of Commerce Bldg., Baltimore, MD 21202. 1977. 359 pp. 13 × 22 cm. Price $24.50.

Identifizierung von Arzneistoffen. By HARRY AUTERHOFF and KARL-ARTUR KOVAR. Wissenschaftliche Verlagsgesellschaft mbH, Postfach 40, 7000 Stuttgart 1, Germany. 1977. 180 pp. 20 × 30 cm. Price DM 32.

Clinical Pharmacokinetics. Proceedings of an International Symposium at Salzgitter-Ringelheim (Germany), June 20 and 21, 1975. Edited by W. A. RITSCHEL. Gustav Fischer Verlag, D-7000 Stuttgart 72, Germany. 1977. 211 pp. 15 × 23 cm. Price DM 48.

Psychodynamics of Drug Dependence. NIDA Research Monograph 12. Edited by JACK D. BLAINE and DEMETRIOS A. JULIUS. National Institute on Drug Abuse, 11400 Rockville Pike, Rockville, MD 20852. 1977. 187 pp. 14 × 23 cm. Available from Superintendent of Documents, U.S. Government Printing Office, Washington, DC 20402.

Manual of Medical Therapeutics. 22nd Ed. Edited by NICHOLAS V. COSTRINI and WILLIAM M. THOMSON. Little, Brown, 34 Beacon St., Boston, MA 02106. 1977. 433 pp. 14 × 22 cm. Price $9.95.

The Total Synthesis of Natural Products. Vol. 3. Edited by JOHN APSIMON. Wiley, 605 Third Ave., New York, NY 10016. 1977. 566 pp. 15 × 23 cm.

Mycotoxic Fungi, Mycotoxins, Mycotoxicoses: An Encyclopedic Handbook. Vol. 1. Edited by THOMAS D. WYLLIE and LAWRENCE G. MOREHOUSE. Dekker, 270 Madison Ave., New York, NY 10016. 1977. 538 pp. 18 × 26 cm. Price $75.00.

Protein Crosslinking: Nutritional and Medical Consequences. Advances in Experimental Medicine and Biology. Vol. 86B. Edited by MENDEL FRIEDMAN. Plenum, 227 W. 17th St., New York, NY 10011. 1977. 740 pp. 16 × 25 cm. Price $59.50.

Protein Crosslinking: Biochemical and Molecular Aspects. Advances in Experimental Medicine and Biology, Vol. 86A. Edited by MENDEL FRIEDMAN. Plenum, 227 W. 17th St., New York, NY 10011. 1977. 760 pp. 16 × 25 cm. Price $59.50.

Plasmids: Medical and Theoretical Aspects. Third International Symposium on Antibiotic Resistance, Castle of Smolenice, Czechoslovakia, 1976. Edited by S. MITSUHASHI, L. ROSIVAL, and V. KRČMÉRY. Springer-Verlag, 175 Fifth Ave., New York, NY 10010. 1977. 489 pp. 16 × 24 cm. Price $44.70.

Microsomes and Drug Oxidations. Proceedings of the Third International Symposium, Berlin, July 1976. Edited by VOLKER ULLRICH, IVAR ROOTS, *et al.* Pergamon, Maxwell House, Fairview Park, Elmsford, NY 10523. 1977. 767 pp. 17 × 25 cm. Price $45.00.

The Specific Treatment of Virus Diseases. By D. J. BAUER. University Park Press, Chamber of Commerce Bldg., Baltimore, MD 21202. 1977. 194 pp. 16 × 24 cm. Price $19.50.

Anticonvulsants. Medicinal Chemistry: A Series of Monographs, Vol. 15. Edited by JULIUS A. VIDA. Academic, 111 Fifth Ave., New York, NY 10003. 1977. 638 pp. 15 × 23 cm.

Cosmetics: What the Ads Don't Tell You. By CAROL ANN RINZLER. Crowell, 10 E. 53rd St., New York, NY 10022. 1977. 212 pp. 15 × 23 cm. Price $9.95.

JULY 1978
VOLUME 67 NUMBER 7

JOURNAL OF PHARMACEUTICAL SCIENCES

MARY H. FERGUSON
Editor

SHELLY ELLIOTT
Production Editor

JANET D. SHOFF
Copy Editor

EDWARD G. FELDMANN
Contributing Editor

SAMUEL W. GOLDSTEIN
Contributing Editor

BELLE R. BECK
Editorial Secretary

DAVID BOHARDT
Director of Publications

L. LUAN CORRIGAN
Assistant Director of Publications

EDITORIAL ADVISORY BOARD

JOHN AUTIAN	HERBERT A. LIEBERMAN
NORMAN R. FARNSWORTH	DAVID E. MANN, JR.
WILLIAM O. FOYE	GERALD J. PAPARIELLO
WILLIAM J. JUSKO	EDWARD G. RIPPIE

The *Journal of Pharmaceutical Sciences* is published monthly by the American Pharmaceutical Association (APhA) at 2215 Constitution Ave., N.W., Washington, DC 20037. Second-class postage paid at Washington, D.C., and at additional mailing office.

All expressions of opinion and statements of supposed fact appearing in articles or editorials carried in this journal are published on the authority of the writer over whose name they appear and are not to be regarded as necessarily expressing the policies or views of APhA.

Offices—Editorial, Advertising, and Subscription: 2215 Constitution Ave., N.W., Washington, DC 20037. Printing: 20th & Northampton Streets, Easton, PA 18042.

Annual Subscriptions—United States and foreign, industrial and government institutions $50, educational institutions $50, individuals *for personal use only* $30; single copies $5. All foreign subscriptions add $5 for postage. Subscription rates are subject to change without notice. Members of APhA may elect to receive the *Journal of Pharmaceutical Sciences* as a part of their annual $70 (foreign $75) APhA membership dues.

Claims—Missing numbers will not be supplied if dues or subscriptions are in arrears for more than 60 days or if claims are received more than 60 days after the date of the issue, or if loss was due to failure to give notice of change of address. APhA cannot accept responsibility for foreign delivery when its records indicate shipment has been made.

Change of Address—Members and subscribers should notify at once both the Post Office and APhA of any change of address.

Photocopying—The code at the foot of the first page of an article indicates that APhA has granted permission for copying of the article beyond the limits permitted by Sections 107 and 108 of the U.S. Copyright Law provided that the copier sends the per copy fee stated in the code to the Copyright Clearance Center, Inc., P. O. Box 765, Schenectady, NY 12301. Copies may be made for personal or internal use only and not for general distribution.

Microfilm—Available from University Microfilms International, 300 N. Zeeb Road, Ann Arbor, MI 48106.

© Copyright 1978. American Pharmaceutical Association, 2215 Constitution Ave., N.W., Washington, DC 20037; all rights reserved.

INFORMATION RELEASE: RAW DATA OR SUMMARY?

Regular readers of this column know that it is not too often that we come down squarely on the same side as the drug industry in commenting on controversial issues.

We do, however, find that this is pretty much the case regarding the current legislative proposals on the subject of disclosure of data developed and used to support the approval of a new drug.

The Drug Regulation Reform Act of 1978 (S.2755; H.R. 11611) includes provisions for the "Disclosure of Reports Contained in a Petition." The "petition" referred to is part of the proposed system for bringing new drugs onto the market; a manufacturer would petition the FDA for establishment of a drug "monograph," the existence of which would be the critical determining factor in approving a drug for marketing. As such, this revised system would replace the present New Drug Application (NDA) procedure.

Under another heading, the legislation specifies that three separate reports—a summary report, a detailed compilation, and "a full report of all data and information from each such investigation"—must be submitted to support the petition. Pundits have labeled the three types of reports as "the one-inch high report, the one-foot high report, and the one-mile high report," respectively.

At any rate, the section dealing with disclosure of reports spells out that the entire content of all these reports would be subject to virtually unrestricted public inspection and review. And that is the proposition with which we find fault.

Over the years, no one has championed the cause of disclosure of drug information more vigorously than APhA. In our own speeches and editorials we have repeatedly urged the drug industry to be more open and informative in revealing pertinent product information for the benefit of practitioners and the patients they serve.

In recent years, there has been a growing trend among a significant number of manufacturers to divulge technical, scientific, and clinical information relating to their products. Some firms have done far better than others in this regard, and, regrettably, there are still some who continue to "stone-wall" on the issue. Consequently, some sort of legislative requirement probably is necessary to bring the laggards into line and to assure that every company will meet at least an acceptable minimum level in releasing pertinent information. For clarification, what we are talking about relates specifically to data supporting the safety and effectiveness of a drug and not to economic, marketing, or "trade secret" information in the normally accepted sense.

The drug industry, and the Pharmaceutical Manufacturers Association in particular, has been screaming that the drug bill goes completely overboard in this regard. They point out that every minute detail of every study would be subject to open examination. Among other things, it is claimed that this would provide a "road map" to competitors both in this country and abroad. Furthermore, it is stated that the privacy of test subjects would be destroyed, and incentives for drug research would be lost.

On the other side, skeptics point out that the drug industry has a notoriously poor record in giving out any more information than the required minimum, that drugs deserve to be treated differently than other commodities of commerce, and that only through scrutiny of the details can one detect either biased conclusions or falsified data.

We have attempted to be objective in our analysis of this issue. Frankly, we aren't able to judge with certainty that release of all test data will result in the rights of test subjects being trampled upon or in the wheels of research coming to a screeching halt.

But more importantly, we are not persuaded that the release of the complete detailed data will serve any public interest purpose. The Food and Drug Administration will have the complete file for its review in verifying that conclusions are supported adequately and that there has been no hanky-panky with regard to what research has in fact been performed.

The information that practitioners—or those to whom they look for guidance such as their professional societies—need in order to make independent judgments concerning the relative merits, usefulness, and limitations of a drug can be fully satisfied from a detailed summary of the sort envisioned in the second, or even the first, report called for in the drug bill.

The PMA has proposed in its testimony on the drug bill that the data disclosure provision be amended to mandate only the release of an appropriately detailed summary. If such information is prepared by the drug sponsor, approved by the FDA, and released prior to the marketing of a new drug, we feel that the needs of the public and the health professions will be adequately served. A broad range of health scientists have already expressed similar views in Congressional testimony. It is our hope, therefore, that this is one point on which cool heads will prevail and this reasonable compromise will be accepted by the bill's proponents. —EGF

JULY 1978
VOLUME 67 NUMBER 7

JOURNAL OF PHARMACEUTICAL SCIENCES

MARY H. FERGUSON
Editor

SHELLY ELLIOTT
Production Editor

JANET D. SHOFF
Copy Editor

EDWARD G. FELDMANN
Contributing Editor

SAMUEL W. GOLDSTEIN
Contributing Editor

BELLE R. BECK
Editorial Secretary

DAVID BOHARDT
Director of Publications

L. LUAN CORRIGAN
Assistant Director of Publications

EDITORIAL ADVISORY BOARD

JOHN AUTIAN	HERBERT A. LIEBERMAN
NORMAN R. FARNSWORTH	DAVID E. MANN, JR.
WILLIAM O. FOYE	GERALD J. PAPARIELLO
WILLIAM J. JUSKO	EDWARD G. RIPPIE

The *Journal of Pharmaceutical Sciences* is published monthly by the American Pharmaceutical Association (APhA) at 2215 Constitution Ave., N.W., Washington, DC 20037. Second-class postage paid at Washington, D.C., and at additional mailing office.

All expressions of opinion and statements of supposed fact appearing in articles or editorials carried in this journal are published on the authority of the writer over whose name they appear and are not to be regarded as necessarily expressing the policies or views of APhA.

Offices—Editorial, Advertising, and Subscription: 2215 Constitution Ave., N.W., Washington, DC 20037. Printing: 20th & Northampton Streets, Easton, PA 18042.

Annual Subscriptions—United States and foreign, industrial and government institutions $50, educational institutions $50, individuals *for personal use only* $30; single copies $5. All foreign subscriptions add $5 for postage. Subscription rates are subject to change without notice. Members of APhA may elect to receive the *Journal of Pharmaceutical Sciences* as a part of their annual $70 (foreign $75) APhA membership dues.

Claims—Missing numbers will not be supplied if dues or subscriptions are in arrears for more than 60 days or if claims are received more than 60 days after the date of the issue, or if loss was due to failure to give notice of change of address. APhA cannot accept responsibility for foreign delivery when its records indicate shipment has been made.

Change of Address—Members and subscribers should notify at once both the Post Office and APhA of any change of address.

Photocopying—The code at the foot of the first page of an article indicates that APhA has granted permission for copying of the article beyond the limits permitted by Sections 107 and 108 of the U.S. Copyright Law provided that the copier sends the per copy fee stated in the code to the Copyright Clearance Center, Inc., P. O. Box 765, Schenectady, NY 12301. Copies may be made for personal or internal use only and not for general distribution.

Microfilm—Available from University Microfilms International, 300 N. Zeeb Road, Ann Arbor, MI 48106.

© Copyright 1978. American Pharmaceutical Association, 2215 Constitution Ave., N.W., Washington, DC 20037; all rights reserved.

INFORMATION RELEASE: RAW DATA OR SUMMARY?

Regular readers of this column know that it is not too often that we come down squarely on the same side as the drug industry in commenting on controversial issues.

We do, however, find that this is pretty much the case regarding the current legislative proposals on the subject of disclosure of data developed and used to support the approval of a new drug.

The Drug Regulation Reform Act of 1978 (S.2755; H.R. 11611) includes provisions for the "Disclosure of Reports Contained in a Petition." The "petition" referred to is part of the proposed system for bringing new drugs onto the market; a manufacturer would petition the FDA for establishment of a drug "monograph," the existence of which would be the critical determining factor in approving a drug for marketing. As such, this revised system would replace the present New Drug Application (NDA) procedure.

Under another heading, the legislation specifies that three separate reports—a summary report, a detailed compilation, and "a full report of all data and information from each such investigation"—must be submitted to support the petition. Pundits have labeled the three types of reports as "the one-inch high report, the one-foot high report, and the one-mile high report," respectively.

At any rate, the section dealing with disclosure of reports spells out that the entire content of all these reports would be subject to virtually unrestricted public inspection and review. And that is the proposition with which we find fault.

Over the years, no one has championed the cause of disclosure of drug information more vigorously than APhA. In our own speeches and editorials we have repeatedly urged the drug industry to be more open and informative in revealing pertinent product information for the benefit of practitioners and the patients they serve.

In recent years, there has been a growing trend among a significant number of manufacturers to divulge technical, scientific, and clinical information relating to their products. Some firms have done far better than others in this regard, and, regrettably, there are still some who continue to "stone-wall" on the issue. Consequently, some sort of legislative requirement probably is necessary to bring the laggards into line and to assure that every company will meet at least an acceptable minimum level in releasing pertinent information. For clarification, what we are talking about relates specifically to data supporting the safety and effectiveness of a drug and not to economic, marketing, or "trade secret" information in the normally accepted sense.

The drug industry, and the Pharmaceutical Manufacturers Association in particular, has been screaming that the drug bill goes completely overboard in this regard. They point out that every minute detail of every study would be subject to open examination. Among other things, it is claimed that this would provide a "road map" to competitors both in this country and abroad. Furthermore, it is stated that the privacy of test subjects would be destroyed, and incentives for drug research would be lost.

On the other side, skeptics point out that the drug industry has a notoriously poor record in giving out any more information than the required minimum, that drugs deserve to be treated differently than other commodities of commerce, and that only through scrutiny of the details can one detect either biased conclusions or falsified data.

We have attempted to be objective in our analysis of this issue. Frankly, we aren't able to judge with certainty that release of all test data will result in the rights of test subjects being trampled upon or in the wheels of research coming to a screeching halt.

But more importantly, we are not persuaded that the release of the complete detailed data will serve any public interest purpose. The Food and Drug Administration will have the complete file for its review in verifying that conclusions are supported adequately and that there has been no hanky-panky with regard to what research has in fact been performed.

The information that practitioners—or those to whom they look for guidance such as their professional societies—need in order to make independent judgments concerning the relative merits, usefulness, and limitations of a drug can be fully satisfied from a detailed summary of the sort envisioned in the second, or even the first, report called for in the drug bill.

The PMA has proposed in its testimony on the drug bill that the data disclosure provision be amended to mandate only the release of an appropriately detailed summary. If such information is prepared by the drug sponsor, approved by the FDA, and released prior to the marketing of a new drug, we feel that the needs of the public and the health professions will be adequately served. A broad range of health scientists have already expressed similar views in Congressional testimony. It is our hope, therefore, that this is one point on which cool heads will prevail and this reasonable compromise will be accepted by the bill's proponents. —EGF

Consideration Fee: View I

It was with great interest that I read the editorial "Why A Consideration Fee?" in the February 1978 issue of the Journal. I was quite shocked to learn that only a relatively small percentage of authors who publish in the Journal actually remit for page charges. I was under the impression that the percentage was higher. I agree wholeheartedly with the editorial in that page charges should actually be an integral part of the research project.

As one who has been associated with institutions that have supported page charges, I feel that the concept of a consideration fee is excellent and serves to distribute more evenly the cost of publication.

It is also difficult for me to understand why 75% of Journal readers are unwilling to pay reasonable subscription costs for personal copies. The charge is not that great.

I normally do not take the time to respond to editorials. However, I felt you might wish to share my comments with some of your colleagues at APhA or with your readers and to let them know that I wholeheartedly endorse the contents of the editorial.

John J. Sciarra
Arnold & Marie Schwartz College of Pharmacy and Health Sciences of Long Island University
Brooklyn, NY 11201

Received April 29, 1978.

Consideration Fee: View II

The February 1978 editorial ("Why A Consideration Fee?") in this Journal by Dr. Mary Ferguson presents a rather cogent argument, from the editor's side, to support the recently instituted $25 manuscript consideration fee. In fairness, we should hear from the other side, namely, those junior and senior researchers trying desperately to keep research projects financially afloat. I think I can speak for this group.

Dr. Ferguson asks the question as to who receives the most benefit from publication of papers. Her response excludes the Journal from this benefit because of a deficit budget, so, in her opinion, benefit accrues to authors and sponsoring institutions. This observation probably is correct but misses a few other important considerations. Could it be that major benefit accrues to APhA as the publisher of the Journal (these benefits may be in terms of prestige and recognition—the same as Dr. Ferguson claims are accrued to authors and sponsoring institutions)? Could it be that benefit accrues to authors who refuse to pay page charges (as Dr. Ferguson explains, 40% of the articles published in *J. Pharm. Sci.* are published without payment of page charges)? Could it also be that in instituting page charges and consideration fees the Journal is alienating those very individuals that it must rely upon for its very existence?

The problem as I see it is whoever said that the Journal should be self-sufficient. Isn't it a reasonable argument that APhA should subsidize the Journal for dissemination of scientific information by APhA members (and nonmembers)? Is it unreasonable for my professional association to provide this subsidy in the amount of $45,000 for 1977 (to use Dr. Ferguson's figures)? This subsidy amounts to $4.50 for each subscribing and, ostensibly, in the main, APhA member. My and my colleague's APhA yearly dues should adequately provide for this subsidy since there are few other benefits that the scientific members of APhA can enjoy. The most apropos analogy would be to consider *American Pharmacy;* surely it publishes at a deficit to provide a needed membership benefit to practitioners of pharmacy.

R. Saul Levinson
Health Sciences Center
University of Oklahoma
Oklahoma City, OK 73190

Received May 10, 1978.

Plant Reidentified

In the August 1977 issue of this Journal, an article entitled "Plant Anticancer Agents III: Isolation of Indole and Bisindole Alkaloids from *Tabernaemontana holstii* Roots" appeared[1]. Since the time of publication, the plant has been reidentified by Dr. Robert E. Perdue, Dr. Arthur S. Barclay, and Sandra Saufferer of the Beltsville Agricultural Research Center, U.S. Department of Agriculture, Beltsville, Md., as *Voacanga thouarsii* R. and S. (Apocynaceae).

David G. I. Kingston
Department of Chemistry
Virginia Polytechnic Institute and State University
Blacksburg, VA 24061

Received May 8, 1978.

[1] D. G. I. Kingston, B. T. Li, and F. Ionescu, *J. Pharm. Sci.*, **66**, 1135 (1977).

Consideration Fee: View I

It was with great interest that I read the editorial "Why A Consideration Fee?" in the February 1978 issue of the Journal. I was quite shocked to learn that only a relatively small percentage of authors who publish in the Journal actually remit for page charges. I was under the impression that the percentage was higher. I agree wholeheartedly with the editorial in that page charges should actually be an integral part of the research project.

As one who has been associated with institutions that have supported page charges, I feel that the concept of a consideration fee is excellent and serves to distribute more evenly the cost of publication.

It is also difficult for me to understand why 75% of Journal readers are unwilling to pay reasonable subscription costs for personal copies. The charge is not that great.

I normally do not take the time to respond to editorials. However, I felt you might wish to share my comments with some of your colleagues at APhA or with your readers and to let them know that I wholeheartedly endorse the contents of the editorial.

John J. Sciarra
Arnold & Marie Schwartz College of Pharmacy and Health Sciences of Long Island University
Brooklyn, NY 11201

Received April 29, 1978.

Consideration Fee: View II

The February 1978 editorial ("Why A Consideration Fee?") in this Journal by Dr. Mary Ferguson presents a rather cogent argument, from the editor's side, to support the recently instituted $25 manuscript consideration fee. In fairness, we should hear from the other side, namely, those junior and senior researchers trying desperately to keep research projects financially afloat. I think I can speak for this group.

Dr. Ferguson asks the question as to who receives the most benefit from publication of papers. Her response excludes the Journal from this benefit because of a deficit budget, so, in her opinion, benefit accrues to authors and sponsoring institutions. This observation probably is correct but misses a few other important considerations. Could it be that major benefit accrues to APhA as the publisher of the Journal (these benefits may be in terms of prestige and recognition—the same as Dr. Ferguson claims are accrued to authors and sponsoring institutions)? Could it be that benefit accrues to authors who refuse to pay page charges (as Dr. Ferguson explains, 40% of the articles published in *J. Pharm. Sci.* are published without payment of page charges)? Could it also be that in instituting page charges and consideration fees the Journal is alienating those very individuals that it must rely upon for its very existence?

The problem as I see it is whoever said that the Journal should be self-sufficient. Isn't it a reasonable argument that APhA should subsidize the Journal for dissemination of scientific information by APhA members (and nonmembers)? Is it unreasonable for my professional association to provide this subsidy in the amount of $45,000 for 1977 (to use Dr. Ferguson's figures)? This subsidy amounts to $4.50 for each subscribing and, ostensibly, in the main, APhA member. My and my colleague's APhA yearly dues should adequately provide for this subsidy since there are few other benefits that the scientific members of APhA can enjoy. The most apropos analogy would be to consider *American Pharmacy;* surely it publishes at a deficit to provide a needed membership benefit to practitioners of pharmacy.

R. Saul Levinson
Health Sciences Center
University of Oklahoma
Oklahoma City, OK 73190

Received May 10, 1978.

Plant Reidentified

In the August 1977 issue of this Journal, an article entitled "Plant Anticancer Agents III: Isolation of Indole and Bisindole Alkaloids from *Tabernaemontana holstii* Roots" appeared[1]. Since the time of publication, the plant has been reidentified by Dr. Robert E. Perdue, Dr. Arthur S. Barclay, and Sandra Saufferer of the Beltsville Agricultural Research Center, U.S. Department of Agriculture, Beltsville, Md., as *Voacanga thouarsii* R. and S. (Apocynaceae).

David G. I. Kingston
Department of Chemistry
Virginia Polytechnic Institute and State University
Blacksburg, VA 24061

Received May 8, 1978.

[1] D. G. I. Kingston, B. T. Li, and F. Ionescu, *J. Pharm. Sci.*, **66**, 1135 (1977).

Consideration Fee: View I

It was with great interest that I read the editorial "Why A Consideration Fee?" in the February 1978 issue of the Journal. I was quite shocked to learn that only a relatively small percentage of authors who publish in the Journal actually remit for page charges. I was under the impression that the percentage was higher. I agree wholeheartedly with the editorial in that page charges should actually be an integral part of the research project.

As one who has been associated with institutions that have supported page charges, I feel that the concept of a consideration fee is excellent and serves to distribute more evenly the cost of publication.

It is also difficult for me to understand why 75% of Journal readers are unwilling to pay reasonable subscription costs for personal copies. The charge is not that great.

I normally do not take the time to respond to editorials. However, I felt you might wish to share my comments with some of your colleagues at APhA or with your readers and to let them know that I wholeheartedly endorse the contents of the editorial.

John J. Sciarra
Arnold & Marie Schwartz College of Pharmacy and Health Sciences of Long Island University
Brooklyn, NY 11201

Received April 29, 1978.

Consideration Fee: View II

The February 1978 editorial ("Why A Consideration Fee?") in this Journal by Dr. Mary Ferguson presents a rather cogent argument, from the editor's side, to support the recently instituted $25 manuscript consideration fee. In fairness, we should hear from the other side, namely, those junior and senior researchers trying desperately to keep research projects financially afloat. I think I can speak for this group.

Dr. Ferguson asks the question as to who receives the most benefit from publication of papers. Her response excludes the Journal from this benefit because of a deficit budget, so, in her opinion, benefit accrues to authors and sponsoring institutions. This observation probably is correct but misses a few other important considerations. Could it be that major benefit accrues to APhA as the publisher of the Journal (these benefits may be in terms of prestige and recognition—the same as Dr. Ferguson claims are accrued to authors and sponsoring institutions)? Could it be that benefit accrues to authors who refuse to pay page charges (as Dr. Ferguson explains, 40% of the articles published in *J. Pharm. Sci.* are published without payment of page charges)? Could it also be that in instituting page charges and consideration fees the Journal is alienating those very individuals that it must rely upon for its very existence?

The problem as I see it is whoever said that the Journal should be self-sufficient. Isn't it a reasonable argument that APhA should subsidize the Journal for dissemination of scientific information by APhA members (and nonmembers)? Is it unreasonable for my professional association to provide this subsidy in the amount of $45,000 for 1977 (to use Dr. Ferguson's figures)? This subsidy amounts to $4.50 for each subscribing and, ostensibly, in the main, APhA member. My and my colleague's APhA yearly dues should adequately provide for this subsidy since there are few other benefits that the scientific members of APhA can enjoy. The most apropos analogy would be to consider *American Pharmacy;* surely it publishes at a deficit to provide a needed membership benefit to practitioners of pharmacy.

R. Saul Levinson
Health Sciences Center
University of Oklahoma
Oklahoma City, OK 73190

Received May 10, 1978.

Plant Reidentified

In the August 1977 issue of this Journal, an article entitled "Plant Anticancer Agents III: Isolation of Indole and Bisindole Alkaloids from *Tabernaemontana holstii* Roots" appeared[1]. Since the time of publication, the plant has been reidentified by Dr. Robert E. Perdue, Dr. Arthur S. Barclay, and Sandra Saufferer of the Beltsville Agricultural Research Center, U.S. Department of Agriculture, Beltsville, Md., as *Voacanga thouarsii* R. and S. (Apocynaceae).

David G. I. Kingston
Department of Chemistry
Virginia Polytechnic Institute and State University
Blacksburg, VA 24061

Received May 8, 1978.

[1] D. G. I. Kingston, B. T. Li, and F. Ionescu, *J. Pharm. Sci.*, **66**, 1135 (1977).

JOURNAL OF PHARMACEUTICAL SCIENCES

JULY 1978
VOLUME 67 NUMBER 7

RESEARCH ARTICLES

Intestinal Absorption of Griseofulvin from a Triolein Digestion Mixture in Rats

JOSEPH A. GRISAFE and WILLIAM L. HAYTON ˣ

Received September 6, 1977, from the *College of Pharmacy, Washington State University, Pullman, WA 99164.* Accepted for publication November 8, 1977.

Abstract □ The intestinal absorption rate of dissolved griseofulvin was determined from: (*a*) an aqueous phase, (*b*) an aqueous phase containing a micellar phase composed of taurodeoxycholate, monoolein, and oleic acid, and (*c*) an aqueous phase containing the micellar phase and emulsified triolein. The triolein digestion mixtures were recirculated through 20-cm segments of *in situ* rat jejunum. Lipid concentrations were maintained constant by infusing the lipids into the digestion mixture at the same rate as they disappeared. Griseofulvin distribution among the aqueous, micellar, and oil phases was determined by solubility and equilibrium dialysis experiments. Analysis with a linear kinetic model indicated that griseofulvin absorption from the micellar and oil phases was negligible compared to its absorption from the aqueous phase.

Keyphrases □ Griseofulvin—GI absorption from aqueous phase and aqueous phases containing triolein digestion mixture, rats □ Triolein digestion mixture—in aqueous phase containing griseofulvin, GI absorption in rats □ Absorption, GI—griseofulvin from aqueous phase and aqueous phases containing triolein digestion mixture, rats □ Lipids—triolein digestion mixture, GI absorption of griseofulvin, rats □ Antifungal agents—griseofulvin, GI absorption from aqueous phase and aqueous phases containing triolein digestion mixture, rats

The literature is replete with examples of the effects of lipids on the oral bioavailability of lipophilic, poorly water-soluble drugs. For example, griseofulvin bioavailability increased with the amount of lipid in the diet of humans (1) and was greater in the rat when coadministered with corn oil (2) or corn oil emulsion (3) than when administered in water. Sulfisoxazole acetyl had greater bioavailability after oral administration in a vegetable oil-in-water emulsion than in water in rats and humans (4) and, compared to water, triolein increased the extent of sulfisoxazole acetyl and dicumarol absorption in rats (5).

Examples of lipids that decreased the bioavailability of lipophilic substances also were reported. Compared to its administration in an aqueous vehicle, chlorophenothane (DDT) absorption appeared to increase when it was administered in corn or olive oil but decreased when given in mineral oil (6). Similarly, sucrose polyester, a nonabsorbable lipid, decreased the absorption of cholesterol from a triolein vehicle when it was included in the triolein as a mixed oil phase. The decrease was linear as the fraction of sucrose polyester in the vehicle increased up to 50% (7).

Consideration of the potential effects of lipids on the absorption of lipophilic substances requires an understanding of the behavior of lipids in the GI tract. Dietary lipids, mainly triglycerides of long chain fatty acids, are emulsified in the gut lumen and hydrolyzed by pancreatic lipase to 2-monoglycerides and fatty acids (8). The 2-monoglycerides may isomerize to 1-monoglycerides (9). The water-insoluble fatty acids and monoglycerides combine with bile salts to form "mixed micelles" (10); they move in this form to the intestinal epithelium where they are absorbed (11). As the fatty acids and monoglycerides are absorbed from the mixed micelle, the bile salts either remain in the lumen to solubilize and transport lipid digestion products (12) or are absorbed, primarily in the ileum by an active transport process (13), and returned to the bile.

Consequently, the lipid digestion mixture of the intestinal lumen can be viewed as a three-phase system: an oil phase consisting primarily of triglycerides; a micellar phase composed of bile salts, fatty acids, and monoglycerides; and an aqueous phase. In this system, lipophilic drugs would probably concentrate in the oil and micellar phases; for example, cholesterol partitions extensively into these phases (14). This study developed and tested a model that describes the absorption of a lipophilic drug from a lipid digestion mixture.

THEORETICAL

The distribution of a poorly water-soluble lipophilic drug among the three phases of a lipid digestion mixture and the potential absorption of drug from each phase is illustrated in Scheme I. Absorption of the drug from all three phases represents the general case; if the case of no absorption is excluded, seven subcases exist for absorption from a single phase or from a combination of phases. The passive transport of drug

0022-3549/78/0700/0895$01.00/0
© 1978, American Pharmaceutical Association

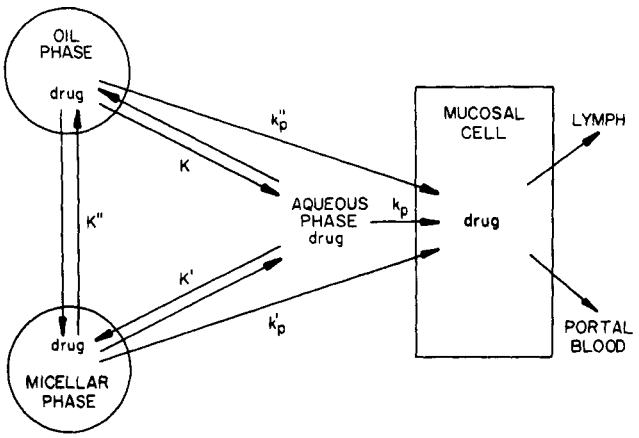

Scheme I—Distribution of a lipophilic drug among the three phases of a lipid digestion mixture with the potential for absorption from each phase. The K, K′, *and* K″ *are apparent partition coefficients for drug between oil and aqueous phases, micellar and aqueous phases, and micellar and oil phases, respectively;* k_p, k_p', *and* k_p'' *are clearance constants for absorption of the drug from the aqueous, micellar, and oil phases, respectively.*

molecules from a single phase across a biological membrane in the direction of a concentration gradient can be described by (15):

$$\frac{dX}{dt} = \frac{-D_m K_m A(C_M - C_S)}{h} \quad \text{(Eq. 1)}$$

where dX/dt is the disappearance rate of drug X from the intestinal lumen (mass/time), D_m is the diffusion coefficient of the drug in the membrane (length^2/time), K_m is the partition coefficient between the membrane and the phase transferring drug X to the membrane, A is the cross-sectional area of the membrane (length^2), and $(C_M - C_S)/h$ is the concentration gradient of the drug across the intestinal mucosa (mass/length^4) at any time.

If it is assumed that the drug is constantly carried from the serosal side of the membrane such that $C_M \gg C_S$ and that A and h are constant throughout the experiment, then:

$$\frac{dX}{dt} = -k_c C_M \quad \text{(Eq. 2)}$$

where k_c is equal to $D_m K_m (A/h)$ and is a clearance constant with the units of flow (length^3/time).

By analogy, the disappearance rate of a lipophilic drug from the intestinal lumen according to the model shown in Scheme I can be described by:

$$\frac{dX}{dt} = (-k_p C_w) - (k_p' C_m) - (k_p'' C_o) \quad \text{(Eq. 3)}$$

where C_w, C_m, and C_o are the drug concentrations in the aqueous, micellar, and oil phases, respectively; and k_p, k_p', and k_p'' are the respective clearance constants. Each clearance constant is a function of four parameters:

$$k_p^i = \frac{D_m K_m^i A^i}{h} \quad \text{(Eq. 4)}$$

Two parameters, D_m and h, are the same for all three clearance constants. The membrane–luminal phase distribution coefficient, K_m^i, and the area of absorbing surface in contact with each luminal phase, A^i, are different for each phase, and they largely determine the relative values of the clearance constants.

The drug concentration in the micellar and oil phases can be related to the aqueous phase concentration by the micellar–aqueous and oil–aqueous partition coefficients:

$$C_m = K' C_w \quad \text{(Eq. 5)}$$

$$C_o = K C_w \quad \text{(Eq. 6)}$$

Substitution of Eqs. 5 and 6 into Eq. 3 and combination of terms give:

$$\frac{dX}{dt} = -[k_p + (k_p' K') + (k_p'' K)] C_w \quad \text{(Eq. 7)}$$

Each phase may be expressed as a fraction, f, of the total volume, V_T:

$$f_w = \frac{V_w}{V_T} \quad \text{(Eq. 8)}$$

$$f_m = \frac{V_m}{V_T} \quad \text{(Eq. 9)}$$

$$f_o = \frac{V_o}{V_T} \quad \text{(Eq. 10)}$$

where V_w, V_m, and V_o are the volumes of the aqueous, micellar, and oil phases, respectively. The total drug concentration, C_T, is then:

$$C_T = (f_w C_w) + (f_m C_m) + (f_o C_o) \quad \text{(Eq. 11)}$$

Substitution of Eqs. 5 and 6 into Eq. 11 gives:

$$C_T = (f_w C_w) + (f_m K' C_w) + (f_o K C_w) \quad \text{(Eq. 12)}$$

and, by rearrangement:

$$C_w = \frac{C_T}{f_w + (f_m K') + (f_o K)} \quad \text{(Eq. 13)}$$

Substitution of Eq. 13 into Eq. 7 for C_w yields:

$$\frac{dX}{dt} = \frac{-[k_p + (k_p' K') + (k_p'' K)] C_T}{f_w + (f_m K') + (f_o K)} \quad \text{(Eq. 14)}$$

Finally, substitution of Eqs. 8–10 for the fractions f_w, f_m, and f_o in Eq. 14 and division by V_T give:

$$\frac{dC_T}{dt} = \frac{-[k_p + (k_p' K') + (k_p'' K)] C_T}{V_w + (V_m K') + (V_o K)} \quad \text{(Eq. 15)}$$

Equation 15 predicts that, in the general case of absorption from all three phases, the rate of decline of the concentration of a lipophilic drug in the intestinal lumen would follow apparent first-order kinetics. A plot of log C_T *versus* time would be linear, and an apparent first-order rate constant could be determined from the slope. It would be a function of the clearance constants, partition coefficients, and phase volumes:

$$k_{app} = \frac{k_p + (k_p' K') + (k_p'' K)}{V_w + (V_m K') + (V_o K)} \quad \text{(Eq. 16)}$$

Less complex models can be developed if absorption occurs from only one or two phases. Some evidence suggests that absorption of lipophilic substances occurs primarily from the micellar or aqueous phase and may not occur directly from the oil phase. For example, salicylamide was absorbed from the aqueous phase after release to that phase from the oil phase in the rat colon (16, 17). Another study indicated that vitamin A acetate was released from the micellar phase, adsorbed to the mucosa of the rat intestine, and then absorbed; oil droplets adsorbed to the mucosa interfered with this process (18). This study also reported that, unlike vitamin A acetate, phenylbutazone was absorbed primarily from the aqueous phase when the vehicle was a three-phase system of oil, micelles, and water. If a drug is not absorbed from a given phase, one subcase of the general model would be appropriate to describe its absorption.

The work described here involved perfusion of a segment of the *in situ* rat small intestine with triolein digestion mixtures containing griseofulvin. The apparent absorption rate constant, k_{app}, for griseofulvin was measured along with the partition coefficients K and K'. These experimentally determined values were used to estimate clearance constants for the intestinal absorption of griseofulvin from the aqueous, micellar, and oil phases.

EXPERIMENTAL

Materials—Oleic acid[1], monoolein[2], triolein[3], sodium taurodeoxycholate[4], and griseofulvin[4] were used as received. All other reagents and solvents were reagent grade.

Intestinal Absorption—Male Sprague–Dawley rats, 180–300 g, were fasted 12–20 hr and then anesthetized with urethan, 1.3 mg/g ip. They were prepared for study of the intestinal absorption of griseofulvin as described previously (19). The abdomen of each rat was opened by a midline incision; a small cannula[5] was inserted into the jejunum, 10 cm

[1] Merck and Co., Rahway, N.J.
[2] Eastman Organic Chemicals, Rochester, N.Y.
[3] Pfaltz and Bauer, Flushing, N.Y.
[4] Sigma Chemical Co., St. Louis, Mo.
[5] Intramedic polyethylene tubing, PE160, 1.14 mm i.d.

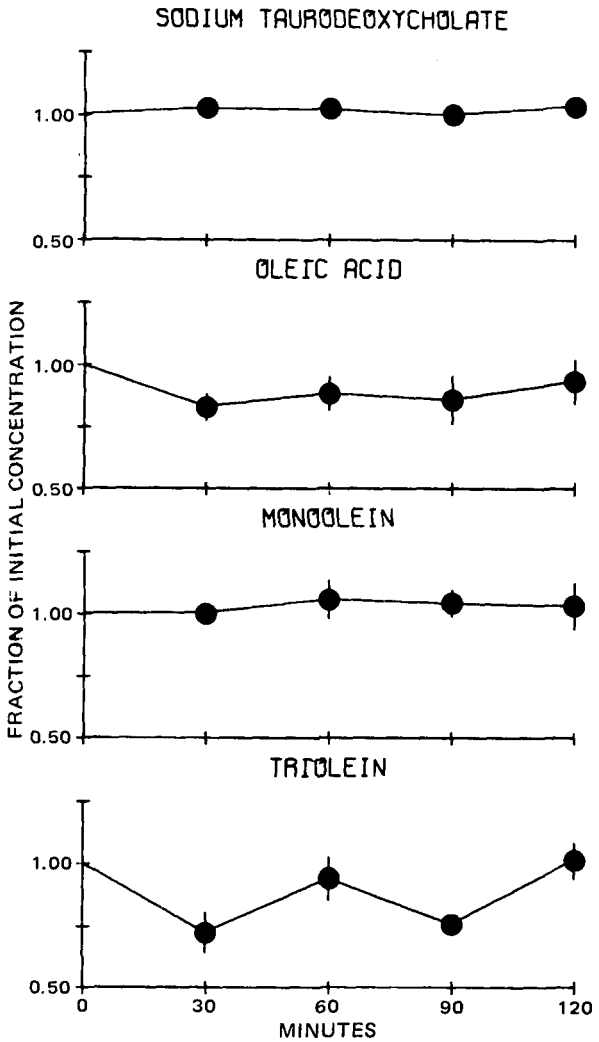

Figure 1—*Fractions of the initial concentration of sodium taurodeoxycholate (8 mM), oleic acid (6 mM), monoolein (3 mM), and triolein (2 g/100 ml) remaining in the intestinal solution as a function of time. Each point represents the mean from six experiments; bars indicate ±1* SE.

distal to the stomach, and tied in place with a silk suture. A second cannula[6] was placed 20 cm distal to the first cannula.

The intestinal segment was washed twice (20) with 10-ml volumes of irrigating solution (21) and then twice with 3-ml volumes of perfusion solution containing all components of the ensuing experiment.

The cephaled cannula was connected to the outlet of a perfusion pump[7] with polyethylene tubing[8], and the caudad cannula was connected to a well-stirred reservoir[9]. The external reservoir was filled with perfusion solution containing griseofulvin (23 μM) in 68 mM sodium phosphate buffer; the buffer, at pH 6.2, was made isotonic with 87 mM sodium chloride. The drug solution was recirculated at 6.5 ml/min through the intestinal segment for approximately 3 min before the zero-time sample was obtained from the reservoir. The experiments were continued for 60–120 min, and samples were withdrawn periodically from the reservoir and subsequently analyzed for griseofulvin.

Throughout the perfusion experiments, the rectal temperature of each rat was maintained at 37 ± 1° by warming the rat on a heating pad when necessary. The volume of the perfusate was held constant by intermittently adding buffer to the reservoir from a buret. The volume tended to decline, because samples were removed and water was absorbed by the intestine. After each experiment, the length of intestine perfused and the volume of buffer added to the reservoir were determined.

[6] Intramedic, PE320, 2.7 mm i.d.
[7] Peristaltic pump model 1201, Harvard Apparatus Co.
[8] Intramedic, PE60, 0.76 mm i.d.
[9] The reservoir was constructed from a 5-ml volumetric flask by adding four 1.5-cm pieces of 3-mm o.d. glass tubing at equally spaced distances around the body of the flask.

Table I—Infusion Rates that Maintain Constant Concentrations of Lipids in the Intestinal Perfusate

Lipid	Infusion Rate[a], μg/min	Intestinal Clearance[b], μl/min/cm
Monoolein, 3 mM	61.0	2.35
Oleic acid, 6 mM	96.4	2.34
Triolein, 2 g/100 ml	778.5	1.45
Sodium taurodeoxycholate, 8 mM	116.2	0.89

[a] Includes replacement of losses due to sampling. Samples of 0.3 ml were removed at 30-min intervals. [b] Calculated by infusion = clearance × concentration in the perfusate. Corrected for removal of samples.

When the lipids were included in the perfusates, they were monoolein (3 mM), oleic acid (6 mM), sodium taurodeoxycholate (8 mM), and triolein (2 g/100 ml). The lipids were infused[10] into the reservoir at a rate equal to their removal rate in samples and the absorption rate by the intestine. By using the infusion rates of the lipids that were determined empirically by preliminary experiments (Table I), it was possible to maintain the concentration of the lipids in the perfusates relatively constant (Fig. 1). The bile salt concentration was sufficient to solubilize the monoglyceride and free fatty acid (22).

Semilogarithmic plots of the fraction of initial griseofulvin concentration *versus* time gave straight lines (Fig. 2) when fitted by the method of least squares. The initial point was omitted from the fit to ensure stationary-state conditions. The absorption rate constants of griseofulvin were determined from the slopes of the fitted lines and were converted to clearance per centimeter of intestine by multiplying the rate constant by the volume of perfusate, correcting for drug removed as samples, and dividing by the length of the intestine.

Triolein–Aqueous Phase Partition Coefficient (K)—Centrifuge tubes were prepared to contain 20 ml of a pH 6.2 aqueous phase containing griseofulvin (23 μM), sodium phosphate buffer (68 mM), sodium taurodeoxycholate (1.2 mM), and sodium chloride (87 mM) and 5 ml of triolein in which griseofulvin (0.58 mM) was dissolved. The mixtures were allowed to equilibrate for 48 hr in an environmental shaker[11] operated at 200 rpm. The tubes were centrifuged[12] at 2500×g for 15 min; the phases were separated, and aliquots of both phases were analyzed for griseofulvin.

Micellar Phase–Aqueous Phase Partition Coefficient (K')—A

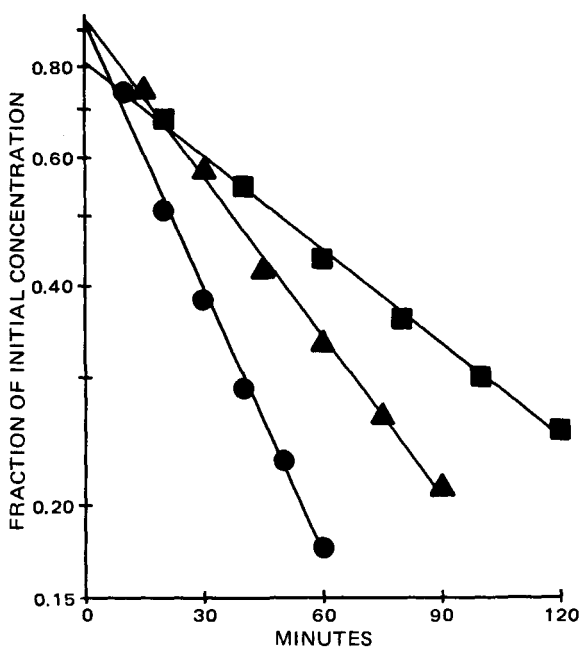

Figure 2—*Disappearance of griseofulvin from perfusate composed of aqueous phase (●), aqueous and micellar phases (▲), or aqueous, micellar, and oil phases (■). Each point represents the mean from six animals.*

[10] Syringe pump model 940, Harvard Apparatus Co.
[11] Model G24, New Brunswick Scientific Co., New Brunswick, N.J.
[12] Model CRU-5000, Damon/IEC Division, Needham Heights, Mass.

Table II—Apparent Partition Coefficients for Griseofulvin

Phases	Apparent Partition Coefficient
Triolein–aqueous[a] (K)	87.7 (9.0)[c]
Micellar[b]–aqueous (K')	65.5[d]
Triolein–micellar (K'')	1.3 (0.1)[c]

[a] Sodium taurodeoxycholate (1.2 mM) in sodium phosphate (68 mM) and sodium chloride (87 mM), pH 6.2. [b] "Mixed micelles" composed of monoolein, oleic acid, and sodium taurodeoxycholate above the CMC. [c] Mean from eight determinations; standard deviation in parentheses. [d] Each point in the line describing the solubility of griseofulvin as a function of the micellar phase fraction (Fig. 3) was the mean from eight determinations.

series of centrifuge tubes was prepared to contain griseofulvin in excess of its solubility and increasing amounts of the micellar phase in an aqueous solution of 68 mM sodium phosphate and 87 mM sodium chloride at pH 6.2. The tubes were equilibrated for 48 hr in an environmental shaker at 200 rpm. They were centrifuged at 2500×g for 15 min, and aliquots of the supernate were analyzed for griseofulvin.

The amount of the micellar phase in an aliquot was calculated by summing the amounts of monoolein, oleic acid, and sodium taurodeoxycholate in the aliquot and subtracting the amount of sodium taurodeoxycholate present as a true solution. The amount of sodium taurodeoxycholate as a true solution was calculated from the reported (23) critical micelle concentration (CMC) of 1.2 mM at 40° in isotonic sodium chloride. It was assumed that the CMC of sodium taurodeoxycholate was not appreciably affected by the inclusion of monoolein and oleic acid in the mixed micellar phase.

In each tube, the ratio of the amount of monoolein, oleic acid, and sodium taurodeoxycholate in the micellar phase was the same. For example, the intestinal perfusates contained 3 mM monoolein, 6 mM oleic acid, and 8 mM sodium taurodeoxycholate; the ratio in the micellar phase was 3:6:6.8. A solution that contained twice the concentration of the micellar phase would be 6 mM monoolein, 12 mM oleic acid, and 14.8 mM sodium taurodeoxycholate, and the ratio in the micellar phase would be 6:12:13.6.

The solubility of griseofulvin in a mixture containing micelles is the sum of the solubilities in the individual phases:

$$S = (S_w f_w) + (S_m f_m) \qquad \text{(Eq. 17)}$$

where S is the solubility in the mixture, S_w and S_m are the respective solubilities in the aqueous and micellar phases, and f_w and f_m are the fractions of the solution as the aqueous and micellar phases, respectively. With the relationships:

$$S_m = S_w K' \qquad \text{(Eq. 18)}$$

$$f_w + f_m = 1 \qquad \text{(Eq. 19)}$$

Equation 17 can be rearranged to:

$$\frac{S}{S_w} = (K' - 1) f_m + 1 \qquad \text{(Eq. 20)}$$

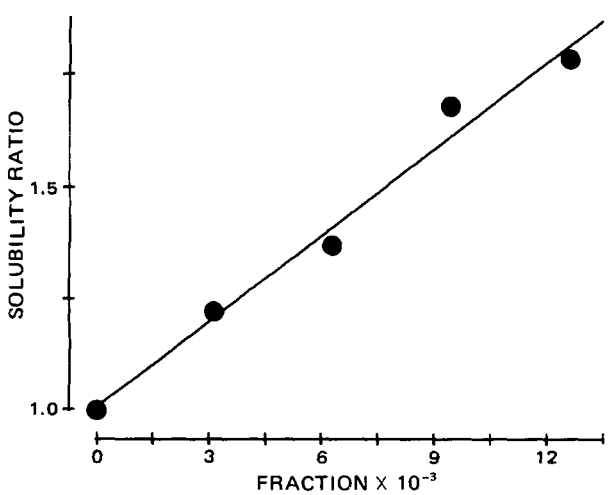

Figure 3—*Apparent solubility of griseofulvin in a mixture containing micelles as a function of the fraction (0–1.2%) of the mixture as the micellar phase. Apparent solubility is expressed as a ratio relative to the solubility of griseofulvin in the aqueous phase.*

Table III—Apparent Intestinal Clearance of Griseofulvin from a Perfusate Containing Various Phases of a Triolein Digestion Mixture[a]

Phase	Intestinal Clearance, µl/min/cm	Intestinal Clearance, % of Aqueous	Gut Length, cm	Water Flux, µl/min/cm
Aqueous[b]	9.72 (1.43)	100.0	19.8 (1.03)	0.46 (0.35)
Aqueous and micellar[c]	5.84 (1.09)[e]	60.1	20.1 (0.86)	0.54 (0.25)
Aqueous, micellar, and oil[d]	3.14 (0.70)[e,f]	32.3	19.9 (0.86)	0.21 (0.21)

[a] Mean from six experiments; standard deviation in parentheses. [b] Sodium taurodeoxycholate (1.2 mM) in sodium phosphate (68 mM) and sodium chloride (87 mM), pH 6.2. [c] Monoolein (3 mM), oleic acid (6 mM), and sodium taurodeoxycholate (8 mM) in sodium phosphate (68 mM) and sodium chloride (87 mM), pH 6.2. [d] Emulsified triolein (2 g/100 ml), monoolein (3 mM), oleic acid (6 mM), and sodium taurodeoxycholate (8 mM) in sodium phosphate. [e] Significantly different from the mean griseofulvin clearance from the aqueous perfusate alone ($p < 0.001$). [f] Significantly different from the mean griseofulvin clearance from perfusate containing the micellar phase ($p < 0.001$).

A plot of the solubility ratio, S/S_w, *versus* the micellar fraction of the mixture yielded a straight line (Fig. 3). The slope of the line gave the micellar phase–aqueous phase partition coefficient.

Triolein–Micellar Phase Partition Coefficient (K'')—A diffusion cell[13] was assembled with a cellulose dialysis membrane and filled with 5 ml of micellar solution and excess griseofulvin on one side (suspension compartment). The other side (emulsion compartment) contained 5 ml of micellar solution with 2% triolein. The membrane allowed passage of griseofulvin but not of triolein. At equilibrium, assay of the contents of the suspension compartment showed that triolein had not crossed the dialysis membrane.

The diffusion cell was equilibrated at 37° in an environmental incubator shaker for 48 hr at 200 rpm. The contents of the suspension compartment were centrifuged at 2500×g for 15 min. Aliquots from both compartments were analyzed for griseofulvin. The griseofulvin solubility attributable to triolein was determined as the difference between the concentration of dissolved griseofulvin in the two compartments. The griseofulvin concentration in triolein divided by the micellar phase concentration (calculated from the total concentration in the suspension compartment and the micellar phase–aqueous phase partition coefficient) gave the triolein–micellar phase partition coefficient.

Analytical Methods—Griseofulvin was determined in the aqueous samples by a spectrofluorometric[14] method (3, 24), which involved extraction of the drug with freshly distilled ether, evaporation of an aliquot of ether to dryness, and reconstitution of the residue with methanol–water (1:1). The methanol–water mixture was washed with hexane, and the fluorescence was determined at activation and emission wavelengths of 298 and 420 nm (uncorrected), respectively. The samples were quenched with 4 drops of concentrated sulfuric acid, and the background fluorescence was determined. The sample fluorescence minus the background fluorescence gave the griseofulvin fluorescence.

Monoolein, oleic acid, and triolein were determined in the rat gut perfusate by a slightly modified spectrophotometric[15] method (25). The lipids were extracted with chloroform and spotted on thin-layer plates[16] 0.25 mm thick. The plates were developed with petroleum ether (bp 30–60°)–ether–methanol–acetic acid (90:7:4:0.5). The lipid spots were visualized with iodine vapor, scraped into tubes, and carbonized in concentrated sulfuric acid at 200° for 45 min. The absorbance of the sulfuric acid was measured at 375 nm.

Sodium taurodeoxycholate was estimated in intestinal perfusate using a crude preparation of the enzyme 3α-hydroxysteroid dehydrogenase (EC 1.1.1.50), obtained from *Pseudomonas testosteroni* (26, 27). The reaction is NAD coupled, and the increase in absorbance at 340 nm was followed spectrophotometrically to completion. The change in absorbance was linearly related to the concentration of sodium taurodeoxycholate over the 0–2 mM range.

[13] Plexiglas; each compartment had a capacity of 10 ml which was exposed to 10 cm² of membrane.

[14] Aminco-Bowman spectrophotofluorometer, American Instrument Co., Silver Spring, Md.

[15] Beckman DU (Beckman Instruments, Fullerton, Calif.) with a Gilford model 2000 multiple-sample recorder (Gilford Instrument Laboratories, Oberlin, Ohio).

[16] Analtech, Newark, Del.

Table IV—Individual Clearance Constants for the Intestinal Absorption of Griseofulvin from Triolein Digestion Mixture

Phase	Clearance, μl/min/cm	Percent of Aqueous Phase
Aqueous	9.72	100
Micellar	-2.31×10^{-2}	−0.24
Oil	1.89×10^{-2}	0.19

RESULTS AND DISCUSSION

Griseofulvin has a slightly greater affinity for triolein than for the micellar phase (Table II). The triolein–micellar partition coefficient (K'') was 1.3 whether measured directly by dialysis or calculated as the ratio of K to K'.

The disappearance of griseofulvin from lipid digestion mixtures composed of one, two, and three phases followed apparent first-order kinetics as predicted by Eq. 15 (Fig. 2). The presence of the micellar and triolein phases reduced significantly the overall clearance of griseofulvin (Table III). The reduced clearance could not be attributed to differences in the length of intestine perfused nor to differences in the rate of water absorption from the perfusate (Table III).

The clearance constants in Table III and the partition coefficients in Table II were used with Eq. 16 to estimate the individual clearance constants for absorption from the micellar and oil phases. Since the volume of the micellar phase was not known, it was approximated by its weight. These calculations suggest that the clearance of griseofulvin from the micellar and oil phases was negligible compared to its clearance from the aqueous phase (Table IV).

For the experimental system studied, the individual clearance constants reflect the area of absorbing surface that each phase contacts and the partitioning of griseofulvin between the absorbing membrane and each phase (Eq. 4). The irregular nature of the surface, covered with villi and microvilli, makes an estimation of the effective area of the surface impossible. Furthermore, it is not possible to estimate the areas of surface contacted by the micellar and oil phases. Thus, whether the lack of absorption from the micellar and oil phases is due to negligible phase and membrane contact or to a small membrane–phase distribution coefficient is not known.

If it is arbitrarily assumed that the area each phase contacts is proportional to its phase volume ratio, the clearances from the micellar and oil phases can be calculated to be −3.70 and 0.95 μl/min/cm, respectively. These clearance values would be observed if the entire perfusate were composed solely of micelles or of oil. The large negative clearance from the micellar phase is, of course, unrealistic. It may be an artifact that results from one or more components of the micellar phase inhibiting the clearance of griseofulvin from the aqueous phase.

In summary, the oral bioavailability of griseofulvin increases when it is administered with triglycerides (1–3). This study shows that the absorption of dissolved griseofulvin by the intestine is slowed in the presence of triglyceride digestion products. The drug concentrates in the micellar and oil phases, and there is negligible absorption from these phases. Thus, the ability of triglycerides to enhance the oral absorption of griseofulvin apparently is due solely to enhanced dissolution (28) and not to enhanced absorption of dissolved drug.

REFERENCES

(1) R. G. Crounse, *J. Invest. Dermatol.*, **37**, 529 (1961).

(2) M. Kraml, J. Dubuc, and D. Beall, *Can. J. Biochem.*, **40**, 1449 (1962).

(3) P. J. Carrigan and T. R. Bates, *J. Pharm. Sci.*, **62**, 1476 (1973).

(4) S. E. Swenson, W. L. DeLorenzo, R. Engelberg, M. Spooner, and L. O. Randell, *Antibiot. Med.*, **2**, 148 (1956).

(5) D. C. Bloedow and W. L. Hayton, *J. Pharm. Sci.*, **65**, 328 (1976).

(6) R. T. Williams, "Detoxication Mechanisms," Wiley, New York, N.Y., 1959, p. 267.

(7) F. H. Mattson, R. J. Jandacek, and M. R. Webb, *J. Nutr.*, **106**, 747 (1976).

(8) P. Desnuelle, *Adv. Enzymol.*, **23**, 129 (1961).

(9) G. Benzonana, B. Entressangles, G. Marchis-Mouren, L. Pasero, L. Sarda, and P. Desnuelle, in "Metabolism and Physiological Significance of Lipids," R. M. C. Dawson and D. N. Rhoades, Eds., Wiley, London, England, 1964, p. 141.

(10) A. F. Hofmann, *Biochem. J.*, **89**, 57 (1963).

(11) A. F. Hofmann, in "Handbook of Physiology: Alimentary Canal," C. F. Code, Ed., American Physiological Society, Washington, D.C., 1968, p. 2507.

(12) J. R. Senior, *J. Lipid Res.*, **5**, 495 (1964).

(13) L. Lack and I. M. Weiner, in "The Bile Acids," vol. II, P. P. Nair and D. Kritchevsky, Eds., Plenum, New York, N.Y., 1973, p. 34.

(14) V. Surpuriya and W. I. Higuchi, *Biochim. Biophys. Acta*, **290**, 375 (1972).

(15) T. R. Bates and M. Gibaldi, in "Current Concepts in the Pharmaceutical Sciences," J. Swarbrick, Ed., Lea & Febiger, Philadelphia, Pa., 1970, pp. 83, 84.

(16) K. Kakemi, H. Sezaki, S. Muranishi, H. Ogata, and S. Isemura, *Chem. Pharm. Bull.*, **20**, 708 (1972).

(17) K. Kakemi, H. Sezaki, S. Muranishi, H. Ogata, and K. Giga, *ibid.*, **20**, 715 (1972).

(18) H. Ogata, K. Kakemi, S. Muranishi, and H. Sezaki, *ibid.*, **23**, 707 (1975).

(19) W. L. Hayton and G. Levy, *J. Pharm. Sci.*, **61**, 367 (1972).

(20) *Ibid.*, **61**, 362 (1972).

(21) J. T. Doluisio, N. F. Billups, L. W. Dittert, E. T. Sugita, and J. V. Swintosky, *J. Pharm. Sci.*, **58**, 1196 (1969).

(22) A. F. Hofmann and B. Borgstrom, *Fed. Proc.*, **21**, 43 (1962).

(23) M. C. Carey and D. M. Small, *J. Colloid Interface Sci.*, **31**, 382 (1969).

(24) V. P. Shah, S. Riegelman, and W. L. Epstein, *J. Pharm. Sci.*, **61**, 634 (1972).

(25) A. Marzo, P. Ghirardi, D. Sardini, and G. Meroni, *Clin. Chem.*, **17**, 145 (1971).

(26) R. H. Palmer, *Methods Enzymol.*, **15**, 280 (1969).

(27) G. M. Murphy, B. H. Billing, and D. N. Baron, *J. Clin. Pathol.*, **23**, 594 (1970).

(28) T. R. Bates, M. Gibaldi, and J. L. Kanig, *J. Pharm. Sci.*, **55**, 901 (1966).

ACKNOWLEDGMENTS

Abstracted from a dissertation submitted by J. A. Grisafe to Washington State University in partial fulfillment of the Doctor of Philosophy degree requirements.

Supported in part by funds provided for biological and medical research by Washington State Initiative Measure No. 171.

J. A. Grisafe is an AFPE Charles J. Lynn Memorial Fellow.

Synthesis and Quantitative Structure–Activity Relationships of Antibacterial 1-(Substituted Benzhydryl)-4-(5-nitro-2-furfurylideneamino)piperazines

D. K. YUNG *x, M. L. GILROY *, and D. E. MAHONY ‡

Received August 8, 1977, from the * *College of Pharmacy, Faculty of Health Professions, and the* ‡ *Department of Microbiology, Faculty of Medicine, Dalhousie University, Halifax, N.S., Canada.* Accepted for publication October 20, 1977.

Abstract □ 1-Benzhydryl -4- (5-nitro-2-furfurylideneamino)piperazine and 11 substituted analogs were prepared and examined for *in vitro* antimicrobial activity. The compounds were active against *Bacillus cereus* 7, *Bacillus megaterium* 122, *Bacillus subtilis* 104, *Clostridium perfringens* 13, and the tetracycline-resistant *Clostridium perfringens* 37. Regression analyses on the antibacterial activity data based on the Hansch approach, using π, π^2, and σ parameters, yielded several statistically significant correlation equations. 1-Benzhydryl-4-(5-nitro-2-furfurylideneamino)piperazine stopped the protein and DNA syntheses in *C. perfringens* 13, as indicated by precipitable radioactivity. The compound, however, showed no effect on the cell wall synthesis in the bacteria.

Keyphrases □ Piperazines, substituted—synthesized, antibacterial and antifungal activity evaluated □ Antibacterial activity—evaluated in various substituted piperazines □ Antifungal activity—evaluated in various substituted piperazines □ Structure–activity relationships—various substituted piperazines evaluated for antibacterial and antifungal activity

Previously (1), 1-benzhydryl-4-(5-nitro-2-furfurylideneamino)piperazine (I*a*) prevented the growth of *Clostridium perfringens* 28 and *Bacillus subtilis* 104. The present study was undertaken to investigate the antibacterial activity of 11 substituted analogs of I*a* (I*b*–I*l*) (Table I) and to correlate the activity with the hydrophobic (π and π^2) and electronic (σ) properties of the substituents. In addition, the effect of the compounds, as represented by I*a*, on the macromolecular and cell wall syntheses of *Clostridium perfringens* 13 was studied.

RESULTS AND DISCUSSION

Chemistry—The synthetic routes to I*a*–I*l* are outlined in Scheme I. The physical properties of I*a*–I*l* and the intermediates II*a*–II*l*, III*a*–III*l*, and IV*a*–IV*l* are summarized in Tables I–IV, respectively.

With the exception of II*a*, II*b*, and II*d*, which were obtained commercially, the substituted benzhydryl chlorides were prepared by treatment of the appropriate benzhydrols with anhydrous hydrogen chloride (2). Those required benzhydrols that were not readily available (Table V) were synthesized by either Grignard reaction of aldehydes or zinc–sodium hydroxide reduction of the corresponding benzophenones (3). 4-*tert*-Butylbenzophenone was prepared by the Friedel–Crafts ketone synthesis (4). The other benzophenones were obtained from commercial sources.

When absolute ethanol was used as the reaction solvent in early attempts to prepare III*f* and III*i*–III*l*, the desired monosubstituted piperazines were obtained in poor yields. Instead, the corresponding benzhydryl ethyl ethers (Table VI) were isolated as the major products in these reactions. In subsequent reactions with chloroform as the reaction solvent, the formation of the undesirable benzhydryl ethyl ethers was not detected. The purity of I*a*–I*l* was established by TLC (silica gel) with benzene–ethyl acetate (3:7) or benzene–acetone (4:1) as the eluant before the microbial evaluations.

The reason for the melting-point discrepancy between the previously prepared I*a* and that prepared in this study is not clear. Satisfactory spectral and analytical data were obtained for both compounds. It was postulated that geometric isomerism might have occurred. However, since the NMR spectra of the two compounds were exactly the same, the likelihood of the two compounds being a pair of *anti*- and *syn*-isomers was small.

Antimicrobial Testing—Compounds I*a*–I*l*, at a concentration of 50 μg/ml, were initially screened for antimicrobial activities against three Gram-positive bacteria, *B. subtilis* 104, *Staphylococcus pyogenes* 11, and *Streptococcus faecalis* 107; six Gram-negative bacteria, *Alcaligenes faecalis* 144, *Escherichia coli* 8, *Proteus vulgaris* 74, *Pseudomonas aeruginosa* 10145; *Salmonella thompson* 140, and *Serratia marcescens* 25; one acid fast bacterium, *Mycobacterium phlei* 111; one anaerobic Gram-positive bacterium, *C. perfringens* 13; and two fungi, *Candida albicans* 48 and *Saccharomyces cerevisiae* 53. The compounds showed activities only against *B. subtilis* 104 and *C. perfringens* 13.

The compounds were studied further to determine their minimum inhibitory concentrations (MIC) against *B. subtilis* 104 and *C. perfringens* 13 as well as *Bacillus cereus* 7, *Bacillus megaterium* 122, and the tetracycline-resistant *Clostridium perfringens* 37. The MIC values are expressed in molar concentrations as log (1/*C*) (Table VII). As a group, the compounds were more inhibitory against the *Clostridium* species than the *Bacillus* species. Compound I*g* was the least active in inhibiting the growth of all five microorganisms tested.

Dimethylformamide was used as the solvent. The effect of this solvent on the bacterial growth was studied prior to the microbiological testings, using *B. subtilis* 104, *Clostridium perfringens* 2, *E. coli* 8, and *Staphylococcus albus* 20 as the representative bacteria. Results indicated that the minimum inhibitory dilution of dimethylformamide in brain heart

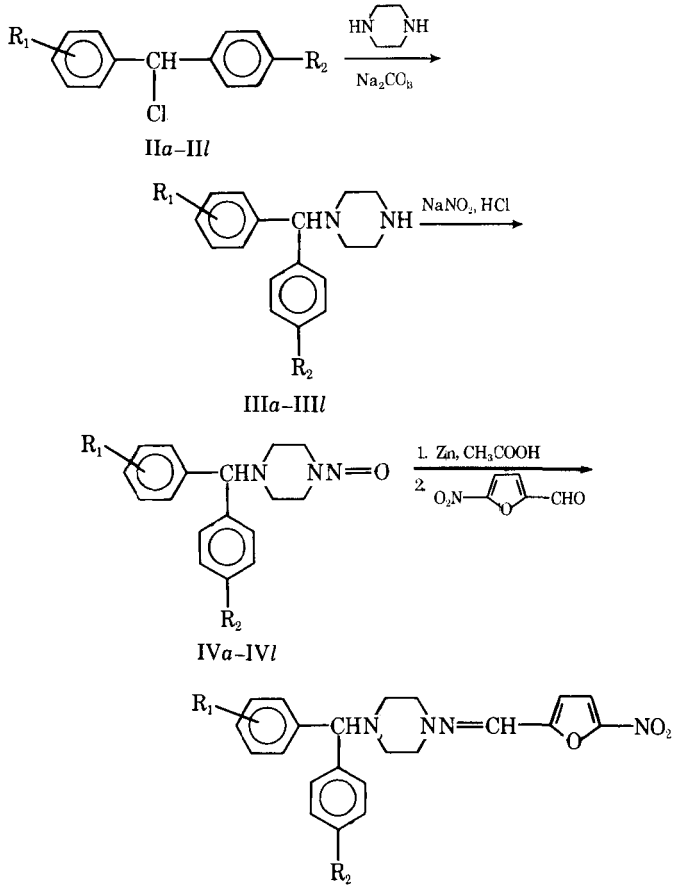

Scheme I

0022-3549/78/0700/0900$01.00/0
© 1978, American Pharmaceutical Association

Table I—1-(Substituted Benzhydryl)-4-(5-nitro-2-furfurylideneamino)piperazines

Compound	R_1	R_2	Yield, %	Melting Point	Recrystallization Solvent	Formula		Analysis, % Calc.	Found
I*a*	4-H	H	74	164.5–165.5°[a]	Ethanol	$C_{22}H_{22}N_4O_3$	C	67.67	67.78
							H	5.68	5.64
							N	14.35	14.02
I*b*	4-Cl	H	37	129–130°	Ether–petroleum ether	$C_{22}H_{21}ClN_4O_3$	C	62.19	62.15
							H	4.98	5.15
							Cl	8.34	8.35
							N	13.19	13.20
I*c*	3,4-Cl_2	H	42	120–122°	Ether–petroleum ether	$C_{22}H_{20}Cl_2N_4O_3$	C	57.52	57.79
							H	4.39	4.43
							Cl	15.44	15.44
							N	12.20	11.90
I*d*	4-Br	H	36	132–134°	Ether–petroleum ether	$C_{22}H_{21}BrN_4O_3$	C	56.30	56.20
							H	4.51	4.62
							Br	17.03	17.37
							N	11.94	11.62
I*e*	4-Cl	Cl	32	106–108°	Ether–petroleum ether	$C_{22}H_{20}Cl_2N_4O_3$	C	57.52	57.21
							H	4.39	4.89
							Cl	15.44	15.15
							N	12.20	11.77
I*f*	4-CH_3	H	30	129–131°	Petroleum ether	$C_{23}H_{24}N_4O_3$	C	68.30	68.43
							H	5.98	6.14
							N	13.85	13.50
I*g*	4-$C(CH_3)_3$	H	69	163–164°	Ethanol	$C_{26}H_{30}N_4O_3$	C	69.93	70.10
							H	6.77	6.93
							N	12.55	12.23
I*h*	3-CH_3	H	20	80–81°	Ether–petroleum ether	$C_{23}H_{24}N_4O_3$	C	68.30	67.85
							H	5.98	6.39
							N	13.85	13.58
I*i*	4-$CH(CH_3)_2$	H	25	163–163.5°	Ethanol	$C_{25}H_{28}N_4O_3$	C	69.42	69.35
							H	6.52	6.61
							N	12.95	12.83
I*j*	4-CH_3	CH_3	42	150–151°	Ethanol	$C_{24}H_{23}N_4O_3$	C	69.38	69.11
							H	5.58	5.59
							N	13.49	13.19
I*k*	2-OCH_3	H	28	130–131°	Ether–petroleum ether	$C_{23}H_{24}N_4O_4$	C	65.70	65.74
							H	5.75	6.13
							N	13.33	13.20
I*l*	4-OCH_3	H	29	129–131°	Ether–petroleum ether	$C_{23}H_{24}N_4O_4$	C	65.70	65.91
							H	5.75	5.89
							N	13.33	13.16

[a] Lit. (1) mp 147–148°.

infusion broth was 1:32. The solvent content in the subsequent test solutions was much lower than this dilution, usually below 1:256.

To ascertain that dimethylformamide does not increase the susceptibility of the bacteria, the MIC of penicillin G sodium against *C. perfringens* 2 was determined using water alone or water–dimethylformamide as the solvent. When the drug was dissolved in water, the MIC was 0.020 ± 0.007 μg/ml; in water–dimethylformamide, the MIC value was 0.016 ± 0.006 μg/ml. There was no statistically significant difference ($p < 0.05$) between the two values. On the basis of this observation, dimethylformamide was considered to be a suitable solvent and the MIC values obtained in the testings were considered a true indication of the antibacterial activities.

Regression Analysis—The relationships between the physicochemical properties and the antibacterial potency of I*a*–I*l* were analyzed by the Hansch approach. The physicochemical parameters were π, π^2, and σ. The π and σ parameter values are given in Table VII. No collinearity was found between π and σ for the compounds studied ($r^2 = 0.16$). Only those regression equations that were shown to be statistically significant ($p < 0.05$) by the F test are listed in Table VIII. The regression coefficients in these equations were found to be significant at the $p < 0.05$ level by the t-test.

In the *B. cereus* 7 system, Eq. 1 best correlated the antibacterial activity data and accounted for 60% ($r^2 = 0.60$) of the variance. For *B. megaterium* 122, the best correlation was obtained with both the π and σ

Table II—Substituted Benzhydryl Chlorides[a]

Compound	R_1	R_2	Yield, %	Melting Point or Boiling Point/mm	Formula		Analysis, % Calc.	Found
II*c*	3,4-Cl_2	H	69	134–136°/0.1	$C_{13}H_9Cl_3$	C	57.49	57.68
						H	3.34	3.59
						Cl	39.17	39.40
II*e*	4-Cl	Cl	63	160–166°/1.5[b]	$C_{13}H_9Cl_3$	—	—	—
II*f*	4-CH_3	H	81	128–132°/1.0[c]	$C_{14}H_{13}Cl$	—	—	—
II*g*	4-$C(CH_3)_3$	H	79	130–135°/0.2[d]	$C_{17}H_{19}Cl$	—	—	—
II*h*	3-CH_3	H	97	100–102°/0.1	$C_{14}H_{13}Cl$	C	77.59	77.89
						H	6.05	6.11
						Cl	16.36	16.16
II*i*	4-$CH(CH_3)_2$	H	71	118–124°/0.1	$C_{16}H_{17}Cl$	C	78.51	78.51
						H	7.00	7.03
						Cl	14.49	14.19
II*j*	4-CH_3	CH_3	94	43.5–44.5°[e]	$C_{15}H_{15}Cl$	—	—	—
II*k*	2-OCH_3	H	68	110–119°/0.1	$C_{14}H_{13}ClO$	C	72.26	72.51
						H	5.63	5.87
						Cl	15.24	15.12
II*l*	4-OCH_3	H	90	61–62°[f]	$C_{14}H_{13}ClO$	—	—	—

[a] 4-Chloro-, 4-bromo-, and benzhydryl chlorides (II*b*, II*d*, and II*a*, respectively) were obtained commercially. [b] Lit. (9) bp 189–193.5°/5 mm. [c] Lit. (4) bp 136°/0.4 mm. [d] Lit. (4) bp 158–160°/1.5 mm. [e] Lit. (3) mp 45–46°. [f] Lit. (10) mp 61°.

Table III—1-(Substituted Benzhydryl)piperazines

Compound	R_1	R_2	Yield, %	Melting Point or Boiling Point/mm	Formula		Analysis, % Calc.	Found
III*a*	4-H	H	52	160–162°	$C_{17}H_{20}N_2$	C	80.91	81.95
						H	7.99	8.05
						N	11.10	10.87
III*b*	4-Cl	H	47	190–192°/1.8	$C_{17}H_{19}ClN_2$	C	71.19	71.08
						H	6.68	6.72
						Cl	12.36	12.15
						N	9.77	9.08
III*c*	3,4-Cl_2	H	37	178–183°/0.6	$C_{17}H_{18}Cl_2N_2$	C	63.56	63.71
						H	5.65	5.80
						Cl	22.07	21.97
						N	8.72	7.95
III*d*	4-Br	H	9	174–176°/0.3	$C_{17}H_{19}BrN_2$	C	61.63	62.11
						H	5.78	5.84
						Br	24.13	23.92
						N	8.46	7.99
III*e*	4-Cl	Cl	51	110.5–111°[a,b]	$C_{17}H_{18}Cl_2N_2$	—	—	—
III*f*	4-CH_3	H	57	168–172°/1.0[c]	$C_{18}H_{22}N_2$	C	81.15	81.43
						H	8.33	8.50
						N	10.52	10.28
III*g*	4-$C(CH_3)_3$	H	74	126–128°[d]	$C_{21}H_{28}N_2$	C	81.77	81.74
						H	9.15	9.05
						N	9.08	8.85
III*h*	3-CH_3	H	53	134–136°/0.3[e]	$C_{18}H_{22}N_2$	—	—	—
III*i*	4-$CH(CH_3)_2$	H	35	186–190°/0.2	$C_{20}H_{26}N_2$	C	81.54	80.80
						H	8.90	8.63
						N	9.52	9.75
III*j*	4-CH_3	CH_3	42	92–94°[f]	$C_{19}H_{24}N_2$	C	81.38	81.69
						H	8.63	8.38
						N	9.99	9.64
III*k*	2-OCH_3	H	71	91–92°[f]	$C_{18}H_{22}N_2O$	C	76.56	76.54
						H	7.85	7.70
						N	9.92	9.28
III*l*	4-OCH_3	H	66	170–175°/0.4[g]	$C_{18}H_{22}N_2O$	—	—	—

[a] Lit. (11) mp 106°. [b] Recrystallized from ether–petroleum ether. [c] Solidified on standing, mp 75.5–77.5°. [d] Recrystallized from *n*-hexane. [e] Lit. (12) bp 150°/0.05 mm. [f] Recrystallized from petroleum ether. [g] Solidified on standing, mp 80–81°. Lit. (13) bp 185–190°/0.5 mm.

Table IV—1-(Substituted Benzhydryl)-4-nitrosopiperazines

Compound	R_1	R_2	Yield, %	Melting Point	Recrystallization Solvent	Formula		Analysis, % Calc.	Found
IV*a*	4-H	H	81	109–110°[a]	Ethanol–water	$C_{12}H_{19}N_3O$	—	—	—
IV*b*	4-Cl	H	92	120–122°	Ethanol	$C_{17}H_{18}ClN_3O$	C	64.65	64.83
							H	5.74	5.87
							Cl	11.22	11.49
							N	13.31	13.10
IV*c*	3,4-Cl_2	H	68	135–136.5°	Ethanol	$C_{12}H_{17}Cl_2N_3O$	C	58.29	57.91
							H	4.89	5.08
							Cl	20.25	20.06
							N	12.00	11.83
IV*d*	4-Br	H	73	128–129.5°	Ethanol	$C_{17}H_{18}BrN_3O$	C	56.68	56.86
							H	5.04	5.18
							Br	22.18	22.32
							N	11.66	11.64
IV*e*	4-Cl	Cl	86	157.5–158.5°	Ethanol–acetone	$C_{17}H_{17}Cl_2N_3O$	C	58.29	58.34
							H	4.89	5.22
							Cl	20.25	19.89
							N	12.00	11.58
IV*f*	4-CH_3	H	94	86–88°	Ethanol	$C_{18}H_{21}N_3O$	C	73.19	73.16
							H	7.17	7.29
							N	14.23	13.84
IV*g*	4-$C(CH_3)_3$	H	77	138–139°	Ethanol–water	$C_{21}H_{27}N_3O$	C	74.74	74.71
							H	8.07	8.05
							N	12.45	12.17
IV*h*	3-CH_3	H	76	88.5–91°	Ethanol–ether	$C_{18}H_{21}N_3O$	C	73.19	73.49
							H	7.17	7.43
							N	14.23	14.21
IV*i*	4-$CH(CH_3)_2$	H	70	88–89.5°	Ethanol–ether	$C_{20}H_{25}N_3O$	C	74.27	73.97
							H	7.79	7.78
							N	12.99	12.86
IV*j*	4-CH_3	CH_3	90	139.5–140.5°	Ethanol–water	$C_{19}H_{23}N_3O$	C	73.75	73.85
							H	7.49	7.39
							N	13.58	13.59
IV*k*	2-OCH_3	H	86	143.5–144.5°	Ethanol	$C_{18}H_{21}N_3O_2$	C	69.43	69.70
							H	6.80	6.74
							N	13.50	13.36
IV*l*	4-OCH_3	H	67	80–81°	Ether–petroleum ether	$C_{18}H_{21}N_3O_2$	C	69.43	69.07
							H	6.80	6.72
							N	13.50	13.18

[a] Lit. (14) mp 110–111°.

Table V—Substituted Benzhydrols [a]

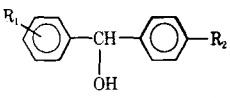

R_1	R_2	Synthetic Method [b]	Yield, %	Melting Point or Boiling Point/mm	Formula
3,4-Cl_2	H	A	65	164–166°/0.3	$C_{13}H_{10}Cl_2O$ [c]
4-Cl	Cl	B	96	91.5–93° [d]	$C_{13}H_{10}Cl_2O$
4-CH_3	H	B	91	53–54° [e]	$C_{14}H_{14}O$
4-$C(CH_3)_3$	H	B	97	79–81° [f]	$C_{17}H_{20}O$
3-CH_3	H	A	81	51–53° [g]	$C_{14}H_{14}O$
4-$CH(CH_3)_2$	H	A	62	53–56° [h]	$C_{16}H_{18}O$
4-CH_3	CH_3	B	96	69–70° [i]	$C_{15}H_{16}O$
2-OCH_3	H	A	53	134.5–135.5° [j]	$C_{14}H_{14}O_2$
4-OCH_3	H	B	97	63–65° [k]	$C_{14}H_{14}O_2$

[a] 4-Chloro, 4-bromo-, and benzhydrols were obtained commercially. [b] A = Grignard reaction; B = zinc–sodium hydroxide reduction. [c] *Anal.*—Calc. for $C_{13}H_{10}Cl_2O$: C, 61.68; H, 3.98; Cl, 28.01. Found: C, 62.02; H, 4.06; Cl, 28.16. [d] Lit. (15) mp 93–93.5°. [e] Lit. (16) mp 53.4–54°. [f] Lit. (4) mp 82°. [g] Lit. (16) mp 54–55°. [h] Lit. (17) mp 59.5–60.5°. [i] Lit. (3) mp 71°. [j] Lit. (3) mp 139°. [k] Lit. (4) mp 59–60°.

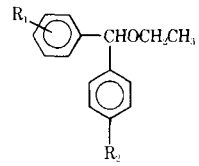

Table VI—Substituted Benzhydryl Ethyl Ethers

R_1	R_2	Yield, %	Boiling Point/mm	n_D^{25}	Formula		Analysis, % Calc.	Found
4-CH_3	H	62	106–112°/0.4	1.5484	$C_{16}H_{18}O$	C	84.91	85.21
						H	8.02	7.99
4-$CH(CH_3)_2$	H	33	123–126°/0.2	1.5414	$C_{18}H_{22}O$	C	84.99	84.81
						H	8.72	8.50
4-CH_3	CH_3	48	120°/0.5	1.5468	$C_{17}H_{20}O$	C	84.95	85.56
						H	8.39	8.48
2-OCH_3	H	96	124°/0.5	1.5559	$C_{16}H_{18}O_2$	C	79.31	79.34
						H	7.49	7.32
4-OCH_3	H	39	146–148°/1.0	1.5565	$C_{16}H_{18}O_2$	C	79.31	78.99
						H	7.49	7.81

terms as indicated by Eq. 4. This equation explained almost 80% (r^2 = 0.790) of the variation in the data. Although the π or σ term in the single-parameter equations (Eqs. 2 and 3) was significant, the r value in each of these equations was inferior to that in Eq. 4. Inclusion of π^2 in Eq. 4 did not improve the correlation coefficient.

In the *B. subtilis* 104 bacterial system, Eq. 5 gave the best correlation, although it explained only 44% (r^2 = 0.438) of the variance. Linear regression with σ was not statistically significant, the r value being only 0.183. Addition of a π^2 term to Eq. 5 did increase the r value to 0.787, but the t-test showed that both terms were not statistically justified. Thus, the electronic characteristic of the substituents, as measured by the σ term, apparently was not important for activity against *B. subtilis* 104. This result is in contrast with the other two *Bacillus* bacterial systems in which the electronic effect of the substituents played a role in the activity of the compounds.

The only equation containing a π^2 term in Table VIII is Eq. 7. This highly significant equation ($F_{2,9}$ = 18.01; $F_{2,9;\alpha=0.001}$ = 16.39) indicated that the activity of the compounds against *C. perfringens* 13 was a parabolic function of π and predicted an ideal lipophilic value (π_0) of 0.456 for this bacterial system. The fact that the single-parameter equation (Eq. 6) with a π term showed a much smaller correlation coefficient than Eq. 7 supported the existence of a parabolic relationship between the hydrophobic property and activity. Equation 8 explained slightly below 70% (r^2 = 0.693) of the variance in the antibacterial activity against *C. perfringens* 37. It can be seen from Eq. 8 that the hydrophobic and electronic natures of the substituents were significant in determining the level of activity of the compounds against this tetracycline-resistant strain of *C. perfringens*.

Effect of Ia on Macromolecular Synthesis in *C. perfringens* 13—The effect of Ia on protein and DNA syntheses in *C. perfringens* 13 is shown in Fig. 1. Based on the total incorporation of radioactive precursors of these macromolecules, as indicated by precipitable radioactivity, both protein and DNA syntheses were stopped by the compound. This cessation of syntheses occurred within 20–30 min after the addition of Ia and was probably immediate.

Effect of Ia on Cell Wall Synthesis in *C. perfringens* 13—To examine any abnormal cellular morphology that might indicate interaction of Ia with cell wall synthesis, *C. perfringens* 13 was grown in brain heart infusion broth containing 10% (w/v) sucrose. Such a medium allowed the development of spheroplasts when the bacteria were treated with penicillin (5) and bacteriocin 28 (6). No spheroplasts or abnormal cell shapes were apparent in experiments with Ia; in conjunction with isotope data

Table VII—Aromatic Substituent Constants and Antibacterial Activities [a] **(Log 1/*C*) of Ia–Il**

Compound	π [b]	σ [c]	*B. cereus* 7	*B. megaterium* 122	*B. subtilis* 104	*C. perfringens* 13	*C. perfringens* 37
Ia	0.00	0.00	6.61	5.10	5.40	6.38	6.38
Ib	0.70	0.23	6.94	4.53	5.44	6.52	6.16
Ic	1.46	0.60	6.68	4.26	4.57	6.07	6.75
Id	0.86	0.23	7.29	4.27	4.88	6.46	6.40
Ie	1.40	0.46	6.37	4.26	4.57	6.28	6.20
If	0.60	−0.17	6.62	4.81	4.81	6.62	6.32
Ig	1.98	−0.20	5.16	4.25	4.25	5.69	4.93
Ih	0.51	−0.07	6.02	4.81	5.41	6.62	6.49
Ii	1.40	−0.15	5.14	4.54	4.84	5.92	5.32
Ij	1.20	−0.34	6.33	4.82	5.12	6.15	5.73
Ik	−0.33	−0.27	6.64	4.83	5.13	6.33	5.81
Il	−0.04	−0.27	6.64	5.13	4.83	6.21	6.33

[a] These values are the average of at least three MIC determinations. [b] Reference 18. [c] Reference 19.

Table VIII—Regression Equations Generated for Ia–Il

System	Equation[a]	r	s	F
B. cereus 7	1. $\log 1/C = -0.670\ (\pm 0.461)\ \pi + 1.287\ (\pm 1.059)\ \sigma + 6.909\ (\pm 0.475)$	0.779	0.450	0.015
B. megaterium 122	2. $\log 1/C = -0.369\ (\pm 0.199)\ \pi + 4.933\ (\pm 0.210)$	0.794	0.209	0.002
	3. $\log 1/C = -0.682\ (\pm 0.578)\ \sigma + 4.637\ (\pm 0.170)$	0.639	0.264	0.025
	4. $\log 1/C = -0.304\ (\pm 0.170)\ \pi - 0.451\ (\pm 0.390)\ \sigma + 4.882\ (\pm 0.175)$	0.889	0.166	0.001
B. subtilis 104	5. $\log 1/C = -0.352\ (\pm 0.281)\ \pi + 5.223\ (\pm 0.296)$	0.662	0.294	0.019
C. perfringens 13	6. $\log 1/C = -0.249\ (\pm 0.221)\ \pi + 6.473\ (\pm 0.233)$	0.621	0.232	0.031
	7. $\log 1/C = -0.384\ (\pm 0.201)\ \pi^2 + 0.350\ (\pm 0.341)\ \pi + 6.415\ (\pm 1.456)$	0.894	0.140	0.001
C. perfringens 37	8. $\log 1/C = -0.505\ (\pm 0.330)\ \pi + 1.300\ (\pm 0.758)\ \sigma + 6.473\ (\pm 0.340)$	0.833	0.322	0.005

[a] $n = 12$.

presented, Ia apparently had no direct action on cell wall synthesis in *C. perfringens* 13.

EXPERIMENTAL[1]

4-*tert*-Butylbenzophenone—This compound was prepared in 42% yield according to the procedure of Hughes *et al.* (4), bp 146–148.5°/0.3 mm [lit. (4) bp 205°/15 mm].

Substituted Benzhydrols (Vc–Vl)—These compounds were synthesized from aldehydes by the Grignard reactions or the by zinc–sodium hydroxide reduction of benzophenones according to Morris and Blake (3).

Substituted Benzhydryl Chlorides (IIc and IIe–IIl)—A modification of the procedure reported by Bateman *et al.* (2) was followed. A solution of the appropriate benzhydrol (0.075 mole) in anhydrous benzene (150 ml), containing suspended calcium chloride (15 g), was saturated with dry hydrogen chloride by passing the gas through the solution for 75 min. The solution was then poured onto fresh calcium chloride (15 g) and saturated again with dry hydrogen chloride for another 75 min. The solution was finally filtered, and the solvent was removed *in vacuo*. The liquid-substituted benzhydryl chlorides were vacuum distilled whereas the solid chlorides were recrystallized.

1-(Substituted Benzhydryl)piperazines (IIIa–IIIl)—These compounds were prepared according to the method of Kitchen and Pollard (7), using chloroform as the reaction solvent instead of absolute ethanol.

1-(Substituted Benzhydryl)-4-nitrosopiperazines (IIIa–IIIl)—To a cold (0–5°) suspension of the appropriate 1-(substituted benzhydryl)-piperazine (0.012 mole) in hydrochloric acid [60% (v/v), 50 ml] was added an aqueous solution (20 ml) of sodium nitrite (0.024 mole), dropwise and with stirring. The reaction mixture was strongly basified with sodium hydroxide and extracted with chloroform. Removal of the solvent *in vacuo* produced yellow crystals of the nitroso compound.

1-(Substituted Benzhydryl)-4-(5-nitro-2-furfurylideneamino)-piperazines (Ia–Il)—To a solution of the appropriate 1-(substituted benzhydryl)-4-nitrosopiperazine (0.014 mole) in acetic acid (60 ml) was added zinc dust (0.07 mole), with stirring, over 20 min at 10°. After the addition was complete, stirring was continued for 1 hr at 10° and for 2 hr at 60°. The reaction mixture was filtered hot; after cooling, the filtrate was strongly basified with sodium hydroxide.

The solution was then extracted with chloroform and, after being dried over anhydrous magnesium sulfate, the chloroform extracts were evaporated *in vacuo*. The resulting residue was redissolved in ethanol (10 ml) and then refluxed, with stirring, with an ethanolic solution (10 ml) of 5-nitro-2-furaldehyde (~0.007 mole) for 30 min. Stirring was continued at room temperature for a further 30 min. The crystals were then filtered, dried, and recrystallized.

5-Nitro-2-furaldehyde—This compound was prepared by the hydrolysis of 5-nitro-2-furaldehyde diacetate (0.007 mole) in sulfuric acid [7% (v/v), 30 ml]. The solution was refluxed with stirring for 1 hr and then poured onto ice. The crude aldehyde thus obtained melted at 32–35° [lit. (8) mp 32–36°] and was used without further purification. 5-Nitro-2-furaldehyde diacetate was purchased commercially.

Antimicrobial Studies[2]—The methods of preparing the microorganisms for evaluation and determining the MIC's of the compounds were described previously (1).

Effect of Ia on Macromolecular Synthesis in *C. perfringens* 13—Protein and DNA syntheses in *C. perfringens* 13 were measured by the incorporation of radioactive precursors of the respective macromolecules, ^{14}C-protein hydrolysate and ^{3}H-thymidine[3]. Labeled protein hydrolysate and thymidine were added to brain heart infusion broth, separately, to obtain final activities of 0.3 μCi/ml. This broth was distributed in 10-ml volumes into sterile test tubes and boiled for 10 min to drive off dissolved oxygen. The cooled tubes were then inoculated with a 1:10 dilution of a 3-hr culture of *C. perfringens* 13 (0.5 ml).

After 60 min of incubation at 37°, broth containing 50 μg of Ia/ml (2 ml) was added to one-half of the culture tubes; the other half received broth only (2 ml) as control cultures. Incubation continued, and a pair of treated and control tubes was removed from the water bath at various times for assay of precipitable radioactivity.

Aliquots of 3 ml of each culture were precipitated with cold trichloroacetic acid [10% (w/v), 3 ml] for 15 min. The precipitate was collected on 2.4-cm glass fiber filter papers and washed five times with cold trichloroacetic acid (5% w/v) and once with ether. The filters were dried, placed in scintillation fluid[4] [2,5-bis[2-(5-*tert*-butylbenzoxazoyl)]thiophene in toluene, 0.4% (w/v), 15 ml], and counted for two 1-min intervals by a liquid scintillation counter[5].

Effect of Ia on Cell Wall Synthesis in *C. perfringens* 13—A 1:10 dilution of a 3-hr culture of the bacteria (0.5 ml) was added to four sterile test tubes containing brain heart infusion broth with sucrose [10% (w/v), 10 ml] that had been boiled for 10 min and cooled. After 60 min of incubation at 37°, 2 ml of Ia in the same broth was added to three of the four tubes, giving final concentrations of 8.3, 4.2, and 1.0 μg/ml. The last tube received the same volume of broth but with no Ia. Samples were

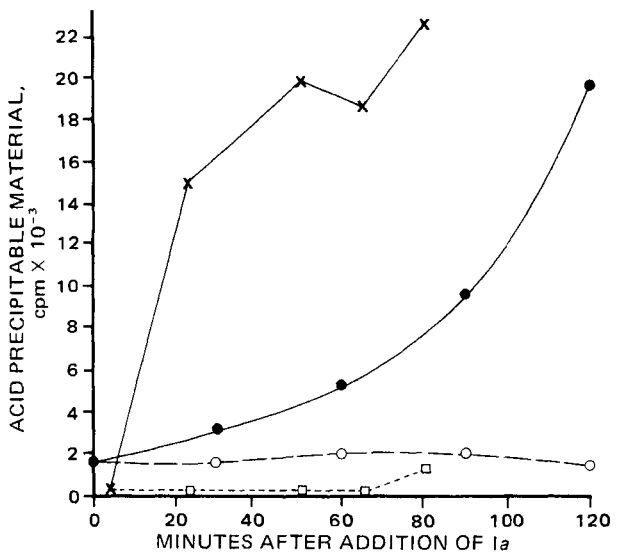

Figure 1—*Effect of Ia on protein and DNA syntheses in* C. perfringens *13 as measured by total uptake of ^{14}C-protein hydrolysate and ^{3}H-thymidine, respectively. Compound was added after 60 min of bacterial growth. Key:* ●, *protein control;* ○, *protein plus Ia;* ×, *DNA control; and* □, *DNA plus Ia.*

[1] Melting points were determined on a Thomas–Hoover capillary melting-point apparatus and are uncorrected. Boiling points are also uncorrected. Elemental analyses were performed by Robertson Laboratory, Florham Park, N.J. IR spectra were recorded on a Perkin-Elmer model 237B spectrophotometer in potassium bromide. A Varian model T-60 spectrometer was used to record the NMR spectra, with deuterated chloroform as the solvent and tetramethylsilane as the internal reference. IR and NMR spectra were in agreement with the assigned structures.

[2] The microorganisms were from the stock culture collections of the Department of Microbiology, Faculty of Medicine, Dalhousie University, Halifax, Nova Scotia.

[3] New England Nuclear.

[4] Packard Instrument Co.

[5] Nuclear Chicago Mark I.

removed from each tube over 2 hr and examined by phase contrast microscopy at a magnification of 1000× for spheroplasts or abnormal cell shapes.

Regression Analysis of Antibacterial Activities—This analysis was carried out by the method of least squares[6].

REFERENCES

(1) D. K. Yung, D. E. Mahony, and L. W. Whitehouse, *J. Pharm. Sci.*, **60**, 386 (1971).

(2) L. C. Bateman, E. D. Hughes, and C. K. Ingold, *J. Chem. Soc.*, **1940**, 1014.

(3) J. F. Morris and J. T. Blake, *J. Am. Chem. Soc.*, **50**, 1811 (1928).

(4) E. D. Hughes, C. K. Ingold, and N. A. Taher, *J. Chem. Soc.*, **1940**, 949.

(5) D. E. Mahony and T. I. Moore, *Can. J. Microbiol.*, **22**, 953 (1976).

(6) D. E. Mahony, M. E. Butler, and R. G. Lewis, *ibid.*, **17**, 1435 (1971).

(7) L. J. Kitchen and C. B. Pollard, *J. Org. Chem.*, **8**, 338 (1943).

(8) P. M. Kochergin and G. A. Karpov, *Khim. Farm. Zh.*, **1967**, 9; through *Pharm. Chem. J.*, **1967**, 8.

(9) W. E. Craig and E. F. Riener, U.S. pat. 2,783,284 (1957); through *Chem. Abstr.*, **51**, 13927b (1957).

(10) J. G. Burr, Jr., and L. S. Ciereszko, *J. Am. Chem. Soc.*, **74**, 5426 (1952).

(11) H. G. Morren, British pat. 817,231 (1959); through *Chem. Abstr.*, **54**, 9970e (1960).

(12) H. G. Morren, Belgium pat. 544,751 (1956); through *Chem. Abstr.*, **54**, 12167c (1960).

(13) H. G. Morren, S. Trolin, R. Denayer, E. Grivsky, and J. Baricq, *Bull. Soc. Chim. Belg.*, **60**, 282 (1951); through *Chem. Abstr.*, **46**, 8661a (1952).

(14) J. W. Cusic and P. Yonan, U.S. pat. 3,265,687 (1966); through *Chem. Abstr.*, **65**, 13764d (1966).

(15) S. Nishida, *J. Org. Chem.*, **32**, 2692 (1967).

(16) V. J. Skiner, Jr., and C. J. Verbanic, *J. Am. Chem. Soc.*, **79**, 369 (1957).

(17) Abbott Laboratories, British pat. 752,332 (1956); through *Chem. Abstr.*, **51**, 5847a (1957).

(18) A. Leo, C. Hansch, and D. Elkins, *Chem. Rev.*, **71**, 525 (1971).

(19) C. Hansch, A. Leo, S. H. Unger, K. H. Kim, D. Nikaitani, and E. J. Lien, *J. Med. Chem.*, **16**, 1207 (1973).

[6] Using the Statistical Package for the Social Sciences, version 600, and the CDC 6400 computer at the Dalhousie University Computer Centre.

ACKNOWLEDGMENTS

Presented at the 37th International Congress of Pharmaceutical Sciences, The Hague, The Netherlands, September 1977.

Supported by Grant MA-5669 from the Medical Research Council of Canada.

The assistance of Miss A. R. Manzer in preparing some intermediates in the chemical synthesis is gratefully acknowledged.

Ball Milling as a Measure of Crushing Strength of Granules

ASHOK MEHTA, M. A. ZOGLIO ˣ, and J. T. CARSTENSEN *

Received April 15, 1977, from *Merrell-National Laboratories, Cincinnati, OH 45215.* Accepted for publication October 5, 1977. *Present address: School of Pharmacy, University of Wisconsin, Madison, WI 53716.

Abstract □ When granules are milled in a ball mill, the size decrease follows a modification of Kick's law. The Briggsian decay constant, here denoted as the attritional crushing strength, shows correlation with the Harwood–Pilpel crushing strength. Both crushing strengths show a correlation with the amount of granulating agent (povidone) added to the granulation, *i.e.*, the more povidone added, the harder the granule.

Keyphrases □ Granules—ball milling as a measure of crushing strength □ Hardness, granule—ball milling as a measure of crushing strength

The measurement of granule hardness is an important parameter in pharmacy research and quality control. In the simplest method, that of Harwood and Pilpel (1, 2), a granule is placed on a supported plane surface and then brought in contact with the flat bottom of a balance pan. Metal shot is placed in the pan until the granule breaks, and the weight of the shot is then determined. This weight is denoted as the crushing strength of the granule.

It was shown previously (3, 4) that the crushing strength obtained by the Harwood–Pilpel method, when used on granules, requires the averaging of many granules because the observed crushing strength is a function of the way in which the granule is positioned under the pan. The method is fully functional once this fact is realized. An average of 20 measurements suffices for good characterization but is somewhat time consuming. Another disadvantage of the Harwood–Pilpel method is that the crushing strength of granules finer than 40 mesh is difficult (impossible) to measure.

Therefore, an alternative method, equally convenient but applicable to all particle sizes, is desirable. This paper describes such a procedure and shows the correlation between it and the method of Harwood and Pilpel (1) for povidone granulations. Its applicability to other granulations (exemplified by a gelatin granulation) is also discussed.

EXPERIMENTAL

A 6.7-cm i.d. × 13.5-cm long ball mill[1] was used. Granulations were made of the compositions shown in Table I; the povidone was added in a 2-propanol solution to a lactose and corn starch mixture. The dried granules were sized, and the 14/20-mesh fraction was used for further study. Granule hardness was determined by the method of Harwood and Pilpel (1, 3, 4). The lactose used had a particle size of 10–20 μm.

In addition, the following method of determining the crushing strength

[1] Fisher Scientific, Pittsburgh, PA 15219.

0022-3549/78/0700/0905$01.00/0

© 1978, American Pharmaceutical Association

removed from each tube over 2 hr and examined by phase contrast microscopy at a magnification of 1000× for spheroplasts or abnormal cell shapes.

Regression Analysis of Antibacterial Activities—This analysis was carried out by the method of least squares[6].

REFERENCES

(1) D. K. Yung, D. E. Mahony, and L. W. Whitehouse, *J. Pharm. Sci.*, **60**, 386 (1971).

(2) L. C. Bateman, E. D. Hughes, and C. K. Ingold, *J. Chem. Soc.*, **1940**, 1014.

(3) J. F. Morris and J. T. Blake, *J. Am. Chem. Soc.*, **50**, 1811 (1928).

(4) E. D. Hughes, C. K. Ingold, and N. A. Taher, *J. Chem. Soc.*, **1940**, 949.

(5) D. E. Mahony and T. I. Moore, *Can. J. Microbiol.*, **22**, 953 (1976).

(6) D. E. Mahony, M. E. Butler, and R. G. Lewis, *ibid.*, **17**, 1435 (1971).

(7) L. J. Kitchen and C. B. Pollard, *J. Org. Chem.*, **8**, 338 (1943).

(8) P. M. Kochergin and G. A. Karpov, *Khim. Farm. Zh.*, **1967**, 9; through *Pharm. Chem. J.*, **1967**, 8.

(9) W. E. Craig and E. F. Riener, U.S. pat. 2,783,284 (1957); through *Chem. Abstr.*, **51**, 13927b (1957).

(10) J. G. Burr, Jr., and L. S. Ciereszko, *J. Am. Chem. Soc.*, **74**, 5426 (1952).

(11) H. G. Morren, British pat. 817,231 (1959); through *Chem. Abstr.*, **54**, 9970e (1960).

(12) H. G. Morren, Belgium pat. 544,751 (1956); through *Chem. Abstr.*, **54**, 12167c (1960).

(13) H. G. Morren, S. Trolin, R. Denayer, E. Grivsky, and J. Baricq, *Bull. Soc. Chim. Belg.*, **60**, 282 (1951); through *Chem. Abstr.*, **46**, 8661a (1952).

(14) J. W. Cusic and P. Yonan, U.S. pat. 3,265,687 (1966); through *Chem. Abstr.*, **65**, 13764d (1966).

(15) S. Nishida, *J. Org. Chem.*, **32**, 2692 (1967).

(16) V. J. Skiner, Jr., and C. J. Verbanic, *J. Am. Chem. Soc.*, **79**, 369 (1957).

(17) Abbott Laboratories, British pat. 752,332 (1956); through *Chem. Abstr.*, **51**, 5847a (1957).

(18) A. Leo, C. Hansch, and D. Elkins, *Chem. Rev.*, **71**, 525 (1971).

(19) C. Hansch, A. Leo, S. H. Unger, K. H. Kim, D. Nikaitani, and E. J. Lien, *J. Med. Chem.*, **16**, 1207 (1973).

[6] Using the Statistical Package for the Social Sciences, version 600, and the CDC 6400 computer at the Dalhousie University Computer Centre.

ACKNOWLEDGMENTS

Presented at the 37th International Congress of Pharmaceutical Sciences, The Hague, The Netherlands, September 1977.

Supported by Grant MA-5669 from the Medical Research Council of Canada.

The assistance of Miss A. R. Manzer in preparing some intermediates in the chemical synthesis is gratefully acknowledged.

Ball Milling as a Measure of Crushing Strength of Granules

ASHOK MEHTA, M. A. ZOGLIO ˣ, and J. T. CARSTENSEN *

Received April 15, 1977, from *Merrell-National Laboratories, Cincinnati, OH 45215.* Accepted for publication October 5, 1977. *Present address: School of Pharmacy, University of Wisconsin, Madison, WI 53716.

Abstract □ When granules are milled in a ball mill, the size decrease follows a modification of Kick's law. The Briggsian decay constant, here denoted as the attritional crushing strength, shows correlation with the Harwood–Pilpel crushing strength. Both crushing strengths show a correlation with the amount of granulating agent (povidone) added to the granulation, *i.e.*, the more povidone added, the harder the granule.

Keyphrases □ Granules—ball milling as a measure of crushing strength □ Hardness, granule—ball milling as a measure of crushing strength

The measurement of granule hardness is an important parameter in pharmacy research and quality control. In the simplest method, that of Harwood and Pilpel (1, 2), a granule is placed on a supported plane surface and then brought in contact with the flat bottom of a balance pan. Metal shot is placed in the pan until the granule breaks, and the weight of the shot is then determined. This weight is denoted as the crushing strength of the granule.

It was shown previously (3, 4) that the crushing strength obtained by the Harwood–Pilpel method, when used on granules, requires the averaging of many granules because the observed crushing strength is a function of the way in which the granule is positioned under the pan. The method is fully functional once this fact is realized. An average of 20 measurements suffices for good characterization but is somewhat time consuming. Another disadvantage of the Harwood–Pilpel method is that the crushing strength of granules finer than 40 mesh is difficult (impossible) to measure.

Therefore, an alternative method, equally convenient but applicable to all particle sizes, is desirable. This paper describes such a procedure and shows the correlation between it and the method of Harwood and Pilpel (1) for povidone granulations. Its applicability to other granulations (exemplified by a gelatin granulation) is also discussed.

EXPERIMENTAL

A 6.7-cm i.d. × 13.5-cm long ball mill[1] was used. Granulations were made of the compositions shown in Table I; the povidone was added in a 2-propanol solution to a lactose and corn starch mixture. The dried granules were sized, and the 14/20-mesh fraction was used for further study. Granule hardness was determined by the method of Harwood and Pilpel (1, 3, 4). The lactose used had a particle size of 10–20 μm.

In addition, the following method of determining the crushing strength

[1] Fisher Scientific, Pittsburgh, PA 15219.

0022-3549/78/0700/0905$01.00/0

© 1978, American Pharmaceutical Association

Table I—Formulas of the Granulations Used for Crushing Strength Studies

Component	Formula I	II	III	IV	V	VI	VII	VIII
Lactose USP	1.75 kg	1.75 kg	1.75 kg	1.75 kg	1.75 kg	1.75 kg	1.75 kg	1.75 kg
Corn starch USP	0.75 kg	0.75 kg	0.75 kg	0.75 kg	0.75 kg	0.75 kg	0.75 kg	0.75 kg
Povidone K29-32[a]	25 g	37.5 g	50 g	62.5 g	75 g	87.5 g	100 g	—
2-Propanol	275 ml	262.5 ml	250 ml	237.5 ml	225 ml	212.5 ml	300 ml	—
Gelatin	—	—	—	—	—	—	—	30 g

[a] General Aniline and Film Corp., New York, NY 10020.

of the granules was used. A weight (w) of 60 g of granules of the 14/20-mesh fraction was charged into the cylinder of the described ball mill. One hundred steel balls, 0.53 cm in diameter, and weighing 0.993 g each, were charged into the cylinder, which was then closed. The ball mill was operated at 120 rpm for a certain time (t min). The material was then sieved, and the amount retained on a 20-mesh screen (w_a g) was determined.

Sieve analysis was performed on the minus 20-mesh fraction (40, 60, 80, and 100 mesh). The weight mean diameter, d_b, of the material passing the 20-mesh screen was determined (by methods described later). Ball milling of a 20/40-mesh cut was also carried out; in this case, a 40-mesh sieve was used to determine w_a.

RESULTS AND DISCUSSION

Kick's law (5, 6) states that the energy, E, expended in milling a material of particle size d' cm into a material of particle size d'' cm is given by:

$$E = -C \ln(d''/d') \qquad \text{(Eq. 1)}$$

where C is a constant particular to the milled material. In the present study, milling was performed on either a 14/20-mesh granule, *i.e.*, a granule with the mean diameter $d_a = 1135$ μm, or a 20/40-mesh granule, *i.e.*, a granule with mean diameter $d_a = 638$ μm. Ball milling produced a fine powder, *i.e.*, a powder passing a 20-mesh screen (when 14/20-mesh granules were milled) or a 40-mesh screen (when 20/40-mesh granules were milled), with a mean weight diameter, d_b, that changed little with time.

If w g of material is milled for t min and it then is determined that w_a g of material of original size remains and that $w_b = w - w_a$ g of fine material has been produced, then:

$$d_a = d' \qquad \text{(Eq. 2)}$$

and:

$$d'' = \frac{(w_a d_a + w_b d_b)}{w} \qquad \text{(Eq. 3)}$$

The energy input is proportional to t, *i.e.*:

$$E = qt \qquad \text{(Eq. 4)}$$

Combining Eqs. 1–4 then gives:

$$\ln\left\{\frac{w_a}{w} + \frac{d_b w_b}{d_a w}\right\} = -kt \qquad \text{(Eq. 5)}$$

where:

$$k = q/C \qquad \text{(Eq. 6)}$$

with k in units of minutes^{-1}. To evaluate k, it is necessary to determine w_a and d_b. Therefore, it is necessary to perform a sieve analysis of the material passing through the 20- (or 40-) mesh sieve at each time point, t.

Table II—Sieve Analysis Data for Formula II (14/20 Mesh) Milled for 2 min

Mesh	Sieve Opening, μm	Amount on Mesh, g	Fraction
20	840	64	0.54
40	420	34	
60	250	3	
80	177	1	0.46
100	149	1	
Pan	0	16	

The data treatment of the results from the four granulations where both 14/20- and 20/40-mesh sieve fractions were studied are listed in Tables II–IV. The sieve analysis data will typically appear as shown in Table II. The parameters of importance are w_a/w, which is the fraction remaining on a 20-mesh screen when a 14/20-mesh granulation is milled (and a 40-mesh sieve when a 20/40-mesh granulation is milled). The value of w_b/w is obtained directly as $1 - (w_a/w)$. The mean particle diameter, d_b, of the fine fraction is obtained by converting the data as they appear in Table II to a fraction smaller than the mean sieve diameter (M μm) and then converting these latter values to normalized standard deviates (τ). A complete set of data of this type corresponding to Formula II, 14/20 mesh, is given in Table III. The columns headed "2 min" in Table III correspond to the data in Table II.

The appropriate fit of the data is log normal (5, 6). Data from other types of fitting are not shown, but it is apparent from the graphical presentation of the results in Fig. 1, as well as from the good correlation coefficients (r^2) shown in Table III, that the data adhere to:

$$\tau = a + b \ln M \qquad \text{(Eq. 7)}$$

where a and b are intercepts and slopes of the log-normal plot. The mean diameter, d_b, is then obtained by equating τ with zero, *i.e.*:

$$\ln d_b = -a/b \qquad \text{(Eq. 8)}$$

The least-squares fit data by this treatment are shown in Table III. Since d_b is (fairly) invariant with time, the data were pooled and the least-squares parameters were obtained for each formula. For Formula II, 14/20 mesh, these parameters are:

$$\tau = 4.0462 - 0.6822 \ln M \qquad r^2 = 0.91 \qquad \text{(Eq. 9)}$$

$$d_b = 376 \pm 6\ \mu\text{m} \qquad \text{(Eq. 10)}$$

The 95% confidence limits for d_b are narrow because the interpolation is close to the average τ value and this proximity is statistically optimum. Table IV lists the d_b values obtained from the four granulations (II, IV, VI, and VIII). In practice, it is time consuming to perform a complete sieve analysis and large sample sizes are required. In actuality, a complete sieve analysis is not necessary. If only w_a is recorded, one can, by iterative procedures, obtain d_b. An example of this approach is shown in Fig. 2, where the data from Formula I are treated according to Eq. 5 by inserting consecutive values of d_b. Underestimation of d_b gives curvature toward the abscissa, and overestimation gives curvature away from the abscissa. Values of k obtained this way or by inserting experimental d_b values in Eq. 5 are shown in Table V.

Ideally, the plots adhering to Eq. 5 should have intercepts of zero and correlation coefficients of $r^2 = 1$. Table V shows the correlation coefficients significant at the 95 or 99% confidence level and intercepts that do not differ significantly ($\alpha = 0.05$) from zero.

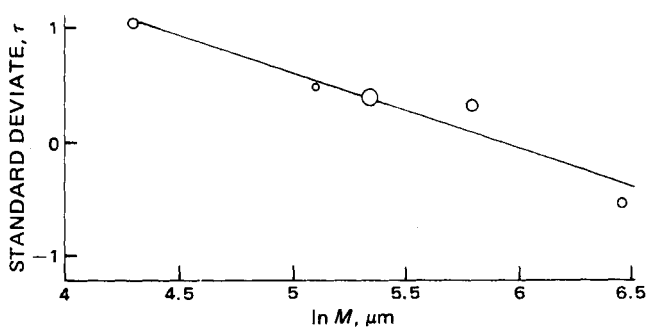

Figure 1—*Log-normal plot of fine fraction from Formula II (14/20 mesh). Each point represents the average of four time points, and the size of the circle represents the range of* t *values it represents.*

Table III—Sieve Analysis as a Function of Time for Formula II [a] (14/20 Mesh)

Mesh Mean, M, μm	Cumulative Fraction below M				τ-Values from Cumulative Fraction Smaller than M			
	2 min	4 min	6 min	8 min	2 min	4 min	6 min	8 min
630	0.69	0.70	0.71	0.72	−0.50	−0.52	−0.56	−0.57
335	0.35	0.37	0.39	0.40	0.37	0.33	0.28	0.38
213	0.32	0.33	0.34	0.35	0.47	0.44	0.40	0.35
163	0.30	0.31	0.32	0.32	0.52	0.50	0.48	0.48
	0.14	0.15	0.15	0.15	1.06	1.05	1.03	1.04
				r^2	0.91	0.92	0.93	0.89
				a	4.03	4.04	4.07	4.04
				b	−0.67	−0.68	−0.69	−0.68
				$\ln d_b$	5.99	5.95	5.89	5.91
				d_b, μm	398	382	360	368

[a] Formula II was studied for 8 min only since only 4% was left on the 20-mesh screen after 8 min.

Table IV—Particle-Size Statistics for Four Granulations

Formula	Povidone, g	Original Mesh Fraction	r^2	a	b	d_b, μm[a]	d_a, μm
II	37.5	14/20	0.91	4.05	−0.68	376 ± 6	1135
IV	62.5	14/20	0.89	4.42	−0.71	507 ± 10	1135
VI	87.5	14/20	0.92	5.03	−0.80	527 ± 7	1135
VIII	Gelatin	14/20	0.95	5.84	−0.93	524 ± 10	1135
II	37.5	20/40	0.95	5.28	−1.00	198 ± 5	630
IV	62.5	20/40	0.92	5.33	−0.98	226 ± 10	630
VI	87.5	20/40	0.90	5.62	−1.07	247 ± 4	630
VIII	Gelatin	20/40	0.91	6.07	−1.08	271 ± 8	630

[a] The 95% confidence limits on the interpolated value for = 0 (see text).

Table V—Attrition Constants and Harwood–Pilpel Crushing Strengths

Formula	Povidone, g	d_a[a], μm	d_b[b], μm	k, min^{-1}	Intercept	r^2	ln Q, g/mg
I	25	1135	100 (250)	(0.195)	−0.002	0.994	4.98
II	37.5	1135	376	0.150	−0.008	0.942	4.90
III	50	1135	470 (450)	(0.087)	0.020	0.997	5.48
IV	62.5	1135	507	0.061	−0.040	0.974	5.50
V	75	1135	540 (500)	(0.060)	0.030	0.990	5.69
VI	87.5	1135	527	0.046	−0.021	0.981	5.72
VII	100	1135	530 (550)	(0.046)	−0.012	0.997	5.94
VIII	Gelatin	1135	524	0.19	−0.007	0.955	6.40
II	37.5	630	198	0.132	−0.069	0.999	
IV	62.5	630	226	0.073	0.048	0.993	
VI	87.5	630	247	0.042	0.031	0.991	
VIII	Gelatin	630	27	0.014	−0.020	0.996	

[a] The 1135 implies that 14/20 material was used; 630 implies that 20/40-mesh material was used. [b] Figures in parentheses imply that the values were obtained through iteration or from iterated values.

The data in Table V are shown graphically in Fig. 3, where Harwood–Pilpel crushing strengths, Q (in grams per milligram), are plotted *versus* attrition constants (in minutes^{-1}) on a ln–ln scale. The data give a least-squares relation of:

$$\ln Q = -0.652 \ln k + 3.808 \qquad \text{(Eq. 11)}$$

with a correlation coefficient of $r^2 = 0.96$, significant for $N = 8$ at the 95% level. Therefore, there is a correlation between Harwood–Pilpel crushing strength and attrition coefficients for at least two granulations, and it is presumably feasible to substitute one for the other as a granule "hardness" test. The advantage of the attrition constant is its lower variance (coefficient of variation of 1–5%) vis-a-vis that of the crushing strength (coefficient of variation of 50–80%).

The practical utility of this correlation is that, if a laboratory has a ball mill, k of a particular mesh is a measure of the crushing strength of the

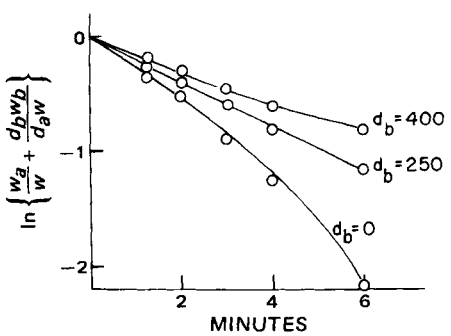

Figure 2—*Estimation of* d_b *via iterative procedure and Eq. 5. Key: lower curve, estimate of* $d_b = 0$*; upper curve, estimate of* $d_b = 400$ *μm; and middle (linear) curve, estimate of* $d_b = 250$ *μm.*

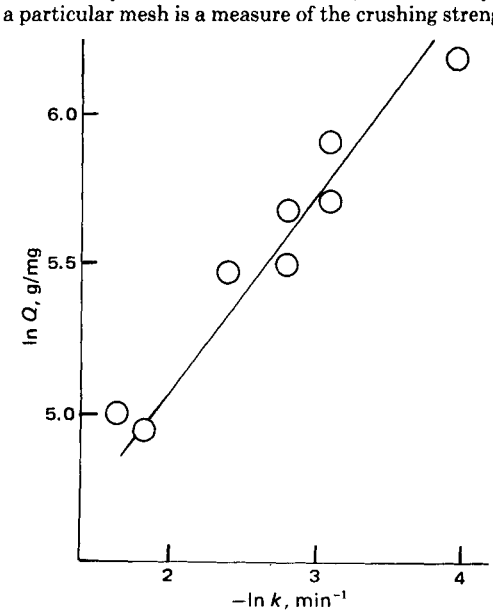

Figure 3—*Correlation between −ln* k *and ln* Q.

granulation and can be used as a process parameter to evaluate batch-to-batch as well as formula-to-formula variation. If this procedure is followed, it is worthwhile at one time (only) to correlate the k values to the Q values for a particular sieve fraction of a particular granulation using the equipment (ball mill, rotations per minute, and steel spheres) desired for the testing.

REFERENCES

(1) C. F. Harwood and N. Pipel, *J. Pharm. Sci.*, **57**, 478 (1968).

(2) J. T. Carstensen, "Theory of Pharmaceutical Systems, II—Heterogeneous Systems," Wiley, New York, N.Y., 1973.

(3) M. A. Zoglio, H. E. Huber, G. Koehne, P. Chan, and J. T. Carstensen, *J. Pharm. Sci.*, **65**, 1205 (1976).

(4) J. T. Carstensen, T. Lai, D. W. Flickner, H. E. Huber,and M. A. Zoglio, *ibid.*, **65**, 992 (1976).

(5) G. Steiner, M. Patel, and J. T. Carstensen, *ibid.*, **63**, 1395 (1974).

(6) E. Parrott, in "The Theory and Practice of Industrial Pharmacy," L. Lachman, H. A. Lieberman, and J. L. Kanig, Eds., Lea & Febiger, Philadelphia, Pa., 1970, p. 102.

General Treatment of Competitive Binding of Small Molecules to Macromolecules as Applied to Dynamic Dialysis: Theoretical Analysis

PETER VENG PEDERSEN

Received June 24, 1977, from the *Department of Pharmacy, University of California, San Francisco, CA 94143.* Accepted for publication October 19, 1977.

Abstract □ A mathematical analysis of the dynamic dialysis process is presented, demonstrating how the process can be applied generally to study competitive and noncompetitive binding between small molecules and macromolecules. A law of mass action model for competitive binding with independent sites and classes with equivalent sites (CIE) is considered as a specific case without loss of generality. The escape profiles of two compounds are calculated to illustrate the effect of an increasing degree of binding competition. Noisy data are generated using the CIE model to test the presented method of estimating competitive binding parameters. The parameters estimated by the nonlinear regression technique came close to the true values, considering the degree of noise added to the exact dialysis data. A transformation approach is presented, enabling initial estimates of the binding parameters in the CIE model to be determined by multiple linear regression, thereby eliminating the main problem in the nonlinear estimation. The presented method of analysis is extended to strongly bound compounds, which also bind significantly to the dialysis membrane.

Keyphrases □ Dynamic dialysis—mathematical analysis, competitive binding of small molecules to macromolecules studied □ Models, mathematical—law of mass action for competitive binding with independent sites and classes with equivalent sites □ Binding, competitive—small molecules to macromolecules, mathematical analysis of dynamic dialysis process

Dynamic dialysis has proven valuable for characterizing interactions of small molecules with macromolecules such as drugs and proteins (1–11). Experimentally, it appears to be the simplest and most convenient method available for determining a complete binding profile (3), and its accuracy seems to be as good as equilibrium dialysis and ultrafiltration methods (3). The main disadvantages of dynamic dialysis are the inaccuracy introduced by the classical data treatment (9, 12), which requires differentiation of discrete data (3), and its limitation to molecules that do not bind or adsorb significantly to the dialysis membrane. However, both disadvantages recently were eliminated by a new approach in the data treatment (12).

This paper presents a mathematical analysis that enables the dynamic dialysis process to be extended to the study of competitive binding between small molecules and macromolecules considering any mathematical model for such interaction.

THEORY

To illustrate the general approach, it is appropriate to consider a law of mass action model with competitive binding, independent sites, and equivalence between sites in the binding classes having multiple sites:

$$\bar{\nu}_i = \sum_{j=1}^{N} n_j k_{ij} c_i \left[1 + \sum_{m=1}^{M} k_{mj} c_m\right]^{-1} \qquad \begin{matrix} i = 1, 2, \ldots, M \\ k_{ij} \geq 0 \end{matrix} \qquad \text{(Eq. 1)}$$

This model will be denoted the general CIE model, where $\bar{\nu}_i$ is the number of moles of the ith small molecules ("ligand") bound per mole of macromolecule, n_j is the number of equivalent binding sites in the jth class of sites, k_{ij} is the association constant for the ith compound's binding to the jth binding class, c_i is the free concentration of the ith compound, N is the number of binding classes, and M is the number of compounds competing in their binding to the macromolecule. Most frequently, $M = 2$. If $M = 1$, the CIE model reduces to the general (IE) model, dealing with the binding of one compound (12).

Cases where the compounds compete in their binding to certain, but not all, of the binding classes also are considered in the CIE model by allowing the association constants to take zero values (*i.e.*, $k_{ij} \geq 0$). For example, Compound 1 may bind to two classes of sites, and Compound 2 may bind to two classes. If the two compounds only compete in their binding for one class (*e.g.*, class two for Compound 1 is the same as class one for Compound 2), this situation is described by $k_{11} > 0$, $k_{12} > 0$, $k_{13} = 0$, $k_{21} = 0$, $k_{22} > 0$, and $k_{23} > 0$. Thus, the actual number of classes is $N = 3$.

According to $\bar{\nu}_i = ([c_i] - c_i)/P$, where $[c_i]$ is the total (free plus bound) molar concentration of the ith compound and P is the total molar concentration of macromolecule, Eq. 1 can be written:

$$[c_i] = c_i \left\{1 + P \sum_{j=1}^{N} n_j k_{ij} \left[1 + \sum_{m=1}^{M} k_{mj} c_m\right]^{-1}\right\} \qquad \begin{matrix} i = 1, 2, \ldots, M \\ k_{ij} \geq 0 \end{matrix} \qquad \text{(Eq. 2)}$$

The dynamic process is characterized by the following relationship:

$$d[c_i]/dt = -K_i c_i \qquad \text{(Eq. 3)}$$

where K_i is the dialysis rate constant for the ith compound. Equations 2 and 3 define the kinetics of dialysis. However, the use of these equations in their present form requires differentiation of discrete data, which introduces substantial errors in the determination of the binding parameters (9, 12).

To avoid such errors, it is necessary to eliminate the variables, c_i, that cannot be measured directly by using a technique similar to that pre-

0022-3549/78/0700/0908$01.00/0

© 1978, American Pharmaceutical Association

granulation and can be used as a process parameter to evaluate batch-to-batch as well as formula-to-formula variation. If this procedure is followed, it is worthwhile at one time (only) to correlate the k values to the Q values for a particular sieve fraction of a particular granulation using the equipment (ball mill, rotations per minute, and steel spheres) desired for the testing.

REFERENCES

(1) C. F. Harwood and N. Pipel, *J. Pharm. Sci.*, **57**, 478 (1968).

(2) J. T. Carstensen, "Theory of Pharmaceutical Systems, II—Heterogeneous Systems," Wiley, New York, N.Y., 1973.

(3) M. A. Zoglio, H. E. Huber, G. Koehne, P. Chan, and J. T. Carstensen, *J. Pharm. Sci.*, **65**, 1205 (1976).

(4) J. T. Carstensen, T. Lai, D. W. Flickner, H. E. Huber,and M. A. Zoglio, *ibid.*, **65**, 992 (1976).

(5) G. Steiner, M. Patel, and J. T. Carstensen, *ibid.*, **63**, 1395 (1974).

(6) E. Parrott, in "The Theory and Practice of Industrial Pharmacy," L. Lachman, H. A. Lieberman, and J. L. Kanig, Eds., Lea & Febiger, Philadelphia, Pa., 1970, p. 102.

General Treatment of Competitive Binding of Small Molecules to Macromolecules as Applied to Dynamic Dialysis: Theoretical Analysis

PETER VENG PEDERSEN

Received June 24, 1977, from the *Department of Pharmacy, University of California, San Francisco, CA 94143.* Accepted for publication October 19, 1977.

Abstract □ A mathematical analysis of the dynamic dialysis process is presented, demonstrating how the process can be applied generally to study competitive and noncompetitive binding between small molecules and macromolecules. A law of mass action model for competitive binding with independent sites and classes with equivalent sites (CIE) is considered as a specific case without loss of generality. The escape profiles of two compounds are calculated to illustrate the effect of an increasing degree of binding competition. Noisy data are generated using the CIE model to test the presented method of estimating competitive binding parameters. The parameters estimated by the nonlinear regression technique came close to the true values, considering the degree of noise added to the exact dialysis data. A transformation approach is presented, enabling initial estimates of the binding parameters in the CIE model to be determined by multiple linear regression, thereby eliminating the main problem in the nonlinear estimation. The presented method of analysis is extended to strongly bound compounds, which also bind significantly to the dialysis membrane.

Keyphrases □ Dynamic dialysis—mathematical analysis, competitive binding of small molecules to macromolecules studied □ Models, mathematical—law of mass action for competitive binding with independent sites and classes with equivalent sites □ Binding, competitive—small molecules to macromolecules, mathematical analysis of dynamic dialysis process

Dynamic dialysis has proven valuable for characterizing interactions of small molecules with macromolecules such as drugs and proteins (1–11). Experimentally, it appears to be the simplest and most convenient method available for determining a complete binding profile (3), and its accuracy seems to be as good as equilibrium dialysis and ultrafiltration methods (3). The main disadvantages of dynamic dialysis are the inaccuracy introduced by the classical data treatment (9, 12), which requires differentiation of discrete data (3), and its limitation to molecules that do not bind or adsorb significantly to the dialysis membrane. However, both disadvantages recently were eliminated by a new approach in the data treatment (12).

This paper presents a mathematical analysis that enables the dynamic dialysis process to be extended to the study of competitive binding between small molecules and macromolecules considering any mathematical model for such interaction.

THEORY

To illustrate the general approach, it is appropriate to consider a law of mass action model with competitive binding, independent sites, and equivalence between sites in the binding classes having multiple sites:

$$\bar{\nu}_i = \sum_{j=1}^{N} n_j k_{ij} c_i \left[1 + \sum_{m=1}^{M} k_{mj} c_m\right]^{-1} \qquad \begin{matrix} i = 1, 2, \ldots, M \\ k_{ij} \geq 0 \end{matrix} \qquad \text{(Eq. 1)}$$

This model will be denoted the general CIE model, where $\bar{\nu}_i$ is the number of moles of the ith small molecules ("ligand") bound per mole of macromolecule, n_j is the number of equivalent binding sites in the jth class of sites, k_{ij} is the association constant for the ith compound's binding to the jth binding class, c_i is the free concentration of the ith compound, N is the number of binding classes, and M is the number of compounds competing in their binding to the macromolecule. Most frequently, $M = 2$. If $M = 1$, the CIE model reduces to the general (IE) model, dealing with the binding of one compound (12).

Cases where the compounds compete in their binding to certain, but not all, of the binding classes also are considered in the CIE model by allowing the association constants to take zero values (*i.e.*, $k_{ij} \geq 0$). For example, Compound 1 may bind to two classes of sites, and Compound 2 may bind to two classes. If the two compounds only compete in their binding for one class (*e.g.*, class two for Compound 1 is the same as class one for Compound 2), this situation is described by $k_{11} > 0$, $k_{12} > 0$, $k_{13} = 0$, $k_{21} = 0$, $k_{22} > 0$, and $k_{23} > 0$. Thus, the actual number of classes is $N = 3$.

According to $\bar{\nu}_i = ([c_i] - c_i)/P$, where $[c_i]$ is the total (free plus bound) molar concentration of the ith compound and P is the total molar concentration of macromolecule, Eq. 1 can be written:

$$[c_i] = c_i \left\{1 + P \sum_{j=1}^{N} n_j k_{ij} \left[1 + \sum_{m=1}^{M} k_{mj} c_m\right]^{-1}\right\} \qquad \begin{matrix} i = 1, 2, \ldots, M \\ k_{ij} \geq 0 \end{matrix} \qquad \text{(Eq. 2)}$$

The dynamic process is characterized by the following relationship:

$$d[c_i]/dt = -K_i c_i \qquad \text{(Eq. 3)}$$

where K_i is the dialysis rate constant for the ith compound. Equations 2 and 3 define the kinetics of dialysis. However, the use of these equations in their present form requires differentiation of discrete data, which introduces substantial errors in the determination of the binding parameters (9, 12).

To avoid such errors, it is necessary to eliminate the variables, c_i, that cannot be measured directly by using a technique similar to that pre-

0022-3549/78/0700/0908$01.00/0

© 1978, American Pharmaceutical Association

sented previously (12). To do so, it is useful to introduce a set of variables, s_i, defined by:

$$s_i = -d[c_i]/dt = K_i c_i \qquad \text{(Eq. 4)}$$

which, when substituted into Eq. 2, yields:

$$[c_i] = f_i = \frac{s_i}{K_i}\left\{1 + P\sum_{j=1}^{N} n_j k_{ij}\left[1 + \sum_{m=1}^{M}\frac{k_{mj}}{K_m}s_m\right]^{-1}\right\}$$
$$i = 1, 2, \ldots, M \qquad \text{(Eq. 5)}$$

For simplicity, and to demonstrate the generality of the following approach, it is convenient to switch to a matrix–vector notation. The system of equations given by Eq. 2 can be represented by:

$$[\mathbf{c}] = \mathbf{f}(\boldsymbol{\theta}, \mathbf{c}) \qquad \text{(Eq. 6)}$$

where $\boldsymbol{\theta}$ is a vector containing the parameters in the model, $[\mathbf{c}] = ([c_1], [c_2], \ldots, [c_M])^T$, $\mathbf{c} = (c_1, c_2, \ldots, c_M)^T$, and $\mathbf{f} = (f_1, f_2, \ldots, f_M)^T$ is the vector of functions describing the relationship between $[c_i]$ and $\mathbf{c}$. The variable $\mathbf{c}$ can, similarly to c_i, be eliminated according to Eq. 4 so that Eq. 6 becomes:

$$[\mathbf{c}] = \mathbf{f}(\boldsymbol{\theta}, \mathbf{D}\mathbf{s}) \qquad \text{(Eq. 7)}$$

where $\mathbf{D} = \text{diag}\,(1/K_1, 1/K_2, \ldots, 1/K_M)$ is the diagonal matrix containing the reciprocal of the dialysis rate constants and $\mathbf{s} = (s_1, s_2, \ldots, s_M)^T$. By taking the total differential of the ith row of Eq. 7, the following relationship is obtained:

$$\frac{d[c_i]}{dt} = \sum_{j=1}^{M}\left(\frac{\partial f_i}{\partial s_j}\right)\frac{ds_j}{dt} = -s_i \qquad \text{(Eq. 8)}$$

which, for $i = 1, 2, \ldots, M$, yields a set of equations:

$$\left(\frac{\partial f_1}{\partial s_1}\right)\frac{ds_1}{dt} + \left(\frac{\partial f_1}{\partial s_2}\right)\frac{ds_2}{dt} + \ldots + \left(\frac{\partial f_1}{\partial s_M}\right)\frac{ds_M}{dt} = -s_1 \qquad \text{(Eq. 9a)}$$

$$\left(\frac{\partial f_2}{\partial s_1}\right)\frac{ds_1}{dt} + \left(\frac{\partial f_2}{\partial s_2}\right)\frac{ds_2}{dt} + \ldots + \left(\frac{\partial f_2}{\partial s_M}\right)\frac{ds_M}{dt} = -s_2 \qquad \text{(Eq. 9b)}$$

$$\vdots \qquad \vdots \qquad \vdots \qquad \vdots$$

$$\left(\frac{\partial f_M}{\partial s_1}\right)\frac{ds_1}{dt} + \left(\frac{\partial f_M}{\partial s_2}\right)\frac{ds_2}{dt} + \ldots + \left(\frac{\partial f_M}{\partial s_M}\right)\frac{ds_M}{dt} = -s_M \qquad \text{(Eq. 9c)}$$

These equations are recognized as a linear matrix–vector system:

$$\mathbf{J}\left(\frac{\mathbf{f}}{\mathbf{s}}\right)\frac{d}{dt}\mathbf{s} = -\mathbf{s} \qquad \text{(Eq. 10)}$$

where $\mathbf{J}$ is the Jacobian matrix of $\mathbf{f}$ with respect to $\mathbf{s}$. Thus, the ijth element of the coefficient matrix is:

$$J_{ij} = \frac{\partial f_i}{\partial s_j} \qquad \text{(Eq. 11)}$$

Equation 10 can be rearranged to give:

$$\frac{d}{dt}\mathbf{s} = -\mathbf{J}^{-1}\left(\frac{\mathbf{f}}{\mathbf{s}}\right)\mathbf{s} \qquad \text{(Eq. 12)}$$

which, subject to:

$$\mathbf{s} = \mathbf{s}_0 \qquad \text{at } t = 0 \qquad \text{(Eq. 13)}$$

constitutes an initial value problem that readily can be solved numerically using a well-established technique (13).

RESULTS AND DISCUSSION

The functional relationship between $[\mathbf{c}]$ and t is defined by Eqs. 7, 12, and 13 in parametric form, with $\mathbf{s}$ as the parametric variable. To get $[\mathbf{c}]$ at t, Eq. 12 is integrated from $t = 0$ to time t and the obtained $\mathbf{s}$ is inserted into Eq. 7 to give $[c]$. The $\mathbf{s}_0 = \mathbf{s}_{t=0}$ required in the integration is obtained from Eq. 7 by solving for $\mathbf{s}_0$ corresponding to $[\mathbf{c}]_{t=0}$. Thus, the complete escape profiles ($[c_i]$ *versus* t) can be calculated when the binding parameters, $\boldsymbol{\theta}$, and the initial total concentrations, $[\mathbf{c}]_{t=0}$, are given.

When $\boldsymbol{\theta}$ is to be determined by the nonlinear regression technique from dynamic dialysis data ($[\mathbf{c}]$ *versus* t), either $[\mathbf{c}]_{t=0}$ or $\mathbf{s}_0$ must be treated as additional unknown parameters to be determined simultaneously with $\boldsymbol{\theta}$. The latter choice ($\mathbf{s}_0$) is computationally most convenient, particularly if $\mathbf{s}$ cannot be expressed explicitly in terms of $[\mathbf{c}]$ and $\boldsymbol{\theta}$ in Eq. 7. The initial estimates of the elements of $\mathbf{s}_0$ required in the curve-fitting procedure are simply obtained according to the definition of $\mathbf{s}$ (Eq. 4) as the absolute values of the initial slopes in the $[c_i]$ *versus* t plots of the data.

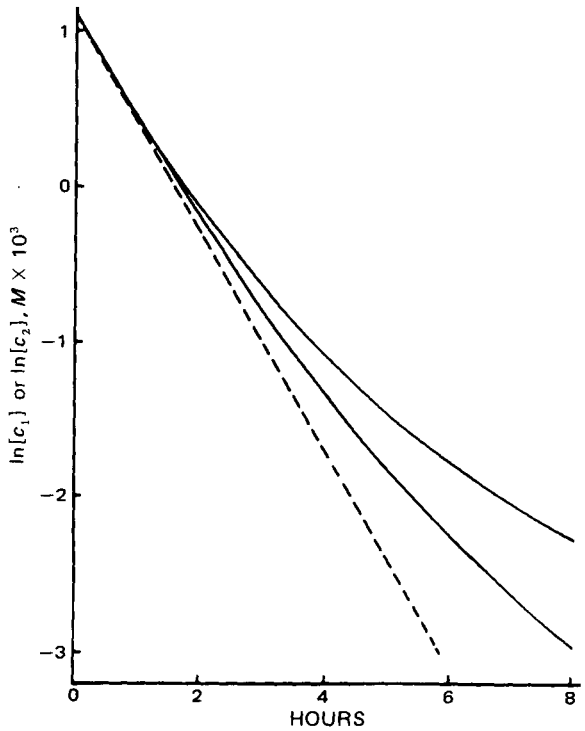

Figure 1—*Theoretical escape curves describing the dynamic dialysis of two compounds competing in their binding to a macromolecular compound according to the CIE model (Eq. 2, M = 2 and N = 1) with one class of sites. The association constant for the two compounds binding to the common binding sites are* $k_1 (= k_{11}) = 5\ mM^{-1}$ *(middle curve) and* $k_2 (= k_{21}) = 10\ mM^{-1}$ *(upper curve). The broken straight line describes the first-order dialysis in the absence of the macromolecular compound. Figures 1–3 show the effect of changing* k_2 *while all other parameters are kept constant:* P = 0.145 mM, n (= n_1) = 2, $K_1 = K_2 = 0.7\ hr^{-1}$, *and* $[c_1]_{t=0} = [c_2]_{t=0} = 3$ mM.

These slopes would normally be determined by extrapolation. To avoid the inconvenience and errors of such extrapolations, it is convenient to define $t = 0$ at the first sampling time. Thus, there is no need to take samples at the very beginning of the experiment, which is very convenient. The accuracy by which the initial slopes are determined does not affect the accuracy of the binding parameters since the slope values are only used as initial guesses for $\mathbf{s}_0$ in the iterative nonlinear estimation.

This treatment (Eqs. 6–13) is completely general and applies to any mathematical model for competitive or noncompetitive binding involving any number of interacting compounds. If the partial derivatives used for the Jacobian matrix (Eq. 11) are not available in an analytical form, they can be evaluated numerically; or if $[\mathbf{c}]$ is not expressed explicitly in the binding model as in Eq. 6, this can also be done numerically. Thus, the method is not restricted by the complexity of the mathematical model for the binding kinetics.

To illustrate this general procedure, consider again the general CIE model (Eq. 2). For this model, the Jacobian matrix is assembled according to Eq. 11 using the following partial derivatives obtained from Eq. 5:

$$\frac{\partial f_i}{\partial s_v} = -\frac{s_i P}{K_v K_i}\sum_{j=1}^{N} n_j k_{ij} k_{vj}\left[1 + \sum_{m=1}^{M}\frac{k_{mj}}{K_m}s_m\right]^{-2}$$
$$i \neq v = 1, 2, \ldots, M \qquad \text{(Eq. 14)}$$

$$\frac{\partial f_i}{\partial s_i} = \frac{1}{K_i} + \frac{P}{K_i}\sum_{j=1}^{N} n_j k_{ij}\left\{1 + \sum_{\substack{m=1 \\ \neq i}}^{M}\frac{k_{mj}}{K_m}s_m\right\}\left[1 + \sum_{m=1}^{M}\frac{k_{mj}}{K_m}s_m\right]^{-2}$$
$$i = 1, 2, \ldots, M \qquad \text{(Eq. 15)}$$

For simplicity, consider the most common case, $M = 2$, with only two compounds competing in their binding to the macromolecule. The inverse of the Jacobian matrix is given by:

$$\mathbf{J}^{-1}\left(\frac{f_1, f_2}{s_1, s_2}\right) = \begin{bmatrix} \frac{\partial f_2}{\partial s_2} & -\frac{\partial f_1}{\partial s_2} \\ -\frac{\partial f_2}{\partial s_1} & \frac{\partial f_1}{\partial s_1} \end{bmatrix} \Big/ \begin{bmatrix} \frac{\partial f_1}{\partial s_1} & \frac{\partial f_1}{\partial s_2} \\ \frac{\partial f_2}{\partial s_1} & \frac{\partial f_2}{\partial s_2} \end{bmatrix} \qquad \text{(Eq. 16)}$$

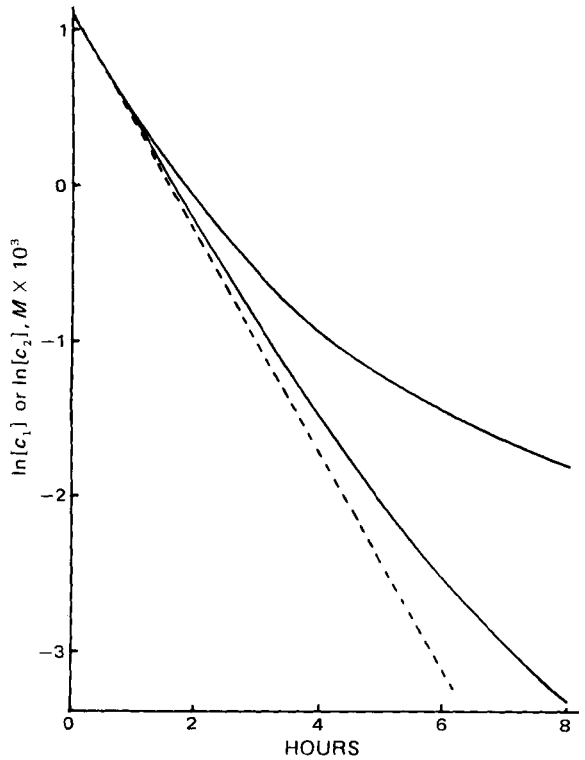

Figure 2—*Theoretical escape curves describing the dynamic dialysis of two compounds competing in their binding to a macromolecular compound according to the CIE model (Eq. 2, M = 2 and N = 1) with one class of sites. The association constant for the two compounds binding to the common binding sites are* k_1 (= k_{11}) = 5 mM^{-1} *(middle curve) and* k_2 (= k_{21}) = 25 mM^{-1} *(upper curve). The broken straight line describes the first-order dialysis in the absence of the macromolecular compound.*

which, when substituted into Eq. 12, yields the following differential equations:

$$\frac{ds_1}{dt} = \frac{-\left(\frac{\partial f_2}{\partial s_2}\right) s_1 + \left(\frac{\partial f_1}{\partial s_2}\right) s_2}{\left(\frac{\partial f_1}{\partial s_1}\right)\left(\frac{\partial f_2}{\partial s_2}\right) - \left(\frac{\partial f_2}{\partial s_1}\right)\left(\frac{\partial f_1}{\partial s_2}\right)} \qquad \text{(Eq. 17)}$$

$$\frac{ds_2}{dt} = \frac{-\left(\frac{\partial f_1}{\partial s_1}\right) s_2 + \left(\frac{\partial f_2}{\partial s_1}\right) s_1}{\left(\frac{\partial f_1}{\partial s_1}\right)\left(\frac{\partial f_2}{\partial s_2}\right) - \left(\frac{\partial f_2}{\partial s_1}\right)\left(\frac{\partial f_1}{\partial s_2}\right)} \qquad \text{(Eq. 18)}$$

where the partial derivatives are given by Eqs. 14 and 15.

The functional relationship among the experimentally available variables $[c_1]$, $[c_2]$, and t is now given in parametric form (with s_1 and s_2 as parameter variables) by Eqs. 5 and 14–18. The procedure by which this functional relationship is established is as follows. Equations 17 and 18 are integrated numerically from $t = 0$ to time t, using an appropriate, well-established technique such as a Runge–Kutta or a multistep method (13).

The obtained s_1 and s_2 values then are substituted into Eq. 5, $i = 1, 2$, to give the $[c_1]$ and $[c_2]$ at that particular time t. This two-step process, when repeated for various t values, defines the $[c_1]$, $[c_2]$ *versus* t functional relationship.

Having defined this relationship, a nonlinear regression technique can be used to estimate the binding parameters by simultaneous curve fitting to experimental $[c_1]$ *versus* t and $[c_2]$ *versus* t dialysis data. The dialysis rate constant, K_i, can be determined from ln (c_i) *versus* t plots in a separate experiment in the absence of the macromolecular compound or it can be determined directly by the nonlinear regression technique by considering K_i as an unknown parameter (12). The initial estimates of $[s_1]_{t=0}$ and $[s_2]_{t=0}$ are obtained graphically as the absolute values of the initial slopes from plots of $[c_1]$ *versus* t and $[c_2]$ *versus* t. As explained, the accuracy of this estimation will not affect the accuracy of the estimated binding parameters.

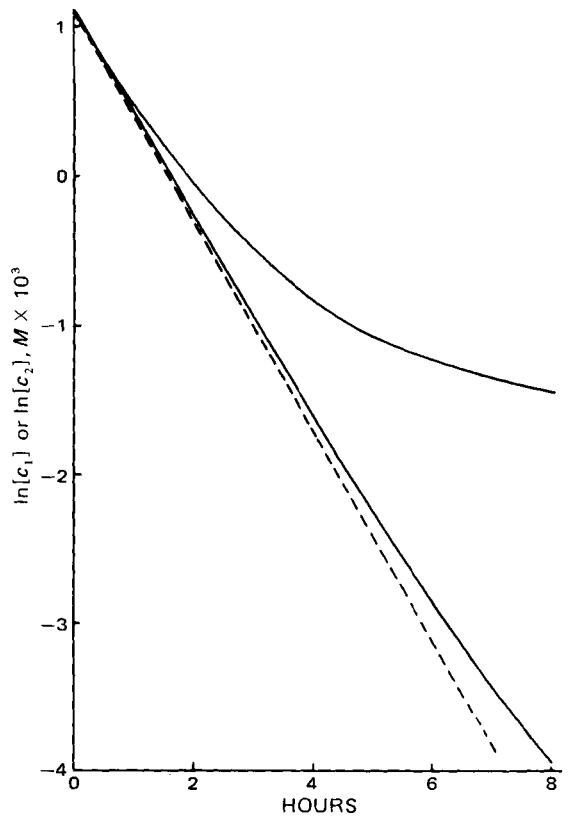

Figure 3—*Theoretical escape curves describing the dynamic dialysis of two compounds competing in their binding to a macromolecular compound according to the CIE model (Eq. 2, M = 2 and N = 1) with one class of sites. The association constant for the two compounds binding to the common binding sites are* k_1 (= k_{11}) = 5 mM^{-1} *(middle curve) and* k_2 (= k_{21}) = 100 mM^{-1} *(upper curve). The broken straight line describes the first-order dialysis in the absence of the macromolecular compound.*

Example of CIE Model with $M = 2$ and $N = 1$—To show the practicality of this approach and to illustrate the dynamic dialysis behavior in a situation with competitive binding, the CIE model in its simplest form ($M = 2$ and $N = 1$) is now considered. The following equations are obtained from Eqs. 5, 14, and 15 with $M = 2$ and $N = 1$:

$$[c_1] = f_1 = \frac{s_1}{k_1} + \frac{nPk_1K_2s_1}{K_1K_2 + k_1K_2s_1 + k_2K_1s_2} \qquad \text{(Eq. 19)}$$

$$[c_2] = f_2 = \frac{s_2}{K_2} + \frac{nPk_2K_1s_2}{K_1K_2 + k_1K_2s_1 + k_2K_1s_2} \qquad \text{(Eq. 20)}$$

$$\frac{\partial f_1}{\partial s_1} = \frac{1}{K_2} + \frac{nPk_1K_2(K_1K_2 + k_2K_1s_2)}{(K_1K_2 + k_1K_2s_1 + k_2K_1s_2)^2} \qquad \text{(Eq. 21)}$$

$$\frac{\partial f_2}{\partial s_2} = \frac{1}{K_2} + \frac{nPk_2K_1(K_1K_2 + k_1K_2s_1)}{(K_1K_2 + k_1K_2s_1 + k_2K_1s_2)^2} \qquad \text{(Eq. 22)}$$

$$\frac{\partial f_1}{\partial s_2} = -\frac{nPk_1K_2k_2K_1s_1}{(K_1K_2 + k_1K_2s_1 + k_2K_1s_2)^2} \qquad \text{(Eq. 23)}$$

$$\frac{\partial f_2}{\partial s_1} = -\frac{nPk_1K_2k_2K_1s_2}{(K_1K_2 + k_1K_2s_1 + k_2K_1s_2)^2} \qquad \text{(Eq. 24)}$$

The dynamic dialysis behavior can now be calculated as discussed using Eqs. 17–24. Three escape profiles were calculated[1] (Figs. 1–3) with the following common parameters: $P = 0.145$ mM; $n = 2$; $K_1 = K_2 = 0.7$ hr^{-1}; $[c_1]_{t=0} = [c_2]_{t=0} = 3$ mM; $k_1 = 5$ mM^{-1}; and $k_2 = 10$, 25, and 100 mM^{-1}. The association constant, k_2, for the competing second compound (top curves in Figs. 1–3) is the only parameter that differs in the three cases.

[1] Calculations were done using an IBM 370 digital computer. The integration of the differential equations was done using a Runge–Kutta algorithm (14). The accuracy of the integration was checked by step reduction. The solution of Eqs. 19 and 20 for s_0 for given values of $[c_1]_{t=0} = [c_2]_{t=0}$ was done using the Newton algorithm.

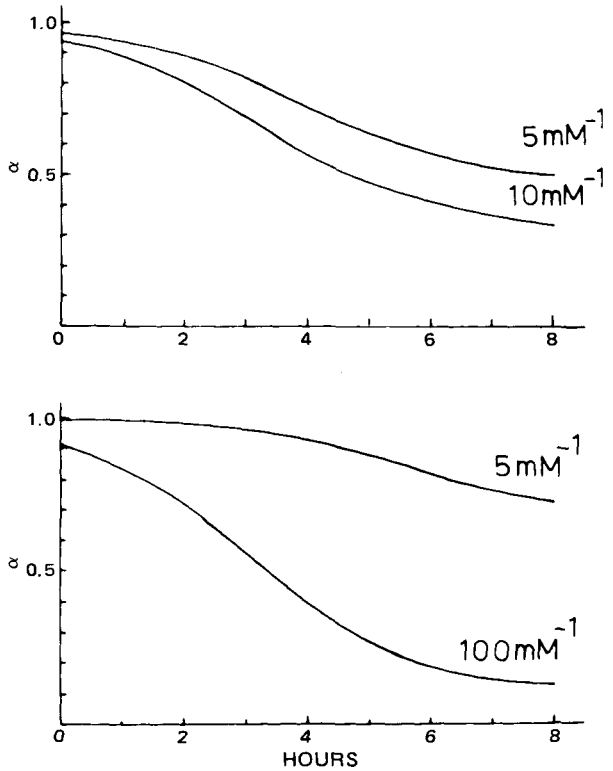

Figure 4—*Calculated variation of the fraction of unbound form* (α = c/[c]) *of two compounds in a dynamic dialysis cell where the compounds compete in their binding to a macromolecular compound according to the CIE binding model (Eq. 2,* M = 2 *and* N = 1*) with one class of sites. The association constant for the binding of the two compounds to the common binding sites are indicated on the curves. The other parameter values are the same for the upper and lower graphs and identical to the parameters in Figs. 1 and 3, respectively.*

Semilogarithmic plots are used to illustrate the effect of binding on the escape of the two compounds from the compartment containing the macromolecular compound. If there is no binding, the escape would be first order and follow the broken line (|slope| = K). The increasing deviation in the slopes of the two dialysis curves observed at decreasing concentrations is expected according to Eq. 4 because of the increased degree of binding at lower concentrations. This deviation becomes more pronounced for the second compound as its association constant increases. The association constant for the first compound is kept constant (k_1 = 5 mM^{-1}) in all three cases. However, the deviation of its escape curve (the middle curves in Figs. 1–3) from that of the broken line becomes less significant as the association constant of the second compound increases. This behavior agrees with the corresponding increased degree of displacement of the first compound as the binding of the second compound to the common binding sites becomes stronger. This pattern in the displacement is clearly seen when the fractions of unbound compounds, α, are plotted *versus* time (the upper and lower graphs in Fig. 4 correspond to Figs. 1 and 3, respectively).

Estimation of Competitive Binding Parameters: A Simple Example—A binding parameter estimation situation was simulated by first calculating 2 × 11 exact dynamic dialysis data points equally spaced over 8 hr, using the CIE model with M = 2, N = 1, P = 0.145 mM, n = 2, k_1 = 5 mM^{-1}, k_2 = 10 mM^{-1}, $[c_1]_{t=0} = [c_2]_{t=0}$ = 3 mM, and $K_1 = K_2$ = 0.7 hr^{-1}. Random deviates from a Gaussian distribution with zero mean and various standard deviations were then added as errors to the exact data[2]. The standard deviations of the Gaussian distribution were chosen so that there was a 95% probability that the relative error would fall within ±5% of the exact value.

The CIE model was then fitted to the noisy data using a general nonlinear regression program, FUNFIT, written for time-sharing use (16). The data were weighted inversely proportional to the observed [c] values according to the theory of least squares (17) since the standard deviations of the errors were chosen proportional to the exact [c] values. It was assumed that the dialysis rate constants K_1 and K_2 were determined in a separate experiment in the absence of the macromolecular compound, so only n, k_1, and k_2 remained to be determined.

[2] The deviates were obtained by the inverse method, using a uniform distribution pseudo-random number generator (15).

Table I—Competitive Binding Parameters Obtained from Simulated Dynamic Dialysis Data Considering the CIE Binding Model (Eq. 2, M = 2 and N = 1)

	n	k_1, mM^{-1}	k_2, mM^{-1}	r
True values[a]	2	5	25	—
Linear regression[b]	3.79	2.76	28.9	—
First nonlinear regression[c]	2.07	5.02	25.3	0.9998
Second nonlinear regression[d]	2	5.15	24.7	0.9997

[a] Values from which exact dynamic dialysis data were calculated and Gaussian noise added to simulate experimental data. [b] Values obtained by the approach described in the *Appendix*. These values were used as initial estimates in the first nonlinear regression. [c] Values obtained by fitting simultaneously by least squares the two regression equations defined by Eqs. 17–24 in dynamic and parametric form to [c_1] *versus* t and [c_2] *versus* t data (Fig. 5). [d] Values were obtained as explained in footnote c, but the value for n was fixed as a constant as the integer value closes to n in the first nonlinear estimation to agree with the binding model.

The difficulty of obtaining good initial parameter estimates is often the main problem in nonlinear parameter estimation. Therefore, it would not simulate a real experimental situation to have *a priori* knowledge about the true parameters in the simulation study. It is shown in the *Appendix* how initial estimates can be obtained for the CIE model by the multiple linear regression technique.

The initial estimates of n_1, k_1, and k_2 were obtained in this way using Eqs. A12–A14, and the estimates of $[s_1]_{t=0}$ and $[s_2]_{t=0}$ were obtained graphically as discussed. Although the linear regression technique itself is not accurate enough to be used as a method for estimating CIE binding parameters, it appears to be valuable to get good initial estimates for the nonlinear estimation (Table I).

The nonlinear regression technique demonstrated very good agreement

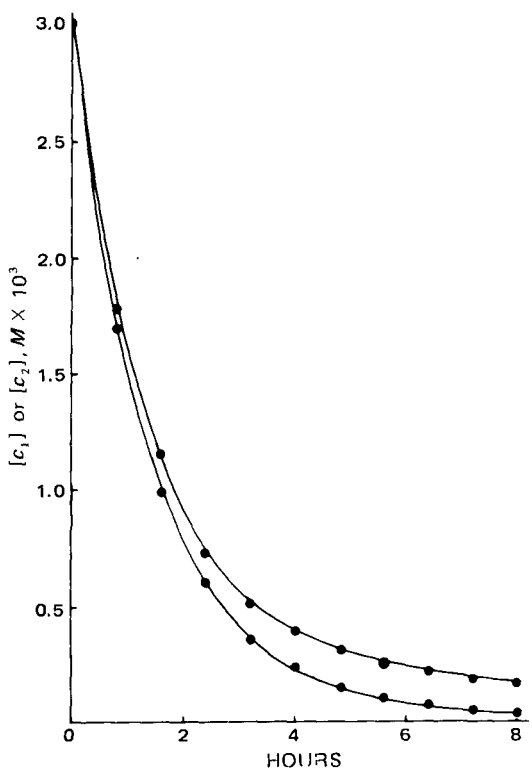

Figure 5—*Simultaneous nonlinear least-squares estimation of competitive binding parameters for two compounds competing in their binding to a macromolecular compound according to the CIE model (Eq. 2,* M = 2 *and* N = 1*). The 2 × 11 dynamic dialysis data points are simulated data with random Gaussian deviates added as noise (for details, see text). The two regression equations fitted simultaneously by least squares to the* [c_1] versus t *and* [c_2] versus t *data are defined in dynamic and parametric form by Eqs. 17–24. The estimated binding parameters are given in Table I.*

between observed and calculated values of the dynamic dialysis data (Fig. 5). The estimated binding parameters came close to the true values, considering the degree of noise added to the true data (Table I).

The dynamic dialysis technique combined with the presented mathematical treatment appears to be a generally applicable and very powerful tool for studying binding interaction between small molecules and macromolecules. However, before the technique can be applied, it is necessary to establish, in the absence of the macromolecular compound, that there is no interaction between the small molecules (*e.g.*, no complexation), in which case Eq. 3 cannot be used. Furthermore, it must be ensured that the experimental conditions are such that the dialysis through the membrane is first order with respect to the free form of the small molecules in the concentration range of interest (3).

If one or more of the small molecules are highly bound, a significant binding to the dialysis membrane may be observed in the preliminary investigations not involving the macromolecular compound and this procedure cannot be applied directly. However, the *Appendix* shows how the method can be extended to include such interactions.

APPENDIX

Equation 5 can, after rearrangement, be written:

$$\frac{P}{\frac{K_i[c_i]}{s_i} - 1} = \sum_{j=1}^{N}\left[\frac{1}{n_j k_{ij}} + \frac{1}{n_j k_{ij}}\sum_{m=1}^{M}\frac{k_{mj}}{K_m}s_m\right] \qquad \text{(Eq. A1)}$$

which is recognized as a linear expression of the form:

$$y_i = a_{oi} + \sum_{m=1}^{M} a_{im}s_m \qquad i = 1, 2, \ldots, M \qquad \text{(Eq. A2)}$$

where:

$$y_i = \frac{P}{\frac{k_i[c_i]}{s_i} - 1} \qquad \text{(Eq. A3)}$$

$$a_{oi} = \sum_{j=1}^{N}\frac{1}{n_j k_{ij}} \qquad \text{(Eq. A4)}$$

$$a_{im} = \sum_{j=1}^{N}\frac{k_{mj}}{n_j k_{ij} K_m} \qquad \text{(Eq. A5)}$$

Thus, multiple linear regression of y_i ($i = 1, 2, \ldots, M$) on s_m ($m = 1, 2, \ldots, M$) yields $M(M + 1)$ regression coefficients, which are functions of the n's, the k's, and the K's only. To evaluate y_i, the K's must be determined in a separate experiment in the absence of the macromolecular compound so that only the n's and k's remain to be determined from Eqs. A4 and A5. The number of parameters is, therefore, $N + (N)(M) = M(N + 1)$ to be determined from $M(M + 1)$ equations (coefficients).

The solution to this system requires that $M(N + 1) \leq M(M + 1)$, *i.e.*, that $N \leq M$, so the multiple linear regression approach cannot be used to estimate the n's and k's in a CIE model if the number of classes is more than the number of competing compounds.

The solution of Eqs. A4 and A5 when $N = M = 2$ is given by:

$$n_1 = \frac{1}{a_{11}K_1} + \frac{1}{a_{21}K_2} \qquad \text{(Eq. A6)}$$

$$n_2 = \frac{1}{a_{12}K_1} + \frac{1}{a_{22}K_2} \qquad \text{(Eq. A7)}$$

$$k_{11} = \frac{a_{21}K_1K_2(a_{11}a_{22} - a_{12}a_{21})}{(a_{11}K_1 + a_{21}K_2)(a_{22}a_{o1} - a_{12}a_{o2})} \qquad \text{(Eq. A8)}$$

$$k_{22} = \frac{a_{12}K_1K_2(a_{11}a_{22} - a_{12}a_{21})}{(a_{12}k_1 + a_{22}K_2)(a_{11}a_{o2} - a_{21}a_{o1})} \qquad \text{(Eq. A9)}$$

$$k_{12} = \frac{a_{21}K_1K_2(a_{11}a_{22} - a_{12}a_{21})}{(a_{11}K_1 + a_{21}K_2)(a_{22}a_{o1} - a_{12}a_{o2})} \qquad \text{(Eq. A10)}$$

$$k_{21} = \frac{a_{11}K_1K_2(a_{11}a_{22} - a_{12}a_{21})}{(a_{11}K_1 + a_{21}K_2)(a_{22}a_{o1} - a_{12}a_{o2})} \qquad \text{(Eq. A11)}$$

where a_{oi} and a_{im} ($i, m = 1, 2$) are the constant term and the mth regression coefficient, respectively, obtained using the ith regression equation defined by Eq. A2. In the specific example already considered ($M = 2, N = 1$), the initial estimates of the binding parameters were obtained using the following equations:

$$n = \frac{1}{K_1a_1} \qquad \text{(Eq. A12)}$$

$$k_1 = \frac{K_1a_1}{a_o} \qquad \text{(Eq. A13)}$$

$$k_2 = \frac{K_2a_2}{a_o} \qquad \text{(Eq. A14)}$$

where the second subscript of the k's and a's has been dropped for simplicity since there is only one class of sites. The linear regression equation used in this case is $y_1 = a_o + a_1s_1 + a_2s_2$, where $y_1 = p/(K_1[c_1]/s_1 - 1)$, from which a_{o1}, a_1, and a_2 were determined using the noisy dialysis data ($[c_1]$ and $[c_2]$ *versus* t). The s_1 and s_2 values would usually be found by fitting an empirical equation[3] to the dialysis data and differentiating this function to get s_1 and s_2 at the various observation times. However, in this simulation, the s_1 and s_2 values were obtained from the exact s values by adding errors in the same way as was done with the $[c_1]$ and $[c_2]$ values.

If a small molecule binds to the dialysis membrane, it can often be considered as a Langmuir-type adsorption phenomenon (5), which is mathematically analogous to binding to a single class of sites and is described by:

$$\bar{\nu}_i^* = \frac{n_i^*k_i'c_i}{1 + k_i'c_i} \qquad \text{(Eq. A15)}$$

where $\bar{\nu}_i^*$ is the amount of the ith compound bound per amount of available membrane material and k_i' is an "association constant" for membrane binding. The quantity n_i^* does not have the same meaning as n previously defined but is introduced to establish a mathematical analogy. Equation A15 may also be written:

$$(c_b)_i = \frac{n_i^*k_i^*c_i}{1 + k_i^*c_i} \qquad \text{(Eq. A16)}$$

where $(c_b)_i$ is the concentration of the bound form of the ith compound and:

$$k_i^* = \frac{k_i'w}{u_iV} \qquad \text{(Eq. A17)}$$

where w is the amount of membrane material available for binding, u_i is the molecular weight of the ith compound, and V is the volume of the dialysis compartment. Equation A16 can, according to Eq. 4, be written:

$$(c_b)_i = g_i = \frac{n_i^*k_i^*s_i}{K_i + k_i^*s_i} \qquad k_i^* \geq 0 \qquad \text{(Eq. A18)}$$

where the function g_i denotes the concentration membrane bound of the ith compound, which must be added to f_i to get $[c_i]$. Therefore, when one or more compounds are bound (adsorbed) significantly to the dialysis membrane, the following two equations:

$$[\mathbf{c}] = \mathbf{f} + \mathbf{g} \qquad \text{(Eq. A19)}$$

$$\frac{d}{dt}\mathbf{s} = -\mathbf{J}^{-1}\left(\frac{\mathbf{f} + \mathbf{g}}{\mathbf{s}}\right)\mathbf{s} \qquad \text{(Eq. A20)}$$

should replace Eqs. 7 and 12, respectively. For the sake of generality, the function g_i may be any binding or adsorption model describing the membrane binding with or without competitive effects. The most accurate way of accounting for the effect of membrane binding is first to determine the membrane binding parameters (n^* and k^* in this case) in the absence of the macromolecular compound in a separate experiment. These parameters can then be fixed as constants in the "correction term," $\mathbf{g}$, when fitting the corrected model (Eq. A19) to reduce the dimensionality of the nonlinear estimation, thereby getting more reliable estimates of the remaining (variable) parameters.

SYMBOLS

a_{im} = mth regression coefficient in ith linear regression equation (Eq. A2) used to obtain initial estimates of binding parameters n's and k's

a_{oi} = constant term in ith linear regression equation (Eq. A2) used to obtain initial estimates of binding parameters n's and k's

$a_o = a_{o1}$ (see a_{oi})

$a_1 = a_{11}$ (see a_{im})

$a_2 = a_{21}$ (see a_{im})

α = fraction unbound ($\alpha = c_i/[c_i]$)

[3] A spline function seems to be the best choice because of its desirable smoothness and flexibility (18).

c_i = free (unbound) molar concentration of ith compound
$\mathbf{c} = (c_1, c_2, \ldots, c_M)^T$ (see c_i)
$[c_i]$ = total (free + bound) molar concentration of ith compound
$[\mathbf{c}] = ([c_1], [c_2], \ldots, [c_M])^T$ (see $[c_i]$)
$(c_b)_i$ = "membrane bound concentration" of ith compound
D = diag$(1/K_1, 1/K_2, \ldots, 1/K_M)$ = diagonal matrix containing reciprocals of dialysis rate constants
f_i = function describing relationship between $[c_i]$ and $\mathbf{c}$ or $[c_i]$ and $\mathbf{s}$
$\mathbf{f} = (f_1, f_2, \ldots, f_M)^T$ (see f_i)
g_i = function describing relationship between $(c_b)_i$ and s_i
$\mathbf{g} = (g_1, g_2, \ldots, g_M)^T$ (see g_i)
i = subscript ($i = 1, 2, \ldots$)
j = subscript ($j = 1, 2, \ldots$)
$\mathbf{J}\left(\frac{\mathbf{f}}{\mathbf{s}}\right)$ = Jacobian matrix of $\mathbf{f}$ with respect to $\mathbf{s}$
J_{ij} = ijth element of Jacobian matrix
k_{ij} = association constant for ith compound's binding to jth class of binding sites on macromolecule
k_i = k_{i1} (see k_{ij})
k_i^* = membrane binding "association constant" of ith compound
K_m = dialysis rate constant for mth compound
m = subscript ($m = 1, 2, \ldots$)
M = number of compounds
n_j = number of binding sites in jth class of sites
n_i^* = mathematical analog to n_i in Langmuir-type membrane "binding" model
n = n_1 (see n_j)
N = number of binding classes
$\bar{\nu}_i$ = number of moles of ith compound ("ligand") bound per mole of macromolecule
$\bar{\nu}_i^*$ = amount of ith compound bound per amount of available membrane material
P = total molar concentration of macromolecular compound
θ = parameter vector containing elements such as n_j, k_{ij}, and P or other parameters used in the particular mathematical model $\mathbf{f}$ describing binding kinetics
r = correlation coefficient
s_i = absolute value of slope in a $[c_i]$ *versus* t plot at time t. This quantity is used as a parameter variable in the parametric representation of the variables $[c_i]$ and t
$\mathbf{s} = (s_1, s_2, \ldots, s_M)^T$ (see s_i)
$\mathbf{s}_0$ = $\mathbf{s}$ evaluated at $t = 0$
t = time
T = transpose
u_i = molecular weight of ith compound
υ = subscript ($\upsilon = 1, 2, \ldots$)
V = volume of dialysis compartment
w = weight of available membrane material
y_i = ith dependent variable in transformed set of linear regression equations (Eq. A2) used to obtain initial estimates of the binding parameters (n's and k's) by multiple linear regression technique

REFERENCES

(1) H. H. Stein, *Anal. Biochem.*, **13**, 605 (1965).
(2) A. Agren, *Acta Pharm. Suec.*, **5**, 37 (1968).
(3) M. C. Meyer and D. E. Guttman, *J. Pharm. Sci.*, **57**, 1627 (1968).
(4) *Ibid.*, **59**, 33 (1970).
(5) *Ibid.*, **59**, 39 (1970).
(6) J. C. Dearden and E. Tomlinson, *J. Pharm. Pharmacol., Suppl.*, **22**, 53S (1970).
(7) M. J. Crooks and K. F. Brown, *J. Pharm. Sci.*, **62**, 1904 (1973).
(8) M. J. Crooks and K. F. Brown, *J. Pharm. Pharmacol.*, **26**, 235 (1974).
(9) I. Kanfer and D. R. Cooper, *ibid.*, **28**, 58 (1976).
(10) S. J. A. Kazmi and A. G. Mitchell, *J. Pharm. Sci.*, **62**, 1299 (1973).
(11) F. Bottari, G. Di Colo, E. Nannipieri, M. F. Saettone, and M. F. Serafini, *ibid.*, **64**, 946 (1975).
(12) P. Veng Pedersen, M. J. Crooks, and K. F. Brown, *J. Pharm. Sci.*, **66**, 1458 (1977).
(13) C. W. Gear, "Numerical Initial Value Problems in Ordinary Differential Equations," Prentice-Hall, Englewood Cliffs, N.J., 1971.
(14) "Handbook of Mathematical Functions," M. Abramowitz and I. A. Stegun, Eds., Dover, New York, N.Y., 1970, p. 897.
(15) *Ibid.*, p. 950.
(16) P. Veng Pedersen, *J. Pharmacokinet. Biopharm.*, **5**, 513 (1977).
(17) Y. Bard, "Nonlinear Parameter Estimation," Academic, New York, N.Y., 1974, p. 57.
(18) J. H. Ahlberg, E. N. Nilson, and J. L. Walsh, "The Theory of Splines and Their Applications," Academic, New York, N.Y., 1967.

Analysis of Steroid Phosphates by High-Pressure Liquid Chromatography: Betamethasone Sodium Phosphate

L. M. UPTON *, E. R. TOWNLEY ˣ, and F. D. SANCILIO ‡

Received July 18, 1977, from the *Physical and Analytical Chemical Research and Development Department, Schering Corporation, Bloomfield, NJ 07003.* Accepted for publication October 25, 1977. *Present address: Seton Hall University, South Orange, NJ 07079. ‡Present address: Burroughs Wellcome Co., Research Triangle Park, NC 27709.

Abstract □ A sensitive, automatable high-pressure liquid chromatographic procedure is presented for the determination of steroid phosphates. Quantitation is described for betamethasone sodium phosphate in dosage forms in the presence of polar excipients. The separation of a multicomponent mixture of steroid phosphates also is reported.

Keyphrases □ Betamethasone sodium phosphate—high-pressure liquid chromatographic analysis in dosage forms □ High-pressure liquid chromatography—analysis, betamethasone sodium phosphate in dosage forms □ Glucocorticoids—betamethasone sodium phosphate, high-pressure liquid chromatographic analysis in dosage forms □ Steroid phosphates, various—high-pressure liquid chromatographic analysis in dosage forms

Steroid phosphates are highly effective anti-inflammatory agents produced in ophthalmic, injectable, and solid dosage forms. Reported analyses utilize spectrophotometric procedures preceded by extraction and/or reaction methods (1–3). These procedures are time consuming and relatively difficult. Two chromatographic methods have been reported: TLC of the methyl ester and ion chromatography (4, 5). This laboratory previously used

0022-3549/78/0700/0913$01.00/0

© 1978, American Pharmaceutical Association

c_i = free (unbound) molar concentration of ith compound
$\mathbf{c} = (c_1, c_2, \ldots, c_M)^T$ (see c_i)
$[c_i]$ = total (free + bound) molar concentration of ith compound
$[\mathbf{c}] = ([c_1], [c_2], \ldots, [c_M])^T$ (see $[c_i]$)
$(c_b)_i$ = "membrane bound concentration" of ith compound
D = diag$(1/K_1, 1/K_2, \ldots, 1/K_M)$ = diagonal matrix containing reciprocals of dialysis rate constants
f_i = function describing relationship between $[c_i]$ and $\mathbf{c}$ or $[c_i]$ and $\mathbf{s}$
$\mathbf{f} = (f_1, f_2, \ldots, f_M)^T$ (see f_i)
g_i = function describing relationship between $(c_b)_i$ and s_i
$\mathbf{g} = (g_1, g_2, \ldots, g_M)^T$ (see g_i)
i = subscript ($i = 1, 2, \ldots$)
j = subscript ($j = 1, 2, \ldots$)
$\mathbf{J}\left(\frac{\mathbf{f}}{\mathbf{s}}\right)$ = Jacobian matrix of $\mathbf{f}$ with respect to $\mathbf{s}$
J_{ij} = ijth element of Jacobian matrix
k_{ij} = association constant for ith compound's binding to jth class of binding sites on macromolecule
k_i = k_{i1} (see k_{ij})
k_i^* = membrane binding "association constant" of ith compound
K_m = dialysis rate constant for mth compound
m = subscript ($m = 1, 2, \ldots$)
M = number of compounds
n_j = number of binding sites in jth class of sites
n_i^* = mathematical analog to n_i in Langmuir-type membrane "binding" model
n = n_1 (see n_j)
N = number of binding classes
$\bar{\nu}_i$ = number of moles of ith compound ("ligand") bound per mole of macromolecule
$\bar{\nu}_i^*$ = amount of ith compound bound per amount of available membrane material
P = total molar concentration of macromolecular compound
θ = parameter vector containing elements such as n_j, k_{ij}, and P or other parameters used in the particular mathematical model $\mathbf{f}$ describing binding kinetics
r = correlation coefficient
s_i = absolute value of slope in a $[c_i]$ *versus* t plot at time t. This quantity is used as a parameter variable in the parametric representation of the variables $[c_i]$ and t
$\mathbf{s} = (s_1, s_2, \ldots, s_M)^T$ (see s_i)
$\mathbf{s}_0$ = $\mathbf{s}$ evaluated at $t = 0$
t = time
T = transpose
u_i = molecular weight of ith compound
υ = subscript ($\upsilon = 1, 2, \ldots$)
V = volume of dialysis compartment
w = weight of available membrane material
y_i = ith dependent variable in transformed set of linear regression equations (Eq. A2) used to obtain initial estimates of the binding parameters (n's and k's) by multiple linear regression technique

REFERENCES

(1) H. H. Stein, *Anal. Biochem.*, **13**, 605 (1965).
(2) A. Agren, *Acta Pharm. Suec.*, **5**, 37 (1968).
(3) M. C. Meyer and D. E. Guttman, *J. Pharm. Sci.*, **57**, 1627 (1968).
(4) *Ibid.*, **59**, 33 (1970).
(5) *Ibid.*, **59**, 39 (1970).
(6) J. C. Dearden and E. Tomlinson, *J. Pharm. Pharmacol., Suppl.*, **22**, 53S (1970).
(7) M. J. Crooks and K. F. Brown, *J. Pharm. Sci.*, **62**, 1904 (1973).
(8) M. J. Crooks and K. F. Brown, *J. Pharm. Pharmacol.*, **26**, 235 (1974).
(9) I. Kanfer and D. R. Cooper, *ibid.*, **28**, 58 (1976).
(10) S. J. A. Kazmi and A. G. Mitchell, *J. Pharm. Sci.*, **62**, 1299 (1973).
(11) F. Bottari, G. Di Colo, E. Nannipieri, M. F. Saettone, and M. F. Serafini, *ibid.*, **64**, 946 (1975).
(12) P. Veng Pedersen, M. J. Crooks, and K. F. Brown, *J. Pharm. Sci.*, **66**, 1458 (1977).
(13) C. W. Gear, "Numerical Initial Value Problems in Ordinary Differential Equations," Prentice-Hall, Englewood Cliffs, N.J., 1971.
(14) "Handbook of Mathematical Functions," M. Abramowitz and I. A. Stegun, Eds., Dover, New York, N.Y., 1970, p. 897.
(15) *Ibid.*, p. 950.
(16) P. Veng Pedersen, *J. Pharmacokinet. Biopharm.*, **5**, 513 (1977).
(17) Y. Bard, "Nonlinear Parameter Estimation," Academic, New York, N.Y., 1974, p. 57.
(18) J. H. Ahlberg, E. N. Nilson, and J. L. Walsh, "The Theory of Splines and Their Applications," Academic, New York, N.Y., 1967.

Analysis of Steroid Phosphates by High-Pressure Liquid Chromatography: Betamethasone Sodium Phosphate

L. M. UPTON *, E. R. TOWNLEY ˣ, and F. D. SANCILIO ‡

Received July 18, 1977, from the *Physical and Analytical Chemical Research and Development Department, Schering Corporation, Bloomfield, NJ 07003.* Accepted for publication October 25, 1977. *Present address: Seton Hall University, South Orange, NJ 07079. ‡Present address: Burroughs Wellcome Co., Research Triangle Park, NC 27709.

Abstract □ A sensitive, automatable high-pressure liquid chromatographic procedure is presented for the determination of steroid phosphates. Quantitation is described for betamethasone sodium phosphate in dosage forms in the presence of polar excipients. The separation of a multicomponent mixture of steroid phosphates also is reported.

Keyphrases □ Betamethasone sodium phosphate—high-pressure liquid chromatographic analysis in dosage forms □ High-pressure liquid chromatography—analysis, betamethasone sodium phosphate in dosage forms □ Glucocorticoids—betamethasone sodium phosphate, high-pressure liquid chromatographic analysis in dosage forms □ Steroid phosphates, various—high-pressure liquid chromatographic analysis in dosage forms

Steroid phosphates are highly effective anti-inflammatory agents produced in ophthalmic, injectable, and solid dosage forms. Reported analyses utilize spectrophotometric procedures preceded by extraction and/or reaction methods (1–3). These procedures are time consuming and relatively difficult. Two chromatographic methods have been reported: TLC of the methyl ester and ion chromatography (4, 5). This laboratory previously used

0022-3549/78/0700/0913$01.00/0

© 1978, American Pharmaceutical Association

Table I—Retention Times for Betamethasone Sodium Phosphate, Its Decomposition Products, and Common Preservatives Used in Formulations

Compound	Retention Time[a], min
Decomposition product	2.5–3.5
Phenol	4.0
Betamethasone sodium phosphate	5.0
Decomposition product	5.5
Betamethasone alcohol	8.0
Decomposition product	11.0
Butylparaben	12.0
Methandrostenolone	15.0

[a] Mobile phase: methanol–0.09 *M* KH_2PO_4 (1:1).

paper chromatography followed by elution of the steroid phosphate and quantitative measurement by colorimetric assay or by an enzymatic–colorimetric analysis.

The present study was undertaken to establish a rapid, reliable, stability-indicating high-pressure liquid chromatographic (HPLC) procedure for steroid phosphates, specifically for betamethasone sodium phosphate in the presence of compounds typically present in formulations. Quantitation of betamethasone sodium phosphate and other steroid phosphates in various formulations was achieved.

EXPERIMENTAL

Apparatus—A liquid chromatograph[1] with a UV absorption detector (254 nm) and a stainless steel column, 30 cm × 4 mm i.d., was used. The column packing[2] was porous silica particles permanently bonded to a monomolecular layer of organosilane. The column was operated at 1200 psi, resulting in a flow rate of 1 ml/min. Each analysis was performed at ambient temperature. Samples were injected with a 5-μl high-pressure syringe[3].

Materials—Acetone[4], methanol[4], butylparaben[5], and methandrostenolone[5] were used as received. The samples of betamethasone sodium phosphate, prednisolone sodium phosphate, dichlorisone sodium phosphate, testosterone sodium phosphate, and 16β-methylprednisone sodium phosphate were obtained in pure form[5].

Mobile Phase—The mobile phase was degassed methanol–0.09 *M* KH_2PO_4[6] (60:40) (Fig. 1). Multicomponent steroid phosphates were separated using methanol–0.09 *M* KH_2PO_4 (1:1) (Fig. 2).

Internal Standard, Reference Standard, and Sample Solutions—The internal standard solution of butylparaben was prepared by dissolving an accurately weighed (~150 mg) quantity of material in acetone in a 50-ml volumetric flask. The reference standard, about 35 mg of betamethasone sodium phosphate, was weighed accurately into each of two 10-ml volumetric flasks and dissolved in water. A response factor solution was prepared by adding 3.0 ml of reference standard solution, 2.0 ml of internal standard solution, and 3.0 ml of water to a stoppered flask. The remaining quantity of reference standard solution was saved for the corrected reference standard weight determination described under *Determination of Corrected Standard Weight*.

The sample solution consisted of an aliquot of sample equivalent to about 10 mg of betamethasone sodium phosphate[7], 2.0 ml of internal standard solution, and water (total of 8.0 ml)[8].

Chromatography—Each of two analyses consisted of an injection of 5 μl of sample solution followed by a 5-μl injection of a reference standard solution into an equilibrated column, using a detector attenuation of 0.64 absorbance unit. Phenol eluted immediately following the solvent. Betamethasone sodium phosphate eluted after 5 min, followed by butylparaben at 12 min (Fig. 1).

[1] Model 841, DuPont, Wilmington, Del.
[2] μBondapak C_{18}, Waters Associates, Milford, Mass.
[3] Model HP-305, Hamilton, Reno, Nev.
[4] Analytical reagent, Mallinckrodt.
[5] Reference standards, Schering Corp., Bloomfield, N.J.
[6] Reagent, Matheson, Coleman and Bell.
[7] Celestone Phosphate Injection, Schering. Label claim of 2.63, 3.95, or 5.26 mg of anhydrous betamethasone sodium phosphate/ml.
[8] The reference standard must be corrected for moisture content using a standard absorptivity figure.

Table II—Method Reproducibility[a]

Sample	Betamethasone Sodium Phosphate[b], mg/ml Assay I	Assay II
1	3.8	3.9
2	3.8	3.9
3	3.7	3.7
4	3.7	3.8
5	3.8	3.8
6	3.7	3.7

[a] Mobile phase: methanol–0.09 *M* KH_2PO_4 (60:40). [b] Each assay result is an average of two injections.

The peak height ratios were used to quantitate the resulting chromatograms. Equation 1 was used to calculate the response factor (*RF*) for the reference standard *versus* the internal standard:

$$RF = \left(\frac{PH_1}{PH_2}\right)\left(\frac{W_{is}}{W_s}\right)(0.133) \qquad \text{(Eq. 1)}$$

where PH_1 is the peak height or area of betamethasone sodium phosphate in the response factor standard solution, PH_2 is the peak height or area of butylparaben in the response factor standard solution, W_{is} is the weight (in milligrams) of butylparaben in the internal standard solution, W_s is the corrected weight (in milligrams) of standard in the reference standard solution, and 0.133 is the combined dilution factor of sample and internal standard solutions ($^1/_{50} \times {}^{10}/_1 \times {}^2/_8 \times {}^8/_3$).

This calculation is repeated for each determination, and an average response factor is used to derive the milligrams of betamethasone sodium phosphate per milliliter of original sample using:

$$\text{mg/ml} = \left(\frac{PH_3}{PH_4}\right)\left(\frac{W_{is}}{RF}\right)\left(\frac{1}{V}\right)(0.04) \qquad \text{(Eq. 2)}$$

where PH_3 is the peak height or area of betamethasone sodium phosphate in the sample solution, PH_4 is the peak height or area of butylparaben in the sample solution, *RF* is the average response factor, *V* is the volume of sample used in the preparation of the sample solution, and 0.04 is the combined dilution factor of sample and internal standard solutions ($^1/_{50} \times {}^2/_8 \times {}^8/_1$).

Determination of Corrected Standard Weight, W_s[8]—Reference standard solution (2.0 ml) is diluted with water to 200 ml in a volumetric flask. The absorbance (A_s) is read at 240 nm; W_s, in milligrams, is calculated in accordance with:

$$W_s = (A_s)(33.67) \qquad \text{(Eq. 3)}$$

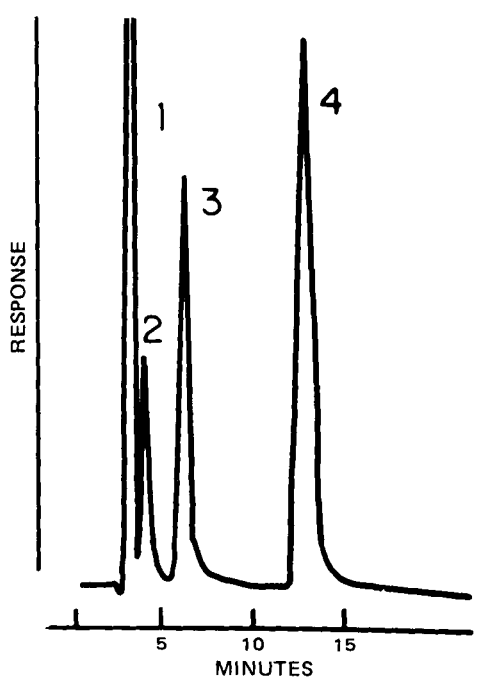

Figure 1—*Chromatogram of betamethasone sodium phosphate formulation. Key: 1, solvent; 2, phenol; 3, betamethasone sodium phosphate; and 4, butylparaben.*

Table III—Comparative Analyses Using Paper Chromatography and HPLC [a]

Sample	Betamethasone Sodium Phosphate, mg/ml	
	HPLC	Paper Chromatography
1	4.2	4.0
2	4.3	4.2
3	4.0	4.0
4	4.2	4.0
5	4.0	4.0
6	4.2	4.2
7	5.4	5.3
8	5.7	5.6
9	5.3	5.3
10	5.4	5.5

[a] Mobile phase: methanol–0.09 *M* KH_2PO_4 (60:40).

where A_s is the absorbance of the sample solution, and 33.67 equals 1000 divided by the absorptivity of betamethasone sodium phosphate which is 29.7.

RESULTS AND DISCUSSION

The polarity of the steroid phosphates necessitated the use of a nonpolar column. The high efficiency of the reversed-phase, small particle-size column enabled resolution of betamethasone sodium phosphate from all of its degradation products and most of the common excipients present in the formulation[7]. Mixtures of several steroid phosphates also were separated readily using the mobile phase indicated previously [methanol–0.09 *M* KH_2PO_4 (1:1)].

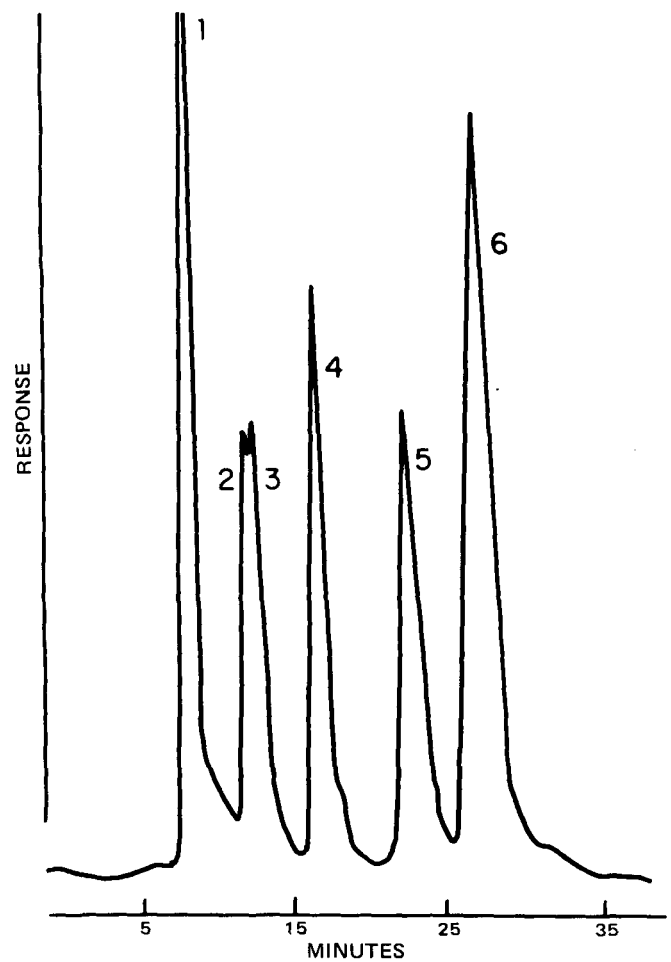

Figure 2—*Chromatogram of a mixture of steroid phosphates. Key: 1, prednisone sodium phosphate; 2, prednisolone sodium phosphate; 3, 16β-methylprednisone sodium phosphate; 4, betamethasone sodium phosphate; 5, testosterone sodium phosphate; and 6, dichlorisone sodium phosphate.*

Table IV—Analysis of Related Formulations

Sample	Percent of Label Strength
	Betamethasone Phosphate[a]
1	97
2	98
3	99
4	100
5	100
	Prednisolone Phosphate[b]
1	100
2	100
3	100
4	102
5	101
	Betamethasone Phosphate with Betamethasone Acetate[c]
1	101
2	100
3	101
4	100
5	103

[a] Ophthalmic solution (0.1%), Schering. [b] Metreton Ophthalmic and Optimyd Ophthalmic, Schering. [c] Celestone Soluspan, Schering.

An acidic mobile phase was utilized to keep the steroid phosphates in the nonionized state. The addition of small quantities of the aqueous component increased both the retention time and the separation of the materials. The optimum resolution and retention times were obtained with a solvent ratio of 13:8 for methanol–0.09 *M* KH_2PO_4.

The internal standard method for the quantitative calculations was chosen to minimize errors resulting from both the apparatus and the injection procedure.

After surveying several compounds, either butylparaben or methandrostenolone was found to be suitable as an internal standard. Each was easily resolved from betamethasone sodium phosphate and was separated from degradation products and excipients. Retention times are presented in Table I.

The plot of the peak height response *versus* the amount of betamethasone sodium phosphate was linear, thus demonstrating that the method can be used for quantitation. This conclusion was obtained after five samples, varying in the quantity of betamethasone sodium phosphate but with a constant concentration of internal standard, were analyzed and did not deviate from the results expected if Beer's law were valid.

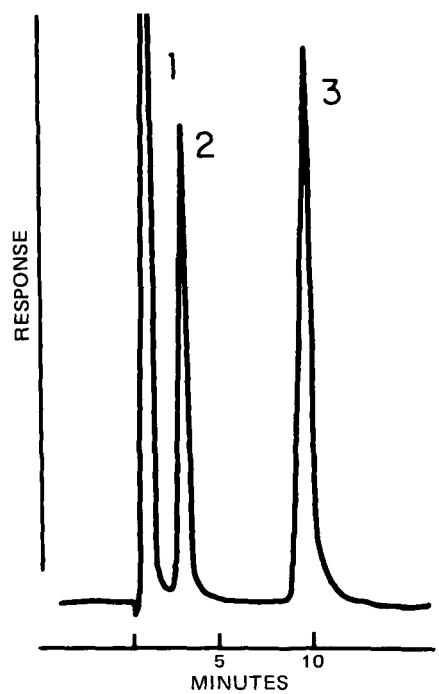

Figure 3—*Chromatogram of a prednisolone sodium phosphate formulation. Key: 1, solvent; 2, prednisolone sodium phosphate; and 3, butylparaben.*

(Similar results were obtained from aged samples of betamethasone sodium phosphate formulations.)

To ensure the usefulness of this technique, pure betamethasone sodium phosphate was degraded by heat, alkalinity, and acidity and the decomposed material was chromatographed. The chromatographic system separated all degradation products and possible manufacturing impurities. The decrease in the peak height upon degradation was not compensated for by an increase in the size of the decomposition peak. Therefore, the primary product, presumed to be the 17-ketone (6), was not detected in this system and was probably retained. Constant amounts of reference standard and internal standard were added to varying amounts of placebo and aged placebo. Recoveries were consistently in the 100% range.

The instrument precision was good at the attenuation used. Duplicate assays were performed for the injection formulation over several days, and the results indicate high reproducibility (Table II) and agreed well with the manufacturer label claims. Comparison of these results with the results obtained with a paper chromatographic assay shows the methods to be equivalent (Table III).

This method can be applied to other steroid phosphate formulations (Fig. 3 and Table IV). HPLC shortens analysis time and is accurate and easy to perform. In addition, it can be easily automated with automatic samplers.

REFERENCES

(1) "The National Formulary," 13th ed., Mack Publishing Co., Easton, Pa., 1970, pp. 90–92.

(2) "The United States Pharmacopeia," 19th rev., Mack Publishing Co., Easton, Pa., 1975, pp. 123–126.

(3) L. Cavatorta, L. Lodi, and R. Rangone, *Farmaco Ed. Prat.*, **25**, 312 (1970).

(4) J. Reiss, *J. Chromatogr.*, **19**, 527 (1965).

(5) W. Beyer and W. Mowzowich, *Ann. N.Y. Acad. Sci.*, **153**, 393 (1968).

(6) D. Guttman and P. Muster, *J. Am. Pharm. Assoc., Sci. Ed.*, **47**, 553 (1958).

ACKNOWLEDGMENTS

The authors express their appreciation to Mr. S. Gruber and Ms. V. Bole for assistance.

Theophylline Bioavailability following Chronic Dosing of an Elixir and Two Solid Dosage Forms

DANNY D. SHEN ˣ, MARK FIXLEY, and DANIEL L. AZARNOFF

Received May 26, 1977, from the *Departments of Medicine and Pharmacology, Clinical Pharmacology–Toxicology Center, Unive sity of Kansas Medical Center, College of Health Sciences and Hospital, Kansas City, KS 66103.* Accepted for publication October 19, 1977.

Abstract □ Theophylline bioavailability following chronic dosing of an elixir and two commercial tablet formulations (I and II) relative to an acute dose of elixir was evaluated in healthy volunteers. Both tablet formulations contained ephedrine. In addition, Tablet I contained hydroxyzine hydrochloride, and Tablet II contained phenobarbital. The mean area under the serum concentration–time curve (*AUC*) calculated either from time $0 \rightarrow \infty$ for a single dose or over one dosing interval after repetitive doses was the highest after chronic administration of the elixir. The *AUC* after chronic elixir, in fact, was statistically different from the values after acute elixir ($p < 0.05$) and Tablet II ($p < 0.05$). There was, however, a large variation in the elimination half-life among the four theophylline treatments. The mean $t_{1/2}$ was the longest after chronic elixir followed by Tablet I, Tablet II, and acute elixir. The *AUC* values for the four treatments, when corrected for differences in $t_{1/2}$, were no longer significantly different, indicating that the extent of theophylline absorption was essentially the same from all three tested products. The time to peak and the peak serum concentration also did not differ among treatments. The prolongation in $t_{1/2}$ following chronic treatment with the elixir and its subsequent shortening during tablet administration suggest an initial inhibition followed by induction of theophylline metabolism. These changes may be due to the prolonged treatment with theophylline itself or the other drug ingredients in the dosage form.

Keyphrases □ Theophylline—bioavailability of commercial elixir and two tablets compared, chronic dosing in humans □ Bioavailability—theophylline, commercial elixir and two tablets compared, chronic dosing in humans □ Relaxants, smooth muscle—theophylline, bioavailability of commercial elixir and two tablets compared, chronic dosing in humans

Literature reports (1, 2) suggested that incomplete bioavailability of theophylline tablets, singly or in combination with ephedrine and sedatives such as phenobarbital or hydroxyzine, may frequently cause therapeutic failures. Theophylline bioavailability after a single oral dose of an elixir and two different combination tablets was essentially complete as compared to intrave. ous aminophylline (3). However, it is not known whether differences in bioavailability for these theophylline formulations occur when given chronically.

Several factors might affect the serum theophylline concentration when it is administered over an extended period. In humans, theophylline is eliminated largely by oxidative microsomal metabolism (4). Drugs frequently combined with theophylline, such as phenobarbital and hydroxyzine, may alter its pharmacokinetics. Cigarette smoking significantly increased the serum clearance of theophylline (5, 6), presumably due to microsomal enzyme induction by the polycyclic aromatic hydrocarbon constituents in the smoke. Theophylline induced its own metabolism in the rat (7), and a similar action could occur in humans.

The present study was designed to ascertain the chronic oral availability of theophylline from previously studied lots of elixir and combination tablet preparations relative to an acute dose of the elixir. In addition, the effects of long-term administration of theophylline and the other drugs in the combination tablets on the disposition kinetics of theophylline were observed.

EXPERIMENTAL

Subjects—Twelve healthy volunteers between 22 and 40 years of age and weighing between 46.2 and 82.4 kg participated. Of the 12 subjects (five men and seven women), only two were habitual smokers, each averaging fewer than 20 cigarettes/day. Written informed consent, a history, a physical examination, and laboratory tests (complete blood count, urinalysis, long-lead II ECG, serum thyroxine, bilirubin, creatinine, glutamic-oxaloacetic transaminase, and alkaline phosphatase) were

0022-3549/78/0700/0916$01.00/0

© 1978, American Pharmaceutical Association

(Similar results were obtained from aged samples of betamethasone sodium phosphate formulations.)

To ensure the usefulness of this technique, pure betamethasone sodium phosphate was degraded by heat, alkalinity, and acidity and the decomposed material was chromatographed. The chromatographic system separated all degradation products and possible manufacturing impurities. The decrease in the peak height upon degradation was not compensated for by an increase in the size of the decomposition peak. Therefore, the primary product, presumed to be the 17-ketone (6), was not detected in this system and was probably retained. Constant amounts of reference standard and internal standard were added to varying amounts of placebo and aged placebo. Recoveries were consistently in the 100% range.

The instrument precision was good at the attenuation used. Duplicate assays were performed for the injection formulation over several days, and the results indicate high reproducibility (Table II) and agreed well with the manufacturer label claims. Comparison of these results with the results obtained with a paper chromatographic assay shows the methods to be equivalent (Table III).

This method can be applied to other steroid phosphate formulations (Fig. 3 and Table IV). HPLC shortens analysis time and is accurate and easy to perform. In addition, it can be easily automated with automatic samplers.

REFERENCES

(1) "The National Formulary," 13th ed., Mack Publishing Co., Easton, Pa., 1970, pp. 90–92.

(2) "The United States Pharmacopeia," 19th rev., Mack Publishing Co., Easton, Pa., 1975, pp. 123–126.

(3) L. Cavatorta, L. Lodi, and R. Rangone, *Farmaco Ed. Prat.*, **25**, 312 (1970).

(4) J. Reiss, *J. Chromatogr.*, **19**, 527 (1965).

(5) W. Beyer and W. Mowzowich, *Ann. N.Y. Acad. Sci.*, **153**, 393 (1968).

(6) D. Guttman and P. Muster, *J. Am. Pharm. Assoc., Sci. Ed.*, **47**, 553 (1958).

ACKNOWLEDGMENTS

The authors express their appreciation to Mr. S. Gruber and Ms. V. Bole for assistance.

Theophylline Bioavailability following Chronic Dosing of an Elixir and Two Solid Dosage Forms

DANNY D. SHEN ˣ, MARK FIXLEY, and DANIEL L. AZARNOFF

Received May 26, 1977, from the *Departments of Medicine and Pharmacology, Clinical Pharmacology–Toxicology Center, Unive sity of Kansas Medical Center, College of Health Sciences and Hospital, Kansas City, KS 66103.* Accepted for publication October 19, 1977.

Abstract □ Theophylline bioavailability following chronic dosing of an elixir and two commercial tablet formulations (I and II) relative to an acute dose of elixir was evaluated in healthy volunteers. Both tablet formulations contained ephedrine. In addition, Tablet I contained hydroxyzine hydrochloride, and Tablet II contained phenobarbital. The mean area under the serum concentration–time curve (*AUC*) calculated either from time $0 \rightarrow \infty$ for a single dose or over one dosing interval after repetitive doses was the highest after chronic administration of the elixir. The *AUC* after chronic elixir, in fact, was statistically different from the values after acute elixir ($p < 0.05$) and Tablet II ($p < 0.05$). There was, however, a large variation in the elimination half-life among the four theophylline treatments. The mean $t_{1/2}$ was the longest after chronic elixir followed by Tablet I, Tablet II, and acute elixir. The *AUC* values for the four treatments, when corrected for differences in $t_{1/2}$, were no longer significantly different, indicating that the extent of theophylline absorption was essentially the same from all three tested products. The time to peak and the peak serum concentration also did not differ among treatments. The prolongation in $t_{1/2}$ following chronic treatment with the elixir and its subsequent shortening during tablet administration suggest an initial inhibition followed by induction of theophylline metabolism. These changes may be due to the prolonged treatment with theophylline itself or the other drug ingredients in the dosage form.

Keyphrases □ Theophylline—bioavailability of commercial elixir and two tablets compared, chronic dosing in humans □ Bioavailability—theophylline, commercial elixir and two tablets compared, chronic dosing in humans □ Relaxants, smooth muscle—theophylline, bioavailability of commercial elixir and two tablets compared, chronic dosing in humans

Literature reports (1, 2) suggested that incomplete bioavailability of theophylline tablets, singly or in combination with ephedrine and sedatives such as phenobarbital or hydroxyzine, may frequently cause therapeutic failures. Theophylline bioavailability after a single oral dose of an elixir and two different combination tablets was essentially complete as compared to intrave. ous aminophylline (3). However, it is not known whether differences in bioavailability for these theophylline formulations occur when given chronically.

Several factors might affect the serum theophylline concentration when it is administered over an extended period. In humans, theophylline is eliminated largely by oxidative microsomal metabolism (4). Drugs frequently combined with theophylline, such as phenobarbital and hydroxyzine, may alter its pharmacokinetics. Cigarette smoking significantly increased the serum clearance of theophylline (5, 6), presumably due to microsomal enzyme induction by the polycyclic aromatic hydrocarbon constituents in the smoke. Theophylline induced its own metabolism in the rat (7), and a similar action could occur in humans.

The present study was designed to ascertain the chronic oral availability of theophylline from previously studied lots of elixir and combination tablet preparations relative to an acute dose of the elixir. In addition, the effects of long-term administration of theophylline and the other drugs in the combination tablets on the disposition kinetics of theophylline were observed.

EXPERIMENTAL

Subjects—Twelve healthy volunteers between 22 and 40 years of age and weighing between 46.2 and 82.4 kg participated. Of the 12 subjects (five men and seven women), only two were habitual smokers, each averaging fewer than 20 cigarettes/day. Written informed consent, a history, a physical examination, and laboratory tests (complete blood count, urinalysis, long-lead II ECG, serum thyroxine, bilirubin, creatinine, glutamic-oxaloacetic transaminase, and alkaline phosphatase) were

0022-3549/78/0700/0916$01.00/0

© 1978, American Pharmaceutical Association

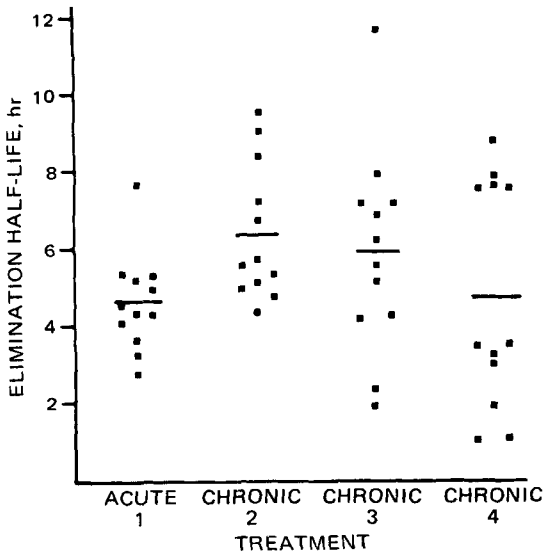

Figure 1—*Comparison of serum theophylline half-life in the 12 volunteers after treatment with an acute dose of the elixir and chronic doses of the elixir and Tablets I and II. The bar represents the mean half-life of each treatment. Key: 1, acute elixir; 2, chronic elixir; 3, chronic Tablet I; and 4, chronic Tablet II.*

obtained before the study, and the results were within normal limits for all volunteers.

Drug Products—Three products containing theophylline were tested: an elixir[1] containing 80 mg of theophylline/15 ml; Tablet I[2], a preparation containing 130 mg of theophylline, 25 mg of ephedrine sulfate, and 10 mg of hydroxyzine hydrochloride; and Tablet II[3], a preparation containing 130 mg of theophylline; 24 mg of ephedrine hydrochloride, and 8 mg of phenobarbital.

Samples of the three preparations were assayed for theophylline content using a previously described high-pressure liquid chromatographic method (8). Theophylline content was within 10% of the label claim for all three dosage forms.

Drug Administration—To minimize any possible alteration of theophylline metabolism by theophylline itself or other drug ingredients in the formulations from influencing the results by a carryover effect, the sequence of administration was not randomized. Accordingly, following a single 130-mg dose of theophylline elixir, the same dosage form was administered for 10 days in a dose of 130 mg at 8-hr intervals. This regimen was followed by an equivalent theophylline dose of Tablets I and II every 8 hr for 10 days each.

A drug-free washout period of at least 21 days followed each 10-day drug administration period. The subjects were forbidden to take other drugs throughout the study and methylxanthine-containing beverages (tea, coffee, cocoa, and cola) on the final 2 days of each treatment period. Compliance was monitored only by verbal questioning.

Blood Sampling—Following the first dose of elixir and on the last day of each 10-day chronic drug administration period, blood samples were drawn at 0, 0.25, 0.5, 0.75, 1.0, 1.5, 2, 3, 4, 6, 8, 10, and 12 hr through an indwelling polytef cannula inserted in an antecubital vein. Subjects were required to fast for at least 12 hr before each blood sampling period.

Analysis of Theophylline—Theophylline concentration in the serum samples was measured by the GLC method of Kowblansky *et al.* (9). The method involves flash heater *N*-butylation of theophylline with 8-chlorotheophylline as an internal standard. The precision of this procedure was estimated by including quadruplicate samples of 1 and 5 μg of theophylline/ml standards in each run. The means of the standards were 0.975 and 4.92 μg with coefficients of variations of 15% (n = 17) and 6.3% (n = 52), respectively.

Pharmacokinetic Analysis—A previous study (10) showed that the pharmacokinetics of theophylline following single intravenous bolus administration can be described by a two-compartment model. However, in the present oral study, a clearly discernible distribution phase was not evident in any serum concentration–time course profile. Therefore, the data were analyzed according to a simple linear one-compartment open model (11), using the iterative nonlinear least-squares regression computer program of Metzler (12). Each data point was weighted by the reciprocal of its observed value.

Theophylline absorption from the various dosage forms was characterized by an apparent first-order absorption rate constant, k_a. In some cases, a more satisfactory fit of the observed data was obtained when an absorption lag time, t_0, was introduced into the model. The serum concentration of drug, C, at any time, t, after a *single* oral dose, D, is described by:

$$C = \frac{FD}{V}\left(\frac{k_a}{k_a - K}\right)\left[e^{-K(t-t_0)} - e^{-k_a(t-t_0)}\right] \qquad \text{(Eq. 1)}$$

where F is the fraction of the oral dose absorbed, V is the apparent volume of distribution, and K is the apparent first-order elimination rate constant.

Half-lives, $t_{1/2}$, were calculated by dividing $\log_e 2$ or 0.693 by its rate constant. Based on the estimates of k_a, K, and t_0, the peak concentration, C_{max}, and time to reach the peak, t_p, following a single dose were calculated according to previously established equations (11).

The equation describing the time course of drug concentration in plasma following the last oral dose at steady state is derived from Eq. 1 by multiplying each exponential term by the multiple-dosing function of Benet (13), *i.e.*, $1/(1 - e^{k_i\tau})$, where k_i is the apparent first-order rate constant in each exponential term (*i.e.*, k_a and K) and τ is the dosage interval (*i.e.*, 8 hr). The peak concentration, C^{∞}_{max}, and time to peak, $t_p{}^{\infty}$, following an oral dose at steady state were calculated (11).

The total area under the serum concentration–time curve (AUC) was estimated by the trapezoidal rule. Extrapolation beyond the last recorded serum concentration, C^*, was calculated by C^*/K.

In theory, the entire AUC (*i.e.*, AUC_∞) for a given drug after a single oral dose is equivalent to the AUC over one dosing interval (*i.e.*, AUC_τ), provided that the bioavailability, F, and serum clearance, KV, remain unchanged during repetitive administration. Since theophylline absorption from a single dose of the elixir previously was found to be complete (3), the relative bioavailability of chronic doses of the elixir and Tablets I and II was evaluated by comparing their AUC_τ values with the AUC_∞ after acute elixir.

The average steady-state serum concentration, $\overline{C}_{ss}$, as proposed by Wagner (14) was calculated by dividing AUC_τ by τ. Based on single-dose serum concentration–time data, $\overline{C}_{ss}$ was predicted by dividing AUC_∞ by τ.

Statistical Analysis—An analysis of variance (15) adapted for single-factor experiments with repeated measures on the same individual was used in the statistical evaluation of AUC and $t_{1/2}$. When significant differences between the products were found, a Newman–Keuls test (15) was carried out to find the source of the difference. Homogeneity of variances was examined by Bartlett's test (14).

RESULTS

The means and standard deviations of the various pharmacokinetic parameters estimated by nonlinear least-squares analysis of serum concentration–time data from both the acute and chronic elixir and the two chronic combination tablet studies are summarized in Table I. The pharmacokinetic parameters derived from the acute dose of elixir were not significantly different [Mann–Whitney test (16), $p > 0.05$] from those of a previous single-dose study with the same lot of elixir in another group of normal volunteers (3).

Substantial variations in the elimination half-lives of theophylline were noted following administration of the four different dosage forms. The half-life values are graphically compared in Fig. 1. The mean elimination half-life of theophylline after an acute dose of elixir for the 12 subjects was 4.62 hr (2.78–7.65 hr) and increased to 6.30 hr (4.36–9.49 hr) following chronic administration of elixir. The prolongation in half-life was inversely correlated with the initial half-life (r = 0.625, $p < 0.05$).

The serum half-life after chronic administration of Tablet I had a mean of 5.84 hr and was quite variable (1.88–11.6 hr). In four of the 12 subjects, the elimination half-life remained prolonged; in the remaining subjects, the half-life values tended to return to initial levels. In fact, the theophylline half-life in two subjects in the latter group decreased to below that after the first dose of elixir.

The final course of treatment with Tablet II, which contained 8 mg of phenobarbital/tablet (daily intake of 24 mg of phenobarbital), further decreased the elimination half-life of theophylline in some subjects. The

[1] Elixophyllin, Cooper Laboratories, Parsippany, NJ 07054 (lot number unavailable).
[2] Marax, lot 45340, Roerig Division, Pfizer, New York, N.Y.
[3] Tedral, lot 0459P034A, Warner-Chilcott Division, Warner-Lambert Co., Morris Plains, N.J.

Table I—Comparison of Serum Pharmacokinetic Parameters among Four Different Theophylline Treatments

Parameter	Acute Elixir	Chronic Elixir	Chronic Tablet I	Chronic Tablet II
Peak serum concentration, μg/ml[a–d]	3.84 ± 0.86[e]	7.08 ± 2.52	5.40 ± 1.41	5.14 ± 1.25
Time to peak, hr[a,d]	1.03 ± 0.65	0.79 ± 0.40	1.22 ± 0.72	1.17 ± 0.73
Absorption lag time, hr[f]	0.19 ± 0.30	0.02 ± 0.06	0.25 ± 0.23	0.17 ± 0.28
Elimination half-life, hr[g]	4.62 ± 1.25	6.30 ± 1.81	5.84 ± 2.62	4.69 ± 2.89
		$p < 0.05$		
AUC, μg hr/ml[b,g,h]	29.4 ± 9.7	41.0 ± 14.2	31.2 ± 9.7	28.3 ± 12.1
		$p < 0.05$		
			$p < 0.05$	
(*AUC*)(*K*), μg/ml[b,d,i]	4.50 ± 1.18	4.94 ± 2.72	4.36 ± 1.97	5.76 ± 4.03

[a] Only the parameters from chronically administered formulations were compared by the analysis of variance. [b] A logarithmic transformation was performed prior to the analysis of variance as suggested by Westlake (17). [c] Corrected to a body weight of 70 kg. [d] No significant difference among products by the analysis of variance. [e] Mean ± *SD*. [f] Due to nonnormal distribution, the means cannot be tested for statistical difference. [g] Comparison by Newman–Keuls range test. [h] *AUC* from either time 0 → ∞ or over one dosing interval. [i] *AUC* corrected for variation in the elimination rate constant.

half-lives of three subjects were reduced to less than 2 hr. The mean for the group was 4.69 hr. In three subjects, the theophylline half-life clearly increased after chronic treatment with elixir and remained elevated throughout the study. In the other subjects, however, either chronic treatment with elixir did not result in a definite increase in half-life or further treatment with Tablets I and II tended to normalize that increase.

The magnitude of change in the elimination half-life between treatments was far greater than the intrasubject or intertreatment variation noted in the preceding acute study (3), where the maximum observed change was no more than ±30% in most subjects.

The group variance in elimination half-life gradually increased during the various treatments. For example, the coefficient of variation for the mean of the half-lives increased by more than twofold, from 27% after an acute dose of elixir to 62% after chronic treatment with Tablet II. When tested for homogeneity, the variance of the elimination half-life during administration of Tablet II was significantly different ($p < 0.05$) than that during the other three treatments. Consequently, the half-life data after Tablet II cannot be included in an analysis of variance of the half-life means. The mean theophylline serum elimination half-lives after acute elixir, chronic elixir, and Tablet I were significantly different ($p < 0.05$). According to the Newman–Keuls test, only the half-life of elimination of theophylline after chronic administration of elixir was significantly longer than that after an acute dose of elixir ($p < 0.05$) (Table I).

The time course of mean serum theophylline concentration following the four dosage treatments is depicted in Fig. 2. The extent of variation in the *AUC* with different treatments is illustrated by a comparison of the predicted and observed average serum theophylline concentrations, $\bar{C}_{ss}$, in Fig. 3. On the average, the *AUC* increased approximately 40% after 10 days of treatment with the elixir when compared to that following the first dose (Table I). Despite substantial changes in the half-life, in most of the 12 volunteers the AUC_τ or $\bar{C}_{ss}$ following the tablet formulations was comparable to the AUC_∞ after an acute dose of elixir.

Westlake (17) suggested use of the logarithm of the *AUC* instead of the untransformed *AUC* in an analysis of variance since the intrasubject variation in the serum clearance of the drug can then be treated as an additive effect due to the subject. When analyzed following transformation, a significant difference ($p < 0.05$) between the mean *AUC* for the four treatments was found (Table I). According to the Newman–Keuls test, the *AUC* after chronic administration of elixir was larger than that after both the acute dose of elixir ($p < 0.05$) and chronic administration of Tablet I ($p < 0.05$).

The increase in *AUC* after chronic treatment with elixir may largely be attributed to the increase in the elimination half-life. Wagner (18) suggested that when analyzing *AUC* data from a comparative bioavailability study, a large intersubject variation in elimination can be corrected by multiplying each subject's *AUC* by the first-order elimination rate constant. When the *AUC* was corrected for the treatment variation in elimination rate and further converted by logarithmic transformation, a statistically significant difference between means was no longer observed ($p > 0.05$).

The absorption rate of theophylline from the elixir and the two combination tablets was reasonably rapid. The mean time to peak was 1.03, 0.791, 1.22, and 1.17 hr for acute and chronic elixir and Tablets I and II, respectively (Table I). There was no significant difference in the time to peak for the chronically administered formulations when tested by the analysis of variance. Neither was there any difference in the peak concentration of theophylline. In some subjects, an absorption lag time from approximately 10 min to as much as 1 hr had to be assigned to obtain a good data fit. These lag times may reflect a real delay in absorption because of gastric emptying of the drug.

DISCUSSION

The present attempt to assess the relative steady-state bioavailability of the three oral theophylline preparations was complicated by the

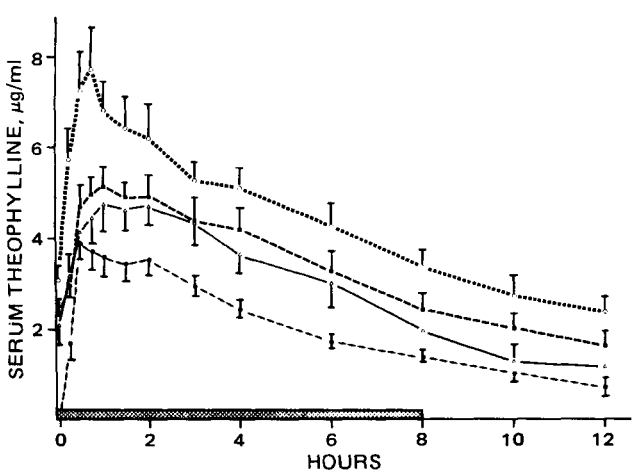

Figure 2—*Serum theophylline concentration after a single administration of 130 mg of theophylline as an elixir (●) and after repetitive administration of the same dose of theophylline in the form of the elixir (○) and commercial Tablets I (■) and II (△). Each point represents the mean and standard error of 12 observations. The individual serum concentrations were normalized to a 70-kg body weight.*

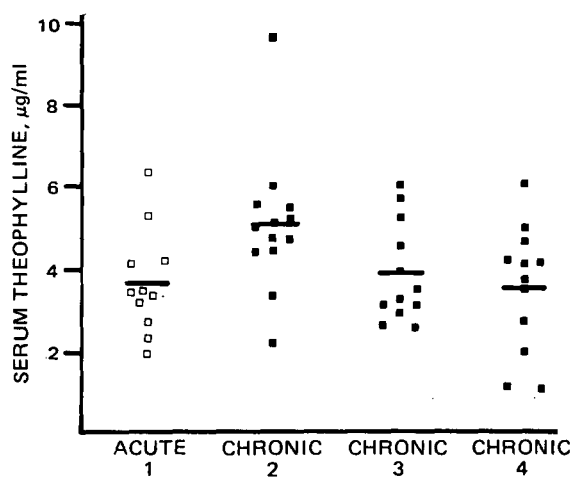

Figure 3—*Average steady-state serum concentration, $\bar{C}_{ss}$, of theophylline during chronic administration of the elixir and commercial Tablets I and II compared to that predicted based on an acute study of the elixir in the 12 volunteers. The bar represents the mean steady-state serum concentration of each treatment. Key: same as Fig. 1.*

marked variation in the elimination half-life of the drug between treatments. However, when individual *AUC* data were corrected for the treatment-dependent change in the elimination half-life, the difference between mean *AUC* values was no longer observed. This result is consistent with the previous single-dose study (3) with the same lots of theophylline products; that study showed that there was no significant difference in relative bioavailability between the elixir and the two theophylline combination tablet formulations. Furthermore, the absorption of theophylline from both the hydroalcoholic solution and tablet preparations was essentially complete when compared to intravenous aminophylline (3).

Although the bioavailability of the three tested products does not appear to be a clinically significant concern in theophylline therapy, the changes in the elimination half-life of the drug observed during the chronic study definitely warrant further investigation. There is no ready explanation for the prolongation in half-life following the 10-day administration of elixir, which was accompanied by an increase in AUC_τ or $\overline{C}_{ss}$. Ingredients in the elixir could have caused an inhibition of theophylline metabolism. The elixir contained 20% (v/v) alcohol and an undisclosed amount of palatable aromatic base (19) for flavoring.

Although inhibition of hepatic microsomal metabolism of drugs has been reported following acute treatment with alcohol (20), the amount of alcohol ingested in each elixir dose (approximately 4 g) was far less than that used in published alcohol–drug interaction studies. Furthermore, long-term administration of alcohol often leads to an opposite effect on drug metabolism, that of microsomal enzyme induction (21). Inhibition of theophylline metabolism because of the alcohol in the elixir preparation is, therefore, an unlikely possibility.

The increase in half-life during repetitive dosing may be a result of nonlinearity in the elimination kinetics of the drug, due perhaps to either self-inhibition or saturation of theophylline metabolism. Although nonlinearity in theophylline elimination kinetics has never been reported, neither has any dose or level dependency study. It may be argued that nonlinearity is an unlikely possibility since similar prolongation in half-life did not occur with other treatments. However, the nonlinearity in theophylline elimination could have been masked by concurrent induction of theophylline metabolism. The mean elimination half-life after both Tablets I and II showed a gradual return to a value comparable to that observed after the initial administration of the elixir. In fact, in a few individuals the elimination half-life was reduced below the baseline value, suggesting that some induction of theophylline metabolism may have occurred.

Theophylline metabolism by rat liver slices was accelerated by pretreatment with phenobarbital and 3-methylcholanthrene (7). On the other hand, pretreatment of male rats with high doses of methylxanthines including theophylline increased hepatic aniline hydroxylase, *p*-nitroanisole demethylase, and aminopyrine demethylase activity (7, 22). Even though a statistically valid comparison of the elimination half-life between treatments with Tablet II and acute elixir cannot be made because of nonhomogeneity of the group variance, the drastic reduction in five of the 12 volunteers strongly suggests that, in certain susceptible individuals, induction of theophylline does occur due to the intake of phenobarbital, hydroxyzine, ephedrine, or a combination thereof. Alternatively, chronic exposure to the drug itself over the three 10-day treatment periods may have resulted in induction.

Concomitant treatment with phenobarbital previously (23) did not cause a statistically significant change in either the half-life or serum clearance of theophylline in 12 male, nonsmoker, healthy volunteers. Induction of theophylline metabolism by smoking, in contrast, is well documented (5, 6) and led to the suggestion (24) that theophylline may be largely metabolized by the cytochrome P-448 system. This system is induced primarily by polycyclic aromatic hydrocarbons and polychlorinated biphenyls.

In a study (4) correlating the urinary excretion of the three major metabolites (3-methylxanthine, 1,3-dimethyluric acid, and 1-methyluric acid) with the serum theophylline concentration, it was concluded that the formation of 3-methylxanthine in humans is the dominant metabolic pathway controlling the serum theophylline concentration. Therefore, it would be of interest to investigate the effect of chronic administration of theophylline on its metabolism, particularly the 1-demethylation to 3-methylxanthine pathway.

In conclusion, since large intersubject variation in the serum theophylline concentration was reported (25) in 83 patients undergoing chronic oral aminophylline therapy, a number of studies attempted to elucidate the underlying factors responsible for this variation (4–6, 23, 24, 26, 27). Although external influences such as differences in dietary and smoking habits are important, individual differences in response to prolonged treatment with theophylline itself or other concurrent drugs may also be a contributing factor.

REFERENCES

(1) H. C. Shirkey, *J. Pediat.*, **76,** 774 (1970).

(2) "Task Force on Prescription Drugs: Final Report," U.S. Department of Health, Education, and Welfare, Washington, D.C., Feb. 7, 1969.

(3) M. Fixley, D. D. Shen, and D. L. Azarnoff, *Am. Rev. Resp. Dis.*, **115,** 955 (1977).

(4) J. W. Jenne, H. T. Nagasawa, and R. D. Thompson, *Clin. Pharmacol. Ther.*, **19,** 375 (1976).

(5) J. Jenne, H. Nagasawa, R. McHugh, F. MacDonald, and E. Wyze, *Life Sci.*, **17,** 195 (1975).

(6) S. N. Hunt, W. J. Jusko, and A. M. Yurchak, *Clin. Pharmacol. Ther.*, **19,** 546 (1976).

(7) S. M. Lohmann and R. P. Miech, *J. Pharmacol. Exp. Ther.*, **196,** 213 (1976).

(8) D. A. Sitar, K. M. Piafsky, R. E. Rangno, and R. I. Ogilvie, *Clin. Chem.*, **21,** 1774 (1975).

(9) J. Kowblansky, B. M. Scheintal, G. D. Cravello, and L. Chafetz, *J. Chromatogr.*, **76,** 467 (1973).

(10) P. A. Mitenko and R. I. Ogilvie, *Clin. Pharmacol. Ther.*, **14,** 509 (1973).

(11) M. Gibaldi and D. Perrier, "Pharmacokinetics," 1st ed., Dekker, New York, N.Y., 1975, p. 33.

(12) C. M. Metzler, Technical Report 7292/69/7293/005, The Upjohn Co., Kalamazoo, Mich., 1969.

(13) L. Z. Benet, *J. Pharm. Sci.*, **61,** 536 (1972).

(14) J. G. Wagner, *Nature*, **207,** 1301 (1965).

(15) B. J. Winer, "Statistical Principles in Experimental Design," 2nd ed., McGraw-Hill, New York, N.Y., 1962, p. 261.

(16) W. J. Dixon and F. J. Massey, Jr., "Introduction to Statistical Analysis," 3rd ed., McGraw-Hill, New York, N.Y., 1969, p. 308.

(17) W. J. Westlake, *J. Pharm. Sci.*, **62,** 1579 (1973).

(18) J. G. Wagner, "Fundamentals of Clinical Pharmacokinetics," 1st ed., Hamilton, Hamilton, Ill., 1975, p. 348.

(19) "Physicians' Desk Reference," 30th ed., Litton Industries, Oradell, N.J., 1976, p. 736.

(20) E. Rubin, H. Gang, P. S. Misra, and C. S. Lieber, *Am. J. Med.*, **49,** 801 (1970).

(21) E. Rubin and C. S. Lieber, *Science*, **172,** 1097 (1971).

(22) H. U. Aeschbacher and H. P. Wurzer, *Toxicol. Appl. Pharmacol.*, **33,** 575 (1975).

(23) K. M. Piafsky, D. S. Sitar, and R. I. Ogilvie, *Clin. Res.*, **23,** 610A (1975).

(24) A. P. Alvares, K. E. Anderson, A. H. Conney, and A. Kappas, *Proc. Natl. Acad. Sci. USA*, **73,** 2501 (1976).

(25) J. W. Jenne, E. Wyze, and F. S. Rood, *Clin. Pharmacol. Ther.*, **13,** 349 (1972).

(26) A. Kappas, K. E. Anderson, A. H. Conney, and A. P. Alvares, *ibid.*, **20,** 643 (1976).

(27) P. G. Welling, L. L. Lyons, W. A. Craig, and G. A. Trochta, *Clin. Pharmacol. Ther.*, **17,** 475 (1975).

ACKNOWLEDGMENTS

Supported by Grant GM 15956 from the U.S. Public Health Service and a grant from Pfizer Laboratories.

Cloprednol Bioavailability in Humans

E. J. MROSZCZAK ˣ, R. RUNKEL, L. J. STRAND, R. V. TOMLINSON, A. FRATIS, and E. SEGRE

Received May 9, 1977, from the *Institutes of Pharmacology and Metabolism and Clinical Medicine, Syntex Research, Palo Alto, CA 94304.* Accepted for publication October 20, 1977.

Abstract □ The bioavailability of cloprednol, a new systemic corticosteroid, was examined in a 12-subject crossover study in which two capsules, a tablet, and a solution were tested. Plasma was analyzed for cloprednol by a GLC–mass spectrometric method. The biological half-life, peak plasma concentration, peak time, plasma concentration at all sampling times, and plasma areas were evaluated for differences ($p \leq 0.05$) in comparisons of pairs among the four formulations. An analysis of variance revealed that cloprednol was absorbed to the same extent from all formulations and rapidly cleared from the plasma with a half-life of 1.86 ± 0.36 (*SD*) hr. All plasma profile parameters from the solid dose formulations were the same, demonstrating bioequivalence in both rate and extent of absorption. Significant differences were observed between the solution and solid dose formulations with respect to peak time, 15-min plasma concentration, and 0–30-min area, indicative of faster absorption from the solution; however, total plasma areas were the same for all four formulations. Comparison of plasma cloprednol levels in this study to those of a prior intravenous–oral dose study suggests that cloprednol was completely bioavailable from all formulations.

Keyphrases □ Cloprednol—bioavailability of various dosage forms in humans □ Bioavailability—cloprednol, various dosage forms in humans □ Glucocorticoids—cloprednol, bioavailability of various dosage forms in humans

Cloprednol (I), 6-chloro-11β,17α,21-trihydroxypregna-1,4,6-triene-3,20-dione, is a new systemic corticosteroid intended for oral use. Although the relative anti-inflammatory potency of cloprednol in patients with rheumatoid arthritis is approximately twice that of prednisolone, the hypothalamic–pituitary–adrenal (HPA) axis function in humans is minimally altered by cloprednol compared to equipotent anti-inflammatory doses of prednisolone, triamcinolone, dexamethasone, and betamethasone (1). Like prednisolone, cloprednol lacks the sodium-retaining properties of hydrocortisone; however, cloprednol may have less of a deleterious effect on nitrogen and calcium excretion than prednisolone (2).

The purpose of the present study was to determine the rate and extent of cloprednol absorption in humans administered various dosage forms. A tablet intended for future phase III studies was compared with two capsules used in early clinical trials and a solution in a 12-subject bioavailability study. In a separate two-subject metabolism study, cloprednol was administered intravenously and orally in solution to determine its absolute bioavailability in humans.

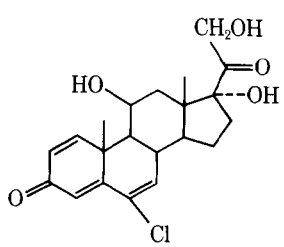

I

Table I—Treatment Schedule [a]

Subjects	Day 1	Day 8	Day 15	Day 22
1, 5, 9	A	B	C	D
2, 6, 10	B	C	D	A
3, 7, 11	C	D	A	B
4, 8, 12	D	A	B	C

[a] A, B, C, and D refer to the formulations described under *Experimental.*

EXPERIMENTAL

Formulations and Dosage—Formulation A was a capsule[1] containing 1.25 mg of cloprednol with starch and lactose as fillers. Formulation B was also a capsule[2] and contained 1.25 mg of cloprednol with starch, lactose, and magnesium stearate as a lubricant. Two capsules were administered to each subject.

Formulation C was a tablet[3] containing 2.50 mg of cloprednol along with starch, lactose, povidone, and magnesium stearate. One tablet was administered to each subject. Formulation D contained 2.50 mg of cloprednol in 100 ml of 15% ethanol–10% citric acid buffer.

Twelve healthy adult male volunteers received 2.5 mg of cloprednol in each of the four dosage forms in an open dose Latin-square study design (3) according to the protocol in Table I. The dose was administered at 8:00 am after a 12-hr fast and immediately followed by 200 ml of water. Subjects remained fasting for 5 hr after dosing, at which time normal meals were resumed. There was an interval of 1 week between drug administrations. Since cloprednol has a short half-life and no residual levels of drug were detected at 24 hr following a dose, 1 week was judged to be a sufficient time to assure no residual effects from prior drug administrations.

In a separate metabolism study, cloprednol was administered intravenously and orally to two subjects. Each dose contained 2.0 mg of drug dissolved in 10 ml of normal saline–ethanol (9:1). The intravenous dose was infused over 5 min, and the oral dose was diluted to 100 ml with water just prior to ingestion. Both subjects received the intravenous dose first, followed by the oral dose 2 weeks later. As already described, subjects fasted overnight, the drug was administered in the morning, and the normal diet was resumed 5 hr later.

Subjects—Subjects in the bioavailability study were normal adult male volunteers between the ages of 26 and 37 years (average 31.8 years); their body weights (69.6–87.7 kg, average 78.2 kg) were within 10% of the normal[4]. Written informed consent was obtained from each subject prior to undergoing baseline evaluation.

Study subjects did not take any medication for 2 weeks prior to the onset of and during the trial. Alcohol ingestion was not permitted from 24 hr before to 48 hr after administration of each formulation. A medical history and complete physical examination were obtained on each subject prior to the study. Routine laboratory profiles including a complete blood count, urinalysis, and chemistry panel were obtained prior to the study and 48 hr after administration of each formulation.

Subjects in the metabolism study were normal adult male volunteers, 30 and 32 years old and weighing 74.1 and 77.3 kg. Other aspects of this study were the same as already described.

Blood Sampling and Processing—In the bioavailability study, heparinized venous blood (10 ml) was obtained just prior to cloprednol administration and at 5, 15, and 30 min and 1, 1.5, 3, 4, 5, 8, 24, and 48 hr after dosing. Blood was centrifuged, and the plasma was separated and frozen prior to assay.

[1] Lot 127.
[2] Lot 144.
[3] Lot 155.
[4] As described in the table of "Desirable Weights of Adults," Metropolitan Life Insurance Co. Statistical Bulletin.

0022-3549/78/0700/0920$01.00/0
© 1978, American Pharmaceutical Association

Table II—Average Plasma Cloprednol Concentrations and Related Parameters Obtained from Normal Adult Subjects following Single Oral Doses of 2.5 mg of Cloprednol

Parameter	Treatment Average A	B	C	D	Probability (among Treatment Averages)
Plasma concentration, ng/ml, at:					
0.25 hr	3.95	1.85	5.65	16.5	<0.001
0.5 hr	33.4	33.8	35.7	43.1	0.503
1.0 hr	39.3	45.0	44.9	36.4	0.045
1.5 hr	31.2	35.7	36.1	28.4	0.017
3.0 hr	17.4	20.5	20.8	17.0	0.156
4.0 hr	12.1	12.0	13.4	10.7	0.066
5.0 hr	8.15	8.35	8.63	7.08	0.415
8.0 hr	2.75	2.41	2.13	3.24	0.377
Peak plasma concentration, ng/ml	41.3	47.0	48.8	44.2	0.378
Peak time, min	49.1	57.3	57.3	35.5	0.008
Area 0–0.5 hr, ng/ml × hr	5.16	4.68	5.87	9.50	0.005
Area 0–1 hr, ng/ml × hr	23.3	24.4	26.0	29.4	0.415
Area 0–1.5 hr, ng/ml × hr	41.0	44.5	46.3	45.5	0.700
Area 0–3 hr, ng/ml × hr	77.5	86.7	88.9	79.6	0.301
Area 0–∞ hr, ng/ml × hr	126	136	138	129	0.692
Biological half-life, hr	1.87	1.76	1.73	2.11	0.062

In the metabolism study, 15-ml blood samples were obtained following both doses. For the intravenous study, blood samples were obtained immediately upon completion of the infusion; thereafter, sampling times were the same as already described.

Assay—An appropriate amount of internal standard (6-fluoro-11β,17α,21-trihydroxypregna-4,6-diene-3,20-dione) was added to each plasma sample to be analyzed. The subsequent analysis consisted of four steps: extraction of plasma with ether (analytical reagent), partial cleanup of the extract by adsorption chromatography on an activated magnesium silicate column[5], formation of the methoxime[6]–trimethylsilyl[7] derivative, and quantitation by GLC–mass spectrometry[8].

A glass GLC column (0.6 m × 2 mm i.d.) was employed with 3% OV-1 (methyl silicone gum) on 60–80-mesh Gas Chrom Q[9]. The operational column temperature was 240°. The mass spectrometer was used in the chemical-ionization mode with methane as the carrier gas and was operated in the multiple-ion detection mode monitoring ions of *m/e* 653 (internal standard) and 667 (cloprednol). This assay was linear from 1 to 100 ng/ml of plasma with an overall coefficient of variation of ±8%.

Data Treatment—Comparisons of the four cloprednol formulations in the bioavailability study were made with respect to the following parameters: biological half-life; time to maximum plasma concentration; maximum plasma concentration; total area under the plasma concentration–time curve (*AUC*) as well as 0–30-, 60-, 90-, and 180-min areas; and plasma concentrations at 15, 30, 60, and 90 min and 3, 4, 5, and 8 hr. The biological half-life was calculated by linear regression on the 3–8-hr (log) plasma concentration values. Sequential areas under the curve were estimated by the trapezoidal rule, while the total area was estimated by the trapezoidal rule up to 8 hr and thereafter by integration using the best fitting exponential decay curve for each subject.

Although the study was of Latin-square design at inception, statistical analysis of the parameters was by randomized block design with subjects as blocks. This method was necessary since two profiles from Subject 12 were missing and one was incomplete. Therefore, none of the data obtained from Subject 12 was used, and analysis appropriate to a replicate Latin-square design was precluded. Subject 4 had one plasma profile completely missing (Formulation D), and values were substituted to include this subject in the randomized block analysis. In instances of missing samples within plasma profiles of other subjects (a total of six other plasma samples), values were substituted to permit analysis of the data. Each missing plasma concentration was estimated using:

$$x_t = (x_{t-1})(\bar{x}_t/\bar{x}_{t-1}) \qquad \text{(Eq. 1)}$$

where x_t is the missing plasma concentration at time t, x_{t-1} is the previous plasma concentration, $\bar{x}_t$ is the average (for the formulation) plasma concentration at time t for all subjects, and $\bar{x}_{t-1}$ is the average (for the formulation) previous plasma concentration for all subjects. The missing profile (Subject 4, Formulation D) was estimated as discussed in Cochran and Cox (4). After the profiles with missing plasma concentrations were "completed" and the missing profile was substituted (resulting in 44 plasma profiles for 11 subjects), statistical analysis was performed. All parameters were evaluated for significant differences ($p \leq 0.05$) in comparisons of pairs among the four formulations using Scheffe's multiple comparison test (5). Data from the two-subject metabolism studies were analyzed and compared to those of the bioavailability study without statistical analysis.

RESULTS AND DISCUSSION

In the bioavailability study, plasma samples were analyzed for cloprednol at 5, 15, and 30 min and 1, 1.5, 3, 4, 5, 8, 24, and 48 hr following each dose. At 5 min, cloprednol was detected in only two samples which contained very low levels (1.1 and 1.4 ng/ml). At 24 hr, only one sample contained measurable levels of cloprednol (3.6 ng/ml); at 48 hr, cloprednol was not detected in any sample. Therefore, the 5-min and 24- and 48-hr samples were not included in the analysis.

Average plasma cloprednol levels obtained for the formulations are plotted in Fig. 1 and are listed in Table II along with other related bioavailability parameters. At 0.25 hr, the average plasma concentration

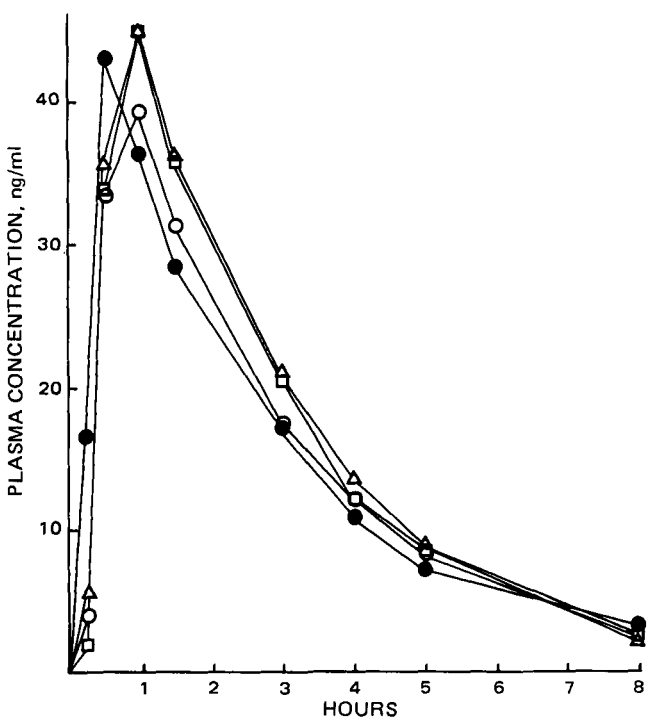

Figure 1—*Average plasma cloprednol concentrations in normal adult subjects following a 2.5-mg oral dose of cloprednol as: Formulation A (two 1.25-mg capsules) (○), Formulation B (two 1.25-mg capsules) (□), Formulation C (one 2.5-mg tablet) (△), and Formulation D (2.5 mg in solution) (●).*

[5] Florisil, J. T. Baker Chemical Co.
[6] Methoxyamine hydrochloride reagent, Eastman Kodak Co.
[7] Trimethylsilylimidazole, Pierce Chemical Co.
[8] Finnigan model 3200 with model 6000 data system.
[9] Applied Science Laboratories.

Table III—Plasma Cloprednol Concentrations Obtained from Two Normal Adult Subjects following an Intravenous and an Oral Dose of 2.0 mg of Cloprednol

Hours	Plasma Concentration, ng/ml			
	Subject 1		Subject 2	
	Intravenous	Oral	Intravenous	Oral
0.12	50.5	—[a]	50.3	—[a]
0.25	30.9	22.4	38.3	9.9
0.5	30.5	32.2	36.8	30.5
1.0	29.5	29.9	24.5	30.1
1.5	22.8	22.7	18.0	19.1
3.0	10.9	14.0	10.1	10.3
5.0	3.9	4.6	4.3	5.9
8.0	2.0	1.7	1.8	1.7
Area 0–∞ hr, ng/ml × hr	97.9	96.7	93.4	87.2

[a] No sample.

observed following a dose in solution was significantly higher (16.5 ng/ml) than that observed after any solid dosage form (1.85–5.65 ng/ml); however, there were no statistically significant plasma concentration differences among the solid dose formulations. At 0.5 hr and all subsequent sampling times, average plasma cloprednol levels were very uniform, and no statistically significant differences among any of the formulations were detected.

Average peak plasma concentrations ranged from 41.3 ng/ml following Capsule A to 48.8 ng/ml after Tablet C; however, no significant differences were detected. Plasma levels peaked earliest (35.5 min) following the solution dose, and this peak was significantly different from peak times observed after Capsule B and Tablet C (57.3 min) but not Capsule A (49.1 min). This result was expected, and the delay in onset of plasma levels following a dose in a solid formulation probably reflects the time required for disintegration and dissolution.

The *AUC* measured from 0 to 0.5 hr was greatest following the solution (9.50 ng/ml × hr) and was significantly different from that observed after Capsule A (5.16 ng/ml × hr) and Capsule B (4.68 ng/ml × hr) but not Tablet C (5.87 ng/ml × hr). All subsequent area calculations were very uniform, and no significant differences among any of the formulations were detected. The total *AUC* ranged from 126 ng/ml × hr for Capsule A to 138 ng/ml × hr following Tablet C. Since total areas were equal, all four formulations were bioequivalent with respect to amount of drug absorbed.

The average biological half-life ranged from 1.73 to 2.11 hr (mean 1.86 ± 0.36 *SD*). No significant differences in half-life were observed among any of the administered formulations.

Cloprednol, 2.0 mg, was also administered intravenously and orally in solution to two subjects. The resultant plasma concentrations and total *AUC* values are listed in Table III. Averaged plasma levels for both subjects are also plotted in Fig. 2. Initial plasma concentrations after an intravenous dose were in excess of those following oral dosing; however, by 0.5 hr, plasma levels following both administration routes were comparable. Since total plasma areas after intravenous and oral dosing were the same, it can be concluded that cloprednol was completely absorbed following an oral dose in solution (the area ratio, $area_{po}/area_{iv}$, calculated for Subject 1 was 0.99; for Subject 2, it was 0.93). The total area after intravenous dosing is compared with total areas observed in the bioavailability study in Table IV. The areas were quite similar, suggesting that cloprednol was completely absorbed from all four formulations administered in the bioavailability study.

The data also demonstrate that there was no appreciable first-pass metabolism or degradation of drug in the gut during absorption. Complete availability can be therapeutically important in patients with liver dysfunction. Variable and unpredictable blood levels of the active moiety of drugs subject to extensive hepatic metabolism during absorption, such as prednisone, have been observed in such patients (6).

These studies were carried out to demonstrate that cloprednol was bioavailable from various solid dose formulations. Furthermore, cloprednol had been administered in capsules during several early preclinical and clinical studies. Capsules A and B were designed to encompass the range of formulations used in these early studies. The tablet was designed for future use in phase III and IV studies. This study demonstrated that cloprednol capsules and tablets were equivalent in terms of the rate and extent of absorption.

No significant drug-related side effects were observed in any subject. All laboratory results for all subjects and test periods were within normal limits, except for an isolated marginally elevated uric acid in one subject noted only prior to the onset of the study and eosinophilia in another subject present before and throughout the study.

Table IV—Comparison of Total Areas following Intravenous and Oral Dosing with Cloprednol

Formulation	Total Area, ng/ml × hr
Intravenous	120[a]
A	126
B	136
C	138
D	129

[a] Total area was obtained by averaging the data from Subjects 1 and 2 in the intravenous metabolism study and multiplying by 2.5/2.0 to adjust for dose.

SUMMARY

Bioequivalence was established for Capsules A and B and Tablet C. There were no statistically significant differences among average plasma concentrations at any sampling time following administration of the two capsules or the tablet. This result illustrates the superimposition principle, which clearly shows that these formulations have equal bioavailabilities (rate and extent of absorption). Furthermore, there were no statistically significant differences in any of the other measured parameters (biological half-life, maximum plasma concentration, time to maximum concentration, and *AUC*'s) following the administration of cloprednol in these solid dose formulations.

A statistically significant difference ($p < 0.001$) between the solution and all of the solid dose formulations was observed with respect to 15-min plasma concentration, where plasma levels were higher following the dose in solution. There was a statistically significant difference ($p = 0.008$) between the solution and both Capsule B and the tablet with respect to the time of maximum concentration, with the solution dose peaking earliest. Finally, there was a significant difference ($p = 0.005$) between the solution and both capsules with respect to the 0–30-min area, with the solution giving the greatest area.

These differences reflect the fact that a drug in solution is immediately available for absorption, whereas a drug in solid form must disintegrate and dissolve prior to absorption. Bioequivalence in the amount of drug absorbed was demonstrated by equal total areas following a dose in solution, capsule, or tablet form. When total areas following intravenous and oral dosing were compared, they were shown to be equivalent, indi-

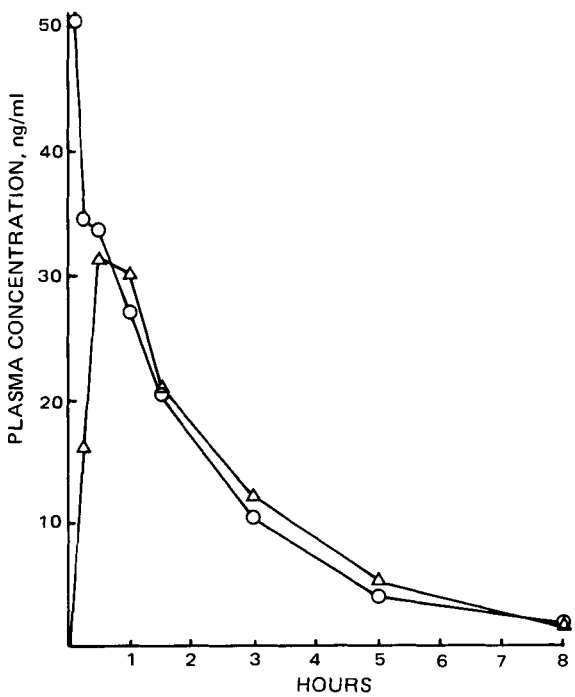

Figure 2—*Average plasma cloprednol concentrations in normal adult subjects following an intravenous (○) and oral (△) solution dose (2.0 mg) of cloprednol.*

cating that the availability of cloprednol from all of the oral dosage forms tested was complete.

REFERENCES

(1) E. Ortega, C. Rodriguez, L. J. Strand, and E. Segre, *J. Int. Med. Res.*, **4**, 326 (1976).

(2) E. Ortega, C. Rodriguez, L. J. Strand, S. Bessler, and E. Segre, *J. Clin. Pharmacol.*, **16**, 122 (1976).

(3) B. J. Winer, "Statistical Principles in Experimental Design," 2nd ed., McGraw-Hill, New York, N.Y., 1962, p. 685.

(4) W. G. Cochran and G. M. Cox, "Experimental Design," 2nd ed., Wiley, New York, N.Y., 1957, p. 110.

(5) H. Scheffe, "The Analysis of Variance," Wiley, New York, N.Y., 1959, p. 68.

(6) L. W. Powell and E. Axelsen, *Gut*, **13**, 690 (1972).

ACKNOWLEDGMENTS

The authors thank B. Amos and J. Smithers of Syntex Research for their assistance in assaying the cloprednol plasma samples.

Quantitative Determination of Prednisone and Prednisolone in Human Plasma Using GLC and Chemical-Ionization Mass Spectrometry

S. B. MATIN ˣ and B. AMOS

Received July 5, 1977, from the *Department of Drug Metabolism, Syntex Research, Palo Alto, CA 94304.* Accepted for publication October 28, 1977.

Abstract □ A method for the quantitative determination of prednisolone and prednisone in human plasma utilizing GLC and chemical-ionization mass spectrometry is described. Corticosteroids are extracted from plasma into ether, and the extract is purified either by passing through a magnesium silicate column or by solvent partitioning. Interference from endogenous hydrocortisone is removed by selective derivatization with Girard Reagent T. Following derivatization, prednisolone can be quantitatively separated from the water-soluble hydrocortisone derivative by simple solvent partitioning. The extracted prednisone and prednisolone are converted to their corresponding methoxyimino trimethylsilyl derivatives, and subjected to GLC–mass spectrometry. Prednisone and prednisolone plasma profiles following a 15-mg oral dose of prednisone in a human volunteer are presented. The method can measure prednisone and prednisolone in plasma at the nanogram per milliliter level.

Keyphrases □ Prednisone—GLC–mass spectrometric analysis in human plasma □ Prednisolone—GLC–mass spectrometric analysis in human plasma □ GLC–mass spectrometry—analyses, prednisone and prednisolone in human plasma □ Glucocorticoids—prednisone and prednisolone, GLC–mass spectrometric analyses in human plasma

The synthetic corticosteroid prednisone and its major metabolite prednisolone are used clinically as anti-inflammatory agents. Previously reported analytical procedures include GLC with flame-ionization detection (1), competitive protein binding assay (2), and radioimmunoassay (3, 4). The GLC method lacks sensitivity and cannot be used to follow plasma levels after the administration of a therapeutic dose.

The radioimmunoassay and competitive protein binding methods provide the required sensitivity for measurement. Specificity is apparently achieved by diluting plasma samples, thereby diluting the interference of cortisone in the prednisone assay and of hydrocortisone in the prednisolone assay. The difficulties and merits of these dilution methods recently were reviewed (5). An alternative method based on paper chromatography followed by radioimmunoassay also was described (6). Paper chromatograms require 24 hr for elution, and R_f values of the compounds of interest are obtained by comparison with R_f values of radioactive standards run on separate paper strips. Although this method has improved specificity, it is cumbersome and lengthy.

Recently, the radioimmunoassay method was used in the analysis of bioavailability and pharmacokinetic samples (7). In these studies, dexamethasone was administered to human volunteers to suppress the secretion of endogenous hydrocortisone and thus increase the specificity of the assay.

This report describes a specific and sensitive analytical method for the determination of prednisone and prednisolone in human plasma. The method is based on GLC and chemical-ionization mass spectrometry with selected ion monitoring. It can be used to study the kinetics of the interconversion of prednisone and prednisolone in humans and to acquire pharmacokinetic and bioavailability data without suppression of endogenous steroid production.

The applicability of the method is shown by the measurement of plasma prednisone and prednisolone levels in a human volunteer after oral administration of 15 mg of prednisone[1].

EXPERIMENTAL

Reagents—Methoxyamine hydrochloride[2], pyridine[2], and trimethylsilylimidazole[2] were used without further purification. Magnesium silicate[3] (60–100 mesh) and (carboxymethyl)trimethylammonium chloride hydrazide[4] (Girard Reagent T) were commercially available. Methoxyamine reagent (4% w/v) was prepared by dissolving methoxyamine hydrochloride in pyridine. Girard Reagent T (10% w/v) was prepared by dissolving it in methanol containing 1% acetic acid.

Instruments—Samples were analyzed on a gas chromatograph–mass spectrometer fitted with a chemical-ionization source and a data system[5]. Methane was used as the carrier (20 ml/min) and as the chemical-ionization reagent gas. The chemical-ionization source pressure was maintained at approximately 1 torr.

[1] Deltasone.
[2] Pierce Chemical Co., Rockford, Ill.
[3] Florisil, Matheson, Norwood, Ohio.
[4] Matheson, Norwood, Ohio.
[5] Finnigan model 3200 with model 6000 data system.

0022-3549/78/0700/0923$01.00/0
© 1978, American Pharmaceutical Association

cating that the availability of cloprednol from all of the oral dosage forms tested was complete.

REFERENCES

(1) E. Ortega, C. Rodriguez, L. J. Strand, and E. Segre, *J. Int. Med. Res.*, **4**, 326 (1976).

(2) E. Ortega, C. Rodriguez, L. J. Strand, S. Bessler, and E. Segre, *J. Clin. Pharmacol.*, **16**, 122 (1976).

(3) B. J. Winer, "Statistical Principles in Experimental Design," 2nd ed., McGraw-Hill, New York, N.Y., 1962, p. 685.

(4) W. G. Cochran and G. M. Cox, "Experimental Design," 2nd ed., Wiley, New York, N.Y., 1957, p. 110.

(5) H. Scheffe, "The Analysis of Variance," Wiley, New York, N.Y., 1959, p. 68.

(6) L. W. Powell and E. Axelsen, *Gut*, **13**, 690 (1972).

ACKNOWLEDGMENTS

The authors thank B. Amos and J. Smithers of Syntex Research for their assistance in assaying the cloprednol plasma samples.

Quantitative Determination of Prednisone and Prednisolone in Human Plasma Using GLC and Chemical-Ionization Mass Spectrometry

S. B. MATIN ˣ and B. AMOS

Received July 5, 1977, from the *Department of Drug Metabolism, Syntex Research, Palo Alto, CA 94304.* Accepted for publication October 28, 1977.

Abstract □ A method for the quantitative determination of prednisolone and prednisone in human plasma utilizing GLC and chemical-ionization mass spectrometry is described. Corticosteroids are extracted from plasma into ether, and the extract is purified either by passing through a magnesium silicate column or by solvent partitioning. Interference from endogenous hydrocortisone is removed by selective derivatization with Girard Reagent T. Following derivatization, prednisolone can be quantitatively separated from the water-soluble hydrocortisone derivative by simple solvent partitioning. The extracted prednisone and prednisolone are converted to their corresponding methoxyimino trimethylsilyl derivatives, and subjected to GLC–mass spectrometry. Prednisone and prednisolone plasma profiles following a 15-mg oral dose of prednisone in a human volunteer are presented. The method can measure prednisone and prednisolone in plasma at the nanogram per milliliter level.

Keyphrases □ Prednisone—GLC–mass spectrometric analysis in human plasma □ Prednisolone—GLC–mass spectrometric analysis in human plasma □ GLC–mass spectrometry—analyses, prednisone and prednisolone in human plasma □ Glucocorticoids—prednisone and prednisolone, GLC–mass spectrometric analyses in human plasma

The synthetic corticosteroid prednisone and its major metabolite prednisolone are used clinically as anti-inflammatory agents. Previously reported analytical procedures include GLC with flame-ionization detection (1), competitive protein binding assay (2), and radioimmunoassay (3, 4). The GLC method lacks sensitivity and cannot be used to follow plasma levels after the administration of a therapeutic dose.

The radioimmunoassay and competitive protein binding methods provide the required sensitivity for measurement. Specificity is apparently achieved by diluting plasma samples, thereby diluting the interference of cortisone in the prednisone assay and of hydrocortisone in the prednisolone assay. The difficulties and merits of these dilution methods recently were reviewed (5). An alternative method based on paper chromatography followed by radioimmunoassay also was described (6). Paper chromatograms require 24 hr for elution, and R_f values of the compounds of interest are obtained by comparison with R_f values of radioactive standards run on separate paper strips. Although this method has improved specificity, it is cumbersome and lengthy.

Recently, the radioimmunoassay method was used in the analysis of bioavailability and pharmacokinetic samples (7). In these studies, dexamethasone was administered to human volunteers to suppress the secretion of endogenous hydrocortisone and thus increase the specificity of the assay.

This report describes a specific and sensitive analytical method for the determination of prednisone and prednisolone in human plasma. The method is based on GLC and chemical-ionization mass spectrometry with selected ion monitoring. It can be used to study the kinetics of the interconversion of prednisone and prednisolone in humans and to acquire pharmacokinetic and bioavailability data without suppression of endogenous steroid production.

The applicability of the method is shown by the measurement of plasma prednisone and prednisolone levels in a human volunteer after oral administration of 15 mg of prednisone[1].

EXPERIMENTAL

Reagents—Methoxyamine hydrochloride[2], pyridine[2], and trimethylsilylimidazole[2] were used without further purification. Magnesium silicate[3] (60–100 mesh) and (carboxymethyl)trimethylammonium chloride hydrazide[4] (Girard Reagent T) were commercially available. Methoxyamine reagent (4% w/v) was prepared by dissolving methoxyamine hydrochloride in pyridine. Girard Reagent T (10% w/v) was prepared by dissolving it in methanol containing 1% acetic acid.

Instruments—Samples were analyzed on a gas chromatograph–mass spectrometer fitted with a chemical-ionization source and a data system[5]. Methane was used as the carrier (20 ml/min) and as the chemical-ionization reagent gas. The chemical-ionization source pressure was maintained at approximately 1 torr.

[1] Deltasone.
[2] Pierce Chemical Co., Rockford, Ill.
[3] Florisil, Matheson, Norwood, Ohio.
[4] Matheson, Norwood, Ohio.
[5] Finnigan model 3200 with model 6000 data system.

0022-3549/78/0700/0923$01.00/0
© 1978, American Pharmaceutical Association

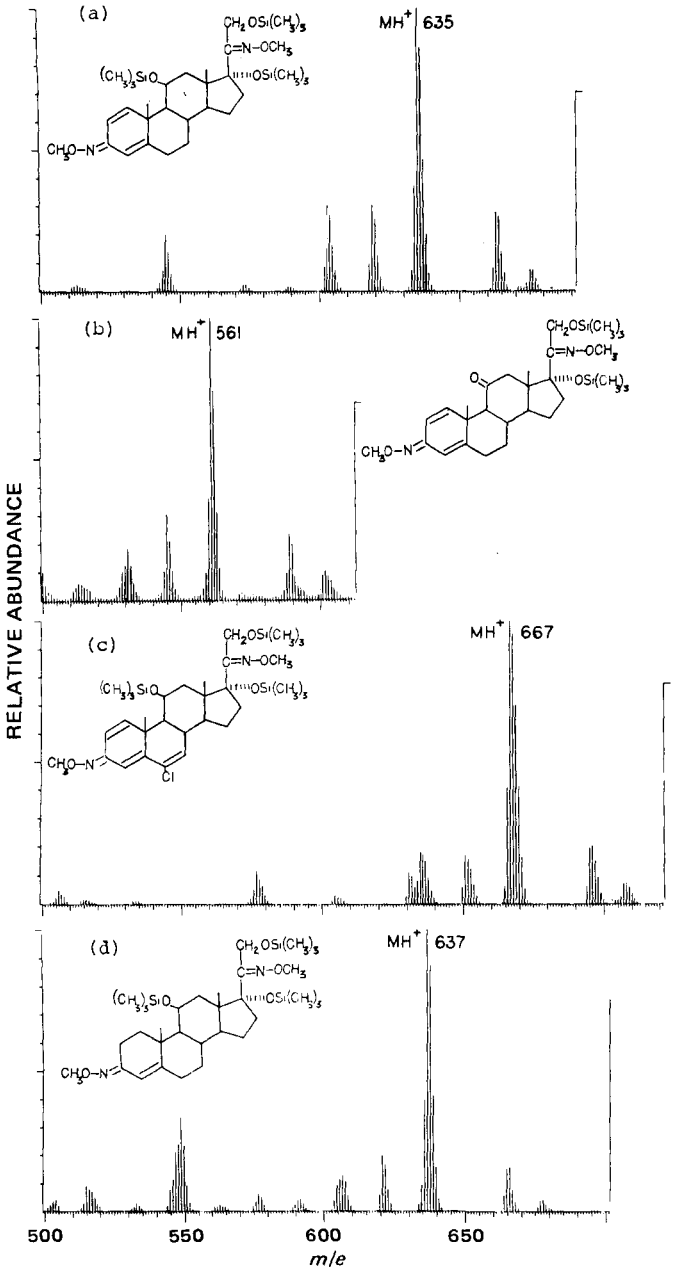

Figure 1—*Methane chemical-ionization mass spectra of methoxyimino trimethylsilyl derivatives of prednisolone (a), prednisone (b), cloprednol (c), and hydrocortisone (d).*

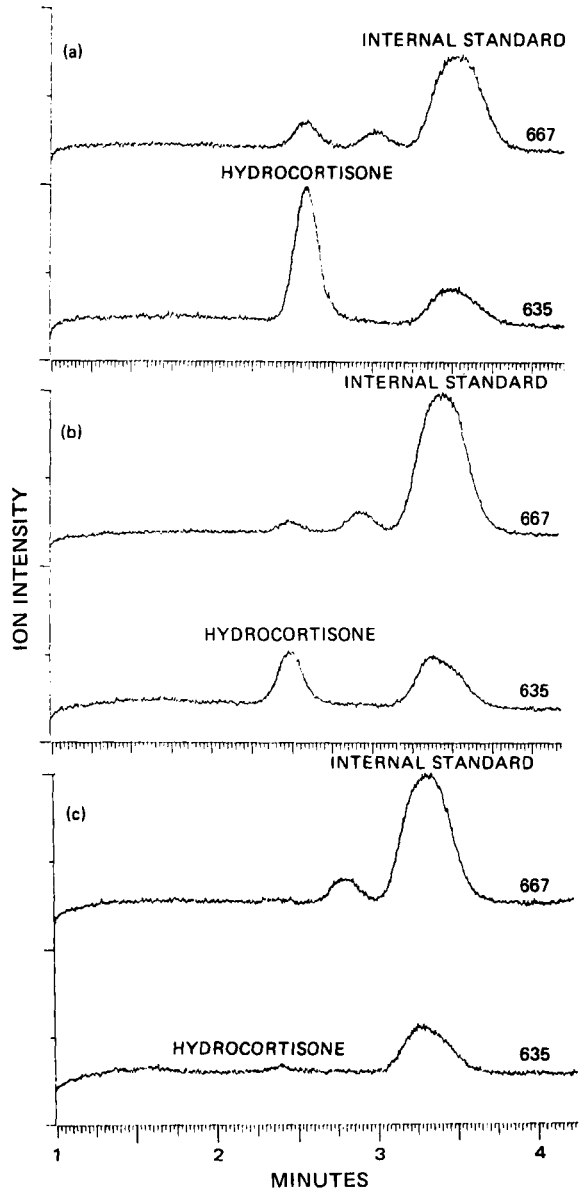

Figure 2—*Selected ion chromatograms depicting the interference of endogenous hydrocortisone at the m/e value (635) and retention time of prednisolone and its selective removal by consecutive Girard reactions. Key:* a, *before reaction;* b, *after first reaction, and* c, *after second reaction.*

GLC was performed on a 60-cm × 2-mm i.d. glass column packed with 3% SP-2250 on 100–120-mesh Supelcoport[6]. Column, injection port, and chemical-ionization source temperatures were maintained at 250, 270, and 120°, respectively. The mass spectrometer was operated in the selected ion recording mode, monitoring ions at *m/e* 561 and 667 or 635 and 667 amu.

Preparation of Magnesium Silicate Column—A 5-mm plug of silanized glass wool was placed in the neck of a disposable glass pipet (Pasteur, 14.5 cm × 7 mm). The pipet was then packed with about 300 mg of magnesium silicate (~2 cm high), and the packing was washed with 3 ml of acetone followed by 3 ml of chloroform. The column was used within 15 min of preparation.

Plasma Sample Preparation—*Method A*—To a 2-ml plasma sample in a 155 × 13-mm culture tube, fitted with a polytef-lined screw cap, were added 100 μl of the internal standard cloprednol (150 ng/100 μl of methanol), 1 ml of water, and 10 ml of ether. The tubes were shaken vigorously for at least 2 min. After centrifugation, the organic layer was transferred to a second tube and evaporated to dryness at 60° under a nitrogen stream.

The residue was transferred to a magnesium silicate column with 3 × 300-μl washes of chloroform. The column was then washed with an additional 1.5 ml of chloroform. The corticoids were eluted from the column with 10 ml of acetone, which was collected and evaporated to dryness at 60° under a nitrogen flow.

The residue was dissolved in 400 μl of Girard Reagent T and allowed to react for 45 min at room temperature. Water, 5 ml, was added, and the solution was extracted twice with 6 ml of dichloromethane–ether (3:7). Layers were separated by centrifugation after each extraction. The extracts were combined and evaporated at 60° under nitrogen. The residue obtained after the evaporation of dichloromethane–ether was taken up in 400 μl of Girard Reagent T, and derivatization was repeated. The residue obtained after the second derivatization was transferred to a 0.3-ml vial[7] with two 300-μl washes of chloroform. The chloroform was evaporated at room temperature under nitrogen after each transfer. This

[6] Supelco, Bellefonte, Pa.

[7] Reactivial.

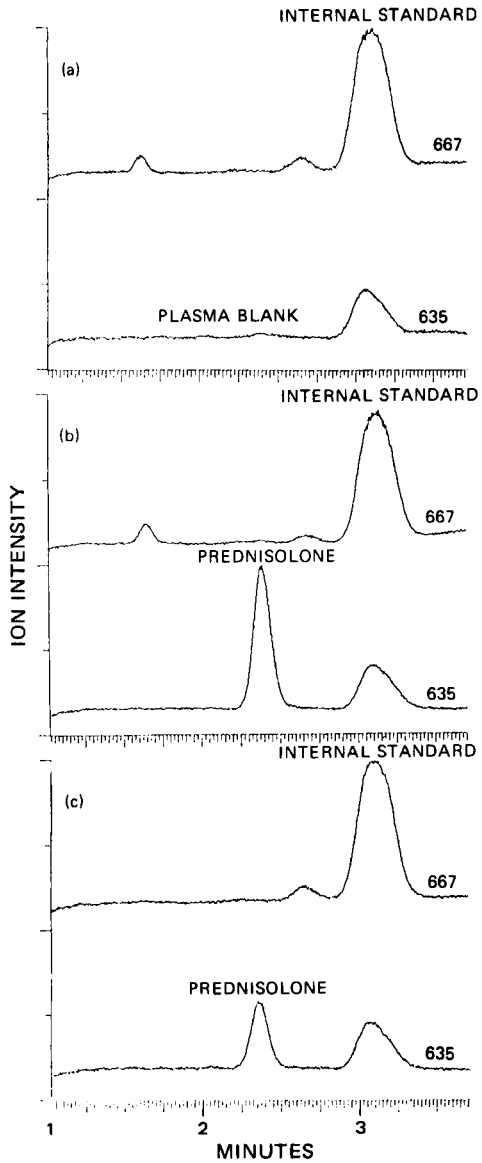

Figure 3—*Selected ion chromatograms of plasma samples obtained from a dosed subject, processed according to Method A and analyzed for prednisolone. Key:* a, *blank plasma;* b, *plasma sample after 15 min; and* c, *plasma sample after 8 hr.*

residue was then subjected to derivatization for GLC–mass spectrometry.

Method B—Corticosteroids were extracted from plasma as described for Method A. The residue obtained after ether evaporation was dissolved in methanol (2 ml) containing 20% (v/v) of 10% aqueous acetic acid. Solvent partitioning was achieved by washing the methanolic solution three times with 3 ml of hexane saturated with methanol–acetic acid. The hexane washings were discarded, and the remaining methanol–acetic acid was evaporated to dryness at 60° under nitrogen. The residue so obtained was reacted with Girard Reagent T as described for Method A, followed by derivatization for GLC–mass spectrometry.

Derivatization for GLC–Mass Spectrometry—Methoxyamine reagent, 50 μl, was added to the residue obtained by either Method A or B. The vial was capped and heated at 120° for 30 min. After cooling, 25 μl of trimethylsilylimidazole was added; the vial was then reheated at 120° for 30 min. Up to 6 μl of this mixture was injected on the GLC–mass spectrometric system for quantitation.

RESULTS AND DISCUSSION

The major requirement in establishing a specific analytical method for prednisolone and prednisone in human plasma is selective removal of the interference by the formed metabolic products and the endogenous

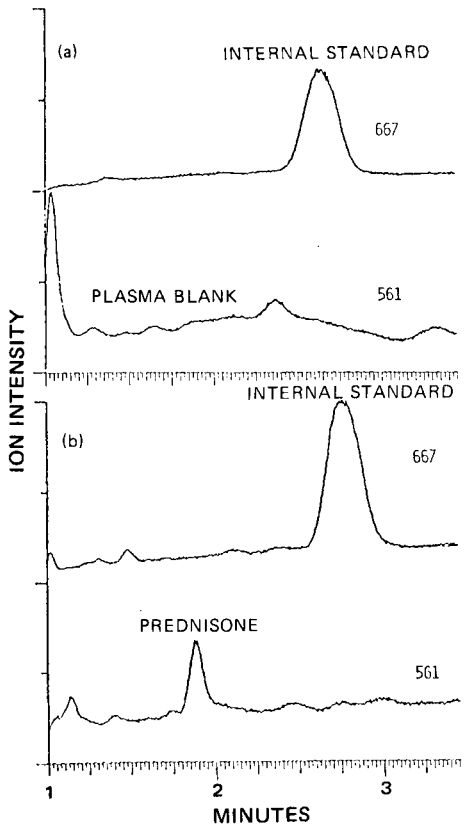

Figure 4—*Selected ion chromatograms of plasma samples obtained from a dosed subject, processed according to Method A and analyzed for prednisone. Key:* a, *blank plasma; and* b, *plasma sample after 1 hr.*

steroids. Most important of these endogenous steroids are hydrocortisone and cortisone. These compounds possess the same functional groups and differ structurally only by the absence of a Δ^1-double bond.

In a recent report on the radioimmunoassay of prednisone and prednisolone, a cross-reactivity on the order of 35% or greater was observed for the 20-hydroxy and the glucuronide metabolites formed from the two compounds (8). The effect of glucuronides on the quantitative results is important since their presence in plasma up to 4 hr after prednisolone administration has been documented (8, 9). Because of these difficulties, previous investigators resorted to chromatography before analysis (6). This alternative is lengthy and difficult and has not increased accuracy (8).

An analytical method was required for studying the pharmacokinetics and interconversion of prednisone and prednisolone in normal subjects as well as in the diseased state without the suppression of endogenous steroids. To achieve this aim, GLC and chemical-ionization mass spectrometry were utilized. Prednisone, prednisolone, and the internal standard cloprednol were derivatized to their corresponding methoxyimine trimethylsilyl derivatives prior to GLC. The chemical-ionization spectra of prednisolone, prednisone, cloprednol, and endogenous steroid hydrocortisone are shown in Fig. 1. These spectra were obtained by derivatizing pure reference compounds and subjecting them to GLC–mass spectrometry under the conditions described.

As expected, because of the presence of several trimethylsilyl groups, the molecular ion for each compound is observed as a multiplet rather than as a single ion. This multiplicity of the molecular ion imposes certain restrictions on the choice of a GLC–mass spectral internal standard. For a deuterium-labeled molecule to serve as an internal standard, it must be substituted with a large number of deuterium atoms so that its molecular ion cluster will not overlap with the molecular ion cluster of the compound under investigation. Although the synthesis of such a compound is possible, the lack of general availability makes this choice less desirable. For this reason, a structurally similar compound, cloprednol, was chosen as the internal standard. It possesses similar functional groups but elutes with a different retention time, thus making it possible to measure the compounds *via* selected ion monitoring (10).

To measure plasma prednisolone levels, it was necessary to separate

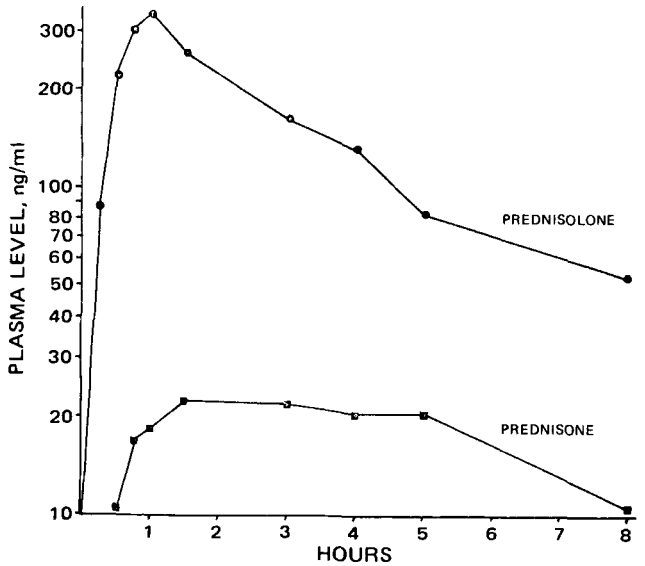

Figure 5—*Plasma prednisone and prednisolone levels achieved after the administration of 15 mg po of prednisone to a human volunteer.*

prednisolone from endogenous hydrocortisone. These two compounds differ by only 2 mass units and, after derivatization to the methoxyimine trimethylsilyl derivatives, their molecular ion clusters overlap each other. Since the basal levels of hydrocortisone change during the day, it is not possible to measure prednisolone in the presence of changing concentrations of hydrocortisone.

Attempts to resolve derivatized prednisolone from hydrocortisone chromatographically for reproducible quantitation at low nanogram levels were not promising. These two compounds could be separated *via* selective derivatization with Girard Reagent T. Derivatization of ketones with Girard Reagent T to form water-soluble products was reported previously (11, 12). The possible application of this reaction in the improvement of the radioimmunoassay for prednisolone also was discussed (13). The reported method does not provide complete separation of hydrocortisone from prednisolone, and extensive modification of the procedure was adopted. It also was necessary to repeat the Girard reaction a second time to remove detectable interference from hydrocortisone (Fig. 2).

Plasma samples to be analyzed could be processed by two alternative procedures, Methods A and B, as described under *Experimental.* Method A was better than Method B in providing less overall background in the mass spectrometer, whereas Method B was simpler and faster. Plasma cleanup procedures similar to Methods A and B previously were reported (1, 14) and were modified for the present study.

The clinical applicability of the developed method was established by the measurement of plasma prednisone and prednisolone levels in a human volunteer after the oral administration of 15 mg of prednisone. Plasma samples were processed *via* either Method A or B, and compounds of interest were measured *via* selected ion monitoring. Figure 3*a* shows the selected ion chromatogram obtained for prednisolone from a blank plasma sample processed according to Method A and then subjected to GLC–mass spectrometry and selected ion monitoring. Figures 3*b* and 3*c* show selected ion chromatograms for prednisolone from plasma samples obtained from a volunteer 15 min and 8 hr after prednisone administration, respectively. The ions selected for measurement were MH^+ 635 for prednisolone and MH^+ 667 for the internal standard.

Figures 4*a* and 4*b* show the selected ion chromatogram obtained for prednisone from a blank plasma sample and a plasma sample from a volunteer 1 hr after drug administration, respectively. Ions selected for measurement were MH^+ 561 for prednisone and MH^+ 667 for the internal standard.

Prednisone and prednisolone could be measured simultaneously in one single analysis. In the present study, however, each compound was monitored separately to gain higher sensitivity.

Plasma concentrations in unknown samples were determined with respect to the calibration curves prepared by plotting the peak height ratio *versus* the amount of compound spiked per milliliter of plasma. The calibration curves prepared for prednisolone (concentration range of 0–150 ng/ml) and prednisone (concentration range of 0–40 ng/ml) were linear. Plasma prednisone and prednisolone levels achieved in a human volunteer after the administration of 15 mg of prednisone are shown in Fig. 5. The two compounds reached peak plasma levels within 2 hr after the administration and then decayed with different apparent half-lives.

REFERENCES

(1) G. E. Bacon, *J. Lab. Clin. Med.*, **73**, 1030 (1969).

(2) A. K. Turner, C. J. Carroll, J. L. Pinkus, D. Charles, and S. C. Chattoraj, *Clin. Chem.*, **19**, 731 (1973).

(3) W. A. Colburn, *Steroids*, **24**, 95 (1974).

(4) W. A. Colburn and R. H. Buller, *ibid*, **21**, 833 (1973).

(5) W. A. Colburn and R. H. Buller, *J. Pharmacokinet. Biopharm.*, **3**, 329 (1975).

(6) A. W. Meikle, J. A. Weed, and F. H. Tyler, *J. Clin. Endocrinol. Metab.*, **41**, 717 (1975).

(7) T. J. Sullivan, M. R. Hallmark, E. Sakmar, D. J. Weidler, R. H. Earhart, and J. G. Wagner, *J. Pharmacokinet. Biopharm.*, **4**, 157 (1976).

(8) S. W. Schalm, W. H. J. Summerskill, and V. L. W. Go, *Mayo Clin. Proc.*, **51**, 761 (1976).

(9) A. A. Sandberg and W. R. Slaunwhite, *J. Clin. Endocrinol. Metab.*, **17**, 1040 (1957).

(10) C. G. Hammer, B. Holmstedt, and R. Ryhage, *Anal. Biochem.*, **25**, 532 (1968).

(11) E. Lederer, *Trav. Members Soc. Chim. Biol.*, **24**, 1149 (1942).

(12) O. H. Wheeler, *Chem. Rev.*, **62**, 205 (1962).

(13) J. C. K. Loo, A. B. Vilim, N. Jordan, and J. Moffatt, *J. Pharm. Sci.*, **65**, 461 (1976).

(14) W. G. Stillwell, A. Hung, M. Stafford, and M. G. Horning, *Anal. Lett.*, **6**, 407 (1973).

ACKNOWLEDGMENTS

Presented at the Pharmaceutical Analysis and Control Section, APhA Academy of Pharmaceutical Sciences, Orlando meeting, November 1976.

The authors thank Dr. James Strand for arranging the clinical study, Ms. Jackie Smithers for the column technique, and Dr. Richard Runkel for support and encouragement.

Kinetic and Mechanistic Studies of Blue Tetrazolium Reaction with Phenylhydrazines

EDWARD R. BIEHL *x, ROBERT WOOTEN *[1], C. T. KENNER *, and ROBERT E. GRAHAM ‡

Received July 11, 1977, from the **Department of Chemistry, Southern Methodist University, Dallas, TX 75275,* and the ‡*Food and Drug Administration, Dallas District, Dallas, TX 75204.* Accepted for publication October 25, 1977.

Abstract □ The reaction kinetics of blue tetrazolium with selected arylhydrazines were investigated under pseudo-first-order conditions. The reaction rate constants were obtained at various temperatures, and the enthalpy (8.4–11.2 kcal/mole) and entropy (−38–−45 eu) of activations were calculated. A Hammett plot yielded a straight line with a slope of 0.52. The reaction was inhibited by atmospheric oxygen and iodine. A free radical mechanism is presented.

Keyphrases □ Blue tetrazolium—reaction with various phenylhydrazines, kinetics and mechanism □ Phenylhydrazines, various—reaction with blue tetrazolium, kinetics and mechanism □ Kinetics and mechanism—reaction of blue tetrazolium with various phenylhydrazines

Blue tetrazolium, 3,3′-[3,3′-dimethoxy(1,1′-biphenyl)-4,4′-diyl]bis(2,5-diphenyl-2*H*-tetrazolium) dichloride (I), has become increasingly important as an assay for both quantitative and qualitative reduction by various reducing agents. These agents reduce I to a highly colored formazan whose concentration is then measured spectrophotometrically.

BACKGROUND

This reduction is useful in many areas (1). For example, in histochemical systems, I may be used as a staining technique for light microscopy (2–4) since few organic compounds are yellow in their oxidized form and highly colored in their reduced form. Compound I gives a deep-blue stain, which is desirable for histological (*i.e.*, cytological) demonstration. In biochemical analysis, tetrazolium salts are used as an activity stain in electrophoretic assay (5) because of their low reduction potential. Clinical investigations of I in studies of bacterial infection (6) and carcinomatous tissues (7) also were reported. However, the high toxicity of I restricts this procedure to *in vitro* systems.

Several reports (8–13) noted the utility of I in corticoidal steroid analysis. USP XIX (14) and NF XIV (15) use a slightly modified procedure of Mader and Buck (8) for corticosteroid analysis in which I oxidizes the α-keto moiety of the C_{17} side chain in strongly alkaline solution and is reduced quantitatively to a highly colored formazan. A recent investigation of the steroid–blue tetrazolium reaction (16) showed that I oxidizes the α-keto moiety of the C_{17} corticosteroid side chain *via* the transfer of an electron pair and a proton from the tetrazolium molecule. A bimolecular mechanism involving a cyclic complex, supported by kinetic data, was presented (16).

The blue tetrazolium determination has been applied most extensively to α-keto systems. However, some nonketo compounds such as polyhydric phenols, quinones, and certain active hydrogen compounds are sufficiently reactive to permit quantitative analysis *via* formazan formation (17). A free radical mechanism was proposed based on similar structural reactivity in the blue tetrazolium reaction to the reaction of the same compounds toward oxygen.

This paper investigates the reactivity of a specific class of nonketo active hydrogen compounds—*viz.*, phenylhydrazines, with I. Rate constants for selected phenylhydrazines at various temperatures, the enthalpy and entropy of activation, and Hammett σ and ρ constants obtained from these kinetic results are reported. A mechanism based on the observed experimental data is proposed to gain an understanding of this system and to predict the reactivity of blue tetrazolium with other hydrazine-related compounds.

[1] Robert A. Welch undergraduate scholar.

EXPERIMENTAL

Apparatus—A UV–visible ratio recording spectrophotometer[2] equipped with water-jacketed cell holders and 1-cm quartz cells, a microbalance[3], a temperature-controlled circulating bath[4], a water-jacketed 40/50 female joint[5], and a gas chromatograph–mass spectrometer[6] containing a 1.2-m column[7] packed with OV-17 on 80–100-mesh Supelcoport were used. A thermocouple[8] was used to determine the difference in temperature between the circulating bath and the cell jackets.

Reagents—Alcohol USP and analytical grade absolute methanol were used as received. Tetramethylammonium hydroxide (II), 1%, was prepared by diluting 5 ml of 10% aqueous[9] II to 50.0 ml with alcohol USP (95% ethanol); 0.25% II in alcohol USP was prepared by diluting 5.00 ml of 1% II with 10.00 ml of alcohol USP. Solutions of I[10] were prepared by dissolving 5.0 mg/ml in absolute methanol.

Arylhydrazine hydrochloride standard solutions contained 0.010 mg of the appropriate phenylhydrazine derivative[11]/ml of alcohol USP, unless otherwise indicated.

Phenylhydrazine Decomposition Study—*In Air*—A 2.5-ml aliquot of phenylhydrazine hydrochloride (0.01 mg/ml of alcohol USP) was mixed with 0.5 ml of 0.5% II, transferred to a cell, and scanned periodically from 300 to 250 nm during 25 min *versus* a reagent blank.

In Nitrogen—The experiment in air was repeated, except that all solutions were purged with nitrogen for 15 min before II was mixed with the phenylhydrazine solution.

Rate Study—All manipulations in the rate study were performed in a nitrogen-filled glove bag. The solutions were purged with nitrogen prior to use; a vacuum was applied to the glove bag during purging. Two water-jacketed ⅁ 40/50 female joints were put in series between the circulating water bath and jacketed cell holder compartment of the spectrophotometer and placed in the glove bag. The solutions were placed in glass-jacketed female joints and allowed to temperature equilibrate for 15 min. Then a 10-ml aliquot of a standard phenylhydrazine hydrochloride solution and a 10-ml blank of alcohol USP were treated with 2.00 ml of I reagent (5 mg/ml) and 0.5 ml of II (0.5%).

Zero time was taken as the time of addition of II to the standard solution. Both solutions were transferred to cells and placed in the spectrophotometer as rapidly as possible, and absorbance readings were taken four times per minute at 525 nm until the reaction essentially reached completion. This procedure was repeated for nine phenylhydrazine derivatives at three different temperatures. Rate constants were calculated as previously described (16).

Determination of Oxidation Products of Phenylhydrazine Salts—At the conclusion of certain kinetic runs, a 5-ml aliquot was drawn from the reaction mixture and subjected to GLC–mass spectral analysis. The mass spectrum obtained for each oxidized phenylhydrazine product was compared with that of an authentic specimen.

Effect of Free Radical Reaction Inhibitor—Three 20.0-ml sets of alcohol USP containing 0, 10.0, and 100 μmoles of iodine and 1.25 μmoles of phenylhydrazine hydrochloride were treated with 2.00 ml of I (5.0 mg/ml) followed by 2.00 ml of 1% II. Each set was run against a reagent blank. Zero time was taken as the time of addition of the 1% II to the standard solution. Both solutions were transferred to cells as rapidly as

[2] Cary model 118.
[3] Mettler model M.
[4] Neslab model RTE-3.
[5] Corning Glass.
[6] DuPont model 321.
[7] Supelco.
[8] Omega Engineering.
[9] Eastman Organic Chemicals.
[10] Dajac Laboratories.
[11] Aldrich Chemical Co.

0022-3549/78/0700/0927$01.00/0
© 1978, American Pharmaceutical Association

Table I—Kinetic Parameters for the Reaction of I with Arylhydrazines, R-$C_6H_4NHNH_2$

R	T, °K	k_0, min^{-1}	$\Delta H^{\ddagger}$, kcal/mole	$\Delta S^{\ddagger}$, eu
3-CH_3	303.53	9.66×10^{-2}	10.04	−38.4
	304.21	4.85×10^{-2}		
	293.29	3.77×10^{-2}		
	293.23	4.86×10^{-2}		
	283.51	2.84×10^{-2}		
	282.92	2.36×10^{-2}		
4-Br	304.02	1.83×10^{-1}	8.31	−42.7
	303.48	1.79×10^{-1}		
	293.38	1.20×10^{-1}		
	293.23	1.17×10^{-1}		
	283.41	6.38×10^{-2}		
	282.92	6.03×10^{-2}		
4-Cl	303.94	1.63×10^{-1}	8.38	−42.7
	303.78	1.67×10^{-1}		
	293.38	9.81×10^{-2}		
	293.58	8.93×10^{-2}		
	283.41	5.76×10^{-2}		
	282.92	5.40×10^{-2}		
3-Br	303.98	2.06×10^{-1}	8.11	−43.1
	304.00	2.05×10^{-1}		
	293.36	1.17×10^{-1}		
	293.58	1.36×10^{-1}		
	283.41	6.99×10^{-2}		
	282.86	7.21×10^{-2}		
3-Cl	303.98	2.01×10^{-1}	7.73	−44.7
	304.00	1.62×10^{-1}		
	293.58	1.05×10^{-1}		
	293.50	1.02×10^{-1}		
	283.41	7.21×10^{-2}		
	282.96	5.99×10^{-2}		
4-CH_3	303.98	6.94×10^{-2}	10.07	−38.7
	304.00	9.58×10^{-2}		
	293.58	3.18×10^{-2}		
	293.42	3.34×10^{-2}		
	283.18	2.30×10^{-2}		
	283.17	2.14×10^{-2}		
3-OCH_3	304.05	8.30×10^{-2}	10.07	−38.4
	304.23	8.83×10^{-2}		
	293.32	4.68×10^{-2}		
	293.37	4.58×10^{-2}		
	282.86	2.42×10^{-2}		
	282.79	2.46×10^{-2}		
H	304.05	7.57×10^{-2}	11.27	−34.8
	304.23	7.30×10^{-2}		
	293.32	3.39×10^{-2}		
	293.34	3.55×10^{-2}		
	282.86	1.59×10^{-2}		
	282.95	1.82×10^{-2}		
4-OCH_3	304.05	9.07×10^{-2}	10.38	−37.3
	304.27	8.87×10^{-2}		
	293.32	4.57×10^{-2}		
	293.32	5.01×10^{-2}		
	282.92	2.18×10^{-2}		
	283.01	2.44×10^{-2}		

possible, and absorbance readings were made each minute at 525 nm for 60 min. The alcohol had been swept with nitrogen for 15 min to minimize oxygen-induced degradation of phenylhydrazine.

RESULTS AND DISCUSSION

Several modifications of the general procedure had to be made in the rate studies of the arylhydrazine–I reaction. The official procedure (14) for the quantitation of corticosteroids calls for very dilute standard solutions, which are very basic [apparent pH ~14 (12)]. The absorptivity of the formazan and its formation rate from freshly prepared solutions of arylhydrazine salts were much higher than solutions that had stood approximately 1 hr before analysis.

UV absorption scans from 200 to 350 nm of arylhydrazine solutions of apparent pH 14 were taken in the presence and absence of atmospheric oxygen. Figure 1 shows a rapid change in the UV spectrum of phenylhydrazine when run under ordinary atmospheric conditions for 25 min. Only slight changes were observed in the UV spectrum (Fig. 1) of a similar solution of phenylhydrazine that had been purged with nitrogen. This result indicates that the decomposition of the hydrazine molecule in basic solution is accelerated by atmospheric oxygen. Hydrazine decomposition was reported previously (18–21) under these conditions and

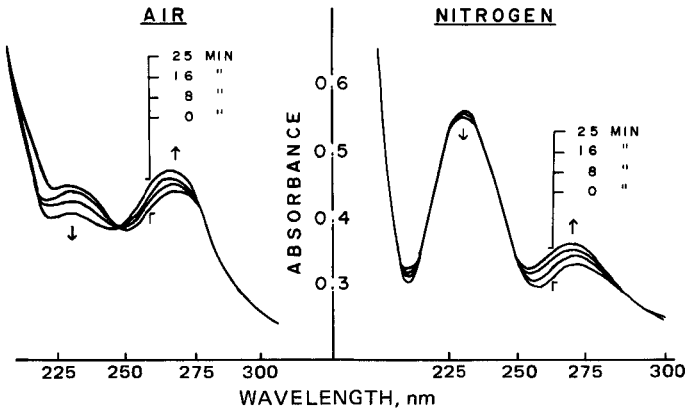

Figure 1—*Effect of oxygen on the UV spectra of phenylhydrazine in basic solution.*

shown to involve the oxidation of the hydrazine moiety *via* a free radical mechanism.

To ensure that all oxidation of phenylhydrazine was from its reaction with the tetrazolium moiety:

1. Fresh hydrazine solutions were prepared prior to taking each set of rate measurements.
2. Hydrazine solutions were made 50% more concentrated.
3. All solutions were purged with nitrogen.
4. All dilutions, pipetting, and mixings were performed under a nitrogen atmosphere.
5. All solutions were allowed to temperature equilibrate prior to mixing.
6. The 0.25% II was used.
7. Four absorbance readings per minute were recorded.

The results of the kinetic studies of the blue tetrazolium reaction with selected phenylhydrazines are shown in Table I. Pseudo-first-order rate constants were observed for all phenylhydrazines during the time interval used in rate calculations. The specific rate constants, k_i, were obtained by performing a least-squares regression on the equation:

$$\ln (1 - A_i/A') = -k_r t_i + E \qquad \text{(Eq. 1)}$$

where A_i is the absorbance at time t_i, A' is the theoretical or optimum absorbance, k_r is the observed rate constant, and E is the intercept. Because of the strong reducing ability of the hydrazine molecule, the reaction essentially reached completion within 20 min for most phenylhydrazines studied. To obtain a maximum number of data points before the reaction reached maximum absorbance, four measurements were made each minute. In each case, a correlation coefficient of 0.99 or greater was observed.

Figure 2 is a typical absorbance plot observed for phenylhydrazines under modified conditions. First-order kinetics were observed in the straight line of negative slope, k_r, and an intercept of zero.

Figure 3 is a Hammett plot of log (k_G/k_H) *versus* σ_G for the reaction of I with substituted phenylhydrazine derivatives at 20°, where k_G and k_H are the specific rate constants for a substituted and unsubstituted phenylhydrazine and σ_G is the substituent constant (22). The ρ value (slope) for this curve is approximately +0.52 (r = 0.8), which reflects the small influence substituents have on the reaction rate. For example, *m*-bromophenylhydrazine, the most reactive substituted phenylhydrazine in this study, reacts only approximately three times faster than phenylhydrazine itself at 20°.

The *meta*- and *para*-isomers of nitrophenylhydrazine and cyanophenylhydrazine also were treated with I. However, suitable kinetic parameters could not be obtained for these compounds since the cyano and nitro substituents are not stable under the extreme basic conditions employed in the blue tetrazolium reaction.

The enthalpy and entropy of activation results are also shown in Table I. These values were obtained by performing a least-squares regression on the equation:

$$\ln (k_r h/kT) = -\Delta H^{\ddagger}/RT + \Delta S^{\ddagger}/R \qquad \text{(Eq. 2)}$$

where k_r is the observed rate constant, h is Planck's constant, k is Boltzman's constant, T is absolute temperature, R is the gas constant, and $\Delta H^{\ddagger}$ and $\Delta S^{\ddagger}$ are the enthalpy and entropy of activation, respectively. Again, first-order kinetics were followed, and a correlation coefficient of 0.99 or greater was observed in each case.

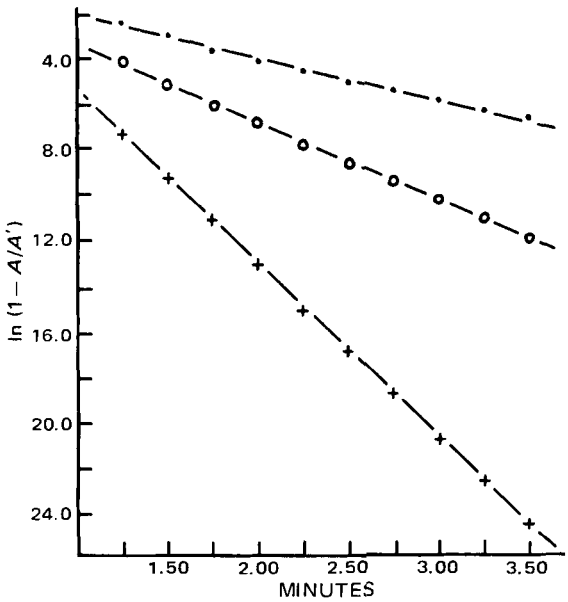

Figure 2—*Reaction rate of phenylhydrazine with I at various temperatures. Key: ●, 10°; ○, 20°; and +, 30°.*

The $\Delta H^{\ddagger}$ values for the phenylhydrazines (8.4–11.2 kcal/mole) were approximately half (17.3–19.8 kcal/mole) of those observed for corticosteroids (16), whereas the $\Delta S^{\ddagger}$ values for the phenylhydrazines (−38–−45 eu) were considerably more negative than those (−8–−12 eu) observed for corticosteroids. This result indicates a more facile transfer of a reduction unit and a more ordered transition state in the I reaction with phenylhydrazine salts as compared with corticosteroids.

GLC–mass spectral analysis of the various reaction mixtures indicated that arylhydrazine salts R–$C_6H_4NHNH_2$ were oxidized to the corresponding arene derivatives R–C_6H_5.

The inhibition of oxygen on the reaction rate and the low $\Delta H^{\ddagger}\rho$ (23) values indicate that the mechanism for the oxidation of phenylhydrazine salts resembles the free radical mechanism proposed previously (17) for active hydrogen compounds. Further evidence for the free radical mechanism was obtained by the study of iodine inhibition on the reaction rate of phenylhydrazine and I. The reaction of blue tetrazolium with 1.25 μmoles of phenylhydrazine containing 10.0 and 100 μmoles of iodine yielded absorbances of 1.222 and 0.692 units, respectively, while the absorbance of a similar solution without iodine was 1.282 units for the same time. The reaction of blue tetrazolium with phenylhydrazine in the two solutions containing iodine was inhibited by 4.7 and 46%. Since iodine is a radical scavenger that inhibits radical reactions and since the reaction rate of phenylhydrazine with blue tetrazolium is inhibited by iodine, the evidence indicates that the oxidation of phenylhydrazine by blue tetrazolium proceeds by a free radical mechanism.

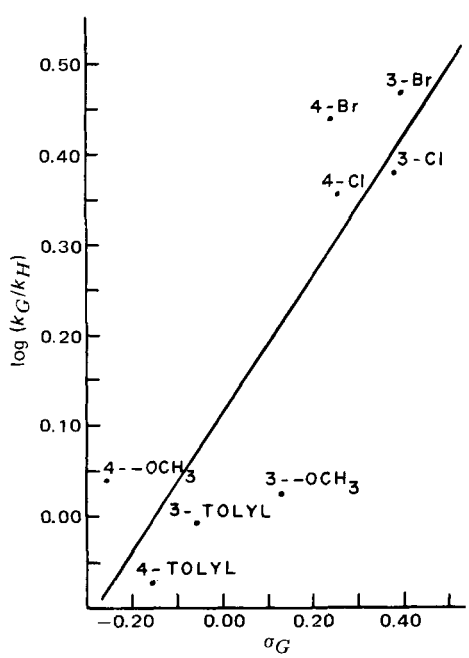

Figure 3—*Effect of substituents on the reaction of phenylhydrazine with blue tetrazolium at 20°.*

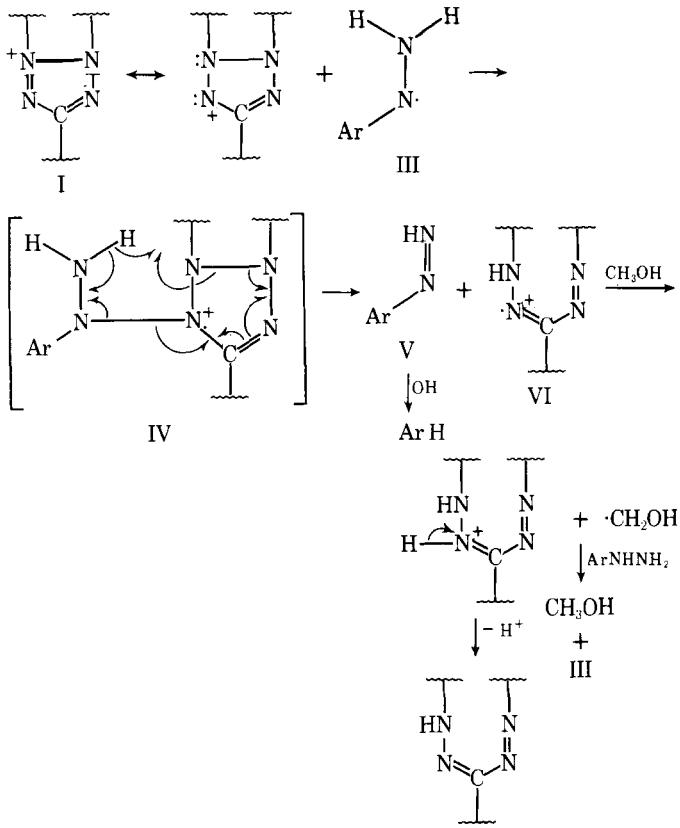

Scheme I

A pictorial description of such a mechanism is illustrated in Scheme I. Initially, a free radical complex, IV, is formed between either the free radical of arylhydrazine, III, and I or vice versa (only the former is shown in Scheme I). Complex IV subsequently decomposes to the aryldiimide V and the free radical derivatives of formazan VI. During the decomposition of IV, a hydrogen atom from the β-nitrogen atom and an electron from the α-nitrogen atom are transferred from the arylhydrazine portion of IV to I. Further decomposition of diimide V yields the corresponding arene derivative; this decomposition in basic solution is very rapid (24). The fate of radical VI is not known accurately, but it might abstract a hydrogen atom from methanol to yield a formazan. The resulting $\cdot CH_2OH$ radical then propagates the chain reaction by reacting with phenylhydrazine to produce III.

In all cases, the theoretical absorbance of formazan, based on transfer of one reduction unit from arylhydrazine to I (10), was observed. Therefore, this method might be feasible for the quantitation of pharmaceuticals containing the hydrazine moiety. The analysis of hydralazine and isoniazid by this proposed method is under investigation.

REFERENCES

(1) F. E. Smith, *Science*, **113**, 751 (1951).

(2) E. Farber and C. D. Louviere, *J. Histochem. Cytochem.*, **4**, 347 (1955).

(3) E. Farber, W. H. Sternberg, and C. E. Dunlap, *ibid.*, **4**, 284 (1956).

(4) E. Shelton and W. C. Schneider, *Anat. Rec.*, **112**, 61 (1952).

(5) J. H. Tyrer, M. S. Eadie, and W. D. Hooper, *J. Chromatogr.*, **39**, 312 (1969).

(6) R. L. Baehner, *Am. J. Dis. Child.*, **128**, 449 (1974).

(7) W. Antopol, S. Glaubach, and L. Goldman, *U.S. Public Health Serv. Public Health Rep.*, **63**, 1231 (1948).

(8) W. J. Mader and R. R. Buck, *Anal. Chem.*, **24**, 665 (1952).

(9) C. A. Johnson, R. King, and C. Vickers, *Analyst*, **85**, 714 (1960).
(10) R. E. Graham, E. R. Biehl, C. T. Kenner, G. H. Luttrell, and D. L. Middleton, *J. Pharm. Sci.*, **64**, 226 (1975).
(11) R. E. Graham, E. R. Biehl, and C. T. Kenner, *ibid.*, **59**, 1152 (1970).
(12) R. E. Graham and C. T. Kenner, *ibid.*, **62**, 103 (1973).
(13) A. S. Meyer and M. C. Lindberg, *Anal. Chem.*, **27**, 813 (1955).
(14) "The United States Pharmacopeia," 19th rev., Mack Publishing Co., Easton, Pa., 1975, p. 622.
(15) "The National Formulary," 14th ed., Mack Publishing Co., Easton, Pa., 1975, p. 976.
(16) R. M. Oteiza, R. S. Wooten, C. T. Kenner, R. E. Graham, and E. R. Biehl, *J. Pharm. Sci.*, **66**, 1385 (1977).
(17) J. E. Sinsheimer and E. F. Salim, *Anal. Chem.*, **37**, 566 (1965).
(18) L. F. Audrieth and B. A. Ogg, "The Chemistry of Hydrazine," Wiley, London, England, 1951, p. 227.
(19) F. D. Chattaway, *J. Chem. Soc.*, **91**, 1323 (1907).
(20) E. J. Cuy and W. C. Bray, *J. Am. Chem. Soc.*, **51**, 1787 (1924).
(21) E. C. Gilbert, *ibid.*, **51**, 2745 (1929).
(22) M. M. Jaffe, *Chem. Rev.*, **53**, 191 (1953).
(23) W. A. Waters, "Mechanism of Oxidation of Organic Compounds," Methuen, London, England, 1964, p. 4.
(24) P. C. Huang and E. M. Kosower, *J. Am. Chem. Soc.*, **90**, 2362 (1968).

ACKNOWLEDGMENTS

Supported in part by Grant N-118 from the Robert A. Welch Foundation, Houston, Tex.

The authors thank Dr. Gabriel D. Castillo of the Food and Drug Administration, Dallas District, for many helpful suggestions.

Pharmacokinetics of Iodoxamic Acid in Rhesus Monkey: Biliary Excretion, Plasma Protein Binding, and Enterohepatic Circulation

SHENG K. LIN *, ALBERT A. MOSS ‡, ROGER MOTSON ‡, and SIDNEY RIEGELMAN *x

Received August 4, 1977, from the **Department of Pharmacy, School of Pharmacy, and the* ‡*Departments of Radiology and Surgery, School of Medicine, University of California, San Francisco, CA 94143.* Accepted for publication October 19, 1977.

Abstract □ The previously reported steady-state method allowed estimation of the capacity-limited pharmacokinetics of the cholangiographic agent, iodipamide. To circumvent the long time period required to establish each steady-state level, a dynamic method was applied to the study of the rate processes involved in the hepatic uptake and biliary excretion of a new cholangiographic agent, iodoxamic acid, in rhesus monkeys. The dynamic method has the advantage that the pharmacokinetic parameters involved in capacity-limited hepatic uptake or biliary excretion can be obtained from a single infusion experiment. The V_{max} was 1.03 ± 0.25 μmoles/kg/min (mean ± *SD*); K_m varied from animal to animal and ranged from 1.5 to 16.4 μ*M*. Protein binding was estimated using equilibrium dialysis. The Freundlich isotherm yielded a linear plot when the natural logarithm of unbound iodoxamic acid concentration in plasma was plotted against the natural logarithm of its blood concentration. The plasma protein binding data also could be fitted to the Langmuir isotherm, presuming two independent classes of binding.

Keyphrases □ Iodoxamic acid—biliary excretion, plasma protein binding, and enterohepatic circulation in rhesus monkeys □ Excretion, biliary—iodoxamic acid in rhesus monkeys □ Binding, plasma protein—iodoxamic acid in rhesus monkeys □ Enterohepatic circulation—iodoxamic acid in rhesus monkeys □ Pharmacokinetics—iodoxamic acid in rhesus monkeys □ Radiopaque media—iodoxamic acid, biliary excretion, plasma protein binding, and enterohepatic circulation in rhesus monkeys

Cholecysto-cholangiographic agents bind significantly to plasma proteins (1–3), and this binding influences their biliary excretion. The role of serum albumin in the hepatic excretion of iodipamide was studied (4), and the binding of iodipamide to albumin retarded iodipamide transfer from plasma to the bile, probably because of competition between albumin and the anion binding protein of the liver.

Previous studies (5, 6) with a steady-state infusion method demonstrated that iodipamide is highly bound to plasma protein and has low blood clearance. Therefore, the unbound fraction of iodipamide is probably the major determinant in its renal and hepatic elimination (7). Although the steady-state method allows extensive analysis of the pharmacokinetics of iodipamide (5, 6), it has the disadvantages that: (*a*) a lengthy time is required to establish each steady-state level; (*b*) the time it takes to reach the steady state increases as one approaches saturation; and (*c*) a series of steady states is required in different experiments in the same animal, but the physiological status of an animal might change between experiments.

To circumvent some of these problems, a dynamic method was used to study the rate processes involved in the biliary excretion and hepatic uptake of a new cholecysto-cholangiographic agent, iodoxamic acid[1] (I), in rhesus monkeys. This method has the advantage that the pharmacokinetic parameters involved in the capacity-limited hepatic uptake or biliary excretion can be obtained from a single experiment.

EXPERIMENTAL

Studies were performed on three healthy rhesus monkeys (one male and two females), 4.5–9.1 kg, restrained in plastic chairs. They were

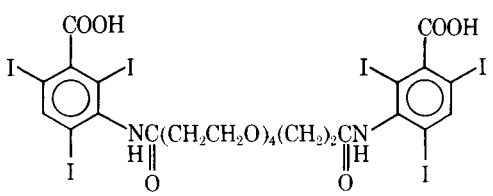

I

[1] Cholovue 40, 3% injection of the meglumine salt, E. R. Squibb and Sons, Inc., Princeton, N.J.

0022-3549/78/0700/0930$01.00/0
© 1978, American Pharmaceutical Association

(9) C. A. Johnson, R. King, and C. Vickers, *Analyst*, **85**, 714 (1960).
(10) R. E. Graham, E. R. Biehl, C. T. Kenner, G. H. Luttrell, and D. L. Middleton, *J. Pharm. Sci.*, **64**, 226 (1975).
(11) R. E. Graham, E. R. Biehl, and C. T. Kenner, *ibid.*, **59**, 1152 (1970).
(12) R. E. Graham and C. T. Kenner, *ibid.*, **62**, 103 (1973).
(13) A. S. Meyer and M. C. Lindberg, *Anal. Chem.*, **27**, 813 (1955).
(14) "The United States Pharmacopeia," 19th rev., Mack Publishing Co., Easton, Pa., 1975, p. 622.
(15) "The National Formulary," 14th ed., Mack Publishing Co., Easton, Pa., 1975, p. 976.
(16) R. M. Oteiza, R. S. Wooten, C. T. Kenner, R. E. Graham, and E. R. Biehl, *J. Pharm. Sci.*, **66**, 1385 (1977).
(17) J. E. Sinsheimer and E. F. Salim, *Anal. Chem.*, **37**, 566 (1965).
(18) L. F. Audrieth and B. A. Ogg, "The Chemistry of Hydrazine," Wiley, London, England, 1951, p. 227.
(19) F. D. Chattaway, *J. Chem. Soc.*, **91**, 1323 (1907).
(20) E. J. Cuy and W. C. Bray, *J. Am. Chem. Soc.*, **51**, 1787 (1924).
(21) E. C. Gilbert, *ibid.*, **51**, 2745 (1929).
(22) M. M. Jaffe, *Chem. Rev.*, **53**, 191 (1953).
(23) W. A. Waters, "Mechanism of Oxidation of Organic Compounds," Methuen, London, England, 1964, p. 4.
(24) P. C. Huang and E. M. Kosower, *J. Am. Chem. Soc.*, **90**, 2362 (1968).

ACKNOWLEDGMENTS

Supported in part by Grant N-118 from the Robert A. Welch Foundation, Houston, Tex.

The authors thank Dr. Gabriel D. Castillo of the Food and Drug Administration, Dallas District, for many helpful suggestions.

Pharmacokinetics of Iodoxamic Acid in Rhesus Monkey: Biliary Excretion, Plasma Protein Binding, and Enterohepatic Circulation

SHENG K. LIN *, ALBERT A. MOSS ‡, ROGER MOTSON ‡, and SIDNEY RIEGELMAN *x

Received August 4, 1977, from the **Department of Pharmacy, School of Pharmacy, and the* ‡*Departments of Radiology and Surgery, School of Medicine, University of California, San Francisco, CA 94143.* Accepted for publication October 19, 1977.

Abstract □ The previously reported steady-state method allowed estimation of the capacity-limited pharmacokinetics of the cholangiographic agent, iodipamide. To circumvent the long time period required to establish each steady-state level, a dynamic method was applied to the study of the rate processes involved in the hepatic uptake and biliary excretion of a new cholangiographic agent, iodoxamic acid, in rhesus monkeys. The dynamic method has the advantage that the pharmacokinetic parameters involved in capacity-limited hepatic uptake or biliary excretion can be obtained from a single infusion experiment. The V_{max} was 1.03 ± 0.25 μmoles/kg/min (mean ± *SD*); K_m varied from animal to animal and ranged from 1.5 to 16.4 μ*M*. Protein binding was estimated using equilibrium dialysis. The Freundlich isotherm yielded a linear plot when the natural logarithm of unbound iodoxamic acid concentration in plasma was plotted against the natural logarithm of its blood concentration. The plasma protein binding data also could be fitted to the Langmuir isotherm, presuming two independent classes of binding.

Keyphrases □ Iodoxamic acid—biliary excretion, plasma protein binding, and enterohepatic circulation in rhesus monkeys □ Excretion, biliary—iodoxamic acid in rhesus monkeys □ Binding, plasma protein—iodoxamic acid in rhesus monkeys □ Enterohepatic circulation—iodoxamic acid in rhesus monkeys □ Pharmacokinetics—iodoxamic acid in rhesus monkeys □ Radiopaque media—iodoxamic acid, biliary excretion, plasma protein binding, and enterohepatic circulation in rhesus monkeys

Cholecysto-cholangiographic agents bind significantly to plasma proteins (1–3), and this binding influences their biliary excretion. The role of serum albumin in the hepatic excretion of iodipamide was studied (4), and the binding of iodipamide to albumin retarded iodipamide transfer from plasma to the bile, probably because of competition between albumin and the anion binding protein of the liver.

Previous studies (5, 6) with a steady-state infusion method demonstrated that iodipamide is highly bound to plasma protein and has low blood clearance. Therefore, the unbound fraction of iodipamide is probably the major determinant in its renal and hepatic elimination (7). Although the steady-state method allows extensive analysis of the pharmacokinetics of iodipamide (5, 6), it has the disadvantages that: (*a*) a lengthy time is required to establish each steady-state level; (*b*) the time it takes to reach the steady state increases as one approaches saturation; and (*c*) a series of steady states is required in different experiments in the same animal, but the physiological status of an animal might change between experiments.

To circumvent some of these problems, a dynamic method was used to study the rate processes involved in the biliary excretion and hepatic uptake of a new cholecysto-cholangiographic agent, iodoxamic acid[1] (I), in rhesus monkeys. This method has the advantage that the pharmacokinetic parameters involved in the capacity-limited hepatic uptake or biliary excretion can be obtained from a single experiment.

EXPERIMENTAL

Studies were performed on three healthy rhesus monkeys (one male and two females), 4.5–9.1 kg, restrained in plastic chairs. They were

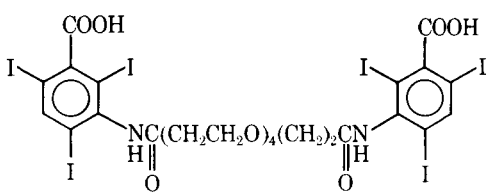

I

[1] Cholovue 40, 3% injection of the meglumine salt, E. R. Squibb and Sons, Inc., Princeton, N.J.

0022-3549/78/0700/0930$01.00/0
© 1978, American Pharmaceutical Association

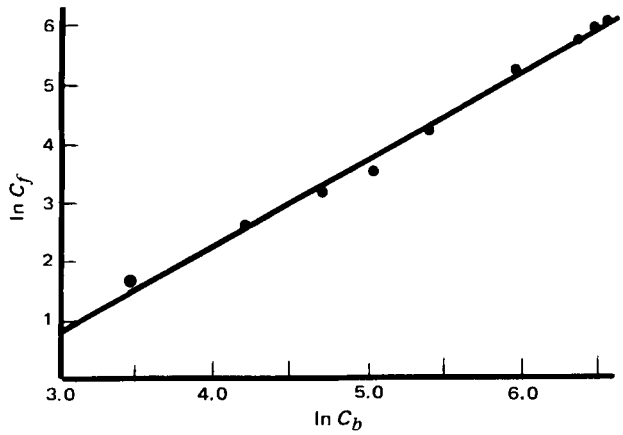

Figure 1—*Plasma protein binding of iodoxamic acid in Monkey A shown as the linear relationship between the natural logarithm of the unbound concentration (ln* C_f) versus *the natural logarithm of the blood concentration (ln* C_b) *of iodoxamic acid.*

prepared as previously described (8) with a T-tube in the common bile duct for bile collection and another T-tube in the duodenum for the recycling of bile salts. All three monkeys were cholecystectomized.

^{125}I-Labeled iodoxamic acid[2] was used in the plasma protein binding study. The ^{125}I-radiopurity was monitored by TLC and was more than 99% pure. Sodium taurocholate[3] was infused into the duodenum 1 hr prior to and throughout each infusion experiment at 5.56 μmoles/kg/min to replace the loss of bile salts from the collection of bile samples (9).

The iodoxamic acid concentrations in the blood, bile, and urine samples were determined by monitoring the iodine content using fluorescent excitation analysis (10), and the ^{125}I-radioactivity was measured using a scintillation spectrometer[4].

Plasma Protein Binding Studies—Appropriate amounts of ^{125}I-iodoxamic acid were added to blood samples obtained from each monkey to achieve the blood iodoxamic acid concentrations, C_b, of 42–912 μ*M*. After equilibration, the plasma was separated from blood cells by centrifugation. Each plasma sample was dialyzed against Krebs–Ringer buffer at 37° for 5 hr using an equilibrium dialysis technique[5]. The equilibrium ^{125}I-concentrations in the buffer and the plasma were measured to obtain the unbound and plasma concentrations of iodoxamic acid. The bound concentration of iodoxamic acid in the plasma was calculated by subtracting the unbound concentration from the plasma concentration of iodoxamic acid.

Lang and Lasser (1) showed that iodipamide binds to albumin but not to globulins in the plasma. Because iodoxamic acid and iodipamide have similar chemical properties, iodoxamic acid was assumed to bind only to albumin. Therefore, the moles of drug bound per mole of plasma protein, r, was calculated by dividing the bound concentration of iodoxamic acid by the albumin concentration in the plasma estimated by electrophoresis (11). A Scatchard plot was constructed by plotting r/C_f *versus* r, where C_f is the unbound concentration of iodoxamic acid in the plasma.

Steady-State Infusion Studies—After loading doses of 25.6 and 77.0 μmoles/kg, meglumine iodoxamate was infused into a monkey at the rates of 0.65 and 2.59 μmoles/kg/min for 120 and 160 min, respectively. In a separate experiment, meglumine iodoxamate was infused at the rates of 1.30 and 1.95 μmoles/kg/min for 160 min each into the same monkey. Blood and bile samples were collected every 20 min throughout the experiment.

Meglumine iodoxamate also was infused (after loading doses of 25.6, 124.9, and 85.0 μmoles/kg) into another monkey at the rates of 0.7, 4.17, and 6.53 μmoles/kg/min, respectively, for 2 hr each. In a separate experiment, meglumine iodoxamate was infused into the same monkey at the rate of 6.53 μmoles/kg/min for 140 min. Throughout each experiment, bile samples were collected at 20- or 30-min intervals. The total volume was recorded, and a 1.0-ml aliquot was used for determinations of biliary iodoxamic acid concentrations; the rest was infused back into the duodenum. In this monkey, no sodium taurocholate was infused during the infusion experiments.

Table I—Freundlich Equation[a] Parameters for Iodoxamic Acid in Monkeys

Monkey	m	A	r^2
A	1.479 (2.9)[b]	−3.671 (6.3)	0.993
B	1.402 (1.6)	−1.370 (2.8)	0.999
C	1.473 (3.0)	−4.366 (5.7)	0.996

[a] $C_f = AC_b^m$. [b] Coefficient of variation in percent.

Dynamic Infusion Studies—In all three monkeys, meglumine iodoxamate was infused at rates varying from 1.20 to 2.60 μmoles/kg/min for 120 min (except in one experiment in one monkey where infusion was for 95 min). To estimate the lag time between the appearance of the drug in the bile canaliculi and at the sampling site, the bile samples were collected every 2 min during the first 30 min. Thereafter, bile samples were collected at 5–15-min intervals until 3–4 hr after the infusion.

Enterohepatic Circulation Studies—A 150-μmole/kg bolus dose of iodoxamic acid was administered into the duodenum of each of two monkeys, and the bile samples were collected every 2 hr for 6 hr.

Pooled bile containing iodoxamic acid collected from infusion experiments was administered as a 75-μmole/kg bolus dose into the duodenum of another monkey. Bile samples were collected every 80–~90 min over 715 min. Sodium taurocholate was infused into the duodenum as previously noted.

Biotransformation Studies—The blood, bile, and urine samples were analyzed for iodoxamic acid and possible metabolites by the following methods.

1. Due to the high iodoxamic acid concentration in the bile and urine samples, these samples were spotted directly on a TLC plate[6] containing a fluorescent pigment[7] and were compared with standard iodoxamic acid and blank bile and urine. The TLC plate was developed with 2-propanol–28% ammonium hydroxide (4:1 v/v) and air dried, and then the spots were visualized under short wavelength UV light to locate iodoxamic acid and possible metabolites by the use of the UV absorption characteristics of the aromatic ring.
2. Blood samples were acidified with 0.1 *N* HCl and extracted with ether. The ether extract was evaporated to dryness with purified nitrogen at room temperature. The residue was redissolved in 20 μl of methanol and spotted on a TLC plate as described for Method 1.

RESULTS

Plasma Protein Binding Studies—Iodoxamic acid was highly bound to plasma protein. As the blood iodoxamic acid concentration increased from 42 to 912 μ*M*, the fraction unbound varied from 6.1 to 41.2%. By using the Freundlich isotherm approach (12), a linear relationship was found when ln C_f was plotted against ln C_b. The data for Monkey A are shown in Fig. 1, and the composite for all monkeys is given in Table I.

When the data were plotted according to the Scatchard equation, a concave descending curve was obtained (Fig. 2), indicating the existence of more than one class of binding sites for iodoxamic acid. By presuming two classes of binding sites that behave independently, r was fitted to C_f according to the Langmuir isotherm equation using the FITFUN program of the PROPHET computer system[8]:

$$r = \frac{n_1 k_1 C_f}{1 + k_1 C_f} + \frac{n_2 k_2 C_f}{1 + k_2 C_f} \qquad \text{(Eq. 1)}$$

where n_1 and n_2 are the number of binding sites for first and second class binding, respectively, and k_1 and k_2 are the association constants of each class of binding. The results are shown in Fig. 3 for the relationship between r and C_f. The computer-estimated binding parameters of the three monkeys are given in Table II. After these parameters were obtained, a theoretical curve was drawn for the relationship of r/C_f *versus* r in the Scatchard plot (Fig. 2), which was resolved into two linear components representing each class of binding.

Steady-State Infusion Studies—The results from steady-state infusion studies are shown in Table III. The data from two independent experiments in each monkey are listed. The biliary excretion rate appears

[2] ^{125}I-meglumine iodoxamate, E. R. Squibb and Sons.
[3] ICN Pharmaceuticals Inc., Cleveland Ohio.
[4] Auto-γ-scintillation spectrometer, model 1185, Searle Analytic Inc., Des Plaines, Ill.
[5] Dianorm, a multiple-equilibrium dialysis system, Innovativ-Medizin AG, Ch-Esslingen, Switzerland.
[6] Silica gel F-254.
[7] EM reagent, West Germany.
[8] The PROPHET system is a specialized computer resource developed by the Chemical/Biological Information Handling Program of the National Institutes of Health. A detailed description of the system features appears in *Proc. Natl. Comput. Conf. Exposition*, **43**, 457 (1974).

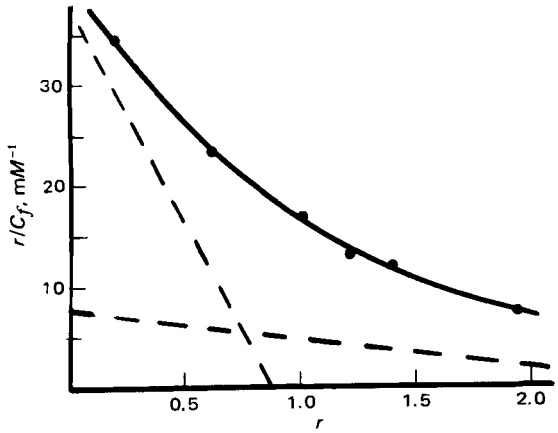

Figure 2—*Scatchard plot of the binding of iodoxamic acid to plasma albumin in Monkey B. Key: ●, data points; —, computer-fitted line presuming two independent binding classes; and – –, computer-resolved linear components representing each class of binding.*

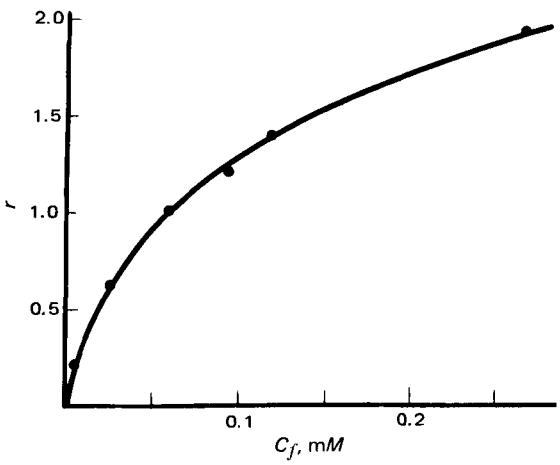

Figure 3—*Relationship between* r *and* C_f *in Monkey C. Key: ●, data points; and —, computer-fitted line presuming two classes of binding according to Eq. 1.*

to increase approximately in proportion to the infusion rates when the low value is compared to the next value listed. However, when intermediate and high infusion rates were utilized, the biliary excretion rates in Monkey C were 1.20, 1.60, and 1.40 μmoles/kg/min; in Monkey D, they were 1.72, 1.12, and 1.44 μmoles/kg/min. Although the data showed variation in biliary excretion, they support the contention that the biliary excretion process or a rate-limiting step prior to excretion appears to be saturable.

Dynamic Infusion Studies—A lag time existed for the bile to flow from the canaliculi to the sampling site, and it was estimated by plotting the cumulative amount of iodoxamic acid excreted in the bile in the first 30 min against time (Fig. 4). The lag time was estimated by extrapolating the initial linear portion to the abscissa; it varied from 5 to ~7 min.

The biliary excretion rate data were plotted against the midpoint of the collection time after correcting for the lag time (Fig. 5).

The blood iodoxamic acid concentration was plotted against time on the same graphs (Fig. 5). Even though two different doses (2.2 and 2.6 μmoles/kg/min) were infused, the maximum biliary excretion rate did not increase proportionately but reached essentially the same plateau value. This result is an indication of the saturation of the biliary excretory mechanism or, alternatively, a hepatic uptake mechanism.

The biliary excretion rate data in the postinfusion period were fitted to the Michaelis–Menten equation against the corresponding unbound concentration of iodoxamic acid at each time using the HYPERBOLIC program of the PROPHET computer system[8] (Fig. 6):

$$RB = \frac{V_m C_f}{K_m + C_f} \qquad \text{(Eq. 2)}$$

where RB is the biliary excretion rate at a given time and V_m and K_m are the maximal biliary excretion rate and the Michaelis–Menten constant, respectively. The parameter estimates are given in Table IV.

Enterohepatic Circulation Studies—The percentages of iodoxamic acid recovered in the bile over 6 hr after an intraduodenal bolus dose of 150 μmoles/kg of meglumine iodoxamate solution were 0.05 and 0.20% in two monkeys. In another monkey, 11.9 hr after a bolus dose of bile containing 75 μmoles/kg, the percent recovery was 1.1%.

Biotransformation Studies—With TLC, iodoxamic acid was found to exist in the blood as the unchanged species. No metabolites were found in the bile. In the urine, two additional spots in very small quantity were found on the thin-layer chromatogram in addition to unchanged iodoxamic acid. These two metabolites had R_f values of 0.48 and 0.23, whereas iodoxamic acid had R_f 0.35. Due to the minute quantity obtained, no attempts were made to identify these metabolites.

DISCUSSION

The goal of the present plasma protein binding studies was to develop a method of estimating the C_f values at various blood or plasma concentrations of iodoxamic acid. The Freundlich empirical relationship that relates the bound and unbound drug concentrations fit the data when log C_f was plotted *versus* log C_b, where C_b is the total blood iodoxamic acid concentration. Normally, one would plot the plasma concentration of the bound drug. However, since the assay results in the measurement of C_b, it is convenient to use this representation so that a direct conversion from C_b to C_f can be made. A virtually identical plot was obtained when log C_f was plotted *versus* log C_p, where C_p is the total plasma iodoxamic acid concentration.

Application of the Freundlich isotherm to the analysis of plasma protein binding data (Table I) shows a relatively small coefficient of variation of the parameter estimates. When analyzed using the Langmuir isotherm, a reasonably good fit was obtained presuming two classes of binding sites and the drug bound solely to plasma albumin (Table II). Two separate studies of iodoxamic acid binding were used with Monkey A, which might have contributed to the observed large coefficients of variation. The data from Monkey B are plotted in Fig. 3 according to the Langmuir equation (Eq. 1) and in Fig. 2 according to the Scatchard relationship. The dashed lines represent the two classes of binding sites.

Rosati *et al.* (13) studied the plasma protein binding of three radiopaques and showed that iodoxamic acid binds slightly less than iodipamide to dog plasma protein. In human serum albumin, the association constant of iodoxamic acid was one-tenth that of iodipamide. The data (13) indicate that iodoxamic acid binds to at least two classes of binding sites in plasma albumin. However, no calculations were reported.

Although the whole blood clearance of drugs varies with dose in capacity-limited processes, the whole blood clearance of iodoxamic acid in the monkeys was calculated by dividing the dose by the area under blood concentrations with time curves in the infusion experiments. The blood clearance of iodoxamic acid was estimated to vary from 1.9 to 14.9 ml/kg/min. These values were much lower than the average hepatic blood flow: 44–50 ml/kg/min (14). Since iodoxamic acid has a high degree of plasma protein binding and low blood clearance, the unbound concentration of iodoxamic acid probably is the major determinant in its hepatic elimination. Therefore, the unbound concentration rather than the blood or plasma concentration of iodoxamic acid was used in the computer fitting of biliary excretion rate data (Eq. 2).

This situation is analogous to comparing the urinary excretion rate to the unbound plasma drug concentration. Even if the blood drug concentration–time profile indicated multiple compartments, the relationship in Eq. 2 nevertheless is applicable and is independent of the distribution into peripheral tissues other than the liver and kidneys.

Rosati *et al.* (13) reported that iodoxamic acid displayed a maximum biliary transport (V_m) value twice that of iodipamide in anesthetized dogs

Table II—Langmuir Equation[a] Parameters for Iodoxamic Acid in Monkeys

Monkey	n_1	k_1, M^{-1}	n_2	k_2, M^{-1}	r^2
A	0.56 (64)[b]	4×10^4 (118)	29.9 (1253)	7.7×10^1 (1351)	0.9850
B	0.46 (34)	5.3×10^4 (31)	4.2 (7)	3.2×10^3 (24)	0.9999
C	0.87 (68)	3.7×10^4 (67)	2.7 (17)	29×10^3 (100)	0.9995

[a] See Eq. 1. [b] Coefficient of variation in percent.

Table III—Relationships among Infusion Rate, R^0, Steady-State Blood Concentration, C_b, Bile Flow, Bile Concentration, and Biliary Excretion Rate, RB, of Iodoxamic Acid

Study	R^0, μmoles/kg/min	C_b[a], μM	Bile Flow[b], ml/min	Bile Concentration[b], mM	RB[b], μmoles/kg/min
Monkey C					
Study 1	0.65	37	0.19	15.1	0.65
	2.60	677[c]	0.27	23.4	1.40
Study 2	1.30	64	0.28	19.3	1.20
	1.95	286	0.32	22.6	1.60
Monkey D[d]					
Study 1	0.71	—[e]	0.14	10.8	0.34
	4.17	—[e]	0.41	18.9	1.72
	6.53	—[e]	0.25	20.1	1.12
Study 2	6.53	—[e]	0.33	19.6	1.44

[a] Mean of at least three determinations. [b] Mean of at least four determinations. [c] The blood concentration in this instance was still increasing at about 10%/hr; however, the biliary excretion rate did not reflect the increase and appeared to be at a steady state. [d] Monkey D died after these two studies. [e] No blood samples were obtained due to dysfunction of the arterial catheter.

(0.91 *versus* 0.48 μmole/kg/min). Evil and Benness (15) also reported that the biliary output of iodoxamic acid (0.74 μmole/kg/min) was more than 50% higher than the iodipamide output (0.46 μmole/kg/min). However, Berk *et al.* (16), using a steady-state infusion method, showed that the biliary transport maximum of 1.60 μmoles/kg/min for iodoxamic acid was only 25% greater than that for iodipamide (1.27 μmoles/kg/min).

In the Rosati *et al.* (13) study, anesthetized dogs were used with no replacement of bile salts, which probably explains why the maximal excretion rates for both iodoxamic acid and iodipamide were lower than those of the Berk *et al.* (16) studies in which unanesthetized dogs with bile salts replacement were used. The Evil and Benness (15) studies also used unanesthetized dogs with bile salts replacement. However, it was not certain whether saturation of biliary excretion was ever reached. In all cases, however, it seems that iodoxamic acid had a higher biliary excretion rate than iodipamide at the same dose levels.

Similar to the previous experiments with dogs (13, 15, 16), the present steady-state infusion experiments in monkeys also demonstrated that the biliary excretion of iodoxamic acid is saturable (Table III). In Monkey C, the infusion of 1.95 μmoles/kg/min resulted in the biliary excretion rate of 1.60 μmoles/kg/min, whereas the infusion of 2.59 μmoles/kg/min resulted in the biliary excretion rate of 1.40 μmoles/kg/min. The fact that slightly lower biliary excretion was obtained following higher infusion rates suggests that biliary excretion was saturated. The reason that the biliary excretion rate following the higher dose was slightly lower than that following the lower dose is unclear. It could be due to day-to-day variations of the animal or the toxicity following the higher dose. Sperber and Sperber (17) showed that the biliary excretion of iodipamide was depressed following excessively high doses in rats.

Present dynamic infusion studies also demonstrated the saturation of biliary excretion of iodoxamic acid (Table IV and Fig. 5). The computer-estimated maximal biliary excretion rate was 0.90 μmole/kg/min (Fig. 6) for Monkey A, a value very close to the actual maximal biliary excretion rate of 1.0 μmole/kg/min (Fig. 5) obtained experimentally. The Michaelis–Menten parameters remained relatively constant following different doses of each animal, *i.e.*, independent of dose (Table IV). The V_m value of 0.66 μmole/kg/min for Monkey A following an excessively high dose (2.60 μmoles/kg/min) was somehow lower than the value of 0.90 μmole/kg/min following an intermediate dose (2.20 μmoles/kg/min) in the same animal. Again, this result could be due to the toxicity following the high dose. The maximum doses in other experiments were below 2.0 μmoles/kg/min. The dynamic method has the important advantage that the pharmacokinetic parameters involved in capacity-limited hepatic uptake or biliary excretion can be obtained from a single experiment.

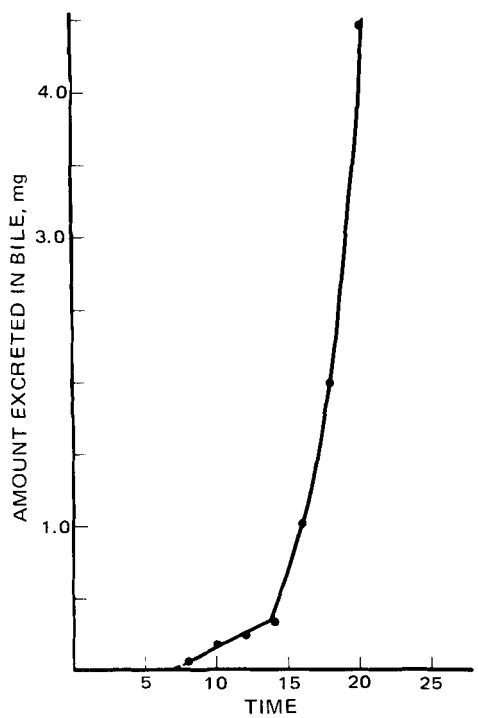

Figure 4—*Cumulative amount of iodoxamic acid excreted in the bile during the initial 20 min in one infusion study in Monkey A.*

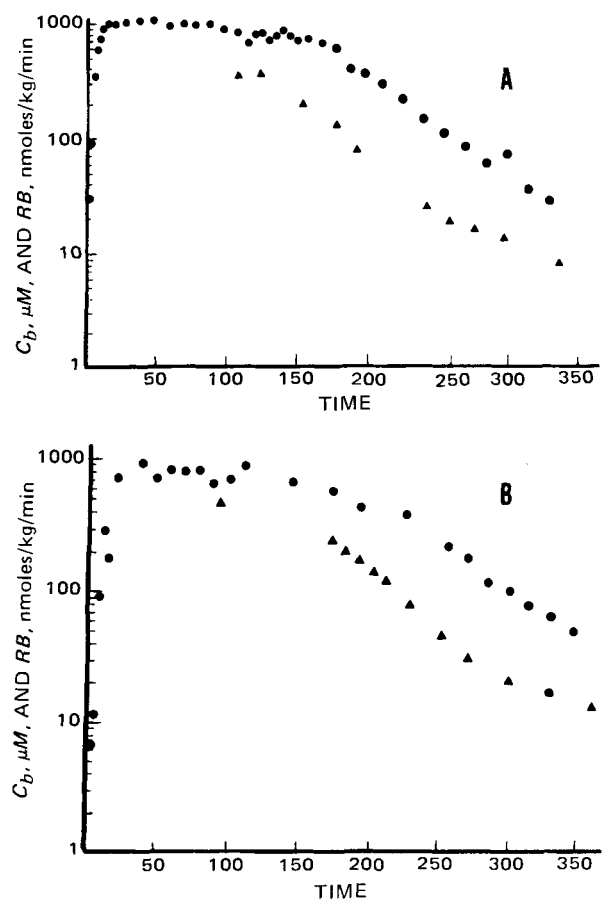

Figure 5—*Semilog plot of the blood concentration (▲) and biliary excretion rate (●) of iodoxamic acid with time following the infusion of 2.20 (A) and 2.60 (B) μmoles/kg/min into Monkey A.*

Table IV—Michaelis-Menten Parameters [a] of Biliary Excretion of Iodoxamic Acid in Monkeys

Parameter	Monkey A	Monkey B	Monkey C
V_m, μmoles/kg/min	0.90 (15) [b]	1.01 (7)	1.28 (20)
	0.66 (6.8)	1.00 (25.5)	1.30 (21.6)
K_m, μM	16.4 (55)	3.5 (30)	1.5 (64)
	11.1 (23.4)	3.10 (54.4)	1.79 (43.9)

[a] Parameter values from two independent studies following different doses in each monkey are listed together. [b] Coefficient of variation in percent.

The overall average maximal biliary excretion rate (V_m) obtained (1.03 μmoles/kg/min) for iodoxamic acid in rhesus monkeys was only slightly (8.4%) higher than the 0.95 μmole/kg/min reported by Wittenberg *et al.* (18) for iodipamide in the same animal species. However, in the cited report (18), there was one study in which an exceptionally high biliary excretion rate was observed (almost three times higher than the other five studies). If this particular study is excluded from the results, the maximal biliary excretion rate becomes 0.64 μmole/kg/min, which is about 61% lower than that of iodoxamic acid in the present studies. In both cases, more iodoxamic acid was excreted in rhesus monkeys than was obtained with iodipamide.

The percentages of iodoxamic acid excreted in the bile following introduction of a meglumine iodoxamate solution into the duodenum indicates that the enterohepatic circulation of iodoxamic acid is insignificant. When the dose of 75 μmoles/kg was given to Monkey C (as the bile containing iodoxamic acid), the percentage of recovery over 11.9 hr was 1.1%. This result is not surprising because of the large molecular weight and polar characteristics of the molecule. Whitney and Cambell (19) reported that the interruption of enterohepatic circulation has no effect on iodipamide excretion in the bile of the rhesus monkey.

TLC revealed that iodoxamic acid existed in the blood and bile as the unchanged species. In the urine, two metabolites were found, one with higher and one with lower polarity. Qualitatively, this finding is consistent with the report of Mutzel *et al.* (20) concerning humans. However, the two metabolites constituted about half of the iodinated compounds in the Mutzel *et al.* (20) studies whereas only very small amounts of these metabolites were found in the urine. Therefore, the metabolism of iodoxamic acid in monkeys is probably closer to that in humans than to that in dogs.

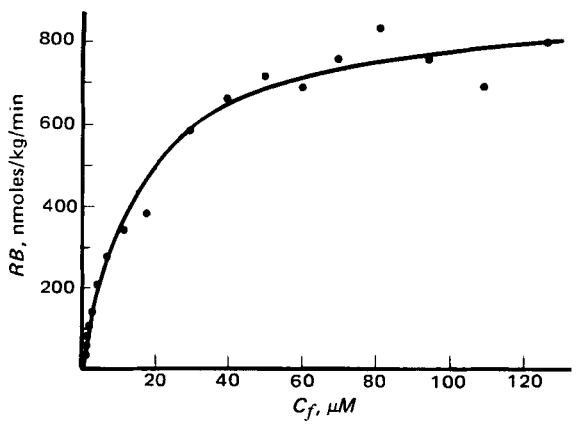

Figure 6—*Relationship between the biliary excretion rate and the unbound concentration of iodoxamic acid in the plasma during the postinfusion period following an infusion of 2.20 μmoles/kg/min into Monkey A. Key: ●, data points; and —, computer-fitted line according to Eq. 2.*

REFERENCES

(1) J. H. Lang and E. C. Lasser, *Invest. Radiol.*, **2**, 396 (1967).

(2) E. C. Lasser, R. S. Farr, T. Fujimagari, and W. N. Tripp, *Am. J. Roentgenol.*, **87**, 338 (1962).

(3) W. R. Cattell, *Invest. Radiol.*, **5**, 473 (1970).

(4) C. S. Song, E. R. Beranbaum, and M. A. Rothschild, *ibid.*, **11**, 39 (1976).

(5) S. K. Lin, A. A. Moss, and S. Riegelman, *ibid.*, **12**, 175 (1977).

(6) S. K. Lin, A. A. Moss, and S. Riegelman, *J. Pharm. Sci.*, in press.

(7) G. R. Wilkinson and D. G. Shand, *Clin. Pharmacol. Ther.*, **18**, 377 (1975).

(8) R. H. Dowling, E. Mack, J. Picott, J. Berger, and D. M. Small, *J. Lab. Clin. Med.*, **72**, 169 (1968).

(9) S. M. Strasberg, K. A. Siminovitch, and R. G. Ilson, *Ann. Surg.*, **180**, 356 (1974).

(10) A. A. Moss, L. Kaufman, and J. A. Nelson, *Invest. Radiol.*, **7**, 335 (1972).

(11) G. Riva, "Das Serumeiweisbild," 2nd ed., Huber, Bern, Switzerland, 1960, p. 257.

(12) H. B. Bull, "Physical Biochemistry," 2nd ed., Wiley, New York, N.Y., 1951, p. 210.

(13) G. Rosati, P. Schiantarelli, and P. Tirone, *Farmaco Ed. Sci.*, **28**, 996 (1973).

(14) A. S. Nies, G. H. Evans, and D. G. Shand, *J. Pharmacol. Exp. Ther.*, **181**, 716 (1973).

(15) C. Evil and G. T. Benness, *Invest. Radiol.*, **11**, 459 (1976).

(16) R. N. Berk, P. M. Loeb, A. Cobo-Frenkel, and J. L. Barnhart, *Radiology*, **119**, 529 (1976).

(17) I. Sperber and G. Sperber, in "Radiocontrast Agents," vol. 1, Section 76, P. K. Knoefel, Section Ed., "International Encyclopedia of Pharmacology and Therapeutics," Pergamon, New York, N.Y., 1971, p. 182.

(18) J. Wittenberg, R. A. Maturi, L. F. Williams, S. K. Teplick, S. R. Preblud, J. J. O'Brien, and D. M. Small, *Invest. Radiol.*, **11**, 45 (1976).

(19) B. Whitney and C. B. Cambell, *ibid.*, **7**, 83 (1972).

(20) W. Mutzel, V. Taenzer, and R. Wolf, *ibid.*, **11**, 598 (1976).

ACKNOWLEDGMENTS

Supported in part by U.S. Public Health Service Grants NIGMS 16496-09 and GM 00728 and in part by a research grant from the San Francisco Academic Senate, University of California.

The authors are grateful to Dr. Thomas N. Tozer for valuable discussions.

Effect of Hydrophilization of Hydrophobic Drugs on Release Rate from Capsules

C. F. LERK ˣ, M. LAGAS, J. T. FELL *, and P. NAUTA

Received May 16, 1977, from the *Laboratory for Pharmaceutical Technology, University of Groningen, Antonius Deusinglaan 2, 9713 AW Groningen, The Netherlands.* Accepted for publication October 19, 1977. *Present address: Department of Pharmacy, University of Manchester, Manchester M13 9PL, England.

Abstract □ The release of poorly soluble hydrophobic drugs from capsules can be improved significantly by the creation of a hydrophilic surface by intensive mixing of the hydrophobic drug with a small amount of a solution of a hydrophilic excipient. This technique was introduced previously for the production of microgranules. The data presented indicate that the hydrophilic material is mechanically distributed over the hydrophobic surface. The creation of hydrophilic capillaries in a capsule or tablet allowed the rapid penetration of the dissolution fluid, resulting in a dispersion of well-wetted particles, so that the maximum surface area of the powder was exposed to the dissolution medium. Moreover, hydrophilization of hydrophobic drugs has the important benefit that the release rate from capsules is independent of the surface tension of the dissolution medium.

Keyphrases □ Hydrophobic drugs—release rate from capsules, effect of hydrophilization □ Drug release—hydrophobic drugs from capsules, effect of hydrophilization □ Hydrophilization—of hydrophobic drugs, effect on release from capsules

Several methods for increasing the dissolution rate of poorly water-soluble drugs are available (1–4). A common approach is to reduce the drug's particle size to expose a greater surface area to the dissolution medium. This approach is, however, not without difficulties. Reducing the particle size leads to increased particle–particle interactions, and the resulting agglomerates may have an effective surface area smaller than anticipated.

If the drug is hydrophobic, particle-size reduction may give greater problems with wetting and liquid penetration into tablets and capsules. Since liquid penetration is the first step in the disintegration and dissolution of tablets and capsules, the overall process may be penetration rate limited. To overcome these problems, diluents and disintegrants are employed (5, 6), or the fine material may be granulated, which will aid in its wetting and promote liquid penetration (7). However, this method apparently would defeat, to some extent, the original object of size reduction.

In an ideal situation, the drug would be released from the dosage form as discrete, well-wetted particles, so that the maximum surface area afforded by the powder would be exposed to the dissolution medium. For hydrophobic materials, such a situation may be difficult; but it may be possible to achieve if the surface properties of the material are changed from hydrophobic into hydrophilic by coating the hydrophobic particles with a hydrophilic material. Such a coating should aid in the penetration of fluid and the wetting of individual particles but should not unduly retard the dissolution rate of the drug.

Coating of particles may be achieved by fluidization techniques (8–11), but problems may arise if the powder is cohesive. In this study, a technique described by de Jong (12) was used, in which a powder and a small amount of binder solution are mixed intensively in a kneading machine or high-speed mixer. The rigorous mixing inhibits agglomeration, resulting in a fine free-flowing powder. Although this method was originally developed for microgranule production, it is claimed that the powder is coated with the binding agent, so hydrophobic substances can be rendered hydrophilic. This study applied this technique to increase the dissolution rate of a hydrophobic, relatively insoluble drug from hard gelatin capsules.

EXPERIMENTAL

Materials—Hexobarbital[1] (Ph. Ned. grade) was chosen as the test drug because it is relatively insoluble in water and exhibits a high contact angle of 88° (13). Prior to use, it was ground in a rotor mill[2] with a 500-μm screen and passed through a centrifugal classifier[3] to remove fines with a particle size under 10 μm. The binders chosen were methylcellulose[4] and hydroxyethylcellulose[5]. Both binders are soluble in water but completely insoluble in alcohol. Hydroxyethylcellulose was passed through a rotor mill[2] fitted with a 200-μm screen. The milled and classified hexobarbital, methylcellulose, and milled hydroxyethylcellulose exhibited mean particle sizes, based on air permeability measurements[6], of 17, 30, and 32 μm, respectively.

Methods—*Treatment of Powders*—Dispersion of the binder over the drug surface was carried out in a small high-speed mixer[7]. Hexobarbital (50 g) was placed in the mixer, 3 ml of an aqueous solution of the binder was added, and the mixer was run for either 2 or 4 min at ~9000 rpm. The mixing was interrupted every 0.5 min to mix, with a spatula, material from deadspots in the mixer.

The material was dried in a tray drier at 50° for 1 hr and screened through a 200-μm sieve. Dry-mixed powders of hexobarbital and binder were prepared using a tumbler mixer[8], running at 90 rpm for 30 min. Hexobarbital was blended with the same amount of methylcellulose or

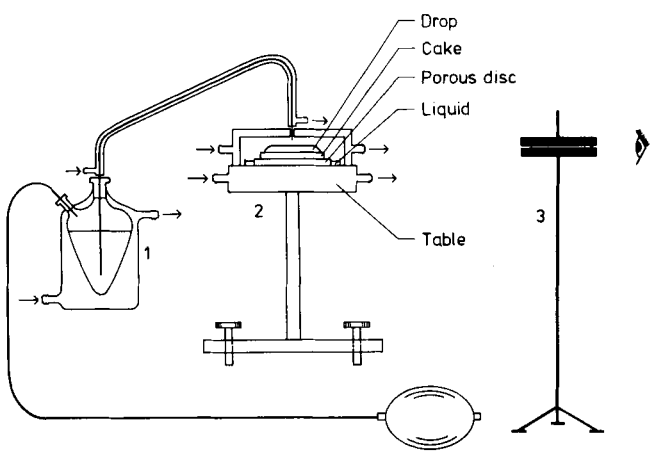

Figure 1—*Schematic diagram of the setup for the contact angle measurement. Key: 1, liquid reservoir water jacketed at 23 and 37°; 2, environmental chamber for drop formation; and 3, cathetometer.*

[1] Brocacef B. V., Maarssen, The Netherlands.
[2] Pulverisette 14002, Fritsch, Idar-Oberstein, West Germany.
[3] Multiplex 100 MZR, Alpine AG, Augsburg, West Germany.
[4] Celacol M20, British Celanese Ltd., Derby, England.
[5] Natrosol 250L, Hercules Inc., Wilmington, Del.
[6] Model 95, Fisher Scientific Co., Pittsburgh, Pa.
[7] MX 32, Braun AG, Frankfurt/M., West Germany.
[8] Turbula, W. A. Bachoven, Basel, Switzerland.

0022-3549/78/0700/0935$01.00/0
© 1978, American Pharmaceutical Association

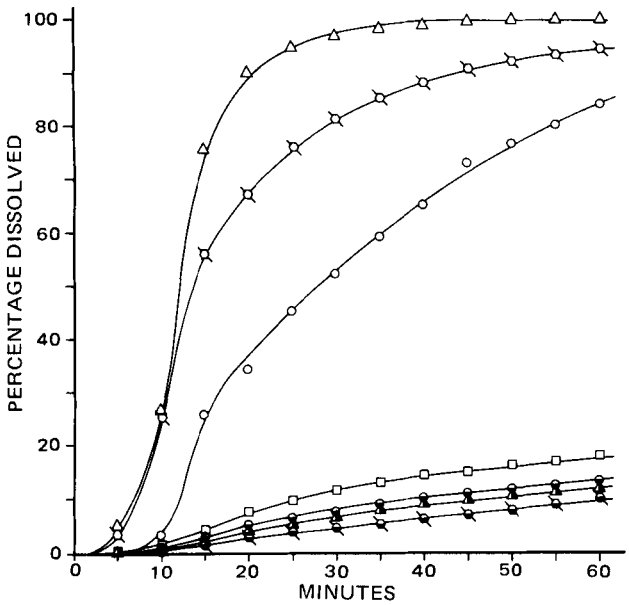

Figure 2—*Release from hard gelatin capsules of hexobarbital, untreated, treated, and mixed with methylcellulose. Key:* □, *untreated;* ◒, *0.06% physical mix;* ▲, *0.18% physical mix;* ◔, *0.30% physical mix; and* ○, △, *and* ◔. *treated for 2 min with 1, 3, and 5% binder solutions, respectively.*

hydroxyethylcellulose as was used for the coating procedure of the drug.

Capsule Filling and Dissolution—The pure drug, the treated drug, or the physical mixes of drug and binder were loosely packed by hand (250 mg) into No. 1 hard gelatin capsules[9], using a manually operated capsule-filling machine[10]. No compression of the powder was made.

Dissolution was carried out in a water-jacketed 1-liter beaker containing 900 ml of distilled water maintained at 37°. The capsule was held in a spiral of stainless steel wire, located centrally, 2 cm above the bottom of the beaker. Stirring was achieved with a 5-cm diameter, three-bladed, right-hand propeller, rotating clockwise at 100 ± 1 rpm 3.5 cm above the capsule.

Samples were taken at 5-min time intervals through membrane filters

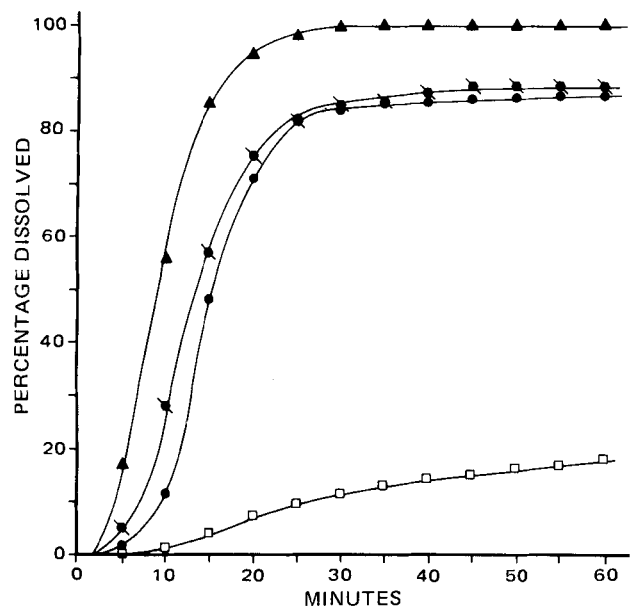

Figure 3—*Release from hard gelatin capsules of hexobarbital, untreated and treated with methylcellulose. Key:* □, *untreated; and* ●, ▲, *and* ◔, *treated for 4 min with 1, 3, and 5% binder solutions, respectively.*

[9] Snap-fit, Capsugel AG, Basel, Switzerland.
[10] Tevopharm, Schiedam, The Netherlands.

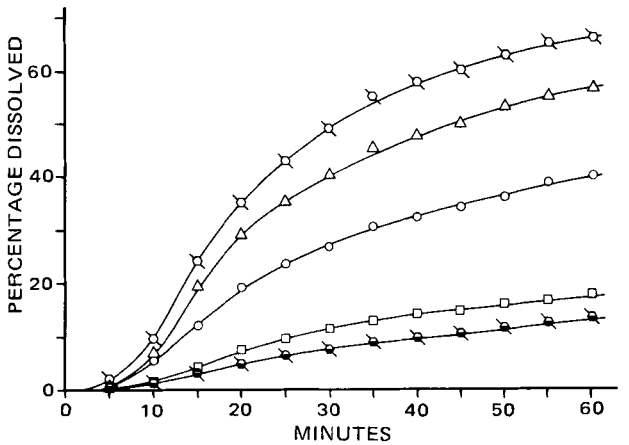

Figure 4—*Release from hard gelatin capsules of hexobarbital, untreated, treated, and mixed with hydroxyethylcellulose. Key:* □, *untreated;* ◔, *0.30% physical mix; and* ○, △, *and* ◔, *treated for 2 min with 1, 3, and 5% binder solutions, respectively.*

(0.8-μm pore diameter), diluted with pH 9.2 borate buffer to a buffer concentration of about 0.05 *M*, and analyzed spectrophotometrically[11] at 245 nm for hexobarbital. Corrections were applied for the samples removed. All release studies were based on six dissolution tests and were highly reproducible. Only average values are reported.

Intrinsic Dissolution Rates—Nondisintegrating disks, 13 mm in diameter, were prepared by compressing 500 mg of the powder at a load of 1500 kg for 5 min in a die and punch assembly. The die served as disk holder and allowed only one face of the disk to be exposed to the dissolution medium. The disk holder was attached to a shaft and was rotated at 100 ± 1 rpm in the center of a water-jacketed beaker containing 500 ml of ethanol maintained at 25°. Samples were taken at 10-min intervals, assayed for hexobarbital by dilution with a fivefold amount of 0.05 *M* borate buffer, and analyzed spectrophotometrically at 245 nm.

Wettability—The wettability of the different powders was characterized by contact angle determinations (13). For this purpose, compacts, 5 cm in diameter, were prepared by compressing about 5 g of the powder at 2000 kg in a die and punch assembly. The compacts were placed on a porous disk partly immersed in the test liquid to saturate the compact, but wetting of the compact surface was avoided (Fig. 1).

As soon as saturation was achieved, the test solution was slowly

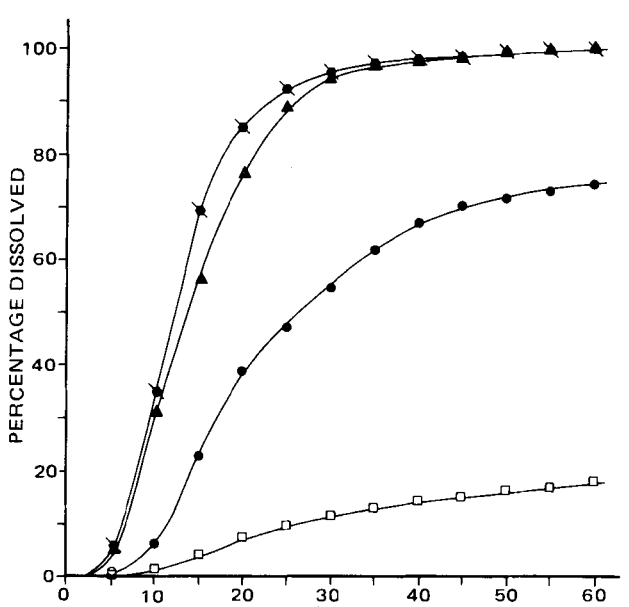

Figure 5—*Release from hard gelatin capsules of hexobarbital, untreated and treated with hydroxyethylcellulose. Key:* □, *untreated; and* ●, ▲, *and* ◔, *treated for 4 min with 1, 3, and 5% binder solutions, respectively.*

[11] Model 25, Beckman Instruments Co., Fullerton, Calif.

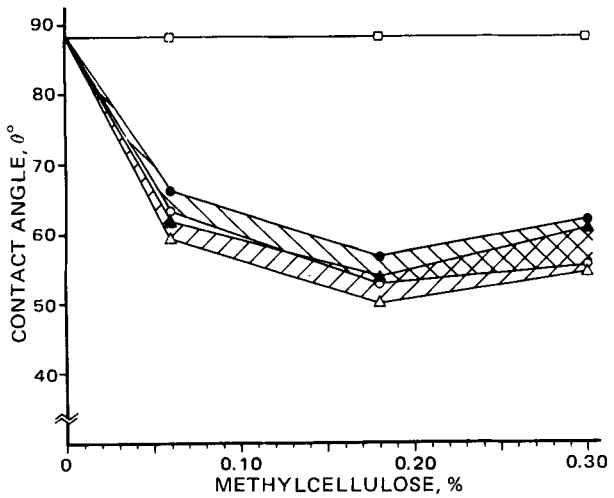

Figure 6—*Relation between percentage of methylcellulose and contact angle of hexobarbital, physically mixed or treated with the binder. Key: □, physical mix; ○ and ●, treated for 2 min; △ and ▲, treated for 4 min; ○ and △, with γ_{LV° = 72.4 dynes/cm; and ● and ▲, with γ_{LV° as given in Table II.*

dropped onto the compact surface; readings of the drop height were taken with a cathetometer[12] until additional drops caused no increase in height. The contact angle was then calculated from the appropriate equations as previously derived (14, 15), extended (16), and successfully adopted for pharmaceutical powders (13). All contact angle measurements were performed at least in duplicate. The reproducibility was better than 1° in each case.

Liquid and Solid Properties—Densities and surface tensions of the liquids and densities of the solids were determined by a balance[13], a tensiometer[14], and an air comparison pycnometer[15], respectively.

RESULTS AND DISCUSSION

Figure 2 shows the effect of the distribution of methylcellulose over the surface of the hexobarbital powder on the release profile of the drug from hard gelatin capsules. Significantly higher release rates were found for the treated hexobarbital than for the pure drug. The hexobarbital treated with 5% methylcellulose solution released the drug slower than when treated with 3% methylcellulose solution. This effect might be due to a large increase in the viscosity of the binder solution with an increasing methylcellulose concentration but also may be caused by thermal gelation

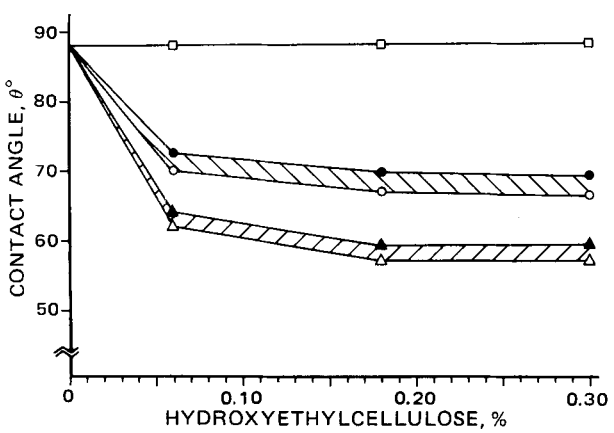

Figure 7—*Relation between percentage of hydroxyethylcellulose and contact angle of hexobarbital, physically mixed or treated with the binder. Key: □, physical mix; ○ and ●, treated for 2 min; △ and ▲, treated for 4 min; ○ and △, with γ_{LV° = 72.4 dynes/cm; and ● and ▲, with γ_{LV° as given in Table II.*

[12] Model 70000, Bouty, Paris, France.
[13] Mohr, G. Kern, Ebingen, West Germany.
[14] Du Noüy, 8600 EE Krüss, Hamburg, West Germany.
[15] Model 930, Beckman Instruments Ned. N.V., Amsterdam, The Netherlands.

Table I—Contact Angles of Cellulose Polymer Solutions on Hexobarbital Measured at 23°

Methylcellulose			Hydroxyethylcellulose		
Concentration, %	γ_{LV°, dynes/cm	θ, degrees	Concentration, %	γ_{LV°, dynes/cm	θ, degrees
0	72.4	88	0	72.4	88
1	45.6	76	1	62.7	87
3	44.6	76	3	62.5	86
5	44.6	76	5	62.3	86

of the methylcellulose at temperatures near 37° during dissolution (17).

The physical mixes exhibited release rates of the same order of magnitude as the pure drug and even showed a slight decrease in rate with an increasing amount of binder. These results indicate that the degree of distribution of a hydrophilic binder over the surface of a hydrophobic drug affects the release rate from capsules. This conclusion is supported by the results shown in Fig. 3. In this study, the hexobarbital powder was intensively mixed with the binder solutions for 8 × 0.5 min instead of 4 × 0.5 min. Comparison of Figs. 2 and 3 shows increased release rates for the drug treated for the longer period.

Distribution of hydroxyethylcellulose over the surface of the hexobarbital powder and blending of the dry binder with the drug resulted in the release rates from capsules shown in Figs. 4 and 5. The data show slightly lower release rates for the physical mixtures than for the pure drug. The release rate increased, over the range studied, with increasing concentrations of hydroxyethylcellulose and with an increasing degree of distribution.

To characterize the wettability of the pure drug by the binder solutions, contact angle measurements were made. Table I presents the contact angles between hexobarbital and solutions of different concentrations of methylcellulose or hydroxyethylcellulose. The results show a decrease in the contact angle from 88° for distilled water to 76° for solutions containing 1–5% methylcellulose. Almost no difference in contact angle was found over a concentration range of 0–5% for solutions of hydroxyethylcellulose. These results imply that neither binder solution would spread spontaneously on hexobarbital since both contact angles were high.

The input of energy from the mixer can, however, promote spreading of the liquid. The success of this operation depends first on factors affecting the spreading such as mixer efficiency, contact angle, and viscosity and second on whether the film is stable when formed and does not "dewet" from the surface (18). This latter factor may be a complex function of the contact angle and the viscosity of the liquid. These arguments are to some extent borne out by the finding that hydroxyethylcellulose, which exhibited higher contact angles and higher surface tensions than the methylcellulose, required greater mixing times to achieve equivalent effects.

To elucidate the mechanism of the change in release rate from capsules, the wettability of pure drug, treated drug, and physical mixtures of drug and binder was determined by contact angle measurement (Figs. 6 and 7). Both the pure drug and the physical mixtures exhibited contact angles of 88°. High-speed mixing of hexobarbital with methylcellulose or hydroxyethylcellulose solutions resulted in decreased contact angles. The contact angles given were calculated on the basis of the surface tension of distilled water and of the solution in the pores of the compact when the maximum amount of binder was dissolved completely from the drug surface (Table II).

As seen from Fig. 7, distribution of 3 ml of 3% methylcellulose over 50 g of hexobarbital powder, corresponding with a weight percentage of 0.18, decreased the contact angle of the drug from 88° to mean values of about 55 and 52° when treated for 4 × 0.5 and 8 × 0.5 min, respectively. Distribution of 3 ml of 5% methylcellulose over the drug resulted in contact

Table II—Surface Tensions of the Solutions in the Pores of the Compacts When the Binder Has Been Completely Dissolved from the Drug Surface

Weight Concentration of Binder on Drug, %[a]	Surface Tension, dynes/cm	
	Methylcellulose	Hydroxyethylcellulose
0	72.4	72.4
0.06	62.4	64.4
0.18	55.4	62.8
0.30	48.6	62.7

[a] Values of 0.06, 0.18, and 0.30% correspond with treatment of 50 g of hexobarbital with 3 ml of 1, 3, and 5% of a binder solution, respectively.

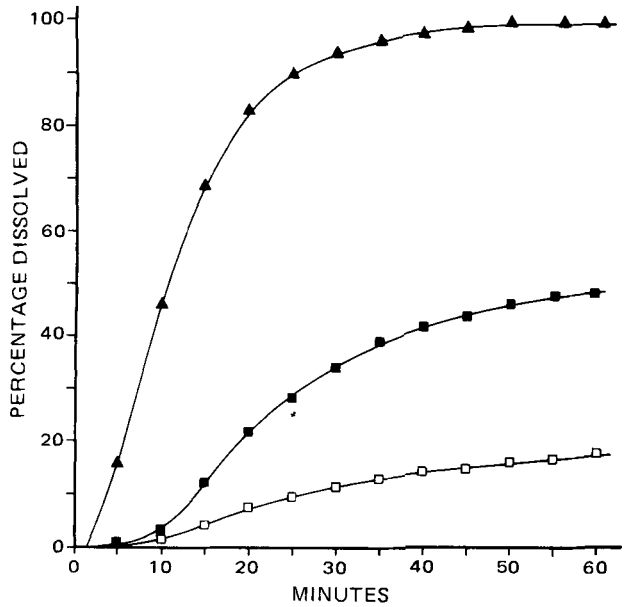

Figure 8—*Release from hard gelatin capsules of pure hexobarbital and hexobarbital treated for 4 min with 3% methylcellulose. Key: □, untreated drug in distilled water, ■, untreated drug in 0.14% methylcellulose; and ▲, treated drug in 0.14% methylcellulose.*

angles of 59 and 58°, respectively. The slight increase in the contact angle found when the concentration of the methylcellulose solution was increased from 3 to 5% was possibly due to the increased viscosity of the binder solution.

Figure 7 shows the change in the contact angle when the drug was treated with hydroxyethylcellulose. The decrease in the contact angle was smaller, compared with a methylcellulose treatment, whereas the difference in contact angles between the powders treated for 4 × 0.5 and 8 × 0.5 min was more pronounced. This result was expected since the hydroxyethylcellulose solution exhibited higher surface tensions and higher contact angles on the drug than the corresponding methylcellulose solutions.

To prove that the increased penetration rates, resulting in increased release rates, were caused primarily by the decreased contact angle of the treated powder and not, or at most to a small extent, to dissolved binder in the pores of the capsule, release rates were measured from capsules filled with pure or treated hexobarbital immersed in water or binder solutions. The concentration of the binder solution was equal to the maximum concentration of binder in the pores of the capsule if all binder had been dissolved from the surface of the treated drug (0.14%). As seen from Fig. 8, the release rate increased when the pure drug was immersed in the methylcellulose solution. The slight decrease in rate observed for the hydroxyethylcellulose solution (Fig. 9) may have been due to a slight increase in solution viscosity. A dramatic increase in release rate was found when the drug had been treated with the binder and immersed in the appropriate binder solution.

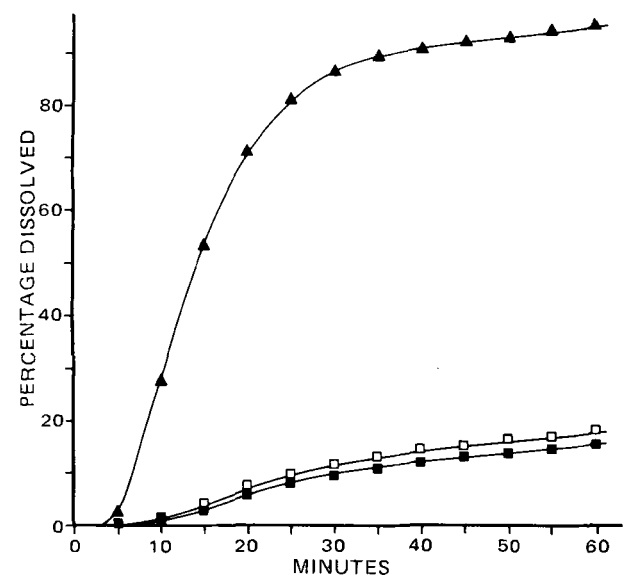

Figure 9—*Release from hard gelatin capsules of pure hexobarbital and hexobarbital treated for 4 min with 3% hydroxyethylcellulose. Key: □, untreated drug in distilled water; ■, untreated drug in 0.14% hydroxyethylcellulose; and ▲, treated drug in 0.14% hydroxyethylcellulose.*

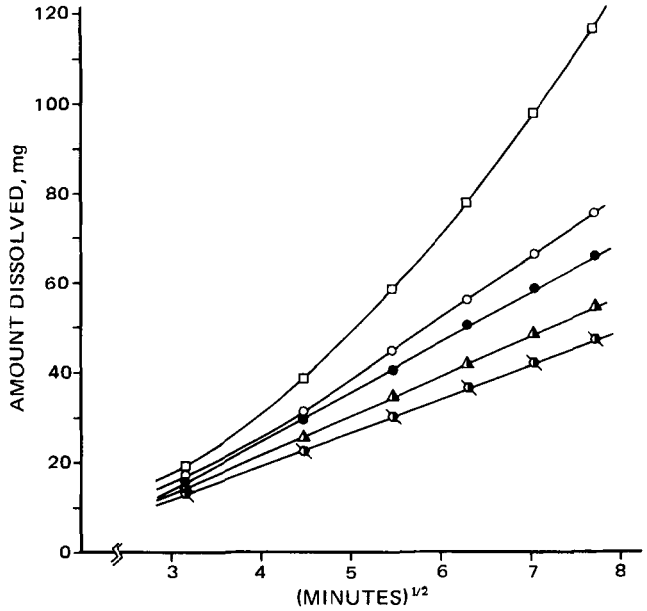

Figure 10—*Dissolution in alcohol from rotating disks of hexobarbital, untreated and treated with hydroxyethylcellulose, as a function of the square root of time. Key: □, untreated; ○ and ●, treated with a 1% binder solution for 2 and 4 min, respectively; ▲, treated with a 3% binder solution for 2 and 4 min, respectively; and ◔, treated with a 5% binder solution for 2 and 4 min, respectively.*

To demonstrate the degree of binder distribution over the drug, the intrinsic dissolution rates of the untreated and treated drugs were measured in ethanol to prevent binder dissolution.

The dissolution rates measured are presented in Fig. 10 as the amount dissolved *versus* the square root of time. The hexobarbital dissolution rates were significantly inhibited on treatment in a high-speed mixer with small amounts of hydroxyethylcellulose solutions. The dissolution rate decreased with increasing mixing times and increasing binder concentrations. A matrix of hydroxyethylcellulose was left when the drug leached out (Fig. 11). The existence of a matrix of hydroxyethylcellulose is consistent with the linear plots obtained when the amount of drug released was plotted as a function of the square root of time (Fig. 10).

The release rate of a strongly hydrophobic drug like hexobarbital from capsules thus can be increased considerably by rendering the hydrophobic surface of the drug hydrophilic. The release rate of a hydrophobic drug from a capsule, however, also can be increased by decreasing the surface tension of the dissolution medium (7). Figure 12 shows the release profiles of pure hexobarbital from capsules immersed in distilled water with varying concentrations of polysorbate 80[16]. As expected, increased release rates were obtained with decreasing surface tensions of the dissolution medium.

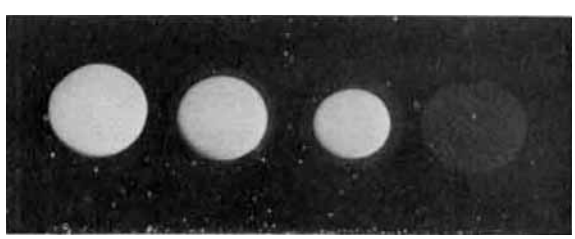

Figure 11—*Photograph of a partly leached matrix of hydroxyethylcellulose.*

[16] Tween 80, Atlas Chemie, Essen, West Germany.

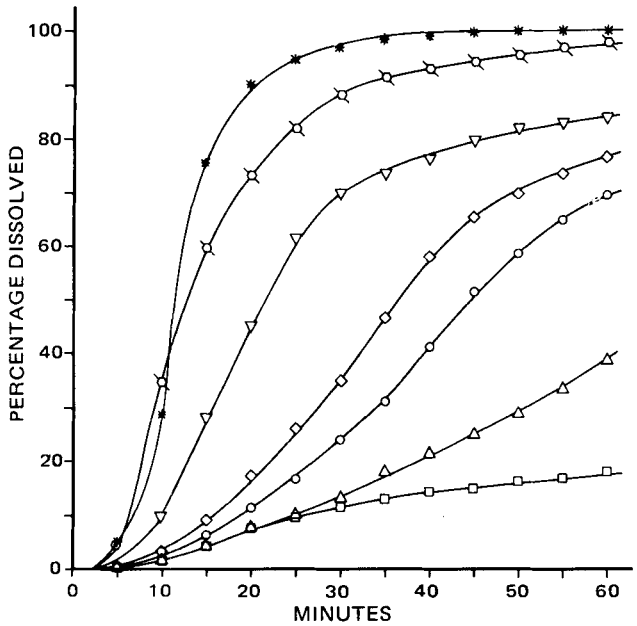

Figure 12—*Release profiles of pure and methylcellulose-treated hexobarbital from hard gelatin capsules in water with varying concentrations of polysorbate 80 at 37°. Key: open symbols, untreated drug; □, 0% polysorbate 80 (γ_{LV}° = 70.1 dynes/cm); △, 0.01% (45.4 dynes/cm); ○, 0.05% (42.7 dynes/cm); ◇, 0.1% (41.4 dynes/cm); ▽, 0.2% (39.3 dynes/cm); ◺, 0.5% (37.7 dynes/cm); and ✱, 0.18% binder-treated drug in solutions with 0–0.5% polysorbate 80.*

According to Finholt and Solvang (19), the surface tension of human gastric juice is nearly independent of pH and secretion rate, having a value between 35 and 50 dynes/cm. Therefore, a mean surface tension of human gastric juice of 43 dynes/cm would require a concentration of 0.05% polysorbate 80. To compare the release rates of pure and treated drug, the release profiles from capsules of hexobarbital, treated as described with a 3% methylcellulose solution and immersed in dissolution media of varying surface tension, are incorporated in Fig. 12. The results show the release rate of the treated drug to be independent of the surface tension of the dissolution medium. Because of the aforementioned differences in the surface tension of human gastric juice, the realization of a release rate from capsules that is independent of the surface tension of the medium is of practical importance, especially where absorption is dissolution rate limited.

REFERENCES

(1) A. H. Goldberg, M. Gibaldi, J. L. Kanig, and M. Mayersohn, *J. Pharm. Sci.*, **55**, 581 (1966).

(2) W. L. Chiou and S. Riegelman, *ibid.*, **58**, 1505 (1969).

(3) M. Gibaldi, S. Feldman, and T. R. Bates, *ibid.*, **60**, 1569 (1971).

(4) R. K. Reddy, S. A. Khalil, and M. W. Gouda, *ibid.*, **65**, 1753 (1976).

(5) J. M. Newton, G. Rowley, and J. F. V. Törnblom, *J. Pharm. Pharmacol.*, **23**, 156S (1971).

(6) J. G. Allen and C. A. Davies, *ibid.*, **27**, 50 (1975).

(7) S. Solvang and P. Finholt, *J. Pharm. Sci.*, **59**, 49 (1970).

(8) D. E. Würster, *J. Am. Pharm. Assoc., Sci. Ed.*, **48**, 451 (1959).

(9) R. E. Singiser and W. Lowenthal, *J. Pharm. Sci.*, **50**, 168 (1961).

(10) H. C. Caldwell and E. Rosen, *ibid.*, **53**, 1387 (1964).

(11) M. J. Robinson, G. M. Grass, and R. J. Lantz, *ibid.*, **57**, 1983 (1968).

(12) E. J. de Jong, *Pharm. Weekbl.*, **104**, 469 (1969).

(13) C. F. Lerk, A. J. M. Schoonen, and J. T. Fell, *J. Pharm. Sci.*, **65**, 843 (1976).

(14) N. W. F. Kossen and P. M. Heertjes, *Chem. Eng. Sci.*, **20**, 593 (1965).

(15) P. M. Heertjes and N. W. F. Kossen, *Powder Technol.*, **1**, 33 (1967).

(16) W. C. Witvoet, Ph.D. thesis, Delft, The Netherlands, 1971.

(17) J. B. Schwartz and T. P. Alvino, *J. Pharm. Sci.*, **65**, 572 (1976).

(18) C. M. Hansen and P. E. Pierce, *Ind. Eng. Chem., Prod. Res. Develop.*, **13**, 218 (1974).

(19) P. Finholt and S. Solvang, *J. Pharm. Sci.*, **57**, 1322 (1968).

ACKNOWLEDGMENTS

The authors thank Mrs. P. Broersma and Mr. K. Zuurman for technical assistance.

Kinetics of Aggregation of Human Platelets

ANWAR B. BIKHAZI *x and GHASSAN E. AYYUB

Received May 25, 1977, from the *School of Pharmacy, American University of Beirut, Beirut, Lebanon.* Accepted for publication November 1, 1977. *Present address: Department of Physiology, School of Medicine, American University of Beirut, Beirut, Lebanon.

Abstract □ A study of the aggregation kinetics of human platelets using an electronic counting device is reported. The experimental data were analyzed quantitatively by a physical model, which assumed that the initial disappearance rate of single platelets *versus* time fitted a second-order type of aggregation with respect to platelet number. The mechanism of aggregation was surface barrier controlled. Thus, the aggregation rate constants in different adenosine diphosphate concentrations (1.5–9.0 μg) were 10–100 times greater than the rate constant (6.6325×10^{-12} cm^3/sec) for a diffusion-controlled process as calculated from Smoluchowski's model. Also, the stability constant values, which were equal to unity in a fast diffusion-controlled mechanism, were smaller in the surface-barrier-controlled process and ranged from 0.00741 to 0.0467. The extent of aggregation was indicated by the calculation of a sticking probability constant as determined by the barrier. Adenosine diphosphate induced a rapid aggregating effect. Prostaglandin E_1 produced the most drastic deaggregating effect as compared to dinoprostone (prostaglandin E_2) and dinoprost (prostaglandin $F_{2\alpha}$). Aspirin completely blocked the aggregating effect of arachidonic acid.

Keyphrases □ Aggregation, platelet—kinetic study, effect of adenosine diphosphate, various prostaglandins, and arachidonic acid □ Kinetics—human platelet aggregation, effect of adenosine diphosphate, various prostaglandins, and arachidonic acid □ Adenosine diphosphate—effect on human platelet aggregation with and without various prostaglandins, kinetic study □ Prostaglandins, various—effect on human platelet aggregation with and without adenosine diphosphate, kinetic study □ Arachidonic acid—effect on human platelet aggregation with and without aspirin, kinetic study

The origin, morphology, chemical composition, lifespan, and role of some endogenous substances on blood coagulation and platelet aggregation have been reported (1–13). Nevertheless, very few quantitative and mechanistic studies have been conducted on human platelet aggregation. The present study was an attempt to develop exper-

© 1978, American Pharmaceutical Association

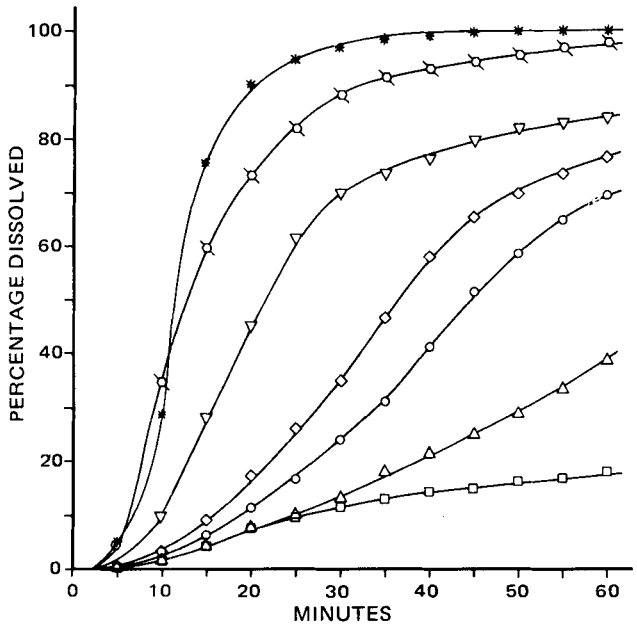

Figure 12—*Release profiles of pure and methylcellulose-treated hexobarbital from hard gelatin capsules in water with varying concentrations of polysorbate 80 at 37°. Key: open symbols, untreated drug; □, 0% polysorbate 80 (γ_{LV}° = 70.1 dynes/cm); △, 0.01% (45.4 dynes/cm); ○, 0.05% (42.7 dynes/cm); ◇, 0.1% (41.4 dynes/cm); ▽, 0.2% (39.3 dynes/cm); ◺, 0.5% (37.7 dynes/cm); and ✱, 0.18% binder-treated drug in solutions with 0–0.5% polysorbate 80.*

According to Finholt and Solvang (19), the surface tension of human gastric juice is nearly independent of pH and secretion rate, having a value between 35 and 50 dynes/cm. Therefore, a mean surface tension of human gastric juice of 43 dynes/cm would require a concentration of 0.05% polysorbate 80. To compare the release rates of pure and treated drug, the release profiles from capsules of hexobarbital, treated as described with a 3% methylcellulose solution and immersed in dissolution media of varying surface tension, are incorporated in Fig. 12. The results show the release rate of the treated drug to be independent of the surface tension of the dissolution medium. Because of the aforementioned differences in the surface tension of human gastric juice, the realization of a release rate from capsules that is independent of the surface tension of the medium is of practical importance, especially where absorption is dissolution rate limited.

REFERENCES

(1) A. H. Goldberg, M. Gibaldi, J. L. Kanig, and M. Mayersohn, *J. Pharm. Sci.*, **55**, 581 (1966).

(2) W. L. Chiou and S. Riegelman, *ibid.*, **58**, 1505 (1969).

(3) M. Gibaldi, S. Feldman, and T. R. Bates, *ibid.*, **60**, 1569 (1971).

(4) R. K. Reddy, S. A. Khalil, and M. W. Gouda, *ibid.*, **65**, 1753 (1976).

(5) J. M. Newton, G. Rowley, and J. F. V. Törnblom, *J. Pharm. Pharmacol.*, **23**, 156S (1971).

(6) J. G. Allen and C. A. Davies, *ibid.*, **27**, 50 (1975).

(7) S. Solvang and P. Finholt, *J. Pharm. Sci.*, **59**, 49 (1970).

(8) D. E. Würster, *J. Am. Pharm. Assoc., Sci. Ed.*, **48**, 451 (1959).

(9) R. E. Singiser and W. Lowenthal, *J. Pharm. Sci.*, **50**, 168 (1961).

(10) H. C. Caldwell and E. Rosen, *ibid.*, **53**, 1387 (1964).

(11) M. J. Robinson, G. M. Grass, and R. J. Lantz, *ibid.*, **57**, 1983 (1968).

(12) E. J. de Jong, *Pharm. Weekbl.*, **104**, 469 (1969).

(13) C. F. Lerk, A. J. M. Schoonen, and J. T. Fell, *J. Pharm. Sci.*, **65**, 843 (1976).

(14) N. W. F. Kossen and P. M. Heertjes, *Chem. Eng. Sci.*, **20**, 593 (1965).

(15) P. M. Heertjes and N. W. F. Kossen, *Powder Technol.*, **1**, 33 (1967).

(16) W. C. Witvoet, Ph.D. thesis, Delft, The Netherlands, 1971.

(17) J. B. Schwartz and T. P. Alvino, *J. Pharm. Sci.*, **65**, 572 (1976).

(18) C. M. Hansen and P. E. Pierce, *Ind. Eng. Chem., Prod. Res. Develop.*, **13**, 218 (1974).

(19) P. Finholt and S. Solvang, *J. Pharm. Sci.*, **57**, 1322 (1968).

ACKNOWLEDGMENTS

The authors thank Mrs. P. Broersma and Mr. K. Zuurman for technical assistance.

Kinetics of Aggregation of Human Platelets

ANWAR B. BIKHAZI *x and GHASSAN E. AYYUB

Received May 25, 1977, from the *School of Pharmacy, American University of Beirut, Beirut, Lebanon.* Accepted for publication November 1, 1977. *Present address: Department of Physiology, School of Medicine, American University of Beirut, Beirut, Lebanon.

Abstract □ A study of the aggregation kinetics of human platelets using an electronic counting device is reported. The experimental data were analyzed quantitatively by a physical model, which assumed that the initial disappearance rate of single platelets *versus* time fitted a second-order type of aggregation with respect to platelet number. The mechanism of aggregation was surface barrier controlled. Thus, the aggregation rate constants in different adenosine diphosphate concentrations (1.5–9.0 μg) were 10–100 times greater than the rate constant (6.6325×10^{-12} cm^3/sec) for a diffusion-controlled process as calculated from Smoluchowski's model. Also, the stability constant values, which were equal to unity in a fast diffusion-controlled mechanism, were smaller in the surface-barrier-controlled process and ranged from 0.00741 to 0.0467. The extent of aggregation was indicated by the calculation of a sticking probability constant as determined by the barrier. Adenosine diphosphate induced a rapid aggregating effect. Prostaglandin E_1 produced the most drastic deaggregating effect as compared to dinoprostone (prostaglandin E_2) and dinoprost (prostaglandin $F_{2\alpha}$). Aspirin completely blocked the aggregating effect of arachidonic acid.

Keyphrases □ Aggregation, platelet—kinetic study, effect of adenosine diphosphate, various prostaglandins, and arachidonic acid □ Kinetics—human platelet aggregation, effect of adenosine diphosphate, various prostaglandins, and arachidonic acid □ Adenosine diphosphate—effect on human platelet aggregation with and without various prostaglandins, kinetic study □ Prostaglandins, various—effect on human platelet aggregation with and without adenosine diphosphate, kinetic study □ Arachidonic acid—effect on human platelet aggregation with and without aspirin, kinetic study

The origin, morphology, chemical composition, lifespan, and role of some endogenous substances on blood coagulation and platelet aggregation have been reported (1–13). Nevertheless, very few quantitative and mechanistic studies have been conducted on human platelet aggregation. The present study was an attempt to develop exper-

© 1978, American Pharmaceutical Association

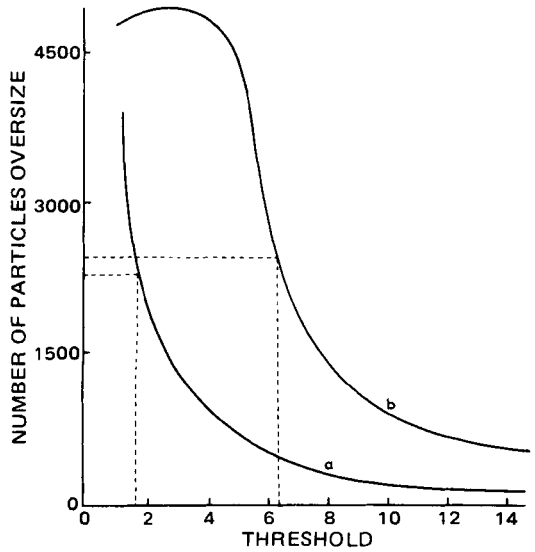

Figure 1—*Cumulative size distribution plot of the number of particles oversize* versus *threshold for polyvinyltoluene–polystyrene latex calibration material. Key: a, 1.15-μm diameter latex; and b, 1.87-μm diameter latex.*

imental techniques to provide data suitable for quantitative treatment and analysis.

EXPERIMENTAL

Particle Counting and Machine Calibration—An electronic counting device[1] was employed for platelet counting. According to estimates of platelet-size distribution (2–4 μm in diameter) (14), a 50-μm aperture opening tube was installed in the machine. Standard monosized calibration materials with a size range of 5–20% of the aperture diameter were used for calibration. The latex particles were dispersed in particle-free normal saline solution and placed on the counter stand for counting. The desired dilutions of the calibration material were made such that, at low threshold values (15), the machine would count at low coincidence factor.

Standard calibration curves were obtained when a plot of the number of particles oversize (15) *versus* threshold were drawn as shown in Figs. 1 and 2. The dotted lines in Figs. 1–4 indicate the threshold values corresponding to 50% of the number of particles in suspension (15) and, thus,

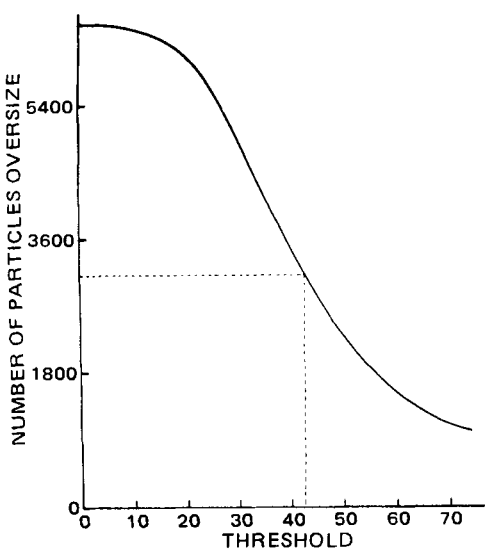

Figure 2—*Cumulative size distribution plot of the number of particles oversize* versus *threshold for polystyrene-divinylbenzene latex of 5.02-μm diameter.*

[1] Coulter counter model A, Coulter Electronics, Hialeah, Fla.

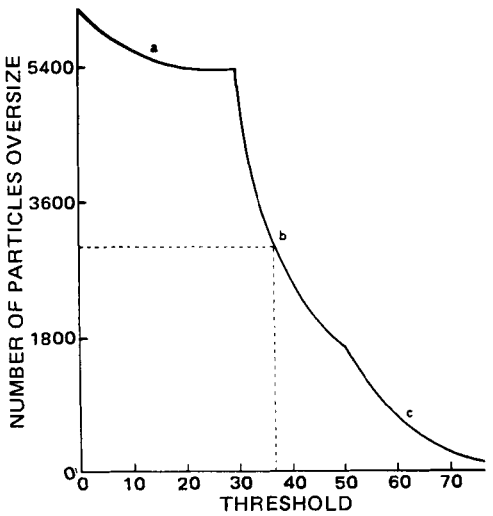

Figure 3—*Cumulative size distribution plot of the number of particles oversize* versus *threshold for human blood cells. Key: a, size distribution for platelets; b, size distribution for red blood cells; and c, size distribution for white blood cells.*

estimate the mean size distribution of particulate matter.

Preparation of Particle-Free Stock Solution—The particle-free stock solution was prepared as follows. Sodium chloride[2], 9 g, was dissolved in 1000 ml of distilled water. A stainless filter holder[3], adapted with a 47-mm, 0.45-μm membrane filter[3] and attached to a vacuum flask, was used for the filtration of the stock solution. The filtrate was refiltered until almost particle free as checked by the counter.

Part of the freshly prepared particle-free stock was used to fill the reservoir of the machine; this procedure was necessary to avoid leakage of particulate matter from the reservoir during flushing of the inner part of the aperture tube. Control studies were run in the following manner. The solution was poured into a clean beaker and then placed on the stand of the counter. Counts were recorded at specific threshold settings and were considered as background counts. The rest of the particle-free stock solution was used as suspending fluid for the calibration material and platelets.

Preparation of Platelet-Rich Plasma—Human blood was collected from the antecubital vein of healthy volunteers, 25–30 years old. The volunteers did not donate blood whenever they were under any type of drug therapy. To nine parts of blood, one part of 3.8% sodium citrate[2] was added. The mixture was then centrifuged[4] at 77×*g* for 15 min. The su-

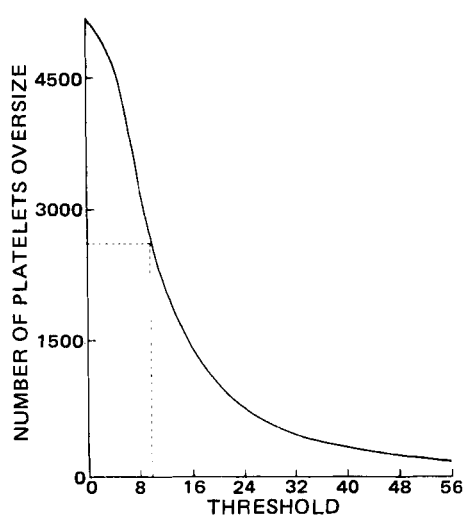

Figure 4—*Cumulative size distribution plot of the number of platelets oversize* versus *threshold for human platelets in platelet-rich plasma.*

[2] E. Merck, Darmstadt, Germany.
[3] Millipore Corp., Bedford, Mass.
[4] International clinical centrifuge model C.L., International Equipment Co., Needham, Mass.

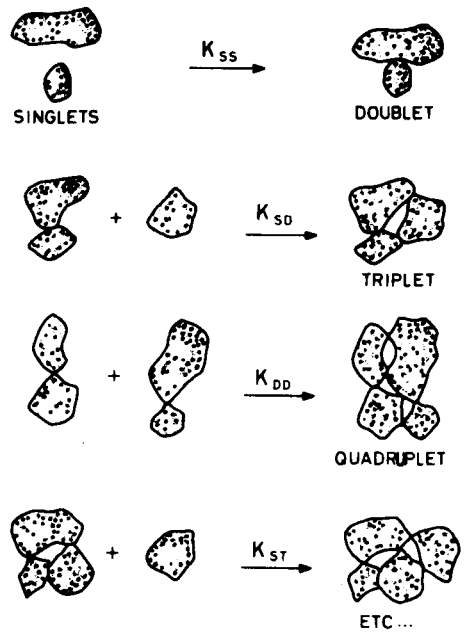

Figure 5—*Proposed model for irreversible aggregation of human platelets.*

pernatant platelet-rich plasma layer was collected. Then 0.5-ml samples of platelet-rich plasma were distributed into carefully cleaned 10-ml erlenmeyer flasks and placed in a water bath[5] maintained at 37°.

Blood Particle Counts—After calibration of the counter, 2 μl of human blood was injected into 80 ml of particle-free normal saline using a microliter syringe[6]. The suspended particles were stirred for 5 sec with a rotary glass stirrer attached to the counter. Counts were estimated per 0.05 ml of the suspension at different thresholds (Fig. 3).

Platelet Counts in Platelet-Rich Plasma—Twenty microliters of platelet-rich plasma was added to 80 ml of particle-free normal saline, and the number of platelets oversize *versus* threshold was estimated in a way similar to that used for blood particle counts (Fig. 4). The dotted lines in Fig. 4 show that threshold 9 was the setting for the average platelet size.

Control Experiments—Control experiments were regularly performed on every blood sample. A platelet-rich plasma sample was placed in an erlenmeyer flask in the water bath. Then 10 μl of normal saline, which was used as a solvent for the compounds to be tested, was added to this control flask. Samples of 10 μl were withdrawn at 0, 15, 30, 45, 60, 75, and 90 sec and added to 80 ml of normal saline to be counted.

Aggregation Experiments—At zero time, the test compounds were added with a microliter syringe to 0.5-ml platelet-rich plasma samples in a water bath at 37°. Sampling and analysis were done in exactly the same manner as described under *Platelet Counts in Platelet-Rich Plasma*. The compounds tested were prepared as follows.

The sodium salt of adenosine 5′-diphosphate[7] was dissolved in normal saline in a concentration of 5 mg/5 ml. The stock solution was frozen, stored at −20°, and thawed when used.

Stock solutions of prostaglindin E_1[8] and dinoprostone[8] (prostaglandin E_2) were prepared by dissolving 2 mg in 0.02% sodium carbonate. The pH was adjusted to 7.35 with a pH meter[9], and the final concentration of each prostaglandin was made up to 2 mg/10 ml with normal saline. Solutions were stored at −20° and thawed only when used.

A stock solution of dinoprost (prostaglandin $F_{2\alpha}$) tromethamine salt[8] was prepared by dissolving a specific weight equivalent to 2 mg of dinoprost acid/10 ml of normal saline. The solution was stored at −20° and thawed only when used.

Arachidonic acid[10] solution was prepared by dissolving 5 μl of arachidonic acid in 0.3 ml of isotonic sodium chloride containing 0.02% sodium carbonate. The final concentration was 15 μg/μl. The solution was stored at −20° and thawed only when used.

[5] Thermocirculator model 1818, Beckman Instruments, Fullerton, Calif.
[6] Hamilton Co., Reno, Nev.
[7] Koch-Light Laboratories, Colnbrook Brecks, England.
[8] The Upjohn Co., Kalamazoo, Mich.
[9] Expandomatic SS-2, Beckman Instruments, Fullerton, Calif.
[10] Sigma Chemical Co., St. Louis, Mo.

Aspirin[2] solution was prepared by dissolving 2.25 mg in 100 ml of normal saline for a final concentration of 2.25 μg/10 μl. The solution was stored at −20° and thawed only when used.

Calculations—*Model*—Figure 5 shows an irreversible particle–particle aggregation model for human platelets. The rate equations for the disappearance of singlets and for the formation of doublets, triplets, *etc.*, may be written as:

$$\frac{d(P_s)}{dt} = -P_s(K_{ss}P_s + K_{sD}P_D + K_{sT}P_T + \ldots) \quad \text{(Eq. 1)}$$

$$\frac{d(P_D)}{dt} = K_{ss}P_s^2 - P_D(K_{sD}P_s + K_{DD}P_D + K_{DT}P_T + \ldots) \quad \text{(Eq. 2)}$$

$$\frac{d(P_T)}{dt} = K_{sD}P_sP_D - P_T(K_{sT}P_s + K_{DT}P_D + K_{TT}P_T + \ldots) \quad \text{(Eq. 3)}$$

where P_s, P_D, and P_T refer to singlet, doublet, and triplet counts, respectively; and K_{ss}, K_{sD}, K_{sT}, K_{DD}, K_{DT}, and K_{TT} are the rate constants of formation of doublets, triplets, and quadruplets. Similar equations can be written for higher aggregates.

Assumptions—

1. Human platelets were assumed to be monodispersed and spherical in shape.
2. The rate constants in the equations were assumed to be equal, thus simplifying the solution of the system of differential equations (16).
3. The experiments were concerned with the initial rapid aggregation of singlets; therefore, the formation rates of triplets and higher aggregates were not being kinetically measured. For this reason, platelets during the experiments were measured at threshold 9 of the machine, corresponding to the number of singlets existing at any time in the platelet-rich plasma sample.

Diffusion-Controlled Case—The rigorous aggregation expression for a monodispersed system was proposed by Smoluchowski (16). If it is assumed that platelets are spherical in nature, then:

$$\frac{d\sum_{k=1}^{\infty} P_k}{dt} = -\frac{1}{2}\sum_{i=1}^{\infty}\sum_{j=1}^{\infty}\frac{4\pi D_{ij}r_{ij}P_iP_j}{W_{ij}} \quad \text{(Eq. 4)}$$

where D_{ij} is the mutual diffusivity of the ith and jth class particles; r_{ij} is the collision radius; W_{ij} is the stability constant; and P_k, P_i, and P_j are platelet counts in classes k, i, and j, respectively. If platelets are assumed to be monodispersed, then the mutual diffusivity, D_{ij}, of two platelets is equal to the sum of the diffusivities of each individual platelet:

$$D_{ij} = D_i + D_j = 2D_i = 2D_s \quad \text{(Eq. 5)}$$

and:

$$r_{ij} = r_i + r_j = 2r_i = 2r_s \quad \text{(Eq. 6)}$$

where D_s and r_s are the diffusivity and radius of a singlet, respectively. Then:

$$K_{ij} = K_{ss} = \frac{4\pi(D_i + D_j)(r_i + r_j)}{W_{ij}} = \frac{16\pi D_s r_s}{W} \quad \text{(Eq. 7)}$$

The Stokes–Einstein relation defines the diffusivity as:

$$D_s = \frac{K_0T}{6\pi n r_s} \quad \text{(Eq. 8)}$$

where K_0 is the Boltzmann constant, T is the absolute temperature, and n is the viscosity of the medium. Combining Eqs. 7 and 8 and substituting for D_s yield:

$$K_{ss} = \frac{8K_0T}{3nW} \quad \text{(Eq. 9)}$$

For a monodispersed system, Eqs. 1 and 4 can be combined to give:

$$\frac{d(P_s)}{dt} = -K_{ss}(P_s)^2 \quad \text{(Eq. 10)}$$

By substituting Eq. 9 into Eq. 10 and integrating, the following expression is obtained:

$$\frac{1}{P_s} = \frac{1}{P_{s0}} + K_{ss}t = \frac{1}{P_{s0}} + \frac{8K_0T}{3nW}t \quad \text{(Eq. 11)}$$

where P_{s0} is the number of singlets at time zero. Equation 11 includes the rate constant K_{ss} for diffusion-controlled aggregation, *i.e.*, when $W = 1$. Thus, K_{ss} has a value of 6.6325×10^{-12} cm^3/sec at 37° for human platelets suspended in plasma having a viscosity equal to 0.0172 poise (17). The value of $W > 1$ explains the experimental deviation of a system from a rapidly aggregating diffusion-controlled process. Instances where

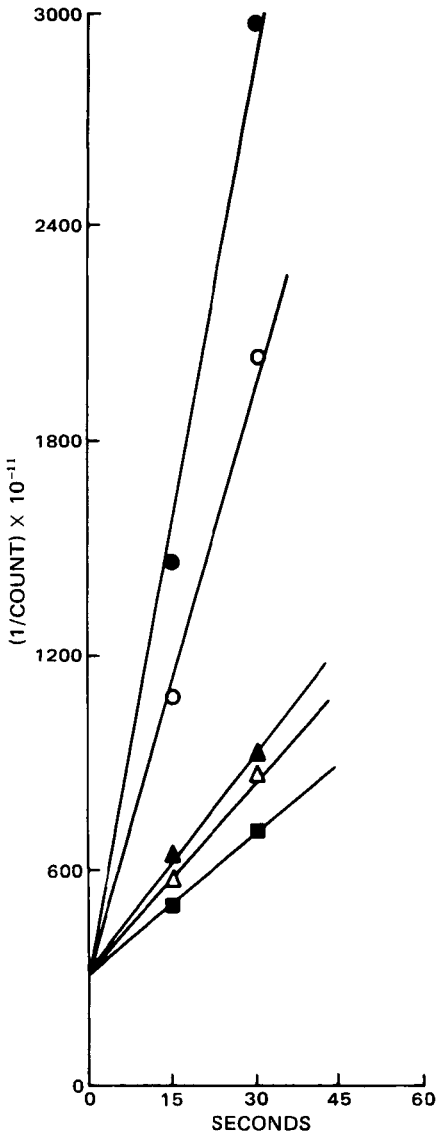

Figure 6—*Plot of 1/platelet count* versus *time for platelet aggregation as induced by adenosine diphosphate. Key (concentrations of adenosine diphosphate per milliliter of platelet-rich plasma):* ■, *1.5 μg;* △, *3 μg;* ▲, *4.5 μg;* ○, *6 μg; and* ●, *9 μg.*

$W < 1$ (18) also can apply for a rapid aggregation process. The half-life of singlet aggregation under the influence of a diffusion-controlled process is calculated from Eq. 11 to be:

$$t_{1/2} = \frac{1}{P_{s0}K_{ss}} = \frac{3nW}{8P_{s0}K_0T} \qquad \text{(Eq. 12)}$$

Surface-Barrier-Controlled Case—Higuchi *et al.* (19) proposed that the rate constant K_{ss} includes the total available surface area of contact between two singlets:

$$K_{ss} = (\text{total available contact area})(D_s + D_s)(\gamma) \qquad \text{(Eq. 13)}$$

Table I—Rate Constants, Half-Lives, and Sticking Probability Factors of Platelet Aggregation in the Presence of Adenosine Diphosphate

Adenosine Diphosphate[a], μg	Rate Constant[b], $K_{ss} \times 10^{-11}$, cm³/sec	Half-Life, $t_{1/2}$, sec	Sticking Probability Factor, $\gamma \times 10^6$/cm/Platelet
1.5	14.20	21.47	0.0993
3.0	19.50	15.64	0.1364
4.5	21.40	14.24	0.1496
6.0	57.56	5.30	0.4025
9.0	89.50	3.40	0.6259

[a] Amount injected into 1 ml of platelet-rich plasma. [b] Rate constant is zero for control experiment.

Table II—Rate Constants, Half-Lives, and Sticking Probability Factors of Platelet Aggregation in the Presence of Adenosine Diphosphate and Prostaglandin E_1

Adenosine Diphosphate[a], μg	Prostaglandin E_1[a], μg	Rate Constant[b], $K_{ss} \times 10^{-11}$, cm³/sec	Half-Life, $t_{1/2}$, sec	Sticking Probability Factor, $\gamma \times 10^6$/cm/Platelet
3.0	0.0	19.50	15.64	0.1364
3.0	0.06	5.20	58.65	0.0363
6.0	0.0	57.56	5.30	0.4025
6.0	0.12	3.88	78.61	0.0271
9.0	0.0	89.50	3.40	0.6259
9.0	0.18	1.03	296.12	0.0072

[a] Amount injected into 1 ml of platelet-rich plasma. [b] Rate constant is zero for control experiments.

where γ, a constant for a given system in which the local curvatures of the contacting surfaces are identical, includes the sticking probability as determined by the barrier. For singlet–singlet interacting particles in a monodispersed system, the total available contacting area for spheres is $16\pi r_s^2$. Then Eq. 13 is written as:

$$K_{ss} = 32\pi r_s^2 D_s \qquad \text{(Eq. 14)}$$

Substituting in Eq. 14 for D_s gives:

$$K_{ss} = \frac{16\gamma K_0 r_s T}{3n} \qquad \text{(Eq. 15)}$$

Thus, Eq. 10 can be evaluated as:

$$\frac{d(P_s)}{dt} = -\frac{16\gamma K_0 r_s T}{3n}(P_s)^2 \qquad \text{(Eq. 16)}$$

The integrated form of Eq. 16 is written as:

$$\frac{1}{P_s} = \frac{1}{P_{s0}} + \frac{16\gamma K_0 r_s T}{3n}t \qquad \text{(Eq. 17)}$$

The rate constant in Eq. 17 is the surface-barrier-controlled rate constant. Any change in the surface barrier is explained by the difference of the sticking probability factor, γ, which is used to determine the degree of the surface-barrier effect on the aggregation of human platelets. From Eq. 17, the half-life of the aggregated particles under the surface-barrier-controlled processes is equal to:

$$t_{1/2} = \frac{1}{P_s K_{ss}} = \frac{3n}{16P_s K_0 r_s T\gamma} \qquad \text{(Eq. 18)}$$

RESULTS

Counter Calibration—Figures 1 and 2 represent calibration curves for calibration material of sizes 1.87, 1.15, and 5.02 μm. The results were employed for the quantitative estimates of human blood cell sizes and human platelet size.

Size Distribution of Human Blood Cells—Figure 3 shows the size distribution of human blood cells. Particulate matter in whole blood was not narrowly distributed. There were approximately three different size distributions, as shown by breaks in the curve. This result was explained on the basis of the differences in the size distributions of platelets, red blood cells, and white blood cells. The machine setting, when counting whole blood cells, differed from that when counting platelets alone (Figs.

Table III—Rate Constants, Half-Lives, and Sticking Probability Factors of Platelet Aggregation in the Presence of Adenosine Diphosphate and Dinoprostone

Adenosine Diphosphate[a], μg	Dinoprostone[a], μg	Rate Constant[b], $K_{ss} \times 10^{-11}$, cm³/sec	Half-Life, $t_{1/2}$, sec	Sticking Probability Factor, $\gamma \times 10^6$/cm/Platelet
3.0	0.0	19.50	15.64	0.1364
3.0	0.6	10.60	28.77	0.0741
6.0	0.0	57.56	5.30	0.4025
6.0	1.2	18.75	16.27	0.1311
9.0	0.0	89.50	3.40	0.6259
9.0	1.8	36.80	8.29	0.2573

[a] Amount injected into 1 ml of platelet-rich plasma. [b] Rate constant is zero for control experiments.

Table IV—Rate Constants, Half-Lives, and Sticking Probability Factors of Platelet Aggregation in the Presence of Adenosine Diphosphate and Dinoprost

Adenosine Diphosphate[a], μg	Dinoprost[a], μg	Rate Constant[b], $K_{ss} \times 10^{-11}$, cm³/sec	Half-Life, $t_{1/2}$, sec	Sticking Probability Factor, $\gamma \times 10^6$/cm/Platelet
3.0	0.0	19.50	15.64	0.1364
3.0	0.6	13.76	22.16	0.0962
6.0	0.0	57.56	5.30	0.4025
6.0	1.2	21.20	14.38	0.1482
9.0	0.0	89.50	3.40	0.6259
9.0	1.8	34.57	8.82	0.2417

[a] Amount injected into 1 ml of platelet-rich plasma. [b] Rate constant is zero for control experiments.

1 and 2). Thus, it was difficult to approximate the average size of human platelets from the a portion in Fig. 3.

Size Distribution of Particles in Platelet-Rich Plasma—Figure 4 represents the size distribution of platelets in platelet-rich plasma. The plot showed a narrow size distribution of platelets. From Figs. 1 and 4, the average diameter of human platelets was calculated to be around 2.15 μm.

Control Studies—These studies were carried out to check the effect of simulating the experimental situations in the absence of an aggregating or deaggregating agent on platelets. Under all experimental conditions, the amount of sodium chloride available in a specific volume of normal saline (10 or 20 μl) injected into 1 ml of platelet-rich plasma had no effect on platelet aggregation. Since control runs for all systems studied showed no aggregation, a plot of 1/platelet count *versus* threshold would show a horizontal line with a slope of zero.

Effect of Adenosine Diphosphate on Platelet Aggregation—Figure 6 shows a plot of 1/platelet count *versus* time in seconds on the effect of different concentrations (1.5, 3.0, 4.5, 6.0, and 9.0 μg/ml of platelet-rich plasma) of adenosine diphosphate on platelet aggregation. The data points were only for the first 30 sec; the results (Table I) showed linearity with all adenosine diphosphate concentrations, agreeing with the theory of Eqs. 10 and 16. With an increase in adenosine diphosphate concentration, the aggregation rate increased drastically.

Effect of Prostaglandins on Platelet Aggregation without and with Adenosine Diphosphate—*Prostaglandin E_1 Alone*—Aggregation was not observed with 0.2 and 0.4 μg of prostaglandin E_1/ml of platelet-rich plasma. Slight deaggregation occurred with platelets originally in

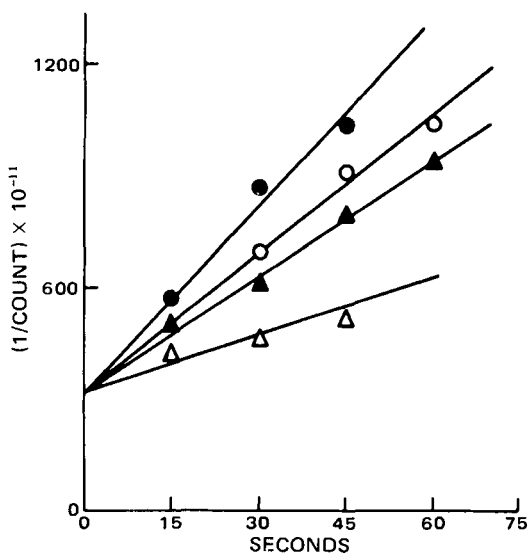

Figure 7—*Plot of 1/platelet count* versus *time for platelet aggregation showing the effect of prostaglandins on adenosine diphosphate-induced platelet aggregation. Key (concentrations per milliliter of platelet-rich plasma): ●, 3 μg of adenosine diphosphate; ○, 3 μg of adenosine diphosphate and 0.6 μg of dinoprost; ▲, 3 μg of adenosine diphosphate and 0.6 μg of dinoprostone; and △, 3 μg of adenosine diphosphate and 0.06 μg of prostaglandin E_1.*

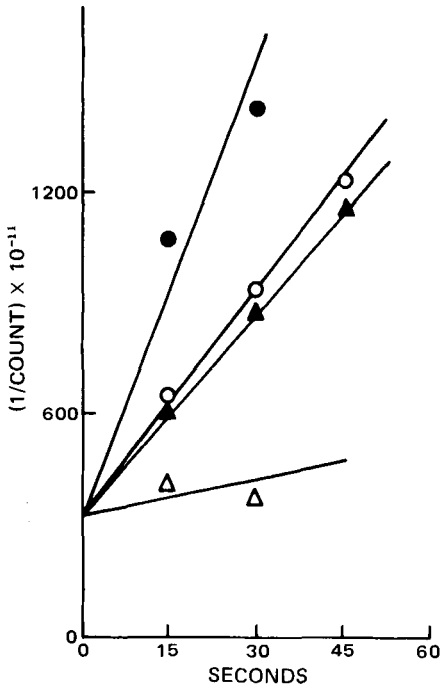

Figure 8—*Plot of 1/platelet count* versus *time for platelet aggregation showing the effect of prostaglandins on adenosine diphosphate-induced platelet aggregation. Key (concentrations per milliliter of platelet-rich plasma): ●, 6 μg of adenosine diphosphate; ○, 6 μg of adenosine diphosphate and 1.2 μg of dinoprost; ▲, 6 μg of adenosine diphosphate and 1.2 μg of dinoprostone; and △, 6 μg of adenosine diphosphate and 0.12 μg of prostaglandin E_1.*

the aggregated state. This result is consistent with the results of the platelet-size distribution (Fig. 4), which did not rule out the possibility of platelets being partly aggregated in the platelet-rich plasma sample.

Dinoprostone Alone—With dinoprostone at 1.0, 2.0, and 4.0 μg/ml of platelet-rich plasma, neither aggregation nor deaggregation of human platelets occurred.

Dinoprost Alone—Dinoprost tromethamine in amounts equivalent to 1.0, 2.0, and 4.0 μg of dinoprost/ml of platelet-rich plasma did not cause aggregation or deaggregation.

Prostaglandin E_1 with Adenosine Diphosphate—Three different concentrations of adenosine diphosphate and prostaglandin E_1 were added per milliliter of platelet-rich plasma to induce aggregation. The concentrations were 3.0 μg of adenosine diphosphate and 0.06 μg of prostaglandin E_1, 6.0 μg of adenosine diphosphate and 0.12 μg of prostaglandin E_1, and 9.0 μg of adenosine diphosphate and 0.18 μg of prostaglandin E_1.

Table II shows the results observed for adenosine diphosphate inducing aggregation without and with prostaglandin E_1. Prostaglandin E_1 induced a deaggregating effect. For example, at 3.0 μg of adenosine diphosphate, the aggregation rate constant was calculated to be 1.95×10^{-10} cm³/sec; in the presence of 0.06 μg of prostaglandin E_1, the rate constant was reduced to 5.2×10^{-11} cm³/sec. This result was similarly observed at 6.0 and 9.0 μg of prostaglandin E_1/ml of platelet-rich plasma. Prostaglandin E_1 had a drastic effect on platelet deaggregation, even in the presence of a strong aggregating agent like adenosine diphosphate.

Dinoprostone with Adenosine Diphosphate—Three different concentrations of adenosine diphosphate and dinoprostone were added per milliliter of platelet-rich plasma. The concentrations were 3.0 μg of adenosine diphosphate and 0.6 μg of dinoprostone, 6.0 μg of adenosine diphosphate and 1.2 μg of dinoprostone, and 9.0 μg of adenosine diphosphate and 1.8 μg of dinoprostone. Table III shows a deaggregating effect of dinoprostone on adenosine diphosphate-induced platelet aggregation. The effect was not as drastic as with prostaglandin E_1, although the amount of prostaglandin E_1 was 10 times less than that of dinoprostone.

Dinoprost Tromethamine with Adenosine Diphosphate—The concentrations of adenosine diphosphate and dinoprost were similar to those used for studying the effect of adenosine diphosphate and dinoprostone. As shown in Tables III and IV, dinoprost had an effect similar to that of

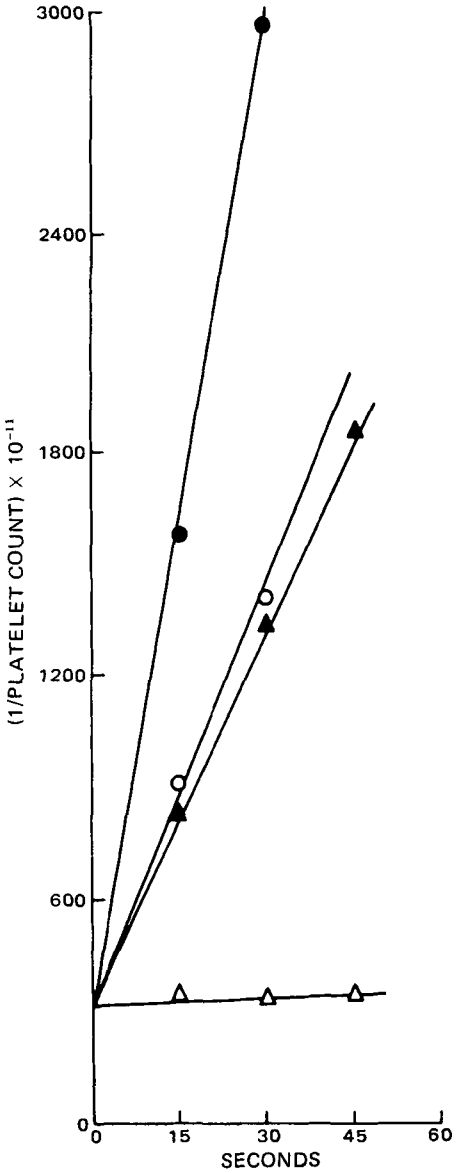

Figure 9—*Plot of 1/platelet count* versus *time for platelet aggregation showing the effect of prostaglandins on adenosine diphosphate-induced platelet aggregation. Key (concentrations per milliliter of platelet-rich plasma):* ●, *9 μg of adenosine diphosphate;* ○, *9 μg of adenosine diphosphate and 1.8 μg of dinoprostone;* ▲, *9 μg of adenosine diphosphate and 1.8 μg of dinoprost; and* △, *9 μg of adenosine diphosphate and 0.18 μg of prostaglandin* E_1.

dinoprostone on adenosine diphosphate-induced platelet aggregation.

Figures 7–9 are comparative plots of 1/platelet count *versus* time on rectangular coordinates, showing the effect of the prostaglandins on platelet aggregation as induced by adenosine diphosphate. Prostaglandin E_1 had the strongest effect followed by dinoprostone and dinoprost. Table V shows the extent of the effect of each prostaglandin on platelet aggregation in the presence of adenosine diphosphate.

Effect of Arachidonic Acid and Aspirin on Platelet Aggregation—Arachidonic acid, a well-known precursor (20) in the biosynthesis of dinoprostone and dinoprost, showed no effect on platelet aggregation at 90, 180, and 360 μg/ml of platelet-rich plasma. But at 540 and 720 μg/ml of platelet-rich plasma, an aggregating effect was observed. The addition of 2.25 μg of aspirin/ml of platelet-rich plasma appeared to block the aggregating effect of arachidonic acid (Fig. 10). This concentration of aspirin was far lower than a sustained blood level concentration for a patient continuously taking 600 mg of the drug three times daily. Table VI shows the rate constants, sticking probability factor, and half-life of the effect of arachidonic acid on platelet aggregation in the absence and presence of aspirin.

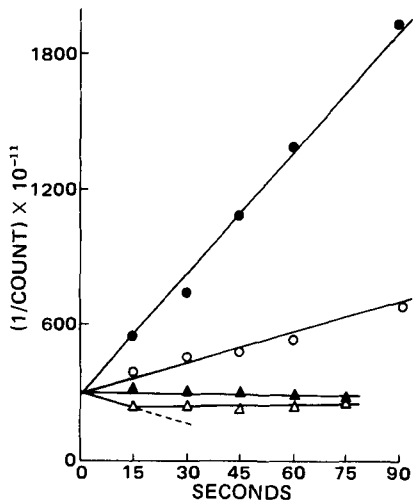

Figure 10—*Plot of 1/platelet count* versus *time of platelet aggregation showing the effect of arachidonic acid in the absence and presence of aspirin. Key (concentrations per milliliter of platelet-rich plasma):* ○, *540 μg of arachidonic acid;* ●, *720 μg of arachidonic acid;* △, *540 μg of arachidonic acid and 2.25 μg of aspirin; and* ▲, *720 μg of arachidonic acid and 2.25 μg of aspirin.*

DISCUSSION

The present approach emphasizes a physical or kinetic description of platelet aggregation and introduces a quantitative method for measuring the aggregation rate of human platelets *in vitro*. This method has one major advantage over the turbidimetric method (9), namely, its sensitivity. The experiments were carried out only for a few minutes, and sampling was done within 15-sec intervals for a series of experiments. Thus, the emphasis was on the initial rate of platelet aggregation utilizing a simplified model (Fig. 5 and Eqs. 11 and 17). Higher order aggregation or deaggregation occurring at longer times is complex, and analysis of the higher order interactions was not attempted. This complexity was apparent in the data obtained after approximately 1-min intervals.

The described process of platelet aggregation most probably occurs by a surface-barrier-controlled mechanism. This hypothesis is, with adenosine diphosphate for example, supported by larger values of the rate constants ranging from 1.42×10^{-10} to 8.95×10^{-10} cm³/sec as compared to 6.6325×10^{-12} cm³/sec for the Smoluchowski approach. The values of these rate constants for the other systems varied from around 10- to 100-fold higher as compared with the rate constant for a diffusion-controlled process (Table V).

It is concluded that platelets suspended in plasma (viscosity of human plasma is 0.0172 poise at 37°) have a low probability of moving under their diffusivities and, thus, aggregating. By calculating the diffusivity of a human platelet with the Stokes–Einstein equation (Eq. 8), a value of 1.226

Table V—Compilation of Rate Constants, Half-Lives, and Sticking Probability Factors of Platelet Aggregation in the Presence of Adenosine Diphosphate and Prostaglandins

Adenosine Diphosphate[a], μg	Prostaglandin[a], μg	Rate Constant[b], $K_{ss} \times 10^{-11}$, cm³/sec	Half-Life, $t_{1/2}$, sec	Sticking Probability Factor, $\gamma \times 10^6$/cm/Platelet
3.0	0.0	19.50	15.64	0.1364
3.0	0.06[c]	5.20	58.65	0.0363
3.0	0.6[d]	10.60	28.77	0.0741
3.0	0.6[e]	13.76	22.16	0.0962
6.0	0.0	57.56	5.30	0.4025
6.0	0.12[c]	3.88	78.61	0.0271
6.0	1.2[d]	18.75	16.27	0.1311
6.0	1.2[e]	21.20	14.38	0.1482
9.0	0.0	89.50	3.40	0.6259
9.0	0.18[c]	1.03	296.12	0.0072
9.0	1.8[d]	36.80	8.29	0.2573
9.0	1.8[e]	34.57	8.82	0.2417

[a] Amount injected into 1 ml of platelet-rich plasma. [b] Rate constant is zero for control experiments. [c] Results for prostaglandin E_1. [d] Results for dinoprostone. [e] Results for dinoprost.

Table VI—Rate Constants, Half-Lives, and Sticking Probability Factors of Platelet Aggregation in the Presence of Arachidonic Acid and Aspirin

Arachidonic Acid[a], μg	Aspirin[a], μg	Rate Constant[b], $K_{ss} \times 10^{-11}$, cm^3/sec	Half-Life, $t_{1/2}$, sec	Sticking Probability Factor, $\gamma \times 10^6$/cm/Platelet
540	0.0	3.18	95.90	0.0222
720	0.0	18.90	16.10	0.1321
540	2.25	−0.24	—	−0.0016
720	2.25	−4.40	—	−0.0307

[a] Amount injected into 1 ml of platelet-rich plasma. [b] Rate constant is zero for control experiments.

$\times 10^{-9}$ cm^2/sec is obtained, which is rather small compared to molecular diffusivities which are usually about 10^{-4}–10^{-6} cm^2/sec. Platelets physically approaching each other may be repulsed or aggregated or aggregates may disperse, depending on the reactivity of their surfaces, which is modulated by the molecular species in the solution.

The surface-barrier process is further supported by calculated values of the stability constant, W, from Eq. 9 showing numbers smaller than 1. Values of the sticking probability constant, γ, were calculated and are reported in Tables I–VI. As reported previously (10), adenosine diphosphate produces an alteration in the platelet membrane surface. Therefore, larger γ values in the presence of adenosine diphosphate probably are the result of a specific modification of the membrane surface reactivity by that compound. More work is needed regarding the biosynthesis of prostaglandins and surface-barrier effects.

The experimental results with prostaglandins and aspirin suggest the following with respect to therapeutics. If it is assumed that the blood volume in an average individual is 5 liters and that a person receiving aspirin or prostaglandin has complete systemic availability of the dose with little or no tissue distribution, the doses of aspirin and prostaglandin E_1 needed to block platelet aggregation completely will be around 10 and 1 mg, respectively. Thus, a combined dose of aspirin and prostaglandin E_1 will have a dual effect in blocking platelet aggregation and possibly thrombus formation.

REFERENCES

(1) E. J. W. Bowle, J. H. Thompson, and C. A. Owen, *Mayo Clin. Proc.*, **40**, 625 (1965).

(2) J. H. Wright, *J. Morphol.*, **21**, 263 (1910).

(3) W. H. Howell and D. D. Donahue, *J. Exp. Med.*, **65**, 177 (1937).

(4) E. Fidlar and E. T. Waters, *ibid.*, **73**, 299 (1941).

(5) B. N. Erickson, H. H. Williams, I. Avrin, and P. Lee, *J. Clin. Invest.*, **18**, 81 (1939).

(6) K. A. Aas and F. H. Gardner, *ibid.*, **37**, 1257 (1958).

(7) A. Gaarder, J. Jonsen, S. Loland, and D. Hellem, *Nature (London)*, **129**, 531 (1961).

(8) R. L. Vigdahl, N. R. Marquis, and P. A. Tavormina, *Biochem. Biophys. Res. Commun.*, **37**, 409 (1969).

(9) D. J. Bouillin, R. A. Green, and S. K. Price, *J. Physiol.*, **221**, 415 (1972).

(10) E. W. Salzman, *N. Engl. J. Med.*, **286**, 358 (1972).

(11) S. Bergstrom, H. Danielsson, and B. Samuelsson, *Biochim. Biophys. Acta*, **90**, 204 (1964).

(12) M. J. Silver, W. Hoch, J. J. Kocsis, and G. M. Ingerman, *Science*, **183**, 1085 (1974).

(13) U. S. Van Euler, F. Dray, and S. M. M. Karim, "Prostaglandins in Documenta Geigy," Ciba-Geigy Ltd., Basel, Switzerland, 1974.

(14) M. M. Wintrobe, "Blood Platelets and Coagulation in Clinical Hematology," 6th ed., Lea & Febiger, Philadelphia, Pa., 1967.

(15) A. B. Bikhazi, J. A. Shiatis, and A. F. Haddad, *J. Pharm. Sci.*, **66**, 181 (1977).

(16) H. R. Kruyt, "Colloid Science," vol. 1, Elsevier, Amsterdam, The Netherlands, 1952.

(17) G. E. Ayyub, M.S. thesis, American University of Beirut, Beirut, Lebanon, 1976.

(18) D. F. Bernstein, Ph.D. dissertation, University of Michigan, Ann Arbor, Mich., 1971.

(19) W. I. Higuchi, R. Okada, G. A. Stelter, and A. P. Lemberger, *J. Pharm. Sci.*, **52**, 49 (1963).

(20) B. B. Vargaftig and P. Zirinis, *Nature New Biol.*, **224**, 114 (1973).

ACKNOWLEDGMENTS

Presented at the Basic Pharmaceutics Section, APhA Academy of Pharmaceutical Sciences, New York meeting, May 1977.

Supported in part by a grant from the University Medical Research Fund, American University of Beirut, Beirut, Lebanon.

The authors thank The Upjohn Co., Kalamazoo, Mich., for providing samples of prostaglandins.

Possible Ion-Pair-Mediated Absorption of Mixidine I: Partitioning and Lethality Studies

W. DOUGLAS WALKLING ˣ, ANTOINETTE C. BONFILIO, and HENRY I. JACOBY

Received August 12, 1977, from the *Research Division, McNeil Laboratories, Inc., Fort Washington, PA 19034.* Accepted for publication October 28, 1977.

Abstract □ Mixidine, a very soluble base which is completely ionized in all physiological fluids, was found to form ion-pairs as demonstrated by its ability to partition into 1-butanol from acidic solutions. A similar relationship was observed for the effect of acids on the absorption of intraduodenally and orally administered solutions of mixidine in rats (as determined by lethality). Studies also demonstrated that the pH-lethality effects were not specific for a particular counterion. Mixidine was more lethal when administered intraduodenally than when administered orally, and the counterions *per se* were not lethal in the doses used.

Keyphrases □ Mixidine—ion-pair formation *in vitro* determined by partitioning, absorption in rats determined by lethality □ Ion-pair formation—mixidine *in vitro*, determined by partitioning □ Absorption—mixidine in rats, determined by lethality □ Vasodilators, coronary—mixidine, ion-pair formation *in vitro* determined by partitioning, absorption in rats determined by lethality

The utilization of ion-pairs, neutral species formed by electrostatic attraction between oppositely charged ions in solution, has been studied as a method for improving drug absorption. The duration of rabbit corneal anesthesia was related to the chloroform–water distribution of dibucaine combined with 10 counterion species (1). The enhanced pharmacological effect of an orally administered quaternary ammonium compound by trichloroacetic acid was related to increases in partition between chloroform or 1-octanol and pH 6 buffer (2).

0022-3549/78/0700/0945$01.00/0

© 1978, American Pharmaceutical Association

Table VI—Rate Constants, Half-Lives, and Sticking Probability Factors of Platelet Aggregation in the Presence of Arachidonic Acid and Aspirin

Arachidonic Acid[a], μg	Aspirin[a], μg	Rate Constant[b], $K_{ss} \times 10^{-11}$, cm^3/sec	Half-Life, $t_{1/2}$, sec	Sticking Probability Factor, $\gamma \times 10^6$/cm/Platelet
540	0.0	3.18	95.90	0.0222
720	0.0	18.90	16.10	0.1321
540	2.25	−0.24	—	−0.0016
720	2.25	−4.40	—	−0.0307

[a] Amount injected into 1 ml of platelet-rich plasma. [b] Rate constant is zero for control experiments.

$\times 10^{-9}$ cm^2/sec is obtained, which is rather small compared to molecular diffusivities which are usually about 10^{-4}–10^{-6} cm^2/sec. Platelets physically approaching each other may be repulsed or aggregated or aggregates may disperse, depending on the reactivity of their surfaces, which is modulated by the molecular species in the solution.

The surface-barrier process is further supported by calculated values of the stability constant, W, from Eq. 9 showing numbers smaller than 1. Values of the sticking probability constant, γ, were calculated and are reported in Tables I–VI. As reported previously (10), adenosine diphosphate produces an alteration in the platelet membrane surface. Therefore, larger γ values in the presence of adenosine diphosphate probably are the result of a specific modification of the membrane surface reactivity by that compound. More work is needed regarding the biosynthesis of prostaglandins and surface-barrier effects.

The experimental results with prostaglandins and aspirin suggest the following with respect to therapeutics. If it is assumed that the blood volume in an average individual is 5 liters and that a person receiving aspirin or prostaglandin has complete systemic availability of the dose with little or no tissue distribution, the doses of aspirin and prostaglandin E_1 needed to block platelet aggregation completely will be around 10 and 1 mg, respectively. Thus, a combined dose of aspirin and prostaglandin E_1 will have a dual effect in blocking platelet aggregation and possibly thrombus formation.

REFERENCES

(1) E. J. W. Bowle, J. H. Thompson, and C. A. Owen, *Mayo Clin. Proc.*, **40**, 625 (1965).

(2) J. H. Wright, *J. Morphol.*, **21**, 263 (1910).

(3) W. H. Howell and D. D. Donahue, *J. Exp. Med.*, **65**, 177 (1937).

(4) E. Fidlar and E. T. Waters, *ibid.*, **73**, 299 (1941).

(5) B. N. Erickson, H. H. Williams, I. Avrin, and P. Lee, *J. Clin. Invest.*, **18**, 81 (1939).

(6) K. A. Aas and F. H. Gardner, *ibid.*, **37**, 1257 (1958).

(7) A. Gaarder, J. Jonsen, S. Loland, and D. Hellem, *Nature (London)*, **129**, 531 (1961).

(8) R. L. Vigdahl, N. R. Marquis, and P. A. Tavormina, *Biochem. Biophys. Res. Commun.*, **37**, 409 (1969).

(9) D. J. Bouillin, R. A. Green, and S. K. Price, *J. Physiol.*, **221**, 415 (1972).

(10) E. W. Salzman, *N. Engl. J. Med.*, **286**, 358 (1972).

(11) S. Bergstrom, H. Danielsson, and B. Samuelsson, *Biochim. Biophys. Acta*, **90**, 204 (1964).

(12) M. J. Silver, W. Hoch, J. J. Kocsis, and G. M. Ingerman, *Science*, **183**, 1085 (1974).

(13) U. S. Van Euler, F. Dray, and S. M. M. Karim, "Prostaglandins in Documenta Geigy," Ciba-Geigy Ltd., Basel, Switzerland, 1974.

(14) M. M. Wintrobe, "Blood Platelets and Coagulation in Clinical Hematology," 6th ed., Lea & Febiger, Philadelphia, Pa., 1967.

(15) A. B. Bikhazi, J. A. Shiatis, and A. F. Haddad, *J. Pharm. Sci.*, **66**, 181 (1977).

(16) H. R. Kruyt, "Colloid Science," vol. 1, Elsevier, Amsterdam, The Netherlands, 1952.

(17) G. E. Ayyub, M.S. thesis, American University of Beirut, Beirut, Lebanon, 1976.

(18) D. F. Bernstein, Ph.D. dissertation, University of Michigan, Ann Arbor, Mich., 1971.

(19) W. I. Higuchi, R. Okada, G. A. Stelter, and A. P. Lemberger, *J. Pharm. Sci.*, **52**, 49 (1963).

(20) B. B. Vargaftig and P. Zirinis, *Nature New Biol.*, **224**, 114 (1973).

ACKNOWLEDGMENTS

Presented at the Basic Pharmaceutics Section, APhA Academy of Pharmaceutical Sciences, New York meeting, May 1977.

Supported in part by a grant from the University Medical Research Fund, American University of Beirut, Beirut, Lebanon.

The authors thank The Upjohn Co., Kalamazoo, Mich., for providing samples of prostaglandins.

Possible Ion-Pair-Mediated Absorption of Mixidine I: Partitioning and Lethality Studies

W. DOUGLAS WALKLING ˣ, ANTOINETTE C. BONFILIO, and HENRY I. JACOBY

Received August 12, 1977, from the *Research Division, McNeil Laboratories, Inc., Fort Washington, PA 19034.* Accepted for publication October 28, 1977.

Abstract □ Mixidine, a very soluble base which is completely ionized in all physiological fluids, was found to form ion-pairs as demonstrated by its ability to partition into 1-butanol from acidic solutions. A similar relationship was observed for the effect of acids on the absorption of intraduodenally and orally administered solutions of mixidine in rats (as determined by lethality). Studies also demonstrated that the pH-lethality effects were not specific for a particular counterion. Mixidine was more lethal when administered intraduodenally than when administered orally, and the counterions *per se* were not lethal in the doses used.

Keyphrases □ Mixidine—ion-pair formation *in vitro* determined by partitioning, absorption in rats determined by lethality □ Ion-pair formation—mixidine *in vitro*, determined by partitioning □ Absorption—mixidine in rats, determined by lethality □ Vasodilators, coronary—mixidine, ion-pair formation *in vitro* determined by partitioning, absorption in rats determined by lethality

The utilization of ion-pairs, neutral species formed by electrostatic attraction between oppositely charged ions in solution, has been studied as a method for improving drug absorption. The duration of rabbit corneal anesthesia was related to the chloroform–water distribution of dibucaine combined with 10 counterion species (1). The enhanced pharmacological effect of an orally administered quaternary ammonium compound by trichloroacetic acid was related to increases in partition between chloroform or 1-octanol and pH 6 buffer (2).

0022-3549/78/0700/0945$01.00/0

© 1978, American Pharmaceutical Association

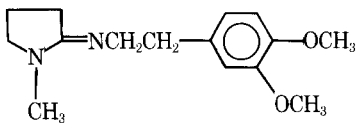

I

The enhancement of the absorption of quaternary ammonium compounds in rat preparations was reported using trichloroacetic acid (3), salicylic acid (3), and decylsulfuric acid (4) as the counterion species.

BACKGROUND

Absorption experiments with ion-pairs have not always resulted in clear pictures of the absorption-enhancing mechanism. One study (5) related apparent ion-pair-mediated absorption more to mucosal binding or mucosal erosion. Apparent site specificity was demonstrated for ion-pair-mediated absorption in rats, *i.e.*, absorption enhancement through the stomach and rectal walls but not through the intestinal wall (6).

Ion-pair-enhanced absorption has become controversial. The absorption of protonated dextromethorphan from the rat stomach was counterion dependent, but dextromethorphan was not absorbed in direct association with the counterion (7). An interfacial tension lowering effect on the gut wall by counterions was proposed as the mechanism for absorption enhancement. Another study (8) supported these conclusions (7) by demonstrating a tetracycline absorption enhancement relationship to surface tension lowering by counterions. However, in a later study (9), bile salts that enhanced isopropamide partitioning failed to increase isopropamide absorption from the rat ileum *in situ*, even when the bile salts were tested above and below their critical micelle concentrations.

Subsequently, Klink and Colaizzi (10) challenged the surface tension lowering theory of Perrin and Vallner (8) by demonstrating increases in the partitioning of several tetracyclines by trichloroacetic acid in acid media.

Mroszczak *et al.* (11) proposed that absorption enhancement, purportedly through ion-pair formation, actually may be caused by the minimization of protein binding of the drug by the counterion. The feasibility of this concept was demonstrated with trichloroacetic acid, a counterion frequently used in ion-pair studies.

More recently, various effects of chloride-ion concentration on the solubility, partitioning, dissolution, and GI absorption of haloperidol, droperidol, and pimozide were reported (12). These observations were explained as interactions among solubilization, precipitation, and ion-pair formation.

A unique aspect of the role of ion-pair formation on the biological activity of methantheline bromide was reported (13); an increase was observed in the lethal intravenous dose of the methantheline bromide solution upon the addition of neutralized trichloroacetic acid. This result was attributed to an increase in drug distribution in the body because of the increased lipophilicity of the ion-pairs.

Although the role of ion-pairs in drug absorption is controversial, the idea of increasing the absorption of a fully ionized, water-soluble drug by forming a neutral lipid soluble complex with a counterion remains intriguing.

Mixidine, 3,4-dimethoxy-*N*-(1-methyl-2-pyrrolidinylidene)benzeneethanamine (I), is a very soluble, surface-active compound and is completely ionized in all physiological fluids. The pKa of mixidine is greater than 12. It is poorly absorbed following oral administration to rats. Consequently, mixidine is an ideal candidate for testing the ion-pair-mediated absorption hypothesis.

This report deals with some preliminary experiments to determine under what conditions a mixidine ion-pair would form and if absorption would be enhanced. Partitioning studies were performed to assess the existence of ion pairs. Rat lethality studies permitted an evaluation of absorption without the intricacies of a quantitative assay in biological fluids.

Originally, mixidine was crystallized as the fumarate salt. Arylsulfonate salts were supplied in the hope that the extremely high ionization of arylsulfonic acids would permit them to function more effectively as ion-pair formers.

EXPERIMENTAL

Partitioning Studies—Citrate–phosphate buffers, with potassium chloride added to adjust ionic strength, were prepared at $\mu = 0.077$ (pH 2.2–3.0), $\mu = 0.157$ (pH 2.2–3.8), and $\mu = 0.344$ (pH 2.2–5.8) according to the method of Elving *et al.* (14). Several organic solvents were screened for their ability to extract mixidine from aqueous solutions, and 1-butanol was the most satisfactory. The buffers were saturated with 1-butanol and vice versa. The concentration of mixidine as mixidine fumarate in the aqueous phase was 5 mg/ml. The phases were combined and agitated for 30 min. The aqueous phase was assayed spectrophotometrically at 275 nm for remaining mixidine.

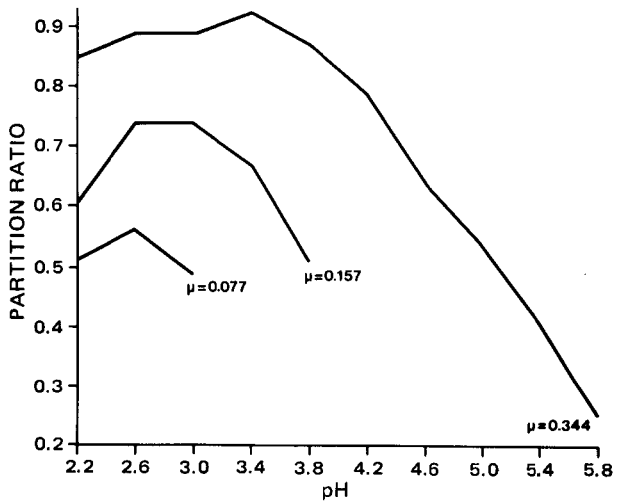

Figure 1—*Effect of pH and ionic strength of citrate–phosphate buffers on mixidine partition ratios between 1-butanol and water.*

A partitioning study with simulated gastric fluid USP without pepsin as the aqueous phase also was performed.

Lethality Studies—Female Sprague–Dawley rats, 150–200 g, were fasted for 24 hr and then lightly anesthetized with ether. For intraduodenal administration, a midline incision was made and the duodenum was identified. The test preparation was administered into the lumen of the duodenum, approximately 1 cm distal to the pylorus, through a 26-gauge needle fitted with a syringe. Reflux of the test preparation into the stomach was prevented by digital occlusion between the injection site and the pylorus.

The incision site was closed with metal wound clips, and the rats were allowed to recover in individual cages. Water was allowed *ad libitum;* food was allowed 4 hr after drug administration. The rats were observed continuously for the 1st hr for signs of drug effects or lethality and then periodically for an additional 5 hr.

For oral administration, unanesthetized rats were used except where noted. Administration of the test preparation was by the standard oral administration technique.

Solution Preparation—Solutions of 75 mg of mixidine/ml for intraduodenal administration and of 100 mg of mixidine/ml for oral administration were prepared by dissolving the mixidine salt or an equivalent mixture of mixidine with an acid in distilled water. To obtain preparations within a wide range of pH values, the pH of the solutions was adjusted with additional amounts of acid. Solutions of pH 5.0 and higher were prepared similarly, except that simulated intestinal fluid USP without pancreatin was used as the solvent.

Doses—Preliminary experiments determined that very acidic solutions

Table I—Mixidine (75 mg/ml) Lethality in Rats following Intraduodenal Administration [a]

Counterion	pH	Dose, mg/kg 1500	750	375	188
Hydrochloride	1.6	3/3	3/3	0/3	0/3
Fumarate	5.0	—	0/3	—	—
Besylate	1.3	—	3/3	—	—
Besylate	2.4	—	2/3	—	—
Besylate	4.0	—	0/3	—	—
Besylate	5.6	—	0/3	—	—
Tosylate	1.3	—	3/3	—	—
Tosylate	2.5	—	3/3	—	—
Tosylate	3.0	—	2/3	—	—
Tosylate	3.6	—	0/3	—	—
Tosylate	4.0	—	0/3	—	—
Tosylate	5.6	—	0/3	—	—

[a] Values are number of deaths per number of rats.

Table II—Mixidine (100 mg/ml) Lethality in Rats following Oral Administration [a]

Counterion	pH	Dose, mg/kg 4000	2000	1000	500
Besylate	1.2	3/3	2/3	0/3	0/3
Besylate	6.2	—	0/3	0/3	0/3
Tosylate	1.3	—	2/3	0/3	0/3
Tosylate	2.1	—	3/3	0/3	0/3
Tosylate	2.5	3/3	2/3	0/3	—
Tosylate	5.0	—	0/3	0/3	0/3
Napsylate	1.2	—	3/3	0/3	0/3
Napsylate	2.5	3/3	3/3	0/3	—

[a] Values are number of deaths per number of rats.

of mixidine administered intraduodenally were always lethal at 750 mg/kg. Similar experiments with oral administration determined that 4000 mg/kg was always lethal. Consequently, studies of the effect of counterion concentrations (as measured by pH) on mixidine lethality were initiated at these doses. For proprietary reasons, more lethality tests were conducted at doses of 2000, 1000, and 500 mg/kg in the oral dose study. All doses were tested on three rats.

Effect of Route and Anesthesia—To ascertain more fully the effects of the route of administration and of anesthesia–surgery on mixidine lethality, a solution containing 150 mg of mixidine/ml as the fumarate at pH 3.7 was administered at 1500 mg of mixidine/kg to four groups of 20 rats each. The groups represented rats dosed orally with mixidine, rats dosed orally with mixidine and receiving the anesthesia–surgery as in intraduodenal administration, rats dosed intraduodenally with mixidine and receiving anesthesia–surgery, and rats dosed intraduodenally with distilled water and receiving anesthesia–surgery.

Effect of Counterions—The lethality of the counterions *per se* was determined with solutions of acids equivalent to 150 mg of mixidine/ml. Rats were dosed intraduodenally with the equivalent of 750 mg of mixidine/kg and orally with the equivalent of 4000 mg of mixidine/kg. All doses were tested on three rats.

RESULTS AND DISCUSSION

Figure 1 illustrates the influence of pH and ionic strength on the 1-butanol–water partitioning of mixidine from pH 2.2 to 5.8. In the citrate–phosphate buffer, counterions facilitated the partition of mixidine into the organic layer. The partition from the citrate–phosphate buffer was maximum in the pH 2.6–3.4 range. Partitioning also depended on ionic strength: the greater the ionic strength, the greater the partitioning. Consequently, partitioning would be expected to change with buffer composition because it would be a function of buffer species, pKa values and concentrations. Figure 1 illustrates that ion-pair-mediated partitioning of mixidine into 1-butanol can occur and that it is influenced by the aqueous phase.

The partition ratio of mixidine (supplied as the fumarate) from simulated gastric fluid USP without pepsin into 1-butanol was 0.381. The simulated gastric fluid USP without pepsin had a pH of 1.26 and an ionic strength of $\mu = 0.697$. At that pH and ionic strength, the partitioning ratio agrees with those reported in Fig. 1.

Rat lethality, following intraduodenal administration, was selected as a rapid screening method for mixidine absorption. The onset of mixidine lethality (respiratory depression) was rapid, often occurring a few minutes after administration. Table I relates the influence of dose, salt form, and pH on rat lethality following intraduodenal administration.

Included in Table I is the response of four dose levels of intraduodenally administered mixidine as a solution in simulated gastric fluid USP without pepsin (pH 1.6). The data show the anticipated response to increasing doses in the rat, *i.e.*, lethality at the higher doses, and no lethality at the lower doses. The minimum lethal dose administered was 750 mg/kg.

Table III—Mixidine Lethality in Rats as a Function of the Route of Administration and the Condition of the Rats

Route	Dose[a]	Anesthesia	Surgery	Lethality[b]
Oral	1500	No	No	4/20
Oral	1500	Yes	Yes	2/20
Intraduodenal	1500	Yes	Yes	20/20
Intraduodenal	0[c]	Yes	Yes	0/20

[a] Milligrams of mixidine per kilogram as the fumarate (pH 3.7). [b] Number of deaths per number of rats. [c] Vehicle only (distilled water).

Table IV—Counterion Lethality in Rats

Counterion[a]	pH	Lethality[b]
Intraduodenal Administration (Equivalent to 750 mg of Mixidine/kg)		
Fumarate[c]	2.3	0/3
Besylate	0.5	0/3
Tosylate	0.5	0/3
Oral Administration (Equivalent to 4000 mg of Mixidine/kg)		
Besylate	0.5	0/3
Tosylate	0.5	0/3
Napsylate	0.5	0/3

[a] Solutions equivalent to 150 mg of mixidine/ml. [b] Number of deaths per number of rats. [c] Suspension.

With the minimum lethal dose as a standard, the influences of salt form and pH were evaluated. The form of mixidine had no measurable effect on lethality. What was important was the effect of pH (counterion concentration) on lethality: the lower the pH, the higher the lethality. To an extent, this pH–lethality relationship follows the pH–partition relationship in 1-butanol where, within limits, a lower pH resulted in greater partitioning. But, unlike the pH–partition relationship which peaked at pH 2.6, lethality increased continuously to the lowest pH tested, 1.3. At the lowest pH values, the increase in lethality was not anticipated from the partitioning ratio. Apparently, the relative affinity for the mixidine ion-pairs is different for the rat duodenum as compared to 1-butanol.

Lethality following oral administration required three to four times more mixidine than lethality following intraduodenal administration. Otherwise, the effects of dose, salt form, and pH were the same as following intraduodenal administration (Table II).

A further examination of the effect of the administration route on the response to mixidine is given in Table III. Orally administered mixidine, whether administered with or without the anesthesia and the surgery necessary for intraduodenal administration, was much less lethal than intraduodenally administered mixidine. Also, a sham operation with the surgery and the anesthesia but without the mixidine was not lethal. Thus, the results demonstrate that intraduodenally administered mixidine does not owe its lethality to anesthesia–surgery and that it is possible that the duodenum is a better absorption site for mixidine in rats.

Although the lethality of the counterions *per se* was not expected to be a problem, solutions of all counterions in distilled water, equivalent to 4000 mg of mixidine/kg po and 750 mg of mixidine/kg id, were tested (Table IV). None of the counterions was lethal. Consequently, the lethalities reported in Tables I–III were due to respiratory depression caused by mixidine and not from any overt property of the counterions.

SUMMARY

If it is assumed that the absorption (cause) and lethality (effect) premise upon which the absorption studies were founded is correct, it appears that mixidine absorption can be facilitated by increasing the counterion concentration, *i.e.*, decreasing the vehicle pH. Consequently, the ion-pair-mediated absorption hypothesis appears to operate, *i.e.*, increased partitioning into a lipophilic phase, 1-butanol, or rat duodenum, with an increased counterion concentration. However, the absorption hypothesis obviously does not operate in the exact manner suggested by ion-pair-mediated partitioning into 1-butanol. The lack of a perfectly parallel relation between 1-butanol partitioning and lethality exists at the highest counterion concentration (lowest pH).

Plasma level studies and pathological examinations are underway and will be reported later.

REFERENCES

(1) M. Aoki and N. Yata, *J. Pharm. Soc. Jpn.*, **86**, 832 (1966).

(2) G. M. Irwin, H. B. Kostenbauder, L. W. Dittert, R. Staples, A. Misher, and J. V. Swintosky, *J. Pharm. Sci.*, **58**, 313 (1969).

(3) M. Gibaldi and B. Grundhofer, *ibid.*, **62**, 343 (1973).

(4) B. W. Masaki, E. J. Lien, and J. A. Biles, *Acta Pharm. Suec.*, **10**, 43 (1973).

(5) K. Kakemi, H. Sezaki, S. Muraniski, and Y. Tsujimura, *Chem. Pharm. Bull.*, **17**, 1641 (1969).

(6) E. Suzuki, M. Tsukigi, S. Muraniski, H. Sezaki, and K. Kakemi, *J. Pharm. Pharmacol.*, **24**, 138 (1972).

(7) G. Fiese and J. H. Perrin, *J. Pharm. Sci.*, **58**, 599 (1969).

(8) J. H. Perrin and J. J. Vallner, *J. Pharm. Pharmacol.*, **22**, 758 (1970).

(9) T. S. Gaginella, P. Bass, J. H. Perrin, and J. J. Vallner, *J. Pharm. Sci.* **62,** 1121 (1973).
(10) P. R. Klink and J. L. Colaizzi, *ibid.*, **62,** 97 (1973).
(11) E. L. Mroszczak, J. Vallner, and J. H. Perrin, *ibid.*, **58,** 1567 (1969).
(12) M. D. Parker, *Diss. Abstr. Int.*, **35,** 1215-B (1974).
(13) J. Newburger and H. B. Kostenbauder, *Life Sci.*, **20,** 627 (1977).
(14) P. J. Elving, J. M. Markowitz, and I. Rosenthal, *Anal. Chem.*, **28,** 1179 (1956).

ACKNOWLEDGMENTS

The authors acknowledge George I. Poos and Richard J. Mohrbacher, McNeil Laboratories, for the synthesis of mixidine fumarate and the preparation of the arylsulfonic acid salts, respectively.

Possible Ion-Pair-Mediated Absorption of Mixidine II: Plasma Levels and Histology

W. DOUGLAS WALKLING ˣ, DONALD G. HOLMES, WILLIAM A. CRESSMAN, ROBERT K. DIX, ELLIOT PIPERNO, and A. HARRIS MOSHER

Received August 12, 1977, from the *Research Division, McNeil Laboratories, Inc., Fort Washington, PA 19034.* Accepted for publication October 28, 1977.

Abstract □ Plasma intact ^{14}C-mixidine levels in rats increased when the drug was administered intraduodenally with 1:3 and 1:5 molar ratios of 2-naphthalenesulfonic acid. Upon histological examination of the duodenums, similar doses of mixidine combined with 2-naphthalenesulfonic acid produced no dose-related lesions. These and previous observations demonstrate that mixidine absorption may be enhanced by ion-pair formation.

Keyphrases □ Mixidine—absorption, effect of intraduodenal administration with various ratios of 2-naphthalenesulfonic acid as counterion □ Absorption—mixidine, effect of intraduodenal administration with various ratios of 2-naphthalenesulfonic acid as counterion □ Ion-pair formation—effect on mixidine absorption, intraduodenal administration with various ratios of 2-naphthalenesulfonic acid as counterion □ Vasodilators, coronary—mixidine, absorption, effect of intraduodenal administration with various ratios of 2-naphthalenesulfonic acid as counterion

The influence of counterions (acids) on the 1-butanol–water partitioning and the lethality in rats of mixidine, a completely ionized base, was reported (1). When the counterion concentration in an aqueous solution of mixidine was increased, mixidine partitioning into 1-butanol increased, as did the lethality of the solution in rats. This concomitant increase in partitioning with an increase in lethality led to the conclusion that mixidine absorption, as measured by lethality, was enhanced by ion-pair formation.

Also reported were the observations that the ion-pair-mediated absorption of mixidine was most easily demonstrated following intraduodenal administration, that counterions *per se* were not lethal, and that the counterions were equivalent in their ability to mediate mixidine absorption at a given pH (1).

In this study, plasma ^{14}C-mixidine levels were followed to determine if a parallel relationship to the effect of counterion concentration on partitioning and lethality occurred. In addition, rats dosed similarly to those in the plasma level study were examined histologically in an effort to show an absence of counterion-related pathology.

EXPERIMENTAL

Plasma Level Studies—*Preparations*—^{14}C-Mixidine fumarate, specific activity of 5.1 μCi/mg, was dissolved in distilled water to yield a salt concentration of 12.6 mg/ml. Rats were dosed with the equivalent of 25 mg of ^{14}C-mixidine/kg (~0.5 ml/rat).

The labeled mixidine was administered alone and in 1:1, 1:3, and 1:5 mixidine to 2-naphthalenesulfonic acid molar ratios. In experiments with 2-naphthalenesulfonic acid, the volumes of the solutions never exceeded 0.5 ml. In one experiment, 2-naphthalenesulfonic acid in a 1:3 drug to adjuvant ratio was neutralized by adding sodium hydroxide equimolar to the 2-naphthalenesulfonic acid.

Administration—Male CFN rats, 180–200 g, were fasted for approximately 17 hr. For oral administration, the rats were dosed *via* stomach tube followed by a 0.5-ml water wash. For intraduodenal administration, the rats were anesthetized with ether and dosed according to the procedure described previously (1).

Three rats were employed for each dose-route combination, except for the mixidine–2-naphthalenesulfonic acid (1:3) combination for intraduodenal administration where four rats were employed.

Analysis—The assay for intact drug was one in which the specificity had been established (2). A 100-μl blood sample was taken from the tail vein and rinsed into 0.5 ml of distilled water. Ten milliliters of chloroform, 1.0 ml of 1.0 *N* NaOH, and 1.0 ml of 0.096 mg of mixidine/ml as the fumarate were added. Then the mixture was agitated and centrifuged.

Table I—Plasma Intact Mixidine Levels (Nanograms per Milliliter) following Oral Administration of ^{14}C-Mixidine (25 mg/kg)

	1:0 Drug–Adjuvant (pH 3.7)				1:1 Drug–Adjuvant (pH 2.5)				1:3 Drug–Adjuvant (pH 1.6)			
Minutes	A	B	C	Mean	A	B	C	Mean	A	B	C	Mean
20	36	31	76	48	33	20	31	28	25	19	27	24
40	32	32	43	36	42	32	27	34	21	30	42	31
60	28	23	40	30	31	30	19	27	30	—	34	32
120	26	163	14	68	31	17	19	22	19	21	21	20
180	49	34	60	48	55	8	59	41	15	18	19	17
240	66	12	28	35	25	15	127	56	12	—	17	14
360	7	1	14	7	8	18	8	11	12	17	18	16

0022-3549/78/0700/0948$01.00/0
© 1978, American Pharmaceutical Association

(9) T. S. Gaginella, P. Bass, J. H. Perrin, and J. J. Vallner, *J. Pharm. Sci.* **62,** 1121 (1973).
(10) P. R. Klink and J. L. Colaizzi, *ibid.*, **62,** 97 (1973).
(11) E. L. Mroszczak, J. Vallner, and J. H. Perrin, *ibid.*, **58,** 1567 (1969).
(12) M. D. Parker, *Diss. Abstr. Int.*, **35,** 1215-B (1974).
(13) J. Newburger and H. B. Kostenbauder, *Life Sci.*, **20,** 627 (1977).
(14) P. J. Elving, J. M. Markowitz, and I. Rosenthal, *Anal. Chem.*, **28,** 1179 (1956).

ACKNOWLEDGMENTS

The authors acknowledge George I. Poos and Richard J. Mohrbacher, McNeil Laboratories, for the synthesis of mixidine fumarate and the preparation of the arylsulfonic acid salts, respectively.

Possible Ion-Pair-Mediated Absorption of Mixidine II: Plasma Levels and Histology

W. DOUGLAS WALKLING ˣ, DONALD G. HOLMES, WILLIAM A. CRESSMAN, ROBERT K. DIX, ELLIOT PIPERNO, and A. HARRIS MOSHER

Received August 12, 1977, from the *Research Division, McNeil Laboratories, Inc., Fort Washington, PA 19034.* Accepted for publication October 28, 1977.

Abstract □ Plasma intact ^{14}C-mixidine levels in rats increased when the drug was administered intraduodenally with 1:3 and 1:5 molar ratios of 2-naphthalenesulfonic acid. Upon histological examination of the duodenums, similar doses of mixidine combined with 2-naphthalenesulfonic acid produced no dose-related lesions. These and previous observations demonstrate that mixidine absorption may be enhanced by ion-pair formation.

Keyphrases □ Mixidine—absorption, effect of intraduodenal administration with various ratios of 2-naphthalenesulfonic acid as counterion □ Absorption—mixidine, effect of intraduodenal administration with various ratios of 2-naphthalenesulfonic acid as counterion □ Ion-pair formation—effect on mixidine absorption, intraduodenal administration with various ratios of 2-naphthalenesulfonic acid as counterion □ Vasodilators, coronary—mixidine, absorption, effect of intraduodenal administration with various ratios of 2-naphthalenesulfonic acid as counterion

The influence of counterions (acids) on the 1-butanol–water partitioning and the lethality in rats of mixidine, a completely ionized base, was reported (1). When the counterion concentration in an aqueous solution of mixidine was increased, mixidine partitioning into 1-butanol increased, as did the lethality of the solution in rats. This concomitant increase in partitioning with an increase in lethality led to the conclusion that mixidine absorption, as measured by lethality, was enhanced by ion-pair formation.

Also reported were the observations that the ion-pair-mediated absorption of mixidine was most easily demonstrated following intraduodenal administration, that counterions *per se* were not lethal, and that the counterions were equivalent in their ability to mediate mixidine absorption at a given pH (1).

In this study, plasma ^{14}C-mixidine levels were followed to determine if a parallel relationship to the effect of counterion concentration on partitioning and lethality occurred. In addition, rats dosed similarly to those in the plasma level study were examined histologically in an effort to show an absence of counterion-related pathology.

EXPERIMENTAL

Plasma Level Studies—*Preparations*—^{14}C-Mixidine fumarate, specific activity of 5.1 μCi/mg, was dissolved in distilled water to yield a salt concentration of 12.6 mg/ml. Rats were dosed with the equivalent of 25 mg of ^{14}C-mixidine/kg (~0.5 ml/rat).

The labeled mixidine was administered alone and in 1:1, 1:3, and 1:5 mixidine to 2-naphthalenesulfonic acid molar ratios. In experiments with 2-naphthalenesulfonic acid, the volumes of the solutions never exceeded 0.5 ml. In one experiment, 2-naphthalenesulfonic acid in a 1:3 drug to adjuvant ratio was neutralized by adding sodium hydroxide equimolar to the 2-naphthalenesulfonic acid.

Administration—Male CFN rats, 180–200 g, were fasted for approximately 17 hr. For oral administration, the rats were dosed *via* stomach tube followed by a 0.5-ml water wash. For intraduodenal administration, the rats were anesthetized with ether and dosed according to the procedure described previously (1).

Three rats were employed for each dose-route combination, except for the mixidine–2-naphthalenesulfonic acid (1:3) combination for intraduodenal administration where four rats were employed.

Analysis—The assay for intact drug was one in which the specificity had been established (2). A 100-μl blood sample was taken from the tail vein and rinsed into 0.5 ml of distilled water. Ten milliliters of chloroform, 1.0 ml of 1.0 *N* NaOH, and 1.0 ml of 0.096 mg of mixidine/ml as the fumarate were added. Then the mixture was agitated and centrifuged.

Table I—Plasma Intact Mixidine Levels (Nanograms per Milliliter) following Oral Administration of ^{14}C-Mixidine (25 mg/kg)

	1:0 Drug–Adjuvant (pH 3.7)				1:1 Drug–Adjuvant (pH 2.5)				1:3 Drug–Adjuvant (pH 1.6)			
Minutes	A	B	C	Mean	A	B	C	Mean	A	B	C	Mean
20	36	31	76	48	33	20	31	28	25	19	27	24
40	32	32	43	36	42	32	27	34	21	30	42	31
60	28	23	40	30	31	30	19	27	30	—	34	32
120	26	163	14	68	31	17	19	22	19	21	21	20
180	49	34	60	48	55	8	59	41	15	18	19	17
240	66	12	28	35	25	15	127	56	12	—	17	14
360	7	1	14	7	8	18	8	11	12	17	18	16

0022-3549/78/0700/0948$01.00/0
© 1978, American Pharmaceutical Association

Table II—Plasma Intact Mixidine Levels (Nanograms per Milliliter) following Intraduodenal Administration of ^{14}C-Mixidine (25 mg/kg)

Minutes	1:0 Drug–Adjuvant (pH 3.7)				1:1 Drug–Adjuvant (pH 2.5)				1:3 Drug–Adjuvant (pH 1.7)				1:5 Drug–Adjuvant (pH 1.3)				Neutralized 1:3 Drug–Adjuvant (pH 3.5)			
	A	B	C	Mean	A	B	C	Mean	A	B	C	D	Mean	A	B	C	Mean	A	B	C	Mean
20	492	410	440	444	227	280	357	305	865	901	510	645	731	1981	2594	772	1782	54	65	44	54
40	329	203	213	248	246	204	266	239	—	—	254	365	310	1395	989	340	908	34	54	39	43
60	247	90	158	165	184	169	190	181	428	401	167	185	296	1034	595	197	609	28	39	33	33
120	105	50	70	75	86	70	78	78	198	168	85	89	135	—	204	—[a]	—	18	15	14	16
180	66	37	37	47	35	23	42	33	130	61	49	46	72	983	111	—	547	8	9	7	8
240	43	38	34	38	23	14	23	20	50	37	40	42	42	—[a]	63	—	—	8	2	6	5
360	27	56	54	46	9	6	9	8	26	28	21	10	21	—	10	—	—	8	2	4	5

[a] Died.

Figure 1—*Plasma intact mixidine levels following intraduodenal administration of ^{14}C-mixidine (25 mg/kg) with various molar ratios of 2-naphthalenesulfonic acid. Key: A, 1:5; B, 1:3; C, 1:1; D, 1:0; and E, neutralized 1:3.*

The aqueous layer was aspirated, and 7 ml was transferred to a counting vial. The chloroform was evaporated, and the residue was redissolved in 0.1 ml of chloroform. A 20% ethanol scintillator was added, and the solution was counted for 10 min. Average efficiencies were determined on all samples.

The samples were collected at 20, 40, 60, 120, 180, 240, and 360 min following administration.

Histological Studies—*Preparations*—The solutions administered to the rats were identical to the solutions employed in the plasma level studies, except that unlabeled mixidine fumarate was used instead of ^{14}C-mixidine fumarate. Each rat received the equivalent of 36 mg of mixidine/kg instead of 25 mg/kg. Molar ratios of 1:0, 1:1, 1:3, and 1:5 mixidine fumarate to 2-naphthalenesulfonic acid were prepared to test the effect of increasing the sulfonic acid dose on the duodenal integrity.

Administration—Male CFN rats, 170–220 g, were fasted for approximately 17 hr. They then were anesthetized with ether and dosed intraduodenally as described for the plasma level studies.

Five rats were examined to evaluate each mixidine to 2-naphthalenesulfonic acid ratio.

Examination—Rats were killed 24 hr after surgery by exsanguination under chloroform anesthesia. GI tracts were opened and examined for gross effects. Tissues with gross lesions were fixed in 10% neutral buffered formalin, paraffin embedded, sectioned at 6 μm, stained with hematoxylin and eosin, and examined histologically.

RESULTS AND DISCUSSION

Plasma intact mixidine concentrations are given in Tables I and II. After oral administration, the plasma intact mixidine levels were low and were essentially equivalent regardless of the amount of 2-naphthalenesulfonic acid. To some degree, this result was anticipated from the lethality studies (1) in which oral doses four times greater than intraduodenal doses were not lethal.

For intraduodenal administration, a vehicle-to-vehicle variation in counterion concentration was detected by differences in the plasma levels

Table III—Histological Examination Results [a]

Mixidine–2-Naphthalene-Sulfonic Acid	Animal	Serositis	Myositis	Enteritis	Granuloma (Foreign Body)
1:0	1	—	—	—	—
	2	—	2	2	—
	3	—	2	2	X
	4	—	—	—	—
	5	—	1	1	—
1:1	6	—	—	—	—
	7	—	—	—	—
	8	1	—	—	—
	9	—	—	—	—
	10	—	—	—	—
1:3	11	—	—	—	—
	12	—	—	—	—
	13	2	2	2	—
	14	—	—	—	—
	15	—	—	—	—
1:5	16	1	1	—	—
	17	—	—	—	—
	18	t	t	—	—
	19	—	—	—	—
	20	3	3	3	X

[a] X = present, t = trace, 1 = slight or small, 2 = moderate, 3 = marked, and 4 = severe.

with 1:5 ≫ 1:3 > 1:1 ≈ 1:0 > neutralized 1:3 for the mixidine to 2-naphthalenesulfonic acid ratios. This result is consistent with the trend observed in the lethality studies.

The 1:5 combination produced lethality in two out of three rats. This finding was not anticipated from the lethality studies in which much higher doses in very acidic solutions failed to produce lethality. Possibly, the extensive absorption of the drug combined with the surgical trauma associated with intraduodenal administration and the prolonged administration of anesthetic was fatal to the animals. This hypothesis was not investigated.

The means of the plasma levels following intraduodenal administration are illustrated in Fig. 1. The figure describes more dramatically the differences in the plasma levels, especially the extremely high levels observed during the 1st hr following administration of the 1:5 mixidine–2-naphthalenesulfonic acid combination.

Of particular interest are the low levels of intact mixidine observed following administration of the sodium hydroxide-neutralized 1:3 mixidine–2-naphthalenesulfonic acid combination. The levels were even lower than with mixidine without adjuvant. It may be postulated that the sodium hydroxide has a greater effect on mixidine absorption across the duodenal wall than just neutralization of the sulfonic acid.

Histologic lesions were present in all groups without any apparent relationship to ratios employed (Table III). Some lesions, such as the foreign body granulomas (trichogranuloma), obviously were related to surgical technique, but the cause of the other lesions could not be ascertained. Certainly, the pathology discovered upon histological examination failed to demonstrate a trend that implicates increases in the doses of 2-naphthalenesulfonic acid with increases in the number and severity of lesions.

It is apparent from the lack of counterion lethality (1) and the absence of counterion-related lesions that dose-related lethality and dose-related plasma intact mixidine levels are the results of increased mixidine absorption across the duodenal wall and are not related to toxic or corrosive effects of the counterions. These observations, coupled with the observation of ion-pair-mediated partitioning of mixidine (1), substantiate the conclusion that mixidine absorption may be ion-pair mediated.

Under the proper circumstances, improved drug absorption through ion-pair mediation across the GI tract may occur. However, the application of ion-pairs to improve the absorption of mixidine or other drugs in humans remains a challenge. Ion-pairs exist only in nonaqueous media. Casually releasing a quantity of drug with counterions into the aqueous GI tract environment is not likely to improve drug absorption, as demonstrated by the oral administration studies.

Increasing the quantity of counterion relative to the quantity of drug to overload the GI tract with counterion presents problems regarding dosage form size, particularly if complete absorption is necessary for the clinical activity of a low potency compound. Also, if ion-pair-mediated absorption is site specific, as it appears to be, then a novel means of delivering the drug and counterion simultaneously to that site must be developed since conventional enteric release dosage forms are generally regarded as problematic. Future studies with ion-pair-enhanced absorption will have to address these problems.

REFERENCES

(1) W. D. Walkling, A. C. Bonfilio, and H. I. Jacoby, *J. Pharm. Sci.*, **67**, 945 (1978).

(2) J. Plostnieks and W. A. Cressman, "Biochemical Research Report No. 50: The Absorption and Excretion of Mixidine-^{14}C Fumarate in Dogs," McNeil Laboratories, Fort Washington, Pa., 1971.

ACKNOWLEDGMENTS

The authors thank Leonard Hecker of McNeil Laboratories for the preparation of the labeled mixidine fumarate.

Simple GLC Analysis of Anticonvulsant Drugs in Commercial Dosage Forms

J. R. WATSON ˣ, R. C. LAWRENCE, and E. G. LOVERING

Received September 28, 1976, from the *Drug Research Laboratories, Health Protection Branch, Ottawa, Ontario, Canada, K1A 0L2.*
Accepted for publication October 27, 1977.

Abstract □ A simple, specific GLC procedure is described for the analysis of one sedative and six anticonvulsant drugs in pharmaceutical dosage forms. Sample aliquots of ethotoin, glutethimide, mephenytoin, methsuximide, and phensuximide were shaken with or extracted into ethyl acetate, diluted with the internal standard (diphenyl phthalate) solution, injected into a gas chromatograph, and eluted from a methylsilicone column. Primidone and phenytoin samples (extracted as the free acid) required derivatization with *N,O*-bis(trimethylsilyl)acetamide prior to chromatography. The same temperature programming conditions and flow rate settings were used for all seven drugs. The GLC results agreed well with those obtained using the pharmacopeial methods.

Keyphrases □ GLC—analyses, various anticonvulsants and one sedative in commercial dosage forms □ Anticonvulsants, various—GLC analyses in commercial dosage forms □ Sedatives—glutethimide, GLC analysis in commercial dosage forms

The pharmacopeial procedures (1–3) for the assay of several important anticonvulsant drugs in commercial dosage forms generally involve multiple steps. The sample preparation and measurement techniques vary, depending on the chemical entity and its associated physicochemical characteristics. UV spectrophotometry is employed for the

0022-3549/78/0700/0950$01.00/0
© 1978, American Pharmaceutical Association

Table III—Histological Examination Results [a]

Mixidine–2-Naphthalene-Sulfonic Acid	Animal	Serositis	Myositis	Enteritis	Granuloma (Foreign Body)
1:0	1	—	—	—	—
	2	—	2	2	—
	3	—	2	2	X
	4	—	—	—	—
	5	—	1	1	—
1:1	6	—	—	—	—
	7	—	—	—	—
	8	1	—	—	—
	9	—	—	—	—
	10	—	—	—	—
1:3	11	—	—	—	—
	12	—	—	—	—
	13	2	2	2	—
	14	—	—	—	—
	15	—	—	—	—
1:5	16	1	1	—	—
	17	—	—	—	—
	18	t	t	—	—
	19	—	—	—	—
	20	3	3	3	X

[a] X = present, t = trace, 1 = slight or small, 2 = moderate, 3 = marked, and 4 = severe.

with 1:5 ≫ 1:3 > 1:1 ≈ 1:0 > neutralized 1:3 for the mixidine to 2-naphthalenesulfonic acid ratios. This result is consistent with the trend observed in the lethality studies.

The 1:5 combination produced lethality in two out of three rats. This finding was not anticipated from the lethality studies in which much higher doses in very acidic solutions failed to produce lethality. Possibly, the extensive absorption of the drug combined with the surgical trauma associated with intraduodenal administration and the prolonged administration of anesthetic was fatal to the animals. This hypothesis was not investigated.

The means of the plasma levels following intraduodenal administration are illustrated in Fig. 1. The figure describes more dramatically the differences in the plasma levels, especially the extremely high levels observed during the 1st hr following administration of the 1:5 mixidine–2-naphthalenesulfonic acid combination.

Of particular interest are the low levels of intact mixidine observed following administration of the sodium hydroxide-neutralized 1:3 mixidine–2-naphthalenesulfonic acid combination. The levels were even lower than with mixidine without adjuvant. It may be postulated that the sodium hydroxide has a greater effect on mixidine absorption across the duodenal wall than just neutralization of the sulfonic acid.

Histologic lesions were present in all groups without any apparent relationship to ratios employed (Table III). Some lesions, such as the foreign body granulomas (trichogranuloma), obviously were related to surgical technique, but the cause of the other lesions could not be ascertained. Certainly, the pathology discovered upon histological examination failed to demonstrate a trend that implicates increases in the doses of 2-naphthalenesulfonic acid with increases in the number and severity of lesions.

It is apparent from the lack of counterion lethality (1) and the absence of counterion-related lesions that dose-related lethality and dose-related plasma intact mixidine levels are the results of increased mixidine absorption across the duodenal wall and are not related to toxic or corrosive effects of the counterions. These observations, coupled with the observation of ion-pair-mediated partitioning of mixidine (1), substantiate the conclusion that mixidine absorption may be ion-pair mediated.

Under the proper circumstances, improved drug absorption through ion-pair mediation across the GI tract may occur. However, the application of ion-pairs to improve the absorption of mixidine or other drugs in humans remains a challenge. Ion-pairs exist only in nonaqueous media. Casually releasing a quantity of drug with counterions into the aqueous GI tract environment is not likely to improve drug absorption, as demonstrated by the oral administration studies.

Increasing the quantity of counterion relative to the quantity of drug to overload the GI tract with counterion presents problems regarding dosage form size, particularly if complete absorption is necessary for the clinical activity of a low potency compound. Also, if ion-pair-mediated absorption is site specific, as it appears to be, then a novel means of delivering the drug and counterion simultaneously to that site must be developed since conventional enteric release dosage forms are generally regarded as problematic. Future studies with ion-pair-enhanced absorption will have to address these problems.

REFERENCES

(1) W. D. Walkling, A. C. Bonfilio, and H. I. Jacoby, *J. Pharm. Sci.*, **67**, 945 (1978).

(2) J. Plostnieks and W. A. Cressman, "Biochemical Research Report No. 50: The Absorption and Excretion of Mixidine-^{14}C Fumarate in Dogs," McNeil Laboratories, Fort Washington, Pa., 1971.

ACKNOWLEDGMENTS

The authors thank Leonard Hecker of McNeil Laboratories for the preparation of the labeled mixidine fumarate.

Simple GLC Analysis of Anticonvulsant Drugs in Commercial Dosage Forms

J. R. WATSON ˣ, R. C. LAWRENCE, and E. G. LOVERING

Received September 28, 1976, from the *Drug Research Laboratories, Health Protection Branch, Ottawa, Ontario, Canada, K1A 0L2.*
Accepted for publication October 27, 1977.

Abstract □ A simple, specific GLC procedure is described for the analysis of one sedative and six anticonvulsant drugs in pharmaceutical dosage forms. Sample aliquots of ethotoin, glutethimide, mephenytoin, methsuximide, and phensuximide were shaken with or extracted into ethyl acetate, diluted with the internal standard (diphenyl phthalate) solution, injected into a gas chromatograph, and eluted from a methylsilicone column. Primidone and phenytoin samples (extracted as the free acid) required derivatization with *N,O*-bis(trimethylsilyl)acetamide prior to chromatography. The same temperature programming conditions and flow rate settings were used for all seven drugs. The GLC results agreed well with those obtained using the pharmacopeial methods.

Keyphrases □ GLC—analyses, various anticonvulsants and one sedative in commercial dosage forms □ Anticonvulsants, various—GLC analyses in commercial dosage forms □ Sedatives—glutethimide, GLC analysis in commercial dosage forms

The pharmacopeial procedures (1–3) for the assay of several important anticonvulsant drugs in commercial dosage forms generally involve multiple steps. The sample preparation and measurement techniques vary, depending on the chemical entity and its associated physicochemical characteristics. UV spectrophotometry is employed for the

0022-3549/78/0700/0950$01.00/0
© 1978, American Pharmaceutical Association

Table I—GLC Data on Anticonvulsant Drugs

Drug	Average Retention Time, min	Relative[a] Retention Time ± % CV	Relative[a] Response Factor ± % CV
Ethotoin	10.86	0.372 ± 1.5	1.549 ± 2.3
Glutethimide	11.69	0.400 ± 0.6	1.118 ± 1.8
Mephenytoin	11.20	0.384 ± 1.9	1.205 ± 2.2
Methsuximide	5.86	0.201 ± 1.1	1.131 ± 0.7
Phensuximide	6.21	0.213 ± 1.3	1.209 ± 1.4
Phenytoin[c]	23.56	0.805 ± 0.4	0.777 ± 0.6
Primidone[c]	11.75	0.402 ± 0.8	0.713 ± 0.8

[a] Relative to the internal standard (diphenyl phthalate average retention time = 29.20 min). [b] Each relative response factor represents the average of five determinations at varying weight levels of drug. [c] Eluted as the silylated derivatives; relative response factors are based on the weight of unsilylated compound.

analysis of glutethimide (a sedative), mephenytoin, methsuximide, phensuximide, and primidone. Phenytoin and its sodium salt in commercial preparations are assayed by nonaqueous titration or gravimetry, and ethotoin is assayed by titrimetric determination of nitrogen.

Even within the same monograph, the methods sometimes differ for the content uniformity and drug content (assay) tests. This situation underscores the need to develop more specific methods, incorporating a single technique and unified approach with the eventual aim of an autosampling setup for the analysis of numerous anticonvulsant drugs in dosage forms. GLC appears to be the method of choice for such analyses because of its resolving power, high sensitivity and specificity, and minimum time requirement.

Many GLC methods (4–16) are concerned with analyses of individual anticonvulsants in biological media only. Recent efforts (17–19) were directed toward establishing a universal GLC system for multiple and reproducible analyses applicable to several antiepileptic drugs. This trend has gained impetus because of economic factors and because the more extensive use of these drugs has increased the necessity of monitoring blood levels on a routine basis.

In this work, a group analytical procedural concept was developed for several anticonvulsant (and one sedative) drugs of similar structure in various dosage forms.

EXPERIMENTAL

Materials and Solutions—The following were used: ethotoin[1], glutethimide[2], mephenytoin[3], methsuximide[2], phensuximide[2], phenytoin[2], phenytoin sodium[4], primidone[2], *N,O*-bis(trimethylsilyl)acetamide[5], and ethyl acetate[6] (ACS reagent grade). The structural integrities of the standard ethotoin, mephenytoin, and phenytoin sodium substances were verified by NMR spectroscopy, and the purities of the compounds were confirmed by TLC.

The internal standard solution was diphenyl phthalate[7] in spectrograde dimethylformamide[8], accurately weighed to contain about 15 mg/ml. Diphenyl phthalate was recrystallized from benzene–cyclohexane (activated charcoal) to give white plates, mp 70–71°.

Sample Preparation: Response Factor Calibration Solutions—*Ethotoin, Glutethimide, Mephenytoin, Methsuximide, and Phensuximide*—For each drug, five separate samples, ranging from about 10 to 15 mg, were weighed accurately into 10-ml flasks and dissolved in ethyl acetate (5 ml). The internal standard solution (1.00 ml) was dispensed into each flask from a 5-ml microburet graduated in 0.01 ml.

Phenytoin and Phenytoin Sodium—For each, five separate samples, ranging from about 10 to 15 mg, were weighed accurately into 30-ml separators and dissolved in 0.1 *N* NaOH (3 ml). After acidification with concentrated hydrochloric acid, the solution was extracted for free phenytoin with 10-, 5-, and 5-ml portions of ethyl acetate; the combined extracts were transferred to a 25-ml flask with a septum seal screw cap[5].

The solvent was removed at 60° under a stream of pure dry nitrogen on a heating block module[5]. The residue in the flask was dissolved in spectrograde dimethylformamide (5 ml) and then treated with *N,O*-bis(trimethylsilyl)acetamide (1.5 ml). The internal standard solution (1.00 ml) was dispensed into the flask, and the mixture was shaken and allowed to stand at ambient temperature for 15 min.

Primidone—Five separate samples, ranging from about 10 to 15 mg, were weighed accurately into 10-ml flasks; each sample was dissolved in spectrograde dimethylformamide (5 ml) and then treated with *N,O*-bis(trimethylsilyl)acetamide (1.5 ml). The internal standard solution (1.00 ml) was dispensed into each flask; each mixture was shaken and heated to 60° on a heating block module for 30 min.

Sample Preparation: Commercial Dosage Forms—*Ethotoin, Glutethimide, Mephenytoin, Methsuximide, and Phensuximide*—Ten capsules were emptied, and their contents were weighed and thoroughly mixed. Ten tablets were selected at random, weighed, and finely powdered. An amount of powder equivalent to about 8–12 mg of drug was weighed accurately into a 10-ml flask and shaken with ethyl acetate (5 ml). The internal standard solution (1.00 ml) was dispensed into the flask from a 5-ml microburet graduated in 0.01 ml.

Samples of oral suspensions (equivalent to 600 mg of drug) were pipetted into a 50-ml volumetric flask and then made up to volume with water. A 1-ml aliquot of this solution was pipetted into a 30-ml separator and extracted successively with 3 × 5-ml portions of ethyl acetate. The combined organic extracts were reduced to about 5 ml under a stream of pure dry nitrogen. The internal standard (1.00 ml) was dispensed into the flasks.

Phenytoin and Phenytoin Sodium—Ten capsules were emptied, and their contents were weighed and thoroughly mixed. An amount of powder (or solution) weighed or measured to be equivalent to about 10–15 mg of labeled active ingredient was transferred to a 30-ml separator and then treated exactly as described for phenytoin and phenytoin sodium response factor calibration solutions.

Primidone—Ten tablets were selected at random, weighed, and finely powdered. An amount of powdered tablet equivalent to about 10–15 mg of drug was weighed accurately into a 10-ml flask, shaken with 5 ml of spectrograde dimethylformamide, and then treated exactly as described for primidone response factor calibration solutions.

GLC—Two microliters of solution (or supernate) was injected into a gas chromatograph[9] (flame-ionization detector) fitted with a U-shaped glass column [1.82 m (6 ft) × 6.4 mm o.d. (4.0 mm i.d.)] packed with 5% OV-101[5] on 100–120-mesh Chromosorb 750[10]. The column was preconditioned at 265° for 18 hr.

Temperature conditions were: column, 150° (5 min) and then programmed to 240° at 3°/min; injector port, 250°; and detector, 250°. Gas flows were: nitrogen, 70 ml/min; hydrogen, 40 ml/min; and air, 380 ml/min.

The detector signal was fed to an electronic integrator[11] with an input signal range capacity of 0–1 v. The gas chromatograph input attenuation was 1×10^{-11} amp/mv, and the integrator attenuation was ×16.

RESULTS AND DISCUSSION

In the described GLC system, only phenytoin and primidone, of the seven drugs examined, required derivatization with *N,O*-bis(trimethylsilyl)acetamide to elute as single sharp peaks. The other compounds do not possess hydrogen atoms of sufficient activity to cause tailing through hydrogen bond adsorptive interactions between the drug and stationary phase. Glutethimide is an apparent anomaly in this respect since, by reason of its imide structure, it would be expected to exhibit chromatographic behavior similar to that of phenytoin.

The relevant GLC data for the drugs investigated are given in Table I. The same methylsilicone column packing material, GLC instrumental

[1] Abbott Laboratories Ltd., Montreal, Quebec, Canada.
[2] United States Pharmacopeia-National Formulary Reference Standard, Rockville, Md.
[3] Aldrich Chemical Co., Milwaukee, Wis.
[4] Parke-Davis & Co., Brockville, Ontario, Canada.
[5] Pierce Chemical Co., Rockford, Ill.
[6] Caledon Laboratories Ltd., Georgetown, Ontario, Canada.
[7] Eastman Kodak Co., Rochester, N.Y.
[8] J. T. Baker Chemical Co., Phillipsburg, N/J.
[9] Bendix series 2500.
[10] Applied Science Laboratories, State College, Pa.
[11] Hewlett-Packard series 3380A reporting integrator.

Table II—GLC *versus* Compendial Assay Results for Commercial Anticonvulsant Drug Dosage Forms

Sample	Labeled Active Ingredient	Dosage Form	Dosage Level, mg/unit	Manufacturer	Percent of Label Claim	
					GLC	Compendial
1	Ethotoin	Tablets	500	O	108.2	107.5[a]
					108.3	108.3
2	Glutethimide	Capsules	500	P	97.9	98.8[b]
					98.7	100.0
3	Glutethimide	Tablets	500	P	101.7	101.2[b]
					99.6	100.9
4	Glutethimide	Tablets	250	P	99.8	96.7[b]
					100.2	96.8
5	Mephenytoin	Tablets	100	Q	101.1	101.3[b]
					100.1	102.0
6	Methsuximide	Capsules	300	R	98.1	97.9[b]
					98.8	96.4
7	Phensuximide	Capsules	500	R	100.0	100.7[b]
					99.9	98.5
8	Phensuximide	Oral suspension	300[c]	R	97.4	99.2[b]
					99.1	97.9
9	Phenytoin	Oral suspension	125[c]	R	100.2	101.9[b]
					100.8	99.2
10	Phenytoin sodium	Capsules	100	R	103.3	103.2[d]
					103.6	101.8
11	Phenytoin sodium	Capsules	30	R	102.0	100.5[d]
					103.1	100.8
12	Phenytoin sodium	Capsules	100	S	99.2	96.6[d]
					98.3	95.7
13	Phenytoin sodium	Capsules	30	S	107.5	105.6[d]
					105.9	104.4
14	Phenytoin sodium	Injection	250[c]	T	105.0	107.1[d]
					104.8	108.1
15	Primidone	Tablets	250	U	100.6	100.4[d]
					99.5	100.4
16	Primidone	Tablets	250	U	101.9	101.5[d]
					101.6	100.8
17	Primidone	Tablets	125	U	102.1	100.4[d]
					100.4	101.1
18	Primidone	Tablets	125	U	100.0	102.1[d]
					101.2	104.5
19	Primidone	Tablets	250	V	100.6	101.7[d]
					103.3	101.6

[a] BP (1973) procedure. [b] NF XIV procedure. [c] In milligrams per 5 ml. [d] USP XIX procedure.

settings, temperature, and gas flow conditions were suitable for the analysis of all seven drugs. The method was designed to use these constant experimental conditions and instrumental parameters to be compatible eventually with an automated analysis.

Each relative response factor represents the average of five determinations at varying weight ratios of compound to internal standard. The values in all cases were calculated and expressed as weight/area in terms of the free drug. Thus, phenytoin and primidone, in agreement with theoretical expectations, gave appreciably lower values since trimethylsilylation confers a significant increase in molecular weight and also results in a larger number of ions being formed at the electrode gap of the flame detector. The accompanying net increase in current manifests itself by a proportional increase in the number of integrator area counts per unit weight of free drug. The low coefficients of variation in response factor values readily attest to the precision of the method over a relatively wide linear range.

In Table II, the percentage of label claim values obtained when the GLC technique was applied to the analysis of commercial formulations of the seven drugs from various manufacturers are compared to those obtained with the pharmacopeial procedures. The good agreement between the two sets of results for each of the 19 samples examined demonstrates the reproducibility and feasibility of the GLC procedure as a reliable monitor of drug content in both solid and liquid dosage forms. The high solubility of primidone in dimethylformamide and of the other six drugs in ethyl acetate permitted ready quantitative extraction of the drugs into the organic solvent.

Complete extraction was confirmed by subjecting the residual aqueous layers and further solvent washings of the insoluble portions of the powders to TLC [layer, fluorescent silica gel (0.25 mm); developing system, chloroform–acetone (9:1); and visualization, shortwave UV light]. In no case was any spot corresponding in R_f value to that of the authentic active ingredient observed. Experimentally determined R_f values were: ethotoin, 0.28; glutethimide, 0.40; mephenytoin, 0.35; phensuximide, 0.44; methsuximide, 0.51; phenytoin, 0.17; and primidone, 0.19.

Gas chromatograms of ethotoin, mephenytoin, methsuximide, phensuximide, glutethimide, phenytoin, and primidone extracted from various types of commercial formulations, treated as described, and diluted with the internal standard solution gave no signals from excipient materials or potential drug impurities. For phenytoin, several congeneric compounds (20) were examined from a qualitative standpoint to establish whether they would interfere with the GLC analysis if present in commercial dosage forms as carryovers during drug synthesis. The compounds examined (after trimethylsilylation) and their retention times relative to diphenyl phthalate were: benzophenone, 0.198; benzil, 0.349; ethyl benzilate, 0.419; and benzilic acid, 0.462. There appears to be little doubt that the associated intermediates of the other six drugs would exhibit analogous differences in elution characteristics to those of the parent drugs because of distinct structural variations, particularly in functional groups.

If desired for any particular analysis, it should be possible to reduce the analytical time considerably by utilizing one of the foregoing drugs as the internal standard.

REFERENCES

(1) "The United States Pharmacopeia," 19th rev., Mack Publishing Co., Easton, Pa., 1975, pp. 379–381, 405, 406.

(2) "British Pharmacopoeia, 1973," Her Majesty's Stationery Office, London, England, 1973, pp. 197, 367, 383.

(3) "The National Formulary," 14th ed., Mack Publishing Co., Easton, Pa., 1975, pp. 298, 299, 409, 458, 570, 571, 574.

(4) K. Sabih and K. Sabih, *Anal. Chem.*, **41**, 1452 (1969).

(5) M. A. Evanson, P. Jones, and B. Darcey, *Clin. Chem.*, **16**, 107 (1970).

(6) T. Chang and A. J. Glazko, *J. Lab. Clin. Med.*, **75**, 145 (1970).

(7) H. J. Kupferberg, *Clin. Chim. Acta*, **29**, 283 (1970).

(8) J. MacGee, *Anal. Chem.*, **42**, 421 (1970).

(9) J. C. Van Meter, H. S. Buckmaster, and L. L. Shelley, *Clin. Chem.*, **16**, 135 (1970).

(10) I. A. Muni, C. H. Altshuler, and J. C. Neicheril, *J. Pharm. Sci.*, **62**, 1820 (1973).
(11) R. J. Perchalski, K. N. Scott, B. J. Wilder, and R. H. Hammer, *ibid.*, **62**, 1735 (1973).
(12) E. A. Fiereck and N. W. Tietz, *Clin. Chem.*, **17**, 1024 (1971).
(13) D. Sampson, I. Harasymiv, and W. J. Hensley, *ibid.*, **17**, 382 (1971).
(14) A. R. Hansen and L. J. Fischler, *ibid.*, **20**, 236 (1974).
(15) N. E. Larsen and J. Naestoft, *J. Chromatogr.*, **92**, 157 (1974).
(16) M. W. Couch, M. Greer, and C. M. Williams, *ibid.*, **87**, 559 (1973).
(17) J. Bonitati, *Clin. Chem.*, **22**, 341 (1976).
(18) R. E. Beam, *Am. J. Med. Technol.*, **40**, 211 (1974).
(19) D. P. Ritz and C. G. Warren, *Clin. Toxicol.*, **8**, 311 (1975).
(20) F. F. Matsui and S. J. Smith, *Z. Anal. Chem.*, **275**, 365 (1975).

ACKNOWLEDGMENTS

The authors are grateful to the following Health Protection Branch laboratories for performing the compendial assays on the commercial dosage forms: Atlantic Regional Laboratories, Halifax, Nova Scotia, for the glutethimide samples; Ontario Regional Laboratories, Toronto, Ontario, for the phenytoin sodium samples; and Central Regional Laboratories, Winnipeg, Manitoba, for the primidone samples.

Synthesis of Spirofluorenes of Biological Interest

MAGID A. ABOU-GHARBIA, T. T. SU, and MADELEINE M. JOULLIÉ ˣ

Received August 29, 1977, from the *Department of Chemistry, University of Pennsylvania, Philadelphia, PA 19104.* Accepted for publication October 25, 1977.

Abstract □ 1′-Substituted spiro[fluorene-9,3′-pyrrolidine-2′,5′-diones], 1′,1‴ - (1,4-piperazinediyldimethylene)bis[spiro[fluorene-9,3′-pyrrolidine-2′,5′-dione]], and 1′-arylspiro[fluorene-9,3′-pyrrolidines] were synthesized from spiro[fluorene-9,3′-tetrahydrofuran-2′,5′-dione]. The rat passive cutaneous anaphylaxis assay showed that one compound possessed slight antiallergic activity. Synthesis of 3-substituted 1-aryl-4-oxospiro[azetidine-2,9′-fluorenes] and 1,1″-*p*-phenylenebis[4-oxospiro[azetidine-2,9′-fluorenes]] was achieved *via* the reaction of appropriate *N*-fluorenylideneanilines with *tert*-butylcyanoketene and cyclopentamethyleneketene, respectively.

Keyphrases □ Spirofluorenes, various—synthesized, evaluated for antiallergic activity □ Fluorene spiro compounds, various—synthesized, evaluated for antiallergic activity □ Antiallergic activity—various spirofluorenes evaluated □ Structure–activity relationships—various spirofluorenes evaluated for antiallergic activity

The fluorene nucleus is a structural unit in several biologically active drugs such as I, which inhibits platelet aggregation (1), or tilorone hydrochloride (II), which exhibits antiviral activity (2).

The marked growth inhibitory effects of certain azaspiranes such as III were first observed in 1963 (3). Many azaspiranes and azaspirodiones have shown a wide span of biological activity (4, 5). These observations and the interest in II and related systems (6–8) prompted the incorporation of the fluorene moiety into selected azaspirodiones and azaspiranes to examine the effect of structural changes on biological activity.

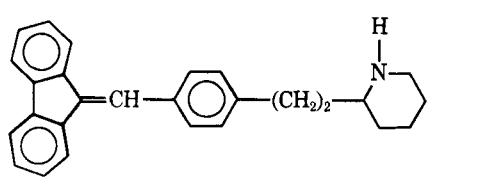

I

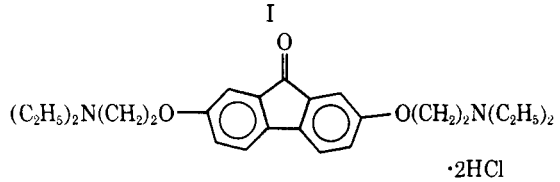

II

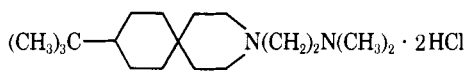

III

DISCUSSION

Spiro[fluorenepyrrolidinediones] VI*a*–VI*e* (Table I) were prepared *via* the reaction of spiro[fluorene-9,3′-tetrahydrofuran-2′,5′-dione] (IV) with different primary amines, followed by cyclization of the intermediate amic acids with acetyl chloride as the dehydrating agent (Scheme I). Attempts to cyclize the intermediate amic acids thermally led to decarboxylation (9).

Spiro[fluorenepyrrolidinediones] VII*a*–VII*c* (Table I) were synthesized *via* the reaction of secondary amines with spiro[fluorene-9,3′-pyrrolidine-2′,5′-dione] (V) and formaldehyde under Mannich conditions.

Compound V was prepared by the ammonolysis of IV and cyclization of the intermediate with acetyl chloride (10).

Alkylation of the potassium salt of V with 2-diethylaminoethyl chloride hydrochloride afforded VIII (Table I) (Scheme I).

Spiro[fluorenepyrrolidines] IX*a* and IX*b* (Table II) were prepared by the reduction of the corresponding diones with lithium aluminum hydride in dry ether for 2 hr [a similar procedure was reported to take 40 hr (11)]. Since the study of azaspiranes revealed that the activity of these compounds is due to the azaspiranyl moiety (12), it was felt that compounds containing two azaspiranyl functions could be of interest to elucidate the relationship between structure and activity among central nervous system (CNS) drugs. Accordingly, the bis[spiro[fluorenepyrrolidinedione]] X (Table II) was prepared from IV, formaldehyde, and piperazine hexahydrate in the presence of *p*-toluenesulfonic acid as the catalyst.

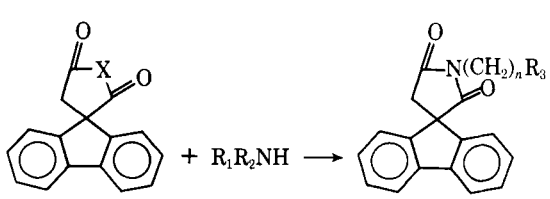

IV: X = O
V: X = NH

VI: *n* = 0
VII: *n* = 1
VIII: *n* = 2

Scheme I

0022-3549/78/0700/0953$01.00/0
© 1978, American Pharmaceutical Association

(10) I. A. Muni, C. H. Altshuler, and J. C. Neicheril, *J. Pharm. Sci.*, **62**, 1820 (1973).
(11) R. J. Perchalski, K. N. Scott, B. J. Wilder, and R. H. Hammer, *ibid.*, **62**, 1735 (1973).
(12) E. A. Fiereck and N. W. Tietz, *Clin. Chem.*, **17**, 1024 (1971).
(13) D. Sampson, I. Harasymiv, and W. J. Hensley, *ibid.*, **17**, 382 (1971).
(14) A. R. Hansen and L. J. Fischler, *ibid.*, **20**, 236 (1974).
(15) N. E. Larsen and J. Naestoft, *J. Chromatogr.*, **92**, 157 (1974).
(16) M. W. Couch, M. Greer, and C. M. Williams, *ibid.*, **87**, 559 (1973).
(17) J. Bonitati, *Clin. Chem.*, **22**, 341 (1976).
(18) R. E. Beam, *Am. J. Med. Technol.*, **40**, 211 (1974).
(19) D. P. Ritz and C. G. Warren, *Clin. Toxicol.*, **8**, 311 (1975).
(20) F. F. Matsui and S. J. Smith, *Z. Anal. Chem.*, **275**, 365 (1975).

ACKNOWLEDGMENTS

The authors are grateful to the following Health Protection Branch laboratories for performing the compendial assays on the commercial dosage forms: Atlantic Regional Laboratories, Halifax, Nova Scotia, for the glutethimide samples; Ontario Regional Laboratories, Toronto, Ontario, for the phenytoin sodium samples; and Central Regional Laboratories, Winnipeg, Manitoba, for the primidone samples.

Synthesis of Spirofluorenes of Biological Interest

MAGID A. ABOU-GHARBIA, T. T. SU, and MADELEINE M. JOULLIÉ ˣ

Received August 29, 1977, from the *Department of Chemistry, University of Pennsylvania, Philadelphia, PA 19104.* Accepted for publication October 25, 1977.

Abstract □ 1′-Substituted spiro[fluorene-9,3′-pyrrolidine-2′,5′-diones], 1′,1‴ - (1,4-piperazinediyldimethylene)bis[spiro[fluorene-9,3′-pyrrolidine-2′,5′-dione]], and 1′-arylspiro[fluorene-9,3′-pyrrolidines] were synthesized from spiro[fluorene-9,3′-tetrahydrofuran-2′,5′-dione]. The rat passive cutaneous anaphylaxis assay showed that one compound possessed slight antiallergic activity. Synthesis of 3-substituted 1-aryl-4-oxospiro[azetidine-2,9′-fluorenes] and 1,1″-*p*-phenylenebis[4-oxospiro[azetidine-2,9′-fluorenes]] was achieved *via* the reaction of appropriate *N*-fluorenylideneanilines with *tert*-butylcyanoketene and cyclopentamethyleneketene, respectively.

Keyphrases □ Spirofluorenes, various—synthesized, evaluated for antiallergic activity □ Fluorene spiro compounds, various—synthesized, evaluated for antiallergic activity □ Antiallergic activity—various spirofluorenes evaluated □ Structure–activity relationships—various spirofluorenes evaluated for antiallergic activity

The fluorene nucleus is a structural unit in several biologically active drugs such as I, which inhibits platelet aggregation (1), or tilorone hydrochloride (II), which exhibits antiviral activity (2).

The marked growth inhibitory effects of certain azaspiranes such as III were first observed in 1963 (3). Many azaspiranes and azaspirodiones have shown a wide span of biological activity (4, 5). These observations and the interest in II and related systems (6–8) prompted the incorporation of the fluorene moiety into selected azaspirodiones and azaspiranes to examine the effect of structural changes on biological activity.

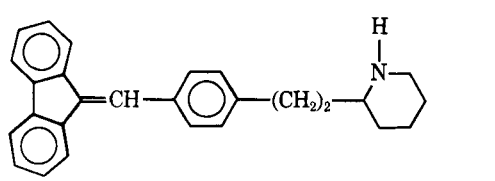

I

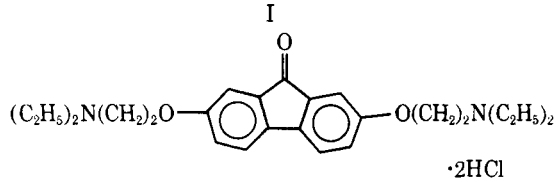

II

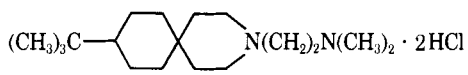

III

DISCUSSION

Spiro[fluorenepyrrolidinediones] VI*a*–VI*e* (Table I) were prepared *via* the reaction of spiro[fluorene-9,3′-tetrahydrofuran-2′,5′-dione] (IV) with different primary amines, followed by cyclization of the intermediate amic acids with acetyl chloride as the dehydrating agent (Scheme I). Attempts to cyclize the intermediate amic acids thermally led to decarboxylation (9).

Spiro[fluorenepyrrolidinediones] VII*a*–VII*c* (Table I) were synthesized *via* the reaction of secondary amines with spiro[fluorene-9,3′-pyrrolidine-2′,5′-dione] (V) and formaldehyde under Mannich conditions.

Compound V was prepared by the ammonolysis of IV and cyclization of the intermediate with acetyl chloride (10).

Alkylation of the potassium salt of V with 2-diethylaminoethyl chloride hydrochloride afforded VIII (Table I) (Scheme I).

Spiro[fluorenepyrrolidines] IX*a* and IX*b* (Table II) were prepared by the reduction of the corresponding diones with lithium aluminum hydride in dry ether for 2 hr [a similar procedure was reported to take 40 hr (11)]. Since the study of azaspiranes revealed that the activity of these compounds is due to the azaspiranyl moiety (12), it was felt that compounds containing two azaspiranyl functions could be of interest to elucidate the relationship between structure and activity among central nervous system (CNS) drugs. Accordingly, the bis[spiro[fluorenepyrrolidinedione]] X (Table II) was prepared from IV, formaldehyde, and piperazine hexahydrate in the presence of *p*-toluenesulfonic acid as the catalyst.

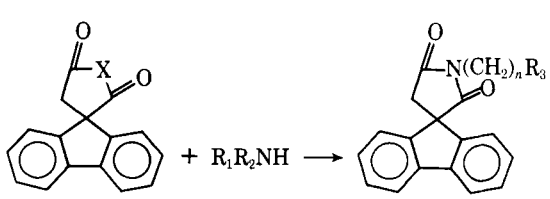

IV: X = O
V: X = NH

VI: *n* = 0
VII: *n* = 1
VIII: *n* = 2

Scheme I

0022-3549/78/0700/0953$01.00/0
© 1978, American Pharmaceutical Association

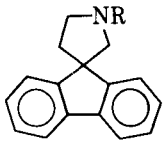

IX*a*: R = 4-$CH_3C_6H_4$
IX*b*: R = 4-FC_6H_4

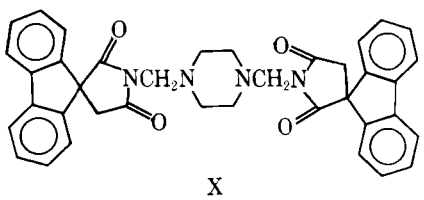

X

Previous interest in ketene chemistry (13–16) led to the preparation of several oxospiro[azetidinefluorenes] (Table III). 1-Aryl-[3-*tert*-butyl-4-oxospiro[azetidine-2,9′-fluorene]-3-carbonitriles (XII*a* and XII*b*) and the corresponding 3-cyclopentamethylene derivative (XII*c*) were synthesized *via* the reaction of *tert*-butylcyanoketene and cyclopentamethyleneketene with *N*-fluorenylidineanilines (XI*a*–XI*c*) (17) (Scheme II).

Since X was the first example of a bis[spiro[fluorenepyrrolidinedione]], some bis[oxospiro[azetidinefluorenes]] (Table III) also were prepared.

1,1″ - *p*-Phenylenebis[3-*tert*-butyl-4-oxospiro[azetidine - 2,9′-fluorene]]-3-carbonitrile (XIII*a*) and the 3-cyclopentamethylene derivative (XIII*b*) were synthesized by the reaction of *N,N*-difluorenylidene-*p*-phenylenediamine (XI*d*) with *tert*-butylcyanoketene and cyclopentamethyleneketene, respectively (Scheme II).

Compounds VI*a*–VI*c*, VII*a*, and VII*b* were tested for antiallergic activity *in vivo* by the rat passive cutaneous anaphylaxis method. Commercial cromolyn sodium[1] was used as the standard, and IgE antibody was used as the sensitizer (subcutaneously injected). Only VI*b* at 5 mg/kg showed antiallergic activity.

From the limited number of compounds tested, the following structure–activity relationship was noted for spiro[fluorenepyrrolidines]:

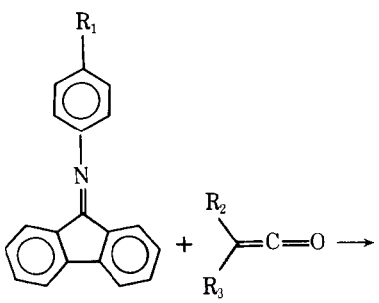

XI*a*: R_1 = Cl
XI*b*: R_1 = CF_3
XI*c*: R_1 = H

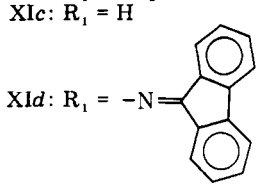

XI*d*: R_1 = –N=

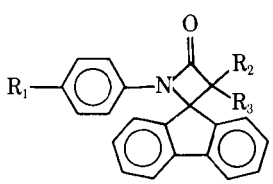

XII*a*: R_1 = Cl, R_2 = $(CH_3)_3C$, R_3 = CN
XII*b*: R_1 = CF_3, R_2 = $(CH_3)_3C$, R_3 = CN
XII*c*: R_1 = H, R_2 = R_3 = $-(CH_2)_5-$

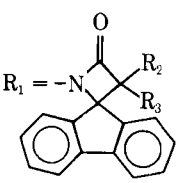

XIII*a*: R_1 = –N, R_2 = $(CH_3)_3C$, R_3 = CN

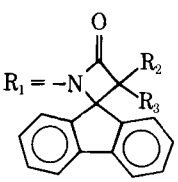

XIII*b*: R_1 = –N, R_2, R_3 = $-(CH_2)_5-$

Scheme II

maximum antiallergic activity is obtained when n = 0 and R is an electron-withdrawing group in the $>N(CH_2)_nR$ moiety.

The other compounds are still under biological testing for possible CNS or anticancer activity.

EXPERIMENTAL

IR spectra were obtained as potassium bromide disks. PMR spectra were recorded using tetramethylsilane as an internal standard. All chemical shifts are given in the δ scale. Mass spectra were determined with an ionizing potential of 30 ev.

Spiro[fluorene-9,3′(2′*H*)-furan-2′,5′(4′*H*)-dione] (IV)—This compound was prepared as the key starting material by condensing fluorenone with ethyl cyanoacetate, using ammonium acetate as the catalyst. Addition of hydrogen cyanide to the fluorenylidineethyl cyanoacetate, followed by hydrolysis to the diacid and cyclization with acetyl chloride, afforded the corresponding cyclic anhydride in a 90% yield (10, 18).

1′-Substituted Spiro[fluorene-9,3′-pyrrolidine]-2′,5′-diones] (VI*a*–VI*e*)—To a hot benzene solution of IV (0.1 mole) was added a solution of the appropriate primary amine (0.1 mole) in benzene. The mixture was refluxed for 1 hr, and the temperature was raised slowly until all of the benzene was removed. Acetyl chloride (50 ml) was added to the remaining solid, and the mixture was refluxed for 2 hr. Excess acetyl chloride was removed under reduced pressure, and the residue was recrystallized from absolute ethanol (Table I).

1′-Substituted Methylspiro[fluorene-9,3′-pyrrolidine]-2′,5′-diones] (VII*a*–VII*c*)—Imide V was prepared by ammonolysis of IV, followed by cyclization of the intermediate amic acid with acetyl chloride (10). Compound V (0.06 mole) was mixed thoroughly with the appropriate secondary amine (0.2 mole), and formaldehyde (1 ml) was added with vigorous stirring.

The white solid that formed was removed by filtration and recrystallized (Table I).

1′-Diethylaminoethylspiro[fluorene-9,3′-pyrrolidine-2′,5′-dione] (VIII)—To a solution of 1.6 g (0.003 mole) of V in 20 ml of *tert*-butyl alcohol was added 1.5 g (0.012 mole) of potassium *tert*-butoxide, and the mixture was refluxed for 5 min. The solvent was removed by distillation, and 1.12 g (0.003 mole) of 2-diethylaminoethyl chloride hydrochloride in 40 ml of dry dimethylformamide was added to the residue.

The mixture was heated to 140–160° for 2 hr, cooled, and poured into ice water with stirring. The solid that formed was separated and recrystallized (Table I).

1′-Arylspiro[fluorene-9,3′-pyrrolidines] (IX*a* and IX*b*)—Lithium aluminum hydride (0.2 g) was dissolved in 30 ml of dry ether, and to this solution was added the appropriate spiro[fluorenepyrrolidinedione] (0.002 mole) over 15 min. The solution was refluxed for 2 hr and then cooled, and the excess lithium aluminum hydride was destroyed. The solution was filtered, washed with water, and dried with anhydrous sodium sulfate. Removal of the solvent yielded the desired azaspiranes (Table II).

1′,1‴- (1,4-Piperazinediyldimethylene)bis[spiro[fluorene-9,3′-pyrrolidine-2′,5′-dione]] (X)—Imide V (1.4 g, 0.006 mole), piperazine hexahydrate (0.6 g, 0.003 mole), and 0.5 ml of formaldehyde were mixed thoroughly. Benzene (30 ml) was added to the solid that formed, and the mixture was refluxed in the presence of a trace of *p*-toluenesulfonic acid for 2 hr. The cooled solution was filtered, and the residue was washed first with a dilute sodium carbonate solution and then with water (Table II).

***N*-Fluorenylidine-*p*-trifluoromethylaniline (XI*b*)**—Boron trifluoride etherate (1.5 ml) was added to a solution of 9 g (0.05 mole) of fluorenone and 12 g (0.08 mole) of freshly distilled *p*-trifluoromethylaniline in 100 ml of chloroform and a few milliliters of ethanol. The solution was refluxed for 15 min, concentrated to 25 ml, and cooled. The resulting yellow needles (15.5 g, 96.2% yield) were recrystallized from chloroform–ethanol (1:1), mp 146–148°.

Anal.—Calc. for $C_{20}H_{12}F_3N$: C, 74.29; H, 3.74; N, 4.33. Found: C, 74.02; H, 3.83; N, 4.30.

3-Substituted 1′-Aryl-4-oxospiro[azetidine-2,9′-fluorenes] (XII*a*–XII*c*) and 1′,1‴-*p*-Phenylenebis[4-oxospiro[azetidine-2,9′-fluorenes]] (XIII*a* and XIII*b*)—Compounds XII*a*, XII*b*, and XIII*a* were prepared by adding the appropriate imine (0.005 mole) to a solution of 2,5-diazido-3,6-bis(*tert*-butyl)-1,4-benzoquinone (1.4 g, 0.005 mole) in 30 ml of dry toluene (19).

The solution was refluxed for 12 hr, allowed to cool, and filtered. The toluene was evaporated under reduced pressure, and the combined solids were recrystallized from appropriate solvents (Table III). Compounds XII*c* and XIII*b* were prepared similarly from the appropriate imine and

[1] Intal R.

Table I—1′-Substituted Spiro[fluorene-9,3′-pyrrolidine-2′,5′-diones]

Compound	R_3	Melting Point[a]	Yield[b], %	IR, ν C=O	NMR ($CDCl_3$), δ	Formula	Analysis[c,d], %	Calc.	Found
VI*a*	4-$CH_3C_6H_4$	190–192°	80	1730, 1700	2.35 (s, 3H), 3.32 (s, 2H), 7–7.3 (m, 12H)	$C_{23}H_{17}NO_2$	C	81.39	81.41
							H	5.05	5.22
							N	4.12	3.97
VI*b*	4-FC_6H_4	204–205°	78	1740, 1700	3.25 (s, 2H), 7.3–7.7 (m, 12H)	$C_{22}H_{14}FNO_2$	C	76.95	77.03
							H	4.10	4.40
							F	5.53	5.47
							N	4.07	3.99
VI*c*	3,4,5-$(OCH_3)_3C_6H_2$	228–229°	79	1770, 1710	3.37 (s, 2H), 3.85 (s, 9H), 6.65 (s, 2H), 7.25–7.9 (m, 8H)	$C_{25}H_{21}NO_5$	C	72.28	71.99
							H	5.10	4.88
							N	3.37	3.21
VI*d*		201–203°	63	1760, 1700	3.4 (s, 2H), 7.25–7.85 (m, 12H)	$C_{21}H_{14}N_2O_2$	C	77.29	77.46
							H	4.32	4.36
							N	8.58	8.29
VI*e*	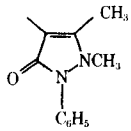	254–256°	83	1730, 1705	—[e]	$C_{26}H_{21}N_3O_3$	C	74.46	74.61
							H	4.86	5.10
							N	9.64	9.62
VII*a*		171–173°	89	1750, 1700	2.7 (t, 4H), 3.25 (s, 2H), 3.8 (t, 4H), 4.6 (s, 2H), 7.3–7.9 (m, 8H)	$C_{21}H_{20}N_2O_3$	C	72.40	72.61
							H	5.79	5.84
							N	8.04	7.92
VII*b*		178–180°	84	1750, 1700	1.55 (broad, 6H), 2.7 (broad, 4H), 3.26 (s, 2H), 4.7 (s, 2H), 7.3–7.7 (m, 8H)	$C_{22}H_{22}N_2O_2$	C	76.28	76.40
							H	6.40	6.48
							N	8.09	7.88
VII*c*		200–202°	66	1750, 1700	1.6 (broad, 4H), 2.6 (broad, 4H), 3.25 (s, 2H), 4.6 (s, 2H), 7.3–7.7 (m, 8H)	$C_{21}H_{20}N_2O_2$	C	75.88	75.99
							H	6.06	5.95
							N	8.43	8.68
VIII	$-N(C_2H_5)_2$	107–109°	53	1760, 1700	0.85–1.1 (t, 6H), 2.4–2.7 (q, 4H), 2.6–2.85 (t, 2H), 3.6–3.9 (t, 2H), 3.25 (s, 2H), 7.35–7.85 (m, 8H)	$C_{22}H_{24}N_2O_2$	C	75.83	75.80
							H	6.94	6.78
							N	8.04	8.05

[a] Melting points are uncorrected. [b] Yield of analytically pure material. [c] Analytical results are within ±0.4% of calculated values. [d] Compounds VI*a*–VI*c* were recrystallized from absolute ethanol, VII*a*–VII*c* were recrystallized from petroleum ether (bp 30–60°)–benzene (1:1), and VIII was recrystallized from petroleum ether (bp 30–60°). [e] Because of the insolubility of VI*e* in suitable solvents, a satisfactory NMR spectrum could not be obtained; *m/e* 435 (M^+).

Table II—Spiro[fluorenepyrrolidines] and Bis[spiro(fluorenepyrrolidinedione)]

Compound	Melting Point[a]	Yield[b], %	IR, ν C=O	NMR ($CDCl_3$), δ	Formula	Analysis[c,d], %	Calc.	Found
IX*a*	179–181°	82	—	2.25 (s, 3H), 2.49–2.25 (t, 2H), 3.9–3.65 (t, 2H), 3.65 (s, 2H), 6.5–7.85 (m, 12H)	$C_{23}H_{21}N$	C	88.71	88.49
						H	6.80	7.03
						N	4.50	4.48
IX*b*	175–177°	85	—	2.27–2.55 (t, 2H), 3.6 (s, 2H), 3.6–3.9 (t, 2H), 6.4–7.9 (m, 12H)	$C_{22}H_{18}FN$	C	83.78	83.52
						H	5.75	6.01
						F	6.02	6.29
						N	4.44	4.23
X	272°	88	1750, 1700	—[e]	$C_{38}H_{32}N_4O_4$	C	74.97	74.68
						H	5.30	5.48
						N	9.20	9.00

[a] Melting points are uncorrected. [b] Yield of analytically pure material. [c] Analytical results are within ±0.4% of calculated values. [d] Compounds IX*a* and IX*b* were isolated analytically pure and not recrystallized. Compound X was recrystallized from dimethyl sulfoxide–benzene (2:1). [e] Because of the insolubility of X in suitable solvents, a satisfactory NMR spectrum could not be obtained; *m/e* 608 (M^+).

Table III—3-Substituted 1-Aryl-4-oxospiro[azetidine-2,9′-fluorenes] and 1,1″-*p*-Phenylenebis[4-oxospiro[azetidine-2,9′-fluorenes]]

Compound	Melting Point[a]	Yield[b], %	IR, ν C=O	NMR ($CDCl_3$), δ	Formula	Analysis[c,d], %	Calc.	Found
XII*a*	188–190°	79	1750	1.15 (s, 9H), 6.85–7.95 (m, 12H)	$C_{26}H_{21}ClN_2O$	C	75.62	75.56
						H	5.12	5.31
						Cl	8.58	8.66
						N	6.78	6.77
XII*b*	143–145°	80	1770	1.17 (s, 9H), 6.95–7.9 (m, 12H)	$C_{27}H_{21}F_3N_2O$	C	72.63	72.42
						H	4.74	4.66
						N	6.27	6.19
XII*c*	195–196°	58	1750	1.15–1.55 (m, 6H), 1.50–1.92 (m, 4H), 6.95–7.05 (m, 5H), 7.30–7.60 (m, 8H)	$C_{26}H_{23}NO$	C	85.45	85.34
						H	6.34	6.25
						N	3.83	3.76
XIII*a*	267–268°	76	1800	0.8 (s, 18H), 6.95–7.55 (m, 20H)[e]	$C_{46}H_{38}N_4O_2$	C	81.38	81.44
						H	5.64	5.77
						N	8.25	8.20
XIII*b*	300°	69	1750	0.30–1.95 (m, 20H), 6.69 (s, 4H), 7.05–7.50 (m, 12H), 7.60–7.92 (m, 4H)	$C_{46}H_{40}N_2O_2$	C	84.63	84.40
						H	6.18	6.01
						N	4.29	4.35

[a] Melting points are uncorrected. [b] Yield of analytically pure material. [c] Analytical results are within ±0.4% of calculated values. [d] Compounds XII*a* and XII*b* were recrystallized from aqueous ethanol, XII*c* was recrystallized from methanol, XIII*a* was recrystallized from acetone, and XIII*b* was recrystallized from chloroform–acetone (1:4). [e] NMR in CF_3CO_2H, *m/e* 678 (M^+).

cyclopentamethyleneketene (generated from α-bromocyclohexanecarboxylic acid bromide, zinc, and diglyme).

REFERENCES

(1) R. D. Mackenzie, T. R. Blohm, E. A. Auxier, J. G. Henderson, and J. M. Steinbach, *Proc. Soc. Exp. Biol. Med.*, **137**, 602 (1971).

(2) E. R. Andrews, R. W. Fleming, J. M. Grisar, J. C. Kihm, D. L. Wenstrup, and G. D. Mayer, *J. Med. Chem.*, **17**, 882 (1974).

(3) L. M. Rice, B. S. Sheth, K. R. Scott, and C. F. Geschickter, *ibid.*, **12**, 126 (1969).

(4) Y. H. Wu, L. E. Allen, H. C. Ferguson, and J. W. Kissel, *ibid.*, **15**, 477 (1972).

(5) V. J. Bauer, B. J. Duffy, D. Hoffman, S. S. Klioze, R. W. Kosley, A. R. McFadden, L. L. Martin, H. H. Ong, and H. M. Geyer, III, *ibid.*, **19**, 1315 (1976).

(6) M. Abou-Gharbia and M. M. Joullié, *J. Pharm. Sci.*, **66**, 1653 (1977).

(7) S. M. Burke and M. M. Joullié, *Synth. Commun.*, **6**, 371 (1976).

(8) S. M. Burke, Ph.D. dissertation, University of Pennsylvania, Philadelphia, Pa., 1977.

(9) D. W. Jones and G. Kneen, *J. Chem. Soc., Perkin I*, **1975**, 171.

(10) C. A. Miller and L. M. Long, *J. Am. Chem. Soc.*, **73**, 489 (1951).

(11) K. E. Eichstadt, J. C. Rapmeyer, R. B. Cook, P. G. Riley, D. P. Davis, and R. A. Wiley, *J. Med. Chem.*, **19**, 47 (1976).

(12) C. H. Grogan, C. F. Geschickter, M. E. Freed, and L. M. Rice, *ibid.*, **8**, 62 (1965).

(13) A. Gomes and M. M. Joullié, *J. Heterocycl. Chem.*, **6**, 729 (1969).

(14) J. M. Bohen and M. M. Joullié, *J. Org. Chem.*, **38**, 2652 (1973).

(15) Z. Lysenko and M. M. Joullié, *ibid.*, **41**, 925 (1976).

(16) Z. Lysenko, M. M. Joullié, I. Miura, and R. Rodebaugh, *Tetrahedron Lett.*, **1977**, 1705.

(17) M. E. Taylor and T. L. Fletcher, *J. Org. Chem.*, **21**, 253 (1956).

(18) L. M. Rice, C. F. Geschickter, and C. H. Grogan, *J. Med. Chem.*, **6**, 388 (1963).

(19) W. Weyler, W. G. Duncan, and H. W. Moore, *J. Am. Chem. Soc.*, **97**, 6187 (1975).

ACKNOWLEDGMENTS

Supported in part by National Institute of Health Grant GM 18028-03.

Effect of Diazepam on Cognition *via* Pupillometry

JEFFREY A. KOTZAN

Received November 29, 1976, from the *School of Pharmacy, University of Georgia, Athens, GA 30602.* Accepted for publication October 25, 1977.

Abstract □ Continuous pupillary readings in response to a random-digit cognition task were obtained for 20 male subjects. Ten subjects were given 10 mg of diazepam, and 10 subjects were given placebos. Additional pupillary curves were recorded for both groups at 1 and 2 hr and compared to the initial curve. Subjects were required to repeat the exact sequence of verbalized randomized digits as a measure of performance. The results indicated that the diazepam treatment group differed significantly from the placebo group in terms of a depressed pupillary response. Furthermore, the performance recall measure was significantly reduced in the diazepam group. The relationships were clarified by an analysis of covariance and variance.

Keyphrases □ Diazepam—effect on recall ability evaluated by pupillometry, humans □ Pupillometry—used to evaluate effect of diazepam on recall ability in humans □ Sedatives—diazepam, effect on recall ability evaluated by pupillometry in humans

Pupillometrics is the aspect of psychology that deals with pupillary alterations elicited by any stimulus other than light (1). Because the pupil of the human eye is innervated by both sympathetic and parasympathetic fibers in close association with the central nervous system, pupillometrics affords an excellent method of observing the effects of many different types of stimuli such as near vision, lid closure, nystagmus, fatigue, color contrast, hippus, psychopathic states, noise, exercise, and drugs on pupil size (2–12). Furthermore, the degree of pupillary dilation has been positively correlated with human cognition and retention. Peavler (9) described a sensitive means of generating pupillary cognition curves by presenting randomized digits verbally to subjects.

Tranquilizers, in addition to their antipsychotic effects, have been correlated with several pupillary responses in humans. The major tranquilizer chlorpromazine produced a miotic effect in relation to dosage form and temporal measures (12). Critical flicker fusion, which is partly a measure of pupillary functions, has been studied extensively (13). Two studies attempted to relate minor tranquilizers, benzodiazepines, to critical flicker fusion with different conclusions (14, 15).

Diazepam was selected for investigation for several reasons. The drug is absorbed rapidly, with peak blood levels occurring in 1–2 hr (16). The diazepam metabolite, desmethyldiazepam, peaks only after repeated doses of several days (17). Furthermore, diazepam and other benzodiazepines have been studied for their relation to motor and cognition tasks, which suggest a relation between pupillary changes and diazepam. For example, auditory reaction times, complex visual reaction times, and their corresponding error rates appear to be increased by the benzodiazepines (18–20). However, simulated car driving tests were not affected by diazepam administration (21).

The hypotheses of this project were that the oral administration of diazepam would affect the pupillary response curve obtained during the execution of a cognition task and would influence the ability of human subjects to perform successfully the task as measured by recall.

EXPERIMENTAL

Twenty male subjects, 18–28 years old, were assigned to either a control or a treatment group. They were instructed to fast for 2 hr prior to the experiment. The treatment subjects allowed their eyes to adapt to the

0022-3549/78/0700/0956$01.00/0

© 1978, American Pharmaceutical Association

cyclopentamethyleneketene (generated from α-bromocyclohexanecarboxylic acid bromide, zinc, and diglyme).

REFERENCES

(1) R. D. Mackenzie, T. R. Blohm, E. A. Auxier, J. G. Henderson, and J. M. Steinbach, *Proc. Soc. Exp. Biol. Med.*, **137**, 602 (1971).

(2) E. R. Andrews, R. W. Fleming, J. M. Grisar, J. C. Kihm, D. L. Wenstrup, and G. D. Mayer, *J. Med. Chem.*, **17**, 882 (1974).

(3) L. M. Rice, B. S. Sheth, K. R. Scott, and C. F. Geschickter, *ibid.*, **12**, 126 (1969).

(4) Y. H. Wu, L. E. Allen, H. C. Ferguson, and J. W. Kissel, *ibid.*, **15**, 477 (1972).

(5) V. J. Bauer, B. J. Duffy, D. Hoffman, S. S. Klioze, R. W. Kosley, A. R. McFadden, L. L. Martin, H. H. Ong, and H. M. Geyer, III, *ibid.*, **19**, 1315 (1976).

(6) M. Abou-Gharbia and M. M. Joullié, *J. Pharm. Sci.*, **66**, 1653 (1977).

(7) S. M. Burke and M. M. Joullié, *Synth. Commun.*, **6**, 371 (1976).

(8) S. M. Burke, Ph.D. dissertation, University of Pennsylvania, Philadelphia, Pa., 1977.

(9) D. W. Jones and G. Kneen, *J. Chem. Soc., Perkin I*, **1975**, 171.

(10) C. A. Miller and L. M. Long, *J. Am. Chem. Soc.*, **73**, 489 (1951).

(11) K. E. Eichstadt, J. C. Rapmeyer, R. B. Cook, P. G. Riley, D. P. Davis, and R. A. Wiley, *J. Med. Chem.*, **19**, 47 (1976).

(12) C. H. Grogan, C. F. Geschickter, M. E. Freed, and L. M. Rice, *ibid.*, **8**, 62 (1965).

(13) A. Gomes and M. M. Joullié, *J. Heterocycl. Chem.*, **6**, 729 (1969).

(14) J. M. Bohen and M. M. Joullié, *J. Org. Chem.*, **38**, 2652 (1973).

(15) Z. Lysenko and M. M. Joullié, *ibid.*, **41**, 925 (1976).

(16) Z. Lysenko, M. M. Joullié, I. Miura, and R. Rodebaugh, *Tetrahedron Lett.*, **1977**, 1705.

(17) M. E. Taylor and T. L. Fletcher, *J. Org. Chem.*, **21**, 253 (1956).

(18) L. M. Rice, C. F. Geschickter, and C. H. Grogan, *J. Med. Chem.*, **6**, 388 (1963).

(19) W. Weyler, W. G. Duncan, and H. W. Moore, *J. Am. Chem. Soc.*, **97**, 6187 (1975).

ACKNOWLEDGMENTS

Supported in part by National Institute of Health Grant GM 18028-03.

Effect of Diazepam on Cognition *via* Pupillometry

JEFFREY A. KOTZAN

Received November 29, 1976, from the *School of Pharmacy, University of Georgia, Athens, GA 30602.* Accepted for publication October 25, 1977.

Abstract □ Continuous pupillary readings in response to a random-digit cognition task were obtained for 20 male subjects. Ten subjects were given 10 mg of diazepam, and 10 subjects were given placebos. Additional pupillary curves were recorded for both groups at 1 and 2 hr and compared to the initial curve. Subjects were required to repeat the exact sequence of verbalized randomized digits as a measure of performance. The results indicated that the diazepam treatment group differed significantly from the placebo group in terms of a depressed pupillary response. Furthermore, the performance recall measure was significantly reduced in the diazepam group. The relationships were clarified by an analysis of covariance and variance.

Keyphrases □ Diazepam—effect on recall ability evaluated by pupillometry, humans □ Pupillometry—used to evaluate effect of diazepam on recall ability in humans □ Sedatives—diazepam, effect on recall ability evaluated by pupillometry in humans

Pupillometrics is the aspect of psychology that deals with pupillary alterations elicited by any stimulus other than light (1). Because the pupil of the human eye is innervated by both sympathetic and parasympathetic fibers in close association with the central nervous system, pupillometrics affords an excellent method of observing the effects of many different types of stimuli such as near vision, lid closure, nystagmus, fatigue, color contrast, hippus, psychopathic states, noise, exercise, and drugs on pupil size (2–12). Furthermore, the degree of pupillary dilation has been positively correlated with human cognition and retention. Peavler (9) described a sensitive means of generating pupillary cognition curves by presenting randomized digits verbally to subjects.

Tranquilizers, in addition to their antipsychotic effects, have been correlated with several pupillary responses in humans. The major tranquilizer chlorpromazine produced a miotic effect in relation to dosage form and temporal measures (12). Critical flicker fusion, which is partly a measure of pupillary functions, has been studied extensively (13). Two studies attempted to relate minor tranquilizers, benzodiazepines, to critical flicker fusion with different conclusions (14, 15).

Diazepam was selected for investigation for several reasons. The drug is absorbed rapidly, with peak blood levels occurring in 1–2 hr (16). The diazepam metabolite, desmethyldiazepam, peaks only after repeated doses of several days (17). Furthermore, diazepam and other benzodiazepines have been studied for their relation to motor and cognition tasks, which suggest a relation between pupillary changes and diazepam. For example, auditory reaction times, complex visual reaction times, and their corresponding error rates appear to be increased by the benzodiazepines (18–20). However, simulated car driving tests were not affected by diazepam administration (21).

The hypotheses of this project were that the oral administration of diazepam would affect the pupillary response curve obtained during the execution of a cognition task and would influence the ability of human subjects to perform successfully the task as measured by recall.

EXPERIMENTAL

Twenty male subjects, 18–28 years old, were assigned to either a control or a treatment group. They were instructed to fast for 2 hr prior to the experiment. The treatment subjects allowed their eyes to adapt to the

0022-3549/78/0700/0956$01.00/0

© 1978, American Pharmaceutical Association

Table I—Mean Number of Correct Responses

Hours	Seven-Digit Task		Nine-Digit Task	
	Diazepam	Placebo	Diazepam	Placebo
0	4.00	4.30	2.00	2.80
1	5.00	4.90	2.00	4.30
2	3.70[a]	6.00[a]	3.20	3.70

[a] t significant at $p = 0.012$.

5-footcandle room illumination level for 3 min. Each placed his head into the chinrest of the pupillometer system[1], which was illuminated by a neutral density wedge tachistoscope[2].

The tachistoscope was activated, and the subjects were instructed to focus their eyes on a single object of the display slide. The illumination of the tachistoscope was adjusted so that the initial pupil diameter measured between 4.5 and 5.5 mm. The entire adjustment procedure required approximately 2–3 additional min.

The experiment commenced when the recorder[3] was initiated. The event marker was programmed for 1-sec intervals. At the beginning of the 4th sec, a series of computer-randomized digits between zero and nine was read in monotone in 1-sec intervals. The subjects kept their eyes fixed on the slide for 20 sec/random set of numbers. The subjects could hear the ticking of the event marker, which served to indicate the beginning and end of the experimental measurement. One set of seven and one set of nine random digits were presented.

Following the 20-sec measurement period in which either the seven- or nine-digit sequence was read, the subjects were instructed to lift their heads from the chinrest and to recall the exact sequence of the numbers. The correct responses were recorded, and each subject was given a 5-mg oral dose of diazepam[4]. (All tablets were from the same lot.)

After 1 hr, the 10 treatment subjects repeated the experimental procedure and were given a second dose of 5 mg of diazepam. One hour later, they repeated the measurement procedures. The final measurement was conducted 2 hr following the initial measurement.

The 10 subjects of the control group were treated identically except that they were given two placebo capsules. The contents of 10-mg chlordiazepoxide[5] capsules were removed and replaced with lactose to serve as placebos.

RESULTS

The ability of the random-digit cognitive task to stimulate pupil dilation was substantiated. Figure 1 displays a typical response pattern, which peaked at 5.8 mm at the 11th sec of the experiment. The pupil diameter remained substantially above the beginning diameter during and following recitation of the randomized digits.

Table I displays the mean correct responses for both the seven- and nine-digit tasks. The performances of the treatment and placebo groups were significantly different at the seven-digit, 2-hr point. The diazepam group was able to recall an average of 3.7 digits, but the placebo group recalled an average of 6.0 digits. A difference in performance was not observed at the nine-digit, 2-hr point.

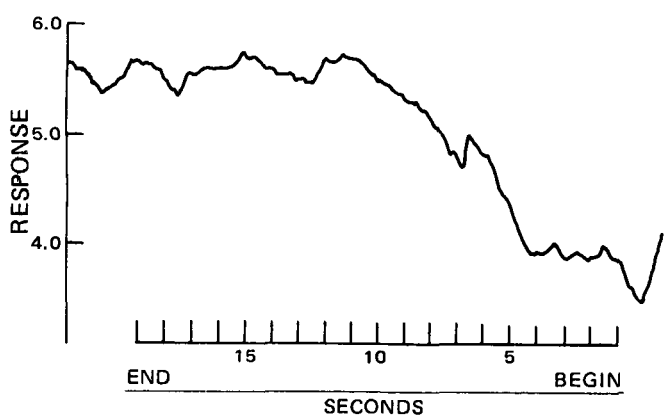

Figure 1—*Example of a pupillary response in millimeters for the 20-sec duration of the experimental observation.*

[1] Polymetric model V11651R, U.S. Testing Co., Hoboken, N.J.
[2] Model 42020, Lafayette Instrument Co., Lafayette, Ind.
[3] Model 680, Leeds and Northrup, North Wales, Pa.
[4] Valium, Roche Laboratories, Nutley, N.J.
[5] Librium, Roche Laboratories, Nutley, N.J.

Table II—Analysis of Variance and Covariance of Pupil Dilation at 11 sec of the Seven-Digit, 2-hr Task

Source of Variation	Sum of Squares	df	Mean Square	F	Significance of F
Covariate: number correct responses	0.183	1	0.183	1.245	0.280
Main effect: drug treatment	0.701	1	0.701	4.758	0.041
Residual	2.504	17	0.147		
Total	3.388	19	0.178		

The pupil dilation data were reduced to machine-readable form and treated to underscore differential treatment effects. First, the entry diameter during the 1st sec of the experiment was subtracted from the remaining seconds of observation. In this manner, differences in initial pupil sizes were removed as contaminating variables. Second, the responses during the initial seven- and nine-digit tasks were respectively subtracted second by second from the measurements of the 1st and 2nd hr. Thus, the analysis focused on measured differences in response patterns between the initial recordings and subsequent recordings of both the placebo and drug treatment groups.

Figure 2 graphically displays the difference between the placebo and treatment groups for the seven-digit task at 2 hr. The diazepam or treatment group showed a recorded value of −0.31 mm during the 8th sec of the experiment. In other words, at this point the average pupil dilation of the treatment group was 0.31 mm less than their response at the initial recording for the 8th sec. The response of the 10 treatment subjects demonstrated less dilation between 3 and 14 sec than did the placebo group. The 10th sec of the treatment group appeared to be an anomaly of the response pattern, although the response remained below the dilation recorded during the initial period.

The data were subjected to a statistical analysis of variance and covariance (22). The correct number of responses was input as the covariate, which removed the effect of the number of correct responses *before* performing an analysis of variance on the pupillary measures.

Table II displays the results of the analysis between the placebo and the drug treatment groups at the 11-sec point of the seven-digit, 2-hr task. The correct number of responses was modestly significant, and its effects were removed before significant differences of pupillary dilation between the treatment and control groups were detected. Table III displays the significance level of the removed covariate and the treatment effect at other seconds of the seven-digit, 2-hr task. The midportion of the experiment proved most significant for this task. By comparison, the nine-digit task at 2 hr did not generate statistically significant differences between the treatment and placebo groups.

DISCUSSION

The lack of difference in dilation at the nine-digit level is not surprising. In an experiment that employed random-digit recall tasks similar to those employed in this experiment, subjects began to overload during the 8th sec of a nine- and 13-digit memory task (9). When overloaded, the pupil

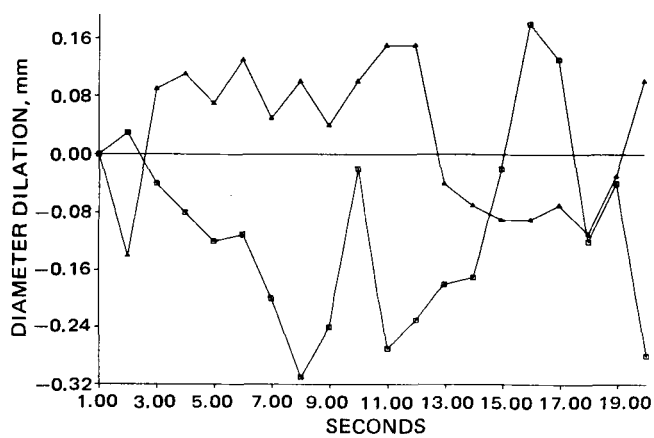

Figure 2—*Mean differential pupillary response of* T_0 *and* T_2 *hr for diazepam subjects (□) and placebo subjects (▲).*

Table III—Significance Level of Treatment and Covariate on Pupil Dilation for the Seven-Digit Task at 2 hr

Seconds	Covariate: Number Correct Responses	Main Effect: Drug Treatment
6	0.090	NS[a]
7	0.028	NS
8	0.160	0.263
9	0.142	NS
10	NS	NS
11	0.280	0.041
12	0.174	0.131
13	NS	NS

[a] NS = not significant.

diameter tended to level. Thus, the lack of significance during the nine-digit task of this experiment was attributed to processing overload. The subjects of both the control and treatment groups began to overload during the 11th sec of the experiment, which rendered further pupillary dilation impossible (23).

The maximum difference between the control and placebo groups was observed at the 11th sec, immediately following the recitation of the last digit. Kahneman *et al.* (24) demonstrated that pupils may continue to dilate following random-digit memory tasks as subjects continue to work on the regrouping of stored information. This fact was substantiated by Peavler (9), who demonstrated that maximum dilation occurred 1–2 sec following stimulation. Therefore, the most significant differential measures were observed at the point where maximum dilation occurred without overload. The differences quickly vanished following the 12th sec, representing a lessening of cognition activity and pupillary dilation.

Variability in measurements was expected. The effects of hippus, eyelid closure, fatigue, and other sources contributed to the variance. Also, blood levels of diazepam are considerably variable at 1 and 2 hr following an oral dose (16). Furthermore, the experiment did not include controls for anxiety levels, which contribute to the response to diazepam (25). Future applications of the cognitive task technique may enhance sensitivity if blood levels and psychological state are evaluated.

The results supported the hypotheses. The group treated with diazepam did not dilate to the degree of the placebo group in response to the seven-digit cognitive task. Additionally, drug administration reduced the ability of the subjects to recall the seven randomized digits.

REFERENCES

(1) E. H. Hess and J. M. Plot, *Science*, **132**, 349 (1960).

(2) O. Lowenstein and I. E. Loesenfeld, in "The Pupil, Muscular Mechanisms," vol. 3, I. E. Davison, Ed., Academic, New York, N.Y., 1963, p. 231.

(3) S. W. Peavler, in "Pupillary Dynamics and Behavior," M. P. Janisse, Ed., Plenum, New York, N.Y., 1974, chap. 6, p. 159.

(4) I. E. Loesenfeld, *Surv. Ophthamol.*, **2**, 291 (1966).

(5) L. S. Rubin, in "Pupillary Dynamics and Behavior," M. P. Janisse, Ed., Plenum, New York, N.Y., 1974, chap. 4, p. 75.

(6) J. C. Nunally, P. D. Cuchnowski, and A. Parker, *Percept. Psychophys.*, **2**, 143 (1967).

(7) H. M. Simpson and M. H. Climan, *Psychophysiology*, **8**, 483 (1971).

(8) R. F. Stanners and D. B. Headley, *ibid.*, **9**, 505 (1972).

(9) S. W. Peavler, *ibid.*, **11**, 559 (1974).

(10) W. W. Tyron, *ibid.*, **12**, 90 (1975).

(11) B. C. Goldwater, *Psychol. Bull.*, **77**, 340 (1972).

(12) V. F. Smolen, H. R. Murdock, W. P. Stoltman, J. W. Clevenger, L. W. Combs, and E. J. Williams, *J. Clin. Pharmacol.*, **15**, 734 (1975).

(13) C. Landis, "An Annotated Bibliography of Flicker Fusion Phenomena," Armed Forces-National Research Council, Ann Arbor, Mich., 1953.

(14) C. M. Idestrom and B. Cadenius, *Psychopharmacologia*, **4**, 235 (1963).

(15) G. Holmberg and U. William-Olsson, *ibid.*, **4**, 402 (1963).

(16) S. A. Kaplan, M. L. Jack, K. Alexander, and R. E. Weinfeld, *J. Pharm. Sci.*, **62**, 1789 (1973).

(17) J. Manto, D. Iisalo, V. Lehtinen, and J. Salminen, *Psychopharmacologia*, **36**, 123 (1974).

(18) M. Ransella, O. Siciliani, L. Burti, and M. Schiavon, *ibid.*, **41**, 81 (1975).

(19) A. J. Bond and M. H. Lader, *ibid.*, **32**, 223 (1973).

(20) S. M. Luria, H. M. Paulson, J. S. Kinney, C. L. McKay, M. S. Strauss, and A. P. Ryann, "Naval Submarine Medical Research Laboratory Report No. 808," Bureau of Medicine and Surgery, Navy Department, Washington, D.C., 1975.

(21) I. Dureman and B. Norrman, *Psychopharmacologia*, **40**, 279 (1975).

(22) N. H. Nie, C. H. Hull, J. G. Jenkins, K. Steinbrenner, and D. N. Bent, "Statistical Package for the Social Sciences," McGraw-Hill, New York, N.Y., 1975 (Release No. 6.00 on Cybernetics 7000).

(23) G. K. Poock, *Percept. Mot. Skills*, **37**, 1000 (1973).

(24) D. Kahneman, L. Onuska, and R. Wolman, *Q. J. Exp. Psychol.*, **20**, 309 (1968).

(25) G. N. Bianchi, M. R. Fennessy, J. Phillips, and B. S. Everitt, *Psychopharmacologia*, **35**, 113 (1974).

ACKNOWLEDGMENTS

Presented at the Economics and Administrative Science Section, APhA Academy of Pharmaceutical Sciences, Orlando meeting, November 1976.

Impurities in Drugs II: Meperidine and Its Formulations

K. M. McERLANE, R. J. WOOD, F. MATSUI ˣ, and E. G. LOVERING

Received June 21, 1977, from the *Drug Research Laboratories, Health Protection Branch, Tunney's Pasture, Ottawa, Ontario, K1A 0L2, Canada.* Accepted for publication November 3, 1977.

Abstract □ Three lots of meperidine hydrochloride, seven lots of meperidine tablets, and 41 lots of meperidine injectables were examined for impurities by TLC. Impurities found were ethyl 1-benzyl-4-phenyl-4-piperidinecarboxylate, methyl 1-methyl-4-phenyl-4-piperidinecarboxylate, ethyl 1-ethyl-4-phenyl-4-piperidinecarboxylate, and three unidentified compounds. Not all impurities were found in every lot of drug investigated, and none of the impurities exceeded a concentration of 1% of the meperidine present.

Keyphrases □ Meperidine—TLC analyses of impurities in bulk drug and dosage forms □ TLC—analyses, impurities in meperidine bulk drug and dosage forms □ Impurities—in meperidine bulk drug and dosage forms, TLC analyses □ Narcotic analgesics—meperidine, TLC analyses of impurities in bulk drug and dosage forms

Impurities in drugs and their formulations may originate as intermediates or by-products during synthesis of the drug substance or as products of degradation during formulation or storage of the finished product, or they may result from drug–excipient interactions. To obtain adequate information on the number and level of impurities

0022-3549/78/0700/0958$01.00/0

© 1978, American Pharmaceutical Association

Table III—Significance Level of Treatment and Covariate on Pupil Dilation for the Seven-Digit Task at 2 hr

Seconds	Covariate: Number Correct Responses	Main Effect: Drug Treatment
6	0.090	NS[a]
7	0.028	NS
8	0.160	0.263
9	0.142	NS
10	NS	NS
11	0.280	0.041
12	0.174	0.131
13	NS	NS

[a] NS = not significant.

diameter tended to level. Thus, the lack of significance during the nine-digit task of this experiment was attributed to processing overload. The subjects of both the control and treatment groups began to overload during the 11th sec of the experiment, which rendered further pupillary dilation impossible (23).

The maximum difference between the control and placebo groups was observed at the 11th sec, immediately following the recitation of the last digit. Kahneman *et al.* (24) demonstrated that pupils may continue to dilate following random-digit memory tasks as subjects continue to work on the regrouping of stored information. This fact was substantiated by Peavler (9), who demonstrated that maximum dilation occurred 1–2 sec following stimulation. Therefore, the most significant differential measures were observed at the point where maximum dilation occurred without overload. The differences quickly vanished following the 12th sec, representing a lessening of cognition activity and pupillary dilation.

Variability in measurements was expected. The effects of hippus, eyelid closure, fatigue, and other sources contributed to the variance. Also, blood levels of diazepam are considerably variable at 1 and 2 hr following an oral dose (16). Furthermore, the experiment did not include controls for anxiety levels, which contribute to the response to diazepam (25). Future applications of the cognitive task technique may enhance sensitivity if blood levels and psychological state are evaluated.

The results supported the hypotheses. The group treated with diazepam did not dilate to the degree of the placebo group in response to the seven-digit cognitive task. Additionally, drug administration reduced the ability of the subjects to recall the seven randomized digits.

REFERENCES

(1) E. H. Hess and J. M. Plot, *Science*, **132**, 349 (1960).

(2) O. Lowenstein and I. E. Loesenfeld, in "The Pupil, Muscular Mechanisms," vol. 3, I. E. Davison, Ed., Academic, New York, N.Y., 1963, p. 231.

(3) S. W. Peavler, in "Pupillary Dynamics and Behavior," M. P. Janisse, Ed., Plenum, New York, N.Y., 1974, chap. 6, p. 159.

(4) I. E. Loesenfeld, *Surv. Ophthamol.*, **2**, 291 (1966).

(5) L. S. Rubin, in "Pupillary Dynamics and Behavior," M. P. Janisse, Ed., Plenum, New York, N.Y., 1974, chap. 4, p. 75.

(6) J. C. Nunally, P. D. Cuchnowski, and A. Parker, *Percept. Psychophys.*, **2**, 143 (1967).

(7) H. M. Simpson and M. H. Climan, *Psychophysiology*, **8**, 483 (1971).

(8) R. F. Stanners and D. B. Headley, *ibid.*, **9**, 505 (1972).

(9) S. W. Peavler, *ibid.*, **11**, 559 (1974).

(10) W. W. Tyron, *ibid.*, **12**, 90 (1975).

(11) B. C. Goldwater, *Psychol. Bull.*, **77**, 340 (1972).

(12) V. F. Smolen, H. R. Murdock, W. P. Stoltman, J. W. Clevenger, L. W. Combs, and E. J. Williams, *J. Clin. Pharmacol.*, **15**, 734 (1975).

(13) C. Landis, "An Annotated Bibliography of Flicker Fusion Phenomena," Armed Forces-National Research Council, Ann Arbor, Mich., 1953.

(14) C. M. Idestrom and B. Cadenius, *Psychopharmacologia*, **4**, 235 (1963).

(15) G. Holmberg and U. William-Olsson, *ibid.*, **4**, 402 (1963).

(16) S. A. Kaplan, M. L. Jack, K. Alexander, and R. E. Weinfeld, *J. Pharm. Sci.*, **62**, 1789 (1973).

(17) J. Manto, D. Iisalo, V. Lehtinen, and J. Salminen, *Psychopharmacologia*, **36**, 123 (1974).

(18) M. Ransella, O. Siciliani, L. Burti, and M. Schiavon, *ibid.*, **41**, 81 (1975).

(19) A. J. Bond and M. H. Lader, *ibid.*, **32**, 223 (1973).

(20) S. M. Luria, H. M. Paulson, J. S. Kinney, C. L. McKay, M. S. Strauss, and A. P. Ryann, "Naval Submarine Medical Research Laboratory Report No. 808," Bureau of Medicine and Surgery, Navy Department, Washington, D.C., 1975.

(21) I. Dureman and B. Norrman, *Psychopharmacologia*, **40**, 279 (1975).

(22) N. H. Nie, C. H. Hull, J. G. Jenkins, K. Steinbrenner, and D. N. Bent, "Statistical Package for the Social Sciences," McGraw-Hill, New York, N.Y., 1975 (Release No. 6.00 on Cybernetics 7000).

(23) G. K. Poock, *Percept. Mot. Skills*, **37**, 1000 (1973).

(24) D. Kahneman, L. Onuska, and R. Wolman, *Q. J. Exp. Psychol.*, **20**, 309 (1968).

(25) G. N. Bianchi, M. R. Fennessy, J. Phillips, and B. S. Everitt, *Psychopharmacologia*, **35**, 113 (1974).

ACKNOWLEDGMENTS

Presented at the Economics and Administrative Science Section, APhA Academy of Pharmaceutical Sciences, Orlando meeting, November 1976.

Impurities in Drugs II: Meperidine and Its Formulations

K. M. McERLANE, R. J. WOOD, F. MATSUI ˣ, and E. G. LOVERING

Received June 21, 1977, from the *Drug Research Laboratories, Health Protection Branch, Tunney's Pasture, Ottawa, Ontario, K1A 0L2, Canada.* Accepted for publication November 3, 1977.

Abstract □ Three lots of meperidine hydrochloride, seven lots of meperidine tablets, and 41 lots of meperidine injectables were examined for impurities by TLC. Impurities found were ethyl 1-benzyl-4-phenyl-4-piperidinecarboxylate, methyl 1-methyl-4-phenyl-4-piperidinecarboxylate, ethyl 1-ethyl-4-phenyl-4-piperidinecarboxylate, and three unidentified compounds. Not all impurities were found in every lot of drug investigated, and none of the impurities exceeded a concentration of 1% of the meperidine present.

Keyphrases □ Meperidine—TLC analyses of impurities in bulk drug and dosage forms □ TLC—analyses, impurities in meperidine bulk drug and dosage forms □ Impurities—in meperidine bulk drug and dosage forms, TLC analyses □ Narcotic analgesics—meperidine, TLC analyses of impurities in bulk drug and dosage forms

Impurities in drugs and their formulations may originate as intermediates or by-products during synthesis of the drug substance or as products of degradation during formulation or storage of the finished product, or they may result from drug–excipient interactions. To obtain adequate information on the number and level of impurities

0022-3549/78/0700/0958$01.00/0

© 1978, American Pharmaceutical Association

Table I—Impurities in Meperidine and Its Formulations

Brand	Form	Dosage	Impurities					
						Unidentified		
			I (R_f 0.75)	II (R_f 0.60)	XI[a] (R_f 0.39)	R_f 0.56	R_f 0.33	R_f 0.25
A	Bulk drug	—	1.0	0.25	—	Tr	—	Tr
A	Bulk drug	—	1.0	Tr	—	—	Tr	—
A	Tablet	50 mg	—	Tr	—	Tr	Tr	Tr
A	Tablet	50 mg	Tr	0.25	+	Tr	0.5	Tr
B	Tablet	50 mg	1.0	0.25	+	Tr	0.5	Tr
B	Injection	75 mg/ml	—	0.5	—	Tr	—	—
C	Injection	75 mg/ml	—	1.0	—	Tr	0.5	—
C	Injection	100 mg/ml	1.0	0.5		Tr	Tr	—
E	Injection	10 mg/ml	0.5	Tr	—	—	—	—
E	Injection	50 mg/ml	—	Tr	—	Tr	—	—
F	Injection	50 mg/ml	—	Tr	—	Tr	—	—
F	Injection	50 mg/ml	—	0.25	+	Tr	0.5	—
I	Injection	75 mg/ml	1.0	0.25	+	Tr	0.25	—

[a] Detected but not quantified.

in pharmaceutical products, it is desirable to examine a substantial number of formulations and drug substances. Chromatographic techniques, geared to the detection of compounds structurally related to the drug, are most suitable for this work. A study of impurities in imipramine and desipramine showed the presence of several compounds related to the drug (1). This paper reports a study of the impurities in meperidine and meperidine formulations.

Meperidine was first synthesized (2) by condensing mechlorethamine with benzyl cyanide, followed by hydrolysis and esterification of the resulting nitrile. Several alternative methods have been developed (3–6). A number of qualitative TLC methods for the determination of meperidine have been published (7–13), but only two (12, 13) deal with impurities in meperidine.

BP (14) monographs for pethidine hydrochloride (meperidine) and its formulations specify a TLC limit test of not more than 1% for unidentified related substances. The USP (15) does not contain specifications for impurities in meperidine hydrochloride.

EXPERIMENTAL

Materials—All drugs and dosage forms were obtained directly from the manufacturers. Meperidine hydrochloride[1], *N*-benzyliminodiacetic acid[2], hexamethylphosphoramide[3], thionyl chloride[4], lithium aluminum hydride[5], sodium amide[6], 10% palladium-on-charcoal[7], absolute ethanol[8], and hydrogen chloride gas[9] were obtained commercially. All other solvents were analytical grade.

Precoated silica gel GF (20 × 20-cm, 0.25-mm) TLC plates[10], 60–200-mesh silica gel for column chromatography, and nylon columns[11] were used. A gas chromatograph[12] equipped with flame-ionization detectors was used with 1.8-m × 0.63-cm o.d., U-shaped glass columns packed with 5% phenylmethyl silicone (OV-25) coated on acid-washed, dimethylchlorosilane-treated, high performance Chromosorb W[13] (100–120 mesh).

Standard Solutions—Two aqueous solutions were prepared, each containing 20 mg of meperidine hydrochloride/ml. To the first solution was added 0.05 mg/ml; to the second was added 0.1 mg/ml of each of the hydrochloride salts of ethyl 1-benzyl-4-phenyl-4-piperidinecarboxylate (I) and ethyl 1-ethyl-4-phenyl-4-piperidinecarboxylate (II). Aliquots of 5 ml of each solution were made basic with 0.5 ml of concentrated ammonium hydroxide and shaken with 2 ml of ether for 15 min. The standard solutions in ether contained 50 mg of meperidine/ml and either 0.125 or 0.250 mg of I and II/ml.

TLC System—The solvent system consisted of ethyl acetate–cyclohexane–methanol–dioxane–water–concentrated ammonium hydroxide (50:50:20:10:1:1). Filter paper-lined TLC tanks were equilibrated with the solvent system for 15 min prior to use. Spots were visualized using UV light at 254 nm and by spraying with dilute potassium iodobismuthate solution.

Extraction from Tablet Formulations—An amount of powdered tablet equivalent to 100 mg of meperidine hydrochloride was weighed into a 10-ml screw-capped culture tube[14] and extracted by shaking[15] for 30 min with 5 ml of distilled water. The aqueous extract was made basic with 0.5 ml of concentrated ammonium hydroxide solution and extracted with 2 ml of ether by shaking for 15 min. Aliquots of the ether layer were applied directly from the culture tubes to the TLC plates.

Extraction from Injectable Formulations—An amount equivalent to 100 mg of meperidine hydrochloride was diluted to 5 ml with distilled water in a screw-capped culture tube, made basic, and then extracted. An aliquot was applied to the TLC plate as already described.

Extraction from Drug Substances—Aqueous solutions were prepared to contain 100 mg of meperidine hydrochloride in 5 ml of distilled water and extracted in the same manner as injectable formulations.

Isolation of Impurities—Meperidine base (3 g) was extracted from Formulation C, 100 mg/ml (Table I), which had been determined by preliminary TLC investigation to contain the largest number and quantities of impurities. The base was generated from bulked injectable formulations, which were made alkaline with concentrated ammonium hydroxide and extracted with 5 × 100 ml of ether.

The ether was evaporated under vacuum. The isolated base was then dissolved in 5 ml of chloroform and adsorbed onto the top of a dry-packed silica gel column, prepared from 200 g of 60–200-mesh silica gel that had been equilibrated with 15% water and packed into a 0.03 × 1-m nylon column by the method of Loev and Snader (16). The silica gel was not equilibrated with the developing solvent as reported in a later publication (17), because the separation at the various bands was adequate when water alone was used.

The solvent system used to elute the drug and impurities on the column was the same as that used for TLC. The location of each compound on the column was established by removing small portions of the silica gel through holes cut into the nylon tube every 1.27 cm and eluting these aliquots with ethanol directly onto a TLC plate. The components were visualized as described for the TLC system.

Sections of the column were excised, and the impurities were eluted by shaking with successive aliquots of ethanol until a drop of the eluate failed to respond to the test for the basic drug substance when examined on a TLC plate. The various fractions were evaporated under vacuum and further purified by preparative TLC with the same solvent system. The residues isolated from the TLC plate were determined to consist of a single component by rechromatographing aliquots with the same TLC system.

[1] USP reference standard.
[2] Aldrich Chemical Co., Milwaukee, Wis.
[3] Eastman Kodak Co., Rochester, N.Y.
[4] J. T. Baker Chemical Co., Phillipsburg, N.J.
[5] Alfa Products, Beverly, Mass.
[6] Fisher Scientific Co., Fair Lawn, N.J.
[7] Koch-Light Laboratories, Colnbrook, England.
[8] Consolidated Alcohols, Toronto, Canada.
[9] Matheson, Toronto, Canada.
[10] Brinkmann Instruments, Toronto, Canada.
[11] ICN Pharmaceuticals, Cleveland, Ohio.
[12] Bendix 2500, Aviation Electric, Montreal, Canada.
[13] Chromatographic Specialties, Brockville, Canada.
[14] Canlab Laboratories, Ottawa, Canada.
[15] Horizontal shaker, Eberbach Corp., Ann Arbor, Mich.

Prior to mass spectral analysis, a portion of the extract was further purified by GLC to remove contaminants originating from the silica gel. The injection port and detector block temperatures were 240°. The column temperatures were adjusted between 160 and 230°, depending on the retention time of the peak of interest. Fractions were collected in dry ice-cooled capillary tubes held over the exit tip of the flame-ionization detector at the retention time established for the compound of interest.

Collections were made, with the hydrogen flame extinguished, until a condensate was visible in the capillary tube. Samples thus collected were reexamined by TLC to ascertain that the compound consisted of a single component with chromatographic characteristics identical to those of the original material.

Screening for Impurities—Aliquots of 10 and 20 μl (0.5 and 1.0 mg, respectively) of the drug or formulation extracts were spotted on the silica gel GF TLC plates adjacent to 10- and 20-μl aliquots of the standard solutions. Impurities were estimated by comparison of the spot diameters and intensities to those of the corresponding spots from the standard solutions. In all cases, 10- and 20-μl aliquots of the aqueous phase prior to being made basic were applied to the chromatoplates to check for the presence of 1-methyl-4-phenyl-4-piperidinecarboxylic acid (III).

Syntheses—Scheme I illustrates the syntheses of the following compounds.

Diethyl N-Benzyliminodiacetate (IV)—A mixture of 45 g of *N*-benzyliminodiacetic acid (V), 39.7 g of concentrated sulfuric acid, and 2 liters of absolute alcohol was refluxed for 24 hr. The solution was concentrated to 500 ml, neutralized with sodium ethoxide, and evaporated to dryness. The residue was treated with ether, filtered to remove inorganic salts, and evaporated to dryness to yield 49 g (87%) of IV; IR (film): λ_{max} 1740 (ester carbonyl) and 3440 cm^{-1} (carboxylic hydroxyl was absent); PMR ($CDCl_3$): 73 (ethyl ester triplet) and 249 (ethyl ester quartet) Hz.

N-Benzylbis(2-hydroxyethyl)amine (VI)—Twenty grams of lithium aluminum hydride was slowly added to a stirred solution of 48 g of IV in 500 ml of dry tetrahydrofuran. The reactants were stirred at room temperature for 1.5 hr and hydrolyzed with 1.0 *N* NaOH until effervescence ceased. The mixture was filtered, and the filtrate was evaporated to yield 26 g (77%) of VI; IR (film): λ_{max} 3370 (hydroxyl) and 1740 cm^{-1} (ester carbonyl was absent); PMR ($CDCl_3$): 181 (hydroxyl protons) Hz (ethyl ester peaks were absent).

N-Benzylbis(2-chloroethyl)amine (VII)—Twenty-five grams of VI was refluxed with 38.9 g of redistilled thionyl chloride in 200 ml of dry chloroform for 1.5 hr. Ether was added to the cooled reaction mixture to induce crystallization. The yield of the hydrochloride salt of VII was 27 g (79%), mp (hydrochloride) 147° [lit. (2) mp 149°].

1-Benzyl-4-phenyl-4-cyanopiperidine (VIII)—A solution of 27 g of the hydrochloride salt of VII in 50 ml of water was made basic with concentrated ammonium hydroxide and extracted into 250 ml of toluene. The toluene was removed and dried with anhydrous sodium sulfate and subsequently mixed with 11.9 g of benzyl cyanide and 12 ml of hexamethylphosphoramide. To the stirred solution was slowly added 10.1 g of sodium amide suspended in 10 ml of dry toluene while the reaction temperature was kept below 10°.

After the addition was complete, the mixture was stirred for 3 hr at room temperature and then diluted with 250 ml of toluene. The organic phase was washed with 3 × 100 ml of water to remove the hexamethylphosphoramide and extracted with 3 × 100 ml of 10% HCl. The aqueous layer was made alkaline with sodium hydroxide and extracted with 2 × 50 ml of toluene. The toluene was dried and evaporated to yield 9.1 g (33%) of VIII, mp (hydrochloride) 255° [lit. (2) mp 259°].

Ethyl 1-Benzyl-4-phenyl-4-piperidinecarboxylate (I)—A solution of 9 g of VIII in 20 ml of 65% (v/v) aqueous sulfuric acid solution was heated at 130–140° for 2 hr. A 1-ml portion of the reaction mixture was removed and neutralized with 1 *N* NaOH, and the liberated base was extracted into 25 ml of chloroform to yield 1-benzyl-4-phenyl-4-piperidinecarboxylic acid (IX). The remainder of the reaction was cooled to 100°, and absolute ethanol was added continuously while distilling off the water–ethanol azeotrope. The rates of addition and distillation were balanced and continued for 24 hr.

The residue was poured onto ice, and the aqueous solution was washed with 2 × 25 ml of ether and then made basic with sodium hydroxide. The product was extracted into 2 × 25 ml of ether, and the ether was dried over anhydrous sodium sulfate and evaporated to yield 4.1 g (36%) of I. It gave a hydrochloride from ethanol–ether, mp 236° [lit. (2) mp 235–238°].

Ethyl 4-Phenyl-4-piperidinecarboxylate (X)—A solution of 1 g of the free base of I in 100 ml of absolute ethanol was hydrogenated at atmospheric pressure with 0.1 g of 10% palladium-on-charcoal catalyst until

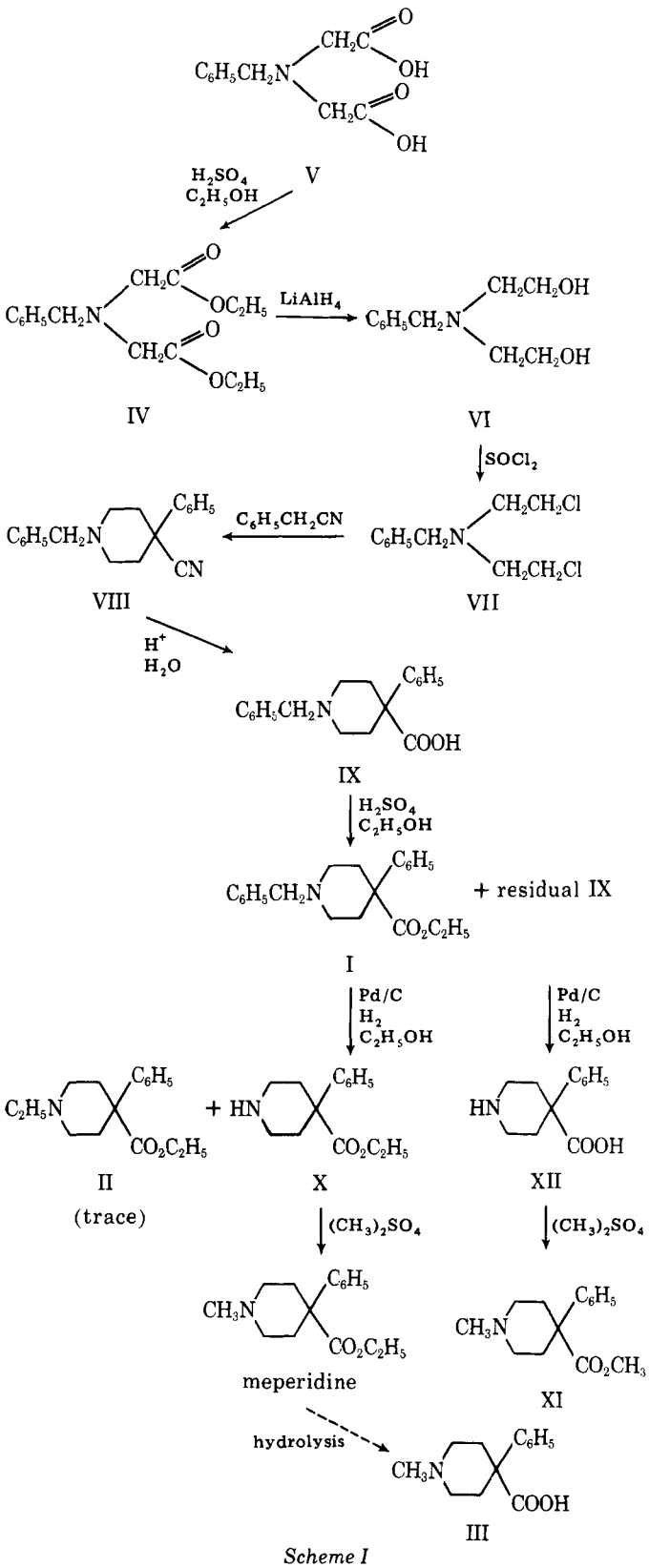

Scheme I

no further hydrogen was absorbed (24 hr). The catalyst was filtered off, the solvent was evaporated, ethanolic hydrochloric acid was added, and the product was recrystallized from ethanol–ether to yield 0.3 g (41%) of the hydrochloride of X, mp 134–137°.

Ethyl 1-Ethyl-4-phenyl-4-piperidinecarboxylate (II)—A solution of 0.1 g of the free base of X in 10 ml of acetone was refluxed for 1 hr in the presence of 0.06 g of anhydrous potassium carbonate and 0.07 g of diethyl sulfate. The reaction mixture was cooled and filtered, and the

filtrate was evaporated under reduced pressure. The residue was dissolved in 25 ml of ether and washed with 2 × 25 ml of 2% potassium hydroxide and subsequently with 2 × 25 ml of water. The ethereal solution was dried with anhydrous sodium sulfate, filtered, and evaporated under reduced pressure to yield 0.08 g (71%) of II, which gave a hydrochloride from ethanol–ether, mp 169° [lit. (18) mp 171°].

Methyl 1-Methyl-4-phenyl-4-piperidinecarboxylate (XI)—A solution of 1 g of meperidine hydrochloride was warmed at 60° in 50 ml of 10 *N* HCl for 12 hr. Then the crystalline solid that separated was filtered off and washed with 2 × 1 ml of water and 3 × 25 ml of ether. The insoluble residue was established by IR and mass spectral analyses to be 1-methyl-4-phenyl-4-piperidinecarboxylic acid hydrochloride (III).

The carboxylic acid (0.7 g) was refluxed for 4 hr with 100 ml of dry methanol, which had been saturated with hydrogen chloride gas. The solvent was removed under vacuum, and the residue was recrystallized from methanol–ether to yield 0.5 g of XI hydrochloride, mp 212° [lit. (5) mp 201–202°].

RESULTS AND DISCUSSION

The TLC R_f values of meperidine, impurities found in formulations, and intermediates in Scheme I are given in Table II. The identities of I, II, and XI were established by TLC, GLC, and mass spectral comparisons to the corresponding authentic materials. TLC showed that a single ether extraction was sufficient for the complete removal of meperidine and its basic associated impurities from formulations. The presence of ether-insoluble impurities was determined by applying aliquots of the aqueous layer remaining after extraction to the TLC plates. No degradation of the drug or associated impurities was observed when extracts were subjected to two-dimensional TLC or when samples were applied to the TLC plates at intervals over 3 hr.

Three lots of meperidine hydrochloride, seven lots of tablets, and 41 lots of injectable preparations from nine manufacturers were examined for impurities. Examples of the products examined and the impurities found are listed in Table I. None of the samples contained III, a hydrolysis product of meperidine. The levels of those impurities not identified were estimated by assuming their TLC response to be equal to that of meperidine. Impurities stated to be present at trace amounts were approximately equal to the minimum detectable quantity established for the impurity or for meperidine.

Attempts to isolate the impurity at R_f 0.33, present in amounts comparable to other impurities, were unsuccessful, possibly because of its volatility. The concentration of XI could not be determined accurately in the presence of meperidine because it overlapped the tailing edge of the meperidine spot in all TLC systems investigated. However, XI was separated from the bulk of meperidine by the column procedure and purified by TLC.

The mechanism by which impurities I, II, and XI would form during synthesis by the routes described previously (2, 3) is not entirely clear. Grew (12) suggested that II and XI might form by an amino–ester exchange; however, the occurrence of I has not been reported previously. It is possible that I, II, and XI could arise as by-products of the synthesis shown in Scheme I. Compound I would be present if incomplete *N*-debenzylation occurred. Compound II may arise during catalytic debenzylation through interaction of the ethanol solvent normally employed, while XI would be produced from residual IX remaining after esterification. This material would then be debenzylated and subsequently methylated at both the nitrogen and carboxylic acid groups during methylation.

Table II—TLC Characteristics of Meperidine and Its Synthetic Intermediates and Impurities

Compound	TLC R_f[a]	TLC Detection Limit[a], μg
V	0.00	—
III	0.00	0.50
X	0.10	—
IX	0.20	—
XI	0.39	0.50
VI	0.42	—
Meperidine	0.47	0.25
II	0.60	0.25
IV	0.70	—
VIII	0.71	—
VII	0.73	—
I	0.75	0.25

[a] Determined on each substance applied separately to the chromatoplate.

REFERENCES

(1) K. M. McErlane, N. M. Curran, and E. G. Lovering, *J. Pharm. Sci.*, **66**, 1015 (1977).

(2) O. Eisleb and O. Schaumann, U.S. pat. 2,167,351 (1939); through *Chem. Abstr.*, **33**, 9442 (1939).

(3) E. E. Smissman and G. Hite, *J. Am. Chem. Soc.*, **81**, 1201 (1959).

(4) H. K. Keyung, *Korean J. Intern. Med.*, **5**, 15 (1962).

(5) H. K. Keyung, *Taehan Nackwa Hakhoe Chapchi*, **6**, 201 (1963).

(6) C. V. Bercz and R. D. Ice, *J. Pharm. Sci.*, **61**, 1316 (1972).

(7) A. Noirfalise, *J. Chromatogr.*, **20**, 61 (1965).

(8) J. L. Emmerson and R. C. Anderson, *ibid.*, **17**, 495 (1965).

(9) F. Reimers, *Arch. Pharm. Chemi*, **78**, 201 (1971).

(10) J. R. Broich, S. Goldner, G. Gourdet, S. Andryauskas, C. J. Umberger, and D. B. Hoffman, *J. Chromatogr.*, **80**, 275 (1973).

(11) A. Alka, M. Karlsson, and T. Kote, *Z. Rechtsmed.*, **75**, 293 (1975).

(12) E. L. Grew, *Chem. Ind.*, **14**, 471 (1970).

(13) B. Ohlson, *Sv. Farm. Tidskr.*, **77**, 635 (1973).

(14) "British Pharmacopoeia 1973," Her Majesty's Stationery Office, London, England, 1973.

(15) "The United States Pharmacopeia," 19th rev., Mack Publishing Co., Easton, Pa., 1975.

(16) B. Loev and K. M. Snader, *Chem. Ind.*, No. 1, 15 (1965).

(17) B. Loev and M. M. Goodman, *ibid.*, **48**, 2026 (1967).

(18) E. Walton and M. B. Green, British pat. 566,307 (1944); through *Chem. Abstr.*, **40**, 6506 (1946).

Pyridinium- and Quinolinium-2-dithioacetic Acid Zwitterions: Antiradiation and Anticancer Activities

WILLIAM O. FOYE ˣ, YEUN JAI LEE, KIRIT A. SHAH, and JOEL M. KAUFFMAN

Received June 21, 1977, from the *Samuel M. Best Research Laboratory, Massachusetts College of Pharmacy, Boston, MA 02215.* Accepted for publication November 2, 1977.

Abstract □ Pyridinium-, quinolinium-, and one pyrimidinium-2-dithioacetic acid zwitterions were prepared by condensation of the *N*-methyl heterocyclic anhydro bases with carbon disulfide. Reaction of the 2-methylpyridine methiodide anhydro base with carbon disulfide resulted in replacement of the 2-methyl group to give the 1-methylpyridinium-2-dithioacetic acid zwitterion. The 1,6-dimethylquinolinium-2-dithioacetic acid zwitterion showed appreciable anticancer activity against P-388 lymphocytic leukemia in mice, but the other zwitterions tested showed no activity. No antiradiation activity was found for 1-methylpyridinium-2-dithioacetic acid zwitterion.

Keyphrases □ Dithioacetic acids, pyridinium and quinolinium—zwitterions synthesized, antitumor and antiradiation activity evaluated □ Zwitterions—pyridinium- and quinolinium-2-dithioacetic acids synthesized, antitumor and antiradiation activity evaluated □ Antitumor activity—various pyridinium- and quinolinium-2-dithioacetic acids evaluated in mice □ Antiradiation activity—1-methylpyridinium-2-dithioacetic acid evaluated in mice □ Structure–activity relationships—various pyridinium- and quinolinium-2-dithioacetic acids evaluated for antitumor and antiradiation activity

Condensation of carbon disulfide with active methylene groups is a method for preparing dithio acids (1). Dithio acid dianions prepared from several cyanomethylene-substituted compounds (2), in particular *N*-cyanoacetylpyrrolidine (3), had appreciable radiation-protective properties. Dithio acids and esters derived from pyridinium ylids also were radiation protective in both mice and bacteria (4).

Antileukemia tests were performed for some dithio acid dianions; although positive activity was not found, it is considered that radiation-protective compounds that may act as DNA-complexing agents should have anticancer potential as well (3). Therefore, synthesis of other dithio acids, particularly those with nitrogen-containing heterocycles, was undertaken to prepare potential antiradiation and anticancer agents.

DISCUSSION

Anhydro bases derived from quaternary pyridinium and quinolinium salts by alkaline treatment react with carbon disulfide to form dithio acids (5, 6). With 2-methylpyridine methiodide (I*a*), carbon disulfide condensation with the anhydro base (I*b*) took place with elimination of the 2-methyl group to give the 1-methylpyridinium-2-dithiocarboxylic acid zwitterion (III, Scheme I). Reaction of I*b* with carbon disulfide was first observed by Schneider *et al.* (7), who obtained a product melting at 186° for which they claimed Structure II.

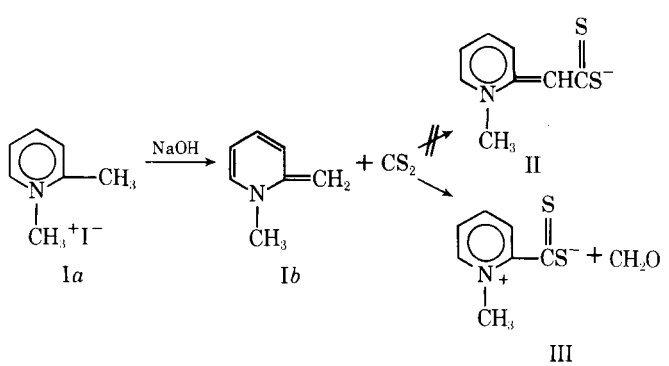

Scheme I

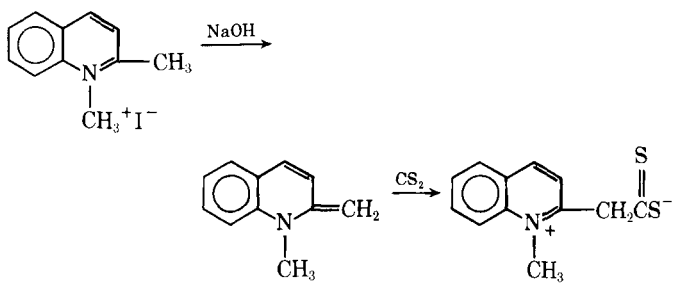

Scheme II

A solution of I*b* was obtained in 20% alkali, and repetition of their reaction in a two-phase aqueous ether system or in a homogeneous aqueous dioxane solution gave an orange product, mp 247–249°. Analytical data did not support Schneider's structure, and NMR analysis showed the complete loss of the C-methyl protons. Both the product and I*a* showed four aromatic ring protons and a singlet for *N*-methyl protons (δ 4.37 ppm in I*a* and 4.11 ppm in the product); only I*a* showed C-methyl protons (δ 2.94 ppm).

Both elemental analysis and NMR data support Structure III for the product, the 1-methylpyridinium-2-dithiocarboxylic acid zwitterion. Mass spectral peaks also corresponded to those expected from III rather than from II. Peaks were observed from measurement at 100, 170, and 235° at *m/e* 76 (CS_2^+), 78, 79 (pyridine$^+$), 92, 93 (*N*-methylpyridine$^+$), 192 (S_6^+), 224 (S_7^+), 256 (S_8^+), and 51 and 148 (polymerized acetylene). No peak was observed at either *m/e* 183 (Structure II) or 169 (Structure III) because of loss of carbon disulfide.

The only other product detected in the reaction was a small quantity of yellow crystals at the interface of the two-phase reaction. Heating this material in dimethylformamide or recrystallization from ethanol converted it to III. Gompper *et al.* (8) found that Schneider's product (II) could be obtained at −30° in acetonitrile.

The same procedure carried out with quinaldine methiodide, however, resulted in the formation of the quinaldinium-2-dithioacetic acid zwitterion (IV, Scheme II) without loss of the 2-methyl group, probably because of greater stability of the quinaldinium anhydro base.

Although condensation of carbon disulfide with the methyl groups of 2,6-dimethylpyridine (2,6-lutidine) and 2-methylquinoline has been claimed to give salts of dithio acids (9), neither 2-methylpyridine, 2,6-lutidine, nor 2,4,6-collidine would react with carbon disulfide in the presence of various concentrations of base. Conversion to the methiodides, however, produced more active methyl groups which did condense with carbon disulfide. The products from 2,6-lutidine and 2,4,6-collidine were the sodium salts of 1-methylpyridinium-2,6-bis(dithioacetic acid) (V) and 1,4-dimethylpyridinium-2,6-bis(dithioacetic acid) (VI) zwitterions, respectively.

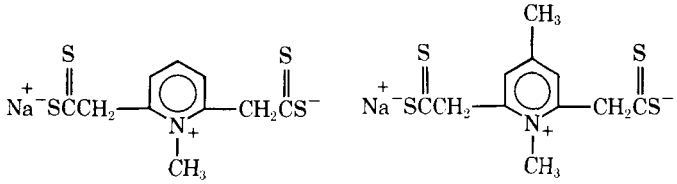

0022-3549/78/0700/0962$01.00/0
© 1978, American Pharmaceutical Association

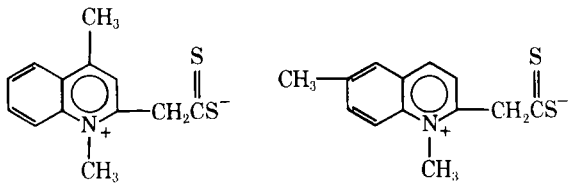

VII VIII

Substitution of the 2- and 6-methyl groups in each compound was confirmed by NMR analysis. 2,6-Lutidine methiodide and V showed three aromatic ring protons (δ 8.10 ppm) and a three-proton singlet (δ 4.20 ppm) for the *N*-methyl. 2,6-Lutidine methiodide also showed a six-proton singlet (δ 3.00 ppm) for the C-methyls, and V showed a four-proton singlet at δ 3.00 ppm.

2,4,6-Collidine methiodide and VI showed two aromatic ring protons (δ 8.10 ppm) and a three-proton singlet (δ 4.20 ppm) for the *N*-methyl. 2,4,6-Collidine methiodide also showed a six-proton singlet (δ 2.82 ppm) for the 2- and 6-methyls and a three-proton singlet (δ 2.50 ppm) for the 4-methyl group. Compound VI showed a three-proton singlet (δ 2.50 ppm) for the 4-methyl but a four-proton singlet (δ 2.85 ppm) for the 2- and 6-methyls.

Condensation of carbon disulfide also occurred with the methiodides of 4-methylquinaldine and 6-methylquinaldine. In both cases, the 2-dithioacetic acid zwitterion (VII and VIII, respectively) was obtained; no bis(dithioacetic acid) was observed. This result is supported by the fact that 4-methylquinaldine condenses with benzaldehyde in the presence of alkali only on the 2-methyl group (10). NMR data could not be obtained because of the insolubility of these compounds.

3-Methylisoquinolinium methiodide underwent condensation with carbon disulfide and alkali to give the expected 2-methylisoquinolinium-3-dithioacetic acid zwitterion (IX, Scheme III).

4,6-Dimethylpyrimidine methiodide also condensed with carbon disulfide to give a mono(dithioacetic acid). On the basis of previous results, anhydro base formation can be assumed to occur on the methyl adjacent to the *N*-methyl group; therefore, the product is 1,4-dimethylpyrimidinium-6-dithioacetic acid zwitterion (X, Scheme IV).

Antiradiation testing[1] was carried out with III in mice at several dosage levels up to 100 mg/kg ip and up to 400 mg/kg po. Radiation dosage was 849 rads of γ-radiation (from a ^{137}Cs-source); no protection of the mice was observed. Details of the testing procedure were described previously (3).

Anticancer screening was done[2] using either L-1210 lymphoid leukemia or P-388 lymphocytic leukemia. Compounds III, VI, and IX were essentially inactive; details regarding dose, tumor system, and survival are listed in Table I. Compound VI, however, showed positive activity in mice with P-388 lymphocytic leukemia, comparable to that from mercaptopurine. Details of the testing procedures were described previously (3).

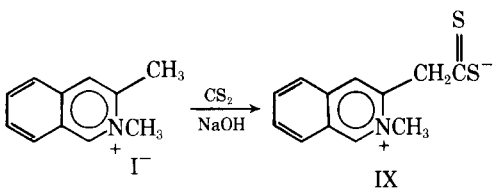

Scheme III

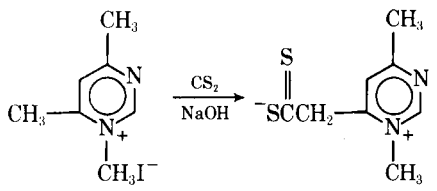

Scheme IV

[1] Antiradiation testing was carried out at the Walter Reed Army Institute of Research. Results were made available through the courtesy of Dr. Marie M. Grenan.

[2] Anticancer screening was carried out by the Division of Cancer Treatment, National Cancer Institute, in accordance with their protocol (11).

Table I—Antitumor Activities in Mice

Compound	Tumor[a]	Dose, mg/kg	Animal Weight Difference (T − C), g	Survival (T/C), %
III	LE	25	−1.8	102
	PS	25	−0.3	95
VI	LE	87.5	−0.4	105
VIII	PS	50	−2.3	126
	PS	100	−1.3	140
IX	PS	100	−1.4	99
6-Mercaptopurine	LE	80	−1.9	156
	LE	160	−3.3	144

[a] LE refers to L-1210 lymphoid leukemia; PS refers to P-388 lymphocytic leukemia.

Antimalarial screening of two compounds was carried out[3] using the blood schizonticidal test in mice infected with *Plasmodium berghei* KBG 173 malaria, according to the procedure of Osdene *et al.* (12). Compounds VII and IX showed essentially no activity at dose levels of 40, 160, and 640 mg/kg.

The antileukemic activity of VIII possibly could be regarded as due to the loss of carbon disulfide, by reversal of the aldol-like condensation, leaving a reactive carbanion which might function similarly to the alkylating agents. Since none of the related structures showed appreciable antileukemic effects and would be expected to undergo the loss of carbon disulfide with similar ease or difficulty, it can be assumed at present that the activity is a function of the dithiocarboxylic acid structure. No previous examples of anticancer activity by dithio acids are known.

EXPERIMENTAL[4]

2-Methylpyridine Methiodide—2-Methylpyridine (20 ml, 0.204 mole) and methyl iodide (16 ml, 0.258 mole) in 125 ml of absolute ethanol were refluxed for 3 hr. Cooling at 5° produced colorless crystals that were recrystallized from absolute ethanol, mp 220–225° [lit. (13) mp 224°]; NMR (dimethyl sulfoxide-d_6): δ 2.94 (s, 3H, 2-CH_3), 4.40 (s, 3H, NCH_3), and 7.9–8.4 (m, 4H, ring H) ppm.

1-Methylpyridinium-2-dithiocarboxylic Acid Zwitterion (III)—To a solution of 2-methylpyridine methiodide (4 g, 0.0163 mole), carbon disulfide (10 ml, 0.166 mole), dioxane (20 ml), and water (10 ml) was added 30 ml of 20% aqueous sodium hydroxide during 0.5 hr at room temperature. The resulting red solution was stirred overnight at room temperature. The red precipitate was filtered, washed with hot water, and dried, giving a 33% yield of orange-brown crystals, mp 247–249°; IR (KBr): 1320 (C=S) and 925 (C=S) cm^{-1}; NMR (dimethyl sulfoxide-d_6); δ 4.4 (s, 3H, NCH_3) and 7.9–8.4 (m, 4H, ring H) ppm; mass spectrum: *m/e* 76 (CS^{+2}), 78, 79 (pyridine$^+$), 92, 93 (*N*-methylpyridine$^+$), 192 (S_6^+), 224 (S_7^+), 256 (S_8^+), and 51 and 148 (polymerized acetylene).

Anal.—Calc. for $C_7H_7NS_2$: C, 49.80; H, 4.14; N, 8.29; S, 37.80. Found: C, 50.08; H, 4.05; N, 8.20; S, 37.50.

GC of the reaction mixture was carried out at 100°, using nitrogen as the carrier with 8% dinonyl phthalate on Chromosorb W and 8% Carbowax 1540 on Chromosorb W columns. A sample was removed from the reaction mixture 15 min after the start of the reaction; it was injected in a solution of either ethanol or methanol. The retention time of one peak was identical to that obtained with 37% formaldehyde solution; the only other peaks were attributable to the alcohol, carbon disulfide, and water.

1-Methylquinolinium-2-dithoacetic Acid Zwitterion (IV)—To a solution of 1-methylquinaldinium iodide (14) (4.85 g, 0.017 mole), dioxane (20 ml), water (10 ml), and carbon disulfide (10 ml, 0.166 mole) was added rapidly 30 ml of saturated sodium hydroxide. A thick red paste formed immediately; an additional 5 ml of water was added, and the mixture was stirred overnight at room temperature. The red solid was filtered and washed with water, mp 185–187°; IR (KBr): 1305 (C=S) and

[3] Antimalarial screening was carried out at the University of Miami; results were made available by the Walter Reed Army Institute of Research.

[4] Melting points were determined with a Mel-Temp capillary melting-point block and are uncorrected. IR spectra were obtained using a Perkin-Elmer model 137B spectrophotometer. NMR spectra were obtained with a Varian A-60 spectrometer using tetramethylsilane as the internal standard. Mass spectra were obtained on a Consolidated Electrodynamics Corp. model 21-110 spectrometer. TLC was carried out using silica gel, and products were detected by exposure to iodine vapor. Elemental analyses were done by F. B. Strauss, Oxford, England, or by Carol K. Fitz, Carlisle, Mass. Organic reagents were obtained from Aldrich Chemical Co. and Fisher Scientific Co.

920 (C=S) cm^{-1}; NMR (dimethyl sulfoxide-d_6): δ 2.55 (s, 2H, 2-CH_2), 4.4 (s, 3H, NCH_3), and 7.9–8.4 (m, 6H, ring H) ppm.

Anal.—Calc. for $C_{12}H_{11}NS_2$: C, 61.80; H, 4.72; N, 6.01; S, 27.46. Found: C, 62.14; H, 4.77; N, 6.20; S, 27.10.

2,6-Dimethylpyridine Methiodide—2,6-Dimethylpyridine (40 ml, 0.37 mole) and methyl iodide (32 ml, 0.32 mole) were added to 250 ml of absolute ethanol. The resulting solution was refluxed for 3 hr and cooled at 5°. The white crystals were recrystallized from absolute ethanol, mp 240–242°; NMR (dimethyl sulfoxide-d_6): δ 3.00 (s, 6H, CH_3), 4.20 (s, 3H, NCH_3), and 8.10 (m, 3H, aromatic H) ppm.

Anal.—Calc. for $C_8H_{12}IN$: C, 38.55; H, 4.81; N, 5.62. Found: C, 38.19; H, 4.97; N, 5.64.

Sodium 1-Methylpyridinium-2,6-bis(dithioacetate) Zwitterion (V)—To a solution of 2,6-dimethylpyridine methiodide (4 g, 0.02 mole), water (10 ml), dioxane (20 ml), and carbon disulfide (10 ml, 0.166 mole) was added 30 ml of 20% sodium hydroxide over 0.5 hr at room temperature. The solution was stirred overnight. A red precipitate was filtered, washed with hot water, and dried in a desiccator, mp 249–250°; IR (KBr): 1335 (C=S) and 935 (C=S) cm^{-1}; NMR (dimethyl sulfoxide-d_6): δ 3.00 (s, 4H, CCH_2), 4.20 (s, 3H, NCH_3), and 8.10 (m, 3H, aromatic H) ppm.

Anal.—Calc. for $C_{10}H_{11}NNaS_4$: C, 40.65; H, 3.41; N, 4.74. Found: C, 41.04; H, 3.46; N, 4.93.

2,4,6-Trimethylpyridine Methiodide—2,4,6-Trimethylpyridine (40 ml, 0.32 mole) and methyl iodide (32 ml, 0.32 mole) were added to 250 ml of absolute ethanol. The resulting solution was refluxed for 3 hr and cooled at 5°. The white crystals were recrystallized from absolute ethanol, mp 209–210°; NMR (dimethyl sulfoxide-d_6): δ 2.50 (s, 3H, 4-CH_3), 2.82 (s, 6H, 2- and 6-CH_3), 4.20 (s, 3H, NCH_3), and 8.10 (s, 2H, aromatic H) ppm.

Anal.—Calc. for $C_9H_{14}IN$: C, 41.06; H, 5.32; N, 5.32. Found: C, 40.95; H, 5.36; N, 5.07.

Sodium 1,4-Dimethylpyridinium-2,6-bis(dithioacetate) Zwitterion (VI)—To a solution of 2,4,6-trimethylpyridine methiodide (4 g, 0.02 mole), water (10 ml), dioxane (20 ml), and carbon disulfide (10 ml, 0.166 mole) was added 30 ml of 20% sodium hydroxide over 0.5 hr at room temperature. The solution was stirred overnight. A red precipitate was filtered, washed with hot water, and dried in a desiccator, mp 188–190°; IR (KBr): 1300 (C=S) and 920 (C=S) cm^{-1}; NMR (dimethyl sulfoxide-d_6): δ 2.50 (s, 3H, 4-CH_3), 2.85 (s, 4H, 2- and 6-CH_2), 4.20 (s, 3H, NCH_3), and 8.10 (s, 2H, aromatic H) ppm.

Anal.—Calc. for $C_{11}H_{12}NNaS_4$: C, 42.69; H, 3.91; N, 4.53. Found: C, 42.45; H, 3.91; N, 4.85.

1,4-Dimethylquinaldinium Iodide—4-Methylquinaldine (25 g, 0.159 mole) and methyl iodide (10 ml, 0.159 mole) were added to 130 ml of butanol. The resulting solution was refluxed for 4 hr and allowed to stand at 5°. The yellow crystals were filtered and recrystallized from propanol, mp 267–268° [lit. (15) mp 263–265°]; NMR (dimethyl sulfoxide-d_6): δ 2.85 (s, 3H, 4-CH_3), 3.00 (d, 3H, 2-CH_3), and 4.40 (s, 3H, NCH_3) ppm.

1,4-Dimethylquinolinium-2-dithioacetic Acid Zwitterion (VII)—To a solution of 1,4-dimethylquinaldinium iodide (5.38 g, 0.017 mole), water (10 ml), dioxane (20 ml), and carbon disulfide (10 ml, 0.166 mole) was added rapidly 30 ml of 30% sodium hydroxide. A thick red paste was formed, and 5 ml of water was added; the mixture was stirred overnight at room temperature. Then the mixture was filtered and washed with hot water and carbon disulfide to give a dark-red powder (2 g, 50% yield), mp 165–167°; IR (KBr): 1300 (C=S) and 920 (C=S) cm^{-1}.

Anal.—Calc. for $C_{13}H_{13}NS_2$: C, 63.15; H, 4.7; N, 5.6; S, 25.9. Found: C, 63.3; H, 5.0; N, 5.6; S, 26.3.

1,6-Dimethylquinaldinium Iodide—To 150 ml of butanol, 6-methylquinaldine (10.05 g, 0.064 mole) and methyl iodide (4 ml, 0.064 mole) were added rapidly. The solution was refluxed for 4 hr, and the resulting mixture was cooled at 5° overnight. Yellow needles were isolated and recrystallized from propanol, mp 251–252° [lit. (16) mp 236–237°]; NMR (dimethyl sulfoxide-d_6): δ 2.55 (s, 3H, 6-CH_3), 3.15 (s, 3H, 2-CH_3), and 4.50 (s, 3H, NCH_3) ppm.

1,6-Dimethylquinolinium-2-dithioacetic Acid Zwitterion (VIII)—To a solution of 1,6-dimethylquinaldinium iodide (3.90 g, 0.013 mole), water (10 ml), dioxane (20 ml), and carbon disulfide (10 ml, 0.166 mole) was added rapidly 30 ml of 30% sodium hydroxide. A dark-red precipitate formed immediately; 5 ml of water was added, and the mixture was stirred overnight at room temperature. The mixture was filtered and washed with hot water and carbon disulfide to give a dark-red powder (1.8 g, 60% yield), mp 191–192°; IR (KBr): 1300 (C=S) and 920 (C=S) cm^{-1}.

Anal.—Calc. for $C_{13}H_{13}NS_2$: C, 63.15; H, 4.7; N, 5.6; S, 25.9. Found: C, 62.9; H, 5.0; N, 5.5; S, 25.6.

2,3-Dimethylisoquinolinium Iodide—3-Methylisoquinoline (36.95 g, 0.258 mole) and methyl iodide (16 ml, 0.258 mole) in 175 ml of butanol were refluxed with stirring for 4 hr and cooled overnight at 5°. The yellow needles were filtered and recrystallized from absolute ethanol, mp 224–225° [lit. (27) mp 219°]; NMR (dimethyl sulfoxide-d_6): δ 2.75 (s, 3H, 3-CH_3) and 4.40 (s, 3H, NCH_3) ppm.

2-Methylisoquinolinium-3-dithioacetic Acid Zwitterion (IX)—To 2,3-dimethylisoquinolinium iodide (4.85 g, 0.017 mole), water (10 ml), dioxane (20 ml), and carbon disulfide (10 ml, 0.166 mole) was added rapidly 30 ml of 30% sodium hydroxide. An orange solid precipitated, 5 ml of water was added, and the mixture was stirred overnight at room temperature. The precipitate was filtered and washed with hot water and carbon disulfide, giving 1.1 g (30% yield) of orange powder, mp 246–250°; IR (KBr): 1020 (C=S) cm^{-1}.

Anal.—Calc. for $C_{12}H_{11}NS_2$: C, 61.8; H, 4.7; N, 6.0; S, 27.4. Found: C, 61.5; H, 4.6; N, 5.8; S, 27.1.

1,4,6-Trimethylpyrimidinium Iodide—4,6-Dimethylpyrimidine (10 g, 0.092 mole) and methyl iodide (6 ml, 0.092 mole) in 100 ml of methanol were refluxed for 3 hr and cooled overnight at 5°. The pale-yellow crystals were filtered and recrystallized from water and methanol–ethyl acetate to give 6 g (40% yield), mp 250–252°; NMR (dimethyl sulfoxide-d_6): δ 2.75 (d, 6H, 4-,6-CH_3), 4.25 (s, 3H, NCH_3), and 8.40 (s, 2H, aromatic H) ppm.

Anal.—Calc. for $C_7H_{11}IN_2$: C, 33.6; H, 4.4; N, 11.2. Found: C, 33.7; H, 4.4; N, 11.0.

1,4-Dimethylpyrimidinium-6-dithioacetic Acid Zwitterion (X)—To a solution of 1,4,6-trimethylpyrimidinium iodide (2.5 g, 0.01 mole), water (5 ml), dioxane (20 ml), and carbon disulfide (5 ml, 0.084 mole) was added rapidly 20 ml of 30% sodium hydroxide. A dark-red solid precipitated, 5 ml of water was added, and the mixture was stirred overnight at room temperature. The product was filtered and washed with water and carbon disulfide, giving 160 mg (10% yield) of dark-red powder, mp 186–187°; IR (KBr): 1300 (C=S) and 865 (C=S) cm^{-1}.

Anal.—Calc. for $C_8H_{10}N_2S_2$: C, 48.5; H, 5.0; N, 14.1. Found: C, 48.8; H, 4.6; N, 13.9.

REFERENCES

(1) H. D. Edwards and J. D. Kendall, U.S. pat. 2,533,233 (1950). M. Brown, U.S. pat. 3,057,875 (1962).

(2) W. O. Foye and J. M. Kauffman, *J. Pharm. Sci.*, **57**, 1611 (1968).

(3) W. O. Foye, Y. H. Lowe, and J. J. Lanzillo, *ibid.*, **65**, 1247 (1976).

(4) W. O. Foye, Y. J. Cho, and K.H. Oh, *ibid.*, **59**, 114 (1970).

(5) "Pyridine and Its Derivatives, Part II," E. Klingsberg, Ed., Interscience, New York, N.Y., 1961, p. 39.

(6) W. O. Foye, *J. Chem. Educ.*, **46**, 841 (1969).

(7) W. Schneider, K. Gaertner, and A. Jordan, *Chem. Ber.*, **57**, 522 (1924).

(8) R. Gompper, B. Wetzel, and W. Elser, *Tetrahedron Lett.*, **53**, 5519 (1968).

(9) F. Scheffer and R. Kickuth, German pat. 1,136,697 (1962).

(10) C. E. Kaslow and R. D. Stayner, *J. Am. Chem. Soc.*, **67**, 1716 (1945).

(11) R. I. Geran, N. H. Greenberg, M. M. MacDonald, A. M. Schumacher, and B. J. Abbott, *Cancer Chemother. Rep., Part 3*, **3**, 1 (1972).

(12) T. S. Osdene, P. B. Russell, and L. Rane, *J. Med. Chem.*, **10**, 431 (1967).

(13) P. Murrill, *J. Am. Chem. Soc.*, **21**, 828 (1899).

(14) O. Doebner and W. von Miller, *Chem. Ber.*, **16**, 2464 (1883).

(15) D. Craig, *J. Am. Chem. Soc.*, **60**, 1458 (1938).

(16) S. Brandes, *J. Prakt. Chem.*, **54**, 460 (1896).

(17) W. H. Mills and J. L. B. Smith, *J. Chem. Soc.*, **121**, 2732 (1922).

ACKNOWLEDGMENTS

Abstracted from theses submitted by Y. J. Lee and K. A. Shah to the Massachusetts College of Pharmacy in partial fulfillment of the Master of Science degree requirements.

Supported by Research Grant RH 00297 from the National Center for Radiological Health, U.S. Public Health Service.

The authors thank Dr. Philip L. Levins, Arthur D. Little, Inc., for the mass spectra.

Effect of Local Anesthetics on Electrically Excitable Bilayer Lipid Membranes

J. PAIEMENT

Received March 22, 1977, from the *Ecole de Pharmacie, Université Laval, Québec, Canada G1K 7P4.* Accepted for publication November 1, 1977.

Abstract □ The effect of three local anesthetics on the action potential of electrically excitable bilayer lipid membranes was studied. The synthetic action potential of bilayers was abolished at drug concentrations roughly identical to those abolishing the action potential in nerves. The threshold depolarizing constant current pulse triggering the synthetic action potential was increased by slightly lower concentrations of these local anesthetics. It is suggested that the anionic channels, which are responsible for the rising phase of the action potential in bilayers, are affected preferentially by these drugs.

Keyphrases □ Anesthetics, local—effect on electrically excitable bilayer lipid membranes □ Lipid membranes, bilayer—electrically excitable, effect of local anesthetics

Action potentials generated in bilayer lipid membranes were like those observed with primitive cells (*Nitella* and ovae): they displayed anion–cation permeability transitions rather than sodium–potassium transitions as in nerves (1). It was hypothesized, however, that regardless of ion selectivity, the gating mechanism, *i.e.*, the molecular mechanism by which excitable membranes open and close for the passage of ions, might be identical in the bilayer and in the nerve (1–4). If this hypothesis is correct, the excitable bilayer should become a valuable asset in elucidating the molecular mode of action of some drugs that modify conduction along the nerve membrane.

While the mechanism of electrical excitability in nerves is still obscure, it is partially understood in bilayers (2–4), and the chemical components of electrical excitability in bilayers are known. Although much basic work is needed to establish the exact nature of the similarities existing between the nerve membrane and the excitable bilayer, it was interesting to compare systematically the effects of some drugs classes on these two systems. Local anesthetics were selected mainly because some available information suggests that these drugs might act (at least in part) on the gating mechanism of excitable membranes (5). This report presents the preliminary findings of this study.

EXPERIMENTAL

Material—The excitability-inducing material was a crude preparation obtained from *Aerobacter cloacae*, grown overnight in an egg white medium and stabilized by pan drying (1). Excitability-inducing material is not a well-defined substance. It is "predominantly a protein oligomer having a maximum specific activity at a molecular weight around 250,000 and a monomeric size presumably as low as 6000; it may also have some associated small molecular weight organic entity"[1]. The potency of this material may vary from batch to batch, and the concentrations necessary to render a bilayer electrically excitable vary accordingly. For a given batch of excitability-inducing material and the given concentration used initially, the concentration of protamine[2] necessary to "interact" with the excitability-inducing material in the bilayer varies little.

The membrane-forming solution contained 25 mg of sphingomyelin[3]/ml of chloroform–methanol–tocopherol[4] (3:2:5).

The 5 m*M* histidine buffer[5], pH 7.0, was prepared from a 0.1 *M* stock solution kept in the refrigerator. The inorganic chemicals used were from the best grade available, and the water was distilled twice.

The excitability-inducing material, protamine, lipids, and local anesthetic[6] solutions were always prepared fresh.

Method—The membranes were prepared by the hairbrush technique across a hole, about 1 mm in diameter, separating two compartments filled with the histidine buffer; one compartment, where all additives were introduced, was arbitrarily defined as the inside. Electrical stimulation and measurement of electrical properties were obtained with a pair of reference calomel electrodes, one on each side of the membrane. The instrumental arrangement, electrical circuits, and technical procedures were described previously (6).

The main steps to obtain an electrically excitable bilayer may be summarized as follows (1, 6, 7).

1. A bimolecular lipid membrane was formed from the membrane-forming solution ["the final compositions of the thinned membranes are unknown but they would be expected to contain both sphingomyelin and tocopherol" (7)], and the specific conductance of the membrane was checked (it had to be around $3–5 \times 10^{-9}$ mho/cm^2).
2. The excitability-inducing material solution was added to the inside compartment to a final concentration of about 0.5×10^{-4} g/ml, and small constant current pulses (with the inside electrode positive) were applied until a significant increase in conductance [to around $3–5 \times 10^{-5}$ mho/cm^2 (7)] was observed (meaning that the excitability-inducing material had adsorbed onto the membrane). Outgoing current pulses helped to drive the excitability-inducing material molecules to the membrane.
3. Potassium sulfate and potassium chloride were added to the inside compartment to final concentrations of 10 and 40 m*M*, respectively. On addition of the salts, a resting potential of more than 50 mv, negative inside, in good analogy with a cell, developed.
4. Constant depolarizing current pulses (inside electrode positive) were applied until the phenomenon of delayed rectification had fully developed (1–2 min) (1).
5. Protamine was carefully titrated into the inside compartment to a final concentration of about 1.5 μg/ml; after the protamine molecules had "interacted" with the excitability-inducing material molecules in the membrane (1–3 min), action potentials could be obtained. The threshold depolarizing constant current pulse necessary to trigger an action potential was then determined, and many action potentials were obtained subsequently to verify that the threshold of excitation did not vary.
6. A local anesthetic was added to the inside compartment to the desired final concentration. After about 1 min, depolarizing currents were applied, and the effects of the drug on the threshold of excitation and on the action potential were noted.

Many experiments were performed with the three local anesthetics. Indeed, "like their counterparts in living systems, [electrically excitable bilayers] are extremely sensitive to small changes in their environment so that experiments must be repeated several times before the main response pattern can be distinguished among the minor fluctuations" (7).

THEORY

Since both the delayed rectification and the action potential occurring in bimolecular lipid membranes must be considered, a brief description

[1] J. Bukovski, Eastern Pennsylvania Psychiatric Institute, Philadelphia, PA 19129, personal communication.

[2] As the sulfate, Schwarz/Mann.

[3] Sigma.

[4] Chloroform, reagent, Merck; methanol, certified, ACS, Fisher; DL-α-tocopherol, Sigma.

[5] L-Histidine, Nutritional Biochemicals.

[6] Procaine hydrochloride USP, New York Quinine and Chemical Works; tetracaine and lidocaine, Pfaltz and Bauer.

0022-3549/78/0700/0965$01.00/0
© 1978, American Pharmaceutical Association

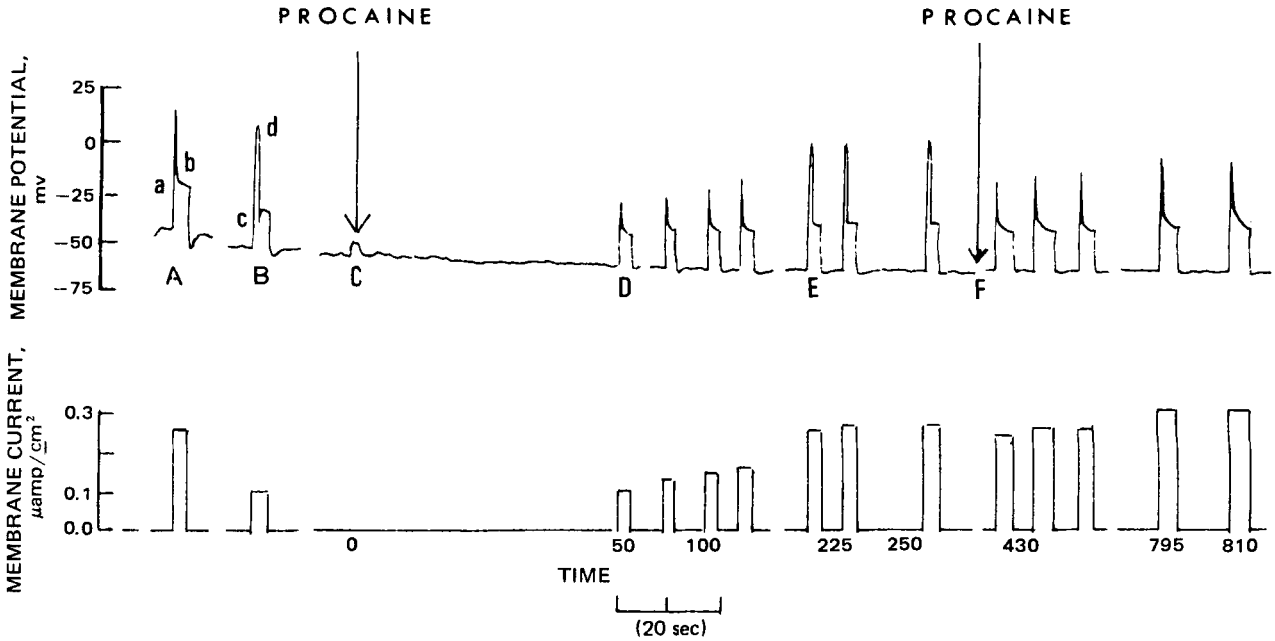

Figure 1—*Effect of procaine on electrically excitable bilayer lipid membranes. At A, only the excitability-inducing material was present in the bilayer, and the phenomenon of delayed rectification was obtained in response to a depolarizing constant current pulse. At B, both excitability-inducing material and protamine were present in the right proportions in the bilayer, and a depolarizing constant current pulse of threshold intensity triggered an action potential. At C, procaine was added to the inside compartment to a final concentration of about 3 mM (arbitrarily chosen as time zero and shown on the time scale). After about 1 min (at D), four successive depolarizing current pulses, of gradually increased size, were applied; the delayed rectification phenomenon was obtained in response to these current pulses. At E, depolarizing pulses of much increased size were applied to the membrane, and action potentials could then be restored. At F, the concentration of procaine was brought to 5 mM, and increasing depolarizing current pulses were applied again; only the delayed rectification phenomenon was obtained in response to these pulses.*

of the main electrical and molecular events thought to underlie these phenomena is presented to help in understanding the effects of the local anesthetics.

Delayed Rectification—After its addition to the inside compartment, the excitability-inducing material goes to the membrane where it adsorbs and, under the proper experimental conditions, forms channels. Its gating characteristics are (1, 7, 8): (*a*) in the absence of an electric field, its channels remain open; but in the presence of a field, they close; (*b*) these channels permit the passage of positive current from the excitability-inducing material-rich side to the other side; and (*c*) the gate selectivity of this particular channel-forming system (both excitability-inducing material and lipids) is cationic and is without discrimination between ions of this class.

Before the addition of the salts, the voltage gradient across the membrane is zero, and the "excitability-inducing material channels" are open and permit an important increase in the specific conductance of the membrane. After the addition of the salts to the inside compartment, some cations (but not anions) escape through the opened channels to reach the outside compartment; as a consequence, a voltage gradient is developed. This voltage gradient, in turn, causes the gates to close.

A depolarizing current, which brings the voltage near zero, causes the gates to reopen; cations then flow from the inside to the outside, and the voltage gradient tends to be restored. This voltage-restoring effect occurs after a small time delay necessary to depolarize the membrane and to open the gates. Experimentally, it is important to note that there is no inflection in the voltage–time curve of the first phase of the phenomenon (a in Fig. 1) and that the rectification process occurs, in a continuous way, all over b (Fig. 1) as the potential moves toward a new equilibrium value.

Action Potential—Protamine "interacts" with *a portion* of the excitability-inducing material channels in the membrane ["it adsorbs in or near the channel" (9)] and changes the selectivity of that portion of the initial excitability-inducing material–lipid system from cationic to anionic (here, also, the selectivity applies to anions as a class). Now, the bilayer has two different kinds of channels, anion selective and cation selective, which behave (kinetically, at least) similarly to the sodium and potassium channels of nerves (1–4, 9).

A depolarizing current of threshold intensity activates the rapid forming anionic gates, allowing the passage of anions and the depolarization of the membrane. The cationic gates (like the potassium gates of nerves) are activated more slowly and manifest their effect after the peak of the action potential has been attained. The fall in potential they initiate acts as a stimulus for the closing of the anionic channels (starting at d in Fig. 1), and the membrane potential is thus restored rapidly. (For simplification, the inactivation of the channels is not considered here.)

In bilayers, anions and then cations flow from the same side of the membrane during the action potential; in nerves, sodium and then potassium flow from opposite sides of the membrane. Experimentally, two inflection points are essential features of the phenomenon: during the rising phase of the action potential (c in Fig. 1) and during the falling phase of the action potential (d in Fig. 1)[7].

RESULTS AND DISCUSSION

The effects of procaine (added to the inside compartment) on the synthetic action potential of bilayers are shown in Fig. 1. At low drug concentrations (0.2–1.0 m*M*), no significant effect could be detected. As the concentration was increased to about 3 m*M*, depolarizing currents of the intensity previously needed for excitation failed to trigger the action potential. Much higher depolarizing currents were then necessary. Upon further increase in the concentration of the local anesthetic (to about 5 m*M*), the synthetic action potential was definitely abolished, regardless of the intensity of the depolarizing currents used.

Careful examination of Fig. 1 reveals, however, that the delayed rectification was not significantly modified, suggesting that the local anesthetic exerted its effects preferentially on the anion-selective channels of the excitable bilayer. (A 50-fold increase in the protamine concentration did not restore the action potential, thus minimizing the possibility that the only effect of the local anesthetic was the competitive displacement of this basic protein from its coupling with the excitability-inducing material and, consequently, the destruction of the anionic gates.) The concentrations of procaine, tetracaine, and lidocaine necessary to abolish the synthetic action potential were 2–5, 0.1–0.25, and 1–5 m*M*, respectively; in nerves, the concentrations of these drugs abolishing the action potential are 3.7, 0.1, and 3.8 m*M* (10).

From these observations, a few analogies between the effects of local anesthetics on excitable bilayers and nerves become apparent. The

[7] The recording paper can be unrolled at a faster rate (by a factor of 5 or 10) during an experiment, which enlarges the time scale and helps in the identification of the two inflection points.

concentrations of these drugs abolishing the synthetic and the nerve action potential are roughly identical. In both cases, the excitation threshold is raised (see Ref. 11 for this effect in nerves). With nerves, it is well established that the sodium channels, responsible for the rising phase of the action potential, are generally more sensitive than the potassium channels to the presence of local anesthetics (10, 12, 13); with excitable bilayers, the observations presented in Fig. 1 suggest that the analogous channels, the anionic channels, responsible for the rising phase of the action potential also are affected preferentially by the presence of the drugs.

At this stage of the investigation, no attempt was made to define the kind of molecular effect local anesthetics might exert on the anionic channels of bilayers [*i.e.*, these drugs, for example, may act directly on these channels or indirectly through an effect on the lipid matrix (14)]. Rather, the hypothesis that local anesthetics may specifically affect the gating mechanism of excitable membranes in general is emphasized. Procaine does exert some effect on the sodium gating currents of nerves (5), thus affecting their molecular mechanism of gate formation. Another observation consistent with this idea is that tetrodotoxin, which exerts its effects on the "component" of the channels responsible for sodium selectivity of nerves [*i.e.*, this poison selectively blocks the sodium conductance (15) without affecting the sodium gating currents (16)] had no effect on the synthetic action potential of bilayers[8] (where different ion selectivities are involved).

REFERENCES

(1) P. Mueller and D. O. Rudin, *Nature*, **213**, 603 (1967).

(2) G. Baumann and P. Mueller, *J. Supramol. Struct.*, **2**, 516 (1974).

(3) P. Mueller, in "MTP International Review of Science, Biochemistry Series: Energy Transducing Mechanisms," vol. 3, E. Racker, Ed., Butterworths, London, England, 1975, pp. 75–120.

(4) P. Mueller, *Ann. N.Y. Acad. Sci.*, **264**, 247 (1975).

(5) R. D. Keynes and E. Rojas, *Proc. Physiol. Soc.*, **28P** (June 1973).

(6) P. Mueller and D. O. Rudin, in "Laboratory Techniques in Membrane Biophysics," H. Passow and R. Stampfli, Eds., Springer-Verlag, Berlin, Germany, 1969, pp. 141–156.

(7) D. R. Kalkwarf, D. L. Frasco, and W. H. Brattain, in "Physical Principles of Biological Membranes," F. Snell *et al.*, Eds., Gordon and Breach, New York, N.Y., 1970, pp. 165–174.

(8) H. Lecar, G. Ehrenstein, and R. Latorre, *Ann. N.Y. Acad. Sci.*, **264**, 304 (1975).

(9) C. W. Cotman and W. B. Levy, in "MTP International Review of Science, Biochemistry Series: Biochemistry of Cell Walls and Membranes," vol. 2, H. L. Kornberg and D. C. Phillips, Eds., Butterworths, London, England, 1975, pp. 187–205.

(10) P. Seeman, *Pharmacol. Rev.*, **24**, 583 (1972).

(11) B. I. Diamond, H. S. Havdala, and H. C. Sabelli, *Anesthesiology*, **43**, 651 (1975).

(12) M. P. Blaustein and D. E. Goldman, *J. Gen. Physiol.*, **49**, 1043 (1966).

(13) P. Arhem and B. Frankenhaeuser, *Acta Physiol. Scand.*, **91**, 11 (1974).

(14) G. Strichartz, in "Progress in Anesthesiology," vol. 1, B. Fink, Ed., Raven, New York, N.Y., 1975, pp. 1–11.

(15) B. Hille, *Nature*, **210**, 1220 (1966).

(16) F. Bezanilla and C. M. Armstrong, *Science*, **183**, 753 (1974).

ACKNOWLEDGMENTS

This work was performed at the Department of Molecular Biology, Eastern Pennsylvania Psychiatric Institute, Philadelphia, Pa. The author thanks Dr. Paul Mueller and Dr. Donald O. Rudin for invaluable help and advice. Thanks are also expressed to Mrs. Patricia Lewis for assistance.

[8] D. O. Rudin, Eastern Pennsylvania Psychiatric Institute, Philadelphia, PA 19129, personal communication.

Binding of Butylated Hydroxyanisole to Human Albumin Using a Novel Dynamic Method

R. EL-RASHIDY and SARFARAZ NIAZI ˣ

Received March 7, 1977, from the *Department of Pharmacy, College of Pharmacy, University of Illinois at the Medical Center, Chicago, IL 60612.* Accepted for publication November 2, 1977.

Abstract □ To study the interaction of butylated hydroxyanisole with various body tissues, a fully automated dynamic method was developed for the determination of plasma protein binding constants at 37°, using membrane filtration equipment designed for dissolution rate studies. Appropriate equations were derived for the calculation of the free drug concentration from comparative diffusion rates across sealed dialysis sacs. A monoexponential equation described the diffusion in the absence of proteins, and a biexponential equation was fitted to diffusion from the drug–protein complex. The Scatchard and double-reciprocal plots were developed for butylated hydroxyanisole. A high degree of reproducibility was obtained for the calculation of protein binding constants ($K = 2.4 - 2.9 \times 10^4$ and $n = 1.4 - 1.32$). The magnitude of these binding-constants suggests that any change in protein binding can have a significant effect on the distribution of butylated hydroxyanisole throughout the body, such as may be brought about by the common variations in the amount ingested.

Keyphrases □ Butylated hydroxyanisole—binding to human albumin studied using membrane filtration equipment □ Binding—butylated hydroxyanisole to human albumin, studied using membrane filtration equipment □ Antioxidants—butylated hydroxyanisole, binding to human albumin studied using membrane filtration equipment

Phenolic antioxidants, butylated hydroxyanisole and butylated hydroxytoluene, are widely used in various products (1) to which the American public is exposed frequently. Although these compounds are generally regarded as safe (GRAS list), they cause enzyme induction (2–9), accumulate in the body tissues (9–13), exhibit dose-dependent elimination (10, 14, 15), affect cellular growth and organization (16–26), and induce various other effects (27). However, no tissue interaction studies have been reported that characterize the toxicity of these compounds.

This paper reports plasma protein binding characteristics of butylated hydroxyanisole using membrane filtration equipment designed for dissolution rate studies. This novel method allows quick estimation of binding parameters at physiological temperature and is totally automated. Because of its advantages over other methods

0022-3549/78/0700/0967$01.00/0

© 1978, American Pharmaceutical Association

concentrations of these drugs abolishing the synthetic and the nerve action potential are roughly identical. In both cases, the excitation threshold is raised (see Ref. 11 for this effect in nerves). With nerves, it is well established that the sodium channels, responsible for the rising phase of the action potential, are generally more sensitive than the potassium channels to the presence of local anesthetics (10, 12, 13); with excitable bilayers, the observations presented in Fig. 1 suggest that the analogous channels, the anionic channels, responsible for the rising phase of the action potential also are affected preferentially by the presence of the drugs.

At this stage of the investigation, no attempt was made to define the kind of molecular effect local anesthetics might exert on the anionic channels of bilayers [*i.e.*, these drugs, for example, may act directly on these channels or indirectly through an effect on the lipid matrix (14)]. Rather, the hypothesis that local anesthetics may specifically affect the gating mechanism of excitable membranes in general is emphasized. Procaine does exert some effect on the sodium gating currents of nerves (5), thus affecting their molecular mechanism of gate formation. Another observation consistent with this idea is that tetrodotoxin, which exerts its effects on the "component" of the channels responsible for sodium selectivity of nerves [*i.e.*, this poison selectively blocks the sodium conductance (15) without affecting the sodium gating currents (16)] had no effect on the synthetic action potential of bilayers[8] (where different ion selectivities are involved).

REFERENCES

(1) P. Mueller and D. O. Rudin, *Nature*, **213**, 603 (1967).

(2) G. Baumann and P. Mueller, *J. Supramol. Struct.*, **2**, 516 (1974).

(3) P. Mueller, in "MTP International Review of Science, Biochemistry Series: Energy Transducing Mechanisms," vol. 3, E. Racker, Ed., Butterworths, London, England, 1975, pp. 75–120.

(4) P. Mueller, *Ann. N.Y. Acad. Sci.*, **264**, 247 (1975).

(5) R. D. Keynes and E. Rojas, *Proc. Physiol. Soc.*, **28P** (June 1973).

(6) P. Mueller and D. O. Rudin, in "Laboratory Techniques in Membrane Biophysics," H. Passow and R. Stampfli, Eds., Springer-Verlag, Berlin, Germany, 1969, pp. 141–156.

(7) D. R. Kalkwarf, D. L. Frasco, and W. H. Brattain, in "Physical Principles of Biological Membranes," F. Snell *et al.*, Eds., Gordon and Breach, New York, N.Y., 1970, pp. 165–174.

(8) H. Lecar, G. Ehrenstein, and R. Latorre, *Ann. N.Y. Acad. Sci.*, **264**, 304 (1975).

(9) C. W. Cotman and W. B. Levy, in "MTP International Review of Science, Biochemistry Series: Biochemistry of Cell Walls and Membranes," vol. 2, H. L. Kornberg and D. C. Phillips, Eds., Butterworths, London, England, 1975, pp. 187–205.

(10) P. Seeman, *Pharmacol. Rev.*, **24**, 583 (1972).

(11) B. I. Diamond, H. S. Havdala, and H. C. Sabelli, *Anesthesiology*, **43**, 651 (1975).

(12) M. P. Blaustein and D. E. Goldman, *J. Gen. Physiol.*, **49**, 1043 (1966).

(13) P. Arhem and B. Frankenhaeuser, *Acta Physiol. Scand.*, **91**, 11 (1974).

(14) G. Strichartz, in "Progress in Anesthesiology," vol. 1, B. Fink, Ed., Raven, New York, N.Y., 1975, pp. 1–11.

(15) B. Hille, *Nature*, **210**, 1220 (1966).

(16) F. Bezanilla and C. M. Armstrong, *Science*, **183**, 753 (1974).

ACKNOWLEDGMENTS

This work was performed at the Department of Molecular Biology, Eastern Pennsylvania Psychiatric Institute, Philadelphia, Pa. The author thanks Dr. Paul Mueller and Dr. Donald O. Rudin for invaluable help and advice. Thanks are also expressed to Mrs. Patricia Lewis for assistance.

[8] D. O. Rudin, Eastern Pennsylvania Psychiatric Institute, Philadelphia, PA 19129, personal communication.

Binding of Butylated Hydroxyanisole to Human Albumin Using a Novel Dynamic Method

R. EL-RASHIDY and SARFARAZ NIAZI ˣ

Received March 7, 1977, from the *Department of Pharmacy, College of Pharmacy, University of Illinois at the Medical Center, Chicago, IL 60612.* Accepted for publication November 2, 1977.

Abstract □ To study the interaction of butylated hydroxyanisole with various body tissues, a fully automated dynamic method was developed for the determination of plasma protein binding constants at 37°, using membrane filtration equipment designed for dissolution rate studies. Appropriate equations were derived for the calculation of the free drug concentration from comparative diffusion rates across sealed dialysis sacs. A monoexponential equation described the diffusion in the absence of proteins, and a biexponential equation was fitted to diffusion from the drug–protein complex. The Scatchard and double-reciprocal plots were developed for butylated hydroxyanisole. A high degree of reproducibility was obtained for the calculation of protein binding constants ($K = 2.4 - 2.9 \times 10^4$ and $n = 1.4 - 1.32$). The magnitude of these binding-constants suggests that any change in protein binding can have a significant effect on the distribution of butylated hydroxyanisole throughout the body, such as may be brought about by the common variations in the amount ingested.

Keyphrases □ Butylated hydroxyanisole—binding to human albumin studied using membrane filtration equipment □ Binding—butylated hydroxyanisole to human albumin, studied using membrane filtration equipment □ Antioxidants—butylated hydroxyanisole, binding to human albumin studied using membrane filtration equipment

Phenolic antioxidants, butylated hydroxyanisole and butylated hydroxytoluene, are widely used in various products (1) to which the American public is exposed frequently. Although these compounds are generally regarded as safe (GRAS list), they cause enzyme induction (2–9), accumulate in the body tissues (9–13), exhibit dose-dependent elimination (10, 14, 15), affect cellular growth and organization (16–26), and induce various other effects (27). However, no tissue interaction studies have been reported that characterize the toxicity of these compounds.

This paper reports plasma protein binding characteristics of butylated hydroxyanisole using membrane filtration equipment designed for dissolution rate studies. This novel method allows quick estimation of binding parameters at physiological temperature and is totally automated. Because of its advantages over other methods

0022-3549/78/0700/0967$01.00/0

© 1978, American Pharmaceutical Association

Table I—Protein Binding Parameters of Butylated Hydroxyanisole

Hours	C_{fo}, mg/ml	D_{fo}, mg	ΣD_s	D_{ti}[a], mg	$\frac{dD_{ti}}{dt}$ [b]	D_b, mg	$1/C_{fi}$[c], M	$\bar{v}$	$1/\bar{v}$	$\bar{v}/C_{fi}$, M
0.0	0.0	0.0	0.0	2.5000	−1.1288	1.68957	1110.52	5.0061	0.1998	5559.41
0.5	0.00331	0.497	0.0	2.0030	−0.9054	1.37175	1425.74	4.0644	0.2460	5794.84
1.0	0.00612	0.918	0.00828	1.5737	−0.7263	1.11770	1973.68	3.3117	0.3020	6536.24
1.5	0.00828	1.242	0.02358	1.2344	−0.5826	0.91341	2803.83	2.7064	0.3695	7588.28
2.0	0.00990	1.485	0.04428	0.9707	−0.4673	0.74892	4058.08	2.2190	0.4506	9004.97
2.5	0.01030	1.545	0.06903	0.8860	−0.3748	0.61247	3290.32	1.8147	0.5510	5971.03
3.0	0.01098	1.647	0.09478	0.7582	−0.3006	0.50481	3551.84	1.4957	0.6686	5312.60
3.5	0.01170	1.755	0.12223	0.6228	−0.2412	0.41950	4426.96	1.243	0.8045	5502.55
4.0	0.01240	1.860	0.15148	0.4885	−0.1934	0.35145	6566.95	1.0413	0.9603	6838.38
4.5	0.01296	1.944	0.18248	0.3735	−0.1552	0.29707	11775.48	0.8802	1.1361	10364.86
5.0	0.01332	1.998	0.21488	0.2871	−0.1245	0.25292	26331.19	0.7494	1.3344	19732.40
5.5	0.01335	2.003	0.24818	0.2488	−0.09983	0.21616	27573.53	0.6405	1.5613	17660.13

[a] $D_{ti} = 2.559e^{-0.44099t}$. [b] $dD_{ti}/dt = -1.12876e^{-0.44099t}$. [c] $k_{12} = 0.6681\ hr^{-1}$; $k_{21} = 0.02226\ hr^{-1}$.

(28–30), this technique is highly recommended for protein binding studies.

EXPERIMENTAL

Materials—Butylated hydroxyanisole[1], human plasma albumin[2], dialysis tubing[3], and monobasic and dibasic potassium phosphates[4] were obtained commercially.

Equipment—Membrane filtration equipment[5] customarily used for dissolution rate studies was modified for protein binding studies (Fig. 1). The modifications included removal of the filter membrane and introduction of a dialysis sac (10.16 × 3.18 cm) sealed on both ends with sterile disposable clamps[3] in the dissolution chamber. In each sac, 10 plastic beads (diameter of 8 mm) were placed to facilitate mixing during agitation.

Each solution chamber was filled with 150 ml of pH 7.4 phosphate buffer, maintained at 37 ± 1°, and 20 plastic beads were added. A sample of 2.5 ml was automatically drawn from the solution chamber every 30 min, and this volume was instantaneously and automatically replaced by phosphate buffer maintained at the same temperature in the external solvent reservoir.

Protein Binding Study—A solution of butylated hydroxyanisole was prepared at 0.5 mg/ml (2.777 mM) in 4% (0.375 mM) albumin in phosphate buffer. A 5-ml aliquot of this solution was placed in the dialysis sac to which 10 plastic beads were added, and the sac was sealed with clamps. The sac was then placed in the solution chamber containing 150 ml of phosphate buffer, and the chamber was rotated at 1.2 rpm (normal peristaltic speed).

A 2.5-ml sample, drawn periodically, was analyzed at 288 nm using a UV spectrophotometer[6]. The standard curve was prepared in phosphate buffer and gave a molar absorptivity of 5×10^3 at $r^2 > 0.99$.

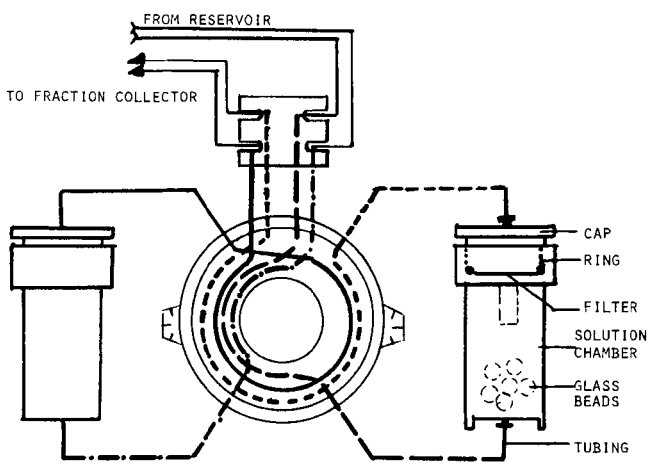

Figure 1—*Flow diagram of solubility simulator.*

[1] BHA, Nutritional Biochemical Corp., Cleveland, OH 44128.
[2] Sigma Chemical Co., St. Louis, MO 63178.
[3] Arthur H. Thomas Co., Philadelphia, Pa.
[4] Fisher Scientific Co., Fair Lawn, N.J.
[5] Sartorius membrane filter, GMbH 34 Göttingen/BRD Postfach, Germany.
[6] Beckman DBGT, Beckman Instruments, Fullerton, Calif.

The total amount of drug bound to proteins can be calculated from:

$$D_t = D_b + D_{fi} + D_{fo} \qquad \text{(Eq. 1)}$$

where D_t is the total drug in the system, D_b is the amount of drug bound, D_{fi} is the amount of free drug in the protein compartment, and D_{fo} is the amount of free drug in the solution chamber.

The loss of drug from the protein compartment takes place due to the equilibration of free drug across the dialysis sac and is expressed as:

$$\frac{dD_{ti}}{dt} = -k_{12}D_{fi} + k_{21}D_{fo} \qquad \text{(Eq. 2)}$$

where k_{12} and k_{21} are first-order mass transport constants as shown in Scheme I, and D_{ti} is the total drug inside the dialysis bag.

$$D_b \rightleftharpoons D_{fi} \underset{k_{21}}{\overset{k_{12}}{\rightleftharpoons}} D_{fo}$$

Scheme I

The values of these rate constants can be determined easily by excluding the protein from the dialysis sac (28); thus:

$$\frac{dD_{ti}}{dt} = \frac{dD_{fi}}{dt} = -k_{12}D_{fi} + k_{21}D_{fo} \qquad \text{(Eq. 3)}$$

which yields the following solution (31):

$$D_{fi} = \frac{D_{fi}{}^0 k_{21}}{k_{12} + k_{21}} + \frac{D_{fi}{}^0 k_{12}}{k_{12} + k_{21}} e^{-(k_{12}+k_{21})t} \qquad \text{(Eq. 4)}$$

where $D_{fi}{}^0 = D_{ti}$ at $t = 0$ and:

$$D_{fo} = \frac{D_{fi}{}^0 k_{12}}{k_{12} + k_{21}} (1 - e^{-(k_{12}+k_{21})t}) \qquad \text{(Eq. 5)}$$

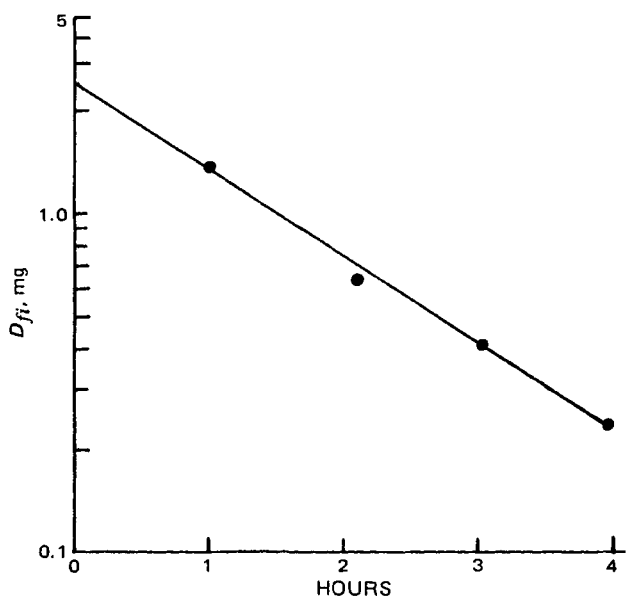

Figure 2—*Loss of free drug from the dialysis sac in the absence of protein.*

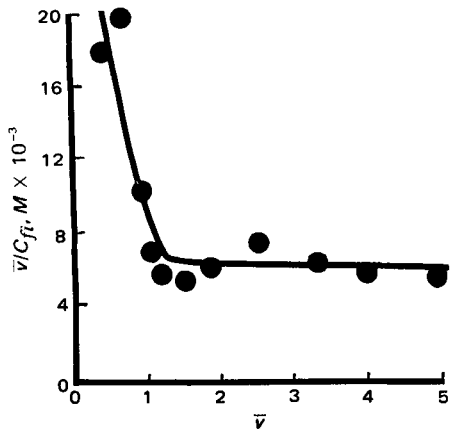

Figure 3—*Scatchard plot. (See text for details.)*

Since D_{fo} can be directly measured as a function of time and:

$$D_{fi} = D_{fi}^0 - D_{fo} \qquad \text{(Eq. 6)}$$

both D_{fi} and D_{fo} are accessible and can be used to calculate the rate constant as shown in Fig. 2, where 2.5 mg of butylated hydroxyanisole was placed inside the dialysis bag and allowed to diffuse.

When the protein is added to the dialysis bag, the total amount of drug inside the bag can be determined by the following mass balance equation:

$$D_{ti} = D_{ti}^0 - D_{fo} - \sum_{i=1}^{n-1} D_{si} \qquad \text{(Eq. 7)}$$

where $\Sigma_{i=1}^{n-1} D_{si}$ is the cumulative amount of drug lost due to preceding samplings of the system.

Table I reports the total drug inside as a function of time. The decrease in the D_{ti} as a function of time, except for D_{si}, can be represented by Eq. 2; thus:

$$D_{fi} = \frac{k_{21} D_{fo} - \dfrac{dD_{ti}}{dt}}{k_{12}} \qquad \text{(Eq. 8)}$$

The term dD_{ti}/dt can be determined either by drawing tangents at specific time function plots or, more appropriately, by fitting to an exponential equation:

$$D_{ti} = \sum_{i=1}^{n} (A_i e^{-a_i t}) \qquad \text{(Eq. 9a)}$$

$$\frac{dD_{ti}}{dt} = \sum_{i=1}^{n} (-A_i a_i e^{-a_i t}) \qquad \text{(Eq. 9b)}$$

where A_i values are constants, a_i values are hybrid rate constants, and t is time. This determination can be accomplished easily by using the desk-top calculater program described by Niazi (32). The data in Table I were fitted by a monoexponential equation:

$$D_{ti} = 2.559e^{-0.4409t} \qquad (r^2 > 0.98) \qquad \text{(Eq. 10)}$$

and:

$$-\frac{dD_{ti}}{dt} = 1.12876e^{-0.4409t} \qquad (r^2 > 0.99) \qquad \text{(Eq. 11)}$$

With this information, all data required for protein binding analysis can be derived as shown in Table I.

RESULTS AND DISCUSSION

Many studies (28–30) reported protein binding parameters using dynamic methods. In some instances, a sink condition is maintained outside the dialysis sac (28) to avoid the necessity of calculating the back-diffusion rate constant. Although the maintenance of sink conditions simplifies the calculations, it leads to cumbersome experimental procedures and definite theoretical errors since some degree of back-diffusion must be assumed no matter how small the outside concentration.

In the approach presented here, the main emphases are on the simplification of experimentation through automation and quick calculations of protein binding parameters using membrane filtration equipment. This equipment maintains the desired temperature (37 ± 1°) throughout the experiment and provides gentle and uniform mixing of solutions, automated sampling at preprogrammed intervals, and simultaneous replacement of the sample volume with the medium; all of these conditions are in a closed system. Further automation can be achieved by hooking the sampling port to a spectrophotometer, which can transmit impulses to a recorder or an appropriate data analyzer system.

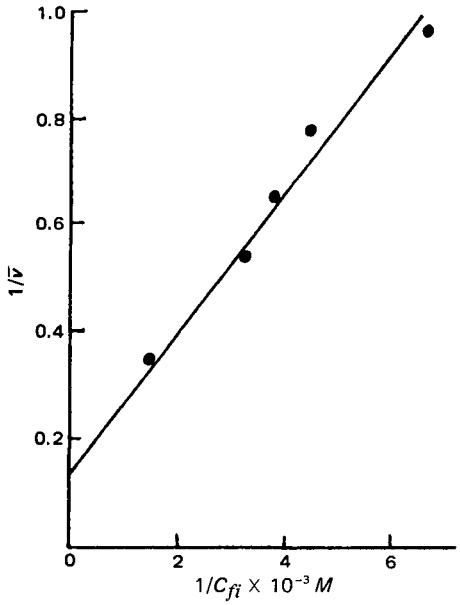

Figure 4—*Double-reciprocal plot using the data points representing the linear part of the Scatchard plot.*

Since the mathematical treatment presented does not require the maintenance of sink conditions, a greater concentration range can be studied. As shown in Table I, the C_{fo}, the outside concentration, varied from 2.62 to about 204% of the inside free concentration, C_{fi}:

$$\% \text{ of } C_{fi} = \frac{C_{fo} \times 5 \times 100}{(D_{ti} - D_{bi})} \qquad \text{(Eq. 12)}$$

Another modification in this method requires accounting for the drug lost from the system because of sampling. Although the total volume sampled each time is small, large numbers of samples can lead to significant errors. For example, after 5.5 hr of sampling, about 10% of the initial amount of drug was removed. If this removal is not considered, the term D_b would be grossly overestimated since it is arrived at by indirect mass balance calculations.

The forward and reverse mass transfer rate constants were obtained by excluding the protein from the sac and fitting the data to Eqs. 4 and 5, using the minicomputer program reported by Niazi (32).

The data fitted to Eq. 4 were plotted in Fig. 2 and showed excellent log linearity ($r^2 > 0.98$). These rate constants were utilized in Eq. 8 to calculate the free drug concentration inside the sac, leading to the complete set of parameters needed for protein binding calculations (Table I):

$$\bar{v}/C_{fi} = nK - K\bar{v} \qquad \text{(Eq. 13)}$$

$$\frac{1}{\bar{v}} = \frac{1}{nKC_{fi}} + \frac{1}{n} \qquad \text{(Eq. 14)}$$

where $\bar{v}$ is the ratio of the moles of drug bound per mole of protein, n is the number of binding sites, and K is the protein binding constant.

The data presented in Table I are plotted according to Eqs. 13 and 14 in Figs. 3 and 4, respectively. Both Scatchard (Eq. 13) and double-reciprocal (Eq. 14) plots gave excellent fits ($r^2 > 0.95$ and $r^2 > 0.98$, respectively). The number of binding sites obtained were 1.40 and 1.32, respectively: K values of 2.4×10^4 and 2.9×10^4 were obtained from Scatchard and double-reciprocal calculations, respectively. The agreement between these two methods of data handling can be considered excellent since the double-reciprocal method normally leads to great variation.

The protein binding constant obtained for butylated hydroxyanisole can be compared with the binding parameters of nafcillin (33), tetracyclines (34), digitoxin (35), digitoxigenin (35), prostaglandins (36), and dimethoxychlorpromazine (37). Most of these drugs show extensive distribution in the body and a wide range of biological half-lives. The magnitude of the binding constant of butylated hydroxyanisole suggests

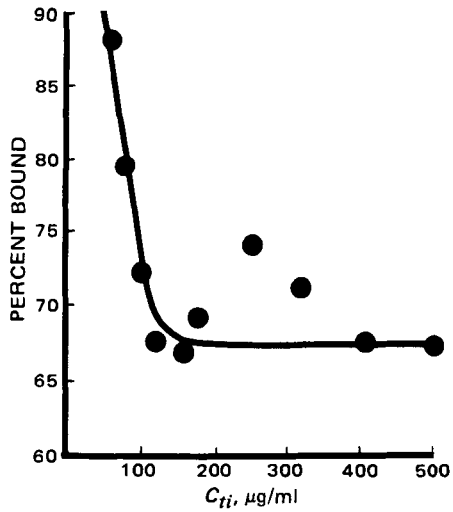

Figure 5—*Percent binding of butylated hydroxyanisole as a function of the total concentration in the protein compartment.*

that any change in protein binding will have a significant effect on the distribution throughout the body (38), such as may be brought about by the variations in the amount of butylated hydroxyanisole ingested.

Figure 5 shows the percent binding of butylated hydroxyanisole as a function of the total concentration in the protein compartment. The minimum binding was about 68% and the maximum binding exceeded 90%. This finding is important since, in normal dosing conditions (2 mg/kg), the total concentration of butylated hydroxyanisole will be well below the range providing minimum binding. For example, a 2-mg/kg dose in a 65-kg individual will give the maximum concentration of about 26 μg/ml, assuming all drug remains in the blood compartment initially. This concentration is well below the concentration at which the percent binding shows a plateau (Fig. 5). Thus, during normal ingestion of butylated hydroxyanisole, a high degree of protein binding can be assumed.

Higher doses of butylated hydroxyanisole have shown nonlinear elimination of the free compound in the urine (15). The increased metabolism can, at least in part, be attributed to possible effects of nonlinearity in protein binding. These studies are currently being conducted and will be reported.

REFERENCES

(1) *WHO Tech. Rep. Ser.*, No. 488, 1971.

(2) A. Takanaka, R. Kato, and Y. Omori, *Shokuhin Eiseigaku Zasshi*, **10**, 260 (1969).

(3) D. M. Conning and T. McElligott, *Proc. Eur. Soc. Study Drug Toxic.*, **11**, 203 (1970).

(4) P. H. Grantham, J. H. Weisburger, and E. K. Weisburger, *Food Cosmet. Toxicol.*, **11**, 209 (1973).

(5) M. A. Cawthrone, J. Bunyan, M. V. Sennitt, and J. Green, *Br. J. Nutr.*, **24**, 357 (1970).

(6) G. Feuer, I. F. Gaunt, L. Goldberge, and F. A. Fairweather, *Food Cosmet. Toxicol.*, **3**, 475 (1965).

(7) I. F. Gaunt, G. Feuer, F. A. Fairweather, and D. Gilbert, *ibid.*, **3**, 443 (1965).

(8) D. Gilbert and L. Goldberg, *ibid.*, **3**, 417 (1965).

(9) *Ibid.*, **5**, 481 (1967).

(10) R. Tye, J. D. Engel, and I. Rapien, *Food Cosmet. Toxicol.*, **3**, 547 (1965).

(11) J. P. Frawley, J. H. Kay, and J. C. Calandra, *ibid.*, **3**, 471 (1965).

(12) P. G. C. van Stratam and H. J. Vos, *ibid.*, **3**, 475 (1965).

(13) A. J. Collings and M. Sharrath, *ibid.*, **8**, 409 (1970).

(14) J. W. Daniel, J. C. Gage, D. J. Jones, and M. A. Stevens, *ibid.*, **5**, 475 (1967).

(15) B. D. Astill, D. Fasseff, and R. L. Roudabush, *Biochem. J.*, **75**, 543 (1960).

(16) A. A. Marino and J. T. Mitchell, *Proc. Soc. Exp. Biol. Med.*, **140**, 122 (1972).

(17) P. A. Riley and P. Seal, *Nature*, **220**, 922 (1968).

(18) B. N. Kaufmann and R. Maier, *Food Cosmet. Toxicol.*, **12**, 33 (1974).

(19) J. E. Baker and J. M. Makie, *J. Econ. Entomol.*, **66**, 765 (1973).

(20) B. E. March, V. Coates, and P. A. Riley, *Science*, **164**, 1398 (1969).

(21) N. K. Clapp, R. L. Tyndall, and R. B. Cumming, *Food Cosmet. Toxicol.*, **11**, 847 (1973).

(22) W. Snipes, S. Person, A. Keith, and J. Cupp, *Science*, **188**, 64 (1975).

(23) S. Elter, M. A. Williams, T. Watkins, and A. D. Keith, *Biochim. Biophys. Acta*, **339**, 190 (1974).

(24) S. M. Metcalfe, *J. Pharm. Pharmacol.*, **23**, 817 (1971).

(25) F. E. Kohn, J. H. Kay, and J. C. Clandra, *Food Cosmet. Toxicol.*, **3**, 377 (1965).

(26) G. Pascal, G. Durand, and E. Penot, *Arch. Sci. Physiol.*, **24**, 37 (1970).

(27) I. F. Gaunt, D. Gilbert, and D. Martin, *Food Cosmet. Toxicol.*, **3**, 445 (1965).

(28) M. C. Meyer and D. E. Guttman, *J. Pharm. Sci.*, **57**, 1627 (1968).

(29) *Ibid.*, **59**, 33 (1970).

(30) *Ibid.*, **57**, 895 (1968).

(31) A. Rescigno and G. Segre, "Drug and Tracer Kinetics," Blaisdell, New York, N. Y., 1971.

(32) S. Niazi, *Comp. Prog. Biomed.*, **7**, 41 (1977).

(33) R. W. Joos and W. H. Hall, *J. Pharmacol. Exp. Ther.*, **166**, 113 (1969).

(34) G. Powis, *J. Pharm. Pharmacol.*, **26**, 113 (1974).

(35) D. S. Lukas and A. DeMartino, *J. Clin. Invest.*, **48**, 1041 (1969).

(36) A. Raz, *Biochem. J.*, **130**, 631 (1972).

(37) S. Gabay and P. C. Huang, in "The Phenothiazines and Structurally Related Drugs," I. S. Forrest, C. J. Carr, and E. Usdin, Eds., Raven, New York, N.Y., 1974.

(38) W. J. Jusko and M. Gretch, *Drug Metab. Rev.*, **5**, 43 (1976).

Molecular Interaction between E-Prostaglandins and Selected Polymers and Its Potential Utilization in Oral Dosage Form Design

HO-LEUNG FUNG * **and MOO J. CHO** ‡x

Received June 22, 1977, from the *Department of Pharmaceutics, School of Pharmacy, State University of New York, Amherst, NY 14260, and the ‡Pharmacy Research Unit, The Upjohn Company, Kalamazoo, MI 49001. Accepted for publication November 3, 1977.

Abstract □ Coacervate formation was observed between some E-prostaglandins and povidone in acetonitrile. This molecular interaction was studied using differential scanning calorimetry, IR spectrophotometry, and light microscopy. The structural requirements for coacervate formation between E-prostaglandins and povidone were investigated. Possible utilization of this molecular interaction in the development of E-prostaglandin formulations was explored. The dissolution rate of some insoluble E-prostaglandin esters increased when they were coprecipitated with povidone and polyethylene glycol. For example, the *p*-hydroxybenzaldehyde semicarbazone ester of 16,16-dimethyldinoprostone dissolved about 200 times faster as a povidone coprecipitate than did the control mixture. Enhancement of the dissolution rate was observed for the povidone coprecipitates of dinoprostone and its *p*-acetylphenyl and β-naphthyl esters but not for the *p*-phenylphenyl ester. Fast dissolving dispersions of the E-prostaglandin esters also could be prepared with the water-insoluble cross-linked polyvinylpyrrolidone. This type of dispersion was nonglassy and easily dispersible in water. Thus, it might have certain advantages over the classical soluble povidone coprecipitates in terms of ease of handling. The degree of enhancement in dissolution of dispersions of cross-linked polyvinylpyrrolidone and E-prostaglandin esters is apparently dependent on the structure of the esters. The potential dissolution enhancement may be related to the strength of the interaction between the macromolecule and the esters, as indicated by the qualitative relationship between the extent of adsorption of the prostaglandins to cross-linked polyvinylpyrrolidone and the dissolution rate enhancement.

Keyphrases □ Prostaglandins, various—molecular interaction with selected polymers, application to oral dosage form design □ Polymers—povidone and cross-linked polyvinylpyrrolidone, molecular interaction with various prostaglandins, application to oral dosage form design □ Molecular interaction—various prostaglandins with selected polymers, application to oral dosage form design

Dinoprostone (prostaglandin E_2) (I) is unstable in aqueous solutions and in the solid state at ambient or elevated temperatures (1–7). Various attempts have been made to improve the solid-state stability of I. These efforts can be broadly classified into two categories: the formulation (or physical admixture) approach and the chemical (or prodrug) approach. Examples of the former technique can be found in the patent literature. It has been claimed that povidone (II) (8), β-cyclodextrin (9), and sodium chloride and succinic acid (10) all stabilize I against dehydration to prostaglandin A_2. The prodrug approach was used to synthesize various higher melting esters; the stability of these derivatives was vastly improved over the parent E-prostaglandins (7).

BACKGROUND

Questions remain regarding the stabilization of I in the solid state. Except for β-cyclodextrin, where clathrate formation appears to be the stabilizing force, the stabilization mechanism for the physical admixture approach is unknown. If I can be stabilized when dispersed in such diverse classes of solids as the ionic sodium chloride, the hydrogen donor succinic acid, and the polymeric dipolar II, then stabilization may be derived from a purely physical dispersion of I in a diluent solid, independent of any chemical interaction between the prostaglandin and the diluent.

The solid-state degradation of I appears to be promoted through its dissolution in its own decomposition product, prostaglandin A_2 (a viscous liquid at room temperature). This mechanism was indicated by the observation of an initial induction period followed by rapid decomposition of I in the solid state (11). The major stabilization mechanism in these systems may then be the physical separation of molecules of I in the diluent so that prostaglandin A_2 can no longer affect the now distant and unreacted I molecules. If this mechanism is correct, then stabilization can, in principle, be achieved with a host of pharmaceutical solids, regardless of their chemical structures. But if stabilization from solid dispersion requires a specific chemical interaction, then the nature of this interaction is of interest so that other nontoxic compounds capable of the same interaction can be systematically screened as I stabilizers.

In the prodrug approach, the improvement of the stability of E-prostaglandins is related directly to the elevation of the melting point of I through prodrug formation: the higher the melting point of the prodrug, the more stable the derivative (7). Unfortunately, a significant increase in the melting point drastically decreases aqueous solubility. This decrease, in turn, probably reduces the dissolution rate, potentially diminishing the *in vivo* oral absorption of the compound.

The following question can then be asked: Is it possible to increase the dissolution rates of the higher melting prodrugs so that both the stability and dissolution criteria can be simultaneously fulfilled? Polymer II is an ideal test compound through which this question may be probed. Its ability to improve the solid-state stability of I is well substantiated (8), and the molecular interaction between II and other organic compounds was studied extensively (12, 13). Also, II can promote the dissolution rate of poorly soluble drugs through the formation of coprecipitates (14). Thus, it appears that II is a unique chemical and may favorably influence both the stability and the dissolution of E-prostaglandins. A cross-linked polyvinylpyrrolidone polymer (III) with extremely limited aqueous solubility is also available. The interaction between this polymer and E-prostaglandins also is of interest.

The present report represents initial attempts to explore the molecular interaction between E-prostaglandins and selected macromolecules. The potential utilization of this interaction in the design of stable and fast dissolving oral dosage forms of E-prostaglandins also was investigated.

EXPERIMENTAL

Reagents and Materials—Methyl (IV), decyl (V), *p*-phenylphenyl (VI), *p*-acetylphenyl (VII), β-naphthyl (VIII), and *p*-hydroxybenzaldehyde semicarbazone (IX) esters of E-prostaglandins were synthesized according to Morozowich (7). The polymers used were II[1], III[2], polyethylene glycol 4000[3], and silanized silica gel 60[4]. The acetonitrile used was distilled in glass[5].

Coacervate Formation—Screening for coacervate formation was carried out by mixing solutions of prostaglandin (10 mg in 1 ml of acetonitrile) and II (100 mg in 1.5 ml of acetonitrile). Coacervate formation was positive when a dense oily layer was formed after mixing. Three different ratios, 1:5, 1:10, and 1:20, of I to II were tested.

Preparation of Coprecipitates of Prostaglandins with II—Coprecipitates of II generally were prepared in a 1:10 ratio of prostaglandin to polymer. The components were separately dissolved in acetonitrile and mixed. The solvent was removed first by a nitrogen stream

[1] Plasdone K 29-32, control No. G-30121B, GAF Corp., New York, NY 10020.
[2] Polyplasdone XL, control No. 906, GAF Corp., New York, NY 10020.
[3] Carbowax 4000, Union Carbide Chemicals, New York, NY 10017.
[4] RP-2, 63–200-μm size, fine free, E.M. Laboratories, Elmsford, NY 10523.
[5] Burdick & Jackson Laboratories, Muskegon, MI 49442.

0022-3549/78/0700/0971$01.00/0
© 1978, American Pharmaceutical Association

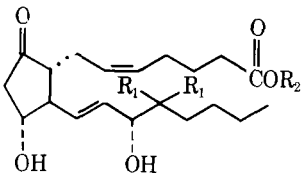

I: $R_1 = R_2 = H$

IV: $R_1 = H$, $R_2 = CH_3$

V: $R_1 = H$, $R_2 = (CH_2)_9CH_3$

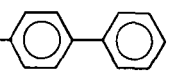

VI: $R_1 = H$, $R_2 =$

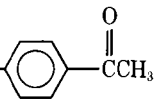

VII: $R_1 = H$, $R_2 =$

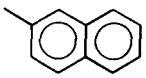

VIII: $R_1 = H$, $R_2 =$

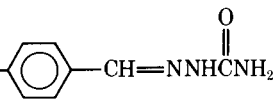

IX: $R_1 = CH_3$, $R_2 =$

and then in a flash evaporator. The glassy film left was scraped from the container.

Preparation of Dispersions of Prostaglandins in III—Dispersions of III were generally prepared in a 1:100 ratio of prostaglandin to III. Compound III was dispersed in acetonitrile to which a solution of prostaglandin in acetonitrile was added. The solvent was then removed in a flash evaporator.

Dissolution Studies—The dissolution apparatus used for UV-absorbing esters consisted of a jacketed beaker maintained at 37 ± 0.5°. The powder was introduced into the dissolution medium (water), and the mixture was stirred at 150 rpm by a magnetic bar. The solution was removed continuously from the dissolution system through a sintered-glass filter of medium porosity *via* a peristaltic pump, passed through a flowcell *placed inside a spectrophotometer*[6], and returned to the dissolution system. The flow rate was approximately 10 ml/min.

The concentrations of prostaglandin esters were monitored at the following wavelengths: VI, 250 nm; VII, 254 nm; VIII, 273 nm; and IX, 282 nm. No rigorous attempts were made to control the particle size of the powders. For I (which has insignificant UV absorption above 240 nm), manual removal of 2-ml aliquots of the dissolution medium at different times was carried out *via* pipets, the tips of which had been wrapped with

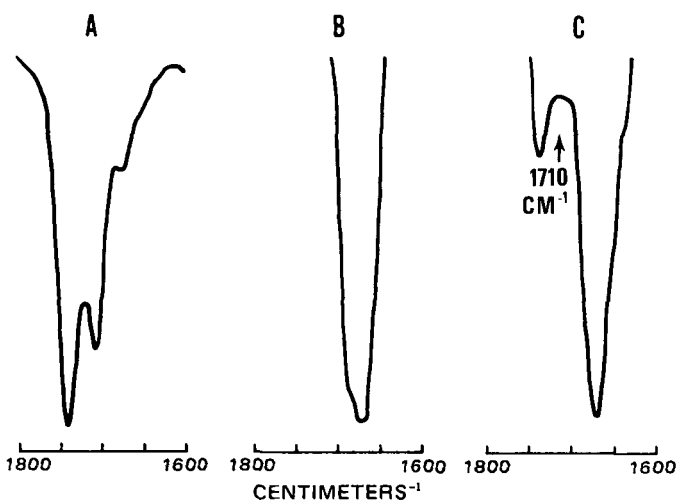

Figure 1—*Absorption peaks due to the carbonyl stretching vibration of I (A), II (B), and a 1:1 coacervate of I and II (C). Spectra were recorded in chloroform.*

[6] Beckman DB-G.

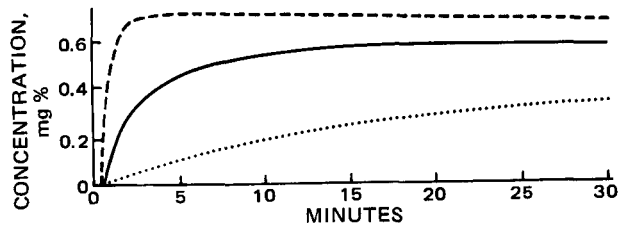

Figure 2—*Dissolution behavior of various forms of VII. Key: - - -, 20.2 mg of a 1:10 coprecipitate of VII and II; —, 20.4 mg of the corresponding physical mixture; and ···, 2.0 mg of pure VII.*

glass wool. When these aliquots were cooled to room temperature, 2 ml of 2 *N* KOH in methanol was added to each tube, and the prostaglandin B_2 formed was measured spectrophotometrically at 280 nm (4). The I concentration was calculated from a calibration plot established with known I concentrations.

Adsorption Studies—Different weights of III were introduced into test tubes or erlenmeyer flasks, and a known volume of the test drug solution in acetonitrile was added and equilibrated with the powder. The equilibrium concentrations of prostaglandin esters, tannic acid, and caffeine in the supernates were determined by UV spectrophotometry. For supernates of I, acetonitrile was removed by a nitrogen stream. The solutions were then reconstituted with methanol and assayed by conversion to prostaglandin B_2 with addition of 2 *N* KOH (4).

RESULTS AND DISCUSSION

Coacervate Formation and Characterization—On mixing solutions of I and II in acetonitrile as described, the mixture became turbid on standing and a dense oily layer settled out. This "oil" could be separated and, by repeated drying in a flash evaporator, "crystallized" into glassy solids. Since the limiting solubility of either I or II in acetonitrile was far in excess over the respective concentration present before mixing, this observation strongly suggested the existence of a molecular interaction between I and II.

The dense oil could be rationalized as being either the stoichiometric complex of I and II or a coacervate formed by the two molecular species. The latter is defined as a colloid-rich layer formed by separation of a macromolecular solution into two phases. A classical example of this phenomenon is the coacervation of gelatin when its solution is mixed with solutions of acacia, alcohol, sodium sulfate, or starch (15). Although the present case involves phase separation from a nonaqueous, albeit polar, medium, the term coacervate is still used because it facilitates conceptualization of the experimental observation.

A number of observations supported the presence of coacervate formation over that of complexation. First, when different weight ratios of I to II (1:5, 1:10, and 1:20) were mixed in acetonitrile, the volume of the dense oil appeared to increase with increasing amounts of II. The actual volumes were much greater than those that could be expected from I and II alone. Thus, the separated phase must have contained significant numbers of solvent molecules, which was consistent with coacervate behavior.

Second, the glassy solids obtained were analyzed with respect to the content of I. The ratios of I to II added to those recovered in the glassy solids were identical within experimental errors; for the ratios added (1:5, 1:10, and 1:20), the ratios recovered were 1:6.6, 1:10.6, and 1:20.0, respectively. If the glassy solids isolated were stoichiometric complexes of I and II, one would reasonably expect a somewhat constant ratio of I to II in the complexes recovered. It could, however, be reasoned that a mixture of stoichiometric complexes was formed and that alteration in the ratio of I to II added would affect the relative contribution of each

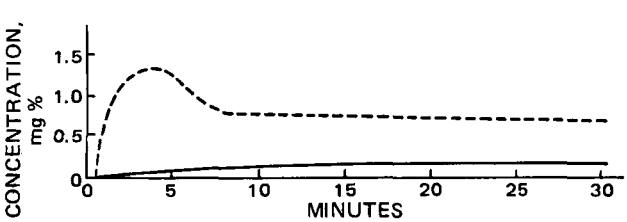

Figure 3—*Dissolution behavior of various forms of VIII. Key: - - -, 21.1 mg of a 1:10 coprecipitate of VIII and II; and —, 22.1 mg of the corresponding physical mixture.*

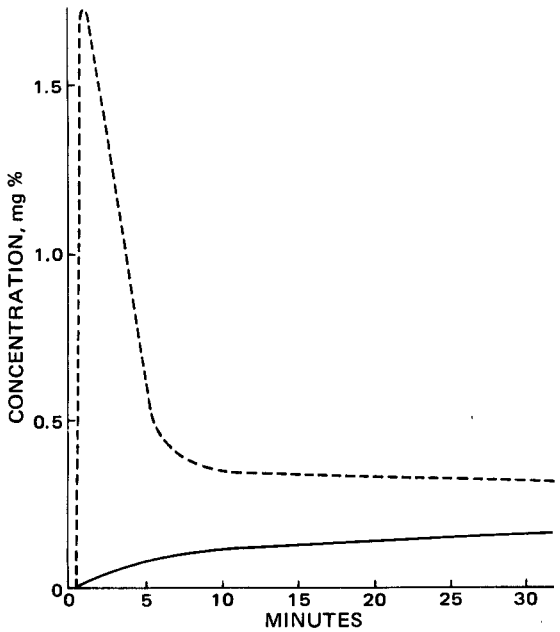

Figure 4—*Dissolution behavior of various forms of IX. Key: - - - , 44.0 mg of a 1:10 coprecipitate of IX and II; and —, 43.8 mg of the corresponding physical mixture.*

stoichiometric complex to the glassy solid, which, in turn, would affect the ratio recovered.

If this were the case, then successive washing of the glassy solids with acetonitrile, particularly those formed from a high ratio of II to I, would change the drug to polymer ratio in the residue solid, because different stoichiometric complexes could be presumed to have different solubilities in acetonitrile. This, however, was not found to be the case. The glassy solid obtained from a 1:20 I to II coacervate was washed with acetonitrile twice. The ratio in the residue solid remained constant at 1:20 after each washing.

Various compounds, including some C_1-esters of I, were tested for coacervate formation with II. Only one weight ratio of test compound to polymer (1:10) was used. Thus, although the presence of coacervation with any one test compound gave a reasonable indication of molecular interaction, the opposite was, of course, not necessarily true. However, because of the similarity in molecular weights of the prostaglandins, those prostaglandins that did form coacervates might have stronger interactions with II than those that did not. Under the conditions used, esters IV–VI and VIII failed to form coacervates with II in acetonitrile while ester IX did.

Nonprostaglandin compounds, such as tannic acid and cholic acid, also

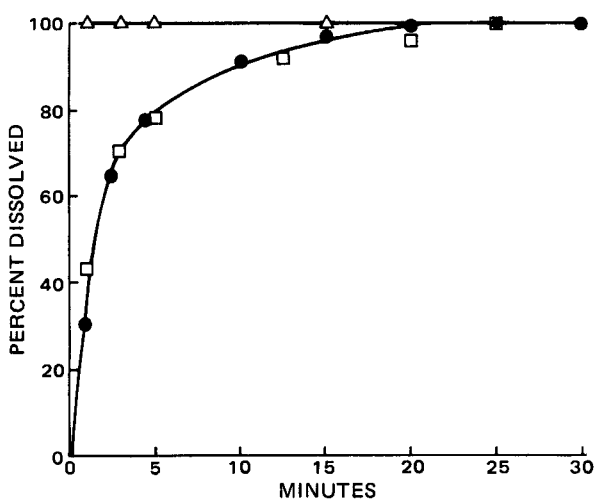

Figure 5—*Dissolution behavior of various forms of I. Key: △, 1.0 g of a 1:100 dispersion of I in III; □, 1.0 g of the corresponding physical mixture; and ●, 10 mg of pure I.*

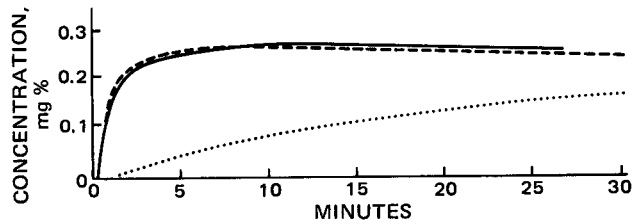

Figure 6—*Dissolution behavior of various forms of VII. Key: - - - , 200 mg of a 1:100 dispersion of VII in III; —, 202 mg of the corresponding physical mixture; and ···, 2.0 mg of pure VII.*

formed coacervates with II in acetonitrile, but acetic acid did not. Since organic acids are known to be strong interactants with II (12), blocking of the COOH group in I by ester formation might have weakened the molecular attraction between the prostaglandin and polymer molecules so that coacervation in acetonitrile was no longer possible. Although IX is also an ester, it possesses three active hydrogen atoms at the semicarbazone moiety. These hydrogen atoms might be able to participate in hydrogen bonding, establishing the interaction of the molecule with II.

Participation of the terminal COOH group of I in the molecular interaction with II was also consistent with the IR data of the I–II (1:1) coacervate. Shown in Fig. 1 are the carbonyl absorption peaks of I, II, and the I–II (1:1) coacervate in chloroform. For I, the absorption peaks due to the carbonyl stretching vibration at 1740 and 1710 cm^{-1} were assigned to the cyclopentanone carbonyl and the carboxylic carbonyl groups of I, respectively (16). The carbonyl group in the pyrrolidone ring of II gave an absorption peak at 1675 cm^{-1}. In the I–II (1:1) coacervate, the carboxylic carbonyl peak at 1710 cm^{-1} became undetectable. This result is consistent with the interpretation that the carboxylic hydrogen participates in the I–II interaction, because proton donation would impart a more carboxylate-like structure to I, shifting the carboxylic carbonyl peak to a lower wave number (17) and causing it to merge with the pyrrolidone peak of II.

The contribution from II toward the molecular interaction can also be examined. Compound II has two potential sites for interaction: the lactam linkage, which is available for hydrogen bonding and dipole–dipole interaction, and the alkyl backbone, which is available for hydrophobic bonding. Caffeine possesses two cyclic amide linkages, and it did not form a coacervate with I. This result is perhaps expected, because caffeine is not a polymer. Differential scanning calorimetry[7] of a 1:1 molar ratio of a I to caffeine mixture and coprecipitate showed, however, that the melting behavior of I was unaffected by caffeine. It appears then that the lactam group in II was not the sole contributor to the I–II interaction; hydrophobic bonding between the alkyl backbones of I and II may also have strengthened the interaction.

From these studies, it is apparent that potential stabilizers of I in the solid state may come from compounds containing a polar portion capable of hydrogen bonding and a nonpolar portion capable of hydrophobic bonding, *e.g.*, dialkyl-substituted amides, long chain esters, and surfactants.

Dissolution of II–Prostaglandin Coprecipitates—Coprecipitates of II and prostaglandin esters were prepared, and their dissolution profiles were determined using the setup described under *Experimental*. Figures 2, 3, and 4 show the representative dissolution curves of the coprecipitates and physical mixtures of II with VII, VIII, and IX, respectively. At least duplicate runs were performed for each compound, and these dissolution curves were all internally consistent. In all dissolution curves, there was an initial lag time of less than 1 min, corresponding to the time required for the dissolution medium to travel from the beaker to the flowcell.

Examination of the dissolution curves shows that, with these esters, the coprecipitates were much faster dissolving than the corresponding control physical mixtures. For example, the dissolution rate of the coprecipitate of IX between 0 and 2 min was about 200 times faster than its physical mixture within the same time interval. The enhancement in dissolution rate was less for esters VII and IX. For VI (absorptivity at 250 nm = 38.0 ml/mg cm in methanol), both the coprecipitate and physical mixture showed negligible absorbance at 250 nm for as long as 40 min after the start of the dissolution runs. The presence of the prostaglandin ester in these samples was confirmed by UV spectrophotometry, suggesting that the lack of absorbance was due to the poor solubility of

[7] DuPont model 900 thermal analyzer.

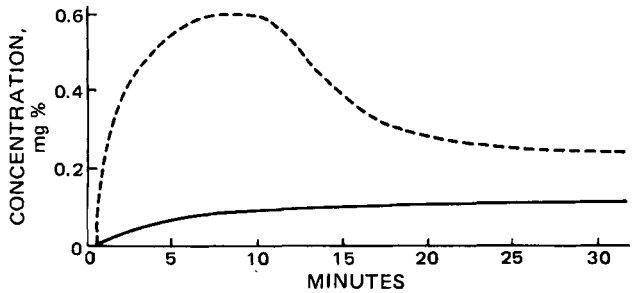

Figure 7—*Dissolution behavior of various forms of IX. Key: - - -, 200 mg of a 1:100 dispersion of IX in III; and —, 202 mg of the corresponding physical mixture.*

this compound even in the coprecipitate rather than to the absence of drug in the samples tested.

The coprecipitate of IX with II was examined under a hot-stage microscope[8], and its melting behavior was compared to its physical mixture. As expected, melting of IX could be distinctly observed in the physical mixture but not in the coprecipitate. The coprecipitate appeared as a homogeneous glassy solid and started to soften at about 180°. These thermal and microscopic data suggested that prostaglandin esters formed solid solutions with II in the coprecipitate. Enhancement of the dissolution of IX also was observed for its coprecipitate with polyethylene glycol 4000 but not for the coprecipitate with silanized silica gel 60[4], a methyl-substituted silica gel used in reversed-phase chromatography (18).

The ineffectiveness of silanized silica gel to improve the dissolution rate of IX suggested that the driving force for dissolution enhancement did not derive entirely from physical adsorption of the prostaglandin ester on the diluent powder matrix. Molecular interactions between the prostaglandin and the diluent, such as those provided by II and polyethylene glycol, appeared to be essential in promoting dissolution of prostaglandin esters in coprecipitates. The influence of particle size on the enhancement of coprecipitate dissolution was not examined.

Dissolution of III–Prostaglandin Dispersions—Polymer III has been used as a tablet disintegrant (19) and as a stabilizer for nitroglycerin in sublingual tablets (20). Unlike ordinary II, a glassy solid very soluble in water and many organic solvents, III is powdery and is insoluble in common solvents. When preparing coprecipitates with II, evaporation of the solvent usually led to formation of a film, which had to be scraped from the surface of the container. The film-like pieces obtained were usually very light and difficult to handle.

In contrast, dispersions of prostaglandins in III were nonglassy and were easier to handle. This type of dispersion has not been reported. It was of interest to explore whether dispersions of prostaglandin esters in III could enhance dissolution as was found for the coprecipitates with II.

Figures 5, 6, and 7 show the dissolution curves of the dispersions and physical mixtures of III with I, VII, and IX, respectively. With I and VII, the dissolution curves of the pure drugs were included for comparison. No appreciable dissolution for pure IX was detected under the experimental conditions. From Fig. 5, it is apparent that dissolution of the dispersion of I with III was extremely fast; complete dissolution was observed at 1 min, which was the first data point obtained. There was essentially no difference between the dissolution profiles of the physical mixture and pure I.

Similarly, the dissolution of the dispersion of IX was significantly enhanced compared to its physical mixture (Fig. 7). The dispersion of IX with III appeared to dissolve more slowly than the coprecipitate of the same drug (Fig. 4). At the same time, however, the III with IX dispersion sample, once dissolved, also precipitated out more slowly than the II with IX system. If the dissolution profiles are indicative of the corresponding absorption rates, then the dispersion of VII with III may be more desirable in oral dosage forms because of its ability to provide a more sustained increase in solubility vis-à-vis the corresponding coprecipitate with II.

In sharp contrast to the dispersions of IX, those of VI, VII (Fig. 6), and VIII provided no noticeable increase in dissolution rates over their respective control physical mixtures. In fact, the dissolution rates of both the dispersions and physical mixtures of VI and VIII were so slow that no detectable absorbance could be measured during the dissolution runs up to 30 min.

[8] Leitz Ortholux microscope equipped with a Mettler FP2 hot stage.

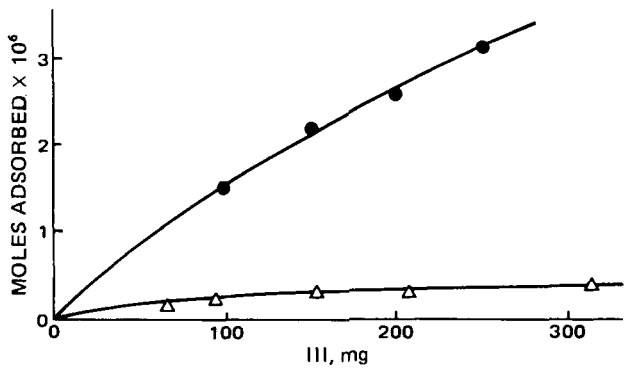

Figure 8—*Adsorption of I and VI–IX as a function of the weight of III in acetonitrile at 25°. Key: ●, adsorption of I; and △, adsorption of IX. Compounds VI–VIII gave no measurable adsorption.*

Correlation between Adsorption of Prostaglandin Esters on III and Dissolution Enhancement—Not all of the coprecipitates and dispersions were capable of enhancing the dissolution of all of the prostaglandins. In coprecipitates with II, the dissolution was not affected in the *p*-phenylphenyl ester. In dispersions with III, the dissolution of three prostaglandin esters (the *p*-phenylphenyl, β-naphthyl, and *p*-acetylphenyl) was not significantly affected by dispersion formation. The substituent apparently played an important role in determining whether coprecipitate and dispersion formulation could affect dissolution favorably. The effect of structure on the dissolution rates of coprecipitates and dispersions has not been reported. This attempt to relate the molecular interactions of various prostaglandin structures with III to the observed dissolution behavior may represent the first study in this area.

Preliminary adsorption studies of prostaglandins with III in acetonitrile revealed that compounds whose dispersions showed enhanced dissolution were also significantly adsorbed onto III. In reverse, prostaglandin esters whose dispersions did not show increased dissolution were not adsorbed by the polymer (Fig. 8). The degree of adsorption was possibly a reasonable reflection of the extent of molecular interaction between the prostaglandins and III because:

1. The adsorption data with III appeared to parallel those on coacervate formation: prostaglandins that showed strong adsorption on III (I and IX) also formed coacervates with II, and vice versa.

2. Tannic acid, a known interactant with II (12), showed extremely strong adsorption on III (Fig. 9) whereas caffeine, a known noninteractant with II (21), did not show any appreciable adsorption.

The adsorption characteristics of tannic acid and I on III (Fig. 9) could be described according to the classical Langmuir adsorption isotherm: $C/N = 1/Km + C/m$, where C is the equilibrium concentration of the adsorbate, N is the number of moles of adsorbate adsorbed per gram of III, K is the Langmuir adsorption constant, and m is the number of moles of adsorbate that 1 g of III can adsorb when the monolayer is complete. The numerical values of K and m were 9.01×10^5 and 1.11×10^{-5} for tannic acid and 1.58×10^4 and 2.34×10^{-5} for I, respectively. Mourey *et al.* (22) recently showed that the molecular interaction between azo

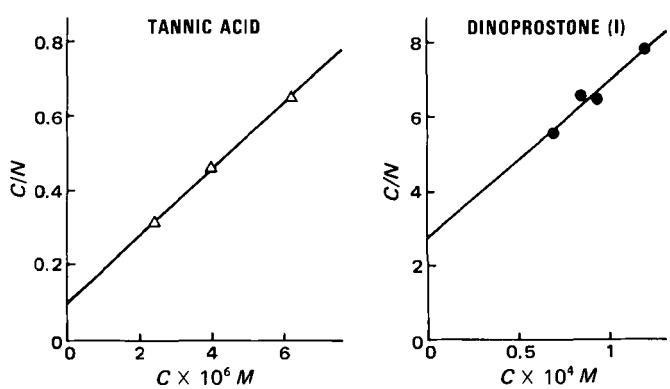

Figure 9—*Langmuir adsorption isotherm of tannic acid and I on III in acetonitrile at 25°.*

compounds and III in aqueous solutions is structure dependent. The presence of polar functional groups (*e.g.*, hydroxyl, amino, carboxylic, and sulfonic groups) in unionized forms facilitates interaction with the polymer.

The thermodynamic driving force for dissolution enhancement in prostanglandin dispersions appeared to derive from molecular interaction (in this case, adsorption) of the prostaglandin with III. This adsorption enabled the breaking up of the crystal lattice of the prostaglandin, thus requiring less energy input for dissolution. When no adsorption took place, the prostaglandin probably precipitated out by itself on evaporation of the acetonitrile, existing as separate particles unassociated with the polymer. These precipitates would essentially have the same physical characteristics as the physical mixtures and, therefore, would not be expected to show enhancement in dissolution.

It appears feasible to predict whether a certain prostaglandin may benefit in dissolution from dispersion formation with III. When a prostaglandin interacts with III, as indicated by significant adsorption, the dispersion formed probably will exhibit an increased dissolution rate. Prostaglandins that show poor interaction with III probably will not improve their dissolution rates through dispersion formation.

REFERENCES

(1) S. Bergström, in "Prostaglandins," Nobel Symposium 2, S. Bergström and B. Samuelsson, Eds., Interscience, New York, N.Y., 1967, p. 21.

(2) S. M. M. Karim, J. Devlin, and K. Hillier, *Eur. J. Pharmacol.*, **4**, 416 (1968).

(3) N. H. Andersen, *J. Lipid Res.*, **10**, 320 (1969).

(4) T. O. Oesterling, presented to the APhA Academy of Pharmaceutical Sciences, Washington, D.C., Apr. 1970.

(5) D. C. Monkhouse, L. Van Campen, and A. J. Aguiar, *J. Pharm. Sci.*, **62**, 576 (1973).

(6) G. F. Thompson, J. M. Collins, and L. M. Schmalzried, *ibid.*, **62**, 1738 (1973).

(7) W. Morozowich, "Abstracts of Papers Presented before the APhA Academy of Pharmaceutical Sciences," vol. 5 (2), 1975, p. 150 (Atlanta, Ga., Nov. 1975).

(8) A. C. O'Rourke and J. S. Kent, U.S. pat. 3,826,823 (to Syntex Inc.) (1974).

(9) M. Hayashi and A. Ishihara, British pat. 1,419,221 (to Ono Pharmaceutical Co.) (1975).

(10) D. C. Monkhouse, U.S. pat. 3,954,787 (to Pfizer Inc.) (1976).

(11) J. T. Carstensen, *J. Pharm. Sci.*, **63**, 1 (1974).

(12) "PVP: An Annotated Bibliography, 1951–1966," vol. 1, General Aniline and Film Corp., New York, N.Y., 1967.

(13) M. J. Cho, A. G. Mitchell, and M. Pernarowski, *J. Pharm. Sci.*, **60**, 720 (1971), and references cited therein.

(14) W. L. Chiou and S. Riegelman, *ibid.*, **60**, 1281 (1971).

(15) A. N. Martin, J. Swarbrick, and A. Cammarata, "Physical Pharmacy," 2nd ed., Lea & Febiger, Philadelphia, Pa., 1973, p. 461.

(16) S. Bergström, R. Ryhage, B. Samuelsson, and J. Sjovall, *J. Biol. Chem.*, **238**, 3555 (1963).

(17) K. Nakanishi, "Infrared Absorption Spectroscopy—Practical," Holden-Day, San Francisco, Calif., 1962, p. 44.

(18) "Products for Chromatography," EM Laboratories, Elmsford, N.Y., 1976, p. 13.

(19) S. S. Kornblum and S. B. Stoopak, *J. Pharm. Sci.*, **62**, 43 (1973).

(20) H.-L. Fung, S. K. Yap, and C. T. Rhodes, *ibid.*, **63**, 1810 (1974).

(21) T. Higuchi and R. Kuramoto, *J. Am. Pharm. Assoc., Sci. Ed.*, **43**, 393 (1954).

(22) T. Mourey, A. P. Carpenter, Jr., S. Siggia, and A. Lane, *Anal. Chem.*, **48**, 1592 (1976).

ACKNOWLEDGMENTS

H.-L. Fung gratefully acknowledges The Upjohn Co. for its generous support of this study, which was carried out while he was an Upjohn Summer Visiting Professor in 1976.

Formation of a Cyclic Derivative of Ethacrynic Acid with Diazomethane

K. K. MIDHA ˣ, J. W. HUBBARD [1], C. CHARETTE, and H. W. JUN *

Received April 25, 1977, from the *Drug Research Laboratories, Health Protection Branch, Health and Welfare Canada, Ottawa, Ontario, K1A 0L2, Canada.* Accepted for publication November 3, 1977. *Present address: School of Pharmacy, University of Georgia, Athens, GA 30601.

Abstract □ Samples of ethacrynic acid were treated with methanol–hydrochloric acid or with diazomethane. GLC and mass spectrometric analysis indicated that the methanol–hydrochloric acid reaction gave the expected methyl ester, whereas diazomethane treatment gave a compound containing an additional 14 mass units. Accurate mass measurement and PMR and IR spectra showed that this product was a cyclic derivative of the methyl ester of ethacrynic acid, methyl 4-(2,3-dihydro-4-ethyl-5-furyl)-2,3-dichlorophenoxyacetate. Either derivatization method can be used for development of an assay for ethacrynic acid.

Keyphrases □ Ethacrynic acid—reaction with methanol–hydrochloric acid or diazomethane, PMR, IR, and GLC–mass spectral analyses of products □ GLC—analysis, derivatives of ethacrynic acid □ Derivatization—ethacrynic acid with methanol–hydrochloric acid or diazomethane, PMR, IR, and GLC–mass spectral analyses of products □ Diuretics—ethacrynic acid, reaction with methanol–hydrochloric acid or diazomethane, PMR, IR, and GLC-mass spectral analyses of products

Ethacrynic acid (I) is a potent, orally active diuretic (1–4) for which a suitable GLC procedure was required for investigating its pharmacokinetic profile in humans. Previously reported analytical procedures involved the administration of ^{14}C-I followed by a tedious workup using TLC or column chromatography (4, 5).

Ethacrynic acid is not amenable to direct GLC analysis, and an approach was to convert it into its methyl ester either by treatment with diazomethane or by reaction with

[1] On leave from the Faculty of Pharmacy, University of Manitoba, Winnipeg, Manitoba, Canada.

0022-3549/78/0700/0975$01.00/0

© 1978, American Pharmaceutical Association

compounds and III in aqueous solutions is structure dependent. The presence of polar functional groups (*e.g.*, hydroxyl, amino, carboxylic, and sulfonic groups) in unionized forms facilitates interaction with the polymer.

The thermodynamic driving force for dissolution enhancement in prostanglandin dispersions appeared to derive from molecular interaction (in this case, adsorption) of the prostaglandin with III. This adsorption enabled the breaking up of the crystal lattice of the prostaglandin, thus requiring less energy input for dissolution. When no adsorption took place, the prostaglandin probably precipitated out by itself on evaporation of the acetonitrile, existing as separate particles unassociated with the polymer. These precipitates would essentially have the same physical characteristics as the physical mixtures and, therefore, would not be expected to show enhancement in dissolution.

It appears feasible to predict whether a certain prostaglandin may benefit in dissolution from dispersion formation with III. When a prostaglandin interacts with III, as indicated by significant adsorption, the dispersion formed probably will exhibit an increased dissolution rate. Prostaglandins that show poor interaction with III probably will not improve their dissolution rates through dispersion formation.

REFERENCES

(1) S. Bergström, in "Prostaglandins," Nobel Symposium 2, S. Bergström and B. Samuelsson, Eds., Interscience, New York, N.Y., 1967, p. 21.

(2) S. M. M. Karim, J. Devlin, and K. Hillier, *Eur. J. Pharmacol.*, **4**, 416 (1968).

(3) N. H. Andersen, *J. Lipid Res.*, **10**, 320 (1969).

(4) T. O. Oesterling, presented to the APhA Academy of Pharmaceutical Sciences, Washington, D.C., Apr. 1970.

(5) D. C. Monkhouse, L. Van Campen, and A. J. Aguiar, *J. Pharm. Sci.*, **62**, 576 (1973).

(6) G. F. Thompson, J. M. Collins, and L. M. Schmalzried, *ibid.*, **62**, 1738 (1973).

(7) W. Morozowich, "Abstracts of Papers Presented before the APhA Academy of Pharmaceutical Sciences," vol. 5 (2), 1975, p. 150 (Atlanta, Ga., Nov. 1975).

(8) A. C. O'Rourke and J. S. Kent, U.S. pat. 3,826,823 (to Syntex Inc.) (1974).

(9) M. Hayashi and A. Ishihara, British pat. 1,419,221 (to Ono Pharmaceutical Co.) (1975).

(10) D. C. Monkhouse, U.S. pat. 3,954,787 (to Pfizer Inc.) (1976).

(11) J. T. Carstensen, *J. Pharm. Sci.*, **63**, 1 (1974).

(12) "PVP: An Annotated Bibliography, 1951–1966," vol. 1, General Aniline and Film Corp., New York, N.Y., 1967.

(13) M. J. Cho, A. G. Mitchell, and M. Pernarowski, *J. Pharm. Sci.*, **60**, 720 (1971), and references cited therein.

(14) W. L. Chiou and S. Riegelman, *ibid.*, **60**, 1281 (1971).

(15) A. N. Martin, J. Swarbrick, and A. Cammarata, "Physical Pharmacy," 2nd ed., Lea & Febiger, Philadelphia, Pa., 1973, p. 461.

(16) S. Bergström, R. Ryhage, B. Samuelsson, and J. Sjovall, *J. Biol. Chem.*, **238**, 3555 (1963).

(17) K. Nakanishi, "Infrared Absorption Spectroscopy—Practical," Holden-Day, San Francisco, Calif., 1962, p. 44.

(18) "Products for Chromatography," EM Laboratories, Elmsford, N.Y., 1976, p. 13.

(19) S. S. Kornblum and S. B. Stoopak, *J. Pharm. Sci.*, **62**, 43 (1973).

(20) H.-L. Fung, S. K. Yap, and C. T. Rhodes, *ibid.*, **63**, 1810 (1974).

(21) T. Higuchi and R. Kuramoto, *J. Am. Pharm. Assoc., Sci. Ed.*, **43**, 393 (1954).

(22) T. Mourey, A. P. Carpenter, Jr., S. Siggia, and A. Lane, *Anal. Chem.*, **48**, 1592 (1976).

ACKNOWLEDGMENTS

H.-L. Fung gratefully acknowledges The Upjohn Co. for its generous support of this study, which was carried out while he was an Upjohn Summer Visiting Professor in 1976.

Formation of a Cyclic Derivative of Ethacrynic Acid with Diazomethane

K. K. MIDHA ˣ, J. W. HUBBARD [1], C. CHARETTE, and H. W. JUN *

Received April 25, 1977, from the *Drug Research Laboratories, Health Protection Branch, Health and Welfare Canada, Ottawa, Ontario, K1A 0L2, Canada.* Accepted for publication November 3, 1977. *Present address: School of Pharmacy, University of Georgia, Athens, GA 30601.

Abstract □ Samples of ethacrynic acid were treated with methanol–hydrochloric acid or with diazomethane. GLC and mass spectrometric analysis indicated that the methanol–hydrochloric acid reaction gave the expected methyl ester, whereas diazomethane treatment gave a compound containing an additional 14 mass units. Accurate mass measurement and PMR and IR spectra showed that this product was a cyclic derivative of the methyl ester of ethacrynic acid, methyl 4-(2,3-dihydro-4-ethyl-5-furyl)-2,3-dichlorophenoxyacetate. Either derivatization method can be used for development of an assay for ethacrynic acid.

Keyphrases □ Ethacrynic acid—reaction with methanol–hydrochloric acid or diazomethane, PMR, IR, and GLC–mass spectral analyses of products □ GLC—analysis, derivatives of ethacrynic acid □ Derivatization—ethacrynic acid with methanol–hydrochloric acid or diazomethane, PMR, IR, and GLC–mass spectral analyses of products □ Diuretics—ethacrynic acid, reaction with methanol–hydrochloric acid or diazomethane, PMR, IR, and GLC-mass spectral analyses of products

Ethacrynic acid (I) is a potent, orally active diuretic (1–4) for which a suitable GLC procedure was required for investigating its pharmacokinetic profile in humans. Previously reported analytical procedures involved the administration of ^{14}C-I followed by a tedious workup using TLC or column chromatography (4, 5).

Ethacrynic acid is not amenable to direct GLC analysis, and an approach was to convert it into its methyl ester either by treatment with diazomethane or by reaction with

[1] On leave from the Faculty of Pharmacy, University of Manitoba, Winnipeg, Manitoba, Canada.

0022-3549/78/0700/0975$01.00/0

© 1978, American Pharmaceutical Association

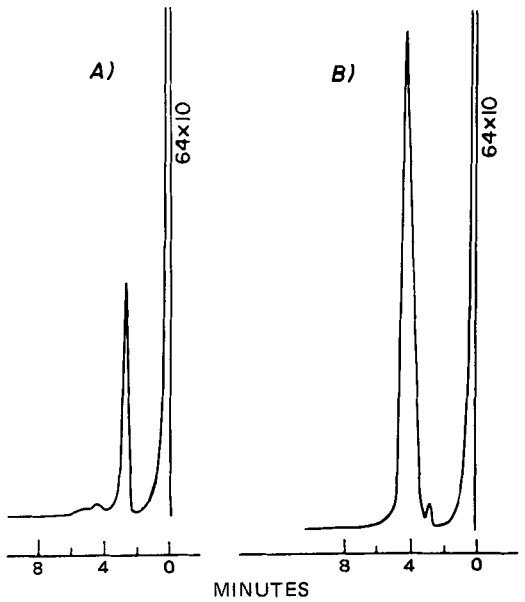

Figure 1—*Typical chromatogram of I when reacted with methanol–hydrochloric acid (A) and when treated with diazomethane (B).*

methanol–hydrochloric acid prior to GLC. The methylation reactions of diazomethane have been reviewed (6–9). The diazomethane treatment of I gave a major product with a different retention time on GLC analysis than that obtained from the methanol–hydrochloric acid reaction. This paper reports characterization of the two products as determined by GLC–mass spectrometry, accurate mass measurement, PMR spectroscopy, and IR spectrophotometry.

EXPERIMENTAL

Reagents and Chemicals—Methanol[2], hydrochloric acid[3], and ether[4] were obtained commercially. Diazomethane was generated using a commercially available kit[5].

GLC—The gas chromatograph[6] was equipped with a flame-ionization detector. The column was coiled glass tubing, 1.83 m (6 ft) long × 2 mm i.d., packed with 2% phenyl methyl silicone fluid[7] (OV-25) on acid-washed, dimethyldichlorosilane-treated, high performance Chromosorb W[7] support (80–100 mesh).

The column was conditioned by maintaining the oven at 300° for 18 hr with a low nitrogen flow. Operating temperatures were: injection port, 250°; column, 225°; and detector, 250°. The nitrogen flow rate was 60 ml/min. Hydrogen and compressed air flow rates were adjusted to give the maximum response.

GLC–Mass Spectrometry—GLC–mass spectrometry was carried out on a mass spectrometer[8] coupled to a gas chromatograph[9] through a two-stage jet separator. The ionization potential was 70 ev. The GLC column and conditions were the same as for direct GLC.

For accurate mass measurement, the sample of reacted product was collected from the detector at its appropriate retention time after extinguishing the flame. The accurate mass was determined on a high-resolution mass spectrometer[10] equipped with a direct insertion inlet and operating at 70 ev with a source temperature of 160°.

PMR—All PMR spectra were recorded[11] at 60 MHz at ambient temperature, using deuterated chloroform as the solvent and tetramethylsilane as the internal standard.

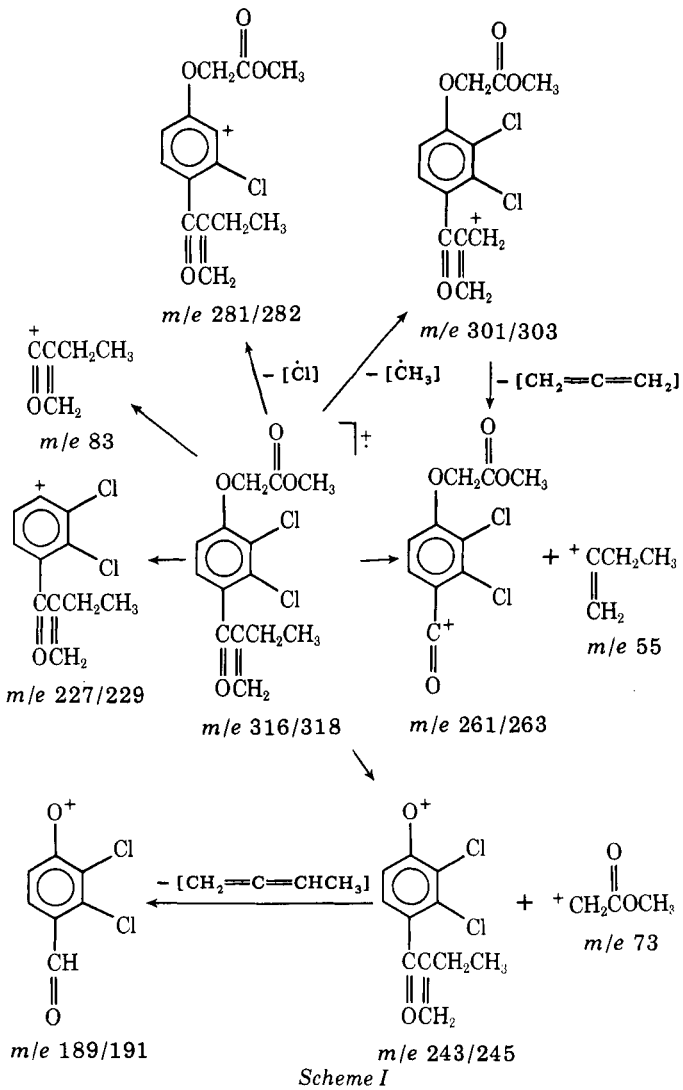

Scheme I

IR—The IR spectra were recorded[12] using solutions in chloroform at ambient temperature.

Methylation—Methyl derivatives were prepared by treating aliquots (0.1–100 mg) of solid I with an excess of ethereal diazomethane[5] at room temperature for 15 min with occasional mixing. Excess diazomethane was evaporated at room temperature under a stream of dry nitrogen.

Alternatively, aliquots of solid I (0.1–100 mg) were treated with 1–5 ml of a methanolic solution of concentrated hydrochloric acid [concentrated hydrochloric acid–methanol (1:4)] for 1 hr at 65°. These solutions were evaporated to dryness at 65° under a stream of dry nitrogen. The residues were dissolved in 0.5 ml of 10 *N* NaOH, extracted[13] with 5 ml of ether for 10 min, and then centrifuged for 10 min at 2500 rpm. The ether layers were transferred to other tubes. The extracts were evaporated to a volume of 100 μl at 45° under a stream of dry nitrogen.

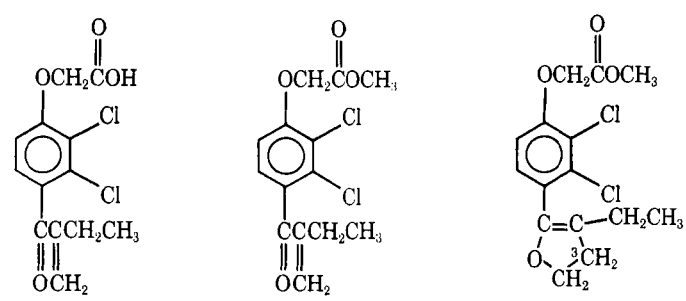

I II III

[2] Burdick and Jackson Laboratories, Muskegon, Mich.
[3] Baker analyzed reagent, Canlab, Montreal, Quebec, Canada.
[4] Anhydrous, Mallinckrodt Chemical Works, Montreal, Quebec, Canada.
[5] Catalog No. 710,025-0, Aldrich Chemical Co., Milwaukee, Wis.
[6] Model 3920, Perkin-Elmer Canada.
[7] Chromatographic Specialties, Brockville, Ontario, Canada.
[8] Hitachi Perkin-Elmer model RMU 6L.
[9] Model 990, Perkin-Elmer Canada.
[10] Varian MAT 311, Varian of Canada, Georgetown, Ontario, Canada.
[11] Varian A-60A, Varian of Canada, Georgetown, Ontario, Canada.
[12] Unicam SP-1000, Canlab, Montreal, Quebec, Canada.
[13] Roto-Rack, Fisher Scientific Co., Montreal, Quebec, Canada.

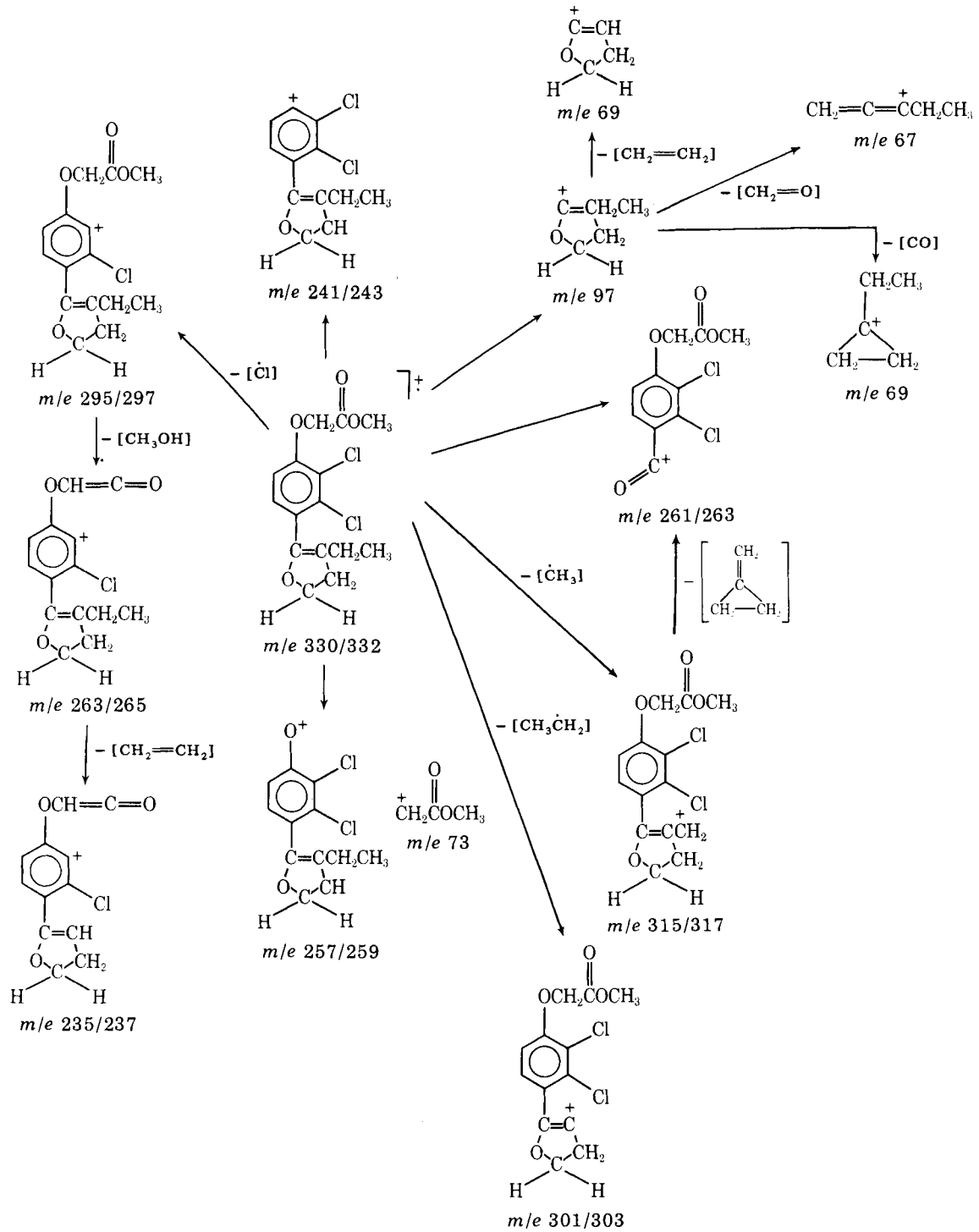

Scheme II

Aliquots (1–2 μl) from either procedure were injected into a gas chromatograph equipped with a flame-ionization detector.

RESULTS AND DISCUSSION

GLC examination of the products obtained from the reaction of I with methanol–hydrochloric acid showed a major peak (97% based on peak area) and a minor peak (≃2% based on peak area) with retention times (R_t) of 2.8 and 4.3 min, respectively (Fig. 1A). The GLC–mass spectrum (Fig. 2A) of the compound giving rise to the major peak showed a molecular ion at *m/e* 316/318 and other diagnostic ions at *m/e* 301/303, 281/283, 261/263, 243/245, 227/229, 189/191, 89, 73, and 55. The formation of these ions is postulated in Scheme I.

The PMR spectrum of this product did not exhibit a singlet at 9.97 ppm for the carboxylic acid proton as observed in the spectrum of I. The only other difference between the spectra was the presence of a singlet (3H) at 3.83 ppm in the spectrum of the product. It was concluded, therefore, that the product was the expected methyl ester (II) of ethacrynic acid.

GLC examination of the product obtained by the reaction of diazomethane with I also gave a major peak (99% based on peak area) but with a retention time of 4.3 min (Fig. 1B) under the same conditions. The GLC–mass spectrum of the compound giving rise to this peak (Fig. 2B) showed an ion of highest mass at *m/e* 330/332 and other ions at *m/e* 315/317, 301/303, 295/297, 263/265, 261/263, 257/259, 241/243, 235/237, 189/191, 97, 73, 69, and 67.

GLC–mass spectral analysis of the compound giving rise to the minor peak (R_t 4.3 min, Fig. 1A) in the methanol–hydrochloric acid reaction of I gave a mass spectrum identical to that shown in Fig. 2B (molecular ion at *m/e* 330/322 and other ions).

The addition of 14 mass units over the molecular weight of II suggested

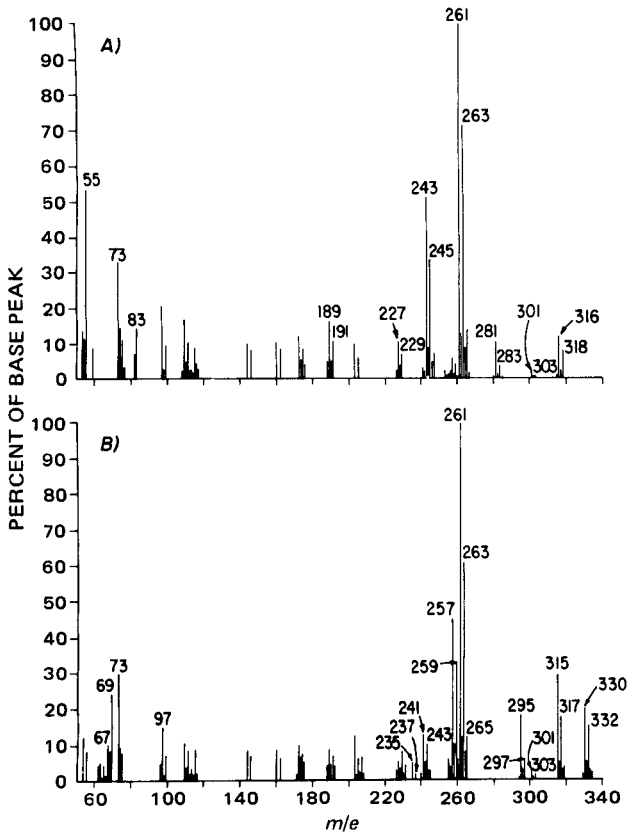

Figure 2—*GLC–mass spectrum (normalized) of the major product obtained from methanol–hydrochloric acid reaction of I (A) and treatment of I with diazomethane (B).*

the addition of an extra methylene unit to the molecule. This structure was supported by an accurate mass determination for $C_{15}H_{16}Cl_2O_4$ from diazomethane-treated I (calc. for $C_{15}H_{16}{}^{35}Cl_2O_4$: 330.0426, found 330.0426; calc. for $C_{15}H_{16}{}^{35}Cl^{37}ClO_4$: 330.0397, found 330.0396).

The IR spectrum of the diazomethane-treated product retained the band at 1765 cm^{-1} (C=O, ester carbonyl), but the strong band at 1670 cm^{-1} (C=O, keto function) in the spectrum of II was replaced by a weaker, broader band at 1690–1710 cm^{-1}.

Significantly, comparison of the PMR spectrum of the diazomethane-treated product with that of II showed the absence of the two singlets at 5.62 and 5.97 ppm, corresponding to the two vinylic protons of II. Instead, the spectrum contained a triplet (2H, J = 8 Hz) centered at 4.57 ppm and a complex multiplet (4H) spread between 1.32 and 2.57 ppm, arising from overlapping signals due to the methylene protons of the ethyl group and two vinyl proton multiplets (Fig. 3).

These IR, PMR, and accurate mass measurement data are consistent with the cyclic Structure III for the diazomethane-treated product. The major ions observed in the mass spectrum can be explained on the basis of this structure as illustrated in Scheme II. The medium intensity band at 1690–1710 cm^{-1} in the IR spectrum is consistent with the ν C=C of a cyclic vinyl ether. An exocyclic cyclopropano keto function would also absorb in this region (10), but the observed band was weaker and broader

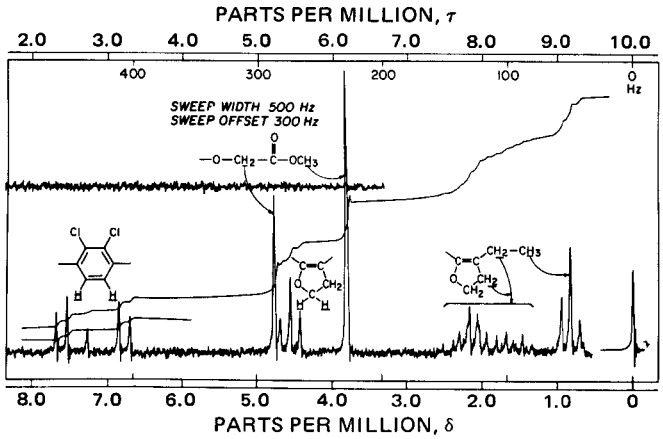

Figure 3—*PMR spectrum (deuterochloroform solution) of the major product obtained from diazomethane treatment of I.*

than the ν C=O of a keto function. Furthermore, there was no evidence of cyclopropano protons in the PMR spectrum.

It was concluded that the major product of the reaction of diazomethane with ethacrynic acid is methyl 4-(2,3-dihydro-4-ethyl-5-furyl)-2,3-dichlorophenoxyacetate (III). An analogous 1,4-addition of methylene occurs when certain α,β-diketones, such as benzil and phenanthraquinone, are allowed to react with diazomethane in the presence of methanol (11).

Either derivatization method appears to be suitable for the development of an assay for I, but the methanol–hydrochloric acid route avoids the hazards implicit in the use of diazomethane.

REFERENCES

(1) W. M. Kirkendall and J. H. Stein, *Am. J. Cardiol.*, **22,** 162 (1968).

(2) K. E. Kim, G. Onesti, J. H. Moyer, and C. Swartz, *ibid.*, **27,** 407 (1971).

(3) J. G. G. Ledingham and R. I. S. Bayliss, *Clin. Pharmacol. Ther.*, **6,** 474 (1965).

(4) K. H. Beyer, J. E. Baer, J. K. Michaelson, and H. F. Russo, *J. Pharmacol. Exp. Ther.*, **147,** 1 (1965).

(5) C. D. Klassen and T. J. Fitzgerald, *ibid.*, **191,** 548 (1974).

(6) J. S. Pizey, "Synthetic Reagents," vol. 2, Wiley, New York, N.Y., 1974, pp. 65–142.

(7) C. D. Gutsche, *Org. React.*, 8, 384 (1954).

(8) B. Eisert, *Z. Angew. Chem.*, **54,** 99 (1941).

(9) L. I. Smith, *Chem. Rev.*, **23,** 193 (1938).

(10) K. Nakanishi, "Infrared Absorption Spectroscopy, Practical," Holden-Day, San Francisco, Calif., 1962, p. 42.

(11) L. F. Fieser and J. L. Hartwell, *J. Am. Chem. Soc.*, **57,** 147 (1935).

ACKNOWLEDGMENTS

The authors thank Dr. I. J. McGilveray and Dr. K. Bailey for helpful discussions and suggestions. They also thank Mr. Walter Miles for accurate mass determinations, Mr. J.-C. Ethier for the GLC–mass spectra, and Mr. Andy Trottier for drafting.

Dissolution Rates of Hydrocortisone and Prednisone Utilizing Sugar Solid Dispersion Systems in Tablet Form

LOYD V. ALLEN, Jr. [x], R. SAUL LEVINSON, and DE DE MARTONO

Received July 20, 1977, from the *College of Pharmacy, Health Sciences Center, University of Oklahoma, Oklahoma City, OK 73190.* Accepted for publication November 3, 1977.

Abstract □ The utilization of ternary sugar solid dispersion systems and the incorporation of these systems into tablet dosage forms were investigated. The dispersion systems were prepared by the fusion method using 50% sucrose–50% mannitol and 50% sorbitol–50% mannitol. Other systems investigated utilized sorbitol, mannitol, and polyethylene glycol 6000 for comparison. The drug component was hydrocortisone or prednisone. The results from a modified NF XIII dissolution rate determination revealed that the mannitol system had the fastest dissolution rate, followed by sorbitol–mannitol, sucrose–mannitol, sorbitol, and, finally, polyethylene gylcol 6000. The corticosteroids were stable and did not decompose during preparation of the dispersion systems or direct compression of the tablets. A short-term stability study revealed that the tablets retained their fast dissolution rates and that the tablet characteristic tests, *i.e.*, tablet hardness, remained unchanged. The use of sugar combinations overcame some difficulties previously reported with single sugar systems.

Keyphrases □ Hydrocortisone—sugar solid dispersions in tablets, dissolution rates and stability □ Prednisone—sugar solid dispersions in tablets, dissolution rates and stability □ Sugar solid dispersions—sucrose, mannitol, and sorbitol in tablets with hydrocortisone and prednisone, dissolution rates and stability □ Dissolution rates—hydrocortisone and prednisone sugar solid dispersions in tablets □ Stability—hydrocortisone and prednisone sugar solid dispersions in tablets □ Tablets—hydrocortisone and prednisone sugar solid dispersions, dissolution rates and stability □ Glucocorticoids—hydrocortisone and prednisone, sugar solid dispersions in tablets, dissolution rates and stability

The corticosteroids are poorly water soluble and have demonstrated unpredictable, irregular dissolution rates (1–5). Solid dispersion techniques have been utilized to reduce the particle size of drugs and to increase their dissolution and absorption rates.

Sugar glass dispersions were used to increase the dissolution rates of some orally administered corticosteroids (6, 7). Some of the most effective sugars used (*e.g.*, sucrose), however, became discolored during the preparation of the melt. This amber discoloration did not appear to affect the dissolution rates of the dispersion systems. Some systems were also hygroscopic and required storage of the prepared materials in a desiccator.

The purposes of the present investigation were to study sugar combinations and other individual sugars in an attempt to overcome discoloration and hygroscopicity and to incorporate the resulting sugar solid dispersion systems into tablet dosage forms and to determine their dissolution rates.

EXPERIMENTAL

Mannitol, sorbitol, and mixtures of 50% sorbitol–50% mannitol and 50% sucrose–50% mannitol were used as the sugar carriers for the dispersion systems. These systems were compared to polyethylene glycol 6000 as a model system. Two orally administered corticosteroids, hydrocortisone and prednisone, were studied.

Preparation of Dispersion Systems—The dispersion systems were parpared by the fusion method as previously described (6). They were prepared in a ratio of 5 mg of the hydrocortisone or prednisone to 95 mg of the individual carrier. The hydrocortisone and prednisone controls were prepared in the same manner, without the melting and quenching procedures. The dispersion systems were stored for 48 hr at 25° in a desiccator before tableting.

A single-punch tablet machine[1] was used to prepare the tablets. The punch faces and die cavity were polished, and the compression pressure was adjusted to produce tablets that would meet USP standards. The formulation for the 200-mg tablets consisted of 2.5% corticosteroid, 47.5% sugar carrier (or 50% dispersion system), 35% dextrose and corn syrup solids[2], 7.5% microcrystalline cellulose[3], and 7.5% stearic acid–palmitic acid derivative[4]. Two batches were prepared for each dispersion system, and two lots of tablets were made from each batch. Therefore, for each dispersion, four lots of tablets were made with 80 tablets in each lot. The tablets were made by the direct compression method.

Tablets from each lot were analyzed for tablet hardness[5], thickness[6], weight[7], disintegration[8], and dissolution[8] and were required to meet the following criteria: hardness, 5–6 kg; thickness, 2.0 mm; weight, 200 mg ± 5%; content uniformity, 95–102%; and disintegration, <5 min.

The prepared tablets and the powdered dispersion systems were individually placed in a modified NF XIII dissolution rate apparatus (6). A 200-mg tablet or 100 mg of powdered sample was placed in the wire basket and lowered into the flask containing 1000 ml of deionized water. The basket was rotated at 100 rpm with a constant temperature of 25°.

A 10-ml volumetric pipet with an attached filter was used to remove a 10-ml sample of the dissolution fluid at 0, 2, 4, 6, 8, and 10 min. The sample was obtained from the same location in the container and transferred to labeled containers. Deionized water, 10 ml, was added to the dissolution container after sampling. Appropriate calculations were made to compensate for replacement of the sample fluid.

The corticosteroid concentration of each sample was analyzed using a UV spectrophotometer[9] (6). The concentrations were converted to percent dissolved and plotted against time t. All determinations were done at least in duplicate.

Short-Term Stability Study—The powdered and tableted dispersion systems were subjected to a short-term stability study at room temperature.

After 30 days of storage, the tablets were subjected to tablet characteristic tests; the dissolution rates of both the powdered melts and the tablets were determined. The results were compared to those obtained from previous experiments.

Corticosteroid Stability Studies—The stability of the corticosteroids during the preparation of the dispersion system and the tablets was studied as previously described (6).

RESULTS

Solid Dispersion Formation—All dispersion systems were relatively easy to prepare. Hydrocortisone and prednisone were miscible with mannitol in the melted state at the preparation temperature (200°). The mannitol dispersion systems were not hygroscopic, did not discolor, were very easy to manipulate, and possessed excellent flow characteristics.

The corticosteroids were only partially miscible with the sorbitol. These

[1] Stokes, Pennsalt Chemical Corp., Warminster, Pa.
[2] Celutab, Penick and Ford Co., Cedar Rapids, Iowa.
[3] Avicel-PH-101, FMC Corp., New York, N.Y.
[4] Sterotex, Capitol City Products Co.
[5] Stokes hardness tester, Pennsalt Chemical Corp., Warminster, Pa.
[6] Ames thickness gauge, Ames Co., Elkhart, Ind.
[7] Mettler H-8 analytical balance, Mettler Instrument Corp., Hightstown, N.J.
[8] Modified NF XIII dissolution rate apparatus, Hansen Research Corp., Los Angeles, Calif.
[9] Beckman ACTA III, Beckman Instruments, Fullerton, Calif.

0022-3549/78/0700/0979$01.00/0
© 1978, American Pharmaceutical Association

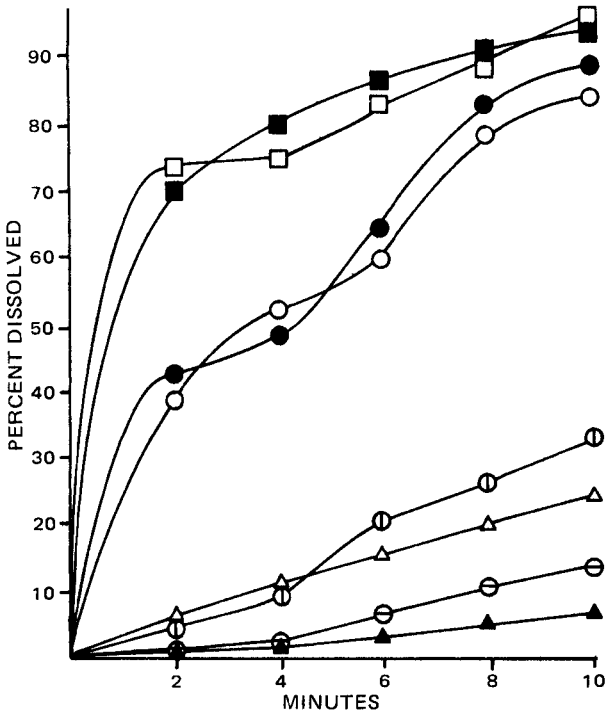

Figure 1—*Dissolution rates of hydrocortisone and prednisone in a sorbitol dispersion. Key for hydrocortisone: △, control powder; ⊖, control tablets; □, dispersion powder; and ○, dispersion tablets. Key for prednisone: ▲, control powder; ⊖, control tablets; ■, dispersion powder; and ●, dispersion tablets.*

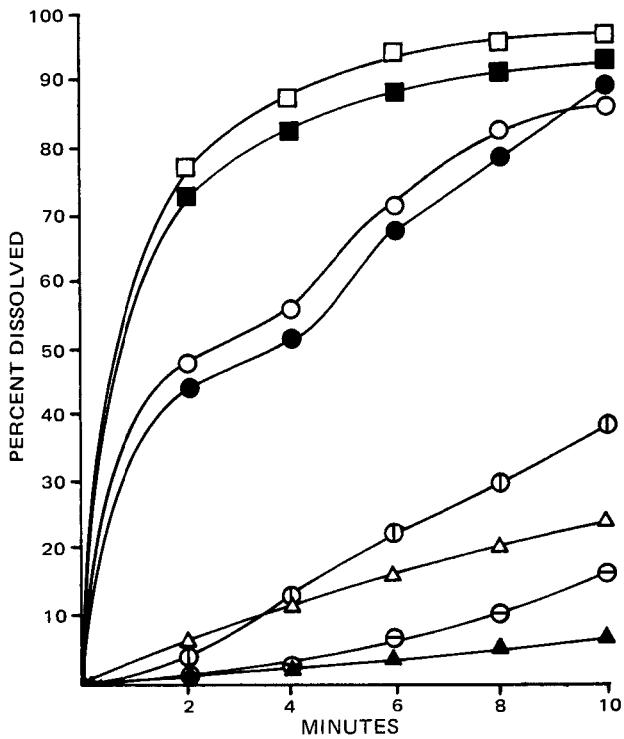

Figure 3—*Dissolution rates of hydrocortisone and prednisone in a sorbitol–mannitol dispersion. Key for hydrocortisone: △, control powder; ⊖, control tablets; □, dispersion powder; and ○, dispersion tablets. Key for prednisone: ▲, control powder; ⊖, control tablets; ■, dispersion powder; and ●, dispersion tablets.*

mixtures were hygroscopic and not as easily manipulated but did not discolor.

Both corticosteroids were miscible with the 50% mannitol–50% sorbitol mixture in the melted state. The addition of the mannitol to the sorbitol greatly improved the properties of these systems because they were easily manipulated, did not discolor, and were only slightly hygroscopic. A slight clumping of the particles could be broken up by a gentle tapping of the sample container; the powder could be seen to flow freely.

The 50% mannitol–50% sucrose mixture had a melting point of 154°, or approximately 14° lower than mannitol alone and about 20° lower than sucrose alone. This melting point resulted in a reduction of the sucrose

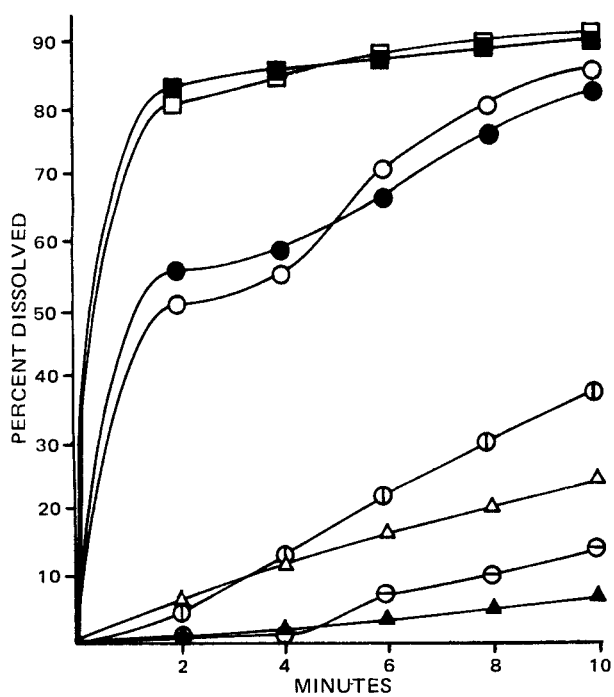

Figure 2—*Dissolution rates of hydrocortisone and prednisone in a mannitol dispersion. Key for hydrocortisone: △, control powder; ⊖, control tablets; □, dispersion powder; and ○, dispersion tablets. Key for prednisone: ▲, control powder; ⊖, control tablets; ■, dispersion powder; and ●, dispersion tablets.*

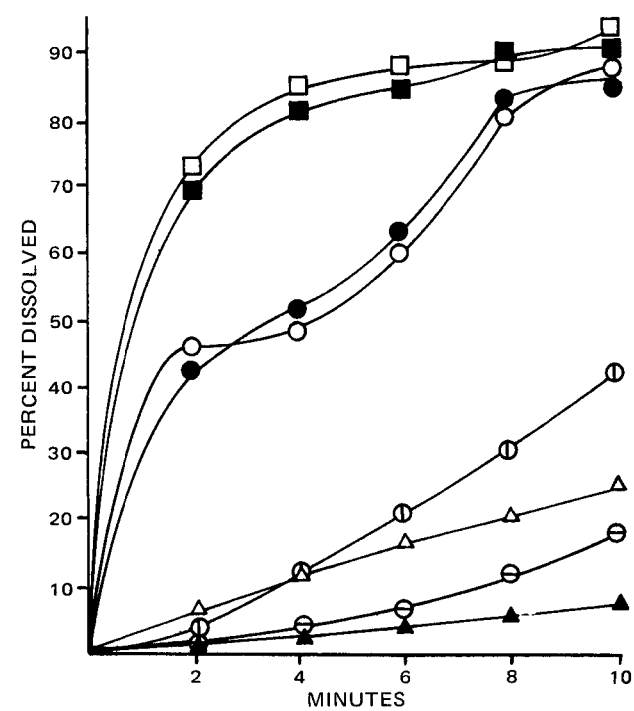

Figure 4—*Dissolution rates of hydrocortisone and prednisone in a sucrose–mannitol dispersion. Key for hydrocortisone: △, control powder; ⊖, control tablets; □, dispersion powder; and ○, dispersion tablets. Key for prednisone: ▲, control powder; ⊖, control tablets; ■, dispersion powder; and ●, dispersion tablets.*

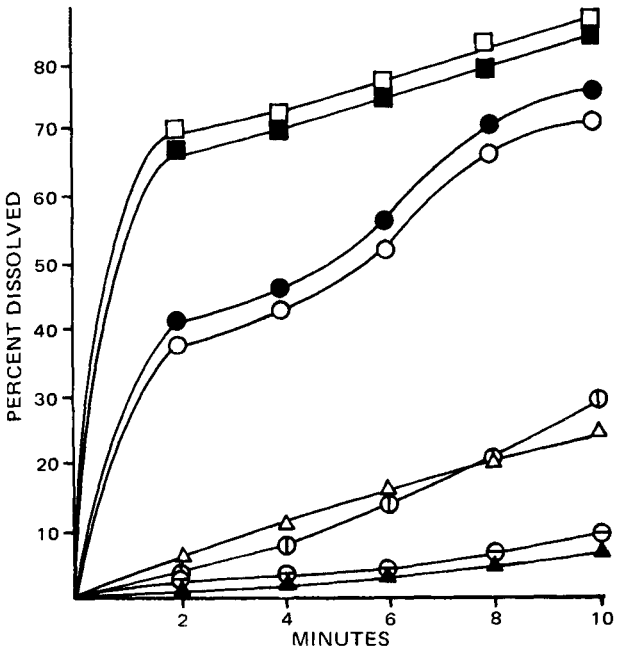

Figure 5—*Dissolution rates of hydrocortisone and prednisone in a polyethylene glycol 6000 dispersion. Key for hydrocortisone: △, control powder; ◑, control tablets; □, dispersion powder; and ○, dispersion tablets. Key for prednisone: ▲, control powder; ⊖, control tablets; ■, dispersion powder; and ●, dispersion tablets.*

discoloration during the preparation of this dispersion system. This mixture was, however, still slightly hygroscopic, but its flow properties were good, resulting in easy manipulation and workability similar to the mannitol–sorbitol mixture.

Hydrocortisone and prednisone were miscible with polyethylene glycol 6000 in the melted state. The physical properties of this dispersion system were very good. The system was heat stable, nonhygroscopic, and easy to manipulate, and it had excellent flow properties.

Dissolution Rate Determinations—As shown in Figs. 1–5, the dissolution rates of both corticosteroids increased markedly in all systems. The mannitol system had the fastest dissolution rate, followed by sorbitol–mannitol, sucrose–mannitol, sorbitol, and, finally, polyethylene glycol 6000.

Samples of the various lots of the powders and the tablets gave similar results. There was no alteration in the dissolution rates of samples subjected to the 30-day short-term stability test.

Stability Studies—Neither hydrocortisone nor prednisone showed any decomposition during the preparation of the melts or the tablets according to the analytical methods used. The tablet characteristic test results remained unchanged after 30 days of storage.

DISCUSSION

The solid dispersion systems demonstrated a fast initial release, followed by a slower, prolonged release of hydrocortisone and prednisone. Similar profiles previously were reported and discussed (6). As expected, the tablets produced slower dissolution rates than the powders.

After about 8 min in the dissolution fluid, the slope of the dissolution curve approached that of the powdered sample. This result indicated that the tablet formulation was effective in breaking up and exposing the system to the dissolution medium.

The control tablets possessed slightly faster dissolution rates than the control powders, probably because of the easier wettability of the steroid particles when encompassed by the hydrophilic tablet excipients. During tablet compression, the adsorbed or entrapped air was removed and, since the excipients were mostly hydrophilic in nature, they assisted in wetting the steroid particles.

The popularity of polyethylene glycol as a carrier was the main reason that the polyethylene glycol 6000 dispersion systems were used as a reference model when comparing the dissolution rates of the sugar dispersions. The sugar dispersions had a faster dissolution rate than the polyethylene glycol dispersions.

The data indicate that mannitol is one of the better sugar carriers, especially since it forms a stable, nonhygroscopic, free-flowing dispersion system. It revealed no discoloration during the preparation of the melt and was miscible with two steroids in the concentration range used.

The use of sugars in dispersion systems is advantageous over other solid dispersion carriers because they are nontoxic, inexpensive, and physiologically acceptable.

REFERENCES

(1) B. E. Ballard and J. A. Biles, *Steroids*, **4**, 273 (1964).

(2) G. Levy, N. A. Hall, and E. Nelson, *Am. J. Hosp. Pharm.*, **21**, 402 (1964).

(3) G. H. Schneller, *Drug Inform. Bull.*, **3**, 100 (1969).

(4) H. C. Shirkey, *J. Pediatr.*, **76**, 774 (1970).

(5) W. E. Hamlin, E. Nelson, B. E. Ballard, and J. G. Wagner, *J. Pharm. Sci.*, **51**, 423 (1962).

(6) L. V. Allen, Jr., V. A. Yanchick, and D. D. Maness, *ibid.*, **66**, 494 (1977).

(7) T. Otto, M.S. thesis, University of Oklahoma, Norman, Okla., 1976.

ACKNOWLEDGMENTS

The authors thank The Upjohn Co. for the corticosteroids.

USP Dissolution III: Semilogarithmic Dissolution Patterns of Tablets in Rotating-Basket Assemblies

J. T. CARSTENSEN *x, J. L. WRIGHT *, KENNETH BLESSEL ‡, and JANE SHERIDAN ‡

Received July 23, 1976, from the **School of Pharmacy, University of Wisconsin, Madison, WI 53716,* and ‡*Hoffmann-La Roche Inc., Nutley, NJ 07110.* Accepted for publication November 7, 1977.

Abstract □ The dissolution of a rapidly soluble, finely subdivided substance in a directly compressed tablet and in a wet granulated tablet was treated experimentally and compared with previous theoretical models. The dissolution curves were sigmoid with a semilogarithmic tail when concentration was plotted *versus* time. As predicted, the slope of the semilogarithmic plots were related to the disintegration decay constant for tablet erosion in the basket.

Keyphrases □ Dissolution—rapidly soluble, finely subdivided substance in directly compressed and wet granulated tablets, compared with previous theoretical models □ Tablets—directly compressed and wet granulated, containing rapidly soluble, finely subdivided substance, dissolution compared with previous theoretical models □ Dosage forms—tablets, directly compressed and wet granulated, containing rapidly soluble, finely subdivided substance, dissolution compared with previous theoretical models

Extensive research has been published recently regarding dissolution rate methodology. Several methods of data treatment exist, but the general plotting modes for tablets have been (*a*) Hixson–Crowell cube root plots with lag time (1, 2), (*b*) σ^{-}-plots (2, 3), (*c*) log-probit plots as suggested by Wagner (4) and Wood (5), and (*d*) Weibull plots as suggested by Langenbucher (6) and Lippman (7). Frequently, dissolution data will fit one of these equations, but there are reported cases (8) where none applies. Whatever the fit may be, little work has been done to explain why dissolution rate profiles in particular situations follow certain patterns.

Part of the dissolution process in the USP dissolution apparatus (or other basket apparatus) takes (or can take) place outside of the basket and part takes place in the basket; the two are not equivalent (9–11). Disintegration also plays a part in dissolution (12, 13). The manner in which this process affects the dissolution of a coarse powder in a nonswellable tablet base has been treated theoretically (14). Since many tablet matrixes exhibit some swelling and since most drug substances are finely subdivided, this special case is treated, experimentally and theoretically, in this report.

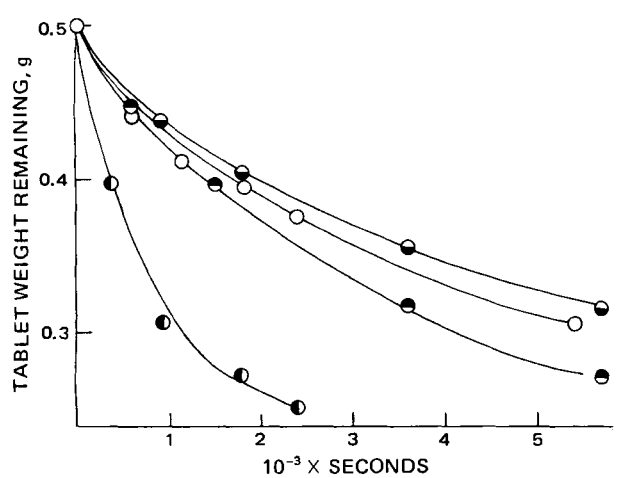

Figure 1—*Weight* versus *time curves of directly compressed tablets. Key:* ◒, *no starch (I);* ○, *10 mg of starch (II);* ◓, *30 mg of starch (III); and* ◐, *50 mg of starch (IV).*

EXPERIMENTAL

Experiments were performed in a USP dissolution rate apparatus operating at 100 rpm at 25°. To test the dissolution of a directly compressed dosage form with varying disintegration times, Formulas I–IV were prepared (Table I). Sufficient powder to make 100 tablets was mixed in a mortar and pestle, and 500-mg portions were weighed and compressed at 5000 lb of force in a hydraulic press. The tablets were 0.582 ± 0.03 cm thick at the crown and 0.25 cm at the edge; the diameter was 1.117 cm. Dissolution was checked in 0.1 *N* HCl at 25°. A volume of 900 ml of liquid was used to dissolve drug from three tablets.

In one set of experiments, the total amount of tablet weight remaining in the basket was determined as a function of time. One tablet was used for each time point. In another set of experiments, the amount of dissolved drug was determined as a function of time by withdrawing samples

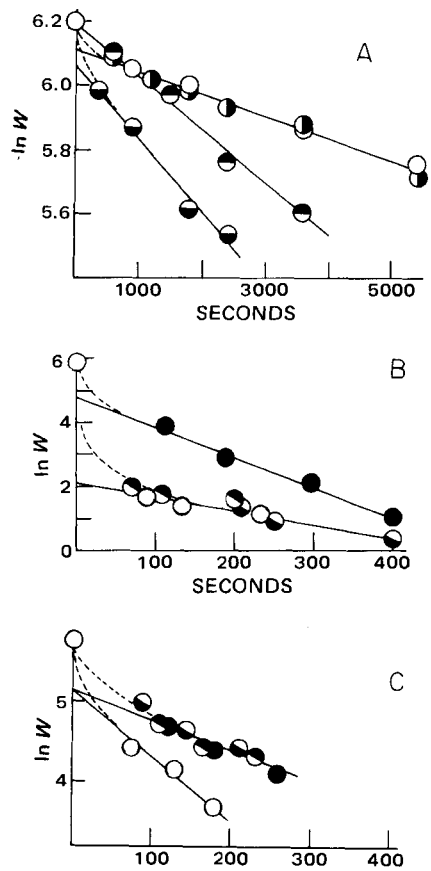

Figure 2—*Plots of ln* W versus t. *A: data from Fig. 1. Key:* ◑, *no starch (I);* ○, *10 mg of starch (II);* ◓, *30 mg of starch (III); and* ◒, *50 mg of starch (IV). B and C: wet granulated tablets (20–30 and 60–80 mesh, respectively). Key:* ○, *no stearic acid (V);* ◑, *1.5 mg of stearic acid (VI);* ◐, *3 mg of stearic acid (VII); and* ●, *9 mg of stearic acid (VIII).*

0022-3549/78/0700/0982$01.00/0
© 1978, American Pharmaceutical Association

Table I—Formulas and Dissolution Parameters of Yellow Tablets

	Amount, mg/Tablet or g/Batch								
	I	II	III	IV	Per Batch	V	VI	VII	VIII
Lactose USP	473.5	463.5	443	423.55	1515	260.31	260.31	260.31	260.31
FD&C Yellow No. 5	1.5	1.5	1.5	1.5	6	1.03	1.03	1.03	1.03
Starch USP (powder)	0	10	30	50	180	31.93	31.93	31.93	
Magnesium stearate	25	25	25	25					
Starch USP (for paste)					45	7.73	7.73	7.73	7.73
Stearic acid						0	1.5	3	9
Total	500	500	500	500	1746	300	301.5	303	309
Disintegration time (D, sec)	2350	1400	750	122	(20–30)	27	63	59	76
					(60–80)	25	28	30	36
SE	47	38	26	5	(20–30)	2	2	3	4
					(60–80)	2	2	2	3

at various times and assaying spectrophotometrically at 420 nm for dye content.

To test the dissolution of wet granulated tablets (with varying USP disintegration test disintegration times), Formulas V–VIII were prepared (Table I). These powders were blended in a planetary mixer, and the starch for paste was dispersed in 100 ml of cold water. The suspension was added to 350 ml of boiling water and formed a gel, which was allowed to cool to 55° and was then added to the blended powders. The wet granules were wet screened through a No. 6 mesh hand screen, dried at 60°, and then classified by sieving. The 20–30- and 60–80-mesh fractions were used. Stearic acid, as a dissolution liquid in chloroform, was added to the dried granules in a small coating pan. The solvent was then removed by hot air.

Tablets of 300 mg, made separately with the 20–30- and 60–80-mesh granules of each of the four formulas, were subjected to dissolution and weight decay studies as described.

RESULTS AND DISCUSSION

A simple, generalized model for the dissolution of a drug in a directly compressed tablet was proposed previously (14). In this model, monodisperse particles of a drug (or model) substance that is coarser than the basket screen are dislodged from a tablet matrix, which, in turn, simply decreases in size with time. This model is realistic in many cases, and some of the data presented here approach this view. Frequently, however, the tablet matrix swells and partially disintegrates prior to erosion (or further, but slower, disintegration), and some of the experimental data generated here follow this pattern. One purpose of this study was to determine whether the predicted correlation between the erosion constant, q (seconds^{-1}), and the semilogarithmic dissolution rate constant, K (seconds^{-1}), which is predicted for the simpler model, also holds for the more complex situation.

If the tablet first swells and flakes off granules rapidly and then disintegrates further in a slower fashion, and if these processes are exponential decay functions, then the weight *versus* time curves of the tablets should be biexponential, *i.e.*, of the nature:

$$W = Q \exp(-qt) + \Gamma \exp(-\alpha t) \qquad \text{(Eq. 1)}$$

where W is the mass of the tablet remaining, Γ and α are attributable to the first rapid disintegration, and Q and q are attributable to the final slower disintegration (erosion) of the tablets in the basket.

Figure 1 shows weight *versus* time plots of the directly compressed tablets, and Fig. 2 shows the data for all tablets tested by semilogarithmic plotting. The parameter values (Q and q) are shown in Table II for all tablets. The goodness of fit is implied by the high correlation coefficients. The value of Γ is obtained as the difference between the original weight and the value of Q. The value for Γ is very small in several cases (*e.g.*, Formulas I, III, and IV); in these instances, the model proposed earlier (14) would hold well. Since this model predicts a correlation between q and K when q is small, it is of interest to see whether this is also the case when q is large and when the weight decay curve is biexponential rather than monoexponential.

For the wet granulated 20–30-mesh tablets, the data relating to the formulas containing stearic acid are clustered together in one group (although there are differences between the three formulations), and they are quite different from the data from the formulation containing no

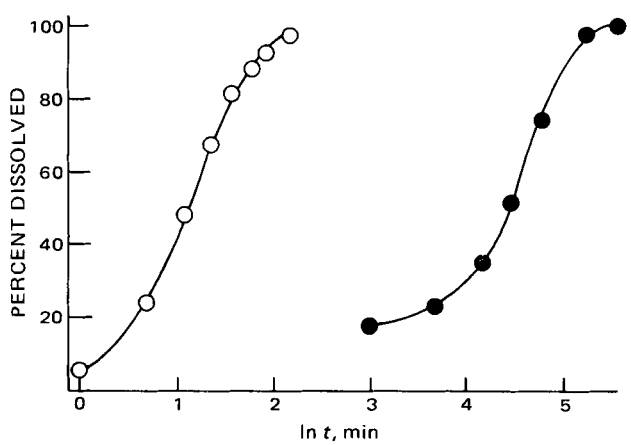

Figure 3—*Plots of* C versus *ln* t *for Formula I* (○) *(no starch) and Formula VIII* (●) *(20–30 mesh, 3% stearic acid).*

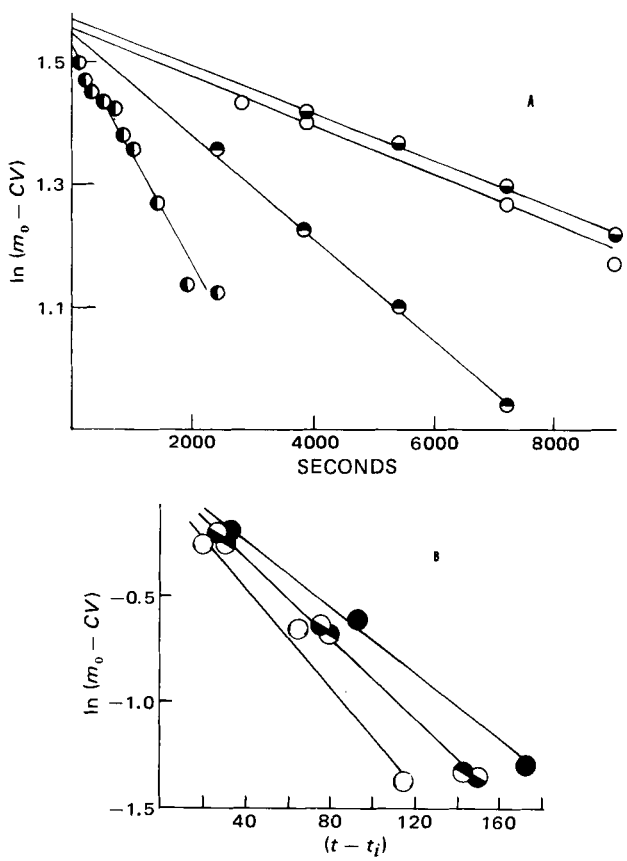

Figure 4—*Plots of ln* ($m_0 - \dot{C}V$) *as a function of time;* m_0 *and* CV *are in milligrams. A: Formulas I–IV. Key:* ◒, *no starch (I);* ○, *10 mg of starch (II);* ◓, *30 mg of starch (III); and* ◑, *50 mg of starch (IV). B: Formulas V–VIII. Key:* ○, *no stearic acid;* ◐, *0.5% stearic acid;* ◑, *1% stearic acid; and* ●, *3% stearic acid.*

Table II—Parameter Values for the Formulas Tested

Formula	Lubricant Level, mg/Tablet	ln W *versus* Time				ln($m_0 - CV$) *versus* Time		
		CR^a	$-q\ 10^3$, sec^{-1}	Q	Γ	CR^a	$K\ 10^3$, sec^{-1}	t_i, sec
I	0	−0.997	0.67	453	47	−0.994	0.038	1630
II	10	−0.998	0.07	459	41	−0.999	0.040	1200
III	30	−0.994	0.17	496	4	−0.950	0.085	599
IV	50	−0.991	0.24	431	69	−0.985	0.170	88
V, 20–30	0	−0.987	7.9	166	134	−0.991	11.8	65
VI, 20–30	1.5	−0.962	3.3	155	145	−0.997	9.4	85
VII, 20–30	3	−0.980	4.7	215	85	−0.998	9.3	62
VIII, 20–30	9	−0.991	4.2	180	120	−0.998	7.9	87
V, 60–80	0	−0.970	12.2	4	296	−0.992	6.3	150
VI, 60–80	1.5	−0.876	2.3	8	292	−0.996	8.3	31
VII, 60–80	3	−0.988	3.4	7	293	−0.973	8.0	65
VIII, 60–80	9	−0.984	9.5	120	180	−0.998	6.1	69

[a] Correlation coefficient.

stearic acid. With tablets made from the 60–80-mesh granules, the formula containing 3% stearic acid is separate from the others, which fall in a clustered group. Apparently, for the larger surface area in the 60–80-mesh granules, more stearic acid is needed to contribute the cohesion necessary to prolong disintegration in the dissolution basket. The argument is not one of monomolecular layers since stearic acid has a close-packed molecular contact area of 20 Å^2 (15). Therefore, it would only take 10^{-5} mole (0.003 mg) to cover a surface area of 10^4 cm^2, the geometric surface area of the 20–30-mesh granules in the 300-mg tablet.

The Γ term is very small in several cases (*e.g.*, Formula III).

The dissolution curves are all typically sigmoid (Fig. 3). The data are presented using ln t (in minutes) as abscissa rather than t, because log-probit plotting is often employed in such situations. In one case (Formula I), the plot is symmetrical about the 50% point (*i.e.*, is log-probit); but in the other case (Formula VIII), it is not.

The tails of all curves are logarithmic time decays (14, 16, 17); *i.e.*, the curves follow:

$$\ln(m_0 - CV) = \ln m_0 - K(t - t_i) \qquad \text{(Eq. 2)}$$

where m_0 is the amount of drug in the tablets originally, C is concentration, V is the volume of dissolving liquid, and t_i is the lag time. This is demonstrated in Fig. 4, and t_i and K values are given in Table II. The goodness of fit is implied by the proximity to unity of the correlation coefficients. Equation 2 obviously holds only for $t > t_i$ (since it otherwise would imply $C = 0$ at $t = t_i$), and t_i will be empirical and may be difficult to reproduce from apparatus to apparatus.

It is difficult to graph q *versus* K because the data fall in two clusters, one with very low q values and one with much higher q values. In Fig. 5, therefore, the correlation of ln K *versus* ln q is shown. The data are grouped as indicated in Fig. 2; the common q value for Formulas VI–VIII is used for the 20–30-mesh fraction, as is the common q value for Formulas V–VII for the 60–80-mesh fraction. The correlation coefficient is 0.985 for the relationship $\ln q = 1.19 \ln K + 1.286$; *i.e.*, q and K correlate but not quite linearly.

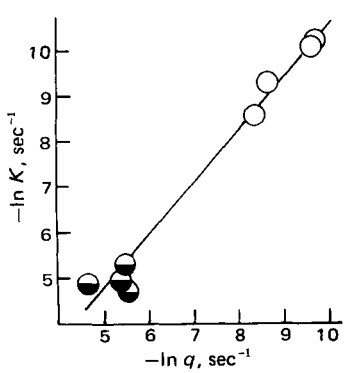

Figure 5—*Correlation between* K *and* q.

REFERENCES

(1) A. W. Hixson and J. H. Crowell, *Ind. Eng. Chem.*, **123,** 923 (1931).

(2) J. T. Carstensen, in "Dissolution Technology," L. Leeson and J. T. Carstensen, Eds., Industrial Pharmaceutical Technology Section, Academy of Pharmaceutical Sciences, American Pharmaceutical Association, Washington, D.C., 1974, p. 189.

(3) T. S. Gaginella, P. G. Welling, and P. Bass, *J. Pharm. Sci.*, **63,** 1849 (1974).

(4) J. Wagner, *ibid.*, **58,** 1253 (1969).

(5) J. H. Wood, "Abstracts of Papers Presented at the 113th Annual Meeting of the American Pharmaceutical Association," Dallas, Tex., Apr. 1966, p. 35.

(6) W. Langenbucher, *J. Pharm. Pharmacol.*, **24,** 979 (1972).

(7) I. Lippmann, in "Dissolution Technology," L. Leeson and J. T. Cartensen, Eds., Industrial Pharmaceutical Technology Section, Academy of Pharmaceutical Sciences, American Pharmaceutical Association, Washington, D.C., 1974, p. 193.

(8) M. J. Taraszka and R. A. Delor, *J. Pharm. Sci.*, **58,** 207 (1969).

(9) R. J. Whithey, *J. Pharm. Pharmacol.*, **23,** 573 (1971).

(10) J. E. Tingstad and S. Riegelman, *J. Pharm. Sci.*, **59,** 692 (1970).

(11) J. E. Tingstad, E. Gropper, L. Lachman, and E. Shami, *ibid.*, **62,** 293 (1973).

(12) J. B. Johnson, P. G. Kennedy, and S. H. Rubin, *ibid.*, **63,** 1931 (1974).

(13) P. L. Madan, *ibid.*, **64,** 1080 (1975).

(14) J. T. Carstensen, J. L. Wright, K. W. Blessel, and J. Sheridan, *ibid.*, **67,** 48 (1978).

(15) N. K. Adam, *Proc. Roy. Soc. (London)*, **A101,** 452 (1922).

(16) J. T. Carstensen, "Pharmaceutics of Solids and Solid Dosage Forms," Wiley, New York, N.Y., 1977, pp. 44, 77.

(17) L. T. Grady, "Abstracts of Papers Presented before the APhA Academy of Pharmaceutical Sciences," vol. 6 (2), 1976, p. 45 (Orlando, Fla., Nov. 1976).

ACKNOWLEDGMENTS

Presented at the APhA Academy of Pharmaceutical Sciences, Orlando meeting, November 1976.

High-Performance Liquid Chromatographic Assay for Suprofen, a Potent New Analgesic, in Plasma

K. B. ALTON [x] **and J. E. PATRICK**

Received August 19, 1977, from *Ortho Pharmaceutical Corporation, Raritan, NJ 08869.* Accepted for publication November 3, 1977.

Abstract □ A simple, rapid, high-performance liquid chromatographic (HPLC) determination of therapeutic levels of suprofen, a potent new analgesic, in human plasma is described. After a simple extraction, the compound is analyzed by HPLC using a reversed-phase column and a UV detector. Quantitation is accomplished using an external standard; peak areas are determined by computer. An average recovery of 80.0 ± 8.5% *SD* of the drug was obtained over the 0.2–20.0-μg/ml range. Maximum sensitivity is approximately 0.1 μg/ml. No interference is encountered from any known metabolite of suprofen.

Keyphrases □ Suprofen—high-performance liquid chromatographic analysis in plasma □ High-performance liquid chromatography—analysis, suprofen in plasma □ Analgesics—suprofen, high-performance liquid chromatographic analysis in plasma

Suprofen, 2-[4-(2-thienoyl)phenyl]propionic acid (I), is a potent inhibitor of prostaglandin synthetase (1) and is currently being studied clinically as a new analgesic agent.

A rapid, precise method for the quantitation of suprofen in plasma was required to determine the pharmacokinetic parameters relating to its absorption, distribution, and elimination in animals and humans.

This paper describes a simple high-performance liquid chromatographic (HPLC) method for the rapid estimation of suprofen in human plasma. The maximum sensitivity is approximately 0.1 μg/ml.

EXPERIMENTAL

Apparatus—The liquid chromatograph[1], equipped with a differential UV detector[2] (254 nm), was operated at ambient temperature. Chromatograms were traced on a strip-chart recorder[3], and peak area integration was performed by computer[4]. Separations were accomplished on a 30.5 × 0.64-cm microparticulate reversed-phase column[5]. A 25-μl syringe[6] was used for the introduction of samples onto the column through a septumless injector[7].

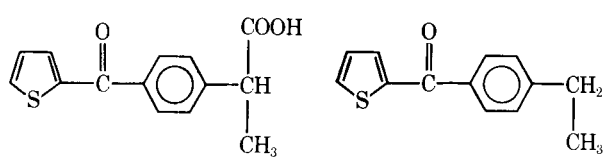

I

II

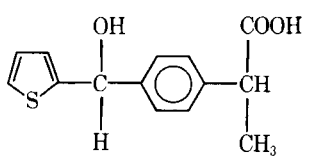

III

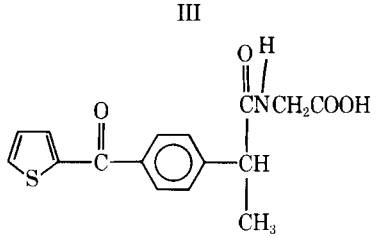

IV

The radioactive content of various samples was determined by liquid scintillation spectrometry. Aliquots of the samples were dissolved in scintillation fluid[8] and assayed for radioactivity in a liquid scintillation spectrometer[9]. Internal standardization was used to determine counting efficiency.

Reagents and Solvents—^{3}H-Suprofen (specific activity of ~65 μCi/mg), unlabeled suprofen (I), and three possible suprofen metabolites, 1-ethyl-4-(2-thienoyl)benzene (II), 2-[4-(α-hydroxy-2-thenyl)phenyl]-propionic acid (III), and 2-[4-(2-thienoyl)phenyl]propionic acid glycine conjugate (IV), were used[10]. All chemicals and reagents, except acetonitrile[11], were reagent grade. Acetonitrile, tetrahydrofuran, and methanol were redistilled before use.

Chromatographic Conditions—The mobile phase was 0.01% (v/v) aqueous acetic acid–acetonitrile (70:30 v/v); the flow was adjusted to 2.5 ml/min, generating a pressure of ~2500 psi. The solvent mixture was prepared daily and degassed under slight vacuum before use.

Extraction Procedure—Aliquots (1.0 ml) of plasma were transferred to 15-ml screw-capped vials (16 × 125 mm), acidified with 3.0 ml of 0.1 *N* HCl, and extracted with 8.0 ml of ether. The phases were separated by centrifugation for 2–3 min at ~1000 rpm, and the organic layer was removed with a Pasteur pipet and then transferred to another 15-ml screw-capped vial.

A second extraction was performed similarly.

The ether layers were pooled for each sample and then taken to dryness under a nitrogen stream in a water bath (40°). An aliquot (2.0 ml) of 1 *N* NaOH was added to the ether residue and mixed with a vortex mixer. The sodium hydroxide solution was then extracted twice with 2.0 ml of ether, and the organic layers were discarded after aspiration. The remaining aqueous fraction was acidified with 3.0 ml of 2 *N* HCl (saturated with sodium chloride), and this mixture again was extracted with 8.0 ml of ether.

The pooled ether extracts were dried over anhydrous sodium sulfate and taken to dryness under nitrogen in a water bath (35°). The residues were transferred with ether to 2.5-ml conical centrifuge tubes and concentrated as already described. The final residue was dissolved in tetrahydrofuran (0.1–0.5 ml) for injection onto the HPLC column.

Extraction Efficiency Studies—The recoveries of both ^{3}H-suprofen and unlabeled suprofen from control plasma samples, prepared to contain known drug concentrations, were investigated in two studies.

In the first study, 0.2 μg of ^{3}H-suprofen (~32,200 dpm) in 10 μl of methanol was added to each of 16 1.0-ml aliquots of control plasma from untreated volunteers. These samples were divided into four equal groups, and total suprofen concentrations of 0.2, 0.5, 1.0, and 5.0 μg/ml were achieved by the subsequent addition of 0, 0.3, 0.8, and 4.8 μg of unlabeled drug from methanolic stock solutions, respectively. The added drug was mixed thoroughly, allowed to equilibrate for 30 min at room temperature, and then extracted as described. Total radioactivity in the final residues (100 μl) was evaluated by assaying aliquots (20 μl) of the tetrahydrofuran solutions for radioactive content.

In a second study, aliquots of methanolic suprofen solutions (described later) were added to four groups, each consisting of at least 10 control

[1] Model ALC 202, Waters Associates, Milford, Mass.
[2] Model 440, Waters Associates, Milford, Mass.
[3] Sevo/riter II, Texas Instruments, Houston, Tex.
[4] Model 3352B, Hewlett-Packard, Avondale, Pa.
[5] μBondapak C_{18}, Waters Associates, Milford, Mass.
[6] Pressure-Lok B-110, Precision Sampling Corp., Baton Rouge, La.
[7] Model U6K, Waters Associates, Milford, Mass.
[8] Prepared from Liquifluor, New England Nuclear, Boston, Mass.
[9] Model SL-30, Teledyne Intertechnique, Westwood, N.J.
[10] Suprofen and its possible metabolite standards were synthesized and supplied by Janssen Pharmaceutica, Beerse, Belgium.
[11] Ninety-nine mole percent pure, Fisher Scientific Co., Fair Lawn, N.J.

0022-3549/78/0700/0985$01.00/0
© 1978, American Pharmaceutical Association

Table I—HPLC Retention Times and Relative Separation (Resolution, *R*) of Suprofen and Three Possible Metabolites

Compound	t_r, min	*R*
I	7.7	—
II	14.8	22.4
III	4.5	16.5
IV	2.9	25

plasma samples (1.0 ml), to achieve final concentrations of 0.2, 0.5, 5.0, and 20.0 μg/ml of plasma. Samples were allowed to equilibrate and were extracted as described.

Since the prepared plasma drug concentrations ranged over two orders of magnitude, varying volumes of the final tetrahydrofuran dilutions were injected for HPLC analysis. When the drug concentration was 0.2 μg/ml, one-fifth (20 μl/100 μl) of the total extract volume was analyzed; at a concentration of 20 μg/ml, only 5 μl from a 500-μl dilution was injected. In general, samples were analyzed in duplicate. Quantitation of recovered suprofen, after separation by HPLC, was accomplished by the use of an external standard method contained in the software of the computer.

Calibration and Standard Preparation—Approximately 0.1 mg of ^{3}H-suprofen was dissolved in 5.0 ml of methanol. Analysis of this solution by HPLC and liquid scintillation spectrometry indicated that the solution contained ~32,200 dpm/0.2 μg/10 μl of solution. Unlabeled suprofen (25 mg) was dissolved in about 10 ml of methanol and diluted to volume in a 25.0-ml volumetric flask to achieve a concentration of 1.0 μg/μl. An aliquot (2.5 ml) of this solution was transferred to another 25.0-ml volumetric flask and then diluted to volume with methanol to obtain a concentration of 0.1 μg/μl. A third stock solution (0.01 μg/μl) was prepared by diluting the last one in the same manner. Three additional standard solutions (0.01, 0.1, and 1.0 μg/μl) were prepared similarly with tetrahydrofuran.

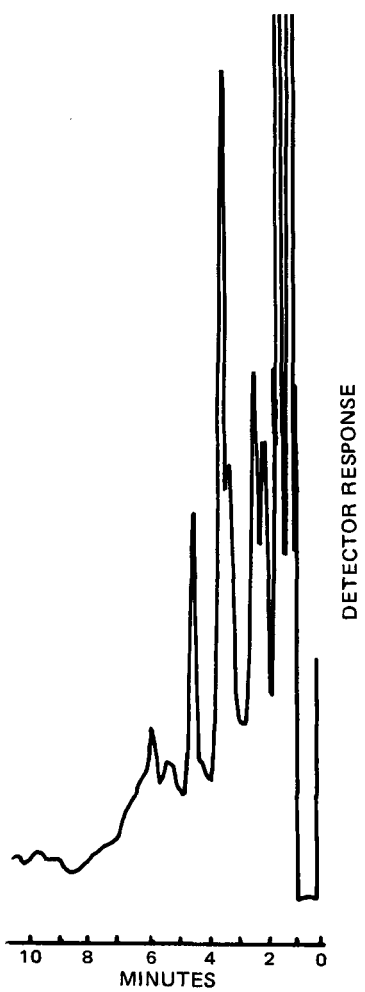

Figure 1—*Chromatogram of a residue from a control plasma sample extracted with ether.*

Table II—Precision and Recovery Data for Both ^{3}H-Suprofen and Unlabeled Suprofen Added to 1.0 ml of Drug-Free Plasma

Initial Concentration Added, μg/ml	*n*	Amount Found, μg/ml ± *SD*	Recovery, % ± *SD*
0.2[a]	4	0.175 ± 0.006	87.3 ± 3.23
0.5[a]	4	0.416 ± 0.007	83.1 ± 1.68
1.0[a]	4	0.727 ± 0.077	72.7 ± 10.6
5.0[a]	4	4.08 ± 0.187	81.6 ± 4.58
			$\bar{\bar{x}}$ = 81.2 ± 4.82
0.2[b]	18	0.158 ± 0.022	79.2 ± 11.0
0.5[b]	18	0.395 ± 0.04	79.0 ± 8.1
5.0[b]	18	4.03 ± 0.32	80.5 ± 6.4
20.0[b]	16	15.9 ± 1.7	80.0 ± 8.49
			$\bar{\bar{x}}$ = 80.0 ± 8.5

[a] Recovery of added ^{3}H-suprofen as determined by liquid scintillation spectrophotometry. [b] Recovery of added unlabeled suprofen as determined by HPLC.

Since the external standard method prepared from the software section of the computer assumes linearity between micrograms injected and peak area (microvolt seconds as reported by the integrating computer), this relationship was initially evaluated by repeated HPLC analyses of 0.2, 0.15, 0.05, 0.025, and 0.01 μg of suprofen in tetrahydrofuran (0.01 μg/μl). Thereafter, an average calibration response factor was established by the computer following triplicate injections of 0.15 μg of suprofen. As a final check, the accuracy of the computer-generated response factor was verified by analyzing known quantities of suprofen (0.05 and 0.2 μg).

Specificity—Assay specificity was determined by injecting a solution containing a mixture of suprofen and its potential metabolites, II–IV (1 μg/μl in methanol), onto the HPLC column.

RESULTS AND DISCUSSION

Ether extracts of control plasma were free of endogenous UV (254 nm) absorbing peaks that interfered with the assay (Fig. 1). Under the chro-

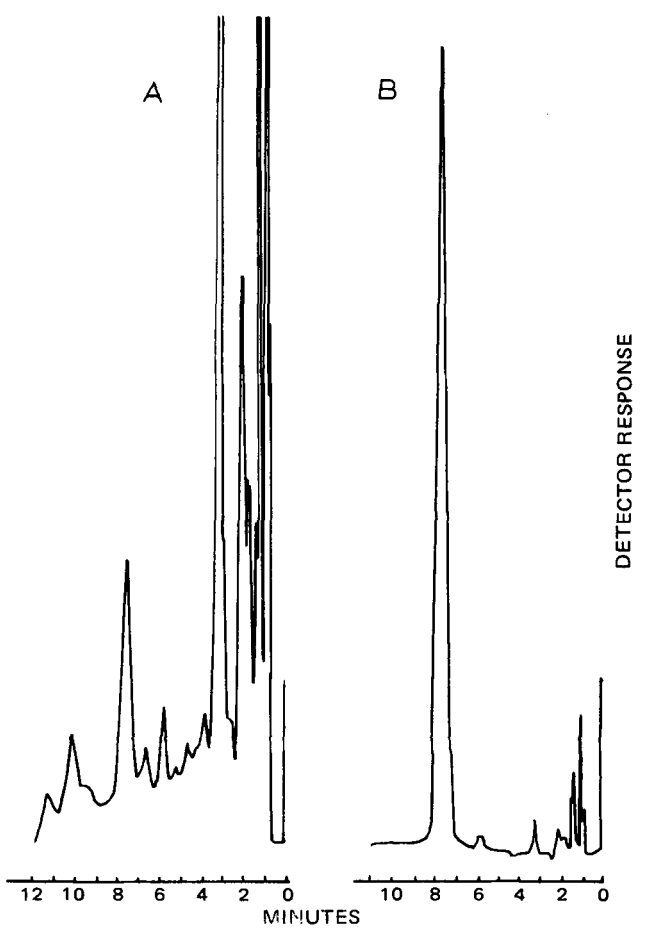

Figure 2—*Chromatograms of ether residues from plasma samples containing 0.2 μg of suprofen/ml (A) and 20 μg of suprofen/ml (B).*

matographic conditions described, baseline resolution between suprofen and the three potential metabolite reference standards was achieved. Retention times and the relative separation of these potential metabolites from suprofen are reported in Table I.

Linear regression analysis of the curve, described by plotting microvolt seconds *versus* micrograms injected, indicated a virtual linear fit of the data ($r^2 = 0.99992$).

The response factor, F_i, generated by the computer is described by $F_i = W_i/A_i$, where W_i is the amount injected and A_i is the area in microvolt seconds. It was shown to be linear over the concentration range evaluated (0.05–0.2 μg/injection). Over a 2-month period of analysis, this response factor demonstrated little change, with a coefficient of variation equal to 2.4% ($n = 23$).

The results from the extracted control plasma to which ^{3}H-suprofen had been added are shown in Table II. The average extraction efficiency based on total recovered radioactivity was 81.2 ± 4.8% *SD*. The average recovery of suprofen from plasma samples to which unlabeled suprofen had been added was 80.0 ± 8.5% *SD* (Table II). Representative chromatograms of extracts from plasma containing 0.2 μg/ml (20 μl from a 100-μl dilution with tetrahydrofuran) and 20.0 μg/ml (5 μl from a 500-μl dilution with tetrahydrofuran) are shown in Fig. 2. A multicomparison analysis of the percent recovery data shown in Table II was performed using the two-tailed Dunnett (2) and Scheffé (3) test. No statistically significant differences were found in extraction efficiencies among the four groups of plasma samples with added suprofen.

These data suggest that there is no concentration dependence in extraction efficiencies over the range of expected plasma drug[12] levels following oral administration of 200 mg of suprofen. The results of this study will be the subject of a separate report.

REFERENCES

(1) P. A. J. Janssen, *Arzneim.-Forsch.*, **25**, 1495 (1975).

(2) C. W. Dunnet, *Biometrics*, **20**, 482 (1964).

(3) H. A. Scheffé, "The Analysis of Variance," Wiley, New York, N.Y., 1959.

ACKNOWLEDGMENTS

The authors thank Dr. E. McGonigle for useful discussions. They are grateful to Dr. J. Heykants and Dr. J. Wynants, Janssen Pharmaceutica, for providing preliminary information concerning plasma levels following oral administration of 100 mg of suprofen to humans and for supplying samples of suprofen and potential metabolites. The authors also thank Dr. H. Weintraub and Dr. L. Abrams, Ortho Pharmaceutical Corp., for providing preliminary information concerning plasma levels of total radioactivity following oral administration of 200 mg of ^{3}H-suprofen (specific activity of ~0.25 μCi/mg) to humans.

[12] Preliminary studies, conducted by Janssen Pharmaceutica and Ortho Pharmaceutical Corp., indicated that peak plasma levels of suprofen, equal to approximately 10–20 μg/ml, would be achieved following the oral administration of 200 mg of suprofen to normal human subjects.

Anticonvulsant and Antiproteolytic Properties of 2,5-Disubstituted Oxadiazoles and Their Inhibition of Respiration in Rat Brain Homogenates

SUNIL K. CHAUDHARY *§, SUSHIL KUMAR *, SURENDRA S. PARMAR ‡x, and MAHIMA CHAUDHARY *§

Received September 12, 1977, from the **Jawahar Lal Nehru Laboratory of Molecular Biology, Department of Pharmacology and Therapeutics, King George's Medical College, Lucknow University, Lucknow 226003, India,* and the ‡*Department of Physiology, School of Medicine, University of North Dakota, Grand Forks, ND 58202.* Accepted for publication November 7, 1977. §Present address: National Institute of Environmental Health Sciences, Research Triangle Park, NC 27709.

Abstract □ Eight 2-(3,4-methylenedioxyphenyl)-5-arylamino-1,3,4-oxadiazoles were synthesized, characterized by their sharp melting points, elemental analyses, and IR spectra, and evaluated for anticonvulsant activity. The protection afforded by oxadiazoles (100 mg/kg ip) against pentylenetetrazol (90 mg/kg sc)-induced convulsions ranged from 50 to 80%. All oxadiazoles inhibited the respiratory activity of rat brain homogenates during oxidation of pyruvate, α-ketoglutarate, and succinate. The presence of added nicotinamide adenine dinucleotide (NAD) to the reaction mixture during oxidation of pyruvate decreased the degree of inhibition. All oxadiazoles possessed antiproteolytic activity that was reflected by their ability to decrease trypsin-induced hydrolysis of bovine serum albumin. Such an inhibition was concentration dependent and ranged from 10.2 to 47.5 and from 15.7 to 71.8% by 0.5 and 1 m*M* oxadiazoles, respectively. All oxadiazoles competitively inhibited *in vitro* succinate dehydrogenase activity of rat brain homogenates.

Keyphrases □ Oxadiazoles, various—synthesized, evaluated for effect on enzyme activity in rat brain homogenates, anticonvulsant activity in mice, and antiproteolytic activity *in vitro* □ Enzyme activity—effect of various oxadiazoles in rat brain homogenates □ Anticonvulsant activity—various oxadiazoles evaluated in mice □ Antiproteolytic activity—various oxadiazoles evaluated *in vitro* □ Structure–activity relationships—various oxadiazoles evaluated for effect on enzyme activity in rat brain homogenates, anticonvulsant activity in mice, and antiproteolytic activity *in vitro*

Earlier studies indicated central nervous system depressant (1, 2), analgesic (3), muscle relaxant (4), and tranquilizing (5, 6) properties of substituted oxadiazoles. The inhibitory effects of 2,5-disubstituted 1,3,4-oxadiazoles on the respiratory activity of rat brain homogenates were reported (7–9). These observations led to the synthesis of 2,5-disubstituted oxadiazoles, which were evaluated for anticonvulsant activity.

In the present study, the ability of these oxadiazoles to inhibit respiratory activity of rat brain homogenates and trypsin activity during hydrolysis of bovine serum albumin was determined to investigate the biochemical mechanism of action for the anticonvulsant activity of these newer substituted oxadiazoles.

0022-3549/78/0700/0987$01.00/0

© 1978, American Pharmaceutical Association

matographic conditions described, baseline resolution between suprofen and the three potential metabolite reference standards was achieved. Retention times and the relative separation of these potential metabolites from suprofen are reported in Table I.

Linear regression analysis of the curve, described by plotting microvolt seconds *versus* micrograms injected, indicated a virtual linear fit of the data ($r^2 = 0.99992$).

The response factor, F_i, generated by the computer is described by $F_i = W_i/A_i$, where W_i is the amount injected and A_i is the area in microvolt seconds. It was shown to be linear over the concentration range evaluated (0.05–0.2 μg/injection). Over a 2-month period of analysis, this response factor demonstrated little change, with a coefficient of variation equal to 2.4% ($n = 23$).

The results from the extracted control plasma to which ^{3}H-suprofen had been added are shown in Table II. The average extraction efficiency based on total recovered radioactivity was 81.2 ± 4.8% *SD*. The average recovery of suprofen from plasma samples to which unlabeled suprofen had been added was 80.0 ± 8.5% *SD* (Table II). Representative chromatograms of extracts from plasma containing 0.2 μg/ml (20 μl from a 100-μl dilution with tetrahydrofuran) and 20.0 μg/ml (5 μl from a 500-μl dilution with tetrahydrofuran) are shown in Fig. 2. A multicomparison analysis of the percent recovery data shown in Table II was performed using the two-tailed Dunnett (2) and Scheffé (3) test. No statistically significant differences were found in extraction efficiencies among the four groups of plasma samples with added suprofen.

These data suggest that there is no concentration dependence in extraction efficiencies over the range of expected plasma drug[12] levels following oral administration of 200 mg of suprofen. The results of this study will be the subject of a separate report.

REFERENCES

(1) P. A. J. Janssen, *Arzneim.-Forsch.*, **25**, 1495 (1975).

(2) C. W. Dunnet, *Biometrics*, **20**, 482 (1964).

(3) H. A. Scheffé, "The Analysis of Variance," Wiley, New York, N.Y., 1959.

ACKNOWLEDGMENTS

The authors thank Dr. E. McGonigle for useful discussions. They are grateful to Dr. J. Heykants and Dr. J. Wynants, Janssen Pharmaceutica, for providing preliminary information concerning plasma levels following oral administration of 100 mg of suprofen to humans and for supplying samples of suprofen and potential metabolites. The authors also thank Dr. H. Weintraub and Dr. L. Abrams, Ortho Pharmaceutical Corp., for providing preliminary information concerning plasma levels of total radioactivity following oral administration of 200 mg of ^{3}H-suprofen (specific activity of ~0.25 μCi/mg) to humans.

[12] Preliminary studies, conducted by Janssen Pharmaceutica and Ortho Pharmaceutical Corp., indicated that peak plasma levels of suprofen, equal to approximately 10–20 μg/ml, would be achieved following the oral administration of 200 mg of suprofen to normal human subjects.

Anticonvulsant and Antiproteolytic Properties of 2,5-Disubstituted Oxadiazoles and Their Inhibition of Respiration in Rat Brain Homogenates

SUNIL K. CHAUDHARY *§, SUSHIL KUMAR *, SURENDRA S. PARMAR ‡x, and MAHIMA CHAUDHARY *§

Received September 12, 1977, from the **Jawahar Lal Nehru Laboratory of Molecular Biology, Department of Pharmacology and Therapeutics, King George's Medical College, Lucknow University, Lucknow 226003, India,* and the ‡*Department of Physiology, School of Medicine, University of North Dakota, Grand Forks, ND 58202.* Accepted for publication November 7, 1977. §Present address: National Institute of Environmental Health Sciences, Research Triangle Park, NC 27709.

Abstract □ Eight 2-(3,4-methylenedioxyphenyl)-5-arylamino-1,3,4-oxadiazoles were synthesized, characterized by their sharp melting points, elemental analyses, and IR spectra, and evaluated for anticonvulsant activity. The protection afforded by oxadiazoles (100 mg/kg ip) against pentylenetetrazol (90 mg/kg sc)-induced convulsions ranged from 50 to 80%. All oxadiazoles inhibited the respiratory activity of rat brain homogenates during oxidation of pyruvate, α-ketoglutarate, and succinate. The presence of added nicotinamide adenine dinucleotide (NAD) to the reaction mixture during oxidation of pyruvate decreased the degree of inhibition. All oxadiazoles possessed antiproteolytic activity that was reflected by their ability to decrease trypsin-induced hydrolysis of bovine serum albumin. Such an inhibition was concentration dependent and ranged from 10.2 to 47.5 and from 15.7 to 71.8% by 0.5 and 1 m*M* oxadiazoles, respectively. All oxadiazoles competitively inhibited *in vitro* succinate dehydrogenase activity of rat brain homogenates.

Keyphrases □ Oxadiazoles, various—synthesized, evaluated for effect on enzyme activity in rat brain homogenates, anticonvulsant activity in mice, and antiproteolytic activity *in vitro* □ Enzyme activity—effect of various oxadiazoles in rat brain homogenates □ Anticonvulsant activity—various oxadiazoles evaluated in mice □ Antiproteolytic activity—various oxadiazoles evaluated *in vitro* □ Structure–activity relationships—various oxadiazoles evaluated for effect on enzyme activity in rat brain homogenates, anticonvulsant activity in mice, and antiproteolytic activity *in vitro*

Earlier studies indicated central nervous system depressant (1, 2), analgesic (3), muscle relaxant (4), and tranquilizing (5, 6) properties of substituted oxadiazoles. The inhibitory effects of 2,5-disubstituted 1,3,4-oxadiazoles on the respiratory activity of rat brain homogenates were reported (7–9). These observations led to the synthesis of 2,5-disubstituted oxadiazoles, which were evaluated for anticonvulsant activity.

In the present study, the ability of these oxadiazoles to inhibit respiratory activity of rat brain homogenates and trypsin activity during hydrolysis of bovine serum albumin was determined to investigate the biochemical mechanism of action for the anticonvulsant activity of these newer substituted oxadiazoles.

0022-3549/78/0700/0987$01.00/0

© 1978, American Pharmaceutical Association

Table I—Physical Constants of 2-(3,4-Methylenedioxyphenyl)-5-arylamino-1,3,4-oxadiazoles

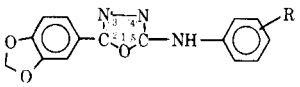

Compound	R	Melting Point[a]	Yield, %	Molecular Formula		Analysis, % Calc.	Found
I	H	224°	60	$C_{15}H_{11}N_3O_3$	C	64.05	64.21
					H	3.91	3.92
					N	14.94	14.68
II	2-CH_3	174°	55	$C_{16}H_{13}N_3O_3$	C	65.08	65.20
					H	4.40	4.36
					N	14.23	14.20
III	4-CH_3	210°	56	$C_{16}H_{13}N_3O_3$	C	65.08	65.00
					H	4.40	4.48
					N	14.23	14.22
IV	2,4-$(CH_3)_2$	170°	48	$C_{17}H_{15}N_3O_3$	C	66.01	65.94
					H	4.85	4.62
					N	13.59	13.67
V	2,6-$(CH_3)_2$	184°	50	$C_{17}H_{15}N_3O_3$	C	66.01	66.20
					H	4.85	4.94
					N	13.59	13.70
VI	2-OCH_3	162°	52	$C_{16}H_{13}N_3O_4$	C	61.73	61.50
					H	4.18	4.20
					N	13.50	13.47
VII	4-OCH_3	214°	54	$C_{16}H_{13}N_3O_4$	C	61.73	61.55
					H	4.18	4.23
					N	13.50	13.36
VIII	4-Cl	274°	57	$C_{15}H_{10}ClN_3O_3$	C	57.05	57.00
					H	3.15	3.26
					N	13.31	13.54

[a] Melting points were taken in open capillary tubes with a partial immersion thermometer and are corrected.

EXPERIMENTAL[1]

1-(3,4-Methylenedioxybenzoyl)-4-substituted Thiosemicarbazides—The various substituted thiosemicarbazides were synthesized and reported previously (10).

2-(3,4-Methylenedioxyphenyl)-5-arylamino - 1,3,4-oxadiazoles (I–VIII)—The various 1-(3,4-methylenedioxybenzoyl)-4-substituted thiosemicarbazides were cyclized to the corresponding 2,5-disubstituted 1,3,4-oxadiazoles following the method of Silberg and Cosma (11). To an ethanolic solution (300 ml) of the appropriate thiosemicarbazide (0.01 mole) was added 5 ml of 4 *N* NaOH, with cooling and shaking, to obtain a clear solution. To this solution was added iodine in 5% KI, gradually with stirring, until the color of the iodine persisted at room temperature.

The mixture was refluxed on a steam bath, and more iodine solution was added carefully until a permanent color of excess iodine was obtained. The reaction mixture was poured over crushed ice (500 g), and the solid mass that separated was filtered, washed first with water and then with hot carbon disulfide, dried, and recrystallized from ethanol in the presence of activated charcoal. Compounds I–VIII (Table I) were characterized by their sharp melting points, elemental analyses, and IR spectra.

The presence of characteristic bands of C=N (1640 cm^{-1}), NH–Ar (1299 cm^{-1}), NH (3300 cm^{-1}), and pentaatomic ring (1389 cm^{-1}) in the IR spectra of 2,5-disubstituted oxadiazoles provided further support for their structures.

Assay of Respiratory Activity of Rat Brain Homogenate[2]—Swiss albino rats, 100–150 g, were kept on an *ad libitum* diet. Rat brains isolated from decapitated animals were homogenized[3] immediately in ice-cold 0.25 *M* sucrose in a ratio of 1:9 (w/v). All incubations were carried out at 37°, and the oxygen uptake was measured by conventional Warburg manometric techniques with air as the gas phase (12).

Fresh brain homogenates, equivalent to 100 mg wet weight, were added to chilled Warburg vessels containing 6.7 m*M* magnesium sulfate, 2 m*M* sodium hydrogen phosphate buffer (pH 7.4), 1 m*M* adenosine monophosphate (sodium salt), 33 m*M* potassium chloride, and 500 μg of cytochrome c in a final volume of 3 ml unless otherwise stated. The central well contained 0.2 ml of 20% KOH. Pyruvate, α-ketoglutarate, and succinate were used at a final concentration of 10 m*M*, while the concentration of nicotinamide adenine dinucleotide (NAD) was 0.5 m*M*.

Compounds I–VIII were dissolved in propylene glycol (100%) and incubated with rat brain homogenates at 37° for 10 min prior to the addition of various substrates. An equal volume of the solvent was added to the control vessels. The oxygen uptake was measured every 10 min for a total of 60 min.

Determination of Anticonvulsant Activity—Anticonvulsant activity was determined in Swiss albino mice, 25–30 g, of either sex. The mice were divided into groups of 10, keeping the group weights as near the same as possible. Each 2-(3,4-methylenedioxyphenyl)-5-arylamino-1,3,4-oxadizole was suspended in 5% aqueous gum acacia to give a concentration of 1% (w/v). The test compounds were injected intraperitoneally in a group of 10 mice at a dose of 100 mg/kg.

Four hours after the administration of the test compounds, the mice were injected subcutaneously with 90 mg of pentylenetetrazol/kg. This dose of pentylenetetrazol produced convulsions in almost all untreated mice and exhibited 100% mortality during 24 hr. However, no mortality was observed during the 24-hr period in animals treated with 100-mg/kg doses of the test compounds alone.

The mice were then observed for 60 min for seizures. An episode of clonic seizure that persisted for at least 5 sec was considered a threshold convulsion. Transient intermittent jerks and tremulousness were not counted. Animals devoid of the threshold convulsion during 60 min were considered protected. The number of animals protected in each group was recorded, and the anticonvulsant activity of I–VIII was represented as percent protection. In the present study, no anticonvulsant activity was observed in animals treated with 5% aqueous gum acacia solution alone. The animals were then observed for 24 hr, and their mortality due to the administration of pentylenetetrazol was recorded.

Assay of Proteolytic Activity of Trypsin—The inhibitory effects of substituted oxadiazoles on the hydrolysis of bovine serum albumin by trypsin were determined by the method reported earlier (13). The reaction mixture consisted of 0.05 *M* tromethamine buffer (pH 8.2), 0.075 mg of crystalline trypsin (1 g is sufficient to hydrolyze 250 g of casein), 3.3×10^{-5} *M* bovine serum albumin, and water in a total volume of 1 ml. All oxadiazoles were dissolved in dimethylformamide and were used at 1×10^{-3} and 5×10^{-4} *M*. An equivalent amount of dimethylformamide, added to the control tubes, had no effect on the activity of trypsin during hydrolysis of bovine serum albumin.

All oxadiazoles were preincubated with trypsin for 10 min prior to the addition of bovine serum albumin, unless otherwise stated, and the reaction mixture was further incubated for 5 min after the addition of bovine serum albumin. The reaction was stopped by the addition of 0.5 ml of 15% (w/v) trichloroacetic acid. The acid-soluble products of protein breakdown obtained after centrifugation were determined by the method of Lowry *et al.* (14). A decrease in the formation of the products of protein breakdown in the presence of the test compounds was used to determine their antiproteolytic activity (14).

Assay of Succinate Dehydrogenase Activity of Rat Brain Homogenate—The method of Kun and Abood (15) was followed for the determination of succinate dehydrogenase activity of rat brain homogenates, using succinate as the substrate and triphenyltetrazolium as a proton acceptor. Tissue homogenates in the presence of succinate in a buffered (pH 7.4) medium reduce the colorless tetrazolium salt to a red-colored water-insoluble formazan. The formazan can be dissolved easily in acetone, which, by precipitating tissue proteins, leaves a colored supernate ready for colorimetric determination.

The reaction mixture in a total volume of 3 ml consisted of 0.2 ml of 0.25 *M* sodium phosphate buffer (pH 7.4), 0.5 ml of 0.2 *M* sodium succinate, 1.0 ml of rat brain homogenates equivalent of 100 mg wet weight of tissue, and 1.0 ml of 0.1% triphenyltetrazolium chloride solution (freshly prepared). After shaking, the tubes were incubated for 30 min at 38°. The various oxadiazoles were dissolved in propylene glycol (100%) and were used at final concentrations of 1 and 2 m*M*.

All oxadiazoles were preincubated for 10 min with rat brain homogenates prior to the addition of succinate, and the reaction was continued for 30 min. The tubes were removed from the constant-temperature bath, and 7 ml of extra pure acetone was added immediately to arrest the enzyme reaction. The precipitate was then centrifuged, and the absorbance of the clear supernate was determined. The color intensity was measured[4]

[1] All compounds were analyzed for their carbon, hydrogen, and nitrogen content. Melting points were taken in open capillary tubes with a partial immersion thermometer and are corrected. IR spectra were taken with a Perkin-Elmer Infracord spectrophotometer model 137, equipped with sodium chloride optics, in potassium bromide films in the 700–3500-cm^{-1} range.

[2] Commercial chemicals were used. Adenosine monophosphate (sodium salt), monosodium α-ketoglutarate, sodium pyruvate, NAD, sodium succinate, and cytochrome c were obtained from Sigma Chemical Co., St. Louis, Mo.

[3] Potter-Elvehjem homogenizer.

[4] Perkin-Elmer spectrophotometer.

Table II—Anticonvulsant Activity of 2-(3,4-Methylenedioxyphenyl)-5-arylamino-1,3,4-oxadiazoles and Their Effect on the Respiratory Activity of Rat Brain Homogenates

Compound	Anticonvulsant Activity[a], % Protection	Pentylenetetrazol Mortality[b], %	Inhibition of Respiratory Activity[c], %			
			Pyruvate		α-Ketoglutarate	Succinate
			−NAD	+NAD		
I	50	50	67.8 ± 1.5	59.3 ± 1.4	37.2 ± 1.2	76.2 ± 1.3
II	50	30	69.5 ± 1.7	60.4 ± 1.6	31.1 ± 1.3	72.0 ± 1.3
III	80	0.0	70.8 ± 1.4	61.5 ± 1.5	49.3 ± 1.3	66.1 ± 1.0
IV	70	0.0	63.8 ± 1.3	50.3 ± 1.5	55.6 ± 0.8	70.6 ± 1.0
V	50	0.0	49.2 ± 1.5	41.6 ± 1.8	37.3 ± 1.3	33.4 ± 1.3
VI	70	0.0	84.5 ± 1.9	75.4 ± 1.8	30.0 ± 1.0	80.7 ± 1.5
VII	60	30	56.6 ± 0.9	50.3 ± 1.3	41.6 ± 1.5	71.1 ± 1.5
VIII	50	50	46.5 ± 1.3	40.6 ± 1.1	28.2 ± 1.3	40.3 ± 1.4

[a] Screening procedures were as described in the text. All substituted oxadiazoles were administered (100 mg/kg ip) 4 hr before the administration of pentylenetetrazol (90 mg/kg sc). [b] Represents pentylenetetrazol-induced mortality during 24 hr in each group of 10 animals. [c] Each experiment was done in duplicate. All values represent the mean of six values of percent inhibition, with the standard error of the mean calculated from three separate experiments. Inhibition was determined by the decrease in oxygen uptake by 100 mg of rat brain weight/hr. The final concentration of pyruvate, α-ketoglutarate, and succinate was 10 m*M*; NAD was used at 0.5 m*M*. All oxadiazoles were used at a final concentration of 2 m*M*. Assay procedures and the contents of the reaction mixture were as indicated in the text.

at 420 nm. An increase in the percent transmission provided a direct measurement of reduced triphenyltetrazolium chloride, which was taken as an index of the enzyme activity. The percent inhibition was calculated from the decrease in the absorbance with 100 mg of fresh tissue weight/30 min.

In addition, kinetic studies were carried out, and the enzyme inhibition by substituted oxadiazoles was determined by using the graphic method of Lineweaver and Burk (16) as modified by Dixon (17). In preincubation studies, rat brain homogenates in the incubation mixture were incubated with or without oxadiazoles at 38° for 10, 20, and 30 min prior to the addition of succinate. The zero-time experiments represent those in which the oxadiazoles and the substrate were added simultaneously to the reaction mixture containing appropriate brain homogenate preparations.

RESULTS

The anticonvulsant activity of the substituted 2-(3,4-methylenedioxyphenyl)-5-arylamino-1,3,4-oxadiazoles is recorded in Table II. The ability of oxadiazoles to provide protection at a dose of 100 mg/kg ip against pentylenetetrazol (90 mg/kg sc)-induced convulsions in mice ranged from 50 to 80%; maximum protection was observed with 2-(3,4-methylenedioxyphenyl)-5-(4-methylphenylamino)-1,3,4-oxadiazole (III). Administration of substituted oxadiazoles also provided significant protection against pentylenetetrazol-induced mortality during 24 hr since no mortality was observed with animals treated with III–VI.

The effects of substituted oxadiazoles on the *in vitro* respiratory activity of rat brain homogenates are shown in Table II. All substituted oxadiazoles inhibited oxidation of both NAD-dependent oxidation of pyruvate and α-ketoglutarate and NAD-independent oxidation of succinate. The maximum inhibition of pyruvate and sodium succinate was observed with 2-(3,4-methylenedioxyphenyl)-5-(2-methoxyphenylamino)-1,3,4-oxadiazole (VI), while 2-(3,4-methylenedioxyphenyl)-5-(2,4-dimethylphenylamino)-1,3,4-oxadiazole (IV) caused maximum inhibition of the oxidation of α-ketoglutarate.

The degree of inhibition by substituted oxadiazoles at a final concentration of 2 m*M* ranged from 46.5 to 84.5, from 28.2 to 55.6, and from 33.4 to 80.7% during oxidation of pyruvate, α-ketoglutarate, and succinate, respectively. It was presumed that endogenous NAD in rat brain homogenates was sufficient for the oxidation of pyruvate and α-ketoglutarate. On the other hand, the presence of added NAD to the reaction mixture not only increased the respiratory activity of rat brain homogenates during pyruvate oxidation but also decreased the inhibitory effectiveness of substituted oxadiazoles (40.6–75.6%).

All substituted oxadiazoles exhibited antiproteolytic activity (Table III). The degree of inhibition of trypsin activity during hydrolysis of bovine serum albumin increased with the increase in the concentration of these substituted oxadiazoles and ranged from 10.2 to 47.5 and from 15.8 to 71.8% at final concentrations of 0.5 and 1 m*M*, respectively. Maximum antiproteolytic activity was observed with 2-(3,4-methylenedioxyphenyl)-5-(2,6-dimethylphenylamino)-1,3,4-oxadiazole (V), while 2-(3,4-methylenedioxyphenyl)-5-(2-methylphenylamino)-1,3,4-oxadiazole (II) provided the least protection against trypsin-induced hydrolysis of bovine serum albumin.

The ability of substituted oxadiazoles to inhibit *in vitro* activity of succinate dehydrogenase activity of rat brain homogenates is recorded in Table IV. All compounds inhibited succinate dehydrogenase activity, and the degree of inhibition increased with the increase in their concentration. The inhibition ranged from 20.0 to 48.6 and from 55.0 to 87.5% at final concentrations of 1 and 2 m*M*, respectively.

The *in vitro* inhibition of succinate dehydrogenase of rat brain homogenates by substituted oxadiazoles was investigated by preincubation studies. Preincubation of these substituted oxadiazoles for varying times prior to the addition of succinate in *in vitro* studies in no way altered the degree of succinate dehydrogenase activity (Table V). These results indicated a rapidly reversible and possibly competitive inhibition by substituted oxadiazoles. This finding was further supported by kinetic studies with 2-(3,4-methylenedioxyphenyl)-5-(4-methoxyphenylamino)-1,3,4-oxadiazole (VII), which revealed the competitive nature of inhibition of rat brain succinate dehydrogenase (Fig. 1). The inhibitor constant, K_i, for VII was 0.015 m*M*.

DISCUSSION

These results indicating the equal effectiveness of substituted oxadiazoles in providing protection against pentylenetetrazol-induced convulsions and pentylenetetrazol-induced 24-hr mortality have failed to provide structure–activity relationships with respect to anticonvulsant

Table III—Effect of 2-(3,4-Methylenedioxyphenyl)-5-arylamino-1,3,4-oxadiazoles on the Inhibition of Trypsin-Induced Hydrolysis of Bovine Serum Albumin

Compound	Inhibition[a], %	
	1×10^{-3} *M*	5×10^{-4} *M*
I	36.3 ± 1.3	31.1 ± 0.8
II	15.8 ± 0.8	10.2 ± 1.2
III	31.4 ± 1.2	20.2 ± 1.4
IV	35.7 ± 1.2	19.7 ± 1.5
V	71.8 ± 1.5	47.5 ± 1.4
VI	50.0 ± 1.2	44.3 ± 1.2
VII	35.0 ± 1.3	18.8 ± 0.8
VIII	25.2 ± 1.2	21.3 ± 1.2

[a] Assay procedures were as indicated in the text. Each experiment was done in duplicate. All values represent the mean of six values of percent inhibition obtained from three separate experiments with the standard error of the mean. Concentrations given were the final concentrations of the oxadiazoles in the reaction mixture.

Table IV—Effect of 2-(3,4-Methylenedioxyphenyl)-5-arylamino-1,3,4-oxadiazoles on the Succinate Dehydrogenase Activity of Rat Brain Homogenates

Compound	Inhibition[a], %	
	2×10^{-3} *M*	1×10^{-3} *M*
I	57.5 ± 0.8	36.0 ± 0.9
II	55.0 ± 1.0	20.0 ± 0.6
III	75.0 ± 1.1	48.6 ± 0.7
IV	65.0 ± 0.6	46.3 ± 0.3
V	50.0 ± 0.5	37.1 ± 0.8
VI	80.0 ± 0.7	38.3 ± 0.4
VII	87.5 ± 0.9	36.5 ± 0.7
VIII	60.0 ± 1.0	40.0 ± 0.6

[a] Contents of the reaction mixture and assay procedures were as described in the text. Each experiment was done in triplicate. All values are the mean of nine values obtained from three separate experiments with the standard error of the mean. Concentrations given were the final concentrations of the oxadiazoles in the reaction mixture.

Table V—Preincubation Studies with 2-(3,4-Methylenedioxyphenyl)-5-arylamino-1,3,4-oxadiazoles during Inhibition of Rat Brain Succinate Dehydrogenase

Compound	Inhibition of Succinate Dehydrogenase[a], %			
	0 min	10 min	20 min	30 min
I	57.2 ± 0.1	57.3 ± 0.8	56.9 ± 0.3	57.4 ± 0.8
II	55.2 ± 0.6	55.6 ± 1.0	54.9 ± 0.6	55.1 ± 0.5
III	75.2 ± 0.7	75.3 ± 0.7	75.8 ± 0.4	75.2 ± 0.4
IV	65.0 ± 0.5	65.9 ± 1.0	65.3 ± 0.4	65.6 ± 0.3
V	50.0 ± 0.8	50.5 ± 0.9	50.0 ± 0.3	50.0 ± 0.8
VI	81.2 ± 0.4	81.7 ± 1.1	81.0 ± 0.2	81.5 ± 0.9
VII	87.5 ± 0.3	87.4 ± 0.6	87.4 ± 0.1	87.2 ± 0.7
VIII	60.3 ± 0.1	60.5 ± 0.1	60.5 ± 0.9	60.4 ± 0.3

[a] Contents of the reaction mixture and the assay procedures were as indicated in the text. The enzyme preparations were incubated with oxadiazoles for 10, 20, and 30 min before the addition of succinate. Zero-time experiments indicate that both succinate and oxadiazoles were added to the reaction mixture containing enzyme preparations simultaneously. All oxadiazoles were used at a final concentration of 2×10^{-3} *M*.

activity (Table I). The data indicate, in general, a trend of more protection from convulsions with less mortality. The unspecific inhibition of both the NAD-dependent and NAD-independent oxidations (Table II) and reversible and competitive inhibition of succinate dehydrogenase in rat brain homogenates (Tables III and IV and Fig. 1) indicated the possible sensitivity of substituted oxadiazoles toward both NADH–CoQ (oxido) reductase (Complex I) and succinate–CoQ (oxido) reductase (Complex II) of the electron transport chain. It is also possible that hydro CoQ–cytochrome c–O_2 (oxido) reductase (Complex III) and/or cytochrome c–O_2 (oxido) reductase (Complex IV) are also susceptible to these substituted oxadiazoles as reported earlier (9).

These substituted oxadiazoles inhibit flavine adenine dinucleotide-dependent oxidation of succinate (NAD-independent) and NAD-dependent oxidations of pyruvate and α-ketoglutarate by rat brain homogenates and thus differ from other anticonvulsants belonging to the group of quinazolones (18), thiazolidones (19), and nitrobenzamides (20) in their ability to inhibit both NAD-dependent and NAD-independent oxidations by rat brain homogenates, as observed with phenothiazines (21) and salicylic acid derivatives (22). The concentration-dependent antiproteolytic activity of the substituted oxadiazoles (Table III) was unrelated to their anticonvulsant activity.

These results failed to provide any relationship between *in vitro* antiproteolytic activity and *in vitro* inhibition of respiratory activity and succinate dehydrogenase activity of rat brain homogenates with anticonvulsant activity. Detailed investigations of the effects of these substituted oxadiazoles on the activity of purified enzyme systems possibly may reflect a biochemical basis for their anticonvulsant activity.

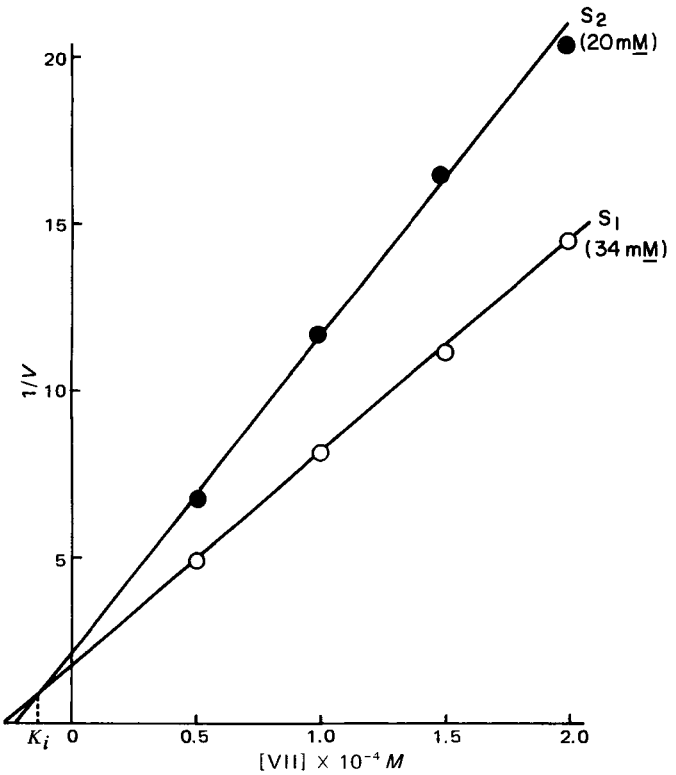

Figure 1—*Kinetic study showing competitive inhibition of rat brain succinate dehydrogenase by VII. The 1/V represents the reciprocal of enzyme activity as described in the text. The concentrations of succinate were 20 and 34 mM. The* K_i *value for VII was 0.015 mM.*

REFERENCES

(1) J. Maillard, M. Vincent, R. Moris, and M. Benard, French pat. M379 (Jan. 1962); through *Chem. Abstr.*, **57**, 15251g (1962).

(2) I. Angelini, L. Angelini, and F. Sparaco, British pat. 1,161,801 (Aug. 1969); through *Chem. Abstr.*, **71**, 112936g (1969).

(3) H. Najer, R. Giudicelli, C. Morel, and J. Menin, *Bull. Soc. Chim. Fr.*, **153**, 9 (1966).

(4) H. L. Yale and K. Losee, *J. Med. Chem.*, **9**, 478 (1966).

(5) J. J. Piala and H. L. Yale, U.S. pat. 3,142,022 (July 1964); through *Chem. Abstr.*, **61**, 8317b (1964).

(6) J. J. Piala and H. L. Yale, U.S. pat. 3,166,566 (Jan. 1965); through *Chem. Abstr.*, **62**, 10444b (1965).

(7) H. H. Singh, S. Nagar, A. Chaudhari, and S. S. Parmar, *Indian J. Pharm.*, **34**, 101 (1972).

(8) H. H. Singh, S. Nagar, A. Chaudhari, and S. S. Parmar, *J. Pharm. Sci.*, **62**, 504 (1973).

(9) S. S. Parmar, P. C. Joshi, B. Ali, and W. E. Cornatzer, *ibid.*, **63**, 872 (1974).

(10) S. S. Parmar, S. K. Chaudhary, M. Chaudhary, A. Chaudhari, and T. K. Auyong, *Proc. West. Pharmacol. Soc.*, **19**, 183 (1976).

(11) A. Silberg and N. Cosma, *Acad. Repub. Pop. Rom. Fil. Cluj Stud. Cercet. Chim.*, **10**, 151 (1969); through *Chem. Abstr.*, **54**, 8794g (1960).

(12) S. K. Chaudhary, S. S. Parmar, M. Chaudhary, and J. P. Barthwal, *J. Pharm. Sci.*, **65**, 1010 (1976).

(13) A. Chaudhari, A. K. Chaturvedi, S. S. Parmar, and S. J. Brumleve, *Res. Commun. Chem. Pathol. Pharmacol.*, **7**, 205 (1974).

(14) O. H. Lowry, N. J. Rosebrough, A. L. Farr, and R. J. Randall, *J. Biol. Chem.*, **193**, 265 (1951).

(15) E. Kun and L. G. Abood, *Science*, **109**, 144 (1949).

(16) H. Lineweaver and D. Burk, *J. Am. Chem. Soc.*, **56**, 658 (1934).

(17) M. Dixon, *Biochem. J.*, **55**, 170 (1953).

(18) S. S. Parmar and P. K. Seth, *Can. J. Biochem.*, **43**, 1179 (1965).

(19) M. Chaudhary, S. S. Parmar, S. K. Chaudhary, A. K. Chaturvedi, and B. V. Rama Sastry, *J. Pharm. Sci.*, **65**, 443 (1976).

(20) S. S. Parmar, C. Dwivedi, B. Ali, and R. S. Misra, *J. Med. Chem.*, **15**, 846 (1972).

(21) P. N. Abadom, K. Ahamad, and P. G. Scholefield, *Can. J. Biochem. Physiol.*, **39**, 551 (1961).

(22) R. Penniall, G. Kalnitsky, and J. I. Routh, *Arch. Biochem. Biophys.*, **64**, 390 (1956).

ACKNOWLEDGMENTS

Supported in part by the Council of Scientific and Industrial Research, New Delhi, India, and by U.S. Public Health Service Grant 7 R01 DA01893 and Grant 5 T01 HL05939-03.

The authors thank Professor K. P. Bhargava and Professor Stanley J. Brumleve for their advice and encouragement. Grateful acknowledgment is made to the State Council of Scientific and Industrial Research, Uttar Pradesh, Lucknow, India, for providing a Research Fellowship to S. Kumar and to the Northwest Area Foundation, St. Paul, Minn., for providing a Hill Professorship to S. S. Parmar.

New Biphenyl Derivatives I: 1-(4-Biphenylyl)-2-phenylethylamines as Potential Antispasmodic and Cardiovascular Agents

RAGAB M. SHAFIK ˣ, RAAFAT SOLIMAN, and AHMED M. M. HASSAN

Received September 13, 1977, from the *Department of Pharmaceutical Chemistry, Faculty of Pharmacy, University of Alexandria, Alexandria, A.R. Egypt.* Accepted for publication November 3, 1977.

Abstract □ A series of 1-(4-biphenylyl)-2-phenylethylamine derivatives was synthesized as potential antispasmodic and cardiovascular agents related to papaverine. Preliminary pharmacological tests, on isolated guinea pig ileum and anesthetized cat blood pressure, showed that the new compounds possess nonspecific inhibitory action on smooth muscles.

Keyphrases □ Biphenyl derivatives, various—synthesized, evaluated for antispasmodic and cardiovascular activity □ 2-Phenylethylamines, substituted—synthesized, evaluated for antispasmodic and cardiovascular activity □ Antispasmodic activity—various substituted 1-(4-biphenylyl)-2-phenylethylamines evaluated □ Cardiovascular activity—various substituted 1-(4-biphenylyl)-2-phenylethylamines evaluated □ Structure–activity relationships—various substituted 1-(4-biphenylyl)-2-phenylethylamines evaluated for antispasmodic and cardiovascular activity

The fact that papaverine (I) has a partially dehydrogenated 1,2-diphenylethylamine (II) moiety in its structure initiated the preparation of some derivatives of II to investigate their biological activities.

Although some investigators (1–8) synthesized substituted II derivatives as possible analgesic agents, the 1-biphenylyl or 2-biphenylyl analogs have not been prepared. The present work dealt with the synthesis of some *N*-alkyl and *N*,*N*-dialkyl derivatives of 1-(4-biphenylyl)-2-phenylethylamine (VI, Scheme I) to determine whether they possessed antispasmodic and/or cardiovascular effects similar to I. The synthesized compounds are listed in Tables I and II.

RESULTS AND DISCUSSION

Synthesis—The synthetic route (Scheme I) began with the preparation of benzyl 4-biphenylyl ketone (III) from phenylacetyl chloride and biphenyl by applying Friedel–Crafts conditions. The key intermediate, 1-(4-biphenylyl)-2-phenylethylamine (VI), was obtained either by the reduction of benzyl 4-biphenylyl ketoxime (IV) with aluminum amalgam in aqueous ethanol or from III through a modified Leuckart–Wallach reaction, *i.e.*, by first isolating the *N*-formyl derivative (V) followed by hydrolysis with concentrated hydrochloric acid.

The *N*-alkyl (IX) and *N*,*N*-dialkyl (XI) derivatives were prepared from the corresponding *N*-acyl (V and VIII) and *N*-acyl-*N*-alkyl (X) analogs, respectively, by reduction with lithium aluminum hydride in absolute ether. The *N*-methyl-*N*-propyl (XI*d*) and *N*,*N*-dimethyl (XI*e*) derivatives also were obtained through the Clarke–Eschweiler reaction by refluxing with a mixture of formaldehyde solution and formic acid. In addition, the *N*-benzoyl (VIII*c*) and *N*-benzoyl-*N*-methyl (X*f*) derivatives were prepared, but attempts to obtain the *N*-benzyl analogs through reduction with lithium aluminum hydride in absolute ether or absolute tetrahydrofuran were unsuccessful.

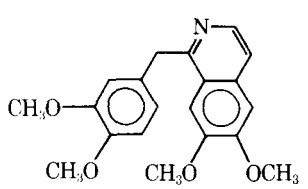

I

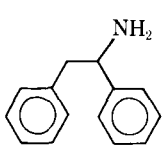

II

The structures of the new compounds were substantiated by IR, PMR, and mass spectrometric studies of representative members of the series. The mass spectrum of the *N*-acetyl derivative (VIII*a*) showed, in addition to the molecular ion peak, significant fragment ion peaks at *m/e* 314 (M − H), 272 (M − CH_3CO), 258 (M − CH_3CONH), 224 (M − $CH_2C_6H_5$), 182 (M − CH_3CO − $CH_2C_6H_5$ + H, base peak), 181 (M − CH_3CO − $CH_2C_6H_5$), and 180 (M − CH_3CO − $CH_2C_6H_5$ − H) and the biphenyl radical peak at 153.

Pharmacology—Testing of the antispasmodic activity of VII, IX*a*, XI*a*, XI*b*, XI*d*, and XI*e* was carried out on isolated guinea pig ileum. All of these compounds inhibited contractions produced by standard submaximal doses of acetylcholine, histamine, or serotonin with no specificity toward any of these spasmogens. The results showed that the tested compounds might possess considerable nonspecific inhibitory action on smooth muscles similar to I (9, 10).

A comparative study of XI*b*, XI*d*, and XI*e* with similar molar concentrations of I was then conducted. The data (Table III) indicated that the *N*,*N*-diethyl (XI*b*) and the *N*,*N*-dimethyl (XI*e*) analogs were more potent smooth muscle inhibitors than I, as shown by their antagonistic effects on acetylcholine-induced contractions.

The cardiovascular activity of IX*a*, XI*a*, XI*b*, XI*d*, and XI*e* was examined using the blood pressure response of chloralose–urethan anesthetized cats. The compounds were injected into the femoral vein, and the blood pressure was recorded from the carotid artery. The experiments revealed a marked hypotensive activity for all tested compounds; the most

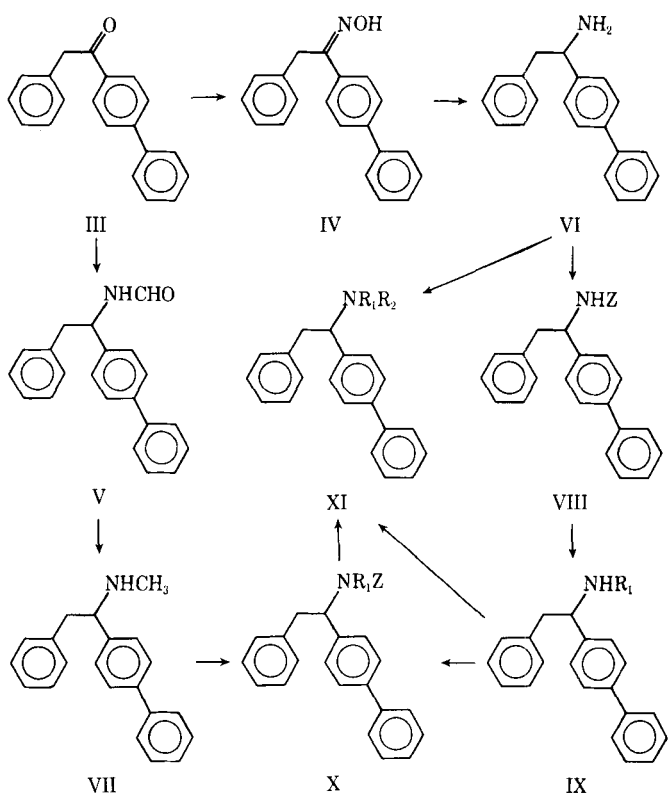

Scheme I

0022-3549/78/0700/0991$01.00/0
© 1978, American Pharmaceutical Association

Table I—*N*-Acyl-1-(4-biphenylyl)-2-phenylethylamines and *N*-Acyl-*N*-alkyl-1-(4-biphenylyl)-2-phenylethylamines

Compound	Z	R_1	Method	Yield, %	Melting Point	Formula	Analysis, %	Calc.	Found
V	—	—	—	65	197–198°[a]	$C_{21}H_{19}NO$	C	83.7	84.0
							H	6.4	6.7
							N	4.6	4.6
VIII*a*	$COCH_3$	—	C	98	204–205°[a]	$C_{22}H_{21}NO$	C	83.8	84.2
							H	6.7	6.3
							N	4.4	4.7
VIII*b*	COC_2H_5	—	D	70	191–192°[a]	$C_{23}H_{23}NO$	C	83.9	84.3
							H	7.0	7.4
							N	4.3	4.7
VIII*c*	COC_6H_5	—	E,F[b]	60, 70	203–205°[c]	$C_{27}H_{23}NO$	C	85.9	86.1
							H	6.1	6.0
							N	3.7	4.2
X*a*	$COCH_3$	CH_3	C	70	130–131°[d]	$C_{23}H_{23}NO$	C	83.9	83.8
							H	7.0	7.0
							N	4.3	4.6
X*b*	$COCH_3$	C_2H_5	C	60	97–98°[d]	$C_{24}H_{25}NO$	C	83.9	83.8
							H	7.3	6.8
							N	4.1	4.5
X*c*	$COCH_3$	n-C_3H_7	C	50	85–87°[e]	$C_{25}H_{27}NO$	C	84.0	83.6
							H	7.6	7.2
							N	3.9	3.9
X*d*	COC_2H_5	CH_3	D	50	112–113°[e]	$C_{24}H_{25}NO$	N	4.1	4.4
X*e*	COC_2H_5	C_2H_5	D	55	217–218°[f]	$C_{25}H_{27}NO$	C	84.0	84.3
							H	7.6	7.5
							N	3.9	4.3
X*f*	COC_6H_5	CH_3	E	50	93–95°[e]	$C_{28}H_{25}NO$	C	85.9	86.2
							H	6.4	6.3
							N	3.6	3.5

[a] Recrystallized from ethanol. [b] Admixture of the products obtained by both methods showed no melting-point depression. [c] Recrystallized from methanol. [d] Recrystallized from petroleum ether (bp 40–60°). [e] Recrystallized from a benzene–petroleum ether mixture (bp 40–60°). [f] Recrystallized from benzene.

pronounced effect was produced by XI*b*. This effect could not be blocked by atropine, which indicated that it was not mediated through cholinergic nerve fibers but might have been due to a direct vasodilating effect on smooth muscles, an effect similar to that known for I (9, 10).

EXPERIMENTAL[1]

Benzyl 4-Biphenylyl Ketone (III)—Under strictly anhydrous conditions, a stirred mixture of biphenyl (15.4 g, 0.1 mole), carbon disulfide (300 ml), and finely powdered anhydrous aluminum chloride (24 g, 0.18 mole) was treated with phenylacetyl chloride (15.4 g, 0.1 mole). The reaction mixture was then refluxed at 50–60° for 6–8 hr. The carbon disulfide was then removed by distillation under reduced pressure, and the residue was decomposed with ice and dilute hydrochloric acid. The solid was triturated with ether, filtered, and recrystallized from ethanol to yield 19.6 g (72%) of product, mp 152–153° [lit. (11) mp 149°, yield 34%]. The IR spectrum showed a peak at 1690 cm^{-1}, indicative of a carbonyl group.

Benzyl 4-Biphenylyl Ketoxime (IV)—A solution of III (2.7 g, 0.01 mole) in ethanol (30 ml) was treated with a solution of hydroxylamine hydrochloride (1.4 g, 0.02 mole) in water (1 ml), followed by a solution of sodium hydroxide (2 g, 0.05 mole) in water (2 ml). The reaction mixture was then refluxed for 5 min, cooled, and poured into 2 *N* HCl (40 ml) with constant stirring. The solid product was filtered, washed several times with distilled water, dried, and recrystallized from methanol. The yield was 2.3 g (83%), mp 163–164°. The IR spectrum showed a broad peak centered at 3500 cm^{-1}, indicative of a hydroxyl group, a peak at 1650 cm^{-1}, indicative of C=N, and a peak at 950 cm^{-1}, indicative of NO.

Anal.—Calc. for $C_{20}H_{17}NO$: C, 83.6; H, 6.0; N, 4.9. Found: C, 83.8; H, 6.0; N, 4.4.

***N*-Formyl-1-(4-biphenylyl)-2-phenylethylamine (V)**—A mixture of III (2.7 g, 0.01 mole) and ammonium formate (2.5 g, 0.04 mole) was fused at 200–220° in an oil bath for 4–6 hr until frothing ceased. The reaction mixture was cooled to room temperature, triturated twice with water, and decanted. The residue was then extracted twice with benzene, and the combined extract was dried over anhydrous sodium sulfate and filtered. The solvent was then removed under reduced pressure, and the product was recrystallized.

1-(4-Biphenylyl)-2-phenylethylamine Hydrochloride (VI)—*Method A*—A solution of 5% aqueous mercuric chloride (100 ml) was added to aluminum foil (6 g) that had been cut into pieces of approximately 2 cm^2. The foil was left in contact with the mercuric chloride solution for 5–10 min to effect amalgamation and then washed with 3 × 250 ml of distilled water. The aluminum amalgam was treated immediately with a solution of IV (2.9 g, 0.01 mole) in ethanol (60 ml), followed by distilled water (60 ml).

The reaction mixture was magnetically stirred at room temperature for 24 hr and then filtered. The solid material on the filter was washed with 2 × 100 ml of ethanol, and the washings were added to the original filtrate. The alcohol was then removed under reduced pressure, and the product was extracted with ether. The ethereal extract was dried over anhydrous sodium sulfate and filtered, and then dry hydrogen chloride gas was slowly bubbled through it. The separated salt was collected and recrystallized.

Method B—A solution of V (3 g, 0.01 mole) in ethanol (20 ml) was treated with concentrated hydrochloric acid (6 ml). The mixture was refluxed for 30 min and then allowed to cool to room temperature. The separated product was collected and recrystallized.

***N*-Acyl-1-(4-biphenylyl)-2-phenylethylamines and *N*-Acyl-*N*-alkyl-1-(4-biphenylyl)-2-phenylethylamines**—*Method C* (*VIII*a, X*a*, X*b*, *and* X*c*)—A mixture of the appropriate amine (VI, VII, IX*a*, and IX*b*, respectively) (0.01 mole), acetic anhydride (6 ml), and anhydrous sodium acetate (0.012 mole) was refluxed for 2 hr. The reaction mixture was allowed to cool to room temperature, poured onto crushed ice, and then neutralized by the addition of solid sodium bicarbonate in portions until effervescence ceased. The acetyl derivative was filtered, washed several times with hot distilled water, dried, and then recrystallized.

Method D (*VIII*b, X*d*, *and* X*e*)—A solution of propionyl chloride (0.015 mole) in benzene (10 ml) was added dropwise to a cooled, magnetically stirred solution of the appropriate amine (VI, VII, and X*a*, respectively) (0.01 mole), in pyridine (10 ml). Cooling was maintained for 2 hr, and then the reaction mixture was refluxed for another 4 hr. The solvents were removed *in vacuo*, and the resulting residue was treated with distilled water (30 ml), filtered, dried, and recrystallized.

Method E (*VIII*c *and* X*f*)—Benzoyl chloride (0.012 mole) was added to a mixture of the appropriate amine (VI and VII, respectively) (0.01 mole), and 4% NaOH (15 ml). The reaction mixture was vigorously shaken for 15 min and then acidified with 10% HCl. The product was filtered, washed several times with distilled water, dried, and recrystallized.

[1] IR spectra were determined on a Beckman IR-33 spectrophotometer with potassium bromide pellets. PMR spectra were determined on a Jeolco C-60 HL spectrometer with tetramethylsilane as the internal standard. The mass spectrum was determined using a du Pont-CEC 492 spectrometer. Melting points were determined in open glass capillaries and are uncorrected. Microanalyses were performed by the Microanalytical Unit, Faculty of Science, University of Cairo, Cairo, A.R. Egypt.

Table II—1-(4-Biphenylyl)-2-phenylethylamine and Its *N*-Alkyl and *N,N*-Dialkyl Derivatives

Compound	R_1	R_2	Yield[a], %	Melting Point	Formula	Analysis, %	Calc.	Found
VI	—	—	60[b], 70[c,d]	273°[e]	$C_{20}H_{20}ClN$	C	77.5	77.4
						H	6.5	6.8
						Cl	11.4	11.0
						N	4.5	4.1
VII	—	—	67	241–242°[e]	$C_{21}H_{22}ClN$	C	77.8	77.6
						H	6.8	7.0
						Cl	11.0	11.2
						N	4.3	4.7
IX*a*	C_2H_5	—	65	270°[e]	$C_{22}H_{24}ClN$	C	78.2	78.6
						H	7.2	6.9
						Cl	10.5	10.9
						N	4.1	4.3
IX*b*	n-C_3H_7	—	75	242–243°[e]	$C_{23}H_{26}ClN$	C	78.5	78.3
						H	7.7	7.6
						Cl	10.1	10.4
						N	4.0	4.5
XI*a*	CH_3	C_2H_5	64	136° dec.[f]	$C_{23}H_{26}ClN$	C	78.5	78.8
						H	7.7	7.7
						Cl	10.1	10.3
						N	4.0	4.0
XI*b*	C_2H_5	C_2H_5	60	166–167° dec.[g]	$C_{24}H_{28}ClN$	C	78.8	79.1
						H	7.7	8.0
						Cl	9.7	9.6
						N	3.8	3.5
XI*c*	C_2H_5	n-C_3H_7	70	167–169° dec.[h]	$C_{25}H_{30}ClN$	C	79.0	79.5
						H	8.0	7.8
						Cl	9.3	9.7
						N	3.7	4.0
XI*d*	CH_3	n-C_3H_7	70, 98[i,d]	196–198° dec.[g]	$C_{24}H_{28}ClN$	C	78.8	78.5
						H	7.7	7.3
						Cl	9.7	10.2
						N	3.8	4.1
XI*e*	CH_3	CH_3	80[i]	239–240°[f]	$C_{22}H_{24}ClN$	C	78.2	78.5
						H	7.2	7.3
						Cl	10.5	10.7
						N	5.1	4.6

[a] Unless otherwise indicated, Method G was used for preparation. [b] Method A. [c] Method B. [d] Admixture of the products obtained by both methods showed no melting-point depression. [e] Recrystallized from ethanol. [f] Recrystallized from a methanol–benzene mixture. [g] Recrystallized from an ethanol–benzene mixture. [h] Recrystallized from an ethanol–ether mixture. [i] Method H.

Method F (VIIIc)—A solution of benzoyl chloride (0.012 mole) in dry benzene (10 ml) was added dropwise to a cooled, magnetically stirred solution of VI (0.01 mole) in pyridine (10 ml). Cooling was maintained for 2 hr, and then the reaction mixture was refluxed for 4 hr. The solvents were removed under reduced pressure, and the residue was treated with water (30 ml), filtered, dried, and recrystallized.

IR spectra of VIII*a*–VIII*c* showed peaks in the region of 3400–3250 cm^{-1}, indicative of NH, and peaks at 1650–1640, 1550–1540, and 1290–1280 cm^{-1}, indicative of amide I, II, and III bands, respectively. IR spectra of X*a*–X*f* revealed a peak at around 1650 cm^{-1}, indicative of a tertiary amide carbonyl group.

For VIII*a*, the PMR spectrum ($CDCl_3$) exhibited peaks at δ 1.86 (s, 3H, methyl), 3.06 (d, 2H, methylene, J = 7 Hz), 5.15 (t, 1H, CH, J = 7 Hz), 5.80 (b, 1H, NH), and 7.25 (m, 14H, aromatic) ppm; mass spectrum: *m/e* (relative intensity) 315 (M^+, 2%), 314 (4), 272 (13), 258 (5), 224 (59), 182 (100), 181 (70), 180 (88), and 153 (59).

Hydrochloride Salts of *N*-Alkyl- and *N,N*-Dialkyl-1-(4-biphenylyl)-2-phenylethylamines—*Method G (VII, IX*a, *IX*b, *XI*a, *XI*b, *XI*c, *and XI*d)—To a magnetically stirred mixture of lithium aluminum hydride (0.05 mole) and absolute ether (300 ml) was added the appropriate *N*-acyl (V, VIII*a*, and VIII*b*) or *N*-acyl-*N*-alkyl (X*a*, X*b*, X*c* or X*e*, and X*d*, respectively) derivative (0.01 mole) under strictly anhydrous conditions. The reaction mixture was refluxed for 24 hr and cooled in an ice bath, and the excess hydride was decomposed by the dropwise addition of 4% NaOH.

The ethereal layer was separated, and the base was extracted with 10% HCl (50 ml). The acid extract was made alkaline with drops of concentrated ammonium hydroxide solution, and the liberated base was dissolved in ether. The ethereal layer was then washed several times with distilled water until free from alkalinity, dried over anhydrous sodium sulfate, and filtered. The hydrochloride salt was obtained by passing dry hydrogen chloride gas through the solution. The product was then recrystallized.

*Method H (XI*d *and XI*e)—A mixture of the appropriate amine hydrochloride (IX*b* and VI, respectively) (0.01 mole), formic acid (98%) (0.05 mole), and formaldehyde solution (38%) (0.022 mole) was refluxed for 12 hr. The reaction mixture was transferred to an evaporating dish and heated on a water bath until most of the unreacted formaldehyde and formic acid were removed. The syrupy residue was treated with formic acid (98%) (0.6 ml) and formaldehyde solution (38%) (0.2 ml) and allowed to evaporate on the water bath until dry. The last traces of water were azeotroped with absolute ethanol and benzene. The hydrochloride salt was prepared in the usual manner and then recrystallized.

IR spectra of VII and IX*a* showed broad peaks centered at the region of 2960–2700 cm^{-1}, indicative of NH_2^+. IR spectra of XII*a*–XI*e* revealed broad peaks centered at the region of 2650–2550 cm^{-1}, indicative of NH^+.

The PMR spectrum of VII ($CDCl_3$) exhibited peaks at δ 2.50 (s, 3H, methyl), 3.27 (d, 2H, methylene), 3.90 (m, 1H, CH), 6.90 (s, 5H, aromatic), 7.40 (m, 9H, aromatic), and 9.20 (b, 2H, NH_2^+) ppm.

Table III—Comparative Study of the Effects of Similar Molar Concentrations[a] of Some Tested Compounds with Papaverine

Compound	Mean Reduction[b] of Response[c], % ± *SE*
I	57.67 ± 1.36
XI*b*	64.00 ± 1.30
XI*d*	30.00 ± 1.18
XI*e*	68.00 ± 1.51

[a] The concentration used was 3×10^{-5} mole/ml. Aqueous solutions were used. [b] Average of three experiments. [c] Concentration produced by acetylcholine (0.2 μg/ml).

REFERENCES

(1) L. H. Goodson, C. J. W. Wiegand, and J. S. Splitter, *J. Am. Chem. Soc.*, **68**, 2174 (1946).

(2) K. Ogiu, H. Fujimura, Y. Yamakawa, and S. Mita, Japanese pat. 2616 (May 25, 1962) (applied July 11, 1958); through *Chem. Abstr.*, **58**, 7866d (1963).

(3) K. Ogiu, H. Fujimura, Y. Yamakawa, and S. Mita, Japanese pat.

4063 (Mar. 4, 1965) (applied Mar. 11, 1961); through *Chem. Abstr.*, **62**, 16119a (1965).

(4) K. Ogiu, H. Fujimura, and S. Mita, Japanese pat. 23,087 (Dec. 23, 1961) (applied Sept. 9, 1958); through *Chem. Abstr.*, **58**, 13843d,e (1963).

(5) E. C. Dodds, W. Lawson, and P. C. Williams, *Nature*, **151**, 614 (1943).

(6) E. C. Dodds, W. Lawson, and P. C. Williams, *Proc. Roy. Soc. (London)*, **B 132**, 119 (1944).

(7) M. Nakazaki, *Chem. Ind. (London)*, **1962**, 1577; through *Chem. Abstr.*, **58**, 1379b (1963).

(8) M. Nakazaki, I. Mita, and N. Toshioka, *Bull. Chem. Soc. Jpn.*, **36**, 161 (1963).

(9) "Textbook of Organic Medicinal and Pharmaceutical Chemistry," 6th ed., C. O. Wilson, O. Gisvold, and R. F. Doerge, Eds., Lippincott, Philadelphia, Pa., 1971, p. 555.

(10) "The Pharmacological Basis of Therapeutics," 4th ed., L. S. Goodman and A. Gilman, Eds., Macmillan, London, England, 1970, pp. 753, 754.

(11) N. Mann, W. Back, and E. Mutschler, *Ger. Arch. Pharm.*, **306**, 625 (1973).

ACKNOWLEDGMENTS

The authors thank Mr. Shaker A. Mousa, Department of Pharmacology, Faculty of Pharmacy, University of Alexandria, Alexandria, A.R. Egypt, for the pharmacological evaluations. The authors are also grateful to Dr. Farouk S. El-Feraly, Department of Pharmacognosy, School of Pharmacy, University of Mississippi, University, MS 38677, for the spectral determinations.

Light-Scattering Studies on Bile Acid Salts II: Pattern of Self-Association of Sodium Deoxycholate, Sodium Taurodeoxycholate, and Sodium Glycodeoxycholate in Aqueous Electrolyte Solutions

YUNIK CHANG * and JOHN R. CARDINAL ˣ

Received July 1, 1977, from the *College of Pharmacy, University of Utah, Salt Lake City, UT 84112.* Accepted for publication November 11, 1977. *Present address: College of Pharmacy, University of Kansas, Lawrence, KS 66044.

Abstract □ The pattern of self-association of the bile salts sodium deoxycholate, sodium glycodeoxycholate, and sodium taurodeoxycholate was investigated in aqueous electrolyte solutions by the light-scattering technique. The turbidity of the bile salt solutions was obtained over the concentration range of 0–20 mg/ml at 25°. These data were analyzed according to a monomer–micellar equilibrium model and a stepwise association model. Comparison of the light-scattering data with these models suggests that the monomer–micellar model may be inappropriate. Analysis of the data according to the stepwise association model suggests that the dihydroxy bile salts associate to form dimers, trimers, and tetramers in addition to a larger aggregate which varies in size depending on the degree of conjugation of the bile salt.

Keyphrases □ Bile salts, dihydroxy—self-association in aqueous electrolyte solutions, turbidimetric study □ Self-association—various dihydroxy bile salts in aqueous electrolyte solutions, turbidimetric study □ Turbidimetry—study of self-association of various dihydroxy bile salts in aqueous electrolyte solutions

The self-association of the dihydroxy bile salts has been studied extensively (1–5). Most often, the association pattern has been interpreted in terms of a monomer–micellar equilibrium model. This model is analogous to that utilized for flexible chain surfactants and involves the existence of a critical micelle concentration (CMC) below which surfactant aggregation is assumed to be negligible (6). Above the CMC, it is assumed that nearly all added surfactant in excess of the CMC associates to form micelles. Appreciable concentrations of intermediate-sized aggregates are presumed absent, and the polydispersity of the micelles is assumed to be small (7).

Previously (8), it was noted that the conditions necessary for the highly cooperative transition observed for flexible chain surfactants may not be met by all molecular structures. For example, rigid, planar aromatic structures such as dyes and purine and pyrimidine bases seem to associate by continuous stepwise self-association in which small aggregates such as dimers, trimers, and tetramers dominate (8). Furthermore, nonrigid aromatic structures such as the antihistamines self-associate in aqueous solution. Attwood and Udeala (9–11) showed that either pattern of association may dominate depending on the specific molecular structure.

The bile salts possess rigid but nonplanar molecular structures. However, unlike the dyes and the purine and pyrimidine bases, which are approximately symmetrical with respect to hydrophobicity on both sides of the ring, the bile salts consist of a rigid, nonplanar, alicyclic ring system in which one face is hydrophobic while the remaining face is hydrophilic because of the presence of either two or three hydroxyl groups. It was argued previously (12) that the association pattern of trihydroxy bile salts is best represented by a model that assumes the existence of some small aggregates such as dimers and trimers in addition to a higher aggregate.

The present paper extends previous work on the self-association of the bile salts to the dihydroxy bile salts including sodium deoxycholate, sodium taurodeoxycholate, and sodium glycodeoxycholate. The variation of the light scattered as a function of bile salt concentration was obtained in 0.15 *M* sodium halides. These data were analyzed in terms of a monomer–micellar equilibrium model and a stepwise association model in which it is assumed that appreciable concentrations of small multimers coexist with large aggregates.

0022-3549/78/0700/0994$01.00/0
© 1978, American Pharmaceutical Association

4063 (Mar. 4, 1965) (applied Mar. 11, 1961); through *Chem. Abstr.*, **62**, 16119a (1965).

(4) K. Ogiu, H. Fujimura, and S. Mita, Japanese pat. 23,087 (Dec. 23, 1961) (applied Sept. 9, 1958); through *Chem. Abstr.*, **58**, 13843d,e (1963).

(5) E. C. Dodds, W. Lawson, and P. C. Williams, *Nature*, **151**, 614 (1943).

(6) E. C. Dodds, W. Lawson, and P. C. Williams, *Proc. Roy. Soc. (London)*, **B 132**, 119 (1944).

(7) M. Nakazaki, *Chem. Ind. (London)*, **1962**, 1577; through *Chem. Abstr.*, **58**, 1379b (1963).

(8) M. Nakazaki, I. Mita, and N. Toshioka, *Bull. Chem. Soc. Jpn.*, **36**, 161 (1963).

(9) "Textbook of Organic Medicinal and Pharmaceutical Chemistry," 6th ed., C. O. Wilson, O. Gisvold, and R. F. Doerge, Eds., Lippincott, Philadelphia, Pa., 1971, p. 555.

(10) "The Pharmacological Basis of Therapeutics," 4th ed., L. S. Goodman and A. Gilman, Eds., Macmillan, London, England, 1970, pp. 753, 754.

(11) N. Mann, W. Back, and E. Mutschler, *Ger. Arch. Pharm.*, **306**, 625 (1973).

ACKNOWLEDGMENTS

The authors thank Mr. Shaker A. Mousa, Department of Pharmacology, Faculty of Pharmacy, University of Alexandria, Alexandria, A.R. Egypt, for the pharmacological evaluations. The authors are also grateful to Dr. Farouk S. El-Feraly, Department of Pharmacognosy, School of Pharmacy, University of Mississippi, University, MS 38677, for the spectral determinations.

Light-Scattering Studies on Bile Acid Salts II: Pattern of Self-Association of Sodium Deoxycholate, Sodium Taurodeoxycholate, and Sodium Glycodeoxycholate in Aqueous Electrolyte Solutions

YUNIK CHANG * and JOHN R. CARDINAL ˣ

Received July 1, 1977, from the *College of Pharmacy, University of Utah, Salt Lake City, UT 84112.* Accepted for publication November 11, 1977. *Present address: College of Pharmacy, University of Kansas, Lawrence, KS 66044.

Abstract □ The pattern of self-association of the bile salts sodium deoxycholate, sodium glycodeoxycholate, and sodium taurodeoxycholate was investigated in aqueous electrolyte solutions by the light-scattering technique. The turbidity of the bile salt solutions was obtained over the concentration range of 0–20 mg/ml at 25°. These data were analyzed according to a monomer–micellar equilibrium model and a stepwise association model. Comparison of the light-scattering data with these models suggests that the monomer–micellar model may be inappropriate. Analysis of the data according to the stepwise association model suggests that the dihydroxy bile salts associate to form dimers, trimers, and tetramers in addition to a larger aggregate which varies in size depending on the degree of conjugation of the bile salt.

Keyphrases □ Bile salts, dihydroxy—self-association in aqueous electrolyte solutions, turbidimetric study □ Self-association—various dihydroxy bile salts in aqueous electrolyte solutions, turbidimetric study □ Turbidimetry—study of self-association of various dihydroxy bile salts in aqueous electrolyte solutions

The self-association of the dihydroxy bile salts has been studied extensively (1–5). Most often, the association pattern has been interpreted in terms of a monomer–micellar equilibrium model. This model is analogous to that utilized for flexible chain surfactants and involves the existence of a critical micelle concentration (CMC) below which surfactant aggregation is assumed to be negligible (6). Above the CMC, it is assumed that nearly all added surfactant in excess of the CMC associates to form micelles. Appreciable concentrations of intermediate-sized aggregates are presumed absent, and the polydispersity of the micelles is assumed to be small (7).

Previously (8), it was noted that the conditions necessary for the highly cooperative transition observed for flexible chain surfactants may not be met by all molecular structures. For example, rigid, planar aromatic structures such as dyes and purine and pyrimidine bases seem to associate by continuous stepwise self-association in which small aggregates such as dimers, trimers, and tetramers dominate (8). Furthermore, nonrigid aromatic structures such as the antihistamines self-associate in aqueous solution. Attwood and Udeala (9–11) showed that either pattern of association may dominate depending on the specific molecular structure.

The bile salts possess rigid but nonplanar molecular structures. However, unlike the dyes and the purine and pyrimidine bases, which are approximately symmetrical with respect to hydrophobicity on both sides of the ring, the bile salts consist of a rigid, nonplanar, alicyclic ring system in which one face is hydrophobic while the remaining face is hydrophilic because of the presence of either two or three hydroxyl groups. It was argued previously (12) that the association pattern of trihydroxy bile salts is best represented by a model that assumes the existence of some small aggregates such as dimers and trimers in addition to a higher aggregate.

The present paper extends previous work on the self-association of the bile salts to the dihydroxy bile salts including sodium deoxycholate, sodium taurodeoxycholate, and sodium glycodeoxycholate. The variation of the light scattered as a function of bile salt concentration was obtained in 0.15 *M* sodium halides. These data were analyzed in terms of a monomer–micellar equilibrium model and a stepwise association model in which it is assumed that appreciable concentrations of small multimers coexist with large aggregates.

0022-3549/78/0700/0994$01.00/0
© 1978, American Pharmaceutical Association

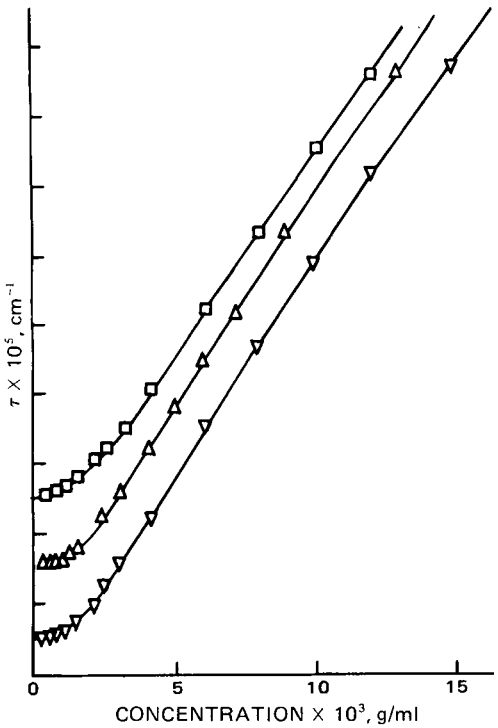

Figure 1—*Turbidity, τ, versus concentration of sodium deoxycholate in 0.15 M sodium fluoride (□), sodium chloride (△), and sodium bromide (▽). Each division on the ordinate represents 10 × 10⁻⁵ cm⁻¹. The intercepts representing the turbidity of the solvent are: sodium bromide, 5.32 × 10⁻⁵ cm⁻¹; sodium chloride, 5.07 × 10⁻⁵ cm⁻¹; and sodium fluoride, 4.85 × 10⁻⁵ cm⁻¹.*

EXPERIMENTAL

Materials—Deoxycholic acid[1] was recrystallized according to the method of Sobotka and Goldberg (13). Glycodeoxycholic acid and taurodeoxycholic acid were synthesized from deoxycholic acid according to the method of Lack *et al.* (14). All bile acids were shown to be free of other bile acids by TLC, using a 100-μg spot (15). In addition, the conjugated bile salts were found to be free of unconjugated glycine and taurine by a similar procedure, using a ninhydrin reagent for development of the chromatogram.

The sodium salts were obtained by titration of aqueous solutions of the acids to pH 10.0 ± 0.2, followed by flash evaporation of the solvent and drying to constant weight in a vacuum oven at 40 ± 2°. Sodium chloride[1] and sodium bromide[1] were reagent grade chemicals and were used as received. Sodium fluoride[1] was also reagent grade but was recrystallized twice from water before use. All water was deionized[2], distilled twice from an all-glass still, and stored in glass containers.

Apparatus—Light-scattering measurements were made with a light-scattering photometer[3] using the small dissymmetry cell[4]. The cell was aligned in the instrument as previously described (12). Refractive index measurements were obtained on a differential refractometer[5]. Temperature control of the refractometer was maintained at 25 ± 0.2° by a circulating water bath[6]. The pH measurements were made with a digital pH meter[7].

Methods—Solutions for the light-scattering measurements were made either by dilution of stock solutions or by direct weighing of the required quantities. All dilutions were made from stock solutions adjusted to pH 10.0 ± 0.1. Particulate-free solutions were obtained by filtration through porous membrane filters[8] (0.22-μm pore diameter) using the technique described previously (12). Membranes were used as received. Various control experiments indicated that detergent abstraction from these membranes was not a problem.

Only solutions that showed a dissymmetry of less than 1.03 were used for the light-scattering measurements. All light-scattering measurements were made at room temperature (24 ± 1°) at 436 nm. Depolarization and fluorescence of the scattered light were negligible.

[1] J. T. Baker Chemical Co., Phillipsburg, N.J.
[2] Model LD-2a, Corning Glass Works, Corning, N.Y.
[3] Brice-Phoenix model BP-2000, Virtus Co., Gardiner, N.Y.
[4] Catalog No. D105, Virtus Co., Gardiner, N.Y.
[5] Model BP-2000-V, Virtus Co., Gardiner, N.Y.
[6] Lauda model K2-R, Brinkmann Instruments, Westbury, N.Y.
[7] Model 110, Corning Glass Works, Corning, N.Y.
[8] Type GS, Millipore Filter Corp., Bedford, Mass.

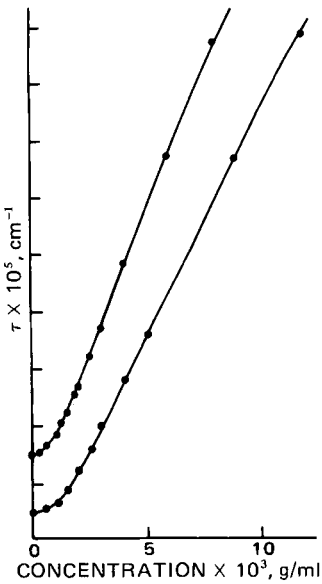

Figure 2—*Turbidity, τ, versus concentration for sodium taurodeoxycholate (upper curve) and sodium glycodeoxycholate (lower curve) in 0.15 M NaCl. The units of the ordinate and the intercepts are as in Fig. 1.*

RESULTS

The turbidity, τ, in centimeters^{-1}, as a function of the sodium deoxycholate concentration in several 0.15 *M* sodium halides is shown in Fig. 1. Figure 2 is a similar plot for sodium taurodeoxycholate and sodium glycodeoxycholate in 0.15 *M* NaCl. The refractive increments, *dn/dc*, for the various bile salts are given in Table I, together with a comparison of the values obtained by previous investigators.

DISCUSSION

To obtain an accurate representation of the self-association pattern of any compound, it is necessary to obtain information about the variation of the monomer concentration, *b*, as a function of the total concentration of the associating species (8, 16). For light scattering, Steiner (16) developed a method for obtaining this information. The weight average molecular weight of all species, M_w, is related to the weight concentration, *c*, in grams per milliliter by:

$$M_0/M_w = 1 + d \ln x/d \ln c \qquad \text{(Eq. 1)}$$

where M_0 is the molecular weight and *x* is the weight fraction of the monomer. The value of M_w can be obtained from the experimental turbidity curve by:

$$\frac{Hc}{\Delta\tau} = \frac{1}{M_w} + 2Bc \qquad \text{(Eq. 2)}$$

where $\Delta\tau$ is the excess turbidity of the solution over the solvent at concentration *c*, *B* is the second virial coefficient, and *H* is an optical constant defined by:

$$H = \frac{32\pi^3 n_0 (dn/dc)^2}{3N_A \lambda_0^4} \qquad \text{(Eq. 3)}$$

Table I—Refractive Index Increments for the Dihydroxy Bile Salts

Solvent	*dn/dc* at 436 nm, ml/g: Sodium Deoxycholate	Sodium Taurodeoxycholate	Sodium Glycodeoxycholate
0.15 *M* sodium fluoride	0.193[a]	—	—
0.15 *M* sodium chloride	0.193	0.171[a] (0.172)[b]	0.193[a] (0.2)[b]
0.15 *M* sodium bromide	0.193	—	—

[a] Present study. [b] Reference 2.

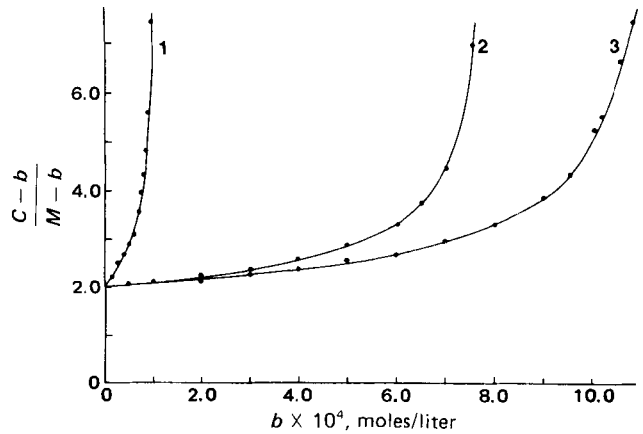

Figure 3—*Average degree of association,* C − b/M − b, versus *the monomer concentration,* b, *for sodium taurodeoxycholate (1), sodium glycodeoxycholate (2), and sodium deoxycholate (3).*

where n_0 is the refractive index of the solvent, dn/dc is the refractive increment of the solute at a constant concentration of added electrolyte, N_A is Avogadro's number, and λ_0 is the wavelength of incident light in vacuum. To obtain M_w by means of Eq. 2, it must be assumed that the second virial coefficient is zero. This approximation can affect the values of M_w calculated at a high concentration but should have relatively minor effects at a low concentration (7). The weight fraction of the monomer, x, can be obtained from:

$$\ln x = \int_0^c [(M_0/M_w) - 1] d \ln c \qquad \text{(Eq. 4)}$$

Given the weight fraction of the monomer, the molar concentration of the monomer, b, at concentration c (grams per milliliter) can be obtained from the relation $b = xc\ 1000/M_0$.

In general, the self-association pattern of a species can be represented by the stepwise addition of monomers to preexisting aggregates. The simplest of such schemes is dimerization, which can be represented by Scheme I:

$$2b \overset{K_2}{\rightleftharpoons} b_2$$

Scheme I

where:

$$K_2 = \frac{b_2}{b^2} \qquad \text{(Eq. 5)}$$

In Scheme I, b_2 is the concentration of dimer and K_2 is the association constant for dimerization. Further steps in this process can be represented by the reactions in Scheme II.

$$b + b_2 \overset{K_3}{\rightleftharpoons} b_3$$

$$b + b_3 \overset{K_4}{\rightleftharpoons} b_4$$

$$b + b_{q-1} \overset{K_q}{\rightleftharpoons} b_q$$

Scheme II

Based on Scheme II, the total equivalent concentration, C, of all species can be defined as:

$$C = b + 2K_2b^2 + 3K_2K_3b^3 + \cdots q \prod_2^q K_q b^q \qquad \text{(Eq. 6)}$$

The total molar concentration, M, of all species can be defined by:

$$M = b + K_2b^2 + K_2K_3b^3 + \cdots \prod_2^q K_q b^q \qquad \text{(Eq. 7)}$$

Finally, the number average degree of association, N_n, for all species excluding the monomer can be defined by:

$$N_n = \frac{C - b}{M - b} \qquad \text{(Eq. 8)}$$

The total equivalent concentration is known from the experimental method. Mukerjee and Ghosh (17) showed that the total molar concentration, M, can be obtained from data on C and b by means of graphical integration according to the following equation:

$$M' - M = 2.303 \int_b^{b'} C\ d \log b \qquad \text{(Eq. 9)}$$

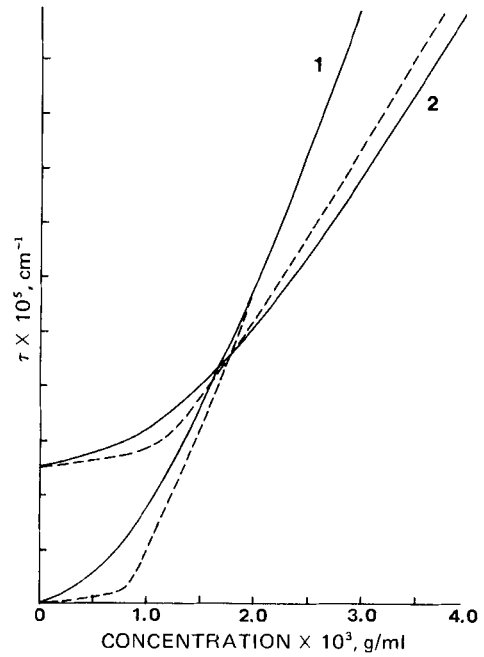

Figure 4—*Comparison of the calculated turbidity (- - -) based on the monomer–micellar model with the experimental curve (—) for sodium taurodeoxycholate (1) and sodium deoxycholate (2) in 0.15* M *NaCl. Each division on the ordinate represents* 2×10^{-5} cm^{-1}. *The intercept for each plot is* 5.07×10^{-5} cm^{-1}.

Monomer-Unique Oligomer Model—Several investigators (1–4) suggested that the dihydroxy bile salts associate in a manner similar to flexible chain surfactants. Under this assumption, the quantities C and M can be defined by:

$$C = b + q\beta_q b^q \qquad \text{(Eq. 10)}$$

$$M = b + \beta_q b^q \qquad \text{(Eq. 11)}$$

where:

$$\beta_q = \prod_2^q K_q$$

By comparison with Scheme II and Eqs. 6–8, it can be seen that, according to this model, N_n should remain nearly zero for all values of b below the CMC. Above the CMC, N_n should rise rapidly and approach a constant value equal to the average aggregation number of the micelles.

Figure 3 shows the variation of N_n with b for all three bile salts in 0.15 M NaCl. For all three bile salts, N_n approaches 2 in dilute solution. For sodium deoxycholate, N_n increases slowly as the monomer concentration increases and then increases rapidly at relatively high values of b. This slow increase in N_n at low values of b is consistent with small aggregate formation in dilute solution (17). For sodium taurodeoxycholate, N_n increases rapidly in dilute solution, suggesting that large aggregates form in relatively dilute solutions. Sodium glycocholate is intermediate between these extremes.

The smallest aggregate formed by all three bile salts is the dimer (Fig. 3). Furthermore, large aggregates must be present to account for the large increase in N_n at the higher concentrations. Thus, the results shown in Fig. 3 are inconsistent with a model that assumes the existence of only monomers plus a unique higher aggregate. This conclusion can also be reached by a comparison of the experimental turbidity curves with those calculated on the basis of a monomer–unique oligomer model. This comparison is shown in Fig. 4 for sodium taurodeoxycholate and sodium deoxycholate. For these calculations, aggregation numbers of 25.3 and 15.9 were used. These values were obtained from the usual Debye plot (12).

Stepwise Association Models—Based on Fig. 3, the limiting size aggregate formed in dilute solution must be the dimer. Moreover, some higher aggregates must form to account for the slowly increasing trend of N_n with b.

Table II—Association Constants, Second Virial Coefficients, and Aggregation Numbers for the Dihydroxy Bile Salts in 0.15 *M* Sodium Halides

Bile Salt and Electrolyte	K_2, liters/mole	K_3, liters/mole	K_4, liters/mole	B, ml-mole/g^2	Aggregation Number
Sodium deoxycholate					
Sodium fluoride	300	810	1360	1.05×10^{-3}	17.7
Sodium chloride	310	870	1290	7.82×10^{-4}	16.7
Sodium bromide	310	710	1130	8.41×10^{-4}	16.0
Sodium glycodeoxycholate					
Sodium chloride	500	780	1370	3.32×10^{-4}	18
Sodium taurodeoxycholate					
Sodium chloride	6820	7160	2.94×10^4	1.23×10^{-4}	25

To determine the nature and size of the higher aggregates formed, the method of Steiner (16) was applied. In this method, it is assumed that aggregate growth occurs in a stepwise fashion such as is given by Eq. 6. According to this method, the weight fraction of the monomer is obtained by the methods described in the previous section. The equilibrium constants K_2, K_3, *etc.*, can be obtained from:

$$[(M_w/xM_0) - 1]/(xc/M_0)$$

$$= 4K_2 + 9K_2K_3(xc/M_0) + \cdots q\prod_2^q K_q(xc/M_0)^{q-2} \quad \text{(Eq. 12)}$$

where K_2 is obtained from the intercept and K_3 is obtained from the limiting slope of a plot made according to Eq. 12. The higher association constants can be obtained by successive applications of Eq. 12.

It was shown previously (9–12) that application of Eq. 12 to light-scattering data of the type generated in the present study leads to a self-consistent set of parameters K_2, K_3, *etc.* In these systems, the association constants were relatively low and little difficulty was encountered in obtaining the values of these constants. In the present systems, however, the turbidity increases rapidly at low concentrations, so small errors in the turbidity can lead to large errors in the derived values of M_w and x. Therefore, it was necessary to develop an iterative technique to obtain K_2, K_3, *etc.*

Based on this procedure, the association constants K_2, K_3, and K_4 shown in Table II were developed. These values were generated from the best smooth curve of plots of both turbidity and molecular weight *versus* concentration. Based on these curves, values of the monomer fraction, x, and the association constants were obtained. The best fits of the association constants were developed by taking advantage of the fact that the slope of the first application of Eq. 12 must be equal to the intercept of the second application, *etc.* Although it is not possible to obtain a direct estimate of the accuracy of these values, the values for sodium deoxycholate are probably somewhat more reliable than those for sodium glycodeoxycholate and sodium taurodeoxycholate because of the slower increase in turbidity with the total concentration.

When an attempt was made to obtain the association constant for the pentamer for each bile salt, the value of the limiting slope was found to be nearly zero. This result suggests that the stability of the pentamer must be small relative to the lower aggregates. This observation that the limiting size of the smaller aggregate does not depend on the degree of conjugation of the bile is consistent with earlier work on the trihydroxy bile salts (12) where the association constants were easier to develop.

At higher values of (xc/M_0), the plots according to Eq. 12 tend to increase rapidly, indicating that some higher aggregates must exist in solution. To determine the size of the higher aggregates, it is assumed that the total equivalent concentration of the dihydroxy bile salts follows a model defined as:

$$C = b + 2K_2b^2 + 3K_2K_3b^3 + 4K_2K_3K_4b^4 + q\beta_q b^q \quad \text{(Eq. 13)}$$

where $q\beta_q b^q$ represents the concentration of the large aggregate. The molecular weight and the second virial coefficient of the large aggregate were obtained from the following equations:

$$\frac{H(c - c')}{(\tau - \tau')} = \frac{1}{M_w} + 2B(c - c') \quad \text{(Eq. 14)}$$

where:

$$c' = b + 2K_2b^2 + 3K_2K_3b^3 + 4K_2K_3K_4b^4 \quad \text{(Eq. 15}a\text{)}$$

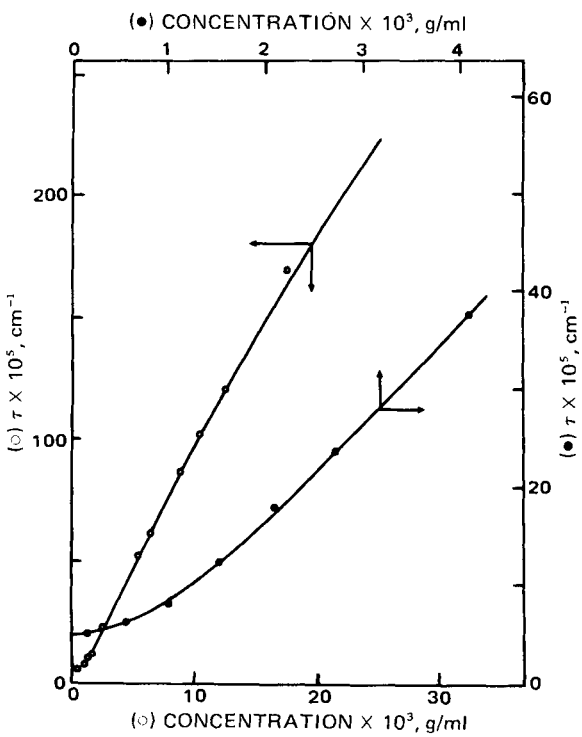

Figure 5—*Comparison of the experimental curve for sodium taurodeoxycholate in 0.15* M *NaCl (—) with the calculated values (○,●) based on the stepwise association model.*

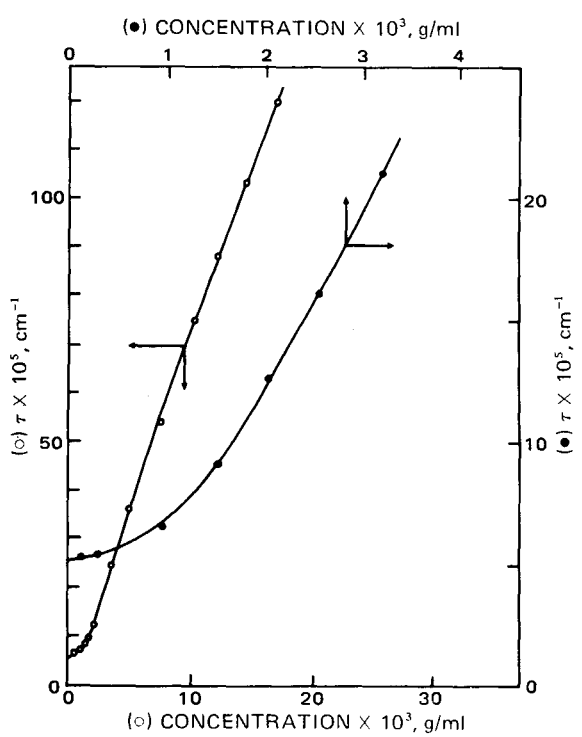

Figure 6—*Comparison of the experimental curve for sodium glycodeoxycholate in 0.15* M *NaCl (—) with the calculated values (○,●) based on the stepwise association model.*

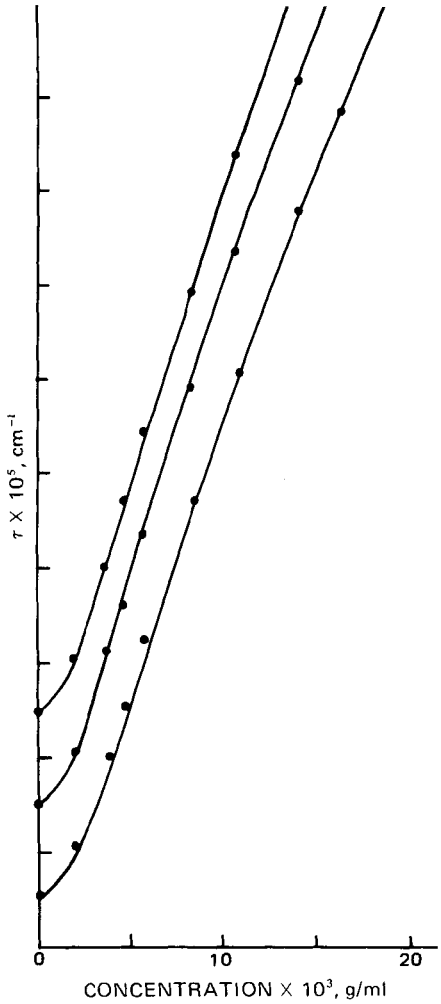

Figure 7—*Comparison of the experimental curves (—) for sodium deoxycholate in 0.15 M sodium halides with the calculated values (●) based on the Vrij–Overbeek treatment of the stepwise association model. Proceeding from top to bottom, the curves represent sodium deoxycholate in sodium fluoride, sodium chloride, and sodium bromide. The units of the ordinate and the intercepts are as given in Fig. 1.*

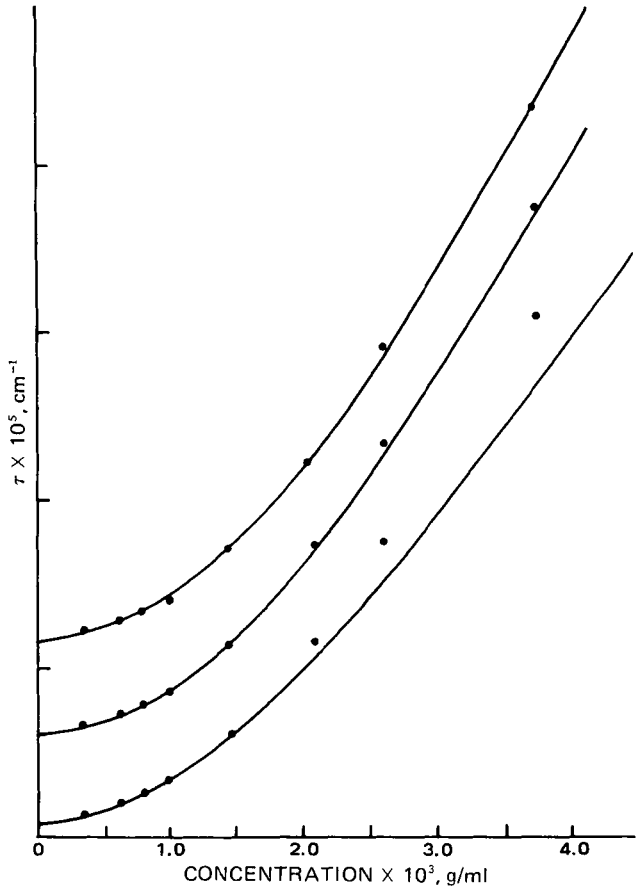

Figure 8—*Plot similar to Fig. 7 for the low concentration region. Each division on the ordinate represents 5 X 10^{-5} cm^{-1}. The intercepts are as given in Fig. 1.*

and:

$$\tau' = \tau_0 + \tau_1 + \tau_2 + \tau_3 + \tau_4 \qquad \text{(Eq. 15}b\text{)}$$

where c represents the total concentration and τ represents the total turbidity at concentration c, τ_0 represents the turbidity of the solvent, and τ_1, τ_2, *etc.*, represent the turbidity of the monomer, dimer, *etc.* The value of τ_0 is obtained experimentally. The values of τ_1, *etc.*, can be calculated according to Eq. 2, assuming that the second virial coefficients are zero. Application of these equations to the light-scattering data leads to the aggregation numbers for the high aggregates shown in Table II. These values are somewhat higher than those obtained previously by application of the usual monomer–micellar model. This trend of higher aggregation numbers from the stepwise association treatment is consistent with the results obtained previously (12, 18).

A comparison between the experimental curves and those calculated on the basis of this model for sodium taurodeoxycholate and sodium glycodeoxycholate is shown in Figs. 5 and 6. The agreement between the experimental curves and the calculated values is excellent in both the low and high concentration regions.

As discussed by Vrij and Overbeek (19), the aggregation numbers shown in Table II are apparent values uncorrected for effects arising from the negative adsorption of the co-ions. These authors (19) developed the necessary procedures to obtain the true aggregation number from the apparent values, provided that the apparent values were obtained in several different sodium halides at the same concentration.

In the present study, sufficient data for application of the procedure of Vrij and Overbeek (19) were obtained only for sodium deoxycholate. When using the apparent aggregation numbers shown in Table II, the true aggregation number was found to be 18.8. Comparisons of the calculated values with the experimental curves for the three electrolytes are shown in Figs. 7 and 8. The agreement seems to be quite good except for sodium bromide, where the calculated values lie somewhat above the experimental curve in the intermediate concentration region. These curves were calculated on the basis of the average values of K_2, K_3, and K_4 for all electrolytes shown in Table II. The lack of agreement of the calculated values with the experimental curve in sodium bromide is consistent with the lower values of K_3 and K_4 found in the sodium bromide system. The reasons for these lower values in this system are not known.

The results obtained in the present study of the dihydroxy bile salts are in agreement with those reported by previous investigators with respect to several points, including that the dihydroxy bile salts associate to form large aggregates, which are substantially larger than those found in the trihydroxy bile salts, and that conjugation affects the size of the higher aggregates, the size decreasing in the order sodium taurodeoxycholate > sodium glycodeoxycholate > sodium deoxycholate. However, in this study, evidence suggests that dimers, trimers, and tetramers are also present. This result should be compared with the results obtained on the trihydroxy bile salts where the evidence suggests that only dimers and trimers are present (12). Also, the association constants are much smaller for the trihydroxy bile salts. Thus, the number of hydroxyl groups on the bile salt molecule seems to affect not only the aggregation number of the higher aggregates but also the type and stability of the small aggregates formed. Any indepth analyses of the pattern of the association constants for the low aggregates would probably be misleading because of the uncertainties in these values for the dihydroxy bile salts.

REFERENCES

(1) D. M. Small, in "The Bile Acids," P. P. Nair and D. Kritchevsky, Eds., Plenum, New York, N.Y., 1971, chap. 8.

(2) J. P. Kratohvil and H. T. DelliColli, *Can. J. Biochem.*, **46**, 443 (1968).

(3) J. P. Kratohvil and H. T. DelliColli, *Fed. Proc.*, **29**, 1335 (1970).
(4) J. P. Kratohvil, *Colloid Polym. Sci.*, **253**, 251 (1975).
(5) K. Fontell, *Kolloid-Z. Z. Polym.*, **244**, 253 (1971).
(6) P. Mukerjee, *Adv. Colloid Interface Sci.*, **1**, 241 (1967).
(7) P. Mukerjee, *J. Phys. Chem.*, **65**, 565 (1972).
(8) P. Mukerjee, *J. Pharm. Sci.*, **63**, 972 (1974).
(9) D. Attwood and O. K. Udeala, *J. Phys. Chem.*, **79**, 889 (1975).
(10) D. Attwood and O. K. Udeala, *J. Pharm. Sci.*, **65**, 1053 (1976).
(11) D. Attwood, *J. Phys. Chem.*, **80**, 1984 (1976).
(12) Y. Chang and J. R. Cardinal, *J. Pharm. Sci.*, **67**, 174 (1978).
(13) H. Sobotka and A. Goldberg, *Biochem. J.*, **26**, 555 (1932).
(14) L. Lack, G. D. Singletary, T. Walker, and F. O. Dorrity, *J. Lipid Res.*, **14**, 367 (1973).
(15) A. F. Hofmann, *ibid.*, **3**, 127 (1962).
(16) R. F. Steiner, *Arch. Biochem. Biophys.*, **39**, 333 (1952).
(17) P. Mukerjee and A. K. Ghosh, *J. Am. Chem. Soc.*, **92**, 6403 (1970).
(18) K. J. Mysels and L. H. Princen, *J. Phys. Chem.*, **63**, 1949 (1959).
(19) A. Vrij and J. T. G. Overbeek, *J. Colloid Sci.*, **17**, 570 (1962).

ACKNOWLEDGMENTS

Abstracted in part from a dissertation submitted by Y. Chang to the University of Utah in partial fulfillment of the Doctor of Philosophy degree requirements.

Supported by the University of Utah Research Committee.

New Opiate–Receptor Model

VERA M. KOLB

Received September 9, 1977, from the *Department of Chemistry and Biochemistry and the School of Medicine, Southern Illinois University, Carbondale, IL 62901.* Accepted for publication November 4, 1977.

Abstract □ A new opiate–receptor model is proposed in which only one conformation of the receptor is needed for binding of both agonists and antagonists. There are two different spacially fixed amine-binding sites in this model: one agonist and one antagonist. The opiates undergo binding to their amine-binding sites *via* the lone electron pair on nitrogen. The role of the *N*-allyl or other such group in imparting antagonist properties is explained in terms of the steric requirements of this group. For this group to be accommodated without imposing severe steric interactions in the rest of the opiate molecule, the piperidine ring must assume a flexible (skew boat) conformation; in this conformation, the *N*-lone-pair electron lobe assumes the characteristic directionality of an antagonist toward its amine-binding site. If the *N*-lone-pair lobe is not rigorously maintained in this direction, the opiate molecule assumes both antagonist and agonist conformations and mixed antagonist–agonist activity is observed. The observed differences in the effect of sodium on the degree of binding of an agonist *versus* an antagonist can be explained in this model by the different effects of sodium on the two amine-binding sites. The antagonist activity of an *N*-methyl antagonist can be rationalized on the basis of the proposed model.

Keyphrases □ Opiate–receptor model—proposed, only one receptor conformation needed for binding both agonists and antagonists □ Model, opiate–receptor—proposed, only one receptor conformation needed for binding both agonists and antagonists □ Binding—opiate agonists and antagonists to receptor, new model proposed

Recently, Snyder and coworkers (1, 2) proposed a model of the opiate receptor to explain structure–activity relationships of opiate agonists and antagonists. They postulated that the receptor can exist in two different conformations: the antagonist conformation (a sodium-binding form) and the agonist conformation (no sodium form). On the basis of the qualitative conformational analysis of a series of opiate agonist and antagonist molecules, the following spacially fixed binding sites on the receptor were proposed (2): lipophilic, amine binding, agonist binding, and specific antagonist binding (Fig. 1).

To account for the observation that substitution of the *N*-methyl of an opiate agonist by an *N*-allyl or *N*-cyclopropylmethyl usually confers antagonist activity, Snyder and coworkers (2) suggested that: "Presumably, the *N*-allyl or other such group interacts with a portion of the opiate receptor regulating antagonist activity." This portion of the receptor in Fig. 1 is the specific antagonist binding site. Their view, therefore, is one interpretation of the data.

BACKGROUND

In the Snyder model, the amine-binding site is defined as the ionic site that interacts with the amine nitrogen. The protonated amine has been considered (3, 4) the active form at the receptor site. From the pKa of morphine (7.88), Beckett and Casy (3) estimated that it would be 80% protonated at physiological pH. However, it is not unreasonable to believe that the unprotonated amine is, in fact, the active species because of the nature of the amine-binding site. In this respect, a relatively high pKa value (a thermodynamic, not kinetic, value) may have an adverse effect on binding.

Figure 1 indicates that, in the Snyder model, the *N*-lone-pair electron lobe of naloxone is pointed away from the amine-binding site, while the *N*-lone-pair lobe of morphine is directed toward this binding site. It seems improbable that interaction between naloxone and the amine-binding site would occur in the juxtaposition shown in this figure. Only if the interaction between the amino nitrogen and the amine-binding site were chemical could a binding interaction in the conformation shown in Fig. 1 be reconcilable, and then only as a minor collision process in a cross-

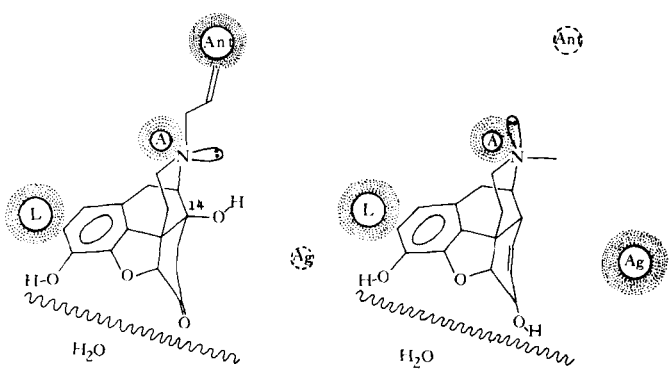

Figure 1—*Snyder's model for binding of naloxone (antagonist) and morphine (agonist) to the receptor. Key: left, naloxone bound to the antagonist conformation of the receptor; right, morphine bound to the agonist conformation of the receptor; L, lipophilic site; A, amine-binding site; Ag, agonist-binding site; and Ant, specific antagonist-binding site.*

0022-3549/78/0700/0999$01.00/0
© 1978, American Pharmaceutical Association

(3) J. P. Kratohvil and H. T. DelliColli, *Fed. Proc.*, **29**, 1335 (1970).
(4) J. P. Kratohvil, *Colloid Polym. Sci.*, **253**, 251 (1975).
(5) K. Fontell, *Kolloid-Z. Z. Polym.*, **244**, 253 (1971).
(6) P. Mukerjee, *Adv. Colloid Interface Sci.*, **1**, 241 (1967).
(7) P. Mukerjee, *J. Phys. Chem.*, **65**, 565 (1972).
(8) P. Mukerjee, *J. Pharm. Sci.*, **63**, 972 (1974).
(9) D. Attwood and O. K. Udeala, *J. Phys. Chem.*, **79**, 889 (1975).
(10) D. Attwood and O. K. Udeala, *J. Pharm. Sci.*, **65**, 1053 (1976).
(11) D. Attwood, *J. Phys. Chem.*, **80**, 1984 (1976).
(12) Y. Chang and J. R. Cardinal, *J. Pharm. Sci.*, **67**, 174 (1978).
(13) H. Sobotka and A. Goldberg, *Biochem. J.*, **26**, 555 (1932).
(14) L. Lack, G. D. Singletary, T. Walker, and F. O. Dorrity, *J. Lipid Res.*, **14**, 367 (1973).
(15) A. F. Hofmann, *ibid.*, **3**, 127 (1962).
(16) R. F. Steiner, *Arch. Biochem. Biophys.*, **39**, 333 (1952).
(17) P. Mukerjee and A. K. Ghosh, *J. Am. Chem. Soc.*, **92**, 6403 (1970).
(18) K. J. Mysels and L. H. Princen, *J. Phys. Chem.*, **63**, 1949 (1959).
(19) A. Vrij and J. T. G. Overbeek, *J. Colloid Sci.*, **17**, 570 (1962).

ACKNOWLEDGMENTS

Abstracted in part from a dissertation submitted by Y. Chang to the University of Utah in partial fulfillment of the Doctor of Philosophy degree requirements.

Supported by the University of Utah Research Committee.

New Opiate–Receptor Model

VERA M. KOLB

Received September 9, 1977, from the *Department of Chemistry and Biochemistry and the School of Medicine, Southern Illinois University, Carbondale, IL 62901.* Accepted for publication November 4, 1977.

Abstract □ A new opiate–receptor model is proposed in which only one conformation of the receptor is needed for binding of both agonists and antagonists. There are two different spacially fixed amine-binding sites in this model: one agonist and one antagonist. The opiates undergo binding to their amine-binding sites *via* the lone electron pair on nitrogen. The role of the *N*-allyl or other such group in imparting antagonist properties is explained in terms of the steric requirements of this group. For this group to be accommodated without imposing severe steric interactions in the rest of the opiate molecule, the piperidine ring must assume a flexible (skew boat) conformation; in this conformation, the *N*-lone-pair electron lobe assumes the characteristic directionality of an antagonist toward its amine-binding site. If the *N*-lone-pair lobe is not rigorously maintained in this direction, the opiate molecule assumes both antagonist and agonist conformations and mixed antagonist–agonist activity is observed. The observed differences in the effect of sodium on the degree of binding of an agonist *versus* an antagonist can be explained in this model by the different effects of sodium on the two amine-binding sites. The antagonist activity of an *N*-methyl antagonist can be rationalized on the basis of the proposed model.

Keyphrases □ Opiate–receptor model—proposed, only one receptor conformation needed for binding both agonists and antagonists □ Model, opiate–receptor—proposed, only one receptor conformation needed for binding both agonists and antagonists □ Binding—opiate agonists and antagonists to receptor, new model proposed

Recently, Snyder and coworkers (1, 2) proposed a model of the opiate receptor to explain structure–activity relationships of opiate agonists and antagonists. They postulated that the receptor can exist in two different conformations: the antagonist conformation (a sodium-binding form) and the agonist conformation (no sodium form). On the basis of the qualitative conformational analysis of a series of opiate agonist and antagonist molecules, the following spacially fixed binding sites on the receptor were proposed (2): lipophilic, amine binding, agonist binding, and specific antagonist binding (Fig. 1).

To account for the observation that substitution of the *N*-methyl of an opiate agonist by an *N*-allyl or *N*-cyclopropylmethyl usually confers antagonist activity, Snyder and coworkers (2) suggested that: "Presumably, the *N*-allyl or other such group interacts with a portion of the opiate receptor regulating antagonist activity." This portion of the receptor in Fig. 1 is the specific antagonist binding site. Their view, therefore, is one interpretation of the data.

BACKGROUND

In the Snyder model, the amine-binding site is defined as the ionic site that interacts with the amine nitrogen. The protonated amine has been considered (3, 4) the active form at the receptor site. From the pKa of morphine (7.88), Beckett and Casy (3) estimated that it would be 80% protonated at physiological pH. However, it is not unreasonable to believe that the unprotonated amine is, in fact, the active species because of the nature of the amine-binding site. In this respect, a relatively high pKa value (a thermodynamic, not kinetic, value) may have an adverse effect on binding.

Figure 1 indicates that, in the Snyder model, the *N*-lone-pair electron lobe of naloxone is pointed away from the amine-binding site, while the *N*-lone-pair lobe of morphine is directed toward this binding site. It seems improbable that interaction between naloxone and the amine-binding site would occur in the juxtaposition shown in this figure. Only if the interaction between the amino nitrogen and the amine-binding site were chemical could a binding interaction in the conformation shown in Fig. 1 be reconcilable, and then only as a minor collision process in a cross-

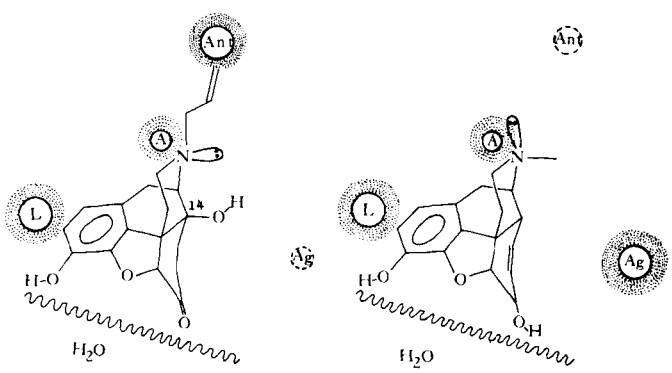

Figure 1—*Snyder's model for binding of naloxone (antagonist) and morphine (agonist) to the receptor. Key: left, naloxone bound to the antagonist conformation of the receptor; right, morphine bound to the agonist conformation of the receptor; L, lipophilic site; A, amine-binding site; Ag, agonist-binding site; and Ant, specific antagonist-binding site.*

0022-3549/78/0700/0999$01.00/0
© 1978, American Pharmaceutical Association

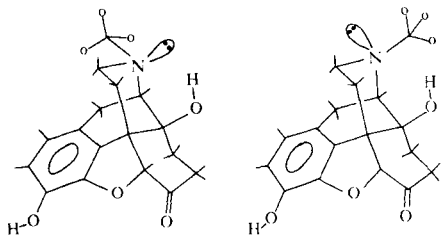

Figure 2—*Some conformations of oxymorphone. Key: left,* N-*methyl equatorial conformation; right,* N-*methyl axial conformation; and small circles, hydrogens of the* N-*methyl group. Other hydrogens are not shown.*

reaction (5). Therefore, if it can be demonstrated that the amine-binding site interacts with the N-lone-pair electron lobe of opiate bases, the Snyder model for the binding of naloxone to the receptor is not tenable.

Figure 1 also shows that, in the Snyder model, specific conformations of morphine and naloxone bind to the receptor and exhibit activity. The reason for the choice of these particular conformations was not made clear. Moreover, these conformations are not the most stable ones (*vide infra*).

While morphine (Fig. 1), oxymorphone (Fig. 2), and levorphanol were depicted by Snyder (1) in conformations in which the N-methyl is axial–chair, conformations in which the N-methyl of these compounds is equatorial–chair should be more stable. Thus, simple Van der Waals calculations indicate that more than 90% of N-methylpiperidine will be in the conformation in which N-methyl is equatorial–chair (6). Also, on the basis of dipole moment measurements on different systems, the axial–equatorial equilibrium for the N-methyl of N-methylpiperidine (in the chair conformation) was determined (ΔG = 1.5 kcal/mole) and showed that the equatorial placement of N-methyl was much preferred (6). Also, X-ray analysis of morphine hydroiodide dihydrate showed the equatorial–chair orientation of the N-methyl (7); however, extrapolation of this result to the solution state would be tenuous.

Loew and Berkowitz (8) showed, by PCILO calculations, that the conformation of N-methylpiperidine in which the N-methyl is axial–chair is less stable by 5.7 kcal/mole than the corresponding equatorial conformer. They also calculated that the axial–chair N-methyl conformer of oxymorphone (Fig. 2) is 12 kcal/mole less stable than the equatorial–chair conformer (8). Finally, there is now very strong experimental evidence that the N-methyl group in N-methylpiperidine prefers the equatorial position by about 3.0 kcal/mole (9).

Loew and Berkowitz (8) concluded that "the energy difference of 5.7 kcal/mole between the best axial and equatorial conformers would make the axial conformer only barely accessible to the drug by interaction in the biophase of the receptor." On this basis, they proposed that the more stable, equatorial–chair conformers of morphine and oxymorphone are most likely to bind to the receptor site. In contrast, the Snyder model indicates that the less stable, N-methyl axial–chair conformations of morphine and oxymorphone bind to the receptor.

On the other hand, with respect to naloxone, Snyder and coworkers (1, 2) considered the equatorial–chair conformation as the most stable (Fig. 1) and the one responsible for binding to the receptor. However, in view of the fact that the N-allyl group of naloxone might sterically influence the relative stabilities of its conformers, a qualitative conformational analysis was performed. As suspected, this steric effect is quite impressive and, surprisingly, it is very apparent in the equatorial–chair conformation while least apparent in the pseudoequatorial–skew boat conformation. The latter, therefore, appears to be the most stable conformation of naloxone. This observation, together with those already noted, led to the proposed new opiate–receptor model.

CONFORMATIONAL ANALYSIS[1]

A molecular model of naloxone was built according to that depicted by the Snyder model (1, 2). In this conformation (Fig. 3, I), the piperidine ring is in the chair conformation and the N-allyl group is equatorial.

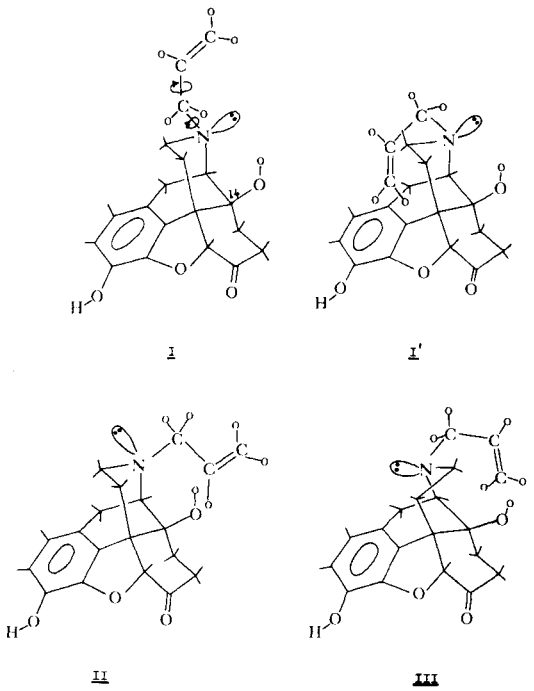

Figure 3—*Some conformations of naloxone. Small circles represent hydrogens of the* N-*allyl and 14-OH. Other hydrogens are not shown. Conformations (except I) are shown to point out the most unfavorable steric interactions.*

Snyder and coworkers (1, 2) referred to this conformation as the one allowing free N-allyl rotation and being the most stable compared to the N-allyl axial–chair conformer (Fig. 3, II) in which N-allyl rotation is reduced by interaction with the 14-OH.

However, careful study of the molecular model of the equatorial–chair rotamers (Fig. 3, I and I') reveals that the stated free rotations around the single bonds, N–C–C=C, are, in fact, subjected to very severe steric interactions. On the contrary, if the piperidine ring assumes the skew boat (flexible) form in which N-allyl is pseudoequatorial (Fig. 3, III), the N-allyl group exhibits virtually complete rotational freedom without introducing any apparently unfavorable interactions (the molecular models illustrate that eclipsing of ring hydrogens is absent in this skew boat form as well as in the chair form).

On these grounds, it is reasonable to conclude that the most stable form of naloxone is the skew boat conformation in which the N-allyl is pseudoequatorial.

Qualitative conformational analysis of other opiate molecules in this study (*vide infra*) was performed by the following method. The equatorial–chair, axial–chair, pseudoequatorial–boat, and pseudoaxial–boat conformations of the drug molecule were built. The N-substituent in each of these four conformations was rotated, and the least stable rotamer was found. The least stable rotamers must be considered because they reduce the overall stability of the system, even though there is an infinite number of more stable rotamers. The order of stability of these conformations was established. (Any conformational analysis book can be used for classifying unfavorable interactions—1,3-interactions, eclipsing, *etc.*—and for evaluating the energies of these interactions as well as the energies of chair–boat interconversion, *etc.*) Numerous examples (5, 10) illustrate the order of magnitude of unfavorable interactions necessary to force the piperidine ring into a boat conformation.

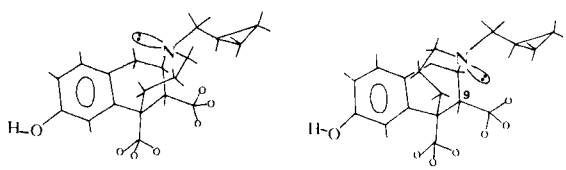

Figure 4—*Some conformations of* trans-*homobenzomorphan cyclazocine homolog. Key: left, conformation with a nonhindered* N-*lone pair; right, conformation with hindered* N-*lone pair; and small circles, methyl hydrogens. Other hydrogens are now shown.*

[1] Qualitative conformational analysis was performed on Japanese HGS Maruzen B models. A quantitative conformational analysis of morphine-type agonists and antagonists by ^{13}C-NMR spectrometry is planned.

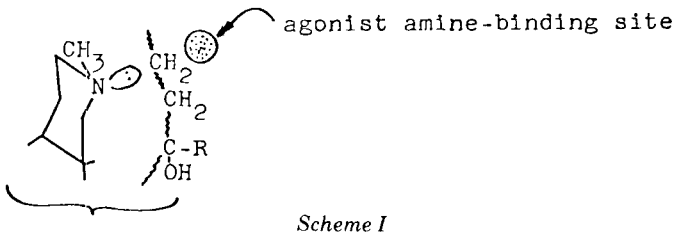

Scheme I

RESULTS AND DISCUSSION

It is reasonable to believe that the most stable form of naloxone is the skew boat conformation in which the *N*-allyl is pseudoequatorial (*vide supra*) and that this form interacts with the receptor. On this basis, the antagonist activity of naloxone may be explained differently from that of the Snyder model. Thus, it is seen from conformation III that the *N*-lone-pair electron lobe is not hindered and is pointed approximately to the left, in a line parallel to one passing through the 3-OH and 6-keto groups. It is proposed that an antagonist amine-binding site is situated in this direction and that the primary action on a receptor by an antagonist may be through its *N*-lone pair that is pointing toward the antagonist amine-binding site. The antagonist effect of naloxone, therefore, would be derived indirectly through the *N*-allyl group whose steric effect forces the *N*-lone pair in the direction of the antagonist amine-binding site[2].

If the *N*-allyl group of naloxone is replaced by an *N*-methyl group, oxymorphone, an agonist, is obtained (Fig. 2). The most stable conformation (*N*-methyl equatorial–chair) of oxymorphone will probably bind to the receptor. The *N*-lone-pair lobe in this conformation is pointed to the right at about 45° from the plane in which the model sits. It is proposed that, in this direction, an agonist amine-binding site is placed and that the *N*-lone-pair lobe of an agonist interacts with this amine-binding site.

Similar conformational analysis of *cis*- and *trans*-homobenzomorphan cyclazocine homologs (*N*-cyclopropylmethylazacycloheptane opiates) is performed by moving the *N*-cyclopropylmethyl group between the axial and equatorial positions (10) and by the easy flipping of the azacycloheptane ring through its conformations, which are known to be flexible (11, 12). Thus, the *trans*-compound (antagonist) exists in two stable conformations (Fig. 4). The *N*-lone-pair electron lobe of one conformer is hindered by the 9-methyl, while the *N*-lone-pair lobe of the other conformer is pointed in the antagonist direction and is not hindered.

The *cis*-isomer assumes the analogous antagonist conformation but can also exist in another stable agonist conformation (Fig. 5). Thus, the *cis*-compound should show mixed activity, as was found to be the case (2). The *trans*-isomer cannot assume this agonist conformation without imposing severe steric restrictions on the 9-methyl group.

The same type of conformational analysis would account for the agonist, antagonist, and mixed activity of levorphanol, etorphine, nalorphine, levallorphan, benzomorphans, pentazocine, cyclazocine, and related compounds.

The introduction of the F-ring (2) or a moiety simulating it into the opiate molecule makes the analysis of the structure–activity relationship more complicated because of the new variables simultaneously introduced. Thus, the observed strong agonist effect imparted by the introduction of an F-ring (2) may compensate or overcome the antagonist effect of the molecule. The strong binding of the F-ring to the agonist

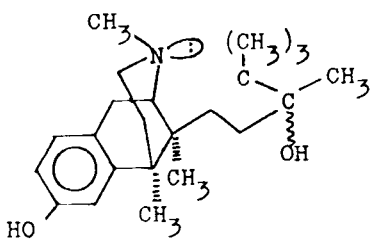

IV

[2] Concrete evidence for the importance of the *N*-lone electron pair orientation in stereospecific opiates for productive interaction with the opiate receptor was reported [B. Belleau, T. Conway, F. R. Ahmed, and A. D. Hardy, *J. Med. Chem.*, 17, 907 (1974)].

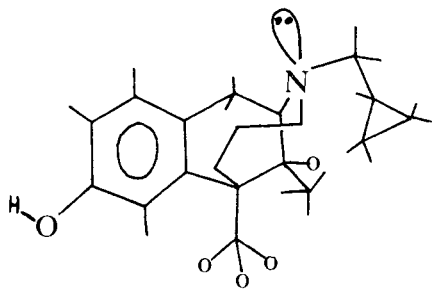

Figure 5—*Agonist conformation of* cis-*homobenzomorphan cyclazocine homolog. Small circles are hydrogens of the* trans-*methyl. Other hydrogens are not shown.*

binding site (Fig. 1) may slightly change the juxtaposition of the molecule with respect to the receptor and shift the *N*-lone-pair lobe away from the antagonist amine-binding site.

Furthermore, it is possible that a long alkyl side chain (*e.g.*, at a carbinol carbon of an *N*-methyloripavine), instead of folding into the F-ring conformation and causing agonist activity, will assume a different conformation that will block the *N*-lone pair of the agonist conformation, thereby obstructing interaction with its amine-binding site (Scheme I). The piperidine ring may flip into a skew boat conformation, which would permit hydrophobic interactions of the *N*-methyl with the alkyl side chain as well as polar interactions of the *N*-lone pair with the antagonist amine-binding site, the overall effect being antagonist activity.

The fact that an *N*-methyl compound has now been found to possess antagonist properties strongly supports the proposed concept. Michne *et al.* (13) reported two isomers, differing only in the chirality of the carbinol carbon, of Compound IV. One isomer (mp 242–247°) showed strong antagonist activity (of at least 60% of the potency of nalorphine). The reversed chirality at the carbinol carbon of the other isomer (mp 219–223°) destroyed the antagonist activity. The large difference in antagonist activity effected merely by a change in chirality at the carbinol carbon can be easily rationalized by Scheme I.

The proposed model was applied to numerous compounds with known activities. In no instance did the model predict antagonist activity for a compound that was an agonist, or *vice versa*, or in any other way fail to explain classic features of opiate pharmacology.

In summary, the salient features of this model are as follows. Only one conformation of the receptor is needed for binding of both agonists and antagonists. While lipophilic and agonist binding sites are the same as in the Snyder model, the amine-binding site and specific antagonist binding site are changed. There are two distinct, spacially fixed, amine-binding sites in this proposed model: one agonist amine-binding site and one antagonist amine-binding site. Agonists and antagonists interact with their respective amine-binding sites *via* the lone-pair electrons on their nitrogen atoms.

In this model, it is suggested that the primary action of an antagonist on the receptor may be through the interaction of the antagonist *N*-lone pair and its amine-binding site and not through lipophilic interaction of the *N*-allyl chain with the specific antagonist binding site. The main role of the *N*-allyl (or *N*-cyclopropylmethyl) chain is to force the *N*-lone-pair lobe of an antagonist molecule in the direction of its amine-binding site. This situation is achieved when the antagonist assumes a geometry in which its piperidine ring is in a flexible (skew boat) conformation and the *N*-allyl chain is pseudoequatorial. The specific antagonist binding site of the Snyder model thus becomes less important, or even not important, for antagonist activity.

Finally, in the proposed model, a change in sodium concentration affects the two amine-binding sites differently, resulting in the observed (1, 2) differences in the effect of sodium on the degree of binding by an agonist *versus* an antagonist.

REFERENCES

(1) S. H. Snyder, *Sci. Am.*, **236**, 44 (1977).

(2) A. P. Feinberg, I. Creese, and S. H. Snyder, *Proc. Natl. Acad. Sci. USA*, **73**, 4215 (1976).

(3) A. H. Beckett and A. F. Casy, *J. Pharm. Pharmacol.*, **6**, 986 (1954).

(4) P. S. Portoghese, *J. Pharm. Sci.*, **55**, 865 (1966).

(5) J. McKenna, in "Topics in Stereochemistry," vol. 5, E. L. Eliel and N. L. Allinger, Eds., Wiley–Interscience, New York, N.Y., 1970, pp. 279, 280.

(6) E. L. Eliel, N. L. Allinger, S. J. Angyal, and G. A. Morrison, "Conformational Analysis," Interscience, New York, N.Y., 1967, pp. 180, 181.

(7) M. Hanack, "Conformation Theory," Academic, New York, N.Y., 1965, p. 322.

(8) G. H. Loew and D. S. Berkowitz, *J. Med. Chem.*, **18**, 656 (1975).

(9) P. J. Crowley, M. J. T. Robinson, and M. G. Ward, *Tetrahedron*, **33**, 915 (1977).

(10) E. L. Eliel, N. L. Allinger, S. J. Angyal, and G. A. Morrison, "Conformational Analysis," Interscience, New York, N.Y., 1967, pp. 244–248.

(11) *Ibid.*, pp. 207, 208.

(12) K. von Bredow, H. Friebolin, and S. Kabuss, in "Conformational Analysis, Scope and Present Limitations," vol. 21, G. Chiurdoglu, Ed., Organic Chemistry, A Series of Monographs, Academic, New York, N.Y., 1971, pp. 51–54.

(13) W. F. Michne, R. L. Salsbury, and S. J. Michalec, *J. Med. Chem.*, **20**, 682 (1977), and references cited therein.

ACKNOWLEDGMENTS

Presented at the national meeting of the American Chemical Society, Chicago, Ill., 1977, Abstract 31 (Medicinal Chemistry).

Supported in part by the University Research Foundation, La Jolla, Calif.

The author is grateful to Dr. Cal Y. Meyers for fruitful discussions and editorial help and to Dr. William F. Michne and Dr. Ernest L. Eliel for valuable suggestions.

Modified Technique Using Perfused Isolated Guinea Pig Lung to Determine Effect of an Aerosol Constituent on Pulmonary Dynamics

ANDREW G. CLAIR and MICHAEL A. BARLETTA ˣ

Received August 5, 1977, from the *Department of Pharmaceutical Sciences, College of Pharmacy and Allied Health Professions, St. John's University, Jamaica, NY 11439.* Accepted for publication November 10, 1977.

Abstract □ Polyethylene glycol 400, a commonly used plasticizer in many cosmetic aerosol hair sprays, was tested to determine its effect on perfusion pressure, perfusion vascular flow rate, and tidal volume in the perfused isolated guinea pig lung. Negative pressure was maintained within the chamber housing the intact lungs, and initial perfusion of the pulmonary vasculature was accomplished *via* the right side of the heart *in situ* after guinea pigs were sacrificed by decapitation. Polyethylene glycol 400 was injected into the pulmonary arterial system in doses of 0.01–30 μg/ml after pretreatment with isoproterenol (1 μg/ml). Isoproterenol was then readministered, followed by nebulized doses of the cosmetic chemical into the trachea at 0.3, 3, and 30% concentrations. Nebulized polyethylene glycol 400 was also administered in 50, 70, and 90% concentrations. Polyethylene glycol 400 significantly increased perfusion pressure and flow rate after injection into the pulmonary arterial system of the isolated lung. In addition, nebulized administration in concentrations of 0.3–30% significantly increased the perfusion flow rate; following the 50–90% nebulized doses, a significant increase in both perfusion pressure and flow rate was observed. Tidal volume decreased, regardless of the route of administration, as increasing doses of the cosmetic constituent were delivered to the isolated lung.

Keyphrases □ Polyethylene glycol 400—effect on pulmonary dynamics in perfused isolated guinea pig lung □ Pulmonary dynamics—effect of polyethylene glycol 400 in perfused isolated guinea pig lung □ Aerosol constituents—polyethylene glycol 400, effect on pulmonary dynamics in perfused isolated guinea pig lung

The relation between inhalation of airborne particles and pulmonary disease has been known for some time (1). Numerous cases of pulmonary thesaurosis were attributed to the inhalation of cosmetic hair sprays, although the question of whether cosmetic aerosols actually cause pulmonary disease is still controversial (2–5). Zuskin and Bouhoys (6) observed, under controlled experimental conditions, that short lasting and significant decreases in the air expiratory flow rate from the lung occurred following acute exposures to various commercial hair sprays. The purposes of this investigation were to develop a simplified, improved version of the perfused isolated guinea pig lung and to employ it as a model by which responses to the administration of a cosmetic constituent (polyethylene glycol 400) could be monitored to determine whether or not it alters pulmonary dynamics.

EXPERIMENTAL

Lung Chamber and Perfusion Apparatus—A modified method of Bhattacharya and Delaunois (7) was used for perfusion of the isolated guinea pig lung. The apparatus that housed the lungs consisted of a cylindrical Plexiglas chamber, 16 cm high and 11 cm wide. Resting within the chamber on three pegs, cemented to and situated in a triangular pattern around the inner wall, was a Plexiglas funnel with its bottom located directly above a glass mason jar. The top of the jar was screwed into the bottom of the chamber with a single hollow nylon nut and bolt.

A Plexiglas elbow and connecting tube, cemented to the exterior bottom of the chamber, led from the inside to the outside through a small hole in the chamber floor. The base of a three-way tube was connected to the outside Plexiglas tube of the elbow. One side of the three-way tube led into a calibrated mercury manometer[1]; the other side was conected to a second three-way tube, which had its base ttached to the expiration outlet of a small animal respirator[2]. The other side of the second three-way tube was connected to the air intake valve of a vacuum pump[3] (Fig. 1).

The chamber's upper end was closed with a Plexiglas plate. A piece of polyethylene tubing[4] that served as the perfusion cannula was passed through a small opening in the top of the chamber. The other end of the tubing was attached to a metal needle (20 gauge), which had the male end of a three-way valve inserted into its base. This valve served as an injection port through which test materials were administered into the pulmonary arterial vasculature of the isolated guinea pig lung.

Perfusion of the pulmonary vasculature was accomplished *via* a solid-state veristaltic pump[5]. It pumped aerated Tyrode solution from

[1] Fisher Scientific Co., Springfield, N.J.
[2] Model V5KG, E&M Instrument Co., Houston, Tex.
[3] Model 0211V45F, Gast Manufacturing Corp., Benton Harbor, Mich.
[4] PE-60 (0.08 cm i.d., 0.12 cm o.d.), Clay Adams, Becton, Dickinson and Co., Parsippany, N.J.
[5] Portable combination pressure/vacuum pump (model 0211-V45F. G8CX), Manostat Corp., New York, N.Y.

0022-3549/78/0700/1002$01.00/0
© 1978, American Pharmaceutical Association

(6) E. L. Eliel, N. L. Allinger, S. J. Angyal, and G. A. Morrison, "Conformational Analysis," Interscience, New York, N.Y., 1967, pp. 180, 181.

(7) M. Hanack, "Conformation Theory," Academic, New York, N.Y., 1965, p. 322.

(8) G. H. Loew and D. S. Berkowitz, *J. Med. Chem.*, **18**, 656 (1975).

(9) P. J. Crowley, M. J. T. Robinson, and M. G. Ward, *Tetrahedron*, **33**, 915 (1977).

(10) E. L. Eliel, N. L. Allinger, S. J. Angyal, and G. A. Morrison, "Conformational Analysis," Interscience, New York, N.Y., 1967, pp. 244–248.

(11) *Ibid.*, pp. 207, 208.

(12) K. von Bredow, H. Friebolin, and S. Kabuss, in "Conformational Analysis, Scope and Present Limitations," vol. 21, G. Chiurdoglu, Ed., Organic Chemistry, A Series of Monographs, Academic, New York, N.Y., 1971, pp. 51–54.

(13) W. F. Michne, R. L. Salsbury, and S. J. Michalec, *J. Med. Chem.*, **20**, 682 (1977), and references cited therein.

ACKNOWLEDGMENTS

Presented at the national meeting of the American Chemical Society, Chicago, Ill., 1977, Abstract 31 (Medicinal Chemistry).

Supported in part by the University Research Foundation, La Jolla, Calif.

The author is grateful to Dr. Cal Y. Meyers for fruitful discussions and editorial help and to Dr. William F. Michne and Dr. Ernest L. Eliel for valuable suggestions.

Modified Technique Using Perfused Isolated Guinea Pig Lung to Determine Effect of an Aerosol Constituent on Pulmonary Dynamics

ANDREW G. CLAIR and MICHAEL A. BARLETTA ˣ

Received August 5, 1977, from the *Department of Pharmaceutical Sciences, College of Pharmacy and Allied Health Professions, St. John's University, Jamaica, NY 11439.* Accepted for publication November 10, 1977.

Abstract □ Polyethylene glycol 400, a commonly used plasticizer in many cosmetic aerosol hair sprays, was tested to determine its effect on perfusion pressure, perfusion vascular flow rate, and tidal volume in the perfused isolated guinea pig lung. Negative pressure was maintained within the chamber housing the intact lungs, and initial perfusion of the pulmonary vasculature was accomplished *via* the right side of the heart *in situ* after guinea pigs were sacrificed by decapitation. Polyethylene glycol 400 was injected into the pulmonary arterial system in doses of 0.01–30 μg/ml after pretreatment with isoproterenol (1 μg/ml). Isoproterenol was then readministered, followed by nebulized doses of the cosmetic chemical into the trachea at 0.3, 3, and 30% concentrations. Nebulized polyethylene glycol 400 was also administered in 50, 70, and 90% concentrations. Polyethylene glycol 400 significantly increased perfusion pressure and flow rate after injection into the pulmonary arterial system of the isolated lung. In addition, nebulized administration in concentrations of 0.3–30% significantly increased the perfusion flow rate; following the 50–90% nebulized doses, a significant increase in both perfusion pressure and flow rate was observed. Tidal volume decreased, regardless of the route of administration, as increasing doses of the cosmetic constituent were delivered to the isolated lung.

Keyphrases □ Polyethylene glycol 400—effect on pulmonary dynamics in perfused isolated guinea pig lung □ Pulmonary dynamics—effect of polyethylene glycol 400 in perfused isolated guinea pig lung □ Aerosol constituents—polyethylene glycol 400, effect on pulmonary dynamics in perfused isolated guinea pig lung

The relation between inhalation of airborne particles and pulmonary disease has been known for some time (1). Numerous cases of pulmonary thesaurosis were attributed to the inhalation of cosmetic hair sprays, although the question of whether cosmetic aerosols actually cause pulmonary disease is still controversial (2–5). Zuskin and Bouhoys (6) observed, under controlled experimental conditions, that short lasting and significant decreases in the air expiratory flow rate from the lung occurred following acute exposures to various commercial hair sprays. The purposes of this investigation were to develop a simplified, improved version of the perfused isolated guinea pig lung and to employ it as a model by which responses to the administration of a cosmetic constituent (polyethylene glycol 400) could be monitored to determine whether or not it alters pulmonary dynamics.

EXPERIMENTAL

Lung Chamber and Perfusion Apparatus—A modified method of Bhattacharya and Delaunois (7) was used for perfusion of the isolated guinea pig lung. The apparatus that housed the lungs consisted of a cylindrical Plexiglas chamber, 16 cm high and 11 cm wide. Resting within the chamber on three pegs, cemented to and situated in a triangular pattern around the inner wall, was a Plexiglas funnel with its bottom located directly above a glass mason jar. The top of the jar was screwed into the bottom of the chamber with a single hollow nylon nut and bolt.

A Plexiglas elbow and connecting tube, cemented to the exterior bottom of the chamber, led from the inside to the outside through a small hole in the chamber floor. The base of a three-way tube was connected to the outside Plexiglas tube of the elbow. One side of the three-way tube led into a calibrated mercury manometer[1]; the other side was conected to a second three-way tube, which had its base ttached to the expiration outlet of a small animal respirator[2]. The other side of the second three-way tube was connected to the air intake valve of a vacuum pump[3] (Fig. 1).

The chamber's upper end was closed with a Plexiglas plate. A piece of polyethylene tubing[4] that served as the perfusion cannula was passed through a small opening in the top of the chamber. The other end of the tubing was attached to a metal needle (20 gauge), which had the male end of a three-way valve inserted into its base. This valve served as an injection port through which test materials were administered into the pulmonary arterial vasculature of the isolated guinea pig lung.

Perfusion of the pulmonary vasculature was accomplished *via* a solid-state veristaltic pump[5]. It pumped aerated Tyrode solution from

[1] Fisher Scientific Co., Springfield, N.J.
[2] Model V5KG, E&M Instrument Co., Houston, Tex.
[3] Model 0211V45F, Gast Manufacturing Corp., Benton Harbor, Mich.
[4] PE-60 (0.08 cm i.d., 0.12 cm o.d.), Clay Adams, Becton, Dickinson and Co., Parsippany, N.J.
[5] Portable combination pressure/vacuum pump (model 0211-V45F. G8CX), Manostat Corp., New York, N.Y.

0022-3549/78/0700/1002$01.00/0
© 1978, American Pharmaceutical Association

Table I—Mean Perfusion Pressure, Flow Rate, and Tidal Volume Expressed as a Percentage of the Control [a] following Intrapulmonary Injection of Polyethylene Glycol 400

	Dose, μg/ml							
	0.01	0.03	0.1	0.3	1	3	10	30
Lungs per experiment [b]	10	10	10	10	10	10	10	9
Perfusion pressure	100.4 ± 4.0 [c]	101.0 ± 4.0	103.0 ± 5.0	111.1 ± 4.1 [d]	114.2 ± 3.0 [e]	117.0 ± 4.0 [e]	119.0 ± 4.0 [e]	124.4 ± 6.0 [e]
Flow rate	102.4 ± 6.0	112.0 ± 8.2	123.0 ± 9.0 [d]	126.0 ± 11.0 [d]	142.0 ± 12.0 [e]	148.4 ± 14.0 [e]	157.0 ± 13.0 [e]	159.4 ± 15.0 [e]
Tidal volume	102.2 ± 4.3	102.4 ± 5.0	103.0 ± 5.0	100.0 ± 5.4	96.0 ± 7.0	91.3 ± 10.0	84.4 ± 10.0	85.2 ± 5.0 [e]

[a] (Final value at each dose/control value) × 100. [b] Lungs pretreated with intrapulmonary injection of 1 μg of isoproterenol/ml. [c] Mean percentage value ± *SEM*. [d] $p < 0.05$. [e] $p < 0.01$.

a bottle maintained in a water bath at 37° past both a pressure transducer[6] and flowmeter[7]. The components of the Tyrode solution (8), in grams per liter, were: sodium chloride, 8.0; potassium chloride, 0.2; magnesium chloride, 0.1; calcium chloride, 0.2; monobasic sodium phosphate, 0.05; sodium carbonate, 1.0; and glucose, 1.0. With the addition of povidone, the Tyrode solution simulated the osmotic pressure of guinea pig serum, previously determined to be 291 mosmoles. Upon exiting from the flowmeter, the fluid flowed through the metal needle before entering the chamber, which was situated in another 37° water bath (Fig. 2).

A central nylon tube and polyethylene cannula protruded downward into the chamber, and the trachea of the isolated lung was sutured onto the polyethylene tube. In passing through the central opening in the top of the chamber, the tracheal cannula bisected a flattened Plexiglas doughnut-shaped structure cemented to its inside. It was continuous with the outside through a hole in the top of the chamber, and into this opening was inserted one end of a length of tubing with a three-way valve attached to its other end. A 10-ml syringe was placed into the injection port of the valve. Encircling the lower edge of the doughnut-shaped structure were 55 pinholes, each having a depth of approximately 0.15 cm, which served as a sprinkler system to moisten the lung continuously during the experiment.

A four-pronged Plexiglas fitting was connected to the upper exposed portion of the nylon tracheal cannula. The fitting was divided by a three-way nylon tube; it ran perpendicular to the chamber and had a small opening located directly above the tracheal cannula. One of the bifurcated ends of the tube was clamped closed, and the other end had an open-ended male adapter[8] attached to it. The base of the three-way tube was connected to one end of a U tube, while the other end of the tube led into a pressure transducer permanently set to the calibration position. Four milliliters of water, always in contact with the transducer, lined the U; the distal portion of tubing was connected to the Plexiglas fitting on top of the chamber. Approximately 18 cm left in the tubing served as pulmonary "dead space" for expired air leaving the lung.

The last projection of the Plexiglas piece extended straight up and was directly in line with the opening in the nylon three-way tube and the tracheal cannula. The ejection outlet of a nebulizer[9] was connected, *via* tubing, to the Plexiglas projection. When the nebulizer was not in operation, a hemostat clamped the tubing closed just above the end of the Plexiglas extension. An air compressor[10] interfaced with an automatic timer[11] enabled the cosmetic chemical to be administered in nebulized form into the respiratory tract of the isolated lung.

Operative Procedure—Male English short hair guinea pigs[12], 800–1200 g and approximately 10 months old, were sacrificed by decapitation and allowed to exsanguinate. A midline incision was made from the abdomen to the cervical region, and the skin was retracted. The diaphragm was then separated from the distal end of the rib cage, and the sternum was removed to expose the heart. The heart was transversely cut in half, and the perfusion cannula was inserted into the pulmonary artery through the right ventricle.

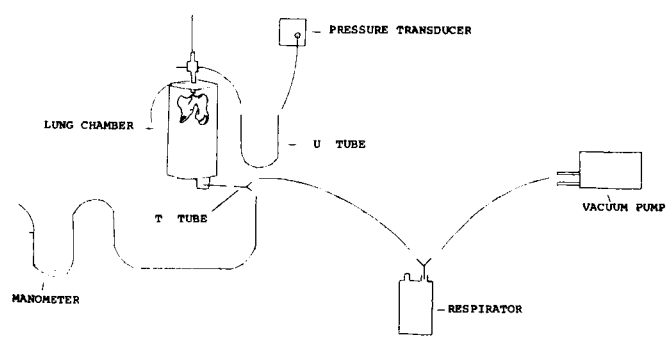

Figure 1—*Withdrawal of air from lung chamber.*

The cannula was then connected to an inverted bottle containing modified Tyrode solution and suspended above the guinea pig to allow for initial *in situ* perfusion of the lung. By blunt dissection, the trachea was isolated and the intact lung was gently lifted and removed from all body connections. The preparation was then placed on a dissecting tray, and the tracheal cannula was inserted into the air passage of the isolated lung. Initial *in situ* perfusion times averaged 200 sec, and the total time for complete removal of the tissue never exceeded 15 min from the time of decapitation.

The nylon end of the tracheal cannula was passed through the central opening in the chamber's top, which was then joined to the main body of the chamber with the double-cannulated lung suspended inside. The perfusion cannula and tracheal cannula were connected to the metal 20-gauge needle and four-pronged fitting, respectively, and the chamber was three-quarters submerged within the water bath.

Treatment—Ten lungs were initially administered 1 ml of a 1-μg/ml solution of isoproterenol[13] into the pulmonary artery, followed by intrapulmonary injections of polyethylene glycol 400[14] in doses of 0.01, 0.03, 0.1, 0.3, 1, 3, 10, and 30 μg/ml (1 ml injected/dose). Following the final intrapulmonary injections of polyethylene glycol 400, 1 ml of a 1-μg/ml solution of isoproterenol was reinjected into the pulmonary artery of the same lung. This injection was followed by three consecutive and separate 10-sec sprays of the cosmetic chemical, in concentrations of 0.3, 3, and 30%, into the trachea of the isolated lung. The air flow rate of the nebulizer was 2.5 liters/min, and it delivered approximately 0.006 g of test material into the lung during a single 10-sec period.

Six lungs were administered 1 ml of a 1-μg/ml solution of isoproterenol into the pulmonary artery, followed by a single 20-sec nebulized administration of polyethylene glycol 400 into the trachea of the lung in concentrations of 50, 70, and 90%.

Throughout any experiment, perfusion pressure and tidal volume were monitored on a physiograph[6]. The pulmonary vascular flow rate was recorded using the flowmeter.

Apparatus Operation—The veristaltic pump, which delivered the perfusion solution to the pulmonary vasculature, was operated at 20–30 mm Hg. As soon as a clear perfusate dripped from the left side of the heart onto the funnel within the chamber, the respirator was switched on. It was used at a setting of 30 ventilations/min with the inspiration to expiration ratio set at 1:1. The vacuum pump was utilized to produce negative alternating pressure within the chamber, simulating intrathoracic pressure, as recorded *via* the mercury manometer. The respirator,

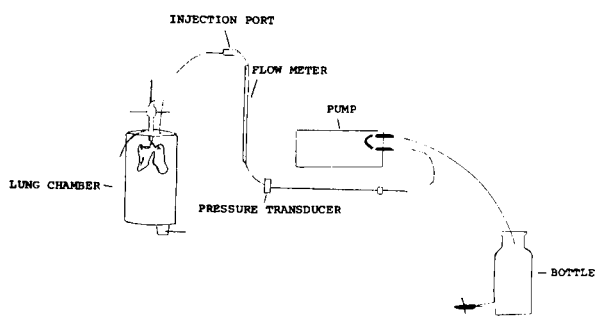

Figure 2—*Path of perfusing solution to lung chamber.*

[6] Narco Biosystems, Houston, Tex.
[7] Roger Gilmont Instruments, Great Neck, N.Y.
[8] Type A, Clay Adams, Becton, Dickinson and Co., Parsippany, N.J.
[9] No. 841 (particle diameter of 1–5 μm), DeVilbiss Co., Somerset, Pa.
[10] Type 501, DeVilbiss Co., Sommerset, Pa.
[11] Universal timer, Dimco-Gray Co., Dayton, Ohio.
[12] Camm Research Institute, Wayne, N.J.
[13] Lot 18123, Vitarine Co., New York, N.Y.
[14] Lot 1043JK, Ruger Chemical Co., New York, N.Y.

Table II—Mean Perfusion Pressure, Flow Rate, and Tidal Volume Expressed as a Percentage of the Control [a] following Nebulized Administration of Polyethylene Glycol 400

	Dose		
	0.3%	3%	30%
Lungs per experiment[c]	10	10	9
Perfusion pressure	99.4 ± 4.0[d]	103.0 ± 6.0	109.0 ± 7.0
Flow rate	99.4 ± 3.0[e]	107.0 ± 4.0[e]	120.1 ± 6.0[f]
Tidal volume	117.0 ± 11.2	115.0 ± 14.2	104.0 ± 17.4

[a] (Final value at each dose/control value) × 100. [b] All results represent the average of three responses. [c] Lungs previously exposed to intrapulmonary injections of polyethylene glycol 400. [d] Mean percentage value ± *SEM*. [e] $p < 0.05$. [f] $p < 0.01$.

Table III—Mean Perfusion Pressure, Flow Rate, and Tidal Volume Expressed as a Percentage of the Control [a] following Nebulized Administration of Polyethylene Glycol 400

	Dose		
	50%	70%	90%
Lungs per experiment[b]	6	6	6
Perfusion pressure	111.3 ± 2.4[c,d]	120.0 ± 6.0[d]	127.0 ± 7.1[d]
Flow rate	111.0 ± 3.0[d]	124.0 ± 5.0[d]	131.3 ± 7.0[d]
Tidal volume	92.1 ± 6.0	96.3 ± 6.2	91.1 ± 8.0

[a] (Final value at each dose/control value) × 100. [b] Lungs pretreated with intrapulmonary injection of 1 μg of isoproterenol/ml. [c] Mean percentage value ± *SEM*. [d] < 0.01.

therefore, served only to stop momentarily the continuous withdrawal of air from the chamber.

In this manner, the lung was able to expand noticeably (as negative pressure within the chamber forced atmospheric air into the lung *via* the adapter located on the four-pronged Plexiglas fitting) and collapse (as the respirator "cut" the continuous evacuation of chamber air). The lung ventilated at a rate dictated by the setting on the respirator, and expired air from the lung was diverted into the water-filled conduit of the U tube.

RESULTS

As a result of the polyethylene glycol 400 injections into the isolated guinea pig lungs, both perfusion pressure and flow rate significantly increased (Table I). Tidal volume decreased approximately 15% in comparison with the control, although it initially increased as a result of the chemical treatment. The flow rate increase was considerably more than that of the increase observed with perfusion pressure.

Nebulized polyethylene glycol 400, delivered into the respiratory tract in a concentration of 0.3–30%, significantly increased the perfusion flow rate (Table II). Perfusion pressure and tidal volume increased and decreased, respectively, as a result of the administrations. The percent decrease in tidal volume never fell below the control value; however, the 30% dosage level response undoubtedly represents a pneumoconstricting reaction since a chemically induced increase in tidal volume (observed after the 0.3 and 3% doses) might be explained on the basis of air entering into and stretching the lung tissue during the nebulizer administration process. Thus, any decrease in tidal volume may be attributed solely to the action of nebulized polyethylene glycol 400 within the airways of the lungs.

The nebulized polyethylene glycol 400 treatment at concentrations of 50–90% magnified those results observed at the lower dosage level (Table III). Perfusion pressure and flow rate both significantly increased, while tidal volume showed a consistent drop, below control values, as a result of the administrations.

DISCUSSION

Data presented here demonstrate that polyethylene glycol 400, when administered into either the arterial or bronchial system of the isolated guinea pig lung, is capable of altering pulmonary dynamics. Such changes may be indicative of one of three factors:

1. The chemical's viscous characteristics, which would tend to "coat" the arterial vessels of the isolated lung or to block the bronchial airways, depending on the route of administration.
2. The chemical's pharmacological activity.
3. The chemical's ability to cause the release of histamine from the connective tissue spaces of the lung or pulmonary circulation.

The third possibility may best explain the observed results. Murray (9) summarized the fate of several vasoactive substances in the pulmonary circulation of experimental animals and found that histamine was not effectively removed or inactivated by the lung. Because these findings hold true in perfusion studies as well, it is conceivable that the cosmetic constituent triggers the release of active histamine from depots in the isolated lung. Histamine and histamine-like effects may explain simultaneously the bronchial and vascular responses observed in the isolated lungs after polyethylene glycol 400 administration. Since overall, in this study, tidal volume consistently decreased, regardless of the route of administration of polyethylene glycol 400, and perfusion pressure and flow rate both increased, histamine's ability to produce constriction of the airways as well as vascular dilatation (in small vessels) and constriction (in large vessels) could be responsible.

It is important to consider, however, that decreases in tidal volume as a result of polyethylene glycol 400 injections into the pulmonary artery represent changes at the alveoli, since the perfusing solution is directed toward them and not the bronchi (10). In addition, because the nebulized particles of the polyethylene glycol 400 sprays are impacted onto the walls of the trachea and are, therefore, not deposited into the airways of the isolated lung, the nebulized effect in comparison to the injected responses is diminished.

As for the other two considerations, the glycols are generally not considered to be pharmacologically toxic (11) and the physical nature of polyethylene glycol 400 probably plays only a minor role, if any, in altering pulmonary dynamics. The findings of Zuskin and Bouhoys (6), noted previously, were postulated to be the result of histamine-induced release caused by cosmetic hair spray exposure; the present results support their supposition. In addition, this modified technique for perfusion of the isolated guinea pig lung apparently offers a simple yet sensitive method by which any agent may be tested for its effect on pulmonary dynamics.

REFERENCES

(1) B. Stuart, *Arch. Int. Med.*, **131**, 60 (1973).

(2) I. Greenfield, *Lancet*, **2**, 412 (1959).

(3) W. K. Morgan, *ibid.*, **2**, 412 (1959).

(4) L. Leonard, *ibid.*, **2**, 412 (1959).

(5) M. Brunner, *J. Am. Med. Assoc.*, **176**, 1055 (1961).

(6) E. Zuskin and A. Bouhoys, *N. Engl. J. Med.*, **290**, 660 (1974).

(7) B. K. Bhattacharya and A. L. Delaunois, *Arch. Int. Pharmacodyn. Ther.*, **101**, 495 (1955).

(8) W. L. M. Perry, "Pharmacological Experiments on Isolated Preparations," 2nd ed., Churchill Livingstone, London, England, 1970, p. 152.

(9) J. F. Murray, "The Normal Lung," Saunders, Philadelphia, Pa., 1976, p. 146.

(10) L. Dautrebande, "Microaerosols," Academic, New York, N.Y., 1962, p. 201.

(11) "The Pharmacological Basis of Therapeutics," 5th ed., L. S. Goodman and A. Gilman, Eds., Macmillan, New York, N.Y., 1975, p. 947.

ACKNOWLEDGMENTS

Presented in part at the Federation of American Societies for Experimental Biology, Chicago meeting, April 1977.

Study of Drug–Protein Binding by Affinity Chromatography: Interaction of Bovine Serum Albumin and Salicylic Acid

NAOMI I. NAKANO ˣ, TAKAYUKI OSHIO, YUKIO FUJIMOTO, and TAKASHI AMIYA

Received March 22, 1977, from *Hokkaido Institute of Pharmaceutical Sciences, Otaru, Japan.* Accepted for publication November 9, 1977.

Abstract □ The affinity chromatographic technique was used to study the interaction of bovine serum albumin and salicylic acid at 3.3 ± 1.1°. Beaded agarose gel, on which the albumin was immobilized by covalent linkage, was packed in a column as an affinity adsorbent. Frontal analysis was performed on this column to evaluate the binding parameters for the interaction. The effect of albumin immobilization on drug binding was investigated by comparing the binding parameters of two affinity adsorbents, directly coupled albumin and albumin coupled through a spacer arm. The latter mode of attachment gave binding characteristics comparable to those of the soluble albumin. The method is simple and precise. The affinity adsorbent can be used repeatedly for many months for various drugs, including those that do not diffuse through dialysis membranes.

Keyphrases □ Salicylic acid—binding to bovine serum albumin, affinity chromatographic study □ Binding, protein—salicylic acid to bovine serum albumin, affinity chromatographic study □ Chromatography, affinity—study of binding of salicylic acid to bovine serum albumin □ Keratolytic agents—salicylic acid, binding to bovine serum albumin, affinity chromatographic study

The interaction of drugs with serum albumin is well known, and its consequences are manifested in various aspects of drug disposition. Recently, it was observed that the displacement of a bound drug from albumin by another drug can have profound pharmacological and toxicological effects in multiple drug therapy (1, 2). The methods of quantitating serum protein binding are numerous (3, 4), but a simple and direct procedure particularly suitable for systems containing more than one drug is not available. The development of such a method through the affinity chromatographic technique was initiated by studying serum albumin–single drug interactions. This report describes the application of this technique for studying interactions of bovine serum albumin and salicylic acid and the evaluation of affinity adsorbents.

The present method differs from gel filtration (5, 6) or other methods (7) employing gel beads in that the protein is immobilized on a gel matrix through covalent linkage and packed in a chromatographic column as an adsorbent; a drug in an appropriate buffer is passed through the column. In gel filtration, the gel is employed to exclude the protein molecule from the gel matrix. Similar use of affinity columns was described previously (8, 9). The interaction between an enzyme and its inhibitor was studied by immobilization of the small inhibitor molecules on a gel matrix. Bovine serum albumin immobilized on agarose was employed in a batchwise procedure in competition with free protein to evaluate the binding parameters for the interactions of hydrocortisone, bilirubin, fatty acids, and tryptophan with several proteins or protein fragments (10).

Although affinity chromatography by means of immobilized albumin has not been employed in quantitative investigations of drug–protein interactions, these interactions were utilized to separate or isolate substances. DL-Tryptophan was resolved successfully on an albumin–agarose column on the basis of differences in the binding of the two optical isomers to albumin (11). The isolation of albumin from serum also was attempted by passing serum samples through a column of affinity adsorbents prepared by coupling to agarose substances known to interact strongly with albumin, such as a dye (12), fatty acids (13), and bilirubin (14).

EXPERIMENTAL

Materials—Agarose[1], bovine serum albumin[2], salicylic acid[3] (recrystallized from hot water), 6-aminohexanoic acid[3], cyanogen bromide[3], sodium azide[3], and *N*-ethyl-*N*-(3-dimethylaminopropyl)carbodiimide hydrochloride[4] were used. Chemicals in the buffer solutions were reagent grade. Water was deionized and double distilled, with the second distillation performed in an all-glass apparatus. Cellulose tubing[5] was used for the equilibrium dialysis study.

Immobilization of Albumin to Agarose—Bovine serum albumin directly coupled to cyanogen bromide-activated agarose (Affinity Adsorbent I) was prepared according to the general method of Axén and Ernback (15). The activation of agarose was carried out at pH 11 for 6 min, and approximately 50 ml of the activated gel was coupled with 2 g of bovine serum albumin at about 3° overnight under constant shaking. The reaction mixture was filtered and extensively washed with 0.1 *M* $NaHCO_3$.

The gel was suspended in 100 ml of 1 *M* ethanolamine hydrochloride (pH 9.4) for 2 hr at room temperature to block the unreacted active groups and packed into a glass column. It was then washed thoroughly to remove the adsorbed albumin with 0.025 *M* $Na_2B_4O_7$–acetic acid containing 1 *M* NaCl (pH 8.5), followed by 0.1 *M* acetate buffer containing 1 *M* NaCl (pH 4.1) and, finally, 0.1 *M* CH_3COONa at the maximum flow rate of the column under gravity.

Bovine serum albumin coupled to cyanogen bromide-activated agarose through a six-carbon-atom spacer (Affinity Adsorbent II) was prepared according to the Kaufman method (16) for the preparation of methotrexate–aminohexylagarose; 50 ml of the cyanogen bromide-activated agarose was reacted with 100 ml of a solution of 0.5 *M* 6-aminohexanoic acid and 0.5 *M* NaCl (pH adjusted to 10 with 2 *N* NaOH) at about 3° for 16 hr. The spacer arm coupled agarose (carboxypentylagarose[6]) thus obtained was extensively washed, and the unreacted groups were blocked as described previously.

After exhaustive washing with 1 *M* HCl, water, 1 *M* NaOH, and then water, the gel was reacted with 1 g of albumin at pH 4.5 in the presence of 0.5 g of the carbodiimide hydrochloride for 16 hr at room temperature. Affinity Adsorbent II thus prepared was subjected to the same treatment as described for Affinity Adsorbent I.

Assay of Coupled Albumin—The determination of the albumin immobilized per milliliter of gravity-packed Affinity Adsorbents I and II was carried out by direct spectrophotometry (17) at 278 nm. An aliquot of adsorbent gel suspension was gravity packed into a previously weighed and graduated column equipped with a sintered-glass disk (G3) to determine the volume of the packed gel under normal column packing. This volume of adsorbent was either dried directly in the column with water–acetone mixtures, as described by Axén and Ernback (15), or freeze

[1] Sepharose 4B, Pharmacia Fine Chemicals, Uppsala, Sweden.
[2] Fraction V, powder lot 243, Miles Laboratories, Elkhart, Ind.
[3] Wako Pure Chemical Industries, Osaka, Japan.
[4] Fluka AG, Buchs SG, Switzerland.
[5] Visking cellulose tubing, size 18/32, Union Carbide Corp., Chicago, Ill.
[6] Carboxypentylagarose is also available under the name CH-Sepharose from Pharmacia Fine Chemicals, Uppsala, Sweden.

0022-3549/78/0700/1005$01.00/0
© 1978, American Pharmaceutical Association

Table I—Column Characteristics

Column	Affinity Adsorbent	Column Dimensions, i.d. × height, cm	Gel Volume, ml	Bovine Serum Albumin, mg/ml of gel	Flow Rate, ml/hr
1	I	0.98 × 29.2	22.0	4.2	4–12
2	I	1.60 × 10.8	21.7	4.1	5.0 or 11.0
3	II	0.79 × 20.1	9.8	8.6	6.6
4	II	0.96 × 27.0	19.6	8.6	6.0
5	II	1.60 × 11.5	23.1	8.6	5.6 or 11.4

dried to determine the corresponding dry weight. Approximately 10 mg of the dried adsorbent was weighed directly into a 1-cm cell and suspended in 3 ml of 50% glycerin.

The turbidity due to the gel beads was balanced at 350 nm against agarose or carboxypentylagarose beads in the reference cell compartment of the spectrophotometer[7] (cells were positioned directly in front of the photomultiplier). Then the difference spectrum was recorded and showed no difference from the spectrum of an albumin solution. A molecular weight of 66,210 (18) was used for bovine serum albumin.

Affinity Chromatography by Frontal Analysis—The column characteristics are listed in Table I. The columns were preequilibrated in a cold room (3.3 ± 1.1°), with buffer flowing for at least 24 hr before the experiment. The buffer employed throughout the binding study was 0.05 *M* tromethamine [tris(hydroxymethyl)aminomethane] containing 0.1 *M* NaCl at pH 7.40 (ionic strength of $\mu = 0.142$). A solution of salicylic acid in the buffer containing 0.004% NaN_3 was applied to a column continuously either by gravity flow or a peristaltic pump[8], and the eluate was collected in 1–6-ml fractions[9], depending on the concentration of salicylic acid, until the concentration in the eluate fractions reached that of the applied solution.

The amount of the drug adsorbed, D_b, by the total amount of albumin immobilized in the column was determined by the equation $D_b = [D_0](V - V_0)$, where $[D_0]$ is the concentration of the drug applied to the column and V_0 and V are eluted volumes of 0.004% NaN_3 and the drug, respectively. The latter values were obtained from the frontal chromatogram as the volumes of eluate corresponding to the concentrations that reached 50% of those of the applied solution. The concentrations of the drug and sodium azide were determined spectrophotometrically[7] at 295 and 247 nm, respectively.

Equilibrium Dialysis—The dialysis tubing was pretreated for 30 min in hot 8% Na_2CO_3 (19) and washed thoroughly with water. Dialysis bags were made from the tubing and soaked in water for about 48 hr at refrigerative temperature. Water was replaced several times during this period until no significant UV absorbance (λ 360–250 nm) was detected. Finally, the bags were soaked and rinsed with the buffer containing 0.004% NaN_3.

Dialysis studies were carried out under the same conditions as the affinity chromatographic studies, using the soluble albumin instead of the immobilized one. Thus, 0.004% NaN_3 was incorporated in the buffer, and experiments were performed at two albumin concentrations (0.45 and 0.8%), corresponding approximately to those of Affinity Adsorbents I and II, respectively. The solution containing the albumin and the drug (5 ml) was placed inside the bag and dialyzed against 50 ml of the buffer system in a 100-ml erlenmeyer flask.

Dialysis was allowed to proceed at 3.3 ± 1.1° for about 16–24 hr under agitation of both the inside and outside solutions by magnetic bars. A small magnetic bar (0.3 × 1.0 cm) was placed inside each bag. Care was taken to arrange the flask on a magnetic stirrer so that neither magnetic bar excessively touched the bag during movement.

The concentration of salicylic acid outside the bag was determined spectrophotometrically at 295 nm. Blank studies with the buffer system alone showed that the absorbance at 295 nm outside of the bag increased by at most 0.003 over that of the buffer system during the equilibration period of over 20 hr, and correction was made for this factor. When the albumin was placed alone inside the bag, no substance that interfered with the salicylic acid assay was dialyzed out of the bag.

Data Analysis—Binding data of a small molecule to a macromolecule are often analyzed according to (20):

$$r = \sum_{i=1}^{m} \frac{n_i K_i [D_0]}{1 + K_i [D_0]} \qquad \text{(Eq. 1)}$$

where r is the molar ratio of bound drug, D_b, to total protein, P_t; n_i is the number of binding sites in the ith class; K_i is the intrinsic binding constant for the sites in the ith class; and $[D_0]$ is the concentration of unbound (free) drug.

For only one class of n binding sites, Eq. 1 reduces to:

$$r = \frac{nK[D_0]}{1 + K[D_0]} \qquad \text{(Eq. 2)}$$

and Eq. 2 is often transformed to the following familiar Scatchard equation (21):

$$\frac{r}{[D_0]} = Kn - Kr \qquad \text{(Eq. 3)}$$

Substituting $(V - V_0)[D_0]/P_t$ for r in the reciprocal of Eq. 2 yields:

$$\frac{1}{(V - V_0)} = \frac{1}{nKP_t} + \frac{1}{nP_t}[D_0] \qquad \text{(Eq. 4)}$$

This form for the value of D_b relates directly to the affinity chromatography frontal analysis data. Thus, a plot of $1/(V - V_o)$ *versus* $[D_0]$ should be linear. The binding constant, K, can be determined from the slope and ordinate intercept of the straight line, and n can be determined from the slope if P_t is known.

When this plot or a plot according to Eq. 3 does not give a straight line, the existence of multiple classes of sites on a protein molecule is assumed and the extrapolation of a Scatchard plot curve to the abscissa and ordinate allows estimation of $\Sigma_{i=1}^{m} n_i$ and $\Sigma_{i=1}^{m} K_i n_i$, respectively (22).

Resolution of K_i and n_i is usually attempted on the assumption that there exist only two classes of sites; K_1, K_2, n_1, and n_2 are calculated by a nonlinear least-squares fit by computer (23). Since this assumption is made only for convenience, in this report the graphically obtainable quantity, $\Sigma_{i=1}^{m} K_i n_i$, the total binding capacity (10), is reported either from the extrapolation of the plots of $r/[D_0]$ *versus* r to the ordinate or from the intercept of the plots of $1/(V - V_0)$ *versus* $[D_0]$ and P_t. The apparent K_1 (app K_1) and n_1 (app n_1) values also were obtained from the limiting linear portions of the plots according to Eqs. 3 and 4 for comparison only.

RESULTS AND DISCUSSION

Concentration-Dependent Elution Profiles—Figure 1 shows typical elution profiles of sodium azide and salicylic acid when salicylic acid solutions of varying concentrations, each containing 0.004% NaN_3, were applied to a column of Affinity Adsorbent II. These elution profiles indicated that the elution volume of 0.004% NaN_3 was independent of salicylic acid concentration but that the elution volume of salicylic acid depended on its own concentration. That the concentration-dependent

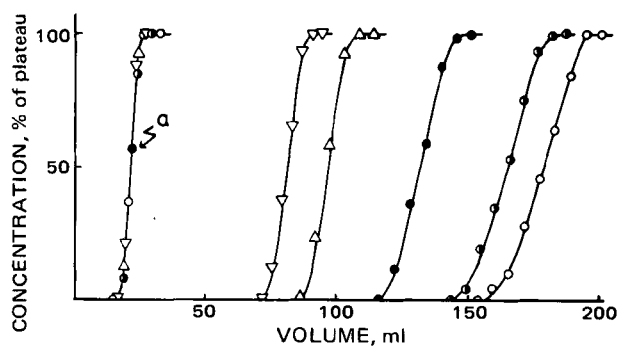

Figure 1—*Concentration-dependent elution profiles of salicylic acid from Column 4 (see Table I for the column characteristics). Key (concentrations of salicylic acid): ○, 1.07 × 10⁻⁵ M; ◑, 1.40 × 10⁻⁵ M; ●, 2.49 × 10⁻⁵ M; △, 5.04 × 10⁻⁵ M; and ▽, 7.10 × 10⁻⁵ M. Curve a is the elution profile of 0.004% NaN_3 incorporated in these salicylic acid solutions.*

[7] Double-beam spectrophotometer, model UV-300, Shimadzu Manufacturing Co., Kyoto, Japan.

[8] P-3, Pharmacia Fine Chemicals, Uppsala, Sweden, or MultiPerpex 2115, LKB, Bromma, Sweden.

[9] Fraction collector model LKB 7000A UltroRac, LKB, Bromma, Sweden, or model SF-160K, Toyo Scientific Co., Tokyo, Japan.

Table II—Binding Parameters for the Interaction of Bovine Serum Albumin with Salicylic Acid

State of Albumin	Buffer	pH	Temperature	$\Sigma K_i n_i \times 10^{-4}, M^{-1}$	app $K_1 \times 10^{-4}, M^{-1}$	app n_1	Method[a]	Reference
Immobilized (Affinity Adsorbent I)	$\mu = 0.143$[b], tromethamine	7.40	3.3 ± 1.1°	7.09	6.03	1.18	AF	This work
Immobilized (Affinity Adsorbent II)	$\mu = 0.143$[b], tromethamine	7.40	3.3 ± 1.1°	9.33	4.73	1.97	AF	This work
Soluble	$\mu = 0.143$[b], tromethamine	7.40	3.3 ± 1.1°	9.83	5.02	1.96	ED	This work
	$\mu = 0.05, 0.04$ *M* phosphate	7.4	4°	1.88[c]	2.44[c]	0.78[c]	ED	29
		7.0	25°	20.9[c]	19.1[c]	1.09[c]	DD	30
	0.016 *M* phosphate + 0.122 *M* NaCl	7.4	25°	15[d]	10[d]	1.5[d]	ED	31
	0.128 *M* phosphate	7.38	37°	5.4[c]	4.82[c]	1.12[c]	DD	32

[a] AF = affinity chromatography, ED = equilibrium dialysis, and DD = dynamic dialysis. [b] μ = ionic strength, including 0.1 *M* NaCl and 0.004% NaN_3. [c] Two classes were assumed; thus, $\Sigma K_i n_i = n_1K_1 + n_2K_2$, app $K_1 = (n_1K_1^2 + n_2K_2^2)/(n_1K_1 + n_2K_2)$, and app $n_1 = [(n_1K_1 + n_2K_2)^2]/(n_1K_1^2 + n_2K_2^2)$ (Ref. 23). [d] Estimated from Scatchard plots.

elution patterns of the drug were primarily the consequence of the specific interaction between the immobilized albumin and salicylic acid was apparent when similar drug solutions were applied to an agarose column. From the column void of albumin, salicylic acid was eluted within experimental error at the elution volume of sodium azide. A similar observation was made with a carboxypentylagarose column, indicating that the six-carbon-atom spacer also contributed little to the observed effect.

When 0.004% NaN_3 alone was applied to a column of albumin-coupled agarose, its elution volume was the same as that of 0.004% NaN_3 added to salicylate solutions of varying concentrations (Fig. 1). Even at a salicylate concentration as high as 1.0×10^{-3} *M*, the elution volume of 0.004% NaN_3 was not significantly influenced. In the absence of salicylic acid, the elution volume of sodium azide from the albumin-coupled column was independent of its concentration (0.004–0.1%). Furthermore, the elution volume of salicylic acid at a relatively low concentration of 2.17×10^{-5} *M* was not altered significantly by 0.004% NaN_3.

These observations suggest that 0.004% NaN_3 does not significantly influence the specific interaction of salicylic acid with albumin immobilized on agarose[10]. Thus, 0.004% NaN_3 was employed as an internal void volume indicator throughout these studies, because the column heights sometimes decreased suddenly for unknown reasons and settled to a constant level during continuous use for several months. The void volume here means the void volume of the column plus the volume of tubing.

Effect of Flow Rate—Investigations concerning the effect of flow rate on the elution profile on Column 5 (Table I) indicated that the elution volumes were unaffected within a range of 5–12 ml/hr, although the sigmoidal elution curve became less steep as the flow rate increased. At a flow rate of 17.6 ml/hr, elution volumes decreased only by about 1.5%, but the gradual saturation of the column was noted. With Column 1, the flow rate of which was not controlled by a peristaltic pump, elution volumes were little affected by the variation in flow rates shown in Table I.

Data Treatment—Figure 2 shows plots of $1/(V - V_0)$ *versus* $[D_0]$ according to Eq. 4 for Columns 1, 2, and 4 (Table I). Points are shown for only low $[D_0]$ data, and the straight lines correspond to the least-squares fit. It is possible to estimate app K_1 and app n_1 from such plots if P_t is known. Equation 4 is thus useful for obtaining these parameters directly from chromatographic data, *i.e.*, the elution volume and concentration of the drug applied to an affinity adsorbent column. If P_t immobilized in each column is known, data obtained from all columns can be presented in the familiar Scatchard form (Eq. 3).

The results of the determination of albumin coupled per milliliter of packed gel (Table I) reveal that nearly twice as much albumin was coupled to agarose through the spacer. Although the direct coupling was undertaken at refrigerative temperature and the carbodiimide coupling was carried out at room temperature, separate carbodiimide coupling reactions showed that the amount of albumin coupled was the same whether carried out overnight at room or refrigerative temperature. Thus, these results may indicate that the direct coupling of the albumin is considerably sterically unfavorable.

Since the total number of moles of albumin, P_t, immobilized on the column and the moles of drug bound, D_b, were known from elution data, the ratio $r = D_b/P_t$ was calculated for each free concentration of drug for all columns and plotted against $r[D_0]$ (Fig. 3). The points all converged into two separate curves, one for Affinity Adsorbent I and the other for II. Even the two different batches of Affinity Adsorbent I (Columns 1 and 2) showed the trend satisfactorily. These results indicated that the albumin coupled through the spacer bound more salicylic acid per mole of albumin than the directly coupled albumin.

Comparison with Equilibrium Dialysis Data—The equilibrium dialysis data obtained under the same conditions as for the affinity chromatographic study for two different soluble albumin concentrations, *i.e.*, one corresponding closely to the concentration of coupled albumin in the packed gel bed of Affinity Adsorbent II (0.8%) and the other corresponding to that of I (0.45%), fell close to the curve for Affinity Adsorbent II (Fig. 3).

Table II summarizes the binding parameters for the interaction of salicylic acid with bovine serum albumin. The parameters from the present studies were obtained from the straight lines drawn by the least-squares method for the linear portion ($r < 1$–1.4) of the Scatchard plots (Fig. 3). The correlation coefficients for the straight lines were greater than 0.98 for the affinity chromatographic studies and 0.96 for the equilibrium dialysis data. Apparent K_1 for Affinity Adsorbent I was greater than that for the Affinity Adsorbent II, although the total binding capacity of I was reduced by about 24% over that of II. Employing a batchwise method with bovine serum albumin directly coupled to agarose, Reed *et al.* (10) similarly noted that the tryptophan binding capacity of immobilized albumin was approximately one-tenth of that of soluble albumin but that the app K_1 was slightly higher than that for soluble albumin.

The role played by the spacer groups in affinity chromatography is largely to relieve the steric hindrance for specific interactions, thereby increasing the capacity of affinity adsorbents (24–27); six-carbon atom chains are generally considered long enough. Good agreement between the data obtained on Affinity Adsorbent II and those of equilibrium dialysis, under controlled experimental conditions, may indicate that the spacer largely eliminates the steric hindrance imposed on the directly coupled albumin and that immobilization of albumin through the spacer

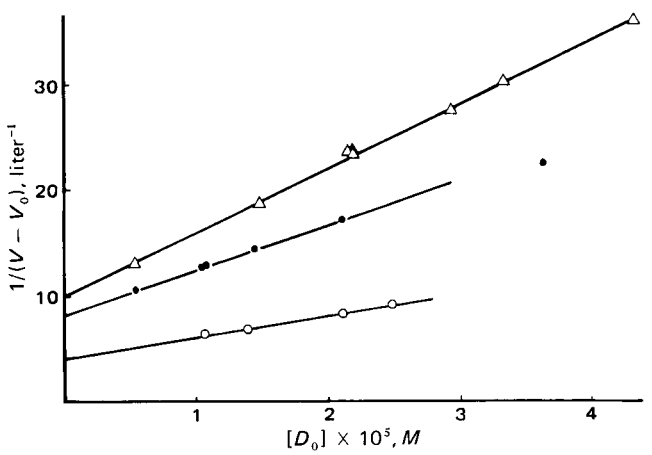

Figure 2—*Plots of* $1/(V - V_0)$ versus $[D_0]$ *according to Eq. 4. Key:* △, *Column 1;* ●, *Column 3; and* ○, *Column 4 (see Table I for the column characteristics).*

[10] This does not mean that sodium azide does not interact with the albumin. In fact, when 0.1% NaN_3 was incorporated in 2.17×10^{-5} *M* salicylic acid, the elution volume of salicylic acid decreased in comparison with that in the absence of sodium azide, indicating that sodium azide may possibly influence salicylate binding at higher concentrations. At 0.004% NaN_3, however, this effect was negligible.

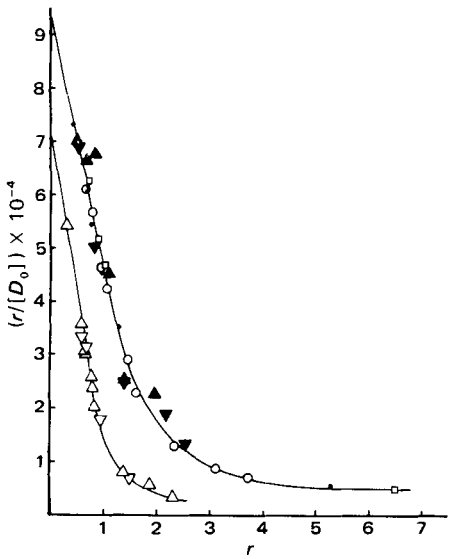

Figure 3—*Scatchard plots for the interaction of salicylic acid with bovine serum albumin at 3.3 ± 1.1°, pH 7.40, and μ = 0.143. Key for affinity chromatographic technique:* △, *Column 1;* ▽, *Column 2;* ●, *Column 3;* ○, *Column 4; and* □, *Column 5 (see Table I for the column characteristics). Key for equilibrium dialysis technique:* ▲, *0.8% bovine serum albumin; and* ▼, *0.45% bovine serum albumin.*

does not significantly impair the binding capacity of the albumin, at least toward salicylic acid.

Table II presents some previously published data for the interaction of bovine serum albumin with salicylate. In spite of the good agreement between the binding parameters obtained by this equilibrium dialysis and affinity chromatographic study employing Affinity Adsorbent II, these parameters are not in agreement with those of other workers. The present app K_1 values, for instance, are generally smaller than those of other workers when the differences in temperature at which the studies were carried out are considered. An exact comparison is not possible because binding parameters are affected not only by temperature but also by the preparation of serum albumin (28), the composition of buffer, the pH and ionic strength of the medium, *etc.* As for the preparation of albumin, the difference in the content of free fatty acids or other impurities tightly bound to albumin or other factors may be responsible for the disparity. Also, the azide incorporated in the present studies might have inhibited salicylate binding, particularly at low salicylate concentrations, although this was not obvious in the affinity chromatographic study.

CONCLUSIONS

Although the conformation on the soluble albumin may not be kept intact after immobilization on agarose, the present study demonstrated that the salicylate binding capacity was not altered significantly by immobilization, particularly through the spacer. It is not the maintenance of conformation upon immobilization that is important in this method but that the drug binding characteristics of immobilized albumin are similar to that of soluble albumin. Thus, Affinity Adsorbent II is better than I for drug binding studies by affinity chromatography. Even if the drug binding capacity is reduced upon immobilization, as with Affinity Adsorbent I, the technique would still be of value in *in vitro* comparison of affinities of drugs toward serum albumin if the degrees of reduction are the same for many drugs.

This method is simple and much more precise than the batchwise method of Reed *et al.* (10), since measurement of the volume of gel suspension, which is essential in the batchwise method, inherently introduces uncertainty about the amount of albumin present. The salicylate binding capacity of immobilized albumin was unaltered for at least 8 months under continuous use. When the columns were not in use for 1 week or more, the buffer was continuously applied at a low flow rate. During the 8 months, many drugs were applied to the columns, but subsequent elution with the buffer after each run apparently left the column unaltered. These observations support the conclusions that albumin itself and the covalent linkage between agarose and albumin are stable and that the conformation of albumin is likely to be restored each time upon elution with the buffer. Therefore, repeated use of the column renders this method economical.

Affinity chromatography facilitates the quantitation of salicylic acid binding by frontal analysis, and the salicylate binding capacity of immobilized bovine serum albumin depends on the mode of immobilization. Many other drugs were tested similarly on these columns, and the data will be published separately. Theoretically, any drug can be studied by this method, provided that the eluate can be assayed for the drug, including drugs that do not diffuse through the dialysis membrane. However, the effect of immobilization of albumin may have to be investigated for each drug. Such studies, in turn, may shed light on the sites of drug interaction on the albumin molecule.

REFERENCES

(1) R. A. O'Reilly, *Ann. N.Y. Acad. Sci.*, **226**, 293 (1973).

(2) H. M. Solomon, in "Handbook of Experimental Pharmacology," vol. 28/1, B. B. Brodie and J. R. Gillette, Eds., Springer-Verlag, Berlin, Germany, 1971, p. 234.

(3) J. Steinhardt and J. A. Reynolds, "Multiple Equilibria in Proteins," Academic, New York, N.Y., 1969, pp. 34–83.

(4) M. C. Meyer and D. E. Guttman, *J. Pharm. Sci.*, **57**, 895 (1968).

(5) J. P. Hummel and W. J. Dreyer, *Biochim. Biophys. Acta*, **63**, 530 (1962).

(6) P. F. Cooper and G. C. Wood, *J. Pharm. Pharmacol.*, **20**, 150S (1968).

(7) W. Scholtan, *Arzneim.-Forsch.*, **14**, 146 (1964).

(8) B. M. Dunn and I. M. Chaiken, *Proc. Natl. Acad. Sci. USA*, **71**, 2382 (1974).

(9) K. Kasai and S. Ishii, *J. Biochem.*, **77**, 261 (1975).

(10) R. G. Reed, T. Gates, and T. Peters, Jr., *Anal. Biochem.*, **69**, 361 (1975).

(11) K. K. Steward and R. F. Doherty, *Proc. Natl. Acad. Sci. USA*, **70**, 2850 (1973).

(12) J. Travis and R. Pannell, *Clin. Chim. Acta*, **49**, 49 (1973).

(13) T. Peters, Jr., H. Taniuchi, and C. B. Anfinsen, Jr., *J. Biol. Chem.*, **248**, 2447 (1973).

(14) M. Hierowski and R. Brodersen, *Biochim. Biophys. Acta*, **354**, 121 (1974).

(15) R. Axén and S. Ernback, *Eur. J. Biochem.*, **18**, 351 (1971).

(16) B. T. Kaufman, in "Methods in Enzymology," vol. 34, W. B. Jakoby and M. Wilchek, Eds., Academic, New York, N.Y., 1974, p. 272.

(17) A. Miyakawa and N. Okuyama, *Seikagaku*, **48**, 413 (1976).

(18) T. Peters, Jr., in "The Plasma Proteins," vol. 1, F. W. Putnum, Ed., Academic, New York, N.Y., 1975, p. 141.

(19) D. Hultmark, K. O. Borg, R. Elofsson, and L. Palmer, *Acta Pharm. Suec.*, **12**, 259 (1975).

(20) G. Scatchard, J. S. Coleman, and A. L. Shen, *J. Am. Chem. Soc.*, **79**, 12 (1957).

(21) G. Scatchard, *Ann. N.Y. Acad. Sci.*, **51**, 660 (1949).

(22) I. M. Klotz and D. L. Hunston, *Biochemistry*, **10**, 3065 (1971).

(23) J. J. Vallner, J. H. Perrin, and S. Wold, *J. Pharm. Sci.*, **65**, 1182 (1976).

(24) P. Cuatrecasas, *J. Biol. Chem.*, **245**, 3059 (1970).

(25) E. Steers, P. Cuatrecasas, and H. Polland, *ibid.*, **246**, 196 (1971).

(26) C. R. Lowe, M. J. Harvey, D. B. Craven, and P. D. G. Dean, *Biochem. J.*, **133**, 499 (1973).

(27) C. R. Lowe and P. D. G. Dean, "Affinity Chromatography," Wiley, New York, N.Y., 1974, p. 23.

(28) R. H. McMenamy, *J. Biol. Chem.*, **240**, 4235 (1965).

(29) C. Davison and P. K. Smith, *J. Pharmacol. Exp. Ther.*, **133**, 161, (1961).

(30) M. C. Meyer and D. E. Guttman, *J. Pharm. Sci.*, **59**, 39 (1970).

(31) T. E. Huntley, J. K. Neitzel, and M. K. Elson, *Biochim. Biophys. Acta*, **490**, 112 (1977).

(32) C. A. Cruze and M. C. Meyer, *J. Pharm. Sci.*, **65**, 33 (1976).

Tissue Culture Cytotoxicity Assay for Cyclophosphamide Metabolites in Rat Body Fluids

FRED A. WEAVER *, ANTHONY R. TORKELSON, WALTER A. ZYGMUNT *, and HENRY P. BROWDER

Received June 8, 1977, from the *Departments of Biologic Research, Medical Research, and Pathology and Toxicology, Mead Johnson Research Center, Evansville, IN 47721.* Accepted for publication November 9, 1977. *Present address: Bioclinical Laboratories, Inc., Evansville, IN 47714.

Abstract □ An *in vitro* cytotoxicity assay for cyclophosphamide metabolites in rat body fluids is described. Of the two tissue culture tumor *cell lines* employed, the Walker-256 rat carcinosarcoma was more sensitive to metabolite levels than the L-1210 mouse lymphocytic leukemia. The Walker-256 system detected cyclophosphamide metabolite levels two orders of magnitude lower than the commonly used 4-(*p*-nitrobenzyl)pyridine analytical procedure.

Keyphrases □ Cyclophosphamide metabolites—*in vitro* cytotoxicity analyses in rat body fluids □ Cytotoxicity—*in vitro* analyses of cyclophosphamide metabolites in rat body fluids □ Metabolites—cyclophosphamide, *in vitro* cytotoxicity analyses in rat body fluids □ Antineoplastic agents—cyclophosphamide, *in vitro* analyses of metabolites in rat body fluids

Cyclophosphamide, a widely used cancer chemotherapeutic agent, is converted to a number of metabolites by liver microsomal enzymes (1). The most commonly used procedure for measuring cyclophosphamide metabolites involves reaction with 4-(*p*-nitrobenzyl)pyridine as an indication of chemical alkylating activity (2, 3). This assay, however, is not sensitive to cyclophosphamide metabolite levels below 10 μg/ml and, in addition, there is no direct correlation between total chemical alkylating activity and cytotoxicity. The cyclophosphamide metabolite acrolein, for example, has no alkylating activity but is highly cytotoxic (4).

Tissue culture systems amenable to measuring the cytotoxicity of drug metabolites involve cells grown in a monolayer (5, 6) or suspension-grown cells in small volume microcells (7). Neither of these procedures can be used for cell culture growth studies involving repeated sampling from individual cultures. This paper reports an *in vitro* cytotoxicity assay for cyclophosphamide metabolites in rat body fluids using two tissue culture-adapted tumor cell lines. The method is sensitive to low levels of cyclophosphamide metabolites, can be employed in growth studies, and may be applicable to the clinical monitoring of cyclophosphamide metabolites in human body fluids.

EXPERIMENTAL

Cell Lines and Culture Techniques—Mouse L-1210 lymphocytic leukemia cells were obtained commercially[1]. Walker-256 (W-256) rat carcinosarcoma cells were isolated from the ascitic fluid of male Sprague–Dawley rats (Harlan strain) bearing the Arthur D. Little strain of the W-256 tumor. After establishment in tissue cultures, W-256 cells retained the ability to induce tumor growth upon reinjection in Sprague–Dawley rats. Both cell lines were grown in media[2] containing 10% fetal calf serum, with penicillin[1] and streptomycin[1] added.

Cultures were passaged three times weekly and maintained in logarithmic growth. Cell density (number of cells per milliliter) and viability were determined in a hemacytometer microscope counting chamber using the trypan blue dye exclusion method (8). Screw-capped, 150-ml, milk dilution bottles containing 5×10^4 cells/ml in 20 ml of medium were placed on their sides and incubated with loose caps in a humidified environment cabinet[3] at 37° in an atmosphere of 5% CO_2–95% air. Cultures were checked routinely for absence of mycoplasma contamination (9).

Body Fluid Collection—Male Sprague–Dawley rats (Harlan strain), 200–250 g, were used. Cyclophosphamide[4] was given at 500 mg/kg ip; 15 min after dosing, blood was taken by cardiac puncture or from the vena cava. Plasma or serum was prepared and pooled from 10–15 rats. Urine was collected from 10–15 dosed or control animals over 24 hr and pooled. Urine creatinine levels were determined by the method of Owen *et al.* (10).

Chemical alkylating activity of body fluids from dosed animals was determined by the 4-(*p*-nitrobenzyl)pyridine method (3), and alkylating activity was expressed relative to 2,2′-dichlorodiethylamine hydrochloride (nornitrogen mustard), an alkylating metabolite of cyclophosphamide (11). Samples frozen at −25° exhibited no change in alkylating activity within 3 months.

Cytotoxicity Assay—The cell density of a 2- or 3-day L-1210 or W-256 culture was determined by counting 1.0 ml of culture with 0.5 ml of 0.1% trypan blue four times in a hemacytometer and averaging the counts. A single starter culture in the medium[2] was then inoculated at 2×10^4 cells/ml, and screw-capped milk dilution bottles were inoculated with 10.0 ml of this starter culture. Various dilutions of rat body fluids previously sterilized with a 0.45-μm pressure filter[5] were added in a constant 2.0-ml volume, using sterile, glass-distilled water as a diluent.

Recovery of radioactivity from filtered urine containing radioactive cyclophosphamide and its metabolites was 87, 93, and 95% in three separate experiments. Recovery from serum was essentially quantitative[6]. Eight milliliters of a medium[2] mixture (single strength to double strength = 3:1) was then added to yield a final 20-ml culture volume at 1×10^4 cells/ml. For plasma samples, the medium mixture also contained heparin sodium to yield a final concentration of 0.1 unit/ml of growth medium to eliminate the fibrinogen → fibrin reaction, which obscures cell counts in the electronic particle counter (see *Results and Discussion*).

In experiments involving fluids from drug-treated animals, appropriate controls were run using identical volumes of fluids from untreated animals. Triplicate cultures were incubated as described for 3 days. At the end of the incubation period, 2.0 ml of each culture was added to 18.0 ml of a 0.9% sodium chloride solution[7], and the final cell density was determined in an electronic particle counter[8]. Each culture was counted four times, and the counts were corrected for coincidence and averaged. Cell growth inhibition is expressed as percent inhibition of final cell density relative to control cultures. Final control cell densities in the absence of body fluids were typically 2×10^5 cells/ml for W-256 and 5×10^5 cells/ml for L-1210.

RESULTS AND DISCUSSION

Cytotoxicity Assay Response to Body Fluids from Untreated Animals—Urine collected from animals dosed with cyclophosphamide was in varying states of hydration because of varied antidiuretic response. The relative concentration of urine components was generally higher in treated than in untreated animals but was not constant between animals treated identically. Consequently, it is not sufficient to express a maximum tolerable level of control urine on a volume basis. It was necessary to measure the creatinine concentration of all urine samples and to ex-

[1] Associated Biomedic Systems.
[2] Roswell Park Memorial Institute 1640.
[3] Wedco.
[4] Cyclophosphamide for injection, a product of Mead Johnson Laboratories.
[5] Millipore.
[6] Unpublished results.
[7] Isoton, Coulter Diagnostics Inc.
[8] Coulter Electronic model B particle counter.

0022-3549/78/0700/1009$01.00/0
© 1978, American Pharmaceutical Association

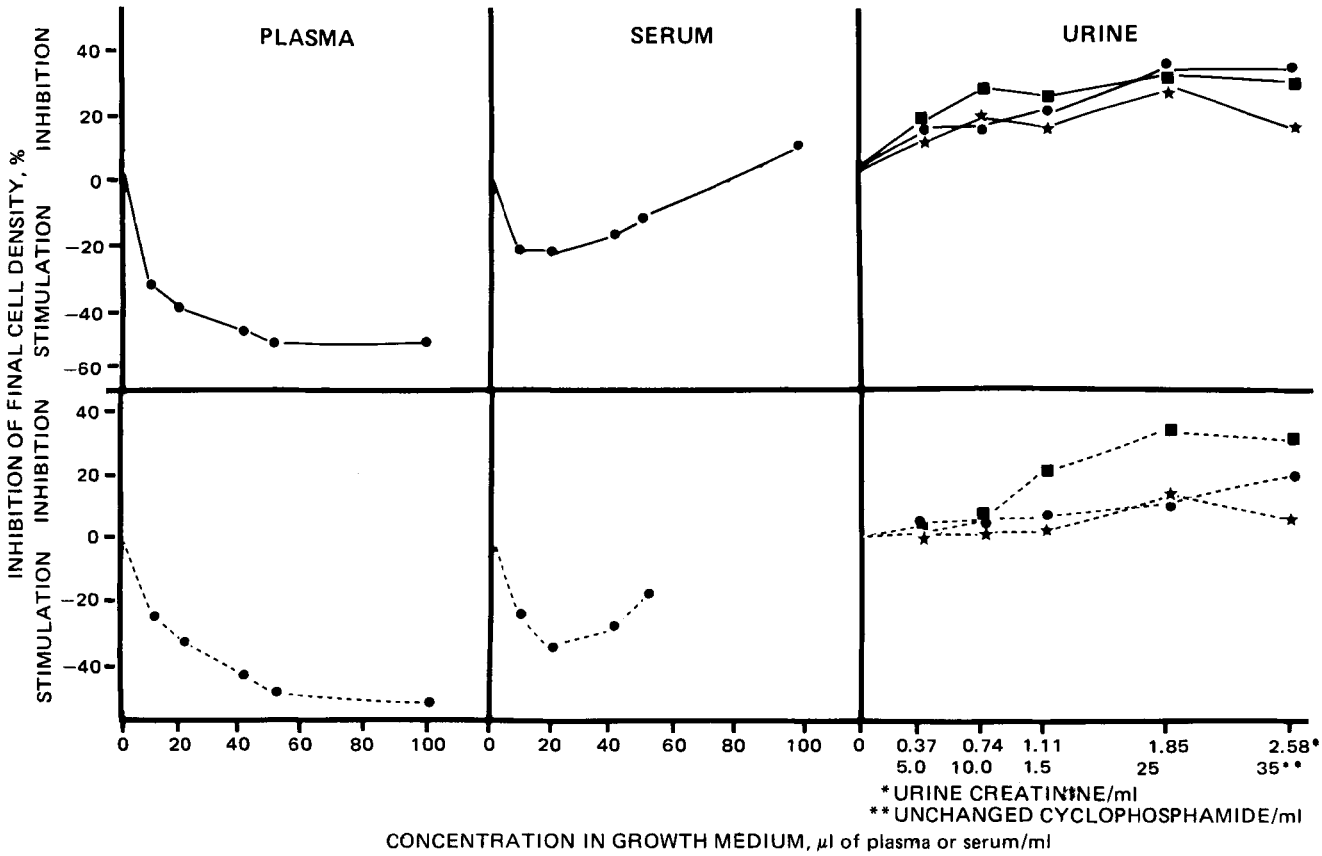

Figure 1—*L-1210* (—) *and W-256* (- - -) *cytotoxicity assays with body fluids from control rats. Unchanged cyclophosphamide was included in urine assays, assuming a complete lack of cyclophosphamide activation in rats dosed with 500 mg of cyclophosphamide/kg ip. Key:* ●, *urine alone;* ★, *unchanged cyclophosphamide alone; and* ■, *urine plus unchanged cyclophosphamide.*

press the maximum tolerable control urine level in the *in vitro* system relative to creatinine levels.

Plasma prepared using edetic acid as an anticoagulant was highly toxic to both L-1210 and W-256 cells, and the toxicity was shown to be due entirely to the edetic acid. Approximately 50% growth inhibition was noted with 120 µg of edetic acid/ml of growth medium. This problem was circumvented by using either 1.0 unit of heparin sodium/ml or 0.2% sodium citrate as the anticoagulant in plasma preparations.

Another problem was encountered with cultures containing added rat plasma. Residual thrombin in the plasma apparently converted fibrinogen present in a fetal calf serum component of the growth medium to the insoluble protein fibrin during culture incubation. The fibrin was then falsely registered during counting with the electronic particle counter, and cell counts were errantly high. The addition of 0.1 unit of heparin sodium/ml of growth medium to the cultures eliminated this problem by inhibiting thrombin activity.

Results of L-1210 and W-256 cytotoxicity assays with control rat plasma, serum, and urine are shown in Fig. 1. Plasma stimulated growth at levels up to 100 µl of plasma/ml of growth medium. Low serum levels stimulated growth, and 100 µl of serum/ml was only slightly inhibitory. Urine was inhibitory, and the maximum tolerable level was arbitrarily set at 25% inhibition of cell growth. This value corresponds to 1.8 µg of urine creatinine/ml, which is approximately 30 µl of urine/ml and is dependent upon the antidiuretic response of individual animals to cyclophosphamide treatment. All further assays using body fluids from cyclophosphamide-treated animals did not exceed 100 µl of plasma or serum/ml or 1.8 µg of urine creatinine/ml.

Since both unchanged cyclophosphamide and its metabolites are very rapidly excreted in the urine (12), it was necessary to determine if any synergistic effect existed between control urine and unchanged cyclophosphamide. Cyclophosphamide was added to control urine at a level assuming a complete lack of *in vivo* activation at a dose of 500 mg of cyclophosphamide/kg (6.25 mg/ml of urine). The results (Fig. 1) confirm earlier reports that low levels of unchanged cyclophosphamide are fairly innocuous *in vitro* (*e.g.*, Ref. 13). No synergistic effect was exhibited by the combination of control urine and unchanged cyclophosphamide.

Cytotoxicity Assay Response to Body Fluids from Drug-Treated Animals—Figure 2 depicts L-1210 and W-256 assays with plasma, serum, and urine from rats dosed with 500 mg of cyclophosphamide/kg ip. The W-256 cells were much more sensitive to cyclophosphamide metabolites than were L-1210 cells. In each case, the response was reasonably linear and precision between triplicate cultures was good. In 10 experiments involving 60 sets of triplicate cultures showing greater than 20% inhibition of growth, the mean percent coefficient of variation was 3.69.

Trypan blue cell viability determinations were made on each of the L-1210 cultures inhibited with cyclophosphamide metabolites in plasma; at each plasma level, viability remained greater than 95%, although growth inhibition was as high as 95%. Use of the electronic particle counter is, therefore, an effective way of estimating viable cell density, even though it does not distinguish between living and dead cells, since

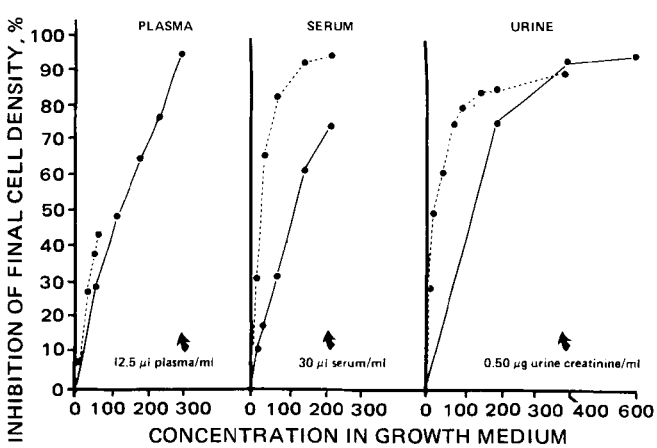

Figure 2—*L-1210* (—) *and W-256* (- - -) *cytotoxicity assays with body fluids from rats dosed with 500 mg of cyclophosphamide/kg ip. Concentration is expressed as 4-*(p-*nitrobenzyl)pyridine alkylating activity equivalents relative to 2,2'-dichlorodiethylamine hydrochloride. Arrows signify the amount of body fluid added to attain the indicated concentration of alkylating activity.*

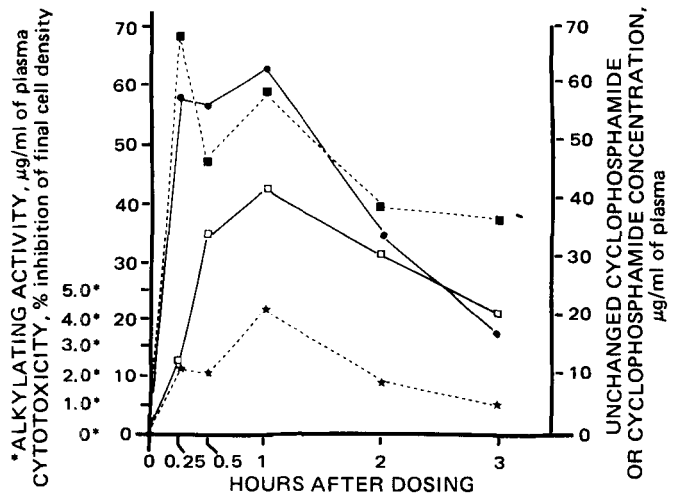

Figure 3—*Rat plasma levels of unchanged cyclophosphamide, cyclophosphamide metabolites, W-256 cytotoxicity (percent inhibition of growth with 10 μl of plasma/ml of growth medium), and chemical alkylating activity at various times after dosing rats with 200 mg of ^{3}H-cyclophosphamide/kg ip. Key: ●, unchanged cyclophosphamide; ■, cyclophosphamide metabolites; □, cytotoxicity (W-256 system); and ★, alkylating activity (2,2′-dichlorodiethylamine hydrochloride equivalents).*

growth-inhibited cells remain viable during the experiment.

To demonstrate a correlation between cytotoxicity and plasma levels of cyclophosphamide metabolites, female Sprague–Dawley rats, 200 g, were dosed with 200 mg of ^{3}H-cyclophosphamide (0.160 μCi/mg randomly labeled in the side chain)/kg ip. Plasma was collected at various times after dosing and pooled (four rats at each time point). The concentration of unchanged cyclophosphamide was determined by extraction with 10% methanol in ethylene dichloride using the method described by Mellett *et al.* (14). Metabolite levels were calculated by subtracting the unchanged cyclophosphamide concentration from the concentration of total radioactivity. Background counts per minute were less than 1% of the total counts.

In vitro cytotoxicity in the W-256 system, using 10 μl of plasma/ml of growth medium, and 4-(*p*-nitrobenzyl)pyridine alkylating activity also were determined. The data presented in Fig. 3 show a close similarity in the time course of occurrence of alkylating activity, *in vitro* W-256 cytotoxicity, and cyclophosphamide metabolite levels in plasma. The initial spike in the curves of unchanged cyclophosphamide and metabolites represents the early appearance in plasma of unchanged cyclophosphamide and metabolites with neither alkylating activity nor cytotoxicity; unchanged cyclophosphamide was nontoxic in the *in vitro* system.

Growth Studies—In drug metabolism studies, it is often desirable to follow the response of culture growth parameters with time. This approach involves repeated sampling from individual cultures and is not possible with monolayer cultures or microcell cultures involving small volumes. The L-1210 and W-256 systems can readily be used in growth studies, as exemplified by the following experiments.

The L-1210 and W-256 growth curves were determined for cultures containing both low and high levels of cyclophosphamide metabolites in rat urine. Figures 4*a* and 4*b* show that, at low levels of cyclophosphamide metabolites, growth remained exponential but with an increased population doubling time. At the higher metabolite levels, L-1210 cells apparently completed less than one full round of division and W-256 cells completed slightly more than one full round of division before the growth curve plateaued. The possible presence of a critical point in the cell growth cycle at which cyclophosphamide metabolites are active awaits further examination with synchronous cultures.

Many drugs preferentially inhibit rapidly dividing cells, and this action is also apparently true of cyclophosphamide metabolites. The W-256 cells were retarded in their growth by a single passage in glutamine-deficient medium that had been aged for 6 months at 4° to allow glutamine decomposition. Dosed rat urine was added to cells at a concentration of 400 ng of alkylating activity equivalents/ml. These "slow-growing" cells completed three rounds of division (Fig. 4*c*), while normal "fast-growing" cells were limited to one division at the same cyclophosphamide metabolite level over an equivalent time period (Fig. 4*b*).

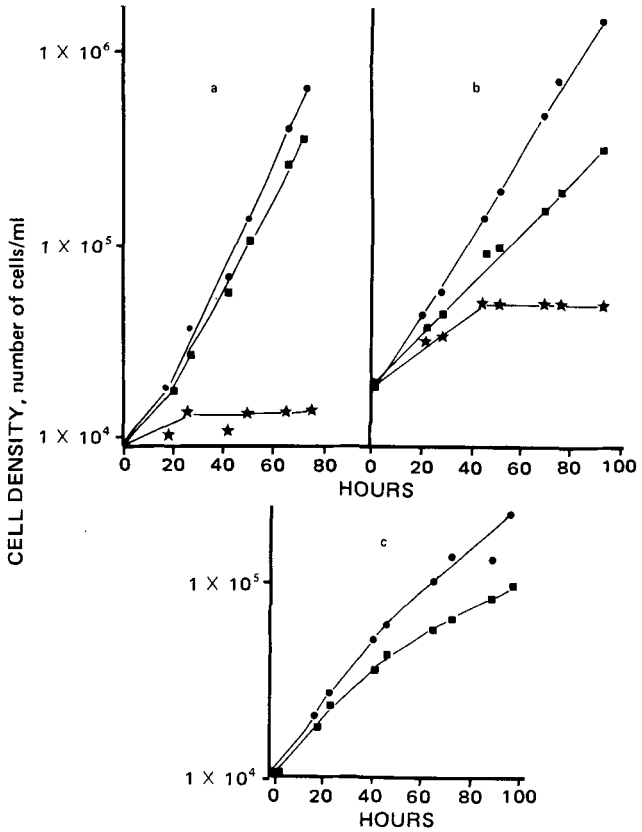

Figure 4—*Cell growth curves at various supplementation levels (concentration in growth medium) of urine from rats dosed with 500 mg of cyclophosphamide/kg ip. Key: a, L-1210; b, W-256; c, W-256 cells whose growth was previously retarded by culturing in glutamine-deficient medium; ●, control; ■, 40 ng of alkylating activity equivalents/ml; and ★, 400 ng of alkylating activity equivalents/ml.*

SUMMARY

The W-256 and L-1210 *in vitro* cytotoxicity assay systems are sensitive to low levels of cyclophosphamide metabolites in rat body fluids. From a consideration of maximum tolerable levels of control body fluids, minimum detectable cyclophosphamide metabolite concentrations, and typical metabolite levels in body fluids from rats dosed with 500 mg of cyclophosphamide/kg, it was estimated that the minimum dosage needed to give detectable metabolite levels in plasma, serum, or urine is ≃5 mg of cyclophosphamide/kg in the W-256 assay system. This dose is equivalent to ≃10 ng of 4-(*p*-nitrobenzyl)pyridine alkylating activity equivalents/ml of growth medium or ≃100 ng of alkylating activity equivalents/ml of body fluid, which is two orders of magnitude more sensitive than the commonly used 4-(*p*-nitrobenzyl)pyridine assay.

This method can be used readily in tissue culture growth studies or drug metabolism studies involving various drugs. The procedure also may be applicable to the clinical measurement of cyclophosphamide metabolite levels in human body fluids after dosing in the normal therapeutic range of 10–15 mg of cyclophosphamide/kg.

REFERENCES

(1) N. E. Sladek, *Cancer Res.*, **31**, 901 (1971).

(2) J. Epstein, R. W. Rosenthal, and R. J. Ess, *Anal. Chem.*, **27**, 1435 (1955).

(3) O. Friedman and E. Boger, *ibid.*, **33**, 906 (1961).

(4) R. A. Alarcon and J. Meienhofer, *Nature New Biol.*, **233**, 250 (1971).

(5) D. Laux and R. N. Lausch, *Antimicrob. Agents Chemother.*, **3**, 407 (1973).

(6) E. Dolfini, A. Martini, M. G. Donelli, L. Morasca, and S. Garattini, *Eur. J. Cancer*, **9**, 375 (1973).

(7) B. J. Phillips, *Biochem. Pharmacol.*, **23**, 131 (1974).

(8) A. J. Girardi, H. McMichale, and W. Henle, *Virology*, **2**, 532 (1956).

(9) "Difco Manual," 9th ed., Difco Laboratories, Detroit, Mich., 1966, pp. 82–90.
(10) H. Mattenheimer, "Micromethods for the Clinical and Biochemical Laboratory," Ann Arbor Scientific, Ann Arbor, Mich., 1970, p. 68.
(11) H. J. Hohorst, A. Ziemann, and N. Brock, *Arzneim.-Forsch.*, **15**, 432 (1965).
(12) A. R. Torkelson, J. A. LaBudde, and J. H. Weikel, Jr., *Drug Metab. Rev.*, **3**, 131 (1974).
(13) N. Brock, *Cancer Chemother. Rep.*, **51**, 315 (1967).
(14) L. B. Mellett, S. M. ElDareer, D. P. Rall, and R. H. Adamson, *Arch. Int. Pharmacodyn. Ther.*, **177**, 60 (1969).

Solubility Studies of Silver Sulfonamides

R. U. NESBITT, Jr. *, and B. J. SANDMANN ˣ

Received August 1, 1977, from the *School of Pharmacy, University of Missouri–Kansas City, Kansas City, MO 64110.* Accepted for publication November 10, 1977. *Present address: Merck Sharp & Dohme Research Laboratories, Rahway, N.J.

Abstract □ The solubilities of silver sulfapyridine, silver sulfamethazine, and silver sulfamethizole as a function of pH were determined in nitric acid–potassium nitrate, acetate, and sulfonic acid buffers. All silver sulfonamides showed an increase in solubility with increasing hydrogen-ion concentration, a behavior which closely paralleled the protonation of the *p*-amino function of the sulfonamide. A silver-ion selective electrode was used to measure silver-ion concentration in solution and the methods of known subtraction and known addition were used to measure total silver. Both silver sulfamethizole and silver sulfamethazine were ionized completely in solution. Silver sulfapyridine was ionized completely only in the more acidic pH 2–3 range. A comparison of the physical properties of the silver salts for which mortality studies were available revealed a unique set of properties for silver sulfadiazine.

Keyphrases □ Silver sulfonamides, various—aqueous solubility, effect of pH □ Solubility, aqueous—various silver sulfonamides, effect of pH □ Antibacterials—various silver sulfonamides, aqueous solubility, effect of pH

While some silver salts have been tested for effectiveness against *Pseudomonas* infections, the unique activity of silver sulfadiazine remains impressive but incompletely explained. The solubility and ionization properties of this compound were reported (1) and the drug was characterized as a practically insoluble salt having a solubility product of 8.1×10^{-12} at 25° and 0.1 *M* ionic strength. In the presence of a nitrate buffer under these experimental conditions, the silver ion was dissociated completely from the sulfadiazine moiety and therefore free to precipitate or complex with any suitable ligand. In the presence of endogenous chloride ion, silver sulfadiazine did not cause the rapid precipitation of silver chloride, under physiological conditions, even though the solubility product of silver chloride was exceeded (2). Further studies of the behavior of silver sulfadiazine in the presence of chloride ion are indicated for a better understanding of this phenomenon.

Other silver sulfonamides have been compared to silver sulfadiazine for anti-infective activity and reaction with human serum and DNA. Differences between the reactions of the other sulfonamides to those of silver sulfadiazine were postulated to relate to the ionization constants for the sulfonamide moieties (2). However, a comparison of the literature values of the amide hydrogen ionization constants with the reported behavior for the reaction of the silver compounds with serum does not indicate that a simple ionization phenomenon is involved. The solubility of these salts should be considered, as well as the tendency of free silver ions to complex with many endogenous biological substances.

This solubility study was undertaken to determine the properties of some silver sulfonamides other than silver sulfadiazine to provide more information about their behavior in aqueous solution. The solubility and ionization properties of silver sulfamethazine, silver sulfamethizole, and silver sulfapyridine are reported. A possible correlation between the physical properties of the silver salts and their biological activity is proposed.

EXPERIMENTAL

Equipment—Potentiometric measurements were made using a pH meter[1], accurate to ±0.001 pH unit, in a thermostated bath regulated at 25 ± 0.1°. Silver-ion concentration was measured with a silver-ion se-

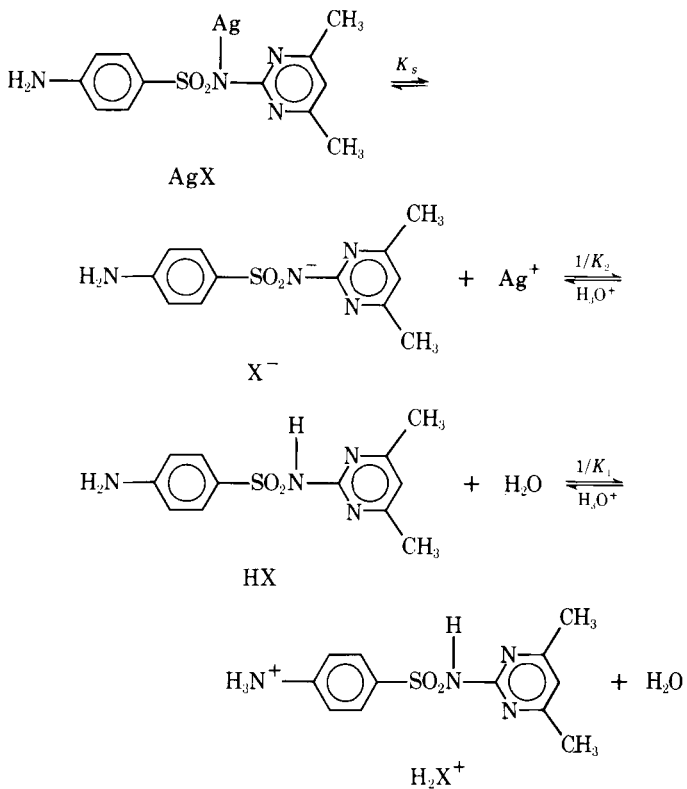

Scheme I—Silver sulfamethazine dissolution

[1] Digital 112 research pH meter, Corning Scientific Instruments, Medfield, Mass.

0022-3549/78/0700/1012$01.00/0
© 1978, American Pharmaceutical Association

(9) "Difco Manual," 9th ed., Difco Laboratories, Detroit, Mich., 1966, pp. 82–90.
(10) H. Mattenheimer, "Micromethods for the Clinical and Biochemical Laboratory," Ann Arbor Scientific, Ann Arbor, Mich., 1970, p. 68.
(11) H. J. Hohorst, A. Ziemann, and N. Brock, *Arzneim.-Forsch.*, **15**, 432 (1965).
(12) A. R. Torkelson, J. A. LaBudde, and J. H. Weikel, Jr., *Drug Metab. Rev.*, **3**, 131 (1974).
(13) N. Brock, *Cancer Chemother. Rep.*, **51**, 315 (1967).
(14) L. B. Mellett, S. M. ElDareer, D. P. Rall, and R. H. Adamson, *Arch. Int. Pharmacodyn. Ther.*, **177**, 60 (1969).

Solubility Studies of Silver Sulfonamides

R. U. NESBITT, Jr. *, and B. J. SANDMANN ˣ

Received August 1, 1977, from the *School of Pharmacy, University of Missouri–Kansas City, Kansas City, MO 64110.* Accepted for publication November 10, 1977. *Present address: Merck Sharp & Dohme Research Laboratories, Rahway, N.J.

Abstract □ The solubilities of silver sulfapyridine, silver sulfamethazine, and silver sulfamethizole as a function of pH were determined in nitric acid–potassium nitrate, acetate, and sulfonic acid buffers. All silver sulfonamides showed an increase in solubility with increasing hydrogen-ion concentration, a behavior which closely paralleled the protonation of the *p*-amino function of the sulfonamide. A silver-ion selective electrode was used to measure silver-ion concentration in solution and the methods of known subtraction and known addition were used to measure total silver. Both silver sulfamethizole and silver sulfamethazine were ionized completely in solution. Silver sulfapyridine was ionized completely only in the more acidic pH 2–3 range. A comparison of the physical properties of the silver salts for which mortality studies were available revealed a unique set of properties for silver sulfadiazine.

Keyphrases □ Silver sulfonamides, various—aqueous solubility, effect of pH □ Solubility, aqueous—various silver sulfonamides, effect of pH □ Antibacterials—various silver sulfonamides, aqueous solubility, effect of pH

While some silver salts have been tested for effectiveness against *Pseudomonas* infections, the unique activity of silver sulfadiazine remains impressive but incompletely explained. The solubility and ionization properties of this compound were reported (1) and the drug was characterized as a practically insoluble salt having a solubility product of 8.1×10^{-12} at 25° and 0.1 *M* ionic strength. In the presence of a nitrate buffer under these experimental conditions, the silver ion was dissociated completely from the sulfadiazine moiety and therefore free to precipitate or complex with any suitable ligand. In the presence of endogenous chloride ion, silver sulfadiazine did not cause the rapid precipitation of silver chloride, under physiological conditions, even though the solubility product of silver chloride was exceeded (2). Further studies of the behavior of silver sulfadiazine in the presence of chloride ion are indicated for a better understanding of this phenomenon.

Other silver sulfonamides have been compared to silver sulfadiazine for anti-infective activity and reaction with human serum and DNA. Differences between the reactions of the other sulfonamides to those of silver sulfadiazine were postulated to relate to the ionization constants for the sulfonamide moieties (2). However, a comparison of the literature values of the amide hydrogen ionization constants with the reported behavior for the reaction of the silver compounds with serum does not indicate that a simple ionization phenomenon is involved. The solubility of these salts should be considered, as well as the tendency of free silver ions to complex with many endogenous biological substances.

This solubility study was undertaken to determine the properties of some silver sulfonamides other than silver sulfadiazine to provide more information about their behavior in aqueous solution. The solubility and ionization properties of silver sulfamethazine, silver sulfamethizole, and silver sulfapyridine are reported. A possible correlation between the physical properties of the silver salts and their biological activity is proposed.

EXPERIMENTAL

Equipment—Potentiometric measurements were made using a pH meter[1], accurate to ±0.001 pH unit, in a thermostated bath regulated at 25 ± 0.1°. Silver-ion concentration was measured with a silver-ion se-

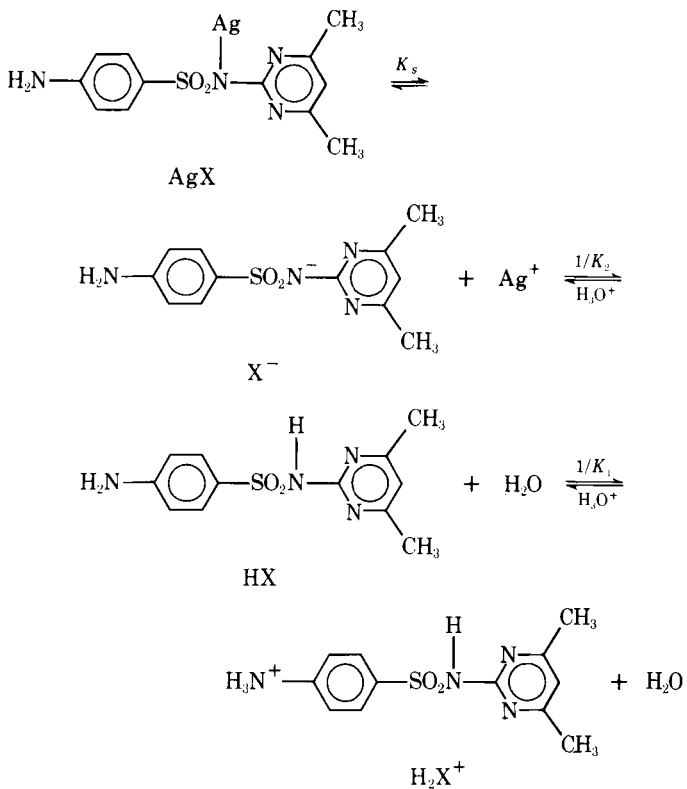

Scheme I—Silver sulfamethazine dissolution

[1] Digital 112 research pH meter, Corning Scientific Instruments, Medfield, Mass.

0022-3549/78/0700/1012$01.00/0
© 1978, American Pharmaceutical Association

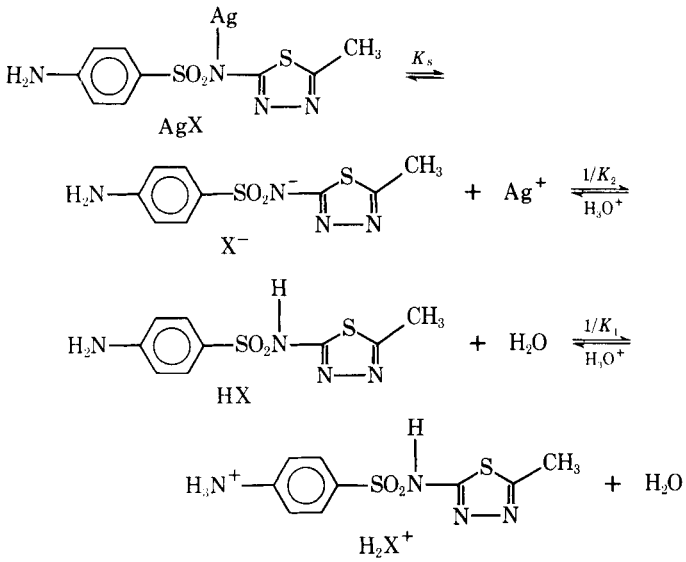

Scheme II—Silver sulfamethizole dissolution

lective electrode[2]. Hydronium-ion concentration was measured with a pH electrode[3]. A double-junction silver chloride reference electrode[4] with a filling solution of 10% KNO_3 was used to eliminate the possible precipitation of silver chloride in the sample solutions.

Reagents—All reagents used were analytical or USP grade, unless otherwise stated. The water had a specific conductivity of $1–10 \times 10^{-7}$ ohm^{-1} cm^{-1}. Silver sulfamethazine, silver sulfapyridine, and silver sulfamethizole were prepared by the method of Rosenzweig and Fuchs (3) and recrystallized from concentrated ammonia (4). The sulfonic acid[5] and acetic acid buffers were prepared with a total molar concentration of 0.05 *M*. The nitric acid buffers were prepared by dilution of 0.1 *M* HNO_3. All buffers were adjusted to an ionic strength of 0.1 *M* with potassium nitrate.

Preparation of Equilibrium Mixtures—Procedures similar to those previously reported were utilized (1). The recrystallized and dried silver sulfonamides were screened through an 80-mesh standard screen[6], and a 100-mg sample was added to either 25 or 27 ml of nitric acid buffer, 27 ml of acetate buffer, or 27 ml of sulfonic acid buffer. For measurement of total silver, 27 ml of buffer was used.

The mixtures were adjusted to a constant ionic strength of 0.1 *M* and placed in paraffin-coated vials with paraffin-sheet[7]-covered rubber closures. The vials were rotated end over end in the thermostated bath until equilibrium solubility was obtained (3–7 days).

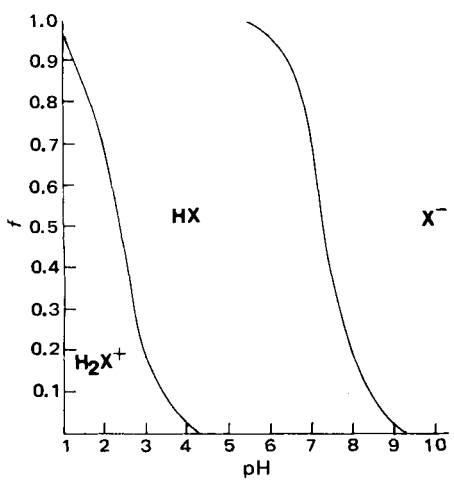

Figure 1—*Distribution diagram: fraction of sulfamethazine present as some particular form, f, as a function of pH; pK_1 = 2.36 and pK_2 = 7.38 (8).*

[2] No. 94-16, Orion Research, Cambridge, Mass.
[3] Triple-Purpose pH electrode, Corning Scientific Instruments, Medfield, Mass.
[4] No. 90-02, Orion Research, Cambridge, Mass.
[5] United States Biochemical Corp., Cleveland, Ohio.
[6] W. S. Tyler Co., Minton, Ohio.
[7] Parafilm, American Can Co., Neenah, Wis.

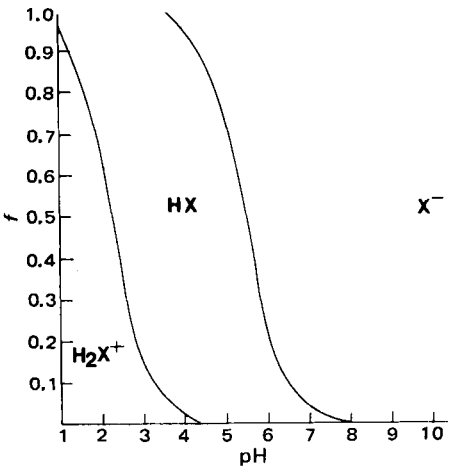

Figure 2—*Distribution diagram: fraction of sulfamethizole present as some particular form, f, as a function of pH; pK_1 = 2.20 and pK_2 = 5.45 (8).*

Measurement of Silver—The equilibrated mixtures were filtered through 20M glass filtering crucibles. The solutions were analyzed at 25 ± 0.1° in paraffin-coated beakers for silver ions with a silver-ion selective electrode[2] standardized at 25 ± 0.1° and 0.1 *M* ionic strength using procedures reported earlier (1, 5, 6).

Measurement of pH—The pH was measured with a pH electrode standardized using buffers meeting National Bureau of Standards requirements (7).

RESULTS AND DISCUSSION

The analytical method and the acid–base properties of silver sulfadiazine were discussed previously (1). Similar systems are proposed for the silver salts of sulfamethazine, sulfamethizole, and sulfapyridine.

The equilibria of the saturated solutions of silver sulfamethazine and silver sulfamethizole (Schemes I and II) are described by Eqs. 1–5:

$$K_s = [Ag^+][X^-] \quad \text{(Eq. 1)}$$

$$\frac{1}{K_2} = \frac{[HX]}{[H_3O^+][X^-]} \quad \text{(Eq. 2)}$$

$$\frac{1}{K_1} = \frac{[H_2X^+]}{[HX][H_3O^+]} \quad \text{(Eq. 3)}$$

$$S = [Ag^+] \quad \text{(Eq. 4)}$$

$$S = [H_2X^+] + [HX] + [X^-] \quad \text{(Eq. 5)}$$

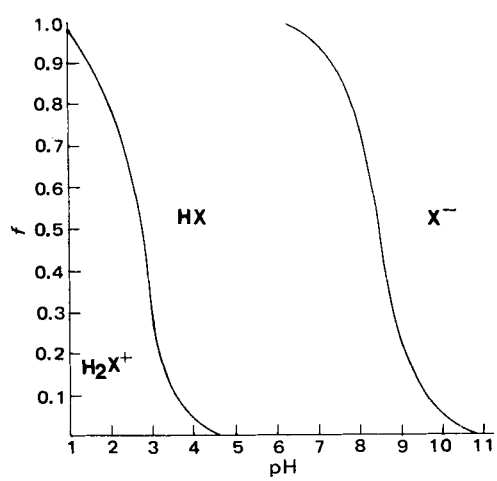

Figure 3—*Distribution diagram: fraction of sulfapyridine present as some particular form, f, as a function of pH; pK_1 = 2.58 and pK_2 = 8.43 (8).*

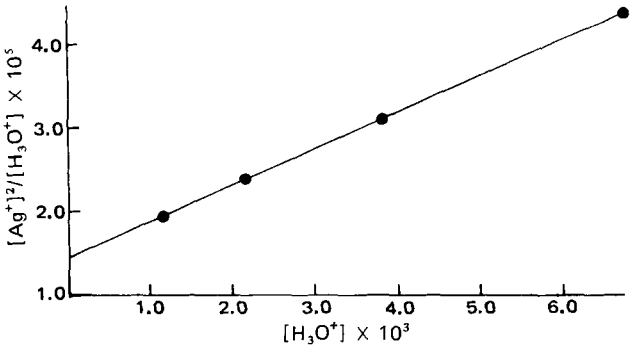

Figure 4—*Equilibrium values of* $[Ag^+]^2/[H_3O^+]$ versus $[H_3O^+]$ *for silver sulfamethazine in nitric acid buffer at 0.1* M *ionic strength and 25 ± 0.1°.*

where S is the total molar solubility of the silver sulfonamide. Substitution of Eqs. 1–4 into Eq. 5 and rearrangement give:

$$S^2 = [Ag^+]^2 = \frac{[H_3O^+]^2K_s}{K_1K_2} + \frac{[H_3O^+]K_s}{K_2} + K_s \qquad \text{(Eq. 6)}$$

which describes the solubility of these silver sulfonamides in terms of only the silver- and hydronium-ion concentrations of the saturated solutions. The parameter K_s is the apparent solubility product, and K_1 and K_2 are the apparent dissociation constants of the N^4- and N^1-hydrogens, respectively. Equation 6 may be simplified by using the limiting conditions of low (2–4) and high (5–9) pH. These approximations were derived by using distribution diagrams for the sulfonamides (Figs. 1 and 2), calculated using ionization constants determined by Bell and Roblin (8), noting which species of sulfonamide was not present in the pH range of interest, and neglecting this term in the mass balance equation (Eq. 5).

In the low pH range, Eq. 6 may be approximated to give:

$$S^2 = [Ag^+]^2 = \frac{[H_3O^+]^2K_s}{K_1K_2} + \frac{[H_3O^+]K_s}{K_2} \qquad \text{(Eq. 7)}$$

by neglecting the X^- species in Eq. 5. This equation may be linearized by dividing both sides by the hydronium-ion concentration, giving:

$$\frac{[Ag^+]^2}{[H_3O^+]} = \frac{[H_3O^+]K_s}{K_1K_2} + \frac{K_s}{K_2} \qquad \text{(Eq. 8)}$$

When $[Ag^+]^2/[H_3O^+]$ is plotted against $[H_3O^+]$, a linear relationship should exist with an intercept of K_s/K_2 and a slope of $(K_s/K_2)(1/K_1)$. From the slope and intercept, K_1 may be determined experimentally.

At the higher pH range (5–9), Eq. 6 may be approximated to give:

$$S^2 = [Ag^+]^2 = \frac{[H_3O^+]K_s}{K_2} + K_s \qquad \text{(Eq. 9)}$$

where the H_2X^+ species in Eq. 6 has been neglected. The application of Eq. 9 to the experimental data in the presence of the acetate and sulfonic acid buffer systems does not adequately represent the system because of apparent complexation of the free silver ion with the buffer. This results in an increased value of the solubility, S, and subsequently a higher value for K_s, the apparent solubility product.

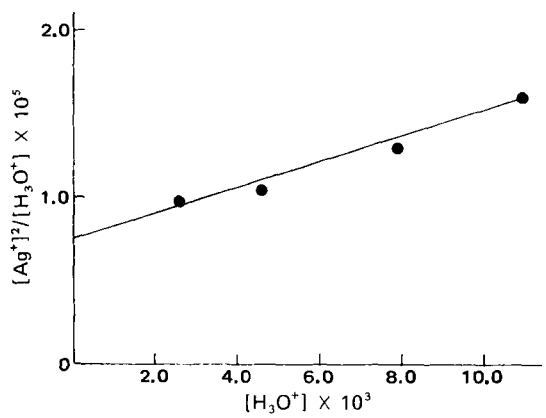

Figure 5—*Equilibrium values of* $[Ag^+]^2/[H_3O^+]$ versus $[H_3O^+]$ *for silver sulfamethizole in nitric acid buffer at 0.1* M *ionic strength and 25 ± 0.1°.*

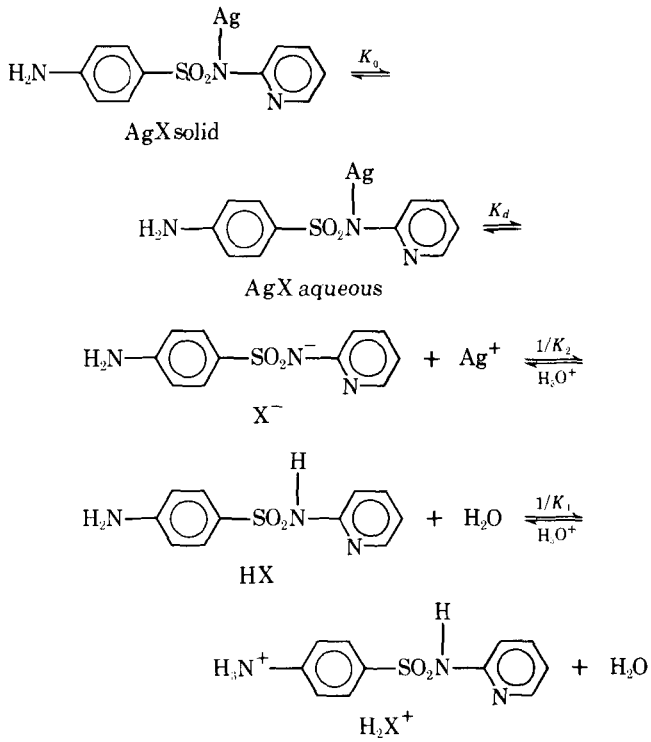

Scheme III—Silver sulfapyridine dissolution

A suitable modification of Eq. 9 to include this complexation may be made by using a conditional solubility product K_s' defined by:

$$K_s' = [Ag^+]'[X^-] \qquad \text{(Eq. 10)}$$

where $[Ag^+]'$ represents the concentration of all silver in solution, irrespective of the form of the silver. Equation 9 may now be rewritten as:

$$S^2 = \frac{[H_3O^+]K_s'}{K_2} + K_s' \qquad \text{(Eq. 11)}$$

where S is the total molar solubility and K_2 is defined by Eq. 2. A plot of S^2 *versus* $[H_3O^+]$ would be expected to be linear with an intercept of K_s' and a slope of K_s'/K_2, from which K_2 may be determined experimentally.

The silver sulfapyridine equilibria shown in Scheme III may be described by the following equations:

$$K_0 = \frac{[AgX]_{(soln)}}{[AgX]_{(s)}} \qquad \text{(Eq. 12)}$$

$$K_d = \frac{[Ag^+][X^-]}{[AgX]_{(soln)}} \qquad \text{(Eq. 13)}$$

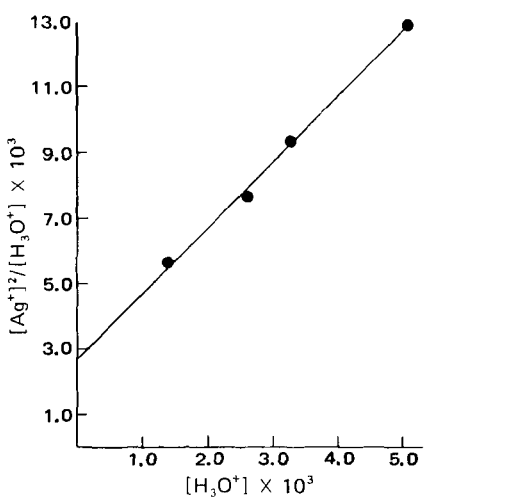

Figure 6—*Equilibrium values of* $[Ag^+]^2/[H_3O^+]$ versus $[H_3O^+]$ *for silver sulfapyridine in nitric acid buffer at 0.1* M *ionic strength and 25 ± 0.1°.*

Table I—Amino pK Values Calculated from Plots of Eq. 9 [a]

Silver Sulfonamide	Experimental $pK_1 \pm SD$	r	p
Silver sulfamethazine	2.47 ± 0.002	0.9998	>0.001
Silver sulfamethizole	2.00 ± 0.01	0.9957	>0.01
Silver sulfapyridine	2.88 ± 0.02.	0.9985	>0.01

[a] Degrees of freedom equals 2.

Table II—Amide pK Values Calculated from Plots of Eq. 11 [a]

Silver Sulfonamide	Experimental $pK_2 \pm SD$	r	p
Silver sulfamethazine	7.29 ± 0.06	0.9779	>0.05
Silver sulfamethizole	5.45 ± 0.06	0.9914	>0.01
Silver sulfapyridine	8.46 ± 0.07	0.9288	>0.1

[a] Degrees of freedom equals 2.

$$K_d K_0 = [Ag^+][X^-] = K_s \quad \text{(Eq. 14)}$$

$$\frac{1}{K_2} = \frac{[HX]}{[H_3O^+][X^-]} \quad \text{(Eq. 2)}$$

$$\frac{1}{K_1} = \frac{[H_2X^+]}{[HX][H_3O^+]} \quad \text{(Eq. 3)}$$

$$S = [Ag^+] + [AgX]_{(soln)} \quad \text{(Eq. 15)}$$

$$S = [H_2X^+] + [HX] + [X^-] + [AgX]_{(soln)} \quad \text{(Eq. 16)}$$

Substituting Eq. 13 into Eq. 15 gives:

$$\frac{S}{[Ag^+]} = 1 + \frac{[X^-]}{K_d} \quad \text{(Eq. 17)}$$

If $S/[Ag^+]$ is plotted against $[X^-]$, a linear plot should result with an intercept of 1 and a slope of $1/K_d$.

Equating Eq. 15 with Eq. 16 gives:

$$[Ag^+] = [H_2X^+] + [HX] + [X^-] \quad \text{(Eq. 18)}$$

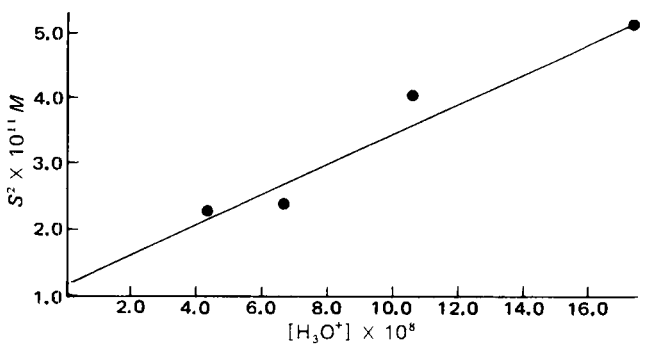

Figure 7—*Equilibrium values of* S^2 versus $[H_3O^+]$ *for silver sulfamethazine in 0.05* M 2-(N-*morpholino*)*propanesulfonic acid buffer at 0.1* M *ionic strength and 25 ± 0.1°.*

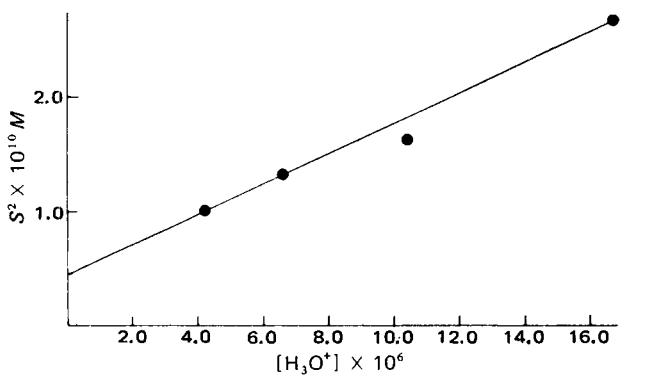

Figure 8—*Equilibrium values of* S^2 versus $[H_3O^+]$ *for silver sulfamethizole in 0.05* M 2-(N-*morpholino*)*propanesulfonic acid buffer at 0.1* M *ionic strength and 25 ± 0.1°.*

Table III—Comparison of Total Silver Sulfamethazine Molar Solubility, *S*, Determined by the Method of Known Subtraction with the Molar Concentration of the Silver Ion Determined by Direct Potentiometry on Identical Samples at 25 ± 0.1°, 0.1 *M* Ionic Strength, in Nitric Acid Buffer

	pH 2.186		pH 3.970	
	$S \times 10^3$	$[Ag^+] \times 10^3$	$S \times 10^4$	$[Ag^+] \times 10^4$
	1.194	1.185	0.992	1.028
	1.191	1.185	0.9689	1.003
	1.191	1.171	0.9813	1.041
	1.218	1.194	1.1010	1.170
	1.194	1.157	0.9945	1.053
	1.204	1.166		
Mean	1.198	1.176	1.010	1.059

Table IV—Comparison of Total Silver Sulfamethizole Molar Solubility, *S*, Determined by the Method of Known Subtraction with the Molar Concentration of the Silver Ion Determined by Direct Potentiometry of Identical Samples at 25 ± 0.1°, 0.1 *M* Ionic Strength, in Nitric Acid Buffer

	pH 1.931		pH 2.565	
	$S \times 10^4$	$[Ag^+] \times 10^9$	$S \times 10^4$	$[Ag^+] \times 10^4$
	4.073	4.052	1.477	1.486
	4.077	4.068	1.491	1.486
	4.088	4.068	1.477	1.492
	4.062	4.036	1.459	1.475
	4.120	4.099	1.482	1.486
	4.080	4.021	1.476	1.475
Mean	4.084	4.057	1.477	1.483

Substituting Eqs. 1–3 into Eq. 18 gives:

$$[Ag^+]^2 = \frac{[H_3O^+]^2 K_s}{K_1 K_2} + \frac{[H_3O^+] K_s}{K_2} \quad \text{(Eq. 19)}$$

Equation 19 describes silver sulfapyridine solubility in terms of only the silver- and hydronium-ion concentrations of the saturated solutions. This equation may be simplified by applying the limiting conditions of low (2–4) and high (5–9) pH, as done previously utilizing the sulfapyridine distribution diagram (Fig. 3) calculated with the values of Bell and Roblin (8). When using these approximations, Eq. 19 reduces to Eq. 7 in the low pH range and to Eq. 9 at the higher pH range. Again Eq. 9 is modified to give Eq. 11 to include the complexation of the silver ion with the sulfonic acid buffer.

Figures 4–6 display linear plots of Eq. 9. The pK_1 values for the amino dissociation constants are summarized in Table I. As shown in Figs. 7–9, plots of the equilibrium values of S^2 *versus* $[H_3O^+]$ are linear. The pK_2 values for the amide dissociation constants are summarized in Table II.

The possibility of intact silver sulfonamide in solution in the lower pH range was investigated. The total molar solubility, S, as determined by the method of known subtraction was compared with the molar concentration of the free silver ion, $[Ag^+]$, by direct potentiometric analysis of identical samples under the given experimental conditions. Only the

Table V—Calculation of the Solubility Product of Silver Sulfamethazine from Eq. 21 at 25 ± 0.1° and 0.1 *M* Ionic Strength

pH	f_0	S^2	K_s [a]
2.174	2.551×10^{-6}	1.477×10^{-6}	3.77×10^{-12}
2.421	6.323×10^{-6}	5.897×10^{-7}	3.72×10^{-12}
2.668	1.455×10^{-5}	2.606×10^{-7}	3.79×10^{-12}
2.934	3.265×10^{-5}	1.151×10^{-7}	3.76×10^{-12}
		Mean	$(3.76 \pm 0.03)10^{-12}$

[a] K_s reported as mean ± *SD*.

Table VI—Calculation of the Solubility Product of Silver Sulfamethizole from Eq. 21 at 25 ± 0.1° and 0.1 *M* Ionic Strength

pH	f_0	S^2	K_s [a]
1.965	1.583×10^{-4}	1.733×10^{-7}	2.74×10^{-11}
2.102	2.526×10^{-4}	1.051×10^{-7}	2.65×10^{-11}
2.345	5.448×10^{-4}	4.693×10^{-8}	2.56×10^{-11}
2.598	1.132×10^{-3}	2.508×10^{-8}	2.85×10^{-11}
		Mean	$(2.70 \pm 0.12)10^{-11}$

[a] K_s reported as mean ± *SD*.

Table VII—Comparison of Total Silver Sulfapyridine Molar Solubility, *S*, Determined by the Method of Known Subtraction with the Molar Concentration of the Silver Ion Determined by Direct Potentiometry on Identical Samples at 25 ± 0.1°, 0.1 *M* Ionic Strength, in Nitric Acid Buffer

	pH 2.294		pH 2.486	
	$S \times 10^3$	$[Ag^+] \times 10^3$	$S \times 10^3$	$[Ag^+] \times 10^3$
	8.973	8.143	5.472	7.425
	8.889	8.018	5.514	7.514
	9.030	8.143	5.579	7.632
	9.030	8.143	5.304	7.484
	8.889	8.018	5.514	7.514
			5.660	7.454
Mean	8.962	8.093	5.508	7.504

Table VIII—Comparison of Total Silver Sulfapyridine Molar Solubility, *S*, Determined by the Method of Known Subtraction with the Molar Concentration of the Silver Ion Determined by Direct Potentiometry on Identical Samples at 25 ± 0.1°, 0.1 *M* Ionic Strength, in Nitric Acid Buffer

	pH 2.583		pH 2.848	
	$S \times 10^3$	$[Ag^+] \times 10^3$	$S \times 10^3$	$[Ag^+] \times 10^3$
	5.366	4.540	3.031	2.954
	5.336	4.488	2.974	2.874
	5.356	4.401	2.866	2.774
	5.346	4.505	2.979	2.863
	5.366	4.470	2.788	2.678
	5.356	4.436		
Mean	5.354	4.473	2.928	2.839

extremes of the low pH range were studied for silver sulfamethazine and silver sulfamethizole. For silver sulfapyridine, the entire low pH range was studied.

When tested by one-way analysis of variance, the means displayed in Tables III and IV were found not to be statistically different at the 1% confidence level. Therefore, in the low pH range, silver sulfamethazine and silver sulfamethizole are completely dissociated and the solubility is given by Eqs. 4 and 5. The solubility product is given by Eq. 1. By substituting Eqs. 2 and 3 into Eq. 5, an expression may be derived giving the ratio, f_0, of the sulfonamide anion to the total solubility, where:

$$f_0 = \frac{[X^-]}{S} = \left(1 + \frac{[H_3O^+]}{K_2} + \frac{[H_3O^+]^2}{K_1K_2}\right)^{-1} \quad \text{(Eq. 20)}$$

Combining this expression with Eqs. 1 and 4 gives:

$$K_s = f_0S^2 \quad \text{(Eq. 21)}$$

Application of Eq. 21 to the experimental data at the low pH range for silver sulfamethazine and silver sulfamethizole is given in Tables V and VI, where f_0 was calculated using the experimentally determined dissociation constants.

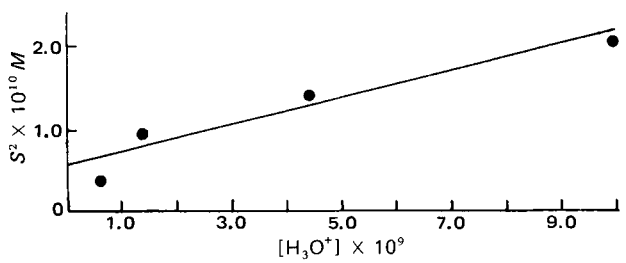

Figure 9—*Equilibrium values of* S^2 versus $[H_3O^+]$ *for silver sulfapyridine in 0.05* M *2-(N-morpholino)propanesulfonic acid buffer at 0.1* M *ionic strength and 25 ± 0.1°.*

Plots of the molar solubility of silver sulfamethazine and silver sulfamethizole over the low pH ranges studied are displayed in Figs. 10 and 11.

As shown in Scheme III, the existence of intact silver sulfapyridine in solution was proposed for the low pH nitric acid buffers. This condition is due to the high solubility of silver sulfapyridine at the low pH values studied, pH 2.294–2.583. This solubility increase is due to the effect of K_2 in Eq. 7, because K_2 is inversely proportional to solubility. The total molar solubility as determined by the method of known subtraction was compared with the molar concentration of free silver ion by direct potentiometric analysis on identical samples under the given experimental conditions for every value in the pH range studied.

When tested by one-way analysis of variance, the means displayed in Tables VII and VIII were statistically different at the 1% confidence level. At the average pH of 2.848, the values of free and total silver are not statistically different, because the decreased solubility of silver sulfapyridine does not allow enough silver or sulfonamide ions in solution to ion pair at pH 2.848. Therefore, in the pH 2.294–2.583 range, the solubility of silver sulfapyridine is given by Eq. 15. Figure 12 displays Eq. 17 ($r = 0.6893$, $p > 0.01$, 15 df), where each value represents greater than the average of five or six determinations. The intercept is 0.93 ± 0.078 SD, and the reciprocal of the slope gives (6.828 ± 2.336 SD) 10^{-9} for K_d. The intercept, 0.93, for Eq. 17 compares well with the expected value of 1, further confirming the assumption of intact silver sulfapyridine in solution in the pH range studied.

The solubility product of silver sulfapyridine is defined by Eq. 14. Substituting Eq. 20 into Eq. 14 gives:

$$K_s = f_0[Ag^+]S \quad \text{(Eq. 22)}$$

Application of Eq. 22 to the experimental data at the low pH range for silver sulfapyridine is illustrated in Table IX. The value of K_0 was found

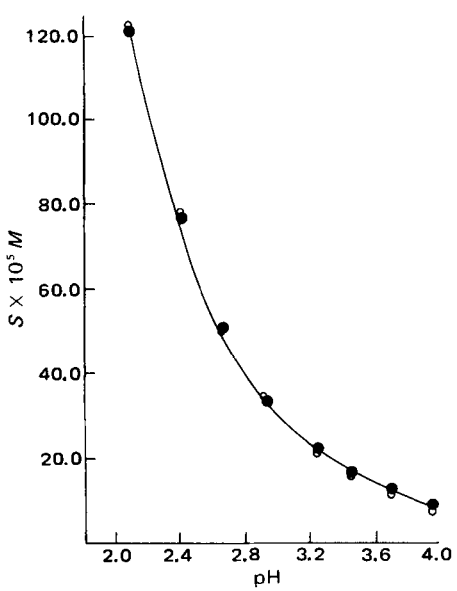

Figure 10—*Molar solubility,* S, *of silver sulfamethazine* versus *pH at 0.1* M *ionic strength and 25 ± 0.1°. Key:* ●, *calculated from Eq. 7; and* ○, *experimental values.*

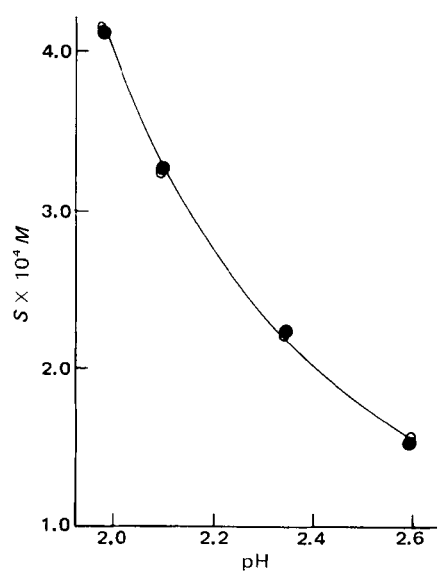

Figure 11—*Molar solubility,* S, *of silver sulfamethizole against pH at 0.1* M *ionic strength and 25 ± 0.1°. Key:* ●, *calculated from Eq. 7; and* ○, *experimental values.*

Table IX—Calculation of the Solubility Product of Silver Sulfapyridine from Eq. 22 at 25 ± 0.1° and 0.1 *M* Ionic Strength

pH	f_0	$[Ag^+]$	S	K_s
2.294	1.418×10^{-7}	8.093×10^{-3}	8.890×10^{-3}	1.02×10^{-11}
2.486	3.066×10^{-7}	5.508×10^{-3}	7.504×10^{-3}	1.27×10^{-11}
2.583	4.480×10^{-7}	4.473×10^{-3}	5.354×10^{-3}	1.07×10^{-11}
2.848	1.184×10^{-6}	2.828×10^{-3}	2.937×10^{-3}	9.80×10^{-12}
			Mean	$(1.09 \pm 0.13)10^{-11}$

[a] K_s reported as mean ± *SD*.

to equal 1.58 ± 0.25 *SD* × 10^{-3} on substitution of the experimentally determined values of K_s and K_d into Eq. 14.

A plot of the molar solubility of silver sulfapyridine over the low pH range is displayed in Fig. 13. The open circles represent experimentally determined values, and the closed circles represent values calculated using Eq. 17 in the form:

$$S = \left(\frac{[H_3O^+]^2 K_s}{K_1 K_2} + \frac{K_s}{K_2}[H_3O^+]\right)^{1/2}\left(1 + \frac{f_0 S}{K_d}\right) \qquad \text{(Eq. 23)}$$

The solubility data obtained may be used to establish a possible correlation between physically measurable properties of the silver salts of certain weak acids and their anti-infective activities. Plots of percent mortality, as reported[8] (9) for burned mice infected with *Pseudomonas aeruginosa*, *versus* log K_s and log K_2 were attempted using data for silver compounds mutually investigated. There was little correlation between percent mortality and log K_s or log K_2 for the silver salts plotted. There was a large disparity in biological effectiveness for silver sulfonamides of similar log K_s values.

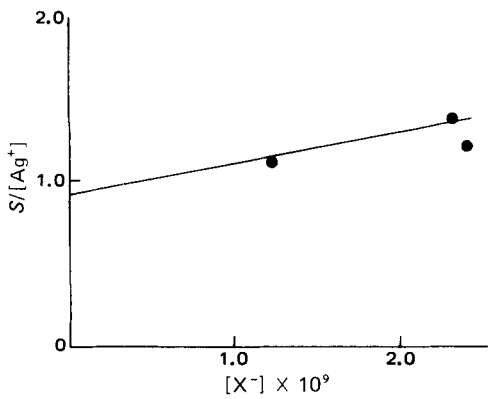

Figure 12—*Equilibrium values of* S/[Ag^+] *against* [X^-] *(sulfapyridine anion) for silver sulfapyridine in nitric acid buffer at 0.1* M *ionic strength and 25 ± 0.1°.*

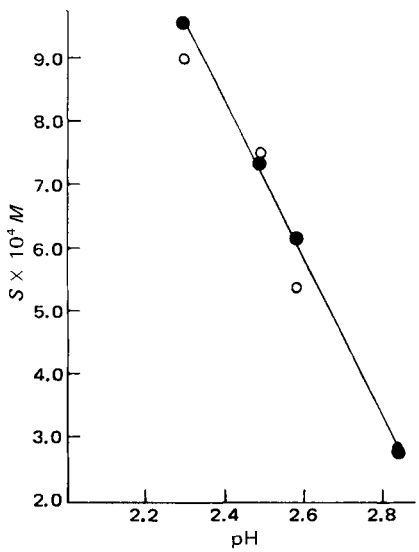

Figure 13—*Molar solubility,* S, *of silver sulfapyridine* versus *pH at 0.1* M *ionic strength and 25 ± 0.1°. Key:* ●, *calculated from Eq. 23; and* ○, *experimental values.*

[8] J. Stanford, Columbia University College of Physicians and Surgeons, New York, N.Y., personal communication, 1976.

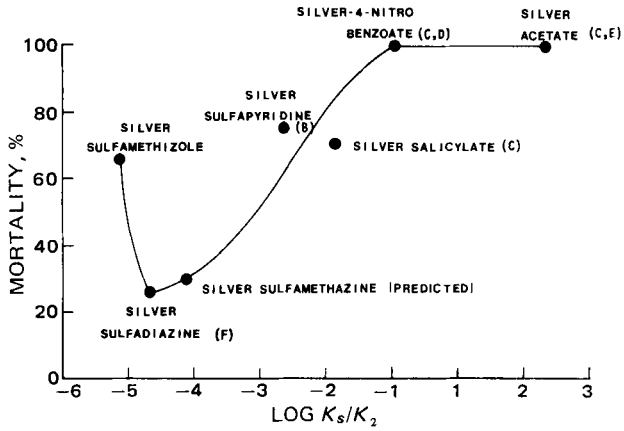

Figure 14—*Percent mortality* versus *log* K_s/K_2. *Percent mortality was taken from Ref. 9, except as indicated. Key: B, percent mortality from J. Stanford (see footnote 8); C,* K_2 *from Ref. 12; D,* K_s *from Ref. 10; E,* K_s *from Ref. 11; and F,* K_s *from Ref. 1.*

However, by combining K_s with K_2, the percent mortality *versus* log K_s/K_2 plot (Fig. 14) reveals a minimum for silver sulfadiazine as compared to other silver salts of weak organic acids. The K_2 values (dissociation constant for monoprotonated acid) and solubility products for silver 4-nitrobenzoate, silver salicylate, and silver acetate are literature values (10–12). The K_2 value for silver sulfadiazine was determined previously (1). The percent mortality value for silver sulfamethazine was predicted using the experimentally determined value for the log K_s/K_2 ratio. For this set of data, the efficacy of silver sulfadiazine in the treatment of burn wound sepsis apparently is directly related to its unique physical–chemical properties, where the dissociation and solubility are involved in providing the most favorable concentration of the silver ion for anti-infective activity.

REFERENCES

(1) R. U. Nesbitt, Jr., and B. J. Sandmann, *J. Pharm. Sci.*, **66**, 519 (1977).

(2) C. L. Fox, Jr., and S. M. Modak, *Antimicrob. Agents Chemother.*, **5**, 582 (1974).

(3) S. Rosenzweig and W. Fuchs, U.S. pat. 2,536,095 (1951).

(4) B. J. Sandmann, R. U. Nesbitt, Jr., and R. A. Sandmann, *J. Pharm. Sci.*, **63**, 948 (1974).

(5) R. A. Durst, in "Ion Selective Electrodes," R. A. Durst, Ed., National Bureau of Standards Special Publication No. 314, U.S. Government Printing Office, Washington, D.C., 1969, pp. 381–385.

(6) *Orion Research Inc. Newsletter*, **1**, 4 (1969).

(7) R. G. Bates, "Determination of pH Theory and Practice," 2nd ed., Wiley, New York, N.Y., 1973, p. 96.

(8) P. H. Bell and R. O. Roblin, Jr., *J. Am. Chem. Soc.*, **64**, 2905 (1942).

(9) W. Stanford, B. W. Rappole, and C. L. Fox, Jr., *J. Trauma*, **9**, 378 (1969).

(10) N. F. Linke, "Solubilities of Inorganic and Metal Organic Compounds," vol. I, 4th ed., Van Nostrand, Princeton, N.J., 1958, p. 48.

(11) J. N. Butler, "Ionic Equilibrium, a Mathematical Approach," Addison-Wesley, Reading, Mass., 1964, p. 468.

(12) A. Albert and E. P. Serjeant, "The Determination of Ionization Constants," Chapman and Hall Ltd., London, England, 1971, chap. 8.

ACKNOWLEDGMENTS

Presented at the Basic Pharmaceutics Section, APhA Academy of Pharmaceutical Sciences, New Orleans meeting, April 1976.

Supported in part by Marion Laboratories.

R. U. Nesbitt, Jr., is a Fellow, Robert Lincoln McNeil Memorial, and a Fellow, American Foundation for Pharmaceutical Education.

Evidence for a Trimodal Pattern of Acetylation of Isoniazid in Uremic Subjects

DENNIS J. CHAPRON *x, M. ROBERT BLUM ‡, and PAUL A. KRAMER *

Received July 18, 1977, from the **School of Pharmacy, University of Connecticut, Storrs, CT 06268, and the Department of Pharmacy, University of Connecticut Health Center, Farmington, CT 06032,* and the ‡*School of Pharmacy, University of North Carolina, Chapel Hill, NC 27514.* Accepted for publication October 25, 1977.

Abstract □ Isoniazid metabolic clearance values were calculated retrospectively and plotted on a frequency distribution histogram. A trimodal distribution pattern was observed. According to a two-allele codominant model, the mean clearance values of the slow and rapid acetylators closely predicted the mean clearance value for the intermediate acetylators. The potential clinical implications of identifying intermediate and rapid acetylators of isoniazid and its use in renal failure are discussed.

Keyphrases □ Isoniazid acetylation—genetic phenotypes determined using metabolic clearance values in humans □ Acetylation—isoniazid in humans, genetic phenotypes determined using metabolic clearance values □ Genetic phenotypes—of isoniazid acetylation in humans, determined using metabolic clearance values □ Metabolic clearance values—used to determine genetic phenotypes of isoniazid acetylation in humans □ Tuberculostatic antibacterials—isoniazid, genetic phenotypes of acetylation determined using metabolic clearance values in humans

Several widely used medications are metabolized by polymorphic acetylation in humans. Such drugs include isoniazid, hydralazine, procainamide, sulfamethazine, sulfapyridine, and dapsone (1–7). Genetic studies demonstrated that the acetylation polymorphism involved is controlled by two allelic genes at a single locus; slow acetylators are homozygous for the gene controlling slow acetylation, and fast acetylators are either heterozygous or homozygous for the gene controlling fast acetylation (1). Furthermore, Schloot *et al.* (8) presented evidence that the quantitative effects of the two alleles (or gene products) were simply additive.

BACKGROUND

Because the therapeutic or toxic response to polymorphically acetylated drugs may differ among the phenotypes, several methods have been developed for acetylator phenotyping in humans. Most procedures can accurately separate fast and slow acetylators, but none can adequately differentiate homozygous and heterozygous fast acetylators (9). For the sake of simplicity, heterozygous and homozygous fast acetylators will be referred to as intermediate and rapid acetylators, respectively.

The lumping of intermediate and rapid acetylators together has an obvious disadvantage, since the two phenotypes may differ with regard to therapeutic or toxic drug response. This difference may be particularly important for isoniazid; it recently was demonstrated (10) that severe hepatotoxic reactions to this drug occur predominately in fast acetylators. However, intermediate and rapid acetylators were not separated in that investigation. Consequently, demonstration of three isoniazid acetylation phenotypes could provide new insights into the nature of isoniazid toxicity.

A preliminary study suggested that metabolic clearance determination may serve as a useful technique for separating intermediate and rapid acetylators (11). Recently, Gold *et al.* (12) reported isoniazid half-lives following intravenous administration to 18 patients with chronic renal insufficiency. By using an antimodal value of 118 min for the isoniazid half-life, they classified 11 patients as apparent slow acetylators and seven as apparent fast acetylators. These isoniazid data allowed for the direct calculation of metabolic clearance.

Furthermore, since acetylation is a major pathway for isoniazid removal from plasma, differences in metabolic clearance between uremic individuals should reflect differences in acetylation capacity. Because isoniazid is not appreciably bound to plasma protein, disease-induced change in plasma proteins would not be expected to alter pharmacokinetic parameters significantly (13). Therefore, the data of Gold *et al.* (12) were evaluated to demonstrate a trimodal acetylation pattern of isoniazid in uremic subjects.

EXPERIMENTAL

Values of $t_{1/2u}$ and V_d (12) were calculated with the assumption that the data obey the kinetics of a one-compartment model. Although biexponential decline would have been observed had more data points been obtained at the early time points, the error involved in assuming monoexponential decay is minimal (14). Thus, metabolic clearance, *MC*, was calculated according to:

$$MC = \frac{0.693 V_d}{t_{1/2u}} \qquad \text{(Eq. 1)}$$

where $t_{1/2u}$ is the isoniazid half-life in uremic subjects and V_d is the volume of distribution of the drug as reported by Gold *et al.* (12). Each clearance value was corrected to body weight.

RESULTS AND DISCUSSION

When the computed metabolic clearance values were plotted on a frequency distribution histogram, a trimodal pattern became apparent, with approximate antimodes at 3.9 and 6.8 ml/min/kg (Fig. 1). The clearance method appears to classify individuals as slow, intermediate, or rapid acetylators. Table I lists the mean metabolic clearance ($\pm SD$) of isoniazid for each acetylator phenotype. In the absence of family data, definitive genotypic classification is not possible.

From the distribution histogram shown in Fig. 1, it is apparent that the clearance method allows for a clearer separation of the three phenotypes than does the half-life method where there is evident confluence of the two phenotypes. Subject 7, listed as a slow acetylator by Gold *et al.* (12), was classified as an intermediate acetylator by the clearance method.

Furthermore, some simple genetic calculations lend support to the observed trimodal distribution of isoniazid metabolic clearance values. The genetics of the polymorphism for isoniazid acetylation in humans assume a two allele codominant model: two alleles, Ac^R (rapid acetylator)

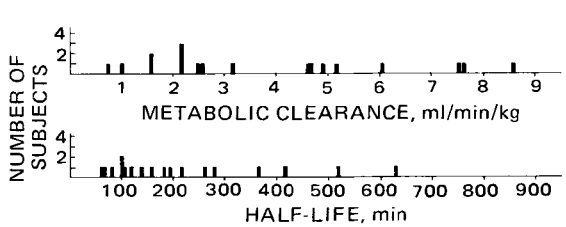

Figure 1—*Distribution of corrected metabolic clearance values and half-lives of isoniazid in 18 uremic patients.*

0022-3549/78/0700/1018$01.00/0
© 1978, American Pharmaceutical Association

Table I—Mean Isoniazid Metabolic Clearance Values as a Function of Acetylator Status

Acetylator Status	Number of Subjects	Isoniazid Clearance ± *SD*, ml/min/kg
Slow	10	2.0 ± 0.8
Intermediate	5	5.1 ± 0.6
Rapid	3	7.9 ± 0.6

and Ac^S (slow acetylator), for one autosomal gene locus (8). Slow acetylators are designated Ac^S/Ac^S, while intermediate and rapid acetylators are designated Ac^R/Ac^S and Ac^R/Ac^R, respectively.

As reported in Table I, the arithmetic mean of the acetylation capacity of the genotype Ac^S/Ac^S is 2.0 ml/min/kg. The value of the allele Ac^S is thus 2.0/2 = 1.0. Genotype Ac^R/Ac^R has the mean value of 7.9 ml/min/kg; for the allele Ac^R, 7.9/2 = 3.95 or approximately 4.0. Since the quantitative effect (or gene product) of the alleles is considered additive, the mean acetylation capacity for the group Ac^R/Ac^S should follow the relationship:

$$\frac{Ac^S/Ac^S}{2} + \frac{Ac^R/Ac^R}{2} = Ac^R/Ac^S \qquad \text{(Eq. 2)}$$

Thus, based on the calculations from the mean slow and rapid acetylator modes, the expected mean acetylation capacity of the heterozygote would be 5.0 ml/min/kg [(2.0/2) + (7.95/2)]. The observed mean value for the intermediate acetylator was 5.10 ml/min/kg, a difference of less than 3% from the expected value of 5.0 ml/min/kg. Although these retrospective data apply only to uremic patients, they do support the concept that acetylation clearance determinations may represent a useful method for identifying slow, intermediate, and rapid acetylators.

Finally, significant amounts of acetylisoniazid appear in the urine of normal subjects following oral administration of isoniazid, approximately 49 and 32% of the dose in fast and slow acetylators, respectively (10). Obviously, kidney failure should reduce significantly the contribution of the renal excretory pathway for acetylisoniazid. Thus, uremic patients receiving isoniazid might accumulate substantial levels of acetylisoniazid and, subsequently, be exposed to excessive amounts of its metabolite, acetylhydrazine. Acetylhydrazine is subsequently oxidized to hepatotoxic substances (15).

None of the published reports of isoniazid kinetics in renal failure examined the possibility of metabolite accumulation (12, 16, 17). There is a great need to study the effects of renal insufficiency on the plasma and urinary excretion kinetics of acetylisoniazid and metabolites and the potential for removal by dialysis. It is also important to investigate the effects of uremia on acetylisoniazid hydrolysis, as well as the oxidative activation of acetylhydrazine to toxic substances.

REFERENCES

(1) D. A. P. Evans, K. A. Manley, and V. A. McKusick, *Br. Med. J.*, **2**, 485 (1960).

(2) D. A. P. Evans and T. A. White, *J. Lab. Clin. Med.*, **63**, 394 (1964).

(3) J. Elson, J. M. Strong, W. K. Lee, and A. Atkinson, *Clin. Pharmacol. Ther.*, **17**, 134 (1975).

(4) D. A. P. Evans, *J. Med. Genet.*, **6**, 405 (1969).

(5) K. V. N. Rao, D. A. Metchison, N. G. K. Nair, K. Prema, and S. P. Tripathy, *Br. Med. J.*, **3**, 495 (1970).

(6) H. Schroder and D. A. P. Evans, *J. Med. Genet.*, **9**, 168 (1972).

(7) R. Gelber, J. H. Peters, G. R. Gordon, A. J. Glazko, and L. Levy, *Clin. Pharmacol. Ther.*, **12**, 225 (1971).

(8) W. Schloot, K. G. Blume, and H. W. Goedde, *Humangenetik*, **4**, 274 (1967).

(9) E. M. Scott, R. C. Wright, and D. D. Weaver, *J. Clin. Invest.*, **48**, 1173 (1969).

(10) J. R. Mitchell, U. P. Thorgeisson, M. Black, J. A. Timbrell, W. R. Snodgrass, W. Z. Potter, D. J. Jollow, and H. R. Keiser, *Clin. Pharmacol. Ther.*, **18**, 70 (1975).

(11) D. J. Chapron and M. R. Blum, *J. Clin. Pharmacol.*, **16**, 338 (1976).

(12) C. H. Gold, N. Buchannan, V. Trigham, M. Viljoen, B. Strickwold, and G. P. Moodley, *Clin. Nephrol.*, **6**, 365 (1976).

(13) H. G. Boxenbaum, I. Bekersky, U. Mattaliano, and S. A. Kaplan, *J. Pharmacokinet. Biopharm.*, **3**, 443 (1975).

(14) H. G. Boxenbaum and S. Riegelman, *ibid.*, **4**, 287 (1976).

(15) S. D. Nelson, J. R. Mitchell, J. A. Timbrell, W. R. Snodgrass, and G. B. Corcoran, *Science*, **193**, 901 (1976).

(16) M. M. Reidenberg, L. Shear, and R. V. Cohen, *Am. Rev. Resp. Dis.*, **108**, 1426 (1973).

(17) D. W. Bowersox, R. H. Winterbauer, C. L. Stewart, O. Burton, and E. Barron, *N. Engl. J. Med.*, **289**, 84 (1973).

ACKNOWLEDGMENTS

Supported in part by Grant 5.171-000-22-1002-35-297 from the University of Connecticut Research Foundation.

Ketonic Oxidation Products of Cyclobarbital

R. BOUCHE *x, M. DRAGUET-BRUGHMANS *, J. P. FLANDRE *, C. MOREAUX ‡, and M. VAN MEERSSCHE ‡

Received July 12, 1977, from the **Laboratoire d'Analyse des Médicaments, Institut de Pharmacie, U.C.L. 7340, 1200 Bruxelles, Belgium,* and the ‡*Unité de Chimie Physique et de Cristallographie, Bâtiment Lavoisier, 1348 Louvain-La-Neuve, Belgium.* Accepted for publication October 25, 1977.

Abstract □ Chemical or biochemical oxidation of cyclobarbital yielded 5-(3-oxo-1-cyclohexen-1-yl)-5-ethyl -2,4,6- (1*H*,3*H*,5*H*)-pyrimidinetrione, and photochemical oxidation gave 5-(6-oxo-1-cyclohexen-1-yl)-5-ethyl-2,4,6-(1*H*,3*H*,5*H*)-pyrimidinetrione. These compounds were isolated and purified by TLC, and their structures were determined by UV, IR, NMR, and mass spectral data; the crystalline structure was determined by X-ray diffraction.

Keyphrases □ Cyclobarbital—oxidation products isolated and identified □ Oxidation—cyclobarbital, products isolated and identified □ Depressants, central—cyclobarbital, oxidation products isolated and identified

The identification of ketonic oxidation products of cyclobarbital[1] [5-(1-cyclohexen-1-yl)-5-ethyl-2,4,6-(1*H*,3*H*,5*H*)-pyrimidinetrione] (I) has been reported by several investigators. Tsukamoto *et al.* (1) isolated a ketonic derivative from rabbit urine; it was identified by UV spectrometry and chemical means as 5-(3-oxo-1-cyclohexen-1-yl)-5-ethyl-2,4,6-(1*H*,3*H*,5*H*)-pyrimidinetrione (II). Later, Goldschmidt and Koss (2) extracted this same product (II) from rat urine, while Willems *et al.* (3) iden-

[1] Phanodorm, British pat. 231,150 (1924) to Farbenfabriken Bayer and Co.

0022-3549/78/0700/1019$01.00/0

© 1978, American Pharmaceutical Association

Table I—Mean Isoniazid Metabolic Clearance Values as a Function of Acetylator Status

Acetylator Status	Number of Subjects	Isoniazid Clearance ± *SD*, ml/min/kg
Slow	10	2.0 ± 0.8
Intermediate	5	5.1 ± 0.6
Rapid	3	7.9 ± 0.6

and Ac^S (slow acetylator), for one autosomal gene locus (8). Slow acetylators are designated Ac^S/Ac^S, while intermediate and rapid acetylators are designated Ac^R/Ac^S and Ac^R/Ac^R, respectively.

As reported in Table I, the arithmetic mean of the acetylation capacity of the genotype Ac^S/Ac^S is 2.0 ml/min/kg. The value of the allele Ac^S is thus 2.0/2 = 1.0. Genotype Ac^R/Ac^R has the mean value of 7.9 ml/min/kg; for the allele Ac^R, 7.9/2 = 3.95 or approximately 4.0. Since the quantitative effect (or gene product) of the alleles is considered additive, the mean acetylation capacity for the group Ac^R/Ac^S should follow the relationship:

$$\frac{Ac^S/Ac^S}{2} + \frac{Ac^R/Ac^R}{2} = Ac^R/Ac^S \qquad \text{(Eq. 2)}$$

Thus, based on the calculations from the mean slow and rapid acetylator modes, the expected mean acetylation capacity of the heterozygote would be 5.0 ml/min/kg [(2.0/2) + (7.95/2)]. The observed mean value for the intermediate acetylator was 5.10 ml/min/kg, a difference of less than 3% from the expected value of 5.0 ml/min/kg. Although these retrospective data apply only to uremic patients, they do support the concept that acetylation clearance determinations may represent a useful method for identifying slow, intermediate, and rapid acetylators.

Finally, significant amounts of acetylisoniazid appear in the urine of normal subjects following oral administration of isoniazid, approximately 49 and 32% of the dose in fast and slow acetylators, respectively (10). Obviously, kidney failure should reduce significantly the contribution of the renal excretory pathway for acetylisoniazid. Thus, uremic patients receiving isoniazid might accumulate substantial levels of acetylisoniazid and, subsequently, be exposed to excessive amounts of its metabolite, acetylhydrazine. Acetylhydrazine is subsequently oxidized to hepatotoxic substances (15).

None of the published reports of isoniazid kinetics in renal failure examined the possibility of metabolite accumulation (12, 16, 17). There is a great need to study the effects of renal insufficiency on the plasma and urinary excretion kinetics of acetylisoniazid and metabolites and the potential for removal by dialysis. It is also important to investigate the effects of uremia on acetylisoniazid hydrolysis, as well as the oxidative activation of acetylhydrazine to toxic substances.

REFERENCES

(1) D. A. P. Evans, K. A. Manley, and V. A. McKusick, *Br. Med. J.*, **2**, 485 (1960).

(2) D. A. P. Evans and T. A. White, *J. Lab. Clin. Med.*, **63**, 394 (1964).

(3) J. Elson, J. M. Strong, W. K. Lee, and A. Atkinson, *Clin. Pharmacol. Ther.*, **17**, 134 (1975).

(4) D. A. P. Evans, *J. Med. Genet.*, **6**, 405 (1969).

(5) K. V. N. Rao, D. A. Metchison, N. G. K. Nair, K. Prema, and S. P. Tripathy, *Br. Med. J.*, **3**, 495 (1970).

(6) H. Schroder and D. A. P. Evans, *J. Med. Genet.*, **9**, 168 (1972).

(7) R. Gelber, J. H. Peters, G. R. Gordon, A. J. Glazko, and L. Levy, *Clin. Pharmacol. Ther.*, **12**, 225 (1971).

(8) W. Schloot, K. G. Blume, and H. W. Goedde, *Humangenetik*, **4**, 274 (1967).

(9) E. M. Scott, R. C. Wright, and D. D. Weaver, *J. Clin. Invest.*, **48**, 1173 (1969).

(10) J. R. Mitchell, U. P. Thorgeisson, M. Black, J. A. Timbrell, W. R. Snodgrass, W. Z. Potter, D. J. Jollow, and H. R. Keiser, *Clin. Pharmacol. Ther.*, **18**, 70 (1975).

(11) D. J. Chapron and M. R. Blum, *J. Clin. Pharmacol.*, **16**, 338 (1976).

(12) C. H. Gold, N. Buchannan, V. Trigham, M. Viljoen, B. Strickwold, and G. P. Moodley, *Clin. Nephrol.*, **6**, 365 (1976).

(13) H. G. Boxenbaum, I. Bekersky, U. Mattaliano, and S. A. Kaplan, *J. Pharmacokinet. Biopharm.*, **3**, 443 (1975).

(14) H. G. Boxenbaum and S. Riegelman, *ibid.*, **4**, 287 (1976).

(15) S. D. Nelson, J. R. Mitchell, J. A. Timbrell, W. R. Snodgrass, and G. B. Corcoran, *Science*, **193**, 901 (1976).

(16) M. M. Reidenberg, L. Shear, and R. V. Cohen, *Am. Rev. Resp. Dis.*, **108**, 1426 (1973).

(17) D. W. Bowersox, R. H. Winterbauer, C. L. Stewart, O. Burton, and E. Barron, *N. Engl. J. Med.*, **289**, 84 (1973).

ACKNOWLEDGMENTS

Supported in part by Grant 5.171-000-22-1002-35-297 from the University of Connecticut Research Foundation.

Ketonic Oxidation Products of Cyclobarbital

R. BOUCHE *x, M. DRAGUET-BRUGHMANS *, J. P. FLANDRE *, C. MOREAUX ‡, and M. VAN MEERSSCHE ‡

Received July 12, 1977, from the **Laboratoire d'Analyse des Médicaments, Institut de Pharmacie, U.C.L. 7340, 1200 Bruxelles, Belgium,* and the ‡*Unité de Chimie Physique et de Cristallographie, Bâtiment Lavoisier, 1348 Louvain-La-Neuve, Belgium.* Accepted for publication October 25, 1977.

Abstract □ Chemical or biochemical oxidation of cyclobarbital yielded 5-(3-oxo-1-cyclohexen-1-yl)-5-ethyl -2,4,6- (1*H*,3*H*,5*H*)-pyrimidinetrione, and photochemical oxidation gave 5-(6-oxo-1-cyclohexen-1-yl)-5-ethyl-2,4,6-(1*H*,3*H*,5*H*)-pyrimidinetrione. These compounds were isolated and purified by TLC, and their structures were determined by UV, IR, NMR, and mass spectral data; the crystalline structure was determined by X-ray diffraction.

Keyphrases □ Cyclobarbital—oxidation products isolated and identified □ Oxidation—cyclobarbital, products isolated and identified □ Depressants, central—cyclobarbital, oxidation products isolated and identified

The identification of ketonic oxidation products of cyclobarbital[1] [5-(1-cyclohexen-1-yl)-5-ethyl-2,4,6-(1*H*,3*H*,5*H*)-pyrimidinetrione] (I) has been reported by several investigators. Tsukamoto *et al.* (1) isolated a ketonic derivative from rabbit urine; it was identified by UV spectrometry and chemical means as 5-(3-oxo-1-cyclohexen-1-yl)-5-ethyl-2,4,6-(1*H*,3*H*,5*H*)-pyrimidinetrione (II). Later, Goldschmidt and Koss (2) extracted this same product (II) from rat urine, while Willems *et al.* (3) iden-

[1] Phanodorm, British pat. 231,150 (1924) to Farbenfabriken Bayer and Co.

0022-3549/78/0700/1019$01.00/0

© 1978, American Pharmaceutical Association

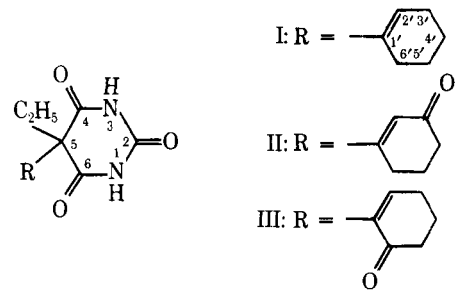

tified 5-(6-oxo-1-cyclohexen-1-yl)-5-ethyl-2,4,6-(1*H*,3*H*,5*H*)-pyrimidinetrione (III) as a degradation product of I using IR, NMR, and mass spectral data.

The purposes of this study were to establish the definitive characteristics of both II and III by physicochemical methods and to prove exclusive production of II or III from I by photochemical, chemical, and human biochemical means.

EXPERIMENTAL

TLC System—Silica gel[2] glass plates (20 × 20 cm, thickness of 0.5 mm) were activated for 1 hr at 100° and used immediately after cooling. A portion (20 mg) of the product, dissolved in a minimum volume of acetone, was deposited in a band 2 cm from the bottom edge of the plate. Ascending development was achieved in a chromatographic tank saturated with chloroform–acetone–methanol [90:10:1 (v/v)].

GLC System[3]—A glass column (2.0 m long and 4.0 mm i.d.) was packed with 3% OV-17[4] on 100–120-mesh Gas Chrom Q[4] and then conditioned at 240° overnight. Chromatographic conditions were: column oven, 230°; injection port and flame-ionization detector, 250°; and nitrogen gas flow, 40 ml/min. A 2-μl aliquot of a 1-mg/ml methanol solution was injected.

UV Spectrophotometry[5]—UV spectra of the derivatives were recorded between 220 and 300 nm with a double-beam spectrophotometer in 1-cm quartz cells. The pH of the solutions was adjusted to 2.0, 10.0, and 13.0 by appropriate buffers. Concentrations were $\sim 10^{-4}$ *M*.

IR Spectrophotometry[6]—IR spectra were recorded in potassium bromide disks (0.5% w/w) and in saturated dichloromethane solutions (cell thickness of 1.0 mm).

Mass Spectrometry[7]—A portion (1.0 mg) of solid substance was injected into the spectrometer. The ionization potential was 70 ev.

Proton NMR Spectroscopy[8]—Spectra were recorded from a saturated solution of deuterated methanol.

X-Ray Diffraction[9]—The diffractometer was a four-circle, punchcard-operated unit. Signal intensities were measured by ω–2θ scanning to $2\theta_{max}$: 110°. Radiation was Cu–K with λ = 1.5418 Å. Structures were resolved by the MULTAN 74 computer program and refined by a full-matrix least-squares procedure[10,11].

Preparation of I—A commercial product[12] was extracted and purified by successive methanol extractions; it was then dried to a constant melting point (170°).

Preparation of II—A portion (500 mg) of I purified by TLC was administered orally to human subjects. Urine was monitored for 24 hr after administration and ether extracted in an acid medium [10% (w/w) sulfuric acid]. The ether fraction was evaporated to dryness and separated by TLC. Four spots appeared at R_f 0.05, 0.07, 0.25, and 0.48. The band corresponding to R_f 0.25 was methanol extracted. After the methanol was evaporated, the residue was purified by fractional sublimation at 200° under 10^{-1} torr.

[2] Silica gel GF_{254}, type 60, Stahl (Merck).
[3] HP 5750 gas chromatograph fitted with a flame-ionization detector.
[4] Applied Science Laboratories.
[5] Perkin-Elmer model 124 UV-visible double-beam spectrophotometer.
[6] Perkin-Elmer model 580 IR spectrophotometer.
[7] LKB model 9000 S mass spectrometer.
[8] Varian model XL 100 NMR spectrometer.
[9] Picker X-ray four-circle diffractometer.
[10] P. Main, H. M. Woolfson, L. Lessinger, G. Germain, and J. P. Declercq, Multan 74, York, England, and Louvain-La-Neuve, Belgium, 1974.
[11] F. R. Ahmed, S. R. Hall, M. E. Pippy, and C. P. Huber, NCR Crystallographic Programs for the IBM/360 System, National Research Council, Ottawa, Canada, 1966.
[12] Phanodome Calcium, Merck, Darmstadt, West Germany.

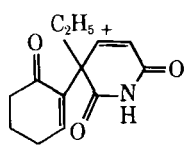
IV: *m/e* 233

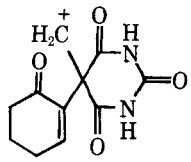
V: *m/e* 235

Preparation of III—One gram of I (acid form) was exposed for 48 hr to 254-nm UV radiation, and the product was purified by TLC. Four spots appeared at R_f 0.13, 0.19, 0.28, and 0.52. The band corresponding to the third spot was methanol extracted. After methanol evaporation, the residue was purified by fractional sublimation at 250° under 10^{-1} torr.

RESULTS AND DISCUSSION

The melting temperature of II, 227°, was in good agreement with the oxidation product melting temperature (222°) reported previously (4), taking into account a possible sublimation of the product. On the other hand, no sudden melting point was observed for III, which decomposed at about 290°. The much lower melting temperature reported in the literature (3, 5) may have been due to impurities or, more probably, to sublimation of III at 255°.

In solution, II and III had the same IR absorption bands as I at 1762, 1740, and 1712 cm^{-1}; this finding supports the integrity of the 2,4,6-(1*H*,3*H*,5*H*)-pyrimidinetrione ring. In addition, these products showed the same spectral changes as I in the UV region, dependent on pH.

Nevertheless, II and III differed from I by an additional absorption band at 218 (II) and 213 (III) nm (pH 2.0), by a fourth band at 1677 (II) and 1670 (III) cm^{-1}, and by an ion molecular peak at *m/e* 250. The additional oxygen atom in the carbonyl group conjugated together with a double bond allows two structure possibilities: the 5-(3-oxo-1-cyclohexen-1-yl) or the 5-(6-oxo-1-cyclohexen-1-yl) substituent. The NMR spectra of I and III were identical with those published (3); the chemical shifts of the olefinic proton were 5.84 and 7.32 ppm, respectively. The olefinic proton chemical shift of II was 6.06 ppm.

The theoretical value of the olefinic proton chemical shift may be calculated for the two possible isomers using the additive increments of

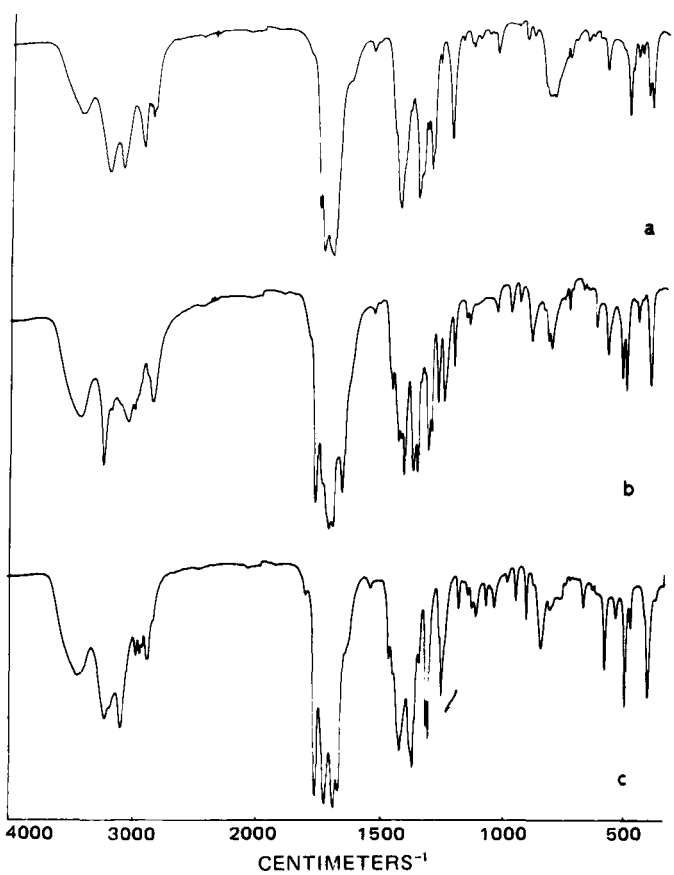

Figure 1—*IR spectra in potassium bromide disks of I (a), II (b), and III (c).*

Table I—Crystal Data of I–III

	I[a]	II	III
Molecular formula	$C_{12}H_6N_2O_3$	$C_{12}H_{14}N_2O_4$	$C_{12}H_{14}N_2O_4$
Molecular weight	236.26	250.25	250.25
System	Monoclinic	Monoclinic	Monoclinic
Space group	C2/c	$P2_1$	$P2_1/c$
Unit cell dimensions, Å or degrees			
a	22.415 (6)	8.822 (3)	9.719 (3)
b	10.770 (6)	10.072 (3)	17.081 (5)
c	10.350 (5)	6.848 (2)	12.273 (4)
β	92.29 (5)	104.07 (2)	143.11 (3)
Unit cell volume, Å^3	2496.6	590.2	1223.0
Number of formula units per cell = z	8	2	4
Density, D_X, g/cm^3	1.258	1.407	1.358

[a] Values from Ref. 12.

Matter *et al.* (6): $\delta = 5.25 + Z_{cis} + Z_{gem} + Z_{trans}$. The Z_{cis} shielding increment corresponding to 2,4,6-(1*H*,3*H*,5*H*)-pyrimidinetrione-5-ethyl radical was estimated at 0.14 when using the olefinic proton chemical shift of I. This procedure provided chemical shifts of 6.21 (II) and 6.95 (III) ppm. Moreover, the NMR spectrum of the olefinic proton of II exhibited a nonresolved multiplet, corresponding to only lone-range coupling. For III, a triplet corresponding to a J_3 coupling constant due to the neighboring methylene was observed. This observation removed any ambiguity about formulas of II and III.

The main difference between the mass spectra of II and III was the presence of two very strong peaks at M − 15 and M − 17 for III (3, 7), which may be explained by formation of radicals IV and V. They arise from a stronger interaction of the cyclohexenyl ring and the ethyl substituent of the 2,4,6-(1*H*,3*H*,5*H*)-pyrimidinetrione ring.

In the solid phase, the IR absorption of these chemically related products showed appreciable differences of the crystalline lattice. In solution, IR spectra of I, II, and III showed the same absorption bands with the same relative intensities at 1760, 1737, and 1712 cm^{-1} and additional bands at 1677 and 1670 cm^{-1} for II and III, respectively. However, the print of these three compounds differed in this latter region when spectra were recorded in potassium bromide disks (Fig. 1).

The very strong intensity of the 1760-cm^{-1} band of II and III suggests a decoupling of the 4,6-carbonyl vibrators (8) arising either from a change in the geometry and rigidity of the 2,4,6-(1*H*,3*H*,5*H*)-pyrimidinetrione ring or from an intermolecular hydrogen bond asymmetry. Moreover, the shift of the absorption band corresponding to the ethylenic carbonyl group, 27 (II) and 7 (III) cm^{-1}, indicates the existence of a hydrogen bond, including an oxygen atom, in II. In a diluted solution, the 3380-cm^{-1} band arose for the three compounds from the free NH valence vibration. As a potassium bromide disk, I gave two broad bands at 3210 and 3090 cm^{-1}, which Bellamy (9) associated with cyclic dimer formation. In the spectrum of III, the same two bands appeared; however, the first was accompanied by a distinct shoulder at 3170 cm^{-1}. This fact may suggest the existence of two different intermolecular hydrogen bonds.

Compound II showed a very strong absorption band at 3230 cm^{-1} with two relatively weak bands at 3170 and 3030 cm^{-1}. Miyazawa (10, 11) studied and solved the problems of the secondary associated amide absorption and, more specifically, of the *cis*-cyclic lactams. He identified the in-plane deformation band as dropping near 1440 cm^{-1}. Therefore, it is possible to consider the absorption band in the 3100-cm^{-1} region as a combination band of the NH in-plane mode and the carbonyl absorption. The existence of two separate bands in this region suggests the existence of two intermolecular bond types, which differ one from another in length and/or NH···O bond angle. This fact must be considered together with the shift of the cyclohexenyl carbonyl vibration frequency. This assignment was confirmed by the partially deuterated product

Table II—Interatomic Lengths[a] of the Carbonyl Groups in II and III[b]

Carbonyl Group Position	II	III
2	1.205	1.203
4	1.201	1.223
6	1.220	1.225
3′[c]	1.229	—
6′[c]	—	1.214

[a] Lengths in angstroms. [b] Results obtained by X-ray diffraction. [c] The 3′- and 6′-carbonyls are the 3-oxo-1-cyclohexen-1-yl and 6-oxo-1-cyclohexen-1-yl carbonyl groups, respectively.

Table III—Intermolecular Hydrogen Bond Characteristics of I–III

	Contact	Length, Å, N···O	Length, Å, NH	Angle, NH···O
I[a]				
$N_1I^b \rightarrow O_2III$	+ + 1 0 1	2.89		
$N_3I \rightarrow O_4III$	+ 1 0 0	2.85		
$N_2II \rightarrow O_2IV$	− − 1 0 2	2.89		
$N_3II \rightarrow O_4IV$	− − 1 0 1	2.85		
$N_1V \rightarrow O_2VII$	+ + 1 0 1	2.89		
$N_3V \rightarrow O_4VII$	+ 1 0 0	2.85		
$N_1VI \rightarrow O_2VIII$	− − 1 0 2	2.89		
$N_3VI \rightarrow O_4VII$	− − 1 0 1	2.85		
II				
$N_1I \rightarrow O_{3'}{}^bII$	+ − + 2 1 2	2.82	1.03	170.5°
$O_6I \rightarrow N_3I$	+ 0 0 1	2.88	0.90	164.5°
$N_3I \rightarrow O_6I$	− 0 0 1	2.88	0.90	164.5°
$O_{3'}{}^bI \rightarrow N_1II$	+ + 2 0 2	2.82	1.03	170.5°
III				
$N_1I \rightarrow O_4IV$	− − 1 0 1	2.99	0.94	167.3°
$O_6I \rightarrow N_3IV$	− − 1 0 1	2.85	0.95	174.5°
$N_3I \rightarrow O_6IV$	+ 1 0 0	2.85	0.95	174.5°
$O_4I \rightarrow N_1IV$	+ 1 0 0	2.99	0.94	167.3°
$N_1II \rightarrow O_4III$	+ − 1 1 0	2.99	0.94	167.3°
$O_6II \rightarrow N_3III$	+ − 1 1 0	2.85	0.95	174.5°
$N_3II \rightarrow O_6III$	− − − 1 1 1	2.85	0.95	174.5°
$O_4II \rightarrow N_1III$	− − − 1 1 1	2.99	0.94	167.3°

[a] Values from Ref. 12. The hydrogen atoms are not positioned. [b] N_1I represents the N_1 atom in the pyrimidinetrione ring, included in the molecule I of the (000) projection of the unit cell.

spectrum; it showed three absorption bands at 2395 (strong), 2340 (weak), and 2235 (medium) cm^{-1}.

The crystalline structure, the spectrometric data confirmation, and the explanation of the thermal behavior differences between II and III are given by X-ray diffraction results (Table I).

The geometry of the two molecules was practically identical. The interatomic length mean value of the CN bond, 1.368 (II) and 1.367 (III) Å, exhibited a certain double bond character according to the observed lengths, 1.47 Å for a single CN bond and 1.352 Å for pyrimidinic CN bonds. On the other hand, the CO bond lengths showed significant differences, taking into account the environment and the existence of the intermolecular hydrogen bonds (Table II).

In II and III, the planes were nearly perpendicular; they formed 78° (II) and 99° (III) dihedral angles. The ethylenic bond occupied a transoide space orientation with regard to the 2,4,6-(1*H*,3*H*,5*H*)-pyrimidinetrione ring, but the angle formed with the plane of this latter ring was 30° larger in III (Structure B) than in II (Structure A) because of electrostatic interaction between the 6-pyrimidinetrione oxygen atom and the 6-oxocyclohexenyl carbonyl group.

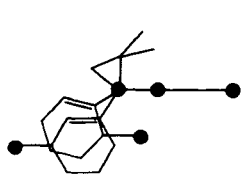

A

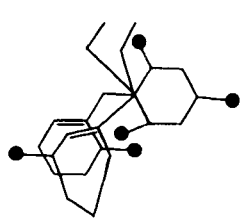

B

With regard to the intermolecular bond, however, the three compounds differed entirely. In I and II, the hydrogen bonds were arranged alternately; they included the 2- and 4-pyrimidinetrione carbonyl groups (I) and the 4-pyrimidinetrione and 3-oxocyclohexenyl carbonyl groups (II). In III, hydrogen bonds generated cyclic structures, analogous to the adenine–thymine configuration in the Watson–Crick model of DNA, which included the 4- and 6-pyrimidinetrione carbonyl groups (Table III), and the molecules formed two linear interlacing chains. The structure's tenseness explains the high melting temperature (>290°) of III.

Concerning the preparation of II and III, the chemical oxidation of I, using *tert*-butyl chromate and the *in vivo* biochemical oxidation by six human subjects, gave exclusively the ketonic derivative II. On the other hand, UV irradiation of I gave III and not II. The results were unambiguous; the compounds were purified by fractional sublimation at 220° and then at 280°. Thus, detection of 0.5% of III in II and vice versa was very easy. Conflicting results (4) were probably due to the use of poorly purified materials.

A yield of oxidation products with different structures as a result of the different experimental conditions may be explained by the reaction mechanisms: a radical reaction for III and a chemical or biochemical mechanism, which implies steric hindrance with regard to enzyme or reactant, for II.

REFERENCES

(1) H. Tsukamoto, H. Yoshimura, and S. Toki, *Chem. Pharm. Bull.*, **4**, 239 (1955).

(2) S. Goldschmidt and F. W. Koss, *Z. Physiol. Chem.*, **316**, 233 (1959).

(3) G. Willems, D. De Backer, R. Bouche, and C. De Ranter, *Bull. Soc. Chim. Belg.*, **82**, 803 (1973).

(4) S. Goldschmidt and F. W. Koss, *Z. Naturforsch.*, **14b**, 68 (1959).

(5) F. Fretwurst, *Arzneim. Forsch.*, **8**, 44 (1958).

(6) U. E. Matter, C. Pascual, E. Pretsch, A. Pross, W. Simon, and S. Sternhell, *Tetrahedron*, **25**, 691 (1969).

(7) W. Arnold and H. F. Grützmacher, *Arch. Toxicol.*, **25**, 200 (1969).

(8) R. Bouche, *Chim. Ther.*, **6**, 676 (1973).

(9) L. J. Bellamy, "The Infrared Spectra of Complex Molecules," vol. I, 3rd ed., Chapman and Hall, London, England, 1975, p. 236.

(10) T. Miyazawa, *J. Mol. Spectrosc.*, **4**, 155 (1960).

(11) *Ibid.*, **4**, 168 (1960).

(12) J. P. Bideau and M. Artaud, *C. R. Acad. Sci. Paris, Ser. C*, **271**, 806 (1970).

Synthesis and Hypotensive Activity of a Series of 2-Substituted 5,6-Dimethoxyindazoles

THOMAS J. SCHWAN ˣ, LeROY J. HONKOMP, CHARLES S. DAVIS, and GUY S. LOUGHEED

Received July 28, 1977, from the *Research and Development Department, Norwich-Eaton Pharmaceuticals Division of Morton-Norwich Products, Inc., Norwich, NY 13815.* Accepted for publication October 18, 1977.

Abstract □ The synthesis and hypotensive activity in the dog of a series of 2-substituted 5,6-dimethoxyindazoles are reported. Structure–activity relationships for this class of compounds are discussed. Indazoles containing the diethylaminoethyl, 3-pyridyl, and hydroxyethyl functions in the 2-position were the most effective in lowering blood pressure for the longest times (>270 min).

Keyphrases □ Indazoles, substituted—synthesized, evaluated for hypotensive activity □ Hypotensive activity—various substituted indazoles evaluated □ Structure–activity relationships—various substituted indazoles evaluated for hypotensive activity

A limited number of 2-substituted indazoles have been subjected to extensive pharmacological screening (1–4). For example, 2-(2-aminoethyl)indazole showed only weak serotonin-like activity and exhibited no appreciable pharmacological responses in smooth muscle tests (5). This report describes the synthesis and results of a pharmacological evaluation of a series of 2-substituted 5,6-dimethoxyindazoles.

EXPERIMENTAL[1]

Chemistry—The majority of the 2-substituted 5,6-dimethoxyindazoles (Ia–Ie, Table I) were synthesized from *N*-substituted 6-nitroveratrylideneamines (IIa–IIe) in refluxing triethyl phosphite (6). These intermediate Schiff bases were conveniently prepared by the acid-catalyzed condensation of 6-nitroveratraldehyde (III) with primary amines

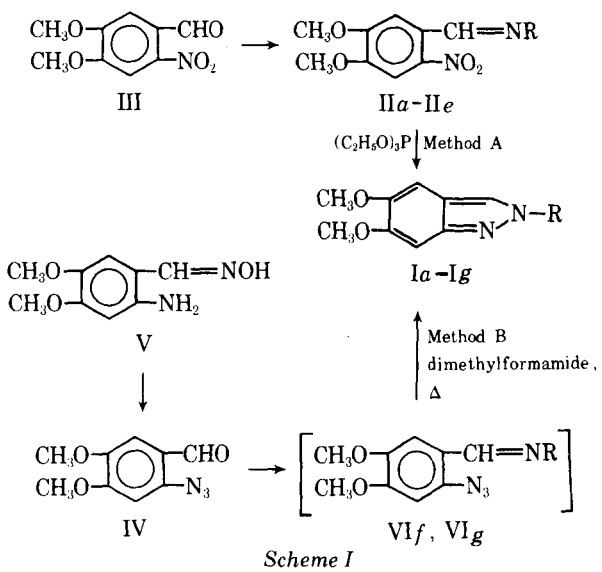

Scheme I

(Scheme I). However, since Schiff bases containing labile hydrogens are susceptible to alkylation by triethyl phosphite or the triethyl phosphate formed during indazole synthesis[2], an alternative route using nonal-

[1] Melting points were determined on a Mel-Temp apparatus, and those below 230° are corrected. IR spectra were determined as Nujol mulls on a Perkin-Elmer 137-B spectrophotometer and were consistent with the assigned structures.

[2] Cadogan *et al.* (6) showed that 2-nitro-4'-hydroxyazobenzene (A) in refluxing triethyl phosphite gave the ethoxy compound (B), presumably by alkylation of the phenol with triethyl phosphate, the oxidation product of the phosphite.

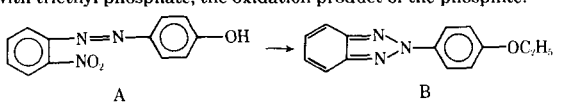

0022-3549/78/0700/1022$01.00/0

© 1978, American Pharmaceutical Association

With regard to the intermolecular bond, however, the three compounds differed entirely. In I and II, the hydrogen bonds were arranged alternately; they included the 2- and 4-pyrimidinetrione carbonyl groups (I) and the 4-pyrimidinetrione and 3-oxocyclohexenyl carbonyl groups (II). In III, hydrogen bonds generated cyclic structures, analogous to the adenine–thymine configuration in the Watson–Crick model of DNA, which included the 4- and 6-pyrimidinetrione carbonyl groups (Table III), and the molecules formed two linear interlacing chains. The structure's tenseness explains the high melting temperature (>290°) of III.

Concerning the preparation of II and III, the chemical oxidation of I, using *tert*-butyl chromate and the *in vivo* biochemical oxidation by six human subjects, gave exclusively the ketonic derivative II. On the other hand, UV irradiation of I gave III and not II. The results were unambiguous; the compounds were purified by fractional sublimation at 220° and then at 280°. Thus, detection of 0.5% of III in II and vice versa was very easy. Conflicting results (4) were probably due to the use of poorly purified materials.

A yield of oxidation products with different structures as a result of the different experimental conditions may be explained by the reaction mechanisms: a radical reaction for III and a chemical or biochemical mechanism, which implies steric hindrance with regard to enzyme or reactant, for II.

REFERENCES

(1) H. Tsukamoto, H. Yoshimura, and S. Toki, *Chem. Pharm. Bull.*, **4**, 239 (1955).

(2) S. Goldschmidt and F. W. Koss, *Z. Physiol. Chem.*, **316**, 233 (1959).

(3) G. Willems, D. De Backer, R. Bouche, and C. De Ranter, *Bull. Soc. Chim. Belg.*, **82**, 803 (1973).

(4) S. Goldschmidt and F. W. Koss, *Z. Naturforsch.*, **14b**, 68 (1959).

(5) F. Fretwurst, *Arzneim. Forsch.*, **8**, 44 (1958).

(6) U. E. Matter, C. Pascual, E. Pretsch, A. Pross, W. Simon, and S. Sternhell, *Tetrahedron*, **25**, 691 (1969).

(7) W. Arnold and H. F. Grützmacher, *Arch. Toxicol.*, **25**, 200 (1969).

(8) R. Bouche, *Chim. Ther.*, **6**, 676 (1973).

(9) L. J. Bellamy, "The Infrared Spectra of Complex Molecules," vol. I, 3rd ed., Chapman and Hall, London, England, 1975, p. 236.

(10) T. Miyazawa, *J. Mol. Spectrosc.*, **4**, 155 (1960).

(11) *Ibid.*, **4**, 168 (1960).

(12) J. P. Bideau and M. Artaud, *C. R. Acad. Sci. Paris, Ser. C*, **271**, 806 (1970).

Synthesis and Hypotensive Activity of a Series of 2-Substituted 5,6-Dimethoxyindazoles

THOMAS J. SCHWAN ˣ, LeROY J. HONKOMP, CHARLES S. DAVIS, and GUY S. LOUGHEED

Received July 28, 1977, from the *Research and Development Department, Norwich-Eaton Pharmaceuticals Division of Morton-Norwich Products, Inc., Norwich, NY 13815.* Accepted for publication October 18, 1977.

Abstract □ The synthesis and hypotensive activity in the dog of a series of 2-substituted 5,6-dimethoxyindazoles are reported. Structure–activity relationships for this class of compounds are discussed. Indazoles containing the diethylaminoethyl, 3-pyridyl, and hydroxyethyl functions in the 2-position were the most effective in lowering blood pressure for the longest times (>270 min).

Keyphrases □ Indazoles, substituted—synthesized, evaluated for hypotensive activity □ Hypotensive activity—various substituted indazoles evaluated □ Structure–activity relationships—various substituted indazoles evaluated for hypotensive activity

A limited number of 2-substituted indazoles have been subjected to extensive pharmacological screening (1–4). For example, 2-(2-aminoethyl)indazole showed only weak serotonin-like activity and exhibited no appreciable pharmacological responses in smooth muscle tests (5). This report describes the synthesis and results of a pharmacological evaluation of a series of 2-substituted 5,6-dimethoxyindazoles.

EXPERIMENTAL[1]

Chemistry—The majority of the 2-substituted 5,6-dimethoxyindazoles (Ia–Ie, Table I) were synthesized from *N*-substituted 6-nitroveratrylideneamines (IIa–IIe) in refluxing triethyl phosphite (6). These intermediate Schiff bases were conveniently prepared by the acid-catalyzed condensation of 6-nitroveratraldehyde (III) with primary amines

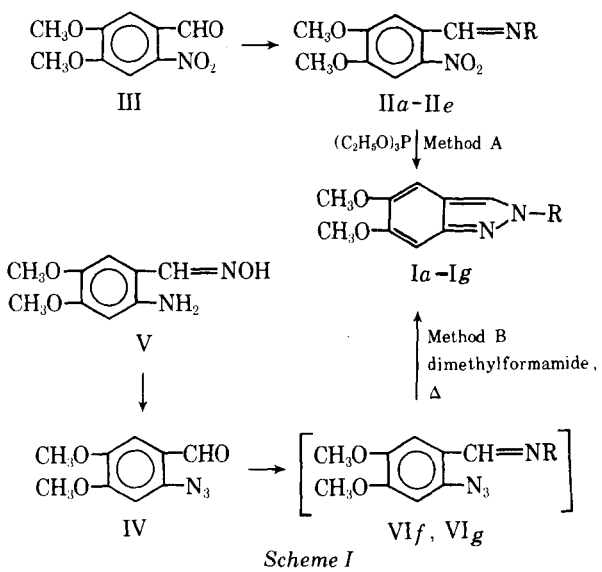

Scheme I

(Scheme I). However, since Schiff bases containing labile hydrogens are susceptible to alkylation by triethyl phosphite or the triethyl phosphate formed during indazole synthesis[2], an alternative route using nonal-

[1] Melting points were determined on a Mel-Temp apparatus, and those below 230° are corrected. IR spectra were determined as Nujol mulls on a Perkin-Elmer 137-B spectrophotometer and were consistent with the assigned structures.

[2] Cadogan *et al.* (6) showed that 2-nitro-4'-hydroxyazobenzene (A) in refluxing triethyl phosphite gave the ethoxy compound (B), presumably by alkylation of the phenol with triethyl phosphate, the oxidation product of the phosphite.

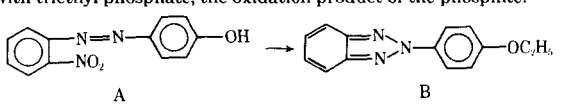

0022-3549/78/0700/1022$01.00/0

© 1978, American Pharmaceutical Association

Table I—Physical and Analytical Data for 2-Substituted 5,6-Dimethoxyindazoles

Compound	R	Recrystallization Solvent[a]	Melting Point	Yield, %[b]	Formula	Analysis, %	Calc.	Found
Ia	$N(CH_3)_2$·HCl	A	195–196°	32	$C_{11}H_{15}N_3O_2$·HCl	C	51.26	51.12
						H	6.26	6.12
						N	16.30	16.34
Ib	$(CH_2)_2N(C_2H_5)_2$·2HCl	A	202–204°	30	$C_{15}H_{23}N_3O_2$·2HCl	C	51.43	51.32
						H	7.19	7.28
						N	12.00	11.88
Ic	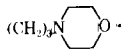	B	238–239°	22	$C_{16}H_{23}N_3O_3$·2HCl	C	50.80	51.04
						H	6.66	6.85
						N	11.11	10.85
Id	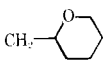	C	95–96°	45	$C_{15}H_{20}N_2O_3$	C	65.20	65.31
						H	7.30	7.08
						N	10.14	9.92
Ie	$CH_2CH_2OCH_3$·HCl	D	160–161°	15	$C_{12}H_{16}N_2O_3$·HCl	C	52.84	53.08
						H	6.28	6.44
						N	10.27	10.37
If	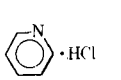	E	243–245°	64	$C_{14}H_{13}N_3O_2$·HCl	C	57.64	57.91
						H	4.84	4.93
						N	14.40	14.35
Ig	CH_2CH_2OH	F	122–124°	57	$C_{11}H_{14}N_2O_3$	C	59.45	59.36
						H	6.35	6.26
						N	12.61	12.57

[a] A = 95% ethanol, B = methanol, C = heptane, D = ethyl acetate, E = 2-ethoxyethanol, and F = toluene. [b] Yield of material from cyclization suitable for biological evaluation (*i.e.*, 95% pure).

kylating conditions was sought. A procedure in which 2-azidobenzylideneamines were thermally decomposed to indazoles was reported by Krbechek and Takimoto (7) and then modified (8). Since this approach required 6-azidoveratraldehyde (IV), a convenient synthesis of large quantities of IV was desired.

Bamberger and Demuth (9) reported the preparation of 2-azidobenzaldehyde by reaction of 2-aminobenzaldoxime with nitrous acid, but attempted utilization of this method for the synthesis of IV from the oxime V (10) gave erratic results. However, addition of an external source of azide ion to the diazotization mixture of V gave the desired azide IV in 70–80% yields (Scheme I).

Acid-catalyzed treatment of IV with amines in dimethylformamide at 90° gave rise to the azides VI*f* and VI*g*, which were not isolated. Conversion to the desired indazoles I*f* and I*g* (Table I) was effected in boiling dimethylformamide (Scheme I). This method, although preferable for the synthesis of indazoles containing labile hydrogens (*e.g.*, I*g*), also was employed for the preparation of I*f*.

N-Substituted 6-Nitroveratrylideneamines (IIa–IIe)—These compounds were synthesized by refluxing equimolar quantities of 6-nitroveratraldehyde and the amine in ethanol for 5 min–1.5 hr, using catalytic amounts of acetic acid. The separated products were suitable for conversion to the desired indazoles. In cases where the product failed to crystallize, the solvent was removed *in vacuo* and the residue was used directly to prepare the indazole.

5,6-Dimethoxy-2-(3-morpholinopropyl)indazole Dihydrochloride (Ic)—A mixture of 127 g (0.376 mole) of 6-nitroveratrylidene-2-(3-morpholinopropyl)amine (IIc) and 144 g (0.867 mole) of triethyl phosphite was refluxed for 4.5 hr. The excess phosphite and phosphates were removed in high vacuum. The residue was dissolved in 300 ml of chloroform. The resulting solution was washed with water, dried, and concentrated to dryness to give the crude indazole.

Treatment of a methanolic solution of the crude product with methanolic hydrogen chloride gave Ic (Table I).

Similarly prepared were I*a* and I*b* (Table I). For I*d* and I*e* (Table I), synthesized using similar conditions, the crude products were purified by passing a benzene solution of the indazole through a column containing neutral alumina. The purified free base of indazole I*e* was converted to the product with ethereal hydrogen chloride.

6-Azidoveratraldehyde (IV)—To 1290 ml of concentrated hydrochloric acid, cooled at −10°, was added rapidly 252 g (1.29 moles) of V (10). While the reaction mixture was maintained at from 0 to −10°, a solution of 97.7 g (1.41 moles) of sodium nitrite in 400 ml of water was added (30 min required). Then the mixture was stirred at from 0 to −15° for an additional 30 min. While the mixture was maintained below 0°, a solution of 83.5 g (1.28 moles) of sodium azide was added cautiously.

After 15 min of stirring, the mixture was diluted with 3.2 liters of cold water. It then was stirred at from 0 to −10° for 1.5 hr; while being maintained at this temperature, a solution of 3.47 liters of 25% sodium hydroxide was introduced. This mixture was stirred at ambient temperature for 15 hr, and the precipitated product was filtered, washed with water, and dried to constant weight to give 207 g (78.1%) of the azide, mp 112–114°. An analytical sample, mp 116–118°, was prepared by recrystallization from 2-propanol; IR: 4.71 (N_3), 6.01 (C=O), and 6.27 (C=C) μm.

Anal.—Calc. for $C_9H_9N_3O_3$: C, 52.17; H, 4.38; N, 20.28. Found: C, 52.12; H, 4.26; N, 20.29.

5,6-Dimethoxy-2-(3-pyridyl)indazole Hydrochloride (If)—A mixture of IV (62 g, 0.300 mole), acetic acid (1 ml), dimethylformamide (250 ml), and 3-aminopyridine (28.2 g, 0.300 mole) was heated at 90° for 3 hr. The dark solution was refluxed for 1 hr and then allowed to stand overnight at room temperature. The dimethylformamide was removed under reduced pressure, and the residue was poured into water (1500 ml). The aqueous solution was extracted with ethyl acetate (4 × 500 ml).

The ethyl acetate extract was dried over sodium sulfate and concentrated to dryness. The resulting oil was dissolved in methanol, decolorized, and filtered. The methanolic filtrate was treated with methanolic hydrogen chloride to give 56 g (64%) of the crude product, which was recrystallized from ethoxyethanol (2500 ml) to yield 34 g of I*f*, mp 230–238° (Table I).

Compound I*g* was prepared in a similar manner from IV. Removal of the dimethylformamide in high vacuum gave the crude product, which was taken up in ethyl acetate, decolorized, and filtered. Removal of the solvent gave the crude product (Table I).

Pharmacology—Indazoles I*a*–I*g* were evaluated for cardiovascular activity in anesthetized dogs at doses ranging from 10 to 100 mg/kg iv using the CARDAMAP procedure (11). Their hypotensive activity is summarized in Table II.

Compounds I*b*–I*d*, I*f*, and I*g* were most effective in lowering blood

Table II—Hypotensive Activity of 2-Substituted 5,6-Dimethoxyindazoles in Dogs

Compound	Dose, mg/kg iv	Blood Pressure, % Change	Duration, min
Ia	10	−16	25
	100	−25	210
Ib	100	−74	270
Ic	10	−34	210
	100	−59	150
Id	100	−70	15
Ie	100	−25	150
If	10	−25	10
	25	−59	>330
	50	−66	>270
	100	−78	>270
Ig	50	−43	15
	100	−84	>270

pressure, but the duration of action of Ib, If, and Ig was considerably greater than that of the other indazoles.

Regarding structure–activity relationships, increasing the distance between the indazole 2-nitrogen and the tertiary amino group of the side chain increased hypotensive activity (Ia *versus* Ib and If). Furthermore, Id, with the alkoxyalkyl moiety as part of the tetrahydropyran ring, was more active than the straight chain compound Ie, although the duration of action of Id was considerably less. Finally, the carbinol Ig exhibited greater hypotensive activity than its *O*-methyl derivative Ie.

REFERENCES

(1) T. J. Schwan, C. S. Davis, and L. J. Honkomp, U.S. pat. 3,966,760 (June 29, 1976).

(2) T. J. Schwan, C. S. Davis, and L. J. Honkomp, U.S. pat. 4,002,657 (Jan. 11, 1977).

(3) T. J. Schwan, C. S. Davis, and L. J. Honkomp, U.S. pat. 4,014,878 (Mar. 29, 1977).

(4) T. J. Schwan, C. S. Davis, and L. J. Honkomp, U.S. pat. 4,014,866 (Mar. 29, 1977).

(5) C. Ainsworth, *J. Am. Chem. Soc.*, **80**, 965 (1958).

(6) J. I. G. Cadogan, M. Cameron-Wood, R. W. Mackie, and R. J. G. Searle, *J. Chem. Soc.*, **1965**, 4831.

(7) L. Krbechek and H. Takimoto, *J. Org. Chem.*, **29**, 1150 (1964).

(8) T. J. Schwan and C. S. Davis, *J. Pharm. Sci.*, **57**, 877 (1968).

(9) E. Bamberger and E. Demuth, *Chem. Ber.*, **34**, 1309 (1901).

(10) A. Rilliet, *Helv. Chim. Acta*, **5**, 547 (1902).

(11) G. V. O'Bleness, R. K. Bickerton, and W. T. Rockhold, *Computer Application Service*, **4**, 69 (1964).

ACKNOWLEDGMENTS

The authors are indebted to Mr. Frederick Abbott for the large-scale synthesis of intermediates and to Mr. Grant Gustin and Mr. Marvin Tefft for the microanalysis.

Colorimetric Determination of Nadolol in Tablets

EUGENE IVASHKIV

Received February 22, 1977, from the *Squibb Institute for Medical Research, New Brunswick, NJ 08903.* Accepted for publication October 25, 1977.

Abstract □ Nadolol was extracted from tablet excipients with an acidic potassium chloride solution. The drug was oxidized with periodic acid, and the resulting aldehyde was reacted with 2,4-dinitrophenylhydrazine to form the corresponding hydrazone. Excess reagent was removed with a cupric chloride solution. The hydrazone was extracted into chloroform, and its absorbance was measured at the 352-nm maximum.

Keyphrases □ Nadolol—colorimetric analysis in tablets □ Colorimetry—analysis, nadolol in tablets □ Antiadrenergic agents—nadolol, colorimetric analysis in tablets

Nadolol [*cis*-5-[3-[(1,1-dimethylethyl)amino]-2-hydroxypropoxy] -1,2,3,4- tetrahydro-2,3-naphthalenediol] (I) is a new β-adrenergic blocking agent (1). A fluorometric determination of nadolol in human serum and urine, with references on clinical uses of the drug, was reported previously (2). The present method involves coupling the carbonyl groups of the periodate-oxidized drug with 2,4-dinitrophenylhydrazine to form a highly colored hydrazone. Procedures for the determination of carbonyl compounds as their 2,4-dinitrophenylhydrazones have been reported (3, 4). In the present paper, a novel elimination of the excess 2,4-dinitrophenylhydrazine with a cupric chloride solution is described.

EXPERIMENTAL

Apparatus—Colorimetric measurements were made with a spectrophotometer[1]. Samples were shaken on a heavy-duty shaker[2]. Screw-top test tubes, 150 mm, with plastic caps were washed as described (2). A centrifuge with stainless steel adapters was used[3].

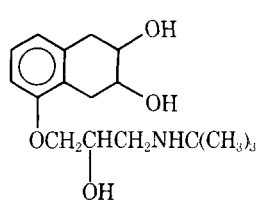

I

Reagents—All chemicals were reagent grade. A 10-ml quantity of 1% sodium metaperiodate[2] was prepared in 0.1 *N* HCl. Sodium arsenite[2] was prepared by dissolution of 0.4 g of the reagent in 9 ml of 0.1 *N* HCl and addition of 1 ml of concentrated hydrochloric acid. Both reagents were prepared daily.

Methanol[2] was purified by refluxing 4 liters with 20 g of 2,4-dinitrophenylhydrazine[4] and 20 ml of hydrochloric acid followed by glass distillation. 2,4-Dinitrophenylhydrazine solution was prepared daily by dissolution of 50 mg of 97% pure reagent in 25 ml of purified methanol containing 0.5 ml of hydrochloric acid. Acidic potassium chloride[5] solution was prepared by dissolution of 50 g of potassium chloride in 950 ml of 0.1 *N* HCl, and 20% cupric chloride[5] was prepared by dissolution of 200 g of cupric chloride dihydrate in distilled water.

Preparation of Standard Assay[6]—Weigh about 40 mg of standard nadolol into a 100-ml volumetric flask. Dissolve and dilute to volume with acidic potassium chloride solution. Dilute 10.0 ml of this solution to 100 ml with acidic potassium chloride.

Assay—*Sample Preparation*—Weigh and finely powder not less than 20 nadolol tablets. Accurately weigh a portion of the powder equivalent to 40 mg of nadolol. Transfer the powdered sample to a 120-ml glass bottle.

Extraction—To each bottle, add 100.0 ml of acidic potassium chloride solution. Cover the bottles with aluminum foil and caps and shake them for 1 hr. Filter the solutions through medium-porosity sintered-glass filters and collect the filtrates in 120-ml glass bottles. Dilute 10.0 ml of the filtrate to 100 ml with acidic potassium chloride solution.

Oxidation and Hydrazone Formation—Pipet 1.0 ml of acidic potassium chloride solution (reagent blank), 1.0 ml of tablet extract, and 1.0 ml of the diluted standard nadolol solution into separate 150-mm, screw-capped, acid-washed test tubes. With an automatic syringe, add 0.10 ml of sodium periodate solution to each tube and mix well on a vortex mixer. Centrifuge the tubes at about 2000 rpm for 2 min.

[1] Beckman DU equipped with a tungsten lamp.
[2] Fisher Scientific Co.
[3] IEP 2741, Scientific Products.
[4] Aldrich.
[5] Mallinckrodt Chemical Works.
[6] Both standard solutions are stable at room temperature for at least 4 weeks.

0022-3549/78/0700/1024$01.00/0

© 1978, American Pharmaceutical Association

pressure, but the duration of action of Ib, If, and Ig was considerably greater than that of the other indazoles.

Regarding structure–activity relationships, increasing the distance between the indazole 2-nitrogen and the tertiary amino group of the side chain increased hypotensive activity (Ia *versus* Ib and If). Furthermore, Id, with the alkoxyalkyl moiety as part of the tetrahydropyran ring, was more active than the straight chain compound Ie, although the duration of action of Id was considerably less. Finally, the carbinol Ig exhibited greater hypotensive activity than its *O*-methyl derivative Ie.

REFERENCES

(1) T. J. Schwan, C. S. Davis, and L. J. Honkomp, U.S. pat. 3,966,760 (June 29, 1976).

(2) T. J. Schwan, C. S. Davis, and L. J. Honkomp, U.S. pat. 4,002,657 (Jan. 11, 1977).

(3) T. J. Schwan, C. S. Davis, and L. J. Honkomp, U.S. pat. 4,014,878 (Mar. 29, 1977).

(4) T. J. Schwan, C. S. Davis, and L. J. Honkomp, U.S. pat. 4,014,866 (Mar. 29, 1977).

(5) C. Ainsworth, *J. Am. Chem. Soc.*, **80**, 965 (1958).

(6) J. I. G. Cadogan, M. Cameron-Wood, R. W. Mackie, and R. J. G. Searle, *J. Chem. Soc.*, **1965**, 4831.

(7) L. Krbechek and H. Takimoto, *J. Org. Chem.*, **29**, 1150 (1964).

(8) T. J. Schwan and C. S. Davis, *J. Pharm. Sci.*, **57**, 877 (1968).

(9) E. Bamberger and E. Demuth, *Chem. Ber.*, **34**, 1309 (1901).

(10) A. Rilliet, *Helv. Chim. Acta*, **5**, 547 (1902).

(11) G. V. O'Bleness, R. K. Bickerton, and W. T. Rockhold, *Computer Application Service*, **4**, 69 (1964).

ACKNOWLEDGMENTS

The authors are indebted to Mr. Frederick Abbott for the large-scale synthesis of intermediates and to Mr. Grant Gustin and Mr. Marvin Tefft for the microanalysis.

Colorimetric Determination of Nadolol in Tablets

EUGENE IVASHKIV

Received February 22, 1977, from the *Squibb Institute for Medical Research, New Brunswick, NJ 08903.* Accepted for publication October 25, 1977.

Abstract □ Nadolol was extracted from tablet excipients with an acidic potassium chloride solution. The drug was oxidized with periodic acid, and the resulting aldehyde was reacted with 2,4-dinitrophenylhydrazine to form the corresponding hydrazone. Excess reagent was removed with a cupric chloride solution. The hydrazone was extracted into chloroform, and its absorbance was measured at the 352-nm maximum.

Keyphrases □ Nadolol—colorimetric analysis in tablets □ Colorimetry—analysis, nadolol in tablets □ Antiadrenergic agents—nadolol, colorimetric analysis in tablets

Nadolol [*cis*-5-[3-[(1,1-dimethylethyl)amino]-2-hydroxypropoxy] -1,2,3,4- tetrahydro-2,3-naphthalenediol] (I) is a new β-adrenergic blocking agent (1). A fluorometric determination of nadolol in human serum and urine, with references on clinical uses of the drug, was reported previously (2). The present method involves coupling the carbonyl groups of the periodate-oxidized drug with 2,4-dinitrophenylhydrazine to form a highly colored hydrazone. Procedures for the determination of carbonyl compounds as their 2,4-dinitrophenylhydrazones have been reported (3, 4). In the present paper, a novel elimination of the excess 2,4-dinitrophenylhydrazine with a cupric chloride solution is described.

EXPERIMENTAL

Apparatus—Colorimetric measurements were made with a spectrophotometer[1]. Samples were shaken on a heavy-duty shaker[2]. Screw-top test tubes, 150 mm, with plastic caps were washed as described (2). A centrifuge with stainless steel adapters was used[3].

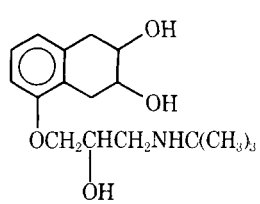

I

Reagents—All chemicals were reagent grade. A 10-ml quantity of 1% sodium metaperiodate[2] was prepared in 0.1 *N* HCl. Sodium arsenite[2] was prepared by dissolution of 0.4 g of the reagent in 9 ml of 0.1 *N* HCl and addition of 1 ml of concentrated hydrochloric acid. Both reagents were prepared daily.

Methanol[2] was purified by refluxing 4 liters with 20 g of 2,4-dinitrophenylhydrazine[4] and 20 ml of hydrochloric acid followed by glass distillation. 2,4-Dinitrophenylhydrazine solution was prepared daily by dissolution of 50 mg of 97% pure reagent in 25 ml of purified methanol containing 0.5 ml of hydrochloric acid. Acidic potassium chloride[5] solution was prepared by dissolution of 50 g of potassium chloride in 950 ml of 0.1 *N* HCl, and 20% cupric chloride[5] was prepared by dissolution of 200 g of cupric chloride dihydrate in distilled water.

Preparation of Standard Assay[6]—Weigh about 40 mg of standard nadolol into a 100-ml volumetric flask. Dissolve and dilute to volume with acidic potassium chloride solution. Dilute 10.0 ml of this solution to 100 ml with acidic potassium chloride.

Assay—*Sample Preparation*—Weigh and finely powder not less than 20 nadolol tablets. Accurately weigh a portion of the powder equivalent to 40 mg of nadolol. Transfer the powdered sample to a 120-ml glass bottle.

Extraction—To each bottle, add 100.0 ml of acidic potassium chloride solution. Cover the bottles with aluminum foil and caps and shake them for 1 hr. Filter the solutions through medium-porosity sintered-glass filters and collect the filtrates in 120-ml glass bottles. Dilute 10.0 ml of the filtrate to 100 ml with acidic potassium chloride solution.

Oxidation and Hydrazone Formation—Pipet 1.0 ml of acidic potassium chloride solution (reagent blank), 1.0 ml of tablet extract, and 1.0 ml of the diluted standard nadolol solution into separate 150-mm, screw-capped, acid-washed test tubes. With an automatic syringe, add 0.10 ml of sodium periodate solution to each tube and mix well on a vortex mixer. Centrifuge the tubes at about 2000 rpm for 2 min.

[1] Beckman DU equipped with a tungsten lamp.
[2] Fisher Scientific Co.
[3] IEP 2741, Scientific Products.
[4] Aldrich.
[5] Mallinckrodt Chemical Works.
[6] Both standard solutions are stable at room temperature for at least 4 weeks.

0022-3549/78/0700/1024$01.00/0

© 1978, American Pharmaceutical Association

Table I—Reproducibility of Results

Tablet Formulation, mg	*RSD*, %[a]
10	1.11
40	0.64
80	0.86
120	0.46

[a] Ten runs of each tablet formulation.

Fifteen minutes after mixing the last tube on the vortex mixer, add 0.20 ml of sodium arsenite solution with an automatic syringe and mix well on the vortex mixer. Five minutes after mixing the last tube on the vortex mixer, add 1.0 ml of 2,4-dinitrophenylhydrazine solution with a volumetric pipet and mix well on the vortex mixer. After 5 min, add 10.0 ml of chloroform to each tube and mix on the vortex mixer for 5 sec.

To each tube add 10.0 ml of 20% cupric chloride, cover the tubes with plastic caps, and shake mechanically for 15 min. Centrifuge the tubes at about 2000 rpm for 5 min. Aspirate completely and discard the top aqueous layer. If needed, aspirate some of the chloroform layer.

Measure the absorbance of the chloroform solutions of the sample and standard in 1-cm cells at the 352-nm maximum with the chloroform reagent blank in the reference cell. Nadolol in an average tablet is calculated from the concentration and absorbance of a nadolol standard.

RESULTS AND DISCUSSION

Experimental results for the oxidation of nadolol with periodate were given previously (2). The 2,4-dinitrophenylhydrazine reagent was optimized by using excess reagent and a proper hydrochloric acid concentration. When less than 0.5 ml or more than 4.0 ml of acid/100 ml of reagent was used, a lower absorbance was obtained. A novel method for eliminating excess 2,4-dinitrophenylhydrazine from the chloroform extracts with cupric chloride was introduced.

Several concentrations of cupric chloride were tried for the elimination of the excess 2,4-dinitrophenylhydrazine. From 10 to 30% cupric chloride solutions were used successfully. Higher than 30% cupric chloride solutions decomposed the oxidation reagent by producing a small amount of iodine, which slightly lowered the absorbance of the solutions and had an adverse effect on reproducibility. Elimination of 2,4-dinitrophenylhydrazine was rapid and occurred within a few minutes, but 15 min of shaking is recommended for reproducible results.

Nadolol 2,4-dinitrophenylhydrazone was stable in chloroform when shaken with cupric chloride solutions. No change in the absorbance was found when chloroform solutions were shaken with 20% cupric chloride solutions for up to 0.5 hr.

Table II—Nadolol in Tablet Formulations

Tablet Formulation, mg	Nadolol, mg/tablet Run 1	Run 2
10	10.04	9.97
40	40.00	40.20
80	80.20	80.00
120	120.80	120.10

The reaction of oxidized nadolol with 2,4-dinitrophenylhydrazine was completed in less than 1 min. The product was stable in the reaction mixture and in chloroform for at least 60 min.

The volume of sample or standard to be oxidized and then reacted with 2,4-dinitrophenylhydrazine should be 1 ml. When samples of more than 2 ml were used, lower absorbances were obtained. At least 30% methanol also was needed in the reaction mixture for maximum color development.

Various solvents were tried for the extraction of nadolol 2,4-dinitrophenylhydrazone from aqueous solutions. Methylene chloride, chloroform, and ethylene chloride produced the same reagent blank and extracted the color completely. No color was extracted with carbon tetrachloride, ether, ethyl acetate, butyl alcohol, and methyl ethyl ketone. Butyl acetate extracted the color completely, but incomplete destruction of 2,4-dinitrophenylhydrazine was obtained. Toluene extracted about 60% of the color.

Nadolol 2,4-dinitrophenylhydrazone–chloroform solutions had a maximum absorption at 352 nm and obeyed Beer's law at least between 0 and 200 μg of nadolol.

Recovery of nadolol was studied by adding the drug to the appropriate placebo tablet. Recoveries from 10-, 40-, 80-, and 120-mg tablets varied between 99.2 and 101.0%. Reproducibility of results was checked by analysis of each tablet formulation 10 times (Table I).

The method has performed reliably for a number of batches of nadolol tablets and, therefore, can be used for manufacturing control. Results from the analysis of some nadolol tablets are given in Table II.

REFERENCES

(1) R. J. Lee, D. B. Evans, S. H. Baky, and R. J. Laffan, *Eur. J. Pharmacol.*, **33**, 371 (1975).

(2) E. Ivashkiv, *J. Pharm. Sci.*, **66**, 1168 (1977).

(3) M. Pesez and J. Bartos, "Colorimetric and Fluorometric Analysis of Organic Compounds and Drugs," Dekker, New York, N.Y., 1974, chap. 8.

(4) H. J. Senf, H. Wollmann, and A. Kreher, *Pharmazie*, **31**, 746 (1976).

New 5-Hydroxy-2-indolecarbohydrazides as Platelet Aggregation Inhibitors in Ethylene Glycol

A. MONGE ˣ, I. GENUA, J. A. PALOP, M. T. MARTINEZ, F. ROLDAN, and J. FERNÁNDEZ

Received May 2, 1977, from the *Departamento de Química Orgánica, Facultad de Farmacia, Universidad de Navarra, Pamplona, Spain.* Accepted for publication October 27, 1977.

Abstract □ The effect of ethylene glycol on blood platelet aggregation was examined using a previously described method. This method also was used to investigate several derivatives of 2-indolecarbohydrazide *in vitro*. All compounds inhibited platelet aggregation induced by collagen, epinephrine, or adenosine diphosphate at concentrations below 5×10^{-4} *M*.

Keyphrases □ Indolecarbohydrazides, various—effect on human platelet aggregation in ethylene glycol *in vitro* □ Platelet aggregation, human—effect of various indolecarbohydrazides in ethylene glycol *in vitro* □ Structure–activity relationships—effect of various indolecarbohydrazides on human platelet aggregation in ethylene glycol *in vitro*

The role of platelets in the formation of thrombi and arterial occlusions and the effect of adenosine diphosphate (ADP) on platelet aggregation are well documented (1). It has been suggested that the inhibition of platelet aggregation may be more useful than standard anticoagulant therapy (2, 3).

0022-3549/78/0700/1025$01.00/0
© 1978, American Pharmaceutical Association

Table I—Reproducibility of Results

Tablet Formulation, mg	*RSD*, %[a]
10	1.11
40	0.64
80	0.86
120	0.46

[a] Ten runs of each tablet formulation.

Fifteen minutes after mixing the last tube on the vortex mixer, add 0.20 ml of sodium arsenite solution with an automatic syringe and mix well on the vortex mixer. Five minutes after mixing the last tube on the vortex mixer, add 1.0 ml of 2,4-dinitrophenylhydrazine solution with a volumetric pipet and mix well on the vortex mixer. After 5 min, add 10.0 ml of chloroform to each tube and mix on the vortex mixer for 5 sec.

To each tube add 10.0 ml of 20% cupric chloride, cover the tubes with plastic caps, and shake mechanically for 15 min. Centrifuge the tubes at about 2000 rpm for 5 min. Aspirate completely and discard the top aqueous layer. If needed, aspirate some of the chloroform layer.

Measure the absorbance of the chloroform solutions of the sample and standard in 1-cm cells at the 352-nm maximum with the chloroform reagent blank in the reference cell. Nadolol in an average tablet is calculated from the concentration and absorbance of a nadolol standard.

RESULTS AND DISCUSSION

Experimental results for the oxidation of nadolol with periodate were given previously (2). The 2,4-dinitrophenylhydrazine reagent was optimized by using excess reagent and a proper hydrochloric acid concentration. When less than 0.5 ml or more than 4.0 ml of acid/100 ml of reagent was used, a lower absorbance was obtained. A novel method for eliminating excess 2,4-dinitrophenylhydrazine from the chloroform extracts with cupric chloride was introduced.

Several concentrations of cupric chloride were tried for the elimination of the excess 2,4-dinitrophenylhydrazine. From 10 to 30% cupric chloride solutions were used successfully. Higher than 30% cupric chloride solutions decomposed the oxidation reagent by producing a small amount of iodine, which slightly lowered the absorbance of the solutions and had an adverse effect on reproducibility. Elimination of 2,4-dinitrophenylhydrazine was rapid and occurred within a few minutes, but 15 min of shaking is recommended for reproducible results.

Nadolol 2,4-dinitrophenylhydrazone was stable in chloroform when shaken with cupric chloride solutions. No change in the absorbance was found when chloroform solutions were shaken with 20% cupric chloride solutions for up to 0.5 hr.

Table II—Nadolol in Tablet Formulations

Tablet Formulation, mg	Nadolol, mg/tablet Run 1	Run 2
10	10.04	9.97
40	40.00	40.20
80	80.20	80.00
120	120.80	120.10

The reaction of oxidized nadolol with 2,4-dinitrophenylhydrazine was completed in less than 1 min. The product was stable in the reaction mixture and in chloroform for at least 60 min.

The volume of sample or standard to be oxidized and then reacted with 2,4-dinitrophenylhydrazine should be 1 ml. When samples of more than 2 ml were used, lower absorbances were obtained. At least 30% methanol also was needed in the reaction mixture for maximum color development.

Various solvents were tried for the extraction of nadolol 2,4-dinitrophenylhydrazone from aqueous solutions. Methylene chloride, chloroform, and ethylene chloride produced the same reagent blank and extracted the color completely. No color was extracted with carbon tetrachloride, ether, ethyl acetate, butyl alcohol, and methyl ethyl ketone. Butyl acetate extracted the color completely, but incomplete destruction of 2,4-dinitrophenylhydrazine was obtained. Toluene extracted about 60% of the color.

Nadolol 2,4-dinitrophenylhydrazone–chloroform solutions had a maximum absorption at 352 nm and obeyed Beer's law at least between 0 and 200 μg of nadolol.

Recovery of nadolol was studied by adding the drug to the appropriate placebo tablet. Recoveries from 10-, 40-, 80-, and 120-mg tablets varied between 99.2 and 101.0%. Reproducibility of results was checked by analysis of each tablet formulation 10 times (Table I).

The method has performed reliably for a number of batches of nadolol tablets and, therefore, can be used for manufacturing control. Results from the analysis of some nadolol tablets are given in Table II.

REFERENCES

(1) R. J. Lee, D. B. Evans, S. H. Baky, and R. J. Laffan, *Eur. J. Pharmacol.*, **33**, 371 (1975).

(2) E. Ivashkiv, *J. Pharm. Sci.*, **66**, 1168 (1977).

(3) M. Pesez and J. Bartos, "Colorimetric and Fluorometric Analysis of Organic Compounds and Drugs," Dekker, New York, N.Y., 1974, chap. 8.

(4) H. J. Senf, H. Wollmann, and A. Kreher, *Pharmazie*, **31**, 746 (1976).

New 5-Hydroxy-2-indolecarbohydrazides as Platelet Aggregation Inhibitors in Ethylene Glycol

A. MONGE ˣ, I. GENUA, J. A. PALOP, M. T. MARTINEZ, F. ROLDAN, and J. FERNÁNDEZ

Received May 2, 1977, from the *Departamento de Química Orgánica, Facultad de Farmacia, Universidad de Navarra, Pamplona, Spain.* Accepted for publication October 27, 1977.

Abstract □ The effect of ethylene glycol on blood platelet aggregation was examined using a previously described method. This method also was used to investigate several derivatives of 2-indolecarbohydrazide *in vitro*. All compounds inhibited platelet aggregation induced by collagen, epinephrine, or adenosine diphosphate at concentrations below 5×10^{-4} *M*.

Keyphrases □ Indolecarbohydrazides, various—effect on human platelet aggregation in ethylene glycol *in vitro* □ Platelet aggregation, human—effect of various indolecarbohydrazides in ethylene glycol *in vitro* □ Structure–activity relationships—effect of various indolecarbohydrazides on human platelet aggregation in ethylene glycol *in vitro*

The role of platelets in the formation of thrombi and arterial occlusions and the effect of adenosine diphosphate (ADP) on platelet aggregation are well documented (1). It has been suggested that the inhibition of platelet aggregation may be more useful than standard anticoagulant therapy (2, 3).

0022-3549/78/0700/1025$01.00/0
© 1978, American Pharmaceutical Association

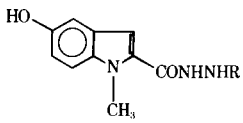

Table I—Effect of the Indolecarbohydrazides on Platelet Aggregation [a]

Compound	R	Final Concentration, *M*	Inhibition, % of Platelet Aggregation Induced by: Collagen	Epinephrine	Adenosine Diphosphate[b]	Adenosine Diphosphate[c]
I	H	5×10^{-4}	38	23	2	20
II	$(CH_3)_2CH$	5×10^{-4}	12	33	5	80–90
		5×10^{-5}				10
III	$CH_3CH_2(CH_3)CH$	5×10^{-4}	15	20	6	80–90
		5×10^{-5}				10
IV	$(CH_3)_2CHCH_2$	5×10^{-4}	30	10	0	90–100
		5×10^{-5}				90
		5×10^{-6}				85
		5×10^{-7}				10
V	$(CH_3)_2CHCH_2(CH_3)CH$	5×10^{-4}	0	11	0	50
		5×10^{-5}				20
VI	$CH_3(CH_2)_8CH_2$	5×10^{-4}	30	0	20	40
VII	$(CH_2)_4CH$	5×10^{-4}	25	30	30	20
VIII	$(CH_2)_5CH$	5×10^{-4}	37	16	34	30–35
IX	$C_6H_5CH_2$	5×10^{-4}	38	25	30	70

[a] The tests were carried out on eight different samples of plasma of apparently healthy humans without measuring maximum and minimum values. [b] Platelet-rich plasma incubated for 90 sec at 37°. [c] Platelet-rich plasma incubated for 5 min at 37°.

Various substances that inhibit platelet aggregation were investigated extensively (3), and several compounds that inhibit the adenosine diphosphate and/or collagen-induced platelet aggregation were described. An obvious relationship between chemical structure and inhibition of platelet aggregation has not been established (4–18).

The present paper describes an alteration in the ability of platelets to agglutinate with adenosine diphosphate, collagen, and epinephrine when a suspension of human thrombin was mixed with new 2-alkyl-1-(1-methyl-5-hydroxy-2-indole)carbohydrazides. Preparation of the hydrazides from ethyl 1-methyl-5-hydroxy-2-indolecarboxylate and their action as monoamine oxidase inhibitors were described previously (19).

EXPERIMENTAL

Samples—Blood was obtained by venipuncture in the forearms of apparently healthy humans. The blood was collected in polyethylene tubes containing a 1:9 volume of 3.8% sodium citrate.

Platelet-rich plasma was obtained by sedimentation and adjustment of platelet-poor plasma to 200,000 platelets/mm^3. Platelet-poor plasma was obtained by centrifugation of citrated blood at 4000 rpm for 30 min.

Compounds—Compounds I–IX (Table I) were described previously (19).

Solvent—Ethylene glycol was used as the solvent.

Aggregative Agents—Adenosine diphosphate (2×10^{-5} *M*), epinephrine (10^{-4} *M*), and collagen (0.2 mg/ml) in pH 7.4 phosphate buffer were used. The collagen solution was incubated at 37° for at least 30 min until opalescence was observed. It was then maintained in ice water at 0° until the end of the test.

Platelet Aggregation—Platelet aggregation was measured by the method of Born and Cross (20), using a platelet aggregation meter[1]. A 0.1-ml aliquot of the test sample dissolved in ethylene glycol was added to a polyethylene cell containing 0.8 ml of platelet-rich citrated plasma. It was incubated for 90 sec at 37°, after which 0.1 ml of adenosine diphosphate, epinephrine, or collagen in saline was added to the platelet-rich citrated plasma.

The final concentration of each sample was 5×10^{-4} *M*. If the product produced inhibition greater than 50% at 5×10^{-4} *M*, tests also were performed with lower concentrations (Table I).

The percent inhibition of aggregation by a test compound was calculated by comparison between the inhibition produced by the solvent (ethylene glycol) and that produced by the test compound.

[1]Evans EEL 169.

RESULTS AND DISCUSSION

Platelet aggregation tests were carried out on new indolecarbohydrazides to study their possible biological action in primary human hemostasis.

Since these compounds are not soluble in water, it was necessary to use a solvent that would not affect the polyethylene tubes, would be soluble in water, and would produce minimum antiaggregative effects. The use of dimethyl sulfoxide (13) was described for tests with male rabbits carried out in a parallel manner to those described here; this solvent, however, inhibited the adenosine diphosphate-induced platelet aggregation at 10^{-1} *M* up to 100% in human plasma.

The action of different solvents on platelet aggregation was determined before the aggregation test to ensure the utilization of a product capable of dissolving the compounds under study. Hexametapol, ethanol, 2-propanol, 1,4-dioxane, tetrahydrofuran, diethylene glycol, dipropylene glycol, and ethylene glycol were tested. The first six solvents were inhibitors, but the inhibitions elicited by dipropylene glycol and ethylene glycol were comparatively much lower.

Ethylene glycol was chosen. When it was added to plasma, the first of the two waves characteristic of epinephrine aggregation disappeared and only the second wave was observed. This second wave is related to the adenosine diphosphate of the platelets (Fig. 1).

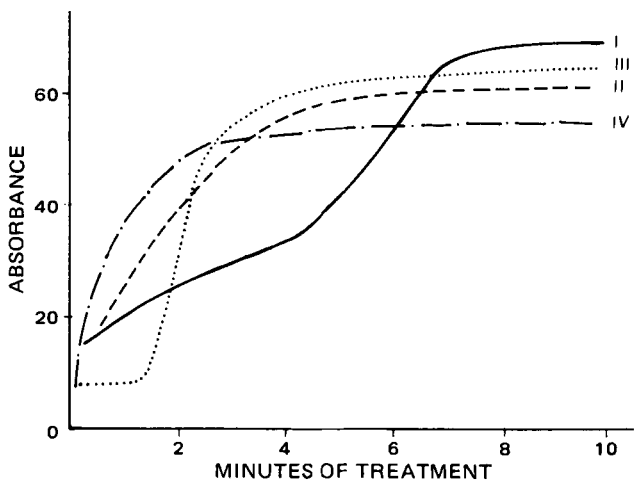

Figure 1—*Aggregation produced by: epinephrine (I) (a double wave is observed); epinephrine after the addition of ethylene glycol to plasma (II) (the disappearance of the double wave is observed without marked inhibition of the aggregation); collagen (III) (three phases are observed: a latent period, rapid aggregation, and then a stationary phase); and collagen after the addition of ethylene glycol to plasma (IV) (the disappearance of the latent period is observed).*

The aggregation curve due to collagen changed when ethylene glycol was added to plasma, and the time lag characteristic of this aggregant disappeared (Fig. 1).

In Table I, the action of indolecarbohydrazides in platelet aggregation is represented with reference to the aggregant adenosine diphosphate (2×10^{-5} *M*), epinephrine (10^{-4} *M*), and collagen (0.2 mg/ml). Platelet-rich plasma was incubated with the compounds for 90 sec at 37°. Inhibition of aggregation at 5×10^{-4} *M* of the compounds is significant (Table I).

When the incubations were carried out for 5 min at 37°, obvious differences were observed in the antiaggregant action of the tested compounds with adenosine diphosphate as the aggregant. Under these conditions, all of the compounds presented a higher capacity of aggregation inhibition. Compound IV at 5×10^{-6} *M* totally inhibited aggregation; *i.e.*, approximately 2 mg of the compound can produce complete platelet aggregation inhibition in humans.

REFERENCES

(1) A. Gaarder, J. Jonsen, S. Laland, A. Hellem, and P. A. Owren, *Nature (London)*, **192**, 531 (1961).

(2) G. W. Schnetzer, *Am. Heart J.*, **83**, 552 (1973).

(3) J. F. Mustard and M. A. Packham, *Pharmacol. Rev.*, **22**, 97 (1970).

(4) P. R. Emmons, M. J. Harrison, A. J. Honour, and J. G. R. Mitchell, *Nature (London)*, **208**, 255 (1965).

(5) A. A. Hassanein, A. G. G. Turpie, G. P. MacNicol, and A. S. Dorglas, *Br. Med. J.*, **5**, 83 (1970).

(6) M. Nakanishi, H. Imamura, and K. Goto, *Yakugaku Zasshi*, **90**, 564 (1970).

(7) J. J. Sixma and A. M. C. Treesnichnigg, *Scand. J. Haematol.*, **8**, 417 (1971).

(8) E. F. Elslager, N. F. Haley, J. R. MacLean, S. C. Perricone, D. Potoczak, H. Veloso, D. Worth, and R. H. Wheelock, *J. Med. Chem.*, **14**, 397 (1971).

(9) H. Ott and G. M. Smith, *Br. J. Pharmacol.*, **43**, 460 (1971).

(10) R. D. Mackenzie, T. R. Blohm, E. M. Auxier, J. M. G. Henderson, and J. M. Steinbach, *Proc. Soc. Exp. Biol. Med.*, **137**, 662 (1971).

(11) G. P. Claxton, J. M. Grisar, E. M. Roberts, and R. W. Fleming, *J. Med. Chem.*, **15**, 500 (1972).

(12) E. Deutsh, K. Lachner, K. Moser, and L. Stockinger, *Thromb. Diath. Hemorrh.*, **26**, 145 (1971).

(13) K. Kikugawa and M. Ichino, *Chem. Pharm. Bull.*, **21**, 1151 (1973).

(14) W. N. Beverung and R. A. Partyka, *J. Med. Chem.*, **18**, 224 (1975).

(15) K. Izuka and K. Kikugawa, *Chem. Pharm. Bull.*, **20**, 614 (1972).

(16) M. H. Maguire, F. Penglis-Caredes, and G. R. Gough, *Experientia*, **30**, 922 (1974).

(17) J. Lasierra Cirujeda *et al.*, *Anal. Real Acad. Farm.*, **2**, 347 (1974).

(18) E. Szarvasi *et al.*, *Eur. J. Med. Chem.*, **11**, 115 (1976).

(19) A. Monge, J. A. Palop, M. T. Martínez, and E. F. Alvarez, *An. Quim.*, **73**, 278 (1977).

(20) G. U. R. Born and M. J. Cross, *J. Physiol.*, **168**, 178 (1963).

ACKNOWLEDGMENTS

Supported by the Subdireccion General de Promocion Científica del Ministerio de Educación y Ciencia.

The authors thank Dr. P. Angulo of Clinica Universitaria, Pamplona, Spain, and Prof. Dr. E. Fernández-Alvarez of Centro Nacional de Química Orgánica, Madrid, Spain, for their helpful discussions and suggestions.

Assay of Mercaptopurine in Plasma Using Paired-Ion High-Performance Liquid Chromatography

JAMES L. DAY ˣ, LAMBROS TTERLIKKIS, RHONDA NIEMANN, ANDREW MOBLEY, and CARLOS SPIKES

Received May 26, 1977, from the *School of Pharmacy, Florida Agricultural and Mechanical University, Tallahassee, FL 32307.* Accepted for publication September 21, 1977.

Abstract □ A sensitive, quantitative, and specific high-performance liquid chromatographic method for mercaptopurine in plasma is described. The analysis, in which mercaptopurine and the internal standard, 6-methylthio-2-hydroxypurine, are chromatographed as ion-pairs with heptane–sulfonic acid, employs a simple and rapid sample preparation based on deproteination using 60% trichloroacetic acid. Quantitation of plasma samples to 0.2 μg of mercaptopurine/ml is reported. The retention times of the major metabolites do not interfere.

Keyphrases □ Mercaptopurine—high-performance liquid chromatographic analysis in plasma □ High-performance liquid chromatography—analysis, mercaptopurine in plasma □ Antineoplastic agents—mercaptopurine, high-performance liquid chromatographic analysis in plasma

To investigate plasma mercaptopurine (I) levels for pharmacokinetic studies, a sensitive and accurate assay was needed that would distinguish I from its metabolites. Several methods have been reported for I in biological fluids, but each has some disadvantages in specificity and sensitivity (1–3).

Recently, a GLC method was described that separates I from its metabolites (4). However, to achieve a sensitivity of 0.5 μg/ml, I must be extracted from a biological sample and then methylated to achieve a sample suitable for assay. The use of cation-exchange high-performance liquid chromatography (HPLC) for the detection, but not the quantification, of I in biological samples was reported (5, 6). The described method is specific and convenient and has sufficient sensitivity to measure accurately concentrations of mercaptopurine normally encountered at therapeutic levels.

EXPERIMENTAL

Reagents—All compounds used in the assay were used as received.

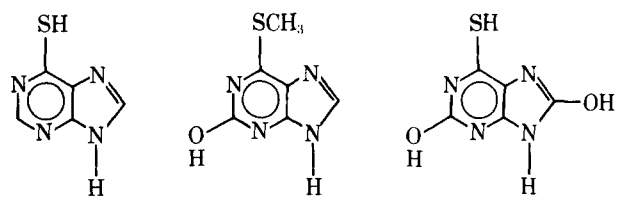

I II III

0022-3549/78/0700/1027$01.00/0

© 1978, American Pharmaceutical Association

The aggregation curve due to collagen changed when ethylene glycol was added to plasma, and the time lag characteristic of this aggregant disappeared (Fig. 1).

In Table I, the action of indolecarbohydrazides in platelet aggregation is represented with reference to the aggregant adenosine diphosphate (2×10^{-5} *M*), epinephrine (10^{-4} *M*), and collagen (0.2 mg/ml). Platelet-rich plasma was incubated with the compounds for 90 sec at 37°. Inhibition of aggregation at 5×10^{-4} *M* of the compounds is significant (Table I).

When the incubations were carried out for 5 min at 37°, obvious differences were observed in the antiaggregant action of the tested compounds with adenosine diphosphate as the aggregant. Under these conditions, all of the compounds presented a higher capacity of aggregation inhibition. Compound IV at 5×10^{-6} *M* totally inhibited aggregation; *i.e.*, approximately 2 mg of the compound can produce complete platelet aggregation inhibition in humans.

REFERENCES

(1) A. Gaarder, J. Jonsen, S. Laland, A. Hellem, and P. A. Owren, *Nature (London)*, **192**, 531 (1961).

(2) G. W. Schnetzer, *Am. Heart J.*, **83**, 552 (1973).

(3) J. F. Mustard and M. A. Packham, *Pharmacol. Rev.*, **22**, 97 (1970).

(4) P. R. Emmons, M. J. Harrison, A. J. Honour, and J. G. R. Mitchell, *Nature (London)*, **208**, 255 (1965).

(5) A. A. Hassanein, A. G. G. Turpie, G. P. MacNicol, and A. S. Dorglas, *Br. Med. J.*, **5**, 83 (1970).

(6) M. Nakanishi, H. Imamura, and K. Goto, *Yakugaku Zasshi*, **90**, 564 (1970).

(7) J. J. Sixma and A. M. C. Treesnichnigg, *Scand. J. Haematol.*, **8**, 417 (1971).

(8) E. F. Elslager, N. F. Haley, J. R. MacLean, S. C. Perricone, D. Potoczak, H. Veloso, D. Worth, and R. H. Wheelock, *J. Med. Chem.*, **14**, 397 (1971).

(9) H. Ott and G. M. Smith, *Br. J. Pharmacol.*, **43**, 460 (1971).

(10) R. D. Mackenzie, T. R. Blohm, E. M. Auxier, J. M. G. Henderson, and J. M. Steinbach, *Proc. Soc. Exp. Biol. Med.*, **137**, 662 (1971).

(11) G. P. Claxton, J. M. Grisar, E. M. Roberts, and R. W. Fleming, *J. Med. Chem.*, **15**, 500 (1972).

(12) E. Deutsh, K. Lachner, K. Moser, and L. Stockinger, *Thromb. Diath. Hemorrh.*, **26**, 145 (1971).

(13) K. Kikugawa and M. Ichino, *Chem. Pharm. Bull.*, **21**, 1151 (1973).

(14) W. N. Beverung and R. A. Partyka, *J. Med. Chem.*, **18**, 224 (1975).

(15) K. Izuka and K. Kikugawa, *Chem. Pharm. Bull.*, **20**, 614 (1972).

(16) M. H. Maguire, F. Penglis-Caredes, and G. R. Gough, *Experientia*, **30**, 922 (1974).

(17) J. Lasierra Cirujeda *et al.*, *Anal. Real Acad. Farm.*, **2**, 347 (1974).

(18) E. Szarvasi *et al.*, *Eur. J. Med. Chem.*, **11**, 115 (1976).

(19) A. Monge, J. A. Palop, M. T. Martínez, and E. F. Alvarez, *An. Quim.*, **73**, 278 (1977).

(20) G. U. R. Born and M. J. Cross, *J. Physiol.*, **168**, 178 (1963).

ACKNOWLEDGMENTS

Supported by the Subdireccion General de Promocion Científica del Ministerio de Educación y Ciencia.

The authors thank Dr. P. Angulo of Clinica Universitaria, Pamplona, Spain, and Prof. Dr. E. Fernández-Alvarez of Centro Nacional de Química Orgánica, Madrid, Spain, for their helpful discussions and suggestions.

Assay of Mercaptopurine in Plasma Using Paired-Ion High-Performance Liquid Chromatography

JAMES L. DAY ˣ, LAMBROS TTERLIKKIS, RHONDA NIEMANN, ANDREW MOBLEY, and CARLOS SPIKES

Received May 26, 1977, from the *School of Pharmacy, Florida Agricultural and Mechanical University, Tallahassee, FL 32307.* Accepted for publication September 21, 1977.

Abstract □ A sensitive, quantitative, and specific high-performance liquid chromatographic method for mercaptopurine in plasma is described. The analysis, in which mercaptopurine and the internal standard, 6-methylthio-2-hydroxypurine, are chromatographed as ion-pairs with heptane–sulfonic acid, employs a simple and rapid sample preparation based on deproteination using 60% trichloroacetic acid. Quantitation of plasma samples to 0.2 μg of mercaptopurine/ml is reported. The retention times of the major metabolites do not interfere.

Keyphrases □ Mercaptopurine—high-performance liquid chromatographic analysis in plasma □ High-performance liquid chromatography—analysis, mercaptopurine in plasma □ Antineoplastic agents—mercaptopurine, high-performance liquid chromatographic analysis in plasma

To investigate plasma mercaptopurine (I) levels for pharmacokinetic studies, a sensitive and accurate assay was needed that would distinguish I from its metabolites. Several methods have been reported for I in biological fluids, but each has some disadvantages in specificity and sensitivity (1–3).

Recently, a GLC method was described that separates I from its metabolites (4). However, to achieve a sensitivity of 0.5 μg/ml, I must be extracted from a biological sample and then methylated to achieve a sample suitable for assay. The use of cation-exchange high-performance liquid chromatography (HPLC) for the detection, but not the quantification, of I in biological samples was reported (5, 6). The described method is specific and convenient and has sufficient sensitivity to measure accurately concentrations of mercaptopurine normally encountered at therapeutic levels.

EXPERIMENTAL

Reagents—All compounds used in the assay were used as received.

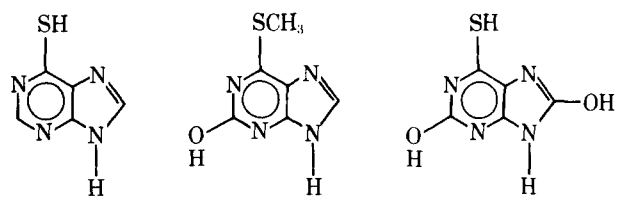

I II III

0022-3549/78/0700/1027$01.00/0

© 1978, American Pharmaceutical Association

Table I—Statistics of Calibration Curve and Reproducibility

Concentration, μg/ml	Mean PHR[a]/ Micrograms of I	*SD*	*CV*, %
0.2	1.355	0.065	4.8
0.5	1.375	0.045	3.3
0.75	1.386	0.021	1.5
1.0	1.380	0.013	0.95

[a] PHR = peak height ratio of I to II. Each value represents the average of five determinations.

The solvents employed were reagent grade and were used without further purification.

Instrumentation—The liquid chromatograph[1] was equipped with a double-beam UV detector and a wavelength kit for monitoring at 313 nm. The stationary phase was a 300 × 4-mm prepacked stainless steel column containing a monomolecular layer of octadecyltrichlorosilane (C_{18}) chemically bonded to a high efficiency porous silica surface[2].

The mobile phase was a paired-ion solution containing 0.005 *M* 1-heptanesulfonic acid sodium salt[3], 1% acetic acid, and 10% methanol in distilled water. It was filtered[4] and then deaerated prior to use by the brief application of a vacuum. The temperature was ambient, and the solvent flow rate was 1.0 ml/min. The amount of sample injected was 10 μl for concentrations of I in the 0.2–1.0-μg/ml range. The detector was set at a sensitivity of 0.005 absorbance unit full scale, and the chart speed was 30.5 cm (12 in.)/hr.

Preparation of Standard Solutions—Mercaptopurine[5], 10.0 mg, was weighed accurately into a 100-ml volumetric flask and dissolved by adding 5 ml of distilled water and 200 μl of 1.0 *N* NaOH and then diluted to volume with Sorensen buffer (7). The final concentration was 100 μg/ml.

The blank was prepared as the standard but without I.

The internal standard, 6-methylthio-2-hydroxypurine[5] (II), 3.0 mg, was weighed accurately into a 100-ml volumetric flask and dissolved in and diluted to volume with methanol. The final concentration was 30 μg/ml.

Procedure—Concentrations of I ranging from 2.0 to 100 μg/ml were prepared by diluting the standard solution with the blank. To 0.5 ml of plasma (heparinized) were added 50 μl of the appropriate dilution of I and 50 μl of the internal standard (II). The solution was mixed[6] for 5 sec and then allowed to equilibrate for 10 min. The solution was then deproteinized by the addition of 100 μl of 60% (w/v) trichloroacetic acid. After being mixed[6] for 15 sec and standing for 2 min, the mixture was centrifuged at 2500 rpm for 10 min.

To 200 μl of the clear supernate was added 10 μl of a 50% (w/v) NaOH solution. After 5 sec of mixing[6], a 10-μl sample was used for analysis. The peak height ratio of I to II was plotted on the ordinate and the amount of I added was plotted on the abscissa to obtain the standard curve; this curve proved to be linear over the range evaluated. The reproducibility and accuracy of the assay method are given in Table I.

RESULTS AND DISCUSSION

Under the chromatographic conditions described, the retention volumes of I and II were 4.6 and 8.4 ml, respectively. Figure 1A shows the chromatogram of rat plasma as a control. Figure 1B shows the chromatogram of plasma containing 0.2 μg of I/ml together with 1.5 μg of II/ml. The chromatogram of 1.0 μg of I/ml in plasma is given in Fig. 1C.

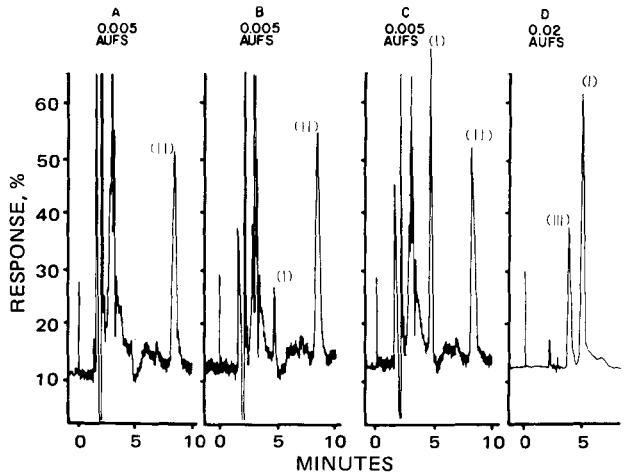

Figure 1—*A: Chromatogram of control plasma. B: Chromatogram of plasma containing 0.2 μg of I/ml and II. C: Chromatogram of plasma containing 1.0 μg of I/ml and II. D: Chromatogram of I in the presence of 6-thiouric acid (III).*

The two major metabolites of I that could interfere in the assay are 6-thiouric acid (III) and 6-methylmercaptopurine. Figure 1D shows that, although 6-thiouric acid comes off before I, it does not interfere. 6-Methylmercaptopurine comes off at a much later time than II.

The data in Table I show a zero coefficient of variation at 1.13 μg/ml when extrapolated by linear regression. The coefficient of variation of the linear regression is −0.985, indicating that the coefficient of variation of the assay is linear with respect to concentration and approaching zero at this point. The sensitivity and reproducibility of this method are better than those previously reported for the determination of I in plasma (1, 2). The lower range of the plasma concentration curve represents over a twofold improvement from that reported using a GLC method (4). The procedure described is currently being employed to obtain concentration–time data for I in animal species.

REFERENCES

(1) T. L. Loo, J. K. Luce, M. P. Sullivan, and E. Frei, *Clin. Pharmacol. Ther.*, **9**, 180 (1968).

(2) J. M. Finkel, *Anal. Biochem.*, **21**, 362 (1967).

(3) J. J. Coffey, C. A. White, A. B. Lesk, W. I. Rogers, and A. A. Serpick, *Cancer Res.*, **32**, 1283 (1972).

(4) D. G. Bailey, T. W. Wilson, and G. E. Johnson, *J. Chromatogr.*, **111**, 305 (1975).

(5) D. J. Nelson, C. J. L. Bugge, H. C. Krasny, and T. P. Zimmerman, *ibid.*, **77**, 181 (1973).

(6) H. J. Breter, *Z. Klin. Chem. Klin. Biochem.*, **12**, 223 (1974).

(7) "Remington's Pharmaceutical Sciences," 14th ed., Mack Publishing Co., Easton, Pa., 1970, p. 1554.

ACKNOWLEDGMENTS

Supported in part by Research Grant RR-08111 from the National Institutes of Health, Minority Biomedical Support Program, and in part by the National Cancer Institute, Bethesda, Md.

The authors thank Mr. Paul Grenier of the Florida A & M University School of Pharmacy for technical assistance.

[1] Model ALC/GPC 244 equipped with a model U6K injector and a model 52110 dual-pen 10-mv Houston recorder, Waters Associates, Milford, Mass.

[2] μBondapak C_{18}, Waters Associates, Milford, Mass.

[3] Eastman Kodak Co., Rochester, N.Y.

[4] Filter apparatus, 47 mm (5.0-μm pore size), Millipore Corp., Bedford, Mass.

[5] Sigma, St. Louis, Mo.

[6] Vortex-Genie, Scientific Industries, Springfield, Mass.

Effect of Concomitant Administration of Magnesium Trisilicate on GI Absorption of Dexamethasone in Humans

VIVIANE F. NAGGAR *, SAID A. KHALIL *x, and M. WAFIK GOUDA ‡

Received August 29, 1977, from the *Department of Pharmaceutics, Faculty of Pharmacy, University of Alexandria, Alexandria, Egypt, and the ‡School of Pharmacy, University of Montana, Missoula, MT 59801. Accepted for publication November 1, 1977.

Abstract □ The oral absorption of dexamethasone in humans was compared to its absorption when coadministered with magnesium trisilicate. The bioavailability of dexamethasone was estimated by measuring the suppressive effect of the drug on the daily excretion of endogenous steroids. Administration of 1 mg of dexamethasone to six healthy male volunteers significantly decreased the urinary excretion of 11-hydroxycorticosteroids. However, the coadministration of magnesium trisilicate with dexamethasone decreased its absorption, as indicated by the increased urinary excretion of 11-hydroxycorticosteroids. The decrease in absorption was attributed to drug adsorption on the antacid surface. These results confirm previous *in vitro* findings.

Keyphrases □ Dexamethasone—absorption in humans, effect of concomitant administration of magnesium trisilicate □ Magnesium trisilicate—effect on dexamethasone absorption, concomitant administration in humans □ Absorption—dexamethasone in humans, effect of concomitant administration of magnesium trisilicate □ Glucocorticoids—dexamethasone, absorption in humans, effect of concomitant administration of magnesium trisilicate □ Antacids—magnesium trisilicate, effect on dexamethasone absorption, concomitant administration in humans

Corticosteroids, being ulcerogenic, are sometimes administered concomitantly with one or more commonly used antacids. Previous *in vitro* experiments (1) showed that a depletion in the concentration of several corticosteroids from their solution was observed in the presence of various antacids or adsorbents. Of the antacids tested, magnesium trisilicate exhibited the highest adsorptive capacity and a rather high affinity for the drugs. Eluting solutions of various pH values simulating the GI tract pH showed no significant release of the corticosteroids from the antacid surface.

Since no information is available on the effect of coadministration of antacids on corticosteroid bioavailability, the previously mentioned *in vitro* interactions were investigated *in vivo*.

BACKGROUND

Synthetic corticosteroid analogs produce a total or partial cessation of adrenal gland activity (2, 3). The decreased function of the gland can be tested by estimating the amount of endogenous corticosteroids secreted in the plasma or excreted in the urine. This principle was useful (2–6) in detecting the absorption of synthetic corticosteroids. Upon oral administration of triamcinolone to human subjects, the production of endogenous corticosteroids decreased, as indicated by their plasma cortisone and urinary 17-hydroxycorticosteroids content (2). On the other hand, urine volume increased. These changes were dose dependent.

The same principle was adopted (4–6) to test the percutaneous absorption of steroids from topically applied preparations. The determination of endogenously produced corticosteroids excreted in the urine can, therefore, be taken as an indication of the bioavailability of synthetic analogs.

The objective of the present work was to study the effect of coadministration of magnesium trisilicate on dexamethasone bioavailability in human subjects, as indicated by their natural corticosteroid daily excretion. Dexamethasone was selected because it was reported to be an effective and potent suppressor of adrenal gland activity (7). Moreover, it exhibited a rather strong interaction *in vitro* with magnesium trisilicate (1).

EXPERIMENTAL

Materials—Hydrocortisone acetate[1], 0.5-mg dexamethasone tablets[2], and magnesium trisilicate (BP) were used.

Methods—Six healthy male volunteers, capable of informed consent, participated in this crossover study. No hypoadrenal or abnormally hyperadrenal subjects were included. The subjects received no corticosteroid therapy within at least 4 weeks before the study and no other drugs during it.

None of the subjects was exposed to recognizable stressful procedures. Food and fluid intake were kept as uniform as possible. The 24-hr urinary excretion of endogenous corticosteroids was determined fluorometrically[3] according to Mattingly (8) subsequent to each of the following treatments: A, 24-hr urine collection with no drug administration; B, administration of 1 mg of dexamethasone with 100 ml of water; and C, concomitant administration of 1 mg of dexamethasone and 5 g of magnesium trisilicate with 100 ml of water.

At least 1 week elapsed between Treatments B and C for any subject. A treatment day began and ended at 11 pm. All administrations of the drug or the drug-antacid combination were at 11 pm (9). At that time, the subjects also emptied their urinary bladders and started to collect urine samples in dark-colored bottles, which were kept in a cool place until urine analysis.

The volume of the thoroughly mixed 24-hr urine of each subject was recorded. The normal daily excretion of endogenous corticosteroids in Subject SK was estimated twice at 1-week intervals. The response to a smaller dose of dexamethasone (0.5 mg) also was studied in the same subject. The steroid values reported are the averages of duplicate determinations.

RESULTS AND DISCUSSION

The daily excretion of endogenous corticosteroids, selected as a measure of the biological availability of dexamethasone in the absence and presence of magnesium trisilicate and referred to for convenience as 11-hydroxycorticosteroids, is shown in Table I. These 11-hydroxycorticosteroids are responsible for the particular reaction in the fluorescent test that is negative for synthetic analogs (8). The amount of free hydrocortisone in the urine, which changes rapidly with changes in adrenal activity, partly determines the magnitude of the 11-hydroxycorticosteroid excretion (8, 10). Therefore, 11-hydroxycorticosteroids are expressed in terms of hydrocortisone equivalents. Similarly to previous reports (8), a linear relationship (between 20 and 100 μg/100 ml) existed in the present study between the intensity of fluorescence and the concentration of hydrocortisone acetate standard.

The urinary excretion of 11-hydroxycorticosteroids for the different subjects (Treatment A) ranged from 250 to 483 μg/24 hr with a mean value of 340 μg/24 hr (Table I). Variation between subjects in the amount of 11-hydroxycorticosteroids excreted, with a relatively high standard deviation, also was found by Mattingly (8). This result was attributed to the different physiological states of individuals. However, the values observed (Table I) fell within normal limits; consequently, the correlation between the urinary excretion of 11-hydroxycorticosteroid values and adrenal activity is acceptable (8). No significant week-to-week variation of 11-hydroxycorticosteroid excretion (360 and 340 μg/24 hr) was observed in Subject SK.

The effects of both 0.5 and 1 mg of dexamethasone administered at 11 pm [period coinciding with the least activity of the adrenal gland (9)] on the excretion of 11-hydroxycorticosteroids were tested in Subject SK. The level of 11-hydroxycorticosteroids in the urine decreased from 340

[1] El-Kahira Pharmaceutical and Chemical Co., Cairo, Egypt.
[2] Dexa-Scheroson, Schering A.G., Berlin, Germany.
[3] Hitachi Perkin-Elmer model 204 fluorescence spectrophotometer.

0022-3549/78/0700/1029$01.00/0
© 1978, American Pharmaceutical Association

Table I—Effect of the Coadministration of Magnesium Trisilicate on the Absorption of Dexamethasone as Determined by the Urinary Excretion of 11-Hydroxycorticosteroids

Subject	Age, years	Weight, kg	Treatment A Excretion, μg/24 hr[a]	Treatment A Urine Volume, ml/24 hr	Treatment B Excretion, μg/24 hr[a]	Treatment B Urine Volume, ml/24 hr	Treatment C Excretion, μg/24 hr[a]	Treatment C Urine Volume, ml/24 hr
SK	44	90	340	1410	37	1735	200	1510
HS	32	60	285	1390	80	1170	280	840
MB	35	60	250	1041	160	1265	220	1115
HB	36	80	380	1500	200	1100	286	780
EB	36	65	483	850	263	1550	480	1160
AH	52	70	300	990	50	1190	240	1050
Mean			340	1197	132	1335	284	1076
SD			83.4	269.1	90.6	250.8	101.5	261.1
Significance[b]					99.9%	N.S.	N.S.	N.S.
Significance[c]							99.5%	99.5%

[a] Concentration of 11-hydroxycorticosteroids in the urine in micrograms per 24 hr expressed in terms of hydrocortisone. [b] Paired *t*-test *versus* Treatment A. [c] Paired *t*-test *versus* Treatment B.

to 117 μg/24 hr with 0.5 mg and to 37 μg/24 hr with 1 mg of dexamethasone. Consequently, 1 mg of the drug was used in Treatment B.

The administration of 1 mg of dexamethasone to each subject (Treatment B) significantly decreased the 11-hydroxycorticosteroid content of the urine (Table I). The difference was statistically significant (>99.9% level). The average amount excreted in 24 hr was approximately 39% of the average amount excreted in the same time when no drug was administered. The administration of dexamethasone in a single oral dose at 11 pm was reported (9) to decrease the level of endogenous corticosteroids well below normal limits. This effect persisted for at least 24 hr, although the dexamethasone biological half-life in plasma is only 170–210 min (11). Normal levels are usually reached again after 24–48 hr (2, 9). In the present study, an increase of urine output in four of six subjects also was observed. However, such an increase was not statistically significant (six subjects).

The results of Treatment C (Table I) show that the coadministration of magnesium trisilicate with dexamethasone decreased the absorption of the latter as reflected by the amounts of 11-hydroxycorticosteroids excreted by the different individuals. The average quantity of 11-hydroxycorticosteroids excreted in the urine after Treatment C was 83.2% of that in Treatment A. On the other hand, the 11-hydroxycorticosteroid excretion in Treatment C was statistically significantly different (>99.5% level) from that in Treatment B. Moreover, urine volume in all subjects decreased in Treatment C compared to Treatment B.

The previous effects indicate a reduced bioavailability of dexamethasone in the presence of magnesium trisilicate, probably due to an adverse interaction in the GI tract leading to a decrease in the amount of the free drug available for absorption. Steroids have been reported to be absorbed by diffusion (12). The more lipoidal the compound, the greater will be its absorption rate. Similar to other steroids, dexamethasone is a nonionizing compound and, consequently, the alkalinity of magnesium trisilicate will not affect its absorption (12). For the same reason, the dissolution rate of the drug will not be influenced. Drug adsorption on the antacid surface seems the most probable cause of the reduced bioavailability (1).

From the present results, it can be concluded that a significant decrease in the bioavailability of dexamethasone results if the drug is coadministered with magnesium trisilicate. These *in vivo* results reflect previous *in vitro* findings.

REFERENCES

(1) V. F. Naggar, M. W. Gouda, and S. A. Khalil, *Pharmazie*, **32**, 778 (1977).

(2) R. B. Scoggins and B. Kliman, *N. Engl. J. Med.*, **273**, 831 (1965).

(3) W. Feinstein and J. J. Sciarra, *J. Pharm. Sci.*, **64**, 1050 (1975).

(4) R. B. Scoggins, *J. Invest. Dermatol.*, **39**, 473 (1962).

(5) K. A. Gill and D. L. Baxter, *Arch. Dermatol.*, **89**, 734 (1964).

(6) M. Kirketerp, *Acta Derm.-Venereol.*, **44**, 54 (1964).

(7) S. Nishida, S. Matsumura, M. Horino, H. Oyama, and A. Tenku, *Steroids*, **28**, 411 (1976).

(8) D. Mattingly, *Lancet*, **2**, 1046 (1964).

(9) T. Nichols, C. A. Nugent, and F. H. Tyler, *J. Clin. Endocrinol.*, **25**, 343 (1965).

(10) C. L. Cope and E. G. Black, *Br. Med. J.*, **2**, 1117 (1959).

(11) J. J. Bunim, R. L. Black, L. Lutwak, R. E. Peterson, and G. D. Whedon, *Arthritis Rheum.*, **1**, 313 (1958).

(12) W. Saski, *J. Pharm. Sci.*, **57**, 836 (1968).

ACKNOWLEDGMENTS

Supported in part by the National Science Foundation under SFC Program Grants OIP73-07437A02 and OIP73-10592A01 (formerly GF39207 and GF38851).

Erythromycin VI: Kinetics of Acid-Catalyzed Hydrolysis of Erythromycin Oxime and Erythromycylamine

TOMISLAV LAZAREVSKI ˣ, GORJANA RADOBOLJA, and SLOBODAN DJOKIĆ

Received June 6, 1977, from the *Research Department, Pliva Pharmaceutical and Chemical Works, L. Ribara 89, 41000 Zagreb, Yugoslavia.* Accepted for publication November 3, 1977.

Abstract □ Kinetic data were obtained, by qualitative and quantitative analysis, of the hydrolytic degradation of erythromycin oxime and erythromycylamine separated by TLC. The pseudo-first-order rate constants were determined at three temperatures (17, 26, and 36°), and the temperature dependency of the reaction was studied. The activation energy for the hydrolysis and methanolysis of the compounds was calculated. The factors contributing to the differences in the reaction rate are discussed.

Keyphrases □ Erythromycin oxime and amine—kinetics of acid-catalyzed hydrolysis □ Kinetics—acid-catalyzed hydrolysis of erythromycin oxime and amine □ Hydrolysis, acid catalyzed—erythromycin oxime and amine, kinetics □ Antibacterials—erythromycin oxime and amine, kinetics of acid-catalyzed hydrolysis

Erythromycin (I*a*) in acidic media rapidly loses its biological activity because of extensive acid-catalyzed transformations (1). These transformations involve the formation of an internal enol ether (I*b*) by addition of the C-6 hydroxyl to the carbonyl at C-9 followed by dehydration. This step is followed by the participation of the C-12 hydroxyl in an irreversible addition to the double bond, giving a spiroketal (II). In a further reaction, the glycosidic linkage at the C-3 position is broken and the sugar cladinose (3-*O*-methylmycarose) (III) and erythralosamine (IV) are obtained. The degradation pathway is presented in Scheme I.

Erythromycin oxime (V) and erythromycylamine (VI) are prepared from erythromycin (2), and their structures differ only at the C-9 position. No information was available regarding the stability of these compounds. The purposes of this investigation were to establish the rates of hydrolysis and methanolysis of V and VI at various temperatures and to compare them with those of erythromycin (3).

EXPERIMENTAL

Apparatus—The light absorption measurements were made on a densitometer[1] using a blue filter of 465-nm wavelength. Temperature control was carried out with thermostats maintained at 17, 26, and 36°. Constant-temperature baths with a mean variation of about 0.1° were used.

Materials—The standards cladinose (III) and methylcladinoside (VII) were prepared by a reported method (4), and their purity was verified by TLC. Other chemicals were analytical grade and were used without further purification.

Kinetic Measurements—Compounds V and VI were hydrolyzed in 0.23% (0.063 *N*) methanolic or aqueous hydrochloric acid at 17, 26, and 36° for 48 hr. The concentration of the investigated substances in acid solutions was 2%. Samples were withdrawn at various times and neutralized immediately with sodium carbonate. The solvent was removed *in vacuo*, and the residue was extracted with chloroform. The extract was dried, concentrated *in vacuo* to a solid, and redissolved in chloroform (10 mg/ml) for TLC analysis.

The chloroform solutions were spotted (10 μl) on 250-μm silica gel F_{254} plates. Components in the hydrolysates were separated on TLC plates by development in chloroform–benzene (19:1) saturated with ammonia vapor and were then visualized as dark-brown spots by spraying with

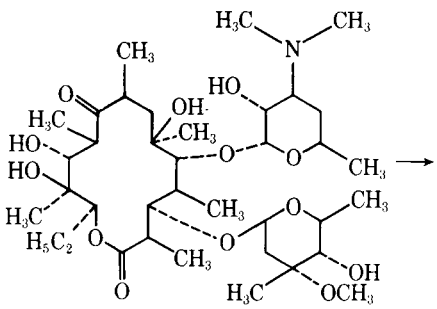

Ia

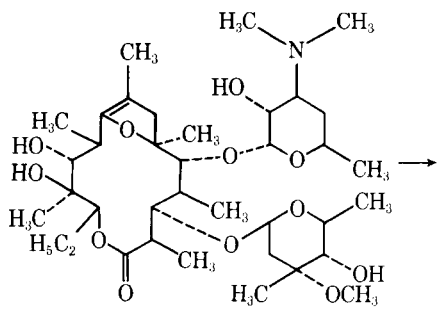

Ib

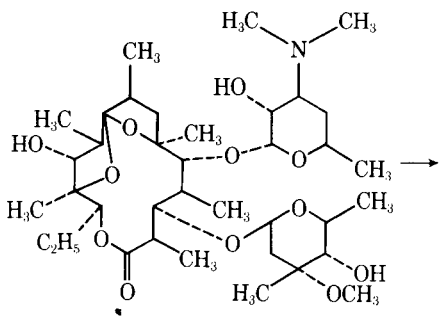

II

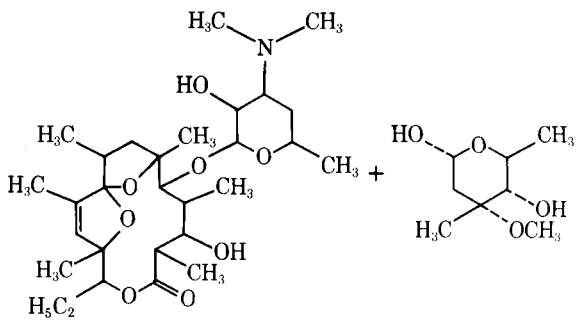

IV III

Scheme I

[1] Model 520A, Photovolt Corp., New York, N.Y.

0022-3549/78/0700/1031$01.00/0
© 1978, American Pharmaceutical Association

Table I—Rate Constants and Energy of Activation for the Acid Solvolysis of Erythromycin Oxime and Erythromycylamine

Compound	Temperature	Rate Constants for Hydrolysis, k, min^{-1}	Rate Constants for Methanolysis, k, min^{-1}	E_a for Hydrolysis, kcal/mole	E_a for Methanolysis, kcal/mole
V	17°	5.23×10^{-4}	2.01×10^{-3}	19.4	24.8
	26°	1.42×10^{-3}	7.50×10^{-3}		
	36°	4.12×10^{-3}	2.94×10^{-2}		
VI	17°	3.69×10^{-4}	1.59×10^{-3}	20.7	22.9
	26°	1.13×10^{-3}	5.11×10^{-3}		
	36°	3.48×10^{-3}	1.77×10^{-2}		

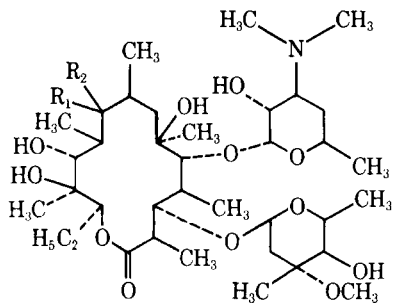

V: R_1R_2 = =NOH
VI: R_1 = H, R_2 = NH_2

phenol–sulfuric acid (5). The assay was based on the densitometric measurements of these spots.

RESULTS AND DISCUSSION

Solvolysis of V and VI with 0.23% HCl in water or methanol at 17, 26, and 36° was monitored by TLC; each degradation product was identified by the corresponding standard. The neutral sugar cladinose was removed by solvolysis. Cladinose (III) and methylcladinoside (VII), formed during the aging of V and VI in acid media (Scheme II), were determined quantitatively by densitometry of TLC plates; the results were used for calculating the velocity constants.

The amounts of sugar liberated during hydrolysis were determined by measuring the light absorbance. Linear calibration curves were obtained by the least-squares method for each sugar, and their equations were used to convert densitometric peak areas into amounts of sugar in the hydrolysate (5). From the amount of sugar, the amount of starting material present at any time was obtained indirectly.

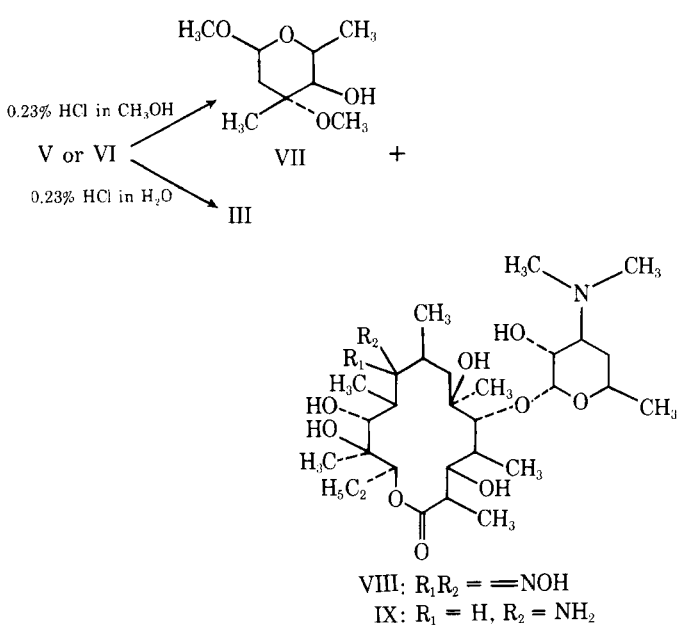

VIII: R_1R_2 = =NOH
IX: R_1 = H, R_2 = NH_2

Scheme II

By plotting the hydrolysis time *versus* the degree of sample conversion, a linear relationship was obtained (Fig. 1). The straight line is a valid proof that the reaction follows first-order kinetics. The equation employed is:

$$k = \frac{2.303}{t} \log \frac{a}{a - x} \qquad \text{(Eq. 1)}$$

where a is the initial amount of sample and x is the amount of hydrolyzed sample at time t.

The values of the velocity constant at three different temperatures are given in Table I. The increased temperature accelerated the degradation rates of V and VI. No difference in the number or identity of the compounds formed was seen at the temperatures studied. The logarithms of the k values were plotted *versus* $1/T$. These Arrhenius plots produced straight lines, allowing the calculation of the activation energy (Table I).

The difference between the reaction rates for the solvolysis of V and VI suggests the influence of the oximino and amino groups at C-9, respectively. Erythromycylamine was slightly more stable than erythromycin oxime. Compared with the parent antibiotic erythromycin, the rate of acid-catalyzed hydrolysis of V and VI is believed to be mainly influenced by different substituents at C-9. Oximino and amino groups do not permit the formation of spiroketal (II), causing a decrease of the reaction rate and an increase of the stability in an acidic medium.

The velocity constants for methanolysis were higher than for hydrolysis because of the different polarity of the solvents. These results are consistent with the mechanism of glycoside hydrolysis (6). Few literature data are available for comparison of the activation energy values. However, the activation energy for the hydrolysis of V and VI agrees well with that calculated from the reported rate constants for inactivation of erythromycin (3).

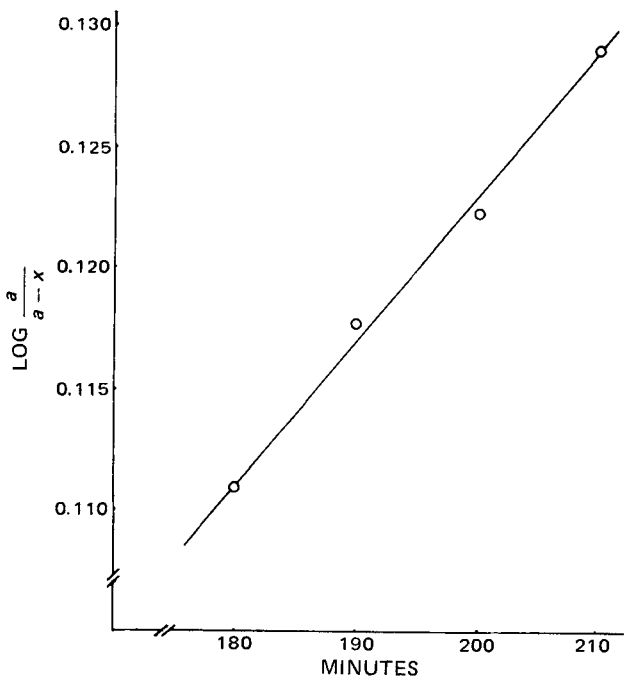

Figure 1—*First-order plot for the hydrolysis of erythromycin oxime in 0.23% aqueous hydrochloric acid at 26°.*

REFERENCES

(1) P. Kurath, P. H. Jones, R. S. Egan, and T. J. Perun, *Experientia*, **27**, 362 (1971).

(2) S. Djokić and Z. Tamburašev, *Tetrahedron Lett.*, **17**, 1645 (1967).

(3) A. P. Kondračeva and B. P. Bruns, *Antibiotiki*, **7**, 511 (1962).

(4) E. H. Flynn, M. V. Sigal, Jr., P. F. Wiley, and K. Gerzon, *J. Am. Chem. Soc.*, **76**, 3121 (1954).

(5) T. Lazarevski, Z. Tamburašev, and S. Djokić, *J. Chromatogr.*, **132**, 309 (1977).

(6) W. G. Overend, C. W. Rees, and J. S. Sequeira, *J. Chem. Soc.*, **1962**, 3429.

ACKNOWLEDGMENTS

The authors thank Miss B. Hruškar for her skillful technical assistance.

Rapid Determination of Atenolol in Human Plasma and Urine by High-Pressure Liquid Chromatography

ORVILLE H. WEDDLE, EDWIN N. AMICK, and WILLIAM D. MASON ˣ

Received March 28, 1977, from the *Pharmacokinetics Laboratory, Schools of Pharmacy and Medicine, University of Missouri–Kansas City, Kansas City, MO 64108.* Accepted for publication November 2, 1977.

Abstract □ A rapid, specific, high-pressure liquid chromatographic determination of atenolol in plasma and urine was developed. This method employs the high sensitivity of fluorescence detection together with selective extraction and reversed-phase chromatography to measure concentrations as low as 20 ng of drug/ml of plasma with a coefficient of variation of 3.91%. The assay is specific enough to be valid in the presence of plasma and urine substances. The detection limit (*i.e.*, three times baseline noise) is 3 ng/ml.

Keyphrases □ Atenolol—high-pressure liquid chromatographic determination in biological fluids □ High-pressure liquid chromatography—analysis, atenolol in biological fluids □ Antiadrenergic agents—atenolol, high-pressure liquid chromatographic determination in biological fluids

Atenolol[1], 4-(2-hydroxy-3-isopropylaminopropoxy)-phenylacetamide (I), is a new β-adrenergic blocking agent. Studies in animals and humans suggest that this drug causes preferential blockade of cardiac β-adrenoreceptors, is free of intrinsic sympathomimetic activity, and is devoid of significant membrane-stabilizing activity (1–5). Initial clinical experience indicates that atenolol may be of value in the treatment of hypertension (6–9).

Previous procedures for the determination of atenolol in plasma and urine employed GLC with electron-capture detection (10, 11) or spectrophotofluorometry (12). The spectrophotofluorometric method is relatively simple but is of questionable specificity, and the detection limit is 50 ng/ml. Although the GLC methods are highly selective and have a detection limit of 20 ng/ml, they are relatively complex and rely on a demanding prechromatography derivatization.

The procedure reported here combines a selective two-step extraction with the separative capability of high-pressure liquid chromatography (HPLC) and the sensitivity of fluorescence detection. The method is rapid and specific, employs an internal standard, and is of sufficient sensitivity (3 ng/ml detection limit) for pharmacokinetic studies.

[1] Burdick and Jackson Laboratories, Muskegon, Mich.

EXPERIMENTAL

Materials—UV grade methanol[1], 1-butanol[1], and hexane[1] were used as obtained, as were reagent grade triethanolamine[2] and 1-heptane sulfonic acid in acetic acid[3]. Water was passed through an ion-exchange bed and then distilled. Atenolol[4] and procainamide[5] were used as obtained.

Apparatus—HPLC was performed in a system consisting of a universal injector[6], a high pressure pump[7], a bonded-phase column[8], and a fluorescence detector[9]. The fluorescence of atenolol was excited at 222 nm. A combination of a 7-54 and a UV 30 filter was used between the flowcell and the photomultiplier tube.

Chromatographic Parameters—The mobile phase was prepared by mixing 2.0 ml of 1-heptane sulfonic acid in acetic acid[3] with 100 ml of 0.1 *M* triethanolamine in distilled water and 1900 ml of methanol. The mobile phase was pumped at 2 ml/min and 20° through a stainless steel column (30.5 cm × 4 mm i.d.) packed with a high efficiency bonded-phase packing. Aliquots of 100–250 μl of the reextraction solution were injected directly on-column through the injector.

Analytical Procedure—*Plasma*—Two 1.0-ml aliquots of each plasma sample were placed in 15-ml screw-topped centrifuge tubes. To each tube were added 0.1 ml of 2.5 *N* NaOH and 5.0 ml of 10% 1-butanol in *n*-hexane. The tubes were vortexed for 30 sec and then centrifuged for 10 min at 2000 rpm. After centrifugation, the organic phase was removed and discarded.

Four milliliters of 50% 1-butanol in *n*-hexane was then added to each tube. This solution contained 50.0 ng of procainamide/ml as an internal standard. The tubes were again vortexed for 30 sec and centrifuged for 10 min at 2000 rpm. This second organic phase was transferred to a second centrifuge tube containing 300 μl of 0.1% acetic acid. After 30 sec of vortexing and 5 min of centrifugation at 2000 rpm, 100–250 μl of the lower (aqueous) phase was withdrawn with a syringe and injected into the injector loop.

The output of the detector was recorded on a chart recorder, and the areas of the atenolol and procainamide peaks were measured. The ratios of the peak areas were converted into plasma atenolol concentrations by comparison with a standard curve.

Urine—Urine, 100 μl, was added to 4.90 ml of 1.52 *M* phosphate buffer (pH 12.3) and mixed thoroughly. Then 1-ml aliquots of this diluted sample were placed in 15-ml centrifuge tubes and assayed by the same

[2] Fisher Scientific Co., St. Louis, Mo.
[3] B7 reagent, Waters Associates, Milford, Mass.
[4] Stuart Pharmaceutical Division of ICI United States, Wilmington, Del.
[5] E. R. Squibb & Sons, Princeton, N.J.
[6] U6K, Waters Associates, Milford, Mass.
[7] Model 6000A, Waters Associates, Milford, Mass.
[8] μBondapak CN, Waters Associates, Milford, Mass.
[9] Schoeffel, FS-970, Westwood, N.J.

0022-3549/78/0700/1033$01.00/0

© 1978, American Pharmaceutical Association

REFERENCES

(1) P. Kurath, P. H. Jones, R. S. Egan, and T. J. Perun, *Experientia*, **27**, 362 (1971).

(2) S. Djokić and Z. Tamburašev, *Tetrahedron Lett.*, **17**, 1645 (1967).

(3) A. P. Kondračeva and B. P. Bruns, *Antibiotiki*, **7**, 511 (1962).

(4) E. H. Flynn, M. V. Sigal, Jr., P. F. Wiley, and K. Gerzon, *J. Am. Chem. Soc.*, **76**, 3121 (1954).

(5) T. Lazarevski, Z. Tamburašev, and S. Djokić, *J. Chromatogr.*, **132**, 309 (1977).

(6) W. G. Overend, C. W. Rees, and J. S. Sequeira, *J. Chem. Soc.*, **1962**, 3429.

ACKNOWLEDGMENTS

The authors thank Miss B. Hruškar for her skillful technical assistance.

Rapid Determination of Atenolol in Human Plasma and Urine by High-Pressure Liquid Chromatography

ORVILLE H. WEDDLE, EDWIN N. AMICK, and WILLIAM D. MASON ˣ

Received March 28, 1977, from the *Pharmacokinetics Laboratory, Schools of Pharmacy and Medicine, University of Missouri–Kansas City, Kansas City, MO 64108.* Accepted for publication November 2, 1977.

Abstract □ A rapid, specific, high-pressure liquid chromatographic determination of atenolol in plasma and urine was developed. This method employs the high sensitivity of fluorescence detection together with selective extraction and reversed-phase chromatography to measure concentrations as low as 20 ng of drug/ml of plasma with a coefficient of variation of 3.91%. The assay is specific enough to be valid in the presence of plasma and urine substances. The detection limit (*i.e.*, three times baseline noise) is 3 ng/ml.

Keyphrases □ Atenolol—high-pressure liquid chromatographic determination in biological fluids □ High-pressure liquid chromatography—analysis, atenolol in biological fluids □ Antiadrenergic agents—atenolol, high-pressure liquid chromatographic determination in biological fluids

Atenolol[1], 4-(2-hydroxy-3-isopropylaminopropoxy)-phenylacetamide (I), is a new β-adrenergic blocking agent. Studies in animals and humans suggest that this drug causes preferential blockade of cardiac β-adrenoreceptors, is free of intrinsic sympathomimetic activity, and is devoid of significant membrane-stabilizing activity (1–5). Initial clinical experience indicates that atenolol may be of value in the treatment of hypertension (6–9).

Previous procedures for the determination of atenolol in plasma and urine employed GLC with electron-capture detection (10, 11) or spectrophotofluorometry (12). The spectrophotofluorometric method is relatively simple but is of questionable specificity, and the detection limit is 50 ng/ml. Although the GLC methods are highly selective and have a detection limit of 20 ng/ml, they are relatively complex and rely on a demanding prechromatography derivatization.

The procedure reported here combines a selective two-step extraction with the separative capability of high-pressure liquid chromatography (HPLC) and the sensitivity of fluorescence detection. The method is rapid and specific, employs an internal standard, and is of sufficient sensitivity (3 ng/ml detection limit) for pharmacokinetic studies.

[1] Burdick and Jackson Laboratories, Muskegon, Mich.

EXPERIMENTAL

Materials—UV grade methanol[1], 1-butanol[1], and hexane[1] were used as obtained, as were reagent grade triethanolamine[2] and 1-heptane sulfonic acid in acetic acid[3]. Water was passed through an ion-exchange bed and then distilled. Atenolol[4] and procainamide[5] were used as obtained.

Apparatus—HPLC was performed in a system consisting of a universal injector[6], a high pressure pump[7], a bonded-phase column[8], and a fluorescence detector[9]. The fluorescence of atenolol was excited at 222 nm. A combination of a 7-54 and a UV 30 filter was used between the flowcell and the photomultiplier tube.

Chromatographic Parameters—The mobile phase was prepared by mixing 2.0 ml of 1-heptane sulfonic acid in acetic acid[3] with 100 ml of 0.1 *M* triethanolamine in distilled water and 1900 ml of methanol. The mobile phase was pumped at 2 ml/min and 20° through a stainless steel column (30.5 cm × 4 mm i.d.) packed with a high efficiency bonded-phase packing. Aliquots of 100–250 μl of the reextraction solution were injected directly on-column through the injector.

Analytical Procedure—*Plasma*—Two 1.0-ml aliquots of each plasma sample were placed in 15-ml screw-topped centrifuge tubes. To each tube were added 0.1 ml of 2.5 *N* NaOH and 5.0 ml of 10% 1-butanol in *n*-hexane. The tubes were vortexed for 30 sec and then centrifuged for 10 min at 2000 rpm. After centrifugation, the organic phase was removed and discarded.

Four milliliters of 50% 1-butanol in *n*-hexane was then added to each tube. This solution contained 50.0 ng of procainamide/ml as an internal standard. The tubes were again vortexed for 30 sec and centrifuged for 10 min at 2000 rpm. This second organic phase was transferred to a second centrifuge tube containing 300 μl of 0.1% acetic acid. After 30 sec of vortexing and 5 min of centrifugation at 2000 rpm, 100–250 μl of the lower (aqueous) phase was withdrawn with a syringe and injected into the injector loop.

The output of the detector was recorded on a chart recorder, and the areas of the atenolol and procainamide peaks were measured. The ratios of the peak areas were converted into plasma atenolol concentrations by comparison with a standard curve.

Urine—Urine, 100 μl, was added to 4.90 ml of 1.52 *M* phosphate buffer (pH 12.3) and mixed thoroughly. Then 1-ml aliquots of this diluted sample were placed in 15-ml centrifuge tubes and assayed by the same

[2] Fisher Scientific Co., St. Louis, Mo.
[3] B7 reagent, Waters Associates, Milford, Mass.
[4] Stuart Pharmaceutical Division of ICI United States, Wilmington, Del.
[5] E. R. Squibb & Sons, Princeton, N.J.
[6] U6K, Waters Associates, Milford, Mass.
[7] Model 6000A, Waters Associates, Milford, Mass.
[8] μBondapak CN, Waters Associates, Milford, Mass.
[9] Schoeffel, FS-970, Westwood, N.J.

0022-3549/78/0700/1033$01.00/0

© 1978, American Pharmaceutical Association

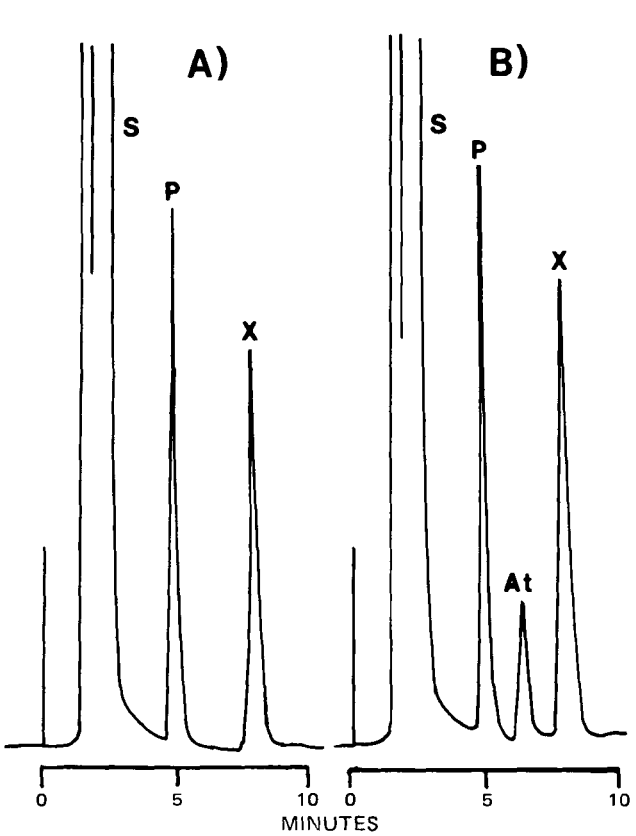

Figure 1—*High-pressure liquid chromatograms of extracts from plasma. Key: A, control plasma; B, plasma containing 40 ng of atenolol/ml; P, procainamide internal standard; S, solvent artifact; X, endogenous material; and At, atenolol.*

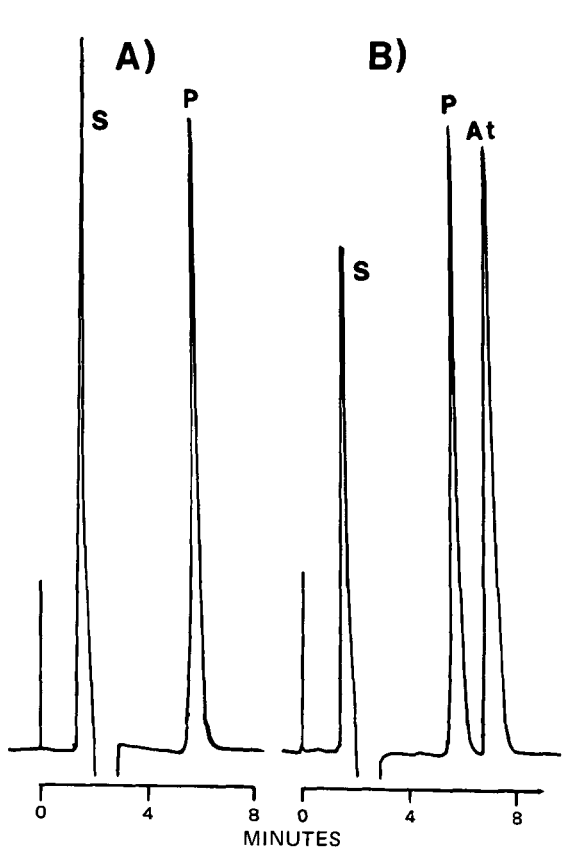

Figure 2—*High-pressure liquid chromatograms of extracts from urine. Key: A, control urine; B, urine containing 20 μg of atenolol/ml; P, procainamide internal standard; S, solvent artifact and endogenous material; and At, atenolol.*

procedure as described for plasma samples, except that the addition of 2.5 *N* NaOH was omitted.

RESULTS AND DISCUSSION

Figure 1 shows chromatograms of pooled plasma samples with and without atenolol. The atenolol peak was well separated from the procainamide internal standard peak and from artifacts. The retention times of procainamide and atenolol were 4.8 and 6.3 min, respectively. An unidentified compound, with a retention time of 7.8 min, was extracted from most plasma samples.

The ratios of the area under the atenolol peak to the area under the procainamide peak varied linearly with atenolol concentration. Analysis of six plasma samples at each concentration, 10, 30, 50, 70, and 100 ng/ml, gave a linear regression coefficient of 0.9967 for line $y = 0.00765x + 0.0057$, where y is the area ratio and x is the atenolol concentration in nanograms per milliliter of plasma. Analysis of six plasma samples of each concentration, 100, 300, 500, 700, and 1000 ng of atenolol/ml, gave a linear regression coefficient of 0.9976 for the line $y = 0.00889x + 0.0959$. The precision and accuracy of these values are given in Table I.

The analysis of 20 plasma samples to which 20 ng of atenolol/ml was added gave a mean of 20.2 ng/ml (range of 18.6–21.7) and a coefficient of variation of 3.91%. Concentrations down to 5 ng/ml can be quantitated with slightly less precision and accuracy. These figures on precision and accuracy relate to the entire analytical procedure, from pipetting the plasma to integrating the chromatogram.

Table I—Precision and Accuracy of Atenolol Measurement by HPLC

Atenolol Added to Plasma, ng/ml	*n*	Average of Calculated Atenolol Concentrations, ng/ml	*SD*	*CV*
1000	5	1000	40.4	4.04
700	6	702	14.2	2.02
500	6	496	25.1	5.07
300	6	303	6.82	2.25
100	6	100.8	2.20	2.88
70	6	67.9	3.35	4.93
50	6	51.5	2.79	5.43
30	6	29.9	1.03	3.44
10	6	10.0	0.90	9.00

The analysis of 25 samples[10] obtained from a clinical study of atenolol demonstrated the applicability of the method for samples from human subjects. The results were in close agreement with those obtained by GLC analysis[10]. In some samples, a small peak on the ascending portion of the atenolol peak was identified as the hydroxy metabolite of atenolol. Although it was not completely separated by the operating conditions, the separation was adequate to prevent interference with the quantitation of atenolol.

The analysis of plasma samples from 30 patients not taking atenolol resulted in no chromatographic peaks that interfered with atenolol or procainamide. In a pharmacokinetic study where the only drug permitted is atenolol, the described procedure is quite specific. Further study is required to determine if other drugs that may be used concomitantly in

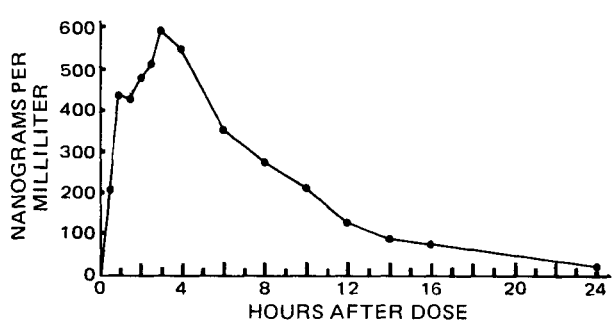

Figure 3—*Atenolol concentration* versus *time curve in a human volunteer following an oral dose of one 100-mg tablet.*

[10] Supplied by ICI United States.

therapy with atenolol, such as diuretics, might cause additional chromatographic peaks and/or interferences. These studies are currently underway.

The analysis of atenolol in urine involves the addition of one step to the analytical procedure: an initial sample dilution. Chromatograms (Fig. 2) of the urine extract were free of interfering peaks and had the same precision and accuracy as comparable concentrations in plasma.

The method was used in the analysis of 768 plasma and 384 urine samples in a pharmacokinetic study over 4 months. A plot of the plasma concentration *versus* time following a 100-mg dose to one volunteer is shown in Fig. 3. Over the 4 months, standard curves were prepared daily. When the same column was used, the day-to-day change in the slope of the standard curve never exceeded 7.2%; however, when new columns were installed, changes up to 15% were observed.

REFERENCES

(1) A. M. Barrett, J. Carter, J. D. Fitzgerald, R. Hull, and D. Lecount, *Br. J. Pharmacol.*, **48**, 340P (1973).

(2) J. Conway and M. Reeves, *Br. Heart J.*, **34**, 963 (1973).

(3) R. Hainsworth, F. Karim, and J. B. Stoker, *Br. J. Pharmacol.*, **48**, 342P (1973).

(4) J. D. Harry, M. F. Knapp, and R. J. Linden, *ibid.*, **48**, 340P (1973).

(5) F. J. Conway, J. D. Fitzgerald, J. McAnish, D. J. Rowlands, and W. T. Simpson, *Br. J. Clin. Pharmacol.*, **3**, 267 (1976).

(6) M. G. Myers, G. R. J. Lewis, J. Steiner, and C. T. Dollery, *Clin. Pharmacol. Ther.*, **19**, 502 (1976).

(7) L. Hansson, H. Alberg, S. Jameson, B. Karlberg, and R. Malmcrona, *Acta Med. Scand.*, **194**, 549 (1973).

(8) J. Sassard, N. Pozet, M. Vincent, and P. Y. Zech, *N. Engl. J. Med.*, **294**, 787 (1976).

(9) A. Amery, L. Billiet, J. V. Joossens, J. Meekers, T. Reybrouk, and W. VanMiechem, *Acta Clin. Belg.*, **28**, 358 (1973).

(10) J. O. Malbica and K. R. Monson, *J. Pharm. Sci.*, **64**, 1992 (1975).

(11) B. Scales and P. B. Copsey, *J. Pharm. Pharmacol.*, **27**, 430 (1975).

(12) C. M. Kaye, *Br. J. Clin. Pharmacol.*, **1**, 84 (1974).

ACKNOWLEDGMENTS

Supported in part by Grant 07-D-000193-01-1 from the Department of Health, Education, and Welfare.

The authors thank Dr. Robert Bell, Dr. Irving Cohen, Dr. Joseph Malbica, and Dr. Robert Simon of ICI United States for assistance.

Benzoyl Peroxide Assay Using High-Pressure Liquid Chromatography

S. OLIVERI-VIGH ˣ and F. T. HAINSWORTH, III

Received August 1, 1977, from the *G. S. Herbert Laboratories, Allergan Pharmaceuticals, Irvine, CA 92713.* Accepted for publication November 9, 1977.

Abstract □ A highly specific assay for benzoyl peroxide was developed using high-pressure liquid chromatography. A concentration curve was recorded from 0.1 to 3.0 μg with a correlation coefficient of 0.9969. The standard deviation for 10 individual analyses of a benzoyl peroxide preparation was ±0.547 (1.80% *RSD*).

Keyphrases □ Benzoyl peroxide—high-pressure liquid chromatographic analysis in bulk drug and commercial preparations □ High-pressure liquid chromatography—analysis, benzoyl peroxide in bulk drug and commercial preparations □ Keratolytic agents—benzoyl peroxide, high-pressure liquid chromatographic analysis in bulk drug and commercial preparations

Benzoyl peroxide is widely used in topical preparations for the treatment of acne. The methods currently available for benzoyl peroxide include titrimetry (1), spectrophotometry (2), and polarography (2). Only polarography is specific for benzoyl peroxide.

The visible absorption curves for benzoyl peroxide and analogous compounds, such as benzaldehyde and benzoic acid, obtained with the spectrophotometric method described in the USP (3) show marked similarity. If benzoyl peroxide is mixed with any of these analogous compounds, an accurate determination of benzoyl peroxide is impossible.

The sodium thiosulfate titration of liberated iodine is a back-titration, which is a limitation in itself. It also does not distinguish the difference between benzoyl peroxide and its chief degradation products, benzoic acid and benzaldehyde, because of the addition of iodine to aromatic double bonds.

The high-pressure liquid chromatographic (HPLC) method described in this paper is specific and provides accurate determinations of benzoyl peroxide, benzoic acid, and benzaldehyde, all with a single injection (Fig. 1).

EXPERIMENTAL

Apparatus—Absorbance measurements were recorded with a spectrophotometer[1] with matched 1-cm path length quartz cells[2]. A high-pressure liquid chromatograph[3] with a UV-visible detector[3] was used with an integrator[3] to separate and quantitate benzoyl peroxide.

Instrument Settings—All separations were run on an octadecylsilane 10-μm reversed-phase column utilizing isocratic elution (1.2 ml/min) with acetonitrile–water (50:50). A detector sensitivity of 0.16 aufs and a chart speed of 20 cm/hr were used.

Reagents—Acetonitrile[4] and deionized water were purified by filtration through a 0.22-μm solvent inert filter.

Procedure—Samples were prepared by taking aliquots of a benzoyl peroxide preparation containing approximately 30.0 mg of benzoyl peroxide and stirring in 75.0 ml of acetonitrile for 5 min. The samples were then filtered through a prewetted 0.22-μm solvent inert filter into a 100-ml volumetric flask and diluted to volume with acetonitrile. Samples were injected *via* a 10.0-μl fixed loop injector, and the UV absorption at 254 nm was used for detection and quantitation.

The concentration curve was prepared by accurately weighing 1.0, 2.0, 5.0, 10.0, 20.0, and 30.0 mg of benzoyl peroxide into 100-ml volumetric flasks and diluting to volume with acetonitrile.

[1] Beckman.
[2] Markson.
[3] Spectra Physics.
[4] Burdick & Jackson.

0022-3549/78/0700/1035$01.00/0

© 1978, American Pharmaceutical Association

therapy with atenolol, such as diuretics, might cause additional chromatographic peaks and/or interferences. These studies are currently underway.

The analysis of atenolol in urine involves the addition of one step to the analytical procedure: an initial sample dilution. Chromatograms (Fig. 2) of the urine extract were free of interfering peaks and had the same precision and accuracy as comparable concentrations in plasma.

The method was used in the analysis of 768 plasma and 384 urine samples in a pharmacokinetic study over 4 months. A plot of the plasma concentration *versus* time following a 100-mg dose to one volunteer is shown in Fig. 3. Over the 4 months, standard curves were prepared daily. When the same column was used, the day-to-day change in the slope of the standard curve never exceeded 7.2%; however, when new columns were installed, changes up to 15% were observed.

REFERENCES

(1) A. M. Barrett, J. Carter, J. D. Fitzgerald, R. Hull, and D. Lecount, *Br. J. Pharmacol.*, **48**, 340P (1973).

(2) J. Conway and M. Reeves, *Br. Heart J.*, **34**, 963 (1973).

(3) R. Hainsworth, F. Karim, and J. B. Stoker, *Br. J. Pharmacol.*, **48**, 342P (1973).

(4) J. D. Harry, M. F. Knapp, and R. J. Linden, *ibid.*, **48**, 340P (1973).

(5) F. J. Conway, J. D. Fitzgerald, J. McAnish, D. J. Rowlands, and W. T. Simpson, *Br. J. Clin. Pharmacol.*, **3**, 267 (1976).

(6) M. G. Myers, G. R. J. Lewis, J. Steiner, and C. T. Dollery, *Clin. Pharmacol. Ther.*, **19**, 502 (1976).

(7) L. Hansson, H. Alberg, S. Jameson, B. Karlberg, and R. Malmcrona, *Acta Med. Scand.*, **194**, 549 (1973).

(8) J. Sassard, N. Pozet, M. Vincent, and P. Y. Zech, *N. Engl. J. Med.*, **294**, 787 (1976).

(9) A. Amery, L. Billiet, J. V. Joossens, J. Meekers, T. Reybrouk, and W. VanMiechem, *Acta Clin. Belg.*, **28**, 358 (1973).

(10) J. O. Malbica and K. R. Monson, *J. Pharm. Sci.*, **64**, 1992 (1975).

(11) B. Scales and P. B. Copsey, *J. Pharm. Pharmacol.*, **27**, 430 (1975).

(12) C. M. Kaye, *Br. J. Clin. Pharmacol.*, **1**, 84 (1974).

ACKNOWLEDGMENTS

Supported in part by Grant 07-D-000193-01-1 from the Department of Health, Education, and Welfare.

The authors thank Dr. Robert Bell, Dr. Irving Cohen, Dr. Joseph Malbica, and Dr. Robert Simon of ICI United States for assistance.

Benzoyl Peroxide Assay Using High-Pressure Liquid Chromatography

S. OLIVERI-VIGH ˣ and F. T. HAINSWORTH, III

Received August 1, 1977, from the *G. S. Herbert Laboratories, Allergan Pharmaceuticals, Irvine, CA 92713.* Accepted for publication November 9, 1977.

Abstract □ A highly specific assay for benzoyl peroxide was developed using high-pressure liquid chromatography. A concentration curve was recorded from 0.1 to 3.0 μg with a correlation coefficient of 0.9969. The standard deviation for 10 individual analyses of a benzoyl peroxide preparation was ±0.547 (1.80% *RSD*).

Keyphrases □ Benzoyl peroxide—high-pressure liquid chromatographic analysis in bulk drug and commercial preparations □ High-pressure liquid chromatography—analysis, benzoyl peroxide in bulk drug and commercial preparations □ Keratolytic agents—benzoyl peroxide, high-pressure liquid chromatographic analysis in bulk drug and commercial preparations

Benzoyl peroxide is widely used in topical preparations for the treatment of acne. The methods currently available for benzoyl peroxide include titrimetry (1), spectrophotometry (2), and polarography (2). Only polarography is specific for benzoyl peroxide.

The visible absorption curves for benzoyl peroxide and analogous compounds, such as benzaldehyde and benzoic acid, obtained with the spectrophotometric method described in the USP (3) show marked similarity. If benzoyl peroxide is mixed with any of these analogous compounds, an accurate determination of benzoyl peroxide is impossible.

The sodium thiosulfate titration of liberated iodine is a back-titration, which is a limitation in itself. It also does not distinguish the difference between benzoyl peroxide and its chief degradation products, benzoic acid and benzaldehyde, because of the addition of iodine to aromatic double bonds.

The high-pressure liquid chromatographic (HPLC) method described in this paper is specific and provides accurate determinations of benzoyl peroxide, benzoic acid, and benzaldehyde, all with a single injection (Fig. 1).

EXPERIMENTAL

Apparatus—Absorbance measurements were recorded with a spectrophotometer[1] with matched 1-cm path length quartz cells[2]. A high-pressure liquid chromatograph[3] with a UV-visible detector[3] was used with an integrator[3] to separate and quantitate benzoyl peroxide.

Instrument Settings—All separations were run on an octadecylsilane 10-μm reversed-phase column utilizing isocratic elution (1.2 ml/min) with acetonitrile–water (50:50). A detector sensitivity of 0.16 aufs and a chart speed of 20 cm/hr were used.

Reagents—Acetonitrile[4] and deionized water were purified by filtration through a 0.22-μm solvent inert filter.

Procedure—Samples were prepared by taking aliquots of a benzoyl peroxide preparation containing approximately 30.0 mg of benzoyl peroxide and stirring in 75.0 ml of acetonitrile for 5 min. The samples were then filtered through a prewetted 0.22-μm solvent inert filter into a 100-ml volumetric flask and diluted to volume with acetonitrile. Samples were injected *via* a 10.0-μl fixed loop injector, and the UV absorption at 254 nm was used for detection and quantitation.

The concentration curve was prepared by accurately weighing 1.0, 2.0, 5.0, 10.0, 20.0, and 30.0 mg of benzoyl peroxide into 100-ml volumetric flasks and diluting to volume with acetonitrile.

[1] Beckman.
[2] Markson.
[3] Spectra Physics.
[4] Burdick & Jackson.

0022-3549/78/0700/1035$01.00/0

© 1978, American Pharmaceutical Association

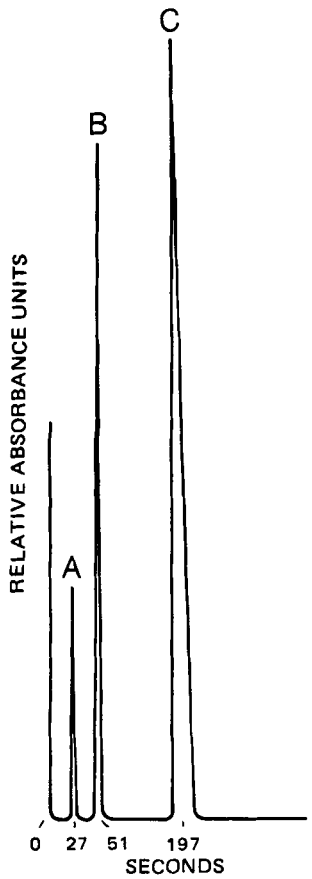

Figure 1—*High-pressure liquid chromatogram for benzoyl peroxide and analogous compounds. Key: A, benzoic acid; B, benzaldehyde; and C, benzoyl peroxide.*

RESULTS

A correlation coefficient of 0.9969 was obtained for the concentration curve, which was linear over the range of 0.1–3.0 μg, when peak areas were plotted *versus* concentration.

Table I—Marketed Product Survey

Product	Benzoyl Peroxide Claimed, %	Benzoyl Peroxide Found by HPLC, %	Benzoic Acid/ Benzaldehyde, %	Product Age, Months
A	5.0	5.15	0.07	6
B	10.0	10.11	0.14	6
C	10.0	10.93	—	3
D	5.0	4.35	0.57	3
E	10.0	8.58	0.12	3
F	10.0	9.27	0.35	3

Reproducibility of the method was checked by taking aliquots of a benzoyl peroxide preparation, equivalent to 30.0 mg of benzoyl peroxide, and working the sample up as described (resulting concentration of 30.0 mg/100 ml). The average value for 10 runs was 30.45 mg of benzoyl peroxide with a standard deviation of ±0.5468 (±1.80% *RSD*). The precision ($ts/\sqrt{N}$ for nine degrees of freedom at the 95% confidence level) was ±1.237 (±4.05% *RSD*).

CONCLUSION

The HPLC method is specific and reproducible and offers greater efficiency over current methods. Once the chromatograph is primed, 20 samples can be run in 1 hr, including a determination for all three compounds per sample. Suitable modifications of the procedure can make it applicable to other preparations of benzoyl peroxide (Table I).

REFERENCES

(1) D. H. Wheeler, *J. Am. Oil Chem. Soc.*, **25**, 144 (1948).
(2) M. P. Gruber and R. W. Klein, *J. Pharm. Sci.*, **56**, 1505 (1967).
(3) "The United States Pharmacopeia," 19th rev., Mack Publishing Co., Easton, Pa., 1975.

ACKNOWLEDGMENTS

The authors thank Emory Smith for preparing the benzoyl peroxide preparations. Special thanks also go to Sue Lloyd for the figure and Heidi Jones for typing.

Rapid and Micro High-Pressure Liquid Chromatographic Determination of Chloramphenicol in Plasma

GEOFFREY W. PENG, M. A. F. GADALLA, and WIN L. CHIOU ˣ

Received July 25, 1977, from the *Clinical Pharmacokinetics Laboratory and the Department of Pharmacy, University of Illinois, Chicago, IL 60612.* Accepted for publication November 3, 1977.

Abstract □ A high-pressure liquid chromatographic method was developed for chloramphenicol in plasma. Plasma samples were deproteinized with 2.5 volumes of acetonitrile, and the supernates were chromatographed on a reversed-phase column, using acidified ethanol–water as the mobile phase and UV spectrophotometry for detection. The sensitivity for accurate quantitation of chloramphenicol was about 2.5 μg/ml in plasma, and concentrations as low as 0.5 μg/ml could be detected. Only about 8 min is needed for each sample. This method is specific, rapid, and sufficiently sensitive and may be useful for clinical monitoring.

Keyphrases □ Chloramphenicol—high-pressure liquid chormatographic analysis in plasma □ High-pressure liquid chromatography—analysis, chloramphenicol in plasma □ Antibacterial–antirickettsials—chloramphenicol, high-pressure liquid chromatographic analysis in plasma

Chloramphenicol is effective against several Gram-negative bacteria and exhibits antirickettsial activity (1). Unfortunately, this antibiotic also depresses the erythropoietic elements of bone marrow and causes prolonged morbidity and high fatality of aplastic anemia (2).

A plasma concentration of 5–10 μg/ml was reported to be clinically effective for veterinary use in dogs (3). Similar data for humans are lacking. In humans, the activity as well as toxicity appears to be dose related (1, 2). For example, 25–30 mg/kg/day was judged to be adequate and 50 mg/

0022-3549/78/0700/1036$01.00/0
© 1978, American Pharmaceutical Association

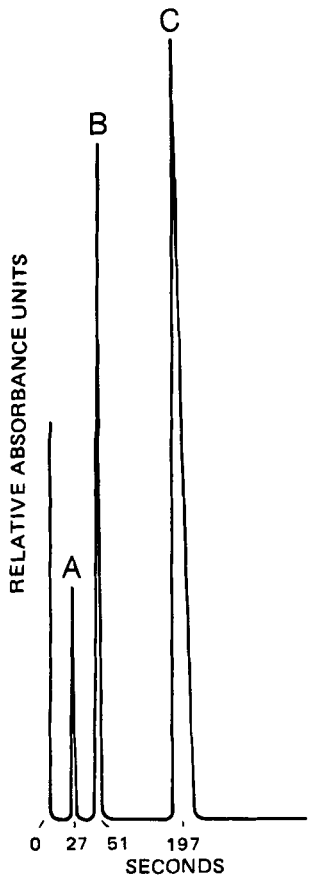

Figure 1—*High-pressure liquid chromatogram for benzoyl peroxide and analogous compounds. Key: A, benzoic acid; B, benzaldehyde; and C, benzoyl peroxide.*

RESULTS

A correlation coefficient of 0.9969 was obtained for the concentration curve, which was linear over the range of 0.1–3.0 μg, when peak areas were plotted *versus* concentration.

Table I—Marketed Product Survey

Product	Benzoyl Peroxide Claimed, %	Benzoyl Peroxide Found by HPLC, %	Benzoic Acid/ Benzaldehyde, %	Product Age, Months
A	5.0	5.15	0.07	6
B	10.0	10.11	0.14	6
C	10.0	10.93	—	3
D	5.0	4.35	0.57	3
E	10.0	8.58	0.12	3
F	10.0	9.27	0.35	3

Reproducibility of the method was checked by taking aliquots of a benzoyl peroxide preparation, equivalent to 30.0 mg of benzoyl peroxide, and working the sample up as described (resulting concentration of 30.0 mg/100 ml). The average value for 10 runs was 30.45 mg of benzoyl peroxide with a standard deviation of ±0.5468 (±1.80% *RSD*). The precision ($ts/\sqrt{N}$ for nine degrees of freedom at the 95% confidence level) was ±1.237 (±4.05% *RSD*).

CONCLUSION

The HPLC method is specific and reproducible and offers greater efficiency over current methods. Once the chromatograph is primed, 20 samples can be run in 1 hr, including a determination for all three compounds per sample. Suitable modifications of the procedure can make it applicable to other preparations of benzoyl peroxide (Table I).

REFERENCES

(1) D. H. Wheeler, *J. Am. Oil Chem. Soc.*, **25**, 144 (1948).
(2) M. P. Gruber and R. W. Klein, *J. Pharm. Sci.*, **56**, 1505 (1967).
(3) "The United States Pharmacopeia," 19th rev., Mack Publishing Co., Easton, Pa., 1975.

ACKNOWLEDGMENTS

The authors thank Emory Smith for preparing the benzoyl peroxide preparations. Special thanks also go to Sue Lloyd for the figure and Heidi Jones for typing.

Rapid and Micro High-Pressure Liquid Chromatographic Determination of Chloramphenicol in Plasma

GEOFFREY W. PENG, M. A. F. GADALLA, and WIN L. CHIOU ˣ

Received July 25, 1977, from the *Clinical Pharmacokinetics Laboratory and the Department of Pharmacy, University of Illinois, Chicago, IL 60612.* Accepted for publication November 3, 1977.

Abstract □ A high-pressure liquid chromatographic method was developed for chloramphenicol in plasma. Plasma samples were deproteinized with 2.5 volumes of acetonitrile, and the supernates were chromatographed on a reversed-phase column, using acidified ethanol–water as the mobile phase and UV spectrophotometry for detection. The sensitivity for accurate quantitation of chloramphenicol was about 2.5 μg/ml in plasma, and concentrations as low as 0.5 μg/ml could be detected. Only about 8 min is needed for each sample. This method is specific, rapid, and sufficiently sensitive and may be useful for clinical monitoring.

Keyphrases □ Chloramphenicol—high-pressure liquid chormatographic analysis in plasma □ High-pressure liquid chromatography—analysis, chloramphenicol in plasma □ Antibacterial–antirickettsials—chloramphenicol, high-pressure liquid chromatographic analysis in plasma

Chloramphenicol is effective against several Gram-negative bacteria and exhibits antirickettsial activity (1). Unfortunately, this antibiotic also depresses the erythropoietic elements of bone marrow and causes prolonged morbidity and high fatality of aplastic anemia (2).

A plasma concentration of 5–10 μg/ml was reported to be clinically effective for veterinary use in dogs (3). Similar data for humans are lacking. In humans, the activity as well as toxicity appears to be dose related (1, 2). For example, 25–30 mg/kg/day was judged to be adequate and 50 mg/

0022-3549/78/0700/1036$01.00/0
© 1978, American Pharmaceutical Association

kg/day was associated with toxicity (4). In adults, peak plasma concentrations of 20–40 μg/ml are reached within 2 hr after oral administration of a 2-g dose, and the drug has a biological half-life of 1.5–3.5 hr (1).

BACKGROUND

An increase in susceptibility to erythropoietic depression was associated with a decrease in chloramphenicol clearance from the blood (5). This effect is especially significant in patients with hepatic impairment, because toxicity occurred more frequently in patients with hepatic cirrhosis (5). Therefore, measurements of biological half-lives or steady-state concentrations of chloramphenicol may permit dosage adjustment to prevent serious toxicity (6). The variable bioavailability of different chloramphenicol preparations (7) also can complicate the dosage regimen required for optimal chemotherapy.

General assays for chloramphenicol were reviewed recently (8, 9). Among the methods for biological specimens, GLC procedures (10, 11) probably are superior in specificity and sensitivity. However, the GLC method using electron-capture detection (10) showed nonlinearity of response toward the methylsilyl derivatives in the range of concentrations encountered clinically. The GLC method using flame-ionization detection (11) required multiple solvent extractions and evaporations to separate chloramphenicol from the biological matrixes and also silylation to make the compounds suitable for chromatography. It used 0.5 ml of plasma or serum and more than 1 hr for the assay of each sample (11).

This report describes a high-pressure liquid chromatographic (HPLC) method for the determination of chloramphenicol in plasma.

EXPERIMENTAL

Apparatus—A high-pressure liquid chromatograph[1] equipped with an injector[2], a reversed-phase column[3], and a spectrophotometric detector attached to an attenuator[4] was used for separation and detection of chloramphenicol.

Reagents—Chloramphenicol[5], alcohol USP, acetonitrile[6], and phosphoric acid[7] were used.

Sample Preparation—Aliquots of plasma samples, 0.2 ml (or less), were vortex mixed with 0.5 ml (or 2.5 volumes) of acetonitrile in 13 × 100-mm culture tubes for about 10 sec and then centrifuged at 2000 rpm for 1 min. The supernates were poured into another set of culture tubes, 20-μl aliquots of which were chromatographed. The supernates could also be injected without transfer into new tubes.

Plasma samples for chloramphenicol analyses were obtained from a human subject after oral dosing of 250 mg of chloramphenicol and from an albino rabbit after intravenous injection of 20 mg of chloramphenicol/kg. Pooled human plasma samples supplemented with chloramphenicol in concentrations up to 50 μg/ml also were analyzed to establish calibration curves.

Chromatographic Conditions—The mobile phase consisted of ethanol–dilute phosphoric acid, prepared by mixing 2 volumes of alcohol USP (95% ethanol) and 8 volumes of 0.05% phosphoric acid (pH 2.5 ± 0.01). The ethanol and dilute phosphoric acid were separately filtered through membrane filters[8] before mixing. The flow rate of the mobile phase was 1.5 ml/min.

The column effluent was monitored by UV absorption at 280 nm. The chromatograms were recorded on a potentiometric recorder[9], and peak height measurements were used for quantitation. For all separations, the column was maintained at a constant 30° temperature in an oven.

RESULTS AND DISCUSSION

Figure 1 shows the chromatograms of chloramphenicol in the plasma of a human subject and of a rabbit receiving this antibiotic. Chromatograms of a human plasma blank before and after addition of chloramphenicol are also shown. Notably, all three chromatograms are quite similar. Chloramphenicol has a retention time of 6 min under the chromatographic conditions.

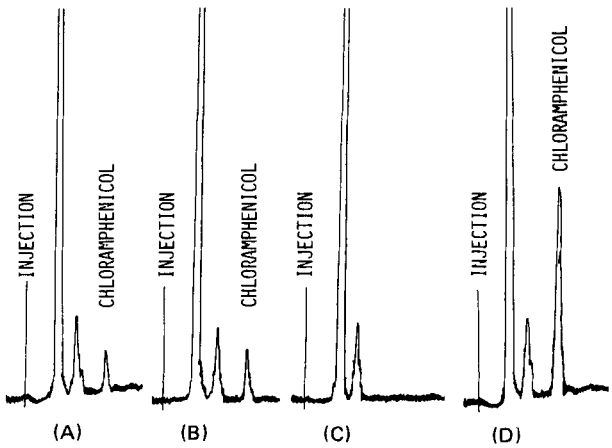

Figure 1—*Chromatograms of chloramphenicol from plasma of a human 1.5 hr after a 250-mg oral dose (A), a rabbit 0.5 hr after 20 mg/kg iv (B), human plasma blank (C), and human plasma supplemented with 35 μg of chloramphenicol/ml (D).*

Plasma samples from rabbits, healthy human subjects, and patients treated with theophylline, procainamide, propranolol, and gentamicin showed no interference with the assay. Plasma samples spiked with salicylates, acetaminophen, phenobarbital, phenytoin, ampicillin, and sulfisoxazole also did not show interference. No peaks that could be assigned to metabolites were observed in chromatograms from plasma drug samples of the human subject and the rabbit.

The major metabolites, the 3-glucuronide and deacylated form of chloramphenicol (1), are more polar than the parent drug. Under the reversed-phase separation conditions, they would probably be eluted early from the column and not interfere with the assay. These metabolites, however, were not investigated in this study.

The linearity of a typical standard curve is summarized in Table I. The response factors (peak height/concentration) were quite constant for all concentrations, even though no internal standard was used. The reproducibility is indicated by a coefficient of variation of 2.24% on replicate analyses of six 20-μg/ml samples. The resolution of separation of the column was good for a prolonged period (longer than 1 year), with occasional cleansing with methanol or dimethyl sulfoxide.

To test the potential use of this HPLC procedure in clinical drug monitoring, plasma samples collected from the rabbit at different times after intravenous chloramphenicol administration were analyzed. Figure 2 shows that the plasma antibiotic concentrations declined rapidly, with a half-life of about 33 min. This biological half-life of chloramphenicol in the rabbit is much shorter than that of 1.5–3.5 hr reported in humans (1).

HPLC has been used for the detection of chloramphenicol and some of its synthetic intermediates in manufacturing (12). However, the application of HPLC to the assay of chloramphenicol in biological specimens was not reported. The proposed method uses acetonitrile to precipitate plasma proteins to obtain a clear supernate after centrifugation. This sample preparation makes the assay fast, simple, and subject to less potential errors. It takes only about 8 min to complete. Since only 20-μl aliquots of the supernate were required for injection, small volumes (10–20 μl) of plasma would be sufficient. Thus, the assay would be particularly valuable for pediatric monitoring.

Table I—Linearity of Calibration Curve of Chloramphenicol

Concentration in Plasma, μg/ml	Peak Height, cm	Response Factor[a]
2.5	0.40	0.160
5.0	0.78	0.156
10.0	1.56	0.156
20.0	3.13[b]	0.157
30.0	4.59	0.153
40.0	6.13	0.153
50.0	7.70	0.154

[a] Response factor = peak height/concentration. [b] Average of six replicate analyses; *SD* = 0.07 cm.

[1] Model 601, Perkin-Elmer Corp., Norwalk, Conn.
[2] Model SVOV-6-IX, Glenco Scientific Co., Houston, Tex.
[3] HC ODS Sil-X-1, Perkin-Elmer Corp., Norwalk, Conn.
[4] Model LC-55, Perkin-Elmer Corp., Norwalk, Conn.
[5] Sigma Chemical Co., St. Louis, Mo.
[6] Burdick & Jackson Laboratory, Muskegon, Mich.
[7] Fisher Scientific Co., Fair Lawn, N.J.
[8] Type HA, 0.45 μm for water; type FH, 0.5 μm for ethanol. Millipore Corp., Bedford, Mass.
[9] Perkin-Elmer Corp., Norwalk, Conn.

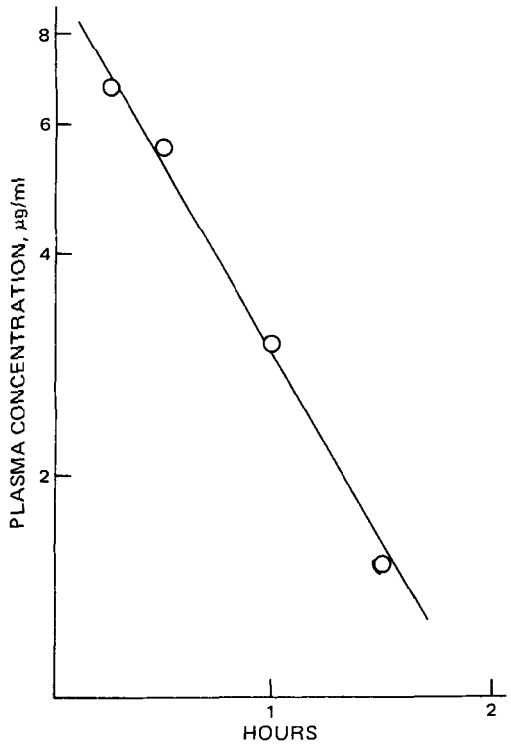

Figure 2—*Plasma concentration profile of chloramphenicol in a rabbit after 20 mg/kg iv.*

The low limit of accurate quantitative measurement of chloramphenicol was about 2.5 μg/ml in plasma when the detector sensitivity was set at 0.004 absorbance unit for full-scale deflection by use of the attenuator. Chloramphenicol at the 0.5-μg/ml level could be detected by the enhancement of the sensitivity to 0.0029 absorbance unit for full-scale deflection. Sample preparation by solvent extraction can improve the low limit of accurate measurement greatly. Sensitivity by solvent extraction depends on the sample size and the volume fraction of the reconstituted solution of the extract injected. For example, by extracting 0.2 ml of plasma with 2.5 ml of ethyl acetate and injecting 20 μl of the 50-μl reconstituted solution of residue from a 2.0-ml aliquot of the organic extract, the low limit of accurate quantitation could be as low as 0.5 μg/ml.

REFERENCES

(1) "The Pharmacological Basis of Therapeutics," L. S. Goodman and A. Gilman, Eds., Macmillan, New York, N.Y., 1975, p. 1183.

(2) A. A. Yunis and G. R. Bloomberg, in "Progress in Hematology," C. V. Moore and E. G. Brown, Eds., Grune and Stratton, New York, N.Y., 1964, p. 138.

(3) H. D. Mercer, J. N. Geleta, J. Kramer, and G. Carter, *J. Am. Vet. Med.*, **158**, 47 (1971).

(4) J. L. Scott, S. M. Finegold, G. A. Belkin, and J. S. Lawrence, *N. Engl. J. Med.*, **272**, 1137 (1965).

(5) L. G. Suhrland and A. S. Weisberger, *Blood*, **34**, 466 (1969).

(6) W. J. Jusko, in "Clinical Pharmacokinetics," G. Levy, Ed., American Pharmaceutical Association, Washington, D.C., 1974, p. 111.

(7) A. J. Glazko, A. W. Kinkel, W. C. Alegnani, and E. L. Holmes, *Clin. Pharmacol. Ther.*, **9**, 472 (1968).

(8) D. Szulczewski and F. Eng, in "Analytical Profiles of Drug Substances," vol. 4, K. Florey, Ed., Academic, New York, N.Y., 1975, p. 47.

(9) M. Margosis, *J. Pharm. Sci.*, **63**, 435 (1974).

(10) G. L. Resnick, D. Corbin, and D. H. Sanberg, *Anal. Chem.*, **38**, 582 (1966).

(11) C. J. Least, Jr., N. J. Weigand, G. F. Johnson, and H. M. Solomon, *Clin. Chem.*, **23**, 220 (1977).

(12) G. Vigh and J. Inczedy, *J. Chromatogr.*, **129**, 81 (1976).

Perfluorooctyl Bromide Concentration in Plasma and Tissues of Beagle Dogs

F. H. LEE, M. SCRIME, and J. EDELSON ˣ

Received August 22, 1977, from the *Department of Drug Metabolism and Disposition, Sterling-Winthrop Research Institute, Rensselaer, NY 12144.* Accepted for publication November 10, 1977.

Abstract □ Plasma levels were determined frequently after single doses of perfluorooctyl bromide were administered to beagle dogs at doses of either 30.8 g/kg po or 3.9 g/kg intratracheally. The apparent first-order half-life during the terminal elimination phase was about 1 day after oral medication and about 7 days after intratracheal administration. Analysis of tissues revealed the highest concentrations of the compound in abdominal fat of dogs autopsied 4 weeks later.

Keyphrases □ Perfluorooctyl bromide—tissue distribution in dogs after oral and intratracheal administration □ Distribution, tissue—perfluorooctyl bromide in dogs after oral and intratracheal administration □ Fluorocarbons—perfluorooctyl bromide, tissue distribution in dogs after oral and intratracheal administration

Liquid fluorocarbon studies provided the stimulus for the development of radiopaque perfluorocarbon compounds (1). The most effective compound tested was perfluorooctyl bromide (I), $C_8F_{17}Br$ (2). Toxicity and efficacy studies indicated a low toxicity and satisfactory radiographic density (3). Concentrated oil-in-water emulsions were found useful for bronchographic examinations in humans and animals (4). The use of I as a diagnostic contrast medium for gastroenterography of laboratory animals was reported (5). Recently, I was reported as a potential antiobesity agent (6).

Some data on the disposition of I after intratracheal administration to rats, dogs, and human subjects were reported (7); the sensitivity of the method did not allow quantitation of I in blood. This report describes studies on the plasma and tissue I concentrations in beagle dogs after oral and intratracheal administrations.

EXPERIMENTAL

Animal Procedure—Following an overnight fast, two groups of beagle dogs of both sexes (Tables I and II) received either a 30.8-g/kg po dose

0022-3549/78/0700/1038$01.00/0
© 1978, American Pharmaceutical Association

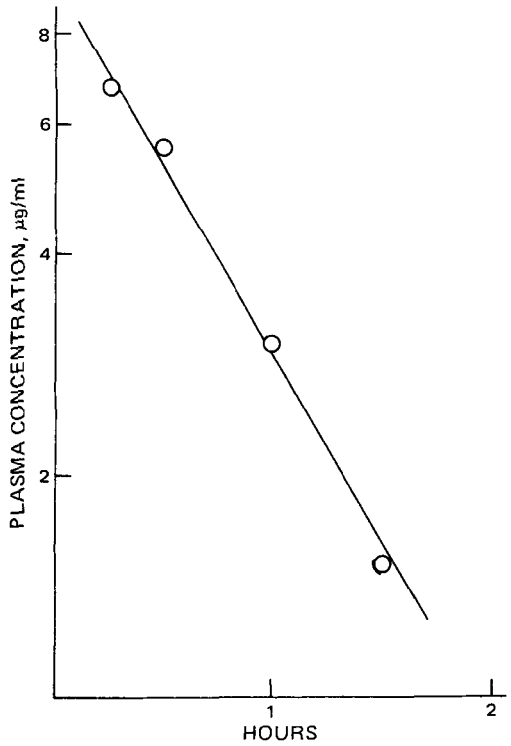

Figure 2—*Plasma concentration profile of chloramphenicol in a rabbit after 20 mg/kg iv.*

The low limit of accurate quantitative measurement of chloramphenicol was about 2.5 μg/ml in plasma when the detector sensitivity was set at 0.004 absorbance unit for full-scale deflection by use of the attenuator. Chloramphenicol at the 0.5-μg/ml level could be detected by the enhancement of the sensitivity to 0.0029 absorbance unit for full-scale deflection. Sample preparation by solvent extraction can improve the low limit of accurate measurement greatly. Sensitivity by solvent extraction depends on the sample size and the volume fraction of the reconstituted solution of the extract injected. For example, by extracting 0.2 ml of plasma with 2.5 ml of ethyl acetate and injecting 20 μl of the 50-μl reconstituted solution of residue from a 2.0-ml aliquot of the organic extract, the low limit of accurate quantitation could be as low as 0.5 μg/ml.

REFERENCES

(1) "The Pharmacological Basis of Therapeutics," L. S. Goodman and A. Gilman, Eds., Macmillan, New York, N.Y., 1975, p. 1183.

(2) A. A. Yunis and G. R. Bloomberg, in "Progress in Hematology," C. V. Moore and E. G. Brown, Eds., Grune and Stratton, New York, N.Y., 1964, p. 138.

(3) H. D. Mercer, J. N. Geleta, J. Kramer, and G. Carter, *J. Am. Vet. Med.*, **158**, 47 (1971).

(4) J. L. Scott, S. M. Finegold, G. A. Belkin, and J. S. Lawrence, *N. Engl. J. Med.*, **272**, 1137 (1965).

(5) L. G. Suhrland and A. S. Weisberger, *Blood*, **34**, 466 (1969).

(6) W. J. Jusko, in "Clinical Pharmacokinetics," G. Levy, Ed., American Pharmaceutical Association, Washington, D.C., 1974, p. 111.

(7) A. J. Glazko, A. W. Kinkel, W. C. Alegnani, and E. L. Holmes, *Clin. Pharmacol. Ther.*, **9**, 472 (1968).

(8) D. Szulczewski and F. Eng, in "Analytical Profiles of Drug Substances," vol. 4, K. Florey, Ed., Academic, New York, N.Y., 1975, p. 47.

(9) M. Margosis, *J. Pharm. Sci.*, **63**, 435 (1974).

(10) G. L. Resnick, D. Corbin, and D. H. Sanberg, *Anal. Chem.*, **38**, 582 (1966).

(11) C. J. Least, Jr., N. J. Weigand, G. F. Johnson, and H. M. Solomon, *Clin. Chem.*, **23**, 220 (1977).

(12) G. Vigh and J. Inczedy, *J. Chromatogr.*, **129**, 81 (1976).

Perfluorooctyl Bromide Concentration in Plasma and Tissues of Beagle Dogs

F. H. LEE, M. SCRIME, and J. EDELSON ˣ

Received August 22, 1977, from the *Department of Drug Metabolism and Disposition, Sterling-Winthrop Research Institute, Rensselaer, NY 12144.* Accepted for publication November 10, 1977.

Abstract □ Plasma levels were determined frequently after single doses of perfluorooctyl bromide were administered to beagle dogs at doses of either 30.8 g/kg po or 3.9 g/kg intratracheally. The apparent first-order half-life during the terminal elimination phase was about 1 day after oral medication and about 7 days after intratracheal administration. Analysis of tissues revealed the highest concentrations of the compound in abdominal fat of dogs autopsied 4 weeks later.

Keyphrases □ Perfluorooctyl bromide—tissue distribution in dogs after oral and intratracheal administration □ Distribution, tissue—perfluorooctyl bromide in dogs after oral and intratracheal administration □ Fluorocarbons—perfluorooctyl bromide, tissue distribution in dogs after oral and intratracheal administration

Liquid fluorocarbon studies provided the stimulus for the development of radiopaque perfluorocarbon compounds (1). The most effective compound tested was perfluorooctyl bromide (I), $C_8F_{17}Br$ (2). Toxicity and efficacy studies indicated a low toxicity and satisfactory radiographic density (3). Concentrated oil-in-water emulsions were found useful for bronchographic examinations in humans and animals (4). The use of I as a diagnostic contrast medium for gastroenterography of laboratory animals was reported (5). Recently, I was reported as a potential antiobesity agent (6).

Some data on the disposition of I after intratracheal administration to rats, dogs, and human subjects were reported (7); the sensitivity of the method did not allow quantitation of I in blood. This report describes studies on the plasma and tissue I concentrations in beagle dogs after oral and intratracheal administrations.

EXPERIMENTAL

Animal Procedure—Following an overnight fast, two groups of beagle dogs of both sexes (Tables I and II) received either a 30.8-g/kg po dose

0022-3549/78/0700/1038$01.00/0
© 1978, American Pharmaceutical Association

Table I—Tissue I Concentrations (Micrograms per Gram) in Beagle Dogs that Received 30.8 g/kg po

Dog (Sex; Weight in kg)	Lung	Abdominal Fat	Mesenteric Lymph	Thoracic Lymph	Adrenal	Ovary	Testes
			1 Week				
1 (M; 10.9)	0.04	5.44	<0.08	<0.18	<0.10	—	<0.05
2 (M; 8.4)	0.03	9.24	0.24	<0.18	<0.10	—	<0.05
3 (M; 9.5)	0.09	5.60	<0.08	1.57	<0.10	—	<0.05
4 (F; 8.4)	0.12	23.9	0,29	<0.18	<0.10	<0.04	—
5 (F; 10.2)	2.4	19.4	0.38	5.06	<0.10	<0.04	—
6 (F; 8.2)	0.06	16.7	0.36	<0.18	<0.10	<0.04	—
Mean ± *SE*[a]	0.46 ± 0.39	13.4 ± 3.1	0.22 ± 0.06	1.16 ± 0.82	<0.10	<0.04	<0.05
			4 Weeks				
7 (M; 7.5)	<0.02	<0.72	<0.08	<0.18	<0.10	—	0.46
8 (M; 9.1)	<0.02	<0.72	<0.08	<0.18	<0.10	—	<0.05
9 (M; 8.4)	0.04	20.6	2.2	2.13	<0.10	—	<0.05
10 (M; 10.3)	0.10	4.67	0.24	<0.18	<0.10	—	<0.05
11 (F; 9.4)	0.06	1.46	0.18	<0.18	<0.10	<0.04	—
12 (F; 12.2)	0.04	<0.72	0.24	<0.18	<0.10	<0.04	—
13 (F; 11.2)	0.07	14.8	1.72	<0.18	<0.10	<0.04	—
14 (F; 8.4)	0.05	<0.72	0.30	<0.18	<0.10	0.54	—
Mean ± *SE*[a]	0.05 ± 0.01	5.37 ± 2.79	0.62 ± 0.30	<0.26	<0.10	<0.13	<0.11

[a] Half of minimum quantifiable level used in calculating mean.

or a 3.9-g/kg intratracheal dose of I[1]. The oral dose was administered *via* a gastric tube. Intratracheal administration was carried out under light thiopental[2] anesthesia (35 mg/kg iv), and a gastric tube was passed into the trachea, reaching a point a few centimeters above the bifurcation of the left and right bronchi.

At intervals, 5 ml of blood was withdrawn from the femoral vein. The blood was collected with potassium oxalate as the anticoagulant and centrifuged promptly at 2500 rpm for 10 min. The plasma was separated, frozen, and stored at −4° until assay.

Three dogs of each sex of the orally dosed group were anesthetized with pentobarbital sodium[2] (45 mg/kg iv) and sacrificed after 7 days; the remaining animals were sacrificed after 28 days. Of the intratracheally dosed animals, two dogs of each sex were sacrificed at 7, 14, and 28 days. At sacrifice, samples of the abdominal fat, gonads, adrenals, mesenteric lymph nodes, thoracic lymph nodes, and lungs were removed and stored at −4° pending assay. Earlier studies demonstrated that the highest levels of I were found in these tissues after tracheal administration (7).

Extraction Procedure—To 1 ml of plasma, 1 ml of *n*-hexane containing either 1.6 μg, for analysis of plasma from orally dosed animals, or 0.41 μg, for analysis of plasma from intratracheally dosed animals, of the internal standard, tetrachlorodifluoroethane[3], was added. The mixture was mechanically shaken for 10 min. After centrifugation at 2500 rpm for 10 min, 2 μl of the organic phase was analyzed by GLC.

From 0.5 to 50 g of tissue sample was homogenized with 0.8–9 parts by weight of water. Homogenates equivalent to 0.1–1 g of tissue samples were extracted with 1 ml of *n*-hexane containing 0.41 μg of the internal standard, and 2 μl of the organic phase was analyzed.

GLC Determination—All assays were performed using a gas chromatograph equipped with a ^{63}Ni-electron-capture detector[4], an automatic

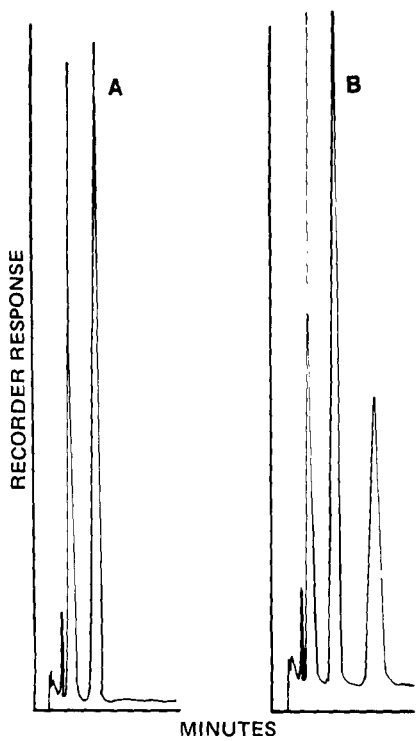

Figure 1—*Chromatogram of extracted dog plasma containing the internal standard (A) and the same sample containing 1.5 μg of I/ml (B).*

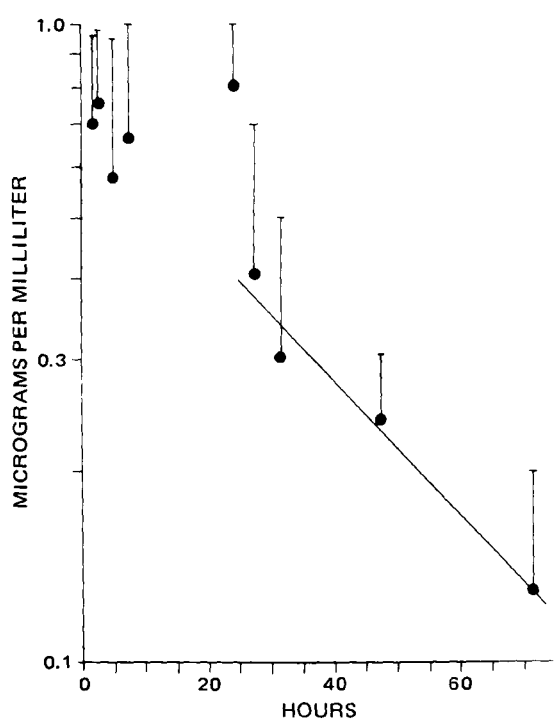

Figure 2—*Plasma concentrations in beagle dogs after oral administration of 30.8 g of I/kg;* n = *14. The vertical bar represents 1* SE.

[1] E. I. du Pont de Nemours, Wilmington, Del.
[2] Abbott, North Chicago, Ill.
[3] Freon 112, E. I. du Pont de Nemours, Wilmington, Del.
[4] Model 5710A, Hewlett-Packard, Avondale, Pa.

Table II—Tissue I Concentrations (Micrograms per Gram) in Beagle Dogs that Received 3.9 g/kg Intratracheally

Dog (Sex; Weight in kg)	Lung	Abdominal Fat	Mesenteric Lymph	Thoracic Lymph	Adrenal	Ovary	Testes
			1 Week				
15 (M; 8.9)	894	613	15.8	58.3	11.1	—	4.10
16 (M; 8.3)	947	286	5.17	13.0	21.1	—	4.84
17 (F; 8.2)	107	250	10.6	<0.18	19.8	3.57	—
18 (F; 7.5)	201	242	4.98	87.6	2.84	3.66	—
Mean ± *SE*[a]	537 ± 222	348 ± 89	9.14 ± 2.57	39.7 ± 20.2	13.7 ± 4.2	3.62 ± 0.04	4.47 ± 0.37
			2 Weeks				
19 (M; 8.6)	12.3	151	0.44	<0.18	<0.10	—	1.64
20 (F; 7.7)	53.4	357	4.25	11.2	1.28	38.9	—
21 (M; 8.4)	12.8	197	1.91	6.63	3.39	—	1.28
22 (F; 7.4)	7.72	189	4.66	6.13	<0.10	<0.04	—
Mean ± *SE*[a]	21.6 ± 10.7	224 ± 46	2.82 ± 1.00	6.01 ± 2.28	1.19 ± 0.79	19.5 ± 19.4	1.46 ± 0.18
			4 Weeks				
23 (M; 8.7)	8.58	151	0.31	4.33	1.39	—	<0.05
24 (M; 8.2)	2.13	49.9	0.58	<0.18	3.78	—	<0.05
25 (F; 7.4)	3.73	61.9	3.50	3.98	<0.10	<0.04	—
26 (F; 6.9)	11.0	58.8	12.4	14.8	1.56	<0.04	—
Mean ± *SE*[a]	6.36 ± 2.07	80.4 ± 23.7	4.20 ± 2.83	5.80 ± 3.15	1.70 ± 0.77	—	—

[a] Half of minimum quantifiable level used in calculating mean.

sampler, and a 1-mv recorder. A 1.54-m × 3-mm presilanized glass column was packed with porous polymer beads[5], 80–100 mesh. The column temperature was 220°, the injection port temperature was 250°, and the temperature of the electron-capture detector was 300°. The carrier gas was a mixture of 7% methane in argon[6], with a flow rate of 40 ml/min. When using these conditions, the retention times of I and tetrachlorodifluoroethane were 6 and 3 min, respectively.

Freshly prepared samples of normal, untreated plasma and tissue containing known amounts of I were used as standards. They were extracted and assayed as described.

RESULTS AND DISCUSSION

Typical chromatograms of plasma extracts are shown in Fig. 1. The relationship between the relative peak size ratio and the I concentration was linear up to 1.5 μg/ml or g; the standard line was computer estimated by a least-squares fit. There was some day-to-day variation in the slopes and intercepts, as can be seen from the standard errors in the equation for the plasma standards line:

$$\text{(peak size ratio)} = (0.0038 \pm 0.008) \times [\text{plasma concentration}] + (0.1294 \pm 0.0362) \quad \text{(Eq. 1)}$$

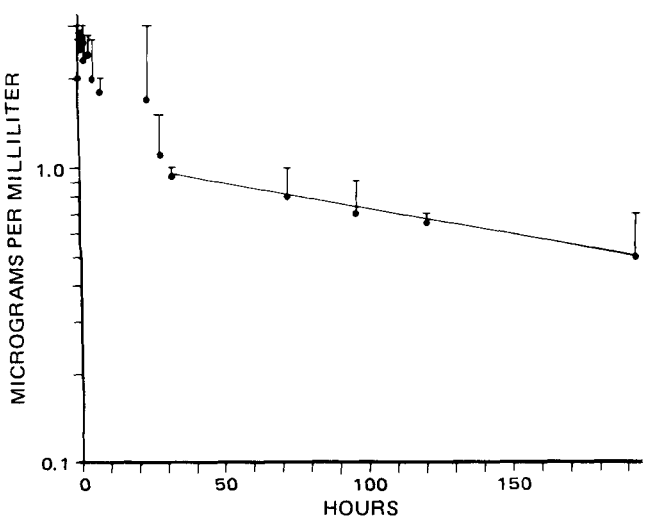

Figure 3—*Plasma concentrations in beagle dogs after intratracheal administration of 3.9 g of I/kg;* n = *12. The vertical bar represents 1* SE.

[5] Porapak QS, Waters, Framingham, Mass.
[6] Linde (Union Carbide), New York, N.Y.

The assay precision within groups of samples augmented with I ranged from 2.9 to 11.1% *SE*, and the accuracy ranged from 10.9% low to 8.5% high. The concentration in the unknowns was calculated from the extracted standards line, which was run on the same day as the samples. The mean minimum quantifiable level, defined as the value whose 80% confidence limit just encompasses zero, was 0.0909 ± 0.0127 μg/ml for 11 different sets of plasma standards. Tissue standards behaved similarly; the minimum quantifiable level value for the tissues was 0.08 ± 0.02 μg/sample analyzed. The recovery of extracted standards, relative to direct standards, was 53.1 ± 4.1%.

The plasma I concentrations in beagle dogs following oral and intratracheal administrations of the liquid are summarized in Figs. 2 and 3, respectively. The apparent first-order terminal phase elimination half-lives of the compound were about 1 day after oral administration and about 7 days after intratracheal administration, as determined by least-squares regression on the data points of the respective terminal phases. At 24 hr after the oral dose and at 1.5 hr after the endotracheal dose, the mean quantities of drug in plasma were 0.34 mg (1.2×10^{-4}% of the administered dose, assuming 45 ml of plasma/kg) and 9.49 mg (3.4×10^{-3}% of the administered dose), respectively.

Some tissue I concentrations after oral and intratracheal routes are summarized in Tables I and II, respectively. After 1 month, the highest concentrations of I administered by both routes were measured in abdominal fat, with mean values of 5.4 μg/g after the oral dose and 80.4 μg/g after the intratracheal dose. The apparent elimination half-life of the intratracheally administered compound in fat was 9.8 days, determined from three data points at 1, 2, and 4 weeks (Table II). In the other tissues, only two data points were available; no half-life estimates were made.

In summary, the developed GLC assay for the determination of I concentrations permitted estimation of apparent first-order terminal elimination half-lives in plasma and selected tissues of beagle dogs that received I by either the oral or intratracheal route.

REFERENCES

(1) D. M. Long, M. Liu, P. S. Szanto, and P. Alrenga, *Chest*, **61S**, 64 (1972).

(2) D. M. Long, M. Liu, P. S. Szanto, and P. Alrenga, *Rev. Surg.*, **29**, 71 (1972).

(3) D. M. Long, M. Liu, P. S. Szanto, D. P. Alrenga, M. M. Patel, M. V. Rios, and L. M. Nyhus, *Radiology*, **105**, 323 (1972).

(4) A. S. Arambulo, M. Liu, A. L. Rosen, G. Dobben, and D. M. Long, *Drug Dev. Commun.*, **1**, 73 (1974).

(5) M. Liu and D. M. Long, *Radiology*, **122**, 71 (1977).

(6) M. Hussain, S. Niazi, A. Arambulo, and D. M. Long, *J. Pharm. Sci.*, **66**, 907 (1977).

(7) M. S. Liu and D. M. Long, *Invest. Radiol.*, **11**, 479 (1976).

ACKNOWLEDGMENTS

The authors thank the Department of Toxicology, Sterling-Winthrop Research Institute, for assistance with the animal studies.

Influence of Partition Coefficient on Intestinal Absorption of Alkylamine Antihistamines

Keyphrases □ Absorption, GI—various alkylamine antihistamines, effect of partition coefficient, rats □ Partition coefficients—various alkylamine antihistamines, effect on GI absorption, rat □ Antihistamines, various alkylamine—GI absorption, effect of partition coefficient, rats

To the Editor:

Prior to initiating studies on the bioequivalence of various brands of chlorpheniramine maleate tablets, it was considered of value first to compare in animals the intestinal absorption of chlorpheniramine with that of brompheniramine and pheniramine to determine the overall absorption characteristics of the therapeutically useful alkylamine antihistamines.

The comparative absorption characteristics of these antihistamines as a group have not been studied in humans or animals, and such information would prove useful in the design of the experimental protocol and the subsequent assessment of bioavailability data in the bioequivalency studies.

The method of Doluisio *et al.* (1) was used to evaluate the intestinal absorption of each drug at pH 6.0. Aqueous phosphate buffer solutions of the maleate salts of pheniramine, chlorpheniramine, and brompheniramine were prepared at 25 mg/100 ml. Because of limited aqueous solubility, the tannate salt of chlorpheniramine was prepared at 7.5 mg/100 ml.

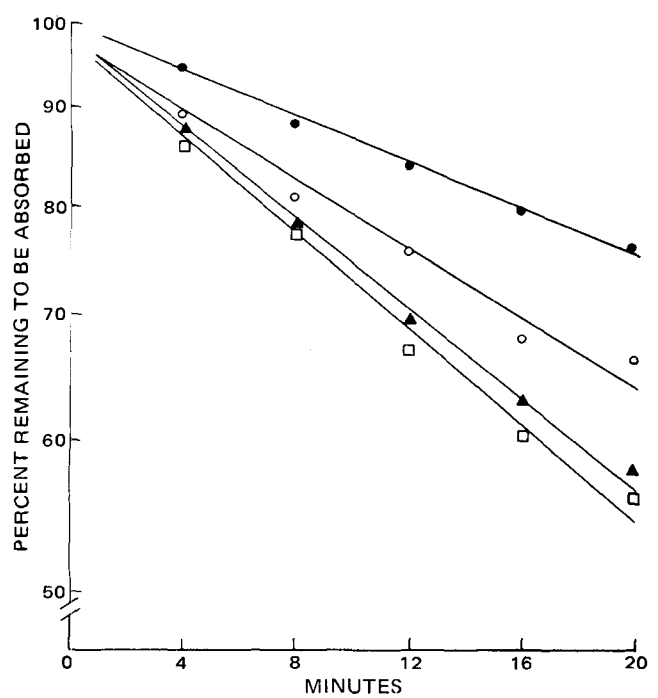

Figure 1—*Percent remaining to be absorbed as a function of time for the intestinal absorption of pheniramine maleate (●), chlorpheniramine tannate (○), chlorpheniramine maleate (▲), and brompheniramine maleate (□). Each data point represents the mean of three determinations.*

Table I—Absorption Half-Lives [a] and Partition Coefficients [b]

Drug	$t_{1/2}$, min	Partition Coefficient (pH 6.0) Heptane	Ether	Carbon Tetrachloride	Partition Coefficient (pH 7.5), Heptane
Pheniramine maleate	49.2	0.01	0.17	0.10	0.33
Chlorpheniramine tannate	32.9	0.10	0.60	1.04	—
Chlorpheniramine maleate	25.2	0.14	0.63	1.21	1.74
Brompheniramine maleate	23.7	0.16	0.64	2.04	3.16

[a] Measured at pH 6.0. [b] Measured at 25°.

The concentrations of the antihistamines in the phosphate buffer were determined by GLC analysis. Aqueous sample, 0.1 ml, was added to 4.0 ml of 0.12% NaOH (pH 12.2) in a 15-ml acid-washed glass centrifuge tube fitted with a polytef-lined cap. For the determination of chlorpheniramine and brompheniramine, 500 μl of chloroform containing 2.4 mg of pheniramine maleate/100 ml (as internal standard) was then added. The tubes were shaken and centrifuged, and 5 μl of the chloroform layer was injected directly onto the column. For the determination of pheniramine, the procedure outlined was repeated except that 500 μl of chloroform containing 5 mg of chlorpheniramine/100 ml (as internal standard) was substituted. The retention times for pheniramine, chlorpheniramine, and brompheniramine were 80, 121, and 153 sec, respectively.

The instrument[1] was equipped with a flame-ionization detector. Peak integration was measured with an electronic integrator[2]. Dual 1.8-m glass columns, 0.6-cm o.d., were packed with 2.5% SE-30 on 80–100-mesh Chromosorb G, DMCS. The nitrogen flow rate was 60 ml/min. Oven, injector, and detector temperatures were maintained at 240, 250, and 250°, respectively.

The results for the absorption of the antihistamines from the rat small intestine are shown in Fig. 1. Each alkylamine derivative was absorbed rather slowly at pH 6.0, with half-lives for first-order disappearance of drug from the lumen ranging from 24 min for brompheniramine to 49 min for pheniramine (Table I). Included in Table I are the heptane–phosphate buffer (pH 6.0) partition coefficients for each drug determined by the method of McMahon (2). As might be inferred from the absorption data of Fig. 1, the values of the partition coefficients were generally quite low at pH 6.0. Similar rank-order correlations were found when ether or carbon tetrachloride was substituted for heptane. As expected for these weakly basic alkylamine antihistamines (pKa = ~9.2), the partition coefficients increased when the pH of the phosphate buffer was increased to 7.5 (Table I).

[1] Hewlett-Packard model 5711A.
[2] Spectra-Physics Autolab Minigrator.

0022-3549/78/0700/1041$01.00/0
© 1978, American Pharmaceutical Association

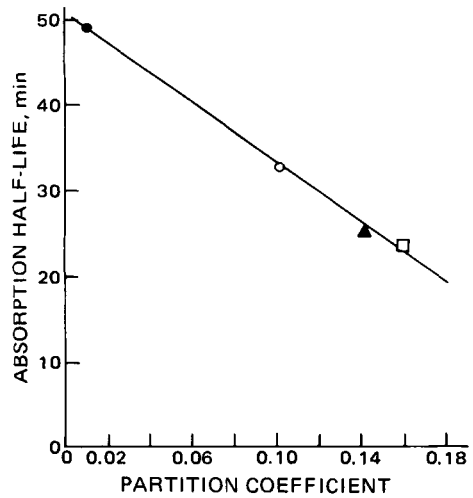

Figure 2—*Absorption half-life as a function of the heptane–phosphate buffer (pH 6.0) partition coefficient for pheniramine maleate (●), chlorpheniramine tannate (○), chlorpheniramine maleate (▲), and brompheniramine maleate (□).*

Of significance was the finding that a plot of the $t_{1/2}$ for disappearance of drug from the lumen as a function of the heptane–phosphate buffer (pH 6.0) partition coefficient was linear with a correlation coefficient of 0.998, as determined from a least-square fit to the observed data (Fig. 2). Our results are in accord with those of Schanker (3) and Kakemi *et al.* (4) who found an excellent correlation of absorption characteristics for a series of barbiturates with their corresponding lipid–water partition coefficients.

Of interest is the comparison of the absorption characteristics of these drugs to the corresponding urinary excretion data observed by Kabasakalian *et al.* (5). They found that the extent of free (unmetabolized) pheniramine excreted in the urine was greater than the extent of free chlorpheniramine excreted which, in turn, was greater than the extent of free brompheniramine excreted. Our current findings support the suggestion by Kabasakalian *et al.* (5) that the more lipid-soluble agents are to a greater extent passively reabsorbed from the kidney tubules back into the blood, allowing for further metabolism and thus resulting in decreased renal excretion of free drug. Therefore, as is true for many drugs, both absorption and excretion profiles of these alkylamine antihistamines follow patterns consistent with their overall lipid solubilities.

(1) J. T. Doluisio, N. F. Billups, L. W. Dittert, E. T. Sugita, and J. V. Swintosky, *J. Pharm. Sci.*, **58**, 1196 (1969).

(2) R. E. McMahon, *J. Med. Pharm. Chem.*, **4**, 67 (1961).

(3) L. S. Schanker, *ibid.*, **2**, 343 (1960).

(4) K. Kakemi, T. Arita, R. Hori, and R. Konishi, *Chem. Pharm. Bull.*, **15**, 1534 (1967).

(5) P. Kabasakalian, M. Taggart, and E. Townley, *J. Pharm. Sci.*, **57**, 621 (1968).

Nathan R. Strahl ˣ
Susan Lopez
College of Pharmacy
University of New Mexico
Albuquerque, NM 87131

Received March 27, 1978.
Accepted for publication April 26, 1978.
Supported in part by National Institutes of Health Grant RR 08139.

Aggregation of Dantrolene to Human Serum Albumin

Keyphrases □ Dantrolene—binding to human serum albumin, fluorescence quenching study, mechanism evaluated □ Binding—dantrolene to human serum albumin, fluorescence quenching study, mechanism evaluated □ Albumin, human serum—binding to dantrolene, fluorescence quenching study, mechanism evaluated □ Relaxants, skeletal muscle—dantrolene, binding to human serum albumin, fluorescence quenching study, mechanism evaluated

To the Editor:

A recent article (1) concerning the interaction of dantrolene, 1-[[5-(4-nitrophenyl)furfurylidine]amino]hydantoin, with human serum albumin reported difficulty saturating the protein with the drug in an aqueous system. Difference spectrophotometric titrations of these two reactants resulted in a continual hyperchromism of the complexed drug's spectral band. A saturation end-point was not reached, even though the dantrolene concentration in all test solutions was increased to its solubility limit ($\sim 1.0 \times 10^{-4}$ *M*) in the pH 7.4 buffered aqueous system. Furthermore, the albumin was not saturated even in solutions that had the protein concentration reduced 100-fold from 1.45×10^{-4} to 1.45×10^{-6} *M*.

Lack of a definite end-point in the titration was attributed to two possible causes: the poor water solubility of dantrolene, limiting the saturation of available binding sites on the albumin; or association between bound and unbound drug molecules, hindering detection of a saturation point. A closer examination of this problem indicates that the latter self-association is most likely.

The purity of dantrolene[1] as the free acid was established by TLC in three different solvent systems: acetone–chloroform (7:3), R_f 0.50; methanol–chloroform (7:3), R_f 0.55; and benzene–methanol (9:1), R_f 0.80. All solvents were the highest grade commercially available.

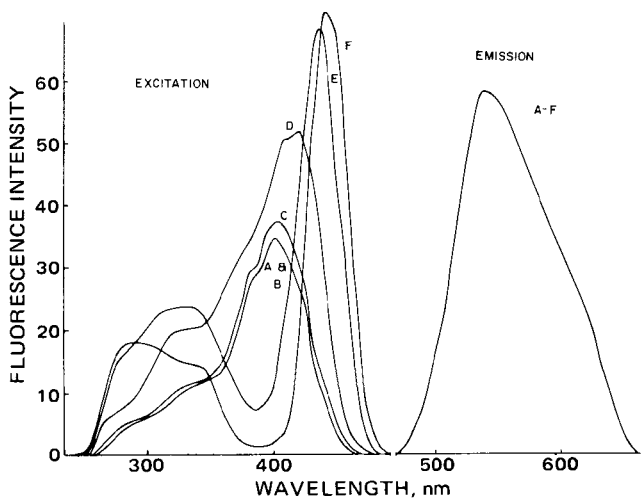

Figure 1—*Corrected fluorescence excitation and emission spectra of dantrolene in chloroform at 3.0×10^{-4} (A), 3.0×10^{-5} (B), 3.0×10^{-6} (C), 3.0×10^{-7} (D), 3.0×10^{-8} (E), and 3.0×10^{-9} (F) M. Instrumental electronic amplification was increased for each spectrum as the concentration was decreased so that the relative band shape and position of each spectrum could be seen.*

[1] Eaton Laboratories, Norwich, N.Y.

0022-3549/78/0700/1042$01.00/0
© 1978, American Pharmaceutical Association

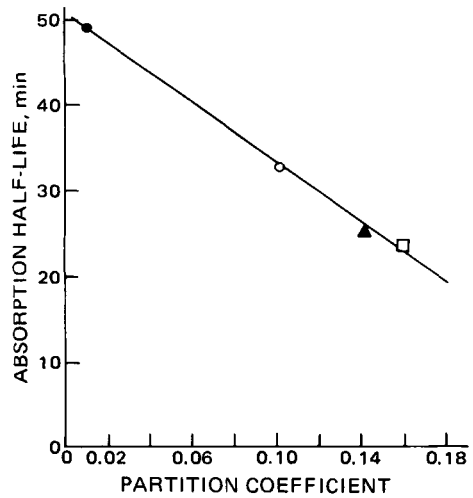

Figure 2—*Absorption half-life as a function of the heptane–phosphate buffer (pH 6.0) partition coefficient for pheniramine maleate (●), chlorpheniramine tannate (○), chlorpheniramine maleate (▲), and brompheniramine maleate (□).*

Of significance was the finding that a plot of the $t_{1/2}$ for disappearance of drug from the lumen as a function of the heptane–phosphate buffer (pH 6.0) partition coefficient was linear with a correlation coefficient of 0.998, as determined from a least-square fit to the observed data (Fig. 2). Our results are in accord with those of Schanker (3) and Kakemi *et al.* (4) who found an excellent correlation of absorption characteristics for a series of barbiturates with their corresponding lipid–water partition coefficients.

Of interest is the comparison of the absorption characteristics of these drugs to the corresponding urinary excretion data observed by Kabasakalian *et al.* (5). They found that the extent of free (unmetabolized) pheniramine excreted in the urine was greater than the extent of free chlorpheniramine excreted which, in turn, was greater than the extent of free brompheniramine excreted. Our current findings support the suggestion by Kabasakalian *et al.* (5) that the more lipid-soluble agents are to a greater extent passively reabsorbed from the kidney tubules back into the blood, allowing for further metabolism and thus resulting in decreased renal excretion of free drug. Therefore, as is true for many drugs, both absorption and excretion profiles of these alkylamine antihistamines follow patterns consistent with their overall lipid solubilities.

(1) J. T. Doluisio, N. F. Billups, L. W. Dittert, E. T. Sugita, and J. V. Swintosky, *J. Pharm. Sci.*, **58**, 1196 (1969).

(2) R. E. McMahon, *J. Med. Pharm. Chem.*, **4**, 67 (1961).

(3) L. S. Schanker, *ibid.*, **2**, 343 (1960).

(4) K. Kakemi, T. Arita, R. Hori, and R. Konishi, *Chem. Pharm. Bull.*, **15**, 1534 (1967).

(5) P. Kabasakalian, M. Taggart, and E. Townley, *J. Pharm. Sci.*, **57**, 621 (1968).

Nathan R. Strahl ˣ
Susan Lopez
College of Pharmacy
University of New Mexico
Albuquerque, NM 87131

Received March 27, 1978.
Accepted for publication April 26, 1978.
Supported in part by National Institutes of Health Grant RR 08139.

Aggregation of Dantrolene to Human Serum Albumin

Keyphrases □ Dantrolene—binding to human serum albumin, fluorescence quenching study, mechanism evaluated □ Binding—dantrolene to human serum albumin, fluorescence quenching study, mechanism evaluated □ Albumin, human serum—binding to dantrolene, fluorescence quenching study, mechanism evaluated □ Relaxants, skeletal muscle—dantrolene, binding to human serum albumin, fluorescence quenching study, mechanism evaluated

To the Editor:

A recent article (1) concerning the interaction of dantrolene, 1-[[5-(4-nitrophenyl)furfurylidine]amino]hydantoin, with human serum albumin reported difficulty saturating the protein with the drug in an aqueous system. Difference spectrophotometric titrations of these two reactants resulted in a continual hyperchromism of the complexed drug's spectral band. A saturation end-point was not reached, even though the dantrolene concentration in all test solutions was increased to its solubility limit ($\sim 1.0 \times 10^{-4}$ *M*) in the pH 7.4 buffered aqueous system. Furthermore, the albumin was not saturated even in solutions that had the protein concentration reduced 100-fold from 1.45×10^{-4} to 1.45×10^{-6} *M*.

Lack of a definite end-point in the titration was attributed to two possible causes: the poor water solubility of dantrolene, limiting the saturation of available binding sites on the albumin; or association between bound and unbound drug molecules, hindering detection of a saturation point. A closer examination of this problem indicates that the latter self-association is most likely.

The purity of dantrolene[1] as the free acid was established by TLC in three different solvent systems: acetone–chloroform (7:3), R_f 0.50; methanol–chloroform (7:3), R_f 0.55; and benzene–methanol (9:1), R_f 0.80. All solvents were the highest grade commercially available.

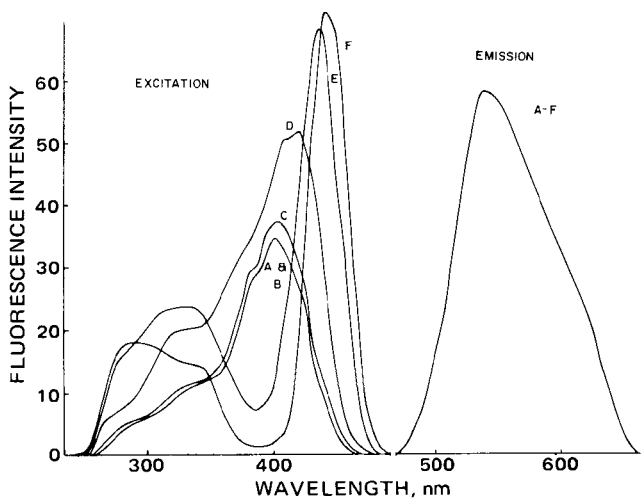

Figure 1—*Corrected fluorescence excitation and emission spectra of dantrolene in chloroform at 3.0×10^{-4} (A), 3.0×10^{-5} (B), 3.0×10^{-6} (C), 3.0×10^{-7} (D), 3.0×10^{-8} (E), and 3.0×10^{-9} (F) M. Instrumental electronic amplification was increased for each spectrum as the concentration was decreased so that the relative band shape and position of each spectrum could be seen.*

[1] Eaton Laboratories, Norwich, N.Y.

0022-3549/78/0700/1042$01.00/0
© 1978, American Pharmaceutical Association

Table I—Corrected Fluorescence Excitation and Emission Maxima of Dantrolene in Solutions of Varying Acidity, Polarity, and Hydrogen Bonding Capability

	Excitation, nm		Emission, nm	
	Monomer	Aggregate	Monomer	Aggregate
Dilute sulfuric acid, pH 3	360	380	520	520
Dilute sodium hydroxide, pH 12	387	387	530	530
Chloroform	390	430	540	540
Nitromethane	400	430	580	580

Anal.—Calc. for $C_{14}H_{10}N_4O_5$: C, 53.45; H, 3.21; N, 17.83. Found: C, 53.53; H, 3.23; N, 17.78.

The corrected fluorescence excitation and emission spectra of dantrolene were recorded on a spectrofluorometer[2] in aqueous solution at pH 3 and 12 and in chloroform and nitromethane.

In aqueous solutions, the dantrolene concentration was varied from 8.0×10^{-9} to 8.0×10^{-5} *M;* in chloroform and nitromethane, the concentrations ranged from 3.0×10^{-9} to 3.0×10^{-4} *M*. The long wavelength excitation and emission spectral maxima of the highest and lowest concentrations of dantrolene employed in these solvents are reported in Table I.

As the dantrolene concentration in chloroform solutions was decreased, the long wavelength excitation maximum shifted from 390 to 430 nm (Fig. 1). Accompanying the shift was a gradual loss in vibrational structure, terminating in the diffuse spectral band with a maximum at 430 nm. Over the same concentration range, the emission spectrum demonstrated no change in band shape or position whether the wavelength of exciting light was 390 or 430 nm.

The shift to longer wavelengths of the corrected excitation spectrum with the subsequent loss of vibrational structure is consistent with the association of molecules in the ground state to form polymeric complexes (usually dimers) containing two or more monomer molecules (2, 3). Such complexes are frequently nonfluorescent (2). This situation is evidently the case with dantrolene since the emission spectrum is not altered in any way by an increase in drug concentration or a change in wavelength of exciting light. Therefore, the emission spectrum with the maximum at 540 nm must be that of the dantrolene monomer.

[2] Perkin-Elmer MPF-4, Perkin-Elmer Corp., Norwalk, Conn.

Results similar to these were obtained for solutions of dantrolene in nitromethane and in aqueous solutions at pH 3. However, in aqueous solutions at pH 12, neither the fluorescence excitation nor emission spectra exhibited any change in band shape or position as the dantrolene concentration in solution was increased. Since dantrolene has a pKa at 7.5[3], this result seems to indicate that the free acid forms polymeric aggregates while the anion does not.

The interaction of dantrolene with human serum albumin is believed to occur through complexation of the anion at a binding site containing both an electropositive and a hydrophobic region (1). If it is assumed that electrostatic attraction between the anion and the electropositive region partially neutralizes the anion, then conditions are suitable for association between unbound molecules of free acid and neutralized, bound anion. An association of this nature would explain why solutions of human serum albumin could not be saturated regardless of their dantrolene concentration.

Such associations of molecules in solution may be due to hydrogen bonding and/or van der Waals interactions. The dependence of aggregate formation upon solution acidity suggests that hydrogen bonding may occur between molecules of the free acid in aqueous solution. Apparently, the dissociable hydrogen with pKa 7.5 may be important not only to the self-association of dantrolene free acid molecules in aqueous solution but to the association of the free acid to previously bound molecules.

(1) J. J. Vallner, L. A. Sternson, and D. L. Parsons, *J. Pharm. Sci.*, **65**, 873 (1976).

(2) C. A. Parker, "Photoluminescence of Solutions," Elsevier, Amsterdam, The Netherlands, 1968, p. 344.

(3) J. Yguerabide, *J. Chem. Phys.*, **49**, 1018 (1968).

A. C. Capomacchia ˣ
J. J. Vallner
L. Boone
Department of Pharmaceutics
School of Pharmacy
University of Georgia
Athens, GA 30602

Received March 6, 1978.
Accepted for publication May 3, 1978.
L. Boone is a NSF/SSTP Participant.

[3] Literature on dantrolene sodium (Dantrium), Eaton Laboratories, Norwich, N.Y.

BOOKS

REVIEWS

Survey of Organic Syntheses, Vol. 2. By CALVIN A. BUEHLER and DONALD E. PEARSON. Wiley-Interscience, 605 Third Ave., New York, NY 10016, 1977. 1105 pp. 16 × 24 cm. Price $25.00.

Every synthetic chemist should appreciate this book, particularly those who are not working in the field but need to plan the synthesis of an organic compound. There is much that recommends this book, notably its convenience in leading one into the vast and seemingly inhibiting realm of the organic chemical literature and the organized way in which functional group preparations are presented.

Volume 2 spans the literature from 1969 to 1975. Over 3000 references from journal articles, reviews, and books are cited. Addenda are included at the end of each chapter, listing references to synthetic methods not available when the chapter was first written.

The organization of this volume is similar to the first volume in that there are 20 chapters, each dealing with different functional groups. Much

Table I—Corrected Fluorescence Excitation and Emission Maxima of Dantrolene in Solutions of Varying Acidity, Polarity, and Hydrogen Bonding Capability

	Excitation, nm		Emission, nm	
	Monomer	Aggregate	Monomer	Aggregate
Dilute sulfuric acid, pH 3	360	380	520	520
Dilute sodium hydroxide, pH 12	387	387	530	530
Chloroform	390	430	540	540
Nitromethane	400	430	580	580

Anal.—Calc. for $C_{14}H_{10}N_4O_5$: C, 53.45; H, 3.21; N, 17.83. Found: C, 53.53; H, 3.23; N, 17.78.

The corrected fluorescence excitation and emission spectra of dantrolene were recorded on a spectrofluorometer[2] in aqueous solution at pH 3 and 12 and in chloroform and nitromethane.

In aqueous solutions, the dantrolene concentration was varied from 8.0×10^{-9} to 8.0×10^{-5} *M;* in chloroform and nitromethane, the concentrations ranged from 3.0×10^{-9} to 3.0×10^{-4} *M*. The long wavelength excitation and emission spectral maxima of the highest and lowest concentrations of dantrolene employed in these solvents are reported in Table I.

As the dantrolene concentration in chloroform solutions was decreased, the long wavelength excitation maximum shifted from 390 to 430 nm (Fig. 1). Accompanying the shift was a gradual loss in vibrational structure, terminating in the diffuse spectral band with a maximum at 430 nm. Over the same concentration range, the emission spectrum demonstrated no change in band shape or position whether the wavelength of exciting light was 390 or 430 nm.

The shift to longer wavelengths of the corrected excitation spectrum with the subsequent loss of vibrational structure is consistent with the association of molecules in the ground state to form polymeric complexes (usually dimers) containing two or more monomer molecules (2, 3). Such complexes are frequently nonfluorescent (2). This situation is evidently the case with dantrolene since the emission spectrum is not altered in any way by an increase in drug concentration or a change in wavelength of exciting light. Therefore, the emission spectrum with the maximum at 540 nm must be that of the dantrolene monomer.

[2] Perkin-Elmer MPF-4, Perkin-Elmer Corp., Norwalk, Conn.

Results similar to these were obtained for solutions of dantrolene in nitromethane and in aqueous solutions at pH 3. However, in aqueous solutions at pH 12, neither the fluorescence excitation nor emission spectra exhibited any change in band shape or position as the dantrolene concentration in solution was increased. Since dantrolene has a pKa at 7.5[3], this result seems to indicate that the free acid forms polymeric aggregates while the anion does not.

The interaction of dantrolene with human serum albumin is believed to occur through complexation of the anion at a binding site containing both an electropositive and a hydrophobic region (1). If it is assumed that electrostatic attraction between the anion and the electropositive region partially neutralizes the anion, then conditions are suitable for association between unbound molecules of free acid and neutralized, bound anion. An association of this nature would explain why solutions of human serum albumin could not be saturated regardless of their dantrolene concentration.

Such associations of molecules in solution may be due to hydrogen bonding and/or van der Waals interactions. The dependence of aggregate formation upon solution acidity suggests that hydrogen bonding may occur between molecules of the free acid in aqueous solution. Apparently, the dissociable hydrogen with pKa 7.5 may be important not only to the self-association of dantrolene free acid molecules in aqueous solution but to the association of the free acid to previously bound molecules.

(1) J. J. Vallner, L. A. Sternson, and D. L. Parsons, *J. Pharm. Sci.*, **65**, 873 (1976).

(2) C. A. Parker, "Photoluminescence of Solutions," Elsevier, Amsterdam, The Netherlands, 1968, p. 344.

(3) J. Yguerabide, *J. Chem. Phys.*, **49**, 1018 (1968).

A. C. Capomacchia ˣ
J. J. Vallner
L. Boone
Department of Pharmaceutics
School of Pharmacy
University of Georgia
Athens, GA 30602

Received March 6, 1978.
Accepted for publication May 3, 1978.
L. Boone is a NSF/SSTP Participant.

[3] Literature on dantrolene sodium (Dantrium), Eaton Laboratories, Norwich, N.Y.

BOOKS

REVIEWS

Survey of Organic Syntheses, Vol. 2. By CALVIN A. BUEHLER and DONALD E. PEARSON. Wiley-Interscience, 605 Third Ave., New York, NY 10016, 1977. 1105 pp. 16 × 24 cm. Price $25.00.

Every synthetic chemist should appreciate this book, particularly those who are not working in the field but need to plan the synthesis of an organic compound. There is much that recommends this book, notably its convenience in leading one into the vast and seemingly inhibiting realm of the organic chemical literature and the organized way in which functional group preparations are presented.

Volume 2 spans the literature from 1969 to 1975. Over 3000 references from journal articles, reviews, and books are cited. Addenda are included at the end of each chapter, listing references to synthetic methods not available when the chapter was first written.

The organization of this volume is similar to the first volume in that there are 20 chapters, each dealing with different functional groups. Much

of the material from Vol. 1 was omitted to avoid needless repetition; however, frequent reference to Vol. 1 material is made and appears as 1 (for volume) followed by the page number. These references to Vol. 1 are found in both chapter contents and text material. New material in Vol. 2 includes the preparation of allenes, cumulenes, orthoesters, orthocarbonates, and ketenimines.

At the start of each chapter is a brief, concise overview of some of the synthetic methods presented in the following text. This overview is pleasantly written and focuses on emergence of new reagents, improvements in methodology, and advantages and disadvantages of alternative methods. In the text that follows, structural formulas are used liberally and references are supplied faithfully. Yields and experimental conditions for many reactions are given. The inclusion of theoretical aspects such as mechanisms, stereochemistry, and substituent effects give the text an added dimension.

The functional group transformations listed involve no more than one or two steps, with emphasis on fundamental aliphatic–aromatic chemistry. Excluded are synthetic preparations of nucleotides, peptides, lipids, and heterocycles, which would have been useful and of more interest to the biochemist.

A rather elaborate reaction index is cross-referenced to Vol. 1. Instructions on the use of the index are provided, but it is somewhat complex to use. The subject index is quite complete; unfortunately, an author index is omitted. The lack of proofreading oversights is notable, and the print and format are good.

Reviewed by A. J. Villani
Research and Development Division
Smith Kline & French Laboratories
Philadelphia, PA 19101

Pharmacology of Steroid Contraceptive Drugs (Monographs of the Mario Negri Institute for Pharmacological Research, Milan, Italy). Edited by S. GARATTINI and H. W. BERENDES. Raven, 1140 Avenue of the Americas, New York, NY 10036. 1977. 391 pp. 16 × 24 cm. Price $28.00.

This book comprises 30 chapters by 91 authors from eight countries. Its purpose was to present current information and opinion concerning steroid contraceptive side effects; that aim has largely been achieved. A third of the references cited were published between 1973 and 1976; some were in press in 1977. Several chapters contain new data not published previously nor in press.

The book consists of articles presenting basic *in vivo* and/or *in vitro* research data, clinical research data, and/or literature reviews concerning specific side effects. Chapter contents vary considerably, because of different types of study presented and types of side effect studied.

Some chapters concern investigations into biochemical mechanisms of action and cellular and subcellular sites of action, aiming to contribute to the data base on which occurrence of various side effects might eventually be explained. Others discuss metabolism and excretion, mainly human, of contraceptive steroids. Also presented are basic and clinical research data concerning steroid contraceptives and lipids. Drug interactions are briefly reviewed, and experiments explaining a mechanism by which rifampin (rifampicin) may decrease contraceptive efficacy are described.

In the chapter Oral Contraceptive Use and Breast Diseases, available data are summarized and the way pointed for future research; other chapters concern basic research on this topic. Concisely reviewed are quite recent data associating liver tumors with oral contraceptive use. Lack of studies concerning endometrial carcinoma and combination-type oral contraceptives and lack of standardized criteria for histological diagnosis of early cervical neoplasia are noted.

Additional chapters concern oral contraceptives and the cardiovascular system. One discusses serial plasma fibrinogen chromatography, a technique that might prove useful in screening women for predisposition to thromboembolism and/or for evaluating thrombogenicity of steroid contraceptive preparations. Others are concerned with hypertension and myocardial infarction; Mann's "Discussion" of a preceding chapter, however, is in poor taste and should not have been included.

A disappointing chapter is Oral Contraceptives—The Clinical Perspective. It merely summarizes, in a less enlightening manner, data already published in 1974 by the Royal College of General Practitioners; that reference, which "contains an extensive bibliography," is the chapter's only citation. Included are comparisons between incidence of several side effects and three dosage ranges of progestogen or of estrogen; since only the lowest dosage range in each case approximates doses found in the majority of oral contraceptive preparations currently available in both England and the United States, the information is of little practical value.

It is somewhat disconcerting to find that although all chapters have numbered references, about half have them numbered based on alphabetical listing of first authors, while in the others they are numbered based on their chronological appearance within the given chapter. This distinction also applies to the references to chapters coauthored or authored, respectively, by the two editors! The titles of journal articles are missing from the references to three of the chapters, and two coauthors cited twice in each of two other chapters have their names spelled differently in the text and/or references to these two chapters.

The index, listing over 800 items, contains insufficient cross-indexing. Norethindrone and norethisterone, for example, are not cross-indexed. Authors apparently used whichever term they preferred, but only those pages on which one or the other appears are listed under that term in the index. Furthermore, in one chapter, norethisterone and norethindrone are mentioned as the fourth and seventh progestogens, respectively, in a list of agents reportedly associated with liver tumors!

The shortcomings of this book really are minor, although the insufficient cross-indexing could present a problem to the student or to someone whose major field of interest is somewhat remote from steroid pharmacology. Its greatest asset is that, in general, it is a rather up-to-date review. A few chapters are somewhat technical and specialized and, therefore, may have a somewhat narrower appeal, to individuals engaged in similar research, for example. Much of the book, however, contains valuable information, usually adequately referenced, for anyone whose interests and/or specific professional duties require knowledge of the potential(?) disadvantages of steroid contraception as well as the advantages.

Reviewed by Audrey S. Bingel
Department of Pharmacognosy and Pharmacology
College of Pharmacy
University of Illinois
Chicago, IL 60612

NEW JOURNALS

Clinical and Experimental Hypertension. Edited by MICHAEL J. ANTONACCIO. Dekker Journals, P.O. Box 11305, Church Street Station, New York, NY 10249. January 1978. 17 × 26 cm. Price $90.00 (6 issues).

Journal of Environmental Science and Health. Part C: Environmental Health Sciences. Edited by Robert J. Rubin. Dekker Journals, P.O. Box 11305, Church Street Station, New York, NY 10249. January 1978. 15 × 22.5 cm. Price $44.00 (4 issues).

of the material from Vol. 1 was omitted to avoid needless repetition; however, frequent reference to Vol. 1 material is made and appears as 1 (for volume) followed by the page number. These references to Vol. 1 are found in both chapter contents and text material. New material in Vol. 2 includes the preparation of allenes, cumulenes, orthoesters, orthocarbonates, and ketenimines.

At the start of each chapter is a brief, concise overview of some of the synthetic methods presented in the following text. This overview is pleasantly written and focuses on emergence of new reagents, improvements in methodology, and advantages and disadvantages of alternative methods. In the text that follows, structural formulas are used liberally and references are supplied faithfully. Yields and experimental conditions for many reactions are given. The inclusion of theoretical aspects such as mechanisms, stereochemistry, and substituent effects give the text an added dimension.

The functional group transformations listed involve no more than one or two steps, with emphasis on fundamental aliphatic–aromatic chemistry. Excluded are synthetic preparations of nucleotides, peptides, lipids, and heterocycles, which would have been useful and of more interest to the biochemist.

A rather elaborate reaction index is cross-referenced to Vol. 1. Instructions on the use of the index are provided, but it is somewhat complex to use. The subject index is quite complete; unfortunately, an author index is omitted. The lack of proofreading oversights is notable, and the print and format are good.

Reviewed by A. J. Villani
Research and Development Division
Smith Kline & French Laboratories
Philadelphia, PA 19101

Pharmacology of Steroid Contraceptive Drugs (Monographs of the Mario Negri Institute for Pharmacological Research, Milan, Italy). Edited by S. GARATTINI and H. W. BERENDES. Raven, 1140 Avenue of the Americas, New York, NY 10036. 1977. 391 pp. 16 × 24 cm. Price $28.00.

This book comprises 30 chapters by 91 authors from eight countries. Its purpose was to present current information and opinion concerning steroid contraceptive side effects; that aim has largely been achieved. A third of the references cited were published between 1973 and 1976; some were in press in 1977. Several chapters contain new data not published previously nor in press.

The book consists of articles presenting basic *in vivo* and/or *in vitro* research data, clinical research data, and/or literature reviews concerning specific side effects. Chapter contents vary considerably, because of different types of study presented and types of side effect studied.

Some chapters concern investigations into biochemical mechanisms of action and cellular and subcellular sites of action, aiming to contribute to the data base on which occurrence of various side effects might eventually be explained. Others discuss metabolism and excretion, mainly human, of contraceptive steroids. Also presented are basic and clinical research data concerning steroid contraceptives and lipids. Drug interactions are briefly reviewed, and experiments explaining a mechanism by which rifampin (rifampicin) may decrease contraceptive efficacy are described.

In the chapter Oral Contraceptive Use and Breast Diseases, available data are summarized and the way pointed for future research; other chapters concern basic research on this topic. Concisely reviewed are quite recent data associating liver tumors with oral contraceptive use. Lack of studies concerning endometrial carcinoma and combination-type oral contraceptives and lack of standardized criteria for histological diagnosis of early cervical neoplasia are noted.

Additional chapters concern oral contraceptives and the cardiovascular system. One discusses serial plasma fibrinogen chromatography, a technique that might prove useful in screening women for predisposition to thromboembolism and/or for evaluating thrombogenicity of steroid contraceptive preparations. Others are concerned with hypertension and myocardial infarction; Mann's "Discussion" of a preceding chapter, however, is in poor taste and should not have been included.

A disappointing chapter is Oral Contraceptives—The Clinical Perspective. It merely summarizes, in a less enlightening manner, data already published in 1974 by the Royal College of General Practitioners; that reference, which "contains an extensive bibliography," is the chapter's only citation. Included are comparisons between incidence of several side effects and three dosage ranges of progestogen or of estrogen; since only the lowest dosage range in each case approximates doses found in the majority of oral contraceptive preparations currently available in both England and the United States, the information is of little practical value.

It is somewhat disconcerting to find that although all chapters have numbered references, about half have them numbered based on alphabetical listing of first authors, while in the others they are numbered based on their chronological appearance within the given chapter. This distinction also applies to the references to chapters coauthored or authored, respectively, by the two editors! The titles of journal articles are missing from the references to three of the chapters, and two coauthors cited twice in each of two other chapters have their names spelled differently in the text and/or references to these two chapters.

The index, listing over 800 items, contains insufficient cross-indexing. Norethindrone and norethisterone, for example, are not cross-indexed. Authors apparently used whichever term they preferred, but only those pages on which one or the other appears are listed under that term in the index. Furthermore, in one chapter, norethisterone and norethindrone are mentioned as the fourth and seventh progestogens, respectively, in a list of agents reportedly associated with liver tumors!

The shortcomings of this book really are minor, although the insufficient cross-indexing could present a problem to the student or to someone whose major field of interest is somewhat remote from steroid pharmacology. Its greatest asset is that, in general, it is a rather up-to-date review. A few chapters are somewhat technical and specialized and, therefore, may have a somewhat narrower appeal, to individuals engaged in similar research, for example. Much of the book, however, contains valuable information, usually adequately referenced, for anyone whose interests and/or specific professional duties require knowledge of the potential(?) disadvantages of steroid contraception as well as the advantages.

Reviewed by Audrey S. Bingel
Department of Pharmacognosy and Pharmacology
College of Pharmacy
University of Illinois
Chicago, IL 60612

NEW JOURNALS

Clinical and Experimental Hypertension. Edited by MICHAEL J. ANTONACCIO. Dekker Journals, P.O. Box 11305, Church Street Station, New York, NY 10249. January 1978. 17 × 26 cm. Price $90.00 (6 issues).

Journal of Environmental Science and Health. Part C: Environmental Health Sciences. Edited by Robert J. Rubin. Dekker Journals, P.O. Box 11305, Church Street Station, New York, NY 10249. January 1978. 15 × 22.5 cm. Price $44.00 (4 issues).

of the material from Vol. 1 was omitted to avoid needless repetition; however, frequent reference to Vol. 1 material is made and appears as 1 (for volume) followed by the page number. These references to Vol. 1 are found in both chapter contents and text material. New material in Vol. 2 includes the preparation of allenes, cumulenes, orthoesters, orthocarbonates, and ketenimines.

At the start of each chapter is a brief, concise overview of some of the synthetic methods presented in the following text. This overview is pleasantly written and focuses on emergence of new reagents, improvements in methodology, and advantages and disadvantages of alternative methods. In the text that follows, structural formulas are used liberally and references are supplied faithfully. Yields and experimental conditions for many reactions are given. The inclusion of theoretical aspects such as mechanisms, stereochemistry, and substituent effects give the text an added dimension.

The functional group transformations listed involve no more than one or two steps, with emphasis on fundamental aliphatic–aromatic chemistry. Excluded are synthetic preparations of nucleotides, peptides, lipids, and heterocycles, which would have been useful and of more interest to the biochemist.

A rather elaborate reaction index is cross-referenced to Vol. 1. Instructions on the use of the index are provided, but it is somewhat complex to use. The subject index is quite complete; unfortunately, an author index is omitted. The lack of proofreading oversights is notable, and the print and format are good.

Reviewed by A. J. Villani
Research and Development Division
Smith Kline & French Laboratories
Philadelphia, PA 19101

Pharmacology of Steroid Contraceptive Drugs (Monographs of the Mario Negri Institute for Pharmacological Research, Milan, Italy). Edited by S. GARATTINI and H. W. BERENDES. Raven, 1140 Avenue of the Americas, New York, NY 10036. 1977. 391 pp. 16 × 24 cm. Price $28.00.

This book comprises 30 chapters by 91 authors from eight countries. Its purpose was to present current information and opinion concerning steroid contraceptive side effects; that aim has largely been achieved. A third of the references cited were published between 1973 and 1976; some were in press in 1977. Several chapters contain new data not published previously nor in press.

The book consists of articles presenting basic *in vivo* and/or *in vitro* research data, clinical research data, and/or literature reviews concerning specific side effects. Chapter contents vary considerably, because of different types of study presented and types of side effect studied.

Some chapters concern investigations into biochemical mechanisms of action and cellular and subcellular sites of action, aiming to contribute to the data base on which occurrence of various side effects might eventually be explained. Others discuss metabolism and excretion, mainly human, of contraceptive steroids. Also presented are basic and clinical research data concerning steroid contraceptives and lipids. Drug interactions are briefly reviewed, and experiments explaining a mechanism by which rifampin (rifampicin) may decrease contraceptive efficacy are described.

In the chapter Oral Contraceptive Use and Breast Diseases, available data are summarized and the way pointed for future research; other chapters concern basic research on this topic. Concisely reviewed are quite recent data associating liver tumors with oral contraceptive use. Lack of studies concerning endometrial carcinoma and combination-type oral contraceptives and lack of standardized criteria for histological diagnosis of early cervical neoplasia are noted.

Additional chapters concern oral contraceptives and the cardiovascular system. One discusses serial plasma fibrinogen chromatography, a technique that might prove useful in screening women for predisposition to thromboembolism and/or for evaluating thrombogenicity of steroid contraceptive preparations. Others are concerned with hypertension and myocardial infarction; Mann's "Discussion" of a preceding chapter, however, is in poor taste and should not have been included.

A disappointing chapter is Oral Contraceptives—The Clinical Perspective. It merely summarizes, in a less enlightening manner, data already published in 1974 by the Royal College of General Practitioners; that reference, which "contains an extensive bibliography," is the chapter's only citation. Included are comparisons between incidence of several side effects and three dosage ranges of progestogen or of estrogen; since only the lowest dosage range in each case approximates doses found in the majority of oral contraceptive preparations currently available in both England and the United States, the information is of little practical value.

It is somewhat disconcerting to find that although all chapters have numbered references, about half have them numbered based on alphabetical listing of first authors, while in the others they are numbered based on their chronological appearance within the given chapter. This distinction also applies to the references to chapters coauthored or authored, respectively, by the two editors! The titles of journal articles are missing from the references to three of the chapters, and two coauthors cited twice in each of two other chapters have their names spelled differently in the text and/or references to these two chapters.

The index, listing over 800 items, contains insufficient cross-indexing. Norethindrone and norethisterone, for example, are not cross-indexed. Authors apparently used whichever term they preferred, but only those pages on which one or the other appears are listed under that term in the index. Furthermore, in one chapter, norethisterone and norethindrone are mentioned as the fourth and seventh progestogens, respectively, in a list of agents reportedly associated with liver tumors!

The shortcomings of this book really are minor, although the insufficient cross-indexing could present a problem to the student or to someone whose major field of interest is somewhat remote from steroid pharmacology. Its greatest asset is that, in general, it is a rather up-to-date review. A few chapters are somewhat technical and specialized and, therefore, may have a somewhat narrower appeal, to individuals engaged in similar research, for example. Much of the book, however, contains valuable information, usually adequately referenced, for anyone whose interests and/or specific professional duties require knowledge of the potential(?) disadvantages of steroid contraception as well as the advantages.

Reviewed by Audrey S. Bingel
Department of Pharmacognosy and Pharmacology
College of Pharmacy
University of Illinois
Chicago, IL 60612

NEW JOURNALS

Clinical and Experimental Hypertension. Edited by MICHAEL J. ANTONACCIO. Dekker Journals, P.O. Box 11305, Church Street Station, New York, NY 10249. January 1978. 17 × 26 cm. Price $90.00 (6 issues).

Journal of Environmental Science and Health. Part C: Environmental Health Sciences. Edited by Robert J. Rubin. Dekker Journals, P.O. Box 11305, Church Street Station, New York, NY 10249. January 1978. 15 × 22.5 cm. Price $44.00 (4 issues).

AUGUST 1978
VOLUME 67 NUMBER 8

JOURNAL OF PHARMACEUTICAL SCIENCES

MARY H. FERGUSON
Editor

SHELLY ELLIOTT
Production Editor

JANET D. SHOFF
Copy Editor

EDWARD G. FELDMANN
Contributing Editor

SAMUEL W. GOLDSTEIN
Contributing Editor

BELLE R. BECK
Editorial Secretary

DAVID BOHARDT
Director of Publications

L. LUAN CORRIGAN
Assistant Director of Publications

EDITORIAL ADVISORY BOARD

JOHN AUTIAN
NORMAN R. FARNSWORTH
WILLIAM O. FOYE
WILLIAM J. JUSKO
HERBERT A. LIEBERMAN
DAVID E. MANN, JR.
GERALD J. PAPARIELLO
EDWARD G. RIPPIE

The *Journal of Pharmaceutical Sciences* is published monthly by the American Pharmaceutical Association (APhA) at 2215 Constitution Ave., N.W., Washington, DC 20037. Second-class postage paid at Washington, D.C., and at additional mailing office.

All expressions of opinion and statements of supposed fact appearing in articles or editorials carried in this journal are published on the authority of the writer over whose name they appear and are not to be regarded as necessarily expressing the policies or views of APhA.

Offices—Editorial, Advertising, and Subscription: 2215 Constitution Ave., N.W., Washington, DC 20037. Printing: 20th & Northampton Streets, Easton, PA 18042.

Annual Subscriptions—United States and foreign, industrial and government institutions $50, educational institutions $50, individuals *for personal use only* $30; single copies $5. All foreign subscriptions add $5 for postage. Subscription rates are subject to change without notice. Members of APhA may elect to receive the *Journal of Pharmaceutical Sciences* as a part of their annual $70 (foreign $75) APhA membership dues.

Claims—Missing numbers will not be supplied if dues or subscriptions are in arrears for more than 60 days or if claims are received more than 60 days after the date of the issue, or if loss was due to failure to give notice of change of address. APhA cannot accept responsibility for foreign delivery when its records indicate shipment has been made.

Change of Address—Members and subscribers should notify at once both the Post Office and APhA of any change of address.

Photocopying—The code at the foot of the first page of an article indicates that APhA has granted permission for copying of the article beyond the limits permitted by Sections 107 and 108 of the U.S. Copyright Law provided that the copier sends the per copy fee stated in the code to the Copyright Clearance Center, Inc., P. O. Box 765, Schenectady, NY 12301. Copies may be made for personal or internal use only and not for general distribution.

Microfilm—Available from University Microfilms International, 300 N. Zeeb Road, Ann Arbor, MI 48106.

© Copyright 1978. American Pharmaceutical Association, 2215 Constitution Ave., N.W., Washington, DC 20037; all rights reserved.

PROPOSITION 13 AND PHARMACEUTICAL SCIENTISTS

There's an old maxim that nobody worries about money except the people who don't have it. The same thing probably can be said about employment.

In recent years, a debate has been raging about whether there is or is not a surplus of practicing pharmacists in the United States. In the view of many educators, the problem is not one of too many pharmacists but rather of mal-distribution or of underutilization. The contrary views are that: (*a*) even if there is a shortage in some isolated geographic area, schools several thousand miles away should not continue to accelerate their enrollments; and (*b*) until meaningful progress is made in expanding practitioner roles, it is foolish to pour out a surplus of graduates who will have no opportunity to fulfill such roles.

But aside from the employment situation at the professional practice level, we also hear occasional stories about unemployment among pharmaceutical scientists. Fortunately, there appears to be no widespread problem in this area. Nevertheless, it is extremely difficult to judge just how prevalent unemployment or marginal employment is among scientists. Lack of hard data can result in giving undue weight to anecdotes about individual scientists who are either without jobs or at best getting along by driving taxicabs.

Given this situation, many of our readers may be interested in a report just recently released concerning a survey conducted by the Commission on Human Resources of the National Research Council. The report is entitled *Science, Engineering, and Humanities Doctorates in the United States: 1977 Profile,* and it presents a comprehensive survey of persons who have earned research doctorates since 1934.

All in all, the picture would have to be rated as "not bad" in terms of the kinds of people who would primarily be identified with the pharmaceutical sciences.

Specifically, at the time the study was conducted—in February 1977—Bureau of Labor Statistics data showed that the U.S. labor force as a whole had an unemployment rate of 8.5 percent, while for U.S. workers with five or more years of college training, the unemployment rate was 2.3 percent.

The NRC report revealed that 2.9 percent of those holding doctorates in humanities were involuntarily unemployed, and the corresponding figure for holders of doctorates in science or engineering was a rather low 1.2 percent.

Moreover, it was found that of the fortunate 98.8 percent with jobs, only 6.2 percent of the doctorate-holders in science or engineering were working in nonscientific fields, and for some of these it was by personal choice rather than necessity.

There are loads of other statistics in this 98-page NRC report covering average salaries by field of employment, employment rates broken down by sex, and assorted other tabulations, but the key figures seem to reveal a rather healthy employment situation.

This effort at assessment seems to be especially timely in view of the recent action by the electorate in the state of California concerning overwhelming adoption of the so-called "Proposition 13." Although this referendum is specifically related to a cutback and ceiling on property taxes, it is being broadly interpreted as symptomatic of a nationwide rebellion of taxpayers. In turn, this is expected to have the effect of concomitant reductions in government spending with consequent contraction of government programs and funding.

The short-term impact will undoubtedly be traumatic for those directly affected. However, some economists believe that such a change of national direction is necessary to bring raging inflation under control and to restore the nation's economy to a solid basis.

The U.S. has never done much about establishing long-term goals and adhering to the programs necessary to reach those objectives. Hence, there have been periodic spurts in which one thing or another becomes the temporary fashion, and things get somewhat out of balance. Government taxation and spending appear to have reached such a high-level mark in the public opinion. Viewed in this light, Proposition 13 represents an effort to restore balance which will stabilize the economy as well as the value of the dollar. In the long run, this can only have a beneficial effect for the great mass of our people by assuring both high employment and stable remuneration.

Pharmacy practitioners as well as pharmaceutical scientists can expect to share in, and to benefit from, such a broad-based result. The NRC report told us where we presently stand; Proposition 13 may give us a hint as to where we are going.

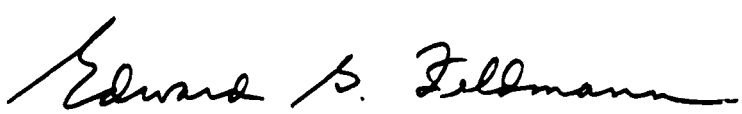

AUGUST 1978
VOLUME 67 NUMBER 8

JOURNAL OF PHARMACEUTICAL SCIENCES

MARY H. FERGUSON
Editor

SHELLY ELLIOTT
Production Editor

JANET D. SHOFF
Copy Editor

EDWARD G. FELDMANN
Contributing Editor

SAMUEL W. GOLDSTEIN
Contributing Editor

BELLE R. BECK
Editorial Secretary

DAVID BOHARDT
Director of Publications

L. LUAN CORRIGAN
Assistant Director of Publications

EDITORIAL ADVISORY BOARD

JOHN AUTIAN
NORMAN R. FARNSWORTH
WILLIAM O. FOYE
WILLIAM J. JUSKO
HERBERT A. LIEBERMAN
DAVID E. MANN, JR.
GERALD J. PAPARIELLO
EDWARD G. RIPPIE

The *Journal of Pharmaceutical Sciences* is published monthly by the American Pharmaceutical Association (APhA) at 2215 Constitution Ave., N.W., Washington, DC 20037. Second-class postage paid at Washington, D.C., and at additional mailing office.

All expressions of opinion and statements of supposed fact appearing in articles or editorials carried in this journal are published on the authority of the writer over whose name they appear and are not to be regarded as necessarily expressing the policies or views of APhA.

Offices—Editorial, Advertising, and Subscription: 2215 Constitution Ave., N.W., Washington, DC 20037. Printing: 20th & Northampton Streets, Easton, PA 18042.

Annual Subscriptions—United States and foreign, industrial and government institutions $50, educational institutions $50, individuals *for personal use only* $30; single copies $5. All foreign subscriptions add $5 for postage. Subscription rates are subject to change without notice. Members of APhA may elect to receive the *Journal of Pharmaceutical Sciences* as a part of their annual $70 (foreign $75) APhA membership dues.

Claims—Missing numbers will not be supplied if dues or subscriptions are in arrears for more than 60 days or if claims are received more than 60 days after the date of the issue, or if loss was due to failure to give notice of change of address. APhA cannot accept responsibility for foreign delivery when its records indicate shipment has been made.

Change of Address—Members and subscribers should notify at once both the Post Office and APhA of any change of address.

Photocopying—The code at the foot of the first page of an article indicates that APhA has granted permission for copying of the article beyond the limits permitted by Sections 107 and 108 of the U.S. Copyright Law provided that the copier sends the per copy fee stated in the code to the Copyright Clearance Center, Inc., P. O. Box 765, Schenectady, NY 12301. Copies may be made for personal or internal use only and not for general distribution.

Microfilm—Available from University Microfilms International, 300 N. Zeeb Road, Ann Arbor, MI 48106.

© Copyright 1978. American Pharmaceutical Association, 2215 Constitution Ave., N.W., Washington, DC 20037; all rights reserved.

PROPOSITION 13 AND PHARMACEUTICAL SCIENTISTS

There's an old maxim that nobody worries about money except the people who don't have it. The same thing probably can be said about employment.

In recent years, a debate has been raging about whether there is or is not a surplus of practicing pharmacists in the United States. In the view of many educators, the problem is not one of too many pharmacists but rather of mal-distribution or of underutilization. The contrary views are that: (*a*) even if there is a shortage in some isolated geographic area, schools several thousand miles away should not continue to accelerate their enrollments; and (*b*) until meaningful progress is made in expanding practitioner roles, it is foolish to pour out a surplus of graduates who will have no opportunity to fulfill such roles.

But aside from the employment situation at the professional practice level, we also hear occasional stories about unemployment among pharmaceutical scientists. Fortunately, there appears to be no widespread problem in this area. Nevertheless, it is extremely difficult to judge just how prevalent unemployment or marginal employment is among scientists. Lack of hard data can result in giving undue weight to anecdotes about individual scientists who are either without jobs or at best getting along by driving taxicabs.

Given this situation, many of our readers may be interested in a report just recently released concerning a survey conducted by the Commission on Human Resources of the National Research Council. The report is entitled *Science, Engineering, and Humanities Doctorates in the United States: 1977 Profile,* and it presents a comprehensive survey of persons who have earned research doctorates since 1934.

All in all, the picture would have to be rated as "not bad" in terms of the kinds of people who would primarily be identified with the pharmaceutical sciences.

Specifically, at the time the study was conducted—in February 1977—Bureau of Labor Statistics data showed that the U.S. labor force as a whole had an unemployment rate of 8.5 percent, while for U.S. workers with five or more years of college training, the unemployment rate was 2.3 percent.

The NRC report revealed that 2.9 percent of those holding doctorates in humanities were involuntarily unemployed, and the corresponding figure for holders of doctorates in science or engineering was a rather low 1.2 percent.

Moreover, it was found that of the fortunate 98.8 percent with jobs, only 6.2 percent of the doctorate-holders in science or engineering were working in nonscientific fields, and for some of these it was by personal choice rather than necessity.

There are loads of other statistics in this 98-page NRC report covering average salaries by field of employment, employment rates broken down by sex, and assorted other tabulations, but the key figures seem to reveal a rather healthy employment situation.

This effort at assessment seems to be especially timely in view of the recent action by the electorate in the state of California concerning overwhelming adoption of the so-called "Proposition 13." Although this referendum is specifically related to a cutback and ceiling on property taxes, it is being broadly interpreted as symptomatic of a nationwide rebellion of taxpayers. In turn, this is expected to have the effect of concomitant reductions in government spending with consequent contraction of government programs and funding.

The short-term impact will undoubtedly be traumatic for those directly affected. However, some economists believe that such a change of national direction is necessary to bring raging inflation under control and to restore the nation's economy to a solid basis.

The U.S. has never done much about establishing long-term goals and adhering to the programs necessary to reach those objectives. Hence, there have been periodic spurts in which one thing or another becomes the temporary fashion, and things get somewhat out of balance. Government taxation and spending appear to have reached such a high-level mark in the public opinion. Viewed in this light, Proposition 13 represents an effort to restore balance which will stabilize the economy as well as the value of the dollar. In the long run, this can only have a beneficial effect for the great mass of our people by assuring both high employment and stable remuneration.

Pharmacy practitioners as well as pharmaceutical scientists can expect to share in, and to benefit from, such a broad-based result. The NRC report told us where we presently stand; Proposition 13 may give us a hint as to where we are going.

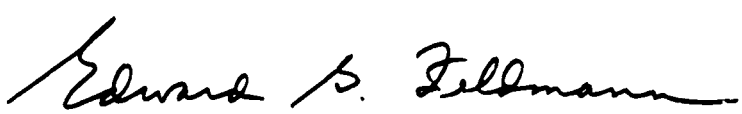

Paraquat in Marijuana

Because of very limited expertise currently available regarding the testing of Paraquat in contaminated marijuana, few laboratories are capable of determining the presence of Paraquat in the marijuana exported from Mexico. In view of the potentially health hazardous nature of the Paraquat, we wish to report a simple TLC procedure for determining its presence in marijuana or plant residue. The publication of this procedure will enable private laboratories to undertake its testing and thus alleviate future problems of a backlog of street specimens contaminated with Paraquat. The sensitivity of the procedure is less than 1 μg.

The procedure is as follows. Approximately 0.1–0.5 g of marijuana (plant material) is transferred to a 25- or 50-ml beaker (the plant material is not powdered or ground; the large size stems, if any, are cut into small pieces) and soaked for about 30 min with 5 ml of extraction solvent (methanol, 99 ml; concentrated hydrochloric acid, 1 ml). The contents are then boiled for about 30 sec on the water bath (if the extraction solvent has been absorbed by the plant material, an additional 3 ml is added prior to boiling the contents) and decanted into a 50-ml nongraduated conical centrifuge tube. This extraction process is repeated an additional three times, using 3–5 ml of the extraction solvent each time. All extracts are decanted into the same 50-ml conical centrifuge tube.

The color of the combined extracts is examined, and 1–2 teaspoonfuls of activated animal charcoal are added, depending on the color intensity of the extract. The test tube is heated to boiling for about 30 sec in the water bath with constant swirling, and the slurry of the extract and charcoal is filtered through Whatman No. 1 filter paper into another 50-ml nongraduated conical centrifuge tube. The tube is washed with 3 ml of boiling extraction solvent and poured through the same filter paper after the original solvent has been filtered.

Three such washings are performed, each with 3–5 ml of extraction solvent. Then the solvent is evaporated to about 50 μl in the drying oven having a horizontal air flow and maintained at 85–90°. The residue along the sides of the tube is washed with about 1 ml of methanol, the contents are mixed on a mechanical mixer, and the sides of the tube are again washed with an additional few drops of methanol. The solvent is evaporated to about 50 μl as described above. The contents are mixed on a mechanical mixer, and the entire extract is spotted on a 20 × 20-cm Gelman precoated silica gel glass microfiber sheet (ITLC type SA) with a layer thickness of 250 μm (if the solvent has entirely evaporated, 50–100 μl of methanol is added to the test tube, depending on the drug residue, the contents are mixed on a mixer, and the entire extract is spotted). A hair dryer or other means of drying may be used while spotting the entire extract onto the TLC plate to keep the size of the spot as small as possible.

Three spots each of 0.5-, 1.0-, and 1.5-μl size of the standard reference solution of Paraquat (1 mg of Paraquat/ml of methanol) are interspaced with five unknown specimens. If possible, two controlled marijuana specimens (0.2 g each) spiked with 1 and 2 μl of the Paraquat reference solution (equivalent to 1 and 2 μg of Paraquat) are carried through the procedure and spotted beside the unknown specimens to calculate semiquantitatively the concentration of Paraquat in unknown specimens. The plate is air dried for about 10 min and then dried in an oven at 85–90° for 5 min before it is placed in 100 ml of developing solvent (concentrated hydrochloric acid, 11 ml; water, 59 ml; acetic acid, 30 ml). The plate is developed up to 15 cm; if, however, a greenish spot or cloud from the plant material is below the 6–7-cm level, development is continued until the spot or cloud passes this level. From 1.5 to 3.5 hr or more may be required.

The plate is then removed from the developing tank and allowed to air dry for about 10–15 min. After heating the plate in the oven for 5 min at 85–90°, it is sprayed with iodoplatinate[1] followed by iodine–potassium iodide[1]. The plate is then allowed to air dry for 5 min and is again sprayed with iodoplatinate. Then it is covered with a paper towel for about 15 min and heated in an oven at 85–90° for about 4–5 min. The standard appears as an oval dark-gray (black) spot after iodoplatinate and as a white trail after heating in the oven for 4–5 min. The unknown specimen does not show the upper dark-gray spot but appears as a white decolorized spot of irregular or oval shape. The black or dark-gray color seen in the unknown specimens after iodoplatinate and iodine–potassium iodide sprays is ignored since it may be due to the reaction of iodoplatinate with plant material.

This solvent system is capable of separating Paraquat from Diaquat. The R_f value of Paraquat is about 0.25–0.40 and that of Diaquat is 0.35–0.45 when the solvent is allowed to travel a definite measured distance; if the solvent is allowed to run for several hours, Paraquat is seen at a distance of about 5.5–7.0 cm and Diaquat is seen at about 8.3 cm. Both of these herbicides form a white trail. However, the Paraquat dark spot is contained within the white trail; the dark spot of Diaquat is separate and is not contained within the white trail. We have been able to analyze 25 specimens/day using this procedure. The procedure is specific and does not give false positives.

K. K. Kaistha
Rahmeh Tadrus
Dennis Wojtulewicz
Dangerous Drugs Commission
Toxicology Laboratories
c/o I.I.T. Research
10 W. 35th Street
Chicago, IL 60616

Received May 22, 1978.

We thank the Chevron Chemical Co., California, for their generous supply of Paraquat and Diaquat, and Jack Gilpin and the management of Dangerous Drugs Commission for their great interest in the Paraquat problem.

[1] K. K. Kaistha and J. H. Jaffe, *J. Pharm. Sci.*, **61**, 679 (1972).

Carcinogenesis: A Coagulation–Coacervation Hypothesis

A recent critical response[1] to a single facet of a new carcinogenesis hypothesis proposed by Ecanow *et al.*[2] gives unwitting and unintended support for the hypothesis.

The essence of the overall concept proposed by Ecanow[3] and later developed with the help of coworkers is that the tumor matrix, which is rich in macromolecules, colloids, and electrolytes, combines with water to form a structured aqueous phase[4]. This phase is in a different thermodynamic state (a coacervated system) than is the normal extracellular aqueous phase[5]. This altered thermodynamic state now exists as a pathological aqueous matrix. It is more highly structured and less polar than the normal bulk water, polar, extracellular matrix[4–6]. When hydrophilic particles or cells with multilayers of strongly adsorbed water (low chemical potential) on their surfaces are aggregated so that the surface water layers are in contact (coagulated state), then the resulting matrix constitutes a coacervate phase[6]. The other aggregated state exists when the particles or cells are held in an open network structure in which the matrix is "normal" polar bulk water (flocculated state). Any event in the body that irreversibly converts the normal equilibrium thermodynamic states of the cells and the extracellular fluids to the coacervated coagulated state produces a pathological condition[4].

The first relevant sentence in the response[1] begins "The Class B particle complexes with the cellular material present . . . ." Thus, the critique of the pathological process begins with the unquestioned acceptance of the fact that the so-called inert particles are indeed capable of complexing with membranes. This is of particular importance because one major question in current oncology concerns the possible role of foreign inert particles found in the normal and

Paraquat in Marijuana

Because of very limited expertise currently available regarding the testing of Paraquat in contaminated marijuana, few laboratories are capable of determining the presence of Paraquat in the marijuana exported from Mexico. In view of the potentially health hazardous nature of the Paraquat, we wish to report a simple TLC procedure for determining its presence in marijuana or plant residue. The publication of this procedure will enable private laboratories to undertake its testing and thus alleviate future problems of a backlog of street specimens contaminated with Paraquat. The sensitivity of the procedure is less than 1 μg.

The procedure is as follows. Approximately 0.1–0.5 g of marijuana (plant material) is transferred to a 25- or 50-ml beaker (the plant material is not powdered or ground; the large size stems, if any, are cut into small pieces) and soaked for about 30 min with 5 ml of extraction solvent (methanol, 99 ml; concentrated hydrochloric acid, 1 ml). The contents are then boiled for about 30 sec on the water bath (if the extraction solvent has been absorbed by the plant material, an additional 3 ml is added prior to boiling the contents) and decanted into a 50-ml nongraduated conical centrifuge tube. This extraction process is repeated an additional three times, using 3–5 ml of the extraction solvent each time. All extracts are decanted into the same 50-ml conical centrifuge tube.

The color of the combined extracts is examined, and 1–2 teaspoonfuls of activated animal charcoal are added, depending on the color intensity of the extract. The test tube is heated to boiling for about 30 sec in the water bath with constant swirling, and the slurry of the extract and charcoal is filtered through Whatman No. 1 filter paper into another 50-ml nongraduated conical centrifuge tube. The tube is washed with 3 ml of boiling extraction solvent and poured through the same filter paper after the original solvent has been filtered.

Three such washings are performed, each with 3–5 ml of extraction solvent. Then the solvent is evaporated to about 50 μl in the drying oven having a horizontal air flow and maintained at 85–90°. The residue along the sides of the tube is washed with about 1 ml of methanol, the contents are mixed on a mechanical mixer, and the sides of the tube are again washed with an additional few drops of methanol. The solvent is evaporated to about 50 μl as described above. The contents are mixed on a mechanical mixer, and the entire extract is spotted on a 20 × 20-cm Gelman precoated silica gel glass microfiber sheet (ITLC type SA) with a layer thickness of 250 μm (if the solvent has entirely evaporated, 50–100 μl of methanol is added to the test tube, depending on the drug residue, the contents are mixed on a mixer, and the entire extract is spotted). A hair dryer or other means of drying may be used while spotting the entire extract onto the TLC plate to keep the size of the spot as small as possible.

Three spots each of 0.5-, 1.0-, and 1.5-μl size of the standard reference solution of Paraquat (1 mg of Paraquat/ml of methanol) are interspaced with five unknown specimens. If possible, two controlled marijuana specimens (0.2 g each) spiked with 1 and 2 μl of the Paraquat reference solution (equivalent to 1 and 2 μg of Paraquat) are carried through the procedure and spotted beside the unknown specimens to calculate semiquantitatively the concentration of Paraquat in unknown specimens. The plate is air dried for about 10 min and then dried in an oven at 85–90° for 5 min before it is placed in 100 ml of developing solvent (concentrated hydrochloric acid, 11 ml; water, 59 ml; acetic acid, 30 ml). The plate is developed up to 15 cm; if, however, a greenish spot or cloud from the plant material is below the 6–7-cm level, development is continued until the spot or cloud passes this level. From 1.5 to 3.5 hr or more may be required.

The plate is then removed from the developing tank and allowed to air dry for about 10–15 min. After heating the plate in the oven for 5 min at 85–90°, it is sprayed with iodoplatinate[1] followed by iodine–potassium iodide[1]. The plate is then allowed to air dry for 5 min and is again sprayed with iodoplatinate. Then it is covered with a paper towel for about 15 min and heated in an oven at 85–90° for about 4–5 min. The standard appears as an oval dark-gray (black) spot after iodoplatinate and as a white trail after heating in the oven for 4–5 min. The unknown specimen does not show the upper dark-gray spot but appears as a white decolorized spot of irregular or oval shape. The black or dark-gray color seen in the unknown specimens after iodoplatinate and iodine–potassium iodide sprays is ignored since it may be due to the reaction of iodoplatinate with plant material.

This solvent system is capable of separating Paraquat from Diaquat. The R_f value of Paraquat is about 0.25–0.40 and that of Diaquat is 0.35–0.45 when the solvent is allowed to travel a definite measured distance; if the solvent is allowed to run for several hours, Paraquat is seen at a distance of about 5.5–7.0 cm and Diaquat is seen at about 8.3 cm. Both of these herbicides form a white trail. However, the Paraquat dark spot is contained within the white trail; the dark spot of Diaquat is separate and is not contained within the white trail. We have been able to analyze 25 specimens/day using this procedure. The procedure is specific and does not give false positives.

K. K. Kaistha
Rahmeh Tadrus
Dennis Wojtulewicz
Dangerous Drugs Commission
Toxicology Laboratories
c/o I.I.T. Research
10 W. 35th Street
Chicago, IL 60616

Received May 22, 1978.

We thank the Chevron Chemical Co., California, for their generous supply of Paraquat and Diaquat, and Jack Gilpin and the management of Dangerous Drugs Commission for their great interest in the Paraquat problem.

[1] K. K. Kaistha and J. H. Jaffe, *J. Pharm. Sci.*, **61**, 679 (1972).

Carcinogenesis: A Coagulation–Coacervation Hypothesis

A recent critical response[1] to a single facet of a new carcinogenesis hypothesis proposed by Ecanow *et al.*[2] gives unwitting and unintended support for the hypothesis.

The essence of the overall concept proposed by Ecanow[3] and later developed with the help of coworkers is that the tumor matrix, which is rich in macromolecules, colloids, and electrolytes, combines with water to form a structured aqueous phase[4]. This phase is in a different thermodynamic state (a coacervated system) than is the normal extracellular aqueous phase[5]. This altered thermodynamic state now exists as a pathological aqueous matrix. It is more highly structured and less polar than the normal bulk water, polar, extracellular matrix[4–6]. When hydrophilic particles or cells with multilayers of strongly adsorbed water (low chemical potential) on their surfaces are aggregated so that the surface water layers are in contact (coagulated state), then the resulting matrix constitutes a coacervate phase[6]. The other aggregated state exists when the particles or cells are held in an open network structure in which the matrix is "normal" polar bulk water (flocculated state). Any event in the body that irreversibly converts the normal equilibrium thermodynamic states of the cells and the extracellular fluids to the coacervated coagulated state produces a pathological condition[4].

The first relevant sentence in the response[1] begins "The Class B particle complexes with the cellular material present . . . ." Thus, the critique of the pathological process begins with the unquestioned acceptance of the fact that the so-called inert particles are indeed capable of complexing with membranes. This is of particular importance because one major question in current oncology concerns the possible role of foreign inert particles found in the normal and

later the tumorous tissue[8]. Our answer is that the particles are capable of combining with membranes to the extent of forming a localized abnormal matrix. Depending on the degree of aqueous matrix distortion, the result can vary from nerve tissue irritation to neoplastic induction.

This abnormal matrix can expand by any of a number of mechanisms. One such mechanism first discussed in physical–chemical phraseology is through an immunologic response[3,4]. An optimum response will inhibit growth, but an excessive response (massive) produces an antibody halo (film) about the particle matrix (antigen). The presence of sufficient numbers of such intermeshed matrixes produces the structured (coagulated) pathological site (*immunosuppression*). This immunological mechanism is presented as plausible in the responding letter[1], and we agree since we originated it[4]. The presence of a virus as being essential in every case of triggering a neoplasm is still widely under investigation. Alternative routes of pathology are also possible, especially considering the fact that tumors can have induction periods of many years.

The abnormal matrix developed by any of the mechanisms would be expected to provide an environment in which the normal biochemical reactions would be radically altered. Further, carcinogenesis in such an abnormal matrix might even be the result of enzyme induction or a damaged feedback mechanism that fails to prevent a continuous production of extracellular macromolecules. The pathological mechanism proposed for the extracellular phase can also occur in the cytoplasm. The gel-like structures of the internal organelles are particularly susceptible to matrix distortion by particles such as chemicals and viruses. These are among the many possibilities that fit the hypothesis. Using this concept of a tumor as cells coagulated in a coacervated matrix suggested the use of matrix structure breakers as therapeutic agents. This approach, consistent with our hypothesis, is showing early promise[7,9,10].

Bernard Ecanow
Bernard H. Gold
Byong H. Moon

University of Illinois at the Medical Center
Chicago, IL 60680
and the
Rush-Presbyterian-St. Luke's Medical Center
Chicago, IL 60612

R. Saul Levinson
University of Oklahoma
Oklahoma City, OK 73118

Received June 2, 1978.

[1] S. Silberberg, *J. Pharm. Sci.*, **67**(5), IV (1978).
[2] B. Ecanow, B. H. Gold, B. H. Moon, and R. S. Levinson, *ibid.*, **67**(1), VIII (1978).
[3] B. Ecanow, U.S. copyright A 825 763 (Ecanow, Skokie, Ill.) (1966).
[4] B. Ecanow and H. Klawans, Jr., in "Models of Human Neurological Disease," H. Klawans, Ed., Excerpta Medica, Amsterdam, The Netherlands, 1974, chap. 9.
[5] H. Takruri, B. Ecanow, and R. Balagot, *J. Pharm. Sci.*, **66**, 283 (1977).
[6] B. Ecanow and B. H. Gold, *Science*, **193**, 919 (1976).
[7] B. Ecanow, B. Gold, and J. McCreery, *Clin. Oncol.*, **3**, 319 (1977).
[8] H. J. P. Ryser, *N. Engl. J. Med.*, **295**, 1485 (1976).
[9] E. Danapoulos and I. Danapoulou, *Clin. Oncol.*, **1**, 341 (1975).
[10] G. Gandhi, S. Anasuya, P. Kawathekar, and K. Krishnamurthy, *J. Surg. Oncol.*, **9**, 139 (1977).

Simplified Drug Transport Scheme

The following suggestions concern the *Theoretical* section of the recent article "Potential of Liquid Membranes for Drug Overdose Treatment: *In Vitro* Studies"[1]:

1. The symbol C_e^o should be C_o.
2. Equation 3 should be clarified.
3. A simplified scheme to describe the transport of acidic drug from the donor phase (pH 2) to the central aqueous phase of liquid membranes (pH 12) should be formulated into at least three major steps:

(*a*) Partition of unionized drug (HA) between the oil phase and the aqueous phase (pH 2):

$$P_{\mathrm{I}} = \frac{C_o}{C_e} \qquad \text{(Eq. 1)}$$

where P_{I} is the apparent partition coefficient of unionized drug (HA) between the oil phase and the aqueous phase (pH 2) and C_o is the concentration of drug in the oil phase of the membrane before diffusion.

(*b*) Diffusion of drug across the membrane.

(*c*) Partition of diffused unionized drug (HA) between the oil phase and the central aqueous phase (pH 12):

$$P_{\mathrm{II}} = \frac{C_{\mathrm{I}}}{C_i} \qquad \text{(Eq. 2)}$$

where P_{II} is the apparent partition coefficient of diffused unionized drug (HA) between the oil phase and the central aqueous phase (pH 12), C_{I} is the concentration of drug in the oil phase of the membrane after diffusion, and C_i is the concentration of drug in the central aqueous phase of the membrane.

Therefore, Fick's law of drug diffusion across the membrane may be written as:

$$\frac{dC_o}{dt} = -DA\frac{\Delta C}{\Delta X} \qquad \text{(Eq. 3)}$$

$$\frac{dC_o}{dt} = \frac{-DA}{\Delta X}(C_o - C_{\mathrm{I}}) \qquad \text{(Eq. 4)}$$

Since $C_o = P_{\mathrm{I}}C_e$ and $C_{\mathrm{I}} = P_{\mathrm{II}}C_i$, then:

$$\frac{dC_eP_{\mathrm{I}}}{dt} = \frac{-DA}{\Delta X}(P_{\mathrm{I}}C_e - P_{\mathrm{II}}C_i) \qquad \text{(Eq. 5)}$$

$$\frac{dC_e}{dt} = \frac{-DA}{\Delta X}\frac{1}{P_{\mathrm{I}}}(P_{\mathrm{I}}C_e - P_{\mathrm{II}}C_i) \qquad \text{(Eq. 6)}$$

If $C_e \gg C_i$ and $P_{\mathrm{I}} \approx P_{\mathrm{II}}$, $(P_{\mathrm{II}}/P_{\mathrm{I}})C_i$ can be negligible. Equation 6 can be written as:

$$\frac{dC_e}{dt} = \frac{-DA}{\Delta X}C_e \qquad \text{(Eq. 7)}$$

$$\frac{dC_e}{dt} = -kC_e \qquad \text{(Eq. 8)}$$

Jiun-Ren Chen
6884 Thomas Drive
Liverpool, NY 13088

Received May 24, 1978.

[1] C.-W. Chiang, G. C. Fuller, J. W. Frankenfeld, and C. T. Rhodes, *J. Pharm. Sci.*, **67**, 63 (1978).

later the tumorous tissue[8]. Our answer is that the particles are capable of combining with membranes to the extent of forming a localized abnormal matrix. Depending on the degree of aqueous matrix distortion, the result can vary from nerve tissue irritation to neoplastic induction.

This abnormal matrix can expand by any of a number of mechanisms. One such mechanism first discussed in physical–chemical phraseology is through an immunologic response[3,4]. An optimum response will inhibit growth, but an excessive response (massive) produces an antibody halo (film) about the particle matrix (antigen). The presence of sufficient numbers of such intermeshed matrixes produces the structured (coagulated) pathological site (*immunosuppression*). This immunological mechanism is presented as plausible in the responding letter[1], and we agree since we originated it[4]. The presence of a virus as being essential in every case of triggering a neoplasm is still widely under investigation. Alternative routes of pathology are also possible, especially considering the fact that tumors can have induction periods of many years.

The abnormal matrix developed by any of the mechanisms would be expected to provide an environment in which the normal biochemical reactions would be radically altered. Further, carcinogenesis in such an abnormal matrix might even be the result of enzyme induction or a damaged feedback mechanism that fails to prevent a continuous production of extracellular macromolecules. The pathological mechanism proposed for the extracellular phase can also occur in the cytoplasm. The gel-like structures of the internal organelles are particularly susceptible to matrix distortion by particles such as chemicals and viruses. These are among the many possibilities that fit the hypothesis. Using this concept of a tumor as cells coagulated in a coacervated matrix suggested the use of matrix structure breakers as therapeutic agents. This approach, consistent with our hypothesis, is showing early promise[7,9,10].

Bernard Ecanow
Bernard H. Gold
Byong H. Moon

University of Illinois at the Medical Center
Chicago, IL 60680
and the
Rush-Presbyterian-St. Luke's Medical Center
Chicago, IL 60612

R. Saul Levinson
University of Oklahoma
Oklahoma City, OK 73118

Received June 2, 1978.

[1] S. Silberberg, *J. Pharm. Sci.*, **67**(5), IV (1978).
[2] B. Ecanow, B. H. Gold, B. H. Moon, and R. S. Levinson, *ibid.*, **67**(1), VIII (1978).
[3] B. Ecanow, U.S. copyright A 825 763 (Ecanow, Skokie, Ill.) (1966).
[4] B. Ecanow and H. Klawans, Jr., in "Models of Human Neurological Disease," H. Klawans, Ed., Excerpta Medica, Amsterdam, The Netherlands, 1974, chap. 9.
[5] H. Takruri, B. Ecanow, and R. Balagot, *J. Pharm. Sci.*, **66**, 283 (1977).
[6] B. Ecanow and B. H. Gold, *Science*, **193**, 919 (1976).
[7] B. Ecanow, B. Gold, and J. McCreery, *Clin. Oncol.*, **3**, 319 (1977).
[8] H. J. P. Ryser, *N. Engl. J. Med.*, **295**, 1485 (1976).
[9] E. Danapoulos and I. Danapoulou, *Clin. Oncol.*, **1**, 341 (1975).
[10] G. Gandhi, S. Anasuya, P. Kawathekar, and K. Krishnamurthy, *J. Surg. Oncol.*, **9**, 139 (1977).

Simplified Drug Transport Scheme

The following suggestions concern the *Theoretical* section of the recent article "Potential of Liquid Membranes for Drug Overdose Treatment: *In Vitro* Studies"[1]:

1. The symbol C_e^o should be C_o.
2. Equation 3 should be clarified.
3. A simplified scheme to describe the transport of acidic drug from the donor phase (pH 2) to the central aqueous phase of liquid membranes (pH 12) should be formulated into at least three major steps:

(*a*) Partition of unionized drug (HA) between the oil phase and the aqueous phase (pH 2):

$$P_{\mathrm{I}} = \frac{C_o}{C_e} \qquad \text{(Eq. 1)}$$

where P_{I} is the apparent partition coefficient of unionized drug (HA) between the oil phase and the aqueous phase (pH 2) and C_o is the concentration of drug in the oil phase of the membrane before diffusion.

(*b*) Diffusion of drug across the membrane.

(*c*) Partition of diffused unionized drug (HA) between the oil phase and the central aqueous phase (pH 12):

$$P_{\mathrm{II}} = \frac{C_{\mathrm{I}}}{C_i} \qquad \text{(Eq. 2)}$$

where P_{II} is the apparent partition coefficient of diffused unionized drug (HA) between the oil phase and the central aqueous phase (pH 12), C_{I} is the concentration of drug in the oil phase of the membrane after diffusion, and C_i is the concentration of drug in the central aqueous phase of the membrane.

Therefore, Fick's law of drug diffusion across the membrane may be written as:

$$\frac{dC_o}{dt} = -DA\frac{\Delta C}{\Delta X} \qquad \text{(Eq. 3)}$$

$$\frac{dC_o}{dt} = \frac{-DA}{\Delta X}(C_o - C_{\mathrm{I}}) \qquad \text{(Eq. 4)}$$

Since $C_o = P_{\mathrm{I}}C_e$ and $C_{\mathrm{I}} = P_{\mathrm{II}}C_i$, then:

$$\frac{dC_eP_{\mathrm{I}}}{dt} = \frac{-DA}{\Delta X}(P_{\mathrm{I}}C_e - P_{\mathrm{II}}C_i) \qquad \text{(Eq. 5)}$$

$$\frac{dC_e}{dt} = \frac{-DA}{\Delta X}\frac{1}{P_{\mathrm{I}}}(P_{\mathrm{I}}C_e - P_{\mathrm{II}}C_i) \qquad \text{(Eq. 6)}$$

If $C_e \gg C_i$ and $P_{\mathrm{I}} \approx P_{\mathrm{II}}$, $(P_{\mathrm{II}}/P_{\mathrm{I}})C_i$ can be negligible. Equation 6 can be written as:

$$\frac{dC_e}{dt} = \frac{-DA}{\Delta X}C_e \qquad \text{(Eq. 7)}$$

$$\frac{dC_e}{dt} = -kC_e \qquad \text{(Eq. 8)}$$

Jiun-Ren Chen
6884 Thomas Drive
Liverpool, NY 13088

Received May 24, 1978.

[1] C.-W. Chiang, G. C. Fuller, J. W. Frankenfeld, and C. T. Rhodes, *J. Pharm. Sci.*, **67**, 63 (1978).

JOURNAL OF PHARMACEUTICAL SCIENCES

AUGUST 1978
VOLUME 67 NUMBER 8

RESEARCH ARTICLES

Controlled Delivery of Theophylline: Chemistry of 7-Acyl- and 7,7′-Acylditheophylline Derivatives

NICHOLAS BODOR ˣ, KENNETH B. SLOAN, YU-NENG KUO, and TAKERU HIGUCHI

Received September 26, 1977, from *INTERx Research Corporation, Lawrence, KS 66044.* Accepted for publication November 16, 1977.

Abstract □ 7-Acyl- and 7,7′-acyldithophylline derivatives were prepared from the reaction of theophylline with acid chlorides. In addition, a novel synthesis of these compounds was developed, which proceeds through an acylonium ion generated under mild conditions. The physical properties and stability of the derivative of choice, 7,7′-succinyldithophylline, depend on the synthetic procedure employed. This compound is a useful controlled-release prodrug of theophylline.

Keyphrases □ Theophylline—various 7-acyl- and 7,7′-acyldithophylline derivatives synthesized, evaluated as prodrugs □ Prodrugs, potential—7,7′-succinyldithophylline synthesized, evaluated □ Relaxants, smooth muscle—theophylline, various 7-acyl- and 7,7′-acyldithophylline derivatives synthesized, evaluated as prodrugs

One widely used treatment for asthma is oral theophylline. Where long-term treatment of asthma is indicated, theophylline therapy has reduced the frequency of acute attacks, the need for concomitant use of other medication such as steroids, and chronic airway obstruction (1). However, in spite of oral theophylline's good bioavailability, problems are associated with its use.

The rather short half-life of theophylline and its narrow therapeutic range [10–20 μg/ml in plasma (2, 3)] make it necessary to administer the drug relatively often, while the peak levels achieved shortly after administration are associated with the observed side effects (2). It has been suggested that a slow-release theophylline preparation that would eliminate round-the-clock dosing every 6 hr would be desirable in the treatment of asthma (3, 4).

There are at least two approaches to developing a slow-release form of any drug: by formulation (4, 5) and by a chemical modification of the drug, a "slow-release prodrug." Because of the well-known problems related to the first approach, the latter approach was chosen.

Theophylline is a fairly water-soluble, polar molecule. It has only one position available for reversible modification, the 7-position. The slow-release approach consisted simply in decreasing the water solubility and dissolution rate by increasing the lipophilicity and the intermolecular forces in the crystals, respectively, of theophylline by acylating the 7-position. Unlike other aliphatic and arylamides, 7-acetyltheophylline (6), the only carefully studied member of this series, hydrolyzes quickly; in this respect, it resembles acid chlorides in its reactivity.

The expected rapid hydrolyses of the 7-acyltheophyllines ensure the equally rapid release of theophylline from the solvated 7-acyltheophyllines; and by using lipophilic acyl portions in the theophylline derivatives, their solubility in water is decreased. Thus, the slow dissolution of the derivatives due to their hydrophobic nature, followed by the quick hydrolysis of the theophylline derivatives once they are in solution, results in a slowly released theophylline.

To confirm this hypothesis, some 7-acyltheophylline derivatives were prepared and their dissolution rates were determined. Based on the dissolution rates, active component content, toxicity, and stability, one derivative, 7,7′-succinyldithophylline, was tested further *in vivo*, and some interesting aspects of its chemistry were explored. 7,7′-Succinyldithophylline, which had a slow dissolution rate yet fast hydrolysis, indeed afforded an excellent slow-release form of theophylline.

EXPERIMENTAL[1]

Preparation of 7,7′-Succinyldithophylline (I)—*Method A*—To 2.03 g (17.0 mmoles) of thionyl chloride were added 2.77 g (38.0 mmoles) of dimethylformamide and 0.83 g (7.0 mmoles) of succinic acid, in that order, at room temperature while nitrogen was bubbled through the reaction mixture; the reaction warmed during the addition of the dimethylformamide. After 0.25 hr, 2.52 g (14.0 mmoles) of theophylline was

[1] All melting points are uncorrected. NMR spectra were run on a Varian T-60 spectrometer, using tetramethylsilane as an internal standard. IR spectra were obtained from a Beckman Acculab 4 spectrophotometer. The UV spectra were recorded on a Cary 14 spectrophotometer. Microanalyses were performed by Midwest Microlab, Indianapolis, Ind. Theophylline was obtained from Knoll, Inc.; unless otherwise specified, all other chemicals were obtained from Aldrich Chemical Co. and all solvents were analytical reagent grade and obtained from Mallinckrodt, Inc.

0022-3549/78/0800-1045$01.00/0
© 1978, American Pharmaceutical Association

added, and the resulting suspension was diluted with 100 ml of dichloromethane. Then 2.82 g (34 mmoles) of pyridine was added dropwise to the well-stirred suspension, causing the suspension to clear gradually and the resulting solution to take on a yellow color. All additions were done at room temperature, and nitrogen was bubbled through the reaction mixture the entire time.

The reaction solution was then protected from atmospheric moisture with a calcium chloride drying tube, and the solution was refluxed overnight with the heating bath temperature at 60–70°. The resulting suspension was filtered, and the residue was washed with dichloromethane to give 1.50 g (50% yield) of I as a white solid whose IR and UV spectra showed no theophylline impurity.

The IR spectrum of I was characterized by three bands at 3160 (m), 1734 (s) (NC=O), and 1540 (m) cm^{-1}. Theophylline itself showed a very broad, intense absorption between 3300 and 2200 cm^{-1} in which it was difficult to pick out a characteristic absorption; it did not show any absorption at 1734 cm^{-1} and showed the 1540-cm^{-1} absorption shifted to 1570 cm^{-1}. The UV spectrum of I in dichloromethane was characterized by a symmetrical band centered at 300 nm with an intensity of $\epsilon = 1.31 \times 10^4$, while theophylline was characterized by a symmetrical band centered at 270 nm with an intensity of 1.0×10^4.

Anal.—Calc. for $C_{18}H_{18}N_8O_6$: C, 48.87; H, 4.10; N, 25.33. Found: C, 49.19; H, 4.11; N, 25.02.

Method B—To 2.04 g (13 mmoles) of ice bath cooled and well-stirred succinyl chloride was added 2.33 g (32 mmoles) of dimethylformamide. This clear colorless solution was stirred for 10 min; then 4.68 g (26 mmoles) of theophylline was added, and the light-yellow suspension was diluted with 100 ml of dichloromethane. Finally, 2.21 g (27 mmoles) of pyridine was added dropwise to the well-stirred suspension. The suspension never did become homogeneous, but it did go from a reddish-orange to a grayish-green color during pyridine addition.

The suspension was gradually allowed to warm to room temperature and was stirred over the weekend at room temperature; the reaction was protected from atmospheric moisture at all times with a calcium chloride drying tube. Then the suspension was filtered, and the residue was washed with 50 ml of dichloromethane to give 4.88 g (85% yield) of I as a yellow solid. The IR spectrum was identical with that of I from Method A; UV (CH_2Cl_2) λ_{max} 300 nm ($\epsilon = 1.28 \times 10^4$). The yellow solid was suspended in refluxing dichloromethane for 2 hr. The hot suspension was filtered to give a yellow solid (4.77 g) which now had λ_{max} 300 nm ($\epsilon = 1.31 \times 10^4$) in dichloromethane.

Anal.—Calc. for $C_{18}H_{18}N_8O_6$: C, 48.87; H, 4.10; N, 25.33. Found: C, 48.44; H, 3.96; N, 25.31.

Method C—To 1.89 g (15.9 mmoles) of well-stirred thionyl chloride at room temperature were added 2.60 g (35.6 mmoles) of dimethylformamide, dropwise, and 0.80 g (8 mmoles) of succinic anhydride. The resulting suspension was stirred at room temperature for 1 hr, during which time it became homogeneous and light yellow in color. Then dichloromethane (50 ml) was added to the solution, followed by 2.70 g (15 mmoles) of theophylline, 50 ml of dichloromethane, and 2.80 g (35 mmoles) of pyridine.

Nitrogen was bubbled through the clear yellow-orange solution for 20 min at room temperature, and the solution was refluxed overnight in a reaction flask equipped with a calcium chloride drying tube. The next day, the resulting suspension was filtered while hot to give 1.70 g (51% yield) of I as a white solid. The IR spectrum was identical to that of I from Method A; UV (CH_2Cl_2) λ_{max} 300 nm ($\epsilon = 1.30 \times 10^4$).

Anal.—Calc. for $C_{18}H_{18}N_8O_6$: C, 48.87; H, 4.10; N, 25.33. Found: C, 48.79; H, 4.08; N, 25.63.

Method D—The same results as Method C were obtained when phosgene in benzene was substituted for thionyl chloride on a molar basis.

Anal.—Calc. for $C_{18}H_{18}N_8O_6$: C, 48.87; H, 4.10; N, 25.33. Found: C, 48.70; H, 3.91; N, 25.61.

In addition to I, the following 7,7′-acylditheophylline compounds were prepared according to Method B:

7,7′-Glutarylditheophylline (II)—mp 229–230°, 84% yield.

Anal.—Calc. for $C_{19}H_{20}N_8O_6$: C, 49.99; H, 4.42; N, 24.56. Found: C, 49.94; H, 4.71; N, 24.84.

7,7′-Adipylditheophylline (III)—mp 238–239°, 82% yield.

Anal.—Calc. for $C_{20}H_{22}N_8O_6$: C, 51.06; H, 4.71; N, 23.82. Found: C, 50.96; H, 4.95; N, 23.80.

7,7′-Terephthaloyldittheophylline (IV)—92% yield.

Anal.—Calc. for $C_{22}H_{18}N_8O_6$: C, 54.10; H, 3.30; N, 22.94. Found: C, 53.40; H, 3.64; N, 22.48.

Preparation of 7-Octanoyltheophylline (VI)—Theophylline (4.5 g, 0.025 mole) was added to 200 ml of anhydrous 1,2-dichloroethane containing 5 ml (0.062 mole) of pyridine. Octanoyl chloride (4.86 g, 0.03 mole) diluted with 50 ml of 1,2-dichloroethane was then added to the solution. The mixture was heated at reflux for 2 hr and cooled to 0°. The precipitate was filtered, and the filtrate was concentrated *in vacuo* to give a white crystalline residue. The crystals were recrystallized from heptane to give 6.2 g (mp 62–63°, 90% yield) of VI.

Anal.—Calc. for $C_{15}H_{22}N_4O_3$: C, 58.81; H, 7.28; N, 18.28. Found: C, 58.68; H, 7.24; N, 18.48.

In a similar manner were prepared the following 7-acyltheophylline derivatives:

7-Decanoyltheophylline (VII)—mp 71–72°, 87% yield.

Anal.—Calc. for $C_{17}H_{26}N_4O_3$: C, 61.06; H, 7.84; N, 16.75. Found: C, 60.99; H, 7.81; N, 16.87.

7-Palmitoyltheophylline (VIII)—mp 92–93°, 88% yield.

Anal.—Calc. for $C_{23}H_{38}N_4O_3$: C, 66.00; H, 9.15; N, 13.38. Found: C, 66.06; H, 9.24; N, 13.41.

7-Cinnamoyltheophylline (IX)—mp 234°, 91% yield.

Anal.—Calc. for $C_{16}H_{14}N_4O_3$: C, 61.93; H, 4.55; N, 18.06. Found: C, 61.76; H, 4.40; N, 18.16.

Preparation of Ethyl 7-Succinyltheophylline (X)—A dichloromethane (125 ml) suspension containing 4.0 g (0.022 mole) of theophylline and 2.25 g (0.022 mole) of triethylamine was added to an ice bath cooled dichloromethane (100 ml) solution of ethyl succinyl chloride (3.6 g, 0.022 mole). The solution was filtered immediately, and the filtrate was concentrated *in vacuo* at room temperature to give a hygroscopic residue, which was suspended in ether (500 ml). The suspension was filtered, and the residue was discarded.

The filtrate was concentrated *in vacuo* to give a white solid, which was triturated with heptane (200 ml). The suspension was filtered, and the residue was dried to give 1.19 g (mp 107–109°, 17% yield) of X; IR (KBr): 1720, 1695, and 1660 (s) (C=O) cm^{-1}; NMR ($CDCl_3$): δ 8.46 (s, 1, N=CHN), 4.06 (q, J = 7 Hz, 2, OCH_2CH_3), 3.73–3.57 (m, 2, CH_2C=ON), 3.57 and 3.37 (two s, 6, NCH_3), 2.83–2.60 (m, 2, CH_2C=OO), and 1.18 (t, J = 7 Hz, 3, CH_3CH_2O) ppm.

Anal.—Calc. for $C_{13}H_{16}N_4O_5$: C, 50.64; H, 5.23; N, 18.17. Found: C, 50.58; H, 5.27; N, 18.28.

Preparation of 7′-*p*-Toluenesulfonyltheophylline (XI)—A tetrahydrofuran (100 ml) suspension containing 1.54 g (0.015 mole) of triethylamine, 2.70 g (0.015 mole) of theophylline, and 2.70 g (0.014 mole) of *p*-toluenesulfonyl chloride was refluxed for 48 hr and then filtered while still warm to remove triethylamine hydrochloride. The filtrate was cooled, and the resulting precipitate was filtered. The residue (2.60 g) was suspended in 50 ml of benzene to remove unreacted theophylline.

The benzene filtrate was concentrated *in vacuo* to give 2.2 g (mp 202–204°, 46% yield) of XI as a white powder; TLC (silica gel, acetone): R_f 0.66; NMR ($CDCl_3$): δ 8.33 (s, 1, N=CHN), 7.78 (*AB* quartet, J = 9 Hz, $\Delta_{AB\nu}$ = 38 Hz, 4, aromatic H), 3.58 and 3.36 (two s, 6, NCH_3), and 2.45 (s, 3, aromatic CH_3) ppm.

Anal.—Calc. for $C_{14}H_{14}N_4O_4S$: C, 50.29; H, 4.22; N, 16.76. Found: C, 50.31; H, 4.15; N, 16.83.

Preparation of 7,7′-Carbonylditheophylline (V)—A chloroform (100 ml) suspension of theophylline (3.60 g, 0.02 mole) was treated with 10.3 g (12 ml, 12.5 mmoles) of 12.5% phosgene in benzene and then with a chloroform (20 ml) solution of pyridine (2.0 g, 0.025 mole). The solution that resulted was allowed to react at room temperature overnight in a tightly sealed reaction flask. The next day, an additional 4 ml of 12.5% phosgene in benzene was added. The suspension was allowed to stir at room temperature overnight, and then it was heated to reflux and quickly filtered while hot.

The residue was dried *in vacuo* over phosphorus pentoxide to give 1.72 g (45% yield) of V as a white powder, which was too unstable upon exposure to the atmosphere to give a satisfactory elemental analysis. The IR spectrum showed complete loss of NH absorption and the appearance of two new carbonyl bands at 1780 and 1750 cm^{-1}; UV (dioxane): λ_{max} 274 nm ($\epsilon = 2.91 \times 10^4$); UV ($CH_2Cl_2$): λ_{max} 270 nm ($\epsilon = 2.96 \times 10^4$). The $t_{1/2}$ dissolution in water was 4.5 min.

NMR Studies—The NMR spectrum were obtained by directly mixing the appropriate reagents on a 0.7–1.0-mmole scale in NMR spin tubes or in small (10 ml) erlenmeyer flasks from which NMR samples were taken when desired. Each reaction was run at least three times with no significant variation in the results. The reaction between dimethylformamide and thionyl chloride in deuterochloroform after 10 min resulted in the formation of very broad absorptions centered in the regions of 660–580 Hz (0.22, relative integration) and 510–460 Hz (0.78) for NCH and of 280–210 Hz (1.3) and 210–150 (4.7) for NCH_3.

The lower field absorption in each set was attributed to the ionic, $(CH_3)_2N$=$CHCl^+$ Cl^-, rather than the covalent, $(CH_3)_2NCHCl_2$, form

Table I—Dissolution of Acyltheophyllines

Compound	$t_{50\%}$	Preparation Method[a]
Theophylline	<10 sec	—
I	1 hr	B
I	22 hr[b]	C
I	22 hr[b]	D
II	45 min	B
IV	3 hr	B
VII	18 hr	B
VIII	60 hr	B
IX	75 hr	B

[a] See *Experimental*. [b] After proper formulation, a half-life of less than 4 hr could be obtained.

of the Vilsmeier reagent obtained. When the reagent was allowed to age, there was a decrease in the contribution of those absorptions attributed to the ionic form.

When an equivalent of succinic anhydride was added to the Vilsmeier reagent, an absorption at 184 Hz was observed. Furthermore, all succinic anhydride went into solution, whereas a dimethylformamide–deuterochloroform solution in the same ratio and volume did not dissolve that much succinic anhydride. Therefore, the absorption at 184 Hz was assigned to the $CH_2C{=}O$ absorption in the intermediate formed between the Vilsmeier reagent and succinic anhydride. As the reaction mixture of dimethylformamide, thionyl chloride, and succinic anhydride was allowed to age, another absorption appeared at 200 Hz. It was identified as due to succinyl chloride by spiking the sample with succinyl chloride. The absorption due to succinyl chloride amounted to 5% after 1 hr, 33% after 16 hr, and 63% after 41 hr.

When one-half equivalent of succinic acid was substituted for succinic anhydride in this reaction, the time course of succinyl chloride formation was much slower; after 16 hr, about 10% succinyl chloride was formed. The $CH_2C{=}O$ absorption due to the remaining succinyl moiety remained at about 185 Hz. But the CH_3N absorption due to dimethylformamide was no longer centered at about 184 Hz but was at 196 Hz instead; with time, it appeared to shift to 205 Hz.

The addition of two equivalents each of theophylline and pyridine to freshly prepared reaction mixtures of dimethylformamide, thionyl chloride, and succinic anhydride resulted in the formation of yellow-orange solutions with very small amounts of solid suspended in them. Almost all theophylline dissolved in each case, but the clear solutions obtained in preparative scale reactions were never obtained, probably because of the difficulty in maintaining anhydrous conditions. Analysis of the NMR spectra of those solutions immediately after they were formed showed, in addition to pyridine, the absorptions due to dimethylformamide (two sharp singlets at 179 and 173 Hz, CH_3N) and a theophylline-containing moiety (two sharp singlets at 218 and 202 Hz, CH_3N), as well as a sharp singlet at 188 Hz and a broad singlet at 152 Hz. The singlet at 188 Hz was identified as succinic anhydride by spiking the sample with succinic anhydride. With time, the broad singlet at 152 Hz became broader and shifted downfield; after 16 hr, it had shifted to 164 Hz. In each case, after about 24 hr, the precipitate obtained was analyzed and found to be 7,7′-succinylditheophylline (I).

Theophylline was not soluble to the same extent in the same mixture of dimethylformamide–deuterochloroform, nor did the addition of pyridine hydrochloride improve theophylline solubility in such a mixture. There was an unidentified reaction between theophylline and the Vilsmeier reagent.

Dissolution Studies—The dissolution studies were conducted directly in accordance with the guidelines set forth in the USP (7). The apparatus and materials employed were within USP requirements.

Table II—Stability of 7,7′-Succinylditheophylline

Preparation Method	Conditions	$\epsilon \times 10^4$ (Percent Decomposition)[a] 1 Week	2 Weeks	3 Weeks
A	60°[b]	1.28 (1.5)	1.25 (4.0)	—
B	60°[b]	0.95 (27)	0.71 (46)	—
C	60°[b]	1.28 (1.5)	1.21 (6.5)	1.16 (10)
	25°, 52% R.H.[c]	1.30 (0)	1.29 (0.7)	—
	40°[b]	1.30 (0)	1.24 (4.5)	1.20 (8)

[a] Samples analyzed in dichloromethane at 300 nm by UV; original transmittance was 1.30 for all samples. [b] Samples stored in sealed ampuls. [c] The relative humidity was maintained in a sealed desiccator with a standard salt solution, and the sample was kept exposed to that atmosphere in the desiccator.

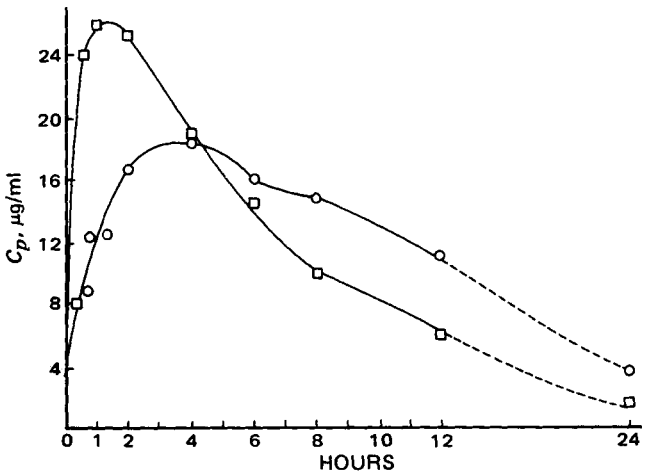

Figure 1—*Bioavailability of theophylline* (□) *and I* (○) *at doses of 30 mg/kg or equivalent.*

The dissolution rates of the theophylline compounds were obtained in 500 ml of distilled water containing 2 drops of polysorbate 80[2] in a standard dissolution pot at 25 ± 0.5° in a constant-temperature water bath. Samples of 100–200-mesh powder of each compound tested were transferred directly into the dissolution medium and stirred with a standard USP stainless steel paddle. The paddle was placed at the center of the 500 ml of dissolution medium and rotated at 100 rpm. After a constant reading was obtained, the solution was sonicated for 15 min to obtain the infinite reading.

All samples were run at least twice. The concentration of each sample in the dissolution medium never exceeded 5% of the solubility of theophylline.

The results of some representative dissolution studies are presented in Table I.

Bioavailability Studies—Beagle dogs of both sexes, 10–15 kg, were fasted for 12 hr prior to use. Theophylline (30 mg/kg) and 7,7′-succinylditheophylline (equivalent to 30 mg of theophylline/kg) were suspended in 5% methylcellulose and administered orally *via* a conventional gastric delivery tube. Each suspended drug solution was prepared immediately prior to administration. Blood (10 ml) was withdrawn from each dog immediately prior to drug administration. Then 10-ml blood samples were obtained at 15, 30, 60, 120, 240, 360, 480, and 720 min after drug administration.

The plasma was separated conventionally and stored in a freezer pending assay. Theophylline concentrations in plasma were determined by the spectrophotometric method of Shack and Waxler (8). Plasma (2 ml) was acidified with 1 *N* HCl to pH 5.5–6 and then was extracted with 20 ml of 5% 2-propanol in chloroform. The organic phase was reextracted with 3 ml of 1 *N* NaOH. The absorbance of the aqueous layer was determined with a 1-cm path length cell in a UV spectrophotometer.

The results of the bioavailability study are presented in Fig. 1. Compound I resulted in therapeutic plasma levels [10–20 μg/ml (2, 3)] essentially for 12 hr, while the same doses of theophylline resulted in toxic blood levels for about 4 hr and dropped below the therapeutic level after 7–8 hr.

Stability Studies—Stability studies were carried out by following the decrease in absorbance due to 7,7′-succinylditheophylline at 300 nm. Table II shows the results of some representative stability studies using five samples for each determination.

RESULTS AND DISCUSSION

Most of the theophylline derivatives (I–XI) were prepared by the reaction of an acid chloride with theophylline in the presence of an acid scavenger, usually pyridine. The compounds thus obtained have characteristic IR, UV, and NMR spectra (Table III). Their elemental analyses are also consistent with the structures indicated. For instance, theophylline itself has a very broad, intense NH absorption between 2400 and 2900 cm^{-1}. That absorption is obviously absent in the derivatives, which instead exhibit a strong carbonyl absorption at about 1730–1760 cm^{-1}.

The UV spectrum of theophylline exhibits a λ_{max} at 273 nm with an

[2] Tween 80.

Table III—Spectral Data for Theophylline Derivatives

Compound	NMR[a] NCHN	NMR[a] $CH_2C{=}ON$	NMR[a] CH_3N	IR[b], C=O
Theophylline	7.83	—	3.63, 3.47	1705, 1660
I	—	—	—	1735, 1705, 1660
II	8.43	3.50	3.60, 3.44	1735, 1716, 1700, 1660
III	—	—	—	1765, 1700, 1650
VI	8.37	3.43, t, J = 7 Hz	3.63, 3.47	—
VII	8.37	3.45, t, J = 7 Hz	3.61, 3.46	1755, 1715, 1670
VIII	8.37	3.41, t, J = 7 Hz	3.61, 3.46	1755, 1715, 1670
IX	8.57	—	3.63, 3.47	1710, 1700, 1665, 1650

[a] NMR spectra were run in deuterochloroform, and chemical shift values (δ) are given in parts per million. [b] IR spectra were run in potassium bromide, and absorption values are in reciprocal centimeters.

ϵ of 1×10^4, while the λ_{max} is shifted to about 298 nm for the monotheophylline derivatives and to slightly longer wavelengths for the ditheophylline derivatives. Comparison of the NMR spectrum of theophylline with the spectra of its derivatives shows that a characteristic change in the chemical shift of the 8-proton occurs [from δ 7.83 to 8.37 ppm in the octanoate VI, for example (Table III)] due to deshielding of the proton by the 7-acyl carbonyl in the derivatives.

The chemical shift of the absorption due to the acyl α-methylene in the 7-acyltheophyllines is more difficult to explain. This methylene absorption is shifted 35–40 Hz downfield from the methylene absorptions in the corresponding acid chlorides. To obtain such a deshielded environment, it appears that it is necessary to invoke a mechanism whereby some charge separation occurs in the ground state of the CN bond (XII). An alternative possibility, in which acylation of the 6-carbonyl takes place to give the conjugated system XIII, would not generate a system with electron-withdrawing properties sufficient to cause the deshielding observed.

Furthermore, if there was enhanced charge separation in the ground state of the CN bond, one might expect elimination of theophylline to occur as readily as in an acid chloride (9), causing the formation of a ketene or, if two theophyllines are eliminated, a diketene-like intermediate, which would then readily polymerize. As a result of this mechanism, water-involved hydrolysis would not be the only route for I decomposition. The stability data presented in Table II suggest that decomposition indeed does not take place in the solid state primarily through a hydrolysis mechanism, since decomposition was not affected by humidity, but through a thermolysis mechanism. The stability data and the NMR spectra tend to support the theory that there is strong charge separation in the N-7 C=O bond of the 7-acyltheophyllines. The cinnamoyl derivative IX does not show this kind of thermal decomposition, obviously because of the lack of the possibility for ketene formation.

Of the monotheophylline derivatives, only NMR and IR data could be obtained for the hexanoyl derivative. The remaining monotheophylline derivatives could be recrystallized from alkanes. The ditheophylline derivatives were not conveniently soluble in any solvent tried. Fortunately, the ditheophylline derivatives could be obtained directly from the reaction mixtures in sufficient purity to establish their dissolution characteristics and other physical-chemical properties.

Table I shows the time course of dissolution of several representative derivatives. There was little effect of pH on the I dissolution rate at pH 2–7 under otherwise identical conditions. The hydrolysis of I under these conditions had a half-life in solution of about 10 sec[3]. The data for V (see *Experimental*) were obtained for the crude reaction product because it was too unstable to survive sieving and had to be stored in a desiccator.

The bioavailability of a slow-release drug depends, in this case, on how long the protected drug remains in the stomach. The time for gastric emptying is, of course, quite variable, so selecting an optimum dissolution half-time for the slow-release theophylline was somewhat arbitrary. However, based on previous work (4), a value of about 2 hr was considered optimal. Compound I contains a greater percentage of theophylline than any other derivative except V. No aryl residue is more than marginally less toxic than succinic acid, and the dissolution study suggests that I can be obtained in a form that has approximately the desired half-life for dissolution. Furthermore, since the dissolution of I was unaffected by pH in the 2–7 range, the I dissolution rate should be reasonably independent of the conditions found in the GI tract.

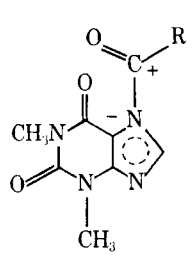

XII

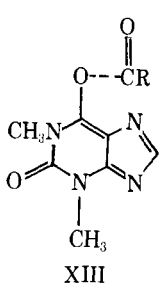

XIII

[3] V. J. Stella, Department of Pharmaceutical Chemistry, University of Kansas, Lawrence, KS 66044, personal communication.

After the preliminary physical-chemical data were determined, *in vivo* data in beagle dogs were obtained for I to assess its utility more thoroughly. The results in Fig. 1 show that I with a half-time of dissolution of 2 hr indeed delivered theophylline in a slow, prolonged manner that resulted in a therapeutic blood theophylline level for a longer time than theophylline itself. A more detailed evaluation of the biopharmaceutics and pharmacokinetics will be presented elsewhere. Based on these data and considerations, I was selected as the best candidate for further evaluation. A successful attempt was made to obtain it in a pure stable form.

The preparation of I from succinyl chloride and theophylline in the presence of a suitable acid scavenger had a number of problems concerned with the physical nature of the product formed. Compound I, prepared in such a manner, was not particularly stable and its dissolution was erratic. These problems are normally overcome by recrystallization, but I was insoluble for all practical purposes in every common solvent. Thus, the crystal form of I that was produced during the synthesis was employed.

The question then became one of how to produce pure stable I with the desired dissolution rate directly from the reaction mixture. Usually, this synthesis is accomplished by adjusting the polarity of the solvent system and the concentration of the reagents so that the formation rate and subsequent precipitation of the product can be controlled. Inherent in this approach is that the reaction proceeds through a clear solution stage or that precipitation of the product is slow enough that it does not occlude unreacted starting materials. This effect could not be accomplished consistently in the preparation of I from theophylline and succinyl chloride.

Alternatively, an attempt was made to prepare I from different reagents. It was suggested that the highly reactive V could react under proper conditions with succinic anhydride, according to Scheme I, but the proper conditions for this exchange could not be found.

A recent patent describing the use of dimethylformamide as a catalyst for the preparation of succinyl chloride from succinic anhydride and phosgene suggested that a heat-labile intermediate was involved in the process (10). It was felt that, under suitable conditions, the intermediate could be caused to react with theophylline in the presence of an acid scavenger to give I. Thus, a mixture of stoichiometric amounts of dimethylformamide, thionyl chloride (Vilsmeier reagent) (11), and succinic anhydride contained only a trace of succinyl chloride initially (by NMR spectroscopy), but increasing amounts of succinyl chloride were observed after several days at room temperature. When the initial mixture of dimethylformamide, thionyl chlorde, and succinic anhydride was immediately allowed to react with theophylline in the presence of pyridine,

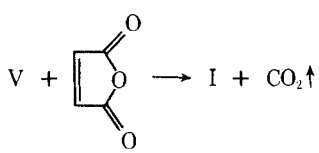

Scheme I

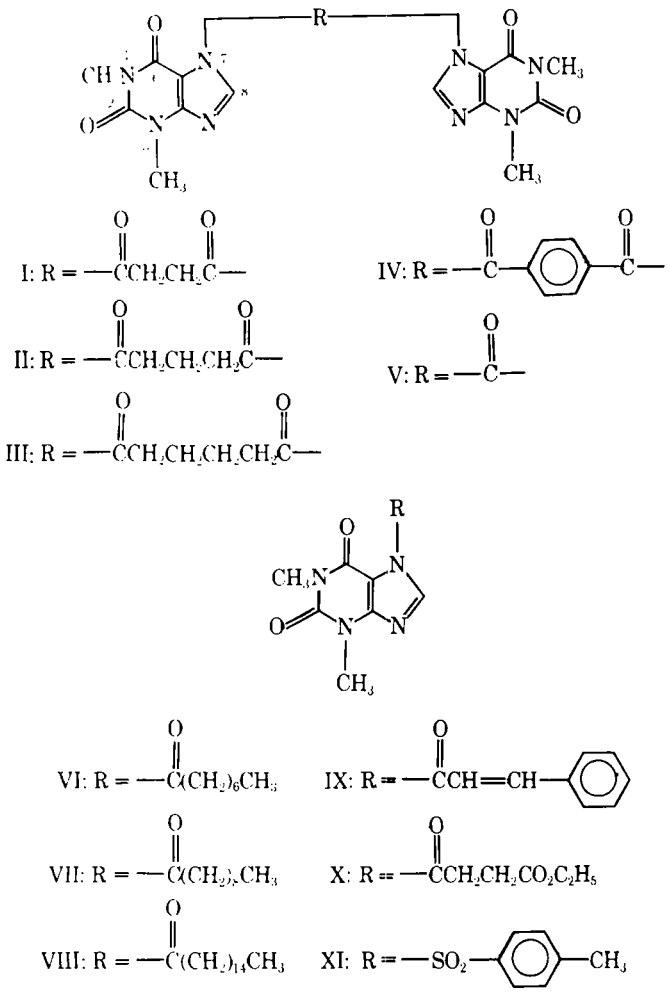

a clear solution was obtained within seconds. This solution did not contain any succinyl chloride (by NMR spectroscopy) and, upon heating, gave I as a precipitate.

The physical properties of I obtained in this manner were quite different from those of I obtained from the reaction of theophylline with succinyl chloride. In the former case, the crystals were visible to the naked eye. In the latter case, the product was an aggregate of amorphous particles. Obviously, these large crystals had a much different dissolution rate (22 hr) compared to the aggregate (1–2 hr). However, by a process of grinding, milling, and formulation, it was possible to convert the long dissolution rate crystals of I to a powder with the desired shorter dissolution rate. The process of converting the crystals of I into a product with a shorter dissolution rate did not perceptibly affect I stability. The stability data for I obtained by the various procedures described under *Experimental* were for forms of I with the same half-life of dissolution (Table II).

The NMR spectrum of the clear solution obtained in the initial stages of the reaction of the Vilsmeier reagent with succinic anhydride and theophylline in the presence of pyridine showed absorptions attributable to dimethylformamide (CH_3N), succinic anhydride ($CH_2C{=}O$), and pyridine and theophylline (CH_3N), as well as a broad absorption centered at 152 Hz. This later absorption and the solubilization of the theophylline in the reaction mixtures suggested that the theophylline absorptions (CH_3N) and the absorption at 152 Hz were due to the CH_3N and $O{=}CCH_2$ protons, respectively, of a soluble form of I or a precursor of I. One logical explanation for this behavior is that the soluble form may be the kinetic product, which would explain why it is necessary to heat

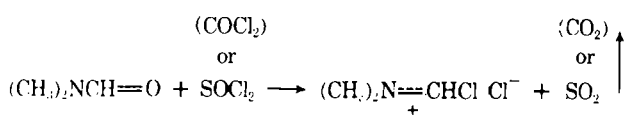

Scheme II

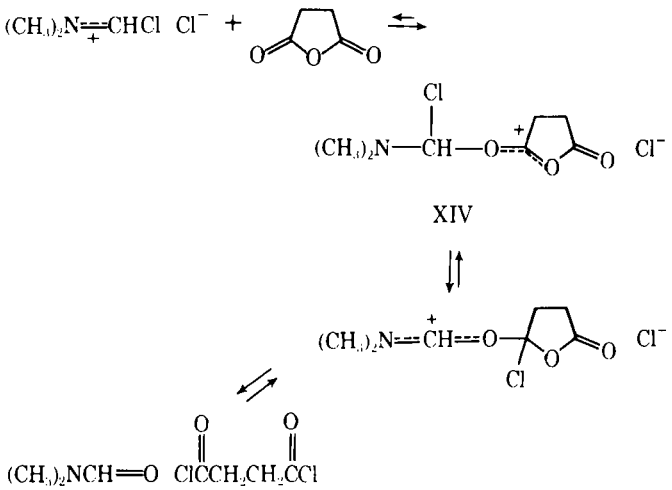

Scheme III

the reaction mixture for a considerable time to convert it to the thermodynamically more stable, insoluble form of I.

In the reaction between dimethylformamide–thionyl chloride, succinic anhydride, theophylline, and pyridine, no cooling was necessary; the reaction had to be refluxed to give good yields of I. The reaction between succinyl chloride, theophylline, and pyridine had to be cooled to obtain comparable yields of less stable I. If the latter reaction was cooled sufficiently (−40°), it occasionally proceeded through a clear solution stage which gradually, upon warming, gave I as a fine precipitate that was more stable than I obtained when the reaction was run at a higher temperature. It seemed reasonable that so much energy was released during the formation of the acylonium ion from succinyl chloride that the kinetic product was immediately converted to the more stable, insoluble form and in the process occluded some theophylline in its crystal lattice. The I thus produced was less stable and dissolved much quicker than I produced *via* the Vilsmeier reagent.

Although succinyl chloride was not detected in the reaction under the experimental conditions, it can be argued that succinyl chloride was produced as a slow step and then reacted quickly with theophylline in the presence of pyridine. This rationale did not fit, however, the observed fact that all theophylline went into solution immediately in a solvent system in which it was otherwise insoluble. Also, theophylline obviously was being converted into a soluble form more quickly than succinyl chloride was being generated; the appearance rate of succinyl chloride was just too slow to account for the rapid reaction observed.

The reaction among dimethylformamide, thionyl chloride, and succinic acid, as followed by NMR, appeared to follow the same course.

The salient features of this unusual reaction with Vilsmeier reagent, succinic anhydride, theophylline, and pyridine are summarized as follows. Thionyl chloride reacts with dimethylformamide to form the Vilsmeier reagent in Scheme II. Then the Vilsmeier reagent reacts as a Lewis acid (12) with succinic anhydride in Scheme III to form the complex XIV, which can undergo a slow equilibrium reaction to give succinyl chloride. The reaction of XIV with pyridine to form the acylonium ion XV and the diacylonium ion XVI (Scheme IV) may be stepwise, with concomitant formation of XVII by trapping the monoacylonium ion with theophylline, or simultaneous, which results in the formation of I directly from XVI.

The reaction took place so quickly that it was not possible to observe any acyl monotheophylline intermediate by NMR spectroscopy. The simultaneous appearance of the NMR absorptions due to dimethylformamide and those attributed to the soluble form of I is compelling evidence that XVII does not represent the structure of the soluble form of I.

SUMMARY

A representative number of 7-acyltheophyllines and 7,7′-acylditheophyllines have been synthesized. One of them (I) has been identified as having properties of dissolution and stability that result in a prolonged controlled release of theophylline *in vivo*. Furthermore, a novel synthesis of I has been developed, which does not involve an acid chloride intermediate but which does appear to proceed through an acylonium ion generated under milder conditions than those obtained when the acylo-

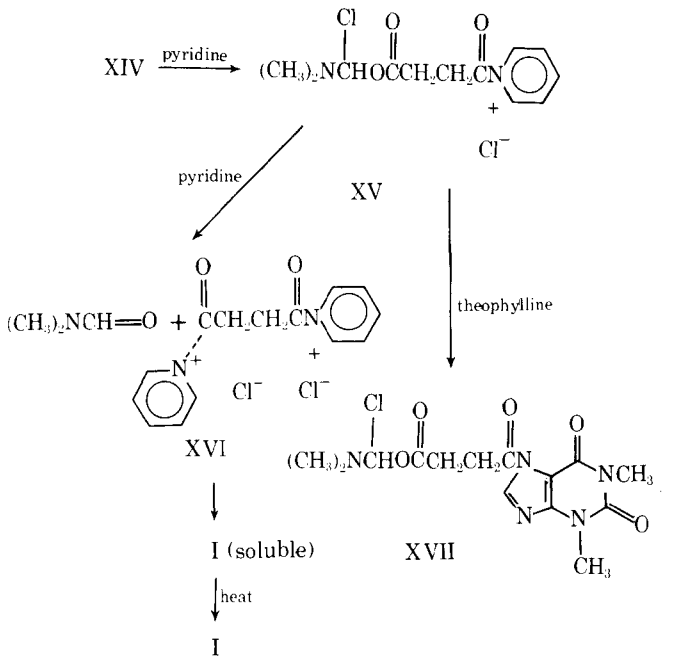

Scheme IV

nium ion is generated from an acid chloride. The crystals of I obtained from this novel synthesis are more stable than those crystals of I obtained when the acid chloride is used in the synthesis of I. In addition, this novel synthesis results in I of consistent physical properties suitable for subsequent formulation.

REFERENCES

(1) H. Salem and R. H. Jackson, *Ann. Allergy,* **32,** 189 (1974).

(2) K. M. Piafsky and R. I. Ogilvie, *N. Engl. J. Med.,* **292,** 1218 (1975).

(3) M. Weinberger and S. Riegelman, *ibid.,* **291,** 151 (1974).

(4) C. Boroda, R. B. Miller, S. T. Leslie, E. G. Nicol, and I. Thomson, *J. Clin. Pharmacol.,* **13,** 383 (1973).

(5) D. McIntosh, *Br. J. Clin. Pract.,* **25,** 233 (1971).

(6) T. Higuchi, H. K. Lee, and I. H. Pitman, *Farm. Aikak.,* **80,** 55 (1971).

(7) "The United States Pharmacopeia," 18th rev., Mack Publishing Co., Easton, Pa., 1970, pp. 934, 935.

(8) J. A. Shack and S. H. Waxler, *J. Pharmacol. Exp. Ther.,* **97,** 283 (1949).

(9) C. W. Bird and D. Y. Wong, *Tetrahedron,* **30,** 2331 (1974).

(10) C. F. Hauser, U.S. pat. 3,810,940 (May 14, 1974).

(11) A. Vilsmeier and A. Haack, *Chem. Ber.,* **60B,** 119 (1927).

(12) G. J. Martin and S. Poignant, *J. Chem. Soc. Perkin Trans. II,* **1974,** 642.

ACKNOWLEDGMENTS

The authors thank D. Wang and V. J. Stella of the Department of Pharmaceutical Chemistry, University of Kansas, Lawrence, KS 66044, and David Walters for technical assistance in the bioavailability and synthetic work, respectively.

Assays and Statistical Analyses for Antibiotic Standards

ELSIE TARCZA ˣ and MARY ANN GARTH

Received July 25, 1977, from the *National Center for Antibiotics Analysis, Food and Drug Administration, Washington, DC 20204.* Accepted for publication November 14, 1977.

Abstract □ Some microbiological assays and statistical analyses of test results used by the National Center for Antibiotics Analysis are described for the establishment of official antibiotic reference standards. Examples are given of both cylinder plate agar diffusion assays and turbidimetric assays. Formulas providing simple and quick analyses of data are shown for calculating potency, determining limits for the potency, and performing validity tests on the results.

Keyphrases □ Microbiological assays—for official antibiotic reference standards, formulas for quick, simple analysis of data □ Antibiotic reference standards, official—microbiological assays, formulas for simple, quick analysis of data

The Food and Drug Administration's National Center for Antibiotics Analysis (NCAA) establishes and maintains official reference standards for all antibiotics subject to certification. When a standard is required for a new antibiotic or when an existing standard must be replaced, NCAA performs a series of assays on representative samples of the proposed batch. The collaboration of other laboratories in assaying samples is requested; the findings are evaluated and certain statistical analyses are performed by NCAA.

In addition, NCAA is frequently called upon to participate and collaborate with other laboratories to establish official standards, such as international standards established by the National Institute for Medical Research in London, England, through the Expert Committee on Biological Standardization of the World Health Organization. Standards are also assayed at the request of the USP and NF.

Kirshbaum *et al.* (1) simplified the bioassay designs described by Bliss (2) and statistical procedures given in USP XV (3). For microbiological assays of antibiotics, they adapted a series of equations to determine potency, error variance, validity, and confidence limits of the assays. This adaptation was published in the USP XVI (4) and is still in use in NCAA laboratories. The calculations are based on a polynomial equation for fitting a line to a parabola. Coefficients and constants are derived from the table of orthogonal polynomials.

METHODS

When evaluating a proposed FDA standard, each participant is supplied with a quantity of the proposed standard and a reference standard and is requested to follow a specific design and to furnish NCAA with the necessary raw data. This design is applied to three-dose assays, where there is a linear response to the log of the dose, where there are parallel

0022-3549/78/0800-1050$01.00/0

© 1978, American Pharmaceutical Association

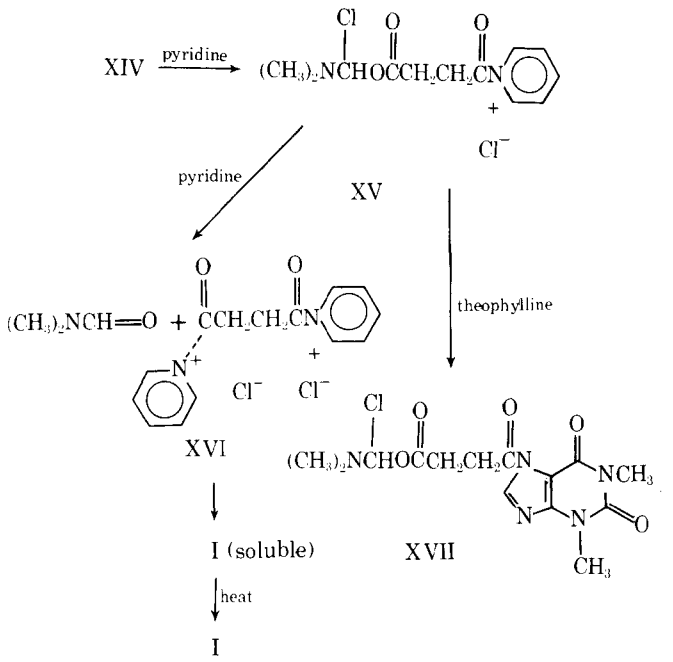

Scheme IV

nium ion is generated from an acid chloride. The crystals of I obtained from this novel synthesis are more stable than those crystals of I obtained when the acid chloride is used in the synthesis of I. In addition, this novel synthesis results in I of consistent physical properties suitable for subsequent formulation.

REFERENCES

(1) H. Salem and R. H. Jackson, *Ann. Allergy,* **32,** 189 (1974).

(2) K. M. Piafsky and R. I. Ogilvie, *N. Engl. J. Med.,* **292,** 1218 (1975).

(3) M. Weinberger and S. Riegelman, *ibid.,* **291,** 151 (1974).

(4) C. Boroda, R. B. Miller, S. T. Leslie, E. G. Nicol, and I. Thomson, *J. Clin. Pharmacol.,* **13,** 383 (1973).

(5) D. McIntosh, *Br. J. Clin. Pract.,* **25,** 233 (1971).

(6) T. Higuchi, H. K. Lee, and I. H. Pitman, *Farm. Aikak.,* **80,** 55 (1971).

(7) "The United States Pharmacopeia," 18th rev., Mack Publishing Co., Easton, Pa., 1970, pp. 934, 935.

(8) J. A. Shack and S. H. Waxler, *J. Pharmacol. Exp. Ther.,* **97,** 283 (1949).

(9) C. W. Bird and D. Y. Wong, *Tetrahedron,* **30,** 2331 (1974).

(10) C. F. Hauser, U.S. pat. 3,810,940 (May 14, 1974).

(11) A. Vilsmeier and A. Haack, *Chem. Ber.,* **60B,** 119 (1927).

(12) G. J. Martin and S. Poignant, *J. Chem. Soc. Perkin Trans. II,* **1974,** 642.

ACKNOWLEDGMENTS

The authors thank D. Wang and V. J. Stella of the Department of Pharmaceutical Chemistry, University of Kansas, Lawrence, KS 66044, and David Walters for technical assistance in the bioavailability and synthetic work, respectively.

Assays and Statistical Analyses for Antibiotic Standards

ELSIE TARCZA ˣ and MARY ANN GARTH

Received July 25, 1977, from the *National Center for Antibiotics Analysis, Food and Drug Administration, Washington, DC 20204.* Accepted for publication November 14, 1977.

Abstract □ Some microbiological assays and statistical analyses of test results used by the National Center for Antibiotics Analysis are described for the establishment of official antibiotic reference standards. Examples are given of both cylinder plate agar diffusion assays and turbidimetric assays. Formulas providing simple and quick analyses of data are shown for calculating potency, determining limits for the potency, and performing validity tests on the results.

Keyphrases □ Microbiological assays—for official antibiotic reference standards, formulas for quick, simple analysis of data □ Antibiotic reference standards, official—microbiological assays, formulas for simple, quick analysis of data

The Food and Drug Administration's National Center for Antibiotics Analysis (NCAA) establishes and maintains official reference standards for all antibiotics subject to certification. When a standard is required for a new antibiotic or when an existing standard must be replaced, NCAA performs a series of assays on representative samples of the proposed batch. The collaboration of other laboratories in assaying samples is requested; the findings are evaluated and certain statistical analyses are performed by NCAA.

In addition, NCAA is frequently called upon to participate and collaborate with other laboratories to establish official standards, such as international standards established by the National Institute for Medical Research in London, England, through the Expert Committee on Biological Standardization of the World Health Organization. Standards are also assayed at the request of the USP and NF.

Kirshbaum *et al.* (1) simplified the bioassay designs described by Bliss (2) and statistical procedures given in USP XV (3). For microbiological assays of antibiotics, they adapted a series of equations to determine potency, error variance, validity, and confidence limits of the assays. This adaptation was published in the USP XVI (4) and is still in use in NCAA laboratories. The calculations are based on a polynomial equation for fitting a line to a parabola. Coefficients and constants are derived from the table of orthogonal polynomials.

METHODS

When evaluating a proposed FDA standard, each participant is supplied with a quantity of the proposed standard and a reference standard and is requested to follow a specific design and to furnish NCAA with the necessary raw data. This design is applied to three-dose assays, where there is a linear response to the log of the dose, where there are parallel

0022-3549/78/0800-1050$01.00/0

© 1978, American Pharmaceutical Association

dose–response lines for the standard and unknown, and where the potency of the unknown is estimated as close to 100% of the standard. The usual instructions are for two weighings daily of the proposed standard to be assayed for 3 days against two weighings of the standard.

Before starting, erlenmeyer flasks used for preparing test solutions are rinsed with distilled water and dried in a hot air oven. The weighed material is dissolved in sufficient solvent to make a convenient stock solution. The same is done with the reference standard. Where possible, only volumetric glassware is used for dilution. All glassware is rinsed with some of the final diluent before use.

If an intermediate dilution is required, only one such dilution is made from each stock solution. With appropriate aqueous solvents, dilutions from the stock concentrations are made to three different concentrations. These concentrations are equally spaced at logarithmic intervals and result in the same number of responses so that a constant may be used in the statistical analyses. These concentrations are referred to as S_1, S_2, and S_3 (low, middle, and high concentrations) for the standard and U_1, U_2, and U_3 (low, middle, and high concentrations) for the unknown.

The method may be a cylinder plate procedure or turbidimetric procedure as described in the CFR (5). In the plate assay procedure, each of the six solutions is put in a coded random pattern into six stainless steel cylinders sitting on the surface of a freshly prepared agar plate containing the test organism. Twelve plates are prepared for each weighing. After overnight incubation, the plates are examined visually. All plates with aberrant or missing values are discarded. Nine plates are chosen at random, and the diameters of the zones of inhibition are measured in millimeters with an appropriate instrument. If any of the six zones of inhibition on one plate must be discarded because of aberrance, the entire plate is discarded and one of the remaining plates is used. If more than three plates are discarded, the assay is considered invalid. If only nine plates are prepared, missing or aberrant readings are replaced by methods described in the USP (6).

In the turbidimetric assay, 60 test tubes are placed in one large spool; test solutions are put in the tubes in a coded random pattern, using 1 ml/tube. Then 9 ml of broth containing the test organism is added, and the spool of tubes is incubated in a 37° constant-temperature circulating water bath. After the incubation period, the spool is removed from the water bath and 0.5 ml of 12% formaldehyde solution is added to each tube. The turbidity is measured with a photoelectric colorimeter. The absorbance readings are decoded, and only three absorbance values are used for each concentration. The other values are used only to replace an aberrant reading.

RESULTS AND DISCUSSION

Example 1—The statistical analysis shown in Table I is for a cylinder plate assay. After the zone sizes are decoded and tabulated, the range of the values of each vertical column is obtained by subtracting the lowest value from the highest. The ratio of the largest range to the sum of the ranges should not exceed the appropriate critical value (0.273 for nine plates; $p = 0.05$). If it does, the readings in the column with the largest range are checked to find the aberrant response. The plate with this reading is replaced by a random selection of one remaining plate. If there are no complete plates to substitute, the assay is not considered valid.

This procedure is continued until the table includes data from nine plates with no missing or aberrant values. If a satisfactory assay has been performed, the three extra plates should ensure that the analyst ends up with nine good plates. The columns of values are totaled both horizontally and vertically.

The log potency, M, is determined from:

$$M = \frac{^{*}(U_1 + U_2 + U_3 - S_1 - S_2 - S_3)}{S_3 + U_3 - S_1 - U_1} \qquad \text{(Eq. 1)}$$

and the percent potency, P, is obtained from:

$$P = 100 \times \text{antilog } M \qquad \text{(Eq. 2)}$$

The numerator constant (*) depends on the ratio between doses (see *Formulas for Determining Potency Constant and* L/2 *Constant for All Three-Dose Assays*).

From Example 1:

$$M = \frac{0.12921\,(119.0 + 126.3 + 132.3 - 119.1 - 126.4 - 132.8)}{132.8 + 132.3 - 119.1 - 119.0}$$

$$= -0.00335 \qquad \text{(Eq. 3)}$$

$$P = 100 \times \text{antilog} - 0.00335 = 99.2\% \text{ or } 636\ \mu\text{g/mg} \qquad \text{(Eq. 4)}$$

Table I—Example 1, Assuming a Potency for the Unknown of 641 μg/mg and a Ratio between Doses of 1.25:1

Plate Number	S1	S2	S3	U1	U2	U3	Plate Sum (T_r)
1	13.3	14.1	14.8	13.2	13.9	15.0	84.3
2	12.7	13.7	14.7	12.9	13.8	14.6	82.4
3	12.9	14.1	14.6	13.1	13.9	14.7	83.3
4	12.9	13.8	14.8	13.2	13.5	14.1	82.3
5	13.6	14.6	14.9	13.8	14.4	14.9	86.2
6	12.8	13.6	14.7	12.9	14.3	14.9	83.2
7	13.6	14.0	14.8	13.2	14.3	14.4	84.3
8	13.7	14.2	14.8	13.0	14.0	14.8	84.5
9	13.6	14.3	14.7	13.7	14.2	14.9	85.4
Sum (T_t)	119.1	126.4	132.8	119.0	126.3	132.3	755.9 (T)
Range	1.0	1.0	0.3	0.9	0.9	0.9	

observed $R = \frac{1.0}{5.0} = 0.2000$ critical $R = 0.273$

The error variance, s^2, from cylinder to cylinder and from plate to plate is determined using:

$$s^2 = \frac{\sum y^2 - \frac{\sum T_r^2}{6} - \frac{\sum T_t^2}{9} + \frac{T^2}{54}}{40} \qquad \text{(Eq. 5)}$$

where:

y = individual response, zone measurement, or single observation

$\sum y^2$ = sum of the squares of all 54 zone sizes

$\frac{\sum T_r^2}{6}$ = sum of the squares of the totals of the horizontal rows divided by the number of treatments (6)

$\frac{\sum T_t^2}{9}$ = sum of the squares of the totals of the vertical columns divided by the number of plates (9)

$\frac{T^2}{54}$ = squares of the sum of the totals of the horizontal rows or the square of the sum of the total of the vertical columns (they should be equal) divided by the number of observations (54)

40 = degrees of freedom

From Example 1:

$$\sum y^2 = 10{,}605.87 \qquad \text{(Eq. 6a)}$$

$$\sum T_r^2 = 63{,}501.00 \qquad \text{(Eq. 6b)}$$

$$\frac{\sum T_r^2}{6} = 10{,}583.5017 \qquad \text{(Eq. 6c)}$$

and:

$$\sum T_t^2 = 95{,}413.59 \qquad \text{(Eq. 7a)}$$

$$\frac{\sum T_t^2}{9} = 10{,}601.51 \qquad \text{(Eq. 7b)}$$

and:

$$T^2 = 571{,}384.81 \qquad \text{(Eq. 8a)}$$

$$\frac{T^2}{54} = 10{,}581.2002 \qquad \text{(Eq. 8b)}$$

Therefore:

$$s^2 = \frac{10{,}605.87 - 10{,}583.3017 - 10{,}601.51 + 10{,}581.2002}{40} \qquad \text{(Eq. 9a)}$$

$$s^2 = \frac{2.0585}{40} = 0.0515 \qquad \text{(Eq. 9b)}$$

(The values obtained for $\sum y^2$, $\sum T_r^2/6$, $\sum T_t^2/9$, and $\sum T^2/54$ should all be quite close numerically.)

To test the assay validity, three equations are used. The value ab is used to test whether the dose–response lines are parallel. The value q is used to test combined curvature in the same direction. The value aq is used to test separate curvatures in opposite directions. The three values obtained from these equations should not exceed the value obtained for three times the error variance, $3s^2$. If any value is greater than three times the error variance, the significant F-test is used to determine validity.

The three values are added and their sum is divided by $3s^2$. This value should not exceed the critical F (2.84). If it does, the assay is not valid and is discarded. Therefore:

$$ab = \frac{[S_1 + U_3 - (S_3 + U_1)]^2}{36} \quad \text{(Eq. 10)}$$

$$q = \frac{[S_1 + U_1 + S_3 + U_3 - 2(S_2 - U_2)]^2}{108} \quad \text{(Eq. 11)}$$

$$aq = \frac{[(U_1 + U_3 + 2S_2) - (S_1 + S_3 + 2U_2)]^2}{108} \quad \text{(Eq. 12)}$$

$$F = \frac{ab + q + aq}{3s^2} \quad \text{(Eq. 13)}$$

From Example 1:

$$ab = \frac{[119.1 + 132.3 - (132.8 + 119.0)]^2}{36} = 0.0044 \quad \text{(Eq. 14)}$$

$$q = \frac{[119.1 + 119.0 + 132.8 + 132.3 - 2(126.4 + 126.3)]^2}{108} = 0.0448 \quad \text{(Eq. 15)}$$

$$aq = \frac{[119.0 + 132.3 + 252.8 - (119.1 + 132.8 + 252.6)]^2}{108} = 0.0015 \quad \text{(Eq. 16)}$$

$$F = \frac{0.0044 + 0.0448 + 0.0015}{0.1545} = 0.3282 \quad \text{(Eq. 17)}$$

Critical $F = 2.84$. The assay is valid.

If the assay is valid, the precision of the assay, C, and the confidence interval, L, are determined next:

$$C = \frac{(S_3 + U_3 - S_1 - U_1)^2}{(S_3 + U_3 - S_1 - U_1)^2 - 147.06s^2} \quad \text{(Eq. 18)}$$

and:

$$\frac{L}{2} = \sqrt{(C - 1)(CM^2 + *)} \quad \text{(Eq. 19)}$$

The confidence interval depends on the precision with which the slope of the dose–response curve has been determined.

From Example 1:

$$C = \frac{(132.8 + 132.3 - 119.1 - 119.0)^2}{(132.8 + 132.3 - 119.1 - 119.0)^2 - 147.06 \times 0.0515} = 1.0105 \quad \text{(Eq. 20)}$$

and:

$$\frac{L}{2} = \sqrt{(1.0105 - 1)[1.0105\,(-0.00335)^2 + 0.02504]} = 0.0162 \quad \text{(Eq. 21)}$$

Finally, the upper and lower 95% confidence limits are computed. There is 95% assurance that the true potency lies between the upper and lower limits, with the best estimate of potency being that derived by the appropriate calculation for potency:

$$X_u = 100 \times \text{antilog}\left(CM + \frac{L}{2}\right) \quad \text{(Eq. 22)}$$

$$X_1 = 100 \times \text{antilog}\left(CM - \frac{L}{2}\right) \quad \text{(Eq. 23)}$$

X_u = percent potency, upper limit of 95% confidence interval (Eq. 24)

X_1 = percent potency, lower limit of 95% confidence interval (Eq. 25)

From Example 1:

$$X_u = 100 \times \text{antilog}\,[1.0105 \times (-0.00335) + 0.0162] = 103.0\% \text{ or } 660\ \mu g/mg \quad \text{(Eq. 26)}$$

$$X_1 = 100 \times \text{antilog}\,[1.0105 \times (-0.00335) - 0.0162] = 95.6\% \text{ or } 613\ \mu g/mg \quad \text{(Eq. 27)}$$

Example 2—The statistical analysis of turbidimetric assays (Table II) is performed in a similar manner. After the absorbance values are decoded, the first three readings are recorded for testing. The range of the values in each vertical column is obtained by subtracting the lowest value from the highest. The ratio of the largest range to the sum of the ranges should not exceed the appropriate critical value (0.389 for three tubes). If it does, the readings in the column with the largest range are checked to find the aberrant response. A reading from another tube of the same dose chosen at random is substituted.

Table II—Example 2, Assuming a Potency for the Unknown of 1000 μg/mg and a Ratio between Doses of 1.25:1[a]

Tube Number	S1	S2	S3	U1	U2	U3
1	32.3	26.8	21.6	33.0	26.1	21.5
2	31.1	25.5	21.0	31.8	26.4	21.0
3	31.9	25.3	21.3	32.2	26.0	21.8
Sum (T_t)	95.3	77.6	63.9	97.0	78.5	64.3
Range	1.2	1.5	0.6	1.2	0.4	0.8

observed $R = \frac{1.5}{5.7} = 0.2632$ critical $R = 0.389$

[a] To simplify calculations, the absorbance readings are recorded as whole numbers instead of thousandths.

This procedure is continued until the table has 18 values with no missing or aberrant readings. If there are no values left to be substituted, the assay is considered invalid.

The log potency, M, and the percent potency, P, are obtained from Eqs. 1 and 2, respectively. From Example 2:

$$M = \frac{0.12921\,(97.0 + 78.5 + 64.3 - 95.3 - 77.6 - 63.9)}{63.9 + 64.3 - 95.3 - 97.0} = -0.0061 \quad \text{(Eq. 28)}$$

$$P = 100 \times \text{antilog} - 0.0061 = 98.6\% \text{ or } 986\ \mu g/mg \quad \text{(Eq. 29)}$$

The error variance, s^2, is determined using:

$$s^2 = \frac{\sum y^2 - \frac{\sum T_t^2}{3}}{12} \quad \text{(Eq. 30)}$$

From Example 2:

$$\sum y^2 = 12{,}967.68 \quad \text{(Eq. 31a)}$$

$$\sum T_t^2 = 38{,}892.80 \quad \text{(Eq. 31b)}$$

$$\frac{\sum T_t^2}{3} = \frac{38{,}892.80}{3} \quad \text{(Eq. 31c)}$$

Therefore:

$$s^2 = \frac{12{,}967.68 - \frac{38{,}892.80}{3}}{12} \quad \text{(Eq. 32a)}$$

$$= \frac{12{,}967.68 - 12{,}964.2667}{12} \quad \text{(Eq. 32b)}$$

$$s^2 = 0.2844$$

(The values obtained for $\sum y^2$ and for $\sum T_t^2/3$ should be very close to each other numerically.)

To test the assay validity as in Example 1, the following equations are used:

$$ab = \frac{[S_1 + U_3 - (S_3 + U_1)]^2}{12} \quad \text{(Eq. 33)}$$

$$q = \frac{[S_1 + U_1 + S_3 + U_3 - 2(S_2 + U_2)]^2}{36} \quad \text{(Eq. 34)}$$

$$aq = \frac{[U_1 + U_3 + 2S_2 - (S_1 + S_3 + 2U_2)]^2}{36} \quad \text{(Eq. 35)}$$

$$F = \frac{ab + q + aq}{3s^2} \quad \text{(Eq. 36)}$$

From Example 2:

$$ab = \frac{[95.3 + 64.3 - (63.9 + 97.0)]^2}{12} = 0.1408 \quad \text{(Eq. 37)}$$

$$q = \frac{[95.3 + 97.0 + 63.9 + 64.3 - 2(77.6 + 78.5)]^2}{36} = 1.9136 \quad \text{(Eq. 38)}$$

$$aq = \frac{[97.0 + 64.3 + 155.2 - (95.3 + 63.9 + 157.0)]^2}{36} = 0.0025 \quad \text{(Eq. 39)}$$

Table III—Potency and $L/2$ Constants for Three-Dose Assay

•	1:1.12	1:1.2	1:1.25	1:1.33	1:1.5	1:1.56	1:2	1:4
P	0.06563	0.10557	0.12921	0.16513	0.23479	0.25749	0.40137	0.80275
$L/2$	0.00646	0.01672	0.02504	0.04090	0.08268	0.09945	0.24165	0.96660

$$F = \frac{0.1408 + 1.9136 + 0.0025}{0.8532} = 2.4108 \quad \text{(Eq. 40)}$$

Critical $F = 3.49$. The assay is valid.

If the assay is valid, the precision, C, is determined:

$$C = \frac{(S_3 + U_3 - S_1 - U_1)^2}{(S_3 + U_3 - S_1 - U_1)^2 - 56.964\, s^2} \quad \text{(Eq. 41)}$$

The confidence interval, L, is determined using Eq. 19.

From Example 2:

$$C = \frac{(63.9 + 64.3 - 95.3 - 97.0)^2}{(63.9 + 64.3 - 95.3 - 97.0)^2 - 56.964 \times 0.2844} = 1.0040 \quad \text{(Eq. 42)}$$

and:

$$\frac{L}{2} = \sqrt{(1.0040 - 1)\,[1.0040\,(-0.0061)^2 + 0.02504]} = 0.0100 \quad \text{(Eq. 43)}$$

Finally, the upper and lower 95% confidence limits are computed using Eqs. 22 and 23. From Example 2:

$$X_u = 100 \times \text{antilog}\,[1.0040 \times (-0.0061) + 0.0100] = 100.9\% \text{ or } 1009\ \mu\text{g/mg} \quad \text{(Eq. 44)}$$

$$X_l = 100 \times \text{antilog}\,[1.0040 \times (-0.0061) - 0.0100] = 96.4\% \text{ or } 964\ \mu\text{g/mg} \quad \text{(Eq. 45)}$$

Formulas for Determining Potency Constant and $L/2$ Constant for All Three-Dose Assays (Plate and Turbidimetric)—Determine the log of the interval of the ratio:

ratio	logarithm of interval between successive log doses (i)
1:1.12	0.04922
1:1.2	0.07918
1:1.25	0.09691
1:1.33	0.12385
1:1.5	0.17609
1:1.56	0.19312
1:2	0.30103
1:4	0.60206

Thus, $P = i(4/3)$ and $(L/2) = i^2(8/3)$ (Table III).

From all of the valid assays, the mean of the potency and 95% confidence limits of the mean are calculated:

$$\text{C.L.} = \overline{X} \pm t\left[\frac{\sqrt{\dfrac{\sum X^2 - \dfrac{(\sum X)^2}{N}}{N-1}}}{\sqrt{N}}\right] \quad \text{(Eq. 46)}$$

where:

C.L. = confidence limits
X = individual result or observation
$\overline{X}$ = mean, or average, of results
t = constant obtained from t table for $N - 1$ degrees of freedom (use a probability = 0.05)
N = number of results

Furthermore:

$$s = \sqrt{\frac{\sum X^2 - \dfrac{(\sum X)^2}{N}}{N-1}} = SD \quad \text{(Eq. 47)}$$

$$s_x = \frac{\sqrt{\dfrac{\sum X^2 - \dfrac{(\sum X)^2}{N}}{N-1}}}{\sqrt{N}} = SDM\ (SEM \text{ or } SE) \quad \text{(Eq. 48)}$$

For example, assume an estimated potency of 800 μg/mg:

assay number	potency
1	812
2	814
3	798
4	830
5	816
6	814

and:

$$\sum X = 4884.0 \quad \text{(Eq. 49)}$$

$$X = 814 \quad \text{(Eq. 50)}$$

$$t = 2.571 \quad \text{(Eq. 51)}$$

$$N = 6 \quad \text{(Eq. 52)}$$

$$\sum X^2 = 3{,}976{,}096.0 \quad \text{(Eq. 53)}$$

$$(\sum X)^2 = (4884.0)^2 = 23{,}853{,}456.0 \quad \text{(Eq. 54)}$$

$$\frac{(\sum X)^2}{N} = 3{,}975{,}576.0 \quad \text{(Eq. 55)}$$

$$\sqrt{N} = 2.4495 \quad \text{(Eq. 56)}$$

The confidence limits are:

$$\text{C.L.} = 814 \pm 2.571\,\frac{\sqrt{\left(\dfrac{3{,}976{,}096 - 3{,}975{,}576}{5}\right)}}{2.4495} \quad \text{(Eq. 57a)}$$

$$\text{C.L.} = 814 \pm 2.571\ (10.198/2.4495) \quad \text{(Eq. 57b)}$$

$$\text{C.L.} = 814 \pm 2.571\ (4.1633) \quad \text{(Eq. 57c)}$$

$$\text{C.L.} = 814 \pm 10.7038 \quad \text{(Eq. 57d)}$$

$$\text{C.L.} = 803\text{–}825 \quad \text{(Eq. 57e)}$$

The six assays, with a mean of 814 μg/mg, have 95% confidence limits of 803–825 μg/mg; *i.e.*, 95% of the time, the mean of six such assays will fall between 803 and 825 μg/mg.

An estimate of the variation of the individual results (X) used in determining the 95% confidence limits is made by computing the coefficient of variation:

$$\%\,CV = \frac{SD}{\text{mean}} \times 100 \quad \text{(Eq. 58a)}$$

$$\%\,CV = \frac{10.198}{814} \times 100 \quad \text{(Eq. 58b)}$$

$$\%\,CV = 1.25 \quad \text{(Eq. 58c)}$$

After the data analysis is completed and a potency is determined, the results and statistical analyses are sent to the participants with a request for their comments. Calculated potency is agreed upon, and the standard then becomes official. Before the advent of these equations, analyses of this kind were performed by statisticians. The use of these formulas has enabled NCAA to analyze the results of this type of studies quickly and simply.

REFERENCES

(1) A. Kirshbaum, B. Arret, and J. Kramer, *Antibiot. Chemother. (Washington, D.C.)*, **6**, 660 (1956).

(2) C. I. Bliss, "The Statistics of Bioassay," Academic, New York, N.Y., 1952.

(3) "The United States Pharmacopeia," 15th rev., Mack Publishing Co., Easton, Pa., 1955, pp. 865–880.

(4) *Ibid.*, 16th rev., 1960, p. 866.

(5) "Code of Federal Regulations," Title 21, Part 436.105, 106, 1978.

(6) "The United States Pharmacopeia," 19th rev., Mack Publishing Co., Easton, Pa., 1975, p. 602.

Equilibrium Penetration of Monolayers VI: Cholesterol–Cetrimonium Bromide System

MARYLYN A. McGREGOR and G. T. BARNES ×

Received September 6, 1977, from the *Department of Chemistry, University of Queensland, St. Lucia, Queensland 4067, Australia.* Accepted for publication November 15, 1977.

Abstract □ Equilibrium surface pressure–area isotherms for the penetration of cholesterol monolayers by the surfactant cetrimonium bromide are presented. From these isotherms, the saturation adsorptions of surfactant for various surface concentrations of cholesterol were calculated. Plots of adsorption against the inverse of the area per cholesterol molecule revealed two linear regions, corresponding to penetration at high and low monolayer areas. At high monolayer areas, surfactant adsorption into accessible areas of the surface was similar to adsorption at a monolayer-free surface. In this region, packing of cholesterol and surfactant molecules on the surface lowered the effective cross-sectional area of the cholesterol molecule. However, at low monolayer areas, adsorption was determined by the size of the surfactant ion and the effective area of the cholesterol molecule was equal to the collapse area of a pure cholesterol monolayer.

Keyphrases □ Cholesterol monolayers—penetration by cetrimonium bromide, equilibrium surface pressure–area isotherms obtained □ Monolayers, cholesterol—penetration by cetrimonium bromide, equilibrium surface pressure–area isotherms obtained □ Cetrimonium bromide—penetration of cholesterol monolayers, equilibrium surface pressure–area isotherms obtained □ Sterols—cholesterol, monolayers penetrated by cetrimonium bromide, equilibrium surface pressure–area isotherms obtained □ Surfactants—cetrimonium bromide, penetration of cholesterol monolayers, equilibrium surface pressure–area isotherms obtained

If a surfactant is injected into the aqueous phase beneath an insoluble monolayer, it usually tends to penetrate the monolayer, forming a mixed film of monolayer substance and surfactant. This tendency is manifest as a rise in surface pressure at a given monolayer area or as an increase in area at constant surface pressure. Because of the significance of monolayer behavior in the Davson–Danielli (1) model for biological membranes, there has been considerable interest in penetration studies with monolayers of substances found in natural membranes and with surfactants of biological significance.

Cholesterol has featured prominently in these studies, as has the surfactant cetrimonium (hexadecyltrimethylammonium) bromide (I), but these two substances were used together only once previously (2). There are significant differences between these earlier results and the data presented here.

The "accessible area" theory, developed to explain the permeation of a monolayer by water evaporating from the subphase (3), was modified to describe the equilibrium penetration of a monolayer by a surfactant (4). It leads to an equation for the adsorption or penetration of surfactant into a monolayer-covered surface, Γ_f:

$$\Gamma_f = \Gamma_w - a_M\Gamma_w(1/\hat{A}_M) \qquad \text{(Eq. 1)}$$

where Γ_w is the adsorption into the accessible area of the surface, a_M is the apparent cross-sectional area of a monolayer molecule, and $\hat{A}_M$ is the area per monolayer molecule. A plot of Γ_f against $(1/\hat{A}_M)$ should be a straight line, and physically reasonable values should be obtained for Γ_w and a_M. In this paper, the measurements reported for the equilibrium penetration of cholesterol monolayers by cetrimonium bromide are analyzed in terms of the accessible area theory.

Table I—Analysis of Penetration Data in Terms of Eq. 1

Region	Γ_w, molecules/nm^2	a_M, nm^2/molecule
Low area	2.36 ± 0.19	0.40 ± 0.04
High area	1.42 ± 0.12	0.27 ± 0.03
Predicted values	1.71 ± 0.20	0.39 ± 0.02

EXPERIMENTAL

The monolayer-forming substance, cholesterol[1], was dissolved in *n*-hexane[2] for spreading. The surfactant, I[3], was found, by surface tension measurements, to have a critical micelle concentration of 0.96 mM (5). Triple-distilled water was used for all substrates and solutions.

The apparatus and techniques were described previously (5). Briefly, a monolayer was spread on a water surface, the surfactant was injected into the subphase and mixed, and the surface was then compressed in steps, with ample time for equilibrium to be established between each step. An equilibrium surface pressure (π)–area per monolayer molecule

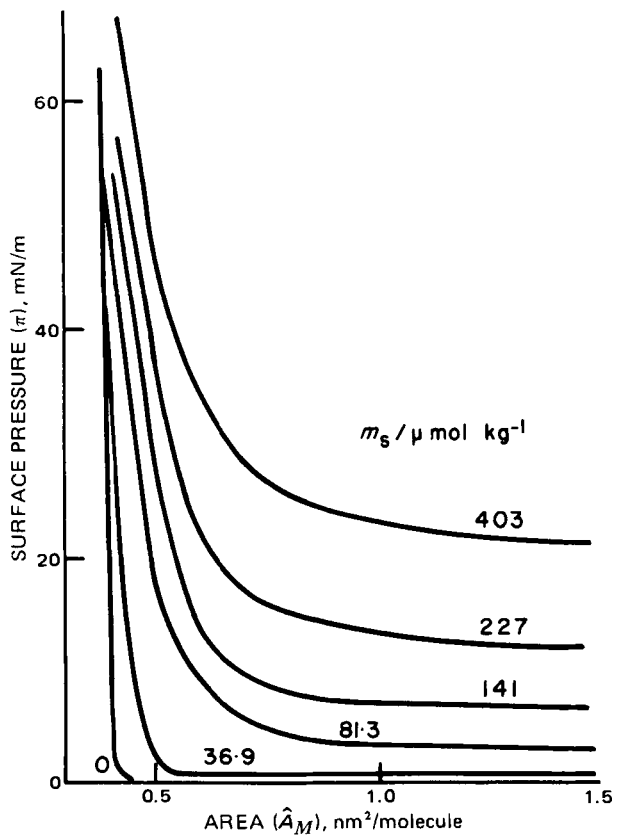

Figure 1—*Surface pressure–area isotherms of cholesterol monolayers on I solutions of various concentrations (T = 298 °K).*

[1] "For Biochemistry" grade, Merck.
[2] Spectroscopic grade, BDH.
[3] "Pro analysi" grade (>99% purity), Merck.

0022-3549/78/0800-1054$01.00/0
© 1978, American Pharmaceutical Association

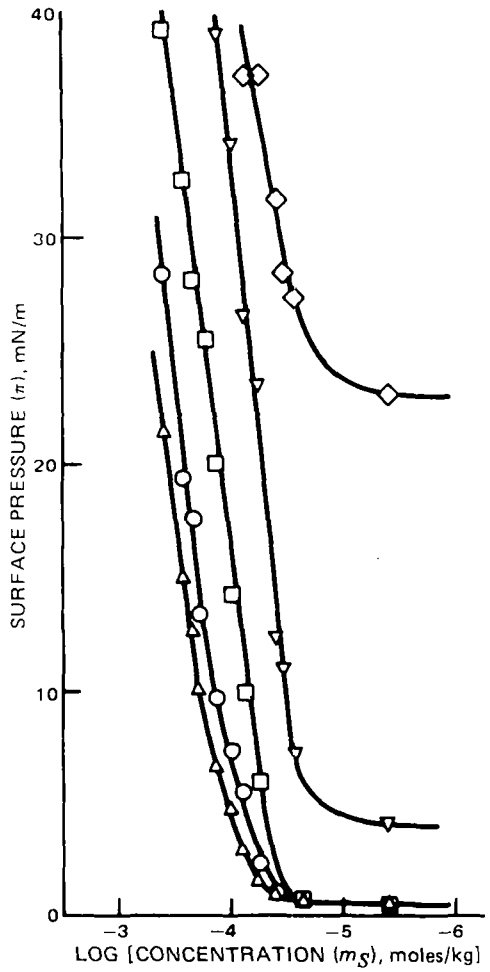

Figure 2—*Surface pressure as a function of I concentration for cholesterol monolayers at 0.4 (◊), 0.45 (▽), 0.55 (□), 0.70 (○), and 1.40 (△) nm²/monolayer molecule.*

($\hat{A}_M$) isotherm was thus obtained for one particular concentration of surfactant, m_S, in the subphase. The concentration of surfactant in such an experiment was determined at the completion of the run by sweeping the monolayer off the surface and measuring the surface tension of the subphase. The surface tension was then compared with a calibration curve (5).

RESULTS AND DISCUSSION

Equilibrium surface pressure–area isotherms for cholesterol with various concentrations of surfactant are shown in Fig. 1. From these curves, plots of surface pressure against log m_S were prepared for selected values of $\hat{A}_M$ (Fig. 2). The curves in Fig. 2 were approximately linear at surface pressures greater than 10 mN/m, indicating saturation adsorption. The slopes of the linear sections, $d\pi/d$ log m_S, were plotted against the area per monolayer molecule, $\hat{A}_M$ (Fig. 3). As expected, the values of $d\pi/d$ log m_S at high areas tended toward the slope for a monolayer-free surface.

Similar experiments with this system were reported (2) but over a narrower range of surfactant concentrations. There are significant differences between the two sets of results. The previous (2) surface pressure–area curves were appreciably more expanded than those shown in Fig. 1, and their monolayers appeared to collapse at 30–36 mN/m and about 0.7 nm²/molecule compared with the collapse pressures of 55–65 mN/m and areas less than 0.5 nm²/molecule reported here. In view of differences in the source of materials and techniques, there can be no firm explanation of these discrepancies. However, the results are consistent with the possibility that Ahmad *et al.* (2) had not allowed sufficient time in the stepwise compression of their monolayers for proper equilibria to be established.

Table II—Determinations of the Cross-Sectional Area of the Surfactant Ion

Cross-Sectional Area of Surfactant Ion, nm²/molecule	Method of Determination	Reference
0.39	Leybold models	5
0.29	Molecular models	6
0.37	Amagat equation	6
0.40	Alexander equation	6
0.37	$1/\Gamma_w$	5
0.42	$1/\Gamma_w$	Present work

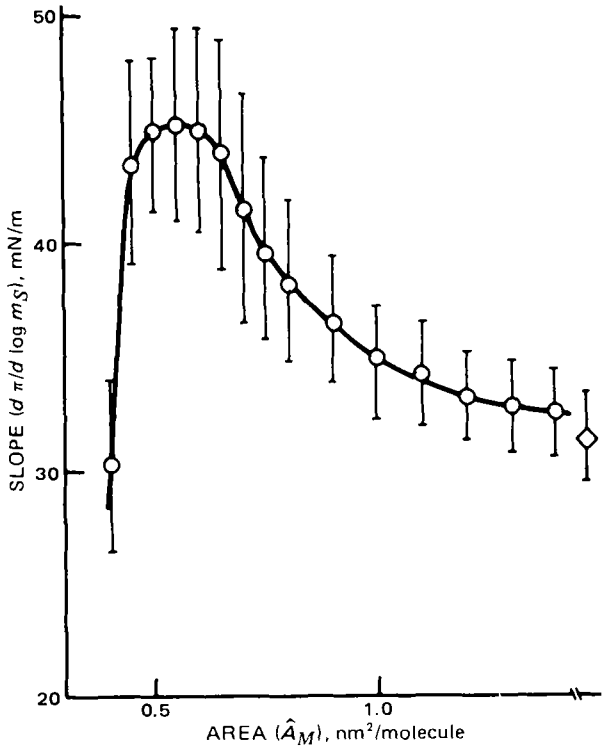

Figure 3—*Slope of the surface pressure–log (surfactant concentration) plot as a function of the area per cholesterol molecule.*

Adsorption values were calculated from the slopes of the linear sections of the π–log m_S curves by using Pethica's modification to the Gibbs ad-

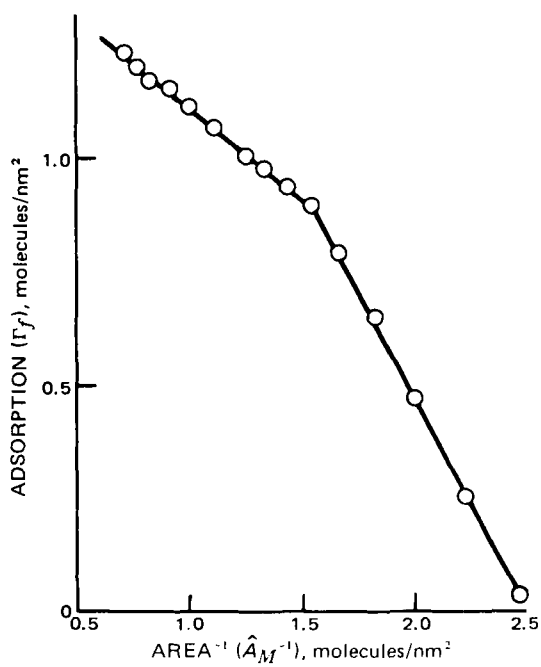

Figure 4—*Adsorption of I into cholesterol monolayers plotted according to Eq. 1.*

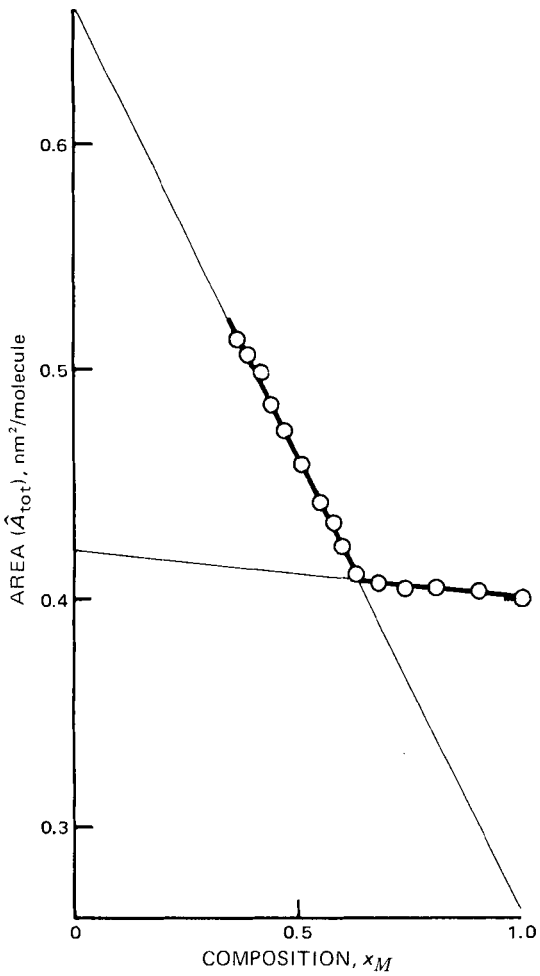

Figure 5—*Total area plotted against mole fraction of monolayer material to determine partial molecular areas.*

sorption isotherm. A plot of adsorption, Γ_S, against the inverse of the area per monolayer molecule, $1/\hat{A}_M$, as required for the accessible area theory (Eq. 1), is given in Fig. 4. Two distinct linear regions can be seen in this plot; for convenience, they will be called the high area region and the low area region. Values of the parameters Γ_w and a_M were determined for both regions using regression analysis (Table I).

The values obtained for Γ_w, the adsorption into the accessible area of the surface, in the two linear regions were similar to those for the octadecanol–I system (5).

In the high area region, Γ_w had practically the same value as Γ_S: the adsorption at a monolayer-free surface (Table I). In this region, the electrostatic forces limiting adsorption at the monolayer-free surface had a similar effect in the presence of the monolayer, even though the average surface concentration of surfactant molecules was less than at the monolayer-free surface. This result suggests that the surfactant is adsorbing or penetrating into large gaps in the monolayer and that the local surface concentration in these gaps is similar to that at a monolayer-free surface.

However, in the low area region, Γ_w was much higher than Γ_S. Here, the data indicate that the surfactant is adsorbed in small holes in the monolayer with only one molecule per hole. Thus, the size of the surfactant molecule is important and $1/\Gamma_w$ (0.42 nm²/molecule) should be a good estimate of the cross-sectional area of the surfactant ion. Table II summarizes values for the cross-sectional areas of the ion. There is reasonable agreement between all values except the second.

Table III—Partial Molecular Areas as Determined from a Plot of Total Area against Composition

Region	$\bar{A}_M$, nm²/molecule	$\bar{A}_S$, nm²/molecule	$\Gamma = 1/\bar{A}_S$, molecules/nm²
Low area	0.40	0.42	2.38
High area	0.26	0.67	1.50

The values obtained for a_M in the two regions differed substantially. At low areas, the value agreed well with the collapse area of cholesterol, 0.39 nm²/molecule. At high areas, the value for a_M was appreciably smaller. Probably the effective cross-sectional area of the monolayer molecule is reduced because the cholesterol is able to fit between the widely spaced surfactant molecules with only a moderate increase in their spacing.

A plot of total area against composition yielded values for the partial molecular areas of the two single components (Fig. 5). Table III summarizes values for the partial molecular areas obtained for both the low and the high area regions. These values agreed well with the corresponding values obtained for $1/\Gamma_w$ and a_M in the two regions. Indeed, it can be shown (7) that $1/\Gamma_w$ and a_M are theoretically identical to the partial molecular areas of surfactant and monolayer, respectively, and that the accessible area theory provides an alternative means of estimating these areas.

The equilibrium penetration of cholesterol monolayers by sodium lauryl sulfate was studied by Pethica (8) and analyzed in terms of the accessible area theory (4). The data were restricted to a region corresponding approximately to the low area region of the present system. Within this region, the two systems are very similar. The value of a_M obtained from Pethica's data was 0.374 nm²/molecule, in reasonable agreement with the value found here; the value of Γ_w again indicated that penetration was primarily determined by the size of the surfactant ion.

Neither Pethica's data nor the data presented here indicate that a complex might be formed between cholesterol and the surfactant. However, complex formation has been suggested between cholesterol and sodium hexadecyl sulfate (9, 10) and for the present system (2). It is likely that the longer chain length of the hexadecyl sulfate ion would lead to a stronger interaction with cholesterol than occurs between the lauryl sulfate ion and cholesterol. Nevertheless, Goddard and Schulman (10) suggested that the interaction is not strong enough for complex formation. Ahmad *et al.* (2), working with the cholesterol–I system, suggested that complex formation could explain the large collapse areas. However, the present data do not show this feature (Fig. 1), and analysis by the accessible area theory gives no indication of complex formation (11).

REFERENCES

(1) H. Davson and J. F. Danielli, "The Permeability of Natural Membranes," 2nd ed., Cambridge University Press, Cambridge, England, 1952.

(2) J. Ahmad, J. A. Mann, and M. J. Povich, *J. Colloid Interface Sci.*, **49**, 1 (1974).

(3) G. T. Barnes, T. I. Quickenden, and J. E. Saylor, *ibid.*, **33**, 236 (1970).

(4) M. A. McGregor and G. T. Barnes, *ibid.*, **49**, 362 (1974).

(5) *Ibid.*, **54**, 439 (1976).

(6) N. D. Weiner and G. Zografi, *J. Pharm. Sci.*, **54**, 436 (1965).

(7) M. A. McGregor and G. T. Barnes, *J. Colloid Interface Sci.*, in press.

(8) B. A. Pethica, *Trans. Faraday Soc.*, **51**, 1402 (1955).

(9) R. Matalon, *J. Colloid Sci.*, **8**, 53 (1953).

(10) E. D. Goddard and J. H. Schulman, *ibid.*, **8**, 309 (1953).

(11) M. A. McGregor and G. T. Barnes, *J. Colloid Interface Sci.*, **62**, 213 (1977).

Pharmacokinetics of Intravenous Erythromycin

P. G. WELLING *§x **and W. A. CRAIG** ‡

Received August 31, 1977, from the *School of Pharmacy, University of Wisconsin, the ‡Madison Veterans Administration Hospital, and the Department of Medicine, School of Medicine, University of Wisconsin, Madison, WI 53706. Accepted for publication November 17, 1977. §Present address: Department of Therapeutics and Clinical Pharmacology, School of Medicine, Queen Elizabeth Hospital, Edgbaston, Birmingham B15 2TH, England.

Abstract □ Erythromycin pharmacokinetics were examined following intravenous infusion to male subjects. The biological half-life of erythromycin in serum was 2 hr in individuals with normal renal function. The half-life varied in cases of reduced renal function, with values of 3.9 and 7.0 hr occurring in two subjects with severe renal impairment. Postinfusion serum erythromycin levels were adequately described by two-compartment model kinetics, and values for the distribution volume of the central compartment and the overall distribution are described. Estimated erythromycin distribution volumes in normal individuals may facilitate calculation of absorption efficiencies of erythromycin and its salts after oral doses.

Keyphrases □ Erythromycin—pharmacokinetics after intravenous administration in humans □ Pharmacokinetics—erythromycin after intravenous administration in humans □ Antibacterials—erythromycin, pharmacokinetics after intravenous administration in humans

Erythromycin is actively cleared from the body by the liver (1), and only 10–15% of the drug is excreted in microbiologically active form by the kidneys (2). Therefore, the half-life of circulating antibiotic should not be influenced significantly by variations in renal function. In an early study (3), the serum half-life of erythromycin increased from 1.5 hr in normal individuals to 4.8–5.8 hr in anuric patients. A preliminary report indicated that the erythromycin half-life increased only to 2.5 hr in severe uremia (4). This value appeared more consistent with the minor contribution by the kidneys to erythromycin clearance.

This report details erythromycin pharmacokinetics following intravenous infusion in individuals with normal and impaired renal function. The major study objectives were to describe erythromycin distribution in the body accurately and to examine the influence of compromised renal function on both its distribution and clearance characteristics.

EXPERIMENTAL

Subjects—Seven male individuals[1] participated. Physical details, creatinine clearance, and serum creatinine values of subjects and also clinical conditions are described in Table I. Creatinine clearance values are the means from five individual determinations (three for Subject 6, one for Subject 7) obtained during 48 hr following erythromycin doses. All individuals had normal liver function, as indicated by blood biochemistry values within the normal range.

Protocols—Subjects 1–6 received 500 mg of erythromycin base equivalents as the lactobionate salt[2], by continuous infusion over 30 min into an arm vein, in a solution of 5% dextrose in water. One month later, Subjects 6 and 7 received 500 mg of erythromycin base equivalents as the glucoheptonate salt[3] in an identical manner. In Subjects 5–7, erythromycin doses were administered 24 hr following dialysis. Infusion was started at approximately 8 am, about 1 hr after breakfast.

Blood samples (5 ml) were taken immediately before the infusion was started, at the end of the infusion, and at 1, 2, 3, 4, 6, 8, 12, and 24 hr after the end of the infusion. Urine was quantitatively collected at intervals during and following the infusion. Erythromycin activity in serum and urine was measured by a standard microbiological cup-plate diffusion method, using *Staphylococcus aureus* (6538P) as the test organism. Subjects received no antibiotic drugs, other than the required doses of erythromycin, for 1 week before and during a study.

Table I—Subject Physical Details

Subject	Age, yr	Weight, kg	Height, m	Cl_{cr}[a], ml/min	C_{cr}[b], mg %	Condition
1	36	75	1.8	118	1.1	Normal
2	52	75	1.6	78	1.1	Diabetic, sebaceous cyst on neck
3	58	52	1.8	105	1.0	Rheumatoid arthritis
4	70	77	1.8	43	2.3	Sclerotic cardiovascular disease, postmyocardial infarction, streptococcal cellulitis, rheumatoid arthritis
5	33	75	1.8	5.3	8.7	Severe hypertension, chronic renal failure (dialysis)
6(a)[c]	41	69	1.7	3.4	10.7	Chronic renal failure, renal transplant recipient with chronic rejection (dialysis)
6(b)[c]	41	69	1.7	3.2	10.3	Chronic renal failure, renal transplant recipient with chronic rejection (dialysis)
7	46	60	1.6	<1.0	17.4	Hypertension, small kidneys with chronic renal failure (dialysis)

[a] Creatinine clearance. [b] Serum creatinine. [c] Subject 6 was studied on two separate occasions.

RESULTS

Individual postinfusion serum erythromycin levels declined in a biphasic manner, as reported previously (2). Serum erythromycin levels are summarized in Table II, and typical serum profiles from two subjects are shown in Fig. 1. This type of profile is consistent with two-compartment model kinetics, with elimination occurring from the central compartment. Serum erythromycin levels were interpreted in terms of this model together with zero-order input (5). The model is depicted in Scheme I; serum erythromycin levels, C, are described by (5, 6):

$$C = \frac{k_0}{V_1 k_{el}}\left[\left(\frac{k_{el}-\beta}{\alpha-\beta}\right)(1-e^{-\alpha T})e^{-\alpha(t-T)} - \left(\frac{k_{el}-\alpha}{\alpha-\beta}\right)(1-e^{-\beta T})e^{-\beta(t-T)}\right] \quad \text{(Eq. 1)}$$

where k_0 is the zero-order rate constant for drug infusion; k_{12}, k_{21}, and k_{el} are first-order rate constants for drug distribution between central

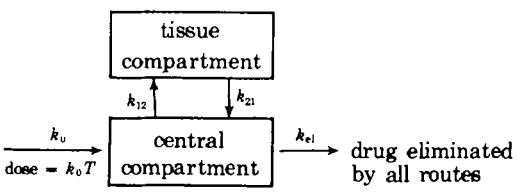

Scheme I

[1] All subjects gave written informed consent. Six were patients in the Madison Veterans Administration Hospital; the other subject was W. A. Craig.
[2] Erythromycin Lactobionate, Abbott Laboratories, North Chicago, IL 60064.
[3] Ilotycin Glucoheptonate, Eli Lilly and Co., Indianapolis, IN 46225.

0022-3549/78/0800-1057$01.00/0
© 1978, American Pharmaceutical Association

Table II—Serum Erythromycin Concentrations

Subject	Serum Erythromycin Concentration								
	0 hr[a]	1 hr	2 hr	3 hr	4 hr	6 hr	8 hr	12 hr	24 hr
1	12.4	6.4	5.0	3.1	1.9	1.2	0.4	—[b]	—
2	9.9	5.0	2.5	2.0	1.3	1.0	0.4	—	—
3	12.2	3.9	2.5	1.3	0.8	0.5	0.2	—	—
4	9.9	4.0	2.0	1.6	1.0	0.6	0.4	—	—
5	7.8	2.5	2.0	1.6	1.2	0.7	0.4	—	—
6(a)	9.9	3.1	2.5	1.4	0.9	0.5	0.4	—	—
6(b)	8.1	2.5	1.6	1.0	0.9	0.6	0.4	0.2	—
7	7.9	4.9	3.8	2.4	2.0	1.6	1.2	1.0	0.2

[a] All sampling times were calculated from the end of infusion. [b] Below limit of detection, 0.1 μg/ml.

and peripheral compartments and also drug elimination, respectively; V_1 is the apparent distribution volume of the central compartment; T is the infusion time; and t is the total time elapsed since the start of the infusion. The complex rate constants α and β are given by:

$$\begin{matrix}\alpha \\ \beta\end{matrix} = 0.5\left[(k_{12} + k_{21} + k_{e1}) \pm \sqrt{(k_{12} + k_{21} + k_{e1})^2 - 4k_{21}k_{e1}}\right] \quad \text{(Eq. 2)}$$

where $\alpha > \beta$ and the elimination half-life is given by $\ln 2/\beta$.

Individual serum data were fitted to Eq. 1 graphically and subsequently by iterative least-squares analysis using the digital computer program NREG (5). Renal clearances of erythromycin were calculated from all urine collection intervals except the −0.5–2-hr interval (Table III).

Urinary recovery data are summarized in Table III, and values of pharmacokinetic parameters are given in Table IV.

A low recovery of erythromycin in 48-hr urine in subjects with normal renal function is consistent with previous reports (2). As renal function deteriorates, urinary recovery of antibiotic is reduced still further and is insignificant in severe uremia. The concentration of antibiotic in urine is also considerably reduced in uremia, although, among the uremic subjects, the concentration of antibiotic in urine was unrelated to urine volume.

Changes in renal function generally had only a small effect on the serum erythromycin half-life. Only Subject 7 showed considerable prolongation of serum levels compared to normal subjects; Subjects 5 and 6 showed a small effect. Uremic subjects tended to have somewhat lower serum erythromycin levels immediately after the end of the infusion. These reduced levels are associated with increased apparent distribution volumes in uremic subjects.

Considerable variation was observed in some pharmacokinetic values (Table IV), particularly the microscopic rate constants k_{12}, k_{21}, and k_{e1}.

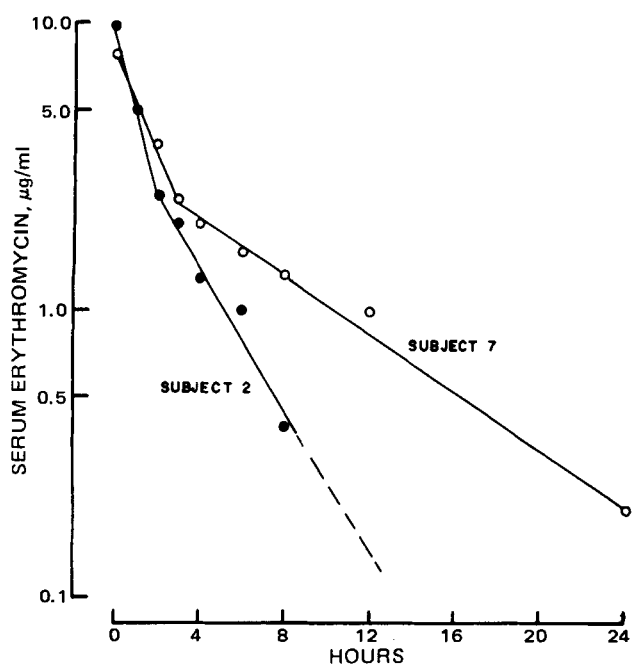

Figure 1—*Serum erythromycin levels in one normal subject and one uremic subject following intravenous infusion. Solid lines are computer lines of best fit using Eqs. 1 and 2. All times are calculated from the end of infusion.*

Table III—Concentrations of Erythromycin and Percentages of Dose Recovered in Urine

Subject		Collection Period, hr						48-hr Urine Volume, liters
		−0.5–2[a]	2–4	4–8	8–12	12–24	24–48	
1	Concentration[b]	125.1	80.7	51.2	12.5	0.1	0.0	2.3
	Percent[c]	8.0	9.2	10.7	11.4	11.4	11.4	
2	Concentration	195.4	60.6	24.9	9.7	0.5	0.0	2.9
	Percent	1.6	2.6	3.4	4.1	4.2	4.2	
3	Concentration	78.5	27.2	—	7.9[d]	0.3	0.0	3.2
	Percent	4.9	6.7	—	7.4	7.4	7.4	
4	Concentration	18.5	—	3.1[d]	0.4	0.0	0.0	2.8
	Percent	1.0	—	1.2	1.2	1.2	1.2	
5	Concentration	6.4	—	2.5[d]	0.3	0.0	0.0	1.4
	Percent	0.2	—	0.3	0.3	0.3	0.3	
6(a)	Concentration	—	—	—	0.8[d]	0.1	0.0	0.8
	Percent	—	—	—	<0.1	<0.1	<0.1	
6(b)	Concentration	—	0.8[d]	—	—	0.4[d]	0.0	0.4
	Percent	—	<0.1	—	—	<0.1	<0.1	
7	Concentration	—	—	—	—	3.1[d]	—	0.02
	Percent	—	—	—	—	<0.1	—	

[a] From the start of infusion until 2 hr postinfusion. [b] Concentration of antibiotic in urine (micrograms per milliliter). [c] Cumulative percent of dose excreted in urine. [d] Combined value for two or more collection intervals.

Subject 7 gave lower values for these constants and also exhibited a lower plasma clearance than all other subjects. It is not clear why these values were different in this subject compared to Subject 6 who had similarly impaired renal function. It is not a dosage form effect since both Subjects 6(b) and 7 received erythromycin glucoheptonate, which should, in any case, release the erythromycin cation in the body in the same way as the lactobionate.

The volume of the central, rapidly equilibrating, compartment increased from 45% of total body weight in normal individuals to 100% in severe uremia. The apparent total distribution of antibiotic, $V_{d(ss)}$, similarly increased from 57 to 109% of body weight. Negative correlations between these distribution parameters and creatinine clearance were quite good, with correlation coefficients of −0.62 ($p < 0.05$) and −0.71 ($p < 0.05$) being obtained for V_1 and $V_{d(ss)}$, respectively.

The very slight dependence of the overall erythromycin clearance on renal function is indicated by the serum and renal clearance values in Table IV. Although the correlation coefficient between erythromycin renal clearance and creatinine clearance was +0.8 ($p < 0.05$), there was no obvious trend in serum clearance values. This result was due to the

Table IV—Values of Pharmacokinetic Parameters

Parameter	Subject							
	1	2	3	4	5	6(a)	6(b)	7
α, hr^{-1}	1.7	0.8	1.4	1.6	2.1	1.2	0.4	0.2
β, hr^{-1}	0.36	0.34	0.35	0.29	0.23	0.33	0.18	0.01
$t_{1/2(elim)}$, hr	1.9	2.0	2.0	2.4	3.0	2.1	3.9	7.0
k_{12}, hr^{-1}	0.34	0.07	0.34	0.52	0.94	0.24	0.05	0.01
k_{21}, hr^{-1}	1.25	0.42	0.59	0.64	0.74	0.51	0.39	0.13
k_{e1}, hr^{-1}	0.49	0.63	0.87	0.71	0.66	0.80	0.30	0.14
V_1, %[a]	45	54	60	50	61	58	83	101
$V_{d(ss)}$[b], %	57	63	95	90	138	85	93	143
Cl_P[c], ml/min	275	428	452	453	502	525	285	141
Cl_R[d], ml/min	21	20	47	1.6	<1.0	<1.0	<1.0	<1.0
r^2[e]	+0.998	+0.991	+0.998	+0.999	+0.998	+0.989	+0.981	+0.992

[a] Calculated from V_1 = dose/$(A + B)$, where A and B are the intercepts on the y ordinate of the fast (α) and slow (β) segments of the biphasic plasma drug decay profile, expressed as percent of total body weight. [b] Overall apparent distribution volume: $V_{d(ss)} = V_1(k_{12} + k_{21})/k_{21}$. [c] Plasma clearance, calculated from $V_1 k_{e1}$. [d] Renal clearance of microbiologically active erythromycin. [e] Coefficient of determination: $(\Sigma obs^2 - \Sigma dev^2)/\Sigma obs^2$.

minor contribution of renal clearance to the overall erythromycin elimination and also to the compensating influences of increasing distribution volumes with decreasing elimination rate constants, both of which are involved in the calculation of serum clearance.

DISCUSSION

The changes in erythromycin elimination characteristics associated with the varying renal function observed support previous contentions that clearance of this antibiotic from the circulation is generally not influenced markedly by renal impairment (3, 4). The regression of β *versus* creatinine clearance was described by the linear expression $y = 0.21 + 0.001x$ ($r = +0.74$, $p < 0.05$), which is numerically similar to the expression reported previously (4); the linear regression of k_{el} *versus* creatinine clearance was described by $y = 0.49 + 0.002x$ ($r = +0.36$, $p > 0.05$).

The large distribution volumes (Table IV) are consistent with reported extensive tissue penetration of erythromycin (7–10). The apparent increase in distribution with decreasing renal function was possibly due to the displacement of this highly protein-bound drug from serum proteins in renal failure, resulting in a larger proportion of drug distributing into extravascular tissues. This phenomenon was demonstrated previously for a number of highly protein-bound drugs both *in vivo* (11, 12) and *in vitro* (13). Application of this concept to erythromycin needs to be verified since protein binding was not measured in the present study.

Although extensive tissue distribution by erythromycin is confirmed by the present data, the degree of tissue penetration is probably considerably underestimated. Drug bound to circulating proteins is not immediately available for extravascular distribution and, provided the drug is not bound to other tissues, the drug concentration in extravascular fluids tends to equilibrate with the concentration of free drug in serum. If the distribution volumes are calculated on this basis, and circulating drug is assumed to be approximately 90% protein bound (14), then calculated volumes are approximately 10 times greater than those given in Table IV. Since erythromycin is sequestered by certain tissues (7) and since there is no information on tissue binding of erythromycin, its true distribution volume cannot be calculated with any accuracy.

Although the calculated distribution volumes in Table IV may be underestimates of true values, they are reasonably consistent among normal individuals (Subjects 1–3) and may thus provide a basis for calculating absolute absorption efficiencies from oral doses of erythromycin or its salts.

REFERENCES

(1) J. B. Hammond and R. S. Griffith, *Clin. Pharm. Ther.*, **2**, 308 (1961).

(2) R. S. Griffith, D. M. Johnstone, and J. W. Smith, *Antibiot. Annu.*, **1953–1954**, 496.

(3) C. M. Kunin and M. Finland, *J. Clin. Invest.*, **38**, 1509 (1959).

(4) P. G. Welling, W. A. Craig, and C. M. Kunin, *Clin. Pharmacol. Ther.*, **18**, 45 (1975).

(5) P. G. Welling, W. R. Shaw, S. J. Uman, F. L. S. Tse, and W. A. Craig, *Antimicrob. Agents Chemother.*, **8**, 532 (1975).

(6) J. G. Wagner, "Fundamentals of Clinical Pharmacokinetics," Drug Intelligence Publications, Hamilton, Ill., 1975, p. 100.

(7) C.-C. Lee, R. C. Anderson, and K. K. Chen, *Antibiot. Chemother.*, **3**, 920 (1953).

(8) C.-C. Lee and R. O. Froman, *ibid.*, **11**, 107 (1960).

(9) R. H. Parker, *Mod. Treatment*, **6**, 1071 (1969).

(10) D. G. Winningham, N. J. Nemoy, and T. A. Stamey, *Nature*, **219**, 139 (1968).

(11) P. G. Welling, W. A. Craig, G. L. Amidon, and C. M. Kunin, *J. Infect. Dis., Suppl.*, **128**, S556 (1973).

(12) P. G. Welling, W. A. Craig, G. L. Amidon, and C. M. Kunin, *Clin. Pharmacol. Ther.*, **15**, 344 (1974).

(13) W. A. Craig, P. G. Welling, J. P. Wagnild, and C. M. Kunin, *Proc. 8th Int. Congr. Chemother., Athens*, **1973**, 722.

(14) R. G. Wiegand and A. H. C. Chun, *J. Pharm. Sci.*, **61**, 425 (1972).

Physicochemical Properties of Amphoteric β-Lactam Antibiotics I: Stability, Solubility, and Dissolution Behavior of Amino Penicillins as a Function of pH

AKIRA TSUJI, EMI NAKASHIMA, SHOICHIRO HAMANO, and TSUKINAKA YAMANA ˣ

Received August 22, 1977, from the *Faculty of Pharmaceutical Sciences, Kanazawa University, Takara-machi, Kanazawa 920, Japan.* Accepted for publication November 16, 1977.

Abstract □ The degradation rate, solubility, and dissolution rate of amino penicillins, amoxicillin, ampicillin, epicillin, and cyclacillin, were determined quantitatively as a function of pH. In the pH range studied, 0.30–10.50, the degradation of amoxicillin and epicillin followed pseudo-first-order kinetics to give the same type of pH–rate profiles as those of ampicillin and cyclacillin. Cyclacillin anhydrate was the most soluble, followed in order by ampicillin anhydrate, ampicillin trihydrate, amoxicillin trihydrate, and epicillin anhydrate. These pH–solubility profiles showed U-shaped curves. The dissolution rate constants from the rotating disk were analyzed by the simultaneous chemical reaction and diffusion models. Their relative bioavailability after a single oral administration was assessed from their physicochemical properties determined *in vitro*.

Keyphrases □ Penicillins, various amino—stability, solubility, and dissolution rates, effect of pH □ Stability—various amino penicillins, effect of pH □ Solubility—various amino penicillins, effect of pH □ Dissolution rates—various amino penicillins, effect of pH □ Antibacterials—various amino penicillins, stability, solubility, and dissolution rates, effect of pH

Amphoteric penicillins like ampicillin, amoxicillin, cyclacillin, and epicillin exhibit a broad spectrum of antibacterial activity, are very acid stable, and are used orally (1). After a single equal oral dose, the peak serum concentration was four times higher for cyclacillin (2) and two times higher for amoxicillin (3–6) than for ampicillin; the peak for epicillin was significantly lower (6).

The physicochemical properties and GI membrane permeabilities of these amphoteric penicillins may cause significant differences in their serum concentrations. An

0022-3549/78/0800-1059$01.00/0

© 1978, American Pharmaceutical Association

minor contribution of renal clearance to the overall erythromycin elimination and also to the compensating influences of increasing distribution volumes with decreasing elimination rate constants, both of which are involved in the calculation of serum clearance.

DISCUSSION

The changes in erythromycin elimination characteristics associated with the varying renal function observed support previous contentions that clearance of this antibiotic from the circulation is generally not influenced markedly by renal impairment (3, 4). The regression of β *versus* creatinine clearance was described by the linear expression $y = 0.21 + 0.001x$ ($r = +0.74$, $p < 0.05$), which is numerically similar to the expression reported previously (4); the linear regression of k_{el} *versus* creatinine clearance was described by $y = 0.49 + 0.002x$ ($r = +0.36$, $p > 0.05$).

The large distribution volumes (Table IV) are consistent with reported extensive tissue penetration of erythromycin (7–10). The apparent increase in distribution with decreasing renal function was possibly due to the displacement of this highly protein-bound drug from serum proteins in renal failure, resulting in a larger proportion of drug distributing into extravascular tissues. This phenomenon was demonstrated previously for a number of highly protein-bound drugs both *in vivo* (11, 12) and *in vitro* (13). Application of this concept to erythromycin needs to be verified since protein binding was not measured in the present study.

Although extensive tissue distribution by erythromycin is confirmed by the present data, the degree of tissue penetration is probably considerably underestimated. Drug bound to circulating proteins is not immediately available for extravascular distribution and, provided the drug is not bound to other tissues, the drug concentration in extravascular fluids tends to equilibrate with the concentration of free drug in serum. If the distribution volumes are calculated on this basis, and circulating drug is assumed to be approximately 90% protein bound (14), then calculated volumes are approximately 10 times greater than those given in Table IV. Since erythromycin is sequestered by certain tissues (7) and since there is no information on tissue binding of erythromycin, its true distribution volume cannot be calculated with any accuracy.

Although the calculated distribution volumes in Table IV may be underestimates of true values, they are reasonably consistent among normal individuals (Subjects 1–3) and may thus provide a basis for calculating absolute absorption efficiencies from oral doses of erythromycin or its salts.

REFERENCES

(1) J. B. Hammond and R. S. Griffith, *Clin. Pharm. Ther.*, **2**, 308 (1961).

(2) R. S. Griffith, D. M. Johnstone, and J. W. Smith, *Antibiot. Annu.*, **1953–1954**, 496.

(3) C. M. Kunin and M. Finland, *J. Clin. Invest.*, **38**, 1509 (1959).

(4) P. G. Welling, W. A. Craig, and C. M. Kunin, *Clin. Pharmacol. Ther.*, **18**, 45 (1975).

(5) P. G. Welling, W. R. Shaw, S. J. Uman, F. L. S. Tse, and W. A. Craig, *Antimicrob. Agents Chemother.*, **8**, 532 (1975).

(6) J. G. Wagner, "Fundamentals of Clinical Pharmacokinetics," Drug Intelligence Publications, Hamilton, Ill., 1975, p. 100.

(7) C.-C. Lee, R. C. Anderson, and K. K. Chen, *Antibiot. Chemother.*, **3**, 920 (1953).

(8) C.-C. Lee and R. O. Froman, *ibid.*, **11**, 107 (1960).

(9) R. H. Parker, *Mod. Treatment*, **6**, 1071 (1969).

(10) D. G. Winningham, N. J. Nemoy, and T. A. Stamey, *Nature*, **219**, 139 (1968).

(11) P. G. Welling, W. A. Craig, G. L. Amidon, and C. M. Kunin, *J. Infect. Dis., Suppl.*, **128**, S556 (1973).

(12) P. G. Welling, W. A. Craig, G. L. Amidon, and C. M. Kunin, *Clin. Pharmacol. Ther.*, **15**, 344 (1974).

(13) W. A. Craig, P. G. Welling, J. P. Wagnild, and C. M. Kunin, *Proc. 8th Int. Congr. Chemother., Athens*, **1973**, 722.

(14) R. G. Wiegand and A. H. C. Chun, *J. Pharm. Sci.*, **61**, 425 (1972).

Physicochemical Properties of Amphoteric β-Lactam Antibiotics I: Stability, Solubility, and Dissolution Behavior of Amino Penicillins as a Function of pH

AKIRA TSUJI, EMI NAKASHIMA, SHOICHIRO HAMANO, and TSUKINAKA YAMANA ˣ

Received August 22, 1977, from the *Faculty of Pharmaceutical Sciences, Kanazawa University, Takara-machi, Kanazawa 920, Japan.* Accepted for publication November 16, 1977.

Abstract □ The degradation rate, solubility, and dissolution rate of amino penicillins, amoxicillin, ampicillin, epicillin, and cyclacillin, were determined quantitatively as a function of pH. In the pH range studied, 0.30–10.50, the degradation of amoxicillin and epicillin followed pseudo-first-order kinetics to give the same type of pH–rate profiles as those of ampicillin and cyclacillin. Cyclacillin anhydrate was the most soluble, followed in order by ampicillin anhydrate, ampicillin trihydrate, amoxicillin trihydrate, and epicillin anhydrate. These pH–solubility profiles showed U-shaped curves. The dissolution rate constants from the rotating disk were analyzed by the simultaneous chemical reaction and diffusion models. Their relative bioavailability after a single oral administration was assessed from their physicochemical properties determined *in vitro*.

Keyphrases □ Penicillins, various amino—stability, solubility, and dissolution rates, effect of pH □ Stability—various amino penicillins, effect of pH □ Solubility—various amino penicillins, effect of pH □ Dissolution rates—various amino penicillins, effect of pH □ Antibacterials—various amino penicillins, stability, solubility, and dissolution rates, effect of pH

Amphoteric penicillins like ampicillin, amoxicillin, cyclacillin, and epicillin exhibit a broad spectrum of antibacterial activity, are very acid stable, and are used orally (1). After a single equal oral dose, the peak serum concentration was four times higher for cyclacillin (2) and two times higher for amoxicillin (3–6) than for ampicillin; the peak for epicillin was significantly lower (6).

The physicochemical properties and GI membrane permeabilities of these amphoteric penicillins may cause significant differences in their serum concentrations. An

0022-3549/78/0800-1059$01.00/0

© 1978, American Pharmaceutical Association

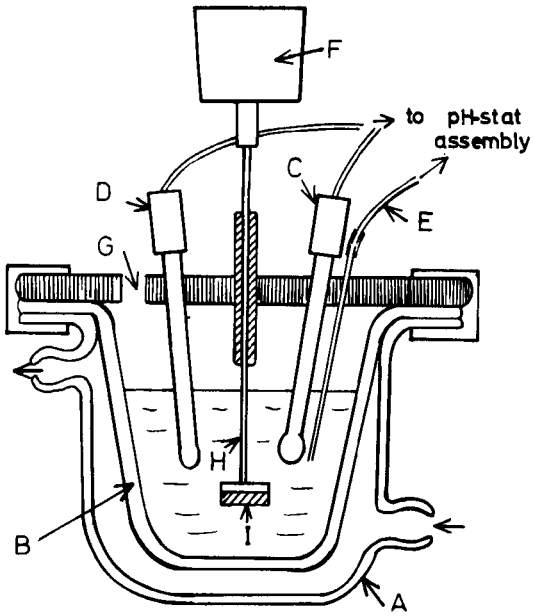

Figure 1—*Apparatus for determination of dissolution rates as a function of solution pH. Key: A, thermostated jacket; B, dissolution vessel; C, glass electrode; D, calomel electrode; E, titration buret; F, speed-controllable synchronous motor; G, sampling hole; H, rotating shaft assembly; and I, sample disk.*

enhanced bioavailability of anhydrous ampicillin compared with the trihydrated product was claimed to be due to its greater solubility and dissolution rate in distilled water (7). Hou and Poole (8) suggested that the rapid attainment of a higher serum level of cyclacillin than ampicillin is related to the difference in their solubilities. A reduction of dose water volume from 250 to 25 ml markedly decreased the serum amoxicillin level, but the ampicillin level was affected only to a small extent (9). This difference was explained by the difference in their water solubility (9).

The literature concerning the comparative absorption properties of the anhydrate and trihydrate forms of ampicillin is conflicting. Recently, Hill *et al.* (10) suggested that ampicillin absorption is not dissolution rate limiting, this suggestion being inconsistent with the previous claim of Poole *et al.* (7).

The objectives of this study were to compare quantitatively the stability, solubility, and dissolution behavior of several amphoteric penicillins as a function of solution pH and to assess the role of physicochemical properties affecting their relative bioavailabilities. The degradation kinetics (11, 12) and pH-dependent solubility (8) of some β-lactam antibiotics were studied extensively previously, but not those of amoxicillin and epicillin. The kinetics of the dissolution of all amino penicillins in the whole pH region have not been studied.

EXPERIMENTAL

Materials—Ampicillin sodium[1] (955 μg/mg), ampicillin anhydrate[1] (1015 μg/mg), ampicillin trihydrate[2] (pure powder), amoxicillin trihydrate[3] (850 μg/mg), cyclacillin anhydrate[1] (999 μg/mg), epicillin sodium[2] (pure powder), and epicillin anhydrate[2] (pure powder) were used as supplied.

[1] Takeda Chemical Industries, Osaka, Japan.
[2] Sankyo Co., Tokyo, Japan.
[3] Fujisawa Pharmaceutical Co., Osaka, Japan.

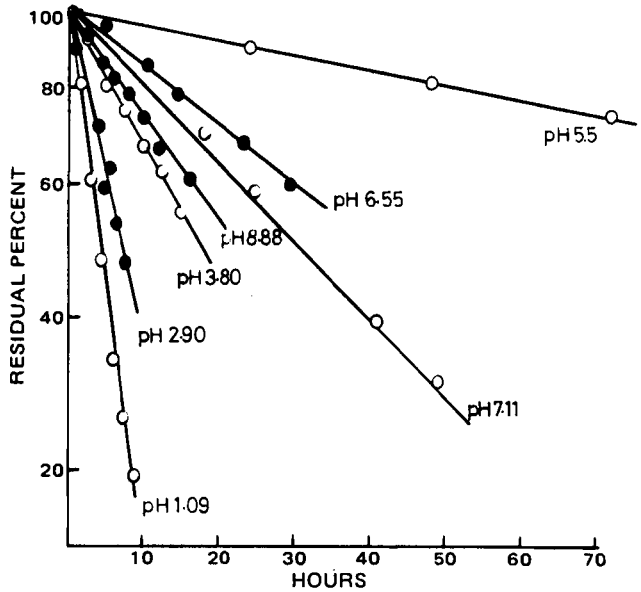

Figure 2—*First-order plots for the degradation of amoxicillin* (○) *and epicillin* (●) *in the buffers of various pH values at 35° and μ = 0.5.*

All other chemicals were reagent grade and were used without further purification.

Procedures—*pKa Determination*—The apparent pKa values of the amphoteric penicillins were determined by potentiometric titration (13) at an ionic strength of 0.5 at 35 and 37°. Twenty milliliters of 1.0×10^{-2} *M* penicillin, adjusted with potassium chloride to a constant ionic strength of 0.5, was titrated[4] with 0.2 *N* HCl (μ = 0.5 with potassium chloride) or 0.2 *N* KOH (μ = 0.5 with potassium chloride). The apparent pKa values of the amphoteric penicillins were computed, from the pH change[5] and the volume of the titrant added, by the equation of Glasstone and Hammel (14).

The values obtained from at least three experiments are listed in Tables I and II, where pK_1 and pK_2 refer to the dissociation of the 3-carboxylic acid and α-amino groups, respectively. The value of pK_3 for the phenolic group of amoxicillin was determined spectrophotometrically (13). The calculation was made from the change in absorbance[6] at 245 nm for 7.50×10^{-5} *M* amoxicillin, adjusted to 0.5 μ with potassium chloride, at various pH values and 37° to give $pK_3 = 9.55 \pm 0.04$.

Solubility—The procedure employed was essentially the same as that described by Hou and Poole (8). Excess penicillin powder was added to a glass-stoppered flask, followed by addition of 0.5 *M* KCl aqueous solution adjusted to the appropriate pH with standard hydrochloric acid or potassium hydroxide solution. The flask was placed in a constant-temperature bath at 37° and mechanically shaken for 2 hr. A sample was taken through a 0.45-μm membrane filter[7], the pH value was measured, and the sample was assayed after appropriate dilution, if necessary, with distilled water.

Amino penicillins were determined by iodometric titration (11) and by UV spectrophotometric measurement at 260 nm for ampicillin and amoxicillin and at 250 nm for epicillin. The penicillin concentration was calculated from respective calibration curves obtained earlier.

Determination of Degradation Rates—The kinetic studies of amoxicillin and epicillin were carried out in the same way as a similar study on ampicillin (11). Degradation was initiated by the addition of a known weight of amoxicillin or epicillin sodium to a buffer solution of 0.5 μ (with potassium chloride), which was preheated to 35°, to make a final concentration of 5×10^{-3} *M*. When the half-life was more than 1 day, the solution was sealed in a 5-ml ampul.

The residual concentration was analyzed by the iodometric titration method described for ampicillin (11). When the solution pH was maintained by means of a pH-stat[8] during the kinetic study, 0.5 *M* KCl

[4] Radiometer ABU12b autoburet, Copenhagen, Denmark.
[5] Radiometer PHM26 pH meter, Copenhagen, Danmark.
[6] Shimadzu UV200S double-beam recording spectrophotometer, Kyoto, Japan.
[7] Sartorius membrane filter GmbH, Göttingen, Germany.
[8] Radiometer pH stat-titrimeter assembly consisting of TTT11 titrator, PHM26 pH meter, and ABU12b autoburet, Copenhagen, Denmark.

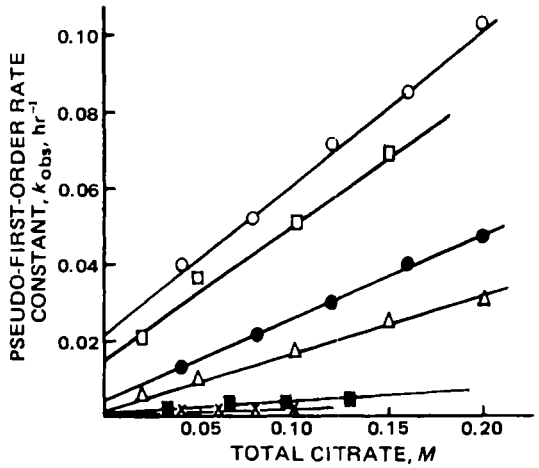

Figure 3—*Plots of the pseudo-first-order rate constant* versus *total citrate buffer concentrations for the degradation of amoxicillin at 35° and μ = 0.5. Key;* ○, *pH 2.80;* □, *pH 3.13;* ●, *pH 3.80;* △, *pH 4.23;* ■, *pH 5.50; and* ×, *pH 6.80.*

aqueous solution containing 1×10^{-4} *M* edetate disodium was used. Edetate disodium was added to avoid possible heavy metal-catalyzed degradation.

The pseudo-first-order rate constants, k_{obs}, were obtained by the least-squares method.

Determination of Dissolution Rates—The procedure for following the dissolution from a rotating disk was similar to that of Nogami *et al.* (15), except for the pH control technique. Figure 1 is a schematic representation of the rotating-disk dissolution apparatus. It consists of four main parts: the outside water-jacketed beaker maintained at 37 ± 0.05°, a stainless steel rotating shaft, a controllable synchronous motor, and pH electrodes. The tip of the titrant delivery tube is connected to the pH-stat assembly.

Disks of 200 mg and 1.0-cm diameter were prepared by compression of the crystals at about 120 kg/cm² in a compression punch-die assembly. When the samples were compressed, phase conversion was not observed from their IR spectra. The disk was stuck to the rotating shaft with an adhesive.

The solutions were sampled periodically, followed by the immediate addition of the same volume of 0.5 *M* KCl, preheated to 37°. The samples were analyzed by the iodometric method and/or by UV spectrophotometry. The penicillin concentration dissolved at each sampling time was corrected for dilution according to:

$$C = C_n^{app} + \sum_{n=1}^{n-1} \frac{V_n^s}{V_T} C_n^{app} \qquad \text{(Eq. 1)}$$

where C_n^{app} and C represent apparent and true concentrations dissolved at the nth sampling time, respectively; and V_T and V_n^s are the volumes of bulk solution and of sampling, respectively.

In most cases, the dissolution medium was recirculated by a peristaltic pump through a 1-cm path length flowcell in a double-beam UV spectrophotometer[6], and the increase in absorbance at 260 nm for ampicillin and amoxicillin and at 250 nm for cyclacillin and epicillin was recorded to give a continuous plot of the amount dissolved *versus* time.

Determination of Diffusion Coefficient—The method was that employed by Goldberg and Higuchi (16), except for the use of a cellulose membrane[9] instead of a silver membrane and two 50-ml conical flasks instead of two 150-ml flasks. The 0.5 *M* KCl containing a penicillin (1×10^{-2} *M*) was placed in one compartment (A) up to the stopcock, while almost the same volume of 0.5 *M* KCl was added to the other compartment (B). The entire cell was then immersed in a constant-temperature water bath.

The solution in Compartment B was stirred with a magnetic stirrer and recirculated for the continuous UV determination by the same procedure used for the dissolution study. The potassium chloride solution was treated to remove air prior to the experiments.

The cell constant was determined at 30 and 37° using 0.5 *M* KCl. The diffusion coefficient of sulfonamide was determined by this apparatus to be 1.28×10^{-5} cm²/sec, in good agreement with the reported value of 1.29×10^{-5} cm²/sec (17).

[9] Visking Co.

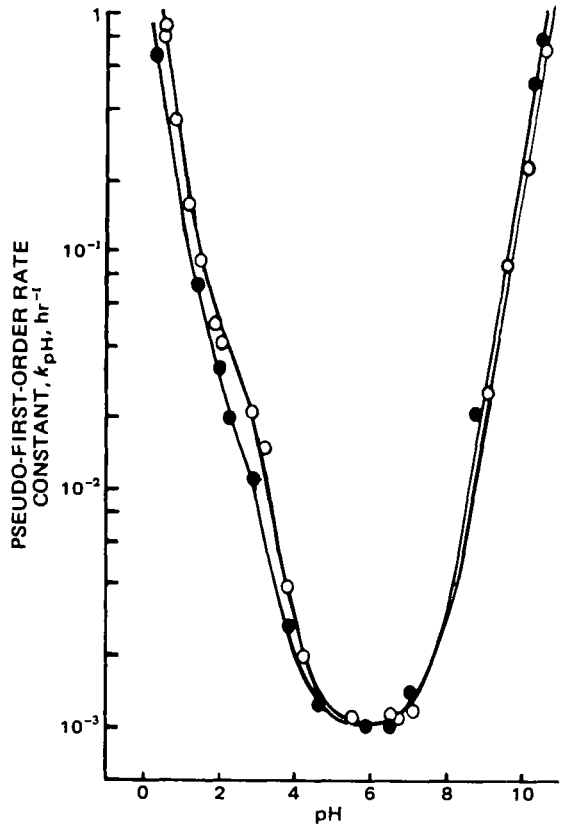

Figure 4—*Log k_{pH}–pH profiles for the degradation of amoxicillin* (○) *and epicillin* (●) *at 35° and μ = 0.5. The points are experimental values. The solid curves were generated from Eq. 2 and parameters listed in Table I.*

RESULTS

Degradation Rate–pH Profiles—The kinetics and mechanism of the degradation of amphoteric penicillins such as ampicillin (11) and cyclacillin (12) were reported previously. At constant pH and with excess buffer, the degradation of amoxicillin and epicillin at a low concentration of 5×10^{-3} *M* followed first-order kinetics (Fig. 2). As observed for ampicillin and cyclacillin, β-lactam cleavage of amoxicillin and epicillin was subjected to general acid–base catalyses. Typical plots of the citrate buffer catalytic effect on the rate of amoxicillin are shown in Fig. 3; a straight line was obtained at every pH. Extrapolation of such plots to zero-buffer concentration provides, as the intercepts, the values of pseudo-first-order rate constants, k_{pH}, corresponding to the non-buffer-catalyzed degradation of β-lactams. The k_{pH} values also were determined by the use of a pH-stat.

The pH dependence curves of k_{pH} of amoxicillin and epicillin are illustrated in Fig. 4, showing the same shape as those for ampicillin (11) and cyclacillin (12). Since there is no break near pK_3 of the log k_{pH}–pH profile of amoxicillin, the dissociation of the phenolic moiety apparently has no effect, as expected, on the β-lactam cleavage.

The rate expression given in Eq. 2 holds for amoxicillin and epicillin, based on the previous claim (12, 18) that the reactive species of penicillins

Table I—Rate Constants[a] for the Degradation of Amino Penicillins and Dissociation Constants at 35° and μ = 0.5

Amino Penicillin	k_H, M^{-1} hr^{-1}	$10^2 k_0$, hr^{-1}	$10^3 k_0'$, hr^{-1}	$10^{-3} k_{OH}$, M^{-1} hr^{-1}	pK_1[b]	pK_2[b]	pK_3[c]
Amoxicillin	1.68	4.19	1.00	1.16	2.63	7.16	9.55
Ampicillin[d]	1.82	5.56	0.750	2.57	—	—	—
Epicillin	1.35	2.08	0.969	1.23	2.77	7.17	—
Cyclacillin[e]	4.61	4.33	2.49	1.10	—	—	—

[a] Rate constants are defined by Eq. 2 and obtained by the least squares analysis. The K_w value used for the calculation was 2.09×10^{-14} at 35° and μ = 0.5 (26). [b] Determined by the potentiometric method. [c] Determined by the UV spectrophotometric method at 37° and μ = 0.5. [d] Values were recalculated according to Eq. 2 for the data reported by Hou and Poole (11). [e] Values were recalculated according to Eq. 2 for the data reported by Yamana *et al.* (12).

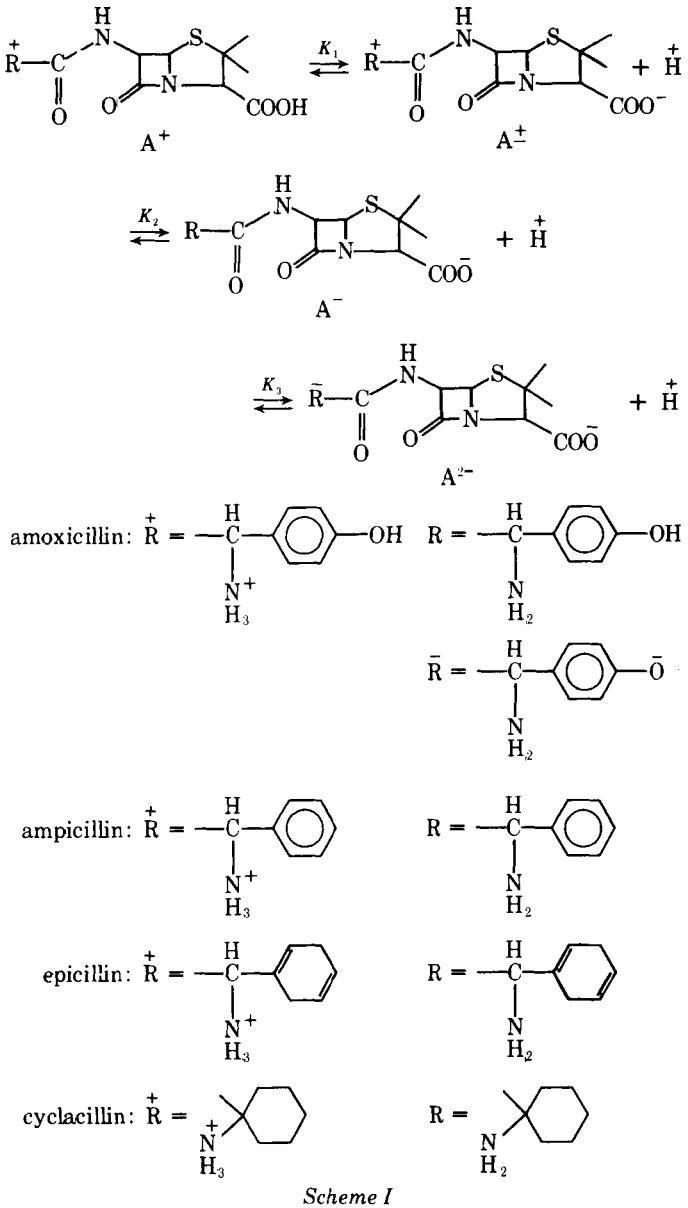

Scheme I

for acid-catalyzed and spontaneous degradations is one with the undissociated 3-carboxylic acid moiety:

$$k_{pH} = (k_H a_{H^+} + k_0)f_{A^+} + (k_0' + k_{OH'}K_w/a_{H^+})(f_{A^\pm} + f_{A^-}) \quad \text{(Eq. 2)}$$

where k_H and k_0 are the second-order rate constant for hydrogen-ion-catalyzed degradation and the first-order rate constant for spontaneous degradation of the cationic species, respectively; k_0' and $k_{OH'}$ are the first- and second-order rate constants for the respective spontaneous and hydroxide-ion-catalyzed degradations of species other than the cationic one, respectively; f_{A^+}, $f_{A^\pm}$, and f_{A^-} represent the mole fractions of the cationic, zwitterionic, and anionic species of amphoteric penicillins, respectively (Scheme I); and K_w is the autoprotolytic constant.

Table I lists these rate constants calculated from the least-squares analysis of the present data for amoxicillin and epicillin, together with the reestimated parameters according to the present kinetic expression of Eq. 2 for ampicillin (11) and cyclacillin (12).

Solubility–pH Profile—The pH–solubility behavior of ampicillin and cyclacillin was studied previously in aqueous buffer solution at 25° and μ = 0.5 (8). For a quantitative comparison of the relative solubility of amphoteric penicillins, the pH–apparent solubility profiles were determined under physiological temperature conditions for these two penicillins and also for amoxicillin and epicillin. The results (Fig. 5) indicate U-shaped pH–solubility curves, with the minimum solubility at the pH near the isoelectric point as observed previously (8).

If the intrinsic solubility of the amphoteric penicillins is due to the solubility, C_0, of the electrically neutral zwitterion ($A^\pm$ in Scheme I), the

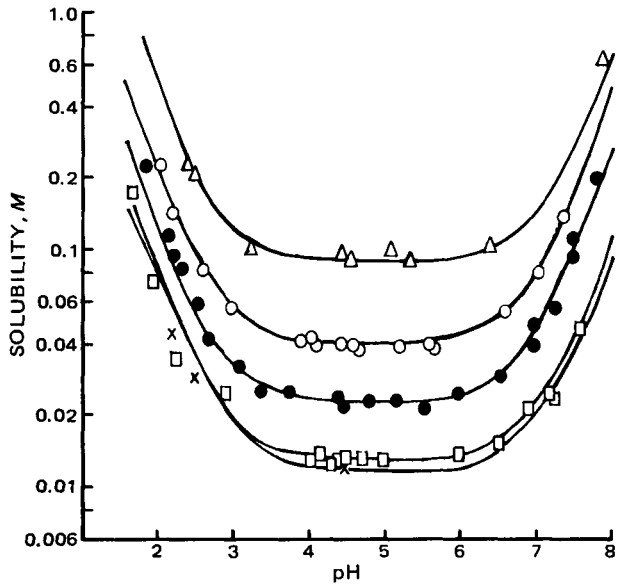

Figure 5—*Solubility–pH profiles of amino penicillins at 37° and μ = 0.5. The points are experimental values. The solid curves were generated from Eq. 3 and parameters listed in Table II. Key; △, cyclacillin anhydrate; ○, ampicillin anhydrate; ●, ampicillin trihydrate; □, amoxicillin trihydrate; and ×, epicillin anhydrate.*

total solubility, C_T, as a function of the solution pH can be expressed as:

$$C_T = C_0\left(\frac{a_{H^+}}{K_1} + 1 + \frac{K_2}{a_{H^+}}\right) \quad \text{(Eq. 3)}$$

The C_0 values estimated from the solubility at the isoelectric point and the dissociation constants under the experimental conditions (37° and μ = 0.5) are listed in Table II. The values of C_0 for ampicillin anhydrate, its trihydrate, and cyclacillin were in good agreement with those in distilled water (10, 19, 20) (Table II). The theoretical curves generated from Eq. 3 fit reasonably the experimental points for all amino penicillins (Fig. 5).

Over the entire pH range investigated, cyclacillin anhydrate was the most soluble and epicillin anhydrate exhibited the lowest solubility, with a sevenfold difference between them. Amoxicillin trihydrate was one-half as soluble as ampicillin trihydrate, which provided an inverse relationship in their comparative serum levels after oral administration (3–6).

The apparent equilibrium solubilities of amoxicillin were determined at 20–50°. Classical van't Hoff plots gave a reasonably good linear relationship (Fig. 6). The value of the heat of solution was calculated from the slope to be 6.2 kcal/mole, being comparable with the 5.4 kcal/mole value reported for ampicillin trihydrate (19).

Dissolution Rates—*Kinetics*—Figure 7 shows typical plots of the concentration, C, of penicillins dissolved *versus* time, t. In all cases, these plots were reasonably linear at an early stage of dissolution, indicating that dissolution follows zero-order kinetics:

$$\left(\frac{dC}{dt}\right)_0 = \frac{S}{V}k_T \quad \text{(Eq. 4)}$$

where S is the area of the solid surface exposed to the solvent, V is the volume of the bulk solution, and k_T is the dissolution rate constant. As shown in Fig. 8, the relationship between the dissolution rate for the unit

Table II—Intrinsic Solubilities and Dissociation Constants of Amino Penicillins at 37° and μ = 0.5

Amino Penicillin	Molecular Weight	Solubility[a], $10^2 C_0$, M	Dissociation Constant pK_1[b]	pK_2[b]	pK_3[c]
Amoxicillin trihydrate	419.4	1.30	2.67	7.11	9.55
Ampicillin anhydrate	349.4	3.97	2.67	6.95	—
Ampicillin trihydrate	403.4	2.23	—	—	—
Epicillin anhydrate	351.4	1.20	2.77[d]	7.17[d]	—
Cyclacillin anhydrate	341.4	8.90	2.64	7.18	—

[a] Defined by Eq. 3. [b] Determined by the potentiometric method. [c] Determined by the UV spectrophotometric method. [d] Determined at 35°.

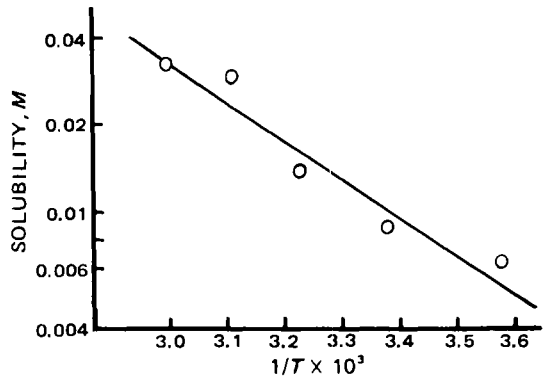

Figure 6—*Plots of the solubility of amoxicillin trihydrate in 0.5 M KCl versus a reciprocal of absolute temperature.*

surface area, $(dC/dt)_0/S$, obtained from the slope of these plots and a reciprocal of V from 20 to 200 ml provided straight lines through the origin in accordance with Eq. 4. With a constant speed of rotation, disk surface area, volume of dissolution medium, and temperature, analyses both by the sampling method and the direct flowcell method gave consistent dissolution rates that were not influenced significantly by the change in the dissolution vessel (Fig. 7).

When the dissolution rate constants, k_T, calculated according to Eq. 4, in 0.5 M KCl were plotted against the square root of the speed of rotation, a good linear relationship was obtained for all antibiotics (Fig. 9). If these dissolution processes from the rotating disk follow the rate-limiting diffusion, the dissolution rate constants can be predicted theoretically as (21):

$$k_T = 0.620D^{2/3}\nu^{-1/6}\omega^{1/2}C_0 \qquad \text{(Eq. 5)}$$

where D is the diffusion coefficient of a drug, ν is the kinematic viscosity of the dissolution medium, and ω is the angular velocity of rotation. With $\nu = 6.99 \times 10^{-3}$ cm²/sec (15) and the values of C_0 listed in Table II, the diffusion coefficients of the amino penicillins in 0.5 M KCl can be calculated from the respective slopes in Fig. 9 according to Eq. 5. The D values thus evaluated (Table III) were in fair agreement with those determined from the diffusion cell method (see *Experimental*). The present value for ampicillin was close to D (25°) = 4.58×10^{-6} cm/sec reported by Padfield and Kellaway (22).

These results strongly indicate that the dissolution of amphoteric penicillins into neutral pH solution is essentially controlled by diffusion of their zwitterionic molecules saturated near the surface of the disk.

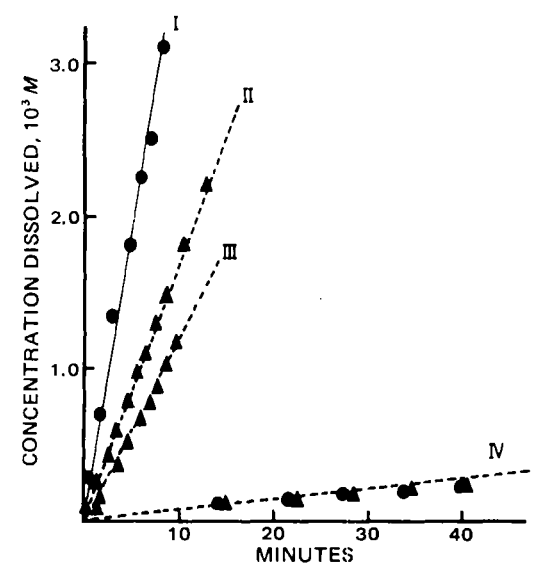

Figure 7—*Dissolution of amino penicillins into 0.5 M KCl at 228 rpm and 37° using the rotating-disk method. Key: cyclacillin anhydrate, I; ampicillin anhydrate, II; ampicillin trihydrate, III; amoxicillin trihydrate, IV; ●, analyzed by iodometry; and ▲, analyzed by UV spectrophotometry. Dotted lines represent the results from the continuous UV determination by means of the flowcell.*

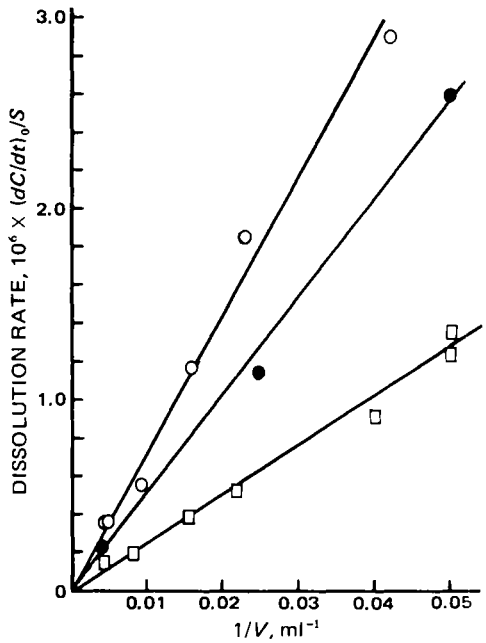

Figure 8—*Plots of the dissolution rate of amoxicillin trihydrate (□), ampicillin trihydrate (●), and ampicillin anhydrate (○) from the unit surface area, $(dC/dt)_0/S$, versus the reciprocal of the volume of the dissolution medium at 228 rpm, 37°, and $\mu = 0.5$.*

Theoretical Consideration of pH-Dependent Dissolution Rate—Dissolution rate constants, k_T, were determined as a function of the bulk solution pH at 228 rpm, 37°, and $\mu = 0.5$ (Fig. 10). The dissolution rate constants increased linearly in an acidic medium below pH 3. Beyond this pH, the rate constants were invariable for every penicillin. These phenomena are consistent with the results obtained for ampicillin by Hill *et al.* (10), who reported that the intrinsic dissolution rates were 10 times

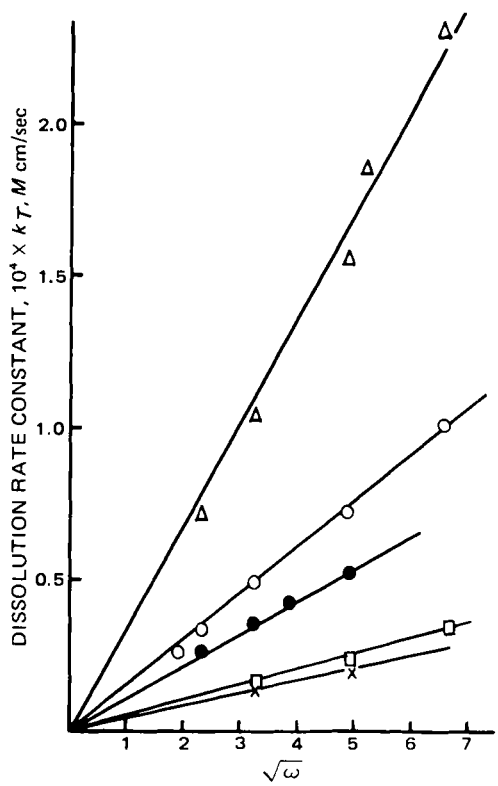

Figure 9—*Effect of stirring speed, $\sqrt{\omega}$, on the dissolution rate of amino penicillins in 0.5 M KCl at 37°. Key: △, cyclacillin anhydrate; ○, ampicillin anhydrate; ●, ampicillin trihydrate; □, amoxicillin trihydrate; and ×, epicillin anhydrate.*

Table III—Theoretical Equations [a] for the Dissolution Rate Constants at 228 rpm and Diffusion Coefficients of Amino Penicillins at 37° and $\mu = 0.5$

Amino Penicillin	Theoretical Equations[b], k_T (theor.), M cm/sec	Diffusion Coefficients, $10^6 \times D$, cm²/sec: Dissolution Rate[c]	Diffusion Cell[d]
Amoxicillin trihydrate	$7.03 \times 10^{-3}(a_{H^+})_h + 2.58 \times 10^{-5} + 1.41 \times 10^{-2}(a_{OH^-})_h$	4.84	3.71
Ampicillin anhydrate	$1.16 \times 10^{-2}(a_{H^+})_h + 7.29 \times 10^{-5} + 1.46 \times 10^{-2}(a_{OH^-})_h$	4.31	4.57
Ampicillin trihydrate	$1.03 \times 10^{-2}(a_{H^+})_h + 5.22 \times 10^{-5} + 1.29 \times 10^{-2}(a_{OH^-})_h$	6.20	4.60
Epicillin anhydrate	$7.05 \times 10^{-3}(a_{H^+})_h + 1.90 \times 10^{-5} + 1.58 \times 10^{-2}(a_{OH^-})_h$	3.45	4.60
Cyclacillin anhydrate	$1.41 \times 10^{-2}(a_{H^+})_h + 1.66 \times 10^{-4} + 1.45 \times 10^{-2}(a_{OH^-})_h$	4.41	4.54

[a] Equation 6. [b] Calculated from Eqs. 6 and 7 with the parameters listed in Tables II and III and those cited in the text. [c] Determined in 0.5 M KCl and used for the calculation of Eqs. 6 and 7. [d] Determined in 0.5 M KCl by means of the diffusion cell apparatus described in the text.

faster in 0.053 N HCl than in distilled water. The rank order of dissolution rates among penicillins was similar to that of their solubilities, but there was a clear difference in the shapes between these two pH profiles.

The complicated and pH-dependent dissolution behavior of amphoteric penicillins can be interpreted by the diffusion layer theory, predicted in terms of: (*a*) drug transfer from a nondisintegrated disk to an aqueous diffusion layer saturated with the drug, (*b*) transfer of the drug from the diffusion layer to the bulk medium, and (*c*) back-diffusion of hydrogen and hydroxide ions and rapid dissociation equilibrium. Scheme II describes qualitatively the steady-state situation of these dissolution processes. The theory leads to Eq. 6 for the steady-state dissolution rate constants of amphoteric penicillins under the sink conditions (see *Appendix*):

$$k_T = \frac{1}{h}\left[D_{H^+}\frac{D_{A^+}C_0}{D_{H^+}K_1 + D_{A^+}C_0}(a_{H^+})_h + D_{A^\pm}C_0 + D_{OH^-}\frac{D_{A^-}K_2C_0}{D_{OH^-}K_w + D_{A^-}K_2C_0}(a_{OH^-})_h \right] \quad \text{(Eq. 6)}$$

where h is the diffusion layer thickness, D's are the diffusion coefficients of species indicated by the subscripts, and $(a_{A^+})_h$ and $(a_{OH^-})_h$ are the hydrogen-ion and hydroxide-ion activities, respectively, in the bulk solution. The effective diffusion boundary layer thickness, h, may be written as (21):

$$h = 1.612 D^{1/3} \nu^{1/6} \omega^{-1/2} \quad \text{(Eq. 7)}$$

By assuming $D_{A^+} = D_{A^\pm} = D_{A^-}$ and employing $D_{H^+} = 4.12 \times 10^{-5}$ cm²/sec (23), $D_{OH^-} = 3.43 \times 10^{-5}$ cm²/sec (24, 25), $K_w = 2.38 \times 10^{-14}$ (26), and the parameters determined in this work (Tables II and III), the theoretical dissolution rate constants, k_T (theor.), for the present experimental conditions of 228 rpm, 37°, and $\mu = 0.5$ can be derived from Eqs. 6 and 7 (Table III). Theoretical curves generated from these equations are illustrated in Fig. 10, indicating a reasonably good agreement with the experimental points for every amino penicillin.

Effect of Ionic Strength, Surfactant, and Temperature—The dissolution rates of amino penicillins were determined in the presence of various amounts of potassium chloride. Figure 11 shows that ionic strength had almost no effect on the dissolution rates of the trihydrate forms of both amoxicillin and ampicillin but that an increase in ionic strength markedly decreased the dissolution rate of ampicillin anhydrate.

The addition of 0.04–0.05 M of surfactants increased the solubility of amino penicillins in most cases and tended to increase the dissolution rate as a result of solubilization (Table IV).

The temperature dependence of the dissolution rate constant, k_T, was investigated for amoxicillin trihydrate. The Arrhenius plot is shown in Fig. 12. The activation energy calculated from the slope was 9.67 kcal/mole. This value is comparable with the 9.09-kcal/mole value determined by Wadke and Reier (27) for ampicillin trihydrate, both energies being reasonable for diffusion-controlled dissolution (27) with the respective heats of solution of 6.2 and 5.4 kcal/mole.

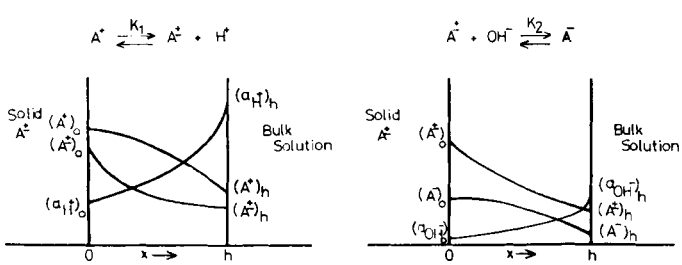

Scheme II—Concentration profiles during dissolution of amino penicillins into acidic medium (left) and alkaline medium (right).

DISCUSSION

The instability of penicillin in acidic solution is well known because of the intramolecular attack of the side-chain amide on the β-lactam moiety. Introduction of an electron-withdrawing group may be expected to reduce such a reaction rate. Since the protonated α-amino group in amoxicillin, ampicillin, epicillin, and cyclacillin plays a powerful electron-attracting role, these amino penicillins are markedly stable to acids, being almost independent of the structure attached to the amino group. The half-lives of the amino penicillins studied were essentially identical, being 15–20 hr at pH 2, 35°, and $\mu = 0.5$; the half life of penicillin G was only 7 min under similar conditions (28). The present results indicate that the extent of the destruction of the β-lactam group of aminopenicillins in the stomach environment is less significant and does not affect their comparative serum levels after oral administration.

The present kinetic analysis of the dissolution of amino penicillins as a function of solution pH supports the mechanism that the transport of amino penicillins from the solid surface to the bulk solution is essentially followed by the simultaneous diffusion and dissociation–equilibrium reaction of the zwitterionic species. The rank order of the dissolution rates of five types of amino penicillins was parallel, over the whole pH region, to that of their solubilities, as expected from the dissolution theory. The serum concentration after a single oral dose with sufficient water decreased in the order of cyclacillin anhydrate > amoxicillin trihydrate > ampicillin anhydrate ≧ ampicillin trihydrate ≧ epicillin anhydrate (2, 6); this pattern did not conform to the solubility order of cyclacillin anhydrate > ampicillin anhydrate > ampicillin trihydrate > amoxicillin trihydrate > epicillin anhydrate.

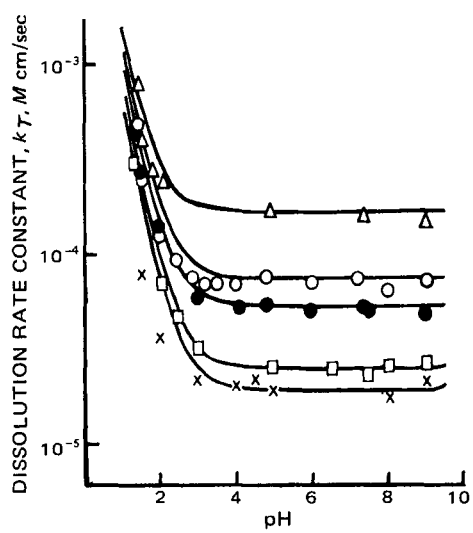

Figure 10—*Log* k_T–*pH profiles for the dissolution of amino penicillins at 228 rpm, 37°, and* $\mu = 0.5$. *The points are experimental values. The solid curves were generated from the theoretical equations listed in Table III. Key:* △, *cyclacillin anhydrate;* ○, *ampicillin anhydrate;* ●, *ampicillin trihydrate;* □, *amoxicillin trihydrate; and* ×, *epicillin anhydrate.*

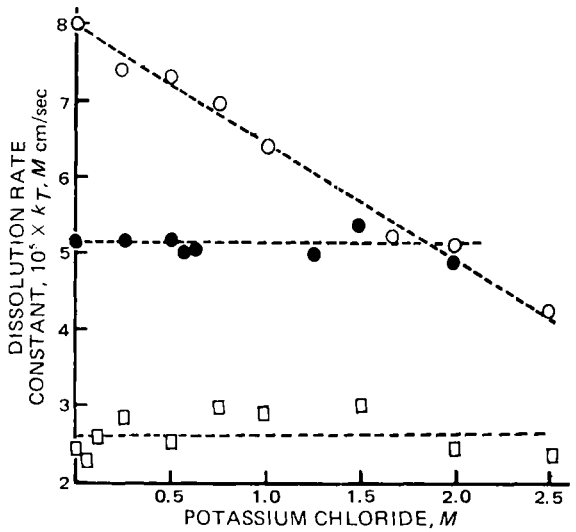

Figure 11—*Effect of ionic strength on the dissolution rate of ampicillin anhydrate* (○), *ampicillin trihydrate* (●), *and amoxicillin trihydrate* (□).

Above pH 3, the dissolution rates from the rotating disks were independent of the pH of the bulk solution; below this pH, the rates markedly increased with the increased acidity of the solution as a result of back-diffusion of the hydrogen ion toward the solid surface. Accordingly, the dissolution of the solids is expected to be fairly rapid under the gastric pH 1–3 conditions. For example, the time for 500 mg of a solid amino penicillin with a 100-cm^2 surface area to dissolve completely in 250 ml of water can be assessed from the present kinetic results, and it is only about 0.5 min at pH 1 and about 3–20 min at pH 3 under the GI agitation condition close to 55 rpm (29).

The amino penicillins, once dissolved, cannot be precipitated at any part of the GI tract, even considering the effect of ionic strength and surfactants such as bile acid. Naturally, administration of amino penicillins with a small amount of water may reduce bioavailability. Welling *et al.* (9) demonstrated that serum ampicillin levels were only slightly affected by fluid volumes, while amoxicillin levels were significantly reduced when 500 mg of each antibiotic was given with 25 ml of water compared to 250 ml of water. This marked effect on amoxicillin level may be related to the 1.7-fold difference in water solubility between ampicillin trihydrate and amoxicillin trihydrate.

The present results on the stability, solubility, and dissolution behavior of amino penicillins suggest that the dissolution of all types of amino penicillins cannot be a rate-determining step of their absorption when they were ingested with sufficient water, so their comparative serum levels may result from their comparative GI membrane permeability. The

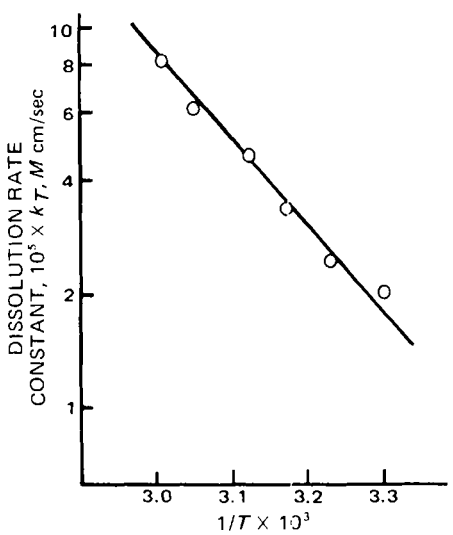

Figure 12—*Plots of the dissolution rate constants at 228 rpm of amoxicillin trihydrate in 0.5* M *KCl* versus *a reciprocal of absolute temperature.*

Table IV—Surfactant Effect on the Dissolution Rate Constants at 228 rpm and Solubilities of Amino Penicillins at 37°

Amino Penicillin	0.04 M Sodium Lauryl Sulfate: Dissolution Rate, $10^5 k_T$, M cm/sec	0.04 M Sodium Lauryl Sulfate: Solubility, $10^2 C_0$, M	0.04 M Cholic Acid: Dissolution Rate, $10^5 k_T$, M cm/sec	0.04 M Cholic Acid: Solubility, $10^2 C_0$, M
Amoxicillin trihydrate	2.67	1.6	--	--
Ampicillin anhydrate	9.63[a]	7.8[a]	9.00	4.40
Ampicillin trihydrate	6.59	3.5	5.44	2.63
Epicillin anhydrate	3.97	2.0	—	—

[a] Sodium lauryl sulfate (0.05 M).

difference in the bioavailability between two different hydrated forms of ampicillin, as observed previously (7), probably results from pharmaceutical formulation factors rather than their physicochemical properties such as solubility and dissolution rate. The conclusion for ampicillin is in agreement with the claim of Hill *et al.* (10) and with the recent *in vivo* observation that there is no significant difference in bioavailability between anhydrous ampicillin and its trihydrate form (10, 30).

APPENDIX: DERIVATION OF EQ. 6

In the acidic region, for the case of $A^{\pm}$ (solid) dissolving in the presence of a_{H^+}, the important equilibrium is:

$$K_1 = \frac{(A^{\pm})a_{H^+}}{(A^+)} \qquad \text{(Eq. A1)}$$

The simultaneous chemical reaction and diffusion model (31) gives the following appropriate differential equation:

$$D_{A^{\pm}}\frac{d^2(A^{\pm})}{dx^2} = -D_{A^+}\frac{d^2(A^+)}{dx^2} = D_{H^+}\frac{d^2a_{H^+}}{dx^2} \qquad \text{(Eq. A2)}$$

The integration of Eq. A2 yields:

$$D_{A^{\pm}}\frac{d(A^{\pm})}{dx} + C_1 = -D_{A^+}\frac{d(A^+)}{dx} + C_2 = D_{H^+}\frac{da_{H^+}}{dx} \qquad \text{(Eq. A3)}$$

where C_1 and C_2 are constants.

By applying proper material balance at $x = h$, $C_2 = 0$ and C_1 becomes:

$$C_1 = \left(D_{H^+}\frac{da_{H^+}}{dx}\right)_{x=h} - \left[D_{A^{\pm}}\frac{d(A^{\pm})}{dx}\right]_{x=h} \qquad \text{(Eq. A4}a\text{)}$$

$$C_1 = \left[D_{A^{\pm}}\frac{d(A^{\pm})}{dx}\right]_{x=0} \qquad \text{(Eq. A4}b\text{)}$$

Therefore, C_1 is the dissolution rate of $A^{\pm}$.

To obtain C_1, further integration of Eq. A3 from $x = h$ to $x = 0$ yields:

$$C_1 = \frac{1}{h}[D_{H^+}(a_{H^+})_h - D_{H^+}(a_{H^+})_0 + D_{A^{\pm}}(A^{\pm})_0 - D_{A^{\pm}}(A^{\pm})_h] \qquad \text{(Eq. A5)}$$

and also, by applying Eq. A1, yields:

$$(a_{H^+})_0 = \frac{D_{H^+}(a_{H^+})_h K_1 + D_{A^+}(A^+)_h K_1}{D_{A^+}(A^{\pm})_0 + D_{H^+}K_1} \qquad \text{(Eq. A6)}$$

Taking the boundary conditions $(A^+)_h = 0$, $(A^{\pm})_h = 0$, and $(A^{\pm})_0 = C_0$, C_1 is reduced to:

$$C_1 = \frac{1}{h}\left[D_{H^+}\frac{D_{A^+}C_0}{D_{H^+}K_1 + D_{A^+}C_0}(a_{H^+})_h + D_{A^{\pm}}C_0\right] \qquad \text{(Eq. A7)}$$

In the basic region, the important equilibrium is:

$$K_2 = \frac{(A^-)K_w}{(A^{\pm})a_{OH^-}} \qquad \text{(Eq. A8)}$$

Similar treatment of the dissolution of zwitterion solid into bulk basic solution gives:

$$C_1 = \frac{1}{h}\left[D_{A^{\pm}}C_0 + D_{OH^-}\frac{D_{A^-}K_2C_0}{D_{OH^-}K_w + D_{A^-}K_2C_0}(a_{OH^-})_h\right] \qquad \text{(Eq. A9)}$$

From Eqs. A7 and A9, the overall rate expression of Eq. 6 can be obtained.

REFERENCES

(1) G. N. Rolinson and R. Sutherland, *Adv. Pharmacol. Chemother.*, **11**, 187 (1973).

(2) Y. Ueda, F. Matsumoto, N. Nakamura, A. Saito, K. Noda, C. Furuya, M. Omori, S. Shimojyo, H. Hanaoka, M. Utsunomiya, and T. Fujinoki, *Jpn. J. Antibiot.*, **23**, 48 (1970).

(3) E. A. P. Croydon and R. Sutherland, *Antimicrob. Agents Chemother. —1970,* **1971**, 427.

(4) R. Sutherland, E. A. P. Croydon, and G. N. Rolinson, *Br. Med. J.*, **3**, 13 (1972).

(5) R. C. Gordon, C. Regamey, and W. M. M. Kirby, *Antimicrob. Agents Chemother.*, **1**, 504 (1972).

(6) A. Philipson, L. D. Sabath, and B. Rosner, *ibid.*, **8**, 311 (1975).

(7) J. W. Poole, G. Owen, J. Silverio, J. N. Freyhof, and S. B. Rosenman, *Curr. Ther. Res. Clin. Exp.*, **10**, 292 (1968).

(8) J. P. Hou and J. W. Poole, *J. Pharm. Sci.*, **58**, 1510 (1969).

(9) P. G. Welling, H. Huang, P. A. Koch, W. A. Craig, and P. O. Madsen, *ibid.*, **66**, 549 (1977).

(10) S. A. Hill, K. H. Jones, H. Seager, and C. B. Taskis, *J. Pharm. Pharmacol.*, **27**, 594 (1975).

(11) J. P. Hou and J. W. Poole, *J. Pharm. Sci.*, **58**, 447 (1969).

(12) T. Yamana, A. Tsuji, and Y. Mizukami, *Chem. Pharm. Bull.*, **22**, 1186 (1974).

(13) A. Albert and E. P. Serjeant, "The Determination of Ionization Constants," Chapman and Hall, London, England, 1971.

(14) S. Glasstone and E. F. Hammel, Jr., *J. Am. Chem. Soc.*, **63**, 243 (1941).

(15) H. Nogami, T. Nagai, and A. Suzuki, *Chem. Pharm. Bull.*, **14**, 329 (1966).

(16) A. H. Goldberg and W. I. Higuchi, *J. Pharm. Sci.*, **57**, 1583 (1968).

(17) S. J. Desai, P. Singh, A. P. Simonelli, and W. I. Higuchi, *ibid.*, **55**, 1224 (1966).

(18) T. Yamana, A. Tsuji, E. Kiya, and E. Miyamoto, *ibid.*, **66**, 861 (1977).

(19) J. W. Poole and C. K. Bahal, *ibid.*, **57**, 1945 (1968).

(20) *Ibid.*, **59**, 1265 (1970).

(21) V. G. Levich, "Physicochemical Hydrodynamics," Prentice-Hall, Englewood Cliffs, N.J., 1962, p. 69.

(22) J. M. Padfield and I. W. Kellaway, *J. Pharm. Pharmacol.*, **27**, 348 (1975).

(23) R. H. Stokes, *J. Am. Chem. Soc.*, **72**, 2243 (1950).

(24) R. N. Bhatia, K. E. Gubbins, and R. D. Walker, *Trans. Faraday Soc.*, **64**, 2091 (1968).

(25) H. R. Bruins, in "International Critical Tables," vol. 5, E. W. Washburn, Ed., McGraw-Hill, New York, N.Y., 1929, p. 68.

(26) H. S. Harned and W. J. Hammer, *J. Am. Chem. Soc.*, **55**, 2194 (1933).

(27) D. A. Wadke and G. E. Reier, *J. Pharm. Sci.*, **61**, 868 (1972).

(28) R. Broderson, *Trans. Faraday Soc.*, **43**, 351 (1947).

(29) A. Hussain, *J. Pharm. Sci.*, **61**, 811 (1972).

(30) P. L. Whyatt, G. W. A. Slywka, A. P. Melikian, and M. C. Meyer, *ibid.*, **65**, 652 (1976).

(31) W. I. Higuchi, E. L. Parrott, D. E. Wurster, and T. Higuchi, *J. Am. Pharm. Assoc., Sci. Ed.*, **47**, 376 (1958).

ACKNOWLEDGMENTS

Presented in part at the 97th annual meeting of the Pharmaceutical Society of Japan, Tokyo, Japan, April 1977.

The authors acknowledge the gifts of amino penicillins from Takeda Chemical Industries and Sankyo Co. They also thank Mr. W.-Z. Hwang and Miss H. Yamazaki for technical assistance.

Determination of Salicylic Acid and Aspirin in Multicomponent Tablets by Liquid Chromatography on a Nonionic Resin

ROBERT G. BAUM and FREDERICK F. CANTWELL ˣ

Received September 26, 1977, from the *Department of Chemistry, University of Alberta, Edmonton, Alberta, Canada T6G 2G2.* Accepted for publication November 18, 1977.

Abstract □ Aspirin and free salicylic acid were determined in combinations containing caffeine, phenacetin, salicylamide, and acetaminophen by liquid chromatography on poly(methyl methacrylate) resin. Precision and accuracy were ±0.6% for aspirin and ±2% for salicylic acid, the latter at levels corresponding to 0.02% of the aspirin content.

Keyphrases □ Aspirin—liquid chromatographic analysis in multicomponent tablets □ Salicylic acid—liquid chromatographic analysis in multicomponent tablets □ Liquid chromatography—analyses, aspirin and salicylic acid in multicomponent tablets □ Analgesics—aspirin and salicylic acid, liquid chromatographic analyses in multicomponent tablets

Of the methods reported for the determination of aspirin and salicylic acid in pharmaceutical preparations, relatively few permit their simultaneous determination. Partition chromatography combined with spectrophotometric measurement has been used for free salicylic acid determination in aspirin products (1–3). Direct spectrophotometry (4) and fluorometric methods (5, 6) also have been used for free salicylic acid determination.

The simultaneous determination of aspirin and salicylic acid has been performed by UV spectrophotometry (7), but this method and methods based on IR spectrophotometry (8) and nonaqueous titration (9) all lack sensitivity for the low levels of salicylic acid present in freshly prepared aspirin tablets. The simultaneous determination of aspirin and salicylic acid based on fluorometric or colorimetric quantitation has been performed on a continuous-flow automated analyzer (10).

GLC separation of aspirin and salicylic acid was achieved on high molecular weight polyethylene glycol containing isophthalic acid and supported on glass microbeads (11). Salicylic acid eluted after aspirin and showed considerable tailing, precluding use of the method for free salicylic acid in tablets. The presence of active

0022-3549/78/0800-1066$01.00/0

© 1978, American Pharmaceutical Association

From Eqs. A7 and A9, the overall rate expression of Eq. 6 can be obtained.

REFERENCES

(1) G. N. Rolinson and R. Sutherland, *Adv. Pharmacol. Chemother.*, **11**, 187 (1973).

(2) Y. Ueda, F. Matsumoto, N. Nakamura, A. Saito, K. Noda, C. Furuya, M. Omori, S. Shimojyo, H. Hanaoka, M. Utsunomiya, and T. Fujinoki, *Jpn. J. Antibiot.*, **23**, 48 (1970).

(3) E. A. P. Croydon and R. Sutherland, *Antimicrob. Agents Chemother. —1970,* **1971**, 427.

(4) R. Sutherland, E. A. P. Croydon, and G. N. Rolinson, *Br. Med. J.*, **3**, 13 (1972).

(5) R. C. Gordon, C. Regamey, and W. M. M. Kirby, *Antimicrob. Agents Chemother.*, **1**, 504 (1972).

(6) A. Philipson, L. D. Sabath, and B. Rosner, *ibid.*, **8**, 311 (1975).

(7) J. W. Poole, G. Owen, J. Silverio, J. N. Freyhof, and S. B. Rosenman, *Curr. Ther. Res. Clin. Exp.*, **10**, 292 (1968).

(8) J. P. Hou and J. W. Poole, *J. Pharm. Sci.*, **58**, 1510 (1969).

(9) P. G. Welling, H. Huang, P. A. Koch, W. A. Craig, and P. O. Madsen, *ibid.*, **66**, 549 (1977).

(10) S. A. Hill, K. H. Jones, H. Seager, and C. B. Taskis, *J. Pharm. Pharmacol.*, **27**, 594 (1975).

(11) J. P. Hou and J. W. Poole, *J. Pharm. Sci.*, **58**, 447 (1969).

(12) T. Yamana, A. Tsuji, and Y. Mizukami, *Chem. Pharm. Bull.*, **22**, 1186 (1974).

(13) A. Albert and E. P. Serjeant, "The Determination of Ionization Constants," Chapman and Hall, London, England, 1971.

(14) S. Glasstone and E. F. Hammel, Jr., *J. Am. Chem. Soc.*, **63**, 243 (1941).

(15) H. Nogami, T. Nagai, and A. Suzuki, *Chem. Pharm. Bull.*, **14**, 329 (1966).

(16) A. H. Goldberg and W. I. Higuchi, *J. Pharm. Sci.*, **57**, 1583 (1968).

(17) S. J. Desai, P. Singh, A. P. Simonelli, and W. I. Higuchi, *ibid.*, **55**, 1224 (1966).

(18) T. Yamana, A. Tsuji, E. Kiya, and E. Miyamoto, *ibid.*, **66**, 861 (1977).

(19) J. W. Poole and C. K. Bahal, *ibid.*, **57**, 1945 (1968).

(20) *Ibid.*, **59**, 1265 (1970).

(21) V. G. Levich, "Physicochemical Hydrodynamics," Prentice-Hall, Englewood Cliffs, N.J., 1962, p. 69.

(22) J. M. Padfield and I. W. Kellaway, *J. Pharm. Pharmacol.*, **27**, 348 (1975).

(23) R. H. Stokes, *J. Am. Chem. Soc.*, **72**, 2243 (1950).

(24) R. N. Bhatia, K. E. Gubbins, and R. D. Walker, *Trans. Faraday Soc.*, **64**, 2091 (1968).

(25) H. R. Bruins, in "International Critical Tables," vol. 5, E. W. Washburn, Ed., McGraw-Hill, New York, N.Y., 1929, p. 68.

(26) H. S. Harned and W. J. Hammer, *J. Am. Chem. Soc.*, **55**, 2194 (1933).

(27) D. A. Wadke and G. E. Reier, *J. Pharm. Sci.*, **61**, 868 (1972).

(28) R. Broderson, *Trans. Faraday Soc.*, **43**, 351 (1947).

(29) A. Hussain, *J. Pharm. Sci.*, **61**, 811 (1972).

(30) P. L. Whyatt, G. W. A. Slywka, A. P. Melikian, and M. C. Meyer, *ibid.*, **65**, 652 (1976).

(31) W. I. Higuchi, E. L. Parrott, D. E. Wurster, and T. Higuchi, *J. Am. Pharm. Assoc., Sci. Ed.*, **47**, 376 (1958).

ACKNOWLEDGMENTS

Presented in part at the 97th annual meeting of the Pharmaceutical Society of Japan, Tokyo, Japan, April 1977.

The authors acknowledge the gifts of amino penicillins from Takeda Chemical Industries and Sankyo Co. They also thank Mr. W.-Z. Hwang and Miss H. Yamazaki for technical assistance.

Determination of Salicylic Acid and Aspirin in Multicomponent Tablets by Liquid Chromatography on a Nonionic Resin

ROBERT G. BAUM and FREDERICK F. CANTWELL ˣ

Received September 26, 1977, from the *Department of Chemistry, University of Alberta, Edmonton, Alberta, Canada T6G 2G2.* Accepted for publication November 18, 1977.

Abstract □ Aspirin and free salicylic acid were determined in combinations containing caffeine, phenacetin, salicylamide, and acetaminophen by liquid chromatography on poly(methyl methacrylate) resin. Precision and accuracy were ±0.6% for aspirin and ±2% for salicylic acid, the latter at levels corresponding to 0.02% of the aspirin content.

Keyphrases □ Aspirin—liquid chromatographic analysis in multicomponent tablets □ Salicylic acid—liquid chromatographic analysis in multicomponent tablets □ Liquid chromatography—analyses, aspirin and salicylic acid in multicomponent tablets □ Analgesics—aspirin and salicylic acid, liquid chromatographic analyses in multicomponent tablets

Of the methods reported for the determination of aspirin and salicylic acid in pharmaceutical preparations, relatively few permit their simultaneous determination. Partition chromatography combined with spectrophotometric measurement has been used for free salicylic acid determination in aspirin products (1–3). Direct spectrophotometry (4) and fluorometric methods (5, 6) also have been used for free salicylic acid determination.

The simultaneous determination of aspirin and salicylic acid has been performed by UV spectrophotometry (7), but this method and methods based on IR spectrophotometry (8) and nonaqueous titration (9) all lack sensitivity for the low levels of salicylic acid present in freshly prepared aspirin tablets. The simultaneous determination of aspirin and salicylic acid based on fluorometric or colorimetric quantitation has been performed on a continuous-flow automated analyzer (10).

GLC separation of aspirin and salicylic acid was achieved on high molecular weight polyethylene glycol containing isophthalic acid and supported on glass microbeads (11). Salicylic acid eluted after aspirin and showed considerable tailing, precluding use of the method for free salicylic acid in tablets. The presence of active

0022-3549/78/0800-1066$01.00/0

© 1978, American Pharmaceutical Association

hydrogens on the carboxyl and phenolic groups requires derivative formation to obtain well-defined GLC peaks (12–14).

Salicylic acid and aspirin were separated by high-performance liquid chromatography on a pellicular strong base anion exchanger at a mobile phase pH of 9.2 (15, 16). Salicylic acid was much more strongly retained than aspirin, but no quantitative data were presented. The two compounds were separated on silica gel adsorbents with various mobile phases (14, 17, 18), and free salicylic acid was determined in aspirin formulations (14).

In the present study, the chromatographic column was packed with a macroporous poly(methyl methacrylate) resin[1] (19). This inexpensive adsorbent has been found useful for the liquid chromatographic analysis of multicomponent analgesic formulations (20). The goal of the present work was the development of a rapid simultaneous chromatographic assay for aspirin and its principal impurity and decomposition product, salicylic acid, in multicomponent analgesic tablets.

EXPERIMENTAL

Apparatus—The liquid chromatograph was assembled from commercially available components (Fig. 1). Two solvent delivery pumps, P1[2] and P2[3], were employed. Glass chromatographic columns[4] were dry packed with <325-mesh macroporous resin. The precolumn, C1, was 5 × 0.28 cm; the analytical column, C2, was 15 × 0.28 cm. The photometric detector was either a UV absorbance detector set at 280 nm[5] or a variable wavelength UV–visible detector[6]. All fittings and polytef tubing were supplied by one manufacturer[7].

The precolumn was connected into the system *via* a rotary injection valve, V1[8], in such a way that, in one valve setting (shown in Fig. 1 as dashed lines), P1 pumped Solvent 1 through the precolumn and the analytical column. At the same time, P2 pumped Solvent 2 to waste. In this configuration, 20 μl of sample solution was injected onto the precolumn by the slider injection valve, V2[9].

After aspirin and salicylic acid eluted from the precolumn, but before any of the other drug components eluted, V1 was switched to the position shown by the solid lines. With V1 in this position, Solvent 1 still flowed through the analytical column, while the precolumn was removed from series and washed with Solvent 2. Immediately after switching V1, the detector sensitivity was changed from 0.01 to 0.64 aufs. To minimize extracolumn band broadening in the polytef tubing associated with V1 and V2, the 0.8-mm i.d. tubing supplied with the valves was replaced with 0.3-mm i.d. tubing.

Chemicals and Reagents—Aspirin[10] and salicylic acid[10] were analyzed by USP methods (1) as 100.0 and 99.6%, respectively. Other drugs and tablet excipients were USP or equivalent grade. Hexane and ethanol were anhydrous reagent grade and were distilled before use. Ether, acetic acid, and dioxane were reagent grade and were used as received.

All mobile phase solvents were prepared volumetrically by transferring measured volumes of a given solvent into a volumetric flask and diluting to volume with hexane. Solvent 1 was 25% ether–10^{-2} *M* acetic acid in hexane. Solvent 2 was 50% ethanol in hexane.

The preparation of <325-mesh resin was described previously (20). The acid washing step in this procedure is necessary to reduce aspirin and salicylic acid tailing.

Tablets, Blank, and Synthetic Mixture—Tablets were purchased at a local pharmacy. The average tablet weight was determined (21), for each product and the tablets were ground to a fine powder. Sample solutions were prepared by weighing a quantity of powdered tablets equivalent to 250 mg of aspirin into 25-ml volumetric flasks, shaking with 10.0 ml of dioxane, and diluting to volume with hexane. Undissolved solids were filtered out by drawing the solution into the sampling valve through a small plug of cotton placed in the inlet tubing.

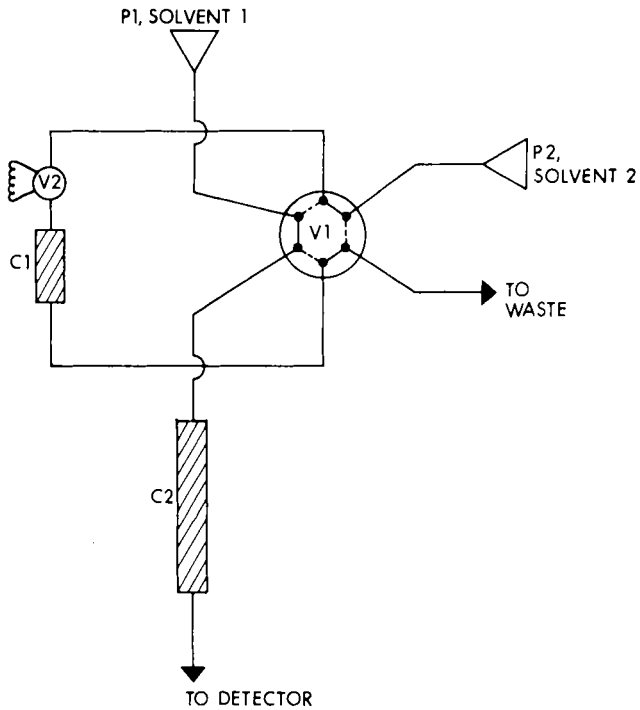

Figure 1—*Diagram of the liquid chromatograph.*

To demonstrate the lack of chromatographic interference by common tablet excipients and likely active ingredients, a blank mixture was prepared containing corn starch, talc, lactose, stearic acid, caffeine, phenacetin, salicylamide, and acetaminophen. A blank solution was prepared by shaking this mixture with dioxane and diluting with hexane as for tablet samples. Quantitative recovery of aspirin and salicylic acid was demonstrated by chromatographing a dioxane–hexane solution of a synthetic mixture containing known amounts of aspirin and salicylic acid along with salicylamide, phenacetin, caffeine, and acetaminophen.

Tablets and the synthetic mixture were analyzed for aspirin and salicylic acid by comparison of peak heights to calibration curves. Calibration curves were obtained by injecting mixtures of the two compounds containing 8.8–11 mg of aspirin/ml and 0.002–0.0065 mg of salicylic acid/ml dissolved in 40% dioxane–hexane. A 20-μl sampling valve was used for all injections. The peak height due to salicylic acid already present in the aspirin was measured by injecting a standard solution of aspirin, and this value was subtracted from that of the standard mixtures to obtain the peak height due to added salicylic acid.

RESULTS AND DISCUSSION

Chromatographic Behavior—Although the detailed mechanism of adsorption of sample molecules on this polyacrylate resin has not yet been elucidated, it is useful to view the resin as a relatively nonpolar adsorbent. Sample molecules interact with the resin *via* dispersion forces, dipole forces, and hydrogen bonding. Mobile phase solvent molecules also interact with the resin and compete with sample molecules for adsorption sites on the resin surface.

A third type of interaction is that between sample molecules and solvent molecules. In contrast to the situation that prevails when using polar adsorbents such as silica gel, it is not possible to neglect the influence of this third type of interaction on the chromatographic retention of a sample molecule. No eluotropic series exists for the nonpolar resin. In fact, it has been shown that for several analgesics the retention volume varies inversely with the solubility of the drug in the mobile phase solvent (20).

Plots of the net retention volumes for five analgesics and salicylic acid *versus* the percent ether in an ether–hexane mobile phase already were presented (20). Previous publications (20, 22) showed how this type of plot may be used to select column length and mobile phase composition to achieve the desired retention and resolution of sample components. Application of this approach to the present problem suggests that base-

[1] Amberlite XAD-7, Rohm & Haas Co., Philadelphia, Pa.
[2] Model CMP-2VK, Laboratory Data Control, Riviera Beach, Fla.
[3] Syringe pump, Perkin-Elmer Corp., Norwalk, Conn.
[4] Type MB, Laboratory Data Control, Riviera Beach, Fla.
[5] Model 230, Spectra Physics, Santa Clara, Calif.
[6] Model 770, Schoeffel Instrument Corp., Westwood, N.J.
[7] Laboratory Data Control, Riviera Beach, Fla.
[8] Model R6031 SVP, Laboratory Data Control, Riviera Beach, Fla.
[9] Model CSV, Laboratory Data Control, Riviera Beach, Fla.
[10] Baker Chemical Co., Phillipsburg, N.J.

Table I—Net Retention Volumes on a 20 × 0.28-cm Column of Macroporous Resin

Compound	Net Retention Volume in 25% Ether[a]	Net Retention Volume in 25% Ether–10^{-2} *M* Acetic Acid
Salicylic acid	2.0	1.84
Aspirin	7.8	6.05
Phenacetin	41	34.2
Salicylamide	44	39.4
Caffeine	100	47.0
Acetaminophen	>150	>150

[a] Values calculated from data in Ref. 20.

line resolution between salicylic acid and the unretained solvent peak and between aspirin and salicylic acid can be achieved on a 20 × 0.28-cm column using 25% ether in hexane as the mobile phase. Predicted retention volumes are given in Table I. Theoretical plate heights calculated on the basis of the six compounds, studied at linear velocities of 0.25 cm/sec, were between 0.1 and 0.17 cm; the void volume for a 20-cm column was 1.7 ml.

With an ether–hexane mobile phase, salicylic acid was the first compound of the six to elute, which is desirable for chromatographic trace analysis (23).

To minimize tailing of aspirin and salicylic acid peaks, 10^{-2} *M* acetic acid was added to the 25% ether mobile phase. The presence of acetic acid had the side effect of reducing the net retention volumes of the six compounds compared to their net retention volumes in 25% ether (Table I). The greatest effect of added acetic acid was on the retention volume of the basic compound caffeine. Retention volumes of salicylic acid and aspirin were affected slightly, and the difference in retention volumes between aspirin and phenacetin, salicylamide, caffeine, and acetaminophen remained very large (Table I).

Because of the large retention volumes of the other drugs, it would be necessary to wait an inordinately long time between sample injections to elute strongly retained components. On the other hand, if these strongly retained components were not allowed to elute between sample injections, they would produce severely drifting baselines as they eluted during later sample chromatograms. One solution to this problem would be a change to a strong eluent such as 50% ethanol in hexane after the elution of aspirin (20). However, the analysis time then would be prolonged both by the time required to elute the strongly retained components with the stronger solvent and by the time required to reequilibrate the resin with 25% ether–10^{-2} *M* acetic acid before making the next injection.

An alternative approach, adopted in this study, is to employ a short column of resin located in series before the analytical column (Fig. 1). With this configuration, the sample solution is injected into the chromatograph with Solvent 1 as the mobile phase. Valve V1 is switched after aspirin has eluted from the precolumn but before any of the other four drugs has eluted from the precolumn. After V1 is switched to the position shown with solid lines in Fig. 1, the salicylic acid and aspirin continue to chromatograph down the analytical column with Solvent 1 mobile phase; the strong eluent Solvent 2 passes through the precolumn, washing off the more strongly retained components. After aspirin has eluted through the detector, V1 is put back to its original setting, and a 5-min equilibration period is allowed before the next injection. The total time between injections is about 15 min.

If the sample contains salicylamide or phenacetin, a small fraction of it may elute from the precolumn along with aspirin and salicylic acid, depending upon precisely when valve V1 is switched. This occurrence presents no problem, however, since these compounds are well resolved from aspirin on the 15-cm column with Solvent 1, and they are eluted completely by the "slug" of ethanol-rich solvent that passes through it when the precolumn is switched back into series.

Analysis of Tablets—Linear calibration curves of peak height at 280 nm *versus* milligrams of compound per milliliter of solution were obtained for both aspirin and salicylic acid. Slopes of the calibration curves were 0.037 and 0.22 absorbance unit/mg/ml for aspirin and salicylic acid, respectively, with relative average deviations for replicate injections of 0.6 and 2%, respectively. In the absence of aspirin, salicylic acid had a slightly longer retention time and a peak height about 14% smaller than when aspirin was present. However, as long as some aspirin was present, the salicylic acid peak was insensitive even to large variations in the amount of aspirin. For this reason, the standards used to construct the calibration curve were mixtures of the two compounds. The presence of other drugs had no effect on the shapes of either the aspirin or salicylic acid peak.

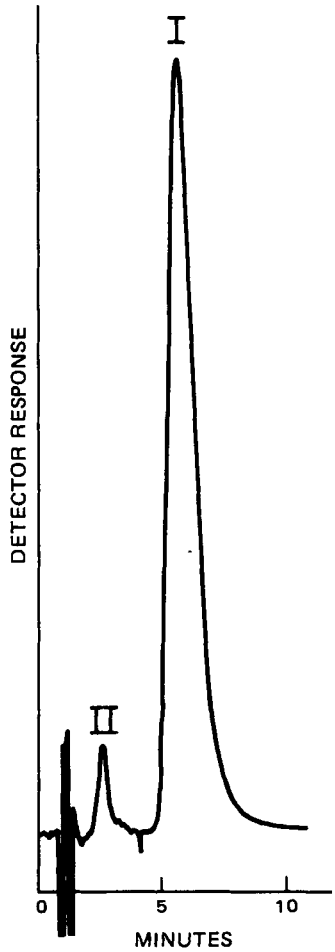

Figure 2—*Typical chromatogram for an aspirin (I) tablet containing 0.028% free salicylic acid (II). The conditions were: pressure, 420 psig; flow rate, 1.35 ml/min; linear velocity, 0.26 cm/sec; detector wavelength, 280 nm; and detector sensitivity, 0.01 aufs for II and 0.64 aufs for I.*

To assess the accuracy of the method, a synthetic mixture containing known amounts of aspirin and salicylic acid, along with salicylamide, phenacetin, caffeine, and acetaminophen, was prepared as already described and analyzed. Assay results for this sample as well as for several commercial tablet preparations are summarized in Table II. Results for the latter are reported on the basis of average tablet weight for each product. The fifth column in Table II gives the salicylic acid as a percentage of the aspirin found in the tablet. Quantitative recovery was observed for both aspirin and salicylic acid in the synthetic mixture. The salicylic acid content of all commercial tablets fell well within the USP limit of 0.3%.

A typical chromatogram of a tablet preparation found to contain 0.090 mg of salicylic acid/tablet and 320 mg of aspirin/tablet is presented in Fig. 2. The negative spike between the salicylic acid and aspirin peaks occurred when the precolumn was taken out of series by switching valve V1.

A problem with all determinations of free salicylic acid in aspirin tablets is the relatively rapid hydrolysis of aspirin in solution to produce additional salicylic acid. Usually, the analysis must be performed as soon as possible after dissolving the sample. In the present method, the salicylic acid concentration increased linearly in the dioxane–hexane sample solutions over at least 5 hr. The generation rate of salicylic acid ranged from 3×10^{-5} mg/ml/hr in Tablet B to 2.4×10^{-4} mg/ml/hr in Tablet A, with the other tablet batches having values between these. All solutions contained 10 mg of aspirin/ml. Thus, if one prepares the standard and sample solution within about 15 min of the injection time, the error in the free salicylic acid determination will be negligible. For the highest accuracy, samples and standards can be chromatographed at various times after preparing their solutions and the results can be extrapolated to zero time. This method was used for the data in Table II.

For comparison with the present method, Tablets A and C were analyzed for free salicylic acid by the official USP method (21). Standards were chosen to bracket the salicylic acid content of the tablets so that quantitative assay values could be obtained. Tablet A contained 0.12 ± 0.005 mg/tablet and Tablet C contained 0.080 ± 0.007 mg/tablet by the USP method. These values are in agreement with those reported in Table II.

Table II—Assay Results for Tablets and Synthetic Mixture

Product	Aspirin, mg/Tablet Label Claim	Aspirin, mg/Tablet Found	Salicylic Acid, mg/Tablet Found	Salicylic Acid, %	Other Drugs Present
A[a]	325	331	0.115	0.035	—
B[b]	325	320	0.090	0.028	—
C[c]	324	323	0.074	0.023	—
D[d]	455	454	0.153	0.034	—
E[e]	455	449	0.082	0.018	Caffeine
F[f]	455	447	0.190	0.043	Caffeine
G[g]	325	310	0.178	0.057	Salicylamide
Synthetic[h] mixture	—	219 (218)	0.126 (0.128)	0.059	Caffeine, phenacetin, acetaminophen, salicylamide

[a] Bayer Aspirin (lot 116NO), Bayer Co., Division of Sterling Drug Ltd., Aurora, Ontario, Canada. [b] Safeway A.S.A. (lot C62A BB), Wes-Pak Products Ltd., North Vancouver, British Columbia, Canada. [c] Lifeprin (lot B48A BA), Stanley Drug Products Ltd., North Vancouver, British Columbia, Canada. [d] Instantine (lot 0920K), Bayer Co., Division of Sterling Drug Ltd., Aurora, Ontario, Canada. [e] Anacin (lot 916 VC), Whitehall Laboratories Ltd., Toronto, Ontario, Canada. [f] C 2 Tablets (lot 154071), Wampole Ltd., Perth, Ontario, Canada. [g] Excedrin (lot 047), Bristol-Meyers Canada Ltd., Toronto, Ontario, Canada. [h] Amount in parentheses is amount added.

The proposed chromatographic method for salicylic acid is significantly more precise and sensitive than the current USP method. This advantage can be further increased by using a detector wavelength nearer the UV absorption maximum of salicylic acid (Fig. 3). At 312 nm, the salicylic acid peak height was over twice its value at 280 nm. The aspirin peak was very small at this wavelength, but this problem can be overcome readily by using a detector sensitivity greater than 1.00 aufs.

Although wavelengths higher than 280 nm appear to be preferable for the analysis of salicylic acid and aspirin, they are not available on most commercial UV absorbance detectors; for this reason, the commonly available wavelength of 280 nm was employed. For comparison, a chromatogram recorded at 254 nm is also included in Fig. 3. This detector wavelength is the most commonly available, but it is considerably less sensitive than 280 nm for detecting salicylic acid.

This method is significantly faster than the USP XIX method for free salicylic acid, and its speed can be increased further by packing the resin in steel columns and using higher pressures to achieve higher mobile phase flow rates. The precolumn is not necessary when analyzing products containing aspirin as the only active ingredient.

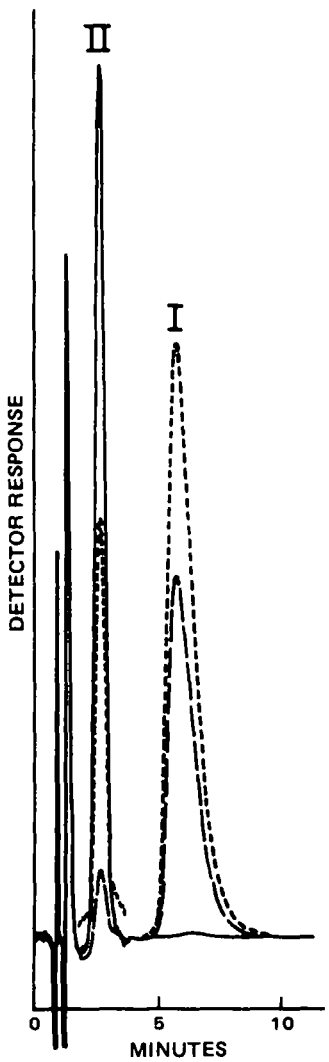

Figure 3—*Chromatogram for a standard solution containing 0.013 mg of salicylic acid (II)/ml and 9.9 mg of aspirin (I)/ml. Detector wavelengths were 254 (– –), 280 (---), and 312 (–·–) nm. Detector sensitivity was 0.01 aufs for II and 1.00 for I. Other conditions were as in Fig. 2.*

REFERENCES

(1) J. D. Weber and J. Levine, *J. Pharm Sci.*, **55**, 78 (1966).
(2) J. Levine and J. D. Weber, *ibid.*, **57**, 631 (1968).
(3) D. E. Guttman and G. W. Salomon, *ibid.*, **58**, 120 (1969).
(4) R. C. Reed and W. W. Davis, *ibid.*, **54**, 1533 (1965).
(5) N. Shane and D. Miele, *ibid.*, **59**, 397 (1970).
(6) N. Shane and R. Stillman, *ibid.*, **60**, 114 (1971).
(7) A. W. Clayton and R. E. Thiers, *ibid.*, **55**, 404 (1966).
(8) G. Kister, M. Ribes, J. Chanal, and A. Catterini, *Ann. Pharm. Fr.*, **34**, 215 (1976).
(9) S.-L. Lin, *J. Pharm. Sci.*, **56**, 1130 (1967).
(10) H. Kubin and H. Gaenshirt, *Pharm. Ind.*, **38**, 224 (1976).
(11) J. G. Nickelly, *Anal. Chem.*, **36**, 2248 (1964).
(12) J. R. Watson, P. Crescuolo, and F. Matsui, *J. Pharm. Sci.*, **60**, 454 (1971).
(13) S. Patel, J. H. Perrin, and J. J. Windheuser, *ibid.*, **61**, 1794 (1972).
(14) S. L. Ali, *J. Chromatogr.*, **126**, 651 (1976).
(15) R. A. Henry and J. A. Schmit, *Chromatographia*, **3**, 116 (1970).
(16) J. A. Schmit, in "Modern Practice of Liquid Chromatography," J. J. Kirkland, Ed., Wiley-Interscience, New York, N.Y., 1971, p. 388.
(17) P. P. Ascione and G. P. Chrekian, *J. Pharm. Sci.*, **64**, 1029 (1975).
(18) K. Harzer and R. Barchet, *Dtsch. Apoth.-Ztg.*, **116**, 1229 (1976).
(19) "Preliminary Technical Notes: Amberlite XAD-7," Rohm & Haas Co., Philadelphia, Pa., 1972.
(20) R. G. Baum and F. F. Cantwell, *Anal. Chem.*, **50**, 280 (1978).
(21) "The United States Pharmacopeia," 19th Rev., Mack Publishing Co., Easton, Pa., 1975.
(22) H. Y. Mohammed and F. F. Cantwell, *Anal. Chem.*, **50**, 491 (1978).
(23) J. J. Kirkland, *Analyst (London)*, **99**, 859 (1974).

ACKNOWLEDGMENTS

Supported by the National Research Council of Canada and the University of Alberta.

Correlation of Aspirin Excretion with Parameters from Different Dissolution Methods

T. E. NEEDHAM ˣ, K. SHAH, J. KOTZAN, and H. ZIA *

Received July 5, 1977, from the *School of Pharmacy, University of Georgia, Athens, GA 30602.* Accepted for publication November 18, 1977. *Present address: University of Isfahan, Isfahan, Iran.

Abstract □ The cumulative urinary excretion of four different aspirin products (two tablets, a capsule, and a timed-release tablet) was determined in a crossover study using five subjects. Comparison of *in vivo* results showed a significant difference in cumulative urinary excretion levels at only 1 hr. The excretion from the two regular tablets was significantly different from the timed-release tablet, but the capsule showed no significant difference from the other three products. Each product was tested in the USP, Levy beaker, and the regular and large magnetic basket dissolution apparatus. Analysis of variance of the *in vitro* results showed a significant difference between the aspirin products and the dissolution methods at selected times. *In vitro* comparison with *in vivo* results for the four products showed that a regression analysis can be used to determine which dissolution methods produce a significant correlation with urinary excretion.

Keyphrases □ Aspirin—excretion in humans correlated with parameters from various *in vitro* dissolution methods □ Excretion—aspirin in humans, correlated with parameters from various *in vitro* dissolution methods □ Dissolution methods, various—*in vitro* parameters correlated with human excretion of aspirin □ Analgesics—aspirin, excretion in humans correlated with parameters from various *in vitro* dissolution methods

The evolution of *in vitro* dissolution testing has introduced a myriad of methods useful mainly for quality control. The acceptance of this testing technique can be measured by its use in quality control and the adoption of an official dissolution apparatus as well as dissolution standards for some USP XVIII (1) drugs. Controversy has marked the official USP test, with suggestions ranging from continued acceptance to replacement by other dissolution methods. The 1980 USP XX is expected to require dissolution standards for all official drugs. The Food and Drug Administration also has reconfirmed the importance of dissolution with the acceptance of this type of *in vitro* testing for demonstrating bioequivalence (2).

With these regulations, comparisons of the different methods for monitoring dissolution become more important. Use of different dissolution methods produced significantly different amounts of drug dissolved at specified times in a dissolution profile (3). The variance produced by these different dissolution methods was not significantly different and was of the same magnitude (3).

The availability of aspirin from different oral brands and formulations was studied (4–8), and bioavailability comparisons were made. Dissolution of various aspirin dosage forms was compared with their *in vivo* absorption or availability (4–7). However, a comparison of different dissolution methods for several types of oral aspirin formulations and their correlation with *in vivo* excretion should provide a means of determining if the selection of an official (and required) dissolution method is necessary or if several methods allow a measure of bioequivalence.

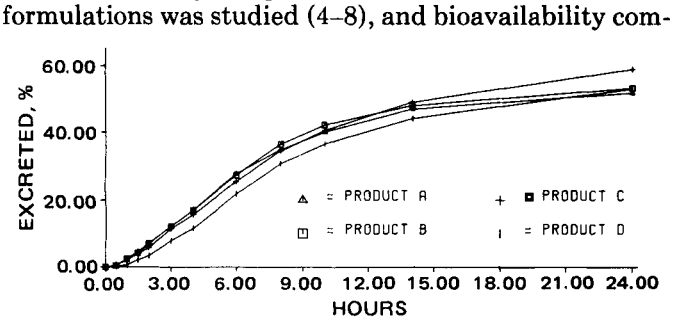

Figure 1—*Cumulative urinary excretion of aspirin from four products.*

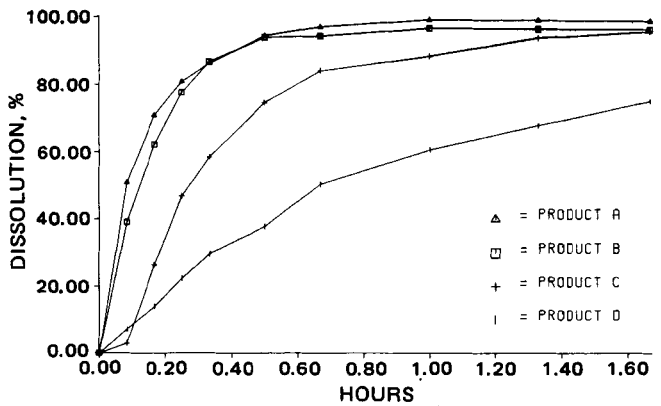

Figure 2—*Comparison of the dissolution profiles of four aspirin products using the USP method.*

EXPERIMENTAL

Aspirin Dosage Forms—Four different dosage forms of aspirin were purchased through local retail outlets. Products A[1] and B[2] were 325-mg tablets, Product C[3] was a 325-mg capsule, and Product D[4] was a 648-mg timed-release tablet.

***In Vitro* Studies**—Four dissolution apparatus were used including: the USP (U) method (1), the modified Levy (L) beaker method (9–11),

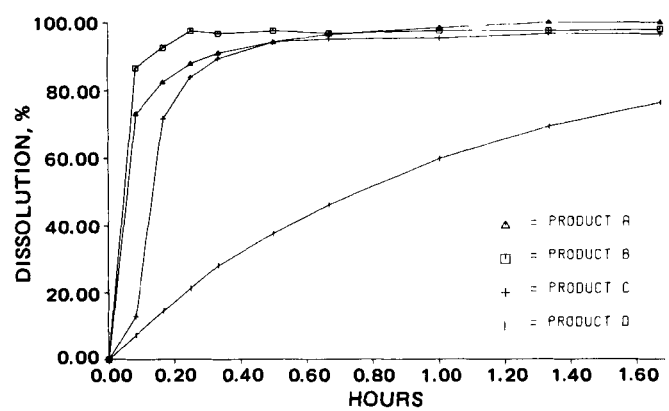

Figure 3—*Comparison of the dissolution profiles of four aspirin products using the modified Levy beaker method.*

[1] Lot 3F10G, Bayer Co., Division of Sterling Drug, New York, NY 10016.
[2] Product 10407-B1 (Lot 694997), Eckerd Drugs, Charlotte, N.C.
[3] Lot 7FF98A, Eli Lilly & Co., Indianapolis, IN 46206.
[4] Lot F3223, Bayer Co., Glenbrook Laboratories, Division of Sterling Drug, New York, NY 10016.

0022-3549/78/0800-1070$01.00/0
© 1978, American Pharmaceutical Association

Table I—Cumulative Percent Urinary Excretion of Four Brands of Aspirin as a Function of Time

Hours	Brands[a] A	B	C	D
0.5	0.53 (0.41)	0.43 (0.28)	0.71 (0.62)	0.22 (0.21)
1.0	2.42 (0.83)	2.45 (1.13)	2.08 (1.13)	0.63 (0.63)
1.5	4.62 (1.51)	4.25 (2.20)	4.02 (1.28)	2.11 (1.56)
2.0	7.20 (2.31)	7.06 (2.66)	5.88 (1.11)	3.44 (1.97)
3.0	12.13 (4.03)	12.24 (5.58)	11.40 (1.98)	7.84 (1.61)
4.0	17.08 (4.97)	16.98 (6.53)	15.74 (1.84)	11.56 (2.41)
6.0	27.71 (5.34)	27.37 (7.59)	25.49 (2.84)	21.84 (4.37)
8.0	34.81 (6.86)	36.52 (7.42)	34.46 (5.04)	30.58 (6.63)
10.0	39.99 (7.67)	41.14 (6.84)	40.53 (5.37)	36.48 (6.05)
14.0	46.93 (7.72)	48.07 (6.69)	49.10 (5.48)	44.12 (4.16)
24.0	51.82 (9.73)	53.26 (5.75)	58.96 (6.28)	55.76 (5.36)

[a] Average percent excreted for five subjects (*SD*).

the regular magnetic basket (R) method (12), and the large magnetic basket (B) method (13). A stirring rate of 75 rpm, a temperature of 37 ± 0.5°, and 600 ml of 0.1 *N* HCl were used. At appropriate times, 1-ml samples were withdrawn and an equal volume of medium was added to the beaker. Samples were analyzed using Trinder's reagent method (14). Each dissolution profile is the average of five separate capsules or tablets.

***In Vivo* Studies**—Five healthy male subjects[5], 21–32 years old and within 90–110% of their ideal body weight, had no history of GI, liver, or kidney disease. Each volunteer was instructed to abstain from all medication, alcohol, and beverages or foods that might interfere with the drug for 1 week before each administration.

Following an overnight fast, each subject was instructed to void his bladder and ingest 250 ml of water. In 1 hr, the 0-hr urine sample was taken, and 650 mg of aspirin was ingested with 250 ml of water. Cumulative urine samples were taken at 0, 0.5, 1, 1.5, 2, 3, 4, 6, 8, 10, 14, and 24 hr and refrigerated immediately. Each subject was instructed to drink 250 ml of water after each urine collection for the first 2 hr. Subjects were allowed to eat after the 2-hr sample.

The four different dosage forms were given to each subject, using a random crossover design with 7 days between administrations. The urine samples were assayed using the described *in vitro* procedure with no variation in urine blanks noted. While the percent of drug excreted in the urine was less than some previous reports (4, 6) because of the inability of Trinder's reagent to react completely with some metabolites of salicylic acid (15), these differences did not affect the interbrand comparisons.

RESULTS AND DISCUSSION

Analysis of *In Vivo* Drug Excretion—Figure 1 and Table I illustrate the cumulative percent of drug excreted in the urine for each dosage form as a function of time. The cumulative percent of drug excreted was transformed using a log arc sine transformation to give homogeneity of variance and additivity of effects (16). These data were analyzed using a 4 (brands) × 5 (subjects) × 11 (sample times) repeated measures ANOV (17).

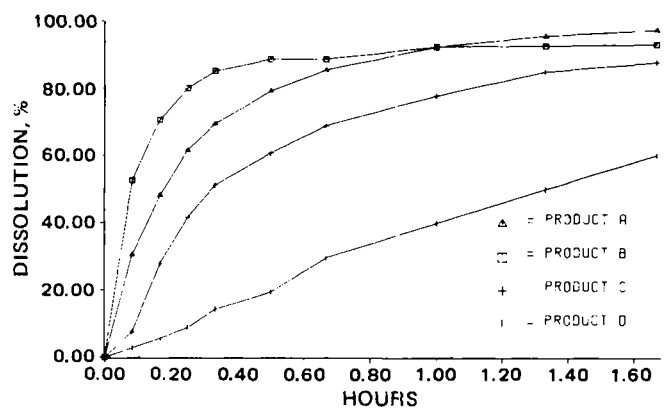

Figure 4—*Comparison of the dissolution profiles of four aspirin products using the regular magnetic basket method.*

[5] Informed consent was obtained from each subject.

Table II shows that the calculated *F* value for subjects of 0.42 and for brands of 2.76 was not significant ($p = 0.05$) across the elapsed time of the experiment. The time–brand interaction was statistically significant. A visual inspection of Fig. 1 shows crossover of the dosage form excretion profiles. Therefore, an analysis of the data at specific sample times was undertaken. These subsequent ANOV's produced a statistically significant *F* value for the different dosage forms administered at only 1 ($F = 5.19$) and 2 ($F = 3.98$) hr, with all other times showing no significant difference (18). This result indicates that absorption is dissolution rate controlled and agrees with the suggestion of Levy and Yacobi (5) that urine collections must be made at times of less than 3 hr to detect meaningful differences.

The Neuman–Keuls (19) analysis of the cumulative amount of drug excreted from each of the different brands further substantiates these conclusions. At 1 hr, a significant difference was found between the two regular tablets (Products A and B) and the timed-release tablet (Product D). The capsule (Product C) showed no statistically significant difference from either the regular tablets or the timed-release tablets. At 2 hr, the Neuman–Keuls analysis showed no significant difference between any of the four brands. This result could be expected since the calculated *F* value is barely larger than the tabular *F* value of 3.24.

Analysis of *In Vitro* Drug Dissolution—The dissolution profiles for the aspirin dosage forms are shown in Figs. 2–5 for each of the four dissolution methods using the same medium and agitation rate. The timed-release tablet dissolved at a slower rate in each apparatus, and the remaining three brands showed a close grouping of their profiles.

The percent of drug dissolved was transformed using a log arc sine transformation to give homogeneity of variance and additivity of effects (16). A 4 (brands) × 4 (methods) × 9 (sample times) with five replications repeated measures analysis of variance (ANOV) was applied to the data and yielded significant differences ($p = 0.05$) among brands, methods, and times (Table III). However, all interaction effects were also significant at this level.

Reducing the analysis to a two-way ANOV at specific sample times presented a better illustration of the results. At the sample times of 5, 40, 60, 80, and 100 min, the calculated *F* values for brands, methods, and the brand–method interaction were all significant ($p = 0.05$). This interaction factor was not significant at sample times of 10, 15, 20, and 30 min, while the calculated *F* values for brands and methods were significant. These results indicate a statistically significant difference between each of the single factors with no crossover between them.

Comparison of the individual dissolution methods at 10, 15, 20, and 30 min to determine which apparatus produced significantly different drug release, as well as comparison of the different dosage forms, was accomplished using the Neuman–Keuls test (19). Table IV demonstrated that for the sample times 10 through 30 min the rank order of drug re-

Table II—Repeated Measures Analysis of Variance for the *In Vivo* Data

Source	*df*	Mean Square	*F*	Probability *F* Exceeded
Subjects	4	0.0456	0.42	0.791
Brands	3	0.2987	2.76	0.088
Error (between)	12	0.1084	—	—
Time	10	5.7079	1351.36	0.000
Time–subjects	40	0.0058	1.38	0.094
Time–brands	30	0.0068	1.60	0.040
Error (within)	120	0.0042	—	—

Table III—Repeated Measures Analysis of Variance of the *In Vitro* Dissolution Data

Source	*df*	Mean Square	*F*	Probability *F* Exceeded
Brands	3	45.67	127.27	0.000
Methods	3	13.62	37.98	0.000
Brands–methods	9	1.43	3.97	0.000
Error	64	0.36	—	—
Time	8	22.49	1860.39	0.000
Time–brands	24	0.75	61.61	0.000
Time–methods	24	0.32	26.64	0.000
Time–brands–methods	72	0.07	5.81	0.000
Error	512	0.01	—	—

leased was B > A > C > D, with significant differences between dosage forms B–C, B–D, A–C, A–D, and C–D.

Investigation of the drug release as a function of the dissolution methods showed more variability through the same timespan. The Levy beaker method showed a significant difference from all of the other methods at the first three times. The Levy method was also different from the two magnetic baskets at 30 min. The USP method showed no statistical difference from the regular magnetic basket at 15, 20, and 30 min and a difference from the large magnetic basket at 20 and 30 min. The two magnetic basket methods were not significantly different in drug released at any of the four times analyzed.

Correlation of *In Vitro* with *In Vivo* Results—Previously (4–7), it was shown that aspirin absorption is dissolution rate controlled. Quantification of dissolution behavior as a means of testing aspirin release from various dosage forms would seem an excellent initial step in assuring drug availability. The ability of a particular dissolution method to show correlation with the urinary excretion of aspirin is an important means of qualifying that procedure for use in quality control testing and/or as an indication of drug bioavailability.

Rank-order correlation of the sequence of dissolution as it relates to the order of urinary excretion for different dosage forms of aspirin can be used to give a preliminary indication of *in vivo–in vitro* correlation.

Figure 1 shows that the order of drug excretion after administration of the different types of aspirin products varied as a function of time. During the first 8 hr, the highest amount of urinary excretion was found for either Product A or B followed by C and then D. At 10 hr after drug administration, the excretion from the highest to the lowest cumulative amount found in the urine was in the order of B > C > A > D. At 14 hr, the order was C > B > A > D; and at the last sampled time, the order was C > D > B > A.

The *in vitro* drug release can be seen in Figs. 2–5. For each of the four dissolution methods, the exact order of drug release from each of the four

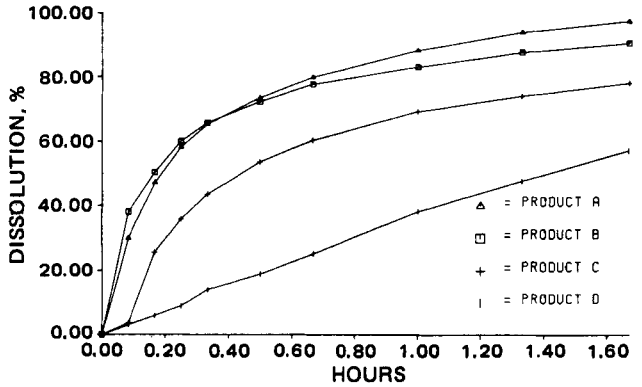

Figure 5—*Comparison of the dissolution profiles of four aspirin products using the large magnetic basket method.*

different dosage forms was somewhat different at the individual sampling times. However, the sequence of drug release varied in only two ways at the representative times of 10, 20, 30, and 40 min. In the order of the highest to the lowest rate of dissolution, B > A > C > D or A > B > C > D.

Table V shows a simple sequential order correlation of the *in vivo* and *in vitro* results. By using the urinary excretion sample times of 1.0, 1.5, 2.0, 3.0, 4.0, and 6.0 hr and the dissolution sample times of 10, 20, 30, and 40 min, many correlations were produced. Consideration of the effect of dissolution on urinary excretion does not seem to affect these correlations. In fact, if the number of simple correlations found for *in vivo* times less than 2 hr are compared to those for the same number of times greater than 2 hr, an equal number of correlations can be seen for each dissolution method. This result indicates that the importance of dissolution rate-controlled absorption is lost with this method of correlation.

To investigate a more quantitative measure of correlation between the transformed data of percent cumulative urinary excretion and the percent drug dissolved for each of the four dosage forms tested, a regression analysis was performed at each *in vivo–in vitro* time shown in Table V, and the *F*-ratio was used to determine significance. Table VI presents the results of the correlation using a linear regression analysis of the averaged transformed data and an *F*-test. The number of significant correlations found for the *in vivo* times of 1.0, 1.5, and 2.0 hr when absorption was dissolution rate controlled were definitely higher than the number found for the *in vivo* times greater than 2 hr for all dissolution methods except the large magnetic basket. The greatest number of correlations was found for the 1-hr urinary excretion and the representative dissolution times. The Levy method showed a significant correlation at all four

Table IV—Significant Differences[a] in *In Vitro* Drug Release Produced by the Products and the Dissolution Methods at Selected Times using a Neuman–Keuls Analysis

	Sample Times															
	10 min				15 min				20 min				30 min			
Products	B	A	C	D	B	A	C	D	B	A	C	D	B	A	C	D
B		—	*	*		—	*	*		—	*	*		—	*	*
A			•	*			*	*			*	*			*	*
C				*				*				*				*
Dissolution methods[b]	L	U	R	B	L	U	R	B	L	U	R	B	L	U	R	B
Levy		*	*	*		*	*	*		*	*	*		—	*	*
USP			—	—			—	*			*	*			*	*
Regular basket				—				—				—				—

[a] The symbol * indicates a significant difference between the brands or methods compared. [b] Four dissolution methods were used: Levy (L), USP (U), regular magnetic basket (R), and large magnetic basket (B).

Table V—Rank-Order Correlations (S) for *In Vivo* Excretion and *In Vitro* Dissolution for Four Brands of Aspirin

	In Vitro Methods															
	USP				Levy				Regular Basket				Large Basket			
In Vivo Time, hr	10 min	20 min	30 min	40 min	10 min	20 min	30 min	40 min	10 min	20 min	30 min	40 min	10 min	20 min	30 min	40 min
1.0	—	S	S	—	S	S	S	S	S	S	S	—	S	—	—	—
1.5	S	—	—	S	—	—	—	—	—	—	—	S	—	S	S	S
2.0	S	—	—	S	—	—	—	—	—	—	—	S	—	S	S	S
3.0	—	S	S	—	S	S	S	S	S	S	S	—	S	—	—	—
4.0	S	—	—	S	—	—	—	—	—	—	—	S	—	S	S	S
6.0	S	—	—	S	—	—	—	—	—	—	—	S	—	S	S	S

Table VI—Correlation [a] of *In Vivo* Excretion and *In Vitro* Dissolution for Four Brands of Aspirin Using Regression Analysis and the *F* Test

	In Vitro Methods															
	USP				Levy				Regular Basket				Large Basket			
In Vivo Time, hr	10 min	20 min	30 min	40 min	10 min	20 min	30 min	40 min	10 min	20 min	30 min	40 min	10 min	20 min	30 min	40 min
1.0	—	—	S	S	S	S	S	S	—	S	S	S	S	S	—	—
1.5	—	—	—	S	S	—	S	S	—	—	—	S	—	—	S	S
2.0	—	—	—	S	—	—	—	—	—	—	—	S	—	S	—	S
3.0	—	—	—	—	S	S	S	S	—	—	—	—	—	—	—	—
4.0	—	—	—	S	—	—	—	—	—	—	—	S	—	S	S	S
6.0	—	—	—	S	—	—	—	—	—	—	—	S	—	S	S	S

[a] S indicates significant correlation at $\alpha = 0.95$.

in vitro times, and the regular magnetic basket showed significant correlations at three of the four times.

In summary, significant differences in the cumulative urinary excretion of the four aspirin products could only be determined at the 1-hr excretion time, although the ANOV indicated a difference at the 2-hr sample time. Statistically significant differences also were found between these four products and between the four dissolution methods at selected times in the dissolution profiles. Attempts to use a simple sequential order correlation showed a random array of significant correlations between *in vitro* data and a number of excretion times that exceeded the limits of dissolution rate-controlled absorption. The regression analysis, on the other hand, showed the best correlation with *in vivo* 1-hr excretion times. This result indicates a need to analyze both *in vitro* and *in vivo* data statistically before selecting the parameters for data correlation. Adoption of this approach shows that, for aspirin, the Levy beaker and regular magnetic basket provide the best correlation with urinary excretion.

REFERENCES

(1) "The United States Pharmacopeia," 18th rev., Mack Publishing Co., Easton, Pa., 1970.

(2) *Fed. Regist.*, **42**, 1624 (Jan. 7, 1977).

(3) T. E. Needham and L. A. Luzzi, *J. Pharm. Sci.*, **63**, 925 (1974).

(4) G. Edenved and R. Elofsson, *Acta Pharm. Suec.*, **12**, 323 (1975).

(5) G. Levy and A. Yacobi, *J. Clin. Pharmacol.*, **15**, 525 (1975).

(6) W. L. Chiou and I. Onyemelukwe, *ibid.*, **14**, 597 (1974).

(7) G. Levy, J. R. Leonards, and J. A. Procknal, *J. Pharm. Sci.*, **54**, 1719 (1965).

(8) A. T. Canada, A. H. Little, and E. L. Creighton, *Can. Ther. Res.*, **19**, 554 (1976).

(9) G. Levy and B. A. Hayes, *N. Engl. J. Med.*, **262**, 1053 (1961).

(10) G. Levy, *J. Pharm. Sci.*, **52**, 1039 (1963).

(11) G. Levy and B. Sahli, *ibid.*, **51**, 58 (1962).

(12) R. E. Shepherd, J. C. Price, and L. A. Luzzi, *ibid.*, **61**, 1152 (1972).

(13) L. A. Luzzi and T. E. Needham, *ibid.*, **62**, 1907 (1973).

(14) P. Trinder, *Biochem. J.*, **57**, 301 (1954).

(15) W. L. Chiou and I. Onyemelukwe, *J. Pharm. Sci.*, **63**, 630 (1974).

(16) C. A. Bennett and N. L. Franklin, "Statistical Analysis in Chemistry and the Chemical Industry," Wiley, New York, N.Y., 1954, p. 355.

(17) P. Sampson, in "Biomedical Computer Programs," W. J. Dixon, Ed., University of California Press, Berkeley, Calif., 1975, pp. 711–783.

(18) "Biomedical Computer Programs," W. J. Dixon, Ed., University of California Press, Berkeley, Calif., 1970, pp. 495–510.

(19) G. W. Snedecor and W. G. Cochran, "Statistical Methods," 6th ed., Iowa State University Press, Ames, Iowa, 1967, p. 273.

Sensitive Electron-Capture GLC Determination of Metoclopramide in Biological Fluids

Y. K. TAM and J. E. AXELSON ×

Received October 3, 1977, from the *Faculty of Pharmaceutical Sciences, University of British Columbia, Vancouver, British Columbia, Canada.* Accepted for publication November 18, 1977.

Abstract □ A highly sensitive and specific electron-capture GLC assay capable of detecting picogram quantities of metoclopramide, a procaine derivative, in biological fluids was developed. This assay consisted of extracting metoclopramide from an alkalinized aqueous layer into benzene. A portion of the organic phase was derivatized with heptafluorobutyric anhydride. Quantitative estimation of the derivative was accomplished by adding diazepam, the internal standard, in benzene (750 ng/ml). A calibration curve was prepared for the plasma extracts. Linearity was observed in the range studied (91–825 ng/ml). No interference from endogenous substances was observed. The minimum detectable amount was 1 pg/injection. The structure of the derivative was confirmed by electron-impact and chemical-ionization mass spectrometry. The applicability of this method was shown by a preliminary study of the elimination kinetics of metoclopramide in rats after a 10-mg/kg iv dose.

Keyphrases □ Metoclopramide—electron-capture GLC analysis in biological fluids □ GLC, electron capture—analysis, metoclopramide in biological fluids □ Antiemetics—metoclopramide, electron-capture GLC analysis in biological fluids

Metoclopramide, 4-amino-5-chloro-2-methoxy-*N*-(2-diethylaminoethyl)benzamide, an antiemetic procaine derivative (1), is currently used in GI diagnostics (2, 3) and in the treatment of various GI disorders (4, 5). Metoclopramide increases the tone and peristalsis of the stomach and the duodenum, distends the duodenal bulb, and im-

0022-3549/78/0800-1073$01.00/0

© 1978, American Pharmaceutical Association

Table VI—Correlation [a] of *In Vivo* Excretion and *In Vitro* Dissolution for Four Brands of Aspirin Using Regression Analysis and the *F* Test

	In Vitro Methods															
	USP				Levy				Regular Basket				Large Basket			
In Vivo Time, hr	10 min	20 min	30 min	40 min	10 min	20 min	30 min	40 min	10 min	20 min	30 min	40 min	10 min	20 min	30 min	40 min
1.0	—	—	S	S	S	S	S	S	—	S	S	S	S	S	—	—
1.5	—	—	—	S	S	—	S	S	—	—	—	S	—	—	S	S
2.0	—	—	—	S	—	—	—	—	—	—	—	S	—	S	—	S
3.0	—	—	—	—	S	S	S	S	—	—	—	—	—	—	—	—
4.0	—	—	—	S	—	—	—	—	—	—	—	S	—	S	S	S
6.0	—	—	—	S	—	—	—	—	—	—	—	S	—	S	S	S

[a] S indicates significant correlation at $\alpha = 0.95$.

in vitro times, and the regular magnetic basket showed significant correlations at three of the four times.

In summary, significant differences in the cumulative urinary excretion of the four aspirin products could only be determined at the 1-hr excretion time, although the ANOV indicated a difference at the 2-hr sample time. Statistically significant differences also were found between these four products and between the four dissolution methods at selected times in the dissolution profiles. Attempts to use a simple sequential order correlation showed a random array of significant correlations between *in vitro* data and a number of excretion times that exceeded the limits of dissolution rate-controlled absorption. The regression analysis, on the other hand, showed the best correlation with *in vivo* 1-hr excretion times. This result indicates a need to analyze both *in vitro* and *in vivo* data statistically before selecting the parameters for data correlation. Adoption of this approach shows that, for aspirin, the Levy beaker and regular magnetic basket provide the best correlation with urinary excretion.

REFERENCES

(1) "The United States Pharmacopeia," 18th rev., Mack Publishing Co., Easton, Pa., 1970.

(2) *Fed. Regist.*, **42**, 1624 (Jan. 7, 1977).

(3) T. E. Needham and L. A. Luzzi, *J. Pharm. Sci.*, **63**, 925 (1974).

(4) G. Edenved and R. Elofsson, *Acta Pharm. Suec.*, **12**, 323 (1975).

(5) G. Levy and A. Yacobi, *J. Clin. Pharmacol.*, **15**, 525 (1975).

(6) W. L. Chiou and I. Onyemelukwe, *ibid.*, **14**, 597 (1974).

(7) G. Levy, J. R. Leonards, and J. A. Procknal, *J. Pharm. Sci.*, **54**, 1719 (1965).

(8) A. T. Canada, A. H. Little, and E. L. Creighton, *Can. Ther. Res.*, **19**, 554 (1976).

(9) G. Levy and B. A. Hayes, *N. Engl. J. Med.*, **262**, 1053 (1961).

(10) G. Levy, *J. Pharm. Sci.*, **52**, 1039 (1963).

(11) G. Levy and B. Sahli, *ibid.*, **51**, 58 (1962).

(12) R. E. Shepherd, J. C. Price, and L. A. Luzzi, *ibid.*, **61**, 1152 (1972).

(13) L. A. Luzzi and T. E. Needham, *ibid.*, **62**, 1907 (1973).

(14) P. Trinder, *Biochem. J.*, **57**, 301 (1954).

(15) W. L. Chiou and I. Onyemelukwe, *J. Pharm. Sci.*, **63**, 630 (1974).

(16) C. A. Bennett and N. L. Franklin, "Statistical Analysis in Chemistry and the Chemical Industry," Wiley, New York, N.Y., 1954, p. 355.

(17) P. Sampson, in "Biomedical Computer Programs," W. J. Dixon, Ed., University of California Press, Berkeley, Calif., 1975, pp. 711–783.

(18) "Biomedical Computer Programs," W. J. Dixon, Ed., University of California Press, Berkeley, Calif., 1970, pp. 495–510.

(19) G. W. Snedecor and W. G. Cochran, "Statistical Methods," 6th ed., Iowa State University Press, Ames, Iowa, 1967, p. 273.

Sensitive Electron-Capture GLC Determination of Metoclopramide in Biological Fluids

Y. K. TAM and J. E. AXELSON ×

Received October 3, 1977, from the *Faculty of Pharmaceutical Sciences, University of British Columbia, Vancouver, British Columbia, Canada.* Accepted for publication November 18, 1977.

Abstract □ A highly sensitive and specific electron-capture GLC assay capable of detecting picogram quantities of metoclopramide, a procaine derivative, in biological fluids was developed. This assay consisted of extracting metoclopramide from an alkalinized aqueous layer into benzene. A portion of the organic phase was derivatized with heptafluorobutyric anhydride. Quantitative estimation of the derivative was accomplished by adding diazepam, the internal standard, in benzene (750 ng/ml). A calibration curve was prepared for the plasma extracts. Linearity was observed in the range studied (91–825 ng/ml). No interference from endogenous substances was observed. The minimum detectable amount was 1 pg/injection. The structure of the derivative was confirmed by electron-impact and chemical-ionization mass spectrometry. The applicability of this method was shown by a preliminary study of the elimination kinetics of metoclopramide in rats after a 10-mg/kg iv dose.

Keyphrases □ Metoclopramide—electron-capture GLC analysis in biological fluids □ GLC, electron capture—analysis, metoclopramide in biological fluids □ Antiemetics—metoclopramide, electron-capture GLC analysis in biological fluids

Metoclopramide, 4-amino-5-chloro-2-methoxy-*N*-(2-diethylaminoethyl)benzamide, an antiemetic procaine derivative (1), is currently used in GI diagnostics (2, 3) and in the treatment of various GI disorders (4, 5). Metoclopramide increases the tone and peristalsis of the stomach and the duodenum, distends the duodenal bulb, and im-

0022-3549/78/0800-1073$01.00/0

© 1978, American Pharmaceutical Association

Table I—Quantitative Estimation of Metoclopramide in Plasma

Amount Added, ng	n^a	Mean Area Ratio	SE
91.636	4	0.232	±0.003
229.090	5	0.544	±0.017
458.180	4	1.099	±0.020
641.450	5	1.596	±0.006
824.723	5	2.061	±0.038

[a] Each n is the average of three determinations.

proves the pyloric activity, thus promoting gastric motility and reducing gastric emptying time (6, 7). This effect of metoclopramide has led to the increased absorption of several drugs—*viz.*, acetaminophen (8), tetracycline (9), pivampicillin (9), and levodopa (10). Moreover, metoclopramide enhanced griseofulvin absorption from solution but depressed its absorption from a suspension (11). Similarly, digoxin absorption from a tablet was reduced, resulting in lowered steady-state blood digoxin levels (12) after concomitant administration of metoclopramide.

Little information pertaining to the pharmacokinetics of this drug is available. Arita *et al.* (13) reported that conjugation is the major metabolic pathway and that deethylation is the major metabolic reaction in rabbits. Four additional metabolites were identified in rat liver slices using mass spectrometry (14). Interspecies variations in elimination kinetics were minimal after various intravenous doses (5–15 mg/kg) (15). However, major interspecies variations were seen after oral administration of a high dose (100 mg/kg).

Tunon *et al.* (16) reported that, after giving rats an intravenous dose (10 mg/kg), the plasma data were best described by a two-compartment kinetic model with an elimination half-life of 13–20 min. Bakke and Segura (15) observed that metoclopramide followed apparent first-order elimination kinetics. The half-life of this drug varies from 13 to 60 min in the rat. This large variation in the reported half-life may be due to the lack of a sensitive assay capable of detecting trace quantities in biological fluids. The purpose of this study, therefore, was to develop a highly sensitive electron-capture GLC assay for metoclopramide capable of detecting trace quantities in small volumes of biological fluids.

EXPERIMENTAL

Materials—The following reagents were used: 1 *N* NaOH[1], benzene[2], 4% ammonium hydroxide[3], heptafluorobutyric anhydride[4] (I), metoclopramide monohydrochloride[5] (II) and diazepam[6].

GLC—A reporting gas–liquid chromatograph[7] equipped with a ^{63}Ni-electron-capture detector and a 1.8-m (6-ft) × 2-mm i.d. glass column, containing 3% OV-17 coated onto 80–100-mesh Chromosorb W, was used. The operating temperatures for routine analysis were: injection port, 250°; oven, 250°; and detector, 350°. The carrier gas (95% argon–5% methane) flow rate was 40 ml/min.

Differential Scanning Calorimetry—A differential scanning calorimeter[8] equipped for effluent gas analysis was employed. All samples were crimped. The rate of temperature increase was 10°/min for each run.

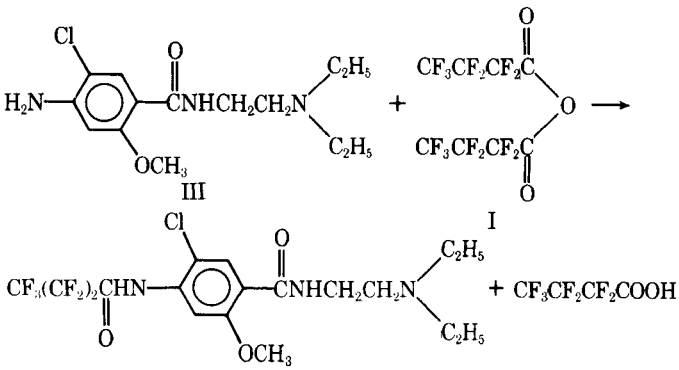

Scheme I

Preparation of Metoclopramide Free Base (III)—About 30 mg of II was dissolved in 1 ml of water and alkalinized by addition of 1 ml of 1 *N* NaOH. The formed free base was extracted repeatedly with 10 ml of benzene until the white precipitate in the aqueous layer disappeared. After the organic layer was removed into a 50-ml erlenmeyer flask, the content was dried under a gentle stream of nitrogen at 60°. The residue was recrystallized three times with benzene and dried at 125° for 2 hr under vacuum.

Extraction Procedure—To 0.1 ml of water, plasma, whole blood, or urine were added various amounts of II (Table I). To each sample, 1 ml of 1 *N* NaOH was added, and the total volume was made up to 2 ml with distilled water (pH 13). The aqueous phase was extracted with 6 ml of benzene. Five milliliters of the organic layer was pipetted into a 15-ml centrifuge tube. One milliliter of benzene containing the internal standard (diazepam, 750 ng/ml) was added, the mixture was dried under a gentle stream of nitrogen, and the residue was reconstituted with 1 ml of benzene.

Derivatization Procedure—Twenty microliters of I was added to the reconstituted solution (Scheme I). After thorough vortexing, the reaction mixture was incubated at 55° for 20 min. The sample was allowed to cool to room temperature, and then excess I was removed by hydrolysis with 0.5 ml of water and neutralization with 0.5 ml of 4% NH_4OH solution. Subsequent to centrifugation, the derivative was pipetted into a 2-ml vial for automatic injection into the gas chromatograph.

GLC–Mass Spectrometry—A computerized gas chromatograph–electron-impact mass spectrometer[9] was used to study the fragmentation pattern of the heptafluorobutyryl derivative. The following conditions were used for the gas chromatograph: injection port temperature, 250°; oven temperature, 250°; and helium (carrier gas) flow rate, 40 ml/min. The 2-m × 2-mm i.d. glass column was packed with 3% OV-17 coated on 80–100-mesh Chromosorb W. For the mass spectrometer, the ionization beam energy was 70 ev, the electron multiplier voltage was 2 kv, the analyzer temperature was 50°, and the separator oven temperature was 200°.

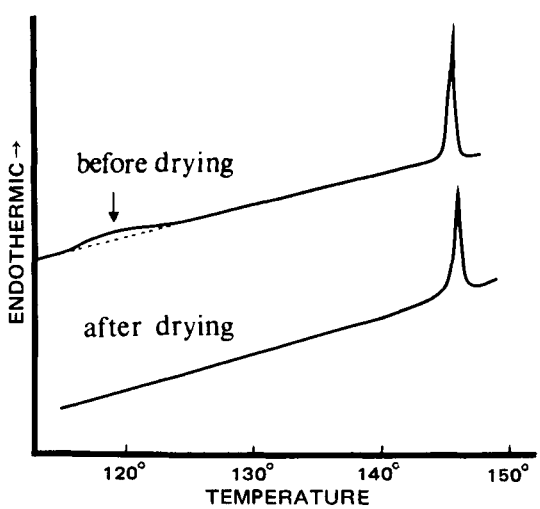

Figure 1—*Differential scanning calorimetry spectra of the free base before and after drying at 125° under vacuum.*

[1] Mallinckrodt Chemical Works, St. Louis, Mo.
[2] Distilled in glass, Caledon, Georgetown, Ontario, Canada.
[3] Reagent ACS code 1293, Allied Chemical Canada Ltd., Claire, Quebec, Canada.
[4] Pierce Chemical Co., Rockford, Ill.
[5] Catalog No. L-593, 856-01F06, Merck Sharp and Dohme Research Laboratories, West Point, Pa.
[6] Lot R-6685, Hoffmann-La Roche, Montreal, Canada.
[7] Hewlett-Packard model 5833A.
[8] Perkin-Elmer model DSC-1B.
[9] Model 3200, Finnigan Corp., Sunnyvale, Calif.

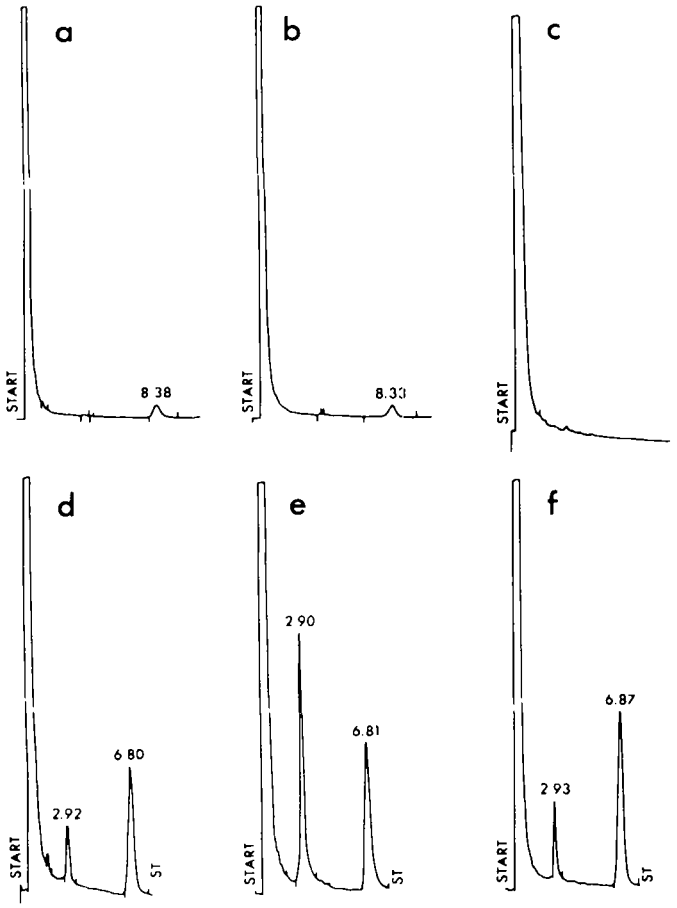

Figure 2—*Sample chromatograms from the extracts of biological specimens. Key:* a, *blank plasma extract;* b, *blank whole blood extract;* c, *blank urine extract;* d, *plasma extract (91.6 pg/injection);* e, *whole blood extract (229 pg/injection); and* f, *urine extract (91.6 pg/injection).*

Chemical-Ionization Mass Spectrometry—A chemical-ionization mass spectrometer[10] was employed to determine the molecular ion of the heptafluorobutyryl derivative. Samples were introduced by the direct probe method. The following conditions were used: probe temperature, 200°; source temperature, 150°; and ionization voltage, 70 v.

Quantitative Analysis—A 1-μl aliquot of the derivative solution was injected into the reporting gas chromatograph equipped with an automatic liquid sampler. Quantitative estimation of III in biological samples was accomplished by plotting the area ratios of the derivative and the internal standard against a series of known concentrations of III.

Animal Studies—An amount of II equivalent to 10 mg of III/kg in 0.9% NaCl was injected into a male Wistar rat (200–300 g) through a cannula inserted into the right jugular vein[11]. A 0.1–0.2-ml blood sample was taken at appropriate time intervals from the cannula, which was exteriorized

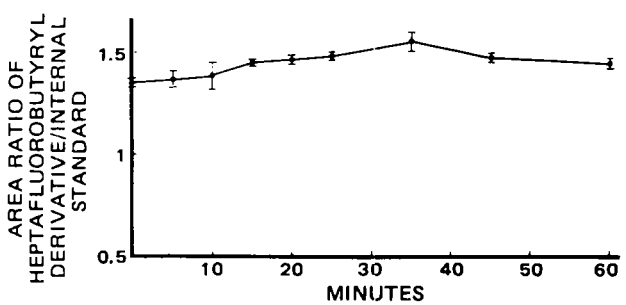

Figure 3—*Kinetics of the derivatizing reaction with respect to time.*

[10] DuPont model 21-490B.
[11] D. Soda, State University of New York at Buffalo, Amherst, NY, 1976.

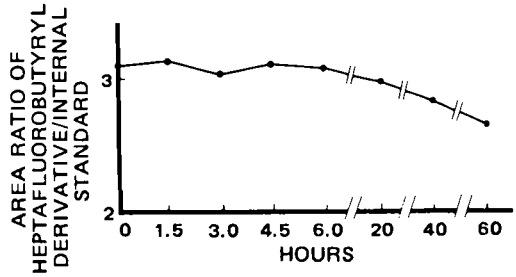

Figure 4—*Stability of the heptafluorobutyryl derivative with time.*

at the nape of the neck. The samples were immediately centrifuged and frozen until analysis. A plasma sample of 20–50 μl was extracted and analyzed as described.

RESULTS AND DISCUSSION

Purity Confirmation—The spectrum from the differential scanning calorimeter showed that II decomposed at 110°. No peaks were observed prior to decomposition, indicating that the purity of the hydrochloride salt was satisfactory.

After recrystallization of the free base from benzene, the differential scanning calorimetry spectra showed that an endothermic peak occurred at 120° before melting. When the samples were dried at 125° under vacuum for 2 hr, the peak disappeared (Fig. 1). It was postulated that benzene, the recrystallizing solvent, was either adsorbed onto or formed a solvate with the free base. The peak at 120° was confirmed to be a volatile substance by coupling the differential scanning calorimeter with effluent gas analysis. No further attempt was made to identify whether the solvent was adsorbed onto or incorporated into the crystal lattice of the free base.

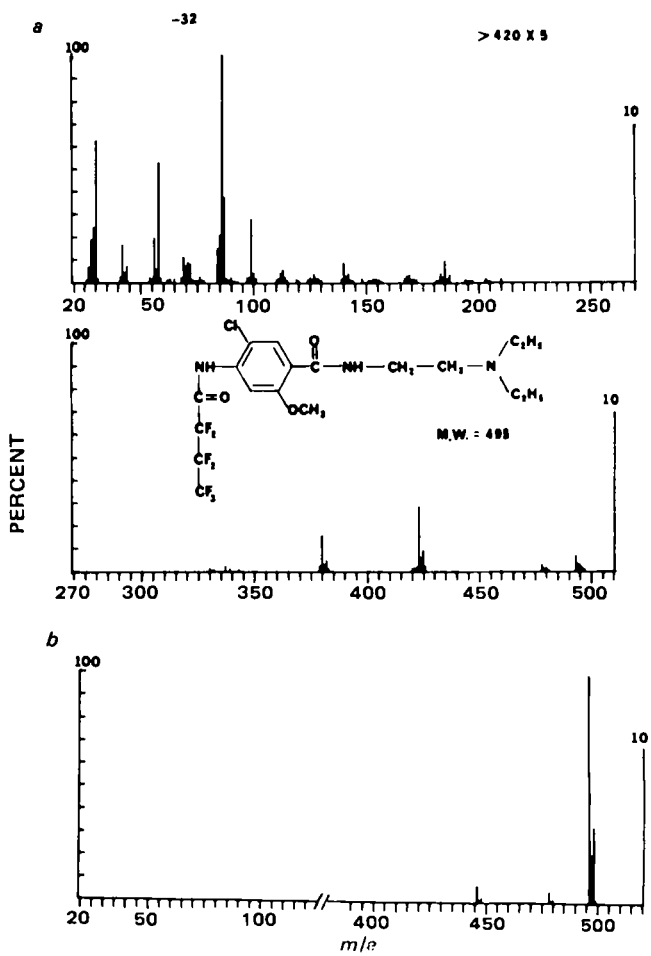

Figure 5—*Electron-impact* (a) *and chemical-ionization* (b) *mass spectra of the heptafluorobutyryl derivative of III extracted from plasma.*

Table II—Percent Recovery after Extraction from Biological Fluids

Metoclopramide Base Equivalent Added, ng	n^a	Plasma Extract		Whole Blood Extract		Urine Extract	
		% Recovered	% Deviation	% Recovered	% Deviation	% Recovered	% Deviation
229.09	5	92.84	±14.23	90.79	±0.84	94.16	±2.10
458.18	5	85.09	±6.35	82.83	±3.35	82.08	±6.55
641.45	5	85.56	±1.65	81.06	±5.54	84.42	±5.54
824.72	5	84.57	±7.75	79.33	±4.40	78.27	±1.04
Average		87.02	±4.49	83.50	±6.06	84.73	±8.00

[a] Each n is the average of three determinations.

GLC—Representative chromatograms from the extracts of the plasma, blood, and urine samples are shown in Fig. 2. A peak at 8.38 min was observed in the chromatograms of the blank plasma and the whole blood (Figs. 2*a* and 2*b*). The unidentified impurity did not interfere with either the derivative of III or the internal standard peak (Figs. 2*d* and 2*e*). No endogenous disturbances were found from the urine extract (Figs. 2*c* and 2*f*). Baseline resolution was achieved between the peaks when the 3% OV-17 column was used.

Chromatographic response was linear in the range studied (91.6–824.7 ng/ml). The calibration curve was obtained by analyzing blank plasma samples spiked with various amounts of the drug (Table I). From the linear regression analysis, the best fit through the data points was described by $y = 0.002508x - 0.019$, with $r^2 = 0.999$.

Reaction Time—The optimum derivatizing time was evaluated by incubating samples containing equivalent amounts of the base with I for various times at 55°. The yield of the derivative, as observed by the area ratio of the derivative to the internal standard, was monitored. No significant difference in response was found throughout the range of reaction time studied (0–60 min) (Fig. 3). To ensure complete derivatization, samples were incubated at 55° for 20 min during current analysis.

Stability of Derivative—As shown in Fig. 4, the area ratios of the derivative to the internal standard did not drop significantly after 20 hr of storage. The areas under the two peaks also did not change perceptibly during that time.

Removal of Excess I—Walle and Ehrsson (17) reported that the presence of trace amounts of a I residue produced chromatographic problems such as spurious peaks and a broad solvent front. Furthermore, excess I caused a huge solvent front, which masked the heptafluorobutyryl derivative peak. Therefore, a method that could remove the excess reagent without diminishing the response of the derivative was necessary.

Walle and Ehrsson (17) suggested two methods: after incubation, dry the reaction mixture by a gentle stream of nitrogen; and hydrolyze excess I with water and neutralize it with aqueous ammonia. The former method decreased the response of the derivative by at least two-thirds when compared to the latter. Both methods were capable of removing excess I. The decrease in response when the former method was applied was probably due to the volatility of the derivative (17), whereas the loss of the derivative from evaporation was minimal with the latter method.

Recovery—A standard curve was prepared by derivatizing a serial dilution of the free base in benzene. After extraction of known quantities of II from biological fluids, the amount of free base recovered in the organic phase was determined by using the free base calibration curve. The average percentages of III recovered from plasma, whole blood, and urine were 87.02, 83.5, and 84.73, respectively (Table II). The respective percentage standard deviations were 4.49, 6.06, and 8.00.

Structural Confirmation of Derivative—The fragmentation patterns of the derivatized free base and plasma extracted from metoclopramide-dosed animals were found to be identical by GLC–mass spectrometry, indicating that III was being analyzed from the plasma samples. Like III (18) and its procaine analogs (19), cleavage occurred at the amine bond (*m/e* 423), as well as the carbonyl–amide bond (*m/e* 99 and 380). The base peak, *m/e* 86, was a result of the cleavage at the carbon–carbon bond beta to the amine nitrogen (Scheme II).

Although a monosubstitution reaction was postulated, the molecular ion was not readily discernible (Fig. 5*a*) from the electron-impact mass spectrum, perhaps because of the high ionization energy of the source. Further investigation is underway to clarify the causative mechanism. Since electron-impact mass spectrometry was not conclusive, chemical-ionization mass spectrometry was employed to reveal the molecular ion. From the chemical-ionization mass spectrum (Fig. 5*b*), a very intense *m/e* 496 peak, which corresponded to the $(MH)^+$ peak, was observed. The other two peaks, *m/e* 478 and 446, were postulated to be $(MH - water)^+$ and $(MH - water - methyl\ alcohol)^+$, respectively.

Animal Data—The applicability of this method was demonstrated by studying the elimination kinetics of III in rats after a 10-mg/kg iv dose. Because of the extremely high sensitivity of this method, only small volumes of plasma (20–50 μl) were required. This method permits serial blood sampling from the same rat over a sufficient period to allow adequate characterization of the pharmacokinetics of III.

Distribution was extremely rapid within the first few minutes after injection. An apparent distribution equilibrium was established at around 16 min. From the semilog plot of the plasma profile (Fig. 6), a linear elimination phase was seen. The half-life calculated was 49.75 ± 8 min.

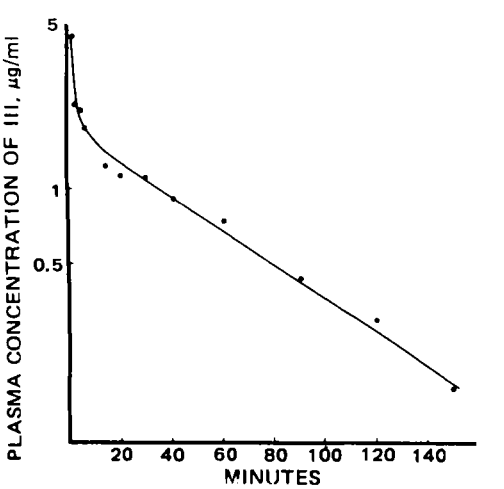

Figure 6—*Representative semilog plot of the plasma profile of III in a rat after a 10-mg/kg iv dose.*

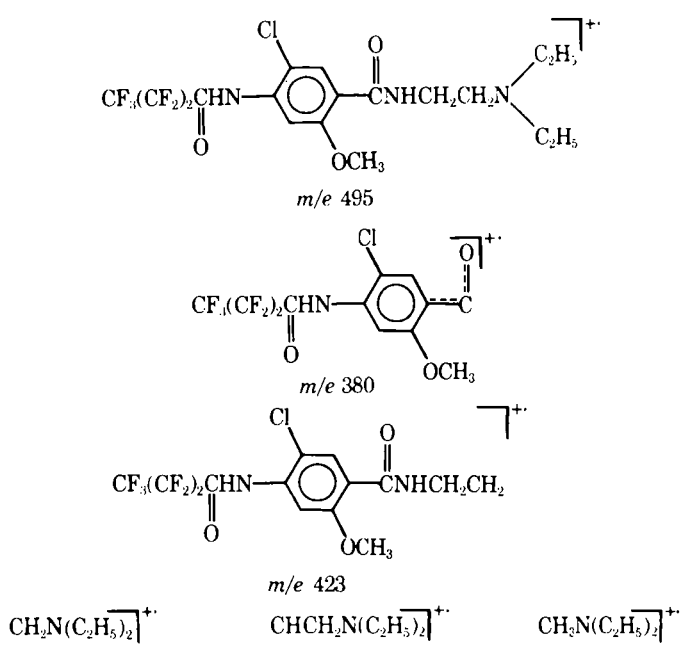

Scheme II

When these results were compared to the pharmacokinetic data obtained by Tunon *et al.* (16), it was found that the "elimination phase" previously reported was actually part of the distribution phase. Therefore, the half-life (13–20 min) calculated was erroneous. This error was due to the use of a relatively insensitive assay that was unable to detect any III after 16 min. The method reported here offers significant superiority over the Bakke and Segura (15) TLC–photodensitometry method. A smaller volume of plasma is required for analysis, thereby obviating the need for the sacrifice of individual rats to obtain data.

REFERENCES

(1) A. J. Handley, *Br. J. Clin. Pract.*, **21**, 460 (1967).

(2) L. Kreel, M. Trott, and T. H. Howells, *Clin. Radiol.*, **23**, 213 (1972).

(3) J. A. H. Davies and T. H. Howells, *Postgrad. Med. J., Suppl. 4*, **49**, 58 (1973).

(4) R. McCallum, A. Ippoliti, C. Cooney, and R. A. L. Sturdevant, *Gastroenterology*, **70**, 962 (1976).

(5) J. A. P. Trafford, A. M. H. Fisher, S. Marshall, and A. H. Douthwaite, *Br. J. Clin. Prac.*, **21**, 457 (1967).

(6) A. G. Johnson, *Gut*, **12**, 421 (1971).

(7) W. B. James and R. Hume, *ibid.*, **9**, 203 (1968).

(8) J. Nimmo, R. C. Heading, P. Tothill, and L. F. Prescott, *Br. Med. J.*, **1**, 587 (1973).

(9) G. Gothoni, P. Pentikainen, H. I. Vapaatalo, R. Hackmen, and K. AF Bjorksten, *Ann. Clin. Res.*, **4**, 228 (1972).

(10) P. T. Mearrick, D. N. Wade, D. J. Birkett, and J. Morris, *Aust. N. Z. J. Med.*, **4**, 144 (1974).

(11) F. Jamali and J. E. Axelson, *J. Pharm. Sci.*, **66**, 1540 (1977).

(12) V. Manninen, A. Apajalahti, J. Melin, and M. Karesja, *Lancet*, **1**, 398 (1973).

(13) T. Arita, R. Hori, K. Ito, K. Ichikawa, and T. Uesugi, *Chem. Pharm. Bull.*, **18**, 1663 (1970).

(14) D. A. Cowan, G. Huizing, and A. H. Beckett, *Xenobiotica*, **6**, 605 (1976).

(15) O. M. Bakke and J. Segura, *J. Pharm. Pharmacol.*, **28**, 32 (1976).

(16) P. E. Tunon, C. Tous, A. Martin, and J. M. Pla'Delfina, *Cienc. Ind. Farm.*, **6**, (1974).

(17) T. Walle and H. Ehrsson, *Acta Pharm. Suec.*, **7**, 389 (1970).

(18) R. Venkataramanan and J. E. Axelson, *J. Pharm. Sci.*, **67**, 201 (1978).

(19) W. A. Garland, W. F. Trager, and S. D. Nelson, *Biomed. Mass Spectrom.*, **1**, 124 (1974).

ACKNOWLEDGMENTS

Supported by University of British Columbia Grant 32-9400, B. C. Heart Foundation Grant 65-0566, and M. R. C. Grant MA-5358.

The authors are grateful to Dr. F. Jamali for his constructive advice and to Dr. F. Abbott of the Faculty of Pharmaceutical Sciences, University of British Columbia, Vancouver, B.C., Canada, Dr. D. Hasman of Cantest Ltd., and Dr. W. Godolphin of Vancouver General Hospital for their help and assistance in the mass spectrometry analysis.

Interaction of Sulindac and Metabolite with Human Serum Albumin

M. A. SHAMS-ELDEEN, J. J. VALLNER ˣ, and T. E. NEEDHAM

Received April 28, 1977, from the *Department of Pharmaceutics, School of Pharmacy, University of Georgia, Athens, GA 30602.* Accepted for publication November 29, 1977.

Abstract □ The binding of the newly developed nonsteroidal anti-inflammatory agent sulindac and its principal active metabolite, sulindac sulfide, to human serum albumin was investigated. With the methods of dialysis, fluorescence quenching, and difference spectrophotometry, it was found that both agents were extensively bound to albumin. The binding affinity of the metabolite was considerably higher than that of sulindac and this effect may be related to its prolonged plasma half-life *versus* the parent drug. Sulindac binding was albumin concentration dependent, which gave rise to an unfamiliar Scatchard analysis of the dialysis data.

Keyphrases □ Sulindac—and metabolite, binding to human serum albumin □ Binding, protein—sulindac and metabolite to human serum albumin □ Anti-inflammatory agents—sulindac and metabolite, binding to human serum albumin

Drug synthesis and testing for the treatment of arthritis are ongoing areas of research. Many nonsteroidal anti-inflammatory agents have been synthesized (1). Recently, sulindac[1], *cis*-5-fluoro-2-methyl-1-[*p*-(methylsulfinyl)-benzylidene]indene-3-acetic acid (I), was developed as a nonsteroidal anti-inflammatory agent (2). The drug is well absorbed after oral administration in all tested species.

Most anti-inflammatory drugs induce some GI side effects. However, sulindac does not induce significant irritative or erosive effects on the GI tracts of healthy subjects (3–8). In humans, the only significant enterohepatic biotransformations undergone by sulindac are irreversible oxidation of its sulfoxide function to sulfone and reversible reduction to sulfide (II) (9–12).

The potency of sulindac is approximately half that of indomethacin, while the safety ratio between the dose causing intestinal perforation or gastric hemorrhage and the anti-inflammatory dose is several times higher for sulindac than for indomethacin. Comparisons of activity were made among the sulfoxide, the sulfide, and the sulfone. The sulfone was not active at high doses in several assays, but the sulfide derivative was generally twice as active as the parent compound and was as active as in-

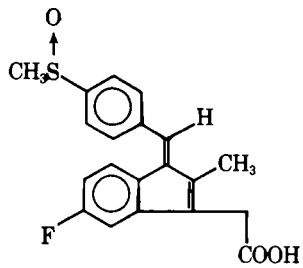

I

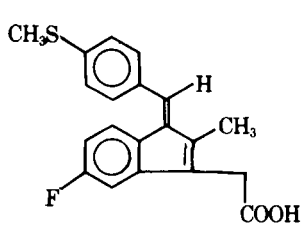

II

[1] Clinoril, MK-231.

0022-3549/78/0800-1077$01.00/0

© 1978, American Pharmaceutical Association

When these results were compared to the pharmacokinetic data obtained by Tunon *et al.* (16), it was found that the "elimination phase" previously reported was actually part of the distribution phase. Therefore, the half-life (13–20 min) calculated was erroneous. This error was due to the use of a relatively insensitive assay that was unable to detect any III after 16 min. The method reported here offers significant superiority over the Bakke and Segura (15) TLC–photodensitometry method. A smaller volume of plasma is required for analysis, thereby obviating the need for the sacrifice of individual rats to obtain data.

REFERENCES

(1) A. J. Handley, *Br. J. Clin. Pract.*, **21**, 460 (1967).

(2) L. Kreel, M. Trott, and T. H. Howells, *Clin. Radiol.*, **23**, 213 (1972).

(3) J. A. H. Davies and T. H. Howells, *Postgrad. Med. J., Suppl. 4*, **49**, 58 (1973).

(4) R. McCallum, A. Ippoliti, C. Cooney, and R. A. L. Sturdevant, *Gastroenterology*, **70**, 962 (1976).

(5) J. A. P. Trafford, A. M. H. Fisher, S. Marshall, and A. H. Douthwaite, *Br. J. Clin. Prac.*, **21**, 457 (1967).

(6) A. G. Johnson, *Gut*, **12**, 421 (1971).

(7) W. B. James and R. Hume, *ibid.*, **9**, 203 (1968).

(8) J. Nimmo, R. C. Heading, P. Tothill, and L. F. Prescott, *Br. Med. J.*, **1**, 587 (1973).

(9) G. Gothoni, P. Pentikainen, H. I. Vapaatalo, R. Hackmen, and K. AF Bjorksten, *Ann. Clin. Res.*, **4**, 228 (1972).

(10) P. T. Mearrick, D. N. Wade, D. J. Birkett, and J. Morris, *Aust. N. Z. J. Med.*, **4**, 144 (1974).

(11) F. Jamali and J. E. Axelson, *J. Pharm. Sci.*, **66**, 1540 (1977).

(12) V. Manninen, A. Apajalahti, J. Melin, and M. Karesja, *Lancet*, **1**, 398 (1973).

(13) T. Arita, R. Hori, K. Ito, K. Ichikawa, and T. Uesugi, *Chem. Pharm. Bull.*, **18**, 1663 (1970).

(14) D. A. Cowan, G. Huizing, and A. H. Beckett, *Xenobiotica*, **6**, 605 (1976).

(15) O. M. Bakke and J. Segura, *J. Pharm. Pharmacol.*, **28**, 32 (1976).

(16) P. E. Tunon, C. Tous, A. Martin, and J. M. Pla'Delfina, *Cienc. Ind. Farm.*, **6**, (1974).

(17) T. Walle and H. Ehrsson, *Acta Pharm. Suec.*, **7**, 389 (1970).

(18) R. Venkataramanan and J. E. Axelson, *J. Pharm. Sci.*, **67**, 201 (1978).

(19) W. A. Garland, W. F. Trager, and S. D. Nelson, *Biomed. Mass Spectrom.*, **1**, 124 (1974).

ACKNOWLEDGMENTS

Supported by University of British Columbia Grant 32-9400, B. C. Heart Foundation Grant 65-0566, and M. R. C. Grant MA-5358.

The authors are grateful to Dr. F. Jamali for his constructive advice and to Dr. F. Abbott of the Faculty of Pharmaceutical Sciences, University of British Columbia, Vancouver, B.C., Canada, Dr. D. Hasman of Cantest Ltd., and Dr. W. Godolphin of Vancouver General Hospital for their help and assistance in the mass spectrometry analysis.

Interaction of Sulindac and Metabolite with Human Serum Albumin

M. A. SHAMS-ELDEEN, J. J. VALLNER ˣ, and T. E. NEEDHAM

Received April 28, 1977, from the *Department of Pharmaceutics, School of Pharmacy, University of Georgia, Athens, GA 30602.* Accepted for publication November 29, 1977.

Abstract □ The binding of the newly developed nonsteroidal anti-inflammatory agent sulindac and its principal active metabolite, sulindac sulfide, to human serum albumin was investigated. With the methods of dialysis, fluorescence quenching, and difference spectrophotometry, it was found that both agents were extensively bound to albumin. The binding affinity of the metabolite was considerably higher than that of sulindac and this effect may be related to its prolonged plasma half-life *versus* the parent drug. Sulindac binding was albumin concentration dependent, which gave rise to an unfamiliar Scatchard analysis of the dialysis data.

Keyphrases □ Sulindac—and metabolite, binding to human serum albumin □ Binding, protein—sulindac and metabolite to human serum albumin □ Anti-inflammatory agents—sulindac and metabolite, binding to human serum albumin

Drug synthesis and testing for the treatment of arthritis are ongoing areas of research. Many nonsteroidal anti-inflammatory agents have been synthesized (1). Recently, sulindac[1], *cis*-5-fluoro-2-methyl-1-[*p*-(methylsulfinyl)-benzylidene]indene-3-acetic acid (I), was developed as a nonsteroidal anti-inflammatory agent (2). The drug is well absorbed after oral administration in all tested species.

Most anti-inflammatory drugs induce some GI side effects. However, sulindac does not induce significant irritative or erosive effects on the GI tracts of healthy subjects (3–8). In humans, the only significant enterohepatic biotransformations undergone by sulindac are irreversible oxidation of its sulfoxide function to sulfone and reversible reduction to sulfide (II) (9–12).

The potency of sulindac is approximately half that of indomethacin, while the safety ratio between the dose causing intestinal perforation or gastric hemorrhage and the anti-inflammatory dose is several times higher for sulindac than for indomethacin. Comparisons of activity were made among the sulfoxide, the sulfide, and the sulfone. The sulfone was not active at high doses in several assays, but the sulfide derivative was generally twice as active as the parent compound and was as active as in-

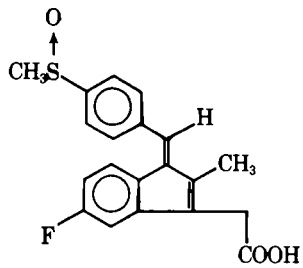

I

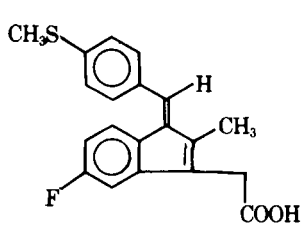

II

[1] Clinoril, MK-231.

0022-3549/78/0800-1077$01.00/0

© 1978, American Pharmaceutical Association

Table I—Results of the Quenching of Native Human Serum Albumin Fluorescence by Sulindac and the Sulfide Derivative

Albumin Concentration, M	Mole ratio, n		Association Constant $\times M^{-1}$
	Sulindac		
1.45×10^{-5}	1.3		1.07×10^{5}
7.25×10^{-6}	3.0		7.78×10^{4}
3.62×10^{-6}	6.0		1.41×10^{5}
1.45×10^{-6}	12.0		6.16×10^{4}
		Average	9.69×10^{4}
	Sulindac Sulfide		
1.45×10^{-5}	1.1		1.94×10^{5}
1.16×10^{-5}	1.1		1.33×10^{5}
5.80×10^{-6}	1.1		1.07×10^{5}
2.89×10^{-6}	1.1		1.07×10^{5}
1.45×10^{-6}	1.0		1.34×10^{5}
		Average	1.35×10^{5}

domethacin (13). Upon administration of the sulfoxide, the sulfide soon appears in the plasma. In humans, the plasma half-life of the metabolically formed sulfide was greater than 18.2 hr whereas that of the parent compound was only 1.5–3 hr (9, 13, 14).

Almost all anti-inflammatory agents are highly bound to serum albumin, and only the unbound fraction exerts the pharmacological effect (15). The binding of a new drug to human serum albumin should be examined, especially if the drug is an acidic molecule, because competitive binding with serum protein among acidic drugs was shown to be significant (16, 17). Indomethacin and phenylbutazone also were shown to compete with concurrently administered acidic drugs. Previous results suggest that sulindac, as well as its active metabolite, may have high binding affinities to human serum albumin (9).

Fluorescence spectroscopy and UV absorption spectroscopy can provide valuable information on the drug–protein interaction (18–21). The interaction of both sulindac and its metabolite with human serum albumin was determined by difference spectrophotometry, fluorescence quenching measurement, and equilibrium dialysis techniques.

EXPERIMENTAL

Materials—Human serum albumin fraction V[2] was used and had been investigated previously for purity. Sulindac[3] and the sulfide[3] derivative were used as supplied. Other materials were reagent grade and were used as supplied. All solutions were prepared in pH 7.4 physiological phosphate buffer.

For the equilibrium dialysis method, rigid acrylic plastic 10-ml dialysis cells were used. The dialysis membranes contained glycerin as a plasticizer, traces of sulfurous compounds, and heavy metal ions (22). Some of these contaminants may have rather drastic effects on protein solutions and were removed before use by subjecting the membranes to each of the following solutions for 1 hr at 80°: 5% Na_2CO_3 in 50 mM edetate, 1% acetic acid, and deionized water (23, 24). Finally, the membranes were washed thoroughly with deionized water several times, stored at 4°, and used within 3 weeks.

Since the sulfide derivative is less water soluble than the parent drug, the stock solutions were prepared with the aid of sodium hydroxide (*i.e.*, deionized water adjusted to pH 9.0–10.0). Further dilution was made with the physiological buffer, which kept the final pH at 7.4.

Fluorescence Quenching—Solutions of albumin, 1.45×10^{-6}–1.45×10^{-5} M, were prepared at ambient temperature, and each solution was carried through the following procedure. The fluorescence intensity of the native protein solution was adjusted to the maximum and recorded[4] at excitation and emission wavelengths of 288 and 331 nm, respectively. Aliquots of 10 μl of sulindac or the sulfide derivative stock solutions were subsequently added to the protein-containing cell to give a final concentration of drug of 6.95×10^{-6}–1.10×10^{-3} M for sulindac and 2.91×10^{-6}–5.88×10^{-5} M for the sulfide derivative. Titration of the fluorescent intensity of the albumin was carried out. At the selected wavelengths, neither sulindac nor the sulfide contributed to the fluorescence.

The protein concentration was kept constant throughout each quenching titration by preparing the drug solution in the protein solution under investigation. Drug–protein ratios in these experiments ranged from 0.50 to 70.4 for sulindac and from 0.20 to 29.50 for the sulfide derivative.

Difference Spectrophotometry—UV-visible spectra of sulindac solutions were recorded[5] and showed maxima at 325 ($a = 1.29 \times 10^4$) and 284 ($a = 1.55 \times 10^4$) nm. For difference spectrophotometric studies, the tandem cell technique was employed (25) in the split beam mode. This technique is capable of measuring small differences from the baseline, due to binding of the small molecule to the protein, provided that both protein and drug concentrations are kept constant in the reference and sample compartments.

The baseline was obtained by placing equal volumes of the protein solution in one cell and buffer in the other cell of the reference beam; the sample compartment contained exactly the same solutions. Difference absorbance curves were recorded by adding drug solution to the buffer cell in the reference beam and the protein cell in the sample beam (equal volumes of the same stock drug solution) to give final concentrations of drug ranging from 3.43×10^{-6} to 3.33×10^{-4} M for sulindac.

To maintain a constant protein concentration throughout the titration, each addition of drug to the protein solution in the sample compartment was accompanied by the concomitant addition of an equal volume of albumin solution at a concentration twice that in the cell (26). Similarly, drug concentration was maintained equivalent in both beams during titration by the addition of an equal volume of buffer to the cell containing drug and buffer in the reference compartment.

Drug–Surfactant Interaction—Difference spectroscopic studies were repeated in an identical manner to that already described, except that 0.025% solutions of cetylpyridinium chloride, sodium lauryl sulfate, or polysorbate 80 were used in place of the protein.

Equilibrium Dialysis—Equilibrium between drug and human serum albumin was carried out in dialysis cells shaken[6] for 16 hr at room temperature. Both drug and protein solutions were placed on the same side of the dialysis membrane, and the phosphate buffer was placed on the other side. Determination of the free drug was carried out spectrophotometrically [the sulfide derivative had a maximum at 345 nm ($a = 1.745 \times 10^4$)].

The sulfide concentration ranged from 5.88×10^{-6} to 4.41×10^{-5} M (drug–protein ratio of 0.31:12.15) while the sulindac concentration ranged from 1.12×10^{-5} to 1.40×10^{-3} M (drug–protein ratio of 0.78:96.93).

RESULTS AND DISCUSSION

Sulindac and the sulfide were shown to interact with albumin by the technique of fluorescence quenching. These measurements were based on the fact that albumin contains a single tryptophan residue that emits radiation at 331 nm when irradiated at 288 nm. The native fluorescence of human serum albumin resides in a single tryptophan residue incorporated into an apparently hydrophobic region of the protein (27). This region is postulated to be a high affinity site, involved in the binding of anionic drugs with the protein. Interaction of drug with this site perturbs the tryptophan environment, decreasing the fluorescent intensity of the protein.

Fluorescence quenching measurements of drug–protein interactions are only sensitive to perturbations in the tryptophan residue or region. Secondary binding sites removed from the fluorescent moiety are not detected (26). Interaction of small molecules with serum albumin resulting in a perturbation of the environment surrounding the tryptophan may be sensed by reduction in fluorescent intensity attributed to the amino acid. Addition of sulindac and the sulfide derivative to albumin solutions of varying concentrations resulted in a quenching of the native fluorescence (Table I).

A typical titration curve for the drug–albumin interaction is shown in Fig. 1. Extrapolation of the linear portion of the curves gave the stoichiometric point from which the mole ratio (n) of the drug bound to protein was obtained (21). Association constants of the interaction of the drug with protein were also calculated (28) from the titration curves

[2] Armour Pharmaceutical Co., Kankakee, Ill.
[3] Merck Sharp & Dohme Research Laboratories.
[4] Perkin-Elmer fluorescence spectrophotometer MPF-4 attached to Perkin-Elmer recorder 56.
[5] Model 118 spectrophotometer, Cary Instruments, Monrovia, Calif.
[6] Wrist-action shaker, Burrell Corp., Pittsburgh, Pa.

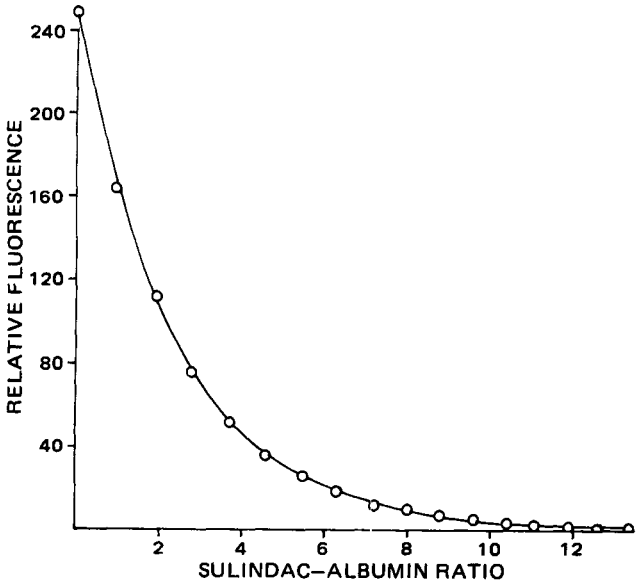

Figure 1—*Example of fluorescence quenching of human serum albumin by sulindac. Albumin concentration was 7.25 × 10^{-6} M.*

(Table I). Table I shows that n for sulindac was albumin concentration dependent; that is, higher molar ratios of bound sulindac to protein were obtained with dilute albumin solutions; n for the sulfide derivative was equal to 1. Attallah and Lata (28) attributed the greater testosterone binding capacity in dilute solutions compared with concentrated solutions of albumin to a configurational change in the protein. Similar observations concerning the binding of small molecules to proteins were made (29–32).

Interactions between serum albumin, sulindac, and the sulfide derivative also were examined by difference spectrophotometry. Difference absorption spectra for the association of sulindac with protein in phosphate buffer (Fig. 2) were characterized by positive peaks at 355 ± 5 and 300 nm and negative peaks at 315 and 282 ± 1 nm. The absorption spectrum of sulindac in the buffer was characterized by peaks at 325 and 284 nm. Families of curves were generated by the incremental addition of sulindac to protein solutions of fixed concentration (7.25 × 10^{-6}, 1.45 × 10^{-5}, 2.89 × 10^{-5}, and 5.79 × 10^{-5} *M*). The sulfide derivative did not produce difference absorption spectra that contained both positive peaks and negative valleys, isosbestic points, or similar shapes with varying protein concentration. Adequate precautions (as described under *Experimental*) were taken to maintain equivalent concentrations of drug and protein in both the sample and the reference beam so that the curves had to be the result of an interaction between sulindac and albumin.

Close examination of the several difference spectral titrations recorded at different protein concentrations suggests that sulindac interacts with

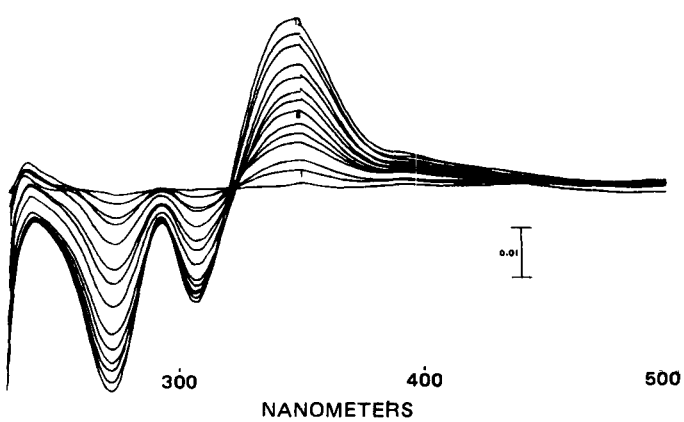

Figure 2—*Difference spectrophotometric titration of 1.45 × 10^{-5} M human serum albumin with sulindac. Each curve represents the addition of 25 μl of 5.62 × 10^{-4} M sulindac to 2 ml (initially) of buffer in the reference compartment and to 2 ml of protein in the sample compartment. The numbers 1, 6, and 13 indicate the number of increments added.*

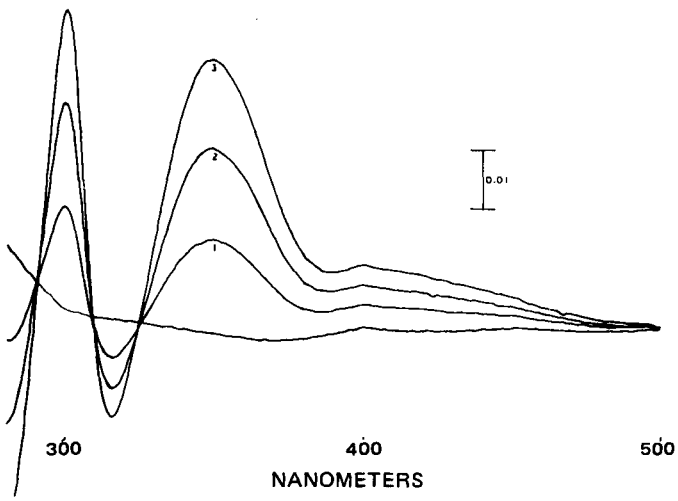

Figure 3—*Difference spectra of the interaction between cetylpyridinium chloride and sulindac. Cetrimide concentration was constant at 0.025%. Sulindac concentrations were 1.37 × 10^{-5} (curve 1), 2.67 × 10^{-5} (curve 2), and 3.91 × 10^{-5} (curve 3) M.*

albumin and that this interaction has no distinct isosbestic point maintained throughout the titrations; however, the absorbance differences have considerable magnitude and are reproducible (Fig. 2).

The difference spectra generated by titrating sulindac in the cationic detergent cetylpyridinium chloride (Fig. 3) were similar to those observed when the drug bound to human serum albumin. Anionic and nonionic detergents did not produce similar spectral differences. Thus, the albumin binding site may be cationic and, possibly, hydrophobic in nature.

Drug binding to proteins often causes small conformational changes. When such changes alter the environment of the protein amino acid residues, spectral shifts are often observed. With sulindac, spectral shifts of the positive absorption around 350 nm indicated that the wavelength also increased as the protein concentration increased. However, upon increasing the sulindac to protein ratio, a spectral shift in the wavelength of the positive peak at 350 nm toward shorter wavelengths was observed. This result may indicate that the sulindac–protein interaction is protein concentration dependent and supports the observation seen with the fluorescence quenching.

On the other hand, although the sulfide derivative is more hydrophobic (less soluble in the phosphate buffer), it failed to produce definite reproducible difference spectra. A possible explanation for the lack of a sulfide difference spectrum may be the difference in structural formula between sulindac and its metabolite. While the parent compound is highly electron donating because of its conjugated double bonds in addition to

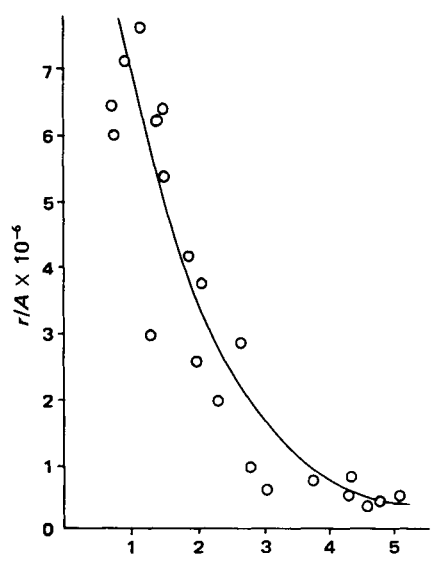

Figure 4—*Scatchard plot of dialysis data for the interaction of sulindac sulfide with human serum albumin (r is moles of drug bound per mole of protein, and A is the free concentration of drug).*

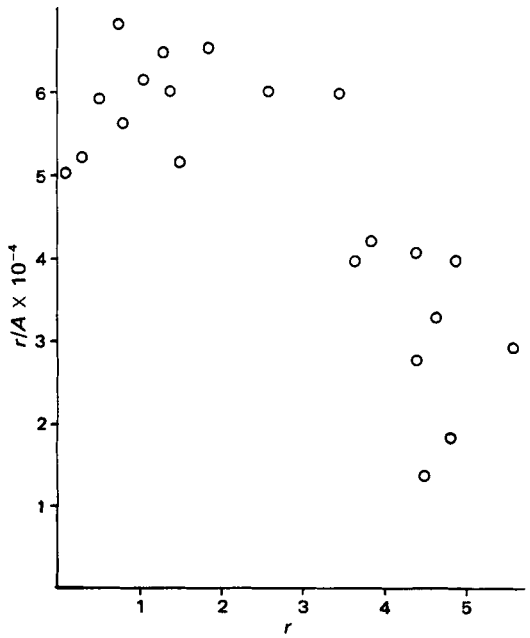

Figure 5—*Scatchard representation of dialysis data obtained for sulindac–albumin interaction. No lines are drawn through the points because these data may represent a cooperative process until* r *becomes greater than 2.*

the sulfoxide and the carbonyl groups, the sulfide metabolite is missing the oxygen atom, which makes it less electron donating.

The interaction between human serum albumin and both sulindac and the sulfide derivative also was examined by equilibrium dialysis. Scatchard plots were constructed for the data from both sulindac and sulfide (Figs. 4 and 5). These Scatchard plots are not the same in shape; however, the total number of binding sites (n_t) for both sulindac and sulindac sulfide is approximately equivalent. The mode of interaction of sulindac with human serum albumin may be different from that of the metabolite because of the difference in the chemical nature of the compounds. Sulindac may open new sites on the albumin molecule up to the r value of 2, in which case a usual Scatchard representation is found (Fig. 5). This behavior may also be explained by the highly electron-donating groups in the sulindac molecule. The association constant for sulindac is approximately 6×10^4. On the other hand, the sulfide derivative has a familiar Scatchard plot (Fig. 4), which shows two sets of binding sites; upon application of a nonbiased statistical technique (33, 34), the parameters are $n_1 = 1.07$, $K_1 = 3.4 \times 10^6$, $n_2 = 3.75$, and $K_2 = 5.7 \times 10^5$.

Quenching fluorescence, spectral differences, and equilibrium dialysis data support the fact that both sulindac and its active metabolite interact with human serum albumin. Fluorescence measurements showed that the binding constant obtained for the sulfide derivative was more than that obtained for the parent compound. This observation was confirmed by the data obtained from the equilibrium dialysis method, where the binding affinity of the sulfide derivative was about 10–100 times greater than sulindac. Meanwhile, some investigators (32) reported that the calculation of association constants from quenching fluorescence yielded values indicative of higher binding affinities than did values obtained by other methods. This observation is also true for sulindac.

In conclusion, sulindac provides some advantages over other known anti-inflammatory drugs. The reversible biotransformation between sulindac and its active metabolite avoids the initial exposure of gastric and small intestinal mucosa to the active form of the drug and also keeps systemic levels of the active drug constant by means of enterohepatic recycling. In addition, the prolonged anti-inflammatory effect of the sulfide derivative can possibly be attributed to its higher binding affinity.

REFERENCES

(1) S. Wong, *Annu. Rep. Med. Chem.*, **10**, 172 (1975).

(2) T. Y. Shen, B. E. Witzel, H. Jones, B. O. Linn, J. McPherson, R. Greenwald, M. Fordice, and A. Jacobs, *Fed. Proc.*, **31**, 577 Abst. (1972).

(3) W. H. Charade and W. A. Peredrico, *Scand. J. Rheumatol.*, **4** (Suppl. 8), Abstract S02-03 (1975).

(4) I. Caruso, M. Fumagalli, F. Montrone, M. Vernazza, and L. Carratelli, *ibid.*, **4** (Suppl. 8), Abstract 097 (1975).

(5) T. C. Highton and R. Jeremy, *ibid.*, **4** (Suppl. 8), Abstract S02-06 (1975).

(6) O. Holopanen and L. Inberg, *ibid.*, **4** (Suppl. 8), Abstract S02-02 (1975).

(7) A. Cohen, *Clin. Pharmacol. Ther.*, **20**, 238 (1976).

(8) C. G. Van Arman, E. A. Risley, and G. W. Nuss, *Fed. Proc.*, **31**, 577, Abstract (1972).

(9) H. B. Hucker, S. C. Stauffer, S. D. White, R. E. Rhodes, B. H. Arison, E. M. Umbenhauer, R. J. Bower, and F. G. McMahon, *Drug Metab. Dispos.*, **1**, 721 (1973).

(10) L. E. Hare, C. A. Ditzler, M. Michens, and D. E. Duggan, *Pharmacologist*, **16**, 221, Abstract 171 (1974).

(11) H. B. Hucker, S. C. Stauffer, R. J. Bower, E. R. Umbenhauer, and F. G. McMahon, *Fed. Proc.*, **31**, 577, Abstract (1972).

(12) D. E. Duggan, K. P. Hooke, R. Carlson, and C. G. Zanarman, *Pharmacologist*, **18**, 164, Abstract 286 (1976).

(13) C. G. Van Arman and E. A. Risley, "Proceedings of a Symposium at the VIII European Rheumatology Congress, Helsinki," 1975, Raven, New York, N.Y., 1976, pp. 9–36.

(14) T. Y. Shen, *ibid.*, pp. 1–8.

(15) B. K. Martin, *Nature*, **207**, 274 (1965).

(16) H. M. Solomon, *Proc. Int. Congr. Pharmacol. 4th*, **4**, 169 (1970).

(17) C. M. Kunin, *J. Lab. Clin. Med.*, **65**, 416 (1965).

(18) C. F. Chignell, *Adv. Drug Res.*, **5**, 55 (1970).

(19) C. F. Chignell, *Life Sci.*, **7**, 1181 (1968).

(20) C. F. Chignell, *Mol. Pharmacol.*, **5**, 244 (1969).

(21) *Ibid.*, **5**, 455 (1969).

(22) W. B. Jakoby, in "Methods in Enzymology," vol. XXII, S. P. Colowick and N. O. Kaplan, Eds., Academic, New York, N.Y., 1971, p. 25.

(23) K. Moldane and L. Grossman, in *ibid.*, vol. XX, p. 72.

(24) K. Moldane and L. Grossman, in *ibid.*, vol. XXI, p. 483.

(25) A. S. Brill and H. E. Sandberg, *Biophys. J.*, **8**, 664 (1968).

(26) J. J. Vallner, L. A. Sternson, and D. L. Parsons, *J. Pharm. Sci.*, **65**, 873 (1976).

(27) J. B. Swaney and I. M. Klotz, *Biochemistry*, **9**, 2570 (1970).

(28) N. A. Attallah and G. F. Lata, *Biochim. Biophys. Acta*, **168**, 321 (1968).

(29) I. M. Klotz and J. Urquhart, *J. Phys. Chem.*, **53**, 100 (1949).

(30) B. Caroll, *J. Am. Chem. Soc.*, **72**, 2763 (1950).

(31) A. Ray, J. A. Reylands, H. Polet, and J. Steinhardt, *Biochemistry*, **5**, 2606 (1966).

(32) W. K. Brunkhorst and E. L. Hess, *Arch. Biochem. Biophys.*, **111**, 54 (1965).

(33) J. H. Perrin, J. J. Vallner, and S. Wold, *Biochim. Biophys. Acta*, **371**, 482 (1974).

(34) J. H. Perrin, J. J. Vallner, and D. Nelson, *Biochem. Pharmacol.*, **24**, 769 (1975).

ACKNOWLEDGMENTS

The authors thank Dr. T. Y. Shen of Merck Research Laboratories for the gift of sulindac and metabolite.

Mechanism of Adsorption of Clindamycin and Tetracycline by Montmorillonite

LINDA S. PORUBCAN *, CARLOS J. SERNA [1], JOE L. WHITE ‡, and STANLEY L. HEM *x

Received September 6, 1977, from the *Department of Industrial and Physical Pharmacy and the [1]Department of Agronomy, Purdue University, West Lafayette, IN 47907. Accepted for publication November 30, 1977.

Abstract □ IR and X-ray analyses of the interaction of clindamycin with montmorillonite indicate that clindamycin is adsorbed by a cation-exchange mechanism under pH conditions favoring the cationic form of the drug and by physical adsorption when the unionized drug is present. This physical adsorption is relatively weak since the drug is readily desorbed by alkaline washing. Tetracycline is adsorbed by cation exchange at low pH values where the +00 species predominates. Complexation with divalent interlayer cations contributes significantly to adsorption at higher pH values where the +−0 and +−− species exist. In a strongly alkaline solution, the 0−− species was not adsorbed in the interlayer space of montmorillonite but rather produced an external calcium–tetracycline complex. This study illustrates the utility of X-ray and IR analyses in elucidating the mechanisms responsible for clay–drug interactions.

Keyphrases □ Clindamycin—adsorption to montmorillonite, IR and X-ray analyses of mechanism □ Tetracycline—adsorption to montmorillonite, IR and X-ray analyses of mechanism □ Montmorillonite—adsorption of clindamycin and tetracycline, IR and X-ray analyses of mechanism □ Adsorption—clindamycin and tetracycline to montmorillonite, IR and X-ray analyses of mechanism □ Antibacterials—clindamycin and tetracycline, adsorption to montmorillonite, IR and X-ray analyses of mechanism □ Clays—montmorillonite, adsorption of clindamycin and tetracycline, IR and X-ray analyses of mechanism

Clays are widely used in pharmaceuticals, and the applications of their properties range from suspending agents (1) to carriers in sustained-release dosage forms (2). Therefore, the possible interactions of clays with drugs is important.

BACKGROUND

Clay–drug systems have been investigated by the use of adsorption isotherms. This classical approach indicates the quantity of compound adsorbed, the rate, and other physical parameters. However, only indirect evidence of the adsorption mechanism can be obtained. Swelling clays, especially montmorillonite, are unique in that their c-axis spacing adapts to the intercalated molecule when internal adsorption occurs. Changes in this parameter can be detected using X-ray diffractometry. In addition, the large internal surface in montmorillonite leads to a high degree of adsorption and permits direct observation of the adsorbate by IR spectroscopy. Perturbations of functional groups in the adsorbed molecules can be observed by IR spectroscopy and give direct information about the adsorption mechanism (3, 4).

Numerous organic molecules can be adsorbed by clays (5). For simple molecules, X-ray and IR methods have been used to elucidate the adsorption mechanisms and have defined the interlayer orientation of the molecule (6–8). Possible mechanisms include hydrogen bonding and van der Waals forces, which are means of physical adsorption, and cation exchange, protonation, and complexation, which are encompassed by chemisorption (9–11). For more complicated molecules, several adsorption mechanisms can operate simultaneously, depending on the pH, concentration, temperature, and interlayer cation (9).

Drug interactions with clays tend to be complex because of the size and structure of the drug molecules. Several papers reported the behavior of various drugs with montmorillonite but did not present direct evidence about the mechanisms (12, 13). To elucidate the adsorption mechanisms responsible for clay–drug interactions, the adsorption of the antibiotics clindamycin and tetracycline by montmorillonite was investigated.

Montmorillonite was chosen as the model clay because it exhibits both a high exchange capacity (80–150 mEq/100 g) (14) and a high surface area (700–800 m^2/g) (5). Other clays used in pharmaceutical systems include kaolin, a member of the kaolinite group, which has a low exchange capacity (3–15 mEq/100 g) (14) and a low surface area (20 m^2/g) (5), and attapulgite, a member of the fibrous pseudolayer clays, which in the pure state has no exchange capacity but possesses a high surface area (200 m^2/g) (15). Adsorption mechanisms of clays are related directly to surface area and/or exchange capacity. Results obtained with montmorillonite should be useful in predicting the adsorption behavior of clay minerals having a lower adsorptive capacity.

EXPERIMENTAL

Materials—All drugs and chemicals were either official or reagent grade. The source of clay was bentonite USP. X-ray diffraction indicated that montmorillonite was the major mineral present and that the bentonite also contained a small quantity of quartz. To study the clay component, which is responsible for the adsorptive properties in bentonite USP, the <2-μm clay fraction was separated by sedimentation and collected.

The clay fraction was concentrated to approximately 5% by evaporation of the water through dialysis tubing. Water removal was facilitated by placing the dialysis bags in an air stream. Bentonite USP is predominantly a sodium montmorillonite (1, 16); however, metal-ion analysis by atomic absorption spectrometry[2] showed that 10% of the exchange capacity is satisfied by divalent cations (7.1% Ca^{2+}, 2.7% Mg^{2+}).

Pure sodium montmorillonite was prepared by adding 1 *N* NaCl to the concentrated montmorillonite suspension until the clay suspension was approximately 2% (w/w). The suspension was stirred, centrifuged, and decanted; the clay was resuspended in 1 *N* NaCl to produce a 2% suspension. This washing procedure was repeated four additional times. Excess salt was removed by repeated washings with deionized water until the addition of silver nitrate to the supernate gave a negative chloride test.

Calcium montmorillonite was prepared in an analogous manner with 1 *N* $CaCl_2$ as the exchanging solution. All clays were stored as concentrated suspensions.

Sample Preparation—Clay suspensions and drug solutions were prepared separately and adjusted with hydrochloric acid or sodium hydroxide to the pH values at which each ionic species of the drug predominated. In very alkaline conditions, the exchangeable calcium in montmorillonite can be replaced to some extent by sodium from the sodium hydroxide solution used to adjust the pH. Lowered drug solubility was encountered at some pH values, resulting in the formation of drug suspensions.

After mixing and correcting for any pH change, the clay–drug system was equilibrated for 1 hr at 37°. The mixtures contained 0.6 mg of clindamycin or 1 mg of tetracycline and 10 mg of montmorillonite/ml of clay–drug suspension. After interaction, aliquots were washed one or five times with deionized water adjusted to the pH of the initial mixture and resuspended to yield a 1% suspension. In every case but that of clindamycin at pH 11.0, no difference was observed between the first and fifth wash.

For comparative purposes, each ionic species for the drugs was maximized by adjusting tetracycline solutions to pH 1.5, 5.0, 8.7, and 11.0 (17, 18) and clindamycin solutions to pH 2.0 and 11.0. Where precipitation occurred, the suspension was filtered to remove solid drug. Evaporation yielded solid drug in the appropriate ionic form.

Tetracycline calcium was obtained by adjusting a tetracycline solution to pH 11.0 and then adding sufficient aqueous calcium chloride to obtain

[1] On leave from Instituto de Edafologia, C.S.I.C., Madrid, Spain.

[2] Model 290B, Perkin-Elmer Corp., Norwalk, Conn.

0022-3549/78/0800-1081$01.00/0
© 1978, American Pharmaceutical Association

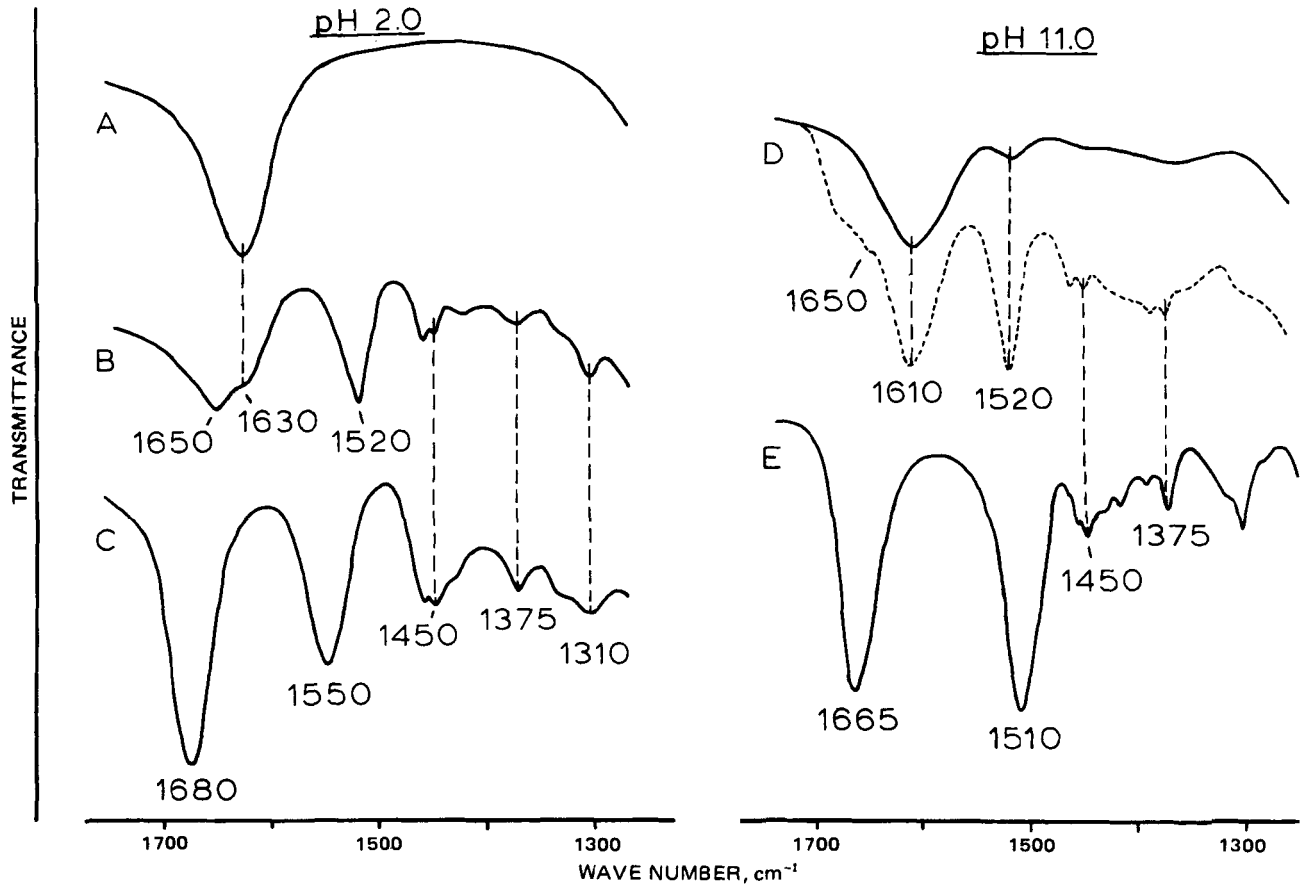

Figure 1—*IR spectra of montmorillonite interacted with clindamycin after five washings. Key: A, montmorillonite; B, clindamycin and montmorillonite, pH 2.0; C, clindamycin, pH 2.0; D, clindamycin and montmorillonite, pH 11.0 (one washing); and E, clindamycin, pH 11.0.*

a 1.5 *M* ratio of calcium to tetracycline. The resulting slurry was lyophilized in the absence of light and stored as a powder.

X-Ray Analysis—For X-ray diffraction[3], 2 ml of the 1% suspension was pipetted onto a glass slide and air dried. This technique produces a preferential orientation of the clay particles parallel to the 001 plane, allowing direct determination of the interlayer spacing. Tetracycline degradation was minimized by avoiding exposure to light and drying under vacuum. Prior to running X-ray diffractograms, all samples were dehydrated under vacuum for 30 min. The vacuum cell containing the samples was transferred to a controlled environment chamber of the X-ray diffractometer, which was constantly purged with a stream of dry nitrogen gas. This dry atmosphere maintained the dehydrated state of the sample.

To draw definite conclusions about the presence and size of the drug molecule in the interlayer space, water must be excluded from the clay–drug system when recording X-ray diffractograms. When drug molecules have been adsorbed onto interlayer clay surfaces, the observed increase in basal spacing compared to that of dehydrated clay will be due only to the dimensions of the adsorbed molecule without any contribution from water.

IR Analysis—Self-supporting clay films were prepared for IR analysis[4] by pipetting appropriate volumes of the 1% suspension onto polyethylene terephthalate[5] film. After air or vacuum drying (in the dark for tetracycline), the clay film was separated from the polymer film by bending both over a sharp 90° corner. The rigidity of the clay film caused it to be detached from the polymer sheet. Clay films of uniform thickness may be readily prepared by this technique.

The clay is free from IR absorption between 3000 and 1300 cm^{-1}, except for a strong water bending vibration at approximately 1630 cm^{-1}, providing a convenient window for the observation of drug absorption bands. The absorption near 1630 cm^{-1} is primarily due to water directly coordinated to the exchangeable cations of the clay (19). Therefore, its absence after drug interaction is a good indication of the replacement of this interlayer cation by the drug. For many drugs, the IR spectrum between 1800 and 1300 cm^{-1} is especially useful because most important absorption bands for potentially interacting functional groups are present in this region.

Tetracycline, tetracycline calcium, and clindamycin were prepared for IR analysis as potassium bromide pellets.

Adsorption Isotherms—Aqueous solutions of clindamycin (>2 mg/ml) were adjusted to pH 2.0 and 11.0. Tritium-labeled clindamycin[6] was added to these solutions, and final dilution adjustments were made to yield stock solutions with a specific concentration of approximately 160,000 dpm/ml. Two aliquots of the aqueous montmorillonite suspensions containing 0.096 g of montmorillonite were diluted (such that the combined volumes of clay and drug solutions would be approximately 90 ml), adjusted to pH 2.0 and 11.0, transferred to 100-ml volumetric flasks containing suitable aliquots of the stock drug solution, and diluted to volume with water of the proper pH.

After thorough shaking, the clindamycin–montmorillonite mixtures were placed in covered jacketed beakers (37°) and stirred continuously for 24 hr. Initial results indicated that equilibrium was attained after approximately 30 min. The initial pH was maintained by adding a minimum volume of hydrochloric acid or sodium hydroxide when necessary. Five-milliliter samples were taken periodically and centrifuged at 6000 rpm for 10 min. The equilibrium solution still containing small amounts of clay was decanted into another centrifuge tube to which a trace of sodium chloride crystals was added to facilitate separation of the clay. The tube was shaken and again centrifuged at 6000 rpm for 30 min.

The equilibrium concentration of the supernate was determined by liquid scintillation spectrometry[7] using a commercially prepared scintillation fluid[8]. Counts were recorded for 10 min or up to 10,000 (±2%), using an external barium-133 standard. In all cases, an appropriate clay blank was used to obtain a background count.

Tetracycline isotherms were obtained similarly. Aqueous stock solutions of tetracycline in the 2–4-mg/ml range were adjusted to pH 1.5, 8.7,

[3] Siemens AG Kristalloflex 4 generator, type F diffractometer, Karlsruhe, West Germany.
[4] Model 180, Perkin-Elmer Corp., Norwalk, Conn.
[5] Mylar.
[6] The Upjohn Co., Kalamazoo, Mich.
[7] Isocap/300 liquid scintillation system, Searle Analytical, Inc., Des Plaines, Ill.
[8] Riafluor, New England Nuclear, Boston, Mass.

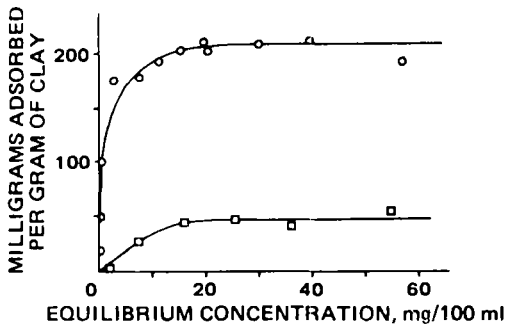

Figure 2—*Adsorption isotherm for clindamycin and montmorillonite. Key:* ○, *pH 2.0; and* □, *pH 11.0.*

and 11.0. Because of lowered tetracycline solubility at pH 5.0, a 0.5-mg/ml stock solution was prepared. Three aliquots of the montmorillonite suspension containing 0.096 g of the clay were diluted as with clindamycin, adjusted to pH 1.5, 8.7, and 11.0, transferred to flasks containing suitable aliquots of the stock tetracycline solution, and diluted to volume with water adjusted to the appropriate pH. For the pH 5.0 drug–clay mixture, 0.0256- and 0.0128-g portions of montmorillonite were treated similarly and added to a proportionately smaller amount of tetracycline.

Equilibrating conditions and sampling procedures were the same as those for clindamycin. Equilibrium concentrations were determined spectrophotometrically[9] with appropriate clay blanks in the reference beam. At pH 11.0, the equilibrium plateau concentrations obtained within the 1st hr were used to construct the adsorption isotherm. This approach was necessary since tetracycline degradation significantly affected the established plateau levels after that time.

RESULTS AND DISCUSSION

Clindamycin—Clindamycin has a pKa of 7.6 and, therefore, exists predominantly as a cation in acidic solutions because of protonation of the tertiary amine and as a neutral species in basic solution.

When clindamycin interacts with montmorillonite at pH 2, interlaminar adsorption is suggested by an increase in the basal spacing of the clay from 9.5 to 13.4 Å, a difference of 3.9 Å. This interlayer spacing is somewhat smaller than the 4.8-Å minimum dimension of clindamycin, as determined by a Corey–Pauling–Kolton (CPK) molecular scale model. Green-Kelley (20) studied a number of organic molecules adsorbed onto the interlayer surface of montmorillonite and noted that the increase in interlayer space could be smaller than the dimension of the adsorbed molecule by as much as 1 Å. Further studies showed that keying or a different geometric packing can occur for the adsorbed molecule, resulting in smaller basal spacings than expected (21). The observed interlaminar spacing is then due to the adsorption of clindamycin and suggests that a single layer has been adsorbed in a parallel orientation.

At pH 11, where clindamycin is uncharged, the basal spacing for the montmorillonite interacted with drug was that of the dehydrated clay, 9.6 Å, indicating no adsorption in the interlayer space by the neutral molecule. The fact that clindamycin was adsorbed in the interlayer space of montmorillonite only as a cationic molecule suggests that the adsorption mechanism at low pH is cation exchange.

Figure 1A shows the IR spectrum of montmorillonite in the range of

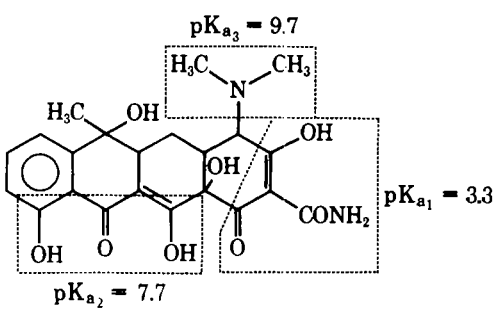

I

[9] Model 124, Perkin-Elmer Corp., Norwalk, Conn.

1800–1300 cm^{-1}; only one absorption band appears at 1630 cm^{-1} because of the bending vibration of water. (In the presence of basic drug solutions, this deformation band shifts to 1610 cm^{-1}, indicating less hydrogen bonding between water molecules.) The IR spectrum of the montmorillonite–clindamycin system at pH 2 shows relatively intense drug absorption bands (Fig. 1B) and confirms that the drug has been adsorbed in the interlaminar space of the clay.

Comparison between absorption bands for the drug alone and those of the adsorbed drug (Figs. 1C and 1B) shows a shift in the position of the amide I band from 1680 to 1650 cm^{-1}. This shift to lower frequency might be interpreted as carbonyl participation in hydrogen bonding with hydroxyl groups of the water coordinated to the interlayer cation or as coordination with the exchangeable ions on the interlayer clay surface (22). However, the interaction is not due to hydrogen bonding because of the irreversible nature of the reaction. On the other hand, coordination can be supported by the decrease in frequency of the amide II band (NH deformation vibration) from 1550 to 1520 cm^{-1}, indicating less restricted NH bending as is the case in the resonance structure favored by a carbonyl coordination. The amide CN and NH stretching vibrations are obscured by the OH stretching vibrations of the clay and adsorbed water and cannot contribute to elucidation of the adsorption mechanism.

Although the amide II shift to lower frequency could support a coordination mechanism, the difference in environment between an adsorbed molecule and a molecule in the pure state might also cause such a shift. Generally, secondary amides in the solid state display an amide II band at higher frequency than when in dilute solution. This effect would correspond to the change in environment and configuration of the drug molecules from an intermolecularly bonded aggregate to almost totally isolated molecules on the clay surface, as indicated by X-ray diffraction data. Thus, the observed perturbations of the amide II and amide I bands may be explained without a covalent interaction occurring between the drug molecule and the clay.

Hydrogen bonding other than with the carbonyl is not an additional stabilizing factor, as evidenced by both irreversible adsorption and the presence of absorption bands at 2960, 2920, and 2870 cm^{-1} due to CH stretching vibrations and at 3370 cm^{-1} due to OH stretching vibrations (not shown in Fig. 1), which are unperturbed compared to their position in the spectrum of the solid drug at pH 2.0.

Both coordination and cation-exchange mechanisms can be supported by the shifts in amide I and II band frequencies and the irreversible nature of the adsorption (as evidenced by identical spectra after one or five washings). However, direct evidence for an exchange mechanism is obtained by noting the low intensity of the water absorption band at 1630 cm^{-1} (Fig. 1B). Since the exchangeable cations are hydrated to a considerable extent, the observed decrease of the associated water absorption band, as compared to that in Fig. 1D (one wash), indicates replacement of the inorganic cation by clindamycin cations.

At pH 11, clindamycin is a neutral species; after several washings, it does not interact significantly with montmorillonite *via* a cation-exchange mechanism, as evidenced by the virtual absence of IR drug absorption bands (Fig. 1E). This result is further supported by the presence of the water absorption band at 1610 cm^{-1} after one washing. The decrease in absorption band intensity with washing indicates that reversible physical adsorption is responsible for drug adsorption on the external clay surface.

Adsorption isotherms of clindamycin adsorbed onto montmorillonite are presented in Fig. 2. The amounts that could theoretically be adsorbed by montmorillonite, calculated on the basis of cation-exchange capacity and external surface area, are listed in Table I. Under acidic conditions, the magnitude of adsorption suggests cation exchange as the adsorption mechanism. The experimental adsorptive capacity greatly exceeds that of the external surface but satisfies 49% of the calculated cation-exchange capacity. The fact that approximately one-half of the theoretical adsorption occurred and the parallel orientation of the adsorbed monolayer, as indicated from X-ray diffraction data, suggest that clindamycin cations are too large to neutralize completely the charge on the internal clay surface. This conclusion is verified by comparing the area of a clindamycin molecule to the area per exchange position on each basal plane surface of the clay. Based on a 190-$Å^2$ planar surface area for clindamycin and 80 $Å^2$ for a montmorillonite exchange site (23), 42% of the interlayer cation-exchange capacity can be satisfied by the cationic drug if it is assumed that the montmorillonite is in the expanded state in the adsorption isotherm experiments.

The data obtained in this study were applied to both the empirical Freundlich equation and the theoretical Langmuir isotherm equation. Conformity to the Freundlich equation was found at pH 2.0 and 11.0. Clindamycin adsorption at pH 2.0 also followed a linear isothermal plot

Table I—Comparison of Observed and Theoretical Adsorption Capacity of Montmorillonite

Adsorbate (Ionic Form)	Maximum Adsorption Capacity, mg of Adsorbate/g of Montmorillonite	Theoretical Adsorption Capacity, mg of Adsorbate/g of Montmorillonite	
		Based on Cation Exchange Capacity	Based on External Surface Area
Clindamycin			
pH 2.0 (+)	210	425	33
pH 11.0 (0)	50	425	33
Tetracycline			
pH 1.5 (+00)	375	481	44
pH 5.0 (+−0)	240	481	44
pH 8.7 (+−−)	80	481	44
pH 11.0 (0−−)	<10	481	44

of the Langmuir equation. At pH 11.0, however, the data did not yield a straight line. Mechanistic interpretations of the Langmuir adsorption equation are difficult and are not entirely agreed upon; however, conformity of the data to the equation usually implies a chemisorption mechanism. Physical adsorption might then be indicated for the neutral molecule since chemisorption is not an apparent mechanism at pH 11.0.

IR and X-ray analyses together show that clindamycin is adsorbed by

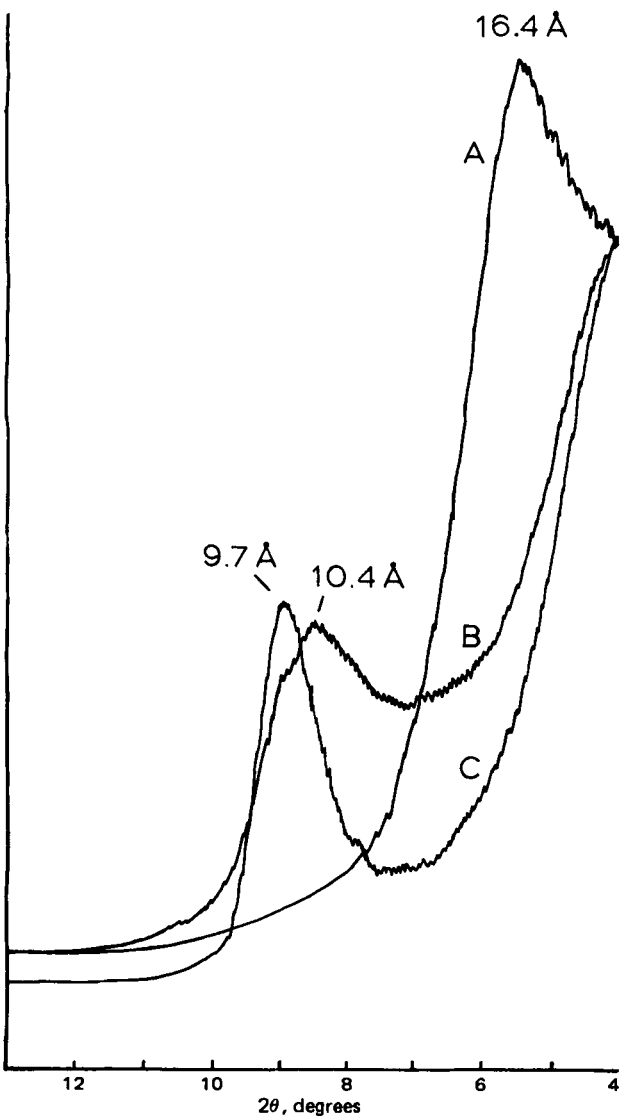

Figure 3—*X-ray diffractograms of montmorillonite interacted with tetracycline at pH 1.5 and 5.0 (A), pH 8.7 (B), and pH 11.0 (C). Curve C is also the diffraction pattern for untreated montmorillonite.*

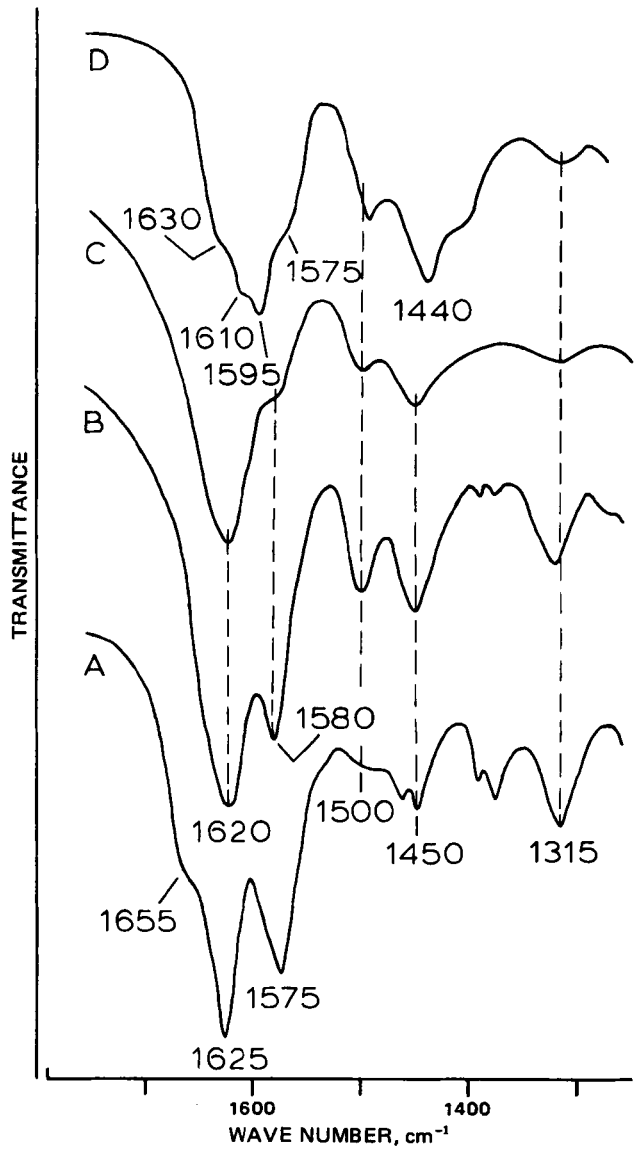

Figure 4—*IR spectra of montmorillonite interacted with tetracycline. Key: A, pH 1.5; B, pH 5.0; C, pH 8.7; and D, pH 11.0.*

a cation-exchange mechanism under pH conditions favoring the cationic form of the drug and by physical adsorption when the nonionized drug is present. Since physical adsorption is relatively weak, the drug is desorbed readily by alkaline washing.

Tetracycline—Tetracycline is ionized throughout the pH range and, as illustrated in Structure I, exists predominantly as a cation, +00, below pH 3.3, a zwitterion, +−0, between pH 3.3 and 7.7, and an anion, +−− or 0−−, above pH 7.7 (19).

The X-ray patterns of montmorillonite interacted with tetracycline at pH 1.5, 5.0, 8.7, and 11.0 are shown in Fig. 3. At pH 1.5 and 5.0, the increase in interlaminar space of 6.8 Å indicates that tetracycline is adsorbed. This dimension is in good agreement with the smallest dimension of tetracycline, 6.3 Å, based on a molecular model and suggests a parallel or slightly tilted orientation of the tetracycline molecules between the clay layers.

At pH 8.7, the X-ray diffractogram shows a diffuse reflection, indicating irregular interlayer spacing. This pattern is characteristic of partial interlayer adsorption (15) and is consistent with the difficulty expected in adsorbing a predominantly negative molecule (+−−) onto the negative clay surface. At pH 11, no increase in interlayer spacing is observed, indicating that the 0−− form of tetracycline is not adsorbed by montmorillonite.

The IR spectrum at pH 1.5, in which the cationic species of tetracycline interacts with montmorillonite (Fig. 4A), shows the presence of tetracycline in the interlaminar space. The IR spectrum of the adsorbed tetracycline does not show any significant shifts compared to the spectrum

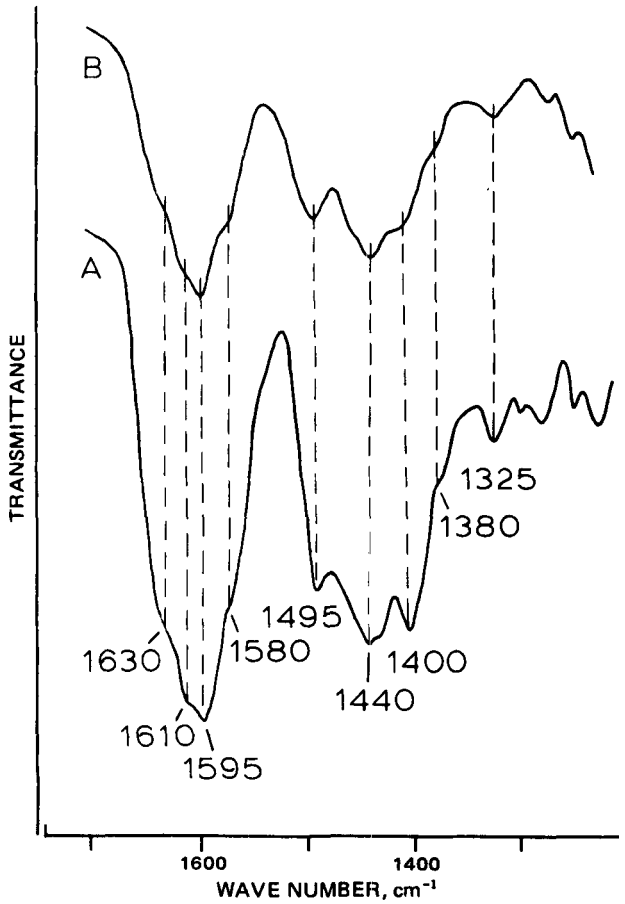

Figure 5—*Role of complexation when tetracycline interacts with montmorillonite. Key: A, calcium–tetracycline complex at pH 11.0; and B, tetracycline interacted with montmorillonite at pH 11.0.*

of tetracycline at pH 1.5, thus indicating no covalent interaction between drug and clay. This result suggests that adsorption occurs by exchange with the interlayer cations. Relative water band intensities are not useful in supporting this mechanism, as with clindamycin, since the water band is obscured by strong drug absorption bands. The higher concentration of tetracycline within the clay layers may also account for the similarity between spectra of the drug and drug interacted with clay. A more crowded drug environment would resemble the solid state more closely and produce an equivalent spectrum.

The IR spectra of tetracycline–montmorillonite equilibrated at pH 5.0 and 8.7 (Figs. 4B and 4C), where the +−0 and +−− forms, respectively, predominate, indicate that tetracycline is adsorbed in the interlayer space. However, spectral shifts suggest that a second mechanism in addition to cation exchange is responsible for adsorption. The carbonyl vibration associated with the ketone and amide I bands occurring at 1660 and 1640 cm^{-1} for tetracycline at pH 5.0 and 8.7, respectively, shifts to a lower frequency and is hidden under the amide II bands when tetracycline interacts with montmorillonite.

A shift of ketone carbonyl vibrations to lower frequency when organic compounds are adsorbed by clay was observed in cases where the carbonyl group was directly coordinated with the interlayer cations or when the carbonyl group hydrogen bonded with hydroxyl groups of the water coordinated to the interlayer cation (24). A shift of the amide I band to lower frequency was discussed previously. Hydrogen bonding of the ketone or amide carbonyl was not appreciable, as evidenced by irreversible adsorption on the montmorillonite. Since calcium comprises 10% of the exchangeable cations, the spectral shifts observed at pH 5.0 and 8.7 can be attributed to drug complexation with the interlayer divalent cations.

Drug absorption bands are observed when tetracycline is interacted with montmorillonite at pH 11 (Fig. 4D). However, the spectrum is significantly different from the spectrum of tetracycline at pH 11. Notably, a shift in the amide I band from 1640 to 1630 cm^{-1} and splitting of the amide II band occur to give absorption bands at 1610 and 1595 cm^{-1}, which suggests a coordination type of interaction (22). This participation of the amide function in the formation of a complex with divalent cations

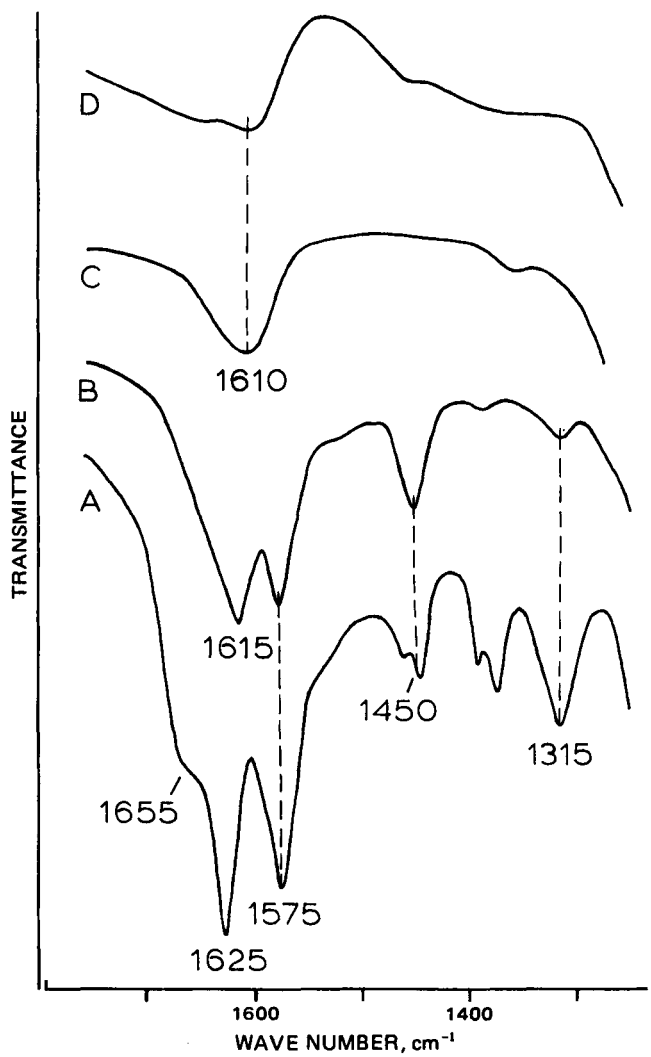

Figure 6—*IR spectra of sodium montmorillonite interacted with tetracycline. Key: A, pH 1.5; B, pH 5.0; C, pH 8.7; and D, pH 11.0.*

at high pH values also was demonstrated in a recent NMR study of tetracycline complexation sites (25).

The presence of calcium in the montmorillonite suggested a comparison to tetracycline calcium. As seen in Fig. 5, the tetracycline in the clay mixture has the same IR spectrum as tetracycline calcium. Since X-ray diffraction showed no increase in interlayer space at pH 11, it was hypothesized that the interaction of the 0−− species leads to the formation of an external calcium–tetracycline complex.

This hypothesis was confirmed by determining the concentration of calcium ion in calcium montmorillonite before and after interaction with tetracycline at pH 11. Only 32% of the original exchangeable calcium was found by atomic absorption spectroscopy after interaction with tetracycline. Therefore, 68% of the calcium must be attributed to the formation of external tetracycline calcium.

To demonstrate that cation exchange is one mechanism responsible for tetracycline adsorption and to determine which cationic species can be adsorbed by cation exchange, the interaction of tetracycline and pure sodium montmorillonite was studied at pH 1.5, 5.0, 8.7, and 11.0. Since the monovalent sodium ion is the only exchangeable cation, the only possible chemisorption mechanism for tetracycline is cation exchange. X-ray diffraction showed an increase in the interlayer space of 7.3 Å at pH 1.5 and an irregular spacing at pH 5.0 (Table II). No increase was observed at pH 8.7 and 11.0.

Adsorption of the drug within the clay at pH 1.5 and 5.0 was confirmed by IR absorption bands corresponding to those of tetracycline at pH 1.5 and 5.0 (Figs. 6A and 6B). Although tetracycline is a neutral molecule at pH 5.0, some degree of adsorption by cation exchange can occur due to the higher acidity of the clay surface (26). No drug absorption bands were seen at pH 8.7 or 11 (Figs. 6C and 6D). The increase in interlayer spacing and the presence of drug absorption bands at pH 1.5 and 5.0 in-

Table II—Interlayer Spacing, Å, of Montmorillonite Interacted with Tetracycline

pH	Montmorillonite	Sodium Montmorillonite	Calcium Montmorillonite
1.5	6.8	7.3	6.7
5.0	6.8	Irregular	5.9
8.7	Irregular	—[a]	Irregular
11.0	—[a]	—[a]	—[a]

[a] Less than 0.35 Å, signifying no interlayer adsorption.

dicate that, in the absence of complexing interlayer cations, adsorption occurs by a cation-exchange mechanism. At higher pH conditions, the anionic species, +−− or 0−−, cannot be adsorbed because of the negative surface of the clay.

The role of complexation in tetracycline adsorption was studied by examining the interaction of tetracycline and calcium montmorillonite, a clay that can interact with tetracycline by both cation exchange and complexation with divalent calcium cation. As seen in Table II, interlayer adsorption occurred at pH 1.5, 5.0, and 8.7, as evidenced by the increase in interlayer spacing. No interlayer adsorption occurred at pH 11. The IR spectrum of tetracycline–calcium montmorillonite at pH 1.5 (Fig. 7A) corresponds to the IR spectrum of tetracycline at pH 1.5, indicating adsorption by cation exchange. The IR spectra at pH 5.0, 8.7, and 11.0 are identical (Fig. 7B) and correspond to the spectrum of tetracycline calcium. Thus, the +−0, +−−, and 0−− species readily form complexes with divalent exchangeable cations. Complexation appears to predominate over a cation-exchange mechanism for the +−0 species.

Adsorption isotherms of the four tetracycline species (Fig. 8) show that the adsorptive capacity of the clay increases as a function of increasing acidity. Since the tetracycline ion develops a stronger cationic character with increasing acidity, a chemisorption mechanism is suggested as responsible for tetracycline–montmorillonite interaction. This hypothesis is further supported at pH 1.5 and 5.0 by the magnitude of adsorption, which considerably surpasses the capacity of the external surface (Table I). The unusual behavior of the pH 11.0 isotherm is probably due to negative adsorption resulting from the repulsion of the doubly charged anion, 0−−, from the negative surface of the clay.

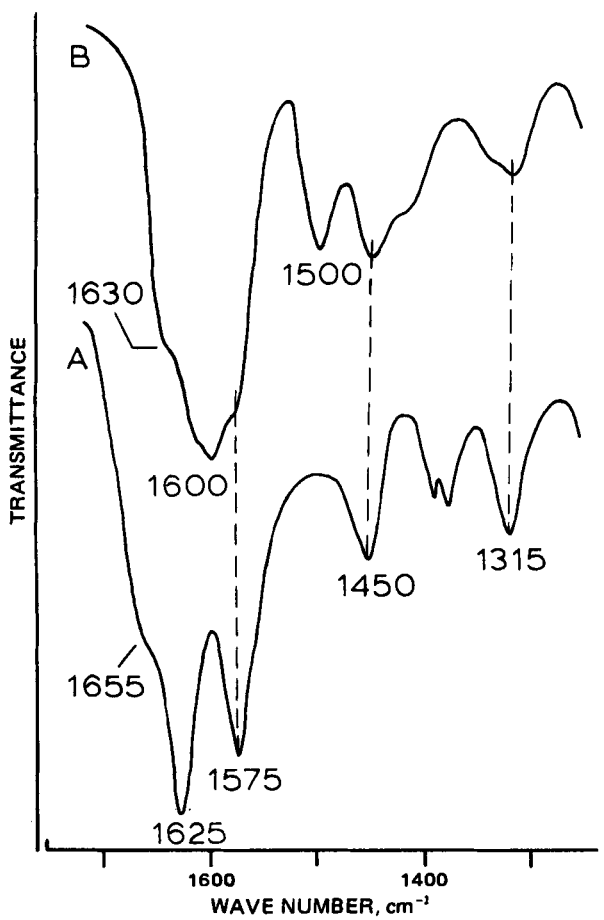

Figure 7—*IR spectra of calcium montmorillonite interacted with tetracycline. Key: A, pH 1.5; and B, pH 5.0, 8.7, and 11.0.*

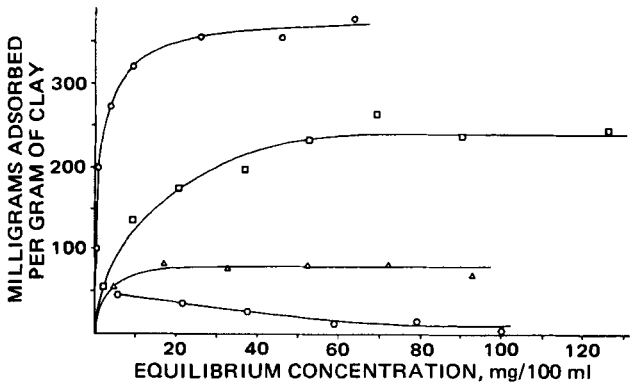

Figure 8—*Adsorption isotherm for tetracycline and montmorillonite. Key: ○, pH 1.5; □, pH 5.0; △, pH 8.7; and ○, pH 11.0.*

Under pH conditions favoring the cationic form of tetracycline, about 375 mg/g of montmorillonite is adsorbed. Clindamycin is adsorbed to a maximum of only 160 mg/g of adsorbent when it exists as a cation. Tetracycline and clindamycin have virtually identical volumes, 944 and 947 Å^3, and very similar planar surface areas, 190 and 150 Å^2, respectively. The greater adsorptive capacity suggests that tetracycline more fully occupies adsorption sites within the interlayer spaces of montmorillonite. This result could be accounted for by assuming a tilted orientation, which permits closer packing than does the parallel orientation of clindamycin. X-ray diffraction evidence supports this orientation since slightly larger c-axis spacings were observed than would be required for a parallel orientation. This orientation would be even more likely if foreshortening of tetracycline bond lengths occurs in the intercalated molecule.

Adsorption isotherms for tetracycline adsorbed onto montmorillonite followed the Freundlich equation for pH 1.5, 5.0, and 8.7. The data obtained at pH 11.0 also yielded a straight line but with a negative slope. Conformity to the Langmuir adsorption equation was observed for the tetracycline isotherms obtained at pH 1.5, 5.0, and 8.7 but not for that at pH 11.0. The linear relationships suggest chemisorption as the mechanism of adsorption for the +00, +−0, and +−− species of tetracycline. A suitable explanation for the adsorption at pH 11.0 is not apparent from the isotherm.

IR spectroscopy and X-ray diffraction show that tetracycline can be adsorbed onto montmorillonite by two mechanisms, cation exchange and complexation, depending upon the ionic species of the drug and the nature of the interlayer cation. At low pH values, where the +00 species exists, cation exchange is the mechanism of adsorption. At slightly acidic pH values, the zwitterion is adsorbed by both cation exchange and complexation. The 0−− species is not adsorbed but rather produces an external calcium–tetracycline complex.

Physical adsorption is not an important factor in tetracycline adsorption since washing does not change the IR spectra of the tetracycline–montmorillonite mixtures.

SUMMARY

The utility of X-ray diffraction and IR spectroscopy in elucidating the mechanisms responsible for clindamycin and tetracycline adsorption by montmorillonite was demonstrated in this study. Montmorillonite is suggested as a model clay for screening clay–drug interactions because it possesses a higher exchange capacity and surface area than other clays used in pharmaceutical systems, thereby undergoing any adsorption reactions to a greater degree than other pharmaceutical clays. In addition, its physical properties such as swelling and formation of self-supporting films make montmorillonite especially suitable for X-ray and IR examination.

The adsorption behavior of sodium montmorillonite showed that adsorption due to complexation with multivalent cations, as occurred with tetracycline, can be eliminated by prior treatment of the clay to replace all multivalent exchangeable cations with monovalent cations.

A full understanding of the adsorption mechanisms involved in clay–drug interactions should permit rational predictions of potential clay–drug interactions based on an understanding of clay properties and drug structures.

REFERENCES

(1) M. Barr, *J. Am. Pharm. Assoc.*, **NS4**, 4 (1964).
(2) J. W. McGinity and J. L. Lach, *J. Pharm. Sci.*, **66**, 63 (1977).
(3) L. H. Little, "Infrared Spectra of Adsorbed Species," Academic, New York, N.Y., 1966.
(4) R. L. Ledoux and J. L. White, *J. Colloid Interface Sci.*, **21**, 127 (1966a).
(5) B. K. G. Theng, "The Chemistry of Clay-Organic Reactions," Adam Hilger, London, England, 1974, pp. 136–210.
(6) J. M. Serratosa, *Clays Clay Miner.*, **14**, 385 (1966).
(7) M. Cruz, J. L. White, and J. D. Russell, *Isr. J. Chem.*, **6**, 315 (1968).
(8) S. Yariv, J. D. Russell, and V. C. Farmer, *ibid.*, **4**, 201 (1966).
(9) G. W. Bailey and J. L. White, *Residue Rev.*, **32**, 29 (1970).
(10) M. M. Mortland, *Clay Miner.*, **6**, 143 (1966).
(11) R. L. Ledoux and J. L. White, *Proc. Int. Clay Conf., Jerusalem*, **1**, 361 (1966).
(12) J. W. McGinity and J. L. Lach, *J. Pharm. Sci.*, **65**, 896 (1976).
(13) L. A. Pinck, W. F. Holton, and F. E. Allison, *Soil Sci.*, **91**, 22 (1961).
(14) R. E. Grim, "Clay Mineralogy," 2nd ed., McGraw-Hill, St. Louis, Mo., 1968, p. 189.
(15) C. J. Serna, G. Van Scoyoc, and J. L. Alrichs, *Am. Miner.*, **62**, 784 (1977).
(16) "United States Dispensatory," 27th ed., Lippincott, Philadelphia, Pa., 1973, p. 182.
(17) K. K. Kalnin'sh and B. G. Belen'kil, *Dan SSSR*, **157**, 619 (1964).
(18) J. L. Colaizzi and P. R. Klink, *J. Pharm. Sci.*, **58**, 1184 (1969).
(19) B. K. G. Theng, "The Chemistry of Clay-Organic Reactions," Adam Hilger, London, England, 1974, p. 18.
(20) R. Green-Kelley, *Trans. Faraday Soc.*, **51**, 412 (1955).
(21) G. W. Brindley and R. W. Hoffmann, *Clays Clay Miner.*, **9**, 546 (1962).
(22) S. A. Tahoun and M. M. Mortland, *Soil Sci.*, **102**, 314 (1966).
(23) R. E. Grim, "Clay Mineralogy," 2nd ed., McGraw-Hill, St. Louis, Mo., 1968, p. 196.
(24) R. L. Parfitt and M. M. Mortland, *Soil Sci. Soc. Am. Proc.*, **32**, 355 (1968).
(25) D. E. Williamson and G. W. Everett, Jr., *J. Am. Chem. Soc.*, **97**, 9 (1975).
(26) M. M. Mortland, J. J. Fripiat, J. Chaussidon, and J. Uytterhoeven, *J. Phys. Chem.*, **67**, 248 (1963).

ACKNOWLEDGMENTS

Supported in part by The Upjohn Co. and a National Institutes of Health biomedical research support grant.

C. J. Serna acknowledges a Fellowship from the Ministerio de Education y Ciencia, Madrid, Spain.

This report is Journal Paper 6865, Purdue University Agricultural Experiment Station, West Lafayette, IN 47907.

Physical Characterization of Erythromycin: Anhydrate, Monohydrate, and Dihydrate Crystalline Solids

P. V. ALLEN, P. D. RAHN, A. C. SARAPU, and A. J. VANDERWIELEN ˣ

Received July 5, 1977, from *The Upjohn Company, Kalamazoo, MI 49001.* Accepted for publication November 16, 1977.

Abstract □ Hot-stage microscopy, thermoanalytical methods, and X-ray powder diffraction were used to demonstrate that crystalline erythromycin dihydrate converts to the crystalline anhydrate *via* a noncrystalline intermediate. X-ray powder diffraction, IR spectral, thermogravimetric, and differential thermal analyses were used to characterize the monohydrate material. The flow interrupt technique, a procedure recently developed to deal with low surface area samples, was employed successfully in obtaining isotherms and specific surface areas for the monohydrate and anhydrate. The relative dissolution rates of the various hydrates were determined in an aqueous solution (0.01 *M* phosphate buffer, pH 7.5) at 37°. The results showed a significant difference in the dissolution rate of the dihydrate compared to the monohydrate and anhydrate.

Keyphrases □ Erythromycin—physical characterization of anhydrate, monohydrate, and dihydrate crystalline solids, dissolution rates in aqueous solution □ Hydrated forms—of erythromycin crystalline solids, physical characterization, dissolution rates in aqueous solution □ Dissolution rates—erythromycin anhydrate, monohydrate, and dihydrate crystalline solids in aqueous solution □ Antibacterials—erythromycin, physical characterization of anhydrate, monohydrate, and dihydrate crystalline solids, dissolution rates in aqueous solution

Erythromycin is a potent antibiotic effective against various microorganisms. Commercial erythromycin is a mixture of several active components. Erythromycin A (I), the major component, is unstable in acidic media. To prevent deactivation of the drug by gastric acid and to facilitate absorption in the small intestine, erythromycin can be administered as enteric-coated tablets, which are stable in acid media but dissolve in intestinal fluids. Once the enteric coating has dissolved, the absorption and therapeutic efficacy of this material may be affected by the physical characteristics of the remaining solid. It has been postulated (1) and demonstrated (2–6) that the bioavailability of various drugs can be influenced by their dissolution rate, particle size, solubility, wettability, and extent of hydration.

Erythromycin exists in many different forms, including at least two hydrates (7, 8) and an anhydrate (7), which can

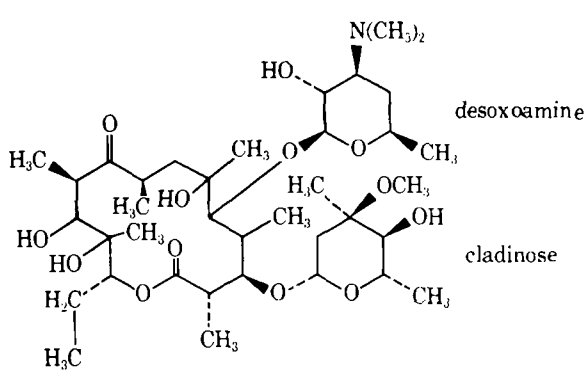

I

© 1978, American Pharmaceutical Association

REFERENCES

(1) M. Barr, *J. Am. Pharm. Assoc.*, **NS4**, 4 (1964).
(2) J. W. McGinity and J. L. Lach, *J. Pharm. Sci.*, **66**, 63 (1977).
(3) L. H. Little, "Infrared Spectra of Adsorbed Species," Academic, New York, N.Y., 1966.
(4) R. L. Ledoux and J. L. White, *J. Colloid Interface Sci.*, **21**, 127 (1966a).
(5) B. K. G. Theng, "The Chemistry of Clay-Organic Reactions," Adam Hilger, London, England, 1974, pp. 136–210.
(6) J. M. Serratosa, *Clays Clay Miner.*, **14**, 385 (1966).
(7) M. Cruz, J. L. White, and J. D. Russell, *Isr. J. Chem.*, **6**, 315 (1968).
(8) S. Yariv, J. D. Russell, and V. C. Farmer, *ibid.*, **4**, 201 (1966).
(9) G. W. Bailey and J. L. White, *Residue Rev.*, **32**, 29 (1970).
(10) M. M. Mortland, *Clay Miner.*, **6**, 143 (1966).
(11) R. L. Ledoux and J. L. White, *Proc. Int. Clay Conf., Jerusalem*, **1**, 361 (1966).
(12) J. W. McGinity and J. L. Lach, *J. Pharm. Sci.*, **65**, 896 (1976).
(13) L. A. Pinck, W. F. Holton, and F. E. Allison, *Soil Sci.*, **91**, 22 (1961).
(14) R. E. Grim, "Clay Mineralogy," 2nd ed., McGraw-Hill, St. Louis, Mo., 1968, p. 189.
(15) C. J. Serna, G. Van Scoyoc, and J. L. Alrichs, *Am. Miner.*, **62**, 784 (1977).
(16) "United States Dispensatory," 27th ed., Lippincott, Philadelphia, Pa., 1973, p. 182.
(17) K. K. Kalnin'sh and B. G. Belen'kil, *Dan SSSR*, **157**, 619 (1964).
(18) J. L. Colaizzi and P. R. Klink, *J. Pharm. Sci.*, **58**, 1184 (1969).
(19) B. K. G. Theng, "The Chemistry of Clay-Organic Reactions," Adam Hilger, London, England, 1974, p. 18.
(20) R. Green-Kelley, *Trans. Faraday Soc.*, **51**, 412 (1955).
(21) G. W. Brindley and R. W. Hoffmann, *Clays Clay Miner.*, **9**, 546 (1962).
(22) S. A. Tahoun and M. M. Mortland, *Soil Sci.*, **102**, 314 (1966).
(23) R. E. Grim, "Clay Mineralogy," 2nd ed., McGraw-Hill, St. Louis, Mo., 1968, p. 196.
(24) R. L. Parfitt and M. M. Mortland, *Soil Sci. Soc. Am. Proc.*, **32**, 355 (1968).
(25) D. E. Williamson and G. W. Everett, Jr., *J. Am. Chem. Soc.*, **97**, 9 (1975).
(26) M. M. Mortland, J. J. Fripiat, J. Chaussidon, and J. Uytterhoeven, *J. Phys. Chem.*, **67**, 248 (1963).

ACKNOWLEDGMENTS

Supported in part by The Upjohn Co. and a National Institutes of Health biomedical research support grant.

C. J. Serna acknowledges a Fellowship from the Ministerio de Education y Ciencia, Madrid, Spain.

This report is Journal Paper 6865, Purdue University Agricultural Experiment Station, West Lafayette, IN 47907.

Physical Characterization of Erythromycin: Anhydrate, Monohydrate, and Dihydrate Crystalline Solids

P. V. ALLEN, P. D. RAHN, A. C. SARAPU, and A. J. VANDERWIELEN ˣ

Received July 5, 1977, from *The Upjohn Company, Kalamazoo, MI 49001.* Accepted for publication November 16, 1977.

Abstract □ Hot-stage microscopy, thermoanalytical methods, and X-ray powder diffraction were used to demonstrate that crystalline erythromycin dihydrate converts to the crystalline anhydrate *via* a noncrystalline intermediate. X-ray powder diffraction, IR spectral, thermogravimetric, and differential thermal analyses were used to characterize the monohydrate material. The flow interrupt technique, a procedure recently developed to deal with low surface area samples, was employed successfully in obtaining isotherms and specific surface areas for the monohydrate and anhydrate. The relative dissolution rates of the various hydrates were determined in an aqueous solution (0.01 *M* phosphate buffer, pH 7.5) at 37°. The results showed a significant difference in the dissolution rate of the dihydrate compared to the monohydrate and anhydrate.

Keyphrases □ Erythromycin—physical characterization of anhydrate, monohydrate, and dihydrate crystalline solids, dissolution rates in aqueous solution □ Hydrated forms—of erythromycin crystalline solids, physical characterization, dissolution rates in aqueous solution □ Dissolution rates—erythromycin anhydrate, monohydrate, and dihydrate crystalline solids in aqueous solution □ Antibacterials—erythromycin, physical characterization of anhydrate, monohydrate, and dihydrate crystalline solids, dissolution rates in aqueous solution

Erythromycin is a potent antibiotic effective against various microorganisms. Commercial erythromycin is a mixture of several active components. Erythromycin A (I), the major component, is unstable in acidic media. To prevent deactivation of the drug by gastric acid and to facilitate absorption in the small intestine, erythromycin can be administered as enteric-coated tablets, which are stable in acid media but dissolve in intestinal fluids. Once the enteric coating has dissolved, the absorption and therapeutic efficacy of this material may be affected by the physical characteristics of the remaining solid. It has been postulated (1) and demonstrated (2–6) that the bioavailability of various drugs can be influenced by their dissolution rate, particle size, solubility, wettability, and extent of hydration.

Erythromycin exists in many different forms, including at least two hydrates (7, 8) and an anhydrate (7), which can

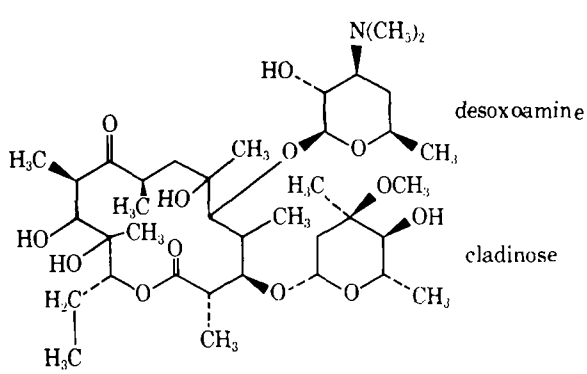

I

© 1978, American Pharmaceutical Association

be differentiated by their X-ray powder diffraction patterns. The present study deals with the effects of hydration and specific surface area on the dissolution rate of erythromycin bulk drug (commercial mixture). Recent literature (9–12) indicates that the thermal behavior of crystalline drugs is not well understood. Consequently, a study of erythromycin's several hydrates was conducted to examine their thermal behavior. Special emphasis was placed on determining melting points and interconversions of the dihydrate, monohydrate, and anhydrate crystalline solids.

EXPERIMENTAL

Materials—The monohydrate and dihydrate were commercially available. The anhydrate was made from the dihydrate by drying 50 g of powdered drug for 1 week at 105° in a vacuum oven. The pressure in the oven was maintained at 5 torr or less. Nitrogen[1] and helium[1] were used in the surface area studies. Commercially available trisodium phosphate, sodium hydroxide, and erythromycin USP grade were used for the dissolution studies. Ammonium nitrate standard was used to calibrate the differential thermal analyzer.

Surface Area Measurements—All measurements were made using a dynamic flow gas adsorption system (13). For the adsorption isotherms, the desired partial pressures, P/P_0, were obtained by using premixed gases (10, 20, and 30% N_2 in helium) where convenient and by manually mixing nitrogen and helium (using the flow controls on the instrument) to obtain the other concentrations. Calibrations were effected using precision sampling gas syringes.

Samples were degassed at 60° for 30 min with a nitrogen flow of 50 ml/min. The adsorption isotherm for the dihydrate was constructed using the continuous flow method. Adsorption isotherms and surface area measurements for the monohydrate and anhydrate were performed using an interrupted flow method (14) to avoid thermal diffusion effects. All surface area values were obtained using a three-point Brunauer, Emmett, and Teller (BET) method (13).

Dissolution Apparatus—The stationary basket rotating paddle (operated at 150 rpm) consisted of the USP rotating paddle apparatus with a 12-mesh basket (Fig. 1). The basket was placed midway between the center and side of the flask, 6.5 cm from the bottom. The basket was similar in dimension to that employed in the USP rotating basket apparatus.

The metal strip at the top of the basket was tapped and screwed onto the basket lid, which was connected to a metal shaft 10 mm in diameter and 15 cm long. The metal shaft was attached to a rabbeted Plexiglas disk by a compression fitting.

The Plexiglas cover for the apparatus was countersunk around the edges so that it rested securely on the 1-liter round-bottom flask. The cover had a hole 2.54 cm in diameter in its center for the shaft of the paddle and two holes 16 mm in diameter for sampling. Another hole 2.54 cm in diameter was countersunk so that the Plexiglas disk fit flush with the cover. This fit allowed the basket to be reproducibly positioned in the flask[2].

Nine hundred milliliters of 0.01 *M* phosphate buffer (pH 7.5) at 37° was used as the dissolution medium.

Dissolution Procedure—Erythromycin bulk drug, 200 ± 6 mg, was packed into a clear gelatin capsule, size 0. Timing of the dissolution run began when the 12-mesh basket containing the capsule was immersed in the dissolution medium with the paddle rotating at 150 rpm. Aliquots of 15 ml were withdrawn with a glass syringe from the flasks at 10, 20, 30, and 60 min and replaced with 15 ml of buffer solution. The samples were immediately filtered through a 0.6-μm filter[3] into a 50-ml centrifuge tube.

The amount of erythromycin in each sample was determined by a procedure similar to the one discussed by Kuzel *et al.* (15). The procedure involves base hydrolysis [using 0.25 *M* NaOH containing 15% (w/w) Na_3PO_4] of the erythromycin by heating the mixture of base solution (2 ml) and sample (10 ml, *qs* to 20 ml) for 15 min at 60°. The absorbance (λ 236 nm) of the cooled sample was determined[4] and compared to the absorbance of a reference solution treated similarly.

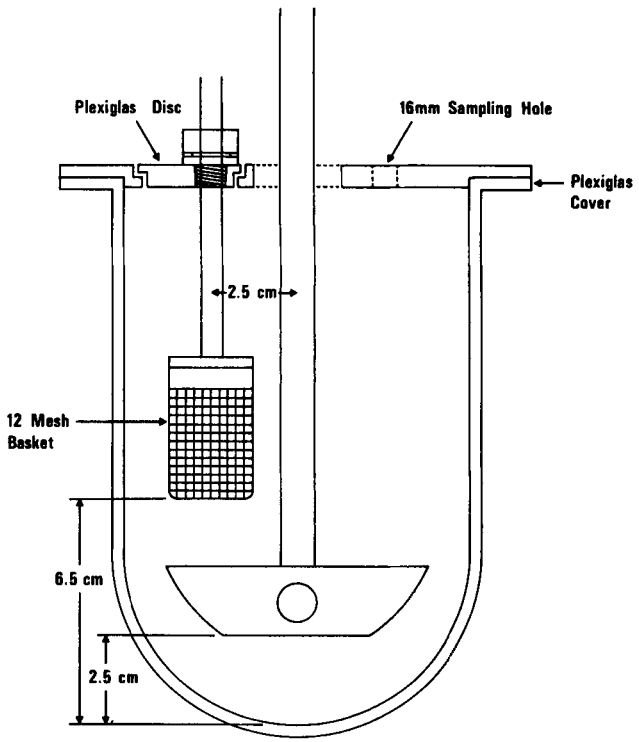

Figure 1—*Stationary basket rotating paddle dissolution apparatus.*

Thermal Analyses—The thermal behavior of erythromycin was examined using a thermal analysis system[5]. The differential thermal analysis (DTA) curves were obtained by using a standard DTA cell with a quick cool assembly. Sample tubes of 2 mm were used for the drug samples and the reference material (glass beads in all cases except one). Samples of ammonium nitrate were used to calibrate the instrument, and dry nitrogen at 50 ml/min was used to flush the DTA cell. Heating rates of 10 and 2°/min were used.

Thermal gravimetric analysis (TGA) were performed on the TGA accessory. A platinum sample pan was cleaned by heating with a Bunsen burner after each experiment. Samples (30–60 mg) were heated at 10°/min in a dry nitrogen atmosphere (flow rate = 50–60 ml/min).

The thermal stability of erythromycin was examined in both air and silicon oil, using a microscope at 125× magnification and a hot stage. Heating rates of 1–3°/min were used, and photomicrographs were taken at 20° intervals and at any significant transition points.

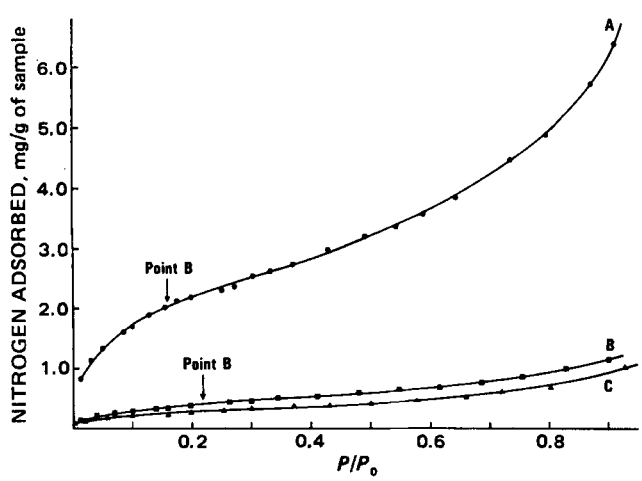

Figure 2—*Adsorption isotherms. Key: A, erythromycin dihydrate; B, erythromycin monohydrate; and C, erythromycin anhydrate.*

[1] Linde Division, Union Carbide Corp.

[2] The basket, lid, and metal shaft may be purchased from Coffman Industries. The basket and paddle were mounted on a Hansen research dissolution apparatus (model 72B-115).

[3] Millipore.

[4] Cary 11 spectrophotometer.

[5] DuPont 990 system including the 951 thermal gravimetric analysis accessory.

Table I—Comparison of Methods for Specific Area Determination on the Same Sample of Erythromycin Dihydrate

Parameter	Nitrogen Adsorption Continuous Flow	Nitrogen Adsorption Interrupted Flow	Krypton Adsorption Continuous Flow
Sample size, g	0.7028	0.0902	0.0902
Measured surface area, m^2	3.68	0.44	0.42
Specific surface area, m^2/g	5.2	4.9	4.7
Correlation coefficient	0.999	0.997	0.999

Table II—Isotherm Data for Erythromycin

Parameter	Dihydrate[a]	Monohydrate	Anhydrate
Specific surface area, m^2/g	6.6 (2.1)	1.3	1.0
Net heat of adsorption, kcal/mole at 298°K	2.4 (2.2)	1.8 ± 0.2	1.7
BET constant	55.0 (41.9)	19.6	17.3
Point B: Predicted	0.19	0.23	0.24
Actual	0.17	0.21	0.23

[a] Values in parentheses are averages of three dihydrate samples with a low measured surface area.

X-ray powder patterns were obtained using a diffractometer and powdered samples. Melt solvate analyses were performed by heating the erythromycin in an evacuated tube attached to a standard 10-cm IR gas cell. Calcium carbide was used as the drying material for the evolved gas, and an IR grating spectrometer was used to record the absorption spectra. A Fourier transform IR spectrometer also was used to identify the various hydrates.

RESULTS AND DISCUSSION

Surface Area—The adsorption isotherms for the erythromycin hydrates were all Type II (Fig. 2) (13), and their BET plots (Fig. 3) all contained linear regions of sufficient breadth to allow surface area determinations using P/P_0 values between 0.1 and 0.3. Samples of the dihydrate were analyzed by the normal continuous flow method with nitrogen as the adsorbate gas (13). This technique also was tried on the monohydrate and anhydrate but was unsuccessful because of thermal diffusion. The flow interrupt technique (14) and continuous flow with krypton as the adsorbate were examined as possible alternatives (Table I). The values obtained were comparable; however, the value obtained by krypton adsorption was slightly lower than expected. In addition, krypton adsorption was very time consuming, rarely requiring less than 10 min and occasionally longer than 2 hr for the higher P/P_0 values required in isotherms. Krypton adsorption peaks showed extensive tailing, making it difficult to determine when adsorption was complete. Therefore, the flow interrupt method was used to determine the surface area of the monohydrate and anhydrate. Adsorption was rapid, and the attainment of an equilibrium was unambiguous at all P/P_0 values since the same procedure was used as for conventional nitrogen adsorption.

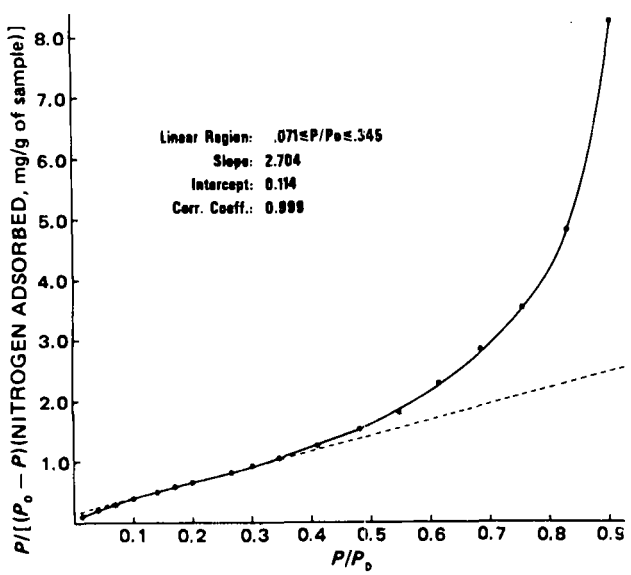

Figure 3—*Typical BET plot.*

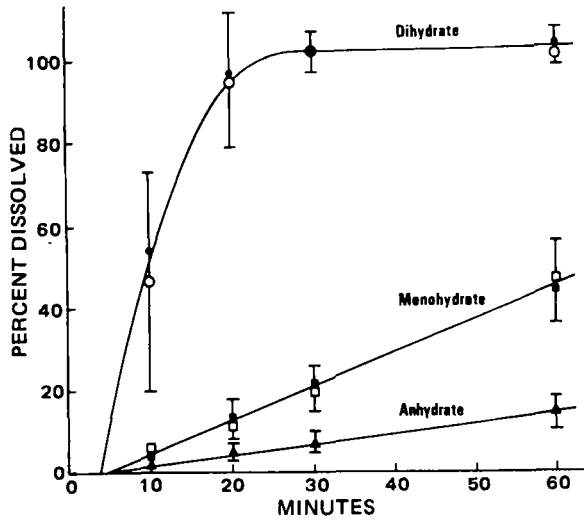

Figure 4—*Dissolution behavior of erythromycin dihydrate, monohydrate, and anhydrate in phosphate buffer (pH 7.5) at 37°. Key: ●, Sample 1; ○, Sample 2; ■, Sample 3; □, Sample 4; and ▲, Sample 5.*

The slope, S, and the extrapolated intercept, I, of the linear portion of the BET plot can then be used to calculate the weight of gas necessary to form a monolayer according to:

$$X_m = \frac{1}{S + I} \quad \text{(Eq. 1)}$$

The net heat of adsorption, ΔH_n, for a material is calculated as follows:

$$\Delta H_n = RT \ln C \quad \text{(Eq. 2)}$$

where C is the BET constant as determined from the BET plot relationship:

$$C = S/I + 1 \quad \text{(Eq. 3)}$$

However, Eqs. 2 and 3 are valid only for systems that are well defined by the BET equation (13). For such systems, the BET constant, C, may be used to predict the location of "point B" (13) (Fig. 2). This point, the beginning of the linear portion of the adsorption isotherm, was believed by Emmett and Brunauer (16) to coincide with the completion of a monolayer of adsorbate gas. A comparison of the predicted and actual point B values (Table II) indicates that the surfaces of all three hydrates are well defined by the BET equation.

The ΔH_n values for the various crystal forms were not significantly different. The small differences observed were most likely due to the amount of surface available, since the ΔH_n values and the BET constant decrease with decreasing specific surface areas.

Dissolution Studies—The results of the dissolution studies of five samples of erythromycin are depicted in Fig. 4. The dissolution curves show that the dissolution rates of the three hydrates differed significantly. The dihydrate was the fastest dissolving material while the anhydrate was less than 20% dissolved after 1 hr. Several physical parameters of the various hydrates, including surface area, net heat of adsorption (ΔH_n), and capsule packing, were examined to determine the reason for the difference in their dissolution behavior.

The results in Table III and Fig. 4 indicate that the surface area did not significantly affect the dissolution rate of erythromycin. For example, there was no difference in the dissolution rate of the two dihydrate samples, even though there was about a 2.5-fold difference in their surface

Table III—Dissolution Rate *versus* Surface Area

Sample	Percent Dissolved 20 min	Percent Dissolved 60 min	Specific Surface Area, m^2/g
1 Dihydrate	97	103	2.2
2 Dihydrate	96	101	5.2
3 Monohydrate	13	45	1.5
4 Monohydrate	11	46	1.2
5 Anhydrate	5	14	1.0

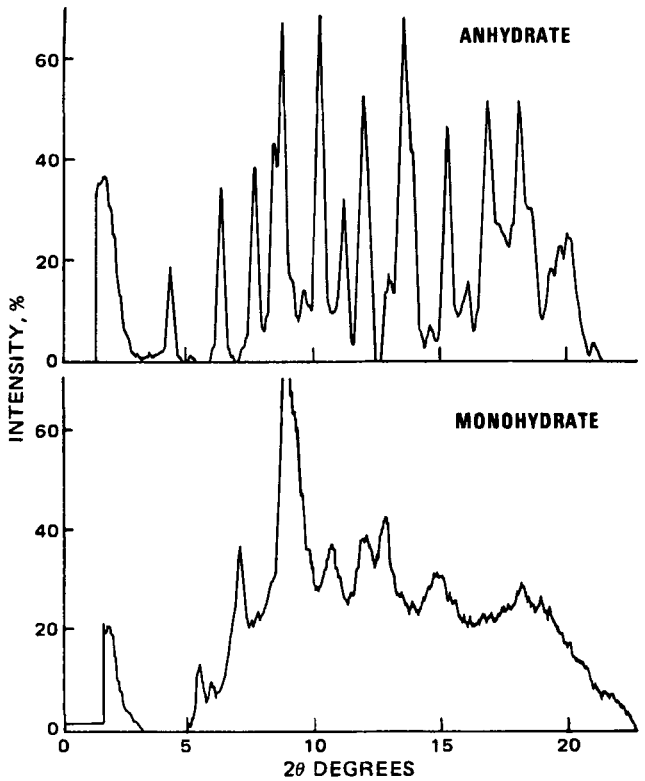

Figure 5—*X-ray powder diffraction pattern of erythromycin anhydrate and monohydrate.*

areas. As mentioned previously, there appeared to be no significant difference in the ΔH_n values of adsorption, and the difference in dissolution rates may be related to particle–particle interactions and/or the wettability of the various crystalline materials.

When performing the dissolution test on the bulk drug samples, the monohydrate and the anhydrate did not disintegrate after the gelatin capsule had dissolved, while both samples of dihydrate dispersed readily throughout the solution immediately after the gelatin capsule dissolved. To determine the effect of capsule packing on the dissolution rate of the bulk drug, 250 mg of several samples was packed into a size 1 capsule (tightly packed) and into a size 0 capsule (capsule full, packed lightly) and compared with the samples run with 200 mg of drug packed into a size 0 capsule (capsule three-fourths full and not packed) (Table IV). An examination of the percent dissolved at 20 and 60 min indicates that there was no significant difference in the dissolution rates for the various drug packings.

Shefter and Higuchi (17) found that the dissolution rate for the hydrate decreased with increasing hydration, as predicted by theory. The experimental design of the present dissolution study approximates the dosage form in which erythromycin is delivered to the small intestine. The sample is not uniformly dispersed in the dissolution medium at the start of the test. Therefore, in the present study, the dissolution rate can be affected not only by the extent of hydration but also by wettability, particle–particle interactions, and surface area.

Table IV—Packing Effects

Sample	Capsule Size[a]	Percent Dissolved 20 min	Percent Dissolved 60 min
Dihydrate	0	87	102
	1	85	101
	0[b]	96	101
Monohydrate (3)	0	9	51
	1	11	43
	0[b]	13	45
Anhydrate	1	10	19
	0[b]	5	14
Monohydrate (4)	0	7	33
	1	13	46
	0[b]	11	46

[a] Samples (250 mg) were tightly packed in the size 1 capsule and loosely packed in the size 0 capsule. [b] Two hundred milligrams of erythromycin in size 0 capsule.

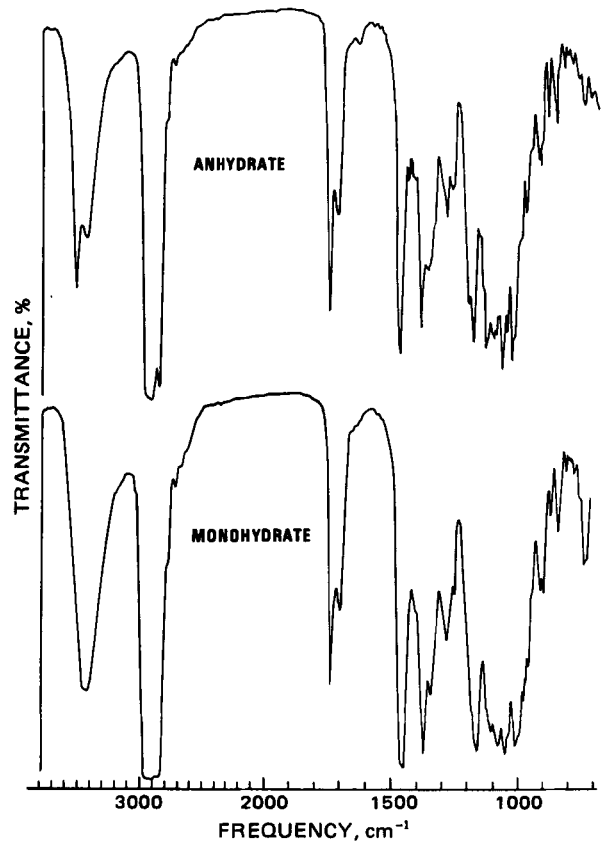

Figure 6—*IR spectrum of erythromycin anhydrate and monohydrate (mineral oil mull preparation).*

The results of Shefter and Higuchi (17) indicate that the dissolution rate of erythromycin is not determined by the extent of hydration under the present conditions. The fact that the monohydrate and the anhydrate did not disintegrate after dissolution of the gelatin capsule is further evidence that the dissolution rates of the various hydrates of erythromycin are most likely related to particle–particle interactions and wettability.

Phase Transitions—The identities of the anhydrate and dihydrate crystalline materials were verified by comparing their X-ray powder diffraction patterns to known references (7). The monohydrate was characterized by its X-ray powder diffraction pattern (Fig. 5), IR spectrum (Fig. 6), and the fact that it contained a stoichiometric amount of water (Table V). The observed weight loss was 2.6% as compared to a

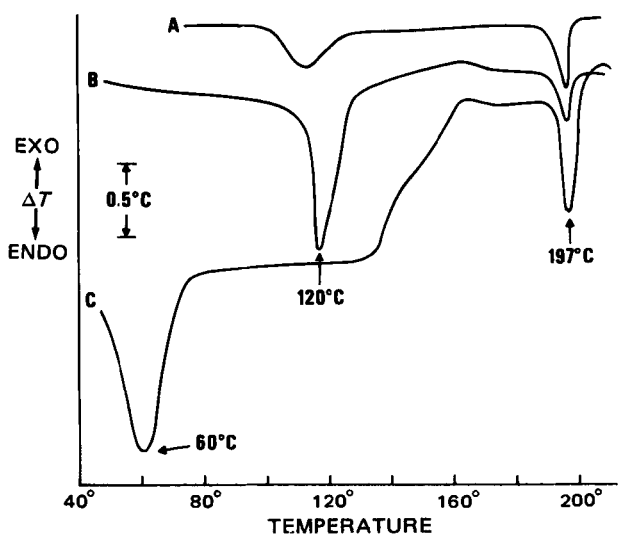

Figure 7—*DTA curves for the erythromycin dihydrate. Key: A, oil mull, nitrogen flow; B, powder sample, nitrogen flow; and C, powder sample, air pressure at 1 torr or less. Heating rate was 10°/min.*

Table V—Thermogravimetric Analysis

Erythromycin		Experimental Temperature Range	Weight Loss, % of Sample
Before Heating	After Heating		
Dihydrate	Dihydrate and amorphous	25–135°	4.6 (average of 6)
	Amorphous	25–135°, 135° for 10 min	4.7
	Anhydrate and amorphous	25–172°	4.6
Monohydrate	Amorphous	25–140°	2.6 (average of 2)
	Amorphous	25–140°, 140° for 10 min	—
	Anhydrate and amorphous	25–180°	2.5
Anhydrate	Anhydrate	25–150°	0.8 ± 0.3

Table VI—Hot-Stage Microscopy Results

Starting Material	Dehydration Temperature Range	Phase Transition to Amorphous	Recrystallization to Anhydrate	Anhydrate Melting
		Air Mount[a]		
Dihydrate	Not observed	129–132°	136–185°	189–192°
Monohydrate	Not observed	124–130°	Not observed	Not observed
Anhydrate	Not observed	Not observed	Not observed	190–193°
		Oil Mount[b]		
Dihydrate	95–130°	Not observed	100–125°	190–195°
Monohydrate	Not observed	114–137°	119–190°	190°
Anhydrate	Not observed	Not observed	Not observed	190–193°

[a] Crystals were exposed to the atmosphere. [b] Crystals were suspended in silicon oil.

theoretical value of 2.4%. Pelizza *et al.* (11) indicated that the monohydrate described previously (8) was the anhydrate containing surface moisture. The present TGA, IR, and X-ray data indicate that the monohydrate is a crystalline material containing one molecule of hydrated water for each molecule of erythromycin. However, the X-ray data (Fig. 5) indicate that the monohydrate does not possess the same degree of crystallinity as the anhydrate.

The results shown in Fig. 7 and Table V demonstrate that erythromycin dihydrate converts to the anhydrate *via* a noncrystalline intermediate when it is heated from 25 to 220° in a dry nitrogen atmosphere as shown by the reactions in Scheme I:

$$A\cdot 2H_2O_{(CS)} \xrightarrow[\text{dehydration}]{\sim 120^\circ} A_{(CS)} + 2H_2O_{(g)}$$

$$A_{(CS)} \xrightarrow{120\text{–}135^\circ} A_{(a)}$$

$$A_{(a)} \xrightarrow{120\text{–}190^\circ} A^{*}_{(CS)}$$

$$A^{*}_{(CS)} \xrightarrow[\text{melting}]{190\text{–}193^\circ} A_{(l)}$$

Scheme I

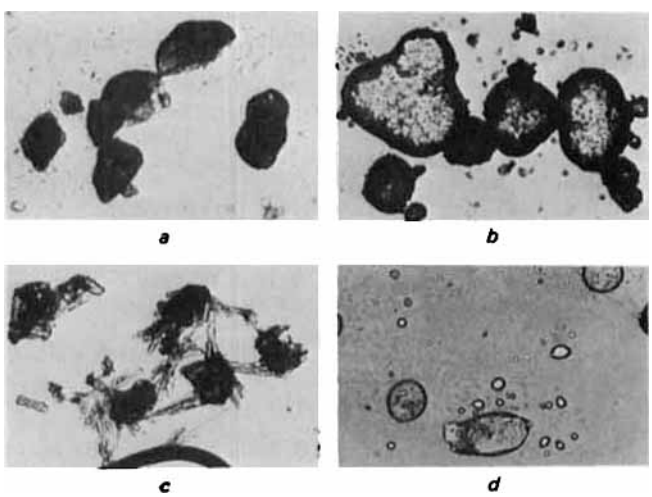

Figure 8—*Photomicrographs of the erythromycin dihydrate taken during the hot-stage microscopy study. Key:* a, *25°, crystalline solid, suspended in oil;* b, *140°, amorphous material, exposed to atmosphere;* c, *180°, crystalline solid, suspended in oil; and* d, *193°, isotropic liquid, suspended in oil.*

where A is erythromycin, a is amorphous, CS is crystalline solid, and l is isotropic liquid. $A^{*}_{(CS)}$ was determined to be the anhydrate crystal form by X-ray diffraction and DTA. The amorphous material was identified by X-ray powder diffraction. The diffraction pattern of amorphous and noncrystalline solids consists of very diffuse reflections since there are no parallel planes of atoms as are normally found in crystalline materials (17). The term amorphous, strictly speaking, means a completely random orientation, which is rarely the case in solid materials. The present study did not establish if the noncrystalline (amorphous) intermediate could be strictly classified as amorphous. However, the material had a glossy appearance, and no reflection planes were observed by X-ray powder diffractometry.

Verification of the dehydration endotherm observed at approximately 120° can be made by the following observations: (*a*) the weight loss (average = 4.65%) is equivalent to the stoichiometric loss of two water molecules, (*b*) a melt solvent analysis shows that the gas evolved is water, and (*c*) the dehydration endotherm (Fig. 7) is pressure dependent, as expected for a reaction involving a volume change.

A careful examination of erythromycin hydrates (Table V) by X-ray powder diffraction showed that the material produced at approximately 135° was amorphous and that the melting reported previously (8, 11, 18, 19) was the formation of a fluid noncrystalline solid and not the formation of an isotropic liquid.

A hot-stage microscopy study was conducted to gain further insight into the thermal behavior of erythromycin. The results (Table VI and Fig. 8) confirm the X-ray, TGA, and DTA findings. The medium used to suspend the erythromycin crystals on the microscope slide had a very pronounced effect on its thermal behavior. The data in Table VI show that when the crystals were left open to the atmosphere, one observed the transition of the dihydrate to an amorphous state and then recrystallization to the anhydrate form. However, when the crystals were covered with silicon oil, the formation of the amorphous state was apparently too rapid to observe (Table VI) since only the formation of the anhydrate was seen. When a DTA of erythromycin dihydrate (Fig. 7, curve A) was performed under similar conditions, the exotherm normally observed between 120 and 190° was not present. The dehydration endotherm was shallow and broad, indicating that recrystallization was probably occurring simultaneously with dehydration.

Table VII—DTA Results: Slow Heating [a]

Starting Material	Dehydration Endotherm[b]	Phase Change Exotherm	Melting Endotherm[b]
Dihydrate	120°	130–185°	192°
Monohydrate	111°	Not observed	185°
Anhydrate	None	None	191°

[a] Heating rate = 2°/min; atmosphere = nitrogen flow. [b] Values reported here are the peak temperatures of the endotherms.

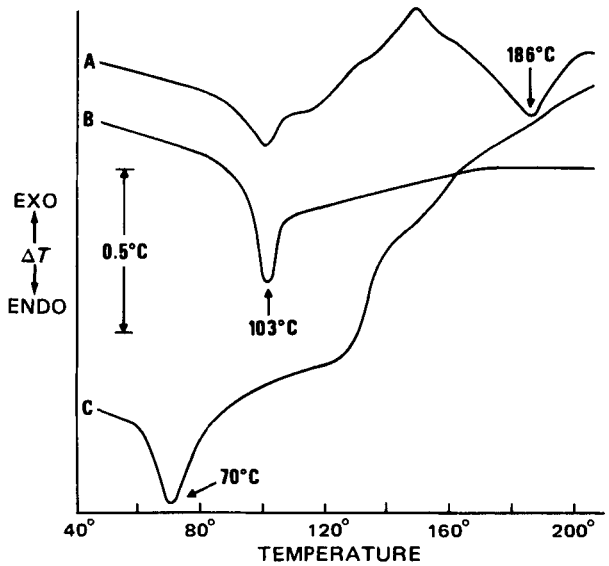

Figure 9—*DTA curves for the erythromycin monohydrate. Key: A, oil mull, nitrogen flow; B, powder sample, nitrogen flow; and C, powder sample, air pressure at 1 torr or less. Heating rate was 10°/min.*

The DTA and hot-stage microscopy studies also were performed on the monohydrate (Figs. 9 and 10). The thermal behavior of the monohydrate in the presence of silicon oil or at slow heating rates (Table VII) is described by the following reactions:

$$A\cdot H_2O \xrightarrow[\text{dehydration}]{\sim 100^\circ} A_{(CS)} + H_2O_{(g)}$$

$$A_{(CS)} \xrightarrow{114\text{–}137^\circ} A_{(a)}$$

$$A_{(a)} \xrightarrow{120\text{–}190^\circ} A^*_{(CS)}$$

$$A^*_{(CS)} \xrightarrow[\text{melting}]{186\text{–}190^\circ} A_{(l)}$$

Scheme II

The main difference observed during the thermal analyses of the monohydrate material was the rate at which the recrystallization occurred. The formation of crystalline material from the amorphous fluid was observed only in oil media (Fig. 10) and during very slow heating on the DTA apparatus (Table VII). Crystalline material did not form in sufficient quantity during the TGA experiments to confirm the presence of the anhydrate. However, the hot-stage microscopy and DTA melting-point data (Tables VI and VII) indicate that the crystalline erythromycin anhydrate was formed.

Hot-stage microscopy and DTA results (Tables VI and VII) for the anhydrate suggest that it is a monotropic crystal form, since the only transition observed was melting (190–193°) to the isotropic liquid of erythromycin. The thermogravimetric results (Table V) indicate that only surface moisture was present, which is further verified by the fact that no dehydration endotherms were observed during the DTA experiments.

SUMMARY AND CONCLUSIONS

Examination of the several physical properties of the dihydrate, monohydrate, and anhydrate indicates that their dissolution rates are probably related to particle–particle interactions and/or wettability of the various hydrates. The anhydrate had the slowest dissolution rate while the dihydrate dissolved very quickly in comparison to the monohydrate and anhydrate. No correlation was observed between the dissolution rate and specific surface area of the drug.

There has been a great deal of confusion concerning the melting point of crystalline solids (8, 9, 11, 12). The present study on erythromycin indicates that the dihydrate and monohydrate convert to the anhydrate (mp 190–193°) *via* an amorphous intermediate. The dihydrate appears

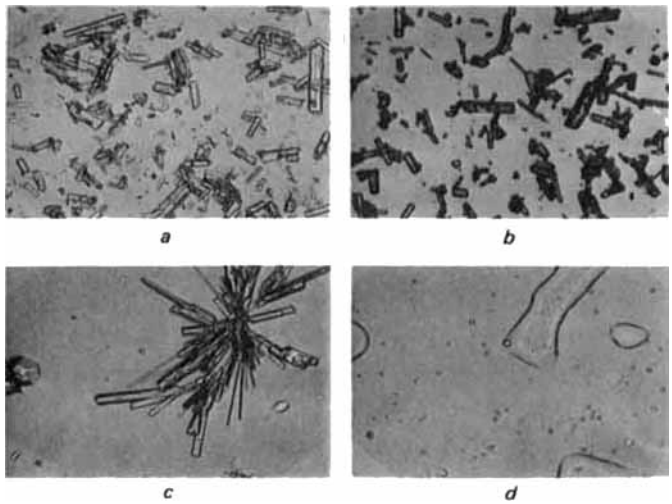

Figure 10—*Photomicrographs of the erythromycin monohydrate taken during the hot-stage microscopy study. Key:* a, *25°, crystalline solid, suspended in oil;* b, *122°, amorphous material, exposed to atmosphere;* c, *180°, crystalline solid, suspended in oil; and* d, *189°, isotropic liquid, suspended in oil.*

to convert readily when it is heated, but the monohydrate converts to the anhydrate only in the presence of silicon oil or if it is heated very slowly. When erythromycin monohydrate was heated at 10°/min, only the formation of the amorphous material was observed. Since the amorphous phase can be described as a fluid whose viscosity varies with temperature (*e.g.*, glass has a viscosity high enough to resemble a solid at ambient temperatures), the phase change from a crystalline solid to a noncrystalline material can be described as a melting point. But if the strict definition of melting is adhered to (*i.e.*, that melting involves the formation of an isotropic liquid), then the melting point observed at 190–193° was the only true melting point observed for the erythromycin forms examined. The change from the amorphous phase to the isotropic liquid involves very low transition energies and, therefore, is very difficult to observe.

It is obvious from this discussion that one must be very careful when assigning the melting point of a crystalline solid. This study shows that the melting point at 130–135° reported for erythromycin dihydrate (19) and monohydrate (8) is the formation of the amorphous phase and not a true melting point. It appears that the anhydrate crystal form is the most stable and that its melting point at 190–193° is the true melting point of crystalline erythromycin base.

REFERENCES

(1) J. T. Carstensen, "Theory of Pharmaceutical Systems," vol. II, Academic, New York, N.Y., 1973, p. 262.

(2) J. H. Fincher, *J. Pharm. Sci.*, **57**, 1825 (1968).

(3) A. J. Aguiar, J. Krc, Jr., A. W. Kinkel, and J. C. Samyn, *ibid.*, **56**, 847 (1967).

(4) A. J. Aguiar, L. M. Wheeler, S. Fusari, and J. E. Zelmer, *ibid.*, **57**, 1844 (1968).

(5) A. J. Aguiar and J. E. Zelmer, *ibid.*, **58**, 983 (1969).

(6) J. W. Poole, G. Owen, J. Silverio, J. N. Feyhof, and S. B. Roseman, *Curr. Ther. Res.*, **10**, 292 (1968).

(7) Eli Lilly Co., U.S. pat. 2,864,817 (Dec. 16, 1958).

(8) M. G. Shtolts, L. K. Shtamm, N. P. Bednyagina, and A. K. Shtolts, *Antibiotiki*, **11**, 291 (1966).

(9) M. A. Moustafa, A. R. Ebian, S. A. Khalil, and M. M. Motawi, *J. Pharm. Pharmacol.*, **23**, 868 (1971).

(10) J. Matsunagan, N. Nambu, and T. Nagai, *Chem. Pharm. Bull.*, **24**, 1169 (1976).

(11) G. Pelizza, M. Nebuloni, and G. G. Gallo, *Farmaco, Ed. Sci.*, **31**, 254 (1976).

(12) J. Haleblian and W. McCrone, *J. Pharm. Sci.*, **58**, 911 (1969).

(13) S. J. Gregg and K. S. W. Sing, "Adsorption Surface Area and Porosity," Academic, New York, N.Y., 1967.

(14) B. G. Tucker, *Anal. Chem.*, **47**, 778 (1975).

(15) N. R. Kuzel, J. M. Woodside, J. P. Caner, and E. E. Kennedy,

Chemotherapy, **4**, 1234 (1954).
(16) P. H. Emmett and S. Brunauer, *J. Am. Chem. Soc.*, **59**, 1553 (1937).
(17) E. Shefter and T. Higuchi, *J. Pharm. Sci.*, **52**, 781 (1963).
(18) J. K. Haleblian, *ibid.*, **64**, 1269 (1975).
(19) E. H. Flynn, M. V. Signal, P. F. Wiley, and K. Gerzon, *J. Am. Chem. Soc.*, **76**, 3121 (1954).

ACKNOWLEDGMENTS

The authors thank D. S. Aldrich for the excellent photomicrographs and K. G. Zipple for obtaining the X-ray diffraction patterns that were used for crystal form identification. They also acknowledge the assistance of C. E. Stiller (surface area determinations) and C. W. Andrews (DTA and TGA analyses of the monohydrate crystal forms).

GLC Determination of Caffeine in Plasma Using Alkali Flame Detection

JORDAN L. COHEN *ˣ, CHI CHENG *, JAMES P. HENRY ‡, and YUEN-LING CHAN *

Received August 15, 1977, from the **School of Pharmacy and the* ‡*School of Medicine, University of Southern California, Los Angeles, CA 90033.* Accepted for publication November 29, 1977.

Abstract □ A rapid, specific, and sensitive GLC assay for caffeine in plasma was developed utilizing alkali flame-ionization detection. The procedure involves the addition of mepivacaine as an internal standard, alkalinization of the sample, and extraction with chloroform. Peak height ratio measurements produced linear standard curves in the 0.25–10.0-μg/ml range. Absolute sensitivity from a 1.0-ml plasma sample was 0.1 μg/ml. The relative standard deviation of a 2.0-μg/ml pooled plasma standard run repeatedly over several months was 5.2%. The method is applicable to time–concentration studies in human and animal plasma following typical oral doses of caffeine.

Keyphrases □ Caffeine—GLC analysis in plasma □ GLC—analysis, caffeine in plasma □ Stimulants, central—caffeine, GLC analysis in plasma

The widespread occurrence of caffeine in popular beverages and over-the-counter medications makes it the drug most consumed by many individuals. The average amount of caffeine in a cup of coffee is about 80–100 mg; however, depending on the manner of preparation, strong coffee can contain as much as 300 mg/cup (1). The amount of caffeine in tea varies considerably, mainly as a function of water temperature and time of contact, with typical averages of 25–50 mg/cup (1). However, caffeine concentrations in tea approach those of coffee when packaged instructions for typical products are followed. Cola and cocoa beverages contain smaller, but substantial, amounts of caffeine.

BACKGROUND

Although caffeine has long been known for its diuretic and central nervous system stimulating activities, many other pharmacological and some toxic effects have been reported, particularly in individuals consuming large quantities. Gilbert (2) reviewed a large number of epidemiologic studies suggesting that ulcers of the stomach and duodenum, carcinomas of the kidney and urinary tract, and certain types of heart disease occur more frequently in individuals ingesting more than 600 mg of caffeine/day. In addition, a large number of symptoms associated with anxiety occur more frequently in this group.

These reports prompted investigations of the relationships among caffeine consumption, adverse effects, and body fluid concentrations. Rather surprisingly, there is a scarcity of published methods suitable for the routine determination of caffeine. The spectrophotometric method of Axelrod and Reichenthal (3) is widely used, as is a modified procedure (4), but these procedures have distinct sensitivity and specificity limitations and are relatively tedious. A GLC method (5) was reported with improved sensitivity, but it suffered from an inadequate internal standard which was added just prior to injection and hampered the reproducibility.

Although several liquid chromatographic methods were reported for theophylline (6, 7), none has been reported specifically for caffeine. Caffeine elutes slowly and broadly in these systems. A radioimmunoassay with a high level of sensitivity recently was reported (8). The inherent specificity of GLC, coupled with the increased sensitivity and selectivity of an alkali flame detector for nitrogen-containing compounds, led to the development of the present assay for caffeine in plasma of animals and humans. Data also are presented that support the application of this method for obtaining plasma time–concentration data on caffeine after ingestion of typical doses.

EXPERIMENTAL

Reagents—Caffeine[1] (purity >99%) was obtained commercially and used directly. A standard stock solution containing 200 μg/ml was prepared in methanol, protected from light, and stored at 4°.

Mepivacaine, the internal standard, was prepared by extraction of the alkalinized commercial dosage form[2] with dichloromethane. The solvent was removed, and the solid was recrystallized from ether, mp 150–152°. A standard stock solution containing 650 μg/ml was prepared in methanol and stored in the same manner as the caffeine stock solution.

Chloroform[3] and methanol[3] were spectral grade. All other reagents were analytical grade and were used as received. Other drugs were commercially available dosage forms.

Standard Curve—Appropriate aliquots of the stock caffeine standard in methanol were added to conical centrifuge tubes, the solvent was evaporated, and 1.0 ml of pooled human plasma was added to produce final concentrations of 0.25, 0.5, 1.0, 5.0, and 10.0 μg/ml. Identical concentrations were used to prepare aqueous standard curves. The tubes were vortexed to dissolve the drug, and the assay was carried out as described later. Standard curves were constructed from peak height ratio measurements of caffeine to internal standard.

Analytical Procedure—To 1.0 ml of plasma or aqueous sample in a 15-ml centrifuge tube were added 25 μl of mepivacaine standard in methanol and 30 μl of 12 *N* NaOH. This solution was vortexed, 10.0 ml of chloroform was added, and the tube was shaken for 15 min. The tube was then centrifuged at 2500 rpm for 10 min, and the aqueous (top) layer was aspirated off. The organic layer was filtered[4] into a 15-ml centrifuge tube and evaporated using a stream of air in a 40° water bath. The residue

[1] Aldrich Chemical Co., Milwaukee, Wis.
[2] Carbocaine Hydrochloride, Winthrop Laboratories, New York, N.Y.
[3] Burdick and Jackson Laboratories, Muskegon, Mich.
[4] Whatman No. 1 filter paper.

0022-3549/78/0800-1093$01.00/0
© 1978, American Pharmaceutical Association

Chemotherapy, **4**, 1234 (1954).
(16) P. H. Emmett and S. Brunauer, *J. Am. Chem. Soc.*, **59**, 1553 (1937).
(17) E. Shefter and T. Higuchi, *J. Pharm. Sci.*, **52**, 781 (1963).
(18) J. K. Haleblian, *ibid.*, **64**, 1269 (1975).
(19) E. H. Flynn, M. V. Signal, P. F. Wiley, and K. Gerzon, *J. Am. Chem. Soc.*, **76**, 3121 (1954).

ACKNOWLEDGMENTS

The authors thank D. S. Aldrich for the excellent photomicrographs and K. G. Zipple for obtaining the X-ray diffraction patterns that were used for crystal form identification. They also acknowledge the assistance of C. E. Stiller (surface area determinations) and C. W. Andrews (DTA and TGA analyses of the monohydrate crystal forms).

GLC Determination of Caffeine in Plasma Using Alkali Flame Detection

JORDAN L. COHEN *ˣ, CHI CHENG *, JAMES P. HENRY ‡, and YUEN-LING CHAN *

Received August 15, 1977, from the **School of Pharmacy and the* ‡*School of Medicine, University of Southern California, Los Angeles, CA 90033.* Accepted for publication November 29, 1977.

Abstract □ A rapid, specific, and sensitive GLC assay for caffeine in plasma was developed utilizing alkali flame-ionization detection. The procedure involves the addition of mepivacaine as an internal standard, alkalinization of the sample, and extraction with chloroform. Peak height ratio measurements produced linear standard curves in the 0.25–10.0-μg/ml range. Absolute sensitivity from a 1.0-ml plasma sample was 0.1 μg/ml. The relative standard deviation of a 2.0-μg/ml pooled plasma standard run repeatedly over several months was 5.2%. The method is applicable to time–concentration studies in human and animal plasma following typical oral doses of caffeine.

Keyphrases □ Caffeine—GLC analysis in plasma □ GLC—analysis, caffeine in plasma □ Stimulants, central—caffeine, GLC analysis in plasma

The widespread occurrence of caffeine in popular beverages and over-the-counter medications makes it the drug most consumed by many individuals. The average amount of caffeine in a cup of coffee is about 80–100 mg; however, depending on the manner of preparation, strong coffee can contain as much as 300 mg/cup (1). The amount of caffeine in tea varies considerably, mainly as a function of water temperature and time of contact, with typical averages of 25–50 mg/cup (1). However, caffeine concentrations in tea approach those of coffee when packaged instructions for typical products are followed. Cola and cocoa beverages contain smaller, but substantial, amounts of caffeine.

BACKGROUND

Although caffeine has long been known for its diuretic and central nervous system stimulating activities, many other pharmacological and some toxic effects have been reported, particularly in individuals consuming large quantities. Gilbert (2) reviewed a large number of epidemiologic studies suggesting that ulcers of the stomach and duodenum, carcinomas of the kidney and urinary tract, and certain types of heart disease occur more frequently in individuals ingesting more than 600 mg of caffeine/day. In addition, a large number of symptoms associated with anxiety occur more frequently in this group.

These reports prompted investigations of the relationships among caffeine consumption, adverse effects, and body fluid concentrations. Rather surprisingly, there is a scarcity of published methods suitable for the routine determination of caffeine. The spectrophotometric method of Axelrod and Reichenthal (3) is widely used, as is a modified procedure (4), but these procedures have distinct sensitivity and specificity limitations and are relatively tedious. A GLC method (5) was reported with improved sensitivity, but it suffered from an inadequate internal standard which was added just prior to injection and hampered the reproducibility.

Although several liquid chromatographic methods were reported for theophylline (6, 7), none has been reported specifically for caffeine. Caffeine elutes slowly and broadly in these systems. A radioimmunoassay with a high level of sensitivity recently was reported (8). The inherent specificity of GLC, coupled with the increased sensitivity and selectivity of an alkali flame detector for nitrogen-containing compounds, led to the development of the present assay for caffeine in plasma of animals and humans. Data also are presented that support the application of this method for obtaining plasma time–concentration data on caffeine after ingestion of typical doses.

EXPERIMENTAL

Reagents—Caffeine[1] (purity >99%) was obtained commercially and used directly. A standard stock solution containing 200 μg/ml was prepared in methanol, protected from light, and stored at 4°.

Mepivacaine, the internal standard, was prepared by extraction of the alkalinized commercial dosage form[2] with dichloromethane. The solvent was removed, and the solid was recrystallized from ether, mp 150–152°. A standard stock solution containing 650 μg/ml was prepared in methanol and stored in the same manner as the caffeine stock solution.

Chloroform[3] and methanol[3] were spectral grade. All other reagents were analytical grade and were used as received. Other drugs were commercially available dosage forms.

Standard Curve—Appropriate aliquots of the stock caffeine standard in methanol were added to conical centrifuge tubes, the solvent was evaporated, and 1.0 ml of pooled human plasma was added to produce final concentrations of 0.25, 0.5, 1.0, 5.0, and 10.0 μg/ml. Identical concentrations were used to prepare aqueous standard curves. The tubes were vortexed to dissolve the drug, and the assay was carried out as described later. Standard curves were constructed from peak height ratio measurements of caffeine to internal standard.

Analytical Procedure—To 1.0 ml of plasma or aqueous sample in a 15-ml centrifuge tube were added 25 μl of mepivacaine standard in methanol and 30 μl of 12 *N* NaOH. This solution was vortexed, 10.0 ml of chloroform was added, and the tube was shaken for 15 min. The tube was then centrifuged at 2500 rpm for 10 min, and the aqueous (top) layer was aspirated off. The organic layer was filtered[4] into a 15-ml centrifuge tube and evaporated using a stream of air in a 40° water bath. The residue

[1] Aldrich Chemical Co., Milwaukee, Wis.
[2] Carbocaine Hydrochloride, Winthrop Laboratories, New York, N.Y.
[3] Burdick and Jackson Laboratories, Muskegon, Mich.
[4] Whatman No. 1 filter paper.

0022-3549/78/0800-1093$01.00/0
© 1978, American Pharmaceutical Association

Table I—Reproducibility of Analysis of Caffeine Added to Plasma[a]

Caffeine Concentration Added, μg/ml	n	Mean Peak Height Ratio (Caffeine to Mepivacaine)	RSD, %
0.25	5	0.210	9.2
0.50	8	0.310	7.5
1.00	8	0.462	7.9
2.00	20	0.837	5.2
5.00	7	1.532	6.9
8.00	5	2.214	5.5
10.00	10	2.905	5.1

[a] Pooled plasma blanks typically demonstrated a caffeine concentration of 0.20 μg/ml.

was reconstituted in 25 μl of methanol and vortexed for 30 sec, and 1–5 μl was injected into the gas chromatograph.

Chromatographic Conditions—Chromatography was performed on a dual-column instrument[5] equipped with an alkali flame-ionization detector. The U-shaped glass column, 182 × 0.25 cm i.d., was packed with 3% OV-17 on 60–80-mesh Chromosorb P[6]. The column oven temperature was 210° (isothermal), and the injector and detector were maintained at 250°. Nitrogen carrier gas, air, and hydrogen flows were 25, 250, and 38 ml/min, respectively. Caffeine eluted at 3.8 min and mepivacaine eluted at 6.5 min under these conditions.

Plasma Time–Concentration Studies—Venous blood samples drawn into heparinized vacuum tubes[7] were collected periodically from normal volunteers following ingestion of varying amounts of coffee containing 350 μg of caffeine/ml (~70 mg/cup). As a part of physiological and histological studies, colonies of mice drank various standard brews of coffee. They were then sacrificed, and the plasma from several animals was pooled for caffeine analysis. Samples were analyzed directly or the separated plasma was frozen until analysis.

RESULTS AND DISCUSSION

Typical chromatograms from the analysis of a human plasma sample and a pooled plasma blank are shown in Fig. 1. The relatively broad peak in the blank eluting after 9.0 min generally was present in all patient samples assayed but did not interfere with the quantitation of caffeine. The small peak eluting at about 3.8 min in the pooled plasma blank was present in all pools and most individual patient blanks and was probably residual caffeine. This peak was not present in mouse plasma blanks or human samples from individuals who had abstained from all caffeine ingestion for 48 hr.

Standard curves from water and pooled plasma were linear up to 10 μg/ml. Based on the unextracted standard curve, the overall efficiency of the extraction was estimated to be 85%. The minimum detectable amount of caffeine over baseline was about 10 ng injected, which provided a practical limit of sensitivity of 0.1 μg/ml for a 1.0-ml plasma sample. This assay is considerably more sensitive than the literature procedure (5) in which a 5.0-ml blood sample was required to produce a reported sensitivity of 0.25 μg/ml using regular flame-ionization detection. This improvement is due mainly to a decrease in background noise seen with the alkali flame detector.

Data from replicate determinations of caffeine added to plasma to produce a working standard curve from 0.25 to 10.0 μg/ml are presented in Table I. Replicate analyses of a spiked 2.0-μg/ml plasma standard over several months produced a relative standard deviation of 5.2%.

Since caffeine is essentially nonionized throughout the physiological pH range, preliminary extractions to allow sample cleanup were not feasible. The relatively high pH used here (>12) was selected primarily to minimize emulsion formation during extraction. Because of the simplicity of the extraction, possible interference, particularly from basic and neutral drugs, was investigated even though no interfering peaks were seen in either pooled or individual plasma blanks.

Lidocaine, procainamide, quinidine, isoniazid, glutethimide, salicylamide, phenylbutazone, and acetaminophen did not interfere at a spiked plasma concentration of 15 μg/ml. As expected, theophylline, theobromine, and the major human caffeine metabolites, methyluric acid, 1-methylxanthine, and paraxanthine (2, 9), also did not interfere under these analytical conditions. Because of the relatively high pH, no other acidic species are anticipated to interfere.

[5] Model 2100, Varian Instruments, Palo Alto, Calif.
[6] Applied Science Laboratories, State College, Pa.
[7] Vacutainers, Becton-Dickinson Co., Rutherford, N.J.

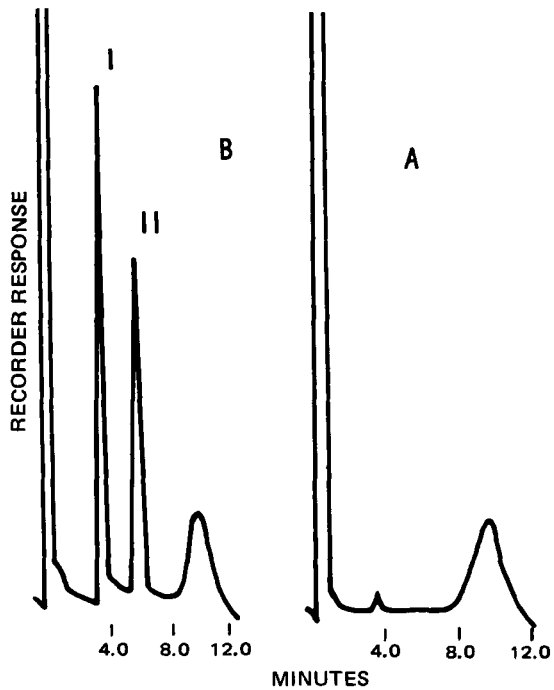

Figure 1—*Gas chromatograms of human plasma samples. Key: A, pooled plasma blank; and B, plasma sample from a normal volunteer containing 5 μg of caffeine/ml (I) and 12 μg of mepivacaine/ml (II).*

The procedure was developed to allow the investigation of plasma time–concentration patterns in humans and mice following various caffeine ingestion patterns. Figure 2 illustrates these profiles for four normal volunteers who consumed varying amounts of coffee through a working day. Peak plasma levels generally occurred 1–2 hr following ingestion, and levels were maintained between 1 and 5 μg/ml for individuals consuming less than 5 cups of coffee per day. This result agrees with previously reported data (5).

The disappearance rate of caffeine from the blood following the absorptive phase varied considerably. In eight subjects, the range in observed half-lives was from 2.1 to 6.5 hr. Literature reports of average terminal phase elimination half-lives of caffeine in humans range from 2.5 (3) to 4.5 (8, 9) hr. Fasting mice appear to absorb and eliminate caf-

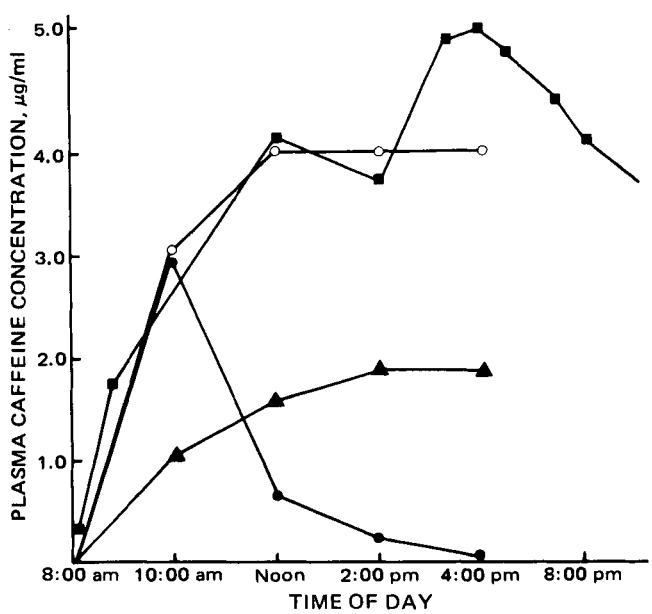

Figure 2—*Caffeine plasma time–concentration curves for four normal volunteers ingesting various amounts of coffee containing 350 μg of caffeine/ml. Key: ●, P-1, 2 cups at 8:00 am; ▲, P-2, approximately 3 cups* ad libitum; *○, P-3, approximately 5 cups* ad libitum; *and ■, P-4, 240 ml at 8:00 am, 11:30 am, and 2:30 pm.*

Table II—Plasma Concentrations in Colonies of Fasted Mice following Ingestion of Caffeine

Minutes	Plasma Caffeine Concentration, μg/ml
0	<0.1
15	5.9
30	1.9
60	1.2

feine more rapidly than humans. Table II indicates some typical plasma level data for a colony of mice fasted overnight and then given approximately 1 mg of caffeine as a single dose in the morning. This dose is equivalent to about 10 cups of coffee for a 70-kg human. Peak absorption occurred within 15 min, and concentrations declined rapidly thereafter. In colonies of nonfasted mice allowed to drink standard brews of coffee (350 μg/ml) *ad libitum*, typical plasma concentrations between drinks were 0.3–1.5 μg/ml throughout the day.

In general, the assay appears to be well suited to the rapid and routine measurement of human or animal plasma caffeine concentrations following administration of caffeine-containing beverages or medications. It is sensitive and highly selective and has permitted a variety of human and animal studies aimed at quantitating plasma concentration–time profiles following varying amounts of caffeine ingestion and correlating them to the possible incidence of adverse effects. The high sensitivity attainable also allows this method to be useful in assessing plasma concentration of caffeine in toxic situations from small volumes of blood.

REFERENCES

(1) R. M. Gilbert, J. A. Marshman, M. Schwieder, and R. Berg, *Can. Med. Assoc. J.*, **114**, 205 (1976).

(2) R. M. Gilbert, in "Research Advances in Alcohol and Drug Problems," vol. 3, Y. Israel, Ed., Wiley, New York, N.Y., 1976, pp. 49–176.

(3) J. Axelrod and J. Reichenthal, *J. Pharmacol. Exp. Ther.*, **107**, 519 (1953).

(4) J. I. Routh, N. A. Shane, E. G. Arredondo, and W. D. Paul, *Clin. Chem.*, **15**, 661 (1969).

(5) F. L. Grab and J. A. Reinstein, *J. Pharm. Sci.*, **57**, 1703 (1968).

(6) L. C. Franconi, G. L. Hawk, B. J. Sandman, and W. G. Haney, *Anal. Chem.*, **48**, 372 (1976).

(7) J. J. Orcutt, P. O. Kozak, S. A. Gillman, and L. H. Cummins, *Clin. Chem.*, **23**, 599 (1977).

(8) C. E. Cook, C. R. Tallent, E. W. Amerson, M. W. Myers, J. A. Kepler, G. F. Taylor, and H. D. Christiansen, *J. Pharmacol. Exp. Ther.*, **199**, 679 (1976).

(9) H. H. Cornish and A. A. Christman, *J. Biol. Chem.*, **228**, 315 (1957).

ACKNOWLEDGMENTS

Presented at the Pharmaceutical Analysis and Control Section, APhA Academy of Pharmaceutical Sciences, New York meeting, May 1977.

Supported in part by Grant HL 17706 from the National Institutes of Health, Bethesda, MD 20014.

GLC Determination of Ticrynafen and Its Metabolites in Urine, Serum, and Plasma of Humans and Animals

BRUCE HWANG ˣ, GEORGE KONICKI, RICHARD DEWEY, and CLARA MIAO

Received June 2, 1977, from the *Research and Development Division, Smith Kline and French Laboratories, Philadelphia, PA 19101.* Accepted for publication November 17, 1977.

Abstract □ A sensitive GLC assay for ticrynafen, a diuretic agent with uricosuric properties, and its two metabolites in urine, serum, and plasma is described. The method employs methylation of carboxylic acid groups and trimethylsilylation of the hydroxyl group on one metabolite that cannot otherwise be separated readily from ticrynafen as a simple methyl ester. Urinary output and serum or plasma levels of ticrynafen and its two metabolites were measured in specimens from human volunteers receiving one 250-mg tablet.

Keyphrases □ Ticrynafen—and metabolites, GLC analyses in biological fluids □ GLC—analysis, ticrynafen and metabolites in biological fluids □ Diuretics—ticrynafen and metabolites, GLC analyses in biological fluids

Ticrynafen [tienilic acid[1] or [2,3-dichloro-4-(2-thienylcarbonyl)phenoxy]acetic acid] (I) is a new potent diuretic agent with uricosuric properties (1–4). A pharmacokinetic study with the ^{14}C-labeled drug in animals (5) and a GLC method (6) for the drug were reported recently. However, the reported GLC method does not distinguish the parent drug from one of its metabolites, [2,3-dichloro-4-(α-hydroxy-2-thienyl)phenoxy]acetic acid (II). The drug is metabolized by two pathways (5): reduction of the ketone function to the corresponding alcohol (II) and oxidation of the thienylcarbonyl moiety to form [2,3-dichloro-4-carboxyphenoxy]acetic acid (III) as shown in Scheme I.

This report describes a procedure capable of measuring

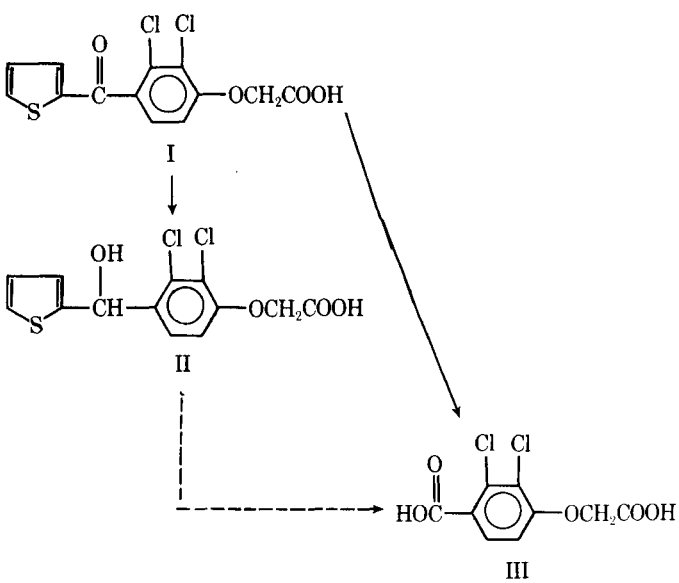

Scheme I

[1] WHO approved name.

© 1978, American Pharmaceutical Association

Table II—Plasma Concentrations in Colonies of Fasted Mice following Ingestion of Caffeine

Minutes	Plasma Caffeine Concentration, μg/ml
0	<0.1
15	5.9
30	1.9
60	1.2

feine more rapidly than humans. Table II indicates some typical plasma level data for a colony of mice fasted overnight and then given approximately 1 mg of caffeine as a single dose in the morning. This dose is equivalent to about 10 cups of coffee for a 70-kg human. Peak absorption occurred within 15 min, and concentrations declined rapidly thereafter. In colonies of nonfasted mice allowed to drink standard brews of coffee (350 μg/ml) *ad libitum*, typical plasma concentrations between drinks were 0.3–1.5 μg/ml throughout the day.

In general, the assay appears to be well suited to the rapid and routine measurement of human or animal plasma caffeine concentrations following administration of caffeine-containing beverages or medications. It is sensitive and highly selective and has permitted a variety of human and animal studies aimed at quantitating plasma concentration–time profiles following varying amounts of caffeine ingestion and correlating them to the possible incidence of adverse effects. The high sensitivity attainable also allows this method to be useful in assessing plasma concentration of caffeine in toxic situations from small volumes of blood.

REFERENCES

(1) R. M. Gilbert, J. A. Marshman, M. Schwieder, and R. Berg, *Can. Med. Assoc. J.*, **114**, 205 (1976).

(2) R. M. Gilbert, in "Research Advances in Alcohol and Drug Problems," vol. 3, Y. Israel, Ed., Wiley, New York, N.Y., 1976, pp. 49–176.

(3) J. Axelrod and J. Reichenthal, *J. Pharmacol. Exp. Ther.*, **107**, 519 (1953).

(4) J. I. Routh, N. A. Shane, E. G. Arredondo, and W. D. Paul, *Clin. Chem.*, **15**, 661 (1969).

(5) F. L. Grab and J. A. Reinstein, *J. Pharm. Sci.*, **57**, 1703 (1968).

(6) L. C. Franconi, G. L. Hawk, B. J. Sandman, and W. G. Haney, *Anal. Chem.*, **48**, 372 (1976).

(7) J. J. Orcutt, P. O. Kozak, S. A. Gillman, and L. H. Cummins, *Clin. Chem.*, **23**, 599 (1977).

(8) C. E. Cook, C. R. Tallent, E. W. Amerson, M. W. Myers, J. A. Kepler, G. F. Taylor, and H. D. Christiansen, *J. Pharmacol. Exp. Ther.*, **199**, 679 (1976).

(9) H. H. Cornish and A. A. Christman, *J. Biol. Chem.*, **228**, 315 (1957).

ACKNOWLEDGMENTS

Presented at the Pharmaceutical Analysis and Control Section, APhA Academy of Pharmaceutical Sciences, New York meeting, May 1977.

Supported in part by Grant HL 17706 from the National Institutes of Health, Bethesda, MD 20014.

GLC Determination of Ticrynafen and Its Metabolites in Urine, Serum, and Plasma of Humans and Animals

BRUCE HWANG ˣ, GEORGE KONICKI, RICHARD DEWEY, and CLARA MIAO

Received June 2, 1977, from the *Research and Development Division, Smith Kline and French Laboratories, Philadelphia, PA 19101.* Accepted for publication November 17, 1977.

Abstract □ A sensitive GLC assay for ticrynafen, a diuretic agent with uricosuric properties, and its two metabolites in urine, serum, and plasma is described. The method employs methylation of carboxylic acid groups and trimethylsilylation of the hydroxyl group on one metabolite that cannot otherwise be separated readily from ticrynafen as a simple methyl ester. Urinary output and serum or plasma levels of ticrynafen and its two metabolites were measured in specimens from human volunteers receiving one 250-mg tablet.

Keyphrases □ Ticrynafen—and metabolites, GLC analyses in biological fluids □ GLC—analysis, ticrynafen and metabolites in biological fluids □ Diuretics—ticrynafen and metabolites, GLC analyses in biological fluids

Ticrynafen [tienilic acid[1] or [2,3-dichloro-4-(2-thienylcarbonyl)phenoxy]acetic acid] (I) is a new potent diuretic agent with uricosuric properties (1–4). A pharmacokinetic study with the ^{14}C-labeled drug in animals (5) and a GLC method (6) for the drug were reported recently. However, the reported GLC method does not distinguish the parent drug from one of its metabolites, [2,3-dichloro-4-(α-hydroxy-2-thienyl)phenoxy]acetic acid (II). The drug is metabolized by two pathways (5): reduction of the ketone function to the corresponding alcohol (II) and oxidation of the thienylcarbonyl moiety to form [2,3-dichloro-4-carboxyphenoxy]acetic acid (III) as shown in Scheme I.

This report describes a procedure capable of measuring

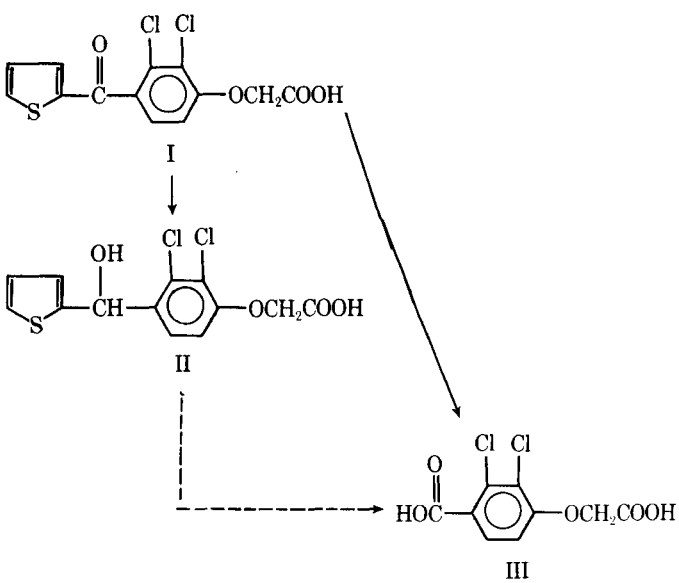

Scheme I

[1] WHO approved name.

© 1978, American Pharmaceutical Association

Table I—Reproducibility and Recovery from Urine Based on Peak Height Ratios

Sample	Extracted			Unextracted		
	I, 10 μg/ml	II, 10 μg/ml	III, 1 μg/ml	I, 10 μg	II, 10 μg	III, 1 μg
Blank	0	0	0	0	0	0
1	1.67	1.15	0.23	2.19	2.64	0.33
2	1.65	1.61	0.23	2.23	2.69	0.31
3	1.51	1.58	0.23	2.03	2.72	0.31
4	1.65	1.66	0.24	2.10	2.78	0.30
5	1.64	1.67	0.22	2.23	2.58	0.33
$\bar{x}$	1.62	1.62	0.23	2.16	2.68	0.32
Sx	0.06	0.04	0.006	0.08	0.06	0.01
$S\bar{x}$	0.03	0.02	0.003	0.04	0.03	0.005
Recovery[a], %	100	84	104			

[a] Recovery = ($\bar{x}$ extracted/$\bar{x}$ unextracted) × 1.39. The factor 1.39 = 9.7/7.0; a 7-ml aliquot was taken from 9.7 ml of the organic layer, which resulted from mixing 10 ml of ether and 3 ml of the aqueous mixture.

I–III simultaneously in urine, serum, or plasma at very low concentrations. Analyses of specimens from human volunteers receiving a single dose of 250 mg of I also are reported.

EXPERIMENTAL

Reagents—The following reagents were used: 1.0 *N* HCl[2], chloroform[3], ether[3], methanol[2], *N*-methyl-*N*-nitroso-*p*-toluenesulfonamide[4], bis-(trimethylsilyl)trifluoroacetamide plus 10% trimethylchlorosilane[5], acetonitrile[6] (dried over molecular sieve 3A), pyridine[7], and boron trifluoride–methanol complex[4].

Preparation of Diazomethane—Diazomethane ethereal solution (~1 mmole/ml) was prepared by mixing 2 g of *N*-methyl-*N*-nitroso-*p*-toluenesulfonamide in 10 ml of ether and 0.2 g of potassium hydroxide in 5 ml of 90% ethanol (10% water) at 0° or below. The mixture was then heated in a water bath (70°), and 6 ml of diazomethane ethereal solution distillate was collected in an ice-cooled test tube. The solution was stored in a freezer until used.

Preparation of Internal Standard Solution—The methyl ester of ethacrynic acid, used as an internal standard for this assay, was prepared by reacting ethacrynic acid with methanol in the presence of boron trifluoride. A 500-μg sample of ethacrynic acid was dissolved in 0.5 ml of methanol and mixed with 25 μl of boron trifluoride–methanol complex. The mixture was kept at 60° for 30 min and evaporated under nitrogen.

To the residue, 1 ml of 5% Na_2CO_3 was added; the product, methyl ethacrynate, was extracted with 2 ml of ether. The organic layer was evaporated to dryness, and the residue was dissolved in 200 ml of acetonitrile (predried over molecular sieves) to give an approximate concentration of 2.5 μg/ml. The structure of the methyl ester was verified by its NMR and mass spectra.

Diazomethane esterification of ethacrynic acid did not provide a suitable standard because diazomethane reacted with the activated double bond in ethacrynic acid to give two products, one of which interfered with the analysis.

Instrumentation—The gas chromatograph[8] was equipped with an on-column injection port, an electron-capture detector, and a 180-cm long, 2-mm i.d. glass column packed with 3% OV-17 on 100–120-mesh

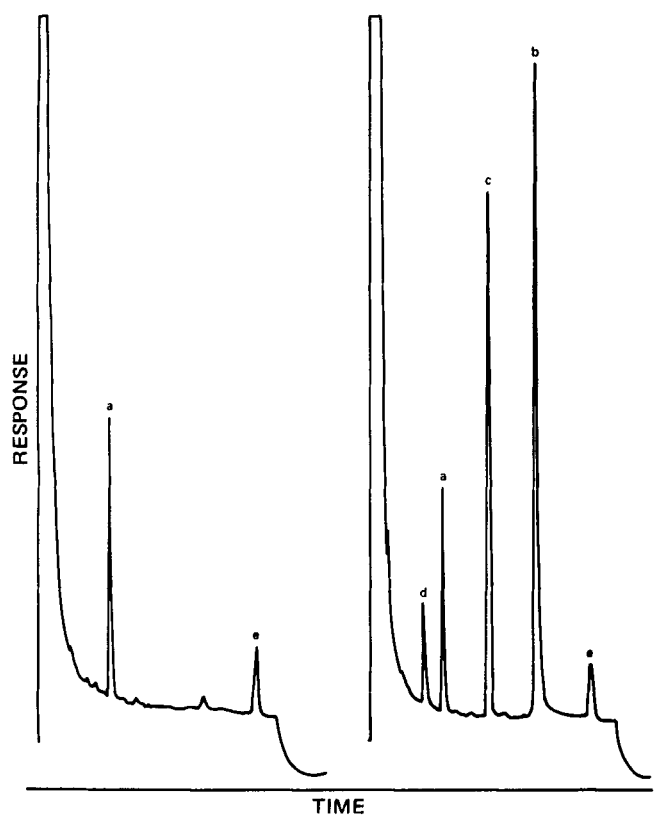

Figure 1—*Typical chromatograms of human urine with internal standard (a). Key: left, control urine; and right, urine containing 10 μg of I/ml (b), 10 μg of II/ml (c), and 1 μg of III/ml (d). Peak e is due to endogenous material in human urine.*

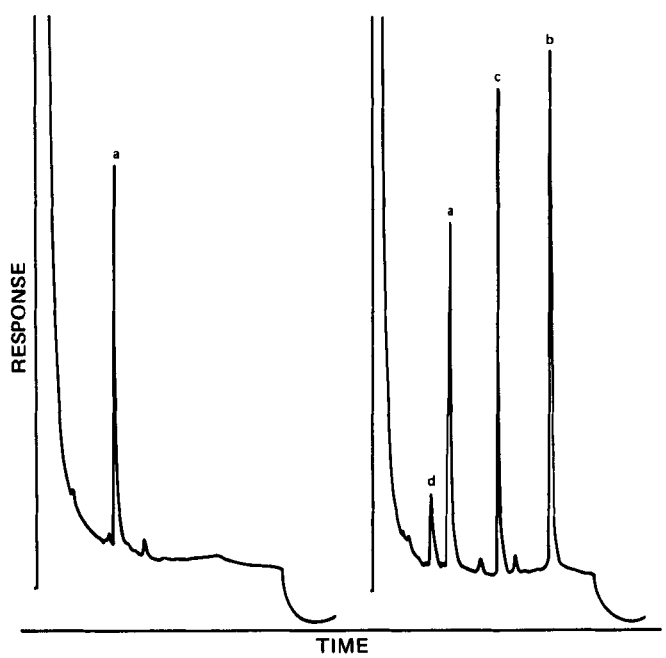

Figure 2—*Typical chromatograms of human plasma with internal standard (a). Key: left, control plasma; and right, plasma containing 5 μg of I/ml (b), 5 μg of II/ml (c), and 0.5 μg of III/ml (d).*

[2] Target electronic grade, Lehigh Valley Chemical Co., Easton, Pa.
[3] Analytical reagent, Mallinckrodt, St. Louis, Mo.
[4] Aldrich Chemical Co., Milwaukee, Wis.
[5] Regisil No. 3, Regis Chemical Co., Morton Grove, Ill.
[6] Fisher Scientific Co., Pittsburgh, Pa.
[7] Burdick & Jackson Laboratories, Muskegon, Mich.
[8] Model 3920B, Perkin-Elmer Corp., Norwalk, Conn.

Table II—Reproducibility and Recovery from Plasma Based on Peak Height Ratios

Sample	Extracted			Unextracted		
	I, 5 μg/ml	II, 5 μg/ml	III, 0.5 μg/ml	I, 5 μg	II, 5 μg	III, 0.5 μg
Blank	0	0	0	0	0	0
1	1.55	1.58	0.20	2.17	2.17	0.28
2	1.51	1.57	0.18	2.10	2.20	0.27
3	1.44	1.57	0.19	2.14	2.14	0.27
4	1.46	1.54	0.19	2.20	2.16	0.27
5	1.54	1.53	0.18	2.12	2.14	0.27
$\bar{x}$	1.50	1.56	0.19	2.15	2.16	0.27
Sx	0.04	0.02	0.007	0.04	0.02	0.004
$S\bar{x}$	0.02	0.01	0.003	0.02	0.01	0.002
Recovery[a], %	97	100	98			

[a] Recovery = ($\bar{x}$ extracted/$\bar{x}$ unextracted) × 1.39. The factor 1.39 = 9.7/7.0; a 7-ml aliquot was taken from 9.7 ml of the organic layer, which resulted from mixing 10 ml of ether and 3 ml of the aqueous mixture.

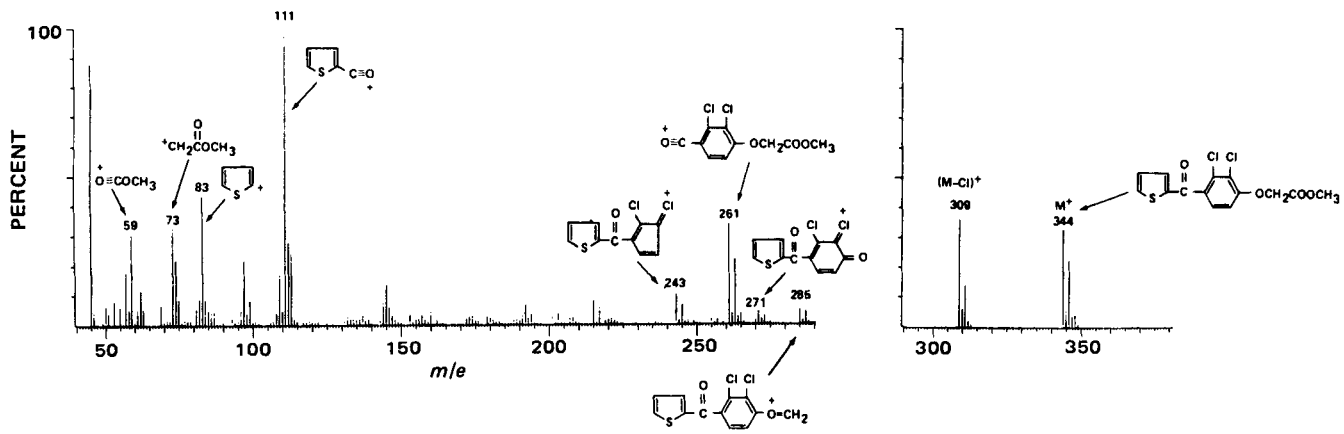

Figure 3—*Mass spectra of ticrynafen methyl ester.*

Gas Chrom Q. The oven temperature was programmed from 230° after 2 min initial temperature time and heated to 282° at the rate of 8°/min. The analysis ended 4 min after the final temperature was reached. Injection port, interface, and detector temperatures were 270, 310, and 300°, respectively. Argon–methane (95:5) was used as a carrier gas at 4.2 kg/cm^2. The detector standing current was 1.0 amp, and attenuation was at 512.

Under these conditions, retention times of the derivatized compounds were: diacid (III), 4 min; internal standard, 5 min; reduced metabolite (II), 8 min; and ticrynafen (I), 10.5 min. Since a urinary component had a retention time of about 15 min, the final temperature had to be maintained until this substance was eluted off the column before the oven was returned to the initial temperature for the next analysis. Temperature settings may have to be adjusted to suit individual columns to obtain good chromatograms.

Extraction and Preparation of Samples for Chromatography—Each 1-ml sample (urine, plasma, or serum) was diluted with 2 ml of 1.0 *N* HCl in a 40-ml centrifuge tube. Ether, 10 ml, was added to each tube, and the tubes were capped and shaken on a rocking mechanical shaker for 45 min. After centrifugation at 2000 rpm for 15 min, 7 ml of the organic layer from each tube was transferred to 12-ml centrifuge tubes. Each extract was cooled in an ice bath for 5 min, 0.5 ml of the diazomethane solution was added, and the tubes were mixed and kept at ice bath temperature for 1 hr.

The tubes were removed from the ice bath to a 40° water bath, and the solvent was evaporated under a constant flow of nitrogen. Aliquots of 1 ml of methanol were used to wash the residue from the wall of each tube, and the methanol also was evaporated to dryness under nitrogen at 40°. Finally, 1 ml of a solution consisting of 75 parts of acetonitrile containing a suitable concentration of the internal standard, 10 parts of pyridine, and 15 parts of the silylating reagent was added to the tube; then the tube was mixed well and sealed with a cap. The samples were ready for analysis after 3 hr. Samples can be kept overnight (or several days) at room temperature.

Method of Quantitation—Suitable ranges of standard solutions of I–III in urine, plasma, or serum were prepared for each group of unknown samples and treated similarly and simultaneously. The standard curves, based on peak height ratio and concentration, were used to quantitate each component. For analysis of samples from subjects receiving 250 mg of I, the appropriate concentration ranges of standard solutions for the standard curves were 1.0–10.0 μg/ml in urine for I and II, 0.25–5.0 μg/ml in urine for III, 0.5–10.0 μg/ml in plasma or serum for I and II, and 0.1–2.0 μg/ml in plasma or serum for III.

GLC–Mass Spectrometry—Mass spectra were obtained on two in-

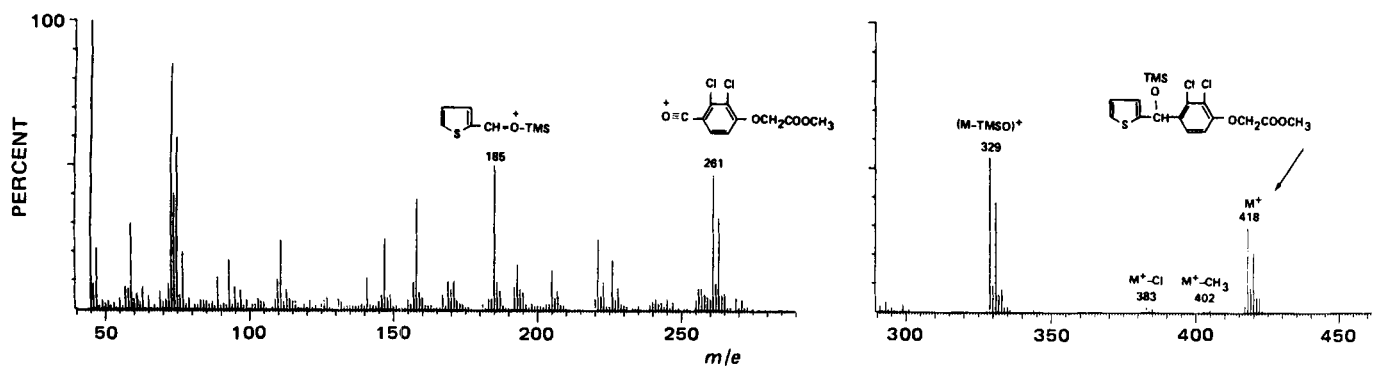

Figure 4—*Mass spectra of methyl ester–trimethylsilyl derivative of II.*

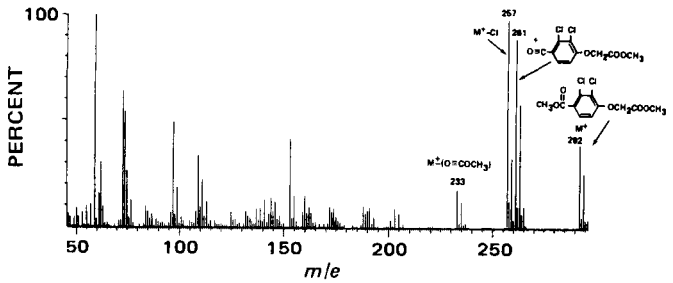

Figure 5—*Mass spectrum of dimethyl ester of III.*

struments using GLC inlets. A 180-cm × 2-mm (i.d.) glass column packed with 3% OV-17 was used on one instrument[9]. The column temperature was programmed from 220 to 275° at 10°/min with a carrier gas helium flow rate of 30 ml/min. The mass spectrometer was operated by autotune software. A 180-cm × 2-mm (i.d.) glass column packed with 3% OV-101 was used on the other instrument[10]. The column temperature was programmed from 210 to 280° at 10°/min with the helium flow rate at 20 ml/min. The mass spectrometer was operated under the following conditions: emission voltage, 70 v; extractor voltage, 5 v; and multiplier, 2200 v. Similar results were obtained from the two instruments.

RESULTS AND DISCUSSION

Linear standard curves were obtained for all compounds. The assay sensitivity was 0.01 μg/ml for each compound in biological fluids using the method described. Peak height of 1% or more of full-scale deflection at an attenuation of 512 was attainable by injecting 1 μl of the final solutions prepared from 1 ml of biological fluids containing 0.01 μg of compounds. Figures 1 and 2 show some typical chromatograms of control urine and plasma containing first the internal standard alone and then all three compounds and the internal standard. Chromatograms of serum samples were similar to those of plasma samples.

Recovery was calculated from the peak height ratio of each component to the internal standard in extracted samples and solutions spiked with each component. The loss of samples during transfer of extracts was considered. As shown in Tables I and II, reproducibility and recovery from urine and plasma were very good. Quantitative recovery and good reproducibility also were observed in every case with serum.

The identity of the three compounds being measured and confirmation of the specificity of analysis were shown by analyzing representative urine

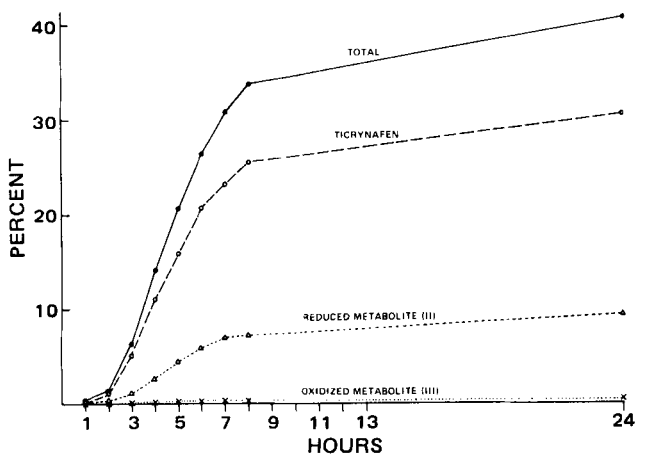

Figure 6—*Average urinary excretion of I–III of eight volunteers receiving 250 mg of ticrynafen (percent of dose excreted, cumulative).*

[9] HP 5992A GC/MS system.
[10] Finnigan model 4000 GC/MS automated system.

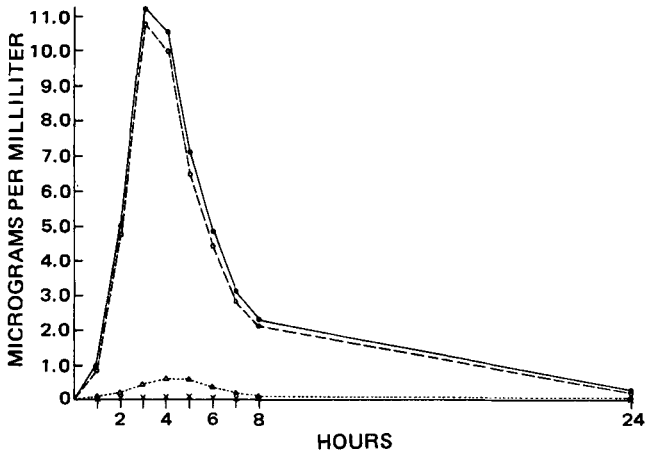

Figure 7—*Average plasma levels of I–III in eight volunteers receiving 250 mg of ticrynafen (data are reported in micrograms of ticrynafen per milliliter or equivalent in the case of the metabolites). Key: ●, total; ○, I; △, II; and ×, III.*

samples by combined GLC–mass spectrometry using the technique described. The spectra obtained from the specimen were identical to those obtained from authentic compounds derivatized by the same procedure. All three compounds gave molecular ions showing two chlorine atoms. Strong fragment ions are in agreement with the structures of derivatized I–III (Figs. 3–5).

The present method was used for the determination of I–III in urine and plasma of eight normal volunteers. Volunteers received a standard waterload of 20 ml/kg, followed by a 250-mg ticrynafen tablet at 9:00 am; water was given hourly (300 ml/hr during the first 15 min of the hour) for the next 7 hr. Results of analysis are shown in Figs. 6 and 7. Average plasma I–III levels peaked between 3 and 4 hr at about 11, 0.7, and 0.07 μg/ml, respectively. Urinary excretions in 24 hr averaged about 40% of the dose. No increase in urinary I–III after enzymatic hydrolysis indicated the absence of glucuronides.

Analyses of two sets of plasma and serum samples from the same blood of two volunteers gave similar results. The method was also suitable for animal urine and serum (or plasma). Analysis of urine and serum samples of a dog administered I, 5 mg/kg iv, showed that the ratios of the levels of II to I in the dog serum and urine were much higher than in humans. The dog excreted 12 and 53% of the dose as I and II, respectively, in the 0–140-min urine collection. No oxidized metabolite (III) was detected in the dog urine or serum samples.

REFERENCES

(1) G. Thuillier, J. Laforest, B. Cariou, P. Bessin, J. Bonnet, and J. Thuillier, *Eur. J. Med. Chem.*, **9**, 625 (1974).

(2) A. Masbernard and C. Guidicelli, *Lyon Med.*, **232**, 165 (1974).

(3) F. Vial, C. Argence, and J. Rulliere, *J. Pharmacol. Clin., Special Issue*, **1976**, 83.

(4) R. M. Stote, A. R. Maass, D. A. Cherril, M. M. A. Begand, and F. Alexander, *ibid.*, **1976**, 19.

(5) Y. Dormard, J. C. Levron, P. Adnot, T. Lebedeff, and G. Enjoubault, *Eur. J. Drug Metab. Pharmacokinet.*, **1**, 41 (1976).

(6) J. P. Desager, M. Vanderbist, B. Hwang, and P. Levandoski, *J. Chromatogr.*, **123**, 379 (1976).

ACKNOWLEDGMENTS

The authors thank Dr. R. Stote, Dr. A. Maass, Mr. R. Familiar, and Ms. I. Snow for drug administration and collection of human and animal specimens. The technical assistance of Miss J. Chwastyk, Mr. K. Dobson, and Mr. F. Havnoonian is gratefully acknowledged. The authors also express appreciation to Dr. B. M. Sutton and Dr. S. Walkenstein for assistance in preparing this manuscript.

Chromatographic Separation and Assay of Morphine in Tablets

I. J. HOLCOMB, R. B. LUERS, and S. A. FUSARI ˣ

Received January 6, 1975, from *Analytical Development, Parke, Davis and Company, Detroit, MI 48232.* Accepted for publication November 29, 1977.

Abstract □ A method specific for the determination of morphine sulfate in tablets was developed. Morphine is separated from the excipient and degradation products by a column chromatographic method. The eluate containing morphine is extracted into an acid solution and determined spectrophotometrically. Recovery from standard solutions is greater than 99%. This method is more specific for the separation and determination of morphine in tablets than is the USP XVIII procedure.

Keyphrases □ Morphine sulfate—chromatographic analysis in tablets □ Chromatography—analysis, morphine sulfate in tablets □ Narcotic analgesics—morphine sulfate, chromatographic analysis in tablets

Previously (1), morphine was separated from degradation products in injectables by a simple, rapid, chromatographic method. The same type of procedure is applicable to the separation of morphine in tablets. The USP XVIII extraction–titrimetric method (2) is time consuming, and small amounts of decomposition products as well as morphine are extracted from tablets.

The purpose of this investigation was to provide a simple, rapid, chromatographic method specific for the separation of morphine from its degradation products in tablets.

EXPERIMENTAL

Reagents—Morphine sulfate and lactose were USP grade. Acid-washed diatomaceous earth[1], sodium chloride, hydrochloric acid, isobutyl alcohol, chloroform, and anhydrous ether were reagent grade. Pseudomorphine base and morphine *N*-oxide were prepared in these laboratories (1).

Apparatus—A 25-mm i.d. × 25-cm long chromatographic column with a polytef stopcock, 1-cm quartz cells, and a spectrophotometer[2] with a recorder[3] were used.

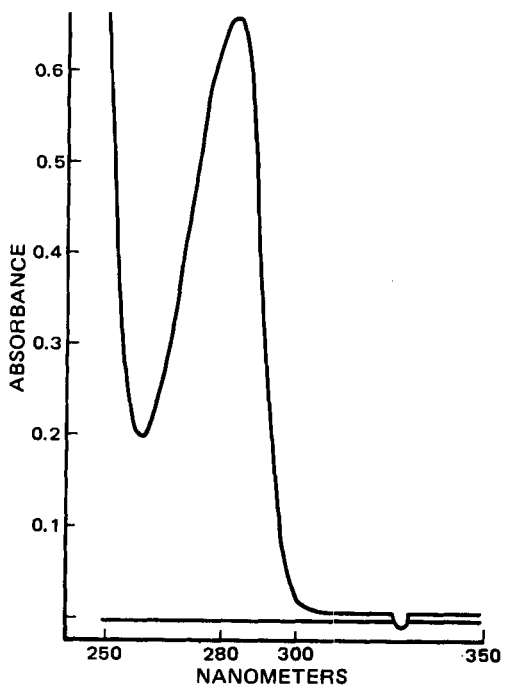

Figure 1—*UV spectrum of morphine sulfate standard, 0.1624 mg/ml, in 0.05 N HCl.*

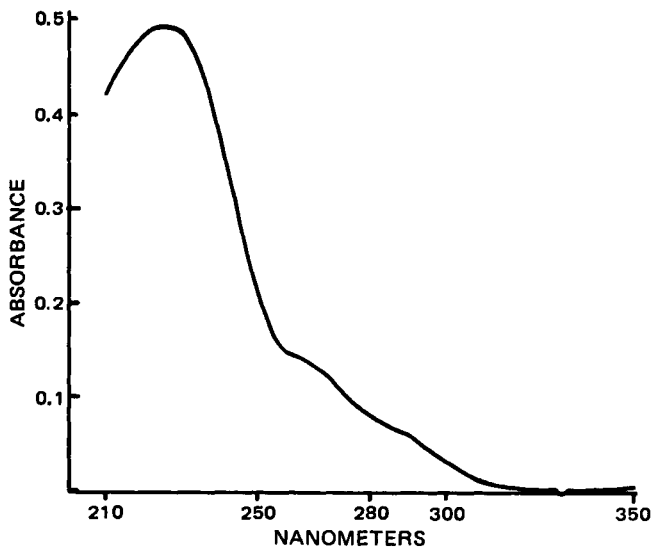

Figure 2—*UV spectrum of pseudomorphine, 0.00746 mg/ml, in 0.05 N HCl.*

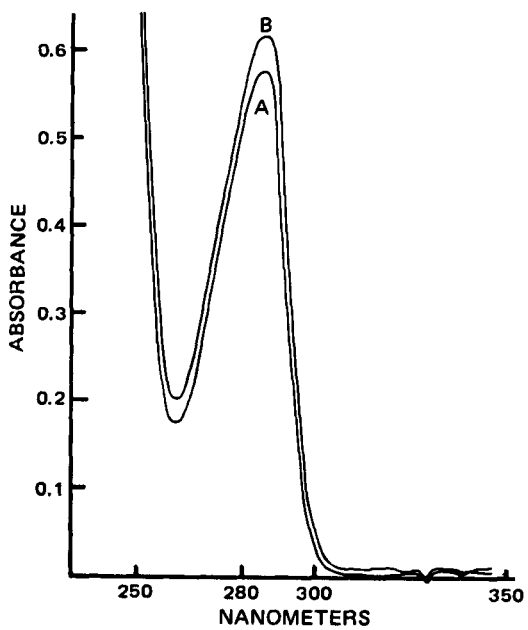

Figure 3—*UV spectra. Key: A, morphine sulfate, 0.1486 mg/ml, in 0.05 N HCl; and B, morphine sulfate, 0.1486 mg/ml, and pseudomorphine, 0.0075 mg/ml, in 0.05 N HCl.*

[1] Celite 545, Johns-Manville Co.

[2] Perkin-Elmer model 124.

[3] Perkin-Elmer model 165.

0022-3549/78/0800-1099$01.00/0
© 1978, American Pharmaceutical Association

Table I—Assay Results on Morphine Tablets

Lot	Date of Manufacture	Milligrams of Morphine Sulfate Found per Tablet (Percent Label Claim)		
		Column Separation Spectrophotometry	Direct Dilution Spectrophotometry	USP XVIII Procedure
10-mg Tablets				
A	1964	10.03 (100.3)	10.50 (105.0)	10.26 (102.6)
B	1966	9.74 (97.4)	10.46 (104.6)	10.28 (102.8)
C	1973	9.55 (95.5)	9.76 (97.6)	9.81 (98.1)
15-mg Tablets				
D	1966	14.40 (96.0)	15.01 (100.1)	15.00 (100.0)
E	1966	15.30 (102.0)	15.68 (104.5)	15.58 (103.9)
30-mg Tablets				
F	1966	29.54 (98.5)	30.72 (102.4)	30.85 (102.8)
G	1968	30.57 (101.9)	31.24 (104.1)	—

Sample Preparation—The weight of 20 tablets was determined, and the tablets were reduced to a fine powder with a mortar and pestle.

Separation—In a 100-ml beaker, 2.0 ml of 1 *M* potassium phosphate buffer (pH 6.5) was mixed with 3 g of diatomaceous earth. The mixture was firmly packed in a chromatographic column with a pledget of glass wool at the base. A quantity of the powdered tablets, accurately weighed and equivalent to about 20 mg of morphine sulfate, was transferred to a 150-ml beaker. Then 1 ml of water was added to dissolve the powder, and 0.5 g of sodium bicarbonate was added and mixed well. Then 3 g of reagent grade acid-washed diatomaceous earth was added and thoroughly mixed. The mixture was transferred to the chromatographic column and packed firmly.

The beaker was wiped with a pledget of glass wool, and the glass wool was placed on the top of the packed column. The column was eluted with 25 ml of reagent grade chloroform, and the eluate was discarded. The column was then eluted with 55 ml of 15% (v/v) isobutyl alcohol in chloroform, and the eluate was collected in a 250-ml separator. A 100-ml volume of ether, water washed prior to use, was added to the eluate in the separator, and the contents were mixed carefully.

The solvent mixture was extracted with three 25-ml portions of 0.05 *N* HCl. The acid phases were collected in a 100-ml volumetric flask, and 0.05 *N* HCl was added to volume and mixed. The spectrum of the acid solution was obtained from 350 to 250 nm, and the absorbance maximum at 285 nm was used to calculate the quantity of morphine sulfate.

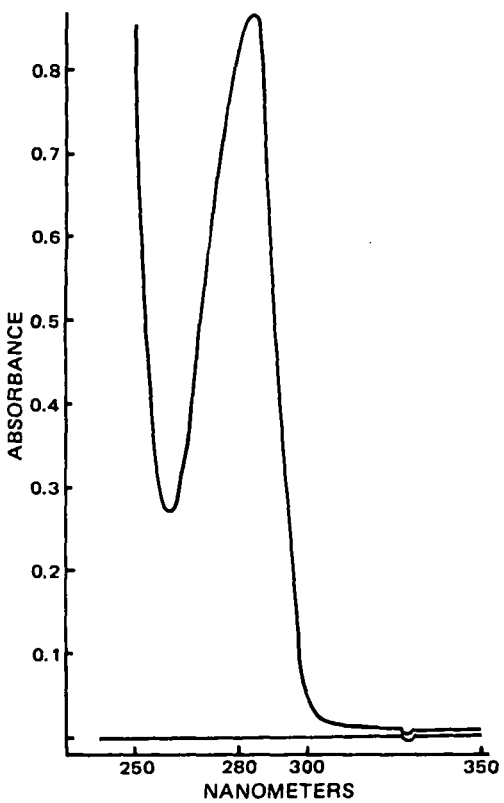

Figure 4—*UV spectrum of morphine eluate from the column chromatographic procedure for morphine tablets (in 0.05 N HCl), Lot C.*

With this chromatographic separation procedure, morphine sulfate standard formulation and tablets were assayed.

Morphine Sulfate Solutions—The excellent recovery of morphine sulfate from standard solutions using this method was established previously (1).

Morphine Sulfate Standard Formulations—Morphine sulfate standard formulations were prepared by mixing weighed quantities of morphine sulfate USP with lactose USP in 100-ml beakers. The following standard formulations were prepared and assayed by the described chromatographic procedure: A, morphine sulfate USP, 19.80 mg, plus lactose USP, 12.20 mg; B, morphine sulfate USP, 19.66 mg plus lactose USP, 15.05 mg; and C, morphine sulfate USP, 18.57 mg, plus lactose USP, 10.80 mg.

UV Spectra of Morphine and Pseudomorphine—The curves in Figs. 1–4 show the spectral differences of morphine and pseudomorphine and demonstrate the effect of pseudomorphine at the morphine maximum at 285 nm. Application of the column chromatographic method separates morphine from pseudomorphine and other degradation products.

Direct Spectrophotometric Examination of Morphine Tablets—Samples from seven lots of morphine sulfate tablets (A–G) from two manufacturers were diluted directly in 0.05 *N* HCl, and spectrophotometric curves were obtained. The purpose of this experiment was to show that interfering substances, which may or may not be decomposition products in morphine tablets, would give assay values (Table I) higher than those obtained using the column chromatographic procedure.

TLC—Separation of morphine in the standard formulation and tablets

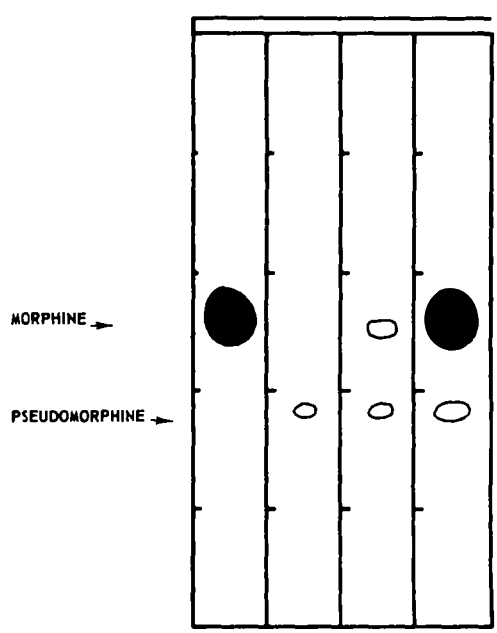

Figure 5—*TLC examination of the fractions obtained using the USP assay for morphine tablets. Key: 1, morphine sulfate; 2, pseudomorphine; 3, alkaline buffer phase after extraction; and 4, chloroform–isobutyl alcohol extract.*

Table II—Recovery of Morphine from Standard Formulations

Standard Formulation	Morphine Sulfate in Standard Formulation, mg	Amount Recovered, mg	Recovery, %
A	19.80	19.70	99.5
B	19.66	19.60	99.7
C	18.57	18.49	99.6

Table III—Content Uniformity Data on Morphine Tablets

Tablet	Milligrams of Morphine Sulfate Found per Tablet (Percent Label Claim) Lot C	Lot E
1	10.05 (100.5)	15.23 (101.5)
2	8.63 (86.3)	15.59 (103.9)
3	10.11 (101.1)	15.12 (100.8)
4	9.90 (99.0)	16.44 (109.6)
5	8.87 (88.7)	16.01 (106.7)
6	9.38 (93.8)	15.06 (100.4)
7	9.18 (91.8)	15.93 (106.2)
8	9.50 (95.0)	15.15 (101.0)
9	9.01 (90.1)	15.62 (104.1)
10	9.29 (92.9)	14.42 (96.1)
Average	9.39 (93.9)	15.45 (103.0)
Range, %	8.63–10.11 (86.3–101.1)	14.42–16.44 (96.1–109.6)

was monitored by TLC. Following the chloroform and chloroform–isobutyl alcohol elutions, the chromatographic columns were eluted with 0.05 *N* HCl in methanol to remove any remaining decomposition products and lactose.

Precoated silica gel GF plates[4] (10 × 20 cm) were used; the mobile phase was chloroform–methanol–diethylamine (80:15:5).

Eluates from the chromatographic columns were concentrated to about 1 ml prior to application to the plates. Aliquots of 20 μl of each concentrate were applied, and the plates were developed for 15 cm from the start. Then the plates were air dried and examined under long and short wavelength UV light.

RESULTS AND DISCUSSION

Extracts from the USP procedure were examined by TLC, and both morphine and pseudomorphine were found (Fig. 5), showing that the USP procedure lacks selectivity. Since most of the tablets were discolored to varying degrees, TLC was performed on the tablets to characterize them. All tablets showed that pseudomorphine was present, and other zones were also present (Fig. 6).

The procedure presented involves the release of morphine as the base with the use of sodium bicarbonate. Chloroform passed through an acidic

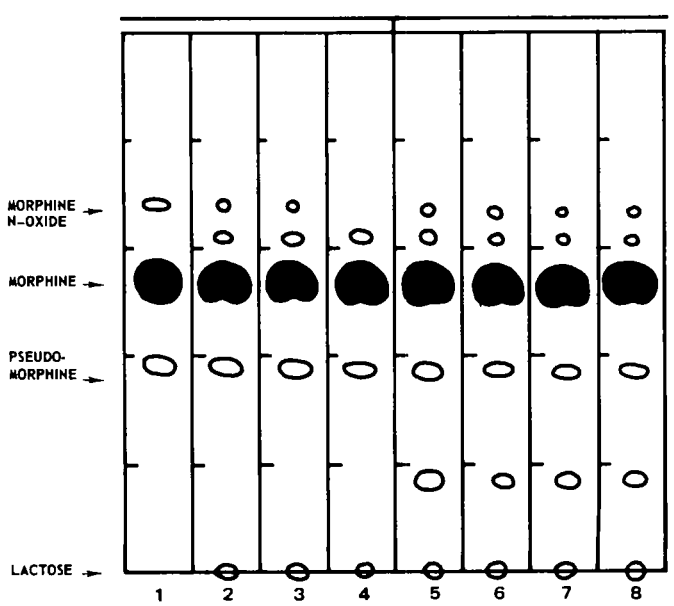

Figure 6—*TLC of morphine tablets. Solutions of tablets in water (10 μl of 60 mg/ml) were chromatographed. Key: 1, standard mixture of morphine sulfate, morphine* N*-oxide, and pseudomorphine; and 2–8, solutions of morphine tablets, Lots A–G.*

[4] Analtech, E. Merck.

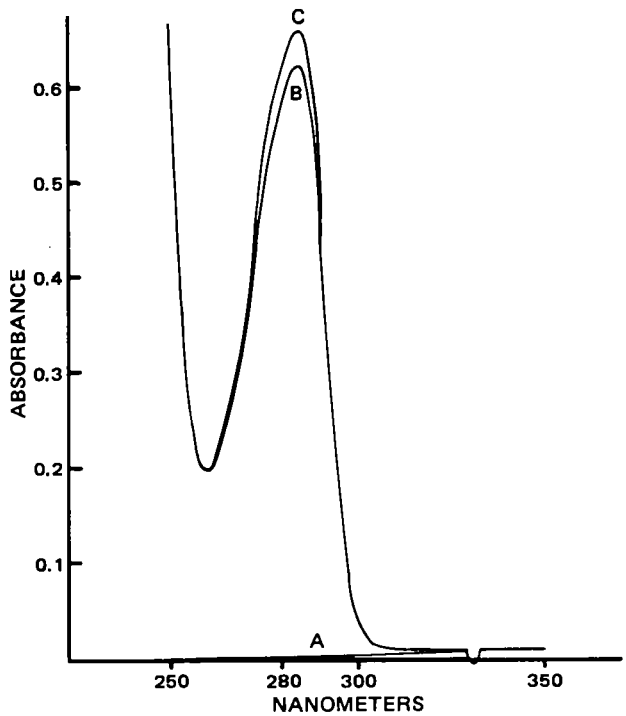

Figure 7—*UV spectra of 0.15 mg of lactose/ml in 0.05* N *HCl (A), Lot E of morphine sulfate tablets via the column chromatographic procedure (B), and Lot E of morphine sulfate tablets via direct dilution and spectrophotometry (C).*

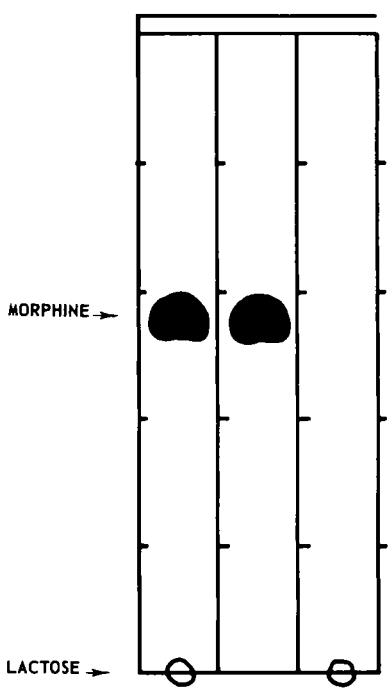

Figure 8—*Chromatogram showing the column separation of morphine in the standard formulation. Key: 1, direct application of standard formulation of morphine sulfate USP and lactose USP; 2, 20 μl of chloroform–isobutyl alcohol eluate; and 3, 20 μl of the 0.05* N *HCl in methanol eluate.*

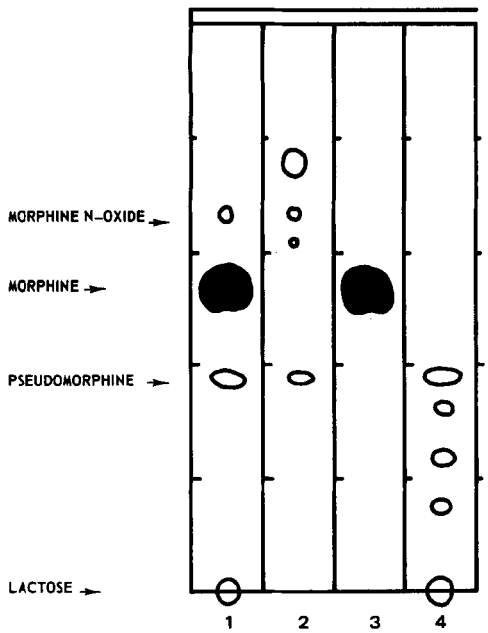

Figure 9—*Chromatogram showing the separation of morphine from decomposition products in morphine tablets. Key: 1, mixture of morphine sulfate, lactose, morphine* N*-oxide, and pseudomorphine; 2, 20 μl of chloroform eluate; 3, 20 μl of chloroform–isobutyl alcohol eluate; and 4, 20 μl of 0.05* N *HCl–methanol eluate.*

trap layer elutes morphine *N*-oxide and other impurities. Morphine, which is partially eluted by the chloroform, is retained by an acidic trap layer (1 *M* phosphate buffer, pH 6.5) and is finally eluted from the column using 15% (v/v) isobutyl alcohol in chloroform. Other tablet ingredients and remaining decomposition products are retained on the column.

On freshly manufactured lots, a direct dilution spectrophotometric assay should be possible. On aged lots, a separation step is necessary (Fig. 7).

The procedure presented was monitored by TLC to check for completeness of separation. In every instance, complete and clean separation of intact morphine was obtained from other substances either present or added (Figs. 8 and 9).

Recovery of morphine from the standard formulations was quantitative (Table II). Morphine was completely and cleanly separated from its decomposition products and lactose (Fig. 9). Seven samples of tablets from two manufacturers were assayed by the column chromatographic procedure (Table I). The results obtained by direct dilution and spectrophotometry (Table I) support the enhancing effect of interfering substances on the morphine assay results as obtained at the maximum at 285 nm. The USP XVIII procedure gave consistently higher assay values than those obtained by the proposed method. The column chromatographic procedure was applied successfully to determine content uniformity of two lots of morphine tablets. Both lots met the USP requirements for content uniformity (Table III).

REFERENCES

(1) I. J. Holcomb, R. B. Luers, and S. A. Fusari, *J. Pharm. Sci.*, **62**, 1504 (1973).

(2) "The United States Pharmacopeia," 18th rev., Mack Publishing Co., Easton, Pa., 1970, p. 439.

Estimation of Adsorption of Drugs and Proteins on Glass Surfaces with Controlled Pore Glass as a Reference

TAKAHARU MIZUTANI ˣ **and AKIRA MIZUTANI**

Received September 2, 1977, from the *Faculty of Pharmaceutical Sciences, Nagoya City University, Mizuho-ku, Nagoya 467, Japan.* Accepted for publication November 15, 1977.

Abstract □ The amount of drugs adsorbed to glass surfaces was studied, with controlled pore glass as a reference standard, by elution of a solution containing each drug on a pore glass column. The amount of basic drugs, such as epinephrine, physostigmine, and atropine, adsorbed was 1.5–2.0 mg/g of controlled pore glass (97 m^2) in a distilled water medium, but this amount in physiological saline or 0.1 *M* tris(hydroxymethyl)aminomethane hydrochloride (pH 8.6) was negligible. Ascorbic acid, barbital, aspirin, sulfamethoxazole, and acetylcholine were minimally adsorbed to the glass in a water medium or a physiological saline medium. Insulin was adsorbed in a water medium and a glycerin isotonic solution medium at pH 2.6; the amount was 5.5–5.9 mg/g of glass. For clarification of the adsorption mechanism of protein drugs, adsorption of proteins such as bovine serum albumin, chymotrypsin, and lysozyme to glass surfaces was investigated under the various conditions. The maximum amounts of proteins adsorbed on 1 g of controlled pore glass in a distilled water medium were 136, 233, and 84 mg, respectively. The two major forces for adsorption of proteins were ionic amine–silanol bonding and a cooperative cohesive force between proteins and glass. The amount of drugs and proteins to be adsorbed on the inner surface of a glass container and conditions for preventing this adsorption are discussed.

Keyphrases □ Adsorption—various drugs and proteins to glass surfaces studied using controlled pore glass, effect of pH □ Glass surfaces—adsorption of various drugs and proteins studied using controlled pore glass

Adsorption of biological materials on glass surfaces is well known, *e.g.*, the blood clotting reaction (1), macrophage adhesion (2), an antigen-coated column (3), and low adhesion of transformed cells (4). Controlled pore glass was developed for exclusion chromatography (5), and adsorption chromatography of proteins on controlled pore glass was recently reported (6, 7). Applications of porous glass as a carrier for immobilized enzyme were investigated, and the forces involved in the reactions between proteins and glass surfaces were suggested to be ionic amine–silanol bonding and hydrogen bonding (8).

Adsorption of biochemical materials on glass was studied (9) to clarify the adsorption mechanisms. It was reported that about 5 μmoles of cationic biological materials, such as basic amino acids and amino sugars, were adsorbed on 1 g of controlled pore glass, which had a large

0022-3549/78/0800-1102$01.00/0
© 1978, American Pharmaceutical Association

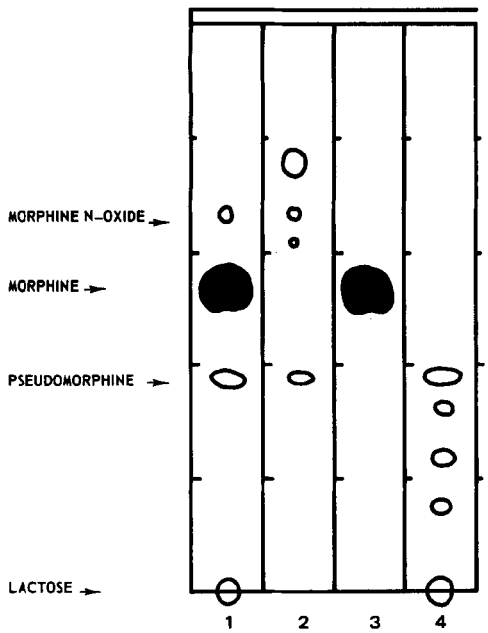

Figure 9—*Chromatogram showing the separation of morphine from decomposition products in morphine tablets. Key: 1, mixture of morphine sulfate, lactose, morphine* N*-oxide, and pseudomorphine; 2, 20 μl of chloroform eluate; 3, 20 μl of chloroform–isobutyl alcohol eluate; and 4, 20 μl of 0.05* N *HCl–methanol eluate.*

trap layer elutes morphine *N*-oxide and other impurities. Morphine, which is partially eluted by the chloroform, is retained by an acidic trap layer (1 *M* phosphate buffer, pH 6.5) and is finally eluted from the column using 15% (v/v) isobutyl alcohol in chloroform. Other tablet ingredients and remaining decomposition products are retained on the column.

On freshly manufactured lots, a direct dilution spectrophotometric assay should be possible. On aged lots, a separation step is necessary (Fig. 7).

The procedure presented was monitored by TLC to check for completeness of separation. In every instance, complete and clean separation of intact morphine was obtained from other substances either present or added (Figs. 8 and 9).

Recovery of morphine from the standard formulations was quantitative (Table II). Morphine was completely and cleanly separated from its decomposition products and lactose (Fig. 9). Seven samples of tablets from two manufacturers were assayed by the column chromatographic procedure (Table I). The results obtained by direct dilution and spectrophotometry (Table I) support the enhancing effect of interfering substances on the morphine assay results as obtained at the maximum at 285 nm. The USP XVIII procedure gave consistently higher assay values than those obtained by the proposed method. The column chromatographic procedure was applied successfully to determine content uniformity of two lots of morphine tablets. Both lots met the USP requirements for content uniformity (Table III).

REFERENCES

(1) I. J. Holcomb, R. B. Luers, and S. A. Fusari, *J. Pharm. Sci.*, **62**, 1504 (1973).

(2) "The United States Pharmacopeia," 18th rev., Mack Publishing Co., Easton, Pa., 1970, p. 439.

Estimation of Adsorption of Drugs and Proteins on Glass Surfaces with Controlled Pore Glass as a Reference

TAKAHARU MIZUTANI ˣ **and AKIRA MIZUTANI**

Received September 2, 1977, from the *Faculty of Pharmaceutical Sciences, Nagoya City University, Mizuho-ku, Nagoya 467, Japan.* Accepted for publication November 15, 1977.

Abstract □ The amount of drugs adsorbed to glass surfaces was studied, with controlled pore glass as a reference standard, by elution of a solution containing each drug on a pore glass column. The amount of basic drugs, such as epinephrine, physostigmine, and atropine, adsorbed was 1.5–2.0 mg/g of controlled pore glass (97 m^2) in a distilled water medium, but this amount in physiological saline or 0.1 *M* tris(hydroxymethyl)aminomethane hydrochloride (pH 8.6) was negligible. Ascorbic acid, barbital, aspirin, sulfamethoxazole, and acetylcholine were minimally adsorbed to the glass in a water medium or a physiological saline medium. Insulin was adsorbed in a water medium and a glycerin isotonic solution medium at pH 2.6; the amount was 5.5–5.9 mg/g of glass. For clarification of the adsorption mechanism of protein drugs, adsorption of proteins such as bovine serum albumin, chymotrypsin, and lysozyme to glass surfaces was investigated under the various conditions. The maximum amounts of proteins adsorbed on 1 g of controlled pore glass in a distilled water medium were 136, 233, and 84 mg, respectively. The two major forces for adsorption of proteins were ionic amine–silanol bonding and a cooperative cohesive force between proteins and glass. The amount of drugs and proteins to be adsorbed on the inner surface of a glass container and conditions for preventing this adsorption are discussed.

Keyphrases □ Adsorption—various drugs and proteins to glass surfaces studied using controlled pore glass, effect of pH □ Glass surfaces—adsorption of various drugs and proteins studied using controlled pore glass

Adsorption of biological materials on glass surfaces is well known, *e.g.*, the blood clotting reaction (1), macrophage adhesion (2), an antigen-coated column (3), and low adhesion of transformed cells (4). Controlled pore glass was developed for exclusion chromatography (5), and adsorption chromatography of proteins on controlled pore glass was recently reported (6, 7). Applications of porous glass as a carrier for immobilized enzyme were investigated, and the forces involved in the reactions between proteins and glass surfaces were suggested to be ionic amine–silanol bonding and hydrogen bonding (8).

Adsorption of biochemical materials on glass was studied (9) to clarify the adsorption mechanisms. It was reported that about 5 μmoles of cationic biological materials, such as basic amino acids and amino sugars, were adsorbed on 1 g of controlled pore glass, which had a large

0022-3549/78/0800-1102$01.00/0
© 1978, American Pharmaceutical Association

surface area (97 m^2/g) and a high flow rate, and that ionic amine–silanol bonding was one major force of the reactions (9).

Standards for pharmaceutical glass containers, in which drugs are stored or maintained, are provided in the USP (10) and the JP (11). However, the kind and amount of drugs adsorbed on the glass surface of a container have not been defined. The purpose of this investigation was to study the kind and amount of some drugs and proteins adsorbed on glass surfaces using controlled pore glass.

EXPERIMENTAL

Methods—The controlled pore glass[1] was composed of 100-μm particles with a pore diameter of 240 Å and a surface area of 97 m^2/g. After being washed with a chromic acid mixture, water, and 60% nitric acid and then washed thoroughly with distilled water to neutrality, the glass was packed in a 0.65 × 11-cm column. Solutions containing a drug or protein, 0.05–0.8 mg/ml, were applied onto the column at a flow rate of 0.5 ml/cm^2/min, and 1.6-ml fractions were collected.

The amount of sample adsorbed on the glass surfaces was estimated from the loss of the sample in the eluate from the solution applied onto the pore glass column; this value was corrected by subtracting the column volume, which was calculated from the void and inner volumes of the column obtained by elution of 0.1 ml of bromphenol blue or dextran marker[2]. The surface areas of the glass tube column and other glassware were neglected because they were very small.

Adsorption experiments were carried out at room temperature, but the adsorption profiles of proteins and basic biological materials at 30° were identical with those at 4°, as described previously (7).

Materials—The drugs and analytical wavelengths were: insulin[3], 280 nm; atropine sulfate[4], 220 nm; barbital[4], 230 nm; epinephrine[5], 280 nm; physostigmine salicylate[6], 260 nm; sulfamethoxazole[7], 300 nm; aspirin[8], 280 nm; acetylcholine[5], 210 nm; and ascorbic acid[4], 290 nm. These drugs were dissolved in distilled water, physiological saline, or pH 8.6 tris(hydroxymethyl)aminomethane hydrochloride buffer in concentrations of 0.05–0.8 mg/ml and loaded on the pore glass column. Insulin was dissolved in a pH 2.6 glycerin isotonic solution.

Bovine serum albumin[9], chymotrypsin[10], and lysozyme[11] were dissolved in water, 6 *M* guanidine hydrochloride[5], or 8 *M* urea[4], and the solution pH was adjusted with 0.1 *N* NaOH or 0.1 *N* HCl to the particular pH as shown in the figures. The concentration of the protein solutions was determined with an extinction coefficient of 6.7 for $E^{1\%}_{1cm}$ of bovine serum albumin (12), 20.7 for chymotrypsin (13), and 26.4 for lysozyme (14) at 280 nm. Succinylated bovine serum albumin was prepared by the method of Habeeb *et al.* (15). The adsorption of leucine and glycine[12] was studied at pH 2.6, 6.0, and 10.3, and the concentration of these amino acids was determined by the color reaction with ninhydrin.

RESULTS AND DISCUSSION

Drug Adsorption—The control experiments illustrated in Figs. 1 and 2 show the eluting position (tube 2) of the dextran marker and bromphenol blue, by which the void and inner volumes of the column were obtained, respectively. Epinephrine in water was eluted at tube 35 (Fig. 1). Epinephrine was eluted at tube 3 in the tris(hydroxymethyl)aminomethane hydrochloride buffer and saline media and was minimally adsorbed to the glass. Epinephrine also was not adsorbed to the glass in the physiological saline containing bisulfite and chlorobutanol.

The adsorption patterns of atropine and physostigmine are shown in Fig. 1. Both drugs were adsorbed to the glass in a water medium, and the amount in a tris(hydroxymethyl)aminomethane hydrochloride buffer medium was lower than that in a water medium. The amount of atropine and physiostigmine adsorbed to the glass in the saline solution was low and negligible. Measurement of absorbance at 295 nm showed that salicylate ions in physostigmine salicylate molecules were not adsorbed to porous glass in water and eluted at tube 2, even though physostigmine was adsorbed and eluted at tube 10 (Fig. 1). Figure 1 also shows the adsorption patterns of insulin in water at pH 2.6 and a pH 2.6 glycerin isotonic solution. Insulin was well adsorbed in both media.

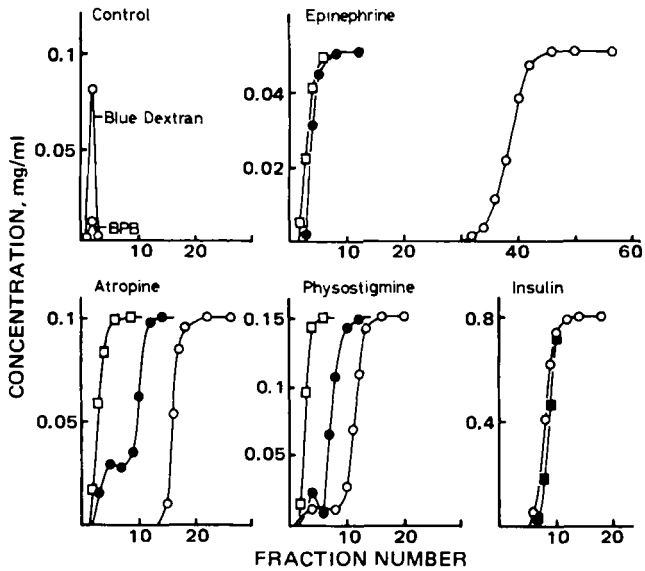

Figure 1—*Adsorption profiles of drugs on controlled pore glass. Key: ○, distilled water; ●, 0.1 M tris(hydroxymethyl)aminomethane hydrochloride, pH 8.6; □, physiological saline; and ■, glycerin isotonic solution. The column size was 0.65 × 11 cm, the fraction volume was 1.6 ml, BPB is bromphenol blue, and blue dextran is a dextran marker of high molecular weight.*

The amounts of drugs adsorbed on 1 g of controlled pore glass are shown in Table I. The adsorption of basic drugs, such as epinephrine, atropine, and physostigmine, to glass surfaces in water was 1.5–2.0 mg (about 3–10 μmoles)/g of glass. The amount of basic drugs adsorbed to the inner surface (50 cm^2) of a glass container (20 ml) in water was about

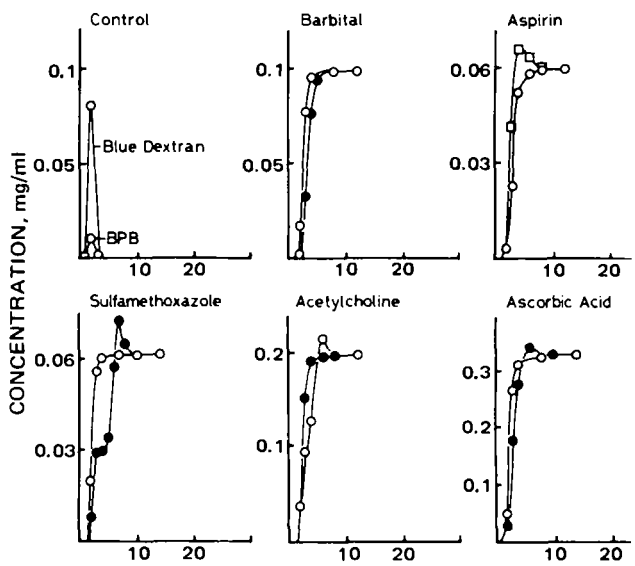

Figure 2—*Elution profiles of drugs on controlled pore glass. Key: ○, distilled water; ●, 0.1 M tris(hydroxymethyl)aminomethane hydrochloride, pH 8.6; and □, physiological saline. The column size was 0.65 × 11 cm, the fraction volume was 1.6 ml, BPB is bromphenol blue, and blue dextran is a dextran marker.*

[1] CPG-10, Electro-Nucleonics, Fairfield, N.J.
[2] Blue Dextran 2000, Pharmacia Fine Chemicals, Uppsala, Sweden.
[3] Fluka AG., Buchs, Switzerland.
[4] Wako Pure Chemicals Ltd., Osaka, Japan.
[5] Katayama Chemical, Osaka, Japan.
[6] E. Merck AG, Darmstadt, Germany.
[7] Shionogi Co. Ltd., Osaka, Japan (see "The Japan Pharmacopoeia," 9th ed., Hirokawa Shoten, Tokyo, Japan, 1976, pp. 370, 371).
[8] Bayer AG, Leberkusen, Germany.
[9] Armour Pharmaceutical Co., Chicago, Ill.
[10] Boehringer GmbH, Mannheim, Germany.
[11] Seikagaku Kogyo Co., Tokyo, Japan.
[12] Ajinomoto Co. Inc., Kawasaki, Japan.

Table I—Amount of Drugs Adsorbed to Glass Surfaces

Drug	Amount, mg/g of Controlled Pore Glass			
	Water	Tris(hydroxy methyl) aminomethane Hydrochloride	Saline	Glycerin Isotonic Solution
Epinephrine	2.00	0.03	0.03	—
Atropine sulfate	1.70	0.70	0.05	—
Physostigmine salicylate	1.54	0.86	0.08	—
Insulin	5.46[a]	—	—	5.95[a]
Barbital	0	0.10	0	—
Aspirin	0	0.03	0	—
Sulfamethoxazole	0	0	0	—
Acetylcholine chloride	0.35	0	0	—
Ascorbic acid	0	0.01	0.03	—

[a] Measured at pH 2.6.

0.1 μg, but the amount in saline was negligible. However, it was also necessary to examine the adsorption of basic drugs that are effective in a microdose. The amount of insulin adsorbed to 1 g of controlled pore glass was 5.5–5.9 mg in water and in the glycerin isotonic solution; 0.3 μg of insulin might be adsorbed on 50 cm^2 of the surface of a glass container.

Elution patterns of nonbasic drugs, such as ascorbic acid, barbital, aspirin, sulfamethoxazole, and acetylcholine, are shown in Fig. 2. The amount of these drugs adsorbed to the glass in water, physiological saline, and 0.1 *M* tris(hydroxymethyl)aminomethane hydrochloride buffer (pH 8.6) was 0–0.3 mg (Table I). It was concluded from these results that basic drugs and proteins were well adsorbed to glass surfaces in water but that neutral or acidic drugs were not adsorbed in water.

Protein Adsorption—To clarify the mechanism of adsorption of insulin, adsorption using bovine serum albumin, chymotrypsin, and lysozyme was studied under various conditions. Adsorption patterns of bovine serum albumin and succinylated bovine serum albumin in distilled water, 8 *M* urea, and 6 *M* guanidine hydrochloride at pH 5.4 are shown in Fig. 3. Serum albumin was not liberated as a milky precipitate in these solutions. The amount of native albumin adsorbed was 136 mg/g of controlled pore glass in water, but the amount of modified albumin adsorbed was 3 mg under the same conditions.

These results showed that one major force of adsorption of proteins on glass surfaces was ionic bonding between amines in the protein molecules and terminal silanol groups on glass surfaces. The amount of bovine serum albumin adsorbed in 8 *M* urea (pH 5.4) was slightly smaller than that in water; therefore, hydrogen bonding seemed to be related to the protein adsorption on the glass. Succinylated albumin was not adsorbed in 8 *M* urea, so modified serum albumin was adsorbed by hydrogen bonding in water.

Meanwhile, the adsorption of native albumin in 6 *M* guanidine hydrochloride (pH 5.4) was lower than that in water, and this phenomenon must be due to inhibition of ionic bonding of proteins to glass by concentrated guanidinium ions. The effect of guanidinium ions on protein adsorption was not so strong that a definite amount of native bovine serum albumin was adsorbed in 6 *M* guanidine hydrochloride. This result is consistent with the previous findings that zwitterions such as amino acids inhibited adsorption but that ammonium ions did not prevent adsorption of proteins (16).

Figure 4 shows adsorption profiles of bovine serum albumin, chymotrypsin, and lysozyme in water at various pH values. Albumin was adsorbed the most at pH 5.4, and the amount adsorbed decreased at above or below this pH. It was concluded from these results that a protein was adsorbed most extensively to glass surfaces at its isoelectric point; this fact was ascertained from adsorption patterns of lysozyme, whose isoelectric point is at pH 10–11 (Fig. 4). Chymotrypsin, having an isoelectric point of pH 8, also was adsorbed the most at neutral pH 8.0 (Fig. 4). Proteins must be adsorbed most extensively to glass at their isoelectric points because of the cooperative aggregative action between glass and proteins, which are most precipitable at their isoelectric points.

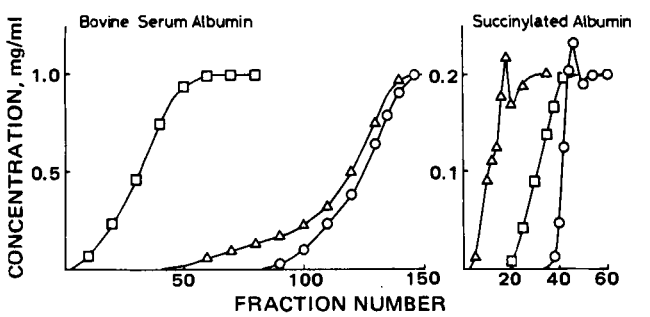

Figure 3—*Adsorption patterns of bovine serum albumin and succinylated albumin in detergent solutions (pH 5.4) on controlled pore glass. Key: ○, distilled water; △, 8 M urea; and □, 6 M guanidine hydrochloride. The fraction volumes were 1.6 ml for bovine serum albumin and 0.52 ml for succinylated albumin.*

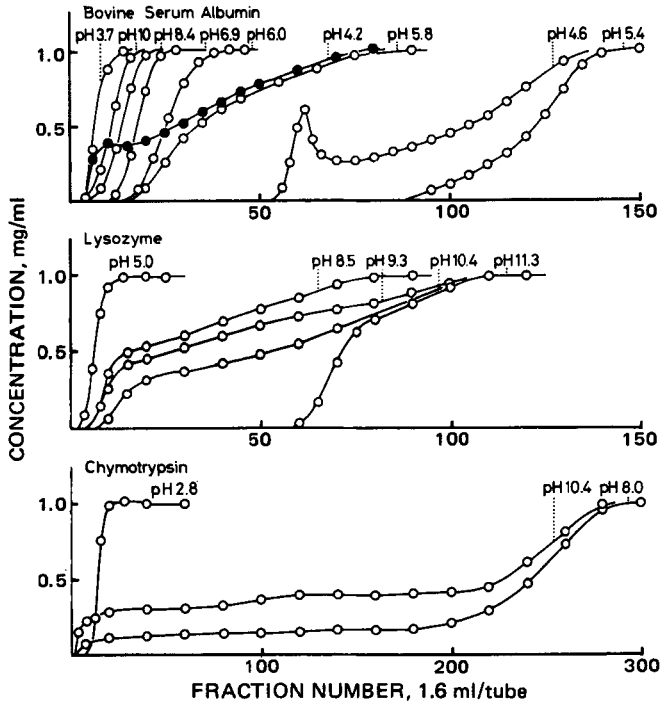

Figure 4—*Adsorption patterns of bovine serum albumin, lysozyme, and chymotrypsin on controlled pore glass at various pH values in distilled water. The column size was 0.65 × 11 cm, and the fraction volume was 1.6 ml.*

The amount of insulin adsorbed at the isoelectric point was not estimated because insulin precipitates at neutral pH. However, the amount adsorbed at the isoelectric point might be more than that at pH 2.6 if insulin were soluble at its isoelectric point. The maximum amounts of proteins adsorbed on 1 g of controlled pore glass were 136 mg (2 μmoles) for bovine serum albumin, 233 mg (9 μmoles) for chymotrypsin, and 84 mg (6 μmoles) for lysozyme. These values might not depend on molecular weights but rather on the amounts of residue for adsorption on the protein surface. These values (2–9 μmoles) of the proteins agreed with the values of 5 μmoles for basic amino acids and amino sugars and of 3–10 μmoles for basic drugs, and these results showed that the glass had adsorption sites of 2–10 μmoles/97 m^2 of surface area. Therefore, one to six molecules were adsorbed on the glass surface having an area of (100 Å)^2.

If the adsorption reactions between proteins and glass surfaces simply depended on ionic amine–silanol bonding, proteins should be adsorbed more at acidic pH, at which proteins would have a positive charge. However, proteins were adsorbed most extensively at their isoelectric points. Therefore, another important factor for adsorption would be the cooperative aggregative force between glass surfaces and proteins. This aggregative force might depend on bondings such as intermolecular forces, hydrogen bonding, and/or hydrophobic bonding, including ionic bonding.

From the values of chymotrypsin (233 mg/g), the amount of proteins adsorbed on the surfaces of a glass container (50 cm^2) and a glass injector was estimated to be more than 12 μg. This 12-μg value must be significant when protein drugs, such as hormones and vaccines, are used in microdoses and accurate doses are required. The purified protein derivative of tuberculin is used at 0.5 μg/ml in phosphate buffer containing sodium chloride, in which proteins are well adsorbed to the glass. The 0.5-μg/ml concentration must be a marginal point not affected by adsorption, and the doses of biologics used at lower concentrations would be ambiguous by adsorption to glass surfaces. The accurate dose of an injection at low

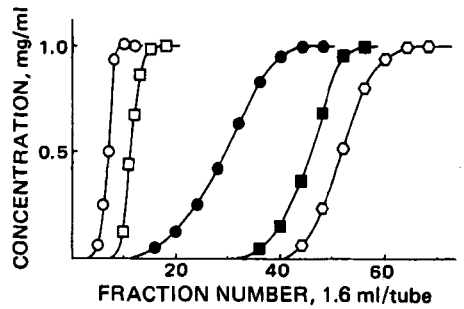

Figure 5—*Adsorption of bovine serum albumin in amino acid solutions. Key:* ○, *0.15* M *glycine, pH 8.0;* ●, *0.15* M *glycine, pH 5.4;* □, *0.15* M *lysine, pH 8.0;* ■, *0.15* M *lysine, pH 5.4; and* ○ *saline, pH 5.4.*

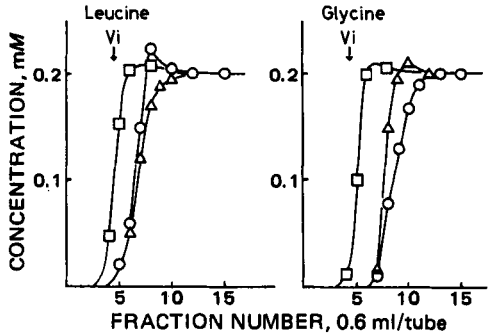

Figure 6—*Adsorption patterns of leucine and glycine on controlled pore glass in water. Key:* ○, *pH 6.0;* △, *pH 2.6;* □, *pH 10.3; and Vi, inner volume of the column. The column size was 0.65 × 11 cm.*

concentrations of biologics must be estimated after evaluating the value of the protein adsorbed to glass containers and injectors.

It was previously shown that the amino acid buffer was the most effective of several buffers for preventing adsorption of albumin on the glass (16). The conditions needed for the solvent to prevent adsorption were examined with bovine albumin, and adsorption patterns in solutions of glycine or lysine are shown in Fig. 5. The amount of albumin adsorbed to the glass in the glycine buffer or the lysine buffer of pH 5.4 was smaller than that in water at pH 5.4 (Fig. 4) and similar to that in saline. The amount in the amino acid buffers of pH 8.0 was smaller than at pH 5.4. The amount of albumin adsorbed to the porous glass in 0.15 *M* glycine of pH 8.0 was the smallest compared to the amounts in lysine and glutamic acid of pH 8.0; therefore, it may be desirable to add glycine to protein drug solutions to prevent protein adsorption. It is also important to select the optimum pH for minimum adsorption of protein drugs in the pH range of retention of drug activity.

It was previously reported that 5 μmoles of basic amino acids was adsorbed on 1 g of controlled pore glass and that the amount of other amino acids was 0.2–0.8 μmole/g of glass (9). In this work, adsorption of leucine and glycine on glass was studied at three pH values. Adsorption patterns of the amino acids in water at pH 2.6, 6.0, and 10.3 are shown in Fig. 6. The amino acids were adsorbed in an acidic solution but not in a basic solution, because the positively charged amino acids in an acidic condition were adsorbed to silanol but the negatively charged amino acids in a basic condition were repulsed by the negatively charged terminal silanol groups on glass surfaces. The amount of leucine and glycine adsorbed at pH 6.0 and 10.3 was 0.2 μmole/g of controlled pore glass. Leucine and glycine were greatly adsorbed to glass at their isoelectric point (pH 6.0). The force of this bonding has not been resolved, but this phenomenon may be correlated with the maximum adsorption of proteins at their isoelectric point and with the prevention of adsorption of proteins.

The amount of samples adsorbed was estimated by the column method, not by a batch operation. The former approach was preferable for the determination of the maximum amount adsorbed, even though the latter approach was preferable for the estimation of the dissociation constant or the reaction rate. The sample solution was eluted from the column with a constant flow rate to normalize the reaction rate.

REFERENCES

(1) J. Schoenmakers, R. Matze, C. Haanen, and F. Zilliken, *Biochim. Biophys. Acta*, **101**, 166 (1965).

(2) P. Lehtinen, J. Pikkarainen, and E. Kulonen, *ibid.*, **439**, 393 (1976).

(3) H. Wigzell and B. Anderson, *J. Exp. Med.*, **129**, 23 (1969).

(4) J. Pouyssegur, M. Willingham, and I. Pastan, *Proc. Natl. Acad. Sci. USA*, **74**, 243 (1977).

(5) W. Haller, *Nature*, **206**, 693 (1965).

(6) H. G. Bock, P. Skene, S. Fleischer, P. Cassidy, and S. Harshman, *Science*, **191**, 380 (1976).

(7) T. Mizutani and A. Mizutani, *J. Chromatogr.*, **120**, 206 (1976).

(8) R. A. Messing, *J. Non-Cryst. Solids*, **19**, 277 (1975).

(9) T. Mizutani and A. Mizutani, *Anal. Biochem.*, **83**, 216 (1977).

(10) "The United States Pharmacopeia," 19th rev., Mack Publishing Co., Easton, Pa., 1975, pp. 642–647.

(11) "The Japan Pharmacopoeia," 9th ed., Hirokawa Shoten, Tokyo, Japan, 1976, pp. 665–667.

(12) G. C. Webster, *Biochim. Biophys. Acta*, **207**, 371 (1970).

(13) M. S. N. Rao and G. Kegeles, *J. Am. Chem. Soc.*, **80**, 5724 (1958).

(14) K. C. Aune and C. Tanford, *Biochemistry*, **8**, 4579 (1969).

(15) A. Habeeb, H. G. Cassidy, and S. J. Singer, *Biochim. Biophys. Acta*, **29**, 587 (1958).

(16) T. Mizutani and A. Mizutani, *J. Chromatogr.*, **111**, 214 (1975).

ACKNOWLEDGMENTS

The authors thank Dr. Y. Kudo for his generous support.

Multicompartment Pharmacokinetic Model of 4′-Demethylepipodophyllotoxin 9-(4,6-*O*-Ethylidene-β-D-glucopyranoside) in Humans

FRANCIS R. PELSOR ˣ, LARRY M. ALLEN *, and PATRICK J. CREAVEN ‡

Received November 13, 1975, from the *National Cancer Institute–Veterans Administration Medical Oncology Branch, Veterans Administration Hospital, Washington, DC 20422.* Accepted for publication November 30, 1977. *Present address: Comprehensive Cancer Center, Division of Oncological Pharmacology, University of Miami School of Medicine, Jackson Memorial Medical Center, Miami, FL 33152. ‡Present address: Grace Cancer Drug Center, Division of Experimental Therapeutics, Roswell Park Memorial Institute, Buffalo, NY 14263.

Abstract □ The formation and elimination of the metabolite of 4′-demethylepipodophyllotoxin 9-(4,6-*O*-ethylidene-β-D-glucopyranoside) (I) were studied in seven patients with advanced cancer who received I intravenously. The plasma concentration–time data best fit a triexponential equation. The volume of the metabolite compartment (27.5 liters) was calculated as a fraction of the extrapolated volume. A larger body clearance (111.7 ml/min) of metabolite as compared to the renal clearance (31.3 ml/min) indicates that the metabolite is lost from the plasma equivalent space by another elimination route. The combination of metabolite data presented here with previously published data for unchanged I leads to a multicompartment model for the distribution, metabolism, and excretion of I and its metabolite. A comparison of algebraically derived model transfer constants with those evaluated by computer fitting the system of differential equations is presented.

Keyphrases □ 4′-Demethylepipodophyllotoxin 9-(4,6-*O*-ethylidene-β-D-glucopyranoside)—and metabolite, pharmacokinetics in humans □ Pharmacokinetics—podophyllotoxin derivative and metabolite in humans □ Antineoplastic agents, potential—podophyllotoxin derivative and metabolite, pharmacokinetics in humans □ Podophyllotoxin derivative and metabolite—pharmacokinetics in humans

The clinical pharmacology of 4′-demethylepipodophyllotoxin 9-(4,6-*O*-ethylidene-β-D-glucopyranoside) (I) in patients with advanced cancer was reported previously (1). The data for the time course of the plasma concentration of I following intravenous administration previously were computer fitted to a biexponential equation, and distribution and elimination parameters were calculated (1, 2). These results established that the turnover of unchanged drug in the peripheral compartment was quite rapid, although the elimination phase was moderately prolonged.

However, urinary excretion of metabolized and unmetabolized I accounted for less than 50% of the administered dose of this highly water-insoluble compound (1, 2). Further study of the disposition of unchanged I showed that extensive degradation to tritiated water, retention in the body, and excretion in feces did not account for this discrepancy (1). Furthermore, because the body clearance equaled the plasma clearance for unchanged I, it was previously concluded that the less than quantitative recovery of radioactivity was due to body sequestering of the metabolite and not of unchanged drug (2).

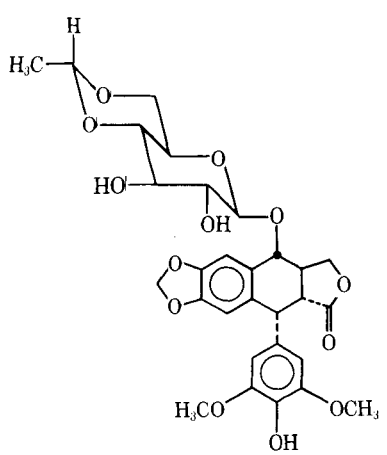

I

To analyze the disposition of I in humans more fully, the kinetics of metabolite formation and elimination were studied and a multicompartment model was developed to describe the disposition of I and its metabolite. Since the chemical identity of the metabolite has not been established, the concentration–time course of the I metabolite in biological fluids was determined by selective extraction of unchanged drug.

To facilitate the derivation of metabolite distribution parameters, the differential equations resulting from the multicompartment model were solved to yield an integrated equation describing the plasma level–time curve of the metabolite after a single intravenous injection of I. These algebraically derived parameters are compared with those obtained by fitting the differential equations.

EXPERIMENTAL

Materials—The reagents were obtained commercially. Compound I[1] was supplied in sealed ampuls ready for intravenous use. Each patient received 250 μCi of 9-^{3}H-I[2] (specific activity of 14.112 mCi/mmole).

Analytical Procedures—The concentration of 9-^{3}H-I and the metabolite in biological fluids was obtained by selective extraction of unchanged drug with chloroform and radioisotope counting as described previously (1). The procedure quantitatively removed unchanged drug without removing the metabolite, as determined by TLC. Further chromatographic analysis of the aqueous phase in several systems confirmed the presence of one major metabolite of I.

Pharmacokinetic Studies—The plasma decay and urinary excretion of I and its metabolite were studied in seven patients who received I, 130–290 mg/m^2 body surface area, during the initial clinical trials of weekly intravenous administration (3). Infusion of the solubilized drug, sample collection, and handling of plasma and urine were described previously (1).

RESULTS

Solution of the differential equations describing the multicompartment model (Scheme I), by the method of Benet (4), yields the following equation, which describes the time course of plasma metabolite con-

[1] VP16-213 (NSC 141540), 100 mg/5 ml, Drug Research and Development, National Cancer Institute, Bethesda, MD 20014.

[2] Supplied by Dr. H. Stähelin, Sandoz Ltd., Basel, Switzerland, through Drug Research and Development, National Cancer Institute, Bethesda, MD 20014.

0022-3549/78/0800-1106$01.00/0
© 1978, American Pharmaceutical Association

Table I—Parameters [a] for the Plasma Concentration of I Metabolite According to Eq. 1

Patient (mg/m²)	Dose, mg	A_1, μg/ml	α, hr^{-1}	A_2, μg/ml	β, hr^{-1}	A_3, μg/ml	γ, hr^{-1}	Area[b], μg hr/ml
NG (130)	205	1.59 (0.16)	2.21 (0.46)	1.31 (13.37)	0.05 (0.12)	0.27 (13.27)	0.08 (1.23)	29.10
KR (170)	255	2.47 (1.25)	0.92 (0.36)	0.63 (4.18)	0.05 (0.12)	1.80 (3.00)	0.15 (0.37)	22.22
TS (170)	230	4.57 (10.06)	0.64 (0.47)	2.60 (0.40	0.04 (0.004)	1.94 (9.81)	0.33 (0.72)	64.31
JB (220)	415	2.02 (0.73)	0.81 (0.47)	0.29 (1.18)	0.02 (0.10)	1.62 (0.64)	0.11 (0.17)	27.35
RJ (220)	363	4.36 (1.72)	0.71 (0.21)	0.46 (0.24)	0.02 (0.01)	3.83 (1.60)	0.20 (0.07)	35.99
HR (290)	400	3.77 (0.36)	1.21 (0.15)	0.47 (0.15)	0.02 (0.007)	3.29 (0.30)	0.16 (0.02)	39.04
KR (290)	425	5.50 (9.18)	0.70 (0.48)	1.47 (1.26)	0.04 (0.03)	3.99 (8.17)	0.30 (0.44)	40.82

[a] Parameters are quoted ± *SE*. [b] $\text{Area}^{0\to\infty} = \int_0^T C_4\,dt + (A_2e^{-\beta T}/\beta)$ (Ref. 8).

Table II—Calculated I Metabolite Distribution and Clearance Parameters

Patient (Body Weight, kg)	V_4[a], liters	Cl_{rm}[b], ml/min	Cl_b[c], ml/min	Urine Excretion (48 hr), % (Found)
NG (62)	15.84	21.83	96.30	15.57 (15.34)
KR (56)	24.43	32.51	109.02	14.58 (14.87)
TS (48)	16.82	26.46	34.57	35.37 (34.92)
JB (75)	54.01	30.01	171.96	7.98 (7.84)
RJ (62)	40.15	41.68	134.48	16.20 (14.94)
HR (48)	19.55	41.01	124.66	15.49 (—)
KR (56)	21.75	26.17	111.06	11.33 (10.82)
Mean ± *SD*[d]	27.51 ± 14.25	31.27 ± 7.67	111.72 ± 41.86	

[a] V_4 calculated according to Eq. 5. [b] $Cl_{rm} = (\Sigma M_u/\int_0^T C_4\,dt)$ (Ref. 12). [c] $Cl_b = (F_m \text{ dose}/\text{area}^{0\to\infty})$, where F_m is the difference between the dose and the fraction recovered unchanged in the urine (2) (Ref. 10). [d] The means of the central, V_1, and peripheral, V_2, compartment volumes and renal clearance of unchanged drug for the seven patients as determined previously (2) are 8.09 ± 2.30 liters, 9.15 ± 3.70 liters, and 11.80 ± 3.90 ml/min, respectively.

centration, C_4, following the single intravenous administration of I:

$$C_4 = -A_1e^{-\alpha t} + A_2e^{-\beta t} + A_3e^{-\gamma t} \qquad \text{(Eq. 1)}$$

where A_2 and A_3 are the zero-time intercepts given by:

$$A_2 = \frac{k_m \text{dose}}{V_4}\,\frac{(k_{21}-\beta)}{(\alpha-\beta)(\gamma-\beta)} \qquad \text{(Eq. 2)}$$

$$A_3 = \frac{k_m \text{dose}}{V_4}\,\frac{(k_{21}-\gamma)}{(\alpha-\gamma)(\beta-\gamma)} \qquad \text{(Eq. 3)}$$

and α, β, and γ are hybrid transfer constants for disposition processes of unchanged drug and metabolite (4). The disposition rate constant, k_{21}, and the rate constant of biotransformation, k_m, were determined previously (2). The parameter A_1 is determined as a function of the rate constants given by:

$$A_1 = \frac{k_m \text{dose}}{V_4}\,\frac{(k_{21}-\alpha)}{(\beta-\alpha)(\gamma-\alpha)} \qquad \text{(Eq. 4)}$$

Graphical estimates of the parameters of Eq. 1 were refined by nonlinear least-squares regression analysis, using the Marquardt–Levenburg method (5) in the computer program package[3] MLAB (6, 7). The computed parameter values and the area under the plasma decay curve are listed in Table I.

The volume of the metabolite compartment, V_4, may be calculated as a fraction of the extrapolated volume (9, 10) using Eq. 5 (see proof in *Appendix*):

$$V_4 = \frac{k_m \text{dose}}{A_2(\alpha-\beta) + A_3(\alpha-\gamma)} \qquad \text{(Eq. 5)}$$

The renal clearance of the metabolite, Cl_{rm}, was evaluated by linear least-squares regression analysis (11) of the cumulative amount excreted on the area under the plasma decay curve at the midpoint of the collection interval (12). The renal excretion rate constant, k_{em}, was calculated by algebraic manipulation of Eq. 6:

$$Cl_{rm} = k_{em}V_4 \qquad \text{(Eq. 6)}$$

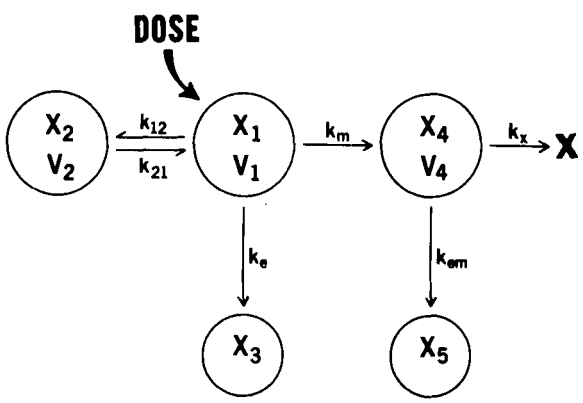

Scheme I—Multicompartment pharmacokinetic model. The parameters k_{12} *and* k_{21} *are the distribution rate constants between the central compartment,* X_1*, with volume* V_1 *and the peripheral compartment,* X_2 *with volume* V_2*;* k_m *is the first-order rate constant of biotransformation;* k_e *and* k_{em} *are urine* (X_3 *and* X_5) *excretion rate constants; and* k_x *is the transfer rate constant for irreversible loss from the metabolite compartment,* X_4*, with volume* V_4.

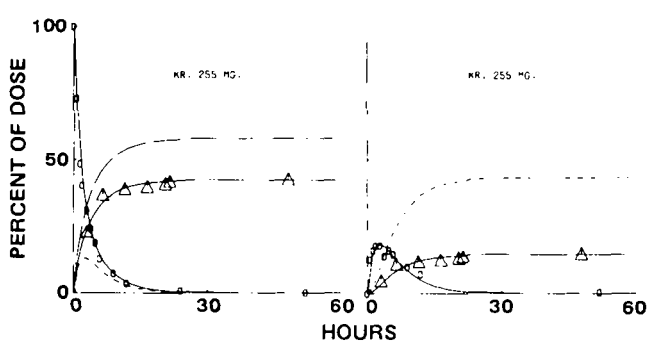

Figure 1—*Left: plot of the distribution, excretion, and metabolism of the percent dose of I. Data points were determined experimentally for serum (○) and urine (△) I concentrations for Patient KR. The theoretical amount of drug in the peripheral compartment,* X_2*, is represented by line ---. The line – – represents the cumulative amount of I metabolized. Right: plot of the formation, disposition, and excretion of the metabolite of I. The symbols ○ and △ represent experimentally determined data points for serum and urine concentrations, respectively. The line --- represents the theoretical amount of depot of I metabolite in body tissues,* X.

[3] Available on a DEC system-10 digital computer, Computer Center, Division of Computer Research and Technology, National Institutes of Health, Bethesda, MD 20014.

Table III—Disposition Rate Constants for the Multicompartment Model [a]

Patient	k_{12}, hr^{-1}	k_{21}, hr^{-1}	k_e, hr^{-1}	k_m, hr^{-1}	k_{em}, hr^{-1}	k_x, hr^{-1}
NG	0.51 (0.02)	0.28 (0.02)	0.05 (0.002)	0.22 (0.009)	0.07 (0.004)	0.31 (0.02)
KR	0.15 (0.01)	0.43 (0.07)	0.14 (0.002)	0.20 (0.004)	0.09 (0.003)	0.26 (0.01)
TS	0.37 (0.02)	0.27 (0.02)	0.10 (0.002)	0.15 (0.004)	0.10 (0.004)	0.06 (0.005)
JB	0.12 (0.01)	0.18 (0.05)	0.06 (0.002)	0.14 (0.008)	0.04 (0.005)	0.28 (0.03)
RJ	0.18 (0.01)	0.16 (0.03)	0.06 (0.002)	0.24 (0.01)	0.07 (0.003)	0.26 (0.02)
HR	0.10 (0.02)	0.02 (0.01)	0.06 (0.003)	0.12 (0.02)	0.14 (0.01)	0.33 (0.09)
KR	0.07 (0.01)	0.14 (0.05)	0.06 (0.001)	0.13 (0.009)	0.09 (0.007)	0.47 (0.05)
Mean ± SD [b]	0.21 ± 0.16	0.21 ± 0.13	0.08 ± 0.03	0.17 ± 0.05	0.08 ± 0.03	0.28 ± 0.12

[a] Results are quoted ± SE of the parameter estimate. [b] The means of the transfer constants for the seven patients as determined previously from the integrated equation (2) are 0.34 ± 0.30, 0.33 ± 0.35, 0.09 ± 0.04, and 0.21 ± 0.05, respectively; those for k_{em} and k_x (see text) are 0.08 ± 0.03 and 0.19 ± 0.09, respectively.

which describes the relationship between the compartment volume and the renal clearance. The difference between the body clearance (renal plus nonrenal) of the metabolite, Cl_b, and the renal clearance was used to determine the rate constant for loss of the metabolite, k_x, to body tissue. Substitution and rearrangement yield:

$$k_x = \frac{Cl_b - Cl_{rm}}{V_4} \qquad \text{(Eq. 7)}$$

The volume and clearance parameters are listed in Table II. The average value and standard deviation of the excretion rate constants as derived here for the metabolite, using Eqs. 6 and 7, are 0.08 ± 0.03 hr^{-1} for k_{em} and 0.19 ± 0.09 hr^{-1} for k_x.

The multicompartment model of I pharmacokinetics, as depicted in Scheme I, was developed by addition of the model for metabolite formation and disposition developed here to the two-compartment open model of unchanged drug distribution and elimination previously described (2). Initial estimates of the rate constants were refined by fitting the parameters of the differential equations to the data calculated as the percent of dose administered. A weighting factor of 1 was used in the weighted least-squares analysis (6, 7). Typical computer fits are shown in Figs. 1 and 2. Table III shows the results of the computer-fitted model parameters for the seven patients as well as the average value of those calculated transfer constants previously published for unchanged drug (2) and obtained here for the metabolite.

DISCUSSION

Compound I is a semisynthetic podophyllotoxin derivative for which the pharmacokinetics of unchanged drug in humans were reported (2). However, because the cumulative excretion of drug is substantially less than the amount of drug administered, of which two-thirds can be accounted for as unchanged drug (1), a multicompartment pharmacokinetic model was developed to ascertain if I or its metabolite was sequestered in the body.

The excellent agreement (Table III) between the calculated values of the transfer constants for unchanged drug previously reported (2) and those obtained here for the metabolite with the disposition constants obtained from fitting the differential equations directly to the data indicates that the drug and its metabolite behave according to the model (Scheme I). According to the model, biotransformation of I occurs only in the central compartment, V_1, in agreement with the previous conclusion obtained from the comparison of body and plasma clearances of unchanged drug (2). The metabolite is distributed into a threefold larger compartment, V_4, which approximates the volume of total body water. From this compartment, the metabolite is eliminated.

Since the renal excretion mechanism is not saturation limited, as indicated by the plot of the urinary excretion rate *versus* the plasma metabolite concentration (13), a nonrenal mechanism for loss of the metabolite must be sought to account for the difference between the amount of the metabolite recovered in the urine (Table II) and the theoretical fraction of I metabolized (2). Furthermore, the larger body clearance of the metabolite as compared to renal clearance (Table II) indicates that the theoretical rate of loss of the metabolite to body tissues is both rapid (Table III) and extensive (Figs. 1 and 2).

In conclusion, the pharmacokinetic analysis of I and its metabolite has identified the metabolite as being retained in the body.

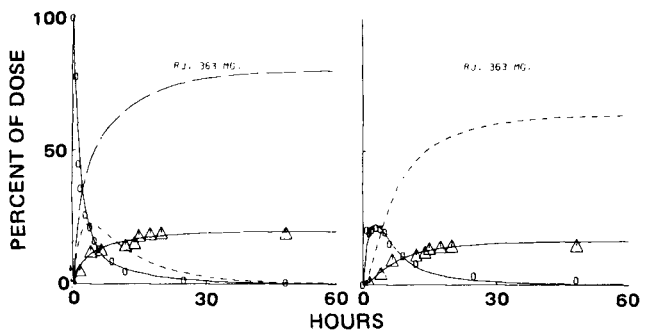

Figure 2—*Same as Fig. 1 but for Patient RJ.*

APPENDIX

Substitutions in Eq. 5 were made from Eqs. 2 and 3, in a manner similar to that reported by Wagner (14), to yield:

$$V_4 = \frac{k_m \text{dose}}{\frac{k_m \text{dose}}{V_4}\frac{(k_{21}-\beta)(\alpha-\beta)}{(\alpha-\beta)(\gamma-\beta)} + \frac{k_m \text{dose}}{V_4}\frac{(k_{21}-\gamma)(\alpha-\gamma)}{(\alpha-\gamma)(\beta-\gamma)}} \qquad \text{(Eq. A1)}$$

$$V_4 = \frac{k_m \text{dose}}{\frac{k_m \text{dose}}{V_4}\left(\frac{(k_{21}-\beta)}{(\gamma-\beta)} - \frac{(k_{21}-\gamma)}{(\gamma-\beta)}\right)} \qquad \text{(Eq. A2)}$$

REFERENCES

(1) P. J. Creaven and L. M. Allen, *Clin. Pharmacol. Ther.*, **18**, 221 (1975).

(2) L. M. Allen and P. J. Creaven, *Eur. J. Cancer*, **11**, 697 (1975).

(3) P. J. Creaven, S. J. Newman, O. S. Selawry, M. H. Cohen, and A. Primack, *Cancer Chemother. Rep.*, **58**, 901 (1974).

(4) L. Z. Benet, *J. Pharm. Sci.*, **61**, 536 (1972).

(5) L. B. Smith, *Commun. ACM*, **13**, 625 (1970).

(6) G. D. Knott and D. K. Reece, in "Proceedings of the ONLINE '72 International Conference," vol. 1, Brunel University, England, 1972, p. 497.

(7) G. D. Knott and R. I. Shrager, *Siggraph.*, **6**, 138 (1972).

(8) J. G. Wagner, "Biopharmaceutics and Relevant Pharmacokinetics," Drug Intelligence Publications, Hamilton, Ill., 1971, p. 298.

(9) J. G. Wagner and J. I. Northam, *J. Pharm. Sci.*, **56**, 529 (1967).

(10) S. Riegelman, J. Loo, and M. Rowland, *ibid.*, **57**, 128 (1968).

(11) N. R. Draper and H. Smith, "Applied Regression Analysis," Wiley, New York, N.Y., 1966, pp. 7–34.

(12) J. G. Wagner, "Biopharmaceutics and Relevant Pharmacokinetics," Drug Intelligence Publications, Hamilton, Ill., 1971, p. 249.

(13) W. J. Jusko and G. Levy, *J. Pharm. Sci.*, **59**, 765 (1970).

(14) J. G. Wagner, "Fundamentals of Clinical Pharmacokinetics," Drug Intelligence Publications, Hamilton, Ill., 1975, p. 103.

ACKNOWLEDGMENTS

Presented in part at the Basic Pharmaceutics Section, APhA Academy of Pharmaceutical Sciences, Atlanta meeting, November 1975.

Solid Dispersion of Pharmaceutical Ternary Systems I: Phase Diagram of Aspirin–Acetaminophen–Urea System

HANY M. EL-BANNA

Received May 2, 1977, from the *Department of Pharmaceutics, Faculty of Pharmacy, University of Alexandria, Alexandria, Egypt.* Accepted for publication December 1, 1977.

Abstract □ The phase diagram of an aspirin–acetaminophen–urea system was constructed. The data obtained by the thermomicroscopic method showed that the binary systems of aspirin–acetaminophen, aspirin–urea, and acetaminophen–urea are simple eutectic mixtures with negligible formation of solid solutions or molecular compounds. The equilateral triangular phase diagram of the ternary system revealed that it forms, upon solidification, solid dispersions of the mechanical mixture type. The ternary eutectic corresponded to a composition of 60% aspirin, 20% acetaminophen, and 20% urea at 72°. The method of calculating the composition of finally solidified melts, lying within any area of the phase diagram, is presented. Use of the phase diagram in selecting the optimum ratio of components to enhance dissolution rates of these drugs may be possible.

Keyphrases □ Solid dispersions—aspirin–acetaminophen–urea ternary system, phase diagram constructed, physical properties evaluated □ Phase diagram—constructed for aspirin–acetaminophen–urea ternary system solid dispersion □ Analgesics—aspirin–acetaminophen–urea ternary system, phase diagram constructed, physical properties evaluated □ Dosage forms—solid dispersions, aspirin–acetaminophen–urea ternary system, phase diagram constructed, physical properties evaluated

Drug–drug and/or drug–adjuvant interactions in solid dosage forms have gained the interest of pharmaceutical research workers in the last two decades. A considerable change in physical properties of drugs such as dissolution rates, equilibrium solubilities, partition coefficients, and, consequently, bioavailability usually occurs if such interactions take place.

Thermal analysis has been used to construct phase diagrams from which interactions in the solid state can be identified. The cooling curve method (1), the thaw–melt method (2–4), the thermomicroscopic method (5–12), the zone-melting method (13), and differential thermal analysis (9, 14) are among the applied thermal techniques. Reviews of these methods were reported previously (3, 15).

BACKGROUND

Phase diagrams of pharmaceutical binary systems were first reported (16) to explain the obvious enhancement in dissolution rate of two sparingly soluble drugs *via* the solid dispersion technique. Since then, there have been other studies on phase diagrams of various drug–inert carrier binary solid dispersion systems (5–12, 15–22). Phase diagrams were used to study the physical nature of solid dispersions of some drug–carrier (8–11) as well as drug–drug (11, 12) binary systems. Phase diagrams of reported binary systems showed simple eutectic mixtures (5, 11, 12, 17, 19, 21), solid solutions (6–8, 18), glass solutions (20), or molecular compounds (9, 10, 22).

Almost all reported work on pharmaceutical solid dispersions is limited to binary systems. However, a solid dispersion may be composed of one or more active ingredients dispersed in one or more inert carriers to obtain ternary and quaternary systems. Although excellent work on ternary systems has been accumulated in metallurgy, geology, and chemistry (15, 23, 24), pharmaceutical solid dispersion ternary systems have not been studied extensively.

In the present study, the phase diagram of an aspirin–acetaminophen–urea system was constructed. Solid dosage forms of aspirin with acetaminophen are common. Trials to improve the dissolution rate of aspirin (25) or acetaminophen (5, 12) using solid dispersions were reported previously. Furthermore, urea is often used as an inert carrier in binary solid dispersion systems. The information from the constructed phase diagram might help explain the dissolution rate behavior of such a combination of drugs.

EXPERIMENTAL

Materials—Aspirin[1] BP (mp 135–136°), acetaminophen[2] NF (mp 167–168°), and urea[3] (GR) (mp 132–134°) were used as obtained.

Procedure—Phase diagrams of the binary systems aspirin–acetaminophen, aspirin–urea, and acetaminophen–urea were made using the thermomicroscopic method. Various combinations of binary mixtures were weighed and thoroughly mixed. Each mixture was carefully melted, resolidified with mild stirring, and then finely powdered.

Thaw and final melting points of each sample were determined using a hot-stage microscope[4]; the temperature was raised 4°/min. Phase diagrams were constructed by plotting both thaw and melting temperatures *versus* the ratio of components (percent weight per weight).

The phase equilibria of aspirin–acetaminophen–urea ternary systems were initially represented by a triangular prism, whose base was an equilateral triangle (composition triangle). Each vertical face of the prism depicted a two-component system. A number of ternary compositions, represented by points lying on lines connecting the apex of the composition triangle (representing urea) with the opposite side of the aspirin–acetaminophen binary system at 10, 20, 40, 50, 60, and 80% (w/w) of acetaminophen, were selected.

For the detection of the lines of intersections of the parts of the liquidus surface, additional compositions were taken on the lines joining the apexes of the triangle with the binary eutectic compositions on the corresponding opposite side. Thaw and final melting points of all selected ternary mixtures were determined as described. Perpendiculars were then erected at the selected points, and the critical points were plotted on these perpendiculars at the corresponding temperatures. Finally, the three binary and one ternary eutectic points, the curves joining them, and the different isothermal lines were projected on an equilateral triangle.

RESULTS AND DISCUSSION

Binary Phase Diagrams—Phase diagrams of aspirin–acetaminophen and aspirin–urea systems are shown in Fig. 1. Binary systems closely approximating theoretical eutectic mixtures were present. Moreover, the eutectic temperatures of aspirin–urea and aspirin–acetaminophen systems were 83 and 109°, respectively, while the eutectic composition was approximately 25% (w/w) aspirin in both systems. The eutectic composition for the acetaminophen–urea system, on the other hand, was 52% acetaminophen and 48% urea at 114°, which closely coincided with the values reported by Goldberg *et al.* (5). No solid solubility or molecular compound formation was evidenced in the three binary systems studied.

Ternary Phase Diagram—The phase equilibria in aspirin–acetaminophen–urea are represented by a triangular prism (Fig. 2). The three vertical faces of the prism depict the three binary systems aspirin–acetaminophen, aspirin–urea, and acetaminophen–urea. Points E_1, E_2, and E_3 are the binary eutectics. The liquidus of the ternary mixtures is formed by the three surfaces: $t_AE_2E_tE_1t_A$, $t_pE_3E_tE_1t_p$, and $t_UE_2E_tE_3t_U$.

Lines E_1E_t, E_2E_t, and E_3E_t are the intersections of the parts of the liquidus surface and correspond to the melting point of the binary eutectics

[1] Bayer, Leverkusen, West Germany.
[2] Courtesy of Alexandria Co. for Pharmaceutical and Chemical Industry, Egypt.
[3] E. Merck, Darmstadt, West Germany.
[4] Microheating table "Boetius," GDR.

0022-3549/78/0800-1109$01.00/0
© 1978, American Pharmaceutical Association

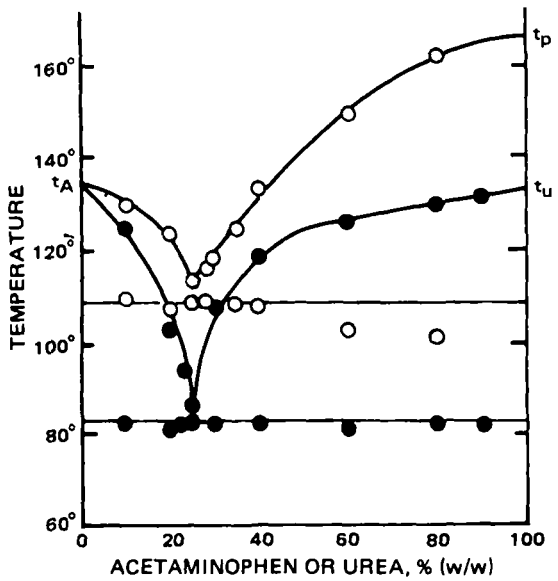

Figure 1—*Phase diagrams of aspirin–acetaminophen* (○), *and aspirin–urea* (●) *binary systems.*

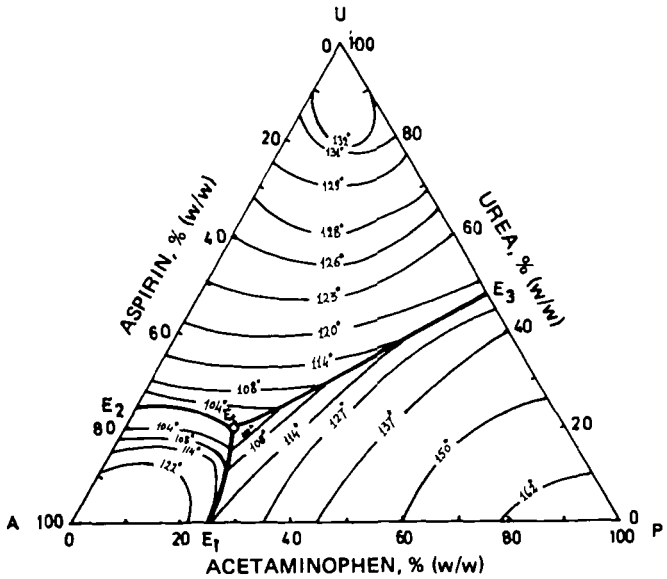

Figure 3—*Equilateral triangular phase diagram of aspirin (A)–acetaminophen (P)–urea (U) system showing isothermal lines.*

in the ternary system. These lines intersect at the common point E_t, which represents the eutectic aspirin–acetaminophen–urea of composition 60:20:20% (w/w) at 72°. This ternary system forms, upon solidification, solid dispersions of the mechanical mixture type (Fig. 2) (23). The solids aspirin, acetaminophen, and urea separate in the pure state, and there is no formation of compounds or solid solutions.

To obtain a convenient picture of the complete phase model, the three binary and the one ternary eutectic points and the curves joining them were projected on a horizontal plane, as shown by the equilateral triangular phase diagram (Fig. 3). Sections taken through the prism at a number of temperatures were projected on the triangle, and isothermal lines were presented as shown in Fig. 3. Eutectic lines E_1E_t, E_2E_t, and E_3E_t as well as lines AE_t, PE_t, and UE_t divide the phase diagram into six areas (24) (Fig. 4). From Fig. 4, it is possible to follow the solidification of any ternary melt having a composition within any of these six areas.

Calculation of the amounts of various solids deposited in such a crystallization process can be illustrated by the following example. On cooling a melt of composition h to a temperature at which the vertical line from h strikes the liquidus surface $t_UE_2E_tE_3t_U$, solid urea (in this case called the primary phase) begins to separate. As cooling proceeds, the composition of the residual liquid follows the linear extension of Uh to q.

On further cooling, solid acetaminophen as well as solid urea start to separate. At the same time, the liquid composition leaves q and alters its course to remain on E_3E_t. Eventually, the temperature of E_t is reached at which the liquid remaining solidifies completely to give the ternary eutectic mixture aspirin–acetaminophen–urea. While this occurs, the temperature must remain constant. The compositions of h, q, and E_t, determined from Fig. 4, are given in Table I.

Suppose that 100 g of the melt of composition h is gradually cooled and that x is the weight of urea deposited from h to q. Of the original 30 g of urea, there is now left in solution $(30 - x)$ g of urea but all of the original 45.5 g of aspirin. Therefore, in the liquid at q, the weight of urea/aspirin $= (30 - x)/45.5$, and this ratio equals 25.5/48 from the known composition of q. Solving for x gives 5.8 g of urea deposited by the time q is reached. The residual solution at q thus contains 45.5 g of aspirin, 24.5 g of acetaminophen, and $(30 - 5.8 = 24.2)$ g of urea.

By similar reasoning, if an additional y g of urea and z g of acetaminophen are deposited from q to E_t, y and z are found from the following equations, which are valid to E_t: weight of urea/aspirin $= 20/60 = (24.2 - y)/45.5$ and weight of acetaminophen/aspirin $= 20/60 = (24.5 - z)/45.5$. Solving for y gives 9.0 g of urea, and solving for z gives 9.3 g of acetaminophen deposited. Consequently, the residual solution now consists of 45.5 g of aspirin, $(24.2 - 9.0 = 15.2)$ g of urea, and $(24.5 - 9.3 = 15.2)$ g of acetaminophen. These are the amounts of the solid components that E_t gives on complete solidification. The finally solidified mixture of composition h, as well as any ternary mixture within area IV (Fig. 4), consists of the surplus component urea, the binary eutectic acetaminophen–urea,

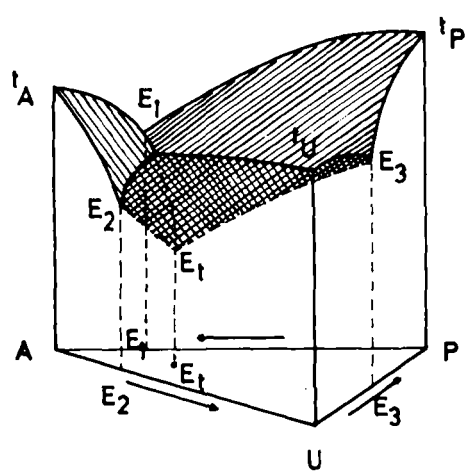

Figure 2—*Model phase diagram of aspirin (A)–acetaminophen (P)–urea (U) system. Key: E_1, aspirin–acetaminophen eutectic; E_2, aspirin–urea eutectic; E_3, acetaminophen–urea eutectic; and E_t, ternary eutectic.*

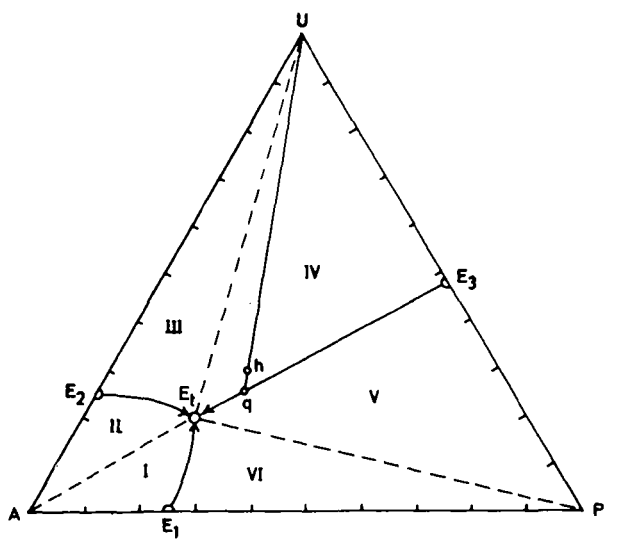

Figure 4—*Phase diagram of aspirin (A)–acetaminophen (P)–urea (U) system showing the final composition of solidified melts of the various areas I–VI. Key: I, A + AP + APU; II, A + AU + APU; III, U + AU + APU; IV, U + PU + APU; V, P + PU + APU; and VI, P + AP + APU.*

Table I—Compositions of h, q, and E_t Determined from Fig. 4

Sample (Melt)	Composition, % (w/w)		
	Aspirin	Acetaminophen	Urea
h	45.5	24.5	30.0
q	48.0	26.5	25.0
E_t	60.0	20.0	20.0

and the ternary eutectic aspirin–acetaminophen–urea. Similarly, the composition of other solidified ternary mixtures within the areas (I–VI) can be estimated (1).

On the other hand, ternary mixtures of compositions along line E_1E_t, E_2E_t, or E_3E_t consist of the binary eutectic aspirin–acetaminophen, aspirin–urea, or acetaminophen–urea, respectively, as well as the ternary eutectic aspirin–acetaminophen–urea when completely solidified. Ternary mixtures of compositions along lines AE_t, PE_t, and UE_t contain no binary eutectics but only the surplus component aspirin, acetaminophen, or urea, respectively, and the ternary eutectic. The ternary mixture of the composition corresponding to point E_t consists only of the ternary eutectic when completely solidified (23).

Information about the composition of solidified melts is useful in explaining dissolution patterns of drugs from binary solid dispersion systems (11, 14). It is hoped, therefore, that the knowledge obtained from the ternary phase diagram of the aspirin–acetaminophen–urea system will help in selection of the optimum ratio of these components (within therapeutic doses) for enhancement of their dissolution rates and improved bioavailability. Dissolution studies on this ternary system will be presented in Part II.

REFERENCES

(1) A. Findlay, "The Phase Rule," 9th ed., Dover, New York, N.Y., 1951, pp. 320, 475.

(2) H. Rheinboldt, *J. Prakt. Chem.*, 111, 242 (1925).

(3) J. K. Guillory, S. L. Hwang, and J. L. Lach, *J. Pharm. Sci.*, **58**, 301 (1969).

(4) K. Sekiguchi, Y. Ueda, and Y. Nakamori, *Chem. Pharm. Bull.*, **11**, 1108 (1963).

(5) A. H. Goldberg, M. Gibaldi, and J. L. Kanig, *J. Pharm. Sci.*, **55**, 482 (1966).

(6) *Ibid.*, **55**, 487 (1966).

(7) A. H. Goldberg, M. Gibaldi, J. L. Kanig, and M. Mayersohn, *J. Pharm. Sci.*, **55**, 581 (1966).

(8) H. M. El-Banna, S. Abd-Elfattah, and N. A. Daabis, *Pharmazie*, **29**, 396 (1974).

(9) N. A. Daabis, S. Abd-Elfattah, and H. M. El-Banna, *ibid.*, **29**, 400 (1974).

(10) H. M. El-Banna, N. A. Daabis, L. M. Mortada, and S. Abd-Elfattah, *ibid.*, **30**, 788 (1975).

(11) S. Abd-Elfattah, N. A. Daabis, and H. M. El-Banna, *Pharm. Ind.*, **38**, 93 (1976).

(12) H. M. El-Banna, A. G. Eshra, and Y. Hammouda, *Pharmazie*, **32**, 511 (1977).

(13) W. G. Pfann, "Zone Melting," 2nd ed., Wiley, New York, N.Y., 1966, pp. 1, 279.

(14) R. F. Schwenker and P. D. Garn, "Thermal Analysis," vol. 2, Academic, New York, N.Y., 1969, p. 829.

(15) W. L. Chiou and S. Riegelman, *J. Pharm. Sci.*, **60**, 1281 (1971).

(16) K. Sekiguchi and N. Obi, *Chem. Pharm. Bull.*, **9**, 866 (1961).

(17) W. L. Chiou, *J. Pharm. Sci.*, **60**, 1406 (1971).

(18) W. L. Chiou and S. Niazi, *ibid.*, **60**, 1333 (1971).

(19) A. M. Agrawal, R. L. Nikore, and A. K. Dorle, *Indian J. Pharm.*, **35**, 41 (1973).

(20) R. N. Gidwani and A. J. Anderson, *Can. J. Pharm. Sci.*, **11**, 118 (1976).

(21) M. P. Summers and R. P. Enever, *J. Pharm. Sci.*, **65**, 1613 (1976).

(22) K. Sekiguchi, N. Obi, and Y. Ueda, *Chem. Pharm. Bull.*, **12**, 134 (1964).

(23) Y. Lakhtin, "Engineering Physical Metallurgy and Heat-Treatment," Mir, Moscow, U.S.S.R., 1974, pp. 138, 139.

(24) W. H. Hamill, R. R. Williams, Jr., and C. MacKay, "Principles of Physical Chemistry," 2nd ed., Prentice-Hall, Englewood Cliffs, N.J., 1966, p. 231.

(25) A. F. Asker and C. W. Whiteworth, *Pharmazie*, **30**, 8 (1975).

ACKNOWLEDGMENTS

Supported in part by the National Science Foundation SFC program, Grants GF 39207 and GF 38251.

The author thanks Dr. Said A. Khalil, Department of Pharmaceutics, Faculty of Pharmacy, University of Alexandria, Alexandria, Egypt, and Dr. M. W. Gouda, School of Pharmacy, University of Montana, Missoula, Mont., for valuable suggestions.

Solid Dispersion of Pharmaceutical Ternary Systems II: Dissolution Studies on Aspirin–Acetaminophen–Urea System

HANY M. EL-BANNA *, SAID A. KHALIL *x, and M. WAFIK GOUDA ‡

Received May 2, 1977, from the *Department of Pharmaceutics, Faculty of Pharmacy, University of Alexandria, Alexandria, Egypt, and the ‡School of Pharmacy, University of Montana, Missoula, MT 59801. Accepted for publication December 1, 1977.

Abstract □ Solid dispersions of an aspirin–acetaminophen–urea ternary system were prepared by the solvent method. The different phases in the solid state of some selected samples were characterized, and their compositions were determined in the light of information deducted from a previously constructed phase diagram. Studies carried out on physically mixed and coprecipitated aspirin–acetaminophen samples in ratios of 2:1, 3:1, and 9:1 without urea revealed that the dissolution rate of both drugs is a function of their concentrations. Aspirin from coprecipitated samples dissolved 1.8–2.6 times as rapidly as the pure drug, while the initial dissolution rate of acetaminophen decreased 10–35%. Simultaneous dissolution rates of aspirin and acetaminophen from the three binary and the ternary eutectics were studied. The dissolution rates of both drugs, except for that of acetaminophen from its binary eutectic with aspirin, obviously improved. Dissolution rates of both drugs from coprecipitated aspirin–acetaminophen (2:1 and 9:1) as a function of the urea concentration also were considered. The mechanism of the observed improvement in their initial dissolution rates and their T_{90} values is described. About a sixfold increase in the dissolution rate of aspirin and about a threefold increase in that of acetaminophen were achieved when both drugs were coprecipitated with 5% urea.

Keyphrases □ Solid dispersions—aspirin–acetaminophen–urea ternary system, dissolution rates □ Dissolution rates—aspirin–acetaminophen–urea ternary system solid dispersions □ Analgesics—aspirin–acetaminophen–urea ternary system, dissolution rates □ Dosage forms—solid dispersions, aspirin–acetaminophen–urea ternary system, dissolution rates

In 1961, Sekiguchi and Obi (1) proposed that particle-size reduction of sparingly soluble drugs *via* solid dispersion techniques resulted in faster dissolution rates. This concept was later applied successfully by others (2). Almost all reports on this technique are limited to binary systems. Different solid dispersions of phenindione were studied (3). Some of these solid dispersions were prepared using random ratios of mixtures of two carriers. However, excellent work on ternary systems in other disciplines (4) stimulated interest in pharmaceutical ternary solid dispersion systems.

Previously (4), the phase diagram of aspirin–acetaminophen–urea was constructed to contribute information regarding the physical nature of this ternary system. The present work concerned the dissolution rates of aspirin and acetaminophen from ternary solid dispersions with urea in ratios chosen in light of the previously constructed phase diagram. Correlation between dissolution rate data and other information from the phase diagram also are discussed.

EXPERIMENTAL

Materials—Aspirin BP, acetaminophen NF, and urea (GR) were used as obtained (4). Absolute ethanol, hydrochloric acid, and sodium hydroxide were analytical grade.

Sample Preparation—The choice of samples of various compositions to study the dissolution rate of both aspirin and acetaminophen from solid dispersions with urea was based on information obtained from the previously constructed phase diagram (4). The solvent method was applied because of possible aspirin decomposition in samples prepared by the melt method (5). IR spectra[1] of aspirin samples, prepared by both the solvent and melt methods, were identical.

Coprecipitates of aspirin and acetaminophen in ratios of 65:35, 75:25, and 90:10 (for simplicity, 2:1, 3:1, and 9:1, respectively) with urea, ranging in concentration from 0.0 to 30% (w/w), were selected. Samples representing the three binary eutectics E_1, E_2, and E_3 of the aspirin–acetaminophen, aspirin–urea, and acetaminophen–urea binary systems, respectively, as well as the ternary eutectic E_t were included for comparison. The coprecipitates were prepared by dissolving the components in the minimum volume of absolute ethanol and evaporating the solvent *in vacuo* at room temperature using a rotary evaporator. The residue was finely ground, sieved to a particle-size range of 80–125 μm, and stored in a desiccator over anhydrous calcium sulfate.

Physical mixtures were prepared by simple mixing of ingredients possessing the same particle-size range (80–125 μm). Pure crystalline aspirin and acetaminophen (80–125 μm) served as controls.

Dissolution Rate Studies—Dissolution rate studies were carried out on samples containing aspirin, acetaminophen, and urea in the various compositions listed in Table I. All samples contained an equivalent of 100 mg of aspirin. Samples I_1–I_4, J_1–J_4, and E_1–E_t contained acetaminophen in quantities equivalent to 53.84, 11.11, and 33.33 mg, respectively. The dissolution fluid consisted of 450 ml of 0.1 *N* HCl maintained at 37° in a 500-ml beaker immersed in a constant-temperature water bath.

The dissolution fluid was stirred by a glass spiral paddle, attached by a ring to a metal rod joined with a side constant-speed motor. With this arrangement, the spiral paddle made 30 up and down movements/min, accompanied by two horizontal rotations through an arc of 180° with each up and down cycle (6). Samples of 2 ml were withdrawn at appropriate time intervals and replaced by an equal volume of dissolution fluid.

Assay Procedure—Samples were transferred to a 50-ml volumetric flask containing 3 ml of distilled water. A 0.5-ml quantity of 50% (w/v) NaOH was added to each flask and mixed thoroughly. After 15 min, 1.5 ml of concentrated hydrochloric acid was added, and the volume was brought to the mark with 0.1 *N* HCl (7). Preliminary investigations showed that only aspirin is hydrolyzed under these conditions. The absorbance of the solution was determined spectrophotometrically[2] at 302 and 242 nm using an appropriate blank.

Equations for determining the concentration of aspirin and acetaminophen as a two-component mixture were derived from the following absorptivity indexes: α_1, 0.552; α_2, 0.265; β_1, 0.657; and β_2, 0.000; α_1 and α_2 are the absorbances of a 1-mg % solution of salicylic acid in 0.1 *N* HCl at 242 and 302 nm, respectively, while β_1 and β_2 are the absorbances of a 1-mg % solution of acetaminophen at the same wavelengths. The following working equations were valid:

$$C_s = 3.770A_2 \qquad \text{(Eq. 1)}$$

$$C_a = \frac{A_1 - 0.552C_s}{0.657} \qquad \text{(Eq. 2)}$$

where C_s is the concentration of salicylic acid (milligrams percent), C_a is the concentration of acetaminophen (milligrams percent), A_1 is the absorbance at 242 nm, and A_2 is the absorbance at 302 nm. Urea did not interfere with the assay under test conditions. All samples were run at least in duplicate.

RESULTS AND DISCUSSION

To elucidate the mechanism involved in the dissolution process of aspirin and acetaminophen from their solid dispersions with urea, samples with compositions lying within the six areas of the previously constructed phase diagram were chosen (4). Accordingly, the compositions

[1] Perkin-Elmer model 237 IR spectrophotometer.
[2] Unicam SP 1800 UV spectrophotometer.

0022-3549/78/0800-1112$01.00/0
© 1978, American Pharmaceutical Association

Table I—Initial and Final Composition of Coprecipitated Samples Employed in the Dissolution Studies

	Composition[a], % (w/w)														
	Initial			Final											
				Solid			Binary Eutectic						Ternary Eutectic		
Sample	A	P	U	A	P	U	A–P		A–U		P–U		A–P–U		
I_1	65.0	35.0	—	—	13.3	—	65.0	21.7	—	—	—	—	—	—	—
I_2	61.8	33.2	5.0	—	11.0	—	46.7	17.3	—	—	—	—	15.0	5.0	5.0
I_3	52.0	28.0	20.0	—	7.6	—	—	—	—	—	3.0	2.3	52.5	17.3	17.3
I_4	45.5	24.5	30.0	—	—	5.8	—	—	—	—	9.3	9.0	45.5	15.2	15.2
J_1	90.0	10.0	—	60.0	—	—	30.0	10.0	—	—	—	—	—	—	—
J_2	85.5	9.5	5.0	56.0	—	—	14.5	4.5	—	—	—	—	15.0	5.0	5.0
J_3	72.0	8.0	20.0	15.2	—	—	—	—	32.8	12.0	—	—	24.0	8.0	8.0
J_4	63.0	7.0	30.0	—	—	8.1	—	—	42.0	14.9	—	—	21.0	7.0	7.0
E_1	75.0	25.0	—	—	—	—	75.0	25.0	—	—	—	—	—	—	—
E_2	75.0	—	25.0	—	—	—	—	—	75.0	25.0	—	—	—	—	—
E_3	—	52.0	48.0	—	—	—	—	—	—	—	52.0	48.0	—	—	—
E_t	60.0	20.0	20.0	—	—	—	—	—	—	—	—	—	60.0	20.0	20.0

[a] A = aspirin, P = acetaminophen, and U = urea.

of the selected finely crystallized solid dispersions were calculated, applying previously discussed principles (4) (Table I).

Although the final physical properties of solid dispersions prepared by the solvent method may differ from those obtained by the melt method (2), the solvent method has been used often in the preparation of solid solutions or mixed crystals of organic or inorganic compounds (8). Moreover, solid dispersions prepared by the solvent method can be characterized and their interactions in the solid state can be identified by phase diagrams constructed by thermal techniques (9). From various areas of the phase diagram, random samples prepared by the solvent method had the same melting characteristics as those obtained by the fusion method.

Simultaneous Dissolution Rate of Aspirin and Acetaminophen as a Function of Their Ratios—Melts or coprecipitates of acetaminophen (10, 11) or aspirin (12) with highly soluble inert carriers were previously reported. In the present work, the dissolution rates of these two drugs were studied simultaneously. Therefore, the effect of each drug on the dissolution behavior of the other was evaluated in their physical mixtures and solid dispersions without a carrier.

Physical mixtures and coprecipitates of aspirin with acetaminophen in ratios of 2:1, 3:1, and 9:1 were prepared, and their dissolution rates were determined. The amounts of aspirin and acetaminophen (in milligrams percent) dissolved as a function of their ratio are shown in Figs. 1 and 2. The relative dissolution rates, obtained by calculating the ratio of the observed rate to the rate of the pure crystalline aspirin or acetaminophen, are shown in Table II.

Physical Mixtures—The dissolution curve of pure crystalline aspirin was linear during the entire experimental time (Fig. 1). Curves of pure acetaminophen showed two linear segments; the initial rates tapered off at a time depending on the amount of the drug in the dissolution medium. When particles of pure aspirin were physically mixed with particles of pure acetaminophen in different ratios, no apparent change in the dissolution rate of aspirin was observed. However, the initial dissolution rate of acetaminophen decreased, ranging from about 30% for the aspirin–acetaminophen 2:1 ratio to 60% for the 9:1 ratio (Table II).

The explanation of these results is probably related to effective, rather than absolute, surface area. Both aspirin and acetaminophen have hydrophobic surfaces, and their particles float on the surface of the dissolution medium during the test. Theoretically, in such a system containing an abundant amount of aspirin particles relative to that of acetaminophen, acetaminophen would not influence the dissolution rate of aspirin particles. However, as a result of a decreasing acetaminophen ratio in the physical mixture, the surface area available to the dissolution fluid decreases and so does the dissolution rate.

Coprecipitates—Aspirin coprecipitated with acetaminophen in a 9:1 ratio exhibited a fast initial dissolution rate (3.25 mg/min), showing an increase 2.6 times greater than that of pure aspirin of comparable particle size (Table II). This sample contained 60% aspirin deposited as a primary phase together with 30% aspirin and 10% acetaminophen in the eutectic (Table I). The small amount of acetaminophen occupied in the interaspirin particulates resulted in decreasing aggregation of aspirin particles, increasing its effective surface area and, consequently, its initial dissolution rate.

This mechanism was confirmed by the 35% decrease of the initial dissolution rate of entrapped acetaminophen particles relative to that of pure crystalline acetaminophen. However, such a decrease in the initial dissolution rate of acetaminophen was still less than that observed with the physically mixed sample of identical composition (Fig. 1). This result was probably due to the relatively better wettability of the nonfloating coprecipitated sample.

The initial dissolution rate of acetaminophen from the coprecipitated aspirin–acetaminophen (2:1 ratio) was reduced to only 10% (Table II). This sample contained 35% acetaminophen (13.3% deposited as a primary phase and 21.7% in the eutectic), holding with it the whole 65% aspirin in the eutectic. In this case, some type of competition possibly existed between the two solutes in the dissolution fluid, decreasing the initial dissolution rate of aspirin (which was still 1.8 times greater than that of pure crystalline aspirin). Consequently, aspirin and acetaminophen in the coprecipitated sample of the 3:1 ratio, consisting mainly of 100% eutectic, exhibited intermediate dissolution behavior. In all studied ratios,

Table II—Relative Dissolution Rates of Aspirin (A) and Acetaminophen (P) as a Function of Their Ratios as Well as from Their Binary and Ternary Eutectics

			Relative Dissolution Rate			
			Aspirin		Acetaminophen	
Sample	Description	Condition	Initial	Limiting	Initial	Limiting
A	A	Crystalline	1.0	1.0	—	—
	A	Coprecipitate	1.4	0.8	—	—
P	P	Crystalline	—	—	1.0	1.0
	P	Coprecipitate	—	—	2.3	1.0
I_1	A_2:P_1	Physical mixture	1.0	1.0	0.7	0.7
E_1	A_3:P_1	Physical mixture	1.0	1.0	0.5	3.5
J_1	A_9:P_1	Physical mixture	1.0	1.0	0.4	2.0
I_1	A_2:P_1	Coprecipitate	1.8	0.8	0.9	10.0
E_1	A_3:P_1	Coprecipitate	2.5	0.8	0.8	3.7
J_1	A_9:P_1	Coprecipitate	2.6	0.8	0.6	4.0
E_2	A_3:U_1	Coprecipitate	5.6	0.6	—	—
E_3	P_1:U_1	Coprecipitate	—	—	2.1	1.0
E_t	A_3:P_1:U_1	Coprecipitate	6.6	0.2	2.3	1.0
E_t	A_3:P_1:U_1	Physical mixture	2.4	0.7	2.2	1.0

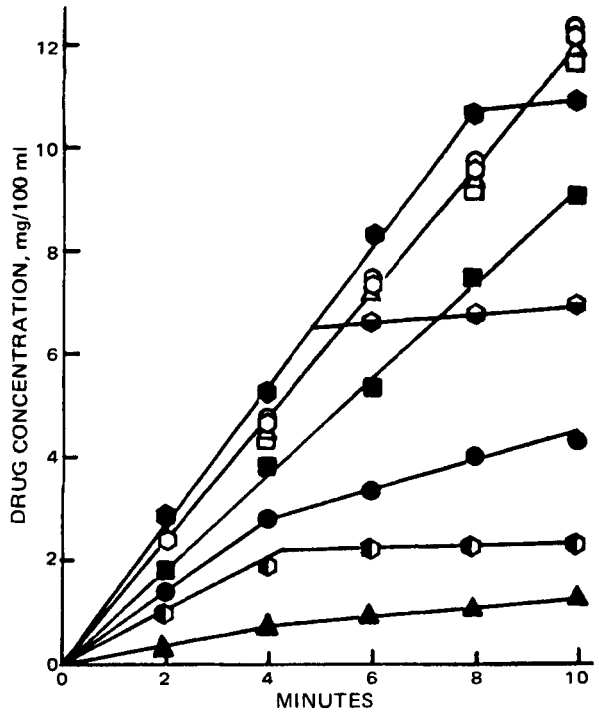

Figure 1—*Dissolution rates of aspirin and acetaminophen as a function of their ratios in physical mixtures. Key: aspirin from 1:0 (○), 2:1 (□), 3:1 (○), and 9:1 (△) ratio and acetaminophen from 0:1 (●, ⊖, and ◐; 54, 33, and 11 mg, respectively, in the dissolution fluid), 2:1 (■), 3:1 (●), and 9:1 (▲) ratios.*

once the second phase of acetaminophen dissolution started, showing high limiting dissolution rates, the dissolution of aspirin tapered off to approximately the same rate as that of the pure crystalline aspirin (Table II).

To see if a relationship existed between the dissolution rate and the aspirin to acetaminophen ratio in both coprecipitated and physically mixed samples, the relative initial dissolution rates were plotted *versus* the weight fraction of acetaminophen in the studied samples (Fig. 3). No linear relationship was observed for aspirin in the coprecipitated samples. Coprecipitation of aspirin with the minimum amount of acetaminophen highly improved its initial dissolution rate, but a further increase in the acetaminophen content decreased such improvement.

On the other hand, acetaminophen showed a linear relationship between its initial dissolution rate and its weight fraction in both coprecipitated and physically mixed samples. Generally, an increase in the acetaminophen content diminished the observed reduction in its initial dissolution rate.

Simultaneous Dissolution Rates of Aspirin and Acetaminophen from Binary and Ternary Eutectics—Figure 4 shows the dissolution rates of aspirin from the eutectics with acetaminophen (E_1) and with urea (E_2) and the ternary eutectic (E_t). For comparative purposes, the dissolution rate of aspirin precipitated from ethanol is also shown. The pure crystalline aspirin sample yielded an initial dissolution rate constant of 1.25 mg/min, while the precipitated sample demonstrated an initial rate constant of 1.7 mg/min, showing an increase of approximately 35%.

Tawashi (13) reported that polymorph I of aspirin, prepared by slow crystallization from its saturated solution in 95% ethanol, was very similar to commercial aspirin in its dissolution rate from tablets and in its X-ray diffraction pattern. The experimental discrepancy between the former study and the present work may be ascribed to differences in the method of aspirin crystallization. The relative initial dissolution rate data (Table II) indicate approximately a sixfold increase in the dissolution rate of aspirin from the eutectic mixture aspirin–urea (3:1) over that of crystalline aspirin, a fourfold increase over that of precipitated aspirin, and a twofold increase over that from the eutectic mixture aspirin–acetaminophen (3:1). However, the highest increase in the initial dissolution rate of aspirin (approximately seven times greater than the crystalline drug) was achieved with the ternary eutectic sample.

These results may reflect the significant reduction in the size of aspirin particulates during sample preparation. In addition to the increase in surface area of aspirin particles, local solubilization by urea appears to

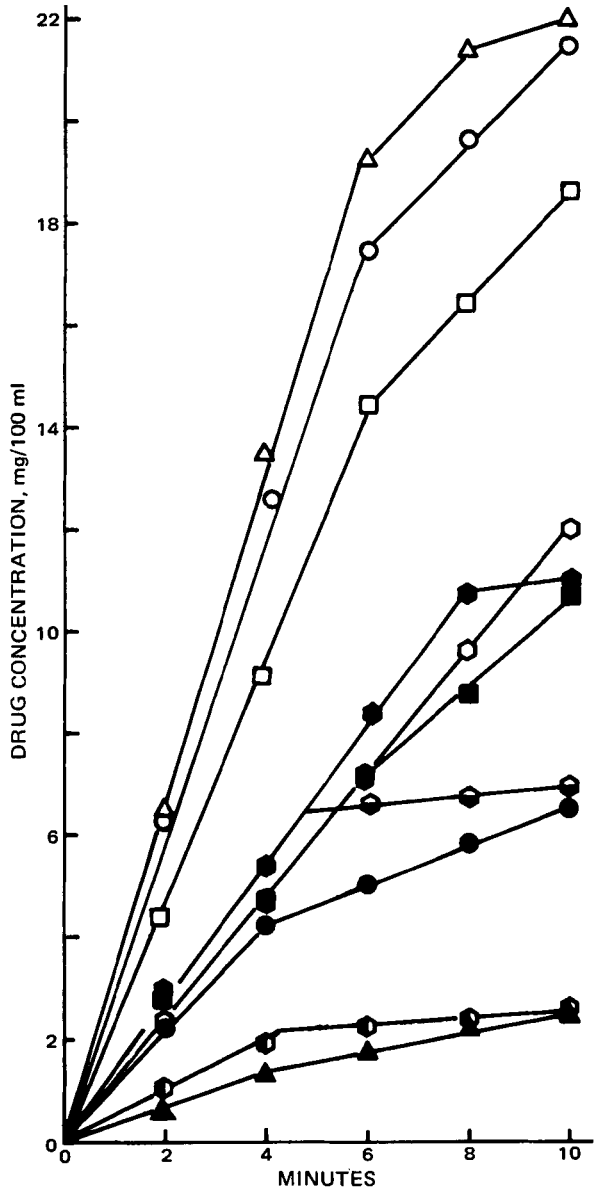

Figure 2—*Dissolution rates of aspirin and acetaminophen as a function of their ratios in coprecipitates. Key: aspirin from 1:0 (○), 2:1 (□), 3:1 (○), and 9:1 (△) ratios; and acetaminophen from 0:1 (●, ⊖, and ◐; 54, 33, and 11 mg, respectively, in the dissolution fluid), 2:1 (■), 3:1 (●), and 9:1 (▲) ratios.*

be responsible for the observed potentiation. The importance of the microenvironmental effect of urea on the dissolution of aspirin may be appreciated by considering the behavior of the physically mixed ternary eutectic sample. The initial dissolution of aspirin from this sample was almost twice as rapid as that of pure crystalline aspirin (Table II) but still lower than that of the coprecipitated sample of the same composition.

The second phase of dissolution of aspirin from the coprecipitated sample aspirin–urea (3:1) and the physically mixed ternary eutectic sample showed relative dissolution rate values favorably comparable to the rate found with the precipitated aspirin. This result suggests that once urea is completely depleted from the diffusion layer immediately surrounding the dissolved solid particles, the dissolution behavior of aspirin from these samples is almost identical. However, the coprecipitated ternary eutectic sample exhibited a much lower limiting dissolution rate.

The relative initial and limiting dissolution rates of acetaminophen from its precipitated sample, the binary eutectic sample with urea (E_3), or the ternary eutectic samples (physically mixed or coprecipitated) showed no significant difference in their dissolution behavior (Table II). These samples yielded an initial dissolution rate constant of 3.2–3.4 mg/min, showing approximately a twofold increase in the dissolution rate

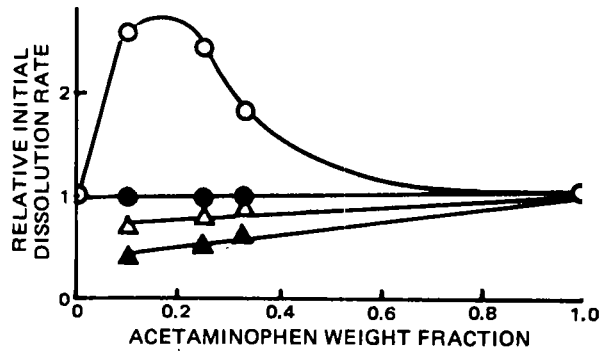

Figure 3—*Relative initial dissolution rates of aspirin and acetaminophen (compared to the crystalline drug) as a function of their weight fraction. Key: ○, aspirin from coprecipitates; ●, aspirin from physical mixtures; △, acetaminophen from coprecipitates; and ▲, acetaminophen from physical mixtures.*

of acetaminophen. In all cases, the second phase of dissolution had a rate constant of 0.1 mg/min, a value quite close to that of pure crystalline acetaminophen of equal particle size.

Goldberg *et al.* (10) reported that there is no evidence of particle-size reduction of acetaminophen by eutectic formation with urea. IR studies on precipitated acetaminophen showed that no ethanol solvates were formed under the present experimental conditions. The observed increase in the initial dissolution rate of acetaminophen, therefore, may be due to coprecipitation and/or better wetting of the drug by urea.

Simultaneous Dissolution Rate of Aspirin and Acetaminophen as a Function of Urea Concentration—The amounts of aspirin and acetaminophen dissolved from the 2:1 and 9:1 ratios as a function of the urea concentration are shown in Figs. 5 and 6, respectively. The relative initial dissolution rates and the time required to dissolve 90% of the drug (designated by T_{90}) were calculated (Table III). In general, the presence of urea in the studied ratios increased the dissolution parameters of both drugs. This result could be attributed mainly to the wetting effect of the highly water-soluble urea in intimate contact with the drugs.

Aspirin–Acetaminophen (2:1 Ratio)—Approximately a sixfold increase in the initial dissolution rate of aspirin from Sample I_2, coprecipitated with 5% urea, over that of pure crystalline aspirin was observed (Table III). This sample also exhibited a threefold increase in the initial dissolution rate of aspirin over that of Sample I_1, free from urea. This potentiation (also shown by the decrease in the T_{90} value from 18 to 8) could be attributed to the participation of urea in depositing a portion of aspirin as the ternary eutectic (Table I), previously shown to exert an accelerated initial dissolution rate (Fig. 4).

A comparison of the relative initial dissolution rates and T_{90} values of the physically mixed and coprecipitated I_2 samples again reflects the significance of solid dispersion in enhancing the dissolution rate of poorly soluble drugs (Table III). Samples I_3 and I_4, containing 20 and 30% urea, respectively, actually had most of their aspirin content in the form of a ternary eutectic (approximately 87 and 76%, respectively, Table I). Consequently, these two samples were expected to exhibit similar initial dissolution rates. However, I_4 showed a T_{90} value almost half that of I_3, probably because of the presence of free urea (6%) in I_4 deposited as a primary phase (Table I).

The dissolution profiles of acetaminophen from the coprecipitated samples, containing urea concentrations of 5–30%, were almost the same, as is evident from their initial relative dissolution rates (Table III).

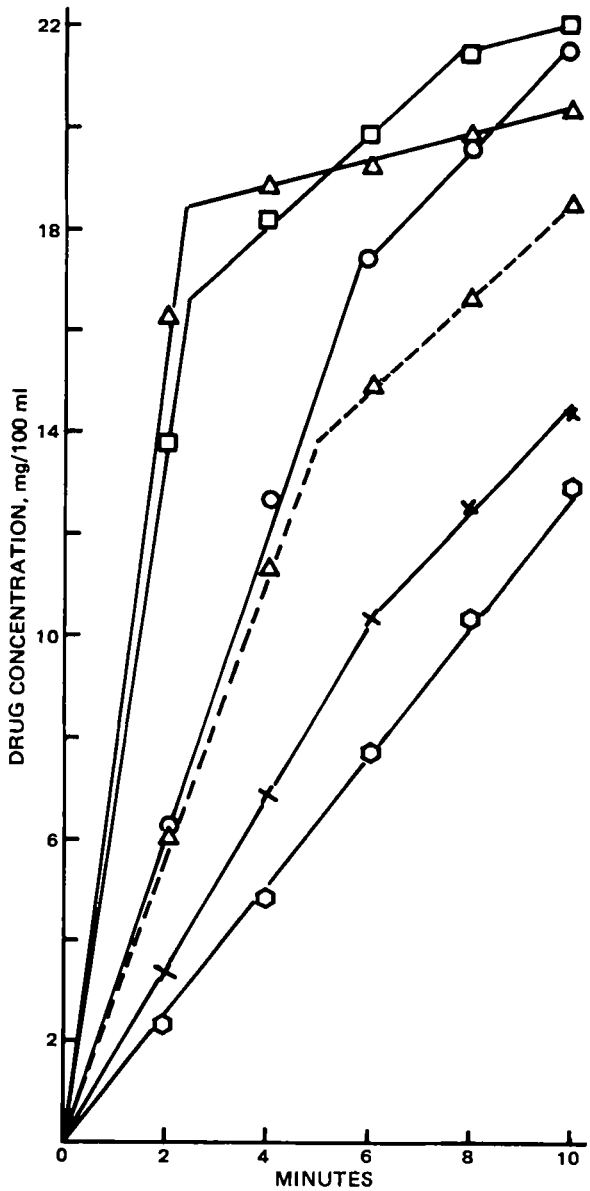

Figure 4—*Dissolution rates of aspirin from binary and ternary eutectics. Key: ○, crystalline aspirin; ×, precipitated aspirin; ○, aspirin–acetaminophen (E_1); □, aspirin–urea (E_2); and △, aspirin–acetaminophen–urea (E_t). The dotted line represents the physical mixture.*

Samples I_3 and I_4 had their acetaminophen content deposited as a ternary eutectic, a binary eutectic with urea, and/or a primary phase (Table I), which were shown to exhibit equal dissolution rates (Table II). The only difference was observed from the relatively high T_{90} value for Sample I_2, which contained approximately half of its acetaminophen in the form

Table III—Relative Initial Dissolution Rates (RIDR) and T_{90} Values of Aspirin (A) and Acetaminophen (P) as a Function of Urea (U) Concentration

A:P Ratio	Sample	[U], %	Condition	[A] RIDR	[A] T_{90}, min	[P] RIDR	[P] T_{90}, min
—	A	—	Crystalline	1.0	18.0	—	—
—	P	—	Crystalline	—	—	1.0	6.8
	I_1	—	Coprecipitate	1.8	15.0	0.9	10.0
	I_2	5	Physical mixture	1.8	10.0	1.4	15.0
2:1	I_2	5	Coprecipitate	5.8	8.0	3.2	7.5
	I_3	20	Coprecipitate	6.8	5.0	3.5	3.0
	I_4	30	Coprecipitate	7.7	2.3	3.7	2.5
	J_1	—	Coprecipitate	2.6	6.5	0.6	6.0
	J_2	5	Coprecipitate	5.8	3.5	1.7	4.0
9:1	J_3	20	Coprecipitate	6.7	5.0	2.0	2.4
	J_4	30	Coprecipitate	6.8	5.0	2.0	2.4

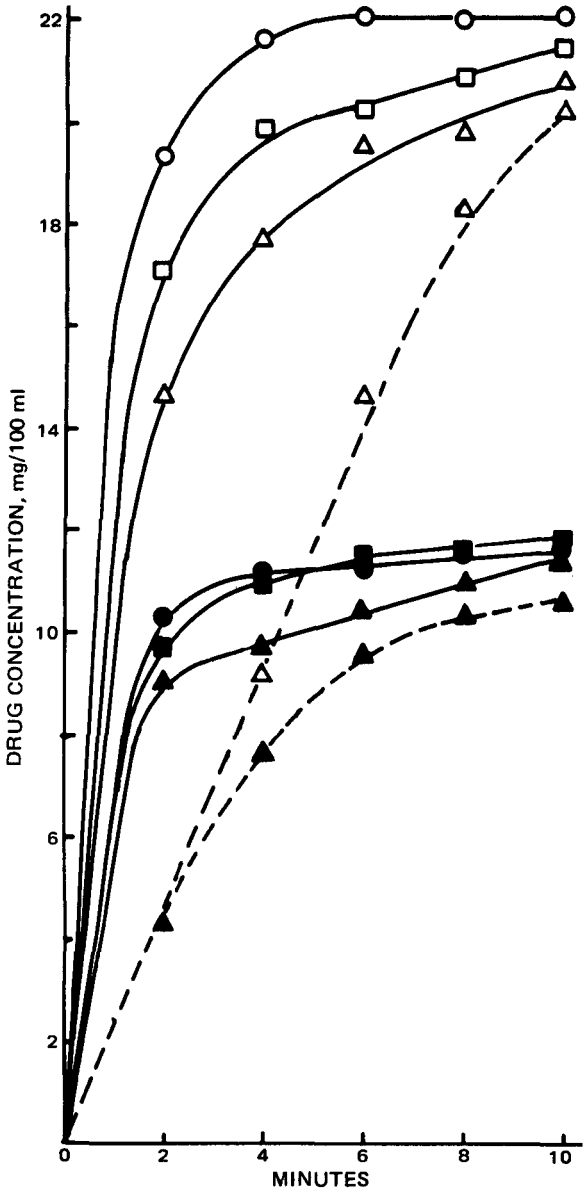

Figure 5—*Dissolution rates of aspirin (open symbols) and acetaminophen (solid symbols) from coprecipitates in 2:1 ratio as a function of urea concentration. Key: △, 5% urea; □, 20% urea; and ○, 30% urea. Dotted lines represent the physical mixture.*

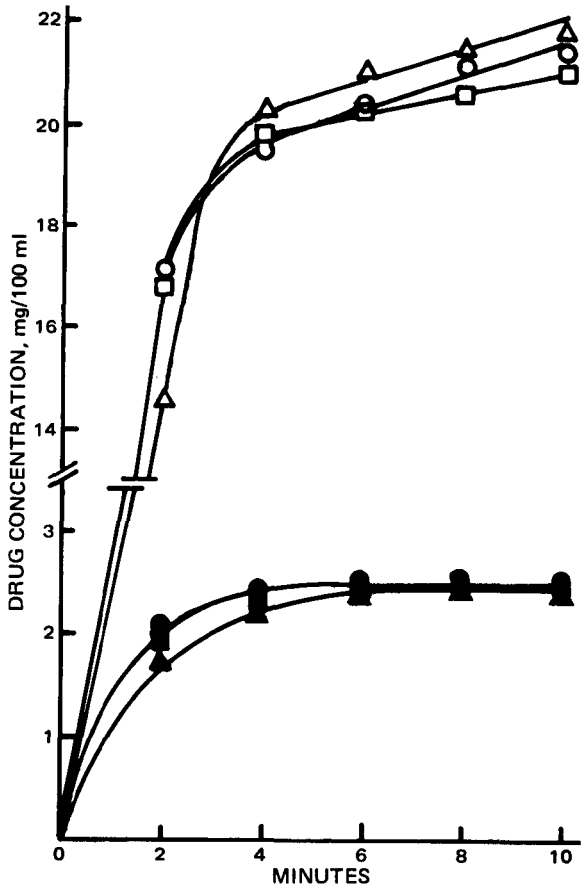

Figure 6—*Dissolution rates of aspirin (open symbols) and acetaminophen (solid symbols) from coprecipitates in 9:1 ratio as a function of urea concentration. Key: △, 5% urea; □, 20% urea; and ○, 30% urea.*

of the binary eutectic with aspirin, previously shown to exert a low acetaminophen dissolution rate (Fig. 2).

Aspirin–Acetaminophen (9:1 Ratio)—Samples I_2 and J_2, coprecipitated with 5% urea, contained an equal proportion of the ternary eutectic (Table I). This composition probably could explain the identical relative initial dissolution rate values of aspirin from both samples (Fig. 6 and Table III). However, the presence of a large amount of aspirin deposited as a primary phase in J_2 would explain the twofold decrease in the T_{90} value in this sample relative to I_2 (Tables I and III).

Samples J_3 and J_4, however, showed similar initial dissolution rates and T_{90} values. Both samples contained more or less equal amounts of the binary eutectic aspirin–urea (3:1) and the ternary eutectic. The possible increase in the dissolution rate due to the presence of free aspirin, deposited as a primary phase in J_3, would make up for the increase resulting from the free urea in J_4.

All of the acetaminophen content in J_3 and J_4 was deposited as the ternary eutectic (Table I), a fact that could explain the identical dissolution behavior of acetaminophen from these samples (Table III and Fig. 6). The acetaminophen content of J_2, on the other hand, was equally distributed between the binary eutectic aspirin–acetaminophen (3:1) and the ternary eutectic. The ternary eutectic would account for the observed increase in the initial dissolution rate of acetaminophen, while the binary eutectic might be responsible for the high T_{90} value relative to the values of J_3 and J_4.

It can be concluded that coprecipitation of aspirin and acetaminophen with only 5% urea markedly improved the dissolution parameters of both drugs. However, a further increase in the urea content (from 5 to 30%) only slightly improved their initial dissolution rates from samples representing the six areas of the phase diagram. Nevertheless, the variation in the T_{90} values of both drugs in these samples was a function of the urea concentration.

The sixfold increase of the initial dissolution rate of aspirin and the threefold increase in that of acetaminophen when aspirin–acetaminophen (2:1) was coprecipitated with 5% (w/w) urea encourage *in vivo* testing of this ternary system. The bioavailability of this combination of drugs is presently under investigation.

Simultaneous dissolution rates of two drugs, possible enhancement in dissolution behavior of one at the expense of the other, and elucidation of possible mechanisms by which accelerated dissolution rates can occur (on the basis of accurate determination of the composition of finally crystallized solid dispersions) are some contributions of the present report. The suggested approach of ternary solid dispersion systems represents a fertile area for possible enhancement of dissolution rates of drug combinations in solid dosage forms and proposes systematic techniques for their evaluation.

REFERENCES

(1) K. Sekiguchi and N. Obi, *Chem. Pharm. Bull.*, **9**, 866 (1961).

(2) W. L. Chiou and S. Riegelman, *J. Pharm. Sci.*, **60**, 1281 (1971).

(3) H. A. Salama, H. O. Ammar, M. A. Kassem, and M. S. El-Ridy, paper presented at XIV Egyptian Conference of Pharmaceutical Sciences, Dec. 1975, p. 39.

(4) H. M. ElBanna, *J. Pharm. Sci.*, **67**, 1109 (1978).

(5) C. C. Edison and M. G. Ines, *An. R. Acad. Farm.*, **40**, 487 (1974).

(6) H. M. El-Banna and A. A. Ismail, *Pharmazie*, **30**, 226 (1975).
(7) K. A. Javaid and D. E. Cadwallader, *J. Pharm. Sci.*, **61**, 1370 (1972).
(8) A. Findlay, "The Phase Rule," 9th ed., Dover, New York, N.Y., 1951, p. 372.
(9) R. N. Gidwani and A. J. Anderson, *Can. J. Pharm. Sci.*, **11**, 117 (1976).
(10) A. H. Goldberg, M. Gibaldi, and J. L. Kanig, *J. Pharm. Sci.*, **55**, 482 (1966).
(11) H. M. El-Banna, A. G. Eshra, and Y. Hammouda, *Pharmazie*, **32**, 511 (1977).
(12) A. F. Asker and C. W. Whitworth, *ibid.*, **30**, 530 (1975).
(13) R. Tawashi, *Science*, **160**, 76 (1968).

ACKNOWLEDGMENTS

Supported in part by the National Science Foundation SFC program, Grants GF 39207 and 38251.

Fluorometric Assay for Urinary Indapamide

PETER E. GREBOW ˣ, JO A. TREITMAN, and ANNE K. YEUNG

Received July 25, 1977, from the *Biochemistry and Drug Disposition Department, USV Pharmaceutical Corporation, Tuckahoe, NY 10707.* Accepted for publication December 1, 1977.

Abstract □ A sensitive fluorescence method for the determination of indapamide was developed. Reaction of indapamide with sodium hydroxide at 100° yielded a fluorescent product, and addition of formaldehyde to the fluorescent product increased its fluorescence intensity by a factor of three. The assay is sensitive to levels of indapamide of 0.025 μg/ml in an aqueous solution, and a linear response between 0.025 and 2.0 μg/ml was observed. The procedure was adapted to the analysis of intact indapamide in urine. Concentrations of indapamide of 0.05 μg/ml can be detected in dogs given 20 mg of the drug.

Keyphrases □ Indapamide—fluorometric analysis in urine □ Fluorometry—analysis, indapamide in urine □ Antihypertensive agents—indapamide, fluorometric analysis in urine

Indapamide, 1-(3-sulfamoyl-4-chlorobenzamido)-2-methylindoline (I), is a new agent for the treatment of mild to moderate hypertension (1–4). Drug levels in biological fluids were measured by TLC with a sensitivity of 0.1 μg/ml (5), and plasma ^{14}C-indapamide concentrations following oral administration of the radiolabeled drug also were determined by TLC (6).

It was considered desirable to investigate other highly sensitive assays amenable to analyzing large numbers of samples from pharmacokinetic studies using the unlabeled drug. Accordingly, a spectrofluorometric assay for indapamide in both aqueous solutions and urine was developed.

EXPERIMENTAL

Materials and Instruments—All fluorescent measurements were performed on a scanning fluorescence spectrophotometer[1]. TLC was performed on 0.25-mm silica gel plates[2].

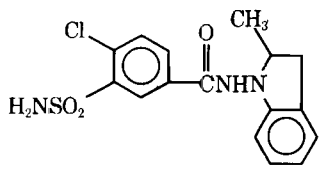

I

[1] Model MPF-2A, Perkin-Elmer Corp., Wilton, Conn.
[2] LQD Quanta, Quantum Industries, Fairfield, N.J.

Indapamide[3] was used without further purification. Indapamide tablets[3] were administered to dogs. Indoline[4], alipamide[5], 2-methylindoline[6], and 1-(3-sulfamoyl-4-chlorobenzoyl)-2-methylindoline[6] were studied as model fluorescent compounds. Methanol and all solvents used in the TLC studies were distilled-in-glass grade[7]. The ether used routinely was anhydrous grade[8], and all other reagents were analytical reagent grade[9].

Aqueous Assay—Indapamide was dissolved in 5.0 ml of 0.005 *N* NaOH containing 3 *M* NaCl. This solution was heated at 100° for 45 min in a water bath in screw-capped culture tubes (16 × 150 mm) with polytef liners. After heating, the tubes were removed and placed in ice water for a few minutes; then 0.2 ml of 37% formaldehyde was added. The tubes were reheated at 100° for 8 min, cooled in ice water for a few minutes, and then allowed to remain at room temperature until read on the fluorescence spectrophotometer.

Duplicate samples were run in all experiments. Reaction blanks were prepared by treating the sodium hydroxide–sodium chloride solution without indapamide identically.

The fluorescence of the samples was measured in quartz cells with a 1-cm path length. The excitation wavelength was 284 nm, and the emission spectrum was scanned for each sample. Both the excitation and emission slit widths were set according to the sensitivity required in the assay. Typical values were 4 nm.

The fluorescence intensity for each sample and blank was calculated by subtracting the fluorescence intensity at 300 nm (the baseline following the Rayleigh–Tyndall scattering peak) from that at 356 nm, where the peak occurs. A corrected sample fluorescence intensity was determined by subtracting the fluorescence intensity of the blank from that of the sample.

Extraction of Urine—Different indapamide concentrations were added to urine, which was then adjusted to pH 2 with 6 *N* HCl. Urine without indapamide was used as a control blank. In 16 × 150-mm screw-capped culture tubes with polytef liners, 6 ml of urine was extracted twice with 3.5 ml of ether. The ether previously was washed with 0.1 *N* NaOH [ether–sodium hydroxide (2:3 v/v)]. The combined ether layers were then extracted twice with 0.05 *M* sodium phosphate, pH 7.4 (16.0 ml, 5.0 ml).

The aqueous layer was discarded, and the ether layer was extracted with 6.0 ml of a 0.005 *N* NaOH–3 *M* NaCl solution. A 5-ml aliquot of the aqueous solution was then transferred into 16 × 150-mm tubes and reacted as described. The fluorescence of each sample was measured, and the absorbance between 280 and 360 nm was measured in random samples to test for interference by light-absorbing compounds.

[3] Servier Laboratories, Neuilly Sur Seine, France.
[4] Eastman Kodak Co., Rochester, N.Y.
[5] Parke-Davis, Ann Arbor, Mich.
[6] USV Pharmaceutical Corp., Tuckahoe, N.Y.
[7] Burdick & Jackson Laboratories, Muskegon, Mich.
[8] Fisher Chemicals, Fair Lawn, N.J.
[9] Mallinckrodt Chemical Works, St. Louis, Mo.

0022-3549/78/0800-1117$01.00/0
© 1978, American Pharmaceutical Association

(6) H. M. El-Banna and A. A. Ismail, *Pharmazie*, **30**, 226 (1975).
(7) K. A. Javaid and D. E. Cadwallader, *J. Pharm. Sci.*, **61**, 1370 (1972).
(8) A. Findlay, "The Phase Rule," 9th ed., Dover, New York, N.Y., 1951, p. 372.
(9) R. N. Gidwani and A. J. Anderson, *Can. J. Pharm. Sci.*, **11**, 117 (1976).
(10) A. H. Goldberg, M. Gibaldi, and J. L. Kanig, *J. Pharm. Sci.*, **55**, 482 (1966).
(11) H. M. El-Banna, A. G. Eshra, and Y. Hammouda, *Pharmazie*, **32**, 511 (1977).
(12) A. F. Asker and C. W. Whitworth, *ibid.*, **30**, 530 (1975).
(13) R. Tawashi, *Science*, **160**, 76 (1968).

ACKNOWLEDGMENTS

Supported in part by the National Science Foundation SFC program, Grants GF 39207 and 38251.

Fluorometric Assay for Urinary Indapamide

PETER E. GREBOW ˣ, JO A. TREITMAN, and ANNE K. YEUNG

Received July 25, 1977, from the *Biochemistry and Drug Disposition Department, USV Pharmaceutical Corporation, Tuckahoe, NY 10707.* Accepted for publication December 1, 1977.

Abstract □ A sensitive fluorescence method for the determination of indapamide was developed. Reaction of indapamide with sodium hydroxide at 100° yielded a fluorescent product, and addition of formaldehyde to the fluorescent product increased its fluorescence intensity by a factor of three. The assay is sensitive to levels of indapamide of 0.025 μg/ml in an aqueous solution, and a linear response between 0.025 and 2.0 μg/ml was observed. The procedure was adapted to the analysis of intact indapamide in urine. Concentrations of indapamide of 0.05 μg/ml can be detected in dogs given 20 mg of the drug.

Keyphrases □ Indapamide—fluorometric analysis in urine □ Fluorometry—analysis, indapamide in urine □ Antihypertensive agents—indapamide, fluorometric analysis in urine

Indapamide, 1-(3-sulfamoyl-4-chlorobenzamido)-2-methylindoline (I), is a new agent for the treatment of mild to moderate hypertension (1–4). Drug levels in biological fluids were measured by TLC with a sensitivity of 0.1 μg/ml (5), and plasma ^{14}C-indapamide concentrations following oral administration of the radiolabeled drug also were determined by TLC (6).

It was considered desirable to investigate other highly sensitive assays amenable to analyzing large numbers of samples from pharmacokinetic studies using the unlabeled drug. Accordingly, a spectrofluorometric assay for indapamide in both aqueous solutions and urine was developed.

EXPERIMENTAL

Materials and Instruments—All fluorescent measurements were performed on a scanning fluorescence spectrophotometer[1]. TLC was performed on 0.25-mm silica gel plates[2].

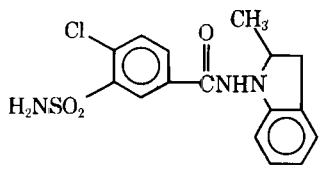

I

[1] Model MPF-2A, Perkin-Elmer Corp., Wilton, Conn.
[2] LQD Quanta, Quantum Industries, Fairfield, N.J.

Indapamide[3] was used without further purification. Indapamide tablets[3] were administered to dogs. Indoline[4], alipamide[5], 2-methylindoline[6], and 1-(3-sulfamoyl-4-chlorobenzoyl)-2-methylindoline[6] were studied as model fluorescent compounds. Methanol and all solvents used in the TLC studies were distilled-in-glass grade[7]. The ether used routinely was anhydrous grade[8], and all other reagents were analytical reagent grade[9].

Aqueous Assay—Indapamide was dissolved in 5.0 ml of 0.005 *N* NaOH containing 3 *M* NaCl. This solution was heated at 100° for 45 min in a water bath in screw-capped culture tubes (16 × 150 mm) with polytef liners. After heating, the tubes were removed and placed in ice water for a few minutes; then 0.2 ml of 37% formaldehyde was added. The tubes were reheated at 100° for 8 min, cooled in ice water for a few minutes, and then allowed to remain at room temperature until read on the fluorescence spectrophotometer.

Duplicate samples were run in all experiments. Reaction blanks were prepared by treating the sodium hydroxide–sodium chloride solution without indapamide identically.

The fluorescence of the samples was measured in quartz cells with a 1-cm path length. The excitation wavelength was 284 nm, and the emission spectrum was scanned for each sample. Both the excitation and emission slit widths were set according to the sensitivity required in the assay. Typical values were 4 nm.

The fluorescence intensity for each sample and blank was calculated by subtracting the fluorescence intensity at 300 nm (the baseline following the Rayleigh–Tyndall scattering peak) from that at 356 nm, where the peak occurs. A corrected sample fluorescence intensity was determined by subtracting the fluorescence intensity of the blank from that of the sample.

Extraction of Urine—Different indapamide concentrations were added to urine, which was then adjusted to pH 2 with 6 *N* HCl. Urine without indapamide was used as a control blank. In 16 × 150-mm screw-capped culture tubes with polytef liners, 6 ml of urine was extracted twice with 3.5 ml of ether. The ether previously was washed with 0.1 *N* NaOH [ether–sodium hydroxide (2:3 v/v)]. The combined ether layers were then extracted twice with 0.05 *M* sodium phosphate, pH 7.4 (16.0 ml, 5.0 ml).

The aqueous layer was discarded, and the ether layer was extracted with 6.0 ml of a 0.005 *N* NaOH–3 *M* NaCl solution. A 5-ml aliquot of the aqueous solution was then transferred into 16 × 150-mm tubes and reacted as described. The fluorescence of each sample was measured, and the absorbance between 280 and 360 nm was measured in random samples to test for interference by light-absorbing compounds.

[3] Servier Laboratories, Neuilly Sur Seine, France.
[4] Eastman Kodak Co., Rochester, N.Y.
[5] Parke-Davis, Ann Arbor, Mich.
[6] USV Pharmaceutical Corp., Tuckahoe, N.Y.
[7] Burdick & Jackson Laboratories, Muskegon, Mich.
[8] Fisher Chemicals, Fair Lawn, N.J.
[9] Mallinckrodt Chemical Works, St. Louis, Mo.

0022-3549/78/0800-1117$01.00/0
© 1978, American Pharmaceutical Association

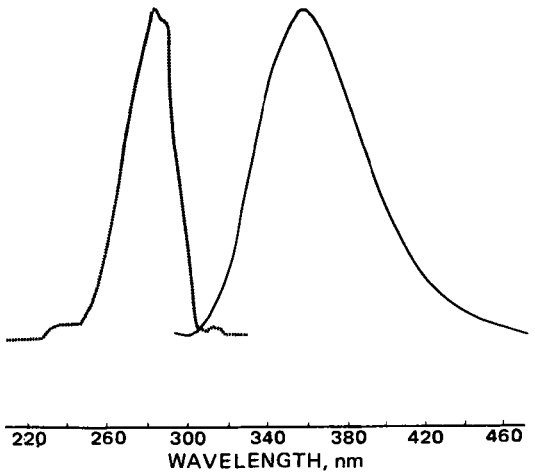

Figure 1—*Excitation (- - -) and emission (—) spectra of indapamide fluorescent product.*

Administration of Indapamide and Specimen Collection—Two male beagle dogs, ~10 kg, received 20 mg of indapamide (tablets) orally. The dogs were housed in metabolism cages that permitted separation of urine and feces. Urine was collected by catheterization before dosing and at 1.0, 2.0, 3.0, 4.0, 5.0, 6.0, 7.0, 8.0, 24.0, and 48.0 hr after dosing to ensure that the bladder was completely emptied at specific time intervals.

The urine collected by catheterization was combined with that collected in the cage pan. The pH and volume of each sample were immediately measured. The samples were kept frozen until they were extracted and assayed as described.

Stability of Indapamide in Urine—The cumulative 24-hr urine sample from an indapamide-treated dog was divided into several aliquots, and these aliquots were frozen. Periodically during 6 months, an aliquot was thawed and assayed as described.

Specificity—The specificity of the fluorescence assay was evaluated by TLC with two solvent systems: A, benzene–acetone (80:20 v/v); and B, benzene–ethyl acetate (60:40 v/v). TLC was performed on the ether extract of a urine sample from a dog given indapamide, and the chromatograms were visualized under a UV lamp (254 nm).

The silica gel corresponding to the observed spots was scraped off the plates, added to a solution of 0.005 *N* NaOH–3 *M* NaCl, and shaken for 15 min. An aliquot of the sodium hydroxide solution was then decanted and reacted at 100° as previously described, and the fluorescence was measured.

RESULTS AND DISCUSSION

Indapamide did not exhibit any significant fluorescence when dissolved in either methanol or 0.1 *N* NaOH. However, heating the alkaline solution produced a fluorescent product with the properties illustrated in Fig. 1 (λ_{ex} = 284 nm and λ_{em} = 356 nm). The excitation and emission spectra of the product of the sodium hydroxide reaction are typical of indoline-like compounds (7–9), suggesting that the nature of indapamide was changed to that of a fluorescent indole-like molecule.

Table I—Fluorescence Intensity Obtained with Different Concentrations of Sodium Hydroxide and Methanol

Concentration[a]	Average Relative Fluorescence Intensity
Sodium hydroxide, *N*	
Water, pH 6	0
1×10^{-3}	20
5×10^{-3}	37
1×10^{-2}	29
5×10^{-2}	21
1×10^{-1}	16
Methanol, % (v/v)	
0	62
20	83
40	48
60	36
80	24
100	9

[a] All solutions contained 3 *M* NaCl and were heated at 100° for 45 min. No formaldehyde was added. Different concentrations of indapamide were used for sodium hydroxide and methanol.

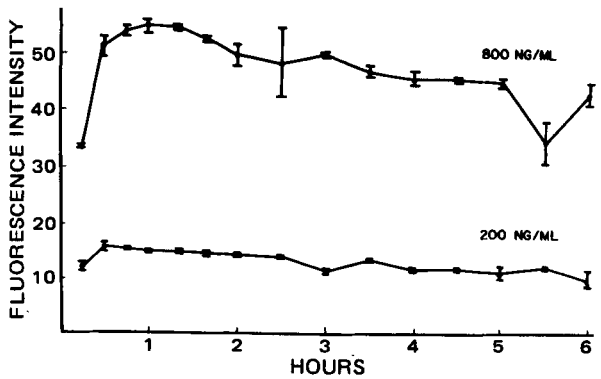

Figure 2—*Effect of heating time for the indapamide (200 and 800 ng/ml)–sodium hydroxide solution on the observed fluorescence intensity.*

Reaction Conditions—The fluorescent yield from the indapamide–sodium hydroxide mixture was further characterized and optimized. A solution of 0.005 *N* NaOH gave the maximum fluorescence intensity when compared with solutions of different concentrations of sodium hydroxide as well as water (Table I). Figure 2 shows the results when the indapamide–sodium hydroxide–sodium chloride solution was heated at 100° for various times without formaldehyde.

A 45-min heating period was selected for convenience; there was only a slight difference between the fluorescence values obtained after either 30 or 60 min at 100°. In subsequent experiments, in which the indapamide concentration was above 1.5 μg/ml, it was necessary to allow the alkaline solutions to react for 60 min at 100°. When a temperature of 50° was used, no fluorescence was observed, indicating that the reaction had not proceeded.

The fluorescence intensity of the product was measured as a function of pH by diluting the reacted solution with an appropriate buffer. No formaldehyde was added. There was no significant change in the fluorescence intensity of the product between pH 3 and 12. Above pH 12 and below pH 3, there was a marked decrease in the fluorescence intensity of the product (Fig. 3).

The effect of methanol on the fluorescent properties of the indapamide product was studied. Dilution of the reacted product with methanol did not decrease the fluorescence, as expected, by the concomitant decrease in concentration (Table II). This result is in contrast to dilution of the reacted product with sodium hydroxide, which did decrease the fluoresence intensity proportionally. When samples containing indapamide and different amounts of methanol in 0.005 *N* NaOH were reacted for 45 min in a 100° water bath, the measured fluorescence intensity decreased as the methanol concentration increased above 20% (Table I). Thus, while methanol enhanced the fluorescence intensity of the reaction product, it decreased the yield of the product if added before heating.

Since the fluorescence intensity of some indole compounds increases in the presence of formaldehyde (8), the addition of formaldehyde to increase the fluorescence of the indapamide product was considered. When 0.1 ml of formaldehyde was added to 5 ml of the indapamide product, the fluorescence was immediately increased by approximately

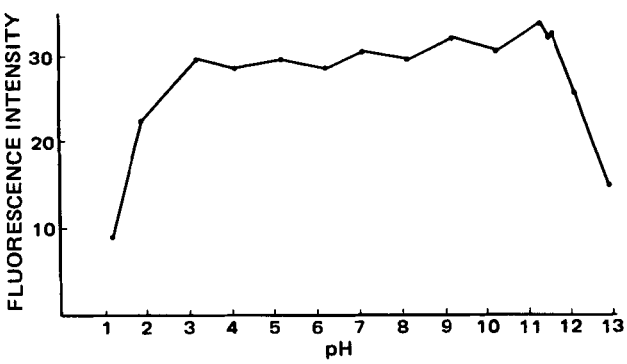

Figure 3—*Effect of pH of the solution, at the time of measurement, on the fluorescence intensity of the fluorescent product of indapamide.*

Table II—Changes in the Fluorescence Intensity of the Indapamide Product upon Dilution with Methanol

Indapamide Concentration, μg/ml	Methanol, %	Fluorescence Intensity
2.0	2.0	59
1.0	51.0	90
0.5	75.5	48
0.05	97.5	4

threefold. Following this addition, the fluorescence continued to increase slightly for 1 hr. However, if the samples were heated at 100° for 8 min after formaldehyde addition, the fluorescence remained stable. Since the addition of 0.2 ml of formaldehyde gave a slightly higher fluorescence intensity, this volume was used.

The fluorescence of the reaction product (after formaldehyde addition) was stable for at least 4 hr and showed very little, if any, decay after 24 hr.

Standard Curve—A standard curve was obtained for indapamide using the optimal procedure developed. Concentrations of indapamide from 0.025 to 20 μg/ml were detected. At concentrations greater than 2.0 μg/ml, there was a negative deviation from linearity, possibly due to an "inner filter effect" (10, 11).

The reproducibility of the assay was demonstrated by three studies performed on 3 successive days. A correlation coefficient of 0.998 was obtained for these values, indicating that the daily calibration curve did not change significantly. The error in the calibration curve ranged between 5 and 10%.

Extraction of Urine—At the onset of the extraction studies with ether, contact with ether limited the fluorescence intensity obtained from the reaction of indapamide with sodium hydroxide. When sodium hydroxide was shaken with ether (taken from a freshly opened can), the ether discarded, and indapamide added to the sodium hydroxide, the fluorescence intensity following reaction was less than 50% of that obtained if there had been no ether contact with the sodium hydroxide. A component of the ether was apparently extracted into the sodium hydroxide and interfered with the assay. This observation was also noted with glass-distilled ether.

If the ether was cleaned by preextraction with 0.1 *N* NaOH prior to use [ether–sodium hydroxide (2:3 v/v)], there was no interference in the procedure. Thus, all ether used in the extraction was so purified. The addition of sodium chloride to the sodium hydroxide solution was necessary to limit ether solubility in the aqueous phase.

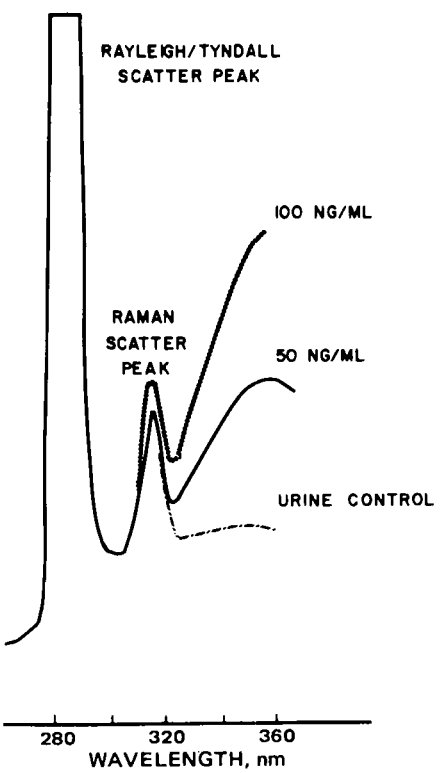

Figure 4—*Fluorescence spectra obtained from extracted dog urine spiked with indapamide before extraction.*

Table III—Efficiency of the Indapamide Extraction

	Indapamide Concentration, μg/ml		
	0.05	0.20	0.80
Fluorescence intensity of extracted sample	23.2 ± 3.1[a]	96.0 ± 3.0	367.0 ± 3.0
Fluorescence intensity of unextracted sample	37.0 ± 1.5	154.0 ± 3.1	574.0 ± 5.7
Percent extracted	62	62	64

[a] Numbers are reported as ±*SEM* (n = 3).

A typical fluorescence spectrum of control dog urine that had gone through extraction and reaction is shown in Fig. 4. The blank spectrum is compared with spectra obtained for urine containing 0.05 and 0.10 μg of indapamide/ml. Similar spectra were obtained with human urine. The absorbance of the control samples between 280 and 360 nm was less than 0.05 for all human urines tested and for most of the dog urines. For those few samples with absorbances slightly greater than 0.05, correction could be made by sample dilution or by calculations described previously (11). The possibility remains that the absorbing material may be partially due to fecal contamination, rather than due to an endogenous material, since the urine passes over the feces in the metabolism cage.

A standard curve was obtained for extracted indapamide by extracting control dog urine that contained different indapamide concentrations and then reacting the solutions as previously described. This standard curve was compared with the standard curve obtained for unextracted samples; the efficiency for this method of extracting indapamide is reported in Table III. The ratio of fluorescence intensity (extracted) to fluorescence intensity (aqueous) defines the extraction efficiency at each concentration and was approximately 62%.

Specificity—The results of the TLC study of urine samples from dogs given indapamide showed that only one spot, corresponding to indapamide, yielded material that was fluorescent under the assay conditions. In addition, the fluorescence spectra obtained from the extracted urine samples from dogs given indapamide were identical to those obtained for aqueous solutions of indapamide.

Urinary Excretion of Indapamide in Dogs—The fluorometric assay was used to study the urinary excretion of indapamide following a 20-mg oral dose to beagles. In two dogs, only 7.2 and 11.2% of the administered indapamide were excreted in the urine as the unchanged drug in the first 24 hr after administration. By 48 hr, these values were increased to only 7.3 and 11.7% of the dose, respectively. These values agree with previous results (5, 6), which indicated that indapamide is extensively metabolized. A representative urinary excretion rate of indapamide from a dog is shown in Fig. 5.

Indapamide stability in urine was tested for 6 months, and the results indicated that urine samples of indapamide can be kept frozen for at least 6 months without any degradation.

Mechanism Studies—The results of these studies have given some preliminary information regarding the product of the indapamide reaction with sodium hydroxide. Alipamide (3-sulfamoyl-4-chlorobenzoic acid-2,2-dimethylhydrazide) did not exhibit any fluorescence when

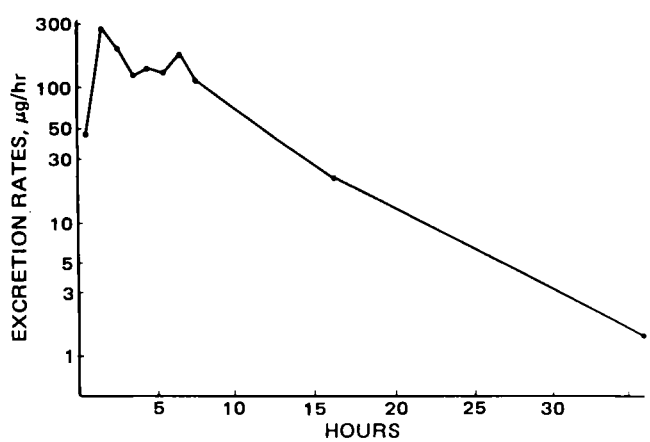

Figure 5—*Urinary excretion rate of indapamide for a dog dosed with 20 mg.*

subjected to the assay conditions, which supported the hypothesis that the indoline group was responsible for the fluorescence observed for indapamide. When 2-methylindoline was dissolved in the 0.005 *N* NaOH–3 *M* NaCl solution, a fluorescence spectrum similar to that of indapamide was observed. Furthermore, either heating at 100° or adding formaldehyde increased the fluorescence intensity of 2-methylindoline by a factor of approximately 1.4 or 2.5, respectively.

Indoline was similarly treated. Indoline possesses fluorescent properties (λ_{ex} = 290 nm and λ_{em} = 356 nm) similar to those described for the indapamide reaction product. Indoline was fluorescent in distilled water, 0.005 *N* NaOH, and methanol. While the fluorescence intensity in water and sodium hydroxide was nearly identical, the fluorescence intensity in methanol was more than 20 times that obtained in the aqueous solutions. Addition of formaldehyde to aqueous solutions of indoline increased the fluorescence intensity approximately threefold. In addition, heating (100° for 45 min) the indoline–sodium hydroxide solution in the absence of formaldehyde increased the fluorescence nearly threefold, while heating indoline in distilled water only slightly increased the fluorescence intensity. Thus, heating of indoline in sodium hydroxide causes a rearrangement to a more fluorescent molecule.

It seems probable that the product of the indapamide–sodium hydroxide reaction may be similar to indoline or 2-methylindoline. All three compounds had a higher fluorescence intensity in methanol (see Table II for indapamide), and their fluorescence intensities increased approximately threefold with the addition of formaldehyde to the aqueous solution.

In alkaline solutions, quenching of the indole fluorescence could result by transfer of the proton from the imino nitrogen of the excited indole molecule to the hydroxide ion of the solvent. The dissociated molecule could then return to the ground state by a radiationless pathway. This mechanism was described by White (12). Formaldehyde may combine with the ring nitrogen of the indole, forming a product that does not dissociate in the excited state. It can then be postulated that this phenomenon occurs when formaldehyde is added to the indapamide product, indoline, or 2-methylindoline, thereby minimizing, to some degree, the quenching by the the aqueous solvent.

Since indapamide, which contains an indoline group, has essentially no intrinsic fluorescence, the reaction with sodium hydroxide must cause this group to be fluorescent. When 1-(3-sulfamoyl-4-chlorobenzoyl)-2-methylindoline (II) was dissolved in sodium hydroxide–sodium chloride, there was no discernible fluorescence. Heating at 100° produced fluorescence, again similar in nature to indapamide, which could also be increased by the addition of formaldehyde. However, after heating for 45 min, the fluorescence intensity was markedly less for II than for indapamide. Continued heating of II for up to 5.5 hr caused a steady increase in its fluorescence intensity. The fluorescence intensity of indapamide did not significantly change under similar conditions (Fig. 2).

One hypothesis is that the amide bond of the molecule is cleaved during the sodium hydroxide reaction, thereby yielding the isolated indoline. (If this were the case, the observed reaction difference between II and indapamide may be explained by the possible greater lability of the amide bond in indapamide as compared to the amide bond of II.) There is evidence (9) that the addition of electronegative substituents to the indole ring will quench the fluorescence of the indole. Thus, if the sulfonamide moiety intramolecularly quenches the fluorescence of the indoline ring, it is easy to see how cleavage of the amide bond could create fluorescence. While the fluorescence of the reaction product appears to be generated from the indoline moiety of the indapamide molecule, it cannot be certain whether the final product is an indoline or whether oxidation to an indole has occurred.

REFERENCES

(1) G. Onesti, D. Lowenthal, M. Affrime, C. Swartz, J. Shirk, R. Mann, and E. Schultz, *Clin. Pharmacol. Ther.*, **21,** 113 (1977).

(2) L. Finch and P. Hicks, *Br. J. Pharmacol.*, **58,** 282P (1976).

(3) J. Kyncl, K. Oheim, T. Seki, and A. Solles, *Arzneim.-Forsch.*, **25,** 1491 (1975).

(4) Y. Seedat and J. Reddy, *Curr. Ther. Res.*, **16,** 275 (1974).

(5) D. Campbell and E. Phillips, *Eur. J. Clin. Pharmacol.*, **7,** 407 (1974).

(6) D. Campbell, A. Taylor, and R. Moore, *Br. J. Clin. Pharmacol.*, **3,** 971P (1976).

(7) S. Udenfriend, "Fluorescence Assay in Biology and Medicine," vol. 1, Academic, New York, N.Y., 1962, pp. 160–177.

(8) S. Udenfriend, "Fluorescence Assay in Biology and Medicine," vol. 2, Academic, New York, N.Y., 1969, pp. 228–237.

(9) R. Cowgill, *Arch. Biochem. Biophys.*, **100,** 36 (1963).

(10) D. Hercules, "Fluorescence and Phosphorescence Analysis," Interscience, New York, N.Y., 1966, p. 49.

(11) E. Kirby, in "Excited States of Proteins and Nucleic Acids," R. Steiner and I. Weinryb, Eds., Plenum, New York, N.Y., 1971, p. 39.

(12) A. White, *Biochem. J.*, **71,** 217 (1959).

ACKNOWLEDGMENTS

Presented in part at the APhA Academy of Pharmaceutical Sciences, New York meeting, May 1977.

Electronic Monitoring of Events within Dynamic Particulate Beds: Conductance and Capacitance Measurements

EDWARD G. RIPPIE ×, DOUGLAS C. KRIESEL *, and HARALD RETTIG ‡

Received July 15, 1976, from the *Department of Pharmaceutics, College of Pharmacy, University of Minnesota, Minneapolis, MN 55455.* Accepted for publication November 15, 1977. *Present address: Abbott Laboratories, North Chicago, IL 60064. ‡Present address: Ciba-Geigy Corp., Basel, Switzerland.

Abstract □ Methods for monitoring mechanical events occurring within particulate solids systems in a dynamic state are described. The electrical conductance and capacitance characteristics of such systems, as they relate to the degree of bed dilation or expansion, extent of interparticulate contact, and intensity of particle motion, were studied and are discussed. To establish the potential of this approach, harmonically vibrated beds of monodispersed conducting spheres were used. A technique, based on the frequency modulation of standard FM broadcast frequency carrier signals, was developed to measure low and high frequency fluctuations in bed capacitance. The electrical conductance of these systems also was determined by both voltage drop and current flow methods. The experimental techniques developed are broadly applicable to various materials and modes of agitation or flow. They permit the evaluation of the time courses of both bed dilation and particle motion which, in turn, are known to determine or modify critically powder flow and mixing behavior.

Keyphrases □ Particulate beds, dynamic—electronic monitoring of mechanical events, conductance and capacitance characteristics evaluated □ Solids—dynamic particulate beds, electronic monitoring of mechanical events, conductance and capacitance characteristics evaluated □ Electronic monitoring—mechanical events in dynamic particulate beds, conductance and capacitance characteristics evaluated

Solids mixing research has concentrated on the development of experimental methodology and the elucidation of the underlying mechanisms responsible for the mixing and segregation characteristics of multiparticulate solids systems (1–4). From these mixing studies at the particulate level, it became evident that much new information could be gained from the quantification of certain fundamental properties of dynamic particle beds. Two kinematic properties in particular that seemed of value to characterize were generalized bed dilation and individual particulate motion. These properties result whenever adjacent regions of a free-flowing multiparticulate system are caused to move relative to each other. This movement occurs when vibration or shear is induced by mixing operations or by processes in which noncohesive powders are made to flow.

An understanding of the extent and time course of bed dilation is important. Both the degree of interparticulate contact and the associated magnitude of the energy barriers that individual particles must overcome in moving past each other are strongly dilation dependent. Moreover, measurements of the intensity of particle motion within a particulate bed provide evidence of the relative kinetic energy content of the particles and their patterns of energy decay through energy-absorbing collisions, particle attrition, and other kinetic energy-consuming interparticulate interactions.

For particles to move past each other without fracturing, they not only require space in which to move but also must possess the energy necessary to overcome interparticulate frictional forces. Because the average particle kinetic energy and the associated degree of bed dilation are frequently strongly coupled, these quantities ideally should be measured simultaneously by techniques that do not perturb the system. Such techniques will be most useful if they possess the following characteristics: a wide range of application capable of providing data on beds having varied particulate compositions and subjected to vibration and/or shear, the ability to detect rapidly occurring changes of very short duration throughout the bulk of a given particulate system, and a high degree of sensitivity to small relative changes in bed characteristics.

Furthermore, the response of any such measurement technique to rapid bed changes should be stable, reproducible, and flat over the range of approximately 20–15,000 Hz. This frequency range should cover adequately the frequency spectrum of events occurring within typical systems. Since, in vibrated beds, the degree of bed expansion and the intensity of particle motion are expected to be approximately periodic functions of time, corresponding to the periodicity of vibration, an ideal measurement technique should permit the resolution of events within the time base of a single vibratory cycle.

The characteristics described as being desirable for monitoring changes in void volume and particulate motion of dynamic multiparticulate solids systems were found in this study to be satisfactorily met by techniques for measurement of their electrical conductance and behavior in a capacitor. This paper describes the operational characteristics of these techniques and illustrates their utility and that of data acquired from vibrated beds of spherical conducting particles of uniform density.

DESIGN CONSIDERATIONS

A bed of electrically conducting particles can be visualized as a three-dimensional network of switches with interconnecting conductors. In a vibrated bed, these switches are constantly being opened and closed as the bed expands and contracts. The conductance is a function not only of the multiplicity of conducting pathways between sensing electrodes placed in such beds but also of the interparticulate contact pressures that determine virtual contact areas between particles and, hence, contact resistances. Changes in bed conductance can be observed from measurements both of voltage drops across the bed and of current flow through the bed under conditions of constant circuit voltage. Both approaches were used in the present studies.

The nature of the dependence of bed conductance on interparticulate contact, assuming any and all contacts are of low resistance, can be seen from a consideration of the probability of electrical continuity through a chain of n particles. If the probability of contact between any two adjacent particles in the chain is p, then the probability of chain conduction is p^{n-1}, provided end particles contact electrodes. In the systems studied, many paths of various lengths (numbers of particles) between the electrodes were possible.

It is characteristic of such systems that, for a fixed interelectrode distance, the number of possible paths of a given length increases as the path length increases. However, since for a given value of p, the probability of conduction per path drops rapidly with increased path length, only the shorter paths contribute significantly to conduction. Calculation of the number of paths as a function of their length was not possible because of random bed packings.

0022-3549/78/0800-1121$01.00/0
© 1978, American Pharmaceutical Association

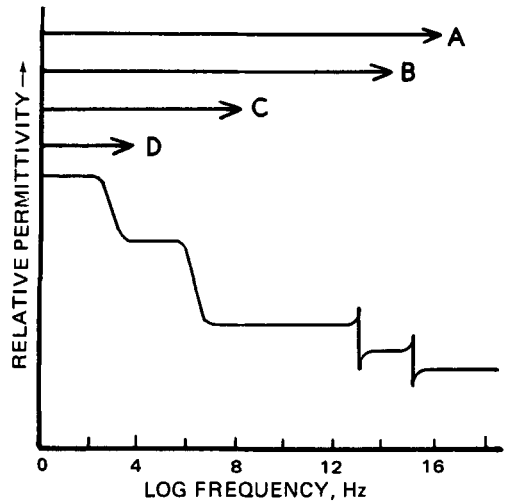

Figure 1—*Dependence of relative permittivity on frequency. Frequency ranges of the contributions to permittivity from electronic (A), atomic (B), dipole (C), and interfacial (D) sources are indicated.*

The probability of conduction through a typical path, 33 particles in length, decreases from 0.725 to 0.194 as p decreases from 0.99 to 0.95. With the probability of adjacent particle contact at 0.5, the probability of electrical continuity drops to 2.33×10^{-10}. Bed conductivity can be expected to reflect small changes in the degree of interparticulate contact when such contacts are highly probable. However, such measurements cannot be expected to reflect unambiguously bed packing densities since, for example, even a hexagonally close packed array of conducting spheres will be nonconducting if uniformly expanded by a minuscule amount.

Consider next the capacitance, C, of a parallel plate condenser which, by definition, is directly proportional to the relative permittivity, ϵ', of a dielectric material placed between the plates (5), as can be seen from:

$$C = \frac{\epsilon_0 \epsilon' A}{d} \qquad \text{(Eq. 1)}$$

where A is the plate area and d is the distance of separation between the plates. Capacitance changes resulting from short- and long-term permittivity changes of liquids, liquid suspensions, and gas–solid mixtures have been determined with the aid of microwave resonance chambers, capacitance bridges, and oscillating circuits (6–9). In contrast, very small, high frequency changes in capacitance were anticipated to occur in the present systems because of changes in the effective distance of separation of the plates, d, rather than changes in permittivity as such. The effective thickness of air separating the plates fluctuates because of changes in the spatial configuration and number of conducting spheres between the plates.

An electric oscillator in its simplest form consists of an inductance coil and a condenser connected end to end. Power losses due to resistance or radiation are compensated by a suitable driving circuit so as to maintain oscillation. The resonant frequency, f, of an electronic oscillator is a function of the capacitance, C, and is given by the expression (10):

$$f = \frac{1}{2\pi\sqrt{LC}} \qquad \text{(Eq. 2)}$$

where L is the inductance. By coupling a capacitor, having the particle bed as its dielectric, into such a circuit, the previously listed design requirements would be met. With the circuit tuned to a nominal frequency of several megahertz, small changes in bed configuration or packing density would result in substantial frequency changes that could be measured accurately. Moreover, rapid changes in capacitance would be readily detectable since the bed would be scanned several million times per second.

Care must be taken, however, when selecting the mean frequency since the permittivities of static dielectrics, air and the container in this case, are a function of frequency (Fig. 1). A frequency of 100 MHz was selected since it falls within both a frequency-independent permittivity region and the commercial FM broadcast band. Relatively inexpensive transmitting and receiving equipment capable of excellent response characteristics is available and can easily be adapted for these studies.

A parallel plate condenser was constructed with plates of a length and width so that a well-defined segment of the bed constituted a major portion of its dielectric medium.

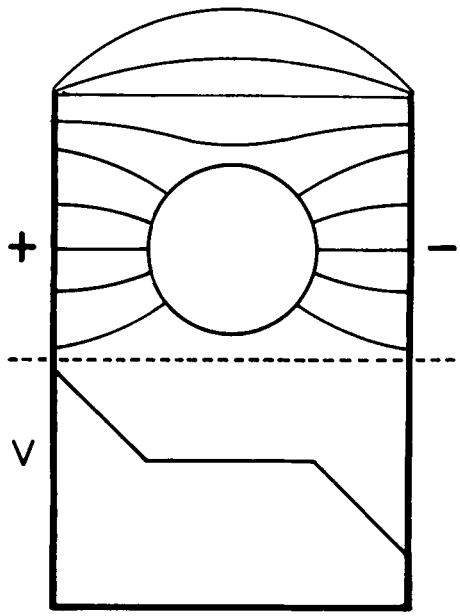

Figure 2—*Top: electrical field pattern for a conducting sphere between two parallel condenser plates. Bottom: potential drop through the center of the sphere and to the surfaces of the plates.*

Figure 2 illustrates the effects of a single spherical conducting particle on the electric field between parallel capacitor plates. The instantaneous effect, at a given time, of a dynamic bed of conducting particles on an otherwise uniform external electric field is vastly more complex. Assuming no electrical contact between conducting spheres comprising the bed, successful theoretical treatments of apparent permittivity are limited to solid–gas volume ratios of 0.25 and less (11). Since the volume fraction of solids in the present systems was estimated to range from approximately 0.5 to 0.7, calculation of capacitance was not feasible.

Further complications arise since interparticulate contacts lead to increased capacitance *via* networks of touching particles. Such clusters behave, in effect, as individual conducting particles of various sizes and configurations. Thus, each particle or electrically connected cluster of particles lying within the condenser alters the electrical field. Changes in bulk density due to bed dilation and changes in the electrically connected clusters due to particle motion, in combination, elicit changes in the effective thickness of the dielectric separating the plates and consequently produce corresponding capacitance changes.

As has been indicated, capacitance changes within an oscillating circuit result in a frequency modulated signal. This signal can be demodulated by an FM detector in standard fashion to yield a signal whose amplitude is proportional to the frequency shift and whose frequency corresponds to the rate (frequency) of modulation of the carrier frequency. Consider a carrier signal having a peak-to-peak amplitude of $2A$ and a phase angle as a function of time, t, as given by θ. The amplitude of the signal, y, is given by (12):

$$y = A \sin\theta = A \sin(\omega_0 t + \varphi) \qquad \text{(Eq. 3)}$$

$$\varphi = \alpha \int_{-\infty}^{t} m(t)\, dt \qquad \text{(Eq. 4)}$$

where ω_0 corresponds to the angular velocity of the electrical vector of the unmodulated carrier. A shift, φ, in phase angle is proportional to the time integral of a modulating signal, $m(t)$, through a constant, α, as shown in Eq. 4. The carrier frequency, f_0, and the instantaneous frequency, f, at any time, t, are given by the following relationships:

$$2\pi f = d\theta/dt = \omega_0 + d\varphi/dt \qquad \text{(Eq. 5)}$$

$$2\pi f_0 = \omega_0 \qquad \text{(Eq. 6)}$$

Thus, combining Eqs. 5 and 6 gives:

$$2\pi(f - f_0) = d\varphi/dt \qquad \text{(Eq. 7)}$$

Differentiating Eq. 2 with respect to capacitance yields:

$$\frac{df}{dC} = \frac{-C^{-3/2}}{4\pi L^{1/2}} \qquad \text{(Eq. 8)}$$

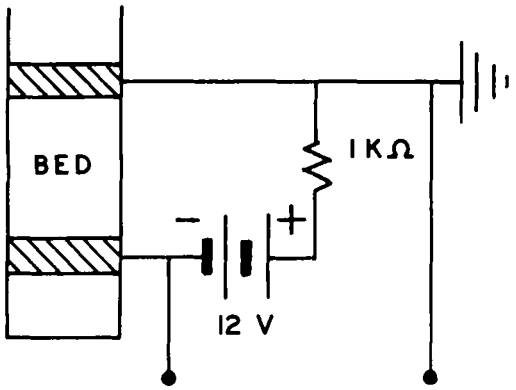

Figure 3—*Electrical circuit used for measurements of both bed voltage drop and conductance.*

If changes in capacitance are small in comparison with total capacitance, Eq. 8 reduces to:

$$\Delta f \cong -K\,\Delta C \qquad \text{(Eq. 9)}$$

where K is a proportionality constant. This condition is satisfied in commercial FM transmission and was valid in the present work.

Combining Eqs. 7 and 9 yields:

$$d\varphi/dt = 2\pi\,\Delta f = -2\pi K\,\Delta C \qquad \text{(Eq. 10)}$$

Integration of Eq. 10 and substitution into Eq. 4 yield the following relationship between capacitance changes and the nature of the modulating signal:

$$\int_{-\infty}^{t} m(t)\,dt \cong -(2\pi K/\alpha)\int_{-\infty}^{t} \Delta C\,dt \qquad \text{(Eq. 11)}$$

Thus, there is a direct relationship between changes in capacitance and the "audio" output of the FM receiver. The demodulation of the carrier signal, having a frequency modulated by the coupled bed capacitor, permits an unambiguous measurement of changes in relative capacitance.

EXPERIMENTAL

Materials and Equipment—A mechanical shaker, designed to generate nearly pure sinusoidal motion, provided the energy input into the particle beds. Previous studies (1–4) were conducted with this equipment and mode of agitation. In this study, the shaker frequency was held at 17.09 Hz while peak-to-peak amplitudes were varied from 0.254 to 0.508 cm.

A 2.54-cm i.d. segmented polycarbonate[1] tube, 20 cm long, was used as the bed container for the conductivity measurements. Segments were 1.6 cm in length; two were brass and served as electrodes. The particulate bed was approximately 12 cm deep, and the electrodes were centered 7.2 and 2.4 cm from the bottom of the bed. Capacitance experiments were conducted on beds of the same depth in 2.54- and 3.18-cm i.d. acrylic[2] tubes, 40 cm long. These tubes were fitted with plungers from the bottom capable of moving the particle bed vertically to position various bed regions within the sensing zone of the capacitor.

The parallel plate capacitor consisted of two copper sheets (1.5 × 7.5 cm) mounted 4.7 cm apart on a rectangular block of acrylic. The block had a central bore, allowing it to be positioned around the cylinder containing the bed. The monodispersed particle beds consisted of 304 g of chrome steel spheres[3], ranging from 0.238 to 0.556 cm in diameter.

Conductance and Capacitance Circuits—Conductance measurements were made using the circuit depicted in Fig. 3. A 12-v dc potential was placed across the bed with a 1-kohm resistor in series. The voltage drop across the bed was measured using a high impedance probe[4] through the dual-trace amplifier[5] of a 50-MHz oscilloscope[6] with a 7-nsec rise time. The probe was connected between the negative pole of the voltage supply and the bed, with the ground connector at ground potential as

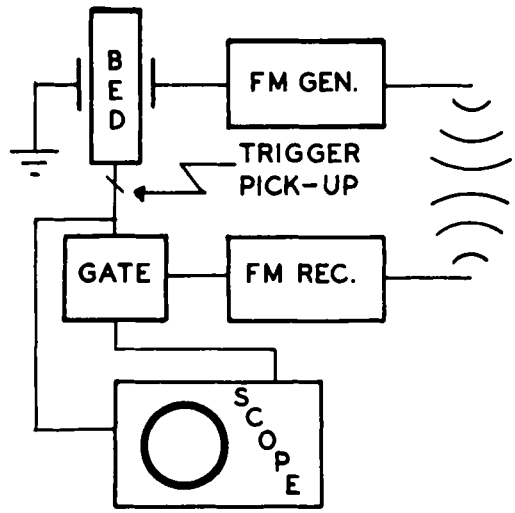

Figure 4—*Block diagram of circuit used for measurements of the particle bed relative capacitance.*

shown in Fig. 3. Current flow measurements were made on the same circuit as was used for voltage drop determinations, using an ac current probe[7] with a current flow amplifier[8]. The probe was placed over the conductor between the 1-kohm resistor and the positive pole of the power supply.

The circuitry employed to monitor capacitance changes is represented by Fig. 4. The bed condenser plates were extended horizontally beyond the diameter of the cylindrical bed container to minimize fringe effects. Acquisition of stray capacitance contributions from the mixer was avoided by placing a grounded aluminum shield in the proximity of the capacitor, isolating it from the shaker. The shield, capacitor, and bed container were mechanically connected and moved together with the same amplitude and frequency.

One plate of the capacitor was grounded, and the other was connected in parallel to the carrier oscillator of an FM transmitter[9]. The carrier frequency was tuned to approximately 100 MHz and broadcast. It was received by a standard FM radio ratio–detector receiver[10]. The resultant "audio" frequency output from the receiver was fed through a gating circuit (Fig. 5; see *Appendix*) and displayed on the oscilloscope. A magnetic pickup coupled with a magnet mounted on and revolving with the shaker flywheel provided a voltage pulse that served as a trigger signal for the oscilloscope and the gating circuit. This arrangement permitted the correspondence between the signal output and the shaker phase angle

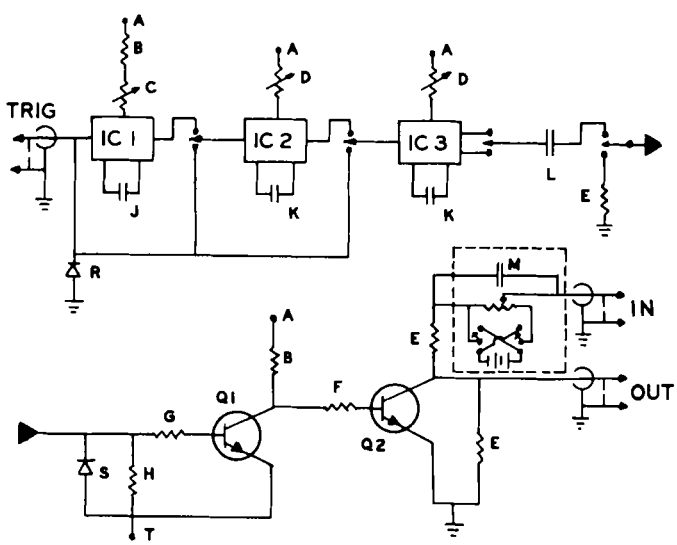

Figure 5—*Circuit diagram of the time delay triggered gate having a wide band frequency pass.*

[1] Lexan, General Electric Co.
[2] Lucite, du Pont.
[3] Atlas Ball Division, SKF Industries.
[4] P 6008 10X probe, Tektronix, Inc.
[5] Type 1A2 plug-in unit, Tektronix, Inc.
[6] Type 547, Tektronix, Inc.
[7] P 6021 current probe and termination, Tektronix, Inc.
[8] Type 134 current probe amplifier, Tektronix, Inc.
[9] Model 1G-37 FM stereo generator, Heath Co.
[10] Model AR-27 FM solid-state receiver, Heath Co.

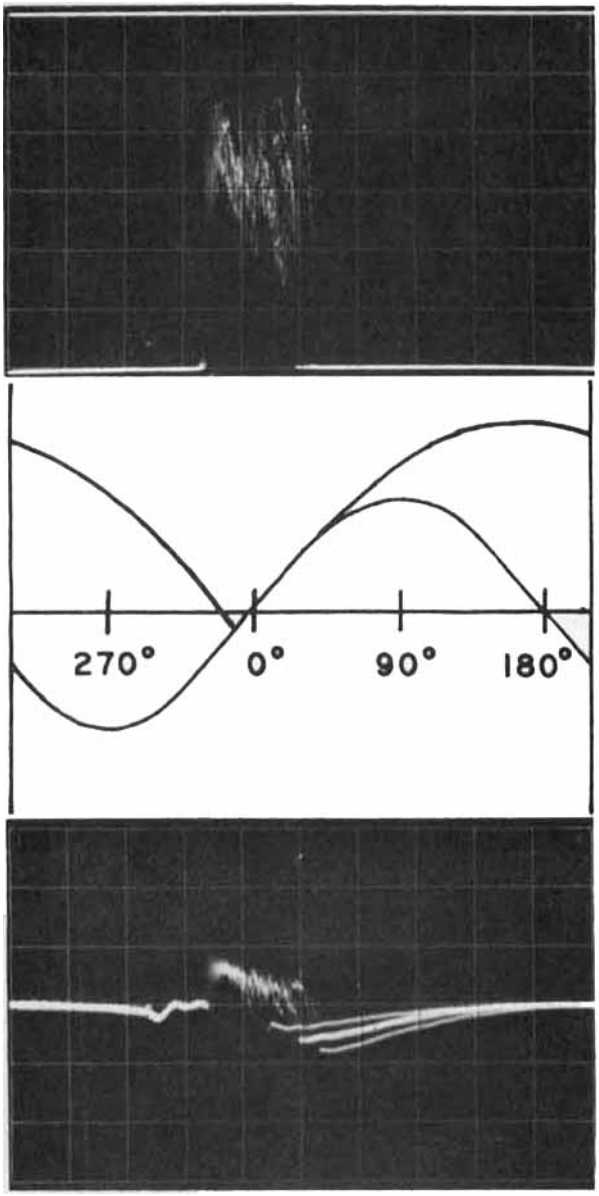

Figure 6—*Relationship of voltage drop (upper trace) and conductance (lower trace) to phase angles and projected free-flight behavior (center curve). Traces show eight cycles each of a bed composed of 0.397-cm diameter steel spheres shaken at a peak-to-peak amplitude of 0.442 cm. Sensitivities are −2 v/div and 1 mamp/div for the upper and lower traces, respectively.*

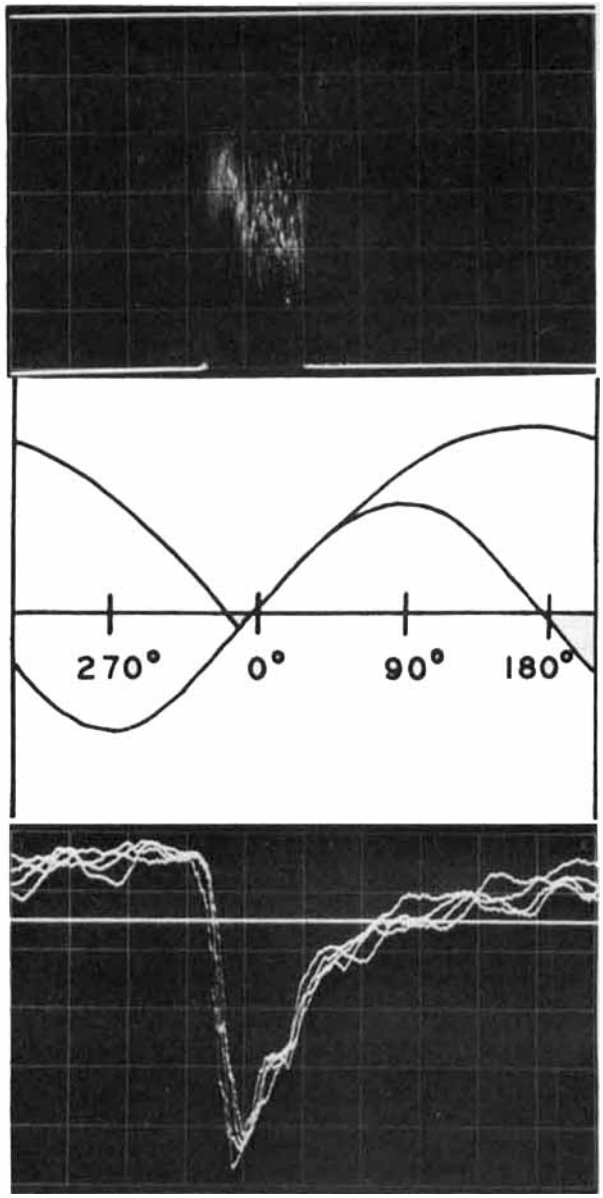

Figure 7—*Relationship of voltage drop (upper trace) and capacitance (lower trace) to phase angles and projected free-flight behavior (center curve). Traces show eight cycles each of a bed composed of 0.397-cm diameter steel spheres shaken at a peak-to-peak amplitude of 0.442 cm. Sensitivities are −2 v/div and 50 mv/div for the upper and lower traces, respectively.*

to be determined. The flywheel was calibrated so that the trigger magnet could be adjusted to produce a voltage pulse at any desired shaker phase angle.

FM receiver output signals were displayed as amplitude *versus* time after suitable amplification or were fed into a spectrum analyzer[11] and displayed on the scope as amplitude *versus* frequency spectra over selected frequency ranges. The frequency spectrum of the signal generated through FM modulation changed continuously during each shaking cycle. For this reason, the gating circuit was designed to permit frequency analysis over selected time intervals of various duration during each cycle.

Signal Processing—Voltages produced during conductance studies were measured using the dual-trace amplifier to display simultaneously the trigger and bed voltage signals. The sweep time of the scope was calibrated so that the full width of the CRT graticule corresponded to one cycle of the shaker. Voltage fluctuations were then displayed at a vertical deflection of 100–200 mv/graticule division. Current flow measurements differed from this system only in that the ac current probe and current probe amplifier were used in place of the voltage probe.

As mentioned previously, bed capacitance was a function of time over the period of a shaking cycle. The FM output signal was observed to vary in voltage by relatively large amounts in cycles (17.09 Hz) corresponding to the frequency of the shaker and to contain relatively high frequency, low amplitude voltage fluctuations. The former signal features varied only slightly from cycle to cycle and were not analyzed for their frequency content.

The FM receiver was tuned to the 100-MHz carrier frequency of the transmitter, using a 1-kHz audio reference signal available in the stereo generator used for transmission. Following tuning, the reference signal was turned off and shaking was begun. Observed audio outputs were thus solely due to fluctuations in capacitance due to the bed. With an open gate, calibration of the graticule was carried out to portray one cycle of agitation in the same manner as described for conductance measurements. All measurements were made with the capacitor centered 5 cm above the bottom of the particle bed.

Higher frequency components of the FM output signal (100 Hz–10 kHz) were examined over the entire agitation cycle. Measurements were

[11] Type 1L5, Tektronix, Inc.

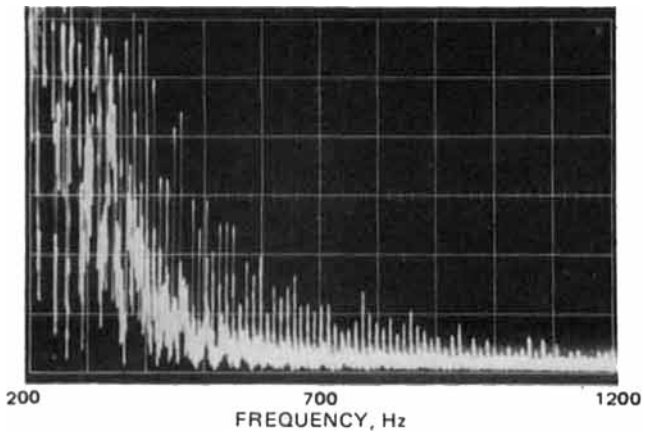

Figure 8—*Spectrum of capacitance changes over the frequency range of 200–1200 Hz. The bed was composed of 0.397-cm diameter steel spheres shaken at a peak-to-peak amplitude of 0.442 cm. Sensitivity is 0.4 v/div.*

made by two procedures. In the first, the spectrum analyzer was set to scan continuously from low to high frequency at rates of 100–200 Hz/sec with a dispersion of 100 Hz/horizontal scale division. Therefore, a single sweep of the CRT beam across the 10 divisions of the graticule provided a frequency scan over a range of 1 kHz. The interval of 200–1200 Hz was selected as being characteristic of this general frequency range, since signal amplitudes were very low above this range.

The second procedure for spectrum analysis was designed to provide information over limited agitation phase intervals and was a modification of the method described for full cycle scans. The gate was set to open for a predetermined 36° interval during each shaking cycle and to pass no signal during the remaining fraction of the cycle. A highpass filter[12] was inserted into the circuit between the FM receiver and the oscilloscope. This filter removed frequencies below 100 Hz and served to eliminate difference frequencies originating with the 17-Hz chopping action of the gate. As before, the spectrum analyzer was set to scan from 200 to 1200 Hz, providing spectral information on the cycle time segment selected. This procedure was used successively to examine piecewise the full shaking cycle. Intensity was displayed as root mean square (rms) voltage at a given frequency, and the spectrum analyzer was frequency and amplitude calibrated using a signal generator[13] and a frequency counter[14].

Conductance and capacitance measurements were recorded on high contrast film[15] using an optically projected graticule. Exposures were made of both single and multiple scans, some of which are included in Figs. 6–9.

RESULTS AND DISCUSSION

The concept of the free-flight trajectory of a nonrebounding particle subjected to vertical harmonic shaking is useful as an idealized model in considering the motion of a particulate bed subjected to a similar agitation (3, 13, 14). In this model, the hypothetical nonrebounding particle follows the vertical sinusoidal motion of the shaker until the downward acceleration of the shaker exceeds that of gravity. At this point, the particle lifts free and follows a free-flight vertical trajectory until it again contacts the shaker. This behavior is illustrated in Fig. 10, which depicts the free-flight trajectories for particles subjected to the same amplitudes as the particle beds under investigation. For comparison, the individual trajectories are drawn to the scale of a single shaker amplitude. Peak-to-peak agitation amplitudes of 0.254, 0.358, 0.442, and 0.508 cm were sufficiently low that bed liftoff and landing fell within a single cycle.

One can obtain an approximate view of general bed behavior by analyzing various periods of the free-flight trajectory. After takeoff, the bed expands rapidly; it then remains more or less in a uniformly expanded state. As the shaker begins its upward movement, the bed quickly collapses and is caught up by the ascending base of the chamber. The actual time required for maximal bed compression also depends on the rate of

[12] Model F 250, Allen Avionics Co.
[13] Model 144 HF sweep generator, Wavetek Co.
[14] Model 390 digital multimeter, Anaconic, Inc.
[15] Type 127, Polaroid.

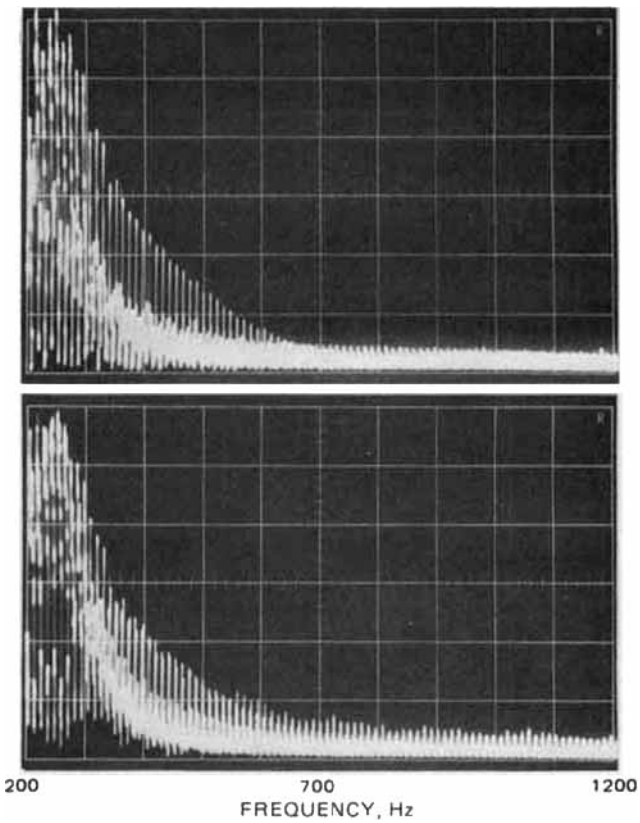

Figure 9—*Spectra of capacitance changes over the frequency range of 200–1200 Hz for 36° phase intervals. Phase intervals are 65–101° for the upper trace and 245–281° for the lower trace, and sensitivities are 50 and 80 mv/div, respectively.*

kinetic energy decay by frictional, intraparticulate acoustic, and other losses. The minimum porosity, corresponding to maximal compression, exists only for an instant during each cycle.

The relationship of voltage drop and current flow traces to the free-flight model is shown in Fig. 6. These tracings indicate the period during which the bed is conducting. Amplification settings were chosen for convenient display. Baseline distortion of the lower trace is an artifact from the current probe. Loss of conduction coincides with the expected time at which bed expansion begins, and its reestablishment occurs near the expected time at which bed compression begins.

A preliminary series of measurements was made at various bed locations and indicated that the upper bed expanded first and was the last to be compressed, whereas the lower bed was expanded for the shortest period of time. This behavior is indicative of frictional wall effects, and measurements of its magnitude are of potential value in quantitating particle–wall interactions.

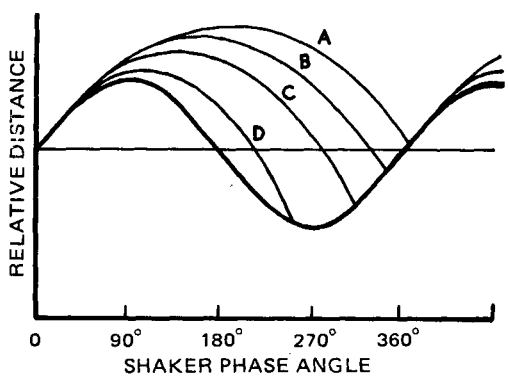

Figure 10—*Free-flight trajectories for a nonrebounding particle subjected to vertical harmonic shaking of various amplitudes. Trajectories are each drawn to the scale of the sine wave. Trajectories are shown for peak-to-peak shaker amplitudes of 0.508 (A), 0.442 (B), 0.358 (C), and 0.254 (D) cm.*

Table I—Shaking-Phase Angles of Bed Conductance Changes

Shaker Amplitude, cm	Sphere Diameter, cm	Phase Angle of Conduction, Ending/Onset	Relative Phase Angle[a] of Particle Bed, Liftoff/Landing
0.254	0.238	31°/262°	6°/−15°
	0.397	51°/239°	−14°/8°
	0.556	41°/254°	−5°/−7°
	0.635	41°/260°	−5°/−13°
0.358	0.238	32°/295°	−7°/9°
	0.397	48°/301°	−23°/3°
	0.556	33°/306°	−8°/−2°
	0.635	38°/306°	−13°/−2°
0.442	0.238	33°/311°	−12°/30°
	0.397	43°/309°	−22°/32°
	0.556	26°/327°	−4°/13°
	0.635	3°/341°	18°/0°
0.508	0.238	33°/353°	−16°/11°
	0.397	31°/357°	−13°/7°
	0.556	34°/344°	−17°/20°
	0.635	20°/348°	−3°/16°

[a] Phase angles of apparent bed liftoff and landing, based on measurements of bed conductance, expressed relative to liftoff and landing phase angles as predicted by free-flight calculations.

Table II—Shaking-Phase Angles of Characteristic Capacitance Changes of Particulate Beds

Shaker Amplitude, cm	Sphere Diameter, cm	Phase Angle at Which Slope Changes[a]	Phase Angle	
			Minimum Capacitance	Maximum Capacitance
0.254	0.238	44°	230°	274°
	0.397	53°	216°	275°
	0.556	37°	188°	270°
	0.635	45°	157°	271°
0.358	0.238	42°	303°	324°
	0.397	43°	272°	322°
	0.556	39°	284°	315°
	0.635	35°	223°	330°
0.442	0.238	35°	306°	353°
	0.397	44°	271°	352°
	0.556	45°	293°	347°
	0.635	40°	250°	322°
0.508	0.238	29°	341°	12°
	0.397	39°	325°	1°
	0.556	30°	326°	4°
	0.635	34°	310°	351°

[a] The phase angle at which the rate of decrease of capacitance decreases, resulting in a slope change in the curve and reflecting a change in bed behavior.

Shaker phase angles corresponding to the termination and onset of bed conductance are listed in Table I. The ascending neutral position of the shaker, midway between its lower and upper extremes of motion, is the designated reference point for phase angle measurements. This reference point is used for both Tables I and II and is the point during the upward motion of the shaker when its acceleration is zero. Identical data on this behavior were obtained from measurements of either amperage or voltage drop; however, voltage measurements were largely used because of the relative ease of reading the scope. Four monodispersed systems were examined at each agitation amplitude.

Column three in Table I consists of number pairs, the first number indicating the phase angle at which conduction was terminated and the second number indicating the angle where conduction was resumed. Thus, the interval between these angles was the time period during which the bed was in an expanded state sufficient to prevent conduction.

Column four in Table I also consists of number pairs, representing the differences in phase angles between measured and predicted bed liftoff and landing. For example, a "0" means that the measured (*via* conductance) and the predicted (*via* the free-flight model) phase angles were the same. If a drop in bed resistance appeared prior to the predicted time, it is indicated by a positive angle; conversely, negative angles signify delayed bed response times. In most cases, bed expansion began slightly later than predicted by the free-flight model. Bed contractions tended to begin earlier than predicted by the model; however, this result is not unexpected since a late liftoff would result in a lower projection velocity.

Figure 7 illustrates the relationships typically observed between the bed voltage drop and the FM receiver output in comparison with the free-flight model. Several features of these scans can be related to the dynamic behavior of the particle bed. The establishment of interparticulate contact, as evidenced by a marked decrease in bed resistance, occurred within the time period when capacitance was increasing abruptly. Keeping in mind the relationship expressed in Eq. 9, such an increase in capacitance would result in lowered carrier frequency and decreased receiver output voltage. This relationship is also dependent on the number of signal inversions occurring in the amplification stages in the receiver.

The phase relationship was established from the receiver circuit schematic and verified experimentally in this study. Consequently, negative FM output voltages signify increased capacitance, and the converse is true for positive signals. The point of greatest capacitance fell very close to the time of predicted complete bed collapse. The characteristic break in the slopes of the capacitance curves coincides closely with a loss of bed conductivity and the free-flight liftoff time. Capacitance decreases gradually to a minimum just before bed collapse begins.

To avoid signal distortions, it was essential that the response of the audio amplifier was linear over the frequency range of interest and, in particular, down to the 17-Hz frequency of the shaker. This response was verified experimentally to hold at the amplification levels employed.

These events are well correlated with the idealized free-flight behavior for the monodispersed system shown; however, segregation behavior of binary systems containing this size particle as the large component showed little or no wall effects (2). Where such effects do occur, predictions of bed behavior based on free-flight considerations are of little value, and measurements of relative bed conductance and capacitance as outlined are necessary. Phase angles corresponding to the times of minimum and maximum capacitance are listed in the last two columns of Table II for various shaker amplitudes and particle sizes. As stated earlier, changes in capacitance can result from either of two mechanisms: a change in the relative bed density or a change in the number or density of interparticulate contacts within the bed. Obviously, both mechanisms must be considered when the data are interpreted.

Decreasing capacitance, for example, can be due to bed expansion and/or loss of interparticulate contact. The lowest trace in Fig. 7 shows that the capacitance decreases in two stages: an initial rapid decrease followed by a more gradual decrease. This behavior is shown by the rising right-hand portion of the trace. The phase angle at which the rate of capacitance decrease changes (decreases) is listed in column three of Table II. The time of this change of slope is shown in Fig. 7 to correspond closely with the time at which conduction ceases, as previously indicated. The initial rapid decrease in capacitance was likely due to a reduction in both cluster size and bed density, while the slower capacitance drop was due primarily to a continuing decrease in bed density.

Before considering the implications of frequencies in the range of 200–1200 Hz in the FM audio signal, it is important to examine the operating characteristics of the spectrum analyzer. The analyzer used was of the real-time type, which performed a continuous frequency analysis of the incoming signal. This examination does not constitute a Fourier analysis but instead indicates the composition of the signal at a given time during the shaking cycle. This composition was verified experimentally by examining single frequency, sinusoidal signals pulsed at 17 Hz by the gate. As mentioned earlier, a highpass filter was used to eliminate the 17-Hz waveform from the signal prior to analysis and also served to eliminate difference frequencies that otherwise originated with the 17-Hz chopping action of the gate. Since the amplitude of these higher frequencies was substantially less than that of the 17-Hz waveform, they are not readily apparent in Fig. 7.

The presence of these higher frequency components in the FM receiver output signal is illustrated by the typical spectrum shown in Fig. 8. Each spike in the figure represents the amplitude–time relationship over the period of a single shaking cycle. The frequency being scanned by the spectrum analyzer, as shown in Fig. 8, is continuously increasing from left to right at the rate of approximately 12 Hz/cycle. The pictured decrease in the magnitude of the capacitance changes at the higher frequencies was characteristic of all systems examined. Except for amplitude scaling, beds contained in the 2.54- and 3.18-cm tubes behaved identically.

Capacitance changes in this frequency range probably are a consequence of correspondingly short-lived changes in the configurations of particle clusters and in particle contact numbers. Such fluctuations at the particulate level are the result of particulate motion. For this reason, it is expected that useful information can be obtained by examining this frequency range over various shaking phase intervals. With the gating technique previously described, the relative magnitude of capacitance changes were analyzed as a function of frequency over various segments of the shaking cycle. Figure 9 shows spectra of 0.397-cm particles, at a

shaking amplitude of 0.442 cm, over two different 36° phase intervals, corresponding to periods of increasing bed expansion and of maximum bed expansion.

Two features of such spectra are worthy of note. As a bed expands, a given particle velocity distribution can be expected to result in increasingly lower frequency signals as interparticulate distances increase. The converse, of course, occurs during bed contraction. Thus, relative shifts in intensity *versus* frequency result from changes in bed density alone. The overall or average changes in intensity of these spectra are indicative of the relative intensities of the particulate motions they reflect and provide a relative measure of particulate kinetic energy.

CONCLUSIONS

It is generally recognized that the principal factors governing the rates of free-flowing solids mixing and segregation and their underlying mechanisms are the degree of bed dilation and the velocity distribution of the component particles (15). In many solids mixing or conveying operations, particle motion and bed dilation are strongly coupled and are the inseparable consequences of vibration and/or shear. The mechanisms by which both mixing and segregation occur under these forms of energy input are incompletely understood. Theories of these kinetic processes are commonly subjected to critical experimental verification based on their predictive capabilities; however, direct experimental evidence concerning other aspects of particle bed dynamics is often lacking.

The rates at which segregation and mixing occur within a vibrated bed are thought to vary considerably during each shaking cycle. Also, it is to be expected that these two processes do not necessarily increase and decrease in their intensities simultaneously or in phase. For these reasons, the kinetic behavior of mixing and segregation in vibrated particulate beds, as typically reported, reflects time-averaged rates that yield apparent rate constants representing minimum absolute values. Phase angles (Tables I and II) corresponding to various features of bed behavior can be used to estimate the time periods during each cycle when mixing and/or segregation primarily occur. Refinement of apparent rate constants to reflect more accurately their virtual values is, therefore, possible.

Data on the higher frequency fluctuations in capacitance that reflect movements of single particles or small clusters of particles may be applied to explain the magnitudes of the adjusted apparent rate constants. The details of such correlations will follow in subsequent reports. While the particles studied here have been idealized in size and shape, the methods discussed may be applied directly to any system of conducting particles and, excluding conductance measurements, can be arranged to apply to nonconducting systems.

APPENDIX

The gating circuit diagrammed in Fig. 5 was designed to pass signals having component frequencies ranging from dc to 50 kHz without distortion. Signals in this band were attenuated uniformly by the gate by a factor of 0.50. By adjusting the variable resistors at IC1 and IC2, the gate could be set to open, following the trigger pulse, after time delays of up to 60 msec. The variable resistor at IC3 permits adjusting the "open" phase of the gate for 2–30 msec.

Integrated circuits, IC1, IC2, and IC3, are type SN74121 monostable multivibrators and the high current switches, Q1 and Q2, are type 2N3642. A list of other components and power requirements as coded in Fig. 5 follows: A, 5-v dc supply; B, 12 kohm; C, 2 kohm; D, 35 kohm; E, 100 kohm (matched); F, 590 ohm; G, 39 kohm; H, 150 kohm; J, 2 μF; K, 1 μF; L, 10 μF; M, 100 pF; R, IN6424; S, IN457; and T, −4.5-v dc supply.

REFERENCES

(1) J. L. Olsen and E. G. Rippie, *J. Pharm. Sci.*, **53,** 147 (1964).

(2) E. G. Rippie, J. L. Olsen, and M. D. Faiman, *ibid.*, **53,** 1360 (1964).

(3) M. D. Faiman and E. G. Rippie, *ibid.*, **54,** 719 (1965).

(4) E. G. Rippie, M. D. Faiman, and M. K. Pramoda, *ibid.*, **56,** 1523 (1967).

(5) J. C. Anderson, "Dielectrics," Chapman and Hall, London, England, 1964.

(6) "High Frequency Dielectric Measurement," J. Chamberlain and G. W. Chantry, Eds., I. P. C. Science and Technology Press, Surrey, England, 1973, pp. 12, 28, 140.

(7) J. M. Dotson, J. H. Holden, C. B. Seibert, H. P. Simons, and L. D. Schmidt, *Chem. Eng.*, **56,** 129 (1949).

(8) P. J. Bakker and P. M. Heertjes, *Br. Chem. Eng.*, **3,** 240 (1958).

(9) D. Geldart and J. R. Kelsey, *Powder Technol.*, **6,** 45 (1972).

(10) V. A. Suprynowicz, "Introduction to Electronics for Students of Biology, Chemistry, and Medicine," Addison-Wesley, Reading, Mass., 1966, pp. 91, 316.

(11) L. K. H. van Beek, *Prog. Dielectr.*, **7,** 105 (1967).

(12) A. B. Carlson, "Communications Systems," 2nd ed., McGraw-Hill, New York, N.Y., 1975, p. 220.

(13) H. Takahashi, A. Suzuki, and T. Tanaka, *Powder Technol.*, **2,** 65 (1969).

(14) W. A. Gray and G. T. Rhodes, *ibid.*, **6,** 271 (1972).

(15) E. G. Rippie, in "The Theory and Practice of Industrial Pharmacy," 2nd ed., L. Lachman, H. A. Lieberman, and J. L. Kanig, Eds., Lea & Febiger, Philadelphia, Pa., 1976, pp. 498–500.

ACKNOWLEDGMENTS

Presented in part at the Basic Pharmaceutics Section, APhA Academy of Pharmaceutical Sciences, Atlanta meeting, November 1975.

Oxidative Degradation of Pharmaceutically Important Phenothiazines I: Isolation and Identification of Oxidation Products of Promethazine

W. J. M. UNDERBERG

Received July 12, 1977, from the *Farmaceutisch Laboratorium, Rijksuniversiteit Utrecht, Catharijnesingel 60, Utrecht, The Netherlands.* Accepted for publication November 17, 1977.

Abstract □ The thermal degradation of promethazine in water in the presence of oxygen was studied. After degradation, the products were isolated by TLC. Identification was carried out by comparison of the isolated compounds with reference compounds. Melting points, spectral data, and polarographic and chromatographic behavior were compared. The following products were identified: 10-methylphenothiazine, phenothiazine, 3*H*-phenothiazine-3-one, phenothiazine 5-oxide, promethazine 5-oxide, 7-hydroxy-3*H*-phenothiazine-3-one, acetaldehyde, formaldehyde, and dimethylamine.

Keyphrases □ Promethazine—oxidative thermal degradation products isolated and identified □ Oxidation—promethazine, thermal degradation products isolated and identified □ Degradation, oxidative thermal—promethazine, products isolated and identified □ Phenothiazines—promethazine, oxidative thermal degradation products isolated and identified □ Antiemetics—promethazine, oxidative thermal degradation products isolated and identified

The separation of phenothiazines and their oxidation products, mostly by TLC or paper chromatography, was described previously (1–10). Details were given about the identity of the products obtained, but the purity of the isolated fractions was unknown. Moreover, many reports (11–23) described the separation of different phenothiazines, also by TLC, paper chromatography, and GLC. These data were used for the development of a method to separate promethazine and its degradation products.

EXPERIMENTAL

Materials—Since promethazine hydrochloride[1] gave a single spot with several TLC solvent systems, it was used as supplied, as were 10-methylphenothiazine[2], phenothiazine[3], 3*H*-phenothiazine-3-one[2], 10-methylphenothiazine 5-oxide[2], and promethazine 5-oxide[1]. Phenothiazine 5-oxide was synthesized according to Pummerer and Gassner (24); 7-hydroxy-3*H*-phenothiazine-3-one was synthesized according to Vidal as modified by Inukai and Ueda (25). All other materials were reagent grade, and deionized water was used throughout.

Methods—Promethazine hydrochloride, 500 mg, was dissolved in 100 ml of water, and oxygen was bubbled through the solution for 30 min. The solution was placed into a screw-capped bottle and kept at 65° in the dark for 48 hr. After cooling to room temperature, the sample was transferred into a separator, made alkaline with 4 *N* NaOH, and extracted with dichloromethane. The remaining water layer was made acid with 4 *N* H_2SO_4 and extracted with dichloromethane.

Both organic phases were applied to a silica gel[4] TLC plate, 0.25 mm thick (26), as zones 15 cm long × 1 cm wide. Dichloromethane was evaporated by heating the plate at the lower side. After equilibration of the plate with the vapor of the solvent for 10 min, the chromatogram was developed for 15 cm, using acetone–6 *N* ammonia (100:2) as the solvent.

During the procedure, the system was protected from light to avoid uncontrolled degradation. After development, the zones on the chromatogram were detected in UV light (254 nm). All compounds except H were derived from the alkaline dichloromethane fraction. Compound H was derived from the acidic dichloromethane fraction.

For the identification of the degradation products, the zones were extracted with either dichloromethane or 96% ethanol. Identification was carried out using data obtained from TLC, GLC, spectroscopy (UV, IR, and mass[5]), polarography, and melting points. For the isolation of Compounds A_1 and A_2, zone A was extracted with dichloromethane. The extract was applied onto a silica gel plate, and the chromatogram was developed for 15 cm with *n*-hexane–chloroform (75:25). Both zones obtained were extracted with dichloromethane, recrystallized from acetone–water (1:1), and dried over 96% H_2SO_4 under reduced pressure in the dark.

Some volatile degradation products were isolated by precipitation as the 2,4-dinitrophenylhydrazones (aldehydes) or 3,5-dinitrobenzamides (amines) (27). Purification was carried out by recrystallization from ether and water. Identification of the volatile compounds was completed using TLC, GLC, spectroscopy, and melting-point data. Moreover, the sample was distilled, and the distillate was subjected to color reactions.

RESULTS AND DISCUSSION

Nine zones could be observed on the chromatogram obtained (Table I). Zone D has the same R_f value as promethazine, zone B was red, and zone H was violet.

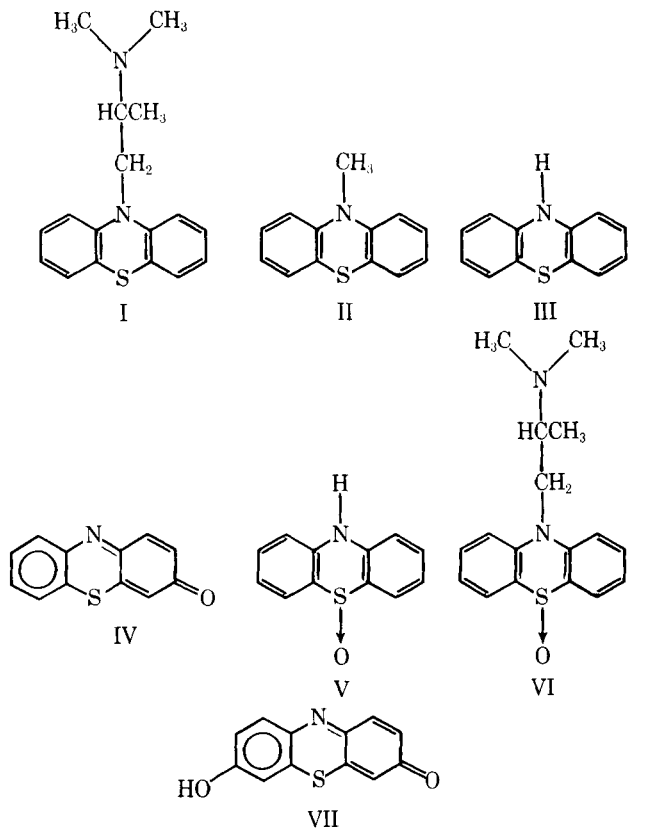

[1] Rhône Poulenc, Paris, France.
[2] Provided by Dr. C. D. M. Ten Berge, Groningen, The Netherlands.
[3] Merck-Schuchardt, Munich, West Germany.
[4] GF 254, E. Merck, Darmstadt, West Germany.
[5] Mass spectra were recorded at the Analytisch-Chemisch Laboratorium, Rijksuniversiteit Utrecht, The Netherlands.

0022-3549/78/0800-1128$01.00/0
© 1978, American Pharmaceutical Association

Table I—TLC [a] Separation of Promethazine and Degradation Products

Zone[b]	R_f	Color in Daylight
A	0.80	Colorless
B	0.72	Red
C	0.61	Colorless
D	0.48	Colorless
E	0.38	Colorless
F	0.28	Colorless
G	0.19	Colorless
H	0.10	Violet
I	0.00	Brownish

[a] The sorbent was silica gel, the solvent was acetone–6 *N* ammonia (100:2), and detection was by UV light (254 nm). [b] All zones except H were extracted from an alkaline medium; H was extracted from an acidic medium.

Table II—R_f Values [a] of Phenothiazone, 10-Methylphenothiazine, and Fraction A

Solvent	Phenothiazine[b]	10-Methylphenothiazine	Fraction A A_1	Fraction A A_2[b]
Acetone–6 *N* ammonia (100:2)	0.76	0.76	0.76	0.76
n-Hexane	0.03	0.17	0.17	0.03
Chloroform	0.65	0.79	0.79	0.65
Toluene	0.54	0.71	0.71	0.54
Dichloromethane	0.81	0.85	0.85	0.81
n-Hexane–acetone (9:1)	0.20	0.42	0.42	0.20
n-Hexane–chloroform (75:25)	0.19	0.44	0.44	0.19

[a] The sorbent was silica gel. [b] Turned green under light.

Table III—R_f Values [a] of 3*H*-Phenothiazine-3-one and Fraction B

Solvent	3*H*-Phenothiazine-3-one	Fraction B
Acetone	0.64	0.64
Acetone–6 *N* ammonia (100:2)	0.69	0.69
Methanol	0.67	0.67
Methanol–6 *N* ammonia (100:2)	0.67	0.67
96% Ethanol	0.61	0.61
96% Ethanol–6 *N* ammonia (100:2)	0.62	0.62
Chloroform	0.17	0.17
n-Hexane	0.00	0.00

[a] The sorbent was silica gel.

Compound D—The R_f values of Compound D in several TLC systems were identical with those of promethazine (I) in the same systems. In all cases, only one spot was observed. The UV spectrum of D in 1 *N* HCl and IR spectrum of D in sodium chloride were identical with those of I in the same media.

Compound A_1—Table II shows that R_f values of Compound A_1 and 10-methylphenothiazine (II) were the same. The melting point of A_1 was 107°, and a mixture of equal parts of A_1 and II melted at 107°.

The UV spectra of A_1 and II in dichloromethane were identical, with a maximum at 255 nm. The IR spectra of both compounds in sodium chloride were also identical. The parent peak of A_1 in the mass spectrum was *m/e* 213, corresponding to the formula $C_{13}H_{11}NS$. The data showed A_1 to be II.

Compound A_2—The R_f values of Compound A_2 and phenothiazine (III) in several chromatographic systems were the same (Table II). The melting point of A_2 was 178–182°, while a mixture of A_2 and III melted at 178–181°.

The UV spectra of A_2 and III in dichloromethane were identical, with a maximum at 255 nm. The IR spectra of both compounds were also identical. The mass spectrum of A_2 showed a parent peak at *m/e* 199, corresponding to the formula $C_{12}H_9NS$. These data led to the conclusion that A_2 was III.

Compound B—Compound B was red, as is 3*H*-phenothiazine-3-one (IV), and was identified according to Roseboom and Fresen (28). The R_f values of B and IV in several systems were identical (Table III). The melting point of B was 146–150°, and the melting point of a mixture of equal parts of B and IV was 149–155°. (The melting point of B was a few degrees below the melting point of IV. The fraction could not be purified by recrystallization.)

Table IV—R_f Values of Phenothiazine 5-Oxide, 10-Methylphenothiazine 5-Oxide, and Fraction C

Sorbent	Solvent	Phenothiazine 5-Oxide	10-Methylphenothiazine 5-Oxide	Fraction C
Silica gel	Acetone–6 *N* ammonia (100:2)	0.59	0.59	0.59
Silica gel	Acetone–water (95:5)	0.75	0.75	0.75
Silica gel	Acetone	0.57	0.57	0.57
Silica gel	Acetone–dichloromethane (6:4)	0.40[a]	0.40[a]	0.40[a]
Alumina, basic	Chloroform	0.23	0.67	0.23

[a] Tailing.

Table V—R_f Values [a] of Promethazine 5-Oxide and Fraction F

Solvent	Promethazine 5-Oxide	Fraction F
Acetone–6 *N* ammonia (100:2)	0.21	0.21
1-Butanol–acetic acid–water (88:5:7)	0.14	0.14
Acetone–water–acetic acid (5:4:1)	0.33	0.33
3 g of ammonium acetate in 20 ml of water and methanol to 100 ml	0.35	0.35

[a] The sorbent was silica gel.

The UV and visible light spectra of B and IV in water were identical, with maxima at 530, 385, and 289 nm. Shoulders were observed at 269 and 238 nm. The IR spectra of both compounds were also identical, with a strong maximum at 1620 cm^{-1} due to the C=O group. The mass spectrum showed a parent peak at *m/e* 213, corresponding to the formula $C_{12}H_7NOS$. These data showed B to be IV.

Compound C—The melting point of Compound C was 257–258.5°. Its UV spectra in acidic and alkaline ethanolic media were identical. The IR spectrum in sodium chloride showed a strong maximum at 973 cm^{-1}. The mass spectrum showed a parent peak at *m/e* 215. Calculation of an exact mass yielded a value of *m/e* 215.0401, corresponding to the formula $C_{12}H_9NOS$. Compound C could be reduced at the dropping mercury electrode with an $E_{1/2}$ of −590 mv *versus* the saturated calomel electrode in 96% ethanol–4 *N* H_2SO_4 (25:75).

The data obtained from the mass spectrum showed C to be an oxidation product of phenothiazine containing one oxygen atom. The data from the UV spectra showed that no hydroxyl group was present, while the IR spectral data indicated the possible presence of an SO group with a maximum at about 1000 cm^{-1} (29). The polarographic behavior of C also indicated the presence of a reducible SO group. The melting point of phenothiazine 5-oxide (V) is 257–258° (30), which was in good agreement with the melting point of C. The mixed melting point of C and V was also 258°. The R_f values of C and V (Table IV) were identical, while 10-methylphenothiazine 5-oxide had a different R_f value in one system. All these data showed C to be V.

Compound F—Zone F showed the strongest absorption under UV light (254 nm) and contained probably the main degradation product. Compound F and promethazine 5-oxide (VI) had the same R_f values in several chromatographic systems (Table V). Compound F melted at 120°, and a mixture of F and VI (1:1) melted at 119–120°.

The UV absorption spectra of F and VI in water were identical, with maxima at 334, 293, 268, and 234 nm, in agreement with the values of Kofoed *et al.* (31). The IR spectra of both compounds were identical as well, with a maximum at 1020 cm^{-1} due to the SO group (29). The mass spectrum of F showed a parent peak at *m/e* 300 in agreement with the formula $C_{17}H_{20}N_2OS$. All these data led to the conclusion that F and VI were identical.

Compound H—After extraction of the original sample in an alkaline medium, the remaining water phase had a violet color, which turned red when acidified. The dye was extracted from the acidic medium with dichloromethane. Chromatographic analysis showed that only one compound was obtained. The melting point of H was above 360°.

Absorption spectra of H in different solvents showed that, when the solutions were made alkaline, the absorption maximum shifted from about 510 to about 600 nm (Table VI) while the extinction of the ethanolic

Table VI—Absorption Maxima of Fraction H in UV and Visible Light

Solvent	λ_{max}, nm
Water, acidic[a]	244, 286, 502
Water, alkaline[b]	278, (510), 590
96% Ethanol, acidic[a]	246, (275), 429, 515
96% Ethanol, alkaline[b]	231, 277, 309, (565), 600
Acetone, acidic[a]	510[c]
Acetone, alkaline[b]	565, 609[c]

[a] Three milliliters of solution plus 1 drop of 6 *N* HCl. [b] Three milliliters of solution plus 1 drop of 6 *N* NaOH. [c] Spectra were recorded in the 330–700-nm region. Numbers in parentheses are shoulders.

Table VII—R_f Values of 7-Hydroxy-3*H*-phenothiazine-3-one and Fraction H

Sorbent	Solvent	7-Hydroxy-3*H*-phenothiazine-3-one	Fraction H
Silica gel	Acetone–water (95:5)	0.42	0.42
Silica gel	Acetone–6 *N* ammonia (100:2)	0.06	0.06
Silica gel	Acetone–6 *N* ammonia (90:10)	0.56	0.56
Silica gel	*n*-Hexane–chloroform (75:25)	0.00	0.00
Alumina, basic	Acetone–6 *N* ammonia (90:10)	0.50	0.50
Alumina, basic	Acetone–water (90:10)	0.37	0.37
Alumina, basic	1. Benzene–acetone (95:5)[a] 2. Benzene–acetone–acetic acid (95:5:5)[a]	0.24	0.24

[a] Subsequent development.

Table VIII—R_f Values[a] of the 2,4-Dinitrophenylhydrazones of Formaldehyde (A), Acetaldehyde (B), and Some Degradation Products of Promethazine (C)

Solvent	A	B	C
Nitrobenzene–cyclohexane (1:2)	0.34	0.43	0.34 0.43
Nitrobenzene–chloroform–*n*-hexane (1:2:8)	0.37	0.49	0.37 0.49

[a] The sorbent was alumina GF 254 (E. Merck, Darmstadt, West Germany).

solution increased by a factor of 4.4. Moreover, the acetone solution showed an intense fluorescence. The mass spectrum showed a parent peak at *m/e* 229, corresponding to the formula $C_{12}H_7NO_2S$.

The data obtained led to the conclusion that the compound was an acid, probably a phenol. Moreover, the spectra indicated a similarity in structure between Compound H and 3*H*-phenothiazine-3-one (IV). Some investigators (25, 32, 33) discussed a compound, 7-hydroxy-3*H*-phenothiazine-3-one (VII), with the same spectral properties and melting point. The R_f values of H and VII in several chromatographic systems were identical (Table VII). The spectra in the UV and visible light region, as well as the IR spectra of both compounds, were identical. The data obtained showed H to be VII.

Compounds E, G, and I were not identified. They only occurred in traces during the degradation of promethazine.

Identification of Volatile Degradation Products—On oxidation of promethazine (with persulfate or on boiling), some volatile degradation products are formed, such as formaldehyde, acetaldehyde, and dimethylamine (34) or acetaldehyde and dimethylamine (35).

Aldehydes—The precipitate of the 2,4-dinitrophenylhydrazones was analyzed chromatographically (Table VIII). GLC analysis on Chromosorb W with 5% SE-30 showed the retention times of the 2,4-dinitrophenylhydrazones to be identical to those of the 2,4-dinitrophenylhydrazones of acetaldehyde and formaldehyde. After distillation of a few milliliters of the original sample, the reaction with chromotropic acid in 96% H_2SO_4 (36) and Schiff's reaction (37), both very selective for formaldehyde, were positive in the distillate.

Finally, GLC analysis of the headspace of the decomposed promethazine solution on Chromosorb WAW DMC-8 with 50% Carbowax 1500 showed a peak with a retention time identical to that of acetaldehyde (formaldehyde is not detectable with a flame-ionization detector). These data showed the volatile aldehydes to be acetaldehyde and formaldehyde.

Table IX—R_f Values[a] of the 3,5-Dinitrobenzamides of Dimethylamine (A) and a Degradation Product of Promethazine (B)

Solvent	A	B
Chloroform–ethanol (99:1)	0.57	0.57
Ethanol–6 *N* ammonia (75:25)	0.53	0.53
1-Butanol–acetic acid–water (4:1:5)	0.76	0.76

[a] The sorbent was silica gel.

Dimethylamine—The R_f values of the 3,5-dinitrobenzamide obtained were identical with those of the 3,5-dinitrobenzamide of dimethylamine (Table IX). The melting point of the isolated compound was 108–112°, and the melting point of a mixture of the isolated and the synthesized compound was 110–112°. The IR spectra of both compounds were identical.

GLC analysis of the headspace of the original sample on Chromosorb WAW DMC-8 with 50% carbowax 1500 showed a peak with the same retention time as dimethylamine. The data obtained led to the conclusion that the isolated amine was dimethylamine.

REFERENCES

(1) F. Eiden and H. D. Stachel, *Dtsch. Apoth. Ztg.*, **103**, 121 (1963).

(2) M. Ferrari and C. E. Toth, *J. Chromatogr.*, **9**, 388 (1962).

(3) H. Eberhardt, O. W. Lerbs, and K. J. Freundt, *Arzneim.-Forsch.*, **13**, 804 (1963).

(4) R. Yamamoto and S. Fujisawa, lecture at the 23rd International Congress of Pharmaceutical Sciences, Munster, West Germany, 1963; through *Int. Pharm. Abstr.*, **1**, 19 (1964).

(5) C. L. Huang and F. L. Sands, *J. Chromatogr.*, **13**, 246 (1964).

(6) C. L. Huang and F. L. Sands, *J. Pharm. Sci.*, **56**, 259 (1967).

(7) *Ibid.*, **57**, 1511 (1968).

(8) S. Seno, W. V. Kessler, and J. E. Christian, *J. Pharm. Sci.*, **53**, 1101 (1964).

(9) E. Jaszsagy-Nagy and I. Elekes, *Pharmazie*, **24**, 337 (1969).

(10) J. Weir and J. Sanford, *J. Pharm. Pharmacol.*, **21**, 169 (1969).

(11) I. B. Eisdorfer and W. Ellenbogen, *J. Chromatogr.*, **4**, 329 (1960).

(12) J. Bäumler and S. Rippstein, *Pharm. Acta Helv.*, **36**, 382 (1961).

(13) M. W. Anders and G. J. Mannering, *J. Chromatogr.*, **7**, 258 (1962).

(14) T. J. Mellinger and C. E. Keeler, *J. Pharm. Sci.*, **51**, 1169 (1962).

(15) K. D. Parker, C. R. Fontan, and P. L. Kirk, *Anal. Chem.*, **34**, 757 (1962).

(16) J. Vecerkova, M. Sulkova, and K. Kacl, *Pharmazie*, **17**, 22 (1962).

(17) W. Paulus, W. Koch, and R. Keymer, *Arzneim.-Forsch.*, **13**, 609 (1963).

(18) A. Noirfalise and M. H. Grosjean, *J. Chromatogr.*, **16**, 236 (1964).

(19) "Chromatographic Data," *ibid.*, **27**, D4 (1965).

(20) B. J. Gudzinowicz, *J. Gas Chromatogr.*, **4**, 110 (1966).

(21) P. N. Moza and G. S. Khajuria, *J. Chromatogr.*, **24**, 261 (1966).

(22) H. Gerlach, *Pharmazie*, **22**, 651 (1967).

(23) I. Zingalis, *J. Chromatogr.*, **31**, 405 (1967).

(24) R. Pummerer and S. Gassner, *Ber. Dtsch. Chem. Ges.*, **46**, 2324 (1913).

(25) K. Inukai and T. Ueda, *Rep. Gov. Ind. Res. Inst. Nagoya*, **1**, 16 (1952); through *Chem. Abstr.*, **50**, 3449g (1956).

(26) J. F. E. Van Kessel, thesis, University of Utrecht, Utrecht, The Netherlands, 1969.

(27) K. Teichert, E. Mutschler, and H. Rochelmeyer, *Dtsch. Apoth. Ztg.*, **100**, 283 (1960).

(28) H. Roseboom and J. A. Fresen, *Pharm. Acta Helv.*, **50**, 55 (1975).

(29) R. J. Warren, I. B. Eisdorfer, W. E. Thompson, and J. E. Zarembo, *J. Pharm. Sci.*, **55**, 144 (1966).

(30) G. Bodea and I. Silberg, *Rev. Chim. Acad. Rep. Pop. Roum.*, **7**, 683 (1962); through *Chem. Abstr.*, **61**, 8161a (1964).

(31) J. Kofoed, C. Fabierkiewicz, and G. W. H. Lucas, *J. Chromatogr.*, **23**, 410 (1966).

(32) H. R. Vidal, *Friedlaender*, **5**, 440 (1897).

(33) D. E. Houston, E. B. Kester, and F. De Eds, *J. Am. Chem. Soc.*, 71, 3819 (1949).
(34) G. M. Nano, P. Sancin, and G. Tappi, *Pharm. Acta Helv.*, 38, 623 (1963).
(35) T. Waaler, *ibid.*, 35, 168 (1960).
(36) F. Feigl, "Spot Tests in Organic Analysis," 6th ed., Elsevier, Amsterdam, The Netherlands, 1960, p. 349.
(37) *Ibid.*, p. 223.

Oxidative Degradation of Pharmaceutically Important Phenothiazines II: Quantitative Determination of Promethazine and Some Degradation Products

W. J. M. UNDERBERG

Received August 8, 1977, from the *Farmaceutisch Laboratorium, Rijksuniversiteit Utrecht, Catharijnesingel 60, Utrecht, The Netherlands.* Accepted for publication December 14, 1977.

Abstract □ Methods for the determination of promethazine and several degradation products, which can be used in kinetic studies, were developed. All determinations were carried out after isolation of the compounds by TLC. Promethazine was determined by oxidation with vanadyl sulfate in an acidic medium. The method was suitable for approximately 3 mg of the compound. 3*H*-Phenothiazine-3-one was determined spectrophotometrically at 492 nm in acetone. The compound could be determined in amounts of 30–40 μg. Promethazine 5-oxide was determined spectrophotometrically using the acid dye method; 100–200 μg could be determined. 7-Hydroxy-3*H*-phenothiazine-3-one could be determined spectrophotometrically at 600 nm after extraction of the other compounds from the solution. The medium had to be alkaline and contain water in a fixed ratio. The method was suitable for 15–30 μg of the compound.

Keyphrases □ Promethazine—polarographic analysis, prepared samples □ Degradation products, various—of promethazine, spectrophotometric analyses, prepared samples □ Polarography—analysis, promethazine, prepared samples □ Spectrophotometry—analyses, various degradation products of promethazine, prepared samples □ Antiemetics—promethazine, polarographic analysis, prepared samples □ Phenothiazines—promethazine, polarographic analysis, various degradation products, spectrophotometric analyses, prepared samples

Previously (1), the isolation and identification of some products formed on storage of promethazine dissolved in water in the presence of oxygen were described. Literature methods for the determination of promethazine are not useful for the study of its degradation kinetics because of interference by the degradation products. Moreover, no suitable methods are available for the determination of the degradation products.

This paper describes suitable methods for the quantitative determination of promethazine, promethazine 5-oxide, 3*H*-phenothiazine-3-one, and 7-hydroxy-3*H*-phenothiazine-3-one. The method for the determination of promethazine is also suitable for other phenothiazine derivatives. All quantitative determinations were carried out after separation by TLC.

EXPERIMENTAL

Materials—All materials were described previously (1).

Preparation of Reagents—The acid mixture contained 16 parts of 4 *N* sulfuric acid mixed with nine parts of 85% phosphoric acid.

To prepare 0.002 *M* ferrous ammonium sulfate, about 0.20 g of ferrous ammonium sulfate was dissolved in 50 ml of water. To the solution were added 62 ml of 4 *N* sulfuric acid and water to a volume of 250.0 ml. The strength of the solution was determined by titration with potassium dichromate.

To prepare 0.005 *M* vanadyl sulfate ($VOSO_4$), about 0.58 g of ammonium vanadate(V) was dissolved in 10 ml of 6 *N* ammonia and 200 ml of water. To the solution were added 250 ml of 4 *N* sulfuric acid and water to a volume of 1 liter. The strength of the solution was determined with the 0.002 *M* ferrous ammonium sulfate.

Acetate buffer, pH 4.6, was prepared by dissolving 26.6 g of sodium acetate in water and adding 15.9 g of 97% acetic acid and water to a volume of 100.0 ml. The pH was adjusted to 4.6.

A saturated solution of tropaeolin 00 in water also was prepared. A sulfuric acid–methanol solution was prepared by mixing one part of 96% sulfuric acid with 99 parts of methanol.

Procedures—For the determination of promethazine, an amount of the sample corresponding to about 3 mg of promethazine was transferred into a separator. Extraction and separation by TLC were carried out as described (1). The zone containing promethazine was transferred into a 50-ml beaker, and 5.00 ml of 0.005 *M* vanadyl sulfate and 25 ml of acid mixture were added. The mixture was stirred until the red color disappeared completely. Excess vanadyl sulfate was determined with 0.002 *M* ferrous ammonium sulfate, with biamperometric determination of the end-point according to Van Pinxteren and Verloop (2) with a potential of 150 mv between the platinum electrodes.

The equivalent weight is the molecular weight divided by 2.

The oxidation mechanism of promethazine was studied using polarography[1] with a platinum electrode as the indicator electrode and a saturated calomel electrode (SCE) as the reference electrode.

After separation by TLC as described previously (1), 3*H*-phenothiazine-3-one was determined. The dye was extracted from the silica gel with acetone. The solution was filtered through a small plug of cotton, and acetone was added to a volume of 10.0 ml. The absorbance of the solution was measured[2] at 492 nm in a 1- or 2-cm cell with acetone as a blank.

The determination of promethazine 5-oxide was carried out using the acid dye method described by Häussler and Hajdú (3). After extraction of the sample and separation by TLC as described previously (1), the zone containing promethazine 5-oxide was transferred into a separator and mixed with 10 ml of pH 4.6 acetate buffer and 5 ml of tropaeolin 00 (Mixture A). A blank was prepared using a zone of the same size from the same chromatogram containing no compounds (Mixture B). Both mixtures were extracted with portions of 5 ml of chloroform until the color of the chloroform phases of both systems was the same. The chloroform phases were filtered through a plug of cotton into 50-ml volumetric flasks, and 3.0 ml of sulfuric acid–methanol and chloroform to a volume of 50.0 ml were added. The absorbance of Mixture A was measured at 545 nm in a 0.5- or 1-cm cell with Mixture B as a blank.

To obtain reproducible results and to lower the blank values, all glassware was cleaned carefully, freshly prepared solvent was used always,

[1] Radiometer polarograph PO3m.
[2] Unicam SP 500 spectrophotometer.

0022-3549/78/0800-1131$01.00/0
© 1978, American Pharmaceutical Association

(33) D. E. Houston, E. B. Kester, and F. De Eds, *J. Am. Chem. Soc.*, 71, 3819 (1949).
(34) G. M. Nano, P. Sancin, and G. Tappi, *Pharm. Acta Helv.*, 38, 623 (1963).
(35) T. Waaler, *ibid.*, 35, 168 (1960).
(36) F. Feigl, "Spot Tests in Organic Analysis," 6th ed., Elsevier, Amsterdam, The Netherlands, 1960, p. 349.
(37) *Ibid.*, p. 223.

Oxidative Degradation of Pharmaceutically Important Phenothiazines II: Quantitative Determination of Promethazine and Some Degradation Products

W. J. M. UNDERBERG

Received August 8, 1977, from the *Farmaceutisch Laboratorium, Rijksuniversiteit Utrecht, Catharijnesingel 60, Utrecht, The Netherlands.* Accepted for publication December 14, 1977.

Abstract □ Methods for the determination of promethazine and several degradation products, which can be used in kinetic studies, were developed. All determinations were carried out after isolation of the compounds by TLC. Promethazine was determined by oxidation with vanadyl sulfate in an acidic medium. The method was suitable for approximately 3 mg of the compound. 3*H*-Phenothiazine-3-one was determined spectrophotometrically at 492 nm in acetone. The compound could be determined in amounts of 30–40 μg. Promethazine 5-oxide was determined spectrophotometrically using the acid dye method; 100–200 μg could be determined. 7-Hydroxy-3*H*-phenothiazine-3-one could be determined spectrophotometrically at 600 nm after extraction of the other compounds from the solution. The medium had to be alkaline and contain water in a fixed ratio. The method was suitable for 15–30 μg of the compound.

Keyphrases □ Promethazine—polarographic analysis, prepared samples □ Degradation products, various—of promethazine, spectrophotometric analyses, prepared samples □ Polarography—analysis, promethazine, prepared samples □ Spectrophotometry—analyses, various degradation products of promethazine, prepared samples □ Antiemetics—promethazine, polarographic analysis, prepared samples □ Phenothiazines—promethazine, polarographic analysis, various degradation products, spectrophotometric analyses, prepared samples

Previously (1), the isolation and identification of some products formed on storage of promethazine dissolved in water in the presence of oxygen were described. Literature methods for the determination of promethazine are not useful for the study of its degradation kinetics because of interference by the degradation products. Moreover, no suitable methods are available for the determination of the degradation products.

This paper describes suitable methods for the quantitative determination of promethazine, promethazine 5-oxide, 3*H*-phenothiazine-3-one, and 7-hydroxy-3*H*-phenothiazine-3-one. The method for the determination of promethazine is also suitable for other phenothiazine derivatives. All quantitative determinations were carried out after separation by TLC.

EXPERIMENTAL

Materials—All materials were described previously (1).

Preparation of Reagents—The acid mixture contained 16 parts of 4 *N* sulfuric acid mixed with nine parts of 85% phosphoric acid.

To prepare 0.002 *M* ferrous ammonium sulfate, about 0.20 g of ferrous ammonium sulfate was dissolved in 50 ml of water. To the solution were added 62 ml of 4 *N* sulfuric acid and water to a volume of 250.0 ml. The strength of the solution was determined by titration with potassium dichromate.

To prepare 0.005 *M* vanadyl sulfate ($VOSO_4$), about 0.58 g of ammonium vanadate(V) was dissolved in 10 ml of 6 *N* ammonia and 200 ml of water. To the solution were added 250 ml of 4 *N* sulfuric acid and water to a volume of 1 liter. The strength of the solution was determined with the 0.002 *M* ferrous ammonium sulfate.

Acetate buffer, pH 4.6, was prepared by dissolving 26.6 g of sodium acetate in water and adding 15.9 g of 97% acetic acid and water to a volume of 100.0 ml. The pH was adjusted to 4.6.

A saturated solution of tropaeolin 00 in water also was prepared. A sulfuric acid–methanol solution was prepared by mixing one part of 96% sulfuric acid with 99 parts of methanol.

Procedures—For the determination of promethazine, an amount of the sample corresponding to about 3 mg of promethazine was transferred into a separator. Extraction and separation by TLC were carried out as described (1). The zone containing promethazine was transferred into a 50-ml beaker, and 5.00 ml of 0.005 *M* vanadyl sulfate and 25 ml of acid mixture were added. The mixture was stirred until the red color disappeared completely. Excess vanadyl sulfate was determined with 0.002 *M* ferrous ammonium sulfate, with biamperometric determination of the end-point according to Van Pinxteren and Verloop (2) with a potential of 150 mv between the platinum electrodes.

The equivalent weight is the molecular weight divided by 2.

The oxidation mechanism of promethazine was studied using polarography[1] with a platinum electrode as the indicator electrode and a saturated calomel electrode (SCE) as the reference electrode.

After separation by TLC as described previously (1), 3*H*-phenothiazine-3-one was determined. The dye was extracted from the silica gel with acetone. The solution was filtered through a small plug of cotton, and acetone was added to a volume of 10.0 ml. The absorbance of the solution was measured[2] at 492 nm in a 1- or 2-cm cell with acetone as a blank.

The determination of promethazine 5-oxide was carried out using the acid dye method described by Häussler and Hajdú (3). After extraction of the sample and separation by TLC as described previously (1), the zone containing promethazine 5-oxide was transferred into a separator and mixed with 10 ml of pH 4.6 acetate buffer and 5 ml of tropaeolin 00 (Mixture A). A blank was prepared using a zone of the same size from the same chromatogram containing no compounds (Mixture B). Both mixtures were extracted with portions of 5 ml of chloroform until the color of the chloroform phases of both systems was the same. The chloroform phases were filtered through a plug of cotton into 50-ml volumetric flasks, and 3.0 ml of sulfuric acid–methanol and chloroform to a volume of 50.0 ml were added. The absorbance of Mixture A was measured at 545 nm in a 0.5- or 1-cm cell with Mixture B as a blank.

To obtain reproducible results and to lower the blank values, all glassware was cleaned carefully, freshly prepared solvent was used always,

[1] Radiometer polarograph PO3m.
[2] Unicam SP 500 spectrophotometer.

0022-3549/78/0800-1131$01.00/0
© 1978, American Pharmaceutical Association

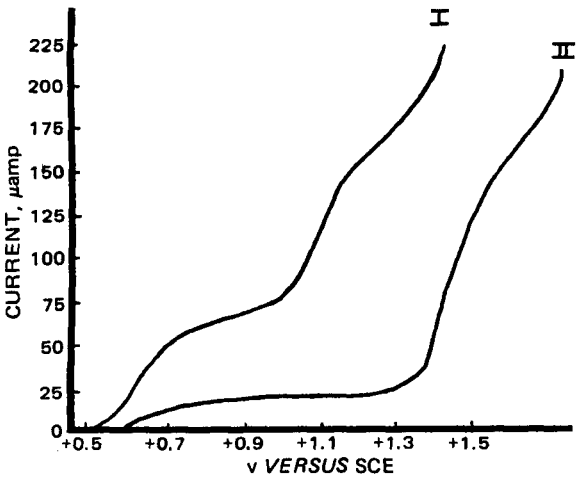

Figure 1—*Voltammogram of promethazine in 4 N sulfuric acid. Key: curve I, 2 × 10⁻⁴ M promethazine hydrochloride in 4 N sulfuric acid; and curve II, 4 N sulfuric acid.*

and the chromatograms were dried with a warm air stream immediately after development.

For the determination of 7-hydroxy-3*H*-phenothiazine-3-one, 3.00 ml of the sample was transferred into a separator, 1.00 ml of 4 *N* sodium hydroxide was added, and the mixture was extracted with dichloromethane until the organic phase remained colorless. The water layer was transferred quantitatively into a volumetric flask, and 96% ethanol was added to a volume of 10.0 ml. The absorbance of the solution was measured at 600 nm in a 1- or 2-cm cell with water as a blank.

RESULTS AND DISCUSSION

The polarogram of the oxidation of promethazine in 4 *N* sulfuric acid showed two steps (Fig. 1). The first was the loss of one electron and the formation of a red-colored radical ($E_{1/2}$ = +0.65 v *versus* the saturated calomel electrode). The second step was the loss of another electron with the formation of a colorless compound (3) ($E_{1/2}$ = +1.02 v *versus* the saturated calomel electrode). Since the radical was unstable, an oxidimetric determination method was used to measure the formation of the colorless product.

The oxidation potential of a mixture of 5.00 ml of 0.005 *M* vanadyl sulfate and 25 ml of acid mixture was +1.03 v *versus* the saturated calomel electrode, which was in good agreement with the $E_{1/2}$ of the second step of the oxidation of promethazine. This result indicated that vanadyl sulfate was adequate for performing the oxidation. Subsequent determinations of promethazine after each step of the isolation procedure showed neither degradation of promethazine during the isolation procedure nor interference from the silica gel in the determination.

Table I gives the results obtained with this method. Moreover, the procedure is suitable for the determination of N-10 substituted phenothiazines in general (Table II). Finally, the oxidation product formed was identified as promethazine 5-oxide according to the procedure described previously (1).

The absorption maximum of 3*H*-phenothiazine-3-one in acetone is 492 nm. With this solvent, the compound could be eluted easily from the silica gel. In the 20–100-μg range, Beer's law was obeyed; the molar absorptivity of 3*H*-phenothiazine-3-one is 7130. Table III shows the results of the determination of 3*H*-phenothiazine-3-one with the procedure described.

Table I—Determination of Promethazine Hydrochloride

Amount, mg	Recovery[a], %
3.00	100
3.04	101
3.01	102
2.99	99
3.02	99
3.08	101
Average ± *SD* = 100.3 ± 1.0%	

[a] Average of three determinations.

Table II—Determination of Several Phenothiazines

Compound	Amount, mg	Recovery, %
Chlorpromazine hydrochloride	3.02	100
Cyanopromazine hydrochloride	3.01	102
Methoxypromazine hydrochloride	2.89	99
Methylpromazine hydrochloride	3.06	101
Promazine hydrochloride	3.12	100
Promethazine hydrochloride	2.99	102
Triflupromazine hydrochloride	3.08	101

Table III—Determination of 3*H*-Phenothiazine-3-one

Amount, μg	Recovery, %
31	90
31	91
50	94
50	91
51	94
70	93
70	93
72	93
Average ± *SD* = 92.4 ± 1.5%	

Table IV—Determination of Promethazine 5-Oxide

Amount, μg	Recovery, %
99	97
99	106
115	101
115	104
149	104
149	103
173	103
173	97
Average ± *SD* = 101.9 ± 3.5%	

Table V—Determination of Promethazine 5-Oxide (150 μg) after Isolation by TLC with Different Solvents

Solvent	Recovery, %
Acetone–6 *N* ammonia (100:2)	102
Methanol–6 *N* ammonia (100:2)	90
Ether–6 *N* ammonia (100:2)	80
Water–6 *N* ammonia (100:2)	79
Methanol–6 *N* ammonia–isopropylamine (100:1:1)	79
No development	81

Promethazine 5-oxide forms an ion-pair with tropaeolin 00 at pH 4.6, extractable with chloroform. Tropaeolin 00 in acidified chloroform–methanol solution has an absorption maximum at 545 nm. Since the ion-pair was destroyed after extraction by adding sulfuric acid–methanol, all determinations were carried out at this wavelength. In the 40–200-μg range of promethazine 5-oxide, Beer's law was obeyed. The molar absorptivity of the ion-pair is 48,590. The molar absorptivity of tropaeolin 00 under the same conditions is 40,400 (3), which shows promethazine and tropaeolin 00 to be present in the complex in a 1:1 ratio. Table IV shows the results of some determinations of promethazine 5-oxide with the described method.

The blank showed an absorbance that could not be neglected. This response sometimes was due to the solvent used in the TLC separation of the compounds, so other solvents were tried. Table V shows that the absorbance of the blank could be decreased to almost zero, but the recovery also decreased. This phenomenon also occurred when promethazine 5-oxide was applied onto a silica gel layer without development of the chromatogram (Table V). Apparently, the extraction of the ion-pair from the sorbent was not complete. Only after developing the chromatogram with acetone–6 *N* ammonia (100:2) were good results obtained (Table VI).

The fact that the acetone–6 *N* ammonia mixture is highly reactive (4) might be an explanation. Possibly, an intermediate formed in the reaction decreases the activity of the sorbent so that a complete extraction can

Table VI—Determination of 7-Hydroxy-3*H*-phenothiazine-3-one

Amount, μg	Recovery, %
16.4	89
18.2	93
18.4	94
19.6	96
24.6	93
27.3	95
27.8	94
29.4	99
Average ± *SD* = 94.1 ± 3.2%	

be carried out. This reactivity is also an explanation for the higher blank values obtained with the solvent acetone–6 *N* ammonia (100:2). One product formed, isopropylamine, also forms a complex with tropaeolin 00 that is extractable with chloroform. The use of freshly prepared solvent, careful cleaning of the glassware, and fast drying of the developed chromatograms were necessary to reduce the absorbance of the blank.

Although 7-hydroxy-3*H*-phenothiazine-3-one was the only compound formed during degradation of promethazine with an absorption maximum at 600 nm in an alkaline medium, the other products and promethazine itself interfered by reducing the compound to the colorless 3,7-dihydroxyphenothiazine. Therefore, the other compounds had to be removed by extraction with dichloromethane from the alkaline medium. The resulting water phase was diluted with 96% ethanol to get a clear solution. In the 5–40-μg range, Beer's law was obeyed. The molar absorptivity of the compound under this condition is 58,900. The results obtained with this method (Table VI) were quite satisfactory, provided that the ratio between water and ethanol in the solvent remained constant.

REFERENCES

(1) W. J. M. Underberg, *J. Pharm. Sci.*, **67**, 1128 (1978).

(2) J. A. C. Van Pinxteren and M. E. Verloop, *Pharm. Weekbl.*, **96**, 545 (1961).

(3) A. Häussler and P. Hajdú, *Arzneim.-Forsch.*, **12**, 411 (1962).

(4) D. C. Borg and G. C. Cotzias, *Proc. Natl. Acad. Sci. USA*, **48**, 617 (1962); through A. H. Beckett and S. H. Curry, *J. Pharm. Pharmacol.*, **15**, 246T (1963).

Oxidative Degradation of Pharmaceutically Important Phenothiazines III: Kinetics and Mechanism of Promethazine Oxidation

W. J. M. UNDERBERG

Received August 8, 1977, from the *Farmaceutisch Laboratorium, Rijksuniversiteit Utrecht, Catharijnesingel 60, Utrecht, The Netherlands.* Accepted for publication December 14, 1977.

Abstract □ The kinetics of the thermal degradation of promethazine in an acidic medium under various conditions were investigated. The degradation of promethazine and the formation of some degradation products were studied under aerobic and anaerobic conditions. The influence of pH, metal ions such as copper(II) and iron(III), and antioxidants was investigated. In an oxygen-saturated medium, promethazine generally followed first-order kinetics. Increasing the pH increased the degradation rate to a limiting value at pH 5. Addition of copper(II) increased the degradation rate over the whole process, while iron(III) caused an increase for only a short time. Ascorbic acid sometimes increased the degradation rate, while higher concentrations of hydroquinone also accelerated the degradation. Pyrosulfite did not have any influence. Under anaerobic conditions, promethazine degraded only in the presence of copper(II) and iron(III) ions. As a result of the studies on the qualitative and quantitative aspects of the oxidation process, a mechanism for the oxidative degradation of promethazine is suggested. Promethazine 5-oxide and a number of degradation products without intact side chains are formed *via* a semiquinone free radical. The influence of several factors on the degradation process is discussed.

Keyphrases □ Promethazine—thermal degradation kinetics in acidic medium, effect of anaerobic and aerobic conditions, pH, metal ions, and antioxidants □ Degradation, thermal—promethazine, kinetics in acidic medium, effect of anaerobic and aerobic conditions, pH, metal ions, and antioxidants □ Oxidation—promethazine, thermal degradation kinetics in acidic medium, effect of anaerobic and aerobic conditions, pH, metal ions, and antioxidants □ Antiemetics—promethazine, thermal degradation kinetics in acidic medium, effect of anaerobic and aerobic conditions, pH, metal ions, and antioxidants □ Phenothiazines—promethazine, thermal degradation kinetics in acidic medium, effect of anaerobic and aerobic conditions, pH, metal ions, and antioxidants

Little information is available on the quantitative aspects of promethazine degradation. Chalabala *et al.* (1) mentioned the stability of a solution containing aminopyrine, trimecaine, and promethazine at pH 5.5–6.0 in the presence of sodium pyrosulfite, thiourea, or sodium formaldehyde sulfoxylate. One study (2) found that promethazine degradation followed first-order kinetics. The degradation rate decreased on changing the pH from 3.0 to 5.0. In another study, the degradation rate of the reaction was reported to be pH independent (3). Other studies (4, 5) also described first-order kinetics for the degradation reaction. However, at pH values over 5.5, degradation no longer followed first-order kinetics (5). Moreover, promethazine was most unstable at pH 4.3.

In this paper, the kinetics of promethazine degradation under varying conditions are described and the degradation mechanism is discussed.

EXPERIMENTAL

Materials—All materials used were described previously (6).

Methods—For the study of promethazine degradation under aerobic conditions, about 50 mg of promethazine hydrochloride, accurately weighed, was dissolved in a few milliliters of water. To the solution were added 12.5 ml of acetate buffer according to Walpole (7) to get the right pH (at 65°), any other necessary additive previously adjusted to the right pH, and water to a volume of 50.0 ml. The solution was saturated with oxygen, and 4 ml was transferred into 10-ml ampuls in an oxygen atmosphere according to a previous method (8). The ampuls were kept at 65° in the dark.

The isolation and determination of promethazine, promethazine 5-oxide, 3*H*-phenothiazine-3-one, and 7-hydroxy-3*H*-phenothiazine-3-one were carried out as described previously (6, 9).

For the study of promethazine degradation under anaerobic conditions, the oxygen was removed by bubbling carbon dioxide through the solution for 5 hr. The degradation was carried out at 100°.

0022-3549/78/0800-1133$01.00/0

© 1978, American Pharmaceutical Association

Table VI—Determination of 7-Hydroxy-3*H*-phenothiazine-3-one

Amount, μg	Recovery, %
16.4	89
18.2	93
18.4	94
19.6	96
24.6	93
27.3	95
27.8	94
29.4	99
Average ± *SD* = 94.1 ± 3.2%	

be carried out. This reactivity is also an explanation for the higher blank values obtained with the solvent acetone–6 *N* ammonia (100:2). One product formed, isopropylamine, also forms a complex with tropaeolin 00 that is extractable with chloroform. The use of freshly prepared solvent, careful cleaning of the glassware, and fast drying of the developed chromatograms were necessary to reduce the absorbance of the blank.

Although 7-hydroxy-3*H*-phenothiazine-3-one was the only compound formed during degradation of promethazine with an absorption maximum at 600 nm in an alkaline medium, the other products and promethazine itself interfered by reducing the compound to the colorless 3,7-dihydroxyphenothiazine. Therefore, the other compounds had to be removed by extraction with dichloromethane from the alkaline medium. The resulting water phase was diluted with 96% ethanol to get a clear solution. In the 5–40-μg range, Beer's law was obeyed. The molar absorptivity of the compound under this condition is 58,900. The results obtained with this method (Table VI) were quite satisfactory, provided that the ratio between water and ethanol in the solvent remained constant.

REFERENCES

(1) W. J. M. Underberg, *J. Pharm. Sci.*, **67**, 1128 (1978).

(2) J. A. C. Van Pinxteren and M. E. Verloop, *Pharm. Weekbl.*, **96**, 545 (1961).

(3) A. Häussler and P. Hajdú, *Arzneim.-Forsch.*, **12**, 411 (1962).

(4) D. C. Borg and G. C. Cotzias, *Proc. Natl. Acad. Sci. USA*, **48**, 617 (1962); through A. H. Beckett and S. H. Curry, *J. Pharm. Pharmacol.*, **15**, 246T (1963).

Oxidative Degradation of Pharmaceutically Important Phenothiazines III: Kinetics and Mechanism of Promethazine Oxidation

W. J. M. UNDERBERG

Received August 8, 1977, from the *Farmaceutisch Laboratorium, Rijksuniversiteit Utrecht, Catharijnesingel 60, Utrecht, The Netherlands.* Accepted for publication December 14, 1977.

Abstract □ The kinetics of the thermal degradation of promethazine in an acidic medium under various conditions were investigated. The degradation of promethazine and the formation of some degradation products were studied under aerobic and anaerobic conditions. The influence of pH, metal ions such as copper(II) and iron(III), and antioxidants was investigated. In an oxygen-saturated medium, promethazine generally followed first-order kinetics. Increasing the pH increased the degradation rate to a limiting value at pH 5. Addition of copper(II) increased the degradation rate over the whole process, while iron(III) caused an increase for only a short time. Ascorbic acid sometimes increased the degradation rate, while higher concentrations of hydroquinone also accelerated the degradation. Pyrosulfite did not have any influence. Under anaerobic conditions, promethazine degraded only in the presence of copper(II) and iron(III) ions. As a result of the studies on the qualitative and quantitative aspects of the oxidation process, a mechanism for the oxidative degradation of promethazine is suggested. Promethazine 5-oxide and a number of degradation products without intact side chains are formed *via* a semiquinone free radical. The influence of several factors on the degradation process is discussed.

Keyphrases □ Promethazine—thermal degradation kinetics in acidic medium, effect of anaerobic and aerobic conditions, pH, metal ions, and antioxidants □ Degradation, thermal—promethazine, kinetics in acidic medium, effect of anaerobic and aerobic conditions, pH, metal ions, and antioxidants □ Oxidation—promethazine, thermal degradation kinetics in acidic medium, effect of anaerobic and aerobic conditions, pH, metal ions, and antioxidants □ Antiemetics—promethazine, thermal degradation kinetics in acidic medium, effect of anaerobic and aerobic conditions, pH, metal ions, and antioxidants □ Phenothiazines—promethazine, thermal degradation kinetics in acidic medium, effect of anaerobic and aerobic conditions, pH, metal ions, and antioxidants

Little information is available on the quantitative aspects of promethazine degradation. Chalabala *et al.* (1) mentioned the stability of a solution containing aminopyrine, trimecaine, and promethazine at pH 5.5–6.0 in the presence of sodium pyrosulfite, thiourea, or sodium formaldehyde sulfoxylate. One study (2) found that promethazine degradation followed first-order kinetics. The degradation rate decreased on changing the pH from 3.0 to 5.0. In another study, the degradation rate of the reaction was reported to be pH independent (3). Other studies (4, 5) also described first-order kinetics for the degradation reaction. However, at pH values over 5.5, degradation no longer followed first-order kinetics (5). Moreover, promethazine was most unstable at pH 4.3.

In this paper, the kinetics of promethazine degradation under varying conditions are described and the degradation mechanism is discussed.

EXPERIMENTAL

Materials—All materials used were described previously (6).

Methods—For the study of promethazine degradation under aerobic conditions, about 50 mg of promethazine hydrochloride, accurately weighed, was dissolved in a few milliliters of water. To the solution were added 12.5 ml of acetate buffer according to Walpole (7) to get the right pH (at 65°), any other necessary additive previously adjusted to the right pH, and water to a volume of 50.0 ml. The solution was saturated with oxygen, and 4 ml was transferred into 10-ml ampuls in an oxygen atmosphere according to a previous method (8). The ampuls were kept at 65° in the dark.

The isolation and determination of promethazine, promethazine 5-oxide, 3*H*-phenothiazine-3-one, and 7-hydroxy-3*H*-phenothiazine-3-one were carried out as described previously (6, 9).

For the study of promethazine degradation under anaerobic conditions, the oxygen was removed by bubbling carbon dioxide through the solution for 5 hr. The degradation was carried out at 100°.

0022-3549/78/0800-1133$01.00/0

© 1978, American Pharmaceutical Association

Table I—Rate Constants k' of Promethazine Degradation at Various Temperatures at pH 4.6

Temperature, °K	k', sec^{-1}
318	3.3×10^{-7}
328	13.6×10^{-7}
338	54.4×10^{-7}
348	218.6×10^{-7}
363	1253.0×10^{-7}

RESULTS

Degradation of Promethazine under Aerobic Conditions—*Influence of Temperature*—At all temperatures, the degradation was first order with respect to promethazine. Table I gives the observed rate constants, k', at various temperatures at pH 4.6. The Arrhenius plot gives an E_a of 30.6 kcal/mole. This energy of activation includes a term for the variation of the oxygen solubility with temperature. The decreased solubility of oxygen with increasing temperature is partially compensated by an increase in solubility because of a higher oxygen pressure above the solution at higher temperatures.

Influence of pH—The pH of the solutions was varied from 1.5 to 6.3; in this region, the solubility of oxygen in water was independent of pH. The degradation followed first-order kinetics at all pH values. Figure 1 shows that the rate constant increased with increasing pH and remained constant above pH 5.

The formation of the degradation products that were quantitated was also pH dependent. Figure 2 shows that the formation of 3*H*-phenothiazine-3-one and promethazine 5-oxide showed maxima at pH 3.2 and 4.3, respectively; the formation of 7-hydroxy-3*H*-phenothiazine-3-one decreased with increasing pH. At pH values over 3, the formation of the latter compound was negligible. These phenomena were not primarily due to decomposition of these products; promethazine 5-oxide was stable at pH 6.3 (Table II), while 3*H*-phenothiazine-3-one only decomposed at low pH values. Evaluation of the intensity of the zone containing phenothiazine and 10-methylphenothiazine on chromatograms of degraded promethazine solutions led to the conclusion that the formation of these compounds increased with increasing pH.

Influence of Metal Ions—Of the metal ions investigated, only copper(II) and iron(III) ions influenced promethazine degradation. Figure 3 shows this influence, which was different for the two metals at pH 3.2. While the k' values increased up to a maximum with an increasing concentration of copper(II) (Fig. 4), only the initial degradation rate increased dramatically with an increasing iron(III) concentration, and after a short time the degradation curves had slopes equal to those obtained when no metal ions were added (Fig. 3). The decrease in the extrapolated intercepts at zero time of the latter part of these curves was proportional to the iron(III) concentration.

Figure 5 shows the influence on the formation of promethazine 5-oxide, and Figs. 6 and 7 show the influence on the 7-hydroxy-3*H*-phenothiazine-3-one and 3*H*-phenothiazine-3-one formation, respectively. From

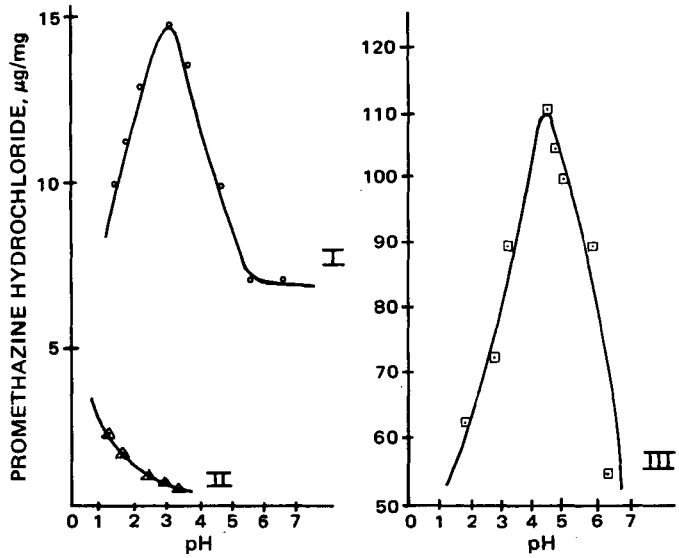

Figure 2—*Influence of pH on the formation of degradation products of promethazine after 25 hr at pH 3.2 under aerobic conditions at 65°. Key: curve I, 3H-phenothiazine-3-one; curve II, 7-hydroxy-3H-phenothiazine-3-one; and curve III, promethazine 5-oxide.*

Table II—Recoveries of 50 μg of Promethazine 5-Oxide after Storage during Specified Times at pH 6.3 and 65°

Time	Recovery, %
0	94
16 hr, 15 min	93
32 hr, 10 min	96
64 hr	98

Figs. 6 and 7, it can be seen that the formation of 3*H*-phenothiazine-3-one and 7-hydroxy-3*H*-phenothiazine-3-one increased with an increasing concentration of the metal ion. With iron(III), this increase only occurred in the initial phase of the process, but the influence of copper(II) was obvious during the whole process. In the presence of copper(II), the formation of promethazine 5-oxide increased (Fig. 5); in the presence of iron(III), the formation of promethazine 5-oxide decreased (Fig. 5).

Evaluation of the zone containing phenothiazine and 10-methylphenothiazine led to the conclusion that the formation of these compounds increased with increasing concentration of copper(II) and iron(III) in the solutions.

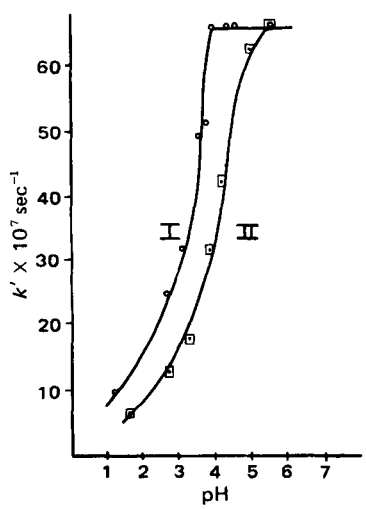

Figure 1—*Influence of pH on the degradation rate k' of promethazine under aerobic conditions at 65°. Key: curve I, no additive; and curve II, 2×10^{-3} M edetate disodium added.*

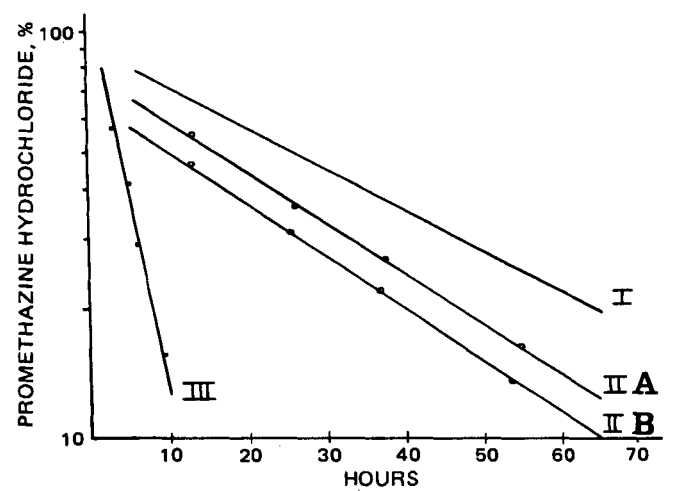

Figure 3—*Influence of copper(II) and iron(III) on the degradation of promethazine at pH 3.2 under aerobic conditions at 65°. Key: curve I, no additive; curve IIA, 10^{-3} M iron(III); curve IIB, 5×10^{-3} M iron(III); and curve III, 5×10^{-3} M copper(II).*

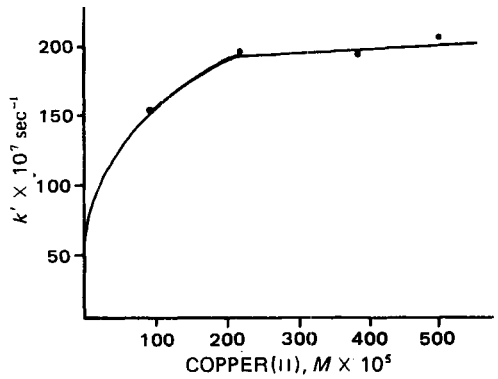

Figure 4—*Influence of copper(II) on the degradation rate* k′ *of promethazine at pH 3.2 under aerobic conditions at 65°.*

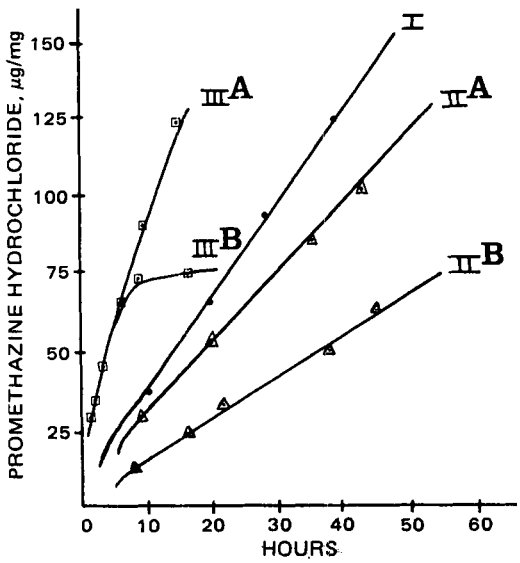

Figure 5—*Influence of copper(II) and iron(III) on the formation of promethazine 5-oxide at pH 3.2 under aerobic conditions at 65°. Key: curve I, no additive; curve IIA, 10^{-4} M iron(III); curve IIB, 10^{-3} M iron(III); curve IIIA, 10^{-4} M copper(II); and curve IIIB, 10^{-3} M copper(II).*

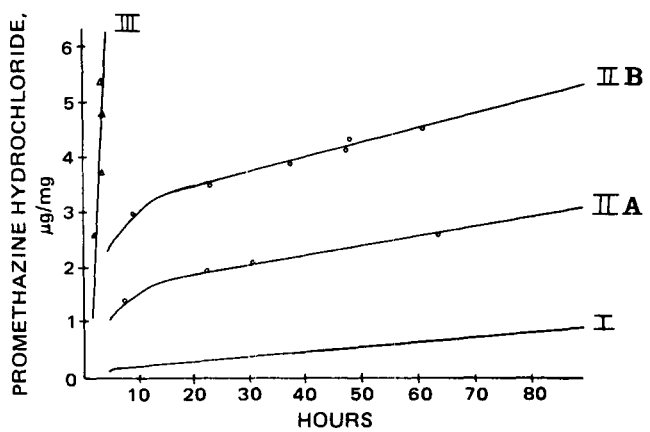

Figure 6—*Influence of copper(II) and iron(III) on the formation of 7-hydroxy-3H-phenothiazine-3-one at pH 3.2 under aerobic conditions at 65°. Key: curve I, no additive; curve IIA, 10^{-3} M iron(III); curve IIB, 5×10^{-3} M iron(III); and curve III, 5×10^{-3} M copper(II).*

Figure 3 shows that the extrapolated intercepts at zero time of the second part of the curves decreased with an increasing iron(III) concentration. For solutions without added iron(III), the intercepts were also below 100%, probably because of contamination of the reagents with very

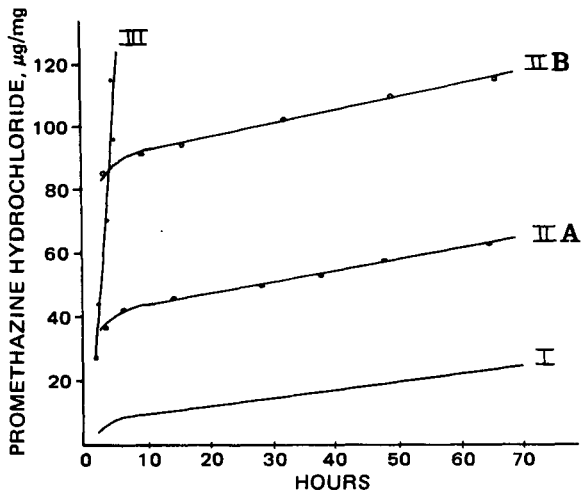

Figure 7—*Influence of copper(II) and iron(III) on the formation of 3H-phenothiazine-3-one at pH 3.2 under aerobic conditions at 65°. Key: curve I, no additive; curve IIA, 10^{-3} M iron(III); curve IIB, 5×10^{-3} M iron(III); and curve III, 5×10^{-3} M copper(II).*

Table III—Influence of Edetate Disodium on the Rate Constant *k′* of Promethazine Degradation at pH 3.2 and 65°

Edetate Disodium, *M*	k', sec^{-1}
0	28.9×10^{-7}
2×10^{-3}	13.9×10^{-7}
10^{-2}	12.8×10^{-7}

low concentrations of iron(III). Promethazine degradation in the presence of edetate disodium was compared with the degradation without this additive. Table III shows that the rate constant decreased on addition of edetate disodium but that the concentration of the additive had no further influence on it. The "zero-time" value of the curves in the presence of edetate disodium was 100%. Moreover, the formation of 3*H*-phenothiazine-3-one was greatly reduced while the amount of 7-hydroxy-3*H*-phenothiazine-3-one was negligible. The formation of promethazine 5-oxide was hardly influenced. The rate constant of promethazine degradation was reduced by edetate disodium at low pH values; at pH 6.3, *k′* had the same value as the standard (Fig. 1). The data available led to the conclusion that the stabilizing effect of edetate disodium on promethazine is due to removal of metal ions, primarily iron(III), from the solutions.

Influence of Antioxidants—Of the antioxidants investigated at pH 3.2, only hydroquinone and ascorbic acid interfered in the oxidation process. Sodium pyrosulfite had no effect under these circumstances.

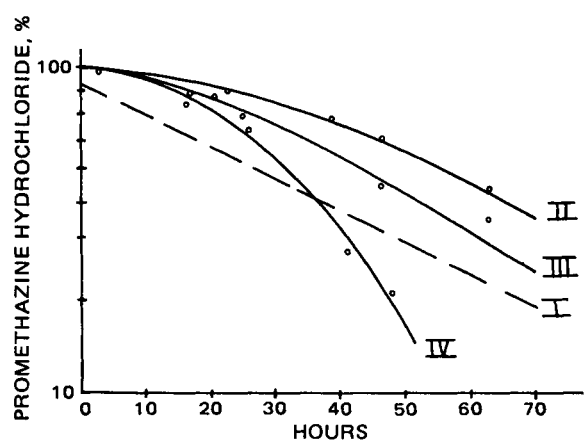

Figure 8—*Influence of hydroquinone on the degradation of promethazine at pH 3.2 under aerobic conditions at 65°. Key: curve I, no additive; curve II, 0.1% hydroquinone; curve III, 0.5% hydroquinone; and curve IV, 1.0% hydroquinone.*

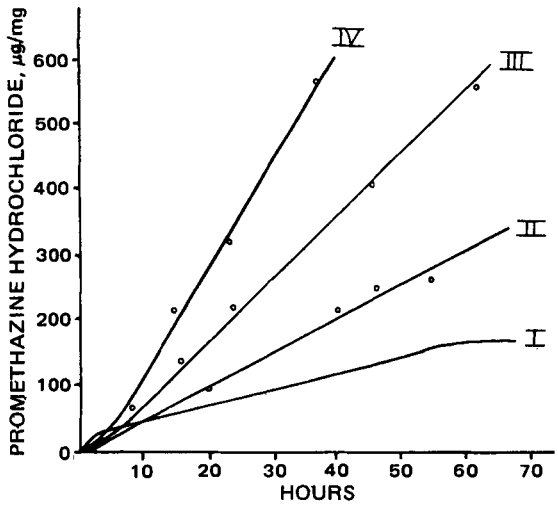

Figure 9—*Influence of hydroquinone on the formation of promethazine 5-oxide at pH 3.2 under aerobic conditions at 65°. Key: curve I, no additive; curve II, 0.1% hydroquinone; curve III, 0.5% hydroquinone; and curve IV, 1.0% hydroquinone.*

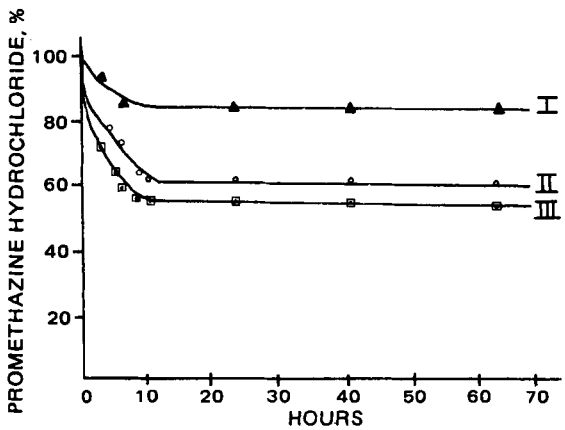

Figure 10—*Influence of copper(II) and iron(III) on the degradation of promethazine at pH 3.2 under anaerobic conditions at 100°. Key: curve I, no additive; curve II, 10^{-3} M iron(III); and curve III, 10^{-3} M copper(II).*

Ascorbic acid had an unpredictable effect on promethazine stability. Sometimes stabilization occurred, but the degradation increased in other cases. This phenomenon is possibly due to the instability of the antioxidant itself at this pH (10).

Figure 8 shows that low concentrations of hydroquinone protected promethazine from degradation. On increasing the concentration, the degradation accelerated and the reaction was not first order.

Figure 9 shows that the formation of promethazine 5-oxide increased dramatically in the presence of hydroquinone while other degradation products hardly were formed.

Degradation of Promethazine under Anaerobic Conditions—Only some initial degradation occurred, probably due to traces of oxygen left in the solution. When this oxygen was consumed, no further degradation took place. This degradation could be suppressed by adding antioxidants such as sodium pyrosulfite, hydroquinone, and ascorbic acid.

Degradation of promethazine under anaerobic conditions occurred in the presence of copper(II) and iron(III) only when these metals were present in the highest oxidation state (Fig. 10). The degradation products formed under these conditions were 10-methylphenothiazine, phenothiazine, and 3*H*-phenothiazine-3-one.

DISCUSSION

Scheme I represents the most probable mechanism for the oxidative degradation of promethazine (I). The first step is the loss of an electron from I to give a semiquinone free radical (II) (11–17). This reaction is reversible. Compound II is only stable under certain conditions. It can lose another electron to give the phenazothionium ion (III), and it can disproportionate to give I and III. Compound III hydrolyzes to promethazine 5-oxide (IV).

Radical II is subjected to another reaction, as shown by Waaler (18). Cleavage of the side chain passes *via* II since IV is the only product with an intact side chain. Waaler (18) found that the products of this reaction are 10-methylphenothiazine, acetaldehyde, and dimethylamine. Previously (6), it was shown that phenothiazine and formaldehyde also are formed. Roseboom and Perrin (19) showed that degradation of 10-methylphenothiazine does not lead to the formation of these products, so it is postulated that cleavage of the side chain of II results in the formation of the intermediate V*a*. This compound can be reduced to give 10-methylphenothiazine (VI); from the rest of the side chain, acetaldehyde (XVI) and dimethylamine (XVII) are formed *via* the carbonium ion XV.

Radical V*a* can undergo mesomerization to give V*b*. This intermediate is subjected to oxidation to give the carbonium ion VII, which can be hydrolyzed to phenothiazine VIII. The rest of the side chain is split off during this process, and formaldehyde (XVIII) is formed. Carbonium ion VII also can be oxidized to give the intermediate IX, which can be hydrolyzed to give the semiquinone radical X and XVIII. Compound X disproportionates to give VIII and phenazothionium ion XI*a*, as shown by Roseboom and Perrin (19). From XI*a*, 3*H*-phenothiazine-3-one (XIII) and 7-hydroxy-3*H*-phenothiazine-3-one (XIV) are formed *via* mesomer XI*b*. Compound XI*a* also undergoes hydrolysis to give phenothiazine 5-oxide (XII).

The influence of such factors as pH, metal ions, and antioxidants on the degradation process will be different for the two parallel reactions of radical II. An increase in pH causes an increase in the value of k'. At lower pH values, the formation of IV also increases. At pH 4.3, a maximum occurs; a further increase in pH greatly reduces the formation of IV. This phenomenon is not due to decomposition of IV, since IV is stable. Moreover, the formation of VI and VIII seems to increase with increasing pH. The explanation is that the cleavage of the side chain, *i.e.*, the formation of V*a* from II, is catalyzed by hydroxide ions in agreement with the findings of Waaler (18). An increase in pH decreases the formation of XIII and XIV, indicating that these compounds are formed under the influence of protons, as also shown by Roseboom and Perrin (19).

The degradation process is highly influenced by copper(II) and iron(III), but other metals do not interfere. Copper(II) catalyzes the formation of radical II from I, shown by the increase of k' and the increase in the formation of IV. Copper(II) ions also influence the formation of radical V*a* from II, shown by the increase of XIII and XIV. Since addition of copper(II) to a solution of I causes the formation of VIII and XIII under anaerobic conditions, copper(II) also promotes the formation of VII and the oxidation of this compound.

The influence of iron(III) on the degradation process is apparently different. There is a dramatic increase in the initial degradation rate on adding iron(III) ions to a solution of I, but the degradation rate after a short time decreases and a first-order reaction occurs with a rate constant equal to k' of the degradation without the addition of iron(III). The initial concentration of iron(III) causes a high oxidation potential and, thus, a high reaction rate. On reduction of iron(III) to iron(II), the oxidation potential decreases, causing a decrease in the degradation rate to the level of the degradation without added iron(III).

This phenomenon cannot be explained by assuming that hydrolysis of iron(III) at pH 3.2 causes precipitation of this ion since solutions of iron(III) with this pH remain clear even after storage. The difference between iron(III) and copper(II) is probably due to the much higher reaction rate of the oxidation of copper(I) to copper(II) under aerobic conditions in comparison to the oxidation of iron(II) to iron(III), which causes a higher oxidation potential in the copper-containing solutions during the whole degradation process.

Iron(III) promotes the cleavage of the side chain and the formation of radical V*a*, as shown by the decrease in the formation of IV, the increase in the formation of products without a side chain, and the occurrence of the latter products under anaerobic conditions. Both the formation of radical V*a* and carbonium ion VII are promoted.

Addition of edetate disodium decreases the rate constant k' of the degradation reaction, especially at lower pH values, while the speed of the formation of IV is almost the same and hardly any XIII and XIV are formed. The explanation of this phenomenon is that low concentrations of iron(III) in the medium catalyze the formation of radical II and the split off of the side chain and, thus, the formation of radical V*a* and other intermediates. The removal of iron(III) from the solution by addition of edetate disodium decreases the degradation and suppresses the cleavage

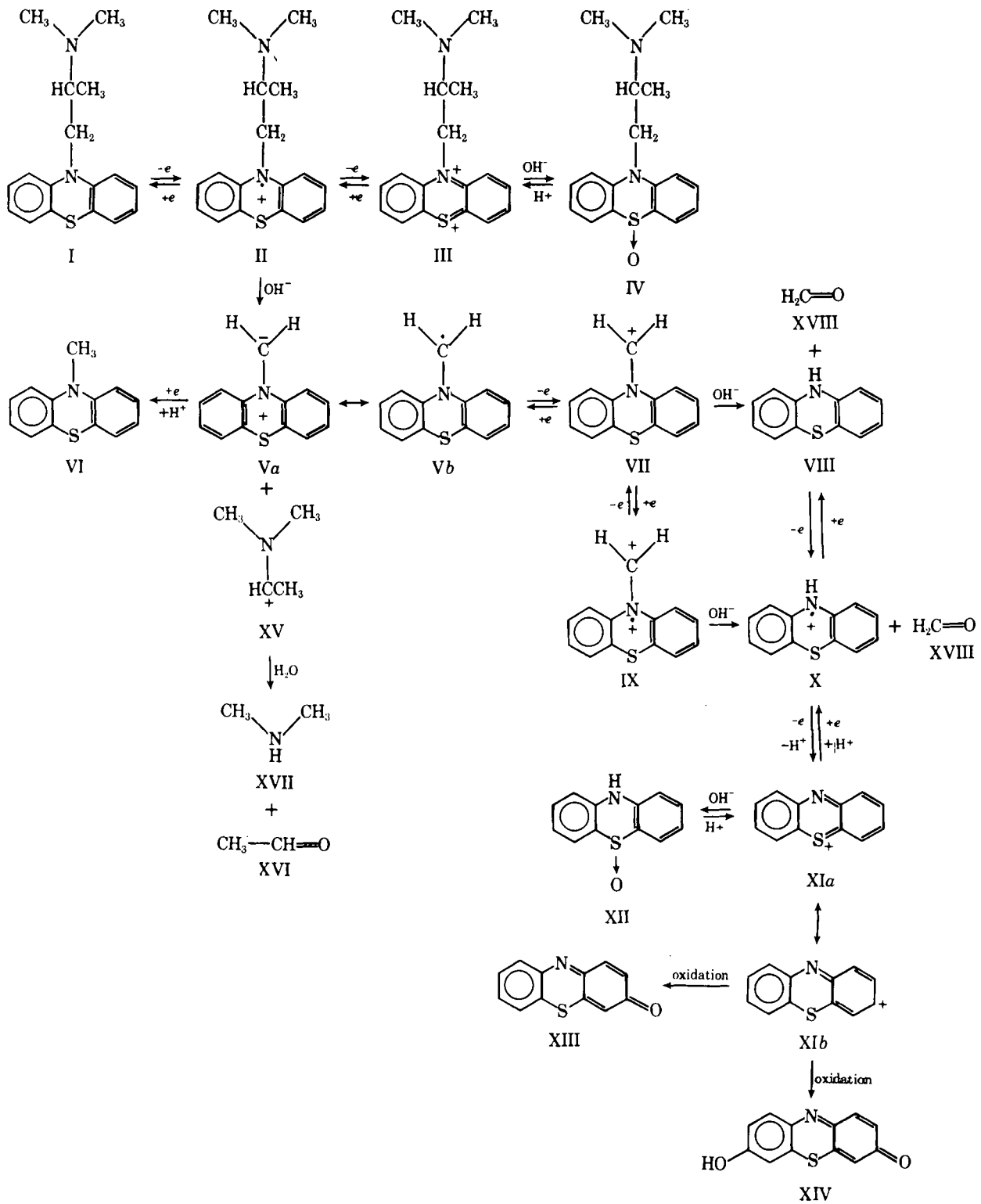

Scheme I

of the side chain so that IV is the main degradation product under these conditions.

Under the influence of hydroquinone, promethazine degradation initially decreases; but when the concentration of the antioxidant is increased, the degradation rate increases. Apparently, the oxidation products of hydroquinone, also being radicals (20), interfere in the redox process by promoting the formation of II and III. Since the formation of radical V*a* is by hydrolysis, the influence of hydroquinone on this reaction is negligible and IV is the main degradation product.

The influence of ascorbic acid on promethazine degradation probably can be explained in the same manner. Kassem *et al.* (10) found that ascorbic acid rapidly decomposes at lower pH values. During this process, radicals are formed that might interfere in the degradation of promethazine.

REFERENCES

(1) M. Chalabala, J. Knapp, and A. Burelova, *Cesk. Farm.*, **17**, 127 (1968); through *Chem. Abstr.*, **69**, 2187c (1968).

(2) J. J. L. Vila and R. Cadorniga Carro, *Chim. Phys. Appl. Prat. Ag. Surface, C. R. Congr. Int. Deterg. 5th*, 305 (1968); through *Chem. Abstr.*, **74**, 45572g (1968).

(3) I. Floderer and V. Horváthy, *Acta Pharm. Hung.*, **35**, 98 (1965); through *Chem. Abstr.*, **63**, 16160c (1965).
(4) B. J. Meakin, D. J. G. Davies, N. Cox, and J. Stevens, *Analyst*, **101**, 720 (1976).
(5) J. Stevens, B. J. Meakin, and D. J. G. Davies, *J. Pharm. Pharmacol.*, **24**, 133P (1972).
(6) W. J. M. Underberg, *J. Pharm. Sci.*, **67**, 1128 (1978).
(7) H. T. S. Britton, "Hydrogen Ions," vol. I, 4th ed., Chapman and Hall, London, England, 1955, p. 357.
(8) W. J. M. Underberg, Ph.D. thesis, University of Utrecht, Utrecht, The Netherlands, 1972.
(9) W. J. M. Underberg, *J. Pharm. Sci.*, **67**, 1131 (1978).
(10) M. A. Kassem, A. A. Kassem, and H. O. Ammar, *Pharm. Acta Helv.*, **44**, 611 (1969).
(11) L. Michaelis, M. P. Schubert, and S. Granick, *J. Am. Chem. Soc.*, **62**, 204 (1940).
(12) S. Granick, L. Michaelis, and M. P. Schubert, *ibid.*, **62**, 1802 (1940).
(13) L. Michaelis, S. Granick, and M. P. Schubert, *ibid.*, **63**, 351 (1941).
(14) D. C. Borg and C. G. Cotzias, *Proc. Natl. Acad. Sci. USA*, **46**, 617 (1962); through A. H. Beckett and S. H. Curry, *J. Pharm. Pharmacol.*, **15**, 246T (1963).
(15) L. H. Piette and I. S. Forrest, *Biochim. Biophys. Acta*, **57**, 419 (1962); through A. H. Beckett and S. H. Curry, *J. Pharm. Pharmacol.*, **15**, 246T (1963).
(16) A. H. Beckett and S. H. Curry, *J. Pharm. Pharmacol.*, **15**, 246T (1963).
(17) A. Feldmeister, R. Schaubman, and H. Howe, *J. Pharm. Sci.*, **54**, 1589 (1965).
(18) T. Waaler, *Pharm. Acta Helv.*, **35**, 168 (1960).
(19) H. Roseboom and J. H. Perrin, *J. Pharm. Sci.*, **66**, 1395 (1977).
(20) D. J. Cram and G. S. Hammond, "Organic Chemistry," 2nd ed., McGraw-Hill, New York, N.Y., 1964, p. 515.

Determination of Ethinyl Estradiol in Human Urine by Radiochemical GLC

FRANCIS R. ZULESKI *, ARTHUR LOH ‡, and FREDERICK J. DI CARLO §x

Received June 6, 1977, from the *Department of Drug Metabolism, Warner-Lambert Research Institute, Morris Plains, NJ 07950.* Accepted for publication December 1, 1977. *Present address: ICI Americas, Wilmington, DE 19897. ‡Present address: Hoffmann-La Roche Inc., Nutley, NJ 07111. §Present address: Office of Toxic Substances, U.S. Environmental Protection Agency, Washington, DC 20460.

Abstract □ A radiochemical GLC analysis was developed for ^{3}H-labeled ethinyl estradiol in human urine. The technique was applied to the unconjugated and aglycone fractions of urine collected from women who were dosed orally with: (*a*) single capsules containing 2.0 mg of ^{3}H-quinestrol (900 μCi) and 2.5 mg of unlabeled quingestanol acetate dissolved in sesame oil and (*b*) single tablets containing 100 μg of ^{3}H-quinestrol (86 μCi). Unconjugated ethinyl estradiol in Day 1 urine collections represented means of 0.02% of the high quinestrol dose and 0.12% of the low dose. Ethinyl estradiol glucuronide in the same collections represented means of 0.55% of the high drug dose and 1.35% of the low dose. The method could detect 1-ng quantities of ^{3}H-ethinyl estradiol and ^{3}H-quinestrol.

Keyphrases □ Ethinyl estradiol—radiochemical GLC analysis in human urine □ Radiochemical GLC—analysis, ethinyl estradiol in human urine □ GLC, radiochemical—analysis, ethinyl estradiol in human urine □ Estrogens—ethinyl estradiol, radiochemical GLC analysis in human urine

Radiochemical GLC (1–14), a system of monitoring the eluates from GLC columns for radioactive compounds, has the capability of detecting only the labeled compounds in complex mixtures of predominantly unlabeled components. Moreover, this system offers flexibility, convenience, specificity, and high sensitivity.

This paper reports a drug metabolism study using radiochemical GLC. Single low doses of ^{3}H-quinestrol (17α-ethinyl estradiol 3-cyclopentyl ether) were administered to women, and their urine was assayed for quinestrol and its metabolite ethinyl estradiol. This biotransformation was described previously (15, 16), but information on the extent of the conversion is lacking.

EXPERIMENTAL

Radioactive Ethinyl Estradiol—Merrill and Vernice (17) described the synthesis of 6,7-^{3}H-ethinyl estradiol with a specific activity of 275 mCi/mmole. Its chemical purity and radiochemical purity were approximately 99%.

Radioactive Quinestrol—The synthesis of this compound (mol. wt. 364.5) from ^{3}H-ethinyl estradiol also was reported previously (17). The oral contraceptive dose consisted of a capsule containing 2.0 mg of ^{3}H-quinestrol (900 μCi) and 2.5 mg of unlabeled quingestanol acetate in 0.2 ml of sesame oil stabilized with 0.05% piperidine. The estrogen replacement dose was a tablet containing 100 μg of ^{3}H-quinestrol (86 μCi).

Radioactivity Measurements—The scintillation counting solution was prepared by dissolving 6 g of 2,5-diphenyloxazole and 100 mg of 1,4-bis[2-(4-methyl-5-phenyloxazolyl)]benzene in 1 liter of ethanol–toluene (17:100). By using internal standardization, 200-μl samples of urine were counted in 20 ml of this solution with a liquid scintillation spectrometer[1] at 4°.

Radiochemical GLC—An oven and proportioning temperature controller[2] were connected to a gas proportional counter[3] by a heated glass-lined metal tube. The operating conditions for the gas chromatograph were: column, 1.8 m coiled glass, 2 mm i.d., 20% SE-30 on 80–100-mesh Gas Chrom Q; carrier gas (helium) flow rate, 50 ml/min; oven temperature, 215°; and injector temperature, 245°. The operating conditions for the gas proportional counter were: quench gas (propane) flow rate, 2.5 ml/min; hydrogen flow rate, 10 ml/min; transfer line temperature, 237°; and oxidizer and reduction furnace temperature, 750°.

Preparation of Standard Curves—Quantitation of ^{3}H-ethinyl estradiol peaks was accomplished by the following absolute calibration method. A stock solution of ^{3}H-ethinyl estradiol in methanol was prepared; its concentration was 140,380 dpm/4.0 μl. From this stock solution, serial twofold dilutions were made to give a set of standards corresponding to 70,190, 35,100, 17,550, and 8775 dpm/4.0 μl. Aliquots (4.0 μl) of the standards were injected into the gas chromatograph so that a standard curve could be constructed by integration (planimetry) of the resultant peaks. Data plotted in this manner yielded acceptable straight lines. However, it was necessary to generate a new curve each day because the slope varied from day to day.

The standard curves from one column are shown in Fig. 1; curve A was obtained on Day 1, curve B on Day 2, curve C on Day 3, and curve D on

[1] Tri-Carb model 3320, Packard Instrument Co., Downers Grove, Ill.
[2] Warner-Chilcott, Morris Plains, N.J.
[3] Model 894, Packard Instrument Co., Downers Grove, Ill.

0022-3549/78/0800-1138$01.00/0
© 1978, American Pharmaceutical Association

(3) I. Floderer and V. Horváthy, *Acta Pharm. Hung.*, **35**, 98 (1965); through *Chem. Abstr.*, **63**, 16160c (1965).
(4) B. J. Meakin, D. J. G. Davies, N. Cox, and J. Stevens, *Analyst*, **101**, 720 (1976).
(5) J. Stevens, B. J. Meakin, and D. J. G. Davies, *J. Pharm. Pharmacol.*, **24**, 133P (1972).
(6) W. J. M. Underberg, *J. Pharm. Sci.*, **67**, 1128 (1978).
(7) H. T. S. Britton, "Hydrogen Ions," vol. I, 4th ed., Chapman and Hall, London, England, 1955, p. 357.
(8) W. J. M. Underberg, Ph.D. thesis, University of Utrecht, Utrecht, The Netherlands, 1972.
(9) W. J. M. Underberg, *J. Pharm. Sci.*, **67**, 1131 (1978).
(10) M. A. Kassem, A. A. Kassem, and H. O. Ammar, *Pharm. Acta Helv.*, **44**, 611 (1969).
(11) L. Michaelis, M. P. Schubert, and S. Granick, *J. Am. Chem. Soc.*, **62**, 204 (1940).
(12) S. Granick, L. Michaelis, and M. P. Schubert, *ibid.*, **62**, 1802 (1940).
(13) L. Michaelis, S. Granick, and M. P. Schubert, *ibid.*, **63**, 351 (1941).
(14) D. C. Borg and C. G. Cotzias, *Proc. Natl. Acad. Sci. USA*, **46**, 617 (1962); through A. H. Beckett and S. H. Curry, *J. Pharm. Pharmacol.*, **15**, 246T (1963).
(15) L. H. Piette and I. S. Forrest, *Biochim. Biophys. Acta*, **57**, 419 (1962); through A. H. Beckett and S. H. Curry, *J. Pharm. Pharmacol.*, **15**, 246T (1963).
(16) A. H. Beckett and S. H. Curry, *J. Pharm. Pharmacol.*, **15**, 246T (1963).
(17) A. Feldmeister, R. Schaubman, and H. Howe, *J. Pharm. Sci.*, **54**, 1589 (1965).
(18) T. Waaler, *Pharm. Acta Helv.*, **35**, 168 (1960).
(19) H. Roseboom and J. H. Perrin, *J. Pharm. Sci.*, **66**, 1395 (1977).
(20) D. J. Cram and G. S. Hammond, "Organic Chemistry," 2nd ed., McGraw-Hill, New York, N.Y., 1964, p. 515.

Determination of Ethinyl Estradiol in Human Urine by Radiochemical GLC

FRANCIS R. ZULESKI *, ARTHUR LOH ‡, and FREDERICK J. DI CARLO §x

Received June 6, 1977, from the *Department of Drug Metabolism, Warner-Lambert Research Institute, Morris Plains, NJ 07950.* Accepted for publication December 1, 1977. *Present address: ICI Americas, Wilmington, DE 19897. ‡Present address: Hoffmann-La Roche Inc., Nutley, NJ 07111. §Present address: Office of Toxic Substances, U.S. Environmental Protection Agency, Washington, DC 20460.

Abstract □ A radiochemical GLC analysis was developed for ^{3}H-labeled ethinyl estradiol in human urine. The technique was applied to the unconjugated and aglycone fractions of urine collected from women who were dosed orally with: (*a*) single capsules containing 2.0 mg of ^{3}H-quinestrol (900 μCi) and 2.5 mg of unlabeled quingestanol acetate dissolved in sesame oil and (*b*) single tablets containing 100 μg of ^{3}H-quinestrol (86 μCi). Unconjugated ethinyl estradiol in Day 1 urine collections represented means of 0.02% of the high quinestrol dose and 0.12% of the low dose. Ethinyl estradiol glucuronide in the same collections represented means of 0.55% of the high drug dose and 1.35% of the low dose. The method could detect 1-ng quantities of ^{3}H-ethinyl estradiol and ^{3}H-quinestrol.

Keyphrases □ Ethinyl estradiol—radiochemical GLC analysis in human urine □ Radiochemical GLC—analysis, ethinyl estradiol in human urine □ GLC, radiochemical—analysis, ethinyl estradiol in human urine □ Estrogens—ethinyl estradiol, radiochemical GLC analysis in human urine

Radiochemical GLC (1–14), a system of monitoring the eluates from GLC columns for radioactive compounds, has the capability of detecting only the labeled compounds in complex mixtures of predominantly unlabeled components. Moreover, this system offers flexibility, convenience, specificity, and high sensitivity.

This paper reports a drug metabolism study using radiochemical GLC. Single low doses of ^{3}H-quinestrol (17α-ethinyl estradiol 3-cyclopentyl ether) were administered to women, and their urine was assayed for quinestrol and its metabolite ethinyl estradiol. This biotransformation was described previously (15, 16), but information on the extent of the conversion is lacking.

EXPERIMENTAL

Radioactive Ethinyl Estradiol—Merrill and Vernice (17) described the synthesis of 6,7-^{3}H-ethinyl estradiol with a specific activity of 275 mCi/mmole. Its chemical purity and radiochemical purity were approximately 99%.

Radioactive Quinestrol—The synthesis of this compound (mol. wt. 364.5) from ^{3}H-ethinyl estradiol also was reported previously (17). The oral contraceptive dose consisted of a capsule containing 2.0 mg of ^{3}H-quinestrol (900 μCi) and 2.5 mg of unlabeled quingestanol acetate in 0.2 ml of sesame oil stabilized with 0.05% piperidine. The estrogen replacement dose was a tablet containing 100 μg of ^{3}H-quinestrol (86 μCi).

Radioactivity Measurements—The scintillation counting solution was prepared by dissolving 6 g of 2,5-diphenyloxazole and 100 mg of 1,4-bis[2-(4-methyl-5-phenyloxazolyl)]benzene in 1 liter of ethanol–toluene (17:100). By using internal standardization, 200-μl samples of urine were counted in 20 ml of this solution with a liquid scintillation spectrometer[1] at 4°.

Radiochemical GLC—An oven and proportioning temperature controller[2] were connected to a gas proportional counter[3] by a heated glass-lined metal tube. The operating conditions for the gas chromatograph were: column, 1.8 m coiled glass, 2 mm i.d., 20% SE-30 on 80–100-mesh Gas Chrom Q; carrier gas (helium) flow rate, 50 ml/min; oven temperature, 215°; and injector temperature, 245°. The operating conditions for the gas proportional counter were: quench gas (propane) flow rate, 2.5 ml/min; hydrogen flow rate, 10 ml/min; transfer line temperature, 237°; and oxidizer and reduction furnace temperature, 750°.

Preparation of Standard Curves—Quantitation of ^{3}H-ethinyl estradiol peaks was accomplished by the following absolute calibration method. A stock solution of ^{3}H-ethinyl estradiol in methanol was prepared; its concentration was 140,380 dpm/4.0 μl. From this stock solution, serial twofold dilutions were made to give a set of standards corresponding to 70,190, 35,100, 17,550, and 8775 dpm/4.0 μl. Aliquots (4.0 μl) of the standards were injected into the gas chromatograph so that a standard curve could be constructed by integration (planimetry) of the resultant peaks. Data plotted in this manner yielded acceptable straight lines. However, it was necessary to generate a new curve each day because the slope varied from day to day.

The standard curves from one column are shown in Fig. 1; curve A was obtained on Day 1, curve B on Day 2, curve C on Day 3, and curve D on

[1] Tri-Carb model 3320, Packard Instrument Co., Downers Grove, Ill.
[2] Warner-Chilcott, Morris Plains, N.J.
[3] Model 894, Packard Instrument Co., Downers Grove, Ill.

0022-3549/78/0800-1138$01.00/0
© 1978, American Pharmaceutical Association

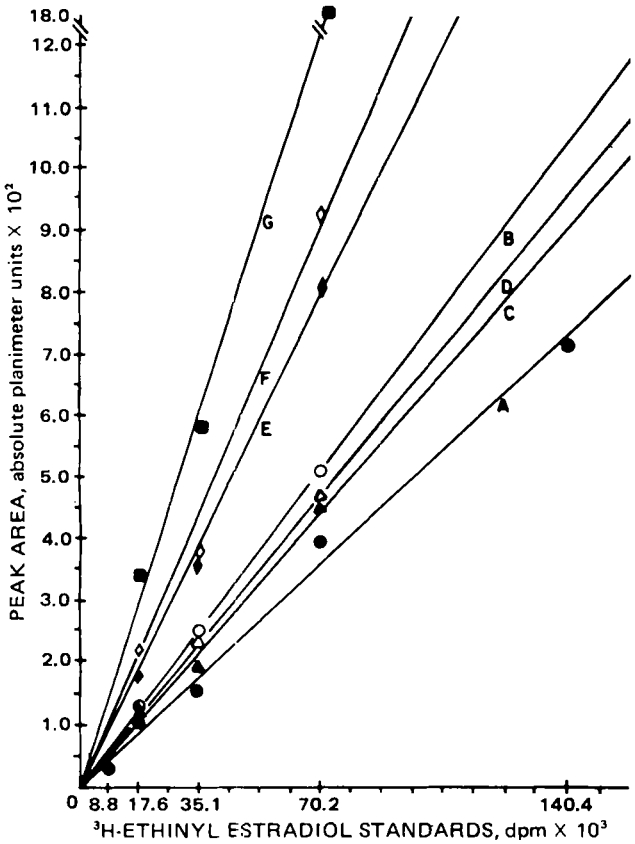

Figure 1—*Representative standard curves used for quantitation of ^3H-ethinyl estradiol in the unconjugated and aglycone fractions.*

Day 6. The second family of curves in Fig. 1 (E, F, and G) was obtained from a second column prepared identically. Their slopes increased in a chronological fashion in contrast to the first family of curves (A, B, C, and D). Sample peaks corresponding to ^3H-ethinyl estradiol were integrated by planimetry, and the disintegrations per minute of tritium present were determined by reference to the appropriate standard curve.

For quantitation of ^3H-quinestrol, a set of five standards was prepared by serial twofold dilutions of a ^3H-quinestrol stock solution with a concentration of 69,600 dpm/2.0 μl. Aliquots (2.0 μl) of the standards (34,800, 17,400, 8700, 4350, and 2175 dpm/2.0 μl) were injected into the gas chromatograph for standard curve preparation. The two standard curves are shown in Fig. 2. Curve A was obtained on Day 1 and curve B on Day 2.

Subjects, Doses, and Urine Collection—Eight healthy women participated in the study after being informed of all potential hazards. Four women (Group I), 21–26 years of age, each were given one capsule of the oral contraceptive formulation. The second four women (Group II), 42–47 years of age, each were given one estrogen replacement tablet. All subjects collected all urine for 24 hr after drug administration. These collections were stored frozen.

Fractionation of Urine—Thirty percent of the 0–24-hr urine collected by each subject was removed for individual fractionation. First each aliquot was concentrated to 30–50 ml by flash evaporation at 40–50° and poured onto an ion-exchange resin[4] column (2.5 × 50 cm). After the column was rinsed with 1 liter of deionized water, the adsorbed materials were eluted with methanol. Thirty fractions (10 ml each) were collected.

In general, a major peak of radioactivity was eluted in tubes 13–26. The contents of these tubes were pooled and evaporated to dryness under nitrogen. After 50 ml of deionized water was added to the residue, the pH was adjusted to 7; then the solution was extracted four times with 30-ml portions of ether to collect unconjugated steroids. The ether extracts were combined and concentrated to 30 ml under nitrogen. A 0.5-ml aliquot was removed and assayed for tritium. After the remaining ether solution was evaporated to dryness under nitrogen, the residue was dissolved in 50 μl of methanol for injection into the system.

[4] Amberlite XAD-2.

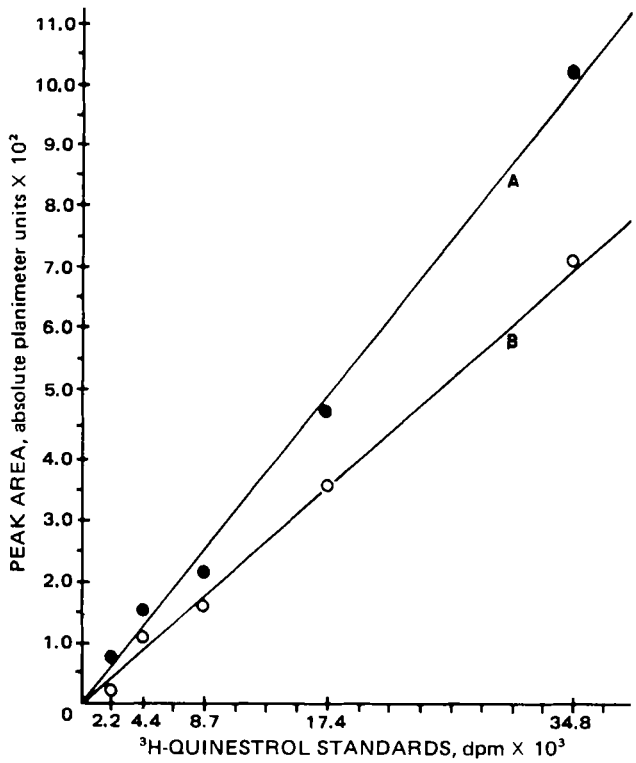

Figure 2—*Representative standard curves used for quantitation of ^3H-quinestrol in the unconjugated and aglycone fractions.*

The aqueous solution remaining after ether extraction was adjusted to pH 5.5 and incubated for 24 hr at 37° with 50,000 units of β-glucuronidase. The solution was then extracted with four 20-ml volumes of ether, and an additional quantity of β-glucuronidase was added to the aqueous phase. Following reincubation, the solution was extracted with ether as already described. The ether extracts were combined, evaporated under nitrogen to 2.0 ml, and chromatographed on a 1 × 36-cm column[5] with methanol as the eluant.

Twenty-five fractions (3.0 ml/9.0 min/fraction) were collected, and a 0.3-ml aliquot of each was assayed for tritium to find the center of the radioactive peak. In general, the peak was located between tubes 6 and 13. The contents of these tubes were pooled and evaporated to 2.0 ml; aliquots were counted to determine ^3H-recovery and injected into the system for analysis.

RESULTS

Standard Curves—The ability of the detector to respond in a proportional manner to tritium became evident from radiochromatograms of serially diluted solutions of ^3H-ethinyl estradiol. Twofold dilutions yielded proportional results with respect to both peak height and peak area (Fig. 3). Under operating conditions that achieved satisfactory resolution, standard curves were developed for ^3H-quinestrol (retention time of 53 min) and ^3H-ethinyl estradiol (retention time of 15 min). The ranges covered were 2175–34,800 dpm for quinestrol and 8775–140,380 dpm for ethinyl estradiol. The curves generated by plotting disintegrations per minute *versus* absolute planimeter units are presented in Figs. 1 and 2.

Reference to Fig. 1 shows clearly that a family of standard curves was obtained from each chromatographic column. Curves A, B, C, and D were developed in that sequence after injecting the indicated quantities of ^3H-ethinyl estradiol onto the same column on different days; curves E, F, and G were developed similarly with another column, presumably identical to the first. The slopes of the curves and, therefore, the sensitivity of the assay varied considerably and indicated the necessity of preparing a standard curve on the same day that the assays were performed to maintain reproducibility within replicates at approximately 5%.

Figure 2 presents two standard curves generated for ^3H-quinestrol on

[5] Sephadex LH-20.

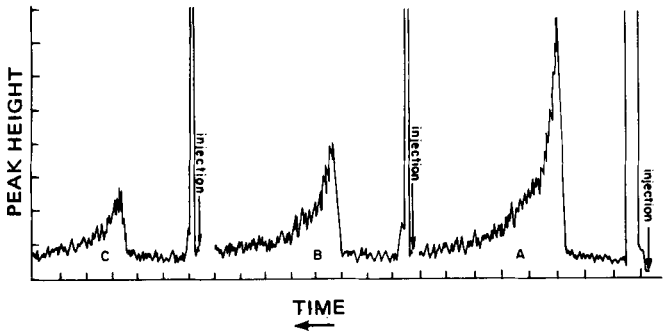

Figure 3—*Radiochromatograms of known ^{3}H-ethinyl estradiol representing serial twofold dilutions for standard curve preparation. The height and area of peak B are one-half those of peak A; peak C has a height and an area that are one-half those of B.*

different days. Like the ^{3}H-ethinyl estradiol curves, they differ markedly, confirming the conclusion that standard curves must be run on the same days as assays.

Urinary Excretion of Radioactivity—Table I shows the quantities of tritium excreted within 24 hr by each subject. The data are expressed in terms of quinestrol equivalents. The mean excretion of the dose was 4.6 ± 0.7% by Group I and 7.7 ± 1.0% by Group II.

Radioactivity in Unconjugated and Aglycone Fractions of Urine—The distribution of tritium between the unconjugated and aglycone urine fractions of each subject is listed in Table II. Each urine specimen contained small quantities (1.7–3.9%) of labeled unconjugated steroids and significant amounts (15.3–54.8%) of labeled steroid glucuronides, including ethinyl estradiol glucuronide (mol. wt. 472.5).

Radiochemical GLC of Urine Fractions—Typical responses following the injection of unconjugated and aglycone fractions appear in Figs. 4 and 5. All fractions showed the presence of only one peak, and the retention time of this peak corresponded to ^{3}H-ethinyl estradiol (Fig. 3). When a stream splitter was used to direct one part of the column effluent into a flame-ionization detector and 10 parts into the gas proportional counter, the mass response showed the presence of several components in addition to ethinyl estradiol. The splitter was not employed for quantitative purposes because steroids adsorb to stainless steel.

Table I—Description of Women and Their Urinary Excretion of Tritium from 0 to 24 hr after Treatment with ^{3}H-Quinestrol

Group	Subject	Age, years	Weight, kg (lb)	Equivalents of Quinestrol in 0–24-hr Urine, μg
I[a]	1	26	50 (111)	115.80
	2	24	89 (196)	68.00
	3	24	63 (138)	70.40
	4	21	49 (107)	113.20
			Mean ± *SE*	91.85 ± 13.10
II[b]	5	45	61 (135)	10.36
	6	45	57 (126)	5.27
	7	47	68 (151)	7.37
	8	42	49 (108)	7.67
			Mean ± *SE*	7.67 ± 1.04

[a] Given capsule containing 2.0 mg of ^{3}H-quinestrol (900 μCi) and 2.5 mg of unlabeled quingestanol acetate. [b] Given tablet containing 100 μg of ^{3}H-quinestrol (86 μCi).

Table II—Recovery of Tritium in the Unconjugated and Aglycone Fractions of Urine

Group	Subject	Tritium in Urine, %	
		Unconjugated	Aglycone
I	1	3.39	42.29
	2	3.07	29.12
	3	3.89	54.77
	4	1.70	17.59
	Mean ± *SE*	3.01 ± 0.47	35.94 ± 8.05
II	5	2.59	37.91
	6	1.80	15.32
	7	3.83	27.47
	8	2.61	34.25
	Mean ± *SE*	2.71 ± 0.42	28.74 ± 4.97

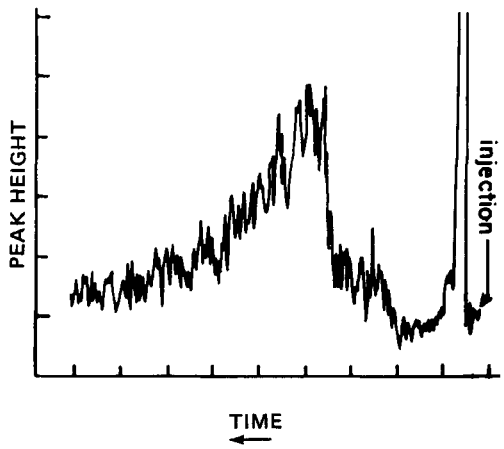

Figure 4—*Typical radiochromatogram of an unconjugated fraction.*

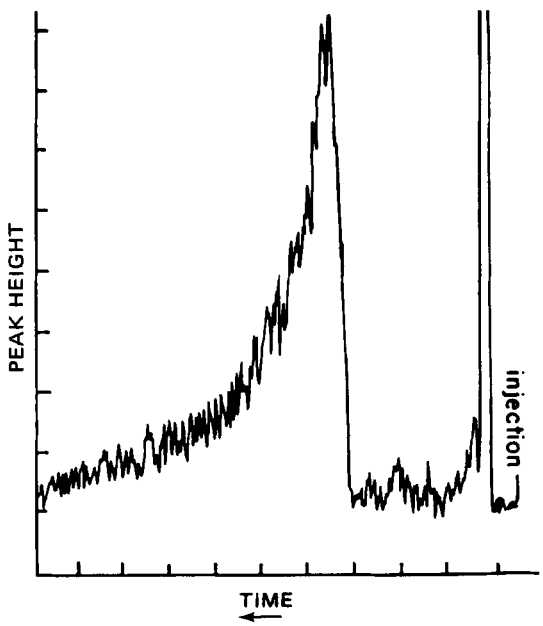

Figure 5—*Typical radiochromatogram of an aglycone fraction.*

Although the ^{3}H-ethinyl estradiol in several unconjugated fractions was represented by small peaks, these peaks were clearly defined and their areas could be measured accurately. With the exception of one fraction, appropriate standard solutions of ^{3}H-ethinyl estradiol were used for calibration so that the area of the metabolite ethinyl estradiol peak was read from a portion of the standard curve that included points on both sides of the metabolite point.

Table III shows the recoveries of tritium as ^{3}H-ethinyl estradiol in the unconjugated and aglycone fractions for both groups. The percentage

Table III—Ethinyl Estradiol Content of Unconjugated and Aglycone Fractions

Group	Subject	Tritium in Fraction as ^{3}H-Ethinyl Estradiol, %	
		Unconjugated	Aglycone
I	1	21.4	74.3
	2	7.8	41.1
	3	12.4	9.4
	4	21.7	30.4
	Mean ± *SE*	15.8 ± 3.4	38.8 ± 13.5
II	5	105.2	59.0
	6	100.1	87.4
	7	23.6	99.6
	8	64.5	61.4
	Mean ± *SE*	73.4 ± 18.9	76.9 ± 9.9

Table IV—Ethinyl Estradiol in Unconjugated and Aglycone Fractions

Group	Subject	Ethinyl Estradiol, μg	
		Unconjugated	Aglycone
I	1	0.68	29.50
	2	0.13	6.59
	3	0.28	2.93
	4	0.34	4.90
	Mean ± *SE*	0.36 ± 0.12	10.98 ± 6.22
II	5	0.23	1.88
	6	0.08	0.57
	7	0.05	1.64
	8	0.10	1.31
	Mean ± *SE*	0.12 ± 0.04	1.35 ± 0.28

recoveries listed are based on the total tritium present in each fraction. For Group I, ^{3}H-ethinyl estradiol constituted approximately 8–22% of the unconjugated fraction; for Group II, the recovery was 24–100%. The aglycone fraction of Group I was composed of 9–74% ethinyl estradiol; again the recovery for Group II was much higher, ranging from 59 to 100%.

Presented in Table IV are the total quantities of ethinyl estradiol found in the unconjugated and aglycone fractions of the urine collected from each subject. The largest amounts of this metabolite were present in the aglycone fraction of every subject. The range for Group I was approximately 3–30 μg; for Group II, it was 0.6–1.9 μg. Unconjugated ethinyl estradiol was found in small amounts: 0.1–0.7 and 0.05–0.2 μg for Groups I and II, respectively. Although more ethinyl estradiol was present in both urine fractions of Group I, the quantities were considerably less than the 20-fold difference in the administered doses. Besides reflecting wide interpersonal differences of the quantities of ethinyl estradiol and its glucuronide excreted by members of a given group, the data show that there were large interpersonal differences in the ratio of these metabolites.

DISCUSSION

The radiochemical GLC unit developed functioned satisfactorily in the present drug metabolism study, making it clear that the method has wide applicability. The instrumentation also can be applied to the assay of body fluids for nonradioactive drugs, drug metabolites, and endogenous compounds after the target compound is derivatized with a radioactive reagent (14).

There are two potential problems with radiochemical GLC. One problem relates to the quantity of radioactivity in the injected aliquot. When this level was too high, radioactivity tended to bleed from the column and to produce a heightened "noisy" baseline, which sometimes persisted for 30 min. This on-column degradation produced a dark, dense plug in the throat of the column. It was impossible to identify the material because it could be dissolved only in concentrated acid. The second problem is the necessity of preparing a standard curve for each day on which assays are performed. The most important operational parameter contributing to the difficulty is the composition of the counting gas. In the described setup, there might have been minor inadvertant differences in mixing the three gases at different times.

Intact quinestrol was not found in the urine of any subject who ingested the compound. In view of the ability of the instrument to detect 1300 dpm of ^{3}H-quinestrol, the specific activities of the administered labeled compound preparations would allow finding 1.3 ng of quinestrol in Group I specimens and 0.68 ng in Group II specimens. Therefore, quinestrol would have submitted to assay if either the Group I fraction had contained the drug to the extent of 0.003% of the dose or the Group II fraction had contained quinestrol to the extent of 0.03% of the dose.

This investigation confirmed the *O*-dealkylation of quinestrol to ethinyl estradiol *in vivo* and quantified this conversion for the first time. This quantification was limited to unconjugated ethinyl estradiol and its glucuronide. The use of reverse isotope dilution in an earlier study (18) indicated that women dosed with ^{3}H-ethinyl estradiol excreted conjugated ethinyl estradiol, 2-methoxy-17α-ethinyl estradiol, 2-hydroxy-17α-ethinyl estradiol 3-methyl ether, and 17αβ-D-homoestradiol.

REFERENCES

(1) F. Drawert and O. Bachmann, *Angew. Chem.*, **75**, 717 (1963).

(2) F. Drawert, A. Rapp, and H. Ullemeyer, *Vitis*, **6**, 177 (1967).

(3) R. Tressl and F. Drawert, *Z. Naturforsch. Teil B*, **26**, 774 (1971).

(4) U. Groth and H.-G. Neumann, *Chem. Biol. Interact.*, **4**, 409 (1971).

(5) I. Hanin, R. Masarel, and E. Costa, *Pharmacologist*, **13**, 242 (1971).

(6) M. Metzler and H.-G. Neumann, *Z. Krebsforsch.*, **76**, 16 (1971).

(7) W. H. Wientjens, T. van der Marel, and E. P. Bennet, *Experientia*, **27**, 373 (1971).

(8) J. R. L. Smith, B. A. J. Shaw, and D. M. Foulkes, *Xenobiotica*, **2**, 215 (1972).

(9) R. Takeda, M. Noto, and M. Murakami, *Clin. Chim. Acta*, **36**, 163 (1972).

(10) H.-G. Newmann and J. Schenk, *Xenobiotica*, **3**, 435 (1973).

(11) A. S. Goldman and D. A. Klingele, *Endocrinology*, **94**, 1 (1974).

(12) K. Buchtela, F. Grass, and G. Muller, *J. Chromatogr.*, **103**, 141 (1975).

(13) A. Kuksis, N. Kovacevic, D. Lau, and M. Vranic, *Fed. Proc.*, **34**, 2238 (1975).

(14) A. Loh, F. R. Zuleski, and F. J. Di Carlo, *J. Pharm. Sci.*, **66**, 1056 (1977).

(15) K. I. H. Williams, D. S. Layne, R. Hobkirk, M. Nilsen, and P. R. Blahey, *Steroids*, **9**, 275 (1967).

(16) D. I. Cargill, B. G. Steinetz, E. Gosnell, V. L. Beach, A. Meli, G. I. Fujimoto, and B. M. Reynolds, *J. Clin. Endocrinol. Metab.*, **29**, 1051 (1969).

(17) E. J. Merrill and G. G. Vernice, *J. Labelled Compd.*, **6**, 266 (1970).

(18) M. T. Abdel-Aziz and K. I. H. Williams, *Steroids*, **15**, 695 (1970).

ACKNOWLEDGMENTS

The authors are indebted to Mr. Edward J. Merrill, their late colleague and friend, of the Warner-Lambert Research Institute for synthesizing radiolabeled quinestrol and for preparing the pharmaceutical dosage forms with the aid of Mr. Alexander Nutzul of the same Institute.

Spectrophotofluorometric Analysis of 3′,4′,7-Tris[*O*-(β-hydroxyethyl)]rutoside in Urine

HENRY S. I. TAN ˣ, PAT J. MOWERY, WOLFGANG A. RITSCHEL, and CHARLES NEU

Received April 21, 1977, from the *College of Pharmacy, University of Cincinnati Medical Center, Cincinnati, OH 45267.* Accepted for publication December 2, 1977.

Abstract □ A sensitive procedure was developed for 3′,4′,7-tris[*O*-(β-hydroxyethyl)]rutoside (I) in urine. The method is based on the fluorescence behavior of the I–aluminum complex in absolute methanol. This complex has activation and emission wavelengths of 420 and 480 nm, respectively. Optimum conditions for the reaction were investigated. The fluorescence was linear (r = 0.998) in the range of 0.1–4.0 μg of I/ml. At concentrations below 0.1 μg/ml, a shift in the emission wavelength was observed. Replicate studies (n = 9) of spiked urine samples, each containing 0.4 μg of I/ml, showed good precision with a relative standard deviation of 0.009. Overall percent recovery (± *SEM*) from five urine samples was 99.5 ± 1.34%. Following a single 500-mg po dose of I to individuals, only traces of I were found in the urine. However, β-glucuronidase treatment of urine resulted in a total cumulative urine excretion of 26.53 mg of I after 78.6 hr.

Keyphrases □ 3′,4′,7-Tris[*O*-(β-hydroxyethyl)]rutoside—spectrophotofluorometric analysis in urine □ Spectrophotofluorometry—analysis, 3′,4′,7-tris[*O*-(β-hydroxyethyl)]rutoside in urine

3′,4′,7-Tris[*O*-(β-hydroxyethyl)]rutoside[1] (I), a bioflavonoid, is widely used in Europe for the treatment of some pathological conditions associated with the increased permeability or fragility of blood capillaries such as varicosis and chronic erythema. For pharmacokinetic studies on I and its dosage forms, a simple, yet sensitive, analytical procedure for I in urine is needed.

Flavonoids form complexes in the presence of aluminum chloride (1). 3′,4′,5,7-Tetrahydroxyflavonol-3-rutinoside, for example, was determined by precipitating the drug–aluminum complex with ammonia, followed by redissolving the complex in acetic acid and measuring absorbance after addition of potassium acetate solution (2).

Previous determinations of I in blood or urine were based on quantitative TLC. Wienert and Gahlen (3) irradiated the chromatogram by UV light and quantitated the spots by visual comparison of the fluorescence produced. Foerster and Ziege (4) sprayed the chromatograms with methanolic aluminum chloride and measured the resulting fluorescence densitometrically. The time required for the elution was 1–6 hr. The UV absorption spectra of the hydroxyethylrutosides were determined in the presence of aluminum chloride (5). Recently, liquid scintillation counting was used to study ^{14}C-I metabolism (6).

This paper reports the spectrophotofluorometric analysis of I in urine based on its complex formation with aluminum chloride in absolute methanol.

EXPERIMENTAL

Apparatus—The following instruments were used: a ratio spectrophotofluorometer[2] with 1-cm cells and excitation exit, emission entrance, and rotary exit slit widths of 2 mm; and an analytical balance[3]. The spectrophotofluorometer was calibrated daily using a solid fluorescence standard[4].

Materials and Reagents—The following were used: I[5] (mp 175°), 0.1 *M* aluminum chloride[6] (anhydrous, reagent grade) in absolute methanol[6] (water content 0.05%), and β-glucuronidase solution, prepared by dissolving 0.139 g of β-glucuronidase[7] (bovine liver, 15–50 U/g) in 10 ml of distilled water.

Preparation of Standard Curve—Weigh accurately ~25 mg of I and dissolve in 100.0 ml of absolute methanol. Prepare standard solutions containing 1–40 μg of I/ml. Pipet 1.0 ml of the standard solution into a 10-ml glass-stoppered volumetric flask, add 6.0 ml of aluminum chloride reagent, and dilute with absolute methanol to the mark. Warm the flask in a constant-temperature water bath at 50° for 15 min, cool to room temperature, and measure the fluorescence at λ_{act} 420 nm and λ_{emis} 480 nm against a blank.

Assay of I in Urine—Pipet 1.0 ml of urine into a 50-ml volumetric flask and dilute to volume with absolute methanol. Pipet 1.0 ml of this solution into a 10-ml glass-stoppered volumetric flask and proceed as described under *Preparation of Standard Curve*, beginning with "... add 6.0 ml of aluminum chloride reagent...."

Assay of I Glucuronide in Urine—Pipet 3.0 ml of urine into a 15-ml glass-stoppered centrifuge tube, add 1.0 ml of β-glucuronidase solution, and incubate in a constant-temperature water bath at 37° for 24 hr. Centrifuge the mixture for 10 min at 2000 rpm, pipet 1.0 ml of the supernate into a 50-ml volumetric flask, and dilute to volume with absolute methanol. Pipet 1.0 ml of the resulting solution into a 10-ml glass-stoppered volumetric flask and proceed as described under *Preparation of Standard Curve*, beginning with "... add 6.0 ml of aluminum chloride reagent...."

RESULTS AND DISCUSSION

In the presence of aluminum chloride, I showed a yellow fluorescence in methanol. The fluorophore had activation and emission maxima of 420 and 480 nm, respectively (Fig. 1). These wavelengths remained

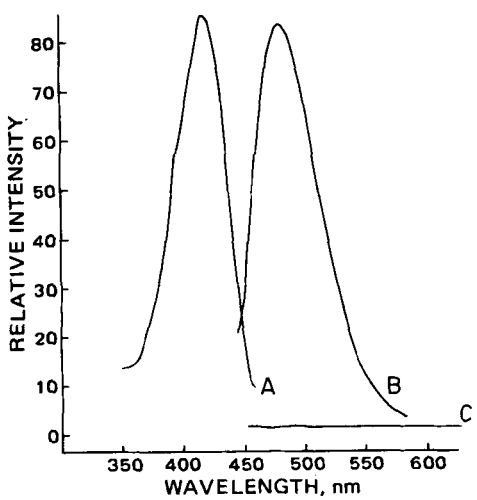

Figure 1—*Activation (curve A) and emission (curve B) spectra of I–aluminum chloride complex. Curve C is emission spectrum of I alone.*

[1] The International Nonproprietary Name is troxerutin.
[2] Aminco-Bowman, Silver Spring, Md.
[3] Model H-18, Mettler Instrument Corp., Princeton, N.J.
[4] Type F53, Carl Zeiss, Inc., New York, N.Y.
[5] Schaper and Brümmer, Salzgitter-Ringelheim, West Germany.
[6] Matheson, Coleman & Bell, Norwood, Ohio.
[7] Worthington Biochemical Corp., Freehold, N.J.

0022-3549/78/0800-1142$01.00/0
© 1978, American Pharmaceutical Association

Table I—Reproducibility of Fluorophore Development of I in Replicate Spiked Urine Samples at 0.4 μg/ml

Sample	Relative Fluorescence[a]
1	43.5
2	43.5
3	43.2
4	44.4
5	43.8
6	43.8
7	44.1
8	43.2
9	43.8
Average	43.7
RSD	0.009

[a] With λ_{act} 420 nm and λ_{emis} 480 nm.

constant as long as the water content in the final test sample was less than 0.2% (v/v). Relatively large percentages of water, however, caused both wavelengths to shift toward shorter wavelengths. For example, at a water concentration of 10%, the activation and emission wavelengths shifted to 355 and 425 nm, respectively.

The concentration optimum of the aluminum chloride reagent was determined by adding varying volumes of 0.1 *M* methanolic aluminum chloride to a series of 10-ml volumetric flasks, each containing 1.0 ml of 0.5 μg of I/ml, and measuring the fluorescence against a blank after diluting each solution to volume with methanol and heating at 50° for 15 min. Each blank contained the same amount of reagent as in the solution studied. The maximum fluorescence was obtained when the concentration of the reagent was 0.06 *M* in the final test solution.

The reaction time and temperature were determined by following the fluorescence development at room temperature, 37°, and 50°. At room temperature, the maximum fluorescence was not obtained even after 100 min (Fig. 2). Heating accelerated the reaction; a heating time of 15 min at 50° was adequate to attain the maximum fluorescence, which remained stable for at least 105 min.

Under the proposed experimental conditions, a linear fluorescence response was obtained from 0.1 to 4.0 μg of I/ml (r = 0.998). At concentrations below 0.1 μg/ml, a shift in the emission wavelength to 465 nm

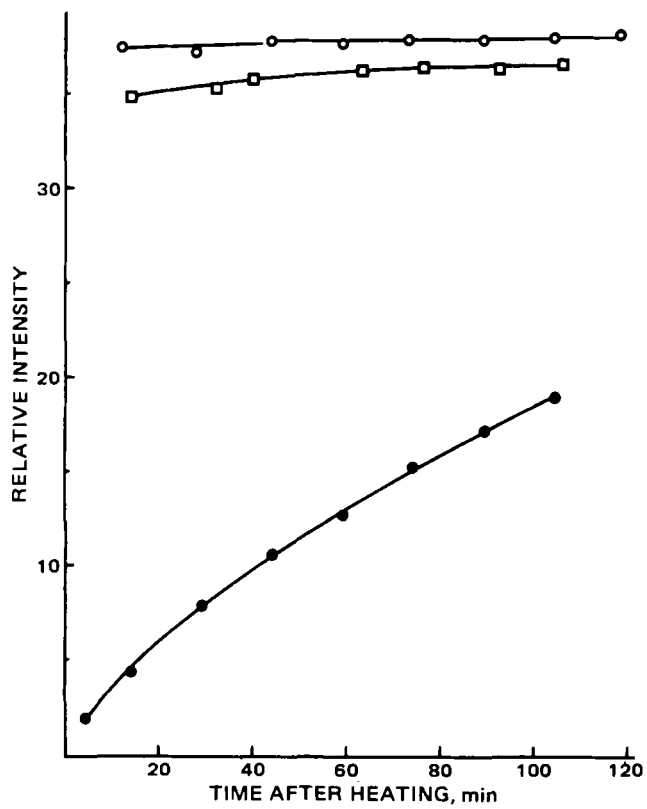

Figure 2—*Effect of heating on the I–aluminum chloride fluorophore. Key: ○, 15 and 30 min at 50°; □, 30 min at 37°; and ●, room temperature with time in hours after mixing.*

Table II—Recovery of I from Spiked Urine Samples

Amount Weighed, mg	Analyzed at Concentration Level, μg/ml	Amount Found, mg	Recovery, %
24.8	0.248	23.5	94.8
24.8	0.496	24.6	99.2
41.6	0.832	41.7	100.2
41.9	0.419	41.9	100.0
51.3	1.026	52.9	103.1
		Average	99.5
		SEM	1.34

was observed. A typical regression equation[8] was $F = 87.13C + 1.51$, where F is the relative fluorescence at λ_{act} 420 and λ_{emis} 480 nm and C is the concentration in micrograms per milliliter. The standard error (n = 5) of the estimates of the slope and the y-intercept were 4.05 and 0.70, respectively.

The reproducibility of the analysis of I in urine was determined by analyzing nine replicate spiked urine samples. At a concentration level of 0.4 μg of I/ml, the coefficient of variation was 0.009 (Table I).

Recovery studies of I from urine samples also were performed. The overall recovery of five spiked urine samples was 99.5% with a standard error of the mean of 1.34% (Table II).

The proposed method was applied to the analysis of I in urine of a human subject following oral I administration. This subject kept the same diet before and during the experiment and took no drugs or vitamins. An aliquot of urine collected before the administration of I (pretreatment urine) was assayed by the proposed method. Negligible fluorescence was observed before and after β-glucuronidase treatment. Therefore, this pretreatment urine served as the blank in subsequent measurements.

After oral administration of a single dose of 500 mg of I to the human subject, only traces of unchanged I were found in the urine. This result is in contrast to the findings of Wienert and Gahlen (3) who, by TLC, did not find traces of I in human urine following a 3600-mg oral dose of I.

When urine of the subject was treated with β-glucuronidase for 24 hr at 37°, following a modified procedure of Griffiths and Smith (7), and then analyzed by the proposed method, a cumulative urinary excretion of 26.53 mg (corresponding to 5.30% of the oral dose) was found in 78.6 hr (Fig. 3). Hackett *et al.* (6) reported that excretion *via* the renal pathway was virtually complete after 48 hr. These workers found, by liquid scintillation analysis, that excretion in human urine accounted for 3.05–5.97% of the administered oral dose of 300 mg of a mixture of *O*-(β-hydroxy-^{14}C-ethyl)rutosides[9].

Studies with ^{14}C-I in rats (5) showed that, following oral administration, two metabolites of I were found in rat urine: the 5′-*O*-glucuronide and a trace of an unidentified 5′-*O*-conjugate. These metabolites do not form fluorescent derivatives with aluminum chloride. No other metabolites of I were reported in rat urine. Although these data are not extrapolatable to humans, the fact that untreated human urine following oral administration of I gave extremely low fluorescence readings whereas the same volume of the same urine after β-glucuronidase treatment showed a tremendous increase in fluorescence at the activation and emission wavelengths of I suggests that the 5′-*O*-glucuronide of I is

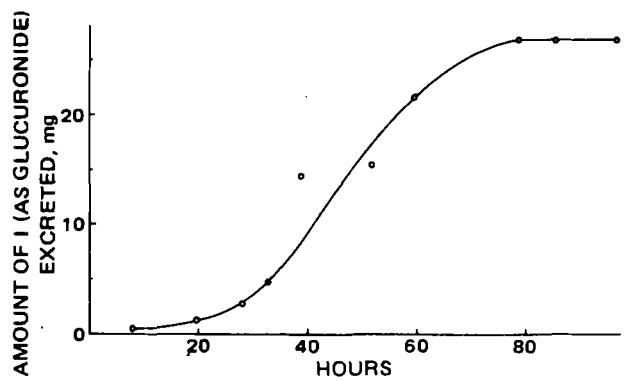

Figure 3—*Cumulative urinary excretion following a single oral dose of 500 mg of I in solution as measured after β-glucuronidase treatment of urine.*

[8] Wang Computer 700C and plotting output writer.
[9] Venuruton, Paroven preparations.

present in human urine. Further evidence was not obtained for the presence of this conjugate in human urine. However, Wienert and Gahlen (3) reported the presence of only one drug-related spot on the thin-layer chromatogram when they analyzed human urine following an intravenous administration of I.

REFERENCES

(1) J. Q. Griffith, C. F. Krewson, and J. Naphski, "Rutin and Related Flavonoids," Mack Publishing Co., Easton, Pa., 1955.

(2) W. L. Porter, D. F. Dickel, and J. F. Couch, *Arch. Biochem.*, **21**, 273 (1949).

(3) V. Wienert and W. Gahlen, *Hautarzt*, **21**, 278 (1970).

(4) H. Foerster and M. Ziege, *Fortschr. Med.*, **89**, 672 (1971).

(5) A. Barrow and L. A. Griffiths, *Xenobiotica*, **4**, 1 (1974).

(6) A. M. Hackett, L. A. Griffiths, A. S. Luyckx, and H. van Cauwenberge, *Arzneim.-Forsch.*, **26**, 925 (1976).

(7) L. A. Griffiths and G. E. Smith, *Biochem. J.*, **128**, 901 (1972).

ACKNOWLEDGMENTS

Presented at the Pharmaceutical Analysis and Control Section, APhA Academy of Pharmaceutical Sciences, New York meeting, 1977.

Nature of Amorphous Aluminum Hydroxycarbonate

CARLOS J. SERNA [1], JOE L. WHITE *, and STANLEY L. HEM ‡×

Received November 7, 1977, from the *Department of Agronomy and the ‡Industrial and Physical Pharmacy Department, School of Pharmacy and Pharmacal Sciences, Purdue University, West Lafayette, IN 47907. Accepted for publication December 6, 1977.

Abstract □ The titration of sodium carbonate with aluminum nitrate is shown to produce amorphous aluminum hydroxycarbonate. This compound is not stoichiometric, although the maximum carbonate to aluminum ratio appears to be 0.5. The pH conditions for achieving the maximum carbonate content are concentration dependent. A model for the particle surface at the solution interface is proposed. This model accounts for the presence of carbonate directly coordinated to the aluminum and carbonate adsorbed by electrostatic forces. Sodium is present in the diffuse layer and is, therefore, not an integral part of the structure.

Keyphrases □ Aluminum hydroxycarbonate, amorphous—prepared by titration of sodium carbonate with aluminum nitrate, physicochemical nature studied, model for particle surface at solution interface proposed □ Antacids—amorphous aluminum hydroxycarbonate, prepared by titration of sodium carbonate with aluminum nitrate, physicochemical nature studied, model for particle surface at solution interface proposed

Aluminum hydroxide gel used as an antacid usually contains carbonate. Carbonate is part of the structure of aluminum hydroxide gel (1) and contributes significantly to the high rate of acid neutralization (2) as well as gel stability (3). Previously, the term carbonate-containing aluminum hydroxide gel was used to describe the highly reactive gels used as antacids (2, 4, 5). However, this gel is now well enough understood to justify its description as amorphous aluminum hydroxycarbonate.

The production of amorphous aluminum hydroxycarbonate is usually performed in basic media to achieve a high concentration of carbonate in the system during precipitation. However, most studies of the hydrolytic precipitation of aluminum hydroxide are performed in acidic media (6, 7). Therefore, a study of the precipitate produced by titrating sodium carbonate with aluminum nitrate was undertaken. Special emphasis was placed on the precipitation conditions favoring the incorporation of carbonate. Further points of interest were the adsorption of sodium cation by the amorphous aluminum hydroxycarbonate and the elution of anions and cations during washing.

Aluminum nitrate was selected as the aluminum salt for precipitation because nitrate does not coordinate with aluminum as does carbonate (5) and, therefore, does not compete with carbonate for adsorption by the gel.

EXPERIMENTAL

Potentiometric titrations were performed by placing 100 ml of either a sodium carbonate or a sodium hydroxide solution in a 400-ml jacketed beaker. The temperature was controlled to ±0.1°, and the solution was stirred[2] at 2000 rpm. Aluminum nitrate solution was added at a controlled rate[3], 2 ml/min. The solution pH was monitored and recorded continuously.

Preliminary experiments were performed to observe the effect of temperature, addition rate, and reactant concentration. Variation of these precipitation factors did not affect the general shape of the titration curves. However, the position of the inflection points was concentration dependent. Excellent reproducibility of titration curves was obtained.

The equivalent aluminum oxide content was determined by chelatometric titration (8). The carbonate content, determined by gasometric displacement using the Chittick apparatus[4] (9), was expressed as the molar ratio of carbonate to aluminum.

IR analysis[5] (10) was performed using potassium bromide pellets after the gel was dried under vacuum at room temperature. All samples were amorphous by X-ray diffraction.

Gels were washed with equal volumes of 0.1 *M* sodium sulfate to determine if the anions in the gel were exchangeable.

The rate of acid reactivity was determined by pH-stat titration at pH 3.0 (11).

The sodium content was determined by atomic absorption spectroscopy[6].

The effect of washing was determined by adding a volume of deionized water equal to the volume of the gel, mixing, and centrifuging. Successive washes were performed by reconstituting the cake with a volume of water equal to the original volume of the gel and repeating the process.

The charge on the gel particles was determined by observing the direction of motion of the particles during electrophoresis[7].

[1] On leave from Instituto de Edafologia, C.S.I.C., Madrid, Spain.

[2] Stedi-Speed stirrer, Fisher Scientific, Pittsburgh, Pa.
[3] Solution metering pump, model 746, Beckman Instruments, Fullerton, Calif.
[4] Sargent-Welch Scientific Co., Skokie, Ill.
[5] Model 180, Perkin-Elmer Corp., Norwalk, Conn.
[6] Model 290B, Perkin-Elmer Corp., Norwalk, Conn.
[7] Zeta meter, Zeta Meter, Inc., New York, N.Y.

0022-3549/78/0800-1144$01.00/0

© 1978, American Pharmaceutical Association

present in human urine. Further evidence was not obtained for the presence of this conjugate in human urine. However, Wienert and Gahlen (3) reported the presence of only one drug-related spot on the thin-layer chromatogram when they analyzed human urine following an intravenous administration of I.

REFERENCES

(1) J. Q. Griffith, C. F. Krewson, and J. Naphski, "Rutin and Related Flavonoids," Mack Publishing Co., Easton, Pa., 1955.

(2) W. L. Porter, D. F. Dickel, and J. F. Couch, *Arch. Biochem.*, **21**, 273 (1949).

(3) V. Wienert and W. Gahlen, *Hautarzt*, **21**, 278 (1970).

(4) H. Foerster and M. Ziege, *Fortschr. Med.*, **89**, 672 (1971).

(5) A. Barrow and L. A. Griffiths, *Xenobiotica*, **4**, 1 (1974).

(6) A. M. Hackett, L. A. Griffiths, A. S. Luyckx, and H. van Cauwenberge, *Arzneim.-Forsch.*, **26**, 925 (1976).

(7) L. A. Griffiths and G. E. Smith, *Biochem. J.*, **128**, 901 (1972).

ACKNOWLEDGMENTS

Presented at the Pharmaceutical Analysis and Control Section, APhA Academy of Pharmaceutical Sciences, New York meeting, 1977.

Nature of Amorphous Aluminum Hydroxycarbonate

CARLOS J. SERNA [1], JOE L. WHITE *, and STANLEY L. HEM ‡×

Received November 7, 1977, from the *Department of Agronomy and the ‡Industrial and Physical Pharmacy Department, School of Pharmacy and Pharmacal Sciences, Purdue University, West Lafayette, IN 47907. Accepted for publication December 6, 1977.

Abstract □ The titration of sodium carbonate with aluminum nitrate is shown to produce amorphous aluminum hydroxycarbonate. This compound is not stoichiometric, although the maximum carbonate to aluminum ratio appears to be 0.5. The pH conditions for achieving the maximum carbonate content are concentration dependent. A model for the particle surface at the solution interface is proposed. This model accounts for the presence of carbonate directly coordinated to the aluminum and carbonate adsorbed by electrostatic forces. Sodium is present in the diffuse layer and is, therefore, not an integral part of the structure.

Keyphrases □ Aluminum hydroxycarbonate, amorphous—prepared by titration of sodium carbonate with aluminum nitrate, physicochemical nature studied, model for particle surface at solution interface proposed □ Antacids—amorphous aluminum hydroxycarbonate, prepared by titration of sodium carbonate with aluminum nitrate, physicochemical nature studied, model for particle surface at solution interface proposed

Aluminum hydroxide gel used as an antacid usually contains carbonate. Carbonate is part of the structure of aluminum hydroxide gel (1) and contributes significantly to the high rate of acid neutralization (2) as well as gel stability (3). Previously, the term carbonate-containing aluminum hydroxide gel was used to describe the highly reactive gels used as antacids (2, 4, 5). However, this gel is now well enough understood to justify its description as amorphous aluminum hydroxycarbonate.

The production of amorphous aluminum hydroxycarbonate is usually performed in basic media to achieve a high concentration of carbonate in the system during precipitation. However, most studies of the hydrolytic precipitation of aluminum hydroxide are performed in acidic media (6, 7). Therefore, a study of the precipitate produced by titrating sodium carbonate with aluminum nitrate was undertaken. Special emphasis was placed on the precipitation conditions favoring the incorporation of carbonate. Further points of interest were the adsorption of sodium cation by the amorphous aluminum hydroxycarbonate and the elution of anions and cations during washing.

Aluminum nitrate was selected as the aluminum salt for precipitation because nitrate does not coordinate with aluminum as does carbonate (5) and, therefore, does not compete with carbonate for adsorption by the gel.

EXPERIMENTAL

Potentiometric titrations were performed by placing 100 ml of either a sodium carbonate or a sodium hydroxide solution in a 400-ml jacketed beaker. The temperature was controlled to ±0.1°, and the solution was stirred[2] at 2000 rpm. Aluminum nitrate solution was added at a controlled rate[3], 2 ml/min. The solution pH was monitored and recorded continuously.

Preliminary experiments were performed to observe the effect of temperature, addition rate, and reactant concentration. Variation of these precipitation factors did not affect the general shape of the titration curves. However, the position of the inflection points was concentration dependent. Excellent reproducibility of titration curves was obtained.

The equivalent aluminum oxide content was determined by chelatometric titration (8). The carbonate content, determined by gasometric displacement using the Chittick apparatus[4] (9), was expressed as the molar ratio of carbonate to aluminum.

IR analysis[5] (10) was performed using potassium bromide pellets after the gel was dried under vacuum at room temperature. All samples were amorphous by X-ray diffraction.

Gels were washed with equal volumes of 0.1 *M* sodium sulfate to determine if the anions in the gel were exchangeable.

The rate of acid reactivity was determined by pH-stat titration at pH 3.0 (11).

The sodium content was determined by atomic absorption spectroscopy[6].

The effect of washing was determined by adding a volume of deionized water equal to the volume of the gel, mixing, and centrifuging. Successive washes were performed by reconstituting the cake with a volume of water equal to the original volume of the gel and repeating the process.

The charge on the gel particles was determined by observing the direction of motion of the particles during electrophoresis[7].

[1] On leave from Instituto de Edafologia, C.S.I.C., Madrid, Spain.

[2] Stedi-Speed stirrer, Fisher Scientific, Pittsburgh, Pa.
[3] Solution metering pump, model 746, Beckman Instruments, Fullerton, Calif.
[4] Sargent-Welch Scientific Co., Skokie, Ill.
[5] Model 180, Perkin-Elmer Corp., Norwalk, Conn.
[6] Model 290B, Perkin-Elmer Corp., Norwalk, Conn.
[7] Zeta meter, Zeta Meter, Inc., New York, N.Y.

0022-3549/78/0800-1144$01.00/0

© 1978, American Pharmaceutical Association

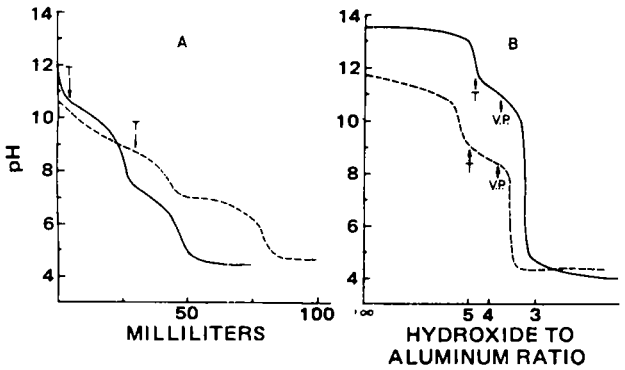

Figure 1—*Effect of concentration on the titration of sodium carbonate (A) or sodium hydroxide (B) with aluminum nitrate. Key: —, 0.5* M; *and - - -, 0.01* M.

RESULTS AND DISCUSSION

Titration Curve—The titration curve of sodium carbonate and aluminum nitrate is shown in Fig. 1A. The curve contains three plateaus and several concentration-dependent inflection points. To establish the role of carbonate in the basic titration curve, a similar titration was conducted with sodium hydroxide and aluminum nitrate (Fig. 1B). Comparison of the curves suggests that the initial decrease in pH observed in the sodium carbonate system was due to the partial neutralization of carbonate anion. A visible precipitate was observed during the first plateau for the sodium carbonate system, but no distinction could be made between turbidity and precipitation.

In contrast, turbidity was noted at the beginning of the second plateau in the sodium hydroxide system, and a visible precipitate was not observed until the end of the second plateau. This result suggests that carbonate was competing with hydroxide during the formation of the initial structure. Thus, when the titration was conducted using a lower concentration of sodium carbonate, the point of precipitation shifted and approached the turbidity point in the sodium hydroxide system. On the other hand, both systems showed the same general titration curve, suggesting that the precipitation mechanism was similar.

Since the hydroxide to aluminum ratio can be determined easily in the titration of sodium hydroxide by aluminum nitrate, an interpretation of the titration curve was based on this system. In basic media, aluminum exists as the aluminate anion, $Al(OH)_4^-$ (12). Consequently, during the first plateau, which extended to a hydroxide to aluminum ratio of 5, the aluminate anion predominated.

Because a large excess of hydroxides was present in the system during the initial phase, a relatively small pH change was observed. As the hydroxide concentration was further reduced by the addition of aluminum

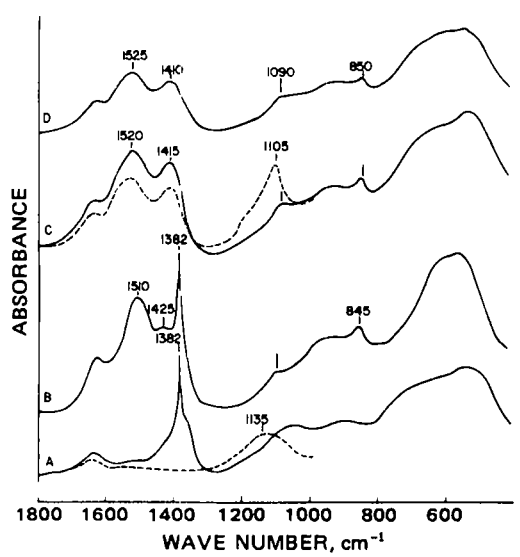

Figure 2—*IR spectra of precipitates at different pH values during titration of 0.5* M *sodium carbonate with 0.5* M *aluminum nitrate. Key: A, pH 4.3; B, pH 4.5; C, pH 6.4; D, pH 9.15; and - - -, IR spectra after three washings with 0.1* M *sodium sulfate.*

Table I—Analysis of the Precipitate at Different Points in the Titration of 0.5 *M* Sodium Carbonate with 0.5 *M* Aluminum Nitrate

Parameter	pH 9.15	7.50	6.40	4.50
Carbonate to aluminum ratio	0.29	0.34	0.54	0.16
Nonbonded carbonate, %	41	38	35	40
T_{50}, min	3.5	3.0	1.0	14.0
Sodium to aluminum ratio	0.113	0.074	0.050	0.040
Apparent charge	—	—	+	+

nitrate, the pH decreased because the free hydroxides combined with aluminum to form aluminate anion.

Turbidity was observed at the beginning of the second plateau (hydroxide to aluminum ratio = 4.6), indicating that polymerization was occurring (6). Aluminate anions react with protons to produce aluminum hydroxide according to the reaction shown in Scheme I:

$$Al(OH)_4^- + H^+ \rightarrow Al(OH)_3 + H_2O$$

Scheme I

Therefore, a visible precipitate was observed at the end of the second plateau (hydroxide to aluminum ratio = 3.8).

Further addition of aluminum nitrate sharply decreased the pH until a hydroxide to aluminum ratio of approximately 3 was reached. The third plateau occurred at this point and continued until enough aluminum nitrate had been added to redissolve the precipitate.

Analysis of Precipitate—The presence of several inflection points and plateaus in the titration curve of sodium carbonate by aluminum nitrate suggests that the precipitate is different at various stages of the titration. Samples were taken at various points in the titration of 0.5 *M* sodium carbonate with 0.5 *M* aluminum nitrate, and the solid product was analyzed. As indicated in Table I, carbonate was present in the solid precipitate throughout the pH range studied. However, the carbonate content increased during the titration until pH 6.4. At this point, the precipitate exhibited a carbonate to aluminum ratio of 0.54. Further addition of aluminum nitrate reduced the carbonate content.

The relationship between the pH and carbonate content of the precipitate was apparent in the IR spectra of the precipitate (Fig. 2). An increase in the relative intensity of the absorption bands associated with carbonate (1525, 1410, 1090, and 850 cm^{-1}) was observed from pH 9.15 to 6.4, in agreement with the chemical analysis (Table I). As previously reported, the splitting of the υ_3 vibration of carbonate (1525 and 1410 cm^{-1}) indicates direct coordination between carbonate and aluminum (1).

At pH 4.5, some carbonate was replaced by nitrate; a sharp absorption band associated with nitrate became apparent at 1382 cm^{-1}. However, the nitrate anion did not appear to be affected directly by the aluminum hydroxide surface since the small difference between the position of the υ_3 vibration for the adsorbed nitrate (1382 cm^{-1}) and the free nitrate anion (1358 cm^{-1}) indicates that an electrostatic attraction occurs (5). Therefore, the nitrate anion can be considered to be acting as a counterion in the diffuse layer (13).

The further addition of aluminum nitrate to pH 4.3 virtually eliminated the presence of carbonate in the precipitate. The IR spectrum shows that only nitrate was present. However, in addition to the sharp absorption band at 1382 cm^{-1}, a new shoulder appeared at 1360 cm^{-1} (Fig. 2). This absorption band may have been due to the presence of a more perturbed form of nitrate located within the Stern layer (13).

The loss of carbonate at low pH must be due to the reaction with protons and is reflected first by the appearance of nitrate as a counterion (pH 4.5) and finally by the presence of more perturbed nitrate (pH 4.3). However, carbonate directly coordinated to aluminum cannot be replaced by nitrate (5).

The behavior of the nitrate anion as observed in Fig. 2 suggests that two types of carbonate must be present in amorphous aluminum hydroxycarbonate: directly coordinated to aluminum and as a counterion. This hypothesis was confirmed by washing the precipitate formed at each pH with a solution of 0.1 *M* sodium sulfate. After three washings, chemical analysis (Table I) showed that approximately 40% of the carbonate was replaced by sulfate in each precipitate. The replaced carbonate is referred to as nonbonded carbonate in Table I.

IR analysis of the precipitate at pH 6.4 after washing with sodium sulfate showed a considerable decrease in the intensity of the absorption bands associated with carbonate at 1520 and 1415 cm^{-1} and the ap-

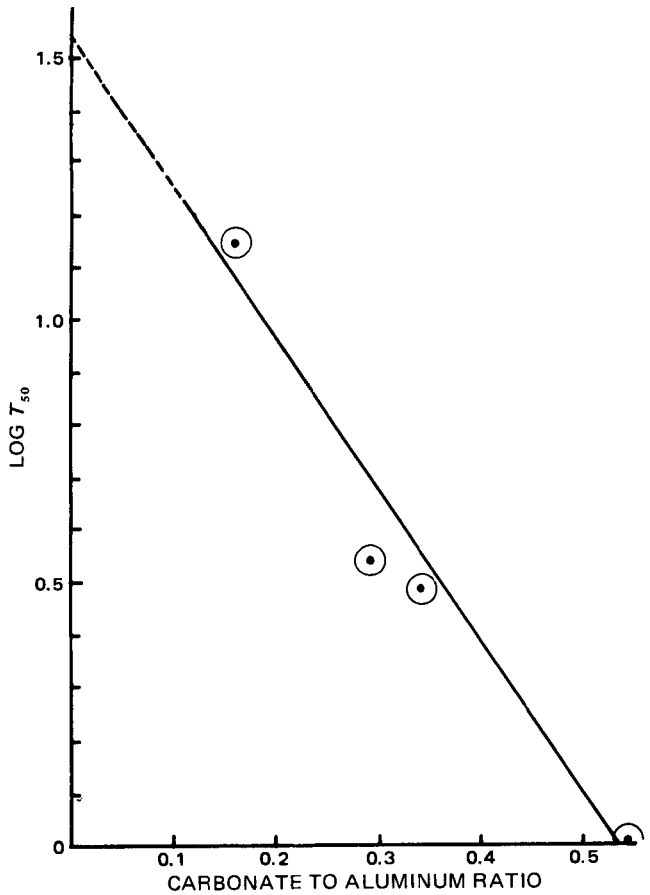

Figure 3—*Relationship between carbonate to aluminum ratio and rate of acid neutralization for precipitates at different pH values during titration of 0.5* M *sodium carbonate with 0.5* M *aluminum nitrate.*

pearance of sulfate absorption bands at approximately 1100 cm^{-1} (Fig. 2). However, when the precipitate containing only nitrate anion (pH 4.3) was washed with sodium sulfate in the same manner, complete removal of the nitrate was observed (Fig. 2). Nitrate interacts by electrostatic forces, so it can be replaced by sulfate, which can coordinate to aluminum (5). Thus, the sodium sulfate treatment replaces electrostatically bound anions.

The rate of acid neutralization of each precipitate was determined by pH-stat titration at pH 3.0 (11). The precipitate at pH 6.4 contained the greatest amount of carbonate and exhibited the most rapid neutralization reaction (Table I). The carbonate to aluminum ratio was directly related to the log of the T_{50} of the neutralization reaction (Fig. 3). Extrapolation suggests that a gel in this series containing no carbonate will have a T_{50} of approximately 35 min. This relatively high reaction rate in the absence

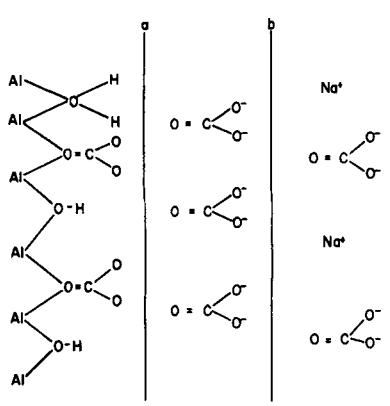

Figure 4—*Proposed structure of amorphous aluminum hydroxycarbonate surface/liquid interface. Key: a, inner Helmholtz plane; and b, outer Helmholtz plane. Water, hydroxides, and protons have not been included.*

Table II—Analysis of Precipitate at pH 6.4 during Titration of 0.5 *M* Sodium Carbonate with 0.5 *M* Aluminum Nitrate after Various Degrees of Washing

Number of Washes	Carbonate to Aluminum Ratio	Sodium to Aluminum Ratio	Particle Charge	T_{50}, min
0	1.22	3.9	−	0.25
1	0.57	0.52	−	0.5
3	0.54	0.05	+	1
5	0.48	0.04	+	1.5
10	0.45	0.03	+	2.5

of carbonate suggests that other factors such as particle size also contribute to the acid neutralization rate.

The sodium content of the precipitates appears to be related to the particle charge (Table I), indicating that sodium is mainly present in the diffuse layer and is, therefore, not specifically adsorbed. This finding is in good agreement with the reported adsorption of divalent cations by aluminum hydroxide from solutions containing 250,000 times more sodium (14).

A model of amorphous aluminum hydroxycarbonate based on the basic titration curve and analysis of the precipitate is presented in Fig. 4. Carbonate is shown coordinated to aluminum by unidentate interaction (5) and present in the Stern layer and the diffuse layer. Sodium is present mainly in the diffuse layer.

Effect of Washing—Previous studies indicated that the washing process had an important effect on the properties of aluminum hydroxide gel (15). The effect of washing on the precipitate containing the greatest carbonate to aluminum ratio (pH 6.4) was studied to test the model structure proposed in Fig. 4. As noted in Table II, a dramatic change occurred in the carbonate content of the precipitate during the first wash. IR analysis also indicated that the nitrate anion was readily removed (Fig. 5). Further washing did not substantially lower the carbonate content of the gel (Table II) and did not alter the carbonate interaction (Fig. 5). This result is in contrast to the behavior of sodium, which was almost completely removed after three washes. Significant amounts of sodium were only present when the particle was negatively charged (up to three washes). The acid neutralization rate decreased during washing. The log of the T_{50} also was related directly to the carbonate to aluminum ratio. This overall behavior agrees well with the model proposed in Fig. 4.

The charge behavior during washing is characteristic of a colloid without permanent charge. This type of colloid has a pH- and concentration-dependent charge that arises from adsorption of ions from solution. The gel particles are positively charged at pH 6.4, but the charge is reversed in concentrated salt solution because of preferential adsorption of anions compressing the double layer (13). As the anions are removed by washing, the gel's positive charge is observed. Therefore the washing process is important because it determines the physical stability of the colloidal particles and, consequently, the rheological properties of the gel.

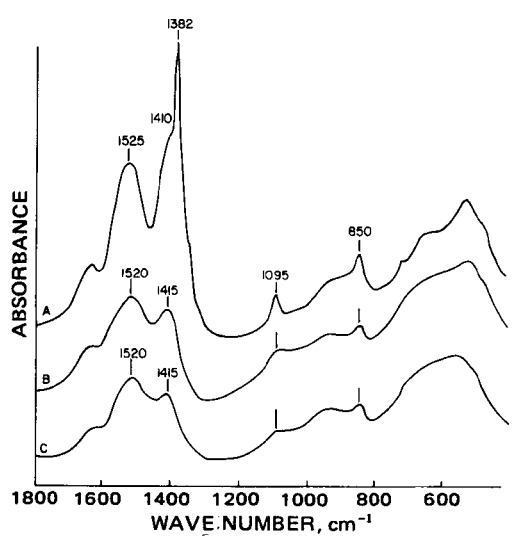

Figure 5—*Effect of washing on the precipitate at pH 6.4 during titration of 0.5* M *sodium carbonate with 0.5* M *aluminum nitrate. Key: A, initial precipitate; B, after three washes; and C, after 10 washes.*

REFERENCES

(1) J. L. White and S. L. Hem, *J. Pharm. Sci.*, **64**, 468 (1975).
(2) N. J. Kerkhof, J. L. White, and S. L. Hem, *ibid.*, **66**, 1533 (1977).
(3) S. L. Hem, E. J. Russo, S. M. Bahal, and R. S. Levi, *ibid.*, **59**, 317 (1970).
(4) C. J. Serna, J. L. White, and S. L. Hem, *ibid.*, **67**, 324 (1978).
(5) C. J. Serna, J. L. White, and S. L. Hem, *Soil Sci. Soc. Am. Proc.*, **41**, 1009 (1977).
(6) A. C. Vermeulen, J. W. Geus, R. J. Stol, and P. L. DeBruyn, *J. Colloid Interface Sci.*, **51**, 449 (1975).
(7) R. J. Stol, A. K. VanMelden, and P. L. DeBruyn, *ibid.*, **57**, 115 (1976).
(8) "The United States Pharmacopeia," 19th rev., Mack Publishing Co., Easton, Pa., 1975, p. 21.
(9) "Official Methods of Analysis of the Association of Official Analytical Chemists," 11th ed., W. Horwitz, Ed., Association of Official Analytical Chemists, Washington, D.C., 1970, p. 139.
(10) S. L. Nail, J. L. White, and S. L. Hem, *J. Pharm. Sci.*, **65**, 231 (1976).
(11) N. J. Kerkhof, R. K. Vanderlaan, J. L. White, and S. L. Hem, *ibid.*, **66**, 1528 (1977).
(12) R. J. Moolenaar, J. C. Evans, and L. D. McKeever, *J. Phys. Chem.*, **74**, 3629 (1970).
(13) D. Eagland, in "Water: A Comprehensive Treatise," vol. 5, F. Franks, Ed., Plenum, New York, N.Y., 1975, pp. 1–74.
(14) D. G. Kinniburgh, J. K. Syers, and M. L. Jackson, *Soil Sci. Soc. Am. Proc.*, **39**, 464 (1975).
(15) R. H. Green and S. L. Hem, *J. Pharm. Sci.*, **63**, 635 (1974).

ACKNOWLEDGMENTS

Supported in part by Barcroft Co. and a National Institutes of Health Biomedical Research Support Grant.

C. J. Serna acknowledges a fellowship from Ministerio de Educacion y Ciencia, Madrid, Spain.

This report is Journal Paper 6947, Purdue University, Agricultural Experiment Station, West Lafayette, IN 47907.

Hepatic Disposition and Biliary Excretion of the Organic Cations Thiazinamium and Thiazinamium Sulfoxide in Rats

KEES NEEF *ˣ, JAN H. G. JONKMAN *, and DIRK K. F. MEIJER ‡

Received July 12, 1977, from the **Department of Pharmaceutical and Analytical Chemistry and the* ‡*Department of Pharmacology, State University of Groningen, Groningen, The Netherlands.* Accepted for publication December 6, 1977.

Abstract □ The disappearance from plasma and the excretion in bile of the monoquaternary thiazinamium (administered as the iodide) and one of its polar metabolites, thiazinamium sulfoxide (also administered as the iodide), were studied in the rat after intravenous injection to obtain more information on hepatic transport mechanisms for organic cations. Both compounds exhibited an extremely rapid plasma disappearance, partly due to a rapid liver uptake. After injection of thiazinamium iodide and thiazinamium sulfoxide iodide, 36 and 47%, respectively, of the administered dose were excreted in bile during 1 hr. TLC analysis of the bile showed at least two unidentified polar metabolites in addition to thiazinamium sulfoxide and only 3.8% unchanged thiazinamium after administration of thiazinamium iodide. The same metabolites were found after injection of thiazinamium sulfoxide iodide. Urinary excretion and intestinal secretion were 18 and 12%, respectively, for thiazinamium sulfoxide iodide and 27 and 9%, respectively, of the dose for thiazinamium iodide. It is concluded that, in spite of unequal physicochemical features, thiazinamium iodide and thiazinamium sulfoxide iodide differ only slightly in hepatic uptake and metabolism.

Keyphrases □ Thiazinamium—tissue distribution and biliary excretion in rats □ Distribution, tissue—thiazinamium in rats □ Excretion, biliary—thiazinamium in rats □ Phenothiazine derivatives—thiazinamium, tissue distribution and biliary excretion in rats

Factors such as molecular weight, polarity, molecular structure, lipophilicity, protein binding, and metabolism were reported (1–3) to influence biliary excretion of drugs. It was suggested (4) that biliary excretion of quaternary ammonium compounds requires a polar organic cation group and a relatively nonpolar ring structure in the molecule.

Thiazinamium (I) iodide is a phenothiazine derivative containing a quaternary ammonium group. No metabolites were detected in rats; no details were provided on biliary excretion of thiazinamium and its metabolites (5). In humans, dogs, and monkeys, one metabolite was detected (6) in bile and urine: thiazinamium sulfoxide (II) (Scheme I, asterisks indicate ^{14}C-label). Introduction of the oxygen in the phenothiazine nucleus results in a much more polar compound (Table I). Therefore, it was of interest to study whether this structural and physicochemical change would result in different hepatic disposition.

^{14}C-Thiazinamium iodide and ^{14}C-thiazinamium sulfoxide iodide were prepared and were used to investigate the distribution, biotransformation, and elimination in rats, with special reference to biliary excretion.

EXPERIMENTAL

Synthesis of ^{14}C-Thiazinamium Iodide—Synthesis of ^{14}C-thiazinamium iodide according to the reaction conditions described by Huang *et al.* (5) resulted in a radiochemical yield of only 8%. The conditions were modified, resulting in the following procedure. Promethazine, 500 mg, was allowed to react for 72 hr at 21° with 251 mg of ^{14}C-methyl iodide (100 μCi total activity) in 25 ml of acetone. After the acetone was removed, the substance was recrystallized (24 hr) in 20 ml of a hot mixture of dichloromethane–benzene (10:9). After drying, a chemically pure product (>99.5%) was obtained (95% yield). TLC analysis showed no radio-

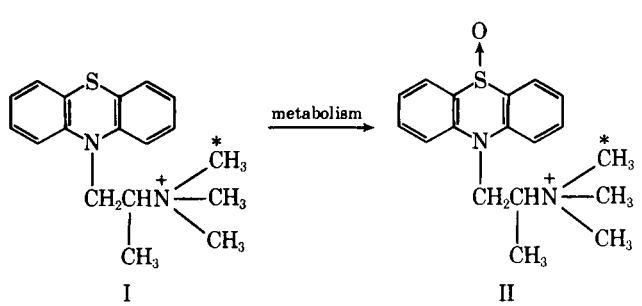

Scheme I

© 1978, American Pharmaceutical Association

REFERENCES

(1) J. L. White and S. L. Hem, *J. Pharm. Sci.*, **64**, 468 (1975).
(2) N. J. Kerkhof, J. L. White, and S. L. Hem, *ibid.*, **66**, 1533 (1977).
(3) S. L. Hem, E. J. Russo, S. M. Bahal, and R. S. Levi, *ibid.*, **59**, 317 (1970).
(4) C. J. Serna, J. L. White, and S. L. Hem, *ibid.*, **67**, 324 (1978).
(5) C. J. Serna, J. L. White, and S. L. Hem, *Soil Sci. Soc. Am. Proc.*, **41**, 1009 (1977).
(6) A. C. Vermeulen, J. W. Geus, R. J. Stol, and P. L. DeBruyn, *J. Colloid Interface Sci.*, **51**, 449 (1975).
(7) R. J. Stol, A. K. VanMelden, and P. L. DeBruyn, *ibid.*, **57**, 115 (1976).
(8) "The United States Pharmacopeia," 19th rev., Mack Publishing Co., Easton, Pa., 1975, p. 21.
(9) "Official Methods of Analysis of the Association of Official Analytical Chemists," 11th ed., W. Horwitz, Ed., Association of Official Analytical Chemists, Washington, D.C., 1970, p. 139.
(10) S. L. Nail, J. L. White, and S. L. Hem, *J. Pharm. Sci.*, **65**, 231 (1976).
(11) N. J. Kerkhof, R. K. Vanderlaan, J. L. White, and S. L. Hem, *ibid.*, **66**, 1528 (1977).
(12) R. J. Moolenaar, J. C. Evans, and L. D. McKeever, *J. Phys. Chem.*, **74**, 3629 (1970).
(13) D. Eagland, in "Water: A Comprehensive Treatise," vol. 5, F. Franks, Ed., Plenum, New York, N.Y., 1975, pp. 1–74.
(14) D. G. Kinniburgh, J. K. Syers, and M. L. Jackson, *Soil Sci. Soc. Am. Proc.*, **39**, 464 (1975).
(15) R. H. Green and S. L. Hem, *J. Pharm. Sci.*, **63**, 635 (1974).

ACKNOWLEDGMENTS

Supported in part by Barcroft Co. and a National Institutes of Health Biomedical Research Support Grant.

C. J. Serna acknowledges a fellowship from Ministerio de Educacion y Ciencia, Madrid, Spain.

This report is Journal Paper 6947, Purdue University, Agricultural Experiment Station, West Lafayette, IN 47907.

Hepatic Disposition and Biliary Excretion of the Organic Cations Thiazinamium and Thiazinamium Sulfoxide in Rats

KEES NEEF *ˣ, JAN H. G. JONKMAN *, and DIRK K. F. MEIJER ‡

Received July 12, 1977, from the **Department of Pharmaceutical and Analytical Chemistry and the* ‡*Department of Pharmacology, State University of Groningen, Groningen, The Netherlands.* Accepted for publication December 6, 1977.

Abstract □ The disappearance from plasma and the excretion in bile of the monoquaternary thiazinamium (administered as the iodide) and one of its polar metabolites, thiazinamium sulfoxide (also administered as the iodide), were studied in the rat after intravenous injection to obtain more information on hepatic transport mechanisms for organic cations. Both compounds exhibited an extremely rapid plasma disappearance, partly due to a rapid liver uptake. After injection of thiazinamium iodide and thiazinamium sulfoxide iodide, 36 and 47%, respectively, of the administered dose were excreted in bile during 1 hr. TLC analysis of the bile showed at least two unidentified polar metabolites in addition to thiazinamium sulfoxide and only 3.8% unchanged thiazinamium after administration of thiazinamium iodide. The same metabolites were found after injection of thiazinamium sulfoxide iodide. Urinary excretion and intestinal secretion were 18 and 12%, respectively, for thiazinamium sulfoxide iodide and 27 and 9%, respectively, of the dose for thiazinamium iodide. It is concluded that, in spite of unequal physicochemical features, thiazinamium iodide and thiazinamium sulfoxide iodide differ only slightly in hepatic uptake and metabolism.

Keyphrases □ Thiazinamium—tissue distribution and biliary excretion in rats □ Distribution, tissue—thiazinamium in rats □ Excretion, biliary—thiazinamium in rats □ Phenothiazine derivatives—thiazinamium, tissue distribution and biliary excretion in rats

Factors such as molecular weight, polarity, molecular structure, lipophilicity, protein binding, and metabolism were reported (1–3) to influence biliary excretion of drugs. It was suggested (4) that biliary excretion of quaternary ammonium compounds requires a polar organic cation group and a relatively nonpolar ring structure in the molecule.

Thiazinamium (I) iodide is a phenothiazine derivative containing a quaternary ammonium group. No metabolites were detected in rats; no details were provided on biliary excretion of thiazinamium and its metabolites (5). In humans, dogs, and monkeys, one metabolite was detected (6) in bile and urine: thiazinamium sulfoxide (II) (Scheme I, asterisks indicate ^{14}C-label). Introduction of the oxygen in the phenothiazine nucleus results in a much more polar compound (Table I). Therefore, it was of interest to study whether this structural and physicochemical change would result in different hepatic disposition.

^{14}C-Thiazinamium iodide and ^{14}C-thiazinamium sulfoxide iodide were prepared and were used to investigate the distribution, biotransformation, and elimination in rats, with special reference to biliary excretion.

EXPERIMENTAL

Synthesis of ^{14}C-Thiazinamium Iodide—Synthesis of ^{14}C-thiazinamium iodide according to the reaction conditions described by Huang *et al.* (5) resulted in a radiochemical yield of only 8%. The conditions were modified, resulting in the following procedure. Promethazine, 500 mg, was allowed to react for 72 hr at 21° with 251 mg of ^{14}C-methyl iodide (100 μCi total activity) in 25 ml of acetone. After the acetone was removed, the substance was recrystallized (24 hr) in 20 ml of a hot mixture of dichloromethane–benzene (10:9). After drying, a chemically pure product (>99.5%) was obtained (95% yield). TLC analysis showed no radio-

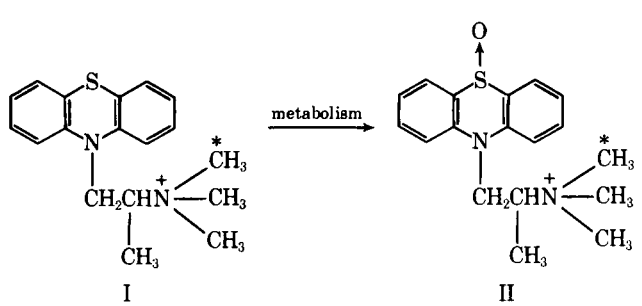

Scheme I

© 1978, American Pharmaceutical Association

chemical impurities. The specific activity was 0.13 μCi/mg (radiochemical yield of 86%, mp 217°).

Synthesis of ^{14}C-Thiazinamium Sulfoxide Iodide—Promethazine hydrochloride, 500 mg, was treated with 360 mg of 30% H_2O_2 in 1.25 g of 30% acetic acid at 40–60° for 1 hr. After extraction with dichloromethane and crystallization in carbon tetrachloride, promethazine sulfoxide was obtained. This product was used for quaternization with ^{14}C-methyl iodide as described for ^{14}C-thiazinamium iodide. No crystallization was necessary because thiazinamium sulfoxide iodide precipitates after its formation in acetone. Washing with acetone gave a chemically pure product (more than 99.5%). The yield was 700 mg (95%), with a specific activity of 0.12 μCi/mg (radiochemical yield of 84%). TLC analysis showed no radiochemical impurities.

Chemical Analysis—The authenticity of the compounds was checked by UV, IR, mass spectrometric, and TLC (methanol–water–ammonia–ammonium acetate, 200:42:6:8) analyses. Purity control was also performed by TLC.

Distribution–Metabolism Studies—Male Wister rats, 250–300 g, were anesthetized with pentobarbital sodium (0.35 ml ip of a 60-mg/ml solution). The animals were intubated and artificially respired. The abdomen was opened, and the bile duct was cannulated with a polyethylene cannula. A similar cannula was placed in the carotid artery for rapid blood sampling. During the experiment, a heating lamp was placed above the animal to maintain normal body temperature (37.8°). Drugs were injected intravenously during 10 sec (vena femoralis).

Immediately after injection, bile samples were collected at 5-min intervals. Blood samples (100 μl) were taken 30, 60, 90, 120, 150, 180, 210, and 240 sec after thiazinamium iodide injection and 30, 60, 90, 120, 180, 240, and 300 sec after thiazinamium sulfoxide iodide injection. After 1 hr, the liver, gut, and kidneys were rapidly removed and stored on ice. Urine was collected from the bladder with a syringe. The administered dose of thiazinamium iodide was 840 nmoles in a 1-ml solution by bolus injection. Thiazinamium sulfoxide iodide was administered in two doses of 2285 and 840 nmoles in separate groups of rats, also by bolus injection. Plasma disappearance rates at two doses of thiazinamium sulfoxide iodide, expressed as the percentage of the dose, were nearly identical. In another group of rats, liver and kidneys were removed 5 min after thiazinamium iodide (dose 840 nmoles) and thiazinamium sulfoxide iodide injection, and total activity in these organs was measured.

In some control experiments, carbon dioxide expired by the rats was trapped in a benzethonium chloride[1]–ethanol mixture to which thymolphthalein was added as indicator. Total absence of radioactivity in this solution indicated that no demethylation of ^{14}C-thiazinamium occurred.

Radiochemical Analysis—Thiazinamium and carbon-14-containing metabolites were determined by liquid scintillation counting (total radioactivity) in plasma, liver, gut, kidneys, bile, and urine. All samples were counted for 10 min, and counting was corrected for quenching by external standardization.

Plasma—Blood samples were heparinized and centrifuged. Then 25 μl of the supernate was mixed with 10 ml of premixed scintillator[2].

Bile—Aliquots of 25 μl were taken for TLC analysis. The remaining part of the samples was mixed with 10 ml of scintillator for counting.

Tissues—Liver, gut, and kidneys were dissected out, weighed, and cut into pieces. The tissues were homogenized with 40 ml of saline, and 0.5 ml of the homogenate was mixed with scintillator for radiochemical analysis.

Urine—An aliquot of 50 μl of urine was mixed with 10 ml of scintillator and counted.

TLC Analysis—Two systems were used to separate and detect the substances under study and their metabolites in bile. System I was the same as mentioned under *Chemical Analysis*, and System II was methanol–chloroform–sodium iodide (20:80:0.5 *M*). Bile samples of 25 μl were applied to silica gel 60 F_{254} alumina plates[3]. The position of the compounds was detected by cutting the plate in 0.5-cm pieces and liquid scintillation counting.

To remove the substances from the silica gel, 0.6 ml of a 10% NaI solution was added to the scintillator. Some plates were scanned[4] for radioactivity. Addition of labeled thiazinamium iodide and thiazinamium sulfoxide iodide to bile and subsequent TLC resulted in only one radioactive spot for each substance.

[1] Hyamine.
[2] Aquasol, New England Nuclear Chemicals.
[3] Merck.
[4] Dünnschicht-Scanner II, Berthold (nr. LB 2723).

Table I—Physicochemical Properties of Thiazinamium and Thiazinamium Sulfoxide

	Thiazinamium	Thiazinamium Sulfoxide
R_f value, TLC (silica gel, chloroform–methanol—0.5 *M* NaI)	0.64	0.50
Protein binding[a] (dialysis), % bound, 60–120 nmoles/ml of plasma	65	20
Lipid solubility[b], % in organic phase, 100 nmoles/ml of aqueous phase	75	3

[a] Protein binding was measured at two concentrations (the initial concentration in plasma is indicated). Percent binding was found to be similar at these concentrations, so values were averaged (n = 6). [b] Mean values of three experiments.

Determination of Lipid Solubility and Protein Binding—Lipid solubility was estimated by partition of the compounds between equal volumes of 1-octanol and a modified Krebs–Ringer solution from which carbon dioxide and sodium bicarbonate were omitted, and the pH was adjusted to 7.4 with sodium hydroxide (7). Recovery of the agents after equilibration was more than 95%. Protein binding was determined by equilibrium dialysis at 37° of 1 ml of defibrinated rat blood plasma and 2 ml of Krebs bicarbonate solution (pH 7.4). Virtually no binding occurred to the dialysis sacs.

RESULTS AND DISCUSSION

Introduction of oxygen by oxidation of the sulfur atom in the phenothiazine nucleus of thiazinamium resulted in a substance with quite different physicochemical features. Table I shows that R_f values with TLC, protein binding, and especially extraction into octanol were considerably lower for the thiazinamium sulfoxide than for the parent compound. Thus, two closely related organic cations with varying polarity due to the ring structure were obtained.

Figure 1 shows that the plasma concentration for both compounds after 4 min was less than 20% of the dose. After 5 min, about 40% of the dose of thiazinamium and thiazinamium sulfoxide was found in the liver and about 20% in the kidneys, expressed as percentage of radioactivity, indicating that the rapid elimination from the blood was predominantly due to uptake in these excretory organs. Despite unequal physicochemical properties, there was no major difference in the plasma elimination rates (Fig. 1), hepatic uptake, or biliary excretion patterns of thiazinamium and thiazinamium sulfoxide. Biliary concentrations were high compared with the plasma levels. This result may be due to both active secretion and diffusion followed by binding to micelles (4, 7, 8). After administration of thiazinamium iodide, TLC analysis of bile with Systems I and II showed at least two metabolites in addition to thiazinamium sulfoxide.

The same metabolites with identical R_f values in both TLC systems were found after injection of thiazinamium sulfoxide iodide. Figure 2 shows that the amount of polar metabolites relative to thiazinamium sulfoxide increased with time. The biliary excretion patterns of thia-

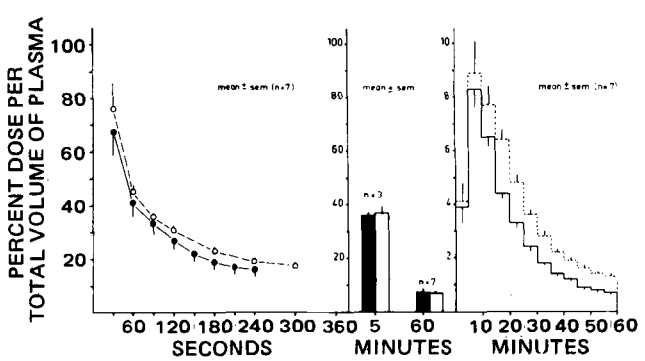

Figure 1—*Plasma disappearance (percent of dose in plasma) (left), hepatic content (percent of dose) 5 and 60 min after injection (middle), and biliary excretion (percent of dose per 5-min fraction, noncumulative) (right) after intravenous administration of thiazinamium iodide (●, ■, —) and thiazinamium sulfoxide iodide (○, □, - - -) (dose = 840 and 2285 nmoles, respectively). Total radioactivity in plasma, liver, and bile is indicated. The substances after injection were assumed to be distributed over the total plasma volume (8% of the body weight), in accordance with the observed plasma concentration at t = 0 from semilogarithmic plots of the plasma curve.*

Table II—Biliary Excretion [a] of Thiazinamium Cation, Thiazinamium Sulfoxide Cation, and Metabolites

Compound	Dose: Thiazinamium Iodide, 840 nmoles	Dose: Thiazinamium Sulfoxide Iodide, 2285 nmoles	Dose: Thiazinamium Sulfoxide Iodide, 840 nmoles
Thiazinamium cation	3.8	—	—
Thiazinamium sulfoxide cation	16.1	30.5	31.8
Metabolite 2	13.1	12.7	20.8
Metabolite 3	2.7	3.6	8.6

[a] Mean values of at least three experiments. Amounts in bile are indicated as percent of the dose excreted in 1 hr (total radioactivity).

zinamium sulfoxide and the two unidentified metabolites (Fig. 3) were very similar after injection of thiazinamium iodide and thiazinamium sulfoxide iodide. Only very small amounts (3.8% of the dose) of unchanged thiazinamium were excreted in bile following administration of thiazinamium iodide (Table II). These results indicate that thiazinamium, after being taken up in the liver, was rapidly oxidized to the sulfoxide and that the additional unknown metabolites may have arisen from biotransformation of this compound.

The present data on the nature of excreted material in bile after administration of thiazinamium iodide contrast with results of Huang *et al.* (5), who suggested that only unchanged thiazinamium is excreted in feces and urine. The distribution of radioactivity after injection of thiazinamium iodide and thiazinamium sulfoxide iodide in some excretory organs, bile, and urine is pictured in Fig. 4. Total recovery in bile, urine, and these organs amounted to 72 and 88% of the dose, respectively. Considerable amounts were detected in kidneys and gut 1 hr after injection. Although the nature of the radioactive material in the kidneys and gut was not studied, its presence probably was related to secretion processes for organic cations in the renal tubuli and in the intestinal mucosa (9).

Schanker (4) proposed that a nonpolar ring system and a polar cationic group would be required for hepatic transport of organic cations from plasma into bile. The present results support this hypothesis concerning the biliary excretion of thiazinamium. The presence of abundant amounts of the more polar thiazinamium sulfoxide in bile indicates that, in spite

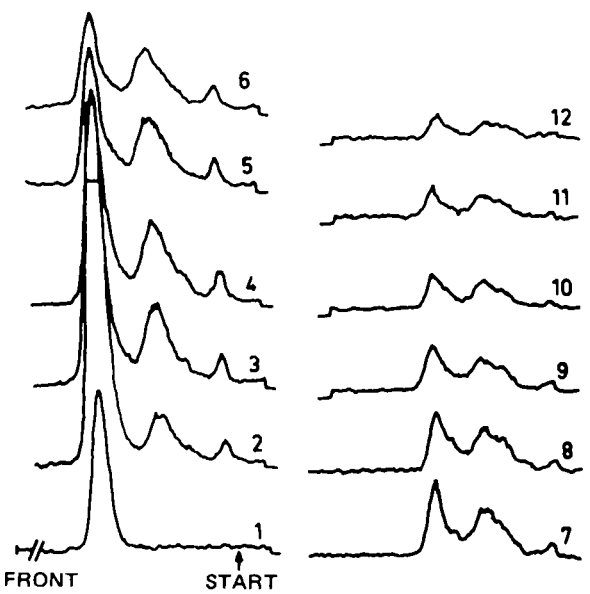

Figure 2—*Example of TLC analysis of 12 5-min bile samples collected after injection of thiazinamium sulfoxide iodide (numbers indicate first to 12th sample). TLC plates were developed with System I and scanned for radioactivity. The major peak (1–6) had an R_f value identical to thiazinamium sulfoxide. The two radioactive spots with lower R_f values probably represent more polar metabolites (Metabolites 2 and 3, Fig. 4). They were not detected when reference compounds thiazinamium iodide and thiazinamium sulfoxide iodide were added to rat bile and chromatographed using the same TLC system.*

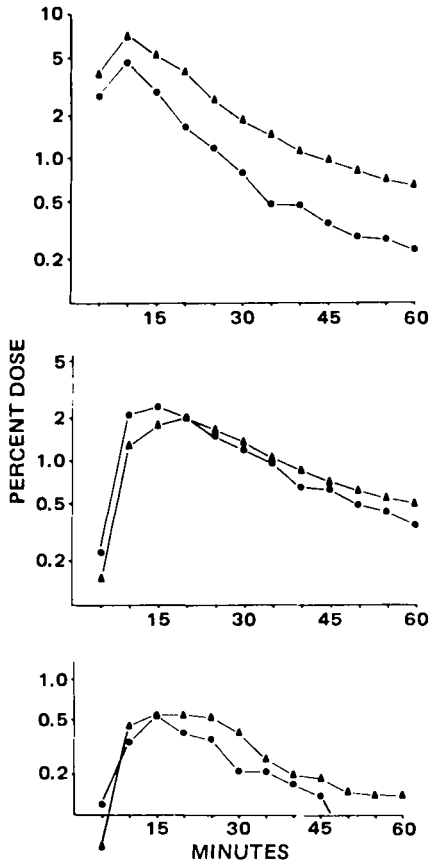

Figure 3—*Biliary excretion patterns (percent of dose per 5-min fraction, noncumulative) of thiazinamium sulfoxide (Metabolite 1) (top), Metabolite 2 (middle), and Metabolite 3 (bottom) after intravenous injection of thiazinamium sulfoxide iodide (▲) (2285 nmoles) and thiazinamium iodide (●) (840 nmoles). The compounds were separated by TLC and quantified by removal from the plates and scintillation counting. The values represent means of at least three experiments.*

of the change in polarity of the ring structure, enough hydrophobic sites remain to guarantee efficient biliary output. The data in Fig. 3 and Table II even suggest a more rapid biliary excretion of material after administration of thiazinamium sulfoxide than with thiazinamium iodide.

Furthermore, the uptake, as indicated by hepatic levels 5 min after injection of the compounds, was very similar, suggesting that the polarity of the ring structure in itself is not a critical factor in hepatic transport of these cations. Although oxidation of the phenothiazine nucleus of thiazinamium does not result in a major change in the hepatic disposition, previous studies with other anticholinergic agents (2), in which the ring structure of the agents was completely removed from the quaternary

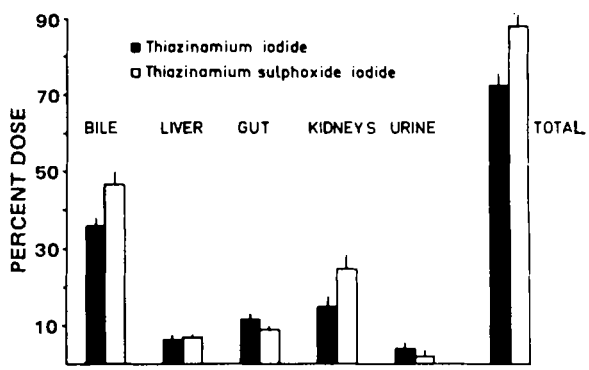

Figure 4—*Distribution of radioactivity 1 hr after intravenous injection of thiazinamium iodide (840 nmoles) and thiazinamium sulfoxide iodide (2285 nmoles). The amounts in the liver, kidneys, and gut and material cumulatively excreted in bile and urine are indicated as percent of administered dose (mean ± SEM, n = 7).*

ammonium part of the molecules by acid hydrolysis, indicate that the presence of a relatively nonpolar lipophilic part in the molecule of organic cations is a prerequisite for efficient biliary excretion.

REFERENCES

(1) P. C. Hirom, R. D. Hughes, and P. Millburn, *Biochem. Soc. Trans.*, **2**, 327 (1974).

(2) D. K. F. Meijer, in "Intestinal Permeation. Proceedings of the Fourth Workshop Conference Hoechst," M. Kramer and F. Lauterbach, Eds., Excerpta Medica, Amsterdam, The Netherlands, 1977, p. 196.

(3) R. L. Smith, in "Handbook of Experimental Pharmacology," vol. XXVIII/1, B. B. Brodie and J. R. Gillette, Eds., Springer-Verlag, Berlin, Germany, 1971, p. 354.

(4) L. S. Schanker, in "The Biliary System," W. Taylor, Ed., Blackwell, Oxford, England, 1965, p. 469.

(5) C. L. Huang, J. A. Yeh, and S. Y. Hsu, *J. Pharm. Sci.*, **59**, 772 (1970).

(6) J. H. G. Jonkman, thesis, State University of Groningen, Groningen, The Netherlands, 1977, pp. 115–303.

(7) D. K. F. Meijer and J. G. Weitering. *Eur. J. Pharmacol.*, **10**, 283 (1970).

(8) U. I. Lavy, W. Hespe, and D. K. F. Meijer, *Naunyn-Schmiedebergs Arch. Pharmacol.*, **275**, 183 (1972).

(9) K. Turnheim and F. O. Lauterbach, *Biochem. Pharmacol.*, **26**, 99 (1977).

ACKNOWLEDGMENTS

The authors thank Mrs. Eily Beerling-v.d. Molen, Dr. Stoffer Reiffers, and Dr. Wim Vaalburg for their advice and help with the synthesis of ^{14}C-labeled compounds and Egbert Scholtens for technical assistance.

Interference in Assays for Hydralazine in Humans by a Major Plasma Metabolite, Hydralazine Pyruvic Acid Hydrazone

PHILLIP A. REECE ˣ, PHILIP E. STANLEY, and RUDOLF ZACEST

Received July 6, 1977, from the *Department of Clinical Pharmacology, The Queen Elizabeth Hospital, Woodville, 5011, South Australia.* Accepted for publication December 9, 1977.

Abstract □ The present study showed that published spectrophotometric and GLC methods for hydralazine in plasma do not distinguish between the drug and a major plasma metabolite, hydralazine pyruvic acid hydrazone. These methods involve the acidic treatment of the sample, which hydrolyzes the hydrazone back to hydralazine. A specific GLC assay for the hydrazone was developed and involves its selective extraction from plasma and transformation to 3-trifluoromethyl-*s*-triazolo[3,4-*a*]phthalazine. This derivative could be sensitively measured by GLC using an electron-capture detector. With this procedure, it was shown that most "apparent hydralazine" in plasma is the hydrazone, which forms rapidly from hydralazine and endogenous pyruvic acid. Previous work indicated that the hydrazone was inactive when administered intravenously to rabbits.

Keyphrases □ Hydralazine—interference in published GLC and spectrophotometric analyses in plasma by major metabolite □ Metabolites—hydralazine pyruvic acid hydrazone, GLC analysis in plasma □ GLC—analysis, hydralazine pyruvic acid hydrazone in plasma □ Antihypertensives—hydralazine, interference in published GLC and spectrophotometric analyses in plasma by major metabolite

The vasodilator hydralazine, 1-hydrazinophthalazine (I), is an effective agent for the treatment of arterial hypertension (1). It undergoes extensive metabolism in humans and animals, and Metabolites II–VIII were identified (1–11). Acetylation was proposed as the major pathway for hydralazine clearance (2–8), where the acetylated drug, 3-methyl-*s*-triazolo[3,4-*a*]phthalazine (III), may be further metabolized to 3-hydroxymethyl-*s*-triazolo[3,4-*a*]-phthalazine (IV) and its glucuronide conjugate (2, 11).

Although hydralazine can form hydrazones readily with compounds having an active carbonyl group, hydralazine pyruvic acid hydrazone, 1-hydrazinophthalazine pyruvic acid hydrazone (II), was identified only as a minor metabolite in rat urine following oral administration of hydralazine (2, 4). Fresh human blood contains pyruvic acid in a concentration of approximately 100 μmoles/liter, which is a considerable excess to the commonly found therapeutic levels of "apparent hydralazine" and appears to favor formation of II. Preliminary findings indicated (12) that plasma apparent hydralazine, or that measured

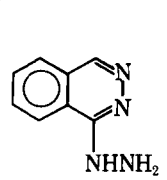

I

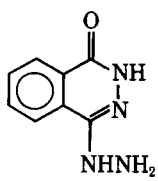

V

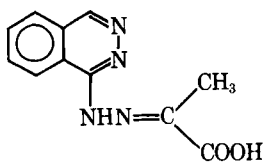

II

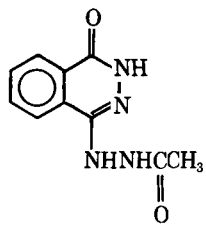

VI

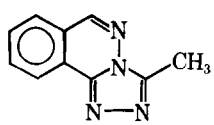

III

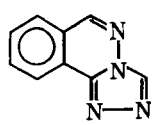

VII

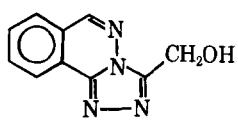

IV

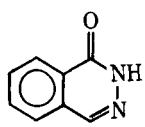

VIII

0022-3549/78/0800-1150$01.00/0

© 1978, American Pharmaceutical Association

ammonium part of the molecules by acid hydrolysis, indicate that the presence of a relatively nonpolar lipophilic part in the molecule of organic cations is a prerequisite for efficient biliary excretion.

REFERENCES

(1) P. C. Hirom, R. D. Hughes, and P. Millburn, *Biochem. Soc. Trans.*, **2**, 327 (1974).

(2) D. K. F. Meijer, in "Intestinal Permeation. Proceedings of the Fourth Workshop Conference Hoechst," M. Kramer and F. Lauterbach, Eds., Excerpta Medica, Amsterdam, The Netherlands, 1977, p. 196.

(3) R. L. Smith, in "Handbook of Experimental Pharmacology," vol. XXVIII/1, B. B. Brodie and J. R. Gillette, Eds., Springer-Verlag, Berlin, Germany, 1971, p. 354.

(4) L. S. Schanker, in "The Biliary System," W. Taylor, Ed., Blackwell, Oxford, England, 1965, p. 469.

(5) C. L. Huang, J. A. Yeh, and S. Y. Hsu, *J. Pharm. Sci.*, **59**, 772 (1970).

(6) J. H. G. Jonkman, thesis, State University of Groningen, Groningen, The Netherlands, 1977, pp. 115–303.

(7) D. K. F. Meijer and J. G. Weitering. *Eur. J. Pharmacol.*, **10**, 283 (1970).

(8) U. I. Lavy, W. Hespe, and D. K. F. Meijer, *Naunyn-Schmiedebergs Arch. Pharmacol.*, **275**, 183 (1972).

(9) K. Turnheim and F. O. Lauterbach, *Biochem. Pharmacol.*, **26**, 99 (1977).

ACKNOWLEDGMENTS

The authors thank Mrs. Eily Beerling-v.d. Molen, Dr. Stoffer Reiffers, and Dr. Wim Vaalburg for their advice and help with the synthesis of ^{14}C-labeled compounds and Egbert Scholtens for technical assistance.

Interference in Assays for Hydralazine in Humans by a Major Plasma Metabolite, Hydralazine Pyruvic Acid Hydrazone

PHILLIP A. REECE ˣ, PHILIP E. STANLEY, and RUDOLF ZACEST

Received July 6, 1977, from the *Department of Clinical Pharmacology, The Queen Elizabeth Hospital, Woodville, 5011, South Australia.* Accepted for publication December 9, 1977.

Abstract □ The present study showed that published spectrophotometric and GLC methods for hydralazine in plasma do not distinguish between the drug and a major plasma metabolite, hydralazine pyruvic acid hydrazone. These methods involve the acidic treatment of the sample, which hydrolyzes the hydrazone back to hydralazine. A specific GLC assay for the hydrazone was developed and involves its selective extraction from plasma and transformation to 3-trifluoromethyl-*s*-triazolo[3,4-*a*]phthalazine. This derivative could be sensitively measured by GLC using an electron-capture detector. With this procedure, it was shown that most "apparent hydralazine" in plasma is the hydrazone, which forms rapidly from hydralazine and endogenous pyruvic acid. Previous work indicated that the hydrazone was inactive when administered intravenously to rabbits.

Keyphrases □ Hydralazine—interference in published GLC and spectrophotometric analyses in plasma by major metabolite □ Metabolites—hydralazine pyruvic acid hydrazone, GLC analysis in plasma □ GLC—analysis, hydralazine pyruvic acid hydrazone in plasma □ Antihypertensives—hydralazine, interference in published GLC and spectrophotometric analyses in plasma by major metabolite

The vasodilator hydralazine, 1-hydrazinophthalazine (I), is an effective agent for the treatment of arterial hypertension (1). It undergoes extensive metabolism in humans and animals, and Metabolites II–VIII were identified (1–11). Acetylation was proposed as the major pathway for hydralazine clearance (2–8), where the acetylated drug, 3-methyl-*s*-triazolo[3,4-*a*]phthalazine (III), may be further metabolized to 3-hydroxymethyl-*s*-triazolo[3,4-*a*]-phthalazine (IV) and its glucuronide conjugate (2, 11).

Although hydralazine can form hydrazones readily with compounds having an active carbonyl group, hydralazine pyruvic acid hydrazone, 1-hydrazinophthalazine pyruvic acid hydrazone (II), was identified only as a minor metabolite in rat urine following oral administration of hydralazine (2, 4). Fresh human blood contains pyruvic acid in a concentration of approximately 100 μmoles/liter, which is a considerable excess to the commonly found therapeutic levels of "apparent hydralazine" and appears to favor formation of II. Preliminary findings indicated (12) that plasma apparent hydralazine, or that measured

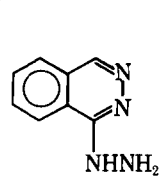

I

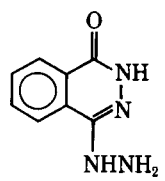

V

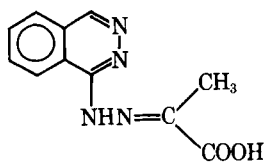

II

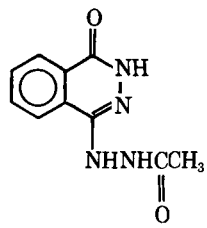

VI

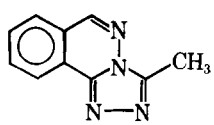

III

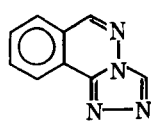

VII

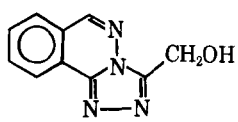

IV

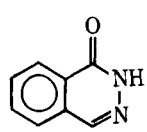

VIII

0022-3549/78/0800-1150$01.00/0

© 1978, American Pharmaceutical Association

$$\text{II} \xrightarrow[H_2O]{\text{acid}} \text{I} + CH_3\overset{\overset{O}{\|}}{C}COOH$$

Scheme I

by the published spectrophotometric (13) and GLC (14) assays, was composed largely of II.

In the present study, methods for plasma hydralazine were examined for specificity using synthesized hydralazine metabolites, and investigations of the significance of plasma II levels were undertaken. Formation of II from I and pyruvic acid in plasma and water and the stability of II in various buffers also were studied.

EXPERIMENTAL

Syntheses—The hydralazine metabolites (II–VIII) were synthesized by published methods (2–11, 15), except 4-hydrazinophthalazin-1(2*H*)-one (V), which was synthesized by refluxing a solution of 1,4-dihydrazinophthalazine sulfate[1] (2.7 g) in water (100 ml) for 30 min. The mixture was concentrated under reduced pressure and cooled to precipitate the desired product (272 mg, 12.5%), mp 155–156°; mass spectroscopy: found *m/e* 176, $C_8H_8N_4O$ requires *m/e* 176 (M^+).

Anal.—Calc. for $C_8H_8N_4O{\cdot}0.5H_2O$: C, 51.9; H, 4.9; N, 30.3. Found: C, 51.9; H, 5.0; N, 30.7.

3-Trifluoromethyl-*s*-triazolo[3,4-*a*]phthalazine (IX) was synthesized by the method of Lesser *et al.* (3).

Apparent Hydralazine Assays—The spectrophotometric hydralazine method of Schulert (13), as modified by Zacest and Koch-Weser (6), was used. The GLC assay of Jack *et al.* (14) was employed without modification; 0.5 ml of plasma was used, and the final residue, after evaporation of the benzene, was dissolved in toluene (1 ml). Replicate samples (1 μl) were injected into the gas–liquid chromatograph[2] with an automatic sample injector[3].

Both chromatographs were equipped with ^{63}Ni-electron-capture detectors. A comparison of the two methods was undertaken by assaying duplicate plasma samples from 94 hypertensive patients receiving chronic oral hydralazine therapy.

Acid Lability of II—At a concentration of 43 μmoles/liter, II was added to Clark–Lubs potassium chloride buffer for pH 1.0 and 2.0; to Clark–Lubs potassium hydrogen phthalate buffer for pH 2.5, 3.0, and 4.0; to Clark–Lubs sodium borate buffer for pH 7.0, 8.0, 9.0, and 10.0; and to aqueous 1 *N* HCl for pH 0.1. The rate and extent of decomposition of II (Scheme I) were determined by UV spectrophotometry at 21° from the absorbance of the peak with $\lambda_{max} \simeq 340$ nm ($\epsilon_{max} \simeq 1.0 \times 10^4$) (Fig. 1). Hydralazine had insignificant absorption at this wavelength. The UV spectrum and melting point of the decomposition product were compared

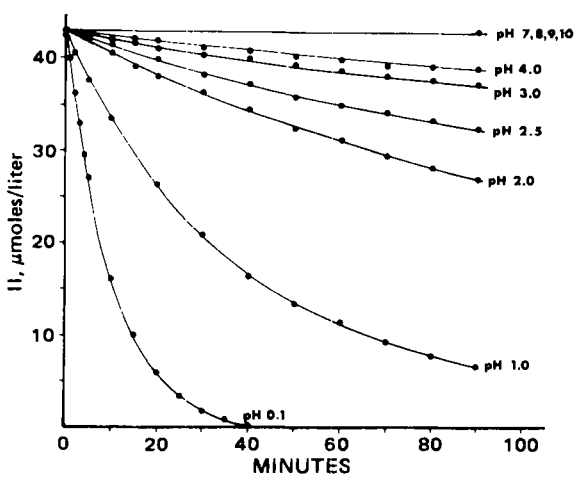

Figure 1—*Stability of II determined by UV spectrophotometry at* $\lambda_{max} \simeq 340$ *nm* ($\epsilon \simeq 1.0 \times 10^4$) *and 21°.*

[1] Ciba-Geigy, Basel, Switzerland.
[2] Packard model 419 or a Pye Series 104.
[3] Packard model 700 or a Pye model S4.

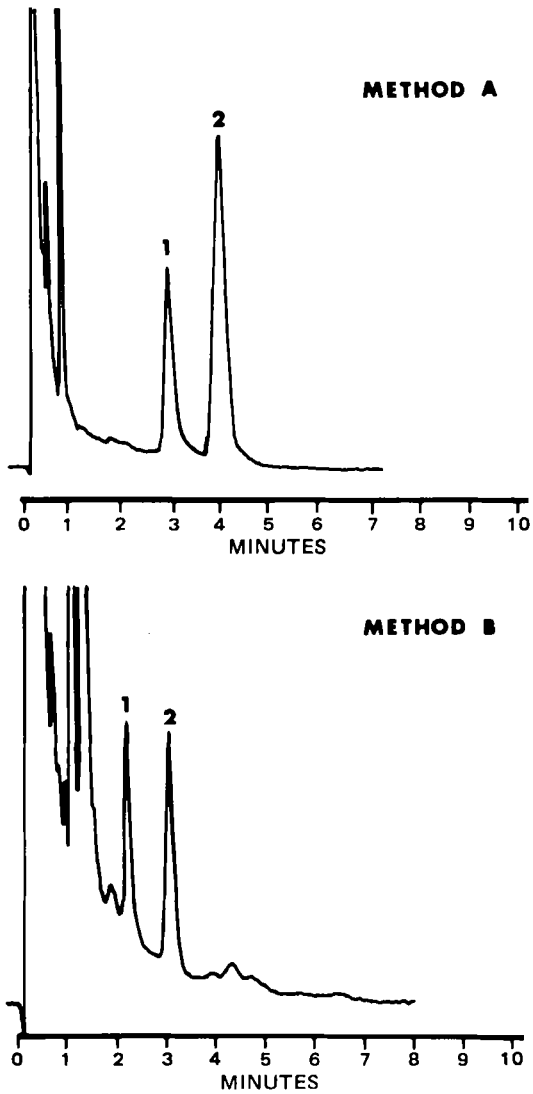

Figure 2—*GLC traces for II assayed by Methods A and B. Key: Peak 1, II; and Peak 2, X (internal standard).*

with those of hydralazine.

Interference of Hydralazine Metabolites in Apparent Hydralazine Assays—Compounds II–V, VII, and VIII were added to separate fresh plasma samples to give a final concentration of 7.5 μmoles/liter and assayed for apparent hydralazine by the spectrophotometric and GLC procedures.

Hydralazine Pyruvic Acid Hydrazone (II) Assays—*Method A*—To 1 ml of plasma, obtained by rapid centrifugation of the blood sample at 4°, was added the internal standard, 4-methylhydralazine pyruvic acid hydrazone (X) (7.5 μmoles/liter). Compound X was synthesized from 4-methylhydralazine[2] and pyruvic acid by the method described for II. Aqueous 4 *N* HCl (45 μl), sodium sulfate (500 mg, pH 3.0), and chloroform (10 ml) were then added. The extraction was performed within 30 sec of acidification by shaking the mixture at 200 rpm for 10 min.

The chloroform layer was then poured into a conical centrifuge tube (the semisolid aqueous mixture adhered to the side of the extraction tube) and evaporated rapidly under a stream of nitrogen at 45°. The residue was treated with trifluoroacetic anhydride (100 μl) at 21° for 5 min. The excess trifluoroacetic anhydride was evaporated under a stream of clean, dry nitrogen. The residue was then dissolved in toluene (1 ml), and 1 μl was injected onto the gas–liquid chromatograph[2] equipped with a ^{63}Ni-electron-capture detector and a 1-m × 2-mm glass column packed with 3% OV-17 on Gas Chrom Q (Fig. 2).

The column flow rate was 50 ml/min (oxygen-free nitrogen), the makeup flow rate was 10 ml/min (nitrogen), the column temperature was 190°, the injector temperature was 220°, and the detector temperature was 300°. The recovery of II (7.5 μmoles/liter) added to plasma and assayed by this method was determined in replicate by comparison with

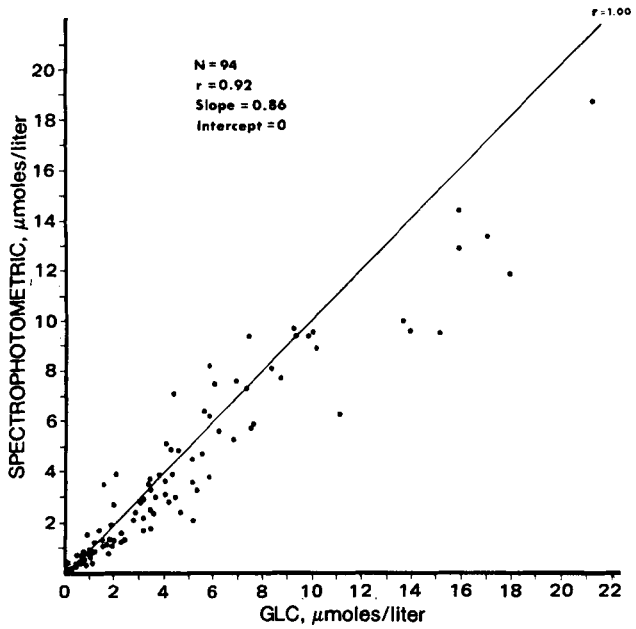

Figure 3—*Comparison of the GLC and spectrophotometric assays for apparent hydralazine in 94 hypertensive patients receiving chronic oral hydralazine therapy.*

the peak obtained for 100 pg of IX injected into the gas chromatograph.

A sample of II was derivatized as described, dissolved in methanol, and injected into a gas chromatograph–mass spectrometer[4]. The total ion current and molecular ion (*m/e* 252) were then monitored. The mass spectrum of the single peak was compared with that of an authentic sample of IX.

Method B—An alternative to Method A was to chromatograph II and the internal standard without prior derivatization. The residue (see *Method A*) was dissolved in methanol (50 μl), and 1 μl was injected into the gas–liquid chromatograph equipped with a 1-m × 2-mm glass column packed with 3% OV-17 on Gas Chrom Q and a nitrogen detector[5]. The flow rates were: nitrogen carrier gas, 35 ml/min; hydrogen, 30 ml/min; and air, 150 ml/min. The temperatures were: column, 245°; injector, 265°; and detector, 270° (Fig. 2).

To check for interference, hydralazine (7.5 μmoles/liter) and its metabolites were added to plasma and samples were assayed for II by Methods A and B.

Formation of II in Plasma and Water—Hydralazine was added to fresh heparinized plasma to give a final concentration of 7.5 μmoles/liter and maintained at 21°. Samples (1 ml) were taken over 4 hr and assayed for II by Method A. Samples were also assayed for apparent hydralazine using the GLC method (14) and for pyruvic acid using a commercially available test kit[6].

The reaction of hydralazine (78 μmoles/liter) with pyruvic acid (12.5 mmoles/liter) in water was monitored by UV spectrophotometry at 21°. The absorbance at $\lambda_{max} \simeq 340$ nm was used to determine the concentration of II in the mixture.

Comparison of Apparent Plasma Hydralazine and II Levels—Samples of plasma from 37 hypertensive patients receiving chronic oral therapy with hydralazine and at steady state (drawn >2 hr after the last dose) were each assayed for II (Methods A and B) and for apparent hydralazine using the spectrometric and/or GLC hydralazine method. The relationship of the concentrations of the two compounds in individual samples was thus obtained.

RESULTS

Comparison of Apparent Hydralazine Assays—A comparison of the spectrophotometric and GLC plasma assays for apparent hydralazine in 94 hypertensive patients receiving chronic oral hydralazine showed that the results from the two methods correlated satisfactorily ($r = 0.92$) (Fig. 3). The line of best fit determined by the method of least squares had a slope of 0.86 and a zero intercept.

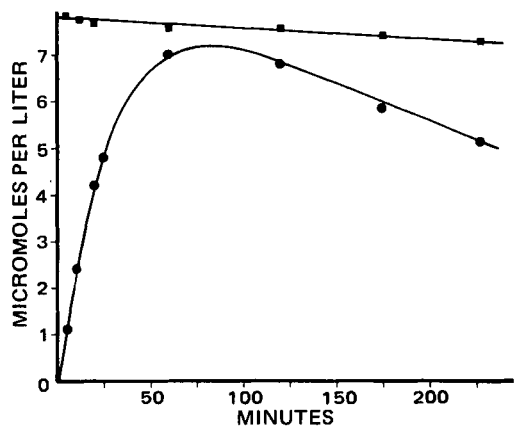

Figure 4—*Formation of II (●) from hydralazine added to fresh plasma containing endogenous pyruvic acid (68 μmoles/liter), and the stability of apparent hydralazine (■) in the same plasma measured by the GLC method of Jack* et al. *(14).*

Acid Lability of II—Compound II, added to plasma to give a concentration of 7.5 μmoles/liter and assayed by the spectrophotometric and GLC methods, gave an apparent hydralazine plasma level of 7.5 μmoles/liter. The other hydralazine metabolites did not interfere. Compound II was converted rapidly to hydralazine at low pH, and hydrolysis in aqueous 1 *N* HCl was complete in 40 min at 21° (Fig. 1). In buffer at pH 3.0, II (43.0 μmoles/liter) decomposed at a rate of 60 nmoles/liter/min. The UV spectrum and melting point of the decomposition product of II were identical with those of hydralazine. During plasma treatment with nitrous acid in the GLC hydralazine assay, the pH of the solution was less than 1 (for 15 min). Similarly, the pH required for the formation of the *p*-hydroxybenzaldehyde derivative in the spectrophotometric assay was 1.5 (70° for 10 min).

II Assays—Treatment of II and its 4-methyl analog with trifluoroacetic anhydride in Method A gave the respective trifluoromethyl-*s*-triazolo[3,4-*a*]phthalazines with GLC retention times of 2.9 and 4.0 min. This conversion was confirmed for II by GLC–mass spectrometry. The mass spectrum of the single product was identical with that of an authentic sample of IX.

Standard curves obtained using Methods A and B for a series of plasma standards were linear over the range of 0.1–10.0 μmoles of II/liter. The coefficient of variation for the 3.0-μmole/liter plasma standard assayed in replicate was 2.0% for Method A and 5.5% for Method B. The mean recovery of II added to plasma (7.5 μmoles/liter) and determined using Method A was 6.9 μmoles/liter (*SD* ±0.1 μmole/liter). Hydralazine was not extracted from the acidified plasma in Methods A and B, and neither it nor the hydralazine metabolites interfered in the assays for II.

Formation of II—Compound II was formed rapidly (Fig. 4) following the addition of hydralazine to fresh human plasma containing endogenous pyruvic acid (68 μmoles/liter). The second-order rate constant for this reaction was 7.4 liters/mole/sec (21°). There was a slight fall (1.5%/hr) in the apparent hydralazine level measured over the same period. The level of II reached a peak and then slowly declined.

The second-order rate constant for the reaction of hydralazine with pyruvic acid in water was 1.9 liters/mole/sec.

Comparison of Apparent Plasma Hydralazine and II Levels—There was good correlation between apparent hydralazine and plasma levels of II ($r = 0.94$, $p = 0.00001$) (Fig. 5). The slope of the line of best fit determined by the method of least squares was 0.94 ± 0.05, and the intercept was not significantly different from zero.

DISCUSSION

The published apparent hydralazine assays employing GLC and UV spectrophotometry correlated well, but both lacked specificity for unmetabolized hydralazine. The interfering metabolite was II, which was unstable at low pH and completely converted to free hydralazine under the conditions of sample treatment (Scheme I).

The recovery of II added to plasma in Method A was high (92%), and decomposition of II at the pH used in the extraction step (pH 3.0) was sufficiently slow (0.15%/min) that it did not interfere in the assay. The derivative obtained in Method A was highly electron capturing, provided

[4] Model AEI MS-30.
[5] Packard model 713.
[6] Boehringer diagnostic kit.

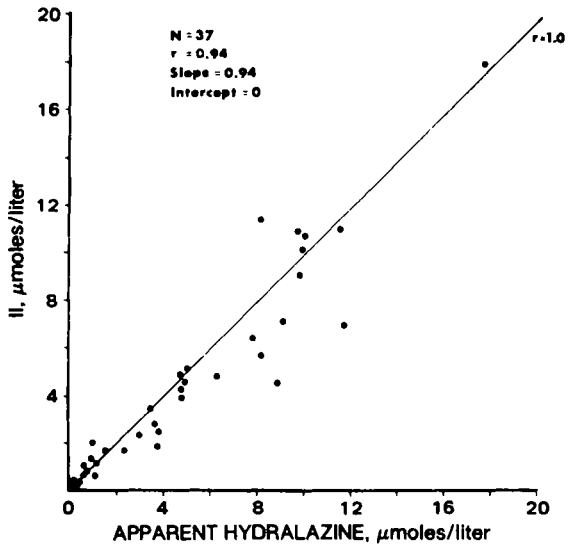

Figure 5—*Comparison of apparent hydralazine (measured by the spectrophotometric and/or GLC hydralazine methods) and II levels at steady state in plasma samples drawn from hypertensive patients receiving chronic oral hydralazine therapy.*

good sensitivity (10 ng/ml), and gave a linear response over the concentration range used. Estimates of the plasma II levels in patients receiving oral hydralazine indicated that more than 90% of the apparent hydralazine measured by the published assays was present as II. These findings are consistent with those of Zak *et al.* (16) who found significantly high levels of "acid-hydrolyzable conjugates" in the plasma of human subjects after oral administration of hydralazine. The discrepancy between II and apparent hydralazine levels in individual samples may be due to other acid-labile hydrazones or free hydralazine itself.

When hydralazine was added to fresh heparinized human plasma containing endogenous pyruvic acid or water containing added pyruvic acid, II formed rapidly. The second-order rate constants (17) for the reaction in each of these systems were 7.4 and 1.9 liters/mole/sec, respectively. The formation rate of II *in vivo* can be expected to be even higher because of the continual replenishment of consumed pyruvic acid and the higher physiological temperature (37°). Therefore, any hydralazine entering the circulation probably would be rapidly metabolized to II and circulate as such. The relative concentrations of pyruvic acid, I, and II in human plasma immediately following administration of the drug by oral and intravenous routes are currently being evaluated.

At present, there is no satisfactory explanation for the slow decline in the level of II (Fig. 4) following its formation from hydralazine. However, the slow decomposition of apparent hydralazine in plasma was observed previously (3, 13, 18).

In parallel with the current findings with hydralazine, Dauphinee *et al.* (17) showed that isoniazid also reacts rapidly with pyruvic acid in water. Comparison with the present work indicated that the rate of this reaction was approximately 100 times slower than that of hydralazine with pyruvic acid in water. This result reflects the lower reactivity of the hydrazide group of isoniazid compared with that of the hydrazino group of hydralazine. Even so, 25% of the total isoniazid in a human subject's plasma was present as unidentified hydrazone 60 min after an oral dose of isoniazid (18).

Compound II did not show any hypotensive activity when administered intravenously to rabbits (12). The lack of hypotensive activity of the metabolite in the rabbit suggests that it may also lack activity in humans.

REFERENCES

(1) "The Pharmacological Basis of Therapeutics," 5th ed., L. S. Goodman and A. Gilman, Eds., Macmillan, New York, N.Y., 1975, p. 705.

(2) K. D. Haegele, H. B. Skrdlant, N. W. Robie, D. Lalka, and J. K. McNay, Jr., *J. Chromatogr.*, **126**, 517 (1976).

(3) J. M. Lesser, Z. H. Israili, D. C. Davis, and P. G. Dayton, *Drug Metab. Dispos.*, **2**, 351 (1974).

(4) W. M. McIsaac and M. Kanda, *J. Pharmacol. Exp. Ther.*, **143**, 7 (1964).

(5) M. M. Reidenberg, D. Drayer, A. L. DeMarco, and C. T. Bello, *Clin. Pharmacol. Ther.*, **14**, 970 (1974).

(6) R. Zacest and J. Koch-Weser, *ibid.*, **13**, 420 (1972).

(7) H. Zimmer, J. McManus, T. Novinson, E. V. Hess, and A. H. Litwin, *Arzneim.-Forsch.*, **20**, 1586 (1970).

(8) H. Zimmer, J. Kokosa, and D. A. Garteiz, *ibid.*, **23**, 1028 (1973).

(9) J. Wagner and P. R. Hedwall, in "Recent Advances in Hypertension," vol. 2, Proceedings of a Symposium held in Monaco, 1975, P. Milliez and M. Safar, Eds., Société Alinéa, Reims, France, 1976, p. 289.

(10) S. B. Zak, T. G. Gilleran, J. Karliner, and G. Lukas, *J. Med. Chem.*, **17**, 381 (1974).

(11) H. Zimmer, R. Glaser, and J. Kokosa, *ibid.*, **18**, 1031 (1975).

(12) P. A. Reece, P. E. Stanley, and R. Zacest, *Clin. Exp. Pharmacol. Physiol.*, in press.

(13) A. R. Schulert, *Arch. Int. Pharmacodyn. Ther.*, **132**, 1 (1961).

(14) D. B. Jack, S. Brechbuhler, P. H. Degen, P. Zbinden, and W. Riess, *J. Chromatogr.*, **115**, 87 (1975).

(15) J. Druey and B. H. Ringier, *Helv. Chim. Acta*, **34**, 195 (1951).

(16) S. B. Zak, G. Lukas, and T. G. Gilleran, *Drug Metab. Dispos.*, **5**, 116 (1977).

(17) K. R. Dauphinee, S. Paynter, and D. W. Russell, *J. Pharm. Pharmacol.*, **27**, 884 (1975).

(18) T. Talseth, *Eur. J. Clin. Pharmacol.*, **10**, 183 (1976).

ACKNOWLEDGMENTS

Abstracted in part from a paper presented at the annual meeting of the Australasian Society of Clinical and Experimental Pharmacologists, November 25, 1976.

Supported in part by a grant from The Queen Elizabeth Hospital Research Foundation Inc.

The authors thank Dr. W. Riess, Research Department, Pharmaceuticals Division, Ciba-Geigy, Basel, Switzerland, for supplying the sample of 4-methyl-1-hydrazinophthalazine; Dr. G. Phillipou for assistance with the GLC–mass spectrometry; and Miss L. Green for technical assistance.

Structure–Toxicity Relationships of Iodinated Aromatic Carbonates and Related Compounds

BARRY N. NEWTON

Received June 8, 1977, from the *Research and Development Department, Lafayette Pharmacal Incorporated, Lafayette, IN 47904.* Accepted for publication December 2, 1977.

Abstract □ Structure–toxicity relationships of iodinated aromatic carbonates, carbamates, and esters are presented. The approximate lethal dose of intraperitoneal injections in mice was used for toxicity determinations. Increasing the alkyl portion of the molecules reduced toxicity. *m*-Amino and *m*-acetamido groups also reduced toxicity. Carbonates were preferred X-ray contrast agents because of their low viscosity and more rapid elimination.

Keyphrases □ Iodinated aromatic compounds, various—toxicity in mice, structure–activity relationships □ Structure–activity relationships—various iodinated aromatic compounds, toxicity in mice □ Radiopaque media—various iodinated aromatic compounds, toxicity in mice, structure–activity relationships

The X-ray visualization of the subarachnoid space from the sacral region through the cervical area is referred to as myelography. Three classes of contrast agents are used for this examination: gas, water-soluble compounds, and oily, water-insoluble compounds.

BACKGROUND

Gas myelography is performed by injecting either air or carbon dioxide into the subarachnoid space, thus providing negative contrast. The interpretation of this examination is difficult, and there is a high incidence of patient headaches (1). For these reasons, gas myelography is used infrequently.

Water-soluble compounds for positive contrast myelography have been used for more than 30 years in Europe. Iodomethane sulfonate was the compound of choice for about three decades, but its use was discontinued because of patient reactions, including convulsions and adhesive arachnoiditis. Other ionic water-soluble salts have been used, but they are not widely accepted because of their side effects. A dimeric compound is available in the United States, but, because of its toxicity, it is recommended only for use in the lumbar sacral region[1] (2, 3).

Nonionic water-soluble radiopaques, prepared by attaching a hydrophilic sugar group to a triiodinated moiety, were first proposed by Hebky and coworkers (4, 5). More recently, this approach was used to design metrizamide, a nonionic water-soluble compound receiving attention as a new myelographic medium (6, 7). To date, metrizamide appears to be the least toxic water-soluble myelographic medium. However, Sackett *et al.* (8) reported that 39% of their patients experienced moderate to severe adverse reactions following metrizamide myelography and that three out of 215 patients had seizures. This report, coupled with other factors, confirms that the ideal myelographic medium has yet to be determined (9).

Oil myelography has dominated the U.S. market since the early 1940's. Iophendylate, ethyl 10-(iodophenyl)undecanoate, has been the preferred contrast agent. During this period, millions of examinations have been performed with a very low incidence of side effects (10). However, since iophendylate is only very slowly eliminated by the body, it is withdrawn from the subarachnoid space at the conclusion of the examination.

While there have been numerous reports concerning new water-soluble compounds, there have been very few reports on new oily materials (11–13). The preparation and toxicity of several oily iodinated organic carbonates were reported elsewhere (14, 15). This paper reports initial structure–toxicity relationships encountered with the carbonates and comparisons with related compounds.

[1] This material has been withdrawn from the market since this article was accepted for publication.

EXPERIMENTAL[2]

Details regarding the preparation of iodinated aromatic carbonates from the pertinent alcohols were given previously (14). The approximate lethal dose (ALD) intraperitoneally in mice was determined by injecting six animals with graduated doses, each dose being 50% higher than the preceding one. With this technique, all doses up to a certain level resulted in survival of the animals while all doses above this level were lethal. The ALD previously (16) was found to agree with the LD_{50} value within the limits of approximately ± 30%.

10-(*p*-Iodophenyl)undecanol (VII)—Ethyl 10-(*p*-iodophenyl)-undecanoate was reduced with lithium aluminum hydride by a known procedure (20). Compound VII was recovered; $n_D^{25} = 1.5238$; mass spectrum: *m/e* (measured mass) 374.1114 (calculated for $C_{17}H_{27}IO$, 374.1108).

Anal.—Calc. for $C_{17}H_{27}IO$: C, 54.53; H, 7.27. Found: C, 54.22; H, 7.56.

***p*-Iodobenzyl Hexanoate (XXIX)**—This compound was prepared by a standard esterification procedure (21); $n_D^{25} = 1.5819$; mass spectrum: *m/e* (measured mass) 332.0264 (calculated for $C_{13}H_{15}IO_3$, 332.0275).

Anal.—Calc. for $C_{13}H_{15}IO_3$: C, 46.98; H, 4.55. Found: C, 46.87; H, 4.94.

Similarly prepared from the appropriate iodinated alcohol and aliphatic acid were XXX and XXXII. For XXX, $n_D^{25} = 1.5454$; mass spectrum: *m/e* (measured mass) 360.0554 (calculated for $C_{15}H_{21}IO_2$, 360.0588).

Anal.—Calc. for $C_{15}H_{21}IO_2$: C, 46.98; H, 4.55. Found: C, 46.87; H, 4.94.

For XXXII, $n_D^{25} = 1.5322$; mass spectrum: *m/e* (measured mass) 388.0900 (calculated for $C_{17}H_{25}IO_2$, 388.0901).

Anal.—Calc. for $C_{17}H_{25}IO_2$: C, 52.57; H, 6.49. Found: C, 52.70; H, 6.77.

The following carbonates were prepared as outlined previously (8): Compound XIII: $n_D^{25} = 1.5431$.

Anal.—Calc. for $C_{12}H_{14}IO_5$: C, 43.11; H, 4.53. Found: C, 42.87; H, 4.40.

Compound XXIV: $n_D^{25} = 1.4806$.

Anal.—Calc. for $C_{12}H_{20}IO_3$: C, 71.14; H, 8.54. Found: C, 71.37; H, 8.65.

Compound XXXV: $n_D^{25} = 1.5369$.

Anal.—Calc. for $C_{14}H_{17}IO_5$: C, 42.86; H, 4.37. Found: C, 43.17; H, 4.45.

The following carbamates were prepared using the procedure for carbonate synthesis.

Compound XXXI, mp 78.6–79.2° (ethanol–water); mass spectrum: *m/e* (measured mass) 347.0353 (calculated for $C_{13}H_{18}INO_2$, 347.0384).

Anal.—Calc. for $C_{13}H_{18}INO_2$: C, 44.95; H, 5.23. Found: C, 44.66; H, 5.11.

Compound XXXIII, mp 92.2–94.2° (hexane); mass spectrum: *m/e* (measured mass) 389.0863 (calculated for $C_{16}H_{24}INO_2$, 389.0854).

Anal.—Calc. for $C_{16}H_{24}INO_2$: C, 49.35; H, 6.22. Found: C, 49.39; H, 6.17.

[2] Melting points were determined on a Buchi capillary apparatus and are uncorrected. IR spectra were recorded on a Beckman IR 33 spectrometer. NMR spectra were taken on a Varian EM 360 spectrometer with tetramethylsilane as the internal standard. Gas chromatograms were obtained on a Hewlett-Packard 5712A chromatograph equipped with a thermal conductivity detector using a 3% SE-30 column. Refractive indexes were determined on a Bausch & Lomb refractometer. Viscosities were determined using an Ostwalt viscometer at 25 ± 1° and an average of three runs. Mass spectra were obtained on a CEC 21-110B double-focusing mass spectrometer with an accelerating potential of 7.5 kv, nominal; an emission current of 100 μmp, regulated; an ionizing voltage of 70 ev; a reservoir temperature of 200°; a source temperature of 175–200°; and a nominal mass resolution of 1/15,000 (17–19). Throughout the program, emphasis was on pure products rather than on improved yields.

0022-3549/78/0800-1154$01.00/0
© 1978, American Pharmaceutical Association

Table I—Approximate Lethal Dose of Iodinated Aromatic Alcohols

Compound	Structure	ALD[a]
I	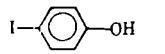	0.7 g/kg
II	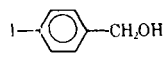	1.0 g/kg
III	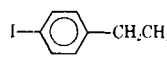	1.0 ml/kg
IV	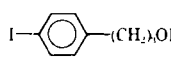	1.0 ml/kg
V	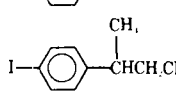	0.5 ml/kg
VI	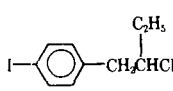	5.5 ml/kg
VII	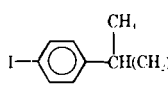	2.2 ml/kg

[a] Compounds with ALD values in grams per kilogram were administered as suspensions in sesame oil (no toxicity from sesame oil alone). Compounds with ALD values in milliliters per kilogram were administered as a neat oil.

Compound XXXIV, mp 113.2–114.4° ($CHCl_3$); mass spectrum: *m/e* (measured mass) 391.0279 (calculated for $C_{14}H_{18}INO_4$, 391.0282).

Anal.—Calc. for $C_{14}H_{18}INO_4$: C, 42.96; H, 4.64. Found: C, 42.61; H, 4.64.

RESULTS AND DISCUSSION

Generally, iodine is incorporated into organic compounds to make them opaque to X-rays. Iodine bound to an aliphatic carbon atom is liberated more easily than aromatically bound iodine. Therefore, the aromatic ring was used to incorporate iodine into the carbonates. Various iodinated aromatic alcohols were used to prepare the carbonates. To gain insight into the toxicity of the carbonates, the ALD of the starting alcohols was determined.

The results of varying the alkyl structure between the iodinated benzene ring and the OH group can be seen in Table I. There was little difference in the ALD values of *p*-iodophenol (I), *p*-iodobenzyl alcohol (II), *p*-iodophenethyl alcohol (III), *p*-iodophenylpropanol (IV), and 3-(*p*-iodophenyl)butanol (V). 2-(*p*-Iodobenzyl)butanol (VI), however, had a disproportionately higher ALD. This difference was not just a result of a higher carbon content in the side chain, because VII has an ALD of only 2.2 ml/kg. The carbon skeleton of VI is the same as that found in iopanoic acid (XL), a relatively nontoxic oral cholecystographic agent (22). The reduced toxicity of IV has been attributed to albumin binding.

Table II—Influence of Ring Substitution on ALD of Iodinated Alcohols

Compound	Structure	ALD, g/kg[a]
II	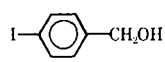	1
VIII	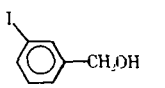	0.75
IX	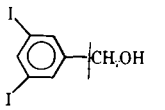	<0.5
X	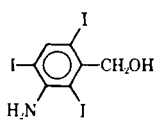	7.5
XI	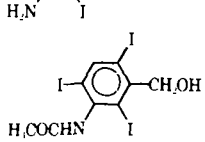	7.5

[a] Administered as suspensions in sesame oil (no toxicity from sesame oil alone).

Table III—Influence of R_2 on ALD of Carbonates

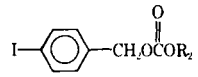

Compound	R_2	ALD, g/kg[a]	u_{25}, cps[b]
XII	C_2H_5	2.74	11.76
XIII	C_4H_9	4.5	14.37
XIV	C_5H_{11}	4.38	—[c]
XV	C_6H_{13}	6.78	18.58
XVI	$CH(C_2H_5)C_3H_7$	4.32	21.69
XVII	C_8H_{17}	>27	22.1
XVIII	$CH_2CH(C_2H_5)C_4H_9$	20.25	33.88

[a] Administered as a neat liquid intraperitoneally in mice. [b] Viscosities were determined on samples containing <5% impurities. [c] Not available.

Table IV—Influence of R_1 on ALD of Carbonates

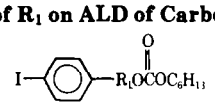

Compound	R_1	ALD, ml/kg[a]
XIX	None	4.5
XV	CH_2	7.0
XX	CH_2CH_2	7.0
XXI	$CH_2CH_2CH_2$	10.2
XXII	$CH(CH_3)CH_2CH_2$	7.0
XXIII	$CH_2CH(C_2H_5)CH_2$	>15

[a] Administered as a neat liquid intraperitoneally to mice.

Substitution on the benzene ring can contribute to reduced toxicity. Thus, the toxicity remained virtually unchanged going from *p*-iodo (II) to *m*-iodo (VIII) to 3,5-diiodobenzyl alcohol (IX) (Table II). However, 3-amino-2,4,6-triiodo- and 3-acetamido-2,4,6-triiodo-substituted benzyl alcohols had much larger ALD values (note X and XI in Table II).

When the iodinated alcohols were converted to carbonates and other related compounds, several interesting structure–activity relationships were found. Generally, an increase in the length of the primary alkyl chain of a carbonate resulted in decreased toxicity. For example, the ethyl carbonate (XII) was more toxic than the butyl carbonate (XIII) (Table III). There was little change in the ALD of the pentyl carbonate (XIV) and 4-substituted hexyl carbonate (XVI). Major toxicity decreases were seen going from *n*-hexyl carbonate (XV) to *n*-octyl carbonate (XVII). Branching of the alkyl portion of the carbonate while holding the carbon content constant reduced the ALD (compare XV with XVI and XVII with XVIII).

The lipophilic character of the carbonates decreases as the chain length decreases. This phenomenon was demonstrated through several examples (23). The decreased lipophilic character results in an increased water solubility and, in turn, may increase the absorption rate. Before a molecule can cross a lipophilic membrane, it must be transported to that membrane. Because of their higher water solubility, the shorter chain members have a greater opportunity to cross the barrier. Thus, the shorter chain compounds may be more toxic because of more rapid transport and absorption.

A good myelographic medium should flow freely within the sub-

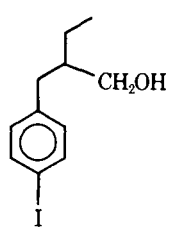

VI

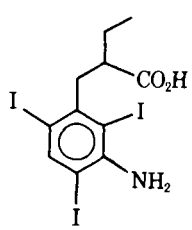

XL

Table V—Influence of Ring Substitution on the Toxicity of Carbonates

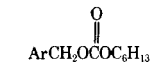

Compound	Ar	ALD[a]
XXIV		4.5 ml/kg
XV	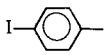	4.8 ml/kg
XXV		4.5 ml/kg
XXVI	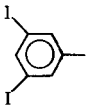	5.0 ml/kg
XXVII	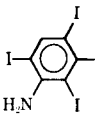	>22.0 g/kg
XXVIII	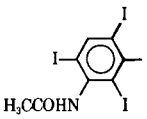	>22.0 g/kg

[a] Administered intraperitoneally in mice. Compounds with ALD values in grams per kilogram were administered as suspensions in sesame oil (no toxicity from sesame oil alone). Compounds with ALD values in milliliters per kilogram were administered as a neat oil.

arachnoid space and thus requires a low viscosity. It should also have a high ALD. Increasing the carbon content of the alkyl portion of the carbonates increases the ALD but results in higher viscosities (Table III). Thus, the least toxic compounds are less suitable as myelographic agents because of their higher viscosity[3].

Variation of the alkyl structure between the benzene ring and the carbonate linkage resulted in less dramatic toxicity changes. Compound XIX (Table IV), where the ring is attached directly to the carbonate linkage, had an ALD of 4.5 ml/kg. Interjection of one, two, and three methylene groups gave only slightly less toxic compounds (compare XV, XX, and XXI, respectively). An α-methyl group also only affected the ALD slightly (compare XXI with XXII). The carbonate (XXIII) prepared from alcohol (VII) showed a large increase in the ALD when compared to the other carbonates in Table IV. Again, however, the high viscosity of this compound precludes its use for myelography.

Variation of ring substitution gave results with the carbonates comparable to those seen with the alcohols. There was little change in toxicity due to the addition of *para*-, *meta*-, or 3,5-disubstituted iodine (compare XXIV, XV, XXV, and XXVI, Table V). Hoppe (24) previously demonstrated the reduction in toxicity resulting from *m*-amino and *m*-acetamido groups. Thus, as expected, *n*-hexyl 3-amino-2,4,6-triiodobenzylcarbonate (XXVII) and *n*-hexyl 3-acetamido-2,4,6-triiodobenzylcarbonate (XXVIII) were far less toxic than just iodinated ring compounds.

When the carbonate linkage was compared with ester and carbamido structures, the toxicity did not change significantly (Table VI). The esters and carbamido compounds were of less interest radiographically, since the esters were more viscous and more slowly eliminated while the carbamido compounds were both solid and more slowly eliminated. Comparing carbonate XIV with ester XXIX and carbonate XV with ester XXX illustrates no real difference between them. Carbamide XXXI is of comparable toxicity with XV. The incorporation of a terminal carboxylic acid in a carbamido structure gave a more toxic compound (compare XXXIII with XXXIV). When an ester linkage was included in the alkyl chain of a carbonate, toxicity decreased (compare XV with XXXV).

[3] A direct correlation between the ALD obtained from intraperitoneal injections in mice and neurotoxicity obtained after intrathecal injections in rats was found. For comparative purposes, the viscosity of ethyl 10-(iodophenyl)undecanoate is 51.04 cps at 25°.

Table VI—ALD of Some Iodinated Carbonates and Related Structures

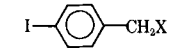

Compound	X	ALD[a], g/kg
XIV	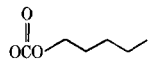	4.38
XXIX	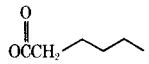	2.94
XV	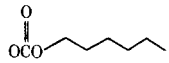	6.78
XXX	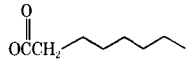	9.66
XXXI	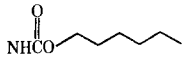	3.4[b]
XVII	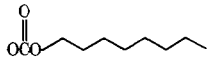	>27
XXXII	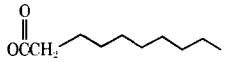	>19.5
XXXIII	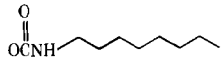	>10.5[b]
XXXIV	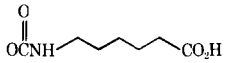	<1[b]
XXXV	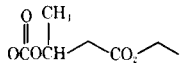	<4.44

[a] Administered intraperitoneally to mice. [b] Administered as suspensions in sesame oil (no toxicity from sesame oil alone).

Several of these compounds are now undergoing more extensive investigation for myelographic and other radiographic applications.

REFERENCES

(1) P. L. Cook, *Br. J. Radiol.*, **49**, 502 (1976).

(2) B. Hammer and H. Scherrer, *Neuroradiology*, **4**, 144 (1972).

(3) L. Irstam and U. Sellden, *Acta Radiol. Diag.*, **16**, 449 (1975).

(4) J. Hebky and V. Jelinek, Czechoslovakian pat., **106**, 426 (1963).

(5) J. Hebky, B. First, J. Polack, and M. Karasek, *Collect. Czech. Chem. Commun.*, **35**, 867 (1970).

(6) T. Almen, *J. Theor. Biol.*, **24**, 216 (1969).

(7) *Acta Radiol. Suppl.*, **1973**, 335.

(8) J. S. Sackett, C. M. Strother, C. E. Quaglieri, M. J. Javard, A. B. Levin, and T. A. Duff, *Radiology*, **123**, 779 (1977).

(9) H. O. Peterson, *ibid.*, **115**, 237 (1975).

(10) K. Y. Chynn, *ibid.*, **109**, 361 (1973).

(11) J. E. Siggins, J. H. Ackerman, and A. A. Larsen, *J. Med. Chem.*, **8**, 728 (1965).

(12) J. H. Ackerman, V. Akullian, C. Moore, and A. A. Larsen, *ibid.*, **9**, 165 (1966).

(13) J. E. Siggins and J. H. Ackerman, *ibid.*, **9**, 973 (1966).

(14) B. N. Newton, *ibid.*, **19**, 1362 (1976).

(15) B. N. Newton, U.S. pat. 4,022,814 (May 10, 1977).

(16) W. B. Deichmann and T. J. LeBlance, *J. Ind. Hyg. Toxicol.*, **25**, 415 (1943).

(17) R. Venkataraghavan, R. D. Board, R. Klimowski, J. W. Amy, and F. W. McLafferty, *Adv. Mass Spectrom.*, **4**, 65 (1967).

(18) R. J. Klimowski and R. N. McLafferty, *Acc. Chem. Res.*, **3**, 158 (1970).

(19) F. W. McLafferty and G. E. VanLear, *Org. Mass Spectrum.*, **2**, 1 (1969).

(20) R. B. Moffett, "Organic Synthesis," coll. vol. IV, Wiley, New York, N.Y., 1963, p. 834.

(21) A. I. Vogel, "Practical Organic Chemistry," 3rd ed., Wiley, New York, N.Y., 1966, p. 1000.

(22) J. O. Hoppe, and S. Archer, *Am. J. Roentgenol.*, **69**, 630 (1953).
(23) C. Hansch, A. R. Steward, S. M. Anderson, and D. L. Bently, *J. Med. Chem.*, 11, 1 (1968).
(24) J. O. Hoppe, in "Medicinal Chemistry," vol. 6, E. E. Campaigne and W. H. Harting, Eds., Wiley, New York, N.Y., 1963, p. 343.

ACKNOWLEDGMENTS

The author thanks Dr. W. S. Bucke and Dr. A. L. Kunz for valuable discussion and support, Barbara Behrmann and Leonard Klein for technical assistance, and Wilma Lotts for help in manuscript preparation.

Quantitative GLC Analysis of Sterols in Biological Samples

S. N. HOOPER and R. F. CHANDLER ˣ

Received May 23, 1977, from the *College of Pharmacy, Faculty of Health Professions, Dalhousie University, Halifax, Nova Scotia, Canada B3H 3J5.* Accepted for publication December 6, 1977.

Abstract □ A GLC method for the quantitative analysis of cholesterol, β-sitosterol, stigmasterol, campesterol, 7-dehydrocholesterol, and dihydrocholesterol in biological samples was developed to screen serum and lipid extracts of heart and liver tissue for these sterols precisely. The addition of the internal standard, cholestane, at the beginning of the procedure led to a reduction in the required sample size and the elimination of several steps. The only critical measurements are those of the biological samples and internal standard.

Keyphrases □ Sterols, various—GLC analyses in biological fluids and extracts □ GLC—analyses. various sterols in biological fluids and extracts

A study involving the feeding of cholesterol and other sterols to large numbers of chicks required a simple, precise method for the qualitative and quantitative analysis of the sterol content of serum, heart, and liver samples. The commonly employed colorimetric methods are subject to several limitations, not least of which is the lack of discrimination among two or more sterols in a single sample (1).

Several GLC methods were reported for the determination of serum cholesterol (2–8); however, a procedure was required to determine quantitatively cholesterol and other sterols in a single sample. Additionally, a small sample size and the least number of manipulations consistent with precise and accurate analysis were desirable objectives.

EXPERIMENTAL

Materials and Chemicals—All solvents were reagent grade. Cholestane[1] and the sterols were dissolved in chloroform, and their purity was checked by GLC. Accuracy was monitored by the daily use of commercial controls[2].

Apparatus—Chromatographs A[3] and B[4], equipped with dual hydrogen flame-ionization detectors and glass columns (3 mm × 2 m), were connected to a recorder fitted with an integrator[5] or an automatic programmable integrator[6] Nitrogen was the carrier gas. All gas flows were adjusted according to recommendations of the manufacturer.

The injection port and detector were set at 300°. Columns were packed with 3% OV-17 on 100–120-mesh Gas Chrom Q[7], 3% SE-30 on 100–120-mesh Gas Chrom Q[8], or 3% SP-2401 on 100–120-mesh Supelcoport[9]. Column temperatures (250–280, 280–300, or 240–250°, respectively) were adjusted to give retention times of less than 10 min for cholesterol. All analyses were isothermal, and the attenuation was adjusted to give near full-scale deflection for the internal standard.

Serum Analysis—Fresh serum (0.1 ml), cholestane standard (200 mg/100 ml, 0.1 ml), 33% KOH aqueous solution (0.2 ml), and ethanol (2.0 ml) were measured into a screw-capped test tube (13 × 100 mm). After mixing[10], the tubes were placed in a shaking water bath[11] at 60° for 2 hr. Following hydrolysis, water (0.5 ml) was added and the cholesterol and cholestane were extracted with hexane (2.0 ml). The hexane fraction was subjected directly to GLC analysis.

Tissue Extracts—Total lipid was determined quantitatively by extracting the weighed hearts and livers according to the method of Bligh and Dyer (9). The lipid subsequently was dissolved in chloroform (5 ml), 0.5 ml was immediately transferred to a screw-capped test tube, and the chloroform was evaporated in a stream of dry nitrogen. The analysis was continued as for serum, care being taken that the amount of lipid was small enough (less than 200 mg) to be saponified by the amount of potassium hydroxide being used. Values were then related to the weight of the tissue lipid.

GLC Analysis—GLC standards containing known amounts of cholestane, cholesterol, and/or β-sitosterol, campesterol, stigmasterol, dihydrocholesterol (cholestanol), and 7-dehydrocholesterol were prepared and analyzed[4,5] at the beginning and end of each day. A correction factor was determined by dividing the sterol concentration found by GLC with the known concentration. Sterol concentration of the serum and tissue samples was determined as follows:

Table I—Analysis of Control Serums

Control Serum	Number of Analyses	Mean ± *SE*
1[a]	41	174.7 ± 2.0
2[b]	37	135.8 ± 3.0

[a] Choles-Trol; reported mean value was 196/100 ml when assayed by the Anderson and Keys modification of the Abell method. [b] Moni-Trol I; reported mean value was 151 mg/100 ml when assayed by the Abell method.

[1] Aldrich Chemical Co., Milwaukee, WI 58233.
[2] Choles-Trol and Moni-Trol I, Dade Division, American Hospital Supply Corp., Miami, FL 33152.
[3] Hewlett-Packard model 5710A.
[4] F&M Scientific 700 laboratory chromatograph.
[5] Fisher Recordall series 100 fitted with disk chart integrator.
[6] Hewlett-Packard model 3380A.
[7] Chromatographic Specialties, Brockville, Ontario, Canada.
[8] Applied Science Laboratories, State College, PA 16801.
[9] Supelco, Inc., Supelco Park, Bellefonte, PA 16823.
[10] Vortex-Geni, Fisher Scientific Co.
[11] Magni Whirl model MSB-1122AA-1.

0022-3549/78/0800-1157$01.00/0
© 1978, American Pharmaceutical Association

(22) J. O. Hoppe, and S. Archer, *Am. J. Roentgenol.*, **69**, 630 (1953).
(23) C. Hansch, A. R. Steward, S. M. Anderson, and D. L. Bently, *J. Med. Chem.*, 11, 1 (1968).
(24) J. O. Hoppe, in "Medicinal Chemistry," vol. 6, E. E. Campaigne and W. H. Harting, Eds., Wiley, New York, N.Y., 1963, p. 343.

ACKNOWLEDGMENTS

The author thanks Dr. W. S. Bucke and Dr. A. L. Kunz for valuable discussion and support, Barbara Behrmann and Leonard Klein for technical assistance, and Wilma Lotts for help in manuscript preparation.

Quantitative GLC Analysis of Sterols in Biological Samples

S. N. HOOPER and R. F. CHANDLER ˣ

Received May 23, 1977, from the *College of Pharmacy, Faculty of Health Professions, Dalhousie University, Halifax, Nova Scotia, Canada B3H 3J5.* Accepted for publication December 6, 1977.

Abstract □ A GLC method for the quantitative analysis of cholesterol, β-sitosterol, stigmasterol, campesterol, 7-dehydrocholesterol, and dihydrocholesterol in biological samples was developed to screen serum and lipid extracts of heart and liver tissue for these sterols precisely. The addition of the internal standard, cholestane, at the beginning of the procedure led to a reduction in the required sample size and the elimination of several steps. The only critical measurements are those of the biological samples and internal standard.

Keyphrases □ Sterols, various—GLC analyses in biological fluids and extracts □ GLC—analyses. various sterols in biological fluids and extracts

A study involving the feeding of cholesterol and other sterols to large numbers of chicks required a simple, precise method for the qualitative and quantitative analysis of the sterol content of serum, heart, and liver samples. The commonly employed colorimetric methods are subject to several limitations, not least of which is the lack of discrimination among two or more sterols in a single sample (1).

Several GLC methods were reported for the determination of serum cholesterol (2–8); however, a procedure was required to determine quantitatively cholesterol and other sterols in a single sample. Additionally, a small sample size and the least number of manipulations consistent with precise and accurate analysis were desirable objectives.

EXPERIMENTAL

Materials and Chemicals—All solvents were reagent grade. Cholestane[1] and the sterols were dissolved in chloroform, and their purity was checked by GLC. Accuracy was monitored by the daily use of commercial controls[2].

Apparatus—Chromatographs A[3] and B[4], equipped with dual hydrogen flame-ionization detectors and glass columns (3 mm × 2 m), were connected to a recorder fitted with an integrator[5] or an automatic programmable integrator[6] Nitrogen was the carrier gas. All gas flows were adjusted according to recommendations of the manufacturer.

The injection port and detector were set at 300°. Columns were packed with 3% OV-17 on 100–120-mesh Gas Chrom Q[7], 3% SE-30 on 100–120-mesh Gas Chrom Q[8], or 3% SP-2401 on 100–120-mesh Supelcoport[9]. Column temperatures (250–280, 280–300, or 240–250°, respectively) were adjusted to give retention times of less than 10 min for cholesterol. All analyses were isothermal, and the attenuation was adjusted to give near full-scale deflection for the internal standard.

Serum Analysis—Fresh serum (0.1 ml), cholestane standard (200 mg/100 ml, 0.1 ml), 33% KOH aqueous solution (0.2 ml), and ethanol (2.0 ml) were measured into a screw-capped test tube (13 × 100 mm). After mixing[10], the tubes were placed in a shaking water bath[11] at 60° for 2 hr. Following hydrolysis, water (0.5 ml) was added and the cholesterol and cholestane were extracted with hexane (2.0 ml). The hexane fraction was subjected directly to GLC analysis.

Tissue Extracts—Total lipid was determined quantitatively by extracting the weighed hearts and livers according to the method of Bligh and Dyer (9). The lipid subsequently was dissolved in chloroform (5 ml), 0.5 ml was immediately transferred to a screw-capped test tube, and the chloroform was evaporated in a stream of dry nitrogen. The analysis was continued as for serum, care being taken that the amount of lipid was small enough (less than 200 mg) to be saponified by the amount of potassium hydroxide being used. Values were then related to the weight of the tissue lipid.

GLC Analysis—GLC standards containing known amounts of cholestane, cholesterol, and/or β-sitosterol, campesterol, stigmasterol, dihydrocholesterol (cholestanol), and 7-dehydrocholesterol were prepared and analyzed[4,5] at the beginning and end of each day. A correction factor was determined by dividing the sterol concentration found by GLC with the known concentration. Sterol concentration of the serum and tissue samples was determined as follows:

Table I—Analysis of Control Serums

Control Serum	Number of Analyses	Mean ± *SE*
1[a]	41	174.7 ± 2.0
2[b]	37	135.8 ± 3.0

[a] Choles-Trol; reported mean value was 196/100 ml when assayed by the Anderson and Keys modification of the Abell method. [b] Moni-Trol I; reported mean value was 151 mg/100 ml when assayed by the Abell method.

[1] Aldrich Chemical Co., Milwaukee, WI 58233.
[2] Choles-Trol and Moni-Trol I, Dade Division, American Hospital Supply Corp., Miami, FL 33152.
[3] Hewlett-Packard model 5710A.
[4] F&M Scientific 700 laboratory chromatograph.
[5] Fisher Recordall series 100 fitted with disk chart integrator.
[6] Hewlett-Packard model 3380A.
[7] Chromatographic Specialties, Brockville, Ontario, Canada.
[8] Applied Science Laboratories, State College, PA 16801.
[9] Supelco, Inc., Supelco Park, Bellefonte, PA 16823.
[10] Vortex-Geni, Fisher Scientific Co.
[11] Magni Whirl model MSB-1122AA-1.

0022-3549/78/0800-1157$01.00/0
© 1978, American Pharmaceutical Association

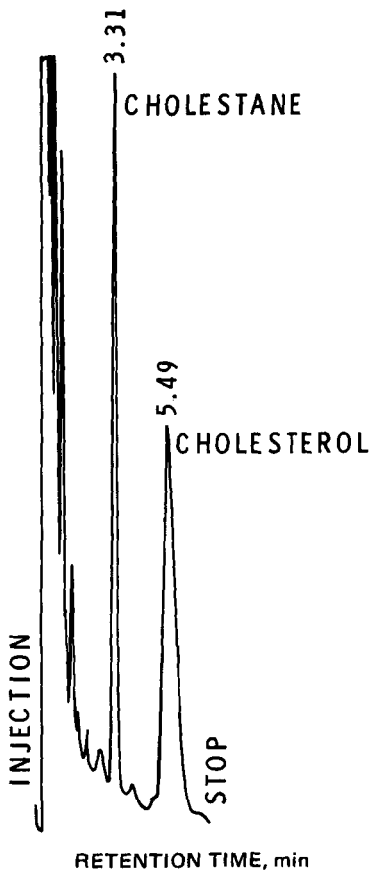

Figure 1—*GLC analysis of heart cholesterol using 3% SE-30 and Chromatograph A.*

$$\text{sterol (mg/100 ml)} = \frac{\text{cholestane concentration (ml/100 ml)}}{\text{counts of GLC peak (cholestane)}} \times \frac{\text{counts of GLC peak (sterol)}}{\text{correction factor}} \quad \text{(Eq. 1)}$$

GLC standards also were injected[3] to program the integrator[6] and then to check the accuracy of the equipment. The integrator subsequently printed the sterol concentrations, in terms of milligrams per 100 ml in the original sample, for all subsequent injections.

RESULTS AND DISCUSSION

Commercially available cholesterol control serums were analyzed with each batch of samples. Values obtained over 15 months with two gas chromatographs, three column phases, and 10 columns are summarized in Table I and testify to the reproducibility of this procedure.

Columns packed with SE-30 (Fig. 1) or OV-17 (Fig. 2) were used interchangeably. While relative retention times differed, there was no evident interference from other components (Fig. 3), except during experiments involving 7-dehydrocholesterol and dihydrocholesterol. Both of these sterols had retention times nearly identical to cholesterol under the experimental conditions. For these sterols, columns packed with SP-2401 were employed (Figs. 4 and 5).

Since a rapid, precise method was needed to conduct numerous, routine determinations of total cholesterol and/or other sterol levels, a programmable automatic integrator[6] was employed. With this apparatus, repeated injections of the same sample varied by less than 1%. The earlier use of a disk-type integrator[5] required more instrument tending and value judgment by the operator; consequently, variations of 5% were observed between repeated injections.

Cholesterol levels as determined by GLC are usually lower than those determined by the standard colorimetric methods, partly because of the greater specificity of the GLC technique (10, 11). The column absorption phenomenon noted previously (2, 8, 11) was observed in this study, even after conditioning and many injections of cholesterol. Consequently, a correction factor, based on the analyses of standards, was determined

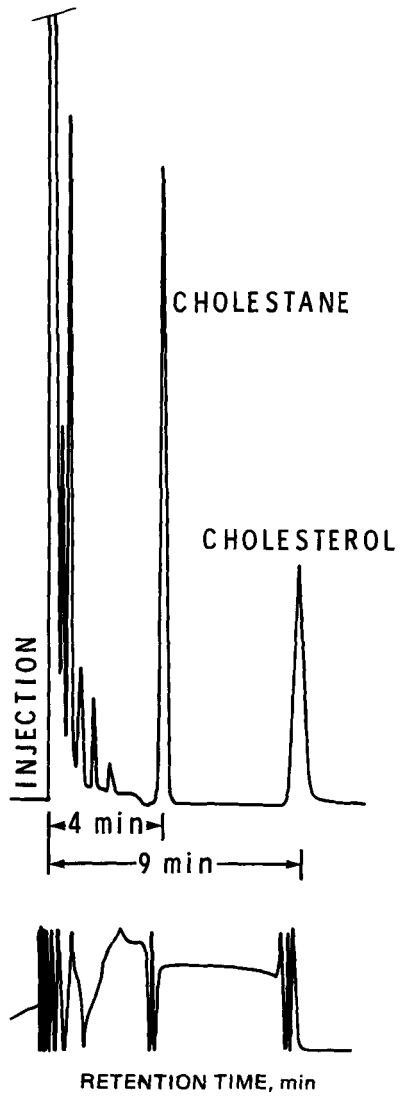

Figure 2—*GLC analysis of chick serum cholesterol using 3% OV-17 and Chromatograph B.*

for each day's set of samples and was further checked during and after each series of analyses. This factor ranged between 0.75 and 0.90 for the disk-type integrator[5]. The calibration of the programmable integrator[6] adjusted the correction factor automatically. When it was determined separately, it was constant at 0.85. Correction factors were similar for the other sterols.

Both samples and standards were kept tightly covered and refrigerated when not in use. Under these conditions, both samples and standards were stable for several weeks, in agreement with those values stated by Tonks (1).

While the use of cholestane as an internal standard was reported previously for cholesterol in serum, it was used only in the final step, necessitating careful measurement of the extraction solvent and extreme care in ensuring complete extraction of cholesterol. In Blomhoff's method (2), the extraction solvent was measured, transferred, and reduced to dryness under nitrogen; the internal standard then was added in chloroform to redissolve the cholesterol. It was found that by adding the cholestane to the accurately measured sample of serum or lipid extract (in the cases of heart and liver tissues), these steps could be eliminated. The complete analysis involved only one test tube and no reduction of solvent. Injections from hexane rather than chloroform also resulted in a cleaner detector and longer column life.

In normal circumstances the hydrolysis time could be greatly decreased (11); however, this project was dealing with artificially high cholesterol levels, and the prolonged hydrolysis period was required. Free sterol concentrations, if desired, could be determined by GLC analysis of the samples prior to hydrolysis.

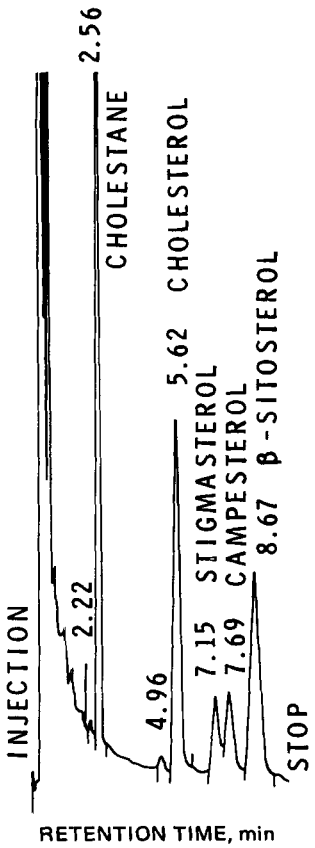

Figure 3—*GLC analysis of a standard solution of some sterols using 3% SP-2401 and Chromatograph A.*

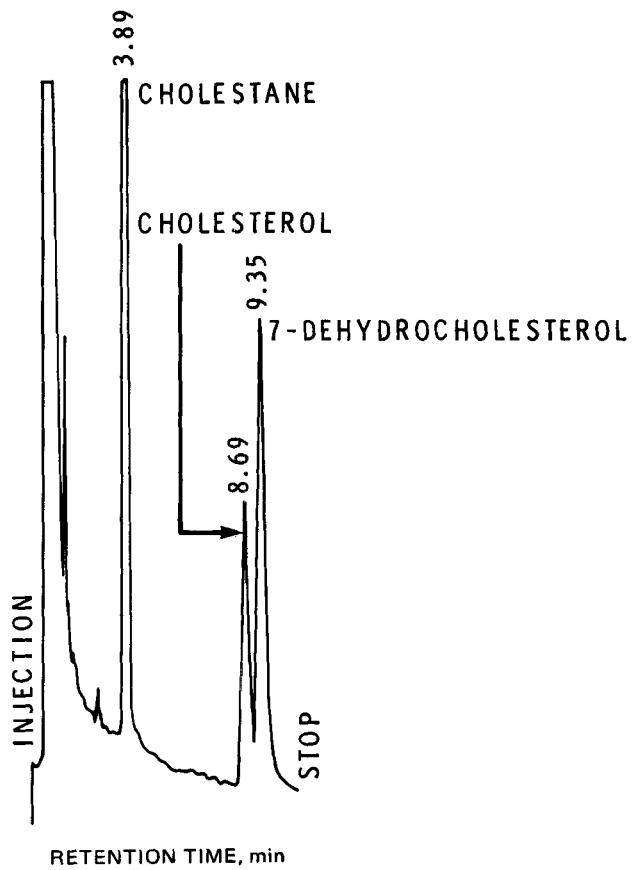

Figure 4—*GLC analysis of 7-dehydrocholesterol and cholesterol in chick serum using 3% SP-2401 and Chromatograph A.*

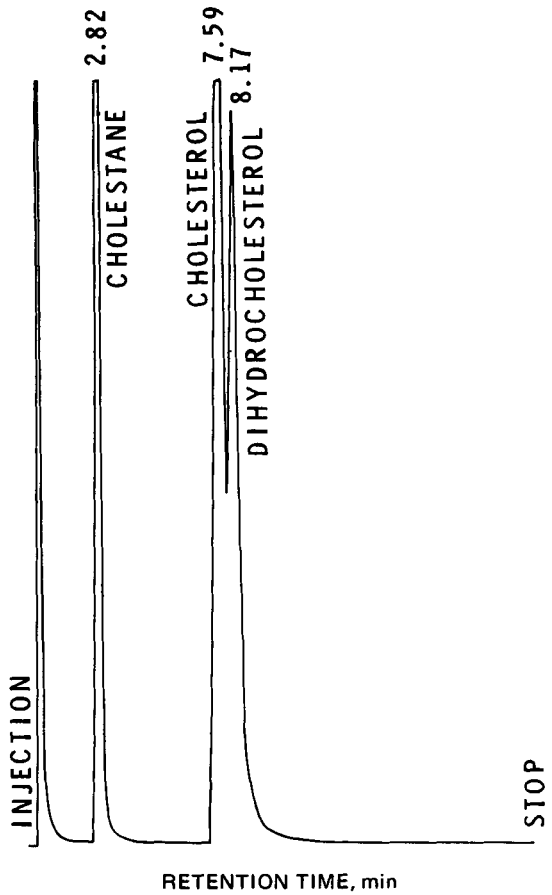

Figure 5—*GLC analysis of dihydrocholesterol and cholesterol in chick serum using 3% SP-2401 and Chromatograph A.*

This method is rapid, precise, and flexible for the qualitative and quantitative analysis of cholesterol and other sterols in biological materials. Except for the amounts of biological sample and internal standard, no other measurements are critical.

REFERENCES

(1) D. B. Tonks, *Clin. Biochem.*, **1**, 12 (1967).

(2) J. P. Blomhoff, *Clin. Chim. Acta*, **43**, 257 (1973).

(3) L. P. Crawley, B. O. Musser, S. Campbell, and W. Faucette, *Am. J. Clin. Pathol.*, **39**, 450 (1963).

(4) H. C. Von Curtius and W. Burgi, *Z. Klin. Chem.*, **4**, 38 (1966).

(5) J. L. Driscoll, D. Aubuchon, M. Descoteaux, and H. F. Martin, *Anal. Chem.*, **43**, 1196 (1971).

(6) J. MacGee, T. Ishikawa, W. Miller, G. Evans, P. Steiner, and C. J. Glueck, *J. Lab. Clin. Med.*, **82**, 657 (1973).

(7) T. T. Ishikawa, J. MacGee, J. A. Morrison, and C. J. Glueck, *J. Lipid Res.*, **15**, 286 (1974).

(8) P. A. Harris and K. L. Harris, *J. Pharm. Sci.*, **63**, 781 (1974).

(9) E. G. Bligh and W. J. Dyer, *Can. J. Biochem. Physiol.*, **37**, 911 (1959).

(10) D. J. Munster, M. Lever, and R. W. Carrell, *Clin. Chim. Acta*, **68**, 167 (1976).

(11) L. Lillienberg and A. Svanborg, *ibid.*, **68**, 223 (1976).

ACKNOWLEDGMENTS

Presented in part at the 23rd Canadian Conference on Pharmaceutical Research, Saskatoon, Canada, 1976, and at the Medicinal Chemistry Section, APhA Academy of Pharmaceutical Sciences, Orlando meeting, 1976.

Supported by the Medical Research Council of Canada, Grant MA-3539.

The authors thank Eli Lilly and Co. Ltd. for the generous supply of cholesterol and β-sitosterol NF.

Differential Pulse Polarographic Determination of Submicrogram Quantities of Carmustine and Related Compounds in Biological Samples

IVAN BARTOŠEK *x, SONIA DANIEL ‡, and STANISLAV SÝKORA ‡

Received June 15, 1977, from the *Istituto di Ricerche Farmacologiche 'Mario Negri,' Via Eritrea, 62, 20157 Milan, Italy, and ‡Bruker Spectrospin Italiana, Via Miglioretti, 2, Milan, Italy. Accepted for publication December 16, 1977.

Abstract □ A polarographic method was developed to determine the antineoplastic agent carmustine and other nitrosoureas, such as *N*-methyl-*N*-nitrosourea and *N*-cyclohexyl-*N*-nitrosourea, in biological fluids at levels well below 1 μg/ml or g. The stability of carmustine in different media was investigated to prevent losses during administration or assay. Examples of nitrosourea determination in biological samples are given.

Keyphrases □ Carmustine—differential pulse polarographic analysis in biological samples □ Nitrosoureas, various—differential pulse polarographic analyses in biological samples □ Polarography, differential pulse—analyses, carmustine and various nitrosoureas in biological samples □ Antineoplastics—carmustine, differential pulse polarographic analysis in biological samples

N-Alkyl-*N*-nitrosoureas and, in particular, carmustine, 1,3-bis(2-chloroethyl)-1-nitrosourea (I), are widely used antineoplastic agents. Unfortunately, their determination in biological samples is hampered by the low sensitivity of the currently used colorimetric method (1, 2). Garrett and Cusimano (3) investigated the polarographic behavior of various *N*-alkyl-*N*-nitrosoureas. Since that time, however, polarographic techniques have been improved considerably (4–6), and their basic sensitivity has been increased by a factor of at least 100, pushing the limits of applicability of polarography far below the microgram level (7, 8). Therefore, the possibility of using polarography for routine assays of I and other nitrosoureas in blood and tissues was investigated.

EXPERIMENTAL

Apparatus—Measurements were made on a modular polarograph[1] with a standard polarographic vessel[2]; for some measurements, the thermostated vessel[2] was used. These vessels require a minimum sample volume of 5 ml; a microcell[1] for 0.5–5 ml also was used with success.

Reagents—All reagents (potassium chloride, hydrochloric acid, citric acid, tartaric acid, ether, and *n*-pentane) were analytical grade. An interfering peak at E = 0.830 v, due to an impurity, appeared in some supplies of the citric acid used as a basic electrolyte; each original bottle had to be checked before use by running a blank polarogram. All solutions were prepared with redistilled water. Tridistilled, commercially supplied mercury was used for the dropping mercury electrode.

Compound I, *N*-cyclohexyl-*N*-nitrosourea (II), and *N*-methyl-*N*-nitrosourea (III) were obtained as lyophilized powders from two sources[3,4]. No difference in quality was observed between the different samples of I as long as the compound was stored in dry plastic bags (with silica gel inserts) at deep-freeze temperatures.

Extraction Procedures—Blood was prevented from clotting by 3.8% sodium citrate (nine parts of blood plus 1 part of citrate solution) and centrifuged (10 min at 3000 rpm) to separate plasma.

Procedure A—Plasma, 1 ml, was mixed with 1 ml of 0.2 *M* citric acid and extracted with 5 ml of *n*-pentane for 1 min. After separation of the two phases, 4 ml of the extract was evaporated directly in the thermostated polarographic vessel at 40° with 5 or 10 ml of 0.2 *M* citric acid.

Procedure B—Plasma, 1 ml, was mixed with 1 ml of 0.2 *M* citric acid and extracted three times with 4 ml of *n*-pentane for 3 min. A 10-ml aliquot of the combined extracts was then evaporated in a test tube with 0.2 *M* citric acid at 40° and submitted to polarography at room temperature.

Polarographic Measurements—Citric acid (0.2 *M*) was used as a basic electrolyte. Dissolved oxygen was removed by bubbling high purity nitrogen gas, passed first through redistilled water to remove all mechanical impurities. A three-electrode arrangement was adopted with a dropping mercury electrode, a platinum auxiliary electrode, and a saturated calomel electrode as reference. The mercury flow rate in the dropping mercury electrode was 1.25 mg/sec, and the height of the mercury column was 120 cm.

The drop time was limited by an electronically controlled hammer; a drop time of 3 sec was optimal. The differential pulse technique was adopted with the pulse height, ΔE, of 100 mv. The sweep normally covered the interval from −250 to −750 mv, and the sweep rate in most cases was 2 mv/sec. The output signal was filtered by a resistance–capacitance filter with a time constant of 0.1 sec. In addition, a gated accumulator was inserted to suppress experimental noise.

RESULTS AND DISCUSSION

Polarographic Properties of Nitrosoureas—The collected data indicate that, qualitatively, I is to some extent representative of all *N*-alkyl-*N*-nitrosoureas and that reduction of I on the dropping mercury electrode is not a simple electrode process. A full interpretation was not attempted, but the data were used to develop a routine analytical method[5].

Figure 1 illustrates the behavior of I in 0.1 *M* KCl acidified to varying degrees with hydrochloric acid. At pH 2.5, there was a single reduction wave (A), whose half-wave potential ($E_{1/2}$), width, and height all depended on pH. At higher pH values, wave A was still present, but a second

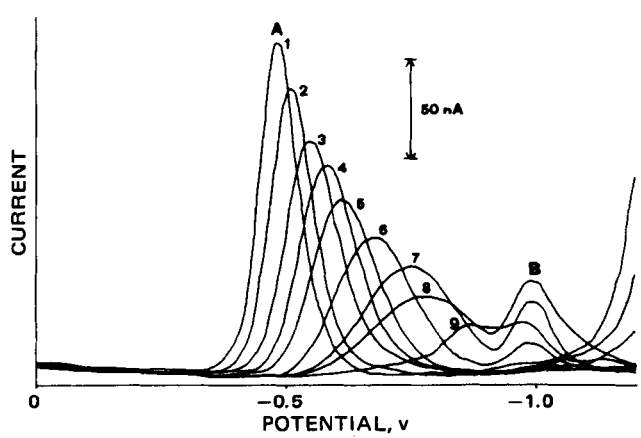

Figure 1—*Polarograms of I, showing dependence on acidity in the 0.1 M KCl–hydrochloric acid basic electrolyte. The concentration of I was* 2×10^{-5} M. *The experimental setup was as described in* Experimental, *except that the differential pulse height was 20 mv and the gated accumulator was not used. Key (pH values): 1, 1.56; 2, 2.00; 3, 2.58; 4, 3.00; 5, 3.50; 6, 4.02; 7, 4.52; 8, 5.02; and 9, 5.70.*

[1] Universal E 310, Bruker Physik AG, 7512 Karsruhe-Rheinstetten, Silberstreifen, West Germany.
[2] Metrohm, Herisau, Switzerland.
[3] National Cancer Institute, Bethesda, Md.
[4] Simes, Milan, Italy.
[5] A detailed analysis of the reduction process will appear elsewhere.

0022-3549/78/0800-1160$01.00/0
© 1978, American Pharmaceutical Association

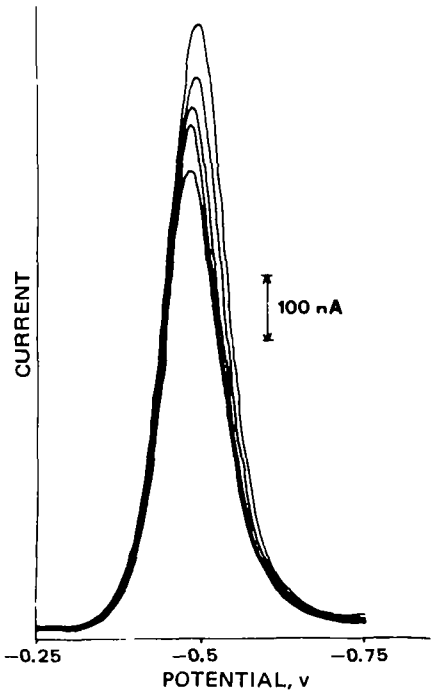

Figure 2—*Polarograms of I, showing dependence on citric acid concentration. The concentration of I was 2 × 10^{-5} M. The experimental setup was as described in* Experimental. *The concentrations of citric acid for the curves (from top to bottom) were 0.025, 0.05, 0.1, 0.2, and 0.5* M.

wave (B) appeared at somewhat more negative potentials. The height and width of wave B also depended on pH, but its position appeared to be nearly constant.

A very tentative interpretation might be that there are two forms (A and B) of I in an equilibrium of the type B + H^+ = A. Form A, prevailing at low pH, is reduced at the mercury electrode in a one-electron process involving H^+ ions. Form B is reduced in a one-electron process that does not involve H^+ ions. For analytical purposes, a single sharp peak at a well-defined position is preferable. The results, therefore, indicate the necessity of a suitable acid buffer.

The choice of buffer was complicated by the fact that the compound behaved somewhat differently when weak acids, such as citric, were used as the basic electrolyte (Fig. 2). Then there was just one peak at about −500 mv, and the pH dependence of the peak parameters was very small. The width of the peak considerably exceeded the value characteristic for a one-electron process, thus indicating a complex electrochemical mechanism. The dependence of the current (I_{500}) on the square root of the height of the mercury column ($\sqrt{h}$) was linear. For a 2 × 10^{-5} *M* solution, the least-squares fit of the data obtained for column heights ranging from 30 to 120 cm gave the relation $I(nA) = 92.978 \cdot \sqrt{h}$ cm − 193.048; the correlation coefficient was $r = 0.998$.

When analyzing low concentrations of I (10^{-7} *M*), the choice of the basic electrolyte was critical for another reason. The buffer itself gave a relatively high background because of the capacitive component of the current, and this background current should be as flat as possible throughout the range of potentials at which the test drug peak appears. The background currents of a number of basic electrolytes were recorded in the range of potentials from −250 to −750 mv at very high sensitivity, and the differences were marked.

The final choice was 0.2 *M* citric acid (an acceptable alternative was tartaric acid). Figure 3 shows the polarograms of I at concentrations ranging from 5 × 10^{-8} to 5 × 10^{-7} *M*. The measurements were made in 5 ml of the basic electrolyte so the smallest quantity measured was about 50 ng. By using a microcell, this figure can be reduced by a factor of about 10. Assays at these levels must be done with the utmost care to avoid impurities (*e.g.*, reagents, water, mercury, and glassware) and any sources of noise (*e.g.*, bad contacts).

At low concentrations, the background current complicates quantitative evaluation of the data. Therefore, a method based on measurements of the current values I_{400}, I_{500}, and I_{600} at potentials of −400, −500, and −600 mv, respectively, was employed.

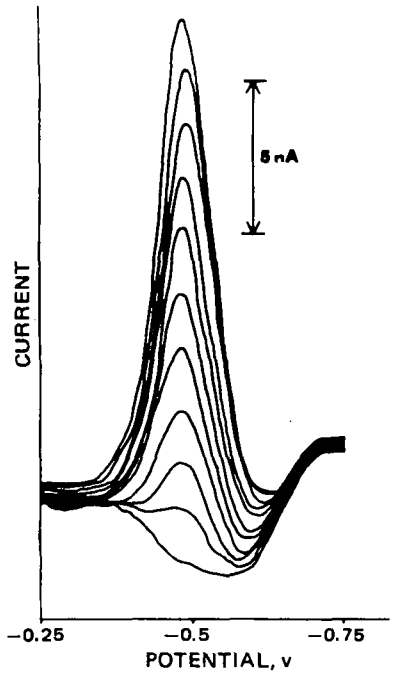

Figure 3—*Calibration curves of I in 0.2* M *citric acid under conditions described in* Experimental. *The concentrations (from bottom to top) were 0 (basic electrolyte), 5 × 10^{-8}, 10^{-7}, 1.5 × 10^{-7}, 2 × 10^{-7}, 2.5 × 10^{-7}, 3 × 10^{-7}, 3.5 × 10^{-7}, 4 × 10^{-7}, 4.5 × 10^{-7}, and 5 × 10^{-7}* M.

The following equation is used for both the sample, *S*, and a blank containing only basic electrolyte, S_0:

$$S \text{ or } S_0 = I_{500} - 0.5 \times (I_{400} + I_{600}) \qquad \text{(Eq. 1)}$$

The difference $s = (S - S_0)$ is then used in empirical calibration graphs; *s* is directly proportional to the concentration of I even at the lowest detectable level. The slope depends, of course, on the experimental setup (capillary, height of the mercury reservoir, drop time, and temperature) so a new calibration is necessary each time any relevant parameter is changed; $s = (K)$ (concentration). In Fig. 3, $k = 0.0355$ amp/mole × $liter^{-1}$. When a calibration graph is not available, the method of standard addition can always be used; but even in this case, the quantity *s* should be used if the concentrations involved are close to the detection limit. Figure 4 gives the polarographic curves of some *N*-alkyl-*N*-nitrosoureas in 0.2 *M* citric acid at a concentration of 10^{-6} *M*. While all nitrosoureas are polarographically active and give rise to peaks between −0.4 and −0.8 v, differences exist between different members of this group.

Thus, assays of II can be made using the same techniques as for I, with the additional advantage of higher sensitivity. On the other hand, the

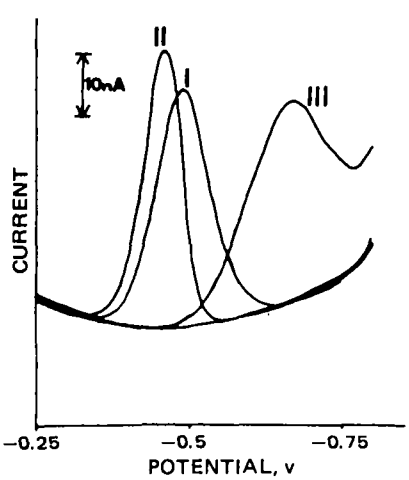

Figure 4—*Polarograms of 10^{-6}* M *I, II, and III in 0.2* M *citric acid under conditions described in* Experimental. *The bottom line is the basic electrolyte.*

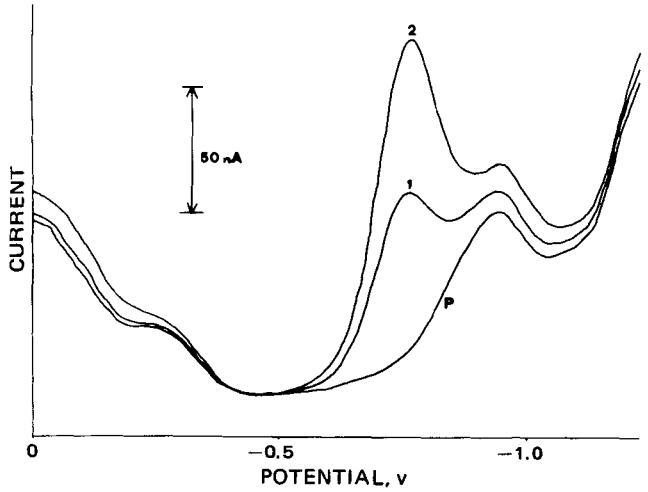

Figure 5—*Polarograms of rat plasma (P) containing 10 (1) and 20 (2) μg of I/ml. The sample was prepared by adding 1 ml of plasma to 9 ml of 0.2* M *citric acid. The conditions were as described in* Experimental, *except that the pulse height was 50 mv and the accumulator was not used.*

peak of III is much broader than that of I and appears at more negative potentials where the reproducibility of the background current is lower because of common impurities in the citric acid. As a result, the sensitivity of III assays is expected to be lower than with I unless the technique is suitably modified.

Stability of I in Various Solutions—Nitrosoureas decompose easily unless the pH values are kept sufficiently low (2, 9, 10). The stability of I in various experimental circumstances was examined to establish reliable time limits for its clinical administration and assay. The pharmaceutical preparation[4] of I was dissolved directly in the unbuffered physiological saline or 5% glucose used for infusion. The pH values of the resulting solution differed considerably from case to case; in several experiments, the pH values remained slightly above 7 and I decomposed completely in less than 1 hr. Therefore, in clinical applications involving infusions of I, pH differences in the unbuffered infusion solutions may be responsible for broad variations in drug delivery and poor reproducibility of the treatment.

On the other hand, no measurable decay was observed in animal plasma buffered with sodium citrate and kept for several weeks at −20°. The half-life of I in citric acid (0.2 *M*) at 0° was about 270 hr; at 20°, it was 16.9 hr. Very slow decay of the compound was observed in ethanol solution acidified by a drop of 1 *M* citric acid per 10 ml; the half-life of I at 20° was between 250 and 300 hr.

Routine Assays of I in Biological Samples—Figure 5 shows the polarogram of 1 ml of plasma, with and without addition of I, measured in 10 ml of 0.2 *M* citric acid. Surprisingly, the peak of I was at −750 mv rather than at the expected −500 mv. A possible explanation is complex formation; preferential binding of I to some plasma proteins has, in fact, been reported (2). However, assay of I in untreated plasma is hindered by the background produced by the plasma itself, which limits the usefulness of the method to concentrations exceeding about 5 μg/ml of plasma. Moreover, it is difficult to eliminate oxygen from the plasma because of foam formation. Foaming may be avoided by denaturing the plasma proteins with 5% $HClO_4$ and removing them by filtration prior to polarography.

The background from blank plasma treated with perchloric acid was, however, exactly the same as when the plasma was not denatured, indicating that it was not due to proteins. The nitrosourea added to the plasma before treatment was no longer detectable in the filtrate, while I added to the filtrate after removal of the proteins gave a peak at its normal position of −500 mv. This result confirms that I forms a strong complex with plasma proteins but, at the same time, precludes any possibility of using denaturation for assay purposes.

An excellent method for solving these problems is to extract the plasma with an apolar organic solvent such as ether or *n*-pentane. After separation of the phases, an aliquot of the organic phase is evaporated in a vessel containing the basic electrolyte (possibly directly in the polarographic cell). There is no detectable background due to the plasma itself. With I, the extraction yield depends on the efficiency and time of shaking.

A simple 1-min extraction (Procedure A) gave yields in the range of 85–90% for ether or *n*-pentane. The standard error of determination of parallel samples extracted with *n*-pentane did not exceed 3.3% within the concentration range studied; the calibration curve was linear. *n*-Pentane is preferred because ether usually contains traces of polarographically active peroxides that interfere with the determination of I. Ether also dissolves considerable amounts of water (7%), which end up in the basic electrolyte and may represent a complication if the final volume is to be kept small (microcell).

Extraction of whole blood directly also was attempted. While the extraction yields were essentially the same as for plasma, difficulties were encountered because of lipids in the blood cells. These were extracted and eventually led to colloid impurities in the solution to be analyzed polarographically. The colloid particles caused severe noise on the dropping mercury electrode unless they were first removed by filtration. The technique finally adopted is simple and quantitative. As described in *Experimental* (*Procedure B*), it consists of removal of the blood cells by centrifugation, triple extraction by *n*-pentane, and evaporation of the organic extract in a vessel containing a known amount of the 0.2 *M* citric acid used as the basic electrolyte.

Disappearance of I from Rat and Mouse Plasma—Male Sprague–Dawley rats[6], 226 ± 3 g, or male Albino Swiss mice CD-1, 20.9 ± 0.6 g, received 10 mg of I/g iv. Groups of animals were killed 2, 5, 10, 20, 30, 60, 90, and 120 min after I administration. Blood was collected (nine parts of blood plus 1 part of 3.8% sodium citrate) and centrifuged at 3000 rpm for 10 min. Prepared plasma was frozen at −20° for further analysis. Before *n*-pentane extraction, plasma samples were thawed at 37° for 5 min. Extraction Procedure B was used to determine the remaining drug. The data are reported in Table I, and kinetic analyses of these data are reported in Table II.

Table I—Disappearance of I from Rat and Mouse Plasma after Administration of 10 mg of the Drug/kg iv

Minutes	Concentration of I, μg/ml of Plasma (Mean ± *SE*) Rat	Mouse
2	2.36 ± 0.41	2.41 ± 0.38
5	1.70 ± 0.18	1.02 ± 0.15
10	0.66 ± 0.04	0.16 ± 0.04
20	0.38 ± 0.02	0.08
30	0.22 ± 0.04	<0.02
60	<0.02	<0.02

Table II—Kinetic Analysis[a] of the Data Reported in Tables I and III

Animal Species	Half-Life, $t_{1/2}$, min	Correlation[b] Coefficient, *r*	Initial Concentration, μg/ml	Volume Distribution, V_d, liters/kg
Rat	8.33 ± 0.14	0.990	2.25 ± 0.22	4.43
Mouse	2.17	0.984	4.57	2.19
Rat liver microsomes	49.74	0.999	40.0	

[a] Standard error is given wherever available. [b] Decay followed first-order kinetics in all cases.

Table III—Disappearance of I after Incubation with Rat Liver Microsomes

Minutes	Concentration of I, μg/ml of Incubation Medium
2	32.1
5	30.1
10	29.6
15	25.8
20	22.4
30	21.3
40	18.8
50	15.5
60	14.5

[6] CD-COBS, Charles River, Italy.

Disappearance of I after Incubation with Rat Liver Microsomes—Rat liver microsomes were prepared according to the standardized technique described previously (11). The incubation medium contained 0.93 μmole of I, 1.5 μmoles of NADP, 50 μmoles of glucose 6-phosphate, 0.7 international unit of glucose 6-phosphate dehydrogenase, 25 μmoles of magnesium chloride, 0.08 *M* phosphate buffer (pH 7.0), and 30 mg of microsomes in a total volume of 5 ml. Samples (1.0 ml) of the incubation medium were taken at different time intervals, acidified with citric acid (0.1 ml of 1 *M* solution), and immediately extracted with 5 ml of *n*-pentane for 10 min at room temperature. The results are reported in Tables II and III.

REFERENCES

(1) T. L. Loo and R. L. Dion, *J. Pharm. Sci.*, **54**, 809 (1965).

(2) T. L. Loo, R. L. Dion, R. L. Dixon, and D. P. Rall, *ibid.*, **55**, 492 (1966).

(3) E. R. Garrett and A. G. Cusimano, *ibid.*, **55**, 702 (1966).

(4) J. B. Flato, *Anal. Chem.* **44**, 75 A (1972).

(5) P. J. Elving, in "Electroanalytical Chemistry," H. W. Nurnberg, Ed., Wiley, London, England, 1974, p. 197.

(6) H. Hoffman and J. Volke, in *ibid.*, p. 287.

(7) A. M. Brooks, J. A. F. De Silva, and R. M. Hackman, *Am. Lab.*, **1974**, 23.

(8) D. J. Pietrzyk, *Anal. Chem.*, **46**, 52 R (1974).

(9) E. R. Garrett, S. Goto, and J. F. Stubbins, *J. Pharm. Sci.*, **54**, 119 (1965).

(10) J. A. Montgomery, R. James, G. S. McCaleb, and T. P. Johnston, *J. Med. Chem.*, **10**, 668 (1967).

(11) D. L. Cinti, P. Moldeus, and J. B. Schenkman, *Biochem. Pharmacol.*, **21**, 3249 (1972).

Automated Potentiometric Procedure for Studying Dissolution Kinetics of Acidic Drugs under Sink Conditions

FRED L. UNDERWOOD *x and DONALD E. CADWALLADER

Received August 4, 1977, from the *Department of Pharmacy, School of Pharmacy, University of Georgia, Athens, GA 30602.* Accepted for publication December 9, 1977. *Present address: College of Pharmacy, University of Arkansas, Little Rock, AR 72201.

Abstract □ An automated potentiometric procedure was used for studying *in vitro* dissolution kinetics of acidic drugs. Theoretical considerations indicated that the pH-stat method could be used to establish approximate sink conditions or, possibly, a perfect sink. Data obtained from dissolution studies using the pH-stat method were compared with data obtained from known sink and nonsink conditions. These comparisons indicated that the pH-stat method can be used to establish a sink condition for dissolution studies. The effective diffusion layer thicknesses for benzoic and salicylic acids dissolving in water were determined, and a theoretical dissolution rate was calculated utilizing these values. The close agreement between the experimental dissolution rates obtained under pH-stat conditions and the theoretical dissolution rates indicated that perfect sink conditions were established under the experimental conditions used.

Keyphrases □ Dissolution kinetics, *in vitro*—acidic drugs, automated potentiometric study, pH-stat method used to establish sink conditions □ Potentiometry, automated—study of *in vitro* dissolution kinetics of acidic drugs, pH-stat method used to establish sink conditions □ pH-stat method—used to establish sink conditions for *in vitro* automated potentiometric study of dissolution kinetics of acidic drugs

Recognition that the availability for GI absorption of drugs in oral solid dosage forms is often reflected by *in vitro* dissolution rates has stimulated the development and use of numerous dissolution rate tests for tablets and capsules. Various types of apparatus have been used to determine dissolution rates of drugs, most of which have been critically reviewed (1–3).

Emphasis has been placed on the need for dissolution systems to be operated under sink conditions, where there is no effective buildup of drug concentration (4, 5). It was suggested that unless sink conditions are embodied in the design of *in vitro* dissolution rate methods, the *in vitro* results may bear little relationship to *in vivo* observations (6). It was also suggested that all dissolution systems should be operated under sink conditions and that systems that do not meet this requirement should either be modified accordingly or discarded (7).

The utility of automatic titration at a stat-pH for studying *in vitro* dissolution rates of acidic and basic drugs was demonstrated previously (8, 9). A pH-stat procedure was used in evaluating antacid products (10, 11). It was thought that the pH-stat method might be used to establish approximate sink conditions or, possibly, a perfect sink during dissolution rate testing.

THEORY

The Noyes–Whitney (12) equation describes the dissolution process:

$$\frac{dW}{dt} = kS(C_{sat} - C_{soln}) \qquad \text{(Eq. 1)}$$

where dW/dt is the dissolution rate, k is a constant, S is the surface area of the dissolving solid, C_{sat} is the concentration of a saturated solution, and C_{soln} is the drug concentration in the solvent at time t. As the C_{soln} increases, the equation predicts that dW/dt decreases. When $C_{sat} \gg C_{soln}$, a sink condition exists; if a buildup of C_{soln} can be prevented, then a sink condition will be maintained.

The total solubility of a weak acid, HA, is the sum of the concentration of the unionized [HA] and the ionized acid [A^-]:

$$C_{sat} = [HA] + [A^-] \qquad \text{(Eq. 2)}$$

and the concentration, C_t(soln), at any time before saturation is:

$$C_t(\text{soln}) = [HA]_t + [A^-]_t \qquad \text{(Eq. 3)}$$

The solubility of the ionized species, A^-, in water is generally much greater than that of the unionized acid, HA. Therefore, for dissolution phenomena involving relatively small quantities of acidic drugs in solution, the concentration of the unionized acid determines the concentration buildup. For example, the solubility of salicylic acid is 1.0 g in 460 ml of water while the solubility of sodium salicylate is 1.0 g in 0.9 ml of water (13).

In dissolution, the sequence of events in Schemes I and II occurs for

0022-3549/78/0800-1163$01.00/0

© 1978, American Pharmaceutical Association

Disappearance of I after Incubation with Rat Liver Microsomes—Rat liver microsomes were prepared according to the standardized technique described previously (11). The incubation medium contained 0.93 μmole of I, 1.5 μmoles of NADP, 50 μmoles of glucose 6-phosphate, 0.7 international unit of glucose 6-phosphate dehydrogenase, 25 μmoles of magnesium chloride, 0.08 *M* phosphate buffer (pH 7.0), and 30 mg of microsomes in a total volume of 5 ml. Samples (1.0 ml) of the incubation medium were taken at different time intervals, acidified with citric acid (0.1 ml of 1 *M* solution), and immediately extracted with 5 ml of *n*-pentane for 10 min at room temperature. The results are reported in Tables II and III.

REFERENCES

(1) T. L. Loo and R. L. Dion, *J. Pharm. Sci.*, **54**, 809 (1965).

(2) T. L. Loo, R. L. Dion, R. L. Dixon, and D. P. Rall, *ibid.*, **55**, 492 (1966).

(3) E. R. Garrett and A. G. Cusimano, *ibid.*, **55**, 702 (1966).

(4) J. B. Flato, *Anal. Chem.* **44**, 75 A (1972).

(5) P. J. Elving, in "Electroanalytical Chemistry," H. W. Nurnberg, Ed., Wiley, London, England, 1974, p. 197.

(6) H. Hoffman and J. Volke, in *ibid.*, p. 287.

(7) A. M. Brooks, J. A. F. De Silva, and R. M. Hackman, *Am. Lab.*, **1974**, 23.

(8) D. J. Pietrzyk, *Anal. Chem.*, **46**, 52 R (1974).

(9) E. R. Garrett, S. Goto, and J. F. Stubbins, *J. Pharm. Sci.*, **54**, 119 (1965).

(10) J. A. Montgomery, R. James, G. S. McCaleb, and T. P. Johnston, *J. Med. Chem.*, **10**, 668 (1967).

(11) D. L. Cinti, P. Moldeus, and J. B. Schenkman, *Biochem. Pharmacol.*, **21**, 3249 (1972).

Automated Potentiometric Procedure for Studying Dissolution Kinetics of Acidic Drugs under Sink Conditions

FRED L. UNDERWOOD *x and DONALD E. CADWALLADER

Received August 4, 1977, from the *Department of Pharmacy, School of Pharmacy, University of Georgia, Athens, GA 30602.* Accepted for publication December 9, 1977. *Present address: College of Pharmacy, University of Arkansas, Little Rock, AR 72201.

Abstract □ An automated potentiometric procedure was used for studying *in vitro* dissolution kinetics of acidic drugs. Theoretical considerations indicated that the pH-stat method could be used to establish approximate sink conditions or, possibly, a perfect sink. Data obtained from dissolution studies using the pH-stat method were compared with data obtained from known sink and nonsink conditions. These comparisons indicated that the pH-stat method can be used to establish a sink condition for dissolution studies. The effective diffusion layer thicknesses for benzoic and salicylic acids dissolving in water were determined, and a theoretical dissolution rate was calculated utilizing these values. The close agreement between the experimental dissolution rates obtained under pH-stat conditions and the theoretical dissolution rates indicated that perfect sink conditions were established under the experimental conditions used.

Keyphrases □ Dissolution kinetics, *in vitro*—acidic drugs, automated potentiometric study, pH-stat method used to establish sink conditions □ Potentiometry, automated—study of *in vitro* dissolution kinetics of acidic drugs, pH-stat method used to establish sink conditions □ pH-stat method—used to establish sink conditions for *in vitro* automated potentiometric study of dissolution kinetics of acidic drugs

Recognition that the availability for GI absorption of drugs in oral solid dosage forms is often reflected by *in vitro* dissolution rates has stimulated the development and use of numerous dissolution rate tests for tablets and capsules. Various types of apparatus have been used to determine dissolution rates of drugs, most of which have been critically reviewed (1–3).

Emphasis has been placed on the need for dissolution systems to be operated under sink conditions, where there is no effective buildup of drug concentration (4, 5). It was suggested that unless sink conditions are embodied in the design of *in vitro* dissolution rate methods, the *in vitro* results may bear little relationship to *in vivo* observations (6). It was also suggested that all dissolution systems should be operated under sink conditions and that systems that do not meet this requirement should either be modified accordingly or discarded (7).

The utility of automatic titration at a stat-pH for studying *in vitro* dissolution rates of acidic and basic drugs was demonstrated previously (8, 9). A pH-stat procedure was used in evaluating antacid products (10, 11). It was thought that the pH-stat method might be used to establish approximate sink conditions or, possibly, a perfect sink during dissolution rate testing.

THEORY

The Noyes–Whitney (12) equation describes the dissolution process:

$$\frac{dW}{dt} = kS(C_{sat} - C_{soln}) \qquad \text{(Eq. 1)}$$

where dW/dt is the dissolution rate, k is a constant, S is the surface area of the dissolving solid, C_{sat} is the concentration of a saturated solution, and C_{soln} is the drug concentration in the solvent at time t. As the C_{soln} increases, the equation predicts that dW/dt decreases. When $C_{sat} \gg C_{soln}$, a sink condition exists; if a buildup of C_{soln} can be prevented, then a sink condition will be maintained.

The total solubility of a weak acid, HA, is the sum of the concentration of the unionized [HA] and the ionized acid [A^-]:

$$C_{sat} = [HA] + [A^-] \qquad \text{(Eq. 2)}$$

and the concentration, C_t(soln), at any time before saturation is:

$$C_t(\text{soln}) = [HA]_t + [A^-]_t \qquad \text{(Eq. 3)}$$

The solubility of the ionized species, A^-, in water is generally much greater than that of the unionized acid, HA. Therefore, for dissolution phenomena involving relatively small quantities of acidic drugs in solution, the concentration of the unionized acid determines the concentration buildup. For example, the solubility of salicylic acid is 1.0 g in 460 ml of water while the solubility of sodium salicylate is 1.0 g in 0.9 ml of water (13).

In dissolution, the sequence of events in Schemes I and II occurs for

0022-3549/78/0800-1163$01.00/0

© 1978, American Pharmaceutical Association

an acid.

$$HA_{solid} \rightleftharpoons HA_{soln}$$

Scheme I

$$HA_{soln} \rightleftharpoons H_3O^+ + A^-$$

Scheme II

The equilibrium of Scheme II is shifted to the right by the automatic titration as shown in Scheme III.

$$H_3O + A^- + NaOH \rightleftharpoons Na^+ + A^- + 2H_2O$$

Scheme III

Therefore, the pH-stat method, operated at 1.5 pH units or more above the pKa of the acid, would keep the dissolving acid in the ionized form (salt). The salt would be much more water soluble than the acid, and this condition would have the same effect as removing the acid as it dissolves, keeping $C_{sat} \ggg C_{soln}$ and thus maintaining a sink condition.

The pH-stat method should not appreciably affect the dissolution rate since the titrant is reacting with the acid dissolved and does not influence the saturated solution layer (diffusion layer) as would a buffer solution. The effect of bases and buffers on the dissolution rate of acidic solids has been studied, and the double film concept of diffusion-controlled dissolution was used to explain the data (14–16). The solid acid dissolves and diffuses toward the bulk solution; simultaneously the base diffuses from the bulk solution toward the solid surface. Neutralization and formation of a salt occur somewhere in the diffusion layers.

The dissolution rate of the acid depends on the diffusion rate of the dissolved acid through the diffusion layer. The buffer has the effect of reducing the distance the acid must diffuse by diffusing toward the acid, thus increasing the dissolution rate. In the pH-stat method, the base is not added until the dissolved acid has diffused through the diffusion layer to the bulk solution. Therefore, in the pH-stat method, the effective film thickness, h, of the diffusion layer should be essentially the same as in the pure water and the dissolution rate should not be affected.

Higuchi *et al.* (16) derived an equation for calculating the thickness:

$$C_1 = \frac{D_{HA}[HA]_o - D_{HA}[HA]_h}{h} \quad \text{(Eq. 4)}$$

where C_1 is the dissolution rate of HA per unit area of the film, D_{HA} is the diffusion coefficient of the acid in pure water, $[HA]_o$ is the concentration of the acid at the solid–liquid interface, $[HA]_h$ is the concentration of the acid in the bulk dissolution medium, and h is the film thickness. Whenever the pH of the dissolution medium is 2 pH units above the pKa of the acid, $[HA] \cong 0$ and Eq. 4 becomes:

$$C_1 = \frac{D_{HA}[HA]_o}{h} \quad \text{(Eq. 5)}$$

The same equation can be derived from the Noyes–Whitney equation as derived from Fick's law of diffusion:

$$\frac{dW}{dt} = \frac{D_{HA}S}{h}(C_s - C) \quad \text{(Eq. 6)}$$

where dW/dt is the dissolution rate, D_{HA} is the diffusion coefficient of the acid HA, $(C_s - C)$ is the concentration difference, S is the surface area, and h is the film thickness. Under sink conditions, $(C_s - C) = C_s$ (saturated concentration of HA) or $[HA]_o$. If $(dW/dt)/S$ = rate per unit area = C_1, then:

$$C_1 = \frac{D_{HA}[HA]_o}{h} \quad \text{(Eq. 7)}$$

During dissolution studies using a pH-stat method, the diffusion layer, h, of the dissolving substance should not be affected if sink conditions exist. If this is true, then the same diffusion layer thickness, h, should be obtained from pH-stat dissolution data as from data obtained using previously reported methods (14–16).

EXPERIMENTAL

Materials—Benzoic acid USP and salicylic acid USP were the acidic drugs studied. Ceresin wax (technical), cyclohexane, octyl alcohol, potassium phosphate (certified), sodium hydroxide, and hydrochloric acid also were used.

Equipment—A pH-stat instrumental setup similar to that of Shah (8) and a dissolution assembly with a 100-mm o.d. round-bottom dissolution vessel covered with a four-neck flask cover, described previously (17), were used. The propeller was centered in the dissolution medium and immersed 2.2 cm below the solvent surface.

Table I—Dissolution of Benzoic and Salicylic Acids (Milligrams) from Nondisintegrating Disks in Sodium Hydroxide Solutions [a]

Dissolution Time, min	Sodium Hydroxide 0.005 N	0.01 N	0.02 N	0.03 N
		Benzoic Acid		
10	64.5	69.0	96.9	110.5
20	126.0	132.5	185.0	218.0
30	180.0	200.4	264.0	324.0
40	246.0	269.4	353.0	430.0
50	302.0	335.5	444.0	541.0
		Salicylic Acid		
10	53.8	59.9	84.8	120.0
20	103.0	112.0	168.0	228.0
30	149.5	168.5	246.5	341.0
40	195.0	225.0	329.0	449.0
50	243.0	278.0	405.0	555.0

[a] All experiments were run at 37° and 100 rpm. Each value is an average of two experiments.

Preparation of Nondisintegrating Disks—Nondisintegrating disks of benzoic acid and salicylic acid were prepared with a hydraulic press[1] by slugging 3.0 g of the compound in a 2.85-cm diameter punch and die set at 1425 kg/cm^2. These disks were mounted on the tapered end of a rubber stopper (3 cm diameter) with ceresin wax. The disks were affixed to the stopper by pouring a small quantity of melted ceresin wax (mp 70–75°) onto the face of the stopper and pressing the disk on the stopper before the wax solidified. The sides of the disks were coated with melted wax using a cotton-tipped applicator; one surface was left exposed. Any wax on the surface of the tablet to be exposed was removed carefully with a knife blade.

Nondisintegrating Disks in Buffer—The dissolution medium used was 400 ml of a pH 6.2 phosphate buffer (buffer capacity of 0.045) at 37°. Two-milliliter samples were taken at appropriate intervals, and the volume of sample was replaced immediately with an equal volume of the buffer. The samples were diluted with buffer, and the absorbance was read on a spectrophotometer[2] at 230 nm. The amount of benzoic acid in solution as a function of time was calculated from a standard Beer's curve of benzoic acid in the buffer. The buffer was used in the reference cell.

Nondisintegrating Disks in Distilled Water with Organic Reservoir—The dissolution medium used was 400 ml of distilled water at 37° overlayed with 350 ml of 1-octanol–cyclohexane (1:1), previously brought to 37° in a constant-temperature water bath. A nonflexible plastic tube (14 cm long × 1.2 cm i.d.) was inserted through a stopper and fitted in one neck of the flask cover. The tube extended through the organic layer into the aqueous phase. Samples of the aqueous layer were taken through this tube with a pipet, and the volume of solvent removed was replaced immediately through the tube, avoiding contact with the organic phase. The organic phase was sampled through one of the other openings in the flask cover, and the volume of liquid removed was replaced immediately.

The stirring blade and shaft from the stirring motor were inserted in the center neck of the flask cover. An additional marine-type propeller, having a stirring diameter of 44 mm, was placed on the shaft and centered in the organic phase. The propeller consisted of three blades, 18 mm in diameter, set at 45° angles to the shaft.

Two-milliliter samples of each phase were taken at appropriate intervals and assayed spectrophotometrically. The samples from the organic phase were diluted with methanol, and the absorbance was measured at 230 nm with methanol as the reference. The aqueous samples were diluted with 0.1 N HCl, and the absorbance was measured at 273 nm using 0.1 N HCl as the reference. The amount of benzoic acid in each layer as a function of time was determined by appropriate calculations from standard curves.

Nondisintegrating Disks in pH-Stat System—A volume of 400 ml of distilled water was placed in the dissolution vessel and brought to 37 ± 0.1° in the constant-temperature bath. The dissolution medium was adjusted to the predetermined experimental stat-pH by the addition of hydrochloric acid or sodium hydroxide. Two-milliliter samples were taken at appropriate intervals, and the volume of sample was replaced immediately with an equal volume of dissolution medium. The benzoic and

[1] Carver model B.
[2] Beckman DU-2.

Table II—Dissolution Rates in Various Sodium Hydroxide Solutions and Effective Film Thicknesses (h) of Benzoic and Salicylic Acids [a]

Sodium Hydroxide, N	Rate, mg/min/cm^2	h, cm × 10^{-3}
	Benzoic Acid	
0.005	0.9399	3.83
0.010	1.0580	3.40
0.020	1.3620	2.64
0.030	1.6951	2.12
	Salicylic Acid	
0.005	0.7431	3.25
0.010	0.8676	2.78
0.020	1.2660	1.91
0.030	1.7235	1.40

[a] Calculated from data presented in Table I.

salicylic acid samples were diluted with 0.1 N HCl, and the absorbances were measured at 273 and 297 nm, respectively, with 0.1 N HCl as the reference. The amount of benzoic or salicylic acid in solution as a function of time was determined by appropriate calculations from standard curves.

Effective Film Thickness of Diffusion Layer in pH-Stat System—Nondisintegrating disks of benzoic and salicylic acids were placed in 400 ml of various concentrations of sodium hydroxide, which were held constant using pH-stat automatic titration. Samples were taken periodically and assayed spectrophotometrically. Dissolution profiles (amount dissolved *versus* time) were prepared for each sodium hydroxide concentration, and the dissolution rates were calculated from the slopes of the line (Table I). The effective film thicknesses were calculated utilizing Eq. 5 (Table II). Diffusion coefficients of 1.2×10^{-5} and 1.13×10^{-5} cm^2/sec for salicylic and benzoic acids, respectively (18), were used in the calculations.

RESULTS AND DISCUSSION

The dissolution rate of a drug from a constant surface area under sink conditions should follow zero-order kinetics as described by Gibaldi and Feldman (6). This relationship can also be derived from the Noyes–Whitney equation, $dW/dt = kS(C_s - C)$, which describes the dissolution process quantitatively. Under sink conditions, the concentration difference, $(C_s - C)$, remain constant, and when a constant surface area is maintained, the equation becomes dW/dt = constant, the equation for a zero-order process.

The dissolution profile for benzoic acid disks at a pH-stat of 6.2 is shown in Fig. 1. The straight-line curve is characteristic of zero-order kinetics and indicative of a sink condition. Straight-line curves were obtained for pH-stats 4.2, 5.2, 7.2, and 8.2 almost identical to the curve

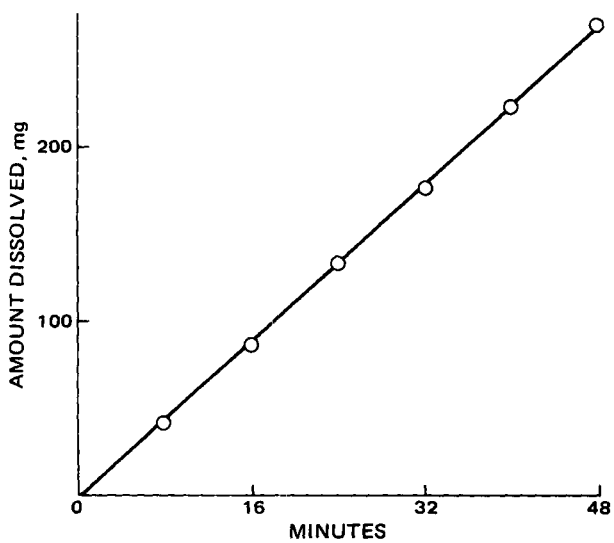

Figure 1—*Dissolution of benzoic acid from a nondisintegrating disk in distilled water (pH-stat 6.2) at 37° and 100 rpm.*

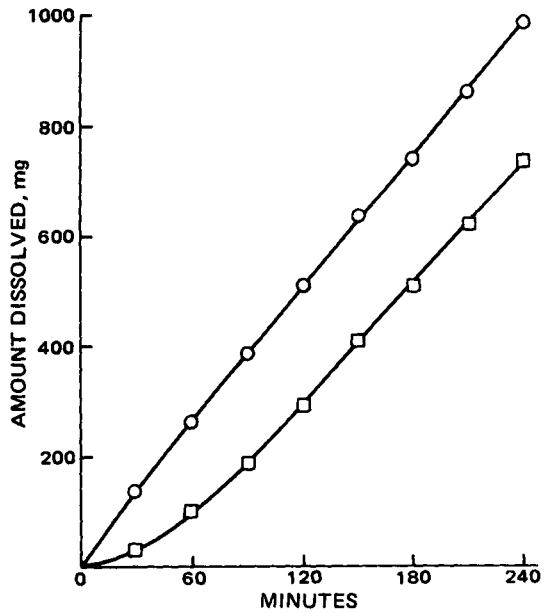

Figure 2—*Dissolution of benzoic acid from a nondisintegrating disk in distilled water having an organic reservoir at 37° and 100 rpm. Key: ○, aqueous plus organic; and □, organic.*

for pH-stat 6.2, which indicated that the dissolution rate was not affected by different pH conditions. Collett *et al.* (9) found that the dissolution of salicylic acid increased in a pH-stat experiment (absence of buffer salts) up to a maximum of pH 3–4. There was no significant difference in dissolution rate from pH 4 to 7.

Further evidence to prove that the pH-stat method actually established sink conditions during dissolution is obtained by comparing the pH-stat method data to data obtained from known sink and nonsink conditions. For this purpose, the dissolution of benzoic acid disks in distilled water at pH-stat 6.2 conditions (Fig. 1) was compared to the dissolution of: (*a*) benzoic acid disks in distilled water overlayed with an organic layer [cyclohexane–1-octanol (1:1)] as a sink (Fig. 2), (*b*) benzoic acid disks in pH 6.2 buffer (Fig. 3), and (*c*) benzoic acid disks in distilled water (Fig. 4).

The dissolution curves obtained using an organic reservoir as a sink (Fig. 2) were the same type as those obtained by Gibaldi and Feldman (6). There was an initial lag period for partitioning of the drug in the organic sink; then the dissolution process followed zero-order kinetics in

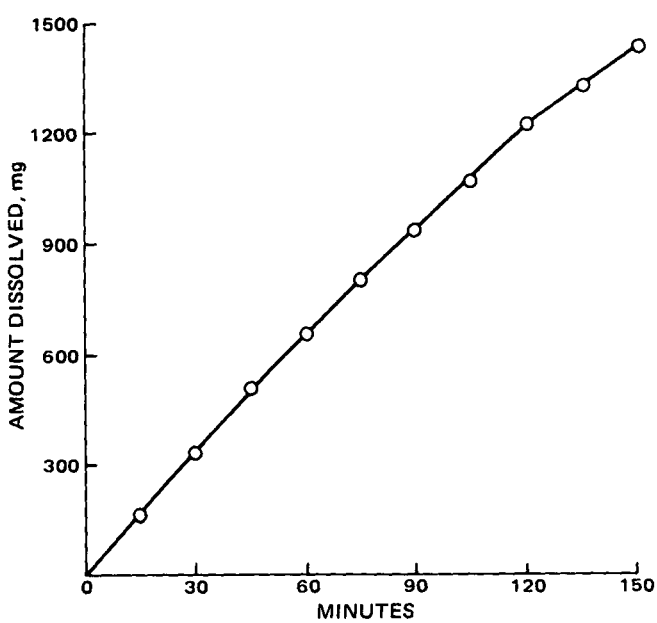

Figure 3—*Dissolution of benzoic acid from a nondisintegrating disk in buffer (pH 6.2) at 37° and 100 rpm.*

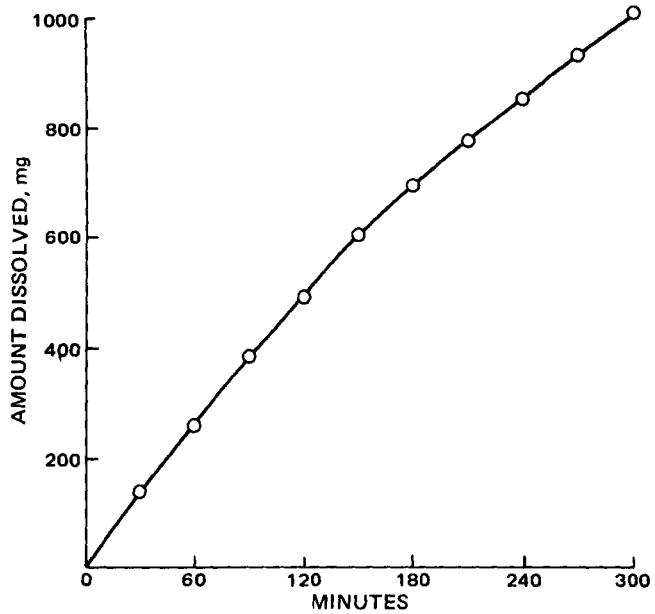

Figure 4—*Dissolution of benzoic acid from a nondisintegrating disk in distilled water at 37° and 100 rpm.*

the sink. The curve for the total amount of drug dissolving followed zero-order kinetics without a lag time (Fig. 2). In the pH-stat method, the straight-line curve was obtained (Fig. 1) without an initial lag period and without the need to analyze two phases.

The dissolution rate in the pH 6.2 buffer (Fig. 3) was much faster than the dissolution rate of a pH-stat of 6.2 (Fig. 1). Bases and buffers increase the dissolution rate of acidic drugs, and this effect was explained by use of the double film concept of diffusion-controlled dissolution (11–13). In this concept, the base diffuses toward the acid at the same time as the acid diffuses toward the bulk medium, having the effect of reducing the diffusion film thickness. This situation would not have been the case in the pH-stat experiment (Fig. 1) since there was essentially no buffer system present in solution.

The dissolution rate also decreased slightly with time in the buffer (Fig. 3) whereas it remained constant for the period studied at pH-stat 6.2 (Fig. 1). A possible reason for this decrease is that the concentration of the buffering compounds in the dissolution medium could retard the dissolution of benzoic acid. As the concentration of benzoic acid in solution increases, there is competition for solvent. Also, the buffer pH decreased slightly as the benzoic acid dissolved, which could have decreased the pH of the diffusion layer next to the benzoic acid and caused a decrease in the dissolution rate. In the pH-stat method, the dissolution medium pH is held constant throughout the experiment.

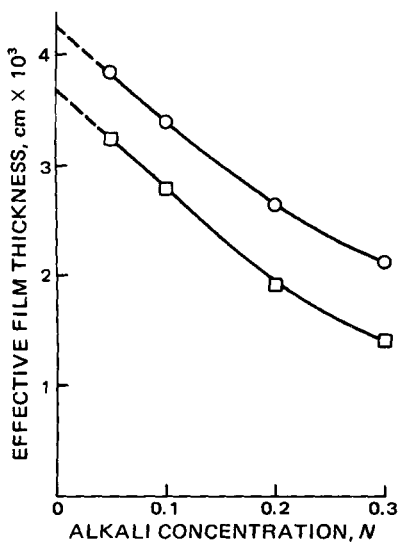

Figure 5—*Effective film thicknesses for dissolution of benzoic acid (○) and salicylic acid (□) in sodium hydroxide solutions.*

Table III—Theoretical and Experimental Dissolution Rates for Benzoic and Salicylic Acids

Compound	h^a, cm × 10^{-3}	Theoretical[b] Dissolution Rate, mg/min/cm²	Experimental[c] Dissolution Rate, mg/min/cm²
Benzoic acid	4.20	0.857	0.845
Salicylic acid	3.68	0.656	0.640

[a] Data obtained from Fig. 5; extrapolated value at zero alkali concentration. [b] Calculated using Eq. 5. [c] Determined at pH-stat 6.2 for benzoic acid and at pH-stat 5.0 for salicylic acid. The rate is the slope of the dissolution curve divided by the surface area of the disk.

When a benzoic acid disk was dissolved in distilled water under the same hydrodynamic conditions, there was a decrease in the dissolution rate with time (Fig. 4). This result is expected for nonsink conditions since the concentration difference is not constant and is decreasing as the benzoic acid dissolves. There is a buildup of benzoic acid in the solution during dissolution, which slows dissolution.

Experimental results indicate that the pH-stat method approximates sink conditions. Since no lag time was involved in establishing the sink, there was at no time a buildup of unionized drug concentration in the dissolution medium. The dissolution rate did not appear to be appreciably affected using the pH-stat method, as was the case when a buffer was used. It appears from these findings that the pH-stat method can be used to establish a perfect sink condition for dissolution studies in distilled water.

If a perfect sink is established in the pH-stat method, the intrinsic dissolution rate should not be affected by the conditions of a pH-stat method and the diffusion layer thickness, h, should remain virtually the same as in distilled water.

Hixson and Baum (15) used various concentrations of sodium hydroxide as the dissolution medium for benzoic acid and calculated the effective film thickness at each concentration. A plot of effective film thickness *versus* initial alkali concentration was extrapolated to zero alkali concentration, and this value was considered as the effective film thickness of the diffusion layer for benzoic acid pellets dissolving in pure water. This general procedure was used in the pH-stat apparatus for benzoic and salicylic acid disks.

A plot of the film thickness *versus* the initial alkali concentration (Fig. 5) extrapolated to a thickness of 3.68 ± 10^{-3} cm for salicylic acid and of 4.2×10^{-3} cm for benzoic acid at zero concentration. This extrapolation should be the diffusion layer thickness of compounds in distilled water according to the concept of Hixson and Baum (15) and should essentially be the thickness of the diffusion layer in the pH-stat method based on the theory that the thickness of the diffusion layer is virtually unaffected by this method.

To test this theory, the extrapolated diffusion layer thicknesses were used to calculate the theoretical dissolution rates of benzoic and salicylic acids and were compared to experimentally determined dissolution rates under the same experimental conditions at pH-stat 6.2 for benzoic acid and at pH-stat 5.0 for salicylic acid (Table III). The theoretical dissolution rates for benzoic acid (0.857 mg/min/cm²) and salicylic acid (0.656 mg/min/cm²) are in close agreement with the experimental rates of 0.845 and 0.640 mg/min/cm², respectively.

These results apparently substantiate the theory that the pH-stat method can be used to establish sink conditions for dissolution studies. Moreover, perfect sink conditions apparently were established under the experimental conditions used.

REFERENCES

(1) J. A. Hersey, *Manuf. Chem. Aerosol News*, **Feb. 1969**, 33.

(2) J. Cooper and J. E. Rees, *J. Pharm. Sci.*, **61**, 1511 (1972).

(3) M. Pernarowski, in "Dissolution Technology," L. J. Leeson and J. T. Carstensen, Eds., APhA Academy of Pharmaceutical Sciences, Washington, D.C., 1974, pp. 58–105.

(4) M. Gibaldi, in "The Theory and Practice of Industrial Pharmacy," L. Lachman, H. A. Lieberman, and J. L. Kanig, Eds., Lea & Febiger, Philadelphia, Pa., 1976, p. 115.

(5) A. C. Shah, C. B. Peot, and J. F. Ochs, *J. Pharm. Sci.*, **62**, 671 (1973).

(6) M. Gibaldi and S. Feldman, *ibid.*, **56**, 1238 (1967).

(7) J. Swarbrick, "Current Concepts in the Pharmaceutical Sciences:

Biopharmaceutics," Lea & Febiger, Philadelphia, Pa., 1970, p. 276.
(8) A. C. Shah, *J. Pharm. Sci.*, **60**, 1564 (1971).
(9) J. H. Collett, J. A. Rees, and N. A. Dickinson, *J. Pharm. Pharmacol.*, **24**, 724 (1972).
(10) W. H. Steinberg, H. H. Hutchins, P. G. Pick, and J. S. Lazar, *J. Pharm. Sci.*, **54**, 761 (1965).
(11) *Ibid.*, **54**, 625 (1965).
(12) A. A. Noyes and W. R. Whitney, *J. Am. Chem. Soc.*, **19**, 930 (1897).
(13) "The Merck Index," 9th ed., Merck & Co., Rahway, N.J., 1976, pp. 1080, 1120.
(14) C. V. King and S. S. Brodie, *J. Am. Chem. Soc.*, **59**, 1375 (1937).
(15) A. W. Hixson and S. J. Baum, *Ind. Eng. Chem.*, **36**, 528 (1944).
(16) W. I. Higuchi, E. L. Parrott, D. Wurster, and T. Higuchi, *J. Am. Pharm. Assoc., Sci. Ed.*, **47**, 376 (1958).
(17) F. L. Underwood and D. E. Cadwallader, *J. Pharm. Sci.*, **65**, 697 (1976).
(18) M. Gibaldi, S. Feldman, and N. Weiner, *Chem. Pharm. Bull.*, **18**, 715 (1970).

ACKNOWLEDGMENTS

Abstracted in part from a dissertation submitted by F. L. Underwood to the Graduate School, University of Georgia, in partial fulfillment of the Doctor of Philosophy degree requirements.

NOTES

Synthesis of Dextroamphetamine Sulfate and Methamphetamine Hydrochloride from D-Phenylalanine

DAVID B. REPKE *x, DALLAS K. BATES ‡, and WILFRED J. FERGUSON §

Received September 19, 1977, from **P.O. Box 899, Los Altos, CA 94022*, the ‡*Department of Chemistry and Chemical Engineering, Michigan Technological University, Houghton, MI 49931*, and §*Research Organics, Inc., Cleveland, OH 44125.* Accepted for publication November 10, 1977.

Abstract □ Starting from D-phenylalanine, dextroamphetamine sulfate and methamphetamine hydrochloride were synthesized. The reaction sequence proceeds through three intermediates, in which the absolute configuration of the asymmetric carbon atom is changed but the relative configuration remains the same. Either product can be obtained from a common intermediate by altering the reductive conditions employed for the removal of a carbamate protecting group.

Keyphrases □ Dextroamphetamine sulfate—synthesized from D-phenylalanine □ Methamphetamine hydrochloride—synthesized from D-phenylalanine □ D-Phenylalanine—starting material for synthesis of dextroamphetamine sulfate and methamphetamine hydrochloride □ Stimulants, central—dextroamphetamine sulfate and methamphetamine hydrochloride, synthesized from D-phenylalanine

Following initial observations on the sympathomimetic properties of amphetamine and related compounds (1–4), the racemate of amphetamine was introduced into clinical medicine for the relief of nasal congestion (5). The (*S*)-(+)-isomers of amphetamine [dextroamphetamine (V)] and methamphetamine (VI) (Scheme I) have been used in the therapy of obesity, narcolepsy, parkinsonism, and certain behavioral disorders (6). Considerable interest also has been generated in the central stimulant properties of these compounds (7).

dl-α-Methylphenethylamine and D-α,*N*-dimethylphenethylamine have been prepared by several routes (4, 8–12). The deuterium-labeled analogs of these compounds also have been synthesized (13, 14). Karrer and Ehrhardt (15) originally prepared V from D-phenylalanine *via* the *N,O*-di-*p*-toluenesulfonate derivative of II. Using a modification of that procedure, Gal (16) recently synthesized the deuterium analog of V and the corresponding (*R*)-(−)-isomer for use as internal standards in GLC–mass spectral studies. An asymmetric synthesis of V also was described (17).

An earlier report (18) presented the synthesis of (*R*)-(−)- and (*S*)-(+)-α-methyltryptamine from the corresponding tryptophan isomers. The present work outlines the application of this method to another aromatic α-amino acid, phenylalanine.

The reaction sequence (Scheme I) is essentially the same

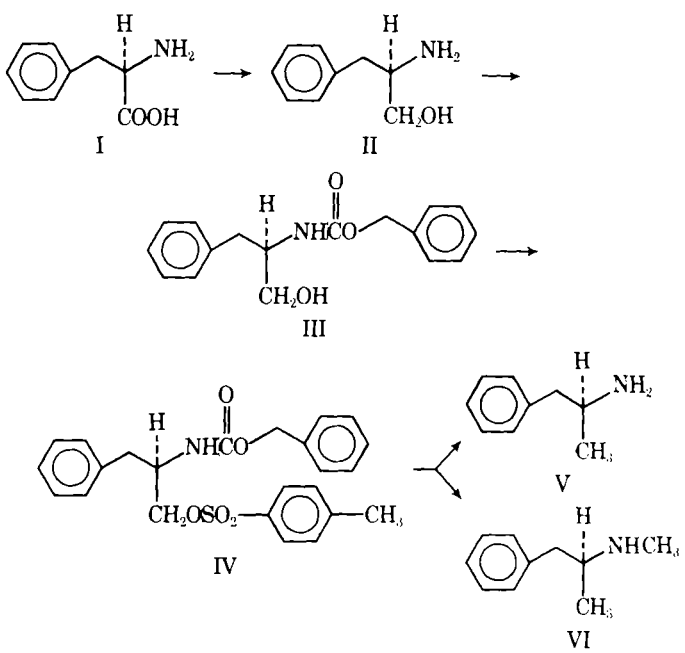

Scheme I

© 1978, American Pharmaceutical Association

Biopharmaceutics," Lea & Febiger, Philadelphia, Pa., 1970, p. 276.
(8) A. C. Shah, *J. Pharm. Sci.*, **60**, 1564 (1971).
(9) J. H. Collett, J. A. Rees, and N. A. Dickinson, *J. Pharm. Pharmacol.*, **24**, 724 (1972).
(10) W. H. Steinberg, H. H. Hutchins, P. G. Pick, and J. S. Lazar, *J. Pharm. Sci.*, **54**, 761 (1965).
(11) *Ibid.*, **54**, 625 (1965).
(12) A. A. Noyes and W. R. Whitney, *J. Am. Chem. Soc.*, **19**, 930 (1897).
(13) "The Merck Index," 9th ed., Merck & Co., Rahway, N.J., 1976, pp. 1080, 1120.
(14) C. V. King and S. S. Brodie, *J. Am. Chem. Soc.*, **59**, 1375 (1937).
(15) A. W. Hixson and S. J. Baum, *Ind. Eng. Chem.*, **36**, 528 (1944).
(16) W. I. Higuchi, E. L. Parrott, D. Wurster, and T. Higuchi, *J. Am. Pharm. Assoc., Sci. Ed.*, **47**, 376 (1958).
(17) F. L. Underwood and D. E. Cadwallader, *J. Pharm. Sci.*, **65**, 697 (1976).
(18) M. Gibaldi, S. Feldman, and N. Weiner, *Chem. Pharm. Bull.*, **18**, 715 (1970).

ACKNOWLEDGMENTS

Abstracted in part from a dissertation submitted by F. L. Underwood to the Graduate School, University of Georgia, in partial fulfillment of the Doctor of Philosophy degree requirements.

NOTES

Synthesis of Dextroamphetamine Sulfate and Methamphetamine Hydrochloride from D-Phenylalanine

DAVID B. REPKE *x, DALLAS K. BATES ‡, and WILFRED J. FERGUSON §

Received September 19, 1977, from **P.O. Box 899, Los Altos, CA 94022*, the ‡*Department of Chemistry and Chemical Engineering, Michigan Technological University, Houghton, MI 49931*, and §*Research Organics, Inc., Cleveland, OH 44125.* Accepted for publication November 10, 1977.

Abstract □ Starting from D-phenylalanine, dextroamphetamine sulfate and methamphetamine hydrochloride were synthesized. The reaction sequence proceeds through three intermediates, in which the absolute configuration of the asymmetric carbon atom is changed but the relative configuration remains the same. Either product can be obtained from a common intermediate by altering the reductive conditions employed for the removal of a carbamate protecting group.

Keyphrases □ Dextroamphetamine sulfate—synthesized from D-phenylalanine □ Methamphetamine hydrochloride—synthesized from D-phenylalanine □ D-Phenylalanine—starting material for synthesis of dextroamphetamine sulfate and methamphetamine hydrochloride □ Stimulants, central—dextroamphetamine sulfate and methamphetamine hydrochloride, synthesized from D-phenylalanine

Following initial observations on the sympathomimetic properties of amphetamine and related compounds (1–4), the racemate of amphetamine was introduced into clinical medicine for the relief of nasal congestion (5). The (*S*)-(+)-isomers of amphetamine [dextroamphetamine (V)] and methamphetamine (VI) (Scheme I) have been used in the therapy of obesity, narcolepsy, parkinsonism, and certain behavioral disorders (6). Considerable interest also has been generated in the central stimulant properties of these compounds (7).

dl-α-Methylphenethylamine and D-α,*N*-dimethylphenethylamine have been prepared by several routes (4, 8–12). The deuterium-labeled analogs of these compounds also have been synthesized (13, 14). Karrer and Ehrhardt (15) originally prepared V from D-phenylalanine *via* the *N,O*-di-*p*-toluenesulfonate derivative of II. Using a modification of that procedure, Gal (16) recently synthesized the deuterium analog of V and the corresponding (*R*)-(−)-isomer for use as internal standards in GLC–mass spectral studies. An asymmetric synthesis of V also was described (17).

An earlier report (18) presented the synthesis of (*R*)-(−)- and (*S*)-(+)-α-methyltryptamine from the corresponding tryptophan isomers. The present work outlines the application of this method to another aromatic α-amino acid, phenylalanine.

The reaction sequence (Scheme I) is essentially the same

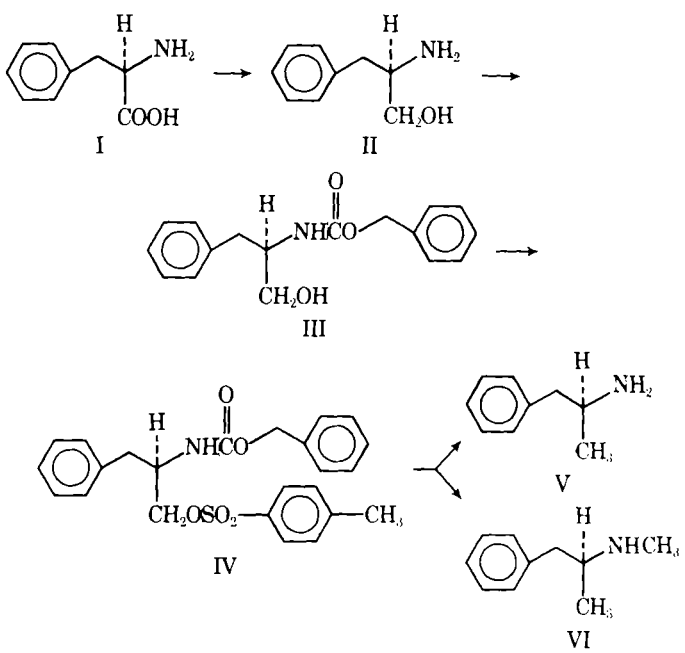

Scheme I

© 1978, American Pharmaceutical Association

as that used previously (18). In contrast to the corresponding indole analog, the *N*-benzyloxycarbonyl-*O*-*p*-toluenesulfonyl intermediate (IV) is a stable, crystalline solid. The substitution of nitrogen with a carbamate group has the advantage of providing either the primary (V) or secondary (VI) amine, depending on the conditions employed for the reduction of IV. Although the preparation of *N*-methylamino acids by lithium aluminum hydride reduction of their *N*-benzyloxycarbonyl derivatives has been known for years (19), this reaction has seldom been applied to other types of amines (20).

EXPERIMENTAL[1]

(*R*)-(+)-2-Amino-3-phenylpropanol (II)—To a suspension of 1.3 g (34 mmoles) of lithium aluminum hydride in 75 ml of anhydrous tetrahydrofuran was added, in portions, 2.1 g (12.7 mmoles) of D-phenylalanine. After the addition, the reaction mixture was refluxed for 20 min and cooled to room temperature. Then the complex and excess reagent were decomposed by dropwise addition of 2 *N* aqueous sodium hydroxide and water. The white solids were collected by filtration and washed with 100 ml of tetrahydrofuran.

The filtrate and washings were combined and concentrated under reduced pressure. The residual clear oil slowly crystallized and was recrystallized from ethyl acetate–hexane, 1.75 g (91%), mp 90–91° [lit. (21) mp 91–92°], $[\alpha]_D$ 23.8° (c 1.0, ethanol) [lit. (19) $[\alpha]_D$ 24.6°].

(*R*)-(+)-*N*-(Benzyloxycarbonyl)-2-amino-3-phenylpropanol (III)–A mixture of 1.5 g (9.9 mmoles) of II and 1.12 g (10.6 mmoles) of sodium carbonate in 25 ml of acetone and 25 ml of water was stirred at room temperature, and 1.5 ml (10.5 mmoles) of benzyl chloroformate was added. The reaction mixture was stirred for 3.0 hr, diluted with 50 ml of water, and acidified (to pH 2) with concentrated hydrochloric acid.

The mixture was shaken with 300 ml of ethyl acetate, and the organic phase was washed with 100 ml of saturated aqueous sodium chloride. After drying (magnesium sulfate), the filtered organic solution was concentrated *in vacuo*. The product was crystallized from ethyl acetate–hexane, 1.5 g (55%), mp 91–92°, $[\alpha]_D$ 41.3° (c 1.0, ethanol).

Anal.—Calc. for $C_{17}H_{19}NO_3$ (mol. wt. 285.35): C, 71.56; H, 6.71; N, 4.91. Found: C, 71.32; H, 6.86; N, 4.74.

(*R*)-(+)-*N*-(Benzyloxycarbonyl)-2-amino-3-phenylpropanol *p*-Toluenesulfonate (IV)—Compound III (1.25 g, 4.4 mmoles) and *p*-toluenesulfonyl chloride (955 mg, 5 mmoles) were dissolved in 100 ml of pyridine. The solution was stored at room temperature with the exclusion of moisture for 4 days. Water (2.0 ml) was added; after 30 min, the solvent was distilled under reduced pressure. The residue was partitioned between 300 ml of ethyl acetate and 75 ml of saturated aqueous sodium bicarbonate, and the organic phase was dried (magnesium sulfate).

After filtration of the drying agent and concentration of the filtrate, the residual semisolid was preparatively chromatographed on two 1-m × 20-cm glass plates coated with 750-μm layers of silica gel GF, using 5% acetone in benzene as the developing solvent. The product band was removed from the plates and eluted with ethyl acetate. Concentration of the eluate afforded a clear syrup, which was crystallized from ethyl acetate–hexane, 985 mg (50%), mp 96–97°, $[\alpha]_D$ 29.7° (c 1.0, ethanol).

Anal.—Calc. for $C_{24}H_{25}NO_5S$ (mol. wt. 439.54): C, 65.58; H, 5.73; N, 3.19. Found: C, 65.77; H, 5.80; N, 2.81.

Dextroamphetamine [(*S*)-(+)-α-Methylphenethylamine] (V) Sulfate—Compound IV (250 mg, 0.568 mmole) and 100 mg of 10% palladium-on-charcoal were mixed in 30 ml of absolute ethanol, and the reaction was shaken under 50 psi of hydrogen for 1.0 hr. The catalyst was removed by filtration[2], and the filtrate was concentrated *in vacuo*. The residue was partitioned between 30 ml of 1 *N* aqueous sodium hydroxide and 200 ml of ethyl acetate. The organic solution was washed with 50 ml of water.

The dried (magnesium sulfate) solution was concentrated under reduced pressure (bath temperature of 25°), and the oily residue was distilled *in vacuo* (Kugelrohr apparatus) at 0.05 mm and 40–60°. The clear distillate was dissolved in 3.0 ml of ether and carefully acidified (to pH 4) by addition of 0.2 *N* H_2SO_4 in ethanol. The white solid was collected by filtration, washed with ether, and dried *in vacuo* to give 40 mg (38%), mp >300°, $[\alpha]_D$ 20.1° (c 1.0, water) [lit. (22) $[\alpha]_D$ 21.5°]. The IR spectrum was identical to that reported for this compound (23).

Methamphetamine [(*S*)-(+)-α,*N*-Dimethylphenethylamine] (VI) Hydrochloride—To a stirred suspension of 200 mg (5.26 mmoles) of lithium aluminum hydride in 5.0 ml of tetrahydrofuran was added a solution of 250 mg (0.568 mmole) of IV in 5.0 ml of tetrahydrofuran. The reaction mixture was refluxed for 30 min and cooled to room temperature, and the complex was decomposed by careful addition of 2 *N* aqueous sodium hydroxide and water. After filtration of the white solids, the filtrate was concentrated *in vacuo*.

The residual oil was distilled *in vacuo* (Kugelrohr apparatus) at 0.05 mm and 40–60°. The distillate was dissolved in 2.0 ml of ether, and the solution was acidified by addition of saturated hydrogen chloride in ether. The crystalline plates were collected by filtration, washed with ether, and dried *in vacuo*, yielding 65 mg (62%), mp 171–173° [lit. (9) mp 172°], $[\alpha]_D$ 15.1° (c 1.0, water) [lit. (24) $[\alpha]_D$ 14–20°]. The IR spectrum was the same as that reported for this compound (23).

[1] The general analytical methods are similar to those described previously (18). IR spectra were obtained on a Perkin-Elmer model 237 spectrophotometer, using potassium bromide disks containing 1% (w/w) sample. Rotational measurements were made on a Perkin-Elmer model 141 polarimeter. Melting points are corrected.

[2] Celite.

REFERENCES

(1) G. Piness, H. Miller, and G. A. Alles, *J. Am. Med. Assoc.*, **94**, 790 (1930).

(2) G. A. Alles, *J. Pharmacol.*, **47**, 339 (1933).

(3) G. A. Alles and M. Prinzmetal, *ibid.*, **48**, 161 (1933).

(4) W. H. Hartung and J. C. Munch, *J. Am. Chem. Soc.*, **53**, 1875 (1931).

(5) C. D. Leake, "The Amphetamines, Their Actions and Uses," Charles C Thomas, Springfield, Ill., 1958.

(6) "The Pharmacological Basis of Therapeutics," 5th ed., L. S. Goodman and A. Gilman, Eds., Macmillan, New York, N.Y., 1975.

(7) B. Weiss and V. G. Laties, *Pharmacol. Rev.*, **14**, 1 (1962).

(8) G. Edeleano, *Chem. Ber.*, **20**, 616 (1887).

(9) H. Emde, *Helv. Chim. Acta*, **12**, 365 (1929).

(10) G. A. Alles, *J. Am. Chem. Soc.*, **54**, 271 (1932).

(11) O. Y. Magidson and G. A. Garkusha, *J. Gen. Chem. (USSR)*, **11**, 339 (1941); through *Chem. Abstr.*, **35**, 5868.

(12) A. Larizza, G. Brancaccio, and A. Segre, *J. Med. Chem.*, **9**, 966 (1966).

(13) B. Lindeke and A. K. Cho, *Acta Pharm. Suec.*, **9**, 363 (1972).

(14) A. F. Fentiman, Jr., and R. L. Foltz, *J. Labelled Compd. Radiopharm.*, **12**, 69 (1976).

(15) P. Karrer and K. Ehrhardt, *Helv. Chim. Acta*, **34**, 2202 (1951).

(16) J. Gal, *J. Labelled Compd. Radiopharm.*, **13**, 3 (1977).

(17) D. E. Nichols, C. F. Barfknecht, D. B. Rusterholz, F. Benington, and R. D. Morin, *J. Med. Chem.*, **16**, 480 (1973).

(18) D. B. Repke and W. J. Ferguson, *J. Heterocycl. Chem.*, **13**, 775 (1976).

(19) P. Karrer and B. J. R. Nicolaus, *Helv. Chim. Acta*, **35**, 1581 (1952).

(20) H. E. Smith, E. P. Burrows, and F.-M. Chen, *J. Org. Chem.*, **40**, 1562 (1975).

(21) J. B. Jones, D. W. Sneddon, and A. J. Lewis, *Biochim. Biophys. Acta*, **341**, 284 (1974).

(22) J. Cymerman Craig, R. P. K. Chan, and S. K. Roy, *Tetrahedron*, **23**, 3573 (1967).

(23) E. C. G. Clarke and J. Berle, "Isolation and Identification of Drugs," Pharmaceutical Press, London, England, 1969.

(24) "The Merck Index," 8th ed., Merck & Co., Rahway, N.J., 1968, p. 332.

Solasodine Stability under Conditions of Saponin Hydrolysis

RUTH SEGAL ˣ, AVIVA BREUER, and ILANA MILO-GOLDZWEIG

Received August 29, 1977, from the *Department of Pharmacognosy, School of Pharmacy, The Hebrew University of Jerusalem, Jerusalem, Israel.* Accepted for publication November 8, 1977.

Abstract □ The extent of formation of solasodiene from solasodine upon treatment with hydrochloric acid under various conditions was determined. The diene formed was assayed by using the characteristic extinction at 236 nm. Diene formation was effected by the acid concentration and the boiling point of the solvent used. Optimal conditions for the hydrolysis of solasodine glycosides are suggested.

Keyphrases □ Solasodine—formation of solasodiene on hydrolysis with hydrochloric acid under various conditions □ Solasodiene—formation from solasodine on hydrolysis with hydrochloric acid under various conditions □ Hydrolysis—solasodine, formation of solasodiene on treatment with hydrochloric acid under various conditions □ Stability—solasodine, formation of solasodiene on hydrolysis with hydrochloric acid under various conditions □ Saponins—solasodine glycosides, formation of solasodiene on hydrolysis with hydrochloric acid under various conditions

Recently (1), solasodine (I) has become a highly valued compound, being a competitor to diosgenin as a precursor of pharmacologically active steroids. Solasodine occurs in different *Solanum* species in glycosidal combination, *i.e.*, as the aglycone of various saponins, and is obtained from the plant extract by acid hydrolysis. Because of the growing demand for raw materials for the synthesis of steroidal hormones, it is important to choose conditions for obtaining optimal yields of solasodine from the plant material.

While deriving solasodine from *S. incanum* (2), it was apparent that the yield was highly influenced by the experimental conditions. Examination of the crude solasodine, obtained after acid hydrolysis of the plant extract, showed that the sapogenin was accompanied by various quantities of a less polar compound (3). This compound proved to be the artifactual dehydration product solasodiene (II). Acids can decompose 3-hydroxy-Δ^5-steroids to the dehydrated $\Delta^{3,5}$-dienes (4).

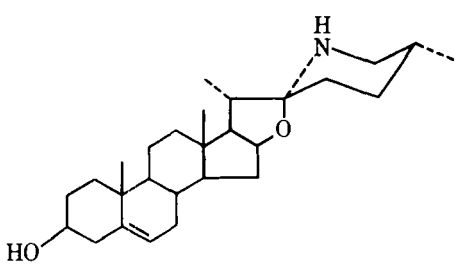

I

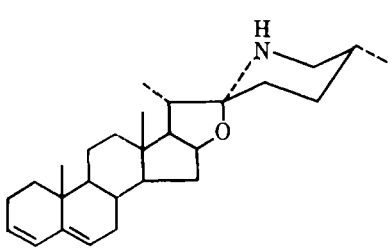

II

The stability of diosgenin under various hydrolytic conditions was investigated thoroughly (4–6). However, no analogous research has been carried out with respect to solasodine, although solasodine is known to give the corresponding diene (7–9).

This paper reports the effect of the acid concentration as well as of the solvent system on solasodine hydrolysis.

RESULTS AND DISCUSSION

Solasodiene (II) was isolated from the reaction of solasodine (I) with ethanolic hydrochloric acid. The compound was identified by its melting point, mass spectrum (M^+ 395), and UV and IR spectra. This compound was identical with the less polar compound obtained in all of the acid-catalyzed reactions of solasodine (same R_f values on TLC, developed in three different solvent systems).

Since the solasodiene obtained after solasodine hydrolysis possesses the characteristic diene chromophore, which is absent in the parent compound, it was possible to monitor its formation by UV spectroscopy. This absorbance followed Beer's law and was scarcely influenced by the coexistence of the corresponding Δ^5-3-ol, *i.e.*, solasodine. The yield, *i.e.*, the extent of the dehydration of solasodine, was evaluated from the absorbance at 236 nm, the molar absorption being 2.07×10^4.

The yields of solasodiene obtained on refluxing solasodine under various conditions are summarized in Table I. The yield of the diene was highly influenced by the acid concentration and by the type of alcohol used. The higher the boiling point of the alcohol, the more diene was obtained. High boiling alcohols, *i.e.*, 1-propanol, bp 97°, and 1-butanol, bp 116°, were used since solasodine hydrochloride is extremely insoluble in water and aqueous alcoholic solutions, the solvents usually used for the extraction and hydrolysis of plant saponins. Even when a low boiling alcohol was used with a high acid concentration (2 *N*), the diene was obtained in a considerable yield.

It seems that the most suitable condition for the saponin hydrolysis is the use of nonaqueous low boiling alcohols and acid concentrations not exceeding 1 *N*.

EXPERIMENTAL

Starting Compound—A commercial sample of solasodine was purified by silica gel column chromatography, using chloroform–methanol

Table I—Yield of Solasodiene from Solasodine [a] upon Boiling [b] with Acid under Various Conditions

Alcohol	Hydrochloric Acid Concentration, *N*	Absorbance at 236 nm [c]	Yield of Solasodiene from Solasodine, %
Methanol	0.5	0.075	1.4
	1	0.13	2.4
	2	0.66	12
Ethanol	0.5	0.09	1.6
	1	0.20	3.7
	2	1.34	25
1-Propanol	0.5	0.29	5.4
	1	0.65	12
	2	2.02	37.5
1-Butanol	0.5	0.34	6.3
	1	1.04	19
	2	2.85	54

[a] Pure solasodine (5 mg) dissolved in 10 ml of alcohol to which concentrated hydrochloric acid was added to give the required concentration. [b] Reflux for 3 hr. [c] UV spectra were measured on Varian Techtron model 635.

0022-3549/78/0800-1169$01.00/0
© 1978, American Pharmaceutical Association

(40:1) as the eluting solvent. The compound was further purified by crystallization from acetone.

TLC—Silica gel 60 F_{254}-precoated aluminum sheets were used with chloroform–methanol (10:1), giving R_f 0.62 for I and R_f 0.8 for II. The spots were visualized by spraying with the following mixture: anisaldehyde (21 ml), phosphomolybdic acid, 10% in methanol (5 ml), acetic acid (45 ml), sulfuric acid (22.5 ml), and methanol (430 ml). The plates were heated to 120–125° and development of color was observed.

Isolation of Solasodiene—Solasodine (400 mg) was dissolved in 100 ml of ethanol, and 24 ml of concentrated hydrochloric acid was then added. The resulting solution was refluxed for 3 hr, cooled, and neutralized with aqueous ammonia, and the methanol was evaporated. The residue was extracted with ether, and the combined extracts were washed with saturated aqueous sodium chloride and then dried over magnesium sulfate. After evaporation of the ether, the mixture was separated by silica gel column chromatography, using chloroform–methanol (40:0.5) as the eluting solvent. Crude solasodiene (25%) was obtained. Crystallization from acetone gave pure solasodiene, mp 173°.

General Procedure for Hydrolysis—Solasodine (0.005 g) was dissolved in methanol, ethanol, 1-propanol, or 1-butanol, and then concentrated hydrochloric acid was added to give the required acid concentration (0.5, 1, and 2 *N* for each alcohol used). The total volume of each solution was 10 ml. The solution was refluxed for 3 hr and neutralized with aqueous ammonia. After evaporation to dryness in a vacuum, a second portion of aqueous ammonia was added, making the reaction mixture alkaline. This mixture was then extracted with ether, and the combined extracts were washed with saturated sodium chloride, dried over magnesium sulfate, and evaporated to dryness. The residue was then diluted with methanol to the required volume for UV spectroscopic reading.

REFERENCES

(1) K. Schreiber, in "The Alkaloids," vol. 10, R. H. F. Manske, Ed., Academic, New York, N.Y., 1968.

(2) D. V. Zaitschek and R. Segal, *Lloydia*, **35**, 192 (1972).

(3) R. Segal, I. Milo-Goldzweig, D. V. Zaitschek, and M. Noam, *Anal. Biochem.*, **84**, 78 (1978).

(4) T. Yamauchi, *Chem. Pharm. Bull.*, **7**, 343 (1959).

(5) W. J. Peal, *Chem. Ind.*, **44**, 1451 (1957).

(6) G. Blunden and C. T. Rhodes, *J. Pharm. Sci.*, **57**, 602 (1968).

(7) K. Syhora, Z. Cekan, S. Hermanek, and J. Trojanek, *Planta Med.*, **10**, 318 (1962).

(8) A. G. Gonzalez, R. Freire, C. B. Francisco, J. A. Salazar, and E. Suarez, *Tetrahedron*, **29**, 1731 (1973).

(9) R. Hardman and T. G. Williams, *Planta Med.*, **29**, 66 (1976).

Analysis of Cefazolin in Serum or Urine

B. KAYE ˣ and P. R. WOOD

Received March 7, 1977, from *Pfizer Central Research, Pfizer Ltd., Sandwich, Kent CT13 9NJ, England.* Accepted for publication November 1, 1977.

Abstract □ A method was developed to determine cefazolin in serum or urine. The drug is extracted from serum or urine with ethyl acetate, separated by TLC, and determined by fluorescence quenching densitometry. The method was developed to study the pharmacokinetics of the compound in humans.

Keyphrases □ Cefazolin—TLC–densitometric analysis in biological fluids □ TLC–densitometry—analysis, cefazolin in biological fluids □ Antibacterials—cefazolin, TLC–densitometric analysis in biological fluids

To carry out pharmacokinetic studies on cefazolin, 7-[1-(1*H*)-tetrazolylacetamido]-3-[2-(5-methyl-1,3,4-thiadiazolyl)thiomethyl]ceph-3-em-4-carboxylic acid (1), an assay was developed to determine antibiotic concentrations in serum and urine. The method provides a convenient alternative to other published procedures (1, 2).

EXPERIMENTAL

Reagents—Ether[1], ethyl acetate[1], chloroform[1], acetic acid[2], 1 *M* HCl, and 0.2 *M* HCl were used.

TLC–Densitometry—Precoated TLC plates[3] (20 × 20 cm) were developed in glass tanks. Solutions were applied to the thin-layer plates using an automatic plate spotter[4]. Plates were scanned using a densitometer[5]. The settings on the instrument were: mode, log −; span, 980; level, e5; damping, 2; rotating-spot diameter, 8 mm; scan speed setting, 3; and chart speed setting, 5.

Analysis of Samples—A sample of serum or urine (1.0 ml diluted 0–500-fold) was pipetted into a 10-ml stoppered tube. The sample pH was adjusted to 2 by adding 1 *M* HCl (250 μl) to serum and 0.2 *M* HCl (250 μl) to urine. The sample was extracted with ethyl acetate (2 × 3 ml), and the combined extracts were evaporated under nitrogen at 37°. The residue in the tube was dissolved in 50 μl of methanol and transferred quantitatively, using a 100-μl syringe, to the origin of the thin-layer plate. The tube was rinsed with methanol (50 μl), and the rinsings also were applied to the respective spot.

The plate was developed for approximately 15 cm in ether, dried at air temperature, and redeveloped again for 15 cm in chloroform–methanol–acetic acid (60:40:5). The drug traveled with an R_f of approximately 0.3, and the drug spot was measured on the densitometer. The area of the peak on the chart recorder was calculated for each spot as the product of peak height and width at half peak height.

Standard Curve—A standard calibration curve was prepared daily for each batch of samples. Aliquots of serum or urine (1.0 ml diluted 0–500-fold) spiked with a range of drug concentrations were processed according to the described method, and peak area was plotted against drug concentration. The standard curve was linear over the 1–8-μg/ml range.

Accuracy and Precision—Control serum samples were spiked with unknown quantities of I. The spiked concentrations and concentrations found (in parentheses) were 6.8 (6.8), 1.4 (1.6), 4.1 (3.8), 8.2 (8.2), 2.7 (2.9), and 5.4 (5.5) μg/ml. Control urine samples spiked with unknown quantities of I also were processed, and the results were 4.2 (4.4), 6.3 (6.2), 2.1 (2.3), 7.4 (7.7), and 3.2 (3.2) μg/ml. Six replicate assays were carried out on serum spiked with I at 4.0 μg/ml. The mean value was 4.1 ± 0.1 (*SD*) μg/ml.

DISCUSSION

The described method gives an accurate means of determining the cefazolin concentration in serum and urine and has been used to study its pharmacokinetics in humans. The homogeneity of the spots corresponding to I in extracts of the serum or urine of subjects given I was established by two-dimensional TLC in chloroform–methanol–acetic acid (60:40:5, R_f 0.3) and 2-propanol–water–acetic acid (28:8:1, R_f 0.5). No metabolites were detected in either system. Data from three subjects

[1] Analar.
[2] General-purpose reagent.
[3] Kieselgel $F60_{254}$, E. Merck, Darmstadt, Germany.
[4] TLC Multi-spotter, Analytical Instrument Specialities, Libertyville, Ill.
[5] TLD 100, Vitatron, Dieren, Holland.

0022-3549/78/0800-1170$01.00/0

© 1978, American Pharmaceutical Association

(40:1) as the eluting solvent. The compound was further purified by crystallization from acetone.

TLC—Silica gel 60 F_{254}-precoated aluminum sheets were used with chloroform–methanol (10:1), giving R_f 0.62 for I and R_f 0.8 for II. The spots were visualized by spraying with the following mixture: anisaldehyde (21 ml), phosphomolybdic acid, 10% in methanol (5 ml), acetic acid (45 ml), sulfuric acid (22.5 ml), and methanol (430 ml). The plates were heated to 120–125° and development of color was observed.

Isolation of Solasodiene—Solasodine (400 mg) was dissolved in 100 ml of ethanol, and 24 ml of concentrated hydrochloric acid was then added. The resulting solution was refluxed for 3 hr, cooled, and neutralized with aqueous ammonia, and the methanol was evaporated. The residue was extracted with ether, and the combined extracts were washed with saturated aqueous sodium chloride and then dried over magnesium sulfate. After evaporation of the ether, the mixture was separated by silica gel column chromatography, using chloroform–methanol (40:0.5) as the eluting solvent. Crude solasodiene (25%) was obtained. Crystallization from acetone gave pure solasodiene, mp 173°.

General Procedure for Hydrolysis—Solasodine (0.005 g) was dissolved in methanol, ethanol, 1-propanol, or 1-butanol, and then concentrated hydrochloric acid was added to give the required acid concentration (0.5, 1, and 2 *N* for each alcohol used). The total volume of each solution was 10 ml. The solution was refluxed for 3 hr and neutralized with aqueous ammonia. After evaporation to dryness in a vacuum, a second portion of aqueous ammonia was added, making the reaction mixture alkaline. This mixture was then extracted with ether, and the combined extracts were washed with saturated sodium chloride, dried over magnesium sulfate, and evaporated to dryness. The residue was then diluted with methanol to the required volume for UV spectroscopic reading.

REFERENCES

(1) K. Schreiber, in "The Alkaloids," vol. 10, R. H. F. Manske, Ed., Academic, New York, N.Y., 1968.

(2) D. V. Zaitschek and R. Segal, *Lloydia*, **35**, 192 (1972).

(3) R. Segal, I. Milo-Goldzweig, D. V. Zaitschek, and M. Noam, *Anal. Biochem.*, **84**, 78 (1978).

(4) T. Yamauchi, *Chem. Pharm. Bull.*, **7**, 343 (1959).

(5) W. J. Peal, *Chem. Ind.*, **44**, 1451 (1957).

(6) G. Blunden and C. T. Rhodes, *J. Pharm. Sci.*, **57**, 602 (1968).

(7) K. Syhora, Z. Cekan, S. Hermanek, and J. Trojanek, *Planta Med.*, **10**, 318 (1962).

(8) A. G. Gonzalez, R. Freire, C. B. Francisco, J. A. Salazar, and E. Suarez, *Tetrahedron*, **29**, 1731 (1973).

(9) R. Hardman and T. G. Williams, *Planta Med.*, **29**, 66 (1976).

Analysis of Cefazolin in Serum or Urine

B. KAYE ˣ and P. R. WOOD

Received March 7, 1977, from *Pfizer Central Research, Pfizer Ltd., Sandwich, Kent CT13 9NJ, England.* Accepted for publication November 1, 1977.

Abstract □ A method was developed to determine cefazolin in serum or urine. The drug is extracted from serum or urine with ethyl acetate, separated by TLC, and determined by fluorescence quenching densitometry. The method was developed to study the pharmacokinetics of the compound in humans.

Keyphrases □ Cefazolin—TLC–densitometric analysis in biological fluids □ TLC–densitometry—analysis, cefazolin in biological fluids □ Antibacterials—cefazolin, TLC–densitometric analysis in biological fluids

To carry out pharmacokinetic studies on cefazolin, 7-[1-(1*H*)-tetrazolylacetamido]-3-[2-(5-methyl-1,3,4-thiadiazolyl)thiomethyl]ceph-3-em-4-carboxylic acid (1), an assay was developed to determine antibiotic concentrations in serum and urine. The method provides a convenient alternative to other published procedures (1, 2).

EXPERIMENTAL

Reagents—Ether[1], ethyl acetate[1], chloroform[1], acetic acid[2], 1 *M* HCl, and 0.2 *M* HCl were used.

TLC–Densitometry—Precoated TLC plates[3] (20 × 20 cm) were developed in glass tanks. Solutions were applied to the thin-layer plates using an automatic plate spotter[4]. Plates were scanned using a densitometer[5]. The settings on the instrument were: mode, log −; span, 980; level, e5; damping, 2; rotating-spot diameter, 8 mm; scan speed setting, 3; and chart speed setting, 5.

Analysis of Samples—A sample of serum or urine (1.0 ml diluted 0–500-fold) was pipetted into a 10-ml stoppered tube. The sample pH was adjusted to 2 by adding 1 *M* HCl (250 μl) to serum and 0.2 *M* HCl (250 μl) to urine. The sample was extracted with ethyl acetate (2 × 3 ml), and the combined extracts were evaporated under nitrogen at 37°. The residue in the tube was dissolved in 50 μl of methanol and transferred quantitatively, using a 100-μl syringe, to the origin of the thin-layer plate. The tube was rinsed with methanol (50 μl), and the rinsings also were applied to the respective spot.

The plate was developed for approximately 15 cm in ether, dried at air temperature, and redeveloped again for 15 cm in chloroform–methanol–acetic acid (60:40:5). The drug traveled with an R_f of approximately 0.3, and the drug spot was measured on the densitometer. The area of the peak on the chart recorder was calculated for each spot as the product of peak height and width at half peak height.

Standard Curve—A standard calibration curve was prepared daily for each batch of samples. Aliquots of serum or urine (1.0 ml diluted 0–500-fold) spiked with a range of drug concentrations were processed according to the described method, and peak area was plotted against drug concentration. The standard curve was linear over the 1–8-μg/ml range.

Accuracy and Precision—Control serum samples were spiked with unknown quantities of I. The spiked concentrations and concentrations found (in parentheses) were 6.8 (6.8), 1.4 (1.6), 4.1 (3.8), 8.2 (8.2), 2.7 (2.9), and 5.4 (5.5) μg/ml. Control urine samples spiked with unknown quantities of I also were processed, and the results were 4.2 (4.4), 6.3 (6.2), 2.1 (2.3), 7.4 (7.7), and 3.2 (3.2) μg/ml. Six replicate assays were carried out on serum spiked with I at 4.0 μg/ml. The mean value was 4.1 ± 0.1 (*SD*) μg/ml.

DISCUSSION

The described method gives an accurate means of determining the cefazolin concentration in serum and urine and has been used to study its pharmacokinetics in humans. The homogeneity of the spots corresponding to I in extracts of the serum or urine of subjects given I was established by two-dimensional TLC in chloroform–methanol–acetic acid (60:40:5, R_f 0.3) and 2-propanol–water–acetic acid (28:8:1, R_f 0.5). No metabolites were detected in either system. Data from three subjects

[1] Analar.
[2] General-purpose reagent.
[3] Kieselgel $F60_{254}$, E. Merck, Darmstadt, Germany.
[4] TLC Multi-spotter, Analytical Instrument Specialities, Libertyville, Ill.
[5] TLD 100, Vitatron, Dieren, Holland.

0022-3549/78/0800-1170$01.00/0

© 1978, American Pharmaceutical Association

Table I—Serum Concentrations (Micrograms per Milliliter) and Urinary Excretion of Cefazolin in Three Subjects Given a Single Intramuscular Dose (8 mg/kg) of Drug

Subject	Hours after Dose[a]								Excretion in 0–24-hr Urine, % of Dose
	0.5	1	1.5	2	4	5.5	7	8	
1	25	30	30	28	14	7.7	3.5	1.8	45
2	39	42	31	29	13	6.4	3.5	1.8	41
3	21	35	32	28	16	11	6.0	5.7	65

[a] No cefazolin was detected at zero hour.

given a single intramuscular dose (8 mg/kg) of cefazolin are shown in Table I.

The procedure is specific in subjects known to be taking only cefazolin but has not been checked to determine whether related compounds may interfere.

The method may have general applicability to other cephalosporins that can be extracted from serum and/or urine and that contain a structural moiety absorbing in the UV spectrum.

REFERENCES

(1) J. S. Wold, *Antimicrob. Agents Chemother.*, 11, 105 (1977).

(2) A. B. C. Yu, C. H. Nightingale, and O. R. Flanagan, *J. Pharm. Sci.*, **66**, 213 (1977).

GLC Assay of Fenclorac in Human Plasma

A. F. DeLONG ˣ, A. POLK, G. MARTIN, R. D. SMYTH *, and N. H. REAVEY-CANTWELL

Received May 11, 1977, from the *Research Division, William H. Rorer, Inc., Fort Washington, PA 19034.* Accepted for publication November 10, 1977. *Present address: Department of Drug Metabolism, Bristol Laboratories, Syracuse, NY 13201.

Abstract □ A simple, sensitive GLC assay for fenclorac is described. Plasma proteins were precipitated with methanol, and the methanolic extract was refluxed with hydrochloric acid to form the methyl esters of fenclorac and the internal standard. The esters were purified by partitioning into benzene. Aliquots of 1 μl of the concentrated benzene phase were injected into the gas chromatograph and quantitated by a ^{63}Ni-electron-capture detector. Recovery of fenclorac from plasma averaged 82 ± 1.6%.

Keyphrases □ Fenclorac—GLC analysis in plasma □ GLC—analysis, fenclorac in plasma □ Anti-inflammatory agents—fenclorac, GLC analysis in plasma

Fenclorac (DL-α,3-dichloro-4-cyclohexylphenylacetic acid) is a potent nonsteroidal anti-inflammatory agent with significant analgesic and antipyretic activities (1–3). In humans and animals, the compound is rapidly absorbed, extensively metabolized, and quantitatively eliminated within 24–48 hr (4, 5). Fenclorac is the primary circulating drug species (>85%) with small amounts of the α-hydroxy metabolite (3-chloro-4-cyclohexylphenylglycolic acid), which has about 0.3 times the anti-inflammatory potency of fenclorac.

A spectrophotometric method (6) was used to quantitate fenclorac in biological samples. However, this method is not specific for the parent drug, and the sensitivity is approximately 1 μg/ml. This report describes a simple, sensitive, specific GLC assay of fenclorac in plasma.

EXPERIMENTAL

Materials—The chemicals and reagents used were: fenclorac diethylammonium salt (I), DL-4′-chloro-α-methyl-4-biphenylglycolic acid (internal standard) (II), GC–spectrophotometric quality benzene and ethyl acetate, and reagent grade methanol and hydrochloric acid.

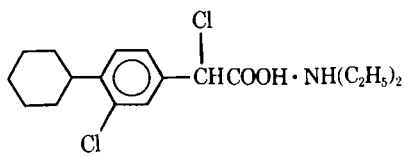

I

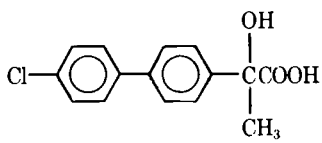

II

Instrumentation—*GLC*—GLC analysis was performed on a gas chromatograph[1] equipped with a ^{63}Ni-electron-capture detector and fitted with a 0.9-m × 2-mm coiled glass column packed with 3% silicone[2] [methyl–cyanopropyl (50:50)] on 80–100-mesh Gas Chrom Q. The column was conditioned at 220° for 18 hr. The methyl esters of fenclorac and the internal standard were formed by refluxing in hydrochloric acid–methanol. Purification and concentration of the resultant product are described later.

The methyl esters of fenclorac and the internal standard were eluted isothermally from the column under the following temperature conditions: column, 220°; injection port, 240°; manifold, 240°; and detector, 300°. Argon (95%)–methane (5%) gas flow was maintained as follows: column, 40 ml/min; and auxiliary, 60 ml/min. Samples (0.5–1.0 μl) were injected manually or with an automatic injector[3].

GLC–Mass Spectrometry—Mass spectra of standards and extracts of plasma were obtained using a GLC–mass spectrometer[4]. A 0.9-m × 2-mm coiled glass column packed with 5% OV-17 on Chromosorb W(HP) was used. The ester fractions were eluted isothermally at 225° with a

[1] Perkin-Elmer model 90013.
[2] Applied Science Laboratories.
[3] Hewlett-Packard model 7076.
[4] Hewlett-Packard model 5930-A.

0022-3549/78/0800-1171$01.00/0

© 1978, American Pharmaceutical Association

Table I—Serum Concentrations (Micrograms per Milliliter) and Urinary Excretion of Cefazolin in Three Subjects Given a Single Intramuscular Dose (8 mg/kg) of Drug

Subject	Hours after Dose[a]								Excretion in 0–24-hr Urine, % of Dose
	0.5	1	1.5	2	4	5.5	7	8	
1	25	30	30	28	14	7.7	3.5	1.8	45
2	39	42	31	29	13	6.4	3.5	1.8	41
3	21	35	32	28	16	11	6.0	5.7	65

[a] No cefazolin was detected at zero hour.

given a single intramuscular dose (8 mg/kg) of cefazolin are shown in Table I.

The procedure is specific in subjects known to be taking only cefazolin but has not been checked to determine whether related compounds may interfere.

The method may have general applicability to other cephalosporins that can be extracted from serum and/or urine and that contain a structural moiety absorbing in the UV spectrum.

REFERENCES

(1) J. S. Wold, *Antimicrob. Agents Chemother.*, 11, 105 (1977).

(2) A. B. C. Yu, C. H. Nightingale, and O. R. Flanagan, *J. Pharm. Sci.*, **66**, 213 (1977).

GLC Assay of Fenclorac in Human Plasma

A. F. DeLONG ˣ, A. POLK, G. MARTIN, R. D. SMYTH *, and N. H. REAVEY-CANTWELL

Received May 11, 1977, from the *Research Division, William H. Rorer, Inc., Fort Washington, PA 19034.* Accepted for publication November 10, 1977. *Present address: Department of Drug Metabolism, Bristol Laboratories, Syracuse, NY 13201.

Abstract □ A simple, sensitive GLC assay for fenclorac is described. Plasma proteins were precipitated with methanol, and the methanolic extract was refluxed with hydrochloric acid to form the methyl esters of fenclorac and the internal standard. The esters were purified by partitioning into benzene. Aliquots of 1 μl of the concentrated benzene phase were injected into the gas chromatograph and quantitated by a ^{63}Ni-electron-capture detector. Recovery of fenclorac from plasma averaged 82 ± 1.6%.

Keyphrases □ Fenclorac—GLC analysis in plasma □ GLC—analysis, fenclorac in plasma □ Anti-inflammatory agents—fenclorac, GLC analysis in plasma

Fenclorac (DL-α,3-dichloro-4-cyclohexylphenylacetic acid) is a potent nonsteroidal anti-inflammatory agent with significant analgesic and antipyretic activities (1–3). In humans and animals, the compound is rapidly absorbed, extensively metabolized, and quantitatively eliminated within 24–48 hr (4, 5). Fenclorac is the primary circulating drug species (>85%) with small amounts of the α-hydroxy metabolite (3-chloro-4-cyclohexylphenylglycolic acid), which has about 0.3 times the anti-inflammatory potency of fenclorac.

A spectrophotometric method (6) was used to quantitate fenclorac in biological samples. However, this method is not specific for the parent drug, and the sensitivity is approximately 1 μg/ml. This report describes a simple, sensitive, specific GLC assay of fenclorac in plasma.

EXPERIMENTAL

Materials—The chemicals and reagents used were: fenclorac diethylammonium salt (I), DL-4′-chloro-α-methyl-4-biphenylglycolic acid (internal standard) (II), GC–spectrophotometric quality benzene and ethyl acetate, and reagent grade methanol and hydrochloric acid.

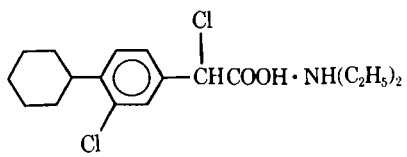

I

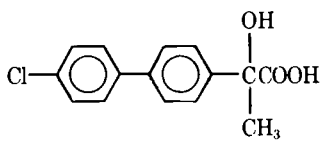

II

Instrumentation—*GLC*—GLC analysis was performed on a gas chromatograph[1] equipped with a ^{63}Ni-electron-capture detector and fitted with a 0.9-m × 2-mm coiled glass column packed with 3% silicone[2] [methyl–cyanopropyl (50:50)] on 80–100-mesh Gas Chrom Q. The column was conditioned at 220° for 18 hr. The methyl esters of fenclorac and the internal standard were formed by refluxing in hydrochloric acid–methanol. Purification and concentration of the resultant product are described later.

The methyl esters of fenclorac and the internal standard were eluted isothermally from the column under the following temperature conditions: column, 220°; injection port, 240°; manifold, 240°; and detector, 300°. Argon (95%)–methane (5%) gas flow was maintained as follows: column, 40 ml/min; and auxiliary, 60 ml/min. Samples (0.5–1.0 μl) were injected manually or with an automatic injector[3].

GLC–Mass Spectrometry—Mass spectra of standards and extracts of plasma were obtained using a GLC–mass spectrometer[4]. A 0.9-m × 2-mm coiled glass column packed with 5% OV-17 on Chromosorb W(HP) was used. The ester fractions were eluted isothermally at 225° with a

[1] Perkin-Elmer model 90013.
[2] Applied Science Laboratories.
[3] Hewlett-Packard model 7076.
[4] Hewlett-Packard model 5930-A.

0022-3549/78/0800-1171$01.00/0

© 1978, American Pharmaceutical Association

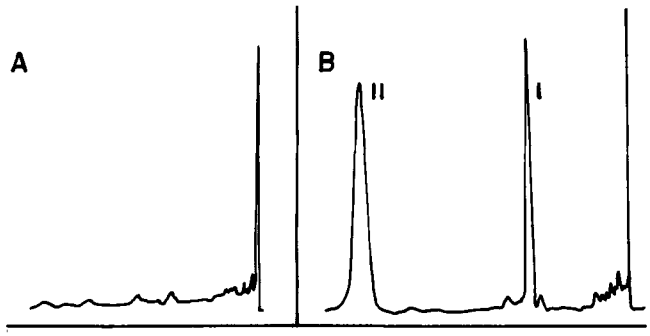

Figure 1—*Chromatograms of derivatized extract of pooled human plasma (A) and derivatized extract of pooled human plasma containing I and II (B).*

helium flow rate of 55 ml/min. The mass spectrometer detector gain was 5, and the ion monitor range was 5 v.

Analytical Procedures—*GLC of Plasma*—Plasma, 200 μl, containing 10 μg of the internal standard was added to a 50-ml, conical, glass-stoppered centrifuge tube. Methanol, 5 ml, was added, and the tube was vortexed for 30 sec and centrifuged[5] for 10 min at 1200×*g*. The methanolic phase was transferred to a 15-ml screw-capped tube, and the plasma residue was reextracted with a second 5-ml aliquot of methanol.

After centrifugation, the methanolic phases were combined, and 200 μl of concentrated hydrochloric acid was added. The tubes were sealed and heated for 1 hr at 100°. The methanolic extract was then transferred to a clean 50-ml, conical, glass-stoppered centrifuge tube containing 5 ml of benzene and 4 ml of water. The tubes were vortexed for 1 min and centrifuged for 20 min at 1200×*g*, and the upper phase was transferred to a 15-ml conical centrifuge tube.

The benzene extract was evaporated to dryness using a 50° water bath and a stream of dry air provided by a manifold apparatus. The dried residue was reconstituted in 100 μl of ethyl acetate, and aliquots were injected into the gas chromatograph. The retention times of fenclorac and the internal standard were 3.3 and 8.0 min, respectively. Plasma standard and unknown samples were processed simultaneously in the manner described.

GLC–Mass Spectrometry of Plasma—Aliquots of 3 ml of plasma, 3 ml of 2 *N* HCl, and 25 ml of ether were added to a 45-ml glass-stoppered centrifuge tube, mixed for 1 min, and centrifuged for 5 min at 2000×*g*. The ether phase was decanted and transferred to a 250-ml round-bottom flask. The remaining residue was reextracted as described, and the ether phases were combined.

The ether extract was evaporated to dryness on a rotary flash evaporator with a 40–50° water bath. The residue was dissolved in 25 ml of methanol with 3 drops of concentrated hydrochloric acid, and the mixture was heated at reflux for 30 min. After cooling, the acid–methanol solution was transferred to a 250-ml separator, the flask was washed with 100 ml of 5% NaCl, and the wash was added to the separator along with 50 ml of benzene. The mixture was shaken for 30 sec and allowed to separate, and the benzene layer was filtered through a 30-g pad of anhydrous sodium sulfate prior to being transferred to a clean 250-ml round-bottom flask.

The aqueous layer was reextracted with benzene as described. The filtered extracts were combined along with 15 ml of benzene, which was used to rinse the sodium sulfate pad. The benzene extract was evaporated to near dryness on a rotary flash evaporator in a 40–50° water bath, and the residue was increased to a final volume of 10 ml with benzene. The concentrated benzene extract was quantitatively applied to a 15 × 450-mm glass column containing 10 g of magnesium silicate[6], which was activated at 130° for 48 hr.

The methyl ester of fenclorac was eluted from the column with 50 ml of benzene–ether (90:10). The column eluate was concentrated to 100 μl in a 40° water bath with dry nitrogen, and aliquots (5 μl) were injected into the gas chromatograph–mass spectrometer. The retention time of the fenclorac methyl ester was obtained from the total ion scan of authentic fenclorac methyl ester samples. Fenclorac was identified in biological fluids by mass spectra obtained at the beginning, middle, and tail of the total ion peak, which had a retention time corresponding to standard fenclorac methyl ester. Confirmation was considered positive when

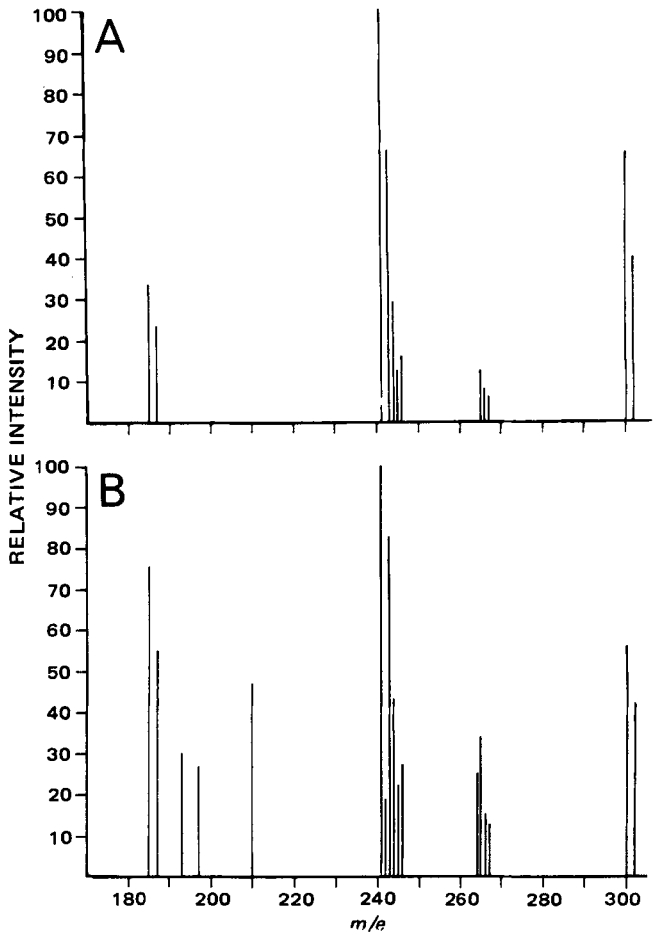

Figure 2—*Mass spectra of methyl ester derivative of fenclorac standard (A) and derivatized extract of plasma obtained from human subjects treated with fenclorac (B).*

two or more prominent ions (*m/e* 300/302 and 241/243) characteristic of fenclorac methyl ester were found to have an intensity greater than twice the intensity observed for the same mass ions in background spectra.

Drug Administration to Humans—Six healthy, normal, male volunteers[7] were administered 200 mg of ^{14}C-fenclorac (specific activity of 0.155 μCi/mg). The subjects, 21–50 years old and 77–86 kg, were fasted for 18 hr prior to receiving a 200-ml dose of a fenclorac solution. Heparinized blood specimens were obtained at appropriate time intervals, and plasma was prepared by centrifugation at 2000×*g* for 10 min. The plasma was frozen immediately and stored at −20° prior to analysis.

Analysis of Radioactivity in Plasma—The determination of radioactivity in plasma samples was described previously (5).

RESULTS AND DISCUSSION

Derivatives of Fenclorac—The trimethylsilyl esters of I and II are readily formed by the use of the derivatizing reagent *N,O*-bis(trimethylsilyl)acetamide[8]. The reaction is complete within 2 min, and the derivatives are stable for up to 8 hr. Peak loss due to nonspecific column adsorption (particularly I) occurs; to obtain linearity, the column must be saturated by multiple injections of I (7).

The methyl ester derivatives of I and II were evaluated by use of the derivatizing reagents boron trifluoride–methanol, hydrochloric acid–methanol, and diazomethane. Under the conditions investigated, the hydrochloric acid–methanol and diazomethane procedures resulted in quantitative production of the methyl esters of I and II, while nonquantitative conversion was obtained with the boron trifluoride–methanol procedure. The kinetics of ester formation were followed using

[5] I.E.C. model K.
[6] Florisil.

[7] Study conducted by Medical and Technical Research Associates at the Massachusetts Correctional Institute, Norfolk, Mass. Informed written consent was obtained.
[8] Pierce Chemical Co., Rockford, Ill.

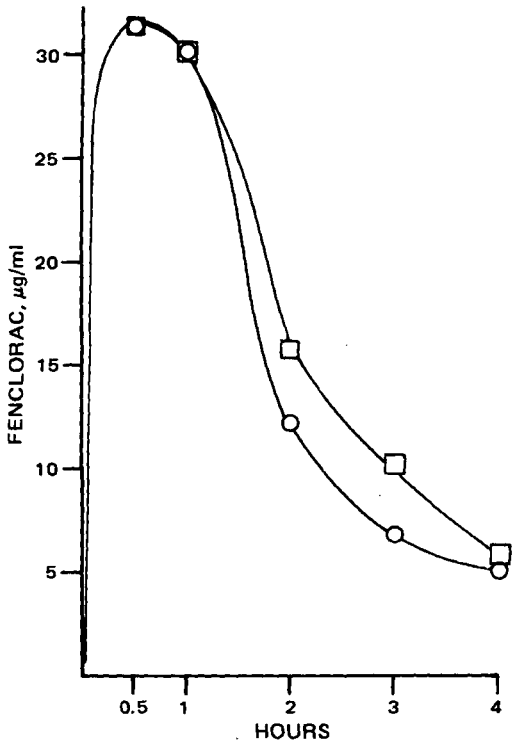

Figure 3—*Plasma fenclorac levels in humans measured by the radioactive (□) and GLC (○) methods.*

^{14}C-labeled I and II and radiochemical TLC. For simplicity, the hydrochloric acid–methanol reflux was used to derivatize I and II for sample analysis.

Analysis of Plasma—The GLC analysis of control human plasma that was carried through the derivatization and extraction procedures is presented in Fig. 1A; very little endogenous plasma constituents could be detected. Figure 1B is a gas chromatogram of the methyl esters of fenclorac (I) and the internal standard (II). The chromatogram was prepared by adding fenclorac and the internal standard to control plasma, which was then carried through the derivatization and extraction procedures. Both fenclorac and the internal standard methyl ester peaks were symmetrical and had retention times of 3.3 and 8.0 min, respectively, at 225°. Plasma samples prepared in this manner were stable for at least 1 week at room temperature.

Assay Sensitivity and Specificity—The standard curve is linear over a plasma concentration range of 0.2–32 μg of fenclorac free acid/ml. Adequate day-to-day reproducibility was indicated by the consistency of the slopes of the standard curves over 4 weeks. The coefficient of variation (*CV*) ranged from 5 to 8%. GLC–mass spectrometric analysis of plasma from drug-treated subjects confirmed that peak I was the fenclorac methyl ester (Fig. 2).

Table I—Recovery of ^{14}C-Fenclorac from Plasma

Plasma Concentration, μg/ml	Recovery, %
0	0
2	84
4	82
8	85
16	81
32	82
Mean ± *SD*	82 ± 1.6

Recovery of Fenclorac from Plasma—Known concentrations of ^{14}C-fenclorac in ethanol were added to pooled normal human plasma. The samples were derivatized, extracted, and concentrated as described under *Experimental*. The mean recovery of added ^{14}C-fenclorac was 82 ± 1.6% over a range of 2–32 μg of compound/ml (Table I).

Analysis of Human Plasma Samples—GLC and analysis of radioactivity were performed on plasma samples obtained from human subjects who received 200 mg of fenclorac. The GLC analysis and total ^{14}C-fenclorac (acid) equivalents were nearly identical for up to 1 hr after oral dosing. From 1 to 4 hr postdose, the GLC analysis was consistently lower than the total radioactivity. This discrepancy could be due to small quantities of circulating metabolite (5) or experimental error.

A typical analysis of human plasma level data is presented in Fig. 3. Analysis of human urine for fenclorac indicated the absence of intact drug. This result was expected since fenclorac is completely biotransformed prior to excretion (5).

REFERENCES

(1) G. W. Nuss, R. D. Smyth, C. H. Breder, M. J. Hitchings, and N. H. Reavey-Cantwell, *Agents Actions*, **6**, 735 (1976).

(2) G. W. Nuss, R. D. Smyth, C. H. Breder, M. J. Hitchings, and N. H. Reavey-Cantwell, *Clin. Res.*, **23**, 584 (1975).

(3) G. W. Nuss, R. D. Smyth, C. H. Breder, M. J. Hitchings, G. N. Mir, and N. H. Reavey-Cantwell, *Fed. Proc.*, **35**, 774 (1976).

(4) R. D. Smyth, A. Polk, A. F. DeLong, R. K. Nayak, and N. H. Reavey-Cantwell, *Clin. Res.*, **23**, 585A (1975).

(5) A. F. DeLong, R. D. Smyth, A. Polk, R. K. Nayak, G. Martin, G. H. Douglas, and N. H. Reavey-Cantwell, *Drug Metab. Dispos.*, **5**, 122 (1977).

(6) J. K. Lee, R. D. Smyth, A. Polk, T. Herczeg, C. T. Tsuei, and N. H. Reavey-Cantwell, *J. Pharm. Sci.*, **66**, 832 (1977).

(7) A. J. Visalli, D. M. Patel, and N. H. Reavey-Cantwell, *ibid.*, **65**, 1686 (1976).

Inhibitors of Polyamine Biosynthesis VI: 2,5-Diamino-2-(cyanomethyl)pentanoic Acid, a Potential Irreversible Inhibitor of Ornithine Decarboxylase

MAHMOUD M. ABDEL-MONEM ˣ **and EZZAT A. MIKHAIL**

Received September 12, 1977, from the *College of Pharmacy, University of Minnesota, Minneapolis, MN 55455.* Accepted for publication November 17, 1977.

Abstract □ (±)-2,5-Diamino-2-(cyanomethyl)pentanoic acid was obtained by the reaction of chloroacetonitrile with the anion obtained by treatment of 3-(benzylideneamino)-2-piperidinone with sodium hydride, followed by hydrolysis in the presence of trifluoroacetic anhydride. The target compound was isolated as the monohydrochloride salt of the lactam. The compound was synthesized as a potential irreversible inhibitor of the enzyme L-ornithine decarboxylase by the mechanism generally known as suicide or K_{cat} inhibition. The synthesized compound produced no inhibition of the enzyme ornithine decarboxylase obtained from rat prostate gland. The inactivity of the target compound is attributed to the hydrophilicity of the cyanomethyl group.

Keyphrases □ (±)-2,5-Diamino-2-(cyanomethyl)pentanoic acid—synthesized, effect on ornithine decarboxylase activity evaluated □ Ornithine decarboxylase activity—effect of (±)-2,5-diamino-2-(cyanomethyl)pentanoic acid □ Pentanoic acid, substituted—synthesized, effect on ornithine decarboxylase activity evaluated □ Enzyme activity—ornithine decarboxylase, effect of (±)-2,5-diamino-2-(cyanomethyl)pentanoic acid □ Structure-activity relationships—(±)-2,5-diamino-2-(cyanomethyl)pentanoic acid, effect on ornithine decarboxylase activity evaluated

Previous reports (1–10) described the synthesis and evaluation of specific inhibitors of the enzyme L-ornithine decarboxylase. The present report describes the synthesis of 2,5-diamino-2-(cyanomethyl)pentanoic acid (VI) and its evaluation as a potential irreversible inhibitor of ornithine decarboxylase from rat prostate gland.

The rationale for the synthesis of VI was based on its potential to produce irreversible inhibition of ornithine decarboxylase, a pyridoxal phosphate enzyme, by the mechanism shown in Scheme I. This mechanism is similar to that proposed for the irreversible inhibition of collagen cross-linking enzymes by β-aminopropionitrile (11).

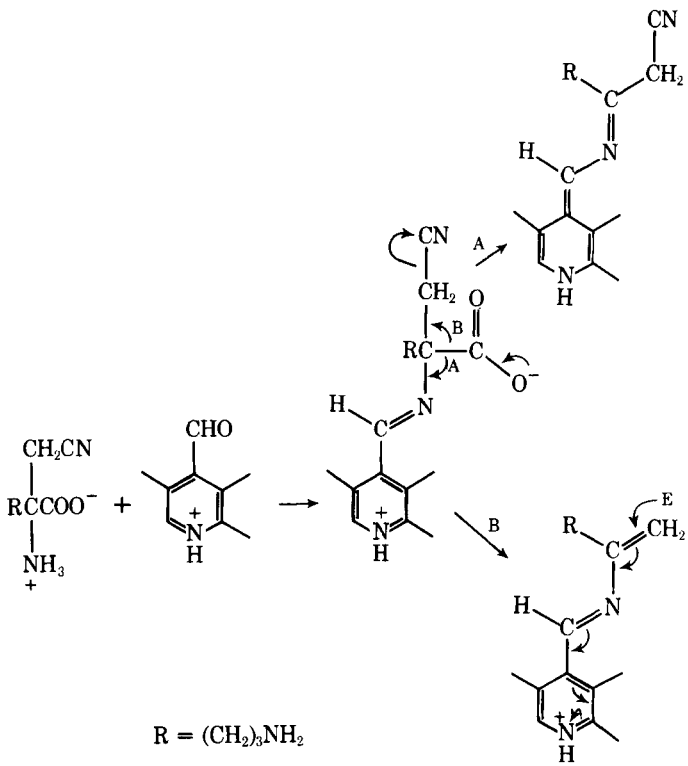

Scheme I

EXPERIMENTAL[1]

Melting points were determined in open capillary tubes and are uncorrected. NMR spectra were taken in deuterochloroform or deuterium oxide, with tetramethylsilane or sodium 2,2-dimethyl-2-silapentane-5-sulfonate as the internal standard, respectively. Mass spectral analyses were performed at 70 ev with a 200° chamber temperature.

3-(Benzylideneamino)-3-(cyanomethyl)-2-piperidinone (II) and 1-(Cyanomethyl) -3- (benzylideneamino) -3- (cyanomethyl)-2-piperidinone (III)—Sodium hydride (0.48 g, 0.01 mole of 50% oil dispersion) was added with stirring to dry tetrahydrofuran (50 ml). A solution of 3-benzylideneamino-2-piperidinone (I, Scheme II) (2.02 g, 0.01 mole) in tetrahydrofuran (80 ml) was added to the suspension. The reaction mixture was heated under reflux for 2 hr, and the reddish solution obtained was cooled to room temperature. Chloroacetonitrile (0.755 g, 0.01 mole) in tetrahydrofuran (10 ml) was added; the mixture was stirred overnight, whereupon its color changed to turbid yellow.

The mixture was filtered through diatomaceous earth[2], and the filtrate was concentrated under reduced pressure at 45°. The residue (2.9 g) was boiled with two separate 300-ml portions of dry benzene, and the combined benzene extract was filtered and concentrated under reduced pressure to 15 ml. The concentrated solution was immediately chromatographed on 15 silica gel plates (20 × 20 cm, 500 μm), using methylene chloride–acetone (8.4:1.6). Zones of R_f 0.3 (II) and 0.7 (III) were separately

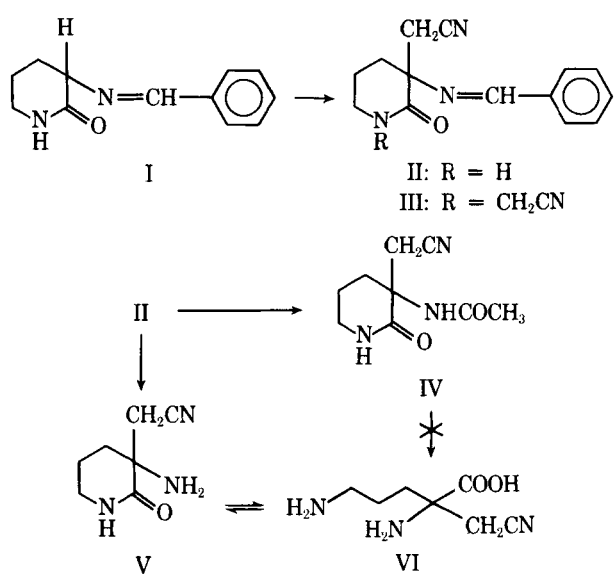

Scheme II

[1] A Thomas-Hoover melting-point apparatus, a Perkin-Elmer 237 or Beckman IR-9 spectrophotometer, a Varian A-60 D NMR spectrometer, an AEI MS-30 mass spectrometer, and a Beckman LS-100C liquid scintillation counter were used. Elemental analysis was performed by MHW Laboratories, Garden City, Mich.

[2] Celite.

0022-3549/78/0800-1174$01.00/0
© 1978, American Pharmaceutical Association

scraped into a sintered-glass funnel, and each was eluted with a mixture of 5% methanol in ethyl acetate (400 ml). The solvent was removed *in vacuo* at 50°, and the oily residue obtained from the R_f 0.3 zone (II) was immediately utilized for the synthesis of V.

Analytical samples of II and III were prepared by rechromatography, and the purified samples were dried *in vacuo* for 48 hr. The yield of crude II was 1.1 g (45.8%); IR (neat): 3300, 2295, 1660, 1575, 750, and 695 cm^{-1}; NMR (deuterochloroform, tetramethylsilane): δ 2.0 (m, 4H), 2.84 (s, 2H), 3.3 (m, 2H), 6.72 (s, 1H), 7.25 and 7.6 (m, 5H), and 8.1 (s, 1H) ppm; high-resolution mass spectrum: 241.1233 (M^+) and 242.1310 (M + 1).

Anal.—Calc. for $C_{14}H_{15}N_3O$: C, 69.73; H, 6.22; N, 17.42. Found: C, 69.89; H, 6.50; N, 16.93.

The yield of crude III was 0.6 g (21.4%); IR (neat): 2265, 2195, 1710, 1610, and 1591 cm^{-1}; NMR (deuterochloroform, tetramethylsilane): δ 4.25 (q, 2H, J = 14 Hz), 8.0 (s, 1H), 2.1 (m, 4H), 2.85 (s, 2H), 3.44 (m, 2H), 7.25, and 7.6 (m, 5H) ppm; mass spectrum: *m/e* 281, 241, 240, 213, 212, and 177 (base peak).

Anal.—Calc. for $C_{16}H_{16}N_4O$: C, 68.57; H, 5.70; N, 20.00. Found: C, 68.37; H, 5.89; N, 19.93.

3-Acetamido-3-(cyanomethyl)-2-piperidinone (IV)—A solution of II (0.12 g, 5 mmoles) in acetic acid (5.0 ml) was heated on a water bath at 60–70° for 30 min. Acetic anhydride (5.0 ml) was added, and the mixture was heated at 50–60° for 45 min. Water (10 ml) was added, and the solution was heated at 80–90° for 1 hr, cooled to room temperature, and extracted with methylene chloride (3 × 10 ml). The aqueous solution was evaporated to dryness under reduced pressure. The residue was triturated with dry ether, and the formed solid was filtered and recrystallized from absolute ethanol–ether (2:1) to afford IV (60 mg, 61% yield), mp 212–214°.

Anal.—Calc. for $C_9H_{13}N_3O_2$: C, 55.37; H, 6.71; N, 21.50. Found: C, 55.45; H, 6.55; N, 21.29.

3-Amino-3-(cyanomethyl)-2-piperidinone Hydrochloride (V)—A solution of II (0.12 g, 5 mmoles) in trifluoroacetic anhydride (5.0 ml) and chloroform (10 ml) was heated under reflux in an oil bath at 70–80° for 1 hr. The reaction mixture was cooled to room temperature and concentrated under vacuum. The residue was treated with dilute hydrochloric acid (10 ml), and the mixture was heated at 40–50° for 30 min, cooled to room temperature, and extracted with methylene chloride. The aqueous solution was evaporated to dryness under reduced pressure.

The formed solid was boiled with absolute ethanol (20 ml) and filtered while hot, and butyl ether (about 10 ml) was added until a slight turbidity was observed. The solution was stored at −20° for 7 days to afford 73.0 mg (76% yield) of V, mp 194–195°; IR (potassium bromide pellet): 3400, 3300, 2650, 3225, 2240, and 1680 cm^{-1}; NMR (deuterochloroform, tetramethylsilane): δ 1.95, 2.20 (d of d, 4H), 216 (m, 4H), 8.4 (s, 1H), and 8.9 (s, 2H) ppm; high-resolution mass spectrum: 153.0892, 152.0813, and 154.0973 emu.

Anal.—Calc. for $C_7H_{12}ClN_3O$: C, 44.32; H, 6.33; N, 22.16. Found: C, 44.33; H, 6.32; N, 22.51.

RESULTS AND DISCUSSION

The target compound I was obtained using the synthesis shown in Scheme II. Compound I was prepared following the procedure described by Abdel-Monem *et al.* (2). It was reacted with sodium hydride, followed by alkylation with chloroacetonitrile to provide the desired product (II) together with III. The ratio of II to III in the product was increased when equimolar molar amounts of the reactants were used.

1-(Cyanomethyl)-3-(benzylideneamino)-2-piperidinone, which would be obtained by *N*-alkylation of I, was not detected in the reaction products, indicating the much greater acidity of the C-3 proton relative to the lactam proton. Compound III is probably formed by the *N*-alkylation of the anion generated from II. The acidity of the lactam proton in II is greater than that in I because of the electron-withdrawing effect of the cyanomethyl substituent at the C-3 position.

Compounds II and III were obtained separately from the mixture of products by preparative TLC, and their identity was confirmed by NMR spectroscopy. The NMR spectrum of III in deuterated chloroform was characterized by the absence of the lactam NH proton, which appeared as a broad singlet at δ 6.72 ppm in the spectrum of II. It also displayed an *AB* quartet centered at δ 4.25 ppm (J = 14 Hz), integrating for two protons, and was assigned to the *N*-cyanomethylene protons. This quartet was absent in the spectrum of II. The two protons of the cyanomethylene group on C-3 appeared as a sharp singlet at δ 2.84 ppm in the spectra of II and III.

Attempts to cleave the benzylidene group by the action of aqueous hydrochloric acid on II to provide the target compound VI were unsuccessful and resulted in the formation of polymers. It was rationalized that the cleavage of the benzylidene group in the presence of an acylating agent might prevent the formation of polymeric products. Indeed, heating II with a mixture of acetic anhydride and acetic acid, followed by the addition of dilute hydrochloric acid, provided IV. Attempts to cleave the acetamido group without the hydrolysis of the cyanomethyl group were not successful. The cleavage of the benzylidene group was also achieved by heating II with trifluoroacetic anhydride under reflux, followed by the addition of dilute hydrochloric acid. However, crystallization of the crude product provided only lactam V and not the expected VI dihydrochloride.

Golankiewicz and Wiewiorowski (12) reported that 3-amino-2-piperidinone was present in equilibrium with 2,5-diaminopentanoic acid in aqueous solutions over pH 3–13 and that the equilibrium was more shifted toward the amino acid at higher pH values. These findings suggest that V will be present in equilibrium with VI in aqueous solutions at pH 7.4. Accordingly, V was used for further biological testing.

Inhibition by V of the enzymatic decarboxylation of L-ornithine by ornithine decarboxylase was measured using extracts of rat prostate glands. The procedures for the tissue extract preparation, enzyme purification, and enzymatic activity assay were described previously (1). In the presence of 2.0×10^{-6} *M* pyridoxal phosphate, the ornithine decarboxylase activity obtained from rat prostate glands had an apparent K_m for L-ornithine of 4.7×10^{-5} *M* and V_{max} value of 0.22 nmole of carbon dioxide/mg of wet tissue/hr. Addition of V in concentrations varying from 1.0×10^{-6} to 1.0×10^{-3} *M* did not suppress the production of ^{14}C-carbon dioxide. Under the same conditions, addition of α-methyl-(±)-ornithine monohydrochloride (1) in concentrations varying from 8.7×10^{-6} to 2.7×10^{-4} *M* significantly suppressed the production of ^{14}C-carbon dioxide. The K_i for α-methyl-(±)-ornithine monohydrochloride was calculated to be 2.0×10^{-5} *M*.

The lack of inhibitory action of V on the enzymatic decarboxylation of L-ornithine was unexpected. The steric bulk of the cyanomethyl group is similar to that of the ethyl group, and replacement of the α-hydrogen in (±)-ornithine with an ethyl group resulted in a compound that retained the necessary features for binding to the active site of the enzyme (2). Therefore, the lack of activity of V could not be attributed to steric interference of the cyanomethyl substituent with binding to the enzyme active site.

In the majority of the previously studied inhibitors of ornithine decarboxylase, the α-hydrogen of the substrate L-ornithine was replaced by an electron-donating hydrophobic alkyl or benzyl group. In VI, the replacement of the α-hydrogen of ornithine with a cyanomethyl group was expected to have opposite effects since this group is hydrophilic and produces a slight electron-withdrawing inductive effect. The inactivity of Compound VI underscores the essentiality of a lipophilic substituent at the α-position of the substrate for enzyme binding. The possible contribution of electronic factors to the inactivity of V could not be ruled out.

REFERENCES

(1) M. M. Abdel-Monem, N. E. Newton, and C. E. Weeks, *J. Med. Chem.*, **17**, 447 (1974).

(2) M. M. Abdel-Monem, N. E. Newton, B. C. Ho, and C. E. Weeks, *ibid.*, **18**, 600 (1975).

(3) M. M. Abdel-Monem, N. E. Newton, and C. E. Weeks, *ibid.*, **18**, 945 (1975).

(4) N. E. Newton and M. M. Abdel-Monem, *ibid.*, **20**, 249 (1977).

(5) C. E. Weeks and M. M. Abdel-Monem, *J. Pharm. Sci.*, **66**, 1586 (1977).

(6) J. J. Ellington and I. L. Honigberg, *J. Org. Chem.*, **39**, 104 (1974).

(7) S. I. Harik and S. H. Snyder, *Biochim. Biophys. Acta*, **327**, 501 (1973).

(8) N. Relyea and R. R. Rando, *Biochem. Biophys. Res. Commun.*, **67**, 392 (1975).

(9) J. S. Heller, E. S. Canellakis, D. L. Bussolotti, and J. K. Coward, *Biochim. Biophys. Acta*, **403**, 197 (1975).

(10) P. S. Mamont, P. Bohlen, P. P. McCann, P. Bey, R. Schuber, and C. Tardif, *Proc. Natl. Acad. Sci. USA*, **73**, 1626 (1976).

(11) R. R. Rando, *Acc. Chem. Res.*, **8**, 281 (1975).

(12) K. Golankiewicz and M. Wiewiorowski, *Acta Biochem. Pol.*, **10**, 443 (1963).

ACKNOWLEDGMENTS

The authors thank Dr. Nancy E. Newton for performing the enzyme assays.

Formation of Thermally Stable Derivatives of Chlordiazepoxide and Its Desmethyl Metabolite for GLC

H. P. GELBKE [x] **and H. J. SCHLICHT**

Received September 22, 1977, from the *Institut für Rechtsmedizin der Universität Heidelberg, Vosstrasse 2, D-6900 Heidelberg, Federal Republic of Germany.* Accepted for publication November 7, 1977.

Abstract □ A derivatization procedure is described for the GLC determination of subnanogram amounts of chlordiazepoxide and nanogram amounts of *N*-desmethylchlordiazepoxide. Treatment with acetic anhydride at elevated temperature eliminates the highly polar and unstable nitrone group of these compounds by rearrangement and acetylation. The mass spectrometric fragmentation pattern of the acetyl derivatives is recorded and interpreted.

Keyphrases □ Chlordiazepoxide—and desmethyl metabolite, derivatization and GLC analyses, bulk drug □ GLC—analyses, chlordiazepoxide and desmethyl metabolite, bulk drug □ Sedatives—chlordiazepoxide and desmethyl metabolite, derivatization and GLC analyses, bulk drug

Although chlordiazepoxide has been used, and sometimes even abused, for many years for the treatment of anxiety, the analytical procedures for its determination in biological material are sometimes unsatisfactory for forensic purposes with respect to practicability, specificity, and/or sensitivity.

BACKGROUND

After publication of a colorimetric assay employing the Bratton–Marshall chromophore (1, 2), several spectrometric procedures were described for the determination of chlordiazepoxide in body fluids with (3, 4) and without (3, 5–8) prior hydrolytic cleavage to the benzophenone derivative. Due to the limited sensitivity of these spectrometric methods, a spectrofluorometric assay was developed (9) and modified (10) for use in pharmacokinetic investigations. Another fluorometric procedure, using fluorophore formation with fluorescamine after acid hydrolysis of chlordiazepoxide, is not sufficiently sensitive for the analysis of biological samples after single-dose administration (11).

Based on several investigations (12, 13), dc polarographic methods were developed for toxicological purposes (14, 15). Later (16), differential pulse polarography was used to measure therapeutic plasma concentrations. A highly sensitive radioimmunoassay (17) also was reported for chlordiazepoxide. Recently (18), benzodiazepines, including chlordiazepoxide, were determined in body fluids by high-pressure liquid chromatography, but the lower detection limit was only 5 μg/ml.

With respect to sensitivity, practicability, specificity, versatility, and general availability to forensic laboratories, GLC is the procedure most suited for identification and quantitation of chlordiazepoxide in biological material. A GLC method for its determination after acid hydrolysis was described (19), but the method lacks specificity because of the measurement of the benzophenone derivative, which also is formed from other benzodiazepines and their metabolites. Several workers also reported GLC data for chlordiazepoxide (20–22), and two procedures for its determination in serum were published (23, 24).

On the other hand, Van der Kleijn *et al.* (25) were not able to measure chlordiazepoxide by GLC, and McMartin and Street (26) observed two GLC peaks for this compound, presumably due to decomposition. Sadée and Van der Kleijn (27) stated that N^4-oxides of benzodiazepines are thermally labile under GLC conditions. Butterfield *et al.* (28) and de Silva *et al.* (29) thoroughly investigated the analysis of benzodiazepines and stated that GLC of chlordiazepoxide does not yield reproducible results. Since similar difficulties were observed in this laboratory, a procedure for derivatization of chlordiazepoxide is presented, enabling the determination of nanogram amounts by GLC.

EXPERIMENTAL

A 100-μl aliquot of freshly prepared methanolic chlordiazepoxide hydrochloride (10–10,000 ng/ml) was evaporated to dryness under a nitrogen stream. Approximately 200 μl of acetic anhydride (p.a. grade) was then added; after thorough mixing, the solution was heated at 100° for 5–10 min. The reagent was removed at room temperature under a nitrogen stream, and the residue was dissolved in an appropriate amount of methanol or hexane.

The gas chromatograph was equipped with ^{63}Ni-electron-capture and nitrogen-sensitive detectors (coiled glass tubes, 180 × 0.3 cm). The stationary phase was 3% SE-30 on 80–100-mesh Chromosorb W/AW-DMCS, the carrier gas was 40 ml of helium/min, and the electron-capture detector purge gas was 70 ml of argon–methane (95:5)/min. The column temperature was 255°, the injection port temperature was 270°, the detector temperature was 310°, and the retention time was 4 min.

Mass spectra were obtained using a gas chromatograph–mass spectrometer with electron-impact ionization.

RESULTS AND DISCUSSION

It can be assumed that the unsatisfactory GLC characteristics of chlordiazepoxide (I) stem from the N^4-oxide group with its thermal instability (27) and high polarity. Therefore, a suitable derivatization procedure should eliminate the nitrone structure. Two procedures were investigated: (*a*) reduction of the nitrone with phosphorus trichloride (30) and (*b*) combined acetylation and rearrangement by treatment with acetic anhydride at elevated temperature (31, 32) as shown in Scheme I. The latter reaction, which was also proposed by Sadée and van der Kleijn (27) for GLC of *N*-methyldemoxepam (without further details being given), yielded satisfactory results and was systematically investigated.

To establish optimal conditions for derivatization, 100, 200, 500, and 1000 ng of I were treated with acetic anhydride (~200 μl) at 100° for 2, 5, 10, 15, 20, and 30 min. The reaction mixture was evaporated to dryness at room temperature under a stream of nitrogen, and the residue was dissolved in 50 or 100 μl of methanol or hexane for GLC. Optimal yields of the acetylated derivatives were obtained for reaction times of 5–10 min, but virtually all of the material was decomposed after 30 min. Formation of the acetylated product was not observed after treatment of I with acetic anhydride at room temperature for 10–60 min.

For structure elucidation, the acetylated product was subjected to GLC–mass spectrometry. The following fragmentation pattern was found: *m/e* 323 (100%, II − CH_3COOH) and 324 (91%, II − CH_3COO) and the corresponding isotope peaks at *m/e* 325 (52%) and 326 (36%). Further fragmentation was negligible, and the M^+ peak was not observed for electron energies varying between 7 and 70 ev.

The lower detection limit for GLC of I after acetylation (SE-30, helium carrier gas, electron-capture detection) was better than 50 pg; under the same conditions without prior derivatization, only 1 ng of I could be detected. Without derivatization, I exhibited broad and unreproducible peaks with helium as the carrier gas. With nitrogen or argon–methane

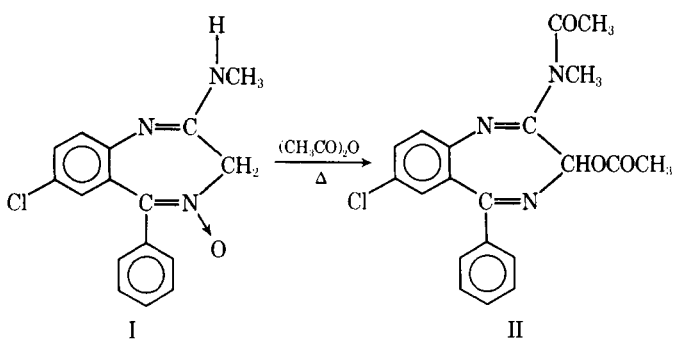

I II

Scheme I

0022-3549/78/0800-1176$01.00/0
© 1978, American Pharmaceutical Association

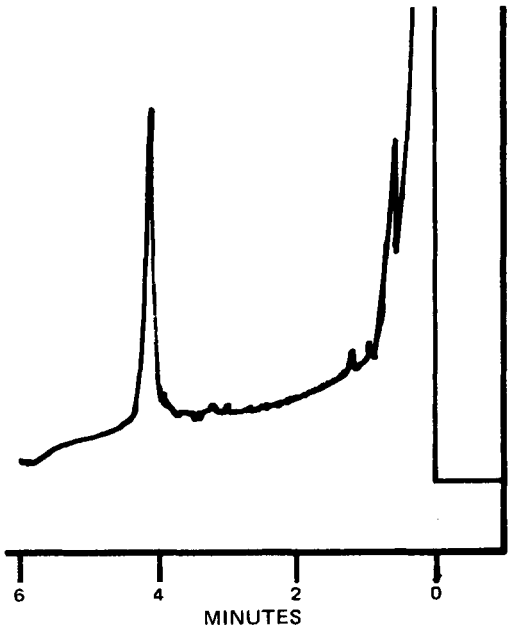

Figure 1—*Gas chromatogram of chlordiazepoxide (100 pg) after acetylation.*

(95:5), GLC was nearly impossible. In contrast, after acetylation, sharp GLC peaks were obtained with helium (Fig. 1) and the use of nitrogen or argon–methane (95:5) led only to a slight peak broadening and an insignificant decrease of sensitivity.

Fifteen samples containing 200 ng of I were acetylated as described. The coefficient of variation of the GLC peaks was ±6.2%; an internal standard was not used. The GLC responses strictly paralleled the amounts of I when 50–1500 ng of I was subjected to GLC after derivatization.

The derivatization procedure described also was applied successfully to *N*-desmethylchlordiazepoxide but not to demoxepam, the corresponding lactam. The lower detection limit for *N*-desmethylchlordiazepoxide after acetylation was about 0.5 ng when subjected to the same GLC conditions as the acetylated derivative of I. The following fragmentation pattern was observed for the diacetyl derivative of *N*-desmethylchlordiazepoxide by GLC–mass spectrometry (electron energies of 20 and 70 ev): *m/e* 369 (M^+, 24%), 327 ($M^+ - CH_2CO$, 23%), 309 ($M^+ - CH_3COOH$, 42%), 298 ($M^+ - CH_2CO - HCO$, 100%), 284 ($M^+ - CH_2CO - CH_3CO$, 57%), 256 ($M^+ - CH_2CO - CH_3CO - CO$, 100%), and 239 (55%). All of these peaks exhibited isotope peaks because of the chlorine atom. This fragmentation pattern corresponds to the ones described by Sadée (33) for 3-acetoxy derivatives of 1,4-benzodiazepin-2-ones but is in contrast to that of I after acetylation.

REFERENCES

(1) J. Bäumler and S. Rippstein, *Helv. Chim. Acta*, **44**, 2208 (1961).

(2) L. O. Randall, *Dis. Nerv. Syst.*, **22** (Suppl. 7), 1 (1961).

(3) K. Besserer, S. Henzler, E. Kohler, and H. J. Mallach, *Arzneim.-Forsch.*, **21**, 2003 (1971).

(4) P. Jatlow, *Clin. Chem.*, **18**, 516 (1972).

(5) D. Smyth and G. W. Pennington, *Arch. Int. Pharmacodyn. Ther.*, **145**, 154 (1963).

(6) G. Kamm and R. Baier, *Arzneim.-Forsch.*, **19**, 213 (1969).

(7) C. S. Frings and P. S. Cohen, *Am. J. Clin. Pathol.*, **56**, 216 (1971).

(8) A. R. E. N. Ossman and A. El Hassany, *Pharmazie*, **31**, 744 (1976).

(9) B. A. Koechlin and L. D'Arconte, *Anal. Biochem.*, **5**, 195 (1963).

(10) M. A. Schwartz and E. Postma, *J. Pharm. Sci.*, **55**, 1358 (1966).

(11) J. T. Stewart and J. L. Williamson, *Anal. Chem.*, **48**, 1182 (1976).

(12) H. Oelschläger, *Arch. Pharm.*, **296**, 396 (1963).

(13) B. Z. Senkowski, M. S. Levin, J. R. Urbigkit, and E. G. Wollish, *Anal. Chem.*, **36**, 1991 (1964).

(14) G. Cimbura and R. C. Gupta, *J. Forensic Sci.*, **10**, 228 (1965).

(15) E. Jacobsen and T. V. Jacobsen, *Anal. Chim. Acta*, **55**, 293 (1971).

(16) M. R. Hackman, M. A. Brooks, J. A. F. de Silva, and T. S. Ma, *Anal. Chem.*, **46**, 1075 (1974).

(17) W. R. Dixon, J. Early, and E. Postma, *J. Pharm. Sci.*, **64**, 937 (1975).

(18) K. Harzer and R. Barchet, *J. Chromatogr.*, **132**, 83 (1977).

(19) J. A. F. de Silva, M. A. Schwartz, V. Stefanovic, J. Kaplan, and L. D'Arconte, *Anal. Chem.*, **36**, 2099 (1964).

(20) L. Kazyak and E. C. Knoblock, *ibid.*, **35**, 1449 (1963).

(21) H. L. Thompson and W. J. Decker, *Am. J. Clin. Pathol.*, **49**, 103 (1968).

(22) H. F. Proelss and H. J. Lohmann, *Clin. Chem.*, **17**, 222 (1971).

(23) I. A. Zingalis, *J. Chromatogr.*, **61**, 237 (1971).

(24) F. L. Vandemark and R. F. Adams, *Chromatogr. Newsl.*, **5**, 4 (1977).

(25) E. Van der Kleijn, G. C. Beelen, and M. A. Frederick, *Clin. Chim. Acta*, **34**, 345 (1971).

(26) C. McMartin and H. V. Street, *J. Chromatogr.*, **22**, 274 (1966).

(27) W. Sadée and E. Van der Kleijn, *J. Pharm. Sci.*, **60**, 135 (1971).

(28) A. G. Butterfield, F. F. Matsui, S. J. Smith, and R. W. Sears, *ibid.*, **66**, 684 (1977).

(29) J. A. F. de Silva, I. Bekersky, C. V. Puglisi, M. A. Brooks, and R. E. Weinfeld, *Anal. Chem.*, **48**, 10 (1976).

(30) L. H. Sternbach, E. Reeder, O. Keller, and W. Metlesics, *J. Org. Chem.*, **26**, 4488 (1961).

(31) S. C. Bell and S. J. Childress, *ibid.*, **27**, 1691 (1962).

(32) L. H. Sternbach, E. Reeder, A. Stempel, and A. I. Rachlin, *ibid.*, **29**, 332 (1964).

(33) W. Sadée, *J. Med. Chem.*, **13**, 475 (1970).

ACKNOWLEDGMENTS

The authors thank Dr. B. Spiegelhalder, Heidelberg, Federal Republic of Germany, for recording and interpreting the mass spectra.

Effect of Changes in Intercompartment Rate Constants on Drug Removal during Hemoperfusion

THOMAS P. GIBSON *[x] and ARTHUR J. ATKINSON, Jr.[‡]

Received August 16, 1977, from the *Section of Nephrology/Hypertension, Department of Medicine, Northwestern University Medical School, Chicago, IL 60611, the Renal Section, [x]V. A. Lakeside Hospital, Chicago, IL 60611, and the [‡]Departments of Medicine and Pharmacology, Northwestern University Medical School, Chicago, IL 60611. Accepted for publication November 18, 1977.

Abstract □ A computer simulation of the effect of changing intercompartment clearance rates on drug removal during hemoperfusion was undertaken. As intercompartment clearance slowed, the fall in plasma levels increased and postperfusion rebound increased, but the total drug removed decreased.

Keyphrases □ Drug removal—during hemoperfusion, effect of changing intercompartment clearance rates, computer simulation □ Clearance rates, intercompartment—effect of changing on drug removal during hemoperfusion, computer simulation □ Pharmacokinetic models—drug removal during hemoperfusion, effect of changing intercompartment clearance rates, computer simulation □ Models, pharmacokinetic—drug removal during hemoperfusion, effect of changing intercompartment clearance rates, computer simulation

Recently (1), the kinetics of intravenous digoxin in dogs before, during, and after resin hemoperfusion were described. There was a rapid curvilinear decline in serum digoxin levels during resin hemoperfusion; but, when hemoperfusion was stopped, serum digoxin levels increased. By 4 hr after hemoperfusion, the increase in digoxin levels was complete. Thereafter, the slope of elimination paralleled the preperfusion slope. A three-compartment open mammillary model (Scheme I) adequately described the kinetics of digoxin distribution and elimination before perfusion, the decline of serum levels during perfusion, and the rebound of digoxin levels after perfusion.

The average volume of distribution, V_d, of digoxin in dogs was found to be 4.3 ± 0.7 liters/kg, most of which (85%) was included in the slowly equilibrating peripheral compartment of the model, V_s (Scheme I). Because the bulk of the body burden of digoxin was sequestered in this large compartment, the effect of changes in the rate of movement of drug from this large compartment, Q_s, to the central compartment, V_c, on the effectiveness of hemodialysis or hemoperfusion was investigated.

EXPERIMENTAL

The experimentally determined pharmacokinetic parameters of one dog are given in Scheme I. For this study, the value of Q_s was either increased or decreased by a factor of 10 from that experimentally observed. Values of V_c, V_s, V_f, Q_F= AND C_h were kept constant, and a simulated perfusion was carried out for 5 hr. For simplicity, C_t was set equal to zero so that concentrations in all model compartments would be equal (18.6 ng/ml) when the distribution equilibrium was reached. All calculations were done with the SAAM 23 program for multicompartment analysis (2).

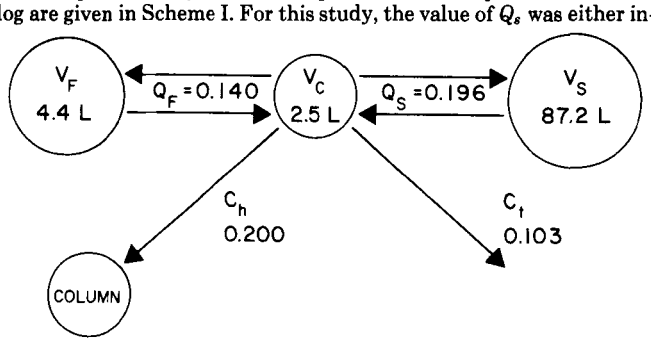

Scheme I—Multicompartment model used to analyze pharmacokinetics of digoxin in dogs. Key: V, volume; Q, intercompartment clearance rate (liters per minute); C, clearance (liters per minute); f, fast; s, slow; c, central; h, hemoperfusion; and t, nonperfusion.

Table I—Changes in Compartment Content of Digoxin with Alterations of Q_s

Parameter	Q_s Fast	Q_s Intermediate	Q_s Slow
Amount removed, μg	777.2	518.9	204.8
Amoung in V_c, μg			
Start	46.5	46.5	46.5
Lowest point	23.8	17.0	4.0
Reequilibration	25.8	32.5	40.5
Amount in V_s, μg			
Start	1621.7	1621.7	1621.7
End	904.7	1182.6	1533.6
Reequilibration	901.4	1140.8	1433.5
Time to 90% reequilibration, min	3	75	705

RESULTS

Results are shown in Fig. 1 and Table I.

In Fig. 1A, Q_s was increased 10-fold over that observed experimentally. With perfusion, there was a linear and concordant fall in digoxin levels in all compartments, much as in a one-compartment model. Although serum digoxin levels only fell from 18.5 to 9.5 ng/ml, 777.2 μg of digoxin was removed (Table I). The postperfusion rebound was 90% complete within 3 min, and levels in V_c reequilibrated at 10.3 ng/ml.

Figure 1B shows the results with the value of Q_s found experimentally. With hemoperfusion, there was a curvilinear decline in serum levels to 6.8 ng/ml. Digoxin levels in V_s and V_f lagged behind the level in V_c, and

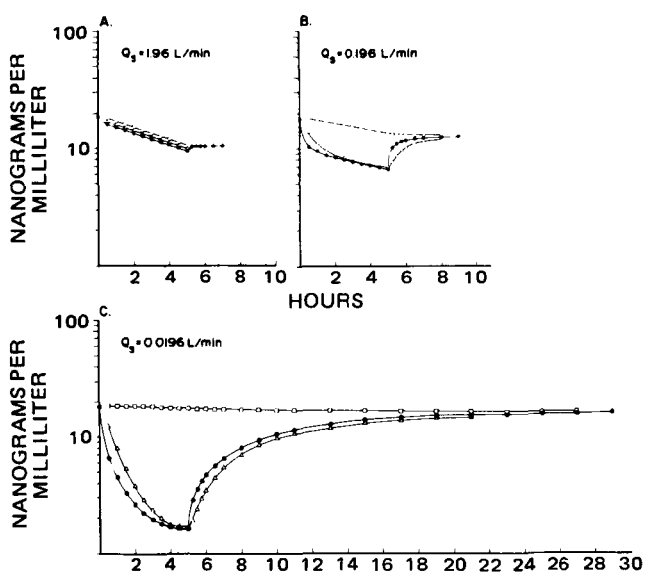

Figure 1—*Effect of altering Q_s on digoxin concentration in V_c (●), V_f (△), and V_s (□) during and after hemoperfusion.*

0022-3549/78/0800-1178$01.00/0
© 1978, American Pharmaceutical Association

only 581.9 μg of digoxin was removed. Seventy-five minutes was required postperfusion before the system reached 90% of equilibration.

In Fig. 1C, Q_s was slowed by a factor of 10. Digoxin levels in V_c and V_f fell rapidly to 1.6 ng/ml, and hemoperfusion in this setting apparently was very effective. However, digoxin levels in V_s fell very slowly, and only 204.8 μg of digoxin was removed. Reequilibration was 90% complete in 705 min.

DISCUSSION

As can be seen in Table I, the amount of digoxin in V_s continued to fall after the completion of perfusion as V_c and V_f were refilled. If the pharmacological effect of digoxin or any other drug takes place in V_s then the adverse effect of those drugs with rapid intercompartment clearances can be rapidly decreased by hemodialysis or hemoperfusion. As Q_s decreases, changes in concentration in V_c will become greater with dialysis or hemoperfusion, but there will be little net reduction in pharmacological effects or total body burden with short perfusion times. However, if the pharmacological effect is in V_c, the toxicity of drugs with slow intercompartment clearances will be rapidly reversed, only to return as this compartment is refilled from V_s.

Schreiner (3) correctly pointed out that the effectiveness of the artificial kidney in removing substances will depend upon the rapid equilibration of the substance with plasma water. However, some nephrologists neglect this fact and feel that V_d *per se* is the rate-limiting factor controlling the effectiveness of drug removal. Clearly, while a large V_d influences the effectiveness of dialysis or hemoperfusion, the rate-limiting step may be the rate of movement of drug from V_s to V_c.

REFERENCES

(1) T. P. Gibson, S. Lucas, H. A. Nelson, A. J. Atkinson, Jr., G. Okita, and P. Ivanovich, *J. Lab. Clin. Med.*, **91**, 673 (1978).

(2) M. Berman and M. F. Weiss, SAAM Manual, PHS Publication 1703, 1967.

(3) G. E. Schreiner, *Arch. Intern. Med.*, **102**, 896 (1958).

ACKNOWLEDGMENTS

Supported by the Medical Research Service of the Veterans Administration and by Grant GM-22371 from the Institute of General Medical Sciences, National Institutes of Health.

A. J. Atkinson, Jr., is a Burroughs Wellcome Scholar in Clinical Pharmacology.

Factors Affecting Homogeneous Precipitation of Aluminum Hydroxide Gel

CARLOS J. SERNA [1], JOE L. WHITE *, and STANLEY L. HEM ‡×

Received November 7, 1977, from the **Department of Agronomy and the* ‡*Industrial and Physical Pharmacy Department, School of Pharmacy and Pharmacal Sciences, Purdue University, West Lafayette, IN 47907.* Accepted for publication December 6, 1977.

Abstract □ The variables affecting homogeneous precipitation in the hydrolysis of aluminum nitrate by sodium carbonate were studied. Increased temperature, decreased concentration of reactants, and decreased rate of addition of titrant favor conditions that achieve homogeneous precipitation. During acid hydrolysis, the nitrate anion was the major anion associated with the gel and only small amounts of carbonate were observed. It is recommended that homogeneous conditions be achieved during the precipitation of aluminum hydroxide gel to improve reproducibility.

Keyphrases □ Aluminum hydroxide gel—factors affecting homogeneous precipitation in hydrolysis of aluminum nitrate by sodium carbonate □ Antacids—aluminum hydroxide gel, factors affecting homogeneous precipitation in hydrolysis of aluminum nitrate by sodium carbonate

The precipitation of aluminum hydroxide gel through the hydrolysis of an aluminum salt is complex. The precipitation method and subsequent treatment have a great effect on the properties of the product (1–4). This variability has been a problem affecting all areas of research and production of aluminum hydroxide gel.

In the titration of aluminum nitrate with sodium hydroxide, polymerization occurs prior to precipitation under homogeneous conditions (5, 6). This was achieved by precipitation under carefully controlled conditions in a specially designed reaction chamber. Precipitation of aluminum hydroxide gel under homogeneous conditions may be important in reducing the variability in precipitation.

Studies were undertaken to determine if homogeneous precipitation conditions could be achieved using standard precipitation equipment. The effect of precipitation variables was then investigated to determine the contribution of each variable in the achievement of a homogeneous reaction.

The system studied was the precipitation of aluminum hydroxide from acidic media (5, 6). However, sodium carbonate was used as the titrant instead of sodium hydroxide because the aluminum hydroxide gels used as antacids usually contain carbonate (7, 8).

EXPERIMENTAL

Potentiometric titrations were performed by placing 100 ml of solution in a 400-ml jacketed beaker. The temperature was controlled to ±0.1°, and the solution was stirred[2] at 2000 rpm. Titrant was added at a controlled rate[3]; the standard rate of addition was 2 ml/min. The solution pH was monitored continuously and recorded. Exact replication of titration curves was obtained when conditions producing homogeneous precipitation were used.

IR analysis[4] (9) was performed on a portion of the aluminum hydroxide, which was washed with three volumes of water to remove excess salts prior to drying under vacuum at room temperature. Spectra were obtained using potassium bromide pellets.

RESULTS AND DISCUSSION

Titration of 0.5 *M* aluminum nitrate by 0.5 *N* NaOH at 22° (Fig. 1)

[1] On leave from Instituto de Edafologia, C.S.I.C., Madrid, Spain.

[2] Stedi-Speed stirrer, Fisher Scientific, Pittsburgh, Pa.

[3] Solution metering pump, model 746, Beckman Instruments, Fullerton, Calif.

[4] Model 180, Perkin-Elmer Corp., Norwalk, Conn.

0022-3549/78/0800-1179$01.00/0
© 1978, American Pharmaceutical Association

only 581.9 μg of digoxin was removed. Seventy-five minutes was required postperfusion before the system reached 90% of equilibration.

In Fig. 1C, Q_s was slowed by a factor of 10. Digoxin levels in V_c and V_f fell rapidly to 1.6 ng/ml, and hemoperfusion in this setting apparently was very effective. However, digoxin levels in V_s fell very slowly, and only 204.8 μg of digoxin was removed. Reequilibration was 90% complete in 705 min.

DISCUSSION

As can be seen in Table I, the amount of digoxin in V_s continued to fall after the completion of perfusion as V_c and V_f were refilled. If the pharmacological effect of digoxin or any other drug takes place in V_s then the adverse effect of those drugs with rapid intercompartment clearances can be rapidly decreased by hemodialysis or hemoperfusion. As Q_s decreases, changes in concentration in V_c will become greater with dialysis or hemoperfusion, but there will be little net reduction in pharmacological effects or total body burden with short perfusion times. However, if the pharmacological effect is in V_c, the toxicity of drugs with slow intercompartment clearances will be rapidly reversed, only to return as this compartment is refilled from V_s.

Schreiner (3) correctly pointed out that the effectiveness of the artificial kidney in removing substances will depend upon the rapid equilibration of the substance with plasma water. However, some nephrologists neglect this fact and feel that V_d *per se* is the rate-limiting factor controlling the effectiveness of drug removal. Clearly, while a large V_d influences the effectiveness of dialysis or hemoperfusion, the rate-limiting step may be the rate of movement of drug from V_s to V_c.

REFERENCES

(1) T. P. Gibson, S. Lucas, H. A. Nelson, A. J. Atkinson, Jr., G. Okita, and P. Ivanovich, *J. Lab. Clin. Med.*, **91**, 673 (1978).

(2) M. Berman and M. F. Weiss, SAAM Manual, PHS Publication 1703, 1967.

(3) G. E. Schreiner, *Arch. Intern. Med.*, **102**, 896 (1958).

ACKNOWLEDGMENTS

Supported by the Medical Research Service of the Veterans Administration and by Grant GM-22371 from the Institute of General Medical Sciences, National Institutes of Health.

A. J. Atkinson, Jr., is a Burroughs Wellcome Scholar in Clinical Pharmacology.

Factors Affecting Homogeneous Precipitation of Aluminum Hydroxide Gel

CARLOS J. SERNA [1], JOE L. WHITE *, and STANLEY L. HEM ‡×

Received November 7, 1977, from the **Department of Agronomy and the* ‡*Industrial and Physical Pharmacy Department, School of Pharmacy and Pharmacal Sciences, Purdue University, West Lafayette, IN 47907.* Accepted for publication December 6, 1977.

Abstract □ The variables affecting homogeneous precipitation in the hydrolysis of aluminum nitrate by sodium carbonate were studied. Increased temperature, decreased concentration of reactants, and decreased rate of addition of titrant favor conditions that achieve homogeneous precipitation. During acid hydrolysis, the nitrate anion was the major anion associated with the gel and only small amounts of carbonate were observed. It is recommended that homogeneous conditions be achieved during the precipitation of aluminum hydroxide gel to improve reproducibility.

Keyphrases □ Aluminum hydroxide gel—factors affecting homogeneous precipitation in hydrolysis of aluminum nitrate by sodium carbonate □ Antacids—aluminum hydroxide gel, factors affecting homogeneous precipitation in hydrolysis of aluminum nitrate by sodium carbonate

The precipitation of aluminum hydroxide gel through the hydrolysis of an aluminum salt is complex. The precipitation method and subsequent treatment have a great effect on the properties of the product (1–4). This variability has been a problem affecting all areas of research and production of aluminum hydroxide gel.

In the titration of aluminum nitrate with sodium hydroxide, polymerization occurs prior to precipitation under homogeneous conditions (5, 6). This was achieved by precipitation under carefully controlled conditions in a specially designed reaction chamber. Precipitation of aluminum hydroxide gel under homogeneous conditions may be important in reducing the variability in precipitation.

Studies were undertaken to determine if homogeneous precipitation conditions could be achieved using standard precipitation equipment. The effect of precipitation variables was then investigated to determine the contribution of each variable in the achievement of a homogeneous reaction.

The system studied was the precipitation of aluminum hydroxide from acidic media (5, 6). However, sodium carbonate was used as the titrant instead of sodium hydroxide because the aluminum hydroxide gels used as antacids usually contain carbonate (7, 8).

EXPERIMENTAL

Potentiometric titrations were performed by placing 100 ml of solution in a 400-ml jacketed beaker. The temperature was controlled to ±0.1°, and the solution was stirred[2] at 2000 rpm. Titrant was added at a controlled rate[3]; the standard rate of addition was 2 ml/min. The solution pH was monitored continuously and recorded. Exact replication of titration curves was obtained when conditions producing homogeneous precipitation were used.

IR analysis[4] (9) was performed on a portion of the aluminum hydroxide, which was washed with three volumes of water to remove excess salts prior to drying under vacuum at room temperature. Spectra were obtained using potassium bromide pellets.

RESULTS AND DISCUSSION

Titration of 0.5 *M* aluminum nitrate by 0.5 *N* NaOH at 22° (Fig. 1)

[1] On leave from Instituto de Edafologia, C.S.I.C., Madrid, Spain.

[2] Stedi-Speed stirrer, Fisher Scientific, Pittsburgh, Pa.

[3] Solution metering pump, model 746, Beckman Instruments, Fullerton, Calif.

[4] Model 180, Perkin-Elmer Corp., Norwalk, Conn.

0022-3549/78/0800-1179$01.00/0
© 1978, American Pharmaceutical Association

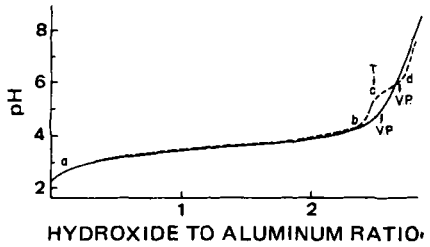

Figure 1—*Effect of temperature on the titration of 0.5 M aluminum nitrate with 0.5 N NaOH at an addition rate of 2 ml/min. Key: —, 22°; ---, 40°; T, turbidity; and VP, visible precipitate.*

resulted in a continuous curve similar to those commonly reported (10). Under these conditions, polymerization and precipitation were not separate processes but occurred simultaneously.

At 40°, a different titration curve, which exhibited two plateaus characteristic of homogeneous precipitation (5, 6), was obtained. Turbidity associated with polymerization of the hydroxyaluminum units occurred at the beginning of the second plateau (hydroxide to aluminum ratio = 2.46). A visible precipitate, indicating the initiation of the precipitation phase, first appeared at the end of this plateau (hydroxide to aluminum ratio = 2.70). In contrast, under nonhomogeneous conditions, turbidity and the formation of a visible precipitate appeared simultaneously at a hydroxide to aluminum ratio of 2.50. Precipitation occurs over a more restricted hydroxide to aluminum ratio and pH under homogeneous conditions and should produce a more uniform product.

The relatively constant pH observed from a to b in Fig. 1 indicates that a strong binding of hydroxides by aluminum is occurring. The reaction during this plateau can be written as shown in Scheme I:

$$XAl^{3+} + YOH^- \rightarrow Al_X(OH)_Y^{3X-Y}$$

Scheme I

This part of the titration does not appear to be affected by precipitation conditions because of the small size of the ionic species formed during this plateau. The hydroxide to aluminum ratio of 2.33 (point b) indicates an average polymeric species consisting of four fused six-member rings with the formula $Al_{16}(OH)_{38}^{10+}$ (10). The titrations now behave differently as polymerization of these primary units occurs under homogeneous conditions, but polymerization and precipitation both proceed simultaneously under nonhomogeneous conditions. Under homogeneous conditions, further addition of sodium hydroxide (b to c) produces a sharp increase in pH, but the solution remains clear. The added hydroxides are neutralizing protons rather than combining with hydroxyaluminum polymeric units.

Turbidity is observed at the beginning of the second plateau (point c). The added hydroxides are adsorbed by the hydroxyaluminum polymers during this plateau. The charge is reduced, and the polymerization of several units occurs. Polymerization increases until the charge on the polymer sheets is reduced enough to permit aggregation, which leads to the formation of a visible precipitate (point d). The pH increases sharply since the added hydroxides are not completely incorporated into the solid phase.

Thus, the polymerization and precipitation phases in the preparation of aluminum hydroxide can be separated using standard laboratory equipment.

In the aluminum nitrate–sodium carbonate system, which is of greater importance for antacids, the effects of temperature, concentration of reactants, and rate of addition of titrant were determined by carefully

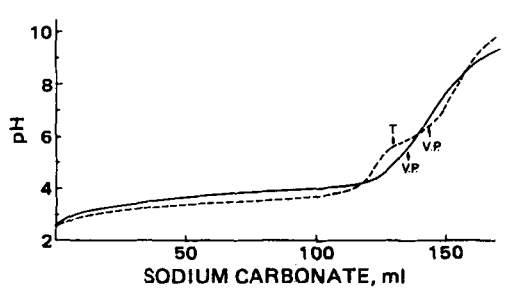

Figure 2—*Effect of temperature on the titration of 0.5 M aluminum nitrate with 0.5 M sodium carbonate at an addition rate of 2 ml/min. Key: —, 23°; ---, 46°; T, turbidity; and VP, visible precipitate.*

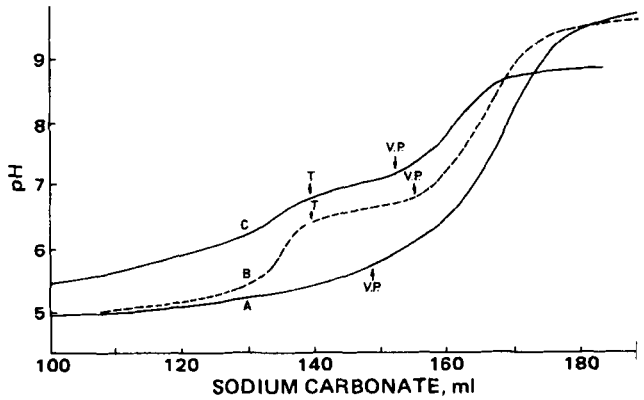

Figure 3—*Effect of concentration and addition rate on the titration of aluminum nitrate with sodium carbonate at 22°. Key: A, 0.1 M aluminum nitrate with 0.1 M sodium carbonate, 5 ml/min; B, 0.1 M aluminum nitrate with 0.1 M sodium carbonate, 2 ml/min; C, 0.005 M aluminum nitrate with 0.005 M sodium carbonate, 5 ml/min; T, turbidity, and VP, visible precipitate.*

varying one factor at a time. The effect of temperature is observed in Fig. 2. The titration curve assumed the characteristics of a homogeneous precipitation as the temperature was increased from 23 to 46°. This result indicates that the increased diffusion rate produces more uniform conditions throughout the reaction medium. Similarly, a decrease in the concentration of the reactants or in the titrant addition rate produced conditions resulting in homogeneous precipitation (Fig. 3).

The important characteristic of a system exhibiting homogeneous precipitation is that every volume of reactant is equally exposed to the titrant, resulting in a controlled process whereby polymerization precedes precipitation. Precipitation conditions should be chosen to achieve homogeneous conditions. However, elevated temperatures are not recommended to produce homogeneous conditions because numerous reports indicated that high temperatures have a deleterious effect on the antacid properties of aluminum hydroxide gel (11, 12).

Comparison of the titration curves utilizing sodium hydroxide or sodium carbonate (Figs. 1 and 2) indicates that a similar reaction occurs in both systems, suggesting that carbonate does not play an important role in the precipitation of aluminum hydroxide from acidic media. Analysis of the precipitate by IR spectroscopy showed that nitrate was the major anion associated with the gel up to pH 8.0, although a small amount of carbonate was also observed. Above this pH, nitrate progressively disappeared, presumably replaced by hydroxides. This result is seen in Fig. 4 where the absorption band at 1382 cm^{-1} is due to nitrate, the bands at 1400 and 1535 cm^{-1} are due to carbonate, and the band at 1635 cm^{-1} is due to water.

Precipitation under homogeneous conditions appears to produce a

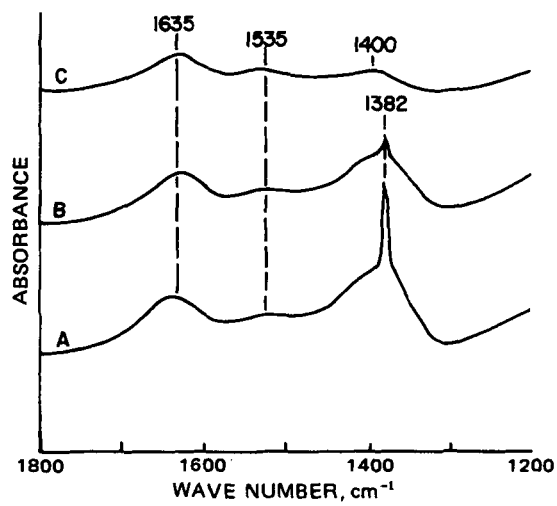

Figure 4—*IR spectra of precipitates at different pH values during titration of 0.1 M aluminum nitrate with 0.1 M sodium carbonate at an addition rate of 2 ml/min at 22°. Key: A, pH 8; B, pH 9; and C, pH 10.*

more consistent product in terms of particle size and charge. Since these properties have important effects on acid reactivity and viscosity, the achievement of homogeneous conditions during precipitation should reduce the variability in the properties of aluminum hydroxide gel. It is recommended that the precipitation system be checked to determine if homogeneous conditions exist by performing an acid titration and determining if polymerization occurs separately from precipitation.

REFERENCES

(1) D. Papee, R. Tertian, and R. Blais, *Bull. Soc. Chim. Fr.*, **1958**, 1301.

(2) P. H. Hsu and T. F. Bates, *Miner. Mag.*, **33**, 749 (1964).

(3) K. Wefers and G. M. Bell, "Alcoa Technical Paper No. 19," Alcoa Research Laboratories, Pittsburgh, Pa., 1972, pp. 1–51.

(4) R. H. Green and S. L. Hem, *J. Pharm. Sci.*, **63**, 635 (1974).

(5) A. C. Vermeulen, J. W. Geus, R. J. Stol, and P. L. DeBruyn, *J. Colloid Interface Sci.*, **51**, 449 (1975).

(6) R. J. Stol, A. K. Van Melden, and P. L. DeBruyn, *ibid.*, **57**, 115 (1976).

(7) J. L. White and S. L. Hem, *J. Pharm. Sci.*, **64**, 468 (1975).

(8) N. J. Kerkhof, J. L. White, and S. L. Hem, *ibid.*, **66**, 1533 (1977).

(9) S. L. Nail, J. L. White, and S. L. Hem, *ibid.*, **65**, 231 (1976).

(10) *Ibid.*, **65**, 1188 (1976).

(11) J. A. Lewis and C. A. Taylor, *J. Appl. Chem.*, **8**, 223 (1958).

(12) D. Cismaru, J. Iordachescu, G. Georgescu, and V. Cristescu, *Rev. Roum. Chim.*, **10**, 803 (1965).

ACKNOWLEDGMENTS

Supported in part by the Barcroft Co. and National Institutes of Health Biomedical Research Support Grant.

C. J. Serna acknowledges a fellowship from Ministerio de Educacion y Ciencia, Madrid, Spain.

This report is Journal Paper 6946, Purdue University, Agricultural Experiment Station, West Lafayette, IN 47907.

Omission of Pepsin from Simulated Gastric Fluid in Evaluating Activated Charcoals as Antidotes

JOHN S. DALY and DAVID O. COONEY ˣ

Received August 23, 1977, from the *Department of Chemical Engineering, Clarkson College of Technology, Potsdam, NY 13676.* Accepted for publication November 30, 1977.

Abstract □ Although simulated gastric fluid USP calls for 3.2 g of pepsin/liter, most researchers omit pepsin when evaluating adsorbents. The present results show that, although pepsin adsorbs strongly to activated charcoal, it does not interfere significantly with the adsorption of a typical drug like sodium salicylate. Therefore, its omission is justified. Gastric mucin also had almost no effect on salicylate adsorption.

Keyphrases □ Pepsin—effect on adsorption of typical drugs to activated charcoal *in vitro* □ Charcoal, activated—adsorption of typical drugs, effect of pepsin *in vitro* □ Adsorption, *in vitro*—typical drugs to activated charcoal, effect of pepsin □ Gastric fluid, simulated—*in vitro* adsorption of typical drugs to activated charcoal, effect of pepsin

An adsorbent like activated charcoal can be evaluated as a potential orally administered poison antidote by dissolving a test substance in simulated gastric fluid, adding the adsorbent, and measuring the amount of drug adsorbed after equilibrium is achieved.

Although simulated gastric fluid USP contains, per liter, 3.2 g of pepsin, 2.0 g of sodium chloride, and 7.0 ml of hydrochloric acid USP (giving a pH of 1.2), it is common practice to omit the pepsin and sodium chloride in preparing simulated gastric fluids. While sodium chloride does not adsorb to materials like activated charcoal, activated charcoal strongly inactivates (1) and strongly adsorbs (2) pepsin. The possibility arises that pepsin would compete with the test substance for available adsorption sites, so its omission from simulated gastric fluid could result in a falsely high value for the amount of drug bound by the adsorbent under actual gastric conditions.

The purpose of this study was to investigate whether the inclusion or omission of pepsin from simulated gastric fluid significantly affects the measured degree of binding of a typical test substance. The omission of gastric mucin is also discussed.

BACKGROUND

The adsorbing ability of substances like activated charcoal has been assessed by dissolving the test drug in distilled water (3, 4). Since pH has a very strong influence on drug adsorption capacities (5–7), the results are not necessarily relevant to what would occur *in vivo*. For this reason, dilute hydrochloric acid solutions (usually 0.1 *M*, pH 1.0) often are used (8–13) as simulated gastric fluid. Such solutions are different from simulated gastric fluid USP in that they do not contain pepsin. Some investigators (11–13) specifically mentioned the deliberate omission of pepsin but did not comment on any possible effect. Apparently, any dilute hydrochloric acid solution of pH 1–2 is considered a valid and equivalent substitute for simulated gastric fluid USP, if not for actual gastric fluid itself.

Piper and Fenton (1) showed substantial inactivation of pepsin dissolved in a pH 1.5 potassium chloride–hydrochloric acid buffer by various adsorbents (charcoal, aluminum hydroxide, and clays). This inactivation was most likely the result of the pepsin having been adsorbed; however, direct evidence of such adsorption was not presented. Lichtwitz and Greef (2) published direct evidence of a substantial adsorption of pepsin onto various similar adsorbents. Thus, pepsin can bind well to several common adsorbents (and rather strongly to activated charcoal in particular).

Based on a molecular weight of pepsin of about 35,000, its equivalent spherical molecular radius is about 20 Å. This radius would allow pepsin to penetrate all macropores (>1000 Å) and a substantial fraction of the micropores in many adsorbent materials. For example, in most typical activated charcoals, about 50–90% of the pore volume resides in the pores of radii greater than 20 Å. Any test drug (*e.g.*, aspirin) would be much smaller in molecular size and could reach the smaller pores (<20 Å radius) where a substantial amount of the internal surface area resides. (Even if the pores of 20 Å radius or less are only 10% of the total pore volume, they would contribute a much larger proportion of the total internal surface area.)

Therefore, pepsin and a typical drug might compete strongly in the

0022-3549/78/0800-1181$01.00/0

© 1978, American Pharmaceutical Association

more consistent product in terms of particle size and charge. Since these properties have important effects on acid reactivity and viscosity, the achievement of homogeneous conditions during precipitation should reduce the variability in the properties of aluminum hydroxide gel. It is recommended that the precipitation system be checked to determine if homogeneous conditions exist by performing an acid titration and determining if polymerization occurs separately from precipitation.

REFERENCES

(1) D. Papee, R. Tertian, and R. Blais, *Bull. Soc. Chim. Fr.*, **1958**, 1301.

(2) P. H. Hsu and T. F. Bates, *Miner. Mag.*, **33**, 749 (1964).

(3) K. Wefers and G. M. Bell, "Alcoa Technical Paper No. 19," Alcoa Research Laboratories, Pittsburgh, Pa., 1972, pp. 1–51.

(4) R. H. Green and S. L. Hem, *J. Pharm. Sci.*, **63**, 635 (1974).

(5) A. C. Vermeulen, J. W. Geus, R. J. Stol, and P. L. DeBruyn, *J. Colloid Interface Sci.*, **51**, 449 (1975).

(6) R. J. Stol, A. K. Van Melden, and P. L. DeBruyn, *ibid.*, **57**, 115 (1976).

(7) J. L. White and S. L. Hem, *J. Pharm. Sci.*, **64**, 468 (1975).

(8) N. J. Kerkhof, J. L. White, and S. L. Hem, *ibid.*, **66**, 1533 (1977).

(9) S. L. Nail, J. L. White, and S. L. Hem, *ibid.*, **65**, 231 (1976).

(10) *Ibid.*, **65**, 1188 (1976).

(11) J. A. Lewis and C. A. Taylor, *J. Appl. Chem.*, **8**, 223 (1958).

(12) D. Cismaru, J. Iordachescu, G. Georgescu, and V. Cristescu, *Rev. Roum. Chim.*, **10**, 803 (1965).

ACKNOWLEDGMENTS

Supported in part by the Barcroft Co. and National Institutes of Health Biomedical Research Support Grant.

C. J. Serna acknowledges a fellowship from Ministerio de Educacion y Ciencia, Madrid, Spain.

This report is Journal Paper 6946, Purdue University, Agricultural Experiment Station, West Lafayette, IN 47907.

Omission of Pepsin from Simulated Gastric Fluid in Evaluating Activated Charcoals as Antidotes

JOHN S. DALY and DAVID O. COONEY ˣ

Received August 23, 1977, from the *Department of Chemical Engineering, Clarkson College of Technology, Potsdam, NY 13676.* Accepted for publication November 30, 1977.

Abstract □ Although simulated gastric fluid USP calls for 3.2 g of pepsin/liter, most researchers omit pepsin when evaluating adsorbents. The present results show that, although pepsin adsorbs strongly to activated charcoal, it does not interfere significantly with the adsorption of a typical drug like sodium salicylate. Therefore, its omission is justified. Gastric mucin also had almost no effect on salicylate adsorption.

Keyphrases □ Pepsin—effect on adsorption of typical drugs to activated charcoal *in vitro* □ Charcoal, activated—adsorption of typical drugs, effect of pepsin *in vitro* □ Adsorption, *in vitro*—typical drugs to activated charcoal, effect of pepsin □ Gastric fluid, simulated—*in vitro* adsorption of typical drugs to activated charcoal, effect of pepsin

An adsorbent like activated charcoal can be evaluated as a potential orally administered poison antidote by dissolving a test substance in simulated gastric fluid, adding the adsorbent, and measuring the amount of drug adsorbed after equilibrium is achieved.

Although simulated gastric fluid USP contains, per liter, 3.2 g of pepsin, 2.0 g of sodium chloride, and 7.0 ml of hydrochloric acid USP (giving a pH of 1.2), it is common practice to omit the pepsin and sodium chloride in preparing simulated gastric fluids. While sodium chloride does not adsorb to materials like activated charcoal, activated charcoal strongly inactivates (1) and strongly adsorbs (2) pepsin. The possibility arises that pepsin would compete with the test substance for available adsorption sites, so its omission from simulated gastric fluid could result in a falsely high value for the amount of drug bound by the adsorbent under actual gastric conditions.

The purpose of this study was to investigate whether the inclusion or omission of pepsin from simulated gastric fluid significantly affects the measured degree of binding of a typical test substance. The omission of gastric mucin is also discussed.

BACKGROUND

The adsorbing ability of substances like activated charcoal has been assessed by dissolving the test drug in distilled water (3, 4). Since pH has a very strong influence on drug adsorption capacities (5–7), the results are not necessarily relevant to what would occur *in vivo*. For this reason, dilute hydrochloric acid solutions (usually 0.1 *M*, pH 1.0) often are used (8–13) as simulated gastric fluid. Such solutions are different from simulated gastric fluid USP in that they do not contain pepsin. Some investigators (11–13) specifically mentioned the deliberate omission of pepsin but did not comment on any possible effect. Apparently, any dilute hydrochloric acid solution of pH 1–2 is considered a valid and equivalent substitute for simulated gastric fluid USP, if not for actual gastric fluid itself.

Piper and Fenton (1) showed substantial inactivation of pepsin dissolved in a pH 1.5 potassium chloride–hydrochloric acid buffer by various adsorbents (charcoal, aluminum hydroxide, and clays). This inactivation was most likely the result of the pepsin having been adsorbed; however, direct evidence of such adsorption was not presented. Lichtwitz and Greef (2) published direct evidence of a substantial adsorption of pepsin onto various similar adsorbents. Thus, pepsin can bind well to several common adsorbents (and rather strongly to activated charcoal in particular).

Based on a molecular weight of pepsin of about 35,000, its equivalent spherical molecular radius is about 20 Å. This radius would allow pepsin to penetrate all macropores (>1000 Å) and a substantial fraction of the micropores in many adsorbent materials. For example, in most typical activated charcoals, about 50–90% of the pore volume resides in the pores of radii greater than 20 Å. Any test drug (*e.g.*, aspirin) would be much smaller in molecular size and could reach the smaller pores (<20 Å radius) where a substantial amount of the internal surface area resides. (Even if the pores of 20 Å radius or less are only 10% of the total pore volume, they would contribute a much larger proportion of the total internal surface area.)

Therefore, pepsin and a typical drug might compete strongly in the

0022-3549/78/0800-1181$01.00/0

© 1978, American Pharmaceutical Association

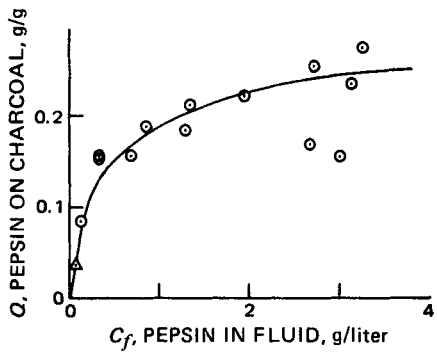

Figure 1—*Isotherm for the binding of pepsin from simulated gastric fluid onto powdered activated charcoal.*

larger pores but not in the smaller pores. The overall degree of competition is uncertain and can only be determined by experiments. To determine the degree to which pepsin adsorption can interfere with, and decrease the extent of, adsorption of a typical drug, the following experiments were conducted.

EXPERIMENTAL

Studies with Pepsin—Pepsin[1], 4 g/liter, was dissolved in a pH 1.2 potassium chloride–hydrochloric acid buffer to give a solution nearly identical to simulated gastric fluid USP. The adsorbent chosen was powdered activated charcoal[2], prepared by washing twice with 6 *M* HCl (to remove leachable inorganic ash), washing six times with distilled water, and drying at 120° for 24 hr.

Aliquots of 10 ml of the pepsin solution were combined with known amounts of the charcoal in glass vials. The vials were then capped and shaken for about 24 hr (prior tests showed that 24 hr is enough to assure nearly complete equilibration). After allowing another 24 hr for the charcoal to settle, the supernates were filtered through 0.45-μm microporous membranes[3]. One milliliter of each of the clear filtrates was combined with 10 ml of a biuret reagent prepared from 10% (w/v) potassium hydroxide–0.5% (w/v) $CuSO_4 \cdot 5H_2O$ (10:1) in distilled water. By reaction with the peptide linkages in the enzyme, this solution produced stable blue-colored complexes, which were assayed colorimetrically at 550 nm. A relation between absorbance and pepsin concentration was established by treating solutions of known pepsin concentrations according to the same procedure (shaking, settling, and filtering). Beer's law was obeyed by this system.

Although these experiments established the adsorption isotherm for pepsin binding to charcoal, the central question is not the extent to which pepsin will adsorb to the charcoal, but whether the adsorption of pepsin would interfere with the adsorption of a typical drug. Solutions of reagent grade sodium salicylate[4] (1 g/liter) in the pH 1.2 buffer were prepared and contacted with the charcoal in the same way as the pepsin solution (as already described) to establish the degree to which salicylate adsorbs to the charcoal. The clear filtrates from the samples were analyzed for salicylate by the colorimetric method (14) involving Trinder's reagent in which the intensity of a purple-colored complex is measured at 540 nm.

Pepsin was then added, at 4 g/liter, to samples containing the salicylate and powdered charcoal. Absorbances were measured at 540 nm after filtration of the supernates and addition of Trinder's reagent to the filtrates. From these measurements, the degree of interference of pepsin with sodium salicylate adsorption was determined.

Studies with Gastric Mucin—Based on the work of Gudiksen (15), Decker *et al.* (16) studied drug adsorption on activated charcoal using a simulated gastric fluid containing 0.5 g of gastric mucin/liter rather than pepsin. To determine if omission or inclusion of gastric mucin in simulated gastric fluid would have any effect on drug adsorption, the experiments with pepsin were repeated with gastric mucin. It was impossible to obtain an adsorption isotherm for the gastric mucin[5] on charcoal because the microporous membranes filtered out the mucin from the supernate. Thus, there appears to be no way of removing the charcoal from the supernate while leaving the mucin behind at its original concentration. It was possible, however, to repeat the interference tests successfully.

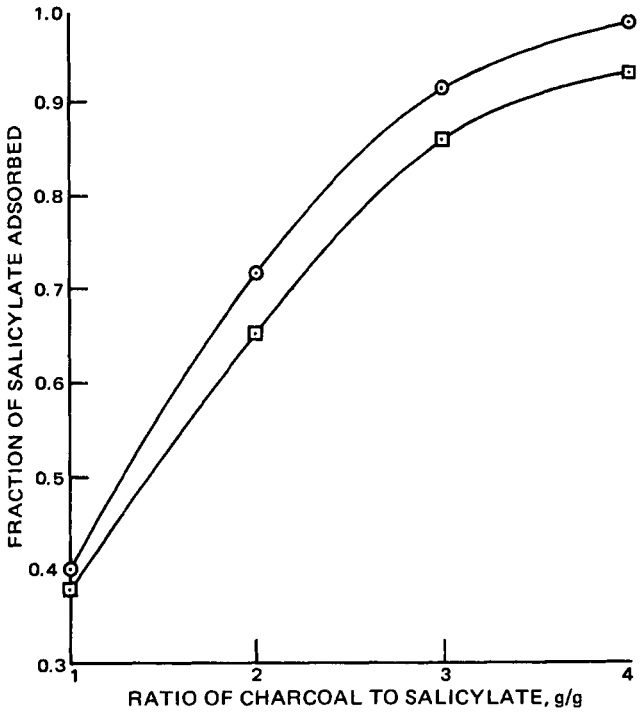

Figure 2—*Salicylate adsorption by charcoal from a 1 g of sodium salicylate/liter solution in the absence of pepsin (○) and in the presence of 4 g of pepsin/liter (□).*

RESULTS AND DISCUSSION

In the experiments designed to determine the degree of pepsin adsorption to charcoal, the amounts were computed for each sample using the mass balance equation $Q = V(C_0 - C_f)/W$, where V is the volume of the aliquot in liters, W is the weight of the charcoal in grams, Q is the weight of pepsin adsorbed on the charcoal (grams per gram), and C_0 and C_f are the initial and final fluid phase pepsin concentrations (grams per liter), respectively. Figure 1 shows the adsorption data obtained, expressed in terms of the quantities Q and C_f. The triangular data point near the origin is the data point of Piper and Fenton (1), computed assuming that the pepsin inactivation observed was due to adsorption and was directly proportional to the extent of such adsorption. While this assumption may not be entirely correct, their data point does fit in reasonably well with the present data.

The scatter in the neighborhood of $C_f = 3$ g/liter occurs because the stock pepsin solution concentration, C_0, was 3.48 g/liter. (The stock pepsin solution was prepared at a nominal 4-g/liter concentration, but the source pepsin was, by the supplier's own assay, only 87% pure.) Thus, to obtain adsorption data at concentrations near 3 g/liter, it was necessary to use very little charcoal and to measure a relatively small change in concentration, $(C_0 - C_f)$, due to adsorption. The greater relative errors in W and $(C_0 - C_f)$ result in larger errors in the Q values in this region.

Studies of the degree of salicylate binding to charcoal and of the extent to which pepsin (at 4-g/liter concentration) interferes with salicylate binding are summarized in Fig. 2. Over the range of the ratio of charcoal to salicylate shown (from 1 to 4 g of charcoal/g of salicylate), the fraction of salicylate adsorbed in the presence of pepsin ranged from about 5 to 9% lower than the fraction of salicylate bound in the absence of pepsin. Clearly, the effect of 4 g of pepsin/liter was not large.

The present studies of the effects of gastric mucin (at 0.5 g/liter) on the binding of salicylate can be summarized as follows. For samples having charcoal to salicylate ratios of 1, 2, 3, and 4, the fractions of salicylate adsorbed in the absence of added mucin were 0.401, 0.717, 0.914, and 0.984, respectively (these data points are shown along the upper line in Fig. 2). With the addition of 0.5 g of gastric mucin/liter to samples

[1] Product P 7012 (twice crystallized), Sigma Chemical Co., St. Louis, Mo.
[2] Norit A, American Norit Co., Jacksonville, Fla.
[3] Amicon Corp., Lexington, Mass.
[4] J. T. Baker Chemical Co., Phillipsburg, N.J.
[5] ICN Pharmaceuticals, Cleveland, Ohio.

having the same charcoal to salicylate ratios, the fractions of salicylate adsorbed were 0.401, 0.711, 0.920, and 0.984, respectively. Clearly, these results show either zero effect, a very slight interference, or a very slight enhancement of adsorption. Overall, no effect of significance can be identified.

CONCLUSIONS

Whether results similar to those obtained using sodium salicylate would be found with other kinds of drugs is, of course, unproved. However, if simple adsorption of the test drug and of the pepsin or gastric mucin is all that occurs, results with other drugs should not be radically different.

However, the question of whether pepsin and/or mucin should be added to simulated gastric fluid to make evaluations more realistic is overshadowed by the implications of data obtained by Andersen (17). He carried out adsorption tests in actual gastric contents (pH 1.5, 60% solids) obtained by aspiration of the stomachs of human volunteers after test meals had been consumed. Values for the amounts of mercuric chloride, barbital, and strychnine adsorbed on charcoal were only about 50–60% of the amounts adsorbed from pH 1.5 hydrochloric acid solutions.

Since the reductions in adsorption were quite large and probably depend on a whole complex array of solid and dissolved materials present in the stomach, it appears that absolute similarity between simulated gastric fluid and actual gastric contents is not achieved simply by adding pepsin and/or mucin to the simulated gastric fluid recipe. Therefore, it is probably just as well to omit both pepsin and mucin in tests involving simulated gastric fluid and to figure, as a rule of thumb, that the amount of drug adsorbed *in vivo* will be roughly half of that adsorbed *in vitro*. The experimental results reported in this paper give one a feeling for the influence of two specific important constituents of actual gastric fluid and indicate that they, at least, are not crucial in affecting adsorption.

REFERENCES

(1) D. W. Piper and B. Fenton, *Am. J. Dig. Dis.*, **6**, 134 (1961).

(2) L. Lichtwitz and E. W. Greef, *Ther. Monatsh.*, **25**, 721 (1911).

(3) A. L. Picchioni, L. Chin, and H. E. Laird, *Clin. Toxicol.*, **7**, 97 (1974).

(4) A. H. Andersen, *Acta Pharmacol.*, **2**, 69 (1946).

(5) L. Chin, A. L. Picchioni, and B. R. Duplisse, *Toxicol. Appl. Pharmacol.*, **16**, 786 (1970).

(6) A. H. Andersen, *Acta Pharmacol.*, **3**, 199 (1947).

(7) D. Henschler, *Arh. Hig. Rada Toksikol.*, **21**, 129 (1970).

(8) R. P. Smith, R. E. Gosselin, J. A. Henderson, and D. M. Anderson, *Toxicol. Appl. Pharmacol.*, **10**, 95 (1967).

(9) M. Manes and J. P. Mann, Jr., *Clin. Toxicol.*, **7**, 355 (1974).

(10) S. Lindenbaum and T. Higuchi, *J. Pharm. Sci.*, **64**, 1887 (1975).

(11) R. C. Oppenheim and N. F. Stewart, *Aust. J. Pharm. Sci.*, **NS4**, 79 (1975).

(12) A. M. Dozzi, A. Leversha, and N. F. Stewart, *Aust. J. Hosp. Pharm.*, **4**, 40 (1974).

(13) C. A. Bainbridge, E. L. Kelly, and W. D. Walkling, *J. Pharm. Sci.*, **66**, 480 (1977).

(14) R. P. MacDonald, in "Standard Methods of Clinical Chemistry," vol. 5, S. Meites, Ed., Academic, New York, N.Y., 1965.

(15) E. Gudiksen, *Acta Physiol. Scand.*, **5**, 39 (1943).

(16) W. J. Decker, H. F. Combs, and D. F. Corby, *Toxicol. Appl. Pharmacol.*, **13**, 454 (1968).

(17) A. H. Andersen, *Acta Pharmacol.*, **4**, 275 (1948).

Synthesis and Antiulcerogenic Evaluation of 2-(Substituted Phenylimino)-2*H*-quinolizines

ROBERT J. ALAIMO ˣ and MARVIN M. GOLDENBERG

Received July 1, 1977, from the *Chemical Research Division and the Biological Research Division, Norwich-Eaton Pharmaceuticals, Division of Morton-Norwich Products, Inc., Norwich, NY 13815.* Accepted for publication November 22, 1977.

Abstract □ The synthesis and antiulcerogenic evaluation of a series of 2-(substituted phenylimino)-2*H*-quinolizines are described. The most active compound, the 4-chlorophenylimido derivative, inhibited ulcer formation by 98%.

Keyphrases □ Quinolizines, substituted phenylimino—synthesized, evaluated for antiulcerogenic activity □ Antiulcerogenic activity—various 2-(substituted phenylimino)-2*H*-quinolizines evaluated □ Structure–activity relationships—various 2-(substituted phenylimino)-2*H*-quinolizines evaluated for antiulcerogenic activity

The synthesis and preliminary pharmacological evaluation of a series of 2-(substituted amino)quinolizinium bromides were reported previously (1, 2). As a continuing part of this investigation, the synthesis and antiulcerogenic testing of a series of 2-(substituted phenylimino)-2*H*-quinolizines (II*a*–II*f*, Table I) are now described. Compounds II*a*–II*f*, when examined for antiulcerogenic action by the modified Shay procedure (2), inhibited ulcer formation as much as 98%.

DISCUSSION

The syntheses of the intermediate compounds, I*a*–I*f*, were described previously (1–3). Their reaction with aqueous sodium hydroxide provided the phenylimino-2*H*-quinolizines (II*a*–II*f*) in high yield (Scheme I). Compounds II*a*–II*f* are the first reported examples of this class of compounds. The elemental analyses and IR and NMR spectra of II*a*–II*f* are consistent with the assigned structures.

For II*a* as an example, the IR spectrum showed strong absorption at 1640, 1560, and 1490 cm^{-1}. These absorptions are characteristic of all other phenylimino-2*H*-quinolizines as well.

The NMR spectral assignment of II*a* was made by use of homonuclear decoupling experiments. The NMR spectrum (dimethyl sulfoxide-d_6) of II*a* showed a *meta* split doublet at 6.22 ppm integrating for one proton, assigned to the proton at position 1. The proton at position 3 appeared as a split doublet (*ortho* and *meta* coupling) at 6.57 ppm. The proton at the 4-position of the quinolizine ring appeared as an *ortho* coupled doublet at 7.89 ppm. The proton at the 6-position appeared as a doublet at 7.85 ppm and showed *ortho* and *meta* splitting.

The proton at the 7-position of the quinolizine ring appeared as a split

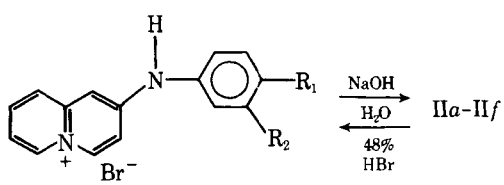

I*a*–I*f*

Scheme I

© 1978, American Pharmaceutical Association

having the same charcoal to salicylate ratios, the fractions of salicylate adsorbed were 0.401, 0.711, 0.920, and 0.984, respectively. Clearly, these results show either zero effect, a very slight interference, or a very slight enhancement of adsorption. Overall, no effect of significance can be identified.

CONCLUSIONS

Whether results similar to those obtained using sodium salicylate would be found with other kinds of drugs is, of course, unproved. However, if simple adsorption of the test drug and of the pepsin or gastric mucin is all that occurs, results with other drugs should not be radically different.

However, the question of whether pepsin and/or mucin should be added to simulated gastric fluid to make evaluations more realistic is overshadowed by the implications of data obtained by Andersen (17). He carried out adsorption tests in actual gastric contents (pH 1.5, 60% solids) obtained by aspiration of the stomachs of human volunteers after test meals had been consumed. Values for the amounts of mercuric chloride, barbital, and strychnine adsorbed on charcoal were only about 50–60% of the amounts adsorbed from pH 1.5 hydrochloric acid solutions.

Since the reductions in adsorption were quite large and probably depend on a whole complex array of solid and dissolved materials present in the stomach, it appears that absolute similarity between simulated gastric fluid and actual gastric contents is not achieved simply by adding pepsin and/or mucin to the simulated gastric fluid recipe. Therefore, it is probably just as well to omit both pepsin and mucin in tests involving simulated gastric fluid and to figure, as a rule of thumb, that the amount of drug adsorbed *in vivo* will be roughly half of that adsorbed *in vitro*. The experimental results reported in this paper give one a feeling for the influence of two specific important constituents of actual gastric fluid and indicate that they, at least, are not crucial in affecting adsorption.

REFERENCES

(1) D. W. Piper and B. Fenton, *Am. J. Dig. Dis.*, **6**, 134 (1961).

(2) L. Lichtwitz and E. W. Greef, *Ther. Monatsh.*, **25**, 721 (1911).

(3) A. L. Picchioni, L. Chin, and H. E. Laird, *Clin. Toxicol.*, **7**, 97 (1974).

(4) A. H. Andersen, *Acta Pharmacol.*, **2**, 69 (1946).

(5) L. Chin, A. L. Picchioni, and B. R. Duplisse, *Toxicol. Appl. Pharmacol.*, **16**, 786 (1970).

(6) A. H. Andersen, *Acta Pharmacol.*, **3**, 199 (1947).

(7) D. Henschler, *Arh. Hig. Rada Toksikol.*, **21**, 129 (1970).

(8) R. P. Smith, R. E. Gosselin, J. A. Henderson, and D. M. Anderson, *Toxicol. Appl. Pharmacol.*, **10**, 95 (1967).

(9) M. Manes and J. P. Mann, Jr., *Clin. Toxicol.*, **7**, 355 (1974).

(10) S. Lindenbaum and T. Higuchi, *J. Pharm. Sci.*, **64**, 1887 (1975).

(11) R. C. Oppenheim and N. F. Stewart, *Aust. J. Pharm. Sci.*, **NS4**, 79 (1975).

(12) A. M. Dozzi, A. Leversha, and N. F. Stewart, *Aust. J. Hosp. Pharm.*, **4**, 40 (1974).

(13) C. A. Bainbridge, E. L. Kelly, and W. D. Walkling, *J. Pharm. Sci.*, **66**, 480 (1977).

(14) R. P. MacDonald, in "Standard Methods of Clinical Chemistry," vol. 5, S. Meites, Ed., Academic, New York, N.Y., 1965.

(15) E. Gudiksen, *Acta Physiol. Scand.*, **5**, 39 (1943).

(16) W. J. Decker, H. F. Combs, and D. F. Corby, *Toxicol. Appl. Pharmacol.*, **13**, 454 (1968).

(17) A. H. Andersen, *Acta Pharmacol.*, **4**, 275 (1948).

Synthesis and Antiulcerogenic Evaluation of 2-(Substituted Phenylimino)-2*H*-quinolizines

ROBERT J. ALAIMO ˣ and MARVIN M. GOLDENBERG

Received July 1, 1977, from the *Chemical Research Division and the Biological Research Division, Norwich-Eaton Pharmaceuticals, Division of Morton-Norwich Products, Inc., Norwich, NY 13815.* Accepted for publication November 22, 1977.

Abstract □ The synthesis and antiulcerogenic evaluation of a series of 2-(substituted phenylimino)-2*H*-quinolizines are described. The most active compound, the 4-chlorophenylimido derivative, inhibited ulcer formation by 98%.

Keyphrases □ Quinolizines, substituted phenylimino—synthesized, evaluated for antiulcerogenic activity □ Antiulcerogenic activity—various 2-(substituted phenylimino)-2*H*-quinolizines evaluated □ Structure–activity relationships—various 2-(substituted phenylimino)-2*H*-quinolizines evaluated for antiulcerogenic activity

The synthesis and preliminary pharmacological evaluation of a series of 2-(substituted amino)quinolizinium bromides were reported previously (1, 2). As a continuing part of this investigation, the synthesis and antiulcerogenic testing of a series of 2-(substituted phenylimino)-2*H*-quinolizines (II*a*–II*f*, Table I) are now described. Compounds II*a*–II*f*, when examined for antiulcerogenic action by the modified Shay procedure (2), inhibited ulcer formation as much as 98%.

DISCUSSION

The syntheses of the intermediate compounds, I*a*–I*f*, were described previously (1–3). Their reaction with aqueous sodium hydroxide provided the phenylimino-2*H*-quinolizines (II*a*–II*f*) in high yield (Scheme I). Compounds II*a*–II*f* are the first reported examples of this class of compounds. The elemental analyses and IR and NMR spectra of II*a*–II*f* are consistent with the assigned structures.

For II*a* as an example, the IR spectrum showed strong absorption at 1640, 1560, and 1490 cm^{-1}. These absorptions are characteristic of all other phenylimino-2*H*-quinolizines as well.

The NMR spectral assignment of II*a* was made by use of homonuclear decoupling experiments. The NMR spectrum (dimethyl sulfoxide-d_6) of II*a* showed a *meta* split doublet at 6.22 ppm integrating for one proton, assigned to the proton at position 1. The proton at position 3 appeared as a split doublet (*ortho* and *meta* coupling) at 6.57 ppm. The proton at the 4-position of the quinolizine ring appeared as an *ortho* coupled doublet at 7.89 ppm. The proton at the 6-position appeared as a doublet at 7.85 ppm and showed *ortho* and *meta* splitting.

The proton at the 7-position of the quinolizine ring appeared as a split

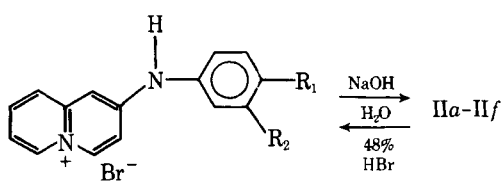

I*a*–I*f*

Scheme I

© 1978, American Pharmaceutical Association

Table I—Antiulcerogenic Evaluation and Physical and Analytical Data for New Compounds

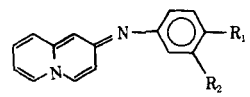

Compound	R_1	R_2	Melting Point	Yield, %	Recrystallization Solvent	Formula		Analysis, % Calc.	Analysis, % Found	Gastric Antiulcerogenic Effect, Inhibition of Control Ulceration[a], %
IIa	Cl	Cl	153–155°	100	Ethyl acetate	$C_{15}H_{10}Cl_2N_2$	C	62.30	62.50	72 (n = 4)
							H	3.49	3.53	
							N	9.69	9.68	
IIb	Cl	H	183–184°	87	Ethanol–water	$C_{15}H_{11}ClN_2$	C	70.73	70.71	98 (n = 5)
							H	4.35	4.28	
							N	11.00	10.90	
IIc	H	CF_3	134–135°	97	Benzene–hexane	$C_{16}H_{11}F_3N_2$	C	66.66	66.79	30 (n = 5)
							H	3.85	3.89	
							N	9.72	9.58	
IId	H	Cl	97–100°	87	Ethanol–water	$C_{15}H_{11}ClN_2 \cdot 3/4\ H_2O$	C	67.16	67.27	48 (n = 5)
							H	4.70	4.80	
							N	10.45	10.30	
IIe	OCH_2CH_3	H	157–159°	100	Benzene–hexane	$C_{17}H_{16}N_2O$	C	77.25	77.23	74 (n = 5)
							H	6.10	5.96	
							N	10.60	10.49	
IIf	CH_3	CH_3	185–187°	89	Benzene–hexane	$C_{17}H_{16}N_2$	C	82.22	81.94	56[b] (n = 5)
							H	6.49	6.34	
							N	11.28	11.20	

[a] The nontreated control group consisted of 21 rats; n = number of rats per group. [b] The dose was 50 mg/kg po; all others were 150 mg/kg po.

triplet at 6.46 ppm with *ortho* and *meta* splitting. A pair of *ortho* split doublets, centered at 7.00 ppm and showing additional *meta* coupling, was assigned to the proton at the 8-position. An *ortho* coupled doublet with *meta* fine structure centered at 7.08 ppm was assigned to the proton at position 9. The protons of the dichloroaniline ring appeared as a *meta* coupled doublet at 6.98 ppm, which was assigned to the proton at the 2′-position. The proton at the 5′-position appeared as an *ortho* coupled doublet at 7.41 ppm, and the proton at the 6′-position appeared as an *ortho* split doublet with additional *meta* splitting.

The NMR spectra of the quinolizine compounds at 60 MHz were all similar and consistent with the assignment based on the decoupling experiments of IIa.

Reaction of the phenylimino-2*H*-quinolizines with 48% hydrobromic acid regenerated the corresponding quinolizinium bromides (Ia–If).

The antiulcerogenic activity of IIa–IIf was determined by use of a slightly modified procedure (1) of Shay *et al.* (4).

Male Sprague–Dawley rats[1], 175–250 g, were fasted 24 hr prior to the experiment; each was dosed with 150 mg of compound/kg po. It was necessary to lower the dose of IIf to 50 mg/kg po because of its toxicity at the higher dose. Ulcerogenesis in the rumen of the rat stomach was graded according to the following scale: 0, no ulceration; 0.5, gray discoloration and thinning of mucosa; 1, hemorrhagic spots; 2, hemorrhagic suffusion; 3, one to five small ulcers (<3 mm); 4, many small ulcers (or one marked ulcer); 5, many ulcers (marked size); and 6, perforated ulcer.

The degree of gastric ulceration in the presence of each compound was compared to the nontreated control and expressed as percent inhibition of control ulceration.

Compounds IIa, IIb, and IIe (Table I) caused marked inhibition of rumenal ulceration in the range of 72–98%. Less inhibition was elicited with IIc, IId, and IIf. The most active compound in inhibiting ulcer formation was IIb, the 4-chloro analog. There was a 50% reduction in antiulcerogenic action when the chlorine atom was in the 3-position. The dichloro-substituted compound (IIa) was somewhat less active than IIb, while the dimethyl-substituted compound (IIf) was not as effective as the 4-ethoxy derivative (IIe). In general, the compounds exerting the greatest inhibition were 3,4-disubstituted (IIa and IIf) or 4-monosubstituted (IIb and IIe). The 3-monosubstituted compounds (IIc and IId) were much less active.

[1] Charles River Breeding Laboratories.

EXPERIMENTAL[2]

A stirred suspension of 2-(3,4-dichloroanilino)quinolizinium bromide (Ia) (23 g, 0.062 mole) in water (1000 ml) was heated to 50°. To the aqueous mixture was added, in portions, a solution of 2 *N* NaOH (400 ml). The solution precipitated a yellow-orange product, and the aqueous mixture was warmed at 50° for 1 hr. After cooling and filtration, the air-dried product weighed 18 g (100%). Recrystallization from ethyl acetate provided analytically pure material (IIa), mp 153–155°; UV: λ_{max} 345 nm ($E^{1\%}_{1cm}$ 740) in 5% ethanol–water. Solubility in water was 180 mg/liter; pKa = 8.9.

All other 2-(substituted phenylimino)-2*H*-quinolizines (IIb–IIf) were prepared similarly. The analytical and physical data for all compounds are shown in Table I (5).

REFERENCES

(1) R. J. Alaimo and M. M. Goldenberg, *J. Pharm. Sci.*, **63**, 1939 (1974).

(2) R. J. Alaimo and M. M. Goldenberg, *J. Med. Chem.*, **18**, 1145 (1975).

(3) R. J. Alaimo, C. J. Hatton, and M. K. Eckman, *ibid.*, **13**, 554 (1970).

(4) H. Shay, S. A. Komarov, S. S. Fels, D. Meranzi, M. Guienstein, and H. Siplet, *Gastroenterology*, **5**, 43 (1945).

(5) R. J. Alaimo, U.S. pat. 3,997,547 (1976).

ACKNOWLEDGMENTS

The assistance of Mr. Arthur Ilse in conducting the biological testing is appreciated. Elemental analyses were performed by Mrs. Cora Jeffrey, and NMR spectra were recorded by Mrs. Connie Lloyd. Homonuclear decoupling experiments were run by Dr. Christian Tanzer of Bruker Instruments, Billerica, MA 01821.

[2] Melting points were determined in open capillary tubes using a Mel-Temp melting-point apparatus and are uncorrected. NMR spectra were obtained on a Varian A-60A instrument with tetramethylsilane as an internal standard. Peak assignments were based on homonuclear decoupling experiments performed on IIa using Bruker WH-270 at Bruker Instruments, Billerica, MA 01821. IR spectra were recorded on a Perkin-Elmer model 137 Infracord. UV spectra were determined on a Perkin-Elmer model 350 spectrophotometer.

High-Pressure Liquid Chromatographic Analysis of a Tetrazolylchromone in Biological Fluids

R. J. HELMS ˣ, I. A. MUNI *, and J. L. LEELING

Received August 17, 1977, from the *Toxicology Department, Miles Laboratories, Inc., Elkhart, IN 46515.* Accepted for publication December 6, 1977. *Present address: J. T. Baker Diagnostics, Bethlehem, Pa.

Abstract □ Biological levels of a tetrazolylchromone were determined by high-pressure liquid chromatography without interference from natural physiological components and metabolic products.

Keyphrases □ Chromone, substituted—high-pressure liquid chromatographic analysis in biological fluids □ High-pressure liquid chromatography—analysis, substituted tetrazolylchromone in biological fluids □ Tetrazolylchromone, substituted—high-pressure liquid chromatographic analysis in biological fluids □ Antiallergic compounds, potential—substituted tetrazolylchromone, high-pressure liquid chromatographic analysis in biological fluids

Substituted chromones have demonstrated potential usefulness as prophylactic adjuncts in management of patients with severe perennial bronchial asthma (1). The sodium salt of 5-(3-*p*-cyanophenoxy-2-hydroxy-1-propoxy)-2-(1*H*-tetrazol-5-yl)chromone[1] (I) is an experimental antiallergic compound whose primary route of administration in humans will probably be inhalation.

For toxicological evaluation of I, an assay was needed for quantitative measurement of unchanged drug in biological fluids. Such an assay was particularly important in inhalation toxicity to establish bioavailability and the dose-dependent nature of drug levels in serum and urine.

Tillman and Whymark (2) reported a spectrophotometric method for the determination of chromones in pharmaceutical preparations. However, this procedure would not be readily adaptable to either biological samples or the potentially large number of samples obtained during a subchronic or chronic toxicity study. TLC was unsuitable as a quantitative tool, and the high molecular weight and variety of polar functional groups precluded the use of GLC.

High-pressure liquid chromatography (HPLC), however, offered the following advantages over other potential methods of analysis: minimal sample preparation, relatively fast separation of the chromone from biological media, and a sensitive absorbance detector. The present report describes the application of HPLC to the analysis of I in biological fluids.

EXPERIMENTAL

Biological Samples—Urine and serum samples obtained during biological disposition studies (3) with 10-mg/kg po or iv doses of ^{14}C-I in rhesus monkeys, beagle dogs, and Charles River COBS-CD rats were assayed radiochemically as well as by HPLC. ^{14}C-I, specific activity of 1.8 μCi/mg, was labeled at the 2-position of the chromone ring and at the tetrazole carbon (asterisks in Structure I).

Apparatus—An HPLC system[2] equipped with a UV detector[3] (254 nm) and attached to a computing integrator[4] was used for the analyses. A 0.45-μm filter system[5] was used to filter mobile phase solvents. A liquid scintillation spectrophotometer[6] was used in radiochemical analyses. Counting was performed for a sufficient time to ensure less than a 2% counting error. All counts per minute were converted to disintegrations per minute after external standardization.

Column—A reversed-phase column[7], 30 × 0.63 cm o.d., with approximately 5000 theoretical plates and a 10-μm nonpolar packing material consisting of a monomolecular layer of octadecyltrichlorosilane was used for the reversed-phase chromatography.

Reagents—Glass-distilled water and methanol[8], the mobile phase solvents, were filtered to remove any particulate matter and to degas the solvents. A paired ion chromatography reagent containing tetrabutylammonium phosphate provided the mobile phase with a large organic counterion (4).

Mobile Phase—One vial of the paired ion reagent[9] was dissolved in 1000 ml of methanol–water (48:52), stirred for 5 min, and filtered through a 0.45-μm filter. The final concentration of the paired ion in solution was 0.005 *M*.

Sample Preparation—Urine, after volume measurement, and serum samples collected at various time intervals were kept frozen until assayed. Prior to HPLC analysis, aliquots of urine samples were centrifuged[10] at 5–10° for 20 min at 10,000 rpm to remove particulate matter. Aliquots (0.5–1.0 ml) of serum samples were pipeted into 12-ml conical-bottom centrifuge tubes. After the addition of equal volumes of methanol, they were mixed on a vortex mixer and centrifuged[10] at 5–10° for 20 min to pack precipitated protein.

In preparation for radiochemical assays, aliquots of urine or serum samples were added directly to the liquid scintillator (5).

Chromatographic Procedure—The mobile phase, containing the paired ion, was set at a flow rate of 1.0 ml/min (inlet pressure of 1400 psig) at ambient temperature. The unattenuated detector signal was fed directly to the computing integrator.

All sample injections (1 μl) were made in triplicate with the flow stopped. Standard samples of I, 2–200 ng/μl, used to establish the standard curve were injected daily to assure that the same detector response and column conditions were maintained. Biological levels of I in standards and samples were calculated using the external standard technique.

Calculations—After samples of I of known concentrations (10 and 30 ng/μl) were injected, the integrator calculated the peak area, based on absorbance, detector response, and a calibration factor (*kf*) using:

$$kf = \frac{\text{area} \times 10^{kf\ \exp}}{\text{concentration}} \qquad \text{(Eq. 1)}$$

After several injections of the standard, a mean *kf* value was calculated and used in Eq. 2 to calculate biological levels of I in unknown samples:

$$\text{concentration} = \frac{\text{area}}{kf \times 10^{kf\ \exp}} \qquad \text{(Eq. 2)}$$

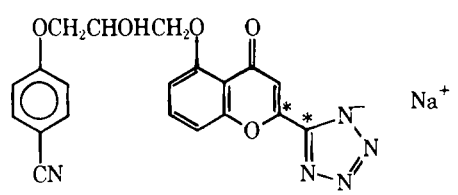

I

[1] Miles Laboratories, Elkhart, Ind.
[2] ALC/GPC 204, Waters Associates, Milford, Mass.
[3] Model 440, Waters Associates, Milford, Mass.
[4] Autolab System I, Spectra-Physics, Santa Clara, Calif.
[5] Millipore Corp., edford, Mass.
[6] Tri-Carb model 3375, Packard Instruments Co., Downers Grove, Ill.
[7] μBondapak C_{18}, Waters Associates, Milford, Mass.
[8] Spectroquality, Matheson, Coleman & Bell, Norwood, Ohio.
[9] PIC Reagent A, Waters Associates, Milford, Mass.
[10] Model RC-2, Ivan Sorvall, Inc., Norwalk, Conn.

0022-3549/78/0800-1185$01.00/0
© 1978, American Pharmaceutical Association

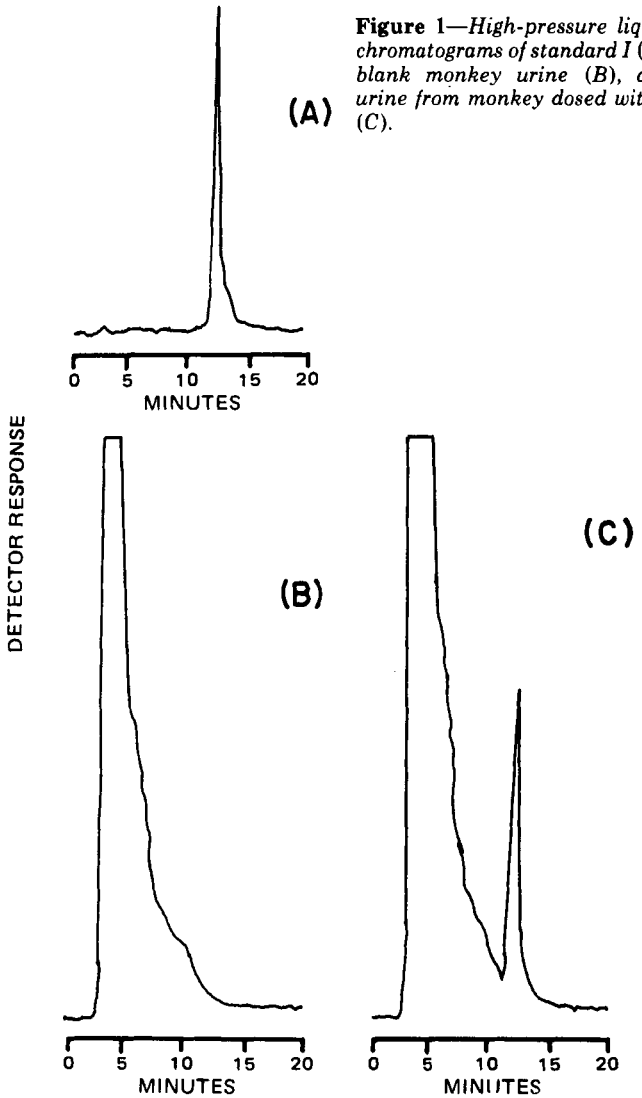

Figure 1—*High-pressure liquid chromatograms of standard I (A), blank monkey urine (B), and urine from monkey dosed with I (C).*

RESULTS AND DISCUSSION

Figure 1 represents typical chromatograms of the standard, urine from undosed monkeys, and urine from monkeys dosed with I. The retention time for I was approximately 11 min. The established techniques separated the chromone from the physiological components of urine and serum from monkeys, dogs, rats, and humans.

Table I—Method Analysis Comparison

Sample[a]	Radiochemical Assay[b], ng Equivalent I/μl	HPLC[b], ng/μl
Dog urine	11.98 ± 0.07	12.02 ± 0.06
Monkey urine	35.71 ± 0.56	36.16 ± 0.11
Rat serum	4.37 ± 0.10	4.18 ± 0.06
Dog serum	3.01 ± 0.08	3.03 ± 0.07

[a] The compound was administered intravenously to dogs and monkeys and orally to rats. [b] The number of replicate assays on the same sample was 10 in the radiochemical system and six in the HPLC system.

The linearity of detector response for I was in the concentration range of 2–200 ng/μl. The sensitivity limit for biological levels of I was 1 ng/μl. The injection technique variation for triplicate 1-μl injections of the same sample was consistently 1–3%. With an appropriate internal standard and/or an automatic injection system, this injection variation could be greatly reduced.

The accuracy of the HPLC method was determined by comparing the computed biological levels of I with those measured by liquid scintillation counting of the same urine and serum samples from monkeys, rats, and dogs dosed with ^{14}C-I. From the biological fluid of each species, the HPLC fraction containing I was collected, analyzed radiochemically, and determined to contain all of the radioactivity of the injected sample. TLC of identical biological samples yielded only one spot. Table I shows that biological concentrations of I, using either method, were not significantly different.

HPLC proved to be a highly sensitive, simple, and fast technique to quantitate I in biological fluids. This method is currently being used to monitor physiological levels of unlabeled I after inhalation of the chromone by monkeys and rats. HPLC can probably be a useful tool for the analysis of other chromone compounds in biological fluids.

REFERENCES

(1) D. L. Francis, J. W. Spicer, W. A. Taylor, and B. T. Warren, presented at the Fifth International Symposium on Medicinal Chemistry, Paris, France, July 1976.

(2) J. Tillman and D. W. Whymark, *Analyst*, **96**, 689 (1971).

(3) I. A. Muni, J. L. Leeling, R. J. Helms, and N. Johnson, Jr., *Toxicol. Appl. Pharmacol.*, **43**, 527 (1978).

(4) D. P. Wittmer, N. O. Nuessle, and W. G. Haney, *Anal. Chem.*, **47**, 1422 (1975).

(5) B. M. Phillips and T. S. Miya, *J. Pharm. Sci.*, **53**, 1098 (1964).

ACKNOWLEDGMENTS

Presented in part at the Federation of American Societies for Experimental Biology, Chicago, Ill., April 1977.

The authors thank Rick Minegar for technical assistance.

Assignment by ^{13}C-NMR Spectroscopy of Configuration at C-5 in 17α-Ethylestran-17β-ol, an Impurity in the Anabolic Steroid Ethylestrenol

ROXANNE DESLAURIERS *, FARIZA HASAN *, BRUCE A. LODGE ‡x, and IAN C. P. SMITH *

Received June 15, 1976, from the *Division of Biological Sciences, National Research Council, Ottawa, Ontario, Canada K1A 0R6, and the ‡Chemical Standard Division, Health Protection Branch, Tunney's Pasture, Ottawa, Ontario, Canada K1A 0L2. Accepted for publication November 21, 1977.

Abstract □ The stereochemistry at C-5 in 17α-ethylestran-17β-ol, found as an impurity in ethylestrenol, was assigned by ^{13}C-NMR spectroscopy. The hydrogen atom attached to C-5 is in the α-configuration. Resonance assignments were confirmed by partial deuteration, off-resonance ^{13}C-(^{1}H)-decoupling, and comparison with model compounds.

Keyphrases □ 17α-Ethylestran-17β-ol—impurity in ethylestrenol, stereochemistry at C-5 assigned □ Ethylestrenol impurity—stereochemistry at C-5 assigned □ Stereochemistry—at C-5 of 17α-ethylestran-17β-ol, impurity in ethylestrenol □ Anabolic steroids—ethylestrenol impurity, stereochemistry at C-5 assigned

Anabolic steroids are used medically for conditions characterized by wastage of protein and bone (1). Because of their particular properties, they are abused nonmedically to increase muscle development and to improve athletic performance (2). Numerous undesirable side effects have been reported (1), but it is not clear whether such side effects are due to the drugs themselves or to impurities.

As part of a screening procedure to isolate and identify impurities in anabolic steroids by GLC, the drug ethylestrenol (17α-ethylestr-4-en-17β-ol) (I) was examined. An impurity that may be present (up to 2%) (3) is 17α-ethylestran-17β-ol (II*a*); the stereochemistry of this compound at C-5 was determined by ^{13}C-NMR spectroscopy. It is reasonable to expect that II*a* will have some hormonal activity of its own (4).

To assist in the elucidation of the ^{13}C-NMR spectrum of II*a*, 17α-ethyl-5α-estran-17β-ol-4,5-d_2 (II*b*) was synthesized from I, and 17α-ethyl-5α-estran-17β-ol-4,5,20,20,21,21,21-d_7 (II*c*) was synthesized from 17α-ethinyl-17β-hydroxyestr-4-ene[1] (III).

EXPERIMENTAL

GLC—A solution of I in acetone (1 mg/ml) was chromatographed on 3% OV-7 on Chromosorb W at 210°. The conditions were: nitrogen carrier gas, 50 ml/min; and flame-ionization detector gases, hydrogen, 45 ml/min, and air, 500 ml/min. Under these conditions, II*a*, present at a level of about 0.7%, separated from I. Retention times were: I, 656 sec; and II*a*, 562 sec. A mass spectrum of II*a* (obtained by GLC–mass spectrometry) showed a molecular ion at *m/e* 290 and many features similar to those of the mass spectrum of I but 2 *m/e* units higher, which suggested that the impurity was the dihydro derivative of I.

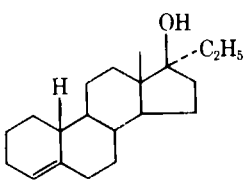

I

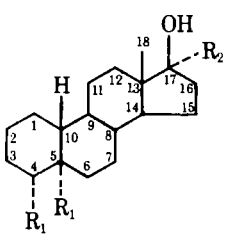

II*a*: R_1 = H, R_2 = C_2H_5
II*b*: R_1 = D, R_2 = C_2H_5
II*c*: R_1 = D, R_2 = C_2D_5

Synthesis of II*a*—Ethylestrenol (200 mg) was dissolved in 200 ml of ethanol and hydrogenated at atmospheric pressure over 10% palladium-on-charcoal (10 mg) for 1 hr. After the catalyst had been removed by filtration, the ethanolic solution was evaporated to dryness, whereupon the product crystallized. Recrystallization from acetone–water gave II*a*, mp 62–63° (86%). The GLC retention time, the mass spectrum, and the IR spectrum of II*a* were identical with those of the impurity isolated from I.

Anal.—Calc. for $C_{20}H_{32}O$: C, 82.1; H, 11.8. Found: C, 82.7; H, 11.7.

Synthesis of II*b*—This synthesis utilized a method similar to that for II*a*, except that deuterium was used in place of hydrogen. The mass spectrum of II*b* showed that at least two atoms of deuterium were incorporated, and the height of the $(M + 1)^+$ peak relative to the M^+ peak suggested that a partial incorporation of a third atom of deuterium occurred. The melting point of II*b* was 62–63°; a mixture of II*a* and II*b* gave the same value, indicative of no configurational heterogeneity.

Synthesis of II*c*—Compound III (200 mg) was reacted with deuterium as for I. The mass spectrum of II*c* showed that at least seven atoms of deuterium were incorporated.

^{13}C-NMR Spectroscopy—^{13}C-NMR spectra were recorded[2] in deuterochloroform with complete proton decoupling. Chemical shifts are expressed with respect to tetramethylsilane with an accuracy of ±0.05 ppm.

DISCUSSION

Three methods were used to assign the ^{13}C-NMR spectra: comparison with model compounds (5, 6) corrected for substituent effects (7), analysis of multiplet splitting in off-resonance decoupled spectra, and measurement of deuterium substitution effect on chemical shifts and resonance intensities.

The ^{13}C-NMR spectrum of II*a* was assigned by comparison with the model compounds 5α- and 5β-androstane (5, 8), 5α-androstane-17α-ol, 5α-androstane-17β-ol (9), 5α-cholestane (5), and *trans-anti-trans*-perhydrophenanthrene (6). 5α- and 5β-Androstane differ in chemical shifts mainly at the resonances for C-19, C-9, C-7, and C-5. Assignments were verified by studying the multiplet structures in off-resonance decoupled spectra as well as by deuterium substitution in II*b* and II*c*.

Off-resonance decoupling should lead to the following multiplet structures for the various carbon resonances in II*a*: singlets, 13 and 17; doublets, 5, 8, 9, 10, and 14; triplets, 1, 2, 3, 4, 6, 7, 11, 12, 15, 16, and 20; and quartets, 18 and 21.

Deuterium substitution is useful for the assignment of possibly ambiguous resonances. Its effects are twofold. There is a substantial decrease in intensity for the substituted carbon because of the extreme lengthening of the spin-lattice relaxation time, T_1, as well as splitting of the resonance into a multiplet pattern because of ^{2}H–^{13}C-spin–spin coupling. In addition, the chemical shift of the deuterated carbon usually differs significantly from that of its protonated analog (10–15). Thus, depending on the signal-to-noise ratio of the ^{13}C-spectrum, the resonance of a deuter-

[1] Organon Ltd., West Hill, Ontario, Canada.

[2] Varian CFT-20 and XL-100 NMR spectrometers, Georgetown, Ontario, Canada.

0022-3549/78/0800-1187$01.00/0
© 1978, American Pharmaceutical Association

Table I—^{13}C-Chemical Shifts of IIa–IIc and the Influence of Deuteration and Off-Resonance Decoupling

Chemical Shifts[a]			Multiplet Structure[b]	Intensity upon Deuterium Substitution[c]	Assignment[d]
IIa	IIb	IIc			
83.52	83.56	83.43	s	d	17
49.86	49.85	49.86	d	—	9
48.55	48.55	48.55	d	—	14
47.46	47.35	47.37	d	d	10
46.52	46.54	46.52	s	—	13
43.34	43.33, 43.27	43.34, 43.31, 43.21	d	d	5
42.29	42.29	42.30	d	—	8
34.56	34.45	34.59, 34.49, 34.43	t	d	4†
34.03	33.93	34.00, 33.94, 33.83	t	d	6†
33.70	33.74	33.69	t	—	16
31.62	31.63	31.63	t	—	7
30.93	30.91	30.94	t	—	1
30.35	30.32	30.33	t	—	12
28.87	28.88	28.54	t	d	20
26.84	26.85, 26.74	26.79	t	d	2*
26.45	26.44, 26.30	26.44, 26.39, 26.35	t	d	3*
25.40	25.40	25.42	t	—	11
23.47	23.48	23.49	t	—	15
14.45	14.45	14.48	q	—	18
7.79	7.83	7.08	q	d	21

[a] In parts per million downfield from the internal standard tetramethylsilane; accuracy of chemical shifts is 0.05 ppm. [b] Multiplet structure in off-resonance decoupled spectrum. [c] If no change was observed, a − sign is indicated; a "d" symbolizes a decrease in intensity. Data are for IIc. [d] The * and † assignments may be reversed.

ated carbon can be completely absent from the spectrum or appear slightly shifted from its usual position with an observable ^{13}C–^{2}H-coupling. With partial deuteration, a resonance from the residual protonated carbon may appear with the usual chemical shift but reduced intensity. The chemical shifts and linewidths of resonances due to carbons adjacent to the position of deuterium incorporation may be affected also (10, 14, 15).

Reduction of the double bond in ethylestrenol in the presence of deuterium gas should lead to deuterium incorporation in IIa at positions 4 and 5 as well as at the adjacent carbons 3, 6, and 10 because of allylic migration. With III, reduction in the presence of deuterium gas should affect C-20, C-21, C-4, and C-5 as well as C-3, C-6, and C-10.

Table I gives the chemical shifts and assignments of the 17α-ethyl-5α-estran-17β-ols studied. The configuration at position 5 is assigned as 5α based on a chemical shift observed at 49.9 ppm attributed to C-9 (in accord with the calculated chemical shift for this position: 5α, 49.9; and 5β, 35.4 ppm). The 5β-isomer is not expected to show any resonance at such a low field. The chemical shifts of C-7 and C-5 are also more in accord with those calculated for the 5α-isomer (C-7, calculated = 32.6, observed = 31.6 ppm; C-5, calculated = 41.9, observed = 43.3 ppm) than for the 5β-isomer (C-7, calculated = 27.1; C-5, calculated = 36.0 ppm).

To assign the remaining resonances in ethyl-5-estran-17β-ol, the multiplet structures of the off-resonance decoupled spectra were evaluated. Two singlets at 46.52 and 83.52 ppm were attributed to C-13 and C-17. Carbon-17 also showed an upfield shift of 0.1 ppm in IIc as a result of deuterium substitution at C-20. The assignments are in good agreement with the values calculated for these carbons (C-13, 45 ppm; C-17, 82 ppm). Two quartets were assigned to C-18 and C-21. Carbon-21 showed a very broad resonance in IIc and was shifted upfield ~0.7 ppm as a result of the deuterium substitution.

The doublets were attributed to C-5, C-8, C-9, C-10, and C-14. Carbon 9 was unperturbed by deuteration, as were C-14 and C-8. The assignments for C-9, C-14, and C-8 (Table I) are in good agreement with the values calculated for these carbons (49.9, 48.8, and 41.4 ppm, respectively). The doublets assigned to C-5 and C-10 both showed decreased intensities in IIb and IIc because of partial deuterium substitution at these carbons. The chemical shift calculated for C-5 of the 5α-isomer (41.9) is in reasonable agreement with the assigned value of 43.3 ppm, whereas the calculated value for the 5β-isomer is 36.0 ppm. The assignment of C-10 (47.5 ppm) corresponds well with that reported for the same carbon in perhydrophenanthrene (48.2 ppm).

Triplet structures in the off-resonance decoupled spectra of C-1, C-2, C-7, C-11, C-12, C-15, and C-16 should be unperturbed by deuteration in IIb and IIc, whereas C-3, C-4, and C-6 should be affected by deuterium incorporation directly at these carbon atoms. Carbon-1 was assigned by comparison with the same carbon in perhydrophenanthrene (30.1 ppm). Carbons-2 and 3 were assigned at 26.5 and 26.8 ppm, respectively, and can be compared to similar positions in perhydrophenanthrene at 27.1 and 26.8 ppm. Both C-2 and C-3 appeared to be affected by deuteration in IIb and IIc, showing decreased resonance intensities and upfield isotope shifts of ~0.1 ppm because of interactions with deuterium on neighboring (vicinal and geminal) carbons.

Carbons-4 and 6 were assigned at 34.56 and 34.03 ppm, respectively, by comparison with perhydrophenanthrene (35.0 and 34.6 ppm); both showed decreased intensities for the residual proton-bearing carbons with upfield shifts of 0.1 ppm because of the presence of neighboring deuterium-substituted carbons. With such small differences in chemical shift between C-2 and C-3 and C-4 and C-6, absolute assignments are difficult and those in Table I may be reversed.

Carbon-7 was assigned by calculating the chemical shift after removal of the 19-CH_3 group from 5α-androstane (calculated = 32.6 ppm, observed = 31.6 ppm). Carbon-13 was calculated in a manner similar to that used for C-7 (calculated = 26.3, observed = 25.4 ppm). Carbon-12 was assigned based on calculation of a γ-substituent effect on 5α-androstane-17β-ol (calculated = 34.4, observed = 30.35 ppm). Carbon-15 was assigned at 23.47 ppm by comparison with a similar position in 5α-cholestane (24.2 ppm) and 5α-androstane-17β-ol (23.4 ppm). Carbon-16 (33.7 ppm) was assigned by calculating either the effect of a hydroxyl substituent at C-17 in 5α-cholestane (calculated = 34.3 ppm) or a β- and γ-alkane substituent effect in 5α-androstane-17β-ol (calculated = 34.6 ppm).

In summary, the chemical shifts assigned to the various carbon atoms of IIa are in complete agreement with the structure of 17α-ethyl-5α-estran-17β-ol and with the hypothetical ^{13}C-spectrum based on contemporary knowledge of the influence of substituents on ^{13}C-chemical shifts.

REFERENCES

(1) "The Extra Pharmacopoeia," Pharmaceutical Press, London, England, 1972, p. 1663.

(2) L. C. Johnson and J. P. O'Shea, *Science*, **164**, 957 (1969).

(3) "British Pharmacopoeia 1973, Addendum 1975," Her Majesty's Stationery Office, London, England, 1975, p. 18.

(4) J. A. Vida, "Androgens and Anabolic Agents," Academic, New York, N.Y., 1969.

(5) J. W. Blunt and J. B. Stothers, *Org. Magn. Reson.*, **9**, 439 (1977).

(6) D. K. Dalling and D. M. Grant, *J. Am. Chem. Soc.*, **96**, 1827 (1974).

(7) J. B. Stothers, "Carbon-13 NMR Spectroscopy," Academic, New York, N.Y., 1972, pp. 65, 66.

(8) H. Eggert and C. Djerassi, *J. Org. Chem.*, **38**, 3788 (1973).

(9) J. W. ApSimon, H. Beierbeck, and J. K. Saunders, *Can. J. Chem.*, **51**, 3874 (1973).

(10) J. B. Stothers, C. T. Tan, A. Nickon, F. Huang, R. Sridhar, and R. Weglein, *J. Am. Chem. Soc.*, **94**, 8581 (1972).

(11) H. N. Colli, V. Gold, and J. E. Pearson, *J. Chem. Soc. Chem. Commun.*, **1973**, 408.
(12) Y. K. Grishin, N. M. Sergeyev, and Y. A. Ustynyuk, *Mol. Phys.*, **22**, 711 (1971).
(13) D. Lauer, E. L. Matell, D. D. Traficante, and G. E. Maciel, *J. Am. Chem. Soc.*, **94**, 5335 (1972).
(14) D. H. Hunter, A. L. Johnson, J. B. Stothers, A. Nickon, J. L. Lambert, and D. F. Covey, *J. Am. Chem. Soc.*, **94**, 8582 (1972).
(15) A. P. Tulloch and M. Mazurek, *J. Chem. Soc. Chem. Commun.*, **1973**, 692.

ACKNOWLEDGMENTS

The authors are grateful to Professors J. B. Stothers and J. Blunt for a critical evaluation of the manuscript.
This paper is NRCC Publication No. 15491.

COMMUNICATIONS

Lack of Influence of Rabbit Nictitating Membrane on Miosis Effect of Pilocarpine

Keyphrases □ Pilocarpine hydrochloride—miosis induction, effect of rabbit nictitating membrane □ Nictitating membrane, rabbit—effect on miosis induction by pilocarpine hydrochloride □ Ophthalmic cholinergics—pilocarpine hydrochloride, effect of rabbit nictitating membrane on miosis induction

To the Editor:

The rabbit frequently is used in ophthalmological research even though it possesses some ocular anatomical dissimilarities to the human. There are differences in the normal tear volume and the tear turnover rate between humans and rabbits (1, 2). A prominently different anatomical feature of the rabbit is the nictitating membrane, a so-called third eyelid. This epithelially covered sheet of cartilaginous tissue retracts into the nasal canthus secondarily to retractions of the globe with contraction of the retractor bulbi muscles (3). Because this membrane is well vascularized and occupies part of the precorneal space, it conceivably could influence the dynamics of instilled material in the eye (3, 4).

Ten New Zealand albino rabbits of either sex, 1.5–2.5 kg, were used in the present study. A 50-μl dose of 2% pilocarpine hydrochloride[1] was administered to the right eye by slightly pulling away the lower eyelid from the globe and allowing the measured drop to fall onto the cornea and collect into the lower conjunctival sac. After a few seconds, the eyelid was carefully returned to its normal position. Pupil diameters were measured under controlled lighting conditions using a micrometer caliper held at a constant distance between the animal's and the observer's eyes.

At the completion of the first experiment, in which the control response to the drug was recorded, the nictitating membranes were surgically removed at the base from the test eyes of all rabbits. After 1 week, the operated animals were handled in the same manner as before and were treated with the same lot of drug as in the first experiment. Pupil size measurements were made in the usual manner for comparison with the previous week's results. The nictitating membrane had no apparent effect on the response parameters of pilocarpine-induced miosis following topical dosing of an aqueous solution (Table I).

These results are surprising for a number of reasons. First of all, the nictitating membrane can be moved approximately halfway across the cornea. In so doing, the membrane occupies a significant portion of the precorneal space. Therefore, one would expect a reduction in the fluid volume in the normal rabbit eye and a concomitant loss of drug available for absorption. However, the movement of the membrane across the eye is accompanied by a retraction of the eye into the orbit. Thus, with its movement, there conceivably could be no net change in the volume of fluid that the rabbit eye can hold.

Second, the membrane is well vascularized and there are many lymphatic nodules in the connective tissue (3). Therefore, the presence of the membrane might provide a competitive depot to channel drug away from the corneal absorption process. Third, tear secretions from the nictitans and Harderian glands containing oil and mucus empty into the nictitating membrane (3). The removal of the membrane carries with it the contribution of the nictitans glandular secretions to the composition of the tears and its possible effect on steady-state tear volume and/or turnover rate. It may be that some of these processes are operative but in effect cancel one another.

An alternative explanation could be that a relative lack of movement of the nictitating membrane occurs throughout drug absorption. We observed that, after dosing, the rabbits may close their eyelids for 15–30 sec but that the membranes remain retracted. Quantitatively, Chrai *et al.* (2) showed that 1 min after dosing a 50-μl aqueous drop, only 28.2% of the original instilled volume remained. Consequently, pilocarpine hydrochloride absorption may be rapid relative to the nictitating membrane activity. Thus, our experiments indicate that the membrane in its fully retracted state has no effect on the response to pilocarpine solution as observed under these

Table I—Miosis Induced by 50 μl of 2% Pilocarpine Hydrochloride Solution in Albino Rabbit Eyes before and after Removal of the Nictitating Membrane

Area under Curve, mm/mm × hr	Peak Intensity[a]	Total Duration, hr	Baseline Diameter, mm
Before Removal of Nictitating Membrane (n = 10)			
0.9194[b] ±0.2058	0.4275 ±0.0445	4.38 ±1.02	4.975 ±0.611
After Removal of Nictitating Membrane (n = 8[c])			
0.9388 ±0.3057	0.3911 ±0.0641	4.32 ±0.96	5.181 ±0.575

[a] Peak intensity = $[(\text{pupil diameter})_{t_0} - (\text{pupil diameter})_{t_{max}}]/(\text{pupil diameter})_{t_0}$. [b] Mean ± *SD*. [c] One rabbit suffered from debilitating diarrhea and another died; therefore, only eight rabbits were used after removal of the nictitating membrane.

[1] Isopto Carpine 2%, Alcon Laboratories, Fort Worth, TX 76101.

0022-3549/78/0800-1189$01.00/0
© 1978, American Pharmaceutical Association

(11) H. N. Colli, V. Gold, and J. E. Pearson, *J. Chem. Soc. Chem. Commun.*, **1973**, 408.
(12) Y. K. Grishin, N. M. Sergeyev, and Y. A. Ustynyuk, *Mol. Phys.*, **22**, 711 (1971).
(13) D. Lauer, E. L. Matell, D. D. Traficante, and G. E. Maciel, *J. Am. Chem. Soc.*, **94**, 5335 (1972).
(14) D. H. Hunter, A. L. Johnson, J. B. Stothers, A. Nickon, J. L. Lambert, and D. F. Covey, *J. Am. Chem. Soc.*, **94**, 8582 (1972).
(15) A. P. Tulloch and M. Mazurek, *J. Chem. Soc. Chem. Commun.*, **1973**, 692.

ACKNOWLEDGMENTS

The authors are grateful to Professors J. B. Stothers and J. Blunt for a critical evaluation of the manuscript.
This paper is NRCC Publication No. 15491.

COMMUNICATIONS

Lack of Influence of Rabbit Nictitating Membrane on Miosis Effect of Pilocarpine

Keyphrases □ Pilocarpine hydrochloride—miosis induction, effect of rabbit nictitating membrane □ Nictitating membrane, rabbit—effect on miosis induction by pilocarpine hydrochloride □ Ophthalmic cholinergics—pilocarpine hydrochloride, effect of rabbit nictitating membrane on miosis induction

To the Editor:

The rabbit frequently is used in ophthalmological research even though it possesses some ocular anatomical dissimilarities to the human. There are differences in the normal tear volume and the tear turnover rate between humans and rabbits (1, 2). A prominently different anatomical feature of the rabbit is the nictitating membrane, a so-called third eyelid. This epithelially covered sheet of cartilaginous tissue retracts into the nasal canthus secondarily to retractions of the globe with contraction of the retractor bulbi muscles (3). Because this membrane is well vascularized and occupies part of the precorneal space, it conceivably could influence the dynamics of instilled material in the eye (3, 4).

Ten New Zealand albino rabbits of either sex, 1.5–2.5 kg, were used in the present study. A 50-μl dose of 2% pilocarpine hydrochloride[1] was administered to the right eye by slightly pulling away the lower eyelid from the globe and allowing the measured drop to fall onto the cornea and collect into the lower conjunctival sac. After a few seconds, the eyelid was carefully returned to its normal position. Pupil diameters were measured under controlled lighting conditions using a micrometer caliper held at a constant distance between the animal's and the observer's eyes.

At the completion of the first experiment, in which the control response to the drug was recorded, the nictitating membranes were surgically removed at the base from the test eyes of all rabbits. After 1 week, the operated animals were handled in the same manner as before and were treated with the same lot of drug as in the first experiment. Pupil size measurements were made in the usual manner for comparison with the previous week's results. The nictitating membrane had no apparent effect on the response parameters of pilocarpine-induced miosis following topical dosing of an aqueous solution (Table I).

These results are surprising for a number of reasons. First of all, the nictitating membrane can be moved approximately halfway across the cornea. In so doing, the membrane occupies a significant portion of the precorneal space. Therefore, one would expect a reduction in the fluid volume in the normal rabbit eye and a concomitant loss of drug available for absorption. However, the movement of the membrane across the eye is accompanied by a retraction of the eye into the orbit. Thus, with its movement, there conceivably could be no net change in the volume of fluid that the rabbit eye can hold.

Second, the membrane is well vascularized and there are many lymphatic nodules in the connective tissue (3). Therefore, the presence of the membrane might provide a competitive depot to channel drug away from the corneal absorption process. Third, tear secretions from the nictitans and Harderian glands containing oil and mucus empty into the nictitating membrane (3). The removal of the membrane carries with it the contribution of the nictitans glandular secretions to the composition of the tears and its possible effect on steady-state tear volume and/or turnover rate. It may be that some of these processes are operative but in effect cancel one another.

An alternative explanation could be that a relative lack of movement of the nictitating membrane occurs throughout drug absorption. We observed that, after dosing, the rabbits may close their eyelids for 15–30 sec but that the membranes remain retracted. Quantitatively, Chrai *et al.* (2) showed that 1 min after dosing a 50-μl aqueous drop, only 28.2% of the original instilled volume remained. Consequently, pilocarpine hydrochloride absorption may be rapid relative to the nictitating membrane activity. Thus, our experiments indicate that the membrane in its fully retracted state has no effect on the response to pilocarpine solution as observed under these

Table I—Miosis Induced by 50 μl of 2% Pilocarpine Hydrochloride Solution in Albino Rabbit Eyes before and after Removal of the Nictitating Membrane

Area under Curve, mm/mm × hr	Peak Intensity[a]	Total Duration, hr	Baseline Diameter, mm
Before Removal of Nictitating Membrane (n = 10)			
0.9194[b] ±0.2058	0.4275 ±0.0445	4.38 ±1.02	4.975 ±0.611
After Removal of Nictitating Membrane (n = 8[c])			
0.9388 ±0.3057	0.3911 ±0.0641	4.32 ±0.96	5.181 ±0.575

[a] Peak intensity = $[(\text{pupil diameter})_{t_0} - (\text{pupil diameter})_{t_{max}}]/(\text{pupil diameter})_{t_0}$. [b] Mean ± *SD*. [c] One rabbit suffered from debilitating diarrhea and another died; therefore, only eight rabbits were used after removal of the nictitating membrane.

[1] Isopto Carpine 2%, Alcon Laboratories, Fort Worth, TX 76101.

0022-3549/78/0800-1189$01.00/0
© 1978, American Pharmaceutical Association

experimental conditions. However, under conditions where the membrane may cover the cornea or by its movement may mechanically remove instilled materials, *e.g.*, suspensions and inserts, absorption kinetics may possibly be altered.

Miller and O'Conner (4) found that dexamethasone sodium phosphate inhibited limbal wound healing in normal rabbit eyes but did not do so when the nictitating membrane had been surgically removed. Our results, as well as the results obtained by Miller and O'Conner, indicate that the influence of the membrane may vary for each preparation and/or experimental condition.

(1) S. Mishima, A. Gasset, and S. D. Klyce, *Invest. Ophthalmol.*, **5**, 264 (1966).

(2) S. S. Chrai, T. F. Patton, A. Mehta, and J. R. Robinson, *J. Pharm. Sci.*, **62**, 1112 (1973).

(3) J. H. Prince, "The Rabbit in Eye Research," Charles C Thomas, Springfield, Ill., 1970, pp. 79–85.

(4) D. Miller and P. O'Conner, *Acta Ophthalmol.*, **55**, 586 (1977).

Louis M. DeSantis
Ronald D. Schoenwald ˣ
New Product Research
Department of Ophthalmology
Alcon Laboratories, Inc.
Fort Worth, TX 76101

Received May 1, 1978.
Accepted for publication June 1, 1978.

Determinations of Amygdalinamide, Amygdalin Acid, and 2-Propanol in Amygdalin Dosage Forms from Mexico

Keyphrases □ Amygdalinamide—synthesized, high-pressure liquid chromatographic analysis in amygdalin dosage forms □ Amygdalin acid—synthesized, high-pressure liquid chromatographic analysis in amygdalin dosage forms □ 2-Propanol—GLC analysis in amygdalin dosage forms □ Impurities—amygdalinamide, amygdalin acid, and 2-propanol, analyses in amygdalin dosage forms □ High-pressure liquid chromatography—analyses, amygdalinamide and amygdalin acid in amygdalin dosage forms

To the Editor:

Assay results for amygdalin dosage forms from Mexico were reported earlier (1). In addition to amygdalin[1] (I), the injectable dosage forms contain significant amounts of amygdalinamide[1] (II) and amygdalin acid[1] (III), hydrolysis products of amygdalin, plus 2-propanol. This communication reports the determination of these three impurities in the amygdalin dosage forms.

Amygdalinamide and amygdalin acid in the amygdalin dosage forms were quantified by an assay that required reference standards of the amide and acid of known purity. Since these standards were unavailable commercially, they were prepared.

Amygdalinamide was prepared from (*R*)-amygdalin by treatment with ammonium hydroxide. The crude product

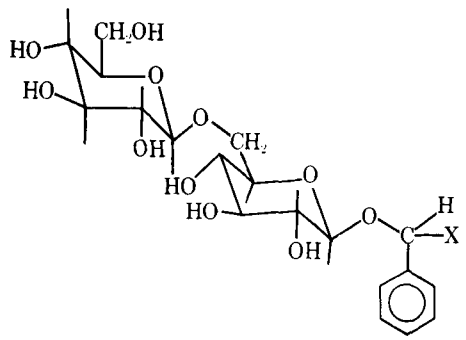

I: X = CN

II: X = C(=O)NH$_2$

III: X = C(=O)OH

was purified by a preparative high-performance liquid chromatographic (HPLC) procedure that used a C_{18}-bonded silica[2] column and an aqueous methanol mobile phase. When this mobile phase was changed to 0.1 *M* KH_2PO_4, the purified amygdalinamide was separated into two major components of nearly equal intensity plus two very minor impurities and a trace of another. On the basis of peak enhancements, these impurities were identified as (*R*)- and (*S*)-amygdalins and amygdalin acid, respectively. Identity of the principal components in purified amygdalinamide was based on spectral evidence. IR data show an intense band near 5.95 μm assigned to the primary amide, broad absorptions between 9 and 10 μm assigned to carbohydrate, and bands near 13.2 and 14.3 μm assigned to phenyl. The ^{1}H-NMR data were consistent with the proposed structure. Only one peak was found in the region where the benzylic protons were expected; its area was one-fifth that of the phenyl protons. The ^{13}C-NMR data were consistent for a mixture of (*R*)- and (*S*)-amygdalinamides. The amide carbon appeared as two bands centering near 136.6 ppm[3], the phenyl carbons appeared as a group of at least six bands centering near 129.4 ppm, and the two anomeric carbons in the glucose moieties appeared as three bands centering near 101.9 ppm. The benzylic carbon was among the nonanomeric glucosido carbons, which appeared as a complex of many bands. These observations were consistent with those reported (2) for a mixture of (*R*)- and (*S*)-amygdalins. GLC–mass spectral analysis of the trimethylsilyl derivative on a phenyl methyl silicone column (OV-17) showed only one major peak; the mass spectral data for this peak were consistent for the proposed structure as the octatrimethylsilyl derivative.

The purity of the amygdalinamide sample was estimated at 90 ± 1.5% on the basis of chromatographic and elemental data and the results of an NMR assay[4] with pyrocatechol[5] as the internal standard.

[1] Amygdalin is mandelonitrile-β-D-glucosido-6-β-D-glucoside (I). Amygdalinamide is mandeloamide-β-D-glucosido-6-β-D-glucoside (II). Amygdalin acid is mandelic acid-β-D-glucosido-6-β-D-glucoside (III). In the amygdalin dosage forms, all three materials exist as nearly equal mixtures of the respective (*R*)- and (*S*)-epimers.

[2] Porasil C_{18}.

[3] Relative to tetramethylsilane as 0.00 ppm.

[4] This assay measured the total amount of phenyls in the sample. Since the HPLC data showed approximately 1% phenyl-containing impurities, this amount was subtracted from the total phenyls to give a sample purity of 90 ± 1.5%, which is consistent with the elemental data. The remainder of the sample was presumed to be 8.5% water, an amount derived by difference.

[5] Pyrocatechol, Aldrich Chemical Co., analyzed 99+% pure based on chromatographic, titrimetric, and elemental data.

0022-3549/78/0800-1190$01.00/0
© 1978, American Pharmaceutical Association

experimental conditions. However, under conditions where the membrane may cover the cornea or by its movement may mechanically remove instilled materials, *e.g.*, suspensions and inserts, absorption kinetics may possibly be altered.

Miller and O'Conner (4) found that dexamethasone sodium phosphate inhibited limbal wound healing in normal rabbit eyes but did not do so when the nictitating membrane had been surgically removed. Our results, as well as the results obtained by Miller and O'Conner, indicate that the influence of the membrane may vary for each preparation and/or experimental condition.

(1) S. Mishima, A. Gasset, and S. D. Klyce, *Invest. Ophthalmol.*, **5**, 264 (1966).

(2) S. S. Chrai, T. F. Patton, A. Mehta, and J. R. Robinson, *J. Pharm. Sci.*, **62**, 1112 (1973).

(3) J. H. Prince, "The Rabbit in Eye Research," Charles C Thomas, Springfield, Ill., 1970, pp. 79–85.

(4) D. Miller and P. O'Conner, *Acta Ophthalmol.*, **55**, 586 (1977).

Louis M. DeSantis
Ronald D. Schoenwald ˣ
New Product Research
Department of Ophthalmology
Alcon Laboratories, Inc.
Fort Worth, TX 76101

Received May 1, 1978.
Accepted for publication June 1, 1978.

Determinations of Amygdalinamide, Amygdalin Acid, and 2-Propanol in Amygdalin Dosage Forms from Mexico

Keyphrases □ Amygdalinamide—synthesized, high-pressure liquid chromatographic analysis in amygdalin dosage forms □ Amygdalin acid—synthesized, high-pressure liquid chromatographic analysis in amygdalin dosage forms □ 2-Propanol—GLC analysis in amygdalin dosage forms □ Impurities—amygdalinamide, amygdalin acid, and 2-propanol, analyses in amygdalin dosage forms □ High-pressure liquid chromatography—analyses, amygdalinamide and amygdalin acid in amygdalin dosage forms

To the Editor:

Assay results for amygdalin dosage forms from Mexico were reported earlier (1). In addition to amygdalin[1] (I), the injectable dosage forms contain significant amounts of amygdalinamide[1] (II) and amygdalin acid[1] (III), hydrolysis products of amygdalin, plus 2-propanol. This communication reports the determination of these three impurities in the amygdalin dosage forms.

Amygdalinamide and amygdalin acid in the amygdalin dosage forms were quantified by an assay that required reference standards of the amide and acid of known purity. Since these standards were unavailable commercially, they were prepared.

Amygdalinamide was prepared from (*R*)-amygdalin by treatment with ammonium hydroxide. The crude product

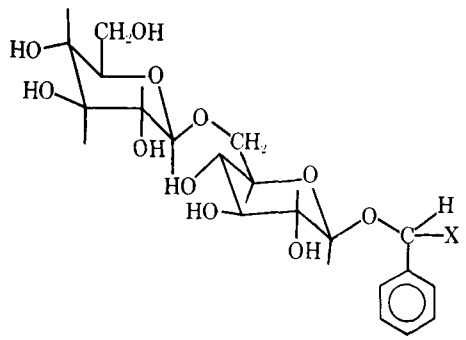

I: X = CN

II: X = C(=O)NH$_2$

III: X = C(=O)OH

was purified by a preparative high-performance liquid chromatographic (HPLC) procedure that used a C_{18}-bonded silica[2] column and an aqueous methanol mobile phase. When this mobile phase was changed to 0.1 *M* KH_2PO_4, the purified amygdalinamide was separated into two major components of nearly equal intensity plus two very minor impurities and a trace of another. On the basis of peak enhancements, these impurities were identified as (*R*)- and (*S*)-amygdalins and amygdalin acid, respectively. Identity of the principal components in purified amygdalinamide was based on spectral evidence. IR data show an intense band near 5.95 μm assigned to the primary amide, broad absorptions between 9 and 10 μm assigned to carbohydrate, and bands near 13.2 and 14.3 μm assigned to phenyl. The ^{1}H-NMR data were consistent with the proposed structure. Only one peak was found in the region where the benzylic protons were expected; its area was one-fifth that of the phenyl protons. The ^{13}C-NMR data were consistent for a mixture of (*R*)- and (*S*)-amygdalinamides. The amide carbon appeared as two bands centering near 136.6 ppm[3], the phenyl carbons appeared as a group of at least six bands centering near 129.4 ppm, and the two anomeric carbons in the glucose moieties appeared as three bands centering near 101.9 ppm. The benzylic carbon was among the nonanomeric glucosido carbons, which appeared as a complex of many bands. These observations were consistent with those reported (2) for a mixture of (*R*)- and (*S*)-amygdalins. GLC–mass spectral analysis of the trimethylsilyl derivative on a phenyl methyl silicone column (OV-17) showed only one major peak; the mass spectral data for this peak were consistent for the proposed structure as the octatrimethylsilyl derivative.

The purity of the amygdalinamide sample was estimated at 90 ± 1.5% on the basis of chromatographic and elemental data and the results of an NMR assay[4] with pyrocatechol[5] as the internal standard.

[1] Amygdalin is mandelonitrile-β-D-glucosido-6-β-D-glucoside (I). Amygdalinamide is mandeloamide-β-D-glucosido-6-β-D-glucoside (II). Amygdalin acid is mandelic acid-β-D-glucosido-6-β-D-glucoside (III). In the amygdalin dosage forms, all three materials exist as nearly equal mixtures of the respective (*R*)- and (*S*)-epimers.

[2] Porasil C_{18}.

[3] Relative to tetramethylsilane as 0.00 ppm.

[4] This assay measured the total amount of phenyls in the sample. Since the HPLC data showed approximately 1% phenyl-containing impurities, this amount was subtracted from the total phenyls to give a sample purity of 90 ± 1.5%, which is consistent with the elemental data. The remainder of the sample was presumed to be 8.5% water, an amount derived by difference.

[5] Pyrocatechol, Aldrich Chemical Co., analyzed 99+% pure based on chromatographic, titrimetric, and elemental data.

0022-3549/78/0800-1190$01.00/0
© 1978, American Pharmaceutical Association

Table I—Assay Results for Amygdalin Ampules[a]

U.S. Customs Group (Seizure Date)	Fill Volume, ml/Ampul	Amygdalin, mg/Ampul	Percent Label (3 g/Ampul)	Amygdalinamide, mg/Ampul	Amygdalin Acid, mg/Ampul	2-Propanol, mg/Ampul
74-2504-10919	9.05	1443	48.1	127	79	48
(12/28/1973)	9.30	1202	40.2	53	149	15
	9.00	1442	48.1	129	80	48
	9.05	1222	40.7	42	128	15
	8.90	1420	47.3	126	78	47
	9.20	1478	49.3	130	80	48
Average	9.08	1368	45.6	101	99	37
SD	0.11	122	4.1	42	31	17
75-2504-10716	10.20	1634	54.5	526	437	66
(11/09/1974)	10.20	1592	53.1	491	413	63
	9.80	1541	51.4	486	402	61
	10.00	1594	53.1	493	417	63
	10.00	1602	53.4	485	406	64
Average	10.06	1592	53.1	496	415	63
SD	0.18	33	1.1	17	14	2
75-2504-11744	10.05	1267	42.2	704	448	157
(05/21/1975)	9.80	1311	43.7	666	430	149
	9.90	1308	43.6	674	436	148
	11.20	1529	51.0	693	471	165
	10.20	1331	44.4	718	468	160
	10.00	1353	45.1	706	443	153
Average	10.19	1350	45.0	694	450	155
SD	0.33	92	3.1	20	17	7
76-2505-11569	9.65	1527	50.9	669	355	171
(04/11/1975)	10.05	1122	37.4	800	372	189
	9.85	1598	53.3	683	392	173
	10.05	1118	37.3	727	336	180
	10.00	1640	54.7	690	392	174
Average	9.92	1401	46.7	714	369	177
SD	0.17	260	8.7	53	24	7

[a] Relative to the weight of amygdalin in the same ampul, the weight of amygdalinamide ranged from 3 to 71%, the weight of amygdalin acid ranged from 5 to 35%, and the weight of 2-propanol ranged from 1 to 17%. Amygdalinamide and amygdalin acid are hydrolysis products believed to have formed during the autoclave process in the manufacturing scheme. 2-Propanol was probably the extraction solvent used to isolate amygdalin from apricot kernels and similar starting materials.

Amygdalin acid was also prepared from (*R*)-amygdalin by treatment with ammonium hydroxide. The crude product was purified by the preparative HPLC procedure used to purify amygdalinamide, except that the mobile phase was altered slightly to optimize separations. IR data for the purified sample showed bands near 6.29 and 7.13 μm assigned to the carboxylate ion, broad absorptions between 9 and 10 μm consistent with carbohydrate, and bands near 13.2 and 14.3 μm assigned to phenyl.

Its ^{1}H-NMR spectrum showed only one peak in the region where benzylic protons were expected; the ratio of its area to the area of the phenyl protons was 1:5. The ^{13}C-NMR data were consistent with a mixture of (*R*)- and (*S*)-amygdalin acids. This conclusion was based on observations that two signals centering near 138.2 ppm were found for the carboxylate carbon, at least five bands centering near 129.1 ppm were found for the phenyl carbons, and at least three peaks centering near 101.7 ppm were found for the two anomeric carbons in the glucose moieties. The benzylic carbon appeared among the nonanomeric glucosido carbons; this pattern was analogous to the benzylic carbons in (*R*)- and (*S*)-amygdalins and (*R*)- and (*S*)-amygdalinamides. These observations were consistent with those reported (2) for mixtures of (*R*)- and (*S*)-amygdalins.

Derivatized as the pertrimethylsilyl derivative and chromatographed on a phenyl methyl silicone (OV-17) column, the epimeric amygdalin acids coeluted. The mass spectral data for this peak were consistent with the proposed structure as the pertrimethylsilyl derivative. Chromatographed on a C_{18}-bonded silica column coupled to a UV detector and with a mobile phase of 0.1 *M* KH_2PO_4, the epimeric acids were readily resolved into two major peaks of nearly equal area plus three very small, faster eluting impurities that were not precursors to the acid.

The purity of the amygdalin acid sample was estimated at 89 ± 2% (free acid) on the basis of chromatographic and elemental data and the results from an NMR assay, the same procedure used to assay the amygdalinamide.

The source and history of the subject amygdalin dosage forms were described previously (1). However, the individual ampuls used in this study were from a different sampling than those used earlier (1), so some discrepancies will be apparent.

Determinations of amygdalinamide and amygdalin acid were based on HPLC analysis on a C_8-bonded silica[6] column with 0.1 *M* KH_2PO_4–methanol (96:4) as the mobile phase. Aliquots of 1.00 ml from each ampul were transferred to separate 25-ml volumetric flasks, which were then filled to the mark with water; 1.00-ml aliquots of the resulting solutions were each mixed with 1.00 ml of an internal standard solution[7] before being injected[8]. The concentrations of amygdalinamide and amygdalin acid per milliliter were determined by the internal standard method; the amide and acid reference standards were those described earlier in this report. The amounts of amygdalinamide and amygdalin acid per ampul were obtained by

[6] Lichrosorb RP8.

[7] This internal standard solution was prepared by dissolving 3.8 mg of 2-acetylbenzoic acid in 50 ml of 10% methanol in water.

[8] Because of lower concentrations of amygdalinamide and amygdalin acid in ampuls from Group 74-2504-10919, 1.00-ml aliquots from these ampul solutions were each transferred to separate 10-ml volumetric flasks. The remainder of the sample preparation procedure was identical to that for other group numbers except that the internal standard solution was prepared with 1.56 mg instead of 3.8 mg of 2-acetylbenzoic acid.

multiplying the ampul solution volume[9] times the respective solute concentration.

To gain a perspective on the relative amounts of amygdalin and the subject hydrolysis products in a given ampul, the amounts of amygdalin in the respective ampuls also were determined by the previously reported procedure (1).

The determination of 2-propanol was based on a GLC procedure with a porous polymer[10] column coupled to a flame-ionization detector. Aliquots of 0.50 ml from each ampul were each mixed with 0.50 ml of an internal standard solution[11] before being injected. The results derived were compared to a working curve obtained from standard solutions containing known amounts of 2-propanol and 2-butanol in water. The amount of 2-propanol in each ampul was calculated by multiplying its concentration times the ampul solution volume.

The amounts of amygdalin, amygdalinamide, amygdalin acid, and 2-propanol per ampul are listed in Table I.

(1) J. Jee, F. Yoshikawa, L. Pont, A. Cheung, and P. Lim, *J. Pharm. Sci.*, **67**, 438 (1978).

(2) T. Cairns, J. Froberg, S. Gonzales, W. Langham, J. Stamp, J. Howie, and D. Sawyer, *Anal. Chem.*, **50**, 438 (1978).

Michael Culcasi
Andrew Cheung
Elaine Shingai
John Jee
Peter Lim ˣ

Life Sciences Division
SRI International
Menlo Park, CA 94025

Received February 17, 1978.

Accepted for publication June 9, 1978.

Supported by Contract N01-CM-33723 from the National Cancer Institute, National Institutes of Health, Bethesda, MD 20014.

The authors thank D. Thomas and L. Cary of SRI International for assistance in mass spectral and NMR determinations and T. Cairns of the Food and Drug Administration for a preprint copy of his paper on "The Analytical Chemistry of Amygdalin."

[9] Each ampul fill volume was determined by carefully scoring the liquid level in each ampul, emptying and drying the ampul, and refilling to the scored mark with water dispensed from a volumetric buret.

[10] Chromosorb 105.

[11] This internal standard solution was prepared by dissolving 400 mg of 2-butanol in 50 ml of water.

Tolbutamide Binding to Plasma Proteins of Young and Old Human Subjects

Keyphrases □ Tolbutamide—plasma protein binding in humans, effect of subject age □ Binding, plasma protein—tolbutamide in humans, effect of subject age □ Age—of subject, effect on plasma protein binding of tolbutamide in humans □ Antidiabetic agents—tolbutamide, plasma protein binding in humans, effect of subject age

To the Editor:

Some evidence supports the view that age may be an important determinant in drug pharmacokinetics and pharmacodynamics (1). Changes in plasma protein binding of some drugs were shown to account for the age-related differences in their pharmacokinetics. Diminished binding of meperidine, phenylbutazone, warfarin, and phenytoin was associated with decreased serum albumin concentrations in elderly subjects (2–5). Tolbutamide is an acidic drug that is highly bound primarily to the albumin fraction of plasma protein (6, 7).

Table I—Effect of Age on Protein and Albumin Concentrations and Unbound Fraction of Tolbutamide [a]

	Young Group (n = 24)	Old Group (n = 19)
Age, years	38.74 ± 10.76	72.05 ± 8.50
Weight, kg	79.37 ± 2.14	74.25 ± 1.91[b]
Serum protein concentration, g/100 ml	7.25 ± 0.11	7.22 ± 0.51
Serum albumin concentration, g/100 ml	5.25 ± 0.54	4.67 ± 0.65[b]
Unbound fraction of tolbutamide[c]	0.032 ± 0.006	0.040 ± 0.007[d]

[a] Mean ± *SD*. [b] Significantly different ($p < 0.01$; t test). [c] Total plasma tolbutamide concentration of 100 μg/ml. [d] Significantly different ($p < 0.001$; t test).

The present study was undertaken to investigate the effect of age on plasma protein binding of tolbutamide. Blood samples were collected from healthy, nonsmoking, drug-free adult males[1]. The subjects were divided into two groups. The young group (n = 24) ranged in age from 23 to 57 years, and the old group (n = 19) ranged in age from 61 to 87 years.

Protein binding studies were carried out in rigid, clear acrylic cells[2] separated into two 1-ml compartments by a cellophane membrane[3]. Plasma (0.9 ml) was placed into one compartment and then spiked with a 10-μl aliquot of ^{35}S-tolbutamide[4] (dissolved in absolute ethanol) to produce a total concentration of 100 μg/ml. A 0.9-ml volume of 0.067 M phosphate buffer (pH 7.4) was placed in the other compartment.

The cells were placed in a metabolic incubator shaker[5] set at 37° and 50 oscillations/min. At equilibrium (16 hr), 50-μl aliquots were sampled from both compartments and counted directly in a liquid scintillation counter[6]. The unbound fraction of tolbutamide was calculated by dividing the amount of radioactivity (counts per minute) in the buffer solution by that of the plasma sample.

While the albumin concentration was decreased ($p < 0.01$) by about 11% in the old group, there was no change in the total protein concentration (Table I). Similar results were observed previously (9, 10), and the lack of change in the total protein concentration was attributed to a rise in globulin concentration with age. The effect of these changes in protein composition on drug binding has not been predictable (11). Table I indicates that the unbound fraction of tolbutamide was increased ($p < 0.001$) by about 25% in the old group. This age-related difference in the plasma protein binding of the drug prompted a study of its pharmacokinetics in the same groups of subjects. Preliminary results indicate that the total plasma clearance and volume of distribution of tolbutamide increased significantly with age (12). These findings may provide a reasonable explanation for the high incidence of hypo-

[1] Volunteer participants in the Baltimore Longitudinal Study of Aging (8) at the Gerontology Research Center, National Institute on Aging, National Institutes of Health, Baltimore, Md.

[2] Fisher Scientific Co., Silver Spring, MD 20910.

[3] Union Carbide Corp., Chicago, IL 60638.

[4] Lot 1076/N19015 (specific activity 4.86 mCi/mmole), Amersham-Searle, Arlington Heights, IL 60005.

[5] Dubnoff, Precision Scientific Co., Chicago, IL 60647.

[6] Packard 2425, Packard Instrument Co., Downers Grove, IL 60515.

0022-3549/78/0800-1192$01.00/0
© 1978, American Pharmaceutical Association

multiplying the ampul solution volume[9] times the respective solute concentration.

To gain a perspective on the relative amounts of amygdalin and the subject hydrolysis products in a given ampul, the amounts of amygdalin in the respective ampuls also were determined by the previously reported procedure (1).

The determination of 2-propanol was based on a GLC procedure with a porous polymer[10] column coupled to a flame-ionization detector. Aliquots of 0.50 ml from each ampul were each mixed with 0.50 ml of an internal standard solution[11] before being injected. The results derived were compared to a working curve obtained from standard solutions containing known amounts of 2-propanol and 2-butanol in water. The amount of 2-propanol in each ampul was calculated by multiplying its concentration times the ampul solution volume.

The amounts of amygdalin, amygdalinamide, amygdalin acid, and 2-propanol per ampul are listed in Table I.

(1) J. Jee, F. Yoshikawa, L. Pont, A. Cheung, and P. Lim, *J. Pharm. Sci.*, **67**, 438 (1978).

(2) T. Cairns, J. Froberg, S. Gonzales, W. Langham, J. Stamp, J. Howie, and D. Sawyer, *Anal. Chem.*, **50**, 438 (1978).

Michael Culcasi
Andrew Cheung
Elaine Shingai
John Jee
Peter Lim ˣ

Life Sciences Division
SRI International
Menlo Park, CA 94025

Received February 17, 1978.

Accepted for publication June 9, 1978.

Supported by Contract N01-CM-33723 from the National Cancer Institute, National Institutes of Health, Bethesda, MD 20014.

The authors thank D. Thomas and L. Cary of SRI International for assistance in mass spectral and NMR determinations and T. Cairns of the Food and Drug Administration for a preprint copy of his paper on "The Analytical Chemistry of Amygdalin."

[9] Each ampul fill volume was determined by carefully scoring the liquid level in each ampul, emptying and drying the ampul, and refilling to the scored mark with water dispensed from a volumetric buret.

[10] Chromosorb 105.

[11] This internal standard solution was prepared by dissolving 400 mg of 2-butanol in 50 ml of water.

Tolbutamide Binding to Plasma Proteins of Young and Old Human Subjects

Keyphrases □ Tolbutamide—plasma protein binding in humans, effect of subject age □ Binding, plasma protein—tolbutamide in humans, effect of subject age □ Age—of subject, effect on plasma protein binding of tolbutamide in humans □ Antidiabetic agents—tolbutamide, plasma protein binding in humans, effect of subject age

To the Editor:

Some evidence supports the view that age may be an important determinant in drug pharmacokinetics and pharmacodynamics (1). Changes in plasma protein binding of some drugs were shown to account for the age-related differences in their pharmacokinetics. Diminished binding of meperidine, phenylbutazone, warfarin, and phenytoin was associated with decreased serum albumin concentrations in elderly subjects (2–5). Tolbutamide is an acidic drug that is highly bound primarily to the albumin fraction of plasma protein (6, 7).

Table I—Effect of Age on Protein and Albumin Concentrations and Unbound Fraction of Tolbutamide [a]

	Young Group (n = 24)	Old Group (n = 19)
Age, years	38.74 ± 10.76	72.05 ± 8.50
Weight, kg	79.37 ± 2.14	74.25 ± 1.91[b]
Serum protein concentration, g/100 ml	7.25 ± 0.11	7.22 ± 0.51
Serum albumin concentration, g/100 ml	5.25 ± 0.54	4.67 ± 0.65[b]
Unbound fraction of tolbutamide[c]	0.032 ± 0.006	0.040 ± 0.007[d]

[a] Mean ± *SD*. [b] Significantly different ($p < 0.01$; t test). [c] Total plasma tolbutamide concentration of 100 μg/ml. [d] Significantly different ($p < 0.001$; t test).

The present study was undertaken to investigate the effect of age on plasma protein binding of tolbutamide. Blood samples were collected from healthy, nonsmoking, drug-free adult males[1]. The subjects were divided into two groups. The young group (n = 24) ranged in age from 23 to 57 years, and the old group (n = 19) ranged in age from 61 to 87 years.

Protein binding studies were carried out in rigid, clear acrylic cells[2] separated into two 1-ml compartments by a cellophane membrane[3]. Plasma (0.9 ml) was placed into one compartment and then spiked with a 10-μl aliquot of ^{35}S-tolbutamide[4] (dissolved in absolute ethanol) to produce a total concentration of 100 μg/ml. A 0.9-ml volume of 0.067 M phosphate buffer (pH 7.4) was placed in the other compartment.

The cells were placed in a metabolic incubator shaker[5] set at 37° and 50 oscillations/min. At equilibrium (16 hr), 50-μl aliquots were sampled from both compartments and counted directly in a liquid scintillation counter[6]. The unbound fraction of tolbutamide was calculated by dividing the amount of radioactivity (counts per minute) in the buffer solution by that of the plasma sample.

While the albumin concentration was decreased ($p < 0.01$) by about 11% in the old group, there was no change in the total protein concentration (Table I). Similar results were observed previously (9, 10), and the lack of change in the total protein concentration was attributed to a rise in globulin concentration with age. The effect of these changes in protein composition on drug binding has not been predictable (11). Table I indicates that the unbound fraction of tolbutamide was increased ($p < 0.001$) by about 25% in the old group. This age-related difference in the plasma protein binding of the drug prompted a study of its pharmacokinetics in the same groups of subjects. Preliminary results indicate that the total plasma clearance and volume of distribution of tolbutamide increased significantly with age (12). These findings may provide a reasonable explanation for the high incidence of hypo-

[1] Volunteer participants in the Baltimore Longitudinal Study of Aging (8) at the Gerontology Research Center, National Institute on Aging, National Institutes of Health, Baltimore, Md.

[2] Fisher Scientific Co., Silver Spring, MD 20910.

[3] Union Carbide Corp., Chicago, IL 60638.

[4] Lot 1076/N19015 (specific activity 4.86 mCi/mmole), Amersham-Searle, Arlington Heights, IL 60005.

[5] Dubnoff, Precision Scientific Co., Chicago, IL 60647.

[6] Packard 2425, Packard Instrument Co., Downers Grove, IL 60515.

0022-3549/78/0800-1192$01.00/0
© 1978, American Pharmaceutical Association

glycemic reactions observed in older patients receiving tolbutamide (13, 14).

(1) D. P. Richey and A. D. Bender, *Annu. Rev. Pharmacol. Toxicol.*, 17, 49 (1977).
(2) L. E. Mather, G. T. Tucker, A. E. Pflug, M. J. Lindop, and C. Wilkerson, *Clin. Pharmacol. Ther.*, 17, 21 (1975).
(3) S. Wallace, B. Whiting, and J. Runcie, *Br. J. Clin. Pharmacol.*, 3, 327 (1976).
(4) M. J. Hayes, M. J. S. Langman, and A. H. Short, *ibid.*, 2, 69 (1975).
(5) *Ibid.*, 2, 73 (1975).
(6) J. Judis, *J. Pharm. Sci.*, 61, 89 (1972).
(7) M. J. Crooks and K. F. Brown, *J. Pharm. Pharmacol.*, 26, 304 (1974).
(8) J. L. Stone and A. H. Norris, *J. Gerontol.*, 21, 575 (1966).
(9) E. Woodford-Williams, A. S. Alvares, D. Webster, B. Landless, and M. P. Dixon, *Gerontologia*, 10, 86 (1964).
(10) A. D. Bender, A. Post, J. P. Meier, J. E. Higson, and G. Reichard, Jr., *J. Pharm. Sci.*, 64, 1711 (1975).
(11) J. Crooks, K. O'Malley, and I. H. Stevenson, *Clin. Pharmacokinet.*, 1, 280 (1976).
(12) A. K. Miller, J. Adir, and R. E. Vestal, *Pharmacologist*, 19, 128 (1977).
(13) P. Gardner, C. J. Goodner, and J. T. Dowling, *J. Am. Med. Assoc.*, 186, 991 (1963).
(14) H. S. Seltzer, *Diabetes*, 21, 955 (1972).

Ann K. Miller
Joseph Adir ˣ
Clinical Pharmacokinetics Laboratory
School of Pharmacy
University of Maryland
Baltimore, MD 21201
Robert E. Vestal *
Gerontology Research Center
National Institute on Aging
National Institutes of Health
Baltimore City Hospitals
Baltimore, MD 21224

Received December 21, 1977.
Accepted for publication May 26, 1978.
*Present address: Veterans Administration Hospital, Boise, ID 83702.

Scatchard Plots with a Positive Slope and Role of Albumin Concentration

Keyphrases □ Scatchard plots—with positive slopes, various drugs, effect of albumin concentration □ Binding, protein—various drugs, Scatchard plots with positive slopes, effect of albumin concentration □ Albumin—effect on drug–protein binding, Scatchard plots with positive slopes

To the Editor:

A recent publication (1) reported Scatchard plots (2) with a positive slope for the binding of three narcotic analgesics and other basic drugs to human albumin. It was implied (1) that such Scatchard plots may be characteristic of organic bases and alkaloids. Positive Scatchard plots have been obtained for hydrocortisone (3), thiopental (4), phenytoin (5, 6), L-tryptophan (5, 6), and 2-(4′-hydroxybenzeneazo)benzoic acid[1] when the protein concentration was varied. Shen and Gibaldi (4) considered some aspects of this problem, but it was not mentioned in a recent review (7). Our own work and the reports listed in Table I suggest that this phenomenon is more common than hitherto supposed and requires explanation.

Two main experimental approaches are used to obtain drug binding data for Scatchard or similar analysis: A, vary the total ligand concentration and use one albumin concentration; and B, vary the albumin concentration and use a single total ligand concentration. Method A is more commonly used and was used in the study of narcotic analgesics (1). The apparent association constant, K, and the number of binding sites, n, derived from data obtained experimentally by Method A are tacitly assumed to be independent of protein concentration.

The positive Scatchard plots obtained for hydrocortisone, thiopental, phenytoin, L-tryptophan, and 2-(4′-hydroxybenzeneazo)benzoic acid indicate that n and/or K (*i.e.*, nK) decrease as the protein concentration increases. Method B was used for ultrafiltration or equilibrium dialysis with these five ligands, so the possibility arises that the results were an artifact of the method. However, this result is unlikely because identical Scatchard plots having the usual negative slopes were obtained experimentally by Methods A and B for both *o*-methyl red (6) and methyl orange[1], using experimental conditions similar to those for phenytoin and L-tryptophan. Previous workers (15, 16) found that nK for methyl orange may be dependent upon protein concentration with bovine albumin, but we have been unable to confirm this finding with human albumin.

Table I lists ligands for which there is an indication that nK may decrease when the protein concentration increases, although many of the data were not reported in a form suitable for Scatchard analysis. Several explanations for these findings are possible.

Commercial albumin preparations contain variable quantities of contaminants, *e.g.*, *N*-acetyl-L-tryptophan and other indoles (23) and fatty acids that may inhibit drug binding. At a constant drug concentration (Method B), the contaminant to ligand ratio increases as the albumin concentration increases and thereby decreases nK. Results with hydrocortisone (3) and 1-dodecanol (12) were attributed to contaminants. The sequential changes of buffer used in the dynamic dialysis technique may remove inhibitors of binding but seem unlikely to account for the results with the narcotic analgesics (1). Scholtan (20) found that drug binding in whole serum with pathologically lowered albumin concentration did not decrease as much as anticipated. Therefore, an increase in nK with lower albumin concentrations cannot be fully explained by dilution of endogenous inhibitory substances since no such dilution would have occurred in whole serum.

Cooperativity was implicated in several unusual ligand–protein interactions (4, 24, 25) and could explain Scatchard plots with positive slopes. However, these cooperative effects all were observed at one protein concentration or, at most, with only a small range of protein concentrations. If cooperativity is responsible, it should be manifest when the albumin concentration, as opposed to the ligand concentration, is varied. However, no such effects were apparent in studies where the ligand concentration was also varied.

[1] Unpublished results.

0022-3549/78/0800-1193$01.00/0
© 1978, American Pharmaceutical Association

glycemic reactions observed in older patients receiving tolbutamide (13, 14).

(1) D. P. Richey and A. D. Bender, *Annu. Rev. Pharmacol. Toxicol.*, 17, 49 (1977).
(2) L. E. Mather, G. T. Tucker, A. E. Pflug, M. J. Lindop, and C. Wilkerson, *Clin. Pharmacol. Ther.*, 17, 21 (1975).
(3) S. Wallace, B. Whiting, and J. Runcie, *Br. J. Clin. Pharmacol.*, 3, 327 (1976).
(4) M. J. Hayes, M. J. S. Langman, and A. H. Short, *ibid.*, 2, 69 (1975).
(5) *Ibid.*, 2, 73 (1975).
(6) J. Judis, *J. Pharm. Sci.*, 61, 89 (1972).
(7) M. J. Crooks and K. F. Brown, *J. Pharm. Pharmacol.*, 26, 304 (1974).
(8) J. L. Stone and A. H. Norris, *J. Gerontol.*, 21, 575 (1966).
(9) E. Woodford-Williams, A. S. Alvares, D. Webster, B. Landless, and M. P. Dixon, *Gerontologia*, 10, 86 (1964).
(10) A. D. Bender, A. Post, J. P. Meier, J. E. Higson, and G. Reichard, Jr., *J. Pharm. Sci.*, 64, 1711 (1975).
(11) J. Crooks, K. O'Malley, and I. H. Stevenson, *Clin. Pharmacokinet.*, 1, 280 (1976).
(12) A. K. Miller, J. Adir, and R. E. Vestal, *Pharmacologist*, 19, 128 (1977).
(13) P. Gardner, C. J. Goodner, and J. T. Dowling, *J. Am. Med. Assoc.*, 186, 991 (1963).
(14) H. S. Seltzer, *Diabetes*, 21, 955 (1972).

Ann K. Miller
Joseph Adir ˣ
Clinical Pharmacokinetics Laboratory
School of Pharmacy
University of Maryland
Baltimore, MD 21201
Robert E. Vestal *
Gerontology Research Center
National Institute on Aging
National Institutes of Health
Baltimore City Hospitals
Baltimore, MD 21224

Received December 21, 1977.
Accepted for publication May 26, 1978.
*Present address: Veterans Administration Hospital, Boise, ID 83702.

Scatchard Plots with a Positive Slope and Role of Albumin Concentration

Keyphrases □ Scatchard plots—with positive slopes, various drugs, effect of albumin concentration □ Binding, protein—various drugs, Scatchard plots with positive slopes, effect of albumin concentration □ Albumin—effect on drug–protein binding, Scatchard plots with positive slopes

To the Editor:

A recent publication (1) reported Scatchard plots (2) with a positive slope for the binding of three narcotic analgesics and other basic drugs to human albumin. It was implied (1) that such Scatchard plots may be characteristic of organic bases and alkaloids. Positive Scatchard plots have been obtained for hydrocortisone (3), thiopental (4), phenytoin (5, 6), L-tryptophan (5, 6), and 2-(4′-hydroxybenzeneazo)benzoic acid[1] when the protein concentration was varied. Shen and Gibaldi (4) considered some aspects of this problem, but it was not mentioned in a recent review (7). Our own work and the reports listed in Table I suggest that this phenomenon is more common than hitherto supposed and requires explanation.

Two main experimental approaches are used to obtain drug binding data for Scatchard or similar analysis: A, vary the total ligand concentration and use one albumin concentration; and B, vary the albumin concentration and use a single total ligand concentration. Method A is more commonly used and was used in the study of narcotic analgesics (1). The apparent association constant, K, and the number of binding sites, n, derived from data obtained experimentally by Method A are tacitly assumed to be independent of protein concentration.

The positive Scatchard plots obtained for hydrocortisone, thiopental, phenytoin, L-tryptophan, and 2-(4′-hydroxybenzeneazo)benzoic acid indicate that n and/or K (*i.e.*, nK) decrease as the protein concentration increases. Method B was used for ultrafiltration or equilibrium dialysis with these five ligands, so the possibility arises that the results were an artifact of the method. However, this result is unlikely because identical Scatchard plots having the usual negative slopes were obtained experimentally by Methods A and B for both *o*-methyl red (6) and methyl orange[1], using experimental conditions similar to those for phenytoin and L-tryptophan. Previous workers (15, 16) found that nK for methyl orange may be dependent upon protein concentration with bovine albumin, but we have been unable to confirm this finding with human albumin.

Table I lists ligands for which there is an indication that nK may decrease when the protein concentration increases, although many of the data were not reported in a form suitable for Scatchard analysis. Several explanations for these findings are possible.

Commercial albumin preparations contain variable quantities of contaminants, *e.g.*, *N*-acetyl-L-tryptophan and other indoles (23) and fatty acids that may inhibit drug binding. At a constant drug concentration (Method B), the contaminant to ligand ratio increases as the albumin concentration increases and thereby decreases nK. Results with hydrocortisone (3) and 1-dodecanol (12) were attributed to contaminants. The sequential changes of buffer used in the dynamic dialysis technique may remove inhibitors of binding but seem unlikely to account for the results with the narcotic analgesics (1). Scholtan (20) found that drug binding in whole serum with pathologically lowered albumin concentration did not decrease as much as anticipated. Therefore, an increase in nK with lower albumin concentrations cannot be fully explained by dilution of endogenous inhibitory substances since no such dilution would have occurred in whole serum.

Cooperativity was implicated in several unusual ligand–protein interactions (4, 24, 25) and could explain Scatchard plots with positive slopes. However, these cooperative effects all were observed at one protein concentration or, at most, with only a small range of protein concentrations. If cooperativity is responsible, it should be manifest when the albumin concentration, as opposed to the ligand concentration, is varied. However, no such effects were apparent in studies where the ligand concentration was also varied.

[1] Unpublished results.

0022-3549/78/0800-1193$01.00/0
© 1978, American Pharmaceutical Association

Table I—Studies Where *nK* Appears to Decrease with an Increase in Plasma Protein Concentration

Drug	Protein[a]	Method[b]	References
Acid Violet 6B	BSA	DS	8[c]
Alprenolol	HSA	ED	9[c]
Bromosulfophthalein	HSA	DF	10
2-Chromonecarboxylic acid	HSA	UF	11[c]
1-Dodecanol	BSA	ED	12
Dodecyl sulfate	BSA	ED	12
Hydrocortisone	HSA	ED	3[c]
2-(4′-Hydroxybenzeneazo)benzoic acid	BSA	DS	13[c]
Lorazepam	BSA	GF, CD	14
Methyl orange	BSA	ED, P	15, 16
Oxazepam	BSA	GF, CD	14
Phenylbutazone	HSA	CD, FP	17[c]
Phenytoin	HSA	ED	5,[c] 6[c]
Progesterone	HSA	ED	18[c]
Thiopental	BSA	UF	4[c]
Salicylate	HSA	CD, FP	17[c]
Sulfadiazine	HSA	ED, CD, FP	17,[c] 19[c]
Sulfamethoxydiazine	HSA, human serum	ED	19,[c] 20
3-Sulfonamido-4-chlorobenzoic acid	HSA	ED	21
Testosterone	BSA	FQ	22
L-Tryptophan	BSA	ED	5,[c] 6[c]

[a] HSA = human serum albumin, and BSA = bovine serum albumin. [b] ED = equilibrium dialysis, DF = diafiltration, UF = ultrafiltration, DS = difference spectrophotometry, GF = gel filtration, CD = circular dichroism, P = polarography, FP = fluorescence polarization, and FQ = fluorescence quenching. [c] Scatchard analysis used.

Protein–protein interaction may decrease *nK* as the albumin concentration increases, and molecular aggregation (4) or some more specific polymerization process may be involved. Several workers (10, 11, 14, 21) viewed albumin polymerization as an explanation for their results but offered no experimental evidence. Commercial preparations of albumin used *in vitro* contain polymers, and the percent of dimers and other oligomers may increase during storage (26). Removal of bovine albumin aggregates was necessary before reliable results could be obtained for 8-anilino-1-naphthalenesulfonate (27).

Westphal and Harding (18) observed that the binding affinity of progesterone was 33% less to the trimeric–polymeric components of human albumin than to the monomer or dimer fractions. Similarly, digitoxin was bound less to the human albumin dimer than to the monomer (28), and excessive concentrations of digitoxin did not influence the monomer to dimer ratio. However, bendazac and phenylbutazone inhibited the heat-induced aggregation of bovine albumin *in vitro* (29).

Several other proteins besides albumin have an affinity for various ligands that is dependent upon protein concentration (30). Hemerythrin monomer has a higher affinity for thiocyanate than does the octamer, and Scatchard plots indicated that this affinity increased with a decreasing protein concentration (30). Studies with the plasma protein apolipoprotein A-1 suggested that the state of association of this protein in aqueous solution largely determines its capacity to bind lipids or other ligands and that only the monomeric apolipoprotein binds lipids readily (31). When a globular protein interacts to form a square planar tetramer, each monomer unit loses 28.6% of accessible surface (32). An ellipsoid molecule like albumin may lose an even greater percent of accessible surface, together with its binding sites, in this way.

The dependence of *nK* upon protein concentration has several implications. Experimentally, the use of a single albumin concentration may be insufficient to characterize a drug–albumin interaction adequately, and the albumin preparation may need to be checked for aggregate content. The dye binding methods used to measure plasma albumin concentrations give erroneously high values at low concentrations (33), and this result is at least partly explicable in terms of the results discussed here.

More *in vivo* information is required on the state of albumin aggregation in health and disease. When the albumin concentration falls because of disease or trauma, an increase in *nK* for some drugs may homeostatically influence the potential increase in the concentration of unbound drug.

(1) J. Judis, *J. Pharm. Sci.*, **66**, 802 (1977).
(2) G. Scatchard, *Ann. N.Y. Acad. Sci.*, **51**, 660 (1949).
(3) W. K. Brunkhorst and E. L. Hess, *Arch. Biochem. Biophys.*, **111**, 54 (1965).
(4) D. Shen and M. Gibaldi, *J. Pharm. Sci.*, **63**, 1698 (1974).
(5) W. E. Lindup, *Biochem. Soc. Trans.*, **3**, 635 (1975).
(6) C. J. Bowmer and W. E. Lindup, *Biochem. Pharmacol.*, **27**, 937 (1978).
(7) J. J. Vallner, *J. Pharm. Sci.*, **66**, 447 (1977).
(8) K. Sekiguchi and M. Iwatsuru, *Yakugaku Zasshi*, **97**, 36 (1977).
(9) C. Appelgren, K. O. Borg, R. Elofsson, and K. A. Johansson, *Acta Pharm. Suec.*, **11**, 325 (1974).
(10) J. S. Crawford, R. L. Jones, J. M. Thompson, and W. D. E. Wells, *Br. J. Pharmacol.*, **44**, 80 (1972).
(11) J. P. Paubel and P. Nivière, *Chim. Ther.*, **8**, 469 (1973).
(12) A. Ray, J. A. Reynolds, H. Polet, and J. Steinhardt, *Biochemistry*, **5**, 2606 (1966).
(13) H. Zia and J. C. Price, *J. Pharm. Sci.*, **64**, 1177 (1975).
(14) W. E. Müller and U. Wollert, *Biochem. Pharmacol.*, **25**, 147 (1976).
(15) I. M. Klotz and J. M. Urquhart, *J. Phys. Colloid Chem.*, **53**, 100 (1949).
(16) B. Breyer and H. H. Bauer, *Aust. J. Chem.*, **6**, 332 (1953).
(17) S. W. Boobis, *Fed. Proc.*, **35**, 664 (1976).
(18) U. Westphal and G. B. Harding, *Biochim. Biophys. Acta*, **310**, 518 (1973).
(19) W. Scholtan, *Macromolek. Chem.*, **54**, 24 (1962).
(20) W. Scholtan, *Arzneim.-Forsch.*, **11**, 707 (1961).
(21) R. Zini, P. d'Athis, A. Hoareau, and J. P. Tillement, *Eur. J. Clin. Pharmacol.*, **10**, 139 (1976).
(22) N. A. Attallah and G. F. Lata, *Biochim. Biophys. Acta*, **168**, 321 (1968).
(23) G. L. K. Bargren and J. I. Routh, *Clin. Biochem.*, **7**, 290 (1974).
(24) F. Karush, *J. Phys. Chem.*, **56**, 70 (1952).
(25) E. Pfaff, M. Schwenk, R. Burr, and H. Remmer, *Mol. Pharmacol.*, **11**, 144 (1975).

(26) T. Peters, *Adv. Clin. Chem.*, **13**, 37 (1970).
(27) D. A. Kolb and G. Weber, *Biochemistry*, **14**, 4476 (1975).
(28) A. Brock, *Acta Pharmacol. Toxicol.*, **38**, 497 (1976).
(29) B. Catanese, A. Rossi, B. Silverstrini, and G. Toschi, *Pharmacol. Res. Commun.*, **816**, 549 (1976).
(30) M. Klapper and I. M. Klotz, *Biochemistry*, **7**, 223 (1968).
(31) L. B. Vitello and A. M. Scanu, *J. Biol. Chem.*, **251**, 1131 (1976).
(32) D. C. Teller, *Nature*, **260**, 729 (1976).
(33) D. C. Cannon, I. Olitzky, and J. A. Inkpen, in "Clinical Chemistry," 2nd ed., R. J. Henry, D. C. Cannon, and J. W. Winkelman, Eds., Harper and Row, London, England, 1974, p. 405.

Christopher J. Bowmer
W. Edward Lindup ˣ
Department of Pharmacology and Therapeutics
University of Liverpool
Liverpool L69 3BX, England

Received December 16, 1977.
Accepted for publication April 27, 1978.

BOOKS

REVIEWS

Advances in General and Cellular Pharmacology. Vol. 1. Edited by TOSHIO NARAHASHI and C. PAUL BIANCHI. Plenum, 227 W. 17th St., New York, NY 10011. 1977. 252 pp. 16 × 23 cm. Price $24.50.

This book is divided into five sections with the titles and authors as follows: Cardiac Cellular Pharmacology, Automaticity in Cardiac Muscle: Its Alteration by Physical and Chemical Imbalances, by Frances M. Wald and J. Thomas Bigger, Jr.; Actions of Opiates and their Antagonists on Cholinergic Transmission in the Guinea Pig Ileum, by Seymour Ehrenpreis; Pharmacology of Heart Cells During Ontogenesis, by Achilles J. Pappano; Analysis of Dose–Response Relationships, by Douglas R. Waud; and Cellular Pharmacology of Ganglionic Transmission, by Syogoro Nishi.

Characteristics of the automaticity in the myocardium after spontaneous diastolic depolarization are included in the first section. The subsection describing depolarization modification by physical and chemical factors contains especially comprehensive information on alterations induced by several cardiac drugs including β-adrenergic blocking agents, lidocaine, phenytoin (diphenylhydantoin), quinidine, procainamide, and digitalis.

Ehrenpreis describes experiments utilizing the electrically stimulated guinea pig ileum. A table listing 12 opiates or their antagonists, relating a correlation between effects on the ileum and analgesic potency, is of interest. A postulated relationship of the prostaglandin system to cholinergic transmission is given special treatment.

A major contribution of the section on ontogenesis is information regarding the effects of autonomic drugs on the physical and mechanical properties of chick embryo hearts. Nicotine and tyramine, thought to act by neurotransmitter release, tetrodotoxin, and the digitalis glycosides were also studied on this test object. In addition, limited experiments on heart cells in culture were described, giving data on a nerve free system.

The section entitled Analysis of Dose–Response Relationships has its forte in the comprehensive presentation of the kinetic approach. Pertinent information on experimental design and statistical evaluation is especially valuable.

Nishi concludes the volume with a section that thoroughly considers postsynaptic muscarinic and nicotinic sites, as well as receptors described as excitatory noncholinoreceptive and inhibitory adrenoceptive sites. A review of presynaptic receptor sites and transmitter liberation is a highlight of this section. Physiopharmacologic characteristics of the postsynaptic membrane are also discussed.

This book is a definite contribution to the pharmacologic literature. The authors are prolific in the reference portion of their sections. The well-documented reviews in each section and the concise presentation of the author's original research are uniformly exceptional throughout this publication. This book is valuable primarily as a reference text across interdisciplinary lines in the biological and physical science areas, and one anticipates future volumes of this quality.

Reviewed by Glenn D. Appelt
School of Pharmacy
University of Colorado
Boulder, CO 80309

Biopharmaceutics and Clinical Pharmacokinetics. By MILO GIBALDI. Lea & Febiger, Washington Square, Philadelphia, PA 19106. 1977. ix + 181 pp. 17.5 × 25.5 cm. Price $8.50.

This book began as a chapter in "Theory and Practice of Industrial Pharmacy" edited by Lachman, Lieberman, and Kanig (Lea & Febiger, 1970). The first edition was a reprint of the chapter in paperback. The second edition retains the advantages of an inexpensive paperback, but it has been considerably expanded and updated. The most useful changes are: division of the book into chapters, addition of many valuable new references, and addition of a significant amount of clinical pharmacokinetic material.

Chapter 1 is a very brief introduction to pharmacokinetics, in which the discussion is restricted to the one-compartment body model. The concepts of drug accumulation and repetitive dosing are also introduced. This chapter could serve as a concise review for a recently graduated pharmacist, but it is not sufficiently detailed to be used alone for the teaching of pharmacokinetics on the undergraduate level.

The next three chapters deal with the GI absorption of drugs. The discussion progresses clearly and logically from biological factors, such as membrane structure, to the role of the dosage form. Chapter 2 reviews membrane structure and function and GI physiology in humans. Chapter 3 discusses such physiochemical factors as pH-partitioning, solubility, and rate of dissolution. Chapter 4 discusses dosage form factors that influence drug dissolution in the GI tract. This chapter contains a survey of several drugs found to present bioavailability problems in humans, with a brief discussion of each drug. This chapter is particularly effective in giving the reader a perspective of the importance of bioavailability testing and control of drug products.

Chapter 5 deals with routes of administration other than oral and discusses relatively recent observations concerning the variability and unreliability of the intramuscular route.

Chapter 6 discusses drug disposition, including tissue distribution, renal excretion, and drug metabolism. Although this chapter is not thorough enough to be used as a sole resource for teaching purposes, it is a suitable review in preparation for the subsequent chapters on the clinical utility of plasma drug concentrations.

Chapter 7, Intersubject Differences in Drug Concentration in Plasma, is an excellent introduction to the complexities one faces in trying to control and adjust drug dosages in individual patients in the real clinical world. Some topics covered are: body weight; sex; age, particularly the newborn; genetic factors; renal, hepatic, and other diseases; and drug interactions. In this chapter, as in Chapter 4, many examples of specific drugs and specific clinical conditions are presented, and the discussion is generously referenced.

The final chapter continues in the drug-by-drug style, with the emphasis on the significance of plasma drug concentrations as guides to efficacy and toxicity. Some of the drugs discussed are warfarin, digoxin, gentamicin, phenytoin, theophylline, salicylate, lidocaine, propranolol, lithium, and nortriptyline. The presentation is clear and to the point, with the added advantage of having practical value in identifying drugs for which monitoring of plasma concentrations may be helpful in guiding therapy.

The book is well written in a very understandable style, with many examples and ample references in each chapter. Although certain chapters would require considerable amplification in the classroom, this book could serve as an inexpensive text for an undergraduate course in bio-

(26) T. Peters, *Adv. Clin. Chem.*, **13**, 37 (1970).
(27) D. A. Kolb and G. Weber, *Biochemistry*, **14**, 4476 (1975).
(28) A. Brock, *Acta Pharmacol. Toxicol.*, **38**, 497 (1976).
(29) B. Catanese, A. Rossi, B. Silverstrini, and G. Toschi, *Pharmacol. Res. Commun.*, **816**, 549 (1976).
(30) M. Klapper and I. M. Klotz, *Biochemistry*, **7**, 223 (1968).
(31) L. B. Vitello and A. M. Scanu, *J. Biol. Chem.*, **251**, 1131 (1976).
(32) D. C. Teller, *Nature*, **260**, 729 (1976).
(33) D. C. Cannon, I. Olitzky, and J. A. Inkpen, in "Clinical Chemistry," 2nd ed., R. J. Henry, D. C. Cannon, and J. W. Winkelman, Eds., Harper and Row, London, England, 1974, p. 405.

Christopher J. Bowmer
W. Edward Lindup ˣ
Department of Pharmacology and Therapeutics
University of Liverpool
Liverpool L69 3BX, England

Received December 16, 1977.
Accepted for publication April 27, 1978.

BOOKS

REVIEWS

Advances in General and Cellular Pharmacology. Vol. 1. Edited by TOSHIO NARAHASHI and C. PAUL BIANCHI. Plenum, 227 W. 17th St., New York, NY 10011. 1977. 252 pp. 16 × 23 cm. Price $24.50.

This book is divided into five sections with the titles and authors as follows: Cardiac Cellular Pharmacology, Automaticity in Cardiac Muscle: Its Alteration by Physical and Chemical Imbalances, by Frances M. Wald and J. Thomas Bigger, Jr.; Actions of Opiates and their Antagonists on Cholinergic Transmission in the Guinea Pig Ileum, by Seymour Ehrenpreis; Pharmacology of Heart Cells During Ontogenesis, by Achilles J. Pappano; Analysis of Dose–Response Relationships, by Douglas R. Waud; and Cellular Pharmacology of Ganglionic Transmission, by Syogoro Nishi.

Characteristics of the automaticity in the myocardium after spontaneous diastolic depolarization are included in the first section. The subsection describing depolarization modification by physical and chemical factors contains especially comprehensive information on alterations induced by several cardiac drugs including β-adrenergic blocking agents, lidocaine, phenytoin (diphenylhydantoin), quinidine, procainamide, and digitalis.

Ehrenpreis describes experiments utilizing the electrically stimulated guinea pig ileum. A table listing 12 opiates or their antagonists, relating a correlation between effects on the ileum and analgesic potency, is of interest. A postulated relationship of the prostaglandin system to cholinergic transmission is given special treatment.

A major contribution of the section on ontogenesis is information regarding the effects of autonomic drugs on the physical and mechanical properties of chick embryo hearts. Nicotine and tyramine, thought to act by neurotransmitter release, tetrodotoxin, and the digitalis glycosides were also studied on this test object. In addition, limited experiments on heart cells in culture were described, giving data on a nerve free system.

The section entitled Analysis of Dose–Response Relationships has its forte in the comprehensive presentation of the kinetic approach. Pertinent information on experimental design and statistical evaluation is especially valuable.

Nishi concludes the volume with a section that thoroughly considers postsynaptic muscarinic and nicotinic sites, as well as receptors described as excitatory noncholinoreceptive and inhibitory adrenoceptive sites. A review of presynaptic receptor sites and transmitter liberation is a highlight of this section. Physiopharmacologic characteristics of the postsynaptic membrane are also discussed.

This book is a definite contribution to the pharmacologic literature. The authors are prolific in the reference portion of their sections. The well-documented reviews in each section and the concise presentation of the author's original research are uniformly exceptional throughout this publication. This book is valuable primarily as a reference text across interdisciplinary lines in the biological and physical science areas, and one anticipates future volumes of this quality.

Reviewed by Glenn D. Appelt
School of Pharmacy
University of Colorado
Boulder, CO 80309

Biopharmaceutics and Clinical Pharmacokinetics. By MILO GIBALDI. Lea & Febiger, Washington Square, Philadelphia, PA 19106. 1977. ix + 181 pp. 17.5 × 25.5 cm. Price $8.50.

This book began as a chapter in "Theory and Practice of Industrial Pharmacy" edited by Lachman, Lieberman, and Kanig (Lea & Febiger, 1970). The first edition was a reprint of the chapter in paperback. The second edition retains the advantages of an inexpensive paperback, but it has been considerably expanded and updated. The most useful changes are: division of the book into chapters, addition of many valuable new references, and addition of a significant amount of clinical pharmacokinetic material.

Chapter 1 is a very brief introduction to pharmacokinetics, in which the discussion is restricted to the one-compartment body model. The concepts of drug accumulation and repetitive dosing are also introduced. This chapter could serve as a concise review for a recently graduated pharmacist, but it is not sufficiently detailed to be used alone for the teaching of pharmacokinetics on the undergraduate level.

The next three chapters deal with the GI absorption of drugs. The discussion progresses clearly and logically from biological factors, such as membrane structure, to the role of the dosage form. Chapter 2 reviews membrane structure and function and GI physiology in humans. Chapter 3 discusses such physiochemical factors as pH-partitioning, solubility, and rate of dissolution. Chapter 4 discusses dosage form factors that influence drug dissolution in the GI tract. This chapter contains a survey of several drugs found to present bioavailability problems in humans, with a brief discussion of each drug. This chapter is particularly effective in giving the reader a perspective of the importance of bioavailability testing and control of drug products.

Chapter 5 deals with routes of administration other than oral and discusses relatively recent observations concerning the variability and unreliability of the intramuscular route.

Chapter 6 discusses drug disposition, including tissue distribution, renal excretion, and drug metabolism. Although this chapter is not thorough enough to be used as a sole resource for teaching purposes, it is a suitable review in preparation for the subsequent chapters on the clinical utility of plasma drug concentrations.

Chapter 7, Intersubject Differences in Drug Concentration in Plasma, is an excellent introduction to the complexities one faces in trying to control and adjust drug dosages in individual patients in the real clinical world. Some topics covered are: body weight; sex; age, particularly the newborn; genetic factors; renal, hepatic, and other diseases; and drug interactions. In this chapter, as in Chapter 4, many examples of specific drugs and specific clinical conditions are presented, and the discussion is generously referenced.

The final chapter continues in the drug-by-drug style, with the emphasis on the significance of plasma drug concentrations as guides to efficacy and toxicity. Some of the drugs discussed are warfarin, digoxin, gentamicin, phenytoin, theophylline, salicylate, lidocaine, propranolol, lithium, and nortriptyline. The presentation is clear and to the point, with the added advantage of having practical value in identifying drugs for which monitoring of plasma concentrations may be helpful in guiding therapy.

The book is well written in a very understandable style, with many examples and ample references in each chapter. Although certain chapters would require considerable amplification in the classroom, this book could serve as an inexpensive text for an undergraduate course in bio-

(26) T. Peters, *Adv. Clin. Chem.*, **13**, 37 (1970).
(27) D. A. Kolb and G. Weber, *Biochemistry*, **14**, 4476 (1975).
(28) A. Brock, *Acta Pharmacol. Toxicol.*, **38**, 497 (1976).
(29) B. Catanese, A. Rossi, B. Silverstrini, and G. Toschi, *Pharmacol. Res. Commun.*, **816**, 549 (1976).
(30) M. Klapper and I. M. Klotz, *Biochemistry*, **7**, 223 (1968).
(31) L. B. Vitello and A. M. Scanu, *J. Biol. Chem.*, **251**, 1131 (1976).
(32) D. C. Teller, *Nature*, **260**, 729 (1976).
(33) D. C. Cannon, I. Olitzky, and J. A. Inkpen, in "Clinical Chemistry," 2nd ed., R. J. Henry, D. C. Cannon, and J. W. Winkelman, Eds., Harper and Row, London, England, 1974, p. 405.

Christopher J. Bowmer
W. Edward Lindup ˣ
Department of Pharmacology and Therapeutics
University of Liverpool
Liverpool L69 3BX, England

Received December 16, 1977.
Accepted for publication April 27, 1978.

BOOKS

REVIEWS

Advances in General and Cellular Pharmacology. Vol. 1. Edited by TOSHIO NARAHASHI and C. PAUL BIANCHI. Plenum, 227 W. 17th St., New York, NY 10011. 1977. 252 pp. 16 × 23 cm. Price $24.50.

This book is divided into five sections with the titles and authors as follows: Cardiac Cellular Pharmacology, Automaticity in Cardiac Muscle: Its Alteration by Physical and Chemical Imbalances, by Frances M. Wald and J. Thomas Bigger, Jr.; Actions of Opiates and their Antagonists on Cholinergic Transmission in the Guinea Pig Ileum, by Seymour Ehrenpreis; Pharmacology of Heart Cells During Ontogenesis, by Achilles J. Pappano; Analysis of Dose–Response Relationships, by Douglas R. Waud; and Cellular Pharmacology of Ganglionic Transmission, by Syogoro Nishi.

Characteristics of the automaticity in the myocardium after spontaneous diastolic depolarization are included in the first section. The subsection describing depolarization modification by physical and chemical factors contains especially comprehensive information on alterations induced by several cardiac drugs including β-adrenergic blocking agents, lidocaine, phenytoin (diphenylhydantoin), quinidine, procainamide, and digitalis.

Ehrenpreis describes experiments utilizing the electrically stimulated guinea pig ileum. A table listing 12 opiates or their antagonists, relating a correlation between effects on the ileum and analgesic potency, is of interest. A postulated relationship of the prostaglandin system to cholinergic transmission is given special treatment.

A major contribution of the section on ontogenesis is information regarding the effects of autonomic drugs on the physical and mechanical properties of chick embryo hearts. Nicotine and tyramine, thought to act by neurotransmitter release, tetrodotoxin, and the digitalis glycosides were also studied on this test object. In addition, limited experiments on heart cells in culture were described, giving data on a nerve free system.

The section entitled Analysis of Dose–Response Relationships has its forte in the comprehensive presentation of the kinetic approach. Pertinent information on experimental design and statistical evaluation is especially valuable.

Nishi concludes the volume with a section that thoroughly considers postsynaptic muscarinic and nicotinic sites, as well as receptors described as excitatory noncholinoreceptive and inhibitory adrenoceptive sites. A review of presynaptic receptor sites and transmitter liberation is a highlight of this section. Physiopharmacologic characteristics of the postsynaptic membrane are also discussed.

This book is a definite contribution to the pharmacologic literature. The authors are prolific in the reference portion of their sections. The well-documented reviews in each section and the concise presentation of the author's original research are uniformly exceptional throughout this publication. This book is valuable primarily as a reference text across interdisciplinary lines in the biological and physical science areas, and one anticipates future volumes of this quality.

Reviewed by Glenn D. Appelt
School of Pharmacy
University of Colorado
Boulder, CO 80309

Biopharmaceutics and Clinical Pharmacokinetics. By MILO GIBALDI. Lea & Febiger, Washington Square, Philadelphia, PA 19106. 1977. ix + 181 pp. 17.5 × 25.5 cm. Price $8.50.

This book began as a chapter in "Theory and Practice of Industrial Pharmacy" edited by Lachman, Lieberman, and Kanig (Lea & Febiger, 1970). The first edition was a reprint of the chapter in paperback. The second edition retains the advantages of an inexpensive paperback, but it has been considerably expanded and updated. The most useful changes are: division of the book into chapters, addition of many valuable new references, and addition of a significant amount of clinical pharmacokinetic material.

Chapter 1 is a very brief introduction to pharmacokinetics, in which the discussion is restricted to the one-compartment body model. The concepts of drug accumulation and repetitive dosing are also introduced. This chapter could serve as a concise review for a recently graduated pharmacist, but it is not sufficiently detailed to be used alone for the teaching of pharmacokinetics on the undergraduate level.

The next three chapters deal with the GI absorption of drugs. The discussion progresses clearly and logically from biological factors, such as membrane structure, to the role of the dosage form. Chapter 2 reviews membrane structure and function and GI physiology in humans. Chapter 3 discusses such physiochemical factors as pH-partitioning, solubility, and rate of dissolution. Chapter 4 discusses dosage form factors that influence drug dissolution in the GI tract. This chapter contains a survey of several drugs found to present bioavailability problems in humans, with a brief discussion of each drug. This chapter is particularly effective in giving the reader a perspective of the importance of bioavailability testing and control of drug products.

Chapter 5 deals with routes of administration other than oral and discusses relatively recent observations concerning the variability and unreliability of the intramuscular route.

Chapter 6 discusses drug disposition, including tissue distribution, renal excretion, and drug metabolism. Although this chapter is not thorough enough to be used as a sole resource for teaching purposes, it is a suitable review in preparation for the subsequent chapters on the clinical utility of plasma drug concentrations.

Chapter 7, Intersubject Differences in Drug Concentration in Plasma, is an excellent introduction to the complexities one faces in trying to control and adjust drug dosages in individual patients in the real clinical world. Some topics covered are: body weight; sex; age, particularly the newborn; genetic factors; renal, hepatic, and other diseases; and drug interactions. In this chapter, as in Chapter 4, many examples of specific drugs and specific clinical conditions are presented, and the discussion is generously referenced.

The final chapter continues in the drug-by-drug style, with the emphasis on the significance of plasma drug concentrations as guides to efficacy and toxicity. Some of the drugs discussed are warfarin, digoxin, gentamicin, phenytoin, theophylline, salicylate, lidocaine, propranolol, lithium, and nortriptyline. The presentation is clear and to the point, with the added advantage of having practical value in identifying drugs for which monitoring of plasma concentrations may be helpful in guiding therapy.

The book is well written in a very understandable style, with many examples and ample references in each chapter. Although certain chapters would require considerable amplification in the classroom, this book could serve as an inexpensive text for an undergraduate course in bio-

pharmaceutics and clinical pharmacokinetics. It would also be useful as a review or first introduction for practicing pharmacists as well as students and practitioners in related health fields.

Reviewed by Randall B. Smith and Lewis W. Dittert
College of Pharmacy
University of Kentucky
Lexington, KY 40506

Pharmacological and Biochemical Properties of Drug Substances, Vol. 1. Edited by MORTON E. GOLDBERG. American Pharmaceutical Association, 2215 Constitution Ave., N.W., Washington DC 20037. 1977. 413 pp 16 × 23 cm. Price $21.00 ($14.00 member rate).

This volume, which promises to be the first of a continuing series, is designed as a companion series to "Analytical Profiles of Drug Substances" edited by Klaus Florey. While Florey's series emphasizes chemical properties of drugs, this volume has the overall objective of reviewing the biological properties of agents that represent prototypes for the major classes of drugs available.

The contents of this initial volume include central nervous system agents (clozapine and pemoline), cardiovascular agents (clonidine and dobutamine), chemotherapeutic agents (amikacin and cefazolin), antiinflammatory agents (fenoprofen, halcinonide, and tolmetin), pulmonary and antiallergy agents (albuterol, cromolyn sodium, and terbutaline), GI agents (cimetidine and prostaglandin analogs), antifertility agents (prostaglandin analogs), and diagnostic agents (metrizamide). The general outline for each monograph consists of a brief discussion of the chemistry of the compound followed by animal pharmacology, toxicology, biopharmaceutics, and clinical pharmacology. The most valuable sections are the discussions of animal and clinical pharmacology.

Most chapters contain extensive tables of data. Some monographs also include descriptions of the agent's effect in pharmacological tests unrelated to its therapeutic indication. This information is particularly interesting because it is often difficult or impossible to extract from the primary literature.

Most monographs, except the monograph on pemoline, contain references into the 1976 and, in some cases, the 1977 literature. All monographs, except the one on clozapine, contain the title of the referenced articles. The volume is relatively free of errors, although the tables on pages 161 and 231 contain ED_{50} values that do not fall within the quoted confidence limits.

As stated above, as well as in the preface of the volume, the editor's objective was to include prototypes for the major classes of drugs available. This reviewer does not believe that drugs such as amikacin, cefazolin, fenoprofen, and tolmetin can be considered as prototypes of classes in keeping with Webster's definition. On the other hand, clonidine and cimetidine certainly would be considered prototypes. Of course, including only true prototypes would lead to a short series of volumes. Followup drugs such as those mentioned are valuable additions to this volume. Their value would be further increased if emphasis were given not only to comparing them with their original commercial target but also to comparing them with other drugs in development by competitors aiming for these same targets.

In summary, the concept of this series promises to be a valuable addition to the pharmaceutical literature. Its success will depend on the discipline of its editor and the objectivity of its authors.

Reviewed by Larry J. Powers
Diamond Shamrock Corporation
T. R. Evans Research Center
Painesville, OH 44077

NOTICES

The Synthesis of Prostaglandins. By ABHIJIT MITRA. Wiley, 605 Third Ave., New York, NY 10016. 1977. 444 pp. 15 × 23 cm.

This book presents a comprehensive review of the new synthetic methods and reactions used to construct prostaglandins, describing in detail almost all of the syntheses of the naturally occurring compounds, thromboxanes, and analogs. Various syntheses are classified according to major synthetic strategies. The individual synthesis is then presented with a brief introduction highlighting the key reaction(s) and followed by a synthetic strategy in the form of a flow diagram that shows the strategic bond disconnections. The actual synthesis is depicted in flowsheet form with extensive footnotes explaining the reactions and their stereochemical outcome if applicable. Both author and subject indexes are included.

Catecholamines of 'Developing 'Brain. Preconditioning of Behavior (Aggression? Anxiety?). By CLARA TORDA. Walters, 101 W. 12th St., New York, NY 10011. 1977. 255 pp. 20 × 28 cm.

Biochemistry. By PAUL JAY FRIEDMAN. Little, Brown, 34 Beacon St., Boston, MA 02106. 1977. 211 pp. 21 × 28 cm. Price $7.95.

Hagers Handbuch der Pharmazeutischen Praxis. Edited by P. H. LIST and L. HÖRHAMMER. Springer-Verlag, 175 Fifth Ave., New York, NY 10010. 1977. 570 pp. 16 × 24 cm. Price $65.20.

Epidemiological Evaluation of Drugs. Edited by F. COLOMBO, S. SHAPIRO, D. SLONE, and G. TOGNONI. PSG, 545 Great Rd., Littleton, MA 01460. 1977. 333 pp. 16 × 24 cm. Price $23.00.

Clinical Psychopharmacology. Edited by JERROLD C. BERNSTEIN. PSG, 545 Great Rd., Littleton, MA 01460. 1977. 154 pp. 15 × 24 cm. Price $12.50.

Peptide Transport and Hydrolysis. Ciba Foundation Symposium 50 (new series). Edited by KATHERINE ELLIOTT and MAEVE O'CONNOR. Elsevier, 52 Vanderbilt Ave., New York, NY 10017. 1977. 385 pp. 16 × 24 cm.

Health and Disease in Tribal Societies. Ciba Foundation Symposium 49 (new series). Elsevier, 52 Vanderbilt Ave., New York, NY 10017. 1977. 344 pp. 16 × 24 cm.

Organic Syntheses. Vol. 57. Edited by CARL R. JOHNSON *et al.* Wiley, 1 Wiley Drive, Somerset, NJ 08875. 2047 pp. 15 × 23 cm. Price $12.95.

Problems of Clinical Pharmacology in Therapeutic Research: Phase 1. Edited by H. P. KUEMMERLE, T. K. SHIBUYA, and E. KIMURA. Urban & Schwarzenberg, 7 E. Redwood St., Baltimore, MD 21202. 1977. 420 pp. 15 × 23 cm. Price $28.50.

Biosynthesis. Vol. 5. A Specialist Periodical Report. Edited by J. D. BU'LOCK, *et al.* The Chemical Society, Burlington House, London, W1V OBN, England, 1977. 318 pp. 13 × 22 cm. Price $45.00. Available from Special Issues Sales, American Chemical Society, 1155 16th St., NW, Washington, DC 20036.

Drug Discrimination and State Dependent Learning. Edited by BENG T. HO, DANIEL W. RICHARDS, III, and DOUGLAS L. CHUTE. Academic, 111 Fifth Ave., New York, NY 10003. 1978. 392 pp. 15 × 23 cm. Price $23.00.

Manual of Anesthesia. By JOHN C. SNOW, Little, Brown, 34 Beacon St., Boston, MA 02106. 1977. 547 pp. 14 × 22 cm. Price $12.50.

Workplace Safety and Health. The Role of Workers' Compensation. By JAMES ROBERT CHELIUS. American Enterprise Institute for Public Policy Research, 1150 17 St., NW, Washington, DC. 20036. 1977. 97 pp. 15 × 23 cm. Price $2.75.

WHO Expert Committee on Specifications for Pharmaceutical Preparations. Twenty-Sixth Report. World Health Organization, 49 Sheridan Ave., Albany, NY 12210. 1977. 53 pp. 13 × 20 cm. Price $2.80.

International Nonproprietary Names (INN) for Pharmaceutical Substances. Cumulative List No. 5. World Health Organization, 49 Sheridan Ave., Albany, NY 12210. 1977. 332 pp. 17 × 24 cm. Price $19.20.

Perspectives in Pharmacy. Edited by ALBERT I. WERTHEIMER and MARGARET L. SCHUBERT. College of Pharmacy, University of Minnesota, Minneapolis, MN 55455. 1977. 84 pp. 15 × 23 cm.

Toxicologic Emergencies. A Handbook in Problem Solving. By LEWIS R. GOLDFRANK and ROBERT KIRSTEIN. Appleton-Century-Crofts, 292 Madison Ave., New York, NY 10017. 1977. 180 pp. Price $9.75.

Physical Chemistry for Students of Pharmacy and Biology. 3rd Ed. By S. C. WALLWORK and D. J. W. GRANT. Longman, 19 W. 44th St., New York, NY 10036. 1977. 607 pp. 14 × 22 cm. Price $18.00.

pharmaceutics and clinical pharmacokinetics. It would also be useful as a review or first introduction for practicing pharmacists as well as students and practitioners in related health fields.

Reviewed by Randall B. Smith and Lewis W. Dittert
College of Pharmacy
University of Kentucky
Lexington, KY 40506

Pharmacological and Biochemical Properties of Drug Substances, Vol. 1. Edited by MORTON E. GOLDBERG. American Pharmaceutical Association, 2215 Constitution Ave., N.W., Washington DC 20037. 1977. 413 pp 16 × 23 cm. Price $21.00 ($14.00 member rate).

This volume, which promises to be the first of a continuing series, is designed as a companion series to "Analytical Profiles of Drug Substances" edited by Klaus Florey. While Florey's series emphasizes chemical properties of drugs, this volume has the overall objective of reviewing the biological properties of agents that represent prototypes for the major classes of drugs available.

The contents of this initial volume include central nervous system agents (clozapine and pemoline), cardiovascular agents (clonidine and dobutamine), chemotherapeutic agents (amikacin and cefazolin), antiinflammatory agents (fenoprofen, halcinonide, and tolmetin), pulmonary and antiallergy agents (albuterol, cromolyn sodium, and terbutaline), GI agents (cimetidine and prostaglandin analogs), antifertility agents (prostaglandin analogs), and diagnostic agents (metrizamide). The general outline for each monograph consists of a brief discussion of the chemistry of the compound followed by animal pharmacology, toxicology, biopharmaceutics, and clinical pharmacology. The most valuable sections are the discussions of animal and clinical pharmacology.

Most chapters contain extensive tables of data. Some monographs also include descriptions of the agent's effect in pharmacological tests unrelated to its therapeutic indication. This information is particularly interesting because it is often difficult or impossible to extract from the primary literature.

Most monographs, except the monograph on pemoline, contain references into the 1976 and, in some cases, the 1977 literature. All monographs, except the one on clozapine, contain the title of the referenced articles. The volume is relatively free of errors, although the tables on pages 161 and 231 contain ED_{50} values that do not fall within the quoted confidence limits.

As stated above, as well as in the preface of the volume, the editor's objective was to include prototypes for the major classes of drugs available. This reviewer does not believe that drugs such as amikacin, cefazolin, fenoprofen, and tolmetin can be considered as prototypes of classes in keeping with Webster's definition. On the other hand, clonidine and cimetidine certainly would be considered prototypes. Of course, including only true prototypes would lead to a short series of volumes. Followup drugs such as those mentioned are valuable additions to this volume. Their value would be further increased if emphasis were given not only to comparing them with their original commercial target but also to comparing them with other drugs in development by competitors aiming for these same targets.

In summary, the concept of this series promises to be a valuable addition to the pharmaceutical literature. Its success will depend on the discipline of its editor and the objectivity of its authors.

Reviewed by Larry J. Powers
Diamond Shamrock Corporation
T. R. Evans Research Center
Painesville, OH 44077

NOTICES

The Synthesis of Prostaglandins. By ABHIJIT MITRA. Wiley, 605 Third Ave., New York, NY 10016. 1977. 444 pp. 15 × 23 cm.

This book presents a comprehensive review of the new synthetic methods and reactions used to construct prostaglandins, describing in detail almost all of the syntheses of the naturally occurring compounds, thromboxanes, and analogs. Various syntheses are classified according to major synthetic strategies. The individual synthesis is then presented with a brief introduction highlighting the key reaction(s) and followed by a synthetic strategy in the form of a flow diagram that shows the strategic bond disconnections. The actual synthesis is depicted in flowsheet form with extensive footnotes explaining the reactions and their stereochemical outcome if applicable. Both author and subject indexes are included.

Catecholamines of 'Developing 'Brain. Preconditioning of Behavior (Aggression? Anxiety?). By CLARA TORDA. Walters, 101 W. 12th St., New York, NY 10011. 1977. 255 pp. 20 × 28 cm.

Biochemistry. By PAUL JAY FRIEDMAN. Little, Brown, 34 Beacon St., Boston, MA 02106. 1977. 211 pp. 21 × 28 cm. Price $7.95.

Hagers Handbuch der Pharmazeutischen Praxis. Edited by P. H. LIST and L. HÖRHAMMER. Springer-Verlag, 175 Fifth Ave., New York, NY 10010. 1977. 570 pp. 16 × 24 cm. Price $65.20.

Epidemiological Evaluation of Drugs. Edited by F. COLOMBO, S. SHAPIRO, D. SLONE, and G. TOGNONI. PSG, 545 Great Rd., Littleton, MA 01460. 1977. 333 pp. 16 × 24 cm. Price $23.00.

Clinical Psychopharmacology. Edited by JERROLD C. BERNSTEIN. PSG, 545 Great Rd., Littleton, MA 01460. 1977. 154 pp. 15 × 24 cm. Price $12.50.

Peptide Transport and Hydrolysis. Ciba Foundation Symposium 50 (new series). Edited by KATHERINE ELLIOTT and MAEVE O'CONNOR. Elsevier, 52 Vanderbilt Ave., New York, NY 10017. 1977. 385 pp. 16 × 24 cm.

Health and Disease in Tribal Societies. Ciba Foundation Symposium 49 (new series). Elsevier, 52 Vanderbilt Ave., New York, NY 10017. 1977. 344 pp. 16 × 24 cm.

Organic Syntheses. Vol. 57. Edited by CARL R. JOHNSON *et al.* Wiley, 1 Wiley Drive, Somerset, NJ 08875. 2047 pp. 15 × 23 cm. Price $12.95.

Problems of Clinical Pharmacology in Therapeutic Research: Phase 1. Edited by H. P. KUEMMERLE, T. K. SHIBUYA, and E. KIMURA. Urban & Schwarzenberg, 7 E. Redwood St., Baltimore, MD 21202. 1977. 420 pp. 15 × 23 cm. Price $28.50.

Biosynthesis. Vol. 5. A Specialist Periodical Report. Edited by J. D. BU'LOCK, *et al.* The Chemical Society, Burlington House, London, W1V OBN, England, 1977. 318 pp. 13 × 22 cm. Price $45.00. Available from Special Issues Sales, American Chemical Society, 1155 16th St., NW, Washington, DC 20036.

Drug Discrimination and State Dependent Learning. Edited by BENG T. HO, DANIEL W. RICHARDS, III, and DOUGLAS L. CHUTE. Academic, 111 Fifth Ave., New York, NY 10003. 1978. 392 pp. 15 × 23 cm. Price $23.00.

Manual of Anesthesia. By JOHN C. SNOW, Little, Brown, 34 Beacon St., Boston, MA 02106. 1977. 547 pp. 14 × 22 cm. Price $12.50.

Workplace Safety and Health. The Role of Workers' Compensation. By JAMES ROBERT CHELIUS. American Enterprise Institute for Public Policy Research, 1150 17 St., NW, Washington, DC. 20036. 1977. 97 pp. 15 × 23 cm. Price $2.75.

WHO Expert Committee on Specifications for Pharmaceutical Preparations. Twenty-Sixth Report. World Health Organization, 49 Sheridan Ave., Albany, NY 12210. 1977. 53 pp. 13 × 20 cm. Price $2.80.

International Nonproprietary Names (INN) for Pharmaceutical Substances. Cumulative List No. 5. World Health Organization, 49 Sheridan Ave., Albany, NY 12210. 1977. 332 pp. 17 × 24 cm. Price $19.20.

Perspectives in Pharmacy. Edited by ALBERT I. WERTHEIMER and MARGARET L. SCHUBERT. College of Pharmacy, University of Minnesota, Minneapolis, MN 55455. 1977. 84 pp. 15 × 23 cm.

Toxicologic Emergencies. A Handbook in Problem Solving. By LEWIS R. GOLDFRANK and ROBERT KIRSTEIN. Appleton-Century-Crofts, 292 Madison Ave., New York, NY 10017. 1977. 180 pp. Price $9.75.

Physical Chemistry for Students of Pharmacy and Biology. 3rd Ed. By S. C. WALLWORK and D. J. W. GRANT. Longman, 19 W. 44th St., New York, NY 10036. 1977. 607 pp. 14 × 22 cm. Price $18.00.

pharmaceutics and clinical pharmacokinetics. It would also be useful as a review or first introduction for practicing pharmacists as well as students and practitioners in related health fields.

Reviewed by Randall B. Smith and Lewis W. Dittert
College of Pharmacy
University of Kentucky
Lexington, KY 40506

Pharmacological and Biochemical Properties of Drug Substances, Vol. 1. Edited by MORTON E. GOLDBERG. American Pharmaceutical Association, 2215 Constitution Ave., N.W., Washington DC 20037. 1977. 413 pp 16 × 23 cm. Price $21.00 ($14.00 member rate).

This volume, which promises to be the first of a continuing series, is designed as a companion series to "Analytical Profiles of Drug Substances" edited by Klaus Florey. While Florey's series emphasizes chemical properties of drugs, this volume has the overall objective of reviewing the biological properties of agents that represent prototypes for the major classes of drugs available.

The contents of this initial volume include central nervous system agents (clozapine and pemoline), cardiovascular agents (clonidine and dobutamine), chemotherapeutic agents (amikacin and cefazolin), antiinflammatory agents (fenoprofen, halcinonide, and tolmetin), pulmonary and antiallergy agents (albuterol, cromolyn sodium, and terbutaline), GI agents (cimetidine and prostaglandin analogs), antifertility agents (prostaglandin analogs), and diagnostic agents (metrizamide). The general outline for each monograph consists of a brief discussion of the chemistry of the compound followed by animal pharmacology, toxicology, biopharmaceutics, and clinical pharmacology. The most valuable sections are the discussions of animal and clinical pharmacology.

Most chapters contain extensive tables of data. Some monographs also include descriptions of the agent's effect in pharmacological tests unrelated to its therapeutic indication. This information is particularly interesting because it is often difficult or impossible to extract from the primary literature.

Most monographs, except the monograph on pemoline, contain references into the 1976 and, in some cases, the 1977 literature. All monographs, except the one on clozapine, contain the title of the referenced articles. The volume is relatively free of errors, although the tables on pages 161 and 231 contain ED_{50} values that do not fall within the quoted confidence limits.

As stated above, as well as in the preface of the volume, the editor's objective was to include prototypes for the major classes of drugs available. This reviewer does not believe that drugs such as amikacin, cefazolin, fenoprofen, and tolmetin can be considered as prototypes of classes in keeping with Webster's definition. On the other hand, clonidine and cimetidine certainly would be considered prototypes. Of course, including only true prototypes would lead to a short series of volumes. Followup drugs such as those mentioned are valuable additions to this volume. Their value would be further increased if emphasis were given not only to comparing them with their original commercial target but also to comparing them with other drugs in development by competitors aiming for these same targets.

In summary, the concept of this series promises to be a valuable addition to the pharmaceutical literature. Its success will depend on the discipline of its editor and the objectivity of its authors.

Reviewed by Larry J. Powers
Diamond Shamrock Corporation
T. R. Evans Research Center
Painesville, OH 44077

NOTICES

The Synthesis of Prostaglandins. By ABHIJIT MITRA. Wiley, 605 Third Ave., New York, NY 10016. 1977. 444 pp. 15 × 23 cm.

This book presents a comprehensive review of the new synthetic methods and reactions used to construct prostaglandins, describing in detail almost all of the syntheses of the naturally occurring compounds, thromboxanes, and analogs. Various syntheses are classified according to major synthetic strategies. The individual synthesis is then presented with a brief introduction highlighting the key reaction(s) and followed by a synthetic strategy in the form of a flow diagram that shows the strategic bond disconnections. The actual synthesis is depicted in flowsheet form with extensive footnotes explaining the reactions and their stereochemical outcome if applicable. Both author and subject indexes are included.

Catecholamines of 'Developing 'Brain. Preconditioning of Behavior (Aggression? Anxiety?). By CLARA TORDA. Walters, 101 W. 12th St., New York, NY 10011. 1977. 255 pp. 20 × 28 cm.

Biochemistry. By PAUL JAY FRIEDMAN. Little, Brown, 34 Beacon St., Boston, MA 02106. 1977. 211 pp. 21 × 28 cm. Price $7.95.

Hagers Handbuch der Pharmazeutischen Praxis. Edited by P. H. LIST and L. HÖRHAMMER. Springer-Verlag, 175 Fifth Ave., New York, NY 10010. 1977. 570 pp. 16 × 24 cm. Price $65.20.

Epidemiological Evaluation of Drugs. Edited by F. COLOMBO, S. SHAPIRO, D. SLONE, and G. TOGNONI. PSG, 545 Great Rd., Littleton, MA 01460. 1977. 333 pp. 16 × 24 cm. Price $23.00.

Clinical Psychopharmacology. Edited by JERROLD C. BERNSTEIN. PSG, 545 Great Rd., Littleton, MA 01460. 1977. 154 pp. 15 × 24 cm. Price $12.50.

Peptide Transport and Hydrolysis. Ciba Foundation Symposium 50 (new series). Edited by KATHERINE ELLIOTT and MAEVE O'CONNOR. Elsevier, 52 Vanderbilt Ave., New York, NY 10017. 1977. 385 pp. 16 × 24 cm.

Health and Disease in Tribal Societies. Ciba Foundation Symposium 49 (new series). Elsevier, 52 Vanderbilt Ave., New York, NY 10017. 1977. 344 pp. 16 × 24 cm.

Organic Syntheses. Vol. 57. Edited by CARL R. JOHNSON *et al.* Wiley, 1 Wiley Drive, Somerset, NJ 08875. 2047 pp. 15 × 23 cm. Price $12.95.

Problems of Clinical Pharmacology in Therapeutic Research: Phase 1. Edited by H. P. KUEMMERLE, T. K. SHIBUYA, and E. KIMURA. Urban & Schwarzenberg, 7 E. Redwood St., Baltimore, MD 21202. 1977. 420 pp. 15 × 23 cm. Price $28.50.

Biosynthesis. Vol. 5. A Specialist Periodical Report. Edited by J. D. BU'LOCK, *et al.* The Chemical Society, Burlington House, London, W1V OBN, England, 1977. 318 pp. 13 × 22 cm. Price $45.00. Available from Special Issues Sales, American Chemical Society, 1155 16th St., NW, Washington, DC 20036.

Drug Discrimination and State Dependent Learning. Edited by BENG T. HO, DANIEL W. RICHARDS, III, and DOUGLAS L. CHUTE. Academic, 111 Fifth Ave., New York, NY 10003. 1978. 392 pp. 15 × 23 cm. Price $23.00.

Manual of Anesthesia. By JOHN C. SNOW, Little, Brown, 34 Beacon St., Boston, MA 02106. 1977. 547 pp. 14 × 22 cm. Price $12.50.

Workplace Safety and Health. The Role of Workers' Compensation. By JAMES ROBERT CHELIUS. American Enterprise Institute for Public Policy Research, 1150 17 St., NW, Washington, DC. 20036. 1977. 97 pp. 15 × 23 cm. Price $2.75.

WHO Expert Committee on Specifications for Pharmaceutical Preparations. Twenty-Sixth Report. World Health Organization, 49 Sheridan Ave., Albany, NY 12210. 1977. 53 pp. 13 × 20 cm. Price $2.80.

International Nonproprietary Names (INN) for Pharmaceutical Substances. Cumulative List No. 5. World Health Organization, 49 Sheridan Ave., Albany, NY 12210. 1977. 332 pp. 17 × 24 cm. Price $19.20.

Perspectives in Pharmacy. Edited by ALBERT I. WERTHEIMER and MARGARET L. SCHUBERT. College of Pharmacy, University of Minnesota, Minneapolis, MN 55455. 1977. 84 pp. 15 × 23 cm.

Toxicologic Emergencies. A Handbook in Problem Solving. By LEWIS R. GOLDFRANK and ROBERT KIRSTEIN. Appleton-Century-Crofts, 292 Madison Ave., New York, NY 10017. 1977. 180 pp. Price $9.75.

Physical Chemistry for Students of Pharmacy and Biology. 3rd Ed. By S. C. WALLWORK and D. J. W. GRANT. Longman, 19 W. 44th St., New York, NY 10036. 1977. 607 pp. 14 × 22 cm. Price $18.00.

SEPTEMBER 1978
VOLUME 67 NUMBER 9

JOURNAL OF PHARMACEUTICAL SCIENCES

MARY H. FERGUSON
Editor

SHELLY ELLIOTT
Production Editor

JANET D. SHOFF
Copy Editor

EDWARD G. FELDMANN
Contributing Editor

SAMUEL W. GOLDSTEIN
Contributing Editor

BELLE R. BECK
Editorial Secretary

DAVID BOHARDT
Director of Publications

L. LUAN CORRIGAN
Assistant Director of Publications

EDITORIAL ADVISORY BOARD

JOHN AUTIAN
NORMAN R. FARNSWORTH
WILLIAM O. FOYE
WILLIAM J. JUSKO
HERBERT A. LIEBERMAN
DAVID E. MANN, JR.
GERALD J. PAPARIELLO
EDWARD G. RIPPIE

The *Journal of Pharmaceutical Sciences* is published monthly by the American Pharmaceutical Association (APhA) at 2215 Constitution Ave., N.W., Washington, DC 20037. Second-class postage paid at Washington, D.C., and at additional mailing office.

All expressions of opinion and statements of supposed fact appearing in articles or editorials carried in this journal are published on the authority of the writer over whose name they appear and are not to be regarded as necessarily expressing the policies or views of APhA.

Offices—Editorial, Advertising, and Subscription: 2215 Constitution Ave., N.W., Washington, DC 20037. Printing: 20th & Northampton Streets, Easton, PA 18042.

Annual Subscriptions—United States and foreign, industrial and government institutions $50, educational institutions $50, individuals *for personal use only* $30; single copies $5. All foreign subscriptions add $5 for postage. Subscription rates are subject to change without notice. Members of APhA may elect to receive the *Journal of Pharmaceutical Sciences* as a part of their annual $70 (foreign $75) APhA membership dues.

Claims—Missing numbers will not be supplied if dues or subscriptions are in arrears for more than 60 days or if claims are received more than 60 days after the date of the issue, or if loss was due to failure to give notice of change of address. APhA cannot accept responsibility for foreign delivery when its records indicate shipment has been made.

Change of Address—Members and subscribers should notify at once both the Post Office and APhA of any change of address.

Photocopying—The code at the foot of the first page of an article indicates that APhA has granted permission for copying of the article beyond the limits permitted by Sections 107 and 108 of the U.S. Copyright Law provided that the copier sends the per copy fee stated in the code to the Copyright Clearance Center, Inc., P. O. Box 765, Schenectady, NY 12301. Copies may be made for personal or internal use only and not for general distribution.

Microfilm—Available from University Microfilms International, 300 N. Zeeb Road, Ann Arbor, MI 48106.

© Copyright 1978. American Pharmaceutical Association, 2215 Constitution Ave., N.W., Washington, DC 20037; all rights reserved.

LOOK WHAT THEY SAY ABOUT US!

During the late 1960s and early 1970s when the image of business, corporations, and the board room world reached its low point on the campuses of American universities, a corporate executive had occasion to visit one of the better-known colleges. He came back with a new realization of the stimulus for much of the restiveness and disdain exhibited by students toward the business community.

"You should hear what they are saying about us," he exclaimed in reference to the lectures being delivered on campus by various social activists. "And look at what they are writing about us!" he gasped, pointing to the handout materials distributed at these lectures.

Although he was a very educated and knowledgeable person, he had just learned a new lesson—one that we all need to be reminded of from time to time. In short, repeating his words: "Look at what they are writing (or saying) about us."

This anecdote came to mind recently as we were searching through copies of the journal *Drug Intelligence & Clinical Pharmacy* for the past year. We were hunting for an article we had earlier read on an entirely different subject, but in the process happened to stumble across three separate items, all on the subject of the responsiveness of the pharmaceutical industry in providing meaningful drug product information to pharmacists.

Item—The August 1977 issue included a communication from two University of Florida pharmacy staff members reporting on their efforts to obtain from drug companies the same information about those firms' products as they supply to physicians. Only one out of twenty firms contacted would agree to send pharmacists the same data that they routinely provide to physicians.

Item—The December 1977 issue contained an article entitled the "Pharmaceutical Industry's Obligation to Clinical Pharmacists," from a hospital center in Brooklyn, New York, which presents, in outline form, the areas of information that the pharmaceutical industry should provide to pharmacists regarding their drug products.

Item—The March 1978 issue carried a report by a community pharmacist from Chicago, Illinois, on his efforts to obtain drug product information from the pertinent manufacturers as part of his personal program to build a professional library of information in his pharmacy. The information he requested was for data on drug absorption, distribution, metabolism, elimination, clinical studies, toxicology, and pharmacokinetics. The responses he received were mixed at best, ranging from plaudits to "It's none of your business." Generally, the replies were sparse and disappointing.

For years, APhA has been urging pharmacists to seek objective data, to study it, and to make decisions, choices, and recommendations based upon facts and not puffery. More and more, pharmacists are trying to follow that advice, as reflected in the three reports cited above.

Many of our readers are either directly or indirectly connected with firms in the drug industry. They may assume that the industry as a whole, or at least the firm with which they are associated, is doing a good job of supplying such data. For purposes of this editorial, we shall not offer any opinion ourselves, but it is revealing to see the published conclusions of the authors of the three above-cited articles. The following excerpts are quoted from those articles in the same order as listed above:

- "If pharmacists are ever going to become patient-oriented drug experts, they should be provided with the necessary information to do so without encountering the lack of interest that is exemplified by the pharmaceutical industry."
- "The pharmaceutical industry must begin to recognize its responsibility to improve patient therapy by providing expanded information to the physicians and pharmacists who monitor it."
- "A note to Industry: Pharmacists do not fill prescriptions *ut dict* anymore. We analyze, check interactions both synergistic and antagonistic, review with doctors and patients the medications, and communicate as professionals. Industry must stop making excuses for their poor contributions to the pharmacist."

The journal in which these articles and excerpts appeared—*Drug Intelligence & Clinical Pharmacy*—is primarily oriented toward pharmacy practitioners. As such, the majority of our readers probably do not review it on a regular basis and would not be aware what many pharmacists are telling each other. Consequently, the purpose of this editorial is simply to afford these readers with an opportunity to see "what they are writing about us" along the line of the anecdote above concerning the miffed corporate executive.

Edward G. Feldmann

SEPTEMBER 1978
VOLUME 67 NUMBER 9

JOURNAL OF PHARMACEUTICAL SCIENCES

MARY H. FERGUSON
Editor

SHELLY ELLIOTT
Production Editor

JANET D. SHOFF
Copy Editor

EDWARD G. FELDMANN
Contributing Editor

SAMUEL W. GOLDSTEIN
Contributing Editor

BELLE R. BECK
Editorial Secretary

DAVID BOHARDT
Director of Publications

L. LUAN CORRIGAN
Assistant Director of Publications

EDITORIAL ADVISORY BOARD

JOHN AUTIAN
HERBERT A. LIEBERMAN
NORMAN R. FARNSWORTH
DAVID E. MANN, JR.
WILLIAM O. FOYE
GERALD J. PAPARIELLO
WILLIAM J. JUSKO
EDWARD G. RIPPIE

The *Journal of Pharmaceutical Sciences* is published monthly by the American Pharmaceutical Association (APhA) at 2215 Constitution Ave., N.W., Washington, DC 20037. Second-class postage paid at Washington, D.C., and at additional mailing office.

All expressions of opinion and statements of supposed fact appearing in articles or editorials carried in this journal are published on the authority of the writer over whose name they appear and are not to be regarded as necessarily expressing the policies or views of APhA.

Offices—Editorial, Advertising, and Subscription: 2215 Constitution Ave., N.W., Washington, DC 20037. Printing: 20th & Northampton Streets, Easton, PA 18042.

Annual Subscriptions—United States and foreign, industrial and government institutions $50, educational institutions $50, individuals *for personal use only* $30; single copies $5. All foreign subscriptions add $5 for postage. Subscription rates are subject to change without notice. Members of APhA may elect to receive the *Journal of Pharmaceutical Sciences* as a part of their annual $70 (foreign $75) APhA membership dues.

Claims—Missing numbers will not be supplied if dues or subscriptions are in arrears for more than 60 days or if claims are received more than 60 days after the date of the issue, or if loss was due to failure to give notice of change of address. APhA cannot accept responsibility for foreign delivery when its records indicate shipment has been made.

Change of Address—Members and subscribers should notify at once both the Post Office and APhA of any change of address.

Photocopying—The code at the foot of the first page of an article indicates that APhA has granted permission for copying of the article beyond the limits permitted by Sections 107 and 108 of the U.S. Copyright Law provided that the copier sends the per copy fee stated in the code to the Copyright Clearance Center, Inc., P. O. Box 765, Schenectady, NY 12301. Copies may be made for personal or internal use only and not for general distribution.

Microfilm—Available from University Microfilms International, 300 N. Zeeb Road, Ann Arbor, MI 48106.

© Copyright 1978. American Pharmaceutical Association, 2215 Constitution Ave., N.W., Washington, DC 20037; all rights reserved.

LOOK WHAT THEY SAY ABOUT US!

During the late 1960s and early 1970s when the image of business, corporations, and the board room world reached its low point on the campuses of American universities, a corporate executive had occasion to visit one of the better-known colleges. He came back with a new realization of the stimulus for much of the restiveness and disdain exhibited by students toward the business community.

"You should hear what they are saying about us," he exclaimed in reference to the lectures being delivered on campus by various social activists. "And look at what they are writing about us!" he gasped, pointing to the handout materials distributed at these lectures.

Although he was a very educated and knowledgeable person, he had just learned a new lesson—one that we all need to be reminded of from time to time. In short, repeating his words: "Look at what they are writing (or saying) about us."

This anecdote came to mind recently as we were searching through copies of the journal *Drug Intelligence & Clinical Pharmacy* for the past year. We were hunting for an article we had earlier read on an entirely different subject, but in the process happened to stumble across three separate items, all on the subject of the responsiveness of the pharmaceutical industry in providing meaningful drug product information to pharmacists.

Item—The August 1977 issue included a communication from two University of Florida pharmacy staff members reporting on their efforts to obtain from drug companies the same information about those firms' products as they supply to physicians. Only one out of twenty firms contacted would agree to send pharmacists the same data that they routinely provide to physicians.

Item—The December 1977 issue contained an article entitled the "Pharmaceutical Industry's Obligation to Clinical Pharmacists," from a hospital center in Brooklyn, New York, which presents, in outline form, the areas of information that the pharmaceutical industry should provide to pharmacists regarding their drug products.

Item—The March 1978 issue carried a report by a community pharmacist from Chicago, Illinois, on his efforts to obtain drug product information from the pertinent manufacturers as part of his personal program to build a professional library of information in his pharmacy. The information he requested was for data on drug absorption, distribution, metabolism, elimination, clinical studies, toxicology, and pharmacokinetics. The responses he received were mixed at best, ranging from plaudits to "It's none of your business." Generally, the replies were sparse and disappointing.

For years, APhA has been urging pharmacists to seek objective data, to study it, and to make decisions, choices, and recommendations based upon facts and not puffery. More and more, pharmacists are trying to follow that advice, as reflected in the three reports cited above.

Many of our readers are either directly or indirectly connected with firms in the drug industry. They may assume that the industry as a whole, or at least the firm with which they are associated, is doing a good job of supplying such data. For purposes of this editorial, we shall not offer any opinion ourselves, but it is revealing to see the published conclusions of the authors of the three above-cited articles. The following excerpts are quoted from those articles in the same order as listed above:

- "If pharmacists are ever going to become patient-oriented drug experts, they should be provided with the necessary information to do so without encountering the lack of interest that is exemplified by the pharmaceutical industry."
- "The pharmaceutical industry must begin to recognize its responsibility to improve patient therapy by providing expanded information to the physicians and pharmacists who monitor it."
- "A note to Industry: Pharmacists do not fill prescriptions *ut dict* anymore. We analyze, check interactions both synergistic and antagonistic, review with doctors and patients the medications, and communicate as professionals. Industry must stop making excuses for their poor contributions to the pharmacist."

The journal in which these articles and excerpts appeared—*Drug Intelligence & Clinical Pharmacy*—is primarily oriented toward pharmacy practitioners. As such, the majority of our readers probably do not review it on a regular basis and would not be aware what many pharmacists are telling each other. Consequently, the purpose of this editorial is simply to afford these readers with an opportunity to see "what they are writing about us" along the line of the anecdote above concerning the miffed corporate executive.

Edward G. Feldmann

JOURNAL OF PHARMACEUTICAL SCIENCES

SEPTEMBER 1978
VOLUME 67 NUMBER 9

RESEARCH ARTICLES

Preparation and Immunological Cross-Reactions of Penicilloic and Penilloic Acids

A. C. MUNRO *, M. G. CHAINEY, and S. R. WORONIECKI ˣ

Received November 22, 1976, from the *Research Division, Beecham Pharmaceuticals, Chemotherapeutic Research Centre, Brockham Park, Betchworth, Surrey, RH3 7AJ, England.* Accepted for publication December 9, 1977. *Present address: Glasgow and West of Scotland Blood Transfusion Service, At Law Hospital, Carluke, Lanarkshire, Scotland.

Abstract □ Methods are described for the preparation of pure crystalline samples of the penicilloic and penilloic acids of penicillin G, carbenicillin, cloxacillin, floxacillin, methicillin, penicillin V, and ticarcillin and the penicilloic acids of amoxicillin, ampicillin, phenethicillin, and propicillin. The interaction between the compounds and rabbit antibenzylpenicilloyl antibodies was evaluated by hemagglutination inhibition measurements. A significant correlation was found in this system between the reactivity of penicilloic acids and the corresponding penilloic acids; on average, the penicilloic acids were more reactive on a molar basis by a factor of 11. The results are discussed in terms of the general immunochemistry and side-chain structure of the parent penicillins.

Keyphrases □ Penicilloic acids, various—synthesized, immunological cross-reactions evaluated *in vitro* □ Penilloic acids, various—synthesized, immunological cross-reactions evaluated *in vitro* □ Immunological cross-reactions—various penicilloic and penilloic acids evaluated *in vitro* □ Antibacterials—various penicilloic and penilloic acids, immunological cross-reactions evaluated *in vitro*

The major degradation products of penicillins are the corresponding penicilloic acids, formed by alkaline hydrolysis of the β-lactam ring (Scheme I). The penicilloic acids thus formed can undergo decarboxylation under relatively mild acidic conditions to yield the corresponding penilloic acids.

BACKGROUND

Penicilloic acids were identified as major metabolites of penicillins in humans (1); they have been used, either individually (2) or in combination with the parent penicillins and penilloic acids, as the "minor determinant mixture" (3) to skin test patients suspected of allergy to penicillin. The minor determinant mixture usually comprises the derivatives of penicillin G (benzylpenicillin), but similar mixtures derived from other penicillins also have been used in human skin tests (4–6).

Although it has not been established how the minor determinants combine with proteins *in vivo* to initiate an immune response of the allergic type, the most common reaction occurring between penicillins and proteins involves a nucleophilic amino group on the protein carrier, yielding a penicilloyl group (Structure A) referred to as the "major determinant." Since the penicilloyl determinant group is frequently implicated in immediate hypersensitivity reactions to penicillin, the immunological cross-reactivity between the penicilloyl groups derived from various therapeutic penicillins is of interest. The interaction between

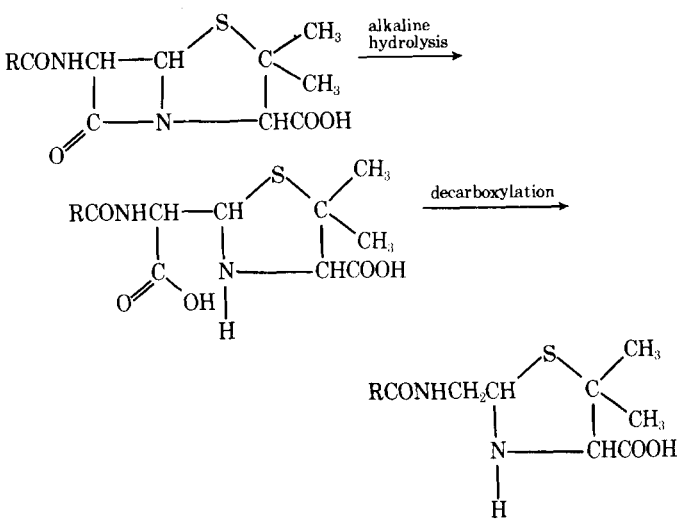

Scheme I

antipenicilloyl antibodies and various penicillins as the penicillins themselves (7), as the derived penicilloic acids (8), or as the penicilloyl derivatives of ε-aminocaproic acid (9) was studied previously.

The preparation of the penicilloic and penilloic acids from penicillin G in pure form was described (2, 10). Detailed methods for the preparation of pure forms of the corresponding materials from other penicillins have been lacking, however, and many *in vitro* and skin test studies utilized chemically uncharacterized materials. The objectives of the present study were to prepare pure samples of the penicilloic and penilloic acids of a number of penicillins and to evaluate their potential to cross-react with benzylpenicilloyl-specific antibodies.

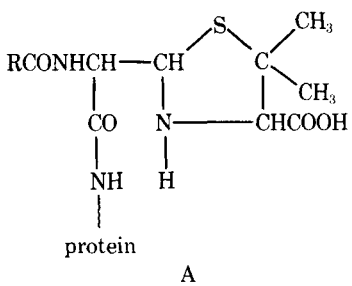

A

0022-3549/78/0900-1197$01.00/0
© 1978, American Pharmaceutical Association

Table I—Penicilloic Acids

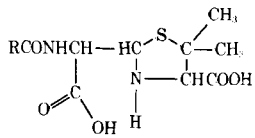

Parent Penicillin	R	Formula		Analysis, % Calc.	Found	Equivalent Weight[a] Calc.	Found	Purity[b], %	$[\alpha]_D$[a]	R_f (TLC)
Amoxicillin	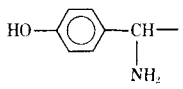	$C_{16}H_{20}N_3NaO_6S \cdot H_2O$	C H N Na S	45.39 5.24 9.92 5.43 7.57	45.34 5.25 9.93 5.69 7.11	141.1	145.4[c]	96.1	+103.8° (c 1.0, water)	0.25
Ampicillin	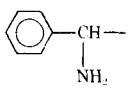	$C_{16}H_{20}N_3NaO_5S \cdot H_2O$	C H N Na S	47.17 5.44 10.31 5.64 7.87	46.79 5.18 10.21 5.74 8.61	135.8	139.1[c]	102.2	+98.1° (c 1.0, water)	0.25
Carbenicillin	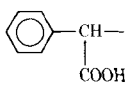	$C_{17}H_{19}N_2O_7S \cdot H_2O$	C H N S	49.33 5.02 6.78 7.76	49.77 5.40 6.77 7.96	137.8	138.4[d]	100.3	−15.1° (c 1.0, methanol)	0.20
Cloxacillin	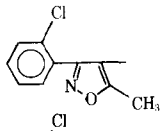	$C_{19}H_{20}ClN_3O_6S \cdot H_2O$	C H Cl N S	48.36 4.70 7.51 8.90 6.79	48.24 4.69 7.28 9.03 6.73	236.0	234.4[d]	109.5	+71.8° (c 1.0, methanol)	0.46
Floxacillin	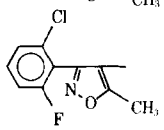	$C_{19}H_{17}ClFN_3Na_2O_6S \cdot 1\frac{1}{2}H_2O$	C H N Na S	42.04 3.71 7.74 8.47 5.91	41.65 3.54 7.53 8.90 6.25	0	0[d]	106.0	+94.5° (c 1.0, water)	0.39
Methicillin	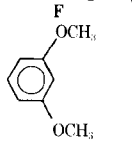	$C_{17}H_{22}N_2O_7S \cdot H_2O$	C H N S	49.03 5.81 6.73 7.70	49.15 5.85 6.71 7.77	208.2	203.8[d]	97.7	+81.2° (c 1.0, methanol)	0.34
Penicillin G	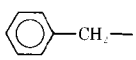	$C_{16}H_{19}N_2NaO_5S \cdot H_2O$	C H N Na S	48.97 5.39 7.14 5.86 8.17	49.09 5.27 7.23 6.01 8.44	392.4	390.5[d]	95.6	+157.1° (c 1.0, water)	0.34
Penicillin V	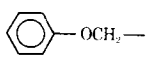	$C_{16}H_{20}N_2O_6S \cdot H_2O$	C H N S	49.73 5.74 7.25 8.30	49.77 5.74 7.08 8.10	193.2	193.9[d]	94.8	+95.6° (c 1.0, methanol)	0.40
Phenethicillin	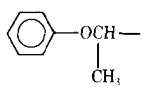	$C_{17}H_{22}N_2O_6S \cdot H_2O$	C H N S	50.09 6.04 7.00 8.01	50.69 5.95 6.95 7.98	200.2	203.2[d]	99.7	+88.6° (c 1.0, methanol)	0.43
Propicillin	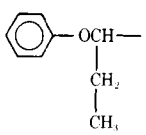	$C_{18}H_{24}N_2O_6S \cdot 1\frac{1}{2}H_2O$	C H N S	51.05 6.43 6.61 7.57	51.03 6.48 6.57 7.20	211.7	210.7[d]	100.4	+67.9° (c 1.0, methanol)	0.46
Ticarcillin	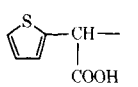	$C_{15}H_{18}N_2O_7S_2 \cdot \frac{1}{2}H_2O$	C H N S	43.79 4.65 6.81 15.59	44.01 4.60 6.85 16.00	137.2	133.5[d]	100.2	−22.3° (c 1.0, water + sodium hydroxide → pH 7.0)	0.21

[a] Corrected for water. [b] From iodometric assay. [c] By nonaqueous titration. [d] By aqueous titration.

EXPERIMENTAL

Materials—The following materials were used: amoxicillin [6-[(−)-α-amino-4-hydroxyphenylacetamido]penicillanic acid trihydrate], ampicillin [6-[D-(−)-α-aminophenylacetamido]penicillanic acid trihydrate], penicillin G [sodium 6-(phenylacetamido)penicillanate], carbenicillin [disodium 6-(α-carboxyphenylacetamido)penicillanic acid], cloxacillin [sodium 6-[3-(2-chlorophenyl)-5-methylisoxazole-4-carboxamido]penicillanate monohydrate], floxacillin [sodium 6-[3-(2-chloro-6-fluorophenyl)-5-methylisoxazole-4-carboxamido]penicillanate monohydrate], methicillin [sodium 6-(2,6-dimethoxybenzamido)penicillanate monohydrate], phenethicillin [potassium 6-(α-phenoxypropionamido)penicillanate], penicillin V[1] [potassium 6-(phenoxyacetamido)penicillanate], propicillin [potassium 6-(α-phenoxybutyramido)penicillanate], and ticarcillin [disodium 6-[2-carboxy-2-(3-thienyl)acetamido]penicillanate]. All penicillins, except penicillin V (phenoxymethylpenicillin), were prepared in these laboratories.

Analytical Methods—Optical rotations were determined for the sodium D-line using a 10-cm cell[2]. Microanalyses were determined on a carbon–hydrogen–nitrogen analyzer[3], IR spectroscopy was carried out with potassium bromide disks[4], and NMR spectra[5] also were obtained.

TLC was performed on silica gel plates[6] with 1-butanol–ethanol–water (2:1:1) as the developing solvent. Detection was carried out with iodine vapor.

[1] Glaxo Limited.

[2] Perkin-Elmer model 141 polarimeter.
[3] Perkin-Elmer model 240.
[4] Perkin-Elmer model 457 spectrophotometer.
[5] Varian A60-A spectrometer.
[6] Eastman Kodak code 13181.

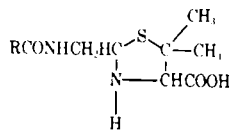

Table II—Penilloic Acids

Parent Penicillin	Formula		Analysis, % Calc.	Found	Equivalent Weight[a,b] Calc.	Found	$[\alpha]_D^b$	R_f (TLC)
Carbenicillin	$C_{16}H_{19}N_2O_5S \cdot \frac{1}{2}H_2O$	C	53.32	53.43	175.7	177.6	+31.8° (c 1.0, water + sodium hydroxide → pH 7.0)	0.54
		H	5.59	5.60				
		N	7.77	7.79				
		S	8.90	8.92				
Cloxacillin	$C_{18}H_{20}ClN_3O_4S$	C	52.72	52.32	409.9	401.4	+94.5° (c 1.0, water + sodium hydroxide → pH 7.0)	0.57
		H	4.92	4.88				
		Cl	8.76	8.58				
		N	10.26	10.18				
		S	7.83	7.77				
Floxacillin	$C_{18}H_{19}ClFN_3O_4S$	C	50.51	50.38	427.9	402.5	+44.6° (c 1.0, methanol)	0.66
		H	4.48	4.46				
		N	9.82	9.59				
		S	7.50	7.84				
Methicillin	$C_{16}H_{22}N_2O_5S$	C	54.22	53.95	354.4	332.0	+15.7° (c 1.0, methanol)	0.52
		H	6.26	6.45				
		N	7.90	7.66				
		S	9.05	8.93				
Penicillin G	$C_{15}H_{19}N_2O_3S \cdot H_2O$	C	55.20	55.38	326.4	319.4	+76.0° (c 1.0, methanol)	0.57
		H	6.79	7.04				
		N	8.58	8.56				
		S	9.82	9.92				
Penicillin V	$C_{15}H_{20}N_2O_4S$	C	55.53	55.42	324.4	323.2	+59.7° (c 1.0, methanol)	0.64
		H	6.21	6.27				
		N	8.66	8.47				
		S	9.88	10.26				
Ticarcillin	$C_{14}H_{18}N_2O_5S_2$	C	46.91	47.19	179.2	180.2	+49.0° (c 1.0, water + sodium hydroxide → pH 7.0)	0.45
		H	5.06	5.12				
		N	7.82	7.92				
		S	17.89	17.77				

[a] By aqueous titration. [b] Corrected for water.

Equivalent weights were determined by either of two methods. In the first method, carboxyl groups were determined by adding a known volume of standard sodium hydroxide to the test compounds, followed by back-titration with standard hydrochloric acid. In the second method, primary and secondary amino groups and metal cations were determined by titrating the test compounds under nonaqueous conditions with standard perchloric acid.

Iodometric assays for assessing the purity of penicilloic acids were carried out as described elsewhere (11), except that the initial alkaline hydrolysis stage was omitted. Values are quoted relative to analytical samples of the parent penicillins assayed by the standard iodometric method (11).

Preparation of Penicilloic Acids—Penicilloic acids were prepared by alkaline hydrolysis of the parent penicillins and isolated as described here. All products were dried *in vacuo* over phosphorus pentoxide. All preparations began with a stirred addition of the parent penicillin to water at ambient temperature. Sufficient 10 *M* NaOH was added to maintain the pH at 12.0 for 1.5 hr, *i.e.*, when the hydrolysis was complete. IR spectral analysis of the isolated compounds showed bands in the region of 1720 (carboxyl C=O), 1670 (amide C=O), and 1600 (aromatic C=C) cm^{-1}. No bands in the 1760–1785-cm^{-1} region (β-lactam C=O) were observed.

Amoxicillin Penicilloic Acid—Amoxicillin trihydrate (50 g) was hydrolyzed in water (500 ml). This solution was filtered, water was added to 1000 ml, and the pH was adjusted to 7.0 by addition of 5 *M* HCl. 2-Propanol (1000 ml) was added slowly with rapid stirring, and the solution was allowed to crystallize at 4°. The product was recovered as the monosodium salt by filtration, washed with cold 2-propanol–water (2:1), and dried, yielding 27 g (59%).

Ampicillin Penicilloic Acid—Ampicillin trihydrate (50 g) was hydrolyzed in water (250 ml). The solution was filtered, and the pH was adjusted to 7.0 by addition of 5 *M* HCl. 2-Propanol (700 ml) was added slowly with rapid stirring, and the resulting solution was allowed to crystallize at 4°. The product was recovered as the monosodium salt by filtration, washed with cold 2-propanol–water (3:1), and dried, yielding 24 g (53%).

Penicillin G Penicilloic Acid—Penicillin G sodium (100 g) was hydrolyzed in water (500 ml). The pH was adjusted to 5.4 by addition of concentrated hydrochloric acid. 2-Propanol (1500 ml) was added slowly with rapid stirring, and the resulting solution was allowed to crystallize at 4°. The product was recovered as the monosodium salt by filtration, washed with cold 2-propanol–water (3:1), and dried, yielding 58 g (55%).

Carbenicillin Penicilloic Acid—Carbenicillin disodium (30 g) was hydrolyzed in water (500 ml). The pH was adjusted to 1.8 by addition of 5 *M* HCl, and the solution was allowed to crystallize at 4°. The product was recovered as the free acid by filtration, washed with cold water, and dried, yielding 9 g (31%).

Cloxacillin Penicilloic Acid—Cloxacillin sodium monohydrate (30 g) was hydrolyzed in water (150 ml). An equal volume of methyl acetate was added, and the pH was adjusted to 2.5 by addition of 5 *M* HCl with stirring. The organic phase was separated, and crystallization immediately occurred. The product was removed by filtration and dissolved in methanol (150 ml), and water (500 ml) was added slowly. The solution was allowed to crystallize at 4°. The product was recovered as the free acid by filtration, washed with cold water, and dried, yielding 14 g (45%).

Floxacillin Penicilloic Acid—Floxacillin sodium monohydrate (15 g) was hydrolyzed in water (250 ml). The pH was adjusted to 7.5 by addition of 5 *M* HCl, and the solution was concentrated by rotary evaporation to 70 ml. 2-Propanol (525 ml) was added slowly with stirring, and the solution was allowed to crystallize at 4°. The product was recovered as the disodium salt by filtration, washed with cold 2-propanol–water (7:1), and dried, yielding 9 g (57%).

Methicillin Penicilloic Acid—Methicillin sodium monohydrate (30 g) was hydrolyzed in water (150 ml). The pH was adjusted to 2.4 with 5 *M* HCl, and a white precipitate formed. The precipitate was then filtered and washed with water. Methyl acetate was added to the precipitate in sufficient quantity to dissolve the solid completely at 35–40°, and the solution was allowed to crystallize at 4°. The product was recovered as the free acid by filtration, washed with cold methyl acetate, and dried.

Phenethicillin Penicilloic Acid—Phenethicillin potassium (22 g) was hydrolyzed in water (110 ml). The pH was adjusted to 7.0 by addition of 5 *M* HCl, and an equal volume of methyl acetate was added. The pH was then adjusted to 2.4 by slow addition of 5 *M* HCl with stirring, and the organic phase was separated and allowed to crystallize at 4°. The product

Table III—Inhibition of Hemagglutination by Penicilloic and Penilloic Acids

Parent Penicillin	Derived Penicilloic Acid: Molar Concentration Giving 50% Inhibition	Derived Penicilloic Acid: K_{rel}	Derived Penilloic Acid: Molar Concentration Giving 50% Inhibition	Derived Penilloic Acid: K_{rel}
Amoxicillin	7.81×10^{-4}	0.0078	—	—
Ampicillin	1.95×10^{-4}	0.0313	—	—
Carbenicillin	3.66×10^{-5}	0.1667	3.91×10^{-4}	0.1875
Cloxacillin	1.46×10^{-4}	0.0418	2.35×10^{-3}	0.0312
Floxacillin	3.91×10^{-4}	0.0156	1.56×10^{-3}	0.0470
Methicillin	3.91×10^{-4}	0.0156	2.35×10^{-3}	0.0312
Penicillin G	6.10×10^{-6}	1.0000	7.33×10^{-5}	1.0000
Penicillin V	1.22×10^{-5}	0.5000	2.93×10^{-4}	0.2502
Phenethicillin	3.66×10^{-5}	0.1667	5.86×10^{-4}	0.1251
Propicillin	7.33×10^{-5}	0.0832	7.81×10^{-4}	0.0939
Ticarcillin	7.81×10^{-4}	0.0078	2.35×10^{-3}	0.0312
Benzylpenicilloyl	5.72×10^{-7}	10.664	—	—

was recovered as the free acid by filtration, washed with cold methyl acetate, and dried, yielding 15.7 g (72%).

Penicillin V Penicilloic Acid—Penicillin V potassium (30 g) was hydrolyzed in water (150 ml). An equal volume of methyl acetate was added, and the pH was adjusted to 2.2 by addition of 5 *M* HCl with stirring. The organic phase was separated and allowed to crystallize at 4°. The product was recovered as the free acid by filtration, washed with cold methyl acetate, and dried, yielding 17 g (57%).

Propicillin Penicilloic Acid—Propicillin potassium (22 g) was hydrolyzed in water (110 ml). An equal volume of methyl acetate was added, and the pH was adjusted to 2.4 by addition of 5 *M* HCl with stirring. The organic phase was separated and dried with magnesium sulfate. After removal of the drying agent, the solution was allowed to crystallize at 4°. The product was recovered as the free acid by filtration, washed with cold methyl acetate, and dried, yielding 15 g (70%).

Ticarcillin Penicilloic Acid—Ticarcillin disodium (20 g) was hydrolyzed in water (100 ml). The pH was adjusted to 2.2 by addition of concentrated hydrochloric acid, and the solution was allowed to crystallize at 4°. The product was recovered as the free acid by filtration, washed with cold water, and dried, yielding 4.0 g (21%).

Preparation of Penilloic Acids—Penilloic acids were prepared by acid decarboxylation of the parent penicilloic acids and isolated as described here. All were dried *in vacuo* over phosphorus pentoxide. IR spectral analysis of the isolated compounds showed bands in the regions of 1720 (carboxyl C=O), 1660 (amide C=O), and 1600 (aromatic C=C) cm^{-1}.

Penicillin G Penilloic Acid—Penicillin G sodium (100 g) was hydrolyzed in water (500 ml). The pH was adjusted to 4.0 by addition of 5 *M* HCl, and an equal volume of ethanol was added. The solution was heated at 70–80° until effervescence ceased while the pH was maintained at 4.0. The solution was filtered and then allowed to cool and crystallize at 4°. The product was recovered as the free acid by filtration, washed with cold ethanol–water (1:1), and dried, yielding 49 g (57%).

Carbenicillin Penilloic Acid—Carbenicillin penicilloic acid (20 g) was added to water (500 ml), and the pH was adjusted to 1.8 by addition of 5 *M* HCl. On heating the suspension at 80°, the penicilloic acid dissolved and effervescence commenced with concomitant precipitation of the penilloic acid. When effervescence ceased, the suspension was cooled. The product was recovered by filtration, washed with cold water, and dried, yielding 11.3 g (65%).

Cloxacillin Penilloic Acid—Cloxacillin penicilloic acid (5 g) was added to a mixture of water (100 ml) and ethanol (100 ml), and the suspension was heated at ~80° until effervescence ceased. The solution was filtered and then allowed to cool and crystallize at 4°. The product was recovered as the free acid by filtration, washed with cold ethanol–water (1:1), and dried, yielding 3.6 g (83%).

Floxacillin Penilloic Acid—Floxacillin sodium monohydrate (20 g) was hydrolyzed in water (100 ml). The solution was diluted to 350 ml (water), and the pH was adjusted to 3.0 by addition of 5 *M* HCl. The solution was heated at ~80° until effervescence ceased while the pH was maintained at <5.0. The pH was finally adjusted to 3.5, and the solution was allowed to crystallize at 4°. The product was recovered as the free acid by filtration, washed with water, and dried, yielding 3.6 g (21%).

Methicillin Penilloic Acid—Methicillin sodium monohydrate (20 g) was hydrolyzed in water (100 ml). The pH was adjusted to 3.0 by addition of 5 *M* HCl, and the solution was heated at 80° while the pH was maintained at <5.0 by further additions of acid. When effervescence ceased, the pH was adjusted to 2.5, ethanol (60 ml) was added, and the solution was allowed to crystallize at 4°. The product was recovered as the free acid by filtration, washed with water–ethanol (2:1), and dried, yielding 6.0 g (36%).

Penicillin V Penilloic Acid—Penicillin V penicilloic acid (5 g) was added to a mixture of ethanol (30 ml) and water (100 ml) and heated at 80° until effervescence ceased. The solution was cooled and allowed to crystallize at 4°. The product was recovered as the free acid by filtration, washed with cold water, and dried, yielding 3.1 g (74%).

Ticarcillin Penilloic Acid—Ticarcillin disodium (25 g) was hydrolyzed in water (250 ml). The pH was adjusted to 2.0 by addition of 5 *M* HCl, and the solution was heated at 80°. Effervescence began and the penilloic acid precipitated; when effervescence ceased, the solution was cooled. The product was recovered by filtration, washed with cold water, and dried, yielding 6.3 g (30%).

Amoxicillin and Ampicillin Penilloic Acids—All attempts to obtain pure samples of these compounds failed. On heating under acidic aqueous conditions, both ampicillin and amoxicillin penicilloic acids were decarboxylated as shown by the evolution of carbon dioxide. The reaction solutions turned yellow, and multiple products, as shown by TLC, were formed. One major product formed was fluorescent; with ampicillin, a compound with identical TLC characteristics was obtained by heating ampicillin itself under acidic conditions.

Phenethicillin and Propicillin Penilloic Acids—Pure crystalline samples of these materials could not be obtained. Both phenethicillin and propicillin penicilloic acids were decarboxylated on heating in acidic aqueous solution as shown by the evolution of carbon dioxide. The reaction products were extracted into methyl acetate and then into aqueous solution by addition of 2 *M* NaOH to pH 6.5. The aqueous phases were lyophilized to give products that were homogeneous by TLC (phenethicillin penilloic acid, R_f 0.64; propicillin penilloic acid, R_f 0.64) but which were not further characterized.

Selective Decarboxylation of Carbenicillin Penicilloic Acid—Carbenicillin disodium (20 g) was hydrolyzed in water (100 ml), and the solution was divided into two portions. To the first portion was added 5 *M* HCl to pH 2.0, and the solution was heated at 80°. The precipitate was removed when effervescence ceased, and TLC confirmed the precipitate to be carbenicillin penilloic acid.

The second portion of the original solution was heated at 100° at pH 12.0 for 1.5 hr, and the pH was maintained by further additions of alkali. TLC of the resulting solution indicated the presence of approximately equal amounts of carbenicillin penicilloic acid and a spot corresponding to penicillin G penicilloic acid. The solution was adjusted to pH 2.0 by addition of 5 *M* HCl and heated at 80° until effervescence ceased. The precipitate was removed and examined, along with the supernate, by TLC. The precipitate contained one major component corresponding to carbenicillin penilloic acid and a trace component corresponding to penicillin G penilloic acid. The supernate contained one major component corresponding to penicillin G penilloic acid and a trace component corresponding to carbenicillin penilloic acid.

***N*-Benzylpenicilloyl ε-Aminocaproic Acid**—The preparation of this compound was described elsewhere (12).

Preparation of Benzylpenicilloyl Antiserums—Benzylpenicilloylated bovine γ-globulin was prepared as described previously (13). New Zealand White rabbits, 2.5 kg, were immunized by 0.5-ml subcutaneous and intramuscular injections of immunogen at a concentration of 10 mg/ml, emulsified in Freund's complete adjuvant, along with 5 × 0.1-ml intradermal injections of immunogen at 10 mg/ml in 0.15 *M* saline. At 2, 4, 5, and 6 months, the animals were each given a booster subcutaneous injection of 2 mg of immunogen in 0.15 *M* saline. Three weeks after the final booster injection, the animals were exsanguinated.

Sensitization of Rabbit Erythrocytes and Standardization of Antiserums for Hemagglutination Studies—The method used to sensitize the rabbit erythrocytes was similar to that described by Thiel *et al.* (14).

Blood from a donor rabbit was mixed with an equal volume of Alsever's solution. The cells were washed three times in pH 7.2 phosphate-buffered saline and made up to 20% in 0.14 *M* barbital[7] buffer, pH 8.5. To 30 ml of the cell suspension was added 1.0 g of penicillin G potassium (benzylpenicillin potassium), followed by incubation at 37° for 1 hr. The cells were washed six times in phosphate-buffered saline containing 1% normal rabbit serum and resuspended to a final concentration of 2% (v/v) in this medium.

[7] Veronal.

Table IV—NMR Spectra for Penilloic Acids

Parent Penicillin	Solvent	Ar	ArC*H*	CH_2CHS	CH_2CHS	OCH_2CO	$(CH_3)_2CCH$	$(CH_3)_2C$	CCH_3
Carbenicillin	Pyridine-d_5 plus deuterium oxide	7.35 (m, 5)	Plus CH_2CHS 5.16 (m, 2)	Plus $(CH_3)_2CCH$ 3.95 (m, 3)	—	—	—	1.70 (d, 6)	–
Cloxacillin	Dimethyl sulfoxide-d_6 plus deuterium oxide	7.54 (s, 4)	—	4.71 (t, 1)	3.26 (d, 2)	—	3.56 (s, 1)	1.39 (d, 6)	2.65 (s, 3)
Floxacillin	Dimethyl sulfoxide-d_6 plus deuterium oxide	7.34 (m, 3)	—	4.72 (t, 1)	Plus $(CH_3)_2CCH$ 3.0–3.7 (m, 3)	—	—	1.40 (d, 6)	2.69 (s, 3)
Methicillin	Dimethyl sulfoxide-d_6 plus deuterium oxide	6.5–7.6 (m, 3)	—	4.77 (t, 1)	Plus $(OCH_3)_2$ plus $(CH_3)_2CCH$ 3.4–4.9	—	—	1.43 (d, 6)	–
Penicillin G	Acetone-d_6 plus deuterium oxide	7.36 (s, 5)	3.61 (s, 2)	4.87 (t, 1)	3.41 (d, 2)	—	3.78 (s, 1)	1.47 (d, 6)	–
Penicillin V	Dimethyl sulfoxide-d_6 plus deuterium oxide	6.8–7.6 (m, 5)	—	4.80 (t, 1)	—	4.53 (s, 2)	Plus CH_2CHS 3.2–3.8	1.42 (d, 6)	–

Cells for control experiments were treated in an identical fashion, except that the penicillin G was omitted.

Serial twofold dilutions of the rabbit antibenzylpenicilloyl antiserums and serums from control nonimmunized rabbits were prepared. To 0.05-ml portions of the appropriate antiserum dilutions were added 0.05 ml of phosphate-buffered saline and 0.05 ml of penicilloylated, or control, erythrocytes. The mixtures were incubated at 37° for 1 hr, and the results were read. From these experiments, an antiserum was selected and used for the inhibition experiments described here at a dilution of 1:50, the highest dilution giving complete agglutination of the benzylpenicilloylated red cell preparation.

Hemagglutination Inhibition by Penicilloic and Penilloic Acids—Samples of the test penicilloic and penilloic acids were prepared as 0.0125 *M* solutions in phosphate-buffered saline containing 1% normal rabbit serum, and serial twofold dilutions of each solution were made. To 0.05-ml portions of each inhibitor dilution was added 0.05 ml of rabbit

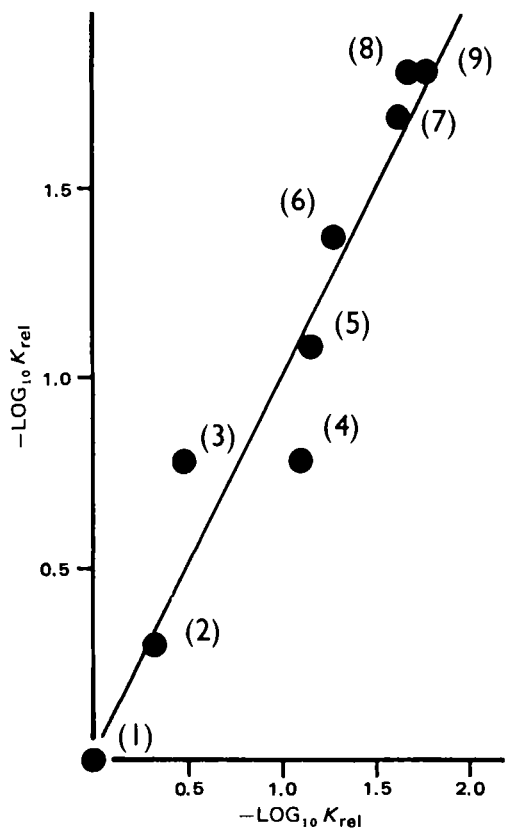

Figure 1—*Correlation (r = 0.967, p < 0.001) between hemagglutination inhibition by penicilloic acids and precipitation inhibition by alkaline hydrolysis products of corresponding penicillins. The $-\log_{10} K_{rel}$ data obtained in this study were plotted* versus *the $-\log_{10} K_{rel}$ data from Nishida* et al. *(8). Key: (1), penicillin G; (2), penicillin V; (3), carbenicillin; (4), phenethicillin; (5), propicillin; (6), cloxacillin; (7), ampicillin; (8), floxacillin; and (9), methicillin.*

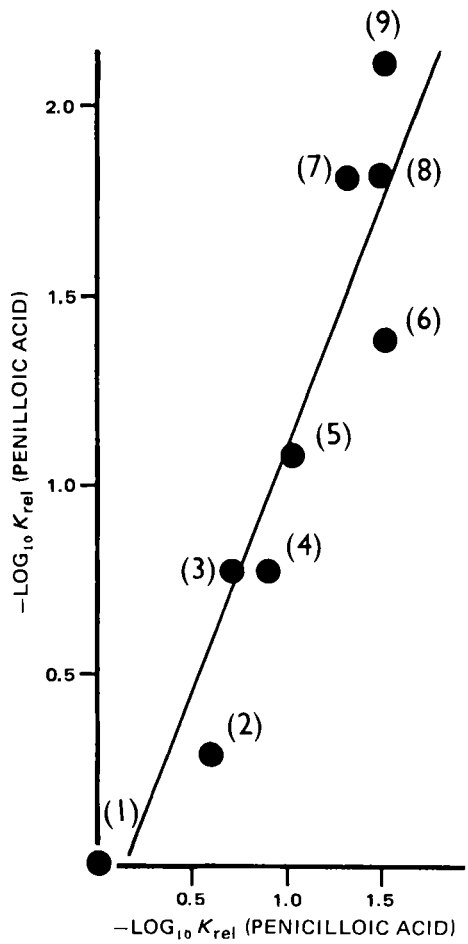

Figure 2—*Correlation (r = 0.937, p < 0.01) between hemagglutination inhibition by penicilloic acids and corresponding penilloic acids. Key to parent penicillins: (1), penicillin G; (2), penicillin V; (3), carbenicillin; (4), phenethicillin; (5), propicillin; (6), cloxacillin; (7), floxacillin; (8), methicillin; and (9), ticarcillin.*

Table V—NMR Spectra for Penicilloic Acids

Parent Penicillin	Solvent	Ar	Ar*CH*	ArCH_2	CHC*HS*	*CH*CHS	*CHCHS*	$(OCH_3)_2$	OCH_2-CO	$(CH_3)_2$-CC*H*	$(CH_3)_2C$	CCH_3
Amoxicillin	Deuterium oxide plus sodium deuteroxide	6.85 (q, 4)	4.45 (s, 1)	—	5.06 (d, 1)	4.22 (d, 1)	—	—	—	3.34 (s, 1)	1.29 (d, 6)	—
Ampicillin	Deuterium oxide	7.55 (s, 5)	5.20 (s, 1)	—	5.07 (d, 1)	4.28 (d, 1)	—	—	—	3.06 (s, 1)	1.05 (d, 6)	—
Carbenicillin	Methanol-d_4	7.45 (s, 5)	4.80 (s, 1)	—	—	—	5.20 (m, 2)	—	—	3.67 (d, 1)	1.36 (q, 6)	—
Cloxacillin	Methanol-d_4	7.53 (s, 4)	—	—	5.03 (d, 1)	4.56 (d, 1)	—	—	—	3.60 (s, 1)	1.43 (d, 6)	2.73 (s, 3)
Floxacillin	Deuterium oxide	7.48 (m, 3)	—	—	5.06 (d, 1)	4.35 (d, 1)	—	—	—	3.46 (s, 1)	1.43 (d, 6)	2.78 (s, 3)
Methicillin	Deuterium oxide plus sodium bicarbonate	6.6–7.7 (m, 3)	—	—	5.59 (d, 1)	4.92 (d, 1)	—	3.89 (s, 6)	—	4.21 (s, 1)	1.61 (d, 6)	—
Penicillin G	Acetone-d_6 plus deuterium oxide	7.36 (s, 5)	—	Plus $(CH_3)_2CCH$ 3.70 (s, 3)	5.18 (d, 1)	4.57 (d, 1)	—	—	—	—	1.40 (d, 6)	—
Penicillin V	Dimethyl sulfoxide-d_6 plus deuterium oxide	6.8–7.6 (m, 5)	—	—	5.10 (d, 1)	4.49 (d, 1)	—	—	4.62 (s, 2)	3.66 (s, 1)	1.40 (d, 6)	—
Phenethicillin	Dimethyl sulfoxide-d_6 plus deuterium oxide	6.8–7.6 (m, 5)	—	—	5.15 (d, 1)	Plus OC*H* 4.4–5.0 (m, 2)	—	—	—	3.71 (s, 1)	Plus $OCHCH_3$ 1.1–1.9 (m, 9)	—
Propicillin	Dimethyl sulfoxide-d_6 plus deuterium oxide	6.8–7.6 (m, 5)	—	—	5.11 (d, 1)	Plus $OCHCH_2CH_3$ 4.3–4.9 (m, 2)	—	—	—	3.69 (s, 1)	Plus $OCHCH_2CH_3$ 0.7–2.2 (m, 11)	—
Ticarcillin	Dimethyl sulfoxide-d_6 plus deuterium oxide	7.34 (m, 3)	Plus *CHCHS* 5.00 (m, 3)	—	—	—	—	—	—	3.54 (d, 1)	1.3 (q, 6)	—

benzylpenicilloyl antiserum at a dilution of 1:50; the mixtures were then incubated at 37° for 1 hr. To each dilution was added 0.05 ml of penicilloylated erythrocytes, and the mixtures were incubated for a further 1 hr at 37°; then the results were read.

All inhibition experiments were carried out simultaneously with the same batch of penicilloylated erythrocytes.

Calculations—For each inhibitor, the dilution and the corresponding concentration giving 50% inhibition of hemagglutination were determined. Values for the relative association constants, K_{rel}, for each inhibitor were calculated as previously described (8), where:

$$K_{rel} = \frac{[\text{reference hapten}]_{50\%}}{[\text{test hapten}]_{50\%}} \qquad \text{(Eq. 1)}$$

In the series of penicilloic acids, the reference hapten chosen was benzylpenicilloic acid; in the series of penilloic acids, benzylpenilloic acid was selected.

RESULTS AND DISCUSSION

Preparation of Penicilloic and Penilloic Acids—The penicilloic acids of a number of penicillins were isolated in pure crystalline form, and the analytical data obtained for these materials are given in Table I. Whereas most compounds were isolated as the free acids, some, notably the penicilloic acids of the amino penicillins amoxicillin and ampicillin, were more readily isolable as the sodium salts.

Under the experimental conditions, it is unlikely that polymers, known to form in concentrated solutions of ampicillin kept at a high pH (15), would have been present in the final preparation. The hydrolysis time was quite short, and workup involved crystallization and washing.

All penicilloic acids examined readily decarboxylated on heating in acidic solution, and several pure penilloic acids were obtained in this fashion. The analytical data obtained for these materials are given in Table II. Whereas most penicilloic acids yielded one main product by this treatment, amoxicillin and ampicillin penicilloic acids yielded multiple products, as shown by TLC analysis. One of these products was of a fluorescent yellow nature, and a fluorescent compound with identical TLC characteristics could be identified in solutions of ampicillin heated under acidic conditions at concentrations of 1 mg/ml.

A second fluorescent component also was formed under these conditions; at ampicillin concentrations of 50 μg/ml, only this second component was formed. The formation of this second component was reported by Jusko (16), who suggested that in solutions of ampicillin penicilloic acid at low pH the 7-carboxyl group could condense with the α-amino group to form a substituted 3,6-diketopiperazine.

The penilloic acids of phenethicillin and propicillin could not be obtained in crystalline form. The products of the decarboxylation of the respective penicilloic acids were purified by extraction procedures and shown to be homogeneous by TLC, with migration characteristics typical of the other penilloic acids. Although these materials were not analyzed further, they were tested by hemagglutination inhibition for comparative purposes.

The decarboxylation of carbenicillin penicilloic acid yielded interesting results; selective removal of the 7-carboxyl group or the side-chain α-carboxyl group could be achieved, depending on the experimental conditions chosen. At low pH values, the 7-carboxyl group was removed to give carbenicillin penilloic acid. This reaction is typical of penicilloic acids, although the mechanism of the decarboxylation involved has not been elucidated (17). However, at higher pH values, the side-chain carboxyl group was selectively removed to yield penicillin G penicilloic acid. This type of reaction appears to occur with carbenicillin itself since penicillin G may be found as an impurity in preparations of this penicillin (18). In terms of the mechanism of removal of the α-carboxyl group, the side chain in carbenicillin corresponds to a substituted phenylmalonic acid (IV), and it has been found[8] that the carboxyl groups in IV and V are susceptible to decarboxylation in the presence of base.

Immunological Cross-Reactivity of Penicilloic and Penilloic Acids—The penicilloic acids isolated were examined for their ability to interact with antibenzylpenicilloyl antibodies by hemagglutination inhibition measurements, and the results are shown in Table III. The interaction between antibenzylpenicilloyl antibodies and the unpurified alkaline hydrolysis products of various penicillins was studied by Nishida *et al.* (8). The results of their studies are in good agreement with those detailed here, and Fig. 1 depicts a significant correlation between both sets of data.

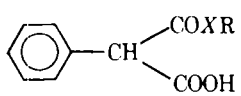

IV: X = NH
V: X = O

The penilloic acids isolated also inhibited antibenzylpenicilloyl antibodies (Table IV); on average, an 11-fold increase in the concentration of a penilloic acid was required to produce the same degree of inhibition as was given by the corresponding penicilloic acid. However, there was a significant correlation between the inhibitory capacities of penicilloic acids and the corresponding penilloic acids (Fig. 2). This result is not unexpected since it is known that the side chain in penicillins (and in cephalosporins) plays an important part in the immunological recognition of the penicilloyl group (19, 20).

A Hansch analysis of the inhibition data obtained in this study was reported recently (21), illustrating the importance of hydrophobic and steric effects on the inhibitory activities of the haptens. The fact that even slight modifications of the side chain of benzylpenicilloic acid, *e.g.*, substitution of α-H by α-NH_2, can markedly affect the reactivity of this hapten toward benzylpenicilloyl antibodies is paralleled by the reported results of skin tests with penicillin-allergic individuals. Parker and Thiel (22) skin tested patients with the penicilloyl polylysine derivatives of penicillin G, phenethicillin, and methicillin, and different patterns of reactivity among patients were observed with the reagents.

Van Dellen *et al.* (6) conducted similar tests with the penicilloyl polylysine derivatives of penicillin G, methicillin, and ampicillin and again a varied pattern of reactivity was found; some patients responded to one reagent, some to two, and only a few to all three. The penicillin G derivatives most frequently gave reactions, resulting in positive skin tests in 90% of the patients; at the other extreme, the ampicillin derivative gave positive skin tests in 22% of the patients.

The same varied pattern has been observed in *in vitro* tests for penicilloyl antibodies from allergic patients. Using the radioallergosorbent test (RAST) technique to measure specific IgE antibodies, Juhlin and Wide (23) found the serum of some penicillin-allergic patients to contain equivalent antibody titers to the penicilloyl groups derived from penicillin G and penicillin V. On the other hand, some patient serums gave considerably higher titers with one or another of the penicillins.

In terms of clinical allergy, it would be tempting to speculate that appropriate side-chain modifications within penicillins and cephalosporins could reduce the risk of hypersensitivity reactions. In this context, cefazolin, a cephalosporin antibiotic containing a tetrazolylacetyl side chain, has been shown (20, 24) to have a low degree of cross-reactivity with penicillin G and cephaloridine in experimental animal models. However, most studies on the cross-reactions between various penicillins and between penicillins and cephalosporins have been related to the cross-reaction with antibenzylpenicilloyl antibodies. The present study is no exception; but to understand the complex events of penicillin allergy in more detail, studies must be extended to those antibodies derived from penicilloyl groups other than penicillin G. The preparation of pure haptens, as described here, may enable such studies to be carried out in a more facile manner.

[8] H. Ferres, Beecham Pharmaceuticals, Walton Oaks, Surrey, England, personal communication.

REFERENCES

(1) M. Cole, M. D. Kenig, and V. A. Hewitt, *Antimicrob. Agents Chemother.*, **1973**, 463.

(2) B. B. Levine and A. P. Redmond, *Int. Arch. Allergy Appl. Immunol.*, **35**, 445 (1969).

(3) B. B. Levine and D. M. Zolov, *J. Allergy*, **43**, 231 (1969).

(4) B. B. Levine, A. P. Redmond, H. E. Voss, and D. M. Zolov, *Ann. N.Y. Acad. Sci.*, **145**, 298 (1967).

(5) H. E. Voss, A. P. Redmond, and B. B. Levine, *J. Am. Med. Assoc.*, **196**, 679 (1966).

(6) R. G. Van Dellen, W. E. Walsh, G. A. Peters, and G. J. Gleich, *J. Allergy*, **47**, 230 (1971).

(7) Y. Horiuchi and K. Shibata, *Int. Arch. Allergy Appl. Immunol.*, **28**, 306 (1965).

(8) K. Nishida, Y. Kinoshita, T. Atsumi, K. Shibata, and Y. Horiuchi, *Immunochemistry*, **9**, 1195 (1972).

(9) T. Atsumi, K. Nishida, Y. Kinoshita, K. Shibata, and Y. Horiuchi, *J. Immunol.*, **99**, 1286 (1967).

(10) R. Mozingo and K. Folkers, in "The Chemistry of Penicillin," H. T. Clarke, J. R. Johnson, and R. Robinson, Eds., Princeton University Press, Princeton, N.J., 1949, pp. 564, 573.

(11) "British Pharmacopoeia 1973," Her Majesty's Stationery Office, London, England, 1973, p. 88.
(12) J. M. Dewdney, H. Smith, and A. W. Wheeler, *Immunology*, **21**, 517 (1971).
(13) H. Smith, J. M. Dewdney, and A. W. Wheeler, *ibid.*, **21**, 527 (1971).
(14) J. A. Thiel, S. Mitchell, and G. W. Parker, *J. Allergy*, **35**, 399 (1964).
(15) H. Bundgaard, *Acta Pharm. Suec.*, **13**, 9 (1976).
(16) W. J. Jusko, *J. Pharm. Sci.*, **60**, 728 (1971).
(17) M. A. Schwartz, *ibid.*, **58**, 643 (1969).
(18) "British Pharmacopoeia 1973," Her Majesty's Stationery Office, London, England, 1973, p. 81.
(19) F. R. Batchelor, J. M. Dewdney, R. D. Weston, and A. W. Wheeler, *Immunology*, **10**, 21 (1966).
(20) S. Kuwahara, Y. Mine, and M. Nishida, *Antimicrob. Agents Chemother.*, **1970**, 374.
(21) A. E. Bird, *J. Pharm. Sci.*, **64**, 1671 (1975).
(22) C. W. Parker and J. A. Thiel, *J. Lab. Clin. Med.*, **62**, 482 (1963).
(23) L. Juhlin and L. Wide, in "Mechanisms in Drug Allergy," C. H. Dash and H. E. H. Jones, Eds., Churchill Livingstone, Edinburgh, Scotland, 1972, p. 139.
(24) Y. Mine and M. Nishida, *J. Antibiot.*, **1970**, 195.

Dequaternization of Curare Bases with Sodium Thiophenoxide and Ethanolamine

JANETTE A. NAGHAWAY and TAITO O. SOINE ˣ

Received August 8, 1977, from the *Department of Medicinal Chemistry, College of Pharmacy, University of Minnesota, Minneapolis, MN 55455.* Accepted for publication December 15, 1977.

Abstract □ To prepare (+)-tubocurine and *O,O*-dimethyl-(+)-tubocurine, the commonly used dequaternization procedures with sodium thiophenoxide and ethanolamine were investigated. The quaternary compounds were (+)-tubocurarine chloride and the chloride and iodide salts of *O,O*-dimethyl-(+)-chondocurarine. The results obtained with ethanolamine indicate that Hofmann elimination is a major pathway and that *N*-demethylation is minor. The elimination products of *O,O*-dimethyl-(+)-chondocurarine iodide with ethanolamine were identified as *O,O*-dimethyltubocurinemethine, *O,O*-dimethyltubocurineisomethine, and *O,O*-dimethyltubocurinedimethine. *N*-Demethylation was the primary reaction with sodium thiophenoxide. Thus, dequaternization of (+)-tubocurarine chloride with sodium thiophenoxide provided (+)-tubocurine which, on diazomethylation, yielded *O,O*-dimethyl-(+)-tubocurine, identical to the compound obtained by *N*-demethylation of *O,O*-dimethyl-(+)-chondocurarine chloride with the same reagent.

Keyphrases □ (+)-Tubocurine—syntheses by dequaternization procedures compared, mechanisms evaluated, products identified □ *O,O*-Dimethyl-(+)-tubocurine—syntheses by dequaternization procedures compared, mechanisms evaluated, products identified □ Dequaternization—of various curare bases, different procedures compared, mechanisms evaluated, products identified □ Curare bases, various—syntheses by dequaternization procedures compared, mechanisms evaluated, products identified

The accepted structure of (+)-tubocurarine chloride (1) was revised to Structure I previously (2). These investigators indicated that (+)-tubocurarine chloride is not a diquaternary compound and that (+)-tubocurine (II) and (+)-chondocurine have identical structures (II) and do not differ as previously reported (3–6). The revelation that (+)-tubocurarine was actually a monoquaternary–monotertiary species suggested that selective monoquaternization of the ditertiary amine, (+)-tubocurine, could provide a pair of isomeric monoquaternary–monotertiary tubocurarines, namely, semisynthetic (+)-tubocurarine and (+)-isotubocurarine chloride. The preparation of the latter was described previously (7). Although (+)-chondocurine [(+)-tubocurine] (II) has been isolated from natural sources (5, 6), the fact that these sources are somewhat inaccessible suggested the generation of II from commercially available I by dequaternization.

Dealkylation of quaternary ammonium salts is a problem that has received considerable attention, but most of the various methods employed (8–16) have limitations. For example, Tomita and Takano (17) showed that the widely used method of heating the quaternary salt in refluxing ethanolamine may lead to extensive Hofmann elimination as well as to *O*-demethylation.

To prepare II, Shamma *et al.* (18) utilized sodium

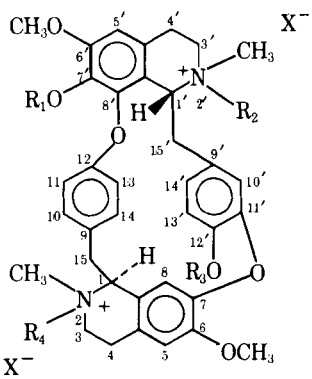

I: $R_1 = R_3 = R_4 = H$, $R_2 = CH_3$, X = Cl
III: $R_1 = R_2 = R_3 = R_4 = CH_3$, X = I
IV: $R_1 = R_2 = R_3 = R_4 = CH_3$, X = Cl

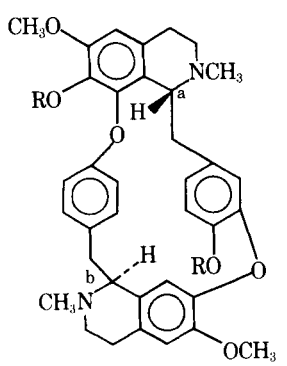

II: R = H, a,b = *R,S*
V: R = CH_3, a,b = *R,S*

0022-3549/78/0900-1204$01.00/0
© 1978, American Pharmaceutical Association

(11) "British Pharmacopoeia 1973," Her Majesty's Stationery Office, London, England, 1973, p. 88.
(12) J. M. Dewdney, H. Smith, and A. W. Wheeler, *Immunology*, **21**, 517 (1971).
(13) H. Smith, J. M. Dewdney, and A. W. Wheeler, *ibid.*, **21**, 527 (1971).
(14) J. A. Thiel, S. Mitchell, and G. W. Parker, *J. Allergy*, **35**, 399 (1964).
(15) H. Bundgaard, *Acta Pharm. Suec.*, **13**, 9 (1976).
(16) W. J. Jusko, *J. Pharm. Sci.*, **60**, 728 (1971).
(17) M. A. Schwartz, *ibid.*, **58**, 643 (1969).
(18) "British Pharmacopoeia 1973," Her Majesty's Stationery Office, London, England, 1973, p. 81.
(19) F. R. Batchelor, J. M. Dewdney, R. D. Weston, and A. W. Wheeler, *Immunology*, **10**, 21 (1966).
(20) S. Kuwahara, Y. Mine, and M. Nishida, *Antimicrob. Agents Chemother.*, **1970**, 374.
(21) A. E. Bird, *J. Pharm. Sci.*, **64**, 1671 (1975).
(22) C. W. Parker and J. A. Thiel, *J. Lab. Clin. Med.*, **62**, 482 (1963).
(23) L. Juhlin and L. Wide, in "Mechanisms in Drug Allergy," C. H. Dash and H. E. H. Jones, Eds., Churchill Livingstone, Edinburgh, Scotland, 1972, p. 139.
(24) Y. Mine and M. Nishida, *J. Antibiot.*, **1970**, 195.

Dequaternization of Curare Bases with Sodium Thiophenoxide and Ethanolamine

JANETTE A. NAGHAWAY and TAITO O. SOINE ˣ

Received August 8, 1977, from the *Department of Medicinal Chemistry, College of Pharmacy, University of Minnesota, Minneapolis, MN 55455.* Accepted for publication December 15, 1977.

Abstract □ To prepare (+)-tubocurine and *O,O*-dimethyl-(+)-tubocurine, the commonly used dequaternization procedures with sodium thiophenoxide and ethanolamine were investigated. The quaternary compounds were (+)-tubocurarine chloride and the chloride and iodide salts of *O,O*-dimethyl-(+)-chondocurarine. The results obtained with ethanolamine indicate that Hofmann elimination is a major pathway and that *N*-demethylation is minor. The elimination products of *O,O*-dimethyl-(+)-chondocurarine iodide with ethanolamine were identified as *O,O*-dimethyltubocurinemethine, *O,O*-dimethyltubocurineisomethine, and *O,O*-dimethyltubocurinedimethine. *N*-Demethylation was the primary reaction with sodium thiophenoxide. Thus, dequaternization of (+)-tubocurarine chloride with sodium thiophenoxide provided (+)-tubocurine which, on diazomethylation, yielded *O,O*-dimethyl-(+)-tubocurine, identical to the compound obtained by *N*-demethylation of *O,O*-dimethyl-(+)-chondocurarine chloride with the same reagent.

Keyphrases □ (+)-Tubocurine—syntheses by dequaternization procedures compared, mechanisms evaluated, products identified □ *O,O*-Dimethyl-(+)-tubocurine—syntheses by dequaternization procedures compared, mechanisms evaluated, products identified □ Dequaternization—of various curare bases, different procedures compared, mechanisms evaluated, products identified □ Curare bases, various—syntheses by dequaternization procedures compared, mechanisms evaluated, products identified

The accepted structure of (+)-tubocurarine chloride (1) was revised to Structure I previously (2). These investigators indicated that (+)-tubocurarine chloride is not a diquaternary compound and that (+)-tubocurine (II) and (+)-chondocurine have identical structures (II) and do not differ as previously reported (3–6). The revelation that (+)-tubocurarine was actually a monoquaternary–monotertiary species suggested that selective monoquaternization of the ditertiary amine, (+)-tubocurine, could provide a pair of isomeric monoquaternary–monotertiary tubocurarines, namely, semisynthetic (+)-tubocurarine and (+)-isotubocurarine chloride. The preparation of the latter was described previously (7). Although (+)-chondocurine [(+)-tubocurine] (II) has been isolated from natural sources (5, 6), the fact that these sources are somewhat inaccessible suggested the generation of II from commercially available I by dequaternization.

Dealkylation of quaternary ammonium salts is a problem that has received considerable attention, but most of the various methods employed (8–16) have limitations. For example, Tomita and Takano (17) showed that the widely used method of heating the quaternary salt in refluxing ethanolamine may lead to extensive Hofmann elimination as well as to *O*-demethylation.

To prepare II, Shamma *et al.* (18) utilized sodium

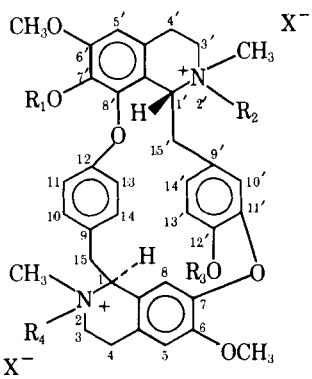

I: $R_1 = R_3 = R_4 = H$, $R_2 = CH_3$, X = Cl
III: $R_1 = R_2 = R_3 = R_4 = CH_3$, X = I
IV: $R_1 = R_2 = R_3 = R_4 = CH_3$, X = Cl

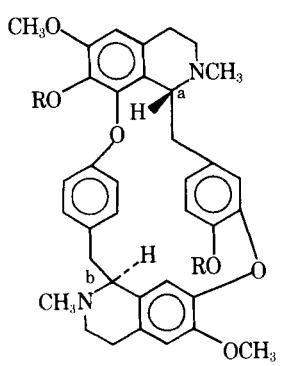

II: R = H, a,b = *R,S*
V: R = CH_3, a,b = *R,S*

0022-3549/78/0900-1204$01.00/0
© 1978, American Pharmaceutical Association

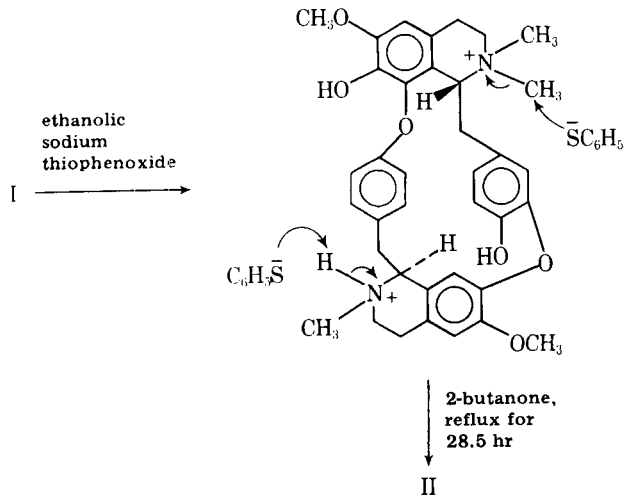

Scheme I

thiophenoxide in refluxing 2-butanone. Marshall *et al.* (19) reported a facile preparation of II from I, as well as an equally successful conversion of *O,O*-dimethyl-(+)-chondocurarine chloride (IV) to *O,O*-dimethyl-(+)-tubocurine (V) using ethanolamine. However, there was marked disagreement in the reported physical constants of II (18, 19). Considering the ultimate necessity to achieve the correct compound in the present study, it was essential to determine which of the two literature procedures of *N*-demethylation was reliable.

DISCUSSION

The sodium thiophenoxide method (18) (Scheme I) was utilized for the preparation of II. Pure II was initially obtained by frictionally induced crystallization from a methanolic solution followed by recrystallization. The melting point of the prepared sample of II and the NMR spectral data were in close agreement with those reported by Bick and Clezy (20) for (+)-chondocurine, although the melting point of II was inexplicably 10° higher than that of Shamma *et al.* (18). In spite of this discrepancy, the spectral evidence seems to substantiate an earlier conclusion that (+)-tubocurine and (+)-chondocurine are identical (2).

The *N*-demethylation of I as described by Marshall *et al.* (19) was carried out by refluxing I in ethanolamine. The physical data secured for the obtained product were in proximity to those reported previously (19). The R_f value (alumina TLC plates) was the same as the reported value and was the same as that obtained for II prepared by the sodium thiophenoxide method. However, visual observation under a UV lamp indicated fluorescence for the ethanolamine reaction product, which was not apparent in the sodium thiophenoxide-generated product. The UV spectrum had maxima at 225 (shoulder), 285, and 305 (shoulder) nm. The shoulder at 305 nm has not been observed in the spectra of the tubocurarine family.

The presence of a mixture of more than one component in the ethanolamine reaction product was made evident by changing the reported developing solvent system (19) and using silica instead of alumina as the TLC medium[1]. This finding was also substantiated by the NMR spectral data, which showed a pair of singlets at δ 2.23 and 2.26 ppm in contrast to the expected singlet for the 2′-NCH_3 resonance at δ 2.25 ppm. The OCH_3 percentage was also less than the theoretical integrated value, and the solubility of the ethanolamine reaction product was greater than that of sodium thiophenoxide-generated II in methanol.

The isolated amounts of II corresponding to the sodium thiophenoxide product and obtained by induced crystallization were inconsistent when the reaction was repeated, and the highest yield was 27%. Attempted separation and identification of components other than II were not successful. However, UV and NMR spectral data provided some evidence of a Hofmann elimination reaction taking place together with the *N*-demethylation reaction. Previous experience with quaternary alkaloids (17) indicated that the use of ethanolamine resulted predominantly in Hofmann elimination and *O*-demethylation.

To shed more light on the problem, the *N*-demethylations of IV and the iodide (III) were investigated. Compound IV, needed for the preparation of V, was obtained in high yield by methylation of I in alkaline medium, followed by exchange of the iodide content by chloride ion with an ion-exchange resin. Compound V was prepared according to the procedure of Shamma *et al.* (18) in about a 70% yield by refluxing a 2-butanone solution of IV with sodium thiophenoxide. The isolated V resisted crystallization with a large number of solvents and solvent mixtures, as reported previously (21). However, preparative TLC was successfully employed for the purification of the desired compound. That the dimethyl ether derivative of (+)-tubocurine was, indeed, in hand was shown both by NMR spectroscopy and diazomethylation of II.

The NMR spectrum of V showed two NCH_3 resonances at δ 2.14 and 2.48 ppm, which integrated for three protons each. The OCH_3 resonances were obtained as two well-integrated and characteristic pairs of singlets at δ 3.69, 3.72, 3.78, and 3.83 ppm. These values are in good agreement with those reported for *O,O*-dimethyl-(+)-chondocurine (20). This report is the first on the physical constants of a pure sample of V. Treatment of sodium thiophenoxide-generated II with an ethereal diazomethane solution provided V in 74% yield. Microanalytical, melting-point, and IR, UV, and NMR spectral comparisons with a sample of V obtained by dequaternization of IV with sodium thiophenoxide showed no significant differences.

The *N*-demethylation of III was carried out as described by Marshall *et al.* (19) by refluxing III with ethanolamine. The physical data obtained for the product were in fair agreement with those reported (19). TLC using alumina revealed a fluorescent spot possessing an R_f value that matched the literature value (19) as well as that obtained for V prepared by either *N*-demethylation of IV with sodium thiophenoxide or diazomethylation of II. However, as before, changing the developing solvent or substituting alumina with silica revealed the presence of a multicomponent mixture.

The UV spectrum showed maxima at 225 (shoulder), 285, and 303 (shoulder) nm. The NMR spectrum was significantly different from that for V, and the predominant signals were those for a singlet $N(CH_3)_2$ resonance at δ 2.27 ppm and a singlet NCH_3 resonance at δ 2.45 ppm. Furthermore, in contrast to the expected 10 aromatic protons, resonances in the aromatic area integrated most nearly for 12 protons. This result suggested that, although a small proportion of V was present, the major components appeared to be elimination products.

Scheme II illustrates the various compounds obtained by separation on TLC (silica), which are, in retrospect, the components of the purported *O,O*-dimethyl-(+)-tubocurine of Marshall *et al.* (19). These are, in addition to small amounts of V, *O,O*-dimethyltubocurinemethine (VI), *O,O*-dimethyltubocurineisomethine (VII), and *O,O*-dimethyltubocurinedimethine (VIII), previously obtained in studies on the diazomethane-induced Hofmann elimination of curare bases (22, 23).

Examination of the NMR spectrum of VI, the major component of the ethanolamine reaction product, indicated the presence of a singlet $N(CH_3)_2$ integrating for six protons and NCH_3 (3H) resonances at δ 2.23 and 2.42 ppm, respectively. Since the chemical shift value of the NCH_3 resonance was in close proximity to the measured value of the 2-NCH_3 resonance in V, III apparently had undergone *N*-demethylation at the N-2 center. On the other hand, the production of an $N(CH_3)_2$ resonance at δ 2.23 ppm suggested a probable elimination at the N-2′ center.

The absence of a strong IR absorption near 880 cm^{-1} excluded styrene as a possible structural representation of VI. The IR spectrum of VI did not show a strong band at 960 cm^{-1} characteristic of *trans*-stilbene, and three UV maxima were detected at 225 (shoulder), 284, and 303 (shoulder) nm. At this point, the identity of VI was ascertained to be that of *O,O*-dimethyltubocurinemethine isolated previously (22, 23). The identity of the two compounds was based on identical IR, UV, and NMR spectra.

Compound VII was recovered in a much smaller yield, and the IR spectrum exhibited styrene absorption at 885 cm^{-1}. The UV maxima corresponding to the styrene fragment in VII were at 262 and 303 nm. The NMR spectrum revealed the presence of two singlets, for the 2′-NCH_3 at δ 2.06 ppm and for the 2-$N(CH_3)_2$ resonance at δ 2.23 ppm, and the *AB* styrene protons were detected between δ 5.08 and 5.54 ppm. These data, combined with the structural decision for VI, suggested that VII was identical to the previously obtained *O,O*-dimethyltubocurineiso-

[1] Such TLC examination on Eastman Chromagram Sheet 6060 silica gel, using a mixture of chloroform–methanol (30:1), provided five spots with R_f values of 0.024, 0.095, 0.21, 0.26, and 0.31. The spot with R_f 0.26 corresponded to that of (+)-tubocurine prepared by the sodium thiophenoxide method. Alternatively, using a mixture of water–propanol (1:4), it was possible to detect four spots with R_f values of 0.06, 0.14, 0.30, and 0.35, of which the one with R_f 0.35 was identical to that of (+)-tubocurine.

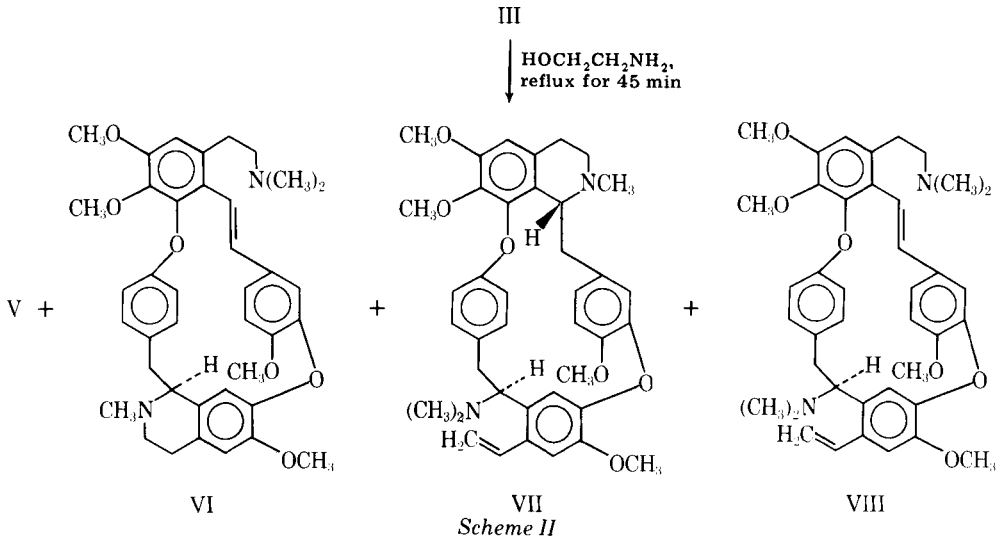

Scheme II

methine (22, 23). The IR, UV, and NMR spectral data were identical and completely in agreement with the assigned identity.

The separation technique employed in these experiments was not able to free VIII from contamination by V. The IR spectrum of the mixture, however, showed characteristic styrene absorption at 885 cm^{-1}. Nevertheless, the identity of VIII in the mixture was established on the basis of UV and NMR spectra which, allowing for the presence of V as a contaminant, were virtually identical to the spectra of pure VIII obtained previously (22, 23). A detailed description of the unique stereochemical pathways undergone by III to provide VI–VIII by the elimination reaction was discussed previously (23).

A review of the work by Marshall *et al.* (19) on the generation of (+)-tubocurine and *O,O*-dimethyl-(+)-tubocurine indicates that the identities of the compounds under question were confirmed solely on the basis of UV spectra that exhibited maxima at 225 and 285 nm. Such confirmation is not convincing because of the presence of these maxima in the spectra of the methine compounds. These investigators (19) converted (+)-tubocurine to the dimethyl ether and indicated that the dimethyl ether was in a state of optical purity identical to the compound obtained by the *N*-demethylation of III. Since our experience indicates considerable difficulty in completely separating V from the methine compounds under the specified conditions of purification, it may be prudent to consider the presence of a mixture of Hofmann elimination compounds together with *N*-demethylated compounds in their products.

A case in point is the proof of structure of V by cleavage with sodium in liquid ammonia. This useful reaction usually gives yields ranging from excellent to nearly quantitative (24–27), although with V the reported yield for the pure cleavage products of V was extremely small (*i.e.*, 1.5%). Consequently, the reported sample of V probably had some of the correct compound and its low percentage presence was reflected by the low percentage yield of its cleavage products. In addition, the microanalytical data presented in support of the molecular formula, $C_{38}H_{42}N_2O_6 \cdot \frac{1}{2}H_2O$, could be misleading because $C_{39}H_{44}N_2O_6 \cdot \frac{1}{2}H_2O$ also has calculated values surprisingly close to those for the suggested compound (Table I).

The information presented in this study leads to the inescapable conclusions that the reaction of quaternary salts with ethanolamine results primarily in a Hofmann elimination reaction and that the dequaternization reaction is secondary. In contrast to ethanolamine, sodium thiophenoxide provides dequaternization in these compounds without significant elimination-type side reactions. The differences in the reported physical constants for (+)-tubocurine seem explicable on the basis of the presented evidence.

Table I—Comparative Microanalytical Data

Molecular Formula		Analysis, % Calc.	Found (19)
$C_{38}H_{42}N_2O_6 \cdot \frac{1}{2}H_2O$	C	72.24	72.40
	H	6.86	6.50
	N	4.43	4.50
$C_{39}H_{44}N_2O_6 \cdot \frac{1}{2}H_2O$	C	72.53	
	H	7.02	
	N	4.34	

EXPERIMENTAL[2]

(+)-Tubocurine (II)—*Method A*—(+)-Tubocurarine chloride (8.0 g, 10.37 mmoles) was treated with sodium thiophenoxide (5.8 g, 43.94 mmoles) according to the procedure of Shamma *et al.* (18). Crystallization of the product from methanol afforded 3.7 g (6.22 mmoles, 60.0%) of II, mp 235–237°[3] [lit. (18, 28, 29) mp 222.5–223.5, 232–234, and 232°, respectively]; $[\alpha]_D^{25}$ + 220° (c 1.0, 0.1 *N* HCl) [lit. (18, 6, 29) $[\alpha]_D$ + 221° (c 1.0, 0.1 *N* HCl), $[\alpha]_D^{24}$ + 200° (c 0.50, 0.1 *N* HCl), and $[\alpha]_D^{18}$ + 220° (c 0.50, 0.1 *N* HCl), respectively]; UV λ_{max} (log ϵ): 225 (4.52) and 281 (3.86) nm; NMR ($CDCl_3$): δ 2.25 (s, 3H, NCH_3), 2.48 (s, 3H, NCH_3), 3.83 (s, 3H, OCH_3), and 3.88 (s, 3H, OCH_3) ppm [lit. (20) chemical shift values for (+)-chondocurine ($CDCl_3$): δ 2.25 (NCH_3), 2.45 (NCH_3), 3.82, and 3.88 (OCH_3) ppm].

Anal.—Calc. for $C_{36}H_{38}N_2O_6$: C, 72.70; H, 6.44; N, 4.70. Found: C, 72.84; H, 6.45; N, 4.44.

Method B—(+)-Tubocurarine chloride (3.2 g, 4.15 mmoles) was refluxed in ethanolamine (40 ml) for 1 hr as described by Marshall *et al.* (19). Solid carbon dioxide was added to the cooled solution, and the resultant precipitate was extracted with ether (8 × 250 ml). The ether solution was dried and evaporated under reduced pressure to yield 2.15 g (87.2%) of a light-yellow solid, mp 166–172° (collapsed at 148°) [lit. (19) mp 164°]; $[\alpha]_D^{25}$ + 77.9 ± 0.2° (c 0.67, pyridine), $[\alpha]_D^{25}$ + 146.8 ± 0.2° (c 0.73, 0.1 *N* HCl), and $[\alpha]_D^{25}$ + 150° (c 0.10, methanol) [lit. (19) $[\alpha]_D^{17}$ + 72° (c 0.67, pyridine), $[\alpha]_D^{17}$ + 144° (c 0.50, 0.1 *N* HCl) and $[\alpha]_D^{17}$ + 153° (c 1.0, methanol)]; R_f 0.78 with fluorescence [alumina and a mixture of chloroform–methanol (10:1)] [lit. (19) R_f 0.78]; UV λ_{max}: 225 and 285 nm (additional UV absorption between 300 and 360 nm that formed a shoulder at 305 nm). TLC examination on silica gel, using chloroform–methanol (10:1), indicated more than one component.

Anal.[4]—Calc. for OCH_3: 10.54. Found: 9.69.

Crystallization of II was induced from a methanolic solution of the reaction product from a number of different efforts in a yield not exceeding 27% of theory. The melting point and UV, IR, and NMR spectra of II obtained in this way were identical to those of II obtained by Method

[2] Melting points were determined on a Mel-Temp melting-point apparatus and are uncorrected. Optical rotations were measured on a Perkin-Elmer 141 polarimeter. Analyses were performed by M-H-W Laboratories, Garden City, Mich. UV spectra were taken in methanol solutions with a Cary 14 recording spectrophotometer. IR spectra were obtained in potassium bromide pellets with a Perkin-Elmer 237 grating IR spectrophotometer. NMR spectra were measured with a Varian Associates model A-60D NMR spectrometer, using tetramethylsilane or sodium 2,2-dimethyl-2-silapentane-5-sulfonate as the internal standard. Mass spectral determinations were performed by the Mass Spectroscopy Laboratory Service, Department of Chemistry, University of Minnesota, Minneapolis, Minn., with a Hitachi Perkin-Elmer RMU-6D mass spectrometer.

TLC was conducted on Eastman Chromagram sheet 6060 silica gel or 6063 alumina with a fluorescent indicator. Visualization was done with both UV lamp and iodine vapor. Brinkmann silica gel HF-254 powder was utilized in preparative TLC and visualization was with the UV lamp. Woelm neutral alumina, activity grade V, was employed in column chromatography. Anion-exchange resin, Amberlite IRA-410 of medium porosity, was supplied by Mallinckrodt Chemical Works. (+)-Tubocurarine chloride was obtained from Sigma Chemical Co., St. Louis, MO 63118; Abbott Laboratories, North Chicago, IL 60064; and Organon Inc., West Orange, NJ 07052.

[3] A sample provided by Dr. Shamma gave mp 227–231° in our apparatus.

[4] Performed by Schwarzkopf Microanalytical Laboratories, Woodside, NY 11377.

A. Further attempts to purify the mother liquors into homogeneous entities by chromatography (column or TLC) or by crystallization were unsuccessful.

Compound III—(+)-Tubocurarine chloride (3.0 g, 3.89 mmoles) was quaternized according to the procedure of Marshall *et al.* (19), using 0.5 *N* ethanolic potassium hydroxide (33 ml) and methyl iodide (4.2 ml). Crystallization from methanol afforded 3.42 g (97%) of III, mp 263–264° [lit. (19, 28, 20) mp 266, 257–267, and 230–240°, respectively]; $[\alpha]_D^{25}$ + 173° (c 1.0, methanol) [lit. (19, 6) $[\alpha]_D$ + 179° (c 1.3, methanol) and $[\alpha]_D^{22}$ + 172° (c 1.02, methanol), respectively].

Anal. Calc. for $C_{40}H_{48}I_2N_2O_6$: C, 52.98; H, 5.33; I, 27.99; N, 3.09. Found: C, 53.11; H, 5.54; I, 28.13; N, 2.90.

Compound IV—The iodide content of III was exchanged for chloride utilizing the following methods.

Method A—Freshly prepared silver chloride (6.0 g) was suspended in a solution of III (2.0 g, 2.21 mmoles) in methanol (270 ml). The suspension was protected from light while stirring for 9 hr. After filtration and evaporation of the solvent under reduced pressure, an off-white colored solid was obtained (1.60 g, 100%), mp 230–231° (with frothing) [lit. (28) mp 236° (effervescence)]; $[\alpha]_D^{25}$ + 156° (c 0.50, H_2O) [lit. (28) $[\alpha]_D$ + 185–195° (c 0.50, H_2O)].

Method B—A methanolic solution of III (1.0 g, 1.10 mmoles in 135 ml) was passed three times through an anion-exchange resin (15 g) column (25 × 1.5 cm) in the chloride cycle. Evaporation of the solvent under reduced pressure provided an off-white solid, which was recrystallized twice from water, mp 225–226° (frothing); $[\alpha]_D^{25}$ + 157.4° (c 0.50, H_2O).

Compound V—Three different approaches were utilized for the preparation of V.

Sodium Thiophenoxide Method—A solution of sodium thiophenoxide (1.73 g, 13.11 mmoles) in absolute ethanol (15 ml) was added to a solution of IV (1.5 g, 2.07 mmoles) in the same solvent (40 ml). The mixture was stirred for 1.75 hr, followed by filtration to remove the precipitated sodium chloride. The precipitate was washed with absolute ethanol; the washings, combined with the filtrate, were then evaporated under reduced pressure. The resulting solid was suspended in 2-butanone (160 ml), freshly distilled from zinc dust, and refluxed under a nitrogen atmosphere for 28.5 hr. Following the removal of the solvent under reduced pressure, water (120 ml) was added and the aqueous suspension was extracted with chloroform (5 × 100 ml).

The residue, obtained from the dried chloroform extract after removal of the solvent under reduced pressure, was treated with 10% HCl and extracted with ether (7 × 100 ml). The aqueous acid layer was neutralized with 10% NaOH and extracted again with chloroform (4 × 150 ml). The chloroform extract was dried and evaporated under reduced pressure to yield a yellow solid (0.90 g, 69.7%), which could not be crystallized from a number of solvents. Bick and Clezy (20) also did not succeed in crystallizing *O,O*-dimethyl-(+)-chondocurine under similar conditions.

The yellow solid was chromatographed on an activity grade V neutral alumina column (30 g), and subsequently the ethyl acetate eluate was purified on 1-mm thick plates (precoated with silica HF-254) using 2.5% aqueous ammonia–ethyl acetate–isopropyl alcohol–methanol (0.7:3:3:4). Half of the applied material was recovered by extraction of the appropriate band on the silica gel plates with methanol–ethyl acetate (1:1). A light-yellow amorphous substance was obtained upon evaporation of the solvent under reduced pressure, mp 115–116.5°; $[\alpha]_D^{25}$ + 189° (c 1.0, methanol); UV λ_{max} (log ϵ): 225 (4.55) and 280 (3.80) nm; NMR ($CDCl_3$): δ 2.14 (s, 3H, NCH_3), 2.48 (s, 3H, NCH_3), 3.69 (s, 3H, OCH_3), 3.72 (s, 3H, OCH_3), 3.78 (s, 3H, OCH_3), and 3.83 (s, 3H, OCH_3) ppm [lit. (20) chemical shift values for *O,O*-dimethyl-(+)-chondocurine ($CDCl_3$): δ 2.18 (NCH_3), 2.50 (NCH_3), 3.70 (OCH_3), and 3.80 (OCH_3) ppm].

Anal. Calc. for $C_{38}H_{42}N_2O_6$: C, 73.26; H, 6.79; N, 4.71. Found: C, 73.46; H, 6.95; N, 4.47.

Diazomethylation Method—An ethereal solution of diazomethane, generated from 0.80 g (7.77 mmoles) of *N*-nitrosomethylurea (30), was added with stirring to an ice-cold solution of II (0.40 g, 0.67 mmole) in methanol (80 ml). The reaction mixture was kept in a freezer for 2 days and then at room temperature for 4 days. A few drops of acetic acid were added to the reaction mixture, and the solvent was evaporated under reduced pressure. The residue was dissolved in water (12 ml) and neutralized with sodium bicarbonate. The aqueous solution was successively extracted with chloroform (4 × 50 ml), dried, and evaporated under reduced pressure.

The residue (0.31 g, 74%) was purified on silica-precoated plates as described for V. The amorphous compound, recovered by extraction with a mixture of methanol–ethyl acetate (1:1) in a 75% yield, gave mp 114–115.5°; $[\alpha]_D^{25}$ + 199.4° (c 1.0, methanol). The IR and UV spectra were the same as those of V prepared by the sodium thiophenoxide method; NMR ($CDCl_3$): δ 2.13 (s, 3H, NCH_3), 2.48 (s, 3H, NCH_3), 3.69 (s, 3H, OCH_3), 3.72 (s, 3H, OCH_3), 3.78 (s, 3H, OCH_3), and 3.83 (s, 3H, OCH_3) ppm; NMR (C_6D_6): δ 2.08 (s, 3H, NCH_3), 2.28 (s, 3H, NCH_3), 3.47, 3.50 (2s, 9H, 3 OCH_3), and 3.67 (s, 3H, OCH_3) ppm [lit. (31) values for *O,O*-dimethyl-(+)-chondocurine (C_6D_6): δ 2.03 (NCH_3), 2.28 (NCH_3), 3.47 (OCH_3), and 3.63 (OCH_3) ppm].

Anal.—Calc. for $C_{38}H_{42}N_2O_6$: C, 73.26; H, 6.79; N, 4.71. Found: C, 73.03; H, 7.01; N, 4.49.

Ethanolamine Method—Compound III (4.72 g, 5.21 mmoles) in ethanolamine (240 ml) was refluxed under nitrogen for 45 min as described by Marshall *et al.* (19). The solution was cooled and treated with an aqueous potassium hydroxide solution (4.56 g in 120 ml). The alkaline solution was extracted with petroleum ether (bp 40–60°, 7 liters). Evaporation of the solvent under reduced pressure yielded 1.55 g (47.8%) of a light-yellow amorphous solid, mp 95° [lit. (19) mp 98°]; $[\alpha]_D^{25}$ + 156° (c 1.25, methanol) [lit. (19) $[\alpha]_D$ + 168° (c 1.25, methanol)]; R_f 0.85 [alumina and chloroform–methanol (10:1)] with fluorescence [lit. (19) R_f 0.89]; UV λ_{max}: 225 and 285 nm (additional absorption between 300 and 360 nm, which formed a shoulder at 303 nm) [lit. (19) λ_{max}: 225 and 286 nm].

TLC on silica gel, using chloroform–methanol (30:1), showed more than one spot. The separation procedure was the same as that applied for V in the sodium thiophenoxide method. Extraction with methanol–ethyl acetate (1:1) provided the following compounds.

1. Compound V. This fraction accounted for 13% of the total recovered material, mp 105–110° (collapsed at 97°) and showed IR and NMR spectra that were the same as those of V prepared by the sodium thiophenoxide method.

2. Compound VI. The slowest moving band on TLC (41% of the total recovered material) had a melting point of 86–90° [lit. (22) mp 90–92.5°]; UV λ_{max} (log ϵ): 225 (4.64) and 284 (4.32) nm with an additional absorption in the 300–360-nm region which formed a shoulder at 303 (4.25) nm [lit. (22) UV λ_{max} (log ϵ): 225 (4.66), 284 (4.34), and shoulder at 303 (4.24) nm]; NMR ($CDCl_3$): δ 2.23 [s, 6H, $N(CH_3)_2$], 2.42 (s, 3H, NCH_3), 3.70 (s, 3H, OCH_3), 3.73 (s, 3H, OCH_3), 3.81 (s, 3H, OCH_3), 3.83 (s, 3H, OCH_3), and 5.76–6.93 (12H, aromatic and olefinic) ppm [lit. (22) NMR ($CDCl_3$): δ 2.28 (s, 6H), 2.46 (s, 3H), 3.73 (s, 3H), 3.77 (s, 3H), 3.85 (s, 3H), 3.88 (s, 3H), and 5.82–7.08 (12H) ppm].

3. Compound VII. The fastest moving band on TLC was obtained in a much smaller yield (5.5% of the total recovered material) and had a melting point of 100–105° [lit. (22) mp 98–104°]; IR (KBr): 885 (styrene) cm^{-1} [lit. (22) IR (KBr): 885 cm^{-1}]; UV λ_{max}: 225 and 262 nm with an additional absorption between 300 and 360 nm, which formed a shoulder at 303 nm [lit. (22) UV λ_{max} (log ϵ): 225 (4.80), 264 (4.48), and shoulder at 303 (4.27) nm]; NMR ($CDCl_3$): δ 2.06 (s, 3H, NCH_3), 2.23 [s, 6H, $N(CH_3)_2$], 3.64 (s, 3H, OCH_3), 3.66 (s, 3H, OCH_3), 3.78 (s, 3H, OCH_3), 3.80 (s, 3H, OCH_3), 5.08–5.54 (2H, the *AB* styrene protons), and 5.78–6.95 (11H, 10 aromatic and the X proton of the styrene product) ppm [lit. (22) NMR ($CDCl_3$): δ 2.10 (s, 3H), 2.25 (s, 6H), 3.66 (s, 3H), 3.68 (s, 3H), 3.81 (s, 3H), 3.83 (s, 3H), 5.10–5.56 (2H), and 5.80–6.95 (11H) ppm].

4. Compound VIII. The intermediate band on TLC had a melting point of 97–110°; IR (KBr): 885 (styrene) cm^{-1}. The UV and NMR spectra were similar to those of a mixture of V and VIII obtained in another experiment (22, 23).

REFERENCES

(1) H. King, *J. Chem. Soc.*, **1935,** 1381.

(2) A. J. Everett, L. A. Lowe, and S. Wilkinson, *Chem. Commun.*, **1970,** 1020.

(3) H. King, *J. Chem. Soc.*, **1948,** 265.

(4) J. D. Dutcher, *J. Am. Chem. Soc.*, **74,** 2221 (1952).

(5) O. Wintersteiner and J. D. Dutcher, *Science*, **97,** 467 (1943).

(6) J. D. Dutcher, *J. Am. Chem. Soc.*, **68,** 419 (1946).

(7) T. O. Soine and J. Naghaway, *J. Pharm. Sci.*, **63,** 1643 (1974).

(8) N. D. V. Wilson and J. A. Joule, *Tetrahedron*, **24,** 5493 (1968).

(9) D. Aumann and L. W. Deady, *Chem. Commun.*, **1973,** 32.

(10) R. O. Hutchins and F. J. Dux, *J. Org. Chem.*, **38,** 1961 (1973).

(11) H. O. House, H. C. Muller, C. G. Pitt, and P. P. Wickham, *ibid.*, **28,** 2407 (1963).

(12) P. A. Bartlet and W. S. Johnson, *Tetrahedron Lett.*, **46,** 4659 (1970).

(13) J. B. Bauman, *J. Org. Chem.*, **36,** 396 (1971).

(14) M. Tomita and T. Ibuka, *J. Pharm. Soc. Jpn.*, **82,** 1652 (1962); through *Chem. Abstr.*, **59,** 2874 (1963).

(15) A. C. Cope, E. Ciganek, L. J. Fleckenstein, and M. A. P. Meisinger, *J. Am. Chem. Soc.*, **82,** 4651 (1960).

(16) V. Simanek and A. Klasek, *Tetrahedron Lett.*, **35**, 3039 (1969).
(17) M. Tomita and Y. Takano, *J. Pharm. Soc. Jpn.*, **80**, 1645 (1960); through *Chem. Abstr.*, **55**, 7452 (1961).
(18) M. Shamma, N. C. Deno, and J. F. Remar, *Tetrahedron Lett.*, **13**, 1375 (1966).
(19) I. G. Marshall, J. B. Murray, G. A. Smail, and J. B. Stenlake, *J. Pharm. Pharmacol.*, **19**, 53-S (1967).
(20) I. R. C. Bick and P. S. Clezy, *J. Chem. Soc.*, **1953**, 3893.
(21) I. R. C. Bick, J. Harley-Mason, N. Sheppard, and M. J. Vernengo, *ibid.*, **1961**, 1896.
(22) J. Naghaway and T. O. Soine, *J. Pharm. Sci.*, **67**, 473 (1978).
(23) J. Naghaway, N. Shaath, and T. O. Soine, *J. Org. Chem.*, **40**, 539 (1975).
(24) M. Tomita, E. Fujita, and F. Murai, *J. Pharm. Soc. Jpn.*, **71**, 226 (1951).
(25) *Ibid.*, **71**, 301 (1951).
(26) *Ibid.*, **71**, 1035 (1951).
(27) M. Tomita, Y. Inubushi, and H. Niwa, *J. Pharm. Soc. Jpn.*, **72**, 213 (1952).
(28) "The Merck Index," 8th ed., Merck and Co., Rahway, N.J., 1968, p. 379.
(29) I. R. C. Bick and P. S. Clezy, *J. Chem. Soc.*, **1960**, 2402.
(30) F. Arndt, "Organic Syntheses," coll. vol. 2, Wiley, New York, N.Y., 1943, p. 165.
(31) J. Baldas, I. R. C. Bick, Q. N. Porter, and M. J. Vernengo, *Chem. Commun.*, **1971**, 132.

Stereospecificity of Esterases Hydrolyzing Oxazepam Acetate

GABOR MAKSAY ˣ, ZSUZSANNA TEGYEY, and LÁSZLÓ ÖTVÖS

Received May 17, 1977, from the *Central Research Institute for Chemistry, Hungarian Academy of Sciences, H-1525 Budapest, Hungary.* Accepted for publication December 19, 1977.

Abstract □ Esterases hydrolyzing the racemic acetate ester of the centrally acting drug oxazepam in mice were examined. Radiolabeled ester administered intravenously was hydrolyzed rapidly in the liver, kidneys, and brain. The distribution of the enzyme activity of liver and brain subcellular fractions was measured. Kinetic data and structure investigation of partially hydrolyzed racemic ester pointed to the stereoselectivity of liver and brain esterases. The preferred hydrolysis of the (*R*)-(−)-isomer in liver homogenates was attributed mainly to microsomal enzymes, while that of the (*S*)-(+)-isomer in brain was considered to be due to the mitochondrial fraction. This phenomenon was a common property of all species tested.

Keyphrases □ Oxazepam acetate—hydrolysis *in vivo* and *in vitro*, stereospecificity of esterases determined □ Hydrolysis—oxazepam acetate *in vivo* and *in vitro*, stereospecificity of esterases determined □ Stereospecificity—esterases hydrolyzing oxazepam acetate *in vivo* and *in vitro* □ Esterases—hydrolyzing oxazepam acetate *in vivo* and *in vitro*, stereospecificity determined □ Tranquilizers—oxazepam, hydrolysis of acetate ester *in vivo* and *in vitro*, stereospecificity of esterases determined □ Enzymes—esterases hydrolyzing oxazepam acetate *in vivo* and *in vitro*, stereospecificity determined

The 1,4-benzodiazepines are effective sedatives and anticonvulsants. The 3-substituted derivatives are less active (1), with the exception of oxazepam (I) and its hydrolyzable compounds. Esters as prodrugs may modify and prolong the pharmacological action of a drug (2), but the succinate half-ester (III) is one of the few derivatives of I that has been tested this way (3). Because of its asymmetric structure, there were stereoselective differences in biological activity (4, 5), ester hydrolysis (6), and serum albumin binding (7, 8).

This paper reports a study of *in vivo* and *in vitro* hydrolysis of oxazepam acetate (II), which has nearly the same pharmacological properties as I (1). Since it hydrolyzes rapidly, its decomposition site was examined down to the subcellular level, and attention was focused on stereospecificity.

EXPERIMENTAL

Animals—Male albino mice, 20–25 g, were used.

Substrates—Oxazepam acetate was obtained by rearrangement of 7-chloro-1,3-dihydro-5-phenyl-2*H*-1,4-benzodiazepine-2-one 4-oxide with acetic anhydride (9). The specific activity of the 2-^{14}C-compound was 3.15 mCi/mmole. β-Naphthyl acetate and physostigmine sulfate were used as received[1].

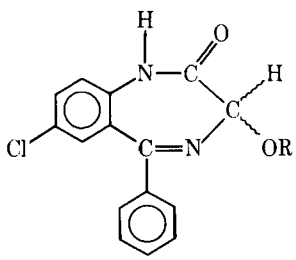

I: R = H
II: R = $COCH_3$
III: R = $COCH_2CH_2COOH$

Pharmacokinetics *In Vivo*—A dose of 11 mg of 2-^{14}C-II/kg iv was administered to mice in 70% aqueous dimethyl sulfoxide (2.5 ml/kg). After decapitation, the brain and blood were immediately homogenized in cold methanol containing nonlabeled I and II in a 50-fold excess. After 5 min of shaking (isotope exchange equilibrium was attained), the samples were centrifuged, and the supernate was then spotted on silica gel thin-layer plates. The developing system was benzene–ether–ethanol (5:5:0.7). The radioactivity of the spots suspended with a gelling agent[2] was measured on a liquid scintillation spectrometer[3].

Tissue Fractionation—The liver and brain were homogenized in 0.25 and 0.32 *M* sucrose, respectively. Fractionation was accomplished by ultracentrifugation[4] with a combination of previous methods (10, 11) according to Scheme I. All fractions were then resuspended in 0.25 and

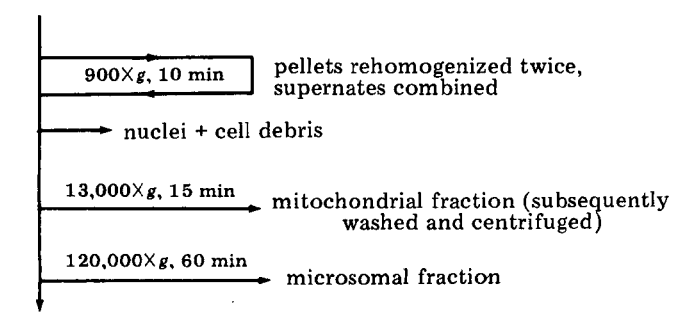

Scheme I

[1] Fluka and Calbiochem.
[2] Aerosil 380, Degussa, Frankfurt am Main, West Germany.
[3] Packard type 3003.
[4] Janetzky type VAC-601.

0022-3549/78/0900-1208$01.00/0
© 1978, American Pharmaceutical Association

(16) V. Simanek and A. Klasek, *Tetrahedron Lett.*, **35**, 3039 (1969).
(17) M. Tomita and Y. Takano, *J. Pharm. Soc. Jpn.*, **80**, 1645 (1960); through *Chem. Abstr.*, **55**, 7452 (1961).
(18) M. Shamma, N. C. Deno, and J. F. Remar, *Tetrahedron Lett.*, **13**, 1375 (1966).
(19) I. G. Marshall, J. B. Murray, G. A. Smail, and J. B. Stenlake, *J. Pharm. Pharmacol.*, **19**, 53-S (1967).
(20) I. R. C. Bick and P. S. Clezy, *J. Chem. Soc.*, **1953**, 3893.
(21) I. R. C. Bick, J. Harley-Mason, N. Sheppard, and M. J. Vernengo, *ibid.*, **1961**, 1896.
(22) J. Naghaway and T. O. Soine, *J. Pharm. Sci.*, **67**, 473 (1978).
(23) J. Naghaway, N. Shaath, and T. O. Soine, *J. Org. Chem.*, **40**, 539 (1975).
(24) M. Tomita, E. Fujita, and F. Murai, *J. Pharm. Soc. Jpn.*, **71**, 226 (1951).
(25) *Ibid.*, **71**, 301 (1951).
(26) *Ibid.*, **71**, 1035 (1951).
(27) M. Tomita, Y. Inubushi, and H. Niwa, *J. Pharm. Soc. Jpn.*, **72**, 213 (1952).
(28) "The Merck Index," 8th ed., Merck and Co., Rahway, N.J., 1968, p. 379.
(29) I. R. C. Bick and P. S. Clezy, *J. Chem. Soc.*, **1960**, 2402.
(30) F. Arndt, "Organic Syntheses," coll. vol. 2, Wiley, New York, N.Y., 1943, p. 165.
(31) J. Baldas, I. R. C. Bick, Q. N. Porter, and M. J. Vernengo, *Chem. Commun.*, **1971**, 132.

Stereospecificity of Esterases Hydrolyzing Oxazepam Acetate

GABOR MAKSAY ˣ, ZSUZSANNA TEGYEY, and LÁSZLÓ ÖTVÖS

Received May 17, 1977, from the *Central Research Institute for Chemistry, Hungarian Academy of Sciences, H-1525 Budapest, Hungary.* Accepted for publication December 19, 1977.

Abstract □ Esterases hydrolyzing the racemic acetate ester of the centrally acting drug oxazepam in mice were examined. Radiolabeled ester administered intravenously was hydrolyzed rapidly in the liver, kidneys, and brain. The distribution of the enzyme activity of liver and brain subcellular fractions was measured. Kinetic data and structure investigation of partially hydrolyzed racemic ester pointed to the stereoselectivity of liver and brain esterases. The preferred hydrolysis of the (*R*)-(−)-isomer in liver homogenates was attributed mainly to microsomal enzymes, while that of the (*S*)-(+)-isomer in brain was considered to be due to the mitochondrial fraction. This phenomenon was a common property of all species tested.

Keyphrases □ Oxazepam acetate—hydrolysis *in vivo* and *in vitro*, stereospecificity of esterases determined □ Hydrolysis—oxazepam acetate *in vivo* and *in vitro*, stereospecificity of esterases determined □ Stereospecificity—esterases hydrolyzing oxazepam acetate *in vivo* and *in vitro* □ Esterases—hydrolyzing oxazepam acetate *in vivo* and *in vitro*, stereospecificity determined □ Tranquilizers—oxazepam, hydrolysis of acetate ester *in vivo* and *in vitro*, stereospecificity of esterases determined □ Enzymes—esterases hydrolyzing oxazepam acetate *in vivo* and *in vitro*, stereospecificity determined

The 1,4-benzodiazepines are effective sedatives and anticonvulsants. The 3-substituted derivatives are less active (1), with the exception of oxazepam (I) and its hydrolyzable compounds. Esters as prodrugs may modify and prolong the pharmacological action of a drug (2), but the succinate half-ester (III) is one of the few derivatives of I that has been tested this way (3). Because of its asymmetric structure, there were stereoselective differences in biological activity (4, 5), ester hydrolysis (6), and serum albumin binding (7, 8).

This paper reports a study of *in vivo* and *in vitro* hydrolysis of oxazepam acetate (II), which has nearly the same pharmacological properties as I (1). Since it hydrolyzes rapidly, its decomposition site was examined down to the subcellular level, and attention was focused on stereospecificity.

EXPERIMENTAL

Animals—Male albino mice, 20–25 g, were used.

Substrates—Oxazepam acetate was obtained by rearrangement of 7-chloro-1,3-dihydro-5-phenyl-2*H*-1,4-benzodiazepine-2-one 4-oxide with acetic anhydride (9). The specific activity of the 2-^{14}C-compound was 3.15 mCi/mmole. β-Naphthyl acetate and physostigmine sulfate were used as received[1].

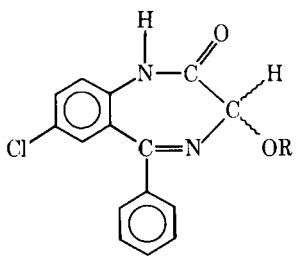

I: R = H
II: R = $COCH_3$
III: R = $COCH_2CH_2COOH$

Pharmacokinetics *In Vivo*—A dose of 11 mg of 2-^{14}C-II/kg iv was administered to mice in 70% aqueous dimethyl sulfoxide (2.5 ml/kg). After decapitation, the brain and blood were immediately homogenized in cold methanol containing nonlabeled I and II in a 50-fold excess. After 5 min of shaking (isotope exchange equilibrium was attained), the samples were centrifuged, and the supernate was then spotted on silica gel thin-layer plates. The developing system was benzene–ether–ethanol (5:5:0.7). The radioactivity of the spots suspended with a gelling agent[2] was measured on a liquid scintillation spectrometer[3].

Tissue Fractionation—The liver and brain were homogenized in 0.25 and 0.32 *M* sucrose, respectively. Fractionation was accomplished by ultracentrifugation[4] with a combination of previous methods (10, 11) according to Scheme I. All fractions were then resuspended in 0.25 and

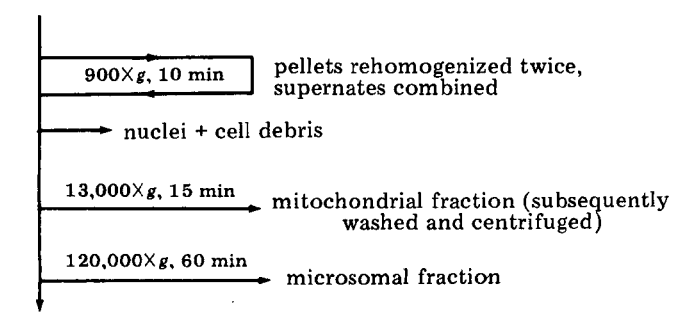

Scheme I

[1] Fluka and Calbiochem.
[2] Aerosil 380, Degussa, Frankfurt am Main, West Germany.
[3] Packard type 3003.
[4] Janetzky type VAC-601.

0022-3549/78/0900-1208$01.00/0
© 1978, American Pharmaceutical Association

Table I—Esterase Activity of Tissues for Oxazepam Acetate [a]

Tissue	v_0
Liver	27.10 ± 4.20
Kidneys	10.57 ± 3.72
Brain	3.02 ± 0.22

[a] Results are averages of three determinations, expressed in nanomoles of II per minute per milligram of protein, at pH 7.5 and 37° in saline.

0.32 *M* sucrose. The protein content of the fractions was determined by the biuret reaction (12).

Esterase Activity—The esterase activity of the tissue homogenates and their subcellular fractions was determined titrimetrically by pH-stat[5] in 20 ml of 0.9% NaCl containing 1–50 mg of protein. The initial concentration of β-naphthyl acetate was 1 m*M*, and that of II was 0.5 m*M*. The initial hydrolysis rate was determined at 37°, and the pH was maintained at 7.5 by addition of 0.01 *N* NaOH.

Preparative Hydrolysis of II—*In vitro* hydrolysis was stopped at 50% conversion, and the remaining ester was extracted by ether and purified on a preparative thin-layer sheet. NMR spectra were obtained[6]. A europium optishift reagent[7] was used for the determination of the ratio of the isomers. Circular dichroism spectra were taken[8] in methanol. Molecular ellipticities (θ_{223}) were calculated at 223 nm.

RESULTS AND DISCUSSION

***In Vivo* Hydrolysis**—The relative tissue binding of I and II in a methanolic homogenate determined by an independent *in vitro* experiment was unity. Therefore, the ratio of radioactivities of the chromatographic spots corresponded to the ratio of the compounds in the tissues. During 30 min, only I and II contributed measurably to the total radioactivity.

Compound II, administered intravenously, hydrolyzed rapidly. Figure 1 shows the logarithm of this ratio as a function of time in brain and blood. At the first experimental point (1 min), the ratio of the concentrations of I and II was about unity. This result suggests an immeasurably rapid, stereospecific hydrolysis of the preferred isomer while the ratio decreases rapidly to 1 (log 1 = 0). Rapid hydrolysis seems to be the reason why II administered orally or intraperitoneally has pharmacological activity similar to I (1); *i.e.*, the ester itself can hardly reach its target organ. Thus, II is not a proper prodrug. However, it is a good model compound for *in vitro* examination of the esterases responsible for the bioactivation of ester-type prodrugs of I.

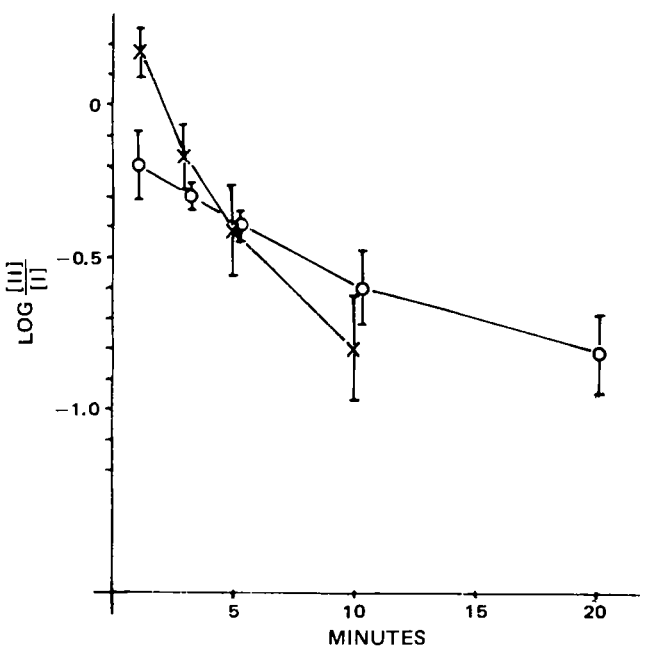

Figure 1—*Ratio of the concentrations of oxazepam acetate to oxazepam in blood (+) and brain (○). Each point represents five animals.*

[5] Radiometer, Copenhagen, Denmark.
[6] Varian XL-100.
[7] Tris[3-(heptafluoropropylhydroxymethylene)-*d*-camphorato]europium (III), Willow-Brook Co.
[8] Jouan-Quetin Dichrographe III.

Table II—Esterase Activity [a] of Liver and Brain Subcellular Fractions

Fraction	Liver		Brain	
	β-Naphthyl Acetate	Oxazepam Acetate	β-Naphthyl Acetate	Oxazepam Acetate
Total homogenate	1143 ± 11	27.1 ± 4.2	74 ± 3	3.02 ± 0.22
Nuclei plus cell debris	349 ± 24	32.9 ± 0.4	50 ± 2	1.88 ± 0.18
Mitochondrial	428 ± 60	46.7 ± 2.3	39 ± 4	2.05 ± 0.15
Microsomal	1810 ± 200	261.7 ± 5.0	125 ± 7	4.71 ± 0.49
Supernate	145 ± 6	2.1 ± 0.3	59 ± 2	5.37 ± 0.40

[a] Results are averages of three determinations in nanomoles of ester per minute per milligram of protein.

***In Vitro* Hydrolysis**—Table I lists the esterase activity of tissue homogenates. Esterase activity of the lungs and blood was not detectable by pH-stat, which does not mean, however, that they had no activity. For example, the hydrolysis of radiolabeled II in serum was detected following chromatographic separation of I. The major part of II decomposed in the liver and kidneys, but esterases also contributed to the process elsewhere. This was especially true for the brain, because its esterases may have modified the effective concentration of the drug at the site of action.

For the detection of stereoselectivity, the whole course of hydrolysis of racemic II was followed by a pH-stat. Titration curves show double exponential character, with a breakpoint at half-conversion of the ester. This phenomenon was significant only for liver and brain homogenates.

Thus, both *in vivo* and *in vitro* kinetic data support the assumption that the esterases in question are stereospecific. Chemical composition and chirality of II isolated by preparative hydrolysis also verify this assumption. The NMR spectrum was identical with the reference substance. On addition of the europium optishift reagent, the proton attached to C-3 (originally at 6.0 ppm) gave two signals of different intensity. With the liver homogenate, the ratio of the isomers was 20:80. The polarimetric rotation results also indicate differing stereospecificities. The $[\alpha]_D$ value of II extracted from liver homogenate was 90°, and that of II extracted from brain homogenate was −56° (c 0.5, dioxane).

Circular dichroism spectra (Fig. 2) show that esterases in liver and brain homogenates had opposite stereospecificity. The spectra were similar to those of oxazepam succinate half-ester (III) (13, 14), and the absolute configuration of the isomers can be established. This identification cannot be approached from the I side because it racemizes rapidly in an aqueous medium (13).

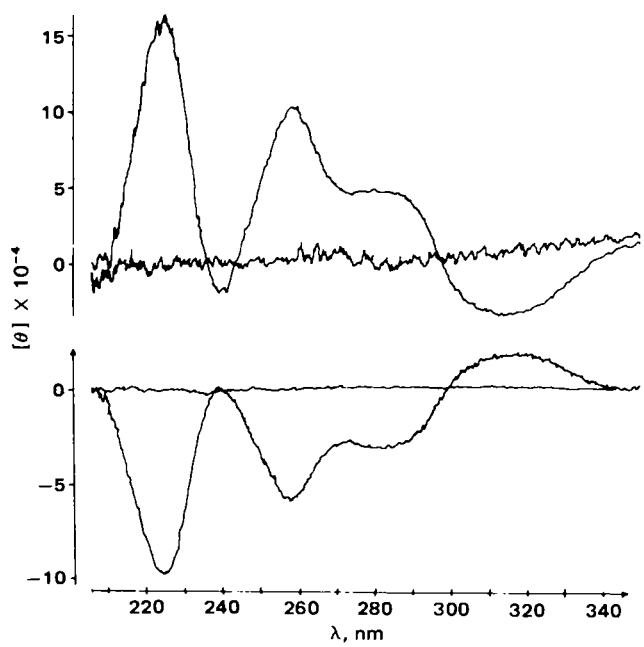

Figure 2—*Circular dichroism spectra of oxazepam acetate partially hydrolyzed by total liver [upper spectrum, (S)-(+)-isomer] and brain [lower spectrum, (R)-(−)-isomer] homogenates.*

Table III—Optical Activity of Partially Hydrolyzed Oxazepam Acetate

Fraction	θ_{223} Liver	θ_{223} Brain
Mitochondrial	19,800	−125,400
Microsomal	42,900	2,310
Soluble	330	−16,500

Stereospecificity was examined in liver and brain homogenates of different species. Indexes of absolute configuration based on the sign of polarimetric rotation of partially hydrolyzed II were (*S*)-(+) in all liver homogenates and (*R*)-(−) in all brain homogenates from mice, rats, chickens, pigs, and cows. These data show that the difference was general for all species tested.

Subcellular Localization of Esterases in Brain and Liver of Mice—The enzymatic activity of the subcellular fractions for oxazepam acetate was determined in a nearly saturated solution of the substrate. Esterase activity was also measured with a nonspecific substrate, β-naphthyl acetate (Table II).

Microsomal proteins had a high specific activity, in agreement with previous findings for the liver (15, 16) and brain (17). Salmona *et al.* (6) reported that III was hydrolyzed only by the 105,000×*g* supernate of mouse liver and kidney homogenate and that the hydrolysis rate of the isomers was different. Compound II hydrolyzed more readily than III, and its stereospecificity was opposite to that of III. Probably this difference was due to different enzymes such as acetic esterases.

For the localization of the different stereoselectivity of brain and liver tissues, the optical activity of II partially hydrolyzed by tissue fractions was measured. Because the 900×*g* pellets formed a rather heterogeneous fraction containing nuclei and cell debris (17), they were excluded from the investigation. Table III lists the molecular ellipticities (θ_{223}) of II.

To estimate the contribution of the fractions to the total stereoselectivity, their participation in the total esterase activity must be considered. The data in Table IV show the total esterase activity of the subcellular fractions calculated for 1 g of wet tissue.

Liver—Microsomal esterases had a decisive role both in activity and selectivity. The soluble fraction had almost no stereoselectivity for racemic II, in contrast to the results of Salmona *et al.* (6) who found this fraction to be selective for the resolved isomers of III.

Brain—Because of its high yield, the crude mitochondrial fraction overcompensated the effect of the microsomal fraction and determined the opposite stereospecificity of brain tissue. De Robertis *et al.* (11) showed that the crude mitochondrial fraction of rat brain contained synaptosomes. Bernsohn *et al.* (17) found that esterase activity of this fraction was related to synaptic membranes. In this case, esterases of the supernate with similar stereospecificity might be of the same origin. At any rate, the phenomenon is not connected with cholinesterases, because physostigmine at up to 2×10^{-3} *M* concentration neither inhibited nor modified stereospecificity.

The opposite stereoselectivity of different organs is an interesting phenomenon. It is similar to earlier findings (18) for the hydrolysis of methyl mandelate by pig liver and pancreas esterases. Peculiarly, however, the stereoselectivity of pig liver was different toward the racemate and the resolved enantiomers (19). To investigate such a possibility, resolution of the isomers of II is in progress. The question arises whether the phenomenon of opposite stereoselectivity exists for other asymmetric esters, which would be significant in the biotransformation of several centrally acting drugs.

Table IV—Total Esterase Activity [a] of the Subcellular Fractions

Fraction	Liver	Brain
Total homogenate	18,420	606.7
Nuclei plus cell debris	1,220	126.0
Mitochondrial	3,060	193.3
Microsomal	9,890	95.1
Soluble	200	126.7

[a] Values are in nanomoles of II per minute per gram of tissue.

REFERENCES

(1) S. C. Bell, R. J. McCaully, C. Gochman, S. J. Childress, and M. J. Gluckman, *J. Med. Chem.*, **11**, 457 (1968).

(2) A. A. Sinkula and S. H. Yalkowsky, *J. Pharm. Sci.*, **64**, 181 (1975).

(3) A. Nudelman, R. J. McCaully, and S. C. Bell, *ibid.*, **63**, 1880 (1974).

(4) E. Mussini, F. Marcucci, R. Fanelli, A. Guaitani, and S. Garattini, *Biochem. Pharmacol.*, **21**, 127 (1972).

(5) L. de Angelis, M. Predominato, and R. Vertua, *Arzneim.-Forsch.*, **22**, 1328 (1972).

(6) M. Salmona, C. Saronio, R. Bianchi, F. Marcucci, and E. Mussini, *J. Pharm. Sci.*, **63**, 222 (1974).

(7) W. E. Müller and U. Wollert, *Res. Commun. Chem. Pathol. Pharmacol.*, **9**, 413 (1974).

(8) W. E. Müller and U. Wollert, *Mol. Pharmacol.*, **11**, 52 (1974).

(9) S. C. Bell and S. J. Childress, *J. Org. Chem.*, **27**, 1691 (1961).

(10) C. Carruthers, D. L. Woornley, A. Baumler, and K. Lilga, *Arch. Biochem. Biophys.*, **87**, 266 (1960).

(11) E. de Robertis, A. P. de Iraldi, G. R. de Lores Anais, and L. Salganicoff, *J. Neurochem.*, **9**, 23 (1962).

(12) M. Ditterbrandt, *Am. J. Clin. Pathol.*, **18**, 439 (1948).

(13) A. Corbella, P. Gariboldi, G. Jommi, A. Forgione, F. Marcucci, P. Martelli, and E. Mussini, *J. Chem. Soc. Chem. Commun.*, **1973**, 721.

(14) V. Šunjic, F. Kajfež, D. Kolbah, and N. Blažević, *Croat. Chem. Acta*, **43**, 205 (1971).

(15) C. Carruthers and A. Baumler, *Arch. Biochem. Biophys.*, **94**, 351 (1961).

(16) A. Omachi, C. P. Barnum, and D. Glick, *Proc. Soc. Exp. Biol. Med.*, **67**, 133 (1948).

(17) J. Bernsohn, K. D. Barron, P. F. Doolin, A. R. Hess, and M. T. Hedrick, *J. Histochem. Cytochem.*, **14**, 455 (1966).

(18) P. Rona and E. Chain, *Biochem. Z.*, **258**, 480 (1933).

(19) P. Rona, R. Ammon, and M. Werner, *ibid.*, **217**, 42 (1930).

ACKNOWLEDGMENTS

The authors are grateful to Dr. Judit Kajtár, Department of Organic Chemistry, Eötvös University of Budapest, for the circular dichroism spectra.

Effects of Short and Medium Chain Fatty Acids on Absorption of Lipophilic Drugs from Perfused Rat Intestine

JOSEPH A. GRISAFE and WILLIAM L. HAYTON ˣ

Received September 26, 1977, from the *College of Pharmacy, Washington State University, Pullman, WA 99164.* Accepted for publication December 20, 1977.

Abstract □ The absorption rates of griseofulvin and prednisolone were measured from solutions that were recirculated through a segment of *in situ* rat jejunum. When premicellar concentrations of butyric, octanoic, or dodecanoic acid were present in the perfusate, the griseofulvin absorption rate decreased while that of prednisolone increased. The fatty acids also increased the absorption rate of water from the perfusate, and the effect of butyric acid was attributed primarily to this increase. The absorption-altering effects of octanoic and dodecanoic acids could not be attributed solely to their effects on water absorption nor to their effects on the surface tension of the perfusate. The effects of octanoic and dodecanoic acids were explained by postulating different rate-limiting barriers to the absorption of prednisolone and griseofulvin.

Keyphrases □ Fatty acids, various—effects on absorption of lipophilic drugs from perfused rat intestine □ Absorption—lipophilic drugs from perfused rat intestine, effects of various fatty acids □ Lipophilic drugs—prednisolone and griseofulvin, effects of fatty acids on absorption from perfused rat intestine □ Griseofulvin—absorption from perfused rat intestine, effects of fatty acids □ Prednisolone—absorption from perfused rat intestine, effects of fatty acids

The presence of a mixed micellar phase composed of sodium taurodeoxycholate, oleic acid, and monoolein in perfusates recirculated through the *in situ* rat intestine reduced the absorption rate of griseofulvin (1). The absorption rate was further reduced when emulsified triolein was included in the perfusate. The reduced absorption rate of griseofulvin was attributed primarily to partitioning of the drug into the micellar and triolein phases from which it was not appreciably absorbed. The griseofulvin absorption rate from the micellar phase was reduced more than could be explained by micellar complexation of the drug. A possible explanation for the additional decrease was that a component of the micellar phase reduced the permeability of the intestinal epithelium. This study, therefore, explored the effects of fatty acids on the permeability of the *in situ* intestinal mucosa.

BACKGROUND

Fatty acids may alter the permeability of the intestinal mucosa to drugs. For example, butyric acid inhibited the absorption of the anionic drugs sulfisoxazole and salicylic acid; it enhanced the absorption of the neutral drugs caffeine and sulfanilamide and of the cationic drugs metoclopramide and quinine (2). Low molecular weight alcohols also appear to alter drug absorption. Hexanol reduced the absorption rate of sulfapyridine and salicylic acid and increased the absorption rate of prednisolone (3). Conversely, the absorption rate of theophylline from the rat intestine was increased by glycerol (4), propylene glycol (4), and ethanol (5).

The intestinal absorption of drugs from perfusates that contained solubilized long chain fatty acids also was investigated. The bile salt sodium taurocholate, alone or together with a low concentration of oleic acid, increased procainamide absorption in the rat; when a high concentration of oleic acid was used, procainamide absorption decreased (6). Furthermore, the absorption of 2-allyloxy-4-chloro-*N*-(2-diethylaminoethyl)benzamide hydrochloride, a drug with a higher chloroform–pH 6.5 phosphate buffer partition coefficient than procainamide, was unchanged by sodium taurocholate and oleic acid (6). These effects were attributed to modification of the permeability of the intestinal membrane and micellar complexation of the drug. However, another study (7) reported that oleic acid, slightly in excess of its solubility, had no detectable effect on the absorption of salicylic acid, salicylamide, and 4-aminoantipyrine.

These results suggest that fatty acids may alter the permeability of the intestinal mucosa to drugs. The direction of the change in permeability appears to depend in part on the properties of the drug. While representative water-soluble drugs have been studied, the effects of fatty acids on the permeability of the intestine to lipophilic drugs have not been well characterized. In this study, the effects of fatty acids on the absorption rates of griseofulvin and prednisolone were examined; both drugs are lipophilic and poorly soluble in water. The fatty acids used were butyric, octanoic, and dodecanoic because they are sufficiently water soluble to be incorporated in perfusate solutions without the aid of bile salts at pH values compatible with the intestine. They also differ in lipophilicity.

EXPERIMENTAL

Materials—Sodium butyrate[1], octanoic acid[2], dodecanoic acid[1], griseofulvin[3], prednisolone[3], and tromethamine[4] were used as received. ^{3}H-Prednisolone[5] was dissolved in alcohol and stored at 5°. The radiochemical purity (>88%) of ^{3}H-prednisolone was determined by TLC on glass plates coated with silica gel G and developed with benzene–2-propanol (4:1). All other reagents and solvents were reagent grade.

Intestinal Clearance—Male Sprague-Dawley rats, 180–360 g, were housed in wire mesh cages in a room maintained at approximately 20° and lighted automatically 12 hr/day. The clearance of prednisolone and griseofulvin from solutions recirculated at 6.5 ml/min through a 20-cm segment of *in situ* jejunum was measured as described previously (1). When fatty acid was present in the perfusate, its concentration was maintained relatively constant by infusing an aqueous solution of the fatty acid into the perfusate. The infusion rate was sufficient to compensate for loss of fatty acid due to absorption by the intestine and removal of samples (Fig. 1). To assure complete solubilization of the fatty acid, the pH of the infused solution was 6.2 for butyrate and octanoate and 8.4 for dodecanoate.

The intestinal solution initially contained either 280 μM prednisolone (0.1 μCi of ^{3}H-prednisolone/ml) or 23 μM griseofulvin. When butyrate or octanoate was studied, the buffer was 68 mM sodium phosphate and was made isotonic with 87 mM sodium chloride. The sodium chloride concentration was not reduced when fatty acid was present. Perfusates that contained dodecanoate were at pH 8.4 in isosmotic tromethamine buffer (250 mM).

The intestinal perfusate was sampled periodically, and the drug concentration was determined. The drugs were absorbed by apparent first-order kinetics (Fig. 2). Semilogarithmic plots of the fraction of initial drug concentration *versus* time gave straight lines when fitted by the least-squares method. The initial point was omitted from the fit to ensure stationary-state conditions. The absorption rate constants were determined from the slopes of the fitted lines.

The absorption rate constants were converted to clearance per centimeter of intestine as described previously (1). The water absorption rate was calculated as $(V_1 + V_2 - V_3)/(XD)$, where V_1 is the volume of buffer added to the drug solution to maintain a constant volume, V_2 is the volume of fatty acid solution infused, V_3 is the total volume of samples, X

[1] Matheson, Coleman and Bell, Norwood, Ohio.
[2] Nu Chek Prep, Elysian, Minn.
[3] Sigma Chemical Co., St. Louis, Mo.
[4] Pfaltz & Bauer, Stamford, Conn.
[5] Amersham/Searle Corp., Des Plaines, Ill.

0022-3549/78/0900-1211$01.00/0
© 1978, American Pharmaceutical Association

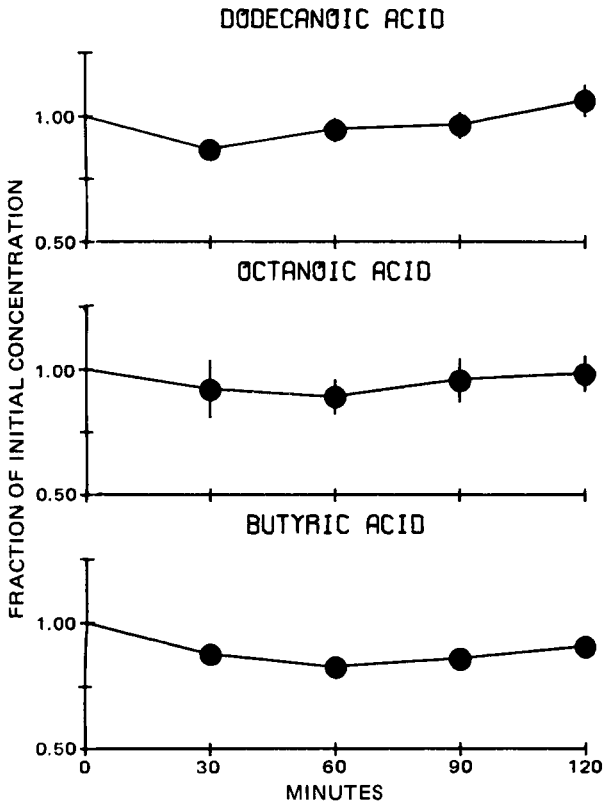

Figure 1—*Fractions of the initial concentration of dodecanoic acid (4 mM), octanoic acid (6 mM), and butyric acid (60 mM) remaining in the intestinal solution as a function of time. Each point represents the mean from six experiments, and bars indicate ±1* SE.

is the length of the intestinal segment, and D is the duration of the experiment. The fatty acid infusion rates were determined experimentally prior to measurement of the drug absorption rate constants (Table I).

Surface Tension—The surface tension of the perfusates was determined by the du Nouy ring detachment method[6]. The surface tension was plotted against the logarithm of the fatty acid concentration, and the critical micelle concentration (CMC) was estimated. Fatty acid concentrations used in the intestinal perfusates were below the CMC.

Analytical Methods—Octanoic and dodecanoic acids were separated and analyzed spectrophotometrically as described previously (1, 8). Butyric acid in 0.3-ml samples of intestinal perfusate was determined by GLC. Samples were mixed with 0.1 ml of aqueous 1-propanol, which was used as an internal standard; approximately 1 μl was injected onto a stainless steel column, 0.31 cm (0.125 in.) o.d. × 1.8 m (6 ft), packed with 80–100-mesh Porapak Q. The temperatures of the injection port, oven, and flame-ionization detector were 250, 230, and 250°, respectively. The flow rates of helium, hydrogen, and air were 55, 65, and 300 ml/min, respectively.

A plot of the ratio of the peak height of butyric acid to that of propanol *versus* butyric acid concentration was linear over the 10–70-m*M* range. Analysis of blank samples of intestinal perfusate did not produce peaks that would interfere with the propanol or butyric acid peaks.

Tritium was determined in intestinal perfusate by mixing 50–200-μl samples with 10 ml of scintillation fluid[7] and counting in a liquid scintillation spectrometer[8]. The counting efficiency of the system was 30–40%; quench corrections were made by the channels-ratio method.

RESULTS AND DISCUSSION

The fatty acids significantly altered the absorption rates of griseofulvin and prednisolone. The disappearance rate of griseofulvin from the intestinal perfusate was decreased significantly by octanoic and dodecanoic acids, but butyric acid produced no detectable effect (Table II). The disappearance rate of prednisolone was increased significantly by the three fatty acids (Table II).

Table I—Infusion Rates that Maintain a Constant Concentration of Fatty Acid in the Intestinal Perfusate

Fatty Acid	Infusion Rate[a], mg/ml	Intestinal Clearance[b], μl/min/cm
Butyric, 60 m*M*	0.92	8.19
Octanoic, 6 m*M*	0.36	20.10
Dodecanoic, 4 m*M*	0.13	7.52

[a] Includes replacement of losses due to sampling. Samples of 0.3 ml were removed at 30-min intervals. [b] Calculated by infusion = clearance × concentration in the perfusate. Corrected for the rate of removal of samples.

One mechanism that accounts for part of the absorption-altering property of the fatty acids involves their effect on the water absorption rate by the intestine. The drug absorption rate is related directly to the water absorption rate through a solvent drag mechanism (4, 5). The absorption rates of both griseofulvin and prednisolone were proportional to the water absorption rates observed (Figs. 3 and 4); griseofulvin was more sensitive than prednisolone to the water flux. All three fatty acids increased the absorption rate of water (Table III), even though they also increased the osmotic pressure of the intestinal perfusate. Thus, the increased absorption rate of prednisolone induced by butyric acid is primarily a secondary effect that results from an increase in the water absorption rate.

When differences in water absorption rates are taken into account, the absorption-altering effects of the fatty acids apparent in Table II are increased for griseofulvin and decreased for prednisolone. However, the absorption-altering effects of octanoic and dodecanoic acids cannot be explained solely by their ability to increase the water absorption rate (Fig. 5). The effects of these fatty acids on absorption appear to involve additional mechanisms.

No significant relationship was observed between the effects of the fatty acids on absorption and their effects on the surface tension of the perfusates (Table II). For example, 4 m*M* dodecanoic acid caused a larger decrease in surface tension than did 24 m*M* octanoic acid, but it had a smaller effect on the absorption rate of the two drugs.

While the fatty acids changed the absorption rates of griseofulvin and prednisolone in opposite directions, the magnitudes of the changes were similar (Table II), especially when the effects of altered water flux were

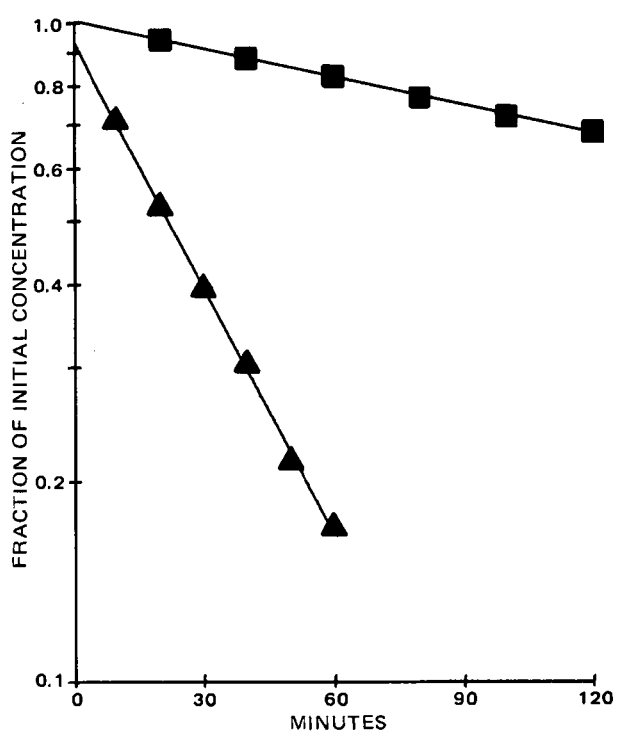

Figure 2—*Disappearance of prednisolone (■) and griseofulvin (▲) from the intestinal perfusate. Initial concentrations were 280 and 23 μM, respectively. Each point is the mean from six experiments.*

[6] Cenco-DuNouy interfacial tensiometer model 70545, Central Scientific Co., Chicago, Ill.
[7] Aquasol, New England Nuclear, Boston, Mass.
[8] Packard Tri-Carb model 3320, Packard Instrument Co., Downers Grove, Ill.

Table II--Effects of Fatty Acids on Perfusate Surface Tension and Intestinal Clearance of Griseofulvin and Prednisolone

Perfusate	Surface Tension Reduction, dynes/cm	Intestinal Clearance, μl/min/cm[a]		Change in Clearance, % of Control			
		Griseofulvin	Prednisolone	Griseofulvin	Prednisolone	Griseofulvin[b]	Prednisolone[b]
pH 6.2 Phosphate buffer							
Control		9.44 (1.19)	1.49 (0.40)	—	—	—	—
Butyric acid, 60 m*M*	0.0	9.50 (0.58)	2.30 (0.40)	1.0	54.4	−27	11
Octanoic acid, 6 m*M*	17.8	8.91 (1.41)	—[c]	−5.6	—[c]	−13	—[c]
Octanoic acid, 12 m*M*	24.7	7.59 (2.59)	—[c]	−19.6	—[c]	−34	—[c]
Octanoic acid, 24 m*M*	31.5	5.47 (0.78)	2.75 (0.28)	−42.1	84.6	−58	58
pH 8.4 Tromethamine buffer							
Control		6.32 (1.13)	1.07 (0.15)	—	—	—	—
Dodecanoic acid, 4 m*M*	48.1	4.20 (0.65)	1.69 (0.31)	−33.5	57.9	−45	31

[a] Mean from six experiments; standard deviation in parentheses. [b] Clearance values adjusted to zero water flux; see Figs. 3 and 4. [c] Not determined.

removed. This similarity suggests that the fatty acids act by changing one aspect of the absorption process and that this change causes the apparent permeability of the intestine to the drugs to change in opposite directions. Thus, griseofulvin and prednisolone possibly are absorbed by two different routes. The change induced by the fatty acids in the intestine augments the route for prednisolone while simultaneously depressing the route for griseofulvin. Although such a mechanism may exist, it is difficult to envisage a specific change in the structure or function of the intestinal epithelium that would plausibly explain the observed effects of the fatty acids.

An alternative explanation for the effects induced by the fatty acids is that the permeability of the mucosa to griseofulvin and prednisolone is controlled by two separate barriers. The permeability of the barrier for prednisolone would then be increased by the fatty acids while the permeability of the barrier for griseofulvin would be decreased. For example, intestinal blood flow or an aqueous unstirred layer could limit the absorption rate of griseofulvin while the permeability of the intestinal epithelium could limit the absorption rate of prednisolone.

The average blood flow rate to the proximal 40% of the small intestine of 258 ± 7-g male Sprague-Dawley rats, anesthetized with 1.3-mg/g doses of urethan, was 1.10 ml/min/g of wet weight (9). The weight of the 20-cm segment perfused in the present study was approximately 1 g; the blood flow rate to the perfused intestine is, therefore, approximately 55 μl/min/cm. However, studies of the blood-to-lumen flux of barbital in the perfused rat ileum revealed that subepithelial capillary blood flow available for transport of absorbed substances amounted to 50.3% of the total blood flow to the intestine (10). Thus, the effective intestinal blood flow to the perfused segment is approximately 28 μl/min/cm. This value is probably an overestimate since equilibration of absorbed drug between erythrocytes and plasma may not be complete during the short time that blood resides in the epithelial capillary. Also, there is the possibility of a countercurrent exchange in the villus that removes drug from the blood exiting the villus (11). The control intestinal clearance of griseofulvin averaged 9.44 μl/min/cm of intestine, and it is possible that griseofulvin clearance was determined primarily by the intestinal blood flow rate. If the fatty acids reduced the blood flow rate through subepithelial capillaries, griseofulvin clearance also would be reduced.

Another potentially important barrier to the intestinal absorption of rapidly absorbed compounds is an unstirred water layer adjacent to the mucosal surface (*e.g.*, 12–14). Estimates of the thickness of this layer are 50–300 μm, depending on the agitation intensity. Water flux across the membrane can affect the thickness of this barrier significantly (15), as can the movement of microvilli (16). A clearance constant for the unstirred layer can be estimated as $D(A/h)$, where D, the diffusion coefficient in water, is 1×10^{-5} cm²/sec; h, the thickness of the unstirred layer, is 50 μm; and A is the surface area of a right cylinder of 0.4-cm diameter. The estimated clearance, 15 μl/min/cm of intestine, is in the range observed for griseofulvin, although the uncertainty in A and h could cause a large error. The fatty acids may have decreased griseofulvin clearance by increasing h, perhaps by stimulating the mucus secretion.

Since the intestinal clearance of prednisolone is considerably less than that of griseofulvin, the primary barrier to prednisolone absorption is probably not blood flow or a stagnant aqueous layer. Thus, a change in these parameters should not have a discernible effect on its absorption. Recent work using the same technique as was used here demonstrated that the permeability of the intestinal epithelium to prednisolone was increased by a number of substances in addition to fatty acids (Table IV). The capacity of the various additives to increase the absorption rate of prednisolone appears to be related directly to the lipophilicity of the additive. Earlier studies with substituted amides and, in particular, di-

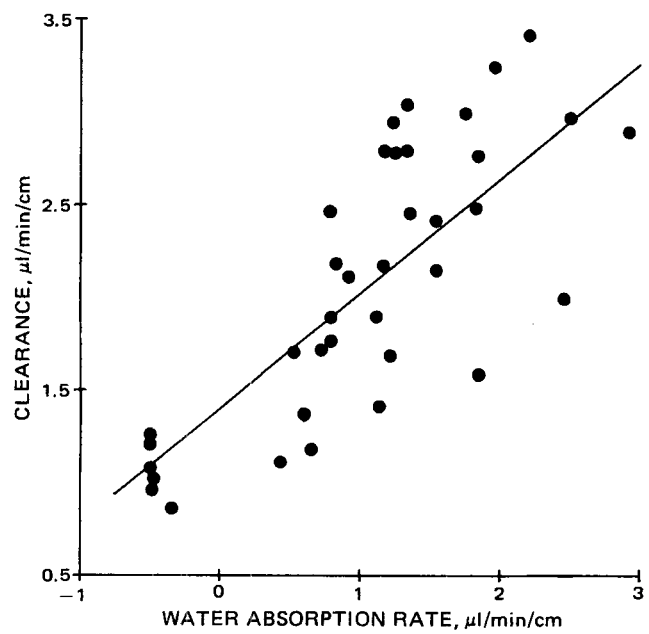

Figure 3—*Clearance of prednisolone* versus *water absorption rate. Each point represents a single experiment. The equation of the line, fit by the least-squares method, is* y = *0.618*x + *1.40.*

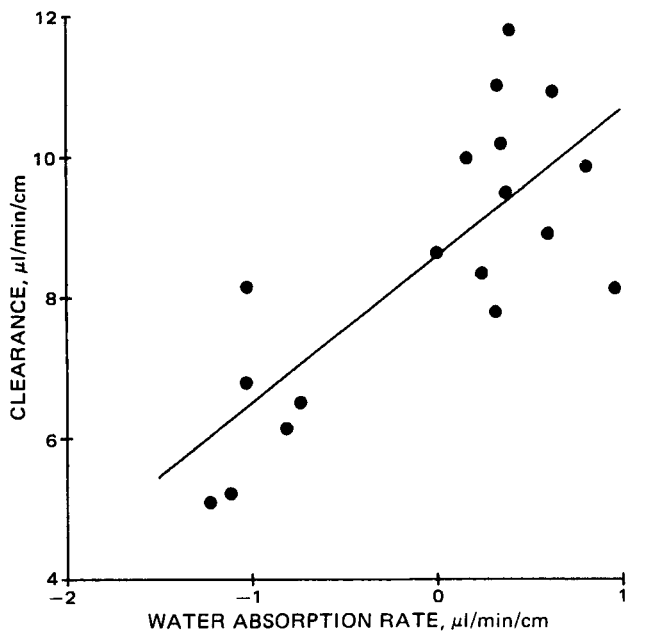

Figure 4—*Clearance of griseofulvin* versus *water absorption rate. Each point represents a single experiment. The equation of the line, fit by the least-squares method, is* y = *2.08*x + *8.58.*

Table III—Effect of Fatty Acids on the Absorption Rate of Water from the Perfused Rat Intestine

	Absorption Rate[a], μl/min/cm of Intestine				
	Control[b]	Control[c]	Butyric Acid[d]	Octanoic Acid[e]	Dodecanoic Acid[f]
Prednisolone	0.70 (0.25)	−0.47 (0.06)	1.20 (0.30)[g]	0.87 (0.19)	−0.23 (0.08)[g]
Griseofulvin	0.41 (0.20)	−0.99 (0.19)	1.55 (0.25)[g]	0.91 (0.35)[g]	−0.25 (0.23)[g]
Mean	0.55 (0.27)	−0.73 (0.31)	1.38 (0.32)[g]	0.89 (0.27)[g]	−0.24 (0.16)[g]

[a] Mean from six experiments with the standard deviation in parentheses. [b] With 68 m*M* sodium phosphate and 87 m*M* sodium chloride, pH 6.2. [c] With 250 m*M* tromethamine, pH 8.4. [d] With 60 m*M* butyric acid in 68 m*M* sodium phosphate, and 87 m*M* sodium chloride, pH 6.2. [e] With 24 m*M* octanoic acid in 68 m*M* sodium phosphate and 87 m*M* sodium chloride, pH 6.2. [f] With 4 m*M* dodecanoic acid in 250 m*M* tromethamine, pH 8.4. [g] Significantly different from the control mean ($p < 0.02$).

propylpropionamide suggest that the absorption-enhancing effect of the additives was due to formation of a complex within a lipid barrier (17, 18). The explanation of complex formation was based on the relatively strong complex ($K_{1:1}$ = 12.5 liters/mole) that was formed in isopropyl myristate by the amides and prednisolone. However, dibutyl sulfoxide forms an even stronger complex ($K_{1:1}$ = 50 liters/mole[9]) with prednisolone in isopropyl myristate while hexanol (3) forms a very weak complex ($K_{1:1}$ = 4.2 liters/mole). The lack of correlation between the association constant for complexation in a lipid environment and the absorption-enhancing effect suggests that complexation may not be the explanation for enhanced prednisolone absorption.

Recent reports on membrane permeability indicate that diffusion across membranes is analogous to diffusion across a polymeric sheet rather than to diffusion within a simple liquid (19, 20). Also, the presence

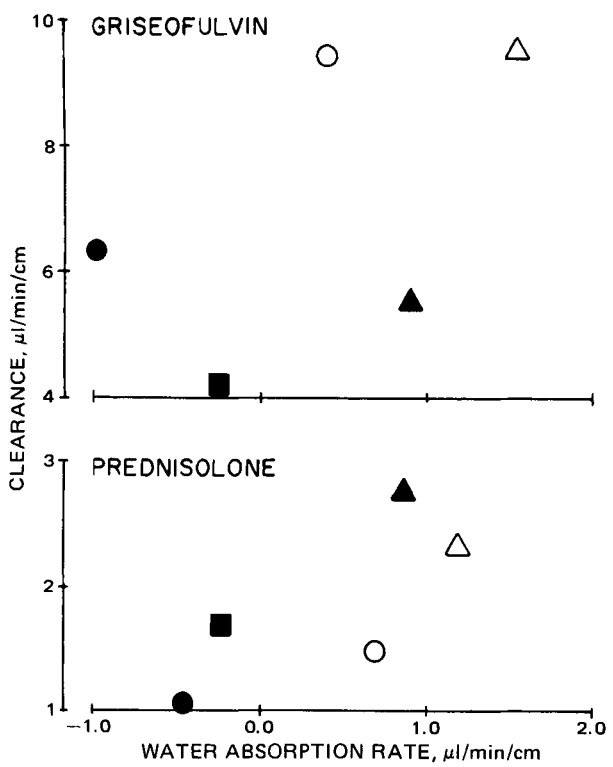

Figure 5—*Clearance of griseofulvin and prednisolone* versus *the water absorption rate. Key:* ○, *68 m*M *sodium phosphate and 87 m*M *sodium chloride, pH 6.2;* ●, *250 m*M *tromethamine, pH 8.4;* △, *60 m*M *butyric acid in 68 m*M *sodium phosphate and 87 m*M *sodium chloride, pH 6.2;* ▲, *24 m*M *octanoic acid in 68 m*M *sodium phosphate and 87 m*M *sodium chloride, pH 6.2; and* ■, *4 m*M *dodecanoic acid in 250 m*M *tromethamine, pH 8.4.*

[9] W. L. Hayton, unpublished data. The phase solubility diagram is curved; analysis of the diagram indicates that two complexes, SL and SL_2, form with association constants of 35 and 4 liters/mole, respectively, at 25°.

Table IV—Effects of Various Additives on the Absorption of Prednisolone and Water from the Perfused Jejunum

Additive[a]	*n*	Intestinal Clearance, % of Control	Water Absorption Rate[b]
Ethanol (3)	4	113	1.98 (0.24)
Butanol (3)	4	123	2.07 (0.71)
Butyric acid	6	154	1.20 (0.30)
Hexanol (3)	5	195	1.98 (0.36)
	4	195	2.26 (0.39)
Dipropylpropionamide (25)	4	171	1.54 (0.23)
Dibutyl sulfoxide[c]	5	170	2.70 (0.70)
Octanoic acid	6	185	0.87 (0.19)
Dodecanoic acid	6	158	−0.23 (0.08)

[a] Reference in parentheses; concentration was approximately 0.5%, except for dodecanoic acid which was 0.08%. [b] Microliters per minute per centimeter of intestine with the standard deviation in parentheses. [c] W. L. Hayton, unpublished data.

of low molecular weight compounds in a membrane, such as general anesthetics, results in an increase in membrane permeability (13). Plasticizers similarly increase the diffusion rate of permeant molecules across synthetic polymeric membranes. It was proposed that plasticizers reduce interchain bonding among polymer molecules, thereby increasing the mobility of permeant molecules within the membrane.

On the basis of differential scanning calorimetry experiments with dipalmitoyllecithin liposomes, it was proposed that compounds such as 1-alkanols, local anesthetics, phenothiazines, and general anesthetics may induce a phase transition in lipid bilayers. The proposed transition is from an organized gel to a randomized liquid crystalline phase (21). When lipophilic small molecules are present, membranes would become more fluid and thinner. It is reasonable to postulate that such changes would also increase membrane permeability. Such a mechanism was proposed to explain the ability of antidiuretic hormone to increase the permeability of the toad urinary bladder to a number of lipophilic solutes (22). Likewise, the effects of temperature on membrane permeability have been attributed in part to a phase transition (23, 24).

A plausible explanation of the effect of the fatty acids on prednisolone absorption is as follows. When the fatty acids are present in the intestinal epithelial cell membranes, they may cause an increase in membrane fluidity and thereby increase the diffusion rate of prednisolone across cell membranes. This explanation accounts for the parabolic relationship

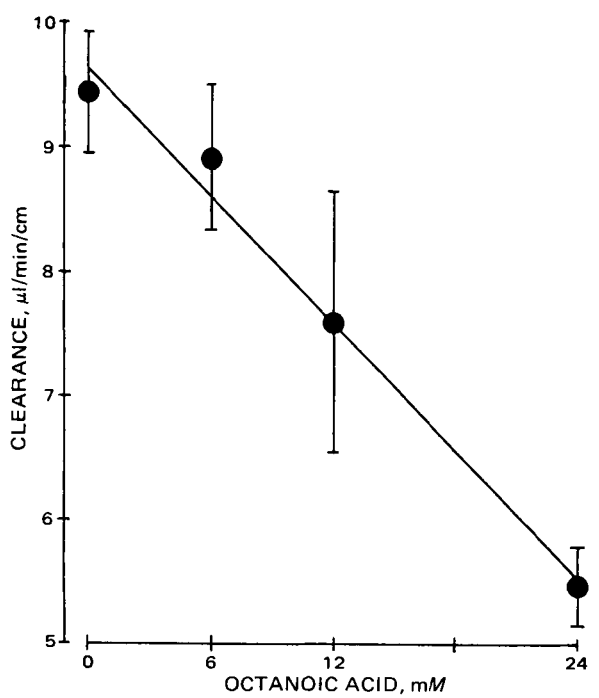

Figure 6—*Effect of various concentrations of octanoic acid on griseofulvin absorption from solutions recirculated through the* in situ *rat jejunum. Each point represents the mean from six experiments, and bars indicate ±1* SE.

between prednisolone clearance and additive concentration (3, 25). Increasing the additive concentration in the perfusate would drive the phase transition to completion, and further increases in the additive concentration would cause proportionately smaller increases in prednisolone clearance. In contrast, the relationship between griseofulvin clearance and additive concentration appears to be linear (Fig. 6), further suggesting that different barriers limit the absorption rate of griseofulvin and prednisolone.

If the effect of the additives listed in Table IV is due to increased membrane fluidity, it may be possible to determine whether the intestinal absorption of any particular compound is rate limited by the cell membranes of the intestinal epithelium. The additives would only increase the absorption rate of those substances whose absorption was membrane rate limited. The effects of one or more of the additives on the absorption of several drugs were observed (3, 17, 18). Prednisolone and closely related prednisone are unique in that they are the only drugs studied whose absorption rate was increased by the additives. Thus, the epithelial cell membrane may not be an important rate-limiting barrier to the absorption of many drugs. *In vitro* and *in situ* studies with rat intestine led to a similar conclusion (26).

In summary, the short and medium chain length fatty acids increase the intestinal absorption rate of prednisolone while they decrease the absorption rate of griseofulvin. The proposed explanation for these effects is that the absorption rate of griseofulvin is limited by the intestinal blood flow rate or an aqueous stagnant layer while the absorption of prednisolone is controlled by the intestinal epithelium. The absorption-altering effects of the fatty acids were attributed to their ability to reduce intestinal blood flow or to increase the thickness of the stagnant layer while simultaneously increasing the permeability of the intestinal epithelium.

REFERENCES

(1) J. A. Grisafe and W. L. Hayton, *J. Pharm. Sci.*, **67**, 895 (1978).

(2) K. Inui, M. Horiguchi, T. Kimura, S. Muranishi, and H. Sezaki, *Chem. Pharm. Bull.*, **22**, 1781 (1974).

(3) W. L. Hayton, *J. Pharm. Sci.*, **64**, 1450 (1975).

(4) R. Koysooko and G. Levy, *ibid.*, **63**, 829 (1974).

(5) J. H. Houston and G. Levy, *ibid.*, **64**, 607 (1975).

(6) K. Inui, M. Shintomi, R. Hori, and H. Sezaki, *Chem. Pharm. Bull.*, **24**, 2504 (1976).

(7) G. Levy and A. Peräla, *J. Pharm. Sci.*, **59**, 874 (1970).

(8) A. Marzo, P. Ghirardi, D. Sardini, and G. Meroni, *Clin. Chem.*, **17**, 145 (1971).

(9) F. Varga and T. Z. Csaky, *Pflugers Arch.*, **364**, 129 (1976).

(10) T. Z. Csaky and F. Varga, *Am. J. Physiol.*, **229**, 549 (1975).

(11) D. Winne, *J. Theor. Biol.*, **53**, 145 (1975).

(12) R. G. Stehle and W. I. Higuchi, *J. Pharm. Sci.*, **56**, 1367 (1967).

(13) N. Bindslev and E. M. Wright, *J. Membr. Biol.*, **29**, 265 (1976).

(14) A. B. R. Thomson and J. M. Dietschy, *J. Theor. Biol.*, **64**, 277 (1977).

(15) K. Green and T. Otori, *J. Physiol. (London)*, **207**, 93 (1970).

(16) B. Sandstrom, *Cytobiology*, **3**, 293 (1971).

(17) W. L. Hayton, G. Levy, and C. G. Regärdh, *J. Pharm. Sci.*, **61**, 473 (1972).

(18) W. L. Hayton and G. Levy, *ibid.*, **61**, 362 (1972).

(19) W. R. Lieb and W. D. Stein, *Nature*, **224**, 240 (1969).

(20) W. R. Lieb and W. D. Stein, *Nature New Biol.*, **234**, 220 (1971).

(21) M. K. Jain, N. Y.-M. Wu, and L. V. Wray, *Nature*, **255**, 494 (1975).

(22) R. J. Pietras and E. M. Wright, *ibid.*, **247**, 222 (1974).

(23) C. H. van Os, M. D. de Jong, and J. F. G. Slegers, *J. Membr. Biol.*, **15**, 363 (1974).

(24) M. E. Dockter and J. A. Magnuson, *Arch. Biochem. Biophys.*, **168**, 81 (1975).

(25) W. L. Hayton and G. Levy, *J. Pharm. Sci.*, **61**, 367 (1972).

(26) M. Gibaldi and B. Grundhofer, *Proc. Soc. Exp. Biol. Med.*, **141**, 564 (1972).

ACKNOWLEDGMENTS

Abstracted from a dissertation submitted by J. A. Grisafe to Washington State University in partial fulfillment of the Doctor of Philosophy degree requirements.

Supported in part by funds provided for biological and medical research by Washington State Initiative Measure No. 171.

J. A. Grisafe is an AFPE Charles J. Lynn Memorial Fellow.

Synthesis and Preliminary Anti-Inflammatory Evaluation of 17β-Amino-3β-methoxy-5-androstene Hydrochloride and Related Derivatives

STEPHEN C. GRIGGS and JOHN A. KING ˣ

Received May 24, 1976, from the *Department of Pharmacy, The Queen's University of Belfast, Belfast BT9 7BL, Northern Ireland.* Accepted for publication December 17, 1976. (Publication delayed at the request of the authors.)

Abstract □ To study the anti-inflammatory properties of 17β-aminosteroids, some 17β-aminoandrostene hydrochlorides based on the 3β-methoxy-5-androstene nucleus were prepared. The syntheses were accomplished *via* a two-stage amination of 3β-methoxy-5-androsten-17-one, involving reduction of an intermediate 17-imine or, for the synthesis of 17β-amino-3β-methoxy-5-androstene, the 17-oxime. The compounds were examined for anti-inflammatory activity in the rat cotton pellet model of inflammation. All tested aminosteroids displayed significant activity. Two compounds also were screened in an adjuvant-induced arthritis model of inflammation and displayed activity.

Keyphrases □ 17β-Aminoandrostenes, substituted—synthesized, evaluated for anti-inflammatory activity in rats □ Anti-inflammatory activity—various substituted 17β-aminoandrostenes evaluated in rats □ Structure–activity relationships—various substituted 17β-aminoandrostenes evaluated for anti-inflammatory activity in rats

Over the past two decades, considerable interest has developed in the synthesis and biological evaluation of aminosteroids (1). The compounds produced have various biological properties including antimicrobial, hypocholesterolemic, hypotensive, and local anesthetic.

Anti-inflammatory activity was established for a series of 16β-amino-17α-hydroxy-20-ketopregnenes using the cotton pellet and foot edema models of inflammation (2). The activity associated with these aminosteroids was not influenced markedly by structural alterations that normally enhance the anti-inflammatory activity of corticosteroids.

0022-3549/78/0900-1215$01.00/0

© 1978, American Pharmaceutical Association

between prednisolone clearance and additive concentration (3, 25). Increasing the additive concentration in the perfusate would drive the phase transition to completion, and further increases in the additive concentration would cause proportionately smaller increases in prednisolone clearance. In contrast, the relationship between griseofulvin clearance and additive concentration appears to be linear (Fig. 6), further suggesting that different barriers limit the absorption rate of griseofulvin and prednisolone.

If the effect of the additives listed in Table IV is due to increased membrane fluidity, it may be possible to determine whether the intestinal absorption of any particular compound is rate limited by the cell membranes of the intestinal epithelium. The additives would only increase the absorption rate of those substances whose absorption was membrane rate limited. The effects of one or more of the additives on the absorption of several drugs were observed (3, 17, 18). Prednisolone and closely related prednisone are unique in that they are the only drugs studied whose absorption rate was increased by the additives. Thus, the epithelial cell membrane may not be an important rate-limiting barrier to the absorption of many drugs. *In vitro* and *in situ* studies with rat intestine led to a similar conclusion (26).

In summary, the short and medium chain length fatty acids increase the intestinal absorption rate of prednisolone while they decrease the absorption rate of griseofulvin. The proposed explanation for these effects is that the absorption rate of griseofulvin is limited by the intestinal blood flow rate or an aqueous stagnant layer while the absorption of prednisolone is controlled by the intestinal epithelium. The absorption-altering effects of the fatty acids were attributed to their ability to reduce intestinal blood flow or to increase the thickness of the stagnant layer while simultaneously increasing the permeability of the intestinal epithelium.

REFERENCES

(1) J. A. Grisafe and W. L. Hayton, *J. Pharm. Sci.*, **67**, 895 (1978).

(2) K. Inui, M. Horiguchi, T. Kimura, S. Muranishi, and H. Sezaki, *Chem. Pharm. Bull.*, **22**, 1781 (1974).

(3) W. L. Hayton, *J. Pharm. Sci.*, **64**, 1450 (1975).

(4) R. Koysooko and G. Levy, *ibid.*, **63**, 829 (1974).

(5) J. H. Houston and G. Levy, *ibid.*, **64**, 607 (1975).

(6) K. Inui, M. Shintomi, R. Hori, and H. Sezaki, *Chem. Pharm. Bull.*, **24**, 2504 (1976).

(7) G. Levy and A. Peräla, *J. Pharm. Sci.*, **59**, 874 (1970).

(8) A. Marzo, P. Ghirardi, D. Sardini, and G. Meroni, *Clin. Chem.*, **17**, 145 (1971).

(9) F. Varga and T. Z. Csaky, *Pflugers Arch.*, **364**, 129 (1976).

(10) T. Z. Csaky and F. Varga, *Am. J. Physiol.*, **229**, 549 (1975).

(11) D. Winne, *J. Theor. Biol.*, **53**, 145 (1975).

(12) R. G. Stehle and W. I. Higuchi, *J. Pharm. Sci.*, **56**, 1367 (1967).

(13) N. Bindslev and E. M. Wright, *J. Membr. Biol.*, **29**, 265 (1976).

(14) A. B. R. Thomson and J. M. Dietschy, *J. Theor. Biol.*, **64**, 277 (1977).

(15) K. Green and T. Otori, *J. Physiol. (London)*, **207**, 93 (1970).

(16) B. Sandstrom, *Cytobiology*, **3**, 293 (1971).

(17) W. L. Hayton, G. Levy, and C. G. Regärdh, *J. Pharm. Sci.*, **61**, 473 (1972).

(18) W. L. Hayton and G. Levy, *ibid.*, **61**, 362 (1972).

(19) W. R. Lieb and W. D. Stein, *Nature*, **224**, 240 (1969).

(20) W. R. Lieb and W. D. Stein, *Nature New Biol.*, **234**, 220 (1971).

(21) M. K. Jain, N. Y.-M. Wu, and L. V. Wray, *Nature*, **255**, 494 (1975).

(22) R. J. Pietras and E. M. Wright, *ibid.*, **247**, 222 (1974).

(23) C. H. van Os, M. D. de Jong, and J. F. G. Slegers, *J. Membr. Biol.*, **15**, 363 (1974).

(24) M. E. Dockter and J. A. Magnuson, *Arch. Biochem. Biophys.*, **168**, 81 (1975).

(25) W. L. Hayton and G. Levy, *J. Pharm. Sci.*, **61**, 367 (1972).

(26) M. Gibaldi and B. Grundhofer, *Proc. Soc. Exp. Biol. Med.*, **141**, 564 (1972).

ACKNOWLEDGMENTS

Abstracted from a dissertation submitted by J. A. Grisafe to Washington State University in partial fulfillment of the Doctor of Philosophy degree requirements.

Supported in part by funds provided for biological and medical research by Washington State Initiative Measure No. 171.

J. A. Grisafe is an AFPE Charles J. Lynn Memorial Fellow.

Synthesis and Preliminary Anti-Inflammatory Evaluation of 17β-Amino-3β-methoxy-5-androstene Hydrochloride and Related Derivatives

STEPHEN C. GRIGGS and JOHN A. KING ˣ

Received May 24, 1976, from the *Department of Pharmacy, The Queen's University of Belfast, Belfast BT9 7BL, Northern Ireland.* Accepted for publication December 17, 1976. (Publication delayed at the request of the authors.)

Abstract □ To study the anti-inflammatory properties of 17β-aminosteroids, some 17β-aminoandrostene hydrochlorides based on the 3β-methoxy-5-androstene nucleus were prepared. The syntheses were accomplished *via* a two-stage amination of 3β-methoxy-5-androsten-17-one, involving reduction of an intermediate 17-imine or, for the synthesis of 17β-amino-3β-methoxy-5-androstene, the 17-oxime. The compounds were examined for anti-inflammatory activity in the rat cotton pellet model of inflammation. All tested aminosteroids displayed significant activity. Two compounds also were screened in an adjuvant-induced arthritis model of inflammation and displayed activity.

Keyphrases □ 17β-Aminoandrostenes, substituted—synthesized, evaluated for anti-inflammatory activity in rats □ Anti-inflammatory activity—various substituted 17β-aminoandrostenes evaluated in rats □ Structure–activity relationships—various substituted 17β-aminoandrostenes evaluated for anti-inflammatory activity in rats

Over the past two decades, considerable interest has developed in the synthesis and biological evaluation of aminosteroids (1). The compounds produced have various biological properties including antimicrobial, hypocholesterolemic, hypotensive, and local anesthetic.

Anti-inflammatory activity was established for a series of 16β-amino-17α-hydroxy-20-ketopregnenes using the cotton pellet and foot edema models of inflammation (2). The activity associated with these aminosteroids was not influenced markedly by structural alterations that normally enhance the anti-inflammatory activity of corticosteroids.

0022-3549/78/0900-1215$01.00/0

© 1978, American Pharmaceutical Association

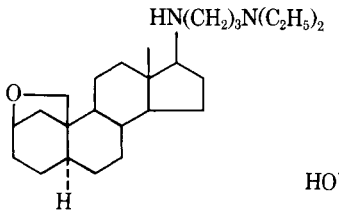

Ia

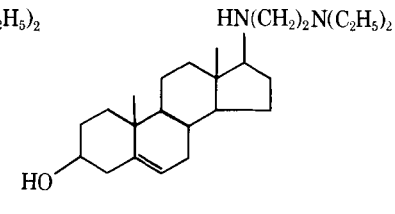

Ib

Filderman and Kovacs (3) studied the anti-inflammatory properties of the azasteroidal glycoside tomatine and noted activity in several inflammation models, including the mouse peritoneal capillary permeability test, a model in which corticosteroids are ineffective. Tomatidine, the aglycone of tomatine, did not exhibit significant anti-inflammatory activity in any of the experimental models.

Several series of aminosteroids, based on various androstane nuclei of differing A- and B-ring functionalities, recently were reported to show anti-inflammatory activity in both intact (4–6) and adrenalectomized rats (7). The compounds, examples of which include 17β-[*N*-(2-diethylaminopropyl)amino]-5α-androstan-2β,19-epoxide (I*a*) and 17β-[*N*-(2-diethylaminoethyl)amino]-3β-hydroxy-5-androstene (I*b*), are characterized by the possession of a 17β-amine function.

The present study investigated the anti-inflammatory activity of androstenes possessing a 17β-amine function, including examination for corticosteroid-like activity. This report describes the synthesis and preliminary anti-inflammatory evaluation of a series of 17β-aminoandrostenes based on the 3β-methoxy-5-androstene nucleus.

DISCUSSION

Synthesis—3β-Methoxy-5-androsten-17-one[1] (II) was utilized as the starting material for the synthesis of the title compounds. Acid-catalyzed condensation of this steroid (II) with the appropriate amines following an established procedure (8) yielded the corresponding 17-iminosteroids (III*a*–III*e*), which were smoothly reduced to the desired 17β-aminosteroids (IV*a*–IV*e*) with lithium aluminum hydride in dioxane (Scheme I). The reduction of 17-iminosteroids with lithium aluminum hydride previously was reported to proceed to the 17β-amino epimer (8).

The intermediate 17-iminosteroids (III*a*–III*e*) were oils or oily solids for which satisfactory elemental analyses could not be obtained. The IR spectra of these compounds were consistent with the assigned structures. In each case, reduction to the desired aminosteroid and hydrochloride formation gave a crystalline product (IV*a*–IV*e*·HCl) whose structure was confirmed by spectral data and elemental microanalyses.

The 17β-aminosteroids IV*a*–IV*e*·HCl (Scheme I) were further characterized by mass spectrometry. The mass spectrum of each compound showed a weak ion signal with an *m/e* value corresponding to the free amine and a strong base peak at *m/e* 316 corresponding to Fragment A, resulting from fission of the amine side chain alpha to the C-17 nitrogen atom (9).

17β-Amino-3β-methoxy-5-androstene hydrochloride (VI·HCl) was

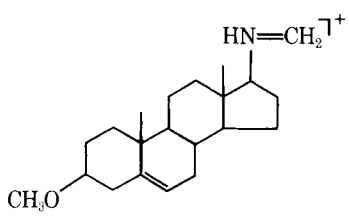

Fragment A

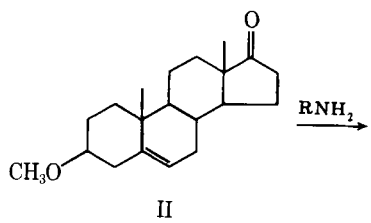

II

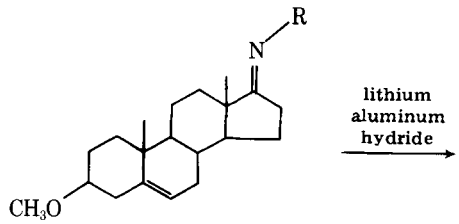

III*a*: R = $CH_2CH_2NH_2$, · 2HCl
III*b*: R = CH_2CH_2OH, · HCl
III*c*: R = $CH_2CH_2OCH_3$, · HCl
III*d*: R = $CH_2CH_2CH_3$, · HCl
III*e*: R = $CH_2CH(CH_3)OH$, · HCl

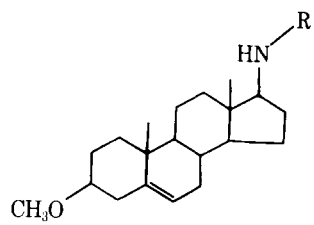

IV*a*–IV*e*

Scheme I

prepared by reduction of oxime V, which was synthesized from II by an established route (10) (Scheme II). Reduction of V with lithium aluminum hydride in dioxane proved unsuitable for the synthesis of the 17β-amine VI, the reaction giving a low yield of the desired compound with, in all cases, several other basic products[2]. Sodium in ethanol reduction of V according to an established procedure (11) and subsequent hydrochloride formation gave a satisfactory yield of the desired VI·HCl.

Biological—The title compounds were examined for anti-inflammatory activity in the rat cotton pellet model of inflammation (12). Male albino rats[3], 100–120 g, were used. Sterilized cotton-wool pellets of known weight (10 mg) were implanted subcutaneously in groups of five rats under ether anesthesia. Four pellets were placed in each animal, one in each groin and one in each axilla. The test compound, as a solution in 5% (w/v) gum acacia, was administered orally to each animal in the group

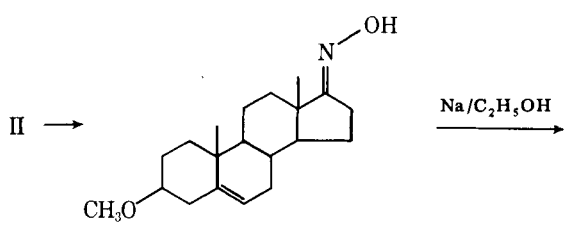

V

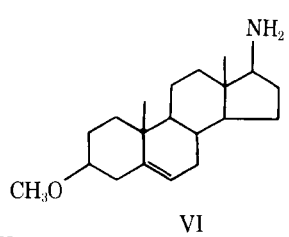

VI

Scheme II

[1] Compound II, mp 142° [lit. (13) mp 142°], was prepared from 3β-hydroxy-5-androsten-17-one 3-tosylate according to the method of Heyl *et al.* (14). Satisfactory analytical data were obtained for all samples prepared.

[2] S. C. Griggs and J. King, to be published.

[3] Wistar strain.

Table I—Anti-Inflammatory Studies: Rat Cotton Pellet Model of Inflammation

Compound[a]	Mean Weight of Granulation Tissue Produced per Pellet, mg ± *SEM*	Mean Inhibition of Granulation Tissue Formation, %
Controls		
Gum acacia (5% w/v)	27.00 ± 4.48	0
Prednisolone	13.35 ± 2.27	50.6
IV*a*·2HCl	13.7 ± 1.6	49.3
IV*b*·HCl	11.65 ± 1.05	57.0
IV*c*·HCl	11.7 ± 2.63	57.0
IV*d*·HCl	14.1 ± 1.74	47.8
IV*e*·HCl	14.7 ± 1.47	45.6
VI·HCl	12.65 ± 2.91	53.2

[a] The dose was 1.0 mg/kg in all cases.

on 4 consecutive days, the first dose being given immediately after implantation of the pellets.

On the 5th day, the rats were killed with chloroform; the pellets were dissected, all fat and extraneous tissue were removed, and the pellets were dried overnight in a hot air oven at 60°. Two groups of control rats received oral doses of either 5% (w/v) gum acacia or prednisolone [suspended in 5% (w/v) gum acacia]. The weight of granulation tissue produced in each pellet was calculated, and the mean value for each group was compared with that of the controls (Table I).

Compounds IV*a*·2HCl and IV*b*·HCl were further assessed for their ability to prevent developing adjuvant arthritis in the rat[4]. Groups of four male inbred rats[5], 120–150 g, were injected with heat-killed *Mycobacterium tuberculosis*[6] (300 μg) suspended in liquid paraffin (0.5 ml). Injections were given intradermally to the plantar aspect of one hindpaw. The volume of each hindpaw (up to the calcaneum and astragalas bones) was measured by displacement of mercury using a plethysmograph coupled to an air-type blood pressure transducer.

The test compound, as a solution in aqueous 0.25% (w/v) hydroxyethylcellulose[7], was administered orally twice daily, at a dose and volume of 1.0 ml/100 g, to each animal in the group for the duration of the experiment. Normal animals without arthritis and arthritic animals, each dosed with hydroxyethylcellulose alone, were included as control groups. A positive control group received indomethacin. The arthritis was allowed to develop for 18 days, and the paw volumes were remeasured. The changes in paw volumes during the experiment were calculated and summed for each group.

The percentage inhibition of developing adjuvant-induced arthritis (Table II) was calculated from:

$$\text{percentage inhibition} = \frac{\Delta V_a - \Delta V_t}{\Delta V_a - \Delta V_c} \times 100 \qquad \text{(Eq. 1)}$$

where ΔV_a is the increase in combined paw volume of arthritic control animals, ΔV_t is the increase in combined paw volume of arthritic animals dosed with the test compound, and ΔV_c is the increase in paw volume of nonarthritic control animals.

All aminosteroids tested displayed at least significant antigranuloma activity ($p > 0.02$) in the rat cotton pellet model. Prednisolone, at the same dose level as the test compounds, produced a similar inhibition of granuloma formation (Table I). Compounds IV*a*·2HCl and IV*b*·HCl were further screened in an adjuvant-induced arthritis model of inflammation. Both compounds displayed anti-inflammatory activity (Table II).

The results clearly establish the 3β-methoxy-5-androstene nucleus as a suitable basis for the synthesis of 17β-aminosteroids with anti-inflammatory activity.

The activity displayed by the compounds tested, including the aminosteroids IV*b*–IV*e*·HCl, each of which possesses a 17β-alkylamine substituent hitherto unassociated with anti-inflammatory activity, and also the primary amine VI·HCl, suggests that the nature of the 17β-alkylamine substituent may be relatively unimportant in determining this biological activity in the 17β-aminosteroids. Quantitative studies may illustrate more clearly the effect of the structure of the 17β-alkylamine substituent on the level of anti-inflammatory activity.

[4] Performed by Allen and Hanburys Ltd.

[5] PVG strain.

[6] Human strains C, DT, PN (Ministry of Agriculture and Fisheries, Weybridge, England).

[7] Natrosol.

Table II—Anti-Inflammatory Studies: Adjuvant-Induced Arthritis Model of Inflammation

Compound	Percentage Reduction in Paw Volume[a]	
	Activity of Test Compound[b]	Activity of Indomethacin[c]
IV*a*·2HCl	70	45
IV*b*·HCl	61	57

[a] Mean of two experiments. [b] The dose was 25 mg/kg po. [c] The dose was 1.0 mg/kg po.

EXPERIMENTAL[8]

The general procedure for the synthesis of the hydrochlorides of aminosteroids IV*a*–IV*e* is shown in Scheme I. A solution of II (5 g, 0.016 mole), the appropriate amine (15 ml), and *p*-toluenesulfonic acid monohydrate (0.2 g) in benzene (200 ml) was refluxed in a Dean–Stark separator until water removal was complete (~6 hr). Solvent removal under reduced pressure gave a viscous oil (~5 g). TLC[9] of the oil indicated the presence of one major component with an R_f value different from that of the starting material.

A solution of the oil in methylene dichloride–methanol (9:1) was chromatographed on silica gel[9] (200 g). Elution with the same solvent gave a pure (as evidenced by TLC) sample of the desired iminosteroid (III*a*–III*e*) as an oil. The IR spectrum of the oil showed major bands at 1675 (C=N) and 1105 (CO) cm^{-1}. A solution of the iminosteroid (4 g, 0.0125 mole) in dry dioxane (50 ml) was slowly added to a stirred slurry of lithium aluminum hydride (2 g) in dioxane (50 ml), and the reaction mixture was stirred at reflux temperature for 48 hr. After this period, aqueous dioxane (50 ml, 50% v/v) was added, and the reaction was left for a further 2 hr. The reaction mixture was then filtered, and the solvent was removed under reduced presure to give an oil. Hydrogen chloride gas was then passed through a solution of the oil in dry ether, and the resultant precipitate was filtered and dried to give IV*a*–IV*e*.

17β-[*N*-(2-Aminoethyl)amino]-3β-methoxy-5-androstene Dihydrochloride (IV*a*·2HCl)—The yield was 2.2 g (31%); recrystallized from ethanol–ether; mp >350° (dec.); $[\alpha]_D^{25}$ −42.1°; IR: 3000–2700 (N^+H_2 stretch, CH), 1600 (N^+H_2 def.), 1105, and 1030 (CO stretch) cm^{-1}; mass spectrum: *m/e* 346 (5), 316 (100), and 30 (100).

Anal.—Calc. for $C_{22}H_{38}N_2O{\cdot}2HCl$: C, 62.98; H, 9.61; N, 6.67. Found: C, 62.74; H, 9.81; N, 6.56.

17β-[*N*-(2-Hydroxyethyl)amino]-3β-methoxy-5-androstene Hydrochloride (IV*b*·HCl)—The yield was 2.4 g (36%); recrystallization from ethanol–ether; mp 265–267° (dec.); $[\alpha]_D^{25}$ −12.1°; IR: 3550 (OH), 3000–2700 (N^+H_2 stretch, CH), 1600 (N^+H_2 def.), 1105, and 1030 (CO stretch) cm^{-1}; mass spectrum: *m/e* 347 (12) and 316 (100).

Anal.—Calc. for $C_{22}H_{37}NO_2{\cdot}HCl$: C, 68.81; H, 9.94; N, 3.64. Found: C, 68.52; H, 10.01; N, 3.51.

17β-[*N*-(2-Methoxyethyl)amino]-3β-methoxy-5-androstene Hydrochloride (IV*c*·HCl)—The yield was 2.6 g (40%); recrystallized from ethanol; mp 300° (dec.); $[\alpha]_D^{25}$ −15.6°; IR: 3000–2700 (N^+H_2 stretch, CH), 1600 (N^+H_2 def.), 1105, and 1030 (CO stretch) cm^{-1}; mass spectrum: *m/e* 361 (3) and 316 (100).

Anal.—Calc. for $C_{23}H_{39}NO_2{\cdot}HCl$: C, 69.40; H, 10.13; N, 3.51. Found: C, 69.12; H, 10.23; N, 3.46.

17β-(*N*-Propylamino)-3β-methoxy-5-androstene Hydrochloride (IV*d*·HCl)—The yield was 2.5 g (40%); recrystallized from ethanol; mp 330° (dec.); $[\alpha]_D^{25}$ −28.09°; IR: 3000–2700 (N^+H_2 stretch, CH), 1600 (N^+H_2 def.), 1105, and 1030 (CO stretch) cm^{-1}; mass spectrum: *m/e* 345 (10), 330 (10), and 316 (100).

Anal.—Calc. for $C_{23}H_{39}NO{\cdot}HCl$: C, 72.30; H, 10.55; N, 3.67. Found: C, 72.15; H, 10.54; N, 3.61.

17β-[*N*-(2-Hydroxypropyl)amino]-3β-methoxy-5-androstene Hydrochloride (IV*e*·HCl)—The yield was 2.4 g (37%); recrystallized

[8] All melting points were obtained using an electrothermal capillary melting-point apparatus and are uncorrected. Elemental analyses were performed by the Microanalytical Laboratories, Chemistry Department, The Queen's University of Belfast. Optical rotations were obtained using a Bellingham and Stanley polarimeter and, unless otherwise stated, refer to 2% (w/v) solutions in methanol. IR spectra were recorded using a Perkin-Elmer 257 grating spectrophotometer and, unless indicated otherwise, refer to pressed potassium bromide disks. Mass spectra were obtained using an AEI MS902 spectrometer operating at 70 ev. The PMR spectrum was obtained using a Varian A-60D spectrometer with chloroform-*d* as the solvent and tetramethylsilane as the internal reference.

[9] TLC was performed using 0.08-cm (0.03-in.) layers of Kieselgel G (Type 60) (E. Merck, Darmstadt, West Germany). Methanol (5% v/v) in methylene dichloride was used as the developing solvent. Column chromatography was performed using silica gel M.F.C., 100–200 mesh (Hopkins and Williams, Essex, England).

from ethanol; mp 285–287° (dec.); IR: 3550 (OH), 3000–2700 (N^+H_2 stretch, CH), 1600 (N^+H_2 def.), 1105, and 1030 (CO stretch) cm^{-1}; mass spectrum: *m/e* 361 (4) and 316 (100).

Anal.—Calc. for $C_{23}H_{39}NO_2$·HCl: C, 69.40; H, 10.13; N, 3.51. Found: C, 69.31; H, 9.97; N, 3.61.

3β-Methoxy-5-androsten-17-one 17-Oxime (V)—A solution of II (5 g, 0.016 mole), sodium acetate (9 g), and hydroxylamine hydrochloride (3 g) in 5% (v/v) aqueous ethanol (80 ml) was refluxed for 4 hr. After sitting at room temperature overnight, the crystalline precipitate was collected and washed with water, giving 4 g (78%) of V. Recrystallization from methanol gave the analytical sample, mp 218–219°; $[\alpha]_D^{25}$ +11.6°; IR: 3500 (OH), 1660 (C=N), 1105, and 1030 (CO stretch) cm^{-1}; PMR ($CDCl_3$): δ 0.92 (s, 3H, C-13 methyl), 1.03 (s, 3H, C-10 methyl), 3.36 (s, 3H, C-3 methoxyl), and 5.35 (broad, 1H, C-6 proton) ppm.

Anal.—Calc. for $C_{20}H_{31}NO_2$: C, 75.66; H, 9.84; N, 4.42. Found: C, 75.69; H, 9.97; N, 4.51.

17β-Amino-3β-methoxy-5-androstene Hydrochloride (VI·HCl)—Sodium (12 g, freshly cut) was added (during 1 hr) in small increments to a refluxing soluton of V (2 g, 0.006 mole) in absolute ethanol (100 ml). After sodium addition, the reaction was stirred at the reflux temperature for 2 hr. The hot mixture was then diluted with warm (60°) water (1 liter) and allowed to stand at room temperature for 24 hr. The resultant solid was dissolved in dry ether, and hydrogen chloride gas was passed through the ethereal solution to give 1.2 g (45%) of VI·HCl. Recrystallizations from ethanol gave the analytical sample, mp 294–296° (dec.); $[\alpha]_D^{25}$ −19.1°; IR: 3200–2800 (N^+H_3 stretch, CH), 1610 (asym. N^+H_3 def.), 1515 (sym. N^+H_3 def.), 1105, and 1030 (CO stretch) cm^{-1}; mass spectrum: *m/e* calc. for $C_{20}H_{33}NO$ (M^+ − HCl): 303.2562. Found: *m/e* 303.2562.

Anal.—Calc. for $C_{20}H_{33}NO$·HCl·C_2H_5OH: C, 68.44; H, 10.44; N, 3.63. Found: C, 68.24; H, 10.40; N, 3.69.

REFERENCES

(1) W. R. Buckett, in "Advances in Steroid Biochemistry and Pharmacology," vol. 3, M. H. Briggs and G. A. Christie, Eds., Academic, London, England, 1972, p. 39.

(2) C. G. Bergstrom, *J. Med. Chem.*, **11**, 875 (1968).

(3) R. B. Filderman and B. A. Kovacs, *Br. J. Pharmacol.*, **37**, 748 (1969).

(4) Y. Nagai, *Chem. Pharm. Bull.*, **17**, 1749 (1969).

(5) P. D. Klimstra, U.S. pat. 3,627,756 (1971).

(6) P. D. Klimstra, U.S. pat. 3,639,598 (1972).

(7) P. D. Klimstra, U.S. pat. 3,636,014 (1972).

(8) R. E. Counsell, P. D. Klimstra, and R. E. Ranney, *J. Med. Chem.*, **5**, 1224 (1962).

(9) H. Budzikiewicz, C. Djerassi, and D. H. Williams, in "Interpretation of Mass Spectra of Organic Compounds," Holden-Day, San Francisco, Calif., 1965, p. 65.

(10) B. M. Regan and F. N. Hayes, *J. Am. Chem. Soc.*, **78**, 639 (1956).

(11) G. R. Pettit, R. L. Smith, A. K. Das Dupta, and J. L. Occolowitz, *Can. J. Chem.*, **45**, 501 (1967).

(12) P. F. D'Arcy, E. M. Howard, P. W. Muggleton, and S. B. Townsend, *J. Pharm. Pharmacol.*, **12**, 659 (1960).

(13) "Dictionary of Organic Compounds," vol. 3, I. Heilbron, A. H. Cook, H. Bunbury, and D. H. Hey, Eds., Eyre and Spottiswoode, London, England, 1965, p. 1642.

(14) F. W. Heyl, M. E. Herr, and A. P. Centolella, *J. Am. Chem. Soc.*, **71**, 247 (1949).

ACKNOWLEDGMENTS

The authors thank Professor and Mrs. P. F. D'Arcy for their valuable assistance with the animal experimentation and Mr. M. Jordan for assistance with the chemical syntheses. Gifts of steroid starting material from Allen and Hanburys Ltd. are also gratefully acknowledged. S. C. Griggs acknowledges the receipt of a Science Research Council postgraduate studentship.

Steady-State Urinary Excretion Method for Determining Bioequivalence of Conjugated Estrogen Products

R. N. JOHNSON ˣ, R. P. MASSERANO, B. T. KHO, and W. P. ADAMS

Received June 18, 1976, from the *Analytical Research and Development Laboratory and the Pharmacy Research and Development Laboratory, Ayerst Laboratories, Inc., Rouses Point, NY 12979.* Accepted for publication December 20, 1977.

Abstract □ The steady-state excretion of conjugated estrogens in the urine of postmenopausal women dosed with conjugated estrogens tablets was studied using a modification of a previously published method. The procedure was used to quantitate the estrogens both before and during conjugated estrogens replacement therapy. The method, which is relatively specific, involves enzyme hydrolysis of urine samples, a number of classical extraction and purification steps, and analysis of the silylated estrogens on a 2.7-m, 1.7% diethylene glycol succinate column using flame-ionization detection. The results indicate that steady-state urinary estrogen excretion levels were obtained within 17 days of dosing. Furthermore, the urinary estrogen excretion profile was significantly different from the composition of the estrogens in the dosage form.

Keyphrases □ Estrogens, conjugated—GLC analyses, steady-state urinary excretion in postmenopausal women □ Excretion, urinary—conjugated estrogens at steady state in postmenopausal women □ GLC—analyses, conjugated estrogens in urine of postmenopausal women

Conjugated estrogen mixtures have been used therapeutically since 1942. However, there is no detailed information concerning the human plasma or urinary levels of these estrogens after administration, primarily because of the lack of sufficiently sensitive and specific analytical methods.

BACKGROUND

Many recent reports focused on the analysis of estriol and other estrogens in pregnancy urine to follow or monitor fetal health (1–5). The urinary estrogen excretion levels in nonpregnant women (6, 7), in postmenopausal women (8–11), and in men (12, 13) were studied. Other investigators studied the types of conjugation of steroids and separated

0022-3549/78/0900-1218$01.00/0

© 1978, American Pharmaceutical Association

from ethanol; mp 285–287° (dec.); IR: 3550 (OH), 3000–2700 (N^+H_2 stretch, CH), 1600 (N^+H_2 def.), 1105, and 1030 (CO stretch) cm^{-1}; mass spectrum: *m/e* 361 (4) and 316 (100).

Anal.—Calc. for $C_{23}H_{39}NO_2$·HCl: C, 69.40; H, 10.13; N, 3.51. Found: C, 69.31; H, 9.97; N, 3.61.

3β-Methoxy-5-androsten-17-one 17-Oxime (V)—A solution of II (5 g, 0.016 mole), sodium acetate (9 g), and hydroxylamine hydrochloride (3 g) in 5% (v/v) aqueous ethanol (80 ml) was refluxed for 4 hr. After sitting at room temperature overnight, the crystalline precipitate was collected and washed with water, giving 4 g (78%) of V. Recrystallization from methanol gave the analytical sample, mp 218–219°; $[\alpha]_D^{25}$ +11.6°; IR: 3500 (OH), 1660 (C=N), 1105, and 1030 (CO stretch) cm^{-1}; PMR ($CDCl_3$): δ 0.92 (s, 3H, C-13 methyl), 1.03 (s, 3H, C-10 methyl), 3.36 (s, 3H, C-3 methoxyl), and 5.35 (broad, 1H, C-6 proton) ppm.

Anal.—Calc. for $C_{20}H_{31}NO_2$: C, 75.66; H, 9.84; N, 4.42. Found: C, 75.69; H, 9.97; N, 4.51.

17β-Amino-3β-methoxy-5-androstene Hydrochloride (VI·HCl)—Sodium (12 g, freshly cut) was added (during 1 hr) in small increments to a refluxing soluton of V (2 g, 0.006 mole) in absolute ethanol (100 ml). After sodium addition, the reaction was stirred at the reflux temperature for 2 hr. The hot mixture was then diluted with warm (60°) water (1 liter) and allowed to stand at room temperature for 24 hr. The resultant solid was dissolved in dry ether, and hydrogen chloride gas was passed through the ethereal solution to give 1.2 g (45%) of VI·HCl. Recrystallizations from ethanol gave the analytical sample, mp 294–296° (dec.); $[\alpha]_D^{25}$ −19.1°; IR: 3200–2800 (N^+H_3 stretch, CH), 1610 (asym. N^+H_3 def.), 1515 (sym. N^+H_3 def.), 1105, and 1030 (CO stretch) cm^{-1}; mass spectrum: *m/e* calc. for $C_{20}H_{33}NO$ (M^+ − HCl): 303.2562. Found: *m/e* 303.2562.

Anal.—Calc. for $C_{20}H_{33}NO$·HCl·C_2H_5OH: C, 68.44; H, 10.44; N, 3.63. Found: C, 68.24; H, 10.40; N, 3.69.

REFERENCES

(1) W. R. Buckett, in "Advances in Steroid Biochemistry and Pharmacology," vol. 3, M. H. Briggs and G. A. Christie, Eds., Academic, London, England, 1972, p. 39.

(2) C. G. Bergstrom, *J. Med. Chem.*, **11**, 875 (1968).

(3) R. B. Filderman and B. A. Kovacs, *Br. J. Pharmacol.*, **37**, 748 (1969).

(4) Y. Nagai, *Chem. Pharm. Bull.*, **17**, 1749 (1969).

(5) P. D. Klimstra, U.S. pat. 3,627,756 (1971).

(6) P. D. Klimstra, U.S. pat. 3,639,598 (1972).

(7) P. D. Klimstra, U.S. pat. 3,636,014 (1972).

(8) R. E. Counsell, P. D. Klimstra, and R. E. Ranney, *J. Med. Chem.*, **5**, 1224 (1962).

(9) H. Budzikiewicz, C. Djerassi, and D. H. Williams, in "Interpretation of Mass Spectra of Organic Compounds," Holden-Day, San Francisco, Calif., 1965, p. 65.

(10) B. M. Regan and F. N. Hayes, *J. Am. Chem. Soc.*, **78**, 639 (1956).

(11) G. R. Pettit, R. L. Smith, A. K. Das Dupta, and J. L. Occolowitz, *Can. J. Chem.*, **45**, 501 (1967).

(12) P. F. D'Arcy, E. M. Howard, P. W. Muggleton, and S. B. Townsend, *J. Pharm. Pharmacol.*, **12**, 659 (1960).

(13) "Dictionary of Organic Compounds," vol. 3, I. Heilbron, A. H. Cook, H. Bunbury, and D. H. Hey, Eds., Eyre and Spottiswoode, London, England, 1965, p. 1642.

(14) F. W. Heyl, M. E. Herr, and A. P. Centolella, *J. Am. Chem. Soc.*, **71**, 247 (1949).

ACKNOWLEDGMENTS

The authors thank Professor and Mrs. P. F. D'Arcy for their valuable assistance with the animal experimentation and Mr. M. Jordan for assistance with the chemical syntheses. Gifts of steroid starting material from Allen and Hanburys Ltd. are also gratefully acknowledged. S. C. Griggs acknowledges the receipt of a Science Research Council postgraduate studentship.

Steady-State Urinary Excretion Method for Determining Bioequivalence of Conjugated Estrogen Products

R. N. JOHNSON ˣ, R. P. MASSERANO, B. T. KHO, and W. P. ADAMS

Received June 18, 1976, from the *Analytical Research and Development Laboratory and the Pharmacy Research and Development Laboratory, Ayerst Laboratories, Inc., Rouses Point, NY 12979.* Accepted for publication December 20, 1977.

Abstract □ The steady-state excretion of conjugated estrogens in the urine of postmenopausal women dosed with conjugated estrogens tablets was studied using a modification of a previously published method. The procedure was used to quantitate the estrogens both before and during conjugated estrogens replacement therapy. The method, which is relatively specific, involves enzyme hydrolysis of urine samples, a number of classical extraction and purification steps, and analysis of the silylated estrogens on a 2.7-m, 1.7% diethylene glycol succinate column using flame-ionization detection. The results indicate that steady-state urinary estrogen excretion levels were obtained within 17 days of dosing. Furthermore, the urinary estrogen excretion profile was significantly different from the composition of the estrogens in the dosage form.

Keyphrases □ Estrogens, conjugated—GLC analyses, steady-state urinary excretion in postmenopausal women □ Excretion, urinary—conjugated estrogens at steady state in postmenopausal women □ GLC—analyses, conjugated estrogens in urine of postmenopausal women

Conjugated estrogen mixtures have been used therapeutically since 1942. However, there is no detailed information concerning the human plasma or urinary levels of these estrogens after administration, primarily because of the lack of sufficiently sensitive and specific analytical methods.

BACKGROUND

Many recent reports focused on the analysis of estriol and other estrogens in pregnancy urine to follow or monitor fetal health (1–5). The urinary estrogen excretion levels in nonpregnant women (6, 7), in postmenopausal women (8–11), and in men (12, 13) were studied. Other investigators studied the types of conjugation of steroids and separated

0022-3549/78/0900-1218$01.00/0

© 1978, American Pharmaceutical Association

steroid conjugates into classes such as glucuronides, mixed glucuronide–sulfates, and sulfates (14–16).

Requirements for added specificity and sensitivity (picograms per milliliter of blood) brought about the use of newer techniques such as mass fragmentography (17, 18) and radioimmunoassay (19, 20). Mass fragmentography may possess the desirable properties required for a blood, plasma, or urine analysis, but major drawbacks are its expense and complexity. While radioimmunoassay may impart the necessary sensitivity required, it may not possess the necessary specificity to distinguish adequately between several structurally related steroids (21, 22). Attempts were made to improve radioimmunoassay specificity by coupling a chromatographic separation prior to quantitative radioimmunoassay (23, 24).

Estimates of bioavailability are conventionally determined from plasma level and/or urinary excretion data of the drug or its metabolite(s). The usual dose of conjugated estrogens is 2.50 mg or less daily on a cyclic schedule. Therefore, total plasma levels of each estrogen would be in the picogram per milliliter range following 2.50 mg po.

Conjugated estrogens prepared from natural sources contain at least nine estrogens (25). Extensive metabolic pathways, which are known only partially (26) or not at all, are possible for each estrogen component. These pathways include interconversion from one estrogen to another (26, 27). Thus, estrogen levels in the plasma or urine cannot be assumed to reflect only unchanged drug. For these reasons, it is believed that a true plasma bioavailability study of conjugated estrogens tablets would be extremely difficult.

An alternative approach, which has several advantages, is to examine the urinary excretion of the estrogens after dosing of subjects to the steady state. The estrogen concentrations in the urine are higher than in the blood, larger amounts of sample are available for analysis, and a direct quantitative comparison can be made between the daily dose and the 24-hr pooled urine samples. Furthermore, a previously developed specific GLC method for the analysis of conjugated estrogens in raw materials and finished dosage forms (25) was available for extensive modification and application.

The objectives of this investigation were to develop a sensitive and specific method to quantitate estrogens in the urine of postmenopausal subjects after dosing to the steady state and to relate the resultant urinary excretion profile to the composition of estrogens in the dosage form.

EXPERIMENTAL

Instrumentation—A research grade gas chromatograph[1] was equipped with a U-shaped racetrack glass column, a flame-ionization detector, and a recorder[2]. The 2.7-m × 3.5-mm i.d. column was silylated and packed with 1.7 ± 0.2% diethylene glycol succinate[3] on 100–120-mesh silanized Gas Chrom Z[3]. Thermogravimetric analysis was used to determine exactly the amount of liquid phase incorporated on the solid support. The column was conditioned with oxygen-free[4] helium carrier gas at 195 ± 5° overnight at ~60–80 ml/min.

Chromatographic Conditions—The following instrumental conditions were used: column oven temperature, 195 ± 5°; detector temperature, 240°; injection port temperature, 225°; helium flow rate, 60–80 ml/min; hydrogen flow rate, 40 ml/min; air flow rate, 1.8 standard cubic feet per hour; and attenuation, 4×10^{-11} amp.

Reagents and Standards—The following reagents and solvents were reagent grade quality or equivalent: absolute ethanol, ethylene dichloride, acetic acid, sodium hydroxide, sodium bicarbonate, anhydrous sodium sulfate, distilled dry chloroform, potassium hydroxide, carbon tetrachloride, and benzene. The nine free estrogens used to establish relative retention times and chromatographic response factors relative to 6-dehydroestrone[5] were house standards[6] that were assayed using phase solubility analysis. All were greater than 98.6% pure, except for 17α-dihydroequilenin, which was 97.2% pure.

Working Enzyme Solution—Sufficient enzyme concentrate[7] was diluted to 100 ml with distilled water to give a working solution containing about 500 ± 50 units of sulfatase/ml and about 2000 ± 200 units of glucuronidase/ml.

Standard Steroid Solutions—Standard solutions of the 10 steroids were prepared in absolute ethanol at the following approximate concentrations: 17α-estradiol, 1 μg/ml; 17β-estradiol, 0.8 μg/ml; 17α-dihydroequilin, 1.6 μg/ml; 17β-dihydroequilin, 1.6 μg/ml; 17α-dihydroequilenin, 1.3 μg/ml; 17β-dihydroequilenin, 1.3 μg/ml; estrone, 9.5 μg/ml; equilin, 3.5 μg/ml; equilenin, 4.0 μg/ml; and 6-dehydroestrone, 12.4 μg/ml.

Standard Solution—Aliquots of 1 ml of each of the 10 standards were pipetted into a 13-ml conical glass centrifuge tube equipped with a polytef-lined screw cap. Just before instrument standardization, the mixture was evaporated to dryness with nitrogen at 40° in a water bath. The residue was dissolved in 50 μl of anhydrous chloroform and 50 μl of silylating agent[8]. The standard was mixed well and allowed to stand for 15 min prior to injection. Silylated standards were prepared fresh daily.

(The very small amounts of the silylated estrogens required that special care be taken to avoid exposure of the sample to moisture.)

Preparation of Urine Extracts—*Hydrolysis*—A 24-hr urine collection was measured for total volume, and a sample was withdrawn for creatinine analysis (28, 29). Although interindividual urinary excretion of creatinine may vary over a wide concentration range, intraindividual excretion rates are relatively constant. By comparing a patient's creatinine levels over several 24-hr collection periods, an assessment of the completeness of a given 24-hr urine pool was made. All urines were refrigerated during the collection process and assayed as soon as possible after receipt. Urine samples were not frozen, and no bacteriostatic agents were added.

The urine pH was adjusted as necessary to pH 5.2 ± 0.2. Two 100.0-ml aliquots were removed from each urine sample and placed in separate 250-ml glass bottles fitted with polytef-lined screw caps. Working enzyme solution (5 ml) was added, and the bottles were flushed with nitrogen and capped immediately. Then the bottle contents were mixed and placed in a 50 ± 1° water bath for 48 hr.

Extraction—Into each bottle, 25.0 ml of ethylene dichloride[9] was pipetted, and the bottle was shaken mechanically for 30 min. The samples were centrifuged for 10 min at about 2200 rpm once, or twice if necessary, to obtain a relatively clear lower layer. The bulk of the urine was aspirated from the samples, and the organic extracts were transferred quantitatively into separate 60-ml glass bottles fitted with polytef-lined screw caps. A 10-ml aliquot of 5% sodium bicarbonate was added, and the bottle was shaken mechanically for 5 min and centrifuged, as already described, to break the emulsion. Most of the aqueous layer was aspirated carefully, and this bicarbonate wash sequence was repeated seven additional times.

The remaining ethylene dichloride extract was filtered through anhydrous sodium sulfate contained in a 4-cm diameter polyethylene funnel plugged with glass wool. Over 20 ml of extract was collected if possible. Then 20.0 ml of extract, or as much as possible, was pipetted into 60-ml glass bottles and evaporated to dryness with nitrogen in a 40° water bath. A 10-ml aliquot of 2 *N* KOH was added, and the mixture was shaken mechanically for 15 min. Then 10 ml of carbon tetrachloride[9] was added, and the bottle was shaken for 5 min and centrifuged for 5 min. Most of the lower organic layer was carefully removed and discarded. The washing sequence was repeated with a second 10-ml portion of carbon tetrachloride.

The remaining basic extract was chilled and, with swirling, brought to pH 1 with 3 *N* HCl. Then 15.0 ml of benzene[9] was added, and the bottle was shaken for 15 min and centrifuged. The lower layer was discarded. The organic layer was treated with three successive 10-ml bicarbonate washes, and then the benzene was filtered through anhydrous sodium sulfate. Over 12 ml was collected if possible.

Benzene extract, 12.0 ml, was pipetted into 13-ml conical glass centrifuge tubes fitted with polytef-lined screw caps. Then 1 ml of the internal standard solution was added, and the mixture was evaporated to dryness with nitrogen at 40°. To the dry residue, 50 μl of anhydrous chloroform and 50 μl of silylating reagent[8] were added. The solution was mixed carefully and allowed to stand for 15 min prior to injection.

(To prevent possible sample composition changes and degradation with time, samples were silylated only as needed. All silylated samples were carefully protected against exposure to moisture.)

Instrument Standardization—About 1–3 μl of silylated standard was injected onto a well-conditioned column, and the identity of the standard estrogen peaks was established by comparing their relative retention times (*RRT*) *versus* 6-dehydroestrone with those indicated in

[1] F&M model 400 equipped with a Keithley 417K electrometer.
[2] Honeywell Electronic 194.
[3] Applied Science Laboratories, State College, Pa.
[4] Oxy-Sorb Trap, Regis Chemical Co., Morton Grove, Ill.
[5] Searle Chemicals, Chicago, Ill.
[6] Ayerst Research Laboratories, Montreal, Quebec, Canada.
[7] Glusulase, Endo Laboratories, Garden City, N.Y.
[8] Regisil [bis(trimethylsilyl)trifluoroacetamide plus 10% trimethylchlorosilane], Regis Chemical Co., Morton Grove, Ill.
[9] Distilled-in-glass solvents, Burdick and Jackson Laboratories, Muskegon, Mich.

Table I—Recoveries of Estrogens from Urine Pool Aliquots Spiked within the Estrogen Concentration Range of Urine Samples after Dosing

Estrogen	Input[a], μg/100 ml	Mean Recovery[b], μg/100 ml	Mean Percentage Recovery	SD	CV, %
Sodium 17α-estradiol sulfate	0.69	0.80	115	0.06	7.4
	1.38	1.39	101	0.06	4.0
	2.76	2.56	92.9	0.33	12.7
	4.14	4.51	109	0.27	6.1
	6.21	6.68	108	0.13	1.9
			105 ± 8.5[c]		
17β-Estradiol	1.12	0.90	80.7	0.06	6.8
	2.24	1.89	84.4	0.13	6.9
	4.48	3.83	85.5	0.37	9.6
	6.72	5.99	89.2	0.30	5.0
	10.08	9.51	94.3	0.26	2.7
			86.8 ± 5.2		
17α-Dihydroequilin	0.54	0.38	71.0	0.10	26.6
	1.08	0.84	77.8	0.02	2.4
	2.16	1.67	77.2	0.06	3.4
	3.24	2.66	82.1	0.16	5.9
	4.86	3.91	80.5	0.10	2.5
			77.7 ● 4.3		
Sodium 17β-dihydroequilin sulfate	1.025	0.74	71.9	0.03	4.1
	2.05	1.45	70.9	0.06	4.4
	4.10	2.80	68.2	0.29	10.3
	6.15	4.83	78.5	0.31	6.3
	9.23	7.19	77.9	0.12	1.6
			73.5 ± 4.5		
17α-Dihydroequilenin	1.44	1.16	80.6	0.06	5.4
	2.88	2.43	84.3	0.04	1.7
	5.76	5.06	87.8	0.33	6.5
	8.64	8.09	93.6	0.34	4.2
	12.96	11.85	91.5	0.28	2.3
			87.6 ± 5.3		
Sodium estrone glucuronide	11.4	9.19	80.6	0.11	1.2
	22.8	18.78	82.4	0.12	0.6
	45.6	38.18	83.7	0.35	0.9
	68.4	55.64	81.3	1.34	2.4
	102.6	85.37	83.2	0.64	0.7
			82.2 ± 1.3		
Sodium equilin glucuronide	0.64	0.38	58.9	0.06	15.3
	1.28	0.79	61.7	0.06	7.7
	2.56	1.79	70.1	0.14	7.7
	3.84	2.70	70.2	0.09	3.4
	5.76	4.24	73.7	0.26	6.1
			66.9 ± 6.3		

[a] Three 100-ml urine aliquots from a male urine pool were spiked at each concentration level with aliquots from a stock solution containing all seven estrogens. [b] Results are corrected by subtraction of background peaks obtained from the corresponding blank urine samples. [c] The grand mean percentage recovery and its standard deviation are reported for each estrogen.

Fig. 1. The sample size and/or instrument attenuation were adjusted so that the larger estrogen peaks were more than 50% of full chart scale.

To determine the response factors, the peak heights were measured carefully. For peaks eluting early and on the tailing portion of the solvent front, an exponential decay of the front was assumed, and peak heights were measured to this drawn line. With the measured peak heights and known concentrations, an estrogen response factor (RF_e) was calculated for each component according to:

$$RF_e = \frac{P_d C_e}{C_d P_e} \qquad \text{(Eq. 1)}$$

where P_d is the peak height of 6-dehydroestrone in the standard, C_d is the micrograms of the internal standard (6-dehydroestrone) in the standard, C_e is the micrograms of estrogen in the standard, and P_e is the peak height of the estrogen peak in the standard. Initially with new columns, two standards were injected in succession to check for system stability and reproducibility. For well-conditioned columns, only single injections of the estrogen standard at the beginning and end of the assay day were required. These RF values were averaged for subsequent calculations.

Chromatographic Analysis—Following system standardization, 1–5 μl of the silylated urinary extracts was injected. The sample estrogen peaks were identified by comparing their RRT values *versus* 6-dehydroestrone with the RRT values generated for the standard. Typical standard and sample RRT values are given in Figs. 1–3. Standard and sample RRT values should agree to within ±2% for a given peak to establish the identity of a sample peak with some confidence. The peak heights of the identified estrogen peaks should then be measured.

The amounts of the individual estrogens present in the 24-hr urine pool, expressed as the sulfate conjugates, were calculated from:

$$\text{weight of conjugated estrogen } (\mu g/24 \text{ hr}) = 1.38\,(RF_e)\,(\text{dilution factor})\,(P_{es})\left[\frac{C_{ds}V_t}{P_d V_a}\right] \qquad \text{(Eq. 2)}$$

where 1.38 is a factor converting free estrogens into the corresponding sodium estrogen sulfate salts, dilution factor is (25 ml/20 ml) (15 ml/12 ml), P_{es} is the peak height of estrogen in the sample, C_{ds} is the micrograms of the internal standard (6-dehydroestrone) in the sample, P_{ds} is the peak height of 6-dehydroestrone in the sample, V_t is the total volume of the 24-hr urine pool in milliliters, and V_a is 100 ml (aliquot of urine taken into assay).

Clinical Study Protocol—Twelve postmenopausal female subjects[10] were selected. The postmenopausal syndrome was established by documented physiological or surgical menopause of not less than 2 years and anestrogenism established by colpocytogram. The average age of the eight physiologically menopausal subjects was 52 years (range of 50–57), and that of the four surgically menopausal subjects was 44 years (range of 37–54). The average weight of all subjects was 62 kg (range of 54–73). All subjects were in good health as established by physical examination, serum biochemistry tests[11], and urinalysis (pH, glucose, and protein)[12].

A 28-day washout period permitted urinary estrogen levels of those subjects previously taking estrogen medication to return to baseline

[10] Each subject signed a voluntary informed consent form.
[11] SMA 12/60.
[12] Combistix, Ames Co., Elkhart, Ind.

Table II—Elution Sequence and Separation of Estrogen Steroids

Component[a]	Relative Retention Time *versus* 6-Dehydroestrone
16-Estratetraene	0.094
17α-Estradiol[b]	0.130
17β-Estradiol[b]	0.154
Estradiol benzoate	0.160
17α-Dihydroequilin[b]	0.166
17β-Dihydroequilin[b]	0.195
Estriol	0.197
17α-Dihydroequilenin[b]	0.342
Methylestradiol methyl ether	0.378
17β-Dihydroequilenin[b]	0.389
3-Desoxyestrone	0.425
Estra-4-ene-3-ol-17-one	0.491
$\Delta^{5,7,9}$-Estratrien-3-ol-17-one	0.624
16-Hydroxyestrone	0.646
17α-Estradiol 17-acetate	0.657
Estrone[b]	0.781
16-Oxo-17β-estradiol	0.782
6-Oxoestradiol	0.805
Equilin[b]	0.875
9-Dehydroestrone	0.914
8-Dehydroestrone	0.953
6-Dehydroestrone	1.00
14-Isoequilenin	1.30
2-Methoxyestrone	1.46
1-Methylestrone	1.58
Equilenin[b]	1.65

[a] All components are eluted as the trimethylsilyl ethers. [b] Components tested for and quantitated in this study.

levels. At the end of this washout period, a 24-hr urine sample was collected from each subject. Each subject then received two 1.25-mg conjugated estrogens tablets[13] daily for 21 days. Each subject was instructed to select a time for dosing each morning and to take the tablets at the same time each morning. On Days 17–19 of the dosing period, three consecutive 24-hr urine samples were collected from each subject. The 24-hr collection period began at the time of dosing. Diet was unrestricted during the study, and each subject was instructed to take no additional medication.

Three subjects who participated in a study at the 2.50-mg dose level participated in a second study at the 1.25-mg dose level. The average age of the two surgically menopausal subjects and one physiologically menopausal subject was 42 years (range of 38–51), and their average weight was 62 kg (range of 55–71). The urinary estrogen levels of these subjects were determined for three consecutive 24-hr urine samples (Days 17–19) during cyclic dosing of one 1.25-mg conjugated estrogens tablet[13]

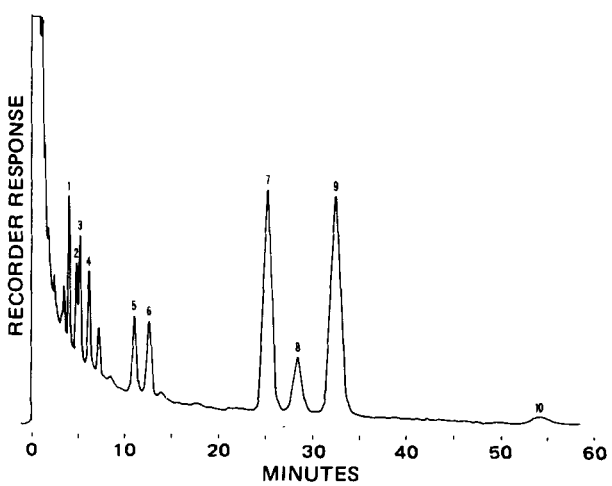

Figure 1—*Separation of the nine estrogen components and the internal standard, 6-dehydroestrone, as the trimethylsilyl ethers. The peaks, together with their relative retention times, are: 1, 17α-estradiol, 0.133; 2, 17β-estradiol, 0.157; 3, 17α-dihydroequilin, 0.167; 4, 17β-dihydroequilin, 0.197; 5, 17α-dihydroequilenin, 0.347; 6, 17β-dihydroequilenin, 0.394; 7, estrone, 0.780; 8, equilin, 0.878; 9, 6-dehydroestrone, 1.00; and 10, equilenin, 1.667.*

[13] Premarin, Ayerst Laboratories, New York, N.Y.

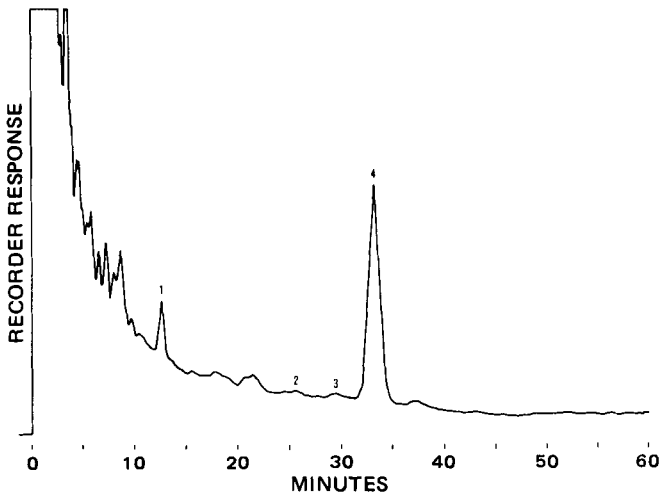

Figure 2—*Chromatogram of the trimethylsilyl ethers of the endogenous estrogens present in the urine of a postmenopausal female. The peaks, identified by comparison of their relative retention times with standards, are: 1, 17β-dihydroequilenin, 0.386; 2, estrone, 0.776; 3, equilin, 0.888; and 4, 6-dehydroestrone, 1.00.*

daily. This study was performed several months after a return from the 2.50-mg daily dose to the 1.25-mg daily dose.

RESULTS AND DISCUSSION

Sample Preparation—Documented steroid decomposition reactions, induced by acid hydrolysis of the conjugates (30, 31), led to the use of mild enzyme hydrolysis of urine samples coupled with controllable classical organic extraction and purification steps. The objective of this study was to determine the total daily amount of estrogens excreted in dosed patients at the steady state. Therefore, there was no need to differentiate between free and conjugated estrogens. The sample preparation used here produced an extract of free estrogens, regardless of the manner or form in which they were excreted.

For long-term storage of urine samples, freezing would be desirable. However, nonfrozen, fresh urine samples yielded higher precision and greater estrogen recoveries than did frozen samples. Therefore, during collection, all samples were stored at 4° without preservatives and were assayed as soon as possible.

The hydrolysis and extraction steps evolved as attempts were made to produce an extract containing reproducible and known recoveries of estrogens, sufficiently free from other urinary components, to allow their separation and quantitation. Following a 48-hr hydrolysis, the estrogen

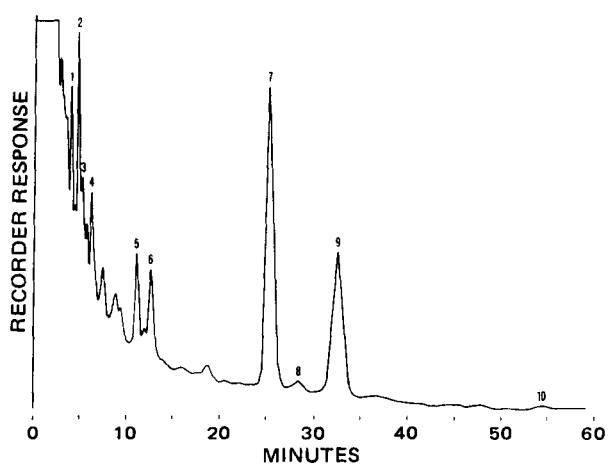

Figure 3—*Chromatogram of the trimethylsilyl ethers of the estrogens present in the urine of a postmenopausal female dosed to the steady state with conjugated estrogens tablets. The peaks, together with their relative retention times* versus *6-dehydroestrone, are: 1, 17α-estradiol, 0.133; 2, 17β-estradiol, 0.157; 3, 17α-dihydroequilin, 0.169; 4, 17β-dihydroequilin, 0.198; 5, 17α-dihydroequilenin, 0.345; 6, 17β-dihydroequilenin, 0.391; 7, estrone, 0.777; 8, equilin, 0.872; 9, 6-dehydroestrone, 1.00; and 10, equilenin, 1.664.*

Table III—Estimated Minimum Quantifiable Estrogen Levels in 24-hr Urine Pools

Sodium Estrogen Sulfate[a]	Minimum Quantifiable Amount[b], μg/24 hr
17α-Estradiol	0.9
17β-Estradiol	1.1
17α-Dihydroequilin	1.4
17β-Dihydroequilin	1.6
17α-Dihydroequilenin	2.8
17β-Dihydroequilenin	2.8
Estrone	5.9
Equilin	2.1
Equilenin	18.7

[a] Although the estrogens are excreted primarily as glucuronides, components are expressed as the sulfate conjugates to aid direct comparison with the tablet content. [b] Based on the amount of estrogen producing a peak 1% of chart scale at 4×10^{-11} amp full scale and an average daily urine volume of 1500 ml. Results represent an average of six separate determinations performed over 3 months.

steroids and other organics were partitioned into ethylene dichloride. This hydrolysis time was based on reported literature times of 24–48 hr (32, 33), together with our own experience and desire to ensure a complete conversion of the estrogen conjugates into the corresponding free steroids. This first partitioning left behind much of the water-soluble organics.

The remaining acids and phenolic acids in the extract, perhaps by weight the largest undesirable fraction, were removed by successive bicarbonate washes. This step also acted to control pH and to minimize steroid decomposition by removing the organic acids. Next, neutral steroids and other organic, nonphenolic by-products were removed by the carbon tetrachloride washes of the formed potassium phenolate salts. The regenerated phenols, washed again with bicarbonate solution, were then ready for GLC analysis. This combination of partitioning and extraction steps gave reproducible recoveries, and the peak patterns obtained for a given assay pair from a urine pool were almost superimposable.

Recovery data were generated for seven of the estrogen steroids (Table I). Ingested estrogen sulfates are excreted as the intact glucuronides, sulfates, free phenols, or mixed glucuronide–sulfate conjugates. Therefore, to show the broad utility of the method and its ability to measure total urinary estrogen excretion regardless of the manner in which the steroid may or may not be conjugated, the recovery studies utilized some of these different conjugate species.

A fresh urine pool was collected from an adult male. The estrogens to be spiked were added to the empty hydrolysis bottles, and the solvent was removed with nitrogen prior to the addition of 100-ml urine aliquots. Three aliquots of the urine pool were assayed at each of the five estrogen concentration ranges together with an unspiked or blank sample. The blank values were subtracted from the found amounts to obtain the recoveries indicated. Although there was a range of recoveries for the group of compounds as a whole, the variation of recoveries for each individual component was acceptable.

In the recovery study reported in Table I and in parallel with an earlier study, when 17α-dihydroequilin, 17β-dihydroequilin, and/or equilin were added to the urine aliquots, their corresponding oxidation products, 17α-dihydroequilenin, 17β-dihydroequilenin, and equilenin, respectively, could be detected and measured. For each estrogen, a relatively constant percentage of the oxidation product was detected. Thus, even with the temperature, nitrogen flushing, pH, and hydrolysis controls used in this method, approximately 12% of the equilin-type compounds was lost through oxidation. Other reported techniques utilizing more vigorous experimental steps, including acid hydrolysis, probably would cause even more significant composition shifts than those observed here.

Analysis—With the large number of known circulating estrogens and estrogen metabolites found in women (5, 34), a technique for resolving potentially complex mixtures of urinary estrogens was needed. For example, when 17β-estradiol was administered to pregnant women, seven individual metabolites were identified (35). Therefore, when patients are placed on conjugated estrogens therapy with drugs containing a mixture of estrogen steroids, the urinary profiles can be expected to contain numerous peaks. However, to keep the project and assay work within reasonable confines, only those estrogens present in the dosage form were quantitated and, without a gas chromatograph–mass spectrometer, no attempt was made to identify other metabolites.

The primary aim in this study was to quantitate the nine known estrogen steroids indicated in Fig. 1. The GLC method published earlier (25) was suitable for analyzing a minimum of nine separate estrogen steroids in dosage forms and appeared promising for use in analyzing urinary estrogen mixtures. The modifications discussed earlier evolved as the procedure was applied to more dilute and complex mixtures. A new internal standard was chosen to elute in one of the relatively few peak-free areas in the chromatograms to allow reproducible quantitation and peak identification.

Figure 1 illustrates the peak pattern obtained for a mixture of estrogen standards at a level approximating that required for the analysis of urine samples from dosed postmenopausal subjects. The amount of material on-column was 15–30 ng for the estrogen diols and 50–250 ng for the estrogen ketones. Because of the baseline obtained, normal disk and digital integration techniques were unsatisfactory for routinely and reproducibly measuring peak areas. Satisfactory quantitation was achieved using peak heights where operator judgment could quickly and reproducibly assign heights to the numerous peaks of interest.

To demonstrate method specificity, 26 different estrogen steroids were analyzed; their retention times were measured relative to 6-dehydroestrone. Except for two pairs whose *RRT* values were within 1% of each other, the procedure provided sufficient resolution for separation and identification of the remaining 22 estrogens. These estrogens, together with their relative retention times *versus* 6-dehydroestrone, are identified in Table II. Although the ultimate in specificity is probably a GLC–mass spectrometry system utilizing either electron impact or chemical ionization together with specific ion detection, such equipment is unavailable to most laboratories.

Method specificity can be expressed in several ways, and frequently a signal twice the noise level is used. However, in working with biological fluids, many unknown components and impurities in trace amounts are retained in the sample. If one reviews a scan of one of these samples, many minor background peaks emerge above the baseline that are of questionable significance. Therefore, a different, more stringent sensitivity estimate was made here to eliminate and identify false positives.

At the normal operating attenuation (4×10^{-11} amp full scale), all peaks less than 1% full scale were considered as background. The amount of estrogen required to produce a peak of this height was estimated from standards injected at the operating attenuation used in the analysis of samples from dosed females. With this quantity of estrogen standard known, an estimate could be made of the minimum amount that could be detected in a 24-hr urine pool. This estimate of method sensitivity was done for nine estrogens (Table III).

Table IV—Endogenous and Steady-State Urinary Estrogen Excretion Levels of 12 Postmenopausal Subjects

Sodium Estrogen Sulfate	Endogenous Level, μg/24 hr	Steady-State Level[a], μg/24 hr			
		Day 17	Day 18	Day 19	Mean
17α-Estradiol	10.0	32.7	30.3	32.0	31.7
17β-Estradiol	9.2	65.8	69.1	67.6	67.5
17α-Dihydroequilin	1.6	26.6	20.2	25.2	24.0
17β-Dihydroequilin	1.3	28.1	25.5	28.5	27.4
17α-Dihydroequilenin	3.9	72.2	66.5	69.4	69.4
17β-Dihydroequilenin	—	—[b]	—[b]	—[b]	—
Estrone	8.1	330.2	341.0	319.9	330.4
Equilin	3.4	15.0	13.3	14.5	14.3
Equilenin	—	—[c]	—[c]	—[c]	—
Total[d]	37.5	549.3	565.7	545.1	553.4

[a] Values are the means for 12 subjects with the exception of estrone and equilin for Days 18 and 19, which are the means for 11 subjects only. Steady-state levels are uncorrected for endogenous levels or the analytical losses reported in Table I. [b] Most peaks masked by urinary impurities. [c] Quantities are below the sensitivity limit of the method. [d] Totals represent the data of 11 subjects only.

Table V—USP XIX and GLC Analyses [a] of 1.25-mg Conjugated Estrogens Tablets [b] USP

Sodium Estrogen Sulfate	GLC Assay		USP XIX Colorimetric Assay [c]	
	mg/Tablet	%	mg/Tablet	%
Estrone	0.773	50.0	0.69	52.3
Equilin	0.403	26.1	0.35	26.4
Equilenin	0.037	2.4		
17α-Estradiol	0.048	3.1		
17β-Estradiol	0.010	0.6		
17α-Dihydroequilin	0.220	14.3		
17β-Dihydroequilin	0.027	1.7		
17α-Dihydroequilenin	0.020	1.3		
17β-Dihydroequilenin	0.008	0.5		
Total	1.546	100.0	1.31	

[a] The two methods give different assay values because of major differences in the analytical methods used. [b] D403 WXA. [c] USP XIX assay includes only the three individual quantitative tests shown.

Urinary Estrogen Levels—The steady-state urinary estrogen excretion after administration of 2.5 mg of conjugated estrogens was determined using the described method. Table IV presents the mean endogenous levels and the mean levels for each estrogen and their total obtained on Days 17, 18, and 19 of the dosing period. The mean of the 3-day excretion is also presented. The total endogenous levels observed were similar to values reported previously (10, 11).

A typical GLC scan of a washout urine sample is shown in Fig. 2. The dosed data clearly indicate the increased quantities of urinary estrogens expected from subjects receiving conjugated estrogens replacement therapy. The absence of an increasing trend in the excretion levels for these 3 successive days establishes that the study was performed under steady-state conditions. Figure 3 is an example of the estrogen excretion patterns found in the dosed subjects.

The USP and GLC assays of the conjugated estrogens tablets are shown in Table V. The mean total recovery of estrogens in the urine was about 17% of the daily ingested amount, based on the GLC assay. This value was obtained after subtraction of the mean endogenous amounts and the amounts of equilenin and 17β-dihydroequilenin sodium sulfates from the tablet content since these estrogens were not quantitated in the urine. The recovery values presented in Table I documented only the general completeness of extraction. Since the predominant conjugates excreted in the urine and their recoveries may vary from those presented, no correction for analytical losses was made to the recovery value of 17%.

Linear pharmacokinetic processes are often assumed in bioavailability and bioequivalence studies. To verify the linear elimination of the conjugated estrogens, the excretion of estrogens was compared in three subjects after dosing to the steady state with 1.25 and 2.50 mg daily. Table VI presents the mean amounts of each estrogen or estrogen metabolite in the urine as a percentage of the dosed amount. With the exception of 17α-estradiol, a close agreement was observed in the percentage excretion of each estrogen or estrogen metabolite at the two dose levels. This agreement indicates the absence of dose dependency within this dosing range, a result anticipated with drugs whose dose is very low. The reason for the decreased 17α-estradiol at the higher dose level is not apparent but may indicate a minor interfering peak in the urine sample of relatively greater importance at the lower dose. The period of time allowed to attain the steady state prohibits obtaining a blank urine immediately prior to sampling, which could eliminate this problem.

The inadequacy of a steady-state urinary excretion method to determine bioavailability is recognized. Neither the rate nor the absolute extent of absorption can be determined. As suggested by the low excretion levels of equilin and 17β-dihydroequilin and the high excretion levels of 17β-estradiol, the complexity in the metabolism of the estrogens results in a urinary estrogen excretion pattern substantially different from that of the composition of conjugated estrogens tablets. Nevertheless, the present method for the first time permits the extent of urinary excretion of seven estrogens to be determined after administration of conjugated estrogens tablets to the steady state.

Relative magnitudes of absorption and elimination half-lives of estrogens may be estimated from recent studies in which estrone sulfate (36) and 17β-estradiol (27) were administered orally and their plasma levels were determined. Estrone sulfate was administered as an oral solution; micronized 17β-estradiol was administered as a tablet. With a one-compartment model with first-order absorption and elimination, approximate ratios of the elimination half-life to the absorption half-life may be estimated at 14 for estrone sulfate and at eight for 17β-estradiol. It is generally recognized that for drugs with long elimination half-lives relative to their absorption half-lives, the steady-state plasma concentrations are relatively insensitive to the absorption rate but do depend on the extent of absorption. Thus, a comparison of the extent of urinary estrogen excretion after administration of conjugated estrogens products from multiple sources should provide one means of assessing their bioequivalence.

Table VI—Percentage Excretion of Individual Estrogens in Three Subjects at the Steady State as a Function of Conjugated Estrogens Dosed

Estrogen	Mean Excretion, % ± SD [a]	
	From 1.25-mg Dose of Conjugated Estrogens USP	From 2.50-mg Dose of Conjugated Estrogens USP
17α-Estradiol [b]	48.6 ± 7.4	36.1 ± 11.6
17β-Estradiol [c]	5.3 ± 0.9	5.1 ± 2.1
17α-Dihydroequilin [b]	5.8 ± 0.4	4.9 ± 3.2
17β-Dihydroequilin [c]	4.7 ± 1.2	5.0 ± 2.5
17α-Dihydroequilenin [c]	16.3 ± 3.9	18.9 ± 9.7
Estrone [b]	25.5 ± 7.2	26.8 ± 13.0
Equilin [b,d]	—	1.9 ± 1.2

[a] Values were calculated from the mean excretion during Days 17–19 for each subject and are uncorrected for endogenous levels or analytical losses. [b] Values are the percentages of the indicated estrogens excreted in the urine relative to the dosed amounts of those estrogens. [c] Values are the percentages of 17β-estradiol, 17β-dihydroequilin, and 17α-dihydroequilenin excreted in the urine relative to the dosed amounts of estrone, equilin, and 17α-dihydroequilin, respectively. A subsequent paper will present evidence suggesting that the major fraction of the former estrogens are derived from the latter. [d] The equilin peak was masked by an interfering peak in two of the three subjects at the 1.25-mg dose.

REFERENCES

(1) V. Ratanasopa, A. Schindler, T. Lee, and W. Hermann, *Am. J. Obstet. Gynecol.*, **99**, 295 (1967).

(2) W. Fischer-Rasmussen, *Dan. Med. Bull. Suppl. II*, **19**, 1 (1972).

(3) A. Howarth and D. Robertshaw, *Clin. Chem.*, **17**, 316 (1971).

(4) Y. Osawa and W. R. Slaunwhite, Jr., *Steroids*, **15**, 73 (1970).

(5) G. Adessi, D. Eichenberger, T. Nhuan, and M. Jayle, *ibid.*, **25**, 553 (1975).

(6) C. Longcope and K. Williams, *J. Clin. Endocrinol. Metab.*, **38**, 602 (1974).

(7) R. Hobkirk, *J. Steroid Biochem.*, **5**, 15 (1974).

(8) G. Goertz, O. Crepy, O. Judas, J. Longchampt, and M. Jayle, *Clin. Chim. Acta*, **51**, 277 (1974).

(9) V. Goebelsmann, *ibid.*, **43**, 285 (1973).

(10) M. Furuhjelm, *Acta Obstet. Gynecol. Scand. Suppl. 7*, **43**, 42 (1964).

(11) G. Dove, F. Morley, A. Batchelor, and S. Lunn, *J. Reprod. Fertil.*, **24**, 1 (1971).

(12) J. Fishman, I. Yoshizawa, and L. Hellman, *Steroids*, **22**, 401 (1973).

(13) H. Kaplan and M. Hreshchyshyn, *Am. J. Obstet. Gynecol.*, **111**, 386 (1971).

(14) M. Matsui, M. Hakozaki, and Y. Kinuyama, *J. Chromatogr.*, **115**, 625 (1975).

(15) M. Levitz and J. Katz, *J. Clin. Endocrinol. Metab.*, **28**, 862 (1968).

(16) R. Haehnel, *J. Steroid Biochem.*, **1**, 299 (1970).

(17) H. Adlercreutz and D. Hunneman, *ibid.*, **4**, 233 (1973).

(18) H. Adlercreutz, M. Tikkanen, and D. Hunneman, *ibid.*, **5**, 211 (1974).

(19) B. Lindberg, E. Johansson, and B. Nilsson, *Acta Obstet. Gynecol. Scand., Suppl.*, **32**, 21 (1974).

(20) B. Desfosses, S. DeLauzon, O. Judas, and M. Jayle, *Steroids Lipids Res.*, **4**, 86 (1973).

(21) A. Bolton and F. Rutherford, *J. Steroid Biochem.*, **7**, 71 (1976).

(22) E. Cerceo and C. Elloso, *Anal. Chem.*, **46**, 1578 (1974).

(23) D. Loriaux, H. Ruder, D. Knab, and M. Lipsett, *J. Clin. Endocrinol. Metab.*, **35**, 887 (1972).

(24) A. Jakobovits, *Kiserl. Orvostud.*, **25**, 275 (1973).

(25) R. Johnson, R. Masserano, R. Haring, B. Kho, and G. Schilling, *J. Pharm. Sci.*, **64**, 1007 (1975).

(26) R. I. Dorfman and F. Ungar, "Metabolism of Steroid Hormones," Academic, New York, N.Y., 1965, chap. 8.

(27) S. S. C. Yen, P. L. Martin, A. M. Burnier, N. M. Czekala, M. O.

Greaney, Jr., and M. R. Callantine, *J. Clin. Endocrinol. Metab.*, **40**, 518 (1975).
(28) S. Pino, J. Benotti, and H. Gardyna, *Clin. Chem.*, **11**, 664 (1965).
(29) M. Metcalf and E. Hunt, *Clin. Biochem.*, **9**, 75 (1976).
(30) C. Muehlbaecher and E. Smith, *Clin. Chem.*, **16**, 158 (1970).
(31) L. Cawley, B. Musser, W. Faucette, S. Beckloff, and H. Learned, *ibid.*, **11**, 1009 (1965).
(32) F. Vandenheuvel, *Can. J. Biochem.*, **45**, 191 (1967).
(33) H. C. Curtius and M. Muller, *J. Chromatogr.*, **30**, 410 (1967).
(34) N. Taylor and C. Shackleton, *Steroids*, **24**, 185 (1974).
(35) R. Hobkirk and M. Nilsen, *J. Clin. Endocrinol. Metab.*, **26**, 625 (1966).
(36) H. J. Ruder, L. Loriaux, and M. B. Lipsett, *J. Clin. Invest.*, **51**, 1020 (1972).

ACKNOWLEDGMENTS

The authors thank Dr. G. Myers for supplying the free estrogens and the estrogen conjugates used in the development of this procedure, Dr. J. Hasegawa for constructive comments and criticism, Mr. R. Haring for work in preparing the high quality column packings required for this work, and Dr. J. Southwick for medical supervision of the subjects.

Characterization of Pharmacologically Important Prototropic Species Derived from a Pyridinemethanol Antimalarial by Electronic Absorption and Fluorescence Spectroscopy

O. J. BOUWSMA, J. T. STEWART, and A. C. CAPOMACCHIA *

Received September 19, 1977, from the *School of Pharmacy, University of Georgia, Athens, GA 30602.* Accepted for publication December 21, 1977.

Abstract □ Variations of the absorption and fluorescence spectra of the experimental antimalarial drug, α-dibutylaminomethyl-2,6-bis(*p*-trifluoromethylphenyl)-4-pyridinemethanol, were investigated throughout the pH region in concentrated sulfuric acid media and in *n*-hexane. The predominant prototropic species at physiological pH is the singly charged cation. In the pH 6–12 region, the structured fluorescence of the monocation is quenched with the concomitant appearance of a diffuse, long wavelength emission while the corresponding absorption spectra shift only slightly to longer wavelengths. Furthermore, the dibutylamino group exhibits an unusually low basicity. This behavior is explained as due to the formation of an intramolecular hydrogen bond in the neutral molecule in the ground and lowest excited singlet states. A similar intramolecular hydrogen bond in the monocation is not spectroscopically visible.

Keyphrases □ Pyridinemethanol, substituted—prototropic species characterized from electronic absorption and fluorescence spectra at various pH values and in *n*-hexane □ Electronic absorption spectroscopy—used to characterize prototropic species of substituted pyridinemethanol at various pH values and in *n*-hexane □ Fluorescence spectroscopy—used to characterize prototropic species of substituted pyridinemethanol at various pH values and in *n*-hexane □ Antimalarial agents, potential—α-dibutylaminomethyl-2,6-bis(*p*-trifluoromethylphenyl)-4-pyridinemethanol, prototropic species characterized from electronic absorption and fluorescence spectra of various pH values and in *n*-hexane

A limited number of pyridinemethanol derivatives have been synthesized and screened for antimalarial activity (1–3). However, most of these compounds demonstrate either little activity or undesirable, toxic side effects (1). One of the few compounds of this class to exhibit antimalarial activity is the investigational drug α-dibutylaminomethyl-2,6-bis(trifluoromethylphenyl) -4- pyridinemethanol (I). It is 22 times more effective than quinine and is active against highly chloroquine-resistant *Plasmodium berghei* in mice (1). Although its specific mechanism of activity is unknown, it may be similar to, but not identical with, that of either chloroquine or quinine (1).

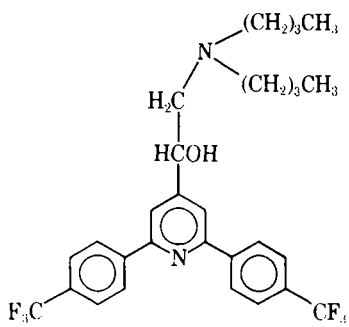

I

Most antimalarial compounds that exert their activity through a mechanism other than disruption of plasmodia nucleotide anabolism have at least one common feature. At physiological pH, these compounds exist as the singly charged cations or, as with chloroquine and quinacrine, as the doubly charged cation (4, 5). The cationic charge is believed to be involved in the binding of acridines, 9-aminoquinolines, and 8-aminoquinolines to parasitic DNA, and this binding is presumed to be related to antimalarial activity (6). Little is known about the mechanism of activity of quinine, alkaloids related to quinine, pyrimidines, quinolinemethanols, and pyridinemethanols. However, the singly charged cations of these agents may bind to plasmodia nuclear proteins, plasmodia DNA, or various enzymes in the metabolic network of these parasites (1, 7).

The present study of the dependence of the electronic spectra on the state of protonation and solvent properties of I was undertaken to elucidate the electronic structures of this compound and ultimately its interaction with native DNA, serum proteins, and selected enzymes.

0022-3549/78/0900-1224$01.00/0
© 1978, American Pharmaceutical Association

Greaney, Jr., and M. R. Callantine, *J. Clin. Endocrinol. Metab.*, **40**, 518 (1975).
(28) S. Pino, J. Benotti, and H. Gardyna, *Clin. Chem.*, **11**, 664 (1965).
(29) M. Metcalf and E. Hunt, *Clin. Biochem.*, **9**, 75 (1976).
(30) C. Muehlbaecher and E. Smith, *Clin. Chem.*, **16**, 158 (1970).
(31) L. Cawley, B. Musser, W. Faucette, S. Beckloff, and H. Learned, *ibid.*, **11**, 1009 (1965).
(32) F. Vandenheuvel, *Can. J. Biochem.*, **45**, 191 (1967).
(33) H. C. Curtius and M. Muller, *J. Chromatogr.*, **30**, 410 (1967).
(34) N. Taylor and C. Shackleton, *Steroids*, **24**, 185 (1974).
(35) R. Hobkirk and M. Nilsen, *J. Clin. Endocrinol. Metab.*, **26**, 625 (1966).
(36) H. J. Ruder, L. Loriaux, and M. B. Lipsett, *J. Clin. Invest.*, **51**, 1020 (1972).

ACKNOWLEDGMENTS

The authors thank Dr. G. Myers for supplying the free estrogens and the estrogen conjugates used in the development of this procedure, Dr. J. Hasegawa for constructive comments and criticism, Mr. R. Haring for work in preparing the high quality column packings required for this work, and Dr. J. Southwick for medical supervision of the subjects.

Characterization of Pharmacologically Important Prototropic Species Derived from a Pyridinemethanol Antimalarial by Electronic Absorption and Fluorescence Spectroscopy

O. J. BOUWSMA, J. T. STEWART, and A. C. CAPOMACCHIA *

Received September 19, 1977, from the *School of Pharmacy, University of Georgia, Athens, GA 30602.* Accepted for publication December 21, 1977.

Abstract □ Variations of the absorption and fluorescence spectra of the experimental antimalarial drug, α-dibutylaminomethyl-2,6-bis(*p*-trifluoromethylphenyl)-4-pyridinemethanol, were investigated throughout the pH region in concentrated sulfuric acid media and in *n*-hexane. The predominant prototropic species at physiological pH is the singly charged cation. In the pH 6–12 region, the structured fluorescence of the monocation is quenched with the concomitant appearance of a diffuse, long wavelength emission while the corresponding absorption spectra shift only slightly to longer wavelengths. Furthermore, the dibutylamino group exhibits an unusually low basicity. This behavior is explained as due to the formation of an intramolecular hydrogen bond in the neutral molecule in the ground and lowest excited singlet states. A similar intramolecular hydrogen bond in the monocation is not spectroscopically visible.

Keyphrases □ Pyridinemethanol, substituted—prototropic species characterized from electronic absorption and fluorescence spectra at various pH values and in *n*-hexane □ Electronic absorption spectroscopy—used to characterize prototropic species of substituted pyridinemethanol at various pH values and in *n*-hexane □ Fluorescence spectroscopy—used to characterize prototropic species of substituted pyridinemethanol at various pH values and in *n*-hexane □ Antimalarial agents, potential—α-dibutylaminomethyl-2,6-bis(*p*-trifluoromethylphenyl)-4-pyridinemethanol, prototropic species characterized from electronic absorption and fluorescence spectra of various pH values and in *n*-hexane

A limited number of pyridinemethanol derivatives have been synthesized and screened for antimalarial activity (1–3). However, most of these compounds demonstrate either little activity or undesirable, toxic side effects (1). One of the few compounds of this class to exhibit antimalarial activity is the investigational drug α-dibutylaminomethyl-2,6-bis(trifluoromethylphenyl) -4- pyridinemethanol (I). It is 22 times more effective than quinine and is active against highly chloroquine-resistant *Plasmodium berghei* in mice (1). Although its specific mechanism of activity is unknown, it may be similar to, but not identical with, that of either chloroquine or quinine (1).

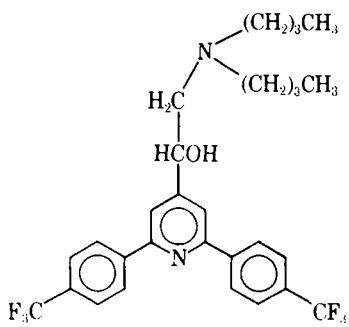

I

Most antimalarial compounds that exert their activity through a mechanism other than disruption of plasmodia nucleotide anabolism have at least one common feature. At physiological pH, these compounds exist as the singly charged cations or, as with chloroquine and quinacrine, as the doubly charged cation (4, 5). The cationic charge is believed to be involved in the binding of acridines, 9-aminoquinolines, and 8-aminoquinolines to parasitic DNA, and this binding is presumed to be related to antimalarial activity (6). Little is known about the mechanism of activity of quinine, alkaloids related to quinine, pyrimidines, quinolinemethanols, and pyridinemethanols. However, the singly charged cations of these agents may bind to plasmodia nuclear proteins, plasmodia DNA, or various enzymes in the metabolic network of these parasites (1, 7).

The present study of the dependence of the electronic spectra on the state of protonation and solvent properties of I was undertaken to elucidate the electronic structures of this compound and ultimately its interaction with native DNA, serum proteins, and selected enzymes.

0022-3549/78/0900-1224$01.00/0
© 1978, American Pharmaceutical Association

Table I—Electronic Absorption ($\lambda\,'L_b$ and $\lambda\,'L_a$) and Fluorescence (λ_f) Maxima of the Dication, Monocation, and Neutral Species of I in Aqueous Media [a]

	λ_a, nm		$\epsilon \times 10^{-3}$, liter/mole/cm	λ_f, nm
	$'L_a$	$'L_b$		
Dication	248 (0–0) 228 (max)	312 (max)	21	380 (max)
Monocation	238 (max)	296 (max) 286 (0–1)	8.5	348 (max)
Neutral species	246 (max)	305 (0–0) 290 (max)	6.5	478 (max)

[a] The dication was determined in 20% H_2SO_4 ($H_0 - 1.5$), the monocation was determined in dilute sulfuric acid at pH 3.0, and the neutral species was determined in dilute sodium hydroxide at pH 12.0. The molar absorptivities (ϵ) were determined at the long wavelength absorption maxima.

EXPERIMENTAL

Apparatus—Electronic absorption spectra were taken in 1-cm silica cells on a spectrophotometer[1]. Fluorescence spectra were recorded with a fluorescence spectrophotometer[2] having monochromators calibrated against the line emission spectrum of xenon. Emission and excitation spectra were corrected for the wavelength response of the light source, monochromators, beam splitter, and phototube by means of a variable resistor-corrected spectrum accessory utilizing an electric cam and rhodamine-B quantum counter. The pH measurements were made on a pH meter[3], employing a silver–silver chloride glass combination pH electrode[4].

Reagents—Compound I was supplied[5] as the hydrochloride salt. Elemental analysis of C,H,Cl,F,N yielded: calculated, 60.57, 5.78, 6.17, 19.82, 4.87; and found: 60.41, 5.62, 6.35, 19.61, 4.98. The melting point (234–235°) agreed with literature values (8, 9). The purity of the compound was verified by TLC in three different solvent systems: benzene–ethanol (9:1), R_f 0.70; chloroform–methanol (9:1), R_f 0.75; and ethanol–petroleum ether (bp 30–60°) (1:9), R_f 0.55.

All solvents were the highest grade commercially available. Acid solutions were prepared from reagent grade sulfuric acid[6] by dilution of the concentrated solution with distilled deionized water. Sodium hydroxide solutions were prepared by dilution, with distilled deionized water, of an 18 *M* solution prepared from USP grade sodium hydroxide pellets[6]. Reagent grade *n*-hexane[6] was used as necessary and did not interfere with the spectroscopic measurements.

Procedures—Ethanol solutions ($\sim 1 \times 10^{-3}$ *M*) of I were delivered from a 100-μl micropipet[7] into 100-ml volumetric flasks containing aqueous solutions at the desired pH. The added 0.1 ml caused negligible volume change. The ethanol solutions were too dilute to affect pH. All solutions were prepared immediately prior to use to remove decomposition errors and errors due to pH changes in poorly buffered solutions in the mid-pH region.

The corrected Hammett acidity scale of Jorgenson and Hartter (10) was employed to calibrate the sulfuric acid solutions. Solutions for the pH region were prepared by dilution of sulfuric acid or sodium hydroxide solution. Buffers were avoided because of their potential interference in fluorometric titrimetry (11). Trifluoroacetic acid was used to generate the dication in *n*-hexane. The hydrochloride salt was neutralized with 0.001 *N* NaOH to form the neutral species. The latter was extracted from solution with ether, allowed to dry, and then dissolved in *n*-hexane. All measurements were conducted at room temperature.

Ground- and excited-state dissociation constants, pKa and pKa*, respectively, were obtained graphically by plotting either the absorbance or relative fluorescence *versus* pH or Hammett acidity.

The ground-state pKa for the equilibrium between the monocation and neutral molecule was obtained potentiometrically. Ethanol solutions of I ($\sim 1 \times 10^{-3}$ *M*) as the hydrochloride salt were diluted with distilled, deionized water until their concentrations were 1×10^{-5} *M*. This procedure was necessary because of the extreme water insolubility of the compound. Three separate 100-ml aliquots of these solutions were titrated with 0.001 *N* NaOH, employing a microsyringe[8]. The pH was monitored during these titrations by the apparatus previously described. The pKa was determined graphically.

[1] Cary 118, Varian Associates, Instrument Division, Palo Alto, Calif.
[2] MPF-4, Perkin-Elmer Corp., Norwalk, Conn.
[3] Corning model 12, Fisher Scientific Co., Pittsburgh, Pa.
[4] Sensorex 5300C, Sensorex, Westminster, Calif.
[5] Walter Reed Army Institute of Research, Walter Reed Army Medical Center, Washington, DC 20012.
[6] J. T. Baker Chemical Co.
[7] Cole-Parmer Instrument Co., Chicago, Ill.
[8] Unimetrics Corp., Anaheim, Calif.

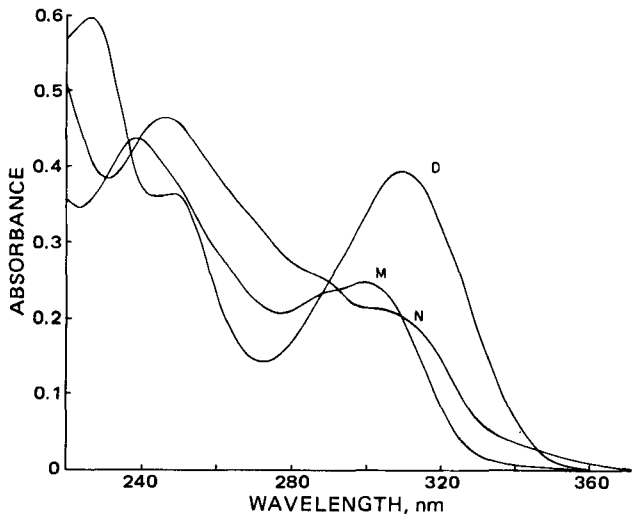

Figure 1—*Electronic absorption spectra of the dication (D), monocation (M), and neutral molecule (N) derived from I in aqueous and sulfuric acid media.*

RESULTS AND DISCUSSION

The electronic absorption and fluorescence maxima of the various prototropic species derived from I are presented in Table I, as are the molar absorptivities (ϵ) at the long wavelength absorption maxima of each species. The electronic absorption and fluorescence spectra of the dication, monocation, and neutral molecule are shown in Figs. 1 and 2, respectively.

For the dication, monocation, and neutral species, there are two distinct long wavelength absorption bands (Fig. 1). Earlier studies on 2-, 3-, and 4-hydroxypyridine derivatives related this two-band system, each band corresponding to a π–π^* transition, to that observed for various *ortho-*, *meta-*, and *para*-substituted benzene derivatives (12–14). The long wavelength band of the latter is the secondary band, while the band at shorter wavelengths is the primary band as designated by Doub and Vandenbelt (15, 16). These assignments correspond to the $'L_b$ and $'L_a$, respectively, in the notation of Klevens and Platt (17) and will be referred to as such here.

Acidity Dependence of Electronic Spectra—The pKa for the equilibrium between the singly charged and neutral species was deter-

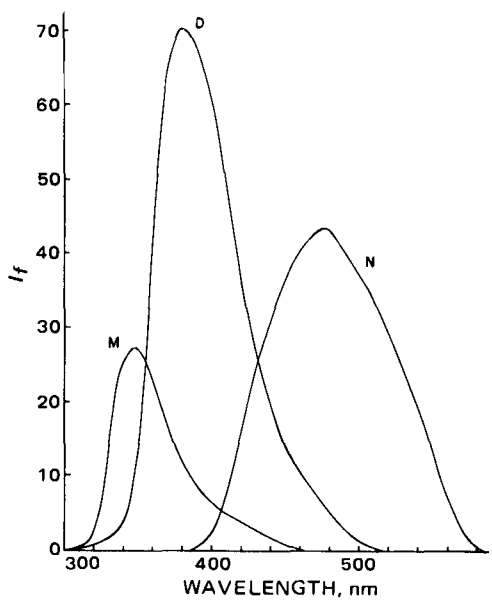

Figure 2—*Fluorescence spectra of the dication (D), monocation (M), and neutral molecule (N) derived from I in aqueous and sulfuric acid media; I_f is the relative fluorescence intensity.*

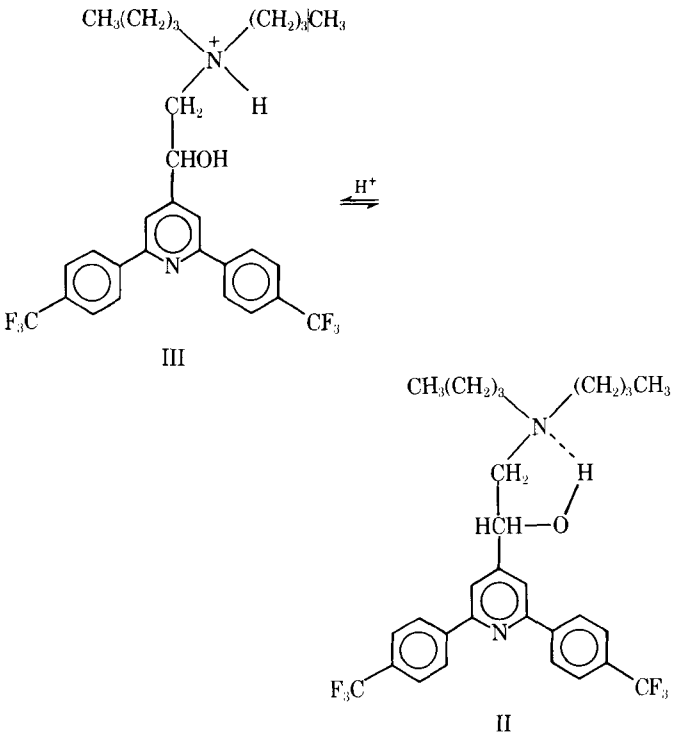

Scheme I

mined potentiometrically to be 8.3. Potentiometry was employed since the spectral band shape and position of the electronic absorption spectra of the monocation and neutral species were too similar to allow the spectroscopic determination of the ground-state dissociation constant. In the pH 3–14 region, the electronic absorption (both $'L_b$ and $'L_a$) and fluorescence maxima of solutions of I shifted to longer wavelengths (Figs. 1 and 2 and Table I) as solution pH was increased. The shift apparently corresponds to protonation of the neutral species, II, to form the monocation, III (Scheme I).

The pKa of the substituted exocyclic amino group relative to that of triethylamine (pKa 10.7) and tripropylamine (pKa 10.6) is anomalously low (18). Its decreased basicity may be the consequence of an intramolecular hydrogen bond between the hydroxyl hydrogen and the lone-pair electrons on the exocyclic nitrogen atom (Structure II). A similar decrease in the basicity of the quinuclidine nitrogen (pKa 8.4) in the neutral molecule of quinine was interpreted as due to an intramolecular hydrogen bond as shown in Structure IV (19). This interpretation also appears valid for II.

This interpretation may also be valid for the antimalarials mefloquine, a quinolinemethanol derivative (pKa 8.6), and 2,8-bis(trifluoromethyl)-4-[(1-hydroxy-3-*N*-*tert*-butylamino)propyl]quinoline[9] (pKa 8.22), which have 4-substituents capable of forming an intramolecular hydrogen bond and also exhibit unusually low pKa values for their exocyclic amino groups (20). Furthermore, it is supported by studies on the solvent dependence of the electronic spectra of all prototropic species derived from I and will be more fully discussed later.

Some differences in the electronic spectroscopy and chemistry of the two compounds (II and IV) can be attributed to the extent the postulated

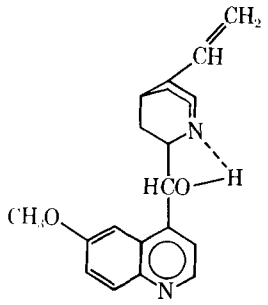

IV

[9] WR 184,806.

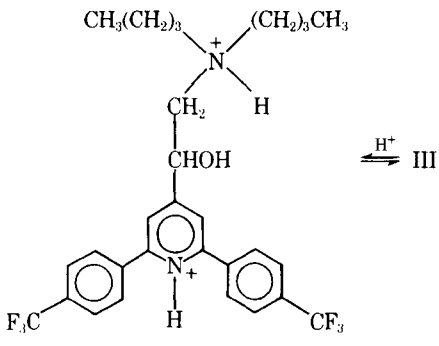

Scheme II

five-membered ring in II interacts with the aromatic portion of the molecule. Of primary importance is the displacement of the electronic spectra of the neutral molecule of I to longer wavelengths relative to its conjugate acid, a phenomenon not observed in the neutral quinine molecule. The shift suggests an interaction of the five-membered ring with the extended pyridinic nucleus. It probably occurs through a stabilization of the neutral compound by hyperconjugation of the substituted carbinol carbon with the π-electron system of the aromatic nucleus. Delocalization of alkyl electrons may be enhanced by the substantial electron-withdrawing effect of the *p*-trifluoromethylphenyl groups in the 2- and 6-positions. The latter is sufficiently strong so that the electronic dipole moment of neutral I is similar to that observed in neutral quinine.

In the lowest excited singlet state, dissociation of the protonated exocyclic amino group occurs in more acidic solutions than when in the ground state (*e.g.*, $pKa = 8.3 \pm 0.1 > pKa^* = 5 \pm 1$). The corresponding prototropic reaction is not observed in quinine since the fluorometric titration follows ground-state titration characteristics. Evidently, the intramolecular hydrogen bond in II is much stronger in the lowest excited singlet state than when in the ground state, thereby reducing to a greater extent the availability of the lone-pair electrons on the exocyclic amino group for protonation. The latter, when considered with the large displacement of the fluorescence spectra, may suggest that the exocyclic amino group is involved in the donation of electronic charge to the aromatic nucleus, more so in the lowest excited singlet state than in the ground state.

Acidic solutions of I have their electronic absorption (both $'L_b$ and $'L_a$) and fluorescence spectra shifted to longer wavelengths as solution acidity is increased from pH 3.0 to $H_0 - 2$ (Figs. 1 and 2 and Table I). In the lowest excited singlet state, the singly charged species is a weaker acid than when in the ground state (*e.g.*, $pKa = 0.0 + 0.1 < pKa^* = 2.5 \pm 0.2$). Studies on aminopyridines and other nitrogen heterocycles suggest that this behavior indicates protonation of the heterocyclic ring nitrogen on III to form the dication V (Scheme II) (21–23).

The low ground-state dissociation constant for the equilibrium between III and V relative to that observed for the dissociation of the pyridinium ion (pKa 5.2) (24) is perhaps the consequence of two related factors. First, protonation of the heterocyclic nitrogen may be sterically hindered by the *p*-trifluoromethylphenyl substituents in the 2- and 6-positions. Studies on 1-phenylpyridine indicate that the phenyl group is coplanar with the pyridine nucleus, a result supported by studies on quinolinemethanol derivatives (1, 25). Moreover, 2,6-diisopropyl- and 2,6-di-*tert*-butylpyridine exhibit a marked steric hindrance to protonation (21). In view of these studies, it seems probable that each *p*-trifluoromethylphenyl group on I is coplanar with the pyridinic moiety, thereby hindering protonation of the heterocyclic nitrogen and contributing to the relatively low basicity of the pyridinic nitrogen. Second, the bandform and position of the wavelength maxima of the $'L_b$ band of the dication (Fig. 1) are similar to those observed for singly charged 2-phenylpyridine. Each of the latter bands lies between the long wavelength absorption bands ($'L_b$) for singly charged pyridine and quinoline (the monocations for each exhibits a λ_{max} at 255 and 330 nm, respectively) (26). Analogous to 2-phenylpyridine as well as biphenyl, the π-electrons of the pyridinic nucleus of I are probably delocalized on the *p*-trifluoromethylphenyl substituents. This configuration would also account for coplanarity of these groups with the pyridine nucleus and tend to deplete the heterocyclic ring nitrogen of electronic charge.

It is difficult to assess the electron-withdrawing inductive and π-electron delocalization effects of the *p*-trifluoromethylphenyl groups on the basicity of the heterocyclic ring nitrogen because of a scarcity of information. However, 2-phenyl substitution in pyridine has a base-

Table II—Long Wavelength Electronic Absorption (^1L_b) and Fluorescence (λ_f) Maxima of the Dication, Monocation, and Neutral Molecule of I in *n*-Hexane

	$\lambda\,^1L_b$, nm	λ_f, nm
Dication	318	385
Monocation	302	342 (0–0) 335 (max)
Neutral species	312	415

weakening effect of 1 log unit relative to pyridine; that of 2-*p*-nitrophenyl substitution is 1.6 log units (24, 25). Moreover, it is plausible to assume that 2-trifluoromethylphenyl substitution will have a base-weakening effect somewhat less than or very near the latter. Therefore, the substituents in the 2- and 6-positions on I cannot decrease basicity more than 3.2 log units. In the 4-position, the substituted carbinol carbon, which can only donate an electronic charge, may increase basicity by no more than 0.7 log unit. [For example, 2-methylpyridine has pKa 5.9. Delocalization of carbinol carbon electrons may be reduced by the electric field effect of the protonated exocyclic nitrogen, but this cannot be assessed at this time (24).] The overall base-weakening effect is approximately 2.5 log units relative to pyridine. Apparently, the low dissociation constant of doubly charged I is due equally to steric hindrance by the 2- and 6-substituents to protonation at the heterocyclic ring nitrogen and to the overall inductive effects and π-electron delocalization over the entire aromatic nucleus.

Solvent Dependence of Electronic Spectra—The Stokes shifts (absorption maxima to fluorescence maxima) of the neutral molecule in aqueous media (Table I) and *n*-hexane (Table II) are almost twice as large as those of the monocation and dication (Table III). Thermal relaxation processes from the Franck–Condon excited state to the thermally relaxed excited state are apparently greater in the neutral molecule than in either of the other species. A similar increase in the Stokes shift was interpreted by Weller (27) as an intramolecular proton transfer in the excited state. Since the hydrogen bonding in the five-membered ring of neutral I qualifies as partial proton transfer, the increase in the Stokes shift of the neutral molecule relative to the monocation and dication appears to be further evidence for the existence of the five-membered hydrogen-bonded substituent in the neutral species.

The shift of the electronic absorption spectra of all prototropic species to shorter wavelengths (increasing energy) upon changing the solvent from *n*-hexane to water suggests that the ground state of all species is stabilized relatively more than the Franck–Condon excited state and is, therefore, more polar (Tables I and II). The magnitude of the shifts for the dication, monocation, and neutral species (0.06, 0.07, and 0.17 μm^{-1}, respectively) suggests that the neutral species is stabilized greater than either the monocation or dication when in the ground state.

The corresponding shifts in the fluorescence spectra are to longer wavelengths (decreasing energy) upon increasing the polarity and hydrogen bonding capability of the solvent. The latter indicates that, in the lowest excited singlet state, all species are stabilized to a greater extent than when in the Franck–Condon ground state and are more polar. The values for the shifts of the dication, monocation, and neutral species are 0.03, 0.05, and 0.21 μm^{-1}, respectively. These values indicate that the neutral molecule also is stabilized to a greater extent than are the monocation and dication when in the lowest excited singlet state.

The greater stabilization of the neutral molecule in both ground and lowest excited singlet states may be due to the conformation change of the 4-substituent upon formation of a five-membered ring. This concept suggests a difference in conformation of the 4-substituent on the neutral and singly charged species, which may be due to a change in solvation of the latter. This notion is supported by the disparity in the Stokes shifts between the neutral molecule and the monocation (Table III). In fact, the similar magnitudes of these shifts for the monocation and dication

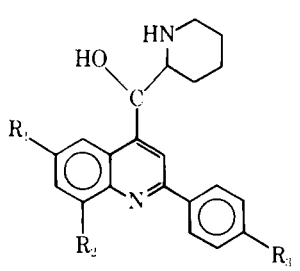

VI

Table III—Stokes Shifts Obtained from the Various Prototropic Species Derived from I in Aqueous Media and *n*-Hexane

	$\Delta\bar{\nu}$, μm^{-1}	
	Aqueous	*n*-Hexane
Dication	0.58	0.52
Monocation	0.62	0.39
Neutral species	1.2	0.80

imply that the 4-substituent on these species is contained in the same solvent cage, which is different from that of the neutral molecule. Evidently, protonation of the neutral species at the exocyclic amino group disrupts the hydrogen-bonded five-membered ring. This rupture results in a reorientation of the solvent cage surrounding the 4-substituent such that the monocation does not engage in an intramolecular hydrogen bond that is observable by the methods employed in this study.

The relevance of the conformation of the 4-substituent in the monocation and neutral species is that a nonaromatic heterocycle, such as the piperidyl moiety in VI, may be necessary for the antimalarial activity of the amino alcohols. It was suggested (28) that amino alcohols similar to I, which possess an amino functional group substituted so that it is free to form an intramolecular hydrogen bond with the nearby carbinol hydroxyl group, owe their antimalarial activity, at least in part, to the formation of a hydrogen-bonded five- or six-membered nonplanar ring.

A more recent and specific study (29) dealt with the conformation of a family (VII*a*–VII*c*) of related antimalarial phenanthrene amino alcohols that have a methanolpiperidine substituent capable of forming an intramolecular hydrogen bond like the one observed in I and IV. The study proposed a model pharmacophore for the singly charged cation, which includes an intramolecular hydrogen bond between a hydrogen atom on the protonated piperidyl nitrogen in VII*a* and VII*b* and the carbinol oxygen atom. Structure VII*c* is said not to form such a hydrogen-bonded ring.

The results presented here for I indicate that the pseudo-oxazole ring system depicted by II is established and spectroscopically visible in the neutral species but not in the singly charged cation, III.

A possible explanation for these results is that the hydrogen bonding of the hydroxyl hydrogen atom with the exocyclic amino group decreases the steric hindrance of this atom with the hydrogens in the 3- and 5-positions on the pyridine ring. This situation could allow the pseudo-oxazole ring system to attain a greater degree of coplanarity with the pyridinic nucleus and thus account for the observed increase in electron delocalization. Protonation of the exocyclic nitrogen atom disrupts the hydrogen-bonded hydroxyl hydrogen from its association with the amino group. The possibility of mutual repulsion of the latter with the hydrogen atoms in either position 3 or 5 on the pyridinic nucleus is now increased and may be responsible for III not forming a ring system like that in II. The monocation, III, may form an out-of-plane hydrogen-bonded ring

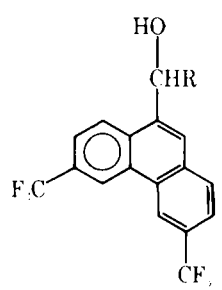

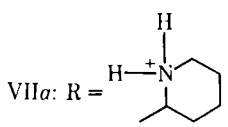

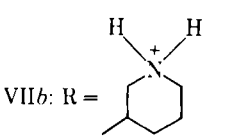

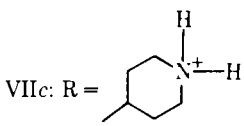

similar to that reported for VII*a* and VII*b*; however, there is no definite spectroscopic evidence of its existence.

REFERENCES

(1) P. E. Thompson and L. M. Werbel, "Antimalarial Agents: Chemistry and Pharmacology," Academic, New York, N.Y., 1972, chap. 8.

(2) P. Blumbergs, M. P. LaMontagne, A. Markovac, J. G. Moehring, A. B. Ash, and C. L. Stevens, *J. Med. Chem.*, **15**, 808 (1972).

(3) A. Markovac, M. P. LaMontagne, P. Blumbergs, A. B. Ash, and C. L. Stevens, *ibid.*, **15**, 918 (1972).

(4) A. Albert, "Selective Toxicity," 4th ed., Metheun & Co., London, England, 1968.

(5) A. C. Capomacchia, J. Casper, and S. G. Schulman, *J. Pharm. Sci.*, **63**, 1272 (1974).

(6) P. E. Thompson and L. M. Werbel, "Antimalarial Agents: Chemistry and Pharmacology," Academic, New York, N.Y., 1972, chaps. 9 and 11.

(7) *Ibid.*, chap. 7.

(8) W. Zecher and F. Krohnke, *Chem. Ber.*, **94**, 690 (1961).

(9) F. Krohnke and W. Zecher, *Angew. Chem., Int. Ed. Engl.*, **1**, 626 (1962).

(10) M. J. Jorgenson and D. R. Hartter, *J. Am. Chem. Soc.*, **85**, 878 (1963).

(11) S. G. Schulman, in "Acid–Base Chemistry of Excited Singlet States: Fundamentals and Analytical Implications, Modern Fluorescence Spectroscopy, Newer Techniques and Applications," E. L. Wehry, Ed., Plenum, New York, N.Y., 1976.

(12) D. E. Metzler and E. E. Snell, *J. Am. Chem. Soc.*, **77**, 2431 (1955).

(13) K. Nakamoto and A. E. Martell, *ibid.*, **81**, 5857 (1959).

(14) *Ibid.*, **81**, 5863 (1959).

(15) L. Doub and J. M. Vandenbelt, *J. Am. Chem. Soc.*, **69**, 2714 (1947).

(16) *Ibid.*, **71**, 2414 (1949).

(17) H. B. Klevens and J. R. Platt, *J. Chem. Phys.*, **17**, 470 (1949).

(18) R. T. Morrison and R. N. Boyd, "Organic Chemistry," 2nd ed., Allyn and Bacon, Boston, Mass., 1966.

(19) S. G. Schulman, R. M. Threatte, A. C. Capomacchia, and W. L. Paul, *J. Pharm. Sci.*, **63**, 876 (1974).

(20) J. M. Grindel, R. S. Rozman, D. M. Leahy, N. A. Molek, and H. H. Gillum, *J. Pharmacol. Exp. Ther.*, **4**, 133 (1976).

(21) S. G. Schulman, A. C. Capomacchia, and M. S. Rietta, *Anal. Chim. Acta*, **56**, 91 (1971).

(22) S. F. Mason, *J. Chem. Soc.*, **1960**, 219.

(23) A. Weller, "Progress in Reaction Kinetics," vol. 1, Pergamon, London, England, 1961.

(24) A. Albert, in "Physical Methods in Heterocyclic Chemistry," vol. I, A. R. Katritsky, Ed., Academic, New York, N.Y., 1963.

(25) P. Krumholz, *J. Am. Chem. Soc.*, **73**, 3487 (1951).

(26) S. F. Mason, in "Physical Methods in Heterocyclic Chemistry," vol. II, A. R. Katritzky, Ed., Academic, New York, N.Y., 1963.

(27) A. Weller, *Z. Elektrochem.*, **60**, 1144 (1960).

(28) C. C. Cheng, *J. Pharm. Sci.*, **60**, 1596 (1971).

(29) G. H. Loew and R. Sahakian, *J. Med. Chem.*, **20**, 103 (1977).

Antitumor Agents XXVIII: Structural Elucidation of the Novel Antitumor Sesquiterpene Lactone, Microlenin, from *Helenium microcephalum*

YASUHIRO IMAKURA, KUO-HSIUNG LEE ˣ, DONALD SIMS, and IRIS H. HALL

Received July 29, 1977, from the *Division of Medicinal Chemistry, School of Pharmacy, University of North Carolina at Chapel Hill, Chapel Hill, NC 27514.* Accepted for publication December 28, 1977.

Abstract □ The structure and stereochemistry of the novel dimeric antitumor sesquiterpene lactone, microlenin, were determined on the basis of ^{1}H-NMR, ^{13}C-NMR, and mass spectral evidence.

Keyphrases □ Microlenin—isolated from *Helenium microcephalum* whole plant extract, structure and stereochemistry determined □ *Helenium microcephalum*—whole plant extract, microlenin isolated, structure and stereochemistry determined □ Antineoplastic agents, potential—microlenin, isolated from *Helenium microcephalum* whole plant extract, structure and stereochemistry determined

A search for ample supplies of helenalin for the purpose of elucidating the structure–activity relationships between sesquiterpene lactones and antitumor activity led to the investigation of the plant *Helenium microcephalum*. Previously, it was reported (1) that this species contains helenalin in good yield. Examination of the whole plant extract revealed that, after the removal of helenalin, the mother liquor had constituents possessing significant inhibitory activity against the Walker 256 carcinosarcoma in rats. Further work with the chloroform extract resulted in the isolation and structure determination of mexicanin-E; microhelenins-A, B, and C (2, 3); and microlenin, a novel antineoplastic principle which resulted in a T/C value of 172 at 2.5 mg/kg/day in Walker 256 carcinosarcoma in Sprague–Dawley rats. The detailed structural determination of microlenin by physical methods is now reported.

RESULTS AND DISCUSSION

Microlenin (1*a*) was isolated by elution with chloroform–ethyl acetate from a silica gel column. Although the structure of microlenin was described previously (4), the stereochemistry and conformational assignments for microlenin require further comments. Microlenin contains an α,β-unsaturated cyclopentenone (IR bands at 1707 and 1580 cm^{-1}; ^{1}H-NMR: doublet of doublets of H_b and H_c at δ 7.84 and 6.02 ppm) and an α,β-unsaturated lactone of the type shown in partial structure A (IR bands at 1756 and 1664 cm^{-1}; narrowly split ^{1}H-NMR doublet of H_j and H_k at δ 6.13 and 5.73 ppm).

The presence of a secondary hydroxyl group (IR band at 3521 cm^{-1};

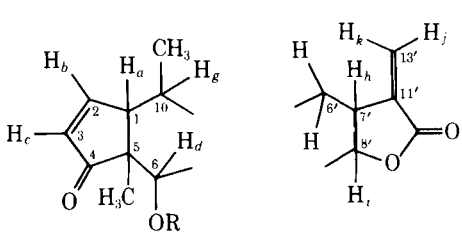

Partial Structure A

0022-3549/78/0900-1228$01.00/0

© 1978, American Pharmaceutical Association

similar to that reported for VII*a* and VII*b*; however, there is no definite spectroscopic evidence of its existence.

REFERENCES

(1) P. E. Thompson and L. M. Werbel, "Antimalarial Agents: Chemistry and Pharmacology," Academic, New York, N.Y., 1972, chap. 8.

(2) P. Blumbergs, M. P. LaMontagne, A. Markovac, J. G. Moehring, A. B. Ash, and C. L. Stevens, *J. Med. Chem.*, **15**, 808 (1972).

(3) A. Markovac, M. P. LaMontagne, P. Blumbergs, A. B. Ash, and C. L. Stevens, *ibid.*, **15**, 918 (1972).

(4) A. Albert, "Selective Toxicity," 4th ed., Metheun & Co., London, England, 1968.

(5) A. C. Capomacchia, J. Casper, and S. G. Schulman, *J. Pharm. Sci.*, **63**, 1272 (1974).

(6) P. E. Thompson and L. M. Werbel, "Antimalarial Agents: Chemistry and Pharmacology," Academic, New York, N.Y., 1972, chaps. 9 and 11.

(7) *Ibid.*, chap. 7.

(8) W. Zecher and F. Krohnke, *Chem. Ber.*, **94**, 690 (1961).

(9) F. Krohnke and W. Zecher, *Angew. Chem., Int. Ed. Engl.*, **1**, 626 (1962).

(10) M. J. Jorgenson and D. R. Hartter, *J. Am. Chem. Soc.*, **85**, 878 (1963).

(11) S. G. Schulman, in "Acid–Base Chemistry of Excited Singlet States: Fundamentals and Analytical Implications, Modern Fluorescence Spectroscopy, Newer Techniques and Applications," E. L. Wehry, Ed., Plenum, New York, N.Y., 1976.

(12) D. E. Metzler and E. E. Snell, *J. Am. Chem. Soc.*, **77**, 2431 (1955).

(13) K. Nakamoto and A. E. Martell, *ibid.*, **81**, 5857 (1959).

(14) *Ibid.*, **81**, 5863 (1959).

(15) L. Doub and J. M. Vandenbelt, *J. Am. Chem. Soc.*, **69**, 2714 (1947).

(16) *Ibid.*, **71**, 2414 (1949).

(17) H. B. Klevens and J. R. Platt, *J. Chem. Phys.*, **17**, 470 (1949).

(18) R. T. Morrison and R. N. Boyd, "Organic Chemistry," 2nd ed., Allyn and Bacon, Boston, Mass., 1966.

(19) S. G. Schulman, R. M. Threatte, A. C. Capomacchia, and W. L. Paul, *J. Pharm. Sci.*, **63**, 876 (1974).

(20) J. M. Grindel, R. S. Rozman, D. M. Leahy, N. A. Molek, and H. H. Gillum, *J. Pharmacol. Exp. Ther.*, **4**, 133 (1976).

(21) S. G. Schulman, A. C. Capomacchia, and M. S. Rietta, *Anal. Chim. Acta*, **56**, 91 (1971).

(22) S. F. Mason, *J. Chem. Soc.*, **1960**, 219.

(23) A. Weller, "Progress in Reaction Kinetics," vol. 1, Pergamon, London, England, 1961.

(24) A. Albert, in "Physical Methods in Heterocyclic Chemistry," vol. I, A. R. Katritsky, Ed., Academic, New York, N.Y., 1963.

(25) P. Krumholz, *J. Am. Chem. Soc.*, **73**, 3487 (1951).

(26) S. F. Mason, in "Physical Methods in Heterocyclic Chemistry," vol. II, A. R. Katritzky, Ed., Academic, New York, N.Y., 1963.

(27) A. Weller, *Z. Elektrochem.*, **60**, 1144 (1960).

(28) C. C. Cheng, *J. Pharm. Sci.*, **60**, 1596 (1971).

(29) G. H. Loew and R. Sahakian, *J. Med. Chem.*, **20**, 103 (1977).

Antitumor Agents XXVIII: Structural Elucidation of the Novel Antitumor Sesquiterpene Lactone, Microlenin, from *Helenium microcephalum*

YASUHIRO IMAKURA, KUO-HSIUNG LEE ˣ, DONALD SIMS, and IRIS H. HALL

Received July 29, 1977, from the *Division of Medicinal Chemistry, School of Pharmacy, University of North Carolina at Chapel Hill, Chapel Hill, NC 27514.* Accepted for publication December 28, 1977.

Abstract □ The structure and stereochemistry of the novel dimeric antitumor sesquiterpene lactone, microlenin, were determined on the basis of ^{1}H-NMR, ^{13}C-NMR, and mass spectral evidence.

Keyphrases □ Microlenin—isolated from *Helenium microcephalum* whole plant extract, structure and stereochemistry determined □ *Helenium microcephalum*—whole plant extract, microlenin isolated, structure and stereochemistry determined □ Antineoplastic agents, potential—microlenin, isolated from *Helenium microcephalum* whole plant extract, structure and stereochemistry determined

A search for ample supplies of helenalin for the purpose of elucidating the structure–activity relationships between sesquiterpene lactones and antitumor activity led to the investigation of the plant *Helenium microcephalum*. Previously, it was reported (1) that this species contains helenalin in good yield. Examination of the whole plant extract revealed that, after the removal of helenalin, the mother liquor had constituents possessing significant inhibitory activity against the Walker 256 carcinosarcoma in rats. Further work with the chloroform extract resulted in the isolation and structure determination of mexicanin-E; microhelenins-A, B, and C (2, 3); and microlenin, a novel antineoplastic principle which resulted in a T/C value of 172 at 2.5 mg/kg/day in Walker 256 carcinosarcoma in Sprague–Dawley rats. The detailed structural determination of microlenin by physical methods is now reported.

RESULTS AND DISCUSSION

Microlenin (1*a*) was isolated by elution with chloroform–ethyl acetate from a silica gel column. Although the structure of microlenin was described previously (4), the stereochemistry and conformational assignments for microlenin require further comments. Microlenin contains an α,β-unsaturated cyclopentenone (IR bands at 1707 and 1580 cm^{-1}; ^{1}H-NMR: doublet of doublets of H_b and H_c at δ 7.84 and 6.02 ppm) and an α,β-unsaturated lactone of the type shown in partial structure A (IR bands at 1756 and 1664 cm^{-1}; narrowly split ^{1}H-NMR doublet of H_j and H_k at δ 6.13 and 5.73 ppm).

The presence of a secondary hydroxyl group (IR band at 3521 cm^{-1};

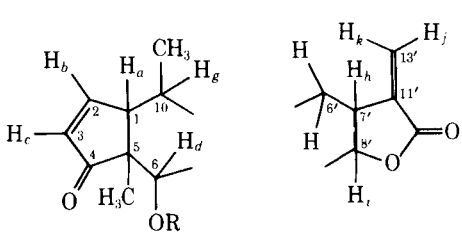

Partial Structure A

0022-3549/78/0900-1228$01.00/0

© 1978, American Pharmaceutical Association

Table I—^{1}H-NMR Spectra of II*b*, III, and I*b* at 100 MHz in Deuterochloroform [a]

Assignment	II*b*	III[b]	I*b*
H-1	3.05 (ddd, 2.0, 3.0, 11.0)	—[d]	3.10 (ddd, 2.0, 3.0, 11.0)
H-2	7.69 (dd, 2.0, 6.0)	7.83 (dd, 2.25, 6.0)	7.67 (dd, 2.0, 6.0)
H-3	6.09 (dd, 3.0, 6.0)	6.28 (dd, 2.25, 6.0)	6.06 (dd, 3.0, 6.0)
H-6	5.41 (br)	—[d]	5.62 (br)
H-7	3.53 (m)	—[d]	2.48 (d, 8.0)
H-8	4.92 (m)	4.64 (m)	4.95 (m)
H-13a	6.46 (d, 3.0)	6.23 (d, 1.5)	
H-13b	6.15 (d, 2.25)	5.70 (d, 1.5)	
H-14[c]	1.27 (d, 7.0)	1.19 (d, 6.0)	1.23 (d, 7.0)
H-15[c]	1.00[c]		0.94
H-7′			3.29 (m)
H-8′			4.71 (m)
H-13′a			6.28 (d, 3.0)
H-13′b			5.52 (d, 3.0)
H-14′			1.18 (d, 7.0)

[a] Values are in parts per million; multiplicities are indicated by the usual symbols: d, doublet; m, multiplet whose center is given; and br, slightly broadened singlet. Unmarked signals are singlets. Figures in parentheses are coupling constants in hertz. [b] The 60-MHz NMR spectrum of III was reported previously (6). [c] Three-proton intensity. [d] Obscured signal.

^{1}H-NMR doublet at δ 5.51 ppm) that disappeared upon addition of deuterated water was confirmed by acetylation of microlenin with acetic anhydride and pyridine. This reaction gave the monoacetate (I*b*) ($C_{31}H_{36}O_8$, high-resolution mass spectrum, mp 278°), which showed the loss of a free hydroxyl in its IR spectrum (carbon tetrachloride). This loss was accompanied by a paramagnetic shift of a signal in its ^{1}H-NMR spectrum from δ 4.20 to 5.62 ppm[1].

A comparison of the chemical shifts and splitting patterns of the ^{1}H-NMR spectra of helenalin acetate (II*b*) (5), mexicanin-E (III) (6–10), and microlenin acetate (I*b*) provided strong evidence for the presence of the partial structure A in I*a* and I*b* (Table I). The ^{1}H-NMR spectrum of I*b* showed the low field doublet of doublets at δ 7.67 ($J_{1,2}$ = 2.0 and $J_{2,3}$ = 6.0 Hz) and 6.06 ($J_{1,3}$ = 3.0 and $J_{2,3}$ = 6.0 Hz) ppm, characteristic of the unsubstituted α,β-unsaturated cyclopentenone found in helenalin (II*a*) and III. The usual narrowly split doublets at δ 6.28 (H_k, J = 3.0 Hz) and 5.52 (H_j, J = 3.0 Hz) ppm due to the α-methylene-γ-lactone moiety of III were also present.

The presence in the ^{1}H-NMR spectrum of one methyl singlet and two methyl doublets led to the postulation of the novel dimeric sesquiterpene lactone structure, I*b*, for microlenin acetate (devoid of stereochemistry). The conclusions that the acetyl side chain was attached to C-6 (with H_d being accounted for by a somewhat broadened singlet at δ 5.62 ppm) and that the lactone rings were closed at C-8 (with multiplet at δ 4.95 ppm) and C-8′ (with multiplet at δ 4.71 ppm) were based on analogous substitution patterns found in other pseudoguaianolides (*i.e.*, II*b* and III).

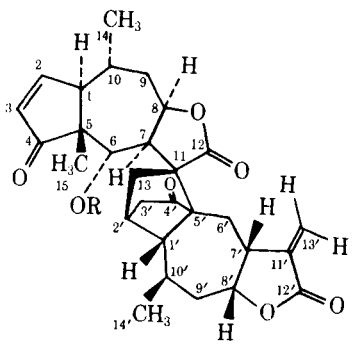

I*a*: R = H
I*b*: R = $COCH_3$

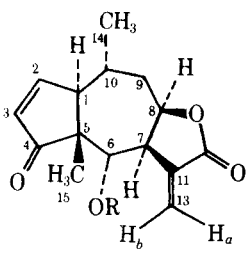

II*a*: R = H
II*b*: R = $COCH_3$

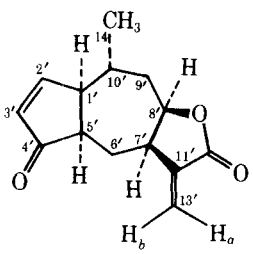

III

Extensive double resonance experiments (Table I) on I*b* led to the assignment of protons that confirmed the carbon skeleton and oxygenation pattern postulated for microlenin. For example, identification of H_a (H-1) as a doublet of doublets of doublets ($J_{1,2}$ = 2.0 Hz, $J_{1,3}$ = 3.0 Hz, and $J_{1,10}$ = 11.0 Hz) at δ 3.10 ppm was achieved by double irradiation at the frequency of H_k and H_c. The location of H_h (H-7′) as a multiplet at δ 3.29 ppm was established by double irradiation at the frequency of H_j and H_k.

Conversely, irradiation at the frequency of H_h collapsed H_j and H_k into singlets and also slightly sharpened the signal of H_i (H-8′) at δ 4.71 ppm. Irradiation at the frequency of H_i converted H_h into a broad doublet of doublets. The foregoing evidence led to the assignment of the partial structure A for I*a*. The remaining three oxygen atoms of the empirical formula of I*a* were derived from a γ-lactone (IR band at 1763 cm^{-1}) and a cyclopentanone (IR band at 1744 cm^{-1}).

The ^{13}C-NMR spectrum (Table II) of I*a* indicated that microlenin contained 29 carbon atoms and possessed the following skeletal systems: seven >CH–; five $-CH_2-$; three each of –CHO–, >C<, and $-CH_3$; two each of –CH=, >C=O, and –C=O(O); and one each of CH_2= and >C=. The extreme similarities of the ^{1}H-NMR (Table I) and ^{13}C-NMR (Table II) parameters of I*a*, I*b*, II*a*, II*b*, and III further strengthened the chemical evidence that microlenin must be derived from helenalin and mexicanin-E. The major differences between the ^{1}H and ^{13}C-NMR spectra of I*a* (or I*b*), II*a* (or II*b*), and III were observed among the proton signals at C-7, C-13a,b, C-2′, and C-3′ and among the carbon signals at C-11, C-13, C-2′, and C-3′ (Tables I and II).

In the ^{13}C-NMR spectrum of microlenin, the carbon signals due to C-11 (singlet), C-13 (triplet), C-2′ (doublet), and C-3′ (triplet) at 67.4, 34.6, 35.5, and 38.2 ppm were observed, respectively. However, in the case of helenalin and mexicanin-E, these characteristic signals [C-11 (singlet), C-13 (triplet), C-2′ (doublet), and C-3′ (doublet)] were seen at 139.8, 129.8,

Table II—^{13}C-NMR Spectra of II*a*, III, and I*a* [a]

Assignment[b]		II*a*	III	I*a*	
C-1	(C-1′)	51.90 d	(45.0 d)	52.9 d	(38.8 d)
C-2	(C-2′)	163.98 d	(166.7 d)	163.9 d	(35.5 d)
C-3	(C-3′)	121.90 d	(132.9 d)	129.4 d	(38.2 t)[g]
C-4	(C-4′)	193.00	(194.3)	215.0[f]	(213.7)[f]
C-5	(C-5′)	57.70	(48.2 d)	57.6	(54.6)
C-6	(C-6′)	79.10 d	(28.0 t)	81.4 d	(26.7 t)
C-7	(C-7′)	52.40 d	(53.6 d)	53.6 d[e]	(53.1 d)[e]
C-8	(C-8′)	74.30 d	(78.9 d)	70.8 d	(76.5 d)
C-9	(C-9′)	40.40 t	(38.7 t)	41.2 t	(41.0 t)
C-10	(C-10′)	26.70 d	(31.7 d)	26.4 d[d]	(26.1 d)[d]
C-11	(C-11′)	139.80	(142.5)	67.4	(140.7)
C-12	(C-12′)	170.20	(170.2)	181.1	(169.1)
C-13	(C-13′)	129.80 t	(121.0 t)	34.6 t[g]	(122.5 t)
C-14	(C-14′)	20.30 q	(21.5 q)	20.1 q[e]	(21.5 q)[e]
C-15		18.80 q		19.7 q	

[a] Run in acetone-d_6–pyridine-d_5 (1:1) on a Varian XL-100 instrument. Unmarked signals are singlets. [b] Assignments based on predicted shifts and comparisons with data in the literature and on file. [c–g] These assignments may be interchanged.

[1] Part of this unusually large shift was attributed to a change of solvent from dimethyl sulfoxide-d_6 to deuterochloroform.

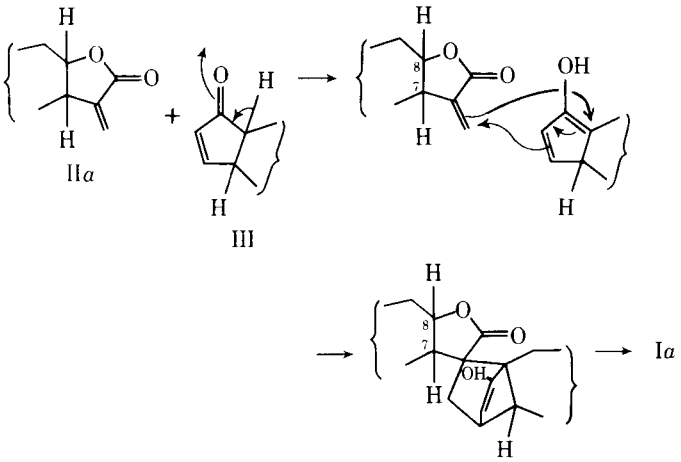

Scheme I

166.7, and 132.9 ppm, respectively. In the ^{1}H-NMR spectrum of I*b*, identification of H_e (H-7) as a broad doublet at 2.48 ppm was achieved by irradiating at frequencies corresponding to those of H_d and H_f. Conversely, irradiation at the frequency of H_e converted a broad singlet at 5.62 ppm (H_d) into a sharp singlet and also sharpened H_f.

These observations allowed expansion of partial structure A to Structure B, which required attachment of the quaternary methyl group to C-5 as in I*a* (devoid of stereochemistry).

The cooccurrence of I*a* with II*a* and III, together with the foregoing evidence, suggested that it had a dimeric sesquiterpene lactone structure resulting from a Diels–Alder-type condensation that involved the 11,13-double bond of helenalin and the enol form of the cyclopentenone ring of a norpseudoguaianolide (mexicanin-E) (Scheme I).

The high-resolution mass spectral data of I*b* (Schemes II–IV) further corroborated these structural assignments. Diagnostically important peaks at *m/e* 95, 96, 123, 124, 232, 305, and 476 indicated the presence of a pseudoguaianolide sesquiterpene lactone bearing oxygen substituents at the 4-, 6-, and 8-positions (11, 12) and a saturated (exocyclic double) bond at C-11 as found in I*b*.

Assignment of the stereochemistry of microlenin was based on two considerations. First, there was the similarity of chemical shifts and coupling constants among microlenin acetate (I*b*), helenalin acetate (II*b*), and mexicanin-E (III). This fact led to the conclusion that microlenin possessed the stereochemistry of helenalin acetate at C-1, C-5, C-6, C-7, and C-8 and that of mexicanin-E at C-1′, C-7′, C-8′, and C-10′. The stereochemistry at C-10 and C-5′ remained undefined. The magnitude of $J_{1,10}$ determined the relative configuration at C-1 and C-10; therefore, if the configuration of H_a was established, the configuration at C-10 would be known. Since $J_{1,10}$ = 11.0 Hz, H_a and H_g must be diaxial as shown in Structure C.

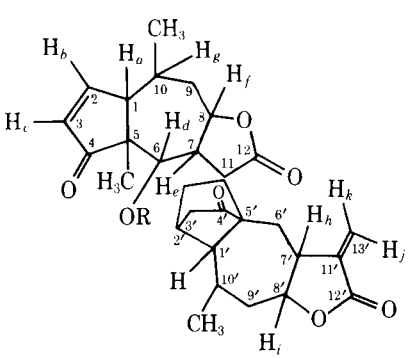

Structure B

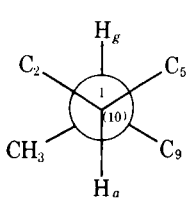

Structure C

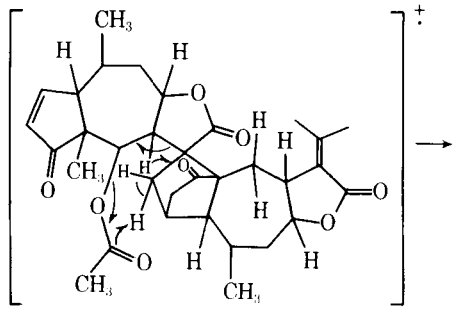

$C_{31}H_{36}O_8$
m/e 536 (1.8%)
Found: 536.2407
Calc.: 536.2408

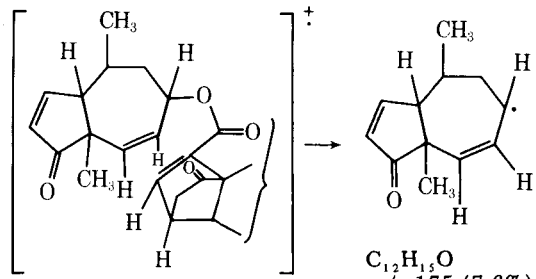

$C_{29}H_{32}O_6$
m/e 476 (10.5%)
Found: 476.2195
Calc.: 476.2199

$C_{12}H_{15}O$
m/e 175 (7.6%)

Scheme II

If the usual assumption is made that the C-7 (C-7′) side chain is equatorial and beta as in all sesquiterpene lactones of known stereochemistry, the value (J = 8.0) of $J_{7,8}$ requires that H_f (C-8) be *cis* to H_e (H-7) and alpha (4); thus, the lactone ring was *cis*-fused. The *cis*-fused α-methylene-γ-lactone ring was confirmed by the magnitude of $J_{7',13a}$ and $J_{7',13'b}$ (<Hz) according to the Samek (13) rule. The stereochemistry at H_d (H-6) was deduced by comparison of the observed coupling constant with that obtained from the dihedral angle in a Dreiding model. The small value ($w_{1/2}$ = 3.0) of $J_{6,7}$ could be explained only by a β-orientation of H_d (C-6).

Second, the stereochemical assignments were based on the biogenetic consideration of the cooccurrence of helenalin and mexicanin-E (which have known absolute configurations) with microlenin. Since helenalin has a conformation closer to a twist-chair rather than a chair form (14), the presence of a *cis*-fused α-methylene-γ-lactone ring in addition to a β-oriented 5-methyl group would produce a severe steric hindrance on the β-face of the molecule. On the other hand, the cycloheptane ring in mexicanin-E adopted a conformation approximately midway between a chair and a twist-chair form (3). Furthermore, it contained one *cis*-fused α-methylene-γ-lactone ring and one *cis*-fused cyclopentenone ring. Consequently, microlenin would be produced by a Diels–Alder-type condensation involving the 11,13-double bond of helenalin, which approached from the α-face of the enolic form of the cyclopentenone ring of mexicanin-E.

This evidence led to the establishment of Structure I*a* for microlenin. Further confirmation of this assignment was achieved by a single-crystal X-ray analysis of microlenin (4).

EXPERIMENTAL[2]

Isolation of Microlenin from *H. microcephalum*—Microlenin was

[2] Unless otherwise specified, melting points were determined utilizing a Thomas-Hoover melting-point apparatus and are uncorrected. Other instruments used were: for specific rotations, Perkin-Elmer model 141 polarimeter (1 = 1 dm); for IR spectra, Perkin-Elmer 257 grating IR spectrometer; for ^{1}H-NMR and ^{13}C-NMR spectra (tetramethylsilane as internal standard), Jeolco (60 MHz) or Varian XL-100 NMR spectrometer; for mass spectra, A.E.I. MS-902 spectrometer (direct inlet at 70 ev); and for optical rotatory dispersion and circular dichroism spectra: Cary model 60 spectrometer. Silica gel (Mallinckrodt CC-7, 200–325 mesh) was used for column chromatography and Merck silica gel G was used for TLC. Detection of components was made by spraying with a 1% $Ce(SO_4)_2$–10% H_2SO_4 solution followed by heating.

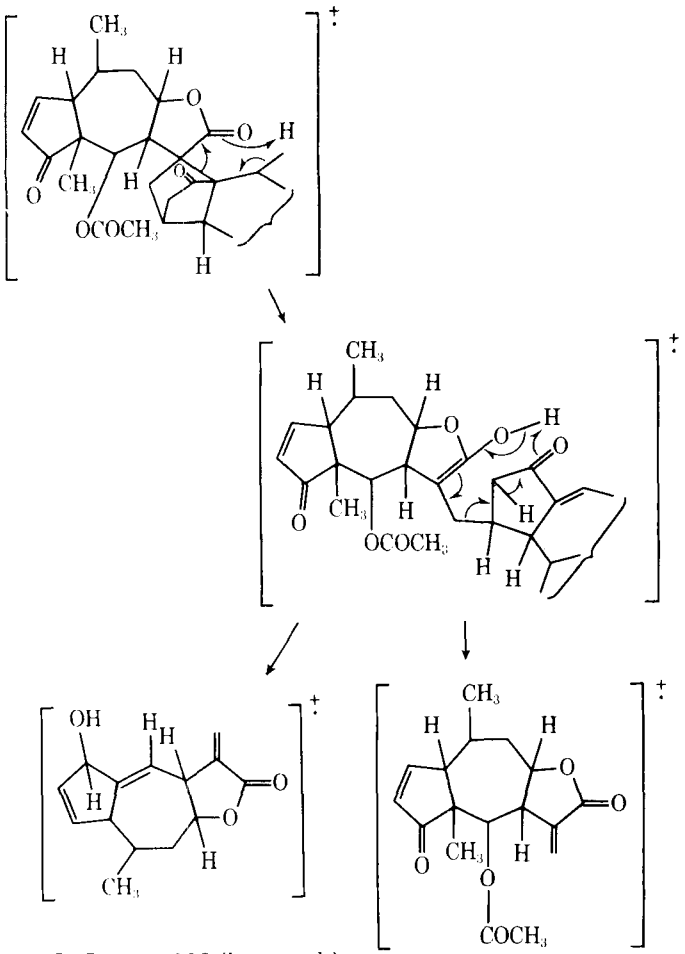

$C_{14}H_{16}O_3$, *m/e* 232 (base peak)
Found: 232.1094
Calc.: 232.1099

$C_{17}H_{21}O_5$, *m/e* 305 (13.9%)
Found: 305.1385
Calc.: 305.1389

Scheme III

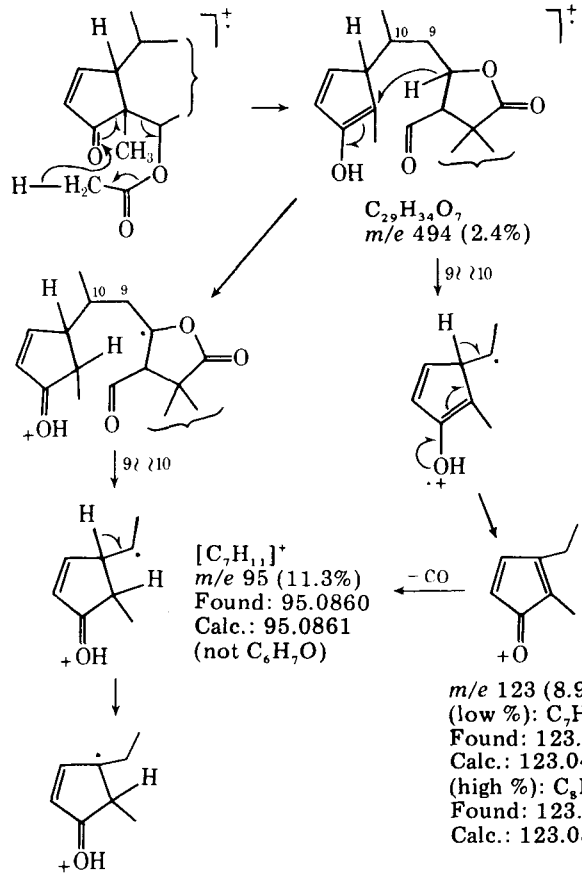

$C_{29}H_{34}O_7$
m/e 494 (2.4%)

$[C_7H_{11}]^+$
m/e 95 (11.3%)
Found: 95.0860
Calc.: 95.0861
(not C_6H_7O)

m/e 123 (8.9%)
(low %): $C_7H_7O_2$
Found: 123.0442
Calc.: 123.0446
(high %): $C_8H_{11}O$
Found: 123.0808
Calc.: 123.0810

$C_8H_{12}O$ *m/e* 124 (7.6%)
(not $C_7H_8O_2$)
Found: 124.0886
Calc.: 124.0888

Scheme IV

isolated by column chromatography and preparative TLC from the chloroform extract of the whole plant of *H. microcephalum*, mp 280° (dec.), $[\alpha]_D^{22}$ +10.0° (c = 1.00, pyridine); IR (potassium bromide pellet): 3521 (OH), 1763 (γ-lactone), 1756, 1664 (α-methylene-γ-lactone), 1744 (cyclopentanone), 1707, and 1582 (cyclopentenone) cm^{-1}; ^{1}H-NMR (100 MHz, dimethyl sulfoxide-d_6): δ 0.75 (3H, s, CH_3-5), 1.07, 1.14 (3H each, d, J = 7.0 Hz, CH_3-10 and CH_3-10′), 5.74 (1H, d, J = 2.0 Hz, H-13′b), 6.03 (1H, dd, J = 3.0 and 6.0 Hz, H-3), 6.14 (1H, d, J = 3.0, H-13′a), and 7.84 (1H, dd, J = 2.0 and 6.0 Hz, H-2) ppm; ^{13}C-NMR [100 MHz, acetone-d_6–pyridine-d_5 (1:1)]: see Table II.

Anal.—Calc. for $C_{29}H_{34}O_7$: C, 70.42; H, 6.93. Found: C, 70.41; H, 7.10.

Acetylation of Microlenin—Acetylation of microlenin (25 mg) with acetic anhydride (0.5 ml) and pyridine (1 ml) at room temperature for 18 hr, followed by usual workup, gave a product (*Ib*). This product was recrystallized from chloroform to give colorless crystals of a monoacetate (19 mg), mp 278° (dec.); IR (chloroform): no OH, 1757 (γ-lactone), 1741, 1662 (α-methylene-γ-lactone), 1715, and 1580 (cyclopentenone) cm^{-1}; mass spectrum: *m/e* (%) 536.2407 (M^+, 1.8), $C_{31}H_{36}O_8$ requires 536.2408; 476.2195 ($M^+ - CH_3COOH$, 10.5), $C_{29}H_{32}O_6$ requires 476.2199; 305.1385 (13.9), $C_{17}H_{21}O_5$ requires 305.1389; 232.1094 (100), $C_{14}H_{16}O_3$ requires 232.1099; 175 (7.6); 124.0886 (7.6), $C_8H_{12}O$ requires 124.0888; 123 [123.0442 (low %), $C_7H_7O_2$ requires 123.0446; 123.0808 (high %), $C_8H_{11}O$ requires 123.0810]; 95.0860 (11.3), C_7H_{11} requires 95.0861; ^{1}H-NMR (100 MHz, deuterochloroform): δ 0.94 (3H, s, CH_3-5), 1.18, 1.23 (3H each d, J = 7.0 Hz, CH_3-10 and CH_3-10′), 1.97 (3H, s, C-6-$OCOCH_3$), 2.48 (1H, d, J = 8.0 Hz, H-7), 3.29 (1H, m, H-7′), 4.71 (1H, m, H-8′), 4.95 (1H, m, H-8), 5.52, 6.28 (1H each, d, J = 3.0, H-13′), 5.62 (1H, s, H-6), 6.06 (1H, dd, J = 3.0 and 6.0 Hz, H-3), and 7.67 (1H, dd, J = 2.0 and 6.0 Hz, H-2) ppm.

REFERENCES

(1) R. Adams and W. Herz, *J. Am. Chem. Soc.*, **71**, 2546 (1949).

(2) K. H. Lee, Y. Imakura, and D. Sims, *J. Pharm. Sci.*, **65**, 1410 (1976).

(3) K. H. Lee, Y. Imakura, D. Sims, A. T. McPhail, and K. D. Onan, *Phytochemistry*, **16**, 393 (1977).

(4) K. H. Lee, Y. Imakura, D. Sims, A. T. McPhail, and K. D. Onan, *J. Chem. Soc. Chem. Commun.*, **1976**, 341.

(5) K. H. Lee, D. C. Anuforo, E. S. Huang, and C. Piantadosi, *J. Pharm. Sci.*, **61**, 626 (1972), and references cited therein.

(6) J. Romo, A. Romo de Vivar, and W. Herz, *Tetrahedron*, **19**, 2317 (1963).

(7) C. N. Caughlan, Mazhar-ul-Hague, and M. T. Emerson, *J. Chem. Soc. Chem. Commun.*, **1966**, 151.

(8) Mazhar-ul-Hague and C. N. Caughlan, *J. Chem. Soc. B*, **1967**, 355.

(9) A. T. McPhail and G. A. Sim, *Tetrahedron*, **29**, 1751 (1973).

(10) Mazhar-ul-Hague, D. Rogers, and C. N. Caughlin, *J. Chem. Soc., Perkin Trans. 2*, **1974**, 223.

(11) L. Tsai, J. Highet, and W. Herz, *J. Org. Chem.*, **34**, 945 (1969).

(12) J. T. Pinhey and S. Sternhell, *Aust. J. Chem.*, **18**, 543 (1965).

(13) Z. Samek, *Tetrahedron Lett.*, **1970**, 671.

(14) Mazhar-ul-Hague and C. N. Caughlan, *J. Chem. Soc. B*, **1969**, 956.

ACKNOWLEDGMENTS

Presented in part at the Medicinal Chemistry Section, APhA Academy of Pharmaceutical Sciences, New Orleans meeting, April 1976.

Supported by grants from the National Cancer Institute (CA-17625)

and the American Cancer Society (CH-19A) to K. H. Lee.

The authors thank Dr. David L. Harris, Department of Chemistry, University of North Carolina, Chapel Hill, for NMR spectra and Dr. David Rosenthal and Mr. Fred Williams, Research Triangle Center for Mass Spectrometry, for mass spectral data. The XL-100 NMR was purchased by grants from the National Science Foundation and the National Institutes of Health to the Chemistry Department, University of North Carolina, Chapel Hill.

Antitumor Agents XXIX: Effects of Eupahyssopin on Nucleic Acid, Protein, Anaerobic, and Aerobic Metabolism of Ehrlich Ascites Tumor Cells

IRIS H. HALL ˣ, KUO-HSIUNG LEE, and SALWA A. EIGEBALY

Received September 30, 1977, from the *Division of Medicinal Chemistry, School of Pharmacy, University of North Carolina at Chapel Hill, Chapel Hill, NC 27514.* Accepted for publication December 28, 1977.

Abstract □ Evidence is presented that the antitumor agent eupahyssopin, a germacranolide, inhibits deoxyribonucleic acid, ribonucleic acid, protein, and cholesterol synthesis of Ehrlich ascites tumor cells in CF_1 male mice. Eupahyssopin appears to bind to nucleotide bases of deoxyribonucleic acid. The drug also inhibits deoxyribonucleic acid and messenger ribonucleic acid polymerase activities and, marginally, thymidylate synthetase activity. Template activity, as regulated by phosphorylation of histones and nonhistones, and cyclic 3′,5′-adenosine monophosphate levels also were affected by drug therapy. Lysosomal enzymes, *e.g.*, deoxyribonuclease and ribonuclease, and cathepsin activities were inhibited by eupahyssopin administration. A number of sulfhydryl-bearing enzymes of the glycolytic and Krebs cycles were inhibited by drug treatment, as were enzymes required for glycogen synthesis and breakdown and for phosphatase hydrolysis. Eupahyssopin also inhibited both basal respiration and coupled oxidative phosphorylation processes of the tumor cell. It was proposed that eupahyssopin, which contains the O=CC=CH_2 as an α-methylene-γ-lactone moiety within its allylic ester side chain, has the ability to undergo a rapid Michael-type addition with sulfhydryl groups of these enzymes and thus to inhibit their activities in a manner analogous to that described for other sesquiterpene antitumor agents containing the O=CC=CH_2 moiety.

Keyphrases □ Eupahyssopin—effects on nucleic acid, protein, anaerobic, and aerobic metabolism of Ehrlich ascites tumor cells □ Metabolism—nucleic acid, protein, anaerobic, and aerobic, in Ehrlich ascites tumor cells, effects of eupahyssopin □ Enzyme activity—Ehrlich ascites tumor cells, effects of eupahyssopin □ Antineoplastic agents, potential—eupahyssopin, effects on nucleic acid, protein, anaerobic, and aerobic metabolism of Ehrlich ascites tumor cells

A new germacranolide, eupahyssopin (I), was isolated from the chloroform extract of the whole plant *Eupatorium hyssopifolium* (1). Its stereochemistry and physical characteristics previously were reported (2). As an antitumor agent, eupahyssopin is active in the Walker 256 carcinosarcoma Sprague–Dawley rat survival system at 2.5 mg/kg/day (T/C = 330), in the P-388 lymphocytic leukemia screen in DBA/2 mice at 25 mg/kg/day (T/C = 132), and in the Lewis lung screen in $C_{57}B1_6$ mice at 25 mg/kg/day (T/C = 147) and caused 93% inhibition of Ehrlich ascites cell growth in CF_1 mice at 25 mg/kg/day (3). The effects of eupahyssopin on nucleic acid, chromatin protein, protein, anaerobic and aerobic glycolysis, and oxidative phosphorylation processes of Ehrlich ascites tumor cells are now reported.

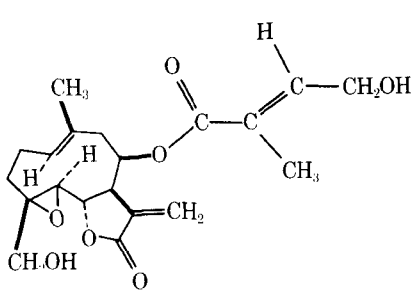

I

EXPERIMENTAL

Male CF_1 mice, ~30 g, were implanted intraperitoneally on Day 0 with 10^6 Ehrlich ascites tumor cells. On Days 7, 8, and 9, the animals were treated with a subacute dose, 0.25 mg ip, of eupahyssopin suspended by homogenization in 0.05% polysorbate 80–water. Animals were sacrificed on the 10th day, and the ascites fluid was collected from the peritoneal cavity. *In vitro* oxidative phosphorylation studies were determined on untreated, harvested, Day 10 Ehrlich ascites cells. The number of tumor cells per milliliter and the 0.4% trypan blue uptake were determined with a hemocytometer.

Incorporation of thymidine into deoxyribonucleic acid was determined by the method of Chae *et al.* (4). One hour prior to animal sacrifice, 10 μCi of [^{14}C-methyl]-thymidine (54 mCi/mmole) was injected intraperitoneally. The deoxyribonucleic acid was isolated, and the carbon-14 content was determined in two parts of toluene, one part of octoxynol, 0.4% 2,5-diphenyloxazole, and 0.01% 1,4-bis[2-(5-oxazolyl)]benzene scintillation fluid and corrected for quenching.

The deoxyribonucleic acid concentration was determined by UV spectrophotometry at 260 nm, using calf thymus deoxyribonucleic acid as a standard. Uridine incorporation into ribonucleic acid was determined in an analogous manner, utilizing 10 μCi of 5-^{3}H-uridine (24.2 Ci/mmole). Ribonucleic acid was extracted by the method of Wilson *et al.* (5). Leucine incorporation into protein was determined by the method of Sartorelli (6), using 1 μCi of 1-^{14}C-leucine (56.9 mCi/mmole). The effects of eupahyssopin on 1-^{14}C-acetic acid (57.8 mCi/mmole) incorporation into cholesterol of Ehrlich ascites cells also were measured (7).

Nuclear deoxyribonucleic acid polymerase activity was determined on isolated nuclei (8). The incubation medium was that of Sawada *et al.* (9), except that 2-^{14}C-deoxyribothymidine triphosphate (45 mCi/mmole) was used and the insoluble nucleic acids were collected on glass fiber paper (GF/F) by vacuum suction. Deoxythymidylate monophosphate and diphosphate kinase activities were determined by the method of Maley and Ochoa (10), which is based on the disappearance of 0.1 μmole of reduced nicotinamide adenine dinucleotide at 340 nm in 20 min. Thymidylate synthetase activity was assayed by the method of Kampf *et al.* (11), utilizing a postmitochondrial (9000×*g* for 10 min) and 5 μCi of 5′-^{3}H-deoxyuridine monophosphate (11 Ci/mmole).

Phosphorylation of histones was determined by injecting intraperitoneally 10 μCi of γ-^{32}P-adenosine triphosphate (7.97 Ci/mmole) 1 hr prior to sacrifice. The nuclei were isolated (8), and the histone chromatin

0022-3549/78/0900-1232$01.00/0
© 1978, American Pharmaceutical Association

and the American Cancer Society (CH-19A) to K. H. Lee.

The authors thank Dr. David L. Harris, Department of Chemistry, University of North Carolina, Chapel Hill, for NMR spectra and Dr. David Rosenthal and Mr. Fred Williams, Research Triangle Center for Mass Spectrometry, for mass spectral data. The XL-100 NMR was purchased by grants from the National Science Foundation and the National Institutes of Health to the Chemistry Department, University of North Carolina, Chapel Hill.

Antitumor Agents XXIX: Effects of Eupahyssopin on Nucleic Acid, Protein, Anaerobic, and Aerobic Metabolism of Ehrlich Ascites Tumor Cells

IRIS H. HALL ˣ, KUO-HSIUNG LEE, and SALWA A. EIGEBALY

Received September 30, 1977, from the *Division of Medicinal Chemistry, School of Pharmacy, University of North Carolina at Chapel Hill, Chapel Hill, NC 27514.* Accepted for publication December 28, 1977.

Abstract □ Evidence is presented that the antitumor agent eupahyssopin, a germacranolide, inhibits deoxyribonucleic acid, ribonucleic acid, protein, and cholesterol synthesis of Ehrlich ascites tumor cells in CF_1 male mice. Eupahyssopin appears to bind to nucleotide bases of deoxyribonucleic acid. The drug also inhibits deoxyribonucleic acid and messenger ribonucleic acid polymerase activities and, marginally, thymidylate synthetase activity. Template activity, as regulated by phosphorylation of histones and nonhistones, and cyclic 3′,5′-adenosine monophosphate levels also were affected by drug therapy. Lysosomal enzymes, *e.g.*, deoxyribonuclease and ribonuclease, and cathepsin activities were inhibited by eupahyssopin administration. A number of sulfhydryl-bearing enzymes of the glycolytic and Krebs cycles were inhibited by drug treatment, as were enzymes required for glycogen synthesis and breakdown and for phosphatase hydrolysis. Eupahyssopin also inhibited both basal respiration and coupled oxidative phosphorylation processes of the tumor cell. It was proposed that eupahyssopin, which contains the O=CC=CH_2 as an α-methylene-γ-lactone moiety within its allylic ester side chain, has the ability to undergo a rapid Michael-type addition with sulfhydryl groups of these enzymes and thus to inhibit their activities in a manner analogous to that described for other sesquiterpene antitumor agents containing the O=CC=CH_2 moiety.

Keyphrases □ Eupahyssopin—effects on nucleic acid, protein, anaerobic, and aerobic metabolism of Ehrlich ascites tumor cells □ Metabolism—nucleic acid, protein, anaerobic, and aerobic, in Ehrlich ascites tumor cells, effects of eupahyssopin □ Enzyme activity—Ehrlich ascites tumor cells, effects of eupahyssopin □ Antineoplastic agents, potential—eupahyssopin, effects on nucleic acid, protein, anaerobic, and aerobic metabolism of Ehrlich ascites tumor cells

A new germacranolide, eupahyssopin (I), was isolated from the chloroform extract of the whole plant *Eupatorium hyssopifolium* (1). Its stereochemistry and physical characteristics previously were reported (2). As an antitumor agent, eupahyssopin is active in the Walker 256 carcinosarcoma Sprague–Dawley rat survival system at 2.5 mg/kg/day (T/C = 330), in the P-388 lymphocytic leukemia screen in DBA/2 mice at 25 mg/kg/day (T/C = 132), and in the Lewis lung screen in $C_{57}B1_6$ mice at 25 mg/kg/day (T/C = 147) and caused 93% inhibition of Ehrlich ascites cell growth in CF_1 mice at 25 mg/kg/day (3). The effects of eupahyssopin on nucleic acid, chromatin protein, protein, anaerobic and aerobic glycolysis, and oxidative phosphorylation processes of Ehrlich ascites tumor cells are now reported.

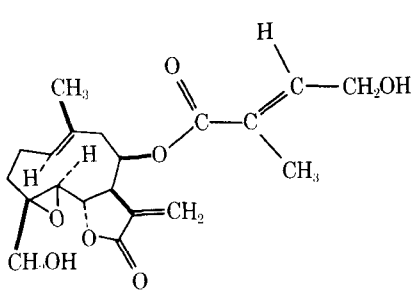

I

EXPERIMENTAL

Male CF_1 mice, ~30 g, were implanted intraperitoneally on Day 0 with 10^6 Ehrlich ascites tumor cells. On Days 7, 8, and 9, the animals were treated with a subacute dose, 0.25 mg ip, of eupahyssopin suspended by homogenization in 0.05% polysorbate 80–water. Animals were sacrificed on the 10th day, and the ascites fluid was collected from the peritoneal cavity. *In vitro* oxidative phosphorylation studies were determined on untreated, harvested, Day 10 Ehrlich ascites cells. The number of tumor cells per milliliter and the 0.4% trypan blue uptake were determined with a hemocytometer.

Incorporation of thymidine into deoxyribonucleic acid was determined by the method of Chae *et al.* (4). One hour prior to animal sacrifice, 10 μCi of [^{14}C-methyl]-thymidine (54 mCi/mmole) was injected intraperitoneally. The deoxyribonucleic acid was isolated, and the carbon-14 content was determined in two parts of toluene, one part of octoxynol, 0.4% 2,5-diphenyloxazole, and 0.01% 1,4-bis[2-(5-oxazolyl)]benzene scintillation fluid and corrected for quenching.

The deoxyribonucleic acid concentration was determined by UV spectrophotometry at 260 nm, using calf thymus deoxyribonucleic acid as a standard. Uridine incorporation into ribonucleic acid was determined in an analogous manner, utilizing 10 μCi of 5-^{3}H-uridine (24.2 Ci/mmole). Ribonucleic acid was extracted by the method of Wilson *et al.* (5). Leucine incorporation into protein was determined by the method of Sartorelli (6), using 1 μCi of 1-^{14}C-leucine (56.9 mCi/mmole). The effects of eupahyssopin on 1-^{14}C-acetic acid (57.8 mCi/mmole) incorporation into cholesterol of Ehrlich ascites cells also were measured (7).

Nuclear deoxyribonucleic acid polymerase activity was determined on isolated nuclei (8). The incubation medium was that of Sawada *et al.* (9), except that 2-^{14}C-deoxyribothymidine triphosphate (45 mCi/mmole) was used and the insoluble nucleic acids were collected on glass fiber paper (GF/F) by vacuum suction. Deoxythymidylate monophosphate and diphosphate kinase activities were determined by the method of Maley and Ochoa (10), which is based on the disappearance of 0.1 μmole of reduced nicotinamide adenine dinucleotide at 340 nm in 20 min. Thymidylate synthetase activity was assayed by the method of Kampf *et al.* (11), utilizing a postmitochondrial (9000×*g* for 10 min) and 5 μCi of 5′-^{3}H-deoxyuridine monophosphate (11 Ci/mmole).

Phosphorylation of histones was determined by injecting intraperitoneally 10 μCi of γ-^{32}P-adenosine triphosphate (7.97 Ci/mmole) 1 hr prior to sacrifice. The nuclei were isolated (8), and the histone chromatin

0022-3549/78/0900-1232$01.00/0
© 1978, American Pharmaceutical Association

protein was extracted by the method of Raineri *et al.* (12). Nonhistone chromatin phosphorylation by a nucleus protein kinase (13) was determined on isolated nuclei (8), utilizing 2 nmoles of γ-^{32}P-adenosine triphosphate (7.97 Ci/mmole). Chromatin protein was collected on nitrocellulose membrane filters (13).

Cyclic 3′,5′-adenosine monophosphate levels were determined by the method of Gilman (14), using ^{3}H(*G*)-cyclic 3′,5′-adenosine monophosphate (39.8 Ci/mmole). Messenger, ribosomal, and hormone sensitive ribonucleic acid polymerase activities were measured by the methods of Anderson *et al.* (15) and Hall *et al.* (16) with 5,6-^{3}H-uridine 5′-triphosphate (35 Ci/mmole). Ammonium sulfate concentrations of 0.3, 0.04, and 0.0 *M* were employed to measure the respective types of ribonucleic acid polymerase activity. Insoluble ribonucleic acid was collected on glass fiber paper (GF/F) by vacuum suction.

The effect of eupahyssopin on hydrolytic enzymes also was determined. Deoxyribonuclease activity was measured at pH 5.0 by a modification of the deDuve method (16). Ribonuclease activity and acid cathepsin activity were determined at pH 5.0 by the methods of Cho-Chung and Gullino (17).

In vitro UV binding studies (18) were conducted with eupahyssopin (0.11 μg/ml) and deoxyribonucleic acid (38 μg/ml) or deoxyriboguanosine monophosphate (38 μg/ml) in 0.1 *M* phosphate buffer, pH 7.2, over a range of 200–340 nm for 24 hr.

The following glycolytic enzymatic activities were determined for both control and treated cells: hexokinase (19), phosphofructokinase (20), aldolase (21), lactic dehydrogenase (22), glucose-6-phosphatase (23), fructose-1,6-diphosphatase (24), phosphorylase *a*, (24), and glycogen synthetase (25), utilizing ^{14}C(*U*)-uridine diphosphate-D-glucose (240 mCi/mmole).

The Krebs cycle dehydrogenase activities of succinic (26) and malic (27) dehydrogenases also were determined. Inorganic phosphate was determined by the method of Chen *et al.* (28), and protein was determined by the method of Lowry *et al.* (29). *In vitro* effects of eupahyssopin (0.2 mg) on Ehrlich ascites tumor cell oxidative phosphorylation were measured in the presence and absence of adenosine diphosphate, utilizing succinate, a flavin adenine dinucleotide-linked dehydrogenase, or α-ketoglutarate, a nicotinamide adenine dinucleotide-linked dehydrogenase, as the substrate (24).

RESULTS

The normal number of Ehrlich ascites cells per milliliter on Day 10 was 223×10^{6}. Eupahyssopin treatment at the subacute dose of 0.25 mg on Days 7, 8, and 9 reduced the cell count by 61%. Drug treatment resulted in no significant difference in the percentage of nonviable cells or in the size or general morphology of the cell as observed by gross microscopy.

For the control animal, the thymidine incorporation into deoxyribonucleic acid was 241,675 dpm/mg of deoxyribonucleic acid. Drug treatment inhibited deoxyribonucleic acid synthesis 69%. Uridine incorporation into ribonucleic acid for the 10-day Ehrlich ascites cells was 39,525 dpm/mg of ribonucleic acid. Eupahyssopin treatment reduced ribonucleic acid synthesis 52%. Leucine incorporation into protein for the control was 4213 dpm/mg of protein. This amount was decreased 42% by drug treatment. Acetic acid incorporation into cholesterol for membrane synthesis for the control was 273,271 dpm/mg of protein. Drug treatment reduced cholesterol synthesis by 76%.

A more detailed examination was made of the enzymes required for the synthesis of deoxyribonucleic acid synthetase. Nuclear deoxyribonucleic acid polymerase activity alpha, beta, and gamma for the control was 7561 dpm/mg of protein. Drug treatment resulted in a 71% reduction in deoxyribonucleic acid polymerase activity. Deoxythymidylate monophosphate kinase activity for the control was 0.413 O.D. (change in absorbance) unit/mg of protein/20 min, and deoxythymidylate diphosphate kinase activity was 0.557 O.D. unit/mg of protein/20 min. Eupahyssopin treatment caused 16 and 12% reductions in deoxynucleotide kinase activities, respectively, which were not significant. Thymidylate synthetase activity for 10-day Ehrlich ascites cells was 103,328 dpm/mg of protein, which was reduced 37% by drug treatment.

In vitro binding studies with deoxyribonucleic acid or deoxyguanosine monophosphate indicated that eupahyssopin interacted with nucleotide bases. Eupahyssopin has an absorption peak at 219–222 nm. After reacting eupahyssopin with deoxyribonucleic acid or deoxyguanosine monophosphate, the absorption peak of eupahyssopin at 219–222 nm immediately disappeared; during 2–20 hr, the magnitude of the absorption of deoxyribonucleic acid at 260 nm or of deoxyguanosine monophosphate at 257 nm increased moderately. Incubation of the drug alone over 24 hr resulted in no change in absorption properties, *e.g.*, magnitude and shift, indicating that the drug was not decomposing.

Messenger (nuclei) ribonucleic acid polymerase activity for the control was 120,811 dpm/mg of protein, whereas ribosomal (nucleolus) ribonucleic acid polymerase activity was 65,460 dpm/mg of protein and hormone-sensitive ribonucleic acid polymerase activity was 46,830 dpm/mg of protein. Treatment with eupahyssopin resulted in a 55% reduction, a 4% reduction, and a 5% increase, respectively, in ribonucleic acid polymerase activities.

Phosphorus incorporation into histone protein for 10-day normal Ehrlich ascites cells was 2954 dpm/mg of chromatin protein, which was reduced 51% by eupahyssopin. Phosphorus incorporation into nonhistone chromatin protein was 9803 dpm/mg of protein. Drug administration reduced the activity of this chromatin protein kinase by 31%. The cyclic 3′,5′-adenosine monophosphate level in the control was 3.65 pmoles/10^{6} cells. Eupahyssopin treatment elevated this cyclic nucleotide level 114%.

The catabolic rate of nucleic acids and proteins also was determined to eliminate the possibility that the drug accelerated hydrolytic enzymatic activity and thus indirectly lowered the incorporation of precursors into nucleic acids and proteins. Deoxyribonuclease activity for the 10-day Ehrlich ascites cells was 35 μg of deoxyribonucleic acid hydrolyzed/mg of protein/30 min, which was inhibited 69% by eupahyssopin administration. Ribonuclease activity for the control was 24 μg of ribonucleic acid hydrolyzed/mg of protein/30 min. Drug treatment reduced this amount 61%. Ten-day tumor cell cathepsin activity was 0.90 mg of protein hydrolyzed/mg of protein/30 min. Eupahyssopin treatment reduced cathepsin activity 83%.

Hexokinase activity for 10-day Ehrlich ascites tumor cells was calculated as a change in absorbance equal to 0.260 O.D. unit/mg of protein/min, based on 500 μmoles of nicotinamide adenine dinucleotide phosphate, which was suppressed 59% by eupahyssopin treatment. Phosphofructokinase activity for the control was 0.176 O.D. unit/mg of protein/min based on 1.125 μmole of reduced nicotinamide adenine dinucleotide; administration of eupahyssopin reduced phosphofructokinase activity 10%. Aldolase activity for the control was 302 mU/mg of protein, which was suppressed 42% by eupahyssopin. Lactic dehydrogenase activity for Ehrlich ascites tumor cells was 0.623 O.D. unit/mg of protein/min based on 0.12 μmole of reduced nicotinamide adenine dinucleotide. Eupahyssopin reduced the activity of this dehydrogenase 50%.

Glucose-6-phosphatase activity for the control was 11.24 μg of phosphate released/mg of protein/15 min. Administration of eupahyssopin reduced glucose-6-phosphatase activity 85%. Fructose-1,6-diphosphatase activity was 29.82 μg of phosphate released/mg of protein/15 min. Drug therapy resulted in 54% reduction. Phosphorylase *a* activity for the control was 5.72 μg of phosphate taken up from the medium/mg of protein/hr; drug treatment reduced phosphorylase *a* activity 58%. Glycogen synthetase activity for the control was 1540 dpm/mg of protein; eupahyssopin reduced glycogen synthesis 57%.

Succinic dehydrogenase activity for the control was 0.069 O.D. unit/mg of protein/min based on 15 μmoles of potassium ferricyanide, which eupahyssopin administration reduced 41%. Malic dehydrogenase activity for 10-day Ehrlich ascites cells was 0.80 O.D. unit/mg of protein/min based on 15 μmoles of reduced nicotinamide adenine dinucleotide. Malic dehydrogenase was suppressed 55% by eupahyssopin treatment.

The basal respiration (state 4) of 10-day Ehrlich ascites tumor cells with sodium succinate as the substrate was 5.273 μl of oxygen/mg of protein/hr; in the presence of adenosine diphosphate (state 3), stimulated respiration or coupled oxidative phosphorylation was 8.752 μl of oxygen/mg of protein/hr. *In vitro* eupahyssopin suppressed state 4 respiration 18% and state 3 respiration 13%. Use of sodium α-ketoglutarate as the substrate resulted in a state 4 respiration of 3.569 μl of oxygen/mg of protein/hr and in a state 3 respiration of 5.156 μl of oxygen/mg of protein/hr. Eupahyssopin inhibited state 4 respiration 41% and state 3 respiration 57% (Tables I and II). The probable significance level (p) was determined by the Student t test (30).

DISCUSSION

Eupahyssopin administration significantly inhibited the synthesis of deoxyribonucleic acids, ribonucleic acids, proteins, and cholesterol in 10-day Ehrlich ascites tumor cells. The synthesis of all of these macromolecules is required for rapidly proliferating cells. One explanation for the reduction of radiolabeled precursor into these macromolecules is that drug treatment accelerated catabolism of the macromolecule. Administration of eupahyssopin did not accelerate the hydrolytic activity of enzymes responsible for catabolism of these macromolecules; rather, the

Table I—*In Vivo* Effects of Eupahyssopin on Nucleic Acid and Protein Metabolism of Ehrlich Ascites Tumor Cells (n = 6)

Parameter	Control, 0.05% Polysorbate 80, $\bar{x} \pm SD$	Percent Control, Treated on Days 7, 8, and 9 with 0.25 mg of Eupahyssopin, $\bar{x} \pm SD$
Thymidine incorporation into deoxyribonucleic acid	100 ± 21	31 ± 13[a]
Uridine incorporation into ribonucleic acid	100 ± 18	48 ± 15[a]
Leucine incorporation into protein	100 ± 13	58 ± 11[a]
Acetic acid incorporation into cholesterol	100 ± 23	24 ± 8[a]
Deoxyribonuclease activity	100 ± 19	31 ± 5[a]
Ribonuclease activity	100 ± 22	39 ± 20[a]
Cathepsin activity	100 ± 19	17 ± 18[a]
Deoxyribonucleic acid polymerase activity	100 ± 5	29 ± 5[a]
Thymidylate monophosphate kinase activity	100 ± 15	84 ± 9
Thymidylate diphosphate kinase activity	100 ± 8	88 ± 22
Thymidylate synthetase activity	100 ± 13	63 ± 7[a]
Messenger ribonucleic acid polymerase activity	100 ± 18	45 ± 16[a]
Ribosomal ribonucleic acid polymerase activity	100 ± 6	96 ± 4
Hormone sensitive ribonucleic acid polymerase activity	100 ± 11	105 ± 20
Phosphorylation of histones	100 ± 8	49 ± 3[a]
Phosphorylation of nonhistones	100 ± 3	69 ± 5[a]
Cyclic 3′,5′-adenosine monophosphate levels	100 ± 5	214 ± 3[a]
Number of tumor cells per milliliter of ascites fluid	100 ± 19	39 ± 10[a]

[a] p = 0.001.

drug inhibited significantly deoxyribonuclease, ribonuclease, and cathepsin activities.

The major site of eupahyssopin inhibition in deoxyribonucleic acid synthesis was the deoxyribonucleic acid polymerase nuclei enzymes, whereas the thymidylate synthetase enzyme appeared to be reduced marginally. The deoxyribonucleotide kinase enzymes were essentially unaffected by drug treatment. Previously (18), it was demonstrated that compounds containing the O=CC=CH_2 system were capable of undergoing a rapid Michael-type addition with biological nucleophiles, *e.g.*, sulfhydryl groups. Both deoxyribonucleic acid polymerase alpha and gamma of the nucleus (31) and thymidylate synthetase possess an exposed sulfhydryl group which can be alkylated (32). Contained in the structure of eupahyssopin is the O=CC=CH_2 system as an α-methylene-γ-lactone and within the allylic ester side chain. The α-methylene-γ-lactone moiety undergoes a rapid-type Michael addition with L-cysteine and reduced glutathione (18). A similar phenomenon occurs with the sesquiterpene lactones, helenalin and tenulin (18, 33).

Cellular proliferation is regulated by phosphorylation of chromatin histones, *i.e.*, the F-1 fraction, by a protein kinase (34). Increased phosphorylation occurs when cyclic- 3′,5′-adenosine monophosphate levels are decreasing and deoxyribonucleic acid polymerase enzymes are increasing in a concentration that would require protein synthesis, *i.e.*, G_1 or early S phase of the cell cycle. Eupahyssopin treatment inhibited phosphorylation of histones and protein synthesis and significantly elevated cyclic-3′,5′-adenosine monophosphate levels. Increased intracellular levels of this cyclic nucleotide are associated with reversal of tumor morphology (35), reduced cellular proliferation, and enhanced cellular differentiation (36).

Nonhistone chromatin protein phosphorylation fluctuates during the cell cycle and parallels ribonucleic acid transcription and cellular differentiation (37). However, in rapidly proliferating lymphocytes, the phosphorylation of a particular fraction (mol. wt. 52,000) was inhibited when cyclic 3′,5′-adenosine monophosphate was present in a high concentration. Inhibition of the phosphorylation of this fraction correlates with the inhibition of cellular proliferation (38). Eupahyssopin treatment inhibited phosphorylation of nonhistone chromatin protein. Other sesquiterpene lactones inhibited chromatin phosphorylation and elevated cyclic 3′,5′-adenosine monophosphate concentrations in tumor cells (33).

Table II—Effects of Eupahyssopin on Anaerobic and Aerobic Metabolism of Ehrlich Ascites Cells

Parameter	Control 0.05% Polysorbate 80, $\bar{x} \pm SD$	Percent Control, Treated on Days 7, 8, and 9 with 0.25 mg of Eupahyssopin, $\bar{x} \pm SD$
In Vivo Enzymatic Assay (n = 6)		
Hexokinase activity	100 ± 8	41 ± 8[a]
Phosphofructokinase activity	100 ± 39	90 ± 15
Aldolase activity	100 ± 7	58 ± 6[a]
Lactic dehydrogenase activity	100 ± 9	50 ± 12[a]
Glucose-6-phosphatase activity	100 ± 23	15 ± 9[a]
Fructose-1,6 diphosphatase activity	100 ± 7	46 ± 4[a]
Phosphorylase a activity	100 ± 15	42 ± 22[a]
Glycogen synthetase activity	100 ± 14	43 ± 10[a]
Succinic dehydrogenase activity	100 ± 16	59 ± 6[a]
Malic dehydrogenase activity	100 ± 2	45 ± 8[a]
In Vitro Oxidative Phosphorylation (n = 8)		
Succinate		
State 3	100 ± 4	87 ± 5[b]
State 4	100 ± 3	82 ± 7[b]
α-Ketoglutarate		
State 3	100 ± 3	53 ± 8[a]
State 4	100 ± 6	59 ± 14[a]

[a] p = 0.001. [b] p = 0.005.

The UV spectral studies suggest that eupahyssopin interacted with the nucleotide bases of deoxyribonucleic acid. The fact that messenger ribonucleotide polymerase activity also was suppressed by drug treatment, indicating that the transcription processes utilizing deoxyribonucleic acid as a template were impaired, supports the idea that the drug binds to nucleotide bases, particularly since rRNA polymerase activity was not affected by drug treatment, which does not require a DNA template at this time. If the drug does bind to nucleotide bases, this binding may also explain the reduction in deoxyribonucleic acid polymerase activity, which also requires an intact DNA template.

Compounds containing the α-methylene-γ-lactone moiety inhibited enzymes of the Embden–Meyerhof and Krebs cycles (24, 38–40). Eupahyssopin inhibited hexokinase, aldolase, lactic dehydrogenase, and glycogen synthetase enzymatic activities but not phosphofructokinase. These enzymes contain sulfhydryl groups (24, 38–40) which can be alkylated by the O=CC=CH_2 moiety. The activities of the hydrolytic enzymes phosphorylase a, glucose-6-phosphatase, and fructose-1,6-diphosphatase were inhibited significantly by eupahyssopin administration. Dehydrogenases of the Krebs cycles also contain sulfhydryl groups in the enzymes and iron inorganic sulfides flavin proteins as integral components of the dehydrogenase enzymes (41). These groups can be subject to alkylation. Both succinic and malic dehydrogenase activities were reduced by drug treatment.

A number of antitumor agents inhibit respiration and oxidative phosphorylation (42). A number of inhibitors of protein synthesis also suppress respiration processes (43). Eupahyssopin inhibited both basal respiration and coupled oxidative phosphorylation or mitochondrial adenosine triphosphate synthesis. This action was more obvious using α-ketoglutarate, a nicotinamide adenine dinucleotide-linked dehydrogenase that contains an iron–sulfur center (44), than with succinate, which is a flavin adenine dinucleotide-linked enzyme.

REFERENCES

(1) K. H. Lee, T. Kimura, M. Okamoto, C. M. Cowherd, A. T. McPhail, and K. D. Onan, *Tetrahedron Lett.*, **14**, 1051 (1976).

(2) K. D. Onan and A. T. McPhail, *J. Chem. Res.*, in press.

(3) I. H. Hall, K. H. Lee, C. O. Starnes, S. A. ElGebaly, T. Ibuka, Y. S. Wu, T. Kimura, and M. Haruna, *J. Pharm. Sci.*, **67**, 1235 (1978).

(4) C. B. Chae, J. L. Irvin, and C. Piantadosi, *Proc. Am. Assoc. Can. Res.*, **9**, 44 (1968).

(5) R. G. Wilson, R. H. Bodner, and G. E. MacHorter, *Biochim. Biophys. Acta*, **378**, 260 (1975).

(6) A. C. Sartorelli, *Biochem. Biophy. Res. Commun.*, **27**, 26 (1967).

(7) G. T. Haven, J. R. Krzemien, and T. T. Nquyea, *Res. Commun. Chem. Pathol. Pharmacol.*, **6**, 253 (1973). F. Wada, K. Hirata, and Y. Sakamoto, *J. Biol. Chem.*, **65**, 171 (1969).

(8) W. C. Hymer and E. L. Kuff, *J. Histochem. Cytochem.*, **12**, 359 (1964).
(9) H. Sawada, K. Tatsumi, M. Sasada, S. Shirakawa, T. Nakumura, and G. Wakisaka, *Cancer Res.*, **34**, 3341 (1974).
(10) F. Maley and S. Ochoa, *J. Biol. Chem.*, **233**, 1538 (1958).
(11) A. Kampf, R. L. Barfknecht, P. J. Schaffer, S. Osaki, and M. P. Mertes, *J. Med. Chem.*, **19**, 903 (1976).
(12) A. Raineri, R. C. Simsiman, and R. K. Boutwell, *Cancer Res.*, **33**, 134 (1973).
(13) Y. M. Kish and L. J. Kleinsmith, *Methods Enzymol.*, **40**, 201 (1975).
(14) A. C. Gilman, *Proc. Natl. Acad. Sci., U.S.A.*, **67**, 305 (1970).
(15) K. M. Anderson, I. S. Mendelson, and G. Guzik, *Biochim. Biophys. Acta*, **383**, 56 (1975). I. H. Hall, G. L. Carlson, G. S. Abernethy, and C. Piantadosi, *J. Med. Chem.*, **17**, 1253 (1974).
(16) I. H. Hall, K. S. Ishaq, and C. Piantadosi, *J. Pharm. Sci.*, **63**, 625 (1974).
(17) Y. S. Cho-Chung and P. M. Gullino, *J. Biol. Chem.*, **248**, 4743 (1973).
(18) I. H. Hall, K. H. Lee, E. C. Mar, C. O. Starnes, and T. G. Waddell, *J. Med. Chem.*, **20**, 333 (1977).
(19) D. G. Walker and J. J. Parry, in "Methods in Enzymology IX," S. P. Colowick and N. O. Kaplan, Eds., Academic, New York, N.Y., 1966, p. 381.
(20) T. E. Mansour, in *ibid.*, p. 430.
(21) P. V. C. Pinto, A. Kaplan, and P. A. Van Dreal, *Clin. Chem.*, **15**, 349 (1969).
(22) M. K. Schwartz and O. Bodausky, in "Methods in Enzymology IX," Academic, New York, N.Y., 1966, p. 294.
(23) M. A. Swanson, *J. Biol. Chem.*, **184**, 647 (1950).
(24) I. H. Hall, K. H. Lee, and S. A. ElGebaly, *J. Pharm. Sci.*, **67**, 552 (1978).
(25) J. A. Thomas, K. K. Schlinder, and J. Larner, *Anal. Biochem.*, **25**, 486 (1968).
(26) D. V. DerVartanian and C. Verger, *Biochim. Biophys. Acta*, **92**, 233 (1964).
(27) S. Ochoa, A. H. Mehler, and A. Kornberg, *J. Biol. Chem.*, **174**, 979 (1948).
(28) P. S. Chen, T. Y. Toribana, and H. Warner, *Anal. Chem.*, **28**, 1756 (1956).
(29) O. H. Lowry, N. J. Rosebrough, A. L. Farr, and R. J. Randall, *J. Biol. Chem.*, **193**, 265 (1951).
(30) G. W. Snedcor, "Statistical Methods," Iowa State College Press, Ames, Iowa, 1956, Section 2.
(31) L. A. Loeb, in "The Enzymes," 3rd ed., P. D. Boyer, Ed., Academic, New York, N.Y., 1974, p. 173.
(32) M. Friedkin, *Adv. Enzymol.*, **38**, 235 (1973).
(33) K. H. Lee, I. H. Hall, E. C. Mar, C. O. Starnes, S. A. ElGebaly, T. G. Waddell, R. I. Hadgraft, C. G. Ruffner, and I. Weidner, *Science*, **196**, 533 (1977).
(34) C. S. Rubin and O. M. Roseu, *Annu. Rev. Biochem.*, **44**, 81 (1975).
(35) V. Stefanovich, *Res. Commun. Chem. Pathol. Pharmacol.*, **7**, 573 (1974).
(36) T. Posternak, *Annu. Rev. Pharmacol.*, **14**, 23 (1974). Y. S. Cho-Chung and P. M. Guillino, *Science*, **183**, 87 (1974).
(37) E. M. Johnson and J. W. Hadden, *Science*, **187**, 1198 (1975).
(38) S. M. Kupchan, D. C. Fessler, M. A. Eakin, and T. J. Giacobbe, *ibid.*, **168**, 376 (1970).
(39) R. L. Hanson, H. A. Landy, and S. M. Kupchan, *ibid.*, **168**, 378 (1970).
(40) C. H. Smith, J. Larner, A. M. Thomas, and S. M. Kupchan, *Biochim. Biophys. Acta*, **276**, 94 (1972).
(41) L. Stryer, "Biochemistry," Freeman, San Francisco, Calif., 1975, p. 32.
(42) M. Gosalvez, R. Garcia-Canero, M. Blanco, and C. Gurmcharri-Lloyd, *Can. Chemother. Rep.*, **60**, 1 (1976).
(43) S. B. Wilson and A. L. Moore, *Biochim. Biophys. Acta*, **292**, 603 (1973).
(44) E. Racker, *Am. Sci.*, **60**, 56 (1972).

ACKNOWLEDGMENTS

Supported by grants from the National Cancer Institute (CA-17625) and the American Cancer Society (CH-19A) to K. H. Lee.

Antitumor Agents XXX: Evaluation of α-Methylene-γ-lactone-Containing Agents for Inhibition of Tumor Growth, Respiration, and Nucleic Acid Synthesis

IRIS H. HALL ˣ, KUO-HSIUNG LEE, CHARLES O. STARNES, SALWA A. ElGEBALY, TOSHIRO IBUKA, YIH-SHIONG WU, TAKEATSU KIMURA, and MITSUMASA HARUNA

Received September 30, 1977, from the *Division of Medicinal Chemistry, School of Pharmacy, University of North Carolina at Chapel Hill, Chapel Hill, NC 27514.* Accepted for publication December 28, 1977.

Abstract □ Evidence is presented that a number of sesquiterpene lactones isolated from plants and synthesized pyrimidines containing the α-methylene-γ-lactone moiety are potent inhibitors of Walker 256 carcinosarcoma and Ehrlich ascites tumor growth and marginal inhibitors of P-388 lymphocytic leukemia and Lewis lung tumor growth. *In vitro* aerobic basal respiration and oxidative phosphorylation processes of Ehrlich ascites cells were inhibited by these agents as well as deoxyribonucleic acid polymerase and thymidylate synthetase enzymatic activities. These studies indicate that the α-methylene-γ-lactone moiety, the β-unsubstituted cyclopentenone ring, and the α-epoxycyclopentanone system are the essential moieties for inhibition of these biochemical parameters.

Keyphrases □ α-Methylene-γ-lactone-containing agents—evaluated for effect on tumor growth, respiration, and nucleic acid synthesis □ Antineoplastic activity—various α-methylene-γ-lactone-containing agents evaluated □ Enzyme activity, tumor—effect of various α-methylene-γ-lactone-containing agents evaluated □ Nucleic acid synthesis, tumor—effect of various α-methylene-γ-lactone-containing agents evaluated □ Structure–activity relationships—various α-methylene-γ-lactone-containing agents evaluated for effect on tumor growth, respiration, and nucleic acid synthesis

Recently (1–13), some sesquiterpene lactones and related analogs were isolated or synthesized. A few of these compounds were shown to be potent antitumor agents of Walker 256 ascites carcinosarcoma (Sprague–Dawley rats at 2.5 mg/kg/day) and Ehrlich ascites tumor (CF_1 male mice at 33.3 mg/kg/day) and marginally active against P-388 lymphocytic leukemia (DBA/2 mice at 25 mg/kg/day) (5, 6). Helenalin, tenulin, and eupahyssopin were

0022-3549/78/0900-1235$01.00/0
© 1978, American Pharmaceutical Association

(8) W. C. Hymer and E. L. Kuff, *J. Histochem. Cytochem.*, **12**, 359 (1964).
(9) H. Sawada, K. Tatsumi, M. Sasada, S. Shirakawa, T. Nakumura, and G. Wakisaka, *Cancer Res.*, **34**, 3341 (1974).
(10) F. Maley and S. Ochoa, *J. Biol. Chem.*, **233**, 1538 (1958).
(11) A. Kampf, R. L. Barfknecht, P. J. Schaffer, S. Osaki, and M. P. Mertes, *J. Med. Chem.*, **19**, 903 (1976).
(12) A. Raineri, R. C. Simsiman, and R. K. Boutwell, *Cancer Res.*, **33**, 134 (1973).
(13) Y. M. Kish and L. J. Kleinsmith, *Methods Enzymol.*, **40**, 201 (1975).
(14) A. C. Gilman, *Proc. Natl. Acad. Sci., U.S.A.*, **67**, 305 (1970).
(15) K. M. Anderson, I. S. Mendelson, and G. Guzik, *Biochim. Biophys. Acta*, **383**, 56 (1975). I. H. Hall, G. L. Carlson, G. S. Abernethy, and C. Piantadosi, *J. Med. Chem.*, **17**, 1253 (1974).
(16) I. H. Hall, K. S. Ishaq, and C. Piantadosi, *J. Pharm. Sci.*, **63**, 625 (1974).
(17) Y. S. Cho-Chung and P. M. Gullino, *J. Biol. Chem.*, **248**, 4743 (1973).
(18) I. H. Hall, K. H. Lee, E. C. Mar, C. O. Starnes, and T. G. Waddell, *J. Med. Chem.*, **20**, 333 (1977).
(19) D. G. Walker and J. J. Parry, in "Methods in Enzymology IX," S. P. Colowick and N. O. Kaplan, Eds., Academic, New York, N.Y., 1966, p. 381.
(20) T. E. Mansour, in *ibid.*, p. 430.
(21) P. V. C. Pinto, A. Kaplan, and P. A. Van Dreal, *Clin. Chem.*, **15**, 349 (1969).
(22) M. K. Schwartz and O. Bodausky, in "Methods in Enzymology IX," Academic, New York, N.Y., 1966, p. 294.
(23) M. A. Swanson, *J. Biol. Chem.*, **184**, 647 (1950).
(24) I. H. Hall, K. H. Lee, and S. A. ElGebaly, *J. Pharm. Sci.*, **67**, 552 (1978).
(25) J. A. Thomas, K. K. Schlinder, and J. Larner, *Anal. Biochem.*, **25**, 486 (1968).
(26) D. V. DerVartanian and C. Verger, *Biochim. Biophys. Acta*, **92**, 233 (1964).
(27) S. Ochoa, A. H. Mehler, and A. Kornberg, *J. Biol. Chem.*, **174**, 979 (1948).
(28) P. S. Chen, T. Y. Toribana, and H. Warner, *Anal. Chem.*, **28**, 1756 (1956).
(29) O. H. Lowry, N. J. Rosebrough, A. L. Farr, and R. J. Randall, *J. Biol. Chem.*, **193**, 265 (1951).
(30) G. W. Snedcor, "Statistical Methods," Iowa State College Press, Ames, Iowa, 1956, Section 2.
(31) L. A. Loeb, in "The Enzymes," 3rd ed., P. D. Boyer, Ed., Academic, New York, N.Y., 1974, p. 173.
(32) M. Friedkin, *Adv. Enzymol.*, **38**, 235 (1973).
(33) K. H. Lee, I. H. Hall, E. C. Mar, C. O. Starnes, S. A. ElGebaly, T. G. Waddell, R. I. Hadgraft, C. G. Ruffner, and I. Weidner, *Science*, **196**, 533 (1977).
(34) C. S. Rubin and O. M. Roseu, *Annu. Rev. Biochem.*, **44**, 81 (1975).
(35) V. Stefanovich, *Res. Commun. Chem. Pathol. Pharmacol.*, **7**, 573 (1974).
(36) T. Posternak, *Annu. Rev. Pharmacol.*, **14**, 23 (1974). Y. S. Cho-Chung and P. M. Guillino, *Science*, **183**, 87 (1974).
(37) E. M. Johnson and J. W. Hadden, *Science*, **187**, 1198 (1975).
(38) S. M. Kupchan, D. C. Fessler, M. A. Eakin, and T. J. Giacobbe, *ibid.*, **168**, 376 (1970).
(39) R. L. Hanson, H. A. Landy, and S. M. Kupchan, *ibid.*, **168**, 378 (1970).
(40) C. H. Smith, J. Larner, A. M. Thomas, and S. M. Kupchan, *Biochim. Biophys. Acta*, **276**, 94 (1972).
(41) L. Stryer, "Biochemistry," Freeman, San Francisco, Calif., 1975, p. 32.
(42) M. Gosalvez, R. Garcia-Canero, M. Blanco, and C. Gurmcharri-Lloyd, *Can. Chemother. Rep.*, **60**, 1 (1976).
(43) S. B. Wilson and A. L. Moore, *Biochim. Biophys. Acta*, **292**, 603 (1973).
(44) E. Racker, *Am. Sci.*, **60**, 56 (1972).

ACKNOWLEDGMENTS

Supported by grants from the National Cancer Institute (CA-17625) and the American Cancer Society (CH-19A) to K. H. Lee.

Antitumor Agents XXX: Evaluation of α-Methylene-γ-lactone-Containing Agents for Inhibition of Tumor Growth, Respiration, and Nucleic Acid Synthesis

IRIS H. HALL ˣ, KUO-HSIUNG LEE, CHARLES O. STARNES, SALWA A. ElGEBALY, TOSHIRO IBUKA, YIH-SHIONG WU, TAKEATSU KIMURA, and MITSUMASA HARUNA

Received September 30, 1977, from the *Division of Medicinal Chemistry, School of Pharmacy, University of North Carolina at Chapel Hill, Chapel Hill, NC 27514.* Accepted for publication December 28, 1977.

Abstract □ Evidence is presented that a number of sesquiterpene lactones isolated from plants and synthesized pyrimidines containing the α-methylene-γ-lactone moiety are potent inhibitors of Walker 256 carcinosarcoma and Ehrlich ascites tumor growth and marginal inhibitors of P-388 lymphocytic leukemia and Lewis lung tumor growth. *In vitro* aerobic basal respiration and oxidative phosphorylation processes of Ehrlich ascites cells were inhibited by these agents as well as deoxyribonucleic acid polymerase and thymidylate synthetase enzymatic activities. These studies indicate that the α-methylene-γ-lactone moiety, the β-unsubstituted cyclopentenone ring, and the α-epoxycyclopentanone system are the essential moieties for inhibition of these biochemical parameters.

Keyphrases □ α-Methylene-γ-lactone-containing agents—evaluated for effect on tumor growth, respiration, and nucleic acid synthesis □ Antineoplastic activity—various α-methylene-γ-lactone-containing agents evaluated □ Enzyme activity, tumor—effect of various α-methylene-γ-lactone-containing agents evaluated □ Nucleic acid synthesis, tumor—effect of various α-methylene-γ-lactone-containing agents evaluated □ Structure–activity relationships—various α-methylene-γ-lactone-containing agents evaluated for effect on tumor growth, respiration, and nucleic acid synthesis

Recently (1–13), some sesquiterpene lactones and related analogs were isolated or synthesized. A few of these compounds were shown to be potent antitumor agents of Walker 256 ascites carcinosarcoma (Sprague–Dawley rats at 2.5 mg/kg/day) and Ehrlich ascites tumor (CF_1 male mice at 33.3 mg/kg/day) and marginally active against P-388 lymphocytic leukemia (DBA/2 mice at 25 mg/kg/day) (5, 6). Helenalin, tenulin, and eupahyssopin were

0022-3549/78/0900-1235$01.00/0
© 1978, American Pharmaceutical Association

shown to be effective inhibitors of deoxyribonucleic acid and protein synthesis, deoxyribonucleic acid polymerase enzymatic activity (5, 6), and basal and adenosine diphosphate stimulation respiration (14) of Ehrlich ascites cells.

A positive correlation between aerobic respiration inhibition and antitumor–antimitotic activity was observed for a number of nonrelated compounds, *e.g.*, a podophyllotoxin derivative[1], ellipticine (15), 4,6-diaminotriazines, methotrexate, naphthoquinone derivatives, tritylthioalanine, carminomycin, piperazinedione (14), 5-fluorinated pyrimidine-6-carboxaldehydes (16), benzamalecene, and triparanol (17). This paper reports a comparison of the effects of sesquiterpene lactones and related analogs on tumor growth, nucleic acid synthesis, and aerobic respiration.

EXPERIMENTAL

***In Vivo* Tumor Screens**—In the Ehrlich ascites screen, 10^6 cells were implanted intraperitoneally on Day 0. Compounds were suspended in 0.05% polysorbate 80 and homogenized to obtain a fine suspension. Each compound was injected intraperitoneally daily (1 mg/day) at 33.3 mg/kg/day into CF_1 male mice (~30 g). On the 7th day, the mice were sacrificed, and the total volume of ascites fluid and packed cell volume (ascites-crit) was determined to calculate the percent inhibition (18). Mercaptopurine was used as a positive standard.

In the Walker 256 ascites carcinosarcoma screen, 10^6 tumor cells were implanted intraperitoneally into Sprague–Dawley male rats (80 ± 10 g). In the P-388 lymphocytic leukemia screen, 10^6 cells were implanted intraperitoneally into DBA/2 male mice (~20 g) on Day 0. In the Lewis lung carcinoma, 2×10^6 cells were implanted intramuscularly in a hindleg of $C_{57}BL/6$ male mice (~25 g). Test compounds were injected intraperitoneally daily at 2.5 mg/kg/day for rats and 25 mg/kg/day for mice. The treated/control (T/C) values for the average days survived were calculated according to National Institutes of Health protocols (19).

The isolation or synthetic methods for the sesquiterpene lactones or related analogs were reported previously and are referred to in Table I under the column noted as "Source of Material."

***In Vitro* Tumor Respiration Studies**—Cells for oxidative phosphorylation studies were collected on the 7th day for Ehrlich ascites tumors and the 10th day for Walker 256 and P-388 tumors. Oxygen consumption was measured with a Clark electrode connected to a Gilson oxygraph. The reaction vessel typically contained 55 μmoles of sucrose, 22 μmoles of monobasic potassium phosphate, 22 μmoles of potassium chloride, 90 μmoles of succinate or 60 μmoles of α-ketoglutarate as the substrate, 2 μmoles of adenosine triphosphate, and 0.75 μmole of the test compound in a total volume of 1.8 ml. After the basal metabolic (state 4) level was obtained, 0.257 μmole of adenosine diphosphate was added to obtain the adenosine diphosphate-stimulated respiration rate (state 3) (20).

Enzyme Studies—*In vitro* DNA polymerase activity of 7-day Ehrlich ascites cells was determined on isolated nuclei from the ascites cells prepared by a literature method (21). The incubation method was that described by Sawada *et al.* (22) except that 2-^{14}C-deoxythymidine triphosphate (1–45 Ci/mmole) was used with 0.75 μmole of test compound in a total volume of 0.35 ml. The insoluble nucleic acids were precipitated with 1 *M* perchloric acid containing 1 mmole of tetrasodium pyrophosphate monohydrate and were collected on glass fiber paper[2] by vacuum suction (22).

In vitro thymidylate synthetase activity was determined by the method of Kampf *et al.* (23), utilizing a postmitochondrial supernate (9000×*g*) from 7-day Ehrlich ascites cells, 0.75 μmole of the test compound, and 5 μCi of ^{3}H-5′-deoxyuridine monophosphate (11 Ci/mmole) in a total volume of 0.1 ml. Preliminary studies indicated that 0.75 μmole *in vitro* resulted in the same magnitude of inhibition of deoxyribonucleic acid polymerase activity as previously demonstrated *in vivo* (5).

RESULTS

All compounds tested in the Ehrlich ascites tumor screen caused at

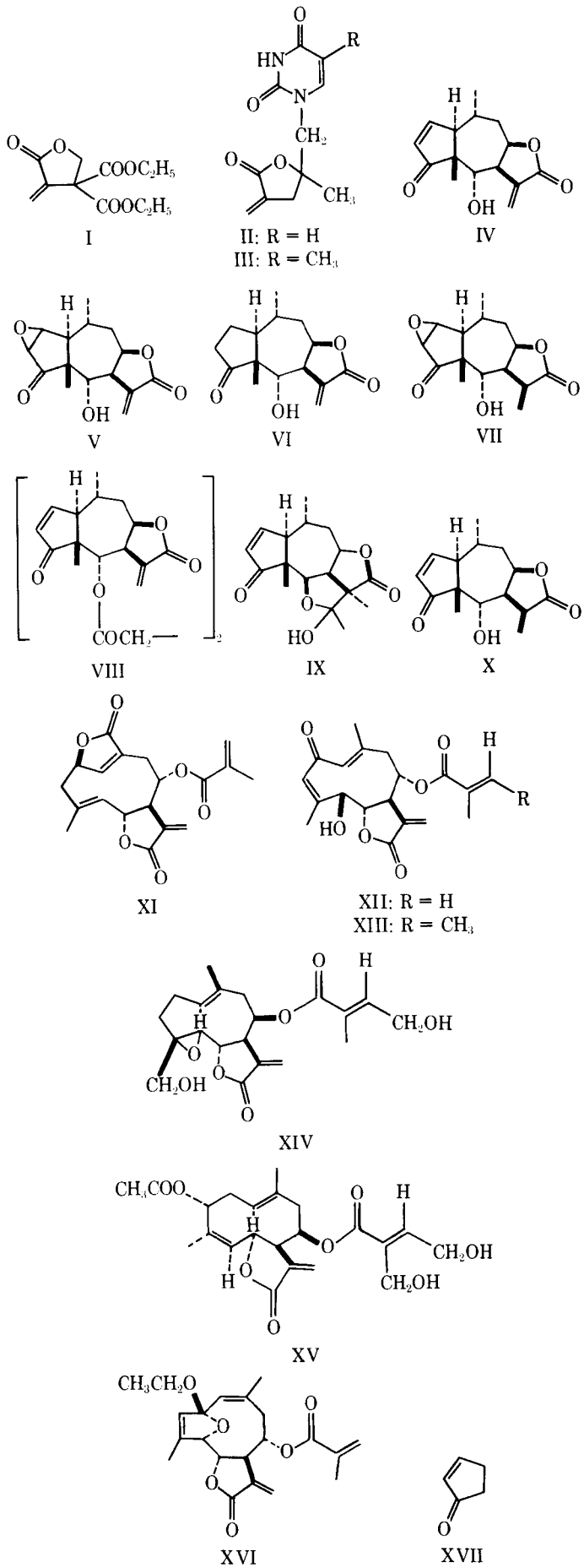

[1] VM-26.
[2] Whatman GF/F.

Table I—Antitumor Activity of Sesquiterpene Lactones and Related Analogs in Rodents

	Compound (n = 6)[a]	*In Vivo* Antitumor Activity: Ehrlich Ascites, % Inhibition	Walker 256 Carcinosarcoma, T/C	Lewis Lung, T/C	P-388 Lymphocytic Leukemia, T/C	Percent Control *In Vitro* Ehrlich Ascites: DNA Polymerase Activity	Thymidylate Synthetase Activity	Source of Material (Reference)
I	α-Methylene-β,β-di(ethoxycarbonyl)-γ-butyrolactone	98	140	—	—	44 ± 11[b]	—	1
II	Uracil lactone	100	131	—	115	29 ± 4[b]	—	2
III	Thymine lactone	99	127	—	127	38 ± 11[b]	79 ± 7[b]	2
IV	Helenalin	99	316	142	127	35 ± 2	49 ± 8[b]	3
V	2,3-Epoxyhelenalin	99	145	—	117	44 ± 4[b]	70 ± 14[b]	4
VI	2,3-Dihydrohelenalin	64	134	—	110	64 ± 19[c]	83 ± 3[b]	4
VII	11,13-Dihydro-2,3-epoxyhelenalin	89	264	—	134	77 ± 11[c]	79 ± 9[b]	4
VIII	Dimeric helenalin[d]	100	187	142	168	39 ± 2[b]	56 ± 2[b]	—
IX	Tenulin	97	266	126	131	83 ± 9[c]	56 ± 11[b]	5
X	Plenolin	100	207	—	138	74 ± 7[b]	73 ± 13[c]	7
XI	Deoxyelephantopin	99	226	—	123	67 ± 7[b]	73 ± 19[e]	8
XII	Molephantin	75	149	80	118	55 ± 6[b]	81 ± 18[f]	9
XIII	Molephantinin	88	397	123	146	37 ± 5[b]	77 ± 9	10
XIV	Eupahyssopin	93	330	132	147	34 ± 5[b]	63 ± 7[b]	11
XV	Eupaformosanin	—	471	—	147	72 ± 10[b]	69 ± 4[b]	13
XVI	Phantomolin	87	378	123	113	38 ± 4[b]	72 ± 14[c]	12
XVII	Cyclopentenone	75	188	—	—	43 ± 4[b]	65 ± 8[b]	—
XVIII	Mercaptopurine	99	—	—	—	—	—	—
XIX	Fluorouracil	—	—	—	186	—	39 ± 7[b]	—
XX	Melphalan	96	317	—	168	—	—	—
XXI	Cyclophosphamide	—	—	140	—	—	—	—
XXII	Iodoacetate	—	—	—	—	41 ± 4[b]	—	—
	0.05% polysorbate 80	0	100	100	100	100 ± 5[g]	100 ± 3[h]	—

[a] n = number of animals per group. [b] $p = 0.001$. [c] $p = 0.005$. [d] The synthesis of VIII is unpublished. [e] $p = 0.010$. [f] $p = 0.025$. [g] 47,424 dpm/mg of DNA. [h] 103,328 dpm/mg of protein.

least 60% inhibition of tumor growth. Compounds I–V, VIII–XI, and XIV inhibited Ehrlich ascites tumor growth greater than 90% (Table I). All compounds tested with the Walker 256 ascites carcinosarcoma were active; *i.e.*, the T/C >125. Compounds VII and IX–XI doubled the life expectancy, and IV, XIII, XIV, and XVI tripled the survival time of these animals; XV improved it four times. Of the compounds tested in the Lewis lung, only IV and VIII were active (T/C = 140 required for activity). In the P-388 lymphocytic leukemia screen, III, IV, VII–X, and XIII–XV demonstrated a T/C >125.

The basal respiration (state 4) was significantly reduced by all compounds tested with both succinate (flavin adenine dinucleotide-linked dehydrogenase) (Table II) and α-ketogluturate (nicotinamide adenine dinucleotide-linked dehydrogenase) for Ehrlich, P-388 leukemia, and Walker 256 cells (Table III). The oxidative phosphorylation processes, *i.e.*, coupled adenosine triphosphate synthesis, were all significantly suppressed by all compounds tested for all three types of cells. *In vitro* deoxyribonucleic acid polymerase activity of Ehrlich ascites cells was inhibited drastically (>50%) by I–V, VIII, XI, XIII, XIV, XVI, XVII, and XXII at 0.75 μmole. *In vitro* thymidylate synthetase activity was inhibited significantly by all compounds tested. Compounds IV, VIII, and IX demonstrated at least 40% inhibition, and XIV, XV, XVII, and XIX showed at least 30% inhibition at 0.75 μmole.

The probable (p) significant difference was determined by the Student t test. Data are expressed in Tables I–III as percent control of average mean and standard deviation.

DISCUSSION

In view of the wide diversity of structural components of I–XVII, it can be surmised that an α-methylene-γ-lactone moiety, a β-unsaturated cyclopentenone ring, or an α-epoxycyclopentanone system is one essential structural requirement for significant *in vivo* antitumor activity in Ehrlich and Walker 256 carcinosarcoma tumors. This conclusion is consistent with the previous observation that any one of these three functions is essentially responsible for the *in vitro* cytotoxic activity against H.Ep-2 cells (4, 24–28).

Compounds IX and X, which contain only the cyclopentenone ring of these three functional groups, must also possess some other characteristic in the molecule that adds to the antitumor activity since they were more active against Walker 256 and Ehrlich ascites tumor growth than the cyclopentenone ring alone (XVII). The presence of the allylic ester side chain, *e.g.*, in the germacranolides, molephantinin (XIII), eupahyssopin (XIV), eupaformosanin (XV), and phantomolin (XVI), may enhance antitumor activity, perhaps facilitating the membrane transport of these

Table II—*In Vitro* Effects of Antitumor Agents on Basal and ADP-Stimulated Respiration (Microliters of Oxygen per Hour per Milligram of Protein) Using Sodium Succinate as the Substrate (Percent Control)

Compound (n = 6)	Walker 256 State 4	Walker 256 State 3	P-388 Leukemia State 4	P-388 Leukemia State 3	Ehrlich Ascites State 4	Ehrlich Ascites State 3
I	47 ± 5[a]	50 ± 4[a]	77 ± 7[a]	70 ± 13[b]	55 ± 8[a]	49 ± 3[a]
II	—	—	—	—	—	—
III	—	—	—	—	74 ± 9[a]	81 ± 7[c]
IV	52 ± 9[a]	73 ± 9[a]	63 ± 14[a]	53 ± 20[a]	72 ± 8[a]	60 ± 8[a]
V	60 ± 9[a]	72 ± 5[a]	69 ± 8[a]	62 ± 17[a]	66 ± 8[a]	77 ± 11[c]
VI	36 ± 10[a]	42 ± 4[a]	83 ± 9	62 ± 13	49 ± 7[a]	59 ± 5[a]
VII	75 ± 14[c]	80 ± 7[c]	87 ± 2[b]	76 ± 3[a]	78 ± 8[a]	84 ± 4[c]
VIII	75 ± 7[a]	80 ± 9[c]	62 ± 13[a]	52 ± 15[a]	59 ± 7[a]	64 ± 6[a]
IX	36 ± 8[a]	70 ± 7[a]	51 ± 9[a]	65 ± 22[c]	52 ± 6[a]	64 ± 5[a]
X	62 ± 7[a]	75 ± 5[a]	62 ± 19[c]	58 ± 16[a]	65 ± 10[a]	52 ± 14[a]
XI	65 ± 6[a]	69 ± 6[a]	73 ± 5[a]	70 ± 8[a]	69 ± 12[a]	75 ± 3[a]
XII	48 ± 5[a]	50 ± 7[a]	69 ± 7[a]	69 ± 6[a]	68 ± 5[a]	55 ± 5[a]
XIII	64 ± 7[a]	82 ± 6[c]	67 ± 17[c]	66 ± 16[c]	64 ± 9[a]	75 ± 8[a]
XIV	—	—	—	—	82 ± 11[c]	87 ± 5[c]
XV	—	—	—	—	69 ± 12[a]	69 ± 9[a]
XVII	—	—	—	—	78 ± 4[c]	74 ± 3[a]
0.05% polysorbate 80	100 ± 5	100 ± 8	100 ± 8	100 ± 11	100 ± 3	100 ± 4
Control	4.494	5.506	4.196	4.532	5.506	6.487

[a] $p = 0.001$. [b] $p = 0.010$. [c] $p = 0.005$.

Table III—*In Vitro* Effects of Antitumor Agents on Basal and ADP-Stimulated Respiration (Microliters of Oxygen per Hour per Milligram of Protein) Using α-Ketoglutarate as Substrate (Percent Control)

Compound (n = 6)	Walker 256		P-388 Leukemia		Ehrlich Ascites	
	State 4	State 3	State 4	State 3	State 4	State 3
I	35 ± 9[a]	43 ± 11[a]	68 ± 8[a]	53 ± 6[a]	46 ± 11[a]	42 ± 12[a]
II	62 ± 4[a]	73 ± 3[a]	55 ± 6[a]	69 ± 3[a]	—	—
III	63 ± 10[a]	71 ± 14[b]	39 ± 9[a]	57 ± 17[a]	—	—
IV	49 ± 21[a]	58 ± 12[a]	70 ± 9[a]	70 ± 6[a]	53 ± 9[a]	66 ± 10[a]
V	52 ± 17[a]	54 ± 17[a]	64 ± 10[a]	95 ± 2	51 ± 9[a]	56 ± 7[a]
VI	49 ± 16[a]	57 ± 17[a]	74 ± 13[b]	85 ± 7[c]	56 ± 10[a]	66 ± 10[a]
VII	54 ± 14[a]	70 ± 17[b]	56 ± 8[a]	78 ± 5[a]	70 ± 5[a]	79 ± 9[b]
VIII	54 ± 16[a]	54 ± 15[a]	41 ± 15[a]	65 ± 4[a]	66 ± 9[a]	18 ± 13[b]
IX	47 ± 9[a]	53 ± 15[a]	59 ± 7[a]	66 ± 13[a]	51 ± 5[a]	55 ± 12[a]
X	67 ± 8[a]	63 ± 10[a]	59 ± 4[a]	82 ± 7[b]	60 ± 10[a]	77 ± 5[b]
XI	57 ± 13[a]	67 ± 15[b]	95 ± 3[a]	58 ± 6[a]	59 ± 12[a]	73 ± 11[b]
XII	55 ± 11[a]	55 ± 14[a]	70 ± 6[a]	68 ± 6[a]	56 ± 18[a]	63 ± 9[a]
XIII	60 ± 31[c]	76 ± 12[b]	61 ± 7[a]	73 ± 13[b]	69 ± 8[a]	67 ± 9[a]
XIV	49 ± 14[a]	46 ± 25[a]	68 ± 9[a]	87 ± 10	59 ± 14[a]	53 ± 8[a]
XV	59 ± 15[a]	52 ± 16[a]	65 ± 10[a]	66 ± 10[a]	52 ± 14[a]	53 ± 8[a]
XVII	—	—	—	—	—	—
0.05% polysorbate 80	100 ± 8	100 ± 7	100 ± 5	100 ± 8	100 ± 5	100 ± 11
Control	2.729	2.691	2.029	1.958	2.525	4.049

[a] $p = 0.001$. [b] $p = 0.005$. [c] $p = 0.010$.

compounds. This possibility is especially obvious with the introduction of the primary alcohol into the side chain (XIV and XV).

Gosalvez *et al.* (29) attempted to correlate antitumor activity with suppression of tumor aerobic respiration in the presence and absence of adenosine diphosphate. With respect to the sesquiterpene lactones or synthetic compounds containing the α-methylene-γ-lactone moiety, there appeared to be a strong positive correlation between antitumor activity and suppression of basal (4) and coupled oxidative phosphorylation processes (3) of Ehrlich and Walker 256 tumor cells with both nicotinamide adenine dinucleotide and flavin adenine nucleotide-linked dehydrogenases. The adenosine triphosphate derived from state 3 respiration is critical in rapidly dividing tumor cells since energy is required for synthetic processes, *e.g.*, nucleic acids, protein, and cellular membranes during G_1 and S phases of the cell cycle.

However, the ability of these compounds to suppress aerobic respiration processes, *i.e.*, states 3 and 4, appeared to exceed their ability to inhibit tumor growth. This observation is confirmed by the fact that these compounds effectively inhibited P-388 leukemic cell respiration but only marginally inhibited P-388 tumor growth. Kupchan *et al.* (30) demonstrated that compounds containing the α-methylene-γ-lactone moiety act as antitumor agents by alkylating sulfhydryl biological nucleophiles by a rapid Michael-type addition. A similar phenomenon was demonstrated *in vitro* with tenulin (IX) and helenalin (IV), indicating that both the α-methylene-γ-lactone and the cyclopentenone moieties act as electrophiles (6). The cytochrome cofactors of the electron transport chain contain iron–sulfur centers or sulfide ions as components of their structure, and a number of Krebs cycle dehydrogenases contain sulfhydryl groups within their structures (31). Theoretically, these compounds can be alkylated by a Michael reaction by these antitumor agents, reducing activity and state 4 respiration.

Compound IV was shown to be an effective inhibitor of nuclei DNA polymerase activity of Ehrlich ascites cells *in vivo* (5). Supposedly, the DNA polymerase alpha and gamma enzymes contain exposed sulfhydryl groups (31) that can be alkylated. From the present study, not only were the compounds containing the α-methylene-γ-lactone moiety inhibitors of deoxyribonucleic acid polymerase activity, but compounds containing only a cyclopentenone ring (IX and X) or an α-epoxycyclopentanone system (VII) were also marginal inhibitors of this enzyme.

Sesquiterpene lactones containing two of these functions were more active than compounds containing only one function in inhibiting deoxyribonucleic acid polymerase activity. Compounds containing the allylic ester side chain (XI–XVI) also demonstrated higher activity, with the exception of XV. Thymidylate synthetase was reported to be a sulfhydryl-bearing enzyme (32). Sesquiterpene lactone and related analogs can significantly inhibit this enzyme but to a slightly less magnitude than the deoxyribonucleic acid polymerase enzymes. All three of these functional moieties appear to be active in the inhibition of thymidylate synthetase activity of tumor cells.

REFERENCES

(1) K. H. Lee, T. Ibuka, S. H. Kim, B. R. Vestal, and I. H. Hall, *J. Med. Chem.*, **18,** 812 (1975).

(2) K. H. Lee, Y. S. Wu, and I. H. Hall, *ibid.*, **20,** 911 (1977).

(3) K. H. Lee and T. A. Geissman, *Phytochemistry*, **8,** 2371 (1970).

(4) K. H. Lee, S. H. Kim, H. Furukawa, and C. Piantadosi, *J. Med. Chem.*, **18,** 59 (1975).

(5) I. H. Hall, K. H. Lee, E. C. Mar, C. O. Starnes, and T. G. Waddell, *ibid.*, **20,** 333, 1977.

(6) I. H. Hall, K. H. Lee, and S. A.ElGebaly, *J. Pharm. Sci.*, **67,** 1232 (1978).

(7) K. H. Lee, T. Ibuka, A. T. McPhail, K. D. Onan, T. A. Geissman, and T. G. Waddell, *Tetrahedron Lett.*, **1974,** 1149.

(8) K. H. Lee, C. M. Cowherd, and M. T. Walo, *J. Pharm. Sci.*, **64,** 1572 (1975).

(9) K. H. Lee, H. Furukawa, M. Kozuka, H. C. Huang, P. A. Luhan, and A. T. McPhail, *J. Chem. Soc. D*, **1973,** 476.

(10) K. H. Lee, T. Ibuka, H. C. Huang, and D. L. Harris, *J. Pharm. Sci.*, **64,** 1077 (1975).

(11) K. H. Lee, T. Kimura, M. Okamoto, C. M. Cowherd, A. T. McPhail, and K. D. Onan, *Tetrahedron Lett.*, **14,** 1041 (1976).

(12) A. T. McPhail, K. D. Onan, K. H. Lee, T. Ibuka, M. Kozuka, T. Shingu, and H. C. Huang, *Tetrahedron Lett.*, **1974,** 2739.

(13) K. H. Lee, T. Kimura, M. Haruna, A. T. McPhail, K. D. Onan, and H. C. Huang, *Phytochemistry*, **16,** 1068 (1977).

(14) K. H. Lee, I. H. Hall, E. C. Mar, C. O. Starnes, S. A. ElGebaly, T. G. Waddell, R. I. Hadgraft, C. G. Ruffner, and I. Weidner, *Science*, **196,** 533 (1977).

(15) M. Gosalvez, M. Blanco, and J. Hunter, *Eur. J. Cancer*, **10,** 567 (1974).

(16) C. Piantadosi, C. S. Kim, and J. L. Irvin, *J. Pharm. Sci.*, **58,** 821 (1969).

(17) S. Aanonson, *Proc. Expt. Biol. Med.*, **136,** 61 (1971).

(18) C. Piantadosi, C. S. Kim, and J. L. Irvin, *J. Pharm. Sci.*, **58,** 821 (1969).

(19) R. I. Geran, N. H. Greenberg, M. M. Macdonald, A. M. Schumacher, and B. J. Abbott, *Cancer Chemother. Rep.* **3,** protocol 1.200, 1.400, and 1.500 (1972).

(20) I. Hall and G. L. Carlson, *J. Med. Chem.*, **19,** 1257 (1976).

(21) W. C. Hymer and E. L. Kuff, *J. Histochem. Cytochem.*, **12,** 359 (1964).

(22) H. Sawada, K. Tatsumi, M. Sadada, S. Shinakawa, T. Nakumura, and G. Wakisaka, *Cancer Res.*, **34,** 3341 (1974).

(23) A. Kampf, R. L. Barfknecht, P. J. Shaffer, S. Osaki, and M. P. Mertes, *J. Med. Chem.*, **19,** 903 (1976).

(24) K. H. Lee, E. S. Huang, C. Piantadosi, J. S. Pagano, and T. A. Geissman, *Cancer Res.*, **31,** 1649 (1971).

(25) K. H. Lee, H. Furukawa, and E. S. Huang, *J. Med. Chem.*, **15,** 609 (1972).

(26) K. H. Lee, R. Meck, C. Piantadosi, and E. S. Huang, *ibid.*, **16,** 299, 1973.

(27) K. H. Lee, *J. Pharm. Sci.*, **62,** 1028 (1973).

(28) K. H. Lee, T. Ibuka, and R. Y. Wu, *Chem. Pharm. Bull.*, **22,** 2206 (1974).

(29) M. Gosalvez, R. Garcia-Vanero, M. Blanco, and C. Gurucharri-

Lloyd, *Cancer Treatment Rep.*, **60**, 1 (1976).
(30) S. M. Kupchan, D. C. Fessler, M. A. Eakin, and T. J. Giacobbe, *Science*, **168**, 376 (1970).
(31) L. A. Loeb, in "The Enzymes," 3rd ed., P. D. Boyer, Ed., Academic, New York, N.Y., 1974, p. 173.
(32) M. Friedkin, *Adv. Enzymol.*, **38**, 235 (1973).

ACKNOWLEDGMENTS

Supported by grants from the American Cancer Society (CH-19A) and the National Cancer Institute (CA-17625 and CA-12360) to K. H. Lee.

The authors thank Professor T. G. Waddell, Department of Chemistry, University of Tennessee at Chattanooga, for a gift of tenulin.

Lyophilization of Sincalide and Correlation of Headspace Relative Humidity with Product Stability

RAYMOND C. HUBER ˣ, A. O. NIEDERMAYER, and AARON L. WEISS

Received June 15, 1977, from the *Squibb Institute for Medical Research, New Brunswick, NJ 08903.* Accepted for publication December 21, 1977.

Abstract □ An optimum freeze-drying cycle was developed for use with industrial equipment in the processing in vials of a product degraded by traces of moisture. The relative humidity of the headspace gas of the vials, which contained only 5 μg of active ingredient, was monitored by a GC method and was then correlated with product stability.

Keyphrases □ Sincalide—lyophilization, optimum cycle developed, vial headspace relative humidity correlated with product stability □ Lyophilization—sincalide, optimum cycle developed, vial headspace relative humidity correlated with product stability □ Humidity, relative—in headspace of lyophilized vials of sincalide, correlated with product stability □ Stability—sincalide, lyophilized, correlated with headspace vial relative humidity

Lyophilization has become a standard procedure for processing labile ingredients in sterile pharmaceutical products. For substances susceptible to hydrolysis, freeze drying assures the final dried formulation a longer shelf-life at higher storage temperatures than would be possible in solution. The process usually yields a sterile plug of powder in a vial as a final product. When the plug has a small mass, it becomes difficult to determine the moisture.

Ordinarily, the freeze-drying process produces a product containing 1% or less moisture (1); in most cases, this amount is not harmful to the product. However, when small quantities of water have a deleterious effect, the moisture content of the product must be reduced to trace quantities. Consequently, alternative approaches must be devised to determine the moisture content present. This report discusses various procedures for the removal of virtually all water from vials by industrial scale lyophilization and a method for determining the trace amount of water remaining in the sealed vials.

The small quantity of sample and the low moisture levels anticipated made the use of the Karl Fischer method inappropriate for water determination without modification. Based on the work of Litchman and Upton (2), the estimation of in-vial water content through headspace GC was developed. This technique allowed headspace relative humidity to be determined without disturbing the sample environment. The headspace humidity value, supplemented by product stability (bioassay), provided the means for process control.

EXPERIMENTAL

Processing (Lyophilization)—Vials (5 ml, 13-mm neck) were filled with 2.1 (±1.5%) ml of a sterile aqueous solution containing 21.43 mg of sodium chloride/ml for a lyophilization trial. About 9000 filled vials were stoppered with siliconed, notched, sterile butyl rubber closures in the raised position; they were then placed in trays and spread through a 90-tray capacity sterile industrial lyophilizer[1] (Lot A). Ten empty vials similarly prepared were also placed in each tray as controls (Lot B).

In addition, "active" vials were each filled with 2.1 ml of an aqueous solution containing 2.5 μg of sincalide[2] (I)/ml and 21.43 mg of sodium chloride/ml. These active vials were placed with the two other categories in trays in the bottom, middle, and top of the lyophilizer (Lot C). Each of the total of 42 trays was numbered and recorded by shelf location.

Prior to filling of the vials, the eutectic temperature of the active solution was found to be −21.8 ± 0.3° by differential scanning calorimetry. This value compared well with the eutectic reported for sodium chloride, −21.6° (3). To ensure freezing of the liquid beyond the effects that supercooling might induce, the shelves of the lyophilizer were held at −60° for 12 hr.

A vacuum was then drawn. The following drying cycle was immediately begun and continued for 72 consecutive hr: −30° (23 hr), +35° (31 hr), and +50° (8 hr). Transitional periods accounted for 10 hr. During the final hour, the temperature was adjusted to +25°. The shelf temperatures and chamber pressures actually obtained during the lyophilization are given in Table I.

At the conclusion of the cycle, with the temperature at +25°, the evacuated chamber was vented with dry nitrogen. As a flushing operation, the venting was followed by a reevacuation and finally by another venting of the chamber with dry nitrogen. At this point, the vials were closed with the stoppers, inside the lyophilizer, under slight vacuum. After stoppering, the chamber was opened, the trays were removed, and the vials were sealed with crimped aluminum caps. Each tray held ~231 vials, and samples were taken at random for moisture determination.

In optimizing the freeze-drying procedure, other cycles were employed. Lots D and E were lyophilized (after freezing) in laboratory equipment[3] for 42.5 hr: −28° (1.5 hr), slow transition (24 hr), and +30° (17 hr). Lot F was lyophilized in laboratory equipment[3] for 72 hr: −30° (24 hr), slow transition (24 hr), +22° (21 hr), and transition to +35° (3 hr). Lot G was lyophilized in the industrial equipment[1] for 72 hr: transition from −45 to −27° (4 hr), −27° (20 hr), slow transition from −27 to +25° (12 hr), +25° (34 hr), and transition to +35° (2 hr). Lot H-1 was lyophilized in laboratory equipment[3] for 72 hr, approximating the cycle of Lot F.

Humidity Determination—The headspace humidity determination was based on the GC estimation of water in a headspace gas sample. The

[1] Model 179FXS350, Hull Corp., Hatboro, Pa.
[2] L-Aspartyl-L-tyrosyl-L-methionylglycyl-L-tryptophyl-L-methionyl-L-aspartylphenyl-L-alaninamide (hydrogen sulfate). The trade name for this gallbladder contractile agent is Kinevac (Squibb).
[3] Model 2004-LLX3, F. J. Stokes Machine Co., Philadelphia, Pa.

0022-3549/78/0900-1239$01.00/0
© 1978, American Pharmaceutical Association

Lloyd, *Cancer Treatment Rep.*, **60**, 1 (1976).
(30) S. M. Kupchan, D. C. Fessler, M. A. Eakin, and T. J. Giacobbe, *Science*, **168**, 376 (1970).
(31) L. A. Loeb, in "The Enzymes," 3rd ed., P. D. Boyer, Ed., Academic, New York, N.Y., 1974, p. 173.
(32) M. Friedkin, *Adv. Enzymol.*, **38**, 235 (1973).

ACKNOWLEDGMENTS

Supported by grants from the American Cancer Society (CH-19A) and the National Cancer Institute (CA-17625 and CA-12360) to K. H. Lee.

The authors thank Professor T. G. Waddell, Department of Chemistry, University of Tennessee at Chattanooga, for a gift of tenulin.

Lyophilization of Sincalide and Correlation of Headspace Relative Humidity with Product Stability

RAYMOND C. HUBER ˣ, A. O. NIEDERMAYER, and AARON L. WEISS

Received June 15, 1977, from the *Squibb Institute for Medical Research, New Brunswick, NJ 08903.* Accepted for publication December 21, 1977.

Abstract □ An optimum freeze-drying cycle was developed for use with industrial equipment in the processing in vials of a product degraded by traces of moisture. The relative humidity of the headspace gas of the vials, which contained only 5 μg of active ingredient, was monitored by a GC method and was then correlated with product stability.

Keyphrases □ Sincalide—lyophilization, optimum cycle developed, vial headspace relative humidity correlated with product stability □ Lyophilization—sincalide, optimum cycle developed, vial headspace relative humidity correlated with product stability □ Humidity, relative—in headspace of lyophilized vials of sincalide, correlated with product stability □ Stability—sincalide, lyophilized, correlated with headspace vial relative humidity

Lyophilization has become a standard procedure for processing labile ingredients in sterile pharmaceutical products. For substances susceptible to hydrolysis, freeze drying assures the final dried formulation a longer shelf-life at higher storage temperatures than would be possible in solution. The process usually yields a sterile plug of powder in a vial as a final product. When the plug has a small mass, it becomes difficult to determine the moisture.

Ordinarily, the freeze-drying process produces a product containing 1% or less moisture (1); in most cases, this amount is not harmful to the product. However, when small quantities of water have a deleterious effect, the moisture content of the product must be reduced to trace quantities. Consequently, alternative approaches must be devised to determine the moisture content present. This report discusses various procedures for the removal of virtually all water from vials by industrial scale lyophilization and a method for determining the trace amount of water remaining in the sealed vials.

The small quantity of sample and the low moisture levels anticipated made the use of the Karl Fischer method inappropriate for water determination without modification. Based on the work of Litchman and Upton (2), the estimation of in-vial water content through headspace GC was developed. This technique allowed headspace relative humidity to be determined without disturbing the sample environment. The headspace humidity value, supplemented by product stability (bioassay), provided the means for process control.

EXPERIMENTAL

Processing (Lyophilization)—Vials (5 ml, 13-mm neck) were filled with 2.1 (±1.5%) ml of a sterile aqueous solution containing 21.43 mg of sodium chloride/ml for a lyophilization trial. About 9000 filled vials were stoppered with siliconed, notched, sterile butyl rubber closures in the raised position; they were then placed in trays and spread through a 90-tray capacity sterile industrial lyophilizer[1] (Lot A). Ten empty vials similarly prepared were also placed in each tray as controls (Lot B).

In addition, "active" vials were each filled with 2.1 ml of an aqueous solution containing 2.5 μg of sincalide[2] (I)/ml and 21.43 mg of sodium chloride/ml. These active vials were placed with the two other categories in trays in the bottom, middle, and top of the lyophilizer (Lot C). Each of the total of 42 trays was numbered and recorded by shelf location.

Prior to filling of the vials, the eutectic temperature of the active solution was found to be −21.8 ± 0.3° by differential scanning calorimetry. This value compared well with the eutectic reported for sodium chloride, −21.6° (3). To ensure freezing of the liquid beyond the effects that supercooling might induce, the shelves of the lyophilizer were held at −60° for 12 hr.

A vacuum was then drawn. The following drying cycle was immediately begun and continued for 72 consecutive hr: −30° (23 hr), +35° (31 hr), and +50° (8 hr). Transitional periods accounted for 10 hr. During the final hour, the temperature was adjusted to +25°. The shelf temperatures and chamber pressures actually obtained during the lyophilization are given in Table I.

At the conclusion of the cycle, with the temperature at +25°, the evacuated chamber was vented with dry nitrogen. As a flushing operation, the venting was followed by a reevacuation and finally by another venting of the chamber with dry nitrogen. At this point, the vials were closed with the stoppers, inside the lyophilizer, under slight vacuum. After stoppering, the chamber was opened, the trays were removed, and the vials were sealed with crimped aluminum caps. Each tray held ~231 vials, and samples were taken at random for moisture determination.

In optimizing the freeze-drying procedure, other cycles were employed. Lots D and E were lyophilized (after freezing) in laboratory equipment[3] for 42.5 hr: −28° (1.5 hr), slow transition (24 hr), and +30° (17 hr). Lot F was lyophilized in laboratory equipment[3] for 72 hr: −30° (24 hr), slow transition (24 hr), +22° (21 hr), and transition to +35° (3 hr). Lot G was lyophilized in the industrial equipment[1] for 72 hr: transition from −45 to −27° (4 hr), −27° (20 hr), slow transition from −27 to +25° (12 hr), +25° (34 hr), and transition to +35° (2 hr). Lot H-1 was lyophilized in laboratory equipment[3] for 72 hr, approximating the cycle of Lot F.

Humidity Determination—The headspace humidity determination was based on the GC estimation of water in a headspace gas sample. The

[1] Model 179FXS350, Hull Corp., Hatboro, Pa.
[2] L-Aspartyl-L-tyrosyl-L-methionylglycyl-L-tryptophyl-L-methionyl-L-aspartylphenyl-L-alaninamide (hydrogen sulfate). The trade name for this gallbladder contractile agent is Kinevac (Squibb).
[3] Model 2004-LLX3, F. J. Stokes Machine Co., Philadelphia, Pa.

0022-3549/78/0900-1239$01.00/0
© 1978, American Pharmaceutical Association

Table I—Details of the Lyophilization Cycle for Production of Vials with Low Relative Humidity (Lots A, B, and C)

Hours	Shelf Temperature	Average Product Temperature	Chamber Pressure, μ	Remarks
0	−55°	−54°	—	Product had been frozen overnight; vacuum in chamber begun
1.5	−26°	−41°	140	
2.5	−25°	−39°	140	
5	−25°	−37°	140	
6	−25°	−37°	140	
9	−25°	−35°	140	
11	−25°	−34°	140	
13	−25°	−32°	140	
24	−25°	−27°	140	Low heat applied to shelves
25	−16°	−23°	—	
26	−4°	−13°	—	
27	2°	−5°	—	
28	9°	−1°	—	
29	33°	15°	140	
30	35°	29°	132	
31	35°	30°	120	
32	36°	33°	110	
33	34°	32°	109	
34	35°	32°	105	
35	34°	32°	100	
36	34°	32°	100	
47	34°	32°	95	
60	34°	33°	95	High heat applied to shelves
61	45°	37°	95	
62	48°	45°	95	
70	52°	47°	96	Shelf cooling applied
72	27°	32°	94	Vacuum discontinued
73	27°	31°	—	Stoppers set into vials

water was quantitated against that found under identical conditions in the headspace of salt solutions prepared to yield a progression of humidities specifically for calibration.

Preparation and Use of Calibration Standards—Four or more saturated aqueous salt solutions were prepared in individual 500-ml septum closure bottles (Table II). Each contained ~100 ml of solution and excess salt. The bottles were sealed at atmospheric pressure and allowed to equilibrate at room temperature for at least 48 hr before use.

The humidity standards were retained equilibrated indefinitely. The creation of a small negative pressure within the bottles following sample withdrawals, however, necessitated readjustment to atmospheric pressure. The momentary insertion of a hypodermic needle into the septum closure of each bottle following a day's use accomplished this readjustment. Reequilibration occurred overnight.

GC—A gas chromatograph[4] equipped with a glass column using on-column injection, a thermal conductivity detector, and a 1-mv recorder[5] constituted the system.

A 1-m glass column, 6 mm i.d., was packed with 50–80-mesh Poropak Q[6]. It was conditioned prior to use according to the manufacturer's instructions. Daily reconditioning for 0.5 hr was generally not necessary but was advisable.

Operating conditions were: column temperature, ~100°[7]; detector temperature, 200°; detector current, >200 mamp; carrier gas, helium, 45–50 ml/min; and gas sample, 0.5 ml.

Sampling—The headspace gas sampling of both calibration standards and samples was accomplished with a gas-tight syringe. For this purpose, a plastic 1-ml tuberculin syringe[8] equipped with a 2.54-cm 26-gauge needle was utilized. The standard gas-tight syringes[9] were unsatisfactory. Excessive deadspace and, more important, the reversible adsorption of moisture by the glass barrel led to cross-contamination and significant analytical bias.

The sampling procedure consisted of two steps. First, the syringe was thoroughly flushed with either dry helium or nitrogen to clear it of atmospheric moisture. Upon expulsion of the drying gas, the syringe needle was plunged through the septum of the vessel to be sampled. Second, the syringe was pumped slowly four or five times, filled to ~0.6 ml, and withdrawn from the sample container. The volume was adjusted to exactly 0.5 ml prior to injection into the chromatograph.

A complete chromatographic run required about 2 min. All GC analyses were in triplicate from each sample, and the average peak height of the three samplings was used in computation. Typical chromatographic curves are displayed in Fig. 1, representing 11 and 75% relative humidities (RH).

Calibration and Quantitation—Headspace gas samples of the calibration standards were taken and chromatographed as specified. A response plot (peak height *versus* relative humidity) was constructed. A typical calibration curve gave a slope of 1.20, an intercept of −0.7, and a correlation coefficient of 0.999. The small variable intercept found may be indicative of constant atmospheric moisture contamination during sampling or simply the experimental error of the method.

Quantitation was achieved by reading the relative humidities of the unknown directly from a calibration curve constructed prior to or immediately following the samples. Because of the sensitivity of the water peak height to changes in experimental conditions, it was imperative that the conditions remain constant throughout the entire calibration–sample sequence.

Precision and Accuracy—The precision of standard or sample replicates varied with relative humidity. At 11% RH, it was within ±4%; at 30% RH, it was ±3%; and at 50% RH, it was ±1%. Precision did not improve greatly at relative humidities above 50%.

The accuracy of the measurements is demonstrated in Table III

Table II—Saturated Salt Solution: Humidity Relationships at 25° (4)

Aqueous Saturated Salt Solution	Headspace Relative Humidity, %
Lithium chloride	11
Calcium chloride hexahydrate	29
Magnesium nitrate hexahydrate	52
Sodium chloride	75

Table III—Atmospheric Relative Humidity Determinations

Percent by GC	Percent by Sling Psychrometry
36	40
44	40
59	62

[4] Model K-2, Burrell Corp., Pittsburgh, Pa.
[5] Brown Instruments, Division of Minneapolis Honeywell Corp., Philadelphia, Pa.
[6] Waters Associates, Framingham, Mass.
[7] The temperature was adjusted so that the retention time to the front of the water peak was 0.6 min.
[8] Stylex tuberculin syringe, no needle, Z020, Pharmaseal Laboratories, Glendale, Calif.
[9] Hamilton.

Table IV—Moisture Content of Formulated Sincalide as a Function of Headspace Relative Humidity

Humidistat Relative Humidity, %	Headspace Relative Humidity (GC), %	Powdered Sample Moisture (TGA), %
0	6	0
11	16	0
23	26	0
33	35	0.01
52	53	0.05
67	69	0.08
79	84	33.8

through a comparison of atmospheric relative humidity measured simultaneously by GC and sling psychrometry.

Equilibrium Moisture Content: Sodium Chloride—Duplicate 1-g samples of lyophilized sodium chloride were weighed accurately and placed in desiccators. Each desiccator contained the appropriate saturated salt solution to maintain the atmosphere within the desiccator at the desired relative humidity. After 25 days at 22°, the samples were again weighed and the percent change in weight from the initial was calculated. The values obtained for the duplicate samples within a desiccator were averaged.

Equilibrium Moisture Content: Sincalide—An electrobalance[10] was used to determine the change in weight of a sample under various humidity conditions. The sample weighing pan was hung from the balance beam into a glass cylinder with two air entry ports and one air exit port. The tare weighing pan was hung in a closed glass cylinder.

To maintain the humidity of the weighing chamber, a compressed air stream was split in two. One stream was passed through a tower containing an indicating desiccant[11] to ensure that the humidity was less than 1%. The second stream was passed through a diffusion tube into a tower containing distilled water. The stream exiting this tower was composed of high relative humidity air. The two flows were then recombined in a desiccator into one stream.

A hygrometer sensing probe[12] was placed in the desiccator for measurement of the relative humidity of the air before it entered the weighing chamber. The humidity of the air was regulated by varying the ratio of the air going through each tower. The air was then passed through a flowmeter and again split into two streams. The two streams were fed through the entry ports into the weighing chamber above and below the sample. The air then passed out through the exit port to a second hygrometer[13] where the humidity was again measured.

A sample of I (approximately 4.5 mg) was placed on the sample pan. Anhydrous air was then passed over the sample for 48 hr to ensure equilibration of the sample with the atmosphere. The sample weight was recorded after equilibration and after each subsequent reequilibration. Low humidity air was then passed into the weighing chamber and equilibrated with the sample. After equilibrium was established, the air entering the weighing chamber was increased to a new relative humidity. The anhydrous weight of the sample was redetermined after equilibration at each relative humidity.

This procedure was repeated for the system without any sample. In the range of 0–60% RH, the blank weight varied up to a maximum of 6.8 μg or approximately 0.2% of the sample weight.

RESULTS AND DISCUSSION

The degradation of I was first studied under conditions of controlled relative humidity. Degradation in excess of 40% after storage of I at 46 and 76% RH was found. Only minor changes were detected at 0% RH[14].

With the role of moisture in I degradation established, the total volatiles in lyophilized plugs of formulated I were determined by thermal gravimetric analysis. The formulated plugs contained sodium chloride, 45 mg, and I, 5.25 μg. per 5-ml vial. The moisture values found in the plugs by thermal gravimetric analysis ranged from 0 to 33.8% (*i.e.*, to 15 mg) (Table IV), but the method was not sensitive enough to differentiate among plugs of the formulation when the moisture present was at the desired very low magnitudes. For example, the moisture present in the plug at 67% RH was only 0.08% or 36 μg of moisture.

Table V—Equilibrium Moisture Contents of Bulk Sincalide (Nonformulated)

Relative Humidity, %	Moisture, %
5	1.6
12	2.2
14	2.8
20	3.6
30	4.2
42	4.8
49	5.2

Table VI—Equilibrium Moisture Contents of Lyophilized Sodium Chloride

Relative Humidity, %	Increase in Weight from Initial, %
0	0.037
11	0.067
23	0.083
33	0.060
42.5	0.022
67	0.068
79	200.0

Theimer and Pavelek (5) used the Karl Fischer method to determine the moisture content in small plugs of lyophilized mannitol and acetylcholine chloride in vials. This work was done on vials containing 0.50–1.63 mg of water each, a much greater amount than is present in the lyophilized formulation of I. Since the precision of the reported data was already inadequate to achieve the accuracy required here and since the precision probably would deteriorate at lower levels, this line of investigation was also not pursued.

The relative humidity of the headspace gas of the vials containing the formulated plug was then explored as an indicator of moisture conditions within a vial. It was assumed that a stable product containing I could be obtained if the relative humidity of the headspace gas was maintained at a low level. Determination of the equilibrium moisture content of I alone was proportional to the relative humidity. The equilibrium moisture content of the sodium chloride in the formulation was essentially independent of the relative humidity at relative humidities of 67% or less. The equilibrium moisture contents of I and sodium chloride at various relative humidities are shown in Tables V and VI, respectively.

The headspace moisture is in equilibrium with the moisture in the plug in a vial. Because of the hygroscopic nature of I compared to the other ingredient, sodium chloride, a relatively larger percent of the moisture in a plug is associated with I. This condition causes I to become vulnerable to degradation by hydrolysis even at exceptionally low levels of moisture in the vials. The level of moisture that may be tolerated in the vials, as shown by the maintenance of the potency of I, was determined by a number of optimizing trials. The trials provided vials containing the formulated product with headspace relative humidities of a few percent to as high as 88%. For example, the relative humidity of the headspace gas in the plant lyophilized vials at the conclusion of the 72-hr cycle described in Table I was determined for the three categories of vials in the chamber. Results are given in Table VII.

As shown, the values for these plant-processed vials were at 5% RH or below. Since the values found for the "active" vials (Lot C) and the pla-

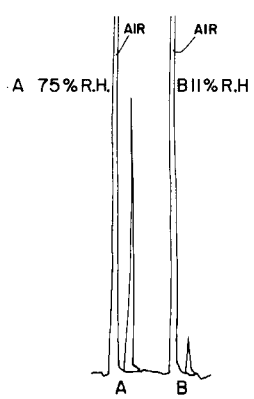

Figure 1—*Typical chromatographic curves.*

[10] Model RG, Cahn Division, Ventron Instruments Corp., Paramount, Calif.
[11] Drierite, Hammond Drierite Co., Zenia, Ohio.
[12] Electric hygrometer, Hygrodynamics, Inc., Silver Spring, Md.
[13] Hygroline, Beckman Instruments, Irvine, Calif.
[14] O. Kocy, Squibb Institute for Medical Research, unpublished data.

Table VII—Relative Humidity of the Headspace Gas in Vials Lyophilized by the Optimum 72-hr Cycle

Lot	Shelf Number in Chamber	Tray Number	Vials Tested per Tray	Relative Humidity in Headspace Gas of Vials[a], %
A	1 (bottom)	1, 4	2	All 3
A	2–11	7, 10, 12, 15, 17, 20, 23, 27, 31, 34, 36, 38	2	All 3
A	12 (top)	42	2	Both 3
B	1	4	3	All 3
B	6	20	4	3, 3, 3, 4
B	12	42	3	4, 4, 3
C	1	4	3	5, 4, 4
C	6	20	4	4, 4, 4, 3
C	12	42	3	4, 3, 4

[a] The nitrogen found was 99.5%/vial.

Table VIII—Comparison of Percent Relative Humidity Found with Potency of Stability Samples in Vials

Months Stored	Sample Lot Number	Storage Temperature	Relative Humidity, % (Number of Replicates in Parentheses)	Sincalide Bioassay, % of Theory Relative to Standard
0	C	—	3–5 (10)	130
9	C	22°	10–17 (10)	105
0	D	—	—	96
12	D	22°	26, 30	98
12	D	40°	25	91
20	D	22°	26–29 (10)	97
20	D	33°	26–29 (10)	91
36	D	22°	26–29 (10)	97
0	E	—	—	121
12	E	22°	22, 34	131
12	E	40°	20	119
20	E	22°	25–27 (10)	119
20	E	33°	26–29 (10)	117
36	E	22°	24–30 (9) 32 (1)	112
0	F	—	—	125
12	F	22°	20–27 (3)	105
12	F	40°	—	98
19	F	22°	20–26 (10)	103
19	F	33°	22–24 (10)	110
36	F	22°	26–30 (10)	98
0	G	—	55–58 (6)	99
6	G	22°	—	81
6	G	40°	—	70
13	G	22°	52–61 (30)	—
16	G	−20°	—	83
16	G	5°	51–59 (10)	84
0	H-1	—	—	106
25	H-1	22°	19–29 (12)	103
3	H-2[a]	22°	46–47 (12)	114
14	H-2[a]	22°	34–35 (4)	94
3	H-3[b]	22°	81–88 (12)	66
14	H-3[b]	22°	54–72 (4)	36

[a] Opened vials of Lot H-1 were subjected to moderate humidity, sealed, stored, and tested at the time period shown. [b] Opened vials of Lot H-1 were subjected to high humidity, sealed, stored, and tested at the time period shown.

cebo vials (Lot A) were virtually no higher than those found for the empty vials (Lot B), drying of the product apparently had reached an end-point and could not be improved by extending the length of the cycle or applying greater heat to the shelves. Although the initial freeze-drying period for the product at −30° might be considered overlong (23 hr), it did allow drying to proceed without collapse of the matrix due to vibration in the lyophilizer and thus afforded a freer flow of vapor from the solids.

Furthermore, with this drying cycle, there was no evidence that the location of the vials in the trays or of the trays on the shelves affected moisture retention. Therefore, the lyophilization cycle was felt to be suitable.

The relative humidity of the headspace gas, reflecting the moisture content of the lyophilized plug within the sealed vials, also correlated well with the stability profile of formulated I.

The bioassay for I consists of determining the potency by giving graded doses of unknown and of reference standard intravenously to anesthetized guinea pigs and statistically comparing the recorded contractile responses of the gallbladder *in situ* (6–8). The special skill and care required by the operator during the *in vivo* assay on the excised animals and the time-consuming nature of the operation made it necessary to use the bioassay as sparingly as possible. In addition, variables inherent in such a bioassay required many replicates to determine accurately the potency of any one sample. Usually, 24 injections had to be made for each bioassay result independent of the administration of the reference standard. Thus, the relative humidity may be a better predictor of stability than any single bioassay value. The substitution may be made in view of the correlation of the relative humidity values and the potency (Table VIII).

Table VIII shows the relationship between the range of the relative humidity values found for the headspace gas of vials and the corresponding bioassays after various periods of stability storage. A minimum potency of 85% of theory by bioassay meets the adopted specification for stability compliance of the product.

As the results indicate, the potency was maintained at approximately the initial activity for at least 18 months at 22° in those instances where the headspace relative humidity for the lot was below 30%. However, activity had decreased at higher humidities. Therefore, an upper limit of not more than 30% RH has been specified for the headspace gas of vials for product acceptance.

REFERENCES

(1) J. A. Bashir and K. E. Avis, *Bull. Parenter. Drug Assoc.*, **27**, 68 (1973).

(2) M. A. Litchman and R. P. Upton, *J. Pharm. Sci.*, **62**, 1140 (1973).

(3) P. DeLuca and L. Lachman, *ibid.*, **54**, 617 (1965).

(4) L. Meites, "Handbook of Analytical Chemistry," 1st ed.,

McGraw-Hill, New York, N.Y., 1963, pp. 3–29.
(5) E. E. Theimer and J. J. Pavelek, *J. Pharm. Sci.*, **57**, 887 (1968).
(6) B. Rubin, S. L. Engel, A. M. Drungis, M. Dzelzkalns, E. O. Grigas, M. H. Waugh, and E. Yiakas, *ibid.*, **58**, 955 (1969).
(7) S. A. Berson and R. S. Yalow, "Peptide Hormones," North-Holland Publishing, Amsterdam, The Netherlands, 1973, chap. 9, pp. 1082–1086.
(8) B. Rubin and S. L. Engel, "Frontiers in Gastrointestinal Hormone Research," Almquist and Wiksell, Stockholm, Sweden, 1973, pp. 41–56.

ACKNOWLEDGMENTS

The authors thank Dr. H. Jacobson and Dr. C. Riffkin for helpful suggestions, Dr. G. Brewer and Dr. I. Gibbs for constructive criticism of the manuscript, and Mrs. Catherine Bucha for capable assistance with the lyophilization trials. The bioassays were performed in the laboratories of Mr. A. Brook and Dr. B. Rubin, and Dr. J. Meyer was helpful in statistically evaluating the results. Additional technical assistance was received from Mrs. M. Bogaczyk and Mr. R. Mark.

GLC–Mass Spectrometry of Several Important Anticancer Drugs I: Pertrimethylsilylation and *O*-Methoxime Formation

ERIC WATSON and KENNETH K. CHAN ˣ

Received July 5, 1977, from the *School of Pharmacy, University of Southern California, Los Angeles, CA 90033.* Accepted for publication January 4, 1978.

Abstract □ Procedures are reported for the formation of pertrimethylsilyl and pertrimethylsilyl methoxime derivatives of the aglycones of doxorubicin, daunorubicin, carminomycin, chromomycin A_3, and mithramycin. The mass spectra are consistent with the formation of these derivatives. Fragmentation patterns highly specific for these derivatives are proposed, and the potential application for the identification of metabolites of these compounds is discussed.

Keyphrases □ Doxorubicin—GLC–mass spectral analysis, bulk drug □ Daunorubicin—GLC–mass spectral analysis, bulk drug □ GLC–mass spectrometry—analyses, doxorubicin, daunorubicin, and other antineoplastic agents, bulk drug □ Antineoplastic agents, various—GLC–mass spectral analyses in bulk drug

Doxorubicin[1,2] (I), daunorubicin[1,3] (II), carminomycin[1,4] (III), chromomycin A_3[1,5] (IV), and mithramycin[1,6] (V) are naturally occurring antibiotics (1–6) which possess significant antineoplastic activities. The first three are structurally related, and the last two differ only in the sugar moieties (6). Both I and V have been marketed in the United States. Of these five drugs, I is the most important clinically and has proven to be extremely effective against various tumors (7–9).

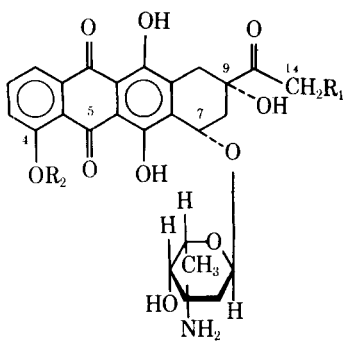

I: R_1 = H, R_2 = CH_3
II: R_1 = OH, R_2 = CH_3
III: R_1 = R_2 = H

The disposition of I and II in animals and humans has been studied in this and other laboratories (1–14). Of major concern has been the development of sensitive, specific analytical procedures for I in physiological fluids and the identification of its metabolites.

GLC–mass spectrometry is one of the most effective instrumental methods for the separation and identification of compounds extracted from biological fluids. The relative retention times and the supplemental mass fragmentographic data provide for the positive characterization of unknown compounds. No reports have yet been published

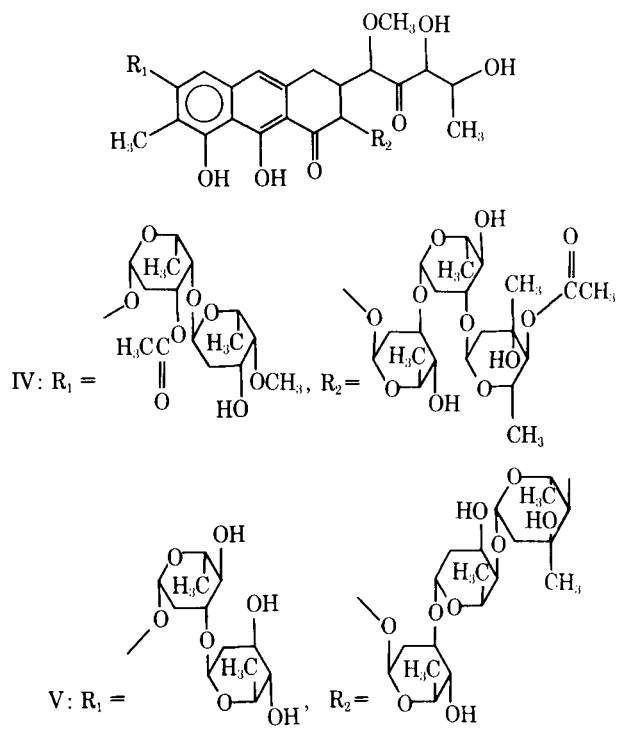

IV: R_1 = , R_2 =

V: R_1 = , R_2 =

[1] Supplied by the Drug Synthesis and Chemistry Branch, Developmental Therapeutics Program, Division of Cancer Treatment, National Cancer Institute, Bethesda, Md.
[2] Adriamycin hydrochloride, NSC-123127, Adria Laboratories.
[3] Daunomycin, rubidomycin, NSC-82151.
[4] NSC-180024.
[5] NSC-58514, Toyomycin, Takeda Chemical Industries, Osaka, Japan.
[6] NSC-143020, Mithracin, Pfizer.

0022-3549/78/0900-1243$01.00/0
© 1978, American Pharmaceutical Association

McGraw-Hill, New York, N.Y., 1963, pp. 3–29.
(5) E. E. Theimer and J. J. Pavelek, *J. Pharm. Sci.*, **57**, 887 (1968).
(6) B. Rubin, S. L. Engel, A. M. Drungis, M. Dzelzkalns, E. O. Grigas, M. H. Waugh, and E. Yiakas, *ibid.*, **58**, 955 (1969).
(7) S. A. Berson and R. S. Yalow, "Peptide Hormones," North-Holland Publishing, Amsterdam, The Netherlands, 1973, chap. 9, pp. 1082–1086.
(8) B. Rubin and S. L. Engel, "Frontiers in Gastrointestinal Hormone Research," Almquist and Wiksell, Stockholm, Sweden, 1973, pp. 41–56.

ACKNOWLEDGMENTS

The authors thank Dr. H. Jacobson and Dr. C. Riffkin for helpful suggestions, Dr. G. Brewer and Dr. I. Gibbs for constructive criticism of the manuscript, and Mrs. Catherine Bucha for capable assistance with the lyophilization trials. The bioassays were performed in the laboratories of Mr. A. Brook and Dr. B. Rubin, and Dr. J. Meyer was helpful in statistically evaluating the results. Additional technical assistance was received from Mrs. M. Bogaczyk and Mr. R. Mark.

GLC–Mass Spectrometry of Several Important Anticancer Drugs I: Pertrimethylsilylation and *O*-Methoxime Formation

ERIC WATSON and KENNETH K. CHAN ˣ

Received July 5, 1977, from the *School of Pharmacy, University of Southern California, Los Angeles, CA 90033.* Accepted for publication January 4, 1978.

Abstract □ Procedures are reported for the formation of pertrimethylsilyl and pertrimethylsilyl methoxime derivatives of the aglycones of doxorubicin, daunorubicin, carminomycin, chromomycin A_3, and mithramycin. The mass spectra are consistent with the formation of these derivatives. Fragmentation patterns highly specific for these derivatives are proposed, and the potential application for the identification of metabolites of these compounds is discussed.

Keyphrases □ Doxorubicin—GLC–mass spectral analysis, bulk drug □ Daunorubicin—GLC–mass spectral analysis, bulk drug □ GLC–mass spectrometry—analyses, doxorubicin, daunorubicin, and other antineoplastic agents, bulk drug □ Antineoplastic agents, various—GLC–mass spectral analyses in bulk drug

Doxorubicin[1,2] (I), daunorubicin[1,3] (II), carminomycin[1,4] (III), chromomycin A_3[1,5] (IV), and mithramycin[1,6] (V) are naturally occurring antibiotics (1–6) which possess significant antineoplastic activities. The first three are structurally related, and the last two differ only in the sugar moieties (6). Both I and V have been marketed in the United States. Of these five drugs, I is the most important clinically and has proven to be extremely effective against various tumors (7–9).

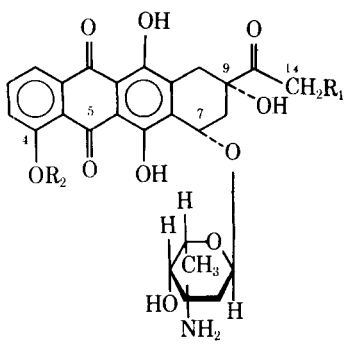

I: R_1 = H, R_2 = CH_3
II: R_1 = OH, R_2 = CH_3
III: R_1 = R_2 = H

The disposition of I and II in animals and humans has been studied in this and other laboratories (1–14). Of major concern has been the development of sensitive, specific analytical procedures for I in physiological fluids and the identification of its metabolites.

GLC–mass spectrometry is one of the most effective instrumental methods for the separation and identification of compounds extracted from biological fluids. The relative retention times and the supplemental mass fragmentographic data provide for the positive characterization of unknown compounds. No reports have yet been published

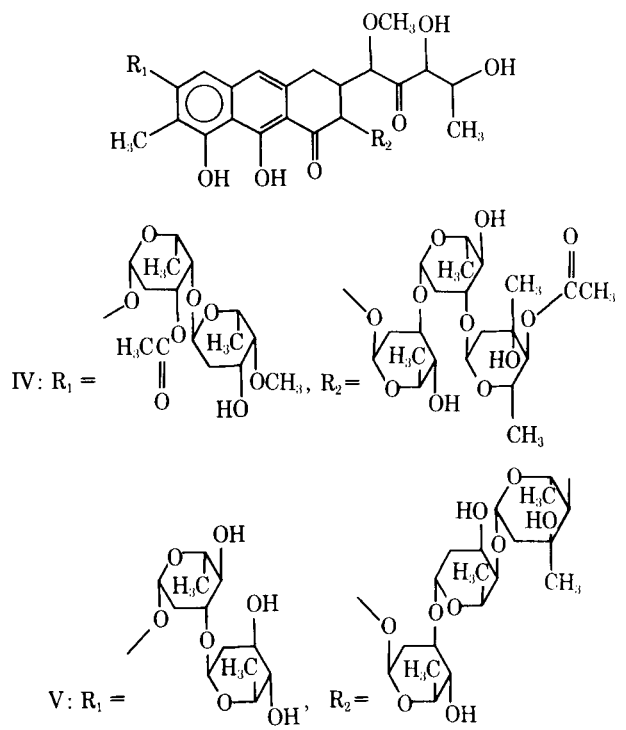

IV: R_1 = , R_2 =

V: R_1 = , R_2 =

[1] Supplied by the Drug Synthesis and Chemistry Branch, Developmental Therapeutics Program, Division of Cancer Treatment, National Cancer Institute, Bethesda, Md.
[2] Adriamycin hydrochloride, NSC-123127, Adria Laboratories.
[3] Daunomycin, rubidomycin, NSC-82151.
[4] NSC-180024.
[5] NSC-58514, Toyomycin, Takeda Chemical Industries, Osaka, Japan.
[6] NSC-143020, Mithracin, Pfizer.

0022-3549/78/0900-1243$01.00/0
© 1978, American Pharmaceutical Association

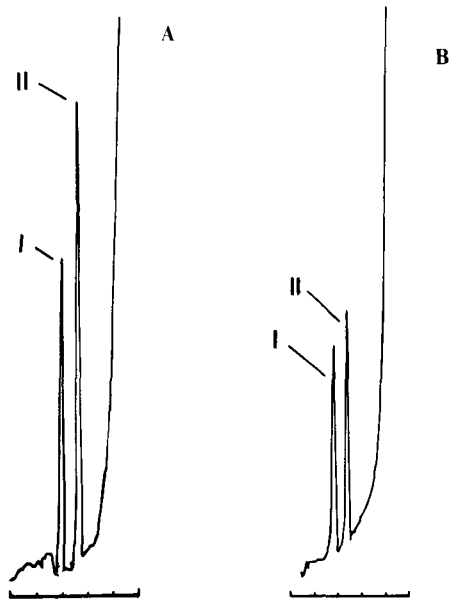

Figure 1—*Chromatograms. A: Peak I = pertrimethylsilyl I aglycone, and peak II = pertrimethylsilyl II aglycone. B: Peak I = pertrimethylsilyl I aglycone methoxime, and peak II = pertrimethylsilyl II aglycone methoxime.*

describing the GLC–mass spectral analysis of I, probably because of the inability to prepare sufficiently volatile and stable derivatives that can be subjected to GLC.

Therefore, the present study was initiated to investigate conditions that would allow the GLC analysis of I and its metabolites and II–V. This report describes two derivatization procedures for the GLC–mass spectral analysis of the aglycones of these anticancer agents. One method used a direct silylation of these aglycones; in the other method, the keto group on the side chain was converted to the methoxime derivative prior to silylation. Mass spectral fragmentations of these compounds are proposed, and the potential application of these methods for the identification of their metabolites is discussed.

EXPERIMENTAL

Instrumental Conditions—A magnetic sector mass spectrometer[7] interfaced with a gas chromatograph was used. The GLC conditions were as follows.

A coiled glass column (92.3 cm × 2 mm i.d.) was packed with 3% OV-101 on 100–120-mesh Gas Chrom Q[8]. The flow rate of the carrier gas (helium) was 22 ml/min. Temperatures were: column, 260°; flash heater, 260°; and molecular separator and restricter, 210°. The operating conditions of the mass spectrometer were: electron energy, 70 ev; ion source temperature, 200°; ionization current, 60 μamp; and accelerating voltage, 3 kv.

Excess reagent was vented to the force-vacuum pump by an all-glass venting system (15). Use of this device considerably reduced contamination problems in the ion source caused by excess silylating agent.

Chemicals and Reagents—Compounds I–V were used without further purification. These compounds were greater than 95% pure as determined by TLC[9]. The aglycones were obtained by heating the parent compounds in 0.1 *N* HCl for 10 min at 95°. This solution was then cooled, and the aglycones were extracted with ethyl acetate. The ethyl acetate was removed by evaporation using dry nitrogen. Methoxylamine hydrochloride[8] and the silylation reagent[10] composed of bis(trimethylsilyl)trifluoroacetamide–trimethylchlorosilane–trimethylsilylimidazole (3:3:2) were obtained commercially. The pyridine[10] was silylation grade.

[7] Varian model CH-7, Springfield, N.J.
[8] Applied Science Laboratories, State College, Pa.
[9] Silica gel GH with chloroform–methanol–acetic acid (80:20:4).
[10] Powersil, Pierce Chemical Co., Rockford, Ill.

Table I—Retention Times of Anthracycline Aglycone Derivatives on 3% OV-101 at 260°

Pertrimethylsilyl Aglycone Derivatives	Retention Time, min
I	5.6
I methoxime	5.6
II	4.6
II methoxime	4.6
III	5.5
III methoxime	5.5
IV/V	6.5
IV/V methoxime	7.2

Preparation of Pertrimethylsilyl and Pertrimethylsilyl Methoxime Derivatives—Approximately 100 μg of each aglycone was reacted with 50 μl of the silylation mixture. After a few minutes, 1–2-μl samples were injected into the gas chromatograph–mass spectrometer. *O*-Methoximes were prepared according to Fales and Luukkainen (16).

The aglycone (200 μg) was reacted with about 5 mg of methoxylamine hydrochloride and 100 μl of pyridine for 45 min at 75°. The pyridine was evaporated using a nitrogen stream. The methoxime derivative was isolated by adding 1 ml of water and extracting with 1 ml of ethyl acetate. The ethyl acetate was evaporated under nitrogen. Silylation was then carried out as already described.

RESULTS AND DISCUSSION

GLC Characteristics—Since the total ion chromatograms of the derivatives following GLC–mass spectrometry were essentially the same, only the chromatograms obtained from the pertrimethylsilyl and pertrimethylsilyl methoxime derivatives of I and II aglycones are illustrated (Fig. 1). The retention times of all derivatives are given in Table I.

All derivatives except two chromatographed as single well-resolved peaks with excellent GLC properties. The pertrimethylsilyl methoxime of the IV/V aglycone reaction mixture contained two peaks. The first peak was the pertrimethylsilyl derivative and the second was the pertrimethylsilyl methoxime derivative, indicating incomplete methoxime formation under the experimental conditions.

The stability of the derivatives during chromatography was dependent on the column condition. Commercially prepared packings containing 3% OV-1, 3% SE-30, 1% JXR, or 3% OV-101 were evaluated for derivative stability. The 3% OV-101 was superior. This particular packing has been in constant use for over 3 months without showing any deterioration.

Derivatization Procedure—All compounds studied contained polar polyhydroxyl groups, making it virtually impossible for them to be chromatographed directly. It was necessary to prepare derivatives with the necessary properties for GLC.

Trifluoroacetic anhydride, pentafluoropropionic anhydride, and acetic anhydride were evaluated as possible derivatization agents. However, none formed volatile derivatives with the I or II aglycone that could be detected following GLC.

In recent years, silyl derivatives have been used for the GLC analyses of extremely polar compounds. Not only does the greatly increased volatility of the silyl derivative lend itself to GLC separation, but the silyl

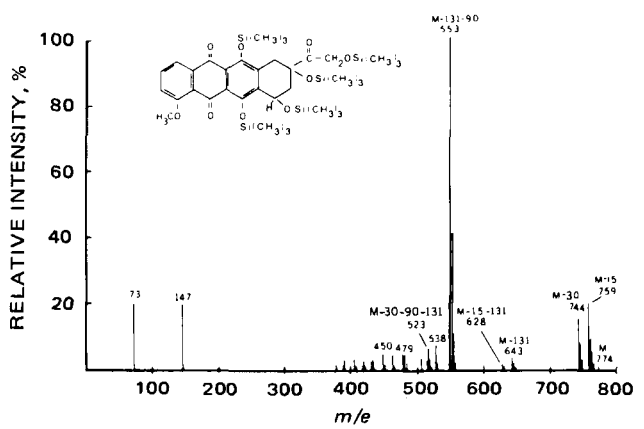

Figure 2—*GLC–mass spectrum of the pertrimethylsilyl I aglycone.*

Table II—Mass Spectral Fragmentations [a] of Pertrimethylsilyl Derivatives of Anthracycline Aglycones

Common Fragmentation	*m/e* (Percent Relative Intensity) I	II	III
M	774 (1)	686 (1)	744 (0)
M − 15	759 (20)	671 (37)	729 (40)
M − 30	744 (15)	656 (45)	714 (90)
M − side chain	643 (5)	643 (2)	701 (0)
M − 15 − side chain	628 (5)	628 (3)	686 (20)
M − 90 − side chain	553 (100)	553 (80)	611 (100)
M − 15 − 90 − side chain	538 (10)	538 (20)	596 (25)
M − 30 − 90 − side chain	523 (10)	523 (20)	581 (50)
$(CH_3)_2SiO^+Si(CH_3)_3$	147 (20)	147 (10)	147 (41)

[a] Only common major fragments are presented.

group appears to direct fragmentation patterns in many instances (17).

Several reagents were evaluated for the extent of pertrimethylsilylation with the I aglycone as the standard. Bis(trimethylsilyl)trifluoroacetamide with 1% trimethylchlorosilane gave a small total ion peak during GLC–mass spectrometry only after the reaction mixture had been heated at 75° for at least 1 hr. With bis(trimethylsilyl)trifluoroacetamide–trimethylchlorosilane (1:1), a large peak was obtained under the same reaction conditions. Since this approach seemed promising, combinations of silylating agents with stronger catalysts were then considered.

A strong, commercially available silylating agent comprised of bis(trimethylsilyl)trifluoroacetamide – trimethylchlorosilane–trimethylsilylimidazole (3:3:2) formed a fully silylated derivative with the I aglycone within a few minutes at room temperature. This reagent was first reported in 1967 for the derivatization of steroids (18), but few reports have described its use. The reagent has several important advantages. First, the use of a solvent is unnecessary since the reagent acts as its own solvent. Second, the derivatization procedure is complete within a few minutes. Third, derivatization leads to a persilylated derivative. The ability of this reagent to silylate all of the hydroxyl groups is extremely critical to evaluating the course of I metabolism by GLC–mass spectrometry, for example, the generation of hydroxyl groups *via* metabolic reactions. Numerous unsuccessful attempts have been made to chromatograph pertrimethylsilyl derivatives of I and II.

The structures of I and II aglycones can be considered somewhat similar to those steroids possessing the 17α,21-dihydroxy-20-keto side chain. The preferred method for the GLC analysis of these compounds is to convert the keto group to the methoxime derivative using methoxylamine, followed by silylation of the remaining hydroxyl group (19). This procedure yields stable volatile derivatives for aglycones of I, II, III, and IV/V with excellent GLC characteristics. The side-chain derivatization also yields useful information concerning the metabolic change of the keto group.

The extent of the I aglycone methoxime formation was evaluated by reacting this derivative with the silylation mixture and monitoring the disappearance of the characteristic *m/e* 553 fragment of the trimethylsilyl derivative. After a reaction time of 45 min at 75°, the *m/e* fragment was negligible. Under these conditions, the methoxime derivatization of IV and V aglycones proceeded to about 70% completion.

The stability of the trimethylsilyl derivative of the I aglycone was

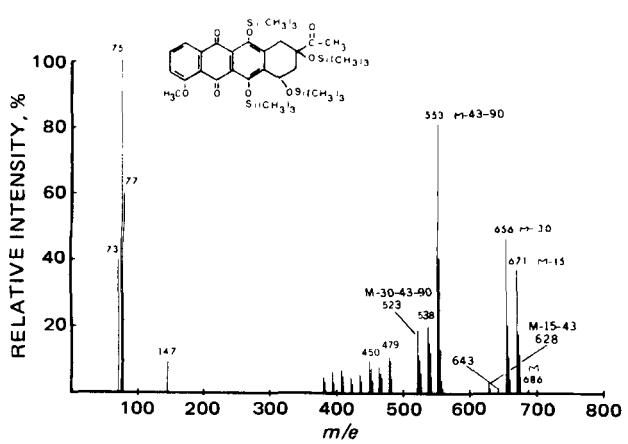

Figure 3—*GLC–mass spectrum of the pertrimethylsilyl II aglycone.*

Table III—Mass Spectral Fragmentations [a] of Pertrimethylsilyl Methoxime Derivatives of Anthracycline Aglycones

Common Fragmentation	*m/e* (Percent Relative Intensity) I	II	III
M	803 (2)	715 (7)	773 (10)
M − 15	788 (100)	700 (45)	758 (45)
M − 30	773 (20)	685 (15)	743 (21)
M − 15 − 90	698 (40)	616 (90)	668 (75)
M − 30 − 90	683 (55)	595 (100)	653 (70)
M − 15 − 90 − 31	667 (15)	579 (42)	637 (36)
M − 30 − 90 − 31	652 (7)	564 (25)	622 (22)

[a] Only common major fragments are presented.

studied by injecting aliquots from the same reaction sample during 24 hr. The reaction with the silylation mixture was complete after 10 min. Allowing the reaction to proceed for up to 1 hr did not significantly increase the total ion response. After 1 hr, a small additional peak, which chromatographed immediately after the pertrimethylsilyl I aglycone, was observed. The height of this peak increased with time. After 24 hr, it equaled that of pertrimethylsilyl I aglycone.

Mass spectral evaluation of this peak indicated that its highest *m/e* fragment was 72 units higher than the highest fragment in the pertrimethylsilyl I aglycone mass spectrum. This component was tentatively identified as the enol pertrimethylsilyl derivative. The experiment was repeated with the pertrimethylsilyl methoxime I aglycone derivative, and no additional component was formed. The derivative remained stable during this period with no signs of degradation.

Mass Spectrometric Characteristics—The mass spectra of silyl ethers of I–V aglycones are shown in Figs. 2–5. Both IV and V aglycones showed identical mass spectra, as expected on the basis of their identical structures.

The mass spectra of these silylated derivatives were characterized by cleavages of methyl radicals (M − 15 and M − 15 − 15), typical of pertrimethylsilyl derivatives (17). With the exception of the IV aglycone, the pertrimethylsilyl derivatives did not show significant amounts of molecular ions. Cleavage of the entire side chain and elimination of silanol appeared to be the favorable processes for the anthracyclines. The latter process is consistent with the fragmentation of pertrimethylsilyl derivatives of polyols. The fragments at *m/e* 147 commonly found for these trimethylsilyl anthracyclines probably represent $(CH_3)_2SiO^+Si(CH_3)_3$, also similar to pertrimethylsilyl derivatives of polyols (20). The common fragmentation patterns of these pertrimethylsilyl derivatives are summarized in Table II.

The mass spectrum of pertrimethylsilyl methoxime derivatives of I aglycone is shown in Fig. 6. Major fragments of pertrimethylsilyl methoxime derivatives of I–III aglycones[11] are summarized in Table III. The spectra indicated that, in all cases, persilylated derivatives were formed and the fragmentation patterns were consistent with the proposed structures. The mass spectrum of pertrimethylsilyl methoxime IV/V aglycones[11] gave a molecular ion at *m/e* 910 (15%) and major fragments at *m/e* 895 (M − 15), 589 (M − side chain), 500 (M − 89 − side chain), and

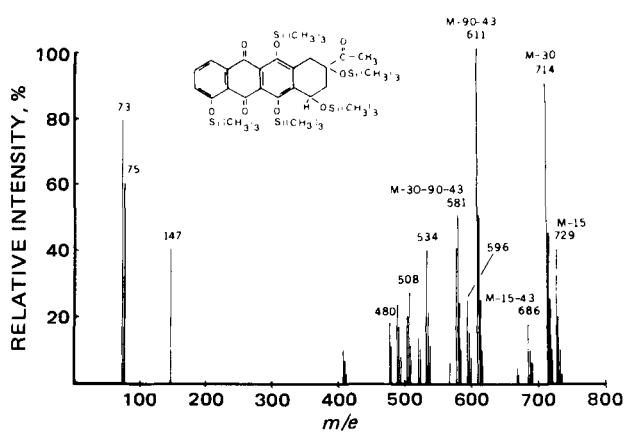

Figure 4—*GLC–mass spectrum of the pertrimethylsilyl III aglycone.*

[11] Mass spectra of these compounds are available from the authors upon request.

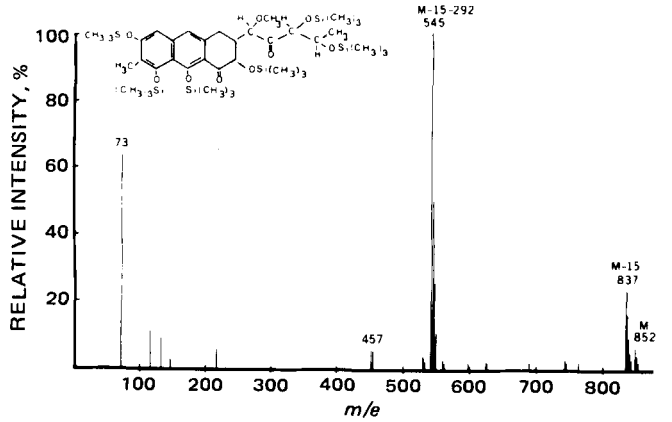

Figure 5—*GLC-mass spectrum of the pertrimethylsilyl IV/V aglycones.*

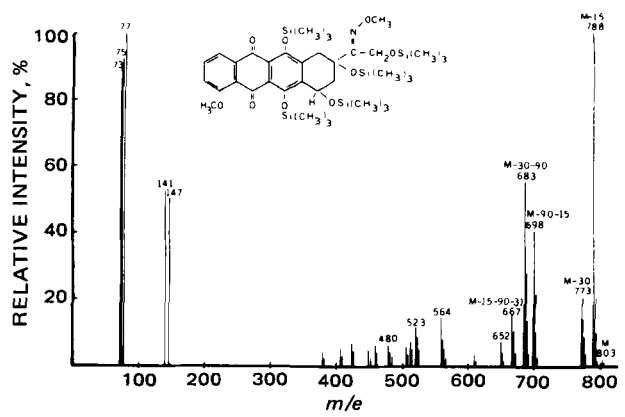

Figure 6—*GLC-mass spectrum of pertrimethylsilyl I aglycone methoxime.*

73 (base peak), all consistent with a bis(*O*-methoxime) pertrimethylsilylated structure.

The most characteristic and, perhaps, diagnostic ion of the silyl ether derivative of anthracycline results from the loss of the side chain at C-9 with simultaneous elimination of silanol. Thus, in the mass spectra of the silyl ethers of I and II aglycones, the ion at *m/e* 553 (Figs. 2–4) is clearly the most dominant. The silyl ether of the III aglycone showed a similar cleavage at C-9 with its corresponding base peak at *m/e* 611. The increase in *m/e* is consistent with the formation of a stable silyl derivative at C-4. The silyl ether of the IV aglycone showed the base at *m/e* 545 formed by the elimination of the side chain at C-3 and a methyl radical. This result indicates that side-chain cleavage is a very favorable process for these silylated compounds regardless of the differences in the side chain. Changes in the ring did not appear to alter this cleavage.

Thus, the fragmentation process is relevant to identifying the metabolite of I. Demethylation of I at C-4, leading to the formation of a phenolic hydroxyl group, was reported (14). The base peak in the spectrum of the pertrimethylsilyl III aglycone is found at *m/e* 611, which is consistent with a stable silyl derivative at C-4. Therefore, the corresponding pertrimethylsilyl metabolite formed from I also should show a similar base peak at *m/e* 611. Moreover, the presence or loss of hydroxyl groups in the ring structure should be reflected in easily identifiable masses from *m/e* 553.

The mass spectra of the methoxime silyl ether derivatives of I–III aglycones are characterized by the presence of a molecular ion and by a series of peaks at M − 15 (CH_3), M − 31 (OCH_3), M − 15 − 90 (CH_3 − trimethylsilanol), and M − 31 − 90 (OCH_3 − trimethylsilanol). Several peaks at lower *m/e* values, representing losses of CH_3 units, are not of diagnostic importance. In contrast to the pertrimethylsilyl ethers of anthracycline aglycones, the methoxime derivatives stabilize the side chain to such an extent that no cleavage is apparent at C-9.

Metabolic reduction of the carbonyl side chains of I and II have been reported to yield the hydroxyl derivatives. Following the fragmentation trend discussed, both of the pertrimethylsilyl derivatives of I and II aglycones should yield a base peak at *m/e* 553. The derivatives obtained by a combination of treatments with the methoxyamine and the above-mentioned silylating agent, giving rise to the pertrimethylsilyl methoxime derivative, should yield identical mass spectra compared to those treated with the silylating agent alone since the lack of the carbonyl group on the side chain should negate the methoxime formation.

A similar approach can be used to probe into the metabolism of IV/V.

The combination of these two derivatization procedures should prove valuable in the identification of the various metabolites of I. Formation of the silyl derivative establishes the extent of metabolism on the ring portion as well as the side chain. Formation of the pertrimethylsilyl methoxime derivative offers corroboration of the identity of the compound.

Investigations are now in progress using the procedures described here to evaluate the metabolism of I in rabbits and in humans. The ease of formation and excellent chromatographic properties of the derivatives, together with their characteristic mass spectra, should make these derivatization procedures valuable for the study of the metabolism of I–V.

REFERENCES

(1) F. Arcamone, G. Cassinelli, G. Fantini, A. Grein, P. Orezzi, C. Pol, and C. Spalla, *Biotechnol. Bioeng.*, **11**, 1101 (1969).

(2) A. Grein, C. Spalla, A. DiMarco, and G. Canevazzi, *Microbiol.*, **11**, 109 (1963).

(3) G. F. Gause, M. G. Brazhnikova, and V. A. Shorin, *Cancer Chemother. Rep.*, **58**, 255 (1974).

(4) S. Tatsuoka, K. Makazawa, A. Miyake, K. Kaziwara, Y. Aramaki, M. Shibata, K. Tanabe, Y. Hamada, H. Hitomi, M. Miyamoto, K. Mizuno, J. Watanabe, M. Ishidate, K. Yokotani, and I. Ishikawa, *Gann*, **49**, Suppl. 23 (1958).

(5) K. V. Rao, W. P. Cullen, and B. A. Sobin, *Antibiot. Chemother. (Basel)*, **12**, 182 (1962).

(6) M. Slavik and S. K. Carter, *Adv. Pharmacol. Chemother.*, **12**, 1 (1975).

(7) A. DiMarco, M. Graetani, and B. Scarpinato, *Cancer Chemother. Rep.*, **53**, 33 (1969).

(8) G. Bonadonna, S. Monfardini, M. DeLena, F. Fossati-Bellani, and G. Baretta, *Cancer Res.*, **30**, 2572 (1970).

(9) S. Monfardini, G. Bonadonna, S. DiPetro, A. Gwindani, F. Fossati-Bellani, and M. DeLena, *Tumori*, **55**, 197 (1969).

(10) F. Arena, N. D. Alessandro, L. Dusonchet, N. Gebbia, F. Gerbasi, M. Palazzoadriano, A. Rainer, L. Rausa, and E. Tubaro, *Arzneim.-Forsch.*, **21**, 1258 (1971).

(11) R. Rosso, C. Ravazzoni, M. Esposito, R. Sala, and L. Santi, *Eur. J. Cancer*, **8**, 455 (1972).

(12) R. S. Benjamin, C. E. Riggs, and N. R. Bachur, *Clin. Pharmacol. Ther.*, **14**, 592 (1973).

(13) N. R. Bachur, R. C. Hildebrand, and R. S. Jaenke, *J. Pharmacol. Exp. Ther.*, **191**, 331 (1974).

(14) S. Takanashi and N. R. Bachur, *Drug Metab. Dispos.*, **4**, 79 (1976).

(15) D. W. Kuehl, G. E. Glass, and F. A. Puglisi, *Anal. Chem.*, **46**, 804 (1974).

(16) H. M. Fales and T. Luukkainen, *ibid.*, **37**, 955 (1965).

(17) H. Budzikiewicz, C. Djerassi, and D. H. Williams, "Mass Spectrometry of Organic Compounds," Holden-Day, San Francisco, Calif., 1967.

(18) E. M. Chambaz and E. C. Horning, *Anal. Lett.*, **1**, 201 (1967).

(19) N. L. Gardiner and E. C. Horning, *Biochim. Biophys. Acta*, **115**, 524 (1966).

(20) D. C. DeJongh, T. Radford, J. D. Hirbar, S. Hanessian, M. Bieber, G. Dawson, and C. C. Sweeley, *J. Am. Chem. Soc.*, **91**, 1728 (1969).

ACKNOWLEDGMENTS

Supported by Contract N01-CM-23241 of the Division of Cancer Treatment, National Cancer Institute.

Applications of Paired Ion High-Pressure Liquid Chromatography to Catecholamines and Phenylephrine

A. G. GHANEKAR and V. DAS GUPTA ˣ

Received June 13, 1977, from the *College of Pharmacy, University of Houston, Houston, TX 77004.* Accepted for publication January 5, 1978.

Abstract □ Paired ion high-pressure liquid chromatography was useful for separating intact catecholamines (epinephrine, isoproterenol, levodopa, and methyldopa) and phenylephrine from some of their decomposition products. Furthermore, methyldopa was separated from either hydrochlorothiazide or levodopa. Under identical conditions without 1-heptanesulfonic acid (a counterion for paired ion chromatography) in the mobile phase, these separations were not possible. Paired ion chromatography also was tried successfully for the quantitative determinations of isoproterenol, levodopa, methyldopa, and phenylephrine in some dosage forms. The results were compared with the results obtained using some literature methods.

Keyphrases □ Catecholamines, various—paired ion high-pressure liquid chromatographic analyses in prepared solutions and dosage forms □ Phenylephrine hydrochloride—paired ion high-pressure liquid chromatographic analysis in prepared solutions and dosage forms □ High-pressure liquid chromatography—analyses, various catecholamines and phenylephrine hydrochloride in prepared solutions and dosage forms

Recently, paired ion high-pressure liquid chromatography (HPLC) has become popular, and the background and theory of this technique were reviewed (1). The quantitative determination of epinephrine by cation-exchange chromatography was reported (2). Watson and Lawrence reported (3–5) the quantitative determinations of catecholamines (epinephrine, isoproterenol, levodopa, and methyldopa) and phenylephrine by GLC, but this method requires derivatization and is lengthy and tedious. Recently, these authors (5) surveyed the literature on catecholamines.

This paper reports the applications of paired ion HPLC to catecholamines and phenylephrine. The catecholamines studied were epinephrine hydrochloride (I), isoproterenol hydrochloride (II), levodopa (III), and methyldopa (IV). The paper reports: (*a*) the separation of intact catecholamines from their decomposition products, (*b*) the separation of levodopa from the structurally related catecholamine methyldopa, (*c*) the separation of methyldopa from hydrochlorothiazide (a common combination product), and (*d*) quantitative determinations of II–IV and phenylephrine (V) in dosage forms using the developed method and literature methods.

EXPERIMENTAL

Chemicals and Reagents—All chemicals and reagents were USP, NF, or ACS grade and were used without further purification. Sodium 1-heptanesulfonate[1] (VI) was used as received.

Apparatus—The high-pressure liquid chromatograph[2] was capable of operating at an inlet pressure of up to 6000 psig. The multiple-wavelength detector[3] was set at 280 nm for all catecholamines except phenylephrine; for phenylephrine, it was set at 273 nm. These are wavelengths of maximum absorption. The detector was attached to a recorder[4] and an integrator[5].

The column[6] (30 cm long × 4 mm i.d.) was used as received.

Chromatographic Solvents—A 20% (v/v) solution of methanol in water containing 2% (v/v) acetic acid was used with or without 0.005 *M* sodium 1-heptanesulfonate. The pH of both solvents was 2.6 ± 0.05.

Chromatographic Conditions—The temperature was ambient. The flow rate was 1.6 ml/min (inlet pressure of approximately 1500 psig) for all catecholamines except levodopa and the levodopa–methyldopa combination for which it was 1.2 ml/min (inlet pressure of approximately 1000 psig). The absorbance unit for full-scale deflection was 0.04 except for levodopa and the levodopa–methyldopa combination for which it was 0.1. The chart speed was 30.5 cm/hr.

Stock Solutions—A 0.1% solution in water of I–V was prepared using a simple solution method. For levodopa and methyldopa, 10 and 3 ml of 0.1 *N* H_2SO_4, respectively, were added per 100 ml of the solution to obtain clear solutions. A commercial[7] 0.1% solution of epinephrine hydrochloride also contained 0.9% NaCl, 0.5% chlorobutanol, and 0.15% $NaHSO_3$. None of these compounds interfered in the assay used.

Standard Solutions—All standard solutions were prepared by diluting 10.0 ml of the stock solution to 100.0 ml with water.

Decomposition of Catecholamines and Phenylephrine—A 5.0-ml quantity of the stock solution was mixed with 5.0 ml of an appropriate solution of sodium hydroxide (0.01, 0.1, or 1 *N*). A sodium hydroxide solution of lower concentration was preferred as long as the mixture became discolored within a few minutes, so the 0.1 *N* solution generally was used. However, for II and V, the 0.01 and 1 *N* solutions were used, re-

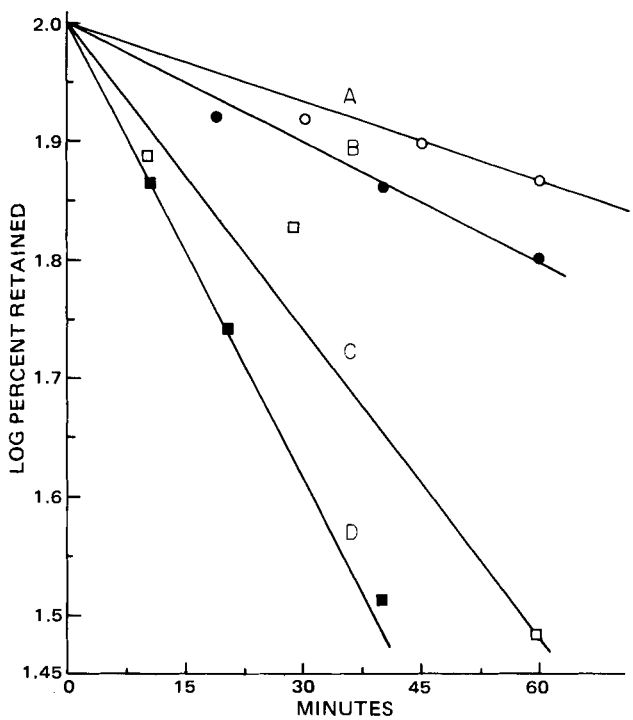

Figure 1—*Plots of log percent retained* versus *time. Key: A, II; B, IV; C, I; and D, III.*

[1] Eastman Kodak Co., Rochester, NY 14650.
[2] Model ALC 202 equipped with a U6K Universal injector, Waters Associates, Milford, Mass.
[3] Spectroflow monitor 770, Schoeffel Instrument Corp., Westwood, N.J.
[4] Omniscribe 5213-12. Houston Instruments, Austin, Tex.
[5] Autolab Minigrator, Spectra-Physics, Santa Clara, Calif.
[6] μBondapak C_{18}, Waters Associates, Milford, Mass.
[7] Parke, Davis & Co., Detroit, Mich.

0022-3549/78/0900-1247$01.00/0
© 1978, American Pharmaceutical Association

Table I—Assay Results on the Dosage Forms and Standard Deviations on I–V

Compound	SD^a, %	Dosage Form Assayed	Results[b], % of Claim
I	0.53	None	—[c]
II	0.84	Injection	100.0[d]
III	0.76	Capsules	100.7[e]
IV	0.83	Tablets	98.4[f]
V	0.98	Nose drops	99.9[g]
IV with hydrochlorothiazide		Tablets	100.2[d]

[a] Based on five injections of the standard solution. [b] Average of two. [c] No dosage form was tested. Only standard deviation was determined. [d] The result with the Kaistha method (6) was 99.6%. [e] The result with the USP method (7) was 100.3%. [f] The result with the USP method (8) was 98.4%. [g] The result with the Koshy and Mitchner method (9) was 99.8%.

spectively. After an appropriate period, the reaction mixture was quenched by adding 5.0 ml of sulfuric acid of an appropriate concentration. The mixture was brought to volume (50.0 ml) with water and assayed as discussed later.

Extraction of Levodopa and Methyldopa from Solid Dosage Forms—Twenty tablets or the contents of 20 capsules were ground to a fine powder, and powder representing 100.0 mg of catecholamine was weighed accurately and transferred to a mortar. Then 10 ml (20 ml for levodopa) of 1:350 sulfuric acid in water was added and mixed thoroughly for 2–3 min. The mixture was brought to volume (100.0 ml) with water and filtered if necessary. The first 10–15 ml of the filtrate was rejected, and then 10.0 ml was diluted to 100.0 ml with water and assayed as discussed later.

Dilutions of Other Dosage Forms—The contents of an isoproterenol hydrochloride injection (contained 0.02% solution of II) were diluted two times with water and assayed as described later. Then 2.0 ml of 0.5% phenylephrine hydrochloride nose drops was diluted to 100.0 ml with water and assayed as described later.

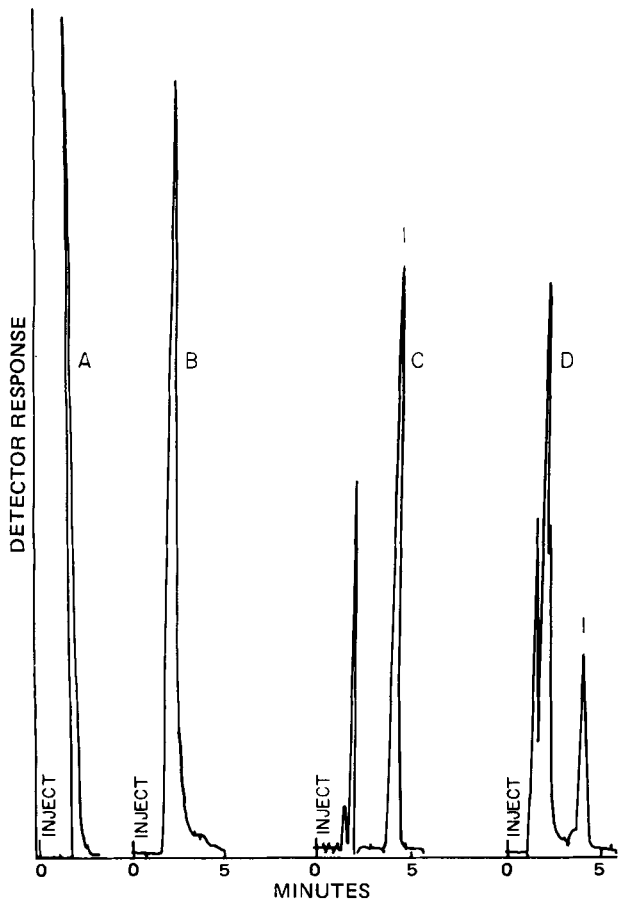

Figure 2—*Sample chromatograms of I (peak 1 is from I). Key: A, from a standard solution using mobile phase without VI; B, from a 1-hr decomposed sample using mobile phase without VI; and C and D, same as A and B, respectively, except that the mobile phase contained VI.*

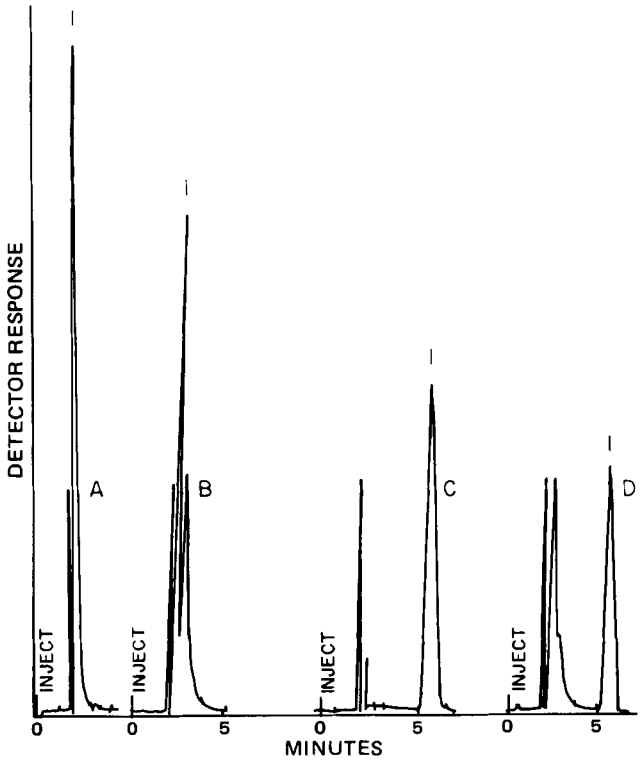

Figure 3—*Sample chromatograms of II (peak 1 is from II). Key: A, from a standard solution using mobile phase without VI; B, from a 1-hr decomposed sample using mobile phase without VI; and C and D, same as A and B, respectively, except that the mobile phase contained VI.*

Assay for All Catecholamines and Phenylephrine—The standard solution (10.0 μl) was injected using the described conditions and solvent containing VI. After the standard eluted out, 10.0 μl of the assay solution was injected. For comparison, this procedure was then repeated using solvent without VI. In another experiment, standard solutions of III and IV were injected together to determine if these two structurally related catecholamines would separate.

Calculations—Since preliminary investigations indicated that concentration (0.5–1.5 μg) was directly related to the peak area, the results were calculated by comparing the peak areas of the standard (A_s) and assay sample (A_a) as follows:

$$\frac{A_a}{A_s} \times 100 = \text{percent of claim} \qquad \text{(Eq. 1)}$$

The results are presented in Table I and Fig. 1. The sample chromato-

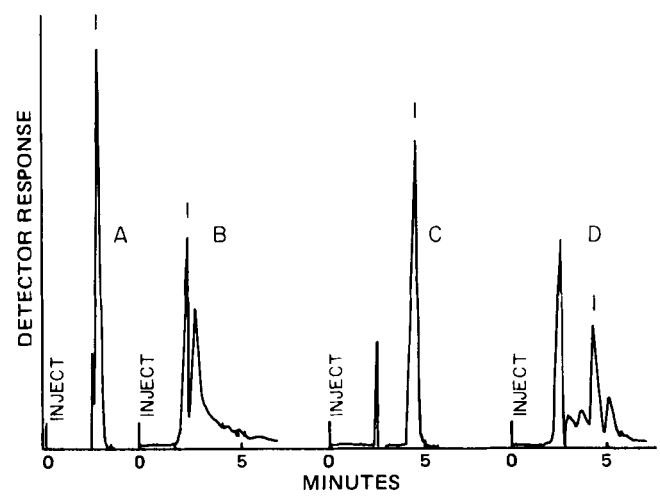

Figure 4—*Sample chromatograms of III (peak 1 is from III). Key: A, from a standard solution using mobile phase without VI; B, from a 1-hr decomposed sample using mobile phase without VI; and C and D, same as A and B, respectively, except that the mobile phase contained VI.*

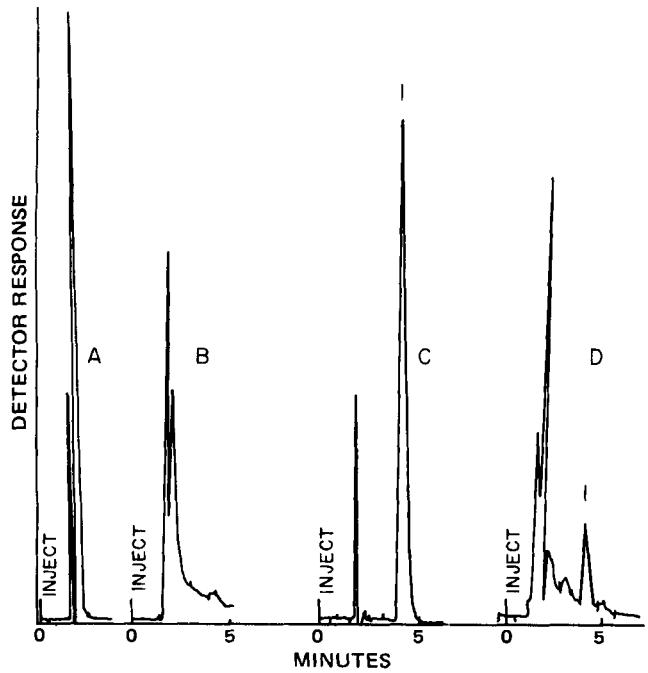

Figure 5—*Sample chromatograms of IV (peak 1 is from IV). Key: A, from a standard solution using mobile phase without VI; B, from a 2-hr decomposed sample using mobile phase without VI; and C and D, same as A and B, respectively, except that the mobile phase contained VI.*

grams (with and without VI in the mobile phase) are presented in Figs. 2–7. The standard deviations on all catecholamines and phenylephrine based on five areas from the identical volumes of the standard solutions are presented in Table I.

RESULTS AND DISCUSSION

Paired ion HPLC was very useful for separating intact catecholamines from some of their decomposition product(s) (Figs. 2–5). However, under identical conditions without VI in the mobile phase, there were no such separations (Figs. 2–5). All catecholamines allowed to react overnight with sodium hydroxide decomposed almost completely except V. The phenylephrine hydrochloride solution did not decompose much (less than 3%) even on reaction with 1 *N* NaOH (Fig. 6) *versus* all catecholamines where the concentrations of sodium hydroxide were lower (0.1 *N* except that for II it was 0.01 *N*).

Decomposition for all catecholamines in the presence of sodium hydroxide appeared to be pseudo first order (Fig. 1). The *K* values at room temperature were estimated to be 0.0197, 0.00506, 0.0301, and 0.00755 min^{-1} for I, II, III, and IV, respectively. Since the kinetic analysis was done for comparison purposes, only readings up to 60 min (40 min for levodopa because of faster decomposition) were treated kinetically. The strength of the sodium hydroxide solution used for isoproterenol was 0.01 *N versus* 0.1 *N* for all other catecholamines. Moreover, the solution of epinephrine (see *Stock Solutions*) contained preservative, which may explain the wider deviations from linearity in Fig. 1. It was not possible to determine the *K* value for V since it did not decompose more than 3% when left overnight in the presence of 1 *N* NaOH or on boiling for 2 hr with 0.1 *N* NaOH.

The results on 10 and 60 min and overnight decomposed samples of I were compared with the results obtained by a cation-exchange[8] method (2). The results were similar, and no new peak was recorded. The other catecholamines did not separate from their decomposition products using the cation-exchange method (2). An overnight decomposed sample of V gave a 97.6% result by the Koshy and Mitchner method (9) *versus* 97.4% by the developed method. The result on an overnight decomposed sample of III was almost 0% by the developed method *versus* 174.5% by the USP method (7) based on UV absorption. On methyldopa, the results on an overnight decomposed sample were 56.4% by the USP colorimetric method (8) and 0% by the developed method.

[8] Zipax SCX (100 cm × 2.1 mm i.d.), DuPont Instruments, Wilmington, Del.

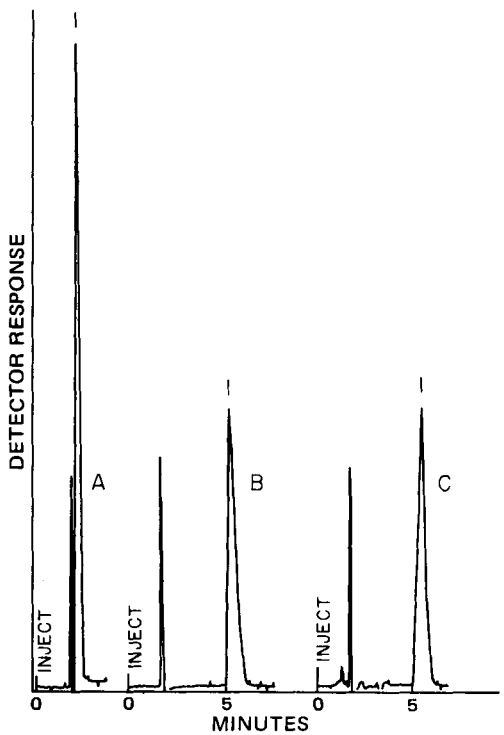

Figure 6—*Sample chromatograms of V (peak 1 is from V). Key: A, from a standard solution using mobile phase without VI; B, from a standard solution using mobile phase with VI; and C, from an overnight decomposed (with 0.1 N NaOH) sample using mobile phase with VI.*

Another advantage of paired ion HPLC appears to be its ability to separate catecholamines from other active ingredient(s). In this study, methyldopa was successfully separated from hydrochlorothiazide (Fig. 7B). The separation without the presence of VI was not as sharp (Fig. 7A) as with VI in the mobile phase (Fig. 7B). Furthermore, only with paired ion HPLC could methyldopa be separated from a structurally related catecholamine, levodopa (Fig. 7D). Without VI, no such separation was possible (Fig. 7C).

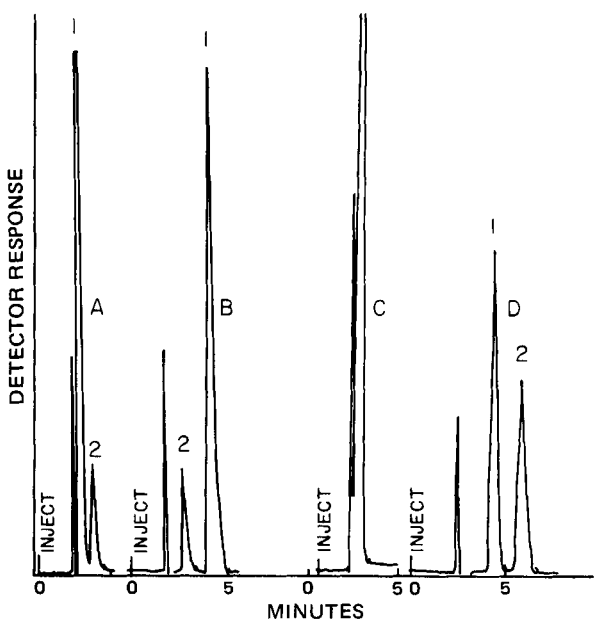

Figure 7—*Sample chromatograms of separation of IV from hydrochlorothiazide and levodopa. Key: A, separation of IV from hydrochlorothiazide using mobile phase without VI (peaks 1 and 2 are from IV and hydrochlorothiazide, respectively); B, same as A except that the mobile phase contained VI; C, separation of IV from III using mobile phase without VI; and D, same as C except that mobile phase contained VI (peaks 1 and 2 are from III and IV, respectively).*

In addition, the new method requires only one solvent–column system for all catecholamines studied and phenylephrine.

The developed method was used for the quantitative determinations of II–V in dosage forms, and the results were in agreement with the results obtained using literature methods (Table I). The presence of methylparaben and propylparaben in the commercial dosage (phenylephrine hydrochloride nose drops) did not interfere (Table I). In all catecholamines studied and phenylephrine, the areas of the peaks were directly related to concentration (range 0.5–1.5 μg). The sensitivity of the method can be further improved by reducing the absorbance unit for full-scale deflection. The standard deviations based on five injections of the standard solution were estimated to be 0.53, 0.84, 0.76, 0.83, and 0.98% for I, II, III, IV, and V, respectively.

REFERENCES

(1) "Paired Ion Chromatography, An Alternative to Ion Exchange," Brochure D61, Waters Associates, Milford, Mass., 1975, p. 3.

(2) C. Fu and M. J. Sibley, *J. Pharm. Sci.*, **66,** 425 (1977).

(3) J. R. Watson, *ibid.*, **63,** 96 (1974).

(4) J. R. Watson and C. R. Lawrence, *J. Chromatogr.*, **103,** 63 (1975).

(5) J. R. Watson and C. R. Lawrence, *J. Pharm. Sci.*, **66,** 560 (1977).

(6) K. K. Kaistha, *ibid.*, **59,** 241 (1970).

(7) "The United States Pharmacopeia," 19th rev., Mack Publishing Co., Easton, Pa., 1975, p. 281.

(8) *Ibid.*, p. 320.

(9) K. T. Koshy and H. Mitchner, *J. Pharm. Sci.*, **52,** 802 (1963).

ACKNOWLEDGMENTS

Abstracted in part from a thesis submitted by A. G. Ghanekar to the University of Houston in partial fulfillment of the Master of Science degree requirements.

The authors thank Merck Sharp & Dohme for a generous supply of methyldopa and Roche Laboratories for levodopa.

High-Performance Liquid Chromatographic Assay of Sulfapyridine and Acetylsulfapyridine in Biological Fluids

JOEL OWERBACH, NOREEN F. JOHNSON, THEODORE R. BATES, HENRY J. PIENIASZEK, Jr., and WILLIAM J. JUSKO *x

Received October 28, 1977, from the *Clinical Pharmacokinetics Laboratory, Department of Pharmaceutics, School of Pharmacy, State University of New York at Buffalo, Amherst, NY 14260.* Accepted for publication December 28, 1977. *Present address: Clinical Pharmacokinetics Laboratory, Millard Fillmore Hospital, Buffalo, NY 14209.

Abstract □ A high-pressure liquid chromatographic method for the sensitive, rapid, and specific determination of sulfapyridine and its *N*-acetyl derivative in plasma and saliva was developed. A cyano-bonded, reversed-phase, high efficiency column was used. The system detected these sulfonamides in serum to 0.25 mg/liter and within only 6 min. Sulfapyridine was separated from its acetyl derivative with little interference from other drugs. The assay reproducibility was within 3%. The assay was highly useful for routine monitoring of patients receiving sulfasalazine for inflammatory bowel disease.

Keyphrases □ Sulfapyridine and acetyl metabolite—high-performance liquid chromatographic analyses in biological fluids □ High-performance liquid chromatography—analyses, sulfapyridine and acetyl metabolite in biological fluids □ Dermatitis suppressants—sulfapyridine and acetyl metabolite, high-performance liquid chromatographic analyses in biological fluids

The measurement of sulfasalazine[1] metabolites in serum is useful for monitoring patients with inflammatory bowel disease (1–4). As a combination drug, sulfasalazine (I) is composed of sulfapyridine (II) azo linked to 5-aminosalicylic acid (IV). The azo linkage is cleaved by bacteria in the colon, releasing II and IV. Compound II metabolizes to acetylsulfapyridine (III), sulfapyridine *O*-glucuronide (VI), and acetylsulfapyridine *O*-glucuronide (VII).

[1] Azulfidine, Pharmacia; SAS-500, Rowell Laboratories; and Rorasul, Rorer.

BACKGROUND

Das and coworkers (1–3) established the relationship among the sulfasalazine metabolites (II, III, VI, and VII) in serum, acetylation phenotype, and sulfasalazine therapeutic efficacy and side effects. Total serum concentrations of II, III, VI, and VII between 20 and 50 mg/liter were associated with disease remission (1). Side effects were more likely to occur in slow acetylators when total sulfapyridine metabolite concentrations were greater than 50 mg/liter (2). Among the several metabolites, only II and III are present in sufficient concentrations in serum (3) and saliva (5) to be important in acetylator phenotyping and to be clinically useful as a guide to dosage adjustment.

Compound I and its metabolites were identified previously by TLC and by colorimetric methods. Schroder and Campbell (6) used TLC to help establish the metabolic pathway of sulfasalazine in humans. Subsequent work by Das and coworkers (1, 2, 4) made use of a modified Bratton–Marshall colorimetric assay (7) that measures only free II. Therefore, all metabolites of II must be hydrolyzed with acid or with enzymes to release free II for quantitation. These hydrolyses require temperature control. It is then necessary to diazotize the free II to produce the color for colorimetric analyses. Two of the several reagent solutions must be made fresh weekly because of their instability. Although the Bratton–Marshall method is reliable for investigative study, the procedural complexity limits its utility for routine clinical monitoring of patient samples on a daily basis and, of course, it is relatively nonspecific.

Current work to identify and quantitate sulfonamides utilizes high-pressure liquid chromatography (HPLC). HPLC was used in measuring I in tablets and powders (8). Sharma *et al.* (9) measured various sulfas and acetyl metabolites in animal urine by HPLC. Cobb and Hill (10) determined the relative retention times of various sulfonamides eluted from an HPLC column. The measurement of II and III from the serum

0022-3549/78/0900-1250$01.00/0

© 1978, American Pharmaceutical Association

In addition, the new method requires only one solvent–column system for all catecholamines studied and phenylephrine.

The developed method was used for the quantitative determinations of II–V in dosage forms, and the results were in agreement with the results obtained using literature methods (Table I). The presence of methylparaben and propylparaben in the commercial dosage (phenylephrine hydrochloride nose drops) did not interfere (Table I). In all catecholamines studied and phenylephrine, the areas of the peaks were directly related to concentration (range 0.5–1.5 μg). The sensitivity of the method can be further improved by reducing the absorbance unit for full-scale deflection. The standard deviations based on five injections of the standard solution were estimated to be 0.53, 0.84, 0.76, 0.83, and 0.98% for I, II, III, IV, and V, respectively.

REFERENCES

(1) "Paired Ion Chromatography, An Alternative to Ion Exchange," Brochure D61, Waters Associates, Milford, Mass., 1975, p. 3.

(2) C. Fu and M. J. Sibley, *J. Pharm. Sci.*, **66,** 425 (1977).

(3) J. R. Watson, *ibid.*, **63,** 96 (1974).

(4) J. R. Watson and C. R. Lawrence, *J. Chromatogr.*, **103,** 63 (1975).

(5) J. R. Watson and C. R. Lawrence, *J. Pharm. Sci.*, **66,** 560 (1977).

(6) K. K. Kaistha, *ibid.*, **59,** 241 (1970).

(7) "The United States Pharmacopeia," 19th rev., Mack Publishing Co., Easton, Pa., 1975, p. 281.

(8) *Ibid.*, p. 320.

(9) K. T. Koshy and H. Mitchner, *J. Pharm. Sci.*, **52,** 802 (1963).

ACKNOWLEDGMENTS

Abstracted in part from a thesis submitted by A. G. Ghanekar to the University of Houston in partial fulfillment of the Master of Science degree requirements.

The authors thank Merck Sharp & Dohme for a generous supply of methyldopa and Roche Laboratories for levodopa.

High-Performance Liquid Chromatographic Assay of Sulfapyridine and Acetylsulfapyridine in Biological Fluids

JOEL OWERBACH, NOREEN F. JOHNSON, THEODORE R. BATES, HENRY J. PIENIASZEK, Jr., and WILLIAM J. JUSKO *x

Received October 28, 1977, from the *Clinical Pharmacokinetics Laboratory, Department of Pharmaceutics, School of Pharmacy, State University of New York at Buffalo, Amherst, NY 14260.* Accepted for publication December 28, 1977. *Present address: Clinical Pharmacokinetics Laboratory, Millard Fillmore Hospital, Buffalo, NY 14209.

Abstract □ A high-pressure liquid chromatographic method for the sensitive, rapid, and specific determination of sulfapyridine and its *N*-acetyl derivative in plasma and saliva was developed. A cyano-bonded, reversed-phase, high efficiency column was used. The system detected these sulfonamides in serum to 0.25 mg/liter and within only 6 min. Sulfapyridine was separated from its acetyl derivative with little interference from other drugs. The assay reproducibility was within 3%. The assay was highly useful for routine monitoring of patients receiving sulfasalazine for inflammatory bowel disease.

Keyphrases □ Sulfapyridine and acetyl metabolite—high-performance liquid chromatographic analyses in biological fluids □ High-performance liquid chromatography—analyses, sulfapyridine and acetyl metabolite in biological fluids □ Dermatitis suppressants—sulfapyridine and acetyl metabolite, high-performance liquid chromatographic analyses in biological fluids

The measurement of sulfasalazine[1] metabolites in serum is useful for monitoring patients with inflammatory bowel disease (1–4). As a combination drug, sulfasalazine (I) is composed of sulfapyridine (II) azo linked to 5-aminosalicylic acid (IV). The azo linkage is cleaved by bacteria in the colon, releasing II and IV. Compound II metabolizes to acetylsulfapyridine (III), sulfapyridine *O*-glucuronide (VI), and acetylsulfapyridine *O*-glucuronide (VII).

[1] Azulfidine, Pharmacia; SAS-500, Rowell Laboratories; and Rorasul, Rorer.

BACKGROUND

Das and coworkers (1–3) established the relationship among the sulfasalazine metabolites (II, III, VI, and VII) in serum, acetylation phenotype, and sulfasalazine therapeutic efficacy and side effects. Total serum concentrations of II, III, VI, and VII between 20 and 50 mg/liter were associated with disease remission (1). Side effects were more likely to occur in slow acetylators when total sulfapyridine metabolite concentrations were greater than 50 mg/liter (2). Among the several metabolites, only II and III are present in sufficient concentrations in serum (3) and saliva (5) to be important in acetylator phenotyping and to be clinically useful as a guide to dosage adjustment.

Compound I and its metabolites were identified previously by TLC and by colorimetric methods. Schroder and Campbell (6) used TLC to help establish the metabolic pathway of sulfasalazine in humans. Subsequent work by Das and coworkers (1, 2, 4) made use of a modified Bratton–Marshall colorimetric assay (7) that measures only free II. Therefore, all metabolites of II must be hydrolyzed with acid or with enzymes to release free II for quantitation. These hydrolyses require temperature control. It is then necessary to diazotize the free II to produce the color for colorimetric analyses. Two of the several reagent solutions must be made fresh weekly because of their instability. Although the Bratton–Marshall method is reliable for investigative study, the procedural complexity limits its utility for routine clinical monitoring of patient samples on a daily basis and, of course, it is relatively nonspecific.

Current work to identify and quantitate sulfonamides utilizes high-pressure liquid chromatography (HPLC). HPLC was used in measuring I in tablets and powders (8). Sharma *et al.* (9) measured various sulfas and acetyl metabolites in animal urine by HPLC. Cobb and Hill (10) determined the relative retention times of various sulfonamides eluted from an HPLC column. The measurement of II and III from the serum

0022-3549/78/0900-1250$01.00/0

© 1978, American Pharmaceutical Association

and saliva of inflammatory bowel disease patients by HPLC has not been reported. This paper reports the development of an HPLC assay for II and III, including comparison to the Bratton–Marshall procedure.

EXPERIMENTAL

Materials—Reagent grade acetic acid, acetic anhydride, dioxane[2], perchloric acid, and sodium hydroxide[3] were used. Pure samples of II[4,5], III, I[4], and sulfamethoxazole[6] were used as standards. Very pure water was used. Reagents were prepared with distilled and deionized water; the HPLC mobile phase was prepared with degassed, distilled, deionized, and filtered water.

Acetylsulfapyridine was prepared in this laboratory using a procedure similar to that described by Sharma *et al.* (9). Pure acetic anhydride, 100 μl, was added dropwise to 100 mg of sulfapyridine in a 10-ml beaker and mixed to wet all of the sulfapyridine. After 50 min, the reaction mixture was rinsed with 40% dioxane–water into a 50-ml volumetric flask. A 2-ml aliquot of 0.1 *N* NaOH was added to the solution to dissolve any remaining sulfapyridine, and enough 40% dioxane–water was added to attain 50 ml. The yield was 97% acetylsulfapyridine and 3% sulfapyridine. The properties of the synthesized acetylsulfapyridine were the same as authentic acetylsulfapyridine[7].

Human plasma was obtained from a hospital blood bank and cleaned of chromatographically interfering substances using activated charcoal. The charcoal was shaken with the plasma for 10 min and then separated from the purified plasma by centrifugation at 20,000 rpm overnight at 10°.

Standards—Standards in distilled, deionized water or in purified plasma were prepared at concentrations of 2.5, 5, 10, 15, 20, and 25 mg/liter by dilutions of a 100- or a 10-mg/liter II and III stock solution (in water or in plasma) in 10-ml volumetric flasks. The standards were frozen in small aliquots (0.65 ml) in 12 × 75-mm glass test tubes covered with plasticized paper[8].

Internal Standard—A 20% perchloric acid–250-mg/liter sulfamethoxazole solution was prepared daily by adding 400 μl of a 60% perchloric acid solution to 800 μl of a 375-mg/liter sulfamethoxazole solution.

Apparatus—A high-performance liquid chromatograph[9] with a 254-nm UV detector and a reversed-phase, high efficiency, CN column[10] (4 mm i.d. × 30 cm) was used. The mobile phase consisted of an aqueous solution of 0.4% sodium acetate and 4% acetic acid. Flow rates varied between 2.0 and 2.3 ml/min under a pressure of approximately 140.6 kg/cm^2. The HPLC attenuation was set between 0.01 and 0.08 with a 1-mv recorder.

Analytical Procedure—Of the 13 sulfonamides tested on the CN column, the retention time of sulfamethoxazole (X), about twice that of II, was the shortest without chromatographically interfering with II or III. Therefore, X was chosen as the internal standard.

To reduce potential serum protein accumulation in the column and to minimize chromatographic interference, protein was precipitated from the samples with a 20% perchloric acid solution containing 250 mg of the internal standard/liter. Plasma standards (three) were used for patient serum samples. Into a 10 × 75-mm glass test tube, 0.02 ml of the perchloric acid–X solution was added to 0.2 ml of the sample or standard. After vortexing and then centrifuging at 2000 rpm for 12 min, the clear supernate was transferred to a clean 10 × 75-mm glass test tube. A 10-μl aliquot of this supernate was injected onto the column.

For patient saliva samples, water standards (three) were used. A 20-μl aliquot of a 250-mg of X/ml aqueous solution was added to 0.2 ml of the sample or standard. Ten microliters of this solution was injected onto the column.

Bratton–Marshall Assay—Compounds II and III also were measured by the Bratton–Marshall assay, modified to yield a three- to fourfold increase in analytical sensitivity over a previous method (7) and to allow convenient second extraction and color development steps for II at room temperature rather than at refrigeration temperatures. Compounds II and III were coextracted from 0.2–1.0 ml of biological specimen (mixed with 1.0 ml of 1 *M* pH 4.8 acetate buffer and 0.5 g of sodium chloride) into 5.0 ml of methyl isobutyl ketone and then reextracted from 3.0 or 4.0 ml of the ketone into 3.0 ml of 2 *N* HCl (acidic phase).

To assay for II, 100-μl quantities of aqueous solutions of sodium nitrite (0.12%), ammonium sulfamate (0.8%), and *N*-(1-naphthyl)ethylenediamine dihydrochloride (0.8%) were added sequentially at 3-min intervals to a 1.0-ml aliquot of the acidic phase. The mixture was stored in the dark for 30 min for maximum color development before measuring absorbance at 540 nm[11]. Total II and III were analyzed similarly after heating a second 1.0-ml aliquot of the acidic phase at 100° for 30 min to effect deacetylation of III.

Recovery—To test for drug recovery after precipitation, concentrations of II, III, and X were analyzed from water, saliva, and 4% human serum albumin in pH 7.4 phosphate-buffered saline and from plasma standards.

Stability—Concentrations of 10 and 20 mg of II and III/liter in plasma were stored at 4° and determined each day for 10 days and at 37° for 48 hr to assess the effect of temperature on short-term stability.

Reproducibility—The reproducibility of determining the concentrations of II and III was obtained by running 20-mg/liter plasma standards, stored in aliquots at 0° in glass tubes, 10 times in 1 day. Furthermore, plasma standards at 10 and 20 mg/liter were run once daily for 10 days over 3.5 weeks. Thus, both the "within" day (intraday) and the "day to day" (interday) variations of the assay could be determined. Measurements were made using peak heights (height of the chromatographic peak) and peak height ratios (drug peak height to internal standard peak height) for comparison as to the most reliable measurement method.

Comparative Assays—Five spiked plasma samples of known concentrations were determined by both the Bratton–Marshall procedure and the HPLC method. To assess clinical reliability, the concentrations of II and III in 35 serum samples from 19 ambulatory patients receiving sulfasalazine were determined independently by both methods. Concentrations of II and III were determined, and the percent acetylation was calculated.

Interferences—The concurrent medications received by the 19 patients were recorded to assess any chromatographic interference that would affect method specificity. Thirteen sulfonamides, sulfasalazine, and 5-aminosalicylic acid also were checked for interference.

RESULTS AND DISCUSSION

Figure 1 shows the typical chromatograms of a 15-mg/liter standard concentration of II and III and a serum sample from a patient receiving 0.5 g of sulfasalazine twice daily. The HPLC method has good specificity, as indicated by the separate peaks for each metabolite and by a lack of overlap with most other drugs taken by the patients as well as with most of the sulfonamides tested on the column. The retention times for II, III, and X varied with the mobile phase flow rate; at a flow rate of 2.20 ml/min, the retention times were 2.8, 4.0, and 4.7 min, respectively.

The concentrations of II and III were derived from a linear regression standard curve using peak height ratio (peak height of II or III to peak height of the internal standard, X). Because of the wide range of II and III concentrations from patient samples, the recorder absorptivity scale was changed by fourfold. Initial studies indicated that the detector response of 2.078, 3.898, and 7.910 correlated fairly well with the changes in the HPLC attenuator of two-, four-, and eightfold, respectively.

Recovery—Since essentially no protein precipitates out of saliva upon addition of 20% perchloric acid, saliva standards were injected directly onto the HPLC column. Saliva standards were compared to water standards, each being injected directly onto the column. The peak heights were nearly equal (saliva II was 103% of water II, and saliva III was 93.6% of water III), and the peak height ratios were identical.

During sample deproteinization, approximately 98, 62, and 71% of II, III, and X, respectively, were recovered from human plasma standards compared to aqueous standards as determined from the slopes of the peak heights (with concentrations of 20 and 50 mg/liter) and from the peak heights themselves. Because of the similar recoveries of III and X during deproteinization, use of the peak height ratio for III is nearly independent of protein concentration. Because II is less bound to serum proteins than X, their peak height ratios may be dependent on protein concentration.

Recoveries of II in 4% human serum albumin appeared to be greater than in water. This result was due to the concentrating effect of precipitating the protein volume out of solution, leaving the free II in a smaller

[2] Fisher Scientific Co., Springfield, N.J.
[3] J. T. Baker Chemical Co., Phillipsburg, N.J.
[4] Pharmacia, Piscataway, N.J.
[5] Eli Lilly and Co., Indianapolis, Ind.
[6] Hoffmann-La Roche, Nutley, N.J.
[7] Provided by Dr. K. M. Das, Albert Einstein College of Medicine, New York, N.Y.
[8] Parafilm.
[9] Model 848, DuPont Instruments, Wilmington, Del.
[10] μBondapak CN, Waters Associates, Milford, Mass.
[11] Beckman DB-6, Beckman Instruments, Fullerton, Calif.

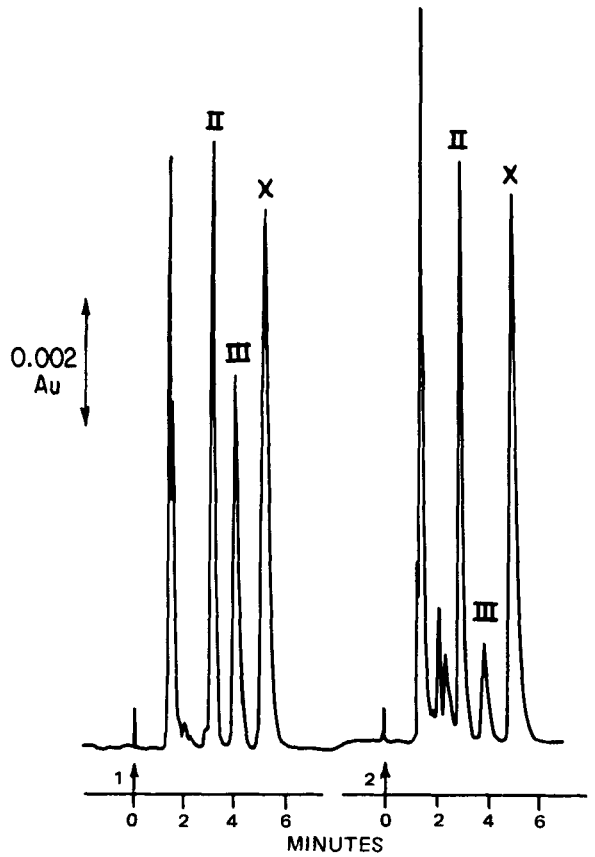

Figure 1—*Chromatogram of sulfapyridine (II), N-acetylsulfapyridine (III), and sulfamethoxazole as the internal standard (X). The arrows denote times of sample injection. Chromatogram 1 was obtained from a standard plasma concentration of 15 mg of II and III/liter. Chromatogram 2 was obtained from a patient sample containing 14.7 mg of II/liter and 3.94 mg of III/liter. The initial peaks are plasma effects.*

supernatant volume. Recoveries of III in 4% human serum albumin were reduced from those in water, although not as much as in plasma (77% in 4% albumin *versus* 62% in plasma). Therefore, to simulate patient samples, standards were made in purified plasma.

Peak height ratios were linearly related to the concentrations of II and III over a range of 2.5–100 mg/liter. Below 6 mg/liter, there was some loss of sensitivity, which could be increased tenfold by decreasing the HPLC attenuation from 0.02 to 0.01 aufs and by increasing injection volume from 10 to 50 μl. This step would allow detection of 0.25 mg of II and III/liter.

Stability—There was less than 3.3% variation in concentrations of II and III stored at 4° and measured once a day on 10 different days. The means and standard deviations determined for the two standard concentrations (10 and 20 mg/liter) tested were 10.4 ± 0.3 and 20.3 ± 0.3 mg/liter for II and 10.1 ± 0.3 and 19.8 ± 0.3 mg/liter for III. Heating a 20-mg/liter sample to 37° did not significantly change the concentration over 48 hr, with the resultant mean concentrations and standard deviations being 21.7 ± 1.5 mg/liter for II and 20.4 ± 0.5 mg/liter for III. Standard plasma samples were stored in glass tubes at 0° until use.

Reproducibility of HPLC Analysis—Table I shows the excellent reproducibility (less than 3% variation) for concentration determinations of both II and III in intraday and interday (over 10 days) determinations using peak height ratios. A 20-mg/liter standard was used for the intraday run, and 10- and 20-mg/liter standards were used for the interday run. Using peak heights alone without the internal standard resulted in variations up to 7% for II and 8% for III for the interday series. As the concentrations of II decreased to less than 5 mg/liter, with a corresponding peak height of 40 mm, the peak height ratio variations increased (5.6% variation at 2.5 mg/liter or at a 20-mm peak height). This ratio variation was also seen with III concentrations less than 10 mg/liter or with less than a 55-mm peak height (6.8% variation at 5 mg/liter or at a 25-mm peak height). The use of peak height ratios and attenuations of the chromatograph and recorder to produce peak heights greater than 25 mm is recommended for optimum results.

Table I—Reproducibility of the HPLC Analysis of II and III by Peak Ratios

Statistical Data	II			III		
	Intraday Series	Interday Series		Intraday Series	Interday Series	
Number	10	10	10	10	10	10
Mean concentration, mg/liter	20.8	10.12	19.92	20.7	10.0	19.99
SD	0.3	0.28	0.31	0.3	0.27	0.35
CV, %	1.5	2.7	1.5	1.5	2.7	1.8

Assay Comparison—Figure 2 compares the results of the HPLC and Bratton–Marshall spectrophotometric analyses of 35 serum samples obtained from patients receiving sulfasalazine maintenance therapy for ulcerative colitis and Crohn's disease. The graphs demonstrate an excellent correlation between concentrations of II and III as determined by the two methods, with respective correlation coefficients of 0.981 and 0.991. In 30 of the 35 assay comparisons, the concentrations of the sum of II and III ("total sulfapyridine") determined by the two procedures were within 20% of each other.

On the average, the HPLC method yielded concentration values lower than those derived from the spectrophotometric method. By regression analysis of the 35 patient serum specimens analyzed by both the HPLC assay and the Bratton–Marshall spectrophotometric assay (Fig. 2), the resulting slopes indicate that the HPLC method concentrations of II and III were 9.2 and 7.7% lower, respectively, than those of the spectrophotometric method. Similarly, when a set of plasma standards was run by both HPLC and the spectrophotometric methods (Table II), the five standards gave slopes indicating that the HPLC method yielded concentrations of II and III 4.5 and 2.7% lower than those of the spectrophotometric method. Compared to the *actual* spiked plasma concentrations listed in Table II, HPLC determinations gave consistently lower values and the spectrophotometric determinations gave consistently higher values. The maximum differences in concentrations between the methods of 5% for the spiked plasma and of 9% for the patient samples are of little clinical significance.

Figure 3 compares the percent acetylation, III × 100%/(II + III), as calculated from the HPLC and Bratton–Marshall assays of 32 patient samples. The average of two samples from each of the 16 patients was used in Fig. 3. There was an excellent correlation between the methods, with a correlation coefficient of 0.994. The HPLC method produced values 5.1% higher than the Bratton–Marshall method. The higher percent acetylation values may reflect the lower concentrations of II obtained using the HPLC method relative to III concentrations. The population was also differentiated by both methods into two distinct groups: rapid acetylators and slow acetylators. There was complete agreement between the assays on which patients were fast and slow acetylators.

Interference—Of all of the patient samples analyzed, only one contained an interfering material, which may have been a metabolite of propoxyphene. The patients sampled were on thiazide diuretics, oral and rectal steroids, vitamins, iron, folic acid, diazepam, meprobamate, oral contraceptives, diphenoxylate hydrochloride[12], diphenhydramine hydrochloride[13], aspirin, and cholestyramine[14]. Of the 13 sulfonamides

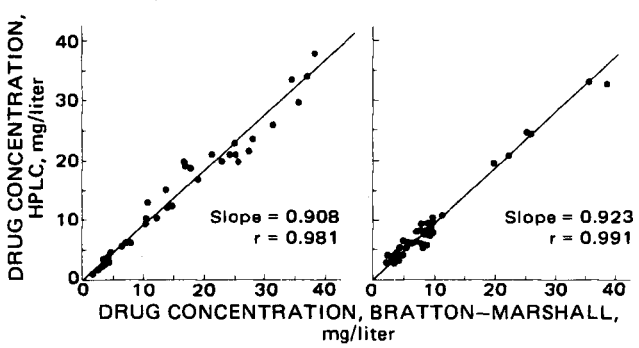

Figure 2—*Correlation between the concentrations of sulfapyridine (left) and acetylsulfapyridine (right) in 35 patient serum specimens as measured by the HPLC assay and the Bratton–Marshall spectrophotometric assay.*

[12] Lomotil, Searle & Co.
[13] Benadryl, Parke, Davis & Co.
[14] Questran, Mead Johnson Laboratories.

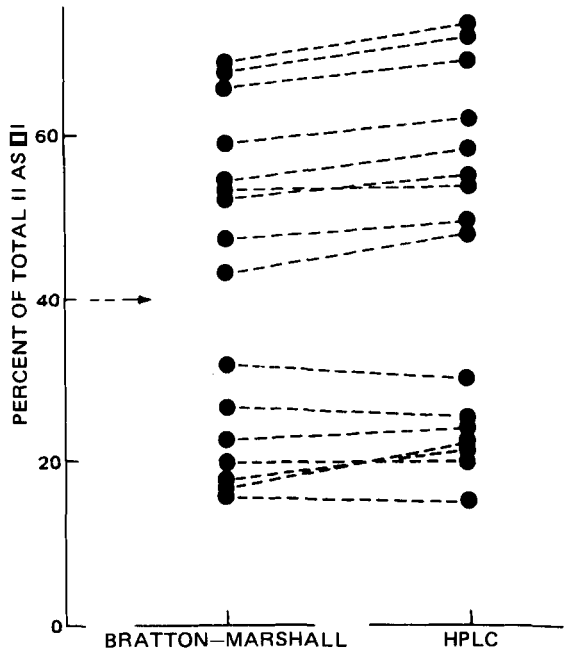

Figure 3—*Acetylation phenotyping in 16 patients by HPLC and the Bratton–Marshall spectrophotometric assay. The points represent the average of two acetylation percent determinations for each patient.*

tested on the column, sulfisomidine, sulfadiazine, sulfamerazine, sulfameter, sulfamethizole, and sulfamethoxypyridazine may interfere. Neither sulfasalazine nor 5-aminosalicylic acid interfered with the assay. Thus, there was minimal interference by other drugs, especially in the actual patient samples.

DISCUSSION

The described method for the HPLC assay of sulfapyridine is useful in the monitoring of patient samples. Although the pharmacokinetic characteristics of sulfasalazine and its clinical toxicity do not necessitate rapid serum level determinations, as may be important with drugs such as theophylline and procainamide, the routine monitoring of a small number of samples is facilitated by a simple method that can be readily added to existing laboratory procedures. Sulfapyridine samples may be injected into the same column and HPLC system as used for procainamide and quinidine with virtually no adjustments (11). Results can be obtained in less than 1 hr.

The method is specific in that it measures III directly whereas the Bratton–Marshall procedure requires hydrolytic cleavage to II and calculation of the amount of II contributed by the acetyl metabolite. Of the concurrent medications given the patients sampled with the HPLC serum level determination and acetylation phenotyping, only one interfered.

An additional feature is the relatively small volume of sample required for the HPLC determination. Less than the 200 μl of plasma may be analyzed if necessary. This advantage is particularly applicable to the pediatric population when only small amounts of serum can be obtained.

Table II—Analysis of Spiked Plasma Standards Containing Mixtures of II and III by the Bratton–Marshall Method and the HPLC Method

II, mg/liter			III, mg/liter		
Bratton–Marshall	Standard	HPLC	Bratton–Marshall	Standard	HPLC
0.53	0.26	0.16	7.81	7.5	7.3
1.05	0.51	0.37	14.90	15.0	15.2
4.24	4.00	3.80	8.13	8.0	7.8
11.60	11.00	10.30	4.44	4.0	3.5
21.70	21.00	20.90	0.94	0	0

The close correlations between the Bratton–Marshall and HPLC assay results clearly demonstrate the utility of the HPLC assay for II, III, and acetylator phenotyping with sulfasalazine. Its superiority over existing methods is evidenced by the small sample volume required, rapid chromatography times, good reproducibility, high sensitivity and specificity, and a minimum of procedural manipulation and technical functions required for analysis. There is the added benefit of minimal environmental pollution in the HPLC method with its lack of organic solvents.

The clinical monitoring of sulfapyridine concentrations and acetylation phenotyping in inflammatory bowel disease patients receiving sulfasalazine is a relatively new advance and has only been extensively reported to date in one series of patients. HPLC analysis facilitates such measurement in patient samples and provides a basis for further clinical research as well as service assay capabilities.

REFERENCES

(1) K. M. Das, M. A. Eastwood, J. P. A. McManus, and W. Sircus, *Gut*, **14**, 631 (1973).

(2) K. M. Das, M. A. Eastwood, J. P. A. McManus, and W. Sircus, *N. Engl. J. Med.*, **289**, 491 (1973).

(3) K. M. Das and R. Dubin, *Clin. Pharmacokinet.*, **1**, 406 (1976).

(4) K. M. Das and M. A. Eastwood, *Clin. Pharmacol. Ther.*, **18**, 514 (1975).

(5) T. R. Bates, H. P. Blumenthal, and H. J. Pieniaszek, Jr., *Res. Commun. Chem. Pathol. Pharmacol.*, **15**, 183 (1976).

(6) H. Schroder and D. E. S. Campbell, *Clin. Pharmacol. Ther.*, **13**, 539 (1972).

(7) K. A. Hansson and M. Sandberg, *Acta Pharm. Suec.*, **10**, 87 (1973).

(8) L. D. Bighley and J. P. McDonnell, *J. Pharm. Sci.*, **64**, 1549 (1975).

(9) J. P. Sharma, E. G. Perkins, and R. F. Bevill, *ibid.*, **65**, 1606 (1976).

(10) P. H. Cobb and G. T. Hill, *J. Chromatogr.*, **123**, 444 (1976).

(11) J. J. Lima and W. J. Jusko, in "Biological/Biochemical Application of Liquid Chromatography," G. L. Hawk, Ed., Dekker, New York, N.Y., 1978.

ACKNOWLEDGMENTS

Supported by Grant 20852 from the National Institute of General Medical Sciences, National Institutes of Health.

High-Pressure Liquid Chromatographic Assays for Clindamycin, Clindamycin Phosphate, and Clindamycin Palmitate

LEO W. BROWN

Received October 19, 1977, from *The Upjohn Company, Kalamazoo, MI 49001.* Accepted for publication January 5, 1978.

Abstract □ High-pressure liquid chromatographic procedures are described for clindamycin, clindamycin palmitate, and clindamycin phosphate as bulk drugs and in formulations. All three procedures utilize a C_{18} reversed-phase chromatographic column with refractive index detection. The mobile phases are hydroalcoholic solutions containing dioctyl sodium sulfosuccinate or disodium ethylenediaminetetraacetate. Separations of related impurities or degradation products also are discussed. The relative standard deviations of the methods range from 0.8 to 1.8%.

Keyphrases □ Clindamycin—base, phosphate, and palmitate, high-pressure liquid chromatographic analyses in bulk drug and dosage forms □ High-pressure liquid chromatography—analyses, clindamycin base, phosphate, and palmitate in bulk drug and dosage forms □ Antibacterials—clindamycin base, phosphate, and palmitate, high-pressure liquid chromatographic analyses in bulk drug and dosage forms

Clindamycin[1] (I) is an antibiotic active against Gram-positive aerobes and very active against both Gram-positive and Gram-negative anaerobic pathogens (1). It is synthesized from lincomycin (II), an antibiotic produced by microbial fermentation. Clindamycin phosphate[1] (III), produced by chemical modification of clindamycin, is used in parenteral preparations. After injection, it is hydrolyzed to the active clindamycin. Clindamycin palmitate[1] (IV) is also produced by chemical modification of clindamycin. The presence of the palmitate group markedly lessens the bitter taste experienced with the parent compound, making it suitable for oral pediatric formulations. Although the ester is not biologically active, it is readily hydrolyzed to the active clindamycin *in vivo* (2).

Clindamycin, clindamycin phosphate, and clindamycin palmitate are presently assayed by GLC and microbiological procedures (3, 4). The GLC procedure for clindamycin involves derivatization with either trifluoroacetic anhydride or acetic anhydride. These procedures separate possible trace contaminants such as epilincomycin (V), epiclindamycin (VI), and clindamycin B (VII) from clindamycin. Clindamycin phosphate is assayed as clindamycin after hydrolysis using alkaline phosphatase. Clindamycin palmitate is derivatized with acetic anhydride and then chromatographed.

High-pressure liquid chromatographic (HPLC) assays for the three clindamycin antibiotics are presented here. Since no derivatization steps are involved, the HPLC assay is simpler and quicker than the GLC procedure.

EXPERIMENTAL

HPLC Conditions—A liquid chromatograph[2] was used with a differential refractometer detector[3]. The column[4] was C_{18} reversed-phase micro silica gel, 30 cm × 3.9 mm. Column pressure was maintained at 42.18 kg/cm^2 (1 ml/min), and a 10-μl injection volume was used with a loop injector[5]. Chart speed was 2.5 cm/5 min, and attenuation on the refractive index detector was 9.6×10^{-5} unit full scale.

Clindamycin Hydrochloride—*Mobile Phase*—One gram of dioctyl sodium sulfosuccinate, 1 ml of formic acid, and 125 ml of water were added to a 500-ml volumetric flask. Methanol was added to volume.

Internal Standard Solution—A chloroform solution containing approximately 5 mg of testosterone propionate/ml was prepared.

Reference Standard and Bulk Drug Preparation—To each of two 4-ml shell vials was added 2 ml of internal standard solution, and the vials then were taken to dryness with a nitrogen stream. To one vial was added approximately 10 mg of clindamycin hydrochloride reference standard, and to the other was added approximately 10 mg of the bulk drug sample, both accurately weighed. Mobile phase, 1 ml, was added to each vial, which was swirled to dissolve the sample and internal standard.

Procedure—The sample and reference solutions were chromatographed using the same chromatographic conditions.

Clindamycin Palmitate Flavored Granules—*Mobile Phase*—One gram of dioctyl sodium sulfosuccinate, 0.77 g of ammonium acetate, 1.0 ml of acetic acid, and 37.5 ml of water were placed in a 500-ml volumetric flask. Methanol was added to volume.

Internal Standard Solution—A chloroform solution was prepared containing approximately 12 mg of methyl palmitate/ml.

Reference Standard Preparation—Approximately 148 mg of clindamycin palmitate hydrochloride reference standard was accurately weighed and transferred to a 32-ml stoppered centrifuge tube. Water, 6 ml, was added to dissolve the sample.

Sample Preparation—Approximately 2.4 g of flavored granules was accurately weighed and transferred to a 32-ml stoppered centrifuge tube. To the tube was added 4.5 ml of water, and the tube was swirled to dissolve the sample.

Procedure—To the sample and reference tubes were added 10.0 ml of internal standard solution and 1.0 ml of 30% (w/v) sodium carbonate solution. The tubes were shaken vigorously for 15 min and then centrifuged at 2500 rpm for 10 min. The top aqueous layer was removed by suction, and a 3-ml aliquot of the chloroform layer was filtered and dried using 1 g of anhydrous sodium sulfate.

A 1-ml aliquot of the dried chloroform layer was transferred to a 4-ml shell vial and evaporated to dryness with a nitrogen stream. Mobile phase, 1 ml, was added to the glass-like residue. The vial was swirled and soni-

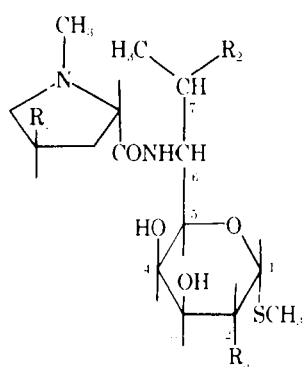

I: R_1 = *n*-propyl, R_2 = (*S*)-Cl, R_3 = OH
II: R_1 = *n*-propyl, R_2 = (*R*)-OH, R_3 = OH
III: R_1 = *n*-propyl, R_2 = (*S*)-Cl, R_3 = phosphate
IV: R_1 = *n*-propyl, R_2 = (*S*)-Cl, R_3 = palmitate
V: R_1 = *n*-propyl, R_2 = (*S*)-OH, R_3 = OH
VI: R_1 = *n*-propyl, R_2 = (*R*)-Cl, R_3 = OH
VII: R_1 = ethyl, R_2 = (*S*)-Cl, R_3 = OH

[1] The USAN name clindamycin phosphate refers to the 2-phosphate, and the generic name clindamycin palmitate refers to the 2-palmitate. Clindamycin is marketed as Cleocin by The Upjohn Co.

[2] DuPont model 830.

[3] Waters model R-401.

[4] Waters μBondapak.

[5] Valco.

0022-3549/78/0900-1254$01.00/0
© 1978, American Pharmaceutical Association

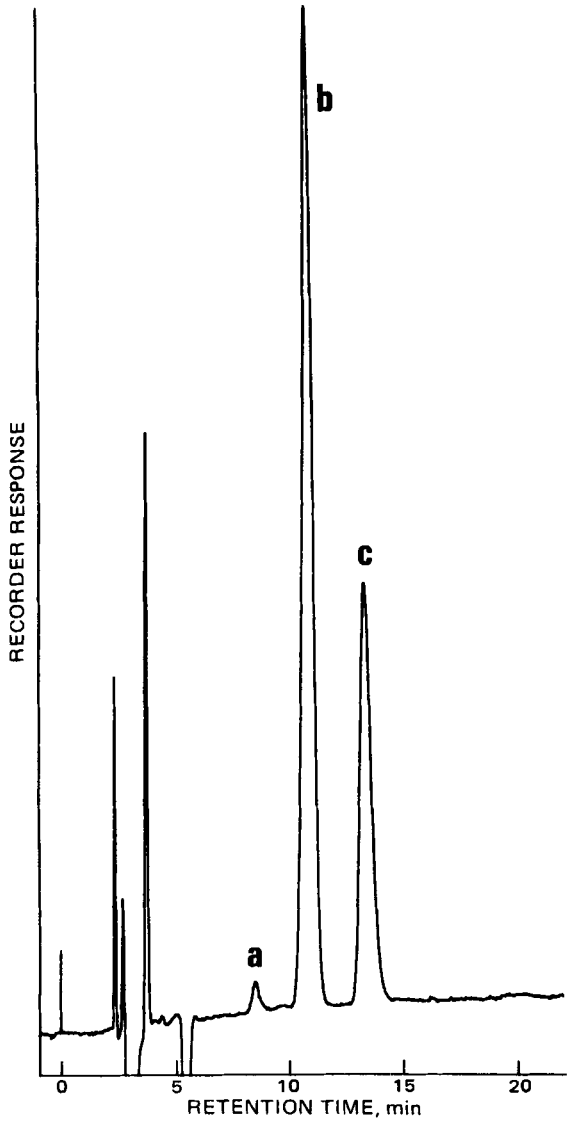

Figure 1—*Chromatogram of clindamycin B (a), clindamycin (b), and testosterone propionate used as the internal standard (c).*

cated to dissolve the residue, and the solution was chromatographed using the conditions already described.

Clindamycin Phosphate Sterile Solution—*Mobile Phase*—One gram of disodium ethylenediaminetetraacetate was added to approximately 200 ml of water in a beaker containing a magnetic stirring bar. The solution was adjusted to pH 5.8 with 5 *N* NaOH. Addition of base caused the disodium ethylenediaminetetraacetate to dissolve slowly. The solution was adjusted with water to 225 ml; then 275 ml of methanol was added, and the solution was mixed thoroughly.

Internal Standard Solution—A methanol–water (55:45) solution containing approximately 20 mg of propylparaben/ml was prepared.

Reference Standard Preparation—Approximately 20 mg of clindamycin phosphate reference was accurately weighed and transferred to a 4-ml shell vial. One milliliter of internal standard solution and 1 ml of methanol–water (55:45) were added and mixed.

Sample Preparation—Sterile solution clindamycin phosphate (3 ml, 150 mg base equivalents of clindamycin/ml) was added to a 25-ml volumetric flask and diluted to volume with methanol–water (55:45). Aliquots of 1 ml of this solution and 1 ml of internal standard solution were added to a 4-ml shell vial.

Procedure—Sample and reference solutions were chromatographed using the chromatographic conditions already described.

RESULTS AND DISCUSSION

Clindamycin Hydrochloride—The assay of clindamycin hydrochloride bulk drug involved no extraction. The compound was simply dissolved in mobile phase containing internal standard and chromatographed. A relative standard deviation of 1.0% was obtained on six samples of various weights. A typical chromatogram for clindamycin is shown in Fig. 1. Formulations of clindamycin for which an extraction step is needed can be assayed by this procedure using the extraction shown under *Experimental* for clindamycin palmitate flavored granules.

Compounds II, V, and VII were separated from clindamycin by this procedure; but VI, a relatively insignificant impurity as determined previously by GLC, was not. Relative retention times of these impurities using the mobile phase for this assay are listed in Table I.

Table I—Relative Retention Times (RRT) of Impurities and Degradation Products of Clindamycin Hydrochloride, Clindamycin Palmitate, and Clindamycin Phosphate Using the Mobile Phases in the *Experimental* Section

Compound	RRT
Clindamycin Hydrochloride	
Lincomycin B hydrochloride	0.49
Epilincomycin hydrochloride	0.55
Lincomycin hydrochloride	0.55
Clindamycin B hydrochloride	0.79
Clindamycin hydrochloride	1.00
Epiclindamycin hydrochloride	1.00
Testosterone propionate (internal standard)	1.25
Clindamycin Palmitate	
Clindamycin hydrochloride	0.23
Palmitic acid	0.44
Clindamycin 4-palmitate	0.59
Methyl palmitate (internal standard)	0.70
Clindamycin 3-palmitate	0.75
Clindamycin 2-palmitate	0.82
Clindamycin 2-palmitate	1.00
Clindamycin Phosphate	
Lincomycin 2-phosphate	0.45
Lincomycin hydrochloride	0.61
Clindamycin 2-phosphate	0.71
Clindamycin 3-phosphate	0.90
Clindamycin 4-phosphate	0.92
Clindamycin 2-phosphate	1.00
Propylparaben (internal standard)	1.29
Clindamycin hydrochloride	1.94

Clindamycin Palmitate Hydrochloride—An extraction step was not necessary to assay clindamycin palmitate hydrochloride bulk drug. A relative standard deviation of 0.8% was obtained on eight samples of bulk drug covering a broad range of sample weights. The mobile phase used for clindamycin palmitate contained a larger percent of methanol than the mobile phase used for clindamycin. The palmitate ester group in clindamycin palmitate increased the retention time, necessitating the use of a less polar mobile phase to give a normal elution time. An extraction was used for the flavored granules formulation of clindamycin palmitate. With a chloroform–sodium carbonate solution, clindamycin palmitate was extracted into the chloroform layer, leaving formulation ingredients such as dye and flavoring agents in the alkaline aqueous layer.

Recovery results on clindamycin palmitate added to the flavored granules placebo formulation are shown in Table II. Recovery was complete, and a relative standard deviation of 1.8% was obtained. The amount of water added to the dry flavored granules in the sample preparation (*Experimental*) was approximately the same as would be present in reconstituted flavored granules, making the procedure applicable to samples before and after reconstitution. A chromatogram of clindamycin

Table II—Recovery Results of Clindamycin Palmitate Added to Flavored Granule Excipients

Clindamycin Palmitate, mg	Excipients, g	Peak Height Ratio/ Weight, g		Recovery, %
149.85	2.309	6.084		98.0
134.20	2.236	6.101		98.3
145.50	2.251	5.999		96.6
152.14	2.279	6.317		101.8
131.12	2.232	6.153		99.1
147.56	2.268	6.209		100.0
			Average	99.0
			RSD	1.8%

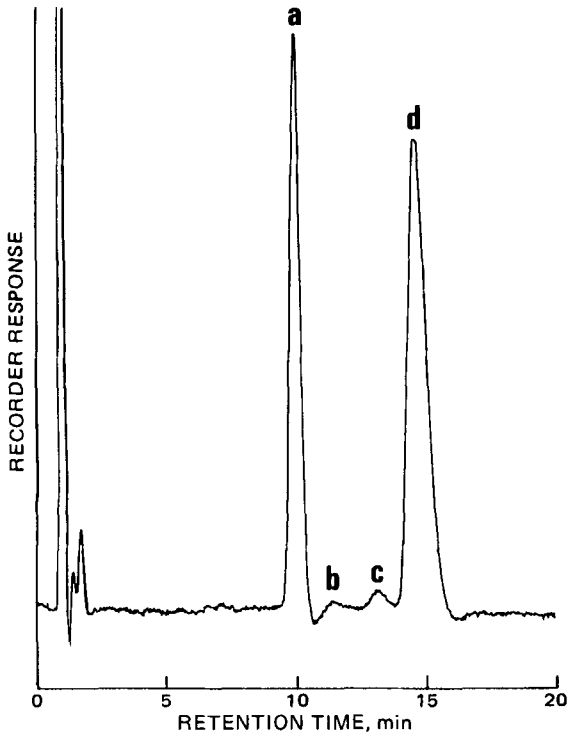

Figure 2—*Chromatogram of methyl palmitate used as the internal standard (a), clindamycin 2-palmitate (b), an unidentified peak (c), and clindamycin 2-palmitate extracted from flavored granules formulation (d).*

palmitate extracted from flavored granules is shown in Fig. 2. HPLC of placebo flavored granules showed no interfering peaks.

Since separation on reversed-phase columns varies from column to column, several columns were tried. Poor separation between methyl palmitate (internal standard) and clindamycin palmitate on a particular column was improved by increasing the water content of the mobile phase. A decrease in the amount of dioctyl sodium sulfosuccinate in the mobile phase decreased the separation. This behavior is due to differences in polarity of methyl palmitate and clindamycin palmitate.

Possible impurities or degradation products of clindamycin palmitate are clindamycin B 2-palmitate, clindamycin 3-palmitate, clindamycin 4-palmitate, epiclindamycin palmitate, clindamycin, and palmitic acid. Authentic samples were used to identify clindamycin B 2-palmitate, clindamycin, and palmitic acid chromatographically. A mixture of clindamycin 2-palmitate, clindamycin 3-palmitate, and clindamycin 4-palmitate was used to demonstrate the separation of these compounds (Fig. 3). The compounds were identified using the GLC procedure (3).

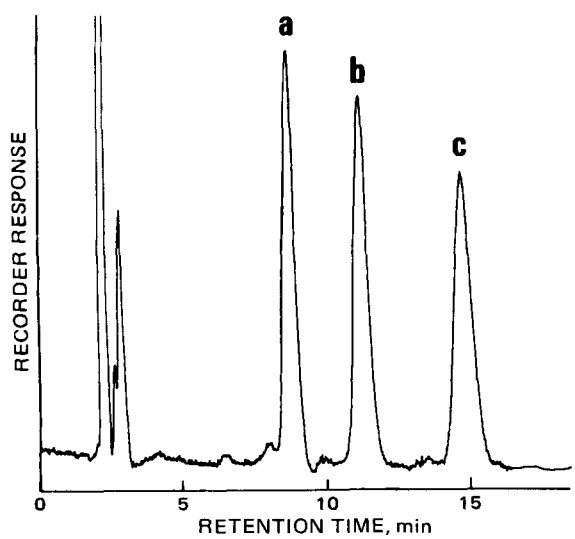

Figure 3—*Chromatogram of clindamycin 4-palmitate (a), clindamycin 3-palmitate (b), and clindamycin 2-palmitate (c).*

Table III—Assay Results on Sterile Solution Clindamycin Phosphate (150 mg Base Equivalents/ml)

Clindamycin Phosphate, mg/ml	Peak Height Ratio		Recovery, %
112.5	0.7487		102.1
127.5	0.8307		99.9
142.5	0.9150		98.5
157.5	1.0262		99.9
172.5	1.1294		97.6
187.5	1.2241		100.1
		Average	99.7
		RSD	1.2%

In Fig. 2, the unidentified peak eluting just prior to the clindamycin palmitate peak may be epiclindamycin palmitate. However, no authentic sample was available to confirm this finding. Although epiclindamycin is not separated from clindamycin (Table I) under conditions of the clindamycin assay, the decreased polarity of clindamycin palmitate may magnify differences in the molecule at the 7-position, thus producing separation. Table I shows the relative retention times of clindamycin palmitate impurities or degradation products using the mobile phase as described under *Experimental.*

Methyl palmitate, used as the internal standard, was chromatographed separately to check for possible impurities in this reagent, and a small amount of methyl stearate was detected in one lot. Methyl stearate has approximately the same retention time as clindamycin palmitate under the chromatographic conditions of this assay.

Clindamycin Phosphate—No extraction was necessary for the assay of sterile solution clindamycin phosphate. The sterile solution was diluted with water–methanol solvent, internal standard was added, and the solution was chromatographed. Assay results on six replicate samples of sterile solution clindamycin phosphate (150 mg clindamycin base equivalents/ml) are shown in Table III. An average recovery of 99.7% of theory was obtained with a relative standard deviation of 1.2%. Results showed linearity over the concentration range studied (75–125% of

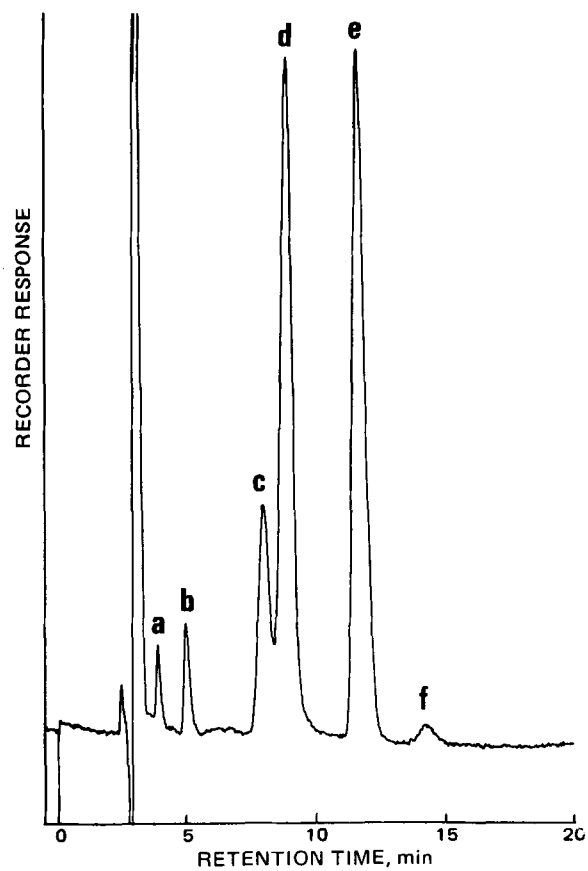

Figure 4—*Chromatogram of lincomycin 2-phosphate (a), benzyl alcohol (b), a mixture of clindamycin 3-phosphate and clindamycin 4-phosphate (c), clindamycin 2-phosphate (d), propylparaben used as the internal standard (e), and clindamycin (f).*

theory). Chromatography of the solution vehicle showed no interfering peaks. Benzyl alcohol, present in the sterile solution as a preservative, can be detected (Fig. 4) and quantitated.

Possible impurities or degradation products of clindamycin phosphate are free clindamycin, clindamycin 3-phosphate, clindamycin 4-phosphate, and clindamycin 2-phosphate. Since clindamycin is produced by chemical modification of lincomycin, the lincomyin analogs of the listed compounds are also possible impurities. Figure 4 shows a chromatogram of clindamycin phosphate with clindamycin, clindamycin 2-phosphate, clindamycin 3-phosphate, and clindamycin 4-phosphate present. Clindamycin 3-phosphate and clindamycin 4-phosphate are almost baseline separated from clindamycin 2-phosphate but are not separated from each other under the assay conditions.

The separation and elution order of the 2-, 3-, and 4-phosphate analogs of clindamycin are dependent on the pH and composition of the mobile phase. Mobile phase containing a greater percent of water causes clindamycin 4-phosphate to be eluted after clindamycin 2-phosphate while clindamycin 3-phosphate is eluted at the same time as clindamycin 2-phosphate. This modified mobile phase also shifts the clindamycin elution to a position before the internal standard peak.

Morozowich and Williams (5) chromatographed the clindamycin phosphate analogs on triethylaminoethylcellulose. The order of elution on the cellulose was 4-, 3-, and 2-phosphates. With the mobile phase of this assay, the relative retention times of possible impurities and degradation products are shown in Table I. If the mobile phase was adjusted to pH 6.0 or higher, the clindamycin phosphate peak tailed badly. If the pH was adjusted to 5.6 or less, the clindamycin phosphate peak broadened on the front side. Use of ammonium nitrate or sodium nitrate in the mobile phase did not improve the chromatography. To compensate for column-to-column variation, the amount of water in the mobile phases used for all three antibiotics was modified to give satisfactory chromatography for any particular column.

REFERENCES

(1) A. A. Forist, R. M. DeHaan, and C. M. Metzler, *J. Pharmacokinet. Biopharm.*, **1**, 89 (1973).

(2) T. F. Brodasky and F. F. Sun, *J. Pharm. Sci.*, **63**, 360 (1974).

(3) L. W. Brown, *ibid.*, **63**, 1597 (1974).

(4) Code of Federal Regulations, Title 21, Part 453, 658 (Apr. 1, 1977).

(5) W. Morozowich and R. G. Williams, *J. Pharm. Sci.*, **64**, 313 (1975).

pH–Solubility Profiles of Organic Carboxylic Acids and Their Salts

Z. T. CHOWHAN

Received October 18, 1977, from the *Institute of Pharmaceutical Sciences, Syntex Research, Palo Alto, CA 94304.* Accepted for publication January 6, 1978.

Abstract □ The solubilities of naproxen, 7-methylsulfinyl-2-xanthonecarboxylic acid, 7-methylthio-2-xanthonecarboxylic acid, and their sodium, potassium, calcium, and magnesium salts were determined as a function of pH. The results on the solubility of naproxen and its salts were in excellent agreement with the theoretical profiles describing the relationship between pH values of the solutions and the dissociation constant of the acid. The solubilities of the two xanthonecarboxylic acids were higher at higher pH values than the values calculated when complete dissociation in solution was assumed. The influence of the salt species on the solubility of organic carboxylic acids, at and above pH values of complete ionization, cannot be predicted even qualitatively from equations used for alkali and alkaline earth metal salts.

Keyphrases □ Solubility—naproxen, two xanthonecarboxylic acids, and various salts, as a function of pH □ Naproxen—and various salts, solubility as a function of pH □ Xanthonecarboxylic acids, substituted—and various salts, solubility as a function of pH □ Anti-inflammatory agents—naproxen and various salts, solubility as a function of pH

Organic carboxylic acids used as medicinal agents generally have poor water solubilities. Since solubility is an important factor in the overall drug absorption process, chemical stability, and formulation of dosage forms, salt-forming agents are used to increase the water solubility. Although salt formation results in an overall increase in solubility, no definitive quantitative methods of predicting the solubility of several salt species of the parent compound are available.

The influence of pH on the solubility of weak electrolytes was reported previously (1–3). The solubility interrelationships of the hydrochloride salt and free base of two amines were investigated extensively (4). Mathematical equations describing the total solubility at an arbitrary pH in terms of the independent solubilities of the hydrochloride and free base species and the dissociation constant of the salt were derived and fitted to the data with good results.

This paper discusses the solubility of three organic carboxylic acids as a function of pH and the salt species. The data were fitted to mathematical relationships similar to those used for organic hydrochlorides (4). The results of the solubility of naproxen and its salts were in excellent agreement with the theory. However, the solubilities of the xanthonecarboxylic acids and their salts were higher at higher pH values than those calculated when complete dissociation in solution was assumed. The effect of the salt species on the solubility of organic carboxylic acids, at and above pH values of complete ionization, cannot be predicted even qualitatively from equations used for alkali and alkaline earth metal salts.

EXPERIMENTAL

Materials—Naproxen [*d*-2-(6-methoxy-2-naphthyl)propionic acid], 7-methylsulfinyl-2-xanthonecarboxylic acid, 7-methylthio-2-xanthonecarboxylic acid, and their sodium salts were at least 99% pure[1]. Other chemicals were analytical reagent grade unless otherwise indicated.

Preparation of Naproxen Potassium—Potassium bicarbonate, 21.7 g, was added to a 500-ml round-bottom flask and dissolved in 26 ml of distilled water. An equimolar quantity of naproxen was added slowly to the flask, and the contents were refluxed for about 2 hr or until all naproxen dissolved. Then the contents of the flask were poured into a petri dish and allowed to crystallize. The crystals were filtered, rinsed with

[1] Institute of Organic Chemistry, Syntex Research, Palo Alto, CA 94304.

0022-3549/78/0900-1257$01.00/0

© 1978, American Pharmaceutical Association

theory). Chromatography of the solution vehicle showed no interfering peaks. Benzyl alcohol, present in the sterile solution as a preservative, can be detected (Fig. 4) and quantitated.

Possible impurities or degradation products of clindamycin phosphate are free clindamycin, clindamycin 3-phosphate, clindamycin 4-phosphate, and clindamycin 2-phosphate. Since clindamycin is produced by chemical modification of lincomycin, the lincomyin analogs of the listed compounds are also possible impurities. Figure 4 shows a chromatogram of clindamycin phosphate with clindamycin, clindamycin 2-phosphate, clindamycin 3-phosphate, and clindamycin 4-phosphate present. Clindamycin 3-phosphate and clindamycin 4-phosphate are almost baseline separated from clindamycin 2-phosphate but are not separated from each other under the assay conditions.

The separation and elution order of the 2-, 3-, and 4-phosphate analogs of clindamycin are dependent on the pH and composition of the mobile phase. Mobile phase containing a greater percent of water causes clindamycin 4-phosphate to be eluted after clindamycin 2-phosphate while clindamycin 3-phosphate is eluted at the same time as clindamycin 2-phosphate. This modified mobile phase also shifts the clindamycin elution to a position before the internal standard peak.

Morozowich and Williams (5) chromatographed the clindamycin phosphate analogs on triethylaminoethylcellulose. The order of elution on the cellulose was 4-, 3-, and 2-phosphates. With the mobile phase of this assay, the relative retention times of possible impurities and degradation products are shown in Table I. If the mobile phase was adjusted to pH 6.0 or higher, the clindamycin phosphate peak tailed badly. If the pH was adjusted to 5.6 or less, the clindamycin phosphate peak broadened on the front side. Use of ammonium nitrate or sodium nitrate in the mobile phase did not improve the chromatography. To compensate for column-to-column variation, the amount of water in the mobile phases used for all three antibiotics was modified to give satisfactory chromatography for any particular column.

REFERENCES

(1) A. A. Forist, R. M. DeHaan, and C. M. Metzler, *J. Pharmacokinet. Biopharm.*, **1**, 89 (1973).

(2) T. F. Brodasky and F. F. Sun, *J. Pharm. Sci.*, **63**, 360 (1974).

(3) L. W. Brown, *ibid.*, **63**, 1597 (1974).

(4) Code of Federal Regulations, Title 21, Part 453, 658 (Apr. 1, 1977).

(5) W. Morozowich and R. G. Williams, *J. Pharm. Sci.*, **64**, 313 (1975).

pH–Solubility Profiles of Organic Carboxylic Acids and Their Salts

Z. T. CHOWHAN

Received October 18, 1977, from the *Institute of Pharmaceutical Sciences, Syntex Research, Palo Alto, CA 94304.* Accepted for publication January 6, 1978.

Abstract □ The solubilities of naproxen, 7-methylsulfinyl-2-xanthonecarboxylic acid, 7-methylthio-2-xanthonecarboxylic acid, and their sodium, potassium, calcium, and magnesium salts were determined as a function of pH. The results on the solubility of naproxen and its salts were in excellent agreement with the theoretical profiles describing the relationship between pH values of the solutions and the dissociation constant of the acid. The solubilities of the two xanthonecarboxylic acids were higher at higher pH values than the values calculated when complete dissociation in solution was assumed. The influence of the salt species on the solubility of organic carboxylic acids, at and above pH values of complete ionization, cannot be predicted even qualitatively from equations used for alkali and alkaline earth metal salts.

Keyphrases □ Solubility—naproxen, two xanthonecarboxylic acids, and various salts, as a function of pH □ Naproxen—and various salts, solubility as a function of pH □ Xanthonecarboxylic acids, substituted—and various salts, solubility as a function of pH □ Anti-inflammatory agents—naproxen and various salts, solubility as a function of pH

Organic carboxylic acids used as medicinal agents generally have poor water solubilities. Since solubility is an important factor in the overall drug absorption process, chemical stability, and formulation of dosage forms, salt-forming agents are used to increase the water solubility. Although salt formation results in an overall increase in solubility, no definitive quantitative methods of predicting the solubility of several salt species of the parent compound are available.

The influence of pH on the solubility of weak electrolytes was reported previously (1–3). The solubility interrelationships of the hydrochloride salt and free base of two amines were investigated extensively (4). Mathematical equations describing the total solubility at an arbitrary pH in terms of the independent solubilities of the hydrochloride and free base species and the dissociation constant of the salt were derived and fitted to the data with good results.

This paper discusses the solubility of three organic carboxylic acids as a function of pH and the salt species. The data were fitted to mathematical relationships similar to those used for organic hydrochlorides (4). The results of the solubility of naproxen and its salts were in excellent agreement with the theory. However, the solubilities of the xanthonecarboxylic acids and their salts were higher at higher pH values than those calculated when complete dissociation in solution was assumed. The effect of the salt species on the solubility of organic carboxylic acids, at and above pH values of complete ionization, cannot be predicted even qualitatively from equations used for alkali and alkaline earth metal salts.

EXPERIMENTAL

Materials—Naproxen [*d*-2-(6-methoxy-2-naphthyl)propionic acid], 7-methylsulfinyl-2-xanthonecarboxylic acid, 7-methylthio-2-xanthonecarboxylic acid, and their sodium salts were at least 99% pure[1]. Other chemicals were analytical reagent grade unless otherwise indicated.

Preparation of Naproxen Potassium—Potassium bicarbonate, 21.7 g, was added to a 500-ml round-bottom flask and dissolved in 26 ml of distilled water. An equimolar quantity of naproxen was added slowly to the flask, and the contents were refluxed for about 2 hr or until all naproxen dissolved. Then the contents of the flask were poured into a petri dish and allowed to crystallize. The crystals were filtered, rinsed with

[1] Institute of Organic Chemistry, Syntex Research, Palo Alto, CA 94304.

0022-3549/78/0900-1257$01.00/0

© 1978, American Pharmaceutical Association

acetone, and dried in a vacuum oven at 50°. The crystals were ground with a pestle and mortar before solubility determinations.

Preparation of Naproxen Calcium—The calcium salt of naproxen was prepared by dissolving 3.5 g of calcium acetate monohydrate in 50 ml of distilled water and adding an equimolar quantity of naproxen sodium dissolved in 25 ml of distilled water. After overnight standing, the precipitate was filtered, washed with one part of water and one part of acetone, and dried in a vacuum oven at 50°.

Preparation of Naproxen Magnesium—The magnesium salt of naproxen was prepared by dissolving 4.2 g of the monohydrated magnesium chloride in 50 ml of distilled water and adding an equimolar quantity of naproxen sodium dissolved in 25 ml of distilled water. After overnight standing, the precipitate was filtered, washed with one part of water and one part of acetone, and dried in a vacuum oven at 50°.

Preparation of Potassium Salts of Xanthonecarboxylic Acids—Potassium bicarbonate, 5 g, was dissolved in 100 ml of distilled water, and 200 ml of 1-propanol was added. An equimolar quantity of the xanthonecarboxylic acid was added and refluxed for 2 hr. Then the reaction mixture was allowed to cool overnight. The crystallized salt was filtered, washed with 1-propanol, and dried in a vacuum oven at 50°.

Preparation of Calcium Salts of Xanthonecarboxylic Acids—The calcium salt of the xanthonecarboxylic acid was prepared by dissolving 2.5 g of the potassium salt in 400 ml of hot distilled water and adding an equimolar quantity of calcium acetate dissolved in 25 ml of distilled water. 1-Propanol, 50 ml, was added to the reaction mixture, and it was then allowed to stand overnight. The crystallized calcium salt was filtered, washed with methanol, and dried in a vacuum oven at 50°.

Preparation of Magnesium Salts of Xanthonecarboxylic Acids—The potassium salt of the xanthonecarboxylic acid, 2.5 g, was dissolved in 400 ml of hot distilled water, and an equimolar quantity of magnesium chloride dissolved in 4 ml of distilled water was added. The crystallized salt was allowed to stand overnight and was then filtered, washed with ethanol, and dried in a vacuum oven at 50°.

Solubility Determinations—The solubility of the carboxylic acids around pH 2.0 was determined by equilibrating the carboxylic acids in dilute hydrochloric acid solutions of different pH values at 25°. Naproxen solubility above pH 4.0 was determined by adding different amounts of dilute sodium hydroxide or dilute potassium hydroxide and equilibrating at 25° to obtain appropriate pH values. The naproxen salts were equilibrated at 25° in water containing small amounts of dilute sodium hydroxide to reach the desired pH values.

The solubility of 7-methylsulfinyl-2-xanthonecarboxylic acid was obtained similarly, except that only potassium hydroxide solution was used to titrate the acid and equilibrated to obtain intermediate pH values.

All four salts of the 7-methylthio-2-xanthonecarboxylic acid were used to obtain the pH profiles. Appropriate amounts of sodium hydroxide solution or dilute hydrochloric acid were used followed by equilibration at 25°. The pH values were determined after equilibrium had been reached.

The samples were prepared in culture tubes, wrapped with aluminum foil, and allowed to equilibrate in a vibromixer[2] at 25°. After equilibration, the samples were filtered through 13-mm diameter and 0.45-μm average pore size filters[3]. The solution pH was determined with a pH meter[4]. The concentrations of the solutions were determined spectrophotometrically. The UV absorbance was determined at 332 nm for naproxen, at 342 nm for 7-methylsulfinyl-2-xanthonecarboxylic acid, and at 262 nm for 7-methylthio-2-xanthonecarboxylic acid.

RESULTS AND DISCUSSION

The pH–solubility profiles for naproxen and its sodium, potassium, calcium, and magnesium salts are given in Fig. 1. The solid data points were obtained by adding appropriate amounts of dilute hydrochloric acid, dilute sodium hydroxide, or dilute potassium hydroxide and equilibrating to reach the final pH values. The open data points were obtained by adding the salts, adjusting the pH values with a small quantity of dilute hydrochloric acid or dilute sodium hydroxide, and then equilibrating.

The lines drawn through the data points were calculated from the simple equilibrium expression based on the dissociation of an organic acid. At any pH, the total concentration of a compound is the sum of the individual concentrations of its respective species. For example, at an intermediate pH, the total concentration of an organic acid is equal to

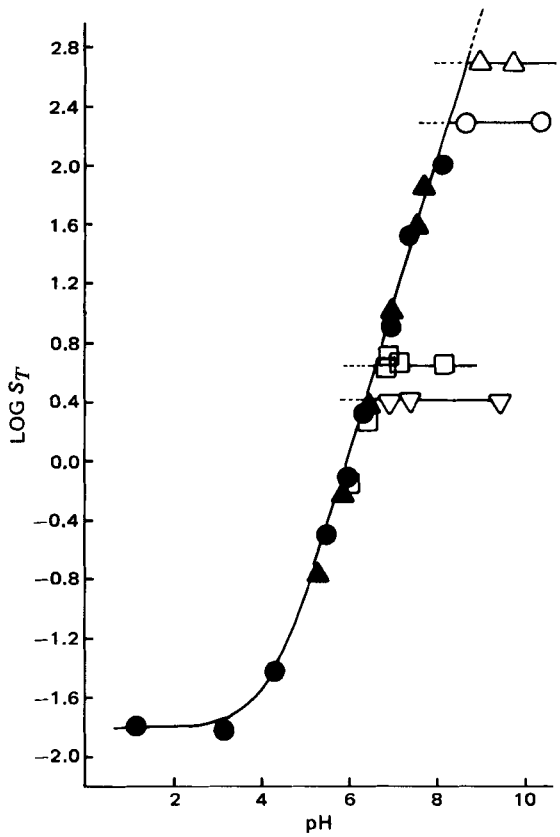

Figure 1—*The pH–solubility profiles for naproxen and its salts at 25°. Symbols represent experimental data: triangles, potassium salt; circles, sodium salt; squares, magnesium salt; and inverted triangles, calcium salt. The lines drawn through the data are theoretical and were calculated using 0.0159 mg/ml as the solubility of the free acid, 507.7 mg/ml as the solubility of the potassium salt, 196.7 mg/ml as the solubility of the sodium salt, 4.4 mg/ml as the solubility of the magnesium salt, 2.55 mg/ml as the solubility of the calcium salt, and 4.15 as the pKa′. Solid symbols indicate that the starting material was the acid, and open symbols indicate that the starting material was the salt.*

[XH] + [X$^-$], where [XH] and [X$^-$] are the concentrations of the unionized and ionized species, respectively. Equations similar to those derived for organic hydrochlorides (4) were used for the calculations at low pH and high pH values. At low pH, the following equations are applicable:

$$S_{T,\mathrm{pH}<\mathrm{pH}_{max}} = [\mathrm{XH}]_s + [\mathrm{X}^-] \qquad \text{(Eq. 1}a\text{)}$$

$$S_{T,\mathrm{pH}<\mathrm{pH}_{max}} = [\mathrm{XH}]_s \left(1 + \frac{K_a'}{[\mathrm{H_3O^+}]}\right) \qquad \text{(Eq. 1}b\text{)}$$

where S_T indicates total solubility, and subscript pH < pH_{max} indicates both that there is a pH of maximum solubility and that this equation is applicable for pH values less than this maximum. The subscript s indicates a saturated species, and K_a' is the apparent dissociation constant.

At high pH, where the solubility of the ionized species is limiting, the following equations hold:

$$S_{T,\mathrm{pH}>\mathrm{pH}_{max}} = [\mathrm{X}^-]_s + [\mathrm{XH}] \qquad \text{(Eq. 2}a\text{)}$$

$$S_{T,\mathrm{pH}>\mathrm{pH}_{max}} = [\mathrm{X}^-]_s \left(1 + \frac{[\mathrm{H_3O^+}]}{K_a'}\right) \qquad \text{(Eq. 2}b\text{)}$$

Equations 1*b* and 2*b* describe an independent curve limited by the solubility of one of the two species. Superposition of these curves produces a pH–solubility profile. The constraint that the solubility of either species cannot be exceeded determines which curve is applicable at a given pH.

At the juncture where two solubility curves (Eqs. 1*b* and 2*b*) intersect, both ionized and unionized species coexist at saturation. At the pH of maximum solubility, Eqs. 1*b* and 2*b* are simultaneously satisfied and can be set equal to one another. However, the resulting equation is of limited practical value because it involves small differences in large numbers (4).

[2] Chempac Inc., Hoboken, NJ 07030.
[3] Metricel GA-6, Gelman Instrument Co., Ann Arbor, MI 48103.
[4] Model 10, Corning Scientific Instruments.

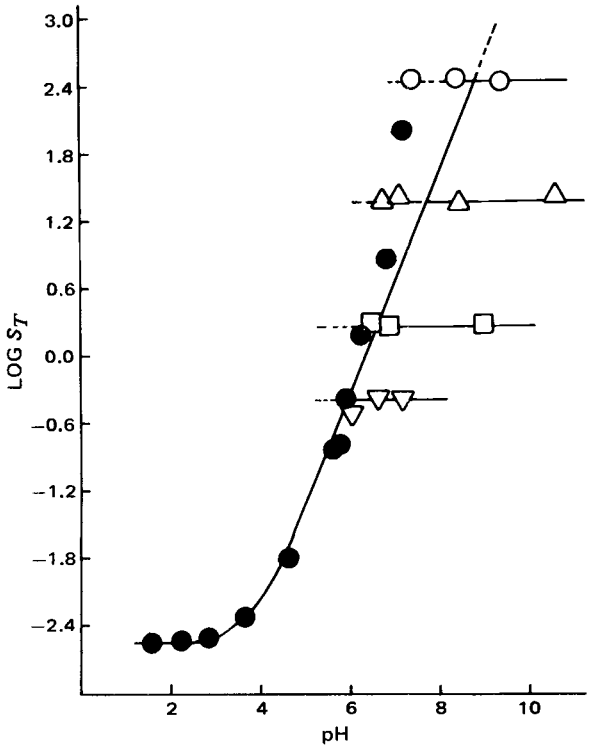

Figure 2—*The pH–solubility profiles for 7-methylsulfinyl-2-xanthonecarboxylic acid and its salts at 25°. Symbols represent experimental data: circles, potassium salt; triangles, sodium salt; squares, calcium salt; and inverted triangles, magnesium salt. The lines drawn through the data are theoretical and were calculated using 0.00274 mg/ml as the solubility of the free acid, 270.0 mg/ml as the solubility of the potassium salt, 23.84 mg/ml as the solubility of the sodium salt, 1.855 mg/ml as the solubility of the calcium salt, 0.35 mg/ml as the solubility of the magnesium salt, and 3.8 as the pKa′. Solid symbols indicate that the starting material was the acid, and open symbols indicate that the starting material was the salt.*

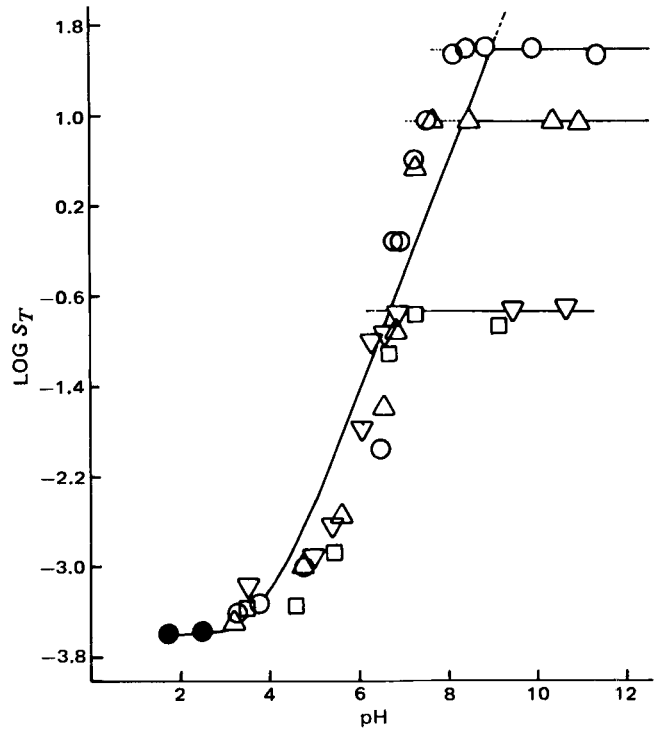

Figure 3—*The pH–solubility profiles for 7-methylthio-2-carboxylic acid and its salts at 25°. Symbols represent experimental data: circles, sodium salt; triangles, potassium salt; squares, magnesium salt; and inverted triangles, calcium salt. The lines drawn through the data are theoretical and were calculated using 0.00026 mg/ml as the solubility of the free acid, 37.2 mg/ml as the solubility of the sodium salt, 8.87 mg/ml as the solubility of the potassium salt, 0.185 mg/ml as the solubility of magnesium and calcium salts, and 3.8 as the pKa′. Solid symbols indicate that the starting material was the acid, and open symbols indicate that the starting material was the salt.*

The pH–solubility profiles for 7-methylsulfinyl-2-xanthonecarboxylic acid and its sodium, potassium, calcium, and magnesium salts are given in Fig. 2. Equations 1*b* and 2*b* were used to calculate the lines. The theoretical lines and the data points show a good fit for lower pH values and for the calcium and magnesium salts. However, the solubilities of the sodium and potassium salts at higher pH values are considerably higher compared to the calculated values.

The solubilities of 7-methylthio-2-xanthonecarboxylic acid and its sodium, potassium, calcium, and magnesium salts are given in Fig. 3. The lines drawn through the data points were calculated as described. Comparisons between theory and experiment indicate some deviations, both at low and high pH values.

Excellent agreement between theory and experiment was obtained for naproxen, although concentrations rather than activities were used in the calculations and pKa′ is not the thermodynamic value. This finding suggests that the higher solubilities of xanthonecarboxylic acids at higher pH values could be due to the complex formation or hydration of the salts. The presence of charged complexes having a different proportion of ions or the presence of undissociated species in solution results in a greater salt solubility than that calculated when complete dissociation in solution is assumed. If this is so, the solubilities predicted by Eq. 1*b* would be lower than the experimental values. Similar deviations were reported (3) for sulfadiazine.

A general prediction of the effect of salt species on the solubility of organic carboxylic acids is not possible (Figs. 1–3). The order of decreasing solubility of naproxen salts is $K^+ > Na^+ > Mg^{2+} > Ca^{2+}$; the order for 7-methylsulfinyl-2-xanthonecarboxylic acid salts is $K^+ > Na^+ > Ca^{2+} > Mg^{2+}$; and the order for 7-methylthio-2-xanthonecarboxylic acid is $Na^+ > K^+ > Ca^{2+} = Mg^{2+}$.

The solubility is determined by the molar free energy change on dissolving a solid in solution. For a monovalent organic salt, this molar free energy change is equal to the molar free energy change of hydration of the cation plus the anion, minus the molar free energy change for the formation of crystal lattice. Mathematically, this change is expressed by:

$$\Delta F_{\text{solution}} = \Delta F_{\text{hx}^-} + \Delta F_{\text{hc}^+} - \Delta F_{\text{lattice}} \qquad \text{(Eq. 3)}$$

where $\Delta F_{\text{solution}}$ is the molar free energy change on dissolving a solid in solution, ΔF_{hx^-} is the molar free energy change of hydration of the anion, ΔF_{hc^+} is the molar free energy change of hydration of the cation, and $\Delta F_{\text{lattice}}$ is the molar free energy change for the formation of the crystal lattice.

Equations describing the change in solubility in a series of similar salts in which the anion is varied and the cation is kept constant, or the cation is varied and the anion is kept constant, were derived (5). These equations represent the differences between two quantities: the change in the hydration energy and the change in the lattice energy. On increasing the value of the radius of the cation at a constant anion radius, both the hydration and the lattice energies decrease. The change in solubility depends on the amount by which these two quantities decrease. If the lattice energy decreases by a larger amount than the hydration energy, a solubility increase occurs. If the lattice energy decreases by a smaller amount than the hydration energy, a solubility decrease occurs. Similar behavior occurs on increasing the radius of the anion at a constant cation radius. For those salts in which the lattice energies are much greater than the hydration energies (and which, as a result, have slight solubility), changes in the ionic radii influence solubility mainly through changes in the lattice energies. Conversely, changes in solubility reflect changes primarily in the hydration energies when the hydration energies are much larger than the lattice energies (highly soluble salts).

The radii of the anions of organic carboxylic acids are large and, based on the calculated changes in solubility of alkali metal salts, the solubility of the potassium salt should be lower than the sodium salt. The data indicate that the solubility of the potassium salts of one of the three carboxylic acids is lower than that of the sodium salt. Similarly, based on the calculated changes in the solubility of alkaline earth metal ions, the solubility of the magnesium salt should be larger than that of the calcium salt. The solubility of the magnesium salt of one of the carboxylic acids is larger than that of the calcium salt. Lower or same solubility of the

magnesium salt of the other two carboxylic acids compared to the calcium salt again suggests that qualitative trends reported for alkali halides or alkaline earth metal salts are not seen in organic carboxylic acid salts.

In view of these results, the equations (5) predicting only qualitatively the solubilities of a series of inorganic salts cannot be used for organic salts. The solubility of several salts of the organic compound of interest should be determined experimentally, and this parameter should be considered in the selection of the most suitable drug entity for further development.

REFERENCES

(1) T. Higuchi, M. Gupta, and L. W. Busse, *J. Am. Pharm. Assoc., Sci. Ed.*, **42**, 157 (1953).

(2) R. Anderson, *Aust. J. Pharm.*, **42**, 919 (1961).

(3) F. S. Hom and J. Autian, *J. Am. Pharm. Assoc., Sci. Ed.*, **45**, 608 (1956).

(4) S. F. Kramer and G. L. Flynn, *J. Pharm. Sci.*, **61**, 1896 (1972).

(5) "Treatise on Analytical Chemistry," I. M. Kolthoff, P. J. Elving, and E. B. Sandell, Eds., The Interscience Encyclopedia, Interscience, New York, N.Y., 1959.

ACKNOWLEDGMENTS

The author thanks Professor G. L. Flynn of the University of Michigan for encouragement and interest in this work. He also thanks R. Pritchard, A. Amaro, T. Rumolo, and E. Linn for the laboratory work.

Preservation of Solubilized and Emulsified Systems I: Correlation of Mathematically Predicted Preservative Availability with Antimicrobial Activity

S. J. A. KAZMI * **and A. G. MITCHELL** ˣ

Received February 14, 1977, from the *Faculty of Pharmaceutical Sciences, University of British Columbia, Vancouver, British Columbia, Canada V6T 1W5.* Accepted for publication January 13, 1978. *Present address: Faculty of Pharmacy, University of El-Fateh, Tripoli, Libya.

Abstract □ Mathematical models were investigated for the distribution and antimicrobial activity of chlorocresol in solubilized and emulsified systems stabilized with a nonionic surfactant. The concentration of free preservative in the solubilized systems was described adequately by an equation widely used to describe the binding of small molecules to macromolecules. For the emulsions, this equation was combined with an expression for the partitioning of the preservative between the oil and water phases. It was confirmed that short-term antimicrobial activity can be related to the free (unbound) preservative concentration in the aqueous phase and that preservative solubilized within the surfactant micelles or partitioned into the oil phase does not contribute to short-term preservation.

Keyphrases □ Chlorocresol—in solubilized and emulsified systems, mathematical model relating phase distribution to antimicrobial activity □ Models, mathematical—relating phase distribution to antimicrobial activity, chlorocresol in solubilized and emulsified systems □ Antimicrobial activity—chlorocresol in solubilized and emulsified systems, related to phase distribution with mathematical model □ Distribution, phase—chlorocresol in solubilized and emulsified systems, related to antimicrobial activity with mathematical model

The ability of preservatives to prevent microbial spoilage of solubilized and emulsified products is normally assessed by empirical tests involving inoculation of the finished product and examination during prolonged storage. Such methods are laborious, time consuming, and usually qualitative.

Mathematical models have been developed that predict the preservative concentration required in a surfactant solution (1–3) or an emulsion (2–9). These models were based on the assumption that antimicrobial activity is a function of the free (unbound or nonmicellar) preservative concentration in the aqueous phase.

Attempts to correlate the predictions made by mathematical equations with the observed antimicrobial activity of preservatives in solubilized systems generally confirmed that the antimicrobial action is largely a function of the free preservative concentration and that preservative associated with the surfactant micelles has little or no activity (10–14).

Although much work has been done on the distribution and antimicrobial activity of preservatives in oil–water systems (15–21), few studies have been made in oil-in-water emulsions stabilized with nonionic surfactants (5, 6). In simple oil-in-water dispersions, the antimicrobial activity appears to depend mainly on the preservative concentration in the aqueous phase while preservative partitioned into the oil phase is biologically inactive. However, Bean *et al.* (18, 20) suggested that preservative adsorbed at the oil–water interface also contributes to the overall activity; an increase in the oil–water ratio results in an increase in interfacial area and, therefore, should enhance the antimicrobial activity. Since the interfacial area in oil-in-water emulsions is much larger than in simple oil-in-water dispersions, antimicrobial activity might increase enormously with an increase in the oil–water ratio.

In this study, a physicochemical and microbiological evaluation of two mathematical models, one for surfactant solutions and the other for emulsions, was made to test their utility. The influence on antimicrobial activity of factors such as surfactant concentration, oil–water ratio, and interfacial area was given particular attention.

THEORETICAL

Garrett (3) suggested that the binding of preservatives with surfactant macromolecules can be quantified using expressions similar to those established for the protein binding of drugs.

Kazmi and Mitchell (1) compared various methods of expressing the interaction of a number of commonly used preservatives with the nonionic surfactant cetomacrogol and found that protein binding equations such

0022-3549/78/0900-1260$01.00/0

© 1978, American Pharmaceutical Association

magnesium salt of the other two carboxylic acids compared to the calcium salt again suggests that qualitative trends reported for alkali halides or alkaline earth metal salts are not seen in organic carboxylic acid salts.

In view of these results, the equations (5) predicting only qualitatively the solubilities of a series of inorganic salts cannot be used for organic salts. The solubility of several salts of the organic compound of interest should be determined experimentally, and this parameter should be considered in the selection of the most suitable drug entity for further development.

REFERENCES

(1) T. Higuchi, M. Gupta, and L. W. Busse, *J. Am. Pharm. Assoc., Sci. Ed.*, **42**, 157 (1953).

(2) R. Anderson, *Aust. J. Pharm.*, **42**, 919 (1961).

(3) F. S. Hom and J. Autian, *J. Am. Pharm. Assoc., Sci. Ed.*, **45**, 608 (1956).

(4) S. F. Kramer and G. L. Flynn, *J. Pharm. Sci.*, **61**, 1896 (1972).

(5) "Treatise on Analytical Chemistry," I. M. Kolthoff, P. J. Elving, and E. B. Sandell, Eds., The Interscience Encyclopedia, Interscience, New York, N.Y., 1959.

ACKNOWLEDGMENTS

The author thanks Professor G. L. Flynn of the University of Michigan for encouragement and interest in this work. He also thanks R. Pritchard, A. Amaro, T. Rumolo, and E. Linn for the laboratory work.

Preservation of Solubilized and Emulsified Systems I: Correlation of Mathematically Predicted Preservative Availability with Antimicrobial Activity

S. J. A. KAZMI * **and A. G. MITCHELL** ˣ

Received February 14, 1977, from the *Faculty of Pharmaceutical Sciences, University of British Columbia, Vancouver, British Columbia, Canada V6T 1W5.* Accepted for publication January 13, 1978. *Present address: Faculty of Pharmacy, University of El-Fateh, Tripoli, Libya.

Abstract □ Mathematical models were investigated for the distribution and antimicrobial activity of chlorocresol in solubilized and emulsified systems stabilized with a nonionic surfactant. The concentration of free preservative in the solubilized systems was described adequately by an equation widely used to describe the binding of small molecules to macromolecules. For the emulsions, this equation was combined with an expression for the partitioning of the preservative between the oil and water phases. It was confirmed that short-term antimicrobial activity can be related to the free (unbound) preservative concentration in the aqueous phase and that preservative solubilized within the surfactant micelles or partitioned into the oil phase does not contribute to short-term preservation.

Keyphrases □ Chlorocresol—in solubilized and emulsified systems, mathematical model relating phase distribution to antimicrobial activity □ Models, mathematical—relating phase distribution to antimicrobial activity, chlorocresol in solubilized and emulsified systems □ Antimicrobial activity—chlorocresol in solubilized and emulsified systems, related to phase distribution with mathematical model □ Distribution, phase—chlorocresol in solubilized and emulsified systems, related to antimicrobial activity with mathematical model

The ability of preservatives to prevent microbial spoilage of solubilized and emulsified products is normally assessed by empirical tests involving inoculation of the finished product and examination during prolonged storage. Such methods are laborious, time consuming, and usually qualitative.

Mathematical models have been developed that predict the preservative concentration required in a surfactant solution (1–3) or an emulsion (2–9). These models were based on the assumption that antimicrobial activity is a function of the free (unbound or nonmicellar) preservative concentration in the aqueous phase.

Attempts to correlate the predictions made by mathematical equations with the observed antimicrobial activity of preservatives in solubilized systems generally confirmed that the antimicrobial action is largely a function of the free preservative concentration and that preservative associated with the surfactant micelles has little or no activity (10–14).

Although much work has been done on the distribution and antimicrobial activity of preservatives in oil–water systems (15–21), few studies have been made in oil-in-water emulsions stabilized with nonionic surfactants (5, 6). In simple oil-in-water dispersions, the antimicrobial activity appears to depend mainly on the preservative concentration in the aqueous phase while preservative partitioned into the oil phase is biologically inactive. However, Bean *et al.* (18, 20) suggested that preservative adsorbed at the oil–water interface also contributes to the overall activity; an increase in the oil–water ratio results in an increase in interfacial area and, therefore, should enhance the antimicrobial activity. Since the interfacial area in oil-in-water emulsions is much larger than in simple oil-in-water dispersions, antimicrobial activity might increase enormously with an increase in the oil–water ratio.

In this study, a physicochemical and microbiological evaluation of two mathematical models, one for surfactant solutions and the other for emulsions, was made to test their utility. The influence on antimicrobial activity of factors such as surfactant concentration, oil–water ratio, and interfacial area was given particular attention.

THEORETICAL

Garrett (3) suggested that the binding of preservatives with surfactant macromolecules can be quantified using expressions similar to those established for the protein binding of drugs.

Kazmi and Mitchell (1) compared various methods of expressing the interaction of a number of commonly used preservatives with the nonionic surfactant cetomacrogol and found that protein binding equations such

0022-3549/78/0900-1260$01.00/0

© 1978, American Pharmaceutical Association

as Eq. 1 could be used to describe the binding data:

$$r = \frac{nK[D_f]}{1 + K[D_f]} \quad \text{(Eq. 1)}$$

where r is the molar ratio of bound preservative to total surfactant, $[D_b]/[M]$; n is the number of independent binding sites on the surfactant molecules; K is the association constant for the binding of a molecule of preservative to one of these sites; and $[D_f]$ is the concentration of free preservative.

Equation 1 can be rearranged as:

$$\frac{r}{[D_f]} = nK - rK \quad \text{(Eq. 2)}$$

According to this simple model, a Scatchard plot (22) of $r/[D_f]$ against r should give a straight line from which the binding constants n and K can be obtained. However, Scatchard plots for the preservative–surfactant systems studied were nonlinear (1).

Failure to obtain a straight line is common in protein binding studies and has been attributed to factors including heterogeneity of binding sites, interaction between sites, and initiation of confirmation changes (23). Hence, the binding constants were determined from the slope of Scatchard plots in the concentration range of free preservative appropriate for antimicrobial activity (1). The total preservative concentration, $[D_t]$, necessary to provide this concentration of free preservative in the aqueous phase of the solubilized system was than calculated using a rearrangement of Eq. 1:

$$[D_t] = [D_f]\left[1 + \frac{nK[M]}{1 + K[D_f]}\right] \quad \text{(Eq. 3)}$$

Expansion of Eq. 1 according to the theory of multiple equilibria (23) with the assumption of two sets of independent binding sites was shown later (2, 9, 24) to characterize the interaction over a wide range of surfactant and preservative concentrations:

$$r = \frac{n_1K_1[D_f]}{1 + K_1[D_f]} + \frac{n_2K_2[D_f]}{1 + K_2[D_f]} \quad \text{(Eq. 4)}$$

where Set 1 has n_1 sites and an association constant K_1 and Set 2 has n_2 sites and an association constant K_2. The molar binding ratio, r, and the equilibrium concentration of free preservative, $[D_f]$, were determined experimentally for various values of $[D_t]$ and $[M]$, and the binding constants were computed from Eq. 4 using a nonlinear regression program to curve fit r as a function of $[D_f]$ (Langmuir-type plot) and $r/[D_f]$ as a function of r (Scatchard plot). Rearrangement of Eq. 4 gives Eq. 5, from which the total preservative concentration can be calculated for any value of $[D_f]$ or $[M]$ (9):

$$[D_t] = [D_f]\left[1 + \frac{n_1K_1[M]}{1 + K_1[D_f]} + \frac{n_2K_2[M]}{1 + K_2[D_f]}\right] \quad \text{(Eq. 5)}$$

The interaction of a preservative with a mixture of two surfactants also can be predicted from the binding constants that characterize the interaction with each surfactant comprising the mixture (2). Nevertheless, as pointed out elsewhere (9), a fit of the experimental data to Eq. 4 does not prove that the surfactant–preservative interaction occurs by any particular mechanism. Although the equations quantify the interaction and permit predictions to be made over a wide range of surfactant and preservative concentrations, caution should be exercised in ascribing a physical mechanism to the interaction based on the numerical values of n and K. Indeed, Schellman *et al.* (25), in discussing the results of their protein binding studies, emphasized the point that only the product nK has theoretical significance without knowledge of the heterogeneity of the binding sites.

As discussed previously (1), since the interaction occurs between the solute and surfactant micelles rather than monomer surfactant molecules, $[M]$ in Eqs. 1–5 should be the concentration of micelles, n the number of binding sites per micelle, and K the association constant for reaction with the micelles. From a practical viewpoint, however, it is more convenient to express $[M]$ in terms of the total surfactant concentration.

Additional terms can be included in Eq. 5 to give Eq. 6, from which the total concentration of preservative, $[D_t]$, can be calculated for emulsions:

$$[D_t] = [D_f]\left[\frac{1 + n_1K_1[M]}{1 + K_1[D_f]} + \frac{n_2K_2[M]}{1 + K_2[D_f]} + K_w{}^oq\right] \Big/ (q + 1) \quad \text{(Eq. 6)}$$

where $K_w{}^o$ is the oil–water partition coefficient and q is the oil–water ratio. In Eq. 6, the term $[M]$ is strictly the concentration of surfactant available in the aqueous phase for interaction with the preservative and not the total concentration.

In a complex dispersion, the total surfactant concentration will not be available for this interaction. For example, some surfactant will be adsorbed at the oil–water interface, some surfactant may partition into the oil phase, and some surfactant will exist in monomer (nonmicellar) form. Each of these factors will reduce the amount of surfactant available for binding with the preservative and may affect the oil–water partition coefficient. The monomer surfactant concentration will be approximately equal to the critical micelle concentration, which for a nonionic surfactant such as cetomacrogol is sufficiently low (26) to be neglected at the surfactant concentrations used in this work.

Garrett (3) suggested that an ultracentrifuge technique be used to determine the "operative partition coefficient" in the actual emulsion system and the equilibrium concentration of surfactant in the aqueous phase as a function of the total surfactant concentration. However, studies using a three-chamber dialysis cell (7), which permitted direct estimation of the distribution of a preservative and surfactant between the oil, micellar, and aqueous phases of an emulsion, demonstrated excellent agreement between observed and predicted values of $[D_b]$ when the initial (*i.e.*, total) surfactant concentration and $K_w{}^o$, obtained by simple partition between the oil and water phases, were substituted into the equation.

In this work, the validity of Eqs. 5 and 6 was first confirmed by physicochemical means. Then the equations were used to calculate the total preservative concentration required in various solubilized and emulsified dispersions to provide a given free preservative concentration in the aqueous phase. The antimicrobial activities of the various dispersions containing different concentrations of total preservative but the same free concentration were then compared by following the death rate of *Escherichia coli* by viable counting using a membrane filtration technique.

EXPERIMENTAL

Materials—Mineral oil (light liquid paraffin BPC[1]), trypticase soy broth[2], trypticase soy agar[2], peptone[3], and reagent grade sodium chloride[4] were used as received. Chlorocresol, cetomacrogol 1000 BPC[5], and silicone rubber membrane were as described previously (24). Deionized glass-distilled water was used throughout, and all studies were carried out at 25°.

Interactions of Chlorocresol with Cetomacrogol—The interaction of chlorocresol with cetomacrogol was studied by equilibrium dialysis, using silicone rubber as the dialysis membrane. The chlorocresol was analyzed spectrophotometrically at 280 nm, and the binding constants (n and K) were computed as described previously (9, 24).

Distribution of Chlorocresol between Mineral Oil and Water and in Mineral Oil Emulsions Stabilized with Cetomacrogol—The experimental procedures for the determination of distribution coefficients and the dialysis technique for studying the distribution of a preservative in emulsions were described previously (7).

Microbiological Procedures—*Sterilization of Experimental Solutions*—Trypticase soy broth and trypticase soy agar were rehydrated and sterilized according to the specifications of the manufacturer. Deionized glass-distilled water, 0.85% saline, and peptone water (peptone, 1.0 g; sodium chloride, 8.5 g, and distilled water to 1 liter) were sterilized by autoclaving at 121° for 15 min. Aqueous chlorocresol solutions and cetomacrogol solutions, with and without chlorocresol, were sterilized by passing the solutions through sterile 0.45-μm filters[6]. Mineral oil was sterilized by dry heat at 160° for 1 hr.

Preparation of Sterile Mineral Oil Emulsions—Sterile mineral oil and cetomacrogol solutions, with or without chlorocresol, were mixed in various ratios and passed through sterile hand homogenizers at least five times to ensure the formation of stable emulsions. All operations were carried out aseptically under a laminar flow hood[7].

For emulsions containing chlorocresol, the mineral oil and cetomacrogol solutions were mixed prior to homogenization and agitated in a

[1] British Drug Houses, Poole, England.
[2] B.V.L., Division of Bioquest.
[3] Difco Laboratories.
[4] Mallinckrodt Chemical Works.
[5] Texofor A1P, Glovers Chemical Ltd., Leeds, England; $CH_3(CH_2)_m = (OCH_2CH_2)_n$ OH, where m may be 15 or 17 and n may be 20–24. The molecular weight was taken as 1300.
[6] HA, Millipore Corp.
[7] Bioquest Biological Cabinet, Division of Bioquest.

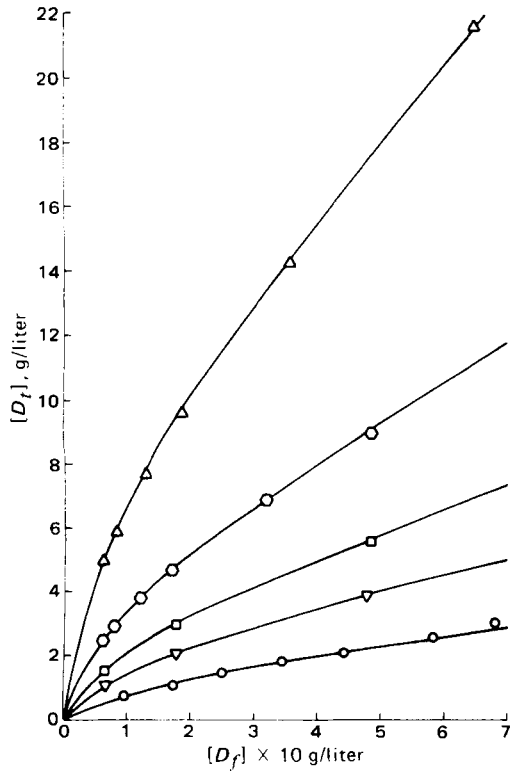

Figure 1—*Variation of free chlorocresol concentration,* $[D_f]$, *with total chlorocresol concentration,* $[D_t]$, *for the interaction of chlorocresol with cetomacrogol. Key [cetomacrogol concentrations (percent)]:* ○, *1.0;* ▽, *2.0;* □, *3.0;* ○, *5.0; and* △, *10.0. The points are experimental; the curves were calculated using Eq. 5 where* $n_1 = 0.697$, $n_2 = 136$, $K_1 = 1.87 \times 10^3$ *liters/mole, and* $K_2 = 2.09$ *liters/mole.*

water bath maintained at 25° for about 3 days to allow the preservative to equilibrate between the various phases of the emulsion.

Organism—Replicate slants of *E. coli* (ATCC 8739) were used in all experiments. The slants were prepared from a single colony and stored in a refrigerator at 4°.

Bacterial Cultures—An aliquot (5 ml) of trypticase soy broth was inoculated from a fresh slant, and the culture was allowed to grow for 12 hr at 37° in an incubator. A 0.2-ml sample of this culture was transferred to 50 ml of fresh trypticase soy broth and incubated at 37° for 12 hr. This final *E. coli* suspension was used to prepare a series of dilutions in trypticase soy broth for the construction of a standard curve of absorbance at 550 nm *versus* the number of viable organisms counted using a pour-plate technique. The purity of the culture was checked using Gram's staining procedures and examination of the growth on MacConkey agar.

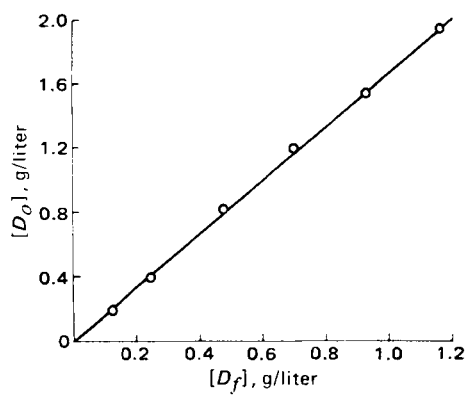

Figure 2—*Concentration of preservative in oil,* $[D_o]$, *as a function of free preservative in the aqueous phase,* $[D_f]$, *for the distribution of chlorocresol between mineral oil and water. The points are experimental; the curve was fitted using least-squares method. The slope =* $1.67 = K_w^o$.

Table I—Comparison of Required with Observed Chlorocresol Concentrations in Mineral Oil Emulsions Stabilized with Cetomacrogol[a]

Oil–Water Ratio	$M \times 10^3$ $[D_t]$ Calculated from Eq. 6	$[D_f]$ Required	$[D_f]$[b] Observed
0.2	27.15	2.45	2.45
0.5	22.54	2.45	2.32
1.0	17.93	2.45	2.35

[a] Cetomacrogol concentration = 23.08×10^{-3} *M*. [b] Mean of three observations.

Preparation of Standard E. coli *Suspension*—An aliquot of the culture was diluted with trypticase soy broth, and the absorbance was measured at 550 nm. From the absorbance and the dilution factor, the concentration of *E. coli* in the culture was determined from the standard curve. The culture was diluted with 0.85% saline to produce the desired number of organisms per milliliter of suspension.

Viable Counting Using Pour-Plate Technique—Culture samples were diluted with an appropriate volume of sterilized 0.85% saline to produce a final count of 50–200 colonies/plate. From these dilutions, 1-ml aliquots were pipetted into each of three petri plates; then 12 ml of sterile trypticase soy agar, kept at 45° in a water bath, was poured into each plate. The plates were rotated to disperse the organisms and incubated for 48 hr at 37°. The colonies were counted using a colony counter[8].

Viable Counting Using Membrane Filtration Technique—A six-place sterility test manifold unit with 47-mm hydrophobic-edge filters[9] (0.45 μm) was used. Details of the filtration assembly, sterilization, and operation are given elsewhere (27). All operations were performed under a laminar flow hood.

Samples were diluted with an appropriate volume of sterile normal saline to produce 100–200 colonies/filter. From these dilutions, 1-ml aliquots were pipetted into funnels containing approximately 10 ml of peptone water, and vacuum was applied immediately to draw the sample through the filter. The filter was washed five times with 25-ml portions of peptone water, and vacuum was applied immediately each time. After filtration, the filter was transferred to trypticase soy agar plates and incubated at 37° for 24 hr; then the colonies were counted. For chlorocresol-treated *E. coli*, the plates were incubated for an additional 12 hr, and colonies were recounted to check for the emergence of new colonies.

Bactericidal Activity of Chlorocresol in Water, Aqueous Solutions of Cetomacrogol, and Mineral Oil Emulsions Stabilized with Cetomacrogol—The aqueous solutions, surfactant solutions, and freshly homogenized emulsions containing chlorocresol were agitated in a water bath maintained at 25° to equilibrate the preservative between the various phases. After about 3 hr, 41.5 ml of each dispersion was inoculated with 0.5 ml of standard *E. coli* culture to give 10^6 organisms/ml. Changes in the preservative concentration, surfactant concentration, and oil–water ratio due to the addition of 0.5 ml of the culture were considered in the experiment design. The solutions were sampled at given time intervals, and viable counts were made using the membrane filtration technique. Controls, consisting of water, aqueous cetomacrogol solutions, and mineral oil emulsions without chlorocresol, were run with each experiment to check the viability of the organism.

RESULTS AND DISCUSSION

Interaction of Chlorocresol with Cetomacrogol—Figure 1 shows the total preservative concentration, $[D_t]$, plotted as a function of free preservative concentration, $[D_f]$, for the interaction of chlorocresol with various cetomacrogol concentrations. The experimentally determined values and the curves calculated by substitution of the binding constants into Eq. 5 agree closely. Hence, using Eq. 5, the total concentration of preservative required in a given surfactant solution can be calculated to provide any desired concentration of free preservative.

Distribution of Chlorocresol between Mineral Oil and Water—Figure 2 shows the chlorocresol concentration in the oil phase, $[D_o]$, plotted as function of the concentration in the aqueous phase, $[D_f]$. A linear relationship between $[D_o]$ and $[D_f]$ indicates that the distribution of chlorocresol between mineral oil and water obeys the simple partition law. The slope of the line gives the partition coefficient, K_w^o. The value

[8] Fisher.
[9] HAEG, Millipore Filter Corp.

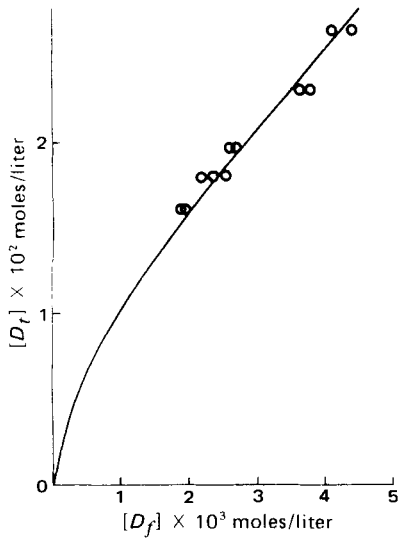

Figure 3—*Variation of free chlorocresol concentration,* $[D_f]$, *in the aqueous phase of an emulsion with total chlorocresol concentration,* $[D_t]$, *for an oil-in-water emulsion containing 50% (v/v) mineral oil emulsified with 3% (w/v) cetomacrogol. The points are experimental; the curve was calculated from Eq. 6.*

of $K_w{}^o$ obtained was 1.67, compared with the value of 1.53 reported previously (20).

Distribution of Chlorocresol in Mineral Oil Emulsions Stabilized with Cetomacrogol—Figure 3 is a plot of the total preservative concentration, $[D_t]$, *versus* the free preservative concentration, $[D_f]$, for the distribution of chlorocresol in mineral oil emulsions of a fixed oil–water ratio. The experimentally determined values and the curve calculated from the experimental value of $K_w{}^o$ and the preservative–surfactant binding constants (n and K) using Eq. 6 agree reasonably well. Close agreement also was found between $[D_f]$ predicted using Eq. 6 and the observed values for the distribution of chlorocresol in mineral oil emulsions of other oil–water ratios (Table I). These results, together with earlier work (7) on the distribution of benzoic acid in both mineral oil and peanut oil emulsions, confirm the validity of Eq. 6. Therefore, the total concentration of preservative required to provide the desired concentration of free preservative in the aqueous phase of an emulsion can be calculated with Eq. 6.

Comparison between Membrane Filtration and Pour-Plate Techniques—The death rate of microorganisms in a given solution can be studied by counting the number of surviving organisms as a function of time. Pour-plate or roll tube methods are often used for the viable counting of microorganisms. These techniques involve dilution of the sample in normal saline or one-fourth strength Ringer's solution and subsequent plating on agar. To follow the death rate of microorganisms in systems containing preservative, large dilutions are required to reduce the preservative concentration, which would otherwise inhibit the microorganism growth upon plating. This dilution is a serious limitation, especially when the death rate is followed to 100% mortality. Since large dilutions are not possible at high mortality levels, the chances of carryover of preservative to the growth medium are great.

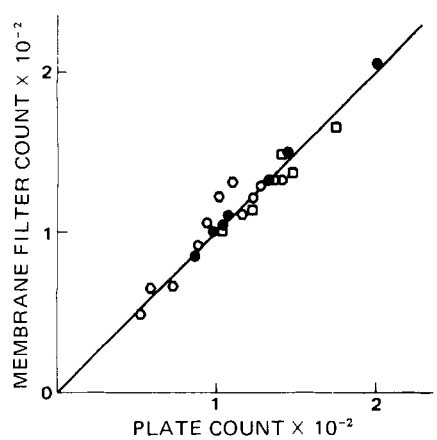

Figure 4—*Comparison between filtration and pour-plate techniques for counting* E. coli. *Different symbols represent separate experiments. The correlation coefficient = 0.95.*

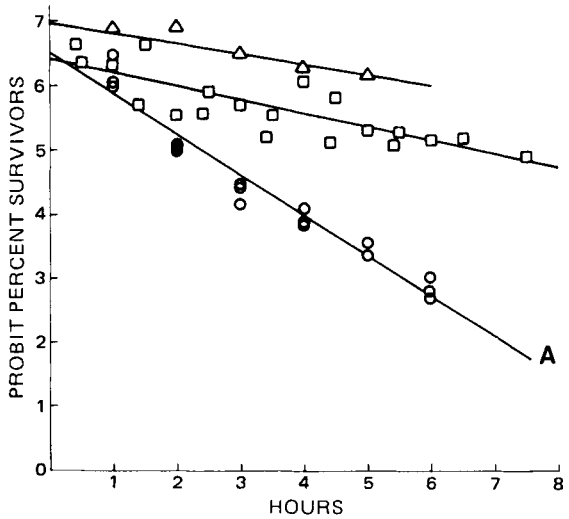

Figure 5—*Probit percent survivors as a function of time for the bactericidal activity of chlorocresol in water against* E. coli. *Key [chlorocresol concentration (percent)]: △, 0.02; □, 0.03; and ○, 0.035.*

The membrane filtration method avoids these problems by rinsing of the test filter with sterile fluid after sample filtration. The test filter is a special type, having a hydrophobic rim approximately 3 mm wide. This rim prevents intrusion of the sample fluid into the area under the sealing edge of the filter holder. All growth-inhibiting residuals are within immediate reach of the rinse fluid and are diluted to the point where they have no discernible effect on culturing. Thus, it is possible to follow the death rate to any desired level of mortality without limiting the sample size and without danger of residual preservative inhibiting microorganism growth.

Figure 4 shows that there was a good correlation between the membrane filtration method and the pour-plate technique for counting *E. coli.*

Bactericidal Activity of Chlorocresol in Water—Figure 5 is a plot of the probit percent survivors *versus* time for the bactericidal activity of chlorocresol in water against *E. coli.* The symbols represent experimental data, while lines were fitted using a desk calculator[10] programmed for linear regression analysis. Increasing the chlorocresol concentration from 0.02 to 0.03% made little change in the *E. coli* death rate. However, at 0.035% chlorocresol, there was a marked increase in the death rate. Since 0.035% chlorocresol produced 99.9% mortality within 6–8 hr, a time suitable for the experimental design, this concentration was selected as a reference standard to which the bactericidal activity of chlorocresol in aqueous cetomacrogol solutions and mineral oil emulsions could be compared. The results of the control experiments are shown in Fig. 6A. The viability of *E. coli* in water remained almost unchanged during the 8 hr.

Bactericidal Activity of Chlorocresol in Aqueous Solutions of Cetomacrogol—Figure 7 shows probit percent survivors plotted as a function of time for the bactericidal activity of chlorocresol in water (curve A) and aqueous solutions of cetomacrogol (curves B′, C′, and D′) against *E. coli.* The aqueous solution contained 0.035% chlorocresol, and surfactant solutions contained sufficient total preservative, as calculated from Eq. 5, to provide a free concentration of 0.035% chlorocresol in the aqueous phase. The symbols represent experimental data, and the lines were fitted using a linear model, Eq. 7 (28), and a computer program (29):

$$Y = \beta_0 + \beta_1 x_1 + \beta_2 x_2 + \beta_3 x_3 + \beta_4 t + \beta_5 x_1 t + \beta_6 x_2 t + \beta_7 x_3 t + \epsilon \quad \text{(Eq. 7)}$$

where β_0 is the intercept of curve A; β_1, β_2, and β_3 are the differences between the intercepts of curves B′ and A, C′ and A, and D′ and A, respectively; β_4 is the slope of curve A; β_5, β_6, and β_7 are the differences in slope between curves B′ and A, C′ and A, and D′ and A, respectively; x's are the

[10] Wang 600.

Table II—Analysis of Survivor-Time Curves for the Antimicrobial Activity of Chlorocresol in Solubilized and Emulsified Systems Compared with an Aqueous Solution, All Containing the Same Initial Concentration of Free Preservative

Parameter from Eq. 7[a]	Parameter Estimate: Solubilized Systems (Fig. 7)	Parameter Estimate: Emulsions (Fig. 8)
β_0	6.50	6.50
β_1	0.09	−0.12
β_2	−0.13	−0.13
β_3	−0.03	0.07
β_4	−0.63	−0.63
β_5	0.18[b]	0.13[c]
β_6	0.31[d]	0.24[d]
β_7	0.28[d]	0.24[d]
$(\beta_5 - \beta_6)$	−0.13[c]	0.11
$(\beta_5 - \beta_7)$	−0.10	0.11
$(\beta_6 - \beta_7)$	0.03	0.00

[a] See text for definitions. [b] $p < 0.0005$. [c] $p < 0.05$. [d] $p < 0.0001$.

dummy variables where $x_1 = 1$ if curve B′ and otherwise is zero, $x_2 = 1$ if curve C′ and otherwise is zero, and $x_3 = 1$ if curve D′ and otherwise is zero; ϵ is a random variable; and t is time.

Table II summarizes the statistical analysis of the intercepts and slopes of the curves in Fig. 7. A Z test (30) was used to test the significance of the model parameters. Differences between the intercepts of surfactant curves B′, C′, and D′ and the intercept of curve A (water) were not significant, while differences between the slopes of curves B′, C′, and D′ with respect to curve A were significant. However, the differences between the slopes of the surfactant curves B′ and D′ $(\beta_5 - \beta_7)$ and of C′ and D′ $(\beta_6 - \beta_7)$ were not significant, although the difference between the slopes of curves B′ and C′ $(\beta_5 - \beta_6)$ was significant.

Comparison with Fig. 5 shows that the three surfactant curves fall between the values of the slopes for 0.030 and 0.035% aqueous chlorocresol solutions; *i.e.*, a difference in $[D_f]$ of 0.005% produced a marked change in the slope. This concentration difference should be contrasted with the large differences between $[D_t]$ for each surfactant concentration, *i.e.*, B′, 0.1743%; C′, 0.4528%; and D′, 0.7324%. The slope of the probit–survivor curve is very sensitive to changes in $[D_f]$ in the concentration range chosen for these experiments (Fig. 5). Therefore, any factor producing a slight change in $[D_f]$ will significantly affect the slope of the survivor–time curve.

The difference between the slopes of curves B′ and C′ in Fig. 7 suggests that increasing the cetomacrogol concentration may decrease bactericidal activity. This decrease could be due to a stimulation of microbial growth (31–35) or protection of the organism by the nonionic surfactant (36–40).

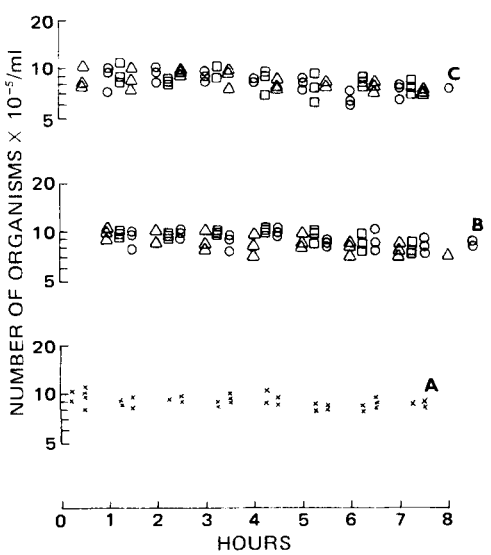

Figure 6—*Semilogarithmic plot of the number of organisms per milliliter as a function of time for the survival of* E. coli. *Key: A, water; B, aqueous cetomacrogol solutions with concentrations of cetomacrogol as in Fig. 1; and C, mineral oil emulsions with values of* q *and* M *as in Fig. 8.*

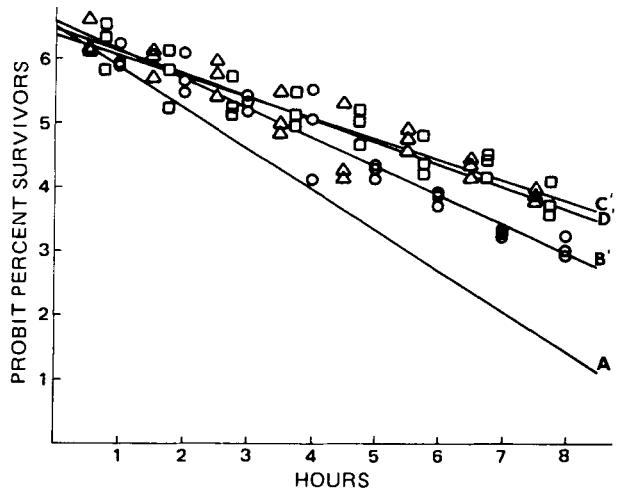

Figure 7—*Probit percent survivors as a function of time for the bactericidal activity of chlorocresol in aqueous cetomacrogol solutions against* E. coli. *Key [cetomacrogol concentration (percent)]: A, 0.0 (from Fig. 5); B, ○, 1.0; C, □, 3.0; and D, △, 5.0. Key [total preservative concentration, $[D_t]$ (percent)]: A, 0.0350; B, 0.1743; C, 0.4528; and D, 0.7314. The initial free preservative concentration, $[D_f]$, = 0.035%. The points are experimental; the lines were fitted using Eq. 7.*

However, the absence of statistically significant differences between the slopes of curves B′ and D′ and curves C′ and D′ indicates that increasing the surfactant concentration is not important, provided $[D_f]$ is the same for each solution. The antimicrobial activity of chlorocresol in each surfactant solution was less than that of the solution in water. Therefore, under the experimental conditions, capacity defined as the ability of the system to resist changes in $[D_f]$ is not important[11]. Moreover, the statistically significant differences between the slopes of curve A (water) and the surfactant curves B′, C′, and D′ indicate, apart from any effect due to the capacity factor, that it is more appropriate to compare the antimicrobial activity of one surfactant solution of preservative with another rather than with that of a solution of the preservative in water.

Bactericidal Activity of Chlorocresol in Mineral Oil Emulsions Stabilized with Cetomacrogol—A realistic test of the theory that preservative activity in emulsions depends on $[D_f]$ is to compare the viability of a given microorganism in various emulsions with the same $[D_f]$ but varying $[D_t]$ values. An equal biological response in emulsions with differing oil–water ratios would then indicate that the antimicrobial activity is essentially a function of $[D_f]$ and that the preservative in the oil phase is biologically inactive. This approach was used in the design of the emulsion experiments in a manner analogous to that used for solubilized systems.

Figure 8 shows probit percent survivors plotted as a function of time for the bactericidal activity of chlorocresol in water (curve A) and mineral oil emulsions of varying oil–water ratios (curves B, C, and D) against *E. coli*. The symbols represent experimental data; the lines were fitted using the linear model, Eq. 7. The initial value of $[D_f]$ was the same for all curves, although the total preservative concentration, $[D_t]$, was varied.

The results of control experiments are shown in Fig. 6C. The viability of *E. coli* in mineral oil emulsions of a varying oil–water ratio, q, remained almost unchanged during the 8-hr interval.

A statistical analysis of the slopes of the curves in Fig. 8 was performed using the method described for Fig. 7 (Table II). Differences between the intercepts of the emulsion curves B, C, and D and the intercept of curve A for aqueous solutions of chlorocresol (β_1, β_2, and β_3, respectively) were not significant. Differences between the slopes of curves B, C, and D and the slope of curve A (β_5, β_6, and β_7, respectively) were significant. However, the differences between the slopes of the emulsion curves $(\beta_5 - \beta_6)$, $(\beta_5 - \beta_7)$, and $(\beta_6 - \beta_7)$ were not significant. This result confirms the suggestion that the antimicrobial activity of chlorocresol in mineral oil emulsions is essentially a function of $[D_f]$.

Additional support for this suggestion comes from a statistical comparison of the survivor–time curves for emulsions B, C, and D (Fig. 8) with the solubilized systems B′, C′, and D′ (Fig. 7) summarized in Table III. None of the intercepts of the emulsion curves differed significantly from

[11] See Part II of this series for a full discussion of this concept.

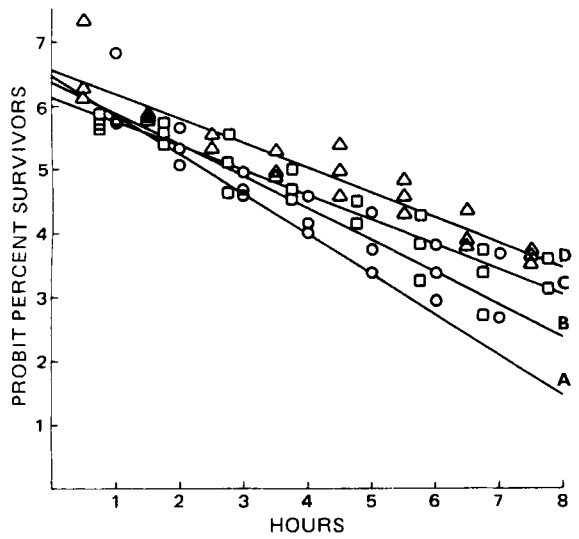

Figure 8—*Probit percent survivors of* E. coli *as a function of time for the bactericidal activity of chlorocresol in water (curve A from Fig. 5) and mineral oil emulsions stabilized with 3.0% (w/v) cetomacrogol. Key (oil–water ratio, q): B, ○, 1.0; C, □, 0.5; and D, △, 0.2. Key [total preservative concentration, $[D_t]$ (percent)]: A, 0.035; B, 0.2557; C, 0.3214; and D, 0.3871. The initial free preservative concentration, $[D_f]$, = 0.035%. The points are experimental; the lines were fitted using Eq. 7.*

the intercepts of the solubilized systems, except for the intercept of emulsion C which differed from that of solubilized system B′. More importantly, differences between the slopes of the survivor–time curves for the emulsions when compared with each solubilized system were not significant, other than the curve for emulsion B which differed in slope from that of solubilized systems C′ and D′.

The preservative activity of the solubilized and emulsified systems was similar, for the short-term bactericidal activity studied, when the dispersions initially contained an equal concentration of free preservative. This was true despite a wide range in the total preservative concentrations, differences in surfactant concentrations, the presence or absence of an oil phase, and variations in the percentage of the oil phase where present. In addition, the results provide striking indirect evidence of the validity of Eqs. 5 and 6 for calculating the total preservative concentration.

The statistically significant differences between the slopes of curve A (water) and emulsion systems B, C, and D again indicate, as was found for solubilized systems, that an emulsion should be compared with other emulsions (Table II) or solubilized systems (Table III) rather than with water (Table II). Although solubilized and emulsified dispersions with the same $[D_f]$ are equitoxic, the present results indicate that they do not have the same activity as a solution of the preservative in water with the same $[D_f]$.

Table III—Comparison of Survivor–Time Curves for the Antimicrobial Activity of Chlorocresol in Emulsified and Solubilized Systems, Each Containing the Same Initial Concentration of Free Preservative

Parameter from Eq. 7[a]	Parameter Estimate		
	B′	C′	D′
β_0	6.59	6.36	6.47
β_1	−0.22	0.01	−0.09
β_2	−0.45[b]	−0.22	−0.32
β_3	−0.02	0.20	0.10
β_4	−0.45	−0.32	−0.34
β_5	−0.05	−0.18[c]	−0.15[c]
β_6	0.06	−0.07	−0.05
β_7	0.06	−0.07	−0.05

[a] Where β_0 = intercepts of curves B′, C′, and D′ (Fig. 7, solubilized systems); β_1 = differences between intercepts of emulsion curve B (Fig. 8) and curves B′, C′, and D′, respectively; β_2 = differences between intercepts of emulsion curve C (Fig. 8) and curves B′, C′, and D′, respectively; β_3 = differences between intercepts of emulsion curve D (Fig. 8) and curves B′, C′, and D′, respectively; β_4 = slopes of curves B′, C′, and D′; β_5 = differences in slope between emulsion curve B and curves B′, C′, and D′, respectively; β_6 = differences in slope between emulsion curve C and curves B′, C′, and D′, respectively; and β_7 = differences in slope between emulsion curve D and curves B′, C′, and D′, respectively. [b] $p < 0.05$. [c] $p < 0.0005$.

The choice of a suitable value of $[D_f]$ depends on whether inhibition or bactericidal activity is desired. Minimum inhibitory concentrations are normally determined in a nutrient growth medium and, as discussed elsewhere (41), the nutritive value of the aqueous phase of a solubilized or an emulsified system is unlikely to be as great as that of nutrient broth or other growth media. Hence, if a minimum inhibitory concentration is used for $[D_f]$, the total concentration calculated from Eq. 5 or 6 should, in most cases, provide free preservative in excess of the minimum concentration necessary to inhibit growth. On the other hand, death or some specified percentage mortality within a finite time is probably a more desirable objective in preservation than simply growth inhibition. Whichever criterion is adopted, substitution of the selected value of $[D_f]$, together with the appropriate constants, into Eq. 5 or 6 will give the total preservative concentration required.

REFERENCES

(1) S. J. A. Kazmi and A. G. Mitchell, *J. Pharm. Pharmacol.*, **23,** 482 (1971).

(2) S. J. A. Kazmi and A. G. Mitchell, *Can. J. Pharm. Sci.*, **11,** 10, (1976).

(3) E. R. Garrett, *J. Pharm. Pharmacol.*, **18,** 589 (1966).

(4) R. A. Anderson and C. E. Chow, *J. Soc. Cosmet. Chem.*, **18,** 207 (1967).

(5) H. S. Bean, G. H. Konning, and S. A. Malcolm, *J. Pharm. Pharmacol., Suppl.*, **21,** 173S (1969).

(6) N. K. Patel and J. M. Romanowski, *J. Pharm. Sci.*, **59,** 372 (1970).

(7) S. J. A. Kazmi and A. G. Mitchell, *ibid.*, **60,** 1422 (1971).

(8) G. H. Konning, *Can. J. Pharm. Sci.*, **9,** 103 (1974).

(9) A. G. Mitchell and S. J. A. Kazmi, *ibid.*, **10,** 67 (1975).

(10) F. D. Pisano and H. B. Kostenbauder, *J. Am. Pharm. Assoc., Sci. Ed.*, **48,** 310 (1959).

(11) S. M. Blaug and S. S. Ahsan, *J. Pharm. Sci.*, **50,** 138 (1961).

(12) A. G. Mitchell, *J. Pharm. Pharmacol.*, **16,** 533 (1964).

(13) W. P. Evans and S. F. Dunbar, "Surface Activity and Microbial Cell," Society of Chemical Industry, London, England, 1965, p. 169.

(14) N. K. Patel, *Can. J. Pharm. Sci.*, **2,** 77 (1967).

(15) F. Atkins, *Manuf. Chem.*, **21,** 51 (1950).

(16) E. R. Garrett and O. R. Woods, *J. Am. Pharm. Assoc., Sci. Ed.*, **42,** 736 (1953).

(17) H. W. Hibbott and J. Monks, *J. Soc. Cosmet. Chem.*, **12,** 2 (1961).

(18) H. S. Bean, J. P. Richards, and J. Thomas, *J. Boll. Chim. Farm.*, **101,** 339 (1962).

(19) H. S. Bean and S. M. Heman-Ackah, *J. Pharm. Pharmacol., Suppl.*, **16,** 58T (1964).

(20) H. S. Bean, S. M. Heman-Ackah, and J. Thomas, *J. Soc. Cosmet. Chem.*, **16,** 15 (1965).

(21) H. S. Bean and S. M. Heman-Ackah, *J. Pharm. Pharmacol., Suppl.*, **17,** 142S (1965).

(22) G. Scatchard, *Ann. N.Y. Acad. Sci.*, **51,** 660 (1949).

(23) J. Steinhardt and J. A. Reynolds, "Multiple Equilibria in Proteins," Academic, New York, N.Y., 1969.

(24) S. J. A. Kazmi and A. G. Mitchell, *J. Pharm. Sci.*, **62,** 1299 (1973).

(25) J. S. Schellman, R. Lumry, and L. T. Sammuels, *J. Am. Chem. Soc.*, **76,** 2808 (1954).

(26) A. G. Mitchell and L. S. C. Wan, *J. Pharm. Sci.*, **53,** 1467 (1964).

(27) "Sterility Testing," MRP-4, Millipore Filter Corp., Bedford, Mass., 1968.

(28) W. Medenhall, "Introduction to Linear Models and the Design and Analysis of Experiments," Duxbury Press, Wadsworth Publishing, Belmont, Calif., 1968, p. 48.

(29) A. J. Barr and J. H. Goodnight, "Statistical Analysis System," Department of Statistics, North Carolina State University, Raleigh, N.C., 1972.

(30) W. Medenhall, "Introduction to Linear Models and the Design and Analysis of Experiments," Duxbury Press, Wadsworth Publishing, Belmont, Calif., 1968, p. 21.

(31) R. J. Dubos and B. D. Davies, *J. Exp. Med.*, **83,** 409 (1946).

(32) W. L. Williams, H. P. Broquist, and E. E. Snell, *J. Biol. Chem.*, **170,** 619 (1947).

(33) A. Bolle and A. Mirimanoff, *J. Pharm. Pharmacol.*, **2,** 685 (1950).

(34) M. G. de Navarre and H. E. Bailey, *J. Soc. Cosmet. Chem.*, **7**, 427 (1956).
(35) M. G. de Navarre, *ibid.*, **8**, 371 (1957).
(36) A. H. Beckett, S. J. Patki, and A. E. Robinson, *Nature*, **181**, 712 (1958).
(37) A. H. Beckett and A. E. Robinson, *Soap Perfum. Cosmet.*, **31**, 454 (1958).
(38) A. H. Beckett, S. J. Patki, and A. E. Robinson, *J. Pharm. Pharmacol.*, **11**, 421 (1959).
(39) D. L. Wedderburn, *J. Soc. Cosmet. Chem.*, **9**, 210 (1958).
(40) J. Judis, *J. Pharm. Sci.*, **51**, 261 (1962).
(41) S. J. A. Kazmi and A. G. Mitchell, *Soap Perfum. Cosmet.*, **45**, 549 (1972).

ACKNOWLEDGMENTS

The authors thank Dr. R. Marks, Biostatistics Unit, Department of Statistics, University of Florida, for assistance with the statistical analysis of the microbiological data.

Preservation of Solubilized and Emulsified Systems II: Theoretical Development of Capacity and Its Role in Antimicrobial Activity of Chlorocresol in Cetomacrogol-Stabilized Systems

S. J. A. KAZMI * and A. G. MITCHELL ˣ

Received June 20, 1977, from the *Faculty of Pharmaceutical Sciences, University of British Columbia, Vancouver, British Columbia, Canada V6T 1W5.* Accepted for publication January 13, 1978. *Present address: Faculty of Pharmacy, University of El-Fateh, Tripoli, Libya.

Abstract □ The preservation of solublized and emulsified disperse systems against microbial spoilage depends on the free (unbound) preservative concentration in the aqueous phase and the capacity of the system. The capacity may be defined as the system's ability to resist losses in free preservative concentration. The theory of capacity is developed quantitatively for solubilized and emulsified systems containing the preservative chlorocresol stabilized by the nonionic surfactant cetomacrogol. Equations are derived for solubilized systems that relate capacity to surfactant concentration and the interaction between the surfactant and the preservative. Additional terms are included in the equations to account for the effects of the oil phase on the capacity of oil-in-water emulsions.

Keyphrases □ Chlorocresol—in solubilized and emulsified systems, role of capacity in antimicrobial activity □ Capacity—theoretical development, role in antimicrobial activity of chlorocresol in solubilized and emulsified systems □ Antimicrobial activity—chlorocresol, role of capacity in solubilized and emulsified systems

For solubilized systems and oil-in-water emulsions stabilized with the nonionic surfactant cetomacrogol, the kill rate of *Escherichia coli* over 6–8 hr depends on the free chlorocresol concentration (1). However, for long-term protection against microbial contamination, the preservative's effectiveness should depend on the capacity of the system in addition to the free preservative concentration.

The term capacity was first used (2) in discussing the antibacterial activity of iodine solubilized by a nonionic surfactant[1]. The saturation solubility of the iodine was used as a measure of capacity. This definition implies that depletion of preservative due to interaction with microorganisms or foreign materials[2], volatilization, chemical decomposition (4), or metabolism by microorganisms (5) will be relatively greater from a solution in water than from a surfactant solution where the micelles act as a reservoir of preservative.

In this paper, the theoretical basis of capacity is developed more fully for solubilized systems and the theory is extended to oil–water dispersions and oil-in-water emulsions. The necessary physicochemical parameters were obtained previously (1, 6).

THEORETICAL

Capacity of Solubilized Systems—For a given loss of preservative, the decrease in concentration of free (unbound or nonmicellar) preservative in a solubilized system is less than from a solution in water and decreases with surfactant concentration. The percent decrease in con-

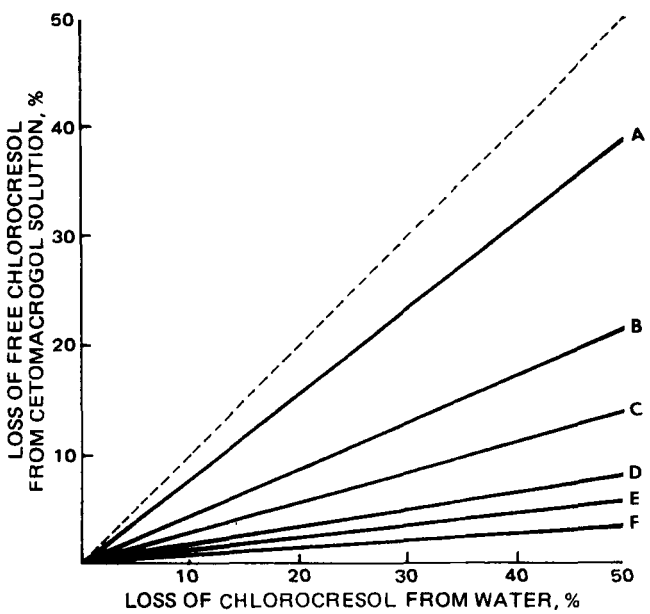

Figure 1—*Correlation between percent loss of chlorocresol from water and free chlorocresol from cetomacrogol solution when equal amounts of chlorocresol are removed from water and the surfactant solution. Key [cetomacrogol concentration (percent)]: A, 0.1; B, 0.5; C, 1.0; D, 2.0; E, 3.0; and F, 4.0 Curves were calculated using Eq. 1.*

[1] Antarox A-400.
[2] See Tables III and IV of Ref. 3.

0022-3549/78/0900-1266$01.00/0
© 1978, American Pharmaceutical Association

(34) M. G. de Navarre and H. E. Bailey, *J. Soc. Cosmet. Chem.*, **7**, 427 (1956).
(35) M. G. de Navarre, *ibid.*, **8**, 371 (1957).
(36) A. H. Beckett, S. J. Patki, and A. E. Robinson, *Nature*, **181**, 712 (1958).
(37) A. H. Beckett and A. E. Robinson, *Soap Perfum. Cosmet.*, **31**, 454 (1958).
(38) A. H. Beckett, S. J. Patki, and A. E. Robinson, *J. Pharm. Pharmacol.*, **11**, 421 (1959).
(39) D. L. Wedderburn, *J. Soc. Cosmet. Chem.*, **9**, 210 (1958).
(40) J. Judis, *J. Pharm. Sci.*, **51**, 261 (1962).
(41) S. J. A. Kazmi and A. G. Mitchell, *Soap Perfum. Cosmet.*, **45**, 549 (1972).

ACKNOWLEDGMENTS

The authors thank Dr. R. Marks, Biostatistics Unit, Department of Statistics, University of Florida, for assistance with the statistical analysis of the microbiological data.

Preservation of Solubilized and Emulsified Systems II: Theoretical Development of Capacity and Its Role in Antimicrobial Activity of Chlorocresol in Cetomacrogol-Stabilized Systems

S. J. A. KAZMI * and A. G. MITCHELL ˣ

Received June 20, 1977, from the *Faculty of Pharmaceutical Sciences, University of British Columbia, Vancouver, British Columbia, Canada V6T 1W5.* Accepted for publication January 13, 1978. *Present address: Faculty of Pharmacy, University of El-Fateh, Tripoli, Libya.

Abstract □ The preservation of solublized and emulsified disperse systems against microbial spoilage depends on the free (unbound) preservative concentration in the aqueous phase and the capacity of the system. The capacity may be defined as the system's ability to resist losses in free preservative concentration. The theory of capacity is developed quantitatively for solubilized and emulsified systems containing the preservative chlorocresol stabilized by the nonionic surfactant cetomacrogol. Equations are derived for solubilized systems that relate capacity to surfactant concentration and the interaction between the surfactant and the preservative. Additional terms are included in the equations to account for the effects of the oil phase on the capacity of oil-in-water emulsions.

Keyphrases □ Chlorocresol—in solubilized and emulsified systems, role of capacity in antimicrobial activity □ Capacity—theoretical development, role in antimicrobial activity of chlorocresol in solubilized and emulsified systems □ Antimicrobial activity—chlorocresol, role of capacity in solubilized and emulsified systems

For solubilized systems and oil-in-water emulsions stabilized with the nonionic surfactant cetomacrogol, the kill rate of *Escherichia coli* over 6–8 hr depends on the free chlorocresol concentration (1). However, for long-term protection against microbial contamination, the preservative's effectiveness should depend on the capacity of the system in addition to the free preservative concentration.

The term capacity was first used (2) in discussing the antibacterial activity of iodine solubilized by a nonionic surfactant[1]. The saturation solubility of the iodine was used as a measure of capacity. This definition implies that depletion of preservative due to interaction with microorganisms or foreign materials[2], volatilization, chemical decomposition (4), or metabolism by microorganisms (5) will be relatively greater from a solution in water than from a surfactant solution where the micelles act as a reservoir of preservative.

In this paper, the theoretical basis of capacity is developed more fully for solubilized systems and the theory is extended to oil–water dispersions and oil-in-water emulsions. The necessary physicochemical parameters were obtained previously (1, 6).

THEORETICAL

Capacity of Solubilized Systems—For a given loss of preservative, the decrease in concentration of free (unbound or nonmicellar) preservative in a solubilized system is less than from a solution in water and decreases with surfactant concentration. The percent decrease in con-

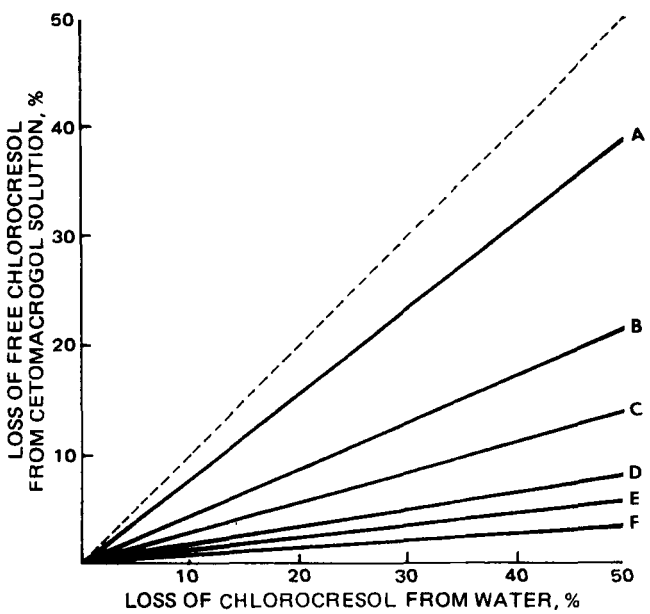

Figure 1—*Correlation between percent loss of chlorocresol from water and free chlorocresol from cetomacrogol solution when equal amounts of chlorocresol are removed from water and the surfactant solution. Key [cetomacrogol concentration (percent)]: A, 0.1; B, 0.5; C, 1.0; D, 2.0; E, 3.0; and F, 4.0 Curves were calculated using Eq. 1.*

[1] Antarox A-400.
[2] See Tables III and IV of Ref. 3.

0022-3549/78/0900-1266$01.00/0
© 1978, American Pharmaceutical Association

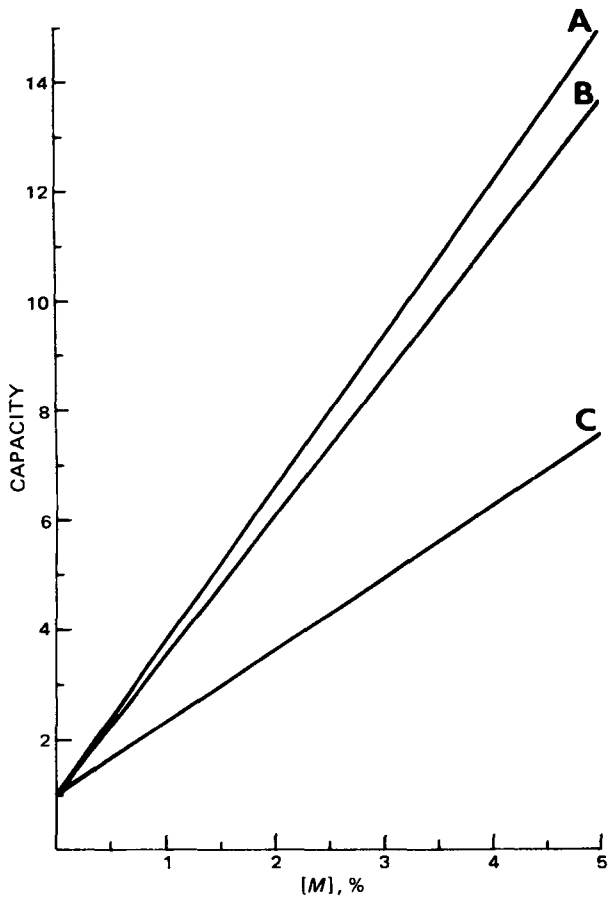

Figure 2—*Capacity as a function of surfactant concentration,* [M], *for the interaction of chlorocresol with: I, where* $n_1 = 0.538$, $n_2 = 142$, $K_1 = 2.12 \times 10^3$ *liters/mole, and* $K_2 = 1.65$ *liters/mole (A); cetomacrogol, where* $n_1 = 0.697$, $n_2 = 136$, $K_1 = 1.87 \times 10^3$ *liters/mole, and* $K_2 = 2.09$ *liters/mole (B); and II, where* $n_1 = 0.432$, $n_2 = 148$, $K_1 = 4.97 \times 10^3$ *liters/mole, and* $K_2 = 3.16$ *liters/mole (C). Curves were calculated using Eq. 8.*

centration of free preservative from a solubilized system is given by:

$$\text{percent decrease} = \{([D_f] - [D_f'])/[D_f]\}100 \qquad \text{(Eq. 1)}$$

where $[D_f]$ is the initial free preservative concentration in a solution that contains an initial total preservative concentration, $[D_t]$; $[D_f']$ is the free preservative concentration remaining after a loss of preservative from solution, $[D_{t1}]$; and $[D_t] - [D_{t1}]$ is the remaining total preservative concentration, $[D_t']$.

The total preservative concentration, $[D_t]$, present initially in the chlorocresol–cetomacrogol system described previously (1) is given by:

$$[D_t] = [D_f]\left[1 + \frac{n_1K_1[M]}{1 + K_1[D_f]} + \frac{n_2K_2[M]}{1 + K_2[D_f]}\right] \qquad \text{(Eq. 2)}$$

where n_1 is the number of independent binding sites on the surfactant molecule of Set 1 and K_1 is the corresponding association constant, n_2 is the number of independent binding sites on the surfactant molecule of Set 2 and K_2 is the corresponding association constant, and $[M]$ is the surfactant concentration. Rearrangement of Eq. 2 gives Eq. 3, from which $[D_f']$ can be obtained:

$$K_1K_2[D_f']^3 + (K_1 + K_2 + n_1K_1K_2[M] + n_2K_1K_2[M] - K_1K_2[D_t'][D_f']^2 + 1\ n_1K_1[M] + n_2K_2[M] - K_1[D_t'] + K_2[D_t'])[D_f'] - [D_t'] = 0 \qquad \text{(Eq. 3)}$$

The roots of Eq. 3 were calculated using the Bairstows method[3].

When equal amounts of chlorocresol are removed from water and a cetomacrogol solution, there is a direct relationship between the loss of preservative from water and the loss of free preservative from the solubilized system (Fig. 1). The slope of the curve increases as the surfactant concentration decreases and approaches that of water, which, with a value of unity, offers no resistance to losses of preservative.

[3] University of British Columbia computer program Z POLY.

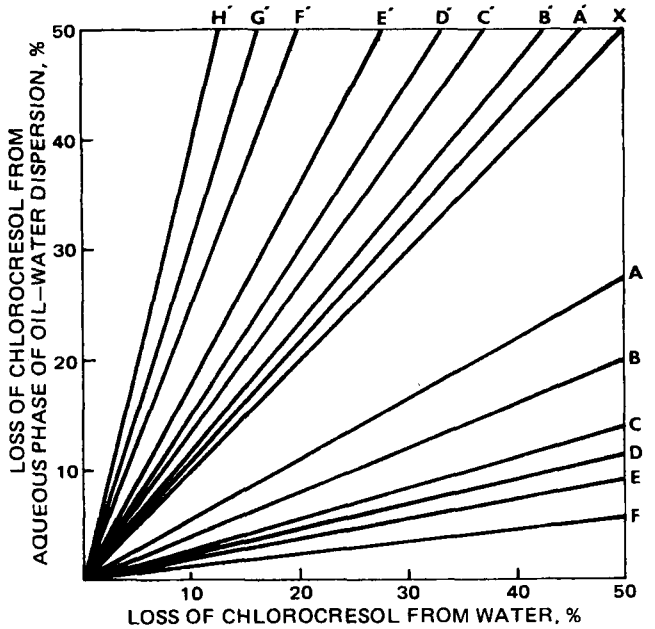

Figure 3—*Comparison between percent loss of chlorocresol from water and the aqueous phase of a hypothetical oil–water dispersion when equal amounts of preservative are removed from water and the dispersion. When* $K_w^o = 0.1$, $q = 0.1$ *(A'), 0.2 (B'), 0.4 (C'), 0.6 (D'), 1.0 (E'), 2.0 (F'), 3.0 (G'), and 5.0 (H'). When* $K_w^o = 1.0$, $q = 0.0$–∞ *(X). When* $K_w^o = 10.0$, $q = 0.1$ *(A), 0.2 (B), 0.4 (C), 0.6 (D), 1.0 (E), and 5.0 (F). Curves were calculated using Eq. 1.*

If capacity is defined as the ability of a system to resist losses in $[D_f]$, then the inverse of the slope of a given curve in Fig. 1 becomes a numerical expression of capacity:

$$\text{capacity} = 1/\text{slope} = \frac{\text{percent loss of preservative from water}}{\text{percent loss of free preservative from solubilized system}} \qquad \text{(Eq. 4)}$$

$$\text{capacity} = \frac{[D_{t1}]/[D_f]}{([D_f] - [D_f'])/[D_f]} \qquad \text{(Eq. 5)}$$

where:

$$[D_{t1}] = [D_t] - [D_t'] \qquad \text{(Eq. 6)}$$

Capacity increases with an increase in the surfactant concentration according to Eq. 4 and Allawala and Riegelman's (2) definition. The relationship between capacity as defined by Eq. 4 and surfactant concentration can be derived from Eqs. 6 and 2:

$$[D_{t1}] = [D_f]\left[1 + \frac{n_1K_1[M]}{1 + K_1[D_f]} + \frac{n_2K_2[M]}{1 + K_2[D_f]}\right] - [D_f']\left[1 + \frac{n_1K_1[M]}{1 + K_1[D_f']} + \frac{n_2K_2[M]}{1 + K_2[D_f']}\right] \qquad \text{(Eq. 7)}$$

Substituting $[D_{t1}]$ from Eq. 7 into Eq. 5 and rearranging give:

$$\text{capacity} = 1 + \left[\frac{n_1K_1}{1 + K_1[D_f] + K_1[D_f'] + K_1^2[D_f][D_f']} + \frac{n_2K_2}{1 + K_2[D_f] + K_2[D_f'] + K_2^2[D_f][D_f']}\right][M] \qquad \text{(Eq. 8a)}$$

$$\text{capacity} = 1 + \left[\frac{n_1K_1}{x_1} + \frac{n_2K_2}{x_2}\right][M] \qquad \text{(Eq. 8b)}$$

where:

$$x_1 = 1 + K_1[D_f] + K_1[D_f'] + K_1^2[D_f][D_f'] \qquad \text{(Eq. 9a)}$$

$$x_2 = 1 + K_2[D_f] + K_2[D_f'] + K_2^2[D_f][D_f'] \qquad \text{(Eq. 9b)}$$

Investigations of the effect of surfactant concentration on the antimicrobial activity of preservatives frequently include solutions of the preservative in water for comparison (1, 2, 7). Because of the difference

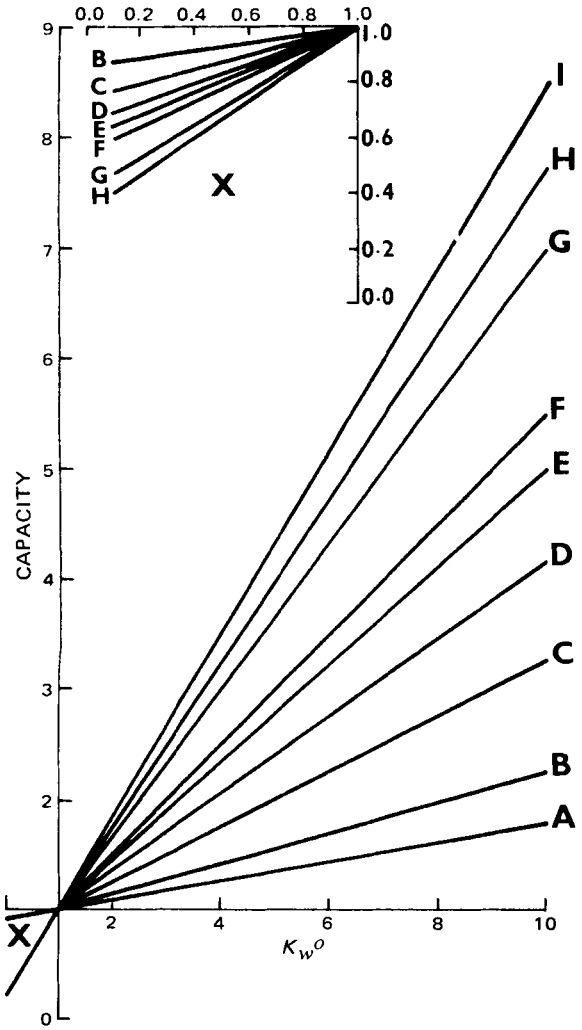

Figure 4—*Capacity as a function of* K_w^o *for the distribution of chlorocresol in hypothetical oil–water dispersions. Key (oil–water ratio): A, 0.1; B, 0.2; C, 0.4; D, 0.6; E, 0.8; F, 1.0; G, 2.0; H, 3.0; and I, 5.0. Curves were plotted according to Eq. 12b.*

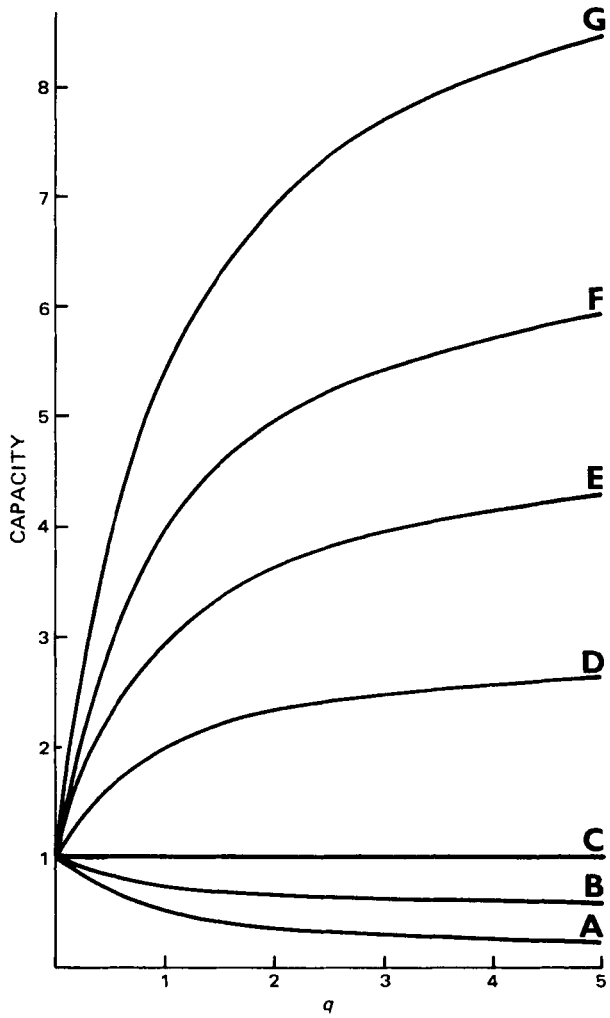

Figure 5—*Capacity as a function of the oil–water ratio,* q, *for the distribution of chlorocresol in hypothetical oil–water dispersions. Key* (K_w^o): *A, 0.1; B, 0.5; C, 1.0; D, 3.0; E, 5.0; F, 7.0; and G, 10.0. Curves were plotted according to Eq. 13.*

in capacity between surfactant solutions and solutions in water, such comparisons may be misleading unless either $[D_f]$ remains comparable throughout the experiment or the duration of the experiment is too short for the capacity of the system to exert an effect. It is better to compare the antimicrobial activity of various solubilized systems having the same initial value of $[D_f]$. During an experiment, changes in $[D_f]$ due to interaction of preservative or surfactant with the microorganisms or other factors will be relatively small, so any enhancement or diminution of activity can be attributed to the differences in surfactant concentration.

The interaction of chlorocresol with cetomacrogol and two other *n*-alkylpolyoxeythylene surfactants, designated[4] I and II, when plotted according to Eq. 8 (Fig. 2) shows that the capacity of the solubilized systems becomes smaller as the ethylene oxide chain length decreases. The efficiency of solubilization decreases with an increase in the number of ethylene oxide units (6).

Capacity of Oil–Water Dispersions—The percent loss of preservative from the aqueous phase of an oil–water dispersion for a given loss of preservative from the total system can be calculated in a similar manner to surfactant solutions, except $[D_f']$ for a given $[D_t']$ is calculated using (8):

$$[D_f'] = \frac{[D_t'](q+1)}{K_w^o q + 1} \qquad \text{(Eq. 10)}$$

where K_w^o is the experimentally determined oil–water partition coefficient and q is the oil–water ratio.

Figure 3 shows a direct relationship between the percent loss of chlorocresol from water and the aqueous phase of hypothetical oil–water dispersions when an equal amount of preservative is removed from water and the oil–water dispersion. The percent loss from the aqueous phase of oil–water dispersions increases with an increase in q when $K_w^o < 1.0$; it is independent of q when $K_w^o = 1.0$ and decreases with an increase in q when $K_w^o > 1.0$. As before, the capacity of a system to resist changes in $[D_f]$ is inversely proportional to the slope of a given line. A slope equal to or greater than one means the system offers no resistance to changes in $[D_f]$.

The relationship between capacity and $K_w^o q$ can be defined as follows. From Eqs. 6 and 10:

$$[D_{t1}] = [D_f]\left[\frac{K_w^o q + 1}{q+1}\right] - [D_f']\left[\frac{K_w^o q + 1}{q+1}\right] \qquad \text{(Eq. 11)}$$

Substituting $[D_{t1}]$ from Eq. 11 into Eq. 5 and rearranging give:

$$\text{capacity} = \frac{K_w^o q + 1}{q+1} \qquad \text{(Eq. 12a)}$$

or:

$$\text{capacity} = \left(\frac{1}{1+q}\right) + \left(\frac{q}{q+1}\right) K_w^o \qquad \text{(Eq. 12b)}$$

The capacity of various hypothetical oil–water dispersions plotted according to Eq. 12*b* is shown in Fig. 4. For a given value of q, the capacity increases when $K_w^o > 1.0$ and decreases when $K_w^o < 1.0$. When $K_w^o = 1.0$, the capacity is independent of q (see also Fig. 5) and its value is unity.

[4] Texofor A16 and Texfor A60, respectively, Glovers Chemicals Ltd., Leeds, England. The general formula of *n*-alkylpolyoxyethylene surfactants is $CH_3(CH_2)_m(OCH_2CH_2)_nOH$, where $m = 15$ and $n = 16$ for A16, $m = 15$ or 17 and $n = 20$–24 for cetomacrogol, and $m = 15$ and $n = 77$ for A60 (6).

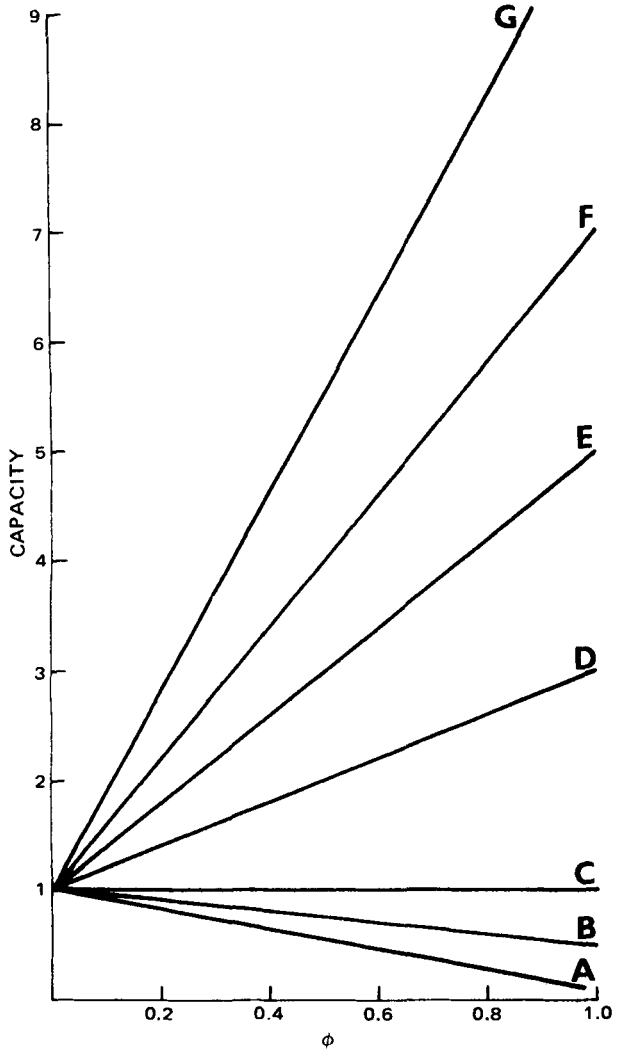

Figure 6—*Capacity as a function of the volume fraction of the oil phase, ϕ, for the distribution of chlorocresol in hypothetical oil–water dispersions. Partition coefficients of curves A–G are as in Fig. 5. Curves were plotted according to Eq. 14.*

Rearrangement of Eq. 12*b* shows that the relationship between capacity and q is nonlinear:

$$\text{capacity} = 1 + \left(\frac{K_w^o - 1}{1 + q}\right) q \qquad \text{(Eq. 13)}$$

Figure 5 shows the curvilinear relationship between capacity and q for various values of K_w^o. The intercept of 1.0 is the capacity of water in the absence of an oil phase. The capacity decreases with an increase in q when $K_w^o < 1.0$, increases with an increase in q when $K_w^o > 1.0$, and is independent of q when $K_w^o = 1.0$.

When q is expressed in terms of the volume fraction of the oil phase, ϕ, Eq. 12*b* becomes:

$$\text{capacity} = 1 + (K_w^o - 1)\phi \qquad \text{(Eq. 14)}$$

where $\phi = q/(q + 1)$.

Equation 14 gives a linear relationship between capacity and ϕ for a given K_w^o (Fig. 6). When ϕ approaches a value of 1.0, the capacity becomes equal to K_w^o. Hence, K_w^o is a measure of the capacity of the oil phase in the absence of an aqueous phase.

Capacity of Emulsions—The method used to calculate the percent loss of chlorocresol from the aqueous phase of an emulsion stabilized with cetomacrogol for a given loss of preservative from the total system is similar to that already given except that $[D_f']$ in Eq. 1 is calculated using:

$$(K_1K_2 + K_w^oqK_1K_2)[D_f']^3 + (K_1 + K_2 + n_1K_1K_2[M] + n_2K_1K_2[M] + K_w^oqK_1 + K_w^oqK_2 - K_1K_2[D_t']q - K_1K_2[D_t'])[D_f']^2 + (1 + n_1K_1[M] + n_2K_2[M] + K_w^oq - K_1[D_t']q - K_1[D_t'] - K_2[D_t']q - K_2[D_t'])[D_f'] - [D_t'](q + 1) = 0 \qquad \text{(Eq. 15)}$$

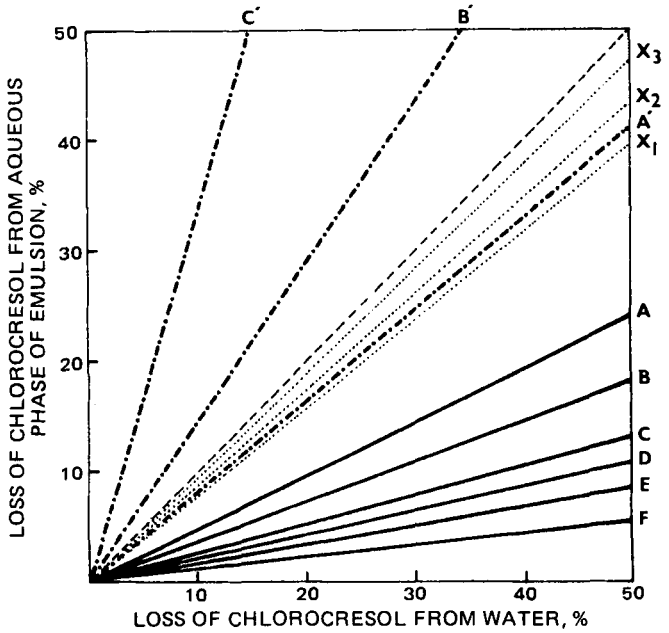

Figure 7—*Comparison between the percent loss of chlorocresol from water and the aqueous phase of a hypothetical oil-in-water emulsion stabilized with 0.1% cetomacrogol when equal amounts of preservative are removed from water and the emulsion. When $K_w^o = 0.1$, q = 0.1 (A'), 1.0 (B'), and 5.0 (C'). When $K_w^o = 1.0$, q = 0.1 (X_1), 1.0 (X_2), and 5.0 (X_3). When $K_w^o = 10.0$, q = 0.1 (A), 0.2 (B), 0.4 (C), 0.6 (D), 1.0 (E), and 5.0 (F). Curves were calculated using Eq. 1.*

which is a rearrangement of (1):

$$[D_t] = [D_f]\left[1 + \frac{n_1K_1[M]}{1 + K_1[D_f]} + \frac{n_2K_2[M]}{1 + K_2[D_f]}\right] / q + 1 \qquad \text{(Eq. 16)}$$

The roots of Eq. 15 were calculated using the Bairstows method[3].

Figure 7 shows a direct relationship between the percent loss of chlorocresol from water and the aqueous phase of hypothetical oil-in-water emulsions stabilized with 0.1% (w/v) cetomacrogol when an equal amount of preservative is removed from water and the emulsion. For a given percent loss of preservative from water, the percent loss from the aqueous phase of the emulsion is a function of q, K_w^o, and $[M]$. As before, the capacity of a system to resist changes in $[D_f]$ is inversely proportional to the slope of a given line. A slope equal to or greater than one means that the system offers no resistance to changes in $[D_f]$.

For a given oil–water ratio, the value of the slope is a function of $[M]$ and K_w^o. Figure 7 shows that for a given $[M]$, an increase in q results in a decrease in the value of the slope when $K_w^o = 10.0$. For the same $[M]$, increasing q results in an increase in the value of the slope when $K_w^o = 0.1$ and $K_w^o = 1.0$. Thus, unlike surfactant and oil–water systems where capacity is determined only by $[M]$ and K_w^oq, respectively, in emulsified systems the capacity is a result of the interaction among the parameters $[M]$, K_w^o, and q.

The relationship between the capacity of oil-in-water emulsions and $[M]$, K_w^o, and q can be derived from Eqs. 6 and 16:

$$[D_{t1}] = \left\{\left[[D_f]\left(1 + \frac{n_1K_1[M]}{1 + K_1[D_f]} + \frac{n_2K_2[M]}{1 + K_2[D_f]} + K_w^oq\right)\right] / (q + 1)\right\} - \left\{\left[[D_f']\left(1 + \frac{n_1K_1[M]}{1 + K_1[D_f']} + \frac{n_2K_2[M]}{1 + K_2[D_f']} + K_w^oq\right)\right] / (q + 1)\right\} \qquad \text{(Eq. 17)}$$

Substituting $[D_{t1}]$ from Eq. 17 into Eq. 5 and rearranging give:

$$\text{capacity} = \left(1 + \frac{n_1K_1[M]}{1 + K_1[D_f] + K_1[D_f'] + K_1^2[D_f][D_f']} + \frac{n_2K_2[M]}{1 + K_2[D_f] + K_2[D_f'] + K_2^2[D_f][D_f'] + K_w^oq}\right) / (q + 1) \qquad \text{(Eq. 18}a\text{)}$$

$$\text{capacity} = \left(1 + \frac{n_1K_1[M]}{x_1} + \frac{n_2K_2[M]}{x_2} + K_w^oq\right) / (q + 1) \qquad \text{(Eq. 18}b\text{)}$$

where x_1 and x_2 are as already defined.

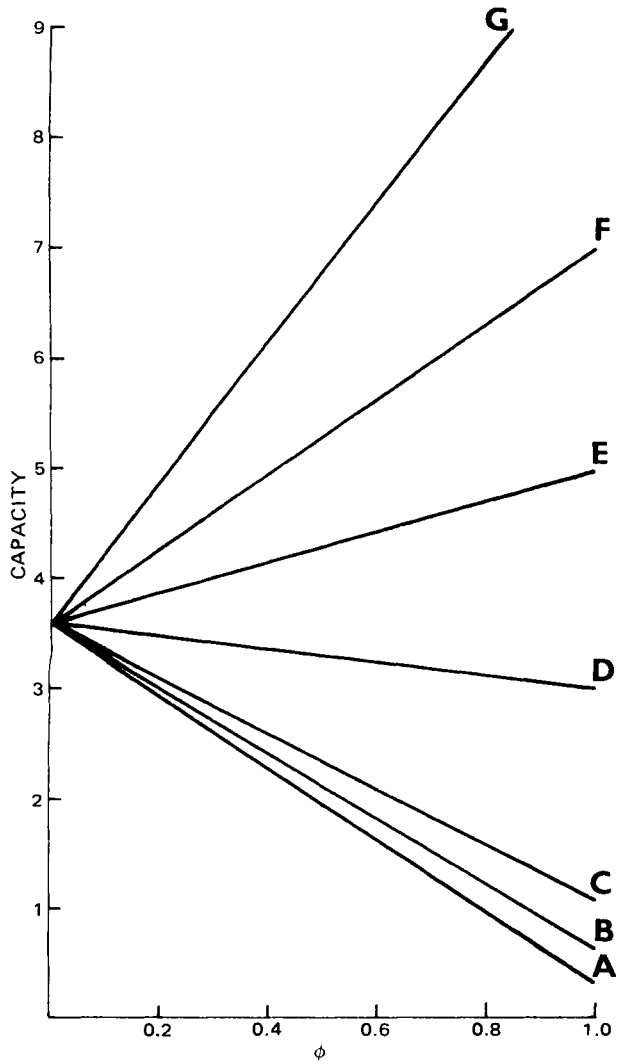

Figure 8—*Capacity as a function of the volume fraction of the oil phase, ϕ, for the distribution of chlorocresol in hypothetical oil-in-water emulsions stabilized with 1.0% (w/v) cetomacrogol. Key (K_w^o): A, 0.1, B, 0.5; C, 1.0; D, 3.0; E, 5.0; F, 7.0; and G, 10.0. Curves were plotted according to Eq. 19.*

When q is expressed in terms of the volume fraction of the oil phase, ϕ, the relation between capacity and $[M]$, $K_w{}^o$, and ϕ is given by:

$$\text{capacity} = \left(1 + \frac{n_1K_1[M]}{x_1} + \frac{n_2K_2[M]}{x_2}\right) - \left(1 + \frac{n_1K_1[M]}{x_1} + \frac{n_2K_2[M]}{x_2} - K_w{}^o\right)\phi \quad \text{(Eq. 19)}$$

Figure 8 shows the results for the distribution of chlorocresol in hypothetical emulsions stabilized with 1.0% (w/v) cetomacrogol plotted according to Eq. 19. The intercept gives the capacity of the aqueous phase (containing surfactant) in the absence of an oil phase; *i.e.*, when $\phi = 0$, the capacity is given by Eq. 8*b*.

At fixed $[M]$, an increase in ϕ decreases the capacity up to a certain value of $K_w{}^o$ (curves A–D, Fig. 8); beyond that value, an increase in ϕ results in an increase in capacity (curves E–G). For all curves, when $\phi \xrightarrow{\lim} 1$, then capacity = $K_w{}^o$, which is the capacity of the oil phase in the absence of an aqueous phase. According to Eq. 19, the overall capacity of the emulsion is determined by two factors: the capacity of the oil phase and the capacity of the surfactant-containing aqueous phase. The capacity of the oil phase is governed by $K_w{}^o$; the capacity of the aqueous phase is controlled by the surfactant concentration, $[M]$, and the binding affinity of the surfactant for the preservative (n's and K's).

If the capacity of the oil phase is less than the capacity of the aqueous surfactant phase, then an increase in ϕ results in a decrease in the overall capacity of the system (curves A–D, Fig. 8). This aspect is further illustrated in Fig. 9, which shows the decrease in capacity with ϕ for mineral oil emulsions (1) stabilized with 3.0% (w/v) cetomacrogol. Conversely, if the capacity of the aqueous phase is less than the capacity of the oil phase, then an increase in ϕ results in an increase in the capacity of the emulsion (curves E–G, Fig. 8). As the capacity of the aqueous phase approaches the capacity of water, *e.g.*, with dilute surfactant solutions [0.1% (w/v) cetomacrogol in Fig. 10], an increase in ϕ results in an increase in the capacity for all values of $K_w{}^o > 1.0$.

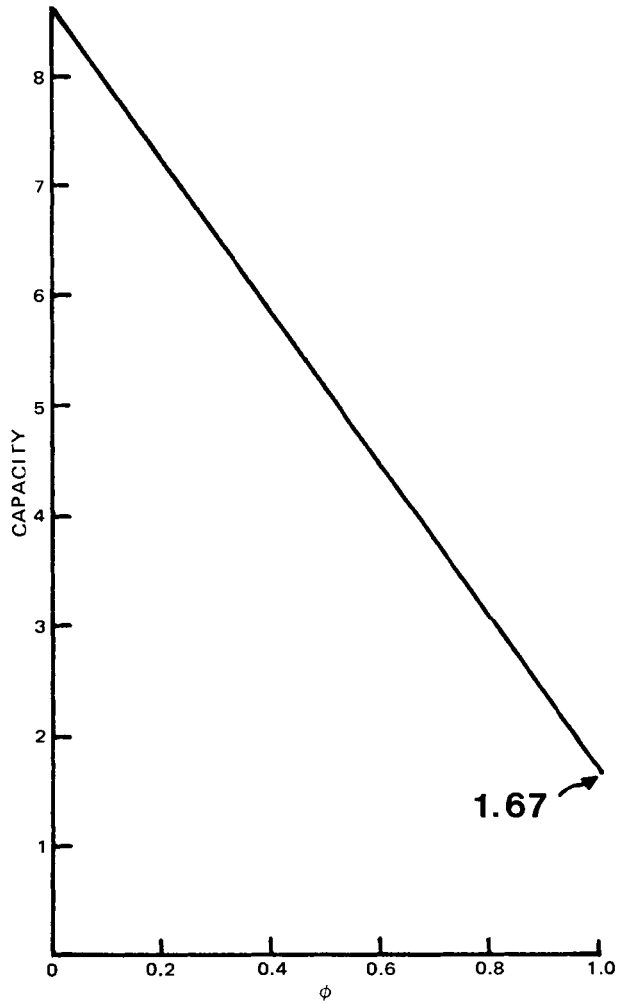

Figure 9—*Capacity as a function of the volume fraction of the oil phase, ϕ, for the distribution of chlorocresol in mineral oil emulsions stabilized with 3.0% (w/v) cetomacrogol, plotted according to Eq. 19, with $K_w{}^o$ (mineral oil) = 1.67.*

CONCLUSIONS

The concept of capacity, defined as the ability of solubilized and emulsified systems to resist losses in the concentration of free preservative, was developed theoretically from equations used previously to quantitate the distribution of chlorocresol in solubilized and emulsified systems stabilized with the nonionic surfactant cetomacrogol. The treatment should apply to other preservative–nonionic surfactant combinations for which the interaction can be described by the same binding expression (6).

The capacity of a system should affect its ability to withstand microbial contamination. High capacity systems should be able to resist losses in preservative concentration due to such factors as: (*a*) adsorption onto, or complexation with, the container and closure surfaces; (*b*) adsorption, absorption, or chemical reaction with contaminants including microorganisms; and (*c*) chemical decomposition and volatilization.

The effectiveness of a preservative in a complex disperse system should depend on the capacity of the system and the concentration of the free preservative. However, the magnitude of the capacity factor's contribution to the overall antimicrobial activity of a preservative will vary according to the testing procedure adopted. Thus, the effect of capacity is likely to become apparent in procedures that involve sampling for

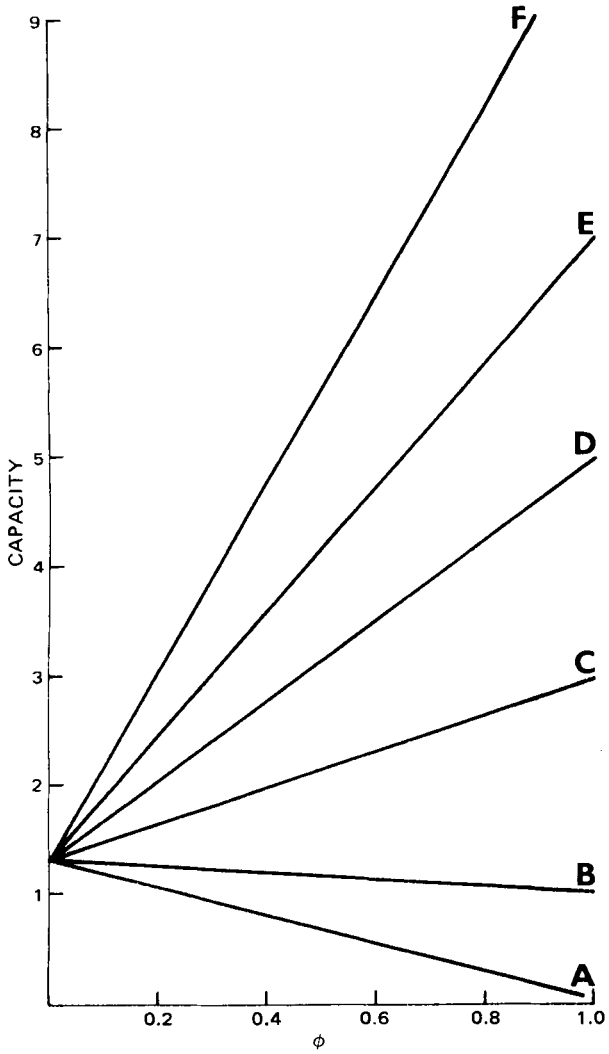

Figure 10—*Capacity as a function of the volume fraction of the oil phase, ϕ, for the distribution of chlorocresol in hypothetical oil-in-water emulsions stabilized with 0.1% (w/v) cetomacrogol. Key* (K_w^o): *A, 0.1; B, 1.0; C, 3.0; D, 5.0; E, 7.0; ad F, 10.0. Curves were plotted according to Eq. 19.*

microorganisms over prolonged periods, *e.g.*, days, weeks, or months [compared with hours as used in Part I (1)], or challenge tests (9, 10) in which the preparation is reinoculated with microorganisms over a long storage period. Such procedures allow time for the preservative to reequilibrate between the various phases following any depletion and for this reequilibration to affect the antimicrobial action. Incomplete understanding of the capacity factor and its significance is a probable reason for some controversy regarding the evaluation of preservative effectiveness in solubilized and emulsified systems.

Capacity equations should be useful in the formulation of high capacity systems containing the least amount of preservative necessary for adequate preservation. In view of the number of variables involved in the preservation of solubilized and emulsified systems, however, a choice of preservative concentration based solely on physicochemical measurements cannot replace a final microbiological evaluation of the product for its ability to withstand microbial contamination. Nevertheless, determination of the appropriate physicochemical parameters provides a logical first step in estimating the total amount of preservative required and should help to avoid much "trial-and-error" formulation when purely microbiological techniques are employed.

REFERENCES

(1) S. J. A. Kazmi and A. G. Mitchell, *J. Pharm. Sci.*, **67**, 1260 (1978).

(2) N. A. Allawala and S. Riegelman, *J. Am. Pharm. Assoc., Sci. Ed.*, **42**, 267 (1953).

(3) H. S. Bean, *J. Soc. Cosmet. Chem.*, **23**, 703 (1972).

(4) A. D. Nair and J. L. Lach, *J. Am. Pharm. Assoc., Sci. Ed.*, **48**, 390 (1959).

(5) W. T. Sokolski, G. G. Chidester, and G. E. Honeywell, *Dev. Ind. Microbiol.*, **3**, 179 (1962).

(6) S. J. A. Kazmi and A. G. Mitchell, *Can. J. Pharm. Sci.*, **11**, 10 (1976).

(7) A. G. Mitchell, *J. Pharm. Pharmacol.*, **16**, 533 (1964).

(8) H. S. Bean, S. M. Heman-Ackah, and J. Thomas, *J. Soc. Cosmet. Chem.*, **16**, 15 (1965).

(9) M. Barnes and G. W. Denton, *Soap Perfum. Cosmet.*, **42**, 729 (1969).

(10) R. A. Cowen and B. Steiger, *J. Soc. Cosmet. Chem.*, **27**, 467 (1976).

ACKNOWLEDGMENTS

The authors thank Dr. A. W. Khanzada, Physics Division, Pakistan Council of Scientific and Industrial Research, for the preparation of various computer programs.

Effect of Surfactants on Percutaneous Absorption of Naproxen I: Comparisons of Rabbit, Rat, and Human Excised Skin

Z. T. CHOWHAN ˣ **and R. PRITCHARD**

Received May 9, 1977, from the *Institute of Pharmaceutical Sciences, Syntex Research, Palo Alto, CA 94304.* Accepted for publication January 12, 1978.

Abstract □ The *in vitro* skin penetration model using excised skin from rats, rabbits, and humans was examined to evaluate the relative effect of surfactants on percutaneous absorption of naproxen. Differences in the magnitude of the effect of surfactants in promoting percutaneous absorption of naproxen through skins of different species were observed. For comparative evaluations of the formulation effects on percutaneous absorption, such as the effect of surfactants, *in vitro* studies with animal skin may not provide information in agreement with *in vitro* human skin.

Keyphrases □ Absorption, percutaneous—naproxen, effect of various surfactants, rabbit, rat, and human skin compared □ Naproxen—percutaneous absorption, effect of various surfactants, rabbit, rat, and human skin compared □ Surfactants, various—effect on percutaneous absorption of naproxen, rabbit, rat, and human skin compared □ Anti-inflammatory agents—naproxen, percutaneous absorption, effect of various surfactants, rabbit, rat, and human skin compared

Surfactants are important adjuvants in the formulation of vehicles for application to the skin. Nonionic surfactants generally have little effect in promoting percutaneous absorption, although numerous reports (1–5) discussed the influence of nonionic surfactants. Long chain alkyl methyl sulfoxides, which are nonionic surfactants, increased the permeability of guinea pig skin for sodium nicotinate and thiourea (6). Among the anionic surfactants, the laurate ion had the greatest effect on the penetration of other solutes (7, 8).

Excised animal (4, 9–11) and human (7, 8) skins have been used in studying the influence of surfactants on percutaneous absorption of water and organic solutes. A definite and reproducible relationship also exists between the excised skin permeabilities of different species. Rabbit skin is consistently more permeable than that of other rodents, pigs, or humans (12). Because of these differences, studies relating the effect of surfactants on percutaneous absorption may be confusing and sometimes contradictory.

This investigation evaluates the effect of surfactants on percutaneous absorption of naproxen through excised human skin. Cream formulations containing 5% naproxen were used to study the effect of selected surfactants on percutaneous absorption through excised human, rat, and rabbit skins. This study suggests that the data on excised skin of laboratory animals may not provide information in agreement with excised human skin concerning the effect of surfactants on percutaneous absorption of compounds similar to naproxen.

EXPERIMENTAL

Materials—The surfactants hexadecylpyridinium chloride[1], triethylammonium lauryl sulfate[2], octylphenoxypolyoxyethanol[3], dioctyl sodium sulfosuccinate[4], sodium lauryl sulfate[5], sodium laurate[6], polysorbate 60[7], polyoxyethylene 23 lauryl ether[8], and methyldecyl sulfoxide[9] were used as received. Hydroxypropylcellulose[10] and carboxyvinyl polymer[11] were used in the preparation of gels. Thimerosal and glycerin were USP grade.

Nonlabeled naproxen[12] was at least 99% pure. The tritiated naproxen was purified by radiochromatography and was at least 98% pure. The two solvent systems used were hexane–ethyl acetate (85:15) and benzene–tetrahydrofuran–acetic acid (90:9:3). All other chemicals were analytical reagent grade unless otherwise indicated.

Preparation of Vehicles—The aqueous gels containing 1% hydroxypropylcellulose were prepared by dispersing the polymer in 5% glycerin and adding it to the aqueous portion containing 0.5% dissolved naproxen. The pH of the solution was adjusted to 6.5. The carboxyvinyl polymer (0.5%) gel was prepared by dispersing the polymer and naproxen in water, adding an equimolar quantity of sodium hydroxide, and adjusting the pH to 6.5.

The cream vehicles were prepared by dissolving 5% naproxen in an equimolar quantity of sodium hydroxide solution. The pH was adjusted to 7.5. The oil phase contained 6% cetyl alcohol, 6% stearyl alcohol, 3% mineral oil, and 4% polysorbate 60. The aqueous and the oil phases were heated to about 70°, and the aqueous phase was added to the oil phase with appropriate stirring. After the formation of the emulsion, the stirring was continued until the temperature of the cream reached 30°.

Excised Human Skin Studies—Whole abdominal skin, obtained at autopsy, was frozen on a glass plate with the epidermal surface flat in contact with the plate. Just prior to an experiment, the frozen skin was dislodged by warming the plate with water. A layer of skin, 0.76 mm thick, was removed[13] from the abdominal side. This procedure allowed removal of the subcutaneous fat without contamination of the intact epidermal surface.

Circular sections having a diameter of 2.2 cm were cut. The dermal side of each section was blotted with tissue[14] paper and then positioned between the two polytef disks of the diffusion cell. The cell design and operation were the same as those reported by Coldman *et al.* (13), except that the exposed surface area for penetration had a diameter of 1.4 cm and an area of 1.54 cm^2. The dose of formulation per cell was 1.4 ml. To prevent evaporation, a glass coverslip was placed over the vehicle and sealed with silicone grease.

A polytef-coated stirring bar attached to a polyethylene sail provided efficient mixing in the sampling chamber, which contained approximately 12 ml of 0.01 *M* phosphate buffer at pH 7.4 with 0.02% thimerosal. The sampling arm was stoppered with a cork to prevent evaporation. The samples (1 ml for radiochemical assay and 3 ml for the spectrophotometric assay) were withdrawn at appropriate times, and the sample volume was replaced by a fresh solution.

By the spectrophotometric method, the absorbance of the samples was recorded at 342 nm. The radioactive counts were measured by a liquid scintillation counter[15]. The composition of the scintillation fluid was 1.4 liters of scintillation grade toluene[16], 1.4 liters of spectrograde *p*-dioxane[1],

[1] Matheson, Coleman & Bell, Norwood, Ohio.
[2] Alcolac Chemical Corp., Baltimore, Md.
[3] Triton X-45, Rohm & Haas Co., Philadelphia, Pa.
[4] American Cyanamid Co., Pearl River, N.Y.
[5] E. I. du Pont de Nemours & Co., Menlo Park, Calif.
[6] Eastman Kodak Co., Rochester, N.Y.
[7] Tween 60, ICI America Inc., Atlas Chemical Division, Wilmington, Del.
[8] Brij 35, ICI America Inc., Atlas Chemical Division, Wilmington, Del.
[9] Institute of Organic Chemistry, Syntex Research, Palo Alto, Calif.
[10] Klucel HF, Hercules Inc., Wilmington, Del.
[11] Carbomer 940, B. F. Goodrich.
[12] *d*-2-(6′-Methoxy-2′-naphthyl)propionic acid, Syntex Research, Palo Alto, Calif.
[13] Model B Dermatome, Paddet-Hood, Division of Kansas City Assemblage Co., Kansas City, MO 64111.
[14] Kimwipes disposal wipers, Kimberly Clark Corp., Neenah, WI 54956.
[15] Unilux II, Nuclear-Chicago, Chicago, IL 60600.
[16] J. T. Baker Chemical Co., Phillipsburg, NJ 08865.

0022-3549/78/0900-1272$01.00/0
© 1978, American Pharmaceutical Association

Table I—Effect of Surfactants on Naproxen Flux through Excised Human Abdominal Skin from Aqueous Gels

Surfactant (Concentration)	Mean Flux, $\mu g/cm^2/hr$	*SD*	Relative Flux
Experiment 1			
No added surfactant (control)	2.82	0.41	1.0
Hexadecylpyridinium chloride (0.5%)	1.26	0.22	0.44
Triethylammonium lauryl sulfate (2%)	2.00	0.81	0.71
Octylphenoxypolyethoxy 5 ethanol (2%)	2.30	0.24	0.82
Dioctyl sodium sulfosuccinate (0.05%)	2.94	0.21	1.04
Experiment 2			
No added surfactant (control)	1.26	0.58	1.0
Sodium lauryl sulfate (4%)	10.45	0.18	8.29
Sodium laurate (4%)	3.17	1.29	2.51
Polysorbate 60 (4%)	1.22	0.11	0.97
Polyoxyethylene 23 lauryl ether (4%)	1.04	0.18	0.83

0.84 liter of methanol[17], 18.2 g of 2,5-diphenyloxazole[18], 0.364 g of 1,4-bis[2-(4-methyl-5-phenyloxazolyl)]benzene[18], 219.2 g of naphthalene[16], and 0.350 g of 2,6-di-*tert*-butyl-4-methylphenol[19].

Excised Rat Skin Studies—Male Sprague–Dawley rats[20], 250–300 g, were employed. Hair was removed[21] between the forelegs and hindlegs on both sides of the spine 1 day prior to the experiment. The rats were killed by exposure to carbon dioxide generated in a chamber from dry ice and water. A 5 × 6-cm piece of skin was excised, and the connective tissue below the dermis was removed. Circular sections having a diameter of 2.21 cm were cut and used in the skin cell. The rest of the procedure was exactly the same as that used for the human skin studies.

Excised Rabbit Skin Studies—Male albino rabbits[22], ~2 kg, were employed. Hair was removed[21] between the forelegs and hindlegs on both sides of the spine 1 day prior to the experiment. The rabbits were killed with an intraperitoneal injection of 2 ml of pentobarbital[23], and a 7 × 8-cm piece of skin was excised. The connective tissue below the dermis was removed. Circular sections having a diameter of 2.21 cm were cut and used in the skin cell. The rest of the procedure was exactly the same as that used for the human skin studies.

RESULTS

The effect of surfactants on percutaneous absorption of naproxen through excised human skin was studied using a simple aqueous gel system. Four skin cells, taken from the same piece of skin, were used for the control and for each surfactant under study. The results of these experiments are given in Table I. For comparison, the mean flux of control in each experiment was taken as one, and the relative flux was then calculated. The concentration of all surfactants was above the critical micelle concentration (CMC).

The effect of nonionic, cationic, and amphoteric surfactants on the relative flux of naproxen was small. The lower relative flux with certain surfactants may be due to the lowering of the thermodynamic activity of naproxen by complexation or other interactions with the skin. Above the CMC, proportionately less surfactant is available for interaction. The anionic surfactants, sodium laurate and sodium lauryl sulfate, increased the *in vitro* flux of naproxen appreciably.

Similar experiments were conducted to study the influence of two surfactants, sodium lauryl sulfate and methyldecyl sulfoxide, at different concentrations. The mean *in vitro* flux was used to calculate the relative flux similarly. The relative flux *versus* surfactant concentration plots are given in Fig. 1. A large increase in flux of naproxen was seen up to 0.2% methyldecyl sulfoxide, above which the relative flux essentially remained constant. This effect appears to be limited by the surfactant solubility in aqueous gel. The effect of sodium lauryl sulfate on the *in vitro* flux of naproxen was less pronounced compared to methyldecyl sulfoxide and appeared linear in the concentration range studied.

The results of the influence of surfactants on excised human skin in a simple aqueous gel vehicle indicated that polysorbate 60 at 4% did not change the *in vitro* flux of naproxen (Table I). For studying selected surfactants from oil-in-water cream vehicles, it was assumed that polysorbate 60 did not alter the *in vitro* flux of naproxen by interaction with the surfactant under study. Sodium lauryl sulfate, sodium laurate, and methyldecyl sulfoxide were studied using excised human, rat, and rabbit skins.

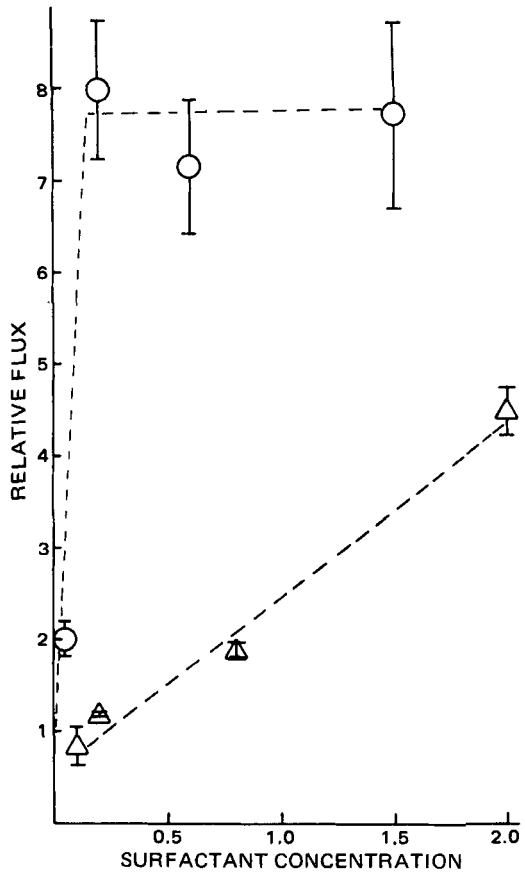

Figure 1—*Effect of surfactant concentration on the* in vitro *relative flux of naproxen (micrograms per milliliter per centimeter hour) through excised human skin from aqueous gels. Key:* ○, *methyldecyl sulfoxide; and* △, *sodium lauryl sulfate. Experimental points are averages of four skin cells, and vertical bars are standard deviations.*

The *in vitro* mean flux of naproxen through excised human, rat, and rabbit skins is given in Table II. The *in vitro* mean flux of the control experiments indicates that the excised human skin was the least permeable and that the excised rabbit skin was most permeable to naproxen. These results are in agreement with the results reported earlier for other solutes (12). Another important difference in the three types of excised skin was in the lag time. The lag time for the human skin was approximately 100 hr; for the rat and rabbit skins, it was about 14 hr. Although excised rat skin was less permeable than excised rabbit skin, the lag time was similar.

For comparing the effect of surfactants on percutaneous absorption through excised human, rat, and rabbit skins, flux relative to the control is given in Table II and Fig. 2. Excised human skin, which was least permeable in control experiments, showed a larger increase in the *in vitro* relative flux due to the presence of these surfactants. On the other hand, excised rabbit skin, which was most permeable in control experiments, showed a moderate increase in the relative flux of naproxen when creams containing these surfactants were tested. The excised rat skin showed a relatively small increase in naproxen flux from creams containing the same surfactants. For example, the influence of 1% methyldecyl sulfoxide on excised human skin in increasing the relative flux was approximately 10-fold, compared to a fourfold increase on excised rabbit skin and only about a 50% increase on excised rat skin.

DISCUSSION

Excised animal skin has been used in studies on percutaneous absorption of drugs and other solutes, possibly because of its ready availability, although it differs significantly from human skin. The skin of

[17] Mallinckrodt Chemical Works, St. Louis, MO 63100.
[18] Arapahoe Chemicals, Division of Syntex Corp., Boulder, CO 80301.
[19] Aldrich Chemical Co., Milwaukee, WI 53210.
[20] Simonsen Laboratories, Gilroy, CA 95020.
[21] Model-A2 animal electric clipper with size 40 blade, John Oster Manufacturing Co., Milwaukee, WI 53200.
[22] L.I.T. Rabbitery, Aptos, CA 95003.
[23] Euthenol.

Table II—Effect of Surfactants on the *In Vitro* Flux of Naproxen through Excised Human, Rat, and Rabbit Skins from an Oil-in-Water Cream Formulation

Surfactant (Concentration)	Excised Human Skin			Excised Rat Skin			Excised Rabbit Skin		
	Mean Flux, $\mu g/cm^2/hr$	*SD*	Relative Flux	Mean Flux, $\mu g/cm^2/hr$	*SD*	Relative Flux	Mean Flux, $\mu g/cm^2/hr$	*SD*	Relative Flux
No added surfactant (control)	1.66	0.49	1	3.75	0.60	1	5.86	0.55	1
Sodium lauryl sulfate (2%)	5.12	1.86	3.09	4.91	0.79	1.31	10.18	4.78	1.74
Sodium laurate (2%)	7.32	3.69	4.41	6.53	0.18	1.74	20.01	9.00	3.41
Methyldecyl sulfoxide (1%)	17.18	4.32	10.35	5.47	0.54	1.46	24.11	10.34	4.11

rodents lacks sweat glands and abounds in hair and hair follicles in contrast to human skin. The thickness of the stratum corneum also varies from species to species. In addition, the absorption of medicaments by way of sweat ducts of human skin has been reported to be negligible as compared to the transepidermal routes (14–16).

The effect of surfactants on percutaneous absorption of several solutes using excised human and animal skin was reported previously (17). Anionic surfactants, sodium laurate and sodium lauryl sulfate, caused continuous damage to the stratum corneum as long as the surfactant solutions remained in contact (17). These surfactants were thought to bind strongly with α-protein, thus causing a reversible denaturation and an uncoiling of the filaments. Membrane expansion, likely hole formation, and loss of water binding capacity are consistent with the reversible $\alpha \rightleftarrows \beta$ conversion of keratin, induced by the strong binding of the surfactant with the protein (18).

Several methods have been used to study the dermatitic effect of nonionic surfactants on rabbit skin (19–22). These studies suggested that nonionic surfactants change the content, composition, and biosynthesis rate of epidermal phospholipids. These results probably indicate changes in epidermal membrane structure since phospholipids are major components of biological membranes.

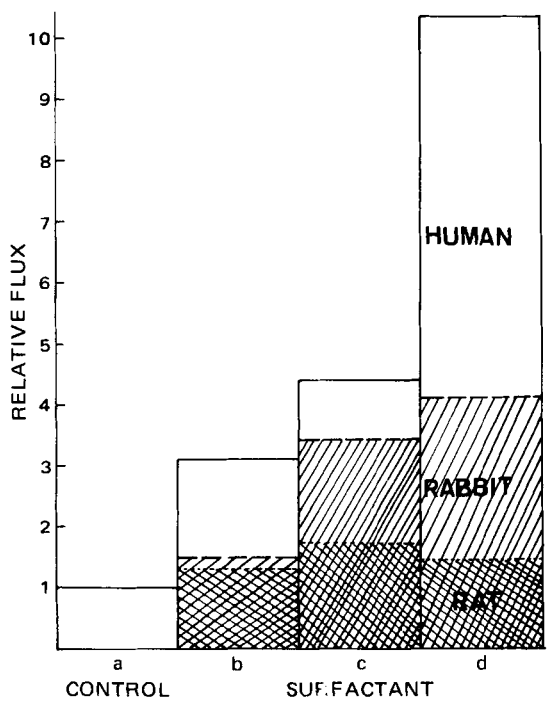

Figure 2—*Relative flux of naproxen through excised human, rabbit, and rat skins, showing the effect of surfactants. Key: a, control; b, 2% sodium lauryl sulfate; c, 2% sodium laurate; and d, 1% methyldecyl sulfoxide.*

The manner in which methyldecyl sulfoxide increases skin permeability is not known. The exact mechanism by which nonionic and anionic surfactants induce permeability changes may differ considerably. However, the net results are damage or disruption of the membrane and permeability changes. Although the mechanism by which a certain class of surfactants changes the permeability of organic solutes may be similar for skins of different species, the magnitude of morphological changes due to damage or disruption of the skin may be different for skins of different species. The results of this study indicate that the excised skin from laboratory animals may lead to erroneous conclusions regarding the effect of surfactants on excised human skin in altering percutaneous absorption of compounds similar to naproxen.

REFERENCES

(1) M. E. Stolar, G. V. Rossi, and M. Barr, *J. Am. Pharm. Assoc., Sci. Ed.*, **49**, 148 (1960).

(2) J. M. Stelzer, Jr., J. L. Colaizzi, and P. J. Wurdack, *J. Pharm. Sci.*, **57**, 1732 (1968).

(3) W. Shen, A. G. Danti, and F. N. Bruscato, *ibid.*, **65**, 1780 (1976).

(4) A. J. Aguiar and M. A. Weiner, *ibid.*, **58**, 210 (1969).

(5) M. Mezei and K. Ryan, *ibid.*, **61**, 1329 (1972).

(6) D. L. Sekura and J. Scala, in "Advances in Biology of Skin," vol. 12, W. Montagna, R. B. Stoughton, and E. J. Van Scott, Eds., Appleton-Century-Crofts, New York, N.Y., 1972, p. 257.

(7) F. R. Bettley, *Br. J. Dermatol.*, **73**, 448 (1961).

(8) F. R. Bettley and E. Donoghue, *Nature*, **185**, 17 (1960).

(9) J. Scala, D. E. McOsker, and H. H. Reller, *J. Invest. Dermatol.*, **50**, 371 (1968).

(10) D. E. Loveday, *J. Soc. Cosmet. Chem.*, **12**, 224 (1961).

(11) P. A. Isherwood, *J. Invest. Dermatol.*, **40**, 143 (1963).

(12) R. T. Tregear, in "Physical Functions of Skin," Academic, New York, N.Y., 1966, pp. 6–13.

(13) M. F. Coldman, B. J. Poulsen, and T. Higuchi, *J. Pharm. Sci.*, **58**, 1098 (1969).

(14) W. B. Shelley and E. M. Melton, *Fed. Proc.*, **6**, 199 (1947).

(15) P. Flesh, S. B. Goldston, and F. Urbach, *Arch. Dermatol. Syphilol.*, **63**, 228 (1951).

(16) G. M. Mackee, F. Hermann, R. L. Baer, and M. B. Sulzberger, *Science*, **98**, 66 (1943).

(17) R. J. Scheuplein and L. Ross, *J. Soc. Cosmet. Chem.*, **21**, 853 (1970).

(18) R. J. Scheuplein and I. H. Blank, *Physiol. Rev.*, **51**, 702 (1971).

(19) M. Mezei, R. W. Sager, W. D. Stewart, and A. I. DeRuyter, *J. Pharm. Sci.*, **55**, 584 (1966).

(20) M. Mezei and R. W. Sager, *ibid.*, **56**, 1604 (1967).

(21) M. Mezei and G. N. White, *ibid.*, **58**, 1209 (1969).

(22) M. Mezei and A. K. Y. Lee, *ibid.*, **59**, 858 (1970).

ACKNOWLEDGMENTS

The authors are grateful to Dr. Boyd J. Poulsen for helpful discussions.

Neuromuscular Block of the Polymyxin Group of Antibiotics

D. V. VISWANATH and H. J. JENKINS ˣ

Received June 17, 1977, from the *Massachusetts College of Pharmacy, Boston, MA 02115.* Accepted for publication January 11, 1978.

Abstract □ The neuromuscular blocking effects of polymyxin and colistin were investigated in the unanesthetized rabbit, in the cat sciatic nerve–tibialis anterior muscle preparation *in vivo*, and in the frog rectus abdominis preparation *in vitro*. These antibiotics, along with certain others used for comparison, produced paralyses of different intensities in rabbits, depending on the dose, with no preceding fasciculation. In this regard, polymyxin was the most potent antibiotic studied. Polymyxin B sulfate (3–5 mg/kg) and colistimethate sodium (60–90 mg/kg) caused a blockade of neuromuscular transmission, partial paralysis of respiration, and hypotension in cats. The intraarterial injection of these antibiotics did not elicit muscle contraction; the response to the intraarterial injection of acetylcholine was reduced or abolished during the block; calcium and epinephrine antagonized the block; posttetanic potentiation occurred; edrophonium and decamethonium produced brief antagonism of the block; neostigmine, tetraethylammonium, and choline were without effect; and tubocurarine accentuated the block. During the block, muscle action potentials were reduced or abolished, and nerve action potentials were unaffected. (Response of the muscle to direct stimulation was reduced compared to the predrug response.) Both agents depressed muscle twitches elicited at the faster rate of stimulation (60/min) while the slow rate twitches (6/min) were hardly depressed. The serum ionic calcium level was not altered significantly by these antibiotics. Thus, the neuromuscular block displayed characteristics of a postsynaptic, nondepolarizing type that was noncompetitive in nature, with possible presynaptic elements and a depressant action on muscle fibers. Both polymyxin and colistin possess transient ganglionic blocking action.

Keyphrases □ Polymyxin—neuromuscular blocking effect in rabbits and cat and frog muscle preparations □ Colistin—neuromuscular blocking effect in rabbits and cat and frog muscle preparations □ Neuromuscular blocking effect—polymyxin and colistin in rabbits and cat and frog muscle preparations □ Antibacterials—polymyxin and colistin, neuromuscular blocking effect in rabbits and cat and frog muscle preparations

Several clinically important antibiotics produce somatic neuromuscular transmission blockade. This effect has been implicated in their paralyzing potentiality. Respiratory and motor paralysis have been observed clinically following the administration of streptomycin, polymyxin, and tetracycline groups of antibiotics to anesthetized and unanesthetized patients (1).

BACKGROUND

The neuromuscular blocking activity of streptomycin, polymyxin, and tetracycline groups of antibiotics has been demonstrated (2). Several studies (3, 4) led to the emergence of the "competitive hypothesis" concerning the mechanism of the neuromuscular blocking action of the streptomycin group of antibiotics. This hypothesis postulates that the antibiotics inhibit prejunctional release of acetylcholine primarily by competing with calcium ions for receptor sites on the motor nerve terminal while decreasing the sensitivity of the motor end-plate to the depolarizing action of acetylcholine.

The mechanism of the neuromuscular blockade produced by the polymyxin antibiotics has not been elucidated (2) and was investigated in this study.

Pittinger *et al.* (1) recently reviewed the clinical occurrences of antibiotic-induced paralysis and abstracted and analyzed the case histories of more than 100 incidences of hazardous antibiotic paralysis. The first clinical cases of respiratory arrest and muscular weakness associated with the administration of polymyxins were reported in 1962, and several such cases have been reported since then. This complication occurred in patients receiving large doses of polymyxin antibiotics, in myasthenic patients, and in some patients receiving routine therapeutic doses of these antibiotics.

Few studies have investigated the neuromuscular blocking effect of the polymyxin antibiotics. The neuromuscular blocking effect of polymyxins was demonstrated in the sciatic–gastrocnemius preparation of rabbits anesthetized with pentobarbital (5, 6). Supramaximal pulses were used at a frequency of 100 (5) and 250/sec (6) for 0.2 sec every 5 or 10 sec for stimulation of the sciatic nerve. Unfortunately, pentobarbital has a neuromuscular blocking effect of its own.

The effect of polymyxin was studied in the urethan-anesthetized rabbit sciatic–gastrocnemius preparation, employing supramaximal stimuli at 10-sec intervals with 0.2-sec bursts at a frequency of 100/sec (7). No correlation with respiratory effects was made because artificial respiration was applied throughout. The effect of the antibiotics was studied with the human intercostal nerve–muscle preparation and stimuli at the rate of 6/min (8).

The neuromuscular blocking action of colistin was studied in single muscle fibers of the rat hemidiaphragm preparation with the microelectrode technique (9). Even very high doses of colistin (1 g/liter) did not produce neuromuscular block. However, a combination of colistin and tubocurarine produced a block.

The response of the neuromuscular junction of the cat is much more similar to that of the human than is the response of the rabbit junction.

This paper reports an investigation of the neuromuscular block of polymyxin and colistin with a view to determining the mechanism of their neuromuscular blocking action and its relationship to the respiratory paralysis accompanying their use.

EXPERIMENTAL

The investigation was carried out on unanesthetized rabbits, the cat sciatic nerve–tibialis anterior muscle preparation *in vivo*, and the frog rectus abdominis preparation *in vitro*.

The paralytic progression patterns of polymyxin, colistin, tetracycline, and oxytetracycline were studied by injecting different doses intravenously through a needle cannula inserted in the marginal ear vein of rabbits. Their effect on serum ionic calcium levels was determined in rabbits from blood samples obtained by intracardiac puncture before and after injection of paralyzing doses of antibiotics. The serum ionic calcium levels were measured with a calcium-selective electrode[1].

Cats of either sex, 2–4 kg, anesthetized with a mixture of chloralose (70 mg/kg ip) and pentobarbital (8 mg/kg ip), were used for the sciatic-tibialis preparation. A schematic representation of the experimental setup in the cat is presented in Fig. 1. The anesthetized cat was placed on the myograph stand, the trachea was cannulated, and artificial respiration was applied when necessary with a small animal respirator. Hindlimbs were immobilized by drills inserted through the lower end of the tibia and condyles of the femur. The lateral popliteal branch of the sciatic nerve was ligated and sectioned, and platinum electrodes were placed on the nerve for stimulation. The electrodes were then connected to the stimulator[2].

The tendon of the tibialis was connected to a force-displacement transducer precalibrated for recording the force of contraction in grams, and the contractions were recorded on a four-channel polygraph. A resting tension of 75 g was maintained on the muscle and tendon. Drugs were injected through a polyethylene cannula into the jugular vein. The carotid artery was cannulated, and the arterial blood pressure was recorded with a pressure transducer. Respiratory movements were recorded with a pneumograph. Muscle action potentials of the tibialis anterior muscle in response to nerve stimulation were recorded with a concentric needle electrode (positioned in the muscle) attached to the high gain preamplifier of the polygraph. Nerve action potentials were recorded similarly with a high gain preamplifier from the lateral popliteal nerve through a shielded platinum electrode placed on the nerve.

[1] Orion.
[2] American Electronics Laboratory (104A).

0022-3549/78/0900-1275$01.00/0
© 1978, American Pharmaceutical Association

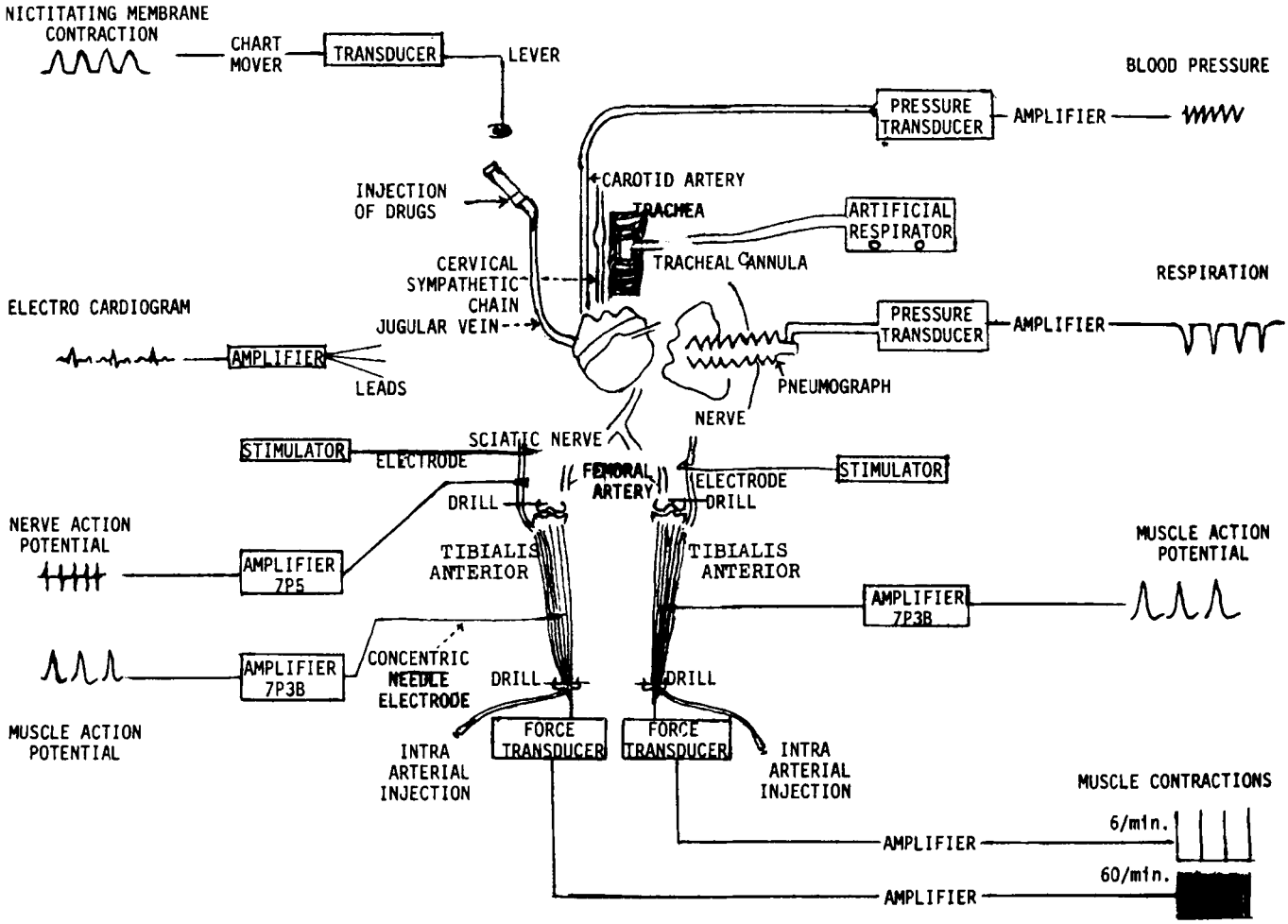

Figure 1—*Experimental setup in the cat.*

In the unilateral preparation, the tibialis twitches of one hindlimb were elicited by stimulating the corresponding (lateral popliteal) nerve with supramaximal pulses of 0.4-msec duration at a frequency of 6/min. In the bilateral preparation, tibialis twitches of both hindlimbs were elicited by stimulating one lateral popliteal nerve at a frequency of 6/min and the other at 60/min. Stimuli to one tibialis muscle were passed through a 1:1 isolation transformer. The tendons of the tibialis muscles were attached to different force–displacement transducers, and the contractions of the muscles were recorded isometrically on the polygraph.

Close-arterial injection of drugs to the tibialis was made according to the method described by Brown (10). Cooling of the tibialis anterior muscles was avoided by allowing warm saline, heated to 37° (by using a constant-temperature circulator[3] with condenser), to soak a thin layer of cotton spread over the muscle. As in similar studies, heat lamps assisted the cat in maintaining body temperature.

The dose of the antibiotic producing a 50% reduction in the amplitude of indirect maximal twitches (ED_{50}) was calculated from data obtained by administering at different times a dose of antibiotic reducing the amplitude of these twitches, slow (6/min) and fast (60/min), to an extent greater than, less than, and approximately 50% of their original value.

Responses to direct stimulation (70–90 v) of the muscle and tetanic stimulation at rates of 50 and 100/sec were determined before and during partial and complete neuromuscular block.

In some experiments, the antagonistic effects of neostigmine methylsulfate, calcium chloride, edrophonium chloride, choline chloride, guanidine hydrochloride, sodium bicarbonate, and potassium chloride on the antibiotic block were studied, as were the effects of tubocurarine chloride and decamethonium bromide.

For the *in vitro* rectus abdominis preparation, the rectus muscle strip was dissected out from the pithed frog and suspended in a tissue chamber filled with frog Ringer solution. The contraction responses of the muscle to acetylcholine were picked up by a transducer and recorded on a polygraph. The antagonism of the response to acetylcholine of increasing concentrations of each antibiotic was determined to establish whether the antagonism was competitive or noncompetitive.

The following drugs were used during the investigation: polymyxin B sulfate, colistimethate sodium, oxytetracycline, tetracycline hydrochloride, acetylcholine chloride, neostigmine methylsulfate (50–100 μg/kg), calcium chloride (10% solution in distilled water) (12–15 mg/kg), edrophonium chloride (100–200 μg/kg), choline chloride (1–5 mg/kg), sodium bicarbonate (2–5 mg/kg), potassium chloride (2–5 mg/kg), epinephrine (8–10 μg/kg), tubocurarine chloride (100–200 μg/kg), and decamethonium bromide (30 μg/kg).

RESULTS

The antibiotics—*viz.*, polymyxin, colistin, tetracycline, and oxytetracycline, produced paralyses of varying intensities in unanesthetized rabbits, according to the antibiotic and the doses used. Polymyxin was the most potent. The animals recovered from the paralysis when the intensity was mild or moderate. The doses of each antibiotic producing head drop and respiratory arrest, respectively, are presented in Table I. Polymyxin was about 70 times less potent than curare and eight times more potent than colistin in these respects.

The progressive paralytic patterns elicited by the antibiotics were determined. Slowing of respiration was observed initially in most animals, followed by the inability to walk, head drop, and loss of the righting reflex. A further decrease in respiratory activity leading to respiratory arrest resulted in death. No fasciculations such as those occurring with decamethonium were observed. Mild asphyxial convulsions occurred in some instances.

In the cat sciatic–tibialis preparation, intravenous injection of polymyxin B sulfate (3–5 mg/kg) and colistimethate sodium (60–90 mg/kg) produced partial to complete abolition of maximal twitches elicited at the rates of 6 and 60/min and partial to complete paralysis of respiration and hypotension (60–70% of predrug pressure level). The onset of the neuromuscular block was rapid and persisted for 30–40 min.

The doses of antibiotics responsible for a 50% block of indirect maximal twitches were determined graphically. The ED_{50} values of polymyxin B

[3] Haake.

Table I—Paralyzing Doses of the Antibiotics in Unanesthetized Rabbits

Dose	Polymyxin B Sulfate, mg/kg	Oxytetracycline, mg/kg	Colistimethate Sodium, mg/kg	Streptomycin, mg/kg	Tubocurarine Chloride, mg/kg
Head drop dose	11.1 ± 1	450 ± 5	90 ± 2	263 ± 3	0.16 ± 0.02
Loss of righting reflex dose	12.2 ± 1	460 ± 5	100 ± 2	273 ± 3	0.22 ± 0.02
Respiratory arrest dose	13.6 ± 1	476 ± 5	112 ± 2	282 ± 3	0.32 ± 0.02
Cardiac arrest dose	13.9 ± 1	477 ± 5	113 ± 2	291 ± 3	—

sulfate were 5.2 mg/kg for twitches elicited at the rate of 6/min and 2.7 mg/kg for twitches elicited at the rate of 60/min. The respective ED_{50} values for colistimethate sodium were 100 and 61 mg/kg. Polymyxin and colistin produced a far greater depression of fast twitches than slow twitches. For example, a dose of polymyxin B sulfate eliciting a 50% block of twitches at a frequency of 6/min produced a 100% block of twitches at 60/min.

Some characteristics of the neuromuscular block of the antibiotics and their comparison with those of curare and decamethonium are summarized in Table II. With polymyxin and colistin, stimulant effects were absent. The response to a tetanic stimulation of 50 and 100/sec, respectively, was not maintained or only partially maintained during partial neuromuscular block; such response was absent or involved an initial twitch only during complete block. Maximal posttetanic potentiation occurred immediately after tetanus during partial neuromuscular block with these antibiotics. Also, during the block, the response to direct stimulation of the muscle was decreased as compared to the predrug response, and the response to intraarterially injected acetylcholine was reduced or abolished. During the abolition, increasing the dose of acetylcholine injected failed to restore the response. The administration of calcium chloride intravenously gave rise to a partial or complete antagonism of the block; neostigmine was without any effect on the block.

During the block, muscle action potentials were reduced or abolished, while nerve action potentials were unaffected.

Intraarterial injection of antibiotic in doses of 1–500 μg elicited no contractions. An intraarterial dose of 500 μg of polymyxin B sulfate (Fig. 2) and 10–20 mg of colistimethate sodium yielded about a 70–80% block of indirectly elicited maximal twitches, an effect that was not spontaneously reversible. However, intraarterial injection of calcium chloride and epinephrine, but not norepinephrine, partially antagonized the block (Fig. 2). Polymyxin produced depression of respiration concomitant with the block of twitches. A 3-mg/kg dose produced slowing and a decrease in depth of respiration of about 30–35% of the original value, while a 5-mg/kg dose produced cessation of respiration. The ED_{50} values of polymyxin B sulfate and colistimethate sodium with respect to respiratory interference were 3.6 and 41 mg/kg, respectively. Cessation of respiration occurred just after the twitches elicited at 60/min were abolished.

The effect of intravenous polymyxin on indirect maximal twitches and on intraarterial acetylcholine-elicited twitches recorded simultaneously appears in Fig. 3. During depression of indirect maximal twitches at 60 and 6/min, respectively, the twitch response to intraarterial acetylcholine was completely abolished. Acetylcholine contractions were depressed more than indirect twitches at various doses of polymyxin. Hence, polymyxins seem to possess a prominent postsynaptic blocking action.

The administration of the same doses of polymyxin produced more pronounced and prolonged neuromuscular block, eventuating often in complete depression of indirect twitches. This cumulative neuromuscular blocking effect of polymyxin was investigated.

A dose of polymyxin of 3 mg/kg, capable of producing a significant block, was used. Doses were repeated when recovery from each preceding dose became apparent. A second injection of the same dose of polymyxin produced a 50–60% greater neuromuscular block than the first, and a third injection produced about a 40–50% greater block than the second. The administration of calcium chloride effectively reversed the cumulative neuromuscular blocking effect of polymyxin. The first injection of polymyxin of 4 mg/kg produced a 43% block of slow twitches and a 100% block of fast twitches. After administration of calcium chloride, the second injection of polymyxin produced only a 5% block of slow twitches and a 55% block of fast twitches.

Polymyxins depressed blood pressure within seconds to minutes of administration. A 4-mg/kg dose of polymyxin B sulfate and 62.5 mg of colistimethate sodium/kg yielded an average decrease in mean arterial blood pressure of about 50% of the predrug level. The blood pressure rose after a few minutes but then fell again and remained 10–15% below the control level. During the reduced arterial pressure, administration of calcium chloride elevated blood pressure (Fig. 4). Sympathetic stimulation and injection of epinephrine also increased this pressure, while vagal stimulation accentuated the polymyxin fall in blood pressure. The contractions of the nictitating membrane obtained by preganglionic cervical sympathetic stimulation were partially abolished by these antibiotics as they exerted their effect to lower arterial blood pressure, while those obtained by intravenous epinephrine were unaffected. The ECG was unaffected during the production of hypotension by these antibiotics.

In the frog rectus abdominis preparation, both polymyxin B sulfate and colistimethate sodium, preadministered, antagonized acetylcholine-induced contractions. Polymyxin at a dose half that of acetylcholine was responsible for a depression of acetylcholine-induced rectus contractions of approximately 35%. At a dose equivalent to the dose of acetylcholine, a depression of approximately 87% occurred; and at a dose twice that of acetylcholine, a depression of approximately 96% occurred. Polymyxins produced no contracture and had no curative effect on acetylcholine contractions. The contraction responses to various doses of acetylcholine were obtained in the presence of increasing concentrations

Table II—Characteristics of the Neuromuscular Block of Polymyxin and Colistin in the Cat Sciatic-Tibialis Preparation

Antibiotic or Other Agent	Stimulant Effects	Response to Tetanic Stimulation		Posttetanic Facilitation of Response	Response to Intra-arterial Acetylcholine	Direct Stimulation of Muscle	Effect of	
		During Partial Paralysis[a]	During Complete Paralysis[a]				Calcium Chloride	Neostigmine
Polymyxin B sulfate and colistimethate sodium	Absent	Partially maintained/ not maintained	Initial twitch/ absent	Present: maximum immediately after tetanus	Reduced or abolished	Decreased response	Partial to complete antagonism	No significant effect
Curare	Absent	Not maintained	Initial twitch/ present	Present: maximum immediately after tetanus	Reduced or abolished	Normal response	No or partial antagonism	Complete antagonism
Decamethonium	Present (facilitation of twitches)	Maintained	Initial twitch/ absent	Absent	Reduced or abolished	Decreased response	No effect	Accentuation
Magnesium	Absent	Maintained	Maintained	Present: maximum immediately after tetanus	Reduced or abolished	Decreased response	Complete or almost complete antagonism	

[a] Indirect maximal twitches.

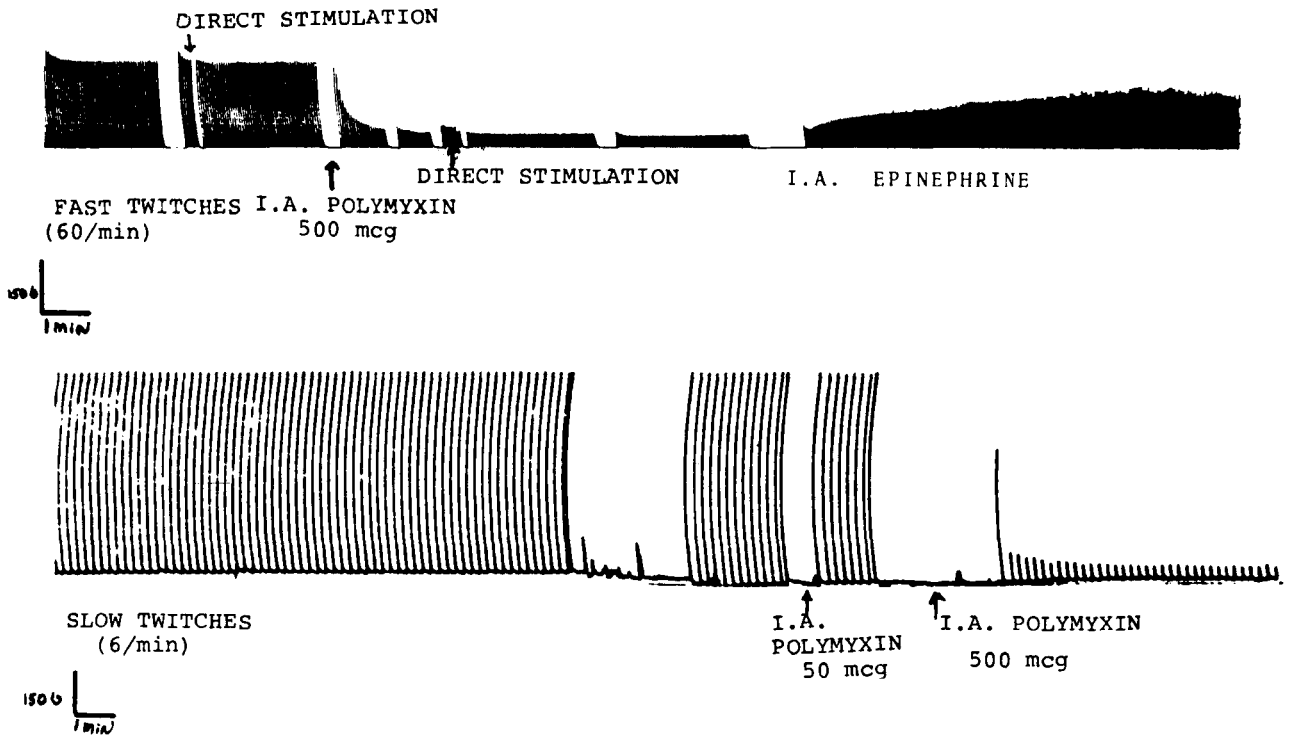

Figure 2—*Effect of intraarterial (I.A.) polymyxin and its antagonism by intraarterial epinephrine.*

of polymyxin and colistin. Each dose–response curve represented a given polymyxin concentration. The decrease in the maximal amplitude of acetylcholine contraction and the flattening of the curves with an increase in polymyxin concentration indicated a noncompetitive antagonism by these antibiotics (Fig. 5).

The effects of polymyxin B sulfate and colistimethate sodium on serum ionic calcium levels in rabbits are given in Table III. These antibiotics in paralyzing doses did not alter the calcium-ion level significantly.

DISCUSSION

The results confirm that polymyxins exert a potent neuromuscular block leading eventually to respiratory arrest. The possible actions at the postsynaptic site, the presynaptic site, and the nerve and muscle investigated show that polymyxin-induced neuromuscular block results from a prominent postsynaptic, nondepolarizing action. This conclusion is based on the following observations.

Polymyxin B sulfate and colistimethate sodium injected intraarterially did not cause contraction of the tibialis muscle in the cat, and these antibiotics elicited neuromuscular block when injected intravenously without any preceding fasciculation or facilitation of twitches, suggesting a nondepolarizing action. A simultaneous study of the effects of the antibiotic on the contraction response of the muscle to close-arterial injection of acetylcholine and on the indirect maximal twitch response elicited by nerve stimulation provides a sensitive means for determining whether the site of the blocking action is presynaptic or postsynaptic (11). During the neuromuscular block of the tibialis preparation in the cat, the contraction response to intraarterial injection of acetylcholine was reduced or abolished and was much more prominently affected than the simultaneously recorded indirect maximal twitches, indicating a significant postsynaptic action. The neuromuscular block was accentuated by curare and was briefly antagonized by edrophonium and decamethonium. Epinephrine and calcium chloride antagonized the neuromuscular block.

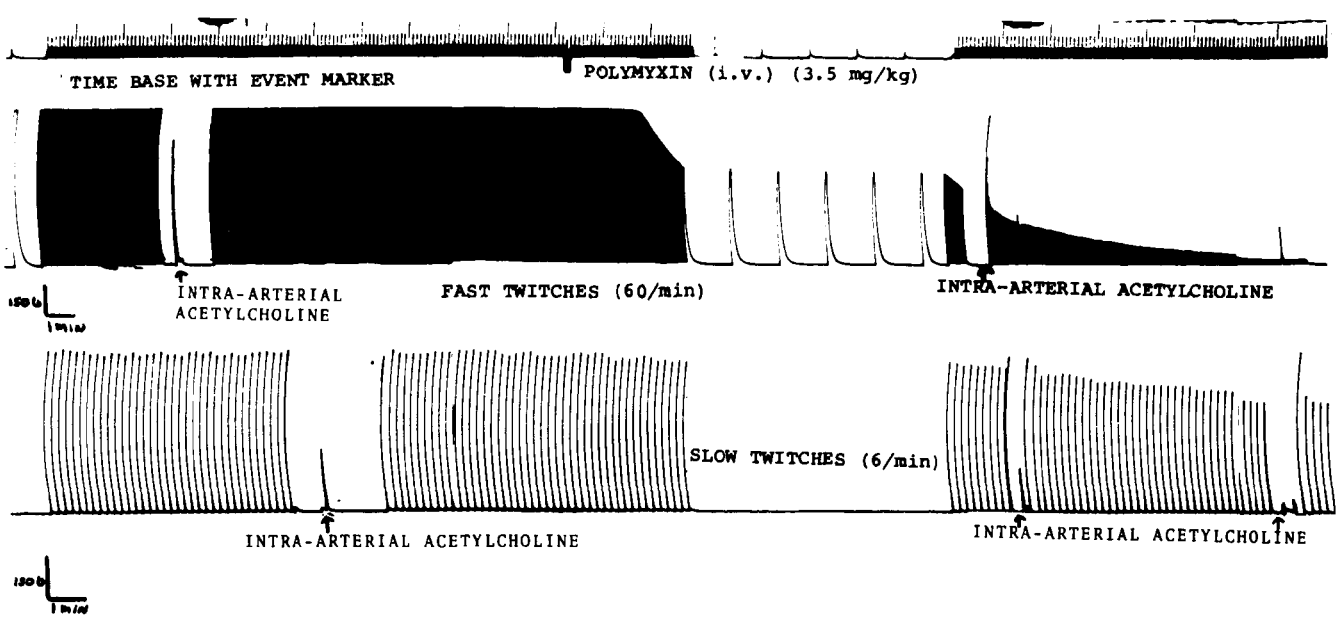

Figure 3—*Effect of intravenous polymyxin on indirect maximal twitches and the response to intraarterial acetylcholine.*

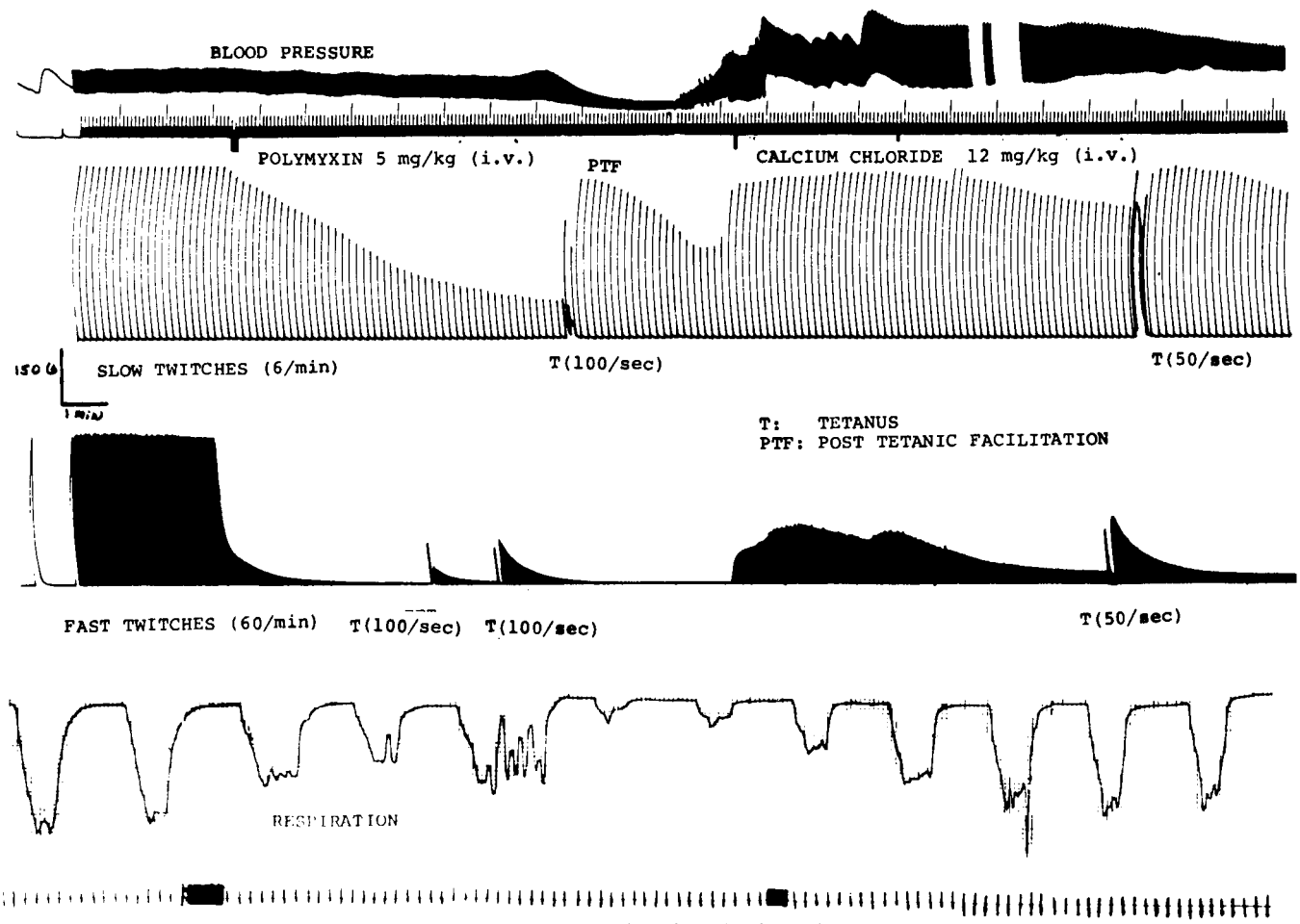

Figure 4—*Effect of calcium chloride on polymyxin-induced depression of maximal twitches, respiration, and blood pressure.*

Polymyxin B sulfate and colistimethate sodium antagonized the acetylcholine response in the frog rectus preparation, *i.e.*, depressed the response of the end-plate to the depolarizing action of applied acetylcholine and did not cause contraction of the rectus muscle by themselves,

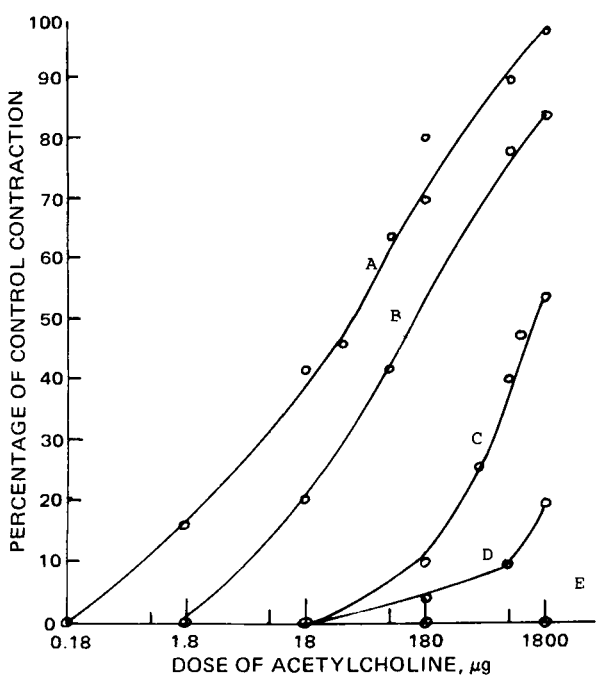

Figure 5—*Antagonism by polymyxin of the acetylcholine-induced contractions of the frog rectus abdominis muscle. Key (dose of polymyxin): A, 0 (control acetylcholine contraction); B, 100 μg; C, 200 μg; D, 300 μg; and E, 500 μg.*

suggesting a postsynaptic, nondepolarizing action. This nondepolarizing, postsynaptic blocking action was determined to be of noncompetitive nature, since:

1. The response to intraarterial acetylcholine in cats, which was abolished during the block, could not be obtained again by increasing the concentration of acetylcholine injected (in contrast to the response to acetylcholine during the curare block).
2. The cumulative log dose–response curve involving the effect of the antibiotics on the acetylcholine-induced frog rectus contraction response showed a decrease of the maximal amplitude and a flattening of the curves, demonstrating a noncompetitive antagonism.
3. Neostigmine did not produce antagonism of the neuromuscular block in cats.

During the block, the muscle action potentials were reduced or abolished while the nerve action potentials were unaffected, thus excluding any action of the antibiotic on the nerve trunk.

During the block of indirect maximal twitches, the response to direct stimulation was decreased as compared with the predrug response. So polymyxin probably acts on muscle fibers by decreasing their direct excitability. Polymyxin probably exerts a presynaptic action, since:

1. The tibialis twitches elicited at 60/min were depressed while twitches elicited at 6/min were unaffected in the bilateral preparation in cats. [The bilateral preparation (in which one sciatic nerve was stim-

Table III—Effect of Polymyxin in Paralyzing Doses on Serum Ionic Calcium Levels in Rabbits [a]

Animal	Calcium-Ion Level, m*M*/liter: Before Drug (pH of Sample)	After Drug (pH of Sample)
1	1.46 (7.33)	1.37 (7.13)
2	1.31 (7.24)	1.40 (7.08)
3	1.34 (7.30)	1.43 (7.14)
4	1.41 (7.37)	1.49 (7.06)
5	0.96 (7.34)	1.26 (7.19)
Mean	1.296 ± 0.176	1.39 ± 0.076

[a] Determined with calcium-selective electrode (Orion model).

ulated at 6/min and the other at 60/min) provides a means for distinguishing pre- and postsynaptic activities. Contractions elicited at the lower rate are blocked preferentially by compounds that act postsynaptically, while contractions elicited at the higher rate are blocked preferentially by compounds that act presynaptically.]

2. The neuromuscular block was antagonized partially or completely by calcium chloride administration.

3. The cumulative neuromuscular blocking effect of polymyxin also was antagonized by calcium chloride administration.

This presynaptic action may involve diminution of the calcium-ion function in the nerve terminal, occasioning a decrease in the mobilization and release of acetylcholine, or it may involve occupation of the superficial neuronal membrane sites by the antibiotics resulting in decreased transmitter release, and these actions could be antagonized by calcium administration.

The characteristics of the neuromuscular block of polymyxin and colistin resembled those of magnesium in its direct effect on muscle fibers, posttetanic response potentiation, and less strikingly, calcium antagonism of the block.

It is concluded that the neuromuscular block of polymyxin B sulfate and colistin results predominantly from their postsynaptic, nondepolarizing action, which is noncompetitive, but also from their action to depress the direct excitability of the muscle fibers and from a presynaptic action resulting in reduced transmitter release. The neuromuscular blocking action does not involve the chelation of calcium ions, since polymyxin in paralyzing doses did not alter significantly the serum calcium-ion level.

REFERENCES

(1) C. B. Pittinger, Y. Elyasa, and R. Adamson, *Anesth. Analg.*, **49**, 487, (1970).

(2) C. B. Pittinger and R. Adamson, *Ann. Rev. Pharmacol.*, **12**, 169 (1972).

(3) V. O. Brazil, *Arch. Int. Pharmacodyn. Ther.*, **79**, 78 (1969).

(4) D. Elmquist and J. O. Josefsson, *Acta Physiol. Scand.*, **54**, 105 (1972).

(5) J. C. Timmerman, J. P. Long, and C. B. Pittinger, *Toxicol. Appl. Pharmacol.*, **1**, 299 (1959).

(6) R. H. Adamson, F. N. Marshall, and J. P. Long, *Proc. Soc. Exp. Biol. Med.*, **165**, 494 (1960).

(7) J. H. Naimen and J. D. Maska, *J. Surg. Res.*, **7**, 199 (1967).

(8) P. B. Sabawalla and B. Dillon, *Anesthesiology*, **20**, 659 (1959).

(9) H. P. McQuillen and L. Engbaek, *Arch. Neurol.*, **32**, 235 (1975).

(10) G. L. Brown, *J. Physiol. (London)*, **92**, 22 (1938).

(11) W. C. Bowman, in "Pharmacometrics," vol. 1, D. R. Lawrence and A. L. Bacharach, Eds., Academic, New York, N.Y., 1964, p. 325.

Influence of High-Viscosity Vehicles on Miotic Effect of Pilocarpine

R. D. SCHOENWALD ˣ, R. L. WARD, L. M. DeSANTIS, and R. E. ROEHRS

Received October 31, 1977, from the *Biopharmaceutics Group and Pharmacology Group, Department of Ophthalmology, Alcon Laboratories, Fort Worth, TX 76101.* Accepted for publication January 12, 1978.

Abstract □ Gel formulations containing 2% pilocarpine hydrochloride were prepared from ethylene maleic anhydride, carbomer, hydroxyethylcellulose, polyacrylamide, ethylhydroxyethylcellulose, hydroxypropylcellulose, and poly(methylvinyl ether–maleic anhydride). The viscosity characteristics of each formulation were evaluated from rheograms developed at 37° using a cone and plate viscometer. Single-point viscosities were determined at room temperature using a single-point rotational viscometer. Plastic viscosity parameters correlated to miosis durations in the rabbit following ophthalmic dosing of 50 μl. Carbomer formulations varying in concentration between 0.9 and 5.0% (w/w) showed a discontinuous relationship when either yield value or plastic viscosity was plotted against miosis durations. At carbomer concentrations above 3%, miosis durations increased 1.5-fold. Above and below this range, plastic parameters did not correlate to miosis duration. It was reasoned that the increased duration was a consequence of the gel's increased yield value such that appreciable *in vivo* thinning of the gel does not take place with eyelid and/or eyeball movements. As a result, the residence time of the drug in the eye would be expected to increase, thus promoting an increased duration.

Keyphrases □ Pilocarpine—miotic effect, influence of various high-viscosity vehicles in rabbits □ Vehicles, high viscosity—influence on miotic effect of pilocarpine in rabbits □ Viscosity, high—in various vehicles, influence on miotic effect of pilocarpine in rabbits □ Miotic effect—of pilocarpine, influence of various high-viscosity vehicles in rabbits □ Ophthalmic cholinergics—pilocarpine, miotic effect, influence of various high-viscosity vehicles in rabbits

Polymers have been added to aqueous solutions of ophthalmic drugs to lengthen the contact time of the drug with the eye. This method is based on the assumption that drug absorption and, hence, duration can be improved.

The use of viscous solutions to prolong the effect of pilocarpine has shown that, in rabbits, large decreases in the drainage rate can be obtained when the viscosity is increased from 1 to 12–15 cps (1). Above this level, however, further increases in viscosity do not appreciably decrease drainage rates. When compared to an aqueous solution of pilocarpine nitrate, the testing of viscous solutions (100 cps) indicated that there is a twofold increase in drug aqueous humor concentration with a 100-fold increase in viscosity at 30 min following dosing to rabbits (2). It was hypothesized that the shear created by blinking resulted in thinning such that a large increase in instilled solution viscosity would not appreciably improve contact time and, therefore, bioavailability (2). For solutions, the approach to increasing bioavailability by increasing the vehicle viscosity is limited.

This study was conducted to determine if high-viscosity polymer systems could overcome the suspected thinning that occurs because of eye movements and/or blinking of the eyelids and prolong pilocarpine effects in the rabbits. Carbomer gel systems were primarily chosen for study because of the possibility of formulating a wide variation of high viscosities.

EXPERIMENTAL

Carbomer Gel Preparation—A series of carbomer[1] gels was pre-

[1] Carbopol 940, B.F. Goodrich.

0022-3549/78/0900-1280$01.00/0

© 1978, American Pharmaceutical Association

ulated at 6/min and the other at 60/min) provides a means for distinguishing pre- and postsynaptic activities. Contractions elicited at the lower rate are blocked preferentially by compounds that act postsynaptically, while contractions elicited at the higher rate are blocked preferentially by compounds that act presynaptically.]

2. The neuromuscular block was antagonized partially or completely by calcium chloride administration.

3. The cumulative neuromuscular blocking effect of polymyxin also was antagonized by calcium chloride administration.

This presynaptic action may involve diminution of the calcium-ion function in the nerve terminal, occasioning a decrease in the mobilization and release of acetylcholine, or it may involve occupation of the superficial neuronal membrane sites by the antibiotics resulting in decreased transmitter release, and these actions could be antagonized by calcium administration.

The characteristics of the neuromuscular block of polymyxin and colistin resembled those of magnesium in its direct effect on muscle fibers, posttetanic response potentiation, and less strikingly, calcium antagonism of the block.

It is concluded that the neuromuscular block of polymyxin B sulfate and colistin results predominantly from their postsynaptic, nondepolarizing action, which is noncompetitive, but also from their action to depress the direct excitability of the muscle fibers and from a presynaptic action resulting in reduced transmitter release. The neuromuscular blocking action does not involve the chelation of calcium ions, since polymyxin in paralyzing doses did not alter significantly the serum calcium-ion level.

REFERENCES

(1) C. B. Pittinger, Y. Elyasa, and R. Adamson, *Anesth. Analg.*, **49**, 487, (1970).

(2) C. B. Pittinger and R. Adamson, *Ann. Rev. Pharmacol.*, **12**, 169 (1972).

(3) V. O. Brazil, *Arch. Int. Pharmacodyn. Ther.*, **79**, 78 (1969).

(4) D. Elmquist and J. O. Josefsson, *Acta Physiol. Scand.*, **54**, 105 (1972).

(5) J. C. Timmerman, J. P. Long, and C. B. Pittinger, *Toxicol. Appl. Pharmacol.*, **1**, 299 (1959).

(6) R. H. Adamson, F. N. Marshall, and J. P. Long, *Proc. Soc. Exp. Biol. Med.*, **165**, 494 (1960).

(7) J. H. Naimen and J. D. Maska, *J. Surg. Res.*, **7**, 199 (1967).

(8) P. B. Sabawalla and B. Dillon, *Anesthesiology*, **20**, 659 (1959).

(9) H. P. McQuillen and L. Engbaek, *Arch. Neurol.*, **32**, 235 (1975).

(10) G. L. Brown, *J. Physiol. (London)*, **92**, 22 (1938).

(11) W. C. Bowman, in "Pharmacometrics," vol. 1, D. R. Lawrence and A. L. Bacharach, Eds., Academic, New York, N.Y., 1964, p. 325.

Influence of High-Viscosity Vehicles on Miotic Effect of Pilocarpine

R. D. SCHOENWALD ˣ, R. L. WARD, L. M. DeSANTIS, and R. E. ROEHRS

Received October 31, 1977, from the *Biopharmaceutics Group and Pharmacology Group, Department of Ophthalmology, Alcon Laboratories, Fort Worth, TX 76101.* Accepted for publication January 12, 1978.

Abstract □ Gel formulations containing 2% pilocarpine hydrochloride were prepared from ethylene maleic anhydride, carbomer, hydroxyethylcellulose, polyacrylamide, ethylhydroxyethylcellulose, hydroxypropylcellulose, and poly(methylvinyl ether–maleic anhydride). The viscosity characteristics of each formulation were evaluated from rheograms developed at 37° using a cone and plate viscometer. Single-point viscosities were determined at room temperature using a single-point rotational viscometer. Plastic viscosity parameters correlated to miosis durations in the rabbit following ophthalmic dosing of 50 μl. Carbomer formulations varying in concentration between 0.9 and 5.0% (w/w) showed a discontinuous relationship when either yield value or plastic viscosity was plotted against miosis durations. At carbomer concentrations above 3%, miosis durations increased 1.5-fold. Above and below this range, plastic parameters did not correlate to miosis duration. It was reasoned that the increased duration was a consequence of the gel's increased yield value such that appreciable *in vivo* thinning of the gel does not take place with eyelid and/or eyeball movements. As a result, the residence time of the drug in the eye would be expected to increase, thus promoting an increased duration.

Keyphrases □ Pilocarpine—miotic effect, influence of various high-viscosity vehicles in rabbits □ Vehicles, high viscosity—influence on miotic effect of pilocarpine in rabbits □ Viscosity, high—in various vehicles, influence on miotic effect of pilocarpine in rabbits □ Miotic effect—of pilocarpine, influence of various high-viscosity vehicles in rabbits □ Ophthalmic cholinergics—pilocarpine, miotic effect, influence of various high-viscosity vehicles in rabbits

Polymers have been added to aqueous solutions of ophthalmic drugs to lengthen the contact time of the drug with the eye. This method is based on the assumption that drug absorption and, hence, duration can be improved.

The use of viscous solutions to prolong the effect of pilocarpine has shown that, in rabbits, large decreases in the drainage rate can be obtained when the viscosity is increased from 1 to 12–15 cps (1). Above this level, however, further increases in viscosity do not appreciably decrease drainage rates. When compared to an aqueous solution of pilocarpine nitrate, the testing of viscous solutions (100 cps) indicated that there is a twofold increase in drug aqueous humor concentration with a 100-fold increase in viscosity at 30 min following dosing to rabbits (2). It was hypothesized that the shear created by blinking resulted in thinning such that a large increase in instilled solution viscosity would not appreciably improve contact time and, therefore, bioavailability (2). For solutions, the approach to increasing bioavailability by increasing the vehicle viscosity is limited.

This study was conducted to determine if high-viscosity polymer systems could overcome the suspected thinning that occurs because of eye movements and/or blinking of the eyelids and prolong pilocarpine effects in the rabbits. Carbomer gel systems were primarily chosen for study because of the possibility of formulating a wide variation of high viscosities.

EXPERIMENTAL

Carbomer Gel Preparation—A series of carbomer[1] gels was pre-

[1] Carbopol 940, B.F. Goodrich.

0022-3549/78/0900-1280$01.00/0

© 1978, American Pharmaceutical Association

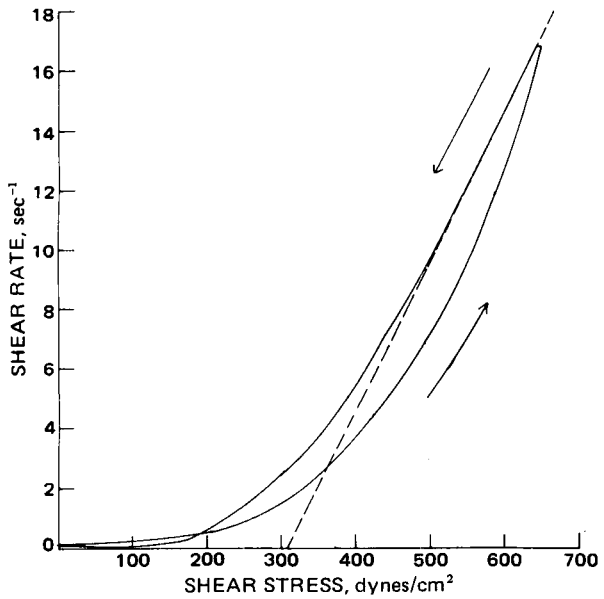

Figure 1—*Rheogram of a 5% carbomer preparation generated at 37°. The arrows indicate the upward and downward curves. When multiplied by the appropriate constants, the intersection of the dashed line with the abscissa represents the plastic yield value, whereas the slope of the line represents the plastic viscosity.*

pared. Each gel contained 2% pilocarpine hydrochloride[2], 0.01% benzalkonium chloride[2], 0.01% edetate disodium[2], 2% mannitol[2], purified water, and sufficient sodium hydroxide[2] to maintain a pH of 5.9–6.2. For gel preparations containing 0.9–2.0% carbomer, the addition of 2% pilocarpine hydrochloride produced a flocculated gel. However, within 24 hr, each mixture formed a cloudy gel. Sodium hydroxide (3 *N*) was added dropwise and stirred into the gel after each addition. As the pH rose above 5 and approached 6, the gels became rigid and clear. Gel preparations containing 2.35–5.0% carbomer did not flocculate upon the addition of pilocarpine hydrochloride. These gels became rigid and clear at lower pH values than those previously described.

Preparation of Other Gels—Ethylene maleic anhydride[3], hydroxyethylcellulose[4], polyacrylamide[5], ethylhydroxyethylcellulose[6], hydroxypropylcellulose[7], and poly(methylvinyl ether–maleic anhydride)[8] were used to prepare gels. Each polymer was hydrated according to the procedure specified in each manufacturer's technical bulletin. A stiff gel was prepared with ethylene maleic anhydride and poly(methylvinyl ether–maleic anhydride) by the addition of 2.3 and 1.6% (w/w) strong ammonia solution[9], respectively. Stiff gels were formed without the addition of base to the other hydrated polymers; however, 3 *N* NaOH was added dropwise to adjust the pH to 5.2.

Two percent pilocarpine hydrochloride, 0.01% benzalkonium chloride, and 2% mannitol were first dissolved in about 10% of the water solution of each formulation and thoroughly incorporated into each gel. The final pH of all formulations ranged between 5.1 and 5.3. Viscosity readings were obtained in 2 days or more following preparation of each gel.

Petrolatum Preparation—A petrolatum ointment was prepared by levigating 2% pilocarpine hydrochloride with 6% mineral oil to produce a viscous but fluid mixture. The homogeneous mixture was then incorporated into petrolatum[10] USP by the method of geometric dilution.

Viscosity Measurements—A cone and plate viscometer[11], equipped with an *x–y* recorder[12] and a constant-temperature water bath[13], was used to generate rheograms at 35° in triplicate for ethylene maleic anhydride and carbomer formulations. The operating conditions were: 60-sec sweep, medium cone, B switch position, and a 2–5× scale reading. Viscosity measurements were made by applying a sufficient quantity of gel from the same syringes as were used to dose rabbits. The cone was brought in contact with the plate and was held stationary for 3–4 min to allow the gel to reach 35°. Standard operating procedures were followed[14].

Single-point viscosity measurements[15] also were made on each gel formulation. Although temperature was not controlled using this instrument, it ranged between 20 and 24°.

Miosis Measurements—New Zealand albino rabbits of either sex, free of gross ocular defects and weighing 1.8–2.5 kg, were positioned into restraining boxes and placed in a room with controlled rheostat lighting. A standard light intensity of 90–110 foot-candles was measured at the position of the rabbits' eyes. All rabbits were acclimated to the laboratory testing conditions for 30 min prior to initiating the study.

Two baseline pupillary diameters were measured to the nearest 0.1 mm with a micrometer[16] held at a fixed distance from each rabbit. All measurements were taken by the same individual. Rabbits were screened for a range in pupillary diameter of 4.0–5.2 mm; all others were excluded from the study.

Fifty microliters[17] of gel was dosed from a 1.0-ml tuberculin syringe. The filled syringes were centrifuged prior to dosing to remove trapped air. The eyelashes of test animals were trimmed to facilitate instillation of the test compounds. In dosing gel preparations, the right lower eyelid was pulled away from the globe and the dose or extruded ribbon was placed lengthwise along the lower portion of the conjunctival sac. The eyelid was immediately returned to its normal position.

Each treatment group consisted of five or six rabbits; no animal was used more than one time. Pupillary measurements were made on the treated eyes every 15 min for 1 hr and then every 30 min until the pupillary diameter returned to ±0.1 mm of the averaged baseline values for each individual rabbit for two successive readings.

The duration of response is defined as the point in time when the pupillary diameter first returned to baseline values. The duration associated with each rabbit was determined, and the results from the treatment group were expressed as an average ±*SD*. No more than two formulations were tested on a given day; however, a control gel formulation was used throughout the studies.

RESULTS

A rheogram, typical for either ethylene maleic anhydride or carbomer preparations, is depicted in Fig. 1. The flow curve for carbomer and ethylene maleic anhydride formulations produced a hysteresis loop in which the plastic downcurve was displaced to the left by a pseudoplastic upcurve. For this study, the limiting linear slope of the downcurve was used to calculate plastic viscosity; a yield value was obtained by extrapolating the linear portion of the downcurve to the shear stress axis. These two parameters, plastic viscosity and yield value, were used for correlation purposes and are listed in Table I along with the single-point viscosity determinations measured on each formulation.

Of the polymer materials tested, only carbomer and ethylene maleic anhydride produced rheograms in which a significant portion of the downcurve was linear, *i.e.*, plastic viscosity. The petrolatum preparation also exhibited plastic viscosity characteristics. Gels made from the other polymer materials produced a pseudoplastic upcurve as well as a hysteresis loop. However, the downcurve was mostly pseudoplastic in nature; a linear portion was not distinct.

Table I lists the viscosities obtained for each preparation. As the percent of carbomer in the preparation increased, the single-point viscosities also increased.

Averaged miosis intensity results in Fig. 2 show a comparison of the 3% carbomer gel formulation, a petrolatum formulation, and an aqueous solution of pilocarpine hydrochloride containing hydroxypropyl methylcellulose[18]. The peak response was lower for the carbomer gel in comparison to the viscous solution or the petrolatum preparation. The time to peak of each preparation was within 30 min of one another; however, the duration associated with the carbomer gel preparation was twice that of the viscous solution and 1.75 times greater than that of the petrolatum preparation.

[2] USP grade.
[3] EMA-91, 3.4 and 5% (w/w), Monsanto Co., St. Louis, Mo.
[4] Natrosol 250G, 12% (w/w), Hercules Inc., Wilmington, Del.
[5] Cyanamer P-250, 9% (w/w), American Cyanamid Co., Wayne, N.J.
[6] Ethulose E1200, 5% (w/w), Chemaster Corp., Long Island City, N.Y.
[7] Klucel HF, 5.5% (w/w), Hercules Inc., Wilmington, Del.
[8] Gantrez AN 179, 10% (w/w), GAF Corp., New York, N.Y.
[9] NF, reagent grade, Mallinckrodt, St. Louis, Mo.
[10] Alcon lot RPA 3658.
[11] Ferranti-Shirley viscometer, Ferranti, Ltd., Manchester, England.
[12] Model HR-92, Houston Instrument Co., Bellaire, Tex.
[13] Haake type K41.
[14] Operating handbook, Ferranti-Shirley viscometer system, Ferranti Bulletin No. B/12587-113.
[15] Spindle No. 7, 20 rpm, Brookfield RVT Synchro-Lectric viscometer, Brookfield Engineering Laboratories, Stoughton, Mass.
[16] Starrett.
[17] Fifty microliters was chosen as a dosing volume because it approximates the length of ribbon commonly used for semisolids.
[18] Isopto Carpine 2%, Alcon lot WBBC.

Table I—Viscosity and Corresponding Rabbit[a] Miosis Durations Obtained for Each Gel Formulation

Polymer and Concentration, % w/w	Plastic Viscosities[b], cps	Yield Value, dynes/cm²	Brookfield RV1[c] Viscosities, cps	Mean Miosis Duration, hr	Area under Response Curve
Carbomer					
0.9	100[d] (22)[e]	2,964 (379)	23,800	6.45 (0.53)	1.35 (0.27)
1.25	207 (21)	3,835 (696)	40,000	6.86 (0.93)	1.45 (0.30)
1.65	270 (31)	6,483 (440)	70,000	5.72 (0.58)	0.927 (0.328)
2.0	359 (21)	7,714 (403)	80,000	5.27 (0.32)	0.899 (0.061)
2.35	369 (63)	8,215 (667)	101,000	6.24 (0.71)	1.18 (0.23)
2.70	421 (50)	9,862 (303)	107,000	5.52 (0.94)	0.979 (0.21)
3.00	603 (24)	11,188 (460)	115,000	8.20 (1.1)	1.58 (0.40)
3.50	490 (59)	10,263 (587)	—	8.43 (1.06)	1.74 (0.33)
4.0	613 (59)	12,318 (453)	118,000	10.09 (1.19)	2.53 (0.47)
4.5	695 (88)	12,685 (686)	118,000	8.11 (0.84)	2.01 (0.279)
5.0	786 (73)	14,227 (838)	129,000	8.84 (1.08)	2.03 (0.20)
Ethylene maleic anhydride					
3.4	384	7,078	123,000	8.50 (0.57)	1.93 (0.30)
5.0	558	11,046	109,000	10.70 (1.58)	2.35 (0.69)
Hydroxyethylcellulose, 12	—	—	171,000	4.93 (0.34)	1.05 (0.16)
Polyacrylamide, 9	—	—	184,000	6.18 (0.87)	1.39 (0.18)
Ethylhydroxyethylcellulose, 5	—	—	92,000	4.55 (0.59)	0.885 (0.216)
Hydroxypropylcellulose, 5.5	—	—	193,000	4.66 (0.31)	0.963 (0.043)
Poly(methylvinyl ether-maleic anhydride), 10	—	—	80,000	5.33 (0.87)	1.021 (0.189)
Petrolatum	—	—	25,000	4.70 (0.71)	1.06 (0.15)

[a] Mean values are averages of six to 10 rabbits. [b] Values were determined from rheograms using a Ferranti-Shirley viscometer at 35°. [c] Single-point determinations were made using a No. 7 spindle at 20 rpm and 20–24°. [d] Mean values are averages of three determinations. [e] Values in parenthesis represent 1 *SD*.

It has been hypothesized that the longer durations achieved with either the carbomer or ethylene maleic anhydride gels can be attributed in part to the gel's longer retention in the conjunctival sac of the rabbit eye. Eye retention of the gel was approximately 4–6 hr. The gradual decline in miosis shown in Fig. 2 is consistent with this finding. The intensity curve associated with carbomer following 6 hr began to decline at a slope approximately parallel to the decline associated with either petrolatum or the viscous solution between 1 and 4 hr. This result indicates that the corneal absorptive phase was over by 6 hr. As observed in Fig. 2, the miosis intensities representing the 3.4% ethylene maleic anhydride preparation nearly identically followed the 3% carbomer preparation; the 5% ethylene maleic anhydride preparation paralleled the 3% carbomer formulation but at values about 10–20% higher.

The longer retention time is considered to be a consequence of the plastic viscosity characteristics of carbomer or ethylene maleic anhydride. Figure 3, which represents the data generated for carbomer preparations, shows that a correlation is apparent when miosis durations are plotted against yield values. Although the relationship did not increase linearly, it was statistically significant [$r = 0.654$, $p < 0.05$ (3)]. When a correlation was tested between plastic viscosity or single-point rotational viscosity and miosis durations, similar results were found.

Figure 3 suggests a discontinuous type of relationship; that is, at a certain point on the abscissa, miosis durations significantly increase. For the yield value data, discontinuity occurred between 9862 and 11,188 dynes/cm² (Table I). An ANOVA was performed on the data as outlined by Hays (4). When all 11 groups were tested for a difference between mean miosis durations, a highly significant result was obtained ($F = 2.63$, $p < 0.01$). The treatment groups were then divided into two distinct groups, those below the discontinuity point (0.9–2.7% carbomer) and those above it (3.0–5.0% carbomer). The miosis duration differences were highly significant ($F = 7.08$, $p < 0.01$). However, statistical differences not related to viscosity also were found within each group (for 0.9–2.7% carbomer, $F = 3.82$; $p < 0.05$; for 3.0–5.0% carbomer, $F = 5.25$, $p < 0.01$). The treatment effect within each group, independent of yield value, could have been due to the relatively small numbers of rabbits used in each treatment group. In addition, as the yield value increased, the plastic viscosity or the single-point rotational viscosity increased linearly (Pearson $r = 0.982$ or 0.970, respectively).

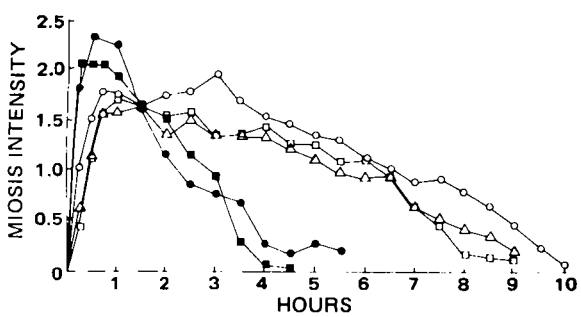

Figure 2—*Averaged (n = 5 or 6) durations of various ophthalmic preparations containing 2% pilocarpine hydrochloride. Each rabbit was dosed topically with 50 µl. The miosis intensity, in millimeters, represents a difference in pupil diameters of time zero and time t. Key: O and □, 5 and 4% ethylene maleic anhydride, respectively; Δ, 3% carbomer; ●, petrolatum; and ■, 2% hydroxypropyl methylcellulose.*

DISCUSSION

Plastic flow occurs as a result of overcoming the weak attraction between dispersed polymer molecules held together by secondary valence forces (5). Below the yield value, the shearing stress produced in a rotational viscometer is not sufficient to bring about flow. But once the shearing stress exceeds that of the yield value, expressed in dynes per square centimeter, the secondary valence forces are no longer capable of holding the molecules in position and the shearing rate increases.

If eye movements or blinking can create a shearing force on viscous formulations when placed in the conjunctival sac, then appreciable thinning should occur once a particular shearing force is reached. Although carbomer and ethylene maleic anhydride could be used to for-

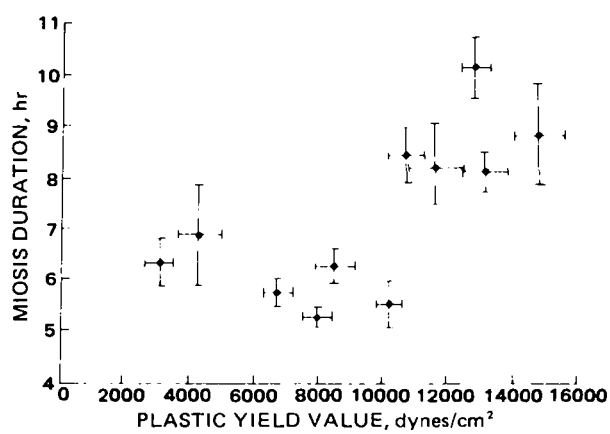

Figure 3—*Effect of plastic yield value (37°, n = 3) on the miosis duration of rabbits (n = 5 or 6) following ophthalmic dosing of 50 µl of carbomer gel preparations containing 2% pilocarpine hydrochloride. Each preparation varied in viscosity as a result of changes in carbomer concentration (0.9–5.0%; see Table I).*

mulate highly viscous, well-retained gels, other highly viscous polymer sols or gels were poorly retained in the rabbit eye and did not produce extended miosis duration. The carbomer data suggest that the increased duration was a result of the increased viscosity of the gels as expressed by a yield value above a certain value corresponding to 2.7–3.0% carbomer. As a consequence, it was not rapidly squeezed out of the eye and a significantly longer duration was achieved.

The viscosities measured with the single-point rotational viscometer did not correlate with miosis duration (Table I). This result illustrates the necessity for constructing a rheogram and identifying specific rheological characteristics that may correlate to the observed phenomenon and perhaps suggest an explanation for the results.

Insight into the mechanism of drug release for ethylene maleic anhydride and carbomer preparations can be speculated upon by analyzing the results of Fig. 2. It is reasoned that the time to peak, t_p, as well as peak miosis intensities, I_{max}, for each preparation are related to the corneal absorption rate; the latter can be altered depending on the degree of control of drug release exerted by the gel systems. The large improvement in eye retention observed for ethylene maleic anhydride and carbomer when compared to a solution dosage form would increase bioavailability, but the effect on t_p and I_{max} would depend on the release characteristics of the gel system.

In general, an improvement in retention followed by an increase in bioavailability could result in: (*a*) a large increase in I_{max} with no change in t_p if drug release from the gel preparations is rapid and uncontrolled, or (*b*) a decrease in I_{max} with a delay in t_p if release from the gel systems is controlled.

The extent of the decrease in I_{max} as well as the delay in t_p depends upon the degree to which the release rate is controlled. It is possible, of course, to decrease significantly or even eliminate the response intensities if the release rate is reduced such that biophasic concentrations are insufficient to invoke a response. This is not of concern here, however.

The miosis intensities observed in Fig. 2 for the gel preparations show a reduced I_{max} and a delayed t_p in comparison to either the solution or petrolatum dosage forms. Consequently, some degree of control of the release rate can be attributed to ethylene maleic anhydride and carbomer. Within the gel, release could be controlled by diffusion and/or slow erosion of the gel surface with time. However, further work is necessary to describe more fully the nature of drug release as well as to estimate the physiological constraints of the precorneal area on the response duration.

REFERENCES

(1) T. F. Patton and J. R. Robinson, *J. Pharm. Sci.*, **64**, 1312 (1975).

(2) S. S. Chrai and J. R. Robinson, *ibid.*, **63**, 1218 (1974).

(3) N. M. Downie and R. W. Heath, in "Basic Statistical Methods," 2nd ed., Harper and Row, New York, N.Y., 1965, p. 154.

(4) W. L. Hays, in "Statistics," Holt, Rinehart and Winston, New York, N.Y., 1963, pp. 371, 372.

(5) A. N. Martin, G. S. Banker, and A. H. C. Chun, in "Advances in Pharmaceutical Sciences," vol. 1, Academic, London, England, 1964, pp. 8–11.

Reaction of Sodium Hydroxymethanesulfonate with Substituted Anilines

MIGUEL G. NEUMANN ˣ and ROBERT A. M. C. DE GROOTE

Received August 9, 1977, from the *Departamento de Química e Física Molecular, Instituto de Física e Química de São Carlos, Universidade de São Paulo, 13560-São Carlos (SP), Brazil.* Accepted for publication January 12, 1978.

Abstract □ The reactions of substituted anilines with sodium hydroxymethanesulfonate to form the anilinomethanesulfonates were studied in 50% ethanol–water at 0–50°. The Arrhenius rate constants were $5.4 \times 10^{10} \exp(-16{,}400/RT)\ M^{-1}\ min^{-1}$ for aniline, $4.8 \times 10^{11} \exp(-17{,}100/RT)\ M^{-1}\ min^{-1}$ for *p*-anisidine, $7.1 \times 10^{9} \exp(-14{,}500/RT)\ M^{-1}\ min^{-1}$ for *p*-toluidine, $1.5 \times 10^{13} \exp(-21{,}100/RT)\ M^{-1}\ min^{-1}$ for *p*-chloroaniline, and $1.1 \times 10^{12} \exp(-19{,}800/RT)\ M^{-1}\ min^{-1}$ for *p*-bromoaniline. Some equilibrium constants and hydrolysis rate constants of the products also were calculated. Hydrolysis rate constants were temperature independent. These reactions had a ρ value of −3.40 in the Hammett equation. The solvent concentrations used proved to be very convenient for obtaining high yields of the aminomethanesulfonates.

Keyphrases □ Anilines, various substituted—kinetics of reaction with sodium hydroxymethanesulfonate, equilibrium and hydrolysis rate constants calculated □ Sodium hydroxymethanesulfonate—kinetics of reaction with various substituted anilines, equilibrium and hydrolysis rate constants calculated □ Kinetics—reaction of various substituted anilines with sodium hydroxymethanesulfonate, equilibrium and hydrolysis rate constants calculated

The sodium salts of substituted methanesulfonic acids are of interest as both synthesis intermediates and pharmacological agents. Sodium *p*-phenetidinomethanesulfonate has been used as an antipyretic, and several other sodium α-aminoalkanesulfonates have antiviral and anticarcinogenic activities (1–3). Industrially, some primary aromatic amines such as aniline and α-naphthylamine have been transformed into their respective sodium methanesulfonates to avoid formation of the diazoamino group (N=NNH) during coupling in the formation of the azo dyes (4, 5). Hydrolysis of those compounds to obtain the desired azo dyes is then performed in appropriate media.

Numerous syntheses of this type of compound were reported (6, 7), but little research has been done on the formation kinetics of these products. Ikeda *et al.* (8) studied the formation of various substituted sodium anilinomethanesulfonates in water but calculated only overall rate constants. The same investigators (9–13) also studied the amine release from different substituted anilinomethanesulfonates in water and its pH dependence. This paper presents the results of research concerning the formation kinetics of anilinomethanesulfonates in mixed ethanol–water solvents at conditions where the syntheses of these compounds are favored.

EXPERIMENTAL

Materials and Apparatus—All reagents were proanalysis grade and were used without further purification except where indicated. The amines proved to be free of any interfering impurities when analyzed by GLC. Toluene did present an impurity peak with a retention time similar to that of aniline, but this impurity was easily removed by distillation.

The formaldehyde content of the mixture was analyzed by the Romijn method, and the metabisulfite content of the initial solutions was determined by iodometric titration.

0022-3549/78/0900-1283$01.00/0

© 1978, American Pharmaceutical Association

mulate highly viscous, well-retained gels, other highly viscous polymer sols or gels were poorly retained in the rabbit eye and did not produce extended miosis duration. The carbomer data suggest that the increased duration was a result of the increased viscosity of the gels as expressed by a yield value above a certain value corresponding to 2.7–3.0% carbomer. As a consequence, it was not rapidly squeezed out of the eye and a significantly longer duration was achieved.

The viscosities measured with the single-point rotational viscometer did not correlate with miosis duration (Table I). This result illustrates the necessity for constructing a rheogram and identifying specific rheological characteristics that may correlate to the observed phenomenon and perhaps suggest an explanation for the results.

Insight into the mechanism of drug release for ethylene maleic anhydride and carbomer preparations can be speculated upon by analyzing the results of Fig. 2. It is reasoned that the time to peak, t_p, as well as peak miosis intensities, I_{max}, for each preparation are related to the corneal absorption rate; the latter can be altered depending on the degree of control of drug release exerted by the gel systems. The large improvement in eye retention observed for ethylene maleic anhydride and carbomer when compared to a solution dosage form would increase bioavailability, but the effect on t_p and I_{max} would depend on the release characteristics of the gel system.

In general, an improvement in retention followed by an increase in bioavailability could result in: (*a*) a large increase in I_{max} with no change in t_p if drug release from the gel preparations is rapid and uncontrolled, or (*b*) a decrease in I_{max} with a delay in t_p if release from the gel systems is controlled.

The extent of the decrease in I_{max} as well as the delay in t_p depends upon the degree to which the release rate is controlled. It is possible, of course, to decrease significantly or even eliminate the response intensities if the release rate is reduced such that biophasic concentrations are insufficient to invoke a response. This is not of concern here, however.

The miosis intensities observed in Fig. 2 for the gel preparations show a reduced I_{max} and a delayed t_p in comparison to either the solution or petrolatum dosage forms. Consequently, some degree of control of the release rate can be attributed to ethylene maleic anhydride and carbomer. Within the gel, release could be controlled by diffusion and/or slow erosion of the gel surface with time. However, further work is necessary to describe more fully the nature of drug release as well as to estimate the physiological constraints of the precorneal area on the response duration.

REFERENCES

(1) T. F. Patton and J. R. Robinson, *J. Pharm. Sci.*, **64**, 1312 (1975).

(2) S. S. Chrai and J. R. Robinson, *ibid.*, **63**, 1218 (1974).

(3) N. M. Downie and R. W. Heath, in "Basic Statistical Methods," 2nd ed., Harper and Row, New York, N.Y., 1965, p. 154.

(4) W. L. Hays, in "Statistics," Holt, Rinehart and Winston, New York, N.Y., 1963, pp. 371, 372.

(5) A. N. Martin, G. S. Banker, and A. H. C. Chun, in "Advances in Pharmaceutical Sciences," vol. 1, Academic, London, England, 1964, pp. 8–11.

Reaction of Sodium Hydroxymethanesulfonate with Substituted Anilines

MIGUEL G. NEUMANN ˣ and ROBERT A. M. C. DE GROOTE

Received August 9, 1977, from the *Departamento de Química e Física Molecular, Instituto de Física e Química de São Carlos, Universidade de São Paulo, 13560-São Carlos (SP), Brazil.* Accepted for publication January 12, 1978.

Abstract □ The reactions of substituted anilines with sodium hydroxymethanesulfonate to form the anilinomethanesulfonates were studied in 50% ethanol–water at 0–50°. The Arrhenius rate constants were $5.4 \times 10^{10} \exp(-16{,}400/RT)\ M^{-1}\ min^{-1}$ for aniline, $4.8 \times 10^{11} \exp(-17{,}100/RT)\ M^{-1}\ min^{-1}$ for *p*-anisidine, $7.1 \times 10^{9} \exp(-14{,}500/RT)\ M^{-1}\ min^{-1}$ for *p*-toluidine, $1.5 \times 10^{13} \exp(-21{,}100/RT)\ M^{-1}\ min^{-1}$ for *p*-chloroaniline, and $1.1 \times 10^{12} \exp(-19{,}800/RT)\ M^{-1}\ min^{-1}$ for *p*-bromoaniline. Some equilibrium constants and hydrolysis rate constants of the products also were calculated. Hydrolysis rate constants were temperature independent. These reactions had a ρ value of −3.40 in the Hammett equation. The solvent concentrations used proved to be very convenient for obtaining high yields of the aminomethanesulfonates.

Keyphrases □ Anilines, various substituted—kinetics of reaction with sodium hydroxymethanesulfonate, equilibrium and hydrolysis rate constants calculated □ Sodium hydroxymethanesulfonate—kinetics of reaction with various substituted anilines, equilibrium and hydrolysis rate constants calculated □ Kinetics—reaction of various substituted anilines with sodium hydroxymethanesulfonate, equilibrium and hydrolysis rate constants calculated

The sodium salts of substituted methanesulfonic acids are of interest as both synthesis intermediates and pharmacological agents. Sodium *p*-phenetidinomethanesulfonate has been used as an antipyretic, and several other sodium α-aminoalkanesulfonates have antiviral and anticarcinogenic activities (1–3). Industrially, some primary aromatic amines such as aniline and α-naphthylamine have been transformed into their respective sodium methanesulfonates to avoid formation of the diazoamino group (N=NNH) during coupling in the formation of the azo dyes (4, 5). Hydrolysis of those compounds to obtain the desired azo dyes is then performed in appropriate media.

Numerous syntheses of this type of compound were reported (6, 7), but little research has been done on the formation kinetics of these products. Ikeda *et al.* (8) studied the formation of various substituted sodium anilinomethanesulfonates in water but calculated only overall rate constants. The same investigators (9–13) also studied the amine release from different substituted anilinomethanesulfonates in water and its pH dependence. This paper presents the results of research concerning the formation kinetics of anilinomethanesulfonates in mixed ethanol–water solvents at conditions where the syntheses of these compounds are favored.

EXPERIMENTAL

Materials and Apparatus—All reagents were proanalysis grade and were used without further purification except where indicated. The amines proved to be free of any interfering impurities when analyzed by GLC. Toluene did present an impurity peak with a retention time similar to that of aniline, but this impurity was easily removed by distillation.

The formaldehyde content of the mixture was analyzed by the Romijn method, and the metabisulfite content of the initial solutions was determined by iodometric titration.

0022-3549/78/0900-1283$01.00/0

© 1978, American Pharmaceutical Association

Table I—Kinetic and Thermodynamic Data for Substituted Anilinomethanesulfonates

Amine	Temperature	Aminomethanesulfonate Solubility, mole/liter	k_f, M^{-1} min^{-1}	K	k_h, min^{-1}
Aniline	1.5°	—	4.1×10^{-3}	(6.1)	7.4×10^{-4}
	9°	0.50	9.6	20	4.8
	15°	0.55	17	35	4.9
	25°	0.73	50	75	6.6
	31.5°	0.89	67	120	5.5
p-Toluidine	1°	0.10	1.3×10^{-2}	(1.7)	(7.5×10^{-3})
	10°	0.19	2.6	18	1.5
	15°	0.23	4.8	25	1.9
	20°	0.27	7.8	40	1.9
	25°	—	9.0	65	1.4
p-Anisidine	10°	0.32	5.6×10^{-2}	(220)	(3.0×10^{-4})
	15°	0.31	5.7	76	7.0
	20°	0.32	10	240	4.0
	25°	0.36	20	2300	0.9
p-Chloroaniline	30°	0.23	1.1×10^{-2}	14	8.0×10^{-4}
	35°	0.35	1.5	90	2.0
	40°	0.39	3.1	520	0.6
	50°	0.46	10.7	3000	0.4
p-Bromoaniline	30°	0.24	0.7×10^{-2}	n.d.[a]	n.d.
	35°	0.21	1.1	n.d.	n.d.
	40°	0.30	2.2	n.d.	n.d.
	50°	0.40	5.2	n.d.	n.d.

[a] n.d. = not determined.

An ultrathermostat and a thermostatic bath were used[1], both assuring temperature accuracy better than 0.2°. GLC was performed on a gas chromatograph[2] using a flame-ionization detector. A 1.5-m long × 3.1-mm o.d. Chromosorb 103 column was used at 180° for aniline and toluidine and at 220° for the other amines.

Procedure—The anilinomethanesulfonates were prepared in the usual way by mixing solutions containing stoichiometric amounts of hydroxymethanesulfonate and the amine (14). The hydroxymethanesulfonate solution was prepared by dissolving the required amount of sodium metabisulfite in a minimal amount of water and adding to it a solution of formol with agitation at room temperature, the total amount of added formaldehyde being equimolar to that of metabisulfite. After diluting and thermostating, the solution was mixed with the same volume of an equimolar solution of the amine in ethanol to obtain the required 50% ethanol–water solvent.

Samples of 2 ml were withdrawn from the reaction vessel at different times, whereupon amine analyses were performed as follows. The sample volume was extracted four times with 5 ml of toluene. The toluene, besides extracting the amine from the aminomethanesulfonate, also stopped the reaction by phase separating the aniline from the hydroxymethanesulfonate. In the analyses of samples where the aminomethanesulfonates had already precipitated, a rapid filtration was performed before extraction. The amine solution in toluene thus obtained was diluted and analyzed by GLC with an internal standard.

RESULTS

The reactions between sodium hydroxymethanesulfonate and various substituted anilines (Scheme I) were studied in 50% ethanol–water.

$$RNH_2 + HOCH_2SO_3^- \rightarrow RNHCH_2SO_3^- + H_2O$$

Scheme I

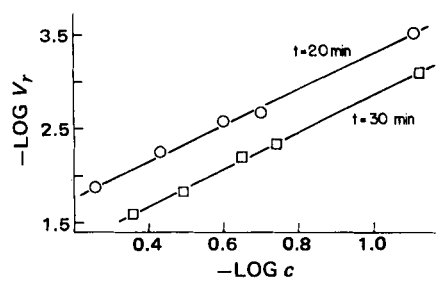

Figure 1—*Reaction order plot for aniline plus hydroxymethanesulfonate at 25° (t_{30} values are displaced in the scale).*

That solvent was chosen for several reasons:

1. The hydroxymethanesulfonate formation reaction is displaced toward its total conversion, avoiding the decomposition (Scheme II) that occurs to some extent in pure water (15).

$$HOCH_2SO_3^- \overset{K_2}{\rightleftharpoons} H_2CO + SO_3^{2-} + H^+$$

Scheme II

In water, the K_2 for aliphatic aldehydes is about 10^{-3}–10^{-4} (16), but it should be less in ethanol–water mixtures because of the higher solvation energy of the ionic products in pure water compared to ethanol–water mixtures.

2. The anilinomethanesulfonates precipitate, keeping the homogeneous phase concentration low enough to neglect their hydrolyses, and are able to reach high conversions without affecting the formation rate.

A second-order reaction rate in aniline plus hydroxymethanesulfonate was found in all cases, although slight deviations from the second-order graph were found occasionally near and after the anilinomethanesulfonate solubility concentrations[3]. This order was also confirmed for the system of aniline plus hydroxymethanesulfonate by performing several runs at 25° and different initial concentrations. Reaction rates, V_r, at 20 and 30 min are shown in Fig. 1. From this graph, a second order can be easily deduced in agreement with results of the individual experiments.

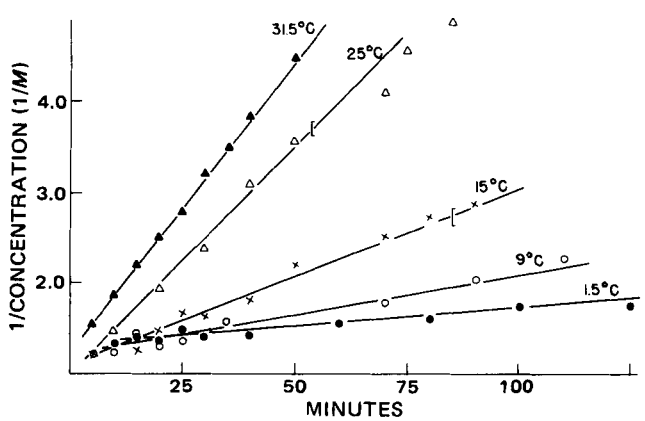

Figure 2—*Second-order plot for the reaction of hydroxymethanesulfonate with aniline at various temperatures; ([) indicates precipitation of the anilinomethanesulfonate.*

[1] ASCA and Sargent model 84805, respectively.
[2] Varian model 2800.
[3] As suggested by the reviewer, these deviations may be due to the constancy of the hydrolysis rate after precipitation of the anilinomethanesulfonate.

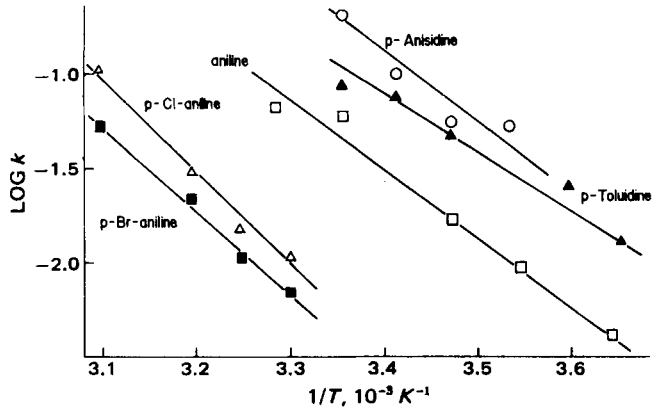

Figure 3—*Arrhenius plot for the reaction of anilines with hydroxymethanesulfonate.*

Figure 2 shows the second-order graph for the reaction of aniline with hydroxymethanesulfonate. Similar graphs were obtained for the other anilines. In Table I, the overall reaction rate constants for these reactions are shown together with the solubilities of the anilinomethanesulfonates, some equilibrium constants, and the hydrolysis reaction rate constants. The equilibrium constants were obtained from the amines limiting concentration and the solubility data using:

$$K = \frac{[RNHCH_2SO_3^-]_\infty}{[RNH_2]_\infty[HOCH_2SO_3^-]_\infty} = \frac{\text{solubility}}{([RNH_2]_\infty)^2} = \frac{k_f}{k_h} \quad \text{(Eq. 1)}$$

Overall hydrolysis reaction rate constants also were obtained using Eq. 1 together with the overall formation reaction rate constants.

Activation energies were obtained for the reactions of the five anilines. Arrhenius plots are shown in Fig. 3. The pH values during the reaction were measured continuously in some runs, and no change could be detected throughout the reaction time. Although these "pH" values cannot be related directly to the conventional acidity of the solutions because the solvents were different from pure water, their invariability should correspond to a constancy of the proton concentration. The measured pH values in 50% ethanol–water mixtures (~7.0) corresponded to proton concentrations higher than those in equivalent true pH's (17).

DISCUSSION

Although it has been postulated that the mechanism for this type of reaction in aliphatic series goes through an immonium ion, $RN^+H_2{=}CH_2$ (18, 19), the results obtained in this work suggest an alternative or collateral pathway for aromatic series under the experimental conditions. The overall kinetic order two is hardly compatible with the Schiff-base mechanism, because in that case the rate-determining step must be the dehydration of the alkylammoniumcarbinol (Scheme III) or the reaction of the immonium ion with sulfite (Scheme IV).

$$RN^+H_2CH_2OH \rightarrow H_2O + RN^+H{=}CH_2$$
Scheme III

$$RN^+H{=}CH_2 + SO_3^{2-} \rightarrow RNHCH_2SO_3^-$$
Scheme IV

Furthermore, in neutral media and nonaqueous solvents, as used here, the dissociation of hydroxymethanesulfonate is greatly reduced compared with the value found in aqueous solutions containing aliphatic amines (19) (pH > 9). Therefore, the concentration of free formaldehyde is largely reduced, allowing a competition between the Schiff-base mechanism with other mechanisms.

It is proposed that the rate-determining step of this alternative mechanism is an S_N2 reaction between the protonated hydroxymethanesulfonate free aniline (Scheme V), followed by deprotonation of the anilinomethanesulfonate through an intermediate involving simultaneous protonation of hydroxymethanesulfonate (Scheme VI).

$$RNH_2 + H_2O^+CH_2SO_3^- \rightarrow RN^+H_2CH_2SO_3^- + H_2O$$
Scheme V

$$RN^+H_2CH_2SO_3^- + HOCH_2SO_3^- \rightarrow RNHCH_2SO_3^- + H_2O^+CH_2SO_3^-$$
Scheme VI

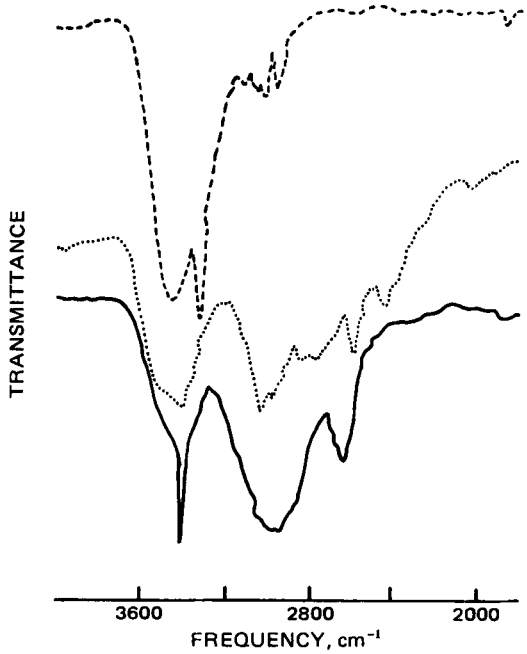

Figure 4—*IR spectra of anilinomethanesulfonate (- - -), the anilinimmethanesulfonate zwitterion (···), and the reaction intermediate (—).*

The anilinimmethanesulfonate deprotonation to the sulfonic group on the hydroxymethanesulfonate ion (Scheme VII) is also possible.

$$RN^+H_2CH_2SO_3^- + HOCH_2SO_3^- \rightarrow RNHCH_2SO_3^- + HOCH_2SO_3H$$
Scheme VII

However, since both acid constants K_a ($HOCH_2SO_3H$) and K_a ($H_2O^+CH_2SO_3^-$) (20) must be similar (~10^{-2} M^{-1}), a rapid equilibrium between both protonated species is established (Scheme VIII) with no effect on the overall kinetics.

$$HOCH_2SO_3H \rightarrow H_2O^+CH_2SO_3^-$$
Scheme VIII

The reaction in Scheme VI can be obtained through a six-membered ring ion-pair such as that shown in Scheme IX.

The existence of this type of ion-pairs was postulated in the hydrolysis of sulfamates (21). In the present case, it can also be inferred from the existence of a similar intermediate found in the reaction of formation of anilinomethanesulfonate when reacting hydroxymethanesulfonate with aniline in an acid medium. In the initial stages of that reaction, a solid precipitates. Upon heating or further addition of hydroxymethanesulfonate, this solid redissolves. When separated, the product presents an IR spectrum with bands corresponding to secondary amine and quaternized nitrogen at ~3400 and 2950 cm^{-1}, respectively.

A similar spectrum was obtained from the reaction of the anilinomethanesulfonate with anilinium chloride;* thus, an ion-pair ($C_6H_5NHCH_2SO_3^-$)($N^+H_3C_6H_5$) does occur during the reaction, that adduct having a spatial configuration similar to I (Scheme IX). The existence of this adduct is further confirmed by the fact that its spectrum is very different from that of anilinimmethanesulfonate hydrochloride (Cl^-)($C_6H_5N^+H_2CH_2SO_3^-$) or the anilinomethanesulfonate ion,

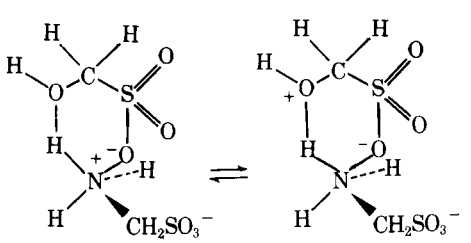

I

Scheme IX

Table II—Maximum Conversion Data for Formation of Anilinomethanesulfonates in 50% Ethanol–Water

Temperature	Anilinomethanesulfonate Maximum Conversion, %	Anilinomethanesulfonate $t_{1/2}$, min	*p*-Toluidinomethanesulfonate Maximum Conversion, %	*p*-Toluidinomethanesulfonate $t_{1/2}$, min	*p*-Anisidinomethanesulfonate Maximum Conversion, %	*p*-Anisidinomethanesulfonate $t_{1/2}$, min
9° (10)	84	100	80	75	96	18
15°	87	60	81	40	94	18
20°	—	—	84	13	96	10
25°	90	20	93	11	99	5
31.5°	92	15	—	—	—	—

$C_6H_5NHCH_2SO_3^-$; its bands are generally displaced with respect to the sum of the latter (Fig. 4).

The mechanism accounting for hydrolysis involves a different pathway with direct anilinomethanesulfonate protonation (Scheme X), as suggested by Kurono *et al.* (13), followed by a direct S_N2 process in which water, acting as a nucleophilic agent, attacks the partially positive methylenic carbon atom (Scheme XI).

$$RNHCH_2SO_3^- + H^+ \rightarrow RN^+H_2CH_2SO_3^-$$

Scheme X

$$RN^+H_2CH_2SO_3^- + H_2O \rightarrow H_2O^+CH_2SO_3^- + RNH_2$$

Scheme XI

The data in Table I for the hydrolysis reactions show that these processes are not temperature dependent or only slightly so. Previous work done on similar systems, but in different solvents, seems to be consistent with these results. The overall hydrolysis rate constants compare rather well with the values found (13) for the reaction in water at pH 7: 2×10^{-3} for the aniline derivative, 6×10^{-3} for the *p*-toluidine derivative, and 1.5×10^{-4} min^{-1} for the *p*-chloroaniline derivative.

The results obtained were also used to set up a linear free energy relationship using the Hammett equation; the corresponding graph is shown in Fig. 5. A ρ value of −3.40 was obtained. This value compares well with that found for the same reaction in water at 37° (13), $\rho = -3.0$. Furthermore, that value also confirms the proposed mechanism and the rate-determining step. Scheme V corresponds to a reaction similar to nucleophilic attack by a base, *i.e.*, aniline in this case. For the ionization equilibrium of substituted anilines in 30% ethanol–water at 25°, a ρ value of −3.44 was reported (22), which also agrees well with the present mechanistic assumption.

Syntheses of Anilinomethanesulfonates—From the data in Table II, the maximum yields under the experimental conditions can be calculated to be always larger than 80% when working at room or higher temperatures for the anilino-, *p*-toluidino-, and *p*-anisidinomethanesulfonates. The time necessary to attain 50% conversion when starting with 1 *M* reagent concentrations also is presented.

The hydrolysis rate was practically temperature independent, which may have been due to the low hydrolysis power of the solvent (50% ethanol–water) and the low solubility of the products in this medium. Therefore, this solvent is recommended for these syntheses in view of the low hydrolysis rate of the anilinomethanesulfonates in comparison with the rather high rate found in pure water (8). When the temperature was increased to about 60°, conversions reached their maximum values in less than 5 min.

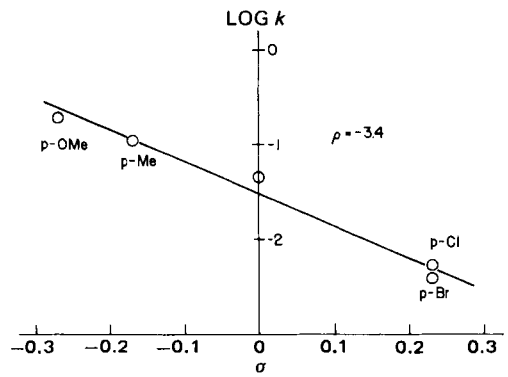

Figure 5—*Hammett plot for the reaction of substituted anilines with hydroxymethanesulfonate.*

REFERENCES

(1) D. M. Greenberg and M. P. Schulman, *Science*, **106**, 271 (1947).

(2) R. L. Thompson, *J. Immunol.*, **55**, 345 (1947).

(3) W. Longeman and G. P. Miori, *Arzneim.-Forsch.*, **5**, 213 (1955).

(4) Ciba Ltd., Swiss pat. 294,228 (1954).

(5) Society pour la Industrie Chimique à Bâle, Swiss pat. 234,786 (1945).

(6) H. Berthold, M. Fedke, and W. Pritakow, East German pat. 84,394 (1971).

(7) A. Rosengren and V. Gasparic, German Offen. 2,343,343 (1971).

(8) K. Ikeda, K. Miyata, T. Iwata, F. Kawata, and K. Kurome, *Chem. Pharm. Bull.*, **18**, 440 (1970).

(9) K. Ikeda, Y. Kurono, and T. Tukamoto, *ibid.*, **20**, 863 (1972).

(10) *Ibid.*, **20**, 1621 (1972).

(11) K. Ikeda and Y. Kurono, *Chem. Pharm. Bull.*, **21**, 1198 (1973).

(12) Y. Kurono, K. Ikeda, and K. Uekama, *ibid.*, **22**, 1264 (1974).

(13) *Ibid.*, **23**, 409 (1975).

(14) L. Neelakantan and W. H. Hartung, *J. Org. Chem.*, **24**, 1943 (1959).

(15) T. D. Stewart and L. H. Donnally, *J. Am. Chem. Soc.*, **54**, 3555 (1932).

(16) M. A. Gubareva, *Zh. Obshch. Khim.*, **17**, 2259 (1947).

(17) M. A. Paul and F. A. Long, *Chem. Rev.*, **57**, 1 (1957).

(18) P. L. Henaff, *C.R.*, **256**, 3090 (1963).

(19) F. H. McMillan and I. C. Pattison, *J. Pharm. Sci.*, **58**, 730 (1969).

(20) A. Albert and E. P. Serjeant, "The Determination of Ionization Constants", Chapman and Hall, London, England, 1971, pp. 82–96.

(21) E. H. White and C. A. Ellinger, *J. Am. Chem. Soc.*, **87**, 5261 (1965).

(22) C. D. Johnson, "The Hammett Equation," University Press, Cambridge, England, 1973, p. 8.

ACKNOWLEDGMENTS

Supported by the Fundação de Amparo à Pesquisa do Estado de São Paulo through Grant 571/76.

Comparative Bioavailability of a Lipophilic Steroid

LARRY S. ABRAMS, HOWARD S. WEINTRAUB ˣ, JAMES E. PATRICK, and J. L. McGUIRE

Received November 22, 1977, from the *Drug Disposition Section, Ortho Pharmaceutical Corporation, Raritan, NJ 08869.* Accepted for publication January 12, 1978.

Abstract □ 17β-Acetoxy-2α-chloro-3-(*p*-nitrophenoxy)imino-5α-androstane (I) is a lipophilic steroid with postimplantive antifertility activity in laboratory animals. The bioavailability of micronized I from solutions and suspensions was compared in four groups of adult female Wistar rats. Each group received varying concentrations of micronized ^{3}H-I (specific activity of 0.38–8.94 μCi/mg) in sesame oil by oral gavage. Samples of whole blood and urine collected following drug administration were assayed for radioactive content. Calculation of the mean area under the blood radioactivity *versus* time curve, when corrected for the quantity of drug administered, indicated that a substantially larger fraction of the dose was absorbed in the two instances where I was present only in solution. A linear relationship between the amount of I absorbed based on whole blood radioactivity and urinary excretion and the administered dose was found primarily for groups receiving the drug in solution. Preliminary results in humans indicate that ^{3}H-I was absorbed to a much greater extent following oral administration of the drug in sesame oil than when admixed with lactose.

Keyphrases □ 17β-Acetoxy-2α-chloro-3-(*p*-nitrophenoxy)imino-5α-androstane—bioavailability from solutions and suspensions in rats and humans □ Bioavailability—substituted androstane from solutions and suspensions in rats and humans □ Steroids, lipophilic—substituted androstane, bioavailability from solutions and suspensions in rats and humans

17β-Acetoxy-2α-chloro-3-(*p*-nitrophenoxy)imino-5α-androstane[1] (I), an *O*-aryl oxime of 2α-chlorodihydrotestosterone, possesses postimplantive antifertility activity in the rat (1, 2) and other laboratory animals[2] following oral administration. The effects of various changes of physical–chemical properties of drug formulations on the bioavailability of drugs were studied for digoxin (3–9), tolbutamide (10), phenylbutazone (11), phenytoin (12, 13), oxytetracycline (14), and chloramphenicol (15). Examples of altered bioavailability due to specific physical–chemical changes include the effects of the particle size of griseofulvin (16, 17), of polymorphs of chloramphenicol (18), of water of hydration of ampicillin (19), and of the acid or salt form of phenylbutazone (20) or phenytoin (21).

Studies of the contragestational potency of I, administered in solution or suspension in various vehicles to animals, suggested that the majority of the biological activity of I resulted from drug in solution in sesame oil at the time of administration[2]. To confirm this hypothesis, a comparative bioavailability study employing solutions and suspensions of I in sesame oil was conducted in rats.

In addition, preliminary data on the comparative bioavailability of I from sesame oil and lactose formulations in normal adult female subjects and on the influence of vehicle on I absorption in Wistar rats are also presented.

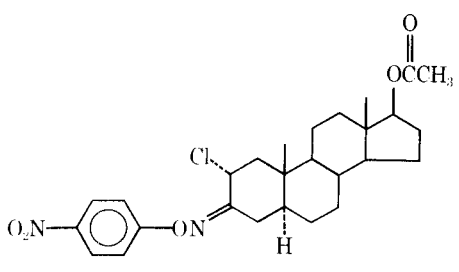

I

EXPERIMENTAL

Comparative Bioavailability Study in Rats—*Preparation of Radiolabeled Suspensions and Solutions*—Unlabeled micronized I was prepared by micronization employing a high-velocity impact mill[3]. Micronized ^{3}H-I (specific activity of 8.94 μCi/mg) was prepared by precipitation of ^{3}H-I[1] (specific activity of 169.5 μCi/mg) and unlabeled micronized I from methylene chloride by the use of hexane.

The radiochemical purity of ^{3}H-I and micronized ^{3}H-I was determined by TLC [250-μm silica gel GF plates with hexane–ethyl acetate (8:2)] to be greater than 95%.

Portions of 2 mg of micronized ^{3}H-I were added to each of four vials containing various amounts of unlabeled micronized I. The powders were mixed gently in each vial, and sesame oil was added slowly with constant stirring to yield a final volume of 2.5 ml.

Aliquots of Solutions A and B were assayed for radioactive content by liquid scintillation spectrometry and for concentration of I using UV absorption spectrometry (at 312 nm). Aliquots of dosage forms C and D were centrifuged (1000 rpm for 5 min), and the resulting supernates were passed through a 0.45-μm filter[4] (cellulose) and then reassayed. The specific activity of ^{3}H-I present in solution in each preparation was determined from the results of the assays for radioactivity and for total I (Table I).

Comparative Absorption Studies—Three adult female Wistar rats[5], 250–275 g, in each of four groups, were fasted 18–22 hr before drug administration and then received 0.6 ml (3.69–3.98 μCi) of the corresponding dose preparation by oral gavage. The rats were placed in metabolism cages for urine and feces collection. Whole blood samples were removed from the tail vein or the orbital plexus at intervals up to 24 hr after drug administration. Aliquots (0.5 ml) of these samples were placed into tissue sample cups[6] immediately after each collection. The samples were subsequently combusted in a tissue oxidizer[7], dissolved in a scintillation cocktail[8], and assayed for radioactive content using a liquid scintillation spectrometer[9].

Internal standardization was used to correct for quenching. The area under the whole blood radioactivity concentration *versus* time curve (*AUC*), from 0 to 24 hr after drug administration to each rat, was then determined. The *AUC*'s were converted (through division by appropriate specific activity) to corrected areas representing mass concentration of I equivalents (I and/or metabolites) *versus* time.

Urine was collected for 48 hr after drug administration. Aliquots of urine (0.5 ml) were added to scintillation cocktail[10] and were assayed for radioactive content.

Influence of Vehicle on ^{3}H-I Absorption—The influence of vehicle on ^{3}H-I absorption was first studied by administering the drug either dissolved in sesame oil or as an aqueous suspension in 0.5% (w/v) methylcellulose and 0.4% (w/v) polysorbate 80. A solution of ^{3}H-I (3.7 μCi, 2.5 mg/kg) in sesame oil (0.4 ml) was orally administered to three rats. To

[1] Synthesized at Ortho Pharmaceutical Corp., Raritan, N.J.
[2] D. W. Hahn, Ortho Pharmaceutical Corp., Raritan, N.J., personal communication.
[3] Trost Inc., Hatboro, Pa.
[4] Millipore.
[5] Royal Heart Laboratories, New Hampton, N.Y.
[6] Combustocones, Packard Instrument Co., Downers Grove, Ill.
[7] Model 306, Packard Instrument Co., Downers Grove, Ill.
[8] Monophase 40, Packard Instrument Co., Downers Grove, Ill.
[9] Model SL-30, Teledyne-Intertechnique, Westwood, N.J.
[10] Scintisol-Complete, Isolab Inc., Akron, Ohio.

0022-3549/78/0900-1287$01.00/0
© 1978, American Pharmaceutical Association

Table I—Comparison of Solutions and Suspensions of ^{3}H-I

Preparation[a]	Micronized ^{3}H-I, mg	Micronized I, mg	Concentration, mg/ml	Activity of[b] Dissolved ^{3}H-I, μCi/ml
Solution A	1.997	0	0.8	6.42
Solution B	2.004	2	1.6	6.20
Suspension C	2.005	18	8	6.63
Suspension D	1.998	38	16	6.13

Group Comparison	Ratio of Activity	Ratio of Mean Area of ^{3}H Activity[c]
A/C	1.93	1.51
A/D	2.62	1.91
B/C	1.86	1.58
B/D	2.53	2.00[d]

[a] Three female Wistar rats per dose group were each administered micronized ^{3}H-I in sesame oil (3.68–3.98 μCi, 0.6 ml) by oral gavage. [b] Aliquots of Solutions A and B were assayed for concentration of radioactivity. Aliquots of Suspensions C and D were centrifuged (1000 rpm for 5 min), and the supernates were assayed. [c] Ratio of uncorrected mean *AUC* values. [d] Statistically significant ($p < 0.05$).

three additional rats, the same dose was administered orally as an aqueous suspension (0.4 ml). Finally, three rats were administered orally ^{3}H-I (9.5 μCi, 75 mg/kg) as an aqueous suspension (0.48 ml). The concentration of radioactivity in whole blood was determined, and the *AUC*, corrected for quantity of administered drug, was calculated.

Comparative Bioavailability Studies in Humans—*Materials*—Compound ^{3}H-I (specific activity of 275 μCi/mg) and unlabeled I were recrystallized together to yield ^{3}H-I with a specific activity of 100.8 μCi/mg. The radiochemical purity of this compound was determined by TLC to be greater than 95%.

The two dosage forms were prepared according to the following procedure. Capsule E, containing 1.0 mg of ^{3}H-I (100 μCi/mg), was prepared by triturating 13.0 mg of ^{3}H-I and 537.0 mg of lactose in a mortar. Aliquots of the resultant blend containing 1.0 mg of ^{3}H-I were then hand packed into white-opaque (No. 4) gelatin capsules.

Capsule F, containing 1.0 mg of ^{3}H-I (100 μCi/mg) dispersed in sesame oil, was prepared by adding 13 mg of ^{3}H-I, dissolved in chloroform, to 3.0 g of sesame oil. The chloroform was then evaporated by heating the mixture to 60° with constant stirring. A suitable volume of sesame oil, containing 1.0 mg of ^{3}H-I, was then injected into each 5-minim, clear, soft gelatin capsule. The capsules were sealed by means of an aqueous gelatin solution. Samples of both dosage formulations were assayed for drug content and tritium activity.

Samples of both formulations were reassayed immediately prior to use for radioactive content, radiochemical purity, and drug content.

Subjects—Two healthy female subjects, LD and MJ, were 40 and 33 years of age, respectively. Their heights were 157 and 168 cm, respectively, and their weights were 60.9 and 58.6 kg, respectively.

Methods—After a 12-hr fast, both subjects were hospitalized and each

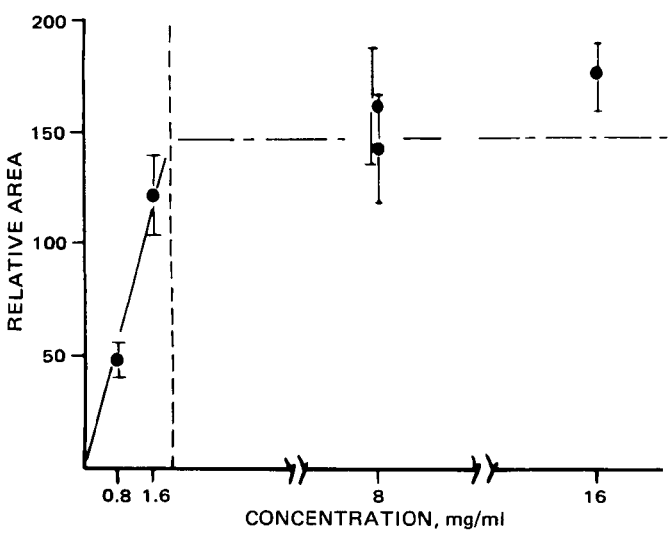

Figure 1—*Absorption of I* versus *concentration administered. Each point represents mean* AUC *converted to area representing mass concentration* versus *time* ± SE *for each group of three rats (Table II). Horizontal dashed line represents an extrapolated line.*

Table II—Absorption of I after Oral Administration in Sesame Oil

Dose Preparation	Concentration in Solution ^{3}H-I, μCi/ml	Concentration in Solution I[a], mg/ml	Concentration in Solution Specific Activity, μCi/mg (Calculated)	Area[b] Mass Concentration × *t*, mg, Mean ± *SE*
A	6.42	0.76	8.44	4.69 ± 8.7
B	6.20	1.83	3.39	122.1 ± 18.0
C	3.32	1.83–2.08[c]	1.60–1.81[c]	163.9 ± 25.3[c]
				144.9 ± 22.4[c]
D	2.45	2.08	1.18	174.9 ± 14.9

[a] Aliquots of Solutions A and B were assayed for concentration of I by UV absorption. Aliquots of Suspensions C and D were centrifuged (1000 rpm for 5 min), and the supernates were filtered and assayed. Filtrate C was lost, and the concentration range from Samples B to D was employed. Refer to footnote *c*. [b] The *AUC* for each rat (expressed in milligrams) was divided by the specific activity for the corresponding dose solution to yield area representing mass concentration *versus* time. [c] Value employed is range based upon results of assay of Solutions B and D. In all cases, the values agree with the known equilibrium solubility of I in sesame oil.

was given a different dosage formulation followed by 240 ml of water. Subject LD received Capsule F. Subject MJ received Capsule E. Water was permitted *ad libitum*, and a normal diet was permitted 6 hr after drug administration.

Venous blood samples were collected into heparinized tubes at 0, 0.5, 1, 2, 4, 6, 8, 10, 12, 16, 20, 24, 30, 36, 48, 60, 72, 96, and 120 hr, at 7, 12, and 14 days, and at selected intervals thereafter. Urine and feces were collected during the day prior to drug administration and daily for 2 weeks thereafter and were frozen immediately.

Two 0.5-ml aliquots of whole blood from each sample were placed into tissue sample cups[6] immediately after each collection. The aliquots were subsequently combusted and assayed for radioactive content. Plasma was separated from the remainder of each whole blood sample and was frozen. Two 0.5-ml aliquots of plasma were subsequently combusted and assayed for radioactive content.

Urine was assayed for radioactive content by the procedure described previously. Each fecal specimen was diluted to a constant volume (500 ml) with methanol–water (1:1 v/v) and homogenized in a blender[11], and aliquots (0.5 ml) were transferred to tissue sample cups[6] and assayed for radioactive content.

RESULTS

Comparative Bioavailability Studies in Rats—For each rat, the concentration of radioactivity determined in samples of whole blood was plotted as a function of time. Radioactivity in whole blood represented the sum of I and/or all of its metabolites at any time. The ratios of the mean area under these curves for any dosage group when compared to the mean for any other group (Table I) were similar to the corresponding ratios of the radioactivity of I dissolved in sesame oil for each dosage form comparison. However, the values obtained for dissolved radioactivity were not proportional to the total amount of I in solution in sesame oil (Table II) and indicated a preferential solubilization of ^{3}H-I.

Calculation of the mean *AUC*, when corrected for the quantity of drug administered (Table II), indicated that a substantially larger fraction of the dose was absorbed in the two instances where I was present only in solution than where I was present in suspension. A linear relationship (Fig. 1) existed between the quantity of I absorbed and the amount of drug present in solution for Solutions A and B (true solutions). This relationship was not apparent for the dosage forms containing I in suspension.

This observation was confirmed upon examination of the total amount of radioactivity excreted in the urine of each group of animals in the first 48 hr after administration of the various dosage forms (Table III). Figure 2 shows the mean mass of I equivalents (I and/or metabolites) excreted for each group of rats as a function of the concentration of I in the dosage forms. A linear relationship was found to exist between the total mass excreted and the concentration of I for dosage forms that were true solutions (A and B) but did not hold where some I was in suspension (C and D).

The relative bioavailability of I following oral drug administration either in solution in sesame oil or in aqueous suspension is presented in

[11] Waring Products Corp., Winstead, Conn.

Table III—Urinary Excretion of I after Oral Administration in Sesame Oil

Dose Preparation	Total Disintegrations per Minute Excreted in 48 hr, Mean ± *SE*	Specific Activity, μCi/mg	Total Micrograms Excreted[a] in 48 hr, Mean ± *SE*	Mean Percent Dose Excreted
A	472,883 ± 58,050	8.44	25.2 ± 3.1	5.2
B	665,000 ± 87,619	3.39	88.4 ± 11.6	9.2
C	595,050 ± 101,416	1.60–1.81[b]	167.5 ± 28.6 148.1 ± 25.2	3.1–3.5[b]
D	318,767 ± 41,128	1.18	121.7 ± 15.7	1.3

[a] Total micrograms excreted in 48 hr for each rat was calculated by the following formula: total dpm excreted × [1000/2,200,000 (specific activity)] = total μg excreted. [b] Theoretical value employed; refer to Table II footnotes *a* and *c* for details.

Table IV—Effect of Different Vehicles on I Bioavailability following Oral Administration in Rats

Vehicle	Dose, mg/kg	Mean *AUC* ± *SE*[a], μg equivalents/ml × hr	Mean *AUC* per Dose ± *SE*
Sesame oil (solution)	2.5[b]	3.92 ± 0.27	1.57 ± 0.11 [c]
0.5% (w/v) methylcellulose and 0.4% (w/v) polysorbate 80 (suspension)	2.5[b]	1.33 ± 0.14	0.53 ± 0.05 [c]
	75[b]	6.53 ± 1.54	0.09 ± 0.02 [d]

[a] *AUC* = area under whole blood drug equivalent concentration (I and/or metabolites) *versus* time curve, determined from the following formula: [*AUC* (μg equivalents/ml × hr)] = [*AUC* (dpm/μl × hr) determined by cut and weight method × 1000 μl/ml]/specific activity of administered I in dpm/μg. [b] $n = 3$. [c] Statistically significant difference ($p < 0.001$) by Student t test (two tail). [d] Statistically significant difference ($p < 0.005$) by Student t test (two tail).

Table IV. Following administration of I in solution in sesame oil, the mean *AUC*, when corrected for the quantity of drug administered, was threefold greater than that following administration of the same dose of I in aqueous suspension ($p < 0.001$). The bioavailability of a 75-mg/kg dose of I was compared with that of a 2.5-mg/kg dose following oral administration of I in aqueous suspension at both doses. The mean *AUC*, when corrected for the quantity of drug administered, was significantly lower ($p < 0.001$) following administration of the 75-mg/kg dose than following administration of the 2.5-mg/kg dose (Table IV).

Comparative Bioavailability Studies in Humans—Absorption of radioactivity was fairly rapid following oral administration of ^{3}H-I in sesame oil to Subject LD. Peak blood levels of total radioactivity occurred within 2 hr after drug administration (Fig. 3). The radioactivity in blood then rapidly decreased to a low level that persisted for more than 120 hr. The apparent half-life of radioactivity in whole blood was estimated to be 63 hr, and the elimination rate constant was calculated to be 0.011 hr^{-1}.

Cumulative elimination of radioactivity in the urine and feces of this subject is shown in Fig. 4. Approximately 45% of the administered dose was eliminated within the 14-day study period, 30% within the first 3 days. Approximately 29% of the administered dose appeared in the urine within the 14-day study period. These calculations were based on an administered dose of 90.2 μCi, the average value obtained from analysis of two similar capsules just prior to the study. By 96 days after drug administration, radioactivity corresponding to approximately 76% of the dose was recovered, with about 49% in the urine. After the initial 2 weeks following drug administration, ~0.5 μCi/day was excreted between Days 15 and 41 and ~0.3 μCi/day was excreted between Days 41 and 60 (Fig. 4).

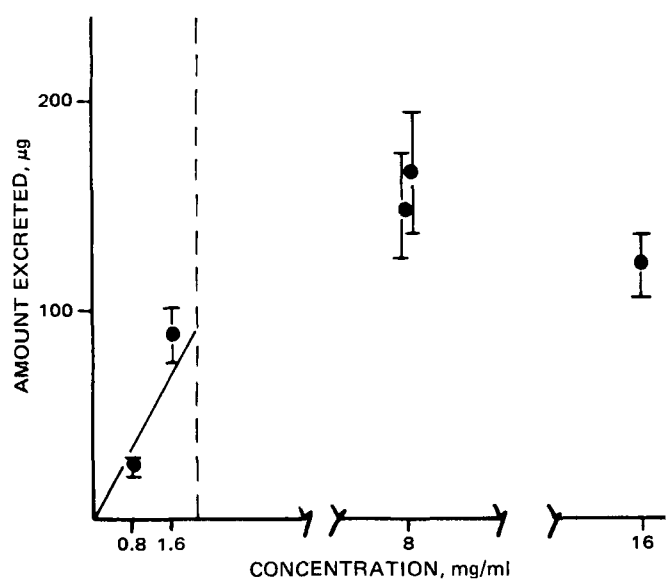

Figure 2—*Urinary excretion of I* versus *concentration administered. Each point represents the mean amount of I and/or metabolites* ± SE *excreted into the urine by 48 hr after drug administration to each group of three rats (Table III).*

Absorption of radioactivity following oral administration of ^{3}H-I, mixed with lactose, to Subject MJ occurred more slowly than in the first subject (Fig. 3). Peak blood levels of radioactivity occurred approximately 10 hr after administration. Furthermore, only low levels of radioactivity were found at all time intervals, *i.e.*, less than 400 dpm/ml.

This subject eliminated approximately 77% of the administered dose within the 9-day study period, 74% within the first 3 days (Fig. 4). Approximately 71% of the total administered dose appeared in feces during the first 10 days. These calculations were based on a dose of 96.2 μCi, the average value obtained from analysis of two similar capsules just prior to the study.

After the first 2 weeks, only trace amounts of radioactivity, slightly above background, were found in the excreta (Fig. 4).

DISCUSSION

Results of the bioavailability study in rats indicated that, for doses of I in sesame oil where all drug was in solution at the time of administration, absorption of radioactivity from ^{3}H-I was proportional to the concentration of the drug present (Fig. 1). When the concentration of I exceeded its equilibrium solubility in sesame oil (2 mg/ml), this relationship was not maintained. If absorption were limited to only that portion of the drug in solution at the time of administration, doses of drug in suspension would yield *AUC* values equivalent to that for Solution B (assuming a constant volume is administered), depicted by the horizontal hatched line in Fig. 1. There appeared to be only a negligible amount of absorption of drug in suspension at the time of administration. Similar conclusions were obtained from a plot of the total mass of I equivalents excreted in the urine *versus* administered dose (Fig. 2).

Studies of the effect of the vehicle employed on I bioavailability indicated that considerably less drug was absorbed from aqueous suspension in methylcellulose than from solution in sesame oil and that absorption of radioactivity following oral administration of aqueous suspensions of ^{3}H-I was not proportional to the administered dose.

The data obtained in humans, although preliminary, indicated that ^{3}H-I absorption from the sesame oil formulation was much greater than that from the lactose formulation. Peak blood levels of radioactivity generated by the oil formulation were 12 times those generated by the

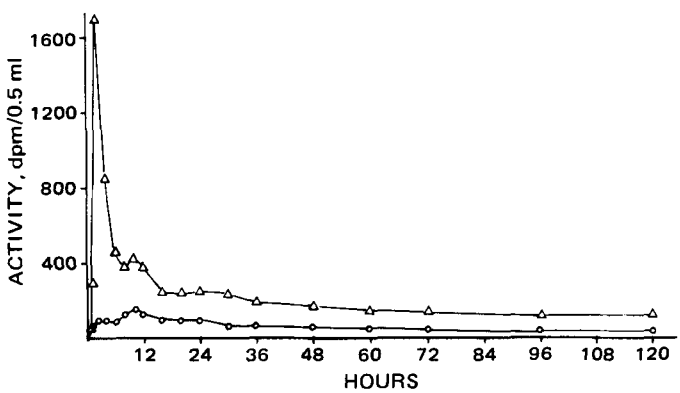

Figure 3—*Radioactivity found at various time intervals in the blood of Subject LD (Δ), who received ^{3}H-I (90.2 μCi, 1.0 mg) dispersed in sesame oil, and Subject MJ (○), who received ^{3}H-I (96.2 μCi, 0.97 mg) admixed with lactose.*

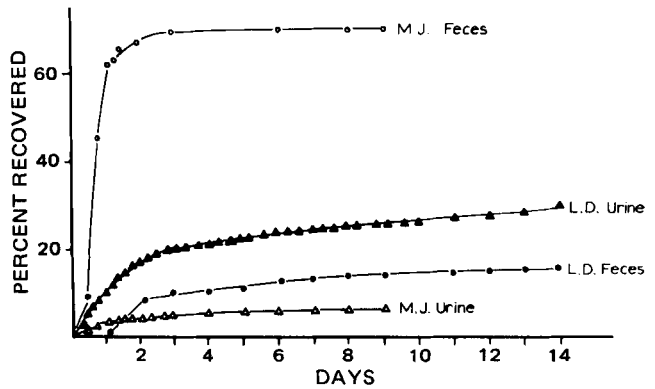

Figure 4—*Cumulative elimination of radioactivity in urine and feces from Subjects LD and MJ.*

lactose formulation, and the areas under the blood level radioactivity curves differed by a factor of four. Furthermore, twice as much radioactivity was excreted in urine as compared to feces in the subject receiving the oil formulation. In the subject receiving the lactose formulation, 12 times as much radioactivity appeared in feces as compared to urine, a likely result of poor absorption.

The data obtained for Subject LD after the initial 2 weeks following drug administration (Fig. 4) suggested that a fraction of the administered radioactivity may have been contained in a deep body compartment from which small amounts were leached out over a prolonged period.

Results of contragestational potency studies in rats employing a 20-mg/ml suspension[2] and the comparative bioavailability studies in rats described in the present report indicated that systemic absorption of biologically effective amounts of I was primarily proportional to the amount of drug in solution at the time of administration. For rats, when the amount of I in the volume of administered sesame oil exceeded the equilibrium solubility of the drug, the expected relationship of systemic absorption and contragestational potency to dose was not maintained.

REFERENCES

(1) D. W. Hahn, G. O. Allen, and F. C. Greenslade, *Fed. Proc.*, **36**, 342 (1977).

(2) A. F. Hirsch, G. O. Allen, B. Wong, S. Reynolds, C. Exarhos, W. Brown, and D. W. Hahn, *J. Med. Chem.*, **20**, 1546 (1977).

(3) J. Lindenbaum, M. H. Mellow, M. O. Blackstone, and V. P. Butler, *N. Engl. J. Med.*, **285**, 1344 (1971).

(4) A. Bertier, A. Redfors, S. Medin, and L. Nyberg, *Lancet*, **2**, 708 (1972).

(5) B. F. Johnson, A. S. E. Fowle, S. Lader, J. Fox, and A. D. Munro-Faure, *Br. Med. J.*, **4**, 323 (1973).

(6) V. Manninen, K. Ojala, and P. Reissel, *Lancet*, **2**, 922 (1972).

(7) T. R. D. Shaw, M. R. Howard, and J. Hamer, *ibid.*, **2**, 303 (1972).

(8) B. Whiting, J. C. Rodger, and D. J. Sumner, *ibid.*, **2**, 922 (1972).

(9) A. Danon, J. Horowitz, A. Ben-Zvi, J. Kaplanski, and S. Glick, *Clin. Pharmacol. Ther.*, **21**, 643 (1977).

(10) A. Varley, *J. Am. Med. Assoc.*, **206**, 1745 (1968).

(11) G. R. VanPetten, H. Feng, R. J. Withey, and H. F. Leytau, *J. Clin. Pharmacol.*, **11**, 177 (1971).

(12) K. S. Albert, E. Sakmar, M. R. Hallmark, D. J. Weidler, and J. G. Wagner, *Clin. Pharmacol. Ther.*, **16**, 727 (1974).

(13) J. H. Tyrer, M. J. Eadie, J. M. Sutherland, and W. D. Hooper, *Br. Med. J.*, **4**, 271 (1970).

(14) D. C. Blair, R. W. Barnes, E. L. Wildner, and W. J. Murray, *J. Am. Med. Assoc.*, **215**, 251 (1971).

(15) A. J. Glazko, A. W. Kinkel, W. C. Aleegnani, and E. L. Holmes, *Clin. Pharmacol. Ther.*, **9**, 472 (1968).

(16) M. Kraml, J. Dubuc, and R. Gaudry, *Antibiot. Chemother. (NY)*, **12**, 239 (1962).

(17) S. S. Davis, *Br. Med. J.*, **1**, 102 (1972).

(18) A. J. Aguiar, J. Krc, Jr., A. W. Kinkel, and J. C. Samyn, *J. Pharm. Sci.*, **56**, 847 (1967).

(19) J. W. Poole, G. Owen, J. Silverio, J. N. Freyhof, and S. B. Rosenman, *Curr. Ther. Res., Clin. Exp.*, **10**, 292 (1968).

(20) L. J. Lesson, *Pharmacology*, **8**, 153 (1972).

(21) A. Glazko, *ibid.*, **8**, 164 (1972).

ACKNOWLEDGMENTS

The authors thank Mr. Gerald F. Eisen and Mr. Timothy J. Kane, III, for technical assistance.

Relative Bioavailability of Meprobamate Tablets in Humans

MARVIN C. MEYER ˣ, ARMEN P. MELIKIAN *, and ARTHUR B. STRAUGHN

Received October 11, 1977, from the *Division of Biopharmaceutics and Pharmacokinetics, Department of Medicinal Chemistry, College of Pharmacy, University of Tennessee Center for the Health Sciences, Memphis, TN 38163.* Accepted for publication January 12, 1978. *Present address: Clinical Pharmacology Department, A. H. Robins Co., Richmond, VA 23220.

Abstract □ The relative bioavailability of 400-mg meprobamate tablets manufactured by 11 different firms was evaluated in two groups of healthy male subjects. Each group of six subjects received a reference standard product and five test products given at 1-week intervals. Plasma meprobamate concentrations at 1, 2, 3, 4, 6, 8, 10, 24, and 32 hr after dosing were determined using a GLC assay. Analysis of variance of the plasma level–time profiles revealed no statistically significant differences between any of the products in terms of plasma levels at the various sample times, time of peak plasma level, peak plasma level, and area under the plasma level–time curve. It was concluded that the 11 400-mg products could be considered bioequivalent.

Keyphrases □ Meprobamate—bioavailability of 11 commercial products in humans □ Bioavailability—meprobamate, 11 commercial products in humans □ Sedatives—meprobamate, bioavailability of 11 commercial products in humans

At present, there are more than 60 manufacturers or distributors of meprobamate products in the United States. Several groups have evaluated the potential of meprobamate products to exhibit bioavailability inequivalence (1–3). However, the bioavailability of meprobamate from tablets obtained from a variety of manufac-

0022-3549/78/0900-1290$01.00/0
© 1978, American Pharmaceutical Association

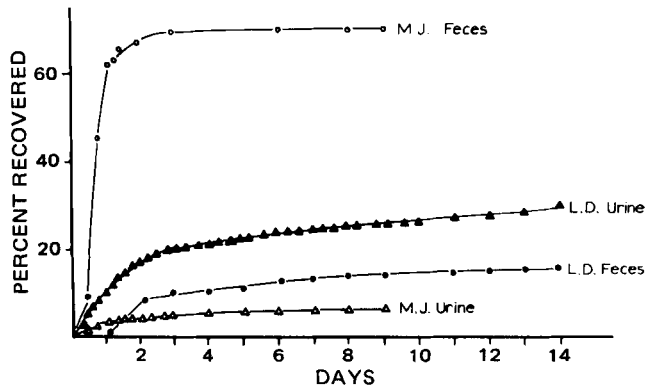

Figure 4—*Cumulative elimination of radioactivity in urine and feces from Subjects LD and MJ.*

lactose formulation, and the areas under the blood level radioactivity curves differed by a factor of four. Furthermore, twice as much radioactivity was excreted in urine as compared to feces in the subject receiving the oil formulation. In the subject receiving the lactose formulation, 12 times as much radioactivity appeared in feces as compared to urine, a likely result of poor absorption.

The data obtained for Subject LD after the initial 2 weeks following drug administration (Fig. 4) suggested that a fraction of the administered radioactivity may have been contained in a deep body compartment from which small amounts were leached out over a prolonged period.

Results of contragestational potency studies in rats employing a 20-mg/ml suspension[2] and the comparative bioavailability studies in rats described in the present report indicated that systemic absorption of biologically effective amounts of I was primarily proportional to the amount of drug in solution at the time of administration. For rats, when the amount of I in the volume of administered sesame oil exceeded the equilibrium solubility of the drug, the expected relationship of systemic absorption and contragestational potency to dose was not maintained.

REFERENCES

(1) D. W. Hahn, G. O. Allen, and F. C. Greenslade, *Fed. Proc.*, **36**, 342 (1977).

(2) A. F. Hirsch, G. O. Allen, B. Wong, S. Reynolds, C. Exarhos, W. Brown, and D. W. Hahn, *J. Med. Chem.*, **20**, 1546 (1977).

(3) J. Lindenbaum, M. H. Mellow, M. O. Blackstone, and V. P. Butler, *N. Engl. J. Med.*, **285**, 1344 (1971).

(4) A. Bertier, A. Redfors, S. Medin, and L. Nyberg, *Lancet*, **2**, 708 (1972).

(5) B. F. Johnson, A. S. E. Fowle, S. Lader, J. Fox, and A. D. Munro-Faure, *Br. Med. J.*, **4**, 323 (1973).

(6) V. Manninen, K. Ojala, and P. Reissel, *Lancet*, **2**, 922 (1972).

(7) T. R. D. Shaw, M. R. Howard, and J. Hamer, *ibid.*, **2**, 303 (1972).

(8) B. Whiting, J. C. Rodger, and D. J. Sumner, *ibid.*, **2**, 922 (1972).

(9) A. Danon, J. Horowitz, A. Ben-Zvi, J. Kaplanski, and S. Glick, *Clin. Pharmacol. Ther.*, **21**, 643 (1977).

(10) A. Varley, *J. Am. Med. Assoc.*, **206**, 1745 (1968).

(11) G. R. VanPetten, H. Feng, R. J. Withey, and H. F. Leytau, *J. Clin. Pharmacol.*, **11**, 177 (1971).

(12) K. S. Albert, E. Sakmar, M. R. Hallmark, D. J. Weidler, and J. G. Wagner, *Clin. Pharmacol. Ther.*, **16**, 727 (1974).

(13) J. H. Tyrer, M. J. Eadie, J. M. Sutherland, and W. D. Hooper, *Br. Med. J.*, **4**, 271 (1970).

(14) D. C. Blair, R. W. Barnes, E. L. Wildner, and W. J. Murray, *J. Am. Med. Assoc.*, **215**, 251 (1971).

(15) A. J. Glazko, A. W. Kinkel, W. C. Aleegnani, and E. L. Holmes, *Clin. Pharmacol. Ther.*, **9**, 472 (1968).

(16) M. Kraml, J. Dubuc, and R. Gaudry, *Antibiot. Chemother. (NY)*, **12**, 239 (1962).

(17) S. S. Davis, *Br. Med. J.*, **1**, 102 (1972).

(18) A. J. Aguiar, J. Krc, Jr., A. W. Kinkel, and J. C. Samyn, *J. Pharm. Sci.*, **56**, 847 (1967).

(19) J. W. Poole, G. Owen, J. Silverio, J. N. Freyhof, and S. B. Rosenman, *Curr. Ther. Res., Clin. Exp.*, **10**, 292 (1968).

(20) L. J. Lesson, *Pharmacology*, **8**, 153 (1972).

(21) A. Glazko, *ibid.*, **8**, 164 (1972).

ACKNOWLEDGMENTS

The authors thank Mr. Gerald F. Eisen and Mr. Timothy J. Kane, III, for technical assistance.

Relative Bioavailability of Meprobamate Tablets in Humans

MARVIN C. MEYER ˣ, ARMEN P. MELIKIAN *, and ARTHUR B. STRAUGHN

Received October 11, 1977, from the *Division of Biopharmaceutics and Pharmacokinetics, Department of Medicinal Chemistry, College of Pharmacy, University of Tennessee Center for the Health Sciences, Memphis, TN 38163.* Accepted for publication January 12, 1978. *Present address: Clinical Pharmacology Department, A. H. Robins Co., Richmond, VA 23220.

Abstract □ The relative bioavailability of 400-mg meprobamate tablets manufactured by 11 different firms was evaluated in two groups of healthy male subjects. Each group of six subjects received a reference standard product and five test products given at 1-week intervals. Plasma meprobamate concentrations at 1, 2, 3, 4, 6, 8, 10, 24, and 32 hr after dosing were determined using a GLC assay. Analysis of variance of the plasma level–time profiles revealed no statistically significant differences between any of the products in terms of plasma levels at the various sample times, time of peak plasma level, peak plasma level, and area under the plasma level–time curve. It was concluded that the 11 400-mg products could be considered bioequivalent.

Keyphrases □ Meprobamate—bioavailability of 11 commercial products in humans □ Bioavailability—meprobamate, 11 commercial products in humans □ Sedatives—meprobamate, bioavailability of 11 commercial products in humans

At present, there are more than 60 manufacturers or distributors of meprobamate products in the United States. Several groups have evaluated the potential of meprobamate products to exhibit bioavailability inequivalence (1–3). However, the bioavailability of meprobamate from tablets obtained from a variety of manufac-

0022-3549/78/0900-1290$01.00/0
© 1978, American Pharmaceutical Association

Table I—*In Vitro* Test Results for 400-mg Meprobamate Tablets [a]

Product Code Number (Study Group)	Assay, % of Label	Mean Percent Dissolved in 30 min
1 (I, II)	102.7	>77.0
2 (I)	97.1	94.2
3 (I)	100.5	100.5
4 (I)	99.3	78.9
5 (I)	106.0	96.9
6 (I)	100.4	81.8
7 (II)	101.5	89.4
8 (II)	106.0	80.9
9 (II)	100.7	72.0
10 (II)	100.9	70.8
11 (II)	95.8	97.2

[a] Manufacturer and lot number are as follows: 1, Wyeth Laboratories, 1751101; 2, ICN Pharmaceuticals, 9031-4XP; 3, Towne, Paulsen and Co., 047544; 4, Stanley Drug Products, 086503; 5, Smith Kline and French Laboratories, 555134; 6, Heather Drug Co., 57023; 7, Lannett Co., 17288; 8, Zenith Laboratories, 3904-670; 9, Westward, 41682; 10, Wallace Laboratories, 5D1008; and 11, Danbury Pharmacal, 10686. All products were obtained from FDA regional offices.

turers has not been well documented. The present study was undertaken to determine the relative bioavailability of 11 meprobamate tablet products.

EXPERIMENTAL

Assay of Plasma Samples—The measurement of plasma meprobamate levels was based on a GLC method developed by Martis and Levy (4). A 0.4–1.5-ml plasma sample was added to 1.0 ml of 0.15 *N* NaOH and 1.0 ml of a 2.5-μg/ml tybamate internal standard solution. The mixture was extracted for 15 min with 5 ml of ether. After centrifugation, 4 ml of the ether phase was removed, evaporated to dryness, and stored at −18° until analysis.

The residue was dissolved in 15–25 μl of ether, and 2 μl was injected into a gas chromatograph[1] equipped with flame-ionization detectors. Glass U-shaped columns (180 mm × 2.5 mm) were packed with 3% SE-30 on 80–100-mesh Gas Chrom Q. Temperatures were 180, 175, and 250° for the injector, oven, and detectors, respectively. Plasma meprobamate concentrations were determined from standard curves of meprobamate to tybamate peak height ratio *versus* meprobamate concentration, prepared over a meprobamate concentration range of 0.5–5.0 μg/ml, using pooled human plasma.

***In Vitro* Tests**—The USP XIX (5) tablet weight variation, product assay, and dissolution tests were performed[2] on each product. Disintegration times also were determined[2] for eight products.

Meprobamate Products—Table I summarizes the meprobamate products evaluated. Eleven single lots of 400-mg tablets were selected.

Clinical Study Protocol—Twelve male volunteers[3] underwent urine analyses as well as hematologic and blood enzyme analyses[4] to ensure that they were in good health. They ranged in age from 22 to 27 years, in height from 175 to 188 cm, and in weight from 70.5 to 95.5 kg. All subjects were within 10% of the ideal weight for their age, sex, height, and build.

The subjects were divided into two groups of six subjects. Each subject received a single 400-mg tablet once a week for 6 consecutive weeks. The administration sequence was based on a crossover matrix designed to minimize the influence of any residual or cumulative effects of the preceding doses (6). Each subject in each group was administered six different meprobamate products, with only Product 1 being common to both test groups as a reference standard.

Each subject was instructed to adhere to a standard protocol and to abstain from any medication during the study period. The tablets were administered in the morning following an overnight fast. No food or liquid, other than water, was permitted until 4 hr following drug ingestion. Blood samples of 10 ml were collected in heparinized containers prior to the dose and at 1, 2, 3, 4, 6, 8, 10, 24, and 32 hr. The blood samples were centrifuged, and the plasma fraction was removed and frozen until assayed.

Statistical Analysis—Four parameters were examined to evaluate the relative bioavailability of the 11 meprobamate products: plasma levels at each sampling time, time of peak plasma level, peak plasma level, and area under the plasma level–time curve (*AUC*). The data for each group were statistically analyzed for differences between products, subjects, and weeks using the *F* ratio test and the Newman–Keuls *a posteriori* test (7). The power of the study design was calculated (8) for $\alpha = 0.05$ and $\beta = 0.2$.

[1] Varian model 2100.
[2] In the laboratories of the U.S. Food and Drug Administration (FDA).
[3] Staff and students of the University of Tennessee Center for the Health Sciences. Each subject gave written informed consent.
[4] SMA 12/60.

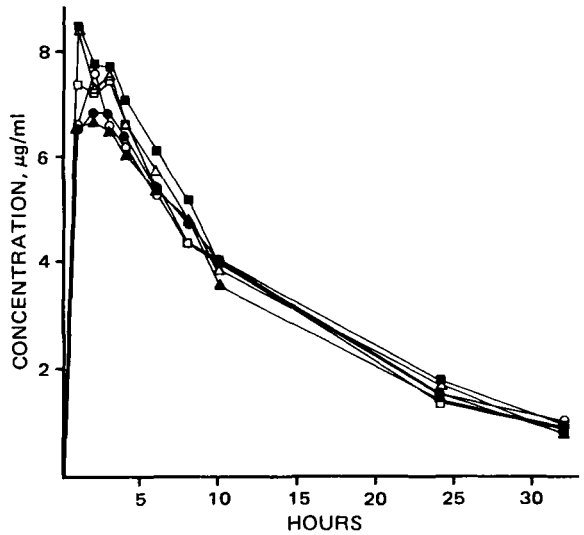

Figure 1—*Mean plasma meprobamate levels for Study Group I. Each data point represents the mean of six subjects. Key: ○, Product 1; ●, Product 2; □, Product 3; ■, Product 4; △, Product 5; and ▲, Product 6.*

RESULTS AND DISCUSSION

***In Vitro* Tests**—Table I summarizes the results of the *in vitro* tests. The meprobamate content of Product 5 (Group I) and Product 8 (Group II) was slightly in excess of the USP XIX (5) limits of 95–105% of labeled content. All 11 products met the USP XIX requirement of 60% dissolution within 30 min, with the mean percent dissolution in 30 min ranging from 71 to 101%. Tablets from eight lots also were tested for disintegration using the USP XIX apparatus. All products tested disintegrated within 5 min.

Plasma Levels—Tables II and III summarize the mean plasma meprobamate levels for each product at each sampling time. These results are shown graphically in Figs. 1 and 2. Analysis of variance for these data indicated no significant differences ($p > 0.05$) among the six products tested in each group in terms of mean plasma levels obtained at each sampling time.

Time of Peak Plasma Level—The mean times of peak plasma meprobamate concentration for the individual products, uncorrected

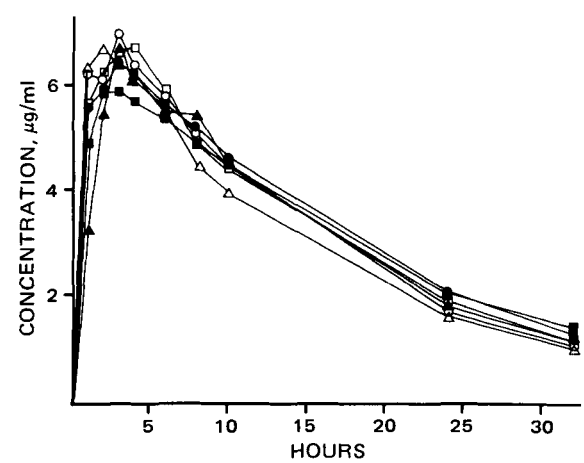

Figure 2—*Mean plasma meprobamate levels for Study Group II. Each data point represents the mean of six subjects. Key: ○, Product 1; ●, Product 7; □, Product 8; ■, Product 9; △, Product 10; and ▲, Product 11.*

Table II—Average Plasma Meprobamate Concentrations [a] of Group I

Product	1 hr	2 hr	3 hr	4 hr	6 hr	8 hr	10 hr	24 hr	32 hr
1	6.68	7.65	6.63	6.25	5.32	4.42	4.03	1.58	1.08
	(20.9)	(7.2)	(7.3)	(12.7)	(14.6)	(11.8)	(14.5)	(23.1)	(17.9)
2	6.60	6.92	6.88	6.45	5.45	4.78	4.10	1.58	0.88
	(19.9)	(15.4)	(13.6)	(5.6)	(13.5)	(27.7)	(22.1)	(21.7)	(46.1)
3	7.48	7.33	7.55	6.73	5.55	4.47	4.13	1.47	1.02
	(12.0)	(18.7)	(14.8)	(18.9)	(28.6)	(32.5)	(29.9)	(38.2)	(36.0)
4	8.57	7.85	7.80	7.17	6.18	5.25	4.05	1.87	1.03
	(27.6)	(27.9)	(19.8)	(15.9)	(15.7)	(11.2)	(31.0)	(32.3)	(42.7)
5	8.50	7.40	7.60	6.67	5.80	4.87	3.93	1.78	0.85
	(19.5)	(24.0)	(19.1)	(21.1)	(19.0)	(25.9)	(27.8)	(39.4)	(41.3)
6	6.65	6.75	6.55	6.12	5.43	4.85	3.65	1.50	0.92
	(33.1)	(18.3)	(24.4)	(19.4)	(15.2)	(27.5)	(28.8)	(36.8)	(48.5)

[a] Average data for six subjects; concentration in micrograms per milliliter. The coefficient of variation in percent is given in parentheses.

Table III—Average Plasma Meprobamate Concentrations [a] of Group II

Product	1 hr	2 hr	3 hr	4 hr	6 hr	8 hr	10 hr	24 hr	32 hr
1	6.25	6.13	7.03	6.43	5.82	5.12	4.52	1.75	1.10
	(45.3)	(39.9)	(37.7)	(27.9)	(22.2)	(21.7)	(17.3)	(32.5)	(28.2)
7	5.62	5.98	6.50	6.28	5.68	5.23	4.68	2.13	1.38
	(36.3)	(32.3)	(23.7)	(19.0)	(22.5)	(17.8)	(27.0)	(26.0)	(37.8)
8	5.70	6.33	6.67	6.77	5.97	4.92	4.42	1.95	1.18
	(41.5)	(37.0)	(32.2)	(22.2)	(26.4)	(35.9)	(40.7)	(35.5)	(19.6)
9	4.90	5.90	5.92	5.73	5.38	4.95	4.43	2.08	1.45
	(43.9)	(32.1)	(21.0)	(26.1)	(25.4)	(39.9)	(49.9)	(42.2)	(50.1)
10	6.40	6.77	6.45	6.33	5.45	4.55	4.00	1.65	1.05
	(33.4)	(21.8)	(24.5)	(26.8)	(28.8)	(28.3)	(27.9)	(38.5)	(30.0)
11	3.27	5.43	6.75	6.20	5.57	5.48	4.57	1.87	1.18
	(28.8)	(33.1)	(27.7)	(26.3)	(17.5)	(22.2)	(19.7)	(31.7)	(36.8)

[a] Average data for six subjects; concentration in micrograms per milliliter. The coefficient of variation in percent is given in parentheses.

for any lag time, are summarized in Table IV. Because the time interval between individual samples was at least 1 hr, the actual peak time may have been overestimated.

In Group I, the time of peak concentration ranged from 1.5 to 2.3 hr. The times of peak concentration in Group II were generally greater, ranging from 1.8 to 3.8 hr. These values are in agreement with other studies that reported peak levels at 1–3 hr after dosing (9). Because of the large coefficient of variation for these mean parameters, no statistically significant differences ($p > 0.05$) were found among products in either test group.

Peak Plasma Level—Table IV summarizes the mean peak concentrations found for the products in each group. These mean levels ranged from 7.4 (Product 6) to 8.9 (Product 4) μg/ml in Group I and from 6.8 (Product 9) to 7.8 (Product 10) μg/ml in Group II. The true peak plasma levels may have been underestimated because of the time interval between successive samples.

Previous studies employing 400-mg single doses of meprobamate reported mean peak plasma levels of 6.0–10.8 μg/ml (9). Blood levels of 5–20 μg/ml usually result during chronic administration of therapeutic doses (10). When expressed as a percentage of the reference standard (Product 1), the peak concentrations ranged from 94.9 to 114.1% in Group I and from 88.3 to 101.3% in Group II. There were no statistically significant differences among the products in either group in terms of peak plasma levels.

Area under Plasma Level–Time Curve (*AUC*)—The trapezoidal rule was used to obtain the individual *AUC* values from 0 to 32 hr. In those instances where plasma concentrations were still measurable at 32 hr, the extrapolated *AUC* was estimated from the following equation:

$$(AUC)_{0-\infty} = (AUC)_{0-32\ hr} + (C_p)_{32\ hr}/K_e \qquad \text{(Eq. 1)}$$

where $(C_p)_{32\ hr}$ is the plasma level at the 32-hr sampling time, and K_e is the elimination rate constant determined from the slope of the terminal portion of the semilog plot of plasma concentration *versus* time.

Table IV summarizes the mean $(AUC)_{0-32\ hr}$ as well as the mean $(AUC)_{0-\infty}$ values for each product. In both groups, neither area showed statistically significant differences ($p > 0.05$) between products. The $(AUC)_{0-\infty}$ values, expressed relative to Product 1, ranged from 94 to 108% in Group I and from 95 to 109% in Group II.

Differences between Subjects and between Weeks—Analysis of variance indicated statistically significant differences ($p < 0.05$) between subjects within each group at all but the 1- and 2-hr sampling times. In Group I, there was also a statistically significant difference ($p < 0.05$) between subjects for the $(AUC)_{0-32\ hr}$ as well as the $(AUC)_{0-\infty}$ but not for the time of peak plasma level or peak level. Group II showed no differences between subjects for time of peak concentration but did for the *AUC* values and peak concentration.

Calculation of individual half-lives following administration of six

Table IV—Mean Peak Concentration, Time of Peak Concentration, and *AUC* for Each Product [a]

Product	Peak Concentration, μg/ml	Time of Peak Concentration, hr	$(AUC)_{0-32\ hr}$, (μg/ml) (hr)	$(AUC)_{0-\infty}$, (μg/ml) (hr)
		Group I		
1	7.8 (6.1)	2.2 (45.4)	103.2 (11.2)	120.2 (12.3)
2	7.6 (11.4)	2.3 (44.3)	103.8 (11.5)	115.0 (13.5)
3	7.9 (12.2)	1.7 (49.0)	105.2 (25.7)	120.5 (26.4)
4	8.9 (20.8)	1.7 (72.7)	114.8 (22.2)	131.2 (26.0)
5	8.8 (17.9)	1.5 (55.8)	109.0 (24.9)	121.7 (25.7)
6	7.4 (18.6)	1.5 (55.8)	98.7 (23.0)	112.5 (26.0)
		Group II		
1	7.7 (24.1)	3.5 (23.9)	110.4 (23.6)	127.2 (26.3)
7	7.3 (14.6)	3.0 (47.1)	115.7 (20.5)	138.9 (21.6)
8	7.4 (18.4)	3.0 (42.2)	112.3 (31.8)	131.9 (28.9)
9	6.8 (24.5)	2.7 (45.4)	110.1 (34.9)	139.0 (37.5)
10	7.8 (16.6)	1.8 (72.5)	103.6 (22.9)	121.0 (24.2)
11	6.9 (23.7)	3.8 (34.7)	108.6 (20.0)	129.1 (24.1)

[a] Average data for six subjects. The coefficient of variation in percent is given in parentheses.

Table V—Power Analysis Table[a]

Parameter	N for 20% Difference		Minimum Detectable Difference, %	
	Group I	Group II	Group I	Group II
1 hr	25	70	44.0	77.3
2 hr	18	50	37.0	60.9
3 hr	10	40	26.8	54.4
4 hr	8	22	23.7	40.8
6 hr	13	20	29.9	38.3
8 hr	22	28	36.3	46.7
10 hr	6	28	19.7	46.3
24 hr	16	24	34.2	42.8
32 hr	45	35	51.9	52.5
Peak level	11	17	27.0	35.5
Time of peak	>150	80	104.7	80.4
$AUC_{0-32\ hr}$	5	14	16.5	32.6
$AUC_{0-\infty}$	6	13	18.3	31.2

[a] Calculated for $\alpha = 0.05$ and $\beta = 0.2$.

products to each subject indicated mean half-lives ranging from 8.9 (*SD* 1.8) to 10.8 (*SD* 1.2) hr for Group I subjects and from 9.7 (*SD* 2.5) to 14.1 (*SD* 4.1) hr for Group II subjects. These data are in agreement with a previous study in which the half-life of meprobamate ranged from 6.4 to 16.6 hr with a mean of 11.3 hr (11). No trends were apparent in half-lives determined for each subject over the 6-week study period, indicating that the weekly administration of the drug had no progressive influence on its metabolism in a given subject.

Statistically significant differences ($p < 0.05$) were also found among study weeks in Group I for the 4-, 10-, and 24-hr sampling times as well as for the *AUC* values. The cause of these differences was not known, but they did not appear to result from any cumulative effect of repeated drug administration. For example, the $(AUC)_{0-32\ hr}$ calculated by week for Group I ranged from 92 to 117 (μg/ml) (hr), with the ranking of the weeks, from lowest *AUC* to highest, being Week 2, 6, 4, 5, 1, and 3.

Data Variability and Power Analysis—To maintain the study design within manageable limits, two groups of six subjects were employed. With the exception of the *AUC* and the drug level at 10 hr for Group I, more than six subjects would have been required to permit a difference of 20% or less to be statistically significant ($p < 0.05$) (Table V). A 20% difference in parameters was selected as the maximum difference allowable and still have the products be considered bioequivalent. For most parameters evaluated, the difference between the reference product and the other products was less than 15%.

There was considerable intersubject variability in the absorption and/or disposition of meprobamate, as may be seen from the coefficients of variation given in Tables II–IV. There was no clear trend to this variability among individual products. In Group I, the reference product (Product 1) was less variable than the other five products tested at several sampling times. However, in Group II, the variability of the data for Product 1 was similar to that of the other five products.

REFERENCES

(1) "Task Force on Prescription Drugs, Final Report," U.S. Department of Health, Education, and Welfare, U.S. Government Printing Office, Washington, D.C., Feb. 7, 1969.

(2) *J. Am. Pharm. Assoc.*, **NS13,** 278 (1973).

(3) *The Academy Reporter* (APhA Academy of Pharmaceutical Sciences), **10,** 6 (1974).

(4) L. Martis and R. H. Levy, *J. Pharm. Sci.*, **63,** 834 (1974).

(5) "The United States Pharmacopeia," 19th rev., Mack Publishing Co., Easton, Pa., 1975, p. 305.

(6) E. G. Williams, *Aust. J. Sci. Res. A*, **2,** 149 (1949).

(7) B. J. Winer, "Statistical Principles in Experimental Design," McGraw-Hill, New York, N.Y., 1971, pp. 185–196.

(8) M. A. Kastenbaum, D. G. Hoel, and K. O. Bowman, *Biometrika*, **57,** 421 (1970).

(9) M. C. Meyer and A. B. Straughn, *J. Am. Pharm. Assoc.*, **NS17,** 173 (1977).

(10) "Physicians' Desk Reference," 29th ed., Medical Economics Co., Oradell, N.J., 1975, p. 1554.

(11) L. E. Hollister and G. Levy, *Chemotherapia*, **9,** 20 (1964).

ACKNOWLEDGMENTS

Supported in part by a contract from the Tennessee Department of Public Health and Food and Drug Administration Contract 223-74-3097.

The authors gratefully acknowledge the support of Mr. H. Bates, Jr., Pharmacist Consultant, Tennessee Department of Public Health, and Dr. R. Mhatre, Food and Drug Administration; the technical assistance of Mrs. Vicki Proefrock and Mrs. Cheryl Quinn; the assistance of Mrs. Ann McEachran in the statistical and computer analysis of the data; and the medical supervision provided by Dr. Philip Lieberman.

New Drug Metabolism Inhibitor of Marine Origin

PUSHKAR N. KAUL ˣ and SHRINIVAS K. KULKARNI

Received November 4, 1977, from the *Marine Pharmacology Laboratories, College of Pharmacy, University of Oklahoma Health Sciences Center, Oklahoma City, OK 73190.* Accepted for publication January 13, 1978.

Abstract □ Dactylyne, an acetylenic dibromochloro ether, was isolated from the sea hare *Aplysia dactylomela* and characterized pharmacologically. It had no direct effect on the cardiovascular, respiratory, and central nervous systems of mice, rats, and guinea pigs. However, a 25-mg/kg ip dose of dactylyne prolonged pentobarbital sleep time in mice by more than 10 hr. This potentiation was subsequently determined to be due to the inhibition of pentobarbital metabolism by dactylyne since the elimination half-life of pentobarbital in the dactylyne-treated mice increased several folds. Dactylyne was nontoxic up to 200 mg/kg iv. The unique structure, high potency, and relatively nontoxic nature of dactylyne make it an interesting pharmacological substance of marine origin.

Keyphrases □ Dactylyne—isolated from *Aplysia dactylomela* sea hare, pharmacological activity in mice, rats, and guinea pigs, effect on drug metabolism in mice □ *Aplysia dactylomela*—sea hare, dactylyne isolated, pharmacological activity in mice, rats, and guinea pigs, effect on drug metabolism in mice □ Metabolism, drug—effect of dactylyne isolated from *Aplysia dactylomela* sea hare

Exploration of the sea as a source of potential drugs is relatively recent. Over the past several years, cardioactive substances (1, 2), anticancer agents (3), and toxins (4) have been isolated from marine invertebrates. Moreover, the extracts of some marine organisms possess potent central nervous system (CNS) depressant activity in laboratory animals (2).

The followup study of bioassay-guided isolation and

0022-3549/78/0900-1293$01.00/0

© 1978, American Pharmaceutical Association

Table V—Power Analysis Table[a]

Parameter	N for 20% Difference		Minimum Detectable Difference, %	
	Group I	Group II	Group I	Group II
1 hr	25	70	44.0	77.3
2 hr	18	50	37.0	60.9
3 hr	10	40	26.8	54.4
4 hr	8	22	23.7	40.8
6 hr	13	20	29.9	38.3
8 hr	22	28	36.3	46.7
10 hr	6	28	19.7	46.3
24 hr	16	24	34.2	42.8
32 hr	45	35	51.9	52.5
Peak level	11	17	27.0	35.5
Time of peak	>150	80	104.7	80.4
$AUC_{0-32\ hr}$	5	14	16.5	32.6
$AUC_{0-\infty}$	6	13	18.3	31.2

[a] Calculated for $\alpha = 0.05$ and $\beta = 0.2$.

products to each subject indicated mean half-lives ranging from 8.9 (*SD* 1.8) to 10.8 (*SD* 1.2) hr for Group I subjects and from 9.7 (*SD* 2.5) to 14.1 (*SD* 4.1) hr for Group II subjects. These data are in agreement with a previous study in which the half-life of meprobamate ranged from 6.4 to 16.6 hr with a mean of 11.3 hr (11). No trends were apparent in half-lives determined for each subject over the 6-week study period, indicating that the weekly administration of the drug had no progressive influence on its metabolism in a given subject.

Statistically significant differences ($p < 0.05$) were also found among study weeks in Group I for the 4-, 10-, and 24-hr sampling times as well as for the *AUC* values. The cause of these differences was not known, but they did not appear to result from any cumulative effect of repeated drug administration. For example, the $(AUC)_{0-32\ hr}$ calculated by week for Group I ranged from 92 to 117 (μg/ml) (hr), with the ranking of the weeks, from lowest *AUC* to highest, being Week 2, 6, 4, 5, 1, and 3.

Data Variability and Power Analysis—To maintain the study design within manageable limits, two groups of six subjects were employed. With the exception of the *AUC* and the drug level at 10 hr for Group I, more than six subjects would have been required to permit a difference of 20% or less to be statistically significant ($p < 0.05$) (Table V). A 20% difference in parameters was selected as the maximum difference allowable and still have the products be considered bioequivalent. For most parameters evaluated, the difference between the reference product and the other products was less than 15%.

There was considerable intersubject variability in the absorption and/or disposition of meprobamate, as may be seen from the coefficients of variation given in Tables II–IV. There was no clear trend to this variability among individual products. In Group I, the reference product (Product 1) was less variable than the other five products tested at several sampling times. However, in Group II, the variability of the data for Product 1 was similar to that of the other five products.

REFERENCES

(1) "Task Force on Prescription Drugs, Final Report," U.S. Department of Health, Education, and Welfare, U.S. Government Printing Office, Washington, D.C., Feb. 7, 1969.

(2) *J. Am. Pharm. Assoc.*, **NS13,** 278 (1973).

(3) *The Academy Reporter* (APhA Academy of Pharmaceutical Sciences), **10,** 6 (1974).

(4) L. Martis and R. H. Levy, *J. Pharm. Sci.*, **63,** 834 (1974).

(5) "The United States Pharmacopeia," 19th rev., Mack Publishing Co., Easton, Pa., 1975, p. 305.

(6) E. G. Williams, *Aust. J. Sci. Res. A*, **2,** 149 (1949).

(7) B. J. Winer, "Statistical Principles in Experimental Design," McGraw-Hill, New York, N.Y., 1971, pp. 185–196.

(8) M. A. Kastenbaum, D. G. Hoel, and K. O. Bowman, *Biometrika*, **57,** 421 (1970).

(9) M. C. Meyer and A. B. Straughn, *J. Am. Pharm. Assoc.*, **NS17,** 173 (1977).

(10) "Physicians' Desk Reference," 29th ed., Medical Economics Co., Oradell, N.J., 1975, p. 1554.

(11) L. E. Hollister and G. Levy, *Chemotherapia*, **9,** 20 (1964).

ACKNOWLEDGMENTS

Supported in part by a contract from the Tennessee Department of Public Health and Food and Drug Administration Contract 223-74-3097.

The authors gratefully acknowledge the support of Mr. H. Bates, Jr., Pharmacist Consultant, Tennessee Department of Public Health, and Dr. R. Mhatre, Food and Drug Administration; the technical assistance of Mrs. Vicki Proefrock and Mrs. Cheryl Quinn; the assistance of Mrs. Ann McEachran in the statistical and computer analysis of the data; and the medical supervision provided by Dr. Philip Lieberman.

New Drug Metabolism Inhibitor of Marine Origin

PUSHKAR N. KAUL ˣ and SHRINIVAS K. KULKARNI

Received November 4, 1977, from the *Marine Pharmacology Laboratories, College of Pharmacy, University of Oklahoma Health Sciences Center, Oklahoma City, OK 73190.* Accepted for publication January 13, 1978.

Abstract □ Dactylyne, an acetylenic dibromochloro ether, was isolated from the sea hare *Aplysia dactylomela* and characterized pharmacologically. It had no direct effect on the cardiovascular, respiratory, and central nervous systems of mice, rats, and guinea pigs. However, a 25-mg/kg ip dose of dactylyne prolonged pentobarbital sleep time in mice by more than 10 hr. This potentiation was subsequently determined to be due to the inhibition of pentobarbital metabolism by dactylyne since the elimination half-life of pentobarbital in the dactylyne-treated mice increased several folds. Dactylyne was nontoxic up to 200 mg/kg iv. The unique structure, high potency, and relatively nontoxic nature of dactylyne make it an interesting pharmacological substance of marine origin.

Keyphrases □ Dactylyne—isolated from *Aplysia dactylomela* sea hare, pharmacological activity in mice, rats, and guinea pigs, effect on drug metabolism in mice □ *Aplysia dactylomela*—sea hare, dactylyne isolated, pharmacological activity in mice, rats, and guinea pigs, effect on drug metabolism in mice □ Metabolism, drug—effect of dactylyne isolated from *Aplysia dactylomela* sea hare

Exploration of the sea as a source of potential drugs is relatively recent. Over the past several years, cardioactive substances (1, 2), anticancer agents (3), and toxins (4) have been isolated from marine invertebrates. Moreover, the extracts of some marine organisms possess potent central nervous system (CNS) depressant activity in laboratory animals (2).

The followup study of bioassay-guided isolation and

0022-3549/78/0900-1293$01.00/0

© 1978, American Pharmaceutical Association

Table I—General Pharmacological Activities of Dactylyne

Treatment	Behavior (Mice)	Ptosis (Mice/Rats)	Hypnosis[a] (Mice)	Spontaneous Motor Activity[b] (Mice)	Motor Activity[c] (Mice)	Temperature (Rats)	Cardiovascular[d]		Intravenous Lethality
							Heart	Blood Pressure	
Saline	Normal, $n = 6$	Absent, $n = 5$	1 ± 0.16 hr, $n = 10$	82 ± 22.5, $n = 6$	303 ± 45, $n = 10$	35.9 ± 0.3°, $n = 5$	None	None	—
Dactylyne (25 mg/kg)	Normal, $n = 6$	Absent, $n = 15$	>10 hr, $n = 20$	88 ± 22.7, $n = 6$ ($p > 0.05$)	274 ± 18, $n = 8$ ($p > 0.05$)	36.1 ± 0.2°, $n = 5$	None	None	>200 mg/kg[e]
Chlorpromazine (3 mg/kg)	Sedated, $n = 6$	—	3 ± 0.66 hr, $n = 10$	40 ± 5.2, $n = 6$	141 ± 38, $n = 6$	33.75 ± 0.3°, $n = 5$	—	—	—

[a] Pentobarbital, 60 mg/kg, was used. [b] In movements per hour per group of three mice. [c] Locomotor activity as mean score per mouse per 10 min. [d] Cardiac activity of dactylyne (10 and 100 μg and 1 mg) was tested on the isolated perfusing guinea pig heart. The effect of dactylyne (up to 1 mg/kg) on mean blood pressure was determined in anesthetized rats and dogs. [e] Doses above 50 mg/kg induced clonic convulsions of short duration on intravenous dactylyne administration. All animals recovered.

purification of extracts from one marine animal, *Aplysia dactylomela*, known commonly as the sea hare, led to the isolation of dactylyne ($C_{15}H_{19}Br_2ClO$) (1), an acetylenic dibromochloro cyclic ether (5). This paper describes the pharmacological characterization and the mechanism of action of this marine-derived novel substance.

EXPERIMENTAL

Although dactylyne was isolated and structurally characterized earlier (6), the compound used in these studies was obtained by an improved method employing chromatography[1] as described elsewhere (5).

Pharmacological Procedures—Male albino Sprague–Dawley rats, 150–200 g, and Swiss–Webster mice, 25–30 g, were maintained on a 12-hr light and dark cycle and given food and water *ad libitum*. Random principle was used in the selection of animals from among acceptable groups as well as in the drug treatments. The Student *t* test was used to test for significance. Each experimental observation was reconfirmed by repeat experiments.

Drug solutions were prepared fresh in saline or distilled water. Dactylyne was dissolved in a few drops of dimethyl sulfoxide and diluted to volume with distilled water. The injection volumes of 1 (mouse) and 0.5 (rat) ml/100 g were kept constant. All drugs were administered intraperitoneally unless indicated otherwise.

Gross Behavior—The gross behavioral scoring method of Irwin (7) was used. Groups of six mice were injected with 25- or 50-mg/kg doses of dactylyne. The changes in the gross behavior produced by dactylyne were compared with those produced by chlorpromazine (3 mg/kg), which served as a standard.

Spontaneous Motor Activity—This test was performed in groups of three mice placed in 600-ml beakers, thereby restricting their locomotor activity (4). The spontaneous head movements and grooming were recorded every minute for 60 min. In this test, the control group invariably showed an activity score of 80–120/hr whereas the chlorpromazine (3 mg/kg) and amphetamine (2 mg/kg) groups showed activities of 40–60 and 140–160/hr, respectively. The activity scores due to dactylyne (25 mg/kg) were compared with these activities.

Locomotor Activity—Motor activity was studied with the help of an actophotometer (8). Groups of six to eight mice each were injected with dactylyne (25 mg/kg), saline (control), and chlorpromazine (3 mg/kg) 30 min prior to measuring their activity. Each mouse was individually placed in the actophotometer, and the activity was recorded for 10 min. Mean scores per mouse in different treatment groups were compared.

In the drug combination studies aimed at understanding the mechanism of action of dactylyne, groups of six to eight mice each received 5-mg/kg doses of either amphetamine or quipazine 30 min after dactylyne. Each mouse was tested in the actophotometer as described.

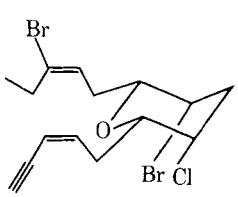

I

Palpebral Response (Ptosis Induction)—The intensity of ptosis was calculated according to the method of Rubin *et al.* (9); the relative degree of ptosis is given scores ranging from 0 to 4. Groups of three to five mice each were given dactylyne (10, 25, or 50 mg/kg ip), saline (control), and reserpine (1 mg/kg ip). The activity was evaluated by summing the scores of each group and expressing these values as percent of reserpine (standard) activity.

Body Temperature Determination—The variation of rectal temperature was recorded by a telethermometer. Three to five rats were used per treatment. The temperatures were recorded every 30 min for 2 hr to note changes. Dactylyne was tested at 25- and 50-mg/kg dose levels.

Anticonvulsant Activity—Groups of five mice each were treated with 25-, 50-, and 100-mg/kg ip doses of dactylyne. Thirty minutes later, pentylenetetrazol (100 mg/kg) was administered. The onset, duration, severity, and death due to convulsions were recorded over 24 hr (10). A group of mice treated with phenobarbital (25 mg/kg) was used as a standard for comparison.

Pentobarbital Hypnosis—The prolongation of pentobarbital-induced hypnosis was carried out in mice (10). Groups of eight to 10 animals each, pretreated with either dactylyne or chlorpromazine (standard), received pentobarbital 30 min later. The onset and duration of sleep due to pentobarbital were noted. Duration of sleep in each animal was recorded as the time elapsing from the loss of the righting reflex to its recovery.

The pentobarbital-induced sleep time experiments were carried out in two sets. In the first set, a fixed dose of dactylyne (25 mg/kg) was followd 30 min later by varying doses of pentobarbital (20, 40, or 60 mg/kg).

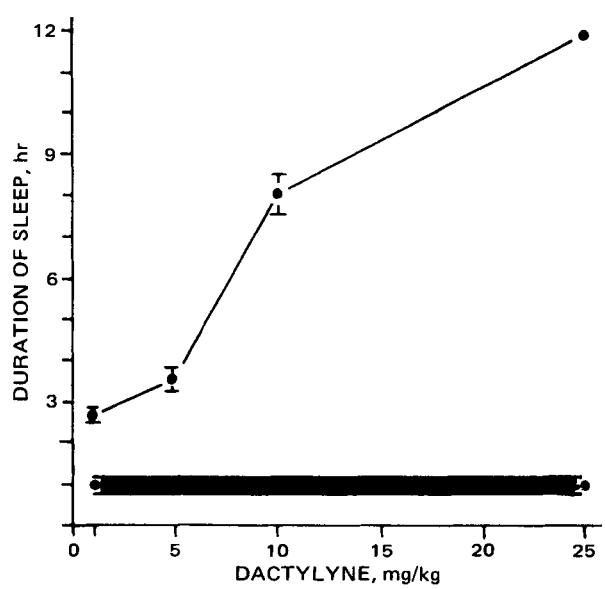

Figure 1—*Effect of increasing doses of dactylyne on pentobarbital-(60 mg/kg) induced hypnosis. Each point is the mean ± SD of eight to 10 animals. The effect was significant ($p < 0.001$) at all dose levels of dactylyne. Key:* ■, *pentobarbital alone; and* —, *pentobarbital plus dactylyne.*

[1] Sephadex LH_{20} columns.

Table II—Effect of Dactylyne on Pentylenetetrazol- (100 mg/kg) Induced Convulsions in Mice

Treatment (*n*)	Dose, mg/kg ip	Convulsions		Death	
		Onset, sec	Severity	*n*	Minutes
Saline (10)	—	48 ± 6.8	+++	10/10	2
Dactylyne (5)	50	49 ± 3.0	+++	5/5	1.5
Dactylyne (5)	100	48 ± 9.3	++	5/5	2.5
Phenobarbital (10)	25	127 ± 57.3	+	1/10	Recovered

In the second set, the dose of dactylyne (1, 5, 10, or 25 mg/kg) was varied and a fixed dose of pentobarbital (60 mg/kg) was injected 30 min later.

Determination of Blood Pentobarbital Levels—Pentobarbital was determined by the modified fluorometric method of Hollister *et al.* (11). To a 0.25–0.5-ml blood sample in a 13-ml screw-capped centrifuge tube was added an equal volume of distilled water. After the pH was adjusted to 5.4 ± 0.2 with 0.25 ml of phosphate buffer, pH 5.3 (27.0 g of monobasic sodium phosphate monohydrate and 1 g of dibasic sodium phosphate/liter), 5 ml of hexane containing 1.5% of isoamyl alcohol was added. The tube was capped and shaken for 10 min at 150 cpm. It was centrifuged for 10 min at 2200 rpm, and a 4-ml aliquot of organic layer then was transferred to another tube containing 3 ml of 0.5 *N* NaOH and shaken for 10 min at 150 cpm. After centrifugation, the fluorescence in the aqueous layer was determined spectrophotofluorometrically at an excitation λ_{max} of 262 nm and an emission λ_{max} of 420 nm.

A standard curve was derived by adding known concentrations (1–5 μg/ml) of pentobarbital sodium to fresh blood samples and processing as described. A blood blank and at least two known concentrations of pentobarbital sodium were carried through the procedure each time. All samples were assayed in replicate sets of two or three.

Disappearance of pentobarbital from the blood was studied in the saline- and dactylyne- (10 mg/kg) treated groups of mice, each receiving 60 mg of pentobarbital sodium/kg ip 30 min after treatment. The animals were sacrificed, and carotid blood samples were collected in heparinized tubes separately from each animal at 5 min and 1, 3, 6, and 24 hr after pentobarbital injection. These collection times were chosen after preliminary experiments so as to reflect the blood levels at the time of sleep onset (3–5 min), at the time of the recovery of the righting reflex in the saline-treated controls (1 hr), and at later times (3, 6, and 24 hr), particularly in the dactylyne-treated mice which slept for much longer periods.

Toxicity Studies—Since the dactylyne supply was limited, only pilot toxicity studies were possible. Groups of three mice were given intravenous doses of 25, 50, 100, 120, 160, and 200 mg of dactylyne/kg, and the gross behavior as well as survival was observed for 48 hr.

Another group of 10 mice was injected with 120 mg of dactylyne/kg ip once a day for 15 days. This dose was selected on the basis that it was larger than the one used in the toxicity study of a well-known enzyme inhibitor proadifen hydrochloride[2] (II) (12). A group of 10 mice, serving as the control, was injected daily with 1 ml of saline/100 g ip. Twenty-four hours after the last dose, all mice were sacrificed. The heart, liver, kidneys, lungs, brain, intestines, stomach, adrenals, and skin were removed and fixed in formalin (10%). Macroscopic and microscopic examinations of the organs were carried out for observation of any possible lesions.

Cardiovascular Activity—With modified Langendorff preparation (4) of the isolated guinea pig heart, varying concentrations (10 and 100 μg and 1 mg) of dactylyne were injected into the perfusion fluid. The effects on the inotropy, chronotropy, and coronary flow were recorded on an amplifier–recorder system. The effect of dactylyne in doses up to 1 mg/kg on mean blood pressure was determined in anesthetized rats and dogs. The animals were anesthetized with urethan (1 g/kg ip) or pentobarbital sodium (45 mg/kg iv). The mean arterial pressure was measured by inserting a cannula into the carotid artery and connecting it to a pressure transducer. One femoral vein was cannulated for drug administration. Electrodes were pinned in the appropriate limbs to provide lead II of the ECG record. Both blood pressure and ECG were monitored continuously.

RESULTS AND DISCUSSION

When freeze dried and redissolved in saline, the aqueous alcoholic crude extract of *A. dactylomela* consistently exhibited a general CNS depressant profile; *i.e.*, it prolonged the pentobarbital sleep time, depressed the body temperature, and decreased the spontaneous and locomotor activities, although only moderately. However, when fractionation of the extract was carried out under the guidance of pentobarbital hypnosis bioassay in mice, the relatively purer fractions became devoid of any significant CNS depressant activity except the potentiation of barbiturate-induced hypnosis. It is possible that the crude extract contained some substance(s) with the CNS depressant activity; but as the purification progressed, the elimination of the substance(s) from the fractions led to a gradually increasing potentiation of pentobarbital hypnosis and, thereby, an improvement in the purity of that component as an index of isolation. The CNS depressant components in the original crude extract were not isolated.

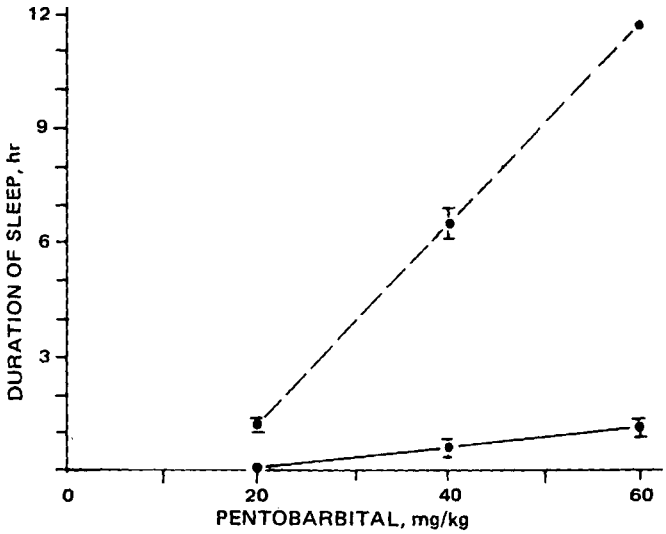

Figure 2—*Effect of a fixed dose (25 mg/kg) of dactylyne on various doses of pentobarbital. Each point is the mean ± SD of six to eight animals. The effect at the nonhypnotic dose of 20 mg of pentobarbital/kg was significant (*$p < 0.001$*). Key: —, pentobarbital alone; and – –, pentobarbital plus dactylyne.*

Dactylyne did not exhibit any significant pharmacological activity of its own in the test systems studied. In doses of 25–50 mg/kg in mice and rats, no major gross behavioral effects were visible. Furthermore, dactylyne did not significantly affect the spontaneous or locomotor activity ($p > 0.05$). Likewise, there was little effect on body temperature of mice (±0.2°) (Table I).

Dactylyne did not significantly modify the stimulant effects of amphetamine ($p > 0.05$) or quipazine ($p > 0.05$). It also failed to protect mice from pentylenetetrazol-induced convulsions (Table II). Neither the onset time nor the severity of convulsions was affected. All mice pretreated with dactylyne died, as did the controls. As expected, the phenobarbital-given mice showed both the delayed onset of convulsion and protection against death.

Dactylyne had no effect on the inotropy, chronotropy, and coronary flow in the isolated perfusing guinea pig heart. Nor did it show any change in the blood pressure or ECG, these effects being observed for 15 min following injections.

The only pronounced activity of dactylyne was a marked prolongation of pentobarbital sleep time in mice. The duration of action of pentobarbital increased with increasing doses of dactylyne (Fig. 1). A significant ($p < 0.001$) prolongation of barbiturate hypnosis was seen even at 1 mg of dactylyne/kg. A dose of 25 mg/kg induced sleep with what was otherwise a nonhypnotic dose of pentobarbital sodium (20 mg/kg) (Fig. 2).

Potentiation of drug activity by another agent is usually a result of receptor sensitization, decreased urinary excretion of the drug, or reduced metabolic inactivation (13, 14). The fact that blood pentobarbital levels in dactylyne-pretreated mice at the time of awakening (16.8 ± 3.99 μg/ml) were nearly the same as those in the control mice (15.9 ± 3.37 μg/ml) rules out the possibility of receptor sensitization. Biliary and urinary excretions together of pentobarbital are limited to 20–30% in most species studied (14). Therefore, if dactylyne should affect kidneys in some manner, reducing the urinary excretion even to the maximum possible extent, one would expect only a marginal increase in the blood pentobarbital levels at any particular time. However, the actual levels in the dactylyne-pre-

[2] SKF 525-A.

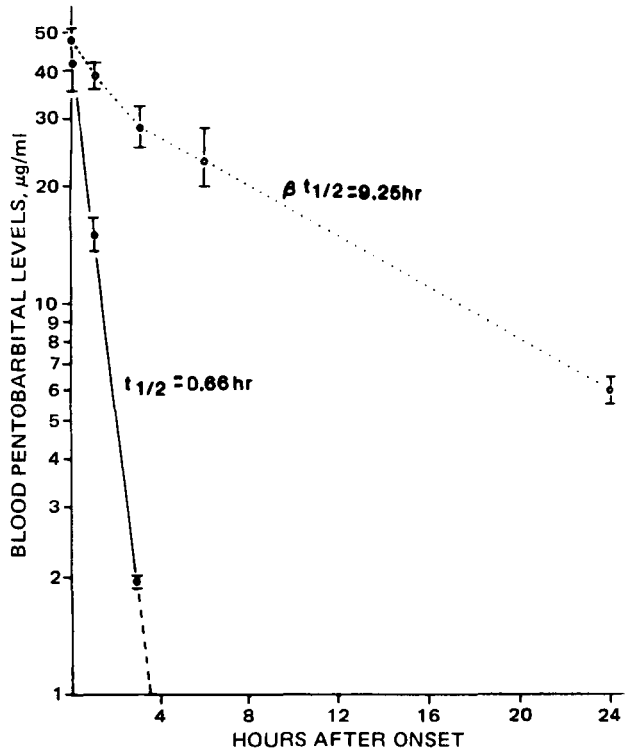

Figure 3—*Disappearance of pentobarbital from the blood of control (saline) and dactylyne- (10 mg/kg) pretreated mice. Each point is the mean ± SD of eight to 10 animals. Key: —, control; and . . . , dactylyne.*

treated mice, for example, at 1 hr following pentobarbital injection were 37.7 ± 3.70 μg/ml as against 15.9 ± 3.3 μg/ml in the saline-pretreated mice, *i.e.*, an increase of more than 100%.

It thus seems reasonable to assume that dactylyne, or perhaps a metabolite, actually inhibits the metabolic elimination of pentobarbital. Figure 3 shows the disappearance of pentobarbital in mice pretreated with dactylyne 30 min prior to pentobarbital administration. Dactylyne increased both the half-life (9.25 *versus* 0.66 hr) and the duration of action of pentobarbital several fold (from 1 to 8 hr).

The inhibition of pentobarbital metabolism by dactylyne apparently is quite analogous to a similar effect of II, except that it is more active on a milligrams per kilogram dose basis. For example, 10 mg of dactylyne/kg prolonged the pentobarbital sleep time from 1 to 8 hr whereas 15 mg of II/kg prolonged the sleep time from only 1 to 6 hr; the molecular weight of dactylyne is only 5% more than that of II. Moreover, dactylyne appeared to be less toxic than II, being nonlethal up to a dose of 200 mg/kg iv; the intravenous LD_{50} of II is 60 mg/kg (12). In the pilot toxicity studies, no gross morphological or histological lesions were found in the body and/or organs of animals treated with 120 mg of dactylyne/kg daily for 15 days.

In conclusion, a substance of marine origin with an ability to inhibit pentobarbital metabolism has been described. Data from further experimentation indicated that dactylyne also potentiated the action of other hypnotics, *e.g.*, phenobarbital and chloral hydrate. The unique structure, high potency, and relatively nontoxic nature of dactylyne make it an interesting pharmacological agent with perhaps a feasible clinical applicability.

REFERENCES

(1) P. N. Kaul, *Proc. Mar. Technol. Soc.*, **1972**, 299.

(2) P. N. Kaul, S. K. Kulkarni, A. J. Weinheimer, F. J. Schmitz, and T. K. B. Karns, *Lloydia*, **40**, 253 (1977).

(3) F. J. Schmitz *et al.*, in "Marine Natural Products Chemistry," D. J. Faulkner and W. H. Fenical, Eds., Plenum, New York, N.Y., 1977, p. 293.

(4) P. N. Kaul, M. R. Farmer, and L. S. Ciereszko, *J. West. Pharmacol. Soc.*, **17**, 294 (1974).

(5) P. N. Kaul, S. K. Kulkarni, F. J. Schmitz, and K. H. Hollenbeak, in "Drugs & Food from the Sea," P. N. Kaul and C. J. Sindermann, Eds., University of Oklahoma Press, Norman, Okla., 1978, p. 99.

(6) F. J. McDonald, D. C. Cambell, D. J. Vanderah, F. J. Schmitz, D. M. Washecbeek, J. E. Burks, and D. van der Helm, *J. Org. Chem.*, **40**, 665 (1975).

(7) S. Irwin, *Psychopharmacologia*, **33**, 222 (1968).

(8) P. B. Dews, *Br. J. Pharmacol.*, **8**, 46 (1953).

(9) B. Rubin, M. H. Malone, M. H. Waugh, and J. C. Burke, *J. Pharmacol. Exp. Ther.*, **120**, 125 (1957).

(10) R. A. Turner, "Screening Methods in Pharmacology," Academic, New York, N.Y., 1965, pp. 69, 164.

(11) L. E. Hollister, S. L. Kanter, and D. J. Clyde, *Clin. Pharmacol. Ther.*, **4**, 612 (1963).

(12) E. Usdin and R. L. S. Amasi, *Psychopharmacol. Serv. Cent. Bull.*, **2**, 17 (1963).

(13) J. Axelrod, J. Reichenthal, and B. B. Brodie, *J. Pharmacol. Exp. Ther.*, **112**, 49 (1954).

(14) F. W. Ossenberg, M. Peignoux, D. Bourdiau, and J. P. Benhamou, *ibid.*, **194**, 111 (1975).

ACKNOWLEDGMENTS

Supported by Office of Sea Grant NOAA Grant 04-158-44062 and by National Institutes of Health Grant GM20250.

The authors appreciate the technical assistance of Ms. Charlene Burns and the pilot histopathological observations of Dr. S. D. Kosanke. Dactylyne was prepared and provided by Dr. K. H. Hollenbeak and Dr. F. J. Schmitz.

Effect of Amitriptyline on Polarography of Chlordiazepoxide

R. RUCKI, A. ROSS ˣ, J. DONAHUE, and S. MOROS

Received October 25, 1977, from the *Quality Control Department, Hoffmann-La Roche Inc., Nutley, NJ 07110.* Accepted for publication January 13, 1978.

Abstract □ With increasing amounts of electroinactive amitriptyline, each of the three chlordiazepoxide reduction waves shifted to more cathodic half-wave potentials and decreased in limiting current. The shift was most pronounced up to the 1:1 mole ratio but continued up to ratios of 200:1. This behavior was observed in several supporting electrolytes and was not due to change in pH since this factor was maintained constant as the amitriptyline concentration was increased. Shifts in $E_{1/2}$ and reductions in limiting current may arise in several ways, such as complex formation between the two drugs or adsorption of the amitriptyline onto the surface of the dropping mercury electrode hindering chlordiazepoxide reduction. Most data point to adsorption as the cause.

Keyphrases □ Amitriptyline—effect on polarographic analysis of chlordiazepoxide, commercial products and synthetic mixtures □ Chlordiazepoxide—polarographic analysis, effect of amitriptyline, commercial products and synthetic mixtures □ Polarography—analysis, chlordiazepoxide, effect of amitriptyline on commercial products and synthetic mixtures □ Tranquilizers—chlordiazepoxide, polarographic analysis, effect of amitriptyline, commercial products and synthetic mixtures □ Antidepressants—amitriptyline, effect on polarographic analysis of chlordiazepoxide, commercial products and synthetic mixtures

Chlordiazepoxide and amitriptyline, in the ratio of 1:2.5, are marketed as a combination product[1]. Since it is well documented that chlordiazepoxide is electrochemically active (1–4) while amitriptyline is not, a study to determine chlordiazepoxide polarographically in this combination was initiated. In synthetic mixtures of the two drugs, the half-wave potentials shifted to more cathodic potentials and the limiting currents decreased for all three chlordiazepoxide waves with increasing concentrations of amitriptyline. Oelschlaeger *et al.* (5), in a paper describing chlordiazepoxide analysis in combinations including several that contained amitriptyline and clidinium bromide, reported a similar effect but attributed it to excipients present in the formulations, apparently being unaware that the change occurs even in their absence.

Shifts in $E_{1/2}$ and decreases in the limiting current of a polarographic wave may be attributed to several factors. One is complex formation between the two drugs. Recently, similar electrochemical evidence was used to show that an interaction exists between chlorpromazine hydrochloride and trifluoperazine hydrochloride and flavin coenzymes (6). The polarography of several charge transfer complexes was studied, and their respective stabilities were determined by measuring the shift in the half-wave potential caused by the electroinactive component (7).

A second possibility is adsorption of amitriptyline onto the dropping mercury electrode surface hindering chlordiazepoxide reduction. Weber *et al.* (8) demonstrated theoretically that the adsorption of an electroinactive substance shifts the half-wave potential and decreases the diffusion current for an irreversible electrode reaction. Subsequently, a theoretical treatment of reversible reactions predicted a decrease in current but no shift in the half-wave potential if the reaction is completely reversible (9). Experimental examples of these predictions also were presented (10, 11).

A more unusual case of a surface-active electroinactive species shifting the half-wave potential and decreasing current but increasing the reversibility of the reaction was reported by McCue and Kennedy (12). They demonstrated that titanium(IV), the polarographically active substance, complexed with procarbazine on the electrode surface, enhancing the reversibility.

The purpose of this study was to distinguish between these possibilities.

EXPERIMENTAL

Apparatus and Equipment—Experiments were performed with a commercial polarograph[2] and x–y recorder[3]. The polarographic cell contained a dropping mercury electrode as the working electrode, a silver–silver chloride reference with a potassium chloride–agar salt bridge, and a platinum wire counterelectrode. In later work, both carbon paste and glassy carbon served as working electrodes. The dropping mercury electrode had an open circuit drop time of 7.13 sec in 0.1 N HCl at a column height of 60 cm and a mercury flow rate of 0.95 mg/sec. All experiments were performed at 25 ± 0.1°. Dissolved air was removed from the solutions by bubbling prepurified nitrogen through the cell for 5 min and passing it over the solution during polarography.

Cyclic voltammetry was performed with the same instrumentation, employing a hanging mercury drop electrode[4] as the working electrode.

Chemicals and Reagents—All chemicals used as supporting electrolytes and for the preparation of buffer solutions were reagent grade. The mercury used in the dropping and hanging mercury electrodes was triple distilled[5]. Chlordiazepoxide hydrochloride[6], amitriptyline hydrochloride[6], clidinium bromide[6], and diazepam[6] were high purity (minimum 99%).

Procedure—The five supporting electrolytes were prepared using double-distilled water: 0.1 N HCl, 0.1 N HCl containing 20% methanol, citrate–phosphate buffer (pH 3.1), phosphate buffer containing 40% methanol (apparent pH 5.1), and citrate–phosphate buffer containing 45% methanol (apparent pH 7.0). Methanol was added to solutions of low pH to prevent polarographic maxima (2). At higher pH values, methanol was added to help maintain chlordiazepoxide and amitriptyline in solution.

Stock solutions (3 mM) of both drugs were prepared in the appropriate supporting electrolyte. These stock solutions were then diluted to obtain the working solutions of 0.6 mM chlordiazepoxide with the various amitriptyline concentrations. In a separate experiment to obtain higher mole ratios of amitriptyline, a 20 mM stock solution of this drug in 0.1 N HCl was made and subsequently diluted with 0.1 mM chlordiazepoxide to produce the appropriate amitriptyline concentration.

For the polarography of chlordiazepoxide alone, another 20 mM stock solution was prepared in 0.1 N HCl. The appropriate aliquots were measured and diluted with additional 0.1 N HCl. In the polarography of the clidinium bromide–chlordiazepoxide and amitriptyline–diazepam combinations, 3 and 3.5 mM stock solutions of the polarographically

[1] Limbitrol, Hoffmann-La Roche Inc., Nutley, NJ 07110.

[2] Princeton Applied Research model 174 polarographic analyzer.
[3] Hewlett-Packard model 7001AM.
[4] Princeton Applied Research model 932.
[5] Bethlehem Apparatus Co., Hellertown, Pa.
[6] Roche Laboratories, Nutley, N.J.

0022-3549/78/0900-1297$01.00/0
© 1978, American Pharmaceutical Association

Table I—Effect of Amitriptyline on Chlordiazepoxide at Various pH Values [a]

Mole Ratio of Amitriptyline to Chlordiazepoxide (0.6 mM)	$-E_{1/2}$, v *versus* Silver–Silver Chloride										Limiting Current, μamp									
	First Wave				Second Wave						First Wave [b]				Second Wave [b]					
	a	pH 1	pH 3	pH 5	pH 7	a	pH 1	pH 3	pH 5	pH 7	a	pH 1	pH 3	pH 5	a	pH 1	pH 3	pH 5
0:1	0.24	0.23	0.42	0.63	0.76	0.59	0.58	0.72	0.88	0.97	2.74	2.42	1.25	1.66	2.92	2.68	1.38	2.04
0.2:1	0.27	0.28	0.45	0.64	0.77	0.62	0.62	0.73	0.89	0.98	2.71	2.30	1.14	1.66	2.74	2.53	1.23	2.02
0.5:1	0.32	0.34	0.50	0.65	0.79	0.66	0.68	0.76	0.89	0.98	2.45	2.22	1.13	1.60	2.54	2.46	1.24	2.06
1:1	0.35	0.39	0.54	0.66	0.86	0.69	0.71	0.78	0.90	1.00	2.42	2.28	1.00	1.48	2.42	2.42	1.14	2.04
1.5:1	0.37	0.41	0.55	0.67	0.88	0.70	0.72	0.79	0.91	1.01	2.40	2.21	0.91	1.41	2.32	2.40	1.09	1.98
2:1	0.38	0.43	0.57	0.68	0.89	0.71	0.73	0.80	0.92	1.01	2.40	2.15	0.87	1.36	2.32	2.37	1.08	1.94
3:1	0.41	0.45	0.59	0.69	0.91	0.72	0.74	0.81	0.92	1.02	2.40	2.10	0.84	1.28	2.40	2.36	1.10	1.86
3.5:1	0.42	0.45	0.59	0.69	0.91	0.72	0.74	0.81	0.92	1.02	2.40	2.08	0.84	1.20	2.42	2.36	1.12	1.80
4:1	0.42	0.45	0.60	0.70	0.92	0.72	0.74	0.81	0.93	1.02	2.40	2.07	0.82	1.19	2.39	2.36	1.12	1.80

[a] Electrolytes used were: a, 0.1 *N* HCl containing 20% methanol; pH 1, 0.1 *N* HCl; pH 3, phosphate–citrate buffer; pH 5, 40% methanolic phosphate buffer; and pH 7, 45% methanolic phosphate–citrate buffer. [b] Overlap precluded accurate current measurements at pH 7.

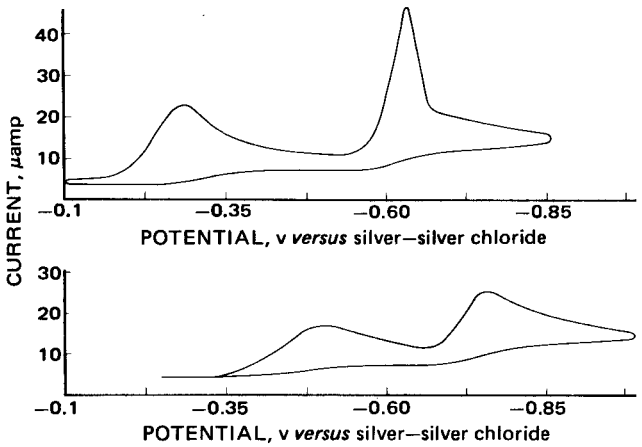

Figure 1—*Cyclic voltammogram of 0.6 m*M *chlordiazepoxide (top scan) and 0.6 m*M *chlordiazepoxide plus 1.2 m*M *amitriptyline (bottom scan) in 0.1* N *HCl. Scan rate was 0.2 v/sec.*

active component were prepared, respectively, in 0.1 *N* HCl. Stock solutions of the inactive component of the same concentrations were also made in 0.1 *N* HCl. Working solutions of 0.6 and 0.7 m*M* chlordiazepoxide and diazepam, respectively, then were prepared with the various concentrations of inactive component.

RESULTS

Chlordiazepoxide Polarography—The polarographic reduction of chlordiazepoxide at the dropping mercury electrode closely resembled the previously reported work (1–4). The compound displayed two well-defined polarographic waves in solutions buffered at apparent pH values from 1 to 7. A third wave appeared at lower pH values but was lost in the electrolyte wave near pH 7. The reduction was pH dependent, as evident from changes in the $E_{1/2}$ of the first wave from −0.23 to −0.76 v and of the second wave from −0.58 to −0.97 v as the pH was raised from 1 to 7.

Plots of $h^{1/2}$ (where h is mercury column height) *versus* the limiting currents of the first two waves were linear, indicating a diffusion-controlled process. Control by diffusion was confirmed by the fact that a 12° rise in temperature increased the limiting current by 20%. Generally, in diffusion-controlled processes, the limiting current increases 1.5%/degree (13).

Cyclic voltammetry studies in 0.1 *N* HCl showed the first two waves to be irreversible (Fig. 1). An electrocapillary curve of a solution containing the drug revealed a large decrease in drop time over a considerable potential range (in comparison to a solution containing only supporting electrolyte), signifying strong adsorption at the electrode. As a result of its surface activity and irreversibility, it would be expected that the half-wave potential would vary with concentration. This view is borne

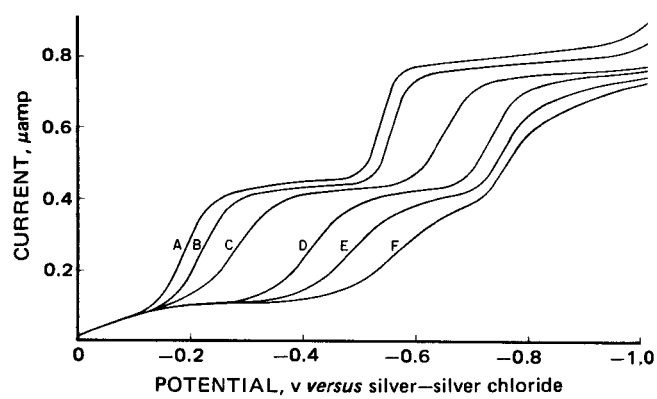

Figure 2—*Effect of amitriptyline on polarography of 0.1 m*M *chlordiazepoxide in 0.1* N *HCl. Key (mole ratio of amitriptyline to chlordiazepoxide): A, no amitriptyline; B, 1:1; C, 2:1; D, 10:1; E, 50:1; and F, 200:1.*

Table II—Effect of Amitriptyline on Chlordiazepoxide at High Mole Ratios [a]

Mole Ratio of Amitriptyline to Chlordiazepoxide (0.1 m*M*)	First Wave			Second Wave		
	$-E_{1/2}$, v	$E_{3/4} - E_{1/4}$, mv	i_{lim}, μamp	$-E_{1/2}$, v	$E_{3/4} - E_{1/4}$, mv	i_{lim}, μamp
0:1	0.17	52	0.312	0.52	28	0.318
1:1	0.21	56	0.312	0.55	31	0.328
5:1	0.37	68	0.240	0.70	42	0.256
10:1	0.39	73	0.240	0.72	45	0.248
25:1	0.44	77	0.240	0.74	50	0.248
50:1	0.47	85	0.240	0.75	52	0.256
100:1	0.50	86	—[b]	0.75	53	0.248
200:1	0.54	87	—[b]	0.75	55	0.240

[a] Supporting electrolyte was 0.1 *N* HCl. [b] It was difficult to measure i_{lim} because wave was merging into second wave.

out experimentally. Up to 0.1 m*M* chlordiazepoxide, the half-wave potentials of the two waves were constant at −0.17 and −0.52 v, respectively. At concentrations greater than 0.1 m*M*, the $E_{1/2}$ values shifted to more cathodic values, becoming −0.32 and −0.69 v, respectively, at 10.0 m*M*.

Effect of Amitriptyline on Chlordiazepoxide Polarography—Amitriptyline was electrochemically inactive in the potential region scanned. However, when solutions of chlordiazepoxide containing amitriptyline were examined in 0.1 *N* HCl containing 20% methanol, the $E_{1/2}$ values of the first two waves shifted to more cathodic potentials and the limiting current decreased as the amitriptyline concentration increased (Table I). The pH of these solutions was confirmed by measurement to be constant, independent of amitriptyline concentration. Therefore, a secondary effect where the base amitriptyline raises the pH, which could cause a shift, can be ruled out.

Similar results (Table I) were obtained in the four other supporting electrolytes used: 0.1 *N* HCl (pH 1), phosphate–citrate buffer (pH 3), phosphate buffer containing 40% methanol (pH 5), and phosphate–citrate buffer containing 45% methanol (pH 7). In each case, as the amitriptyline mole ratio increased, the shift increased and the limiting current decreased. This shift was most pronounced up to the 1:1 mole ratio, slowed in the rate of increase beyond this region, but still occurred up to 200:1 ratios (Fig. 2). The $E_{3/4} - E_{1/4}$ values also increased, indicating that the electrode reaction was becoming more irreversible (Table II).

At a 2:1 mole ratio, the reduction was still diffusion controlled; but in the cyclic scan (Fig. 1), the two peaks were broader and moved to more negative potentials with peak currents lower than those of the scan of chlordiazepoxide alone, indicative of increased irreversibility (14).

Electrocapillary curves of amitriptyline solutions showed a larger decrease in drop time over a similar potential range than did chlordiazepoxide solutions (Fig. 3). Attempts to eliminate the strong adsorption between amitriptyline and the dropping mercury electrode by replacing it with solid electrodes and to study the possibility of interaction between the two drugs without this interfering factor were successful.

A single wave was observed for chlordiazepoxide solutions in the −0.7–−0.8-v region, close to the electrolyte current cutoff, on both glassy carbon and carbon paste electrodes. The wave was reproducible and better defined on the glassy carbon electrode. Within the reproducibility of the measurement, the presence of amitriptyline did not affect the $E_{1/2}$ of the chlordiazepoxide wave.

Other Polarographic Systems—Diazepam, another common benzodiazepine, underwent a similar $E_{1/2}$ shift and decrease in the limiting current of its lone polarographic wave in the presence of increasing amitriptyline concentrations (Table III). Electroinactive clidinium bromide exhibited the same effect as amitriptyline on the polarography of chlordiazepoxide, although it was somewhat reduced in extent (Table IV). Clidinium bromide also was adsorbed onto the dropping mercury electrode, as evident from its electrocapillary curve (Fig. 3).

Table III—Effect of Amitriptyline on Polarography of Diazepam [a]

Mole Ratio of Amitriptyline to Diazepam (0.7 m*M*)	$-E_{1/2}$, v	i_{lim}, μamp
0:1	0.62	2.42
0.1:1	0.62	2.40
0.5:1	0.64	2.35
1:1	0.65	2.34
1.5:1	0.66	2.32
2:1	0.67	2.29
3:1	0.68	2.26

[a] Supporting electrolyte was 0.1 *N* HCl containing 20% methanol.

DISCUSSION

The electrochemical properties of chlordiazepoxide, *i.e.*, the shift of the half-wave potential to more negative values with increasing pH and chlordiazepoxide concentration, the limiting currents of the waves being diffusion controlled, drug adsorption onto the dropping mercury electrode, and the irreversibility of the two waves, were reported previously (4). With ac polarography, a strong adsorption between the drug and mercury was established, and the $E_{1/2}$ shift was attributed to the electrode being completely covered with a monomolecular layer of adsorbed material when the chlordiazepoxide concentration was above 0.1 m*M* (4). A further increase in concentration produced the shift; below 0.1 m*M*, however, the $E_{1/2}$ remained constant.

The presence of amitriptyline increased the irreversibility of the chlordiazepoxide reduction waves. This effect by amitriptyline could be explained by either its surface activity or interaction with chlordiazepoxide. However, enhancement of reversibility by complexation at the electrode surface, as described by McCue and Kennedy (12), probably was not occurring in this case.

Amitriptyline is very strongly adsorbed onto the dropping mercury electrode. Since adsorption of electroinactive substances can influence the half-wave potential of irreversible systems (8, 10–12) and reduce the limiting current of irreversible systems (12), this adsorption probably is the basis for the action of amitriptyline. If chlordiazepoxide concentrations greater than 0.1 m*M* exhibit shifts in half-wave potential, then it is reasonable to expect that higher concentrations of a more surface-active compound will show a similar, or greater, effect. Comparison of several examples of adsorption *versus* complexation gives even greater evidence that an electrode surface phenomenon occurred.

In the proposed interaction between chlorpromazine hydrochloride and flavin mononucleotide, the $E_{1/2}$ of the flavin coenzyme changed only 40 mv in a 1000:1 mole ratio of the two when the coenzyme concentration was 10^{-4} *M* (6). Peover (7) measured a $E_{1/2}$ shift of 20 mv when a 500-fold excess of electroinactive hexamethylbenzene complexed 0.7 m*M* chloranil and an 80-mv shift when a 750-fold excess of hexamethylbenzene complexed 0.6 m*M* dichlorodicyanoquinone. On the other hand, only 0.2 m*M* of surface-active procarbazine displaced the half-wave potential of 0.6 m*M* titanium(IV) by 130 mv (12). The $E_{1/2}$ of 1 m*M* lead(II) was transposed 360 mv when the concentration of surface-active polyoxyethylene lauryl ether was increased from 2×10^{-6} to 10^{-3} *M* (11). The present experimental values are certainly more in line with an adsorption phenomenon: 160-mv shift for a 1:1 mole ratio of 0.6 m*M* amitriptyline and chlordiazepoxide in 0.1 *N* HCl.

Table IV—Effect of Clidinium Bromide on Polarography of Chlordiazepoxide [a]

Mole Ratio of Clidinium Bromide to Chlordiazepoxide (0.6 m*M*)	First Wave		Second Wave	
	$-E_{1/2}$, v	i_{lim}, μamp	$-E_{1/2}$, v	i_{lim}, μamp
0:1	0.23	2.54	0.58	2.70
0.2:1	0.24	2.53	0.59	2.60
1:1	0.26	2.45	0.63	2.52
2:1	0.28	2.44	0.65	2.50
3:1	0.29	2.46	0.67	2.54

[a] Supporting electrolyte was 0.1 *N* HCl.

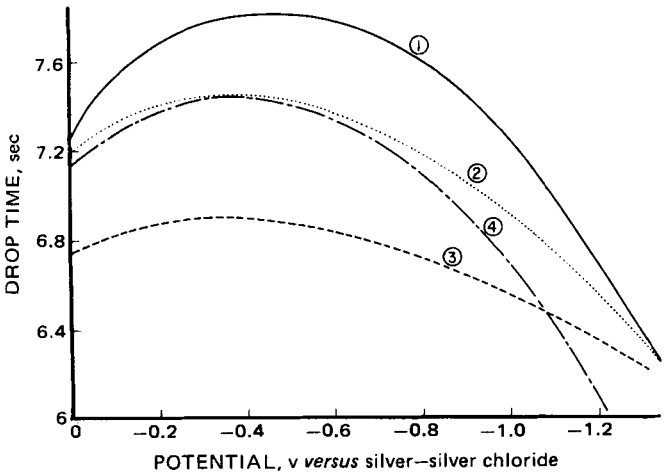

Figure 3—*Electrocapillary maximum curves of 0.1* N *HCl (curve 1), 0.8 mM chlordiazepoxide in 0.1* N *HCl (curve 2), 0.8 mM amitriptyline in 0.1* N *HCl (curve 3), and 0.8 mM clidinium bromide in 0.1* N *HCl (curve 4).*

Other polarographic systems, *i.e.*, amitriptyline with diazepam and clidinium bromide with chlordiazepoxide, underwent similar $E_{1/2}$ shifts and reductions in limiting current. The action of surface-active excipients on the polarography of chlordiazepoxide was studied by Oelschlaeger *et al.* (5) who showed that they all produced, to various degrees, results similar to the action of amitriptyline. It is highly unlikely that all of these dissimilar chemicals would form complexes with chlordiazepoxide.

Solid electrode evidence also points to adsorption as the underlying cause. The $E_{1/2}$ of the single chlordiazepoxide wave observed on carbon electrodes, where no adsorption is expected, was not significantly affected by the presence of amitriptyline in ratios as high as 2:1 of amitriptyline to chlordiazepoxide. On the dropping mercury electrode, the $E_{1/2}$ shift with amitriptyline concentration was most pronounced with ratios below 2:1. Thus, a solution interaction between amitriptyline and chlordiazepoxide appears improbable. If such an interaction exists, it does not significantly contribute to the observed polarographic phenomena.

REFERENCES

(1) H. Oelschlaeger, *Arch. Pharm.*, **296**, 396 (1963).

(2) B. Z. Senkowski, M. S. Levin, J. R. Urbigkit, and E. G. Wollish, *Anal. Chem.*, **36**, 1991 (1964).

(3) H. Oelschlaeger, J. Volke, H. Hoffmann, and E. Kurek, *Arch. Pharm.*, **300**, 250 (1967).

(4) E. Jacobsen and T. V. Jacobsen, *Anal. Chim. Acta*, **55**, 293 (1971).

(5) H. Oelschlaeger, E. Kurek, F. I. Sengun, and J. Volke, *Z. Anal. Chem.*, **282**, 123 (1976).

(6) L. De Lisser-Mathews and A. Khalaj, *J. Pharm. Sci.*, **65**, 1758 (1976).

(7) M. E. Peover, *Trans. Faraday Soc.*, **60**, 417 (1964).

(8) J. Weber, J. Koutecky, and J. Koryta, *Z. Elektrochem.*, **63**, 583 (1959).

(9) J. Koutecky and J. Weber, *Coll. Czech. Chem. Commun.*, **25**, 1423 (1960).

(10) M. Loshkarev and A. Kryukova, *Zh. Fiz. Khim.*, **31**, 452 (1957).

(11) N. Tanaka, R. Tamanushi, and A. Takanishi, *Coll. Czech. Chem. Commun.*, **25**, 3016 (1960).

(12) J. McCue and J. Kennedy, *J. Electrochem. Soc.*, **122** (2), 221 (1975).

(13) L. Meites, "Polarographic Techniques," 2nd ed., Interscience, New York, N.Y., 1965, p. 139.

(14) R. N. Adams, "Electrochemistry at Solid Electrodes," Dekker, New York, N.Y., 1969, pp. 136, 137.

High-Pressure Liquid Chromatographic Separation and Determination of Anomeric Forms of Streptozocin in a Powder Formulation

PHILIP J. OLES

Received September 15, 1977, from *The Upjohn Company, Kalamazoo, MI 49001.* Accepted for publication January 20, 1978.

Abstract □ A high-pressure liquid chromatographic assay for streptozocin in a sterile powder formulation (1.0 g/vial) is described. The method effectively separates the α- and β-anomeric forms of streptozocin. Quantitative results are presented for the drug based on the use of an internal standard and peak height measurements.

Keyphrases □ Streptozocin—high-pressure liquid chromatographic analysis and separation of anomers in a commercial dosage form □ High-pressure liquid chromatography—analysis and separation of anomers of streptozocin in a commercial dosage form □ Antineoplastic agents—streptozocin, high-pressure liquid chromatographic analysis and separation of anomers in a commercial dosage form

Streptozocin is used for the treatment of malignant insulinoma. An assay was sought for this drug that would satisfy quality control requirements with respect to accuracy, precision, and specificity. The described high-pressure liquid chromatographic (HPLC) technique separates the two anomeric forms of streptozocin, 2-deoxy-2-(3-methyl-3-nitrosoureido)-α(and β)-D-glucopyranose. The mutarotation of streptozocin was studied by using HPLC and optical rotation. With these data, the optimum experimental conditions could be chosen for routine assay of both bulk drug and formulated product.

EXPERIMENTAL

Apparatus—A commercial liquid chromatograph[1] was used at an ambient temperature with UV detection at 254 nm. The column was stainless steel (type 316), 4 × 300 mm, prepacked with 10-μm microparticulate C_{18} bonded to silica gel[2]. Chromatographic recordings were made with a standard 1-mv, commercially available recorder[3].

Reagents and Solutions—The mobile phase was 0.1 *M* acetic acid in water–methanol (97:3). The pH was adjusted to 4.0 with 50% NaOH. The internal standard was a 2-mg/ml solution of potassium acid phthalate. A 1-mg/ml reference standard solution of streptozocin was prepared in 0.1 *M* acetate buffer (pH 4.0). Exactly 5.0 ml of this reference standard solution and 5.0 ml of the internal standard solution were mixed

[1] Model ALC202, Waters Associates, Milford, Mass.
[2] μBondapak C_{18}, Waters Associates, Milford, Mass.
[3] Model HP7123A, Hewlett-Packard, Palo Alto, Calif.

0022-3549/78/0900-1300$01.00/0
© 1978, American Pharmaceutical Association

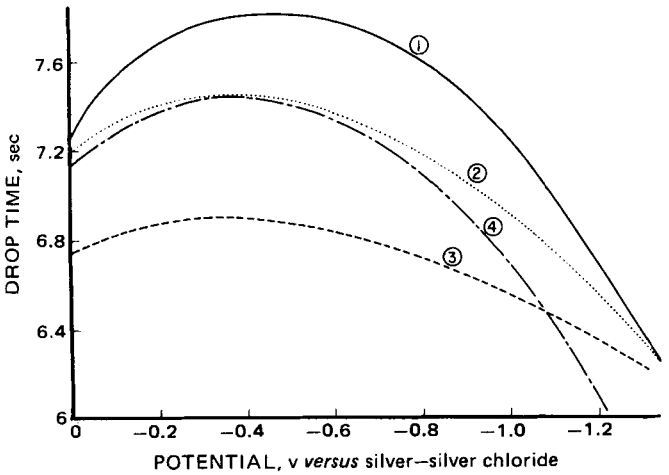

Figure 3—*Electrocapillary maximum curves of 0.1* N *HCl (curve 1), 0.8 mM chlordiazepoxide in 0.1* N *HCl (curve 2), 0.8 mM amitriptyline in 0.1* N *HCl (curve 3), and 0.8 mM clidinium bromide in 0.1* N *HCl (curve 4).*

Other polarographic systems, *i.e.*, amitriptyline with diazepam and clidinium bromide with chlordiazepoxide, underwent similar $E_{1/2}$ shifts and reductions in limiting current. The action of surface-active excipients on the polarography of chlordiazepoxide was studied by Oelschlaeger *et al.* (5) who showed that they all produced, to various degrees, results similar to the action of amitriptyline. It is highly unlikely that all of these dissimilar chemicals would form complexes with chlordiazepoxide.

Solid electrode evidence also points to adsorption as the underlying cause. The $E_{1/2}$ of the single chlordiazepoxide wave observed on carbon electrodes, where no adsorption is expected, was not significantly affected by the presence of amitriptyline in ratios as high as 2:1 of amitriptyline to chlordiazepoxide. On the dropping mercury electrode, the $E_{1/2}$ shift with amitriptyline concentration was most pronounced with ratios below 2:1. Thus, a solution interaction between amitriptyline and chlordiazepoxide appears improbable. If such an interaction exists, it does not significantly contribute to the observed polarographic phenomena.

REFERENCES

(1) H. Oelschlaeger, *Arch. Pharm.*, **296**, 396 (1963).

(2) B. Z. Senkowski, M. S. Levin, J. R. Urbigkit, and E. G. Wollish, *Anal. Chem.*, **36**, 1991 (1964).

(3) H. Oelschlaeger, J. Volke, H. Hoffmann, and E. Kurek, *Arch. Pharm.*, **300**, 250 (1967).

(4) E. Jacobsen and T. V. Jacobsen, *Anal. Chim. Acta*, **55**, 293 (1971).

(5) H. Oelschlaeger, E. Kurek, F. I. Sengun, and J. Volke, *Z. Anal. Chem.*, **282**, 123 (1976).

(6) L. De Lisser-Mathews and A. Khalaj, *J. Pharm. Sci.*, **65**, 1758 (1976).

(7) M. E. Peover, *Trans. Faraday Soc.*, **60**, 417 (1964).

(8) J. Weber, J. Koutecky, and J. Koryta, *Z. Elektrochem.*, **63**, 583 (1959).

(9) J. Koutecky and J. Weber, *Coll. Czech. Chem. Commun.*, **25**, 1423 (1960).

(10) M. Loshkarev and A. Kryukova, *Zh. Fiz. Khim.*, **31**, 452 (1957).

(11) N. Tanaka, R. Tamanushi, and A. Takanishi, *Coll. Czech. Chem. Commun.*, **25**, 3016 (1960).

(12) J. McCue and J. Kennedy, *J. Electrochem. Soc.*, **122** (2), 221 (1975).

(13) L. Meites, "Polarographic Techniques," 2nd ed., Interscience, New York, N.Y., 1965, p. 139.

(14) R. N. Adams, "Electrochemistry at Solid Electrodes," Dekker, New York, N.Y., 1969, pp. 136, 137.

High-Pressure Liquid Chromatographic Separation and Determination of Anomeric Forms of Streptozocin in a Powder Formulation

PHILIP J. OLES

Received September 15, 1977, from *The Upjohn Company, Kalamazoo, MI 49001.* Accepted for publication January 20, 1978.

Abstract □ A high-pressure liquid chromatographic assay for streptozocin in a sterile powder formulation (1.0 g/vial) is described. The method effectively separates the α- and β-anomeric forms of streptozocin. Quantitative results are presented for the drug based on the use of an internal standard and peak height measurements.

Keyphrases □ Streptozocin—high-pressure liquid chromatographic analysis and separation of anomers in a commercial dosage form □ High-pressure liquid chromatography—analysis and separation of anomers of streptozocin in a commercial dosage form □ Antineoplastic agents—streptozocin, high-pressure liquid chromatographic analysis and separation of anomers in a commercial dosage form

Streptozocin is used for the treatment of malignant insulinoma. An assay was sought for this drug that would satisfy quality control requirements with respect to accuracy, precision, and specificity. The described high-pressure liquid chromatographic (HPLC) technique separates the two anomeric forms of streptozocin, 2-deoxy-2-(3-methyl-3-nitrosoureido)-α(and β)-D-glucopyranose. The mutarotation of streptozocin was studied by using HPLC and optical rotation. With these data, the optimum experimental conditions could be chosen for routine assay of both bulk drug and formulated product.

EXPERIMENTAL

Apparatus—A commercial liquid chromatograph[1] was used at an ambient temperature with UV detection at 254 nm. The column was stainless steel (type 316), 4 × 300 mm, prepacked with 10-μm microparticulate C_{18} bonded to silica gel[2]. Chromatographic recordings were made with a standard 1-mv, commercially available recorder[3].

Reagents and Solutions—The mobile phase was 0.1 *M* acetic acid in water–methanol (97:3). The pH was adjusted to 4.0 with 50% NaOH. The internal standard was a 2-mg/ml solution of potassium acid phthalate. A 1-mg/ml reference standard solution of streptozocin was prepared in 0.1 *M* acetate buffer (pH 4.0). Exactly 5.0 ml of this reference standard solution and 5.0 ml of the internal standard solution were mixed

[1] Model ALC202, Waters Associates, Milford, Mass.
[2] μBondapak C_{18}, Waters Associates, Milford, Mass.
[3] Model HP7123A, Hewlett-Packard, Palo Alto, Calif.

0022-3549/78/0900-1300$01.00/0
© 1978, American Pharmaceutical Association

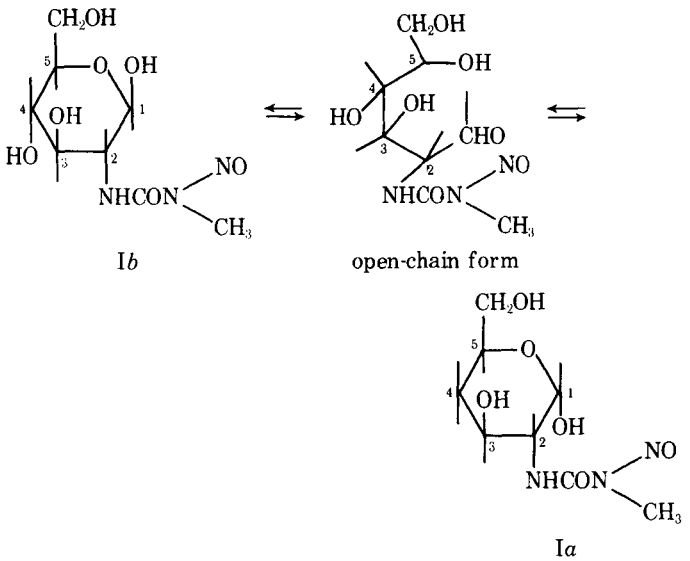

Scheme I

in a suitable container, and the resultant solution served as the standard preparation; 60–90 min elapsed before injection.

Sample Preparation—*Bulk Drug*—A 1-mg/ml solution of streptozocin bulk drug was prepared in 0.1 *M* acetate buffer (pH 4.0). Exactly 5.0 ml of this sample preparation and 5.0 ml of the internal standard solution were mixed in a suitable container, and the resultant solution served as the sample preparation; 60–90 min elapsed before injection.

Sterile Powder—Distilled water, 10–15 ml, was added to the vial to dissolve the contents. This solution was transferred quantitatively to a 1-liter volumetric flask and diluted to volume with water. Exactly 5.0 ml of this sample preparation and 5.0 ml of the internal standard solution were mixed in a suitable container, and the resultant solution served as the sample preparation.

HPLC—Approximately 4 μl of a prepared sample was injected onto the column. The chromatograph was operated at 0.5 ml/min (about 1500 psig) with the detector set at 0.16 absorbance unit full scale. The retention times of the β-anomer, α-anomer, and internal standard were 5, 7, and 21 min, respectively.

Calculations—The amount of streptozocin was calculated by the internal standard–reference standard method using peak height ratios. The peak heights of both anomeric forms of streptozocin were added together in the calculation.

RESULTS AND DISCUSSION

Streptozocin is produced primarily in the α- (Ia) or β- (Ib) form. A typical chromatogram of a freshly prepared solution of streptozocin is shown in Fig. 1A. Subsequent chromatograms of the same solution at various time intervals are shown in Figs. 1B–1D. When the second eluting peak was trapped and reinjected after about 5 min, the chromatogram shown in Fig. 2A resulted. A subsequent injection of the trapped fraction after about 60 min resulted in the chromatogram shown in Fig. 2B.

The phenomenon responsible for this chromatographic behavior is mutarotation of the glucopyranose ring (Scheme I). To assign correctly the proper anomeric form to each peak, the mutarotation reaction of two lots of bulk drug was followed using a polarimeter[4]. Each lot, when freshly prepared as a solution, was composed of principally one form or the other as shown by the chromatograms. The mutarotation reaction followed the time pathway depicted in Fig. 3. Lot A had the higher positive specific rotation, which is generally considered to be attributed to the α-anomer conformation (1). Lot A, when chromatographed, was observed to be primarily composed of the second eluting fraction. Therefore, the order of elution is considered to be the β-anomer first followed by the α-anomer. The mutarotation reaction arrived at an equilibrium state after approximately 60–90 min. The composition of the mixture at equilibrium,

Table I—Recovery of Streptozocin from Spiked Excipients

Added, g/Vial	Found, g/Vial	Recovery, %
0.799	0.802	100.4
0.899	0.879	97.8
0.998	0.985	98.7
1.098	1.073	97.7
1.198	1.180	98.5
	Average	98.6
	RSD	1.1

Table II—Assay Results for Streptozocin in a Sterile Powder

Vial	Found, g/Vial	Percent of Theory
1	0.961	96.1
2	0.977	97.7
3	0.956	95.6
4	0.958	95.8
5	0.955	95.5
	Average	96.1
	RSD	0.9

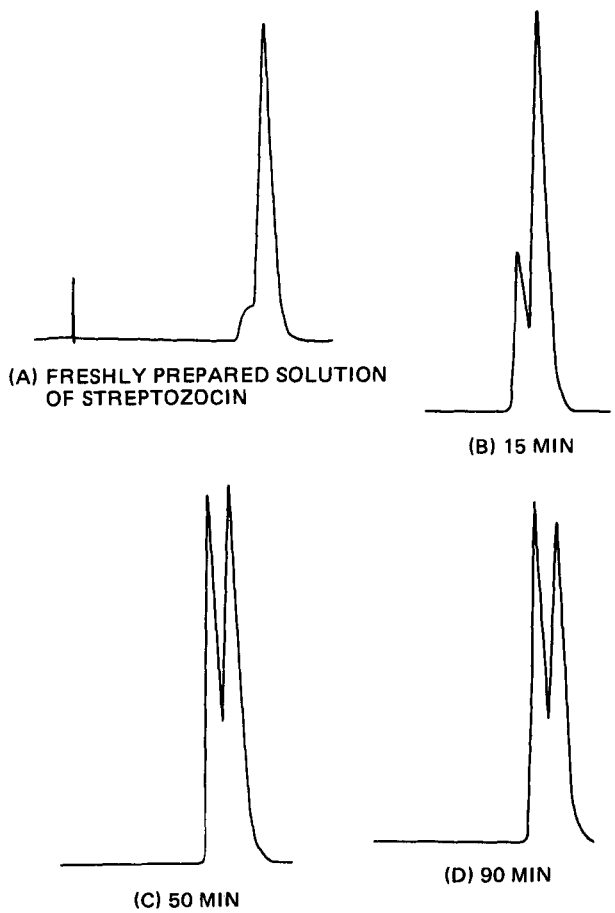

Figure 1—*Mutarotation of streptozocin in aqueous solution as observed by HPLC.*

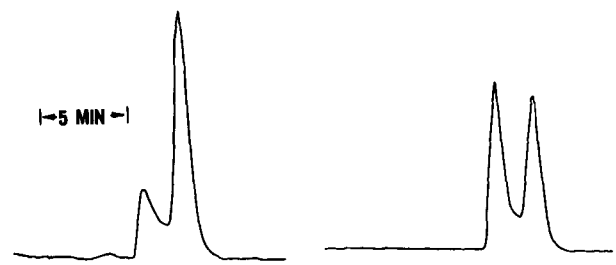

Figure 2—*Chromatograms of second HPLC fraction of streptozocin.*

[4] Model 141, Perkin-Elmer, Norwalk, Conn.

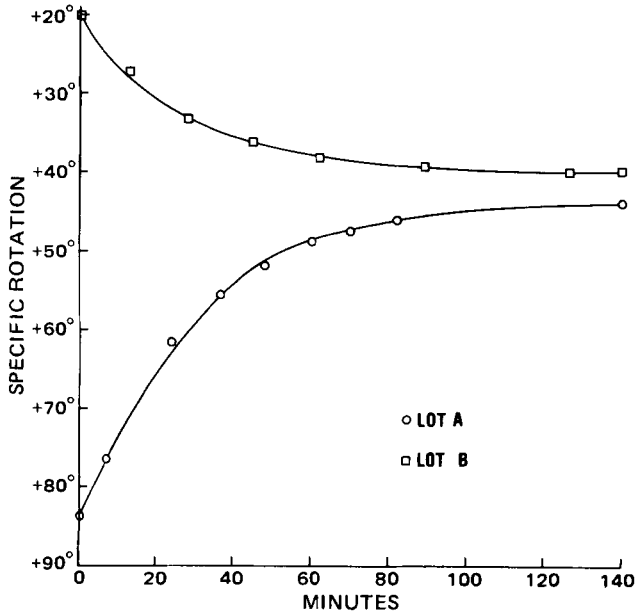

Figure 3—*Change in specific rotation of two anomeric forms of streptozocin with time.*

determined by HPLC using peak area integration, was approximately 1:1. There was a slight pH dependence upon the rate of attainment of equilibrium (Fig. 4).

When streptozocin is formulated as a sterile powder, the drug is in solution for 4–6 hr before freeze drying. Therefore, irrespective of the form of the drug used in manufacture, the product contains the equilibrium mixture of the α- and β-anomers.

The different anomeric forms of streptozocin show different response factors when peak height measurements are used for quantitative analysis. Therefore, when standard preparations or bulk drug sample preparations are chromatographed, 60–90 min should elapse before injection.

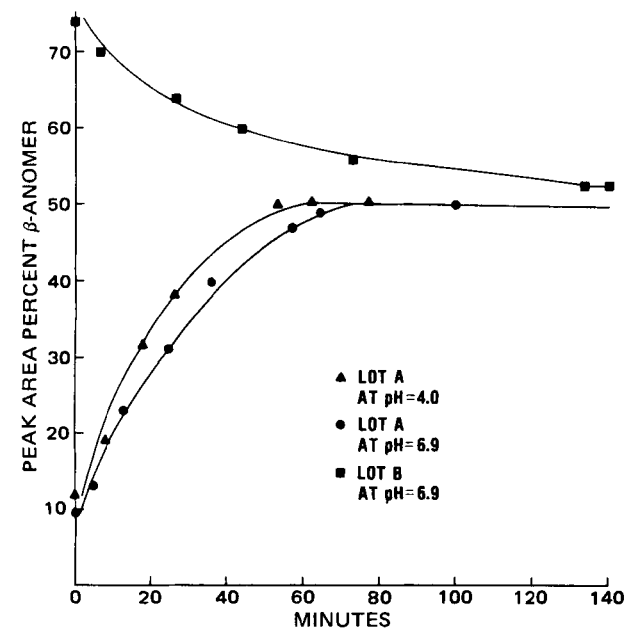

Figure 4—*Change in solution composition of the two forms of streptozocin with time.*

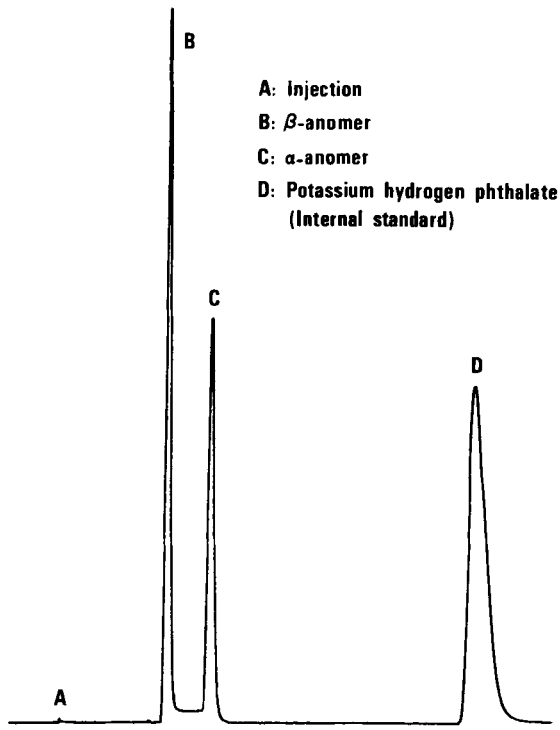

Figure 5—*Chromatogram of streptozocin and internal standard.*

This procedure will ensure that all measurements are taken with the equilibrium mixture of the α- and β-anomers.

A series of placebos consisting of sodium citrate–citric acid was spiked with different amounts of streptozocin to demonstrate the recovery and precision of the chromatographic procedure (Table I). A typical chromatogram is shown in Fig. 5.

These results illustrate the effectiveness of the HPLC procedure for the quality control of the drug, both in bulk and formulation. Streptozocin is not stable for an appreciable time in unbuffered aqueous solution. In buffered solutions, it is stable at room temperature for several days but decomposes rapidly above 70°. Literature reports concerning the degradation of *N*-nitrosamines (2) and *N*-nitrosamides (3) suggest that the majority of degradation products arising from streptozocin have lost the *N*-nitroso group, *i.e.*, the UV chromophore. Similar results also were attained in this laboratory for the degradation of *N*-nitrosoureas.

This effect was verified experimentally by heating a solution of streptozocin at 80° for 30 min and then analyzing an aliquot of the solution for the drug. While the peak heights of the streptozocin anomers decreased significantly (~16%), extraneous peaks due to degradation products were not present in the chromatogram. Furthermore, UV results of the solution for streptozocin were in agreement with the HPLC results for the same solution. Although these data support the UV assay as a specific stability-indicating assay, the HPLC assay was adopted since it provides additional information with respect to the α- and β-anomer composition of bulk drug and product.

Assay results for streptozocin in a sterile-powder, 1 g/vial, are given in Table II.

REFERENCES

(1) "Basic Principles of Organic Chemistry," J. D. Roberts and M. C. Caserio, Eds., W. A. Benjamin, New York, N.Y., 1965, p. 623.

(2) E. H. White and K. W. Field, *J. Am. Chem. Soc.*, **97**, 2148 (1975).

(3) E. H. White, *ibid.*, **77**, 6011 (1955).

USP Dissolution IV: Comparison of Methods

J. T. CARSTENSEN ˣ, TOM YU-FUN LAI, and V. K. PRASAD *

Received August 18, 1977, from the *School of Pharmacy, University of Wisconsin, Madison, WI 53706.* Accepted for publication January 20, 1978. *Present address: Biopharmaceutics Laboratory, Food and Drug Administration, Washington, D.C.

Abstract □ The hydrodynamics of four dissolution apparatus—*viz.*, the USP basket, the USP paddle, the stationary basket–spinning filter, and the USP disintegration apparatus, were characterized. At higher velocities, the relationship between the intrinsic dissolution rate constant and linear velocity was parabolic rather than linear.

Keyphrases □ Dissolution—hydrodynamics of four different types of apparatus compared □ Apparatus, dissolution—hydrodynamics of four different types compared □ Hydrodynamics—four different types of dissolution apparatus compared

There has been an abundance of literature regarding dissolution apparatus in the past 15 years. A good survey of methods was given by Pernarowski (1) who noted over 150 different apparatus designs. Since many dissolution curves are obtained under these conditions, methods are needed whereby one could grossly correlate data obtained by one method to those obtained by another. One purpose of this study was to suggest such an approach.

A direct approach is, of course, to standardize a test and to make it "official." This approach was attempted in NF XIV and USP XVIII and XIX. Nevertheless, results obtained with different pieces of apparatus or different operators frequently differ. One purpose of this study was to suggest an approach for normalization of results obtained with the same apparatus design but different pieces of equipment.

The drive toward standardization in recent years has tentatively narrowed down to the following three methods: the USP basket apparatus (2), the paddle apparatus (3), and the stationary basket–rotating filter method (4).

Dissolution theories based on Noyes–Whitney (5), Nernst–Brunner (6), and Hixson–Crowell (7) treatments result in "intrinsic dissolution rate constants," k (centimeters per second). These constants equal D/h, where D is the diffusion coefficient (square centimeters per second) and h is the thickness of the diffusion layer about the dissolving particle. Within the limitation of these approaches, the layer thickness is a function of the hydrodynamics of the system (8–10). Therefore, one would not expect identical dosage forms to give identical dissolution curves in the three apparatus.

However, a rank-order correlation between dissolution rates and liquid velocities would be expected. To establish this correlation, it was necessary to establish that there is a relationship between the dissolution rate constant and liquid velocity (8).

In this study, this concept was carried further. Directly measured liquid velocities were compared with dissolution rate constants to establish a functionality over a wider range of velocities. This information then was used to establish the velocity in various spots by the inverse technique—*viz.*, by measuring the dissolution rate constants of oxalic acid in various spots of the apparatus.

Table I—USP Basket Positions

Position	R, cm	H, cm	θ[a]
1	0–1	2	—
2	5	2	90°, 180°, 270°
3	3.15	−0.9	90°, 180°, 270°
4	0–1	0	—
5	3	2	180°
6	5	11	90°, 180°, 270°
7	0.7–1	2	—
8	1–1.31	2	—

[a] Three angles denote that three tablets were placed in individual positions as indicated.

EXPERIMENTAL

Oxalic acid tablets were prepared at 4535 kg (10,000 lb) force on a hydraulic press, using a flat-faced tablet punch and die with a flat steel plate as the lower retainer. The tablets were 1.13 cm in diameter and 0.33 cm in height and weighed 0.500 g. When tablets were to be suspended in the liquid, a piece of nylon string was placed on the retaining plate, producing a tablet on a string, which could then be suspended in the liquid at a desired position. In certain cases (paddle method), the positioning was done *via* a glass capillary.

The following methods were studied: USP rotating basket (50, 100, and 150 rpm); USP proposed paddle method (3) (50, 100, and 150 rpm); rotating filter–stationary basket method (4); and USP disintegration apparatus (2). The dimensions of the vessel used for USP basket and paddle methods are shown in Fig. 1*a* and Table I. A polar cylindrical coordinate system as shown in Fig. 1*b* was used.

The positions tested with the USP basket method are shown in Table II and Figs. 2 and 3. It was determined earlier (11) that agitation in the USP basket method does not ensure homogeneity of the liquid. The method used here was as follows. A volume of 900 ml of 0.1 N HCl was placed in the dissolution vessel, which was located in a constant-temperature bath at 25°. One-half hour at 25° was allowed for temperature calibration, and the tablets (3) were placed at the desired position(s). A timer was started simultaneously. After t sec, the tablet was removed and

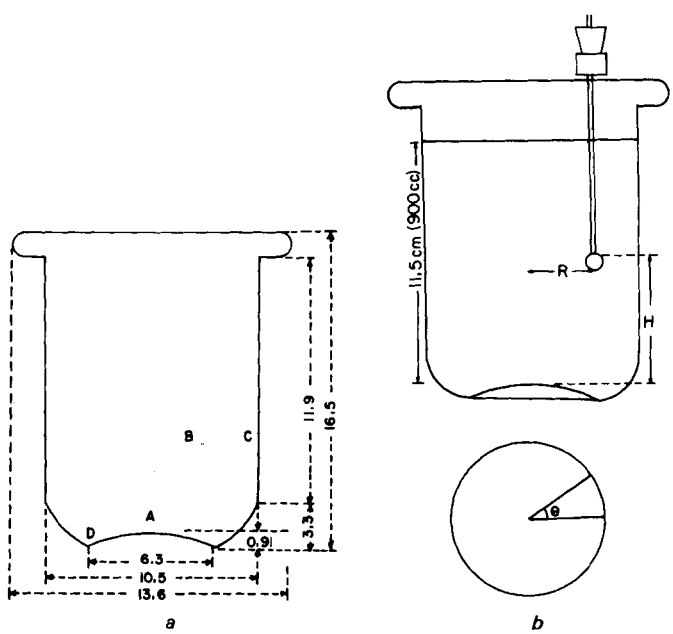

Figure 1—*Dimensions* (a) *and descriptive coordinates* (b) *of the vessel used in the USP apparatus.*

0022-3549/78/0900-1303$01.00/0
© 1978, American Pharmaceutical Association

Table II—Positions of Tablets in the Paddle Apparatus

Position	R, cm	H, cm	θ^a
1	3.15	−0.9	90°, 180°, 270°
2	0–1	0	—
3	5	4.5	90°, 180°, 270°
4	3	4.5	180°
5	5	11	90°, 180°, 270°

[a] Three angles denote that three tablets were placed in individual positions as indicated.

the entire content of the dissolution vessel was determined by spectrophotometry at 255 nm.

The experiment was then repeated for various time periods, t, to produce a dissolution curve of concentration, C (milligrams per milliliter), *versus* t (seconds). This method is obviously more cumbersome than taking samples at a particular place in the liquid at various times (and maintaining the same bulk liquid throughout the experiment), but the external liquid is not homogeneous in the early phases of dissolution in the USP basket method (11).

With the proposed USP paddle method, the tablets were held in position by capillary glass tubes. A special means of introducing the tablet was needed when it was underneath the paddle; two curved capillaries with a string running through both allowed the tablet to be pulled into position rapidly. The adequacy of the agitation in the paddle method was first determined (11) by sampling and assaying the entire content at several time and position points. The sampling positions used are shown in Fig. 3. Dissolution rates were determined in the positions shown in Fig. 4.

To validate the velocities obtained for dissolution data, the following crude, but direct, method was used. Scarlet red dye[1] was dissolved in cyclohexyl chloride, which has a density matching that of water at 25°. A drop of this solution was introduced at the various test points, and the

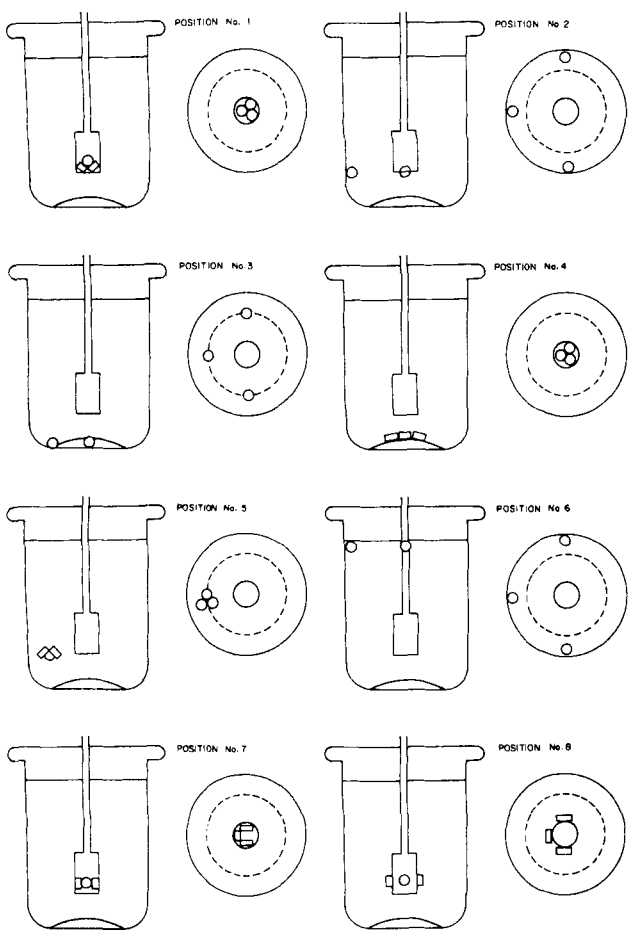

Figure 2—*Positions tested in the USP basket study.*

[1] Sudan IV.

Table III—Intrinsic Dissolution Rate Constants, k, and Corresponding Liquid Velocities, v, for Four Dissolution Methods

Method	Position	Condition, rpm	10^3k, cm/sec[a]	v, cm/sec[b]
USP basket	1	50	1.3 ± 0.06	4.1
	2	50	0.93 ± 0.04	2.4
	3	50	0.71 ± 0.10	1.6
	4	50	0.80 ± 0.10	1.9
	5	50	0.95 ± 0.05	2.5
	6	50	0.92 ± 0.02	2.4
	7	50	1.8 ± 0.2	6.9
	8	50	1.85 ± 0.5	7.2
	1	100	1.7 ± 0.07	6.3
	2	100	0.95 ± 0.08	2.5
	3	100	0.92 ± 0.02	2.4
	4	100	1.17 ± 0.06	3.5
	5	100	1.00 ± 0.03	2.7
	6	100	0.90 ± 0.08	2.3
	7	100	1.7 ± 0.15	6.3
	8	100	2.40 ± 0.07	10.8
	1	150	2.2 ± 0.20	9.4
	2	150	1.05 ± 0.05	2.9
	3	150	1.02 ± 0.04	2.8
	4	150	1.50 ± 0.06	5.1
	5	150	1.19 ± 0.05	3.6
	6	150	0.95 ± 0.02	2.5
	7	150	2.8 ± 0.3	13.8
	8	150	3.30 ± 0.14	17.9
	1 (bottom)	50	1.9 ± 0.2	7.5
	2	50	1.6 ± 0.2	5.7
	3	50	2.1 ± 0.1	8.7
	4	50	1.90 ± 0.03	7.5
	5	50	1.8 ± 0.1	6.9
	6 (free bottom)	50	1.8 ± 0.1	6.9
	1 (bottom)	100	2.90 ± 0.04	14.7
	2	100	2.4 ± 0.1	10.8
	3	100	3.6 ± 0.3	20.6
	4	100	3.5 ± 0.3	19.7
	5	100	3.0 ± 0.2	15.4
	6 (free bottom)	100	2.5 ± 0.1	11.6
	1	150	4.1 ± 0.3	25.3
	2	150	3.1 ± 0.2	16.3
	3	150	4.2 ± 0.2	26.3
	4	150	3.8 ± 0.3	22.5
	5	150	3.5 ± 0.2	19.7
	6 (free bottom)	150	3.3 ± 0.2	17.9
Rotating filter	Inside basket	300	2.00 ± 0.03	8.1
	Bottom rim	300	1.9 ± 0.2	7.5
	Inside basket	600	2.9 ± 0.2	14.6
	Bottom rim	600	3.0 ± 0.3	15.4
USP disintegration	Inside tubes	—	2.9 ± 0.2	14.6
	Bottom of beaker	—	1.4 ± 0.2	4.6

[a] Limits shown are 95% confidence interval. [b] According to Eq. 4a in the form: $\ln v = 1.587 \ln k + 11.957$.

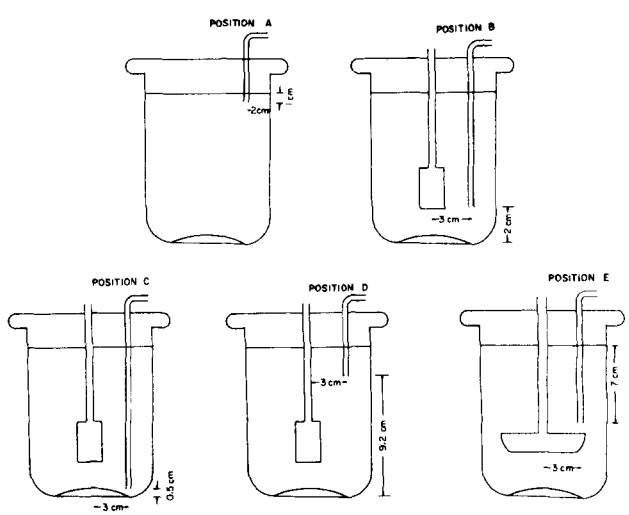

Figure 3—*Sampling positions in the USP basket apparatus (A–D) and paddle method (E).*

Table IV—Observed and Calculated Velocities and Dissolution Rate Constants for Four Dissolution Methods

Method	Position	Condition, rpm	Velocity, cm/sec		ln $v°$	10^3k, cm/sec	$7 + \ln k$
			Observed, $v°$	Calculated			
USP basket	8	50	4.6	5.2	1.53	1.85	0.71
	8	100	9.9	10.5	2.29	2.40	0.97
	8	150	16.1	15.7	2.78	3.3	1.29
Rotating filter		300	7.1	6.2	1.96	2.0	0.79
		600	8.4	8.4	2.13	1.9	0.43
USP paddle	1	50	8.2	—	2.10	1.9	0.73
	1	100	14.5	—	2.67	2.9	1.16
	3	50	8.1	—	2.09	2.1	0.83
	3	100	15.7	—	2.75	3.6	1.37
	4	50	9.4	—	2.24	1.9	0.73
	5	50	6.6	—	1.89	1.8	0.68
	5	150	18.8	—	2.93	3.5	1.35
USP disintegration	Inside tubes	—	—	16.1	2.78	2.9	1.16
	Outside tubes	—	—	6.4	1.85	1.4	0.43

time required for one rotation was noted. Many trials are needed to get the correct path, since the path followed by the drop must be as close to a circle as possible.

With the stationary basket–rotating filter apparatus (4), the adequacy of mixing was first determined as already described. The dissolution rates were then determined with the tablet inside the basket and with the tablet outside the basket (on the bottom close to the rim) at 300 and 600 rpm.

With the USP disintegration apparatus, the adequacy of mixing was first ascertained as already described. The dissolution rates were then determined with the tablets in the tubes (three tablets were placed, one each, in alternating tubes) and with the tablets outside the tube–basket assembly. A volume of 800 ml of 0.1 *N* HCl was used in a 1000-ml beaker (10-cm diameter). At the lowest part of the downstroke, the mesh was 2.5 cm above the bottom. Samples of 4 ml were used for assay.

In all described experiments, at least eight time points were used to calculate the dissolution rate constants.

The dissolution of two dosage forms—*viz.*, 50-mg nitrofurantoin tablets and capsules[2], was then determined in the four apparatus with the prescribed procedures. With the capsules, two antifloating devices were used[2]: a copper coil (with four coilings) of the outer dimensions of the capsule into which the capsule fits snugly, and a 6-mesh steel basket 2 cm in diameter. (This basket can be separated into two halves and is held together by a clip.)

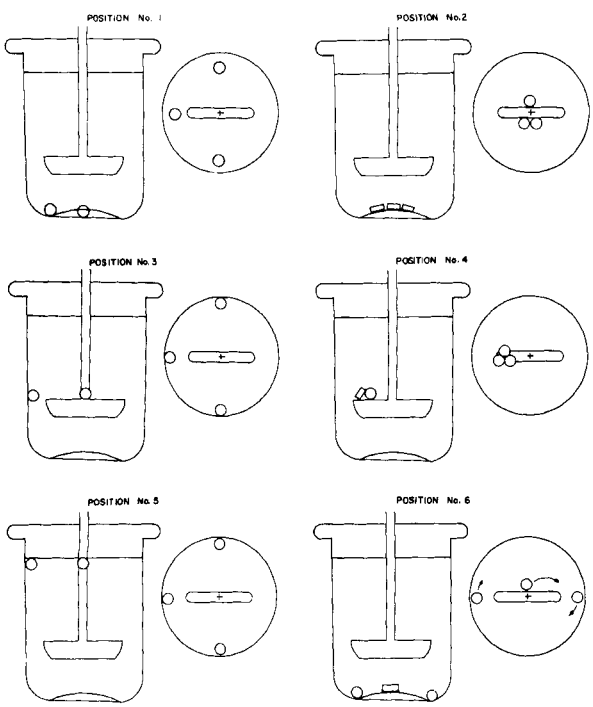

Figure 4—*Tablet positions in the USP paddle method.*

[2] Supplied by the Biopharmaceutics Laboratory, Food and Drug Administration, Washington, D.C.

The rotations per minute were checked and verified in all cases by means of a strobe light.

RESULTS AND DISCUSSION

The intrinsic dissolution rate constants were obtained from concentration *versus* time curves by the method of Lai and Carstensen (12) (Table III). The method is a modification of the Hixson–Crowell law; but where the Hixson–Crowell law assumes the particles to be isometric, the modified method (12) takes into account the change in the shape factor as a function of time.

Carstensen and Dhupar (8) studied the k values *versus* v in a rather narrow column; v was kept fairly low to avoid turbulence. In the study reported here, the dissolution apparatus had large diameters and larger k (and v) values. Because of the larger diameter, the higher v values do not necessarily imply turbulent flow conditions. Table IV lists the velocities obtained experimentally by the dye method and the k values. The linearity found between k and v at low v values (8) fails at higher v values (Fig. 5).

The first point then is to establish a correlation between v and k at these higher velocities. Therefore, the experimentally found velocity values were compared with theoretical figures. For the USP basket and spinning filter methods, this comparison was done as follows. If v denotes the laminar velocity of an incompressible fluid in steady motion between two infinitely long concentric rotating cylinders of radii R_1 and R_2 (where $R_2 > R_1$) at a point that is r cm removed from the concentric axis, it can be shown (13) that:

$$v = Ar + (B/r) \qquad \text{(Eq. 1)}$$

If the outer cylinder is stationary while the inner cylinder moves so that the surface velocity is Ω, then Eq. 1 is subject to the following boundary conditions:

$$\Omega = AR_1 + (B/R_1) \qquad \text{(Eq. 2}a\text{)}$$

$$0 = AR_2 + (B/R_2) \qquad \text{(Eq. 2}b\text{)}$$

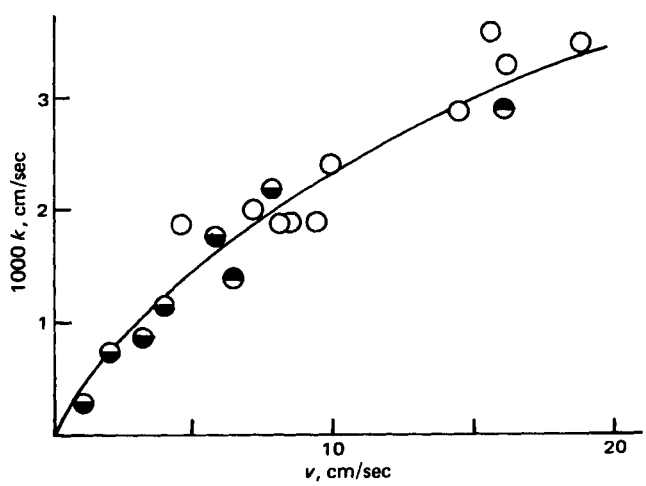

Figure 5—*Dissolution data from USP basket and paddle and rotating filter method* (○), *USP disintegration apparatus* (◓), *and data reported by Carstensen and Dhupar* (8) (◒).

Table V—Dissolution Parameters of Nitrofurantoin Tablets and Capsules

Method	K, 10^3, sec^{-1} Tablet	K, 10^3, sec^{-1} Capsule	v, cm/sec	Position
USP basket				
50 rpm	0.025	0.050	7	7, 8 average
100 rpm	0.033	0.080	8	7, 8 average
150 rpm	0.026	0.084 0.075	16	7, 8 average
Paddle: cage				
50 rpm	0.012 0.018	0.025 0.045	7.5	1 (bottom)
100 rpm	0.03	0.13	14.7	1 (bottom)
150 rpm	0.25	0.27	17.9	1 (bottom)
Paddle: coil				
50 rpm	0.022	0.012	7.5	1 (bottom)
100 rpm	0.075	0.13	14.7	1 (bottom)
150 rpm	0.20	0.24	17.9	1 (bottom)
USP disintegration	0.97	0.043	14.6	In tube
Rotating filter				
300 rpm	0.047 0.023	0.015	8.1	In basket
600 rpm	0.058	0.30 0.25	14.5	In basket

The last equation assumes that no slip occurs. This principle is directly applicable to the rotating basket. It also applies to the rotating filter method because the filter can be viewed as the inner cylinder and the beaker can be viewed as the outer cylinder (R_2 = 5 cm). If one assumes that the major contribution of medium movement at the site of the basket is due to the filter body (R_1 = 2.5 cm), as demonstrated in Fig. 6, while the major contribution of the medium movement at the bottom rim is due to the filter base (R_1 = 4.5 cm), then Eq. 1 can be solved for these two positions at various numbers of rotations per minute of the filter.

Solving for tablets inside the basket at 300 rpm gives $v = (53.25/r) - 2.13r$; at 600 rpm, $v = (106.5/r) - 4.26r$. Obtaining A and B values for the bottom rim gives $v = (200/r) - 8r$ at 300 rpm and $v = (400/r) - 16r$ at 600 rpm.

If one takes 3.75 as r for the basket and 4.5 cm as r for the bottom rim position (Fig. 6), the medium velocity at the two positions can be predicted. The predicted values are given in Table IV.

Table IV also lists the observed velocities obtained using the dye method in the paddle apparatus. To estimate the velocities in the USP dissolution apparatus, the following simplified model was used. If the entire rack (Fig. 6) of the disintegration apparatus does not cause any displacement of medium, then the average relative velocity of the rack moving through the medium is 6.4 cm/sec (calculated from the fact that the rack moves at a rate of 32 cpm and moves 6 cm in half of a cycle). During the downstroke, the solid portion of the base (Fig. 7) of the rack displaces 256 ml in 0.94 sec. This volume of medium has to move through the tubes and through the side of the rack.

The beaker is 10 cm in diameter while the base of the rack is 9 cm in diameter, giving an area of 15 cm^2 between the rack base and the side wall of the beaker. The total cross section of the six tubes is 21 cm^2 less 8 cm^2 due to the wire mesh, *i.e.*, a total of 13 cm^2. Therefore, the 256 ml of medium has to travel through about 28 cm^2 in 0.94 sec, creating an upward medium velocity of 9.7 cm/sec, while the rack moves downward at 6.4 cm/sec; *i.e.*, the relative velocity is 16.1 cm/sec between the base of the rack and the medium. The reverse would happen during the upward stroke, resulting in the same relative velocity.

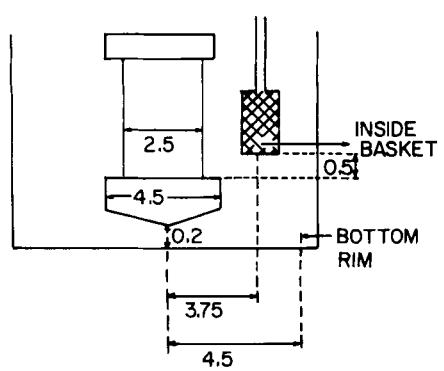

Figure 6—*Dimensions (in centimeters) of rotating filter apparatus.*

Table VI—Mean Deviation of Assays from True Value[a]

Method	Position	Temperature	Number of Determinations, n	Mean Deviation, % (p = 0.95)
Paddle, 50 rpm	Average of all[a]	25°	17	4.2 ± 1.8
Paddle, 100 rpm	Average of all[a]	25°	20	3.1 ± 0.9
Paddle, 150 rpm	Average of all[a]	25°	20	6.0 ± 2.0
Paddle, 50 rpm	Average of all[a]	37°	7	6.7 ± 4.0
Rotating filter[b]	A	25°	9	10 ± 3
Rotating filter[b]	Filter	25°	7	13 ± 3
Rotating filter[b]	E	25°	9	2.8 ± 1.6
USP disintegration		25°	5.3	5.3 ± 2.8

[a] If a sample is taken at random from the liquid during the first 4 min of dissolution, the deviation from the true content will be as shown. [b] Both 300- and 600-rpm figures are included.

There is good correlation between the observed values (*i.e.*, the values from the dye method) and the calculated values in the five cases where comparison is possible (USP basket method and spinning filter method). The first five entries in Table IV give the following least-squares fit:

$$v_{calc} = 0.96v_{obs} + 0.37 \quad (r = 0.989, n = 5) \qquad \text{(Eq. 3)}$$

The slope does not differ significantly from 1.00 (p = 0.01), and the intercept does not differ significantly from zero (p = 0.01). Therefore, it is felt that the dye method yields results in good agreement with theory. At the higher k values that apply here, as mentioned, k is not linear when plotted *versus* v. A plot of ln k *versus* ln v is shown in Fig. 8 and the least-squares fit is:

$$\ln k = (0.63 \pm 0.20) \ln v - (7.53 \pm 0.57) \quad (r = 0.85, n = 15) \qquad \text{(Eq. 4a)}$$

Equation 4*a* may be written as:

$$k = 0.00054(v^{0.63}) \qquad \text{(Eq. 4b)}$$

and the curve shown in Fig. 5 is indeed this correlation. At low v values, the previously reported linear data (8) fit well with Eq. 4*b*. Both the linear model and the one outlined here assume that $k = 0$ at $v = 0$, which cannot be strictly correct since there will always be some finite dissolution rate even under stagnant hydrodynamic conditions.

It is expected from hydrodynamic theory (14) that the diffusion layer thickness, h, relates to the liquid velocity by the relation:

$$h = \Gamma v^{-1/n} \qquad \text{(Eq. 5)}$$

where Γ is a proportionality constant and n has a value between 1 and 2. Since $k = D/h$, it would be expected that:

$$k = \beta v^{1/n} \qquad \text{(Eq. 6)}$$

and Eq. 4*a* substantiates this assumption; β is here a proportionality constant.

It is now possible to list velocities calculated from dissolution rate constants in all positions of the four apparatus tested, and this is done in the last column of Table III.

It was stated previously (15) that, *e.g.*, 100 rpm in the paddle method corresponded to 150 rpm in the basket method which, in turn, corresponded to 600 rpm in the spinning filter method. The spinning filter method yields a velocity of 14–15 cm/sec, the basket method in and at the basket (positions 7 and 8, respectively) yields a velocity of 14–18 cm/sec at 150 rpm, and the paddle method at the bottom (either confined or free, *i.e.*, position 1 or 6, respectively) yields a velocity of 12–15 cm/sec at 100 rpm. This result substantiates such rules in the sense that the dissolution is considered from a point of view that disregards disintegration effects. These effects were discussed elsewhere (16).

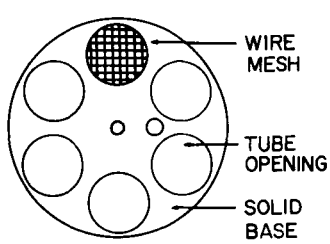

Figure 7—*USP disintegration apparatus rack.*

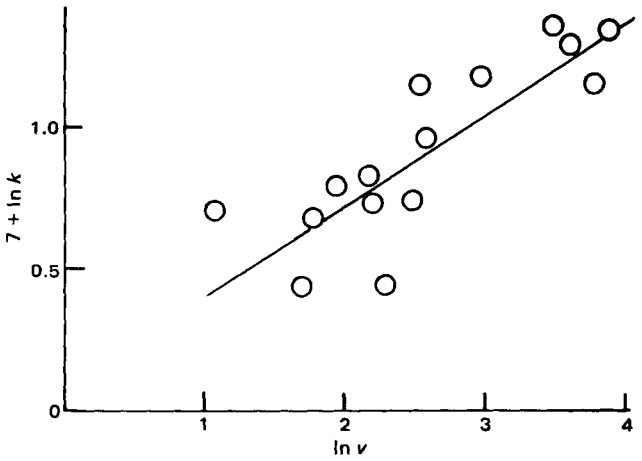

Figure 8—*Dissolution data from dissolution apparatus reported here plotted according to Eq. 4a.*

The effect of liquid velocity on the dissolution of nitrofurantoin from two dosage forms (capsules and tablets) was checked by conducting dissolution tests with all mentioned methods. All (except one) sets of data adhered to a σ^{-}-type plot (17) of the type:

$$\ln(m/m_0) = -Kt + Q \qquad \text{(Eq. 7)}$$

where m is mass undissolved, the zero subscript implies the initial condition, K is a dissolution constant (seconds^{-1}), and Q is a constant. The value of K depends both on dissolution and on how well the dissolution apparatus disintegrates the dosage unit, and Q depends on dissolution only (16). Table V lists K values from the data. There is a correlation between K and v (correlation coefficient of 0.432, which is significant for $n = 29$ at $p = 0.95$), but it is not sufficiently exacting to allow correlation from method to method. The different methods undoubtedly act differently regarding the disintegration of the dosage unit. The fact that the correlation is real, however, makes it a sound basis for calibration or correlation between different pieces of the same apparatus.

The heterogeneity of the dissolution medium reported earlier for the USP basket method (8) is not nearly as pronounced in the other apparatus studied. The paddle apparatus in particular gives good homogeneity (Table VI).

REFERENCES

(1) M. Pernarowski, in "Dissolution Technology," L. Leeson and J. T. Carstensen, Eds., Industrial Pharmaceutical Technology Section, Academy of Pharmaceutical Sciences, American Pharmaceutical Association, Washington, D.C., 1974, p. 102.

(2) "The United States Pharmacopeia," 19th rev., Mack Publishing Co., Easton, Pa., 1975, p. 651.

(3) USP XX Comment Proof, Jan. 17, 1977, **1**, 976 (15) (1977).

(4) A. C. Shah, C. B. Peot, and J. F. Ochs, *J. Pharm. Sci.*, **62**, 671 (1973).

(5) A. A. Noyes and W. R. Whitney, *J. Am. Chem. Soc.*, **19**, 930 (1897).

(6) W. Nernst, *Z. Phys. Chem. (Leipzig)*, **47**, 52 (1904).

(7) A. W. Hixson and J. H. Crowell, *Ind. Eng. Chem.*, **23**, 923 (1931).

(8) J. T. Carstensen and K. Dhupar, *J. Pharm. Sci.*, **65**, 1634 (1976).

(9) J. T. Carstensen and M. Patel, *ibid.*, **64**, 1770 (1975).

(10) M. Patel and J. T. Carstensen, *ibid.*, **64**, 1651 (1975).

(11) J. T. Carstensen, T. Lai, and V. K. Prasad, *ibid.*, **66**, 607, (1977).

(12) T. Y.-F. Lai and J. T. Carstensen, *Int. J. Pharm.*, **1**, 33 (1978).

(13) G. I. Taylor, *Phil. Trans.*, **223 A**, 289 (1928).

(14) V. G. Levich, "Physicochemical Hydrodynamics," Prentice-Hall, Englewood Cliffs, N.J., 1962, p. 342.

(15) M. Pernarowski, in "Dissolution Technology," L. Leeson and J. T. Carstensen, Eds., Industrial Pharmaceutical Technology Section, Academy of Pharmaceutical Sciences, American Pharmaceutical Association, Washington, D.C., 1974, p. 88.

(16) J. T. Carstensen, J. Wright, K. Blessel, and J. Sheridan, *J. Pharm. Sci.*, **67**, 48 (1978).

(17) J. T. Carstensen, in "Dissolution Technology," L. Leeson and J. T. Carstensen, Eds., Industrial Pharmaceutical Technology Section, Academy of Pharmaceutical Sciences, American Pharmaceutical Association, Washington, D.C., 1974, p. 192.

ACKNOWLEDGMENTS

Abstracted in part from a dissertation submitted by T. Y.-F. Lai to the University of Wisconsin in partial fulfillment of the Master of Science degree requirements.

Supported by Grant 223-76-3020 from the Food and Drug Administration.

Quantitative TLC Determination of Propranolol in Human Plasma

B. W. HADZIJA ˣ and A. M. MATTOCKS

Received December 12, 1977, from the *School of Pharmacy, University of North Carolina, Chapel Hill, NC 27514.* Accepted for publication January 20, 1978.

Abstract □ A spectrodensitometric assay was developed for propranolol based on measurement of the absorbance of the drug on silica gel plates irradiated at 288 nm. Quantities as low as 0.010 μg can be detected, and a linear relationship was obtained between 0.010 and 0.400 μg. The percent recovery from plasma spiked with known amounts of the drug was 90.0–102.0. This procedure was used to determine propranolol in the plasma of patients receiving therapeutic doses of the drug.

Keyphrases □ Propranolol—TLC analysis in plasma □ TLC—analysis, propranolol in plasma □ Cardiac depressants—propranolol, TLC analysis in plasma

Propranolol produces a specific blockade of β-adrenergic receptors with minimal intrinsic activity, resulting in an effect on the cardiovascular system. It is capable of suppressing heart rate and contractility and of increasing vasoconstriction in those beds where there may be some degree of masked β-adrenergic vasodilator effect. It is used for the treatment of angina pectoris and in cardiac arrhythmias, hypertrophic subaortic stenosis, pheochromocytoma, and digitalis-induced ventricular tachycardia.

Propranolol is presently receiving much attention in the treatment of essential hypertension associated with a high cardiac output or high plasma angiotensin levels (1, 2).

BACKGROUND

To follow the pharmacokinetics of this drug and to understand the mechanism of its action, plasma propranolol levels are determined. The low levels and the wide variability of plasma propranolol concentrations

0022-3549/78/0900-1307$01.00/0
© 1978, American Pharmaceutical Association

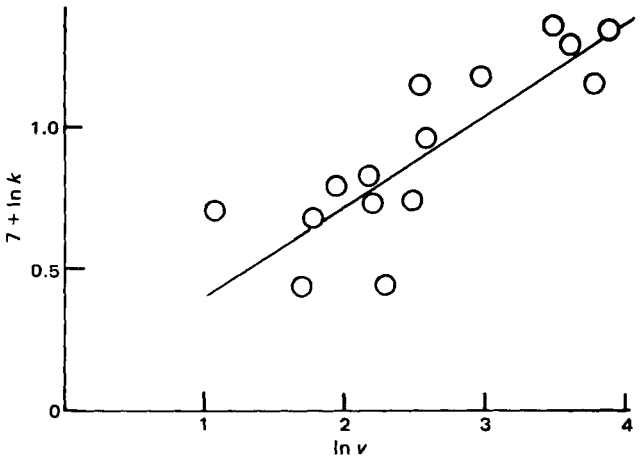

Figure 8—*Dissolution data from dissolution apparatus reported here plotted according to Eq. 4a.*

The effect of liquid velocity on the dissolution of nitrofurantoin from two dosage forms (capsules and tablets) was checked by conducting dissolution tests with all mentioned methods. All (except one) sets of data adhered to a σ^{-}-type plot (17) of the type:

$$\ln(m/m_0) = -Kt + Q \qquad \text{(Eq. 7)}$$

where m is mass undissolved, the zero subscript implies the initial condition, K is a dissolution constant (seconds^{-1}), and Q is a constant. The value of K depends both on dissolution and on how well the dissolution apparatus disintegrates the dosage unit, and Q depends on dissolution only (16). Table V lists K values from the data. There is a correlation between K and v (correlation coefficient of 0.432, which is significant for $n = 29$ at $p = 0.95$), but it is not sufficiently exacting to allow correlation from method to method. The different methods undoubtedly act differently regarding the disintegration of the dosage unit. The fact that the correlation is real, however, makes it a sound basis for calibration or correlation between different pieces of the same apparatus.

The heterogeneity of the dissolution medium reported earlier for the USP basket method (8) is not nearly as pronounced in the other apparatus studied. The paddle apparatus in particular gives good homogeneity (Table VI).

REFERENCES

(1) M. Pernarowski, in "Dissolution Technology," L. Leeson and J. T. Carstensen, Eds., Industrial Pharmaceutical Technology Section, Academy of Pharmaceutical Sciences, American Pharmaceutical Association, Washington, D.C., 1974, p. 102.

(2) "The United States Pharmacopeia," 19th rev., Mack Publishing Co., Easton, Pa., 1975, p. 651.

(3) USP XX Comment Proof, Jan. 17, 1977, **1**, 976 (15) (1977).

(4) A. C. Shah, C. B. Peot, and J. F. Ochs, *J. Pharm. Sci.*, **62**, 671 (1973).

(5) A. A. Noyes and W. R. Whitney, *J. Am. Chem. Soc.*, **19**, 930 (1897).

(6) W. Nernst, *Z. Phys. Chem. (Leipzig)*, **47**, 52 (1904).

(7) A. W. Hixson and J. H. Crowell, *Ind. Eng. Chem.*, **23**, 923 (1931).

(8) J. T. Carstensen and K. Dhupar, *J. Pharm. Sci.*, **65**, 1634 (1976).

(9) J. T. Carstensen and M. Patel, *ibid.*, **64**, 1770 (1975).

(10) M. Patel and J. T. Carstensen, *ibid.*, **64**, 1651 (1975).

(11) J. T. Carstensen, T. Lai, and V. K. Prasad, *ibid.*, **66**, 607, (1977).

(12) T. Y.-F. Lai and J. T. Carstensen, *Int. J. Pharm.*, **1**, 33 (1978).

(13) G. I. Taylor, *Phil. Trans.*, **223 A**, 289 (1928).

(14) V. G. Levich, "Physicochemical Hydrodynamics," Prentice-Hall, Englewood Cliffs, N.J., 1962, p. 342.

(15) M. Pernarowski, in "Dissolution Technology," L. Leeson and J. T. Carstensen, Eds., Industrial Pharmaceutical Technology Section, Academy of Pharmaceutical Sciences, American Pharmaceutical Association, Washington, D.C., 1974, p. 88.

(16) J. T. Carstensen, J. Wright, K. Blessel, and J. Sheridan, *J. Pharm. Sci.*, **67**, 48 (1978).

(17) J. T. Carstensen, in "Dissolution Technology," L. Leeson and J. T. Carstensen, Eds., Industrial Pharmaceutical Technology Section, Academy of Pharmaceutical Sciences, American Pharmaceutical Association, Washington, D.C., 1974, p. 192.

ACKNOWLEDGMENTS

Abstracted in part from a dissertation submitted by T. Y.-F. Lai to the University of Wisconsin in partial fulfillment of the Master of Science degree requirements.

Supported by Grant 223-76-3020 from the Food and Drug Administration.

Quantitative TLC Determination of Propranolol in Human Plasma

B. W. HADZIJA ˣ and A. M. MATTOCKS

Received December 12, 1977, from the *School of Pharmacy, University of North Carolina, Chapel Hill, NC 27514.* Accepted for publication January 20, 1978.

Abstract □ A spectrodensitometric assay was developed for propranolol based on measurement of the absorbance of the drug on silica gel plates irradiated at 288 nm. Quantities as low as 0.010 μg can be detected, and a linear relationship was obtained between 0.010 and 0.400 μg. The percent recovery from plasma spiked with known amounts of the drug was 90.0–102.0. This procedure was used to determine propranolol in the plasma of patients receiving therapeutic doses of the drug.

Keyphrases □ Propranolol—TLC analysis in plasma □ TLC—analysis, propranolol in plasma □ Cardiac depressants—propranolol, TLC analysis in plasma

Propranolol produces a specific blockade of β-adrenergic receptors with minimal intrinsic activity, resulting in an effect on the cardiovascular system. It is capable of suppressing heart rate and contractility and of increasing vasoconstriction in those beds where there may be some degree of masked β-adrenergic vasodilator effect. It is used for the treatment of angina pectoris and in cardiac arrhythmias, hypertrophic subaortic stenosis, pheochromocytoma, and digitalis-induced ventricular tachycardia.

Propranolol is presently receiving much attention in the treatment of essential hypertension associated with a high cardiac output or high plasma angiotensin levels (1, 2).

BACKGROUND

To follow the pharmacokinetics of this drug and to understand the mechanism of its action, plasma propranolol levels are determined. The low levels and the wide variability of plasma propranolol concentrations

0022-3549/78/0900-1307$01.00/0
© 1978, American Pharmaceutical Association

Table I—Reproducibility of Recovery of Propranolol from Spiked Human Plasma (1 ml)

Amount Added, μg[a]	Mean Recovery	Recovery ± CV, %
0.010	0.0094	94.0 ± 2.4
0.020	0.019	95.0 ± 4.9
0.040	0.036	90.0 ± 1.9
0.080	0.073	91.3 ± 1.9
0.120	0.114	95.0 ± 2.7
0.160	0.154	96.3 ± 1.8
0.200	0.204	102.0 ± 1.6

[a] Six samples were determined in each case.

(0.010–0.500 μg/ml) in different subjects after administration necessitated the development of rapid, specific, and sensitive methods for its analysis in biological specimens so that dosage adjustments for the individual patient could be made.

In previous studies, fluorometric methods were applied to the determination of propranolol (3–5), but they had high and variable blank values which, when subtracted from plasma readings, caused considerable variation in results (6). GLC (7, 8) and GLC–mass spectrometric (9, 10) analyses also were reported. Although these methods may be useful for drug quantitation, they require derivatization techniques and often are difficult as well as time consuming because of the slow elution of contaminant peaks, which limits the frequency of sample injection. The most recent GLC method (11) increased the speed of elution of contaminant peaks by using a different derivative and internal standard.

A TLC method, published recently (12), consists of extraction of propranolol and one of its metabolites from biological fluids, separation, and direct measurement of the fluorescence of the spots on the plate. The extraction of propranolol from plasma was only 70%. Fluorescence was achieved by spraying the developed plates with citric acid solution. The plates had to be scanned while still wet from the spraying, a fact that may result in unreliable readings if there is any delay in scanning.

This paper reports a highly sensitive and specific TLC method for the rapid estimation of propranolol in human plasma. The drug is extracted from plasma, separated on silica gel plates, and measured directly by UV absorption. With this method, propranolol concentrations as low as 0.010 μg may be measured accurately, and as many as six samples and three standards can be chromatographed simultaneously on a single plate.

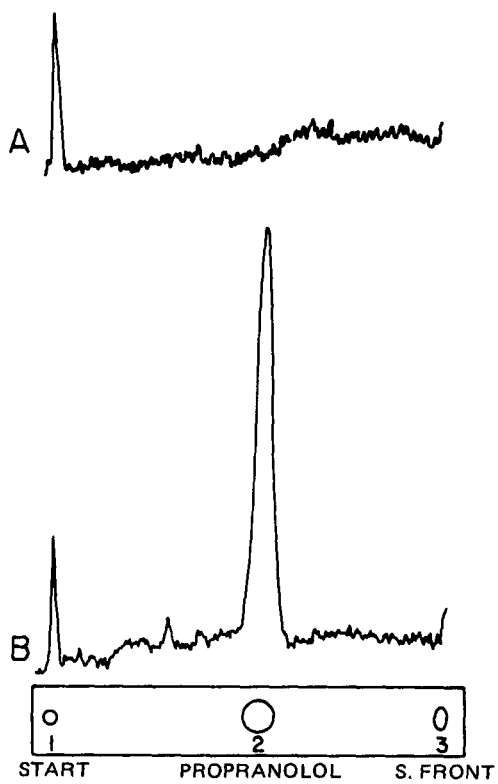

Figure 1—*Chromatograms of plasma samples from a patient before (A) and after (B) an oral dose of propranolol.*

EXPERIMENTAL

Reagents—Propranolol hydrochloride was used for method development[1]. The compound was dissolved in and diluted with methanol to appropriate concentrations (expressed as the free base). All solvents were spectroanalyzed grade, which is especially important to this method. Other chemicals were analytical grade. The developing solvent was methanol–28% aqueous ammonium hydroxide (100:1.5).

Instrumentation—A spectrodensitometer[2] in combination with an integrator[3] and strip-chart recorder[4] was used.

Standard Solutions—The stock solution was prepared as a 1-mg/ml solution in methanol. A standard solution (100 μg/ml) was prepared by diluting 5 ml of the stock solution to 50 ml with methanol. Appropriate volumes were used on the TLC plates to give a series of spots of propranolol in the 0.010–0.400-μg range.

Plasma Extraction—A volume of 1.0 ml of plasma was pipetted into a 20-ml glass centrifuge tube with a polytef-lined screw cap. A 0.5-ml aliquot of 0.5 *N* NaOH and 4 ml of dichloromethane were added, and the tube was shaken for 10 min mechanically. The tube was then centrifuged briefly to separate the layers, the organic phase was transferred to another tube, and extraction of the aqueous layer was repeated with an additional 4 ml of the solvent. The tube with the combined organic phases was immersed in a water bath at 45°, and the solvent was evaporated to dryness under a nitrogen stream.

The solid residue was dissolved in 50 μl of methanol, and suitable aliquots, 5–10 μl, were spotted on a TLC plate[5] along with a series of extracts from plasma spiked with known amounts of propranolol covering at least three concentrations in the 0.010–0.400-μg/ml range. The samples were applied with an automatic spotter[6] supplied with temperature and speed control or by hand using 10-μl syringes[7]. Prior to use, the plates were activated at 105° for 20 min or were used directly from a freshly opened package.

The chromatograms were developed at room temperature in a glass tank by the ascending technique in the developing solvent and were removed from the chamber after the solvent reached a height of 15 cm (~40 min). The solvent system was freshly prepared each day and allowed to equilibrate for 30 min prior to use. After development, the plate was air dried prior to scanning.

The densitometric measurements were performed using the reflectance mode on the scanner, and the plates were scanned at 25 mm/min at the absorption maximum of propranolol (288 nm).

A series of spiked plasma samples in the 0.010–0.400-μg range was run to establish the relation between peak areas (square millimeters) and concentration for the method. The assay result for each sample was calculated by dividing the propranolol peak area of the sample by that of the standard with the closest area and multiplying the ratio by a known concentration of the standard.

Recovery Experiments—The recovery of propranolol from spiked plasma was determined by comparison of the absorbance peak areas from spiked plasma with those of the standard solutions spotted directly on the same TLC plate.

Patient Plasma Samples—Eight hospitalized patients were treated with 120 mg of propranolol hydrochloride[8] daily given orally in three 40-mg doses. Blood samples were drawn 1 week after the start of the treatment at 2 hr after the morning dose. Blood (3–4 ml) was collected in heparinized tubes and centrifuged to separate the plasma. Plasma samples were stored in a refrigerator for not more than 24 hr before analysis.

RESULTS AND DISCUSSION

Plasma Propranolol Determination—Chromatograms of plasma samples from a patient before and after an oral dose of propranolol are shown in Fig. 1. In the chromatogram of the blank plasma, there were no interfering peaks in the region of propranolol. The R_f value of propranolol on the plates was 0.53 in the solvent used. Chromatogram B shows that none of the metabolites of propranolol usually formed after oral administration (13) interfered. Either the extraction procedure used does not

[1] Gift of Ayerst Laboratories, New York, N.Y.
[2] UV-VIS-2 chromatograph scanner, Farrand.
[3] CDS 101 chromatography data system, Varian.
[4] Model 100, Farrand.
[5] Silica gel 60 glass plates, 20 × 20 cm, 0.25 mm, E. Merck Laboratories.
[6] Multi-Spotter, Analytical Instrument Specialties.
[7] Hamilton.
[8] Inderal tablets, 40 mg, Ayerst Laboratories.

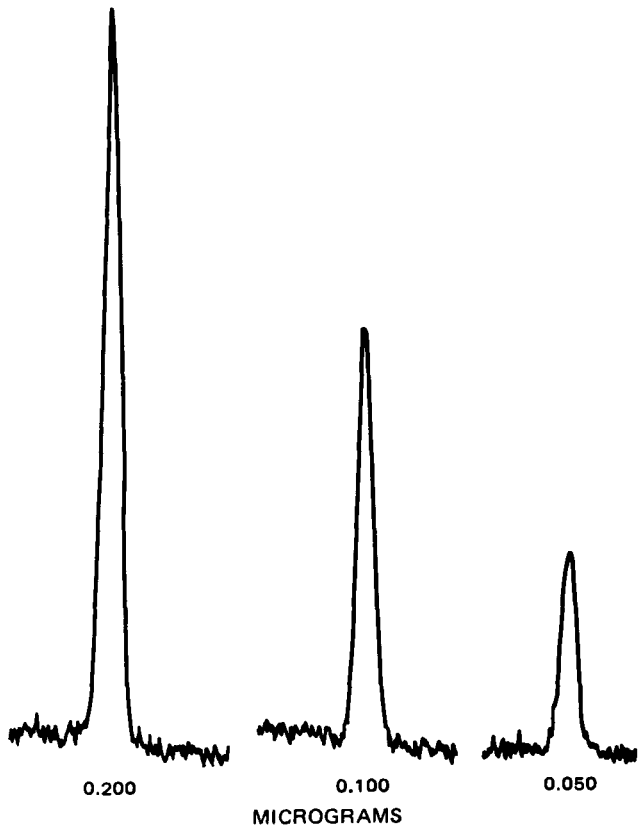

Figure 2—*Typical TLC chromatogram scans obtained with spiked plasma samples.*

extract the metabolites from the plasma or the metabolites do not absorb at 288 nm.

The curve obtained from determinations of known propranolol concentrations in spiked plasma and measurement of the areas under the peaks was linear within the range of 0.010–0.400 μg of drug/ml. The minimum measurable concentration was about 0.010 μg/ml.

Typical TLC chromatogram scans obtained with spiked plasma samples are shown in Fig. 2.

The reproducibility and recovery results from a normal range of plasma concentrations are given in Table I. The recovery varied from 90 to 102%. It is recommended that both the methanol standards, spotted directly on the plate, and the extracts from spiked plasma specimens be determined routinely and concurrently with plasma samples from patients containing unknown quantities of propranolol. This practice enables the detection of incomplete extraction or possible contamination of the observed spots with unknown plasma components.

Application to Clinical Samples—This method is applicable to plasma samples from patients (Table II). Large variations in plasma levels between individuals receiving the same dosage of the drug were reconfirmed.

In all of these assays, 1-ml plasma samples were used. Lower volumes can be used successfully by spotting larger aliquots of the redissolved residue.

Table II—Plasma Propranolol Concentration in Patients following Oral Dose of 40-mg Propranolol Tablets

Patient	Propranolol, μg/ml[a]
AG	0.085
PS	0.017
MD	0.107
MM	0.039
BH	0.149
FS	0.103
CS	0.128
PJ	0.045

[a] At 2 hr after dosing in all cases.

The described TLC method has several advantages over previously reported assays; it is specific, highly sensitive, and fast. About 30 samples can be determined within 8 hr by one person. Its specificity is of particular importance for plasma level studies since the drug is separated from possible interfering substances and is determined directly on the separation medium.

The method sensitivity could probably be increased by measuring the fluorescence of propranolol and keeping other parts of the procedure the same. This increase can be achieved readily with the fluorescence attachments supplied for most spectrodensitometers. At present, the UV absorbance method is as sensitive as is needed.

REFERENCES

(1) "The Pharmacological Basis of Therapeutics," L. S. Goodman and A. Gilman, Eds., Macmillan, New York, N.Y., 1971, p. 565.

(2) "Physicians' Desk Reference," Medical Economics Co., Oradell, N.J., 1976, p. 591.

(3) D. G. Shand, E. M. Nuckolls, and J. A. Oates, *Clin. Pharmacol. Ther.*, **11**, 112 (1970).

(4) E. R. Garrett and K. Schnelle, *J. Pharm. Sci.*, **60**, 833 (1971).

(5) P. K. Ambler, B. N. Singh, and M. Lever, *Clin. Chim. Acta*, **54**, 373 (1974).

(6) E. DiSalle, K. M. Baker, S. R. Bareggi, W. D. Watkins, C. A. Chidsey, A. Frigerio, and P. L. Morselli, *J. Chromatogr.*, **84**, 347 (1973).

(7) T. Walle, *J. Pharm. Sci.*, **63**, 1885 (1974).

(8) D. A. Saelens, T. Walle, and P. J. Privitera, *J. Chromatogr.*, **123**, 185 (1976).

(9) T. Walle, J. Morrison, K. Walle, and E. Conradi, *ibid.*, **114**, 351 (1975).

(10) H. Ehrsson, *J. Pharm. Pharmacol.*, **28**, 662 (1976).

(11) R. E. Kates and C. L. Jones, *J. Pharm. Sci.*, **66**, 1490 (1977).

(12) M. Schäfer, H. E. Geissler, and E. Mutschler, *J. Chromatogr.*, **143**, 607 (1977).

(13) T. Walle and T. E. Gaffney, *J. Pharmacol. Exp. Ther.*, **182**, 83 (1972).

ACKNOWLEDGMENTS

Supported by Grant 1-0-101-4501-VC 784-2311 from the University of North Carolina at Chapel Hill.

Substituent Constant for Drug Design Studies Based on Properties of Organic Electron Donor–Acceptor Complexes

ROY FOSTER *, RICHARD M. HYDE ‡x, and DAVID J. LIVINGSTONE *

Received April 11, 1977, from the **Chemistry Department, University of Dundee, Dundee, Scotland,* and the ‡*Wellcome Research Laboratories, Beckenham, Kent, England.* Accepted for publication January 17, 1978.

Abstract □ A new model chemical system based on organic electron donor–acceptor complexes is described. From values of equilibrium constants measured by an NMR technique, a predictable parameter for use in quantitative structure–activity relationship techniques is discussed.

Keyphrases □ Electron donor–acceptor complexes—as model system for structure–activity relationships □ Complexes, electron donor–acceptor—as model system for structure–activity relationships □ Structure–activity relationships—model system based on electron donor–acceptor complexes □ Models, chemical—for structure–activity relationships based on electron donor–acceptor complexes

In quantitative structure–activity relationships, a regression equation relating biological activity to chosen physicochemical properties is derived for a test set of compounds (1). If the properties are predictable, the regression equation may be used to predict the activities of other analogs prior to their synthesis. Physicochemical properties can best be predicted for substitution in the benzene ring, and the availability of accurately measurable substituent constants is crucial to the prediction of biological activity in these circumstances.

BACKGROUND

The approach can be described as semiempirical, and biological activity may be predicted when no mechanistic knowledge of the biosystem is available. Hence, a regression equation should never in itself be regarded as evidence for the involvement of a particular mechanistic step.

Nevertheless, it is desirable that the physicochemical model systems on which the substituent constants are based should be chosen for their relevance to biological systems. The most commonly used substituent constants (2, 3) are π (4), σ (5), F (6), R (6), and the bulk constant R_D (7). Although other model systems have often been used to provide information for predictive equations, they are rarely as useful as π and σ. In the present work, a model system based on the weak intermolecular interactions between organic electron donors and electron acceptors is proposed, and its potential uses are discussed.

Complexes of this type are often referred to as charge transfer complexes (8–10) because of a commonly observed property, *i.e.*, an electronic absorption attributable to an intermolecular charge transfer transition. However, charge transfer forces are only one component of the total molecular interaction in the ground state, and it is this total interaction that is measured and is of interest as a possible model system.

This type of interaction in biosystems (*vide infra*) has received considerable interest (11–13), and it is now proposed that a substituent constant should be defined as a measure of the capacity of a group to modify the stability of an electron donor–acceptor complex. To achieve this aim, it was necessary to choose a suitable model system, and the formation of complexes between a common acceptor and a series of monosubstituted benzenes was selected for this purpose.

The acceptor chosen was 1,3,5-trinitrobenzene (I), a sufficiently good electron acceptor to give measurable equilibrium constants with most monosubstituted benzenes. An aprotic solvent, carbon tetrachloride, was chosen to minimize undesirable solute–solvent hydrogen bonding effects. Such equilibrium constants can be determined by an NMR technique.

The model system should provide substituent constants applicable to a wide variety of environments. Some data demonstrating the effect of changing the common acceptor or the solvent are given under *Results*.

With this model system, a substituent constant, κ, is defined as:

$$\kappa = \log K_X - \log K_H \qquad \text{(Eq. 1)}$$

where K_X is the equilibrium constant for the formation of a complex between I and an x-substituted benzene and K_H is the equilibrium constant for the formation of a complex between I and benzene. The assumption has usually been made that equilibria of this type involve the formation of a 1:1 complex as shown in Scheme I:

$$A + D \rightleftharpoons AD$$

Scheme I

for which an equilibrium constant K_1 may be defined as:

$$K_1 = \frac{[AD]}{[A][D]} = \frac{[AD]}{([A]_0 - [AD])([D]_0 - [AD])} \qquad \text{(Eq. 2)}$$

where concentration terms with a subscript zero represent the total (free and complexed) concentration of that particular component. However, under the normal experimental conditions—*viz.*, $[D]_0 \gg [A]_0$, at least for π-donor–π^*-acceptor interactions the overall equilibrium may be better represented by assuming that not only a 1:1 complex but also a termolecular complex, AD_2, is formed. It may be written as shown in Scheme II:

$$AD + D \rightleftharpoons AD_2$$

Scheme II

and occur in addition to the first equilibrium (Scheme I). This second equilibrium constant, K_2, may be defined as:

$$K_2 = \frac{[AD_2]}{[AD][D]} \qquad \text{(Eq. 3)}$$

If this second equilibrium is ignored and the whole system is treated as if only the first equilibrium occurs, then experimental data yield a value for the association constant that is not equal to K_1. This value is termed the apparent association constant, K_{app}. There is little doubt that many literature values claimed to be K_1 values are really K_{app} values. Thus, Eq. 1 should be more correctly written as:

$$\kappa = \log_{10} K_{app,x} - \log_{10} K_{app,H} \qquad \text{(Eq. 4)}$$

If the difference between the chemical shift of the proton singlet absorption of I in a solution where the donor concentration is $[D]_0$ and the chemical shift of I in a solution containing no donor is Δ, it may be shown that (14):

$$\Delta/[D]_0 = -K_{app}\Delta + K_{app}\Delta_0 \qquad \text{(Eq. 5)}$$

where Δ_0 is the chemical shift of the measured nucleus that the complex would have in solution, if there were no dissociation, relative to the chemical shift of the same nucleus in completely uncomplexed I in solution.

A plot of $\Delta/[D]_0$ *versus* Δ gives a straight line of gradient $-K_{app}$ and an intercept with the ordinate of $(K_{app}\Delta_0)$, from which K_{app} and Δ_0 may be evaluated. In practice, a least-squares computer program is used to obtain these two parameters.

The determination of K_{app} for complexes formed between electron donors and the acceptor 2,3,5,6-tetrafluoro-*p*-benzoquinone (II) may be similarly determined from observations of the chemical shift of the ^{19}F-singlet absorption of II.

EXPERIMENTAL

The values of K_{app} were obtained from measurements of the variation in the line positions of a nuclear magnetic resonance in the acceptor as

0022-3549/78/0900-1310$01.00/0
© 1978, American Pharmaceutical Association

Table I—Benzene Concentrations ($[D]_0$) and Chemical Shift Differences (Δ) of I

$[D]_0 \times 10^2$, moles/kg	Δ, Hz	$\Delta/[D]_0$, Hz kg/mole
4.00	2.3	57.5
11.76	6.5	55.27
24.98	13.1	52.24
49.18	23.0	46.77
57.47	25.9	45.07
33.57	17.0	50.64
18.75	10.0	53.33
40.60	19.6	48.28
	$K_{app} = 0.53 \pm 0.06$	
	$\Delta_0 = 112 \pm 12$	

Table II—Benzene Concentrations ($[D]_0$) and Chemical Shift Differences (Δ) of I

$[D]_0 \times 10^2$, moles/kg	Δ, Hz	$\Delta/[D]_0$, Hz kg/mole
8.11	4.6	56.72
21.78	11.5	52.80
43.19	20.7	47.93
30.22	15.2	50.30
38.78	18.8	48.48
17.59	9.5	54.01
56.80	25.7	45.25
	$K_{app} = 0.54 \pm 0.06$	
	$\Delta_0 = 109 \pm 11$	

the concentration of the electron donor was varied under the conditions $[D]_0 \gg [A]_0$.

Solutions of different donor concentrations (~0.05–0.8 *M*), but of approximately constant acceptor concentration (~10^{-3} *M*), were prepared gravimetrically using a stock solution of acceptor, with all concentrations of donor being expressed in moles per kilogram. The carbon tetrachloride solutions also contained 2% (v/v) tetramethylsilane. Measurements were made at 90.0000 MHz for the ^{1}H-resonances and at 63.5305 MHz for the ^{19}F-resonances.

The line positions of the ^{1}H-resonance of I and the ^{19}F-resonance of II were measured four times with respect to the internal reference for each solution. Where the solvent was carbon tetrachloride, tetramethylsilane was used as the internal reference; for cyclohexane solutions, the ^{1}H-resonance of the solvent itself was used. The arithmetic mean of the measurements of the line position for a given solution was taken; in all cases, the individual line positions were within ±0.1 Hz of this mean.

Under the conditions of these experiments, the values of K_{app} were independent of the particular internal reference used (15).

All measurements were made at 33.4 ± 0.1°. This temperature was maintained by a built-in temperature control and checked before and after each set of measurements with an external copper–constantan thermocouple in a dummy tube. At least two separate determinations of K_{app} were made for each system. Tables I and II contain typical data for two such determinations for the benzene–I system.

RESULTS

Tables I and II show data and the computed parameters for two separate determinations of K_{app} for the benzene–I system in carbon tetrachloride at 33.4°. The combined data gave the following values of K_{app} and Δ_0 by least-squares treatment: $K_{app} = 0.53 \pm 0.03$ kg/mole and $\Delta_0 = 111 \pm 7$ Hz.

In Fig. 1, the equilibrium constants, K_{app}, for complex formation between I and a set of monosubstituted benzenes are compared with constants for complex formation between II and the same monosubstituted benzenes in the same solvent. The line shown is the least-squares fit straight line ($r = 0.97$). A comparison of equilibrium constants for interactions between I and a set of monosubstituted benzenes in carbon tetrachloride with the corresponding constants for the interactions in cyclohexane is shown in Fig. 2. The least-squares fit straight line has a correlation coefficient of 0.99.

Table III shows the values of K_{app}, $\log_{10}K_{app}$, and κ obtained for 26 monosubstituted benzenes in the chosen model system. Table IV shows the results of a comparison of κ with four commonly used substituent constants.

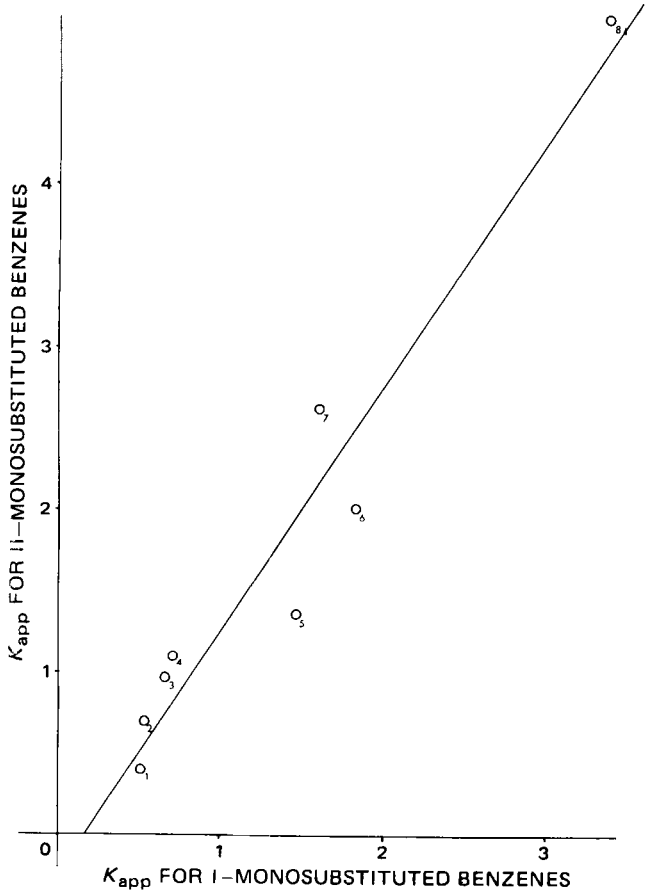

Figure 1—*Correlation between II complexes and the corresponding I complexes with the following monosubstituted benzenes: 1, Cl; 2, H; 3, CH_3; 4, CH_2CH_3; 5, OCH_3; 6, $COOCH_2CH_3$; 7, $COCH_3$; and 8, $N(CH_2CH_3)_2$.*

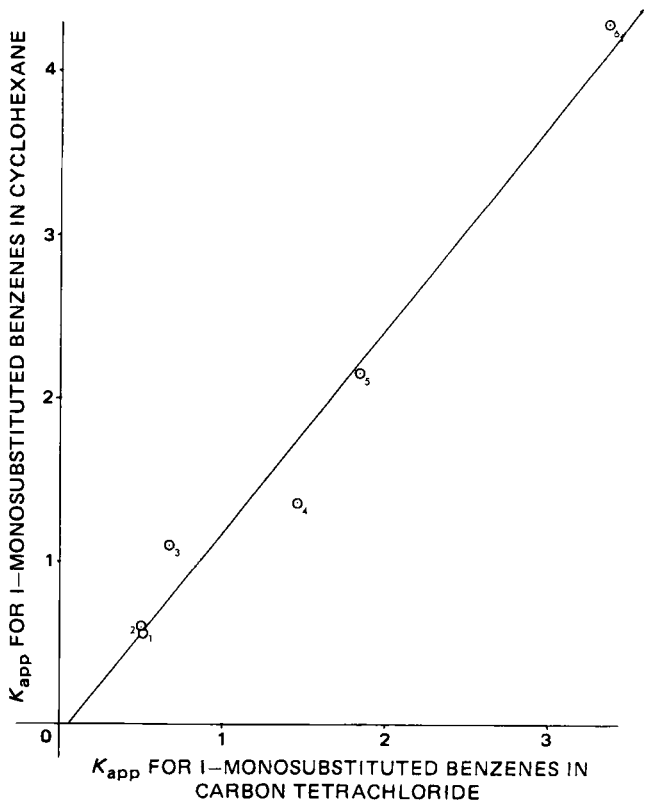

Figure 2—*Correlation between I complexes in cyclohexane and the corresponding complexes in carbon tetrachloride with the following monosubstituted benzenes: 1, Cl; 2, H; 3, CH_3; 4, OCH_3; 5, $COOCH_2CH_3$; and 6, $N(CH_2CH_3)_2$.*

Table III—Measured Association Constants (Moles per Kilogram) for I Complexes of Monosubstituted Benzene Donors in Carbon Tetrachloride at 33.5°

Substituent	K_{app}	$Log_{10}K_{app}$	κ
H[a]	0.53	−0.28	0.00
CH_3[a]	0.67	−0.17	0.11
CH_2CH_3[b]	0.71	−0.15	0.13
$CH_2CH_2CH_3$[b]	0.58	−0.24	0.04
$CH(CH_3)_2$[b]	0.61	−0.22	0.06
CF_3[c]	0.43	−0.37	−0.09
OCH_3[e]	1.46	0.16	0.44
NH_2[d]	2.38	0.38	0.66
NO_2[c]	0.96	−0.02	0.26
Br[e]	0.53	−0.28	0.00
CN[c]	0.90	−0.05	0.23
$CH_2CH_2CH_2CH_3$[b]	0.62	−0.21	0.07
$C(CH_3)_3$[b]	0.45	−0.35	−0.07
C_6H_5[e]	1.48	0.17	0.45
OH[e]	1.31	0.12	0.40
OCH_2CH_3[e]	1.25	0.10	0.38
CHO[e]	1.14	0.06	0.34
$COCH_3$[e]	1.60	0.20	0.48
$COOCH_3$[e]	1.65	0.22	0.50
$COOCH_2CH_3$[e]	1.83	0.26	0.54
$NHCH_3$[d]	2.80	0.45	0.73
$NHCH_2CH_3$[d]	3.20	0.51	0.79
SCH_3[e]	1.31	0.12	0.40
F[e]	0.36	−0.44	−0.16
Cl[e]	0.51	−0.29	−0.01
I[e]	0.54	−0.27	−0.01

[a] From Ref. 14. [b] From Ref. 16. [c] From Ref. 17. [d] From Ref. 18. [e] Present work.

DISCUSSION

It is apparent from the high linear correlation shown in Fig. 1 that the relative values of equilibrium constants of donors are independent of the choice between acceptor I and acceptor II. Likewise, Fig. 2 indicates that the relative values of the equilibrium constants are independent of the particular "inert" solvent used. Thus, it is possible to change both solvent and common acceptor while still retaining a substituent constant well correlated with the original. This finding suggests that the values of κ do not reflect undesirable specific solvent–solute or donor–acceptor interactions to an unacceptable extent.

In addition to the validity of the model system, a substituent constant intended for use in quantitative structure–activity relationships should be judged by four criteria prior to its adoption. These criteria are: plausibility, predictability, availability, and orthogonality. The substituent constant κ is now considered in the light of these criteria.

Plausibility—The involvement of electron donor–acceptor interactions in molecular processes of relevance to the biophase was suggested previously (11, 12, 19). In the work of Cilento and Tedeschi (20), for example, on the system glyceraldehyde 3-phosphate dehydrogenase–NAD, absorptions assignable to charge transfer transitions were observed in the UV spectrum. There is also evidence of the relevance of electron donor–acceptor interactions to some processes involving biological macromolecules and exogenous species (*i.e.*, drug molecules). Hetnarski and O'Brien (21) postulated the involvement of electron donor–acceptor interactions in the action of some arylmethyl carbamates as inhibitors of cholinesterase. Measurements of the UV spectra of the compounds themselves provided results consistent with this theory.

Large numbers of naturally occurring moieties exist whose properties suggest their suitability for participation in electron donor–acceptor complexes. Of the protein residues alone, potential electron donors are aspartate, glutamate, cystine, methionine, and tyrosine; potential electron acceptors are cysteine, arginine, and lysine. Other groups such as histidine, asparaginine, and tryptophan may act as both electron donors and acceptors.

Interactions between a drug molecule and any of these species could, in principle, be involved in either the formation of a drug–receptor complex or drug transport to the site of action. Although the possibility of such a direct relationship between molecular processes in the biosystem and the physicochemical model is desirable, it should not be a *sine qua non* in assessing plausibility. It would have been sufficient to justify an electron donor–acceptor parameter if it could merely be regarded as a "probe" for more fundamental properties, *i.e.*, if it could be postulated that fundamental properties contributing to log $K_{app}(\kappa)$ might also be of relevance to biological molecular interactions.

In both respects, there are grounds to regard κ as a highly plausible substituent constant for quantitative structure–activity relationship studies.

Table IV—Results of Regression Analysis: Correlation Matrix for the Parameter Set for the 26 Substituents in Table III[a]

	F	R_D	R
R_D	−0.37		
R	0.34	0.05	
π	−0.22	0.58	0.39

[a] The best equations of the analysis are:

$\kappa = -0.186\ (0.05)\pi + 0.34$
$r = 0.634 \quad F = 16.09$

$\kappa = -0.330\ (0.03)\pi + 0.037\ (0.004)R_D + 0.059$
$r = 0.935 \quad F = 79.68$

$\kappa = -0.323\ (0.03)\pi - 0.036\ (0.07)R$
$0.037\ (0.004)R_D + 0.054$
$r = 0.936 \quad F = 51.42$

Predictability—The κ values described are derived from monosubstituted benzenes. Their applicability to polysubstituted ring systems has not yet been assessed. Early results indicate that relative log K_{app} values for members of some congeneric series may be derivable from the original data base using simple additivity rules. This may be partly attributable to the fact that the π-electron system as a whole contributes to binding, whereas the effect of the substituent relative to a particular position in the ring is important for a quantity such as σ. The treatment of some diverse sets of electron donor–acceptor complex data by Charton (22–24) using linear free energy relationships is encouraging in this context.

Availability—Values of $\log_{10}K_{app}$ (hence κ) can be easily and accurately measured using an NMR spectrometer. Substituent constants based on 26 monosubstituted benzenes are quoted here, and work is being performed on polysubstituted benzenes.

Orthogonality—To assess whether a new parameter contributes anything extra to existing parameter sets, regression analyses must be performed. If the new parameter correlates with a single well-used parameter, then it clearly has little to offer. If it is completely orthogonal even to a linear combination of all of the parameters in a working set (3), then it can be used as an addition to the set. If, however, it is uncorrelated with any one parameter but correlated with a linear combination of two or more, then it might be considered as a replacement for the "two or more" in situations where a paucity of compounds in the test set limits the number of parameters.

A commonly used set of parameters is: π, derived from octanol–water partition coefficients (4); F and R, field and resonance components, respectively, of Hammett's σ constants (6); and R_D, the molar refraction (7), which is currently used as a bulk parameter.

Regression analysis was performed on the data for the substituent set in Table III to assess the orthogonality of κ with respect to π, F, R, and R_D (Table IV). For the set of 26 substituted benzenes studied, κ is well correlated with a linear combination of π and R_D.

The significance of this equation is such that κ may be said to contribute little extra information to the linear combination of π and R_D for this data set. Thus, in general, κ would not be used as an addition to the above-mentioned four-parameter set unless a correlation matrix for a real subset of compounds indicated the contrary. However, for situations where the number of parameters that may be used is restricted by statistical considerations, κ might be considered as a replacement for π and R_D. Thus, κ–σ regressions may be of value in these circumstances.

REFERENCES

(1) C. Hansch and T. Fujita, *J. Am. Chem. Soc.*, **86**, 1616 (1964).

(2) C. Hansch, A. Leo, S. H. Unger, K. H. Kim, D. Nikaitani, and E. J. Lien, *J. Med. Chem.*, **16**, 1207 (1973).

(3) F. E. Norrington, R. M. Hyde, S. G. Williams, and R. Wootton, *J. Med. Chem.*, **18**, 604 (1975).

(4) T. Fujita, J. Iwasa, and C. Hansch, *J. Am. Chem. Soc.*, **86**, 5175 (1964).

(5) L. P. Hammett, "Physical Organic Chemistry," McGraw-Hill, New York, N.Y., 1940, pp. 184–199.

(6) C. G. Swain and E. C. Lupton, Jr., *J. Am. Chem. Soc.*, **90**, 4328 (1968).

(7) A. I. Vogel, *J. Chem. Soc.*, **1948**, 607, and following papers.

(8) R. Foster, "Organic Charge-Transfer Complexes," Academic, New York, N.Y., 1969.

(9) R. Foster and C. A. Fyfe, in "Progress in Nuclear Magnetic Res-

onance Spectroscopy," vol. 4, J. W. Emsley, J. Feeney, and L. H. Sutcliffe, Eds., Pergamon, New York, N.Y., 1969, chap. 1.
(10) R. Foster, *Ind. Chim. Belg.*, **37**, 547 (1972).
(11) P. H. Doukas, in "Drug Design," vol. V, E. J. Ariens, Ed., Academic, New York, N.Y., 1975, chap. 4.
(12) A. Szent-Gyorgyi, "Introduction to a Submolecular Biology," Academic, New York, N.Y., 1960.
(13) A. Szent-Gyorgyi, "Bioelectronics," Academic, New York, N.Y., 1968, chaps. 2 and 3.
(14) R. Foster and C. A. Fyfe, *Trans. Faraday Soc.*, **61**, 1626 (1965).
(15) R. Foster and D. R. Twiselton, *Recl. Trav. Chim. Pays-Bas Belg.*, **89**, 1020 (1970).
(16) P. H. Emslie, R. Foster, I. Horman, J. W. Morris, and D. R. Twiselton, *J. Chem. Soc. B*, **1969**, 1161.
(17) J. W. Morris, Ph.D. thesis, University of St. Andrews, Scotland, 1968.
(18) R. Foster and J. W. Morris, *J. Chem. Soc. B*, **1970**, 703.
(19) S. Shifrin, *Biochim. Biophys. Acta*, **81**, 205 (1964).
(20) G. Cilento and P. Tedeschi, *J. Biol. Chem.*, **236**, 907 (1961).
(21) B. Hetnarski and R. D. O'Brien, *J. Med. Chem.*, **18**, 29 (1975).
(22) M. Charton, *J. Org. Chem.*, **31**, 2991 (1966).
(23) *Ibid.*, **31**, 2996 (1966).
(24) *Ibid.*, **33**, 3878 (1968).

ACKNOWLEDGMENTS

The authors thank Dr. P. J. Goodford for advice and criticism and Mr. J. A. Chudek for assistance.

Interactions between Polymyxin B and Divalent Nickel in Near-Neutral Aqueous Media

MORTON L. BARR and KENNETH KUSTIN ˣ

Received September 12, 1977, from the *Department of Chemistry, Brandeis University, Waltham, MA 02154.* Accepted for publication January 24, 1978.

Abstract □ Stopped-flow and temperature-jump methods were used to determine the complexation constants for the reactions of polymyxin B with Ni^{2+} at 25° and 0.1 *M* ionic strength [$N(CH_3)_4NO_3$]. At pH 6.4–7.1 and with the ligand in excess, the formation of a 1:1 metal–ligand complex according to the reaction scheme $Ni^{2+} + H_3L^{3+} \rightleftarrows NiH_3L^{5+}$ and $Ni^{2+} + H_4L^{4+} \rightleftarrows NiH_3L^{5+} + H^+$ (k_1 and k_1' are respective forward rate constants; k_{-1} and k_{-1}' are respective reverse rate constants) is consistent with the data. The determined rate constants are $k_1 = (3.8 \pm 0.2) \times 10^3$ M^{-1} sec^{-1} and $k_{-1} = (1.2 \pm 0.1) \times 10^{-1}$ sec^{-1}. Upper and lower limits for k_1' of 2.4 and 0.6 M^{-1} sec^{-1}, respectively, were set. The stability constant ($K_1 = k_1/k_{-1}$) of the 1:1 complex determined by potentiometric titration is $(3.3 \pm 0.1) \times 10^4$ *M*; the four pKa values of polymyxin B agree with the literature values. At pH 7.1–7.9 and with the metal ion in excess, the described scheme and a binuclear complex reaction step, $Ni^{2+} + NiHL^{3+} \rightleftarrows Ni_2HL^{5+}$ (k_2 is the forward rate constant; k_{-2} is the reverse rate constant), fit the data. Upper and lower limits for k_2 of 1×10^4 and 3×10^3 M^{-1} sec^{-1}, respectively, were set for the formation of the binuclear complex. Comparison with model system complex formation rate constants indicates that the forward rate constants evaluated in this study are enhanced. This effect may be interpreted in terms of an internal conjugate base mechanism.

Keyphrases □ Polymyxin B—complexation with nickel(II) in aqueous media, effect of pH and ligand concentration □ Nickel(II)—complexation with polymyxin B in aqueous media, effect of pH and ligand concentration □ Complexation—polymyxin B and nickel(II) in aqueous media, effect of pH and ligand concentration □ Antibacterials—polymyxin B, complexation with nickel(II) in aqueous media, effect of pH and ligand concentration □ Metals—nickel(II), complexation with polymyxin B in aqueous media, effect of pH and ligand concentration

Polymyxin B is a surface-active polypeptide antibiotic exhibiting potent bactericidal activity against most Gram-negative bacilli (1). The addition of polymyxin B to cell suspensions of these bacilli results in a leakage from the cells of pentose, phosphate, and substances with absorption maxima at 260 nm (1, 2). The mechanism of action is thought to involve combination of the antibiotic with charged groups on the cell membrane surface, resulting in disorganization of the membrane structure (1–3). The bactericidal activity of polymyxin B is influenced strongly by various metal ions in several complicated modes of interaction (1, 2).

The proposed structure of polymyxin B is shown in Structure I and Fig. 1 (4, 5). Polymyxin B is a cyclic hexapeptide with a tripeptide side chain *N*-acylated by 6-methyloctanoic acid (polymyxin B_1) or isooctanoic acid (polymyxin B_2); it is a mixture of B_1 and B_2 in the ratio 65:35, respectively (6). Each component has one D-amino

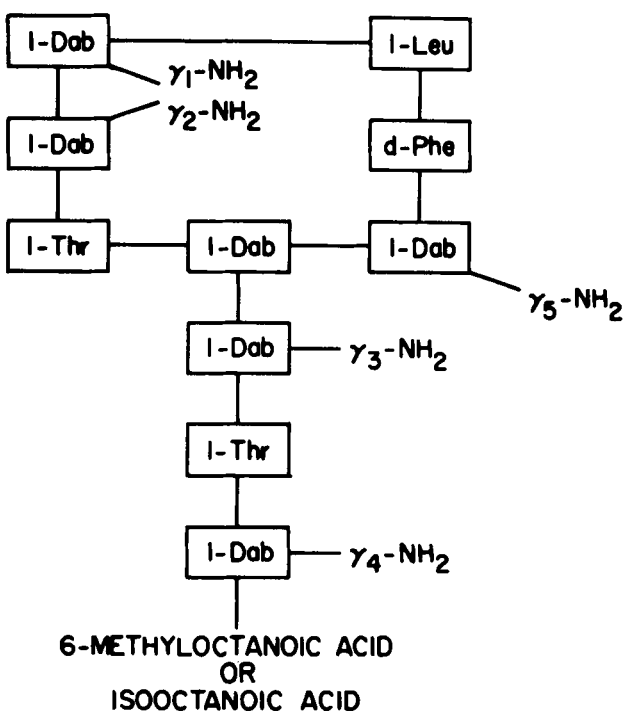

I: Amino acid sequence of polymyxin B. Key: l-Dab, *l*-α,γ-diaminobutyric acid; l-Thr, *l*-threonine; d-Phe, *d*-phenylalanine; and l-Leu, *l*-leucine.

0022-3549/78/0900-1313$01.00/0
© 1978, American Pharmaceutical Association

onance Spectroscopy," vol. 4, J. W. Emsley, J. Feeney, and L. H. Sutcliffe, Eds., Pergamon, New York, N.Y., 1969, chap. 1.
(10) R. Foster, *Ind. Chim. Belg.*, **37**, 547 (1972).
(11) P. H. Doukas, in "Drug Design," vol. V, E. J. Ariens, Ed., Academic, New York, N.Y., 1975, chap. 4.
(12) A. Szent-Gyorgyi, "Introduction to a Submolecular Biology," Academic, New York, N.Y., 1960.
(13) A. Szent-Gyorgyi, "Bioelectronics," Academic, New York, N.Y., 1968, chaps. 2 and 3.
(14) R. Foster and C. A. Fyfe, *Trans. Faraday Soc.*, **61**, 1626 (1965).
(15) R. Foster and D. R. Twiselton, *Recl. Trav. Chim. Pays-Bas Belg.*, **89**, 1020 (1970).
(16) P. H. Emslie, R. Foster, I. Horman, J. W. Morris, and D. R. Twiselton, *J. Chem. Soc. B*, **1969**, 1161.
(17) J. W. Morris, Ph.D. thesis, University of St. Andrews, Scotland, 1968.
(18) R. Foster and J. W. Morris, *J. Chem. Soc. B*, **1970**, 703.
(19) S. Shifrin, *Biochim. Biophys. Acta*, **81**, 205 (1964).
(20) G. Cilento and P. Tedeschi, *J. Biol. Chem.*, **236**, 907 (1961).
(21) B. Hetnarski and R. D. O'Brien, *J. Med. Chem.*, **18**, 29 (1975).
(22) M. Charton, *J. Org. Chem.*, **31**, 2991 (1966).
(23) *Ibid.*, **31**, 2996 (1966).
(24) *Ibid.*, **33**, 3878 (1968).

ACKNOWLEDGMENTS

The authors thank Dr. P. J. Goodford for advice and criticism and Mr. J. A. Chudek for assistance.

Interactions between Polymyxin B and Divalent Nickel in Near-Neutral Aqueous Media

MORTON L. BARR and KENNETH KUSTIN ˣ

Received September 12, 1977, from the *Department of Chemistry, Brandeis University, Waltham, MA 02154.* Accepted for publication January 24, 1978.

Abstract □ Stopped-flow and temperature-jump methods were used to determine the complexation constants for the reactions of polymyxin B with Ni^{2+} at 25° and 0.1 *M* ionic strength [$N(CH_3)_4NO_3$]. At pH 6.4–7.1 and with the ligand in excess, the formation of a 1:1 metal–ligand complex according to the reaction scheme $Ni^{2+} + H_3L^{3+} \rightleftarrows NiH_3L^{5+}$ and $Ni^{2+} + H_4L^{4+} \rightleftarrows NiH_3L^{5+} + H^+$ (k_1 and k_1' are respective forward rate constants; k_{-1} and k_{-1}' are respective reverse rate constants) is consistent with the data. The determined rate constants are $k_1 = (3.8 \pm 0.2) \times 10^3$ M^{-1} sec^{-1} and $k_{-1} = (1.2 \pm 0.1) \times 10^{-1}$ sec^{-1}. Upper and lower limits for k_1' of 2.4 and 0.6 M^{-1} sec^{-1}, respectively, were set. The stability constant ($K_1 = k_1/k_{-1}$) of the 1:1 complex determined by potentiometric titration is $(3.3 \pm 0.1) \times 10^4$ *M*; the four pKa values of polymyxin B agree with the literature values. At pH 7.1–7.9 and with the metal ion in excess, the described scheme and a binuclear complex reaction step, $Ni^{2+} + NiHL^{3+} \rightleftarrows Ni_2HL^{5+}$ (k_2 is the forward rate constant; k_{-2} is the reverse rate constant), fit the data. Upper and lower limits for k_2 of 1×10^4 and 3×10^3 M^{-1} sec^{-1}, respectively, were set for the formation of the binuclear complex. Comparison with model system complex formation rate constants indicates that the forward rate constants evaluated in this study are enhanced. This effect may be interpreted in terms of an internal conjugate base mechanism.

Keyphrases □ Polymyxin B—complexation with nickel(II) in aqueous media, effect of pH and ligand concentration □ Nickel(II)—complexation with polymyxin B in aqueous media, effect of pH and ligand concentration □ Complexation—polymyxin B and nickel(II) in aqueous media, effect of pH and ligand concentration □ Antibacterials—polymyxin B, complexation with nickel(II) in aqueous media, effect of pH and ligand concentration □ Metals—nickel(II), complexation with polymyxin B in aqueous media, effect of pH and ligand concentration

Polymyxin B is a surface-active polypeptide antibiotic exhibiting potent bactericidal activity against most Gram-negative bacilli (1). The addition of polymyxin B to cell suspensions of these bacilli results in a leakage from the cells of pentose, phosphate, and substances with absorption maxima at 260 nm (1, 2). The mechanism of action is thought to involve combination of the antibiotic with charged groups on the cell membrane surface, resulting in disorganization of the membrane structure (1–3). The bactericidal activity of polymyxin B is influenced strongly by various metal ions in several complicated modes of interaction (1, 2).

The proposed structure of polymyxin B is shown in Structure I and Fig. 1 (4, 5). Polymyxin B is a cyclic hexapeptide with a tripeptide side chain *N*-acylated by 6-methyloctanoic acid (polymyxin B_1) or isooctanoic acid (polymyxin B_2); it is a mixture of B_1 and B_2 in the ratio 65:35, respectively (6). Each component has one D-amino

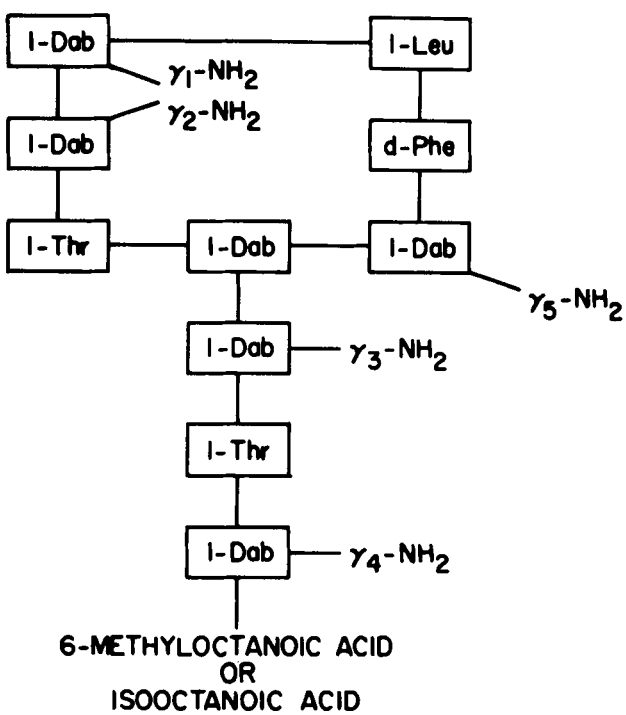

I: Amino acid sequence of polymyxin B. Key: l-Dab, *l*-α,γ-diaminobutyric acid; l-Thr, *l*-threonine; d-Phe, *d*-phenylalanine; and l-Leu, *l*-leucine.

0022-3549/78/0900-1313$01.00/0
© 1978, American Pharmaceutical Association

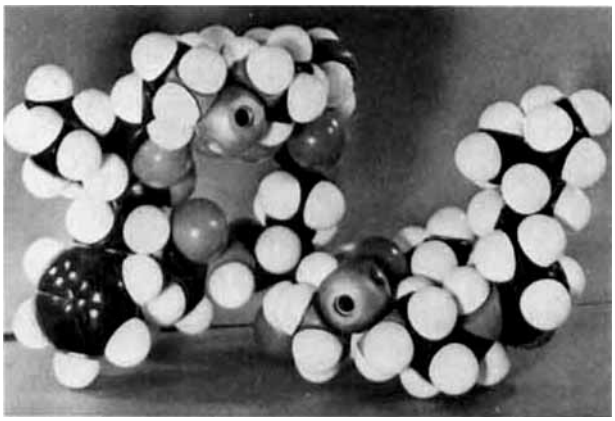

Figure 1—*Corey–Pauling model of one configuration for the bimetallic polymyxin B complex. The metal ions are represented by the gray octahedral units.*

acid (phenylalanine) and six residues of α,γ-diaminobutyric acid, which are responsible for its complexation behavior toward the divalent transition metal ions. From this behavior, it will be shown that polymyxin B represents a physiologically active analog of the simple polyamines, of which the complexation properties with transition metal ions are well known (7, 8).

EXPERIMENTAL

Reagent grade nickel(II) nitrate hexahydrate[1], phenol red (phenolsulfonphthalein), and *p*-nitrophenol[2] were used without further purification. Tetramethylammonium nitrate[2] was used as the supporting electrolyte in all studies, because preliminary investigations indicated complex formation to occur between polymyxin and the alkali metal ions. The nitrate salt was twice recrystallized from 75% aqueous ethanol and dried *in vacuo* under phosphorus pentoxide.

Polymyxin B was obtained commercially as the sulfate[3]; the peptide was dissolved in a minimum amount of distilled water, precipitated as the free base by passing gaseous ammonia through the solution at −5°, centrifuged, filtered on a fritted Büchner funnel, and washed three times with cold water. The light, fluffy white precipitate was then suspended in water and twice lyophilized. The stoichiometric amount of hydrochloric acid was added, and the solution was again twice lyophilized.

The resulting pentahydrochloride migrated identically with an authentic sample of polymyxin B[4] when placed on a thin-layer plate in the solvent system 1-butanol–pyridine–acetic acid–water (30:20:5:24). Both materials migrated as single components. The optical rotatory dispersion curves of the nickel complexes of the two materials also compared favorably in the 350–600-nm region. The chloride content of polymyxin B (pentahydrochloride) was confirmed by the Volhard method. Elemental analysis corresponded to $C_{56}H_{98}N_{16}$, as predicted.

In addition to the characteristic UV absorption near 260 nm, polymyxin B revealed an anomalous absorption tailing into the visible region, with a maximum near 280 nm. Thus, solutions of polymyxin with a concentration greater than 10^{-3} *M* exhibited a yellow hue. This apparent impurity was not detected within the experimental error of elemental analysis and was not removed by treatment of polymyxin B on chromatographic columns of Sephadex G-15 or G-25, Biorex-70 cation-exchange resin, and diethylaminoethylcellulose anion-exchange resin. Attempts to remove this impurity by countercurrent distribution in 1-butanol–pyridine–acetic acid–water (8:2:1:9) (5), in which polymyxins B_1 and B_2 were separated, were unsuccessful. Emission spectra of the purified pentahydrochloride confirmed the absence of metal ions. Therefore, if an impurity was indeed present, its concentration was sufficiently small not to preclude the experimental studies undertaken.

Stock solutions of nickel nitrate and indicators were prepared by weight. The nickel content of the stock solutions was confirmed by complexometric titration with ethylenediaminetetraacetic (edetic) acid

[1] Fisher.
[2] Eastman.
[3] Calbiochem.
[4] Supplied by Dr. R. O. Studer, Hoffmann–La Roche, Basel, Switzerland.

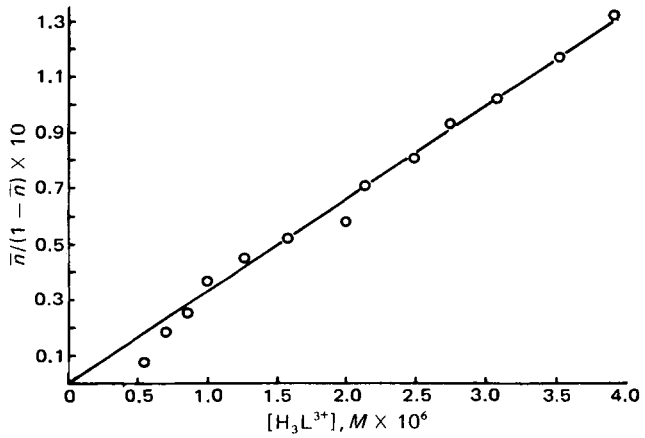

Figure 2—*Plot of* $\bar{n}/(1-\bar{n})$ versus *free ligand species concentration. The straight line was obtained by least-squares data analysis. (Data points close to the origin appear to lie on a curve. However, these points are collected at the start of the titration and have a higher intrinsic relative error. The apparent curvature actually reflects greater scatter and not a systematic trend.)*

with murexide as the indicator (9). Solutions to be studied were prepared by mixing the desired volumes of stock solutions with weighed amounts of polymyxin B and tetramethylammonium nitrate. All pH values were measured to ±0.02 pH unit. Hydrogen-ion concentrations were obtained by dividing the measured hydrogen-ion activity by $\gamma_{\pm} = 0.739$ from the Davies equation (10). The temperature in all experiments was 25 ± 1°. Commercially available distilled water was used in all experiments.

The stopped-flow and temperature-jump apparatuses were described previously (11–14). In the stopped-flow studies, one syringe contained polymyxin solution and the other contained Ni(II). Both syringes contained the same concentrations of the supporting electrolyte, indicator, and hydrogen ion (adjusted by dropwise addition of dilute acid and base). The pH values reported were determined shortly after mixing. Blank experiments of *p*-nitrophenol with nickel and polymyxin gave no discernible effects in the concentration and time ranges studied. However, blank experiments yielded relaxation effects on the temperature-jump apparatus with phenol red and polymyxin, as well as with phenol red and nickel. The former effect can be attributed to complexation of the polypeptide with the indicator, perhaps as in the case of bovine serum albumin with phenol red (15). Nickelous ion complexes with certain pH indicators (16, 17).

The acid dissociation constants of polymyxin B and the stability constant of the polymyxin–Ni(II) complex were determined by potentiometric titration using the Bjerrum technique (18, 19).

RESULTS

Equilibrium Studies—Polymyxin B has five titratable ammonium protons; these amino groups serve as metal binding sites. The number of ligand protons displaced during complexation with nickel cannot be determined clearly in a restricted pH titration range. Furthermore, formation of binuclear and higher order nickel complexes with polymyxin is possible.

Consequently, an unambiguous analysis of the titration data for the nickel–polymyxin system is difficult to achieve. Moreover, both nickel(II) and copper(II) ions, when complexed to di- and oligopeptides, labilize peptide protons (20–23). This effect also was observed in the stability constant determination of Cu(II)–polymyxin (24). Thus, any interpretation of the titration data must consider these factors as in the following treatment.

Under the conditions of excess polymyxin and $6.3 < pH < 7.1$, the initial assumption made was that only a 1:1 complex is formed in which nickel is bound either to H_3L^{3+} or H_2L^{2+}. This assumption is based on two considerations. It is very unlikely that H_5L^{5+} and H_4L^{4+} will bind strongly to nickelous ion on grounds of electrostatic repulsion. Model studies strongly suggest that ring strain and rotational barriers preclude a complexed species in which nickel is simultaneously attached to four or five γ-NH_2 groups.

For the 1:1 complex system, a plot of $\bar{n}/(1-\bar{n})$ *versus* free binding species concentration (where $\bar{n}$ is the average number of ligand molecules bound per metal ion) yields a slope equal to the stability constant. Attempts were also made to fit the data with higher order and binuclear

Table I—Equilibrium Data at 25° and 0.1 *M* Ionic Strength [a]

Acid Dissociation of Polymyxin B			
pKa_1	pKa_2	pKa_3	pKa_4
7.99 (±0.01)	8.71 (±0.02)	9.09 (±0.04)	9.43 (±0.03)

Acid Dissociation of Indicators [b]	
Indicator	K_{In}, *M*
Phenol red	1.26×10^{-8}
p-Nitrophenol	7.08×10^{-8}

[a] Stability constant of polymyxin B–Ni(II) complex ($\log K_1$) = 4.52 (±0.01). [b] I. M. Kolthoff, *J. Phys. Chem.*, **34**, 1466 (1930).

complexes. Within experimental error, the values of the equilibrium quotients corresponding to these complexes approach zero. The best fit of calculated *versus* observed values of $\bar{n}$ was obtained when the binding form of polymyxin was H_3L^{3+} and not H_4L^{4+} or H_2L^{2+}. A plot of $\bar{n}/(1-\bar{n})$ *versus* $[H_3L^{3+}]$ is shown in Fig. 2, from which $K_1 = (3.3 \pm 0.1) \times 10^4\ M^{-1}$.

The relatively simple system consisting of protonated ligand, free metal ion, and complex does not fit the data above pH 7.1. The assumption of higher order (*e.g.*, bis) complexes does not improve the fit. It is reasonable to assume that, as the pH is raised, new nickel(II) species will be present. However, inclusion of these species invalidates the Bjerrum method, necessitating that several assumptions be made to analyze the data.

As a consequence of the ligand's relatively high affinity for the metal ion and its excess concentration, hydrolyzed nickel(II) is not important when $\bar{n} = 1$. Data fitting was then attempted with binuclear and deprotonated complexes, singly and together. For a deprotonated complex, an adjustable parameter was introduced, representing the relative concentrations of deprotonated and protonated complex species. The agreement between observed and calculated $\bar{n}$ was not improved by inclusion of adjustable parameters, and quantitative equilibrium data for the system nickel(II)–polymyxin above pH 7.1 were not obtained.

Unlike the stability constant determination, the measurement of the acid dissociation constants of polymyxin was straightforward. In the pH titration range studied (6.0–10.0), four acid dissociation constants were determined, leading to formation of the fully deprotonated peptide. The results for the pKa and stability constant determinations are reported in Table I.

Kinetic Studies—The conditions chosen for the initial kinetic studies allow the least ambiguous calculation of equilibrium concentrations necessary for interpretation of the data. These calculations were performed with the Newton–Raphson iteration method. Less desirable, but useful, are experiments in which pseudo-first-order conditions prevail and the metal ion is in excess. The metal-ion concentration is approximately equal to the total stoichiometric amount, and the concentrations of other species are calculated accordingly.

For the stopped-flow data, evaluation was achieved by employing close-to-equilibrium analysis. Therefore, only the last portion of each reaction trace was used in determining the relaxation time, τ. Use was made of the stoichiometric equilibrium constants in Table I and the concentrations in Table II in calculating these relaxation times. The experimental values of τ (Table II) were obtained by averaging at least five experimental values (12, 14). The deviations were usually less than ±10% in these averaged relaxation times. The exponentiality of the last portion of the reaction was confirmed by semilogarithmic plots of concentration *versus* time. Long-term stability in the kinetic (and also the equilibrium) studies was established by the absence of baseline drift for times longer than the lapsed time between solution preparation and data collection.

The most favorable experimental conditions are slightly acid pH and excess ligand since the equilibrium parameters under these conditions are known. For these solutions, the reaction consistent with the stopped-flow data is shown in Scheme I.

$$\begin{array}{ccccc} Ni^{2+} + H_3L^{3+} & \underset{k_{-1}}{\overset{k_1}{\rightleftharpoons}} & NiH_3L^{5+} & & \\ K_{a0}\ \Big\downarrow & & & & \\ Ni^{2+} + H_4L^{4+} & \underset{k'_{-1}}{\overset{k'_1}{\rightleftharpoons}} & NiH_3L^{5+} & + & H^+ \end{array}$$

Scheme I

Scheme I is characterized by a single relaxation time for which:

$$1/\tau S = k'_1 + k_1 R/S \qquad \text{(Eq. 1)}$$

Table II—Stopped-Flow Data at 25° and 0.1 *M* Ionic Strength [a]

$[Ni(II)]_0$ [b] $\times 10^3\ M$	$[Polymyxin]_0$ $\times 10^3\ M$	pH	τ, sec, Experimental	τ, sec, Calculated
0.513	1.08	7.10	3.7	4.2
0.720	1.07	7.18	3.3	3.3
1.04	0.935	7.00	3.4	3.4
1.03	2.00	7.00	3.4	3.3
0.260	0.659	6.98	6.2	6.1
0.781	2.10	6.96	4.0	4.0
0.260	1.21	6.71	7.7	6.8
0.520	0.972	6.71	5.4	6.0
0.208	0.755	6.72	7.0	7.1
0.520	0.915	6.48	7.1	7.0
1.04	1.02	6.48	5.7	5.7
0.513	1.03	6.45	6.9	6.8
3.00	0.254	7.90	0.29	0.34
5.00	0.267	7.85	0.25	0.26
10.0	0.321	7.60	0.21	0.19
3.00	0.203	7.58	0.49	0.52
7.00	0.287	7.45	0.23	0.31
5.00	0.282	7.45	0.33	0.41
10.0	0.287	7.44	0.24	0.24
20.0	0.373	7.34	0.22	0.15
5.00	0.287	7.33	0.44	0.51
10.0	0.279	7.32	0.32	0.29
20.0	0.239	7.26	0.23	0.19
7.00	0.455	7.11	0.52	0.54

[a] Using *p*-nitrophenol as indicator at $1.73 \times 10^{-5}\ M$ when Ni(II) is in excess and at $4.32 \times 10^{-5}\ M$ when polymyxin is in excess. [b] The subscript refers to total stoichiometric concentration.

where R and S are defined in the *Appendix*. These terms arise from coupling of Scheme I to the faster indicator and ligand protolytic equilibria. A plot of $1/\tau S$ against R/S yields $k_1 = (3.8 \pm 0.2) \times 10^3\ M^{-1}\ sec^{-1}$ (Fig. 3). The value of k'_1 is unobtainable from Fig. 3, however, and only upper and lower limits of $0.6 < k'_1 < 2.4\ M^{-1}\ sec^{-1}$ can be determined. The reverse rate constant k_{-1} could be calculated from the relation $k_{-1} = k_1K_1$; however, a direct experimental determination of this constant is preferable.

To determine k_{-1} directly, attack of H_4L^{4+} on Ni^{2+} was neglected. There remains only one reaction in Scheme I, in which H_3L^{3+} is the only attacking ligand species. The $1/\tau$ expression for this reaction is given in Eq. 2, where α arises from the faster protolytic equilibria:

$$1/\tau = k_{-1} + k_1([Ni^{2+}]\alpha + [H_3L^{3+}]) \qquad \text{(Eq. 2)}$$

and is also given in the *Appendix*. A plot of Eq. 2 yields $k_1 = (3.5 \pm 0.2) \times 10^3\ M^{-1}\ sec^{-1}$ and $k_{-1} = 1.2 \pm 0.1\ sec^{-1}$ (Fig. 4). The ratio of these rate constants, $2.9 \times 10^4\ M^{-1}$, is in good agreement with the value of $3.3 \times 10^4\ M^{-1}$ obtained for the stability constant by potentiometric titration. The two values of k_1 determined agree within experimental error.

Under the conditions of these experiments, polymyxin exists primarily as the fully protonated species, H_5L^{5+}. With ethylenediamine (25) and related systems (8, 26), protonated forms of the ligand react several orders of magnitude slower than the corresponding neutral species. Therefore, for ligand species with all amine binding sites protonated, the reaction rates should be even slower, if not negligible, within experimental error. Thus, protonated forms of polymyxin other than those included in Scheme I were assumed not to be important attacking forms of the ligand. As previously mentioned, polymyxin has multiple binding sites. Therefore, as in the equilibrium studies, an attempt was made to fit the data to a mechanism whereby an additional metal ion is consumed. This mechanism was inconsistent with the data in the acid pH region and with the ligand in excess.

Although the equilibrium data in slightly basic media could not be successfully determined, the lack of these data does not preclude a kinetic study in the same media. Under pseudo-first-order conditions with the metal in excess, the approximations $\Sigma[\text{ligand species}] \ll [Ni^{2+}] \sim [Ni^{2+}]_0$ are valid, and the interpretation is simplified. The last 12 experiments of Table II were run under these assumptions. Several reaction schemes were applied to these data; Scheme II yielded the best fit.

$$\begin{array}{ccccccc} Ni^{2+} + H_3L^{3+} & \underset{k_{-1}}{\overset{k_1}{\rightleftharpoons}} & NiH_3L^{5+} & & & & \\ & & \Big\downarrow K_{a3},\ K_{a4} & & & & \\ Ni^{2+} + NiHL^{3+} & + & 2H^+ & \underset{k_{-2}}{\overset{k_2}{\rightleftharpoons}} & Ni_2HL^{5+} & + & 2H^+ \end{array}$$

Scheme II

Table III—Rate Constants for Ni(II)–Polymyxin B at 25° and 0.1 *M* Ionic Strength

Method	k_1 (M^{-1} sec^{-1})	k_1' (M^{-1} sec^{-1})	k_2 (M^{-1} sec^{-1})	k_{-1} (sec^{-1})
Stopped flow (excess ligand), M + L ⇄ ML	$3.5\ (\pm1.2) \times 10^3$	—	—	$1.2\ (\pm0.1) \times 10^{-1}$
Stopped flow (excess ligand), M + L = ML M + HL = ML + H	$3.8\ (\pm0.2) \times 10^3$	<2.4 >0.6	—	—
Stopped flow (excess metal)	$4.3\ (\pm0.2) \times 10^3$	—	$\leq 1 \times 10^4$ $\geq 3 \times 10^3$	—
Temperature jump (excess metal)	$\sim 6.0 \times 10^3$[a]	—	—	—

[a] Value represents a composite rate constant; see text.

The observed reciprocal relaxation time is related to the concentration variables according to:

$$(1/\tau)S' = k_2 + k_1R'/S' \qquad \text{(Eq. 3)}$$

where R' and S' are given in the *Appendix*. A plot of Eq. 3 yields $k_1 = (4.3 \pm 0.2) \times 10^3\ M^{-1}\ sec^{-1}$ (Fig. 5). The value of k_2 is unobtainable from Fig. 5, and only upper and lower limits of $1 \times 10^4 > k_2 > 3 \times 10^3\ M^{-1}\ sec^{-1}$ can be determined.

To calculate the concentrations of $NiHL^{3+}$ and Ni_2HL^{5+}, required in Eq. 3, it is necessary to know the values of the complex acid dissociation constants as well as the stability constant K_2 for bimetallic complex formation. Since these constants are not known, estimates were used as initial trial values in a computerized data-fitting routine. Subsequent variation of these parameters by a factor of 10 above and below the initial values resulted in a variation in the rate constants of ±20%, with little sensitivity toward the assumed value of $K_2 \simeq 4 \times 10^3\ M$.

Rate constants for polymyxin complexation with nickelous ion are summarized in Table III.

To confirm the veracity of this treatment, another method was used. Temperature-jump experiments were carried out on slightly alkaline solutions containing excess metal with phenol red as the indicator. Although the approximations required to apply Eq. 3 are not as valid as in the stopped-flow experiments, good agreement was obtained between observed and calculated values of the relaxation times. The value of the rate constant for the formation of the 1:1 complex, k_1, was $6 \times 10^3\ M^{-1}$ sec^{-1}, which is in reasonable accord with the value obtained by stopped flow.

DISCUSSION

Equilibrium Studies—In the pH 6.4–7.1 range, the potentiometric titration data indicate essentially a 1:1 complex between nickelous ion and polymyxin. Although it was determined that the ligand binding species is represented by H_3L^{3+}, it is impossible from the potentiometric data to determine directly which γ-NH_2 groups participate in complex formation. Model studies strongly suggest that complex formation between nickel and the γ_1- and γ_2-NH_2 groups on the cyclic portion of polymyxin has the minimum ring strain and rotational barrier, although other possible structures can be postulated.

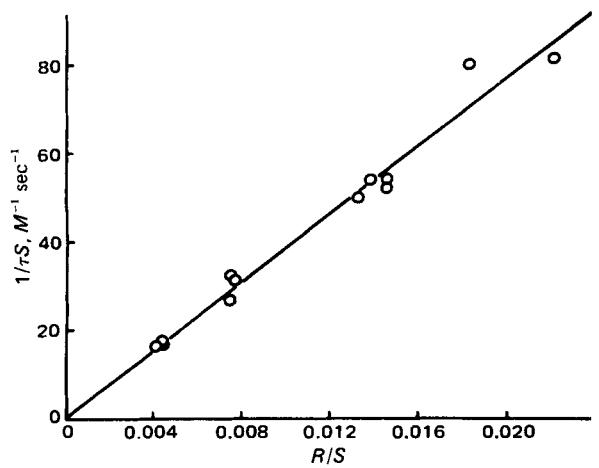

Figure 3—*Plot of* $1/\tau S$ versus R/S. *The straight line was obtained by least-squares data analysis, calculated from the concentrations and relaxation times given in Table II.*

Table IV—Rate Constant Ratios for Selected Ni(II)–Ligand Systems[a]

$Ligand_i/Ligand_j$	f	$f \times k_i/k_j$
$Malonate^{2-}$/H $malonate^-$	1/2	11
$Oxalate^{2-}$/H $oxalate^-$	1/2	8
$Cysteine^{2-}$/H $cysteine^-$	1	10
$H\ II^{3-}/H_2\ II^{2-}$	1	4
III^-/H III	1	13
IV/H IV^+	1/2	120
V/H V^+	1/2	980
$H\ VI^+/H_2\ VI^{2+}$	2/3	64
$H_2\ VII^{2+}/H_3\ VII^{3+}$	2/3	61
H_3L^{3+}/H_4L^{4+}	1/2	800[b]
H_3L^{3+}/H_4L^{4+}	1/2	3300[c]

[a] The statistical factor, f, takes into account the difference in the number of ligand donor atoms initially available for complex formation. Rate constants may be found in Ref. 31. Abbreviations used are: II, 4,5-dihydroxybenzene-1,3-disulfonic acid; III, pyridinedicarboxylic acid; IV, 2-aminomethylpyridine; V, ethylenediamine; VI, triethylenetetraamine; VII, tetraethylenepentaamine; and H_3L^{3+} and H_4L^{4+}, protonated polymyxin species. [b] Ratio corresponds to upper limit of k_1'. [c] Ratio corresponds to lower limit of k_1'.

The fact that no evidence was found for a binuclear complex in the nickel–polymyxin system below pH 7.1 is consistent with the results for the Cu(II)–polymyxin study (24), in which the data were successfully fit to a monocopper complex up to pH 8. Above pH 7.1, the equilibrium studies imply, and the stopped-flow studies confirm, that a binuclear species is present.

In the copper–polymyxin study, a $CuHL^{3+}$ species is postulated to exist, in which copper is attached to two γ-NH_2 groups and two peptide nitrogens. Such a complex species was not detected in the nickel–polymyxin system in near-neutral media. Under similar concentration conditions (excess polymyxin, basic pH), nickelous ion, unlike cupric ion, may prefer to form different order metallic complexes with polymyxin (27, 28). It is not likely that the data above pH 7.1 represent slow hydrolysis of peptide bonds as determined for certain oligopeptides (29), because the solutions were stable during the experiments (*vide supra*).

It is thus concluded that, below pH 7.1 and with the ligand in excess, polymyxin forms a 1:1 complex with nickelous ion in which the ligand binding species is H_3L^{3+}.

Kinetic Studies—The 1:1 complex NiH_3L^{5+} is formed by attack on nickel of polymyxin as either H_3L^{3+} or H_4L^{4+}. The positive charges of these ligand species are so high that the very fact of forming a complex is interesting, as is the magnitude of the formation rate constant. Most neutral ligands have rate constants in the range of $1.6–5.0 \times 10^3\ M^{-1}\ sec^{-1}$ for nickel complex formation (30, 31). One possible exception is ethylenediamine. For this ligand, $k_1 = 3.5 \times 10^5\ M^{-1}\ sec^{-1}$; a special complex formation mechanism has been proposed for such a comparatively large rate constant. To determine whether polymyxin has special kinetic properties, the "normal" mechanism of complex formation should first be considered.

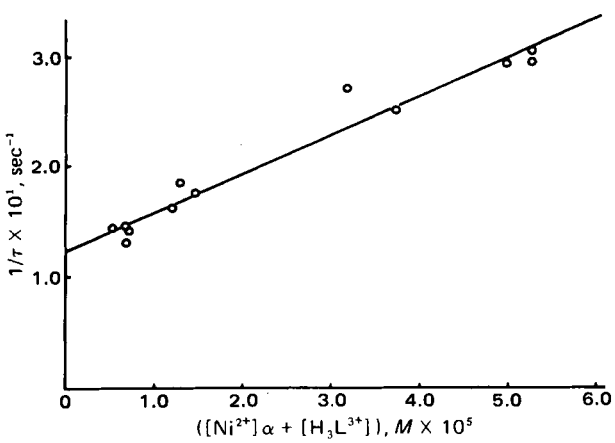

Figure 4—*Plot of* $1/\tau$ versus $[Ni^{2+}]\alpha + [H_3L^{3+}]$. *The straight line was obtained by least-squares data analysis.*

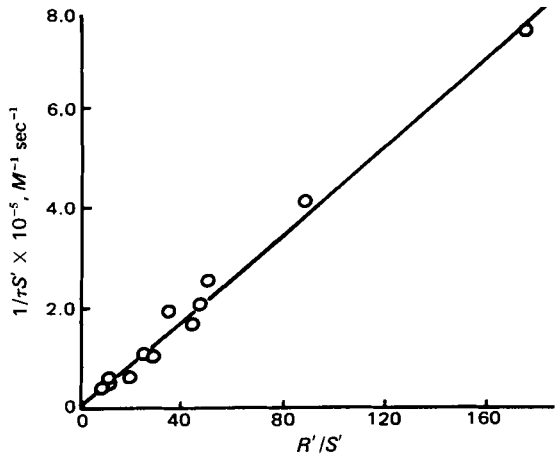

Figure 5—*Plot of* $1/\tau S'$ versus R'/S'. *The straight line was obtained by least-squares data analysis, calculated from the concentrations and relaxation times given in Table II.*

The normal (or eigen) substitution mechanism consists of rapid formation of an ion-pair between the aquometal ion and ligand followed by rate-determining water loss from the metal ion's inner coordination sphere (31). If there are no appreciable changes in the structures of the ion-pair or the solvent cage around the reactants, this mechanism predicts that the ratio of rate constants for two ligands having different charges by virtue of differing protonation should be approximately seven. Ratios for several ligands are listed in Table IV. Many systems have modest ratios in conformance with this mechanism. The rate constant ratios for methylaminopyridine, the polyamines, and polymyxin are considerably larger. This difference suggests anomalous complexation behavior.

For the polyamines, substitution was described in terms of an internal conjugate base mechanism (7), where hydrogen bonding between basic amine donor atoms and water molecules in the metal ion's inner coordination sphere results in enhanced formation rate constants. The clearest indicator of anomalous behavior is a larger than normal substitution rate constant, shown only by ethylenediamine (7). This result recently was reinterpreted (32). However, the new analysis leaves the result unchanged: the reaction between Ni^{2+} and ethylenediamine is anomalously rapid regardless of mechanistic assignment. Amino acids also often have rate constant ratios considerably different from those expected on electrostatic grounds. However, the apparent unreactivity of the zwitterionic form is responsible for this effect (33).

If the value of $k_1 = 3.8 \times 10^3\ M^{-1}\ sec^{-1}$ for complexation of H_3L^{3+} with Ni^{2+} corresponds to normal substitution, then the ligand acts as an electrically neutral species in which the ligand's metal binding site is uncharged. The ligand's formal charge of +3 must then be so remote from this active site that it does not influence the complex formation rate. Addition of one more proton to form H_4L^{4+} places two positive charges on each binding site of only one pair of potential binding groups. Ring closure requires proton loss, but this step would not be expected to be rate determining (7, 25). Hence, it is difficult to see why the reaction of H_4L^{4+} should be so slow compared with H_3L^{3+}.

To act as a neutral ligand, the effective charge differs from the formal charge through either remoteness from the metal binding site or screening. The polypeptide structure may form a barrier that partially shields the metal binding site from the positive charges. However, the high charge and rapid exchange of the protons with solvent, which ensures a random distribution of charge over the entire polymyxin molecule, would make that type of screening unlikely. Therefore, the polymyxin H_3L^{3+} species probably has a high complex formation rate constant because it follows the internal conjugate base mechanism.

In the polymyxin species H_4L^{4+}, an internal conjugate base effect is improbable since only one nitrogen donor is initially available for complexation with Ni(II). The limits set for the forward rate constant, $0.6 < k_1' < 2.4\ M^{-1}\ sec^{-1}$, suggest that H_4L^{4+} attacks nickelous ion as a relatively highly charged ligand. No evidence suggests that H_4L^{4+} attack on Ni(II) follows an abnormal substitution pathway. In fact, the experimentally determined range of k_1 suggests that this ligand species has an effective charge of approximately three based on the normal substitution mechanism.

At basic pH and excess Ni(II), a second complex between polymyxin B and nickelous ion is formed and is of the type Ni_2HL^{5+}. The attacking ligand species in this complexation reaction is $NiHL^{3+}$, in which two protons from the previously formed NiH_3L^{5+} complex have dissociated. If the range of k_2 ($3 \times 10^3 < k_2 < 1 \times 10^4\ M^{-1}\ sec^{-1}$) for complexation of this ligand species with Ni(II) corresponds to an effective ligand charge, q, of $0 < q < +1$, as would be predicted if the metal center in $NiHL^{3+}$ is sufficiently remote or screened from the complexing ligand site (*cf.*, Fig. 1), then the observed upper limit for k_2 is abnormally large, suggesting the presence of an internal conjugate base effect as discussed for the 1:1 complex.

The antibiotic activity of polymyxin B has been investigated (1–3). Metal-ion binding affects antibiotic activity in several ways; chelation may even enhance efficacy. An example is the use of metal-impregnated cellulose as a stratum for antibiotic attachment (34). Polymyxin attached to celluloses treated with various metal ions retained its antimicrobial activity. Since only a portion of the polymyxin binding sites would be attached to the cellulose-bound metal ion, this result cannot be used to infer whether the site of metal binding and the site or sites of antimicrobial activity are the same.

The present results show that polymyxin is rapidly reactive toward metal ions (relatively high k_1 and k_2) and that it can simultaneously bind two metal centers (K_2). Whether, as a class of compounds, the antibiotics exhibit all these characteristics has not been demonstrated; such reactivity patterns, however, if present, would help explain several features of antimicrobial activity such as the bactericidal ability of polymyxin while on insolubilized strata.

APPENDIX

Under the experimental conditions of slightly acid pH and excess ligand, where Scheme I prevails, the relaxation spectrum is calculated from the solution of a single linear differential rate equation. To obtain this differential equation in one variable, it is sufficient to apply mass balance on the ligand, metal, indicator, and proton together with the expanded protolytic equilibrium quotients for the ligand and indicator. Well-known procedures incorporating these 10 relations yield Eqs. 1 and 2. The previously undefined terms are:

$$R = [Ni^{2+}]\alpha + [H_3L^{3+}] + \frac{1}{K_1} \qquad \text{(Eq. A1)}$$

$$S = [Ni^{2+}]\alpha_2 + [H_4L^{4+}] + \frac{[NiH_3L^{5+}]\alpha_1 + [H^+]}{K_1K_{a2}} \qquad \text{(Eq. A2)}$$

$$\alpha = \left(\beta + \frac{[H_3L^{3+}]}{K_{a2}} + 4\frac{[H^+][H_3L^{3+}]}{K_aK_{a2}}\right)\Big/\sigma \qquad \text{(Eq. A3)}$$

$$\sigma = \left(\frac{[H_3L^{3+}]}{K_{a2}} + 2\frac{[H^+][H_3L^{3+}]}{K_{a1}K_{a2}}\right)\left(\frac{[H^+]}{K_{a2}} + 2\right) + \left(\beta - \frac{[H_3L^{3+}]}{K_{a2}}\right)\left(1 + \frac{[H^+]}{K_{a2}} + \frac{[H^+]^2}{K_{a1}K_{a2}}\right) \qquad \text{(Eq. A4)}$$

$$\beta = \frac{K_{In} + [H^+] + [In^-]}{K_{In} + [H^+]} \qquad \text{(Eq. A5)}$$

$$\alpha_1 = \left(\frac{[H^+]}{K_{a2}} + 2\frac{[H^+]^2}{K_{a1}K_{a2}}\right)\Big/\sigma \qquad \text{(Eq. A6)}$$

$$\alpha_2 = \left(\beta + 2\frac{[H^+][H_3L^{3+}]}{K_{a1}K_{a2}}\right)\Big/\rho \qquad \text{(Eq. A7)}$$

$$\rho = \left(\beta + 2\frac{[H_3L^{3+}]}{[H^+]}\right)\left(1 + \frac{[H^+]}{K_{a1}} + \frac{K_{a2}}{[H^+]}\right) + \left(\frac{[H^+][H_3L^{3+}]}{K_{a1}K_{a2}} - \frac{[H_3L^{3+}]}{[H^+]}\right)\left(1 + \frac{2K_{a2}}{[H^+]}\right) \qquad \text{(Eq. A8)}$$

Under conditions of slightly basic pH and excess metal ion, where reaction Scheme II prevails, the relaxation spectrum is calculated analogously from the solution of two linear and independent differential rate equations in two variables. Assuming separability of the two possible relaxation effects as described in the text, the previously undefined terms are:

$$R' = [Ni^{2+}]\alpha_3 + [H_3L^{3+}] + \alpha_4/K_1 \qquad \text{(Eq. A9)}$$

$$S' = [Ni^{2+}]\alpha_5 + [NiHL^{3+}] \qquad \text{(Eq. A10)}$$

$$\alpha_3 = \left(\beta + \gamma + \frac{[H_3L^{3+}]}{K_{a2}} + 4\frac{[H^+][H_3L^{3+}]}{K_{a1}K_{a2}}\right)\Big/\sigma' \qquad \text{(Eq. A11)}$$

$$\gamma = \frac{[NiH_3L^{5+}]K_{a3}}{[H^+]^2} \qquad \text{(Eq. A12)}$$

$$\sigma' = \left(\frac{[H_3L^{3+}]}{K_{a2}} + 2\frac{[H_3L^{3+}][H^+]}{K_{a1}K_{a2}}\right)\left(\frac{[H^+]}{K_{a2}} + 2\right) + \left(\beta + \gamma - \frac{[H_3L^{3+}]}{K_{a2}}\right)\left(1 + \frac{[H^+]}{K_{a2}} + \frac{[H^+]}{K_{a1}K_{a2}}\right) \quad \text{(Eq. A13)}$$

$$\alpha_4 = \gamma\left(\frac{[H^+]}{K_{a2}} + 2\frac{[H^+]^2}{K_{a1}K_{a2}}\right)\Big/\sigma' + 1 \quad \text{(Eq. A14)}$$

$$\alpha_5 = 2\frac{[NiH_3L^{5+}]}{[H^+]}\left(\frac{[H^+]}{K_{a2}} + 2\frac{[H^+]^2}{K_{a1}K_{a2}}\right)\Big/\sigma'\rho' - 1/\rho' \quad \text{(Eq. A15)}$$

$$\rho' = 1 + \frac{[H^+]}{K_{a4}} + \frac{[H^+]^2}{K_{a3}K_{a4}} \quad \text{(Eq. A16)}$$

In deriving Eqs. A9–A16, the reasonable assumptions were made that, under the experimental conditions, $K_{a3}/[H^+]$ and $K_{a3}K_{a4}/[H^+] \ll 1$.

REFERENCES

(1) B. A. Newton, *Bacteriol. Rev.*, **20,** 14 (1956).

(2) M. R. W. Brown and J. Melling, *J. Gen. Microbiol.*, **59,** 263 (1969).

(3) C. HsuChen and S. Feingold, *Biochemistry*, **12,** 2105 (1973).

(4) K. Vogler and R. O. Studer, *Experientia*, **22,** 345 (1966).

(5) K. Vogler, *Helv. Chim. Acta*, **48,** 1161 (1965).

(6) W. Hausmann and L. C. Craig, *J. Am. Chem. Soc.*, **76,** 4892 (1954).

(7) R. W. Taylor, H. K. Stepien, and D. B. Rorabacher, *ibid.*, **13,** 1282 (1974).

(8) D. W. Margerum, D. B. Rorabacher, and J. F. G. Clarke, Jr., *Inorg. Chem.*, **2,** 667 (1963).

(9) G. Schwarzenbach, "Die Komplexometrische Titration," 4th ed., Ferdinand Enke, Verlag Stuttgart, West Germany, 1960, pp. 75, 76.

(10) C. W. Davies, *J. Chem. Soc.*, **1938,** 2093.

(11) D. S. Honig, K. Kustin, and J. F. Martin, *Inorg. Chem.*, **11,** 1895 (1972).

(12) K. Kustin and D. L. Toppen, *ibid.*, **12,** 1404 (1973).

(13) H. L. Fritz and J. H. Swinehart, *ibid.*, **12,** 1259 (1973).

(14) M. L. Barr, K. Kustin, and S.-T. Liu, *ibid.*, **12,** 1486 (1973).

(15) U. Kragh-Hansen and J. V. Moller, *Biochim. Biophys. Acta*, **295,** 438 (1973).

(16) H. Katz and K. Kustin, *ibid.*, **313,** 235 (1973).

(17) R. Karpel, Ph.D. thesis, Brandeis University, Waltham, Mass., 1970.

(18) K. Kustin and S.-T. Liu, *J. Chem. Soc., Dalton Trans.*, **1973,** 278.

(19) F. S. C. Rossotti and H. Rossotti, "The Determination of Stability Constants," McGraw-Hill, New York, N.Y., 1961, chap. 5.

(20) E. B. Paniago and D. W. Margerum, *J. Am. Chem. Soc.*, **94,** 6704 (1972).

(21) E. J. Billo and D. W. Margerum, *ibid.*, **92,** 6811 (1970).

(22) G. K. Pagenkopf and D. W. Margerum, *ibid.*, **90,** 6963 (1968).

(23) R. F. Pasternack, M. Angwin, and E. Gibbs, *ibid.*, **92,** 5878 (1970).

(24) H. Brintzinger, *Helv. Chim. Acta*, **86,** 744 (1961).

(25) L. Kirschenbaum and K. Kustin, *J. Chem. Soc. A*, **1970,** 684.

(26) R. F. Pasternack and K. Kustin, *J. Am. Chem. Soc.*, **90,** 2295 (1968).

(27) J. E. Gorton and R. F. Jameson, *J. Chem. Soc. A*, **1968,** 2615.

(28) L. G. Sillén, *Acta Chem. Scand.*, **8,** 299 (1954).

(29) M. K. Kim and A. E. Martell, *J. Am. Chem. Soc.*, **89,** 5138 (1967).

(30) M. Eigen and R. G. Wilkins, "The Kinetics and Mechanisms of Formation of Metal Complexes," vol. 49, Advances in Chemistry Series, American Chemical Society, Washington, D.C., 1965, p. 55.

(31) K. Kustin and J. Swinehart, *Prog. Inorg. Chem.*, **13,** 107 (1970).

(32) R. B. Jordan, *Inorg. Chem.*, **15,** 748 (1976).

(33) J. C. Cassatt and R. G. Wilkins, *J. Am. Chem. Soc.*, **90,** 6045 (1968).

(34) J. F. Kennedy, S. A. Barker, and A. Zamir, *Antimicrob. Agents Chemother.*, **6,** 777 (1974).

ACKNOWLEDGMENTS

Supported by U.S. Public Health Service Research Grant GM 08893-11.

The authors thank Dr. H. Meienhofer for use of his countercurrent distribution apparatus.

High-Performance Liquid Chromatographic and TLC Determinations of Desacetylvinblastine Amide (Vindesine) and Its Monosulfate Salt

R. L. HUSSEY [x] **and W. M. NEWLON**

Received May 18, 1977, from the *Lilly Research Laboratories, Eli Lilly and Company, Indianapolis, IN 46206.* Accepted for publication November 16, 1977.

Abstract □ High-performance liquid chromatographic and TLC methods were developed for the determination of desacetylvinblastine amide base (vindesine), a chemically modified *Catharanthus* alkaloid presently in clinical evaluation. Both methods permit the detection of 6,7-dihydrovindesine and vindesine N_b'-oxide, the principal by-products in the chemical conversion of vinblastine to vindesine. The methods are applicable to both the sulfate salts and the free bases of the chemical substances described.

Keyphrases □ Vindesine—high-performance liquid chromatographic and TLC analyses, bulk drug □ High-performance liquid chromatography—analysis, vindesine in bulk drug □ TLC—analysis, vindesine in bulk drug □ Alkaloids, *Catharanthus*—vindesine, high-performance liquid chromatographic and TLC analyses, bulk drug

Chemical modification of vinblastine, a clinically effective alkaloid of the Apocynaceae family (1), genus *Catharanthus,* provided the agent desacetylvinblastine amide (vindesine) sulfate (2, 3), which has been in clinical evaluation for antitumor activity since 1975. High-performance liquid chromatographic (HPLC) and TLC methods were developed to determine vindesine free base (I) and/or its monosulfate salt in the presence of two principal by-products (3) obtained during semisynthesis. The first by-product, 6,7-dihydrovindesine (II), is generated in the Raney nickel hydrogenolysis step of the vindesine preparation; the second, vindesine N_b'-oxide (III), is the product of air oxidation of vindesine (Scheme I).

An HPLC method was developed to provide a quantitative assay of I in the final stages of raw material purification. TLC (4, 5) was used in a supplementary, semiquantitative manner.

EXPERIMENTAL

Equipment—The liquid chromatograph[1] was equipped with a UV spectrometer[2] set at 280 nm and a 3.9 × 30-cm stainless steel column containing chemically bonded octadecylsilane on silica[3]. The detector was set with a sensitivity of 1.00 absorbance unit full scale. A strip recorder allowing variable input[4] was employed. Data acquisition and computation were handled by on-line computation[5].

The scanning UV–visible TLC reflectance densitometer[6] was set at 280 nm in the ratio density mode. Commercially available plates[7] of silica gel F-254 and nonfluorescent silica were both employed as alternative detection systems for II and III. The TLC plate was used for making a photographic record, and the nonfluorescent plate was used for semiquantitation in conjunction with the densitometer.

Reagents—Two HPLC solvent systems were employed. The primary system was methanol–water–diethylamine (1000:600:3). The flow rate was adjusted to 1.5 ml/min; the elution volumes from solvent breakthrough were 3.0, 10.9, 13.5, and 20.1 ml for III, I, II, and the internal standard phenanthrene[8], respectively. For the quantitation of I in high levels of II, methanol–water–diethylamine (835:600:3) was employed with a flow rate of 1.5 ml/min. For the latter solvent system, the elution volumes from solvent breakthrough were 3.1, 20.2, 25.6, and 32.8 ml, respectively. In both cases, the column dead volume was 3.2 ml.

Ether–methanol–40% aqueous methylamine (20:4:1) was employed as the TLC solvent system. The average R_f values found for III, I, and II were 0.36, 0.57, and 0.74, respectively.

HPLC Determination of I Raw Material Base and/or Monosulfate—Three replicates of each standard and sample were used for each assay result. The number of replicates chosen for the assay assured that each result would be within ±2% of the true value at the 95% confidence level. Each accurately weighed sample (5 mg) was quantitatively transferred to a 5-ml glass-stoppered flask. Three milliliters of the internal standard was added [45 mg of phenanthrene (IV), reagent grade, prepared in 100 ml of methanol]. To aid the otherwise slow dissolution, 10 sec of sonic vibration was employed.

Aliquots of 20 μl of each sample or standard solution were injected onto the column of the liquid chromatograph. The peak areas (PA) of I and the internal standard were measured by on-line computation. The ratio of each sample (or standard) area to the internal standard was then obtained: $(PA_{sample}/PA_{internal\ standard}) = R$. A five-point calibration was periodically obtained (0–10 mg/3 ml) to verify linearity and passage of concentration through the origin of response. Routinely, however, the

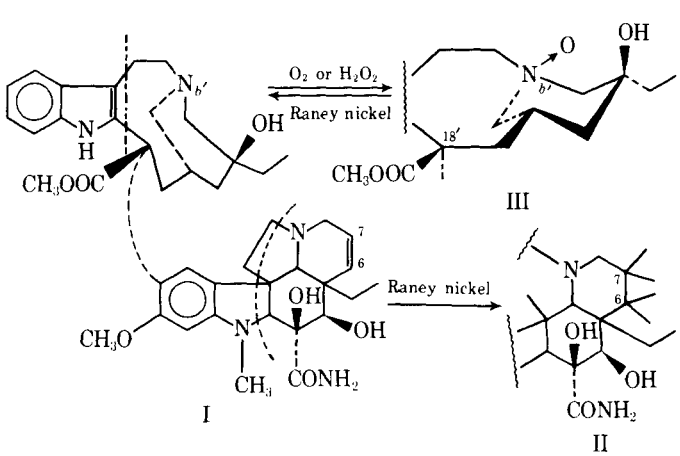

Scheme I

[1] Waters model 6000A.
[2] Varian Vari-Chrom VUV-10.
[3] Waters μBondapak C_{18} No. 27324.
[4] Fisher Recordall series 5000.
[5] Dual Hewlett-Packard 2100 RTE System.
[6] Schoeffel SD3000.
[7] E. Merck.
[8] Aldrich Chemical.

0022-3549/78/0900-1319$01.00/0
© 1978, American Pharmaceutical Association

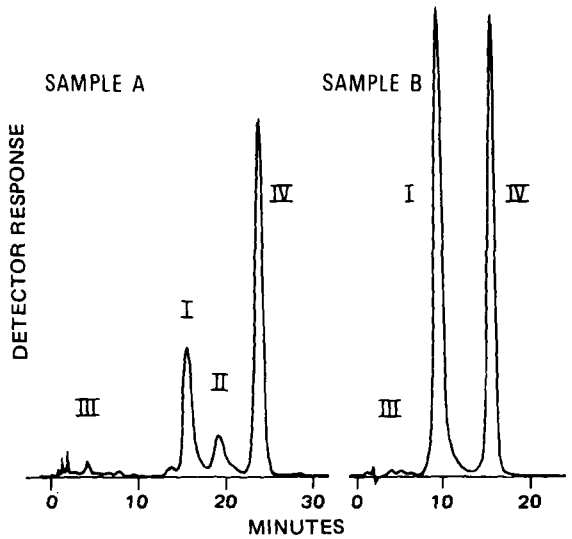

Figure 1—*HPLC separations. Key: Sample A, a sample before prepurification run in the secondary solvent system; and Sample B, a finished I sulfate run in the primary solvent system. The elution times shown are measured from the time of injection.*

purity of each sample was obtained in the following manner:

$$\frac{\text{average sample ratio, } R_{\text{sample}}}{\text{average standard ratio, } R_{\text{standard}}} \frac{\text{mg standard}}{\text{mg sample}} \times \% \text{ purity of standard} = \% \text{ purity of sample} \quad \text{(Eq. 1)}$$

TLC of I Raw Material Base and/or Monosulfate—The I base and/or monosulfate was prepared at a concentration of 20 mg/ml in methanol. This solution was used in two ways. A precoated F-254 plate was spotted with 10 μl of the methanol solution, and a nonfluorescent plate was spotted with 2 μl. Both plates were developed in the aforementioned developing solvent. An equilibration time of just 5 min was employed in a lined tank.

Following development, a photograph was taken of the fluorescent plate, and a TLC reflectance absorbance scan (ratio mode, 280 nm) was taken of the nonfluorescent plate. The linearity of response to concentration was checked periodically from 0 to 20 μg. In most cases, however, the scanned plate was judged on total peak area. In other cases, II was spotted alongside the sample at an equivalent of 5% (1 mg/ml), and a direct semiquantitation was made on a linear response basis.

RESULTS AND DISCUSSION

Both the HPLC and TLC procedures showed the presence of II and III. The HPLC method was linear in response for both the monosulfate salt and the base from 0 to 2.8 mg/ml. For the monosulfate salt, data based on 25 separately weighed samples gave a relative standard deviation of 0.89%. For the free base, the relative standard deviation was 0.99%, also based on 25 separately weighed samples. Methanol solutions of both the sulfate and base proved stable for 18 hr, thus allowing easy automation.

Typical liquid chromatograms are shown in Fig. 1. By-product II was present only in crude vindesine preparations prior to prepurification by preparative high-pressure silica gel chromatography. The secondary solvent system described in *Experimental* was used for the crude vindesine preparations but required a longer assay time. The primary solvent system would have clearly detected II, but the separation would not have been as great. This latter solvent system is of advantage for purified preparations where II is absent since it requires a shorter assay time. The small minor peaks following III were due to compounds of undetermined structure. Phenanthrene (IV), the internal standard for the HPLC analysis, was not used in the TLC semiquantitation.

For very pure finished formulations, 0.5 *M* potassium phosphate buffer can be used instead of diethylamine in the mobile solvent for HPLC. Some additional methanol must be added to the mobile system to reduce the tailing caused by the lowered pH, but the octadecylsilane column packing then has a longer life. With diethylamine, a column life of 3 weeks has been obtained; with the phosphate buffer, a life of several months is obtained.

The TLC procedure was useful principally as a fast, corroboratory check. Thin-layer densitometry still does not have the accuracy or precision of HPLC analysis.

REFERENCES

(1) I. S. Johnson, J. G. Armstrong, M. Gorman, and J. P. Burnett, Jr., *Cancer Res.*, **23**, 1390 (1963).

(2) G. J. Cullinan, K. Gerzon, G. A. Poore, and M. J. Sweeney, XIth International Cancer Congress, Abstract Panel 14, paper 137, Florence, Italy, Oct. 23, 1975.

(3) C. J. Barnett, G. J. Cullinan, K. Gerzon, R. C. Hoying, W. E. Jones, W. M. Newlon, G. A. Poore, R. L. Robison, M. J. Sweeney, G. C. Todd, R. W. Dyke, and R. L. Nelson, *J. Med. Chem.*, **21**, 88 (1978).

(4) I. M. Jakovljevic, L. D. Seay, and R. W. Shaffer, *J. Pharm. Sci.*, **53**, 553 (1964).

(5) N. J. Cone, R. Miller, and N. Neuss, *ibid.*, **52**, 688 (1963).

ACKNOWLEDGMENTS

The authors thank Dr. C. J. Barnett for preparation of purified 6,7-dihydrovindesine and Dr. K. Gerzon for the preparation of vindesine N_b'-oxide. Thanks also are given to Dr. E. C. Rickard and Dr. J. Zynger for the use of their statistical evaluation procedure, to Mr. J. J. Osborne for assistance in performing the assays described, and to Dr. K. Gerzon for review of this article.

Selective Demethylation of Polymethoxyxanthones with Aqueous Piperidine

R. K. CHAUDHURI *§x, **F. ZYMALKOWSKI** *§, and **S. GHOSAL** ‡

Received April 18, 1977, from the *Pharmazeutisches Institut der Universität Bonn, Kreuzbergweg 26, 53 Bonn 1, F.R. Germany, and the ‡Pharmaceutical Chemistry Research Laboratory, Department of Pharmaceutics, Banaras Hindu University, Varanasi-5, India. Accepted for publication December 19, 1977. §Present address: Pharmazeutisches Institut, ETH-Zentrum Clausiusstrasse 25, CH-8092 Zurich, Switzerland.

Abstract □ Data are presented for selective demethylation of eight polymethoxyxanthones with aqueous piperidine. Clarification and rationalization of the present and previous observations are made. The mechanism is defined in terms of both resonance effects and steric factors.

Keyphrases □ Xanthones, various polymethoxy—selective demethylation with aqueous piperidine □ Polymethoxyxanthones, various—selective demethylation with aqueous piperidine □ Demethylation, selective—various polymethoxyxanthones with aqueous piperidine

Interest in selective demethylation of polymethoxyxanthones stems from its use in structure elucidation (allocation of hydroxy–methoxy substituents) and in the synthesis of naturally occurring xanthones (1). Demethylation of 1-methoxyxanthones, with added methoxy groups in the A and B rings, with aluminum chloride produced 1-hydroxy derivatives (2). However, mixtures resulted with this reagent if the methyl ethers were sensitive to acidic reagents (1). Demethylation with basic reagents, on the other hand, was thought to involve 3- and/or 6-methoxy groups since oxygen functions *para* to the carbonyl group of the xanthone nucleus are poorest in electrons. Accordingly, demethylation of 2,3-dimethoxy-, 2,3,4-trimethoxy-, and 1-hydroxy-3,4,7-trimethoxyxanthones with either aqueous piperidine or tetramethylammonium hydroxide under reflux furnished the corresponding 3-hydroxy derivatives (3).

Some anomalies, however, were created by a subsequent report (4) that demethylation with aqueous piperidine was not entirely selective since the reaction was dependent on the number and position of methoxy groups in the xanthone nucleus and on the extent of heating with the demethylating agent. Thus, 1,2,3-trimethoxyxanthone was reported (4) to give 1-methoxy-2,3-dihydroxyxanthone instead of the expected 1,2-dimethoxy-3-hydroxyxanthone. Likewise, 2,3,4-trimethoxyxanthone, contrary to the earlier study (3), was reported to furnish 2-hydroxy-3,4-dimethoxyxanthone, 1,7-dimethoxyxanthone gave 1-hydroxy-7-methoxyxanthone, and 1,8-dimethoxy- and 1,3,5-trimethoxyxanthones were unreactive (4). The purposes of this paper are to sort out the anomalies and to propose a plausible mechanism of this demethylation reaction.

EXPERIMENTAL

Compounds—Xanthones III and VI–VIII were available from previous investigations of *Canscora decussata* (5), *Polygala arillata* (6), and *Swertia bimaculata* (7). Xanthones I, IV, and V were prepared by using previously reported (2, 8) procedures; xanthone II was obtained from the present investigation.

Reaction—In a typical experiment, 1,3-dimethoxyxanthone (I), 0.30 g, in piperidine (6 ml) and water (6 ml) was refluxed for 60 hr. The cooled mixture was poured into 4 *N* HCl. The resulting suspension was extracted with chloroform (3 × 100 ml). The chloroform layer was washed with 2 *N* HCl and water and dried with anhydrous magnesium sulfate. Evaporation of the solvent gave a residue (0.26 g), which showed three major spots on TLC on silica gel G[1]: R_f 0.78, 0.19, and 0.12 [solvent of benzene–acetic acid (20:1); iodine vapor was used for staining].

The xanthones were separated into homogeneous entities by column chromatography over silica gel[2] (60–120 mesh). Benzene and benzene–ethyl acetate (90:10) were used as eluents. The benzene eluates afforded the unchanged parent compound (0.024 g), followed by 1-hydroxy-3-methoxyxanthone (0.132 g), and 1,3-dihydroxyxanthone (0.033 g). The benzene–ethyl acetate eluates gave a brown polymeric compound (0.028 g). The other xanthones (II–VIII), when treated and processed similarly, also afforded unchanged material (8–20%) and some polymeric compounds (5–15%) in addition to the hydroxymethoxyxanthones (Table I).

RESULTS AND DISCUSSION

Xanthones I–VIII, when refluxed (40–60 hr) with aqueous piperidine, yielded unchanged starting material and intractable polymeric compounds in addition to the selectively demethylated hydroxymethoxyxanthones (Table I). The time of heating produced significant effects only with VIII. Thus, 40 hr of refluxing afforded the corresponding 1,6-dihydroxyxanthone, while 60 hr resulted in the corresponding 1,3,6-trihydroxy derivative. The identity of the compounds was established on the basis of UV absorption (5, 9) and PMR (5, 8, 10) spectra and by direct comparison with authentic samples where possible.

These results indicate that demethylation of 1-methoxy-, 1,3-dimethoxy-, and those xanthones containing added methoxy group(s) in the B ring (5- and/or 7-position) would take place preferentially at the 1-position. With a preformed 1-hydroxy substituent or in the absence of an oxygen function at the 1-position, the 3-position would be demethylated. In consonance with this conclusion, 1-hydroxy-3-methoxyxanthone and 2,3,4-trimethoxyxanthone produced 1,3-dihydroxyxanthone and 2,4-dimethoxy-3-hydroxyxanthone, respectively.

With an added methoxy group at the 2-position, the demethylation occurred at this position. Thus, 1,2,3-trimethoxyxanthone and 1,2,3,4,7-pentamethoxyxanthone produced 1,3-dimethoxy-2-hydroxyxanthone and 1,4,7-trimethoxy-2,3-dihydroxyxanthone, respectively. A small amount of 1-methoxy-2,3-dihydroxyxanthone was also produced from the first compound, thereby supporting a previous report (4). A methoxy group flanked by *ortho*-substituents may be pushed out (1, 11) of the benzene ring and its behavior modified accordingly.

A pleasing double application of the demethylation was accomplished in the synthesis of 1,6-dihydroxy-3,5,7-trimethoxy- and 1,3,6-trihydroxy-5,7-dimethoxyxanthones by varying the heating time. The 1- and 6-methoxy groups were preferentially demethylated within 40 hr of heating; with 60 hr of heating, the 3-methoxy group was demethylated. These xanthones were encountered among about two dozen compounds of this class found in *C. decussata* Schult (Gentianaceae) (11).

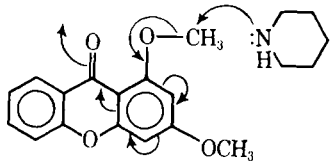

IX

[1] E. Merck, Darmstadt, West Germany.
[2] British Drug Houses or Woelm Pharma GmbH & Co.

0022-3549/78/0900-1321$01.00/0
© 1978, American Pharmaceutical Association

Table I—Selective Demethylation of Polymethoxyxanthones

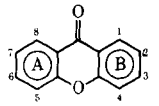

Compound	Substituents	Demethylation Substituents	Yield, %
I	1,3-$(OCH_3)_2$	1-OH-3-OCH_3	44
		1,3-$(OH)_2$	11
II	1-OH-3-OCH_3	1,3-$(OH)_2$	65
III	1,3,5-$(OCH_3)_3$	1-OH-3,5-$(OCH_3)_2$	40
		1,3-$(OH)_2$-5-OCH_3	8
IV	1,3,7-$(OCH_3)_3$	1-OH-3,7-$(OCH_3)_2$	45
		1,3-$(OH)_2$-7-OCH_3	10
V	2,3,4-$(OCH_3)_3$	2,4-$(OCH_3)_2$-3-OH	52
VI	1,2,3-$(OCH_3)_3$	1,3-$(OCH_3)_2$-2-OH	55
		1-OCH_3-2,3-$(OH)_2$	5
VII	1,2,3,4,7-$(OCH_3)_5$	1,4,7-$(OCH_3)_3$-2,3-$(OH)_2$	38
VIII	1,3,5,6,7-$(OCH_3)_5$	1,6-$(OH)_2$-3,5,7-$(OCH_3)_3$	22
		1,3,6-$(OH)_3$-5,7-$(OCH_3)_2$	36

The ease of *O*-demethylation is a function of resonance and steric factors. In compounds that are sterically less strained (I–IV), preferential demethylation occurs at C-1, followed by C-3 (and C-6), as could have been predicted on the basis of resonance factors (IX). Furthermore, since C-1 is more hindered than C-3 and C-6, the former should demethylate more readily. The selective demethylation at C-3 in V is caused by the relief of steric strain. However, this reaction can be explained as well in terms of simple resonance. In compounds having substitution at three or four adjacent carbon atoms, as in VI–VIII, the relief of steric strain is so important that it takes precedence over resonance effects, and one observes *O*-demethylation at C-2, C-3, and C-6, with C-2 demethylation being caused by the relief of steric strain.

REFERENCES

(1) F. M. Dean, in "The Total Synthesis of Natural Products," vol. I, J. ApSimon, Ed., Wiley–Interscience, New York, N.Y., 1973, p. 534.

(2) G. H. Stout and W. J. Balkenhal, *Tetrahedron*, **25**, 1947 (1969).

(3) A. J. Quillinan and F. Scheinmann, *J. Chem. Soc. Perkin 1*, **1973**, 1329.

(4) O. R. Gottlieb, A. A. Mesquita, T. J. Nagen, and P. Ferreirs, *Rev. Lat. Quim.*, **5**, 140 (1974).

(5) S. Ghosal, R. K. Chaudhuri, and K. R. Markham, *J. Chem. Soc. Perkin 1*, **1974**, 2538.

(6) S. Ghosal, S. Bannerjee, R. B. P. S. Chauhan, and R. S. Srivastava, *ibid.*, **1977**, 740.

(7) S. Ghosal, P. V. Sharma, and R. K. Chaudhuri, *Phytochemistry*, **14**, 2671 (1975).

(8) O. R. Gottlieb, M. T. Magalhaes, M. Camey, A. A. L. Mesquita, and D. de Barros Correa, *Tetrahedron*, **22**, 1777 (1966).

(9) T. J. Mabry, K. R. Markham, and M. B. Thomas, in "The Systematic Identification of Flavonoids," Springer Verlag, New York, N.Y., 1970, p. 35.

(10) D. Barraclough, H. D. Locksley, F. Scheinmann, M. T. Magalhaes, and O. R. Gottlieb, *J. Chem. Soc. B*, **1970**, 603.

(11) S. Ghosal, K. Biswas, and R. K. Chaudhuri, *J. Chem. Soc. Perkin 1*, **1977**, 1597.

ACKNOWLEDGMENTS

R. K. Chaudhuri thanks the Alexander von Humboldt Foundation and Deutsche Forschungsgemeinschaft for the award of a postdoctoral fellowship (1975–1976) and a postdoctoral research associateship (1977), respectively. The authors thank the reviewer for his valuable suggestion regarding the mechanism of this demethylation reaction.

South American Plants III: Isolation of Fulvoplumierin from *Himatanthus sucuuba* (M. Arg.) Woodson (Apocynaceae)

GEORGIA PERSINOS PERDUE ˣ and RALPH N. BLOMSTER *

Received October 3, 1977, from *Natural Products Advocates, Rockville, MD 20852.* Accepted for publication January 4, 1978. *Present address: School of Pharmacy, University of Maryland, Baltimore, MD 21201.

Abstract □ The bark of *Himatanthus sucuuba* was screened for pharmacological and anticancer activities. The lactone, fulvoplumierin ($C_{14}H_{12}O_4$), was isolated from the *n*-hexane fraction. The identity was proven by elemental analysis and IR, mass spectral, and melting-point determinations. Reference samples were used for comparison.

Keyphrases □ Fulvoplumierin—isolated from *Himatanthus sucuuba* bark, evaluated for pharmacological and anticancer activity □ *Himatanthus sucuuba*—fulvoplumierin isolated from bark, evaluated for pharmacological and anticancer activity □ Antineoplastic activity—fulvoplumierin isolated from *Himatanthus sucuuba* bark, evaluated

In the search for new drugs from plants growing in the Upper Amazon Valley in Peru, several hundred species were evaluated for antitumor[1] and other pharmacological activities[2]. Plants with known medicinal folk uses received priority.

One plant, "bellaco caspi," *Himatanthus sucuuba* (M. Arg.) Woodson (Apocynaceae)[3], has several uses. Infusions, decoctions, and poultices prepared from the stem bark are used as a vermifuge and laxative and for treating arthritis, "tumors," boils, hernias, and swellings. A 50% ethanol–water extract of the stem bark showed anti-inflammatory activity in the carrageenan-induced edema method and was marginally active against the human epidermoid carcinoma of the nasopharynx (KB) test system. Frac-

[1] Tests were performed at the Drug Evaluation Branch, Drug Research and Development Division of the Cancer Treatment, National Cancer Institute, National Institutes of Health, Bethesda, MD 20014.

[2] All tests were performed at the Natural Products Research Laboratories, Rockville, MD 20851.

[3] The plant was collected in Peru in April 1968. Identification was made by Dr. J. J. Wurdak, Smithsonian Institution, Washington, D.C. A herbarium specimen was deposited at the Smithsonian Institution.

0022-3549/78/0900-1322$01.00/0

© 1978, American Pharmaceutical Association

Table I—Selective Demethylation of Polymethoxyxanthones

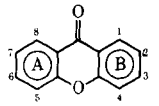

Compound	Substituents	Demethylation Substituents	Yield, %
I	1,3-$(OCH_3)_2$	1-OH-3-OCH_3	44
		1,3-$(OH)_2$	11
II	1-OH-3-OCH_3	1,3-$(OH)_2$	65
III	1,3,5-$(OCH_3)_3$	1-OH-3,5-$(OCH_3)_2$	40
		1,3-$(OH)_2$-5-OCH_3	8
IV	1,3,7-$(OCH_3)_3$	1-OH-3,7-$(OCH_3)_2$	45
		1,3-$(OH)_2$-7-OCH_3	10
V	2,3,4-$(OCH_3)_3$	2,4-$(OCH_3)_2$-3-OH	52
VI	1,2,3-$(OCH_3)_3$	1,3-$(OCH_3)_2$-2-OH	55
		1-OCH_3-2,3-$(OH)_2$	5
VII	1,2,3,4,7-$(OCH_3)_5$	1,4,7-$(OCH_3)_3$-2,3-$(OH)_2$	38
VIII	1,3,5,6,7-$(OCH_3)_5$	1,6-$(OH)_2$-3,5,7-$(OCH_3)_3$	22
		1,3,6-$(OH)_3$-5,7-$(OCH_3)_2$	36

The ease of *O*-demethylation is a function of resonance and steric factors. In compounds that are sterically less strained (I–IV), preferential demethylation occurs at C-1, followed by C-3 (and C-6), as could have been predicted on the basis of resonance factors (IX). Furthermore, since C-1 is more hindered than C-3 and C-6, the former should demethylate more readily. The selective demethylation at C-3 in V is caused by the relief of steric strain. However, this reaction can be explained as well in terms of simple resonance. In compounds having substitution at three or four adjacent carbon atoms, as in VI–VIII, the relief of steric strain is so important that it takes precedence over resonance effects, and one observes *O*-demethylation at C-2, C-3, and C-6, with C-2 demethylation being caused by the relief of steric strain.

REFERENCES

(1) F. M. Dean, in "The Total Synthesis of Natural Products," vol. I, J. ApSimon, Ed., Wiley–Interscience, New York, N.Y., 1973, p. 534.

(2) G. H. Stout and W. J. Balkenhal, *Tetrahedron*, **25**, 1947 (1969).

(3) A. J. Quillinan and F. Scheinmann, *J. Chem. Soc. Perkin 1*, **1973**, 1329.

(4) O. R. Gottlieb, A. A. Mesquita, T. J. Nagen, and P. Ferreirs, *Rev. Lat. Quim.*, **5**, 140 (1974).

(5) S. Ghosal, R. K. Chaudhuri, and K. R. Markham, *J. Chem. Soc. Perkin 1*, **1974**, 2538.

(6) S. Ghosal, S. Bannerjee, R. B. P. S. Chauhan, and R. S. Srivastava, *ibid.*, **1977**, 740.

(7) S. Ghosal, P. V. Sharma, and R. K. Chaudhuri, *Phytochemistry*, **14**, 2671 (1975).

(8) O. R. Gottlieb, M. T. Magalhaes, M. Camey, A. A. L. Mesquita, and D. de Barros Correa, *Tetrahedron*, **22**, 1777 (1966).

(9) T. J. Mabry, K. R. Markham, and M. B. Thomas, in "The Systematic Identification of Flavonoids," Springer Verlag, New York, N.Y., 1970, p. 35.

(10) D. Barraclough, H. D. Locksley, F. Scheinmann, M. T. Magalhaes, and O. R. Gottlieb, *J. Chem. Soc. B*, **1970**, 603.

(11) S. Ghosal, K. Biswas, and R. K. Chaudhuri, *J. Chem. Soc. Perkin 1*, **1977**, 1597.

ACKNOWLEDGMENTS

R. K. Chaudhuri thanks the Alexander von Humboldt Foundation and Deutsche Forschungsgemeinschaft for the award of a postdoctoral fellowship (1975–1976) and a postdoctoral research associateship (1977), respectively. The authors thank the reviewer for his valuable suggestion regarding the mechanism of this demethylation reaction.

South American Plants III: Isolation of Fulvoplumierin from *Himatanthus sucuuba* (M. Arg.) Woodson (Apocynaceae)

GEORGIA PERSINOS PERDUE ˣ and RALPH N. BLOMSTER *

Received October 3, 1977, from *Natural Products Advocates, Rockville, MD 20852.* Accepted for publication January 4, 1978. *Present address: School of Pharmacy, University of Maryland, Baltimore, MD 21201.

Abstract □ The bark of *Himatanthus sucuuba* was screened for pharmacological and anticancer activities. The lactone, fulvoplumierin ($C_{14}H_{12}O_4$), was isolated from the *n*-hexane fraction. The identity was proven by elemental analysis and IR, mass spectral, and melting-point determinations. Reference samples were used for comparison.

Keyphrases □ Fulvoplumierin—isolated from *Himatanthus sucuuba* bark, evaluated for pharmacological and anticancer activity □ *Himatanthus sucuuba*—fulvoplumierin isolated from bark, evaluated for pharmacological and anticancer activity □ Antineoplastic activity—fulvoplumierin isolated from *Himatanthus sucuuba* bark, evaluated

In the search for new drugs from plants growing in the Upper Amazon Valley in Peru, several hundred species were evaluated for antitumor[1] and other pharmacological activities[2]. Plants with known medicinal folk uses received priority.

One plant, "bellaco caspi," *Himatanthus sucuuba* (M. Arg.) Woodson (Apocynaceae)[3], has several uses. Infusions, decoctions, and poultices prepared from the stem bark are used as a vermifuge and laxative and for treating arthritis, "tumors," boils, hernias, and swellings. A 50% ethanol–water extract of the stem bark showed anti-inflammatory activity in the carrageenan-induced edema method and was marginally active against the human epidermoid carcinoma of the nasopharynx (KB) test system. Frac-

[1] Tests were performed at the Drug Evaluation Branch, Drug Research and Development Division of the Cancer Treatment, National Cancer Institute, National Institutes of Health, Bethesda, MD 20014.

[2] All tests were performed at the Natural Products Research Laboratories, Rockville, MD 20851.

[3] The plant was collected in Peru in April 1968. Identification was made by Dr. J. J. Wurdak, Smithsonian Institution, Washington, D.C. A herbarium specimen was deposited at the Smithsonian Institution.

0022-3549/78/0900-1322$01.00/0

© 1978, American Pharmaceutical Association

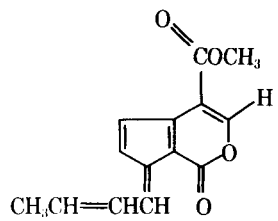

I

tionation of the stem bark was undertaken to isolate the active agent(s).

EXPERIMENTAL[4]

The coarsely ground stem bark (2 kg) of *H. sucuuba* was extracted continuously for 24 hr using a soxhlet apparatus with *n*-hexane. The *n*-hexane extract was concentrated *in vacuo* and refrigerated. Two additional *n*-hexane extracts were similarly prepared from the marc. The combined extracts were concentrated *in vacuo* and refrigerated.

A yellow-orange compound (500 mg), which separated out on standing, was removed by filtration and dried. This compound was dissolved in hot *n*-hexane, and the undissolved portion was dissolved in chloroform and reduced *in vacuo*. Orange crystals (150 mg) formed and were recrystallized from hot ethanol. They proved to be the known compound fulvoplumierin (I), mp 149–150° [lit. (1–3) mp 151–152°].

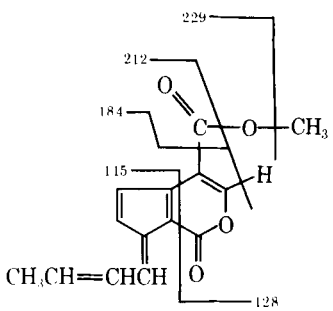

II

Further evidence for the assigned structure of I was derived from mass spectrometric analysis. The parent ion (*m/e* 224) was also the base peak in the mass spectrum. The remaining major ions were accounted for by commonly encountered fragmentation pathways and rearrangements to II (Table I).

Anal.—Calc. for $C_{14}H_{12}O_4$: C, 68.85; H, 4.95. Found: C, 68.64; H, 4.98.

An IR spectrum was superimposable with that of an authentic reference sample of fulvoplumierin[5].

Table I—Fragmentation Ions of Fulvoplumierin

m/e	Relative Intensity, %	Postulated Fragmentation Pattern
244	100	M^+
243	60	M − 1
229	20	M − CH_3
212	70	M − CH_3OH
184	40	*m/e* 212 − CO
156	50	*m/e* 184 − CO
128	75	—
115	25	Loss of pyrone ring

DISCUSSION

Fulvoplumierin, a lactone previously isolated from the root bark of *Plumeria acutifolia* L. (1, 2) and the stem bark of *P. rubra* L., was isolated from *H. sucuuba*. It was devoid of pharmacological activities. The present investigation establishes the first occurrence of this compound in this genus.

REFERENCES

(1) H. Grumbach, H. Schmid, and W. Bencze, *Experientia*, **8**, 224 (1952).

(2) H. Schmid and W. Bencze, *Helv. Chim. Acta*, **36**, 205 (1953).

(3) E. V. Rao and T. S. R. Anjaneyulu, *Indian J. Pharm.*, **29**, 273 (1967).

[4] Elemental analysis was performed by Geller Laboratories, Saddle River, N.J. Melting points were taken on a Mel-Temp apparatus and are uncorrected. IR and mass spectra were determined using a Beckman IR-8 and an LKB-9000 mass spectrophotometer, respectively.

[5] Supplied by Prof. Dr. H. Schmid, Universitat Zurich, and E. Venkata Rao, Andhra University, Waltair, India.

Synthesis and Antimicrobial Properties of 3-Substituted 1,2-Benzisothiazole 1,1-Dioxides

GERALD L. BACHMAN ˣ, JOSEPH W. BAKER, and DANIEL P. ROMAN

Received October 21, 1977, from the *Monsanto Company, St. Louis, MO 63166.* Accepted for publication December 28, 1977.

Abstract □ Twenty aromatic alcohols and thiols were derivatized by reaction with 3-chloro-1,2-benzisothiazole 1,1-dioxide. The resulting 3-substituted 1,2-benzisothiazole 1,1-dioxides were tested against *Staphylococcus aureus, Salmonella typhosa,* and *Aspergillus niger,* and their activities were compared with the activities of the precursors.

Keyphrases □ 1,2-Benzisothiazole 1,1-dioxides, 3-substituted—synthesized, evaluated for antibacterial and antifungal activity □ Antibacterial activity—various 3-substituted 1,2-benzisothiazole 1,1-dioxides evaluated □ Antifungal activity—various 3-substituted 1,2-benzisothiazole 1,1-dioxides evaluated □ Structure–activity relationships—various 3-substituted 1,2-benzisothiazole 1,1-dioxides evaluated for antibacterial and antifungal activity

The herbicidal and fungicidal activities of some 3-substituted 1,2-benzisothiazole 1,1-dioxides were reported previously (1, 2). This paper is concerned with the preparation and antimicrobial activity of a series of these

0022-3549/78/0900-1323$01.00/0

© 1978, American Pharmaceutical Association

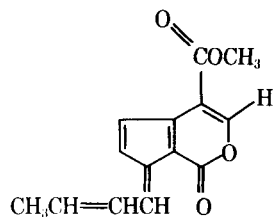

I

tionation of the stem bark was undertaken to isolate the active agent(s).

EXPERIMENTAL[4]

The coarsely ground stem bark (2 kg) of *H. sucuuba* was extracted continuously for 24 hr using a soxhlet apparatus with *n*-hexane. The *n*-hexane extract was concentrated *in vacuo* and refrigerated. Two additional *n*-hexane extracts were similarly prepared from the marc. The combined extracts were concentrated *in vacuo* and refrigerated.

A yellow-orange compound (500 mg), which separated out on standing, was removed by filtration and dried. This compound was dissolved in hot *n*-hexane, and the undissolved portion was dissolved in chloroform and reduced *in vacuo*. Orange crystals (150 mg) formed and were recrystallized from hot ethanol. They proved to be the known compound fulvoplumierin (I), mp 149–150° [lit. (1–3) mp 151–152°].

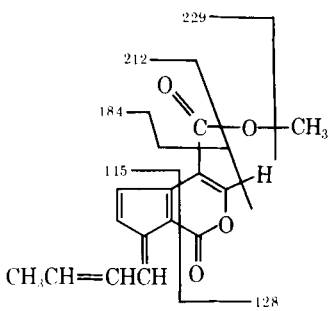

II

Further evidence for the assigned structure of I was derived from mass spectrometric analysis. The parent ion (*m/e* 224) was also the base peak in the mass spectrum. The remaining major ions were accounted for by commonly encountered fragmentation pathways and rearrangements to II (Table I).

Anal.—Calc. for $C_{14}H_{12}O_4$: C, 68.85; H, 4.95. Found: C, 68.64; H, 4.98.

An IR spectrum was superimposable with that of an authentic reference sample of fulvoplumierin[5].

Table I—Fragmentation Ions of Fulvoplumierin

m/e	Relative Intensity, %	Postulated Fragmentation Pattern
244	100	M^+
243	60	M − 1
229	20	M − CH_3
212	70	M − CH_3OH
184	40	*m/e* 212 − CO
156	50	*m/e* 184 − CO
128	75	—
115	25	Loss of pyrone ring

DISCUSSION

Fulvoplumierin, a lactone previously isolated from the root bark of *Plumeria acutifolia* L. (1, 2) and the stem bark of *P. rubra* L., was isolated from *H. sucuuba*. It was devoid of pharmacological activities. The present investigation establishes the first occurrence of this compound in this genus.

REFERENCES

(1) H. Grumbach, H. Schmid, and W. Bencze, *Experientia*, **8**, 224 (1952).

(2) H. Schmid and W. Bencze, *Helv. Chim. Acta*, **36**, 205 (1953).

(3) E. V. Rao and T. S. R. Anjaneyulu, *Indian J. Pharm.*, **29**, 273 (1967).

[4] Elemental analysis was performed by Geller Laboratories, Saddle River, N.J. Melting points were taken on a Mel-Temp apparatus and are uncorrected. IR and mass spectra were determined using a Beckman IR-8 and an LKB-9000 mass spectrophotometer, respectively.

[5] Supplied by Prof. Dr. H. Schmid, Universitat Zurich, and E. Venkata Rao, Andhra University, Waltair, India.

Synthesis and Antimicrobial Properties of 3-Substituted 1,2-Benzisothiazole 1,1-Dioxides

GERALD L. BACHMAN ˣ, JOSEPH W. BAKER, and DANIEL P. ROMAN

Received October 21, 1977, from the *Monsanto Company, St. Louis, MO 63166.* Accepted for publication December 28, 1977.

Abstract □ Twenty aromatic alcohols and thiols were derivatized by reaction with 3-chloro-1,2-benzisothiazole 1,1-dioxide. The resulting 3-substituted 1,2-benzisothiazole 1,1-dioxides were tested against *Staphylococcus aureus, Salmonella typhosa,* and *Aspergillus niger,* and their activities were compared with the activities of the precursors.

Keyphrases □ 1,2-Benzisothiazole 1,1-dioxides, 3-substituted—synthesized, evaluated for antibacterial and antifungal activity □ Antibacterial activity—various 3-substituted 1,2-benzisothiazole 1,1-dioxides evaluated □ Antifungal activity—various 3-substituted 1,2-benzisothiazole 1,1-dioxides evaluated □ Structure–activity relationships—various 3-substituted 1,2-benzisothiazole 1,1-dioxides evaluated for antibacterial and antifungal activity

The herbicidal and fungicidal activities of some 3-substituted 1,2-benzisothiazole 1,1-dioxides were reported previously (1, 2). This paper is concerned with the preparation and antimicrobial activity of a series of these

0022-3549/78/0900-1323$01.00/0

© 1978, American Pharmaceutical Association

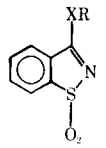

Table I—3-Substituted 1,2-Benzisothiazole 1,1-Dioxides [a]

Compound	R	X	Melting Point	Yield, %	Formula	Analysis, %	Calc.	Found
I	C_6H_5	O	181–183° [b]	89.7	$C_{13}H_9NO_3S$	S	12.40	12.40
II	2-ClC_6H_4	O	196–197° [c]	70.9	$C_{13}H_8ClNO_3S$	Cl	12.07	12.10
						N	4.77	4.79
III	4-ClC_6H_4	O	174–175°	80.5	$C_{13}H_8ClNO_3S$	Cl	12.07	12.10
						N	4.77	4.88
IV	3-$CF_3C_6H_4$	O	126–127°	58.7	$C_{14}H_8F_3NO_3S$	C	51.54	51.14
						H	2.16	2.29
						N	4.29	4.27
V	2,4-$Cl_2C_6H_3$	O	205–206°	76.7	$C_{13}H_7Cl_2NO_3S$	C	47.57	47.63
						H	2.15	2.31
						Cl	21.61	21.60
VI	2,4,6-$Cl_3C_6H_2$	O	278–279°	33.2	$C_{13}H_6Cl_3NO_3S$	C	43.06	43.02
						H	1.67	1.64
						N	3.86	3.56
VII	2,4,5-$Cl_3C_6H_2$	O	192–197°	24.0	$C_{13}H_6Cl_3NO_3S$	Cl	29.33	29.30
						N	3.86	4.01
						S	8.84	8.91
VIII	2,3,4,5,6-Br_5C_6	O	261–270°	31.9	$C_{13}H_4Br_5NO_3S$	C	23.88	23.88
						H	0.62	0.69
						Br	61.11	61.00
IX	2,3,4,5,6-Cl_5C_6	O	272–273°	56.0	$C_{13}H_4Cl_5NO_3S$	Cl	41.08	40.90
						N	3.28	3.38
						S	7.43	7.30
X	2-Cyclopentyl-4-ClC_6H_3	O	201–202°	33.2	$C_{18}H_{16}ClNO_3S$	C	59.74	60.14
						H	4.46	4.59
						N	3.87	3.85
XI	2-Cyclohexyl-4-ClC_6H_3	O	202–204°	32.0	$C_{19}H_{18}ClNO_3S$	N	3.73	4.00
						S	8.53	8.65
XII	2-Biphenyl	O	206–208°	56.0	$C_{19}H_{13}NO_3S$	N	4.19	4.34
						S	9.56	9.26
XIII	2-Benzyl-4-ClC_6H_3	O	173–174°	78.5	$C_{20}H_{14}ClNO_3S$	C	62.58	62.66
						H	3.68	3.74
						Cl	9.24	9.30
XIV	2-*sec*-Butyl-4,6-$NO_2C_6H_2$	O	134–135°	74.0	$C_{17}H_{15}N_3O_7S$	C	50.36	50.53
						H	3.73	3.61
						N	10.37	10.51
XV	C_6H_5	S	224–225° [d]	87.0	$C_{13}H_9NO_2S_2$	C	56.71	56.61
						H	3.29	3.06
						N	5.09	5.04
XVI	4-ClC_6H_4	S	205–207°	77.4	$C_{13}H_8ClNO_2S_2$	C	50.40	50.53
						H	2.60	2.71
						Cl	11.44	11.50
XVII	2,3,4,5,6-Cl_5C_6	S	290–291°	50.0	$C_{13}H_4Cl_5NO_2S$	C	34.88	34.66
						H	0.90	0.85
						N	3.13	3.18
XVIII	2-Pyridyl	S	194–196°	78.2	$C_{12}H_8N_2O_2S_2$	C	52.15	52.38
						H	2.92	3.08
						S	23.20	23.54
XIX	2-Pyridyl *N*-oxide	S	184° (dec.)	65.7	$C_{12}H_8N_2O_3S_2$	C	49.30	49.11
						H	2.76	2.50
						N	9.58	9.63
XX	8-Quinonyl	O	242–246°	95.0	$C_{16}H_{10}N_2O_3S$	N	9.03	8.83
						S	10.33	9.94

[a] All compounds were recrystallized from toluene, except IX which was recrystallized from xylene, XIV from ether, XIX from acetic acid, and XX from tetrahydrofuran. [b] Lit. (4) mp 182°. [c] Lit. (2) mp 196–197°. [d] Lit. (5) mp 219.0–219.5°.

pseudosaccharin ethers and thioethers.

RESULTS AND DISCUSSION

It is sometimes possible to derivatize a biologically active compound and thereby obtain a compound with more desirable physical properties while maintaining or improving the activity of the parent. If such chemically modified compounds are transformed to the parent compound before they elicit a pharmacological response, they are often referred to as prodrugs (3). On this premise, 20 pseudosaccharin derivatives (Table I) were prepared and tested against *Staphylococcus aureus*, *Salmonella typhosa*, and *Aspergillus niger*. These results were compared with those of the parent compounds, which were evaluated under identical conditions (Table II).

Derivatives XV and XVI had significantly greater activity (equivalent response at one-hundredth the concentration) against *S. aureus* and *A. niger* than their thiophenol precursors. Conversely, significantly lower activity (100-fold higher concentration required for equivalent response) was found with XI and XVII against *S. aureus*, with XIII and XIV against *S. typhosa*, and with IX, XI, and XIII against *A. niger*. The other pseudosaccharin derivatives were active at concentrations within a factor of ±10 of the precursors.

EXPERIMENTAL[1]

General Synthetic Procedure—A mixture of 5 g (0.025 mole) of pseudosaccharin chloride (5), 2.6 g (0.025 mole) of triethylamine, 0.025

[1] Melting points were taken on a Fisher-Johns melting-point apparatus and are corrected. IR spectra were recorded on a Beckman IR-5 spectrophotometer.

Table II—Antimicrobial Activity [a]

Compound	*S. aureus*	*S. typhosa*	*A. niger*
I	T	T	T
II	T	T	T
III	T	T	T
IV	T	T	T
V	T	T	T
VI	100T	T	100T
VII	100T	10T	100T
VIII	M	T	T
IX	M	10	T[b]
X	100T	T	10T
XI	+[b]	+	+[b]
XII	+	+	T
XIII	100T	+[b]	+[b]
XIV	M	T[b]	10T
XV	10T[c]	+	10T[c]
XVI	100T[c]	+	10T[c]
XVII	T[b]	T	T
XVIII	10T	T	T
XIX	M	M	M
XX	M	10T	100T

[a] The + represents growth at a dilution of 1×10^3; T, 10T, 100T, and M represent no growth at dilutions of 1×10^3, 1×10^4, 1×10^5, and 1×10^6, respectively. [b] The alcohol or thiol precursor showed equivalent response at one-hundredth the concentration. [c] The thiol precursur showed equivalent response at a 100-fold higher concentration.

mole of an alcohol or thiol, and 100 ml of toluene was stirred at reflux for 1–2 hr (Scheme I). The mixture was filtered free of by-product triethylamine hydrochloride, and the solvent was evaporated from the filtrate. The residue was recrystallized from the solvent indicated in Table I. The absence of carbonyl absorptions in the IR spectra confirmed that the compounds were not the *N*-substituted saccharin derivatives (6).

Antimicrobial Test Procedure—The derivatives were screened against *S. aureus* (ATCC 6538), *S. typhosa* (ATCC 6539), and *A. niger* (SN 111).

Stock solutions were prepared by dissolving 100 mg of the test compound in 10 ml of acetone, alcohol, or other solvent. The stock solutions

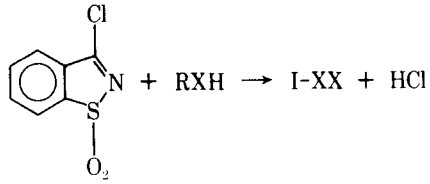

Scheme I

were diluted serially by pipetting 2 ml of the stock solutions into 18 ml of sterile agar to obtain a 1×10^3 dilution and continuing in the same manner for dilutions up to 1×10^6.

The agar was poured into petri dishes, allowed to harden, and spot inoculated with 1 drop of a cell suspension of the appropriate organism, prepared by suspending the growth from an agar slant culture in 10 ml of distilled water. The bacteria were incubated for 48 hr, and the *A. niger* was incubated for 5 days before examination for growth. The results reported are the minimum concentrations of the test compound that completely inhibited organism growth.

REFERENCES

(1) S. Seki, Y. Sekizawa, K. Nishibata, T. Watanabe, T. Kikuchi, H. Igarashi (to Meiji Confectionary Co.), U.S. at. 3,629,428 (Dec. 21, 1971).

(2) J. W. Baker and G. L. Bachman (to Monsanto Co.), U.S. pat. 3,673,200 (June 27, 1972).

(3) A. Albert, "Selective Toxicity," Wiley, New York, N.Y., 1965.

(4) J. R. Meadow and E. E. Reid, *J. Am. Chem. Soc.*, **65**, 457 (1943).

(5) J. R. Meadow and J. C. Cavagnol, *J. Org. Chem.*, **17**, 488 (1952).

(6) H. Hettler, *Tetrahedron Lett.*, **15**, 1793 (1968).

ACKNOWLEDGMENTS

The authors are grateful to P. D. McDonald and J. R. Wiedemann for the microbiological evaluations.

Constituents of *Spartina cynosuroides:* Isolation and ^{13}C-NMR Analysis of Tricin

J. BHATTACHARYYA, D. STAGG, N. V. MODY, and D. H. MILES ˣ

Received October 25, 1977, from the *Department of Chemistry, Mississippi State University, Mississippi State, MS 39762.* Accepted for publication January 4, 1978.

Abstract □ Tricin was isolated from the aerial parts of the marsh plant *Spartina cynosuroides*, which yielded a fraction enriched in antileukemic activity. The ^{13}C-NMR spectrum of tricin is discussed.

Keyphrases □ Tricin—isolated from *Spartina cynosuroides* aerial parts, ^{13}C-NMR spectral analysis □ *Spartina cynosuroides*—tricin isolated from aerial parts, ^{13}C-NMR spectral analysis

The giant cordgrass, *Spartina cynosuroides*[1] (Graminae), is the second most abundant plant in the salt marshes of Southern and Southeastern United States. A preliminary study (1) involved the primary production and decomposition of *S. cynosuroides* and the food value of this plant to marsh and estuarine organisms. The analysis of the volatile constituents of this plant was reported (2). Apart from a superficial study (3), no report of a detailed chemical investigation of the organic constituents of *S. cynosuroides* has appeared.

DISCUSSION

The 95% ethanolic extract of the aerial parts of *S. cynosuroides* showed high activity[2] against P-388 lymphocytic leukemia in BDF_1 mice. The activity[3] was considerably enriched in the chloroform extract at pH 4 of the acid-soluble part of the crude ethanolic extract. Column chromatography of the active extract yielded a yellow compound (M^+ 330), mp 288–290° dec., which gave a triacetate derivative, mp 254–256°, and was

[1] The plant material was identified by Dr. Sidney McDaniel, Department of Botany, Mississippi State University, Mississippi State, Miss. A voucher (preserved) specimen (SM-181) is available for inspection at the Herbarium of the Department of Botany, Mississippi State University.

[2] Percent T/C 146 at a dose level of 400 mg/kg against the National Cancer Institute murine P-388 lymphocytic leukemia system.

[3] Percent T/C 172 at a dose level of 400 mg/kg.

0022-3549/78/0900-1325$01.00/0
© 1978, American Pharmaceutical Association

Table II—Antimicrobial Activity [a]

Compound	*S. aureus*	*S. typhosa*	*A. niger*
I	T	T	T
II	T	T	T
III	T	T	T
IV	T	T	T
V	T	T	T
VI	100T	T	100T
VII	100T	10T	100T
VIII	M	T	T
IX	M	10	T[b]
X	100T	T	10T
XI	+[b]	+	+[b]
XII	+	+	T
XIII	100T	+[b]	+[b]
XIV	M	T[b]	10T
XV	10T[c]	+	10T[c]
XVI	100T[c]	+	10T[c]
XVII	T[b]	T	T
XVIII	10T	T	T
XIX	M	M	M
XX	M	10T	100T

[a] The + represents growth at a dilution of 1×10^3; T, 10T, 100T, and M represent no growth at dilutions of 1×10^3, 1×10^4, 1×10^5, and 1×10^6, respectively. [b] The alcohol or thiol precursor showed equivalent response at one-hundredth the concentration. [c] The thiol precursur showed equivalent response at a 100-fold higher concentration.

mole of an alcohol or thiol, and 100 ml of toluene was stirred at reflux for 1–2 hr (Scheme I). The mixture was filtered free of by-product triethylamine hydrochloride, and the solvent was evaporated from the filtrate. The residue was recrystallized from the solvent indicated in Table I. The absence of carbonyl absorptions in the IR spectra confirmed that the compounds were not the *N*-substituted saccharin derivatives (6).

Antimicrobial Test Procedure—The derivatives were screened against *S. aureus* (ATCC 6538), *S. typhosa* (ATCC 6539), and *A. niger* (SN 111).

Stock solutions were prepared by dissolving 100 mg of the test compound in 10 ml of acetone, alcohol, or other solvent. The stock solutions

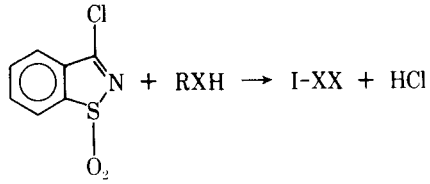

Scheme I

were diluted serially by pipetting 2 ml of the stock solutions into 18 ml of sterile agar to obtain a 1×10^3 dilution and continuing in the same manner for dilutions up to 1×10^6.

The agar was poured into petri dishes, allowed to harden, and spot inoculated with 1 drop of a cell suspension of the appropriate organism, prepared by suspending the growth from an agar slant culture in 10 ml of distilled water. The bacteria were incubated for 48 hr, and the *A. niger* was incubated for 5 days before examination for growth. The results reported are the minimum concentrations of the test compound that completely inhibited organism growth.

REFERENCES

(1) S. Seki, Y. Sekizawa, K. Nishibata, T. Watanabe, T. Kikuchi, H. Igarashi (to Meiji Confectionary Co.), U.S. at. 3,629,428 (Dec. 21, 1971).

(2) J. W. Baker and G. L. Bachman (to Monsanto Co.), U.S. pat. 3,673,200 (June 27, 1972).

(3) A. Albert, "Selective Toxicity," Wiley, New York, N.Y., 1965.

(4) J. R. Meadow and E. E. Reid, *J. Am. Chem. Soc.*, **65**, 457 (1943).

(5) J. R. Meadow and J. C. Cavagnol, *J. Org. Chem.*, **17**, 488 (1952).

(6) H. Hettler, *Tetrahedron Lett.*, **15**, 1793 (1968).

ACKNOWLEDGMENTS

The authors are grateful to P. D. McDonald and J. R. Wiedemann for the microbiological evaluations.

Constituents of *Spartina cynosuroides:* Isolation and ^{13}C-NMR Analysis of Tricin

J. BHATTACHARYYA, D. STAGG, N. V. MODY, and D. H. MILES ˣ

Received October 25, 1977, from the *Department of Chemistry, Mississippi State University, Mississippi State, MS 39762.* Accepted for publication January 4, 1978.

Abstract □ Tricin was isolated from the aerial parts of the marsh plant *Spartina cynosuroides*, which yielded a fraction enriched in antileukemic activity. The ^{13}C-NMR spectrum of tricin is discussed.

Keyphrases □ Tricin—isolated from *Spartina cynosuroides* aerial parts, ^{13}C-NMR spectral analysis □ *Spartina cynosuroides*—tricin isolated from aerial parts, ^{13}C-NMR spectral analysis

The giant cordgrass, *Spartina cynosuroides*[1] (Graminae), is the second most abundant plant in the salt marshes of Southern and Southeastern United States. A preliminary study (1) involved the primary production and decomposition of *S. cynosuroides* and the food value of this plant to marsh and estuarine organisms. The analysis of the volatile constituents of this plant was reported (2). Apart from a superficial study (3), no report of a detailed chemical investigation of the organic constituents of *S. cynosuroides* has appeared.

DISCUSSION

The 95% ethanolic extract of the aerial parts of *S. cynosuroides* showed high activity[2] against P-388 lymphocytic leukemia in BDF_1 mice. The activity[3] was considerably enriched in the chloroform extract at pH 4 of the acid-soluble part of the crude ethanolic extract. Column chromatography of the active extract yielded a yellow compound (M^+ 330), mp 288–290° dec., which gave a triacetate derivative, mp 254–256°, and was

[1] The plant material was identified by Dr. Sidney McDaniel, Department of Botany, Mississippi State University, Mississippi State, Miss. A voucher (preserved) specimen (SM-181) is available for inspection at the Herbarium of the Department of Botany, Mississippi State University.

[2] Percent T/C 146 at a dose level of 400 mg/kg against the National Cancer Institute murine P-388 lymphocytic leukemia system.

[3] Percent T/C 172 at a dose level of 400 mg/kg.

0022-3549/78/0900-1325$01.00/0
© 1978, American Pharmaceutical Association

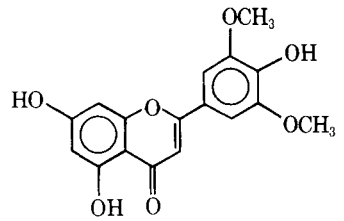

I

identical by mixed melting-point, IR, UV, and NMR comparisons with an authentic[4] sample of tricin (I) (4, 5).

The ^{13}C-NMR spectrum of tricin was taken in dimethyl sulfoxide-d_6 with tetramethylsilane as the internal standard, and the chemical shifts corresponding to the various carbon atoms in the molecule are given in Table I. The chemical shifts were assigned by comparison with the data published (6) for other flavonoid compounds. The shift for C-7 and C-2 can be interchanged. The relative lowfield shifts of C-10 and C-1′ carbons are probably due to the deshielding effect caused by the interaction of the solvent molecules dimethyl sulfoxide-d_6 with the hydroxyl functions *ortho* and *para* to C-10 and C-1′, respectively.

Table I—^{13}C-NMR Chemical Shift Assignments for Tricin

Carbon	Chemical Shift, ppm	Carbon	Chemical Shift, ppm
2	164.0	9	161.3
3	103.6	10	120.8
4	181.6	1′	139.7
5	157.2	2′, 6′	104.3
6	98.7	3′, 5′	148.0
7	163.5	4′	164.0
8	94.1	OCH_3	56.3

EXPERIMENTAL

Air-dried and ground tops of *S. cynosuroides* (10.0 kg) were extracted with 95% ethanol for 24 hr, and the extract was concentrated *in vacuo*. The gummy residue (Fraction A) was treated with 5% acetic acid (2000 ml) and stirred thoroughly. The acidic solution was then filtered through a bed of diatomaceous earth[5], and the filtrate was cooled in ice. Basification of the filtrate with ammonium hydroxide to pH 4 gave a precipitate, which was thoroughly extracted with chloroform. The organic layer was then washed free from acid, dried over anhydrous sodium sulfate, and distilled *in vacuo* to give a dark residue (Fraction B, 15 g).

Tricin—Fraction B was dissolved in chloroform (100 ml) with a few drops of methanol and then chromatographed in a column (50 × 2.5 cm) of silica gel G. Fractions of 500 ml each were eluted successively with chloroform (10 liters) and chloroform–ethanol (99:1, 10 liters). Fractions eluted with chloroform–ethanol (99:1, 5 liters), upon evaporation, gave a yellowish-brown residue (0.5 g). This residue was crystallized several times from chloroform–methanol to give a yellow powder, mp 288–290° dec.

Tricin Triacetate—Tricin (0.066 g, 1.02 mmoles) was treated with acetic anhydride (1 ml) and dry pyridine (1 ml) for 16 hr at room temperature. After the usual workup, the residue was crystallized from ethyl acetate as white needles (0.045 g), mp 263–265° dec.

[4] Kindly supplied by Dr. J. B. Harborne, Department of Botany, University of Reading, Reading, England.

[5] Celite.

REFERENCES

(1) E. P. Odum and A. A. de la Cruz, *AIBS Bull.*, **13**, 39 (1963).

(2) N. V. Mody, J. Bhattacharyya, D. H. Miles, and P. A. Hedin, *Phytochemistry*, **13**, 1175 (1974).

(3) L. R. Brown, *Bull. Georgia Acad. Sci.*, **21**, 20 (1963).

(4) T. J. Mabry, K. R. Markham, and M. B. Thomas, "The Systematic Identification of Flavonoids," Springer, Heidelberg, West Germany, 1970.

(5) J. Gripenberg, in "The Chemistry of Flavonoid Compounds," T. A. Geissman, Ed., Macmillan, New York, N.Y., 1962, p. 426.

(6) K. R. Markham and B. Ternai, *Tetrahedron*, **32**, 2607 (1976).

ACKNOWLEDGMENTS

Supported by Grant 3-ROI-CA-13268 from the National Cancer Institute, National Institutes of Health, Bethesda, MD 20014.

The authors thank Dr. S. W. Pelletier of the Institute for Natural Products Research, Athens, GA 30602, for the NMR spectra. They also thank Dr. Armanda de la Cruz and Dr. Sidney McDaniel for collection of plant material.

Sex Differences in Plasma Half-Life of Dextrorphan in Rats Administered Dextromethorphan

GOLLAMUDI RAMACHANDER *x, K. R. BAPATLA ‡, and JANE FRANCES EMELE

Received April 1, 1977, from the *Consumer Products Group, Warner-Lambert Company, Morris Plains, NJ 07950.* Accepted for publication December 15, 1977.

*Present address: Department of Medicinal Chemistry, College of Pharmacy, University of Tennessee Center for the Health Sciences, Memphis, TN 38163. ‡Present address: Cooper Laboratories Inc., Cedar Knolls, NJ 07927.

Abstract □ Male and female rats exhibited striking differences in their ability to metabolize dextromethorphan. Upon oral administration of this drug, the plasma half-life of dextrorphan, a major biotransformation product formed by *O*-demethylation, was 40 min in the female rat and 18.5 min in the male.

Keyphrases □ Dextromethorphan—metabolism in male and female rats compared □ Dextrorphan—plasma half-life in male and female rats compared □ Metabolism—dextromethorphan in male and female rats compared □ Antitussives—dextromethorphan, metabolism in male and female rats compared

Investigations in these laboratories on the bioavailability of dextromethorphan hydrobromide, a nonnarcotic antitussive agent, revealed striking differences between male and female rats in their metabolism rates. Upon oral administration, it is rapidly metabolized, the main routes of biotransformation being *O*- and *N*-demethylation, followed by conjugation of the desmethyl metabolites to glucuronides and sulfates (1–5).

Determination of the plasma levels of dextrorphan (*d*-3-hydroxy-*N*-methylmorphinan), the *O*-demethylated metabolite, previously (6) was employed to evaluate the bioavailability of dextromethorphan hydrobromide in

0022-3549/78/0900-1326$01.00/0

© 1978, American Pharmaceutical Association

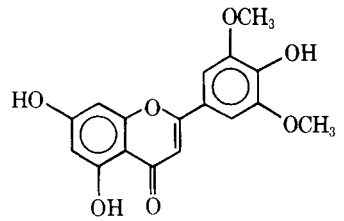

I

identical by mixed melting-point, IR, UV, and NMR comparisons with an authentic[4] sample of tricin (I) (4, 5).

The ^{13}C-NMR spectrum of tricin was taken in dimethyl sulfoxide-d_6 with tetramethylsilane as the internal standard, and the chemical shifts corresponding to the various carbon atoms in the molecule are given in Table I. The chemical shifts were assigned by comparison with the data published (6) for other flavonoid compounds. The shift for C-7 and C-2 can be interchanged. The relative lowfield shifts of C-10 and C-1′ carbons are probably due to the deshielding effect caused by the interaction of the solvent molecules dimethyl sulfoxide-d_6 with the hydroxyl functions *ortho* and *para* to C-10 and C-1′, respectively.

Table I—^{13}C-NMR Chemical Shift Assignments for Tricin

Carbon	Chemical Shift, ppm	Carbon	Chemical Shift, ppm
2	164.0	9	161.3
3	103.6	10	120.8
4	181.6	1′	139.7
5	157.2	2′, 6′	104.3
6	98.7	3′, 5′	148.0
7	163.5	4′	164.0
8	94.1	OCH_3	56.3

EXPERIMENTAL

Air-dried and ground tops of *S. cynosuroides* (10.0 kg) were extracted with 95% ethanol for 24 hr, and the extract was concentrated *in vacuo*. The gummy residue (Fraction A) was treated with 5% acetic acid (2000 ml) and stirred thoroughly. The acidic solution was then filtered through a bed of diatomaceous earth[5], and the filtrate was cooled in ice. Basification of the filtrate with ammonium hydroxide to pH 4 gave a precipitate, which was thoroughly extracted with chloroform. The organic layer was then washed free from acid, dried over anhydrous sodium sulfate, and distilled *in vacuo* to give a dark residue (Fraction B, 15 g).

Tricin—Fraction B was dissolved in chloroform (100 ml) with a few drops of methanol and then chromatographed in a column (50 × 2.5 cm) of silica gel G. Fractions of 500 ml each were eluted successively with chloroform (10 liters) and chloroform–ethanol (99:1, 10 liters). Fractions eluted with chloroform–ethanol (99:1, 5 liters), upon evaporation, gave a yellowish-brown residue (0.5 g). This residue was crystallized several times from chloroform–methanol to give a yellow powder, mp 288–290° dec.

Tricin Triacetate—Tricin (0.066 g, 1.02 mmoles) was treated with acetic anhydride (1 ml) and dry pyridine (1 ml) for 16 hr at room temperature. After the usual workup, the residue was crystallized from ethyl acetate as white needles (0.045 g), mp 263–265° dec.

[4] Kindly supplied by Dr. J. B. Harborne, Department of Botany, University of Reading, Reading, England.

[5] Celite.

REFERENCES

(1) E. P. Odum and A. A. de la Cruz, *AIBS Bull.*, **13**, 39 (1963).

(2) N. V. Mody, J. Bhattacharyya, D. H. Miles, and P. A. Hedin, *Phytochemistry*, **13**, 1175 (1974).

(3) L. R. Brown, *Bull. Georgia Acad. Sci.*, **21**, 20 (1963).

(4) T. J. Mabry, K. R. Markham, and M. B. Thomas, "The Systematic Identification of Flavonoids," Springer, Heidelberg, West Germany, 1970.

(5) J. Gripenberg, in "The Chemistry of Flavonoid Compounds," T. A. Geissman, Ed., Macmillan, New York, N.Y., 1962, p. 426.

(6) K. R. Markham and B. Ternai, *Tetrahedron*, **32**, 2607 (1976).

ACKNOWLEDGMENTS

Supported by Grant 3-ROI-CA-13268 from the National Cancer Institute, National Institutes of Health, Bethesda, MD 20014.

The authors thank Dr. S. W. Pelletier of the Institute for Natural Products Research, Athens, GA 30602, for the NMR spectra. They also thank Dr. Armanda de la Cruz and Dr. Sidney McDaniel for collection of plant material.

Sex Differences in Plasma Half-Life of Dextrorphan in Rats Administered Dextromethorphan

GOLLAMUDI RAMACHANDER *x, K. R. BAPATLA ‡, and JANE FRANCES EMELE

Received April 1, 1977, from the *Consumer Products Group, Warner-Lambert Company, Morris Plains, NJ 07950.* Accepted for publication December 15, 1977.

*Present address: Department of Medicinal Chemistry, College of Pharmacy, University of Tennessee Center for the Health Sciences, Memphis, TN 38163. ‡Present address: Cooper Laboratories Inc., Cedar Knolls, NJ 07927.

Abstract □ Male and female rats exhibited striking differences in their ability to metabolize dextromethorphan. Upon oral administration of this drug, the plasma half-life of dextrorphan, a major biotransformation product formed by *O*-demethylation, was 40 min in the female rat and 18.5 min in the male.

Keyphrases □ Dextromethorphan—metabolism in male and female rats compared □ Dextrorphan—plasma half-life in male and female rats compared □ Metabolism—dextromethorphan in male and female rats compared □ Antitussives—dextromethorphan, metabolism in male and female rats compared

Investigations in these laboratories on the bioavailability of dextromethorphan hydrobromide, a nonnarcotic antitussive agent, revealed striking differences between male and female rats in their metabolism rates. Upon oral administration, it is rapidly metabolized, the main routes of biotransformation being *O*- and *N*-demethylation, followed by conjugation of the desmethyl metabolites to glucuronides and sulfates (1–5).

Determination of the plasma levels of dextrorphan (*d*-3-hydroxy-*N*-methylmorphinan), the *O*-demethylated metabolite, previously (6) was employed to evaluate the bioavailability of dextromethorphan hydrobromide in

0022-3549/78/0900-1326$01.00/0

© 1978, American Pharmaceutical Association

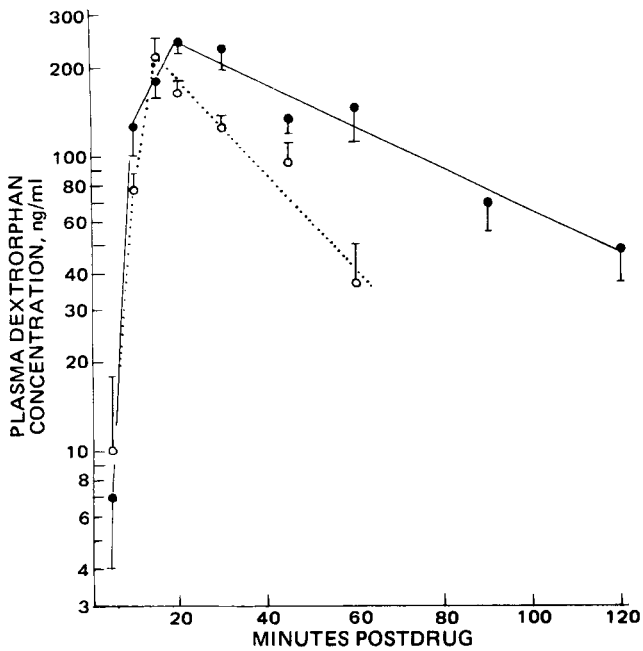

Figure 1—*Concentrations of dextrorphan in the plasma of male (○) and female (●) rats administered dextromethorphan hydrobromide (10 mg/kg po). Each point on the graph represents the mean ± SE of 10 female or four to seven male rats. The numbers of male rats were five at 5, 15, 45, and 60 min; seven at 10 and 20 min; and four at 30 min. The two groups differed significantly at 10 and 20 min ($p < 0.05$) and 30 and 60 min ($p < 0.01$). The data with female rats were reported by Ramachander* et al. *(15).*

humans. This report describes the differences in the plasma half-life of dextrorphan between male and female rats.

EXPERIMENTAL

Materials—Dextromethorphan hydrobromide[1], dextrorphan[1], spectroquality ethyl acetate[2], and analytical reagent grade *n*-hexane[3] were used.

Treatment of Animals—Groups of Sprague–Dawley rats, females (160–200 g) and males (150–200 g), were maintained on a standard laboratory diet for 1 week prior to use. After fasting for 18 hr, they received by stomach tube an aqueous solution of dextromethorphan hydrobromide, 10 mg/kg.

Blood samples were withdrawn into heparinized tubes by cardiac puncture immediately prior to drug administration and at various intervals thereafter (Fig. 1). Plasma was separated by centrifugation and analyzed for dextrorphan. Plasma obtained from one rat was employed to obtain one experimental dextrorphan concentration. Each reported value was derived from 10 female or four to seven male rats.

Determination of Dextrorphan in Plasma—The previously reported procedure (6) was employed. Plasma (3.0 ml) was adjusted to pH 9.5 by the addition of about 0.6 ml of saturated sodium carbonate solution and extracted with 15 ml of ethyl acetate. The mixture was centrifuged, and 12 ml of the organic layer was shaken with 3.0 ml of 1.0 *N* HCl. The acid layer was separated, and its fluorescence was measured in a fluorescence spectrophotometer[4]. The fluorescence and excitation wavelengths were 310 and 280 nm, respectively, and the slit dials were set to a bandpass of 8 nm for excitation and 5 nm for fluorescence. The dextrorphan concentration in the samples was read from a calibration curve whose validity was determined by including three to four known concentrations of the drug added to rat plasma with each series of unknowns.

Plasma half-lives were estimated by obtaining the slope of the line by the method of least squares, when ln C_p is plotted *versus t*, and dividing the absolute values of the slope into 0.693 (7).

RESULTS AND DISCUSSION

After oral administration of dextromethorphan hydrobromide (10 mg/kg) to male rats, dextrorphan appeared in plasma in 5 min (10 ng/ml), reached peak levels at 15 min (213 ng/ml), and declined thereafter (Fig. 1). The previously reported (6) average level of dextrorphan in the plasma of female rats was 7 ng/ml at 5 min, attained a maximum of 245 ng/ml at 20 min, and fell thereafter. The plasma dextrorphan concentrations in the female rats were significantly higher at 10 and 20 min ($p < 0.05$) and at 30 and 60 min ($p < 0.01$) than in the male rats; the average differences at these sampling times were 50, 81, 103, and 108 ng/ml, respectively. The plasma half-life of dextrorphan was 40 min in the female rats and 18.5 min in the males.

The observed differences in the plasma half-lives of dextrorphan between male and female rats are probably attributable to sex-dependent differences in glucuronidation, but the contribution of other sex-related factors in drug metabolism may be involved. Female rats are known to metabolize xenobiotics more slowly than male rats (8). The ability of hepatic microsomes to form *O*-aminophenol glucuronide *in vitro* was four times greater in male rats than in female rats (9). Progesterone glucuronide formation *in vitro* was faster and occurred in significantly greater quantities in male rats than in females (10).

Substantial sex-dependent differences in the metabolism of drugs also occur in humans. The metabolism of nicotine was reported (11) to differ between male and female smokers. Serum aspirin esterase activity was significantly higher in men than in women (12). The half-life of antipyrine was 30% longer in males than in females (13). In light of such evidence, it appears noteworthy to determine the clinical significance of the observed differences in the plasma half-lives of dextrorphan between male and female rats. At a dose of 2.0 mg/kg, this metabolite was reported (14) to possess antitussive activity comparable to that of dextromethorphan in the dog.

REFERENCES

(1) J. J. Kamm, A. B. Taddeo, and E. J. Van Loon, *J. Pharmacol. Exp. Ther.*, **158**, 437 (1967).

(2) K. Willner, *Arzneim.-Forsch.*, **12**, 26 (1963).

(3) C. Elison and H. Elliott, *J. Pharmacol. Exp. Ther.*, **144**, 265 (1964).

(4) A. Brossi, O. Hafliger, and O. Schneider, *Arzneim.-Forsch.*, **5**, 62 (1955).

(5) R. Versie, A. Noirsfalise, M. Niven, and R. Malchair, *Ann. Med. Leg. Criminol. Police Sci.*, **42**, 561 (1962).

(6) G. Ramachander, F. D. Williams, and J. F. Emele, *J. Pharm. Sci.*, **66**, 1047 (1977).

(7) J. G. Wagner, *J. Pharmacokinet. Biopharm.*, **1**, 165 (1973).

(8) R. Kato, *Drug Metab. Rev.*, **3**, 1 (1974).

(9) J. K. Inscoe and J. Axelrod, *J. Pharmacol. Exp. Ther.*, **129**, 128 (1960).

(10) L. G. S. Rao and W. Taylor, *Biochem. J.*, **96**, 172 (1965).

(11) A. H. Beckett, J. W. Gorrod, and P. Jenner, *J. Pharm. Pharmacol.*, **23**, 62S (1971).

(12) R. Menguy, L. Desbaillets, Y. F. Masters, and S. Okabe, *Nature*, **239**, 102 (1972).

(13) K. O'Malley, J. Crooks, E. Duke, and I. H. Stevenson, *Br. Med. J.*, **3**, 607 (1971).

(14) W. M. Benson, P. F. Stefko, and L. O. Randall, *J. Pharmacol. Exp. Ther.*, **109**, 189 (1953).

(15) G. Ramachander, F. D. Williams, and J. F. Emele, *J. Pharm. Sci.*, **67**, 761 (1978).

ACKNOWLEDGMENTS

The authors thank Dr. Herbert A. Lieberman for interest in this work.

[1] Hoffmann-La Roche, Nutley, N.J.
[2] Matheson, Coleman and Bell, Norwood, Ohio.
[3] Mallinckrodt Chemical Works, St. Louis, Mo.
[4] Perkin-Elmer model MPF-3.

Comparison of *In Vitro* Dissolution and *In Vivo* Bioavailability of Methaqualone Tablets in Humans

ROGER G. STOLL ˣ, GEORGE C. CHAO, HARVEY J. HOYT, and AVRAHAM YACOBI

Received October 20, 1977, from the *Department of Biopharmaceutical Sciences, Arnar-Stone Laboratories, McGaw Park, IL 60085.* Accepted for publication January 4, 1978.

Abstract □ Two methaqualone tablets that exhibited different *in vitro* dissolution rates were administered to 11 normal healthy male volunteers. Serial blood samples were withdrawn following administration of each tablet, and plasma methaqualone concentrations were determined by an established spectrophotofluorometric assay. Both tablets produced virtually identical plasma concentration *versus* time profiles in humans, and no statistically significant differences in either the rate or extent of drug absorbed were detected. The results indicate that there is no correlation between *in vivo* bioavailability and the modified NF *in vitro* dissolution test used.

Keyphrases □ Methaqualone—two tablets, *in vitro* dissolution compared to *in vivo* bioavailability in humans □ Dissolution, *in vitro*—methaqualone, two tablets, compared to *in vivo* bioavailability in humans □ Bioavailability, *in vivo*—methaqualone, two tablets in humans, compared to *in vitro* dissolution □ Hypnotic-sedatives—methaqualone, two tablets, *in vitro* dissolution compared to *in vivo* bioavailability in humans

Methaqualone [2-methyl-3-*o*-tolyl-4(3*H*)-quinazolinone], a sedative-hypnotic (1), is very slightly soluble in water (2). In humans, it is metabolized by the liver and excreted in the urine and feces (3, 4). Peak plasma concentrations of methaqualone are achieved 1.5–3 hr after oral administration of most tablet dosage forms (5–8). Following administration of 300-mg methaqualone tablets, peak plasma concentrations of about 3.0 μg/ml have been achieved (6, 7).

In recent *in vitro* dissolution rate studies using a modified NF dissolution rate procedure, several lots of methaqualone tablets[1] did not meet existing dissolution rate specifications. These tablets had been aged at room temperature for approximately 2 years. Chemburkar *et al.* (8) previously reported that the standard dissolution rate testing procedures might not correlate with the *in vivo* performance of methaqualone tablets. Therefore, the study reported here was undertaken to substantiate these findings for the particular formulation. More importantly, if present compendial dissolution rate standards cannot be correlated with the *in vivo* bioavailability of methaqualone tablets, the tests probably should be revised.

EXPERIMENTAL

In a two-way crossover study, 11 healthy, nonobese male subjects[2], 20–28 years old and 61–89 kg (mean 71 kg), were randomly selected by sequential admission. The subjects were instructed not to consume any drugs (including enzyme inducers) for at least 30 days preceding the study or alcoholic beverages during the entire study.

One methaqualone tablet (A or B) was given together with 240 ml of water in the morning after an overnight fast (12 hr). The subjects were allowed a standard diet 4 hr following drug ingestion. Blood samples, 8 ml, were obtained in heparinized syringes just prior to drug administration (0 hr) and at 0.5, 1, 2, 3, 4, 6, 8, 12, 16, and 24 hr after drug ingestion.

[1] Sopor, Arnar-Stone Laboratories, McGaw Park, Ill.
[2] All subjects were paid and signed a written consent form.

Table I—Dissolution Rate of Methaqualone Tablets

Tablet	Tablet Content, mg of Methaqualone	Dissolution Rate, % per 20 min	Dissolution Rate, % per 30 min
A	303	65.4	98.2
B	304	39.0	53.9
NF specifications		70.0	—

Plasma was immediately separated and frozen until assayed. A washout period of 1 week was allowed between the two treatment phases.

Concentrations of methaqualone in plasma were determined in duplicate by a spectrophotofluorometric procedure (9). A comparison of the spectrophotofluorometric procedure with GLC showed very low plasma concentrations of circulating metabolites of methaqualone during multiple-dose regimens (7). Therefore, the spectrophotofluorometric method was sufficiently specific for methaqualone for single-dose bioavailability studies (7). In this study, each concentration of methaqualone in plasma was corrected for the blank concentration of the 0-hr sample. For the analysis of variance test, a statistical package (10) was used to detect the significance of several sources of variability at the 0.05 level.

The dissolution test was done with the NF rotating-basket assembly set at 100 rpm, using 900 ml of dilute hydrochloric acid (17 ml of concentrated hydrochloric acid/2000 ml of aqueous solution) at 37°. This method is similar to the Method I dissolution test of the NF (2), except that the hydrochloric acid concentration in the NF test is 1/2000. Dissolution data for the methaqualone tablets tested in this study are shown in Table I.

RESULTS AND DISCUSSION

Table II lists the average plasma concentrations found for the two methaqualone tablets after oral administration to 11 fasted volunteers. There were no statistically significant differences in plasma concentrations (as determined by analysis of variance) at any sampling time following Tablets A and B. Likewise, no statistically significant differences in peak plasma concentration, time of peak plasma concentrations, and area under the plasma concentration–time curve (*AUC*) between 0 and 24 hr were found for the two tablets.

An additional important factor in any bioavailability study is the variability in plasma concentrations associated with any given drug treatment. The magnitude of the standard deviations associated with each mean value was comparable for both tablets (Table II). Furthermore, the subject population tested was sufficient to detect at least a 25% difference between treatment means for peak concentration and *AUC* at the 5% significance level with 95% certainty if such differences existed ($\alpha = 0.05$ and $\beta = 0.05$). Therefore, the power of the test was within established standards for bioavailability testing.

No significant trends were associated with the period and subject effects. Statistically significant differences among subjects (intersubject variability) are quite common to most bioavailability studies, and the effects noted for the 4–16-hr sampling time and the 0–24-hr *AUC* are to be expected.

Because of the usual subject population and study condition differences, it serves no useful purpose to attempt to demonstrate exact numerical correlation with reported plasma level data. Nonetheless, the general magnitude of the numbers found in this study was consistent with previous reports. For a 300-mg dose, peak concentrations of 3 μg/ml at 1.5–2 hr have been obtained generally (6, 7). The *AUC* (0–24 hr) obtained for Tablets A and B was, however, higher than a previously reported *AUC* (0–24 hr) value of 26.7 μg/ml × hr (7). Unless a common lot of drug or reference solutions is tested by both laboratories, no absolute conclusions can be drawn from these comparisons.

0022-3549/78/0900-1328$01.00/0
© 1978, American Pharmaceutical Association

Table II—Mean Individual Plasma Concentration Parameters for Methaqualone and Analysis of Variance for Each Indicated Parameter

Hours	Plasma Concentration, μg/ml (Mean ± SD)[a] Tablet A	Tablet B	Statistical Significance[b] Treatment Effect	Period Effect	Subject Effect
0.5	1.27 ± 1.27	1.35 ± 0.936	NS	NS	NS
1.0	3.10 ± 1.05	3.30 ± 1.09	NS	NS	NS
2.0	3.52 ± 0.863	3.29 ± 0.552	NS	NS	NS
3.0	2.93 ± 0.647	2.78 ± 0.572	NS	NS	NS
4.0	2.36 ± 0.575	2.30 ± 0.480	NS	NS	0.05
6.0	1.64 ± 0.366	1.59 ± 0.369	NS	NS	0.01
8.0	1.39 ± 0.287	1.43 ± 0.378	NS	NS	0.05
12.0	1.14 ± 0.265	1.17 ± 0.354	NS	NS	0.05
16.0	1.04 ± 0.279	1.02 ± 0.289	NS	0.05	0.05
24.0	0.848 ± 0.214	0.815 ± 0.253	NS	NS	NS
Peak concentration[c]	3.97 ± 0.718	3.70 ± 0.664	NS	NS	NS
Peak time, hr	1.82 ± 0.750	1.36 ± 0.664	NS	NS	NS
AUC[cd], (μg hr)/ml	34.6 ± 6.17	34.2 ± 8.00	NS	NS	0.05

[a] Average of 11 subjects. [b] A statistical package (10) was used to detect the significance of the factors at the 0.05 level. [c] A difference of 25% in overall means can be detected with $\alpha = 0.05$ and $\beta = 0.05$. [d] Area under plasma concentration–time curve from 0 to 24 hr.

The two methaqualone tablets tested in this study were bioequivalent. Thus, the currently used dissolution test did not accurately reflect the *in vivo* performance of methaqualone tablets. Since a dissolution test serves no useful purpose unless it reflects the potential safety or efficacy of a drug product, this study indicates that a new testing procedure is required.

Both tablets did not meet the existing NF dissolution rate standard (Table I). However, Tablet A could readily be considered an appropriate reference standard since the product met all NDA specifications. Furthermore, the data clearly show that changes of more than 50% in the *in vitro* dissolution rate of a tablet dosage form produced no apparent significant effect *in vivo*. Additionally, Chemburkar *et al.* (8) indicated that the dissolution rate test that most closely correlated with *in vivo* bioavailability was an extremely slow 2-rpm procedure. Based on their report plus the findings in this paper, serious considerations should be given toward revision of the current NF dissolution rate standards for methaqualone tablets.

REFERENCES

(1) A. H. Amin, D. R. Meta, and S. S. Samartha, *Progr. Drug Res.*, **14**, 218 (1970).

(2) "The National Formulary," 14th ed., Mack Publishing Co., Easton, Pa., 1975, pp. 432, 434, 892, 1049.

(3) J. A. Cella, *J. Pharm. Sci.*, **63**, 627 (1974).

(4) S. S. Brown and S. Goenechea, *Clin. Pharmacol. Ther.*, **14**, 314 (1973).

(5) "The Pharmacological Basis of Therapeutics," 5th ed., L. Goodman and A. Gilman, Eds., Macmillan, New York, N.Y., 1975, p. 130.

(6) R. N. Morris, G. A. Gunderson, S. W. Babcock, and J. F. Zaroslinski, *Clin. Pharmacol. Ther.*, **13**, 719 (1972).

(7) R. K. Nayak, R. D. Smyth, J. H. Chamberlain, A. Polk, A. F. Delong, T. Herczeg, P. B. Chemburkar, R. S. Joslin, and N. H. Reavey-Cantwell, *J. Pharmacokinet. Biopharm.*, **2**, 107 (1974).

(8) P. B. Chemburkar, R. D. Smyth, J. D. Buehler, P. B. Shah, R. S. Joslin, A. Polk, and N. H. Reavey-Cantwell, *J. Pharm. Sci.*, **65**, 529 (1976).

(9) S. S. Brown and G. A. Smart, *J. Pharm. Pharmacol.*, **21**, 466 (1969).

(10) A. J. Barr, J. H. Goodnight, J. P. Sall, and J. T. Helwig, in "The User's Guide to SAS 76," SAS Inc., Raleigh, N.C., 1976.

Binding of Drugs to Ion-Exchange Resins in Simulated Gastric Fluid

V. KHOUW, H. G. GILES ˣ, and E. M. SELLERS

Received July 5, 1977, from the *Clinical Pharmacology Program, Clinical Institute, Addiction Research Foundation, Toronto, Ontario, M5S 2S1, Canada*, and the *Departments of Medicine and Pharmacology, University of Toronto, Toronto, Canada.* Accepted for publication December 21, 1977.

Abstract □ The binding of 13 frequently abused drugs to two ion-exchange resins was studied in simulated gastric fluid. The results were compared with those previously obtained with activated charcoal as the adsorbent. The ion-exchange resins adsorbed the drugs more slowly than activated charcoal, and the binding capacities of the resins were inferior. These ion-exchange resins are unlikely to be very useful in removing drugs from the stomach.

Keyphrases □ Binding—various drugs to two ion-exchange resins in simulated gastric fluid, compared to previous results with charcoal □ Ion-exchange resins—binding of various drugs in simulated gastric fluid, compared to previous results with charcoal □ Adsorption—various drugs to two ion-exchange resins in simulated gastric fluid, compared to previous results with charcoal

The effective removal of drugs from the blood of animals and humans by hemoperfusion is well established (1). In the early work, use was made of the irreversible binding of drugs to activated charcoal by nonspecific surface adsorption. Charcoal hemoperfusion is not currently employed, however, since Hagstram *et al.* (2) documented platelet adsorption and the release of particles of charcoal into blood. More recently, coated activated charcoal (3)

0022-3549/78/0900-1329$01.00/0

© 1978, American Pharmaceutical Association

Table II—Mean Individual Plasma Concentration Parameters for Methaqualone and Analysis of Variance for Each Indicated Parameter

Hours	Plasma Concentration, μg/ml (Mean ± SD)[a] Tablet A	Tablet B	Statistical Significance[b] Treatment Effect	Period Effect	Subject Effect
0.5	1.27 ± 1.27	1.35 ± 0.936	NS	NS	NS
1.0	3.10 ± 1.05	3.30 ± 1.09	NS	NS	NS
2.0	3.52 ± 0.863	3.29 ± 0.552	NS	NS	NS
3.0	2.93 ± 0.647	2.78 ± 0.572	NS	NS	NS
4.0	2.36 ± 0.575	2.30 ± 0.480	NS	NS	0.05
6.0	1.64 ± 0.366	1.59 ± 0.369	NS	NS	0.01
8.0	1.39 ± 0.287	1.43 ± 0.378	NS	NS	0.05
12.0	1.14 ± 0.265	1.17 ± 0.354	NS	NS	0.05
16.0	1.04 ± 0.279	1.02 ± 0.289	NS	0.05	0.05
24.0	0.848 ± 0.214	0.815 ± 0.253	NS	NS	NS
Peak concentration[c]	3.97 ± 0.718	3.70 ± 0.664	NS	NS	NS
Peak time, hr	1.82 ± 0.750	1.36 ± 0.664	NS	NS	NS
AUC[cd], (μg hr)/ml	34.6 ± 6.17	34.2 ± 8.00	NS	NS	0.05

[a] Average of 11 subjects. [b] A statistical package (10) was used to detect the significance of the factors at the 0.05 level. [c] A difference of 25% in overall means can be detected with $\alpha = 0.05$ and $\beta = 0.05$. [d] Area under plasma concentration–time curve from 0 to 24 hr.

The two methaqualone tablets tested in this study were bioequivalent. Thus, the currently used dissolution test did not accurately reflect the *in vivo* performance of methaqualone tablets. Since a dissolution test serves no useful purpose unless it reflects the potential safety or efficacy of a drug product, this study indicates that a new testing procedure is required.

Both tablets did not meet the existing NF dissolution rate standard (Table I). However, Tablet A could readily be considered an appropriate reference standard since the product met all NDA specifications. Furthermore, the data clearly show that changes of more than 50% in the *in vitro* dissolution rate of a tablet dosage form produced no apparent significant effect *in vivo*. Additionally, Chemburkar *et al.* (8) indicated that the dissolution rate test that most closely correlated with *in vivo* bioavailability was an extremely slow 2-rpm procedure. Based on their report plus the findings in this paper, serious considerations should be given toward revision of the current NF dissolution rate standards for methaqualone tablets.

REFERENCES

(1) A. H. Amin, D. R. Meta, and S. S. Samartha, *Progr. Drug Res.*, **14**, 218 (1970).

(2) "The National Formulary," 14th ed., Mack Publishing Co., Easton, Pa., 1975, pp. 432, 434, 892, 1049.

(3) J. A. Cella, *J. Pharm. Sci.*, **63**, 627 (1974).

(4) S. S. Brown and S. Goenechea, *Clin. Pharmacol. Ther.*, **14**, 314 (1973).

(5) "The Pharmacological Basis of Therapeutics," 5th ed., L. Goodman and A. Gilman, Eds., Macmillan, New York, N.Y., 1975, p. 130.

(6) R. N. Morris, G. A. Gunderson, S. W. Babcock, and J. F. Zaroslinski, *Clin. Pharmacol. Ther.*, **13**, 719 (1972).

(7) R. K. Nayak, R. D. Smyth, J. H. Chamberlain, A. Polk, A. F. Delong, T. Herczeg, P. B. Chemburkar, R. S. Joslin, and N. H. Reavey-Cantwell, *J. Pharmacokinet. Biopharm.*, **2**, 107 (1974).

(8) P. B. Chemburkar, R. D. Smyth, J. D. Buehler, P. B. Shah, R. S. Joslin, A. Polk, and N. H. Reavey-Cantwell, *J. Pharm. Sci.*, **65**, 529 (1976).

(9) S. S. Brown and G. A. Smart, *J. Pharm. Pharmacol.*, **21**, 466 (1969).

(10) A. J. Barr, J. H. Goodnight, J. P. Sall, and J. T. Helwig, in "The User's Guide to SAS 76," SAS Inc., Raleigh, N.C., 1976.

Binding of Drugs to Ion-Exchange Resins in Simulated Gastric Fluid

V. KHOUW, H. G. GILES ˣ, and E. M. SELLERS

Received July 5, 1977, from the *Clinical Pharmacology Program, Clinical Institute, Addiction Research Foundation, Toronto, Ontario, M5S 2S1, Canada*, and the *Departments of Medicine and Pharmacology, University of Toronto, Toronto, Canada.* Accepted for publication December 21, 1977.

Abstract □ The binding of 13 frequently abused drugs to two ion-exchange resins was studied in simulated gastric fluid. The results were compared with those previously obtained with activated charcoal as the adsorbent. The ion-exchange resins adsorbed the drugs more slowly than activated charcoal, and the binding capacities of the resins were inferior. These ion-exchange resins are unlikely to be very useful in removing drugs from the stomach.

Keyphrases □ Binding—various drugs to two ion-exchange resins in simulated gastric fluid, compared to previous results with charcoal □ Ion-exchange resins—binding of various drugs in simulated gastric fluid, compared to previous results with charcoal □ Adsorption—various drugs to two ion-exchange resins in simulated gastric fluid, compared to previous results with charcoal

The effective removal of drugs from the blood of animals and humans by hemoperfusion is well established (1). In the early work, use was made of the irreversible binding of drugs to activated charcoal by nonspecific surface adsorption. Charcoal hemoperfusion is not currently employed, however, since Hagstram *et al.* (2) documented platelet adsorption and the release of particles of charcoal into blood. More recently, coated activated charcoal (3)

0022-3549/78/0900-1329$01.00/0

© 1978, American Pharmaceutical Association

Table I—Kinetic Studies

Drug	Resin 1 Initial $t_{1/2}$, min	Resin 1 Linear Interval, min	Resin 1 Correlation Coefficient	Resin 1 % Free at End of Linear Interval	Resin 1 % Free Final	Resin 1 Time of Finish, min	Resin 2 Initial $t_{1/2}$, min	Resin 2 Linear Interval, min	Resin 2 Correlation Coefficient	Resin 2 % Free at End of Linear Interval	Resin 2 % Free Final	Resin 2 Time of Finish, min
Amitriptyline	15.4	30	0.993	20.2	1.2	120	9.7	60	0.998	1.2	1.2	60
Aspirin (acetylsalicylic acid)	23.5	20	0.999	49.6	1.6	240	18.0	90	0.999	2.7	2.7	90
Chlordiazepoxide	36.7	45	0.968	40.3	19.1	240	20.3	60	0.999	11.6	2.3	240
Secobarbital	11.5	15	0.997	40.0	2.0	150	11.7	30	0.996	16.0	0.8	90

and two ion-exchange resins (4) were employed in hemoperfusion to circumvent the deleterious properties of plain, activated charcoal. The ion-exchange resins[1] are hard, insoluble spheres of porous polystyrene. They are hydrophobic and have large surface areas.

Although effective in hemoperfusion, the ion-exchange resins have not been tested for the removal of drugs from the stomach. If the resins are effective in this regard, they may be useful in the management of drug overdose. The binding of drugs *in vitro* to two ion-exchange resins was examined and compared to results previously obtained with activated charcoal (5).

EXPERIMENTAL

The studies were carried out by dissolving 0–10 mg of the drugs in 25 ml of simulated gastric fluid (5) at pH 1.3. Resin 1 or 2 was added to the solution, the solutions were incubated with shaking at 37° in a metabolic shaker, and the resin was allowed to settle. Free drug concentrations in the supernate were determined spectrophotometrically by comparison with standard curves.

RESULTS AND DISCUSSION

In general, the log drug concentration *versus* time profiles (Fig. 1) for the drugs showed two-mode relationships (least-squares analysis). From these relationships, the half-life of disappearance of each drug may be estimated (Table I). Without exception, the drug adsorption rate onto Resin 2 was faster than onto Resin 1, reflecting the larger surface area of Resin 2 (1). In comparison, however, drug adsorption onto activated charcoal under identical circumstances is so fast that the drug concentration in the supernate after 2 min of incubation is below the lower limit of the spectrophotometric assay.

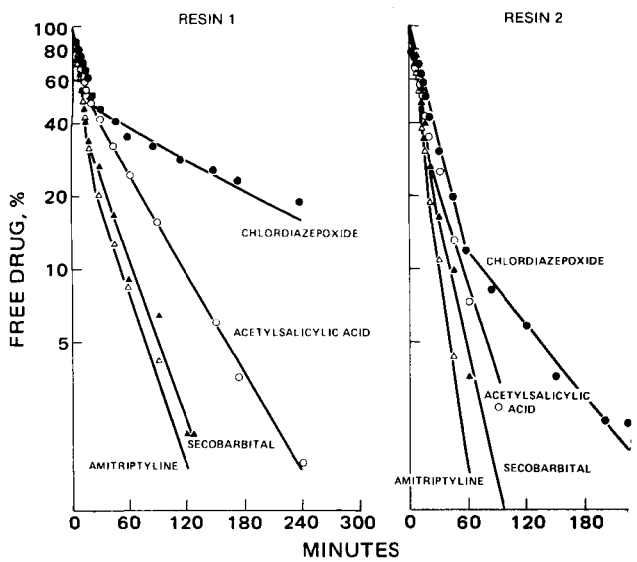

Figure 1—*Binding of drugs to ion-exchange resins in simulated gastric fluid.*

[1] Resin 1 was Amberlite XAD-2, 330 m^2/g; and Resin 2 was Amberlite XAD-4, 750 m^2/g. They were obtained from BDH Chemicals, Toronto, Ontario, Canada, and manufactured by Rohm and Haas, Philadelphia, Pa.

Table II—Comparison of Binding Capacities

Drug	Binding Capacity, mg/g: Resin 2	Binding Capacity, mg/g: Activated Charcoal
Amitriptyline	35	133
Amobarbital	43	51
Aspirin (acetylsalicylic acid)	54	262
Chlordiazepoxide	47	157
Chlorpromazine	40	—
Diazepam	50	136
Glutethimide	43	252
Methaqualone	39	179
Pentobarbital	55	103
Phenobarbital	49	70
Propoxyphene hydrochloride	26	127
Propoxyphene napsylate	28	137
Secobarbital	55	124

By employing the Langmuir equation, the binding capacities of Resin 2 were determined (5) (Table II). Comparison with previously obtained data with activated charcoal as the adsorbent (5) indicates that activated charcoal has a far higher binding capacity for the drugs studied.

These ion-exchange resins offer neither the advantage of rate nor extent of the drug adsorption shown by activated charcoal and are unlikely to be very useful in reducing the adsorption of drugs from the stomach.

REFERENCES

(1) J. L. Rosenbaum, *Ind. Eng. Chem. Prod. Res. Dev.*, **14**, 99 (1975).

(2) K. Hagstram, L. Larrson, and H. Thysell, *Acta Med. Scand.*, **180**, 593 (1966).

(3) T. M. S. Chang, J. F. Coffey, C. Lister, E. Taroy, and A. Stark, *Trans. Am. Soc. Artif. Intern. Organs*, **19**, 87 (1973).

(4) J. L. Rosenbaum, M. S. Kramer, and R. Raja, *Arch. Intern. Med.*, **136**, 263 (1976).

(5) E. M. Sellers, V. Khouw, and L. Dolman, *J. Pharm. Sci.*, **66**, 1640 (1977).

ACKNOWLEDGMENTS

The authors thank Hoffmann–La Roche Ltd., Vaudreuil, Quebec, Canada, for the benzodiazepines; Eli Lilly, Scarborough, Ontario, Canada, for aspirin (acetylsalicylic acid) and propoxyphene; Novopharm, Scarborough, Ontario, Canada, for amitriptyline and chlorpromazine; Abbott, Montreal, Quebec, Canada, for barbiturates; Charles E. Frosst and Co., Dorval, Quebec, Canada, for methaqualone; and Ciba Pharmaceuticals, Dorval, Quebec, Canada, for glutethimide.

Fluorometric Assay for Measuring Biological Half-Life of Coralyne Sulfoacetate in Dogs and Monkeys

JOE M. FINKEL ˣ **and DONALD L. HILL**

Received May 31, 1977, from *Kettering-Meyer Laboratory, Southern Research Institute, Birmingham, AL 35205.* Accepted for publication December 19, 1977.

Abstract □ A spectrophotofluorometric assay for coralyne sulfoacetate was developed. Coralyne was extracted from serum samples with *n*-butyl alcohol, and the drug concentrations were determined fluorometrically at 475 nm when the extract was excited at 325 nm. A biphasic serum decay curve for coralyne was observed for both dogs and monkeys. The biological half-lives for the two phases were 20 and 196 min in dogs and 15 and 142 min in monkeys.

Keyphrases □ Coralyne sulfoacetate—fluorometric analysis in serum □ Fluorometry—analysis, coralyne sulfoacetate in serum □ Antineoplastic agents, potential—coralyne sulfoacetate, fluorometric analysis in serum

Coralyne and some of its derivatives exhibit activity against leukemia L-1210 and P-388 in mice (1, 2). The basis for the biological activity of coralyne may be formation of intercalated complexes with cellular DNA (3, 4). The physiological distribution and metabolic fate of ^{14}C-coralyne in CDF_1 mice and Sprague–Dawley rats were reported (5), as was a preclinical toxicological evaluation of coralyne in dogs and monkeys (6).

The present paper reports serum levels and biological half-lives for coralyne in dogs and monkeys, as determined by a new fluorometric assay.

EXPERIMENTAL

Instrumentation—Fluorescence measurements were made with a spectrophotofluorometer[1] and an *x–y* recorder. The following instrument settings were used for all measurements: slit arrangement, No. 4; photomultiplier shutter, 4 mm; and sensitivity control, 40. Stainless-steel mirrors were inserted in the cell compartment to increase the amount of radiation reaching the photomultiplier tube.

Reagents—Various concentrations of coralyne sulfoacetate[2] in water or *n*-butyl alcohol saturated with water were prepared daily from a stock solution of 100 μg/ml.

Phosphate-buffered saline, 0.05 *M*, pH 7.4, was prepared by the addition of 2.6 g of monobasic sodium phosphate monohydrate and 11.5 g of dibasic sodium phosphate anhydrous to 9.0 g of sodium chloride. The mixture was dissolved and diluted to 1000 ml with water.

Coralyne extractions were made with *n*-butyl alcohol[3] saturated with water.

Analytical Procedures—Serum (0.2 ml) was diluted with an equal volume of phosphate-buffered saline and extracted with 2 ml of *n*-butyl alcohol. The fluorescence of the organic extract was measured at 475 nm with an excitation wavelength of 325 nm. Coralyne concentrations in serum were determined by comparison of the relative fluorescence intensity of extracts of serum to which 1–100 ng/ml of coralyne in *n*-butyl alcohol had been added. The fluorescence observed was proportional to concentration in the range of 10–1000 ng/ml of serum. Pretreatment serum from each animal served as blanks.

Recovery Studies—A 2-ml aliquot of coralyne standard in *n*-butyl alcohol (1–100 ng/ml) was manually shaken with 0.2 ml of serum plus 0.2 ml of pH 7.4 buffer or with 0.4 ml of pH 7.4 buffer in a 12-ml screw-capped centrifuge tube for 1 min and centrifuged at 1640×*g* for 10 min. The organic phase was removed, and its fluorescence intensity was determined as previously described. The fluorescence intensities of these extracts were compared with the intensities of corresponding coralyne standards in *n*-butyl alcohol.

Table I—Values for Selected Pharmacokinetic Parameters for Dogs and Monkeys Receiving a Single Intravenous Dose of Coralyne Sulfoacetate

Animal Model	Decay Phase, min	Pharmacokinetic Parameters[a] y Intercept, μg/ml	Rate Constant (Slope)	$t_{0.5}$, min
Dog	0–60 (α)	3.5, 2.4	−0.0328, −0.0365	21, 19
	90–300 (β)	0.29, 0.25	−0.0044, −0.0030	159, 232
Monkey	0–60 (α)	5.9, 3.3	−0.0483, −0.0439	14, 16
	90–300 (β)	0.22, 0.24	−0.0048, −0.0050	144, 140

[a] Values for individual dogs and monkeys are presented.

Animal Studies—Two female beagle dogs, 10 and 12 kg, and two female rhesus monkeys, 4 and 5 kg, each received a single dose (10 mg/kg iv) of coralyne sulfoacetate. The injection solution (10 mg/ml) was prepared in the phosphate-buffered saline immediately prior to administration. Blood samples were collected at 11 time intervals up through 6 hr after treatment and placed in an ice bath. Each animal served as its own control.

The serum samples were assayed within 3–5 hr after collection. Although the drug remained stable during its storage in an ice bath, longer storage periods required prior extraction into *n*-butyl alcohol.

TLC—Coralyne metabolites soluble in *n*-butyl alcohol might interfere with the fluorometric assay. To determine if such metabolites appeared in the serum, 100- or 500-μl aliquots of the alcohol extract from each sample of serum were spotted on TLC sheets[4]. The sheets were developed in a solvent of chloroform–methanol–acetic acid (80:19:1 v/v/v). Coralyne was located at R_f 0.45 on the sheets under UV light (366 nm).

RESULTS AND DISCUSSION

Fluorescence Studies—Coralyne sulfoacetate showed fluorescence in a neutral or acidic aqueous solution. A twofold increase of fluorescence intensity was observed when coralyne was dissolved in *n*-butyl alcohol. The maximum excitation occurred at 325 nm; at that wavelength, the maximum fluorescence was 475 nm. Preliminary studies indicated that the drug was unstable in 0.1 *N* NaOH but stable in 0.1 *N* HCl, ethanol, and *n*-butyl alcohol at room temperature. The relative fluorescence intensity was linear with the concentration of the drug in *n*-butyl alcohol in the range of 1–100 ng/ml.

The relative fluorescence intensities of a coralyne standard (1 μg/ml) as extracted from pH 7.4 phosphate-buffered saline and from serum were 44.8 ± 0.64 and 33.5 ± 1.0, respectively. These values, the averages of three determinations, were corrected for background interferences of 0.25 ± 0.02 for extracts from the buffer and 1.47 ± 0.03 for extracts from serum. The saturated *n*-butyl alcohol gave a fluorescence background of 0.24 ± 0.02. Concentrations of coralyne in serum as low as 10 ng/ml were detected. The extraction efficiency of coralyne from serum was 67% when compared with a coralyne standard in *n*-butyl alcohol.

Applications—Serum levels of coralyne were analyzed by computer programs. The exponential parameters were estimated by curve stripping of the data as described by Sedman and Wagner (7). After preliminary resolution into individual exponential components, the data were analyzed by a weighted, nonlinear, least-squares program and were fitted to the biexponential equation $C = Ae^{-\alpha t} + Be^{-\beta t}$, where C was the drug concentration in serum, A and B were coefficients, and α and β were rate constants representing the slopes of the two phases.

[1] Aminco-Bowman, American Instrument Co.

[2] Supplied by Drug Research and Development, Division of Cancer Treatment, National Cancer Institute.

[3] Analyzed reagent, J. T. Baker Chemical Co.

[4] Gelman Type SA ITLC.

0022-3549/78/0900-1331$01.00/0
© 1978, American Pharmaceutical Association

The serum decay curves for coralyne in dogs and monkeys exhibited a rapid distribution phase followed by a much slower second phase. Pharmacokinetic values derived by computer analysis are summarized in Table I. Values for the first phase were similar to those derived for rats given an intravenous dose of coralyne (5). As observed for rats, however, a distribution phase may be missing, because distribution of the dose in the total body water of dogs and monkeys would produce a larger serum concentration (15 μg/ml) at t_0 (y intercept).

In dog serum, but not monkey serum, a faintly fluorescent metabolite of coralyne appeared after 45 min at R_f 0.80. This nonpolar metabolite may be the same as that observed in the bile of rats (5). Based on TLC using 10–50-fold more extract than was used to detect coralyne, the contribution of fluorescence of this metabolite to total fluorescence is small.

REFERENCES

(1) K. Y. Zee-Cheng, K. D. Paull, and C. C. Cheng, *J. Med. Chem.*, **17**, 347 (1974).

(2) R. K. Y. Zee-Cheng and C. C. Cheng, *ibid.*, **19**, 882 (1976).

(3) K. Y. Zee-Cheng and C. C. Cheng, *J. Pharm. Sci.*, **62**, 1572 (1973).

(4) W. D. Wilson, A. N. Gough, J. J. Doyle, and M. W. Davidson, *J. Med. Chem.*, **19**, 1261 (1976).

(5) J. Plowman, R. L. Cysyk, and R. N. Adamson, *Xenobiotica*, **6**, 281 (1976).

(6) T. R. Castles, J. S. Hicks, J. L. Sanyer, and C. C. Lee, Society of Toxicology (Abstr.), No. 177, 145 (1976).

(7) A. J. Sedman and J. G. Wagner, *J. Pharm. Sci.*, **65**, 1006 (1976).

ACKNOWLEDGMENTS

Supported by Contract NO1-CM-43780 from the Division of Cancer Treatment, National Cancer Institute, National Institutes of Health.

The authors thank Mrs. Sheila Campbell for assistance.

Rapid Determination of Gold in Whole Blood of Arthritis Patients Using Flameless Atomic Absorption Spectrophotometry

MICHAEL J. BARRETT, ROY DeFRIES *, and WILLIAM M. HENDERSON ˣ

Received July 14, 1977, from the *Department of Pharmaceutics and Pharmacy Practice, College of Pharmacy, North Dakota State University, Fargo, ND 58102.* Accepted for publication December 9, 1977.

*Present address: School of Medicine, Southern Illinois University, Carbondale, IL 62901.

Abstract □ An assay for gold in whole blood of arthritis patients was developed using the graphite furnace atomic absorption spectrophotometer. This method involves no pretreatment of the whole blood except for simple dilution, thereby eliminating some variables and saving laboratory time and expense.

Keyphrases □ Gold—atomic absorption spectrophotometric analysis in whole blood □ Atomic absorption spectrophotometry—analysis, gold in whole blood □ Metals—gold, atomic absorption spectrophotometric analysis in whole blood

Gold salts have been used in rheumatoid arthritis for over 40 years, but few concise and accurate assays for the determination of gold in biological fluids have been developed. Since varying amounts of gold are found in the red blood cells of some patients receiving chrysotherapy (1, 2), an analysis of whole blood rather than blood fractions should be used to determine optimally the total gold content in the circulation.

Most methods of gold analysis (*i.e.*, chemical, UV emission, spectrography, polarography, and neutron activation) require extensive laboratory work to remove interfering fractions and repeated extractions (3, 4). Neutron activation analysis for the estimation of gold is the most sensitive method available (5); but since samples must be dried, sealed, irradiated for several hours, and cooled for several days, there is a possibly prohibitive time delay in reporting results. Furthermore, the assay requires expensive neutron sources with licensed operators and multichannel analyzers, both of which are relatively unavailable (5). This assay is beyond the capabilities of most clinical laboratories, thus rendering it rather impractical (4).

The lack of simple and accurate assay techniques for gold in biological fluids made it difficult to determine absorption, distribution, deposition, and excretion throughout dosing intervals and inhibited evaluation of the pharmacology and the pharmacodynamics of gold (4, 6–8). Atomic absorption spectrophotometric results compare well with those of neutron activation analysis (5), and its simplicity, speed, and range make it ideal for clinical work.

EXPERIMENTAL

Apparatus—The analysis was done using an atomic absorption spectrophotometer[1] with a graphite furnace accessory[2]. Power for the furnace was supplied by a controller[2] with a temperature ramp accessory[2] (Table I) to minimize elemental loss due to rapid gross temperature changes. All samples were injected *via* an automatic sampling system[3]. Since the instrument digital readout did not respond rapidly enough to the atomization signal, a strip-chart recorder[4] was implemented. The chosen emission source was a hollow cathode lamp[5].

Reagents and Standards—The water used in all dilutions was previously deionized by passage through a mixed-bed, ion-exchange column[6] with subsequent filtration through a 5-μm membrane filter[7] to remove any dislodged resin and other particulates.

[1] Perkin-Elmer model 403.
[2] Perkin-Elmer model HGA-2100.
[3] Perkin-Elmer model AS-1.
[4] Perkin-Elmer model 36.
[5] Perkin-Elmer Intensitron (No. 303-6031).
[6] Barnstead Ultrapure (No. D0809).
[7] Metricel.

0022-3549/78/0900-1332$01.00/0

© 1978, American Pharmaceutical Association

The serum decay curves for coralyne in dogs and monkeys exhibited a rapid distribution phase followed by a much slower second phase. Pharmacokinetic values derived by computer analysis are summarized in Table I. Values for the first phase were similar to those derived for rats given an intravenous dose of coralyne (5). As observed for rats, however, a distribution phase may be missing, because distribution of the dose in the total body water of dogs and monkeys would produce a larger serum concentration (15 μg/ml) at t_0 (y intercept).

In dog serum, but not monkey serum, a faintly fluorescent metabolite of coralyne appeared after 45 min at R_f 0.80. This nonpolar metabolite may be the same as that observed in the bile of rats (5). Based on TLC using 10–50-fold more extract than was used to detect coralyne, the contribution of fluorescence of this metabolite to total fluorescence is small.

REFERENCES

(1) K. Y. Zee-Cheng, K. D. Paull, and C. C. Cheng, *J. Med. Chem.*, **17**, 347 (1974).

(2) R. K. Y. Zee-Cheng and C. C. Cheng, *ibid.*, **19**, 882 (1976).

(3) K. Y. Zee-Cheng and C. C. Cheng, *J. Pharm. Sci.*, **62**, 1572 (1973).

(4) W. D. Wilson, A. N. Gough, J. J. Doyle, and M. W. Davidson, *J. Med. Chem.*, **19**, 1261 (1976).

(5) J. Plowman, R. L. Cysyk, and R. N. Adamson, *Xenobiotica*, **6**, 281 (1976).

(6) T. R. Castles, J. S. Hicks, J. L. Sanyer, and C. C. Lee, Society of Toxicology (Abstr.), No. 177, 145 (1976).

(7) A. J. Sedman and J. G. Wagner, *J. Pharm. Sci.*, **65**, 1006 (1976).

ACKNOWLEDGMENTS

Supported by Contract NO1-CM-43780 from the Division of Cancer Treatment, National Cancer Institute, National Institutes of Health.

The authors thank Mrs. Sheila Campbell for assistance.

Rapid Determination of Gold in Whole Blood of Arthritis Patients Using Flameless Atomic Absorption Spectrophotometry

MICHAEL J. BARRETT, ROY DeFRIES *, and WILLIAM M. HENDERSON ˣ

Received July 14, 1977, from the *Department of Pharmaceutics and Pharmacy Practice, College of Pharmacy, North Dakota State University, Fargo, ND 58102.* Accepted for publication December 9, 1977.

*Present address: School of Medicine, Southern Illinois University, Carbondale, IL 62901.

Abstract □ An assay for gold in whole blood of arthritis patients was developed using the graphite furnace atomic absorption spectrophotometer. This method involves no pretreatment of the whole blood except for simple dilution, thereby eliminating some variables and saving laboratory time and expense.

Keyphrases □ Gold—atomic absorption spectrophotometric analysis in whole blood □ Atomic absorption spectrophotometry—analysis, gold in whole blood □ Metals—gold, atomic absorption spectrophotometric analysis in whole blood

Gold salts have been used in rheumatoid arthritis for over 40 years, but few concise and accurate assays for the determination of gold in biological fluids have been developed. Since varying amounts of gold are found in the red blood cells of some patients receiving chrysotherapy (1, 2), an analysis of whole blood rather than blood fractions should be used to determine optimally the total gold content in the circulation.

Most methods of gold analysis (*i.e.*, chemical, UV emission, spectrography, polarography, and neutron activation) require extensive laboratory work to remove interfering fractions and repeated extractions (3, 4). Neutron activation analysis for the estimation of gold is the most sensitive method available (5); but since samples must be dried, sealed, irradiated for several hours, and cooled for several days, there is a possibly prohibitive time delay in reporting results. Furthermore, the assay requires expensive neutron sources with licensed operators and multichannel analyzers, both of which are relatively unavailable (5). This assay is beyond the capabilities of most clinical laboratories, thus rendering it rather impractical (4).

The lack of simple and accurate assay techniques for gold in biological fluids made it difficult to determine absorption, distribution, deposition, and excretion throughout dosing intervals and inhibited evaluation of the pharmacology and the pharmacodynamics of gold (4, 6–8). Atomic absorption spectrophotometric results compare well with those of neutron activation analysis (5), and its simplicity, speed, and range make it ideal for clinical work.

EXPERIMENTAL

Apparatus—The analysis was done using an atomic absorption spectrophotometer[1] with a graphite furnace accessory[2]. Power for the furnace was supplied by a controller[2] with a temperature ramp accessory[2] (Table I) to minimize elemental loss due to rapid gross temperature changes. All samples were injected *via* an automatic sampling system[3]. Since the instrument digital readout did not respond rapidly enough to the atomization signal, a strip-chart recorder[4] was implemented. The chosen emission source was a hollow cathode lamp[5].

Reagents and Standards—The water used in all dilutions was previously deionized by passage through a mixed-bed, ion-exchange column[6] with subsequent filtration through a 5-μm membrane filter[7] to remove any dislodged resin and other particulates.

[1] Perkin-Elmer model 403.
[2] Perkin-Elmer model HGA-2100.
[3] Perkin-Elmer model AS-1.
[4] Perkin-Elmer model 36.
[5] Perkin-Elmer Intensitron (No. 303-6031).
[6] Barnstead Ultrapure (No. D0809).
[7] Metricel.

0022-3549/78/0900-1332$01.00/0

© 1978, American Pharmaceutical Association

Table I—Preset Conditions on the Temperature Controller and Ramp Accessory

Parameter	Temperature	Cycle Time[a], sec	Ramp Time, sec
Dry	125°	30	10
Char	800°	90	10
Atomize	2200°	5	0

[a] Includes ramp time for that step.

Table II—Precision of the Gold Analysis at Different Whole Blood Concentrations [a]

Actual, μg/dl	Observed[b], μg/dl	*CV*, %
100	112.6	10.4
300	289.2	5.1
500	493.4	1.8

[a] Using an average calibration curve selected from actual data. [b] Mean of 18 determinations from 3 separate days.

All standards were prepared by the addition of atomic absorption standards[8] to quantities of blank human whole blood. To separate 20-ml aliquots of whole blood were added 20, 60, and 100 μl of 1000-ppm standards, making the final concentrations of the standard gold–whole blood solutions 1, 3, and 5 ppm, respectively.

The atomic absorption spectrophotometer settings were: emission wavelength, 242.8 nm; slit width, 7 nm; lamp current, 10 mamp; argon flow rate, 40 ml/min; and water flow rate, 2–2.5 liters/min.

Procedure—All patient blood samples were received in glass tubes[9] with edetic acid as the anticoagulant. Each sample was both vortexed and inverted gently to distribute the formed constituents evenly throughout, and then a 500-μl portion was withdrawn using a micropipet[10]. This portion was placed in a polypropylene centrifuge tube[11] containing 9.5 ml of the deionized, distilled water. The resulting mixture was then vortexed for 10 sec to ensure complete dispersion and hemolysis of the blood.

The procedure was repeated for all patient and standard samples. The final step involved placing diluted samples, done in duplicate, into sampling cups from which the automatic sampling system withdrew 20 μl for each determination.

RESULTS AND DISCUSSION

The study was conceived to develop a simple, rapid method of determining blood gold levels in arthritis patients and to improve clinician monitoring of chrysotherapy.

Since chrysotherapy is becoming more widely used in the treatment of active rheumatoid arthritis, the clinician needs to be able to adjust the dosing based on blood level data rather than subjective data such as patient opinion and range of motion evaluation. If the patient shows no clinical improvement when therapeutic blood levels (300–600 μg/dl) are reached, therapy can be stopped rather than continued in the hope of subjective improvement.

Study data also indicate that a considerable portion of the so-called therapeutic failures may be due to undetected subtherapeutic blood gold levels. Reproducible quantitative detection of gold at picogram levels was attained (Table II) without complicated analytical procedures involving extraction, chelate formation, and sample transfers. Gold concentrations (300–600 μg/dl) in the normal therapeutic range do not require procedures sensitive to picogram levels. Clinically useful analytical procedures must be simple, specific, and capable of being performed rapidly.

Operation of the atomic absorption spectrometer in the therapeutic gold concentration range results in a good signal-to-noise ratio with suitable amplitude of the recorder response for data reduction.

The preset conditions on the controller[2] (Table I) for the programmed temperature time cycles were critical to the assay precision and accuracy. The cycle timing primarily affected the assay sensitivity, while the assay reproducibility was primarily affected by the temperature settings.

[8] Fisher Scientific (1000 ppm).
[9] Vacutainers, Becton-Dickinson Co.
[10] Eppendorf, Brinkmann.
[11] Nalgene.

Table III—Example of Individualized Patient Blood Level Analysis

Standard Curve Data	
Concentration, ppm	Absorbance Units
1	11
1	11
3	32
3	33
5	52
5	53
Slope	10.375
Y-Intercept	0.875
SE	0.165
Correlation coefficient	0.999
Confidence limits	9.915–10.835
Patient Data	
Patient name	Doe, John
Time	Hour 4
Sample date	3/29/76
Gold concentration (whole blood), μg/dl	411
Error, %	1.659
Average absorbance	43.5

Table IV—Example of Cumulative Blood Level Data for Physician from One Dosing Interval (1 Week)

Time	Date Drawn	Whole Blood Level, μg/dl
Hour 0	3/29/76	213
Hour 1	3/29/76	469
Hour 2	3/29/76	430
Hour 3	3/29/76	425
Hour 4	3/29/76	411
Day 1	3/30/76	293
Day 2	3/31/76	258
Day 3	4/1/76	230
Day 4	4/2/76	194

Volunteer blood and a suitable commercial source of whole blood were used to run whole blood standard curve samples and were compared. There was no difference in instrumental response to freshly drawn or commercial standard curve whole blood samples at any time. The use of different anticoagulants such as edetate disodium, ammonium pyrrolidinedithiocarbamate, heparin, citrates, and oxalates did not alter the test results. Therefore, the whole human blood used for blank determinations could be used with the usual anticoagulants employed by commercial blood suppliers. Anticoagulant citrate phosphate dextrose solution was used in the human whole blood units.

The standard curve was linear from 0 to 600 μg/dl. If the standard curve correlation coefficient (Table III) was less than 0.950, the calibration procedure was repeated. If a patient's whole blood gold level was outside the limits of the chosen standard (roughly the normal therapeutic blood level range), the whole blood sample was diluted more or less than the standard procedure (0.5 ml of whole blood diluted with 9.5 ml of water) to bring the absorbance values within the specified range.

The analytical procedure developed utilizes an ordinary whole blood sample with routinely used anticoagulants, one dilution with water, mixing, and injection into the instrument. The method meets the clinically desirable parameters of simplicity, speed, appropriate sensitivity, and presentation of the data in a format[12] suitable for research (Table III) or clinical (Table IV) utilization.

REFERENCES

(1) P. M. Smith, E. M. Smith, and N. L. Gottlieb, *J. Lab. Clin. Med.*, **82**, 930 (1973).

(2) A. Lorber, *Clin. Pharmacokinet.*, **2**, 127 (1977).

(3) D. J. Pole, N. D. H. Balazs, and J. Maseri, *Med. J. Aust.*, **2**, 1181 (1971).

(4) A. Lorber, R. L. Cohen, C. C. Chang, and H. E. Anderson, *Arthritis Rheum.*, **11**, 170 (1968).

(5) A. A. Dietz and H. M. Rubinstein, *Ann. Rheum. Dis.*, **32**, 124

[12] Copy of computer program is available on request.

(1973).
(6) M. Harth, D. S. M. Haines, and D. C. Bondy, *Am. J. Clin. Pathol.*, **59**, 423 (1973).
(7) H. T. Smart and D. J. Campbell, *Can. J. Pharm. Sci.*, **6**, 303 (1971).
(8) N. L. Gottlieb, E. M. Smith, and P. M. Smith, *Arthritis Rheum.*, **15**, 16 (1972).

ACKNOWLEDGMENTS

Supported in part by a grant from the North Dakota Chapter of the Arthritis Foundation.

The authors thank Blood Services of North Dakota, Inc., Fargo, N.D., for supplying units of human whole blood; and Dr. John Magness of the Dakota Clinic, Fargo, N.D., for assistance.

Synthesis and β-Adrenergic Blocking Action of a New Thiazolylthiopropanolamine Derivative

YOUICHI HARA ˣ, ETSURO SATO, AKIRA MIYAGISHI, AKIRA AISAKA, and TOSHIHIKO HIBINO

Received September 14, 1977, from the *Research and Development Center, Pharmaceuticals Division, Sumitomo Chemical Co., Ltd., Takatsukasa 4-2-1, Takarazuka, Hyogo, Japan.* Accepted for publication January 11, 1978.

Abstract □ The synthesis of (±)-2-(3′-*tert*-butylamino-2′-hydroxypropylthio)-4-(5′-carbamoyl-2′-thienyl)thiazole hydrochloride is described. The new compound antagonized the cardiovascular effects, such as positive chronotropic, positive inotropic, or depressor arterial blood pressure responses, elicited by intravenous isoproterenol; it was 9–14 times as potent as propranolol in anesthetized open chest dogs. The oral administration of the compound reduced isoproterenol tachycardia in conscious dogs. It was about five times as potent as propranolol in this test, with maximal action after 1 hr, and its duration was significantly longer than that of propranolol.

Keyphrases □ Thiazolylthiopropanolamine derivative—synthesized, β-adrenergic blocking activity evaluated in dogs □ β-Adrenergic blocking activity—thiazolylthiopropanolamine derivative evaluated in dogs

Many amino alcohol derivatives have been described to have a β-blocking action, and some have been of interest for the treatment of angina pectoris and cardiac arrhythmias (1). Most compounds available for clinical use belong to the aryloxypropanolamine series, which is considered the second generation of β-blocking agents, in contrast with the arylethanolamine series, which includes original β-blocking agents such as dichloroisoproterenol and pronethalol (2).

During a search for drugs affecting the peripheral autonomic nervous system, various compounds with an *N*-substituted thiopropanolamine moiety attached to a heterocyclic nucleus were synthesized and tested for β-blocking action as well as the other pharmacological actions. A new compound, (±)-2-(3′-*tert*-butylamino-2′-hydroxypropylthio)-4- (5′-carbamoyl-2′-thienyl)thiazole hydrochloride[1] (VI), showed remarkable β-blocking action with low toxicity and was virtually devoid of other pharmacological actions.

The present report describes the chemical synthesis and β-blocking activity of this derivative compared with that of propranolol (3) in *in vivo* experiments.

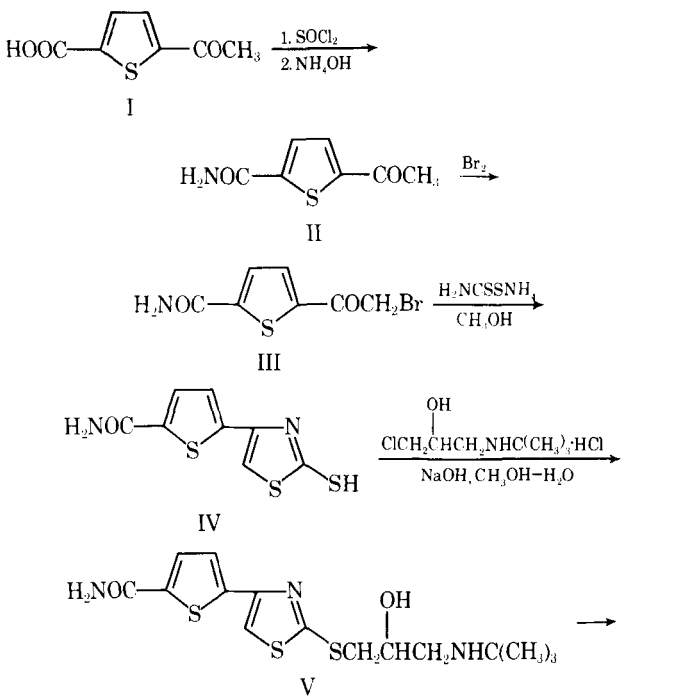

Scheme I

EXPERIMENTAL[2]

Chemistry—Reaction of 5-carboxy-2-acetylthiophene (I, Scheme I) (4) with thionyl chloride in toluene and successive treatment with aqueous ammonia furnished the carbamoyl derivative (II), which was converted to its monobromide (III). Reaction of the bromide with ammonium dithiocarbamate resulted in isolation of 2-mercapto-4-(5′-carbamoyl-2′-thienyl)thiazole (IV). Condensation of IV with 1-chloro-3-*tert*-butylaminopropanol hydrochloride (5) by means of base in an equivalent mixture of methanol and water provided 2-(3′-*tert*-butylamino-2′-hydroxypropylthio)-4-(5′-carbamoyl-2′-thienyl)thiazole (V), from which its crystalline hydrochloride (VI) was derived.

5-Carbamoyl-2-acetylthiophene (II)—To a suspension of I, 22 g (0.129 mole) of thionyl chloride in 200 ml of toluene was added dropwise with vigorous stirring. The mixture was heated under a gentle reflux for 2 hr and evaporated *in vacuo* to dryness. The residue was dissolved in 150 ml of toluene again and treated with aqueous ammonia below 10°.

The white precipitate was collected by suction filtration, washed with water, and dried, yielding 20 g (92.8%), mp 226–228° (methanol); NMR:

[1] S-596.

[2] Melting points were obtained on a Thomas-Hoover capillary melting-point apparatus and are uncorrected. IR spectra were determined in mineral oil mulls on a Hitachi EPI-G3 IR spectrometer. NMR spectra were taken in deuterated dimethyl sulfoxide on a Varian Associates T-60 instrument with tetramethylsilane as the internal standard.

0022-3549/78/0900-1334$01.00/0
© 1978, American Pharmaceutical Association

(1973).
(6) M. Harth, D. S. M. Haines, and D. C. Bondy, *Am. J. Clin. Pathol.*, **59**, 423 (1973).
(7) H. T. Smart and D. J. Campbell, *Can. J. Pharm. Sci.*, **6**, 303 (1971).
(8) N. L. Gottlieb, E. M. Smith, and P. M. Smith, *Arthritis Rheum.*, **15**, 16 (1972).

ACKNOWLEDGMENTS

Supported in part by a grant from the North Dakota Chapter of the Arthritis Foundation.

The authors thank Blood Services of North Dakota, Inc., Fargo, N.D., for supplying units of human whole blood; and Dr. John Magness of the Dakota Clinic, Fargo, N.D., for assistance.

Synthesis and β-Adrenergic Blocking Action of a New Thiazolylthiopropanolamine Derivative

YOUICHI HARA ˣ, ETSURO SATO, AKIRA MIYAGISHI, AKIRA AISAKA, and TOSHIHIKO HIBINO

Received September 14, 1977, from the *Research and Development Center, Pharmaceuticals Division, Sumitomo Chemical Co., Ltd., Takatsukasa 4-2-1, Takarazuka, Hyogo, Japan.* Accepted for publication January 11, 1978.

Abstract □ The synthesis of (±)-2-(3′-*tert*-butylamino-2′-hydroxypropylthio)-4-(5′-carbamoyl-2′-thienyl)thiazole hydrochloride is described. The new compound antagonized the cardiovascular effects, such as positive chronotropic, positive inotropic, or depressor arterial blood pressure responses, elicited by intravenous isoproterenol; it was 9–14 times as potent as propranolol in anesthetized open chest dogs. The oral administration of the compound reduced isoproterenol tachycardia in conscious dogs. It was about five times as potent as propranolol in this test, with maximal action after 1 hr, and its duration was significantly longer than that of propranolol.

Keyphrases □ Thiazolylthiopropanolamine derivative—synthesized, β-adrenergic blocking activity evaluated in dogs □ β-Adrenergic blocking activity—thiazolylthiopropanolamine derivative evaluated in dogs

Many amino alcohol derivatives have been described to have a β-blocking action, and some have been of interest for the treatment of angina pectoris and cardiac arrhythmias (1). Most compounds available for clinical use belong to the aryloxypropanolamine series, which is considered the second generation of β-blocking agents, in contrast with the arylethanolamine series, which includes original β-blocking agents such as dichloroisoproterenol and pronethalol (2).

During a search for drugs affecting the peripheral autonomic nervous system, various compounds with an *N*-substituted thiopropanolamine moiety attached to a heterocyclic nucleus were synthesized and tested for β-blocking action as well as the other pharmacological actions. A new compound, (±)-2-(3′-*tert*-butylamino-2′-hydroxypropylthio)-4- (5′-carbamoyl-2′-thienyl)thiazole hydrochloride[1] (VI), showed remarkable β-blocking action with low toxicity and was virtually devoid of other pharmacological actions.

The present report describes the chemical synthesis and β-blocking activity of this derivative compared with that of propranolol (3) in *in vivo* experiments.

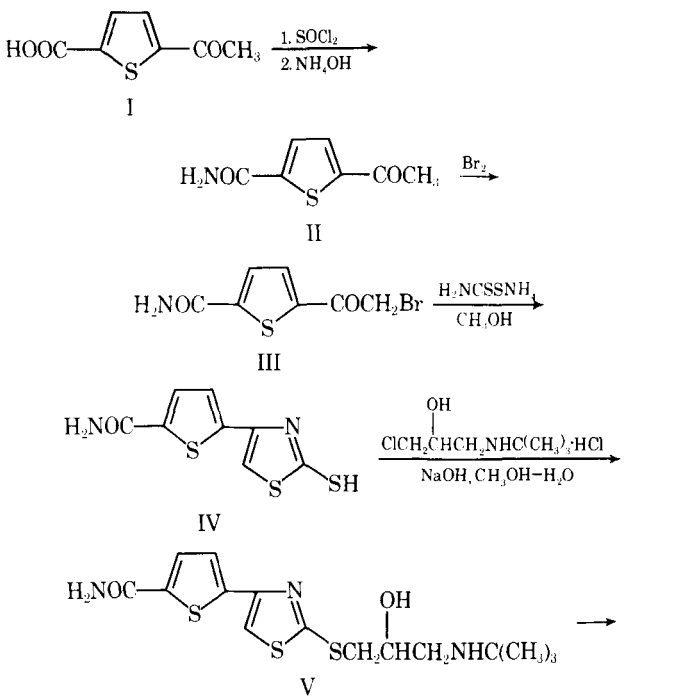

Scheme I

EXPERIMENTAL[2]

Chemistry—Reaction of 5-carboxy-2-acetylthiophene (I, Scheme I) (4) with thionyl chloride in toluene and successive treatment with aqueous ammonia furnished the carbamoyl derivative (II), which was converted to its monobromide (III). Reaction of the bromide with ammonium dithiocarbamate resulted in isolation of 2-mercapto-4-(5′-carbamoyl-2′-thienyl)thiazole (IV). Condensation of IV with 1-chloro-3-*tert*-butylaminopropanol hydrochloride (5) by means of base in an equivalent mixture of methanol and water provided 2-(3′-*tert*-butylamino-2′-hydroxypropylthio)-4-(5′-carbamoyl-2′-thienyl)thiazole (V), from which its crystalline hydrochloride (VI) was derived.

5-Carbamoyl-2-acetylthiophene (II)—To a suspension of I, 22 g (0.129 mole) of thionyl chloride in 200 ml of toluene was added dropwise with vigorous stirring. The mixture was heated under a gentle reflux for 2 hr and evaporated *in vacuo* to dryness. The residue was dissolved in 150 ml of toluene again and treated with aqueous ammonia below 10°.

The white precipitate was collected by suction filtration, washed with water, and dried, yielding 20 g (92.8%), mp 226–228° (methanol); NMR:

[1] S-596.

[2] Melting points were obtained on a Thomas-Hoover capillary melting-point apparatus and are uncorrected. IR spectra were determined in mineral oil mulls on a Hitachi EPI-G3 IR spectrometer. NMR spectra were taken in deuterated dimethyl sulfoxide on a Varian Associates T-60 instrument with tetramethylsilane as the internal standard.

0022-3549/78/0900-1334$01.00/0
© 1978, American Pharmaceutical Association

2.55 (s, 3H, acetyl) and 7.82 (*AB*q, J_{AB} = 4 Hz, δ_{AB} = 3 Hz, 2H, 3,4-H on the thiophene) ppm; IR: 3400, 3180 (NH), 1660 (C=O), and 1640 (amide) cm^{-1}.

Anal.—Calc. for $C_7H_7NO_2S$: C, 49.70; H, 4.14; N, 8.28; S, 18.94. Found: C, 49.51; H, 4.20; N, 8.30; S, 19.00.

5-Carbamoyl-2-bromoacetylthiophene (III)—Compound II, 21.9 g (0.131 mole), was dissolved in 350 ml of hot acetic acid; bromine, 21.9 g (0.136 mole), was added dropwise at 80°. After the addition was complete, the resulting solution was maintained at the same temperature for 1.5 hr, evaporated to half, and filtered.

The product was washed with water thoroughly and dried, yielding 26.2 g (80.6%), mp 198–199° dec. (acetic acid); NMR: 4.80 (s, 2H, bromoacetyl) and 7.85 (*AB*q, J_{AB} = 4 Hz, δ_{AB} = 6 Hz, 2H, 3,4-H on the thiophene) ppm; IR: 3400, 3170 (NH), and 1670 (amide and bromoacetyl) cm^{-1}.

Anal.—Calc. for $C_7H_6BrNO_2S$: C, 33.87; H, 2.42; N, 5.65; S, 12.90. Found: C, 33.68; H, 2.40; N, 5.75; S, 12.70.

2-Mercapto-4-(5'-carbamoyl-2'-thienyl)thiazole (IV)—To a solution of 15.6 g (0.138 mole) of ammonium dithiocarbamate in 145 ml of methanol was added 26.2 g (0.106 mole) of III in 260 ml of dimethylformamide, dropwise, under 5°. The resulting mixture was stirred at room temperature for 3 hr and heated under reflux for a further 2 hr. Water, 150 ml, was added and the mixture was cooled at 0° overnight.

The precipitate was collected by suction filtration, washed with water, and dried, yielding 19.6 g (76.7%), mp 263–265° dec. (dimethylformamide–water); NMR: 7.30 (s, 1H, 5-H on the thiazole) and 7.68 (*AB*q, J_{AB} = 4 Hz, δ_{AB} = 5 Hz, 2H, 3,4-H on the thiophene) ppm; IR: 3400 (NH) and 1630 (amide) cm^{-1}.

Anal.—Calc. for $C_8H_6NOS_3$: C, 39.67; H, 2.48; N, 11.57; S, 39.67. Found: C, 39.75; H, 2.50; N, 11.75; S, 39.38.

2-(3'-tert-Butylamino-2'-hydroxypropylthio)-4-(5'-carbamoyl-2'-thienyl)thiazole (V)—To a solution of 3.2 g (0.0132 mole) of IV in 20 ml of 0.3% aqueous sodium hydroxide was added 1.26 g (0.008 mole) of 1-chloro-3-*tert*-butylaminopropanol hydrochloride (5) in 20 ml of methanol while the temperature was maintained at 20°. The reaction solution was stirred at room temperature for 4 hr and then condensed to half *in vacuo*. The residual solution was mixed with 100 ml of water and extracted with chloroform.

The chloroform extract was washed with water, dried, and evaporated *in vacuo* to give a residue, 4.8 g. This residue was recrystallized from chloroform–light petroleum ether to yield 4.0 g (74.3%) of V as needles, mp 148–149°; IR: 3350, 3320, 3200 (OH, NH), and 1650 (amide) cm^{-1}.

Anal.—Calc. for $C_{15}H_{21}N_3O_2S_3$: C, 48.52; H, 5.66; N, 11.32; S, 25.88. Found: C, 48.31; H, 5.42; N, 11.15; S, 25.00.

Treatment of this material with concentrated hydrochloric acid (aqueous) in methanol and subsequent recrystallization from methanol–water (1:1) provided its hydrochloride (VI) in an 80% yield, mp 234–235.5° dec.; NMR: 1.35 (s, 9H, *tert*-butyl), 3.20 (m, 2H), 3.52 (m, 3H), 4.25 (m, 1H), 7.70 (*AB*q, J_{AB} = 8 Hz, δ_{AB} = 8 Hz, 2H, 3,4-H on the thiophene), and 8.00 (s, 1H, 5-H on the thiazole) ppm.

Anal.—Calc. for $C_{15}H_{21}N_3O_2S_3 \cdot HCl$: C, 44.12; H, 5.39; N, 10.29; S, 23.53. Found: C, 43.87; H, 5.37; N, 10.26; S, 23.24.

Biological Evaluation—For the estimation of β-blocking activities of VI and propranolol, *in vivo* studies were carried out in pentobarbital-anesthetized, bilaterally vagotomized, open chest dogs. Doses of 0.3 μg of isoproterenol/kg were given; responses on heart rate, cardiac contractile force, and arterial blood pressure were recorded. Compound VI or propranolol was intravenously administered at 15-min intervals in increasing doses. Isoproterenol was injected 5 min after a dose of the blocking agents, and the sequence was continued until nearly total suppression of the cardiovascular effects of isoproterenol was achieved.

The oral β-blocking activities of VI and propranolol were examined in conscious beagle dogs. The ECG and heart rate were recorded from needle electrodes inserted through the skin of limbs. Dogs fasted for 24 hr were dosed orally with either VI (0.1 or 0.5 mg/kg) or propranolol (0.5 or 2.5 mg/kg). Each dose of a blocking agent, with lactose and starch (1:1) as the vehicle, was administered in a gelatin capsule. Intravenous isoproterenol (0.3 or 0.5 μg/kg) challenges were repeated at 20- or 40-min intervals for 3 hr, and all experiments were terminated 24 hr after oral dosing.

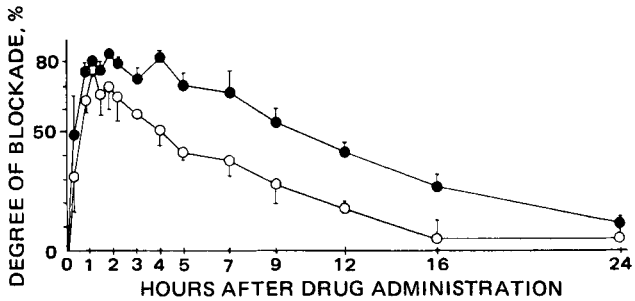

Figure 1—*Time–effect curves for β-adrenergic blocking activity of VI and propranolol, given orally, on the positive chronotropic responses to 0.3 μg of isoproterenol/kg iv in conscious beagle dogs. Each point represents the mean value ± SE from three experiments. Key: ●, VI, 0.5 mg/kg; and ○, propranolol, 2.5 mg/kg.*

RESULTS AND DISCUSSION

The β-blocking activities of VI and propranolol in the anesthetized dogs were evaluated following cumulative intravenous administration (0.3–10 and 10–300 μg/kg, respectively). Dose–response curves for VI for inhibition of the isoproterenol challenge were parallel to those for propranolol. Both drugs showed similar antagonistic effect on the chronotropic, inotropic, and depressor responses of isoproterenol, but the effect of VI was more potent than that of propranolol.

The following estimates of intravenous ED_{50} values were obtained for VI and propranolol: 3.1 and 40.5 μg/kg against the chronotropic response to 0.3 μg of isoproterenol/kg, 2.9 and 41.5 μg/kg against the inotropic response, and 2.5 and 24.0 μg/kg against the depressor response, respectively. Thus, VI appears to be 9–14 times as potent as propranolol. In conscious beagle dogs, VI or propranolol antagonized the tachycardia produced by repeated intravenous injection of isoproterenol. Typical results are shown in Fig. 1. Compound VI was about five times as potent as propranolol in this test, with maximal action after 1 hr. The duration of the β-blockade after VI was significantly longer than after propranolol.

Compound VI blocks the explored classical responses associated with β-adrenergic stimulation, *i.e.*, isoproterenol-induced cardiac stimulation and vascular relaxation. Thus, VI, like propranolol, is a β-adrenergic blocking agent with no special selectivity for a particular type of β-receptor (6). However, VI possesses no intrinsic sympathomimetic activity, as indicated by tachycardia in reserpinized rats, and does not show membrane-stabilizing properties such as local anesthetic and antiarrhythmic activities[3]. The LD_{50} values of VI in mice were 86 mg/kg iv, more than 360 mg/kg ip, and more than 5000 mg/kg po; the propranolol values were 23, 120, and 320–420 mg/kg, respectively. Thus, VI is one of the most specific β-adrenergic blocking agents with low toxicity and the least other pharmacological activities.

REFERENCES

(1) A. C. Dornhorst, *Ann. N.Y. Acad. Sci.*, **139**, 968 (1967).

(2) A. M. Barrett, "Drug Design," vol. III, J. Ariens, Ed., Academic, New York, N.Y., 1972, p. 205.

(3) J. W. Black, W. A. M. Duncan, and R. G. Shanks, *Br. J. Pharmacol.*, **25**, 577 (1965).

(4) S. F. Thomas and J. E. McClesky, *J. Heterocycl. Chem.*, **3**, 104 (1966).

(5) V. R. Gaetner, *Tetrahedron*, **23**, 2123 (1967).

(6) A. M. Lands, A. Arnold, J. P. McAuliff, F. P. Luduena, and T. G. Brown, *Nature*, **214**, 597 (1967).

ACKNOWLEDGMENTS

The authors thank Dr. H. Nakatani, Dr. S. Okano, and Dr. S. Aono, Sumitomo Chemical Co., for valuable advice and encouragement.

[3] Unpublished data.

Selenium Heterocycles XXII: Synthesis and Antibacterial and Antifungal Activities of Arylsulfonyl-1,2,3-selenadiazoles

I. LALEZARI ˣ, A. SHAFIEE, J. KHORRAMI, and A. SOLTANI

Received September 12, 1977, from the *Department of Chemistry and the Department of Industrial Pharmacy, College of Pharmacy, Tehran University, Tehran, Iran.* Accepted for publication January 11, 1978.

Abstract □ Series of 4-arylsulfonylmethyl-1,2,3-selenadiazoles, 4-(1-arylsulfonylethyl)-1,2,3-selenadiazoles, and 4-alkyl (or aryl) -5-arylsulfonyl-1,2,3-selenadiazoles were synthesized. 4-(3-Pyridyl)-5-phenylsulfonyl-1,2,3-selenadiazole exhibited the highest activity of growth inhibition against some bacteria and fungi.

Keyphrases □ 1,2,3-Selenadiazoles, various substituted—synthesized, antibacterial and antifungal activities evaluated □ Antibacterial activity—various substituted 1,2,3-selenadiazoles evaluated □ Antifungal activity—various substituted 1,2,3-selenadiazoles evaluated □ Structure–activity relationships—various substituted 1,2,3-selenadiazoles evaluated for antibacterial and antifungal activities

Recently, the antibacterial activity of series of 4-pyridyl-1,2,3-thiadiazoles, 4-pyridyl-1,2,3-selenadiazoles, and related 1,4-diselenafulvenes was reported (1). However, 4-substituted (1,2,3-selenadiazol-5-yl)carbamic acid esters and their sulfur analogs did not show significant antibacterial activity (2). Similarly, although selenosemicarbazide and its acyl derivatives exhibited potent antibacterial activity, the corresponding sulfur analogs were inactive (3).

The purpose of the present work was to study the influence of the sulfone group on the antibacterial and antifungal activities of the 1,2,3-selenadiazole ring system.

DISCUSSION

Chemistry—The selenium dioxide oxidation of the appropriate α-methyl or methylene aldehyde or ketone semicarbazones, as described previously (4–6), was used for the synthesis of arylsulfonyl-1,2,3-selenadiazoles. Chloroacetaldehyde or the appropriate α-chloroketones were condensed with sodium salts of benzenesulfinic acid or *p*-toluenesulfinic acid to give the desired carbonyl compounds (Scheme I). Semicarbazones of the carbonyl compounds reacted with selenium dioxide in hot acetic acid to afford the corresponding 1,2,3-selenadiazoles IV*a*, IV*d*–IV*q* (Scheme I), IV*b*, IV*c*, V*a*, V*b* (Scheme II), and V*c* (Scheme III). With the acetonylarylsulfonylsemicarbazones, isomeric 1,2,3-selenadiazoles V*a*–IV*b* and V*b*–IV*c* were obtained. In both cases, the isomers were separated easily by repeated crystallization (Scheme II).

All other 1,2,3-selenadiazoles were prepared similarly. With the 4-pyridyl-1,2,3-selenadiazoles, the reaction mixture was neutralized and

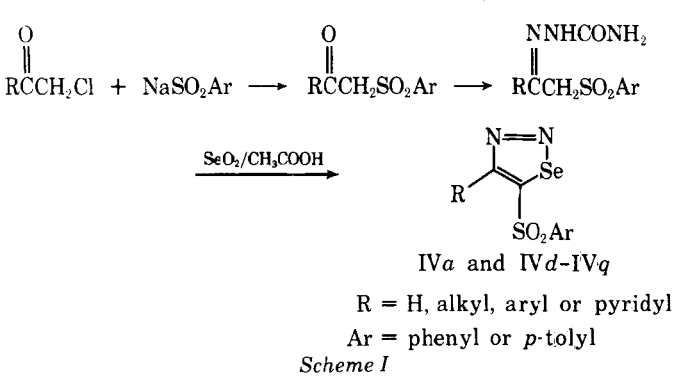

IV*a* and IV*d*–IV*q*

R = H, alkyl, aryl or pyridyl

Ar = phenyl or *p*-tolyl

Scheme I

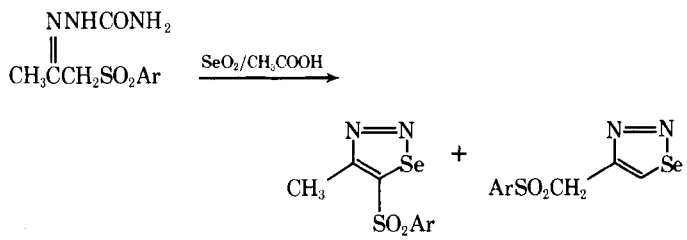

IV*b* and IV*c* V*a* and V*b*

Scheme II

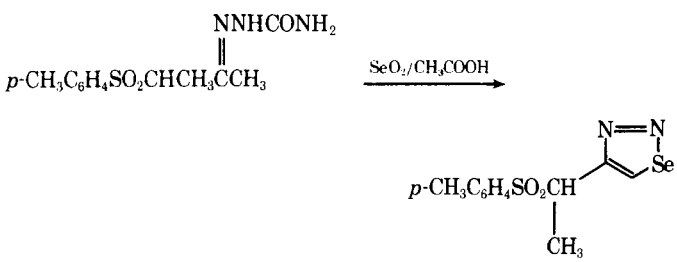

V*c*

Scheme III

the crude compounds were purified by crystallization from aqueous ethanol. All 1,2,3-selenadiazoles prepared are listed in Table I.

An attempt to prepare arylsulfonylacetylenes by mild pyrolysis of arylsulfonyl-1,2,3-selenadiazoles failed. However, photolysis of 4-methyl-5-*p*-toluenesulfonyl-1,2,3-selenadiazole (IV*c*) and 4-phenyl-5-*p*-toluenesulfonyl-1,2,3-selenadiazole (IV*e*) in benzene afforded good yields of the corresponding acetylenes, VI*a* and VI*b* (Scheme IV). Compounds unsubstituted at the 5-position polymerized with these conditions and did not lead to the formation of the desired acetylenes.

Mass spectra of 5-unsubstituted 1,2,3-selenadiazoles showed a very weak parent molecular ion, and an M − SO_2 fragment was common in these molecules. 4,5-Disubstituted compounds also had a very weak parent molecular ion, and the base peak was M − (SO_2 + N_2). Ions corresponding to the arylacetylenes existed in both series.

Biological Activity—Compounds listed in Table II were tested against *Bacillus subtilis* (NCTC 3910), *Sarcina lutea* (ATCC 9341), *Staphylococcus aureus* (ATCC 6538), and *Escherichia coli* (ATCC 4352). Nitrofurazone was used as the control. The compounds were dissolved in pure acetone and diluted to 1% (w/v). Standard paper disks of 6-mm

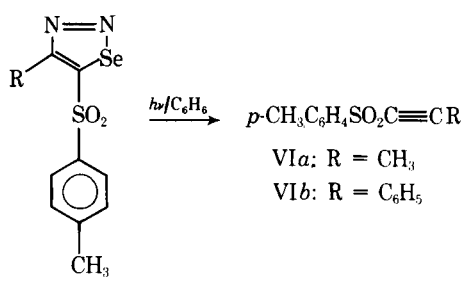

VI*a*: R = CH_3

VI*b*: R = C_6H_5

IV*c* and IV*e*

Scheme IV

0022-3549/78/0900-1336$01.00/0
© 1978, American Pharmaceutical Association

Table I—Arylsulfonyl-1,2,3-selenadiazoles

Compound	R	Ar	Yield, %	Melting Point	Formula	Analysis, %	Calc.	Found
IV*a*	H	*p*-$CH_3C_6H_4SO_2$	48	129–131°	$C_9H_8N_2O_2SSe$	C	37.63	37.71
						H	2.78	2.80
IV*b*	CH_3	$C_6H_5SO_2$	63	76–78°	$C_9H_8N_2O_2SSe$	C	37.63	37.56
						H	2.78	2.75
IV*c*	CH_3	*p*-$CH_3C_6H_4SO_2$	56	64–65°	$C_{10}H_{10}N_2O_2SSe$	C	39.86	39.68
						H	3.32	3.28
IV*d*	C_6H_5	$C_6H_5SO_2$	38	163–165°	$C_{14}H_{10}N_2O_2SSe$	C	48.13	48.21
						H	2.86	2.78
IV*e*	C_6H_5	*p*-$CH_3C_6H_4SO_2$	76	130–135°	$C_{15}H_{12}N_2O_2SSe$	C	49.56	49.77
						H	3.30	3.33
IV*f*	*p*-ClC_6H_4	*p*-$CH_3C_6H_4SO_2$	59	110–115°	$C_{15}H_{11}ClN_2O_2SSe$	C	45.28	45.33
						H	2.76	2.69
IV*g*	*p*-BrC_6H_4	*p*-$CH_3C_6H_4SO_2$	66	108–113°	$C_{15}H_{11}BrN_2O_2SSe$	C	40.72	41.01
						H	2.48	2.53
IV*h*	*m*-$NO_2C_6H_4$	$C_6H_5SO_2$	53	125–128°	$C_{14}H_9N_3O_4SSe$	C	42.63	42.50
						H	2.28	2.30
IV*i*	*p*-$NO_2C_6H_4$	$C_6H_5SO_2$	46	130–135°	$C_{14}H_9N_3O_3SSe$	C	42.63	42.77
						H	2.28	2.31
IV*j*	*m*-$NO_2C_6H_4$	*p*-$CH_3C_6H_4SO_2$	79	128–132°	$C_{15}H_{11}N_3O_4SSe$	C	44.11	44.12
						H	2.69	2.75
IV*k*	*p*-$NO_2C_6H_4$	*p*-$CH_3C_6H_4SO_2$	77	164–166°	$C_{15}H_{11}N_3O_4SSe$	C	44.11	44.20
						H	2.69	2.68
IV*l*	2-Pyridyl	$C_6H_5SO_2$	60	107–110°	$C_{13}H_9N_3O_2SSe$	C	44.57	44.68
						H	2.57	2.61
IV*m*	3-Pyridyl	$C_6H_5SO_2$	63	75–77°	$C_{13}H_9N_3O_2SSe$	C	44.57	44.59
						H	2.57	2.39
IV*n*	4-Pyridyl	$C_6H_5SO_2$	61	161–165°	$C_{13}H_9N_3O_2SSe$	C	44.57	44.44
						H	2.57	2.60
IV*o*	2-Pyridyl	*p*-$CH_3C_6H_4SO_2$	76	118–120°	$C_{14}H_{11}N_3O_2SSe$	C	46.15	46.10
						H	3.02	2.98
IV*p*	3-Pyridyl	*p*-$CH_3C_6H_4SO_2$	78	139–140°	$C_{14}H_{11}N_3O_2SSe$	C	46.15	46.22
						H	3.02	3.11
IV*q*	4-Pyridyl	*p*-$CH_3C_6H_4SO_2$	70	142–145°	$C_{14}H_{11}N_3O_2SSe$	C	46.15	46.29
						H	3.02	3.13
V*a*	$C_6H_5SO_2CH_2$	H	26.5	147–151°	$C_9H_8N_2O_2SSe$	C	37.63	37.71
						H	2.78	2.66
V*b*	*p*-$CH_3C_6H_4SO_2CH_2$	H	44	148–150°	$C_{10}H_{10}N_2O_2SSe$	C	39.86	40.07
						H	3.32	3.28
V*c*	*p*-$CH_3C_6H_4SO_2CH(CH_3)$	H	58	137–139°	$C_{11}H_{12}N_2O_2SSe$	C	40.72	40.88
						H	2.48	2.53

diameter were immersed in the solution and placed on an inoculated assay medium surface[1].

The compounds were also tested against *Candida albicans* (ATCC 10231), *Aspergillus niger* (ATCC 16404), and *Penicillium notatum*[2]. Nystatin[3] was used as the control. Compounds were dissolved in dimethylformamide and diluted with hot culture medium (BBL Sabouraud dextrose agar medium). Concentrations of 10 and 25 mg of each compound/ml were used.

The antibacterial and antifungal activities are reported in Tables II and III, respectively. Most of the compounds tested were as active as the control compounds.

EXPERIMENTAL[4]

5-*p*-Toluenesulfonyl-1,2,3-selenadiazole (IV*a*)—α-*p*-Toluenesulfonyl acetaldehyde semicarbazone, 5.1 g (0.02 mole), was dissolved in 25 ml of boiling acetic acid. To the hot solution, 2 g (0.02 mole) of selenium dioxide was added; then the reaction mixture was stirred and gently heated until gas evolution ceased. The dark-brown mixture was heated with charcoal, filtered, and diluted with water. The precipitate was recrystallized from aqueous ethanol to give 3.22 g (58%) of cream needles, mp 129–131°; mass spectra: *m/e* 287 (M^+), 195 M − (SO_2, N_2), and 180 M − (Se, N_2); NMR (deuteriochloroform): δ 2.53 (s, 3H, CH_3), 7.3–8.0 (q, 4H, C_6H_4), and 8.9 (s, 1H, CH) ppm.

All 4-aryl-1,2,3-selenadiazoles reported in Table I were prepared similarly (Schemes I–III).

4-Phenylsulfonylmethyl-1,2,3-selenadiazole (V*a*)—Acetonylphenylsulfone semicarbazone, 5.1 g (0.02 mole), was dissolved in 25 ml of boiling acetic acid. To the hot solution, 2 g (0.02 mole) of selenium dioxide was added; then the reaction mixture was stirred until the vigorous reaction ceased.

The mixture was gently refluxed for 1 hr to complete the reaction. Charcoal was added, and the solution was filtered hot. To the filtrate, 15 ml of acetone was added; the mixture was then allowed to stand overnight at room temperature. The precipitate was filtered, and the mother liquor was worked up separately to afford IV*b*. The precipitate was recrystal-

Table II—Antibacterial Activity[a]

Compound	Average Inhibition Zone Diameter, mm			
	B. subtilis	*S. lutea*	*Staph. aureus*	*E. coli*
IV*a*	8	12	16	7
IV*b*	–	8	–	–
IV*c*	9	12	8	16
IV*d*	12	12	20	–
IV*e*	15	13	19	–
IV*g*	10	10	10	10
IV*h*	15	10	14	15
IV*j*	12	11	12	16
IV*k*	10	15	15	16
IV*l*	13	14	20	–
IV*m*	22	23	23	–
IV*o*	13	15	20	–
IV*p*	7	8	11	–
V*a*	10	8	10	7
V*b*	–	–	–	8
V*c*	8	8	–	–
Nitrofurazone	17	18	17	17

[a] – = inactive.

[1] AAM antibiotic assay medium, "The British Pharmacopoeia," 1968.

[2] This microorganism was obtained from the Department of Parasitology, Public Health Institute, Tehran, Iran.

[3] Mycostatin lot 2090a, potency 4858 U/mg, Squibb.

[4] Melting points were taken on a Kofler hot-stage microscope and are uncorrected. Mass spectra were recorded on a Varian Matt 311 instrument. IR spectra were recorded with a Leitz model III instrument, and NMR spectra were recorded with a Varian T60A instrument. Aldehydes, ketones, and their semicarbazones were prepared by known methods.

Table III—Antifungal Activity [a]

Compound	*C. albicans*		*P. notatum*		*A. niger*	
	10 μg/ml	25 μg/ml	10 μg/ml	25 μg/ml	10 μg/ml	25 μg/ml
IV*a*	+	+	+	+	+	+
IV*b*	−	−	−	−	−	−
IV*c*	+	+	+	+	+	+
IV*d*	+	+	+	+	+	+
IV*e*	−	+	+	+	+	+
IV*g*	−	−	−	−	−	−
IV*h*	−	−	−	−	+	+
IV*j*	−	−	−	−	−	−
IV*k*	−	−	−	−	−	−
IV*l*	+	+	+	+	+	+
IV*m*	−	−	+	+	+	+
IV*o*	−	+	+	+	+	+
IV*p*	−	−	+	+	+	+
V*a*	+	+	+	+	+	+
V*b*	−	−	−	−	−	−
V*c*	−	−	−	−	−	−
Nystatin	+	+	+	+	+	+

[a] − = inactive.

lized from hot acetone to give 1.5 g (26.5%) of white needles, mp 147–151°; mass spectra: *m/e* 287 (M^+), 233 M − (SO_2), 195 M − (SO_2, N_2), and 180 M − (Se, N_2); NMR (deuteriochloroform): δ 5.1 (s, 2H, CH_2), 7.4–7.7 (m, 5H, C_6H_5), and 9.45 (s, 1H, CH) ppm.

4-Methyl-5-phenylsulfonyl-1,2,3-selenadiazole (IV*b*)—The mother liquor from the preparation of V*a* was diluted with an excess of water. After refrigeration, it gave 3.5 g of brownish crystals, which were recrystallized from diluted acetone to give 3.1 g (54%) of IV*b*, mp 76–78°; mass spectra: *m/e* 278 (M^+), 195 M − (SO_2,N_2) and 180 M − (Se, N_2); NMR (deuteriochloroform): δ 2.88 (s, 3H, CH_3) and 7.3–8.1 (m, 5H, C_6H_5) ppm.

The isomeric compounds V*b* and IV*c* were prepared similarly. The ratio of V*b* to IV*c* was 44:56 (Table I).

Photolysis of Disubstituted-1,2,3-selenadiazoles—p-*Toluenesulfonylpropyne* (*VI*a)—4-Methyl-5-*p*-toluenesulfonyl-1,2,3-selenadiazole (IV*c*), 3 g (0.01 mole), in 90 ml of dry benzene was photolyzed during 6 hr using a 100-w high-pressure mercury lamp. The solution was filtered and evaporated at low pressure, and the crystalline residue was recrystallized from petroleum ether to give 0.81 g (42%) of white crystals, mp 96–97° [lit. (7) mp 98–99°]; IR: λ_{max} 2200 (C≡C), 1328, 1291, 1152, 1087, 818, and 706 cm^{-1}.

Anal.—Calc. for $C_{10}H_{10}O_2S$: C, 61.85; H, 5.15. Found: C, 61.99; H, 5.17.

p-*Toluenesulfonylacetylene* (*VI*b)—Photolysis of IV*e* as indicated for the preparation of VI*a* afforded 64% of the desired compound, mp (petroleum ether) 79–81° [lit. (8) mp 80–81°]; IR: 2109 (C≡C) cm^{-1}.

Anal.—Calc. for $C_{15}H_{12}O_2S$: C, 70.31; H, 4.53. Found C, 70.22; H, 4.40.

REFERENCES[5]

(1) I. Lalezari, A. Shafiee, and S. Yazdany, *J. Pharm. Sci.*, **63**, 628 (1974).

(2) A. Shafiee, I. Lalezari, S. Yazdany, F. M. Shahbazian, and T. Partovi, *ibid.*, **65**, 304 (1976).

(3) A. Shafiee, I. Lalezari, S. Yazdany, and A. Pournorouz, *ibid.*, **62**, 839 (1973).

(4) I. Lalezari, A. Shafiee, and M. Yalpani, *Tetrahedron Lett.*, **1969**, 5105.

(5) I. Lalezari, A. Shafiee, and M. Yalpani, *Angew. Chem.*, **82**, 484 (1970).

(6) I. Lalezari, A. Shafiee, and M. Yalpani, *J. Org. Chem.*, **36**, 2838 (1971).

(7) L. Maioli, G. Modena, and P. E. Todesco, *Boll. Sci. Fac. Chim. Ind. Bologne*, **18**, 66 (1960); through *Chem. Abstr.*, **56**, 5872 (1962).

(8) S. I. Miller, C. Arzech, C. A. Welch, G. R. Zeigler, and I. I. Dickstein, *J. Am. Chem. Soc.*, **84**, 2020 (1962).

ACKNOWLEDGMENTS

Supported by a grant from the Tehran University Research Council.

[5] For Part XXI of this series, see A. Shafiee, I. Lalezari, and F. Savabi, *Synthesis*, 1977, 764.

Effect of Dissolved Oxygen Levels on Oxidative Degradation of Pyrogallol

ANTHONY PALMIERI, III

Received September 16, 1977, from the *School of Pharmacy, University of Wyoming, Laramie, WY 82071.* Accepted for publication January 10, 1978.

Abstract □ Pyrogallol decomposition in aqueous systems with various dissolved oxygen levels was studied. The reduced dissolved oxygen levels were produced by deaeration *via* gas permeation. Dissolved oxygen levels were determined using a dropping mercury electrode polarograph. Degradation rates, T_{90}, and relative protection indexes are discussed. Even at dissolved oxygen levels of less than 0.05 ppm, some decomposition of pyrogallol occurred, indicating nonoxidative pathways or the necessity of total removal of dissolved oxygen to afford complete protection. Apparently, reducing the level of dissolved oxygen is a viable alternative to stabilization of aqueous pyrogallol solutions, since the T_{90} was increased from 1.9 days in water with dissolved oxygen levels of 9.05 ppm to 114.4 days in water with dissolved oxygen levels of less than 0.05 ppm.

Keyphrases □ Pyrogallol—oxidative degradation in aqueous systems, effect of dissolved oxygen levels □ Degradation, oxidative—pyrogallol in aqueous systems, effect of dissolved oxygen levels □ Oxidative degradation—pyrogallol in aqueous systems, effect of dissolved oxygen levels □ Antibacterials, topical—pyrogallol, oxidative degradation in aqueous systems, effect of dissolved oxygen levels

An important factor in drug stabilization is reduction of oxidative degradation. The sensitivity of several drugs to oxidative degradation was studied previously (1–5), and several techniques were used to inhibit this degradative pathway (6). Autoxidation of pharmaceuticals was described as a process mediated by free radicals: initiation, propagation *via* free radicals, and termination of the reaction to form inactive products (7).

If molecular oxygen, necessary for the propagation step, were substantially reduced, oxidative processes might be significantly reduced or eliminated. Therefore, the propagation step assumes major importance in free radical-

0022-3549/78/0900-1338$01.00/0

© 1978, American Pharmaceutical Association

Table III—Antifungal Activity [a]

Compound	*C. albicans*		*P. notatum*		*A. niger*	
	10 μg/ml	25 μg/ml	10 μg/ml	25 μg/ml	10 μg/ml	25 μg/ml
IV*a*	+	+	+	+	+	+
IV*b*	−	−	−	−	−	−
IV*c*	+	+	+	+	+	+
IV*d*	+	+	+	+	+	+
IV*e*	−	+	+	+	+	+
IV*g*	−	−	−	−	−	−
IV*h*	−	−	−	−	+	+
IV*j*	−	−	−	−	−	−
IV*k*	−	−	−	−	−	−
IV*l*	+	+	+	+	+	+
IV*m*	−	−	+	+	+	+
IV*o*	−	+	+	+	+	+
IV*p*	−	−	+	+	+	+
V*a*	+	+	+	+	+	+
V*b*	−	−	−	−	−	−
V*c*	−	−	−	−	−	−
Nystatin	+	+	+	+	+	+

[a] − = inactive.

lized from hot acetone to give 1.5 g (26.5%) of white needles, mp 147–151°; mass spectra: *m/e* 287 (M^+), 233 M − (SO_2), 195 M − (SO_2, N_2), and 180 M − (Se, N_2); NMR (deuteriochloroform): δ 5.1 (s, 2H, CH_2), 7.4–7.7 (m, 5H, C_6H_5), and 9.45 (s, 1H, CH) ppm.

4-Methyl-5-phenylsulfonyl-1,2,3-selenadiazole (IV*b*)—The mother liquor from the preparation of V*a* was diluted with an excess of water. After refrigeration, it gave 3.5 g of brownish crystals, which were recrystallized from diluted acetone to give 3.1 g (54%) of IV*b*, mp 76–78°; mass spectra: *m/e* 278 (M^+), 195 M − (SO_2,N_2) and 180 M − (Se, N_2); NMR (deuteriochloroform): δ 2.88 (s, 3H, CH_3) and 7.3–8.1 (m, 5H, C_6H_5) ppm.

The isomeric compounds V*b* and IV*c* were prepared similarly. The ratio of V*b* to IV*c* was 44:56 (Table I).

Photolysis of Disubstituted-1,2,3-selenadiazoles—p-*Toluenesulfonylpropyne* (*VI*a)—4-Methyl-5-*p*-toluenesulfonyl-1,2,3-selenadiazole (IV*c*), 3 g (0.01 mole), in 90 ml of dry benzene was photolyzed during 6 hr using a 100-w high-pressure mercury lamp. The solution was filtered and evaporated at low pressure, and the crystalline residue was recrystallized from petroleum ether to give 0.81 g (42%) of white crystals, mp 96–97° [lit. (7) mp 98–99°]; IR: λ_{max} 2200 (C≡C), 1328, 1291, 1152, 1087, 818, and 706 cm^{-1}.

Anal.—Calc. for $C_{10}H_{10}O_2S$: C, 61.85; H, 5.15. Found: C, 61.99; H, 5.17.

p-*Toluenesulfonylacetylene* (*VI*b)—Photolysis of IV*e* as indicated for the preparation of VI*a* afforded 64% of the desired compound, mp (petroleum ether) 79–81° [lit. (8) mp 80–81°]; IR: 2109 (C≡C) cm^{-1}.

Anal.—Calc. for $C_{15}H_{12}O_2S$: C, 70.31; H, 4.53. Found C, 70.22; H, 4.40.

REFERENCES[5]

(1) I. Lalezari, A. Shafiee, and S. Yazdany, *J. Pharm. Sci.*, **63**, 628 (1974).

(2) A. Shafiee, I. Lalezari, S. Yazdany, F. M. Shahbazian, and T. Partovi, *ibid.*, **65**, 304 (1976).

(3) A. Shafiee, I. Lalezari, S. Yazdany, and A. Pournorouz, *ibid.*, **62**, 839 (1973).

(4) I. Lalezari, A. Shafiee, and M. Yalpani, *Tetrahedron Lett.*, **1969**, 5105.

(5) I. Lalezari, A. Shafiee, and M. Yalpani, *Angew. Chem.*, **82**, 484 (1970).

(6) I. Lalezari, A. Shafiee, and M. Yalpani, *J. Org. Chem.*, **36**, 2838 (1971).

(7) L. Maioli, G. Modena, and P. E. Todesco, *Boll. Sci. Fac. Chim. Ind. Bologne*, **18**, 66 (1960); through *Chem. Abstr.*, **56**, 5872 (1962).

(8) S. I. Miller, C. Arzech, C. A. Welch, G. R. Zeigler, and I. I. Dickstein, *J. Am. Chem. Soc.*, **84**, 2020 (1962).

ACKNOWLEDGMENTS

Supported by a grant from the Tehran University Research Council.

[5] For Part XXI of this series, see A. Shafiee, I. Lalezari, and F. Savabi, *Synthesis*, 1977, 764.

Effect of Dissolved Oxygen Levels on Oxidative Degradation of Pyrogallol

ANTHONY PALMIERI, III

Received September 16, 1977, from the *School of Pharmacy, University of Wyoming, Laramie, WY 82071.* Accepted for publication January 10, 1978.

Abstract □ Pyrogallol decomposition in aqueous systems with various dissolved oxygen levels was studied. The reduced dissolved oxygen levels were produced by deaeration *via* gas permeation. Dissolved oxygen levels were determined using a dropping mercury electrode polarograph. Degradation rates, T_{90}, and relative protection indexes are discussed. Even at dissolved oxygen levels of less than 0.05 ppm, some decomposition of pyrogallol occurred, indicating nonoxidative pathways or the necessity of total removal of dissolved oxygen to afford complete protection. Apparently, reducing the level of dissolved oxygen is a viable alternative to stabilization of aqueous pyrogallol solutions, since the T_{90} was increased from 1.9 days in water with dissolved oxygen levels of 9.05 ppm to 114.4 days in water with dissolved oxygen levels of less than 0.05 ppm.

Keyphrases □ Pyrogallol—oxidative degradation in aqueous systems, effect of dissolved oxygen levels □ Degradation, oxidative—pyrogallol in aqueous systems, effect of dissolved oxygen levels □ Oxidative degradation—pyrogallol in aqueous systems, effect of dissolved oxygen levels □ Antibacterials, topical—pyrogallol, oxidative degradation in aqueous systems, effect of dissolved oxygen levels

An important factor in drug stabilization is reduction of oxidative degradation. The sensitivity of several drugs to oxidative degradation was studied previously (1–5), and several techniques were used to inhibit this degradative pathway (6). Autoxidation of pharmaceuticals was described as a process mediated by free radicals: initiation, propagation *via* free radicals, and termination of the reaction to form inactive products (7).

If molecular oxygen, necessary for the propagation step, were substantially reduced, oxidative processes might be significantly reduced or eliminated. Therefore, the propagation step assumes major importance in free radical-

0022-3549/78/0900-1338$01.00/0

© 1978, American Pharmaceutical Association

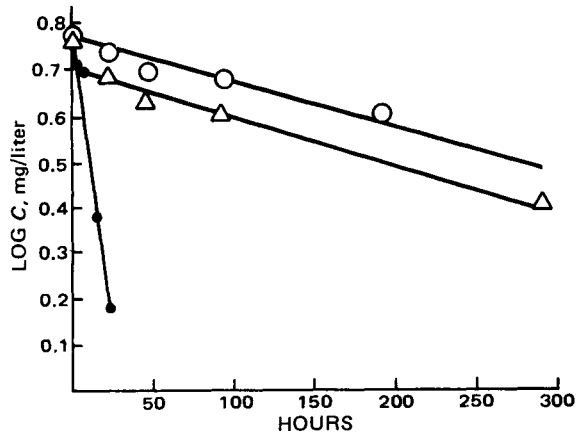

Figure 1—*Comparative degradation of pyrogallol at 30° in various dissolved oxygen levels. Key (dissolved oxygen level): ○, trace; △, 0.48 ppm; and ●, 9.05 ppm.*

mediated reactions for pharmaceutical systems such as pyrogallol decomposition.

The effect of dissolved oxygen concentration on the autoxidation reaction is not readily apparent. Shou (8) indicated that oxygen levels are not usually considered since it is difficult to alter the oxygen concentration with present equipment.

Because of its rapidity of oxidation, pyrogallol (1,2,3-trihydroxybenzene) was used as a model drug system to investigate the effect of a reduced molecular oxygen level of the solvent on the degradation process.

EXPERIMENTAL

Preparation of Deoxygenated Water—The method of reducing the dissolved oxygen levels of the water was described by Palmieri *et al.* (6). Essentially, distilled, deionized water was passed through a gas permeator[1] at various pressures and for various times to lower dissolved oxygen levels.

Dissolved oxygen levels (parts per million) were determined[2] on an average of 15–25 samples using a dropping mercury microelectrode polarograph with a rated sensitivity of ±0.01 ppm. Because of this sensitivity, any reading less than 0.05 ppm was considered to be a trace amount.

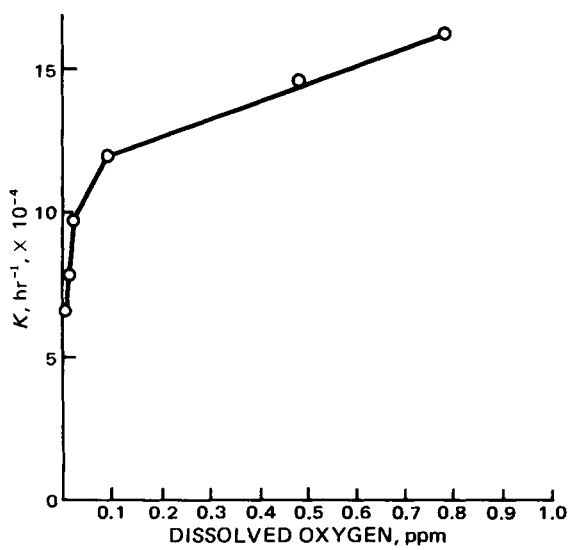

Figure 2—*Effect of oxygen concentration on degradation rate of pyrogallol at 30°.*

[1] Permasep, DuPont, Wilmington, Del.

[2] Model 106 dissolved oxygen analyzer, Delta Scientific Corp., Lindenhurst, N.J.

Table I—Comparative Degradation of Protected and Unprotected Systems of Pyrogallol at 30°

Dissolved Oxygen Level, ppm	K, mg/liter × 10^{-4} × days^{-1}	T_{90}, hr	Protection Index[a]
9.05	557.5	1.9	1.0
0.05–0.78	14.6	72.8	38.19
Trace	10.2	114.4	54.66

[a] Ratio of K rates relative to unprotected system.

Preparation and Analysis of Model Drug—Deoxygenated water prepared at various pressure ratings was employed as the solvent for the model drug system at an initial concentration of 6 mg of pyrogallol/liter. Distilled, deionized water was used to prepare the control sample. Each 30-ml vial was filled to capacity, capped with a polytef-coated screw cap, and sealed with six coats of a high melting wax to prevent oxygen intrusion. After labeling, the vials were stored in a dark, constant-temperature apparatus at 30° for the duration of the study. Unopened vials were removed periodically and assayed for pyrogallol content.

Pyrogallol was assayed according to the procedure of Grant and Patel (9). At preselected intervals, a 3-ml sample of pyrogallol solution was withdrawn, and 6 ml of a 1% vanillin solution in 70% H_2SO_4 was added. The absorbance was determined spectrophotometrically after 18 min against an appropriate blank at 520 nm. A control sample was assayed concurrently.

RESULTS AND DISCUSSION

Table I summarizes the data. There is a rank-order correlation of dissolved oxygen levels and degradation rates. Comparison of the time for 10% degradation (T_{90}) showed that systems with trace levels of dissolved oxygen had greatly increased protection. However, even systems of less than 1 ppm dissolved oxygen exhibited degradation. This result is explainable since pyrogallol may degrade by a nonoxidative process. Many chemicals having primarily oxidative pathways for degradation also degrade by other means. The degradation rates, however, were considerably less and appeared to "stabilize" or proceed at a slower rate after a slight initial degradation (Fig. 1).

Removal of most of the dissolved oxygen in the solvent should retard reaction kinetics since the molecular oxygen concentration affects the propagation step. However, because susceptible systems may degrade by a secondary pathway if oxygen is not readily available, the removal of molecular oxygen might not afford complete protection.

Figure 2 appears to substantiate the hypothesis of nonoxidative degradation of pyrogallol since even extremely low levels of dissolved oxygen (0.01 ppm) did not completely halt degradation. Apparently, with the total removal of molecular oxygen, only a minimum rate of degradation or maximum stability can be attained. The significant reduction in degradation may be due to the depletion of molecular oxygen in the reaction.

As seen in Table I, the relative protection index of deaerated systems was greater than that of the control. An indication of the protection afforded *via* gas permeation is the relative protection ratio. This 55-fold increase in stability is significant in that the drug solution might be stable enough for a commercially viable product.

REFERENCES

(1) T. Higuchi and L. C. Schroeter, *J. Pharm. Sci.*, **48**, 535 (1959).

(2) G. J. West and T. D. Whitter, *Pharm. J.*, **185**, 248 (1960).

(3) E. S. Barron, R. H. DeMeio, and F. Klemperer, *J. Biol. Chem.*, **112**, 624 (1936).

(4) A. Weissberger, J. E. LuValle, and D. S. Thomas, Jr., *J. Am. Chem. Soc.*, **65**, 1934 (1943).

(5) H. Nord, *Acta Chem. Scand.*, **9**, 442 (1955).

(6) A. Palmieri, J. M. Lausier, and A. N. Paruta, *Drug Dev. Commun.*, **2**, 171 (1976).

(7) L. Lachman, *D.&C.I.*, **102**, 36 (1968).

(8) S. A. Shou, *Am. J. Hosp. Pharm.*, **17**, 153 (1960).

(9) J. Grant and J. Patel, *Anal. Biochem.*, **28**, 139 (1969).

ACKNOWLEDGMENTS

Adapted in part from a thesis submitted to the University of Rhode Island in partial fulfillment of the Master of Science degree requirements.

GLC Determination of Atenolol and β-Blocking Agents in Biological Fluids

SUK HAN WAN ˣ, ROBERT F. MARONDE, and SHAIKH B. MATIN *

Received May 27, 1977, from the *Schools of Pharmacy and Medicine, Clinical Pharmacology Section, University of Southern California, Los Angeles, CA 90033.* Accepted for publication January 10, 1978. *Present address: Department of Drug Metabolism, Syntex Research, Palo Alto, CA 94304.

Abstract □ A rapid, sensitive, and specific method of analysis for atenolol is described. Metoprolol is used as the internal standard. Atenolol and metoprolol are extracted into 1-butanol–benzene. Interfering components present in plasma and urine, but not discolored saliva, are removed during an acid wash and reextraction into ether. Drug and internal standard are converted to the pentafluoropropionate derivatives, which are quantitated by GLC with electron-capture detection and characterized by chemical-ionization mass spectrometry. The method should be applicable to measurement of other β-adrenergic blocking agents with similar structures.

Keyphrases □ Atenolol—GLC analysis in biological fluids □ GLC—analysis, atenolol in biological fluids □ Antiadrenergic agents—atenolol, GLC analysis in biological fluids

Recently, some β-adrenergic receptor blocking agents having similar structures and physicochemical properties were synthesized. Atenolol[1], 4-[2-hydroxy-3-(1-methylethyl)aminopropoxy]benzeneacetamide (I), differs from most compounds in this group by having a polar acetamide substituent that confers low partitioning into organic solvents. Thus, extraction procedures used in the analysis of β-blockers such as propranolol, alprenolol, and pronethanol must be modified considerably for application to polar compounds like atenolol.

A fluorescence assay for atenolol is rapid but lacks specificity and sensitivity (1). GLC methods (2, 3) have improved both specificity and sensitivity. A disadvantage in these methods is that the derivatizing agent used, heptafluorobutyric anhydride, must be prepared by a lengthy refluxing process because the commercially available compound is unsuitable. Moreover, the background becomes excessive at low tissue levels, resulting in high variability and low accuracy and reproducibility.

The described GLC method is rapid, specific, and sensitive to 10 ng of atenolol/ml of biological fluid. It can also be used for the analysis of other β-blocking agents such as propranolol and metoprolol. GLC coupled with a chemical-ionization mass spectrometer was used to characterize the derivatives formed.

EXPERIMENTAL

Reagents—Commercially available pentafluoropropionic anhydride[2] was used as the derivatization reagent. Sodium hydroxide (5 *N*), sulfuric acid (0.2 *N*), and pH 8 phosphate buffer (0.067 *M*) were prepared with deionized water[3]. Glass-distilled[4] 1-butanol, benzene, hexane, and ethyl acetate were used. Spectrophotometric grade pyridine[5] and nanograde ether[6] were used without prior distillation. Metoprolol[7], 1-[4-(2-methoxyethyl)phenoxy]-3-[(1-methylethyl)amino]-2-propanol (II), 50 ng in 0.1 ml of water, was used as the internal standard. Standard aqueous solutions were prepared every 2 weeks and were kept at 4°.

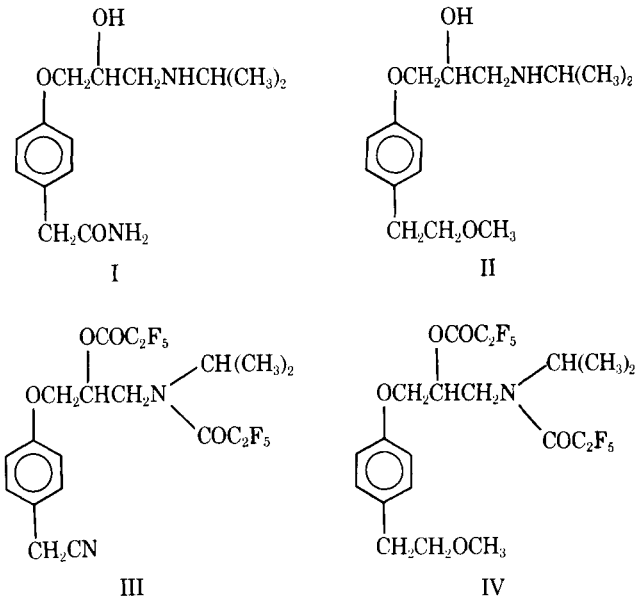

Glassware—The glassware was cleaned by soaking in 10% nitric acid overnight. It was then washed and dried by heating at approximately 400° for 3 hr.

Extraction and Derivatization—To 1 ml of standard solution, plasma, saliva, or appropriately diluted urine in a 7-ml, polytef-faced, screw-capped test tube were added 50 ng of the internal standard and 0.1 ml of 5 *N* NaOH. Atenolol and metoprolol were extracted into 5 ml of a solution of 30% benzene in 1-butanol by shaking for 15 min. The two liquid phases were separated by centrifugation, and the organic layer was transferred to another tube containing 1 ml of 0.2 *N* H_2SO_4. After shaking and centrifugation, the aqueous layer was transferred to a third tube. The solution was made basic by addition of 0.2 ml of 5 *N* NaOH, and the compounds of interest were extracted into 5 ml of ether. The ether layer was transferred to a clean tube and evaporated to dryness at 70° under a nitrogen stream.

To the residue were added 0.5 ml of hexane, 0.025 ml of ethyl acetate containing 1.5% pyridine, and 0.025 ml of pentafluoropropionic anhydride. The tube was capped and heated at 70° for 15 min. At the end of this reaction time, solvents and excess pentafluoropropionic anhydride were removed by flushing with nitrogen. To the residue were added 1 ml of phosphate buffer and 0.05 ml of hexane, and the contents of the capped tube were mixed on a vortex mixer for 15 sec. The phases were then separated by centrifugation, and 1–3 μl of the hexane layer was injected into the gas chromatograph.

GLC Conditions—A gas chromatograph[8] equipped with a ^{63}Ni-detector was used. The glass column, 180 cm × 2 mm i.d., was packed with 100–120-mesh Gas Chrom Q coated with 3% OV-1[9]. The carrier gas was 5% methane in argon, and the flow rate was maintained at 30 ml/min. Injector port, column, and detector temperatures were maintained at 190, 190, and 300°, respectively.

Mass Spectrometric Conditions—A gas chromatograph interfaced with a chemical-ionization mass spectrometer[10] was used in the characterization of atenolol and metoprolol derivatives. The GLC column was

[1] Imperial Chemical Industries Ltd., Macclesfield, England.
[2] PCR Inc., Gainesville, Fla.
[3] Millipore, Bedford, Mass.
[4] Burdick & Jackson, Muskegon, Mich.
[5] Aldrich Chemical Co., Milwaukee, Wis.
[6] Mallinckrodt Chemical Works, St. Louis, Mo.
[7] A. B. Hassle, AB Astra, Sweden.
[8] Hewlett-Packard model 5710A.
[9] Applied Science Laboratories, State College, Pa.
[10] Finnigan model 3200.

0022-3549/78/0900-1340$01.00/0
© 1978, American Pharmaceutical Association

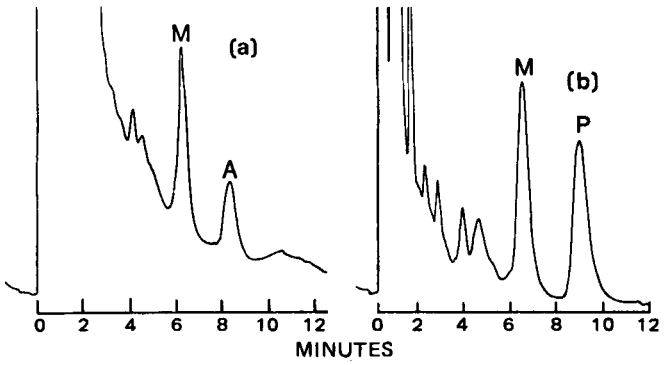

Figure 1—(a) *Spiked plasma sample containing 40 ng of atenolol and 50 ng of metoprolol/ml of sample. Injection volume was 2 μl; attenuation was 32. Key: peak M, metoprolol; and peak A, atenolol.* (b) *Spiked plasma sample containing 60 ng of metoprolol and 50 ng of propranolol/ml of sample. Injection volume was 2 μl; attenuation was 64. Key: peak M, metoprolol; and peak P, propranolol.*

maintained at 160°. Methane was both the carrier and reagent gas. The chemical-ionization source was operated at 250°, and pressure was maintained at 1 torr.

RESULTS AND DISCUSSION

Under the described GLC conditions, metoprolol and atenolol eluted with retention times of 6.5 and 8.5 min, respectively (Fig. 1*a*). Blank plasma and urine samples from healthy volunteers did not contain any interfering peaks with retention times similar to atenolol or metoprolol (Fig. 2). However, discolored saliva samples contained multiple interfering peaks, and such samples could not be analyzed by this technique. Standard curves were obtained by spiking plasma, saliva, or urine with known amounts of atenolol and measuring the peak height ratios of atenolol to metoprolol. The standard curves were linear in the range of 10–500 ng of atenolol/ml of sample.

The coefficients of variation at 10 and 100 ng/ml were 8.50 and 5.43%, respectively (n = 5). The daily variability was determined from the slopes and intercepts of five standard curves and indicated only minor fluctuations (Table I). The slopes of standard curves from water or biological fluids were similar, indicating little difference in extractability of drug from aqueous solutions of different composition. No interference was observed for plasma and urine samples from patients with renal failure who were receiving other medication including guanethidine, furosemide, clonidine, hydrochlorothiazide, digoxin, allopurinol, methyldopa, and hydralazine (Fig. 3).

The pentafluoropropyl derivative of atenolol, when subjected to chemical-ionization mass spectrometry, provided an M + H ion at mass 541 (Fig. 4*a*). The mass of this ion is consistent with Structure III and is confirmed to be the molecular ion by the presence of M + 29 = 569 and M + 41 = 581 ions, the characteristic ions formed with methane under chemical-ionization conditions. The structure of III is further supported by the formation of the doubly derivatized side chain with mass 408. The thermal conversion of the amide moiety of atenolol to cyanide under GLC conditions was reported previously (2).

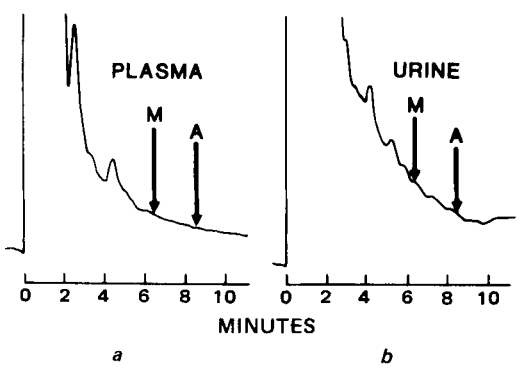

Figure 2—*Blank plasma and urine samples from healthy volunteers. Injection volume was 2 μl; attenuation was 32. Arrows M and A indicate retention times of metoprolol and atenolol, respectively.*

Table I—Daily Variability in Slopes and Intercepts of Standard Curves in Water (Atenolol Concentration of 10–100 ng/ml)

Day	Slope	Intercept
1	0.00635	−0.007
2	0.00628	0.000
3	0.00695	−0.010
4	0.00705	0.008
5	0.00634	0.008
Mean (*SE*)	0.00659 (0.00017)	0.000 (0.0037)

Figure 4*b* shows the chemical-ionization mass spectrum of derivatized metopropolol (IV). The compound formed an abundant ion at mass 528, which was equivalent to the loss of the CH_3OH molecule from the protonated compound (M + H = 560). The presence of a small peak at 560 supports this observation. The formation of doubly derivatized metoprolol is established by the formation of an ion at mass 408 and an ion at mass 396.

The solvent mixture used in the first extraction step was similar to that described by Scales and Copsey (2) who used 1-butanol containing 30% cyclohexane and obtained an overall extraction efficiency of 55% for atenolol (2). The acid wash reduced background detector response and variability of measurement at low drug levels. Ether was used in the final extraction step because it was readily evaporated and expedited sample

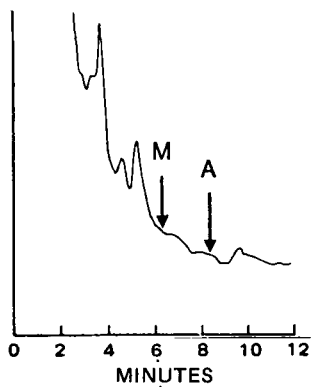

Figure 3—*Blank plasma from a subject with renal failure and receiving clonidine, hydrochlorothiazide, hydralazine, and insulin. Injection volume was 1.8 μl; attenuation was 16. Arrows M and A indicate retention times of metoprolol and atenolol, respectively.*

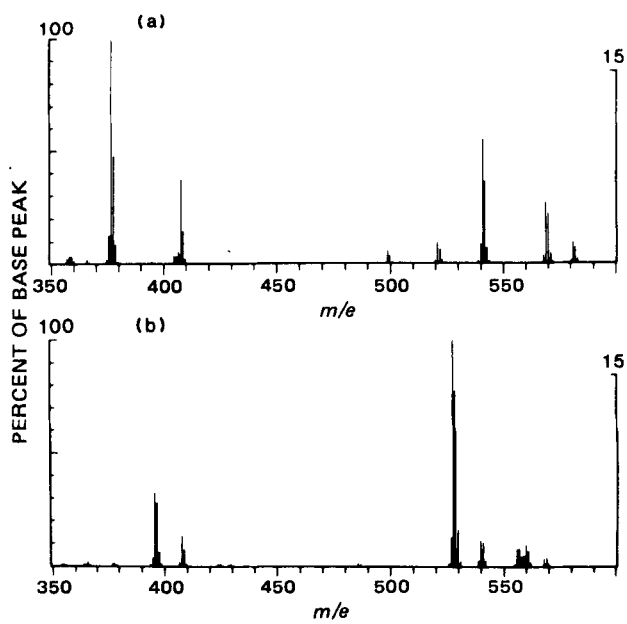

Figure 4—*Chemical-ionization mass spectrum of pentafluoropropionate derivatives of atenolol* (a) *and metoprolol* (b).

preparation. In this method, urea in urine did not interfere with derivatization by pentafluoropropionic anhydride, and it was unnecessary to destroy urea by incubation with urease (3). Derivatization of atenolol and metoprolol with pentafluoropropionic anhydride yielded products with good GLC properties, low retention times, and high electron-capture response. Back-extraction procedures ensured removal of extraneous components which normally take a long time to elute, reducing the time between injections to 15 min.

The method was applicable to the measurement of propranolol, which had a retention time of 9 min (Fig. 1*b*).

REFERENCES

(1) C. M. Kaye, *Br. J. Clin. Pharmacol.*, **1**, 84 (1974).

(2) B. Scales and P. B. Copsey, *J. Pharm. Pharmacol.*, **27**, 430 (1975).

(3) J. O. Malbica and K. R. Monson, *J. Pharm. Sci.*, **64**, 1992 (1975).

New Compounds: Antitumor Activity of 3β-Hydroxy-13α-amino-13,17-seco-5α-androstan-17-oic-13,17-lactam 4-[*p*-[Bis(2-chloroethyl)amino]phenyl]butyrate

P. CATSOULACOS *x, D. POLITIS *, L. BOUTIS ‡, and A. PAPAGEORGIOU ‡

Received October 21, 1977, from the **Department of Chemistry, Nuclear Research Center "Demokritos," Aghia Paraskevi Attikis, Greece,* and the ‡*Theagenion Cancer Institute, Thessaloniki, Greece.* Accepted for publication January 6, 1978.

Abstract □ 3β-Hydroxy-13α-amino-13,17-seco-5α-androstan-17-oic-13,17-lactam 4-[*p*-[bis(2-chloroethyl)amino]phenyl]butyrate was prepared by reacting 4-[*p*-[bis(2-chloroethyl)amino]phenyl]butyryl chloride hydrochloride with 3β-hydroxy-13α-amino-13,17-seco-5α-androstan-17-oic-13,17-lactam. The cytostatic action of the ester was investigated on two tumor systems (B16 melanoma on C57 bl mice and T8-Guerin on rats).

Keyphrases □ 3β-Hydroxy-13α-amino-13,17-seco-5α-androstan-17-oic-13,17-lactam ester of chlorambucil—synthesized, antineoplastic activity evaluated, mice and rats □ Chlorambucil, 3β-hydroxy-13α-amino-13,17-seco-5α-androstan-17-oic-13,17-lactam ester—synthesized, antineoplastic activity evaluated, mice and rats □ Antineoplastic activity—3β-hydroxy-13α-amino-13,17-seco-5α-androstan-17-oic-13,17-lactam ester of chlorambucil evaluated in mice and rats

3β - Hydroxy-13α-amino-13,17-seco-5α-androstan-17-oic-13,17-lactam *p*-[bis(2-chloroethyl)amino]phenylacetate exhibited significant antitumor activity against P-388 and L-1210 leukemia in mice (1) and T8-Guerin, B16 melanoma, and Theagenion-Bahner angiosarcoma (2).

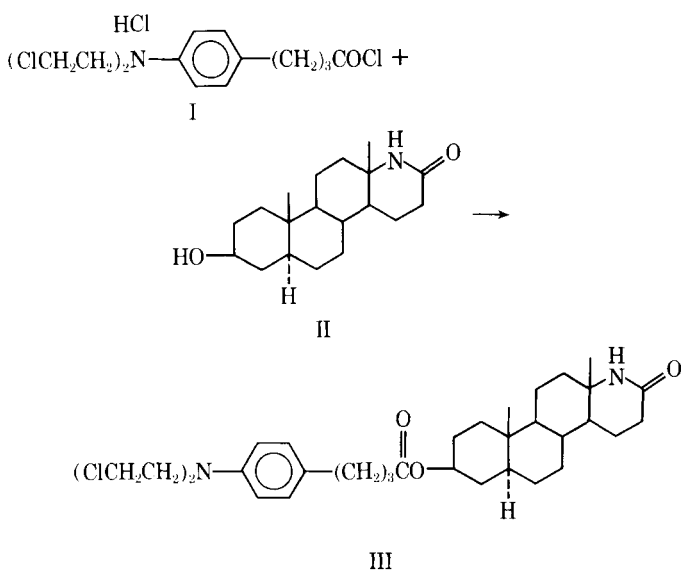

Scheme I

Table I—Effect of III on T8-Guerin Tumor and B16 Melanoma

Treatment	Number of Animals	Mean Survival of Noncured Animals, Days	Survivors
T8-Guerin Tumor (on Wistar Rats)			
Controls	10	55	0/10
Chlorambucil, 12.5 mg/kg ip			
Day 2	5	—	5/5
Days 2 and 10	4	65	3/4
Day 10	5	66	1/5
Days 10 and 20	5	60	1/5
III, 70 mg/kg ip			
Day 2	4	54	1/4
Days 1 and 10	5	60	3/5
Day 10	7	58	2/7
Days 10 and 20	4	76	3/4
B16 Melanoma (on C57 Black Mice)			
Controls	10	30	0/10
Chlorambucil, 12.5 mg/kg ip			
Day 2	5	52	0/5
Days 2 and 10	5	49	0/5
Day 10	5	43	0/5
Days 10 and 20	5	56	0/7
III, 70 mg/kg ip			
Day 2	7	48	0/7
Days 2 and 10	9	44	0/9
Day 10	6	47	0/6
Days 10 and 20	5	57	0/5

This fact created an interest in this compound that led to the synthesis of a number of derivatives (3–5).

DISCUSSION

These findings prompted the study of compounds that might have a favorable ratio between lethal and minimum effective doses and at the same time a lower toxicity than the nitrogen mustards. Therefore, 3β-hydroxy-13α-amino-13,17-seco-5α-androstan-17-oic-13,17-lactam 4-[*p*-[bis(2-chloroethyl)amino]phenyl]butyrate (III, Scheme I) was synthesized by the action of 4-[*p*-[bis(2-chloroethyl)amino]phenyl]butyryl chloride hydrochloride (I) on 3β-hydroxy-13α-amino-13,17-seco-5α-androstan-17-oic-13,17-lactam (II) (6).

Compound III was isolated in pure form after silica gel column chromatography. It gave a 50% increased lifespan over controls in the treatment of L-1210 leukemia in mice by the intraperitoneal, subcutaneous, and oral routes. In contrast, unmodified steroidal esters were inactive

0022-3549/78/0900-1342$01.00/0

© 1978, American Pharmaceutical Association

preparation. In this method, urea in urine did not interfere with derivatization by pentafluoropropionic anhydride, and it was unnecessary to destroy urea by incubation with urease (3). Derivatization of atenolol and metoprolol with pentafluoropropionic anhydride yielded products with good GLC properties, low retention times, and high electron-capture response. Back-extraction procedures ensured removal of extraneous components which normally take a long time to elute, reducing the time between injections to 15 min.

The method was applicable to the measurement of propranolol, which had a retention time of 9 min (Fig. 1*b*).

REFERENCES

(1) C. M. Kaye, *Br. J. Clin. Pharmacol.*, **1**, 84 (1974).

(2) B. Scales and P. B. Copsey, *J. Pharm. Pharmacol.*, **27**, 430 (1975).

(3) J. O. Malbica and K. R. Monson, *J. Pharm. Sci.*, **64**, 1992 (1975).

New Compounds: Antitumor Activity of 3β-Hydroxy-13α-amino-13,17-seco-5α-androstan-17-oic-13,17-lactam 4-[*p*-[Bis(2-chloroethyl)amino]phenyl]butyrate

P. CATSOULACOS *x, D. POLITIS *, L. BOUTIS ‡, and A. PAPAGEORGIOU ‡

Received October 21, 1977, from the **Department of Chemistry, Nuclear Research Center "Demokritos," Aghia Paraskevi Attikis, Greece,* and the ‡*Theagenion Cancer Institute, Thessaloniki, Greece.* Accepted for publication January 6, 1978.

Abstract □ 3β-Hydroxy-13α-amino-13,17-seco-5α-androstan-17-oic-13,17-lactam 4-[*p*-[bis(2-chloroethyl)amino]phenyl]butyrate was prepared by reacting 4-[*p*-[bis(2-chloroethyl)amino]phenyl]butyryl chloride hydrochloride with 3β-hydroxy-13α-amino-13,17-seco-5α-androstan-17-oic-13,17-lactam. The cytostatic action of the ester was investigated on two tumor systems (B16 melanoma on C57 bl mice and T8-Guerin on rats).

Keyphrases □ 3β-Hydroxy-13α-amino-13,17-seco-5α-androstan-17-oic-13,17-lactam ester of chlorambucil—synthesized, antineoplastic activity evaluated, mice and rats □ Chlorambucil, 3β-hydroxy-13α-amino-13,17-seco-5α-androstan-17-oic-13,17-lactam ester—synthesized, antineoplastic activity evaluated, mice and rats □ Antineoplastic activity—3β-hydroxy-13α-amino-13,17-seco-5α-androstan-17-oic-13,17-lactam ester of chlorambucil evaluated in mice and rats

3β - Hydroxy-13α-amino-13,17-seco-5α-androstan-17-oic-13,17-lactam *p*-[bis(2-chloroethyl)amino]phenylacetate exhibited significant antitumor activity against P-388 and L-1210 leukemia in mice (1) and T8-Guerin, B16 melanoma, and Theagenion-Bahner angiosarcoma (2).

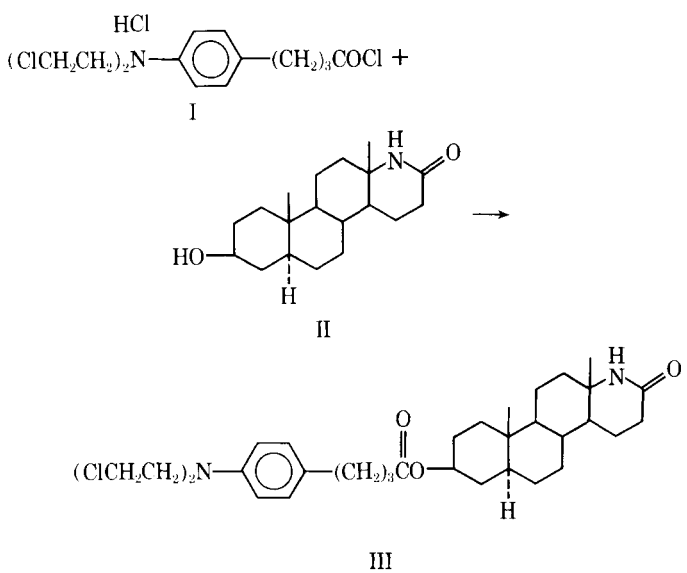

Scheme I

Table I—Effect of III on T8-Guerin Tumor and B16 Melanoma

Treatment	Number of Animals	Mean Survival of Noncured Animals, Days	Survivors
T8-Guerin Tumor (on Wistar Rats)			
Controls	10	55	0/10
Chlorambucil, 12.5 mg/kg ip			
Day 2	5	—	5/5
Days 2 and 10	4	65	3/4
Day 10	5	66	1/5
Days 10 and 20	5	60	1/5
III, 70 mg/kg ip			
Day 2	4	54	1/4
Days 1 and 10	5	60	3/5
Day 10	7	58	2/7
Days 10 and 20	4	76	3/4
B16 Melanoma (on C57 Black Mice)			
Controls	10	30	0/10
Chlorambucil, 12.5 mg/kg ip			
Day 2	5	52	0/5
Days 2 and 10	5	49	0/5
Day 10	5	43	0/5
Days 10 and 20	5	56	0/7
III, 70 mg/kg ip			
Day 2	7	48	0/7
Days 2 and 10	9	44	0/9
Day 10	6	47	0/6
Days 10 and 20	5	57	0/5

This fact created an interest in this compound that led to the synthesis of a number of derivatives (3–5).

DISCUSSION

These findings prompted the study of compounds that might have a favorable ratio between lethal and minimum effective doses and at the same time a lower toxicity than the nitrogen mustards. Therefore, 3β-hydroxy-13α-amino-13,17-seco-5α-androstan-17-oic-13,17-lactam 4-[*p*-[bis(2-chloroethyl)amino]phenyl]butyrate (III, Scheme I) was synthesized by the action of 4-[*p*-[bis(2-chloroethyl)amino]phenyl]butyryl chloride hydrochloride (I) on 3β-hydroxy-13α-amino-13,17-seco-5α-androstan-17-oic-13,17-lactam (II) (6).

Compound III was isolated in pure form after silica gel column chromatography. It gave a 50% increased lifespan over controls in the treatment of L-1210 leukemia in mice by the intraperitoneal, subcutaneous, and oral routes. In contrast, unmodified steroidal esters were inactive

0022-3549/78/0900-1342$01.00/0

© 1978, American Pharmaceutical Association

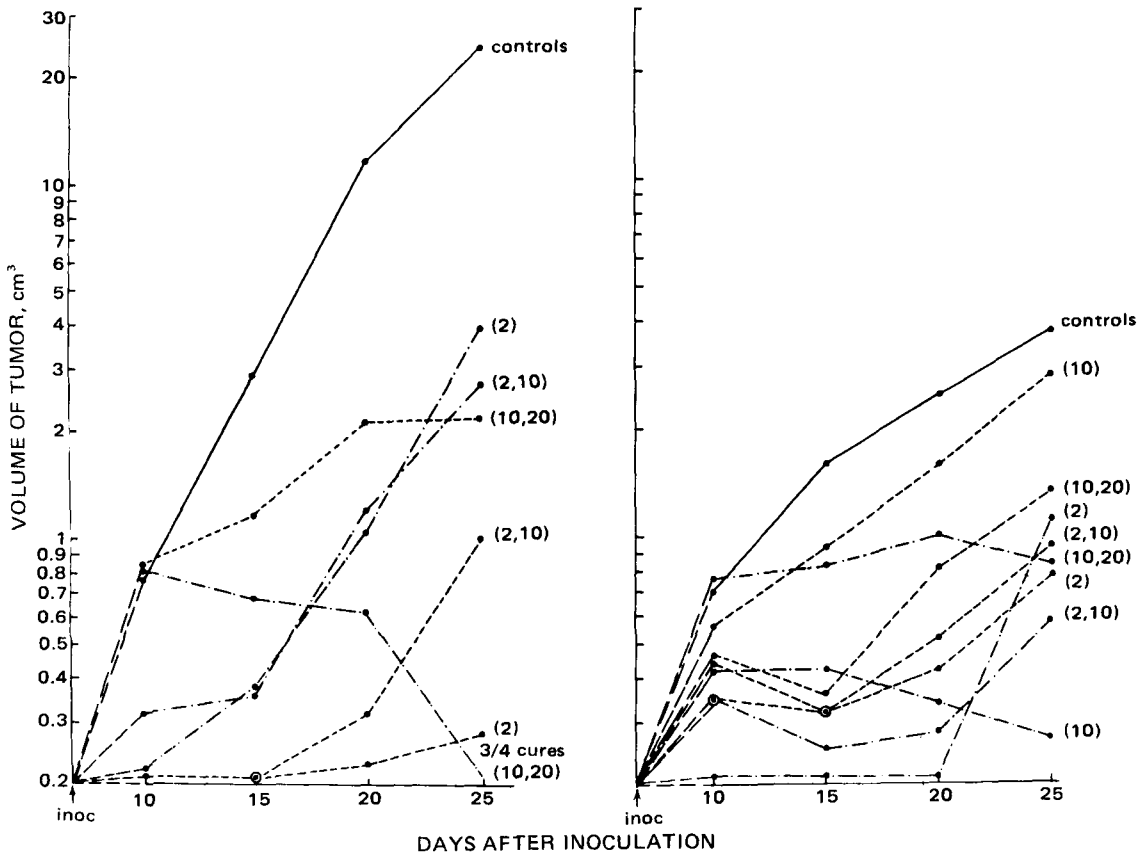

Figure 1—*Tumor growth curves of T8-Guerin tumor (left) and B16 melanoma (right) after treatment with chlorambucil and III. Key: —, controls; - - -, chlorambucil, 12.5 mg/kg ip; and –·–, ester, 70 mg/kg ip. Numbers in parentheses are the days after tumor inoculation.*

in L-1210 leukemia (7). The cytostatic action of III was investigated on two tumor systems (B16 melanoma on C57 bl mice and T8-Guerin tumor on rats).

Compounds II, III, and chlorambucil [4-[*p*-[bis(2-chloroethyl)amino]phenyl]butyric acid] were used as 1–5-mg/ml suspensions in corn oil in various dose schedules. For rats and mice, the LD_{50} (30 days) of III was 120 mg/kg after intraperitoneal injection. Compound II had no direct cytostatic effect on the tumors. The results of treatment of T8-Guerin tumor and B16 melanoma with III and chlorambucil are shown in Table I and Fig. 1.

Both III and chlorambucil, when given to animals with growing tumors, gave an increased lifespan. Clinical observations on the response of the animals and of the tumors and pathological studies revealed about the same antineoplastic activity of both chlorambucil and III but more potent early toxic effects of chlorambucil; the action of III was more prolonged.

EXPERIMENTAL[1]

To a solution of 7 g of II in 250 ml of dry benzene was added 9 g of I. The mixture was heated under reflux under nitrogen for 24 hr. Then the reaction mixture was concentrated under reduced pressure. The remaining residue was dissolved in chloroform, chromatographed on a silica gel column, and eluted with chloroform.

After solvent evaporation, the residue was crystallized from ethyl acetate–*n*-hexane to give 8.5 g (62%) of III, mp 118–121°; IR: ν_{max} 3145, 3030 (NH), 1715 ($COOCH_2$), 1670 (NHCO), 800, and 700 (aromatic ring) cm^{-1}; NMR: τ 9.2 (18-CH_3), 8.85 (19-CH_3), 5.25 (C_3-H), 3.45 (NH), 6.3 [$N(CH_2CH_2)_2$], 7.6 [$(CH_2)_3$] and the four aromatic protons at ~3; mass spectrum: molecular ion M^+ 590.

Anal.—Calc. for $C_{33}H_{48}Cl_2N_2O_3$: C, 67.01; H, 8.12; N, 4.73. Found: C, 67.15; H, 7.71; N, 4.47.

REFERENCES

(1) G. L. Wampler and P. Catsoulacos, *Cancer Treat. Rep.*, **61**, 37 (1977).

(2) P. Catsoulacos and L. Boutis, *Cancer Chemother. Rep.*, **57**, 365 (1973).

(3) P. Catsoulacos and L. Boutis, *Eur. J. Med. Chem.*, **9**, 211 (1974).

(4) P. Catsoulacos, L. Boutis, and K. Dimitropoulos, *ibid.*, **11**, 189 (1976).

(5) P. Catsoulacos and G. L. Wampler, *Eur. J. Med. Chem.*, in press.

(6) P. Catsoulacos and L. Boutis, *Chimie Ther.*, **8**, 215 (1973).

(7) M. E. Wall, S. Abernethy, Jr., F. I. Carroll, and D. J. Taylor, *J. Med. Chem.*, **12**, 810 (1969).

[1] Melting points were determined on a Gallenkamp melting-point apparatus and are uncorrected. IR spectra were recorded with a Perkin-Elmer 521 in solid phase potassium bromide. NMR spectra were determined with a Varian Associates A-60 instrument, using deuterochloroform as a solvent and tetramethylsilane as the internal standard. Elemental analyses were performed by the Analytical Laboratory of the Chemistry Department, Nuclear Research Center "Demokritos."

Scatchard Plot Analysis of Ligand–Erythrocyte Interactions

Keyphrases □ Scatchard plots—constructed from ligand–erythrocyte interaction data, use of binding capacities evaluated □ Ligand–erythrocyte interactions—Scatchard plots constructed from data, use of binding capacities evaluated □ Erythrocyte–ligand interactions—Scatchard plots constructed from data, use of binding capacities evaluated □ Binding capacities—use in Scatchard plots constructed from ligand interaction data evaluated

To the Editor:

Over the past few years, several different methods have been used to construct Scatchard plots from ligand–erythrocyte interaction data. For example, a 1% concentration of protein, determined by the biuret reaction, with an assumed molecular weight of 69,000 was used (1) to construct Scatchard plots of a drug–erythrocyte interaction[1]. More common is the use of the binding capacity of the erythrocytes (2, 3) based on the Rosenthal plot (4). The binding capacity is defined as the product of the number of binding sites and the macromolecule concentration. Such a plot may be necessary to describe binding by systems such as plasma that contain more than one species of binding macromolecules with different concentrations. It does not appear necessary, however, to use binding capacities to describe ligand–erythrocyte interactions.

Data from ligand–erythrocyte interactions have been reported as molecules of ligand bound per erythrocyte (5). This use of erythrocyte concentration is more accurate than the commonly used volume per volume concentration of packed red blood cells. The amount of extracellular fluid trapped between packed erythrocytes varies from 1 to 9%, depending on the speed and length of time of centrifugation (6). Thus, the number of erythrocytes per milliliter of packed erythrocytes also varies with the method of centrifugation. Reliable red cell counts are obtainable with an automated counter[2] (7). Data reported in this way can be analyzed by use of the Scatchard plot (8).

Reversible, noninteracting binding of a ligand by a macromolecular binding site is described by:

$$A + S \overset{k}{\leftrightarrow} D_b$$

Scheme I

where A is the concentration of the free ligand, S is the concentration of the free site, D_b is the concentration of the ligand–site complex, and k is the intrinsic association constant. Thus:

$$k = \frac{D_b}{AS} \qquad \text{(Eq. 1)}$$

and:

$$D_b = kAS \qquad \text{(Eq. 2)}$$

Let S_t be the total concentration of the binding site in the system. Then:

$$S_t = D_b + S \qquad \text{(Eq. 3)}$$

When the system consists of a ligand and erythrocytes, S_t, in molecules per milliliter, equals C_t, the concentration of erythrocytes in cells per milliliter, with the assumption that all erythrocytes are identical in composition. One molecule of any particular site on an erythrocyte is equivalent to one erythrocyte cell. This situation is analogous to the molar concentration of any particular site on a protein molecule being equivalent to the molar concentration of the protein. Therefore:

$$S = C_t - D_b \qquad \text{(Eq. 4)}$$

Substitution of Eq. 4 into Eq. 2 yields:

$$\frac{D_b}{C_t} = \frac{kA}{1 + kA} \qquad \text{(Eq. 5)}$$

When the erythrocytes contain more than one site per cell, the total concentration of ligand bound, $(D_b)_t$, is the summation of the concentrations bound to each site. Thus, by grouping identical sites:

$$\frac{(D_b)_t}{C_t} = r = \sum_{i=1}^{m} \frac{n_i k_i A}{1 + k_i A} \qquad \text{(Eq. 6)}$$

where n_i is the number of identical sites of class i per erythrocyte.

Equation 6 is of the form normally used to analyze Scatchard plots. However, in a Scatchard plot of ligand–erythrocyte interaction data, r is in units of molecules of drug bound per milliliter divided by the number of cells per milliliter while A is in its normal molar concentration unit. From such a plot, values of k_i are obtained in the usual units of M^{-1} and the number of binding sites per cell of each class is obtainable. Such a plot has the additional value of allowing one to postulate which intracellular component(s) of the erythrocyte is involved in the interaction. For example, if a linear Scatchard plot is obtained with an x intercept of approximately 2.8×10^8, it is reasonable to postulate a ligand interaction with a single site on hemoglobulin since there are approximately 280 million hemoglobulin molecules per erythrocyte (9).

In conclusion, the use of binding capacities apparently is not necessary in the study of ligand–erythrocyte interactions. With the assumption that the erythrocytes are identical, the concentration of sites per cell is analogous to the concentration of sites per molecule of protein. If the erythrocytes are sufficiently different so that this method does not hold true, then any results obtained by any method of analysis will have little meaning.

(1) C. A. Cruze and M. C. Meyer, *J. Pharm. Sci.*, **65**, 33 (1976).
(2) S. M. Wallace and S. Riegelman, *ibid.*, **66**, 729 (1977).
(3) A. B. Combs and S. N. Giri, *ibid.*, **62**, 631 (1973).
(4) H. E. Rosenthal, *Anal. Biochem.*, **20**, 525 (1967).
(5) T. Kondo and M. Tomizawa, *J. Pharm. Sci.*, **57**, 1246 (1968).
(6) "Scientific Tables," 7th ed., K. Diem and C. Lentner, Eds., Ciba-Geigy, Basel, Switzerland, 1970, p. 614.
(7) R. S. Hillman and C. A. Finch, "Red Cell Manual," 4th ed., F. A. Davis Co., Philadelphia, Pa., 1974, p. 53.

[1] M. C. Meyer, College of Pharmacy, University of Tennessee Center for the Health Sciences, Memphis, Tenn., personal communication, Oct. 28, 1977.
[2] Coulter.

0022-3549/78/0900-1344$01.00/0
© 1978, American Pharmaceutical Association

(8) G. Scatchard, *Ann. N.Y. Acad. Sci.*, **51**, 660 (1949).
(9) "Scientific Tables," 7th ed., K. Diem and C. Lentner, Eds., Ciba-Geigy, Basel, Switzerland, 1970, p. 360.

D. L. Parsons
J. J. Vallner ˣ
Department of Pharmaceutics
School of Pharmacy
University of Georgia
Athens, GA 30602

Received May 24, 1978.
Accepted for publication July 17, 1978.

Site Dependence for Topical Absorption of Nitroglycerin in Rats

Keyphrases □ Nitroglycerin—percutaneous absorption in rats, effect of application site □ Absorption, percutaneous—nitroglycerin in rats, effect of application site □ Vasodilators, coronary—nitroglycerin, percutaneous absorption in rats, effect of application site

To the Editor:

Topical nitroglycerin ointment produces clinically significant reductions in the frequency and severity of exercise-induced angina attacks (1, 2) and reductions in heart workload and determinants of myocardial oxygen consumption (3). This dosage form enjoys a growing popularity because it provides sustained hemodynamic effects (4), its administration is noninvasive, and unabsorbed drug can be removed conveniently.

Little is known about the physical and physiological factors that influence percutaneous nitroglycerin absorption. Such information is important with nitroglycerin since systemic availability is the primary goal of topical application. Furthermore, because of the relatively short nitroglycerin elimination half-life (5), the percutaneous absorption rate becomes the limiting kinetic factor and essentially determines the plasma concentration–time profile after topical drug application ["flip-flop pharmacokinetics" (6)]. The application mode and the topical preparation vehicle are important factors to consider with nitroglycerin ointment.

This communication describes the effect of the ointment application site on nitroglycerin absorption in the rat. The results may have important bearing not only on the most effective use of nitroglycerin ointment for systemic effects but also on the choice of proper animal models for screening topically delivered drugs.

Male Sprague-Dawley rats[1], 280–390 g, were used. Fifteen to eighteen hours prior to an experiment, the intended dosing site was clipped and shaved with an electric razor[2]. The animal was returned to a cage with free access to water only. The skin was examined under low power magnification for damage resulting from shaving or scratching, and the animal was not used if the skin barrier was disrupted.

A cannula[3] was implanted in the right jugular vein under ether anesthesia and kept patent with heparin sodium (20 U/ml) in normal saline. The animal was loosely restrained to expose the dosing site. Light ether anesthesia was maintained for the remainder of the 4-hr experiment to preclude movements that could result in removal or contamination of the applied dose. Experiments were conducted at ambient temperatures (21–24°). Doses were applied to a 3 × 3-cm area centered midline and midway between the sternum and penis (abdominal site) or midline and 6 cm up from the tail connection (back site).

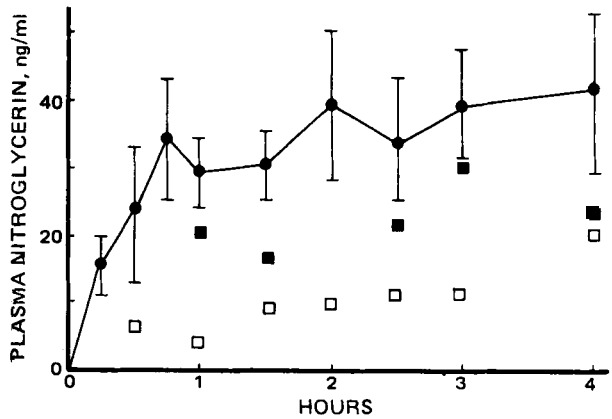

Figure 1—*Plasma nitroglycerin concentrations in rats after application of 2% nitroglycerin ointment. Key: ●, shaved abdominal surface (mean ± SEM, n = 6, 20 mg of nitroglycerin/kg); and ■ and □, back area after stripping with adhesive tape (results from two animals, 14 mg of nitroglycerin/kg).*

At appropriate intervals, 0.5 ml of blood was sampled *via* the implanted cannula. Plasma (200 μl) was stabilized against rapid degradation of nitroglycerin by the addition of 10 μl of 1.0 *N* $AgNO_3$ and assayed for intact nitroglycerin by the specific electron-capture GLC procedure of Yap *et al.* (7). The lower limit of quantitation in this experiment was 1.0 ng of nitroglycerin/ml of plasma.

Nitroglycerin was applied to the shaved back in a variety of doses and dosage forms. Plasma nitroglycerin levels could not be detected after topical application of a 2% nitroglycerin commercial ointment[4] (7 and 14 mg/kg) or a 6.9% nitroglycerin alcohol solution (8, 15, and 20 mg/kg). Each test group consisted of at least two animals. Oral dosing of rats with nitroglycerin at 7 mg/kg gives peak plasma concentrations up to about 10 ng/ml (8).

The tissue on the underside of the animal was of distinctly different character and strength than the dorsal region. Application of 2% nitroglycerin ointment to the shaved abdominal surface showed rapid drug absorption into the systemic circulation, with peak plasma levels ranging between 30 and 40 ng/ml (Fig. 1).

Considerable documentation is available describing the role of the stratum corneum as a drug penetration barrier (9). Comparative photomicrographs of histologic preparations[5] of back and abdominal tissue sections from a rat show a marked difference in the epidermis between the two sites (Fig. 2). The number of layers and relative depth of cornified tissue on the back area are significantly greater than on the abdomen.

If the stratum corneum represents a barrier to nitro-

[1] Blue Spruce Farms, Altamont, N.Y.
[2] Lady Remington MS-120, Sperry Remington, Bridgeport, CT 06602.
[3] Intramedic 7410, Clay-Adam, Parsippany, NJ 07054.
[4] Lot T4808 Nitro-bid Ointment, Marion Laboratories, Kansas City, MO 64137.
[5] Sections taken from a 295-g animal, fixed in formalin, and stained with eosin.

0022-3549/78/0900-1345$01.00/0
© 1978, American Pharmaceutical Association

(8) G. Scatchard, *Ann. N.Y. Acad. Sci.*, **51**, 660 (1949).
(9) "Scientific Tables," 7th ed., K. Diem and C. Lentner, Eds., Ciba-Geigy, Basel, Switzerland, 1970, p. 360.

D. L. Parsons
J. J. Vallner ˣ
Department of Pharmaceutics
School of Pharmacy
University of Georgia
Athens, GA 30602

Received May 24, 1978.
Accepted for publication July 17, 1978.

Site Dependence for Topical Absorption of Nitroglycerin in Rats

Keyphrases □ Nitroglycerin—percutaneous absorption in rats, effect of application site □ Absorption, percutaneous—nitroglycerin in rats, effect of application site □ Vasodilators, coronary—nitroglycerin, percutaneous absorption in rats, effect of application site

To the Editor:

Topical nitroglycerin ointment produces clinically significant reductions in the frequency and severity of exercise-induced angina attacks (1, 2) and reductions in heart workload and determinants of myocardial oxygen consumption (3). This dosage form enjoys a growing popularity because it provides sustained hemodynamic effects (4), its administration is noninvasive, and unabsorbed drug can be removed conveniently.

Little is known about the physical and physiological factors that influence percutaneous nitroglycerin absorption. Such information is important with nitroglycerin since systemic availability is the primary goal of topical application. Furthermore, because of the relatively short nitroglycerin elimination half-life (5), the percutaneous absorption rate becomes the limiting kinetic factor and essentially determines the plasma concentration–time profile after topical drug application ["flip-flop pharmacokinetics" (6)]. The application mode and the topical preparation vehicle are important factors to consider with nitroglycerin ointment.

This communication describes the effect of the ointment application site on nitroglycerin absorption in the rat. The results may have important bearing not only on the most effective use of nitroglycerin ointment for systemic effects but also on the choice of proper animal models for screening topically delivered drugs.

Male Sprague-Dawley rats[1], 280–390 g, were used. Fifteen to eighteen hours prior to an experiment, the intended dosing site was clipped and shaved with an electric razor[2]. The animal was returned to a cage with free access to water only. The skin was examined under low power magnification for damage resulting from shaving or scratching, and the animal was not used if the skin barrier was disrupted.

A cannula[3] was implanted in the right jugular vein under ether anesthesia and kept patent with heparin sodium (20 U/ml) in normal saline. The animal was loosely restrained to expose the dosing site. Light ether anesthesia was maintained for the remainder of the 4-hr experiment to preclude movements that could result in removal or contamination of the applied dose. Experiments were conducted at ambient temperatures (21–24°). Doses were applied to a 3 × 3-cm area centered midline and midway between the sternum and penis (abdominal site) or midline and 6 cm up from the tail connection (back site).

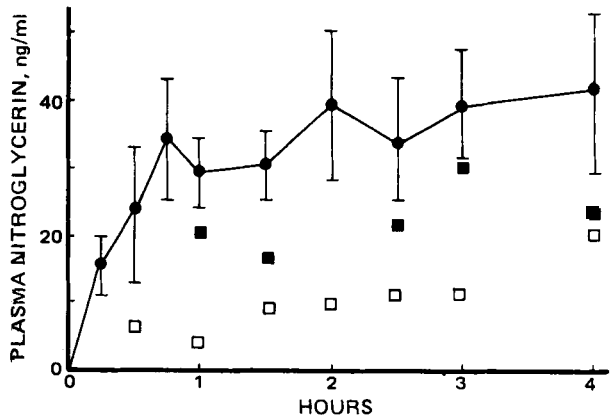

Figure 1—*Plasma nitroglycerin concentrations in rats after application of 2% nitroglycerin ointment. Key: ●, shaved abdominal surface (mean ± SEM, n = 6, 20 mg of nitroglycerin/kg); and ■ and □, back area after stripping with adhesive tape (results from two animals, 14 mg of nitroglycerin/kg).*

At appropriate intervals, 0.5 ml of blood was sampled *via* the implanted cannula. Plasma (200 μl) was stabilized against rapid degradation of nitroglycerin by the addition of 10 μl of 1.0 *N* $AgNO_3$ and assayed for intact nitroglycerin by the specific electron-capture GLC procedure of Yap *et al.* (7). The lower limit of quantitation in this experiment was 1.0 ng of nitroglycerin/ml of plasma.

Nitroglycerin was applied to the shaved back in a variety of doses and dosage forms. Plasma nitroglycerin levels could not be detected after topical application of a 2% nitroglycerin commercial ointment[4] (7 and 14 mg/kg) or a 6.9% nitroglycerin alcohol solution (8, 15, and 20 mg/kg). Each test group consisted of at least two animals. Oral dosing of rats with nitroglycerin at 7 mg/kg gives peak plasma concentrations up to about 10 ng/ml (8).

The tissue on the underside of the animal was of distinctly different character and strength than the dorsal region. Application of 2% nitroglycerin ointment to the shaved abdominal surface showed rapid drug absorption into the systemic circulation, with peak plasma levels ranging between 30 and 40 ng/ml (Fig. 1).

Considerable documentation is available describing the role of the stratum corneum as a drug penetration barrier (9). Comparative photomicrographs of histologic preparations[5] of back and abdominal tissue sections from a rat show a marked difference in the epidermis between the two sites (Fig. 2). The number of layers and relative depth of cornified tissue on the back area are significantly greater than on the abdomen.

If the stratum corneum represents a barrier to nitro-

[1] Blue Spruce Farms, Altamont, N.Y.
[2] Lady Remington MS-120, Sperry Remington, Bridgeport, CT 06602.
[3] Intramedic 7410, Clay-Adam, Parsippany, NJ 07054.
[4] Lot T4808 Nitro-bid Ointment, Marion Laboratories, Kansas City, MO 64137.
[5] Sections taken from a 295-g animal, fixed in formalin, and stained with eosin.

0022-3549/78/0900-1345$01.00/0
© 1978, American Pharmaceutical Association

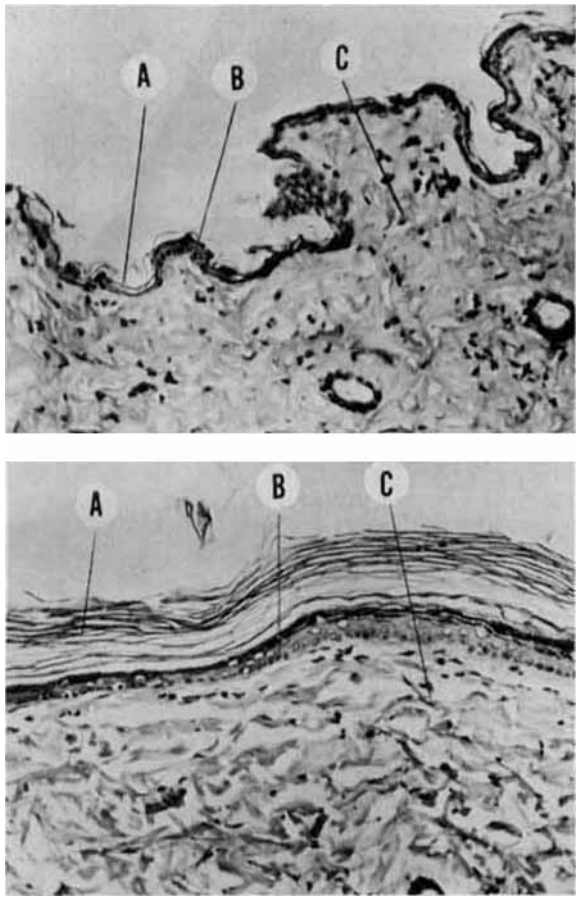

Figure 2—*Photomicrographs of rat skin tissue sections. Key: upper panel, abdominal area; lower panel, back area; A, cornified tissue; B, viable epidermis; and C, dermis.*

glycerin transdermal absorption, then removal of a portion of the barrier should increase nitroglycerin absorption. Classic stripping technique with adhesive tape (10) was used to eliminate the thick, brown, desquamating skin layer at the dorsal site. Care was taken to prevent exposure of the underlying viable epidermis or dermal capillaries. Application of the 2% nitroglycerin ointment then yielded significant drug absorption (Fig. 1).

The present data strongly suggest the presence of a site dependence for topical absorption of nitroglycerin in the rat. The evidence also implicates the stratum corneum as a barrier contributing to the lack of systemic availability from the back. Other factors, such as variations in local blood flow, may play a role in the observed site dependency. Site variations in blood perfusion have been suggested to explain differences in absorption after intramuscular injection (11). Craig *et al.* (12) showed recently that the percutaneous absorption of a cholinesterase inhibitor was a function of skin temperature. This effect was rationalized on the basis of temperature-dependent changes in skin blood flow. In the present experiment, there might have been intrinsic differences in blood perfusion at the two sites. Local changes in skin perfusion might have been induced by the stripping maneuver, thereby increasing drug absorption.

For practical reasons, many drug screening studies of topical absorption utilize the back of the rat as the primary testing site (13–16). This study shows that drug absorption from this location may be poor, even for a relatively nonpolar compound such as nitroglycerin. Lack of penetration of a drug from the back does not necessarily imply poor absorption from topical application when the drug is delivered through other skin areas.

Variations in penetration rates were demonstrated for full thickness human cadaver skin isolated from different sites (17). Regional variations in percutaneous penetration of hydrocortisone (18) and pesticides (19) in humans were reported. No reports document relationships between plasma concentrations and changes in dosing site for topically applied nitroglycerin in humans. The clinical implications of the present laboratory findings are unknown.

(1) J. O. Parker, R. J. Augustine, J. P. Burton, R. O. West, and P. W. Armstrong, *Am. J. Cardiol.*, **38**, 162 (1976).

(2) M. E. Davidov and W. J. Mroczek, *Angiology*, **27**, 205 (1976).

(3) P. W. Armstrong, M. T. Matthew, K. Boroomand, and J. O. Parker, *Am. J. Cardiol.*, **38**, 474 (1976).

(4) S. G. Meister, T. R. Engel, N. Guiha, C. M. Furr, G. S. Feitosa, K. Hart, and W. S. Frankl, *Br. Heart J.*, **38**, 103 (1976).

(5) M. G. Bogaert and M. T. Rosseel, *J. Pharm. Pharmacol.*, **24**, 737 (1972).

(6) M. Gibaldi and D. Perrier, "Pharmacokinetics," Dekker, New York, N.Y., 1975, p. 35.

(7) P. S. K. Yap, E. F. McNiff, and H.-L. Fung, *J. Pharm. Sci.*, **67**, 582 (1978).

(8) P. S. K. Yap and H.-L. Fung, *ibid.*, **67**, 584 (1978).

(9) R. J. Scheuplein and I. H. Blank, *Physiol. Rev.*, **51**, 702 (1971).

(10) S. Monash and H. Blank, *J. Invest. Dermatol.*, **78**, 710 (1958).

(11) L. S. Cohen, J. E. Rosenthal, and D. W. Horner, *Am. J. Cardiol.*, **29**, 520 (1972).

(12) F. N. Craig, E. G. Cummings, and V. M. Sim, *J. Invest. Dermatol.*, **68**, 357 (1977).

(13) C. L. Keen and L. S. Hurley, *Am. J. Clin. Nutr.*, **30**, 528 (1977).

(14) D. H. Moore, L. F. Chasseaud, D. Bucke, and P. C. Risdall, *Food Drug Cosmet. Toxicol.*, **14**, 189 (1976).

(15) M. J. Bartek, J. A. LaBudde, and H. I. Maibach, *J. Invest. Dermatol.*, **58**, 114 (1972).

(16) E. Gross, M. Kiese, and K. Resag, *Arch. Toxikol.*, **18**, 331 (1960).

(17) F. N. Marzulli, *J. Invest. Dermatol.*, **39**, 387 (1962).

(18) F. S. Feldman and H. I. Maibach, *ibid.*, **91**, 661 (1965).

(19) H. I. Maibach, R. J. Feldman, T. H. Milby, and W. F. Serat, *Arch. Environ. Health*, **23**, 208 (1971).

Stephen T. Horhota
Ho-Leung Fung [x]

Department of Pharmaceutics
School of Pharmacy
State University of New York at Buffalo
Amherst, NY 14260

Received May 10, 1978.

Accepted for publication June 22, 1978.

Supported in part by National Institutes of Health General Support Grant RR05454-15.

The assistance of Dr. Peter Nickerson, Department of Pathology, State University of New York at Buffalo, is greatly appreciated.

Direct Heating of Samples

In reference to the paper[1] "Effect of Vehicles and Other Active Ingredients on Stability of Hydrocortisone," one important point should be made.

In the *Preparation of Assay Solution* section, the sample mixture was heated to boiling on a hot plate. No data were shown to verify that direct heating is harmless to the integrity of hydrocortisone in the sample mixture. In a stability study, the proper preparation of the assay solution from a dosage form is a key factor in obtaining meaningful and reliable data. Therefore, a stability test of hydrocortisone in the sample mixture by direct heating is necessary to be sure the reported data are accurate.

Jivn Ren Chen
6884 Thomas Drive
Liverpool, NY 13088

Received June 8, 1978.

[1] V. D. Gupta, *J. Pharm. Sci.*, **67**, 299 (1978).

1978 Drug Regulation Reform Act

At the recent annual meeting of the National Association of Boards of Pharmacy[1], a presentation dealt with the Drug Regulation Reform Act of 1978 (H.R. 11611 and S. 2755, 95th Congress, Second Session). Unfortunately, program scheduling did not allow for a question and answer period.

The speaker alleged that a major reason for revising the Food, Drug, and Cosmetic Act was to update the current law, making it more reflective of recent advances in medical science and technology. A similar justification has been offered by Secretary of Health, Education, and Welfare Joseph Califano[2]. One then wonders why this proposed legislation continues to recognize as official the anachronistic Homeopathic Pharmacopeia and the "drug entities" and "drug products" contained therein.

The "Section by Section Analysis" of the Act contains such mystifying statements as "Homeopathy is analogous to (but in fact quite distinct from) the theory of immunization." Subpart 8, Sec. 145 (b) of the Act states: "Any drug entity or drug product that is represented to be a homeopathic drug entity or homeopathic drug product shall . . . (3) meet the standards and specification set forth for such drug entity or drug product in the official Homeopathic Pharmacopeia as of the date of enactment of this title." This Pharmacopeia, in fact, contains no standards and specifications. The seventh edition (1964), which appears to be the latest edition, bears no relationship to a book of standards. It is more reminiscent of an early 19th century drug compendium.

The Analysis also states: "By restricting the definition of homeopathic drugs to drugs in the official Homeopathic Pharmacopeia on the date of enactment, the bill assures that future homeopathic preparations will be processed through the monograph system." This presumably means that all new homeopathic preparations will be subjected to the same rigorous requirements (IND's, NDA's, proof of efficacy, *etc.*) that affect all new drug products used in allopathic medicine. Why not require proof of efficacy of homeopathic preparations currently on the market?

The Analysis Report further states that "homeopathic drugs have never been fully subjected to the requirements of the current FD and C Act, and should be distinguished from allopathic drugs under the Drug Regulatory Reform Act. Any other approach would probably not be cost-effective in protecting the public health, given the present role of homeopathic medicine in the United States." This, in my view, is poor justification for retaining the official status of the Homeopathic Pharmacopeia.

Martin I. Blake
College of Pharmacy
University of Illinois at
the Medical Center
Chicago, IL 60612

Received July 3, 1978.

[1] 74th Annual Meeting, NABP, New Orleans, La., Apr. 22–26, 1978.
[2] "Section by Section Analysis, Drug Regulation Reform Act of 1978," Department of Health, Education, and Welfare, Washington, D.C., Preface, pp. 122–125.

Propoxyphene Bioavailability

After having written three letters to the authors requesting additional data and having received no response, and having been very disturbed even by the initial publication of this article, I find it necessary to respond to the tactics employed in the article "Generic Propoxyphene: Need for Clinical Bioavailability Evaluation"[1].

Not only was the conclusion "clearly" not supported by the data, but the clever manner of presenting the data to disguise the fact that they were dealing with laboratory formulations proved confusing to the public, to the press, and to state and federal legislators. Careful examination of the article was necessary to determine that: (*a*) the article was not dealing with marketed generic formulations, and (*b*) the conclusion was totally unsupported since the studies dealt only with laboratory lots. If the claim is to be made that bioavailability testing should be required, then data *must* be presented from marketed generic products to support this conclusion. I strongly believe such data do not exist.

Furthermore, I believe that politically oriented articles such as this one have no place in a scientific journal. I have made three attempts to obtain the formulation information supposedly available on request, but these data have not been supplied. I trust that the publication of this letter will bring forth the data, but I believe the damage has already been done and cannot be repaired.

I find it comforting that the MAC Board, state legislators considering DPS legislation, and the Division of Biopharmaceutics at FDA were not swayed by these tactics.

Donald H. Chmielewski
Technical Information Service
Philips Roxane Laboratories
Columbus, OH 43216

Received July 3, 1978.

[1] K. A. DeSante, R. G. Stoll, D. G. Kaiser, and A. R. DiSanto, *J. Pharm. Sci.*, **66**, 1713 (1977).

Direct Heating of Samples

In reference to the paper[1] "Effect of Vehicles and Other Active Ingredients on Stability of Hydrocortisone," one important point should be made.

In the *Preparation of Assay Solution* section, the sample mixture was heated to boiling on a hot plate. No data were shown to verify that direct heating is harmless to the integrity of hydrocortisone in the sample mixture. In a stability study, the proper preparation of the assay solution from a dosage form is a key factor in obtaining meaningful and reliable data. Therefore, a stability test of hydrocortisone in the sample mixture by direct heating is necessary to be sure the reported data are accurate.

Jivn Ren Chen
6884 Thomas Drive
Liverpool, NY 13088

Received June 8, 1978.

[1] V. D. Gupta, *J. Pharm. Sci.*, **67**, 299 (1978).

1978 Drug Regulation Reform Act

At the recent annual meeting of the National Association of Boards of Pharmacy[1], a presentation dealt with the Drug Regulation Reform Act of 1978 (H.R. 11611 and S. 2755, 95th Congress, Second Session). Unfortunately, program scheduling did not allow for a question and answer period.

The speaker alleged that a major reason for revising the Food, Drug, and Cosmetic Act was to update the current law, making it more reflective of recent advances in medical science and technology. A similar justification has been offered by Secretary of Health, Education, and Welfare Joseph Califano[2]. One then wonders why this proposed legislation continues to recognize as official the anachronistic Homeopathic Pharmacopeia and the "drug entities" and "drug products" contained therein.

The "Section by Section Analysis" of the Act contains such mystifying statements as "Homeopathy is analogous to (but in fact quite distinct from) the theory of immunization." Subpart 8, Sec. 145 (b) of the Act states: "Any drug entity or drug product that is represented to be a homeopathic drug entity or homeopathic drug product shall . . . (3) meet the standards and specification set forth for such drug entity or drug product in the official Homeopathic Pharmacopeia as of the date of enactment of this title." This Pharmacopeia, in fact, contains no standards and specifications. The seventh edition (1964), which appears to be the latest edition, bears no relationship to a book of standards. It is more reminiscent of an early 19th century drug compendium.

The Analysis also states: "By restricting the definition of homeopathic drugs to drugs in the official Homeopathic Pharmacopeia on the date of enactment, the bill assures that future homeopathic preparations will be processed through the monograph system." This presumably means that all new homeopathic preparations will be subjected to the same rigorous requirements (IND's, NDA's, proof of efficacy, *etc.*) that affect all new drug products used in allopathic medicine. Why not require proof of efficacy of homeopathic preparations currently on the market?

The Analysis Report further states that "homeopathic drugs have never been fully subjected to the requirements of the current FD and C Act, and should be distinguished from allopathic drugs under the Drug Regulatory Reform Act. Any other approach would probably not be cost-effective in protecting the public health, given the present role of homeopathic medicine in the United States." This, in my view, is poor justification for retaining the official status of the Homeopathic Pharmacopeia.

Martin I. Blake
College of Pharmacy
University of Illinois at
the Medical Center
Chicago, IL 60612

Received July 3, 1978.

[1] 74th Annual Meeting, NABP, New Orleans, La., Apr. 22–26, 1978.
[2] "Section by Section Analysis, Drug Regulation Reform Act of 1978," Department of Health, Education, and Welfare, Washington, D.C., Preface, pp. 122–125.

Propoxyphene Bioavailability

After having written three letters to the authors requesting additional data and having received no response, and having been very disturbed even by the initial publication of this article, I find it necessary to respond to the tactics employed in the article "Generic Propoxyphene: Need for Clinical Bioavailability Evaluation"[1].

Not only was the conclusion "clearly" not supported by the data, but the clever manner of presenting the data to disguise the fact that they were dealing with laboratory formulations proved confusing to the public, to the press, and to state and federal legislators. Careful examination of the article was necessary to determine that: (*a*) the article was not dealing with marketed generic formulations, and (*b*) the conclusion was totally unsupported since the studies dealt only with laboratory lots. If the claim is to be made that bioavailability testing should be required, then data *must* be presented from marketed generic products to support this conclusion. I strongly believe such data do not exist.

Furthermore, I believe that politically oriented articles such as this one have no place in a scientific journal. I have made three attempts to obtain the formulation information supposedly available on request, but these data have not been supplied. I trust that the publication of this letter will bring forth the data, but I believe the damage has already been done and cannot be repaired.

I find it comforting that the MAC Board, state legislators considering DPS legislation, and the Division of Biopharmaceutics at FDA were not swayed by these tactics.

Donald H. Chmielewski
Technical Information Service
Philips Roxane Laboratories
Columbus, OH 43216

Received July 3, 1978.

[1] K. A. DeSante, R. G. Stoll, D. G. Kaiser, and A. R. DiSanto, *J. Pharm. Sci.*, **66**, 1713 (1977).

Direct Heating of Samples

In reference to the paper[1] "Effect of Vehicles and Other Active Ingredients on Stability of Hydrocortisone," one important point should be made.

In the *Preparation of Assay Solution* section, the sample mixture was heated to boiling on a hot plate. No data were shown to verify that direct heating is harmless to the integrity of hydrocortisone in the sample mixture. In a stability study, the proper preparation of the assay solution from a dosage form is a key factor in obtaining meaningful and reliable data. Therefore, a stability test of hydrocortisone in the sample mixture by direct heating is necessary to be sure the reported data are accurate.

Jivn Ren Chen
6884 Thomas Drive
Liverpool, NY 13088

Received June 8, 1978.

[1] V. D. Gupta, *J. Pharm. Sci.*, **67**, 299 (1978).

1978 Drug Regulation Reform Act

At the recent annual meeting of the National Association of Boards of Pharmacy[1], a presentation dealt with the Drug Regulation Reform Act of 1978 (H.R. 11611 and S. 2755, 95th Congress, Second Session). Unfortunately, program scheduling did not allow for a question and answer period.

The speaker alleged that a major reason for revising the Food, Drug, and Cosmetic Act was to update the current law, making it more reflective of recent advances in medical science and technology. A similar justification has been offered by Secretary of Health, Education, and Welfare Joseph Califano[2]. One then wonders why this proposed legislation continues to recognize as official the anachronistic Homeopathic Pharmacopeia and the "drug entities" and "drug products" contained therein.

The "Section by Section Analysis" of the Act contains such mystifying statements as "Homeopathy is analogous to (but in fact quite distinct from) the theory of immunization." Subpart 8, Sec. 145 (b) of the Act states: "Any drug entity or drug product that is represented to be a homeopathic drug entity or homeopathic drug product shall . . . (3) meet the standards and specification set forth for such drug entity or drug product in the official Homeopathic Pharmacopeia as of the date of enactment of this title." This Pharmacopeia, in fact, contains no standards and specifications. The seventh edition (1964), which appears to be the latest edition, bears no relationship to a book of standards. It is more reminiscent of an early 19th century drug compendium.

The Analysis also states: "By restricting the definition of homeopathic drugs to drugs in the official Homeopathic Pharmacopeia on the date of enactment, the bill assures that future homeopathic preparations will be processed through the monograph system." This presumably means that all new homeopathic preparations will be subjected to the same rigorous requirements (IND's, NDA's, proof of efficacy, *etc.*) that affect all new drug products used in allopathic medicine. Why not require proof of efficacy of homeopathic preparations currently on the market?

The Analysis Report further states that "homeopathic drugs have never been fully subjected to the requirements of the current FD and C Act, and should be distinguished from allopathic drugs under the Drug Regulatory Reform Act. Any other approach would probably not be cost-effective in protecting the public health, given the present role of homeopathic medicine in the United States." This, in my view, is poor justification for retaining the official status of the Homeopathic Pharmacopeia.

Martin I. Blake
College of Pharmacy
University of Illinois at
the Medical Center
Chicago, IL 60612

Received July 3, 1978.

[1] 74th Annual Meeting, NABP, New Orleans, La., Apr. 22–26, 1978.
[2] "Section by Section Analysis, Drug Regulation Reform Act of 1978," Department of Health, Education, and Welfare, Washington, D.C., Preface, pp. 122–125.

Propoxyphene Bioavailability

After having written three letters to the authors requesting additional data and having received no response, and having been very disturbed even by the initial publication of this article, I find it necessary to respond to the tactics employed in the article "Generic Propoxyphene: Need for Clinical Bioavailability Evaluation"[1].

Not only was the conclusion "clearly" not supported by the data, but the clever manner of presenting the data to disguise the fact that they were dealing with laboratory formulations proved confusing to the public, to the press, and to state and federal legislators. Careful examination of the article was necessary to determine that: (*a*) the article was not dealing with marketed generic formulations, and (*b*) the conclusion was totally unsupported since the studies dealt only with laboratory lots. If the claim is to be made that bioavailability testing should be required, then data *must* be presented from marketed generic products to support this conclusion. I strongly believe such data do not exist.

Furthermore, I believe that politically oriented articles such as this one have no place in a scientific journal. I have made three attempts to obtain the formulation information supposedly available on request, but these data have not been supplied. I trust that the publication of this letter will bring forth the data, but I believe the damage has already been done and cannot be repaired.

I find it comforting that the MAC Board, state legislators considering DPS legislation, and the Division of Biopharmaceutics at FDA were not swayed by these tactics.

Donald H. Chmielewski
Technical Information Service
Philips Roxane Laboratories
Columbus, OH 43216

Received July 3, 1978.

[1] K. A. DeSante, R. G. Stoll, D. G. Kaiser, and A. R. DiSanto, *J. Pharm. Sci.*, **66**, 1713 (1977).

OCTOBER 1978
VOLUME 67 NUMBER 10

JOURNAL OF PHARMACEUTICAL SCIENCES

MARY H. FERGUSON
Editor

SHELLY ELLIOTT
Production Editor

JANET D. SHOFF
Copy Editor

EDWARD G. FELDMANN
Contributing Editor

SAMUEL W. GOLDSTEIN
Contributing Editor

BELLE R. BECK
Editorial Secretary

DAVID BOHARDT
Director of Publications

L. LUAN CORRIGAN
Assistant Director of Publications

EDITORIAL ADVISORY BOARD

JOHN AUTIAN
HERBERT A. LIEBERMAN
NORMAN R. FARNSWORTH
DAVID E. MANN, JR.
WILLIAM O. FOYE
GERALD J. PAPARIELLO
WILLIAM J. JUSKO
EDWARD G. RIPPIE

The *Journal of Pharmaceutical Sciences* is published monthly by the American Pharmaceutical Association (APhA) at 2215 Constitution Ave., N.W., Washington, DC 20037. Second-class postage paid at Washington, D.C., and at additional mailing office.

All expressions of opinion and statements of supposed fact appearing in articles or editorials carried in this journal are published on the authority of the writer over whose name they appear and are not to be regarded as necessarily expressing the policies or views of APhA.

Offices—Editorial, Advertising, and Subscription: 2215 Constitution Ave., N.W., Washington, DC 20037. Printing: 20th & Northampton Streets, Easton, PA 18042.

Annual Subscriptions—United States and foreign, industrial and government institutions $50, educational institutions $50, individuals *for personal use only* $30; single copies $5. All foreign subscriptions add $5 for postage. Subscription rates are subject to change without notice. Members of APhA may elect to receive the *Journal of Pharmaceutical Sciences* as a part of their annual $70 (foreign $75) APhA membership dues.

Claims—Missing numbers will not be supplied if dues or subscriptions are in arrears for more than 60 days or if claims are received more than 60 days after the date of the issue, or if loss was due to failure to give notice of change of address. APhA cannot accept responsibility for foreign delivery when its records indicate shipment has been made.

Change of Address—Members and subscribers should notify at once both the Post Office and APhA of any change of address.

Photocopying—The code at the foot of the first page of an article indicates that APhA has granted permission for copying of the article beyond the limits permitted by Sections 107 and 108 of the U.S. Copyright Law provided that the copier sends the per copy fee stated in the code to the Copyright Clearance Center, Inc., P. O. Box 765, Schenectady, NY 12301. Copies may be made for personal or internal use only and not for general distribution.

Microfilm—Available from University Microfilms International, 300 N. Zeeb Road, Ann Arbor, MI 48106.

© Copyright 1978. American Pharmaceutical Association, 2215 Constitution Ave., N.W., Washington, DC 20037; all rights reserved.

IRS'S MYOPIC VIEW OF RESEARCH

Deep in the forest, a dead tree topples over and falls to the ground. The resultant sudden disturbance caused by the impact of the tree hitting the ground sets air waves in motion. However, many technically trained people contend that there is no *sound* because this happened far out of earshot. In the absence of an ear to hear, they say there is no such thing as "sound."

We are inclined to draw a similar conclusion with respect to research.

In our view, research is more than simply performing certain manipulative functions off somewhere in a laboratory. Embodied in the concept of research is the element of recording results, interpreting the findings, and communicating the conclusions.

Now we come to the point of this editorial. Specifically, the all-knowing, all-seeing "feds"—affectionately referred to as "big brother" and formally known as the Internal Revenue Service—have their own view of what constitutes research.

For over a hundred years, the American Chemical Society has enjoyed the status of a tax-exempt organization. For many years, the American Institute of Physics has been similarly classified. The tax codes list these as "501(c)(3) organizations." Moreover, the tax codes are rather persnickety about what such organizations may or may not do without running afoul of the law.

From what we know, both the ACS and the AIP have carefully abided by these stipulations and have principally devoted themselves to operating scientific conferences and meetings at which their members can verbally present papers reporting on their research and to publishing a spectrum of scientific journals through which chemists and physicists can communicate written reports of their research findings.

It is estimated that these two societies publish about 90 percent of the physics and chemistry journals in the United States; AIP has 40 different scholarly journals and ACS has 18.

Anyone having the remotest connection with publications—even if it is simply buying a daily newspaper or magazine at the corner newsstand—is aware that publication costs have skyrocketed in recent years. This is due to big jumps in the cost of paper stock, in the cost of printing, in the cost of postage, and in just about every other aspect of publication production. Simultaneously, circulations of most journals have been dropping, which has escalated a cost squeeze into a serious cost crunch for virtually all technical and scientific periodicals.

Indeed, one of the saving features that has kept most of these journals and their sponsoring publishers afloat has been their tax-exempt status.

But the IRS has a well-deserved reputation for being able to extract "blood from a turnip," so not surprisingly its covetous eye has fallen on these organizations and specifically their publication programs. The ax fell recently when IRS notified the two organizations that it was revoking their tax-exempt status on grounds that they are no longer research organizations.

Apparently, the IRS ruling is based on its view that a scientific organization does research, while the ACS and AIP role in publishing research results is not regarded as scientific, or at least a part of the research process.

This strikes us as an astonishing conclusion for a number of reasons. For example, about five years ago other branches of the federal government concluded that publication of findings and results is such an integral part of research that government grants and contracts would recognize the payment of page charges as a legitimate line item cost in research funding proposals. The same thinking and philosophy has long recognized the similar need to provide travel allowances in order to present verbal reports of research findings.

Although this initial IRS attack is directed at the chemistry and physics societies, other scientific and technical organizations are closely watching the proceedings. If the IRS challenge is successful here, it will undoubtedly be broadened to all other groups in a similar position and functioning in a similar manner.

This prospect has triggered predictions that the effects will be to doom the majority of the scholarly scientific periodicals now published in the United States. We are generally skeptical of such ominous predictions because they are often made more in self-serving interest of persuading opinion than as objective prognostication. However, in this instance, we are fearful that the predictions are not exaggerated one bit—indeed, they are right on target!

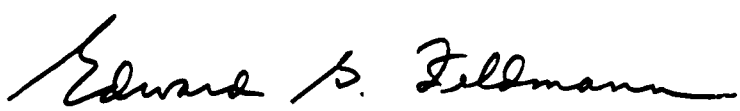

OCTOBER 1978
VOLUME 67 NUMBER 10

JOURNAL OF PHARMACEUTICAL SCIENCES

MARY H. FERGUSON
Editor

SHELLY ELLIOTT
Production Editor

JANET D. SHOFF
Copy Editor

EDWARD G. FELDMANN
Contributing Editor

SAMUEL W. GOLDSTEIN
Contributing Editor

BELLE R. BECK
Editorial Secretary

DAVID BOHARDT
Director of Publications

L. LUAN CORRIGAN
Assistant Director of Publications

EDITORIAL ADVISORY BOARD

JOHN AUTIAN
NORMAN R. FARNSWORTH
WILLIAM O. FOYE
WILLIAM J. JUSKO
HERBERT A. LIEBERMAN
DAVID E. MANN, JR.
GERALD J. PAPARIELLO
EDWARD G. RIPPIE

The *Journal of Pharmaceutical Sciences* is published monthly by the American Pharmaceutical Association (APhA) at 2215 Constitution Ave., N.W., Washington, DC 20037. Second-class postage paid at Washington, D.C., and at additional mailing office.

All expressions of opinion and statements of supposed fact appearing in articles or editorials carried in this journal are published on the authority of the writer over whose name they appear and are not to be regarded as necessarily expressing the policies or views of APhA.

Offices—Editorial, Advertising, and Subscription: 2215 Constitution Ave., N.W., Washington, DC 20037. Printing: 20th & Northampton Streets, Easton, PA 18042.

Annual Subscriptions—United States and foreign, industrial and government institutions $50, educational institutions $50, individuals *for personal use only* $30; single copies $5. All foreign subscriptions add $5 for postage. Subscription rates are subject to change without notice. Members of APhA may elect to receive the *Journal of Pharmaceutical Sciences* as a part of their annual $70 (foreign $75) APhA membership dues.

Claims—Missing numbers will not be supplied if dues or subscriptions are in arrears for more than 60 days or if claims are received more than 60 days after the date of the issue, or if loss was due to failure to give notice of change of address. APhA cannot accept responsibility for foreign delivery when its records indicate shipment has been made.

Change of Address—Members and subscribers should notify at once both the Post Office and APhA of any change of address.

Photocopying—The code at the foot of the first page of an article indicates that APhA has granted permission for copying of the article beyond the limits permitted by Sections 107 and 108 of the U.S. Copyright Law provided that the copier sends the per copy fee stated in the code to the Copyright Clearance Center, Inc., P. O. Box 765, Schenectady, NY 12301. Copies may be made for personal or internal use only and not for general distribution.

Microfilm—Available from University Microfilms International, 300 N. Zeeb Road, Ann Arbor, MI 48106.

© Copyright 1978. American Pharmaceutical Association, 2215 Constitution Ave., N.W., Washington, DC 20037; all rights reserved.

IRS'S MYOPIC VIEW OF RESEARCH

Deep in the forest, a dead tree topples over and falls to the ground. The resultant sudden disturbance caused by the impact of the tree hitting the ground sets air waves in motion. However, many technically trained people contend that there is no *sound* because this happened far out of earshot. In the absence of an ear to hear, they say there is no such thing as "sound."

We are inclined to draw a similar conclusion with respect to research.

In our view, research is more than simply performing certain manipulative functions off somewhere in a laboratory. Embodied in the concept of research is the element of recording results, interpreting the findings, and communicating the conclusions.

Now we come to the point of this editorial. Specifically, the all-knowing, all-seeing "feds"—affectionately referred to as "big brother" and formally known as the Internal Revenue Service—have their own view of what constitutes research.

For over a hundred years, the American Chemical Society has enjoyed the status of a tax-exempt organization. For many years, the American Institute of Physics has been similarly classified. The tax codes list these as "501(c)(3) organizations." Moreover, the tax codes are rather persnickety about what such organizations may or may not do without running afoul of the law.

From what we know, both the ACS and the AIP have carefully abided by these stipulations and have principally devoted themselves to operating scientific conferences and meetings at which their members can verbally present papers reporting on their research and to publishing a spectrum of scientific journals through which chemists and physicists can communicate written reports of their research findings.

It is estimated that these two societies publish about 90 percent of the physics and chemistry journals in the United States; AIP has 40 different scholarly journals and ACS has 18.

Anyone having the remotest connection with publications—even if it is simply buying a daily newspaper or magazine at the corner newsstand—is aware that publication costs have skyrocketed in recent years. This is due to big jumps in the cost of paper stock, in the cost of printing, in the cost of postage, and in just about every other aspect of publication production. Simultaneously, circulations of most journals have been dropping, which has escalated a cost squeeze into a serious cost crunch for virtually all technical and scientific periodicals.

Indeed, one of the saving features that has kept most of these journals and their sponsoring publishers afloat has been their tax-exempt status.

But the IRS has a well-deserved reputation for being able to extract "blood from a turnip," so not surprisingly its covetous eye has fallen on these organizations and specifically their publication programs. The ax fell recently when IRS notified the two organizations that it was revoking their tax-exempt status on grounds that they are no longer research organizations.

Apparently, the IRS ruling is based on its view that a scientific organization does research, while the ACS and AIP role in publishing research results is not regarded as scientific, or at least a part of the research process.

This strikes us as an astonishing conclusion for a number of reasons. For example, about five years ago other branches of the federal government concluded that publication of findings and results is such an integral part of research that government grants and contracts would recognize the payment of page charges as a legitimate line item cost in research funding proposals. The same thinking and philosophy has long recognized the similar need to provide travel allowances in order to present verbal reports of research findings.

Although this initial IRS attack is directed at the chemistry and physics societies, other scientific and technical organizations are closely watching the proceedings. If the IRS challenge is successful here, it will undoubtedly be broadened to all other groups in a similar position and functioning in a similar manner.

This prospect has triggered predictions that the effects will be to doom the majority of the scholarly scientific periodicals now published in the United States. We are generally skeptical of such ominous predictions because they are often made more in self-serving interest of persuading opinion than as objective prognostication. However, in this instance, we are fearful that the predictions are not exaggerated one bit—indeed, they are right on target!

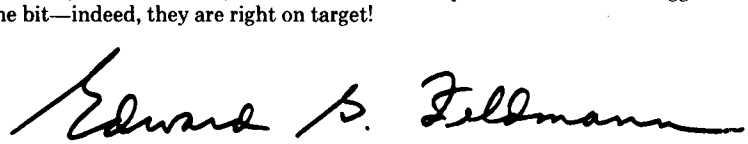

JOURNAL OF PHARMACEUTICAL SCIENCES

OCTOBER 1978
VOLUME 67 NUMBER 10

RESEARCH ARTICLES

Progestin Permeation through Polymer Membranes I: Diffusion Studies on Plasma-Soaked Membranes

GAYLEN M. ZENTNER, JOHN R. CARDINAL ˣ, and SUNG WAN KIM

Received August 18, 1977, from the *Department of Pharmaceutics, College of Pharmacy, University of Utah, Salt Lake City, UT 84112.* Accepted for publication February 15, 1978.

Abstract □ The potential of several commercially available polymeric materials for use in controlled-release drug delivery devices was investigated. Progesterone was used as a model hydrophobic drug. The progesterone permeation rates through polydimethylsiloxane, two polyether urethanes, a hydroxyethyl methacrylate, a polyether urethane–polydimethylsiloxane blend, and a cellulosic membrane were determined. The permeabilities were obtained on nonsoaked membranes and on membranes soaked in plasma for varying times. The purpose of the plasma soaks was to examine the effects of lipid absorption and degradative processes within the membrane on progesterone permeability. This study identified several polymers that show potential for use in controlled-release drug delivery devices. The plasma treatment studies showed that several polymers may not be acceptable. The plasma soak studies were interpreted in terms of the mechanisms of drug permeation through the membranes.

Keyphrases □ Polymer membrane, various—permeabilities to progesterone, effect of soaking in plasma, potential for use in controlled-release drug delivery devices □ Progesterone—permeability through various polymer membranes, effect of soaking in plasma □ Delivery devices, controlled release—various polymer membranes evaluated, permeability to progesterone, effect of soaking in plasma □ Diffusion—progesterone through various polymer membranes, effect of soaking in plasma □ Dosage forms—controlled-release delivery devices, various polymer membranes evaluated, permeability to progesterone, effect of soaking in plasma

Recently, attention has been directed toward the use of polymeric materials to control the release of drugs for extended periods *in vivo*. Some applications of these materials have been the controlled release of contraceptive steroids (1–3), anti-inflammatory agents (4), antihistamines (5), narcotic antagonists (6), inorganic fluorides (7, 8), and antitumor agents (9).

Much of the previous work on controlled-release drug delivery devices utilized polydimethylsiloxane (silicone rubber) because of its biocompatibility and its high permeability to hydrophobic drugs (10, 11). However, this polymer has several disadvantages for certain applications. It is weakly permeable to hydrophilic drugs, especially charged species (12), and tends to absorb large quantities of lipids from biological fluids (13–15). Lipid absorption may cause a decrease in the release rate of drugs as a function of time when controlled-release devices are implanted in body tissues (16, 17).

Other polymers that can be utilized in controlled-release drug delivery devices have been evaluated. The class of polymers known as the hydrogels has shown promise. These polymers can be utilized to control the release of both hydrophobic and hydrophilic drugs, and the release rates can be varied over a wide range by changes in the monomer composition and cross-linker percent (4, 5, 7, 9, 18).

In the present study, the potential use of several commercially available polymeric materials in controlled-release drug delivery devices was investigated. Progesterone was used as a model hydrophobic drug. The rate of permeation of progesterone through several polymeric films was determined on both water-swollen membranes and water-swollen membranes pretreated by soaking in plasma for varying periods. The purpose of the plasma soaks was to examine the effects of lipid absorption and/or any other effects of these biological fluids on the permeability of drug molecules. The results were interpreted in terms of the mechanisms of drug permeation through the films.

EXPERIMENTAL

Materials—Progesterone[1] and 1,2-^{3}H-progesterone[2] were used as received. The polymer films investigated were polydimethylsiloxane[3] (silicone rubber), two polyether urethanes (polyurethane I[4] and polyurethane II[5]), a polyether urethane–polydimethylsiloxane polymer blend[6], a regenerated cellulosic material[7], and a hydroxyethyl methacrylate[8] (hydrogel).

[1] Steraloids Inc., Wilton, N.H.
[2] New England Nuclear, Boston, Mass.
[3] Dow Corning Co., Midland, Mich.
[4] Biomer, Ethicon Co., Somerville, N.J.
[5] Pellethane, The Upjohn Co., Stanford, Conn.
[6] Avcothane, AVCO Everett Research Laboratories, Everett, Mass.
[7] Cuprophan, Vital Assists Inc., Littleton, Colo.
[8] Courtesy of Hydron Laboratories, New Brunswick, N.J.

0022-3549/78/1000-1347$01.00/0
© 1978, American Pharmaceutical Association

The cellulosic, polydimethylsiloxane, and polyurethane II films were obtained from the manufacturer. The polyurethane I and the polyether urethane–polydimethylsiloxane blended films were prepared by solvent casting using dimethylacetamide and tetrahydrofuran, respectively, with vacuum drying. Polyhydroxyethyl methacrylate films were prepared by a free radical polymerization using 7.84 mmoles of azobis(methylisobutyrate)/liter of monomer as the initiator. The initiator was prepared by the method of Mortimer (19). The polymerizations were carried out between glass plates at 60° for 24 hr. The monomer solutions were mixed with 40% (v/v) water prior to polymerization. Cross-linked hydrogels, containing 0.75 and 3.75 mole % ethylene glycol dimethacrylate[9] as the cross-linker, were prepared similarly, except that the initial monomer solution contained 40% (v/v) ethylene glycol.

Plasma was prepared by centrifugation of a 9:1 mixture of bovine blood with 3.8% sodium citrate and was stored in glass containers at −15°.

Methods—All polymer films, except the hydrogels, were wiped with methanol–water (50:50) to remove surface contaminants. The films then were immersed immediately in a large volume of deionized water to equilibrate for 24 hr at room temperature (24 ± 1°). The hydrogels were transferred directly from the polymerization mold into a large volume of deionized water, which was changed twice daily. The gels were equilibrated at room temperature until the weight fraction of water was constant.

Films receiving plasma treatment were transferred from the water equilibration baths into 20 ml of plasma at room temperature. The plasma was changed daily to minimize bacterial contamination. The polymer films were rinsed with deionized water at the same time the plasma was changed to reduce bacterial problems. After the plasma soaks, the polymer films were rinsed and reequilibrated with deionized water at room temperature for 24 hr.

The diffusion coefficients of progesterone in the polymer films were determined in a glass diffusion cell with two compartments of equal volume (176 ml). The membrane was clamped between the compartments and was not supported. Each compartment was stirred continuously at 1600 rpm by externally mounted constant-speed synchronous motors. A ±10% change in the stirring speed did not affect the observed permeabilities. Initially, one chamber was filled with deionized water. The second chamber was filled with an aqueous solution containing 11.2 μg of unlabeled progesterone/ml together with an appropriate amount of the labeled steroid.

Progesterone permeation through the membranes was followed by determining the increase in radioactivity in the initially progesterone-free compartment. Samples of approximately 0.1 ml were withdrawn and weighed in tared vials. Scintillation fluid[10], 10 ml, was added to each vial, and the concentration was determined using a liquid scintillation spectrometer[11].

The partition coefficients were measured by a solution depletion technique. For several membranes, the partition coefficients were dependent on the solute concentration in the aqueous phase. For this reason, the partition coefficients were measured under conditions such that the ratios of the volume of membrane to the volume of solution and the initial bulk concentration of progesterone were similar to those used in the diffusion experiments. The bulk solutions were allowed to equilibrate with the membrane until a constant concentration was obtained. The equilibrium concentrations were obtained from measurements of the radioactivity in the aqueous phase by scintillation counting as already described.

The approximate thicknesses of the films were: polyhydroxyethyl methacrylate, 0.07 cm; polyurethane I, 0.025 cm; polyurethane II, 0.013 cm; polydimethylsiloxane, 0.016 cm; polyether urethane–polydimethylsiloxane, 0.016 cm; and the cellulosic membrane, 0.0029 cm. The accurate thickness of the wet membranes used in the calculation of the diffusion coefficient was determined by direct measurement using a light wave micrometer[12] accurate to 2.5×10^{-5} cm at the minimum allowable pressure (60 g). Because of the low pressures involved in these measurements, film deformation should be minimal.

RESULTS AND DISCUSSION

The membranes were chosen because of their potential for use in drug delivery systems. Polyurethanes I and II are commercially available copolymers of urethane and ethylene glycol. These membranes have been considered for use in artificial hearts and other implant devices. The hydrogels have shown potential for use as controlled-release drug delivery devices (4, 5, 7, 9). These membranes are biocompatible, and the permeability of solutes can be varied over a wide range by changes in the monomer composition and percent cross-linker (18).

Polydimethylsiloxane was utilized in previous studies on controlled-release drug delivery systems for steroids (1–3). The polymer blend of polydimethylsiloxane and polyurethane may offer some advantages not shared by the individual polymers. The cellulosic film was included as a model membrane because solutes permeate this membrane by diffusion through pores in the polymer network.

The diffusion coefficients for progesterone in the various membranes were calculated by means of the following relationship, which was derived elsewhere (20):

$$\ln\left(1 - \frac{2C_t}{C_0}\right) = -\left(\frac{1}{V_1} + \frac{1}{V_2}\right)\frac{AUt}{l} \qquad \text{(Eq. 1)}$$

where C_t is the concentration of progesterone at time t, C_0 is the initial concentration of progesterone, V_1 and V_2 are the compartment volumes (176 ml), A is the membrane area (14.2 cm²), l is the wet membrane thickness, and U is the permeability, which is defined as:

$$U = DK_d \qquad \text{(Eq. 2)}$$

Table I—Diffusion Coefficients, Partition Coefficients, and Permeabilities for Progesterone in Polydimethylsiloxane, Polyurethane I, and Polyurethane II at 25°

Membrane	Plasma Soaking Time	D, cm²/sec	K_d	$U \times 10^7$, cm²/sec
Polydimethylsiloxane	0	$2.15 \times 10^{1-8}$	180[a]	38.5
	1 hr[b]	2.30×10^{-8}		41.5
	24 hr[b]	2.10×10^{-8}		37.7
	3 days[b]	2.41×10^{-8}		43.5
	7 days[b]	2.30×10^{-8}		41.4
	9 days	2.79×10^{-8}		50.2
Polyurethane I	0	4.75×10^{-10}	2110[a]	10.0
	24 hr	4.35×10^{-10}		9.18
	4 days	3.95×10^{-10}		8.33
	7 days	2.82×10^{-10}		5.95
	16 days	6.17×10^{-10}		13.0
	1 hr[b]	4.40×10^{-10}		9.28
	14 days[b]	4.50×10^{-10}		9.50
Polyurethane II	0	6.5×10^{-12}	5000[a]	0.33
	0	5.0×10^{-12}		0.25
	1 hr	4.2×10^{-12}		0.21
	24 hr	4.2×10^{-12}		0.21
	24 hr	5.1×10^{-12}		0.26
	3 days	9.4×10^{-12}		0.47
	7 days	11.3×10^{-12}		0.57

[a] Average values. [b] At 5°.

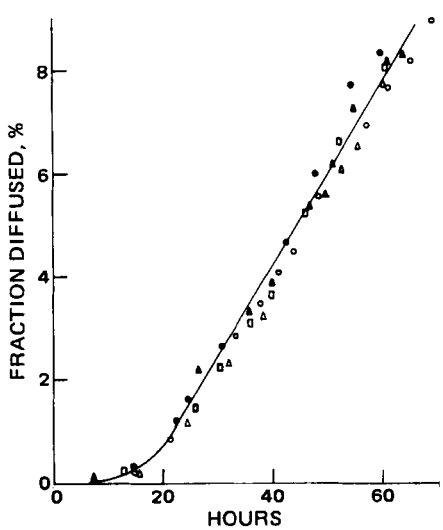

Figure 1—*Fraction of drug diffused* versus *time for progesterone permeation through hydroxyethyl methacrylate without cross-linker. Key (plasma soak times): △, no soak; ○, 1 day; □, 3 days; ●, 7 days; and ▲, 14 days.*

[9] Monomer Polymer Laboratories, Philadelphia, Pa.
[10] Aquasol, New England Nuclear, Boston, Mass.
[11] Model 3390, Packard Instrument Co., Downers Grove, Ill.
[12] Van Keuren Co., Watertown, Mass.

Table II—Diffusion Coefficients, Partition Coefficients, and Permeabilities for Progesterone in Hydrogels at 25°

Membrane	Plasma Soaking Time, days	$D \times 10^9$	K_d	$U \times 10^7$, cm²/sec
Hydroxyethyl methacrylate	0	4.38[a]	120	5.59
	1	3.95	133	5.07
	3	4.60	124	5.91
	7	4.41	134	5.67
	14	4.57	131	5.87
Hydroxyethyl methacrylate plus 0.75% ethylene glycol dimethacrylate	0	3.82[b]	134	5.19
	1	3.50	135	4.76
	3	3.76	139	5.13
	7	3.92	139	5.33
	14	3.34	133	4.54
Hydroxyethyl methacrylate plus 3.75% ethylene glycol dimethacrylate	0	0.34[c]	211	0.71
	1	0.43	161	0.76
	3	0.43	174	0.77
	7	0.40	186	0.71
	14	0.42	155	0.74

[a] Calculated with an average K_d of 128. [b] Calculated with an average K_d of 136. [c] Calculated with an average K_d of 177.

where D is the diffusion coefficient, and K_d is the partition coefficient. The values of U, K_d, and D for the various polymer membranes are shown in Tables I–III. Figures 1–3 are plots of the fraction of drug diffused against time for progesterone permeation through the membranes polyhydroxylethyl methacrylate, polyurethane I, and polyurethane II, respectively.

The permeabilities of the nonsoaked membranes varied from about 40×10^{-7} cm²/sec for silicone rubber to about 0.2×10^{-7} cm²/sec for polyurethane II. The membrane diffusion coefficients varied over a much wider range, from about 2×10^{-8} cm²/sec for silicone rubber to about 4×10^{-12} cm²/sec for polyurethane II. For all membranes, the diffusion coefficients were calculated on the basis of the average value of K_d obtained from all experiments with that polymer. In all cases except polyurethane II, the values of K_d were in good agreement for any given membrane irrespective of the prior treatment of the membrane. With polyurethane II, the values of K_d tended to vary over a wide range and were independent of the prior treatment of the membrane. The value of K_d obtained for polydimethylsiloxane was higher by a factor of about three compared to values reported previously (3, 11).

As mentioned under *Experimental*, the values of K_d were dependent on the concentration of progesterone in the bulk solution; K_d tended to increase as the bulk concentration decreased. This result may have been due to adsorption of the solute at the membrane surface. Previous K_d values (3, 11) were obtained from saturation solubilities whereas the present values were obtained at bulk concentrations considerably below saturation and are not directly comparable with those obtained previously.

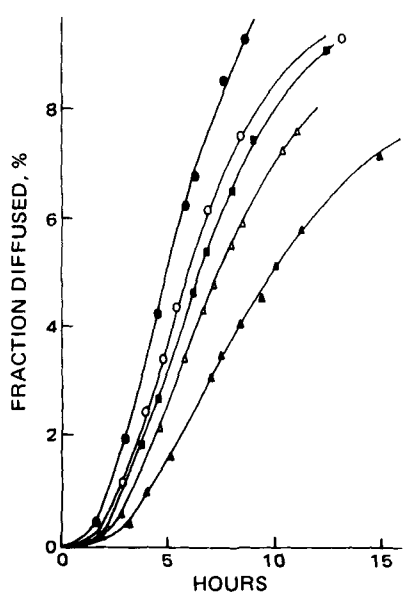

Figure 2—*Fraction of drug diffused* versus *time for progesterone permeation through polyurethane I. Key (plasma soak times): ○, no soak; ■, 1 day; △, 3 days; ▲, 7 days; and ●, 16 days.*

Table III—Plasma Soaking Times and Permeation Coefficients for Progesterone in the Polyether Urethane–Polydimethylsiloxane Blend and Regenerated Cellulose at 25°

Membrane	Plasma Soaking Time	$U \times 10^7$, cm²/sec
Polyether urethane–polydimethylsiloxane blend	0	2.00
	4 days	1.83
	7 days	1.88
Regenerated cellulose	0	3.61
	1 hr	3.98
	24 hr	3.67
	3 days	3.79
	6.3 days	4.17

The value obtained for progesterone permeability in polydimethylsiloxane was intermediate to values obtained previously (3, 11, 12, 21). Literature values varied from 6×10^{-7} cm²/sec (12) to 390×10^{-7} cm²/sec (11). These differences could arise from differences in the membranes, diffusion layer effects, or temperature. The values in the present study were obtained at 25°; previous work was at 37°.

The polydimethylsiloxane used contained a filler of unknown concentration. The presence of a filler can have dramatic effects on drug permeability in this membrane (22, 23). Drug permeability varies with both the concentration of the filler and the concentration of drug in the donor medium (23). Therefore, it is difficult to compare the values of the permeability obtained in the present study with those in previous reports. Nevertheless, progesterone permeability in polydimethylsiloxane apparently decreases in the presence of filler (3, 11, 12, 21).

Diffusion layer effects also are important in the characterization of membrane permeability (24). Although no attempt was made to characterize the thickness of the aqueous diffusion layers, the effects arising from these layers are expected to be minimal for all membranes except polydimethylsiloxane and cellulose. For this reason, the membrane permeabilities given in Tables I–III must be considered as apparent values, which include effects that arise predominantly from the membrane but may have some contribution from the aqueous diffusion layers. This conclusion is based on reasonable estimates of diffusion layer thicknesses obtained previously (25, 26) using diffusion cells similar to those used in this study. Furthermore, diffusion layer effects should not dramatically alter conclusions reached in the present study regarding the effects of plasma soaking on membrane permeability, which are of primary interest.

To investigate the potential of these polymers for use in drug delivery devices in greater detail, the effects of plasma soaking on the membrane permeabilities were investigated. The plasma soaking studies simulate two possible effects of long-term use *in vivo*: the effects of lipid absorption by the membrane and the effects arising from degradative processes within the membrane.

Molecules permeate the cellulosic membrane *via* microscopic channels

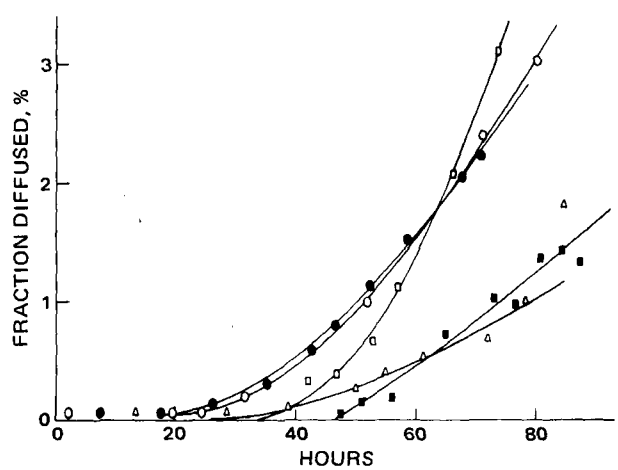

Figure 3—*Fraction of drug diffused* versus *time for progesterone permeation through polyurethane II. Key (plasma soak times): ●, no soak; ○, 5 hr; △, 1 day; □, 3 days; and ■, 7 days.*

(pores) throughout the polymer network (27). The permeation rate is governed primarily by the molecular weight of the solute (28). For a molecule with the molecular weight of progesterone, a diffusion coefficient of approximately 6×10^{-7} cm^2/sec is predicted (29). Although several attempts were made to obtain the partition coefficient of progesterone in the membrane, reproducible values could not be obtained. The trend of the values suggested, however, that K_d was less than one. This value is consistent with the arguments of Ginsburg and Katchalsky (25), who suggested that K_d values for highly water-swollen membranes of the cellulosic type may be equated to the volume fraction of water in the membrane. For the cellulosic membranes used in the present study, this value is approximately 0.67 (30). The K_d values for hydrophilic solutes such as urea and sucrose were quite close to this value (30, 31).

If it is assumed that the approximation suggested by Ginsburg and Katchalsky (25) also holds for hydrophobic solutes such as progesterone, then the value of D calculated from the average of the permeability values shown in Table III is 5.7×10^{-7} cm^2/sec. This value is in agreement with that calculated above for the diffusion coefficient of progesterone assuming that the solute permeates the cellulosic membrane *via* the pore mechanism. As seen from the values shown in Table III, the plasma soaks had no detectable effect on the measured progesterone permeability through this membrane. These results suggest that any absorbed or adsorbed species arising from the plasma treatments do not block the pores or markedly alter the effective pore size of this membrane.

The mechanism of progesterone permeation through hydrogel membranes depends on the equilibrium water content and the nature and chain length of the cross-linker. Progesterone permeation through hydroxyethyl methacrylate without cross-linker occurs predominantly *via* the pore mechanism (18). In the hydroxyethyl methacrylate membranes cross-linked with a high concentration of ethylene glycol dimethacrylate, progesterone permeation appears to occur by a process in which solution and diffusion of the progesterone in the polymer network control the permeation (18). As seen from Table II and Fig. 1, plasma soaking had little or no effect on the observed permeabilities of either the polymer without cross-linker or the membrane containing a high concentration of the cross-linker, ethylene glycol dimethacrylate. The concentration of ethylene glycol dimethacrylate was in the region where the solution and diffusion mechanism is operative.

An attempt was made to determine if the hydrogel membranes absorb lipoidal species. Measurements of the increase in weight of the polymer subsequent to the plasma soaks were taken. This technique previously was used to determine the uptake of lipids by various polymers (32). For the hydrogel membranes, the weight of the wet membrane decreased subsequent to the plasma soakings. However, the weight of these membranes returned to their initial values (prior to the plasma soaks) following a 24-hr soak in deionized water. These results suggest that the hydrogels absorbed little or no lipoidal species during the 2-week interval of plasma treatment, probably because of the low interfacial energy of these polymers (33). Since the permeabilities remained unchanged over this time, these results also suggest that no hydrolytic degradation occurred that affected the permeability of these membranes to progesterone. Finally, the results obtained with the hydrogels without cross-linker are consistent with the results of the studies on the cellulosic membranes in that the permeability of a pore-type polymer was not affected by plasma soaking.

Solute permeation through polydimethylsiloxane occurs by the solution and diffusion mechanism. The permeation rate is strongly related to the partition coefficient of the solute in the membrane (34). Lacey and Cowsar (11) demonstrated this effect for the permeation of steroids through polydimethylsiloxane. Moreover, the polymer chains of this membrane show high flexibility, as reflected in the high permeabilities of gases through this polymer (34).

Several investigators (13–15) measured the uptake of lipids by polydimethylsiloxane and showed that implants took up appreciable quantities, 0.1–16% (w/w), of lipoidal substances. The amounts absorbed seemed to be independent of time. Lipid uptake did not appreciably affect the permeability of polydimethylsiloxane (Table I). This result is in agreement with those of several previous investigators (13, 14) who showed that lipid uptake by polydimethylsiloxane did not appreciably affect the physical properties of this polymer. Based on these results, it appears that the slowly decreasing *in vivo* release rates of progestins (16, 17) from polydimethylsiloxane implants *in vivo* are not related to the lipid uptake by the membrane.

Previous studies (35, 36) established that solutes permeate polyurethanes by solution and diffusion in the polymer network. However, unlike polydimethylsiloxane or the hydrogels, which have uniform properties throughout, polyurethane membranes consist of regions of varying hydrophobicity and hydrophilicity. Presumably, this variation arises from the organization of the urethane segments and the polyethylene glycol segments of the copolymer, respectively. The polyurethanes strongly absorb lipoidal species from biological fluids. For example, polyurethanes absorbed large quantities of lipid from micellar solutions and the percent uptake was highest when the volume percent of hydrophilic groupings was near 50% (37). In another study (32), polyurethane I absorbed large quantities of lipid both *in vivo* and from simulated biological fluids *in vitro*. In addition, the mechanical properties of this polymer are affected by long-term soaking in either water or the simulated biological fluid.

The results in Table I and Fig. 2 indicate that long-term plasma soakings altered the permeability of polyurethane I. The progesterone permeability of this polymer decreased continuously for plasma soaking times up to 1 week. This decrease in permeability may have resulted from lipid uptake by the hydrophobic regions of the copolymer. This lipid probably decreased the free volume of the polymer available for progesterone permeation. Lipid uptake seemed to affect only the diffusion coefficient while K_d was relatively constant. This finding suggests that lipid uptake may not affect the overall hydrophobicity of the polymer but may affect the segmental motion of the polymer chains in the hydrophobic regions. For periods of plasma soaking greater than about 1 week, the permeability of polyurethane I to progesterone increased to values greater than those found in the non-plasma-treated membrane. This increase in diffusivity of the progesterone is believed to be related to the hydrolytic breakdown of the polymer and is consistent with the loss in the mechanical properties of this polymer as discussed by Andrade *et al.* (32).

Support for this interpretation of the effects of lipid absorption on progesterone permeation through polyurethane I can be inferred from studies performed using membranes soaked at 5°. Under these conditions, the plasma soakings had no effect on the progesterone permeation rate for soaking periods of up to 2 weeks. Polyurethanes soaked in water, lactated Ringers solution, and plasma for approximately 2 weeks at 5° gained the same amount of weight irrespective of the liquid (38). This result suggests that lipoidal species are not strongly absorbed at this temperature.

The results of the studies on the effects of plasma soaking on the permeation of progesterone through polyurethane II (Table I and Figs. 2 and 3) present a very different pattern from polyurethane I. The diffusion coefficients varied widely and seemed to be independent of plasma soaking time. These variations are believed to arise from the method of casting this polymer. Polyurethane II is a thermal-casted polymer whereas polyurethane I is solvent cast. As a result of the thermal-casting procedure, it is believed that large inhomogeneities arise during the cooling of the polymer. These inhomogeneities may account for the large variations in D and K_d obtained, even though all membranes were cut from the same polymer films.

Although systematic studies on the mechanism of solute permeation through the polyether urethane–polydimethylsiloxane blend are not available, it is anticipated that solutes permeate by solution and diffusion in the polymer network. Lipid absorption by this membrane is known to occur; however, the amounts and composition of the lipids absorbed differ from those absorbed by polyurethane I (32). The polymer blend absorbs primarily cholesterol esters whereas polyurethane I absorbs primarily free cholesterol.

The effects of plasma soaking on progesterone permeation through the polymer blend are shown in Table III. Plasma soaking times of up to 1 week had no effect on the membrane permeability.

Although studies on the effects of lipid absorption on the mechanical properties of this membrane are not available, it might be anticipated, based on the polyurethane I studies, that long-term exposure of the blended polymer to plasma may increase the permeability of the membrane due to the hydrolytic breakdown of the polyurethane component.

CONCLUSIONS

All of the polymers studied are apparently sufficiently permeable to be of use in controlled-release drug delivery systems. The permeation rates of the model hydrophobic drug, progesterone, through these membranes vary by about two orders of magnitude and, thus, allow great latitude in the release rate of a hydrophobic drug for a given application. However, based on the plasma soaking studies, the polyurethanes and, possibly, the polyether urethane–polydimethylsiloxane blend appear to yield varying release rates, depending on the length of the plasma soaks. The varying release rates arise from the effects of lipid uptake by the membrane and from degradative processes within the membrane. These

results suggest that these polymers may be of questionable value for use in controlled-release drug delivery systems. For the membrane polyurethane I, this conclusion is expected to be valid for hydrophobic molecules in general; however, this conclusion may not be valid for uncharged water-soluble molecules, which probably permeate the membrane through the more hydrophilic regions of the polymer. These regions may not be as greatly affected by lipid absorption; therefore, polyurethane I may be suitable for short-term delivery (less than 2 weeks) of uncharged water-soluble drugs.

From the analysis of the studies of the effects of plasma soaking of the membranes in terms of mechanisms of solute permeation, the following generalizations were reached:

1. For membranes that are porous in nature, lipid absorption should not alter membrane permeability drastically, provided that the solute is small relative to the average pore size of the membrane.
2. When solutes permeate the membrane by solution and diffusion and the membrane is homogeneous, lipid absorption should not alter the membrane permeability drastically.
3. Lipid absorption may lead to significant alteration in membrane permeability for copolymers having regions or domains that differ in their degree of hydrophobicity.
4. Polymers subject to hydrolytic degradation appear to be poor candidates for use in controlled-release drug delivery systems.

Finally, it can be concluded that polydimethylsiloxane, cellulosic membranes, and the hydrogels offer strong potential for use in controlled-release drug delivery systems *in vivo*. The permeation rate of hydrophobic solutes through polydimethylsiloxane and the cellulosic membrane is relatively high. The permeability of the uncross-linked hydrogels is somewhat less; the permeation rate can be varied over approximately an order of magnitude, depending on the nature and concentration of the cross-linking agent.

REFERENCES

(1) P. J. Dzuik and B. Cook, *Endocrinology*, **78**, 208 (1966).

(2) T. J. Roseman and W. I. Higuchi, *J. Pharm. Sci.*, **59**, 353 (1970).

(3) T. J. Roseman, *ibid.*, **61**, 46 (1972).

(4) J. M. Anderson, T. Koinis, T. Nelson, M. Horst, and D. S. Love, in "Hydrogels for Medical and Related Applications," J. D. Andrade, Ed., Symposium Series 31, American Chemical Society, Washington, D.C., 1976, p. 167.

(5) W. R. Good, presented at 5th Midland Macromolecular Institute Symposium on Polymeric Drug Delivery Systems, Midland, Mich., 1976.

(6) R. A. Abrahams and S. H. Ronel, *J. Biomed. Mater. Res.*, **9**, 355 (1975).

(7) D. R. Cowsar, O. R. Tarwater, and A. C. Tanquary, in "Hydrogels for Medical and Related Applications," J. D. Andrade, Ed., Symposium Series 31, American Chemical Society, Washington, D.C., 1976, p. 180.

(8) B. D. Halpern, O. Solomon, L. Kopec, E. Korostoff, and J. L. Ackerman, in "Controlled Release Polymeric Formulations," D. R. Paul and F. W. Harris, Eds., Symposium Series 33, American Chemical Society, Washington, D.C., 1976, p. 135.

(9) J. Drobnik, P. Spacek, and O. Wichterle, *J. Biomed. Mater. Res.*, **8**, 45 (1974).

(10) T. J. Roseman, in "Controlled Release of Biologically Active Agents," A. C. Tanquary and R. E. Lacey, Eds., Plenum, New York, N.Y., 1974, p. 99.

(11) R. E. Lacey and D. R. Cowsar, in *ibid.*, p. 117.

(12) E. R. Garrett and P. B. Chemburkar, *J. Pharm. Sci.*, **57**, 949 (1968).

(13) J. W. Swanson and J. E. LeBeau, *J. Biomed. Mater. Res.*, **8**, 353 (1974).

(14) W. D. Meester and A. B. Swenson, *ibid.*, **6**, 193 (1972).

(15) M. M. McHenry, E. A. Smeloff, W. Y. Fong, G. E. Miller, Jr., and P. M. Ryan, *J. Thorac. Cardiovasc. Surg.*, **59**, 413 (1970).

(16) A. S. Lifchez and A. Scommegna, *Fertil. Steril.*, **21**, 426 (1970).

(17) G. Benagiano, M. Erimini, C. C. Chang, K. Sundaram, and F. A. Kincl, *Acta Endocrinol.*, **63**, 29 (1970).

(18) G. M. Zentner, J. R. Cardinal, and S. W. Kim, *J. Pharm. Sci.*, **67**, 1352 (1978).

(19) G. A. Mortimer, *J. Org. Chem.*, **30**, 1632 (1964).

(20) M. Y. Mah, Master's thesis, University of Utah, Salt Lake City, Utah, 1972.

(21) P. Kratochvil, G. Benagiano, and F. A. Kincl, *Steroids*, **15**, 505 (1970).

(22) C. F. Most, *J. Appl. Polym. Sci.*, **14**, 1019 (1970).

(23) G. L. Flynn and T. J. Roseman, *J. Pharm. Sci.*, **60**, 1788 (1971).

(24) G. L. Flynn, S. H. Yalkowsky, and T. J. Roseman, *ibid.*, **63**, 479 (1974).

(25) B. Z. Ginsburg and A. Katchalsky, *J. Gen. Physiol.*, **47**, 303 (1963).

(26) R. G. Stehle and W. I. Higuchi, *J. Pharm. Sci.*, **61**, 1931 (1972).

(27) L. C. Craig and H. Chen, *Proc. Natl. Acad. Sci. USA*, **69**, 702 (1972).

(28) W. M. Muir, R. A. Gray, J. M. Courtney, and P. D. Ritchie, *J. Biomed. Mater. Res.*, **7**, 3 (1973).

(29) P. C. Farrell and A. L. Babb, *ibid.*, **7**, 272 (1973).

(30) B. K. Fritzinger, S. K. Brauman, and D. J. Lyman, *ibid.*, **5**, 3 (1971).

(31) C. K. Colton, K. A. Smith, E. W. Merrill, and P. C. Farrell, *ibid.*, **5**, 459 (1971).

(32) J. D. Andrade, W. L. Hufferd, and D. J. Lyman, Technical Progress Report on Contract E (11-1)-2147 for the United States Energy Research and Development Administration.

(33) J. D. Andrade, *Med. Instrum.*, **1**, 110 (1973).

(34) J. Crank and G. S. Park, "Diffusion in Polymers," Academic, New York, N.Y., 1968.

(35) D. J. Lyman, *Trans. Am. Soc. Artif. Intern. Organs*, **10**, 17 (1964).

(36) D. J. Lyman and S. W. Kim, *Biomater. Med. Devices Artif. Organs*, **1**, 431 (1973).

(37) H. E. Marsh, Jr., G. C. Hsu, C. J. Wallace, and D. H. Blankenhorn, *Polym. Sci. Technol.*, **7**, 33 (1975).

(38) J. Moacanin, R. F. Fedors, J. D. Ingham, and E. F. Cuddihy, Annual Progress Report on Contract 1200-160 (1974) for National Heart and Lung Institute.

ACKNOWLEDGMENTS

Presented in part at the Basic Pharmaceutics Section, APhA Academy of Pharmaceutical Sciences, New Orleans meeting, April 1976.

Supported by National Institutes of Health Grant HD-09791.

The authors thank Dr. D. E. Gregonis and Dr. J. D. Andrade for their contributions and Mr. Tom Kessler for assistance.

Progestin Permeation through Polymer Membranes II: Diffusion Studies on Hydrogel Membranes

GAYLEN M. ZENTNER, JOHN R. CARDINAL, and SUNG WAN KIM ˣ

Received August 18, 1977, from the *Department of Pharmaceutics, College of Pharmacy, University of Utah, Salt Lake City, UT 84112.* Accepted for publication December 5, 1977.

Abstract □ The potential use of hydrogels in controlled-release drug delivery systems for contraceptive steroids was investigated. The permeabilities, diffusion coefficients, and partition coefficients for progesterone were determined for hydrogels made from hydroxyethyl methacrylate containing varying amounts of ethylene glycol dimethacrylate and tetraethylene glycol dimethacrylate. In addition, copolymers of hydroxyethyl methacrylate with methoxyethyl methacrylate and methoxyethoxyethyl methacrylate were investigated. The results were interpreted in terms of the mechanisms of permeation of progesterone through the hydrogels. This study showed that progesterone permeated these membranes primarily through loose pores in the hydrogel network except at high concentrations of the cross-linker, ethylene glycol dimethacrylate, where dissolution and diffusion of the progesterone in the polymer network was the dominant mechanism.

Keyphrases □ Polymer membranes—permeabilities, diffusion coefficients, and partition coefficients for progesterone permeation through various hydrogels, potential for use as controlled-release drug delivery devices □ Progesterone—permeabilities, diffusion coefficients, and partition coefficients for permeation through various hydrogels □ Hydrogels, various—permeabilities, diffusion coefficients, and partition coefficients for progesterone permeation, potential for use as controlled-release drug delivery devices □ Delivery devices, controlled release—various hydrogel membranes evaluated, permeability to progesterone □ Diffusion coefficients—for progesterone permeation through various hydrogels □ Dosage forms—controlled-release delivery devices, various hydrogel membranes evaluated, permeability to progesterone □ Progestins—progesterone, permeabilities, diffusion coefficients, and partition coefficients for permeation through various hydrogels

Hydrogels are polymeric materials that absorb large quantities of water while remaining insoluble. These polymers exhibit low interfacial free energies with aqueous solutions and only a weak tendency to adsorb biological species such as platelets and proteins. As a result, hydrogels show good biocompatibility and are strong candidates for use as biomedical implant devices (1).

Hydrogels have potential for use in the controlled release of drugs and were investigated in delivery systems for antibiotics (2, 3), steroids (4), inorganic fluoride (5), antitumor agents (6), and narcotic antagonists (7). Hydrogels can be used to control the release of both hydrophobic and hydrophilic drugs, and the release rate can be controlled by variations in the nature and concentration of the cross-linker and by the use of copolymers.

In the present study, the use of hydrogels in the delivery of contraceptive steroids was investigated with progesterone as a model hydrophobic drug. Hydrogels were prepared from hydroxyethyl methacrylate containing varying amounts of ethylene glycol dimethacrylate and tetraethylene glycol dimethacrylate as cross-linking agents. Copolymers of hydroxyethyl methacrylate, methoxyethyl methacrylate, and methoxyethoxyethyl methacrylate also were prepared. The permeability of these polymers to progesterone was determined, and the results were interpreted in terms of the mechanisms of drug permeation through the hydrogels. These studies should provide insight into the general mechanism of permeation of hydrophobic drugs through hydrogels as well as valuable information for the development of these polymers for drug delivery systems.

EXPERIMENTAL

Materials—All hydrogels were prepared by free radical polymerization, using azobis(methylisobutyrate) at a concentration of 7.84 mmoles/liter of monomer as the initiator. The preparation of the initiator followed the procedure given by Mortimer (8). Hydroxyethyl methacrylate[1] was used as received. Methoxyethyl methacrylate and methoxyethoxyethyl methacrylate were synthesized from methyl methacrylate[2] by transesterification with the appropriate alcohol (9). Ethylene glycol dimethacrylate[3] and tetraethylene glycol dimethacrylate[4] were purified by base extraction to remove inhibitors and then distilled prior to use.

The hydrogel membranes prepared from hydroxyethyl methacrylate were synthesized by mixing the required amount of cross-linker and monomer with 45% (v/v) deionized water prior to polymerization between sealed glass plates at 60° for 24 hr. The copolymers of hydroxyethyl methacrylate with methoxyethyl methacrylate or methoxyethoxyethyl methacrylate were prepared by mixing the required amount of monomer with deionized water and polymerizing under the same conditions. The amounts of water added were the maximum amounts that would yield a single solubilized phase as reported by Gregonis *et al.* (9).

Comonomer solutions capable of solubilizing 20% water or greater on a volume basis were prepared similarly. Comonomer solutions solubilizing less than 20% water were polymerized under the same conditions except that polyethylene plates were used in place of the glass plates to facilitate polymer removal from the mold. All hydrogels were equilibrated with water prior to use. For the diffusion experiments, unlabeled progesterone[5], radiolabeled progesterone[6] (1,2-^{3}H-progesterone), and the scintillation fluid[7] were used as received.

Methods—The diffusion experiments were carried out at room temperature, 24 ± 1°, in an all-glass cell composed of two compartments of equal volume (176 ml). The membrane was clamped in place between these compartments. Each compartment was continuously stirred at 1600 rpm by externally mounted constant-speed synchronous motors[8]. A 10% change in the stirring rate did not affect the observed permeabilities.

For each experiment, one compartment was filled initially with deionized water. The remaining compartment was filled with an aqueous solution containing unlabeled progesterone at 11.2 μg/ml and an appropriate amount of the labeled steroid. The increase in radioactivity in the initially progesterone-free compartment was followed by withdrawing microliter quantities of solution. The solution withdrawn was placed in tared scintillation vials and weighed, 10 ml of scintillation fluid was added, and the samples were counted in a scintillation counter[9].

Partition coefficients were determined by a solution depletion technique in which 15 ml of a labeled solution of progesterone was allowed to equilibrate with a known volume of membrane. The equilibrium concentrations of progesterone in the bulk solutions were obtained as already described.

Membrane thicknesses, ~0.07 cm, were measured on water-swollen membranes using a lightwave micrometer[10]. The measurements were made at the minimum allowable pressure for this instrument (60 g). The

[1] Courtesy of Hydron Laboratories, New Brunswick, N.J.
[2] Aldrich Chemical Co., Milwaukee, Wis.
[3] Monomer Polymer Laboratories, Philadelphia, Pa.
[4] Polysciences, Warrington, Pa.
[5] Steraloids, Inc., Pauling, N.Y.
[6] New England Nuclear, Boston, Mass.
[7] Aquasol, New England Nuclear, Boston, Mass.
[8] Precision stirrer, Curtis Matheson Scientific, Denver, Colo.
[9] Model 3385, Packard Instrument Co., Downers Grove, Ill.
[10] Van Kueren Co., Watertown, Mass.

0022-3549/78/1000-1352$01.00/0
© 1978, American Pharmaceutical Association

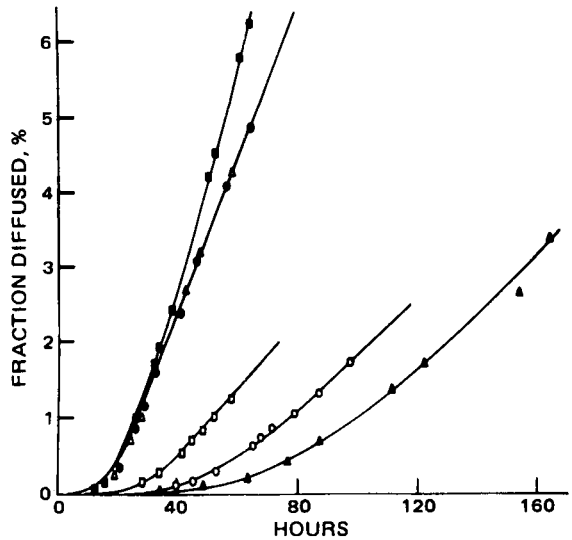

Figure 1—*Fraction of progesterone released* versus *time for progesterone permeation through hydroxyethyl methacrylate cross-linked with ethylene glycol dimethacrylate. Key (mole percent cross-linker):* ■, *0;* ●, *0.56;* △, *0.75;* □, *2.30;* ○, *3.75; and* ▲, *5.25.*

error resulting from these measurements probably varies depending on the properties of the hydrogel but is believed to be small.

Hydration and water fraction values were obtained using the technique described by Wisniewski *et al.* (10).

RESULTS

Figures 1 and 2 show the effects of the cross-linker percentage on the fraction of drug diffused *versus* time for polyhydroxyethyl methacrylate membranes containing varying amounts of ethylene glycol dimethacrylate and tetraethylene glycol dimethacrylate as cross-linking agents. As the cross-linker percentage increased, the fraction of drug diffused decreased. At equivalent mole percents, membranes cross-linked with tetraethylene glycol dimethacrylate showed greater permeabilities than membranes cross-linked with ethylene glycol dimethacrylate.

Figure 3 shows the effects of variations in the monomer composition on the fraction of progesterone diffused as a function of time. Variations in the monomer composition led to changes in the water content, W_f, defined as the weight fraction of water in the swollen gel. The water contents of these membranes are shown in Table I. As the water content

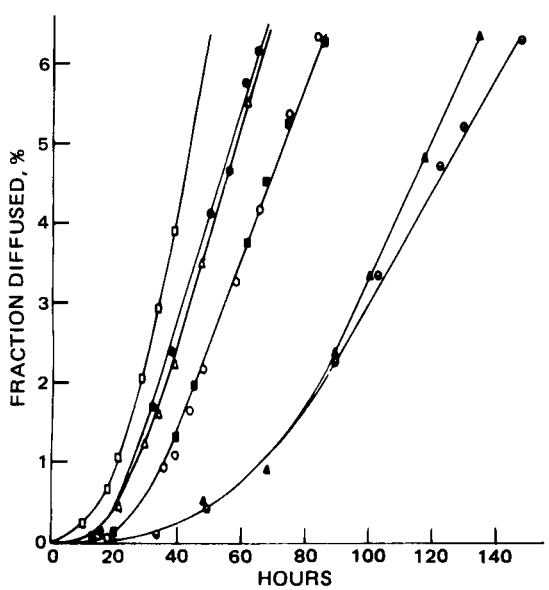

Figure 2—*Fraction of progesterone released* versus *time for progesterone permeation through hydroxyethyl methacrylate cross-linked with tetraethylene glycol dimethacrylate. Key (mole percent cross-linker):* ●, *0;* □, *0.25;* △, *0.46;* ○, *0.92;* ■, *1.84;* ▲, *3.22; and* ⊖, *4.60.*

Table I—Diffusion Coefficients, Partition Coefficients, Water Contents, and Permeabilities for Progesterone in Copolymers of Hydroxyethyl Methacrylates

Membrane	$D \times 10^9$, cm²/sec	K_d	W_f	$U \times 10^7$, cm²/sec
Methoxyethoxyethyl methacrylate	12.7	130	0.723	16.6
34% Hydroxyethyl methacrylate–66% methoxyethoxyethyl methacrylate	7.67	129	0.504	9.86
Hydroxyethyl methacrylate	4.38	129	0.423	5.63
80% Hydroxyethyl methacrylate–20% methoxyethyl methacrylate	0.98	156	0.340	1.53
67% Hydroxyethyl methacrylate–33% methoxyethyl methacrylate	0.90	192	0.308	1.75

of the membrane increased, the fraction of drug diffused also increased.

The diffusion coefficients for progesterone in these membranes were obtained through the use of (11):

$$\ln\left(1 - \frac{2C_t}{C_0}\right) = -\left(\frac{1}{V_1} + \frac{1}{V_2}\right)\frac{AUt}{l} \qquad \text{(Eq. 1)}$$

where C_t is the concentration of progesterone at time t, C_0 is the initial progesterone concentration, V_1 and V_2 are the compartment volumes (176 ml), A is the membrane area (14.2 cm²), l is the wet membrane thickness, and U is the permeability, which is defined as:

$$U = DK_d \qquad \text{(Eq. 2)}$$

where D is the diffusion coefficient and K_d is the partition coefficient. The permeability, U, can be obtained from the linear portion of a plot of $\ln(1 - 2C_t/C_0)$ *versus* t. The effects of variations in the monomer composition of the membrane on the diffusion coefficient, D, are shown in Table I; D decreased as the water content of the membrane decreased. The effects of variations in the cross-linker percentage on D are shown in Table II; D decreased as the cross-linker percentage increased. As seen from Tables I and II, the partition coefficients for progesterone were not strongly dependent on the composition of the membrane.

DISCUSSION

Mechanisms of Solute Permeation through Polymer Membranes—Solute transport through polymeric membranes is generally

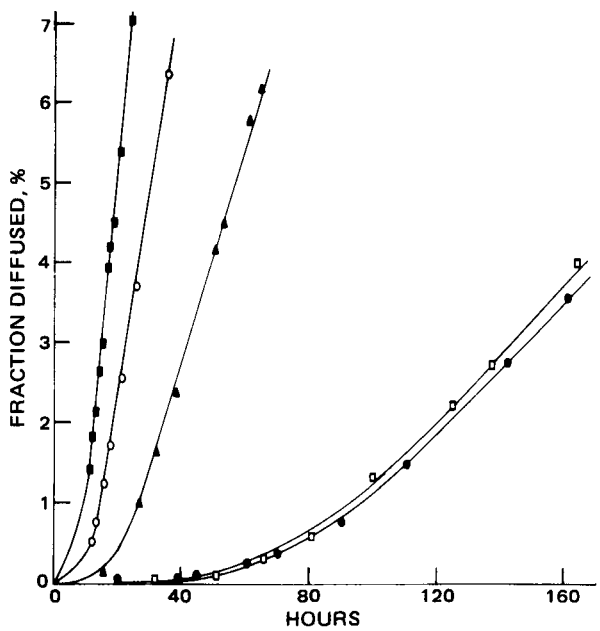

Figure 3—*Fraction of progesterone released* versus *time for progesterone permeation through methoxyethoxyethyl methacrylate* (■), *34% hydroxyethyl methacrylate–66% methoxyethoxyethyl methacrylate* (○), *hydroxyethyl methacrylate* (▲), *80% hydroxyethyl methacrylate–20% methoxyethyl methacrylate* (□), *and 67% hydroxyethyl methacrylate–33% methoxyethyl methacrylate* (○).

Table II—Diffusion Coefficients, Partition Coefficients, Water Contents, and Permeabilities for Progesterone in Cross-Linked Hydroxyethyl Methacrylate Membranes

Mole Percent Cross-Linker	$D \times 10^9$, cm²/sec	K_d	W_f	$U \times 10^7$, cm²/sec
	Ethylene Glycol Dimethacrylate			
0	4.38	129	0.423	5.62
0.56	2.57	151	0.410	3.89
0.75	2.57	151	0.403	3.89
2.30	1.08	151	0.376	1.63
3.75	0.72	161	0.355	1.16
5.25	0.64	232	0.348	1.48
	Tetraethylene Glycol Dimethacrylate			
0	4.38	129	0.423	5.62
0.25	4.76	147	0.414	6.99
0.46	3.82	149	0.418	5.70
0.92	3.28	137	0.408	4.48
1.84	3.30	140	0.398	4.63
3.22	2.10	152	0.383	3.20
4.60	1.27	184	0.368	2.34

described in terms of two mechanisms (12–14). In the "pore" mechanism, solutes are presumed to permeate the membrane by diffusion through microchannels or pores within the membrane structure. The rate at which solutes permeate the membrane is controlled primarily by the pore size of the membrane and the molecular volume of the solute (12). Cellulosic membranes exhibit this type of flow (12–14).

The other mechanism is the solution–diffusion or partition mechanism. In this type of permeation, solutes transverse the membrane by a process involving solute dissolution in the membrane structure followed by solute diffusion along and between the polymer segments that make up the membrane structure (13). The physical–chemical properties of the solute and the membrane play a dominant role in determining membrane permeability; the molecular volume of the solute is of secondary importance. Polyether urethane exhibits this type of permeation (13, 14).

These two mechanisms represent the extreme or limiting types of permeation. For any given membrane, permeation probably occurs by both mechanisms; however, one of the two will usually dominate. The permeation of progesterone through hydrogel membranes can be described in terms of the mechanisms described and, depending on the membrane composition, either the pore mechanism or the partition mechanism dominates.

Effects of Equilibrium Water Content—The effects of the equilibrium water content on the mechanism of progesterone permeation through hydrogel membranes were analyzed according to the methods outlined by Yasuda *et al.* (15, 16). When solutes permeate water-swollen membranes primarily by a porous mechanism, the following relationship should hold (15, 16):

$$\ln \frac{D}{D_0} = \frac{-\beta X(1-\alpha)}{1+\alpha X} \qquad \text{(Eq. 3)}$$

where $X = (1-H)/H$, $\alpha = V_f/V_w$, $\beta = V^*/V_w$, D_0 is the diffusion coefficient of progesterone in pure water, V_w is the free volume in a unit volume of pure water, V_f is the free volume in a unit volume of polymer, V^* is a characteristic volume parameter that describes the diffusion of the permeant molecule in the membrane, and H is the membrane hydration defined by the ratio (concentration of water in membrane/concentration of water in bulk). Equation 3 can be rearranged as follows to yield a linear plot:

$$\left(\ln \frac{D}{D_0}\right)^{-1} = \frac{-1}{\beta(1-\alpha)} X^{-1} - \frac{\alpha}{\beta(1-\alpha)} \qquad \text{(Eq. 4)}$$

A plot of the experimental values for the copolymer membranes according to Eq. 4 is shown in Fig. 4. A value of 7×10^{-6} cm²/sec was used for D_0 (17). As discussed by Yasuda *et al.* (15, 16), the linearity of the plot shown in Fig. 4 suggests that the structural factors for these water-swollen hydrogels are similar and that the permeation of progesterone occurs predominately through the porous regions of the network. Based on this plot, it appears that the dominant mechanism for the hydrogel membranes listed in Table I is the porous mechanism. However, as pointed out by Yasuda *et al.* (15, 16), this result does not imply that these membranes contain rigid pores of the type normally attributed to cellulosic membranes; rather, it suggests that the network is loose and that "fluctuating pores" are present.

Effect of Cross-Linking Agent—Figure 5 is a plot of the mole percent of cross-linking agent *versus* the diffusion coefficient of progesterone

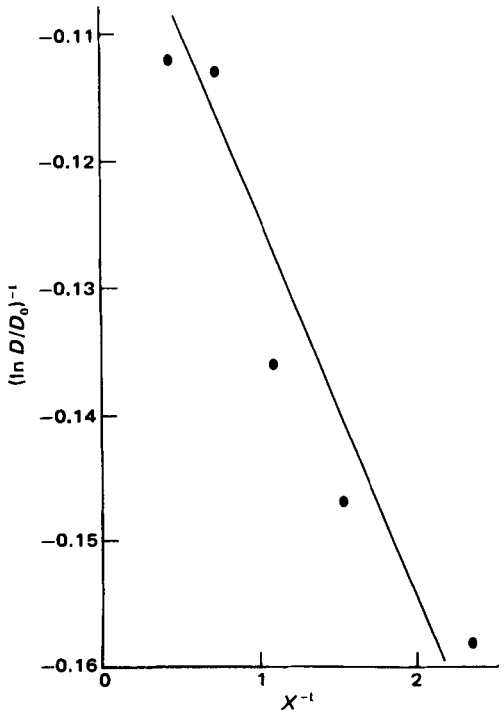

Figure 4—*Plot of* $(\ln D/D_0)^{-1}$ versus X^{-1} *for hydrogels swollen to different equilibrium water concentrations.*

for the hydrogel membranes described in Table II. As the mole percent of the cross-linking agent tetraethylene glycol dimethacrylate, decreased, the diffusion coefficient for progesterone increased linearly. The shape of this curve is in striking contrast to that shown for the cross-linking agent ethylene glycol dimethacrylate. At high concentrations of ethylene glycol dimethacrylate, the diffusion coefficient of progesterone was relatively independent of the mole percent of this cross-linker. However, at low concentrations of ethylene glycol dimethacrylate, the diffusion coefficient increased linearly with decreases in the concentration of the cross-linker. Thus, low concentrations of the cross-linker ethylene glycol dimethacrylate affect the diffusion coefficient of progesterone in the same way as the cross-linker tetraethylene glycol dimethacrylate.

As shown previously, the dominant mechanism of solute permeation through the uncrosslinked polyhydroxyethyl methacrylate membrane is permeation through "fluctuating pores" in the membrane. The effect of the cross-linking agent tetraethylene glycol dimethacrylate and low

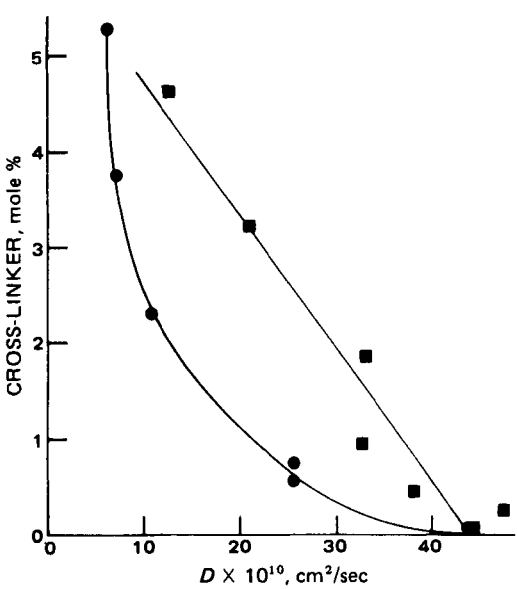

Figure 5—*Mole percent cross-linker* versus *diffusion coefficient. Key:* ●, *ethylene glycol dimethacrylate; and* ■, *tetraethylene glycol dimethacrylate.*

concentrations of the cross-linking agent ethylene glycol dimethacrylate must be to decrease the size of these fluctuating pores with ethylene glycol dimethacrylate, producing a much greater effect than tetraethylene glycol dimethacrylate. This conclusion is consistent with the fact that tetraethylene glycol dimethacrylate is a longer chain length cross-linker. The abruptly increasing slope in the plot of mole percent cross-linker *versus* D for ethylene glycol dimethacrylate shown in Fig. 5 suggests that a change in mechanism occurs in this region such that at high concentrations of this cross-linker the solution–diffusion mechanism is dominant. As discussed in the section on the mechanism of solute permeation through polymer membranes, when the solution–diffusion mechanism is dominant, the diffusion coefficient is controlled primarily by interactions between the solute and the polymer segments of the membrane. The relative constancy of the diffusion coefficients for progesterone with variations in the ethylene glycol dimethacrylate cross-linker percentage in the high concentration region of the plot in Fig. 5 is consistent with this behavior. At intermediate concentrations of this cross-linker, both mechanisms of solute permeation probably contribute to the observed permeability of these membranes.

It is not possible to provide direct proof of the mechanisms outlined for the effects of cross-linker percentage on solute permeation through these membranes. Proof of the proposed mechanisms can only arise from an extensive study of the permeation of a wide variety of solutes in which both the physical-chemical nature and the molar volume of the solute are varied. However, the interpretations presented here are consistent with the shapes of the curves shown in Fig. 5 and with previous studies of the mechanism of solute permeation through polymer membranes (12–14) including hydrogels (10, 15, 16, 18).

REFERENCES

(1) J. D. Andrade, *Med. Instrum.*, **1**, 110 (1973).

(2) M. Tollar, M. Stol, and K. Kliment, *J. Biomed. Mater. Res.*, **3**, 305 (1969).

(3) V. Majkus, F. Horakova, F. Vymola, and M. Stol, *ibid.*, **3**, 443 (1969).

(4) J. M. Anderson, T. Koinis, T. Nelson, M. Horst, and D. S. Love, in "Hydrogels for Medical and Related Applications," J. D. Andrade, Ed., Symposium Series 31, American Chemical Society, Washington, D.C., 1976, p. 167.

(5) D. R. Cowsar, O. R. Tarwater, and A. C. Tanquary, in *ibid.*, p. 180.

(6) J. Drobnik, P. Spacek, and O. Wichterle, *J. Biomed. Mater. Res.*, **8**, 45 (1974).

(7) R. A. Abrahams and S. H. Ronel, *ibid.*, **9**, 355 (1975).

(8) G. A. Mortimer, *J. Org. Chem.*, **30**, 1632 (1964).

(9) D. E. Gregonis, C. M. Chen, and J. D. Andrade, in "Hydrogels for Medical and Related Applications," J. D. Andrade, Ed., Symposium Series 31, American Chemical Society, Washington, D.C., 1976, p. 88.

(10) S. J. Wisniewski, D. E. Gregonis, S. W. Kim, and J. D. Andrade, in *ibid.*, p. 80.

(11) M. Y. Mah, Master's thesis, University of Utah, Salt Lake City, Utah, 1972.

(12) L. C. Craig and W. Konigsberg, *J. Phys. Chem.*, **65**, 116 (1961).

(13) D. J. Lyman and S. W. Kim, *J. Polym. Sci., Symp.*, **41**, 139 (1973).

(14) D. J. Lyman and S. W. Kim, *Biomater. Med. Devices Artif. Organs*, **1**, 431 (1973).

(15) H. Yasuda, C. E. Lamaze, and L. D. Ikenberry, *Makromol. Chem.*, **118**, 19 (1968).

(16) H. Yasuda, C. E. Lamaze, and A. Peterlin, *J. Polym. Sci., A-2*, **9**, 1117 (1971).

(17) N. F. H. Ho, L. Suhardja, S. Hwang, E. Owada, A. Molokhia, G. L. Flynn, W. I. Higuchi, and J. Y. Park, *J. Pharm. Sci.*, **65**, 1578 (1976).

(18) R. Y. S. Chen, *Polym. Prepr.*, **15** (2), 387 (1974).

ACKNOWLEDGMENTS

Presented in part at the Basic Pharmaceutics Section, APhA Academy of Pharmaceutical Sciences, New Orleans meeting, April 1976.

Supported by National Institutes of Health Grant HD-09791.

The authors thank Dr. D. E. Gregonis and Dr. J. D. Andrade for their contributions and Mr. Darryl D. Ivanson for assistance.

Comparison of Effects of Quinidine and Dihydroquinidine on Canine Heart

TIBOR BALAZS *x, EUGENE HERMAN *, and JOHN ATKINSON ‡

Received August 22, 1977, from the **Division of Drug Biology and the* ‡*Division of Mathematics, Food and Drug Administration, Washington, DC 20204.* Accepted for publication January 26, 1978.

Abstract □ Various cardiac effects of quinidine and dihydroquinidine were tested in isolated dog hearts and *in vivo* in dogs. No significant differences were found in the negative inotropic, chronotropic, and dromotropic effects. Dihydroquinidine was more potent than quinidine in decreasing coronary arterial pressure.

Keyphrases □ Quinidine—various cardiac effects on isolated heart and *in vivo* in dogs, compared to dihydroquinidine □ Dihydroquinidine—various cardiac effects on isolated heart and *in vivo* in dogs, compared to quinidine □ Cardiac effects, various—quinidine and dihydroquinidine compared in isolated heart and *in vivo* in dogs □ Antiarrhythmic agents—quinidine and dihydroquinidine, various cardiac effects compared in isolated heart and *in vivo* in dogs

Pharmaceutical preparations of the antiarrhythmic quinidine may contain other cinchona alkaloids, of which dihydroquinidine is present in the highest concentration. The dihydroquinidine content of 40 tested commercial samples of quinidine ranged from 3 to 22% (1). USP XIX specifies that the dihydroquinidine content of quinidine gluconate or sulfate USP should not exceed 20% of the total alkaloids.

Both quinidine and dihydroquinidine have qualitatively similar cardiac pharmacological actions (2–5), but their potencies may differ. The intravenous median lethal dose of dihydroquinidine in mice was about 18% lower than that of quinidine (4). The hypotensive effects of the alkaloids after intravenous administration were about equal in anesthetized cats. The threshold dose of dihydroquinidine required to raise the intensity of electrical stimulation to produce ventricular fibrillation in cats was about one-third of that of quinidine. A recent study with these alkaloids in rats revealed no differences in acute intravenous toxicities or in potencies to suppress electrically induced ventricular fibrillation (6). Limited clinical data indicate that dihydroquinidine has a greater antiarrhythmic effect (2, 3).

Since both alkaloids have several cardiac effects that

0022-3549/78/1000-1355$01.00/0

© 1978, American Pharmaceutical Association

concentrations of the cross-linking agent ethylene glycol dimethacrylate must be to decrease the size of these fluctuating pores with ethylene glycol dimethacrylate, producing a much greater effect than tetraethylene glycol dimethacrylate. This conclusion is consistent with the fact that tetraethylene glycol dimethacrylate is a longer chain length cross-linker. The abruptly increasing slope in the plot of mole percent cross-linker *versus* D for ethylene glycol dimethacrylate shown in Fig. 5 suggests that a change in mechanism occurs in this region such that at high concentrations of this cross-linker the solution–diffusion mechanism is dominant. As discussed in the section on the mechanism of solute permeation through polymer membranes, when the solution–diffusion mechanism is dominant, the diffusion coefficient is controlled primarily by interactions between the solute and the polymer segments of the membrane. The relative constancy of the diffusion coefficients for progesterone with variations in the ethylene glycol dimethacrylate cross-linker percentage in the high concentration region of the plot in Fig. 5 is consistent with this behavior. At intermediate concentrations of this cross-linker, both mechanisms of solute permeation probably contribute to the observed permeability of these membranes.

It is not possible to provide direct proof of the mechanisms outlined for the effects of cross-linker percentage on solute permeation through these membranes. Proof of the proposed mechanisms can only arise from an extensive study of the permeation of a wide variety of solutes in which both the physical-chemical nature and the molar volume of the solute are varied. However, the interpretations presented here are consistent with the shapes of the curves shown in Fig. 5 and with previous studies of the mechanism of solute permeation through polymer membranes (12–14) including hydrogels (10, 15, 16, 18).

REFERENCES

(1) J. D. Andrade, *Med. Instrum.*, **1**, 110 (1973).

(2) M. Tollar, M. Stol, and K. Kliment, *J. Biomed. Mater. Res.*, **3**, 305 (1969).

(3) V. Majkus, F. Horakova, F. Vymola, and M. Stol, *ibid.*, **3**, 443 (1969).

(4) J. M. Anderson, T. Koinis, T. Nelson, M. Horst, and D. S. Love, in "Hydrogels for Medical and Related Applications," J. D. Andrade, Ed., Symposium Series 31, American Chemical Society, Washington, D.C., 1976, p. 167.

(5) D. R. Cowsar, O. R. Tarwater, and A. C. Tanquary, in *ibid.*, p. 180.

(6) J. Drobnik, P. Spacek, and O. Wichterle, *J. Biomed. Mater. Res.*, **8**, 45 (1974).

(7) R. A. Abrahams and S. H. Ronel, *ibid.*, **9**, 355 (1975).

(8) G. A. Mortimer, *J. Org. Chem.*, **30**, 1632 (1964).

(9) D. E. Gregonis, C. M. Chen, and J. D. Andrade, in "Hydrogels for Medical and Related Applications," J. D. Andrade, Ed., Symposium Series 31, American Chemical Society, Washington, D.C., 1976, p. 88.

(10) S. J. Wisniewski, D. E. Gregonis, S. W. Kim, and J. D. Andrade, in *ibid.*, p. 80.

(11) M. Y. Mah, Master's thesis, University of Utah, Salt Lake City, Utah, 1972.

(12) L. C. Craig and W. Konigsberg, *J. Phys. Chem.*, **65**, 116 (1961).

(13) D. J. Lyman and S. W. Kim, *J. Polym. Sci., Symp.*, **41**, 139 (1973).

(14) D. J. Lyman and S. W. Kim, *Biomater. Med. Devices Artif. Organs*, **1**, 431 (1973).

(15) H. Yasuda, C. E. Lamaze, and L. D. Ikenberry, *Makromol. Chem.*, **118**, 19 (1968).

(16) H. Yasuda, C. E. Lamaze, and A. Peterlin, *J. Polym. Sci., A-2*, **9**, 1117 (1971).

(17) N. F. H. Ho, L. Suhardja, S. Hwang, E. Owada, A. Molokhia, G. L. Flynn, W. I. Higuchi, and J. Y. Park, *J. Pharm. Sci.*, **65**, 1578 (1976).

(18) R. Y. S. Chen, *Polym. Prepr.*, **15** (2), 387 (1974).

ACKNOWLEDGMENTS

Presented in part at the Basic Pharmaceutics Section, APhA Academy of Pharmaceutical Sciences, New Orleans meeting, April 1976.

Supported by National Institutes of Health Grant HD-09791.

The authors thank Dr. D. E. Gregonis and Dr. J. D. Andrade for their contributions and Mr. Darryl D. Ivanson for assistance.

Comparison of Effects of Quinidine and Dihydroquinidine on Canine Heart

TIBOR BALAZS *x, EUGENE HERMAN *, and JOHN ATKINSON ‡

Received August 22, 1977, from the **Division of Drug Biology and the* ‡*Division of Mathematics, Food and Drug Administration, Washington, DC 20204.* Accepted for publication January 26, 1978.

Abstract □ Various cardiac effects of quinidine and dihydroquinidine were tested in isolated dog hearts and *in vivo* in dogs. No significant differences were found in the negative inotropic, chronotropic, and dromotropic effects. Dihydroquinidine was more potent than quinidine in decreasing coronary arterial pressure.

Keyphrases □ Quinidine—various cardiac effects on isolated heart and *in vivo* in dogs, compared to dihydroquinidine □ Dihydroquinidine—various cardiac effects on isolated heart and *in vivo* in dogs, compared to quinidine □ Cardiac effects, various—quinidine and dihydroquinidine compared in isolated heart and *in vivo* in dogs □ Antiarrhythmic agents—quinidine and dihydroquinidine, various cardiac effects compared in isolated heart and *in vivo* in dogs

Pharmaceutical preparations of the antiarrhythmic quinidine may contain other cinchona alkaloids, of which dihydroquinidine is present in the highest concentration. The dihydroquinidine content of 40 tested commercial samples of quinidine ranged from 3 to 22% (1). USP XIX specifies that the dihydroquinidine content of quinidine gluconate or sulfate USP should not exceed 20% of the total alkaloids.

Both quinidine and dihydroquinidine have qualitatively similar cardiac pharmacological actions (2–5), but their potencies may differ. The intravenous median lethal dose of dihydroquinidine in mice was about 18% lower than that of quinidine (4). The hypotensive effects of the alkaloids after intravenous administration were about equal in anesthetized cats. The threshold dose of dihydroquinidine required to raise the intensity of electrical stimulation to produce ventricular fibrillation in cats was about one-third of that of quinidine. A recent study with these alkaloids in rats revealed no differences in acute intravenous toxicities or in potencies to suppress electrically induced ventricular fibrillation (6). Limited clinical data indicate that dihydroquinidine has a greater antiarrhythmic effect (2, 3).

Since both alkaloids have several cardiac effects that

0022-3549/78/1000-1355$01.00/0

© 1978, American Pharmaceutical Association

Table I—Average Values (Percent of Control) by Dose Level for Contraction Force, Arterial Pressure, and Heart Rate in Isolated Dog Hearts: Quinidine Tartrate (I) and Dihydroquinidine Tartrate (II)

Dose, mg	Contraction Force		Arterial Pressure		Heart Rate	
	I	II	I	II	I	II
5	106.8	106.8	98.7	93.8	85.9	85.5
10	82.2	95.5[a]	84.8	73.8	80.2	86.5
20	84.8	78.2	81.4	65.4[a]	86.9	87.9
LSD[b]	10.1		11.6		5.7	

[a] Difference between drugs is statistically significant ($p = 0.05$) at this dose level. [b] Least significant difference.

have not been compared previously, the effects on heart rate (chronotropic), force of contraction (inotropic), ventricular conduction velocity (dromotropic), and coronary arterial pressure were chosen as ways to compare their potencies.

EXPERIMENTAL

Materials—Quinidine tartrate and dihydroquinidine tartrate were prepared[1] as described by Smith *et al.* (1) and were found to contain 65 and 67% of the respective alkaloid. Quinidine was free of any dihydroquinidine and contained not more than traces of other cinchona alkaloids. Dihydroquinidine did not contain any quinidine.

Testing in Isolated Dog Hearts—Adult beagle dogs of each sex were anesthetized with pentobarbital sodium (30 mg/kg), and a polyethylene catheter was inserted into the right femoral artery for rapid blood removal. Clotting was prevented by injecting 1000 units of heparin sodium/kg into the femoral vein. Respiration was maintained with a positive pressure respirator[2].

The chest was opened by a midline incision, and all major branches of the ascending aorta except the brachiocephalic trunk were ligated. The latter vessel was cannulated with a short stainless steel cannula connected by tubing to a pump oxygenator system. The descending aorta was then ligated, and the heart was removed from the chest cavity quickly, placed into a chamber of the pump–oxygenator system, and perfused at a constant flow with approximately 500 ml of autologous blood maintained at 35°.

The perfusion pressure (coronary arterial pressure) was continuously monitored *via* a needle-tipped catheter inserted into the perfusion circuit and connected to a pressure transducer. Needle electrodes were inserted into the ventricles to monitor the heart rate. The contraction force was measured by a Walton–Brodie strain gauge sutured to the left ventricle.

After a 30-min stabilization period, the heart preparations were treated over a 30–60-sec period with 5, 10, or 20 mg of quinidine or dihydroquinidine, calculated as the free base, dissolved in 5 ml of physiological saline. These doses were chosen to cover the range from therapeutic to toxic levels. The effect of each level was determined in five separate experiments. All experiments were terminated 60 min after dosing. An analysis of variance was conducted for heart rate, contraction force, and coronary arterial pressure. In each of these three analyses of variance, the effects of drug dose and time were considered, together with the interactions of these effects.

Testing in Anesthetized Dogs—A pool of 12 beagle dogs of both sexes, 7–12 kg, was used. Eight dogs (Group 1) were used to compare the effects of the pure alkaloids in a crossover test. Four dogs from Group 1 and the four remaining dogs were used to compare the effects of a mixture of 25% dihydroquinidine and 75% quinidine with pure quinidine (Group 2). Nine dogs (Group 3) were used to test the effects of a mixture of equal concentrations of the alkaloids. At least 1 week elapsed before an individual dog was used again.

Dogs were anesthetized with pentobarbital sodium. One percent drug solutions of each drug in physiological saline, prepared by gentle heating, were infused into the cephalic vein in the foreleg at a rate of 5 mg/kg/min for 10 min. ECG's (lead II) were recorded at 50 mm/sec prior to and at 1-min intervals during the infusions. The duration of QRS complexes was calculated (mean of three values for each minute). A regression analysis of response *versus* time of infusion was conducted for each infusion.

RESULTS

Both alkaloids affected the contraction force of the isolated heart, resulting initially in a dose-related negative inotropic effect (Fig. 1). The recovery rates were comparable at each dose level for both alkaloids during the first 15 min. Thereafter, the contraction force increased above control levels at the 5-mg doses, remained close to the baseline level at the 10-mg doses, and tended to remain below control values at the 20-mg doses.

The inotropic effects of dihydroquinidine were greater at 10 mg and lower at 20 mg than those of quinidine. However, only the differences at 10 mg were statistically significant. A statistically significant interaction occurred between dose and drug. This result can be seen from the averages in Table I, since the lowest values occurred at 10 mg for quinidine (I) and 20 mg for dihydroquinidine (II). The effect of dose, therefore, was considered separately for each drug, and the least significant difference between drugs for a dose level was determined. The analysis of variance summary is shown in Table II.

The coronary arterial pressure decreased in a dose-related manner during the 1st min after dosing (Table I). Recovery occurred within 5 min at 5 mg but was slower for the 10- and 20-mg doses; only partial recovery occurred with dihydroquinidine. The mean coronary pressure values for the 1-hr experiment were lower, in a dose-related fashion, for dihydroquinidine and were significantly different from those for quinidine at 20 mg (Fig. 2). The analyses of variance are given in Table II.

The heart rate was decreased 10–20% throughout the 1-hr period at each level of each alkaloid (Tables I and II). These findings imply that

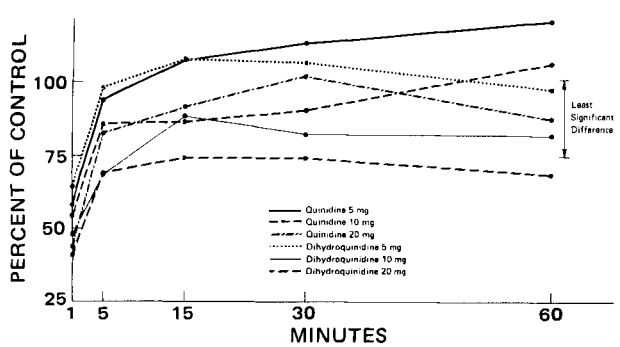

Figure 1—*Effects of the alkaloids on the contraction force in isolated dog hearts. (Each point represents mean values from five hearts.)*

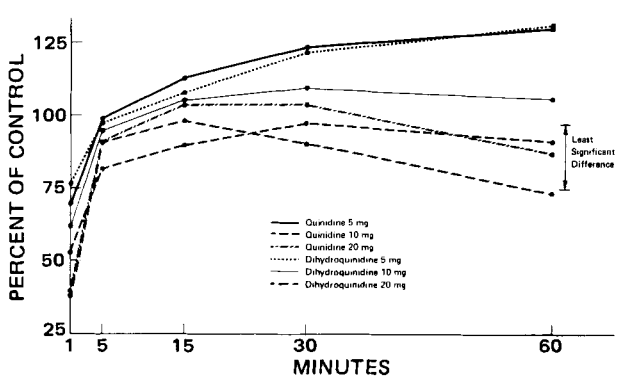

Figure 2—*Effects of the alkaloids on the coronary arterial pressure in isolated dog hearts. (Each point represents mean values from five hearts.)*

[1] The drugs were prepared by M. Maienthal, Division of Drug Chemistry, Food and Drug Administration, Washington, DC 20204, and analyzed by Susan Barkan of the same Division.

[2] Harvard.

Table II—Analysis of Variance [a] for Contraction Force, Arterial Pressure, and Heart Rate

Source of Variation	Degrees of Freedom	Force of Contraction		Arterial Pressure		Heart Rate	
		MS	*F*	*MS*	*F*	*MS*	*F*
Drug	1	182	—	4245	10.11**[b]	199	1.99
Dose	2	8468	6.54	7005	16.61***	212	2.12
Drug × dose	2	1294	4.08*	319	—	157	1.57
Time	4	13205	41.67***	10219	24.94**	76	—
Drug × time	4	44	—	461	1.10	3	—
Dose × time	8	838	2.64	190	—	9	—
Drug × dose × time	8	61	—	156	—	37	—
Error	120	317	—	420	—	100	—

[a] *MS* = mean square; *F* = *F* value. [b] As large or larger difference could occur from chance alone; * = less than 5% of the time, ** = less than 1% of the time, and *** = less than 0.1% of the time.

Table III—Effect of Quinidine Tartrate (I), Dihydroquinidine Tartrate (II), and Their Combinations on the Duration of QRS in Dogs

Group	Number of Dogs	I, %[a]	QRS Increase, msec		I + II		QRS Increase, msec	
			Mean	*SE*	%[a]	%[a]	Mean	*SE*
1	8	100	23.4	3.6	0	100	24.2	4.2
2	9	100	22.4	3.4	50	50	31.2	3.6
3	8	100	21.2	3.4	75	25	28.8	7.0

[a] The concentrations of the drugs are expressed as percentages of the salts.

the changes in the contraction force and coronary pressure are independent of the negative chronotropic effect.

Infusion of the drug solution in anesthetized dogs produced a slight tachycardia during the 1st min, followed by a slight bradycardia throughout the dosing period. Sinus rhythm was maintained, and arrhythmia did not occur. The duration of the QRS complex increased throughout the infusions. Response *versus* time of infusion curves constructed for each of the individual dog exposures from Group 1 revealed that all regressions were significant, with the highest values reached or maintained at the end of dosing. The mean time for maximal effect on the QRS duration was 8.9 min for quinidine and 9.0 min for dihydroquinidine. The maximum QRS less the predose QRS was used to assess the effect (Table III). Differences in effects of dihydroquinidine and quinidine solutions were not statistically significant.

DISCUSSION

Some cardiac effects of quinidine and dihydroquinidine alkaloids were used to compare their potencies. The effect on ventricular conduction velocity, a negative dromotropic effect, as measured by the duration of the QRS complex, represents a major pharmacological action, which is correlated with blood levels of quinidine (7). The negative inotropic effect is, in part, a consequence of the decreased conduction rate since it leads to a reduction of the synchrony of contraction. This effect and also the effect on the coronary pressure represent toxic and, in part, independent effects. This autonomy may explain the greater potency of dihydroquinidine in one parameter, coronary pressure, in the *in vitro* assay.

Similarly, such an explanation might also be applicable to the findings of Scott *et al.* (4) who reported that dihydroquinidine produced a greater antifibrillatory, *i.e.*, negative bathmotropic, effect in cats. Their data demonstrate that the two alkaloids can induce equal systemic hypotensive effects but with different bathmotropic effects. However, the recent data of Dietmann *et al.* (6) on the lack of significant differences in the negative bathmotropic effects of these two alkaloids in rats raise the possibility of species differences in sensitivity. Differences in the pharmacokinetic patterns of dihydroquinidine and quinidine might be one mechanism to explain divergent species effects.

While data are not available for cats and rats, no significant differences were found in humans in the distribution and elimination kinetics of these two alkaloids (8). In view of previous data (6, 8) and the data reported here, a level of 20% dihydroquinidine in pharmaceutical preparations of quinidine is acceptable pharmacologically. However, in view of the earlier data for cats (4) and humans (3) indicating a significantly greater antiarrhythmic potency of dihydroquinidine, a reexamination of the therapeutic effects of these alkaloids in humans appears to be in order.

REFERENCES

(1) E. Smith, S. Barkan, B. Ross, M. Maienthal, and J. Levine, *J. Pharm. Sci.*, **62,** 1151 (1973).

(2) T. Lewis, A. N. Drury, A. M. Wedd, and C. C. Iliescu, *Heart*, **9,** 207 (1922).

(3) F. Alexander, H. Gold, L. N. Katz, R. L. Levy, R. Scott, and P. D. White, *J. Pharmacol. Exp. Ther.*, **90,** 191 (1947).

(4) C. Scott, R. C. Anderson, and K. K. Chen, *ibid.*, **84,** 184 (1945).

(5) W. Model, S. J. Shane, C. Dayrit, and H. Gold, *Fed. Proc. Fed. Am. Soc. Exp. Biol.*, **8,** 320 (1949).

(6) K. Dietmann, W. Bartsch, and M. Gutekunst, *Arzneim.-Forsch.*, **27,** 589 (1977).

(7) R. H. Heissenbuttel and J. T. Bigger, *Am. Heart J.*, **80,** 453 (1970).

(8) C. T. Ueda, B. J. Williamson, and B. S. Dzindzio, *Res. Commun. Chem. Pathol. Pharmacol.*, **14,** 215 (1976).

ACKNOWLEDGMENTS

The authors thank Mr. Joseph Levine (retired), formerly Director, Division of Drug Chemistry, Food and Drug Administration, for bringing the problem to their attention.

Instability of Digoxin in Acid Medium Using a Nonisotopic Method

SALEH A. H. KHALIL ˣ **and SAWSAN EL-MASRY**

Received March 12, 1977, from *the Faculty of Pharmacy, University of Alexandria, Alexandria, Egypt.* Accepted for publication January 30, 1978.

Abstract □ A selective nonisotopic assay was used to investigate the digoxin hydrolysis rates at 37 ± 0.1° over the pH 1.1–2.2 range. The colorimetric method adopted is based on the use of a xanthydrol reagent after extraction with chloroform. The spectrofluorometric method specified in the dissolution test for digoxin tablets was nonspecific because of digoxigenin interference. Digoxin hydrolysis followed specific acid hydrolysis, and K values of the apparent first-order reaction varied from 0.0357 to 0.0027 min^{-1} over the pH range used. The effect of the dissolution medium on digoxin stability during the dissolution tests of the tablets also was studied. Water (the BP medium) and 0.6% HCl (the USP medium) were compared using the fluorometric method and the xanthydrol method. In the USP medium (pH 1.3), no hydrolysis was revealed by the fluorometric estimation whereas the xanthydrol method showed about 74% hydrolysis. In water, the two methods revealed no hydrolysis. The extent of hydrolysis after 1 hr in the USP medium was studied using three brands of digoxin tablets of differing dissolution characteristics. The fast dissolving brand showed relatively more hydrolysis than the slow dissolving tablets.

Keyphrases □ Digoxin—hydrolysis at gastric pH, colorimetric analysis □ Hydrolysis—digoxin at gastric pH, colorimetric analysis □ Colorimetry—analysis, digoxin, using xanthydrol reagent, aqueous acidic solutions □ Stability—digoxin at gastric pH, colorimetric analysis □ Cardiotonic agents—digoxin, hydrolysis at gastric pH, colorimetric analysis

The acid hydrolysis of digitalis glycosides was the subject of many studies. As early as 1897, it was observed that a decrease in the efficacy of the glycosides occurred after prior incubation with acidic gastric juices (1, 2). Later studies confirmed the *in vitro* hydrolysis of the glycosides in acid media, as determined by TLC separation followed by colorimetric estimation or by an isotopic technique (3–5).

Kuhlmann *et al.* (6), using ^3H-digoxin, found that the glycoside was rapidly hydrolyzed in the pH 1–2 range; at higher pH values, digoxin was stable. The present work examined digoxin hydrolysis rates at 37 ± 0.1° within the pH 1.1–2.2 range by a specific nonisotopic colorimetric method. The effect of the BP and USP dissolution media (specified for dissolution of digoxin tablets) on digoxin stability also was studied using three brands of digoxin tablets of differing dissolution properties.

EXPERIMENTAL

Materials—Digoxin powder BP[1], digoxigenin[2], and digitoxose[3] were used as received. Buffer solutions[4] (pH 1.1–2.2 ± 0.05, as measured by a digital pH meter[5]) and an acid pepsin solution (BPC, 1968) were used. For the xanthydrol reagent, 0.1 ml of a 10% solution of xanthydrol in methanol[6] was mixed with 1.0 ml of hydrochloric acid and diluted with acetic acid to 100 ml.

Three brands of digoxin tablets were used in dissolution studies. Brand A was a fast dissolving formulation prepared by coprecipitation of digoxin with polyethylene glycol 6000 in a ratio of 1:50 from an ethanol–chloroform mixture (1:2 v/v). Brands B[7] and C[8] were commercial lots.

Table I—Results of Replicate Assays of Synthetic Mixtures of Digoxin, Digitoxose, and Digoxigenin by the Fluorometric Method (1) and Modified Xanthydrol Method (2)

Composition, mg %			Hydrolysis, %	Digoxin Found, mg %[a]	
Digoxin	Digitoxose	Digoxigenin		1	2
1.00	0.000	0.000	0	1.001	1.020
0.90	0.057	0.050	10	1.007	0.889
0,75	0.142	0.125	25	1.013	0.760
0.50	0.285	0.250	50	0.997	0.493
0.00	0.570	0.500	100	1.005	0.000

[a] Average of four replicates (±1.8%).

Analyses of Synthetic Mixtures of Digoxin, Digoxigenin, and Digitoxose—To check the suitability of the method for stability studies, synthetic mixtures containing digoxin, digoxigenin, and digitoxose, in proportions corresponding to varying percentages of hydrolysis, were analyzed. Two methods were used:

Spectrofluorometric Determinations (7)—The procedure adopted was essentially as described in the USP for the determination of digoxin during the dissolution test of the tablets (8). Fluorescence was measured with a spectrofluorometer[9].

Modified Xanthydrol Method (9)—The sample to be assayed (10–50 μg) was diluted to 15 ml with water and extracted with chloroform (3 × 10 ml). Each chloroform extract was washed with the same 5-ml aliquot of water, and the combined chloroform extract was evaporated. Xanthydrol reagent (5 ml) was added, and the tube was placed in a boiling water bath for 3 min and cooled in an ice bath for 5 min. After cooling, the color intensity was measured after 20 min at 530 nm[10] against a blank. A standard was assayed simultaneously.

Stability Studies—These studies were carried out at 37 ± 0.1° using digoxin solutions of initial concentrations of 0.5–2.0 mg %. The media used were buffer solutions (pH 1.1–2.2), 0.1 N HCl (pH 1.1), 0.6% HCl (pH 1.3, the USP dissolution medium for digoxin tablets), and an acid pepsin solution (pH 1.3) of the BPC 1968. At specified time intervals, aliquots were assayed by the modified xanthydrol method. To stop the acid hydrolysis during the procedure, the sample withdrawn was added to water containing a few drops of ammonia TS before extraction with chloroform as already described.

Dissolution Test—The dissolution test of three brands of digoxin tablets was performed using the rotating-basket dissolution apparatus[11] of USP XIX (8). Following either the USP or BP (addendum 1975) methods, the percentages of digoxin remaining in solution after 1 hr were determined. In addition to the fluorometric method specified in both monographs, the digoxin content also was determined by the modified xanthydrol method.

To determine the dissolution rate in both the USP and BP media (0.6% HCl and water, respectively), six tablets were used; the volume of the dissolution medium was 600 ml. Aliquots were withdrawn at 15, 30, 45, and 60 min, filtered through a membrane filter[12] (0.2-μm mean pore diameter), and assayed by both the fluorometric and modified xanthydrol methods. Fresh aliquots of the dissolution medium were added at each sampling time to maintain a constant volume.

[1] Burroughs Wellcome, Kent, England.
[2] Control No. 90106, Boehringer Mannheim GMBH, West Germany.
[3] L. Light & Co., Colnbrook, England.
[4] Clark-Lub (potassium chloride–hydrochloric acid) buffer solutions.
[5] Model pH N75, Tacussel Electronique, France.
[6] E. Merck, Darmstadt, West Germany.
[7] Lanoxin tablets, batch No. 2042 X, Burroughs Wellcome, Kent, England.
[8] Digoxin tablets, batch No. 58, The Alexandria Co. for Pharmaceuticals and Chemical Industries, Alexandria, Egypt.
[9] Perkin-Elmer model 204 fluorescence spectrophotometer.
[10] Spekol spectrocolorimeter, Carl-Zeiss, Germany.
[11] Erweka Apparatebau GMBH, D-6056 Heusenstamm, West Germany.
[12] Sartorius membrane filter GMBH, 34 Gottingen, West Germany.

0022-3549/78/1000-1358$01.00/0
© 1978, American Pharmaceutical Association

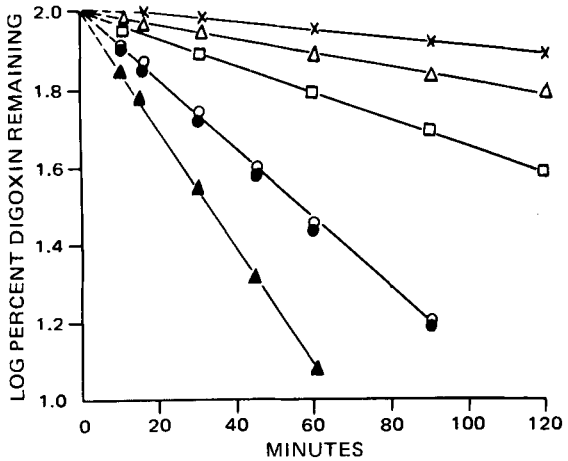

Figure 1—*First-order plot of digoxin stability at 37° in the following media: ▲, 0.1 N HCl, pH 1.1; ○, 0.6% HCl, pH 1.3; ●, acid pepsin solution, pH 1.3; □, buffer, pH 1.7; △, buffer, pH 2.0; and ×, buffer, pH 2.2.*

All three brands tested complied with the USP requirement for content uniformity.

RESULTS AND DISCUSSION

Method Selectivity—Of the nonisotopic assays for digoxin, the fluorometric method is the most sensitive. However, as with some colorimetric methods for digoxin (10), it lacks specificity. Wells *et al.* (7) reported that the sugar digitoxose did not influence the spectrofluorometric analysis of digoxin and digitoxin. They compared the fluorescence of digoxigenin and digitoxigenin with that of the parent glycosides and found identical spectra and equivalent fluorescence intensity when calculated on a molar basis.

The results obtained in the present work (Table I) confirm the findings of Wells *et al.* (7). The fluorometric method did not differentiate between the intact glycoside and its hydrolytic product digoxigenin in the synthetic mixtures tested. Irrespective of the extent of hydrolysis in the mixtures, the "apparent" digoxin contents recovered were almost the same. Even in the synthetic mixture containing no digoxin (corresponding to 100% hydrolysis), the percentage of apparent digoxin found was the same as in the unhydrolyzed mixture (Table I).

The modified xanthydrol method proved to be more selective; the percentages of digoxin recovered were in good agreement with the digoxin contents in the mixtures. Since the xanthydrol reagent reacts with the digitoxose moiety, any "free" digitoxose from hydrolysis should be separated from the intact digoxin to avoid interference. This separation was accomplished in the extraction step with chloroform, and any free digitoxose was retained in the aqueous phase. The modified xanthydrol method, although less sensitive than the fluorometric and isotopic methods, requires no TLC separation. It is simpler and less time consuming.

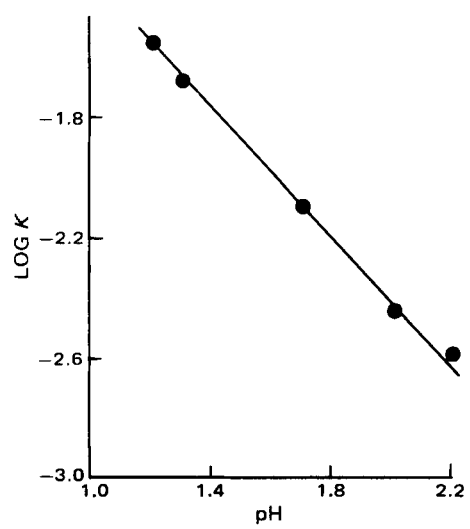

Figure 2—*Log K-pH plot for digoxin at 37°.*

Table II—Values of the Rate Constant (K) and Half-Life ($t_{1/2}$) of Digoxin Hydrolysis in Various Media at 37 ± 0.1°

Medium	K, min^{-1}	$t_{1/2}$, min
0.1 *N* HCl (pH 1.1)	0.0357	19.4
0.6% HCl (pH 1.3)[a]	0.0216	32.1
Acid pepsin solution (pH 1.3)[b]	0.0205	33.8
Buffer (pH 1.3)	0.0209	33.2
Buffer (pH 1.7)	0.0080	86.6
Buffer (pH 2.0)	0.0035	198.0
Buffer (pH 2.2)	0.0027	256.7

[a] The USP dissolution medium for digoxin tablets. [b] BPC (1968).

Table III—Results of Dissolution Testing of Three Brands of Digoxin Tablets in the BP Medium (Water) and USP Medium (0.6% HCl) Using the Modified Xanthydrol Method[a]

Brand	$t_{90\%}$ in Water, min	Digoxin Recovered after 1 hr, % In Water	In 0.6% HCl
A	13.8	101.4	24.9
B	30.0	96.8	26.2
C	45.5	92.6	38.5

[a] Average of three runs.

Stability Testing—Figure 1 shows the apparent first-order plots for digoxin hydrolysis within the pH 1.1–2.2 range. The calculated rate constant, K, and the half-lives, $t_{1/2}$, are shown in Table II. The results of stability testing did not significantly differ with the change in the initial digoxin concentration over the 0.5–2.0 mg % range. Within the pH range studied, digoxin was significantly hydrolyzed; the hydrolysis rate was pH dependent. The calculated half-lives ranged from 19.4 min to about 4.3 hr.

The presence of pepsin in the acid pepsin solution (pH 1.3) had an insignificant effect on the hydrolysis rate. At pH 1.3, the rate constant was 0.0216 min^{-1} in the buffer compared to 0.0205 min^{-1} in the acid pepsin solution (Table II). A plot of log K *versus* pH gave a straight line (Fig. 2) with a slope −1.01 (least-squares method), suggesting a specific acid catalysis.

The present results are in fair agreement with the findings of Kuhlmann *et al.* (6) who studied ^{3}H-digoxin hydrolysis at 37° by TLC followed by an isotopic technique. Their reported half-life in 0.1 *N* HCl was about 13 min, compared with 19.4 min in the present study. They also reported 18% hydrolysis after 30 min at pH 2.0, compared with 14.6% found in the present work.

Dissolution Studies—The results are shown in Fig. 3 and Table III. With the fluorometric method, almost identical dissolution plots were obtained for the same brand whether the medium was water or 0.6% HCl (Fig. 3*a*). Since significant hydrolysis was found in 0.6% HCl (Fig. 1) by the modified xanthydrol method, it follows that the fluorometric method failed to reveal the hydrolysis during dissolution testing.

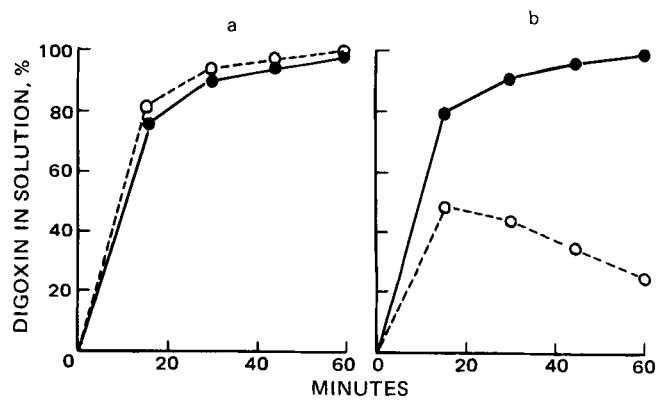

Figure 3—*Results of dissolution rate experiments of digoxin tablets, Brand B, using the spectrofluorometric method (a) and the modified xanthydrol method (b). Dissolution media used were water (●) and 0.6% HCl (○).*

Because of the nonselectivity of the fluorometric method, previously reported dissolution profiles in water and acidic media (11, 12) were almost identical. In the present work, however, this was not the case when the modified xanthydrol method was used. As shown in Fig. 3*b*, the percentage of digoxin in solution was significantly reduced in the USP medium. After 1 hr, only about 26% of the labeled digoxin remained. This result is in agreement with the value obtained from the stability studies at pH 1.3 where 27.5% hydrolysis occurred after 1 hr (Fig. 1). In water (the BP medium), no apparent hydrolysis took place.

Table III compared the amounts of digoxin recovered after 1 hr of dissolution of the tablets following the BP and USP monographs. The brands of digoxin tablets used had differing release profiles since their dissolution plots in water and the calculated $t_{90\%}$ (Table III) varied significantly. The extent of hydrolysis in the USP medium was dependent on the brand used; the fast dissolving Brand A showed more hydrolysis than Brand C (Table III).

Although the type of adjuvants used in the tablet formulations might have an effect, it is believed that the digoxin release rate from the tablets is the rate-determining factor in controlling the *in vitro* hydrolysis of the released digoxin. From the foregoing, it is concluded that digoxin undergoes rapid hydrolysis in acid solutions. As was shown by TLC separation (6), the main hydrolysis product is digoxigenin. Since the latter possesses only about one-tenth the cardioactivity of the parent glycoside (13), it follows that some loss of therapeutic efficacy may result if digoxin is exposed for a sufficient time to the acidic pH of the gastric juice. Normally, gastric pH may reach 1–2 (14, 15); but in hyperacidic patients as in Zollinger–Ellison syndrome (16), gastric pH may fall below 1. Under such conditions, some hydrolysis may occur.

Clark and Kalman (17) found 32 and 40% digoxin breakdown products in the urine of two patients but only 0–1% in four others. This result may be attributed to variations in the gastric pH since a decrease in the pH from 2.2 to 1.1 produced about a 13-fold increase in the value of K (Table II). Some reports indicated significant differences in serum digoxin levels between volunteers (18, 19). Since the gastric pH values were not given, the observed differences could be partly due to variations in the gastric pH of the volunteers.

REFERENCES

(1) P. Deucher, *Dtsch. Arch. Klin. Med.*, **58**, 47 (1897).

(2) C. L. Lhota, *Arch. Int. Pharmacodyn. Ther.*, **23**, 307 (1913).

(3) F. Svec, *Arch. Exp. Pathol. Pharmakol.*, **185**, 57 (1937).

(4) K. Kasahara and A. Ruiz-Torres, *Klin. Wochenschr.*, **47**, 1109 (1969).

(5) M. H. Gault, J. D. Charles, D. L. Sugden, and D. C. Kepkay, *J. Pharm. Pharmacol.*, **29**, 27 (1977).

(6) J. Kuhlmann, U. Abshagen, and N. Rietbrock, *Arch. Pharmacol.*, **276**, 149 (1973).

(7) D. Wells, B. Katzung, and F. H. Meyers, *J. Pharm. Pharmacol.*, **13**, 389 (1961).

(8) "The United States Pharmacopeia," 19th rev., Mack Publishing Co., Easton, Pa., 1975, p. 149.

(9) K. Jensen, *Arch. Pharm. Chem. Sci. Ed.*, **1**, 55 (1973).

(10) S. El-Masry and S. A. H. Khalil, *J. Pharm. Pharmacol.*, **27**, 35 P (1975).

(11) A. C. Caws, D. J. Jenkins, and J. A. McCrerie, *Postgrad. Med. J., Suppl. 6*, **50**, 37 (1974).

(12) D. A. Cowan and A. H. Beckett, *ibid.*, **50**, 52 (1974).

(13) G. Kroneberg, *Arch. Exp. Pathol. Pharmakol.*, **237**, 222 (1959).

(14) M. H. Sleisenger and J. S. Fordtran, "Gastrointestinal Disease—Pathophysiology–Diagnosis–Management," Saunders, Philadelphia, Pa., 1973, p. 720.

(15) G. J. Milton-Thompson, D. J. A. Williams, and J. J. Misiwicz, *Lancet*, **1**, 693 (1974).

(16) E. H. Ellison and S. D. Wilson, *Ann. Surg.*, **160**, 512 (1964).

(17) D. R. Clark and S. M. Kalman, *Drug Metab. Dispos.*, **2**, 148 (1974).

(18) D. H. Huffman, C. V. Manion, and D. L. Azarnoff, *J. Pharm. Sci.*, **64**, 433 (1975).

(19) J. Lindenbaum, *Clin. Pharmacol. Ther.*, **17**, 296 (1975).

ACKNOWLEDGMENTS

Presented in part at the 113th British Pharmaceutical Conference, St. Andrews, Scotland, September 1976.

The authors thank Dr. Ibrahim Abdullah, Chairman of the Alexandria Co. for Pharmaceuticals and Chemical Industries, for facilities and Professor Said A. Khalil for use of the spectrofluorometer.

Plasma Propranolol Levels in Beagle Dogs after Administration of Propranolol Hemisuccinate Ester

Y. GARCEAU, I. DAVIS, and J. HASEGAWA ˣ

Received August 16, 1977, from the *Biopharmacy Section, Pharmacy Research and Development Division, Ayerst Laboratories, Inc., Rouses Point, NY 12979.* Accepted for publication January 26, 1978.

Abstract □ The hemisuccinate ester of propranolol was administered to beagle dogs to test its applicability as a potential prodrug of propranolol. Following oral administration of propranolol hemisuccinate, plasma propranolol levels were eight times higher than after an equivalent dose of propranolol hydrochloride. The hemisuccinate was absorbed rapidly, with peak plasma levels observed at 0.5–1 hr. Following intravenous dosing, the disappearance half-life of the prodrug from the plasma was 0.5 hr while the propranolol half-life was 1.7 hr. This study demonstrated the potential usefulness of the prodrug approach when a highly metabolized drug such as propranolol is protected from first-pass elimination.

Keyphrases □ Propranolol—plasma levels after administration of hemisuccinate in dogs □ Plasma levels—propranolol after administration of hemisuccinate in dogs □ Prodrugs, potential—propranolol hemisuccinate, plasma levels in dogs □ Cardiac depressants—propranolol, plasma levels after administration of hemisuccinate in dogs

Propranolol (I) is a commonly used β-adrenergic receptor blocking drug. When compared to intravenous administration, the bioavailability of an oral propranolol dose is low and varies widely from patient to patient. This variation has been attributed to extensive first-pass elimination of the drug (1).

Several metabolites of propranolol have been identified (2–8). The major metabolites are propranolol *O*-glucuronide, *p*-hydroxypropranolol and its glucuronide conjugate, and naphthoxylactic acid. One major site of propranolol metabolism is the GI tract since *p*-hydroxypropranolol is detected after oral, but not after intravenous, adminis-

0022-3549/78/1000-1360$01.00/0

© 1978, American Pharmaceutical Association

Because of the nonselectivity of the fluorometric method, previously reported dissolution profiles in water and acidic media (11, 12) were almost identical. In the present work, however, this was not the case when the modified xanthydrol method was used. As shown in Fig. 3*b*, the percentage of digoxin in solution was significantly reduced in the USP medium. After 1 hr, only about 26% of the labeled digoxin remained. This result is in agreement with the value obtained from the stability studies at pH 1.3 where 27.5% hydrolysis occurred after 1 hr (Fig. 1). In water (the BP medium), no apparent hydrolysis took place.

Table III compared the amounts of digoxin recovered after 1 hr of dissolution of the tablets following the BP and USP monographs. The brands of digoxin tablets used had differing release profiles since their dissolution plots in water and the calculated $t_{90\%}$ (Table III) varied significantly. The extent of hydrolysis in the USP medium was dependent on the brand used; the fast dissolving Brand A showed more hydrolysis than Brand C (Table III).

Although the type of adjuvants used in the tablet formulations might have an effect, it is believed that the digoxin release rate from the tablets is the rate-determining factor in controlling the *in vitro* hydrolysis of the released digoxin. From the foregoing, it is concluded that digoxin undergoes rapid hydrolysis in acid solutions. As was shown by TLC separation (6), the main hydrolysis product is digoxigenin. Since the latter possesses only about one-tenth the cardioactivity of the parent glycoside (13), it follows that some loss of therapeutic efficacy may result if digoxin is exposed for a sufficient time to the acidic pH of the gastric juice. Normally, gastric pH may reach 1–2 (14, 15); but in hyperacidic patients as in Zollinger–Ellison syndrome (16), gastric pH may fall below 1. Under such conditions, some hydrolysis may occur.

Clark and Kalman (17) found 32 and 40% digoxin breakdown products in the urine of two patients but only 0–1% in four others. This result may be attributed to variations in the gastric pH since a decrease in the pH from 2.2 to 1.1 produced about a 13-fold increase in the value of K (Table II). Some reports indicated significant differences in serum digoxin levels between volunteers (18, 19). Since the gastric pH values were not given, the observed differences could be partly due to variations in the gastric pH of the volunteers.

REFERENCES

(1) P. Deucher, *Dtsch. Arch. Klin. Med.*, **58**, 47 (1897).

(2) C. L. Lhota, *Arch. Int. Pharmacodyn. Ther.*, **23**, 307 (1913).

(3) F. Svec, *Arch. Exp. Pathol. Pharmakol.*, **185**, 57 (1937).

(4) K. Kasahara and A. Ruiz-Torres, *Klin. Wochenschr.*, **47**, 1109 (1969).

(5) M. H. Gault, J. D. Charles, D. L. Sugden, and D. C. Kepkay, *J. Pharm. Pharmacol.*, **29**, 27 (1977).

(6) J. Kuhlmann, U. Abshagen, and N. Rietbrock, *Arch. Pharmacol.*, **276**, 149 (1973).

(7) D. Wells, B. Katzung, and F. H. Meyers, *J. Pharm. Pharmacol.*, **13**, 389 (1961).

(8) "The United States Pharmacopeia," 19th rev., Mack Publishing Co., Easton, Pa., 1975, p. 149.

(9) K. Jensen, *Arch. Pharm. Chem. Sci. Ed.*, **1**, 55 (1973).

(10) S. El-Masry and S. A. H. Khalil, *J. Pharm. Pharmacol.*, **27**, 35 P (1975).

(11) A. C. Caws, D. J. Jenkins, and J. A. McCrerie, *Postgrad. Med. J., Suppl. 6*, **50**, 37 (1974).

(12) D. A. Cowan and A. H. Beckett, *ibid.*, **50**, 52 (1974).

(13) G. Kroneberg, *Arch. Exp. Pathol. Pharmakol.*, **237**, 222 (1959).

(14) M. H. Sleisenger and J. S. Fordtran, "Gastrointestinal Disease—Pathophysiology–Diagnosis–Management," Saunders, Philadelphia, Pa., 1973, p. 720.

(15) G. J. Milton-Thompson, D. J. A. Williams, and J. J. Misiwicz, *Lancet*, **1**, 693 (1974).

(16) E. H. Ellison and S. D. Wilson, *Ann. Surg.*, **160**, 512 (1964).

(17) D. R. Clark and S. M. Kalman, *Drug Metab. Dispos.*, **2**, 148 (1974).

(18) D. H. Huffman, C. V. Manion, and D. L. Azarnoff, *J. Pharm. Sci.*, **64**, 433 (1975).

(19) J. Lindenbaum, *Clin. Pharmacol. Ther.*, **17**, 296 (1975).

ACKNOWLEDGMENTS

Presented in part at the 113th British Pharmaceutical Conference, St. Andrews, Scotland, September 1976.

The authors thank Dr. Ibrahim Abdullah, Chairman of the Alexandria Co. for Pharmaceuticals and Chemical Industries, for facilities and Professor Said A. Khalil for use of the spectrofluorometer.

Plasma Propranolol Levels in Beagle Dogs after Administration of Propranolol Hemisuccinate Ester

Y. GARCEAU, I. DAVIS, and J. HASEGAWA ˣ

Received August 16, 1977, from the *Biopharmacy Section, Pharmacy Research and Development Division, Ayerst Laboratories, Inc., Rouses Point, NY 12979.* Accepted for publication January 26, 1978.

Abstract □ The hemisuccinate ester of propranolol was administered to beagle dogs to test its applicability as a potential prodrug of propranolol. Following oral administration of propranolol hemisuccinate, plasma propranolol levels were eight times higher than after an equivalent dose of propranolol hydrochloride. The hemisuccinate was absorbed rapidly, with peak plasma levels observed at 0.5–1 hr. Following intravenous dosing, the disappearance half-life of the prodrug from the plasma was 0.5 hr while the propranolol half-life was 1.7 hr. This study demonstrated the potential usefulness of the prodrug approach when a highly metabolized drug such as propranolol is protected from first-pass elimination.

Keyphrases □ Propranolol—plasma levels after administration of hemisuccinate in dogs □ Plasma levels—propranolol after administration of hemisuccinate in dogs □ Prodrugs, potential—propranolol hemisuccinate, plasma levels in dogs □ Cardiac depressants—propranolol, plasma levels after administration of hemisuccinate in dogs

Propranolol (I) is a commonly used β-adrenergic receptor blocking drug. When compared to intravenous administration, the bioavailability of an oral propranolol dose is low and varies widely from patient to patient. This variation has been attributed to extensive first-pass elimination of the drug (1).

Several metabolites of propranolol have been identified (2–8). The major metabolites are propranolol *O*-glucuronide, *p*-hydroxypropranolol and its glucuronide conjugate, and naphthoxylactic acid. One major site of propranolol metabolism is the GI tract since *p*-hydroxypropranolol is detected after oral, but not after intravenous, adminis-

0022-3549/78/1000-1360$01.00/0

© 1978, American Pharmaceutical Association

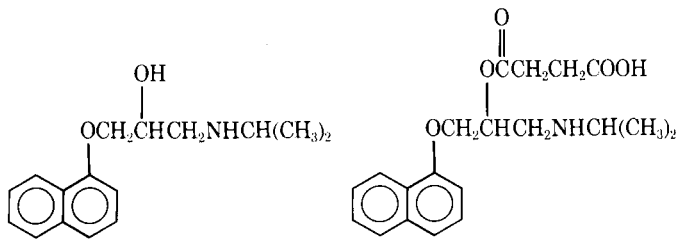

I II

tration. There is evidence that glucuronide conjugation of some drugs occurs, at least in part, in the gut wall (9, 10).

The use of a propranolol prodrug could lead to improved bioavailability. The hemisuccinate ester of propranolol (II) was selected as a potential prodrug and tested in beagle dogs. The hypothesis was that propranolol hemisuccinate administration would make it possible to bypass glucuronide formation during absorption. Propranolol would subsequently be released in the blood by prodrug hydrolysis. The results of this investigation are reported in this paper.

EXPERIMENTAL

Study Protocols—Four blood level studies were conducted. In each study, propranolol or its hemisuccinate ester was administered as the hydrochloride salt. The same beagle dogs were used in all studies.

Study 1—Four female beagle dogs, ~10 kg, were given 80 mg po of propranolol hydrochloride (8 mg/kg) or an equivalent dose of the ester prodrug. The animals were divided into two groups of two, each group receiving the drugs according to a crossover design. The entire experiment was repeated twice. At least 1 week elapsed between each dosing. At regular intervals after dosing, blood samples (10 ml) were obtained in tubes containing edetic acid (9 mg/tube) and centrifuged. The plasma was frozen immediately after preparation, and the samples were analyzed for free propranolol within 1 week.

Study 2—The same four beagle dogs were given a 20-mg iv bolus dose of propranolol hydrochloride on 1 experimental day and an equivalent dose of the prodrug 1 week later. Blood samples were processed as in Study 1, and plasma was analyzed for free propranolol.

Study 3—Two female beagle dogs were given 13.4 mg po of propranolol hemisuccinate ester (equivalent to 10 mg of propranolol hydrochloride). Blood samples were obtained and treated as in Study 1.

Study 4—Four female beagle dogs were given propranolol hemisuccinate intravenously and orally. The dogs were divided into groups of two, each group receiving each dosing regimen according to a crossover design. The oral dose consisted of 107 mg, and the intravenous dose consisted of 26.7 mg of propranolol hemisuccinate. Blood samples were collected as in Study 1, and plasma was analyzed for free propranolol and unchanged propranolol hemisuccinate.

Dosage Forms—Propranolol hydrochloride was given orally as two 40-mg tablets[1]. Propranolol hydrochloride injectables were prepared in saline at 3 mg/ml. Propranolol hemisuccinate was given in capsules of 107 or 13.4 mg (equivalent to 80 or 10 mg of propranolol hydrochloride, respectively). Propranolol hemisuccinate injectables were prepared in saline at 9 mg/ml.

Analytical Methods—Free propranolol was analyzed by a TLC–fluorometric procedure (11). Plasma samples of 2 ml were mixed with 2 ml of pH 10 buffer[2] and extracted with 25 ml of ether. A 20-ml aliquot from the ether phase was evaporated to dryness, and the dry residue was dissolved in 100 μl of ethanol. Aliquots of 25 μl were spotted on silica gel[3] TLC plates along with standard solutions of propranolol.

The plates were developed in a saturated tank containing methanol–concentrated ammonium hydroxide (100:0.4). After development, the plates were dried and sprayed with 50% propylene glycol in water. They were then read in the fluorescence mode of a spectrodensitometer[4], with excitation at 290 nm and emission at 365 nm. The limit of reliable quantitation was 2 ng of propranolol/ml of plasma. The R_f value of propranolol was 0.34, and the method was free of interference from all known metabolites of propranolol and from propranolol hemisuccinate.

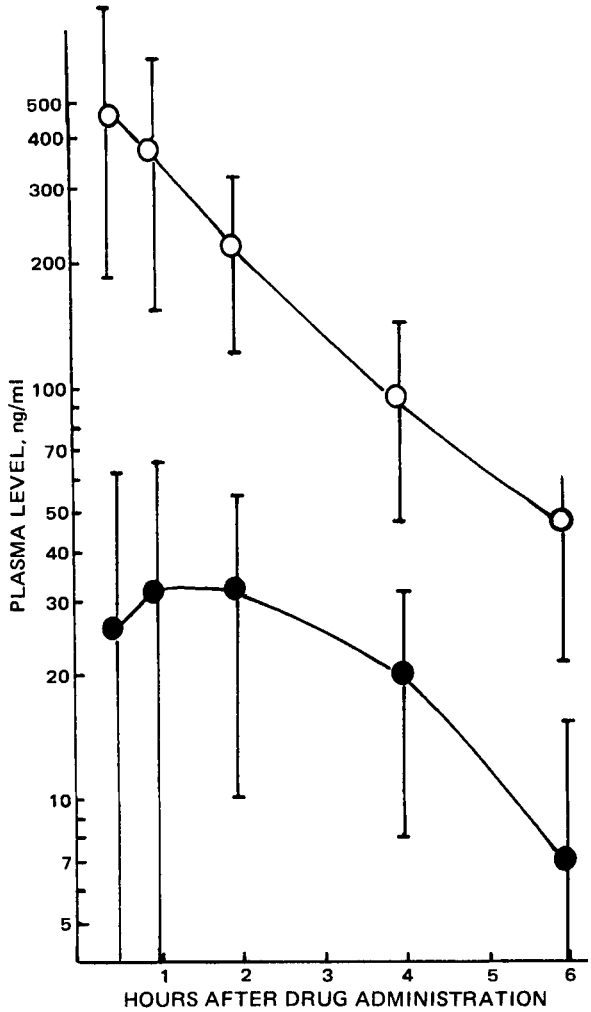

Figure 1—*Mean plasma propranolol levels* (±SD, n = 8) *following 80 mg po of propranolol hydrochloride* (●) *and 107 mg po of propranolol hemisuccinate* (○) *to beagle dogs.*

Propranolol hemisuccinate also was analyzed by a TLC–fluorometric procedure. Plasma samples, 2 ml, were mixed with 2 ml of pH 4 buffer[5] and extracted with 40 ml of methylene chloride. A 30-ml aliquot from the organic phase was evaporated to dryness, and the residue was dissolved in 100 μl of ethanol. Aliquots of 25 μl were spotted on silica gel[6] TLC plates along with standard solutions of propranolol hemisuccinate.

The plates were developed in a saturated tank containing isopropyl alcohol–benzene–water–formic acid (55:40:5:3). After development, the plates were dried and sprayed with 50% propylene glycol in water. They were read in the fluorescence mode of a spectrodensitometer[4], with excitation at 290 nm and emission at 365 nm. The limit of reliable quantitation was 25 ng/ml of plasma. The R_f value of propranolol hemisuccinate was 0.50 while that of propranolol was 0.37. The method was free of interference from propranolol metabolites.

Stability of Propranolol Hemisuccinate—The hemisuccinate hydrolyzed slowly to propranolol in stored plasma. The hydrolysis half-life was 14 hr at room temperature (21°) and 34 days at −20°. The time required to process and extract plasma samples in the assay varied from 30 to 45 min.

To determine how much propranolol was obtained from *in vitro* hydrolysis, plasma samples were spiked with propranolol hemisuccinate and subjected to the analytical procedure for free propranolol; 5% of the ester hydrolyzed to propranolol during sample preparation and analysis.

[1] Inderal, Ayerst Laboratories.
[2] Anachemia, R-1280.
[3] E. Merck.
[4] Schoeffel, SD 3000.
[5] Anachemia, R-1180.
[6] Macherey-Nagel.

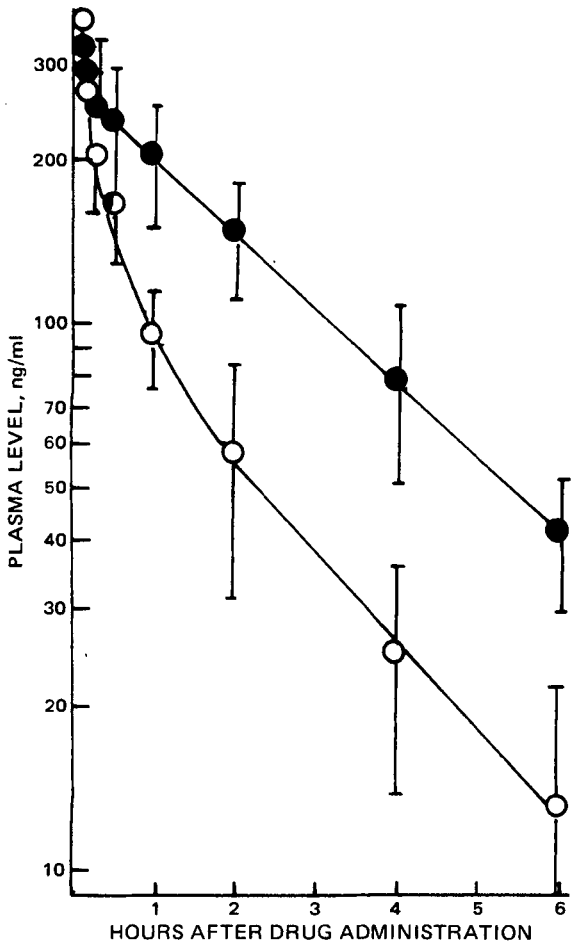

Figure 2—*Mean plasma propranolol levels* (±SD, n = 4) *following 20 mg iv of propranolol hydrochloride* (●) *and 26.7 mg iv of propranolol hemisuccinate* (○) *to beagle dogs.*

Therefore, to ensure that analytical data would not be biased significantly as a result of *in vitro* hydrolysis, plasma samples were processed and analyzed promptly in all experiments.

The hydrolysis rates of propranolol hemisuccinate were determined in buffer at 37°. In pH 7.3 buffer, the hydrolysis half-life was 4.7 hr. In pH 2 buffer, no hydrolysis was observed after 5 days of incubation.

Synthesis of Propranolol Hemisuccinate—The hemisuccinate of propranolol was synthesized from propranolol hydrochloride and succinic anhydride, mp 112–114°; IR (mineral oil mull): 1750 (ester function) and 1720 (free carboxyl function) cm^{-1}. The NMR scan of propranolol hemisuccinate was similar to that of propranolol except for a broad peak at 2.5 ppm which corresponded to the succinate group.

Anal.—Calc. for $C_{20}H_{25}NO_5 \cdot HCl$: C, 60.67; H, 6.61; N, 3.53. Found: C, 60.97; H, 6.96; N, 3.51.

RESULTS AND DISCUSSION

Study 1—Mean plasma levels (n = 8) of propranolol after 80 mg po of propranolol hydrochloride and an equivalent dose of hemisuccinate to beagle dogs are given in Fig. 1. Propranolol concentrations were considerably higher following prodrug administration. The mean area under the plasma level–time curve (*AUC*, 0–6 hr) was 1075 ng/ml × hr (*SD* 445, *CV* 41%) after the hemisuccinate ester and 132 ng/ml × hr (*SD* 87, *CV* 65%) after propranolol hydrochloride. Analysis of variance revealed that difference to be highly significant ($p < 0.01$). In addition, intersubject variation in plasma propranolol levels was reduced following prodrug administration, as evidenced by the smaller coefficient of variation calculated from the *AUC* values.

Absorption of the prodrug and its conversion to propranolol were rapid, peak plasma levels of propranolol being reached between 0.5 and 1 hr after administration of the hemisuccinate. Since blood sampling was terminated at 6 hr after dosing, only a few points were available for calculating half-lives. Based on these values, the disappearance half-life of propranolol was 1.8 hr after oral propranolol hydrochloride and 1.7 hr after oral prodrug administration.

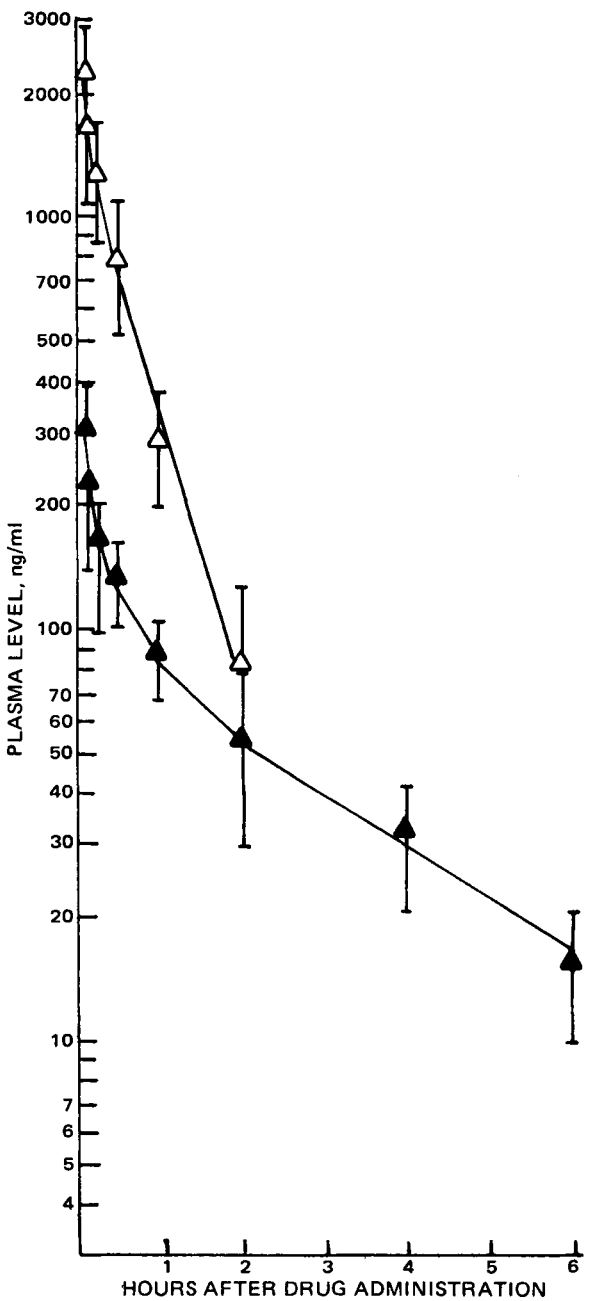

Figure 3—*Mean plasma levels* (±SD, n = 4) *of propranolol hemisuccinate* (△) *and propranolol* (▲) *following 26.7 mg iv of propranolol hemisuccinate to beagle dogs. Levels of propranolol hemisuccinate were below the limit of reliable quantitation (25 ng/ml) in the 4- and 6-hr postdosing plasma samples.*

Study 2—Mean plasma propranolol levels (n = 4) following 20 mg iv of propranolol hydrochloride and an equivalent dose of hemisuccinate to beagle dogs are shown in Fig. 2. Again, conversion of the prodrug to propranolol was fast, high levels of propranolol being found 5 min after intravenous administration. The mean plasma level–time curve of propranolol after intravenous prodrug showed two phases: an initial phase with a half-life of 0.3 hr and a late phase with a half-life of 1.9 hr. The plasma level–time curve after intravenous propranolol was also biphasic, with a late phase half-life of 2.3 hr.

Plasma propranolol levels were lower following intravenous prodrug administration. The mean *AUC* was 367 ng/ml × hr (*SD* 70, *CV* 19%) after propranolol hemisuccinate and 746 ng/ml × hr (*SD* 192, *CV* 27%) after propranolol hydrochloride. It is difficult to explain this observation because too little is known of the distribution, elimination, and metabolism of the prodrug.

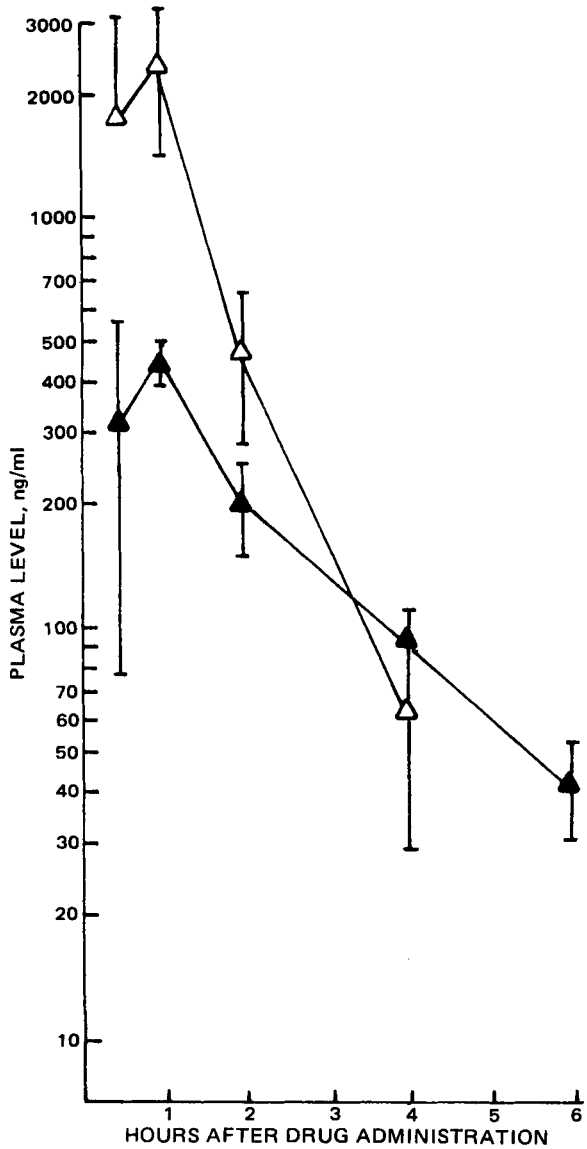

Figure 4—*Mean plasma levels* (±SD, n = 4) *of propranolol hemisuccinate* (△) *and propranolol* (▲) *following 107 mg po of propranolol hemisuccinate to beagle dogs. Levels of propranolol hemisuccinate were below the limit of reliable quantitation (25 ng/ml) in the 6-hr postdosing plasma samples.*

Study 3—Two dogs were given 13.4 mg po of propranolol hemisuccinate (equivalent to 10 mg of propranolol hydrochloride), and their plasma propranolol levels were compared to those obtained after 80 mg of propranolol hydrochloride (Table I). In Dog C, the *AUC* values were 101 and 92 ng/ml × hr after administration of the prodrug and propranolol hydrochloride, respectively; in Dog B, the *AUC* values were 114 and 168 ng/ml × hr, respectively. Although only two dogs were tested, results indicate that a dose of prodrug one-eighth that of propranolol hydrochloride gave comparable levels of free propranolol.

Study 4—In this experiment, plasma unchanged propranolol hemisuccinate levels as well as plasma propranolol levels were measured following intravenous and oral administrations of the prodrug to dogs. The intravenous dose was equivalent to 20 mg, and the oral dose was equivalent to 80 mg of propranolol hydrochloride. Results are given in Figs. 3 and 4, respectively.

Table I—Plasma Propranolol Levels (Nanograms per Milliliter) following 80 mg po of Propranolol Hydrochloride and 13.4 mg po of Propranolol Hemisuccinate to Beagle Dogs

Dog	Hours after Dosing[a] 0.5	1	2	4	6	*AUC*, 0–6 hr, ng/ml × hr
	After Propranolol Hydrochloride					
B	10	38	51	26	9	168
C	18	44	24	7	0	92
	After Propranolol Hemisuccinate					
B	84	42	15	9	0	114
C	10	50	27	9	0	101

[a] No drug was detected at 0 hr.

Following intravenous dosing, the disappearance of propranolol hemisuccinate was biphasic, with a late phase half-life of 0.5 hr; that of propranolol was also biphasic, with a late phase half-life of 2.3 hr. Virtually no prodrug was detected in the blood 4 hr after administration. In contrast, significant propranolol levels were still present 6 hr after dosing with the prodrug.

Following oral administration, plasma unchanged propranolol hemisuccinate levels peaked early (0.5–1 hr postdosing), and levels were negligible 6 hr after dosing. This result suggested rapid absorption and conversion of the prodrug. The half-life of propranolol hemisuccinate disappearance was 0.7 hr, and that of propranolol was 2.0 hr. Plasma propranolol levels peaked at 1 hr and were still substantial 6 hr after dosing. As an index of the amount of the prodrug absorbed orally, the area under the mean plasma level–time curve of propranolol hemisuccinate (3474 ng/ml × hr) after oral dosing was compared to that after intravenous dosing (1234 × 4 = 4936 ng/ml × hr corrected dose). About 70% of the oral dose of the prodrug was absorbed.

REFERENCES

(1) A. S. Nies and D. G. Shand, *Circulation*, **52**, 6 (1975).

(2) P. A. Bond, *Nature*, **213**, 721 (1967).

(3) J. W. Paterson, M. E. Conolly, and C. T. Dollery, *Pharmacol. Clin.*, **2**, 127 (1970).

(4) G. L. Tindell, T. Walle, and T. E. Gaffney, *Life Sci.*, **11**, 1029 (1972).

(5) T. Walle and T. E. Gaffney, *J. Pharmacol. Exp. Ther.*, **182**, 83 (1972).

(6) T. Walle, J. I. Morrison, and G. L. Tindell, *Res. Commun. Chem. Pathol. Pharmacol.*, **9**, 1 (1974).

(7) H. Ehrsson, *J. Pharm. Pharmacol.*, **27**, 971 (1975).

(8) T. Walle, E. C. Conradi, K. Walle, and T. E. Gaffney, Federation of American Society for Experimental Biology, 60th annual meeting, Anaheim, Calif., Apr. 1976, Abstract 2537.

(9) W. H. Barr and S. Riegelman, *J. Pharm. Sci.*, **59**, 154 (1970).

(10) B. N. LaDu, H. G. Mandel, and E. L. Way, "Fundamentals of Drug Metabolism and Drug Disposition," Williams & Wilkins, Baltimore, Md., 1971, chap. 10.

(11) Y. Garceau, I. Davis, and J. Hasegawa, *J. Pharm. Sci.*, **67**, 826 (1978).

ACKNOWLEDGMENTS

The authors thank Dr. D. Chin and Dr. J. Wetzel for help in designing the protocol and supervising drug administration, Dr. L. Humber for synthesizing the hemisuccinate ester of propranolol, and Dr. C. Orzech and Mr. R. Daley for interpretation of NMR and IR data.

Simple Procedure for Determining Octanol–Aqueous Partition, Distribution, and Ionization Coefficients by Reversed-Phase High-Pressure Liquid Chromatography

STEFAN H. UNGER ˣ, JAMES R. COOK, and JOHN S. HOLLENBERG

Received November 14, 1977, from the *Institute of Organic Chemistry, Syntex Research, Palo Alto, CA 94304.* Accepted for publication January 30, 1978.

Abstract □ The described simple, accurate, and precise reversed-phase high-pressure liquid chromatographic procedure is in excellent agreement with 1-octanol shake-flask partition or distribution coefficients over a 3.5 log range. A chemically bonded octadecylsilane support is persilated and coated with 1-octanol. With 1-octanol-saturated buffers as mobile phases, a stable baseline (compared to 1-octanol adsorbed on silica) is obtained rapidly, and the log relative retention times are highly correlated with unit slope to log distribution or partition coefficients obtained from the classical shake-flask procedures. Only relatively basic, unhindered pyridines deviate, probably because of binding with residual silinol sites. In addition, if the apparent pKa or pK_a^b of an ionizable compound lies within the pH operating range of the column support, the apparent pKa or pK_a^b usually can be determined simultaneously with log P by measuring the log distribution coefficient at several pH values. The procedure gives rapid results, requires little material, and can tolerate impurities.

Keyphrases □ Partition coefficients—various compounds, high-pressure liquid chromatographic determination □ Distribution coefficients—various compounds, high-pressure liquid chromatographic determination □ Ionization coefficients—various compounds, high-pressure liquid chromatographic determination □ High-pressure liquid chromatography—determination, partition, distribution, and ionization coefficients for various compounds

There is considerable interest in determining octanol–aqueous partition coefficients in the emerging area of rational drug design (1). Therefore, a reversed-phase high-pressure liquid chromatographic (HPLC) procedure was sought that would be accurate *vis á vis* standard shake-flask octanol–aqueous partition coefficients; precise, *i.e.*, reproducible from day to day; rapidly set up, *i.e.*, baseline rapidly established; and not especially temperature sensitive.

BACKGROUND

The shake-flask procedure (2) is considered the standard reference procedure, but it suffers from several problems. It is time consuming and subject to purity, stability, and mass balance problems. Moreover, it requires handling relatively large quantities of odiferous 1-octanol.

A reversed-phase TLC procedure was described (3), which is more suitable to determining large numbers of analogs. However, the preparation of standardized plates and the necessity of running several dilution series of mobile phases—to detect hydrogen-bonding effects—detract from this procedure. Procedures were reported that used reversed-phase HPLC to measure lipophilicity (4, 5). These procedures (acetonitrile–buffer solutions on octadecylsilane bonded packings) are fast and accurate and avoid purity and stability problems, but octadecylsilane is more like an alkane than an alcohol phase. Therefore, the differential effects of hydrogen bonding limit use of these procedures to close analogs (6).

Hulshoff and Perrin (7) compared reversed-phase HPLC and TLC procedures and also investigated oleyl alcohol supported on Porasil C[1] as an HPLC procedure to measure the lipophilicities of a series of benzodiazepines. Likewise, Mirrlees *et al.* (8) used 1-octanol supported on Hyflo supercel[2] and compared some of the earlier work on reversed-phase TLC and HPLC. Henry *et al.* (9) compared various HPLC techniques such as C-18 Corasil[1] and 1-octanol and squalene on Corasil II and Porasil A. These procedures (8, 9), using 1-octanol physically adsorbed on a solid support, would be close to ideal (a physically bonded "octanol"-like alcohol with the hydroxyl end free). However, attempts to obtain a stable baseline were unsuccessful in this laboratory and others[3].

Since 1-octanol itself is very lipophilic [log $P_{octanol}$ = 3.15 (1)], it should bond strongly to octadecylsilane and give a stable column with minimal free silinol sites (5). Providing that the aqueous mobile phase is saturated with octanol, a system much like that of the octanol–aqueous shake-flask system should result.

EXPERIMENTAL

C-18 Corasil, 37–50 μm, was persilated by the method of McCall (5) and dry packed in stainless steel tubing (2 mm i.d.) in lengths of ~3, 10, and 50 cm. A precolumn of silica gel (70–230 mesh) with dimensions of 9 mm i.d. × 8.5 cm also was prepared. Both columns were loaded with 99.97% (certified) 1-octanol by injecting directly into the column under pressure until droplets appeared. The columns were mounted on a high-pressure liquid chromatograph and flushed with octanol-saturated water (or buffer, 0.01 M) until the eluate appeared clear. The analytical column was then attached to the 254-nm UV detector, and elution was continued until a stable baseline was obtained (~30–45 min). All solutions were first filtered[4] to reduce contamination or column clogging.

Samples were dissolved in octanol-saturated buffer and/or a minimal amount of methanol, and a 25-μl injection loop was used. Elution times, t_x, were measured with a stopwatch; methanol in octanol-saturated buffer served as a suitable nonretained compound to define t_0, the dead volume; pyridine N-oxide or formamide also can be used. Then, $k' = (t_x - t_0)/t_0$. Sample concentrations were adjusted so that relative peak areas remained approximately constant. Column length and flow rate (~1–2 ml/min) were selected for analytical convenience.

In other respects, the procedure follows published methods (5, 8, 9). The same octadecylsilane columns were used with 25% (w/w) methanol–buffer as the mobile phase to demonstrate the effects of octanol[5]. All experiments were performed at ambient temperature (25 ± 1°). The pH of the eluate was determined using aqueous buffers; addition of octanol at saturation had no effect on pH.

Log D or log P (distribution or partition) coefficients for unknowns were determined by interpolation from the standard regression line between shake-flask log D or log P and log k'. Daily standards were highly correlated with each other; different column lengths were correlated with a slope close to 1.0 but with a significant intercept because of a constant increase in log k' with column length.

Shake-flask measurements were made with the same solutions as used in HPLC following the general procedure of Fujita *et al.* (2). Hexaldehyde was measured by vapor phase chromatography at two dilutions because of poor UV absorption.

RESULTS AND DISCUSSION

The effects of ionization and the differential effects of hydrogen bonding are unfortunately ignored in many new methods for determining partition coefficients. If one is cognizant of the effects of ionization, one can simply use the distribution coefficient D in place of the partition

[1] Waters Associates.
[2] Johns-Manville.
[3] P. J. Taylor, I.C.I. Ltd., Macclesfield, England, personal communication.
[4] Millipore.
[5] See I. T. Harrison, W. Kurz, I. J. Massey, and S. H. Unger, *J. Med. Chem.*, 21 588 (1978).

0022-3549/78/1000-1364$01.00/0
© 1978, American Pharmaceutical Association

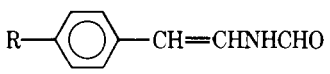

I

coefficient P (10); however, one must correct:

$$P = [\text{octanol}]/[\text{aqueous}]\ (1 - \alpha) = D/(1 - \alpha) \qquad \text{(Eq. 1)}$$

for relative differences in hydrogen-bonding effects when comparing different experimental procedures (6).

This correction is demonstrated in Fig. 1 where log k' determined on octadecylsilane–25% (w/w) methanol–pH 7.00 phosphate buffer is plotted *versus* log P determined by the new HPLC procedure on the same columns for some tuberin [*N*-(β-styryl)formamide] analogs (I)[5]. The neutral substituents are highly linear between the two systems; however, the hydrogen-bonding substituents fall off of this line. Therefore, octadecylsilane–25% (w/w) methanol does *not* correctly represent the partitioning behavior of these compounds *vis á vis* an octanol–aqueous system. On the other hand, the excellent agreement between log P determined by octanol-coated octadecylsilane using HPLC and the classical shake-flask values in the identical solvents is shown in Table I.

A comparison of a large number of standards is given in Table II. Several shake-flask values were redetermined in the same solvent system as used in HPLC to have an accurate comparison. Since pH 7.00 (0.01 *M*) buffer was used, some compounds (*e.g.*, *p*-nitrophenol) were ionized and some were not. Therefore, since linear correlation was obtained, this procedure is sensitive to distribution as well as partition effects.

The wide range of substituent groups, both hydrogen-bond donors and acceptors, clearly demonstrates the excellent modeling of the shake-flask procedure. Of all classes of compounds studied thus far, only two gave poor agreement between the two methods. The relatively unhindered basic pyridines (pyridine, 3-picoline, 4-picoline, and 2-amino-4-picoline) deviated considerably and were retained on the column much longer than expected. This result can probably be attributed to bonding with residual

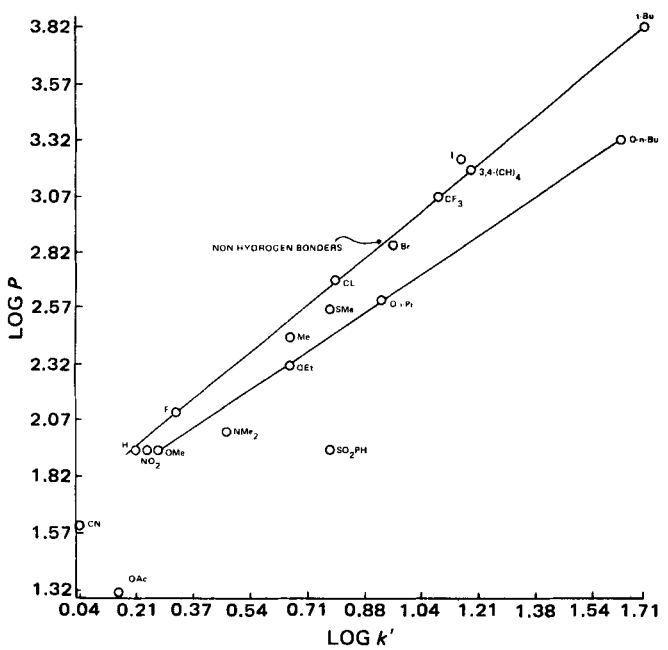

Figure 1—*Partitioning behavior of tuberins in two HPLC systems. The vertical axis gives log* P *determined on octanol-coated octadecylsilyl-bonded support with octanol saturated pH 7.00 (0.01* M*) phosphate buffer as the mobile phase. The horizontal axis gives log* k′ *determined on the same octadecylsilyl-bonded support but with 25% (w/w) methanol in pH 7.00 (0.001* M*) phosphate buffer and no octanol. Note the deviation of hydrogen-bonded substituents between the two systems. Key (R in Structure I): t-Bu,* tert*-butyl; O-n-Bu, butoxy; I, iodo; 3,4-(CH)4, 3,4-benzo (the β-naphthyl analog); CF3, trifluoromethyl; Br, bromo, CL, chloro; O-i-Pr, isopropoxy; SMe, methylthio; Me, methyl; OEt, ethoxy; SO2PH, phenylsulfono; F, fluoro; NMe2, dimethylamino; H, unsubstituted; NO2, nitro; OMe, methoxy; CN, cyano; and OAc, acetoxy.*

Table I—Agreement between Shake-Flask and HPLC Log *P* Values in Tuberin Series and for Naproxen [a]

R (Structure I)	Log $P_{\text{shake flask}}$	Log P_{HPLC}
Unsubstituted	1.93 ± 0.01	1.95[b]
Methoxy	1.92 ± 0.02	1.94[b]
Cyano	1.58 ± 0.01	1.62[b]
Acetoxy	1.40 ± 0.01	1.32[b]
Naproxen[c]	3.18[d]	3.20 ± 0.01

[a] With pH 7.00 (0.01 *M*) phosphate buffer; ambient temperature. [b] The standard deviation of regression between log P and log k' for standards is 0.03, omitting tuberins. [c] (+)-6-Methoxy-α-methylnaphthaleneacetic acid. [d] See Table II, footnote *b*.

silinol sites. For example, different batches of persilated octadecylsilane gave somewhat different log D values for these compounds, while all other compounds behaved as expected.

The other class of deviants, also recognized by Mirrlees *et al.* (8), are the very lipophilic acids or bases, which can still have significant partitioning of the ionized species. Generally, very poor peak shapes were obtained with such compounds. The solution to this problem would be to work at more propitious pH values to drive the ionization completely in one direction. If peak shape is not a problem, however, and the apparent pKa is between 2 and 8 (the pH operating range of octadecylsilyl-bonded supports), then both log P and pKa can be determined simultaneously by measuring log D at several pH values. Horváth *et al.* (11) reported a similar procedure using standard octadecylsilane columns. Since $P = D\ [(K_a/H) + 1]$ for acids and $P = D\ [(H/K_a{}^b) + 1]$ for bases, then for acids:

$$D = P + K_a(-D/H) \qquad \text{(Eq. 2}a\text{)}$$

and for bases:

$$D = P + (1/K_a{}^b)\ (-DH) \qquad \text{(Eq. 2}b\text{)}$$

where the distribution coefficient D (from interpolation using standards) is correlated *versus* $(-D/H)$ or $(-DH)$ by ordinary least squares. To determine the intercept P and the slope K_a (or $1/K_a{}^b$) most accurately, measurements should be taken near pH 2 and approximately the pKa for acids and near pH 8 and the $pK_a{}^b$ for bases. Since D appears on both sides of Eqs. 2*a* and 2*b*, propagation of errors in D make the standard

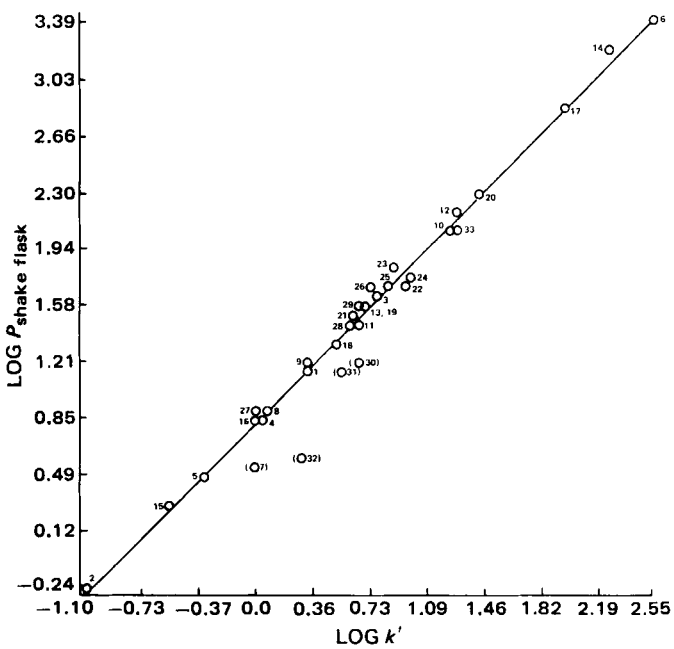

Figure 2—*Comparison of log* $P_{shake\ flask}$ *with log* k′ *determined by octanol-coated octadecylsilyl-bonded support with octanol-saturated pH 7.00 (0.01* M*) phosphate buffer as the mobile phase. Compounds are numbered as in Table II. Note the excellent agreement over 3.5 log* P *units, except for unhindered pyridines, which can be attributed to specific binding to residual silinol sites. Correlation is for Eq. 4.*

Table II—Shake-Flask and HPLC Partition and Distribution Coefficients at pH 7.00 for Standard Compounds

Number	Name	Log $P^{a,b}$	Log $k'^{a,c}$
1	Acetanilide	1.16 ± 0.02 (3)	0.322 ± 0.001 (2)
2	Acetone	−0.24 (1)	−1.097 (1)
3	Acetophenone	1.66 ± 0.08 (3)	0.782 ± 0.02 (3)
4	2-Acetylpyridine	0.85 ± 0.03 (4)[d]	0.047 (1)
5	4-Acetylpyridine	0.48 ± 0.01 (4)[d]	−0.328 (1)
6	Acridine	3.39 (1)	2.554 (1)
7	2-Amino-4-picoline	0.56 ± 0.03 (6)[d]	−0.0127 (1)
8	Aniline	0.93 ± 0.05 (3)	0.0614 (1)
9	*o*-Anisidine	1.23 ± 0.04 (4)[d]	0.335 ± 0.005 (2)
10	Anisole	2.08 ± 0.04 (3)	1.250 (1)
11	Benzaldehyde	1.45 ± 0.03 (2)	0.656 ± 0.007 (4)
12	Benzene	2.15 ± 0.01 (3)	1.262 ± 0.01 (2)
13	Benzonitrile	1.56 ± 0.00 (2)	0.688 (1)
14	Benzophenone	3.18 (1)	2.272 (1)
15	2-Butanone	0.28 ± 0.02 (2)	−0.540 ± 0.008 (2)
16	Catechol	0.86 ± 0.02 (2)	−0.006 ± 0.02 (3)
17	Chlorobenzene	2.84 (1)	1.966 (1)
18	2-Chloropyridine	1.34 ± 0.02 (4)[d]	0.515 (1)
19	4-Cyanophenol	1.58 ± 0.04 (2)	0.667 (1)
20	*N,N*-Dimethylaniline	2.30 ± 0.01 (3)	1.430 (1)
21	*m*-Dinitrobenzene	1.49 ± 0.00 (2)	0.614 ± 0.006 (2)
22	2-Ethylpyridine	1.69 ± 0.08 (5)[d]	0.962 ± 0.09 (3)
23	4-Fluorophenol	1.79 ± 0.03 (2)	0.888 (1)
24	Hexaldehyde	1.78 (2)[d]	0.984 (1)
25	2,6-Lutidine	1.68 ± 0.15 (4)[d]	0.842 ± 0.1 (3)
26	4-Nitrophenol	1.68 ± 0.01 (3)	0.741 (1)
27	2-Pentanone	0.91 ± 0.03 (4)[d]	−0.0105 (1)
28	Phenol	1.48 ± 0.02 (5)	0.609 ± 0.009 (3)
29	Phenylacetonitrile	1.56 (1)	0.654 ± 0.03 (2)
30	3-Picoline	1.20 ± 0.02 (3)	0.654 (1)
31	4-Picoline	1.18 (1)	0.533 (1)
32	Pyridine	0.63 ± 0.02 (4)	0.301 (1)
33	Quinoline	2.04 ± 0.02 (4)	1.290 (1)

[a] Average ± *SD* (number of determinations or dilutions). [b] Values from Pomona College Medicinal Chemistry Project (Claremont, Calif.), unless otherwise indicated. Corrected for ionization using pKa corrected to 25° (A. Albert and E. P. Serjeant, "Ionization Constants of Acids and Bases," Wiley, New York, N.Y., 1962). [c] Octadecylsilane coated with octanol, using octanol-saturated pH 7.00 (0.01 *M*) phosphate buffer as the mobile phase; ambient temperature. Each point is the average of at least two injections. Number in parentheses is the number of independent determinations on different columns. All data were related back to a single set of conditions by simple linear regression using overlapping series of compounds. [d] This work; same solutions and temperatures (25 ± 1°) as HPLC work.

least-squares estimates of errors in P and K somewhat biased (the estimates of P and K are correct). However, in practice, fitting experimental data to the nonlinear form $\log D = \log P - \log [1 + (K_a/H)]$, where the error analysis is correct, gives virtually identical errors as found in the linearized Eqs. 2*a* and 2*b*. Therefore, propagation of error does not appear to be serious. [Note that $s_{\log y} = (0.4343 s_y)/y$, where s is the standard deviation (12)]. Furthermore, for any two pH values, the following equations can be derived:

$$K_a = H_1H_2(D_1 - D_2)/(H_1D_2 - H_2D_1) \quad \text{(Eq. 3a)}$$

$$s_{K_a} = [1/(H_1D_2 - H_2D_1)^2][(D_1 - D_2)^2(H_2^4D_1^2s_{H_1}^2 + H_1^4D_2^2s_{H_2}^2) + H_1^2H_2^2(H_1 - H_2)^2(D_2^2s_{D_1}^2 + D_1^2s_{D_2}^2)]^{1/2} \quad \text{(Eq. 3b)}$$

$$K_a{}^b = (D_1 - D_2)/(H_1D_1 - H_2D_2) \quad \text{(Eq. 3c)}$$

$$s_{K_a{}^b} = [1/(H_1D_1 - H_2D_2)^2][(D_1 - D_2)^2(D_1^2s_{H_1}^2 + D_2^2s_{H_2}^2) + (H_1 - H_2)^2(D_2^2s_{D_1}^2 + D_1^2s_{D_2}^2)]^{1/2} \quad \text{(Eq. 3d)}$$

and the standard deviation in K_a can be estimated by propagation of error. The results also agree closely with those of ordinary least squares near the pKa.

Some comparisons of pKa values determined by the reversed-phase HPLC and other procedures are given in Table III. The procedure is clearly sufficiently accurate for quantitative structure–activity studies and requires only a small amount of material, which can be impure if the impurity separates from the main peak. To increase the degrees of freedom, each observation (injection) can be used instead of averages. Errors for pKa are slightly larger than those for log P by the HPLC procedure, but they are comparable to other methods. Furthermore, this result is not always found in other series of compounds.

The overall correlation between log $P_{\text{shake flask}}$ and log k', including

Table III—Comparison of Log P and Apparent $pK_a^{\text{Octanol/Water}}$ Determined Simultaneously by HPLC with Literature Values

Compound	HPLC[a] pKa	HPLC[a] Log P	Literature[b] pKa	Literature[b] Log P
Naproxen	4.28 ± 0.02[c]	3.21 ± 0.01[c]	4.53 ± 0.06[c,d]	3.18
	4.21 ± 0.02[e]	3.20 ± 0.01[e]	4.39 ± 0.02[d,e]	
			4.15[f]	
			4.57[c,g]	
			4.6	
Benzoic acid	4.33 ± 0.02[c]	1.78 ± 0.01[c]	4.20[c]	1.87
	4.38 ± 0.03[e]	1.77 ± 0.01[e]	4.18	
Salicylic acid	3.52 ± 0.03[c]	2.00 ± 0.01[c]	3.00	2.23 ± 0.03[h]
	3.29 ± 0.03[e]	2.18 ± 0.01[e]		
p-Toluic acid	4.30 ± 0.09[c]	2.22 ± 0.02[c]	4.37	2.27
	4.41 ± 0.01[e]	2.26 ± 0.01[e]		

[a] Three or four injections at each of two to four pH values at indicated ionic strength; each injection was converted to log D (then D) by use of standards and used to fit Eq. 1*a*. [b] See Table II, footnote *b*. The pKa values corrected to 25° from Albert and Serjeant or G. Kortüm, W. Vogel, and K. Andrussow, "Dissociation Constants of Organic Acids in Aqueous Solution," Butterworths, London, England, 1961, unless otherwise indicated. [c] $n = 0.1$. [d] Spectrophotometric. [e] $\mu = 0.01$. [f] Titration in water; 25°. [g] Titration in ethanol, extrapolated to 0% ethanol. [h] Average of three literature values.

all points (Fig. 2), is given by:

$$\log P = 1.025\ (0.061) \log k' + 0.797\ (0.061) \quad \text{(Eq. 4)}$$

$$n = 33 \quad s = 0.127 \quad r = 0.987 \quad F_{1,31} = 1167$$

where F is the overall F test for the regression, and the 95% confidence limits on the regression coefficients are given in parentheses. Omitting the relatively unhindered pyridine, 3- and 4-picolines, and 2-amino-4-picoline yields:

$$\log P = 1.002\ (0.025) \log k' + 0.853\ (0.026) \quad \text{(Eq. 5)}$$

$$n = 29 \quad s = 0.051 \quad r = 0.998 \quad F_{1,27} = 6643$$

The compounds 2-ethylpyridine and quinoline deviate by 2.48 and 2.07 *SD*, respectively, from calculated values. These compounds are slightly more hindered and weaker bases than pyridine and the picolines. Omitting these two compounds yields:

$$\log P = 1.008\ (0.020) \log k' + 0.857\ (0.021) \quad \text{(Eq. 6)}$$

$$n = 27 \quad s = 0.040 \quad r = 0.999 \quad F_{1,25} = 10{,}533$$

All points are now less than 2 *SD* from calculated values using Eq. 6, and hindered, weakly basic pyridines such as 2,6-lutidine and acridine are easily accommodated by this equation. Thus, essentially perfect agreement between shake-flask and reversed-phase HPLC procedures using octanol over a log D range of 3.5 units is obtained. Only small, basic, unhindered pyridines deviate, presumably because of binding to residual silinol sites. Since most drugs are considerably larger, this deviation should not pose a practical limitation. Furthermore, it seems only prudent that at least one member of a potentially suspect series should be determined by classical procedures and the agreement with the reversed-phase HPLC values established. Finally, other reversed-phase packing materials from other sources were not investigated; presumably, they would differ in the extent of free silinol sites after persilation (5).

REFERENCES

(1) A. Leo, C. Hansch, and D. Elkins, *Chem. Rev.*, **71**, 525 (1971).

(2) T. Fujita, J. Iwasa, and C. Hansch, *J. Am. Chem. Soc.*, **86**, 5175 (1964).

(3) G. L. Biagi, A. M. Barbaro, M. F. Bamba, and M. C. Guerra, *J. Chromatogr.*, **41**, 371 (1969).

(4) W. J. Haggerty, Jr., and E. A. Murrill, *Res./Dev.*, **25**, 30 (1974).

(5) J. M. McCall, *J. Med. Chem.*, **18**, 549 (1975).

(6) T. Fujita, T. Nishioka, and M. Nakajima, *ibid.*, **20**, 1071 (1977).

(7) A. Hulshoff and J. H. Perrin, *J. Chromatogr.*, **129**, 263 (1976).

(8) M. S. Mirrlees, S. J. Moulton, C. T. Murphy, and P. J. Taylor, *J.*

Med. Chem., **19**, 615 (1976).
(9) D. Henry, J. H. Block, J. L. Anderson, and G. R. Carlson, *ibid.*, **19**, 619 (1976).
(10) R. A. Scherrer and S. M. Howard, *ibid.*, **20**, 53 (1977).
(11) C. Horváth, W. Melander, and I. Molnár, *Anal. Chem.*, **49**, 142 (1977).
(12) W. E. Deming, "Statistical Adjustment of Data," Dover, New York, N.Y., 1943, p. 45.

ACKNOWLEDGMENTS

The authors thank Dr. David Johnson, Dr. Richard Runkel, and Dr. David Robertson for permission to cite their pKa determinations on naproxen and Dr. Richard Jones for access to his NLNMRQ modification of Metzler's (Upjohn) NONLIN program.

This paper is contribution 500 from the Syntex Institute of Organic Chemistry.

Substituted Tetralins VI: Tentative Assignment of Absolute Stereochemistry of 1-Methyl-1-phenyl-1,2,3,4-tetrahydro-3-naphthoic Acid and *N,N*,1-Trimethyl-1-phenyl-1,2,3,4-tetrahydro-3-naphthylamine Isomers

D. R. GALPIN, E. M. KANDEEL, and A. R. MARTIN *x

Received November 21, 1977, from the *College of Pharmacy, Washington State University, Pullman, WA 99164.* Accepted for publication January 31, 1978. *Present address: Department of Pharmaceutical Sciences, College of Pharmacy, University of Arizona, Tucson, AZ 85721.

Abstract □ The absolute configurations of the enantiomers of *N,N*,1-trimethyl-*cis*- and *trans*-1-phenyl-1,2,3,4-tetrahydro-3-naphthylamines (I*a* and I*b*) were assigned tentatively from the circular dichroism spectrum of a bridged ketone derived by cyclization of optically active 1-methyl-*cis*-1-phenyl-1,2,3,4-tetrahydro-3-naphthoic acid (II*a*). Thus, (−)-II*a* and the corresponding amine, (−)-I*a*, were assigned the (2*S*, 4*R*)-configuration. Epimerization of (−)-II*a* through its methyl ester yielded the *trans*-acid, (−)-II*b*, which established the absolute configuration of (−)-II*b* and the corresponding amine, (−)-I*b*, as (2*R*, 4*R*).

Keyphrases □ Tetralins, substituted—absolute configurations of enantiomers of 1-methyl-1-phenyl-1,2,3,4-tetrahydro-3-naphthoic acid and *N,N*,1-trimethyl-1-phenyl-1,2,3,4-tetrahydro-3-naphthylamine assigned □ Naphthoic acids and naphthylamines, substituted—absolute configurations of enantiomers assigned □ Stereochemistry—substituted naphthoic acids and naphthylamines, absolute configurations assigned

Previous publications described the synthesis of racemic *N,N*,1-trimethyl - 1 - phenyl-1,2,3,4-tetrahydro-3-naphthylamine diastereoisomers (I*a* and I*b*) (1) and the precursors 1-methyl-1-phenyl-1,2,3,4-tetrahydro-3-naphthoic acids (II*a* and II*b*) (2). Since various aminotetralin structures (1) exhibit analgesic (3–5) and/or analgesic antagonist (6) properties in animals, it was desirable to resolve some of the more active racemic compounds and to establish the absolute configuration of the enantiomers. Moreover, the precursor acids are potentially stereoselective anti-inflammatory analgesics.

This report describes the resolution of the diastereoisomeric acids (±)-II*a* and (±)-II*b*, the stereospecific conversion of each enantiomer to the corresponding *N,N*-dimethylamino derivatives, and the tentative assignment of absolute stereochemistry of the acids and amines.

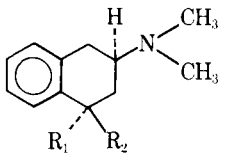

I*a*: $R_1 = CH_3$, $R_2 = C_6H_5$
I*b*: $R_1 = C_6H_5$, $R_2 = CH_3$

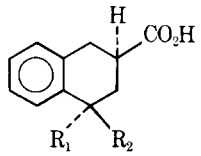

II*a*: $R_1 = CH_3$, $R_2 = C_6H_5$
II*b*: $R_1 = C_6H_5$, $R_2 = CH_3$

DISCUSSION

Stereochemical relationships among stereoisomers I*a*–I*b* and II*a*–II*b* were elucidated by resolution of the acids and stereospecific conversion of II*a* and II*b* to the corresponding amines. Thus, racemic II*a* and II*b* were resolved by fractional recrystallization of their (+)-dehydroabietylamine salts. Each enantiomer was converted to the corresponding primary amine *via* the Curtius reaction. Subsequent Eschweiler–Clarke methylation afforded the tertiary amines. In this manner, (−)-I*a* was obtained from (−)-II*a*, (−)-I*b* was obtained from (−)-II*b*, *etc.*

The absolute configurations of the enantiomeric *cis*-acids, (−)-II*a* and (+)-II*a*, were determined by investigating the spectral properties of the bridged ketone (+)-7,12-dihydro-12-methyl-6,12-methanodibenzo[*a*,*d*]cycloocten-5(6*H*)-one [(+)-III], prepared by cyclization of (−)-II*a* in anhydrous hydrogen fluoride. This cyclization previously was employed to assign the relative stereochemistry of racemic II*a* and II*b* (2).

The absolute configuration of (+)-III was determined from its circular dichroism spectrum (Fig. 1), which exhibited a strong positive Cotton effect for the carbonyl $n \rightarrow \pi^*$ transition. The assignment was made on the basis of the octant rule for aryl ketones developed by Snatzke (7). The aryl ketone chirality rule is an extension of the chirality rules for conjugated enones (7, 8), wherein conjugation of the π-bonds of the aromatic ring with the carbonyl group is formally considered to comprise a combination of both *cisoid*- and *transoid*-enone contributions. In aryl ketones, the *cisoid*- and *transoid*-enone contributions predict the same sign of their Cotton effects and thus reinforce each other.

The aryl ketone chirality rule was employed to predict successfully the sign of the $n \rightarrow \pi^*$ Cotton effect for a wide variety of aryl ketones for which absolute configurations were established independently by chemical synthesis and/or X-ray crystallography. The rule was shown to hold for flavanones (9, 10), α-tetralones (11, 12), respirones and related 9,9′-spirobifluorenone derivatives (13), 1-oxo[2.2]*p*-cyclophanes (14), and 1-oxo[2.2]*m*-cyclophanes (15). In fact, a literature search through August 1977 revealed only one partial exception to the rule, a series of 6-bromo-7-oxoditerpenoids containing an aromatic C-ring (16) for which

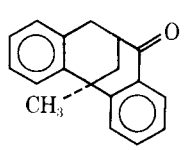

III

0022-3549/78/1000-1367$01.00/0
© 1978, American Pharmaceutical Association

Med. Chem., **19**, 615 (1976).
(9) D. Henry, J. H. Block, J. L. Anderson, and G. R. Carlson, *ibid.*, **19**, 619 (1976).
(10) R. A. Scherrer and S. M. Howard, *ibid.*, **20**, 53 (1977).
(11) C. Horváth, W. Melander, and I. Molnár, *Anal. Chem.*, **49**, 142 (1977).
(12) W. E. Deming, "Statistical Adjustment of Data," Dover, New York, N.Y., 1943, p. 45.

ACKNOWLEDGMENTS

The authors thank Dr. David Johnson, Dr. Richard Runkel, and Dr. David Robertson for permission to cite their pKa determinations on naproxen and Dr. Richard Jones for access to his NLNMRQ modification of Metzler's (Upjohn) NONLIN program.

This paper is contribution 500 from the Syntex Institute of Organic Chemistry.

Substituted Tetralins VI: Tentative Assignment of Absolute Stereochemistry of 1-Methyl-1-phenyl-1,2,3,4-tetrahydro-3-naphthoic Acid and *N,N*,1-Trimethyl-1-phenyl-1,2,3,4-tetrahydro-3-naphthylamine Isomers

D. R. GALPIN, E. M. KANDEEL, and A. R. MARTIN *x

Received November 21, 1977, from the *College of Pharmacy, Washington State University, Pullman, WA 99164.* Accepted for publication January 31, 1978. *Present address: Department of Pharmaceutical Sciences, College of Pharmacy, University of Arizona, Tucson, AZ 85721.

Abstract □ The absolute configurations of the enantiomers of *N,N*,1-trimethyl-*cis*- and *trans*-1-phenyl-1,2,3,4-tetrahydro-3-naphthylamines (I*a* and I*b*) were assigned tentatively from the circular dichroism spectrum of a bridged ketone derived by cyclization of optically active 1-methyl-*cis*-1-phenyl-1,2,3,4-tetrahydro-3-naphthoic acid (II*a*). Thus, (−)-II*a* and the corresponding amine, (−)-I*a*, were assigned the (2*S*, 4*R*)-configuration. Epimerization of (−)-II*a* through its methyl ester yielded the *trans*-acid, (−)-II*b*, which established the absolute configuration of (−)-II*b* and the corresponding amine, (−)-I*b*, as (2*R*, 4*R*).

Keyphrases □ Tetralins, substituted—absolute configurations of enantiomers of 1-methyl-1-phenyl-1,2,3,4-tetrahydro-3-naphthoic acid and *N,N*,1-trimethyl-1-phenyl-1,2,3,4-tetrahydro-3-naphthylamine assigned □ Naphthoic acids and naphthylamines, substituted—absolute configurations of enantiomers assigned □ Stereochemistry—substituted naphthoic acids and naphthylamines, absolute configurations assigned

Previous publications described the synthesis of racemic *N,N*,1-trimethyl - 1 - phenyl-1,2,3,4-tetrahydro-3-naphthylamine diastereoisomers (I*a* and I*b*) (1) and the precursors 1-methyl-1-phenyl-1,2,3,4-tetrahydro-3-naphthoic acids (II*a* and II*b*) (2). Since various aminotetralin structures (1) exhibit analgesic (3–5) and/or analgesic antagonist (6) properties in animals, it was desirable to resolve some of the more active racemic compounds and to establish the absolute configuration of the enantiomers. Moreover, the precursor acids are potentially stereoselective anti-inflammatory analgesics.

This report describes the resolution of the diastereoisomeric acids (±)-II*a* and (±)-II*b*, the stereospecific conversion of each enantiomer to the corresponding *N,N*-dimethylamino derivatives, and the tentative assignment of absolute stereochemistry of the acids and amines.

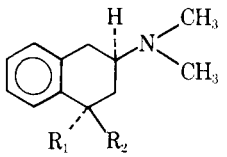

I*a*: $R_1 = CH_3$, $R_2 = C_6H_5$
I*b*: $R_1 = C_6H_5$, $R_2 = CH_3$

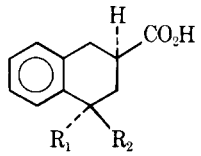

II*a*: $R_1 = CH_3$, $R_2 = C_6H_5$
II*b*: $R_1 = C_6H_5$, $R_2 = CH_3$

DISCUSSION

Stereochemical relationships among stereoisomers I*a*–I*b* and II*a*–II*b* were elucidated by resolution of the acids and stereospecific conversion of II*a* and II*b* to the corresponding amines. Thus, racemic II*a* and II*b* were resolved by fractional recrystallization of their (+)-dehydroabietylamine salts. Each enantiomer was converted to the corresponding primary amine *via* the Curtius reaction. Subsequent Eschweiler–Clarke methylation afforded the tertiary amines. In this manner, (−)-I*a* was obtained from (−)-II*a*, (−)-I*b* was obtained from (−)-II*b*, *etc.*

The absolute configurations of the enantiomeric *cis*-acids, (−)-II*a* and (+)-II*a*, were determined by investigating the spectral properties of the bridged ketone (+)-7,12-dihydro-12-methyl-6,12-methanodibenzo[*a*,*d*]cycloocten-5(6*H*)-one [(+)-III], prepared by cyclization of (−)-II*a* in anhydrous hydrogen fluoride. This cyclization previously was employed to assign the relative stereochemistry of racemic II*a* and II*b* (2).

The absolute configuration of (+)-III was determined from its circular dichroism spectrum (Fig. 1), which exhibited a strong positive Cotton effect for the carbonyl $n \rightarrow \pi^*$ transition. The assignment was made on the basis of the octant rule for aryl ketones developed by Snatzke (7). The aryl ketone chirality rule is an extension of the chirality rules for conjugated enones (7, 8), wherein conjugation of the π-bonds of the aromatic ring with the carbonyl group is formally considered to comprise a combination of both *cisoid*- and *transoid*-enone contributions. In aryl ketones, the *cisoid*- and *transoid*-enone contributions predict the same sign of their Cotton effects and thus reinforce each other.

The aryl ketone chirality rule was employed to predict successfully the sign of the $n \rightarrow \pi^*$ Cotton effect for a wide variety of aryl ketones for which absolute configurations were established independently by chemical synthesis and/or X-ray crystallography. The rule was shown to hold for flavanones (9, 10), α-tetralones (11, 12), respirones and related 9,9′-spirobifluorenone derivatives (13), 1-oxo[2.2]*p*-cyclophanes (14), and 1-oxo[2.2]*m*-cyclophanes (15). In fact, a literature search through August 1977 revealed only one partial exception to the rule, a series of 6-bromo-7-oxoditerpenoids containing an aromatic C-ring (16) for which

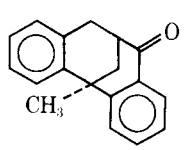

III

0022-3549/78/1000-1367$01.00/0
© 1978, American Pharmaceutical Association

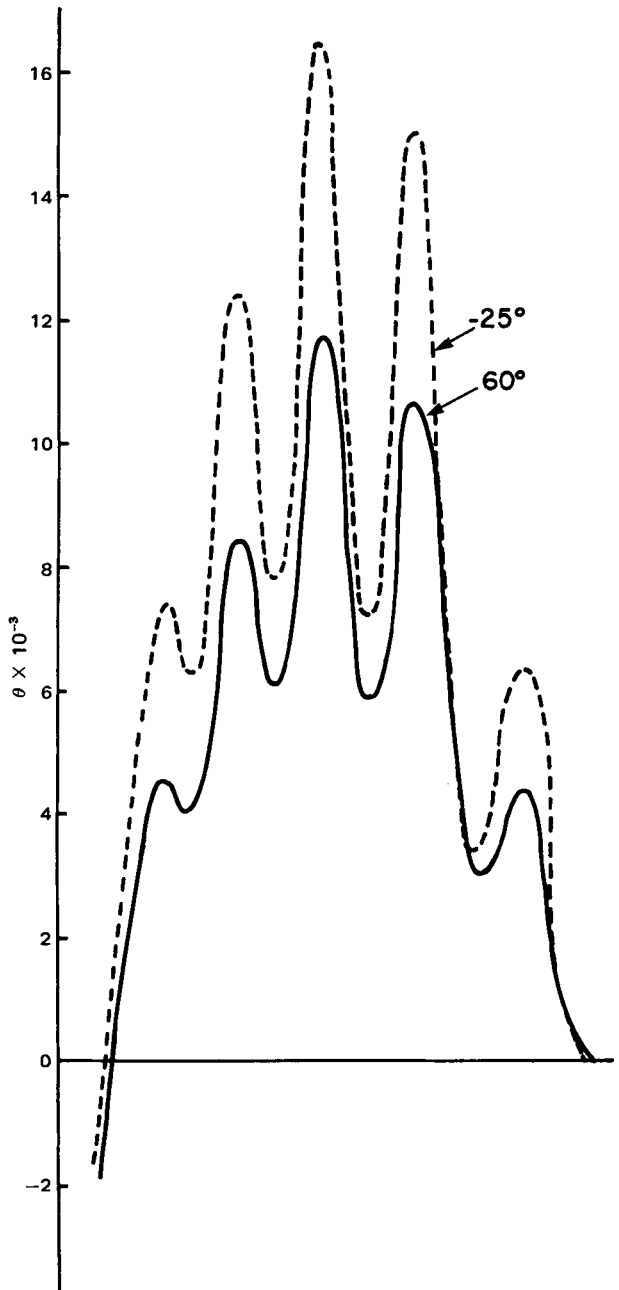

Figure 1—*Circular dichroism curves (isooctane) of (+)-(III) at 60° (—) and at −25° (- - -).*

the rule predicts the correct sign of the Cotton effect of the $n \rightarrow \pi^*$ transition but fails to provide a reliable guide to the orientation of the α-bromo substituent.

An examination of a Dreiding model of III reveals that the preferred conformation of this molecule is one where both nonaromatic rings are in half-chair conformations with all vicinal hydrogen atoms staggered. Deviation from this conformation leads to the eclipsing of several bonds. In this preferred conformation, the octant rule for aryl ketones predicts the absolute configuration of (+)-III to be (6*S*, 12*S*). Furthermore, the nonconjugated aromatic ring is oriented in a pseudoaxial conformation with respect to the aryl ketone system and thus lies in a positive octant to reinforce the positive Cotton effect. Comparative depictions are shown in Fig. 2. Since (+)-III was derived from (−)-II*a* with retention of the configuration (1), the absolute configuration of (−)-II*a* is (2*S*, 4*R*).

Because some conformational mobility is possible for (+)-III, it was necessary to establish that the fully staggered conformation dominated the sign of the Cotton effect. A temperature study in isooctane at three

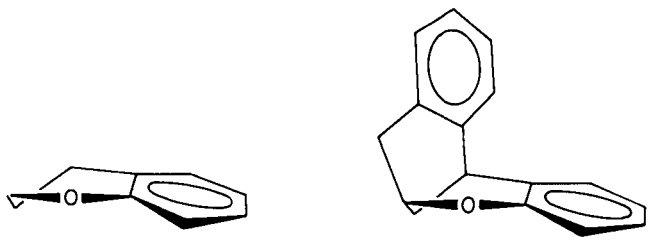

Figure 2—*Projection drawing showing a conformation of aryl ketones which produces a (+)-Cotton effect [after Snatzke (8)] and (+)-III in the preferred conformation.*

different temperatures supported this conclusion. The high- and low-temperature circular dichroism curves are shown in Fig. 1. (An intermediate curve at 25°, which lies between those presented, was omitted for clarity. The data, however, are given under *Experimental*.)

Inspection of the curves reveals that the Cotton effect increases as the temperature is decreased, which is consistent with the argument that the preferred conformation is determining the sign. This result could also be interpreted on the basis of increased solvation (17), where the more solvated species gives rise to a positive Cotton effect. However, the lack of a hypsochromic shift and the more prominent fine structure observed with decreasing temperature suggest that solvation effects are minimal over the temperature range examined (17). A similar enhancement of the carbonyl Cotton effect and its fine structure in 1-tetralone compounds upon lowering the temperature also was attributed to changes in conformer populations (18). By comparison, a slight blue shift is accompanied by a loss of fine structure when the solvent is changed from isooctane to methanol (see *Experimental*).

Separate equilibrations of the methyl esters of both (−)-II*a* and (−)-II*b* with sodium methoxide in refluxing methanol yielded identical results. The equilibrium mixture of esters had a *cis* to *trans* ratio of approximately 40:60, as judged from the optical rotation of the mixture and integration of the signals of the nonequivalent ester methyl groups in the NMR spectrum. The optical rotation of the mixture indicated that the (−)-*cis*-ester epimerized to the (−)-*trans*-isomer. This configurational relationship was confirmed with the isolation of (−)-II*b* from the mixture of acids obtained following hydrolysis of the equilibrium products of the ester of (−)-II*a*. Thus, the absolute configuration of (−)-II*b* and the stereochemically related amine (−)-I*b* is (2*R*, 4*R*).

An X-ray crystallographic investigation of the hydrobromide salt of (+)-I*b* is in progress. Also in progress is the synthesis of sufficient quantities of I*a* and I*b* enantiomers for analgesic and analgesic antagonist evaluation.

EXPERIMENTAL

Melting points were obtained on a melting block and are uncorrected. Elemental analyses were within ±0.4% of theory. NMR spectra were obtained[1] in carbon tetrachloride with tetramethylsilane as an internal reference. Optical rotations were measured in a 1-dcm cell in a half-shade polarimeter[2] at ambient temperatures and are probably accurate to 3°. The diastereoisomeric salts were subjected to differential thermal analysis to establish purity.

(+)-Dehydroabietylamine—Crude (+)-dehydroabietylamine was purified by its conversion to the acetate salt, which was recrystallized to a constant melting point according to the literature procedure (19), mp 45° [lit. (19) mp 44–45°].

(−)-1-Methyl-*trans*-1-phenyl-1,2,3,4-tetrahydro-3-naphthoic Acid [(−)-II*b*]—To a solution of 2.50 g (9 mmoles) of (+)-dehydroabietylamine (19) dissolved in 210 ml of boiling ethanol was added 2.40 g (9 mmoles) of II*b*. The solution was chilled, and the precipitate was collected and dried to give 4.8 g of a mixture of the diastereomeric salts. Fractional recrystallization from 95% ethanol yielded 2.0 g of white needles, mp 186.5–187°.

The dehydroabietylamine salt was shaken gently with a mixture of 40 ml of 10% sodium carbonate and 100 ml of ether until the solid had dis-

[1] Varian T-60 spectrometer.

[2] Dubosq-Pellin precision model. Although this instrument is graduated to 0.01° (using the vernier scale), inability to perceive a difference in the halves covered a range as high as 0.20°. If it is assumed that the midpoint of this range could be estimated with an accuracy of 0.05°, specific rotations would be in error by 2.5° at the lowest concentrations employed.

solved. The aqueous layer was separated and extracted twice with small portions of ether. After acidification, the aqueous phase was extracted twice with ether; the combined ether extracts were washed once with water and dried over anhydrous sodium sulfate. Solvent removal gave crystals of (−)-II*b*, which were recrystallized from 95% ethanol, mp 177.5–178.5°, $[\alpha]_D^{26}$ −100° (c 5, carbon tetrachloride).

(+)-1- Methyl-*trans*-1-phenyl-1,2,3,4-tetrahydro-3-naphthoic Acid [(+)-II*b*]—The mother liquors remaining from the isolation of the dehydroabietylamine salt of (−)-II*b* were diluted intermittently with water over several days; each addition generated the formation of crystals. When a sufficient quantity accumulated, it was isolated and recrystallized from 95% ethanol to give 1.5 g of white crystals, mp 162°. The free acid was recovered in the same manner as described for the (−)-isomer, producing 0.7 g of white needles, mp 175–176°, $[\alpha]_D^{27}$ +96° (c 5, carbon tetrachloride).

(−)-1-Methyl-*cis*-1-phenyl-1,2,3,4-tetrahydro-3-naphthoic Acid [(−)-II*a*]—A mixture of diastereomeric dehydroabietylamine salts of II*a* was obtained and resolved in the same manner as described for II*b*. The first salt isolated and purified had a melting point of 184–186° and yielded (−)-II*a* as an amorphous powder, mp 94–105°, $[\alpha]_D^{25}$ −33° (c 3, carbon tetrachloride).

(+)-1-Methyl-*cis*-1-phenyl-1,2,3,4-tetrahydro-3-naphthoic Acid [(+)-II*a*]—The second salt obtained from the mother liquors of the isolation of (−)-II*a* was purified by recrystallization (ethanol) to yield white needles, mp 167–168°. Liberation of the free acid gave (+)-II*a* as an amorphous powder, mp 95–105°, $[\alpha]_D^{27}$ +30° (c 3, carbon tetrachloride).

(+)- and (−)-7,12-Dihydro-12-methyl-6,12-methanodibenzo[*a,d*]cyclooctene-5(6*H*)-one [(+)- and (−)-III]—The cyclization of 0.3 g of (−)-II*a* in 20 g of anhydrous hydrogen fluoride in a procedure identical to that described previously (2) for the synthesis of racemic ketone III yielded 0.25 g of (+)-III as colorless crystals, mp 145–146°, $[\alpha]_D^{27}$ +96° (c 2, methanol). Compound (−)-III was prepared in an identical fashion from (+)-II*a*, mp 145–146°, $[\alpha]_D^{26}$ −97° (c 3, carbon tetrachloride).

Epimerization of (−)-II*a*—This method was employed to isomerize both (−)-II*a* and (−)-II*b* and yielded the same results in each case. The procedure for (−)-II*a* is described.

A solution of 0.3 g of (−)-II*a* in 30 ml of absolute methanol containing 1 ml of sulfuric acid was refluxed overnight. The reaction solution was diluted with cold water and extracted twice with small portions of carbon tetrachloride. The combined extracts were washed once with 5% sodium bicarbonate and once with water and dried over anhydrous sodium sulfate. Removal of solvent yielded a viscous oil, $[\alpha]_D^{25}$ −20° (c 5, carbon tetrachloride). The NMR spectrum exhibited a methyl group signal at δ 3.60 ppm; no signal for an acid proton was detected. The methyl ester of (−)-II*b* prepared in a similar fashion showed an NMR signal for the ester methyl group at δ 3.55 ppm, $[\alpha]_D^{26}$ −94° (c 4, carbon tetrachloride).

The ester was dissolved in 25 ml of a solution of sodium methoxide (prepared by adding a small piece of sodium metal to freshly distilled, magnesium-dried methanol) and refluxed for 10 hr. The resulting mixture of esters of (−)-II*a* and (−)-II*b* was isolated as described for the ester of (−)-II*a*. The NMR spectrum of this mixture displayed nonequivalent signals of the methyl groups for the two isomers for both the ester and C-4 methyl functions. Integration of the ester methyl signals indicated an isomer composition of approximately 60% *trans*–40% *cis*. The specific rotation ($[\alpha]_D^{26}$ −60.2°) of the crude reaction workup was also consistent with this isomer ratio.

This mixture of esters was hydrolyzed by refluxing for 2 hr in a basic solution of methanol–water. The system was cooled, acidified to pH 2, and extracted three times with small portions of carbon tetrachloride. The combined extracts were washed twice with water and dried over anhydrous sodium sulfate. After removing the solvent, the white solid residue was dissolved in a minimal quantity of boiling ether, diluted with an equal amount of petroleum ether, and chilled. The colorless crystals of (−)-II*b*, which deposited, had a melting point of 174–177° and $[\alpha]_D^{26}$ −93.3° (c 2, carbon tetrachloride). The NMR spectrum showed essentially pure *trans*-acid; no *cis*-isomer was detected.

Circular Dichroism Spectra of (+)-III—The circular dichroism spectra were obtained on a recording spectropolarimeter[3] in spectrograde solvents. The room temperature spectra were measured in 1.0–0.010-cm cells at 0.5 mg/ml. The temperature study was conducted in a 5.0-cm jacketed cell connected to a thermostated bath regulated to ±0.1°; concentrations ranged from 0.1 to 0.01 mg/ml. Data are expressed in values of $[\theta] \times 10^{-3}$ for the maxima (λ) and the points of inflection (λ_i).

With methanol at 25°, c = 0.506: 382.5 (0), 375i (+1.42), 355i (8.39), 339 (+13.3), 328 (+13.0), 307.5 (0), 290 (−4.41), 283 (0), 262 (+42.6), 247 (0), and 215 (123).

With isooctane at 25°, c = 0.53: 387.5 (0), 376 (+4.92), 367.5 (+2.90), 358.5 (+11.6), 350.5 (+5.90), 344 (+12.7), 335 (+6.10), 329 (+9.08), 321 (+4.03), 317.5 (+4.64), 308.5 (0), 290 (−9.18), 277.5 (0), 264–260 (+43.5) (shoulder), 254 (+57.6), 242 (0), 224 (−89.8), 218 (−70.2), and 215 (−84.3).

With isooctane at 60°, c = 0.106: 388 (0), 376 (+4.45), 367.5 (+2.95), 358.5 (+10.7), 350.5 (+5.95), 343 (+11.8), 335 (+6.09), 329.5 (+8.57), 320 (+4.07), 317 (+4.35), 308 (0), 290 (−8.24), 277.5 (0), 264 (+40.8) (shoulder), 254 (+55.8), and 250 (+44.4).

With isooctane at −25°, c = 0.0106: 388 (0), 376 (+6.41), 367.5 (+3.42), 358.4 (+15.1), 350.5 (+7.16), 343 (+16.6), 335 (+7.77), 329 (+12.5), 321.5 (+6.18), 317 (+7.49), 308 (0), 291.5 (−6.74), 277.5 (0), and 275 (+9.83).

(−)-*N,N*,1-Trimethyl-*trans*-1-phenyl - 1,2,3,4 - tetrahydro - 3-naphthylamine Hydrochloride [(−)-I*b*]—A mixture of 0.8 g (3 mmoles) of (−)-II*b* and 1 ml of freshly distilled thionyl chloride was refluxed 4 hr. The excess thionyl chloride was removed *in vacuo* (aspirator), leaving the acid chloride. Then the acid chloride was dissolved in 5 ml of dry reagent grade acetone. The solution was chilled in an ice bath and, with vigorous stirring, a chilled solution of 0.2 g (3 mmoles) of sodium azide in 1 ml of water was added over 1 min. The mixture was stirred for 10 min, 10 ml of cold water was added, and the crude azide was extracted into dry xylene. The extract was washed with saturated sodium chloride solution and then filtered through anhydrous magnesium sulfate.

Rearrangement of the azide to the isocyanate was accomplished by applying vacuum (aspirator) to the xylene solution contained in a 50-ml flask and stirring vigorously with a magnetic stirrer. The evolution of nitrogen was in evidence for about 2 hr. The vacuum was then removed, the flask was fitted with a reflux condenser, and the solution was heated to the boiling point. Xylene was then distilled off *in vacuo*, yielding the isocyanate. Concentrated hydrochloric acid (5 ml) was added cautiously to the isocyanate; after the exothermic reaction subsided, the brownish solution was refluxed overnight. Distilled water was then added, and the solution was extracted with ether. The acidic aqueous solution was then evaporated, and the residue was dissolved in 10% KOH and extracted twice with ether.

The ether extracts were combined and dried over anhydrous potassium carbonate, and the ether was distilled to yield the primary amine. The crude amine was dissolved in 1 ml (2 mmoles) of 90% formic acid, 1 ml of 37% formaldehyde was then added, and the mixture was refluxed for 8 hr. After the mixture cooled, 0.5 ml of concentrated hydrochloric acid was added, and the mixture was evaporated *in vacuo* (aspirator) to dryness. To the residue was added 10% KOH, and the mixture was extracted twice with ether.

The ether extracts were combined, dried over anhydrous potassium carbonate, and decanted to a dry flask. Dry ethereal hydrogen chloride was added to the dry ether solution of the amine, causing 0.4 g (45%) of the hydrochloride salt (−)-I*b* to precipitate as yellowish-white needles, mp 221–223° (from chloroform–ether), $[\alpha]_D^{27}$ −104° (c 3, methanol).

Anal.—Calc. for $C_{19}H_{24}ClN$: C, 75.60; H, 8.01; N, 4.64. Found: C, 75.15; H, 7.85; N, 4.82.

(+)-*N,N*,1-Trimethyl-*trans*-1-phenyl - 1,2,3,4-tetrahydro-3-naphthylamine Hydrochloride [(+)-I*b*]—With the same procedure employed for the preparation of (−)-I*b*, 0.8 g (29 mmoles) of (+)-II*b* gave 0.4 g (45%) of (+)-I*b* as yellowish-white needles, mp 220–222° (from chloroform–ether), $[\alpha]_D^{27}$ +106° (c 3, methanol).

Anal.—Calc. for $C_{19}H_{24}ClN$: C, 75.60; H, 8.01; N, 4.64. Found: C, 75.56; H, 7.88; N, 4.43.

(−)- *N,N*,1-Trimethyl-*cis*-1-phenyl-1,2,3,4-tetrahydro-3-naphthylamine Hydrochloride [(−)-I*a*]—Treatment of 0.78 g (28 mmoles) of (−)-II*a* by the same procedure used to prepare (−)-I*b* gave 0.39 g (45%) of (−)-I*a*, mp 252–255° (chloroform–ether), $[\alpha]_D^{27}$ −99.5° (c 3, methanol).

Anal.—Calc. for $C_{19}H_{24}ClN$: C, 75.60; H, 8.01; N, 4.64. Found: C, 75.28; H, 8.14; N, 4.56.

(+)-*N,N*,1-Trimethyl-*cis*-1-phenyl-1,2,3,4-tetrahydro-3-naphthylamine Hydrochloride [(+)-I*a*]—Treatment of 0.72 g (26 mmoles) of (+)-II*a* by the same procedure used to prepare (−)-I*b* gave 0.31 g (44%) of (+)-I*a*, mp 252–255° (from chloroform–ether), $[\alpha]_D^{27}$ +101° (c 3, methanol).

Anal.—Calc. for $C_{19}H_{24}ClN$: C, 75.60; H, 8.01; N, 4.64. Found: C, 75.42; H, 8.06; N, 4.61.

[3] Cary 60, equipped with a 6001 CD attachment.

REFERENCES

(1) E. M. Kandeel and A. R. Martin, *J. Med. Chem.*, **16**, 947 (1973).

(2) E. M. Kandeel, J. L. Anderson, J. H. Block, A. I. White, and A. R. Martin, *J. Pharm. Sci.*, **61**, 1231 (1972).

(3) A. R. Martin, A. P. Parulkar, D. J. Gusseck, L. J. Anderson, G. L. Grunewald, and A. I. White, *ibid.*, **58**, 340 (1969). V. S. Pai, A. P. Parulkar, A. R. Martin, and A. I. White, *ibid.*, **60**, 201 (1971).

(4) J. Maillard, M. Langlois, P. Delaunay, T. V. Van, J. Chenu, R. Morin, M. Benharkate, C. Manuel, and F. Motosso, *J. Med. Chem.*, **15**, 1123 (1972).

(5) M. E. Freed, J. R. Potoski, E. H. Freed, G. L. Conklin, and J. L. Malis, *ibid.*, **16**, 595 (1973). M. E. Freed, J. R. Potoski, E. H. Freed, G. L. Conklin, and S. C. Bell, *ibid.*, **19**, 476 (1976).

(6) D. S. Fries and D. J. Bertelli, MEDI 24, presented at the 174th ACS National Meeting, Chicago, Ill., Aug. 1977.

(7) G. Snatzke, *Tetrahedron*, **21**, 439 (1965).

(8) *Ibid.*, **21**, 413 (1965).

(9) W. Gaffield and A. C. Weiss, Jr., *Chem. Commun.*, **1968**, 29.

(10) W. Gaffield, *Tetrahedron*, **26**, 4093 (1970).

(11) F. Zymalkowski and E. Dornhege, *Justus Liebigs Ann. Chem.*, **728**, 144 (1969).

(12) J. M. Luche, A. Marquet, and G. Snatzke, *Tetrahedron*, **28**, 1677 (1972).

(13) G. Haas, P. B. Hulbert, W. Klyne, V. Prélog, and G. Snatzke, *Helv. Chim. Acta*, **54**, 491 (1971).

(14) H. Falk, P. Reich-Rohrwig, and K. Schlögl, *Tetrahedron*, **26**, 511 (1970).

(15) K. Mislow, M. Brzechffa, H. W. Gschwend, and R. T. Puckett, *J. Am. Chem. Soc.*, **95**, 621 (1973).

(16) R. C. Cambie, D. R. Crump, W. A. Denny, and T. J. Fullerton, *Aust. J. Chem.*, **24**, 1237 (1971).

(17) K. M. Wellman, P. H. A. Laur, W. S. Briggs, A. Moscowitz, and C. Djerassi, *J. Am. Chem. Soc.*, **87**, 66 (1965).

(18) J. Barry, H.-B. Kagan, and G. Snatzke, *Tetrahedron*, **27**, 4737 (1971).

(19) W. J. Gottstein and L. C. Cheney, *J. Org. Chem.*, **30**, 2072 (1965).

ACKNOWLEDGMENTS

Presented in part at the 167th ACS National Meeting, Los Angeles, Calif., March 1974, MEDI 45. At that time, the stereochemistry of (−)-*Ib* was erroneously assigned as (2*S*, 4*S*).

Abstracted in part from the thesis submitted by E. M. Kandeel to Washington State University in partial fulfillment of the Doctor of Philosophy degree requirements.

Supported by Grants MH21009 from the National Institute of Mental Health and DA00117 from the National Institute on Drug Abuse.

Pharmacokinetics of Drug Permeation through Human Skin

S. K. CHANDRASEKARAN ˣ, W. BAYNE, and J. E. SHAW

Received August 8, 1977, from *Alza Research, Palo Alto, CA 94304.* Accepted for publication January 30, 1978.

Abstract □ Based on sorption and permeation characteristics of scopolamine in human skin *in vitro* and drug elimination kinetics obtained from pharmacokinetic studies, a mathematical model was developed for estimating and optimizing the temporal pattern of scopolamine delivery from a transdermal therapeutic system through human skin *in vivo*. Experimentally measured scopolamine delivery *in vivo* conformed to this model.

Keyphrases □ Permeation, cutaneous—scopolamine, mathematical model for pharmacokinetics in human skin □ Scopolamine—cutaneous permeation, mathematical model for pharmacokinetics in human skin □ Pharmacokinetics—cutaneous permeation of scopolamine, mathematical model for human skin □ Dosage forms—transdermal therapeutic system for scopolamine delivery, mathematical model for pharmacokinetics □ Anticholinergics—scopolamine, cutaneous permeation, mathematical model for pharmacokinetics in human skin

Considerable attention has been focused on drug permeation through skin *in vitro* (1–3). The principal resistance to drug permeation through intact human skin resides within the stratum corneum, which is comprised of dead, partially desiccated, keratinized epidermal cells (3). Transdermal permeation of drugs occurs by Fickian diffusion, with most of the gradient in drug concentration across the entire skin being localized within the stratum corneum (3). There is an experimentally observed disparity between the steady-state diffusivity of the drug in skin and the unsteady-state value computed from transient (time-lag) permeation measurements. This discrepancy can be reconciled using the dual-sorption model, which invokes the coexistence of dissolved and mobile sorbed molecules in equilibrium with site-bound and immobile molecules within the skin (4).

Little effort has been directed to a quantitative understanding of drug permeation through skin *in vivo*, correlation with *in vitro* skin permeation, and a quantitatively understood application of transdermal drug permeation principles to systemic drug administration. The purpose of this study was to examine the kinetics of scopolamine sorption and permeation in human skin to achieve predictable transdermal drug delivery under clinical conditions.

THEORY

***In Vitro* Skin Permeation**—Previously (4), the basic validity of the dual-mode sorption model was demonstrated in the analysis of the permeation characteristics of scopolamine through human skin *in vitro*. The model postulates that sorption occurs by two mechanisms, the first mechanism being a simple dissolution producing mobile and freely diffusible molecules and the second being an adsorption process producing nonmobile molecules that do not participate in the diffusion process. If it is assumed that exchange between mobile and immobile species is rapid compared with the diffusion process and, thus, that a local equilibrium exists between the mobile and immobilized species, the drug concentration in the skin is governed by (4):

$$\left[1 + \frac{C_1^* b^*/k_D}{(1 + C_D b^*/k_D)^2}\right] \frac{\partial C_D}{\partial t} = D \frac{\partial^2 C_D}{\partial x^2} \qquad \text{(Eq. 1)}$$

where the second term within brackets on the left-hand side arises as a consequence of drug immobilization.

Pharmacokinetics—*Oral*—For scopolamine administered orally, the plasma concentration can be represented adequately by a two-compartment pharmacokinetic model after the completion of absorption (5):

$$C_p = Ae^{-at} + Be^{-bt} \qquad \text{(Eq. 2)}$$

0022-3549/78/1000-1370$01.00/0

© 1978, American Pharmaceutical Association

REFERENCES

(1) E. M. Kandeel and A. R. Martin, *J. Med. Chem.*, **16**, 947 (1973).

(2) E. M. Kandeel, J. L. Anderson, J. H. Block, A. I. White, and A. R. Martin, *J. Pharm. Sci.*, **61**, 1231 (1972).

(3) A. R. Martin, A. P. Parulkar, D. J. Gusseck, L. J. Anderson, G. L. Grunewald, and A. I. White, *ibid.*, **58**, 340 (1969). V. S. Pai, A. P. Parulkar, A. R. Martin, and A. I. White, *ibid.*, **60**, 201 (1971).

(4) J. Maillard, M. Langlois, P. Delaunay, T. V. Van, J. Chenu, R. Morin, M. Benharkate, C. Manuel, and F. Motosso, *J. Med. Chem.*, **15**, 1123 (1972).

(5) M. E. Freed, J. R. Potoski, E. H. Freed, G. L. Conklin, and J. L. Malis, *ibid.*, **16**, 595 (1973). M. E. Freed, J. R. Potoski, E. H. Freed, G. L. Conklin, and S. C. Bell, *ibid.*, **19**, 476 (1976).

(6) D. S. Fries and D. J. Bertelli, MEDI 24, presented at the 174th ACS National Meeting, Chicago, Ill., Aug. 1977.

(7) G. Snatzke, *Tetrahedron*, **21**, 439 (1965).

(8) *Ibid.*, **21**, 413 (1965).

(9) W. Gaffield and A. C. Weiss, Jr., *Chem. Commun.*, **1968**, 29.

(10) W. Gaffield, *Tetrahedron*, **26**, 4093 (1970).

(11) F. Zymalkowski and E. Dornhege, *Justus Liebigs Ann. Chem.*, **728**, 144 (1969).

(12) J. M. Luche, A. Marquet, and G. Snatzke, *Tetrahedron*, **28**, 1677 (1972).

(13) G. Haas, P. B. Hulbert, W. Klyne, V. Prélog, and G. Snatzke, *Helv. Chim. Acta*, **54**, 491 (1971).

(14) H. Falk, P. Reich-Rohrwig, and K. Schlögl, *Tetrahedron*, **26**, 511 (1970).

(15) K. Mislow, M. Brzechffa, H. W. Gschwend, and R. T. Puckett, *J. Am. Chem. Soc.*, **95**, 621 (1973).

(16) R. C. Cambie, D. R. Crump, W. A. Denny, and T. J. Fullerton, *Aust. J. Chem.*, **24**, 1237 (1971).

(17) K. M. Wellman, P. H. A. Laur, W. S. Briggs, A. Moscowitz, and C. Djerassi, *J. Am. Chem. Soc.*, **87**, 66 (1965).

(18) J. Barry, H.-B. Kagan, and G. Snatzke, *Tetrahedron*, **27**, 4737 (1971).

(19) W. J. Gottstein and L. C. Cheney, *J. Org. Chem.*, **30**, 2072 (1965).

ACKNOWLEDGMENTS

Presented in part at the 167th ACS National Meeting, Los Angeles, Calif., March 1974, MEDI 45. At that time, the stereochemistry of (−)-*Ib* was erroneously assigned as (2*S*, 4*S*).

Abstracted in part from the thesis submitted by E. M. Kandeel to Washington State University in partial fulfillment of the Doctor of Philosophy degree requirements.

Supported by Grants MH21009 from the National Institute of Mental Health and DA00117 from the National Institute on Drug Abuse.

Pharmacokinetics of Drug Permeation through Human Skin

S. K. CHANDRASEKARAN ˣ, W. BAYNE, and J. E. SHAW

Received August 8, 1977, from *Alza Research, Palo Alto, CA 94304.* Accepted for publication January 30, 1978.

Abstract □ Based on sorption and permeation characteristics of scopolamine in human skin *in vitro* and drug elimination kinetics obtained from pharmacokinetic studies, a mathematical model was developed for estimating and optimizing the temporal pattern of scopolamine delivery from a transdermal therapeutic system through human skin *in vivo*. Experimentally measured scopolamine delivery *in vivo* conformed to this model.

Keyphrases □ Permeation, cutaneous—scopolamine, mathematical model for pharmacokinetics in human skin □ Scopolamine—cutaneous permeation, mathematical model for pharmacokinetics in human skin □ Pharmacokinetics—cutaneous permeation of scopolamine, mathematical model for human skin □ Dosage forms—transdermal therapeutic system for scopolamine delivery, mathematical model for pharmacokinetics □ Anticholinergics—scopolamine, cutaneous permeation, mathematical model for pharmacokinetics in human skin

Considerable attention has been focused on drug permeation through skin *in vitro* (1–3). The principal resistance to drug permeation through intact human skin resides within the stratum corneum, which is comprised of dead, partially desiccated, keratinized epidermal cells (3). Transdermal permeation of drugs occurs by Fickian diffusion, with most of the gradient in drug concentration across the entire skin being localized within the stratum corneum (3). There is an experimentally observed disparity between the steady-state diffusivity of the drug in skin and the unsteady-state value computed from transient (time-lag) permeation measurements. This discrepancy can be reconciled using the dual-sorption model, which invokes the coexistence of dissolved and mobile sorbed molecules in equilibrium with site-bound and immobile molecules within the skin (4).

Little effort has been directed to a quantitative understanding of drug permeation through skin *in vivo*, correlation with *in vitro* skin permeation, and a quantitatively understood application of transdermal drug permeation principles to systemic drug administration. The purpose of this study was to examine the kinetics of scopolamine sorption and permeation in human skin to achieve predictable transdermal drug delivery under clinical conditions.

THEORY

***In Vitro* Skin Permeation**—Previously (4), the basic validity of the dual-mode sorption model was demonstrated in the analysis of the permeation characteristics of scopolamine through human skin *in vitro*. The model postulates that sorption occurs by two mechanisms, the first mechanism being a simple dissolution producing mobile and freely diffusible molecules and the second being an adsorption process producing nonmobile molecules that do not participate in the diffusion process. If it is assumed that exchange between mobile and immobile species is rapid compared with the diffusion process and, thus, that a local equilibrium exists between the mobile and immobilized species, the drug concentration in the skin is governed by (4):

$$\left[1 + \frac{C_1^* b^*/k_D}{(1 + C_D b^*/k_D)^2}\right] \frac{\partial C_D}{\partial t} = D \frac{\partial^2 C_D}{\partial x^2} \qquad \text{(Eq. 1)}$$

where the second term within brackets on the left-hand side arises as a consequence of drug immobilization.

Pharmacokinetics—*Oral*—For scopolamine administered orally, the plasma concentration can be represented adequately by a two-compartment pharmacokinetic model after the completion of absorption (5):

$$C_p = Ae^{-at} + Be^{-bt} \qquad \text{(Eq. 2)}$$

0022-3549/78/1000-1370$01.00/0

© 1978, American Pharmaceutical Association

The urinary excretion rate is given by:

$$R_o = k_E C_p V \qquad \text{(Eq. 3)}$$

where V is the volume of distribution given by:

$$V = \frac{T}{A + B} \qquad \text{(Eq. 4)}$$

and k_E is the elimination rate constant given by:

$$k_E = \frac{ab(A + B)}{Ab + Ba} \qquad \text{(Eq. 5)}$$

Intravenous—During a constant rate intravenous infusion of scopolamine in a two-compartment pharmacokinetic model, the drug excretion rate can be represented by (6):

$$R_I = I\left[1 + \left(\frac{k_E - a}{a - b}\right)e^{-bt} - \left(\frac{k_E - b}{a - b}\right)e^{-at}\right] \qquad \text{(Eq. 6)}$$

After the constant rate infusion, the drug excretion rate is given by:

$$R_I^* = I\left[\left(\frac{k_E - b}{a - b}\right)\left(1 - e^{-at^*}\right)e^{-a(t-t^*)} - \left(\frac{k_E - a}{a - b}\right)(1 - e^{-bt^*})e^{-b(t-t^*)}\right] \qquad \text{(Eq. 7)}$$

where t^* is the termination time of the infusion.

Transdermal Therapeutic System—This system is a multilayer laminate comprised of a drug reservoir, containing scopolamine in a polymeric gel, sandwiched between an impermeable backing membrane and a rate-controlling microporous membrane. On the dermal side of the rate-controlling membrane is an adhesive gel containing scopolamine; this gel layer serves both as an adhesive to secure the system on the skin surface and as an additional drug reservoir to provide an initial priming dose of drug prior to the controlled input of drug to the skin surface (7).

The transport characteristics of scopolamine from the system are determined by molecular diffusion through the various elements of the multilayer laminate. During the priming dose period, drug diffusion from the contact adhesive layer dominates the temporal pattern of drug release. However, during steady-state delivery, rate limitation or control is resident in the microporous membrane.

The scopolamine delivery rate from the system can be adequately approximated by (7):

$$R_S = G + He^{-ht} \qquad \text{(Eq. 8)}$$

where G, h, and H are constants. The first term on the right-hand side represents the steady-state delivery rate; the second term represents the temporal pattern of drug release during the priming dose period.

Mathematical Model—The delivery of scopolamine from a transdermal therapeutic system into and across human skin *in vivo* has been modeled, assuming that drug transport occurs by normal Fickian diffusion, with partition equilibrium of penetrant being maintained at the interlayer boundaries.

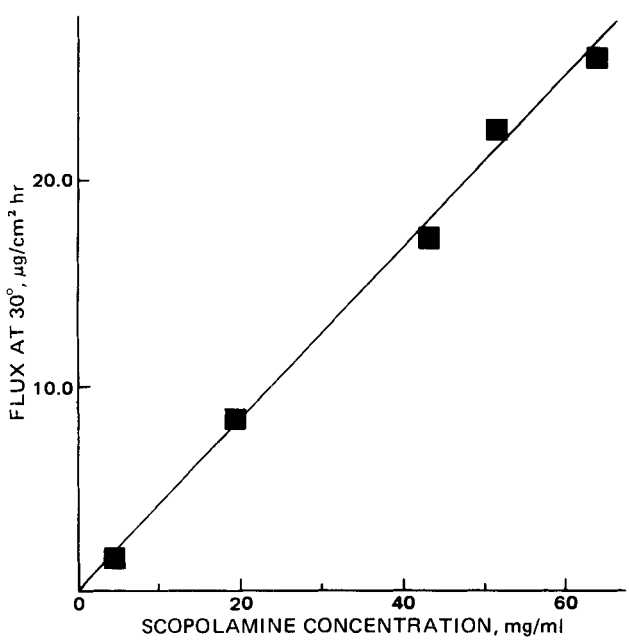

Figure 1—*Effect of concentration on scopolamine flux through human epidermis (epidermis A).*

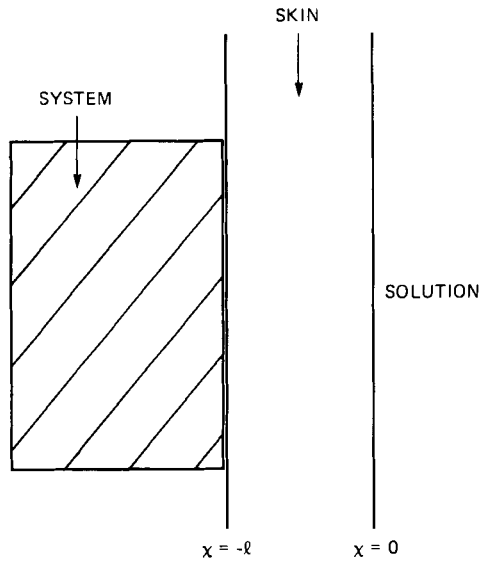

Scheme I—Diagram of system placed on skin.

With reference to Scheme I and the assumption that infinite sink conditions are maintained on the dermal side of the skin, the scopolamine concentration in the skin is given by (4):

$$\frac{\partial C_D}{\partial t} = \frac{D}{\left[1 + \frac{C_I^* b^*/k_D}{(1 + C_D b^*/k_D)^2}\right]}\frac{\partial^2 C_D}{\partial x^2} \qquad \text{(Eq. 9)}$$

with boundary conditions:

$$C_D = 0 \qquad \text{at } x \text{ and } t = 0$$

$$C_D = 0 \qquad \text{at } x = 0 \text{ and } t$$

$$\frac{-D}{\left[1 + \frac{C_I^* b^*/k_D}{(1 + C_D b^*/k_D)^2}\right]}\left.\frac{dC_D}{dx}\right|_{x=-l} = f(t) \qquad \text{at } x = -l \text{ and } t > 0$$

where $f(t) = G + He^{-ht}$.

To provide mathematical simplicity to obtain an analytical solution, it is assumed that, based on experimental data:

$$\frac{C_I^* b^*/k_D}{(1 + C_D b^*/k_D)^2} \simeq \text{constant} = R \qquad \text{(Eq. 10)}$$

Under these conditions, the analytical solution of Eq. 9 is:

$$C_D = \frac{2}{l}\sum_{n=1}^{\infty}(-1)^{n-1}e^{-\alpha(2n-1)^2 t} \sin\frac{(2n-1)\pi x}{2l}\left[\frac{G}{\alpha(2n-1)^2}(e^{(2n-1)^2\alpha t} - 1) + \frac{H}{(2n-1)^2\alpha - h}(e^{[(2n-1)^2\alpha - h]t} - 1)\right] \qquad \text{(Eq. 11)}$$

where $\alpha = \pi^2 D/[4l^2(R + 1)]$.

From mass balance considerations, the drug accumulation in the systemic circulation equals the input of drug *in vivo* minus the excretion of drug *in vivo* and is given by:

$$\frac{dC_p V}{dt} = \frac{D}{R + 1}\left.\frac{dC_D}{dx}\right|_{x=0} - k_E C_p V \qquad \text{(Eq. 12)}$$

where dC_D/dx is the derivative of Eq. 1 with respect to x.

Therefore:

$$\frac{dC_p V}{dt} = k_E C_p V = \frac{4}{\pi}\alpha\sum_{n=1}^{\infty}(-1)^{n-1}(2n-1)e^{-\alpha(2n-1)^2 t} \times\left[\frac{G}{\alpha(2n-1)^2}(e^{(2n-1)^2\alpha t} - 1) + \frac{H}{(2n-1)^2\alpha - h}(e^{[(2n-1)^2\alpha - h]t} - 1)\right] \qquad \text{(Eq. 13)}$$

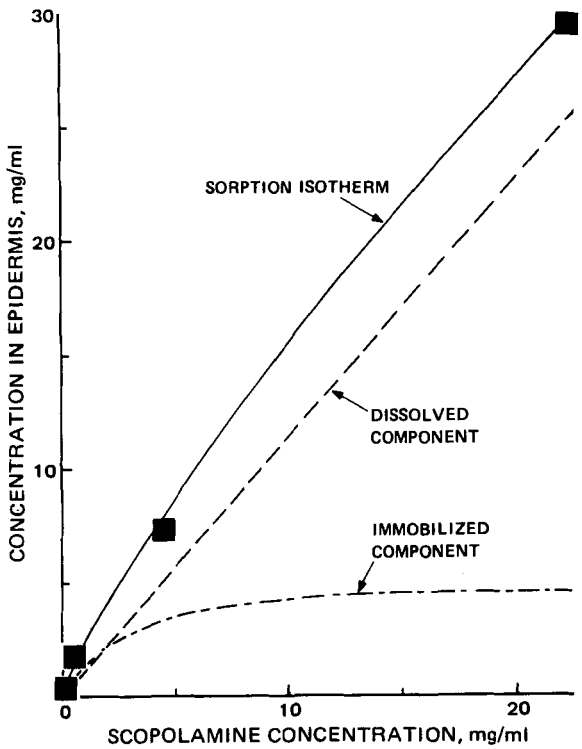

Figure 2—*Scopolamine sorption isotherm in human epidermis* in vitro.

The solution of Eq. 13 is given by:

$$C_pV = \frac{4}{\pi}\alpha e^{-k_E t}\sum_{n=1}^{\infty}(-1)^{n-1}(2n-1) \times\left[\frac{G}{\alpha(2n-1)^2}\left(\frac{e^{k_E t}}{k_E}-\frac{e^{[k_E-\alpha(2n-1)^2]t}}{k_E-\alpha(2n-1)^2}-\frac{1}{k_E}+\frac{1}{k_E-\alpha(2n-1)^2}\right)+\frac{H}{(2n-1)^2\alpha-h}\left(\frac{e^{(k_E-h)t}}{k_E-h}-\frac{e^{[k_E-\alpha(2n-1)^2]t}}{k_E-\alpha(2n-1)^2}-\frac{1}{k_E-h}+\frac{1}{k_E-\alpha(2n-1)^2}\right)\right] \quad \text{(Eq. 14)}$$

From Eqs. 3 and 14, under transdermal drug administration, the model predicts that the urinary drug excretion rate is given by:

$$R_E = \frac{4\alpha}{\pi}k_E\sum_{n=1}^{\infty}(-1)^{n-1}(2n-1) \left[\frac{G}{\alpha(2n-1)^2}\left(\frac{1}{k_E}-\frac{e^{-\alpha(2n-1)^2t}}{k_E-\alpha(2n-1)^2}-\frac{e^{-k_E t}}{k_E}+\frac{e^{-k_E t}}{k_E-\alpha(2n-1)^2}\right)+\frac{H}{(2n-1)^2\alpha-h}\left(\frac{e^{-ht}}{k_E-h}-\frac{e^{-\alpha(2n-1)^2t}}{k_E-\alpha(2n-1)^2}-\frac{e^{-k_E t}}{k_E-h}+\frac{e^{-k_E t}}{k_E-\alpha(2n-1)^2}\right)\right] \quad \text{(Eq. 15)}$$

In the unit of large values for time t:

$$R_E = \frac{4\alpha}{\pi}k_E\sum_{n=1}^{\infty}(-1)^{n-1}\frac{G}{(2n-1)\alpha k_E} = G \quad \text{(Eq. 16)}$$

which implies that, under steady-state conditions, the urinary drug excretion rate will be constant and equal to the steady-state drug input rate.

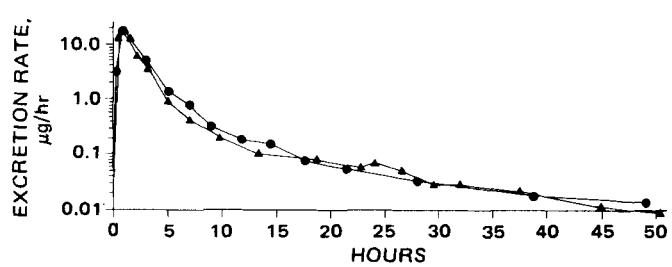

Figure 3—*Urinary excretion rates for scopolamine.*

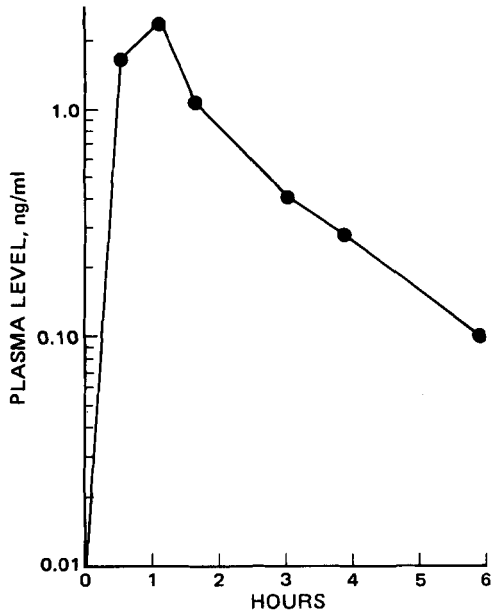

Figure 4—*Plasma levels following oral dose of 906 μg of scopolamine (base).*

After the termination of transdermal scopolamine administration, assuming a linear drug concentration gradient in the skin, the urinary drug excretion rate is given by (8, 9):

$$R_E^* = \alpha\beta k_E\sum_{n=0}^{\infty}\frac{1}{(2n+1)}\sin\left(\frac{2n+1}{2}\right) \times\pi\left[\frac{e^{-(2n+1)^2\alpha t}-e^{-k_E t}}{k_E-(2n+1)^2\alpha}\right] \quad \text{(Eq. 17)}$$

where $\beta = (16lC_D^*)/\pi^3$.

EXPERIMENTAL

***In Vitro* Skin Permeation**—Details of the experimental apparatus and technique were described previously (1, 4). Skin from Caucasian cadavers was in most instances excised from the inner surface of the thigh; samples were preserved in heat-sealed plastic bags, stored at 4° prior to use. Permeation experiments were conducted in glass permeation cells, with concentrated radiolabeled drug confined in one compartment in contact with the stratum corneum surface of the tissue and drug-free solution in the other compartment. Periodic sampling of the downstream solution and assay of drug content by liquid scintillation counting permitted determination of the amount and rate of drug permeation as a function of time.

Equilibrium sorption isotherms were determined by equilibrating a measured weight of isolated epidermis in a relatively large volume of radiolabeled drug solution of known concentration for about 24 hr at 30

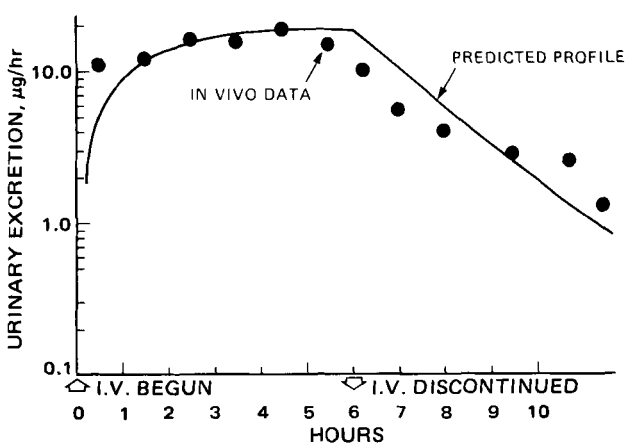

Figure 5—*Urinary excretion of scopolamine base during and following an intravenous infusion.*

Table I—Scopolamine Diffusion Coefficients (Epidermis A)

Scopolamine Solution Concentration, C, mg/ml	Steady-State Diffusion Coefficient, D_{SS}, $cm^2/sec \times 10^{10}$	Time-Lag Diffusion Coefficient, D_{TL}, $cm^2/sec \times 10^{10}$
64.0	5.0	3.6
51.4	5.2	—
43.1	4.8	—
19.5	5.0	2.5
4.4	4.6	1.5

± 0.1°, removing the tissue from the solution, digesting it in a proteolytic solvent, and subsequently scintillation counting the resulting solution for total drug present in the tissue.

Pharmacokinetics—A sensitive and specific assay for scopolamine in plasma and urine was developed to follow the drug input rate into the systemic circulation (5). The assay utilized a stable isotope-substituted internal standard in conjunction with GLC–mass spectrometry and involved monitoring a fragment produced under electron-impact ionization of the heptafluorobutyryl derivative of scopolamine formed from the base-catalyzed hydrolysis of scopolamine.

RESULTS

***In Vitro* Skin Permeation**—The transdermal steady-state flux of scopolamine as a function of concentration of the aqueous solution contacting the stratum corneum surface of the skin is shown in Fig. 1. The *in vitro* flux of scopolamine showed a linear increase with increasing concentration, with the flux approximating 26 $\mu g/cm^2$ hr at a concentration of 64 mg/ml. The two components of the equilibrium sorption isotherm are shown in Fig. 2. The values of the constants k_D, C_I^*, and b^* were 1.1 and 5.0 μg/ml and 0.56 ml/mg, respectively.

The steady-state diffusivity was then determined by dividing the measured steady-state *in vitro* transdermal flux by the computed gradient in the epidermis of dissolved drug. The apparent time-lag diffusivity was determined in the usual manner from the plot of cumulative drug permeating the skin *versus* time after exposure to the drug-containing solution. The results of these computations are presented in Table I.

Pharmacokinetics—Pharmacokinetic studies were performed to establish the absorption, metabolism, and excretion of scopolamine following oral administration of ~900 μg of free base, intramuscular administration of 200 μg of scopolamine hydrobromide, and intravenous infusion at 20.6 μg/hr. The urinary excretion profiles for two subjects and the plasma scopolamine levels for one of these subjects following oral administration of scopolamine are presented in Figs. 3 and 4. The computed instantaneous clearance for scopolamine is about 120 ml/min, indicating that glomerular filtration is the prime mode of clearance. The total amount of scopolamine excreted from both subjects was 4–5% of the orally administered dose. With a nonlinear regression analysis, the urinary excretion profile can be related to a two-compartment pharmacokinetic model (Scheme II) (5) and Eq. 2, where A = 35.0 μg/hr, B = 0.3 μg/hr, a = 0.67 hr^{-1}, and b = 0.07 hr^{-1}.

Following intramuscular or intravenous administration of scopolamine, the total amount of scopolamine excreted was about 10% of the administered dose; the clearance of drug from the plasma again approximated the glomerular filtration rate. With the two-compartment pharmacokinetic model constants computed following oral administration, good agreement was obtained between the predicted urinary excretion profile

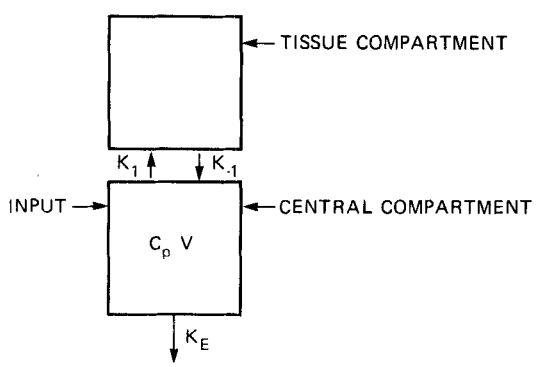

Scheme II—Two-compartment pharmacokinetic model for scopolamine.

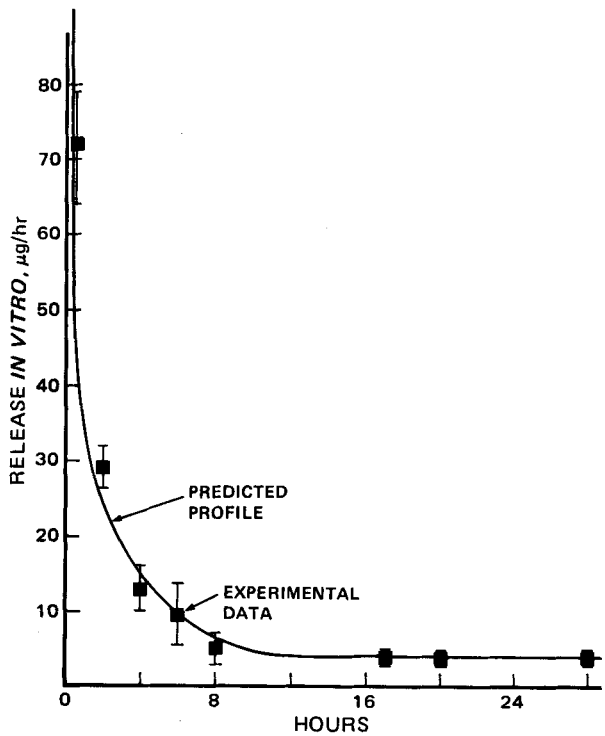

Figure 6—*Scopolamine release rate profile (average ± SD, n = 10): comparison of theory and experiment.*

using Eqs. 6 and 7 and the experimentally measured profile following intravenous infusion (Fig. 5). The results indicate the validity of the pharmacokinetic model and the consistency in the parameters obtained for different routes of scopolamine administration.

Transdermal Therapeutic System–Scopolamine *In Vitro*—A typical *in vitro* release rate–time profile of scopolamine from a transdermal therapeutic system into an infinite sink at isotonic and isothermal conditions is shown in Fig. 6. The data points represent values experimentally measured, and the solid line represents the profile predicted by theory (7). When the release rate–time profile was approximated using Eq. 8, the values of the constants G, H, and h were found to be 3.8 and 150 $\mu g/cm^2$ hr and 1.3 hr^{-1}, respectively.

Transdermal Therapeutic System–Scopolamine *In Vivo*—For the prediction of scopolamine permeation through human skin *in vivo* on the basis of *in vitro* permeation measurements, it was assumed that the stratum corneum thickness was 40 μm and that the average steady-state scopolamine diffusivity was 5 × 10^{-10} cm^2/sec (1, 4). From the two-compartment pharmacokinetic model, the elimination rate constant was estimated using Eq. 5 to be 0.62 hr^{-1}. The predicted urinary excretion rate profile for a single 24-hr application of the transdermal therapeutic system is shown in Fig. 7.

To follow the drug input rate to the systemic circulation *in vivo*, the urinary excretion rate of scopolamine was monitored. Since only 10% of the drug is recovered in the urine in the free form following intramuscular

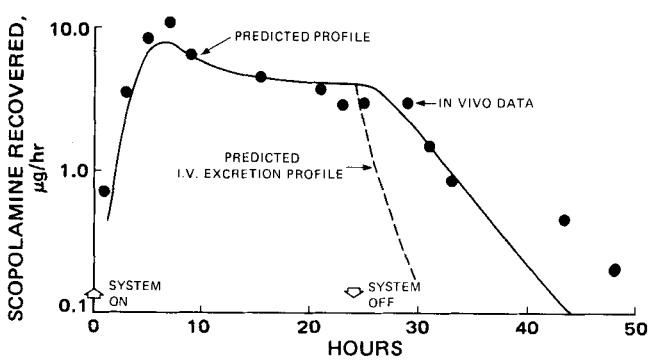

Figure 7—*Scopolamine excretion rate: comparison of theory and* in vivo *data.*

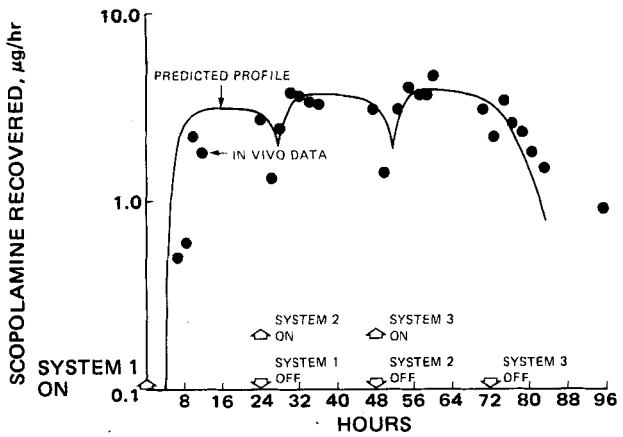

Figure 8—*Scopolamine excretion rate after multiple applications: comparison of theory and* in vivo *data.*

or intravenous administration of scopolamine, it was assumed that a similar recovery would be obtained during transdermal administration. The measured urinary excretion rate of scopolamine for a single 24-hr application of the transdermal system is also shown in Fig. 7.

In Fig. 8, the predicted urinary excretion rate profile of scopolamine for three successive 24-hr applications of the transdermal system in different skin sites is compared with *in vivo* data. Again, the agreement between theory and experiment is good. After system removal, the predicted profile underestimates the rate experimentally measured at the lower values of the urinary excretion rate. These deviations are most likely caused by the permeation of immobilized drug occurring at these late time periods.

CONCLUSIONS

A mathematical model was developed for estimating the temporal pattern of scopolamine delivery from a transdermal therapeutic system through human skin *in vivo*. The model, in turn, was useful in optimizing the design of the therapeutic system, especially in regard to the provision of the priming dose of drug that serves to saturate the immobilization sites for scopolamine within the stratum corneum and, hence, permits rapid establishment of a steady state in the urinary excretion rate of the drug (Fig. 9).

The present transdermal therapeutic system is 2.5 cm^2 in area, and its strength is specified by its temporal pattern of drug release: 200 μg priming dose, 10 μg/hr for 72 hr. Results of large-scale clinical studies indicated that the system is a safe and effective dosage form for systemic administration of scopolamine for prevention of motion-induced nausea (10). The temporal pattern of systemic delivery permits the antiemetic activity of scopolamine to be realized, with minimal incidence of other parasympatholytic effects of the drug.

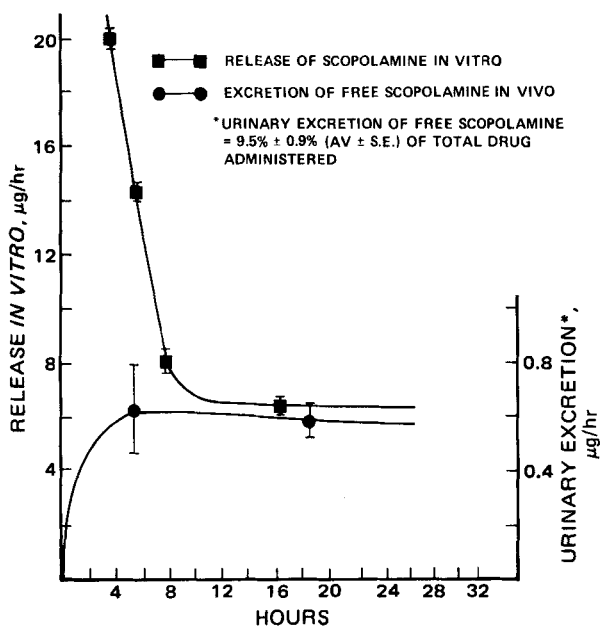

Figure 9—*Functionality of transdermal therapeutic system-scopolamine* in vitro *(average ± SE, n = 6) and* in vivo *(average ± SE, n = 15).*

SYMBOLS

A = constant
a = constant
B = constant
b = constant
b^* = Langmuir's affinity constant
C = concentration
C_D = mobile concentration
C_D^* = mobile concentration at termination of transdermal administration
C_I = immobilized concentration
C_I^* = Langmuir's saturation constant
C_p = plasma concentration
D = diffusion coefficient
D_{SS} = steady-state diffusion coefficient
D_{TL} = time-lag diffusion coefficient
G = constant
h = constant
H = constant
I = infusion rate
k_D = partition coefficient
k_E = elimination rate constant
l = thickness
R = constant
R_E = urinary excretion rate after transdermal administration
R_I = urinary excretion rate after intravenous administration
R_o = urinary excretion rates after oral administration
R_S = transdermal therapeutic system release rate
t = time
T = oral dose
V = volume of distribution
x = distance
$\alpha = [\pi^2 D/4l^2(R+1)]$
$\beta = (16lC_D^*/\pi^3)$

REFERENCES

(1) A. S. Michaels, S. K. Chandrasekaran, and J. E. Shaw, *AIChEJ*, **21**, 985 (1975).

(2) E. R. Cooper, *J. Pharm Sci.*, **65**, 1396 (1976).

(3) R. J. Scheuplein and I. H. Blank, *Physiol. Rev.*, **51**, 702 (1971).

(4) S. K. Chandrasekaran, A. S. Michaels, P. Campbell, and J. E. Shaw, *AIChEJ*, **22**, 828 (1976).

(5) W. F. Bayne, F. T. Tao, and N. Crisologo, *J. Pharm. Sci.*, **64**, 288 (1975).

(6) J. G. Wagner, "Biopharmaceutics and Relevant Pharmacokinetics," Drug Intelligence Publications, Hamilton, Ill., 1971, pp. 295, 296.

(7) S. K. Chandrasekaran and J. E. Shaw, "Design of Transdermal Therapeutic Systems," Contemporary Topics in Polymer Science, vol. 2, Plenum, New York, N.Y., 1977, pp. 291–305.

(8) H. S. Carslaw and J. C. Jaeger, "Conduction of Heat in Solids," Oxford University Press, London, England, 1959, pp. 97, 98.

(9) J. Crank, "The Mathematics of Diffusion," Oxford University Press, London, England, 1970, pp. 45, 46.

(10) J. E. Shaw, W. Bayne, and L. Schmitt, *Clin. Pharmacol. Ther.*, **19**, 115 (1976).

Enhancement of Bioavailability of a Hydrophobic Amine Antimalarial by Formulation with Oleic Acid in a Soft Gelatin Capsule

V. STELLA *, J. HASLAM ‡x, N. YATA *§,
H. OKADA *¶, S. LINDENBAUM *, and T. HIGUCHI *‡

Received November 30, 1977, from the *Department of Pharmaceutical Chemistry, University of Kansas, Lawrence, KS 66045, and the ‡INTERx Research Corporation, Lawrence, KS 66044. Accepted for publication January 30, 1978. §Present address: Faculty of Pharmaceutical Sciences, Osaka University, Osaka, Japan. ¶Present address: Takeda Chemical Industries, Osaka, Japan.

Abstract □ The relative availability of the orally administered hydrophobic antimalarial α-(dibutylaminomethyl)-6,8-dichloro-2-(3′,4′-dichlorophenyl)-4-quinolinemethanol (I) from two dosage forms was determined in beagle dogs. Compound I was soluble in oleic acid to the extent of 23.5% (w/w), and oleic acid was suitable for encapsulation in soft gelatin capsules. The availability of I formulated as its hydrochloride salt in a standard hard gelatin capsule formulation was significantly lower than that of I formulated in a soft gelatin capsule with oleic acid as the solvent. A 20% solution of I in oleic acid (soft gelatin capsules) maintained at 23° provided 4% of the oleic acid ester of I within 1 month. Further reaction, however, was not seen over 2 years.

Keyphrases □ α-(Dibutylaminomethyl)-6,8-dichloro-2-(3′,4′-dichlorophenyl)-4-quinolinemethanol—bioavailability from two dosage forms compared, dogs □ Bioavailability—quinolinemethanol antimalarial from two dosage forms compared, dogs □ Antimalarials—α-(dibutylaminomethyl)-6,8-dichloro-2-(3′,4′-dichlorophenyl)-4-quinolinemethanol, bioavailability from two dosage forms compared, dogs

The antimalarial compound α-(dibutylaminomethyl)-6,8-dichloro-2-(3′,4′-dichlorophenyl)-4-quinolinemethanol[1] (I) as its hydrochloride salt was effective in both animals and humans against chloroquinone-resistant strains of malaria (1–4). Because of the extremely low solubility of I (5), leading to poor bioavailability, large doses of the drug are required to achieve effective blood levels. Typical dosage regimens required to obtain a significant therapeutic effect consisted of 250 mg of the hydrochloride in a hard gelatin capsule formulation[2] administered orally three times a day for 6 days. The large recovery of I in fecal matter from rats given I hydrochloride orally (6) and its low aqueous solubility suggested that the bioavailability of I from its current dosage form was probably poor.

Attempts to improve the bioavailability of I by preparing more water-soluble salt forms, a method successfully employed previously to enhance the water solubility of a hydrophobic amine antimalarial drug (7), were unsuccessful[3]. This paper reports a promising formulation of I utilizing oleic acid as a solvent in a soft gelatin capsule.

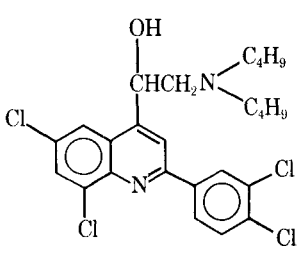

I

EXPERIMENTAL

Materials—The free base was prepared by treating a methanol solution of I hydrochloride with sodium hydroxide. The precipitated free base was filtered and dried at 50° under vacuum. Oleic acid was obtained commercially[4].

Aqueous Solubility of I Hydrochloride—Excess I hydrochloride was agitated in a thermostated dissolution apparatus at 25° in water for varying times. A portion of the supernate was filtered, and the absorbance was measured[5] at 272 nm. The hydrochloride solubility was approximately 1 mg/liter. Very poor reproducibility was obtained in the solubility measurements because I tended to plate out on the walls of the dissolution apparatus and spectrophotometer cells (8), and the solid undissolved material recovered from the aqueous suspension was not the hydrochloride but the free base. Subsequent determination of the aqueous solubility of I showed it to be also approximately 1 mg/liter.

Formulation and Stability of I in an Oleic Acid Solvent—Compound I in oleic acid was soluble to the extent of 23.5% (w/w). Hand-filled soft gelatin capsules[6] were prepared using a 20% (w/w) solution of I in oleic acid. The capsules were weighed before and after injecting the liquid formulation so that the dose contained in each capsule could be determined. Each capsule could hold about 80 mg of I. These hand-filled capsules were prepared just before dosing of the dogs.

A stability study of I in oleic acid was carried out on a small batch of the soft gelatin capsule formulation[7]. At temperatures of 40° and higher, three degradation products were observed with TLC; however, at 23° over 2 years, only one of these degradation products was observed. This product was the ester formed between oleic acid and I. Analysis by high-pressure liquid chromatography (HPLC) showed that about 4% of this ester had formed in a short period after preparation of a small batch of capsules (1 month), but analysis at 1 and 2 years showed no further increase in the amount of the ester formed.

Standard Gelatin Capsule Formulation—Hard gelatin capsules containing 250 mg of I as its hydrochloride in a solid formulation were obtained[7]. The capsules were the standard formulation of I hydrochloride used in a number of clinical trials. Analysis for I in the capsules showed them to contain the labeled amount of I as its hydrochloride.

***In Vivo* Absorption Studies**—Four female (Dogs 1–4 in Fig. 1) and one male (Dog 5 in Fig. 1) beagle dogs received either 250 mg of I as its hydrochloride (equivalent to 234 mg of I) in the standard hard gelatin capsule or 234 mg of I in a total of three oleic acid soft gelatin hand-filled capsules.

The dogs were fasted overnight prior to dosing. After administration of either the soft or hard gelatin capsule, 200 ml of water was given through a gastric tube. The dogs were allowed water *ad libitum* during the study. At predetermined times, 5-ml blood samples were removed and assayed for I by HPLC. After a 3-week lapse, the dogs were given the other dosage form.

Assay of I in Blood—The 5-ml blood samples were discharged immediately into 15-ml glass (polytef-lined screw-capped) centrifuge tubes. The blood was mixed with 2 drops of 15% ethylenediaminetetraacetic

[1] The Walter Reed designation for the hydrochloride salt of this compound is WR30090. This compound is currently undergoing testing by the Walter Reed Army Medical Center. Compound I hydrochloride was obtained from the Walter Reed Army Medical Center under Contract DADA17-73-C-3125.

[2] Control No. E-310, Lafayette Pharmacal.

[3] Unpublished results.

[4] Emersol 633LL, Emery Industries.

[5] Cary model 15 recording spectrophotometer, Varian Associates.

[6] Red oblong capsules (9.5 minims).

[7] A batch of 1000 capsules was prepared at Banner Gelatin Products Corp., Chatsworth, Calif.

0022-3549/78/1000-1375$01.00/0
© 1978, American Pharmaceutical Association

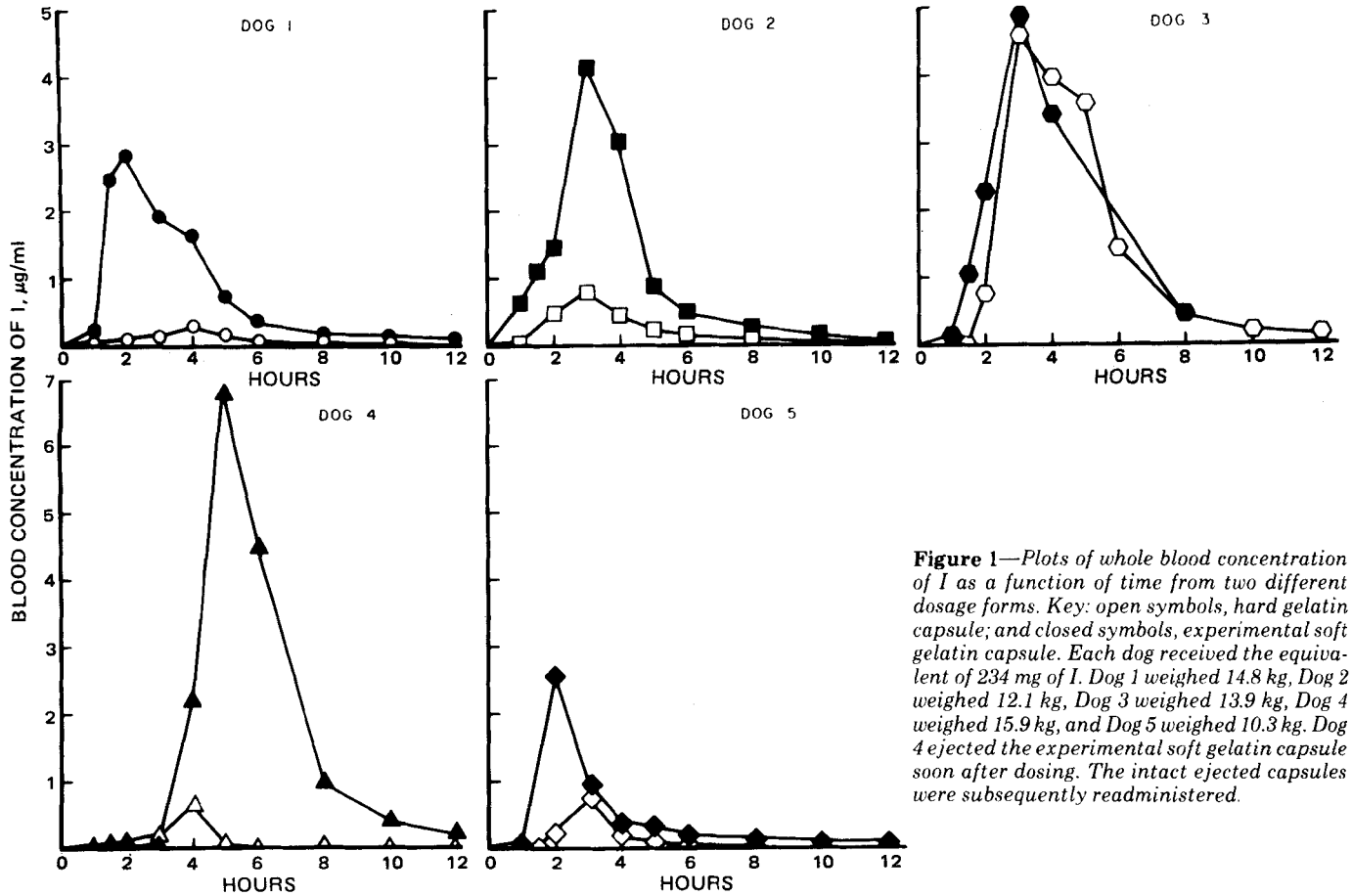

Figure 1—*Plots of whole blood concentration of I as a function of time from two different dosage forms. Key: open symbols, hard gelatin capsule; and closed symbols, experimental soft gelatin capsule. Each dog received the equivalent of 234 mg of I. Dog 1 weighed 14.8 kg, Dog 2 weighed 12.1 kg, Dog 3 weighed 13.9 kg, Dog 4 weighed 15.9 kg, and Dog 5 weighed 10.3 kg. Dog 4 ejected the experimental soft gelatin capsule soon after dosing. The intact ejected capsules were subsequently readministered.*

acid solution previously added to the centrifuge tube. Reagent grade ether, 5 ml, was then added to the centrifuge tube, which was shaken vigorously on a wrist-action shaker with modified, 17.8-cm long rocker arms to hold the centrifuge tubes horizontally.

After 1 hr of continuous shaking, the tubes were removed and centrifuged for 10 min at approximately 5000×*g*. The centrifuge tubes were then immersed in a dry ice–acetone bath to freeze the aqueous layer. The ether layer, about 4 ml, was decanted into a 15-ml conical glass centrifuge tube. The extraction was repeated using the same procedure. Then the ether layer from the second extraction (about 5 ml) was added to the ether from the first extraction, and both were evaporated at room temperature to about one-third of the original volume[8].

The extraction procedure was repeated a third time, and the ether layer (5 ml) was added to the ether from the previous extraction steps. The total ether extracts then were evaporated under vacuum, one tube at a time, by tipping the tube nearly horizontal to prevent bumping. The centrifuge tubes were then placed in a vacuum desiccator over calcium chloride, and the contents were dried completely overnight under vacuum in the dark. Okada *et al.* (9) noted the rapid photolytic degradation of I in organic solvents. The solid material remaining from the ether extracts was dissolved, just prior to analysis, in 100 μl of 20% chloroform–80% heptane (all chemicals were standard reagent grade). Usually 5 or 10 μl of this solution was then injected onto the HPLC column.

A high-pressure liquid chromatograph[9] equipped with a 280-nm UV detector was used. The column was 1.8 mm i.d. stainless steel, 50 cm long, with a silica stationary phase[10].

Several different mobile phases were used, without success, to find conditions yielding a good separation of I free base from the other blood components for as many as 400 injections. However, a system was developed in which one column could be used for 400 injections; but after approximately 40 injections, the composition of the mobile phase needed to be changed slightly to retain good peak separation.

The mobile phase used with a fresh column was 10% (v/v) methanol in the stock solvent [20% (v/v) dioxane–heptane]. The mobile phase was dried over anhydrous sodium sulfate and then degassed to achieve reproducible results. As the column was used, the separation of I from the blood components became poorer and the amount of methanol was decreased to give a good separation. The sensitivity also decreased. A column was used until the methanol concentration was decreased to just less than 3%. A standard concentration of I in 20% (v/v) chloroform–heptane was injected before and after each blood sample as the external standard. The average area of the standard peaks was used to define the column sensitivity for that particular run.

The recovery of I from spiked blood samples was determined using this extraction procedure. The recovery of I was 80% for samples containing 20 ng or more of I in 5 ml of whole blood.

RESULTS AND DISCUSSION

The potential for utilizing a carboxylic acid as a solvent for preparing a solution dosage form of I was recognized when I was found to be extremely soluble in butyric acid and other low molecular weight carboxylic acids. Because of its low volatility and physiological compatibility, oleic acid was chosen as the solvent for a soft gelatin formulation of I. As stated under *Experimental*, I was soluble in oleic acid to the extent of 23.5% (w/w) and formed only a small amount of a degradation product over 2 years of storage at room temperature.

The degradation product was shown by TLC[11] to be the oleic acid ester of I. The identity was confirmed by synthesizing an authentic sample of the ester and comparing its chromatographic properties to those of the formed product. The ester formed to the extent of 4% in 1 month and maintained that level for up to 2 years at 23°. The fact than an equilibrium appeared to be reached could be explained by one of two mechanisms. The product may have formed due to small quantities of oleic anhydride or other reactive species originally present in the oleic acid. Or the esterification may have been simply due to the reaction of I with oleic acid to form the ester and a corresponding amount of water and this reaction rapidly established an equilibrium. Experiments carried out to determine which mechanism applied were inconclusive.

[8] Rotary Evapo-Mix (test tube model).
[9] Model 4000, Varian Associates.
[10] Corasil II, Waters Associates.

[11] Analtech silica gel 250 GF plates, developed from the upper layer of hexane–acetone–ammonium hydroxide (80:14:6) and detected by a UV lamp (254 nm).

Table I—Twelve-Hour Area under the Blood Level *versus* Time Curve (AUC_0^{12}) Comparison for the Hard *versus* Soft Gelatin Capsule Formulations of I

Number	AUC_0^{12} (Hard Gelatin Capsule), μg hr/ml	AUC_0^{12} (Soft Gelatin Capsules), μg hr/ml	$\frac{AUC_0^{12} \text{ (Hard Gelatin Capsule)}}{AUC_0^{12} \text{ (Soft Gelatin Capsules)}}$
1	0.99	9.02	0.11
2	2.46	12.18	0.20
3	16.53	17.53	0.94
4	0.94	18.96	0.05
5	1.38	5.19	0.27
$\bar{x} \pm SD$	4.46 ± 6.77	12.58 ± 5.76 ($p < 0.05$)[b]	0.31 ± 0.36
$\bar{x} \pm SD$[a]	1.44 ± 0.71[a]	11.33 ± 5.83[a] ($p < 0.01$)[b]	0.16 ± 0.10[a]

[a] Numbers refer to the mean and standard deviation values if the data in each column for Dog 3 are disregarded. The AUC_0^{12} for Dog 3 given the hard gelatin capsule could be rejected using the Q test. [b] The AUC_0^{12} for the soft gelatin capsule formulation is significantly different from the AUC_0^{12} at the level indicated using the Student t test.

The results of the blood level–time studies for each dog for the two formulations are given in Fig. 1. Table I summarizes the area under the curve (AUC) data for the blood level–time profile. Also included is the relative AUC for the hard gelatin capsule *versus* the soft gelatin capsule formulation. Compound I was delivered significantly more efficiently from the oleic acid solvent soft gelatin capsule than from the hard gelatin capsule. For both formulations, there appears to be a significant lag time of 1–3 hr for I absorption.

The oleic acid formulation of the hydrophobic drug, I, in a soft gelatin capsule allowed the poorly water-soluble drug to enter the GI tract in a readily dispersible form, providing for more rapid and complete drug absorption. The mechanism for the increased I bioavailability can be postulated to be the emulsification of the oleic acid by the GI contents, resulting in the release of I which is then rapidly absorbed. Whether the drug is carried along by oleic acid absorption or whether it is actually released from oleic acid and subsequently absorbed is not known.

In summary, it appears that I as its hydrochloride is poorly bioavailable from its standard hard gelatin capsule formulation relative to I formulated in a soft gelatin capsule utilizing oleic acid as a solvent. The poor bioavailability of I from the hard gelatin capsule is probably due to its low aqueous solubility combined with a poor formulation design.

REFERENCES

(1) D. F. Clyde, V. C. McCarthy, C. C. Rebert, and R. M. Miller, *Antimicrob. Agents Chemother.*, **3**, 220 (1973).

(2) C. J. Canfield, A. P. Hall, S. MacDonald, D. A. Neuman, and J. A. Shaw, *ibid.*, **3**, 224 (1973).

(3) D. C. Martin, J. A. Arnold, D. F. Clyde, M. A. Ibrahim, P. E. Carson, K. H. Rieckmann, and R. Willerson, Jr., *ibid.*, **3**, 214 (1973).

(4) J. Y. Mu, Z. H. Israili, and P. G. Dayton, *Drug Metab. Dispos.*, **3**, 198 (1975).

(5) A. P. Simonelli, Report No. 1 to U.S. Army Medical Research and Development Command, Contract DADA17-71-C-2002, Jan. 1972.

(6) F. H. Ryer and J. B. Sullivan (Hazleton Laboratories, Inc., Falls Church, Va.), Report No. 1 to U.S. Army Medical Research and Development Command, Aug. 5, 1968.

(7) S. Agharker, S. Lindenbaum, and T. Higuchi, *J. Pharm. Sci.*, **65**, 747 (1976).

(8) K. Thakker, Ph.D. dissertation, University of Kansas, Lawrence, Kans., 1976.

(9) H. Okada, V. Stella, J. Haslam, and N. Yata, *J. Pharm. Sci.*, **64**, 1665 (1975).

ACKNOWLEDGMENTS

Supported by Contract DADA17-73-C-3125, Department of the Army, U.S. Army Medical Research and Development Command (Paper 1490 in the Malarial Publication Series) and by National Institutes of Health Grant GM22357.

Heterocyclic Tricycles as Potential CNS Agents I: 4-Aminoalkylindeno[1,2-*c*]pyrazoles

THOMAS L. LEMKE *[x], MICHAEL B. CRAMER [‡], and K. SHANMUGAM *

Received November 7, 1977, from the **Department of Medicinal Chemistry and Pharmacognosy and the* [‡]*Department of Pharmacology, College of Pharmacy, University of Houston, Houston, TX 77004.* Accepted for publication January 31, 1978.

Abstract □ Series of 4-(3-dimethylaminopropyl)-4-hydroxyindeno[1,2-*c*]pyrazoles and 4-(1-methyl-4-piperidyl)-4-hydroxyindeno[1,2-*c*]pyrazoles were synthesized and identified. The compounds were evaluated as potential CNS agents using spontaneous and forced motor activity in mice as an initial test. 2-Ethyl-3-methyl-4-(1-methyl-4-piperidyl)-4-hydroxyindeno[1,2-*c*]pyrazole possessed significant biological activity.

Keyphrases □ Indenopyrazoles, substituted—synthesized, evaluated for CNS activity in mice □ CNS activity—evaluated in substituted indenopyrazoles in mice □ Structure–activity relationships—substituted indenopyrazoles evaluated for CNS activity in mice □ Heterocycles, tricyclic—substituted indenopyrazoles synthesized, evaluated for CNS activity in mice

Since the introduction of chlorpromazine, a potent central nervous system (CNS) depressant of the phenothiazine class, numerous tricyclic analogs have been investigated. Modification of the side chain and the central ring of the phenothiazines resulted in discovery of additional CNS depressants as well as CNS stimulants. A limited number of investigations involved replacement of one of the benzene rings with heterocyclic aromatic rings. The syntheses of 4-(3-dimethylaminopropylidene)-9,10-dihydro-4*H*-benzo[4,5]cyclohepta[1,2-*b*]thiophene (I) derivatives (1) and 2-methyl-4-(3′-dimethylaminopropylidene)-9,10-dihydro-4*H*-benzo[5,6]cyclo-

© 1978, American Pharmaceutical Association

Table I—Twelve-Hour Area under the Blood Level *versus* Time Curve (AUC_0^{12}) Comparison for the Hard *versus* Soft Gelatin Capsule Formulations of I

Number	AUC_0^{12} (Hard Gelatin Capsule), μg hr/ml	AUC_0^{12} (Soft Gelatin Capsules), μg hr/ml	$\frac{AUC_0^{12} \text{ (Hard Gelatin Capsule)}}{AUC_0^{12} \text{ (Soft Gelatin Capsules)}}$
1	0.99	9.02	0.11
2	2.46	12.18	0.20
3	16.53	17.53	0.94
4	0.94	18.96	0.05
5	1.38	5.19	0.27
$\bar{x} \pm SD$	4.46 ± 6.77	12.58 ± 5.76 ($p < 0.05$)[b]	0.31 ± 0.36
$\bar{x} \pm SD$[a]	1.44 ± 0.71[a]	11.33 ± 5.83[a] ($p < 0.01$)[b]	0.16 ± 0.10[a]

[a] Numbers refer to the mean and standard deviation values if the data in each column for Dog 3 are disregarded. The AUC_0^{12} for Dog 3 given the hard gelatin capsule could be rejected using the Q test. [b] The AUC_0^{12} for the soft gelatin capsule formulation is significantly different from the AUC_0^{12} at the level indicated using the Student t test.

The results of the blood level–time studies for each dog for the two formulations are given in Fig. 1. Table I summarizes the area under the curve (AUC) data for the blood level–time profile. Also included is the relative AUC for the hard gelatin capsule *versus* the soft gelatin capsule formulation. Compound I was delivered significantly more efficiently from the oleic acid solvent soft gelatin capsule than from the hard gelatin capsule. For both formulations, there appears to be a significant lag time of 1–3 hr for I absorption.

The oleic acid formulation of the hydrophobic drug, I, in a soft gelatin capsule allowed the poorly water-soluble drug to enter the GI tract in a readily dispersible form, providing for more rapid and complete drug absorption. The mechanism for the increased I bioavailability can be postulated to be the emulsification of the oleic acid by the GI contents, resulting in the release of I which is then rapidly absorbed. Whether the drug is carried along by oleic acid absorption or whether it is actually released from oleic acid and subsequently absorbed is not known.

In summary, it appears that I as its hydrochloride is poorly bioavailable from its standard hard gelatin capsule formulation relative to I formulated in a soft gelatin capsule utilizing oleic acid as a solvent. The poor bioavailability of I from the hard gelatin capsule is probably due to its low aqueous solubility combined with a poor formulation design.

REFERENCES

(1) D. F. Clyde, V. C. McCarthy, C. C. Rebert, and R. M. Miller, *Antimicrob. Agents Chemother.*, **3**, 220 (1973).

(2) C. J. Canfield, A. P. Hall, S. MacDonald, D. A. Neuman, and J. A. Shaw, *ibid.*, **3**, 224 (1973).

(3) D. C. Martin, J. A. Arnold, D. F. Clyde, M. A. Ibrahim, P. E. Carson, K. H. Rieckmann, and R. Willerson, Jr., *ibid.*, **3**, 214 (1973).

(4) J. Y. Mu, Z. H. Israili, and P. G. Dayton, *Drug Metab. Dispos.*, **3**, 198 (1975).

(5) A. P. Simonelli, Report No. 1 to U.S. Army Medical Research and Development Command, Contract DADA17-71-C-2002, Jan. 1972.

(6) F. H. Ryer and J. B. Sullivan (Hazleton Laboratories, Inc., Falls Church, Va.), Report No. 1 to U.S. Army Medical Research and Development Command, Aug. 5, 1968.

(7) S. Agharker, S. Lindenbaum, and T. Higuchi, *J. Pharm. Sci.*, **65**, 747 (1976).

(8) K. Thakker, Ph.D. dissertation, University of Kansas, Lawrence, Kans., 1976.

(9) H. Okada, V. Stella, J. Haslam, and N. Yata, *J. Pharm. Sci.*, **64**, 1665 (1975).

ACKNOWLEDGMENTS

Supported by Contract DADA17-73-C-3125, Department of the Army, U.S. Army Medical Research and Development Command (Paper 1490 in the Malarial Publication Series) and by National Institutes of Health Grant GM22357.

Heterocyclic Tricycles as Potential CNS Agents I: 4-Aminoalkylindeno[1,2-*c*]pyrazoles

THOMAS L. LEMKE *[x], MICHAEL B. CRAMER [‡], and K. SHANMUGAM *

Received November 7, 1977, from the **Department of Medicinal Chemistry and Pharmacognosy and the* [‡]*Department of Pharmacology, College of Pharmacy, University of Houston, Houston, TX 77004.* Accepted for publication January 31, 1978.

Abstract □ Series of 4-(3-dimethylaminopropyl)-4-hydroxyindeno[1,2-*c*]pyrazoles and 4-(1-methyl-4-piperidyl)-4-hydroxyindeno[1,2-*c*]pyrazoles were synthesized and identified. The compounds were evaluated as potential CNS agents using spontaneous and forced motor activity in mice as an initial test. 2-Ethyl-3-methyl-4-(1-methyl-4-piperidyl)-4-hydroxyindeno[1,2-*c*]pyrazole possessed significant biological activity.

Keyphrases □ Indenopyrazoles, substituted—synthesized, evaluated for CNS activity in mice □ CNS activity—evaluated in substituted indenopyrazoles in mice □ Structure–activity relationships—substituted indenopyrazoles evaluated for CNS activity in mice □ Heterocycles, tricyclic—substituted indenopyrazoles synthesized, evaluated for CNS activity in mice

Since the introduction of chlorpromazine, a potent central nervous system (CNS) depressant of the phenothiazine class, numerous tricyclic analogs have been investigated. Modification of the side chain and the central ring of the phenothiazines resulted in discovery of additional CNS depressants as well as CNS stimulants. A limited number of investigations involved replacement of one of the benzene rings with heterocyclic aromatic rings. The syntheses of 4-(3-dimethylaminopropylidene)-9,10-dihydro-4*H*-benzo[4,5]cyclohepta[1,2-*b*]thiophene (I) derivatives (1) and 2-methyl-4-(3′-dimethylaminopropylidene)-9,10-dihydro-4*H*-benzo[5,6]cyclo-

© 1978, American Pharmaceutical Association

Table I—1- and 2-Alkyl-3-substituted Indeno[1,2-*c*]pyrazol-4(1*H*)-ones

Compound	R_1	R_2	Melting Point	Yield, %[a]	Molecular Formula	Analysis, %	Calc.	Found
VI*a*	CH_3	C_6H_5	192–193°[b]	54	$C_{17}H_{12}N_2O$	C	78.44	78.58
						H	4.65	4.69
						N	10.76	10.74
VI*b*	C_2H_5	C_6H_5	136°[b]	45	—		—	—
VI*c*	$(CH_3)_2CH$	C_6H_5	176–177°[b]	38	$C_{19}H_{16}N_2O$	C	79.14	79.02
						H	5.59	5.61
						N	9.72	9.74
VI*d*	CH_3	$(CH_3)_3C$	147°[b]	46	$C_{15}H_{16}N_2O$	C	74.97	74.86
						H	6.71	6.72
						N	11.66	11.70
VI*e*	C_2H_5	$(CH_3)_3C$	116–118°[b]	50			—	—
VI*f*	$(CH_3)_2CH$	$(CH_3)_3C$	86°[b]	35	$C_{17}H_{20}N_2O$	C	76.09	76.13
						H	7.51	7.53
						N	10.44	10.44
VI*g*	CH_3	CH_3	140–142°[c]	19	$C_{12}H_{10}N_2O$	C	72.70	72.51
						H	5.08	5.12
						N	14.13	13.96
VI*h*	C_2H_5	CH_3	110°[d]	17	$C_{13}H_{12}N_2O$	C	73.56	73.69
						H	5.70	5.79
						N	13.20	13.18
VI*i*	$(CH_3)_2CH$	CH_3	145–146°[c]	23	$C_{14}H_{14}N_2O$	C	74.31	74.17
						H	6.24	6.25
						N	12.38	12.42
VII*a*	CH_3	CH_3	167°[c]	28	$C_{12}H_{10}N_2O$	C	72.70	72.46
						H	5.08	5.14
						N	14.13	14.16
VII*b*	C_2H_5	CH_3	94–96°[d]	26	$C_{13}H_{12}N_2O$	C	73.56	73.60
						H	5.70	5.72
						N	13.20	13.26
VII*c*	$(CH_3)_2CH$	CH_3	108–110°[d]	17	$C_{14}H_{14}N_2O$	C	74.31	74.25
						H	6.24	6.25
						N	12.38	12.41

[a] Yield of VI*a*–VI*i* and VII*a*–VII*c* from V*a*–V*c*. [b] From 95% ethanol. [c] From ethanol. [d] From cyclohexane.

Table II—1- and 2-Ethyl-3-substituted 4-Alkylamino-4-hydroxyindeno[1,2-*c*]pyrazoles

Compound	R_2	Melting Point	Yield, %	Molecular Formula	Analysis, %	Calc.	Found
VIII*a*	C_6H_5	174–177°[a]	71	$C_{23}H_{27}N_3O$	C	76.41	74.46
					H	7.53	7.58
					N	11.62	11.66
VIII*b*	$(CH_3)_3C$	125–126°[a]	73	$C_{21}H_{31}H_3O$	C	73.85	73.81
					H	9.15	9.16
					N	12.30	12.24
VIII*c*	CH_3	139°[b]	46	$C_{18}H_{25}N_3O$	C	72.21	72.23
					H	8.42	8.42
					N	14.03	14.02
IX*a*	C_6H_5	249–252°[a]	54	$C_{24}H_{27}N_3O$	C	77.18	76.97
					H	7.29	7.33
					N	11.24	11.16
IX*b*	$(CH_3)_3C$	141–149°[b]	48	$C_{22}H_{31}N_3O$	C	74.74	74.55
					H	8.84	8.90
					N	11.89	11.83
IX*c*	CH_3	158–161°[c]	51	$C_{19}H_{25}N_3O$	C	73.28	73.08
					H	8.09	8.13
					N	13.49	13.44
X	—	124–126°[d]	79	$C_{18}H_{25}N_3O$	C	72.21	72.13
					H	8.42	8.45
					N	14.03	14.00
XI	—	211–213°[b]	58	$C_{19}H_{25}N_3O$	C	73.28	73.27
					H	8.09	8.12
					N	13.49	13.51

[a] From 95% ethanol. [b] From cyclohexane. [c] From ethyl acetate. [d] From benzene–cyclohexane.

hepta[1,2-*d*]thiazole, imidazole, and oxazole (II*a*–II*c*) derivatives (2) were reported. Both series are analogs of the antidepressant amitriptyline.

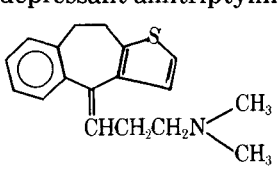

I

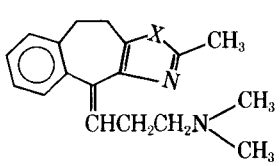

II*a*: X = S
II*b*: X = N
II*c*: X = O

The present investigation concerned the effect of novel heterocyclic tricyclic nuclei as potential CNS agents; synthesis, identification, and evaluation of substituted indeno[1,2-*c*]pyrazoles are reported.

EXPERIMENTAL[1]

Chemistry—The indeno[1,2-*c*]pyrazol-4(1*H*)-ones (V*a*–V*c*, Scheme

Melting points were taken with a Thomas-Hoover Unimelt capillary apparatus and are uncorrected. NMR data were recorded on a Varian Associates model EM-360 spectrophotometer with tetramethylsilane as an internal standard. Merck silica gel 60 (70–230 mesh) was used for column chromatography. Elemental analyses were performed by Atlantic Microlab Inc., Atlanta, Ga.

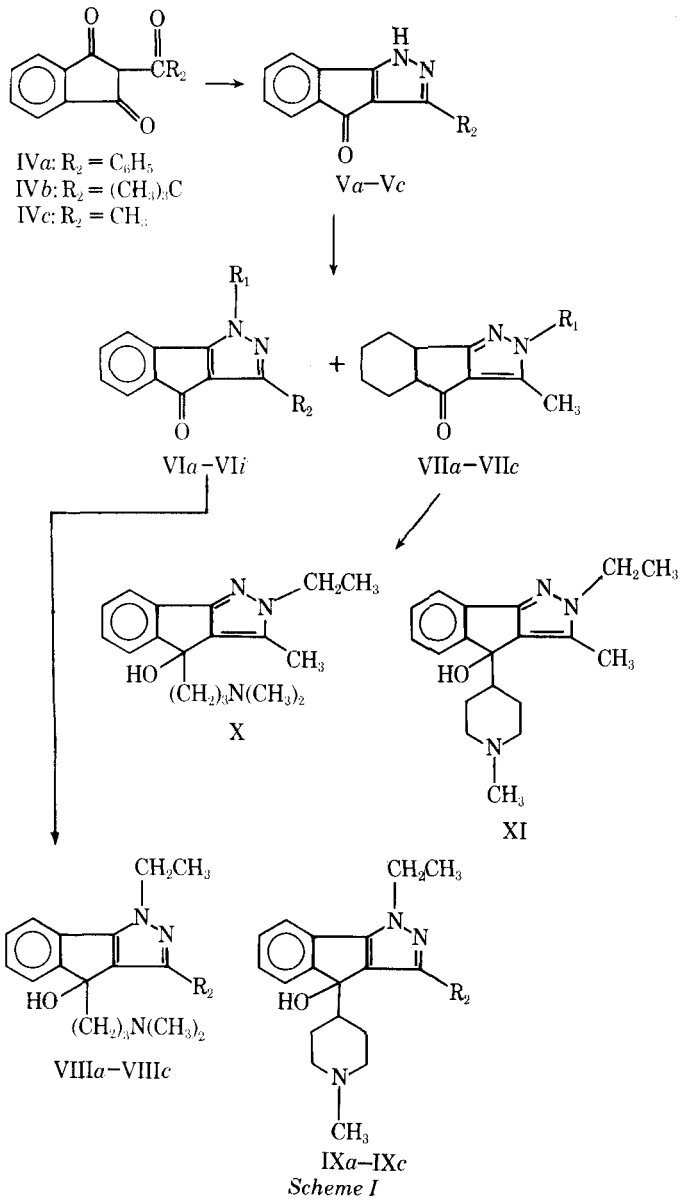

Scheme I

I) were prepared from the corresponding triketones (IV*a*–IV*c*) through the one- or two-step addition of hydrazine (3–6). Alkylation of the sodium salts of V*a*–V*c* with alkyl halides resulted in the preparation of 1-alkyl-3-substituted indeno[1,2-*c*]pyrazol-4(1*H*)-ones (VI*a*–VI*i*) when R_2 was *tert*-butyl or phenyl and the 1- and 2-alkyl-3-methylindeno[1,2-*c*]pyrazol-4(1*H*)-ones (VII*a*–VII*c*) when R_2 was methyl. The 1-ethyl- and 2-ethyl-3-substituted indeno[1,2-*c*]pyrazol-4(2*H*)-ones were converted to the 4-alkylated products (VIII*a*–VIII*c*, IX*a*–IX*c*, X, and XI) *via* reaction with Grignard reagents (Scheme I).

Table III—NMR Data for 1- and 2-Alkyl-3-substituted Indeno[1,2-*c*]pyrazol-4(1*H*)-ones

Compound	R_1			R_2
	CH_3	CH_2	CH	
VI*a*	3.85 (s)			6.90–8.24 (m) (C_6H_5)
VI*d*	3.92 (s)			1.38 (s) [$(CH_3)_3C$]
VI*g*	3.87 (s)			2.28 (s) (CH_3)
VII*a*	3.79 (s)			2.35 (s) (CH_3)
VI*b*	1.48 (t)	4.10 (q)		6.78–8.30 (m) (C_6H_5)
VI*e*	1.52 (t)	4.20 (q)		1.38 (s) [$(CH_3)_3C$]
VI*h*	1.50 (t)	4.17 (q)		2.29 (s) (CH_3)
VII*b*	1.43 (t)	4.02 (q)		2.41 (s) (CH_3)
VI*c*	1.62 (d)		4.60 (m)	6.80–8.38 (m) (C_6H_5)
VI*f*	1.59 (d)		4.60 (m)	1.39 (s) [$(CH_3)_3C$]
VI*i*	1.60 (d)		4.57 (m)	2.32 (s) (CH_3)
VII*c*	1.48 (d)		4.30 (m)	2.39 (s) (CH_3)

Table IV—LD_{50}, ED_{50}, and Safety Indexes of Indenopyrazole Derivatives

Compound	LD_{50}[a]	ED_{50}[a,b]	Safety Index (LD_{50}/ED_{50})
VIII*a*	148.2 (No interval)	42.3 (16.9–105.8)	3.50
VIII*b*	420.6 (268.9–657.9)	70.0 (45.2–108.5)	6.01
VIII*c*	468.6 (398.3–551.4)	>187.4	<2.5
IX*a*	168.3 (136.1–208.2)	89.0 (40.0–197.9)	1.89
IX*b*	318.6 (257.4–394.3)	86.2 (63.4–117.2)	3.70
IX*c*	421.9 (358.6–496.4)	>168.8	<2.5
X	449.3 (398.8–507.1)	104.2 (49.6–218.8)	4.32
XI	571.7 (383.2–853.0)	32.4 (12.0–87.5)	17.6
Haloperidol	49.7 (37.7–65.6)	1.55 (0.603–3.98)	32.1

[a] In milligrams per kilogram intraperitoneally (95% confidence interval in parentheses). [b] Determined using data on depression of spontaneous activity (Table V).

1-Ethyl-3-phenylindeno[1,2-*c*]pyrazol-4(1*H*)-one (VI*b*)—To 3 liters of 10% NaOH was added 18.7 g (0.075 mole) of V*a* (4), and the mixture was heated to boiling. Charcoal was added, the solution was filtered while hot, and the filtrate was cooled to yield 13.4 g (67%) of sodium 3-phenylindeno[1,2-*c*]pyrazol-4(1*H*)-one, mp >300°. The dried salt (0.05 mole) in 200 ml of ethanol was treated with 20.8 g of ethyl bromide (0.2 mole) and heated under reflux for 16 hr. The solution was filtered and cooled, and the crystalline product was collected by filtration. The residue was recrystallized from 95% ethanol.

A similar procedure was used to synthesize VI*a* and VI*c*–VI*f*. Melting points, recrystallization solvents, and yields are listed in Table I.

1-Ethyl-3-methylindeno[1,2-*c*]pyrazol-4(1*H*)-one (VI*h*) and 2-Ethyl-3-methylindeno[1,2-*c*]pyrazol-4(1*H*)-one (VII*b*)—To 3 liters of boiling 10% NaOH was added slowly 27.6 g (0.15 mole) of V*c* (6). After complete solution, the reaction mixture was boiled for 0.5 hr, filtered, and cooled. Then the solid was collected and dried to yield 19.1 g (62%) of sodium 3-methylindeno[1,2-*c*]pyrazol-4(1*H*)-one, mp >300°. The salt (10.3 g, 0.05 mole), 16.4 g (0.15 mole) of ethyl bromide, and 200 ml of ethanol were heated under reflux for 48 hr. The reaction mixture was filtered, concentrated *in vacuo*, diluted with 100 ml of water, and extracted with chloroform.

The combined chloroform extracts were dried. Solvent removal re-

Table V—Effects of Indenopyrazole Derivatives on Spontaneous Motor Activity in Mice

Compound	Dose[a] (*n*)	Activity Counts[b]	Percent of Control
Control[c]	— (18)	168.2 ± 21.3	100
VIII*a*	14.8 (6)	73.0 ± 19.9[d]	43.4
	29.6 (6)	100.5 ± 13.5	59.8
	59.3 (6)	68.3 ± 22.1[d]	40.6
VIII*b*	42.0 (6)	104.7 ± 40.6	62.2
	84.1 (6)	94.5 ± 24.7	56.2
	168.2 (6)	14.7 ± 5.4[d]	8.7
VIII*c*	46.9 (6)	280.2 ± 51.1[d]	166.6
	93.7 (6)	177.7 ± 46.1	105.6
	187.4 (6)	160.0 ± 32.0	95.1
IX*a*	16.8 (6)	164.0 ± 39.9	97.5
	33.7 (6)	162.3 ± 45.5	96.5
	67.3 (6)	109.8 ± 51.9	65.3
IX*b*	31.9 (6)	235.2 ± 49.8	139.8
	63.7 (6)	130.2 ± 34.1	77.4
	127.4 (6)	28.3 ± 11.1[d]	16.8
IX*c*	42.2 (6)	133.7 ± 42.6	79.5
	84.4 (6)	263.7 ± 145.9	156.8
	168.8 (6)	142.0 ± 44.1	84.4
X	45.0 (5)	119.8 ± 35.6	71.2
	89.9 (6)	145.0 ± 76.4	86.2
	179.9 (6)	66.2 ± 39.7	39.3
XI	57.2 (6)	55.7 ± 9.9[d]	33.1
	114.3 (6)	27.8 ± 7.2[d]	16.5
	228.7 (6)	31.2 ± 8.1[d]	18.5
Haloperidol	2.5 (3)	36.0 ± 22.0	21.4
	5.0 (3)	1.7 ± 0.9	1.0
	10.0 (3)	0.3 ± 0.3	0.18

[a] In milligrams per kilogram intraperitoneally; doses are 10, 20, and 40% of the LD_{50}. Number of mice tested is given in parentheses. [b] Activity counts (±*SE*) during 15-min test period. Drug was administered 40 min prior to initiation of activity counts. [c] Administered solvent instead of drug. [d] p *versus* control < 0.05 according to the Student t test.

Table VI—Effects of Indenopyrazole Derivatives on Forced Motor Activity in Mice

Compound	Dose[a] (*n*)	Third Trial[b]	Fourth Trial[b]	Percent of Control
VIII*a*	14.8 (6)	179.6 ± 13.0	170.1 ± 20.9	94.7
	29.6 (6)	205.2 ± 17.3	181.6 ± 10.6	88.5
	59.3 (6)	204.1 ± 13.1	113.7 ± 20.4[c]	55.7
VIII*b*	42.0 (6)	203.1 ± 23.7	191.4 ± 24.7	94.2
	84.1 (6)	222.6 ± 20.8	164.8 ± 44.1	74.0
	168.2 (6)	200.5 ± 18.5	59.5 ± 10.3[c]	29.7
VIII*c*	46.9 (6)	197.1 ± 18.2	152.2 ± 16.4	77.2
	93.7 (6)	215.9 ± 22.5	177.0 ± 16.1	82.0
	187.4 (6)	212.4 ± 15.8	175.6 ± 12.5	82.7
IX*a*	16.8 (6)	206.5 ± 8.9	203.8 ± 9.4	98.7
	33.7 (6)	223.7 ± 23.1	167.5 ± 13.9	74.9
	67.3 (6)	187.9 ± 15.4	146.1 ± 30.3	77.8
IX*b*	31.9 (6)	206.1 ± 22.2	187.7 ± 35.2	91.1
	63.7 (6)	208.8 ± 12.1	159.3 ± 19.7	76.3
	127.4 (6)	216.5 ± 23.2	127.4 ± 32.3[c]	58.8
IX*c*	42.2 (6)	193.2 ± 12.5	215.3 ± 22.7	111.4
	84.4 (6)	192.5 ± 11.1	184.7 ± 14.7	95.9
	168.8 (6)	211.6 ± 19.1	153.4 ± 28.1	72.5
X	45.0 (5)	207.9 ± 39.7	235.5 ± 27.7	113.3
	89.9 (6)	210.7 ± 21.3	215.4 ± 21.9	102.2
	179.9 (6)	191.0 ± 32.1	144.0 ± 35.7	75.4
XI	57.2 (6)	212.8 ± 16.2	215.9 ± 16.5	101.5
	114.3 (6)	195.1 ± 10.0	164.5 ± 21.4	84.3
	228.7 (6)	258.0 ± 14.7	115 ± 16.5[c]	44.8

[a] In milligrams per kilogram intraperitoneally; doses are 10, 20, and 40% of the LD_{50}. Number of mice tested is given in parentheses. [b] Seconds (± *SE*) mice remained on rotating rod. No drug was administered prior to the third (control) trial. Drug was administered 30 min prior to the fourth trial. [c] *p versus* control < 0.05 according to the Student *t* test.

Table VII—Effects of Indenopyrazole Derivatives on Rectal Temperature of Mice

Compound	Dose[a] (*n*)	Predrug[b]	Postdrug[b]	Change *versus* Control
VIII*a*	14.8 (6)	36.3 ± 0.2	35.3 ± 0.4[c]	−1.10
	29.6 (6)	36.4 ± 0.2	36.2 ± 0.4	−0.25
	59.3 (6)	36.7 ± 0.2	34.0 ± 0.4[c]	−2.70
XI	57.2 (6)	36.7 ± 0.2	36.4 ± 0.3	−0.25
	114.3 (6)	36.5 ± 0.3	35.3 ± 0.5[c]	−1.25
	228.7 (6)	36.1 ± 0.2	34.2 ± 0.5[c]	−1.92
VIII*b*	42.0 (6)	37.3 ± 0.8	36.5 ± 0.7	−0.83
	84.1 (6)	37.3 ± 0.3	35.4 ± 0.5[c]	−1.83
	168.2 (6)	35.9 ± 0.3	33.1 ± 0.2[c]	−2.83
X	45.0 (5)	35.8 ± 0.1	35.9 ± 0.4	+0.10
	89.9 (6)	35.0 ± 0.4	36.5 ± 0.4[c]	+1.50
	179.9 (6)	35.4 ± 0.3	33.8 ± 0.4[c]	−1.67
IX*b*	31.9 (6)	37.3 ± 0.2	37.0 ± 0.4	−0.25
	63.7 (6)	37.0 ± 0.3	36.5 ± 0.4	−0.50
	127.4 (6)	36.8 ± 0.2	34.2 ± 0.3[c]	−2.67
VIII*c*	46.9 (6)	37.7 ± 0.2	37.5 ± 0.7	−0.16
	93.7 (6)	37.5 ± 0.3	37.0 ± 0.3	−0.50
	187.4 (6)	37.0 ± 0.2	36.5 ± 0.3	−0.50
IX*c*	42.2 (6)	37.1 ± 0.1	37.3 ± 0.2	+0.25
	84.4 (6)	36.9 ± 0.2	37.1 ± 0.3	+0.17
	168.8 (6)	37.2 ± 0.2	35.6 ± 0.6[c]	−1.58
IX*a*	16.8 (6)	36.9 ± 0.3	37.0 ± 0.5	+0.08
	33.7 (6)	37.0 ± 0.3	37.3 ± 0.3	+0.25
	67.3 (6)	37.1 ± 0.2	35.7 ± 0.3[c]	−1.42

[a] In milligrams per kilogram intraperitoneally; doses are 10, 20, and 40% of the LD_{50}. Number of mice tested is given in parentheses. [b] Degrees (± *SE*) rectally. Predrug values were used as controls; postdrug temperature was taken 25 min after drug administration. [c] *p versus* control < 0.05 according to the Student *t* test.

sulted in recovery of 5.7 g of oil, which was chromatographed on 700 g of silica gel (on a 6 × 117-cm column) and eluted with chloroform; 100–150-ml fractions were collected. Compound VII*b* was eluted first, followed by VI*h*. The compounds were individually recrystallized as indicated in Table I.

A similar procedure was used to synthesize VI*g*, VI*i*, VII*a*, and VII*c*. Melting points, recrystallization solvents, and yields are listed in Table I.

1-Ethyl-3-phenyl-4-(3-dimethylaminopropyl)-4-hydroxyindeno[1,2-*c*]pyrazole (VIII*a*)—To 0.96 g (0.04 g atom) of magnesium and 25 ml of previously distilled tetrahydrofuran (dried over sodium hydride), stirred and maintained under nitrogen, was added dropwise 4.86 g (0.04 mole) of 3-dimethylaminopropyl chloride in 43 ml of tetrahydrofuran. The reaction was initiated with the aid of gentle heating and a few drops of methyl iodide. Grignard formation took 7 hr. To the reaction flask was added dropwise 5.48 g (0.02 mole) of VI*b* in 75 ml of tetrahydrofuran with stirring at 25°.

Following the addition, the reaction was heated under reflux for 3 hr and stirred at 25° for 12 hr. The reaction mixture was concentrated under reduced pressure, treated with 100 ml of 10% ammonium chloride, and stirred for 12 hr. Then the mixture was extracted with chloroform, and the combined extracts were dried. Solvent removal resulted in recovery of 5.1 g of VIII*a*.

A similar procedure was used for the synthesis of VIII*b*, VIII*c*, IX*a*–IX*c*, X, and XI. The melting points, recrystallization solvents, and yields are listed in Table II.

Pharmacological Evaluation—Acute 72-hr lethality was determined for each drug in male Swiss-Webster mice[2], 16–24 g. The LD_{50} values were determined using the method of Weil (7). All subsequent testing was done using three dose groups: 10, 20, and 40% of the LD_{50}. Rectal temperatures were measured using a telethermometer[3].

[2] Texas Inbred Mice Co., Houston, Tex.
[3] Yellow Springs Instrument Co., Yellow Springs, Ohio.

Effects on forced and spontaneous motor activity were determined as previously reported (8). The ED_{50} values for effects on spontaneous activity were determined by the method of Litchfield and Wilcoxon (9).

RESULTS AND DISCUSSION

The alkylation of Va–Vc with various alkyl halides to yield the 1-alkyl derivatives was uneventful when R_2 was the sterically large phenyl or *tert*-butyl group. This alkylation was successful when 3-methylindeno[1,2-*c*]pyrazol-4(1*H*)-one was alkylated since VI*a*–VI*i* and VII*a*–VII*c* formed. The isomers were separated by chromatography, and the products were identified by proton NMR spectroscopy.

As indicated in Table III, the protons of the alkyl at position 2 in VII*a*–VII*c* are shielded with respect to the protons of the alkyl at position 1 in VI*a*–VI*i*. The 1-methyl protons appear at approximately δ 3.9 ppm while the 2-methyl in VII*a* appears at δ 3.8 ppm. A similar trend is seen for the methyl and methylene protons in VI*b*, VI*c*, and VI*h* with respect to VII*b* and the methyl and methine protons in VI*c*, VI*f*, and VI*i* with respect to VII*c*.

As shown in Table IV, LD_{50} values in mice ranged from 148.2 (VIII*a*) to 571.7 (XI) mg/kg. 2-Ethyl-3-methyl-4-(1-methyl-4-piperidyl)-4-hydroxyindeno[1,2-*c*]pyrazole (XI) was the only one of the series to cause a significant depression of spontaneous motor activity at all doses tested (Table V). The safety index (LD_{50}/ED_{50}) for this compound was 17.6, remarkably higher than any other compound in the series although lower than that of haloperidol. Of the remaining compounds, VIII*b* and IX*b* depressed spontaneous activity, but the effect was significant only at the highest dose. Compounds VIII*a* and VIII*c* also produced significant decreases in spontaneous activity, but the dose–response relationship was inconsistent.

Statistically significant depression of forced motor activity was seen with VIII*a*, XI, VIII*b*, and IX*b*, but only at the highest dose tested (Table VI). The series of compounds tended to decrease rectal temperature, with XI and VIII*b* producing a clear dose-related decrease statistically significant at the middle and high doses (Table VII).

Of the compounds in this series, XI is the most appropriate candidate for further evaluation. Its high safety index, along with its preferential effect on spontaneous motor activity relative to that on forced motor activity, suggests potential utility as a psychotropic agent. A positional isomer of XI, IX*c*, was without noticeable biological activity.

REFERENCES

(1) J. M. Bastian, A. Ebnother, E. Jucker, E. Rissi, and A. P. Stoll, *Helv. Chim. Acta*, **54**, 277 (1971).

(2) E. E. Galantay, R. Simpson, G. Corriveau, M. Denzer, D. C. Knorr, R. J. Strohschein, N. A. Paolella, Y. Uike, J. H. Gogerty, E. A. Ryan, and L. C. Iorio, *J. Med. Chem.*, **17**, 1316 (1974).

(3) R. A. Braun and W. A. Mosher, *J. Am. Chem. Soc.*, **80**, 4919 (1958).

(4) R. A. Braun and W. A. Mosher, *J. Org. Chem.*, **24**, 648 (1959).

(5) R. A. Braun and W. A. Mosher, *J. Am. Chem. Soc.*, **80**, 2749 (1958).

(6) W. A. Mosher and T. E. Banks, *J. Heterocycl. Chem.*, **8**, 1005 (1971).

(7) C. S. Weil, *Biometrics*, **8**, 249 (1952).

(8) T. L. Lemke and M. B. Cramer, *J. Med. Chem.*, **19**, 122 (1976).

(9) J. T. Litchfield, Jr., and F. Wilcoxon, *J. Pharmacol. Exp. Ther.*, **96**, 99 (1949).

ACKNOWLEDGMENTS

The authors thank Mrs. Deborah Jones for manuscript preparation.

Interactions of Caffeine and Theophylline with *p*-Cresol: UV Studies

NADHIM I. AL-ANI and HANNA N. BORAZAN ˣ

Received August 31, 1977, from the *Department of Pharmaceutical Chemistry, College of Pharmacy, University of Baghdad, Baghdad, Republic of Iraq.* Accepted for publication February 1, 1978.

Abstract □ UV absorption studies demonstrated the formation of weakly bonded charge transfer complexes between caffeine and theophylline with *p*-cresol in chloroform. The transitions involved were detected at wavelengths longer than those of the single pure substances. Equilibrium constants from the Benesi–Hildebrand equation could be measured together with other thermodynamic constants and molar extinction coefficients. In general, the equilibrium constants were very small while the entropies of formation were quite high. Even though the equilibrium constants of caffeine–*p*-cresol were independent of wavelength over a narrow range, the apparent enthalpies of formation of both complexes indicated wavelength dependence.

Keyphrases □ Caffeine—formation of charge transfer complexes with *p*-cresol, UV absorption study □ Theophylline—formation of charge transfer complexes with *p*-cresol, UV absorption study □ *p*-Cresol—formation of charge transfer complexes with caffeine and theophylline, UV absorption study □ Complexes, charge transfer—formed by caffeine and theophylline with *p*-cresol, UV absorption study

Phenols (1–4) and the purine and pyrimidine bases (5, 6) form charge transfer complexes with many organic compounds. The formation of these complexes between nucleic acid bases and catechol or epinephrine in aqueous solutions containing 0.1 *N* HCl was demonstrated (7–9). Evidence for the formation of charge transfer complexes between isoproterenol and nucleic acid bases in different solvents was described[1] (10). It was hypothesized (7–10) that the charge transfer phenomenon between the nucleic acid bases and catechol or catechol-containing substances might be involved in the mechanism of action of the biogenic amines at the molecular level as well as in their storage in the storage granules at the adrenal medulla and other nerve endings (11).

The present study concerns interactions of caffeine and theophylline with *p*-cresol in chloroform. The contribution of the aromatic nucleus is important information in tracing the mechanism of the formation of complexes between drugs having this nucleus and their receptors and may help explain the mechanism of action of the phenol-containing drugs. Chloroform was chosen as the solvent because of the solubility of the substances studied and the desire to exclude solvent effects in the formation of the complexes.

[1] Unpublished data.

0022-3549/78/1000-1381$01.00/0

© 1978, American Pharmaceutical Association

Effects on forced and spontaneous motor activity were determined as previously reported (8). The ED_{50} values for effects on spontaneous activity were determined by the method of Litchfield and Wilcoxon (9).

RESULTS AND DISCUSSION

The alkylation of Va–Vc with various alkyl halides to yield the 1-alkyl derivatives was uneventful when R_2 was the sterically large phenyl or *tert*-butyl group. This alkylation was successful when 3-methylindeno[1,2-*c*]pyrazol-4(1*H*)-one was alkylated since VIa–VIi and VIIa–VIIc formed. The isomers were separated by chromatography, and the products were identified by proton NMR spectroscopy.

As indicated in Table III, the protons of the alkyl at position 2 in VIIa–VIIc are shielded with respect to the protons of the alkyl at position 1 in VIa–VIi. The 1-methyl protons appear at approximately δ 3.9 ppm while the 2-methyl in VII*a* appears at δ 3.8 ppm. A similar trend is seen for the methyl and methylene protons in VI*b*, VIc, and VI*h* with respect to VII*b* and the methyl and methine protons in VIc, VI*f*, and VI*i* with respect to VII*c*.

As shown in Table IV, LD_{50} values in mice ranged from 148.2 (VIII*a*) to 571.7 (XI) mg/kg. 2-Ethyl-3-methyl-4-(1-methyl-4-piperidyl)-4-hydroxyindeno[1,2-*c*]pyrazole (XI) was the only one of the series to cause a significant depression of spontaneous motor activity at all doses tested (Table V). The safety index (LD_{50}/ED_{50}) for this compound was 17.6, remarkably higher than any other compound in the series although lower than that of haloperidol. Of the remaining compounds, VIII*b* and IX*b* depressed spontaneous activity, but the effect was significant only at the highest dose. Compounds VIII*a* and VIII*c* also produced significant decreases in spontaneous activity, but the dose–response relationship was inconsistent.

Statistically significant depression of forced motor activity was seen with VIII*a*, XI, VIII*b*, and IX*b*, but only at the highest dose tested (Table VI). The series of compounds tended to decrease rectal temperature, with XI and VIII*b* producing a clear dose-related decrease statistically significant at the middle and high doses (Table VII).

Of the compounds in this series, XI is the most appropriate candidate for further evaluation. Its high safety index, along with its preferential effect on spontaneous motor activity relative to that on forced motor activity, suggests potential utility as a psychotropic agent. A positional isomer of XI, IX*c*, was without noticeable biological activity.

REFERENCES

(1) J. M. Bastian, A. Ebnother, E. Jucker, E. Rissi, and A. P. Stoll, *Helv. Chim. Acta*, **54**, 277 (1971).

(2) E. E. Galantay, R. Simpson, G. Corriveau, M. Denzer, D. C. Knorr, R. J. Strohschein, N. A. Paolella, Y. Uike, J. H. Gogerty, E. A. Ryan, and L. C. Iorio, *J. Med. Chem.*, **17**, 1316 (1974).

(3) R. A. Braun and W. A. Mosher, *J. Am. Chem. Soc.*, **80**, 4919 (1958).

(4) R. A. Braun and W. A. Mosher, *J. Org. Chem.*, **24**, 648 (1959).

(5) R. A. Braun and W. A. Mosher, *J. Am. Chem. Soc.*, **80**, 2749 (1958).

(6) W. A. Mosher and T. E. Banks, *J. Heterocycl. Chem.*, **8**, 1005 (1971).

(7) C. S. Weil, *Biometrics*, **8**, 249 (1952).

(8) T. L. Lemke and M. B. Cramer, *J. Med. Chem.*, **19**, 122 (1976).

(9) J. T. Litchfield, Jr., and F. Wilcoxon, *J. Pharmacol. Exp. Ther.*, **96**, 99 (1949).

ACKNOWLEDGMENTS

The authors thank Mrs. Deborah Jones for manuscript preparation.

Interactions of Caffeine and Theophylline with *p*-Cresol: UV Studies

NADHIM I. AL-ANI and HANNA N. BORAZAN ˣ

Received August 31, 1977, from the *Department of Pharmaceutical Chemistry, College of Pharmacy, University of Baghdad, Baghdad, Republic of Iraq.* Accepted for publication February 1, 1978.

Abstract □ UV absorption studies demonstrated the formation of weakly bonded charge transfer complexes between caffeine and theophylline with *p*-cresol in chloroform. The transitions involved were detected at wavelengths longer than those of the single pure substances. Equilibrium constants from the Benesi–Hildebrand equation could be measured together with other thermodynamic constants and molar extinction coefficients. In general, the equilibrium constants were very small while the entropies of formation were quite high. Even though the equilibrium constants of caffeine–*p*-cresol were independent of wavelength over a narrow range, the apparent enthalpies of formation of both complexes indicated wavelength dependence.

Keyphrases □ Caffeine—formation of charge transfer complexes with *p*-cresol, UV absorption study □ Theophylline—formation of charge transfer complexes with *p*-cresol, UV absorption study □ *p*-Cresol—formation of charge transfer complexes with caffeine and theophylline, UV absorption study □ Complexes, charge transfer—formed by caffeine and theophylline with *p*-cresol, UV absorption study

Phenols (1–4) and the purine and pyrimidine bases (5, 6) form charge transfer complexes with many organic compounds. The formation of these complexes between nucleic acid bases and catechol or epinephrine in aqueous solutions containing 0.1 *N* HCl was demonstrated (7–9). Evidence for the formation of charge transfer complexes between isoproterenol and nucleic acid bases in different solvents was described[1] (10). It was hypothesized (7–10) that the charge transfer phenomenon between the nucleic acid bases and catechol or catechol-containing substances might be involved in the mechanism of action of the biogenic amines at the molecular level as well as in their storage in the storage granules at the adrenal medulla and other nerve endings (11).

The present study concerns interactions of caffeine and theophylline with *p*-cresol in chloroform. The contribution of the aromatic nucleus is important information in tracing the mechanism of the formation of complexes between drugs having this nucleus and their receptors and may help explain the mechanism of action of the phenol-containing drugs. Chloroform was chosen as the solvent because of the solubility of the substances studied and the desire to exclude solvent effects in the formation of the complexes.

[1] Unpublished data.

0022-3549/78/1000-1381$01.00/0

© 1978, American Pharmaceutical Association

Solvation interactions are very weak in chloroform (12). Naturally, these interactions affect the equilibrium constant and heat of formation of complexes (13). Moreover, interactions between a drug and its receptor may occur in nonaqueous and low polar environments.

Preliminary IR studies revealed hydrogen-bonded complexes between caffeine and *p*-cresol and theophylline and *p*-cresol. Further UV absorption studies indicated the formation of charge transfer complexes between them. It was possible to calculate various thermodynamic parameters together with molar absorptivities of the complexes at various wavelengths of the charge transfer absorption regions.

EXPERIMENTAL

p-Cresol[2] was purified by distillation twice under reduced pressure in a nitrogen environment at 120–130° after being passed through anhydrous calcium chloride to remove moisture. The middle fraction of each distillate was used. *p*-Cresol is very sensitive to light, oxygen, and moisture. An increase in UV absorbance was observed at longer wavelengths after storage for a short time even when the proper precautions were taken, *e.g.*, storage in dark-brown bottles and under vacuum in a desiccator. Therefore, *p*-cresol was used on the day measurements were taken to avoid photooxidation and water contamination.

Caffeine USP[3] and theophylline[4] were dried under reduced pressure in a vacuum drying apparatus at the boiling point of absolute alcohol and water, respectively. Chloroform[5] was double distilled and dried over aluminum oxide. All chemicals were kept in dark-brown bottles in a refrigerator.

Concentrated solutions were prepared by weighing the chemicals. Solutions of the combinations studied contained a fixed concentration of caffeine or theophylline, 0.02 *M*, with varying concentrations of *p*-cresol, 0.4–1.0 *M*, in chloroform. Solutions were prepared by the dilution method from the concentrated standard solutions and kept in a refrigerator. The measurements were taken within 10 hr in an air-conditioned room (~22°) with subdued lighting.

Measurements were performed by fixing wavelengths to minimize errors attributed to the steepness of the absorption spectrum. Rectangular cells of 1-cm path length with stoppers were used.

The spectrophotometer[6] was calibrated by an oxide film[7] each day. When working at temperatures lower than 15°, the cell compartment of the instrument was flushed with nitrogen gas to avoid water condensation at the cell surface. A thermostated cell holder was connected to a constant-temperature circulator and refrigerator[8] to work at constant and different temperatures.

The baseline was recorded before taking the spectra of a given set of solutions with chloroform in the sample and the reference cells. The spectrum of a complex was detected at wavelengths longer than those of the single pure substances having identical concentrations as those in the mixture. A mixture was measured within approximately 10 min after mixing the solutions and placing the cell in the thermostated cell holder for equilibration.

RESULTS

The absorption spectra of *p*-cresol, caffeine, and theophylline in chloroform were temperature dependent. The absorbance increased as the temperature increased. Two opposing effects must be considered in explaining the hyperchromicity: the dilution resulting from the increase in the volume of solution and the dissociation of self-associated species.

Comparison of the absorption spectra of solutions containing single pure substances with those of the mixtures (Fig. 1) reveals that the absorption spectra of the mixtures shifted toward longer wavelengths with an increase in absorbance, indicating complex formation. Accordingly,

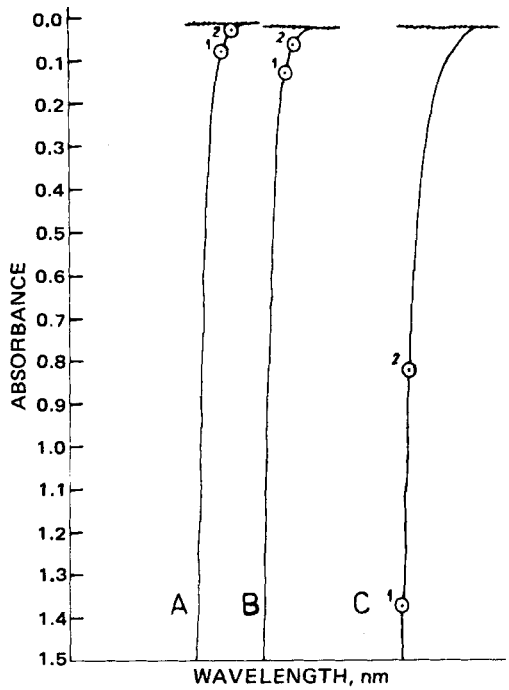

Figure 1—*Absorption spectra of chloroform solutions of* 2×10^{-2} M *caffeine (A), 1.0* M *p-cresol (B), and a mixture containing both concentrations of caffeine and* p*-cresol (C) at 7°. Points 1 and 2 represent the absorption at 308 and 310 nm, respectively, from the baseline (—).*

the absorbance of a complex at a given wavelength and temperature was estimated from the difference in absorbance between the mixture and the sum of the absorbances of the single pure substances, at identical concentrations as those in the mixture, at the same wavelength and temperature. The analytical wavelengths were chosen such that the absorbance of the complex was quite large and that of the pure components was as small as possible to minimize complications in measuring thermodynamic parameters arising from absorption of the free components.

The equilibrium constants of caffeine–*p*-cresol and theophylline–*p*-cresol complexes were calculated from a simple mathematical model by assuming the formation of a 1:1 complex:

$$A + D = AD \qquad \text{(Eq. 1)}$$

and by the application of the Benesi–Hildebrand equation:

$$\frac{[A_0]}{A_\lambda^{AD}} = \frac{1}{\epsilon_\lambda^{AD}} + \frac{1}{K_c^{AD}\epsilon_\lambda^{AD}[D_0]} \qquad \text{(Eq. 2)}$$

where $[A_0]$ and $[D_0]$ are the initial concentrations of the reactant species A and D, respectively; A_λ^{AD} is the absorbance of the complex at the wavelength λ; ϵ_λ^{AD} is the molar absorptivity; and K_c^{AD} is the equilibrium constant. The values of K_c^{AD} and ϵ_λ^{AD} can be obtained graphically from the slope and intercept of a plot of $[A_0]/A_\lambda^{AD}$ *versus* $1/[D_0]$, with $[A_0]$ kept constant and as small as possible compared to $[D_0]$ such that $[D_0] \simeq [D]$, where $[D]$ represents the concentration of free D.

The standard free energy, ΔG^0, standard enthalpy, ΔH^0, and standard entropy, ΔS^0, changes of the reactions can be calculated from the following well-known thermodynamic equations:

$$\Delta G^0 = -RT \ln K_c^{AD} \qquad \text{(Eq. 3)}$$

$$\log K_c^{AD} = -\frac{\Delta H^0}{2.303RT} + \text{constant} \qquad \text{(Eq. 4)}$$

$$\Delta G^0 = \Delta H^0 - T\,\Delta S^0 \qquad \text{(Eq. 5)}$$

where R is the gas constant and T is absolute temperature.

Representative plots of Eqs. 2 and 4 are presented in Figs. 2 and 3, respectively. To minimize experimental errors, the slopes and intercepts were calculated by the method of least squares.

The thermodynamic parameters together with molar absorptivities at the wavelengths are presented in Table I. In Table I and Fig. 2, the molar absorptivities represent average values obtained from working at different temperatures since only slight variations were observed that

[2] Searls Co., Hopkin and Williams Chemical Co., Chadwell Heath, Essex, England.
[3] Nutritional Biochemical Corporation (N.B.C.), Cleveland, Ohio.
[4] E. Merck, Darmstadt, West Germany.
[5] Carlo Erba, Milan, Italy.
[6] Model 402, Perkin-Elmer UV–visible spectrophotometer.
[7] Holmium.
[8] Model FK2, Haake Instrument Co.

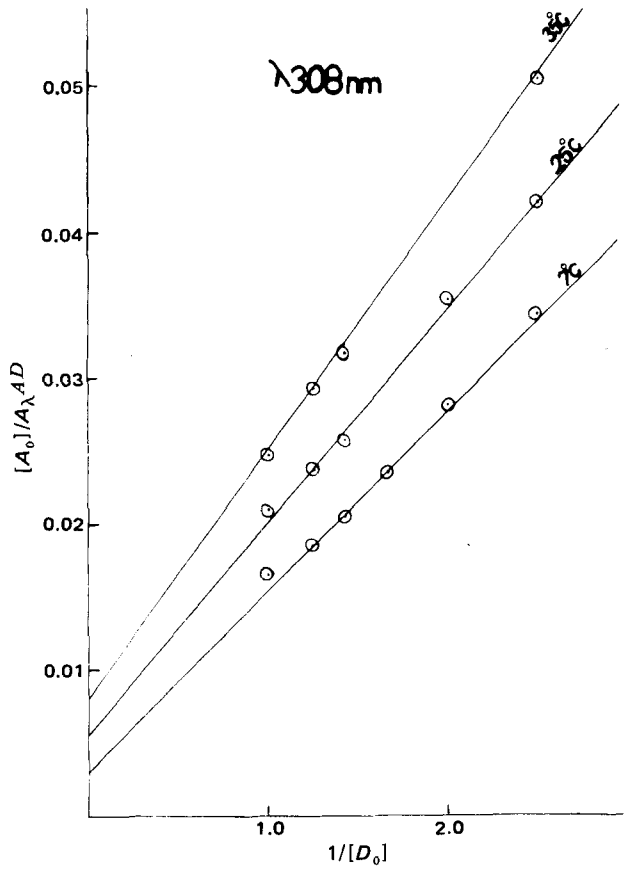

Figure 2—*Plots of* $[A_0]/A_\lambda^{AD}$ versus $1/[D_0]$ *of* p-*cresol solutions containing caffeine in chloroform at different temperatures. The total concentration of caffeine,* $[A_0]$, *was* 2×10^{-2} M; *the total concentration of* p-*cresol,* $[D_0]$, *was 0.4–1.0* M; A_λ^{AD} *represents the absorbance of the complex at the wavelength. Curves have the same intercepts as those of 7°, but they were separated to avoid crowding.*

could be attributed to experimental errors (indicating temperature independence). The equilibrium constants of the caffeine–*p*-cresol complex were wavelength independent; an increase of 2.4% was observed from 310 to 308 nm (Table I). However, with theophylline–*p*-cresol, the equilibrium constants decreased by about 35% over the same wavelength change, indicating wavelength dependence.

The greater dependence of the equilibrium constant of caffeine–*p*-cresol on temperature compared to theophylline–*p*-cresol (Table I) should reflect a greater change in its heat of formation. Although the limit of accuracy is relatively large in measuring enthalpies of formation of both complexes, the results (Table I) could indicate differences in heats of formation of both complexes as well as wavelength dependence.

Even though these reactions are exothermic, as evident from the sign of enthalpy, the free energy changes were observed to be positive since all equilibrium constants were less than unity. Thermodynamically, these reactions are not that favored. The high decrease in entropy of formation of these reactions accounts for the increase in ΔG^0 values and for the extent of complex formation and indicates a high degree of order and great specificity in these complexes as well as great changes in the structure of the solvent. In general, a correlation seems to exist between equilibrium constants and Gibbs free energy with the heat of formation and entropy changes of these complexes (Table I).

DISCUSSION

In forming charge transfer complexes, phenols (2–4) and the purine and pyrimidine bases (5, 6) were considered to act as electron donors. However, the nucleic acid bases were assumed to act as electron acceptors in their interactions with catechol or catechol-containing substances in aqueous or aqueous–alcoholic solutions containing 0.1 *N* HCl (7–10). Therefore, the experimental results presented here can be explained on the basis of formation of charge transfer complexes between caffeine and theophylline with *p*-cresol.

Table I—Equilibrium Constants, *K*, Standard Free Energy, ΔG^0, Standard Enthalpy, ΔH^0, and Standard Entropy, ΔS^0, Changes Associated with the Interactions of Caffeine and Theophylline with *p*-Cresol in Chloroform together with Molar Absorptivities, ϵ, at Different Wavelengths, λ

Temperature ±0.5°	K, M^{-1} ±0.01	ΔG^0, cal/mole	ΔH^0, cal/mole	ΔS^0, cal/degree/mole
		Caffeine–*p*-Cresol		
7°	0.25	774 ± 20		
25°	0.21	926 ± 30	−1966 ± 650	−9.8 ± 2.2
35°	0.18	1054 ± 30		
		λ = 308 nm; ε = 325.7		
7°	0.26	760 ± 20		
25°	0.20	945 ± 30	−2421 ± 500	−11.3 ± 1.7
35°	0.17	1082 ± 35		
		λ = 310 nm; ε = 188.3		
		Theophylline–*p*-Cresol		
6°	0.19	910 ± 30		
18°	0.17	1012 ± 34	−1281 ± 170	−7.9 ± 0.6
37°	0.15	1154 ± 40		
		λ = 308 nm; ε = 297.6		
6°	0.13	1149 ± 43		
18°	0.11	1261 ± 53	−1510 ± 70	−9.5 ± 0.3
37°	0.10	1444 ± 62		
		λ = 310 nm; ε = 260.4		

Quantum mechanical calculations, involving the π-system, of the highest occupied and lowest empty molecular orbitals of xanthine (14) and tyramine (15) indicated that xanthine could be a better electron donor and an acceptor. The electron-donor ability of xanthine seems to exceed its electron acceptability relative to tyramine. It is difficult to assign the donor or acceptor molecule since adjustments of all energy levels accompany electron transfer. Furthermore, the actual situation could be different, and other electrons might be involved in charge transfer, although the π-electrons have relatively lower ionization potentials than those of the lone-pair electrons of oxygen and nitrogen (16).

The increase in equilibrium constants by methylation can be explained on the basis of the inductive effect of the methyl group, which increases the availability of the π-electrons, under the assumption that caffeine and theophylline act as electron donors. If it is assumed that caffeine and theophylline are electron acceptors, then the presence of an extra methyl group in caffeine will increase its basicity relative to theophylline, resulting in a decrease in association with *p*-cresol, a result opposite to what is observed experimentally.

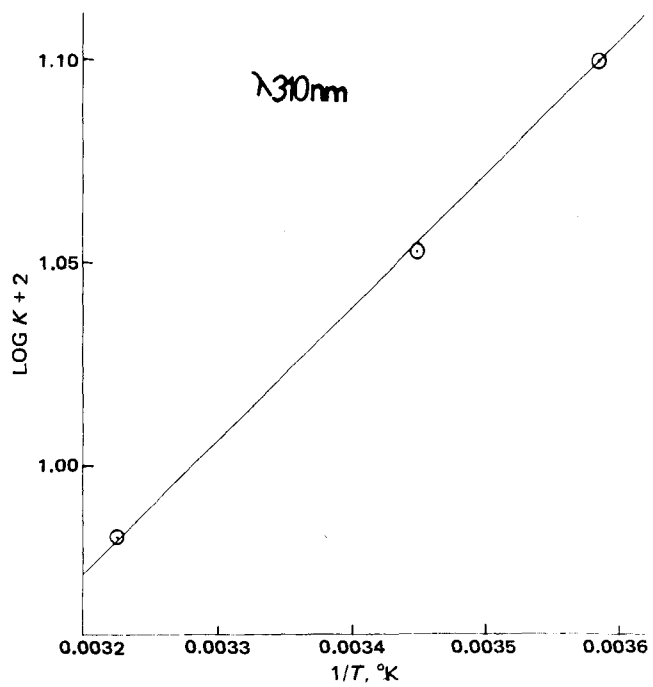

Figure 3—*Log* K *of the theophylline–*p*-cresol interaction* versus 1/T.

The correlation observed in the present work between the heat and entropy of formation of the complexes is consistent with previous observations (7–9, 17, 18) in that a higher heat of a reaction usually accompanies a greater loss in entropy (greater order in the final complex). No correlations were observed, however, between the equilibrium constant and ΔG^0 values with ΔH^0 or ΔS^0 (7–9).

The possible wavelength dependence of ΔH^0 (Table I) can be explained as being due to the formation of complexes having different stoichiometries (19) since the apparent ΔH^0 values determined experimentally are actually functions of ΔH^0 values of different associated forms. Furthermore, the wavelength dependence of the equilibrium constant can be explained by the formation of more than one complex, while wavelength independence was attributed to formation of one type of complex (20, 21). The thermodynamic parameters presented here were measured over a narrow range of wavelengths, and further experimental data can clarify the problem of the wavelength dependence of the equilibrium constant and ΔH^0.

Caffeine and theophylline form complexes and self-associate in different solvents (17, 22–28). It is difficult, however, to propose geometries for the associated forms from UV data alone. Based on IR measurements, Sellini *et al.* (29) presented evidence, supported by PMR studies, for the formation of a hydrogen-bonded, cyclic, and planar dimer between 9-ethyladenine and *p*-cresol in chloroform. Moreover, IR measurements in the present work revealed hydrogen bonds between caffeine and *p*-cresol, theophylline and *p*-cresol, and the self-associated species. Several models for geometries of the associated forms, having predominantly planar structures, were proposed[9]. The electron donor–acceptor theory of hydrogen bonding was proposed previously (30). Thus, the experimental results are consistent.

It may be concluded that the discovery of a charge transfer phenomenon among these systems should help in understanding the mechanism of action of drugs having the phenolic nucleus in the living system at the molecular level.

REFERENCES

(1) G. Cilento and K. Zinner, in "Molecular Associations in Biology," B. Pullman, Ed., Academic, New York, N.Y., 1968, pp. 311–313.

(2) M. A. Slifkin, "Charge Transfer Interactions of Biomolecules," Academic, London, England, 1971, pp. 138–172.

(3) G. Cilento and M. Berenholc, *Biochim. Biophys. Acta*, **94,** 271 (1965).

(4) C. Helene, T. Montenay-Garestier, and J. L. Dimicoli, *ibid.*, **254,** 349 (1971).

(5) M. A. Slifkin, "Charge Transfer Interactions of Biomolecules," Academic, London, England, 1971, pp. 76–95.

(6) R. Foster, "Organic Charge Transfer Complexes," Academic, London, England, 1969, p. 350.

(7) F. A. Al-Obeidi, M.S. thesis, University of Baghdad, Baghdad, Iraq, 1975.

(8) F. A. Al-Obeidi and H. N. Borazan, *J. Pharm. Sci.*, **65,** 892 (1976).

(9) *Ibid.*, **65,** 982 (1976).

(10) H. M. Taha, M.S. thesis, University of Baghdad, Baghdad, Iraq, 1976.

(11) A. Pletscher, M. Da Prada, K. H. Berneis, H. Steffen, B. Lutold, and H. G. Weder, in "Advances in Cytopharmacology," vol. 2, B. Ceccarelli, F. Clementi, and J. Meldolesi, Eds., Raven, New York, N.Y., 1974, p. 257.

(12) Y. Kyogoku, R. C. Lord, and A. Rich, *J. Am. Chem. Soc.*, **89,** 496 (1967).

(13) R. S. Mulliken, *J. Phys. Chem.*, **56,** 801 (1952).

(14) R. Foster, "Organic Charge Transfer Complexes," Academic, London, England, 1969, p. 338.

(15) M. Kumbar and D. V. S. Sankar, *Res. Commun. Chem. Pathol. Pharmacol.*, **5,** 45 (1973).

(16) B. Pullman, *J. Chem. Phys.*, **43,** S233 (1965).

(17) T. Higuchi and D. A. Zuck, *J. Am. Pharm. Assoc., Sci. Ed.*, **42,** 138 (1953).

(18) R. Foster, "Organic Charge Transfer Complexes," Academic, London, England, 1969, p. 207.

(19) *Ibid.*, p. 174.

(20) C. C. Thompson, Jr., and P. A. D. de Maine, *J. Phys. Chem.*, **69,** 2766 (1965).

(21) G. D. Johnson and R. E. Bowen, *J. Am. Chem. Soc.*, **87,** 1655 (1965).

(22) H. N. Borazan, Ph.D. thesis, University of California, San Francisco, Calif., 1969.

(23) F. M. Goyan and H. N. Borazan, *J. Pharm. Sci.*, **57,** 861 (1968).

(24) H. Weil-Malherbe, *Biochem. J.*, **40,** 351 (1946).

(25) T. Higuchi and J. L. Lach, *J. Am. Pharm. Assoc., Sci. Ed.*, **43,** 527 (1954).

(26) M. Blake and L. E. Harris, *ibid.*, **41,** 527 (1952).

(27) D. Guttman and T. Higuchi, *ibid.*, **46,** 4 (1957).

(28) W. O. Emery and C. D. Wright, *J. Am. Chem. Soc.*, **43,** 2323 (1921).

(29) H. Sellini, J. C. Maurizot, J. L. Dimicoli, and C. Helene, *FEBS Lett.*, **30,** 219 (1973).

(30) H. Ratajczak and W. J. Orville-Thomas, *J. Chem. Phys.*, **58,** 911 (1973).

ACKNOWLEDGMENTS

Abstracted in part from a dissertation submitted by N. I. Al-Ani to the University of Baghdad in partial fulfillment of the Master of Science degree requirements.

The authors thank Professor Hatif H. Al-Jalil for encouragement. They also thank the University of Baghdad for financial support of this work.

[9] To be published.

Hardness Increase Induced by Partial Moisture Loss in Compressed Tablets and Its Effect on *In Vitro* Dissolution

Z. T. CHOWHAN ˣ **and L. PALAGYI**

Received July 28, 1977, from the *Institute of Pharmaceutical Sciences, Syntex Research, Palo Alto, CA 94304.* Accepted for publication February 1, 1978.

Abstract □ The hardness increase induced by partial moisture loss in compressed tablets was studied. Several factors such as the type and percentage of the excipient, the water solubility and hygroscopicity of the excipient or drug, and the influence of frequently used binders were investigated. The results indicate that the tablets increased in hardness by the recrystallization of the soluble excipient or the soluble drug in the void spaces. This recrystallization occurred because of the moisture loss after expulsion of the solution of the excipient or drug in the void spaces on compression. The large increase in hardness induced by the partial moisture loss did not decrease *in vitro* dissolution appreciably. This result was clearly different from the hardness increase caused by higher compression loads in the absence of a moisture-induced effect, which showed a decrease in the *in vitro* dissolution as the hardness was increased.

Keyphrases □ Tablets, compressed—effect of partial moisture loss on hardness and *in vitro* dissolution □ Hardness—compressed tablets, effect of partial moisture loss □ Dissolution, *in vitro*—compressed tablets, effect of partial moisture loss □ Dosage forms—compressed tablets, effect of partial moisture loss on hardness and *in vitro* dissolution

It is generally recognized that the granulation moisture content should be adjusted to an optimal range to obtain desirable compaction properties. The optimal range, however, depends on the nature and absorptivity of the drug and excipients. Therefore, it is imperative that the beneficial effects of moisture such as the improvement in compaction properties, alleviation of static charge, and improved cohesion to reduce demixing and the deleterious effects such as the reduction in flow rate and sticking of material to punches are balanced.

BACKGROUND

To study the mechanism by which moisture in powders increases compaction, sodium chloride, a cubic crystalline material capable of being compressed directly to form coherent compacts without added excipients, was used (1, 2). It was concluded that the increase in strength of the compacts on drying of the remaining moisture was due to recrystallization at the crystal boundaries and in the voids.

In a similar study (3), the effect of moisture on the flow and compression properties of phenacetin, acetaminophen, and dextrose monohydrate without the addition of excipients was reported. These results suggested that the increase in strength of the compacts on drying was in the same order as their solubility. It was concluded that substances with low water solubility would show little, if any, increase in compact strength due to the loss of moisture on drying.

Naproxen, a nonsteroidal anti-inflammatory agent, has very low water solubility. The tablet formulation contains about 66% drug, 10% starch, 18% lactose, and 0.2% magnesium stearate. The wet granulation is carried out with a povidone solution in methanol–water. An unusual increase in hardness of these tablets was noticed recently in this laboratory, a few hours after manufacturing. Preliminary investigations suggested that this increase was related to the moisture content of the granulation.

This paper discusses the hardness increase phenomenon in compressed tablets induced by the partial moisture loss during equilibration under ambient room conditions. The effects of drugs, excipients, and binders on the moisture-induced hardness increase were examined and related to *in vitro* dissolution. The data suggest that the increase in hardness of compressed tablets, induced by the partial moisture loss, has very little effect on the *in vitro* dissolution of the drugs studied. Since the moisture-induced hardness increase in compressed tablets does not affect *in vitro* dissolution, a test indicative of *in vivo* bioavailability, an upper limit on stability hardness would be unnecessary and meaningless.

EXPERIMENTAL

Materials—Sodium benzoate[1], starch[2], povidone[3], lactose[4], magnesium stearate[1], dextrose[5], acacia[5], and hydroxypropyl methylcellulose[6] were all USP grade. Microcrystalline cellulose[7] and methanol were NF grade. FD&C Yellow No. 5[8] was used as a coloring agent. Naproxen[9] and naproxen sodium[9] were at least 99% pure. All other chemicals were analytical reagent grade, unless otherwise indicated.

Granulation Preparation—The granulations were prepared by wet granulation. The powders, except magnesium stearate, were mixed in a small planetary-type mixer[10] for 5 min. The granulating solution was added while mixing and was mixed for 5 min. The wet granulation was passed through a No. 12 mesh screen and dried in trays in a forced air drying oven at 50° until the desired moisture level was reached. The dry granulation was screened through a No. 14 mesh screen and mixed with magnesium stearate in a mixer for 2 min. At the end of mixing, the granulation was stored in tightly closed glass jars; the moisture content was determined prior to compression.

The granulating solutions were prepared in the usual fashion. The dye was first dissolved in water and mixed with the cosolvents, if required. The binder was then added and mixed until dissolved. Starch paste was prepared by boiling the water and then mixing with the dye and starch.

Compression—Tablets were compressed with a single-punch machine[11] to a targeted hardness of 10 Strong–Cobb units. The punches and die were 0.95-cm diameter and flat faced. The tablet weight was adjusted to contain 200 mg of active drug. An instrumented single-punch machine[11] was used for a compression load *versus* hardness experiment.

Moisture Determination—The granulation moisture was determined with a moisture balance[12] by exposure to a 125-w IR lamp for 15 min at the 90-v setting. The weight loss on drying, in percent, was read directly from this instrument. The tablets were first ground with a mortar and pestle, and the same procedure for moisture determination was followed.

Hardness Determination—The initial hardness was determined immediately after compression. The tablets were placed in open trays exposed to ambient room conditions (20°, 35–40% relative humidity) and in "filled to capacity and tightly closed" glass bottles. The samples stored in open trays were allowed to equilibrate and reach maximum hardness. For each hardness determination[13], 10 tablets were tested and the mean was calculated.

***In Vitro* Dissolution**—The dissolution apparatus consisted of a 1-liter beaker and a stirrer driven by a synchronous motor at 120 rpm. The beaker, containing 600 ml of 0.1 *M* phosphate buffer (pH 7.4), was maintained at 37° in a constant-temperature water bath. For naproxen sodium and sodium benzoate, the dissolution medium was distilled water.

[1] Mallinckrodt Chemical Works, St. Louis, MO 63160.
[2] Staley Manufacturing Co., Decatur, Ill.
[3] G.A.F. Corp., New York, N.Y.
[4] Lactose Regular, Foremost Food Co., San Francisco, CA 94104.
[5] J. T. Baker Chemical Co., Phillipsburg, NJ 08865.
[6] E-15 Premium, Dow Chemical Co., Midland, Mich.
[7] FMC Corp., American Viscose Division, Marcus Hook, Pa.
[8] Warner Jenkinson Manufacturing Co., St. Louis, Mo.
[9] Syntex Research, Palo Alto, CA 94304.
[10] Kitchen Aid, model K5-A, Hobart Manufacturing Co., Troy, Ohio.
[11] Stokes model E.
[12] Cenco, Central Scientific Co., Chicago, IL 60623.
[13] Heberlein hardness tester, Herberlein and Co., AG, Switzerland, or Stokes hardness tester, F.J. Stokes Machine Co., Philadelphia, Pa. The Stokes hardness tester was only used where the Heberlein hardness tester went off scale; hardness was converted to Strong–Cobb units by running a correlation between the two instruments.

0022-3549/78/1000-1385$01.00/0
© 1978, American Pharmaceutical Association

Table I—Tablet Formulations

Formulation	Ingredients as Percent of Total Tablet Weight[a]												Tablet Weight, mg
	Naproxen	Naproxen Sodium	Sodium Benzoate	Starch	Lactose	Microcrystalline Cellulose	Dextrose	Povidone	Acacia	Hydroxypropyl Methylcellulose	Methanol	Water	
A	65.79	—	—	10.00	18.72	—	—	5.26	—	—	10.26	10.26	380
B	73.96	—	—	10.07	9.82	—	—	5.92	—	—	10.26	10.26	338
C	70.51	—	—	10.00	14.00	—	—	5.26	—	—	10.26	10.26	355
D	59.25	—	—	9.96	25.83	—	—	4.73	—	—	10.26	10.26	422
E	65.79	—	—	10.00	23.98	—	—	—	—	—	—	20.52	380
F	65.79	—	—	10.00	21.98	—	—	—	—	2.00	10.26	10.26	380
G	65.79	—	—	10.00	18.98	—	—	—	5.0	—	—	20.52	380
H	65.79	—	—	10.00	—	—	18.72	5.26	—	—	10.26	10.26	380
I	65.79	—	—	10.00	—	18.72	—	5.26	—	—	10.26	10.26	380
J	—	65.79	—	10.00	—	18.72	—	5.26	—	—	—	20.52	380
K	—	—	65.79	10.00	—	18.72	—	5.26	—	—	10.26	10.26	380

[a] The percentage of magnesium stearate was 0.20 and the percentage of FD&C Yellow No. 5 was 0.03 in all formulations.

A stainless steel paddle, 2.5 × 7.6 cm, was mounted in the middle of a stainless steel shaft and used as a stirrer. The distance between the bottom of the beaker and the bottom of the stirrer was kept constant at 2.5 cm.

At zero time, a tablet was dropped into the stirred dissolution medium. Then 1-ml samples were withdrawn at 5-min intervals and filtered through a medium sintered-glass funnel. The absorbance[14] of the naproxen samples was measured at 332 nm after appropriate dilution. The absorbance of sodium benzoate was measured at 275 nm. Each time point represented the mean of three determinations.

RESULTS AND DISCUSSION

Several tablet formulations were prepared (Table I). Tablets were compressed from granulations containing different moisture contents; they were obtained by drying the wet granulation in a forced air convection oven at 50° to desired moisture levels, mixing with the lubricant, equilibrating in tightly closed containers, and determining moisture contents. No apparent change in moisture content was observed due to compression. After compression and after exposure to ambient room conditions, the tablets were tested for hardness and for *in vitro* dissolution. The difference between the mean hardness before and after exposure to ambient room conditions represented an increase in hardness induced by the partial moisture loss.

The results of hardness increase induced by the partial moisture loss from naproxen tablets, using Formulation A (Table I), are given in Fig. 1. At and below 2% moisture, the tablet hardness did not increase on equilibration. Above 2% moisture, hardness increased as the moisture content increased. An increase in hardness of about 24 Strong–Cobb units occurred at 3.5% moisture. Above 4% moisture, cohesion of the granulation inside the hopper prevented uniform filling in the die. Moreover, the moisture content of the granulation reduced the contact between the die walls and the granulation on compression and caused excessive water lubrication effect.

The *in vitro* dissolution of the tablets after compression and after hardness increase, as a function of the initial moisture content, is also given in Fig. 1. A large increase in hardness at 3 and 3.5% moisture did not affect the *in vitro* dissolution at 5 and 10 min. This result suggests that the hardness increase of these tablets induced by the partial moisture

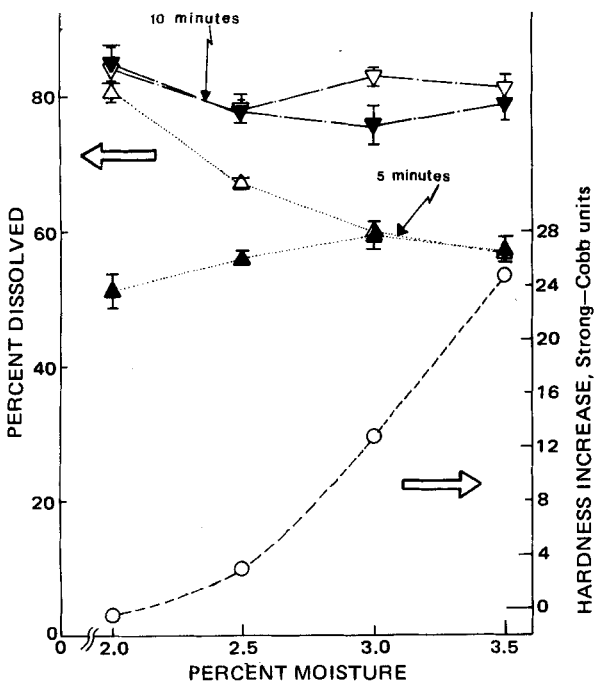

Figure 1—*Effect of hardness increase induced by partial moisture loss on dissolution of naproxen tablets (Table I, Formula A). Key: ○, hardness* versus *percent moisture plot; △ and ▽, dissolution of tablets immediately after compression; and ▲ and ▼, dissolution of tablets after hardness increase. Vertical lines represent standard deviations; the absence of vertical lines indicates that the standard deviation was too small to be shown.*

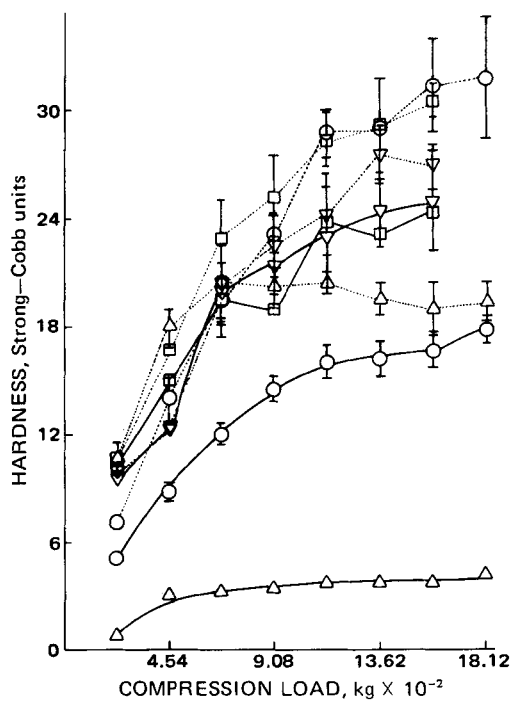

Figure 2—*Effect of compression load on hardness of naproxen tablets (Table I, Formula A) at different moisture contents. Key: —, compression load* versus *hardness profiles immediately after compression; . . . . , compression load* versus *hardness profiles after exposure to ambient room conditions; ▽, 2.0% moisture; □, 2.3% moisture; ○, 3.2% moisture; and △, 4.0% moisture. Vertical lines represent standard deviations; the absence of vertical lines indicates that the standard deviation was too small to be shown.*

[14] Unicam recording spectrophotometer.

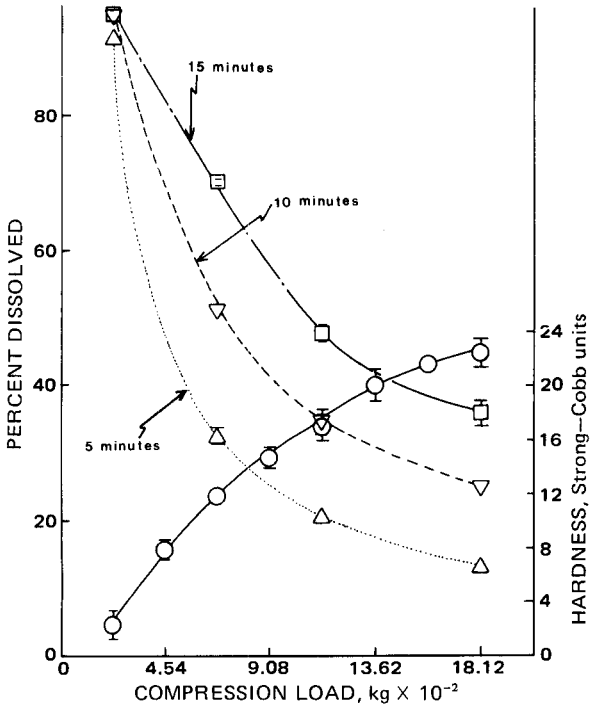

Figure 3—*Effect of compression load on hardness and* in vitro *dissolution of naproxen tablets compressed to contain 0.2% moisture. Key:* ○, *hardness* versus *compression load profile; and* △, ▽, *and* □, *dissolution at various time points* versus *compression load profiles.*

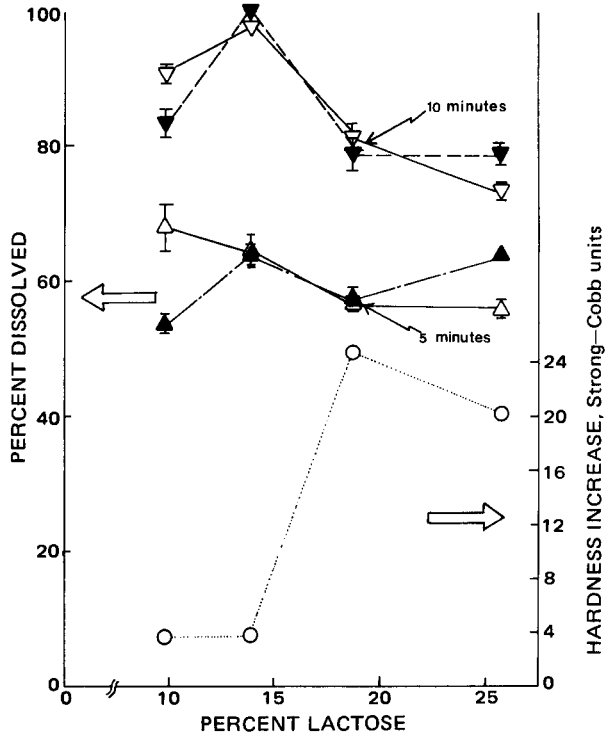

Figure 4—*Effect of percent lactose in naproxen tablets on hardness increase induced by the partial moisture loss and* in vitro *dissolution. The moisture content of the granulation was 3.5%. Key:* ○, *percent lactose* versus *hardness increase plot;* △ *and* ▽, *dissolution of tablets immediately after compression; and* ▲ *and* ▼, *dissolution of tablets after hardness increase. Vertical lines represent standard deviations; the absence of verticle lines indicates that the standard deviation was too small to be shown.*

loss has no effect on *in vitro* dissolution. At a moisture content where no increase in hardness occurred, the *in vitro* dissolution at 5 min was lower after equilibration at ambient room conditions than initially. However, the *in vitro* dissolution under both conditions was the same at 10 min.

The relationship between hardness and compression load of the tablets prepared from Formulation A containing varying moisture content is given in Fig. 2. The hardness of the tablets containing varying moisture content increased as the compression load increased. At all compression loads, as the moisture content increased, the hardness of the tablets decreased. Under normal conditions, as the compression load increases, the porosity of tablets decreases. In the presence of moisture, the void spaces in the tablets probably become filled with the solution of the water-soluble excipient. This phenomenon is dependent on the moisture content and the applied compression load.

At higher moisture contents, as the compression load increases, the liquid driven out of the void spaces forms a continuous film at the die wall. This film acts as a lubricant and results in reduced contact between the tablet granulation and the die wall. The compression load *versus* hardness profile before exposure to ambient room conditions at 4% moisture illustrates this point. It was not possible to compress tablets of reasonable hardness from the granulation containing 4% moisture, even at high compression loads. However, when the moisture content was reduced to 3.2%, the hardness increased as the compression load increased. This result was due to the reduced amount of expelled liquid after filling the void spaces, thus allowing higher contact between the tablet granulation and the die wall. These data reaffirm the importance of controlling the moisture content of the granulation to optimize compression properties.

Figure 2 also gives the compression load *versus* hardness profiles after the tablets were exposed to ambient room conditions. At 2% moisture, a significant increase in hardness did not occur, even at higher compression loads. However, at 2.3% moisture, higher compression loads resulted in hardness increases after equilibration under ambient room conditions. Around compression loads greater than 1000 kg, a small increase in moisture content resulted in some expulsion of saturated solution in the void spaces, which, upon recrystallization, resulted in increased tablet strength. This phenomenon of increased tablet strength after exposure to ambient room conditions was observed at lower compression loads as the moisture content increased.

The granulations from Formulation A were dried to contain 0.2% moisture, and tablets were compressed at different compression loads. Plots of the compression load, hardness, and *in vitro* dissolution are given in Fig. 3. As the compression load increased, the tablet hardness increased and the percent drug dissolved decreased. The hardness increase caused by the compression load in the absence of a moisture-induced effect must be clearly distinct from the hardness increase caused by the partial moisture loss after compression. The data in Fig. 3 indicate that tablets compressed at very low moisture content increased in hardness as the compression load increased and show a remarkable decrease in *in vitro* dissolution. However, the results in Fig. 1 show that the tablets compressed at higher moisture contents, *i.e.*, above 2%, increased in hardness after exposure to ambient room conditions. The increase depended on the initial moisture content and did not decrease *in vitro* dissolution.

Apparently, granulations containing moisture above a certain level, on compression, force solution of the soluble excipient and binder into the void spaces. Recrystallization of the dissolved excipient from the binding solution results in the formation of bridges at the point of contact, resulting in an increase in hardness. Under these circumstances, one should expect a dependence of the hardness increase on the percent of water-insoluble excipient in the formulation containing a water-insoluble drug.

In Formulation A, lactose was varied (Formulations B–D) at a moisture content where it was known that hardening would occur. The plot of the percent lactose *versus* the hardness increase induced by the partial moisture loss (Fig. 4) confirms the importance of the percentage of water-soluble excipient in the formulation. The maximum hardness increase occurred at lactose concentrations that allowed optimum recrystallization in the void spaces, thus giving strength to the tablets. The results of the *in vitro* dissolution *versus* lactose percentage are also given in Fig. 4. Similar *in vitro* dissolution before and after exposure to ambient room conditions reaffirms that the hardness increase induced by the partial moisture loss has no effect on the *in vitro* dissolution.

For a water-insoluble drug, the excipient may play an important role in the moisture-induced hardness increase and *in vitro* dissolution of the drug. In Formulation A, lactose was replaced by microcrystalline cellulose (Formulation I). The results of the hardness increase and *in vitro* dissolution as a function of the initial moisture percentages are given in Fig. 5. Since microcrystalline cellulose is insoluble in water, no excipient

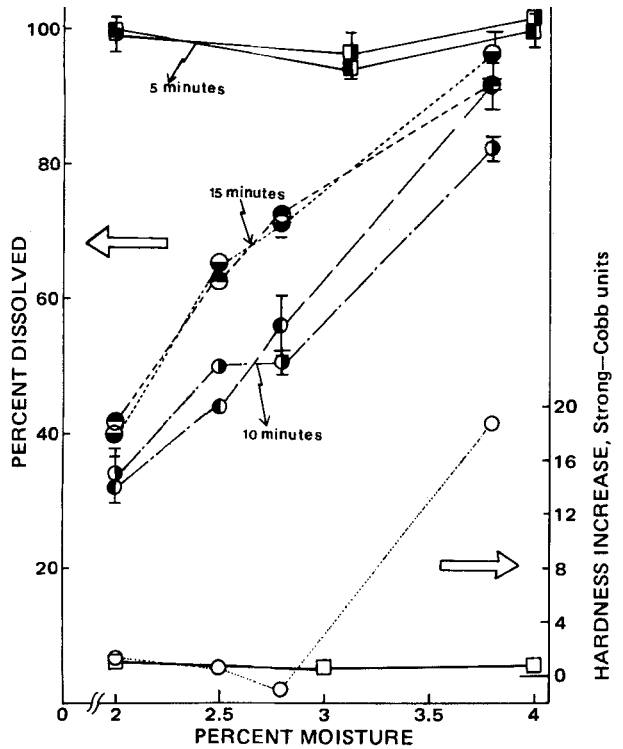

Figure 5—*Effect of excipients on hardness increase induced by the partial moisture loss and* in vitro *dissolution of naproxen tablets. Key:* ○ *and* □, *effect of dextrose and microcrystalline cellulose on moisture-induced hardness increase, respectively;* ◨, ◑, *and* ◓, in vitro *dissolution of tablets immediately after compression; and* ◧, ◐, *and* ◒, *dissolution of tablets after hardness increase. Vertical lines indicate standard deviations; the absence of vertical lines indicates that the standard deviation was too small to be shown.*

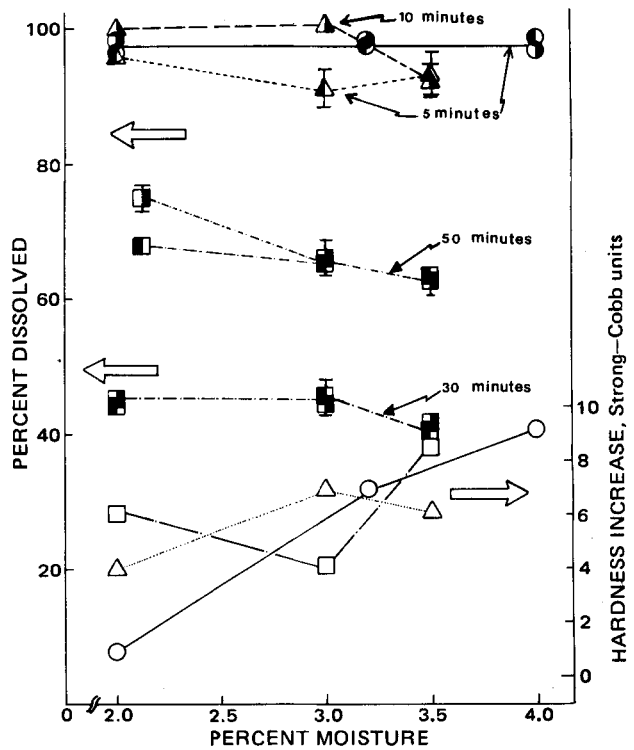

Figure 6—*Effect of binders on hardness incease induced by the partial moisture loss and* in vitro *dissolution of naproxen tablets. Key: circles, starch paste; squares, acacia solution; triangles, hydroxypropyl methylcellulose solution;* ○, □, *and* △, *hardness increase* versus *percent moisture plots;* ◑, ◨, *and* ▲ in vitro *dissolution immediately after compression; and* ◐, ◧, *and* ◭, in vitro *dissolution after hardness increase. Vertical lines represent standard deviations; the absence of vertical lines indicate that the standard deviation was too small to be shown.*

recrystallization was expected and no increase in hardness occurred. This study confirms that when povidone is used as a binder in these formulations, it does not increase tablet strength because it does not crystallize. The replacement of lactose by microcrystalline cellulose also decreased disintegration time, resulting in rapid *in vitro* dissolution. Almost 100% of the drug dissolved at the end of 5 min.

The results of the effect of the replacement of lactose by dextrose (Formulation H) in Formulation A are given in Fig. 5. The hardness of the tablets with an initial moisture percentage of 3.8 increased after room temperature exposure. The granulation containing moisture between the last two data points was not tested. Therefore, the moisture-induced hardness increase probably started anywhere between these two data points. The hardened tablets showed a small decrease in *in vitro* dissolution.

The percent drug dissolved increased as the moisture content at the time of compression increased. The amount of moisture in the granulation affected drug dissolution by its effect on disintegration time. The average disintegration time for 2% moisture-containing tablets was 17 min, compared to the 7 min for the 3.8% moisture case. Although the hardness of 3.8% moisture-containing tablets after exposure increased significantly, the disintegration time did not change. The decrease in disintegration time and the increase in *in vitro* dissolution as a function of moisture content suggest that as the moisture contents increase, saturated solution of dextrose filled the void spaces on compression, thus allowing the liquid to penetrate into the tablets and resulting in an increase in *in vitro* dissolution.

Another parameter that may have considerable bearing on the phenomenon of hardness increase induced by moisture is the choice of binders used in the wet granulation procedure. The strength of the crystalline bridges depends not only on the amount of water-soluble excipient deposited in the void spaces between water-insoluble drug but also on the crystallization rate. Besides povidone (Formulation A), other frequently used binders such as starch paste (Formulation E), hydroxypropyl methylcellulose (Formulation F), and acacia (Formulation G) were investigated. The results of the hardness increase as a function of moisture content at the time of compression are given in Figs. 1 and 6.

At 2% moisture, the largest hardness increase occurred with acacia, while starch paste and hydroxypropyl methylcellulose did not cause a significant increase. At higher moisture contents, povidone caused a larger increase in hardness compared to other binders. The *in vitro* dissolution before and after exposure to ambient room conditions for all binders was similar (Figs. 1 and 6). However, considerable differences in the dissolution rate with different binders are evident. Starch paste and hydroxypropyl methylcellulose gave excellent *in vitro* dissolution, while acacia slowed the dissolution rate considerably (Fig. 6). These differences in dissolution rate are directly related to the effect of binders on disintegration time.

To confirm that the phenomenon of hardness increase induced by moisture is not specific to naproxen, a water-soluble compound, sodium benzoate and a water-insoluble excipient, microcrystalline cellulose, were studied (Formulation K) (Fig. 7). This formulation could be compressed at higher moisture contents. The hardness increase induced by the partial moisture loss occurred at a higher moisture content. Dissolution before and after exposure to ambient room conditions changed only slightly.

Obviously, if the water-soluble drug or the water-soluble excipient in the granulation does not recrystallize in the void spaces on compression, the moisture-induced phenomenon of hardness increase would not occur (Fig. 8). The granulations contained a soluble drug, naproxen sodium, and an insoluble excipient, microcrystalline cellulose. Naproxen sodium absorbs water, and the percentage of water absorbed is proportional to the relative humidity of the surrounding atmosphere. The hardness increase did not occur after storage under various conditions. *In vitro* dissolution also remained similar after overnight drying at 80°.

CONCLUSION

The results of this study suggest that the tablet hardness increase induced by partial moisture loss occurs because of recrystallization of water-soluble excipients or a water-soluble drug that is expelled into the void spaces on compression. The extent of the hardness increase depends on the specific combination of the drug and excipients, and their physical

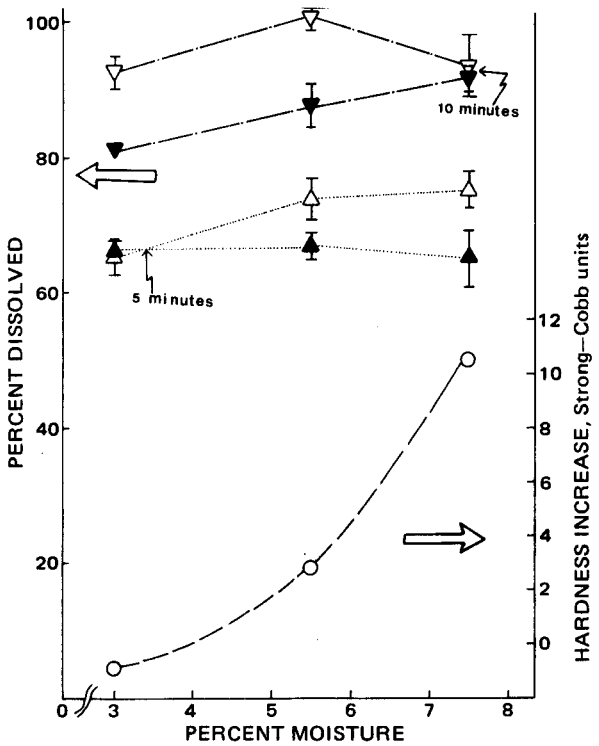

Figure 7—*Effect of hardness increase induced by the partial loss of moisture on the* in vitro *dissolution of compressed tablets prepared from sodium benzoate and microcrystalline cellulose. Key:* ○, *hardness increase* versus *percent moisture plot;* △ *and* ▽, in vitro *dissolution immediately after compression; and* ▲ *and* ▼, in vitro *dissolution after hardness increase. Vertical lines represent standard deviations; the absence of vertical lines indicates that the standard deviation was too small to be shown.*

properties such as aqueous solubility, crystalline properties, and hygroscopicity. These data indicate that this phenomenon could be avoided by careful selection of excipients. No significant decrease in *in vitro* dissolution occurs as a result of the hardness increase induced by the moisture content. However, in the absence of the moisture-induced phenomenon, when moisture contents of the granulations are low, hardness produced by the use of higher compression induces a considerable decrease in *in vitro* dissolution.

Specifications for the hardness of compressed tablets are generally established for two unrelated reasons. A minimum hardness limit is needed to ensure that the tablets resist chipping, abrasion, and breakage during packaging, storage, transportation, and handling prior to use. A maximum hardness limit for tablets is intended to ensure proper dissolution of the drug.

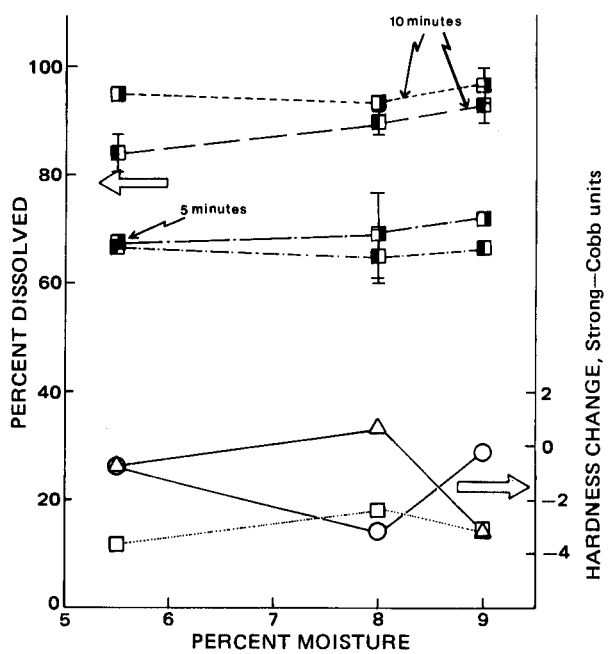

Figure 8—*Effect of moisture on hardness and* in vitro *dissolution of naproxen sodium tablets containing microcrystalline cellulose. Key:* ○, *change in hardness after exposure to ambient conditions;* △, *change in hardness after exposure in a desiccator;* □, *change in hardness after overnight drying at 80°;* ■, in vitro *dissolution immediately after compression; and* ◧, in vitro *dissolution after overnight drying at 80°. Vertical lines represent standard deviations; the absence of vertical lines indicates that the standard deviation was too small to be shown.*

Since the important parameter, *in vitro* dissolution of the tablets, is related to the moisture content of the granulation and the hardness of the tablets at the time of compression, an *in vitro* dissolution specification would ensure that the tablets did meet the moisture and hardness requirements as well. Therefore, it is recommended that the moisture content of the granulation and the initial hardness of the tablets be used as in-process controls. A lower limit of hardness should be established to ensure resistance of the tablets to abrasion, *etc.*

REFERENCES

(1) E. Shotton and J. E. Rees, *J. Pharm. Pharmacol. Suppl.*, **18**, 1960 (1966).

(2) J. E. Rees and E. Shotton, *J. Pharm. Sci.*, **60**, 1704 (1971).

(3) N. A. Armstrong and R. V. Griffith, *Pharm. Acta Helv.*, **45**, 692 (1970).

Hemodynamic Alterations in Isoproterenol-Induced Cardiac Arrhythmias in Corticoid-Treated Rats

MICHAEL A. BARLETTA ˣ, DAVID LEHR, and GIANCARLO GUIDERI

Received September 8, 1977, from the *Department of Pharmaceutical Sciences, College of Pharmacy and Allied Health Professions, St. John's University, Jamaica, NY 11439.* Accepted for publication February 2, 1978.

Abstract □ Hemodynamic alterations were studied to determine their role in isoproterenol-induced cardiac arrhythmias in the desoxycorticosterone acetate–saline-treated rat. Since epinephrine, a catecholamine possessing an α-adrenergic receptor agonist component, was considerably less potent as an arrhythmogenic agent, an elevation in blood pressure was thought to be protective against arrhythmias. Both albuterol, a β_2-adrenergic agonist, alone and epinephrine administered following tolazoline, an α-adrenergic blocking agent, decreased blood pressure to that of isoproterenol but failed to elicit significant arrhythmias. Phenylephrine administered prior to isoproterenol resulted in significant arrhythmias despite the maintenance of mean blood pressure at normal levels. The study shows that blood pressure alterations are not important in the etiology of isoproterenol-induced arrhythmias in the corticoid-pretreated rat.

Keyphrases □ Cardiac arrhythmias—isoproterenol induced, effect of hemodynamic alterations, rats treated with desoxycorticosterone acetate □ Isoproterenol-induced cardiac arrhythmias—effect of hemodynamic alterations in rats treated with desoxycorticosterone acetate □ Desoxycorticosterone acetate—pretreatment, effect of hemodynamic alterations on isoproterenol-induced cardiac arrhythmias

Previous research reported that low, normally nontoxic doses of isoproterenol administered to desoxycorticosterone acetate–saline-pretreated rats resulted in severe cardiac arrhythmias, frequently causing death by ventricular fibrillation within 15 min (1). The extraordinary potentiation of acute isoproterenol toxicity (20,000 times) induced by corticoid treatment in animals also was thought to be related to isoproterenol aerosol deaths in asthmatic patients (2). This relationship was made since most patients were severe asthmatics concurrently on long-term prednisone therapy and isoproterenol. This theory was further supported by findings that showed that the fluorocarbon aerosol propellant at levels found in these aerosol products was not arrhythmogenic in the asthmatic patient (3).

BACKGROUND

Many theories were suggested to explain the arrhythmogenic action of isoproterenol in corticoid-treated rats (4–6). The most interesting involved the synergistic alteration of myocardial electrolytes, involving depletion of potassium and magnesium and a gain of sodium associated with isoproterenol and desoxycorticosterone (7). These effects were thought to be associated with the inhibition of membrane function and an arrhythmogenic liability.

The role of blood pressure variations in cardiac rhythm disturbances was studied extensively in hydrocarbon–catecholamine-induced arrhythmias. Although arrhythmogenicity of epinephrine was not related to the height of its blood pressure elevation, arrhythmias disappeared when blood pressure was reduced (8). Intracardiac tension was thought to favor the development of ventricular arrhythmias and ventricular fibrillation. An adrenolytic substituted benzodioxane reversed epinephrine's pressor response and prevented ventricular fibrillation (9). An elevation of blood pressure might be involved in epinephrine's arrhythmogenic action.

Further studies (10, 11) showed that large doses of tolazoline and dibenamine, beyond those necessary to reversal, were able to protect against cyclopropane–epinephrine arrhythmias but that the artificial elevation of blood pressure by using a regulator or compression of the aorta caused a reappearance of these arrhythmias. Normal sinus rhythm and multifocal ventricular tachycardia were induced by varying mechanically the systemic blood pressure during constant epinephrine infusions, but ventricular fibrillation could not be induced (12).

Several studies (13, 14) showed that elevation of blood pressure by 50–100 mm Hg above normal by using a dextran infusion or narrowing the aorta did not influence the fibrillation threshold in the normal anesthetized cat. However, the production of hypertension by the same procedure in the failing heart did decrease the fibrillation threshold. By using cyclopropane–isoproterenol-induced arrhythmias, the effect of blood pressure variation on the arrhythmogenic threshold dose of this catecholamine was studied (15). Changes in systemic blood pressure (decreased from 30 to 60 mm Hg by bleeding or increased 30 mm Hg or more by aortic constriction) had no effect on the arrhythmogenic threshold dose of isoproterenol, which indicates that blood pressure was not an important factor in these arrhythmias.

In addition, bilateral vagotomy or the minimum blocking dose of atropine did not protect against arrhythmias in epinephrine–cyclopropane arrhythmias, nor did bilateral vagotomy alter the effect of aortic occlusion in inducing irregularities after small protective doses of dibenamine (11). Dawes (16) and Katz (17) agreed that blood pressure is not a crucial factor in hydrocarbon–catecholamine-induced arrhythmias and that arrhythmias often are independent of blood pressure variations. Nevertheless, these changes are among the many contributory factors in the production of cardiac arrhythmias.

It was suggested (18) that blood pressure lowering by isoproterenol may decrease coronary flow and that the cardiac stimulatory effects of isoproterenol greatly increase the oxygen requirements of the myocardial fibers. Increased oxygen requirements, together with a decreased coronary flow, lead to hypoxia and thereby myocardial damage. Although hypoxia may be important in the initiation of cellular damage and death, there is controversy as to whether hypoxia is important in the production of arrhythmias.

Szekeres and Papp (19) found a decrease in the fibrillation threshold of cats and dogs administered an oxygen (5–10%)–nitrogen (90–95%) mixture. Turnbull *et al.* (20), however, found no effect on the fibrillation threshold in dogs that had inhaled gas mixtures of various oxygen content, including those used by Szekeres and Papp (19).

The present study was undertaken to evaluate further the importance of hemodynamic alterations associated with isoproterenol in corticoid–isoproterenol arrhythmias.

EXPERIMENTAL

Male albino rats (362) of the Wistar strain, 250–350 g, were divided into four groups. Animals in Group A (desoxycorticosterone acetate–saline) were implanted subcutaneously with a 25-mg desoxycorticosterone acetate pellet in the axillary region while under tribromoethanol anesthesia (25 mg/100 g ip) and were maintained thereafter on 1% saline. Animals in Group B (desoxycorticosterone acetate) were implanted with the same dose of desoxycorticosterone acetate but were maintained on tap water instead of saline. Animals in Group C (saline rats) were maintained on 1% saline instead of tap water. Group D (normal), untreated rats were maintained on tap water and were control animals. All rats had free access to drinking fluid and standard laboratory chow.

At predetermined intervals within 14–20 days, individual rats from these four groups were anesthetized with allobarbital–urethan (0.7 ml/kg ip) and prepared for the recording of blood pressure and ECG. All animals were ventilated artificially with a small respirator. Blood pressure was measured from the left carotid artery with a transducer. The standard limb leads on the ECG were recorded continually on a magnetic tape system. The chest lead selected was obtained by inserting an 18-gauge needle subcutaneously to the left of the sternum so that its tip reached the third intercostal space.

Blood pressure and ECG tracings were monitored on the oscilloscope

0022-3549/78/1000-1390$01.00/0
© 1978, American Pharmaceutical Association

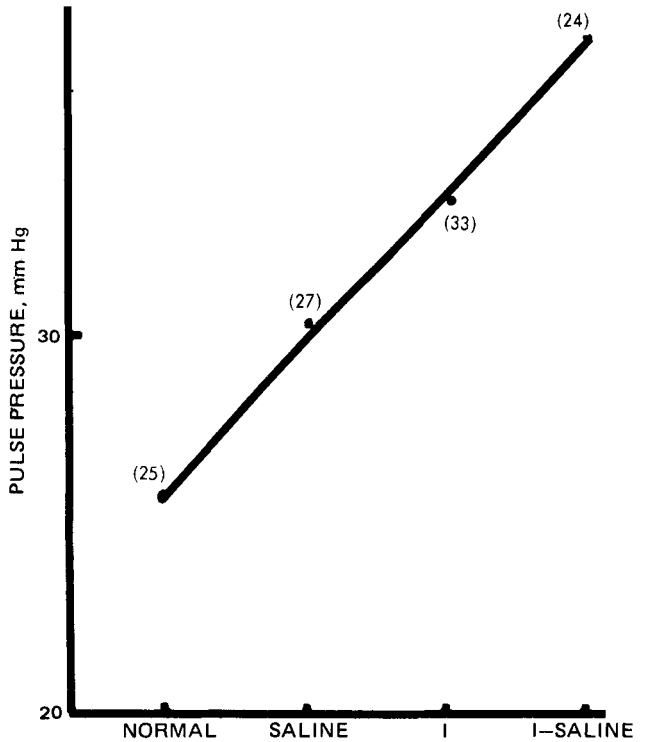

Figure 1—*Pulse pressures associated with the various animal groups.*

screen of a recorder and inscribed intermittently on photorecording paper. Following a 20–30-min stabilization, a single dose of isoproterenol hydrochloride, 10–1000 μg/kg, was injected subcutaneously; each animal was monitored continuously for 30 min and intermittently thereafter for a maximum of 1 or 2 hr.

To record the ECG in conscious, unrestrained rats, 16 desoxycorticosterone acetate–saline rats were prepared several days prior to the experiment in the following manner. Under tribromoethanol anesthesia, fine polytef-coated silver wires were passed under the skin by means of a trochar from each limb to the base of the neck. There the four wires were fixed by a small plaster of Paris cast sutured to the skin in such a manner that long protruding ends of the very flexible wire could be connected to the recording system without substantial restriction or discomfort to the animal. The polytef insulation had been removed from the limb end of the wires, and these terminals had been coated with silver–silver chloride. Statistical significance was determined using the Student *t* test. All animal groups were statistically compared to Group D (normal) rats.

RESULTS

Effect of Treatments—The various animal groups, normal, saline, desoxycorticosterone acetate, and desoxycorticosterone acetate–saline, showed little changes in resting mean blood pressure and heart rate. However, in the desoxycorticosterone acetate–saline group, pulse pressure was increased to the highest extent of all the treatment regimens (Fig. 1).

Effect of Isoproterenol on ECG—The injection of isoproterenol in normal and saline rats did not produce significant ECG changes. In desoxycorticosterone acetate and desoxycorticosterone acetate–saline rats, isoproterenol elicited pronounced ECG alterations and ventricular arrhythmias exemplified by S-T junctional changes, P-R interval prolongation, and higher degrees of A-V block, atrial flutter, and fibrillation.

Ventricular arrhythmias included multifocal premature contractions, coupled ectopic beats (primarily bigemini), ventricular tachycardia, and ventricular fibrillation, which was usually preceded by a short run of ventricular tachycardia or by a single extrasystole. Table I shows that the incidence of ventricular fibrillation was directly proportional to the dose of isoproterenol, reaching a maximum at 150 μg/kg. The comparative incidence of arrhythmias produced by isoproterenol in the four experimental groups showed that desoxycorticosterone acetate (I) animals were far more sensitive to isoproterenol than normal and saline groups, while

Table I—Effect of Isoproterenol on ECG, Heart Rate, and Mean Blood Pressure in the Normal, Saline, I, and I-Saline Rats

Isoproterenol Dose, μg/kg	Treatment	*n*	Arrhythmias		Heart Rate, Beats/min		Blood Pressure	
			Vent.[a]	Fib.[b]	Control, Mean ± *SE*	After Isoproterenol, Mean ± *SE*	Control, Mean ± *SE*	After Isoproterenol, Mean ± *SE*
100	Normal	10	0	0	371.8 ± 11.0	397.2 ± 9.9	122.1 ± 5.2	63.0 ± 4.9[c]
100	Saline	24	2	1	392.1 ± 7.6	415.8 ± 7.3[c]	138.3 ± 3.0	66.3 ± 2.9[c]
100	I	12	7	3	374.3 ± 8.6	407.1 ± 10.6[c]	123.6 ± 5.4	54.7 ± 4.1[c]
100	I–saline	12	12	9	375.4 ± 10.0	402.0 ± 12.0	111.7 ± 0.7	56.4 ± 4.4[c]
150	Normal	10	1	0	359.5 ± 10.3	399.1 ± 9.8[c]	128.8 ± 5.4	57.8 ± 2.8[c]
150	Saline	17	0	0	413.2 ± 7.0	447.8 ± 6.7[c]	145.4 ± 4.4	66.7 ± 2.8[c]
150	I	18	7	5	384.7 ± 6.7	423.8 ± 4.9[c]	134.8 ± 3.4	56.3 ± 2.3[c]
150	I–saline	33	33	26	382.1 ± 6.7	425.1 ± 4.5[c]	125.5 ± 5.6	60.1 ± 3.3[c]
300	Normal	9	1	0	382.2 ± 12.2	414.7 ± 11.2	123.4 ± 5.9	53.8 ± 3.5[c]
300	Saline	17	2	0	397.2 ± 7.9	432.0 ± 7.1	134.0 ± 4.3	60.5 ± 3.3[c]
300	I	11	7	1	401.2 ± 7.3	425.1 ± 7.7	146.0 ± 5.5	62.5 ± 5.1[c]
300	I–saline	12	12	8	378.4 ± 14.2	408.6 ± 12.9	117.7 ± 3.0	45.8 ± 2.2[c]

[a] Ventricular arrhythmias. [b] Ventricular fibrillation. [c] $p < 0.05$.

Table II—Effect of Isoproterenol on ECG, Heart Rate, and Blood Pressure in I–Saline Rats

Isoproterenol Dose, μg/kg	n	Arrhythmias		Heart Rate, Beats/min		Blood Pressure	
		Vent.[a]	Fib.[b]	Control, Mean ± SE	After Isoproterenol, Mean ± SE	Control, Mean ± SE	After Isoproterenol, Mean ± SE
10	9	2	1	373.9 ± 12.0	388.4 ± 13.5	132.4 ± 4.5	77.3 ± 4.4[c]
30	11	8	4	363.9 ± 10.3	381.8 ± 10.6	118.8 ± 6.9	64.0 ± 7.1[c]
60	11	10	5	383.3 ± 12.5	402.7 ± 13.3	131.1 ± 8.8	60.5 ± 6.4[c]
100	12	12	9	375.4 ± 10.0	402.0 ± 12.0	111.7 ± 10.6	56.4 ± 4.4[c]
150	33	33	26	382.1 ± 6.7	425.1 ± 4.5[c]	125.5 ± 5.6	60.1 ± 3.3[c]
300	12	12	8	378.4 ± 14.2	408.6 ± 12.9	117.7 ± 3.0	45.8 ± 2.2[c]
400	14	11	6	366.0 ± 11.5	394.3 ± 12.1	128.1 ± 4.5	55.5 ± 5.3[c]
1000	12	9	3	376.6 ± 7.9	420.4 ± 10.3[c]	130.5 ± 6.0	52.3 ± 4.2[c]
				Unanesthetized			
10	5	5	1	359.2 ± 24.9	536.2 ± 19.0		
30	5	5	2	359.0 ± 9.2	536.2 ± 11.2		
60	4	4	4	396.0 ± 32.3	533.5 ± 5.9		
150	2	2	2	373.0 ± 7.1	518.0 ± 18.0		

[a] Ventricular arrhythmias. [b] Ventricular fibrillation. [c] $p < 0.05$.

Table III—Effect of Adrenergic Agents on the ECG, Heart Rate, and Mean Blood Pressure in I–Saline Rats

Treatment	Dose, mg/kg	n	Arrhythmias		Heart Rate, Beats/min			Blood Pressure, mm Hg		
			Vent.[a]	Fib.[b]	Control[c], Mean ± SE	Control[d], Mean ± SE	Maximum Effect, Mean ± SE	Control[c], Mean ± SE	Control[d], Mean ± SE	Maximum Effect, Mean ± SE
Isoproterenol	0.150	33	33	26	382.1 ± 6.7	—	425.1 ± 4.5	125.5 ± 5.6	—	60.1 ± 3.3[e]
Isoproterenol	0.130	12	12	8	378.4 ± 14.2	—	408.6 ± 12.9	117.7 ± 3.0	—	50.3 ± 8.8[e]
Epinephrine	0.202	6	0	0	408.4 ± 10.0	—	414.2 ± 9.6	134.7 ± 7.5	—	152.0 ± 5.7[e]
Levarterenol	0.125	4	0	0	386.5 ± 15.2	—	418.5 ± 9.4	128.7 ± 9.4	—	181.2 ± 13.9[e]
Albuterol	0.156	5	1	0	409.2 ± 24.9	—	413.0 ± 20.1	133.0 ± 8.5	—	68.8 ± 5.4[e]
Albuterol	0.312	4	0	0	354.8 ± 9.4	—	356.2 ± 6.2	126.0 ± 4.1	—	62.8 ± 1.4[e]
Albuterol	1.560	5	2	1	432.6 ± 20.9	—	451.0 ± 21.2	144.0 ± 11.1	—	78.4 ± 5.4[e]
Tolazoline	8.500	5	5	4	345.8 ± 13.0	368.4 ± 15.4	382.2 ± 15.2	136.6 ± 6.9	123.6 ± 5.7	53.2 ± 4.7[e]
Isoproterenol	0.150									
Tolazoline	8.500	5	1	0	449.4 ± 5.8	425.8 ± 2.6	433.8 ± 6.1	133.6 ± 7.7	105.6 ± 13.5[e]	71.8 ± 7.2[e]
Epinephrine	0.202									
Tolazoline	8.500	5	0	0	400.2 ± 11.4	398.6 ± 9.1	401.8 ± 7.8	149.2 ± 9.4	137.2 ± 8.5	103.8 ± 14.6[e]
Epinephrine	1.360									
Tolazoline	8.500	5	1	0	394.6 ± 9.1	394.4 ± 8.9	412.4 ± 7.8	141.6 ± 9.2	126.4 ± 4.0	140.6 ± 4.4[e]
Levarterenol	0.125									
Tolazoline	8.500	5	0	0	387.2 ± 10.1	396.8 ± 14.7	399.4 ± 10.6	134.8 ± 7.8	119.2 ± 7.4	95.4 ± 10.3[e]
Epinephrine	0.202									
Levarterenol	0.125									
Phenylephrine	1.500	5	5	5	414.8 ± 7.2	407.6 ± 11.5	427.0 ± 2.4	136.2 ± 5.3	175.4 ± 10.0[e]	120.0 ± 13.0[e]
Isoproterenol	0.150									
Phenylephrine	3.000	5	5	3	421.2 ± 16.0	413.2 ± 10.2	441.4 ± 12.8	122.0 ± 4.1	177.0 ± 7.3[e]	105.0 ± 4.5[e]
Isoproterenol	0.150									

[a] Ventricular arrhythmias. [b] Ventricular fibrillation. [c] No drug treatment. [d] Following first drug treatment. [e] $p < 0.05$.

desoxycorticosterone acetate (I)–saline animals were most sensitive to isoproterenol, with a majority of the animals experiencing ventricular fibrillation (Table I).

Effect of Isoproterenol on Heart Rate—The maximum chronotropic effect of various doses of isoproterenol in anesthetized desoxycorticosterone acetate (I) rats is illustrated in Table II. No significant difference was encountered in the control heart rate of either group, but isoproterenol induced an increase in heart rate in anesthetized desoxycorticosterone acetate (I)–saline rats at all doses. However, a significant difference from control animals could only be detected at 150 and 100 μg/kg and at all dosages in unanesthetized animals.

Effect of Isoproterenol on Blood Pressure—The data presented demonstrate that 100, 150, and 300 μg of isoproterenol/kg in all treatment groups produced a significant fall in blood pressure (Table I). When increasing dosages of isoproterenol were administered to desoxycorticosterone acetate (I)–saline rats, a significant consistent fall in blood pressure was observed at all doses (Table II).

Substitution of Epinephrine for Isoproterenol—Epinephrine bitartrate was employed instead of isoproterenol to determine whether another catecholamine possessing a potent β-adrenergic agonist component would produce arrhythmias in desoxycorticosterone acetate–saline rats. Under allobarbital–urethan anesthesia, no arrhythmias were elicited in rats treated with 202 μg of epinephrine/kg (equivalent to 150 μg of isoproterenol/kg) or in an additional group of animals treated with repeated doses of epinephrine up to a total of 4.0 mg/kg.

Since epinephrine is both an α- and a β-adrenergic receptor agonist, 10 desoxycorticosterone acetate–saline-pretreated, anesthetized rats were injected subcutaneously with the α-receptor blocking agent tolazoline (8.5 mg/kg). Ten minutes later, half of these animals were injected subcutaneously with 202 μg/kg; the remainder received 1.36-mg/kg doses of epinephrine. By this technique, it was expected that the unopposed β-adrenergic activity of epinephrine might elicit arrhythmias. However, essentially no cardiac irregularities were encountered, although both doses of epinephrine elicited hypotension instead of hypertension, which indicates effective blockade of vascular α-receptors by tolazoline (Table III). The same tolazoline pretreatment did not prevent ventricular arrhythmias and death in fibrillation in an additional group of desoxycorticosterone acetate (I)–saline rats injected with 150 μg of isoproterenol/kg (Table III).

A similar experiment was carried out in 40 conscious unrestrained rats pretreated for 3 weeks with desoxycorticosterone acetate–saline, using identical dosages of tolazoline and epinephrine. Fourteen animals in this group died within 1 hr in ventricular fibrillation. Thus, on the weight basis, epinephrine appeared to possess a weaker arrhythmogenic potential than isoproterenol, which became manifest only in the absence of anesthesia.

When levarterenol hydrochloride was substituted for isoproterenol in a dose of 125 μg/kg (equivalent to 150 μg of isoproterenol/kg), it increased heart rate and blood pressure but did not produce ventricular arrhythmias or fibrillation (Table III). When levarterenol was administered in the presence of α-adrenergic blockage (tolazoline, 8.5 mg/kg, administered prior to levarterenol), it likewise produced minor ventricular arrhythmias and no ventricular fibrillation (Table III).

Blood Pressure Alterations by Phenylephrine—Since isoproterenol normally caused a fall in blood pressure, it was of interest to determine whether arrhythmias could be induced by isoproterenol when blood pressure was maintained above 100 mm Hg. Therefore, phenylephrine, an α-adrenergic agonist with minimal cardiac stimulatory effect, was injected, and when the animals were clearly hypertensive (3–5 min), isoproterenol was administered (Table III). In these rats, isoproterenol consistently induced ventricular arrhythmias and ventricular fibrillation, although the mean blood pressure was maintained at normotensive levels of 105 and 120 mm Hg (Table III).

Blood Pressure Alteration with Albuterol—Albuterol, a β_2-agonist with preferential ability to activate vascular and bronchial smooth muscle rather than cardiac muscle, afforded the opportunity to produce hypotension with minor cardiac stimulatory effects. As expected, the administration of albuterol in doses equivalent to 0.15, 0.30, and 1.5 mg of isoproterenol/kg caused a fall in blood pressure comparable to isoproterenol and did not consistently produce arrhythmias or ventricular fibrillation (Table III).

DISCUSSION

It was surprising that epinephrine did not elicit cardiac arrhythmias in the anesthetized desoxycorticosterone acetate–saline rats since the arrhythmogenic properties of this agent closely resembled those of isoproterenol in many standard methods for the production of arrhythmias. This result may indicate the effect of general anesthesia and membrane depressants in protecting against these arrhythmias. Epinephrine also differed from isoproterenol because it inconsistently produced ventricular fibrillation in the conscious desoxycorticosterone acetate–saline animals and only if they had been previously treated with tolazoline. This finding, that epinephrine elicited arrhythmias only after α-adrenergic blockade, points to the importance of β-adrenergic stimulation in the genesis of these arrhythmias. Since α-adrenergic stimulants increase the fibrillation threshold (21), the α-adrenergic component of epinephrine may have exerted an antiarrhythmic action. Therefore, blockade of α-receptors by tolazoline would allow the predominance of β-activation and the emergence of ventricular arrhythmias and fibrillation.

β-Adrenergic stimulation produces, among other effects, myocardial ischemic changes and hypotension. In these experiments, desoxycorticosterone acetate and desoxycorticosterone acetate–saline rats appeared to be more sensitive to the ischemic changes induced by isoproterenol, because the most consistent, earliest, and prominent ECG change observed was a depression of the S-T junction. Myocardial ischemia probably increased the likelihood of rhythm irregularities in these animals because it enhances pacemaker activity (22, 23), slows conduction, and increases the dispersion of recovery of excitability in ventricular muscle (24).

Epinephrine, on the other hand, failed to produce ischemic changes as evidenced by the absence of S-T junctional depression. This difference between isoproterenol and epinephrine may have been due to elevation of blood pressure by the latter, which may have increased coronary perfusion and thus prevented the manifestation of ischemia. It was of interest to determine the role of blood pressure in the etiology of these arrhythmias, and two series of experiments were performed.

In the first experiments, albuterol, an agent more selective toward vascular than cardiac β-receptors (25, 26), produced hypotension comparable to that of isoproterenol without S-T junctional depression and did not elicit ventricular fibrillation. However, with a larger dose of this agent, one instance of ventricular fibrillation was obtained, probably as a consequence of a loss of its β-receptor selectivity. In the second set of experiments, when isoproterenol was administered in the presence of phenylephrine, mean blood pressure did not fall below levels to impair adequate coronary perfusion. Nonetheless, it consistently elicited a depression of the S-T junction as well as ventricular fibrillation. These results led to the same conclusion reached by other investigators: that blood pressure changes do not play a major role in the genesis of rhythm disturbances.

REFERENCES

(1) G. Guideri, M. Barletta, and D. Lehr, *Cardiovasc. Res.*, **8**, 775 (1974).

(2) D. Lehr, *N. Engl. J. Med.*, **287**, 987 (1974).

(3) C. T. Dollery, F. M. Williams, and G. I. Draffen, *Clin. Pharmacol. Ther.*, **15**, 596 (1974).

(4) Santagati, *Arch. De Vecchi Anat. Pathol.*, **49**, 467 (1967).

(5) H. Selye, *Circ. Res.*, **6**, 168 (1958).

(6) D. G. Wenzel and L. G. Stark, *Am. Heart J.*, **69**, 780 (1965).

(7) G. Guideri, M. Barletta, R. Chau, M. Green, and D. Lehr, "Recent Advances in Studies on Cardiac Structure and Metabolism," vol. 10, University Park Press, Baltimore, Md., 1975, p. 661.

(8) A. G. Levy, *Heart*, **5**, 299 (1914).

(9) T. C. R. Shen and R. Mari, *Arch. Int. Pharmacodyn. Ther.*, **64**, 58 (1940).

(10) G. K. Moe and S. D. Malton, *J. Pharmacol. Exp. Ther.*, **94**, 319 (1948).

(11) M. Nickerson and C. Nomaguchi, *ibid.*, **95**, 1 (1949).

(12) P. E. Dresel, K. L. MacConnel, and M. Nickerson, *Circ. Res.*, **8**, 948 (1960).

(13) A. Fronek and V. Ganz, *ibid.*, **8**, 175 (1960).

(14) L. Szekeres and J. G. Papp, *Prog. Drug Res.*, **12**, 293 (1968).

(15) P. E. Dresel, C. Hart, and C. R. Stromblad, *Circ. Res.*, **140**, 67 (1963).

(16) G. S. Dawes, *Pharmacol. Rev.*, **4**, 43 (1952).

(17) R. L. Katz, *Anesthesiology*, **26**, 289 (1965).

(18) G. Rona, C. I. Chappel, and D. S. Kahn, *Am. Heart J.*, **66**, 389 (1963).

(19) L. Szekeres and J. G. Papp, "Experimental Cardiac Arrhythmias Anti-Arrhythmic Drugs," Adademiai Kiado, Budapest, Hungary, 1971.

(20) A. D. Turnbull, L. D. MacLean, and A. R. Dobel, *J. Thorac.*

Cardiovasc. Surg., **50**, 842 (1966).
(21) J. G. Papp and L. Szekeres, *Eur. J. Pharmacol.*, **3**, 414 (1968).
(22) B. F. Hoffman and P. F. Cranefield, "Electrophysiology of the Heart," McGraw-Hill, New York, N.Y., 1960, p. 323.
(23) R. Kaufmann and U. Theophile, *Pfluegers Arch. Ges. Physiol.*, **297**, 174 (1967).
(24) D. H. Singer, R. Lazzara, and B. F. Hoffman, *Circ. Res.*, **21**, 537 (1967).
(25) V. A. Cullum, J. B. Farmer, D. Jack, and G. P. Levy, *Br. J. Pharmacol.*, **35**, 141 (1969).
(26) C. Kofi, J. M. Ekue, R. G. Shanks, and S. A. Zaidi, *ibid.*, **39**, 184 (1970).

Nitroglycerin Stability in Polyethylene Glycol 400 and Povidone Solutions

PORNPIMOL SUPHAJETTRA, JOHN H. STROHL, and JAMES K. LIM ˣ

Received May 26, 1977, from the *School of Pharmacy, West Virginia University, Morgantown, WV 26506.* Accepted for publication February 2, 1978.

Abstract □ The stability of solutions of nitroglycerin in several common pharmaceutical solvents and compounds used as tablet excipients was investigated using a UV spectrophotometric assay. Included in the study were povidone (I), polyethylene glycol 400 (II), and solvents such as absolute alcohol, propylene glycol, and glycerol. At the elevated temperatures of the accelerated stability studies, only II demonstrated a considerable adverse effect on the stability of the nitroglycerin solution. It is postulated that a "reaction compound" was formed between nitroglycerin and II which regenerated nitroglycerin depending on hydrolysis conditions. Based on the Arrhenius equation and with initial rates of up to 6 hr of degradation, the predicted stability for a II solution of nitroglycerin in terms of its 10% decomposition at 25° was approximately 7 days.

Keyphrases □ Nitroglycerin—stability in polyethylene glycol 400 and povidone solutions □ Stability—nitroglycerin in polyethylene glycol 400 and povidone solutions □ Polyethylene glycol 400—nitroglycerin solutions, stability □ Povidone—nitroglycerin solutions, stability □ Vasodilators, coronary—nitroglycerin, stability in polyethylene glycol 400 and povidone solutions

The problems encountered with nitroglycerin tablet stability, contributing to a loss of content uniformity (1) and possible potency variation, were the direct result of a measurable vapor pressure of nitroglycerin at room temperature (2). Attempts to overcome these difficulties included changes in the material of the nitroglycerin dosage form container and its cap liner (2). However, nitroglycerin volatilization still was not controlled effectively (3).

Reformulation of the tablet by incorporating "fixatives" (4–7) and changing the manufacturing process from molding to direct compression (8) were other attempts to control this physical problem. These steps were demonstrated to reduce successfully nitroglycerin volatility. For instance, polyethylene glycol 400 (II) (4) and povidone (I) (5, 6) have been employed as fixatives or stabilizing agents in nitroglycerin tablets to reduce volatility and thus maintain content uniformity and potency. A combination of I and microcrystalline cellulose (7), used as stabilizers, was demonstrated to be even more effective (3). The evaluation of these reformulated tablets was based on content uniformity and various physical tests, such as hardness, disintegration, and volatility, as well as exposure to several extreme conditions.

The current study was conducted to investigate the possible chemical interactions between nitroglycerin in solution and I and II since no such data were reported previously. If I or II exerted a detrimental effect, further studies would be conducted to predict nitroglycerin stability in the particular solvent.

EXPERIMENTAL

Nitroglycerin Stock Solution—*Preparation*—A 5-g portion of nitroglycerin mixture powder[1] in lactose was weighed and placed in a suitable separator. Chloroform[2], 10 ml, and 50 ml of deionized distilled water were added and the mixture was shaken gently for about 5 min to extract the nitroglycerin. The lower chloroform layer containing the extracted nitroglycerin was filtered[3].

The chloroform solvent was evaporated by blowing nitrogen gas on the surface until a constant weight of the pale-yellow viscous liquid of nitroglycerin was obtained. A sufficient volume of absolute alcohol was added to the weighed residue to obtain a nitroglycerin stock solution of approximately 1.0 mg/100 μl.

Standardization—This step was based on the USP method (9) with slight modifications. A standard solution of potassium nitrate was prepared by dissolving about 80 mg of potassium nitrate pellets[4], accurately weighed, with 1 ml of deionized distilled water in a 100-ml volumetric flask. Sufficient acetic acid[5] was then added to volume and mixed. A 100-μl volume of nitroglycerin solution to be standardized was withdrawn accurately and placed in a 100-ml volumetric flask containing 1 ml of acetic acid.

After the addition of 2 ml of phenoldisulfonic acid reagent, the mixture was shaken vigorously on a mechanical shaker for 3 min and allowed to stand at room temperature for another 15 min. Approximately 25 ml of deionized distilled water was added to dilute the reaction mixture before the addition of 10 ml of strong ammonia solution[5] and its final dilution to volume with deionized distilled water. Concurrently, 1 ml of the previously prepared standard potassium nitrate solution was pipetted into a 100-ml volumetric flask and treated similarly for the analysis as in the sample.

The absorbances at 410 and 600 nm of both solutions were determined simultaneously against a reagent blank. The strength of the nitroglycerin stock solution was then calculated from the equation:

$$\text{mg}/100\ \mu\text{l} = 0.749C[(A_{410} - A_{600})_U/(A_{410} - A_{600})_S] \quad \text{(Eq. 1)}$$

where 0.749 is a factor for relating the nitrate content of potassium nitrate to that of nitroglycerin, C is the potassium nitrate concentration in milligrams per milliliter in the potassium nitrate standard solution, and the subscripts U and S refer to the nitroglycerin sample and the potassium nitrate standard, respectively.

[1] S.D.M. No. 17, ICI America Inc., Wilmington, Del.
[2] ACS grade, Allied Chemical Corp., Morristown, N.J.
[3] Whatman filter paper No. 2.
[4] NF XI, Matheson, Coleman & Bell, Norwood, Ohio.
[5] ACS grade, Fisher Scientific Co., Fair Lawn, N.J.

0022-3549/78/1000-1394$01.00/0
© 1978, American Pharmaceutical Association

Cardiovasc. Surg., **50**, 842 (1966).
(21) J. G. Papp and L. Szekeres, *Eur. J. Pharmacol.*, **3**, 414 (1968).
(22) B. F. Hoffman and P. F. Cranefield, "Electrophysiology of the Heart," McGraw-Hill, New York, N.Y., 1960, p. 323.
(23) R. Kaufmann and U. Theophile, *Pfluegers Arch. Ges. Physiol.*, **297**, 174 (1967).
(24) D. H. Singer, R. Lazzara, and B. F. Hoffman, *Circ. Res.*, **21**, 537 (1967).
(25) V. A. Cullum, J. B. Farmer, D. Jack, and G. P. Levy, *Br. J. Pharmacol.*, **35**, 141 (1969).
(26) C. Kofi, J. M. Ekue, R. G. Shanks, and S. A. Zaidi, *ibid.*, **39**, 184 (1970).

Nitroglycerin Stability in Polyethylene Glycol 400 and Povidone Solutions

PORNPIMOL SUPHAJETTRA, JOHN H. STROHL, and JAMES K. LIM ˣ

Received May 26, 1977, from the *School of Pharmacy, West Virginia University, Morgantown, WV 26506.* Accepted for publication February 2, 1978.

Abstract □ The stability of solutions of nitroglycerin in several common pharmaceutical solvents and compounds used as tablet excipients was investigated using a UV spectrophotometric assay. Included in the study were povidone (I), polyethylene glycol 400 (II), and solvents such as absolute alcohol, propylene glycol, and glycerol. At the elevated temperatures of the accelerated stability studies, only II demonstrated a considerable adverse effect on the stability of the nitroglycerin solution. It is postulated that a "reaction compound" was formed between nitroglycerin and II which regenerated nitroglycerin depending on hydrolysis conditions. Based on the Arrhenius equation and with initial rates of up to 6 hr of degradation, the predicted stability for a II solution of nitroglycerin in terms of its 10% decomposition at 25° was approximately 7 days.

Keyphrases □ Nitroglycerin—stability in polyethylene glycol 400 and povidone solutions □ Stability—nitroglycerin in polyethylene glycol 400 and povidone solutions □ Polyethylene glycol 400—nitroglycerin solutions, stability □ Povidone—nitroglycerin solutions, stability □ Vasodilators, coronary—nitroglycerin, stability in polyethylene glycol 400 and povidone solutions

The problems encountered with nitroglycerin tablet stability, contributing to a loss of content uniformity (1) and possible potency variation, were the direct result of a measurable vapor pressure of nitroglycerin at room temperature (2). Attempts to overcome these difficulties included changes in the material of the nitroglycerin dosage form container and its cap liner (2). However, nitroglycerin volatilization still was not controlled effectively (3).

Reformulation of the tablet by incorporating "fixatives" (4–7) and changing the manufacturing process from molding to direct compression (8) were other attempts to control this physical problem. These steps were demonstrated to reduce successfully nitroglycerin volatility. For instance, polyethylene glycol 400 (II) (4) and povidone (I) (5, 6) have been employed as fixatives or stabilizing agents in nitroglycerin tablets to reduce volatility and thus maintain content uniformity and potency. A combination of I and microcrystalline cellulose (7), used as stabilizers, was demonstrated to be even more effective (3). The evaluation of these reformulated tablets was based on content uniformity and various physical tests, such as hardness, disintegration, and volatility, as well as exposure to several extreme conditions.

The current study was conducted to investigate the possible chemical interactions between nitroglycerin in solution and I and II since no such data were reported previously. If I or II exerted a detrimental effect, further studies would be conducted to predict nitroglycerin stability in the particular solvent.

EXPERIMENTAL

Nitroglycerin Stock Solution—*Preparation*—A 5-g portion of nitroglycerin mixture powder[1] in lactose was weighed and placed in a suitable separator. Chloroform[2], 10 ml, and 50 ml of deionized distilled water were added and the mixture was shaken gently for about 5 min to extract the nitroglycerin. The lower chloroform layer containing the extracted nitroglycerin was filtered[3].

The chloroform solvent was evaporated by blowing nitrogen gas on the surface until a constant weight of the pale-yellow viscous liquid of nitroglycerin was obtained. A sufficient volume of absolute alcohol was added to the weighed residue to obtain a nitroglycerin stock solution of approximately 1.0 mg/100 μl.

Standardization—This step was based on the USP method (9) with slight modifications. A standard solution of potassium nitrate was prepared by dissolving about 80 mg of potassium nitrate pellets[4], accurately weighed, with 1 ml of deionized distilled water in a 100-ml volumetric flask. Sufficient acetic acid[5] was then added to volume and mixed. A 100-μl volume of nitroglycerin solution to be standardized was withdrawn accurately and placed in a 100-ml volumetric flask containing 1 ml of acetic acid.

After the addition of 2 ml of phenoldisulfonic acid reagent, the mixture was shaken vigorously on a mechanical shaker for 3 min and allowed to stand at room temperature for another 15 min. Approximately 25 ml of deionized distilled water was added to dilute the reaction mixture before the addition of 10 ml of strong ammonia solution[5] and its final dilution to volume with deionized distilled water. Concurrently, 1 ml of the previously prepared standard potassium nitrate solution was pipetted into a 100-ml volumetric flask and treated similarly for the analysis as in the sample.

The absorbances at 410 and 600 nm of both solutions were determined simultaneously against a reagent blank. The strength of the nitroglycerin stock solution was then calculated from the equation:

$$\text{mg}/100\ \mu\text{l} = 0.749C[(A_{410} - A_{600})_U/(A_{410} - A_{600})_S] \quad \text{(Eq. 1)}$$

where 0.749 is a factor for relating the nitrate content of potassium nitrate to that of nitroglycerin, C is the potassium nitrate concentration in milligrams per milliliter in the potassium nitrate standard solution, and the subscripts U and S refer to the nitroglycerin sample and the potassium nitrate standard, respectively.

[1] S.D.M. No. 17, ICI America Inc., Wilmington, Del.
[2] ACS grade, Allied Chemical Corp., Morristown, N.J.
[3] Whatman filter paper No. 2.
[4] NF XI, Matheson, Coleman & Bell, Norwood, Ohio.
[5] ACS grade, Fisher Scientific Co., Fair Lawn, N.J.

0022-3549/78/1000-1394$01.00/0
© 1978, American Pharmaceutical Association

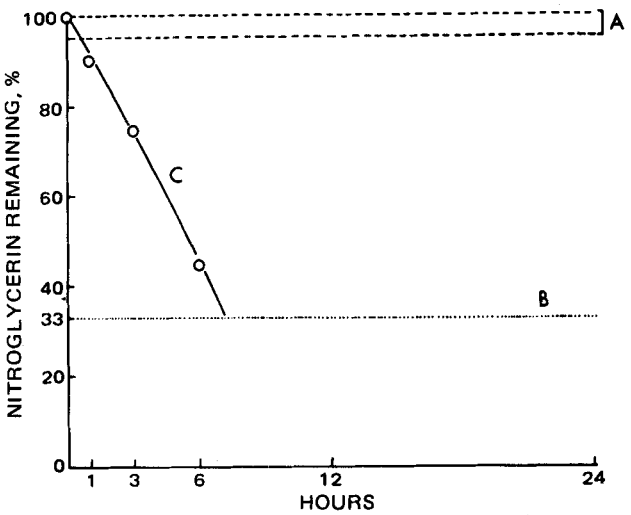

Figure 1—*Percentage of nitroglycerin remaining as a function of time in various solvent solutions at 80 ± 0.5° determined by UV spectrophotometry. Key: A, percentage range of nitroglycerin remaining in absolute alcohol, alcohol–water, glycerin, propylene glycol, and povidone; B, lower limit for the assay; and C, curve for percent nitroglycerin remaining in polyethylene glycol 400 solution.*

Analytical Method—The UV kinetic assay developed by Fung *et al.* (10) was employed in most determinations for nitroglycerin in aqueous solutions. A 1-ml volume of aqueous nitroglycerin solution was mixed with 3 ml of 0.05 *M* NaOH in methanol in a 1-cm cell. The determinations were made on a spectrophotometer[6] at the maximum at 336 nm. From these values, the amount of nitroglycerin was determined subsequently from calibration graphs made with nitroglycerin in the corresponding solvents.

In studies with I and II, the analysis was repeated using 0.1 *M* NaOH and the maximum absorbance readings obtained at 328 nm (11). This slightly modified procedure was based on a later report (11). However, no significant differences in the results were observed. In addition, a colorimetric method, involving an alkaline hydrolysis of nitroglycerin and subsequent diazotization and coupling of the nitrites formed with *N*-(1-naphthyl)ethylenediamine dihydrochloride (12), was performed on these test samples. Only I and II were analyzed by both the modified UV procedure and the Bell method since they represented those compounds that previously showed either an adverse effect or no effect on nitroglycerin stability in solution.

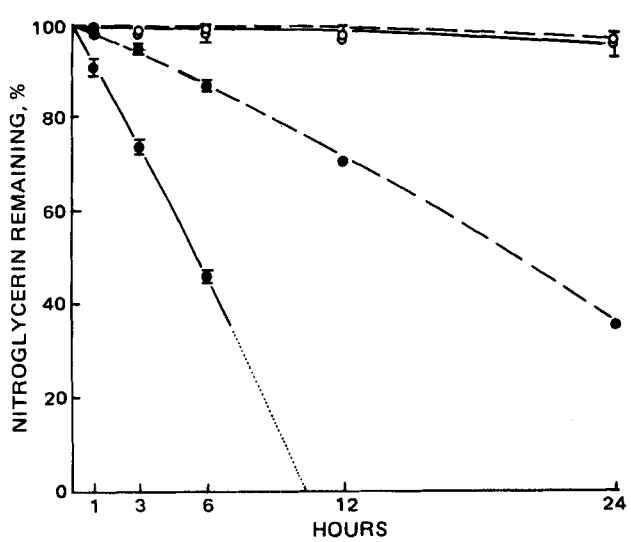

Figure 2—*Percentage of nitroglycerin remaining in povidone (○) and polyethylene glycol 400 (●) solutions as a function of time at 80 ± 0.5° compared using the spectrophotometric (—) and colorimetric (– –) methods.*

[6] Cary model 118, Varian Instruments Division, Palo Alto, Calif.

Table I—Percentage of Nitroglycerin Remaining in Polyethylene Glycol 400 and Povidone Solutions as a Function of Time at 80 ± 0.5°

Solvent	Method[a]	Hours 1	3	6	12	24
Polyethylene glycol 400	A	90.05	74.53	44.63	<33.00	<33.00
	B	99.73	95.62	88.03	69.92	34.96
Povidone	A	99.01	97.86	97.81	96.72	95.08
	B	99.57	98.81	98.03	97.37	96.55

[a] A = UV kinetic assay (10). B = colorimetric method (12).

Stability of Nitroglycerin Solutions—Samples containing the equivalent amount of 3 mg of nitroglycerin, as accurately transferred from the alcoholic stock solution, and 0.4 ml of the various solvents were subjected to a water bath temperature of 80 ± 0.5°. The solvents included absolute alcohol[7], water, glycerin[2], propylene glycol[8], polyethylene glycol 400[9], and alcohol–water (1:1) containing 10% (w/v) povidone[10]. All were used without further purification. At the end of 0, 1, 3, 6, 12, and 24 hr, flasks containing these mixtures were withdrawn from the water bath and adjusted to 10 ml with deionized distilled water. The percent nitroglycerin remaining in the different solvents was calculated and plotted as a function of time.

Nitroglycerin Degradation Kinetics in II—Replicate volumes containing the same quantities of nitroglycerin and II as used in the previous experiment were placed in 10-ml volumetric flasks. These flasks were subjected to both ambient room temperature and water bath temperatures of 40, 50, 60, and 70 ± 0.5°. Flasks were removed at 0, 1, 3, 6, 12, and 24 hr and subsequently diluted to volume with deionized distilled water.

Graphs of the percent nitroglycerin remaining as plotted against time for the various temperatures were obtained. Straight lines were drawn through the initial linear plots corresponding up to 6 hr of study. The slopes, representing the estimates of specific rates or rate constants, k, obtained within this initial period of nitroglycerin degradation were employed to construct the Arrhenius plot.

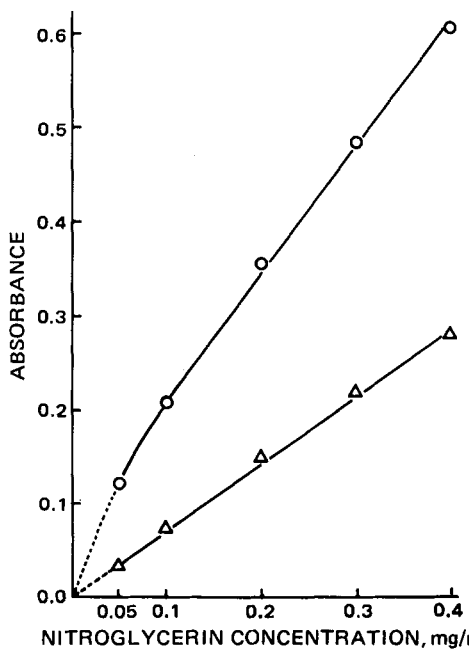

Figure 3—*Plot of absorbances as a function of nitroglycerin concentration in polyethylene glycol 400 solution. Key: ○, maximum absorbance determined at 336 nm by the spectrophotometric assay; and △, absorbance at 550 nm obtained by the colorimetric method.*

[7] U.S.I. absolute pure ethyl alcohol USP–NF reagent.
[8] Laboratory grade, Fisher Scientific Co., Fair Lawn, N.J.
[9] USP grade, Ruger Chemical Co., Irvington-On-Hudson, N.Y.
[10] Plasdone C-15, GAF Corp., New York, N.Y.

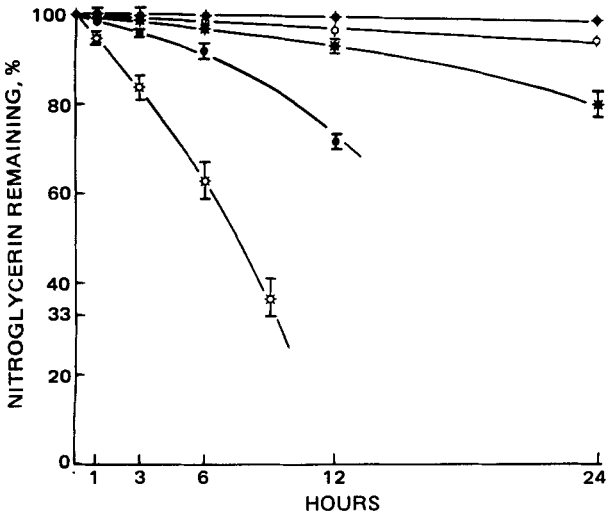

Figure 4—*Percentage of nitroglycerin remaining as a function of time in polyethylene glycol 400 solution at different temperatures as determined by the spectrophotometric method. Key: ◆, room temperature (~25°); ○, 40°; ✱, 50°; ●, 60°; and ☼, 70 ± 0.5°.*

RESULTS AND DISCUSSION

Nitroglycerin stability in the presence of various solvents as determined by the Fung UV kinetic assay (10, 11) is represented schematically in Fig. 1. Absolute alcohol, alcohol-water (1:1), glycerin, propylene glycol, and 10% (w/v) povidone exerted no deleterious effects on nitroglycerin stability. Not less than 95% of the original nitroglycerin remained after 24 hr under conditions of the specified accelerated stability studies with these solvents. However, under identical conditions and in a solution of II, the amount of nitroglycerin decreased considerably with time.

It is postulated that a "reaction compound" was formed between nitroglycerin and II which increased in amount with time. This reaction could result in a reduced amount of free nitroglycerin molecules determinable by the Fung method. The assay of nitroglycerin in this solvent by the Bell method (12), employing sodium hydroxide in place of strontium hydroxide as the hydrolyzing agent, confirmed the marked reduction of assayable nitroglycerin occurring with II (Table I and Fig. 2). However, the amount of nitroglycerin remaining in II after exposure to heat when determined by the Fung method was comparatively lower than that obtained by the Bell colorimetric method. This difference could be attributed partly to the more drastic hydrolysis procedure employed in the Bell method, which resulted in a relatively greater breakdown of the reaction compound, releasing more free nitroglycerin, and, consequently, a higher recovery for the analysis.

Based on the calibration plot obtained by the Fung method in contrast to that obtained by the Bell method, the absorbance below 0.2 (Fig. 3), corresponding to approximately 0.1 mg of nitroglycerin/ml (in this case, 33% nitroglycerin) remaining could not be validly correlated with concentration. Consequently, no plots were included in the graphs (Figs. 1 and 2) representing determinations at 12 and 24 hr for the nitroglycerin solution in II since they showed absorbance readings of 0.1334 and 0.0952, respectively.

The stability of a nitroglycerin solution in II represented in terms of percent nitroglycerin remaining as a function of time for up to 24 hr is shown in Fig. 4. Decomposition is presumed to be complex because of the nonlinear curves becoming especially noticeable after 6 hr. Thus, for each temperature studied, straight lines were drawn through only the initial parts of the plots to derive the specific rates, k. An Arrhenius plot (Fig. 5) then was obtained using these values and gave a linear correlation coefficient of 0.994.

The calculated $t_{90\%}$, which corresponds to the time for 10% nitroglycerin decomposition, was estimated to be 7.4 days based on $k_{40°}$ and $k_{50°}$ values of 0.250 and 0.625%/hr, respectively. This value agrees favorably with that obtained for nitroglycerin samples of similar composition when subjected to actual ambient room temperature conditions. The observed $t_{90\%}$ value for nitroglycerin where temperature varied between 20 and 24° was approximately 10 days.

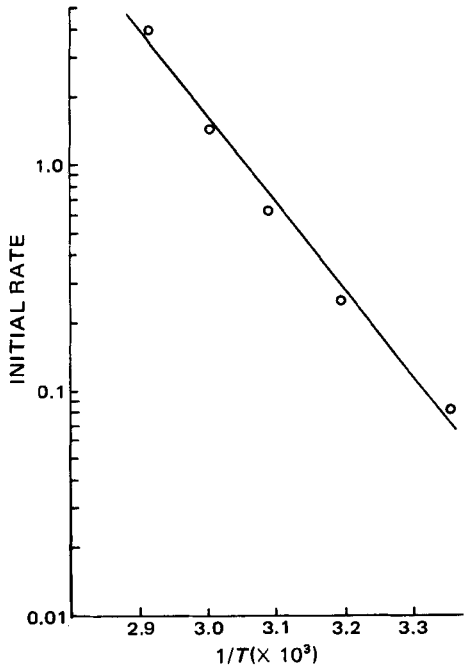

Figure 5—*Arrhenius plot for initial degradation rates of nitroglycerin in polyethylene glycol 400 solution as a function of temperature.*

In conclusion, on the basis of these experimental data obtained for a simple solution of nitroglycerin in II, extra care should be observed when formulating liquid pharmaceutical dosage forms of similar compositions. A tablet dosage form of nitroglycerin, formulated with markedly lower proportions of either II or polyethylene glycol 4000 and subjected to 37° and at 85% relative humidity for up to 39 months, was reported to exhibit good stability (13).

REFERENCES

(1) S. A. Fusari, *J. Pharm. Sci.*, **62,** 122 (1973).

(2) B. A. Edelman, A. M. Contractor, and R. F. Shangraw, *J. Am. Pharm. Assoc.*, **NS 11,** 30 (1971).

(3) B. Dorsch and R. F. Shangraw, *Am. J. Hosp. Pharm.*, **32,** 795 (1975).

(4) S. A. Fusari, *J. Pharm. Sci.*, **62,** 2012 (1973).

(5) W. H. Hargrove, *Tile and Till*, **59,** 65 (1973).

(6) H. L. Fung, S. K. Yap, and C. T. Rhodes, *J. Pharm. Sci.*, **65,** 558 (1976).

(7) F. W. Goodhart, H. Gucluyildiz, R. E. Daly, L. Chafetz, and F. C. Ninger, *ibid.*, **65,** 1466 (1976).

(8) M. D. Richman, C. D. Fox, and R. F. Shangraw, *ibid.*, **54,** 447 (1965).

(9) "The United States Pharmacopeia," 19th rev., Mack Publishing Co., Easton, Pa., 1975.

(10) H. L. Fung, P. Dalecki, E. Tse, and C. T. Rhodes, *J. Pharm. Sci.*, **62,** 696 (1973).

(11) S. K. Yap, C. T. Rhodes, and H. L. Fung, *Am. J. Hosp. Pharm.*, **32,** 1039 (1075).

(12) F. K. Bell, *J. Pharm. Sci.*, **53,** 752 (1964).

(13) S. A. Fusari, "Formulary Monograph," Parke, Davis, Detroit, Mich., 1977.

ACKNOWLEDGMENTS

Presented at the Basic Pharmaceutics Section, APhA Academy of Pharmaceutical Sciences, New York meeting, May 1977.

Abstracted in part from a thesis submitted by P. Suphajettra to West Virginia University in partial fulfillment of the Master of Science degree requirements.

Supported in part by a grant from the Aerosol Division, Chemical Specialties Manufacturers Association, New York, N.Y.

The authors thank Dr. John Gruninger, Chemistry Department, and Dr. Louis C. Martinelli, School of Pharmacy, for helpful discussions.

Semiautomated System for High-Pressure Liquid Chromatographic Determination of Dissolution Rate of Fludrocortisone Acetate Tablets

HAMED M. ABDOU ˣ, THERESE M. AST, and FRANCIS J. CIOFFI

Received September 12, 1977, from the *Methods Development and Technical Standards Department, E. R. Squibb & Sons, Inc., New Brunswick, NJ 08903.* Accepted for publication February 2, 1978.

Abstract □ A new semiautomated high-pressure liquid chromatographic (HPLC) system is described to determine the dissolution rate of fludrocortisone acetate tablets. The system uses a miniaturized dissolution basket and shaft assembly having the same geometry as that given in USP XIX. This reduced size permits use of smaller volumes of dissolution medium, allowing most very low dose oral solid dosage forms to be handled. The USP dissolution kettle was also replaced with a new miniaturized vessel that continuously filters the sample solution before it enters the flow system. Volumes of dissolution medium as small as 15 ml can be accommodated, depending on the sensitivity of the assay employed and the solubility of the drug substance under study. The concentration of fludrocortisone acetate in solution was monitored by a new HPLC system employing a reversed-phase column compatible with the aqueous dissolution medium used. A comparative dissolution study of different lots was made using different basket rotation speeds.

Keyphrases □ Fludrocortisone acetate—tablets, dissolution, high-pressure liquid chromatographic analysis □ Dissolution, *in vitro*—fludrocortisone acetate tablets, high-pressure liquid chromatographic analysis □ High-pressure liquid chromatography—analysis, dissolution of fludrocortisone acetate tablets □ Adrenocortical steroids—fludrocortisone acetate tablets, dissolution, high-pressure liquid chromatographic analysis

Fludrocortisone acetate (9α-fluoro-11β,17α,21-trihydroxy-4-pregnane-3,20-dione), a potent adrenocortical steroid (1), is usually administered as 0.1-mg tablets. The USP XIX dissolution apparatus could not be used to investigate its dissolution characteristics because of the resulting very low concentration of the active ingredient in the 900 ml of solvent specified. Under these conditions, none of the available methods, UV (1), blue tetrazolium (2), nydrazid (2), and 4-aminoantipyrine (3), has the sensitivity required for reliable quantitative analysis. The same difficulty exists in dissolution studies of other pharmaceutical formulations administered in very low doses, *e.g.*, estrogens, thyroxine fractions, digoxin, and digitoxin tablets. Since such a large volume of dissolution fluid is specified by the compendia mainly to minimize the effect of the concentration gradient on the dissolution rate, it seemed logical that the volume could be reduced significantly while still maintaining sink conditions[1].

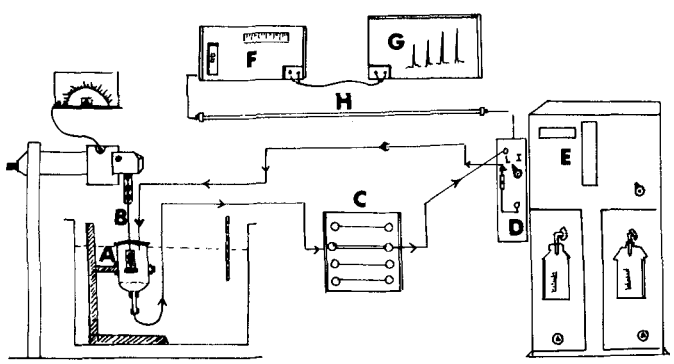

Figure 1—*Flow diagram for semiautomated system for the HPLC determination of the dissolution rate of fludrocortisone acetate tablets.*

Table I—Comparison between USP XIX and Miniaturized Basket and Drive Shaft Assembly [a]

Component	USP XIX	Miniaturized Version
Material	40-mesh, type 316 stainless steel	40-mesh, type 316 stainless steel
Shaft	26 mm × 30 cm	Upper part, 6.4 mm × 7.5 cm; lower part, 4 mm × 7.5 cm
Basket	25 × 36.6 mm	10 × 15.6 mm

[a] Details of the new design are shown in Fig. 2.

To accomplish this volume reduction, some basic modifications had to be made in the USP XIX dissolution apparatus. These modifications included the design of a miniaturized basket, drive shaft assembly, and dissolution vessel. A semiautomated high-pressure liquid chromatographic (HPLC) system also was developed to monitor the fludrocortisone acetate in solution based on the HPLC assay of fludrocortisone acetate recently developed.

EXPERIMENTAL

Apparatus—The system is modular, with the components arranged as shown in Fig. 1. The dissolution vessel (A) consists of a 30-ml glass filter funnel[2] with 2–2.5-μm diameter pores. This filter funnel is connected to a glass U tube *via* a vinyl polymer[3] sleeve and is fitted with a polytef[4] disk cover (3.8 cm i.d.) that has two circular openings. The first opening (6.7 mm i.d.), in the center, is for the basket drive shaft; the second opening (2 mm i.d.), to one side of the cover, is for the return line polyethylene probe from the HPLC injector.

The basket drive shaft assembly (B) consists of a miniaturized version[5] with the same geometry as the USP XIX assembly (Table I and Fig. 2). A proportioning pump[6] (C) was used to circulate the dissolution medium through the injector valve (D), the HPLC instrument, and back to the dissolution vessel. The HPLC instrument[7] (E) consisted of a fixed volume mobile phase reservoir (200 ml), a nitrogen cylinder to maintain system pressure, and a UV monitor operated at 254 nm. The detector (F) output was displayed on a 10-mv recorder[8] (G).

The HPLC column (H) was packed with reversed-phase packing material[9]; the mobile phase consisted of 50 ± 2% acetonitrile[10] in water, pumped at a pressure of 1000 psi, which resulted in a flow rate of 1.2–1.4 ml/min. The HPLC instrument was equipped with a 20-μl loop injector[11], the inlet of which was connected to a 0.065-mm i.d. proportioning pump tube. The outlet was connected to a polyethylene tube, positioned about 2 cm below the surface of the dissolution medium *via* a plastic nipple, which replaced the injector syringe.

[1] Defined as not allowing the concentration of the active ingredients in solution to exceed 10% of saturation level.
[2] Thomas Catalog No. 5221-B30, type 20VF.
[3] Tygon.
[4] Teflon.
[5] Made for Squibb by the Hanson Research Corp., Northridge, Calif.
[6] Technicon pump II, Technicon Instruments, Tarrytown, N.Y.
[7] Chromatronix 3100, Spectra-Physics, Santa Clara, Calif.
[8] Model 410, Pharmacia Fine Chemicals, Piscataway, N.J.
[9] C_{18}-μBondapak, Waters Associates, Milford, Mass.
[10] UV grade distilled in glass, Burdick and Jackson.
[11] Chromatronix and HPSV-20, Spectra-Physics, Santa Clara, Calif.

0022-3549/78/1000-1397$01.00/0
© 1978, American Pharmaceutical Association

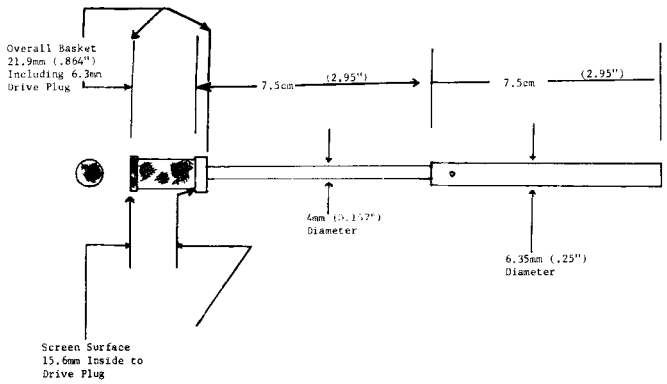

Figure 2—*Design and measurements of the miniaturized dissolution basket and shaft assembly.*

Solutions—The standard stock solution was 0.08 mg of fludrocortisone acetate/ml in acetonitrile. The working standard solutions were three aqueous solutions of standard stock solution accurately prepared to contain 3.5, 1.5, and 0.8 μg/ml.

Procedure—A system suitability test was performed by injecting the working standard solution (3.5-μg/ml level) at least three times. The relative standard deviation did not exceed 2.5%. The dissolution medium was 30 ml of distilled water, which was pipetted into the filter funnel, kept at 37 ± 0.1°, and circulated through the loop injector valve at 1.5 ml/min. One tablet was introduced into the dissolution basket, which was then immersed into the dissolution medium to a depth of 0.6 ± 0.2 cm from the bottom of the dissolution vessel.

The basket was rotated at 125 rpm; after each 15-min interval, a 20-μl aliquot of the sample solution was injected into the chromatograph by turning the injection valve from the "load" position to the "inject" position. After complete dissolution was reached, the polyethylene sampling probe was transferred from the dissolution vessel consecutively to the three working standard solutions. Each standard solution was chromatographed twice.

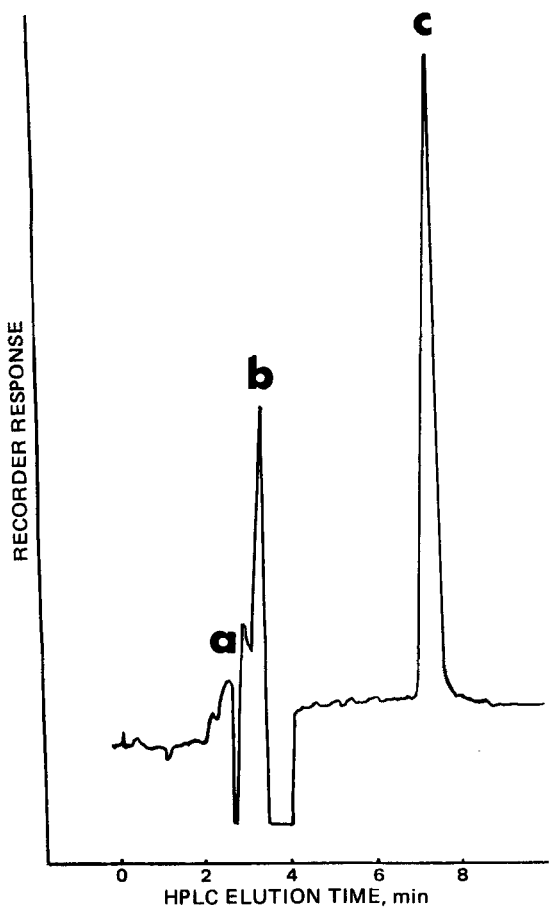

Figure 3—*Chromatogram obtained during the determination of the dissolution rate of fludrocortisone acetate tablets. Key: a, solvent; b, tablet excipients; and c, fludrocortisone acetate (~3.3 μg/ml).*

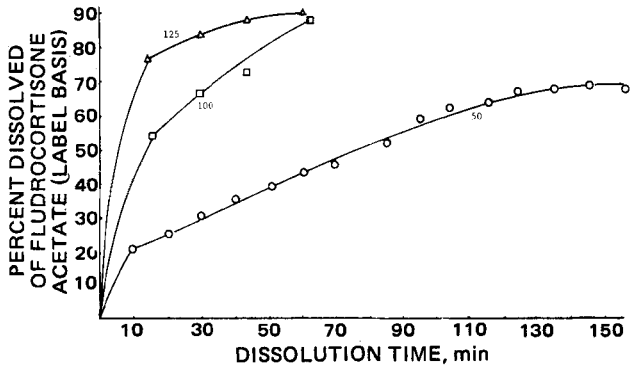

Figure 4—*Comparison between the dissolution rate of fludrocortisone acetate at different rotation speeds. Each point is an average of six tablets of the same lot. Key: ○, 50 rpm; □, 100 rpm; and △, 125 rpm.*

RESULTS AND DISCUSSION

The major difficulty in determining the dissolution rate of fludrocortisone acetate tablets was its very low concentration of active ingredient (0.1 mg/tablet). Therefore, to obtain a measurable concentration in solution, it was necessary to reduce drastically the volume of the dissolution medium recommended by the compendia. A 30-ml volume was used, which was enough to maintain sink conditions and still provide a reasonable concentration for HPLC analysis. Furthermore, the use of such a small volume of dissolution medium alleviated the homogeneity problem usually encountered with the 900-ml compendial system, especially with such low dosage forms.

A reduced version of the USP XIX dissolution system had to be designed to use such a small volume of dissolution medium. The size of the dissolution vessel can be changed on an individual basis to accommodate larger volumes of dissolution medium, depending on the solubility of the active ingredient, to ensure the maintenance of sink conditions. The use of downward direction solvent flow was necessitated by the need for simultaneous sample filtration. The prescribed slow flow rate also helped to maintain a hydrodynamic condition as close as possible to that encountered in the compendial system.

The described miniaturized dissolution assembly is generally applicable to all solid dosage forms containing very low concentrations of active ingredients, *e.g.*, estrogens, thyroxine fractions, digoxin, and digitoxin tablets. Neither the blue tetrazolium nor the nydrazid assay has enough sensitivity to measure fludrocortisone acetate in the very low concentration range encountered in this study (30% dissolution = 1 μg/ml). The 4-aminoantipyrine method described in the USP XIX for content uniformity analysis also lacks the sensitivity required for these low concentrations. The HPLC assay used in this study has a sensitivity of about 0.5 μg/ml, which is more than adequate.

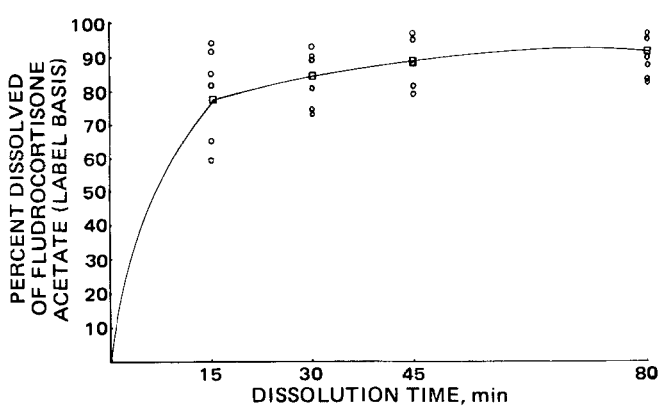

Figure 5—*Dissolution rate of six individual tablets of Lot 1 in distilled water at 125 rpm. Key: ○, individual tablet; and □, average of six tablets.*

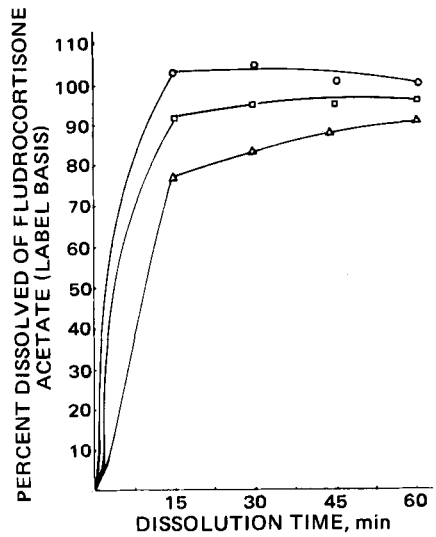

Figure 6—*Comparison between the dissolution rate of different lots of commercial fludrocortisone acetate tablets at 125 rpm in distilled water. Each point is an average of six tablets. Key: △, Lot 1; □, Lot 2; and ○, Lot 3.*

The linearity of the fludrocortisone acetate chromatographic response was checked within a concentration range of 0.8–4.0 μg/ml, equivalent to 25–120% of tablet potency. The response was linear (r = 0.999). The average relative standard deviation for triplicate injections of each standard level varied from 1 to 3%. Figure 3 shows a sample chromatogram from an actual tablet dissolution run. In studying the dissolution rate of fludrocortisone acetate tablets, three different basket rotation speeds were investigated: 50, 100, and 125 rpm. Figure 4 shows that for the same lot the dissolution rate significantly increased with an increase in basket rotation speed.

To compare the dissolution characteristics of different lots, six tablets of each of three different lots were tested in water at 125 rpm. Figure 5 shows the spread in dissolution behavior between different tablets of the same lot, and Fig. 6 compares the dissolution profiles of different lots. In all cases, DT_{50}[12] was less than 15 min while DT_{85}[13] varied between 12 and 37 min. Although the assay values of the three lots were above 95% of the label value, Lot 3 did not reach 90% dissolution even after 2 hr. These tablet-to-tablet and lot-to-lot variations in dissolution characteristics are thought to be due to differences in tablet uniformity.

REFERENCES

(1) "Analytical Profiles of Drug Substances," vol. 3, K. Florey, Ed., Academic, New York, N.Y., 1974, p. 282.

(2) "Pharmaceutical Analysis," T. Higuchi and E. Brochmann-Hanssen, Eds., Interscience, New York, N.Y., 1961, p. 70.

(3) E. P. Schulz, M. A. Diaz, G. Lopez, L. M. Guerrero, H. Barrera, A. L. Pereda, and A. Aguilera, *Anal. Chem.*, **36**, 1634 (1964).

[12] DT_{50} is the time required for 50% of the label value of the drug to go into solution.

[13] DT_{85} is the time required for 85% of the label value of the drug to go into solution.

Bioavailability of Sulfonamide Suspensions I: Dissolution Profiles of Sulfamethizole Using Paddle Method

JEFFREY D. STRUM *, JOHN L. COLAIZZI *, THOMAS J. GOEHL ‡, JAMES M. JAFFE *, WILLIAM H. PITLICK *, VINOD P. SHAH §, and ROLLAND I. POUST *x

Received September 19, 1977, from the **Department of Pharmaceutics and the* ‡*Department of Medicinal Chemistry, University of Pittsburgh, Pittsburgh, PA 15261,* and the §*Division of Biopharmaceutics, Food and Drug Administration, Washington, DC 20204.* Accepted for publication February 2, 1978.

Abstract □ A comparative bioavailability study was performed using two commercially available, chemically equivalent brands of sulfamethizole suspension. One gram of each suspension was administered to 12 different subjects following a completely randomized crossover design. Serum levels and derived pharmacokinetic parameters were compared statistically. There were no significant differences in the extent of sulfamethizole absorption from the two suspensions as evidenced by the area under the serum level–time curves. Significant differences ($p < 0.05$) in the mean serum levels at 0.5 and 0.75 hr and differences in C_{max} and t_{max} indicated that the absorption rate differed for the two products. *In vitro* tests including particle-size analysis and dissolution studies were performed. The size-frequency distribution of particles in the suspensions was studied using a resistance particle counter. The dissolution characteristics of the two products were studied using the Food and Drug Administration's paddle method and the spin-filter apparatus. Suspension A had a significantly greater amount of drug dissolved at 15 and 30 min using either method. It also had a greater percentage of particles at the smaller size range, indicating that the greater dissolution rate may be related directly to the decreased particle size. A comparison of the *in vivo* and *in vitro* results demonstrated a definite rank-order correlation between the dissolution performance of the two suspensions and the *in vivo* parameters reflecting the absorption rate. Suspension A had a greater amount of drug dissolved at 15 and 30 min and resulted in higher serum levels at 0.5 and 0.75 hr, a higher C_{max}, and a shorter t_{max}.

Keyphrases □ Sulfamethizole—bioavailability in humans and *in vitro* dissolution, two suspensions compared □ Bioavailability—sulfamethizole, two suspensions compared □ Dissolution, *in vitro*—sulfamethizole, two suspensions compared □ Antibacterials—sulfamethizole, bioavailability in humans and *in vitro* dissolution, two suspensions compared

In vitro dissolution testing can be a valuable tool for predicting or assuring the *in vivo* performance of a dosage form if appropriate correlation has been established. Several methods are employed for measuring the dissolution of the common solid dosage forms, capsules and tablets. For a drug to be absorbed, the solid dosage form must first undergo disintegration, deaggregation, and then dissolution of drug particles. The size of drug particles in the postdisintegration state affects the dissolution rate.

Suspension dosage forms correspond to the postdisin-

0022-3549/78/1000-1399$01.00/0
© 1978, American Pharmaceutical Association

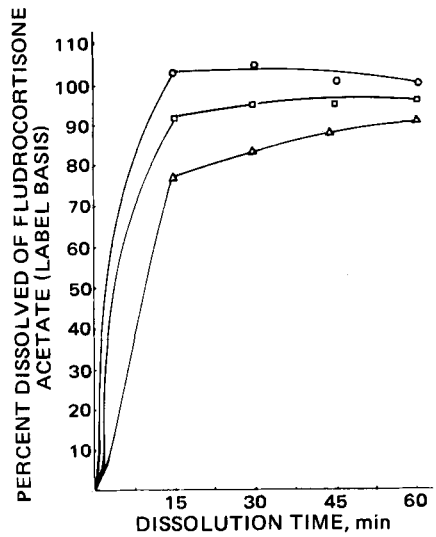

Figure 6—*Comparison between the dissolution rate of different lots of commercial fludrocortisone acetate tablets at 125 rpm in distilled water. Each point is an average of six tablets. Key: △, Lot 1; □, Lot 2; and ○, Lot 3.*

The linearity of the fludrocortisone acetate chromatographic response was checked within a concentration range of 0.8–4.0 μg/ml, equivalent to 25–120% of tablet potency. The response was linear (r = 0.999). The average relative standard deviation for triplicate injections of each standard level varied from 1 to 3%. Figure 3 shows a sample chromatogram from an actual tablet dissolution run. In studying the dissolution rate of fludrocortisone acetate tablets, three different basket rotation speeds were investigated: 50, 100, and 125 rpm. Figure 4 shows that for the same lot the dissolution rate significantly increased with an increase in basket rotation speed.

To compare the dissolution characteristics of different lots, six tablets of each of three different lots were tested in water at 125 rpm. Figure 5 shows the spread in dissolution behavior between different tablets of the same lot, and Fig. 6 compares the dissolution profiles of different lots. In all cases, DT_{50}[12] was less than 15 min while DT_{85}[13] varied between 12 and 37 min. Although the assay values of the three lots were above 95% of the label value, Lot 3 did not reach 90% dissolution even after 2 hr. These tablet-to-tablet and lot-to-lot variations in dissolution characteristics are thought to be due to differences in tablet uniformity.

REFERENCES

(1) "Analytical Profiles of Drug Substances," vol. 3, K. Florey, Ed., Academic, New York, N.Y., 1974, p. 282.

(2) "Pharmaceutical Analysis," T. Higuchi and E. Brochmann-Hanssen, Eds., Interscience, New York, N.Y., 1961, p. 70.

(3) E. P. Schulz, M. A. Diaz, G. Lopez, L. M. Guerrero, H. Barrera, A. L. Pereda, and A. Aguilera, *Anal. Chem.*, **36**, 1634 (1964).

[12] DT_{50} is the time required for 50% of the label value of the drug to go into solution.

[13] DT_{85} is the time required for 85% of the label value of the drug to go into solution.

Bioavailability of Sulfonamide Suspensions I: Dissolution Profiles of Sulfamethizole Using Paddle Method

JEFFREY D. STRUM *, JOHN L. COLAIZZI *, THOMAS J. GOEHL ‡, JAMES M. JAFFE *, WILLIAM H. PITLICK *, VINOD P. SHAH §, and ROLLAND I. POUST *x

Received September 19, 1977, from the **Department of Pharmaceutics and the* ‡*Department of Medicinal Chemistry, University of Pittsburgh, Pittsburgh, PA 15261,* and the §*Division of Biopharmaceutics, Food and Drug Administration, Washington, DC 20204.* Accepted for publication February 2, 1978.

Abstract □ A comparative bioavailability study was performed using two commercially available, chemically equivalent brands of sulfamethizole suspension. One gram of each suspension was administered to 12 different subjects following a completely randomized crossover design. Serum levels and derived pharmacokinetic parameters were compared statistically. There were no significant differences in the extent of sulfamethizole absorption from the two suspensions as evidenced by the area under the serum level–time curves. Significant differences ($p < 0.05$) in the mean serum levels at 0.5 and 0.75 hr and differences in C_{max} and t_{max} indicated that the absorption rate differed for the two products. *In vitro* tests including particle-size analysis and dissolution studies were performed. The size-frequency distribution of particles in the suspensions was studied using a resistance particle counter. The dissolution characteristics of the two products were studied using the Food and Drug Administration's paddle method and the spin-filter apparatus. Suspension A had a significantly greater amount of drug dissolved at 15 and 30 min using either method. It also had a greater percentage of particles at the smaller size range, indicating that the greater dissolution rate may be related directly to the decreased particle size. A comparison of the *in vivo* and *in vitro* results demonstrated a definite rank-order correlation between the dissolution performance of the two suspensions and the *in vivo* parameters reflecting the absorption rate. Suspension A had a greater amount of drug dissolved at 15 and 30 min and resulted in higher serum levels at 0.5 and 0.75 hr, a higher C_{max}, and a shorter t_{max}.

Keyphrases □ Sulfamethizole—bioavailability in humans and *in vitro* dissolution, two suspensions compared □ Bioavailability—sulfamethizole, two suspensions compared □ Dissolution, *in vitro*—sulfamethizole, two suspensions compared □ Antibacterials—sulfamethizole, bioavailability in humans and *in vitro* dissolution, two suspensions compared

In vitro dissolution testing can be a valuable tool for predicting or assuring the *in vivo* performance of a dosage form if appropriate correlation has been established. Several methods are employed for measuring the dissolution of the common solid dosage forms, capsules and tablets. For a drug to be absorbed, the solid dosage form must first undergo disintegration, deaggregation, and then dissolution of drug particles. The size of drug particles in the postdisintegration state affects the dissolution rate.

Suspension dosage forms correspond to the postdisin-

0022-3549/78/1000-1399$01.00/0
© 1978, American Pharmaceutical Association

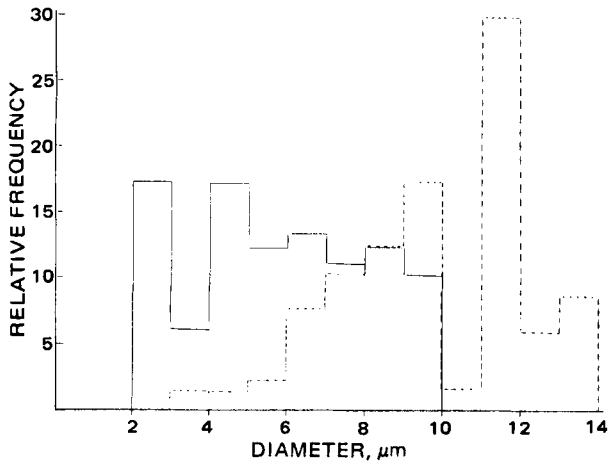

Figure 1—*Particle-size distribution of Suspensions A (—) and B (- - -).*

tegration stage of tablets and capsules, and drug particle dissolution is a prerequisite to bioavailability. Suspensions thus share the dissolution process as an absorption process rate-limiting step with tablets and capsules. Because of the difficulties in handling suspensions by methods primarily designed for tablets or capsules, few research efforts have concentrated on dissolution rate profiles for suspensions. Previous studies (1, 2) emphasized the need to determine the dissolution characteristics of suspension dosage forms. Recently, the dissolution rate profile of steroid suspensions was determined using the spin-filter apparatus (2).

This report presents the methodology for determining the dissolution rate profiles of suspensions using the Food and Drug Administration's (FDA) two-bladed paddle method. The feasibility and reproducibility of the method were demonstrated by determining the dissolution profile of two commercial, chemically equivalent sulfamethizole suspensions. Correlation studies with *in vivo* data and with data generated using the spin-filter method and particle-size measurements also are reported. The paddle method is simple, inexpensive, reproducible, and easily adaptable to the USP basket apparatus.

EXPERIMENTAL

***In Vivo* Study Protocol**—Twelve healthy, normal adult male volunteers, 20–34 years of age and weighing 60–89 kg, each received a 1-g dose of two different commercial chemically equivalent sulfamethizole suspensions, A[1] and B[2], followed by 120 ml of distilled water. The suspensions were administered in a completely randomized crossover design with a 2-week rest between doses.

All subjects fasted for 10 hr before and 3 hr following drug administration.

Blood samples (6 ml) were drawn using evacuated glass containers[3] at 0, 0.25, 0.50, 0.75, 1, 1.5, 2, 2.5, 3, 4, 5, 6, 7, 8, and 10 hr. The samples were centrifuged[4] at 3500 rpm, and the serum was separated and frozen until analyzed.

Particle-Size Analysis—The particle-size analysis was performed using a resistance particle counter[5] equipped with a triple manometer and a 50-μm aperture tube. The instrument was calibrated with 3.40-μm polystyrene microspheres supplied by the manufacturer. Initial sizing estimates were obtained with a microscope[6] equipped with a calibrated ocular micrometer[6]. Preliminary particle-size studies also were performed using 100- and 200-μm aperture tubes.

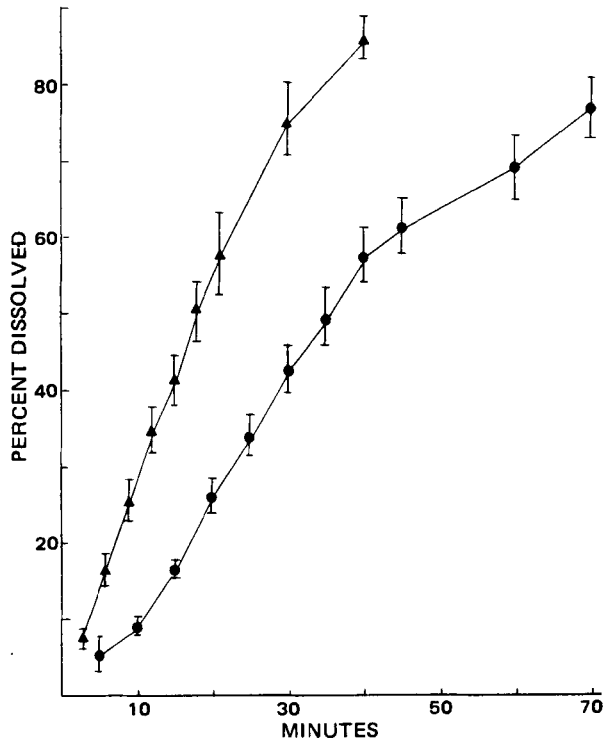

Figure 2—*Mean percent dissolved (±SE) of two commercial sulfamethizole suspensions using the FDA paddle method. Key: ▲, Suspension A; and ●, Suspension B.*

Dilutions of the commercial suspensions (1:50,000) were prepared in a 1% sodium chloride solution saturated with sulfamethizole[7] and containing 0.01% polysorbate 80[8]. The diluent was filtered through a series of membrane filters[9] to eliminate all particles above 0.22 μm in size. To determine the effect of excipient particles on the sizing procedure, an additional set of dilutions (1:50,000) was prepared in the electrolyte–surfactant diluent containing no sulfa drug. All particle counts were corrected for background and coincidence.

Dissolution: Paddle Method—Dissolution profiles of 12 500-mg samples of each suspension were determined at 37° in 900 ml of pH 7.2 phosphate buffer using the FDA paddle method (3) at 25 rpm. Preliminary studies indicated that the dissolution of the suspension samples was too rapid to measure at paddle speeds greater than 25 rpm. The apparatus consists of a cylindrical 1000-ml round-bottom flask[10] secured in a multiple-spindle dissolution drive apparatus[11] and immersed in a controlled temperature bath[12] maintained at 37°. The paddle was positioned to extend to exactly 2.5 cm above the flask bottom.

The suspension was introduced carefully into the flask bottom using a 10-ml glass syringe with an attached 19-cm needle[13]. Paddle rotation was engaged and controlled at a constant 25 rpm using a dissolution stirrer drive[11]. Initial dissolution trials indicated that Suspension A dissolved at a greater rate than Suspension B. On the basis of the data from the preliminary trials, the following sampling schedules were established: Suspension A, 3, 6, 9, 12, 15, 18, 21, 30, and 40 min; and Suspension B, 5, 10, 15, 20, 25, 30, 35, 40, 45, 60, and 70 min.

Samples of 2 ml of the dissolution medium were withdrawn (and replaced with an equal volume of drug-free buffer) in a 5-ml glass syringe through an attached 8.9-cm 20-gauge stainless steel needle[14] secured to the cover of the dissolution flask and positioned to extend 5.2 cm into the dissolution medium. Initially, samples were drawn simultaneously from three different needle depths (5.2, 6.7, and 9.0 cm) to determine if the drug was uniformly dissolved in the area of the sampling needle. The

[1] Thiosulfil, lot 1BBW, Ayerst Laboratories, New York, N.Y.
[2] Proklar, lot 107514, Westerfield Division of O'Neal, Jones, & Feldman, Cincinnati, Ohio.
[3] Vacutainers, silicone-coated interior, Becton Dickinson & Co., Rutherford, N.J.
[4] IEC HN-S centrifuge, Damon/IEC Division, Needham Heights, Mass.
[5] Model ZB counter, Coulter Electronics, Hialeah, Fla.
[6] Fisher Scientific Co., Pittsburgh, Pa.
[7] Sulfamethizole, lot R15917B, Ayerst Laboratories, New York, N.Y.
[8] Tween 80, ICI America, Wilmington, Del.
[9] Millipore Corp., Bedford, Mass.
[10] Kimbel Glass No. 33710-51.
[11] Model 53, Spec. 72B, Hanson Research Corp., Northridge, Calif.
[12] Blue M Electric Co., Blue Island, Ill.
[13] Travenol Laboratories, Morton Grove, Ill.
[14] Pitkin spinal needle, Becton Dickinson & Co., Rutherford, N.J.

Table I—*In Vitro* Dissolution Performance (Mean Percent Dissolved ± *SD*) of Two Sulfamethizole Suspensions

Minutes	Dissolution Method	Suspension A	Suspension B	Statistical Evaluation
15	Paddle[a]	41.67 ± 10.72	16.92 ± 4.64	$p < 0.05$
30	Paddle[a]	75.68 ± 16.07	43.29 ± 11.27	$p < 0.05$
15	Spin filter[b]	72.38 ± 4.27	54.39 ± 6.69	$p < 0.05$
30	Spin filter[b]	92.11 ± 3.05	76.57 ± 7.39	$p < 0.05$

[a] Twelve trials. [b] Six trials.

samples were immediately filtered through a 13-mm, 0.2-μm membrane filter[15] and analyzed for sulfamethizole using the Bratton and Marshall (4) colorimetric method.

Dissolution: Spin Filter—The dissolution profiles of six 500-mg samples of each suspension were determined at 37° in 900 ml of pH 7.2 phosphate buffer at 100 rpm using the rotating filter–stationary basket apparatus described by Shah *et al.* (5). Initial studies indicated that filter speeds greater than 100 rpm resulted in a dissolution rate that was too rapid to measure. The basket was removed for all dissolution trials. The sampling schedule was established on the basis of preliminary trials as described for the paddle method. Samples of 2 ml were withdrawn through the pilot tube into 5-ml glass syringes and analyzed for sulfamethizole using the Bratton and Marshall (4) colorimetric method.

Analysis of *In Vivo* Samples—All *in vivo* serum samples were analyzed for sulfamethizole content by high-pressure liquid chromatography (HPLC). The serum sample (0.2 ml) was transferred to a 1-ml vial[16] containing 5 μl of an internal standard, and 0.1 ml of 14% trichloroacetic acid was added. The samples were mixed[17] and then centrifuged[18] at 2500 rpm for 15 min. A 5-μl aliquot of the clear supernate then was injected onto the column. A linear calibration curve was observed in the 1–90-μg/ml range with an estimated precision of ±2% (*RSD*).

The modular high-pressure liquid chromatograph consisted of a constant-flow pump[19], a valve-type injector[20], a fixed wavelength (254 nm) UV detector[21], and a strip-chart recorder[22]. The stainless steel column (3.9 nm × 30 cm) was packed with fully porous 10-μm silica particles to which was chemically bonded a monomolecular layer of octadecylsilane[23].

Adequate separation of the serum components and unmetabolized drug was achieved using a mobile phase of acetonitrile–1% acetic acid (22:78) and a flow rate of 1.5 ml/min. The column temperature was maintained at 32° by inserting the column into a glass sleeve immersed in a constant-temperature water bath[24].

A stock solution of sulfamethizole[25] was prepared by dissolving 100 mg of sulfamethizole in 0.1 *N* NaOH and adjusting to volume in a 100-ml volumetric flask. Plasma standards were prepared by transferring the appropriate volume of the stock solution to control plasma. Calibration curves were obtained daily. The internal standard stock solution was prepared by transferring 300 mg of sulfamethoxazole[26] to a 100-ml volumetric flask and diluting to volume with 0.1 *N* NaOH.

Data Analysis—The number of drug particles for each size range was determined by subtracting the particle count due to excipients from the total particle count. The number distribution was then converted to a weight distribution (6), and the percent oversize at each size interval was calculated and plotted against the midpoint of the size interval on log probability paper. The mean diameter was determined from the equation for the fitted linear regression line.

The dissolution data for the two suspensions were treated by converting observed drug concentrations at each sampling time to amounts dissolved and, in turn, to percents dissolved. The mean percent dissolved and standard deviation were calculated for each sampling time for the two brands. Values at common sampling times were compared statistically using the Student *t* test.

The peak serum concentration, C_{max}, and time of the peak concentration, t_{max}, were obtained from the individual serum level *versus* time curves. The area under the curve (*AUC*) values were calculated according to the trapezoidal rule and corrected for the area beyond the last data point. The individual *AUC* values were then "normalized" (7) by multiplying the calculated *AUC* by the K_E value obtained from the terminal linear portion of the serum level *versus* time curves. The *in vivo* performance of the two suspensions was statistically compared by analyzing the individual values for C_{max}, t_{max}, K_E, normalized *AUC*, and serum levels at each sampling time using a *t* test for matched pairs.

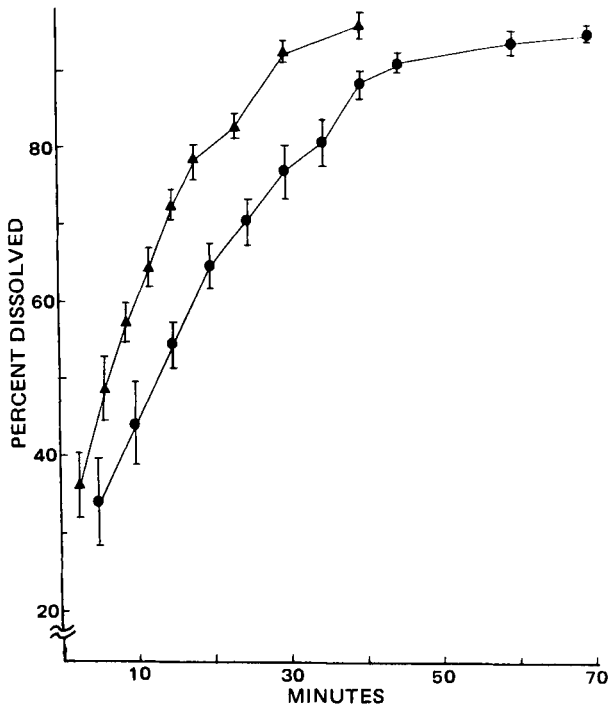

Figure 3—*Mean percent dissolved (±SE) of two commercial sulfamethizole suspensions using the spin-filter method. Key: ▲, Suspension A; and ●, Suspension B.*

RESULTS

An initial microscopic examination of the suspensions indicated that most particles had diameters of 10 μm or less, with no particle diameter exceeding 24 μm (Fig. 1). Data obtained using the 100- and 200-μm aperture tubes indicated that the particles were distributed almost entirely between 2 and 15 μm, with only an insignificant number of counts occurring beyond 15 μm. The particle distribution according to number was converted to a weight distribution to provide an appropriate relationship with the weight of suspension dissolved or absorbed. Particles in Suspension B had a geometric mean diameter of 8.69 ± 1.37 μm, while particles in Suspension A had a geometric mean diameter of 4.90 ± 1.5 μm.

Analysis of the dissolution data obtained using both the paddle method and the spin-filter apparatus demonstrated a substantial difference in the dissolution characteristics of Suspensions A and B. A statistically significant difference ($p < 0.05$) existed between the two suspensions for the percent of drug dissolved at the 15- and 30-min sampling times using both methods (Table I). The entire dissolution profiles of both products are shown in Figs. 2 and 3 for the two methods. An analysis of the amount of drug dissolved at the three different sampling depths indicated that there was no statistically significant difference in drug concentration at those depths.

Figure 4 illustrates the mean serum values for both suspensions at each of the 14 sampling times. A summary of the *in vivo* results and statistical evaluation appears in Table II. Statistically significant differences between the two suspensions were noted when individual values for C_{max}, t_{max}, and serum concentrations at 0.5 and 0.75 hr were analyzed. The results indicated that Suspension A administration resulted in significantly higher serum levels at 0.5 and 0.75 hr and a higher peak concentration, C_{max}, at an earlier time, t_{max}. There were no significant differences in the values for *AUC*, K_E, and serum concentrations at the remaining sampling times. These results indicated that the differences were related to the rate rather than the extent of absorption.

[15] Gelman Instrument Co., Ann Arbor, Mich.
[16] Reacti-Vials, No. 13261, Pierce, Inc., Rockford, Ill.
[17] Vortex-Genie, Fisher Scientific Industries, Springfield, Mass.
[18] IEC EXD centrifuge 460G, Damon/IEC Division, Needham Heights, Mass.
[19] Model M-6000A chromatography pump, Waters Associates, Milford, Mass.
[20] Model U6K universal injector, Waters Associates, Milford, Mass.
[21] Model 440 absorbance detector, Waters Associates, Milford, Mass.
[22] Varian A-25 dual-channel strip-chart recorder, Varian Associates, Walnut Creek, Calif.
[23] Prepacked μBondapak C_{18}, Waters Associates, Milford, Mass.
[24] Braun Thermonix II, Bronwill Scientific Co., Rochester, N.Y.
[25] Powder lot R15917B, Ayerst Laboratories, New York, N.Y.
[26] Powder lot 708115, Roche Chemical Division, Nutley, N.J.

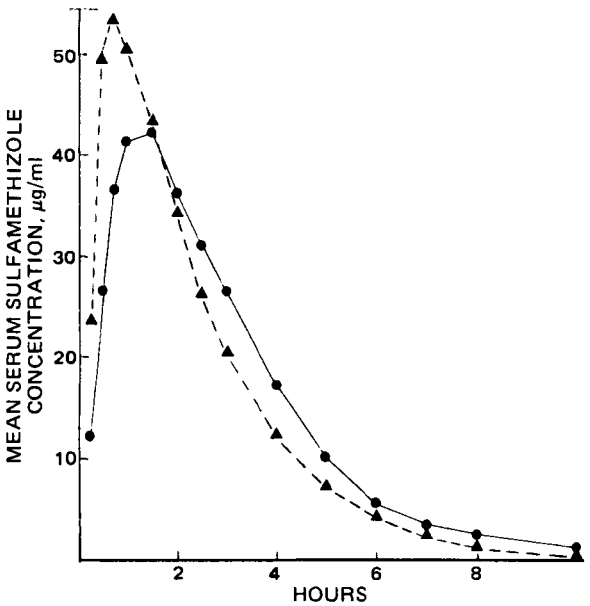

Figure 4—*Mean serum concentrations for 12 subjects for two different brands of sulfamethizole suspension. Key: ▲, Suspension A; and ●, Suspension B.*

DISCUSSION

A statistical evaluation of the results indicated that the absorption rate for Suspension A was greater than that for Suspension B. There were no statistical differences in the extent of drug absorption from the two suspensions.

Suspension A had a significantly greater amount of drug dissolved at 15 and 30 min using either the FDA paddle method or the spin-filter apparatus. Suspension A also had a greater percentage of particles at the smaller size range, indicating that the greater dissolution rate may be directly related to the decreased particle size.

A comparison of the *in vivo* and *in vitro* results demonstrated a definite rank-order correlation between the dissolution performance of the two suspensions and the *in vivo* parameters reflecting the absorption rate. The product with the greater amount of drug dissolved at 15 and 30 min (Suspension A) also resulted in higher serum levels at 0.5 and 0.75 hr, a higher C_{max}, and a shorter t_{max}. This result indicated that the absorption rates of these two suspensions were directly related to the dissolution process.

Table II—*In Vivo* Parameters (Mean ± *SD*) Derived from Serum Levels of Unchanged Drug

Parameter	Treatments		Statistical Evaluation
	Suspension A	Suspension B	
Serum level at 0.5 hr, μg/ml	49.55 ± 25.13	26.95 ± 16.20	$p < 0.05$
Serum level at 0.75 hr, μg/ml	53.60 ± 19.90	36.88 ± 15.24	$p < 0.05$
C_{max}, μg/ml	62.88 ± 14.94	48.34 ± 11.27	$p < 0.05$
t_{max}, hr	0.958 ± 0.520	1.67 ± 0.778	$p < 0.05$
Normalized *AUC*, μg/ml	74.76 ± 10.50	71.98 ± 16.72	$p > 0.05$[a]
K_E, hr^{-1}	0.4997 ± 0.0843	0.4814 ± 0.0812	$p > 0.05$[a]

[a] Not statistically significant.

REFERENCES

(1) T. R. Bates, H. A. Rosenberg, and A. V. Tembo, *J. Pharm. Sci.*, **62,** 2057 (1973).

(2) S. A. Howard, J. W. Mauger, and L. Phusanti, *ibid.*, **66,** 557 (1977).

(3) "Conditions for Marketing of Digoxin Products," *Fed. Regist.*, **39,** 2478 (1974).

(4) A. C. Bratton and E. K. Marshall, Jr., *J. Biol. Chem.*, **128,** 537 (1939).

(5) A. C. Shah, C. B. Peot, and J. F. Ochs, *J. Pharm. Sci.*, **62,** 671 (1973).

(6) A. N. Martin, J. Swarbrick, and A. Cammarata, "Physical Pharmacy," 2nd ed., Lea & Febiger, Philadelphia, Pa., 1973, p. 475.

(7) J. G. Wagner, "Fundamentals of Clinical Pharmacokinetics," 1st ed., Drug Intelligence Publications, Hamilton, Ill., 1975, p. 348.

ACKNOWLEDGMENTS

Supported by Contract 223-76-3010 from the Food and Drug Administration.

The authors thank Mrs. Kathy Weyant and Mr. Chan-Loi Yong for assistance.

Interaction of Cromolyn Sodium in Aqueous Solution with Magnesium Ions

G. D. WOODARD *, R. McDONALD *, and J. S. G. COX ‡x

Received February 14, 1977, from *McCrone Research Associates Ltd., London NW3 5BG, England, and the ‡Pharmaceutical Division, Fisons Ltd., Loughborough, Leicestershire, England. Accepted for publication February 2, 1978.

Abstract □ The interaction of the antiasthmatic drug cromolyn sodium with Mg^{2+} ions in solution was studied. Selective ion electrode and torsion viscometer measurements were used to establish the degree of interaction. At the concentrations studied, the cromolyn ion had no more affinity for Mg^{2+} than SO_4^{2-}. However, thixotropic gels were formed between 4×10^{-2} *M* cromolyn sodium and 4×10^{-4} *M* Mg^{2+}. At lower concentrations of Mg^{2+}, viscosity still increased significantly. However, when the cromolyn concentration was lowered, the increase in viscosity was much less marked.

Keyphrases □ Cromolyn sodium—interaction with magnesium ions in solution □ Magnesium ions—interaction with cromolyn sodium in solution □ Antiasthmatic agents—cromolyn sodium, interaction with magnesium ions in solution □ Metals—magnesium ions, interaction with cromolyn sodium in solution

Cromolyn sodium[1] represents a new pharmacological approach to allergic disease, particularly asthma (1). As is often the case, new and useful drugs are in widespread use before there is any clear understanding of their mechanism of action; this situation is particularly true of cromolyn sodium. However, it seems well accepted that cromolyn sodium does not interfere with antigen–antibody reactions and that it probably acts on the biochemical events in the mast cell that follow the antigen–antibody interaction on the membrane (2).

BACKGROUND

Several investigators (3, 4) explained its mechanism of action on the basis of the role of bivalent ions, especially calcium. However, until recently, these hypotheses arose more from the knowledge that calcium and magnesium play a key role in antigen-induced secretion of histamine from mast cells rather than any direct studies on the interaction of calcium and magnesium ions on cromolyn. By using calcium ionophores (substances that transport calcium across biological membranes and other organic phases), further understanding has been gained of the complex biochemical nature of histamine release from mast cells (5–7).

It seems that the primary event after union of antigen with mast cell-fixed antibody may be an increase in the mast cell membrane permeability to calcium, which promotes entry of calcium into the cell. The movement of calcium ions from the extracellular to the intracellular compartment of mast cells is sufficient to stimulate metabolically intact cells to secrete histamine. The calcium ionophore provides an alternative route for calcium to enter into mast cells, by passing the calcium-gating mechanism operated by the antigen–antibody reaction.

Although a preliminary study (8) suggested that the ionophore-induced release of histamine from rat mast cells could be inhibited by cromolyn, more extensive experiments did not demonstrate any effect (9). Cromolyn probably acts by blocking the antigen-induced transport of calcium either directly or indirectly. Binding of cromolyn to Ca^{2+} could not be demonstrated by various sensitive physical techniques (10); the effect in calcium influx is probably indirect.

As part of a study of the cromolyn ion, various metal-ion salts were prepared, including cromolyn magnesium. This salt was selected following difficulties in the preparation of a clear 2% (approximately 4×10^{-2} *M*) cromolyn sodium solution for clinical investigation of rhinitis. In spite of the use of purified water BP for clinical trial supplies, faintly opalescent solutions were obtained frequently. In subsequent investigations involving analysis of purified water BP for heavy metals, the level of Mg^{2+} was found to be important. At low concentrations of Mg^{2+} (10^{-5}–10^{-6} *M*), opalescent solutions were obtained; the highest Mg^{2+} concentration studied (4×10^{-4} *M*) in a 4×10^{-2} *M* cromolyn sodium solution caused the solution to gel after 2 or 3 hr at room temperature, so that a 1.27-cm diameter tube of solution could be laid on its side before the gel slid down the tube. At this point, there was no sign of visible precipitate and it took about 48 hr before it was detectable. As either the cromolyn or Mg^{2+} concentration was reduced, the "gel" was more fluid. However, if the temperature was reduced, the gel consistency could be increased.

It was decided to follow up these initial interesting observations since the Mg^{2+}–cromolyn interaction might be of some biological significance. The purpose of this study was to investigate the gelling of cromolyn sodium solutions by Mg^{2+}. This interaction was investigated directly by comparative results between binding effects of sulfate and cromolyn for magnesium ions (selective ion electrode measurements) and apparent viscosity measurements of cromolyn sodium solutions in the presence of varying amounts of magnesium acetate (torsion viscometry).

EXPERIMENTAL

Selective Ion Electrode Measurements—A divalent metal electrode was used to detect Mg^{2+}. Magnesium acetate (10^{-1}–10^{-4} *M*, depending on the experiment) was added to sodium sulfate solutions (10^{-2}–10^{-3} *M*) to standardize the ion scale on the pH meter[2]. After calibration, magnesium acetate (10^{-1} or 10^{-2} *M*) was titrated into sodium sulfate (10^{-2} or 10^{-3} *M*) to confirm the meter settings, followed by replicate titrations of magnesium acetate into cromolyn solutions.

The meter was calibrated to read directly the *known* magnesium concentrations of the sulfate standards. This step assumed that all magnesium ions were free, not bound to sulfate ions, which was correct for the lower concentrations (10^{-4} *M*). At higher concentrations (10^{-3} *M*), sulfate did bind a small amount of magnesium. Thus, all results for the cromolyn ion are comparative between the binding effects of sulfate and cromolyn for magnesium ions.

Only water that complied with the requirements of the BP for purified water was used; it could not contain more than 0.04 ppm of Mg^{2+}. It was freshly distilled from a neutral glass still fitted with an efficient device to prevent the entrainment of droplets and was used within 4 hr.

The first series of experiments (Series A) used dilute (10^{-3} *M* Na_2SO_4–10^{-3} *M* cromolyn) solutions, and the electrode responded to the H^+ concentration formed from carbonic acid, arising from dissolved carbon dioxide in the distilled water. To avoid this problem, 10^{-4} *M* sodium carbonate was used to maintain the pH close to or slightly above 7.

Series A calibration solutions were 10^{-4} *M* $Mg(CH_3COO)_2$–10^{-4} *M* Na_2CO_3–10^{-3} *M* Na_2SO_4 and 10^{-3} *M* $Mg(CH_3COO)_2$–10^{-4} *M* Na_2CO_3–10^{-3} *M* Na_2SO_4. Series A titrations were 10^{-2} *M* $Mg(CH_3COO)_2$ into 10^{-3} *M* Na_2SO_4–10^{-4} *M* Na_2CO_3 and 10^{-2} *M* $Mg(CH_3COO)_2$ into 10^{-3} *M* cromolyn–10^{-4} *M* Na_2CO_3.

The second set of experiments used a more concentrated solution (10^{-2} *M*), which approached the 4×10^{-4} *M* Mg^{2+}–4×10^{-2} *M* cromolyn solutions in which gelling had been found. To avoid severe Na^+ interference, the cromolyn concentration was 10^{-2} *M* (~0.5%). Even at this concentration, there was some Na^+ interference, and it was not possible to calibrate the meter to read the free Mg^{2+} concentration directly. Nevertheless, it was possible to obtain comparative results between the binding of Mg^{2+} by cromolyn and by sulfate. In these experiments, since carbonic acid was not a problem, it was not necessary to use a dilute sodium carbonate solution.

Series B calibration solutions were 10^{-3} *M* $Mg(CH_3COO)_2$–10^{-2} *M* Na_2SO_4 and 10^{-2} *M* $Mg(CH_3COO)_2$–10^{-2} *M* Na_2SO_4. Series B titrations

[1] Disodium cromoglycate, Intal, Fisons.

[2] Model 7030, Electronic Instruments Ltd., Chertsey, Surrey, England.

0022-3549/78/1000-1403$01.00/0
© 1978, American Pharmaceutical Association

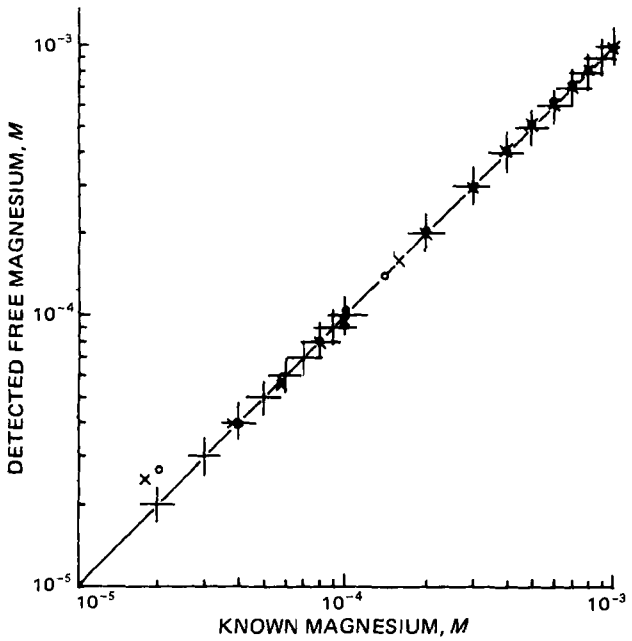

Figure 1—*Titration of 10^{-2} M magnesium acetate with 10^{-4} M sodium sulfate (×) or 10^{-3} M cromolyn (○) (Series A).*

were 10^{-1} *M* $Mg(CH_3COO)_2$ into 10^{-2} *M* Na_2SO_4 and 10^{-1} *M* $Mg(CH_3COO)_2$ into 10^{-2} *M* cromolyn. A volume of 50 ml of solution was used in these experiments, and the solution was stirred continuously to ensure homogeneity. All experiments were replicated.

A final series (C and D) of selective ion electrode measurements was made on fixed, more concentrated solution; the Mg^{2+} concentration was monitored as a function of time. These experiments covered the concentration at which gelling had previously been observed, *i.e.*, 4×10^{-4} *M* Mg^{2+}–4×10^{-2} *M* cromolyn.

The fixed composition experiments, where the free magnesium concentration was monitored with time, were: Series C, 4×10^{-4} *M* $Mg(CH_3COO)_2$–10^{-2} *M* Na_2SO_4 and 4×10^{-4} *M* $Mg(CH_3COO)_2$–10^{-2} *M* cromolyn; and Series D, 4×10^{-4} *M* $Mg(CH_3COO)_2$–4×10^{-2} *M* Na_2SO_4 and 4×10^{-4} *M* $Mg(CH_3COO)_2$–4×10^{-2} *M* cromolyn. The concentration of 4×10^{-4} *M* $(CH_3COO)_2$ closely corresponds with 10 ppm of Mg^{2+}, and 4×10^{-2} *M* cromolyn is close to 2%. At these concentrations, the solution was known to gel.

Series C and D experiments were performed in quadruplicate because the reproducibility was poor.

Viscosity Measurements—Since the solutions were known to be thixotropic, a torsion viscometer[3] was used that had an additional scale at the top of the torsion wire. This scale enabled the torsion to be applied to the wire without disturbing the solution prior to measurement and, therefore, avoided a reduction in the solution's apparent viscosity. The wire (38 cm; 36 swg[4]) and cylinder (41.5 mm diameter) were chosen to give maximum sensitivity in the range of 15–300 cps. The cylinder was covered by approximately 1 cm of solution, and the temperature was controlled at 21° by a water jacket fed from a thermostated bath.

To operate the viscometer, the top of the torsion wire was rotated 180° while the flywheel on the lower end, a few centimeters above the cylinder, was clamped. The flywheel was released, and the overswing (swing exceeding the offset 180°) was noted. The viscosity was derived from the overswing by calibrating the viscometer with water–glycerol mixtures.

For most experiments, the viscosity was measured 1 min after inserting the freshly prepared solution into the viscometer. After 5 min, the viscosity was remeasured, the solution was stirred thoroughly, and a further measurement was taken. The solution was left undisturbed for a fixed time, and the 5-min procedure was repeated. This reading was the time since the thixotropic solution was last stirred but the actual elapsed time was longer. This procedure was repeated at intervals. A few experiments were undertaken with calcium ions present to see if they caused a similar effect.

[3] Laboratory model VS-010, A. Gallenkamp & Co., London EC2 PER, England.

[4] Standard wire gauge, British Standards Institute.

Table I—Variation in Apparent Free Magnesium-Ion Concentration with Time[a]

Series C[b]		Series D[c]	
Time	× 10^{-4} *M* Mg^{2+}	Time	× 10^{-4} *M* Mg^{2+}
1 min	4.0 (4.0–4.1)	1 min	4.0 (3.9–4.1)
10 min	4.0 (3.9–4.0)	10 min	4.0 (3.9–4.0)
2 hr	3.1 (3.0–3.2)	6 hr	2.9 (2.4–3.2)
24 hr	3.1 (2.9–3.2)	24 hr	2.6 (2.1–3.0)
2 days	2.7 (2.4–2.9)	2 days	2.4 (1.9–2.9)

[a] Calculation of the two correlation coefficients on a semilogarithmic scale for linearization gives $r = -0.94$ for C and $r = -0.97$ for D. [b] Using 4×10^{-4} *M* $Mg(CH_3COO)_2$–10^{-2} *M* cromolyn. [c] Using 4×10^{-4} *M* $Mg(CH_3COO)_2$–4×10^{-2} *M* cromolyn.

RESULTS

Interaction between Cromolyn and Magnesium Ions—The results of titrating 10^{-2} *M* $Mg(CH_3COO)_2$ into 10^{-3} *M* Na_2SO_4–10^{-4} *M* Na_2CO_3 and the corresponding titration into 10^{-3} *M* cromolyn–10^{-4} *M* Na_2CO_3 are shown in Fig. 1. The results down to 4×10^{-5} *M* closely follow a 45° slope, which indicates that the actual magnesium-ion concentration and the measured free magnesium-ion concentration as measured at 2×10^{-5} *M* actual Mg^{2+} may result from a low level of divalent metal impurity (the electrode detected all divalent metals). There is no difference between the cromolyn and sulfate lines in Fig. 1 and, therefore, cromolyn has no more affinity for magnesium than sulfate at these concentrations.

Figure 2 shows the titration of 10^{-2} *M* $Mg(CH_3COO)_2$ into 10^{-2} *M* Na_2SO_4 or 10^{-2} *M* cromolyn. The instrument was calibrated at the 10^{-2} *M* Na_2SO_4 point, so the sodium sulfate line passes through this point. It does not pass through the 10^{-3} *M* point because the interference from sodium ions could not be entirely compensated by instrumental settings. The significant fact is that the cromolyn points show little deviation from the sulfate points. If anything, more magnesium is detected with cromolyn than with sulfate, probably because sulfate ions bind a small amount of magnesium. Above 10^{-3} *M*, sulfate binds magnesium to a small extent. It can be concluded that, at these concentrations, cromolyn ions bind magnesium equal to or less than sulfate.

The fixed composition results are shown in Table I. All results were normalized to equivalent sulfate solutions measured throughout the experiments at the same time as the cromolyn solutions. Table I shows that the free magnesium-ion concentration fell with time and that this change was detected long before any precipitate was seen. Means of four values are quoted because the reproducibility was poor; ±20% was the order of variation about the mean for the extreme results of the four. A reduction in free magnesium-ion concentration is to be expected as soon as precipitation occurs.

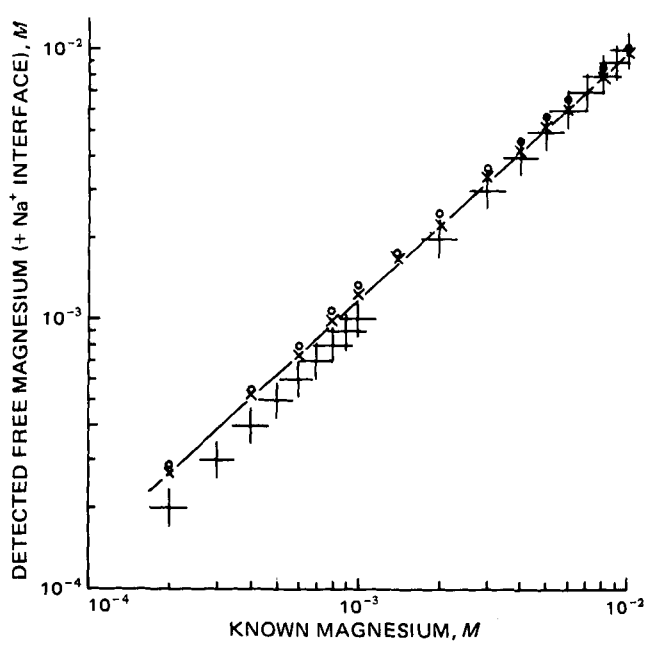

Figure 2—*Titration of 10^{-2} M magnesium acetate with 10^{-2} M sodium sulfate (×) or cromolyn (○) (series B).*

Table II—Change of Viscosity with Time

$\times 10^{-2}$ M Cromolyn	4	4	4		4		4		4		4		4
$\times 10^{-4}$ M Mg^{2+}	0	0	1.2		2.4		4		4		2		
											Together with 1.2×10^{-4} M Ca^{2+}		2.5×10^{-4} M Ca^{2+} Alone
Stirred–Unstirred	U[a]	S	U	S[b]	U	S	U	S	U	S	U	S	U
Time (t)	Viscosity, cps												
1 min	<8	<8	<8	<8	<8		<8		14		<8		<8
5 min	8	8	8		8		19		26	15	10		8
15 min	8	8	9.5		11	10	240	20	106	22	1	14	8
40 min	10	8	15	12	21	10	500	46	260	29	24	16	8
60 min	10	8	19	14	24	10			500	34	39	18	8
16 hr	13	8	38	14	250	28					150	31	8
48 hr	16	8	61	14	500	130					280	33	8

[a] Unstirred for time t. [b] These solutions were stirred for 1 min immediately after the unstirred measurement and the viscosity was remeasured.

Viscosity Measurements—The viscosity measurements and assessments are shown in Tables II and III. The viscosity of 4×10^{-2} M cromolyn solutions at room temperature changed little in 48 hr, but the addition of 1.2×10^{-4} M Mg^{2+} produced a noticeable effect. With 4×10^{-4} M Mg^{2+}, the viscosity increased rapidly; after 1 hr, the solution had quite definitely gelled. A reduction in the cromolyn concentration markedly reduced the increase in viscosity; 10^{-2} M cromolyn–4×10^{-4} M Mg^{2+} only slightly increased in viscosity after 18 hr.

However, an increase in the magnesium-ion concentration in the more dilute cromolyn solutions did increase the viscosity; *e.g.*, with 10^{-2} M cromolyn–9.6×10^{-4} M Mg^{2+}, the viscosity noticeably increased. If part of the magnesium was replaced by calcium, the solutions behaved as though only magnesium at the reduced concentration was present; the calcium ions had no effect. All solutions were thixotropic and showed much lower viscosity after stirring (Table II).

DISCUSSION

The specific ion electrode measurements in which Mg^{2+} was titrated into cromolyn sodium solutions showed that cromolyn ions had no more tendency to bind magnesium than did sulfate during the first 20 min after mixing, the time taken for a single titration. The fixed composition experiments showed that the free magnesium-ion concentration did fall with time, and this effect was detectable up to 48 hr before any precipitate of cromolyn magnesium was seen.

The viscosity experiments clearly showed that 4×10^{-2} M cromolyn with 1.2×10^{-4}, 2.4×10^{-4}, and 4×10^{-4} M Mg^{2+} increased in viscosity; at 4×10^{-4} M Mg^{2+}, the effect was sufficiently marked to describe the solution as gelled. The time for gelling to be detected was only 10 min for 4×10^{-4} M Mg^{2+} and up to 1 hr for 1.2×10^{-4} M Mg^{2+}. When the concentration of cromolyn was lowered, the increase in viscosity was much less marked. With 10^{-2} M cromolyn and 4×10^{-4} M Mg^{2+} at room temperature, it took 18 hr for a change in viscosity to be noticed. Even then, the increase was slight in contrast to the gelling with 4×10^{-2} M cromolyn. At 5°, the 10^{-2} M cromolyn–4×10^{-4} M Mg^{2+} solution did gel after 48 hr.

Table III—Change of Viscosity with Time for Solutions Stored at Room Temperature

$\times 10^{-2}$ M Cromolyn	1	4	1
$\times 10^{-4}$ M Mg^{2+}	4	4	9.6
Hours since Solution Prepared	Viscosity Assessment		
1	NCD[a]	Slight gel	NCD
2	NCD	Slight gel	NCD
18	Very slight increase in viscosity	Stiff gel	Gelled
42	Very slight increase in viscosity	Stiff gel	Less gelled, precipitating

[a] No change detected.

A 4×10^{-2} M cromolyn solution with 4×10^{-4} M Mg^{2+} was supersaturated with respect to cromolyn magnesium, and a faint precipitate of this salt was seen after 48 hr. When observed microscopically, the crystals of cromolyn magnesium were exceptionally elongated and appeared to be branched. These extremely thin, thread-like crystals interwove, and the branches appeared to interconnect at several points. Prior to this precipitate being detected either by slight cloudiness of the solution or microscopically with crossed polars, the nuclei of the salt must be forming and, as they grow, must take up this thread-like, interwoven structure. The growth of such a fine structure would increase the solution viscosity.

However, the rapidity of the gelling and slowness of the precipitate to form suggest that a simple, very fine thread-like network is not the only mechanism involved in the first stage of gelling. It seems unlikely that if it could form in a matter of minutes, it would take 48 hr to grow to a microscopically detectable size. The sharp dependence of gelling on the cromolyn concentration, even though it is in large excess over magnesium, strongly suggests that these ions, in excess of those needed to bond with Mg^{2+}, are involved in gelling.

REFERENCES

(1) J. S. G. Cox, *Nature (London)*, **216**, 1328 (1967).

(2) J. C. Foreman and L. G. Garland, *Br. Med. J.*, **1**, 820 (1976).

(3) J. W. Kerr, M. Govindaraj, and K. R. Patel, *ibid.*, **2**, 139 (1970).

(4) T. S. C. Orr, D. E. Hall, and A. C. Allison, *Nature (London)*, **236**, 350 (1972).

(5) J. C. Foreman, J. L. Mongar, and B. D. Gomperts, *ibid.*, **245**, 249 (1973).

(6) D. E. Cochrane and W. W. Douglas, *Proc. Natl. Acad. Sci. USA*, **71**, 408 (1974).

(7) R. P. Siraganian, A. Kulczycki, G. Mendoza, and H. Metzger, *J. Immunol.*, **115**, 1599 (1975).

(8) H. G. Johnson and M. K. Bach, *ibid.*, **114**, 514 (1975).

(9) L. C. Garland and J. L. Mongar, *Int. Arch. Allergy Appl. Immunol.*, **50**, 27 (1976).

(10) A. C. Spataro and H. B. Bosmann, *Biochem. Pharmacol.*, **25**, 505 (1976).

Disposition of Norgestimate in the Presence and Absence of Ethinyl Estradiol after Oral Administration to Humans

HOWARD S. WEINTRAUB ˣ, LARRY S. ABRAMS, JAMES E. PATRICK, and J. L. McGUIRE

Received November 22, 1977, from *Ortho Pharmaceutical Corporation, Raritan, NJ 08869.* Accepted for publication February 2, 1978.

Abstract □ The disposition of radioactivity following oral administration of ^{14}C-norgestimate was compared to that following administration of the drug in combination with ^{3}H-ethinyl estradiol in humans. Seven normal, healthy female subjects were each administered one capsule orally containing ^{14}C-norgestimate either alone (74.4 μCi, 0.50 mg) or in combination (73.5 μCi, 0.49 mg) with ^{3}H-ethinyl estradiol (103 μCi, 0.14 mg) in polyethylene glycol 400. Peak levels of radioactivity due to carbon-14 and tritium in plasma occurred within 2 hr after drug administration, followed by distribution and elimination phases. The mean apparent elimination half-life and mean cumulative elimination of radioactivity in the urine and feces following ^{14}C-norgestimate administration were not significantly different than those following administration of the combination dose. Approximately 50% of the administered radioactivity due to carbon-14 was excreted in the urine following administration of ^{14}C-norgestimate both in the presence and absence of coadministered ^{3}H-ethinyl estradiol.

Keyphrases □ Norgestimate—disposition after oral administration alone and combined with ethinyl estradiol in humans □ Disposition—norgestimate after oral administration alone and combined with ethinyl estradiol in humans □ Progestins—norgestimate, disposition after oral administration alone and combined with ethinyl estradiol in humans

Norgestimate[1], *d*-17β-acetoxy-13β-ethyl-17α-ethynyl-4-gonene-3-one oxime (I), is a lipophilic steroid with progestational and antifertility activity in a number of laboratory animal species (1, 2). It is currently being studied in humans as a low dose oral contraceptive in combination with ethinyl estradiol (3–5). Drug disposition studies in rats, dogs, and monkeys were conducted previously (6), and the metabolism of ^{14}C-norgestimate in humans was briefly described (7).

The present study determined the absorption characteristics of ^{14}C-norgestimate in humans following oral administration of the compound alone or in combination with ^{3}H-ethinyl estradiol. Preliminary information on the pharmacokinetics and disposition of the progestin was also obtained.

EXPERIMENTAL

Materials—^{14}C-Norgestimate (specific activity ~150 μCi/mg) was synthesized[2], and its radiochemical purity was determined by TLC to be greater than 95%. ^{3}H-Ethinyl estradiol[3] was mixed with unlabeled ethinyl estradiol and repurified. The resulting compound (specific activity ~714 μCi/mg) had a radiochemical purity of >95%.

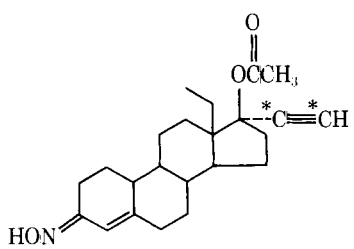

I: * = position of ^{14}C-label

[1] Ortho Pharmaceutical Corp., Raritan, N.J.
[2] Roussel UCLAF, Paris, France.
[3] New England Nuclear Corp., Boston, Mass.

Table I—Subjects Enrolled

Dosage Form Administered	Subject	Age, years	Height, cm	Weight, kg
^{14}C-Norgestimate	PP	35	163	67.3
	KC	33	160	75.9
	MS	40	163	59.5
	JG	40	159	67.7
^{14}C-Norgestimate and ^{3}H-ethinyl estradiol	KB	29	163	55.0
	LS	37	163	56.8
	KK	35	164	57.0

Samples of whole blood, plasma, and fecal homogenate were combusted in a tissue oxidizer[4], and the radioactive content[5] was determined by liquid scintillation spectrometry[6]. Internal standardization was used to correct for quenching. The efficiency of the tissue oxidizer was determined by combusting known amounts of radioactivity.

A radiochromatogram scanner[7] was used to determine the radiochemical purity of the isotope. Blenders[8] were employed to homogenize feces.

Dosage Forms—The dosage forms were prepared in the following manner. Polyethylene glycol 400 (1.5 ml) was added to a solution containing 3.0 mg of ^{14}C-norgestimate in 2.0 ml of alcohol USP. For coadministration of ^{3}H-ethinyl estradiol, polyethylene glycol 400 (1.5 ml) was added to a solution containing 3.0 mg of ^{14}C-norgestimate and 0.841 mg of ^{3}H-ethinyl estradiol in 2.0 ml of alcohol USP. The alcohol was then evaporated by heating the mixtures at 60° with constant stirring for 3 hr.

A 0.25-ml aliquot of polyethylene glycol 400 containing either 0.5 mg of ^{14}C-norgestimate or 0.5 mg of ^{14}C-norgestimate and 0.14 mg of ^{3}H-

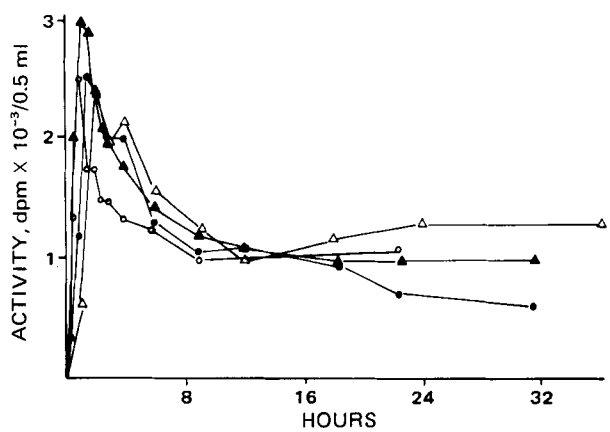

Figure 1—*Radioactivity in plasma following oral administration of ^{14}C-norgestimate (74.4 μCi, 0.50 mg) in polyethylene glycol 400 (0.25 ml) in soft gelatin capsules to Subjects PP (△), MS (▲), JG (●), and KC (○).*

[4] Model 306, Packard Instruments, Downers Grove, Ill.
[5] Carbon-14 content dissolved in Permafluor V and Carbo-Sorb; tritium content dissolved in Monophase-40. These scintillation cocktails were obtained from Packard Instruments, Downers Grove, Ill.
[6] Model SL-30, Intertechnique Inc., Westwood, N.J.
[7] Model 7200, Packard Instruments, Downers Grove, Ill.
[8] Waring Products Corp., Winsted, Conn.

0022-3549/78/1000-1406$01.00/0
© 1978, American Pharmaceutical Association

Table II—Apparent Half-Life of Radioactivity Due to Carbon-14 in Plasma and Elimination Rate Constant following Oral Administration of ^{14}C-Norgestimate

^{14}C-Norgestimate Alone[a]			^{14}C-Norgestimate and ^{3}H-Ethinyl Estradiol[b]		
Subject	Half-Life of Radioactivity Due to Carbon-14, hr	Elimination Rate Constant, hr^{-1}	Subject	Half-Life of Radioactivity Due to Carbon-14, hr	Elimination Rate Constant, hr^{-1}
PP	45	0.015	KB	49	0.014
MS	58	0.012	LS	56	0.012
JG	71	0.010	KK	59	0.012
KC	64	0.011			
Mean ± *SE*	59.5 ± 5.5	0.012 ± 0.001	Mean ± *SE*	54.7 ± 3.0	0.013 ± 0.001
Range	45 – 71	0.010–0.015	Range	44 – 59	0.012–0.014

[a] ^{14}C-Norgestimate (74.4 μCi, 0.50 mg) in polyethylene glycol 400 (0.25 ml) in soft gelatin capsule. [b] ^{14}C-Norgestimate (73.5 μCi, 0.49 mg) in combination with ^{3}H-ethinyl estradiol (103 μCi, 0.14 mg) in polyethylene glycol 400 (0.25 ml) in soft gelatin capsule.

ethinyl estradiol was injected into each preweighed 6-minum soft gelatin capsule. The capsules were then reweighed to confirm the quantity of added solution and were sealed by means of an aqueous gelatin solution.

One representative capsule of each dosage form was assayed for radiochemical purity, radioactive content due to carbon-14 (and tritium), and drug content immediately prior to initiating the clinical trials. The radiochemical purity was greater than 95%, and the capsules contained 73.5 μCi (0.49 mg) of ^{14}C-norgestimate and 103 μCi (0.14 mg) of ^{3}H-ethinyl estradiol in the combination and 74.4 μCi (0.50 mg) of ^{14}C-norgestimate in the norgestimate alone capsule.

Subjects—Seven healthy female subjects (Table I) reported that they had not taken any steroid for at least 3 months prior to the study and had taken no other medication for at least 2 weeks prior to the study. Assay of radioactivity in whole blood, plasma, urine, and fecal samples from the subjects, obtained 1–3 days prior to initiation of the study, indicated the presence of only background levels of radioactivity.

Methods—After a fast of at least 8 hr, the subjects each ingested one norgestimate capsule or a capsule containing norgestimate and ethinyl estradiol followed by 240 ml of water. Water was permitted *ad libitum*, and a normal diet was permitted commencing 4 hr after drug administration.

Venous blood was collected into heparinized tubes at 0, 0.5, 1, 1.5, 2, 2.5, 3, 4, 6, 9, 12, 16, 18, 24, 36, 48, 72, 96, and 120 hr and at 7 and 14 days. Single urine and fecal samples were collected on the day prior to drug administration, and all urine and feces were collected for 2 weeks thereafter. Urine and feces were frozen immediately after collection.

Two 0.5-ml aliquots of whole blood from each blood sample were placed into tissue sample cups[9] immediately after each collection. The aliquots were subsequently combusted and assayed for radioactive content. Plasma was separated from the remainder of each whole blood sample, and both the plasma and red cell pellets were frozen. Two 0.5-ml aliquots of plasma were subsequently combusted and assayed for radioactive content.

Estimation of the half-life of total radioactivity and its corresponding elimination rate constant was made from a linear regression analysis of the terminal exponential phase of a plot of the logarithm of radioactivity in plasma *versus* time.

Each fecal specimen was diluted to a constant volume (500 ml) with methanol–water (1:1) and homogenized, and aliquots (0.5 ml) were removed and assayed for radioactive content.

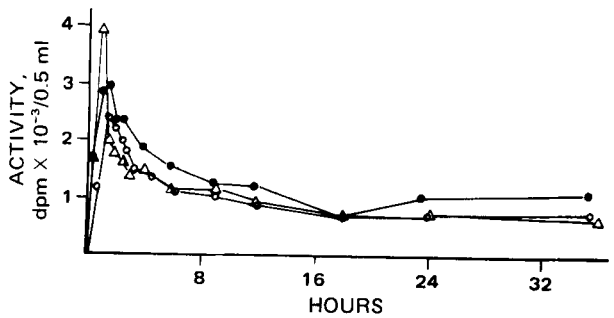

Figure 2—*Radioactivity in plasma following oral administration of ^{14}C-norgestimate (73.5 μCi, 0.49 mg) and ^{3}H-ethinyl estradiol (103 μCi, 0.14 mg) in polyethylene glycol 400 (0.25 ml) in soft gelatin capsules to Subjects KB (●), LS (△), and KK (○).*

[9] Combustocones, Packard Instruments, Downers Grove, Ill.

RESULTS

Absorption of radioactivity after oral administration of ^{14}C-norgestimate alone or in combination with ethinyl estradiol in all seven subjects was rapid. Peak levels of total radioactivity in plasma occurred within 2 hr, followed by distinct distribution and elimination phases (Figs. 1 and 2). The half-life of radioactivity in plasma due to carbon-14 was 45–71 hr (mean ± *SE* = 59.5 ± 5.5 hr) following administration of ^{14}C-norgestimate alone and 49–59 hr (mean ± *SE* = 54.7 ± 3.0 hr) after administration of the drug in combination with ^{3}H-ethinyl estradiol (Table II). The mean elimination rate constants were 0.012 and 0.013 hr^{-1}, respectively (Table II). The apparent half-life of radioactivity in plasma due to tritium was 45–84 hr (mean ± *SE* = 60.4 ± 12.1 hr), and the mean elimination rate constant for tritium was 0.012 hr^{-1}.

Cumulative elimination of radioactivity due to carbon-14 in the urine and feces is summarized in Tables III and IV. Following oral administration of ^{14}C-norgestimate, approximately 64–94% (mean ± *SE* = 83.5 ± 7.0%) of the administered radioactivity due to carbon-14 was eliminated within the 2 week-collection period. About 45–49% (mean ± *SE* = 46.8 ± 1.0%) of the radioactivity was excreted in the urine, while 16–49% (mean ± *SE* = 36.8 ± 7.3%) was recovered in the feces.

Following oral administration of ^{14}C-norgestimate in combination with ^{3}H-ethinyl estradiol, approximately 82–89% (mean ± *SE* = 85.6 ± 2.1%) of the administered radioactivity due to carbon-14 was eliminated during 2 weeks. About 35–49% (mean ± *SE* = 43.6 ± 4.4%) was excreted in the urine while 39–47% (mean ± *SE* = 41.9 ± 2.5%) was recovered in the feces. Approximately 64–90% (mean ± *SE* = 77.7 ± 7.4%) of the administered radioactivity due to tritium was eliminated within the collection period. Approximately 30–50% (mean ± *SE* = 43.5 ± 6.5%) of the radioactivity due to tritium was excreted in the urine, while 14–49% (mean ± *SE* = 34.2 ± 10.3%) was found in the feces.

DISCUSSION

The disposition of radioactivity following oral administration of ^{14}C-norgestimate was compared to that following administration of the drug in combination with ^{3}H-ethinyl estradiol in normal healthy adult female subjects. The mean apparent elimination half-life and mean cumulative elimination of radioactivity in the urine and feces following ^{14}C-norgestimate administration were not significantly different than those following the combination dose. These data are in general agreement with findings following oral administration of other radiolabeled progestins to human subjects (8, 9).

Table III—Cumulative Elimination of Radioactivity Due to Carbon-14 in Urine and Feces following Oral Administration of ^{14}C-Norgestimate[a]

Cumulative Percent Dose Eliminated	Subject PP	MS	JG	KC	Mean ± *SE*
During first 3 days	44	83	70	40	59.5 ± 10.5
During first 7 days	78	94	89	60	80.3 ± 7.5
During first 14 days	83	94	93	64	83.5 ± 7.0
In urine	45	45	49	48	46.8 ± 1.0
In feces	38	49	44	16	36.8 ± 7.3

[a] ^{14}C-Norgestimate (74.4 μCi, 0.50 mg) in polyethylene glycol (0.25 ml) in soft gelatin capsule.

Table IV—Cumulative Elimination of Radioactivity Due to Carbon-14 in Urine and Feces following Oral Administration of ^{14}C-Norgestimate in Combination with ^{3}H-Ethinyl Estradiol [a]

Cumulative Percent Dose Eliminated	Subject KB	LS	KK	Mean ± *SE*
During first 3 days	40.4	50.6	50.4	47.1 ± 3.4
During first 7 days	82.8	78.7	79.3	80.3 ± 1.3
During first 14 days	85.3	81.8	89.4	85.6 ± 2.1
In urine	46.4	35.0	49.4	43.6 ± 4.4
In feces	38.9	46.8	40.0	41.9 ± 2.5

[a] ^{14}C-Norgestimate (73.5 μCi, 0.49 mg) in combination with ^{3}H-ethinyl estradiol (103 μCi, 0.14 mg) in polyethylene glycol 400 (0.25 ml) in soft gelatin capsule.

Cumulative elimination of radioactivity in the seven subjects indicates that approximately half of the dose was excreted in the urine during the 14-day collection period, suggesting that a substantial fraction of the administrered radioactivity was absorbed. It cannot be assumed that the radioactivity recovered in the feces necessarily represents unabsorbed drug since studies with intravenously administered ^{14}C-norgestimate in dogs and rats demonstrated substantial biliary secretion of norgestimate and/or its metabolites (6). Estimates of the apparent half-life of radioactivity due to carbon-14 in the present study were consistent with those reported previously for dogs, rats, and monkeys (6).

REFERENCES

(1) A. P. Shroff, C. H. Harper, G. O. Allen, and R. P. Blye, *J. Med. Chem.*, **16**, 113 (1973).

(2) D. W. Hahn, G. O. Allen, and J. L. McGuire, *Pharmacologist*, **18**, 250 (1976).

(3) J. J. Calderoń-Maŕques, R. A. Alcańtara, and J. J. Osterman, "VIII World Congress of Gynecology and Obstetrics, Abstracts," Mexico, Oct. 1976, Excerpta Medica, Princeton, N.J., p. 252.

(4) C. B. Alejandro, Z. A. Ernestina, and C. C. Jorge, *ibid.*, p. 249.

(5) B. Rubio-Lotvin and R. Gonzalez-Ansorena, *ibid.*, p. 249.

(6) L. S. Abrams, H. S. Weintraub, and J. E. Patrick, *Fed. Proc.*, **36**, 1030 (1977).

(7) J. E. Patrick, K. B. Alton, N. Hetyei, and C. Shaw, *Pharmacologist*, **18**, 153 (1976).

(8) K. Fotherby, "Proceedings 5th International Congress of Pharmacology," San Francisco, 1972, vol. 1, Karger, Basel, Switzerland, 1973, p. 230.

(9) K. Fotherby, *Adv. Steroid Biochem. Pharmacol.*, **3**, 67 (1972).

ACKNOWLEDGMENTS

Presented in part at the Basic Pharmaceutics Section, APhA Academy of Pharmaceutical Sciences, Orlando meeting, November 1976.

The authors thank Mr. Gerald F. Eisen and Mr. Timothy J. Kane for assistance.

Molecular Connectivity Study of Muscarinic Receptor Affinity of Acetylcholine Antagonists

LEMONT B. KIER *x and LOWELL H. HALL ‡

Received December 5, 1977, from the **Department of Pharmaceutical Chemistry, Medical College of Virginia, Richmond, VA 23298*, and the ‡*Department of Chemistry, Eastern Nazarene College, Quincy, MA 02170.* Accepted for publication February 3, 1978.

Abstract □ A correlation between three molecular connectivity indexes and the muscarinic receptor affinity of 104 acetylcholine antagonists was found. Analysis of structure from these indexes reveals not only the importance of the onium and the bulky portions of the molecule but also their virtual independence of each other on the affinity. Analysis of the onium group portion of the molecules indicates that its contribution to the experimental affinity is virtually constant through a variety of structural variations. The influence of the bulky side chains, in contrast, is quite structure dependent. The equation relating connectivity indexes to muscarinic affinity of antagonists is capable of predicting the affinity of other antagonists as well as a number of agonist molecules.

Keyphrases □ Molecular connectivity indexes—various acetylcholine antagonists, correlated to muscarinic receptor affinity □ Muscarinic receptor affinity—various acetylcholine antagonists, correlated to molecular connectivity indexes □ Acetylcholine antagonists, various—molecular connectivity indexes correlated to muscarinic receptor affinity □ Topological indexes—molecular connectivity correlated to muscarinic receptor affinity of various acetylcholine antagonists □ Structure–activity relationships—molecular connectivity indexes of various acetylcholine antagonists correlated to muscarinic receptor affinity

Since the early observation that atropine is a competitive antagonist of acetylcholine muscarinic action, many molecules have been synthesized in efforts to develop clinically useful drugs. The most potent agents possess an onium group (usually quaternary) and a relatively bulky moiety bridged to the nitrogen by a three- to five-carbon chain. This bulky moiety is presumed to increase the affinity of the molecule by interacting through van der Waals forces beyond the region of the muscarinic receptor (1). Some similarities between antagonists and acetylcholine structure were summarized (2).

BACKGROUND

Several studies were directed toward a definition of the structural similarities and differences between muscarinic agonists and antagonists. Burgen (3) suggested that the onium group plays a major role in drug–receptor interaction among agonists while the bulky side-chain moiety is the salient feature for activity among antagonists. Increased drug–receptor interaction at the bulky side chain presumably weakens the interaction at the onium group, giving rise to a diminished agonist but predominant antagonist effect.

Barlow *et al.* (4) tested agonist and antagonist molecules and concluded that changes in the structure of the onium group produce similar effects on affinity for both series. In contrast to Burgen's (3) proposal, this view advocates a comparable role for the onium group among agonists and antagonists.

A subsequent study (5) on more than 100 acetylcholine analogs revealed that changes in the molecule affinity as the onium group was modified were not entirely independent of the bulky side chain. However, the interdependence of onium and the bulky side chain was not marked. Other factors could be operating besides binding influences, including realignment at the receptor due to onium group changes, leading to altered affinity.

Goldstein *et al.* (6) stated that competitive antagonism could result from an interaction at a different receptor near the acetylcholine receptor (7). The antagonist–receptor interaction would modify the agonist re-

0022-3549/78/1000-1408$01.00/0

© 1978, American Pharmaceutical Association

Table IV—Cumulative Elimination of Radioactivity Due to Carbon-14 in Urine and Feces following Oral Administration of ^{14}C-Norgestimate in Combination with ^{3}H-Ethinyl Estradiol [a]

Cumulative Percent Dose Eliminated	Subject KB	LS	KK	Mean ± *SE*
During first 3 days	40.4	50.6	50.4	47.1 ± 3.4
During first 7 days	82.8	78.7	79.3	80.3 ± 1.3
During first 14 days	85.3	81.8	89.4	85.6 ± 2.1
In urine	46.4	35.0	49.4	43.6 ± 4.4
In feces	38.9	46.8	40.0	41.9 ± 2.5

[a] ^{14}C-Norgestimate (73.5 μCi, 0.49 mg) in combination with ^{3}H-ethinyl estradiol (103 μCi, 0.14 mg) in polyethylene glycol 400 (0.25 ml) in soft gelatin capsule.

Cumulative elimination of radioactivity in the seven subjects indicates that approximately half of the dose was excreted in the urine during the 14-day collection period, suggesting that a substantial fraction of the administrered radioactivity was absorbed. It cannot be assumed that the radioactivity recovered in the feces necessarily represents unabsorbed drug since studies with intravenously administered ^{14}C-norgestimate in dogs and rats demonstrated substantial biliary secretion of norgestimate and/or its metabolites (6). Estimates of the apparent half-life of radioactivity due to carbon-14 in the present study were consistent with those reported previously for dogs, rats, and monkeys (6).

REFERENCES

(1) A. P. Shroff, C. H. Harper, G. O. Allen, and R. P. Blye, *J. Med. Chem.*, **16**, 113 (1973).

(2) D. W. Hahn, G. O. Allen, and J. L. McGuire, *Pharmacologist*, **18**, 250 (1976).

(3) J. J. Calderoń-Maŕques, R. A. Alcańtara, and J. J. Osterman, "VIII World Congress of Gynecology and Obstetrics, Abstracts," Mexico, Oct. 1976, Excerpta Medica, Princeton, N.J., p. 252.

(4) C. B. Alejandro, Z. A. Ernestina, and C. C. Jorge, *ibid.*, p. 249.

(5) B. Rubio-Lotvin and R. Gonzalez-Ansorena, *ibid.*, p. 249.

(6) L. S. Abrams, H. S. Weintraub, and J. E. Patrick, *Fed. Proc.*, **36**, 1030 (1977).

(7) J. E. Patrick, K. B. Alton, N. Hetyei, and C. Shaw, *Pharmacologist*, **18**, 153 (1976).

(8) K. Fotherby, "Proceedings 5th International Congress of Pharmacology," San Francisco, 1972, vol. 1, Karger, Basel, Switzerland, 1973, p. 230.

(9) K. Fotherby, *Adv. Steroid Biochem. Pharmacol.*, **3**, 67 (1972).

ACKNOWLEDGMENTS

Presented in part at the Basic Pharmaceutics Section, APhA Academy of Pharmaceutical Sciences, Orlando meeting, November 1976.

The authors thank Mr. Gerald F. Eisen and Mr. Timothy J. Kane for assistance.

Molecular Connectivity Study of Muscarinic Receptor Affinity of Acetylcholine Antagonists

LEMONT B. KIER *x and LOWELL H. HALL ‡

Received December 5, 1977, from the **Department of Pharmaceutical Chemistry, Medical College of Virginia, Richmond, VA 23298*, and the ‡*Department of Chemistry, Eastern Nazarene College, Quincy, MA 02170.* Accepted for publication February 3, 1978.

Abstract □ A correlation between three molecular connectivity indexes and the muscarinic receptor affinity of 104 acetylcholine antagonists was found. Analysis of structure from these indexes reveals not only the importance of the onium and the bulky portions of the molecule but also their virtual independence of each other on the affinity. Analysis of the onium group portion of the molecules indicates that its contribution to the experimental affinity is virtually constant through a variety of structural variations. The influence of the bulky side chains, in contrast, is quite structure dependent. The equation relating connectivity indexes to muscarinic affinity of antagonists is capable of predicting the affinity of other antagonists as well as a number of agonist molecules.

Keyphrases □ Molecular connectivity indexes—various acetylcholine antagonists, correlated to muscarinic receptor affinity □ Muscarinic receptor affinity—various acetylcholine antagonists, correlated to molecular connectivity indexes □ Acetylcholine antagonists, various—molecular connectivity indexes correlated to muscarinic receptor affinity □ Topological indexes—molecular connectivity correlated to muscarinic receptor affinity of various acetylcholine antagonists □ Structure–activity relationships—molecular connectivity indexes of various acetylcholine antagonists correlated to muscarinic receptor affinity

Since the early observation that atropine is a competitive antagonist of acetylcholine muscarinic action, many molecules have been synthesized in efforts to develop clinically useful drugs. The most potent agents possess an onium group (usually quaternary) and a relatively bulky moiety bridged to the nitrogen by a three- to five-carbon chain. This bulky moiety is presumed to increase the affinity of the molecule by interacting through van der Waals forces beyond the region of the muscarinic receptor (1). Some similarities between antagonists and acetylcholine structure were summarized (2).

BACKGROUND

Several studies were directed toward a definition of the structural similarities and differences between muscarinic agonists and antagonists. Burgen (3) suggested that the onium group plays a major role in drug–receptor interaction among agonists while the bulky side-chain moiety is the salient feature for activity among antagonists. Increased drug–receptor interaction at the bulky side chain presumably weakens the interaction at the onium group, giving rise to a diminished agonist but predominant antagonist effect.

Barlow *et al.* (4) tested agonist and antagonist molecules and concluded that changes in the structure of the onium group produce similar effects on affinity for both series. In contrast to Burgen's (3) proposal, this view advocates a comparable role for the onium group among agonists and antagonists.

A subsequent study (5) on more than 100 acetylcholine analogs revealed that changes in the molecule affinity as the onium group was modified were not entirely independent of the bulky side chain. However, the interdependence of onium and the bulky side chain was not marked. Other factors could be operating besides binding influences, including realignment at the receptor due to onium group changes, leading to altered affinity.

Goldstein *et al.* (6) stated that competitive antagonism could result from an interaction at a different receptor near the acetylcholine receptor (7). The antagonist–receptor interaction would modify the agonist re-

0022-3549/78/1000-1408$01.00/0

© 1978, American Pharmaceutical Association

Table I—Calculated Antagonist Affinities and χ Variables for $R_1CH_2CH_2R_2$

Compound	R_1[a]	R_2[b]	$^4\chi_{PC}$	$^1\chi^v$	$^3\chi_C{}^v$	Log K Obs.	Log K Calc.	Log K Result
1	CH_3CH_2O	D	1.966	5.060	0.577	3.974	4.378	−0.404
2		G	1.436	5.059	0.757	4.72	4.221	0.351
3		H	1.655	5.646	0.577	4.007	4.297	−0.290
4	$CH_3CH_2CH_2$	C	1.832	4.896	0.757	4.399	4.476	−0.077
5		D	1.966	5.483	0.577	4.588	4.487	0.101
6		F	1.655	5.569	0.577	4.370	4.277	0.093
7		G	1.436	5.481	0.757	4.815	4.330	0.485
8		H	1.655	6.069	0.577	4.546	4.406	0.140
9	$C_6H_5CH_2COO$	A	1.527	5.328	1.451	4.533	5.290	−0.757
10		B	2.234	5.916	1.162	5.093	5.584	−0.491
11		C	2.609	6.503	0.933	5.379	5.710	−0.331
12		D	2.743	7.091	0.754	5.785	5.721	0.064
13		E	2.213	6.589	0.933	5.084	5.435	−0.351
14		F	2.433	7.176	0.754	5.568	5.511	0.057
15		G	2.213	7.089	0.933	5.194	5.564	−0.370
16		H	2.433	7.676	0.754	5.525	5.639	−0.114
17	$C_6H_5CH_2CH_2O$	A	1.183	5.355	1.392	4.702	4.960	−0.258
18		B	1.890	5.942	1.103	5.167	5.254	−0.087
19		C	2.265	6.530	0.875	5.415	5.380	0.035
20		D	2.399	7.118	0.695	5.758	5.391	0.367
21		E	1.869	6.616	0.875	5.224	5.105	0.119
22		F	2.088	7.203	0.695	5.431	5.181	0.250
23		G	1.869	7.116	0.875	5.369	5.234	0.135
24		H	2.088	7.703	0.695	5.507	5.310	0.197
25	$C_6H_5CH_2CH_2CH_2$	A	1.183	5.778	1.392	5.180	5.069	0.111
26		B	1.890	6.365	1.103	5.549	5.363	0.186
27		C	2.265	6.953	0.875	5.735	5.489	0.246
28		D	2.399	7.540	0.695	5.849	5.500	0.349
29		E	1.869	7.038	0.875	5.602	5.214	0.388
30		F	2.088	7.626	0.695	5.651	5.290	0.361
31		G	1.869	7.538	0.875	5.686	5.343	0.343
32		H	2.088	8.126	0.695	5.467	5.419	0.048
33	$C_6H_{11}CH_2COO$	A	1.527	6.289	1.537	5.067	5.653	−0.586
34		B	2.234	6.876	1.249	5.517	5.947	−0.430
35		C	2.609	7.464	1.020	5.569	6.073	−0.504
36		D	2.743	8.051	0.840	5.630	6.084	−0.454
37		E	2.213	7.549	1.020	5.433	5.798	−0.365
38		F	2.433	8.137	0.840	5.635	5.874	−0.239
39		G	2.213	8.049	1.020	5.429	5.927	−0.498
40		H	2.433	8.637	0.840	5.432	6.003	−0.571
41	$C_6H_{11}CH_2CH_2O$	A	1.183	6.315	1.478	5.282	5.323	−0.041
42		B	1.890	6.903	1.190	5.657	5.617	0.040
43		C	2.265	7.491	0.961	5.783	5.743	0.040
44		D	2.399	8.078	0.781	5.912	5.755	0.157
45		E	1.869	7.576	0.961	5.616	5.468	0.148
46		F	2.088	8.164	0.781	5.729	5.544	0.185
47		G	1.869	8.076	0.961	5.731	5.597	0.134
48		H	2.088	8.664	0.781	5.725	5.673	0.052
49	$C_6H_{11}CH_2CH_2CH_2$	A	1.183	6.738	1.478	5.387	5.432	−0.045
50		B	1.890	7.326	1.190	5.841	5.726	0.115
51		C	2.265	7.913	0.961	5.878	5.852	0.026
52		D	2.399	8.501	0.781	5.921	5.864	0.057
53		E	1.869	7.999	0.961	5.728	5.577	0.151
54		F	2.088	8.586	0.781	5.814	5.653	0.161
55		G	1.869	8.499	0.961	5.933	5.706	0.227
56		H	2.088	9.086	0.781	6.025	5.782	0.243
57	$(C_6H_5)_2CHCOO$	A	2.549	7.398	1.587	7.159	6.771	0.388
58		B	3.256	7.985	1.298	7.578	7.065	0.513
59		C	3.631	8.573	1.069	7.584	7.191	0.393
60		D	3.765	9.160	0.890	7.367	7.202	0.165
61		E	3.235	8.659	1.069	7.440	6.916	0.524
62		F	3.454	9.246	0.890	7.558	6.992	0.566
63		G	3.235	9.159	1.069	7.260	7.045	0.215
64		H	3.454	9.746	0.890	7.015	7.121	−0.106
65	$(C_6H_5)_2CHCH_2O$	A	2.131	7.398	1.569	6.413	6.433	−0.020
66		B	2.838	7.985	1.280	6.693	6.727	−0.034
67		C	3.213	8.573	1.051	6.543	6.853	−0.310
68		D	3.347	9.160	0.872	6.374	6.864	−0.490
69		E	2.816	8.659	1.051	6.507	6.578	−0.071
70		F	3.165	9.236	1.244	6.589	7.247	−0.658
71		G	2.816	9.159	1.051	6.182	6.707	−0.525
72		H	3.036	9.746	0.872	6.131	6.783	−0.652

(continued)

Table I—*Continued*

Compound	R_1[a]	R_2[b]	$^4\chi_{PC}$	$^1\chi^v$	$^3\chi_C^v$	Log K Obs.	Log K Calc.	Log K Result
73	$(C_6H_5)_2CHCH_2CH_2$	A	2.131	7.820	1.569	7.015	6.542	0.473
74		B	2.838	8.408	1.280	7.270	6.836	0.434
75		C	3.213	8.995	1.051	7.091	6.962	0.129
76		D	3.347	9.583	0.872	6.712	6.973	−0.261
77		E	2.816	9.081	1.051	6.788	6.687	0.101
78		F	3.036	9.669	0.872	6.858	6.763	0.095
79		G	2.816	9.581	1.051	6.664	6.816	−0.152
80		H	3.036	10.169	0.872	6.579	6.892	−0.313
81	$(C_6H_5)_2C(OH)COO$	A	4.313	7.505	1.713	8.511	8.288	0.223
82		B	5.020	8.093	1.424	8.934	8.582	0.352
83		C	5.395	8.680	1.195	8.957	8.708	0.249
84		D	5.529	9.268	1.016	8.682	8.719	−0.037
85		E	4.998	8.766	1.195	8.585	8.433	0.152
86		F	5.218	9.354	1.016	8.652	8.509	0.143
87		G	4.998	9.266	1.195	8.034	8.562	−0.528
88		H	5.218	9.854	1.016	8.012	8.638	−0.626
89	$(C_6H_{11})_2CHCOO$	A	2.549	9.299	1.752	7.686	7.482	0.204
90		B	3.256	9.886	1.463	7.723	7.776	−0.053
91		C	3.631	10.474	1.234	8.083	7.902	0.181
92		D	3.765	11.061	1.055	8.068	7.913	0.155
93		E	3.235	10.560	1.234	8.093	7.627	0.466
94		F	3.454	11.147	1.055	8.260	7.703	0.557
95		G	3.235	11.060	1.234	8.117	7.756	0.361
96		H	3.454	11.647	1.055	7.692	7.832	−0.140
97	$(C_6H_{11})CHCH_2O$	A	2.131	9.299	1.744	7.254	7.158	0.096
98		B	2.838	9.886	1.455	7.615	7.452	0.163
99		C	3.213	10.474	1.226	7.574	7.578	−0.004
100		D	3.347	11.061	1.047	7.354	7.589	−0.235
101		E	2.816	10.560	1.226	7.541	7.303	0.238
102		F	3.036	11.147	1.047	7.206	7.379	−0.173
103		G	2.816	11.060	1.226	7.296	7.432	−0.136
104		H	3.036	11.647	1.047	6.600	7.508	−0.908

[a] The molecular formula for each R_1 group is given only for the first compound of each set. It is understood that the subsequent compounds have the same R_1, until a new formula is given. [b] Symbols for the onium groups are as follows: A, $N(CH_3)_3$; B, $N(CH_3)_2C_2H_5$; C, $N(C_2H_5)_2CH_3$; D, $N(C_2H_5)_3$; E, $N(CH_2)_4CH_3$; F, $N(CH_2)_4C_2H_5$; G, $N(CH_2)_5CH_3$; and H, $N(CH_2)_5C_2H_5$.

ceptor, thereby reducing the affinity of the agonist–receptor interaction.

Aside from the question of the interrelation of onium and the side chain in determining affinity, the question of the overall structure–activity effects on affinity has not been evaluated quantitatively. Relationships between affinity and molar volume, osmotic coefficients, and ion-pair formation energies were studied (7–9). Parallel physical properties were considered, leading to the general conclusion that size influences hydrophobic bonding, resulting in increased measured affinity.

EXPERIMENTAL

The work of Abramson *et al.* (5) on a large series of antagonists and agonists provides the best data for a quantitative structure–activity study and a consideration of some conflicting views. Qualitative observations on the structure–activity relationships of more than 100 compounds, mostly antagonists, were made relative to the affinities at the guinea pig ileum.

In the present study, 104 optically inactive antagonists reported by Abramson *et al.* (5) were considered. The structural analysis was made using the molecular connectivity method (10); this method was employed previously (11–15) to study the structure–activity relationships of various biologically active molecules.

RESULTS

The connectivity indexes for the 104 antagonist molecules were searched, using regression analysis, for the best three indexes correlating with affinity (expressed as log K). The best equation was:

$$\log K = 0.749\ (\pm 0.002)\,{}^4\chi_{PC} + 0.258\ (\pm 0.001)\,{}^1\chi^v + 1.340\ (\pm 0.015)\,{}^3\chi_C^v + 0.827\ (\pm 0.33) \quad \text{(Eq. 1)}$$

$$r = 0.962 \quad s = 0.331 \quad n = 104 \quad F = 417 \quad p < 0.001$$

The equation accounts for 93% of the variation in log K, and the standard deviation is less than 7% of the range of log K values in the study (Table I). Only two molecules, Compounds 9 and 104, are predicted by the equation to have a residual greater than 2 *SD*. The correlation matrix is shown in Table II. The indexes used in the regression search include $^0\chi$, the path terms of orders 1 through 4, $^3\chi_C$, $^4\chi_{PC}$, and the corresponding valence terms.

The three indexes in the equation are weighted counts of subgraphs of a specific type. The $^1\chi^v$ index refers to subgraphs of one bond in which the bridged atoms are described by their valence, δ^v, according to the prescription $\delta^v = Z^v - h$, where Z^v is the number of valence electrons in the atom and h is the number of hydrogens bonded to the atom but suppressed in forming the graph. The $^3\chi_C^v$ index describes subgraph fragments in which three bonds converge at one atom. The atoms are described by their δ^v in the computation. The $^4\chi_{PC}$ index quantitates the subgraph fragments that would be identical to the isopentane molecular skeleton. The atom δ values are based on adjacency.

The first two indexes in the equation cross correlate to an extent of 0.65. This low order is not negligible but arises as a consequence of the nature of the molecules under study. Increases in $^1\chi^v$ generally arise from an increase in the number of atoms in the molecule. Increases in the $^4\chi_{PC}$ index reflect an increase in branching in the molecule. In the set of molecules chosen, these structural changes parallel each other to the extent reflected by the cross-correlation value of 0.65. The change in one index accounts for 42% of the variation in the other index.

The indexes in the equation describe specific subgraphs irrespective of their degree of statistical cross correlations. In a multiple index relationship for a structurally similar set of molecules, this result is not unexpected. Nevertheless, the relative amount of information conveyed

Table II—Correlation Matrix for Equation Variables

	$^1\chi^v$	$^4\chi_{PC}$
$^1\chi^v$		
$^4\chi_{PC}$	0.65	
$^3\chi_C^v$	0.25	0.20

Table III—Connectivity Indexes and Log *K* Contributions of Onium Group Models

Group Model	$^4\chi_{PC}$ Analysis n^a	$^4\chi_{PC}$	Average	$^1\chi^v$	$^3\chi_C{}^v$ Analysis n	$^3\chi_C{}^v$	Average	Calculated Log *K* Contribution
$C_2H_5N(CH_3)_3$	3	1.061	0.354	2.221	4	1.274	0.319	3.902
$C_2H_N(CH_3)_2C_2H_5$	6	1.707	0.285	2.808	4	0.986	0.247	4.151
$C_2H_5N(CH_3)(C_2H_5)_2$	9	2.030	0.226	3.396	4	0.757	0.189	4.238
$C_2H_5N(C_2H_5)_3$	12	2.121	0.177	3.983	4	0.577	0.144	4.216
$C_2H_5N(CH_2)_4CH_3$	9	1.634	0.182	3.481	4	0.757	0.189	3.963
$C_2H_5N(CH_2)_4C_2H_5$	12	1.811	0.151	4.069	4	0.577	0.144	4.006
$C_2H_5N(CH_2)_5CH_3$	9	1.634	0.182	3.981	4	0.757	0.189	4.092
$C_2H_5N(CH_2)_5C_2H_5$	12	1.811	0.151	4.569	4	0.577	0.144	4.135

[a] n = number of terms.

by each index in a successful correlation with a property affords an opportunity for meaningful structural analysis and possible prediction.

The equation is statistically significant above the 99.9% level; $F = 416.5 > 6.04 = F(100,3,0.001)$. The addition of the second variable, $^4\chi_{PC}$, to the one-variable equation based on $^1\chi^v$ is statistically significant above the 99.9% level; $F = 145.2 > 11.9 = F(101,1,0.001)$. So also is the addition of the third variable, $^3\chi_C{}^v$; $F = 121.1 > 11.8 = F(100,1,0.001)$.

Random Number Analysis—When a regression equation is obtained from a search of several variables, a question can be raised about possible random correlations (16). In this study, this question was approached with a direct investigation of correlations based on replacement of the 22 χ terms with random numbers. The regression search program was used to find the best set of three variables against the affinity data in the same manner as was done using χ indexes. For each set of random numbers, 1540 triplets of variables were considered. The highest correlation coefficient, r_{max}, was recorded. The procedure was repeated 100 times with different sets of random numbers for all 22 variables. The highest r_{max} value found was 0.45, and the average was 0.25. Four values of r_{max} were in the range 0.35–0.45, 35 were between 0.25 and 0.35, 60 were between 0.15 and 0.25, and one was below 0.15.

In a further study, the three χ terms found to correlate with log *K*, $^4\chi_{PC}$, $^1\chi^v$, and $^3\chi_C{}^v$, were regressed against 100 sets of random numbers in place of log *K*. The highest correlation coefficient found was 0.35, and the average value was 0.16. Ten values lay in the range 0.25–0.35, 43 lay between 0.15 and 0.25, and 47 were between 0.05 and 0.15.

These studies clearly indicate that the set of three χ terms reported here do not correlate with sets of random numbers. Rather, the three terms in concert reflect the systematic variation of log *K* with the molecular structure. In addition, the χ terms yield a regression vastly superior to sets of random numbers. These results further support the conclusion that the correlation reported here is a systematic relation.

Analysis—The best variables as shown in the equation of correlation are no longer than three path lengths (three contiguous bonds as found in the $^4\chi_{PC}$ subgraphs). Indexes reflecting subgraphs through four path lengths were searched in the regression analysis. Additional regression analyses revealed no significant role for indexes based on paths of length five and six.

Among these structures, this finding leads to the conclusion that important structural features may be found at either end of the molecule and are not connected through the length of the molecule. Molecular connectivity provides a partial statement of the real structure of these molecules since the conformation is not dealt with by this method. Thus, the separate ends of the molecule, revealed by molecular connectivity to be important, may in fact be physically quite close because of forces influencing the conformational preference of the molecule. Molecular connectivity speaks to sequential attachment of atoms through formal bonds, not transspatial nonbonded forces and interactions.

The finding of a separate role for the two ends of the molecule, in the sense just described, prompted an additional study to analyze separately the onium group and the side chain for further structural information.

Onium Group—For convenience in analyzing the eight onium group variants, a truncated model of the onium groups in which the bulky side chain was replaced in each case by an ethyl group was used. Table III lists the values of the three connectivity indexes, the number of subgraph terms contributing to each index, and the average value of the subgraphs. The data illustrate a number of structure–activity relationship conclusions about the onium groups and affinity.

The first four onium groups in Table III are a homologous series formed by successively replacing an *N*-methyl group with an ethyl group. The number of subgraphs composing the $^4\chi_{PC}$ index increased by three through this series. However, the numerical values of the subgraph contributions, as illustrated by the average value, decreased in this progression. The net effect was a modest increase in the value of $^4\chi_{PC}$ after the second compound.

The $^3\chi_C{}^v$ terms reveal a different trend in Table III for the first four cases. The number of subgraph terms composing this index in each case was constantly four, while the average value declined numerically. Thus, the $^3\chi_C{}^v$ indexes decreased with successive ethyl group replacement.

The $^1\chi^v$ indexes increased through this series, reflecting the addition of one carbon atom in each case. Thus, a summation of these three connectivity indexes, weighted by the coefficients in the regression equation, reveals a contribution to the log *K* values from the onium group. As can be seen in the last column of Table III, this contribution was quite similar across the series. The numerical range for the first four cases (and indeed all eight cases) was within the standard deviation of the equation.

An analysis of all eight onium group models in Table III gives the same conclusion. The contributions to log *K* from increasing the number of atoms was offset by a decline in the $^3\chi_C{}^v$ terms and a leveling out of the values of the $^4\chi_{PC}$ terms. The net result was a relatively constant contribution to log *K* by the onium group, irrespective of the increase in size or complexity.

Side Chain—The bulky side chain was treated similarly by analyzing the individual connectivity indexes for truncated models of the side chains found in this study. The truncation model utilized an ethyl group

Table IV—Connectivity Indexes and Log *K* Contributions of Side-Chain Models

Group Model	$^4\chi_{PC}$ Analysis n^a	$^4\chi_{PC}$	Average	$^1\chi^v$	$^3\chi_C{}^v$ Analysis n	$^3\chi_C{}^v$	Average	Calculated Log *K* Contribution
$CH_3CH_2OC_2H_5$	0	0	0	1.992	0	0	0	1.341
$CH_3CH_2CH_2C_2H_5$	0	0	0	2.414	0	0	0	1.450
$C_6H_5CH_2COOC_2H_5$	5	0.777	0.155	4.022	2	0.177	0.089	2.684
$C_6H_5CH_2CH_2OC_2H_5$	3	0.433	0.144	4.049	1	0.118	0.118	2.354
$C_6H_5CH_2CH_2CH_2C_2H_5$	3	0.433	0.144	4.471	1	0.118	0.118	2.463
$C_6H_{11}CH_2COOC_2H_5$	5	0.777	0.155	4.982	2	0.263	0.132	3.047
$C_6H_{11}CH_2CH_2OC_2H_5$	3	0.433	0.144	5.009	1	0.204	0.204	2.717
$C_6H_{11}CH_2CH_2CH_2C_2H_5$	3	0.433	0.144	5.432	1	0.204	0.204	2.826
$(C_6H_5)_2CHCOOC_2H_5$	17	1.799	0.106	6.091	4	0.313	0.078	4.165
$(C_6H_5)_2CHCH_2OC_2H_5$	13	1.381	0.106	6.091	3	0.295	0.098	3.828
$(C_6H_5)_2CHCH_2CH_2C_2H_5$	13	1.381	0.106	6.514	3	0.295	0.098	3.937
$(C_6H_5)_2C(OH)COOC_2H_5$	32	3.563	0.111	6.199	7	0.439	0.063	5.683
$(C_6H_{11})_2CHCOOC_2H_5$	17	1.799	0.106	7.992	4	0.478	0.120	4.877
$(C_6H_{11})_2CHCH_2OC_2H_5$	13	1.381	0.106	7.992	3	0.469	0.156	4.552

[a] n = number of terms.

Table V—Prediction of Antagonist Affinities

Molecule	$^4\chi_{PC}$	$^1\chi^v$	$^3\chi_C{}^v$	Experimental Log K	Calculated Log K
$C_6H_5(CH_2)_4N(CH_3)_3$	1.183	5.278	1.392	4.771	4.949
$C_6H_5(CH_2)_6N(CH_3)_3$	1.183	6.278	1.392	5.393	5.198
$C_6H_5(CH_2)_4N(C_2H_5)_3$	2.399	7.040	0.695	5.480	5.371
$C_6H_5(CH_2)_6N(C_2H_5)_3$	2.399	8.040	0.695	5.970	5.629
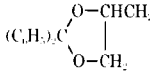	3.541	7.584	1.744	8.020	7.773

Table VI—Prediction of Agonist Affinities

Molecule	$^4\chi_{PC}$	$^1\chi^v$	$^3\chi_C{}^v$	Experimental Log K	Calculated Log K
$C_2H_5OCH_2CH_2N(CH_3)_3$	0.750	3.298	1.274	4.074	3.947
$C_2H_5OCH_2CH_2N(CH_3)_2C_2H_5$	1.457	3.885	0.986	3.887	4.242
$C_2H_5OCH_2CH_2CH_2N(C_2H_5)_2CH_3$	1.832	4.473	0.757	3.735	4.368
$C_2H_5OCH_2CH_2N(CH_2)_4CH_3$	1.436	4.559	0.757	4.026	4.093
$C_2H_5OCH_2CH_2N(CH_2)_4C_2H_5$	1.665	5.146	0.577	3.883	4.167
$C_2H_5CH_2CH_2CH_2N(CH_3)_3$	0.750	3.721	1.274	3.733	4.056
$C_2H_5CH_2CH_2CH_2N(CH_3)_2C_2H_5$	1.457	4.308	0.986	3.970	4.351
$C_2H_5CH_2CH_2CH_2N(CH_2)_4CH_3$	1.436	4.981	0.757	4.165	4.202

terminating the molecule in place of the ethylonium group found in each actual compound. The data for analysis are summarized in Table IV.

The major variation of affinity with molecular structure was associated with side-chain variation (Table IV). This influence was paralleled by all three connectivity indexes in Table IV. The major fraction of the variation was described by the $^1\chi^v$ contribution. The range of $^1\chi^v$ contributions was about 2 log K units while the contributions from $^3\chi_C{}^v$ and $^4\chi_{PC}$ ranged over 0.5 and 0.7 log K unit, respectively.

A more specific analysis of the data can be made in terms of structural features contributing to affinity. The replacement of methylene by an ether oxygen decreased the value of $^1\chi^v$ by 0.422. This difference reflected the observations that the ether side chains had a slightly lower affinity than the alkyl side chains. Cyclohexyl substituents gave $^1\chi^v$ values 0.96 higher than phenyl substituents, mirroring the trend in affinities.

The replacement of a methyl hydrogen in the hydrocarbon or ether series by a phenyl or cyclohexyl increased the affinity significantly. This effect was described principally by the increase in $^1\chi^v$. However, when both groups appeared on the same carbon, additional $^4\chi_{PC}$ and $^3\chi_C{}^v$ subgraphs were generated, giving an increase in affinity greater than anticipated based on the individual contributions. This observation was properly accounted for by Eq. 1 and corresponded to a reported observation (5), but here it was in quantitative form.

Prediction of Antagonist Affinities—The value of the structural descriptions encoded in Eq. 1 lies in the ability to predict the affinities of antagonists not included in the original regression analysis. Accordingly, the χ indexes were calculated for five additional antagonists and the log K values were computed from Eq. 1 (Table V). The predicted values of the affinities were within the standard deviation of the equation.

Prediction of Agonist Affinities—As a further test of Eq. 1 and to determine whether comparable structural features govern the affinities of agonists, Eq. 1 was used to predict the affinities of five agonists and three partial agonists. The results (Table VI) reveal good predictions in almost every case. The standard deviation was within the standard deviation of the original equation.

DISCUSSION

Based on a quantitative structure–activity relationship accounting for 93% of the variation in the log K values for 104 molecules, certain general conclusions about structure and affinity can be made. The affinity of the antagonists in Table I depends on a specific combination of molecular size, branching, and heteroatom composition.

The onium group contribution to the affinity of the molecule is essentially constant, despite structural changes such as size and cyclization (Table III). The variation in the onium group contribution to log K ranges from 3.902 to 4.238 for the eight variations in this study. This range coincides with the standard deviation in the equation.

The same kind of analysis applied to the onium groups of the agonists in Table VI also reveals a fairly constant contribution to the log K values. Furthermore, these onium group contributions are the same as those found among the antagonists. This finding is quite compatible with the views of Barlow *et al.* (4).

The principal influence on the affinity of antagonists arises from structural variation in the side chain. This finding is evident from Table V, which depicts the contributions from 14 different side chains in the study.

The close predictions for antagonists and agonists in Tables V and VI indicate that the molecular connectivity indexes in the equation correctly describe the structural influences governing the affinity.

REFERENCES

(1) A. Bebbington and R. W. Brimblecombe, *Adv. Drug Res.*, **2**, 143 (1965).

(2) R. W. Brimblecombe, "Drug Actions on Cholinergic Systems," University Park Press, Baltimore, Md., 1974.

(3) A. S. V. Burgen, *Br. J. Pharmacol. Chemother.*, **25**, 4 (1965).

(4) R. B. Barlow, K. A. Scott, and R. P. Stephenson, *ibid.*, **21**, 509 (1963).

(5) F. B. Abramson, R. B. Barlow, M. G. Mustafa, and R. P. Stephenson, *Br. J. Pharmacol.*, **37**, 207 (1969).

(6) A. Goldstein, L. Arnow, and S. Kalman, "Principles of Drug Action," Harper and Row, New York, N.Y., 1968.

(7) R. B. Barlow, B. M. Lowe, J. D. Pearson, H. M. Rendall, and G. M. Thompson, *Mol. Pharmacol.*, **7**, 357 (1971).

(8) R. B. Barlow and F. M. Franks, *Br. J. Pharmacol.*, **49**, 480 (1973).

(9) R. B. Barlow, *ibid.*, **51**, 413 (1974).

(10) L. B. Kier and L. H. Hall, "Molecular Connectivity in Chemistry and Drug Research," Academic, New York, N.Y., 1976.

(11) L. B. Kier, L. H. Hall, W. J. Murray, and M. Randic, *J. Pharm. Sci.*, **64**, 1971 (1975).

(12) W. J. Murray, L. B. Kier, and L. H. Hall, *J. Med. Chem.*, **19**, 573 (1976).

(13) T. DiPaolo, L. B. Kier, and L. H. Hall, *Mol. Pharmacol.*, **13**, 31 (1977).

(14) L. B. Kier, L. H. Hall, and T. DiPaolo, *J. Theoret. Biol.*, **67**, 585 (1977).

(15) L. H. Hall and L. B. Kier, *J. Pharm. Sci.*, **66**, 642 (1977).

(16) J. G. Topliss and R. J. Costello, *J. Med. Chem.*, **15**, 1066 (1972).

Fluorescence–TLC Densitometric Determination of Diazepam and Other 1,4-Benzodiazepines in Serum

SY-RONG SUN

Received November 4, 1977, from the *Pharmaceutical Products Division, Abbott Laboratories, North Chicago, IL 60064.* Accepted for publication February 6, 1978.

Abstract □ A sensitive fluorescence–TLC densitometric procedure was developed for the specific determination of diazepam (I) and its two metabolites, desmethyldiazepam (II) and oxazepam (III), in serum. After extraction from serum with benzene, the compounds were separated by TLC and converted with a sulfuric acid spray to greenish-yellow fluorescence spots with R_f values of 0.72, 0.43, and 0.17, respectively. Quantitation of the TLC plate was accomplished by scanning with a densitometer at 380 nm. The sensitivities of the assay were 18 (I), 6 (II), and 5 (III) ng/ml of serum. This procedure also was applicable to other 1,4-benzodiazepines in biological fluids.

Keyphrases □ Diazepam—fluorescence–TLC densitometric analysis in serum □ Desmethyldiazepam—fluorescence–TLC densitometric analysis in serum □ Oxazepam—fluorescence–TLC densitometric analysis in serum □ Fluorescence–TLC densitometry—analyses, diazepam, desmethyldiazepam, and oxazepam in serum □ Sedatives—diazepam, fluorescence–TLC densitometric analysis in serum

Diazepam and its metabolites have been determined in biological fluids primarily by electron-capture GLC (1–9). Clifford and Smyth (10) reviewed the determination of some 1,4-benzodiazepines and their metabolites in body fluids by different instrumental analyses. Other investigators (11, 12) studied the fluorescence properties of some 1,4-benzodiazepines in acidic solutions. Recently, TLC procedures for the determination of diazepam (I) and its metabolites, desmethyldiazepam (II) and oxazepam (III), were reported (13–16). Measurements were taken directly from an unstained thin-layer plate to diffuse-light reflectance of I–III at their UV absorption maxima.

The following new fluorescence–TLC method is capable of measuring low levels of I–III in serum. Compounds I–III are converted to greenish-yellow fluorescence spots on TLC plates by a sulfuric acid spray and measured densitometrically. A similar fluorescence technique for the determination of chlordiazepoxide and its metabolites in serum was reported (17). Strojny *et al.* (16) also examined several fluorescent derivatives by TLC densitometry, but their procedure was less sensitive because of the use of a second monochromator rather than a filter as in the present study.

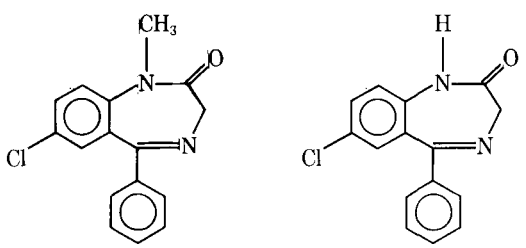

I

II

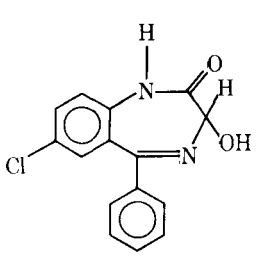

III

EXPERIMENTAL

Reagents and Materials—Diazepam[1] (I), desmethyldiazepam[2] (II), and oxazepam[3] (III) were used as supplied. The other chemicals were analytical reagent grade. TLC plates[4] (20 × 20 cm) were used as supplied.

Apparatus—A two-speed reciprocating shaker[5] and a refrigerated centrifuge[6] were used. Sample solutions in the test tubes were mixed[7]. Samples were spotted on TLC plates with an automatic TLC spotter[8] using polytef-tipped 50-μl syringes[9]. A TLC sprayer[10] was used for the sulfuric acid spray on the plates.

Preparation of Serum Standards—Five serum standards were extracted for each eight unknown samples. Serum standards contained I, II, and III at 0.60, 0.20, and 0.20 μg/ml, respectively, in the first standard; 0.30, 0.10, and 0.10 μg/ml, respectively, in the second standard; 0.15, 0.05, and 0.05 μg/ml, respectively, in the third standard; and 0.075, 0.025, and 0.025 μg/ml, respectively, in the fourth standard. The fifth standard was the serum blank[11]. The first serum standard was prepared by spiking the serum blank with primary standard solutions of I–III each at 100 μg/ml in methanol.

Extraction Procedure—To 2 ml of serum sample or standard in a 20-ml screw-capped test tube were added 1 ml of 0.1 *M* K_2HPO_4 and 5 ml of benzene. The tube was shaken reciprocally at 80 cpm for 10 min. After centrifugation at 3000 rpm for 5 min at 10°, 4 ml of the benzene layer was transferred to a 15-ml conical test tube and evaporated to dryness at 40° with filtered air. The residue was reconstituted with 1 ml of methanol and dried at 40° with filtered air; then 50 μl of methanol was added and mixed.

The entire amount was taken up in a 50-μl syringe and spotted on a TLC plate using an automatic TLC spotter. The heating region of the automatic spotter was set at 35–40°. Thirteen samples (eight unknowns and five standards) were spotted on each TLC plate. A horizontal line was scribed 2.5 cm from the top of the plate, and the plate was developed to the line with chloroform–2-propanol–ammonium hydroxide (95:5:0.5).

After the plate was dried overnight at room temperature, it was stood vertically and sprayed about six times with 7 *N* H_2SO_4. The acid was sprayed across the plate at a distance of about 15.2 cm (6 in.) from it and at the rate of about 5 sec/spray. The spots were located with long wavelength UV light[12]. The compounds appeared as greenish-yellow fluorescence spots with R_f values of 0.72, 0.43, and 0.17 for I, II, and III, respectively.

Densitometry—The TLC plate was scanned at 100 mm/min in a direction perpendicular to the direction of development with a densitom-

[1] 7-Chloro-1,3-dihydro-1-methyl-5-phenyl-2*H*-1,4-benzodiazepin-2-one, lot 309039, Hoffmann–La Roche, Nutley, N.J.
[2] 7-Chloro-1,3-dihydro-5-phenyl-2*H*-1,4-benzodiazepin-2-one, lot 101-294, Hoffmann–La Roche, Nutley, N.J.
[3] 7-Chloro-1,3-dihydro-3-hydroxy-5-phenyl-2*H*-1,4-benzodiazepin-2-one, Wyeth, Philadelphia, Pa.
[4] Silica gel GF (250 μm), Analtech, Newark, Del.
[5] Eberbach Corp., Ann Arbor, Mich.
[6] Sorvall Inc., Newtown, Conn.
[7] Vortex Genie, model K-55-GT, Scientific Industries, Springfield, Mass.
[8] Analytical Instrument Specialties, Libertyville, Ill.
[9] Scientific Products, McGaw Park, Ill.
[10] Sprayon power unit, Sprayon Products, Cleveland, Ohio.
[11] K-N Enterprises Inc., Skokie, Ill.
[12] UV Viewbox, Ultra-Violet Products, San Gabriel, Calif.

0022-3549/78/1000-1413$01.00/0
© 1978, American Pharmaceutical Association

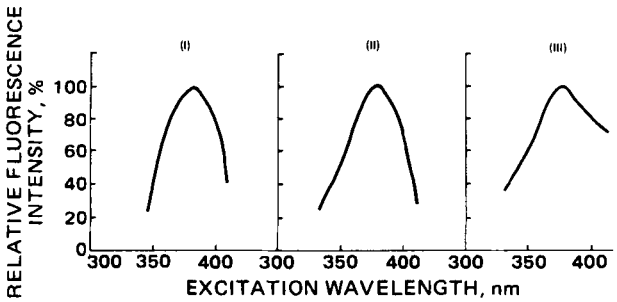

Figure 1—*Fluorescence excitation spectra of I–III.*

eter[13] fitted with a barrier filter (FL 43) in the compartment of the measuring head. The TLC plate was irradiated in the reflectance mode using a xenon lamp as the light source at the maximum excitation wavelength of 380 nm. (See *Results and Discussion.*) The slit width was 0.5 × 12 mm. The chart speed of the recorder was 10 mm/min. The high voltage potential on the photomultiplier tube was set at 2, and the gain was set at 20 on the arbitrary scale of the instrument[14]. Each spot on the TLC plate was manually located to give maximum response.

RESULTS AND DISCUSSION

The excitation spectra for the fluorescence spots (Fig. 1) were constructed by plotting the relative fluorescence intensity (as measured by the peak heights) at different excitation wavelengths. The maximum excitation wavelength was 380 nm for I–III. This wavelength was used for the assay.

Reproducibility of the assay was tested by assaying serum samples from 0.05 to 0.60 μg/ml. Relative standard deviations in a triplicate study on a single TLC plate for I, II, and III ranged from 1.1 to 15.1, from 2.0 to 6.3, and from 9.1 to 12.2%, respectively. Assay of triplicate serum samples on three TLC plates showed relative standard deviations of 0.8–20.2, 9.8–12.4, and 2.4–19.9% for I, II, and III, respectively, indicating larger variabilities among plates. However, the serum standards must be extracted and spotted along with the unknowns on each TLC plate.

Recoveries were 96.4 ± 0.7% (mean ± *SD*) for triplicate I serum samples at 0.6 μg/ml, 87.8 ± 4.3% for triplicate II serum samples at 0.2 μg/ml, and 87.3 ± 3.9% for triplicate III serum samples at 0.2 μg/ml. These values were calculated by comparing the peak height responses between the extracted serum samples and the theoretical amount of pure drug spotted on the TLC plate. The R_f values for I, II, and III were 0.72, 0.43, and 0.17, respectively. Typical TLC densitometric tracings are shown in Fig. 2.

The sensitivity limits of the assay were about 18, 6, and 5 ng/ml of serum for I, II, and III, respectively. These values were calculated by fitting a regression line to the standard curve and taking the 95% confidence interval of the y-intercept (in peak height). The calculated sensitivity was the x-value (in concentration) corresponding to the upper part of this interval of the y-intercept. In calculating the sensitivity for diazepam, the linear portion of the curve (the first four points only) was used.

The accuracy of the assay was tested by determining seven unknown spiked serum sample. The unknown serum concentrations were calculated from the standard curves obtained from the five serum standards extracted and spotted on the same TLC plate. The average percent differences between the observed and theoretical concentrations for serum samples from 0.025 to 0.600 μg/ml were 4.2, 4.3, and 5.6% for I, II, and III, respectively, indicating good accuracy. This precision was partly due to the use of an automatic TLC spotter. This device allowed the simultaneous uniform spotting of all 13 samples within 15 min.

Assay of control serum sample from a commercial source[11] showed a small background peak in the area of each compound (Fig. 2). Therefore, serum samples obtained from volunteers were assayed and compared. The background peaks from different subjects varied and generally were smaller than the background peak of the commercial source[11]. Thus, to compensate for the background variability, the concentration from 0 hr was subtracted from all values in the calculation.

This analytical method was used for the measurement of serum diazepam and metabolite concentrations in normal human subjects after

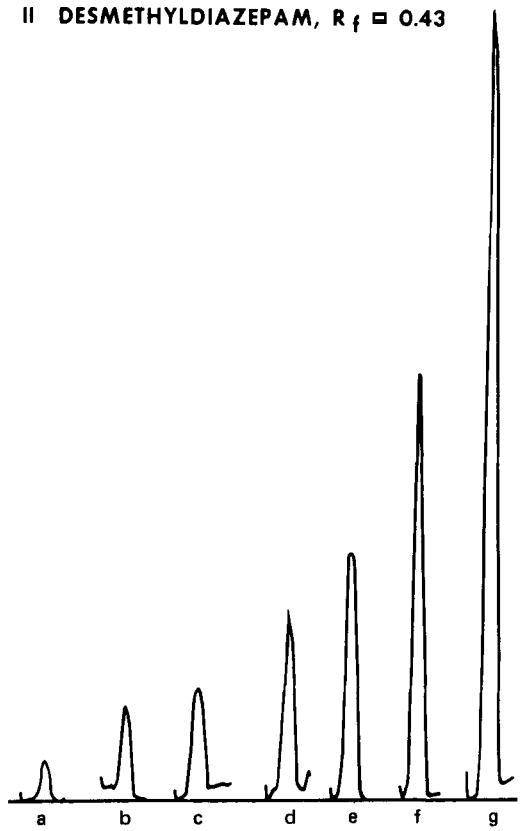

Figure 2—*TLC densitometric tracings of serum extracts containing I–III. Key: a, serum blank; b, serum standard containing 0.019 μg of I/ml, 0.006 μg of II/ml, and 0.006 μg of III/ml; c, serum standard containing 0.038 μg of I/ml, 0.012 μg of II/ml, and 0.012 μg of III/ml; d, serum standard containing 0.075 μg of I/ml, 0.025 μg of II/ml, and 0.025 μg of III/ml; e, serum standard containing 0.15 μg of I/ml, 0.05 μg of II/ml, and 0.05 μg of III/ml; f, serum standard containing 0.30 μg of I/ml, 0.10 μg of II/ml, and 0.10 μg of III/ml; and g, serum standard containing 0.60 μg of I/ml, 0.20 μg of II/ml, and 0.20 μg of III/ml.*

oral administration of diazepam tablets[15] in a single 10-mg dose. The subjects were fasted for 12 hr prior to dosing. The drug was administered with 120 ml (4 oz) of water. A serum concentration–time curve for one subject is shown in Fig. 3. The peak serum diazepam concentration occurred at 20 min and was 0.47 μg/ml. Desmethyldiazepam levels slowly increased throughout the duration of blood sampling. These values agreed with the ranges reported earlier (18). Oxazepam was not detected in this subject.

The results of this study indicate that the developed fluorescence–TLC method can be employed to quantitate diazepam and its metabolite (desmethyldiazepam) serum levels in a single-dose diazepam bioavail-

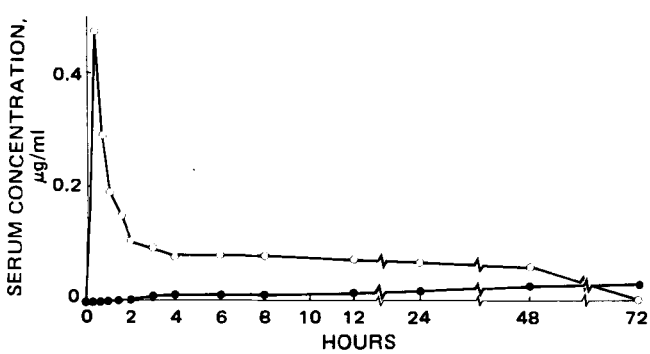

Figure 3—*Serum levels of I (○) and II (●) in one subject after receiving a 10-mg oral dose of diazepam.*

[13] Zeiss PMQ II chromatogram spectrophotodensitometer, Carl Zeiss, Oberkochen, West Germany.
[14] Zeiss PMI indicator.

[15] Valium, Roche, 5 mg/tablet, lot 6259-04165.

ability study. These fluorescent characteristics by a sulfuric acid spray on the TLC plate also were observed for other 1,4-benzodiazepines and were applied for the determination of chlordiazepoxide and its metabolites in serum (17). When chloroform–2-propanol–ammonium hydroxide (95:5:0.5) is used for separation, some 1,4-benzodiazepines have different fluorescence colors under long wavelength UV light after a sulfuric acid spray with R_f values of 0.32 (chlordiazepoxide, blue fluorescence), 0.19 (demoxepam, yellowish green), 0.38 (nitrazepam, blue), 0.73 (medazepam, blue), 0.74 (prazepam, blue), and 0.06 (*p*-hydroxydesmethyldiazepam, yellow). If chloroform–methanol–acetic acid (85:15:1) is used, these compounds have similar fluorescence characteristics after a sulfuric acid spray and their R_f values are 0.79 (diazepam), 0.73 (desmethyldiazepam), 0.65 (oxazepam), 0.68 (chlordiazepoxide), 0.66 (demoxepam), 0.72 (nitrazepam), 0.77 (major spot of medazepam which has a very small spot at R_f 0.14), 0.79 (prazepam), and 0.56 (*p*-hydroxydesmethyldiazepam). By the combined use of these solvent systems and the characteristic fluorescence colors, this procedure should be applicable for the general screening test of some 1,4-benzodiazepines in both serum and urine samples.

REFERENCES

(1) J. A. F. de Silva, M. A. Schwartz, V. Stefanovic, J. Kaplan, and L. D'Arconte, *Anal. Chem.*, **36**, 2099 (1964).

(2) J. A. F. de Silva, B. A. Koechlin, and G. Bader, *J. Pharm. Sci.*, **55**, 692 (1966).

(3) J. A. F. de Silva and C. V. Puglisi, *Anal. Chem.*, **42**, 1725 (1970).

(4) F. Marcuss, R. Fonelli, and E. Mussini, *J. Chromatogr.*, **37**, 318 (1968).

(5) A. Berlin, B. Siwers, S. Agurell, A. Hiort, F. Sjögvist, and S. Ström, *Clin. Pharmacol. Ther.*, **13**, 733 (1972).

(6) R. Erkkola, L. Kangas, and A. Pekkarinen, *Acta Obstet. Gynecol. Scand.*, **52**, 167 (1973).

(7) L. Kangas, A. Pekkarinen, C. Sourander, and E. Raijola, *Ann. Clin. Res., Suppl. 11*, **6**, 12 (1974).

(8) J. Hendel, *Acta Pharmacol. Toxicol.*, **37**, 17 (1975).

(9) J. A. F. de Silva, I. Bekersky, C. V. Puglisi, M. A. Brooks, and R. E. Weinfeld, *Anal. Chem.*, **48**, 10 (1976).

(10) J. M. Clifford and W. F. Smyth, *Analyst*, **99**, 241 (1974).

(11) J. Braun, G. Caille, and E. A. Martin, *Can. J. Pharm. Sci.*, **3**, 65 (1968).

(12) G. Caille, J. Braun, D. Gravel, and R. Plourde, *ibid.*, **8**, 42 (1973).

(13) N. Wad, H. Rosenmund, and E. Hanifl, *J. Chromatogr.*, **128**, 231 (1976).

(14) N. Wad and E. Hanifl, *ibid.*, **143**, 219 (1977).

(15) S. Ebel and H. Kusmaul, *Arch. Pharm.*, **307**, 230 (1974).

(16) N. Strojny, K. Bratin, M. A. Brooks, and J. A. F. de Silva, *J. Chromatogr.*, **143**, 363 (1977).

(17) S. Sun, "APhA Annual Meeting Abstract," vol. 7, No. 1, American Pharmaceutical Association, Washington, D.C., 1977, p. 194. S. Sun, *J. Pharm. Sci.*, **67**, 639 (1978).

(18) S. A. Kaplan, M. L. Jack, K. Alexander, and R. E. Weinfeld, *J. Pharm. Sci.*, **62**, 1789 (1973).

ACKNOWLEDGMENTS

The author gratefully acknowledges the technical assistance of M. Leveque.

Facile Separation of Sulfonamides from Their Degradates by Liquid–Liquid Extraction

D. W. FINK ˣ, R. P. MARTIN *, and J. BLODINGER

Received August 31, 1977, from the *Merck Sharp & Dohme Research Laboratories, Rahway, NJ 07065.* Accepted for publication February 6, 1978. *Present address: New Research Facility, Ortho Pharmaceutical Co., Raritan, NJ 08869.

Abstract □ Regulation of acidity for protonation of the free N^4-amine can provide for the selective liquid–liquid extraction isolation of a sulfonamide from its degradation products. This principle is applied for the stability-indicating determination of sulfacetamide in the presence of sulfanilamide, sulfaquinoxaline in feed, and sulfabromomethazine in dosage forms. In solution, sulfabromomethazine can exhibit photodecomposition to sulfamethazine. The mean relative errors of the these methods and the precision, represented by relative standard deviations, are each typically <2%.

Keyphrases □ Sulfonamides, various—separated from degradation products by liquid–liquid extraction □ Degradation products of various sulfonamides—separated from parent compounds by liquid–liquid extraction □ Liquid–liquid extraction—separation of various sulfonamides from degradation products □ Antibacterials—various sulfonamides, separation from degradation products by liquid–liquid extraction

Although most sulfonamides are highly stable, they can degrade (almost exclusively) by acid-catalyzed hydrolysis of the sulfur–nitrogen bond (1–7) or, occasionally, by cleavage of the nitrogen–carbon bond (1). Hence, any stability-indicating analysis for these drugs in formulations should discriminate between the intact sulfonamide and both sulfanilic acid and sulfanilamide as potential hydrolytic degradates.

BACKGROUND

Applications of separation techniques to the sulfonamides have long been of interest because of the similar chemical and physical properties of these drugs and their use in combinations. Typically, sulfonamides have been separated by TLC, and many very exacting quantitative procedures for determining mixtures of these drugs using this technique have been published. Among those studies that present data for sulfanilamide (*e.g.*, 8, 9) are evaluations of new spray reagents (10, 11) and various stationary phases (12).

Of the GLC methods, those procedures that measure the relevant amine generated from acidic sulfonamide hydrolysis (4–7) are not directly applicable for stability studies; only the methods that derivatize the intact drug (13–18) are appropriate. Some recently published high-pressure liquid chromatographic (HPLC) sulfonamide separations make use of adsorption (19, 20), ion-exchange (21, 22), ion-pair partition (23, 24), and reversed-phase (25) modes.

For stability studies of sulfonamides, simple liquid–liquid extraction is an attractive alternative to some of those tedious or time-consuming approaches. In particular, quantitative TLC methods are lengthy and require careful attention to technique to obtain good precision. The extraction is also convenient because it neither requires the derivatization essential for GLC nor relies on instrumentation, and it can be combined with standard (*e.g.*, Bratton–Marshall) analytical measurements for the sulfonamides. Although other solvents also may be satisfactory, a mixed chloroform–1% dimethylformamide solvent was selected as the organic phase to demonstrate the feasibility of this approach. The aqueous phase

0022-3549/78/1000-1415$01.00/0

© 1978, American Pharmaceutical Association

ability study. These fluorescent characteristics by a sulfuric acid spray on the TLC plate also were observed for other 1,4-benzodiazepines and were applied for the determination of chlordiazepoxide and its metabolites in serum (17). When chloroform–2-propanol–ammonium hydroxide (95:5:0.5) is used for separation, some 1,4-benzodiazepines have different fluorescence colors under long wavelength UV light after a sulfuric acid spray with R_f values of 0.32 (chlordiazepoxide, blue fluorescence), 0.19 (demoxepam, yellowish green), 0.38 (nitrazepam, blue), 0.73 (medazepam, blue), 0.74 (prazepam, blue), and 0.06 (*p*-hydroxydesmethyldiazepam, yellow). If chloroform–methanol–acetic acid (85:15:1) is used, these compounds have similar fluorescence characteristics after a sulfuric acid spray and their R_f values are 0.79 (diazepam), 0.73 (desmethyldiazepam), 0.65 (oxazepam), 0.68 (chlordiazepoxide), 0.66 (demoxepam), 0.72 (nitrazepam), 0.77 (major spot of medazepam which has a very small spot at R_f 0.14), 0.79 (prazepam), and 0.56 (*p*-hydroxydesmethyldiazepam). By the combined use of these solvent systems and the characteristic fluorescence colors, this procedure should be applicable for the general screening test of some 1,4-benzodiazepines in both serum and urine samples.

REFERENCES

(1) J. A. F. de Silva, M. A. Schwartz, V. Stefanovic, J. Kaplan, and L. D'Arconte, *Anal. Chem.*, **36**, 2099 (1964).

(2) J. A. F. de Silva, B. A. Koechlin, and G. Bader, *J. Pharm. Sci.*, **55**, 692 (1966).

(3) J. A. F. de Silva and C. V. Puglisi, *Anal. Chem.*, **42**, 1725 (1970).

(4) F. Marcuss, R. Fonelli, and E. Mussini, *J. Chromatogr.*, **37**, 318 (1968).

(5) A. Berlin, B. Siwers, S. Agurell, A. Hiort, F. Sjögvist, and S. Ström, *Clin. Pharmacol. Ther.*, **13**, 733 (1972).

(6) R. Erkkola, L. Kangas, and A. Pekkarinen, *Acta Obstet. Gynecol. Scand.*, **52**, 167 (1973).

(7) L. Kangas, A. Pekkarinen, C. Sourander, and E. Raijola, *Ann. Clin. Res., Suppl. 11*, **6**, 12 (1974).

(8) J. Hendel, *Acta Pharmacol. Toxicol.*, **37**, 17 (1975).

(9) J. A. F. de Silva, I. Bekersky, C. V. Puglisi, M. A. Brooks, and R. E. Weinfeld, *Anal. Chem.*, **48**, 10 (1976).

(10) J. M. Clifford and W. F. Smyth, *Analyst*, **99**, 241 (1974).

(11) J. Braun, G. Caille, and E. A. Martin, *Can. J. Pharm. Sci.*, **3**, 65 (1968).

(12) G. Caille, J. Braun, D. Gravel, and R. Plourde, *ibid.*, **8**, 42 (1973).

(13) N. Wad, H. Rosenmund, and E. Hanifl, *J. Chromatogr.*, **128**, 231 (1976).

(14) N. Wad and E. Hanifl, *ibid.*, **143**, 219 (1977).

(15) S. Ebel and H. Kusmaul, *Arch. Pharm.*, **307**, 230 (1974).

(16) N. Strojny, K. Bratin, M. A. Brooks, and J. A. F. de Silva, *J. Chromatogr.*, **143**, 363 (1977).

(17) S. Sun, "APhA Annual Meeting Abstract," vol. 7, No. 1, American Pharmaceutical Association, Washington, D.C., 1977, p. 194. S. Sun, *J. Pharm. Sci.*, **67**, 639 (1978).

(18) S. A. Kaplan, M. L. Jack, K. Alexander, and R. E. Weinfeld, *J. Pharm. Sci.*, **62**, 1789 (1973).

ACKNOWLEDGMENTS

The author gratefully acknowledges the technical assistance of M. Leveque.

Facile Separation of Sulfonamides from Their Degradates by Liquid–Liquid Extraction

D. W. FINK ˣ, R. P. MARTIN *, and J. BLODINGER

Received August 31, 1977, from the *Merck Sharp & Dohme Research Laboratories, Rahway, NJ 07065.* Accepted for publication February 6, 1978. *Present address: New Research Facility, Ortho Pharmaceutical Co., Raritan, NJ 08869.

Abstract □ Regulation of acidity for protonation of the free N^4-amine can provide for the selective liquid–liquid extraction isolation of a sulfonamide from its degradation products. This principle is applied for the stability-indicating determination of sulfacetamide in the presence of sulfanilamide, sulfaquinoxaline in feed, and sulfabromomethazine in dosage forms. In solution, sulfabromomethazine can exhibit photodecomposition to sulfamethazine. The mean relative errors of the these methods and the precision, represented by relative standard deviations, are each typically <2%.

Keyphrases □ Sulfonamides, various—separated from degradation products by liquid–liquid extraction □ Degradation products of various sulfonamides—separated from parent compounds by liquid–liquid extraction □ Liquid–liquid extraction—separation of various sulfonamides from degradation products □ Antibacterials—various sulfonamides, separation from degradation products by liquid–liquid extraction

Although most sulfonamides are highly stable, they can degrade (almost exclusively) by acid-catalyzed hydrolysis of the sulfur–nitrogen bond (1–7) or, occasionally, by cleavage of the nitrogen–carbon bond (1). Hence, any stability-indicating analysis for these drugs in formulations should discriminate between the intact sulfonamide and both sulfanilic acid and sulfanilamide as potential hydrolytic degradates.

BACKGROUND

Applications of separation techniques to the sulfonamides have long been of interest because of the similar chemical and physical properties of these drugs and their use in combinations. Typically, sulfonamides have been separated by TLC, and many very exacting quantitative procedures for determining mixtures of these drugs using this technique have been published. Among those studies that present data for sulfanilamide (*e.g.*, 8, 9) are evaluations of new spray reagents (10, 11) and various stationary phases (12).

Of the GLC methods, those procedures that measure the relevant amine generated from acidic sulfonamide hydrolysis (4–7) are not directly applicable for stability studies; only the methods that derivatize the intact drug (13–18) are appropriate. Some recently published high-pressure liquid chromatographic (HPLC) sulfonamide separations make use of adsorption (19, 20), ion-exchange (21, 22), ion-pair partition (23, 24), and reversed-phase (25) modes.

For stability studies of sulfonamides, simple liquid–liquid extraction is an attractive alternative to some of those tedious or time-consuming approaches. In particular, quantitative TLC methods are lengthy and require careful attention to technique to obtain good precision. The extraction is also convenient because it neither requires the derivatization essential for GLC nor relies on instrumentation, and it can be combined with standard (*e.g.*, Bratton–Marshall) analytical measurements for the sulfonamides. Although other solvents also may be satisfactory, a mixed chloroform–1% dimethylformamide solvent was selected as the organic phase to demonstrate the feasibility of this approach. The aqueous phase

0022-3549/78/1000-1415$01.00/0

© 1978, American Pharmaceutical Association

is regulated in the pH 0–4 range to give selectivity to the extraction. The primary application is for the stability-indicating determination of sulfonamides in formulations.

The relatively rapid hydrolysis of sulfacetamide can be a problem, especially with some commercial ophthalmic and dermatological solutions and tablets. The methods used for the stability-indicating determination of this drug include the thin-layer technique (26), a selective colorimetric procedure (27), adsorption column chromatographic separation (28), and HPLC (20). Unlike most other sulfonamides, sulfacetamide undergoes hydrolysis at its more labile nitrogen–carbonyl bond. Nevertheless, the amino-bearing product of this degradation, in common with conventional sulfonamide hydrolysis, is sulfanilamide. Accordingly, sulfacetamide provides one example of the application of the liquid–liquid partitioning system as a convenient alternative to other methods. The determination of sulfaquinoxaline in feed and of sulfabromomethazine in a paste and a powder formulation is also presented. In addition, a photodegradation study of sulfabromomethazine is described.

EXPERIMENTAL

Reagents—Chloroform[1], hydrochloric acid[1], and dimethylformamide[2] were used as received. The sulfonamides[3] also were used without further purification.

Determination of Distribution Ratios—Each sulfonamide was dissolved in water and diluted to 5.00×10^{-5} *M*. The pH was regulated by addition of hydrochloric acid and measured in some solutions on a pH meter[4]. A 20-ml aliquot of each solution was shaken at room temperature with an equal volume of a mixed solvent of 1% (v/v) dimethylformamide in chloroform for 0.5 hr. Sulfonamide concentration in the aqueous phase was then determined colorimetrically with the Bratton–Marshall reaction; the concentration in the organic phase also was determined similarly after evaporation of the organic solvent.

Sulfabromomethazine Photolysis—The photolytic degradation of sulfabromomethazine in ethanol (0.33 mg/ml) was studied under UV irradiation in 10-cm cells equipped with quartz windows[5] in a test chamber[6] for 24 days. Liquid chromatography of the solution was performed[7] according to a procedure described by Kram (22). A 50-cm × 2.1-mm i.d. anion-exchange[8] column was used with a flow rate of ~1 ml/min obtained with 700 psig. A 25-ml aliquot of the ethanol solution also was concentrated to 2 ml, 20 μl was spotted on a 20 × 20-cm fluorescent silica gel TLC plate[9], and the chromatogram was developed to 10 cm with a mobile phase of 50% ethyl acetate–50% chloroform.

Sulfabromomethazine Determinations—*Powder Formulation*—The following procedure was applied to a powder formulation containing sodium citrate, sodium carbonate, and edetate disodium in addition to the drug. A sample taken to provide 800 mg of sulfabromomethazine sodium was dissolved in 500 ml of 0.01 *N* NaOH and diluted to 1 liter with water. A 5.00-ml aliquot of this 5×10^{-3} *N* NaOH solution was diluted to 500.0 ml with water for analysis. A sulfabromomethazine sodium analytical standard of known concentration (8.00×10^{-3} mg/ml) was prepared in the same solvent and processed similarly.

To 20.0 ml of the sample and working standard was added 5.0 ml of 3 *N* HCl for pH regulation (pH 0.22), and the sample was partitioned in three successive equilibrations of 15, 15, and 10 ml with fresh chloroform–1% dimethylformamide. The solvents were equilibrated in 50-ml centrifuge tubes on a mechanical shaker for 10 min. The organic extracts were collected, combined, and diluted to 50.0 ml with the same solvent. A 20.0-ml aliquot of this solution was back-extracted into 15.0 ml of 0.1 *N* NaOH, 2 ml of 10% fluoroboric acid was added to 10.0 ml of this aqueous solution, and the sulfonamide was determined by the conventional Bratton–Marshall colorimetric procedure (29).

Paste Formulation—This procedure was applied to a sulfabromomethazine paste formulation that also contained mineral oil, benzyl alcohol, and a thickener[10]. The immiscibility of this formulation with water and its viscosity decreased the extraction efficiency of the drug into aqueous 0.1 *N* NaOH; this problem was overcome by the use of petroleum ether in the extraction.

[1] J. T. Baker "analyzed" reagent.
[2] Mallinckrodt analytical reagent.
[3] Merck Reference Standard, American Cyanamid (USP), Matheson, Coleman & Bell (USP), and Eastman Kodak Co.
[4] Orion model 801.
[5] Coleman.
[6] Envira-Lite model TRLC 2001.
[7] DuPont model 830 liquid chromatograph.
[8] DuPont Zipax SAX.
[9] E. Merck silica gel 60 F-254.
[10] Bentone 38, an organically modified montmorillonite clay, NL Industries.

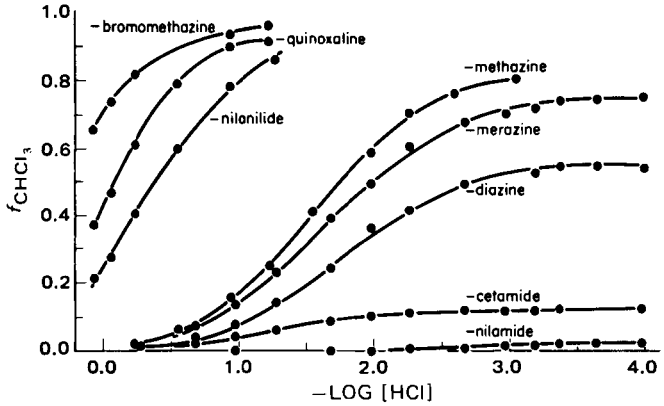

Figure 1—*Distribution ratios of selected sulfonamides into chloroform–1% dimethylformamide as a function of the acidity of the aqueous phase. The fraction in the organic phase, f_{CHCl_3}, is plotted* versus *log [HCl].*

A sample of paste taken to contain 300 mg of sulfabromomethazine sodium was treated with 15 ml of petroleum ether and 15 ml of 0.1 *N* NaOH, and the basic aqueous extracts from three successive extractions with 15.0 ml of fresh solvent were combined and diluted to 1000 ml with water. A 5.00-ml aliquot of this solution was diluted to 250.0 ml with water for analysis. To 20.0 ml of the sample was added 5.0 ml of 3 *N* HCl for pH regulation, and the sample and standard were treated as described for the powder formulation.

Determination of Sulfaquinoxaline in Feed—Sulfaquinoxaline was extracted from the feed sample into aqueous sodium hydroxide solution as prescribed in standard feed procedures (30, 31). To a 50-ml aliquot of the aqueous extract was added 15 ml of 1.2 *N* HCl, and the sample was diluted to 100 ml with water. After centrifugation, 3 g of sodium chloride was added to a portion of the sample, which was equilibrated in three successive extractions of 15, 15, and 10 ml with fresh organic mixed solvent. The combined extracts were diluted to 50.0 ml with the solvent, and a 25.0-ml aliquot was back-extracted into 15.0 ml of 0.1 *N* NaOH; then 10 ml was acidified with 2 ml of 10% fluoroboric acid prior to colorimetric measurement.

Determination of Sulfacetamide in Presence of Sulfanilamide—To a 10.0-ml aliquot of a solution containing ~0.25 mg of sulfacetamide/ml was added 10.0 ml of 0.06 *M* HCl. The sample was diluted to 100.0 ml with water, and a 10.0-ml aliquot was partitioned once with 15.0 ml of the chloroform–1% dimethylformamide mixed solvent. A 10.0-ml portion of the organic phase was evaporated under nitrogen, and the residue was dissolved in water for colorimetric measurement. The analytical reference standard sulfacetamide was treated similarly. In this procedure, the chloroform extract was taken to dryness in lieu of back-extraction into 0.1 *N* NaOH as in the sulfabromomethazine and sulfaquinoxaline procedures because of the rapid hydrolysis of the amide nitrogen–carbon bond at high pH.

RESULTS

Distribution Ratios—The distribution ratios of eight different sulfonamides between chloroform–1% dimethylformamide and water at room temperature at a concentration of 5.00×10^{-5} *M* are presented in Fig. 1 as a function of the acidity of the aqueous phase. Total recovery from both phases was typically 100 ± 3% for each drug over the pH range studied. As the pH was decreased, a greater portion of each sulfonamide remained in the aqueous phase.

Sulfabromomethazine Photolysis—The retention times of sulfabromomethazine and sulfamethazine were 9.2 and 2.2 min, respectively, using a mobile phase containing 0.1 *M* sodium nitrate and 0.01 *M* sodium borate. They increased to 64 and 5.3 min, respectively, when the nitrate concentration was reduced to 0.01 *M*. The chromatogram of the irradiated sample revealed a degradate that eluted with a retention time equal to that of sulfamethazine.

This identification was confirmed by TLC. In the described system, sulfamethazine appeared at R_f 0.56 and sulfabromomethazine appeared at 0.71. The irradiated sample exhibited two spots with the indicated R_f values corresponding to the presence of both compounds, while a control solution stored in the dark yielded the sulfabromomethazine spot only.

Sulfabromomethazine Determinations—Accuracy was measured

Table I—Sulfabromomethazine Determinations in Powder and Paste

Sample Taken			Amount Found		
Decomposition Product		Sulfabromo-		Sulfabromo-	Relative
Compound	Grams	methazine, g	$A_{547\,nm}$	methazine, g	Error, %
		Powder Formulation			
None	—	0.794	0.498	—[a]	—
	—	0.794	0.498	—	—
Sulfanilamide	0.0822	0.794	0.492	0.784	−1.26
	0.0822	0.794	0.505	0.805	1.39
Sulfanilic acid	0.0790	0.794	0.498	0.794	0.00
	0.0790	0.794	0.497	0.792	−0.25
Sulfamethazine	0.0834	0.794	0.499	0.796	0.25
	0.0834	0.794	0.498	0.794	0.00
		Paste Formulation			
None	—	None	0.008	<0.007	—
	—	None	0.002	<0.007	—
	—	None	0.002	<0.007	—
Sulfanilamide	0.0370	None	0.002	<0.007	—
	0.0407	None	0.002	<0.007	—
	0.0336	0.3067	0.366	0.304	−0.98
	0.0320	0.2956	0.359	0.298	0.68
Sulfanilic acid	0.0390	None	0.002	<0.007	—
	0.0504	None	0.002	<0.007	—
	0.0283	0.3000	0.366	0.304	1.33
	0.0281	0.2843	0.342	0.284	0.00
Sulfamethazine	0.0376	None	0.006	<0.007	—
	0.0392	None	0.008	<0.007	—
	0.0347	0.3202	0.392	0.325	1.56
	0.0350	0.2952	0.362	0.300	1.70

[a] Used as the analytical reference standard for the powder determinations.

with unmedicated powder spiked at 71.0% (w/w) sulfabromomethazine sodium by the addition of an aqueous solution of the drug to the sample during extraction. The average of four analyses was 71.0% sulfabromomethazine sodium, with a relative standard deviation of 0.2%. For the paste, the accuracy of this method was estimated by analyses for unmedicated paste spiked at 65.0 ± 1.0% sulfabromomethazine sodium by the addition of a weighed amount of the analate to individual samples of the unmedicated paste. The mean relative error from six measurements was 1.2%.

For estimates of precision, the range of four analyses of a complete water-soluble powder formulated to contain 71.4% sulfabromomethazine sodium was 1.3%. Similarly, the relative standard deviation from six measurements of a paste prepared to contain 65.0% (w/w) drug was 1.4%.

Sulfanilic acid, sulfanilamide, or sulfamethazine (the probable decomposition products of sulfabromomethazine sodium that respond to the Bratton–Marshall reaction) was added to the unmedicated powder and paste formulations at a concentration level corresponding to ~10% (w/w) of the nominal sulfabromomethazine sodium concentration in a complete formulation. Analyses by this procedure (Table I) demonstrate that the presence of these possible decomposition products neither significantly increases the background absorbance contributed by unmedicated paste nor affects the analysis of medicated formulations, confirming the efficiency of the isolation of the parent drug from its decomposition products by this procedure.

Sulfaquinoxaline in Feed—Four unmedicated feeds (a broiler feed and a turkey feed, each in both mash and pelleted forms) were spiked with a combination representing both 0.0100% sulfanilic acid and 0.0100% sulfanilamide by the addition of an aqueous solution of these sulfonamides to the feed during extraction. The absorbances from these feeds analyzed by the present procedure were equal to the background absorbance from unmedicated feed analyzed similarly (0.007–0.009 absorbance unit). These concentrations correspond to the quantitative hydrolysis of all sulfaquinoxaline in a feed containing ~0.035% drug; a typical drug concentration in feed for coccidiosis is 0.0125%. These results confirm that the procedure is not affected by the presence of sulfanilic acid or sulfanilamide in the feed matrix.

Unmedicated feeds were spiked at three concentration levels (0.0100, 0.0125, and 0.0150%) with sulfaquinoxaline. To each of these concentrations was also added either sulfanilic acid or sulfanilamide equal to 10% (w/w) of the sulfaquinoxaline concentration. The resulting analyses (Table II) demonstrate that the determination of sulfaquinoxaline is independent of the presence of these added compounds.

The accuracy and range of linearity of this procedure are represented by the mean relative error of 1.1% from 28 measurements of four feeds spiked with 0.0100–0.0150% sulfaquinoxaline. The precision of the method is estimated by the relative standard deviations of 1.2 and 1.5% from 12 determinations on each of two complete feeds formulated with sulfaquinoxaline at the 0.01 and 0.015% levels, respectively.

Sulfacetamide Determinations—Analyses of eight synthetic aqueous mixtures of sulfacetamide and sulfanilamide, covering the range of 2–8% (w/w) of the decomposition product, averaged 100.5% of the known sulfacetamide concentration with a relative standard deviation of <1% (Table III).

DISCUSSION

The separations are based on the effect of protonation of the free amino group at pH < 3 on the distribution ratios (32–35). The low basicity of

Table II—Analyses of Feeds Spiked with Sulfaquinoxaline, Sulfanilic Acid, and Sulfanilamide

Feed[a]	Sulfaquinoxaline Added, %	Sulfanilamide Added, %	Sulfanilic Acid Added, %	$A_{550\,nm}$	Sulfaquinoxaline Found, %	Relative Error, %
Broiler mash	0.0100	—	—	0.221	0.0103	3.0
Turkey mash	0.0100	0.00100	—	0.221	0.0103	3.0
Broiler pellets	0.0100	—	0.00100	0.219	0.0102	2.0
Turkey pellets	0.0125	—	—	0.270	0.0124	−0.8
Broiler mash	0.0125	0.00125	—	0.275	0.0126	0.8
Turkey mash	0.0125	—	0.00125	0.279	0.0127	1.6
Broiler pellets	0.0150	—	—	0.328	0.0149	−0.7
Turkey pellets	0.0150	0.00150	—	0.333	0.0151	0.7
Broiler mash	0.0150	—	0.00150	0.335	0.0152	1.3
Standard 0.0100% SQ				0.214		
Standard 0.0125% SQ				0.271		
Standard 0.0150% SQ				0.331		

[a] Each sample contained 5.00 g of feed.

Table III—Determination of Sulfacetamide [a] in the Presence of Sulfanilamide

Sulfanilamide Added [b]	$A_{540\ nm}$ [c]	Sulfacetamide Found, mg/ml	Relative Error, %
1.71	0.543	0.237	−0.4
1.71	0.549	0.240	0.8
3.41	0.543	0.237	−0.4
3.41	0.550	0.240	0.8
5.12	0.543	0.237	−0.4
5.12	0.548	0.239	0.4
8.53	0.557	0.243	2.1
8.53	0.552	0.241	1.3

[a] Each solution contained 0.238 mg of sulfacetamide/ml. [b] Percent of sulfacetamide (w/w). [c] Sulfacetamide standard $A_{540} = 0.545$.

this group results from its *para*-orientation to the SO_2 function. At a pH above the pKa of the free N^4-amine, the sulfonamide is uncharged and, therefore, more lipophilic than at a pH below this pKa where the sulfonamide is cationic (Fig. 1). Sulfanilic acid does not partition into chloroform–1% dimethylformamide in the pH range presented in Fig. 1 because of the strong acidity of the SO_3H substituent. In addition, because the organic phase in this system is a binary solvent mixture and each component can form hydrogen bonds, the partition properties of these sulfonamides also depend on charge, structure, and the ability to hydrogen bond with the solvents.

Photolytic loss of halogen from the aromatic ring (36) is demonstrated by the two uncorrelated chromatographic systems in this study of the degradation of sulfabromomethazine to sulfamethazine. Not only are the systems based on different chromatographic properties (ion exchange and adsorption), but the relative mobilities of the two sulfonamides are inverted between the systems as well. These results underscore the need for distinguishing sulfamethazine from sulfabromomethazine in a stability-indicating determination of this halogen-containing sulfonamide.

This separation was easily effected with the present liquid–liquid partitioning system, which provides remarkable selectivity between sulfabromomethazine and sulfamethazine despite their structural similarity. Figure 1 illustrates that the halogenated sulfonamide is much more soluble in the organic solvent than its photolytic degradate. In this procedure, pH 0.22 ($[H+] = 0.6\ M$) is selected for the separation of sulfabromomethazine from its possible interfering decomposition products. After this separation, the analate is back-extracted into 0.1 *N* NaOH for measurement. The low sensitivity of this procedure to sulfanilic acid, sulfanilamide, and sulfamethazine is demonstrated by the results of Table I.

In the pH range of Fig. 1, the maximum fraction of sulfacetamide to partition into the organic phase was 11% (between pH 2 and 4). At higher pH, this fraction decreased in a sigmoid fashion to $f = 0$ at pH 7 with an inflection at 5.5%, occurring at pH 5.40, the pKa of the sulfonamido proton on this molecule (37). At pH 2.2 ($[H+] = 6 \times 10^{-3}\ M$), sulfanilamide remained quantitatively in the aqueous phase, providing adequate conditions for determining the parent drug by comparison to a reference standard which was similarly processed through the partitioning operation (Table III).

The two official AOAC methods for the determination of sulfaquinoxaline in feed (30, 31) are not stability indicating because they rely on a Bratton–Marshall reaction without prior separation. Depending on conditions, hydrolysis of sulfaquinoxaline can yield either sulfanilic acid or sulfanilamide. The other amine that can result from hydrolysis, 2-aminoquinoxaline, is a heterocycle that does not respond to the Bratton–Marshall reaction. In the present method, the liquid–liquid partitioning step separates sulfanilic acid and sulfanilamide from sulfaquinoxaline. The pH of the aqueous phase is adjusted to ~1 for this separation (Fig. 1), and sodium chloride is added to inhibit the emulsion formation. In addition, the extension of this general technique to parts-per-million concentration level feed preparations is demonstrated by this application.

The trisulfapyrimidines in Fig. 1 reflect the effect of methyl substitution on these partitioning properties. The fractions in the organic phase where these curves level off (at pH 3–4) increase in the order sulfadiazine (0.53) < sulfamerazine (0.73) < sulfamethazine (0.80). Schumacher and Nagwekar (35), in a study to correlate partition coefficients with the transfer of drugs across biological membranes, found the same trend with increasing methyl substitution in a pH 4.3 acetate buffer–1-octanol system.

Sulfonamide transport across biological membranes has been studied extentively *in vitro via* partition coefficient measurements relative to the acidity of the sulfonamido group. In the original study (33), Bell and Roblin were unable to discern a relationship between bacteriostatic activity and the pKb of the free amino group because of the small variation of this constant among the sulfonamides. They did not consider the combined effect of this protonation and molecular structure on partitioning properties (Fig. 1). Fujita and Hansch (38) emphasized the importance of hydrophobic character on correlations with biological activity for these drugs. Because it is probable that the free amino group is the reactive center in the biochemical mechanism (32–34, 39, 40), it would be interesting to consider possible structure–activity correlations with reference to the equilibrium at this weakly basic site (Fig. 1).

It should also be feasible to develop meaningful HPLC separations based on distribution ratios in this pH range. Henry *et al.* (41) recently used this approach to correlate reversed-phase HPLC retention volumes of sulfonamides at pH 4.0 with log *P*, pKa, and biological activity. However, even if not applied to other studies, the present simple separation procedure is decidedly more convenient for analytical purposes than the many variations of more cumbersome chromatographic techniques reported previously.

REFERENCES

(1) S. Searles and S. Nukina, *Chem. Rev.*, **59,** 1077 (1959).

(2) J. March, "Advanced Organic Chemistry: Reactions, Mechanisms, and Structure," McGraw-Hill, New York, N.Y., 1968, p. 373.

(3) P. D. Carpenter and M. Lennon, *J. Chem. Soc. Chem. Commun.*, **1973,** 664.

(4) J. W. Turczan, *J. Pharm. Sci.*, **57,** 142 (1968).

(5) A. Fravolini and A. Begliomini, *J. Assoc. Offic. Anal. Chem.*, **52,** 767 (1969).

(6) S. Crisp, *Analyst*, **96,** 671 (1971).

(7) D. G. Hemphill, *Diss. Abstr.*, **27,** 3008B (1967).

(8) H. R. Klein and W. J. Mader, *J. Pharm. Sci.*, **60,** 448 (1971).

(9) R. A. de Zeeuw, *Anal. Chem.*, **40,** 2134 (1968).

(10) S.-C. Lee, *J. Chromatogr.*, **93,** 480 (1974).

(11) M. I. Walash and S. P. Agarwal, *J. Pharm. Sci.*, **61,** 277 (1972).

(12) Y.-T. Lin, K.-T. Wang, and T.-I. Yang, *J. Chromatogr.*, **20,** 610 (1965).

(13) W. J. A. VandenHeuvel and V. F. Gruber, *ibid.*, **112,** 513 (1975).

(14) N. Nose, S. Kobayashi, A. Hirose, and A. Watanabe, *ibid.*, **123,** 167 (1976).

(15) O. Gyllenhall and H. Ehrsson, *ibid.*, **107,** 327 (1975).

(16) R. J. Daun, *J. Assoc. Offic. Anal. Chem.*, **54,** 1277 (1971).

(17) E. Röder and W. Stuthe, *Z. Anal. Chem.*, **266,** 358 (1973).

(18) M. Ervik and K. Gustavii, *Anal. Chem.*, **46,** 39 (1974).

(19) P. H. Cobb and G. T. Hill, *J. Chromatogr.*, **123,** 444 (1976).

(20) M. H. Penner, *J. Pharm. Sci.*, **64,** 1017 (1975).

(21) R. B. Poet and H. H. Pu, *ibid.*, **62,** 809 (1973).

(22) T. C. Kram, *ibid.*, **61,** 254 (1972).

(23) S. C. Su, A. V. Hartkopf, and B. L. Karger, *J. Chromatogr.*, **119,** 523 (1976).

(24) B. L. Karger, S. C. Su, S. Marchese, and B.-A. Persson, *J. Chromatog. Sci.*, **12,** 678 (1974).

(25) J. P. Sharma, E. G. Perkins, and R. F. Bevill, *J. Pharm. Sci.*, **65,** 1606 (1976).

(26) M. P. Gruber and R. W. Klein, *ibid.*, **57,** 1212 (1968).

(27) E. Schleider, D. M. Eno, J. A. Feldman, and A. M. Galinsky, *ibid.*, **58,** 1258 (1969).

(28) E. J. Wojtowicz, *ibid.*, **59,** 240 (1970).

(29) A. C. Bratton and E. K. Marshall, *J. Biol. Chem.*, **128,** 537 (1939).

(30) C. R. Szalkowski, *J. Assoc. Offic. Anal. Chem.*, **56,** 758 (1973).

(31) "Official Methods of Analysis," Association of Official Analytical Chemists, Washington, D.C., 11th ed., 1970, p. 748, 38.139; 12th ed., 1975, p. 800, 42.168.

(32) J. K. Seydel, *J. Pharm. Sci.*, **57,** 1455 (1968).

(33) P. H. Bell and R. O. Roblin, Jr., *J. Am. Chem. Soc.*, **64,** 2905 (1942).

(34) M. Yoshioka, K. Hamamoto, and T. Kubota, *Nippon Kagaku Zasshi*, **84,** 412 (1963).

(35) G. E. Schumacher and J. B. Nagwekar, *J. Pharm. Sci.*, **63,** 240 (1974).

(36) J. G. Calvert and J. N. Pitts, Jr., "Photochemistry," Wiley, New

York, N.Y., 1966, pp. 522–528.
(37) G. L. Biagi, A. M. Barbaro, M. C. Guerra, C. C. Forti, and M. E. Fracasso, *J. Med. Chem.*, **17**, 28 (1974).
(38) T. Fujita and C. Hansch, *ibid.*, **10**, 991 (1967).
(39) L. Doub, in "Kirk-Othmer Encyclopaedia of Chemical Technology," vol. 19, 2nd ed., H. F. Mark, J. J. McKetta, Jr., and D. F. Othmer, Eds., Interscience, New York, N.Y., 1969, p. 275.
(40) J. K. Seydel, *Mol. Pharmacol.*, **2**, 259 (1966).
(41) D. Henry, J. H. Block, J. L. Anderson, and G. R. Carlson, *J. Med. Chem.*, **19**, 619 (1976).

Simultaneous Solubilization of Steroid Hormones I: Estrogens and C_{21} Steroids

T. LÖVGREN ˣ, B. HEIKIUS, B. LUNDBERG, and L. SJÖBLOM

Received September 27, 1977, from the *Department of Biochemistry and Pharmacy, Åbo Akademi, Porthansgatan 3, 20500 Åbo 50, Finland.* Accepted for publication February 6, 1978.

Abstract □ The simultaneous solubilization of some estrogens and C_{21} steroids in aqueous polysorbate 40, tetradecyltrimethylammonium bromide, and sodium lauryl sulfate was studied. The less soluble estrogen estradiol was solubilized independently of the C_{21} steroids. The micellar solubilities of ethinyl estradiol and both corticosterone and hydrocortisone were independent of the presence of each other while the solubility of 11α-hydroxyprogesterone was enhanced by ethinyl estradiol. The solubilizations of ethinyl estradiol and the two C_{21} steroids, progesterone and 21-hydroxyprogesterone, were dependent on each other so that a varying amount of the steroid solubilized first was precipitated by an excess of the second steroid. If saturated solutions of the two steroids were mixed, no precipitation occurred. A possible mechanism for the simultaneous solubilization of steroids and its relation to structure are discussed.

Keyphrases □ Steroid hormones, various—simultaneous solubilization in aqueous surfactants □ Estrogens, various—simultaneous solubilization in aqueous surfactants □ Solubilization, simultaneous—various steroid hormones in aqueous surfactants

Micellar solubilization of drugs in aqueous solutions is well documented, and pharmaceutical systems have utilized surfactants for many years (1–3). Steroid hormones often have low aqueous solubility (3), and surfactants have been used to increase it. As early as 1944, it was noted that bile salts enhance the water solubility of steroid hormones (4). Since that time, the effect of steroid structure on solubilization and the maximum solubilization of steroids in solutions of surfactants have been investigated (5–9). Later reports described the micellar solubilization of testosterone (10–17) and the solubilization of steroids by lysophosphatidylcholine (18).

This study investigated the simultaneous solubilization of estrogens and C_{21} steroids in aqueous solutions of sodium lauryl sulfate, tetradecyltrimethylammonium bromide, and polysorbate 40. The study was undertaken to determine whether the steroids can be incorporated independently in the micelles as if separate loci for solubilization are involved or if an interaction occurs between the steroids that influences their solubility and can be related to chemical structure.

EXPERIMENTAL

Materials—The steroid hormones[1] were used as received after their melting points were found to be in good agreement with published values. Sodium lauryl sulfate[2] was purified by recrystallization from alcohol. Tetradecyltrimethylammonium bromide[3] and polysorbate 40[4] were used as received.

Solubilization Experiments—Solubilities were determined by equilibration of several concentrations of the aqueous surfactant with the steroids, followed by spectrophotometric analyses of suitably diluted aliquots as described previously (6). To two series of 5-ml ampuls, each containing the surfactant of known concentration, a sufficient amount of estrogen, *e.g.*, estradiol, or C_{21} steroid, *e.g.*, progesterone, was added to ensure an excess at equilibrium. The ampuls were closed and shaken mechanically in a thermostat at 20° (40° for sodium lauryl sulfate) for 72 hr until equilibrium was reached.

The contents of the ampuls then were filtered[5] or centrifuged to remove the undissolved steroid. The UV absorbance of the steroids was used to calculate the amount solubilized. To the estrogen-saturated surfactant solutions, an excess of C_{21} steroid was added; to the C_{21} steroid-saturated solutions, an excess of estrogen was added. The ampuls again were closed and shaken mechanically for 72 hr until equilibrium was reached. The undissolved steroid was removed, and the UV absorbance of the solutions was used to calculate steroid concentrations.

The UV absorbance of the solutions was recorded at around 280 nm for the estrogens and 240 nm for the C_{21} steroids with a spectrophotometer[6], using silica cells of 10- and 1.0-mm path length. Reference solutions containing known amounts of steroid were prepared in all surfactant solutions investigated to ascertain the possible influence of the solvent on the absorbance and for calculation of the molar absorptivity of the steroids. The simultaneous solubilization of two steroids in the same surfactant solution did not affect the molar absorptivity of each steroid.

RESULTS AND DISCUSSION

When various concentrations of polysorbate 40, tetradecyltrimethylammonium bromide, and sodium lauryl sulfate were saturated first with progesterone and then with estradiol and *vice versa*, the results were the same as if the solubilization had been done independently. The micelles of the colloids can solubilize the two steroids simultaneously without affecting their micellar solubility. In all cases, the amount of steroids solubilized increased linearly with the surfactant concentration. The amount of solubilized steroid can be calculated from the solubilization capacities measured previously (2, 3).

The micellar solubility of ethinyl estradiol is within the same range as that of progesterone in ionic surfactants and is considerably larger in nonionic surfactants (2, 3, 9). With progesterone and ethinyl estradiol as the estrogen component, the solubilization no longer occurred independently. The steroid added first to saturate the colloid solution pre-

[1] Fluka AG, Switzerland.

[2] Koch-Light Laboratories.
[3] K & K Laboratories.
[4] Tween 40, Atlas Chemical Industries.
[5] Schleicher & Schüll.
[6] Beckman DU-2.

0022-3549/78/1000-1419$01.00/0
© 1978, American Pharmaceutical Association

York, N.Y., 1966, pp. 522–528.
(37) G. L. Biagi, A. M. Barbaro, M. C. Guerra, C. C. Forti, and M. E. Fracasso, *J. Med. Chem.*, **17**, 28 (1974).
(38) T. Fujita and C. Hansch, *ibid.*, **10**, 991 (1967).
(39) L. Doub, in "Kirk-Othmer Encyclopaedia of Chemical Technology," vol. 19, 2nd ed., H. F. Mark, J. J. McKetta, Jr., and D. F. Othmer, Eds., Interscience, New York, N.Y., 1969, p. 275.
(40) J. K. Seydel, *Mol. Pharmacol.*, **2**, 259 (1966).
(41) D. Henry, J. H. Block, J. L. Anderson, and G. R. Carlson, *J. Med. Chem.*, **19**, 619 (1976).

Simultaneous Solubilization of Steroid Hormones I: Estrogens and C_{21} Steroids

T. LÖVGREN ˣ, B. HEIKIUS, B. LUNDBERG, and L. SJÖBLOM

Received September 27, 1977, from the *Department of Biochemistry and Pharmacy, Åbo Akademi, Porthansgatan 3, 20500 Åbo 50, Finland.* Accepted for publication February 6, 1978.

Abstract □ The simultaneous solubilization of some estrogens and C_{21} steroids in aqueous polysorbate 40, tetradecyltrimethylammonium bromide, and sodium lauryl sulfate was studied. The less soluble estrogen estradiol was solubilized independently of the C_{21} steroids. The micellar solubilities of ethinyl estradiol and both corticosterone and hydrocortisone were independent of the presence of each other while the solubility of 11α-hydroxyprogesterone was enhanced by ethinyl estradiol. The solubilizations of ethinyl estradiol and the two C_{21} steroids, progesterone and 21-hydroxyprogesterone, were dependent on each other so that a varying amount of the steroid solubilized first was precipitated by an excess of the second steroid. If saturated solutions of the two steroids were mixed, no precipitation occurred. A possible mechanism for the simultaneous solubilization of steroids and its relation to structure are discussed.

Keyphrases □ Steroid hormones, various—simultaneous solubilization in aqueous surfactants □ Estrogens, various—simultaneous solubilization in aqueous surfactants □ Solubilization, simultaneous—various steroid hormones in aqueous surfactants

Micellar solubilization of drugs in aqueous solutions is well documented, and pharmaceutical systems have utilized surfactants for many years (1–3). Steroid hormones often have low aqueous solubility (3), and surfactants have been used to increase it. As early as 1944, it was noted that bile salts enhance the water solubility of steroid hormones (4). Since that time, the effect of steroid structure on solubilization and the maximum solubilization of steroids in solutions of surfactants have been investigated (5–9). Later reports described the micellar solubilization of testosterone (10–17) and the solubilization of steroids by lysophosphatidylcholine (18).

This study investigated the simultaneous solubilization of estrogens and C_{21} steroids in aqueous solutions of sodium lauryl sulfate, tetradecyltrimethylammonium bromide, and polysorbate 40. The study was undertaken to determine whether the steroids can be incorporated independently in the micelles as if separate loci for solubilization are involved or if an interaction occurs between the steroids that influences their solubility and can be related to chemical structure.

EXPERIMENTAL

Materials—The steroid hormones[1] were used as received after their melting points were found to be in good agreement with published values. Sodium lauryl sulfate[2] was purified by recrystallization from alcohol. Tetradecyltrimethylammonium bromide[3] and polysorbate 40[4] were used as received.

Solubilization Experiments—Solubilities were determined by equilibration of several concentrations of the aqueous surfactant with the steroids, followed by spectrophotometric analyses of suitably diluted aliquots as described previously (6). To two series of 5-ml ampuls, each containing the surfactant of known concentration, a sufficient amount of estrogen, *e.g.*, estradiol, or C_{21} steroid, *e.g.*, progesterone, was added to ensure an excess at equilibrium. The ampuls were closed and shaken mechanically in a thermostat at 20° (40° for sodium lauryl sulfate) for 72 hr until equilibrium was reached.

The contents of the ampuls then were filtered[5] or centrifuged to remove the undissolved steroid. The UV absorbance of the steroids was used to calculate the amount solubilized. To the estrogen-saturated surfactant solutions, an excess of C_{21} steroid was added; to the C_{21} steroid-saturated solutions, an excess of estrogen was added. The ampuls again were closed and shaken mechanically for 72 hr until equilibrium was reached. The undissolved steroid was removed, and the UV absorbance of the solutions was used to calculate steroid concentrations.

The UV absorbance of the solutions was recorded at around 280 nm for the estrogens and 240 nm for the C_{21} steroids with a spectrophotometer[6], using silica cells of 10- and 1.0-mm path length. Reference solutions containing known amounts of steroid were prepared in all surfactant solutions investigated to ascertain the possible influence of the solvent on the absorbance and for calculation of the molar absorptivity of the steroids. The simultaneous solubilization of two steroids in the same surfactant solution did not affect the molar absorptivity of each steroid.

RESULTS AND DISCUSSION

When various concentrations of polysorbate 40, tetradecyltrimethylammonium bromide, and sodium lauryl sulfate were saturated first with progesterone and then with estradiol and *vice versa*, the results were the same as if the solubilization had been done independently. The micelles of the colloids can solubilize the two steroids simultaneously without affecting their micellar solubility. In all cases, the amount of steroids solubilized increased linearly with the surfactant concentration. The amount of solubilized steroid can be calculated from the solubilization capacities measured previously (2, 3).

The micellar solubility of ethinyl estradiol is within the same range as that of progesterone in ionic surfactants and is considerably larger in nonionic surfactants (2, 3, 9). With progesterone and ethinyl estradiol as the estrogen component, the solubilization no longer occurred independently. The steroid added first to saturate the colloid solution pre-

[1] Fluka AG, Switzerland.

[2] Koch-Light Laboratories.
[3] K & K Laboratories.
[4] Tween 40, Atlas Chemical Industries.
[5] Schleicher & Schüll.
[6] Beckman DU-2.

0022-3549/78/1000-1419$01.00/0
© 1978, American Pharmaceutical Association

Table I—Influence of the Addition Order on Solubilization Capacities of Surfactants for Steroids

Order of Addition of Steroid		Moles of Steroid per Mole of Surfactant[a]					
		I		II		III	
First	Second	First	Second	First	Second	First	Second
Progesterone	Estradiol	0.037	0.013	0.16	0.068	0.24	0.025
Estradiol	Progesterone	0.013	0.037	0.068	0.16	0.025	0.24
Progesterone	Ethinyl estradiol	0.0015	0.18	0.0032	0.27	0.024	0.13
Ethinyl estradiol	Progesterone	0.034	0.037	0.068	0.13	0.052	0.24
Ethinyl estradiol	11α-Hydroxyprogesterone	0.18	0.028	0.27	0.20	0.13	0.33
11α-Hydroxyprogesterone	Ethinyl estradiol	0.026	0.18	0.15	0.27	0.31	0.13
Estradiol	17α-Hydroxyprogesterone	0.037	0.0072	0.16	0.043	0.24	0.090
17α-Hydroxyprogesterone	Estradiol	0.0072	0.037	0.043	0.16	0.090	0.24
Estradiol	21-Hydroxyprogesterone	0.037	0.11	0.16	0.43	0.24	0.38
21-Hydroxyprogesterone	Estradiol	0.11	0.037	0.43	0.16	0.38	0.24
21-Hydroxyprogesterone	Ethinyl estradiol	0.039	0.18	0.099	0.27	0.076	0.13
Ethinyl estradiol	21-Hydroxyprogesterone	0.032	0.11	0.068	0.43	0.052	0.38
11,21-Dihydroxyprogesterone	Ethinyl estradiol	0.12	0.18	0.60	0.27	0.42	0.13
Ethinyl estradiol	11,21-Dihydroxyprogesterone	0.18	0.12	0.27	0.60	0.13	0.42
Hydrocortisone	Ethinyl estradiol	0.057	0.18	—	—	—	—
Ethinyl estradiol	Hydrocortisone	0.18	0.057	—	—	—	—

[a] I = polysorbate 40, II = tetradecyltrimethylammonium bromide, and III = sodium lauryl sulfate.

cipitated during the saturation with the second steroid. This reaction was confirmed by visual inspection of the ampuls, which showed a milky precipitate upon addition of the second steroid. The amount of precipitate increased at higher colloid concentrations.

When a progesterone-saturated solution of polysorbate 40 was equilibrated with an excess of ethinyl estradiol, 96% of the solubilized progesterone precipitated while the estrogen component was solubilized maximally (Fig. 1).When the saturation was done in the opposite order (Fig. 2), 81% of the ethinyl estradiol precipitated and progesterone was solubilized maximally. At polysorbate 40 concentrations above 25 m*M*, progesterone solubilization tended to increase in the presence of the second steroid (Fig. 1).

If an excess of both steroids was added at the same time, progesterone was solubilized maximally while the micellar solubility of ethinyl estradiol dropped to 19% of its maximal value, in agreement with the result obtained when it was added as the first component (Figs. 1 and 2). When equal volumes of polysorbate 40 solutions equilibrated with an excess of progesterone and ethinyl estradiol were mixed and shaken for 48 hr, no precipitation occurred and the absorbance of the steroids in solution dropped to exactly half of the value before mixing.

In tetradecyltrimethylammonium bromide, 98% of the solubilized progesterone precipitated on addition of an excess of ethinyl estradiol, which, in turn, was solubilized maximally (Fig. 3). Saturation in the opposite sequence resulted in a 75% precipitation of ethinyl estradiol, but progesterone reached only 83% of its maximal saturation (Fig. 4). The solubilization loci in the micelles contained some ethinyl estradiol even in the presence of excess progesterone. In fact, ethinyl estradiol was more soluble in tetradecyltrimethylammonium bromide solutions than progesterone (2, 3). In spite of this fact, upon simultaneous addition of an excess of the two steroids, progesterone was solubilized maximally while ethinyl estradiol reached only 25% saturation (Figs. 3 and 4), the same level reached as when ethinyl estradiol was added first.

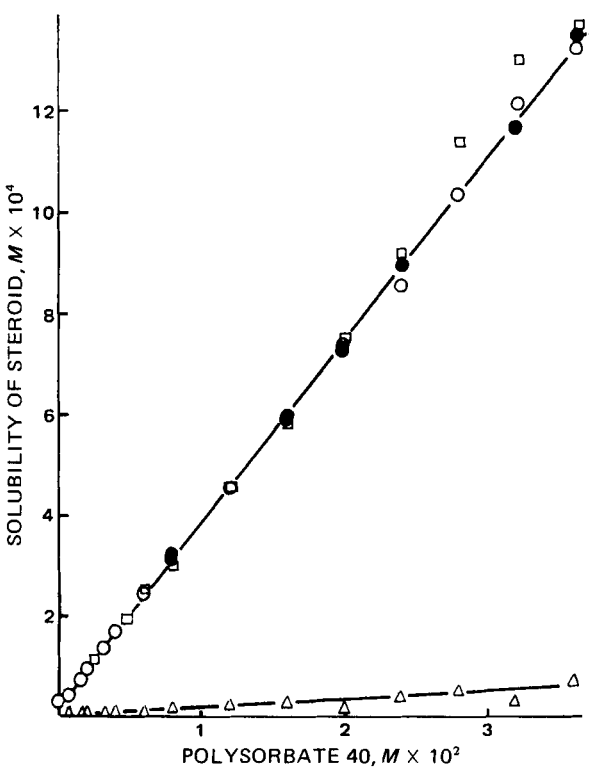

Figure 1—*Solubility of progesterone in aqueous solutions of polysorbate 40. Key:* ○, *progesterone only;* △, *progesterone first and ethinyl estradiol second;* □, *ethinyl estradiol first and progesterone second; and* ●, *progesterone and ethinyl estradiol at the same time.*

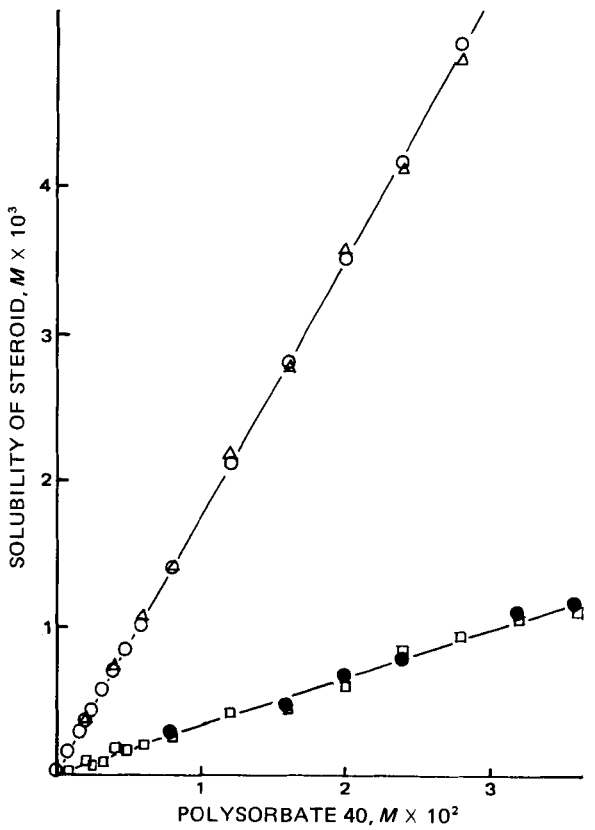

Figure 2—*Solubility of ethinyl estradiol in aqueous solutions of polysorbate 40. Key:* ○, *ethinyl estradiol only;* △, *progesterone first and ethinyl estradiol second;* □, *ethinyl estradiol first and progesterone second; and* ●, *progesterone and ethinyl estradiol at the same time.*

Table II—Solubilization Capacities of Surfactants for Progesterone and Ethinyl Estradiol when the Steroids Were Added at the Same Time

Steroid	Moles of Steroid per Mole of Surfactant[a]		
	I	II	III
Progesterone	0.037	0.16	0.24
Ethinyl estradiol	0.034	0.068	0.016

[a] See footnote *a*, Table I.

In a solution of the anionic colloid, sodium lauryl sulfate, 90% of the solubilized progesterone precipitated on saturation with ethinyl estradiol, which was solubilized maximally (Fig. 5). If, in turn, an excess of progesterone was added to solutions previously saturated with ethinyl estradiol, 60% of the estrogen component precipitated while progesterone reached a maximal saturation level. At higher colloid concentrations, progesterone solubility tended to increase (Fig. 5).

When an excess of both components was added simultaneously, progesterone reached complete saturation while ethinyl estradiol solubility was 12% of its maximal value (Figs. 5 and 6). With simultaneous addition, ethinyl estradiol solubility in a sodium lauryl sulfate solution was considerably lower than if it were added first and progesterone second. This result was probably influenced by the micellar solubility of the steroids (2, 3, 9). Ethinyl estradiol is less soluble than progesterone in sodium lauryl sulfate while the opposite is true of tetradecyltrimethylammonium bromide and polysorbate 40 solutions.

Ethinyl estradiol was solubilized maximally in tetradecyltrimethylammonium bromide solutions if 11α-hydroxyprogesterone was the second steroid. Ethinyl estradiol solubilization did not depend on the addition order, and it obviously was not forced out from the micellar phase by 11α-hydroxyprogesterone. The two other surfactants behaved similarly in respect to these two steroids. 11α-Hydroxyprogesterone solubility increased about 19% when it was added to an ethinyl estradiol-saturated tetradecyltrimethylammonium bromide solution. Evidently, ethinyl estradiol affected the micellar volume of the colloid and more 11α-hydroxyprogesterone was solubilized. Similar results were obtained in solutions of the other two colloids, although the increase in solubility was considerably smaller.

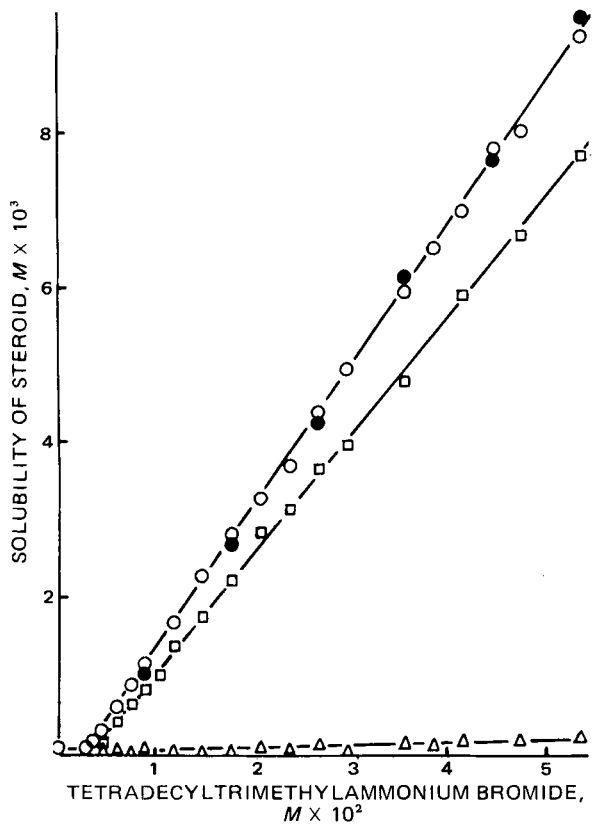

Figure 3—*Solubility of progesterone in aqueous solutions of tetradecyltrimethylammonium bromide. Key: ○, progesterone only; △, progesterone first and ethinyl estradiol second; □, ethinyl estradiol first and progesterone second; and ●, progesterone and ethinyl estradiol at the same time.*

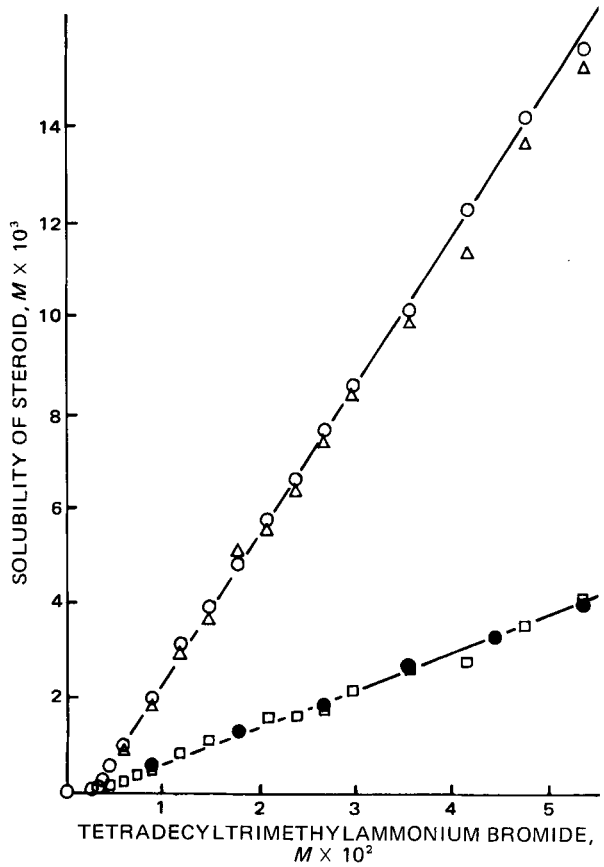

Figure 4—*Solubility of ethinyl estradiol in aqueous solutions of tetradecyltrimethylammonium bromide. Key: ○, ethinyl estradiol only; △, progesterone first and ethinyl estradiol second; □, ethinyl estradiol first and progesterone second; and ●, progesterone and ethinyl estradiol at the same time.*

The micellar solubility of 17α-hydroxyprogesterone and 21-hydroxyprogesterone (11-desoxycorticosterone) in tetradecyltrimethylammonium bromide was tested by adding estradiol as the first or second component. No deviation was found based on the addition order. The steroids were solubilized independently.

Obvious deviations again were obtained in solutions of all three surfactants if ethinyl estradiol was the estrogen component and 21-hydroxyprogesterone was the second steroid. In polysorbate 40, an excess of ethinyl estradiol precipitated about 65% of the solubilized 21-hydroxyprogesterone and reached maximal solubility. If the opposite order of addition was used, an excess of 21-hydroxyprogesterone precipitated 82% of the solubilized ethinyl estradiol and reached maximal micellar solubility. In tetradecyltrimethylammonium bromide solutions, 77% of the solubilized 21-hydroxyprogesterone precipitated when ethinyl estradiol was added second while 75% of the ethinyl estradiol precipitated when the addition order was reversed. When an excess of ethinyl estradiol was added to a 21-hydroxyprogesterone-saturated sodium lauryl sulfate solution, 80% of the first added component precipitated. In the opposite case, 60% of the ethinyl estradiol precipitated.

Compared to 21-hydroxyprogesterone, corticosterone has an additional hydroxyl group at C-11. When corticosterone and ethinyl estradiol were used as the steroids, no deviation from normal micellar solubility was observed independent of the addition order and the surfactant used. The presence of a hydroxyl group at C-11 seems to be important for solubilization independent of ethinyl estradiol. Hydrocortisone (11,17,21-trihydroxyprogesterone), which was tested only in polysorbate 40, showed a similar behavior—*viz.*, the steroids were solubilized independently.

The solubilization capacities of the surfactants for the steroids were calculated from all experiments (Tables I and II).

The results of the present investigation clearly demonstrate that steroids can be solubilized according to different mechanisms, although the exact mechanism has not been defined. Previous investigations showed

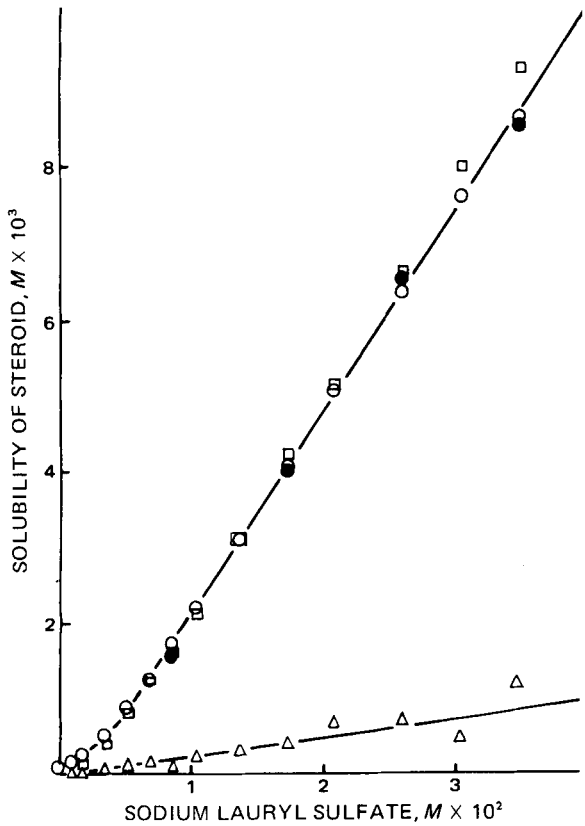

Figure 5—*Solubility of progesterone in aqueous solutions of sodium lauryl sulfate. Key:* ○, *progesterone only;* △, *progesterone first and ethinyl estradiol second;* □, *ethinyl estradiol first and progesterone second; and* ●, *progesterone and ethinyl estradiol at the same time.*

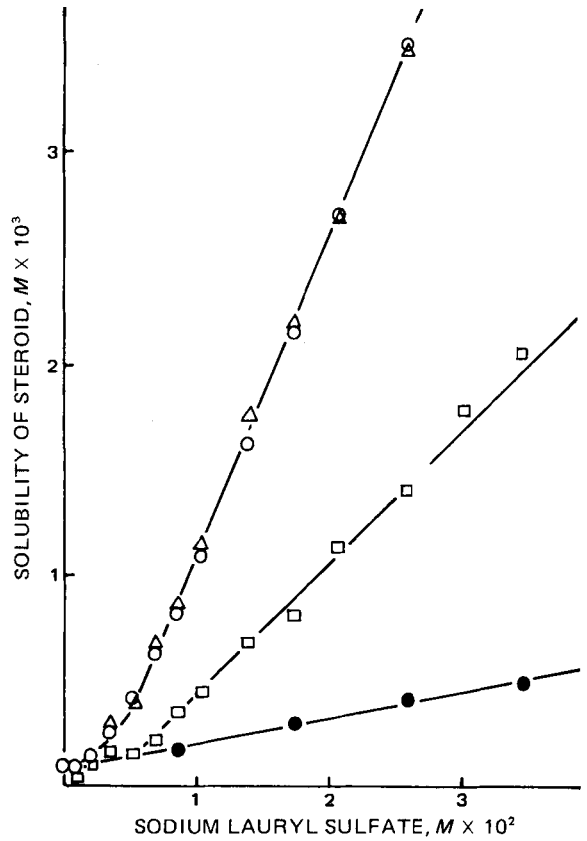

Figure 6—*Solubility of ethinyl estradiol in aqueous solutions of sodium lauryl sulfate. Key:* ○, *ethinyl estradiol only;* △, *progesterone first and ethinyl estradiol second;* □, *ethinyl estradiol first and progesterone second; and* ●, *progesterone and ethinyl estradiol at the same time.*

that the solubilization capacities of ionic surfactants are generally of the same order of magnitude for different steroids, except for the estrogens, while nonionic surfactants have lower capacities (2, 3). For estrogens, the difference is rather small. This finding could also indicate that estrogens are solubilized in a different way compared to the other steroids. The whole steroid molecule determines its micellar solubility (2).

In the present study, the pairs estradiol and progesterone, ethinyl estradiol and 11α-hydroxyprogesterone, estradiol and 17α-hydroxyprogesterone, estradiol and 21-hydroxyprogesterone, ethinyl estradiol and corticosterone, and ethinyl estradiol and hydrocortisone were solubilized independently of one another and most likely by different mechanisms. However, ethinyl estradiol affected the solubilization of progesterone and 21-hydroxyprogesterone, which appeared as a precipitation of the first added steroid from the steroid-saturated solution as the second steroid was added in excess. The same type of mechanism of solubilization probably was involved. The first added steroid was in equilibrium between the micellar and the nonmicellar phases as the excess of undissolved steroid was removed.

In the case where the steroid solubilization mechanism was the same, the equilibrium of the first added steroid was disturbed in the presence of an excess of the second steroid. As a consequence, a new equilibrium had to be reached, including both steroids, and the first steroid had to precipitate partly. When an excess of both steroids was added simultaneously, an equilibrium was reached that usually corresponded to the conditions observed when progesterone was added as the second component.

Apparently, all three surfactants favored progesterone. It is difficult to explain this observation. The entropy for progesterone solubilization by nonionic surfactants was shown to be positive (19). The configuration entropy of the solubilized molecules increases because of the breakup of the water structure surrounding nonpolar groups, which thus controls solubilization. Introduction of an ethinyl group to the D ring of estradiol increases the net dipole moment of the molecule (18). As a consequence, the solubilization is enhanced (2, 18) and influences the mechanism of solubilization of C_{21} steroids, except those with a hydroxyl group at C-11. The position of a substituent is thus important for solubilization.

Work on the simultaneous solubilization of steroid hormones is in progress, and the equilibria will be discussed considering thermodynamic arguments.

REFERENCES

(1) J. Swarbrick, *J. Pharm. Sci.*, **54**, 1229 (1965).

(2) L. Sjöblom, in "Solvent Properties of Surfactant Solutions," K. Shinoda, Ed., Dekker, New York, N.Y., 1967, p. 189.

(3) P. H. Elworthy, A. T. Florence, and C. B. Macfarlane, "Solubilization by Surface-Active Agents," Chapman and Hall, London, England, 1968.

(4) D. K. Madan and D. E. Cadwallader, *J. Pharm. Sci.*, **62**, 1567 (1973).

(5) A. Cantarow, A. E. Rakoff, K. E. Paschkis, and L. P. Hansen, *Endocrinology*, **35**, 129 (1944).

(6) L. Sjöblom, *Acta Acad. Aboensis, Math. Phys.*, **20** (14) (1956).

(7) L. Sjöblom and N.-O. Sundblom, *Acta Chem. Scand.*, **18**, 1996 (1964).

(8) C. Blomqvist and L. Sjöblom, *ibid.*, **18**, 2404 (1964).

(9) L. Sjöblom, in "Surface Chemistry," P. Ekwall, K. Groth, and V. Runnström-Reio, Eds., Munksgaard, Copenhagen, Denmark, 1965, p. 210.

(10) A. L. Thakkar and N. A. Hall, *J. Pharm. Sci.*, **56**, 1121 (1967).

(11) *Ibid.*, **57**, 1394 (1968).

(12) *Ibid.*, **58**, 68 (1969).

(13) A. L. Thakkar and P. B. Kuehn, *J. Pharm. Sci.*, **58**, 850 (1969).

(14) N. H. Choulis, *Can. J. Pharm. Sci.*, **5**, 59 (1970).

(15) K. J. Simons and C. T. Rhodes, *Pharmazie*, **26**, 623 (1971).

(16) L. Martis, N. A. Hall, and A. L. Thakkar, *J. Pharm. Sci.*, **61**, 1757 (1972).

(17) L. H. Loh, M. H. Coulis, and C. T. Rhodes, *Can. J. Pharm. Sci.*, **8**, 93 (1973).

(18) M. M. Gale and L. Saunders, *Biochim. Biophys. Acta*, **248**, 466 (1971).

(19) B. W. Barry and D. I. D. El Eini, *J. Pharm. Pharmacol., Suppl.*, **26**, 87 P (1974).

Fate of ^{14}C-3-Methylamino-1,2,3,4-tetrahydrocarbazole Hydrochloride in Rats and Dogs

I. A. MUNI *, J. L. LEELING ˣ, and N. JOHNSON, Jr.

Received April 15, 1977, from the *Toxicology Department, Miles Laboratories, Inc., Elkhart, IN 46515.* Accepted for publication February 6, 1978. *Present address: Industrial Bio-Test, Decatur, IL 62526.

Abstract □ The fate of ^{14}C-3-methylamino-1,2,3,4-tetrahydrocarbazole hydrochloride, a potential psychotherapeutic agent, was studied in rats and dogs. Rats were given a single oral or intraperitoneal dose while dogs received the drug either orally or intravenously. Radioactivity in plasma samples and excreta was determined by liquid scintillation counting. In addition, ^{14}C-levels in various rat tissues were estimated. The drug appeared to be well absorbed in both species. ^{14}C-Levels were highest in liver and lung and lowest in plasma. Excretion was primarily urinary and was more complete within the first 96 hr in the rat than in the dog, which suggested a longer ^{14}C-half-life in the dog. No evidence was seen that the drug was demethylated.

Keyphrases □ ^{14}C-3-Methylamino-1,2,3,4-tetrahydrocarbazole hydrochloride—distribution and excretion in rats and dogs □ Distribution—^{14}C-3-methylamino-1,2,3,4-tetrahydrocarbazole hydrochloride in rats and dogs □ Excretion—^{14}C-3-methylamino-1,2,3,4-tetrahydrocarbazole hydrochloride in rats and dogs □ Psychotherapeutic agents, potential—3-methylamino-1,2,3,4-tetrahydrocarbazole hydrochloride, ^{14}C-labeled, distribution and excretion in rats and dogs

Derivatives of aminotetrahydrocarbazole possess antidepressant activity in experimental animals and humans (1) and cardiotonic activity in laboratory animals (2). One such compound, of interest for psychotherapeutic applications, is 3-methylamino-1,2,3,4-tetrahydrocarbazole hydrochloride (I). As part of the drug development process, a study of the biological fate of this compound, ^{14}C-labeled (* in Structure I), was carried out in rats and dogs.

EXPERIMENTAL

Synthesis and Dose—Compound ^{14}C-I, mp 306–309°, was prepared from *U*-^{14}C-phenylhydrazine hydrochloride using the synthesis described by Schut (3). The initial specific activity was 2.39 μCi/mg. Radiochemical purity was demonstrated by ascending paper chromatography [methanol–water–pyridine (20:5:1)].

In all experiments, specific activities and doses of I were expressed as free base equivalents. All animals received a single dose of ^{14}C-I as a freshly prepared solution in isotonic saline. Rats received 10 mg (11.95 μCi)/kg po or ip, and dogs were given 2 mg (4 μCi)/kg po or iv.

Animals—Charles River COBS(CD) male rats, 135–170 g, and male mongrel dogs, 7–14 kg, were assigned at random (4) to experimental groups. Animals dosed orally were fasted 16 hr overnight prior to dosing, and food was not reintroduced until 2 hr after dosing. Drinking water was available *ad libitum*. After drug administration, all animals were placed in individual metabolism cages.

Rat Studies—Fifteen rats with ligated bile ducts were assigned to groups of three each. The animals were decapitated by group 0.5, 1, 2, 4, and 8 hr after oral administration of ^{14}C-I. At death, the GI tracts were ligated at the distal end of the esophagus and at the ileocecal junction. Water was added to each GI tract to a final volume of 50 ml, and each mixture was homogenized in a blender.

In tissue distribution experiments, 30 rats were divided into groups of three each. After oral administration of ^{14}C-I, rats were killed by group at the following intervals: 10, 20, 30, and 45 min and 1, 1.5, 2, 4, 8, and 24 hr. Samples of adrenal, dorsal aorta, brain, perirenal fat, heart, kidney, liver, lung, plasma, and spleen were obtained immediately and stored frozen for subsequent analysis. An additional three rats were killed, and their tissues were used to provide undosed, control data.

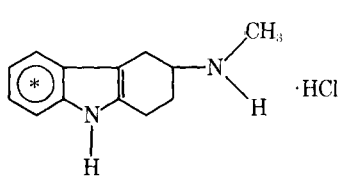

I

Table I—GI Absorption of ^{14}C-I by Rats with Ligated Bile Ducts

Hours	Percent of ^{14}C-Dose Absorbed[a]
1	30.99 ± 8.12
2	47.81 ± 9.42
4	61.08 ± 9.64
8	81.44 ± 5.82

[a] Mean ± *SEM* (n = 3). The percent of dose absorbed was calculated by subtracting the disintegrations per minute remaining in the GI tract at each time interval from the disintegrations per minute in the dose, then dividing by the disintegrations per minute in the dose, and multiplying the result by 100.

Twelve rats in groups of six were given ^{14}C-I: one group orally and the other intraperitoneally. Urine and feces were collected daily through 96 hr. Excreta collected prior to dosing served as controls. After volume measurement, urine samples were stored frozen. Feces were dried, powdered, and weighed.

Dog Studies—Twelve dogs were assigned to groups of six each. One group received ^{14}C-I orally while the other group received the drug *via* the cephalic vein. Heparinized syringes were used to obtain blood samples at 10, 20, and 40 min and 1, 2, 4, 8, and 24 hr after dosing. Plasma samples derived from these blood samples were stored frozen for subsequent analysis. All urine and feces voided were collected daily during the 4-day experiment and were stored as already described. Control plasma, urine, and fecal samples were obtained from each dog prior to the study.

Radiochemical Assays—Aliquots of plasma, urine, or GI tract homogenate samples were added to liquid scintillator[1] (5) and counted directly. A sample oxidizer[2] was used to combust aliquots of fecal and rat tissue samples to $^{14}CO_2$, which was collected in a mixture of trapping reagents[3].

All samples were counted in a liquid scintillation spectrometer[4] for 10 min or 10,000 counts. Counting efficiencies were determined by external standardization, and all counts per minute were converted to disintegrations per minute.

Metabolism Studies—Metabolism experiments of a limited scope were run on 0–24-hr urine obtained during the rat and dog excretion studies. These urine samples were pooled by species; 20-ml aliquots of each, adjusted to pH 9.5, were extracted using 1.5 × 8.5-cm columns of a nonionic resin[5]. After a 10-ml water wash, radioactivity was eluted by two successive 10-ml volumes of ethyl acetate. One drop of 0.1 *N* HCl was added to ethyl acetate eluates pooled by species, which were then evaporated to dryness under a nitrogen stream. Radioactivity in the water-wash fraction was discarded. With this technique, 96 ± 2% *SEM* of ^{14}C-I added to control rat or dog urine could be recovered.

The samples were reconstituted in 0.2 ml of chloroform–methanol (1:1 v/v), 1–5-μl aliquots of which were injected into a gas chromatograph equipped with a dual flame-ionization detector system[6]. Separations were carried out on a 0.9-m glass column of 3% OV-17 on 100–120-mesh Gas Chrom Q. The column temperature was 175° (isothermal), and helium at 37 ml/min was the carrier gas. The retention time of I under these conditions was 7 min. Similarly, the retention time of 3-amino-1,2,3,4-

[1] XDC.
[2] Tri-Carb model 306, Packard Instrument Co., Downers Grove, Ill.
[3] Carbosorb and Permafluor V, Packard Instrument Co., Downers Grove, Ill.
[4] Tri-Carb model 3375, Packard Instrument Co., Downers Grove, Ill.
[5] Drug-Skreen (XAD-2), Brinkmann Instruments, Westbury, N.Y.
[6] Model 2740, Varian Instruments Co., Palo Alto, Calif.

0022-3549/78/1000-1423$01.00/0
© 1978, American Pharmaceutical Association

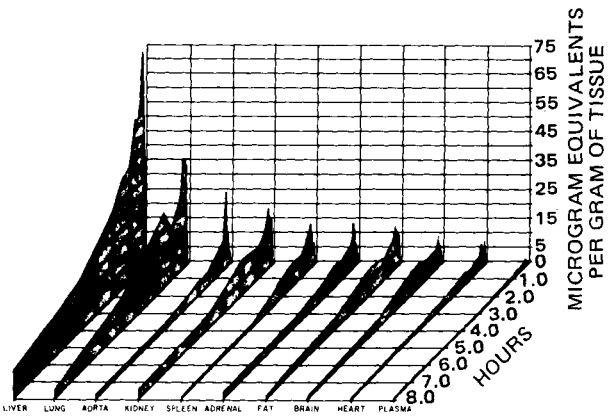

Figure 1—*Tissue levels of undifferentiated carbon-14 in the rat after a single 10-mg/kg po dose of ^{14}C-I.*

tetrahydrocarbazole was 5.9 min. A standard curve, linear from 0 to 4 mg, was obtained with I.

RESULTS AND DISCUSSION

GI absorption experiments in rats (Table I) indicate that I is well absorbed.

The distribution of carbon-14 in rat tissues after a single oral dose is illustrated (through 8 hr) in Fig. 1. While it is recognized that radiochemical measurements include metabolites as well as the original drug, for convenience the levels of undifferentiated carbon-14 in tissues are expressed as microgram equivalents of I per gram or milliliter. In general, tissue ^{14}C-levels maximized within 20–30 min after oral administration, declined for a short time, and then increased again until a second peak (lower than the first and probably representing the appearance of metabolites and/or drug redistribution). The highest ^{14}C-levels were seen in liver and lung tissues. Tissue distribution of I was typical of other strong bases, which tend to distribute in intracellular water, since tissue to plasma ^{14}C-ratios were high. Tissue ^{14}C-levels declined rapidly after 90 min in at least pseudo-first-order fashion, resulting in an average tissue ^{14}C-biological half-life estimate of about 3.1 hr.

Plasma ^{14}C-levels in dogs after oral or intravenous administration of ^{14}C-I are illustrated in Fig. 2. After oral administration, plasma levels were maximal at 4 hr (3 hr later than the rat). Although rats received a fivefold larger dose than dogs, the maximum average ^{14}C-level in the rat was only about three times greater than in the dog.

Excretion data obtained from rats and dogs dosed either orally or parenterally with ^{14}C-I are summarized in Table II. Rats excreted about 79% (orally) and 87% (intraperitoneally) of the dose within 96 hr, and 85 (orally)–92% (intraperitoneally) of the 96-hr total was passed in the first

Table II—Urinary and Fecal Excretion of Carbon-14 by Rats and Dogs after Single Oral or Parenteral Doses of ^{14}C-I

Species	Accumulated Percent Dose Excreted[a] Oral	Parenteral[b]
Rat urine		
24 hr	48.48 ± 4.76	61.61 ± 5.36
96 hr	55.39 ± 5.00	64.90 ± 4.98
Rat feces		
24 hr	19.17 ± 1.53	18.66 ± 1.48
96 hr	24.02 ± 1.57	22.33 ± 1.69
Rat total		
24 hr	67.65 ± 3.63	80.27 ± 4.52
96 hr	79.41 ± 2.78	87.23 ± 3.64
Dog urine		
24 hr	31.31 ± 7.91	37.41 ± 4.36
96 hr	44.21 ± 8.83	51.74 ± 5.49
Dog feces		
24 hr	4.70 ± 0.74	4.58 ± 1.69
96 hr	13.96 ± 0.89	13.80 ± 0.91
Dog total		
24 hr	36.01 ± 7.60	41.99 ± 4.27
96 hr	58.17 ± 9.02	65.54 ± 4.91

[a] Mean ± *SEM* (n = 6). [b] Intraperitoneal administration was used for rats and intravenous administration was used for dogs.

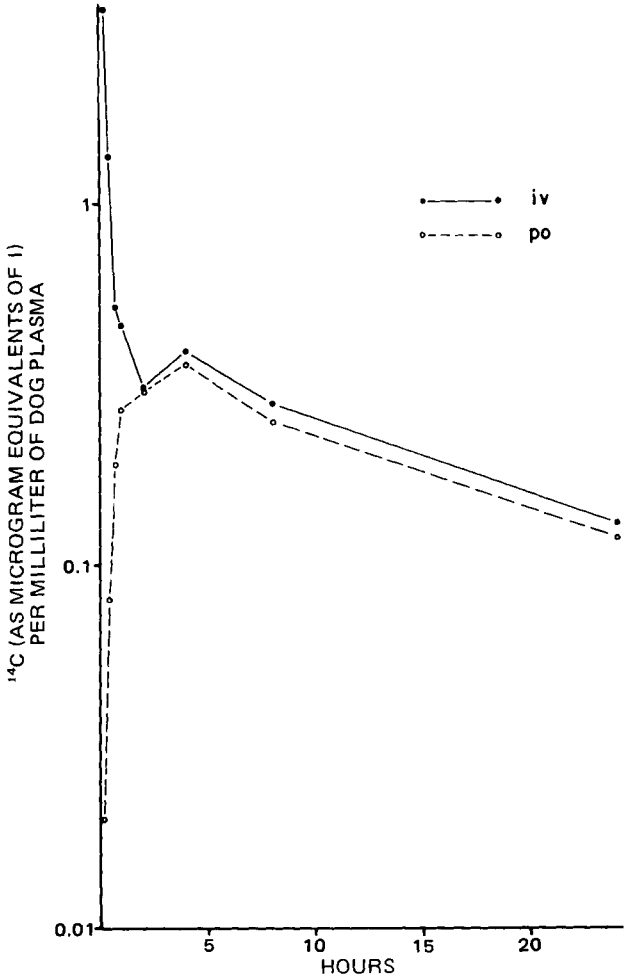

Figure 2—*Semilogarithmic plot of plasma levels of undifferentiated carbon-14 in the dog after a single oral or intravenous dose of ^{14}C-I.*

24 hr. Dogs excreted only about 58% (orally) and 66% (intravenously) of the dose within 96 hr with 62 (orally)–64% (intravenously) of the 96-hr total excreted the 1st day. These data suggest a longer whole body ^{14}C-half-life in the dog. In both species, urine was the preferred route of ^{14}C-excretion. In neither species was the quantity of carbon-14 excreted in urine after oral or parenteral administration statistically different (Student t test), which further indicates that I was well absorbed.

The metabolism of cyclindole, 3-dimethylamino-1,2,3,4-tetrahydrocarbazole, was reported previously (6). This compound, which differs from I only by having an additional N-methyl group, is metabolized primarily by demethylation and/or formation of 7-hydroxylated derivatives. Since I is a metabolite of cyclindole, their hydroxylation patterns should be similar. However, the reference hydroxylated compounds, 3-methylamino- and/or 3-amino-7-hydroxy-1,2,3,5-tetrahydrocarbazole, were not available for GLC comparison with compounds in urine extracts. Therefore, the thrust of the present metabolism experiments was toward identification of unchanged I, its demethylated analog, if present, and any other metabolites sufficiently volatile that derivatization was not required for GLC detection (*i.e.*, nonphenolic metabolites).

About 66 and 68% of the carbon-14 was extractable from rat and dog urine, respectively, using nonionic resin columns. Since the polarity of compounds affects their extraction from the nonionic resin, the 30–35% of urinary carbon-14 not retained by the resin suggests excretion of a metabolite(s) relatively more polar than I by both species, which could be the glucuronic or sulfuric acid conjugates of hydroxylated I.

From the results of radiochemical and GLC analyses, it was estimated that 32 and 28% of a single ^{14}C-I dose administered to rats and dogs, respectively, was excreted unchanged in urine within 96 hr. The remainder of the extractable carbon-14 was probably 7-hydroxylated metabolite(s). While the N-demethylated analog of I was not detected in urinary extracts from either species, the possibility that the demethylated, hydroxylated derivative of I was formed cannot be totally dismissed.

REFERENCES

(1) D. M. Gallant, M. P. Bishop, and R. Guerrero-Figueroa, *Curr. Ther. Res.*, **14**, 61 (1972).

(2) A. Mooradian, A. G. Hlavac, P. E. Dupont, M. R. Bell, and A. A. Alousi, *J. Med. Chem.*, **18**, 640 (1975).

(3) R. N. Schut, *Chem. Abstr.*, **70**, P106382M (1969).

(4) G. W. Snedecor and W. G. Cochran, "Statistical Methods," 6th ed., Iowa State University Press, Ames, Iowa, 1969, pp. 69, 70.

(5) B. M. Phillips and T. S. Miya, *J. Pharm. Sci.*, **53**, 1098 (1964).

(6) D. P. Benziger, K. G. Balfour, and J. Edelson, *Drug Metab. Dispos.*, **5**, 239 (1977).

ACKNOWLEDGMENTS

Presented in part at the 10th American Chemical Society Great Lakes Regional Meeting, Evanston, Ill., June 1976.

The authors thank Mr. Rick Minegar and Mr. Larry Craigo for technical assistance and Dr. John Van Dyke for preparation of the ^{14}C-labeled compound.

Radioimmunoassay for Danazol in Human and Monkey Plasma

J. E. PETERSON ˣ, M. E. KING, W. F. BANKS, J. F. BAKER, A. F. JENSEN, R. W. ROSS, Jr., S. CLEMANS, and J. EDELSON

Received December 12, 1977, from the *Department of Drug Metabolism and Disposition and the Department of Biometrics, Sterling-Winthrop Research Institute, Rensselaer, NY 12144.* Accepted for publication February 7, 1978.

Abstract □ A sensitive method is described for the radioimmunoassay of danazol in monkey and human plasma. Antiserum was developed in rabbits, and a second antibody was used to separate bound from free danazol. The radioimmunoassay was specific for danazol, and the limit of detection ranged from 1.4 to 2.8 ng/ml. Exogenous danazol could be quantitated accurately in both monkey and human plasma. The radioimmunoassay results agreed with values obtained by inverse isotope dilution after intravenous administration of ^{14}C-danazol to monkeys. The assay was used successfully to measure danazol in plasma from human volunteers receiving 200 mg of danazol.

Keyphrases □ Danazol—radioimmunoassay in human and monkey plasma □ Radioimmunoassay—danazol in human and monkey plasma □ Anterior pituitary suppressants—danazol, radioimmunoassay in human and monkey plasma

Danazol[1] (17α-pregna-2,4-dien-20-yno[2,3-*d*]isoxazol-17-ol), a novel steroid, lacks estrogenic or progestational activity upon oral administration but has markedly attenuated androgenic potential (an "impeded" androgen) (1). It inhibits either pituitary gonadotropin synthesis or release in rodents (1, 2), monkeys (3), and humans (4). In males, it depresses the sperm count (5); in women, danazol relieves the symptomatology of endometriosis (6) and may be valuable in the management of benign breast disorders (7).

Limited studies have appeared on plasma danazol concentrations (8, 9). The present report describes a sensitive and accurate method for the measurement of danazol in plasma of both monkeys and humans.

EXPERIMENTAL

Preparation of Antidanazol Serum—The danazol hapten[2] was conjugated with ϵ-amino groups of lysine residues in bovine serum albumin by a carbodiimide condensation (10). A trinitrobenzenesulfonic acid determination (11) indicated that approximately nine hapten molecules were conjugated to each albumin. The hapten–protein conjugate (1.0–2.0 mg) was emulsified in complete Freund's adjuvant[3] and injected intradermally at multiple sites along the dorsal surfaces of three Dutch belted rabbits (12). Booster immunizations of the conjugate in incomplete Freund's adjuvant were administered at approximately 3-week intervals. The rabbits were bled *via* the marginal ear vein.

Preparation of Second Antibody—Anti-rabbit γ-globulin was prepared by repeated subcutaneous injection at monthly intervals of rabbit γ-globulin[4], 100 μg, emulsified in complete Freund's adjuvant to an adult goat. The goat was bled 2 weeks after each immunization. The dilution of the second antibody was 1:16, as determined by a progesterone assay[5] according to the procedure of Midgley *et al.* (13).

Solutions—Iodination buffer contained 0.5 *M* Na_2HPO_4–0.5 *M* NaH_2PO_4 (4:1), adjusted to a final pH of 7.5. Dilute iodination buffer was the same buffer diluted 1:10 with water. Phosphate-buffered saline was made by dissolving 24.51 g of sodium chloride, 1.77 g of monobasic sodium phosphate monohydrate, 3.21 g of dibasic sodium phosphate, and 0.285 g of thimerosal[6] in 3 liters of water and adjusting to pH 7.0. The assay buffer solution contained 0.1% (w/v) gelatin dissolved in phosphate-buffered saline.

Radioiodination—A methyl tyrosinate derivative of danazol[7] (I) was radioiodinated at room temperature by a modification of the method of Greenwood and Hunter (14). Iodination buffer (50 μl) was mixed with 5 μl of a methanol solution of I (1 mg/ml) in a vial. Sodium ^{125}I-iodide[8] (1.0 mCi) was added, the vial was stoppered, and the contents were mixed gently. Chloramine-T[9], 30 μg in 15 μl of dilute iodination buffer, was added, and the reaction mixture was agitated for 2 min. The reaction was stopped by addition of 60 μg of sodium metabisulfite in 30 μl of dilute iodination buffer.

Transfer solution (100 μl), containing 16% (w/v) sucrose dissolved in the assay buffer solution, was added, and the contents of the vial were layered on a 0.5 × 20-cm anion exchange[10] column equilibrated with the assay buffer solution. The vial was rinsed with 70 μl of a solution containing 8% (w/v) sucrose dissolved in the assay buffer, which was then added to the column. The column eluate was collected in 1.0-ml fractions, which were counted to determine the radioactivity profile.

Extraction Procedure—A methanol solution containing 20 μg of hydrocortisone (2 mg/ml) and 40,000 dpm of 1,2-^{3}H-progesterone[11] (40 Ci/mmole) was added to a set of 15 × 85-mm disposable glass tubes, and the solvent was evaporated in a 45° water bath under a nitrogen stream. Plasma (0.5 ml), containing known or unknown amounts of danazol, and water (0.5 ml) were added to the tubes and they were mixed. The mixture was allowed to remain either at room temperature for 2 hr or at 4° overnight. Then *n*-hexane[12] (5 ml) was added to each tube, and the tubes were shaken mechanically for 5 min.

[1] Danocrine, Winthrop Laboratories, New York, N.Y.

[2] 17-Hydroxy-17α-pregn-4-en-20-yno[2,3-*d*]isoxazol-6-ylideneaminoxyacetic acid.

[3] Difco Laboratories, Detroit, Mich.

[4] Fraction II, Miles Laboratories, Kankakee, Ill.

[5] J. E. Peterson and G. D. Niswender, unpublished data.

[6] Sigma Chemical Co., St. Louis, Mo.

[7] Methyl 4-hydroxy-α-[[[[[(17α)-17-hydroxypregna-2,4-dien-20-yno[2,3-*d*]-isoxazol-6-ylidene]amino]oxy]acetyl]amino]benzenepropanoate.

[8] New England Nuclear, Boston, Mass.

[9] Eastman Kodak, Rochester, N.Y.

[10] QAE-Sephadex, Q-25-120, Sigma Chemical Co., St. Louis, Mo.

[11] New England Nuclear, Boston, Mass.

[12] Nanograde, Mallinckrodt, St. Louis, Mo.

0022-3549/78/1000-1425$01.00/0

© 1978, American Pharmaceutical Association

REFERENCES

(1) D. M. Gallant, M. P. Bishop, and R. Guerrero-Figueroa, *Curr. Ther. Res.*, **14**, 61 (1972).

(2) A. Mooradian, A. G. Hlavac, P. E. Dupont, M. R. Bell, and A. A. Alousi, *J. Med. Chem.*, **18**, 640 (1975).

(3) R. N. Schut, *Chem. Abstr.*, **70**, P106382M (1969).

(4) G. W. Snedecor and W. G. Cochran, "Statistical Methods," 6th ed., Iowa State University Press, Ames, Iowa, 1969, pp. 69, 70.

(5) B. M. Phillips and T. S. Miya, *J. Pharm. Sci.*, **53**, 1098 (1964).

(6) D. P. Benziger, K. G. Balfour, and J. Edelson, *Drug Metab. Dispos.*, **5**, 239 (1977).

ACKNOWLEDGMENTS

Presented in part at the 10th American Chemical Society Great Lakes Regional Meeting, Evanston, Ill., June 1976.

The authors thank Mr. Rick Minegar and Mr. Larry Craigo for technical assistance and Dr. John Van Dyke for preparation of the ^{14}C-labeled compound.

Radioimmunoassay for Danazol in Human and Monkey Plasma

J. E. PETERSON ˣ, M. E. KING, W. F. BANKS, J. F. BAKER, A. F. JENSEN, R. W. ROSS, Jr., S. CLEMANS, and J. EDELSON

Received December 12, 1977, from the *Department of Drug Metabolism and Disposition and the Department of Biometrics, Sterling-Winthrop Research Institute, Rensselaer, NY 12144.* Accepted for publication February 7, 1978.

Abstract □ A sensitive method is described for the radioimmunoassay of danazol in monkey and human plasma. Antiserum was developed in rabbits, and a second antibody was used to separate bound from free danazol. The radioimmunoassay was specific for danazol, and the limit of detection ranged from 1.4 to 2.8 ng/ml. Exogenous danazol could be quantitated accurately in both monkey and human plasma. The radioimmunoassay results agreed with values obtained by inverse isotope dilution after intravenous administration of ^{14}C-danazol to monkeys. The assay was used successfully to measure danazol in plasma from human volunteers receiving 200 mg of danazol.

Keyphrases □ Danazol—radioimmunoassay in human and monkey plasma □ Radioimmunoassay—danazol in human and monkey plasma □ Anterior pituitary suppressants—danazol, radioimmunoassay in human and monkey plasma

Danazol[1] (17α-pregna-2,4-dien-20-yno[2,3-*d*]isoxazol-17-ol), a novel steroid, lacks estrogenic or progestational activity upon oral administration but has markedly attenuated androgenic potential (an "impeded" androgen) (1). It inhibits either pituitary gonadotropin synthesis or release in rodents (1, 2), monkeys (3), and humans (4). In males, it depresses the sperm count (5); in women, danazol relieves the symptomatology of endometriosis (6) and may be valuable in the management of benign breast disorders (7).

Limited studies have appeared on plasma danazol concentrations (8, 9). The present report describes a sensitive and accurate method for the measurement of danazol in plasma of both monkeys and humans.

EXPERIMENTAL

Preparation of Antidanazol Serum—The danazol hapten[2] was conjugated with ϵ-amino groups of lysine residues in bovine serum albumin by a carbodiimide condensation (10). A trinitrobenzenesulfonic acid determination (11) indicated that approximately nine hapten molecules were conjugated to each albumin. The hapten–protein conjugate (1.0–2.0 mg) was emulsified in complete Freund's adjuvant[3] and injected intradermally at multiple sites along the dorsal surfaces of three Dutch belted rabbits (12). Booster immunizations of the conjugate in incomplete Freund's adjuvant were administered at approximately 3-week intervals. The rabbits were bled *via* the marginal ear vein.

Preparation of Second Antibody—Anti-rabbit γ-globulin was prepared by repeated subcutaneous injection at monthly intervals of rabbit γ-globulin[4], 100 μg, emulsified in complete Freund's adjuvant to an adult goat. The goat was bled 2 weeks after each immunization. The dilution of the second antibody was 1:16, as determined by a progesterone assay[5] according to the procedure of Midgley *et al.* (13).

Solutions—Iodination buffer contained 0.5 *M* Na_2HPO_4–0.5 *M* NaH_2PO_4 (4:1), adjusted to a final pH of 7.5. Dilute iodination buffer was the same buffer diluted 1:10 with water. Phosphate-buffered saline was made by dissolving 24.51 g of sodium chloride, 1.77 g of monobasic sodium phosphate monohydrate, 3.21 g of dibasic sodium phosphate, and 0.285 g of thimerosal[6] in 3 liters of water and adjusting to pH 7.0. The assay buffer solution contained 0.1% (w/v) gelatin dissolved in phosphate-buffered saline.

Radioiodination—A methyl tyrosinate derivative of danazol[7] (I) was radioiodinated at room temperature by a modification of the method of Greenwood and Hunter (14). Iodination buffer (50 μl) was mixed with 5 μl of a methanol solution of I (1 mg/ml) in a vial. Sodium ^{125}I-iodide[8] (1.0 mCi) was added, the vial was stoppered, and the contents were mixed gently. Chloramine-T[9], 30 μg in 15 μl of dilute iodination buffer, was added, and the reaction mixture was agitated for 2 min. The reaction was stopped by addition of 60 μg of sodium metabisulfite in 30 μl of dilute iodination buffer.

Transfer solution (100 μl), containing 16% (w/v) sucrose dissolved in the assay buffer solution, was added, and the contents of the vial were layered on a 0.5 × 20-cm anion exchange[10] column equilibrated with the assay buffer solution. The vial was rinsed with 70 μl of a solution containing 8% (w/v) sucrose dissolved in the assay buffer, which was then added to the column. The column eluate was collected in 1.0-ml fractions, which were counted to determine the radioactivity profile.

Extraction Procedure—A methanol solution containing 20 μg of hydrocortisone (2 mg/ml) and 40,000 dpm of 1,2-^{3}H-progesterone[11] (40 Ci/mmole) was added to a set of 15 × 85-mm disposable glass tubes, and the solvent was evaporated in a 45° water bath under a nitrogen stream. Plasma (0.5 ml), containing known or unknown amounts of danazol, and water (0.5 ml) were added to the tubes and they were mixed. The mixture was allowed to remain either at room temperature for 2 hr or at 4° overnight. Then *n*-hexane[12] (5 ml) was added to each tube, and the tubes were shaken mechanically for 5 min.

[1] Danocrine, Winthrop Laboratories, New York, N.Y.

[2] 17-Hydroxy-17α-pregn-4-en-20-yno[2,3-*d*]isoxazol-6-ylideneaminoxyacetic acid.

[3] Difco Laboratories, Detroit, Mich.

[4] Fraction II, Miles Laboratories, Kankakee, Ill.

[5] J. E. Peterson and G. D. Niswender, unpublished data.

[6] Sigma Chemical Co., St. Louis, Mo.

[7] Methyl 4-hydroxy-α-[[[[[(17α)-17-hydroxypregna-2,4-dien-20-yno[2,3-*d*]-isoxazol-6-ylidene]amino]oxy]acetyl]amino]benzenepropanoate.

[8] New England Nuclear, Boston, Mass.

[9] Eastman Kodak, Rochester, N.Y.

[10] QAE-Sephadex, Q-25-120, Sigma Chemical Co., St. Louis, Mo.

[11] New England Nuclear, Boston, Mass.

[12] Nanograde, Mallinckrodt, St. Louis, Mo.

0022-3549/78/1000-1425$01.00/0

© 1978, American Pharmaceutical Association

Table I—Relative Affinities of Danazol, Related Compounds, and Native Steroids to the Antiserum

Compound	Relative Affinity
Danazol	1.00
Ethisterone (17-hydroxy-17α-pregn-4-en-20-yn-3-one)	0.055
2-Aminomethylene-17-hydroxy-17α-pregn-4-en-20-yn-3-one	0.031
17-Hydroxy-2α-hydroxymethyl-17α-pregn-4-en-20-yn-3-one	<0.031
17-Hydroxy-3-oxo-17α-pregna-1,4-dien-20-yne-2-carboxyaldehyde	<0.015
6β,17-Dihydroxy-17α-pregn-4-en-20-yn-3-one	<0.015
17-Hydroxy-2-hydroxymethyl-17α-pregna-1,4-dien-20-yn-3-one	<0.015
6β,17-Dihydroxy-2α-hydroxymethyl-17α-pregn-4-en-20-yn-3-one	<0.003
17α-Pregn-4-en-20-yno[2,3-*d*]isoxazol-6β,11β,17-triol	0.001
Testosterone (17β-hydroxy-4-androsten-3-one)	0.004
Progesterone (4-pregnene-3,20-dione)	<0.004
Estradiol [1,3,5(10)-estratriene-3,17β-diol]	<0.004
Androstenedione (4-androstene-3,17-dione)	<0.004
Hydrocortisone (11β,17,21-trihydroxy-4-pregnene-3,20-dione)	<0.006

The aqueous phase of each sample was frozen in a dry ice–acetone bath, and the hexane phase was decanted into another tube. The hexane extraction was repeated two additional times. The combined hexane extracts were evaporated to approximately 5 ml, and 1 ml of distilled water was added to the tubes. The tubes were mixed for 1 min, the aqueous phase was frozen in dry ice–acetone, and the hexane was decanted into a clean set of 15 × 85-mm tubes. Then the hexane was evaporated to dryness, and 20 μl of absolute alcohol was added to each tube.

The tubes were shaken, and 1 ml of assay buffer was added. Then the tubes were mixed, covered, and allowed to remain overnight at 4°. Recovery of ^{3}H-progesterone was determined by counting 300 μl of this solution and used to estimate the extraction efficiency of danazol.

Radioimmunoassay—The radioimmunoassay for danazol was similar to assays previously reported for other steroids (15). Duplicate samples of the plasma extracts at 100 and 200 μl were added to disposable culture tubes (12 × 75 mm). The samples were diluted to 500 μl with assay buffer; 200 μl of antidanazol serum, at a dilution of 1:2000 in nonimmune normal rabbit serum, was then added. Radioiodinated I, 100 μl, prepared by diluting the eluate from the ion-exchange column with assay buffer to 25,000–30,000 cpm/100 μl, was added.

All assay tubes were incubated for 4–6 hr at 4°, followed by addition of 200 μl of appropriately diluted second antibody. Incubation was continued for an additional 12–18 hr. At the end of the incubation period, 2.5 ml of cold phosphate-buffered saline was added, and the tubes were centrifuged at 2500 rpm for 30 min; the supernates were decanted, and the precipitates were counted. Duplicate standards with 0.1–100 ng of danazol were included in each assay.

Human Study—Ten healthy female volunteers received a 200-mg danazol capsule orally following an overnight fast. Blood samples (5 ml) were drawn into an oxalated tube at 0, 1, 2, 4, 6, 8, 12, 16, 20, and 24 hr. The blood samples were centrifuged promptly to separate the plasma, which was frozen until analyzed.

Monkey Study—An intravenous dose was prepared by dissolving 6.0 mg of ^{14}C-danazol[13] in absolute ethanol–physiological saline (1:1) to a final specific activity of 1.2×10^8 dpm/ml (1.37 mg/ml). Three rhesus monkeys received approximately 1 ml of this solution *via* the saphenous vein at a dose level of 0.31 mg/kg. Blood samples were removed from the femoral vein at intervals from 5 min to 3 hr. The samples were immediately centrifuged, and plasma was obtained. The plasma samples were frozen until assayed.

Inverse Isotope Dilution Technique—A measured amount (100–500 μl) of each monkey plasma sample was added to 1 ml of water, followed by 20 μg of nonradioactive danazol dissolved in chloroform (1 mg/ml). Each sample was extracted with hexane (2 × 10 ml), and the organic layer was separated from the aqueous phase as already described. The combined hexane extracts were evaporated to dryness under air, and the residue was dissolved in 50 μl of chloroform. The entire solution was injected into a liquid chromatograph using the following conditions: column, 5 μm silica[14] (4.2 × 150 mm); pressure, 500 psi; mobile phase, 3% (v/v) 2-propanol in redistilled pentane; and detector, UV, 254 nm.

The danazol fraction of each sample was collected and evaporated under air, and the residue was dissolved in 2 ml of methanol. A 1-ml aliquot was transferred to a counting vial containing 10 ml of scintillation fluid[15] and counted. The remaining methanol was evaporated to dryness under air. The residue was dissolved in 50 μl of chloroform and reinjected into the liquid chromatograph, using conditions similar to those described, with chloroform as the mobile phase. The danazol fraction of each sample was collected in a counting vial and evaporated. Methanol (1 ml) and 10 ml of scintillation fluid were added to the residue, and the solutions were counted.

Several blank samples were collected between injections and similarly counted. The average of these blanks was taken as the background counting rate for a given series of injections.

A set of direct standards was prepared in chloroform such that a 10-μl sample of each would contain an amount of danazol varying from 0.1 to 20 μg. These standards were injected onto the liquid chromatograph, and a standard curve was prepared prior to the injection of each set of experimental samples. Danazol recovery in each experimental sample was quantitated, using peak height, with reference to the standard curve.

The specific activity (disintegrations per minute per microgram) of the danazol in the second injection of each sample was calculated and used to determine the number of disintegrations per minute of intact danazol per milliliter of monkey plasma. The specific activity of the dose of danazol was then used to convert to nanograms per milliliter.

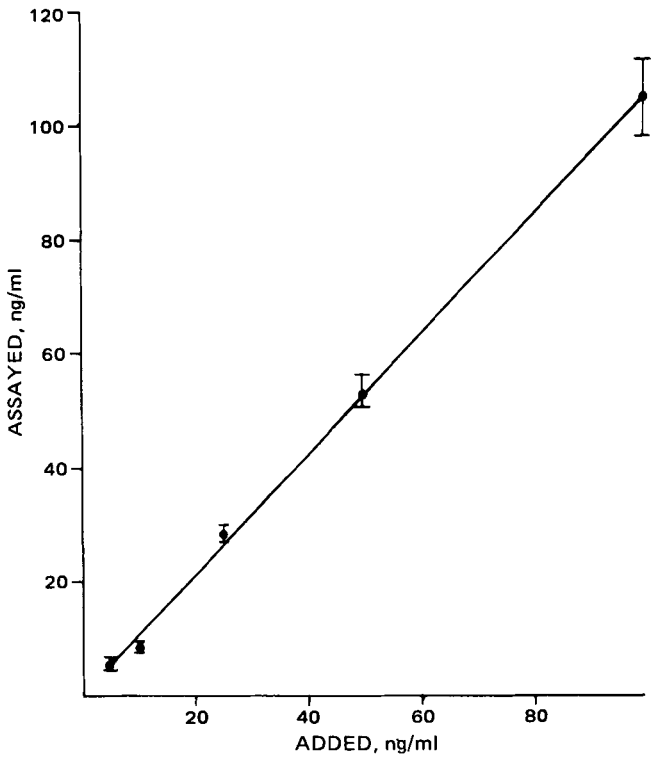

Figure 1—*Correlation of exogenous danazol added to human plasma with mean values obtained by radioimmunoassay. Slope = 1.055, intercept = 0.069, and* r *(correlation coefficient) = 0.999. The vertical line represents 2* SE (n = *8).*

RESULTS AND DISCUSSION

All three rabbits produced antiserums within 2 months that bound radioiodinated I at an initial dilution (200 μl) of 1:400 or greater. The dilution required to bind 40–50% of the radioactive I was 1:2000, equivalent to a 1:10,000 final dilution in the assay tube.

[13] Lot 61004, 13.4 mCi/mmole, Pathfinder Labs, St. Louis, Mo.

[14] Lichrosorb, E. M. Laboratories, Elmsford, N.Y.

[15] Biofluor, New England Nuclear, Boston, Mass.

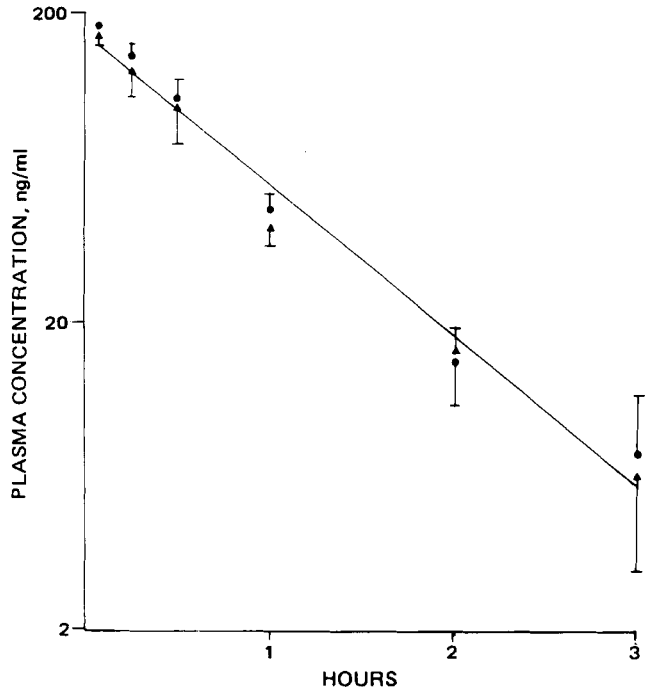

Figure 2—*Mean concentration of danazol in monkey plasma after 0.31 mg of danazol/kg iv. Key: ●, values obtained by radioimmunoassay; and ▲, values obtained by the inverse isotope dilution technique. The vertical line represents 1* SE *(n = 3).*

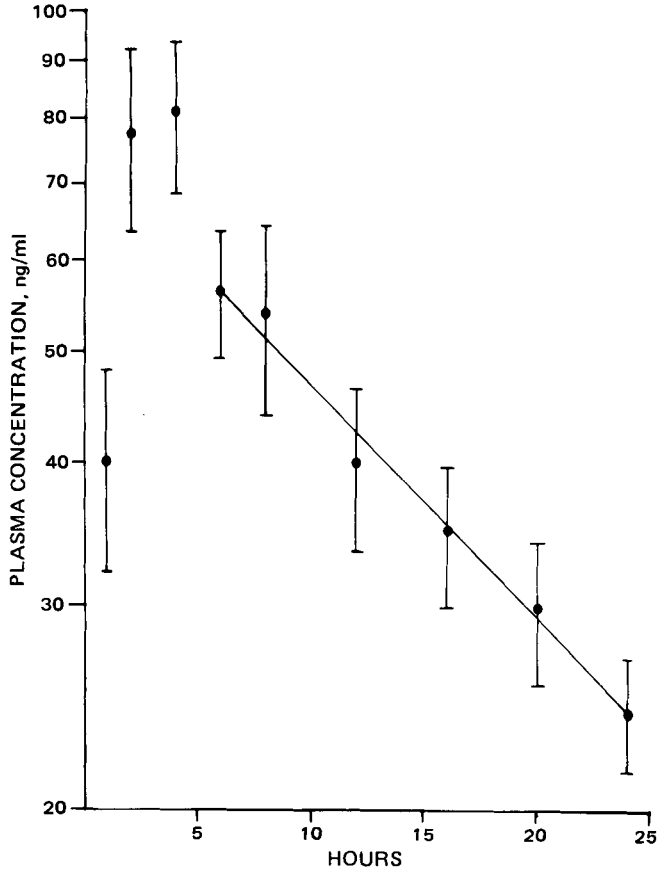

Figure 3—*Mean danazol concentration in plasma of women who received a single 200-mg capsule of danazol. The vertical line represents 2* SE *(n = 10).*

The specificity of antiserums from three rabbits on three different bleeding dates was assessed by determining the ability of naturally occurring steroids and compounds related to danazol (16) to compete with radioiodinated I for binding to the antibody. The amounts of each steroid required for 50% displacement of radioactivity were determined by comparison with the danazol standard curves to arrive at a relative affinity (17). The antiserum from one bleeding, exhibiting the least cross reactivity, was selected for all subsequent work. The relative affinities of potentially competitive steroids with this antiserum are shown in Table I. The only tested steroid to show significant binding activity was ethisterone (5.5%).

Sensitivity is defined as the smallest amount of steroid that can be measured in an aliquot of biological fluid. Sensitivity, S, may be expressed as:

$$S = \frac{2SD}{RF} \times 100 \qquad \text{(Eq. 1)}$$

where R is the fraction recovered, F is the fraction of the extracted steroid used in the assay, and SD is the standard deviation of the mean of the zero-time plasmas (18). The mean recovery, as estimated from ^{3}H-progesterone extraction efficiency, was 73.4 ± 0.63% (n = 88) from human plasma and 71.2 ± 0.46% (n = 18) from monkey plasma. The extraction properties of danazol and progesterone are similar; the mean recovery of ^{14}C-danazol from human plasma was 73.9 ± 0.35% (n = 6). The human plasma blank values gave a limit of detection of 1.40 ng/ml for the 100-μl aliquot and of 1.42 ng/ml for the 200-μl aliquot. The monkey plasma blank values gave 2.81 and 2.60 ng/ml for the 100 and 200-μl aliquots, respectively.

The within- and between-assay precision was evaluated by duplicate measurements of identical samples in the same assay and in replicate assays. The coefficient of variation, CV, can be estimated using (19):

$$CV = \sqrt{\frac{\sum d^2}{2n}} \qquad \text{(Eq. 2)}$$

where:

$$d = \frac{\text{highest value of each duplicate}}{\text{lowest value of each duplicate}} - 1 \times 100 \qquad \text{(Eq. 3)}$$

and n is the number of duplicate determinations.

The within-assay coefficient of variation ranged from 5.7 to 15.1% with a mean of 9.6%. The between-assay coefficient of variation ranged from 8.7 to 23.3% with a mean of 17.6%. There were no differences between monkey and human plasmas. These values are within the range reported for other steroid assays (17).

Exogenous danazol was quantitated accurately when varying amounts were added to human plasma, extracted, and assayed in the danazol radioimmunoassay (Fig. 1). A similar correlation was found for monkey plasma: slope, 0.981; intercept, 3.91; and correlation coefficient, 0.999. A comparison of the results of the radioimmunoassay with values obtained by the inverse isotope dilution technique on plasma from three monkeys that had been injected with ^{14}C-danazol showed excellent agreement (Fig. 2). The apparent first-order elimination half-life for the first 3 hr was 37 min.

The mean concentration of danazol in the plasma of 10 female volunteers receiving 200 mg of danazol is shown in Fig. 3. The apparent first-order elimination half-life of danazol was 14.7 hr as determined by least-squares regression on the data points of the terminal phase.

REFERENCES

(1) G. O. Potts, A. L. Beyler, and H. P. Schane, *Fertil. Steril.*, **25**, 367 (1974).

(2) V. P. Dixit and N. K. Lohiya, *ibid.*, **26**, 68 (1975).

(3) H. P. Schane and G. O. Potts, *ibid.*, **25**, 363 (1974).

(4) R. B. Greenblatt, W. P. Dmowski, V. B. Mahesh, and H. F. L. Scholer, *ibid.*, **22**, 102 (1971).

(5) R. D. Skoglund and C. A. Paulsen, *Contraception*, **7**, 357 (1973).

(6) W. B. J. Schuyler, *J. Maine Med. Assoc.*, **67**, 47 (1976).

(7) R. H. Asch and R. B. Greenblatt, *Am. J. Obstet. Gynecol.*, **127**, 130 (1977).

(8) J. E. Creange and G. O. Potts, *Steroids*, **23**, 411 (1974).

(9) C. Davison, W. Banks, and A. Fritz, *Arch. Int. Pharm. Ther.*, **221**, 294 (1976).

(10) B. F. Erlanger, *Pharmacol. Rev.*, **25**, 271 (1973).

(11) A. F. S. A. Habeeb, *Anal. Biochem.*, **14**, 328 (1966).

(12) J. Vaitukaitis, J. B. Robbins, E. Neischlag, and G. T. Ross, *J. Clin. Endocrinol. Metab.*, **33**, 988 (1971).

(13) A. R. Midgley, Jr., R. W. Rebar, and G. D. Niswender, *Acta Endocrinol. Suppl.*, **142**, 247 (1969).
(14) F. C. Greenwood and W. M. Hunter, *Biochem. J.*, **89**, 114 (1963).
(15) G. D. Niswender and A. R. Midgley, in "Immunologic Methods in Steroid Determination," F. G. Peron and B. V. Caldwell, Eds., Plenum, New York, N.Y., 1970, pp. 149–173.
(16) D. Rosi, H. C. Neumann, R. G. Christiansen, H. P. Schane, and G. O. Potts, *J. Med. Chem.*, **20**, 349 (1977).
(17) G. E. Abraham, *J. Clin. Endocrinol. Metab.*, **29**, 866 (1969).
(18) G. E. Abraham, *Acta Endocrinol. Suppl.*, **183**, 1 (1974).
(19) G. W. Snedecor, *Biometrics*, **8**, 85 (1952).

ACKNOWLEDGMENTS

The authors thank M. Graham, S. Thorpe, and C. Barnick for technical assistance. They are also grateful to R. G. Christiansen and his associates for providing samples of related steroids.

Simulated Respiratory System for *In Vitro* Evaluation of Two Inhalation Delivery Systems Using Selected Steroids

JOHN J. SCIARRA ˣ and ANTHONY CUTIE

Received November 29, 1976, from the *Arnold and Marie Schwartz College of Pharmacy and Health Sciences of Long Island University, Brooklyn, NY 11201.* Accepted for publication February 7, 1978.

Abstract □ A simulated respiratory system was developed for the *in vitro* evaluation of two differently designed oral inhalation delivery systems. The deposition properties of a newly designed delivery system used for triamcinolone acetonide were compared to the more conventional, commercially available adapter utilized for an aerosol containing beclomethasone dipropionate. The simulated respiratory system was constructed so that the delivered dose of active ingredient could be classified into two fractions: the fraction that would be deposited in the oral cavity and throat and the fraction that would reach the desired site of activity in the respiratory tract. Based on this method, the newly designed system delivered more than 95% of the labeled dose to the desired site. The beclomethasone dipropionate aerosol system, which was observed to discharge the active ingredient with a greater intensity, delivered approximately 40% of the labeled dose. The particle-size distribution of the dose dispensed from the newly designed delivery system attached to the triamcinolone acetonide aerosol was determined using an impactor technique. No effort was made to correlate these results with an *in vivo* response.

Keyphrases □ Respiratory system, simulated—developed for *in vitro* evaluation of inhalation delivery systems □ Delivery systems, inhalation—evaluated *in vitro* using simulated respiratory system □ Inhalation delivery systems—evaluated *in vitro* using simulated respiratory system

Oral aerosol products used by inhalation are intended to deliver the active ingredient in the desired particle-size range to the proper portion of the respiratory system. In many instances, however, a fairly high percentage of formulation is retained in the oral adapter, mouth, and back of the throat instead of obtaining the desired deep penetration into the bronchi. This problem was discussed by Hayton (1). Since this loss is fairly consistent, many commonly used aerosol products contain an increased amount of active ingredient in the formulation so that the proper dose is delivered to the desired site of activity.

Various methods are useful for determining the dose of an aerosol delivered through an oral adapter in the desired portions of the lungs. Karig *et al.* (2) developed a compartmentalized lung chamber that could simulate different sized lung bronchi. They established an *in vitro* method for evaluating the penetration of solid particles in the lungs using several different aerosol generators. An air flow rate, based on a vacuum of 30.4 cm Hg, could be used to evaluate several different types of aerosols. The chamber size was based on literature values for the size of the human respiratory tract. Both solution- and suspension-type aerosols were studied, and it was concluded that it was possible to compare solution aerosols to suspension aerosols and to determine differences in their deposition.

The purpose of this study was to develop a suitable method for evaluating various oral adapters. In particular, the method should be capable of classifying the dispensed dose into a fraction that would be trapped in the oral cavity (mouth) and throat and a fraction that would reach the lungs. An artificial or simulated respiratory system was designed and constructed. A newly developed, different type of oral adapter, which may be capable of delivering a greater percentage of the active ingredient to the desired site, was attached to an aerosol product containing triamcinolone acetonide as the model drug and evaluated using the simulated respiratory system. For comparison, an aerosol product using a conventional oral adapter was also evaluated using the simulated respiratory system.

EXPERIMENTAL

Design of Simulated Respiratory System—The simulated respiratory system (Fig. 1) was made of glass and was scaled to twice the relative dimensions of a normal respiratory system. It was designed to follow the normal structure of the respiratory system. The entrance to the simulated respiratory system opened into an area similar to the oral cavity. This area then opened into three separate chambers: the chamber above the opening represented the nasal passageway; another opening, below and to the left, represented the esophagus; and the third opening represented the entrance to the lungs. Removable ground-glass stoppers were fitted at the opening located at the base of the unit (esophagus) and to the simulated nasal passageway.

The simulated respiratory system was then fitted to a modified particle-size impactor[1] capable of classifying particles from 0.5 to 32 μm. However, the six stages of the impactor were removed, and only the last stage (0.5-μm size) was used. The portion of the simulated respiratory system representing the opening to the lungs was fitted to the opening of the impactor, and a vacuum was applied through this "lung" opening.

[1] Cascade impactor, model CI-S-6, Scientific Advances, Columbus, Ohio.

0022-3549/78/1000-1428$01.00/0
© 1978, American Pharmaceutical Association

(13) A. R. Midgley, Jr., R. W. Rebar, and G. D. Niswender, *Acta Endocrinol. Suppl.*, **142**, 247 (1969).
(14) F. C. Greenwood and W. M. Hunter, *Biochem. J.*, **89**, 114 (1963).
(15) G. D. Niswender and A. R. Midgley, in "Immunologic Methods in Steroid Determination," F. G. Peron and B. V. Caldwell, Eds., Plenum, New York, N.Y., 1970, pp. 149–173.
(16) D. Rosi, H. C. Neumann, R. G. Christiansen, H. P. Schane, and G. O. Potts, *J. Med. Chem.*, **20**, 349 (1977).
(17) G. E. Abraham, *J. Clin. Endocrinol. Metab.*, **29**, 866 (1969).
(18) G. E. Abraham, *Acta Endocrinol. Suppl.*, **183**, 1 (1974).
(19) G. W. Snedecor, *Biometrics*, **8**, 85 (1952).

ACKNOWLEDGMENTS

The authors thank M. Graham, S. Thorpe, and C. Barnick for technical assistance. They are also grateful to R. G. Christiansen and his associates for providing samples of related steroids.

Simulated Respiratory System for *In Vitro* Evaluation of Two Inhalation Delivery Systems Using Selected Steroids

JOHN J. SCIARRA ˣ and ANTHONY CUTIE

Received November 29, 1976, from the *Arnold and Marie Schwartz College of Pharmacy and Health Sciences of Long Island University, Brooklyn, NY 11201.* Accepted for publication February 7, 1978.

Abstract □ A simulated respiratory system was developed for the *in vitro* evaluation of two differently designed oral inhalation delivery systems. The deposition properties of a newly designed delivery system used for triamcinolone acetonide were compared to the more conventional, commercially available adapter utilized for an aerosol containing beclomethasone dipropionate. The simulated respiratory system was constructed so that the delivered dose of active ingredient could be classified into two fractions: the fraction that would be deposited in the oral cavity and throat and the fraction that would reach the desired site of activity in the respiratory tract. Based on this method, the newly designed system delivered more than 95% of the labeled dose to the desired site. The beclomethasone dipropionate aerosol system, which was observed to discharge the active ingredient with a greater intensity, delivered approximately 40% of the labeled dose. The particle-size distribution of the dose dispensed from the newly designed delivery system attached to the triamcinolone acetonide aerosol was determined using an impactor technique. No effort was made to correlate these results with an *in vivo* response.

Keyphrases □ Respiratory system, simulated—developed for *in vitro* evaluation of inhalation delivery systems □ Delivery systems, inhalation—evaluated *in vitro* using simulated respiratory system □ Inhalation delivery systems—evaluated *in vitro* using simulated respiratory system

Oral aerosol products used by inhalation are intended to deliver the active ingredient in the desired particle-size range to the proper portion of the respiratory system. In many instances, however, a fairly high percentage of formulation is retained in the oral adapter, mouth, and back of the throat instead of obtaining the desired deep penetration into the bronchi. This problem was discussed by Hayton (1). Since this loss is fairly consistent, many commonly used aerosol products contain an increased amount of active ingredient in the formulation so that the proper dose is delivered to the desired site of activity.

Various methods are useful for determining the dose of an aerosol delivered through an oral adapter in the desired portions of the lungs. Karig *et al.* (2) developed a compartmentalized lung chamber that could simulate different sized lung bronchi. They established an *in vitro* method for evaluating the penetration of solid particles in the lungs using several different aerosol generators. An air flow rate, based on a vacuum of 30.4 cm Hg, could be used to evaluate several different types of aerosols. The chamber size was based on literature values for the size of the human respiratory tract. Both solution- and suspension-type aerosols were studied, and it was concluded that it was possible to compare solution aerosols to suspension aerosols and to determine differences in their deposition.

The purpose of this study was to develop a suitable method for evaluating various oral adapters. In particular, the method should be capable of classifying the dispensed dose into a fraction that would be trapped in the oral cavity (mouth) and throat and a fraction that would reach the lungs. An artificial or simulated respiratory system was designed and constructed. A newly developed, different type of oral adapter, which may be capable of delivering a greater percentage of the active ingredient to the desired site, was attached to an aerosol product containing triamcinolone acetonide as the model drug and evaluated using the simulated respiratory system. For comparison, an aerosol product using a conventional oral adapter was also evaluated using the simulated respiratory system.

EXPERIMENTAL

Design of Simulated Respiratory System—The simulated respiratory system (Fig. 1) was made of glass and was scaled to twice the relative dimensions of a normal respiratory system. It was designed to follow the normal structure of the respiratory system. The entrance to the simulated respiratory system opened into an area similar to the oral cavity. This area then opened into three separate chambers: the chamber above the opening represented the nasal passageway; another opening, below and to the left, represented the esophagus; and the third opening represented the entrance to the lungs. Removable ground-glass stoppers were fitted at the opening located at the base of the unit (esophagus) and to the simulated nasal passageway.

The simulated respiratory system was then fitted to a modified particle-size impactor[1] capable of classifying particles from 0.5 to 32 μm. However, the six stages of the impactor were removed, and only the last stage (0.5-μm size) was used. The portion of the simulated respiratory system representing the opening to the lungs was fitted to the opening of the impactor, and a vacuum was applied through this "lung" opening.

[1] Cascade impactor, model CI-S-6, Scientific Advances, Columbus, Ohio.

0022-3549/78/1000-1428$01.00/0
© 1978, American Pharmaceutical Association

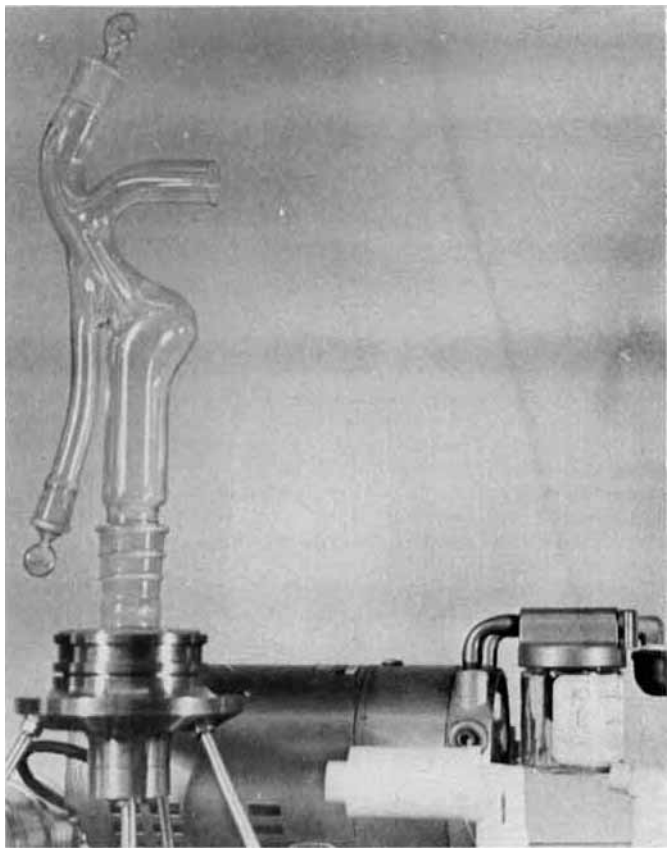

Figure 1—*Simulated respiratory system.*

A vacuum pump was connected to the impactor by a "T" valve (Fig. 1).

For this study, an air flow equivalent to a vacuum of about 75 mm Hg (19.8 liters/min) was utilized to simulate normal inspiration pressure (3, 4). Air flows equivalent to a vacuum of 50 mm Hg (16.9 liters/min) and 25 mm Hg (13.2 liters/min) also were utilized to determine the effect of air flow upon the dispensing characteristics of the product as it flowed through the oral adapter. A glass fiber filter was fitted onto the base of the simulated respiratory system so that all material reaching this point was collected. Spectrophotometric analysis of the material on this filter indicated the amount of active ingredient assumed to reach the desired site of activity.

Evaluation of Newly Designed Oral Adapter—An aerosol product containing triamcinolone acetonide[2] was fitted with an oral adapter (Fig. 2). This adapter consists of a mechanical breakup fitting through which the dose is dispensed into a relatively large chamber and allows for the expansion of the liquefied gas propellant and dispersion of the active ingredient. The product exits through a narrow opening intended to be placed into the patient's mouth. In this study, this opening was placed into the entrance of the simulated respiratory system.

The methodology used in studying the two aerosol products was varied to some extent to compensate for differences in oral inhalation delivery systems and in the apparent solubility of the steroids in the methanol–water solutions.

Assay for Triamcinolone Acetonide—A standard UV spectral curve for triamcinolone acetonide was prepared by dissolving triamcinolone acetonide, 97.2% purity (used as reference standard), in a 6% methanol–water solution (spectroanalytical grade). Six dilutions of this solution were made to obtain varying concentrations of triamcinolone acetonide. The solutions were read[3] at 237 nm. A linear curve was obtained indicating compliance with the Beer–Lambert law.

Triamcinolone Acetonide Delivered through Valve Stem (No Oral Adapter)—The amount of triamcinolone acetonide delivered through the valve stem was determined by making an incision across the plastic valve stem (notch) and inverting the unit into 6 ml of methanol contained in a glass beaker. The aerosol unit was then actuated 3, 6, 9, 12, and 18 times (at least 1-min intervals between actuations) into the methanol, which was then diluted with distilled water to 100 ml. The propellant was allowed to escape from the solution, and each solution was read[3] at 237 nm.

Table I—Triamcinolone Acetonide Actuation Delivered through Simulated Respiratory System at Various Air Flows [a]

Number of Actuations	Amount Delivered to Simulated Respiratory System		Amount Retained in Simulated Oral Cavity		Amount Retained in Oral Inhalation Adapter	
	±2 μg	±4% [b]	±2 μg	±4% [b]	±2 μg	±4% [b]
			At 75 mm Hg			
6	105	52.5	—[c]	—[c]	98	49
12	100	50.0	—[c]	—[c]	—	—
18	100	50.0	—[c]	—[c]	—	—
			At 50 mm Hg			
9	96.6	48.3	3.4	1.7	100	50
			At 25 mm Hg			
9	94.3	47.2	5.7	2.8	100	50

[a] Average of three determinations. [b] Calculated on the basis of 200 μg/actuation delivered through valve. [c] Negligible amount, could not be determined.

Triamcinolone Acetonide Delivered through Oral Adapter—Before proceeding with this determination, a sample of triamcinolone aerosol was dispensed directly onto the glass fiber placed over the lowest stage of the impactor (0.5-μm stage). The aerosol product was fitted with a regular aerosol actuator, and the product was actuated 6, 12, and 18 times directly onto the glass fiber filter. A vacuum of 75 mm Hg was used to collect all active ingredients and to allow for complete vaporization of the propellant. The glass fiber filter was then placed into 6 ml of methanol and gently swirled to aid extraction of the active ingredient. The solution was diluted to 100 ml with distilled water and read at 237 nm. This procedure also was carried out in a vacuum of 400 mm Hg.

The amount of triamcinolone acetonide delivered through the newly designed oral adapter was determined by dispensing 6, 12, and 18 doses directly onto the lowest stage of the impactor fitted with a glass fiber filter paper, as previously described. A vacuum of 75 mm Hg was used. The filter paper was then removed and placed into 6 ml of methanol, and the mixture was swirled to aid extraction. The solution was diluted to 100 ml with distilled water and read at 237 nm. The impactor base was rinsed with 6 ml of methanol, diluted to 100 ml with distilled water, and read at 237 nm. The amount of steroid found on the base was added to the amount collected on the glass fiber.

The simulated respiratory system was then placed over the lower stage of the impactor, and the procedure was repeated by dispensing the triamcinolone aerosol through the simulated respiratory system. Six, 12, and 18 doses were dispensed into the simulated respiratory system at a vacuum of 75 mm Hg. The material collected in the glass fiber filter was determined using the spectrophotometric procedure. The oral adapter was rinsed with methanol, and the amount of active ingredient was determined spectrophotometrically. To determine any possible effect of

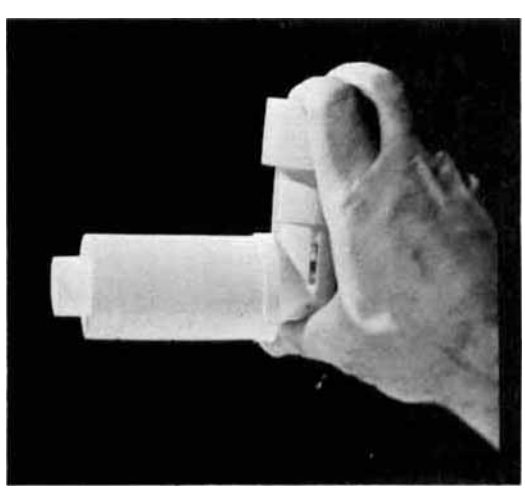

Figure 2—*Newly designed aerosol oral adapter.*

[2] Aristocort Aerosol, Lederle Laboratories, Pearl River, N.Y.
[3] Spectronic 200, Bausch & Lomb Optical Co., Rochester, N.Y.

Table II—Beclomethasone Dipropionate Actuation Delivered through Simulated Respiratory System at Various Air Flows [a]

Number of Actuations	Amount Delivered to Simulated Respiratory System		Amount Retained in Simulated Oral Cavity	
	±2 μg	±4% [b]	±2 μg	±4% [b]
	At 75 mm Hg			
15	20.90	41.8	29.10	58.2
20	20.32	40.6	29.68	59.4
30	18.75	37.5	31.25	62.5
	At 50 mm Hg			
15	22.0	44.0	28.0	56.0
20	21.5	43.0	28.5	57.0
30	20.6	41.2	29.4	58.8
	At 25 mm Hg			
15	16.7	33.4	33.3	66.6
20	18.8	37.6	31.2	62.4
30	20.6	41.2	29.4	56.8

[a] Average of three determinations. [b] Calculated on the basis of a labeled amount of 50 μg/actuation. From 2.9 to 3.5% of active ingredient remained trapped in the oral adapter.

air flow through the simulated respiratory system, the procedure was repeated at vacuums of 50 and 25 mm Hg.

Triamcinolone Acetonide Delivered through Conventional Actuator—The newly designed oral adapter was removed from the aerosol, and the valve stem was fitted with a conventional actuator. Nine doses of the aerosol were dispensed into the simulated respiratory system attached to the impactor, and the amount of triamcinolone acetonide delivered was determined spectrophotometrically as previously indicated.

Evaluation of Conventional Oral Adapter—A commercially available aerosol containing beclomethasone dipropionate fitted with a conventional oral adapter[4] was used for comparison with the newly designed oral adapter.

Assay for Beclomethasone Dipropionate—A standard UV spectral curve, using a reference sample of beclomethasone dipropionate (98.0%) in 50% methanol–water, was established at 239 nm. Beer–Lambert curves were prepared using 6 and 12% methanol–water solutions, but subsequent studies showed that these percentages of alcohol were inadequate to dissolve appreciable quantities of beclomethasone dipropionate.

Beclomethasone Dipropionate Dispensed through Valve Stem—The procedure described for triamcinolone acetonide was used for this determination. The delivery of the labeled amount (50 μg/actuation) was verified by making an incision across the plastic dip tube, inverting the aerosol, and actuating the metered valve 15, 20, 30, and 60 times into 50 ml of methanol, which was subsequently diluted to 100 ml with distilled water. The propellant was allowed to vaporize, and the solutions were read spectrophotometrically at 239 nm.

To verify that the propellant was not solubilized and contributing to the total absorbance of these solutions, the beclomethasone dipropionate aerosol was actuated for 15, 20, 30, and 60 times into a 1000-ml Florence flask that had its neck removed so atomization could be accomplished with minimum loss of active ingredient. The contents of the flask were

Table III—Dose of Triamcinolone Acetonide Dispensed through Conventional Actuator and Reaching Simulated Respiratory System [a]

Vacuum, mm Hg	Retained Dose in Simulated Respiratory System (Esophagus Portion), %	Dose Reaching Simulated Respiratory Portion, %	Average, %
75	47.5	52.5	—
75	51.6	48.4	—
75	40.1	59.9	53.6
50	46.6	53.4	—
50	49.9	50.1	—
50	48.3	51.7	51.7
25	44.9	55.1	—
25	46.6	53.4	—
25	48.3	51.7	53.4

[a] Average of two determinations.

[4] Becotide Aerosol, Allen and Hanburys, Ltd., London, England.

Table IV—Amount of Triamcinolone Acetonide Delivered through Valve Stem [a]

Number of Actuations	Absorbance at 237 nm	Triamcinolone Acetonide per Actuation, μg	Percent Recovered per Actuation [b]
3	0.21	210	105.0
6	0.41	205	102.5
9	0.59	197	98.5
12	0.78	195	97.5
18	1.20	200	100.0

[a] Average of two determinations. [b] Label indicated 200 μg of triamcinolone acetonide/actuation.

removed with 50 ml of methanol, diluted to 100 ml with distilled water, and read spectrophotometrically at 239 nm.

Beclomethasome Dipropionate Delivered through Simulated Respiratory System—The beclomethasone dipropionate aerosol was then actuated 15, 20, and 30 times through the entire simulated respiratory apparatus at air flows equivalent to vacuums of 25, 50, and 75 mm Hg. The material collected in the simulated esophagus was removed by washing with 50 ml of methanol. The 50 ml of methanol containing the active ingredient was diluted to 100 ml with distilled water and read at 239 nm. The oral adapter was also assayed for active ingredient by rinsing with methanol as previously indicated.

RESULTS AND DISCUSSION

The results indicate the applicability of the simulated respiratory system in determining the efficiency of certain oral inhalation adapters. The simulated respiratory system constructed was scaled to twice the relative dimensions of a normal respiratory system to accommodate the oral adapter from the aerosol product as well as to allow for a greater atomization and dispersion of the sample. The system was designed to follow the normal structure of the respiratory system and, in particular, the upper respiratory tract (nasal passage), the back of the mouth, and the esophagus. In this way, the system was capable of separating the dispensed dose into two fractions: the fraction trapped in the simulated oral cavity and throat and the fraction reaching the simulated desired site.

Of particular interest is the fact that the particles emitted into the simulated respiratory system can be classified into two broad ranges. These ranges include those particles small enough to be carried by the airstream into the respiratory system and those particles that may be trapped in the back of the throat. The latter may be due to the particle size itself or to the velocity with which the spray is emitted through the oral inhalation adapter.

In this simulated respiratory system, the entrance into the respiratory system is separated from the opening to the esophagus. It is anticipated that material adhering to the back of the unit would collect in the simulated esophagus area rather than be transferred to the area having the direct opening to the lungs. By attaching the simulated respiratory system to a modified particle-size impactor, a uniform air flow would be obtained through the simulated respiratory system when a vacuum is applied to the outlet of the impactor. By adjusting the vacuum at several different levels, varying air flows through the simulated respiratory system could be achieved. This system also allowed for the determination of the effect of inhalation pressure on the amount of dispensed dose collected in each fraction since these determinations could be carried out at varying pressures.

The glass simulated respiratory system allowed for the classification of particles (Tables I and II). To evaluate this system further, two aerosol inhalation products were studied. The triamcinolone acetonide aerosol

Table V—Dose of Triamcinolone Acetonide per Actuation Delivered through Oral Inhalation Adapter [a]

Number of Actuations	Absorbance at 237 nm	Triamcinolone Acetonide Delivered per Actuation, μg	Percent Recovered per Actuation [b]
6	0.20	100.0	100.0
12	0.39	97.5	97.5
18	0.60	100.0	100.0

[a] Average of three determinations at vacuum of 75 mm Hg. [b] Label indicated that 100 μg/actuation would be delivered through the oral inhalation adapter.

Table VI—Amount of Beclomethasone Dipropionate Delivered through Valve Stem [a]

Number of Actuations	Absorbance at 239 nm	Beclomethasone Dipropionate per Actuation, μg	Percent Recovered per Actuation [b]
15	0.250	52.1	104.2
20	0.535	52.5	104.6
30	0.490	51.0	102.0
60	0.975	49.8	99.8

[a] Average of two determinations. [b] Label indicated 50 μg of beclomethasone dipropionate/actuation.

was selected on the basis of the newly designed oral inhalation adapter used with the product. This adapter decreased spray velocity as it was emitted from the valve stem. Beclomethasone dipropionate aerosol was fitted with a conventional oral inhalation adapter and was studied to determine the usefulness of the simulated respiratory system in evaluating the dispensing characteristics of the two adapters.

The spray emitted from the newly designed oral adapter was of decreased velocity since very little, if any, of the droplets were trapped in the simulated esophagus portion of the simulated respiratory system (Table I). Approximately 100% of the delivered dose reached the simulated respiratory system. When the newly designed oral adapter fitted to the triamcinolone aerosol was replaced with a conventional actuator, only about 50% of the delivered dose reached the simulated respiratory system (Table III). These results clearly indicate that the newly designed adapter reduces the velocity of the emitted dose and allows the dose to be carried in the airstream to the simulated respiratory system. These values can be compared to approximately 58–62% of the delivered dose of beclomethasone dipropionate trapped in the simulated esophagus portion of the simulated respiratory system (Table II). With both products, the amount trapped in the simulated esophagus and oral cavity of the simulated respiratory system increased as the vacuum (air flow) was decreased from 75 to 25 mm Hg (Tables I and II).

Another important aspect in determining the effectiveness of the particles being delivered through an aerosol system is a determination of the amount of active ingredient remaining behind in the oral inhalation adapter. As can be seen from Table I, approximately 50% of the dose delivered through the valve stem (Table IV) actually was emitted through the newly designed oral inhalation adapter. This value of 50% retention in the adapter was consistent based on the analysis of at least 10 units. Table IV indicates the amount of triamcinolone dispensed through the valve stem (~200 μg), and Table V shows that approximately 100 μg of active ingredient actually was delivered through the oral inhalation adapter to the entrance to the simulated respiratory system. Approximately 50 μg of beclomethasone dipropionate was delivered through the valve stem when actuated directly into methanol (Table VI), and approximately the same amount was delivered through the commercially available adapter when actuated onto the Florence flask (Table VII).

Table VII—Recovery of Beclomethasone Dipropionate Delivered through Commercially Available Adapter Using Florence Flask as Collection Chamber [a]

Number of Actuations	Absorbance at 239 nm	Beclomethasone Dipropionate per Actuation, μg	Percent Recovered per Actuation [b]
15	0.225	46.9	97.8
20	0.325	50.8	101.6
30	0.490	51.0	102.0

[a] Average of three determinations. [b] Label indicated 50 μg of beclomethasone dipropionate/actuation.

Table VIII—Amount of Triamcinolone Acetonide Recovered from Glass Fiber Filter Paper [a]

Number of Actuations	Absorbance at 237 nm	Triamcinolone Acetonide per Actuation, μg	Percent Recovered per Actuation [b]
3	0.20	200	100.0
6	0.38	190	95.0
9	0.59	197	98.5
12	0.76	190	95.0
18	1.20	200	100.0

[a] Average of two determinations. Label indicated 200 μg of triamcinolone acetonide/actuation. [b] Similar results were obtained at vacuums of 75 and 400 mm Hg.

The reliability of the analytical procedures was determined in several ways (Tables VI and VIII). The values for the triamcinolone acetonide and beclomethasone dipropionate corresponded to the labeled quantities of active ingredient indicated for each product.

No essential change in the quantity of steroid extracted from the glass fiber filter was noted as the vacuum was varied (Table VIII). Therefore, it was assumed that the steroid did not escape through the collection filter at high pressures and that the steroid was not misdirected from the filter at lower pressures. A vacuum of 75 mm Hg was selected since it simulated the normal lung inspiration capacity. These results also indicated that there was no interference in the spectrophotometric reading by either the propellant or any methanol-soluble extractive from the filter paper.

CONCLUSIONS

On the basis of the results, this simulated respiratory system can be used to evaluate the deposition properties of the dose delivered through the oral inhalation adapter. The newly designed adapter delivered almost 100% of the dose dispensed from the adapter while the commercially available adapter delivered about 38–42% of the spray through the simulated respiratory system. This newly designed oral inhalation adapter can be useful in delivering a greater portion of the emitted dose to the desired area of the respiratory system.

REFERENCES

(1) W. L. Hayton, *J. Am. Pharm. Assoc.*, **NS 16,** 201 (1976).

(2) A. W. Karig, G. E. Peck, and G. J. Sperandio, *J. Pharm. Sci.*, **62,** 811 (1973).

(3) J. S. G. Cox, J. E. Beach, A. M. J. N. Blair, A. J. Clarke, J. King, T. B. Lee, D. E. E. Loveday, G. F. Moss, T. S. C. Orr, J. T. Ritchie, and P. Sheard, *Adv. Drug Res.*, **5,** 115 (1970).

(4) A. C. Guyton, "Textbook of Medical Physiology," 2nd ed., Saunders, Philadelphia, Pa., 1961, p. 517.

ACKNOWLEDGMENTS

Presented at the Industrial Pharmaceutical Technology Section, APhA Academy of Pharmaceutical Sciences, Orlando meeting, November 1976.

Thiazole Derivatives as Potential Chemotherapeutic Agents: Homolytic Arylation of Thiazole with Phenylazotriphenylmethane

G. FENECH ˣ, A. CHIMIRRI, and R. FICARRA

Received April 14, 1977, from the *Istituto di Chimica Farmaceutica, Università di Messina, Via dei Verdi, 98100 Messina, Italy.* Accepted for publication February 7, 1978.

Abstract □ The homolytic arylation of thiazole with phenylazotriphenylmethane (as a free radical source) was carried out to explore the potential chemotherapeutic activity of the resulting triphenylmethyl derivatives. The experimental data differed from similar results on other isosteric heterocycles: one compound only was obtained, having both phenyl and triphenylmethyl groups in the heterocyclic nucleus. The structure of 2-phenyl-5-triphenylmethylthiazole was established by IR, ^{1}H-NMR, and mass spectroscopy. In particular, the mass spectral investigation indicated the cleavage of the 2,3- and 4,5-ring bonds, in contrast with the usual behavior of other thiazole derivatives with no triphenylmethyl substituent.

Keyphrases □ Thiazole—homolytic arylation with phenylazotriphenylmethane, 2-phenyl-5-triphenylmethylthiazole synthesized □ 2-Phenyl-5-triphenylmethylthiazole—synthesized by homolytic arylation of thiazole with phenylazotriphenylmethane □ Arylation, homolytic—thiazole with phenylazotriphenylmethane, 2-phenyl-5-triphenylmethylthiazole synthesized

In the synthesis of thiazole derivatives potentially useful as drugs, research has focused on specifically substituted 2,5-thiazole derivatives. Therapeutic activity related to the thiazole nucleus varies according to both type and position of the substituent; in fact, several derivatives are chemotherapeutic (1–6), hypnotic (7, 8), anesthetic (9, 10), and anti-inflammatory (11) agents.

The chemotherapeutic action is usually related to an electron-withdrawing group on C-5, while the activity is inhibited by introducing a methyl substituent in the 4-position (2). A methyl group on C-4 and an electron-donor group on C-5 promote either a sedative–hypnotic or anesthetic action[1]. A substituent on C-2 has neither determining nor selective influence on the activity.

The present work investigated the influence of the triphenylmethyl substituent on the potential chemotherapeutic activity of the thiazole nucleus. Homolytic arylation of thiazole with phenylazotriphenylmethane as a free radical source yielded 2-phenyl-5-triphenylmethylthiazole (I). The triphenylmethyl group could be relevant for its electronic characteristics and because of its steric effects. In fact, triphenylmethylpenicillin (14) exhibits high resistance to penicillinase.

From a synthetic standpoint, the preparation of I was compared with the syntheses of other arylating agents (15–20) and isosteric five- and six-membered heterocycles such as furan, thiophene, and pyridine (21–25). The reaction could proceed either by addition of the radical species followed by oxidation of the two dihydro derivative isomers obtained with *o*-chloranil, with furan and thiophene (21, 22), or by addition and spontaneous oxidation, as with pyridine (23–25), whose C-2 and C-5 positions have different electronic densities as in thiazole.

[1] A 4-methyl-5-nitro-substituted derivative is, on the contrary, an antipsychotic agent (12); 2,4-diamino-5-phenylthiazole is an analeptic drug (13).

EXPERIMENTAL

Phenylazotriphenylmethane—The Gomberg reaction (26) with bromotriphenylmethane and phenylhydrazine resulted in an almost quantitative yield of phenylazotriphenylmethane. Although alternative methods were proposed (27–29), this reaction was preferred because of its excellent yield and the easy spontaneous oxidation of the starting hydrazo compound, which prevents the use of oxidative agents.

Decomposition of Phenylazotriphenylmethane in Thiazole—A 0.487-g portion of phenylazotriphenylmethane (100:1) was added to 10 ml of thiazole. The mixture was refluxed for 24 hr at 75°, and the reagent decomposed to give the two radicals (30). The resulting clear solution was allowed to evaporate for several days at room temperature. After complete evaporation of the thiazole, the resulting sticky mixture was washed repeatedly with ether. A slightly soluble, whitish compound was separated, mp 175–180° (yield 15%). Its slight solubility in ether caused some losses; however, any other solvent either led to a less pure product or rapidly dissolved it. A similar procedure, using a smaller amount of thiazole, led to resinous products that were not easily identifiable.

Anal.—Calc. for $C_{28}H_{21}NS$: C, 83.35; H, 5.25; N, 3.47; S, 7.93. Calc. for $C_{28}H_{23}NS$: C, 82.94; H, 5.72; N, 3.45; S, 7.89. Found: C, 82.80; H, 5.29; N, 3.48; S, 7.68.

TLC—A chloroform solution containing 25 mg/ml was prepared. TLC was carried out on silica gel[2] 60 F_{254} plates with chloroform–methanol (9:1 v/v) as the eluent. Only one spot was detected, R_f 0.67.

Spectral Data—The IR spectrum[3] was measured as a mineral oil mull. The ^{1}H-NMR spectrum was recorded at room temperature on a spectrometer[4] from a solution in deuterochloroform with tetramethylsilane as the internal standard; chemical shifts are in δ (parts per million). A double-focusing mass spectrometer[5] was used. The most relevant fragments of 2-phenyl-5-triphenylmethylthiazole were: *m/e* 404 (20%), 403 (100), 371 (10), 327 (20), 326 (100), 300 (30), 299 (100), 267 (40), 243 (30), 223 (50), 222 (50), 221 (100), 210 (30), 190 (80), 179 (60), 178 (100), 166 (60), 165 (100), 121 (100), 104 (70), 103 (40), 102 (20), 77 (60), 57 (30), 51 (30), and 45 (30).

RESULTS AND DISCUSSION

Homolytic arylation of the thiazole nucleus gave only one compound, and it contained both phenyl and triphenylmethyl groups. The position of substituents and the type of heterocyclic ring (thiazole or dihydrothiazole) were determined by elemental analysis, TLC behavior, negative reaction with *o*-cloranil, and spectral data.

The IR spectrum was of little diagnostic significance, and the main absorption frequencies (centimeters^{-1}) were assigned by comparison with those of unsubstituted thiazole, phenylazotriphenylmethane, and other arylthiazoles (31): 3042 (ν-CH), 1590 and 1485 (ν-C=N and ν-C=C), 1265–1072 (δ-CH), 760, 752, 740, 700, and 690 (γ-CH) cm^{-1}.

The ^{1}H-NMR spectrum excluded the possibility that the synthesized product was a thiazolidine derivative, all resonance signals falling in the characteristic region of aromatic protons (7.49s, 7.88m, 7.35m, and 7.25s ppm). Furthermore, the presence in the thiazole ring of the phenyl and triphenylmethyl groups, on C-2 and C-5, respectively, was established on the following grounds.

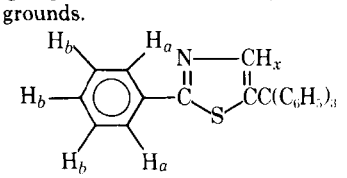

I

[2] Merck.
[3] Perkin-Elmer model 257.
[4] Varian T-60 A (60 MHz).
[5] Varian CH7.

0022-3549/78/1000-1432$01.00/0
© 1978, American Pharmaceutical Association

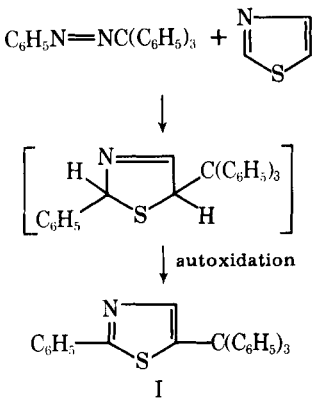

I

Scheme I

The chemical shift at 7.49 ppm can be attributed to proton H_x on C-4 (I), whereas it is found at 7.86 ppm (31) in the unsubstituted thiazole. If the inductive effects of the electronegative substituents in the ring were considered by themselves, this absorption should take place at lower fields. However, the molecular models show that this proton is shielded by the ring current of a phenyl ring of the triphenylmethyl substituent at C-5, thus shifting to higher fields. If the triphenylmethyl group were in the 4-position, for the same effect, the proton at C-5 could not fall at 7.49 ppm but at a higher value than that found in unsubstituted thiazole, *i.e.*, 7.27 ppm.

The singlet at 7.25 ppm is due to the triphenylmethyl group, not only because a sharp singlet occurs at the same position in bromotriphenylmethane but also because the integrated signal corresponds to the theoretical data.

Moreover, the H_a protons of the phenyl group are observed at a lower field (7.88 ppm) than those related to the H_b protons (7.35 ppm). Their different resonances confirm the 2-position for the phenyl substituent; consequently, its *ortho*-protons, in deuterochloroform, are deshielded, as observed (31), on account of the nitrogen anisotropy and of the π-electron deficiency at the 2-position of thiazole. If the phenyl were in the 5-position, its protons should have originated a singlet. On the other hand, this group could not be on C-4 because of steric hindrance of the large triphenylmethyl group on C-5. On these grounds, it was established that the synthesis proceeded according to Scheme I.

Further data from the mass spectral investigation support these conclusions. The peak of the molecular ion is found at *m/e* 403, in agreement with the molecular weight of the phenyltriphenylmethylthiazole, thus excluding a dihydrothiazole derivative.

The base peak at *m/e* 326 corresponds to $(M^+ - C_6H_5\cdot)$: *m/e* 403 − 77. The phenyl radical loss originates from the triphenylmethyl group, no cleavage with loss of a phenyl radical being reported (32) to occur from phenyl-substituted thiazoles. Moreover, this fragmentation mode is confirmed by the *m/e* 210 $[SCC(C_6H_5)_2]^+$, 178 $[CC(C_6H_5)_2]^+$, 121 $(C_6H_5CS)^+$, and 103 $(C_6H_5CN)^+$ peaks. The first ones arise from phenyl radical loss from the triphenylmethyl group; the latter peaks confirm that

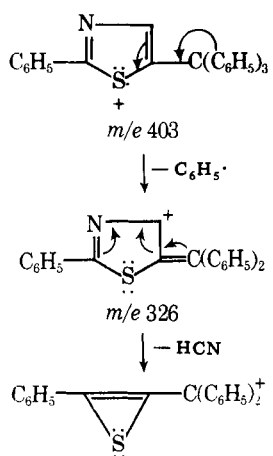

Scheme II

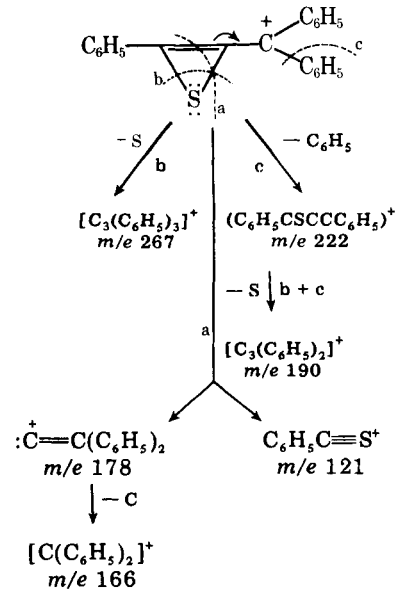

Scheme III

a phenyl radical is still bound to the thiazole C-2 (between N and S), according to previous reports (32) dealing with 2-phenylthiazoles.

To establish the true position of the triphenylmethyl group, the $(M^+ - C_6H_5 - HCN)^+$ peak at *m/e* 299 proved essential. As mentioned previously, when a phenyl substituent is attached to C-2, HCN can never originate from thiazole fragmentation by 1,2- and 3,4-bond cleavage, according to the Clarke *et al.* process (33), as confirmed both on 2-deuterothiazole (34, 35) and on other thiazole derivatives (36, 37). On the contrary, the cleavage of the ring atoms occurred at the 2,3- and 4,5-bond sites, as already established (38) for 2,5-diphenyl-1,3,4-oxadiazole. Therefore, the triphenylmethyl substituent competes with the bond ring cleavage typical of the thiazole nucleus (39). As a consequence, a thiirene derivative at *m/e* 299 is obtained (Scheme II), which allows assignment of the triphenylmethyl group to the 5-position of the thiazole ring, thus confirming the previously assigned structure of the synthesized product.

The peaks at *m/e* 121, 178, and 166 are of high intensity and could arise from the thiirene ion (Scheme III) according to pathway a, while peaks at *m/e* 267, 222, and 190 could follow routes b, c, and b + c. The peak at *m/e* 210 $[SCC(C_6H_5)_2]^+$ could also arise from the same thiirene ionic species.

Most of the above fragments could also originate from the $(M - C_6H_5)^+$ ion by an alternative thiazole cleavage according to Scheme IV, a or d, as observed (37) for alkylthiazoles; however, it would then not be possible to explain the peak at *m/e* 299. Therefore, the bond cleavages take place according to Schemes II and III.

Following the observation that the thiazole nucleus fragments in a different manner from the scheme proposed previously (33–37), further investigations were directed to examine whether other peaks could originate by cleavage of the 1,2- and 3,4-ring bonds of the thiazole. The fairly abundant *m/e* 103 peak $(C_6H_5C{\equiv}N)$ confirms such a cleavage. The fragment can originate by preliminary expulsion of the *m/e* 243 $[C(C_6H_5)_3]^+$ followed by the typical cleavage depicted in Scheme V (33), as confirmed by the presence of peaks at *m/e* 57 and 45, usually found

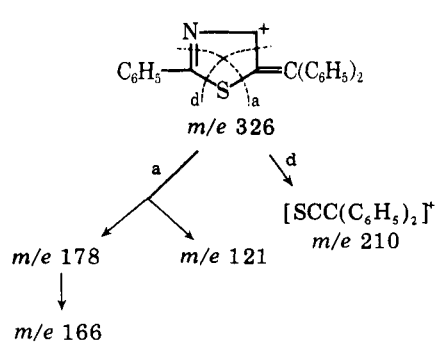

Scheme IV

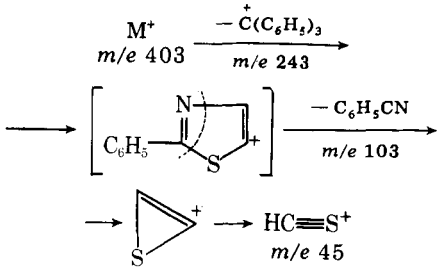

Scheme V

in thiazole derivatives with electron-withdrawing groups on C-5 or C-2 (36). The two peaks at *m/e* 77 and 51 can be attributed to the $C_6H_5^+$ and $C_4H_3^+$ radical ions.

REFERENCES

(1) A. Burger, "Medicinal Chemistry", 3rd ed., Wiley–Interscience, New York, N.Y., 1970, pp. 542, 575, 589.

(2) M. Robba and R. C. Moreau, *Ann. Pharm. Fr.*, **22,** 201 (1964).

(3) A. D. Bortwich, M. W. Foxton, B. Y. Gray, G. I. Gregory, P. W. Seale, and W. K. Warburton, *J. Chem. Soc. Perkin Trans. 1,* **1973,** 2769.

(4) Y. Hasegawa, *Chem. Abstr.*, **80,** 117149y (1974).

(5) S. Ueno, T. Ohtake, Y. Suzuki, K. Satomi, and A. Sasaki, *ibid.*, **81,** 21795a (1974).

(6) Y. Hasegawa, M. Dohya, S.Hohjo, H. Kawada, E. Yoshinaga, and H. Ito, *ibid.*, **81,** 34527q (1974).

(7) U. H. Lindberg, *ibid.*, **76,** 148733f (1972).

(8) G. Herbertz, German Offen. 2,236,796 (1974); through *Chem. Abstr.*, **80,** 120915a (1974).

(9) Meiji Confectionary Co., Fr. 2,039,748 (1971), through *Chem. Abstr.*, **75,** 112867t (1971).

(10) K. Naber, D. Maroske, K. H. Bichler, and T. H. Thaut, *Chem. Abstr.*, **76,** 68117t (1972).

(11) Z. S. Ariyan and W. A. Harrison, German Offen. 2,331,246 (1974); through *Chem. Abstr.*, **80,** 95929y (1974).

(12) Z. S. Ariyan and W. A. Harrison, German Offen. 2,350,223 (1974), U.S. Appl. 295,503 (1972); through *Chem. Abstr.*, **81,** 96459c (1974).

(13) A. Burger, "Medicinal Chemistry," 3rd ed., Wiley–Interscience, New York, N.Y., 1970, p. 1407.

(14) E. G. Brain, F. P. Doyle, K. Hardy, A. A. W. Long, M. D. Mehta, D. Miller, J. H. C. Nayler, M. J. Soulal, E. R. Stove, and G. R. Thomas, *J. Chem. Soc.*, **1962,** 1445.

(15) D. H. Hey, *ibid.*, **1934,** 1966.

(16) W. S. Grieve and D. H. Hey, *ibid.*, **1934,** 1797.

(17) A. W. Johnson, *ibid.*, **1946,** 895.

(18) J. Degani, M. Pallotti, and A. Tundo, *Ann. Chim.*, **51,** 434 (1961).

(19) L. Benati and M. Tiecco, *Bol. Sci. Fac. Chim. Ind. Bologna,* **24,** 225 (1966).

(20) H. J. M. Dou, G. Vernin, and J. Metzger, *Tetrahedron Lett.*, **1967,** 2223.

(21) C. M. Camaggi, R. Leardini, M. Tiecco, and A. Tundo, *J. Chem. Soc. B,* **1969,** 1251.

(22) L. Benati, N. La Barba, M. Tiecco, and A. Tundo, *ibid.*, **1969,** 1253. *Ibid.*, **1970,** 1443.

(23) R. Huisgen and H. Nakaten, *Ann.*, **1954,** 70.

(24) D. H. Hey, C. J. M. Stirling, and G. H. Williams, *J. Chem. Soc.*, **1955,** 3963.

(25) R. Grashey and R. Huisgen, *Chem. Ber.*, **92,** 2641 (1959).

(26) M. Gomberg, *ibid.*, **30,** 2044 (1897).

(27) A. Baeyer and V. Villiger, *ibid.*, **35,** 3017 (1902).

(28) E. Popper, *ibid.*, **55,** 1822 (1922).

(29) R. Meyer and W. Gerloff, *ibid.*, **58,** 2440 (1925).

(30) H. Willand, E. Popper, and H. Seefried, *ibid.*, **55,** 1816 (1922).

(31) G. Vernin, J. P. Aune, H. J. N. Dou, and J. Metzger, *Bull. Soc. Chim. Fr.*, **1967,** 4253.

(32) J. P. Aune and J. Metzger, *ibid.*, **1972,** 3536.

(33) G. M. Clarke, R. Grigg, and D. H. Williams, *J. Chem. Soc. (B),* **1966,** 339.

(34) R. G. Cooks, I. Howe, S. W. Tam, and D. H. Williams, *J. Am. Chem. Soc.*, **90,** 4064 (1968).

(35) I. N. Bojesen, J. H. Hog, J. T. Nielsen, I. B. Petersen, and K. S. Schaumburg, *Acta Chem. Scand.*, **25,** 2739 (1971).

(36) A. Friedmann, G. Salmone, G. Curet, R. Phan Tan Luu, and J. Metzger, *C. R. Acad. Sci. Paris,* **269c,** 273 (1969).

(37) R. Tabacchi, *Helv. Chim. Acta,* **57,** 324 (1974).

(38) J. L. Cotter, *J. Chem. Soc.*, **1964,** 5491.

(39) H. Budzikiewicz, C. Djerassi, and D. H. Williams, "Mass Spectrometry of Organic Compounds," Holden-Day, London, England, 1967, p. 634.

Improved Synthesis of *N*-(2,6-Dimethylphenylcarbamoylmethyl)iminodiacetic Acid and Analogs

H. DONALD BURNS *x, DAVID T. SOWA, and LUIGI G. MARZILLI

Received November 21, 1977, from the *Division of Nuclear Medicine and Department of Chemistry, Johns Hopkins University, Baltimore, MD 21218.* Accepted for publication February 21, 1978.

*Present address: Department of Radiation Therapy and Nuclear Medicine, Hahnemann Medical College, Philadelphia, PA 19102.

Abstract □ A new synthesis of *N*-(2,6-dimethylphenylcarbamoylmethyl)iminodiacetic acid directly from nitrilotriacetic acid was developed. Six analogs also were synthesized. Their technetium Tc 99m complexes were prepared and characterized. Electrophoresis and chromatography were used to determine the radiochemical purity of each complex.

Keyphrases □ *N*-(2,6-Dimethylphenylcarbamoylmethyl)iminodiacetic acid—and analogs, synthesized, ^{99m}Tc-complexes prepared □ Technetium Tc 99m complexes—various substituted iminodiacetic acids prepared □ Iminodiacetic acids, substituted—synthesized, ^{99m}Tc-complexes prepared □ Radiopharmaceuticals, potential—^{99m}Tc-complexes of various substituted iminodiacetic acids prepared

In recent years, considerable attention has been given to the development of new γ-emitting radiopharmaceuticals for the evaluation of the hepatobiliary function. Currently, the only commercially available agent of this type is rose bengal sodium I 131 (1). The relatively poor physical characteristics of iodine-131 have hindered the widespread use of this radiopharmaceutical.

DISCUSSION

Because of the nearly ideal physical properties of technetium Tc 99m and its widespread availability in most nuclear medicine laboratories,

0022-3549/78/1000-1434$01.00/0

© 1978, American Pharmaceutical Association

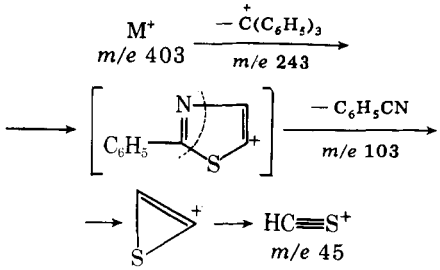

Scheme V

in thiazole derivatives with electron-withdrawing groups on C-5 or C-2 (36). The two peaks at *m/e* 77 and 51 can be attributed to the $C_6H_5^+$ and $C_4H_3^+$ radical ions.

REFERENCES

(1) A. Burger, "Medicinal Chemistry", 3rd ed., Wiley–Interscience, New York, N.Y., 1970, pp. 542, 575, 589.

(2) M. Robba and R. C. Moreau, *Ann. Pharm. Fr.*, **22,** 201 (1964).

(3) A. D. Bortwich, M. W. Foxton, B. Y. Gray, G. I. Gregory, P. W. Seale, and W. K. Warburton, *J. Chem. Soc. Perkin Trans. 1,* **1973,** 2769.

(4) Y. Hasegawa, *Chem. Abstr.*, **80,** 117149y (1974).

(5) S. Ueno, T. Ohtake, Y. Suzuki, K. Satomi, and A. Sasaki, *ibid.*, **81,** 21795a (1974).

(6) Y. Hasegawa, M. Dohya, S.Hohjo, H. Kawada, E. Yoshinaga, and H. Ito, *ibid.*, **81,** 34527q (1974).

(7) U. H. Lindberg, *ibid.*, **76,** 148733f (1972).

(8) G. Herbertz, German Offen. 2,236,796 (1974); through *Chem. Abstr.*, **80,** 120915a (1974).

(9) Meiji Confectionary Co., Fr. 2,039,748 (1971), through *Chem. Abstr.*, **75,** 112867t (1971).

(10) K. Naber, D. Maroske, K. H. Bichler, and T. H. Thaut, *Chem. Abstr.*, **76,** 68117t (1972).

(11) Z. S. Ariyan and W. A. Harrison, German Offen. 2,331,246 (1974); through *Chem. Abstr.*, **80,** 95929y (1974).

(12) Z. S. Ariyan and W. A. Harrison, German Offen. 2,350,223 (1974), U.S. Appl. 295,503 (1972); through *Chem. Abstr.*, **81,** 96459c (1974).

(13) A. Burger, "Medicinal Chemistry," 3rd ed., Wiley–Interscience, New York, N.Y., 1970, p. 1407.

(14) E. G. Brain, F. P. Doyle, K. Hardy, A. A. W. Long, M. D. Mehta, D. Miller, J. H. C. Nayler, M. J. Soulal, E. R. Stove, and G. R. Thomas, *J. Chem. Soc.*, **1962,** 1445.

(15) D. H. Hey, *ibid.*, **1934,** 1966.

(16) W. S. Grieve and D. H. Hey, *ibid.*, **1934,** 1797.

(17) A. W. Johnson, *ibid.*, **1946,** 895.

(18) J. Degani, M. Pallotti, and A. Tundo, *Ann. Chim.*, **51,** 434 (1961).

(19) L. Benati and M. Tiecco, *Bol. Sci. Fac. Chim. Ind. Bologna,* **24,** 225 (1966).

(20) H. J. M. Dou, G. Vernin, and J. Metzger, *Tetrahedron Lett.*, **1967,** 2223.

(21) C. M. Camaggi, R. Leardini, M. Tiecco, and A. Tundo, *J. Chem. Soc. B,* **1969,** 1251.

(22) L. Benati, N. La Barba, M. Tiecco, and A. Tundo, *ibid.*, **1969,** 1253. *Ibid.*, **1970,** 1443.

(23) R. Huisgen and H. Nakaten, *Ann.*, **1954,** 70.

(24) D. H. Hey, C. J. M. Stirling, and G. H. Williams, *J. Chem. Soc.*, **1955,** 3963.

(25) R. Grashey and R. Huisgen, *Chem. Ber.*, **92,** 2641 (1959).

(26) M. Gomberg, *ibid.*, **30,** 2044 (1897).

(27) A. Baeyer and V. Villiger, *ibid.*, **35,** 3017 (1902).

(28) E. Popper, *ibid.*, **55,** 1822 (1922).

(29) R. Meyer and W. Gerloff, *ibid.*, **58,** 2440 (1925).

(30) H. Willand, E. Popper, and H. Seefried, *ibid.*, **55,** 1816 (1922).

(31) G. Vernin, J. P. Aune, H. J. N. Dou, and J. Metzger, *Bull. Soc. Chim. Fr.*, **1967,** 4253.

(32) J. P. Aune and J. Metzger, *ibid.*, **1972,** 3536.

(33) G. M. Clarke, R. Grigg, and D. H. Williams, *J. Chem. Soc. (B),* **1966,** 339.

(34) R. G. Cooks, I. Howe, S. W. Tam, and D. H. Williams, *J. Am. Chem. Soc.*, **90,** 4064 (1968).

(35) I. N. Bojesen, J. H. Hog, J. T. Nielsen, I. B. Petersen, and K. S. Schaumburg, *Acta Chem. Scand.*, **25,** 2739 (1971).

(36) A. Friedmann, G. Salmone, G. Curet, R. Phan Tan Luu, and J. Metzger, *C. R. Acad. Sci. Paris,* **269c,** 273 (1969).

(37) R. Tabacchi, *Helv. Chim. Acta,* **57,** 324 (1974).

(38) J. L. Cotter, *J. Chem. Soc.*, **1964,** 5491.

(39) H. Budzikiewicz, C. Djerassi, and D. H. Williams, "Mass Spectrometry of Organic Compounds," Holden-Day, London, England, 1967, p. 634.

Improved Synthesis of *N*-(2,6-Dimethylphenylcarbamoylmethyl)iminodiacetic Acid and Analogs

H. DONALD BURNS *x, DAVID T. SOWA, and LUIGI G. MARZILLI

Received November 21, 1977, from the *Division of Nuclear Medicine and Department of Chemistry, Johns Hopkins University, Baltimore, MD 21218.* Accepted for publication February 21, 1978.

*Present address: Department of Radiation Therapy and Nuclear Medicine, Hahnemann Medical College, Philadelphia, PA 19102.

Abstract □ A new synthesis of *N*-(2,6-dimethylphenylcarbamoylmethyl)iminodiacetic acid directly from nitrilotriacetic acid was developed. Six analogs also were synthesized. Their technetium Tc 99m complexes were prepared and characterized. Electrophoresis and chromatography were used to determine the radiochemical purity of each complex.

Keyphrases □ *N*-(2,6-Dimethylphenylcarbamoylmethyl)iminodiacetic acid—and analogs, synthesized, ^{99m}Tc-complexes prepared □ Technetium Tc 99m complexes—various substituted iminodiacetic acids prepared □ Iminodiacetic acids, substituted—synthesized, ^{99m}Tc-complexes prepared □ Radiopharmaceuticals, potential—^{99m}Tc-complexes of various substituted iminodiacetic acids prepared

In recent years, considerable attention has been given to the development of new γ-emitting radiopharmaceuticals for the evaluation of the hepatobiliary function. Currently, the only commercially available agent of this type is rose bengal sodium I 131 (1). The relatively poor physical characteristics of iodine-131 have hindered the widespread use of this radiopharmaceutical.

DISCUSSION

Because of the nearly ideal physical properties of technetium Tc 99m and its widespread availability in most nuclear medicine laboratories,

0022-3549/78/1000-1434$01.00/0

© 1978, American Pharmaceutical Association

a search has been underway to develop ^{99m}Tc-labeled hepatobiliary radiopharmaceuticals. ^{99m}Tc-Complexes of the following ligands have been suggested for the evaluation of hepatobiliary function: dihydrothioctic acid (2), mercaptoisobutyric acid (3), penicillamine (4), tetracycline (5), pyridoxylideneglutamate (6, 7), and *N*-(2,6-dimethylphenylcarbamoylmethyl)iminodiacetic acid (I) (8). The most promising of these hepatobiliary radiopharmaceuticals appears to be the ^{99m}Tc-complex of I.

Callery *et al.* (9) first prepared I as a lidocaine analog with an iminodiacetic acid functional group capable of forming a stable complex with ^{99m}Tc. The rapid and extensive biliary excretion of ^{99m}Tc-I after intravenous injection into mice led to intensive investigation of this complex as a potential hepatobiliary radiopharmaceutical. The original synthesis of I required 48 hr and involved treatment of 2,6-xylidine with chloroacetyl chloride to form 2-chloro-2′,6′-dimethylacetanilide. Nucleophilic displacement of the chloride ion by the nitrogen of iminodiacetic acid gave I in an overall yield of 20%.

As part of a study relating molecular structure to biliary excretion of ^{99m}Tc-radiopharmaceuticals (10), a new one-step synthesis of I was developed. The synthesis involves reaction of a pyridine solution of nitrilotriacetic acid monoanhydride (generated *in situ* by treatment of nitrilotriacetic acid with acetic anhydride in anhydrous pyridine) with 2,6-xylidine for 1 hr at 100°. By using this synthesis, I was obtained in a 69% yield with a total working time of less than 4 hr.

A series of analogs of I (II–VII, Table I) subsequently was prepared by substituting the appropriate amine for 2,6-xylidine. These analogs were prepared both to find a better hepatobiliary agent and to aid in studies of the chemistry and nature of ^{99m}Tc-I.

The ^{99m}Tc-complexes of these compounds were prepared by stannous chloride reduction of pertechnetate ion ($^{99m}TcO_4^-$) in an aqueous solution of the appropriate compound. Electrophoresis was used to evaluate the radiochemical purity of each complex. The two most common radiochemical impurities encountered in ^{99m}Tc-radiopharmaceuticals are unreduced pertechnetate ion and reduced hydrolyzed technetium (TcO_2). Electrophoresis easily separated these two impurities from most complexes. Since ^{99m}Tc-IX migrates the same distance on electrophoresis as TcO_4^-, chromatography (silica gel–acetone) was used to evaluate purity in this case.

On this chromatographic system, the complex remained at the origin while pertechnetate migrated with the solvent front. In all cases, a radiochemical purity of at least 98% was obtained. The stabilities of the complexes were evaluated by serial electrophoreses. No significant decomposition was detected for at least 4 hr after preparation. Animal biodistribution studies on the ^{99m}Tc-complexes are currently in progress and will be reported elsewhere.

^{99m}Tc-VII, which appears to have a higher uptake in the GI tract of mice than ^{99m}Tc-I, may prove to be a useful hepatobiliary agent.

EXPERIMENTAL[1]

***N*-(2,6-Dimethylphenylcarbamoylmethyl)iminodiacetic Acid (I)**—*Method A*—A suspension of nitrilotriacetic acid (5.0 g, 26 mmoles) in 40 ml of anhydrous pyridine was placed in a three-necked round-bottom flask equipped with a nitrogen inlet tube, a condensor, a calcium sulfate drying tube, and a thermometer. After flushing with nitrogen, the suspension was heated at 50° for 10 min, at which time most of the nitrilotriacetic acid had dissolved. Acetic anhydride (3.25 g, 31 mmoles) was added, and the solution was heated at 100° for 30 min. After cooling to 50°, 2,6-dimethylaniline was added and the solution was again heated at 100° for 1 hr.

Evaporation of the pyridine *in vacuo* left a yellow oil, which was dissolved in a minimal amount of aqueous ammonia. The solution was extracted three times with an equal volume of ether and then treated with decolorizing carbon[2]. After filtering, the near colorless solution was acidified to pH 3, resulting in formation of a white precipitate. Recrystallization from ethanol–water yielded 3.0 g (39.2%) of white needles, mp 211–213°; IR (mineral oil): 3310 (NH) and 1660–1720 (broad, acid and amide C=O) cm^{-1}; PMR (dimethyl sulfoxide-d_6): δ 2.14 (s, 6H, Ar-CH_3), 3.50 (s, 2H, $NCOCH_2N$), 3.58 (s, 4H, NCH_2CO), and 7.04 (s, 3H, Ar-H) ppm.

[1] Proton magnetic resonance (PMR) spectra were obtained on a Perkin-Elmer Hitachi R12A spectrometer with chemical shifts reported relative to tetramethylsilane. IR spectra were obtained on a Pye-Unicam SP1000 spectrophotometer. Melting points were determined in a Mel-Temp apparatus and are uncorrected. Elemental analyses were performed by Robertson Microanalytical Laboratory, Florham Park, N.J.

[2] Norit, Fisher Scientific, Fair Lawn, N.J.

Table I—Synthetic Analogs of *N*-(2,6-Dimethylphenylcarbamoylmethyl)iminodiacetic Acid

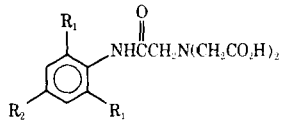

Compound	R_1	R_2	Yield, %	Technetium Complexes: Electrophoresis, R_s[a]	Technetium Complexes: Chromatography, R_f
I	CH_3	H	69	0.68	0
II	H	H	61	0.68	0
III	H	CH_3	50	0.66	0
IV	CH_3	Br	48	0.65	0
V	H	NO_2	31	0.66	0
VI	H	COOH	70	0.98	0
VII	H	I	62	0.65	0
TcO_2				0	0
TcO_4^-				1	1

[a] See *Experimental* for explanation.

Anal.—Calc. for $C_{14}H_{18}N_2O_5$: C, 57.13; H, 6.16; N, 9.52. Found: C, 57.19; H, 6.19; N, 9.50.

Method B—This method was the same as Method A, except that the molar ratio of acetic anhydride to nitrilotriacetic acid was increased from 1.2:1 to 1.5:1. Reaction of nitrilotriacetic acid (5.0 g, 26 mmoles), acetic anhydride (3.98 g, 39 mmoles), and 2,6-dimethylaniline yielded (after recrystallization) 5.24 g (69%) of I.

***N*-(Phenylcarbamoylmethyl)iminodiacetic Acid (II)**—Compound II was prepared by Method A from nitrilotriacetic acid (5.0 g, 26 mmoles), acetic anhydride (3.25 g, 31 mmoles), and aniline (2.42 g, 26 mmoles). After recrystallization from ethanol–water, 4.25 g (61%) of II was obtained, mp 153° dec.; IR (mineral oil): 3370 (NH) and 1670–1720 (broad, acid and amide C=O) cm^{-1}; PMR (dimethyl sulfoxide-d_6): δ 3.50 (s, 2H, NCH_2CON), 3.58 (s, 4H, NCH_2CO_2), and 7.4 (multiplet, 5H, Ar-H) ppm.

Anal.—Calc. for $C_{12}H_{14}N_2O_5 \cdot H_2O$: C, 50.70; H, 5.67; N, 9.85. Found: C, 50.35; H, 5.72; N, 9.92.

***N*-(4-Methylphenylcarbamoylmethyl)iminodiacetic Acid (III)**—Reaction of nitrilotriacetic acid (15.29 g, 0.08 mole), acetic anhydride (12.25 g, 0.12 mole), and *p*-toluidine (8.57 g, 0.08 mole) (Method B) gave III. Recrystallization from ethanol–water yielded 11.1 g (49.6%) of white crystalline III, mp 205.5–206°; IR (mineral oil): 3300 (NH) and 1720 and 1690 (C=O) cm^{-1}; PMR (dimethyl sulfoxide-d_6): δ 2.23 (s, 3H, $ArCH_3$), 3.45 (s, 2H, $NCOCH_2N$), 3.53 (s, 4H, NCH_2CO_2), 7.10 (d, 2H, Ar-H), and 7.45 (d, 2H, Ar-H) ppm.

Anal.—Calc. for $C_{13}H_{16}N_2O_5$: C, 55.71; H, 5.75; N, 9.99. Found: C, 55.95; H, 5.55; N, 10.29.

***N*-(4-Bromo-2,6-dimethylphenylcarbamoylmethyl)iminodiacetic Acid (IV)**—Reaction of nitrilotriacetic acid (4.47 g, 0.023 mole), acetic anhydride (3.58 g, 0.035 mole), and 4-bromo-2,6-dimethylaniline hydrobromide (5.53 g, 0.023 mole) (Method B) yielded (after recrystallization from ethanol–water) 4.16 g (47.7%) of IV, mp 198–199° dec.; IR (mineral oil): 3310 (NH) and 1680–1720 (broad, acid and amide C=O) cm^{-1}; PMR: δ 2.22 (s, 6H, $ArCH_3$), 3.36 (s, 2H, NCH_2CON), 3.49 (s, 4H, NCH_2CO_2), and 7.23 (s, 2H, Ar-H) ppm.

Anal.—Calc. for $C_{14}H_{17}BrN_2O_5 \cdot H_2O$: C, 42.98; H, 4.89; N, 7.16. Found: C, 42.90; H, 4.56; N, 7.24.

***N*-(4-Nitrophenylcarbamoylmethyl)iminodiacetic Acid (V)**—Reaction of nitrilotriacetic acid (15.0 g, 0.078 mole), acetic anhydride (11.94 g, 0.117 mole), and 4-nitroaniline (10.77 g, 0.078 mole) (Method B) followed by recrystallization from ethanol–water resulted in formation of 7.49 g (31%) of V, mp 250° dec.; IR (mineral oil): 3200 (NH) and 1690 and 1720 (C=O) cm^{-1}; NMR: δ 3.58 (s, 6H, NCH_2CO), 7.88 (d, 2H, Ar-H), and 8.22 (d, 2H, Ar-H) ppm.

Anal.—Calc. for $C_{12}H_{13}N_3O_7$: C, 46.31; H, 4.21; N, 13.50. Found: C, 46.04; H, 4.50; N, 13.50.

***N*-(4-Carboxyphenylcarbamoylmethyl)iminodiacetic Acid (VI)**—Reaction of nitrilotriacetic acid (5.0 g, 26 mmoles) and acetic anhydride (3.25 g, 26 mmoles) (Method A) gave (after recrystallization from ethanol–water) 5.67 g (70.3%) of VI, mp 227–229°; IR (mineral oil): 3350 (weak, NH) and 1690 (acid and amide C=O) cm^{-1}; PMR (dimethyl sulfoxide-d_6): δ 3.58 (s, 6H, NCH_2CO), 7.73 (d, 2H, Ar-H), and 7.97 (d, 2H, Ar-H) ppm.

Anal.—Calc. for $C_{13}H_{14}N_2O_7 \cdot H_2O$: C, 48.90; H, 4.74; N, 8.78. Found: C, 48.80; H, 4.65; N, 8.61.

***N*-(4-Iodophenylcarbamoylmethyl)iminodiacetic Acid (VII)**—Compound VII was obtained from nitrilotriacetic acid (4.47 g, 0.023 mole), acetic anhydride (3.58 g, 0.035 mole), and 4-iodoaniline (5.12 g, 0.023 mole) (Method B). Recrystallization from 80% aqueous ethanol yielded white crystals, 5.62 g (62%), mp 194° dec.; IR (mineral oil): 3300 (NH) and 1710 and 1675 (C=O) cm^{-1}; PMR (dimethyl sulfoxide-d_6): δ 3.51 (s, 2H, NCH_2CON), 3.55 (s, 4H, NCH_2CO_2), 7.48 (d, 2H, Ar-H), and 7.60 (d, 2H, Ar-H) ppm.

Anal.—Calc. for $C_{12}H_{13}IN_2O_5$: C, 36.75; H, 3.34; N, 7.14. Found: C, 36.73; H, 3.51; N, 7.25.

Preparation of ^{99m}Tc-Complexes—A solution of 10 mg of compound in 0.5 ml of 0.1 *N* NaOH was prepared, and the pH was adjusted to 5–5.5 with 0.05 *N* HCl. After addition of 0.3 ml of generator eluate (obtained by saline elution of a 500-mCi ^{99}Mo–^{99m}Tc generator[3] at a specific concentration of 10–20 mCi/ml), the solution was purged with nitrogen for 5 min, and 0.1 ml of freshly prepared stannous chloride dihydrate solution (250 μg/ml in 0.001 *N* HCl) was then added. The solution was kept at room temperature for 20 min prior to use.

Electrophoresis and Chromatography[4]—Electrophoresis was performed on paper[5] at constant voltage (600 v, 30 min) with a 0.01 *M* sodium bicarbonate buffer (pH 7). Under these conditions, $^{99m}TcO_4^-$ migrated approximately 13 cm. A pertechnetate standard was utilized with all samples. The distance each complex migrated was determined by scanning the dried paper with a chromatogram scanner equipped with a 2.54-cm sodium iodide detector and a collimator, which consisted of 0.635 cm of lead with a 2.54-cm × 30-mm slit. The results obtained on any given electrophoragram were expressed as the following ratio:

$$R_s = \frac{\text{distance migrated by complex}}{\text{distance migrated by } ^{99m}TcO_4^-} \quad \text{(Eq. 1)}$$

These R_s values were essentially independent of the distance migrated by the pertechnetate ion over a range of at least 11–15 cm.

[3] E. R. Squibb & Sons, Princeton, N.J.

[4] Chromatography was performed on Eastman 13181 silica gel eluted with acetone.

[5] Whatman 3MM.

REFERENCES

(1) G. V. Taplin, O. M. Meridith, and H. Kade, *J. Lab. Clin. Med.*, **45**, 665 (1955).

(2) A. K. Tonkin and F. H. Deland, *J. Nucl. Med.*, **15**, 539 (1974).

(3) T. H. Lin, A. Khentigan, and H. S. Winchell, *ibid.*, **15**, 613 (1974).

(4) G. T. Krishnamurthy, M. Tubis, and J. S. Endow, *ibid.*, **13**, 447 (1972).

(5) M. K. Dewanjee, C. Fliegel, and S. Treeves, *ibid.*, **15**, 176 (1974).

(6) R. J. Baker, J. C. Bellen, and P. M. Ronai, *ibid.*, **16**, 720 (1975).

(7) P. M. Ronai, R. J. Baker, and J. C. Bellery, *ibid.*, **16**, 728 (1975).

(8) E. Harvey, M. Loberg, and M. Cooper, *ibid.*, **16**, 533 (1975).

(9) P. S. Callery, W. F. Faith, and M. D. Loberg, *J. Med. Chem.*, **19**, 962 (1976).

(10) H. D. Burns, L. G. Marzilli, D. Sowa, D. Baum, and H. N. Wagner, Jr., *J. Nucl. Med.*, **18**, 624 (1977).

ACKNOWLEDGMENTS

Supported in part by U.S. Public Health Service Grant GM-10548 and the Biomedical Research Support Program.

Dissolution Profiles of Drugs from Tablets

NOBUYUKI KITAMORI ˣ and KATSUMI IGA

Received January 3, 1977, from the *Pharmaceutical Research Laboratories, Central Research Division, Takeda Chemical Industries, Ltd., Yodogawa-ku, Osaka, 532, Japan.* Accepted for publication February 15, 1978.

Abstract □ A theoretical equation to describe the drug dissolution from a tablet was derived by combining an equation for the disintegration rate of a tablet with an equation for the dissolution of particles. The theory is based on the assumptions that: (*a*) dissolution occurs only from the particles released in a medium by tablet disintegration, (*b*) the number of particles released into a medium obeys the equation $N = N_0(T/T_d)^m$, and (*c*) the dissolution of particles, which are spherical in shape, is represented by the equation previously given by Brooke. Tablet dissolution *versus* time plots, obtained by calculating the equation with a computer, gave an S-shaped curve between the dissolution curve for particles starting at time zero and the curve for particles starting at the tablet disintegration time. The joint influences of disintegration and particle dissolution on the overall tablet dissolution profile also were examined. When dissolution of powders was rapid, disintegration of a tablet directly influenced its dissolution. When powders intrinsically dissolved slowly, the effect of disintegration on the tablet dissolution profile was slight.

Keyphrases □ Dissolution, tablet—theoretical equation derived, effects of tablet disintegration and particle dissolution □ Disintegration, tablet—effects on dissolution, theoretical equation derived □ Tablet dissolution—theoretical equation derived, effects of tablet disintegration and particle dissolution

The dissolution rate of a drug from its solid dosage forms is important relative to bioavailability since dissolution is usually the rate-limiting process in the absorption of poorly soluble drugs.

The overall dissolution profiles for solid dosage forms can be obtained from dissolution tests (1–3). The dissolution data obtained may involve factors related to the drug dissolution rate, the drug particle size (distribution), and the disintegration rate of the dosage forms. The effect of these factors on the dissolution profiles is so complex that no satisfactory quantitative evaluation of the dissolution properties of solid dosage forms is obtained from a measured dissolution profile.

Attempts to describe dissolution profiles include empirical functions that enable representation of the actual results with a minimum number of parameters (4–8). However, the values of the parameters of the distribution function employed give no useful information about the improvement of tablet dissolution.

Theoretical considerations of powder dissolution in relation to particle-size distribution were first attempted by Higuchi and coworkers (9, 10). A more exact equation then was developed that permits calculation of the dissolution profiles of log-normal powders with or without a computer (11–13). Later, a simple relationship was found between the tablet disintegration rate and time (14).

To evaluate tablet dissolution quantitatively, an equation was derived in the present study by combining an equation for tablet disintegration with an equation for

0022-3549/78/1000-1436$01.00/0

© 1978, American Pharmaceutical Association

Anal.—Calc. for $C_{13}H_{14}N_2O_7 \cdot H_2O$: C, 48.90; H, 4.74; N, 8.78. Found: C, 48.80; H, 4.65; N, 8.61.

***N*-(4-Iodophenylcarbamoylmethyl)iminodiacetic Acid (VII)**—Compound VII was obtained from nitrilotriacetic acid (4.47 g, 0.023 mole), acetic anhydride (3.58 g, 0.035 mole), and 4-iodoaniline (5.12 g, 0.023 mole) (Method B). Recrystallization from 80% aqueous ethanol yielded white crystals, 5.62 g (62%), mp 194° dec.; IR (mineral oil): 3300 (NH) and 1710 and 1675 (C=O) cm^{-1}; PMR (dimethyl sulfoxide-d_6): δ 3.51 (s, 2H, NCH_2CON), 3.55 (s, 4H, NCH_2CO_2), 7.48 (d, 2H, Ar-H), and 7.60 (d, 2H, Ar-H) ppm.

Anal.—Calc. for $C_{12}H_{13}IN_2O_5$: C, 36.75; H, 3.34; N, 7.14. Found: C, 36.73; H, 3.51; N, 7.25.

Preparation of ^{99m}Tc-Complexes—A solution of 10 mg of compound in 0.5 ml of 0.1 *N* NaOH was prepared, and the pH was adjusted to 5–5.5 with 0.05 *N* HCl. After addition of 0.3 ml of generator eluate (obtained by saline elution of a 500-mCi ^{99}Mo–^{99m}Tc generator[3] at a specific concentration of 10–20 mCi/ml), the solution was purged with nitrogen for 5 min, and 0.1 ml of freshly prepared stannous chloride dihydrate solution (250 μg/ml in 0.001 *N* HCl) was then added. The solution was kept at room temperature for 20 min prior to use.

Electrophoresis and Chromatography[4]—Electrophoresis was performed on paper[5] at constant voltage (600 v, 30 min) with a 0.01 *M* sodium bicarbonate buffer (pH 7). Under these conditions, $^{99m}TcO_4^-$ migrated approximately 13 cm. A pertechnetate standard was utilized with all samples. The distance each complex migrated was determined by scanning the dried paper with a chromatogram scanner equipped with a 2.54-cm sodium iodide detector and a collimator, which consisted of 0.635 cm of lead with a 2.54-cm × 30-mm slit. The results obtained on any given electrophoragram were expressed as the following ratio:

$$R_s = \frac{\text{distance migrated by complex}}{\text{distance migrated by } ^{99m}TcO_4^-} \quad \text{(Eq. 1)}$$

These R_s values were essentially independent of the distance migrated by the pertechnetate ion over a range of at least 11–15 cm.

[3] E. R. Squibb & Sons, Princeton, N.J.

[4] Chromatography was performed on Eastman 13181 silica gel eluted with acetone.

[5] Whatman 3MM.

REFERENCES

(1) G. V. Taplin, O. M. Meridith, and H. Kade, *J. Lab. Clin. Med.*, **45**, 665 (1955).

(2) A. K. Tonkin and F. H. Deland, *J. Nucl. Med.*, **15**, 539 (1974).

(3) T. H. Lin, A. Khentigan, and H. S. Winchell, *ibid.*, **15**, 613 (1974).

(4) G. T. Krishnamurthy, M. Tubis, and J. S. Endow, *ibid.*, **13**, 447 (1972).

(5) M. K. Dewanjee, C. Fliegel, and S. Treeves, *ibid.*, **15**, 176 (1974).

(6) R. J. Baker, J. C. Bellen, and P. M. Ronai, *ibid.*, **16**, 720 (1975).

(7) P. M. Ronai, R. J. Baker, and J. C. Bellery, *ibid.*, **16**, 728 (1975).

(8) E. Harvey, M. Loberg, and M. Cooper, *ibid.*, **16**, 533 (1975).

(9) P. S. Callery, W. F. Faith, and M. D. Loberg, *J. Med. Chem.*, **19**, 962 (1976).

(10) H. D. Burns, L. G. Marzilli, D. Sowa, D. Baum, and H. N. Wagner, Jr., *J. Nucl. Med.*, **18**, 624 (1977).

ACKNOWLEDGMENTS

Supported in part by U.S. Public Health Service Grant GM-10548 and the Biomedical Research Support Program.

Dissolution Profiles of Drugs from Tablets

NOBUYUKI KITAMORI ˣ and KATSUMI IGA

Received January 3, 1977, from the *Pharmaceutical Research Laboratories, Central Research Division, Takeda Chemical Industries, Ltd., Yodogawa-ku, Osaka, 532, Japan.* Accepted for publication February 15, 1978.

Abstract □ A theoretical equation to describe the drug dissolution from a tablet was derived by combining an equation for the disintegration rate of a tablet with an equation for the dissolution of particles. The theory is based on the assumptions that: (*a*) dissolution occurs only from the particles released in a medium by tablet disintegration, (*b*) the number of particles released into a medium obeys the equation $N = N_0(T/T_d)^m$, and (*c*) the dissolution of particles, which are spherical in shape, is represented by the equation previously given by Brooke. Tablet dissolution *versus* time plots, obtained by calculating the equation with a computer, gave an S-shaped curve between the dissolution curve for particles starting at time zero and the curve for particles starting at the tablet disintegration time. The joint influences of disintegration and particle dissolution on the overall tablet dissolution profile also were examined. When dissolution of powders was rapid, disintegration of a tablet directly influenced its dissolution. When powders intrinsically dissolved slowly, the effect of disintegration on the tablet dissolution profile was slight.

Keyphrases □ Dissolution, tablet—theoretical equation derived, effects of tablet disintegration and particle dissolution □ Disintegration, tablet—effects on dissolution, theoretical equation derived □ Tablet dissolution—theoretical equation derived, effects of tablet disintegration and particle dissolution

The dissolution rate of a drug from its solid dosage forms is important relative to bioavailability since dissolution is usually the rate-limiting process in the absorption of poorly soluble drugs.

The overall dissolution profiles for solid dosage forms can be obtained from dissolution tests (1–3). The dissolution data obtained may involve factors related to the drug dissolution rate, the drug particle size (distribution), and the disintegration rate of the dosage forms. The effect of these factors on the dissolution profiles is so complex that no satisfactory quantitative evaluation of the dissolution properties of solid dosage forms is obtained from a measured dissolution profile.

Attempts to describe dissolution profiles include empirical functions that enable representation of the actual results with a minimum number of parameters (4–8). However, the values of the parameters of the distribution function employed give no useful information about the improvement of tablet dissolution.

Theoretical considerations of powder dissolution in relation to particle-size distribution were first attempted by Higuchi and coworkers (9, 10). A more exact equation then was developed that permits calculation of the dissolution profiles of log-normal powders with or without a computer (11–13). Later, a simple relationship was found between the tablet disintegration rate and time (14).

To evaluate tablet dissolution quantitatively, an equation was derived in the present study by combining an equation for tablet disintegration with an equation for

0022-3549/78/1000-1436$01.00/0

© 1978, American Pharmaceutical Association

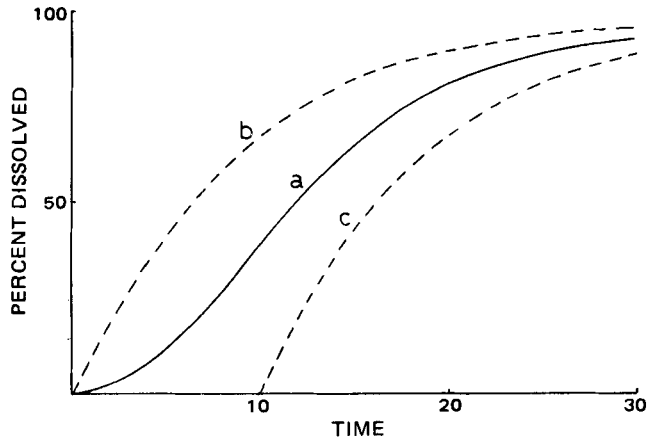

Figure 1—*Typical dissolution profile of a tablet.*

particle dissolution. The joint effect of disintegration and particle dissolution on the overall tablet dissolution profile was examined by calculating the equation with a computer.

THEORETICAL

Consider a tablet containing spherical drug particles whose diameters, a_0, follow a log-normal distribution. The probability function, f, of ln a_0 is given by:

$$f = \frac{1}{\sigma\sqrt{2\pi}} \exp[-(\ln M - \ln a_0)^2/2\sigma^2] \qquad \text{(Eq. 1)}$$

where M is the geometrical mean of a_0, and σ is the standard deviation.

Assume that the dissolution of a tablet occurs only from drug particles released from the tablet *via* disintegration or deaggregation. Assume that the release rate of particles into a medium is expressed, on the numbers basis, by the simple equation derived by Kitamori and Shimamoto (14):

$$N = N_0(T/T_d)^m \qquad \text{(Eq. 2)}$$

where N is the number of primary drug particles released from the tablet or granules *via* disintegration, N_0 is the total number of drug particles within the tablet, T is time ($0 \le T \le T_d$), T_d is disintegration time, and m is a constant concerned with the tablet disintegration rate.

A small number, dN, of particles released within a very narrow interval of time, dT, centered at T is given by:

$$dN = N_0(m/T_d{}^m)T^{m-1}\,dT \qquad \text{(Eq. 3)}$$

As the particles in the tablet distribute log-normally, the particles of very small number, dN, also follow the same log-normal distribution. If these particles dissolve isotropically under sink conditions, their weight undissolved at time t is given by the dissolution equation of log-normal powders derived by Brooke (11, 12), with time $t - T$ in place of time t because the particles start dissolving at time T, and is expressed by:

$$dW_t = \int_{\ln[(2k_i/p)(t-T)]}^{\infty} pV_{(t-T)}f\,dN\,d(\ln a_0) \qquad \text{(Eq. 4)}$$

where $V_{(t-T)}$ is the volume of undissolved particles initially having a_0 diameter at time t and is expressed by:

$$V_{(t-T)} = \frac{\pi}{6}[a_0 - (2k_i/p)(t-T)]^3 \qquad \text{(Eq. 5)}$$

Substituting $N_0(m/T_d{}^m)T^{m-1}\,dT$ into dN in Eq. 4 yields:

$$dW_t = \int_{\ln[(2k_i/p)(t-T)]}^{\infty} pV_{(t-T)}N_0f(m/T_d{}^m)T^{m-1}\,d(\ln a_0)\,dT \qquad \text{(Eq. 6)}$$

When $t < T_d$, the total weight of undissolved solid after time t is given by an integration of Eq. 6 with respect to T between time zero and t:

$$W_t = \int_0^t \int_{\ln[(2k_i/p)(t-T)]}^{\infty} pV_{(t-T)}N_0f(m/T_d{}^m)T^{m-1}\,d(\ln a_0)\,dT \qquad \text{(Eq. 7)}$$

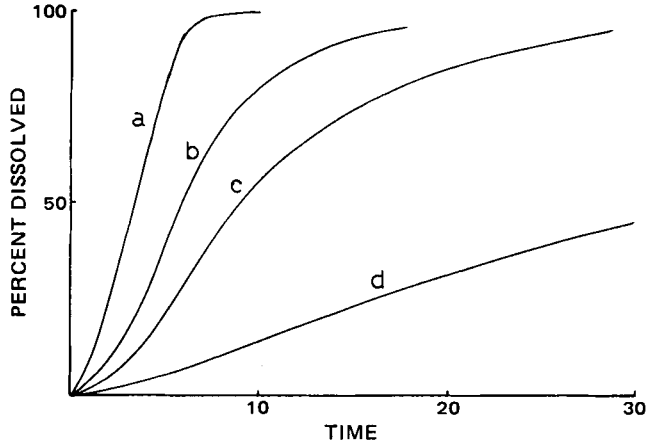

Figure 2—*Effect of the intrinsic dissolution rate of the particles before inclusion in tablets on the dissolution profiles of tablets. Key: a,* $k_i/pM = 0.333$; *b,* $k_i/pM = 0.0667$; *c,* $k_i/pM = 0.0333$; *and d,* $k_i/pM = 0.00667$. *Other variables are the same;* $\sigma = 0.5$, $T_d = 5.0$, *and* $m = 1.0$.

The total weight of the particles released from the tablet *via* tablet disintegration after time t is given by:

$$W_t{}^0 = N_0(t/T_d)^m \int_{-\infty}^{\infty} pV_0f\,d(\ln a_0) \qquad \text{(Eq. 8)}$$

Then the equation for the weight fraction dissolved before disintegration time is:

$$S_t = (W_t{}^0 - W_t)/W_0 \qquad \text{(Eq. 9a)}$$

$$S_t = (t/T_d)^m - \frac{\int_0^t \int_{\ln[(2k_i/p)(t-T)]}^{\infty} pV_{(t-T)}N_0(m/T_d{}^m)T^{m-1}f\,d(\ln a_0)\,dT}{\int_{-\infty}^{\infty} pN_0V_0f\,d(\ln a_0)} \qquad \text{(Eq. 9b)}$$

where W_0 is the initial weight of the particles in a tablet and is expressed by:

$$W_0 = \int_{-\infty}^{\infty} pV_0N_0f\,d(\ln a_0) \qquad \text{(Eq. 10)}$$

When $t > T_d$, the equation for the weight fraction dissolved is:

$$S_t = (W_0 - W_t)/W_0 \qquad \text{(Eq. 11a)}$$

$$S_t = 1 - \frac{\int_0^{T_d} \int_{\ln[(2k_i/p)(t-T)]}^{\infty} pV_{(t-T)}N_0(m/T_d{}^m)T^{m-1}f\,d(\ln a_0)\,dT}{\int_{-\infty}^{\infty} pV_0N_0f\,d(\ln a_0)} \qquad \text{(Eq. 11b)}$$

In double integrations in Eqs. 9*b* and 11*b*, the integral with respect to ln a_0 can be evaluated numerically by introducing a standard normal distribution, $F(x) = \int \exp(-x^2/2)/\sqrt{x}\,dx$, but the integral with respect to T cannot be solved directly. In this paper, these double integrations were approximated by the trapezoidal rule and numerically evaluated with a digital computer (see *Appendix* for details).

RESULTS AND DISCUSSION

When a tablet is placed in a medium according to the USP–NF dissolution test, dissolution occurs from its surface; granules are produced after its disintegration, and drug primary particles ultimately are released (5). In the disintegration–dissolution model described in this paper, it was assumed that the dissolution from drug primary particles produced after disintegration is the major route of tablet dissolution since the surface areas available for dissolution of poorly soluble drugs in a tablet or in granules are smaller than those in drug primary particles and can be neglected.

The calculation of the dissolution of a tablet with k_i/pM[1] = 0.133, σ

[1] It can be seen from Eq. A2 in the *Appendix* that k_i/pM is a variable for the tablet dissolution equation.

Table I—Dissolution Patterns for Tablets with T_d = 5.0, m = 1.0, σ = 0.5, and different k_i/pM Values

	Percent Dissolved at Time				
k_i/pM	5.0	10.0	15.0	20.0	30.0
0.0333	22.88	56.11	75.28	85.99	95.27
0.0667	39.47	80.63	93.60	97.72	99.63
0.1333	60.02	95.66	99.38	99.88	99.97
0.3333	82.04	99.87	99.99	99.99	99.99

Table II—Dissolution Patterns for Tablets with T_d = 5.0 and m = 1.0 Containing the Constituent Drug Particles with k_i = 0.1, p = 1.5, M = 1.0, and Different Standard Deviations

	Percent Dissolved at Time				
σ	5.0	10.0	15.0	20.0	30.0
0[a]	62.86	99.53	99.99	—	—
0.05	62.60	99.46	99.99	—	—
0.1	61.81	99.24	99.99	—	—
0.3	53.68	95.12	99.70	99.98	99.99
0.5	39.47	80.63	93.60	97.72	99.63
0.7	23.82	55.64	72.75	82.47	91.94

[a] Since Eq. 9*b* or 11*b* does not hold for σ = 0, the dissolution pattern for the tablet containing monosized drug was calculated at σ = 0.0001.

= 0.5, T_d = 10.0, and m = 1.0 gave an S-shaped curve (a) as shown in Fig. 1. The curve located between the dissolution profile (b) for the log-normal drug powder before inclusion in a tablet (k_i/pM = 0.133 and σ = 0.5) started at time zero, and the profile (c) for the same powder started at the disintegration time of the tablet. Since the particles start dissolving when they are released from the tablet according to the disintegration–dissolution model, the dissolution of a tablet is slower than the dissolution of the powder before inclusion in the tablet and faster than the dissolution of the same powder started at the disintegration time of the tablet.

The intrinsic dissolution rate (or solubility), the particle size (distribution), and the disintegration rate primarily determine the tablet dissolution profile. Their effect on the overall tablet dissolution profile can be examined by the computer calculation of the proposed equation.

First, the dissolution of the drug powder before inclusion in a tablet is essential for the dissolution of the tablet. Since S_t is a function of k_i/pM ($\propto \tau/M$) and not of k_i or M separately (see *Appendix*), an increase in k_i/pM can result from an increase in k_i or a decrease in the particle size of drug particles. The variation in the dissolution profile of a tablet with the value of k_i/pM is demonstrated in Fig. 2, where the tablets have the same disintegration time, 5.0, and the same coefficient of disintegration pattern, m = 1.0. A decrease in k_i/pM corresponds with the slower slope of the dotted curves so that the S-shaped curve located between both of them lies stretched. The relationship between amount dissolved and time is much less complicated for a powder than for a tablet, which must first disintegrate. Some typical results of dissolution of the tablet with T_d = 5.0, m = 1.0, and σ = 0.5 and different k_i/pM values are listed in Table I.

The standard deviations of the size distribution of particles before inclusion in a tablet should also affect the dissolution profile of the tablet. The calculated results for different drug powder distributions are shown in Table II. The calculated dissolution is not so sensitive to the distribution for smaller σ. For rather large standard deviations, however, the slower the calculated dissolution, the more broadly the drug particles

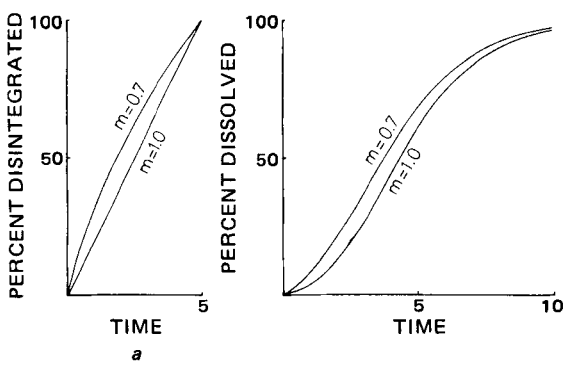

Figure 3—*Effect of the coefficient of disintegration,* m, *on the tablet dissolution profile. Variables are* k_i/pM = *0.133,* σ = *0.5, and* T_d = *5.0.*

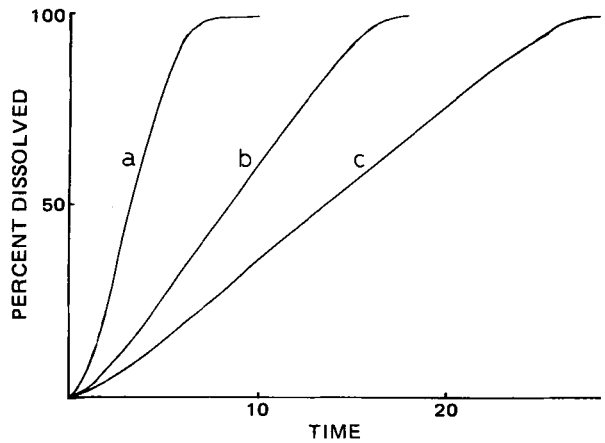

Figure 4—*Effect of disintegration time on the dissolution profiles of tablets. Key: a,* T_d = *5.0; b,* T_d = *15.0; and c,* T_d = *25.0. Other variables are the same;* k_i/pM = *0.333,* σ = *0.5, and* m = *1.0.*

distribute. This behavior is similar to the powder dissolution reported by Brooke (11).

The release profile of drug particles from a tablet varies with the value of the constant m in Eq. 2 as shown in Fig. 3*a*. In accordance with the change in the disintegration pattern, the dissolution profile of the tablet varies as shown in Fig. 3*b*. The shape of the dissolution curves for tablets is reflected by the value of the constant m. The value of m lies between 0.7 and 1.0; but, experimentally (14), the constant m ordinarily is almost unity so that the evaluation of tablet dissolution can be performed with m = 1.0.

The disintegration equation can be applied to the disintegration not only into particles but also into granules. In dissolution, however, a tablet must disintegrate into primary particles because of the assumption. Although a tablet disintegrates rapidly into granules, the surface area available for drug dissolution is so small that the dissolution would not be so fast unless primary particles are produced from the granules. From this point of view, the tablet that should have the fast dissolution rate must disintegrate in a medium into constituent particles.

With the assumption of Eq. 2, the disintegration time of a tablet also affects the tablet dissolution profile. The effect of the disintegration time of tablets on their dissolution profiles is shown in Fig. 4. An increase in disintegration time means an increase in the distance between both dissolution curves for particles before inclusion in a tablet starting at time zero and starting at its disintegration time, so an S-shaped dissolution curve of a tablet between them lies stretched and becomes straightened.

It is of interest to examine the joint influence of disintegration rate and particle dissolution rate on the overall tablet dissolution profile. Dissolution profiles with different T_d and k_i/pM values are shown in Fig. 5. Two pairs of curves, a and a′ and b and b′, are the dissolution profiles with different T_d values (T_d = 15.0 for a and b and 5.0 for a′ and b′) and equal k_i/pM values (k_i/pM = 0.333 for a and a′ and 0.0667 for b and b′). For

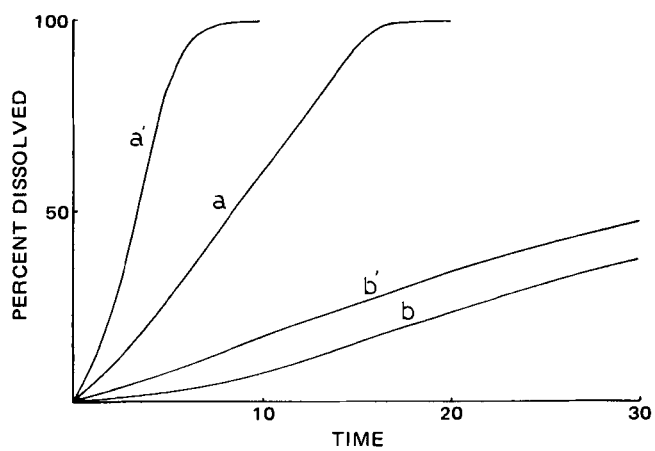

Figure 5—*Joint influence of the disintegration rate of a tablet and the dissolution rate of the constituent particles on the tablet dissolution profile.*

drugs that intrinsically dissolve slowly ($k_i/pM = 0.0667$), a decrease in disintegration time cannot greatly improve the tablet dissolution (curve b → b'), whereas the effect is great for fast dissolving drugs ($k_i/pM = 0.333$, curve a → a'). The T_d and k_i/pM values influence an overall dissolution profile in different ways, so that the evaluation of the dissolution properties of solid dosage forms merely from an overall dissolution profile might lead to an erroneous conclusion. Therefore, to evaluate the dissolution properties of solid dosage forms, disintegration measurements and dissolution tests of the powder before or after inclusion in a tablet should be carried out separately.

The developed equation is based on the simple disintegration–dissolution model. Actually, more complex factors may affect tablet dissolution. For instance, disintegration is not always the deaggregation into primary particles and particle-size distribution is not always log-normal. The equation also would not be applied to the case where drug particle-size distribution changes after compression. In spite of such restrictions, the proposed equation might still be useful to predict or examine tablet dissolution.

APPENDIX

Let the integration with respect to $\ln a_0$ in Eqs. 9*b* and 11*b* be $I(T)$:

$$I(T) = \frac{\int_{\ln[(2k_i/p)(t-T)]}^{\infty} pV_{(t-T)}N_0 f(m/T_d{}^m)T^{m-1}\, d(\ln a_0)}{\int_{-\infty}^{\infty} pN_0 v_0 f\, d(\ln a_0)} \quad \text{(Eq. A1)}$$

By letting $(m/T_d{}^m)T^{m-1} = r(T)$ and $(2k_i/p)(t - T) = \tau(T)$ for simplification and employing the method similar to that used by Brooke (11), Eq. A1 becomes:

$$I(T) = r(T)\left\{\left[1 - F\left(\frac{\ln[\tau(T)/M] - 3\sigma^2}{\sigma}\right)\right]\right.$$
$$-3[\tau(T)/M]\exp(-5\sigma^2/2)\left[1 - F\left(\frac{\ln[\tau(T)/M] - 2\sigma^2}{\sigma}\right)\right]$$
$$+3[\tau(T)/M]^2\exp(-4\sigma^2)\left[1 - F\left(\frac{\ln[\tau(T)/M] - \sigma^2}{\sigma}\right)\right]$$
$$\left.-[\tau(T)/M]^3\exp(-9\sigma^2/2)\left[1 - F\left(\frac{\ln[\tau(T)/M]}{\sigma}\right)\right]\right\} \quad \text{(Eq. A2)}$$

For numerical computation of $I(T)$, the following approximation (15) was used for $F(x)$:

$$F(x) = 1 - \frac{1}{\sqrt{2\pi}}\exp(-x^2/2)(ay + by^2 + cy^3 + dy^4 + ey^5) \quad \text{(Eq. A3)}$$

where $y = 1/(1 + 0.2316419x)$, $a = 0.319381530$, $b = -0.356563782$, $c = 1.781477937$, $d = -1.821255978$, and $e = 1.330274429$. Finally, Eqs. 9*b* and 11*b* can be given by:

$$\int_0^t I(T)\, dT \qquad (t < T_d)$$
$$\int_0^{T_d} I(T)\, dT \qquad (t \geq T_d)$$

For numerical computation, it can be approximated by the trapezoidal rule based on dividing T_d by a large number of n; for $t < T_d$:

$$\int_0^t I(T)\, dT \fallingdotseq \frac{h}{2}[(I_0 + I_{n'}) + 2(I_1 + I_2 + \ldots + I_{n'-1})] \quad \text{(Eq. A4)}$$

for $t \geq T_d$:

$$\int_0^{T_d} I(T)\, dT \fallingdotseq \frac{h}{2}[(I_0 + I_n) + 2(I_1 + I_2 + \ldots + I_{n-1})] \quad \text{(Eq. A5)}$$

where $I_i = I(T_i)$ $(i = 0, 1, 2, \ldots.)$, $h = T_d/n$, $n' = (nt)/T_d$, and $T_n = T_d$.

The double integration is evaluated practically by dividing disintegration time into about 500 intervals.

REFERENCES

(1) J. B. Johnson, P. G. Kennedy, and S. H. Rubin, *J. Pharm. Sci.*, **63**, 1931 (1974).
(2) A. C. Shah, C. Peot, and J. F. Ochs, *ibid.*, **62**, 671 (1973).
(3) A. C. Shah and J. F. Ochs, *ibid.*, **63**, 110 (1974).
(4) M. Gibaldi and S. Feldman, *ibid.*, **56**, 1238 (1967).
(5) J. G. Wagner, *ibid.*, **58**, 1253 (1969).
(6) F. Langenbucher, *J. Pharm. Pharmacol.*, **24**, 979 (1972).
(7) M. Behr, J. Dietrich, P. J. Mehta, D. Reher, and H. Sucker, *Pharm. Ind.*, **35**, 210 (1973).
(8) F. Langenbucher, *ibid.*, **38**, 472 (1976).
(9) W. I. Higuchi and E. N. Hiestand, *J. Pharm. Sci.*, **52**, 67 (1963).
(10) W. I. Higuchi, E. L. Rowe, and E. N. Hiestand, *ibid.*, **52**, 162 (1963).
(11) D. Brooke, *ibid.*, **62**, 795 (1973).
(12) *Ibid.*, **63**, 344 (1974).
(13) P. Veng Pedersen and K. F. Brown, *J. Pharm. Sci.*, **64**, 1192 (1975).
(14) N. Kitamori and T. Shimamoto, *Chem. Pharm. Bull.*, **24**, 1789 (1976).
(15) "Handbook of Mathematical Functions with Formulas, Graphs, and Mathematical Tables," M. Abramowitz and I. A. Stegun, Eds., National Bureau of Standards, Washington, D.C., 1965.

Conductivity of Drugs Used for Iontophoresis

L. P. GANGAROSA ˣ, N. H. PARK, B. C. FONG, D. F. SCOTT, and J. M. HILL

Received December 12, 1977, from the *Departments of Oral Biology–Pharmacology and Cell and Molecular Biology, Medical College of Georgia, Augusta, GA 30902.* Accepted for publication February 21, 1978.

Abstract □ The electrical conductivities of drugs were measured *in vitro* using a conductivity MHO-meter. These experiments indicate that local anesthetics, vasoconstrictors, some corticosteroids, several anticancer drugs, and several antiviral agents are suitable for iontophoresis. The contribution to conductivity of buffers and nonspecific ions in the same solution with the drug also was defined.

Keyphrases □ Conductivity, electrical—various drugs measured *in vitro*, suitability for iontophoresis □ Iontophoresis suitability—various drugs, electrical conductivity measured *in vitro*

Iontophoresis is a simple, well-documented method of drug application for medication of tissues (1). It assures the penetration of electrically charged drugs into surface tissues. It is possible to medicate electrically any surface tissue with drugs having a positive or negative charge (1). The technique involves transporting selected ions electrically into a tissue by passing a direct electrical current through a medicating solution and the patient, using selected electrode polarity.

BACKGROUND

Iontophoresis has many advantages as a drug administration method. Systemic toxicity is virtually eliminated since only a minute amount of

0022-3549/78/1000-1439$01.00/0

© 1978, American Pharmaceutical Association

drugs that intrinsically dissolve slowly ($k_i/pM = 0.0667$), a decrease in disintegration time cannot greatly improve the tablet dissolution (curve b → b'), whereas the effect is great for fast dissolving drugs ($k_i/pM = 0.333$, curve a → a'). The T_d and k_i/pM values influence an overall dissolution profile in different ways, so that the evaluation of the dissolution properties of solid dosage forms merely from an overall dissolution profile might lead to an erroneous conclusion. Therefore, to evaluate the dissolution properties of solid dosage forms, disintegration measurements and dissolution tests of the powder before or after inclusion in a tablet should be carried out separately.

The developed equation is based on the simple disintegration–dissolution model. Actually, more complex factors may affect tablet dissolution. For instance, disintegration is not always the deaggregation into primary particles and particle-size distribution is not always log-normal. The equation also would not be applied to the case where drug particle-size distribution changes after compression. In spite of such restrictions, the proposed equation might still be useful to predict or examine tablet dissolution.

APPENDIX

Let the integration with respect to $\ln a_0$ in Eqs. 9*b* and 11*b* be $I(T)$:

$$I(T) = \frac{\int_{\ln[(2k_i/p)(t-T)]}^{\infty} pV_{(t-T)}N_0 f(m/T_d{}^m)T^{m-1}\, d(\ln a_0)}{\int_{-\infty}^{\infty} pN_0 v_0 f\, d(\ln a_0)} \quad \text{(Eq. A1)}$$

By letting $(m/T_d{}^m)T^{m-1} = r(T)$ and $(2k_i/p)(t - T) = \tau(T)$ for simplification and employing the method similar to that used by Brooke (11), Eq. A1 becomes:

$$I(T) = r(T)\left\{\left[1 - F\left(\frac{\ln[\tau(T)/M] - 3\sigma^2}{\sigma}\right)\right]\right.$$
$$-3[\tau(T)/M]\exp(-5\sigma^2/2)\left[1 - F\left(\frac{\ln[\tau(T)/M] - 2\sigma^2}{\sigma}\right)\right]$$
$$+3[\tau(T)/M]^2\exp(-4\sigma^2)\left[1 - F\left(\frac{\ln[\tau(T)/M] - \sigma^2}{\sigma}\right)\right]$$
$$\left.-[\tau(T)/M]^3\exp(-9\sigma^2/2)\left[1 - F\left(\frac{\ln[\tau(T)/M]}{\sigma}\right)\right]\right\} \quad \text{(Eq. A2)}$$

For numerical computation of $I(T)$, the following approximation (15) was used for $F(x)$:

$$F(x) = 1 - \frac{1}{\sqrt{2\pi}}\exp(-x^2/2)(ay + by^2 + cy^3 + dy^4 + ey^5) \quad \text{(Eq. A3)}$$

where $y = 1/(1 + 0.2316419x)$, $a = 0.319381530$, $b = -0.356563782$, $c = 1.781477937$, $d = -1.821255978$, and $e = 1.330274429$. Finally, Eqs. 9*b* and 11*b* can be given by:

$$\int_0^t I(T)\, dT \qquad (t < T_d)$$
$$\int_0^{T_d} I(T)\, dT \qquad (t \geq T_d)$$

For numerical computation, it can be approximated by the trapezoidal rule based on dividing T_d by a large number of n; for $t < T_d$:

$$\int_0^t I(T)\, dT \fallingdotseq \frac{h}{2}[(I_0 + I_{n'}) + 2(I_1 + I_2 + \ldots + I_{n'-1})] \quad \text{(Eq. A4)}$$

for $t \geq T_d$:

$$\int_0^{T_d} I(T)\, dT \fallingdotseq \frac{h}{2}[(I_0 + I_n) + 2(I_1 + I_2 + \ldots + I_{n-1})] \quad \text{(Eq. A5)}$$

where $I_i = I(T_i)$ $(i = 0, 1, 2, \ldots.)$, $h = T_d/n$, $n' = (nt)/T_d$, and $T_n = T_d$.

The double integration is evaluated practically by dividing disintegration time into about 500 intervals.

REFERENCES

(1) J. B. Johnson, P. G. Kennedy, and S. H. Rubin, *J. Pharm. Sci.*, **63**, 1931 (1974).
(2) A. C. Shah, C. Peot, and J. F. Ochs, *ibid.*, **62**, 671 (1973).
(3) A. C. Shah and J. F. Ochs, *ibid.*, **63**, 110 (1974).
(4) M. Gibaldi and S. Feldman, *ibid.*, **56**, 1238 (1967).
(5) J. G. Wagner, *ibid.*, **58**, 1253 (1969).
(6) F. Langenbucher, *J. Pharm. Pharmacol.*, **24**, 979 (1972).
(7) M. Behr, J. Dietrich, P. J. Mehta, D. Reher, and H. Sucker, *Pharm. Ind.*, **35**, 210 (1973).
(8) F. Langenbucher, *ibid.*, **38**, 472 (1976).
(9) W. I. Higuchi and E. N. Hiestand, *J. Pharm. Sci.*, **52**, 67 (1963).
(10) W. I. Higuchi, E. L. Rowe, and E. N. Hiestand, *ibid.*, **52**, 162 (1963).
(11) D. Brooke, *ibid.*, **62**, 795 (1973).
(12) *Ibid.*, **63**, 344 (1974).
(13) P. Veng Pedersen and K. F. Brown, *J. Pharm. Sci.*, **64**, 1192 (1975).
(14) N. Kitamori and T. Shimamoto, *Chem. Pharm. Bull.*, **24**, 1789 (1976).
(15) "Handbook of Mathematical Functions with Formulas, Graphs, and Mathematical Tables," M. Abramowitz and I. A. Stegun, Eds., National Bureau of Standards, Washington, D.C., 1965.

Conductivity of Drugs Used for Iontophoresis

L. P. GANGAROSA ˣ, N. H. PARK, B. C. FONG, D. F. SCOTT, and J. M. HILL

Received December 12, 1977, from the *Departments of Oral Biology–Pharmacology and Cell and Molecular Biology, Medical College of Georgia, Augusta, GA 30902.* Accepted for publication February 21, 1978.

Abstract □ The electrical conductivities of drugs were measured *in vitro* using a conductivity MHO-meter. These experiments indicate that local anesthetics, vasoconstrictors, some corticosteroids, several anticancer drugs, and several antiviral agents are suitable for iontophoresis. The contribution to conductivity of buffers and nonspecific ions in the same solution with the drug also was defined.

Keyphrases □ Conductivity, electrical—various drugs measured *in vitro*, suitability for iontophoresis □ Iontophoresis suitability—various drugs, electrical conductivity measured *in vitro*

Iontophoresis is a simple, well-documented method of drug application for medication of tissues (1). It assures the penetration of electrically charged drugs into surface tissues. It is possible to medicate electrically any surface tissue with drugs having a positive or negative charge (1). The technique involves transporting selected ions electrically into a tissue by passing a direct electrical current through a medicating solution and the patient, using selected electrode polarity.

BACKGROUND

Iontophoresis has many advantages as a drug administration method. Systemic toxicity is virtually eliminated since only a minute amount of

0022-3549/78/1000-1439$01.00/0

© 1978, American Pharmaceutical Association

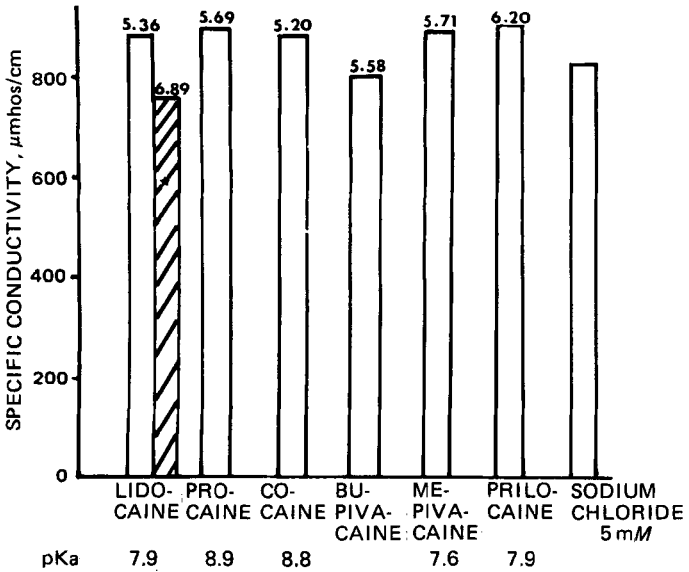

Figure 1—*Specific conductivities of several local anesthetics. The numbers above the bars are pH values of local anesthetic solution. The concentration of local anesthetics was 10 mM.*

drug is delivered. Nevertheless, a relatively high drug concentration is administered locally (2). Patient acceptance is excellent, and fear of administration is eliminated, especially in comparison to administration by syringe and needle.

Iontophoresis is a method of choice for the administration of pilocarpine in a diagnostic test for cystic fibrosis (3) and of lidocaine and epinephrine for external ear canal anesthesia (4). Loose deciduous teeth have been extracted following a profound surface anesthesia induced by iontophoretic application of a local anesthetic (2% lidocaine) containing epinephrine (1:50,000) to the oral mucosa (5). Iontophoresis also has been used to administer vasodilators such as methacholine and histamine for peripheral vascular disease (6).

Iontophoresis frequently has been used in dentistry as a method of choice to aid in the penetration of fluoride ions for the treatment of exposed ultrasensitive (hypersensitive) dentin (7–10). Treatment of recurrent herpes labialis using idoxuridine iontophoresis results in abortion of the lesions and rapid healing (2, 11). Other uses of iontophoresis in medicine have been reviewed (1).

Several conditions are necessary for iontophoretic medication to be achieved. The drug should be charged or modified to carry a charge, and the area medicated must be at a body surface. The drug is applied under an electrode of the same polarity; a return electrode, opposite in charge to the drug, is placed at an indifferent site on the body. Then current is allowed to flow below the level of the pain threshold for an appropriate time (2).

This paper reports on the electrical characteristics of various drugs so that proper conditions for use may be achieved. The drugs studied include local anesthetics, vasoconstrictors, corticosteroids, antiviral agents (including some nucleosides and nucleotides), and anticancer agents.

EXPERIMENTAL

Apparatus—A lectro MHO-meter[1] equipped with a conductivity measuring cell[2] and a pH-millivolt meter[3] were used.

Chemicals—Local anesthetics were lidocaine hydrochloride[4], procaine hydrochloride[5], cocaine hydrochloride[6], bupivicaine hydrochloride[7], mepivacaine hydrochloride[8], and prilocaine hydrochloride[9]. Vasoconstrictors were epinephrine bitartrate[7], levarterenol bitartrate[7], and

[1] Model MC-1, Mark IV, Lab-Line Instruments, Melrose Park, Ill.
[2] Model 3403, Yellow Spring Instrument Co., Melrose Park, Ill.
[3] Model 701, Orion Research, Cambridge, Mass.
[4] Xylocaine Hydrochloride Monohydrate, Astra Pharmaceutical Products, Worcester, Mass.
[5] Novocaine Hydrochloride, Medical College of Georgia Pharmacy, Augusta, Ga.
[6] Medical College of Georgia Pharmacy, Augusta, Ga.
[7] Sterling-Winthrop Research Institute, Rensselaer, N.Y.
[8] Carbocaine Hydrochloride, Sterling-Winthrop Research Institute, Rensselaer, N.Y.
[9] *Citant Hydrochloride*, Astra Pharmaceutical Products, Worcester, Mass.

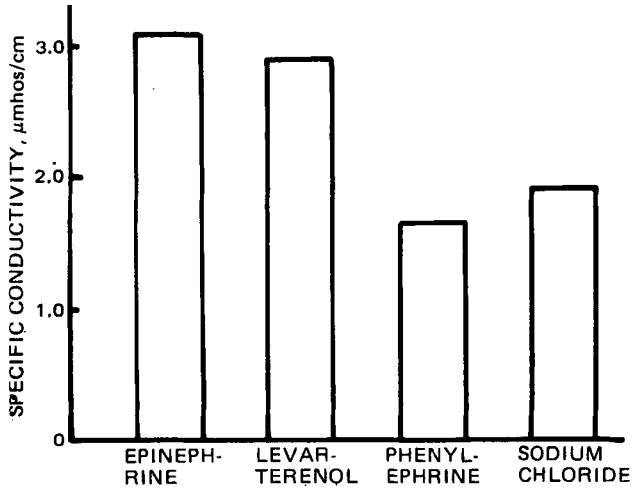

Figure 2—*Specific conductivities of vasoconstrictors. The concentration studied was 0.12 mM (about 1:25,000). The concentration of sodium chloride was the same as that of vasoconstrictors.*

phenylephrine hydrochloride[10]. Corticosteroid hormones were hydrocortisone sodium succinate[11], methylprednisolone sodium succinate[12], and hydrocortisone sodium phosphate[13]. Anticancer drugs were methotrexate[14], cyclophosphamide[15], bleomycin[16], and doxorubicin[17].

Nucleotides were adenosine 5′-monophosphate (AMP)[18], adenosine 5′-diphosphate (ADP)[18], adenosine 5′-triphosphate (ATP)[18], adenosine 3′,5′-cyclic monophosphate (cAMP)[18], uridine 5′-diphosphate (UDP)[18], uridine 5′-triphosphate (UTP)[18], and thymidine 5′-monophosphate (TMP)[18]. Antiviral agents were idoxuridine[19], vidarabine[20], thymine arabinoside[21], vidarabine monophosphate[22], and phosphonoacetic acid[23].

Conductivity Measurement Procedures—Various concentrations of chemicals were prepared with double-distilled water. Some chemicals were dissolved in buffers having different pH values. The prepared solutions were placed in a water bath (25°) for maintaining the temperature of chemical solutions. An aliquot of the solution was taken for measuring the specific conductivity, using the lectro MHO-meter, and the remaining portion of the solution was used for the pH determination.

Specific conductivity, k, was measured by direct reading of the lectro MHO-meter. The formula for calculating k is $k = (l/A)\,L$, where l/A is the conductivity cell constant (l is the distance in centimeters between the electrodes and A is the area in square centimeters of the electrode) and L is the conductivity in reciprocal ohms. Equivalent conductance was calculated from the specific conductivity by using $\Lambda = (k \times 1000)/C$, where Λ is the equivalent conductance, k is the specific conductivity, and C is the concentration of electrolyte (molar).

RESULTS

Figure 1 shows the specific conductivities of several local anesthetics tested at a concentration of 10 mM (sodium chloride measured at 5 mM is shown for reference). The specific conductivities ranged from 800 to 900 μmhos/cm. If one considers the pKa values of local anesthetics (lower line of Fig. 1) and the pH of the local anesthetic solutions (above the bars), it can be calculated that almost all of the local anesthetic molecules were ionized. When the pH of the lidocaine solution was increased from 5.36 to 6.89 by adding 1 mM NaOH (crosshatched bar of Fig. 1), the specific conductivity of the solution was decreased by 15%, indicating that the

[10] Neosynephrine Hydrochloride, Sterling-Winthrop Research Institute, Rensselaer, N.Y.
[11] Solu-Cortef, The Upjohn Co., Kalamazoo, Mich.
[12] Solu-Medrol, The Upjohn Co., Kalamazoo, Mich.
[13] Merck Sharp & Dohme, West Point, Pa.
[14] American Cyanamid Co., Pearl River, N.Y.
[15] Cytoxan, Mead Johnson Laboratories, Evansville, Ind.
[16] Blenoxane, Bristol Laboratories, Syracuse, N.Y.
[17] Adria Laboratories, Wilmington, Del.
[18] Sigma Chemical Co., St. Louis, Mo.
[19] Calbiochem, La Jolla, Calif.
[20] Ara-A, Parke-Davis & Co., Ann Arbor, Mich.
[21] Ara-T, a gift of Dr. Glenn Gentry, University of Mississippi, Jackson, Miss.
[22] Ara-AMP, Parke-Davis, Ann Arbor, Mich.
[23] PAA, Abbott Laboratories, Chicago, Ill.

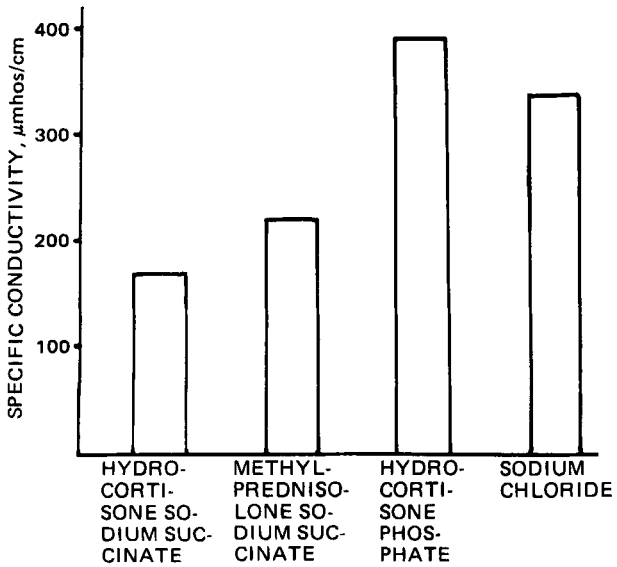

Figure 3—*Specific conductivities of some charged steroids. The concentration of steroids and sodium chloride was 2.0 m*M.

concentration of ionized lidocaine molecules was decreased by alkalization.

Figure 2 shows the specific conductivity of epinephrine bitartrate, levarterenol bitartrate, phenylephrine hydrochloride, and sodium chloride at 0.12 m*M*. This vasoconstrictor concentration is effective for iontophoresis in clinical practice. The conductivities of the two bitartrates were higher than the conductivity of the same concentration of sodium chloride, probably because of the presence of the divalent anion.

Figure 3 shows the specific conductivities of 2.0 m*M* steroids and sodium chloride. Hydrocortisone phosphate had the highest conductivity, methylprednisolone sodium succinate was intermediate, and hydrocortisone sodium succinate had the lowest. Hydrocortisone and methylprednisolone were nonconductive (data not shown).

Since some steroid solutions contain buffers, *e.g.*, phosphate buffer, the specific conductivity of the solution includes the conductivity of the buffer system. An experiment was performed to determine whether drug conductivity can be calculated by determining the conductivities of the drug and buffer followed by subtraction of the conductivity of the buffer alone. An additional amount of phosphate buffer, exactly as specified by the manufacturer, was added to the steroid–buffer solution, and the specific conductivity of the resultant solution as well as that of the buffer alone was measured.

When the same amount of phosphate buffer was added to the methylprednisolone sodium succinate–buffer solution, the conductivity was approximately increased by the conductivity of the phosphate buffer alone (Fig. 4). The pH of each of the three solutions was the same (7.0). The result indicates that there is no interaction between steroid and phosphate buffer and that each ion acts independently in terms of its contribution to conductivity.

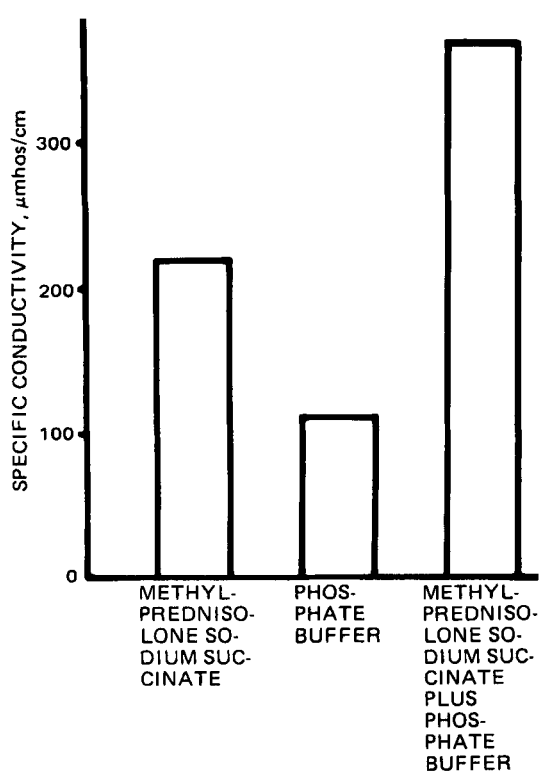

Figure 4—*Effect of phosphate buffer on the specific conductivity of methylprednisolone sodium succinate at 2.0 m*M.

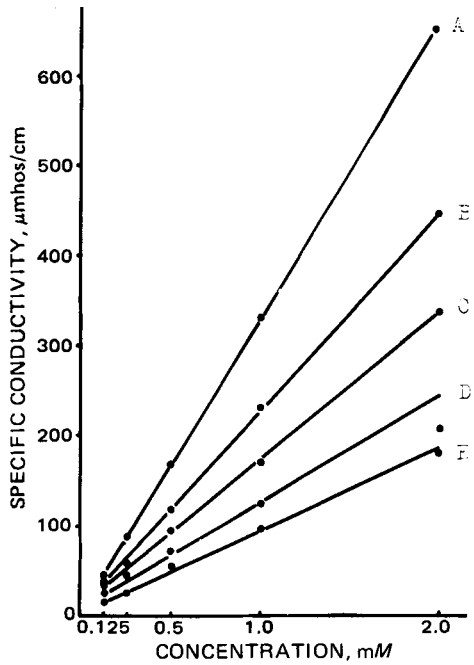

Figure 5—*Specific conductivities of anticancer drugs. Key: A, methotrexate; B, cyclophosphamide; C, sodium chloride; D, bleomycin; and E, doxorubicin.*

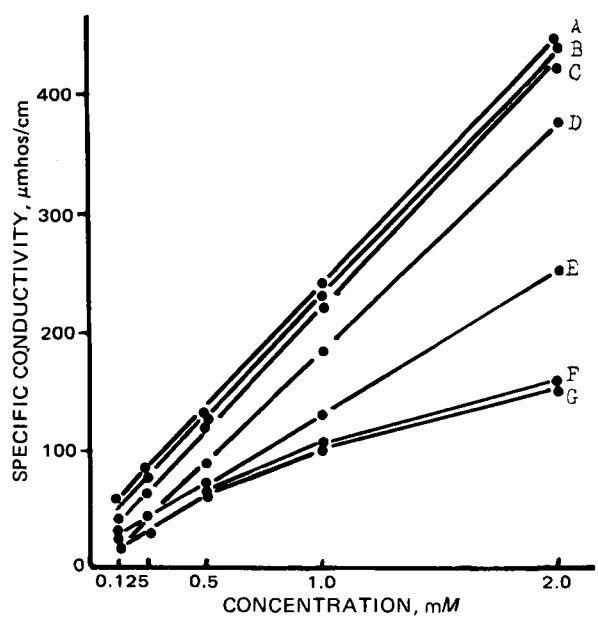

Figure 6—*Specific conductivities of nucleotides. Key: A, uridine 5′-triphosphate; B, adenosine 5′-triphosphate; C, adenosine 5′-diphosphate; D, uridine5′-diphosphate; E, thymidine 5′-monophosphate; F, adenosine 3′,5′-cyclic monophosphate; and G, adenosine 5′-monophosphate.*

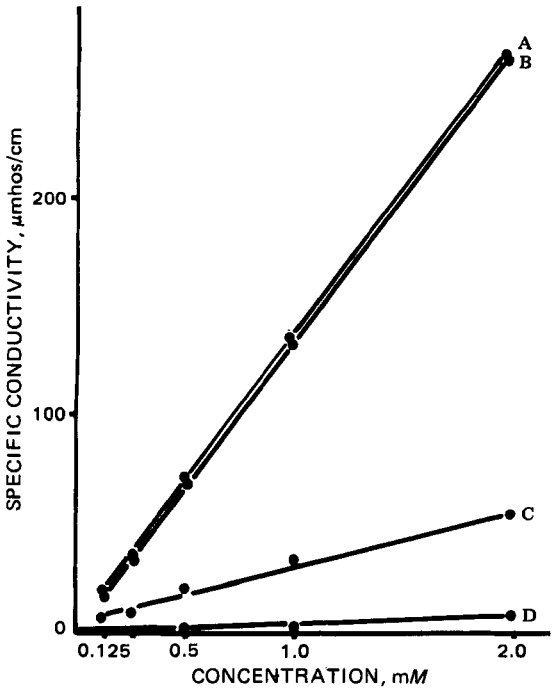

Figure 7—*Specific conductivities of antiviral agents. Key: A, phosphonoacetic acid; B, vidarabine monophosphate; C, idoxuridine; and D, vidarabine and thymine arabinoside. The conductivity of idoxuridine was measured in tromethamine buffer.*

Figure 5 is a plot of drug concentration *versus* specific conductivity for several anticancer drugs. A similar plot for sodium chloride is included for comparison. Drugs tested showed high conductivities. Methotrexate had the highest conductivity since it included a glutamate residue with two negative centers.

Figure 6 illustrates conductivity–concentration plots for several nucleotides. These compounds were studied because of their relationship to antiviral and anticancer drugs. The highly charged phosphate compounds showed high conductivities. The di- and triphosphates were more conductive than monophosphates. All nucleosides tested were nonconductive (data not shown).

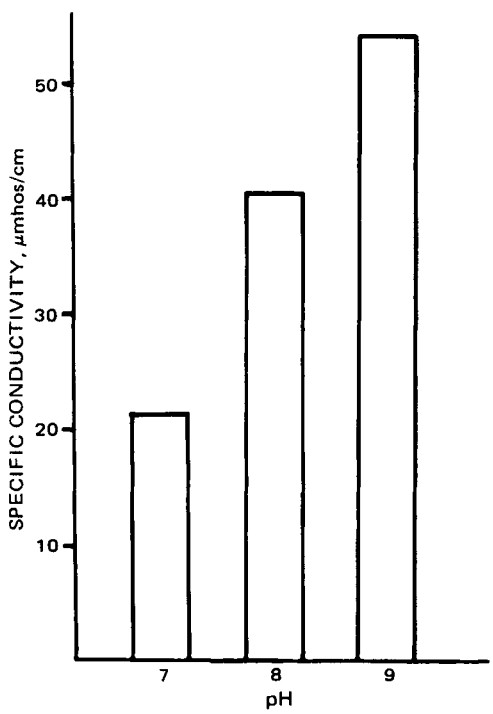

Figure 8—*Specific conductivity of idoxuridine at different pH values. Idoxuridine was dissolved in 0.02* M *tromethamine buffer solutions at pH 7, 8, and 9.*

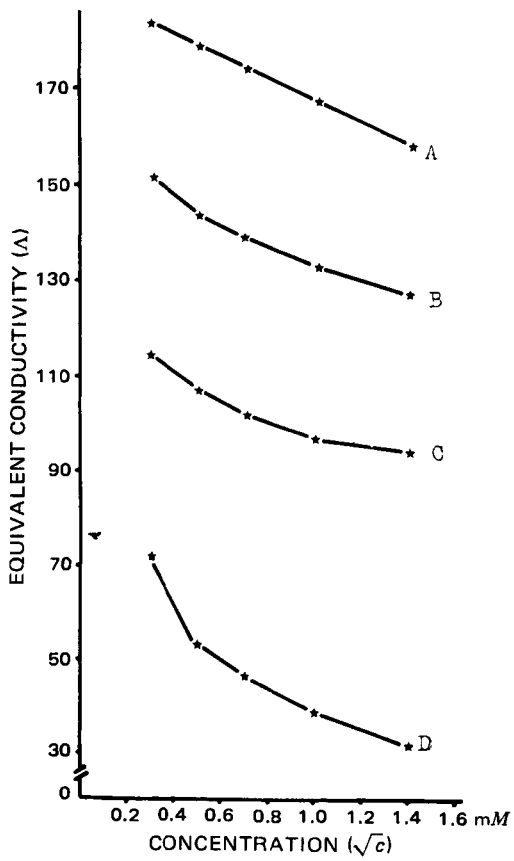

Figure 9—*Plot of equivalent conductivity,* Λ, versus $\sqrt{c}$ *for sodium chloride (A), vidarabine monophosphate (B), lidocaine (C), and idoxuridine (D). The value of* Λ *was calculated by the equation described in the text.*

Figure 7 illustrates the conductivities of several antiviral agents. Nucleoside analogs such as vidarabine, thymine arabinoside, and idoxuridine had almost no conductivity. However, the highly charged vidarabine monophosphate and phosphonoacetic acid had very high conductivities. When idoxuridine was dissolved in 0.02 *M* tromethamine buffer (pH 9.0), the conductivity of idoxuridine itself was highly increased by six times. As the pH increased, the conductivity of idoxuridine also increased (note the conductivity of the buffer alone at each pH subtracted) (Fig. 8). At pH 9, idoxuridine showed the highest conductivity. These data are consistent with the weak acid nature of idoxuridine (pKa 8.20).

Figure 9 shows the equivalent conductance, Λ, plotted against concentration for sodium chloride, vidarabine monophosphate, lidocaine, and idoxuridine. Sodium chloride solution formed a straight-line relationship when Λ was plotted against the square root of the concentration, $\sqrt{c}$; this relationship is typical of strong electrolytes, and the data agree with literature values (12). Idoxuridine showed the curvilinear pattern of a weak electrolyte while vidarabine monophosphate and lidocaine were intermediate.

DISCUSSION

Many drugs are appropriately charged for iontophoretic administration. Conductivity experiments conducted *in vitro* indicate which drugs are the best candidates for iontophoresis. Furthermore, the electrical properties of solutions with altered pH values and buffers added can be defined.

A literature search resulted in only one reference on the conductivity of drugs; it indicated that cocaine had 0.6 of the "tissue velocity" of sodium chloride (13). The conditions under which this measurement was made were not found. The present study reports the specific conductivity of a number of drugs of practical or theoretical usefulness for treatment of conditions or diseases of humans using iontophoresis as the administration method. The tissue to be treated must be at or near a body surface.

Drugs considered eligible for iontophoretic administration include local anesthetics (1, 4, 5) and anti-inflammatory (1), antiviral (2, 14, 15), and anticancer (16) agents.

All of the commonly used local anesthetic hydrochloride salts showed excellent conductivities. The conductivity of 10 m*M* lidocaine hydrochloride was about equal to that of 5.0 m*M* NaCl. Vasoconstrictors were also highly conductive; the conductivity of epinephrine bitartrate was greater than that of sodium chloride. Since local anesthetics and epinephrine are positively charged drugs, both can be introduced under the positive electrode (anode). The drugs can be properly balanced in concentration to obtain optimal vasoconstriction as well as deep topical anesthesia. In this clinic, 2% lidocaine with 1:12,500–1:50,000 epinephrine has been adequate for oral mucosa, ear canal, and skin anesthesia. The choice of epinephrine concentration depends on the vascularity of the tissue. One study (4) recommended 1:2000 epinephrine for ear canal anesthesia, but 1:12,500 was effective in this clinic.

Hydrochloride salts of local anesthetics conduct best at pH ~5. This pH keeps almost all local anesthetic molecules in the positively charged form. Increasing the pH tends to lower the conductivity by converting positively charged molecules to unionized molecules. However, iontophoresis of local anesthetics can be performed successfully even when the pH is close to the pKa since there will be adequate numbers of local anesthetic ions to carry the current.

Steroids are usually uncharged unless they have been chemically modified for high water solubility (intravenous use). Three anti-inflammatory steroids found to be highly conductive are methylprednisolone sodium succinate, hydrocortisone sodium succinate, and hydrocortisone phosphate. Since they are marketed for intravenous use, the solutions contain buffers to bring the solutions to proper pH and osmolarity. The present data indicate that highly ionic drug and buffer ions conduct current independently, each ion contributing to conductivity according to physicochemical factors operating in the solution of strong electrolytes. This conclusion was demonstrated by the finding that the buffer conductivity was equal to the conductivity of buffer in the mixture (Fig. 4).

The presence of buffer or salt ions is a negative factor for iontophoresis of moderate to strong electrolytes since extraneous ions compete with drug ions for the current. Nevertheless, iontophoresis seems to be successful when extraneous ions are present. It is preferable that more than one-half of the conductivity be due to drug ions. Aphthous ulcers, poison ivy, inflamed arthritic joints, and uninfected sores were treated successfully with the steroid iontophoresis.

A number of useful anticancer drugs have high conductivities, and iontophoresis of these drugs directly into the lesion may offer a new approach to treatment when surgical excision is impossible. This experimental hypothesis has not been tested, but studies with the closely related antiviral drugs indicate that experiments with anticancer chemotherapy using iontophoresis should be performed.

Nucleotides were tested for conductivity because of their chemical similarity to antiviral drugs. While nucleosides were nonconductive, the phosphorylated nucleotides were highly conductive because of the presence of phosphate groups. Triphosphates were about equal in conductivity to diphosphates, while monophosphates were less conductive. Adenosine monophosphate was almost equal in conductivity to sodium chloride at equal concentration. On the basis of these experiments, it was predicted that the antiviral nucleoside analogs (idoxuridine, thymine arabinoside, and vidarabine) would be nonconductive and that their respective nucleotide analogs would be highly conductive. These predictions, except for idoxuridine, were verified by the conductivity experiments; idoxuridine acts as a weak acid and becomes more conductive as the pH is increased. Experiments in mice (2, 14) showed that idoxuridine concentration in skin could be greatly increased by iontophoresis in comparison to topical administration. Both cathodal and anodal iontophoresis increased the skin penetration, but cathodal iontophoresis was ~20% more effective than anodal.

Subsequent experiments on penetration of uncharged compounds (tritiated water and thymidine) (17) indicated that sodium or chloride iontophoresis will carry other compounds in solution into the tissues, a process known as electro-osmosis. Anodal iontophoresis of idoxuridine is effective because of electro-osmosis while cathodal iontophoresis may act by both electro-osmosis and introduction of negative idoxuridine ions. On this basis, the commercial preparation of idoxuridine was applied at the anode to herpes simplex viral lesions of the lip (11). In all patients, the treatment was effective in aborting the viral lesions. In conjunction with medical specialists, herpes simplex viral lesions of the skin (recurrent or disseminated) and of the anus were treated successfully.

Many other agents could be suggested for iontophoresis. For example, antibacterial and antifungal agents may be introduced into localized lesions of skin more effectively than by topical administration and more safely than by systemic administration.

REFERENCES

(1) R. Harris, "Therapeutic Electricity and Ultraviolet Radiation," 2nd ed., S. Licht, Ed., Baltimore, Md., 1967, chap. 4, p. 156.

(2) J. M. Hill, L. P. Gangarosa, and N. H. Park, *Ann. N.Y. Acad. Sci.*, **284,** 604 (1977).

(3) L. E. Gibson and R. E. Cooke, *Pediatrics*, **23,** 545 (1959).

(4) M. Comeau, R. Brummett, and J. Vernon. *Arch. Otolaryngol.*, **98,** 114 (1973).

(5) L. P. Gangarosa, Sr., *J. Am. Dent. Assoc.*, **88,** 125 (1974).

(6) T. W. Stone, *J. Pharm. Pharmacol.*, **24,** 318 (1972).

(7) E. M. Collins, *Dent. Dig.*, **68,** 360 (1962).

(8) H. M. Scott, *J. Dent. Child.*, **29,** 225 (1962).

(9) K. S. Murthy, S. T. Talim, and I. Singh, *Oral Surg. Oral Pathol. Oral Med.*, **36,** 448 (1973).

(10) L. P. Gangarosa and N. H. Park, *J. Prosth. Dent.*, **39,** 173 (1978).

(11) L. P. Gangarosa, H. W. Merchant, N. H. Park, and J. M. Hill, *J. Dent. Res.*, **56,** B194 (1977).

(12) N. A. Lange, "Handbook of Chemistry," Handbook Publishers, Sandusky, Ohio, 1949, p. 1411.

(13) S. Leduc, "Electric Ions and Their Use in Medicine," Redman, London, England, 1908.

(14) L. P. Gangarosa, N. H. Park, and J. M. Hill, *Proc. Soc. Exp. Biol. Med.*, **154,** 439 (1977).

(15) N. H. Park, L. P. Gangarosa, and J. M. Hill, *ibid.*, **156,** 326 (1977).

(16) J. M. Hill, L. P. Gangarosa, and N. H. Park, *Am. Assoc. Cancer Res.*, **18,** 41 (1977).

(17) N. H. Park, L. P. Gangarosa, and J. M. Hill, *Proc. Southeast. Sec. Soc. Exp. Biol. Med.*, **1,** 16 (1976).

ACKNOWLEDGMENTS

The authors thank Mr. Robert Faircloth for assistance.

Supported in part by National Institutes of Health Grant 1-R01 DE 04917-01.

Simultaneous Determination of Niacin, Niacinamide, Pyridoxine, Thiamine, and Riboflavin in Multivitamin Blends by Ion-Pair High-Pressure Liquid Chromatography

R. L. KIRCHMEIER [x] **and R. P. UPTON**

Received December 14, 1977, from *Quality Control, Special Testing and Analytical Development Laboratories, Pfizer Inc., Groton, CT 06340.* Accepted for publication February 8, 1978.

Abstract □ A high-pressure liquid chromatographic procedure for the simultaneous determination of niacin, niacinamide, pyridoxine, thiamine, and riboflavin was developed and applied to the analysis of multivitamin blends for these water-soluble vitamins. Reversed-phase ion-pair chromatography, using sodium hexanesulfonate as the counterion, was employed. Analysis time is shortened considerably and precision is improved by the application of this analytical technique as compared to the current official methods of analysis. Involved sample pretreatment is not required.

Keyphrases □ Vitamins, various—simultaneous high-pressure liquid chromatographic analyses in multivitamin preparations □ High-pressure liquid chromatography—simultaneous analyses of various vitamins in multivitamin preparations

Methods currently used for the analysis of niacin, niacinamide, pyridoxine, thiamine, and/or riboflavin in multivitamin preparations involve the application of derivatization and measurement of total UV absorption (1, 2), polarography (3, 4), GLC (5), electrophoretic analysis (6), TLC (7, 8), colorimetry (9, 10), or fluorometry (11). Several of these methods are accurate (1, 2, 10, 11); however, they are complicated, and strict attention must be paid to the preparation of reagents (because of their instability or caustic properties) to obtain meaningful analytical data. Two methods (1, 5) are not capable of distinguishing between niacin and niacinamide.

The specificity and quantitative accuracy of several methods with respect to the determination of water-soluble vitamins in multivitamin preparations are doubtful (7–10). None of the procedures referenced is amenable to the simultaneous determination of niacin, niacinamide, pyridoxine, thiamine, and riboflavin, and most are relatively time consuming. For these reasons, the feasibility of using high-pressure liquid chromatography (HPLC) was examined.

EXPERIMENTAL

Equipment—An HPLC pump[1] at a flow rate of 0.5 ml/min and a loop injector[2] (50-μl volume loop) were used. Eluates were monitored at 270 nm with a variable wavelength detector[3]. A 30-cm × 4-mm i.d. stainless steel column[4] was packed with porous silica particles averaging <10 μm in diameter chemically bonded to a monomolecular layer of octadecyltrichlorosilane.

Materials and Reagents—USP–NF reference standards were used for standard solutions of niacin, niacinamide, pyridoxine, thiamine, and riboflavin. Sodium hexanesulfonate[5] was obtained commercially and used without further purification.

Mobile Phase Preparation—The mobile phase was prepared by mixing 250 ml of reagent grade methanol with 750 ml of a 0.005 *M* solution of sodium hexanesulfonate containing 1% (v/v) acetic acid in a 1-liter erlenmeyer flask. Prior to use, the mobile phase was degassed by vacuum filtration through a 5-μm pore, 47-mm diameter, polytef filter[6].

Standard Curves—Mixed standard solutions were prepared in the aqueous portion of the mobile phase to contain 0.0125–0.110 mg of niacin and niacinamide/ml, 0.0033–0.026 mg of pyridoxine/ml, 0.0016–0.0110 mg of thiamine/ml, and 0.0020–0.019 mg of riboflavin/ml. A 50-μl aliquot of each standard mixture was injected, and observed peak heights at 270 nm were plotted *versus* concentration for each water-soluble vitamin.

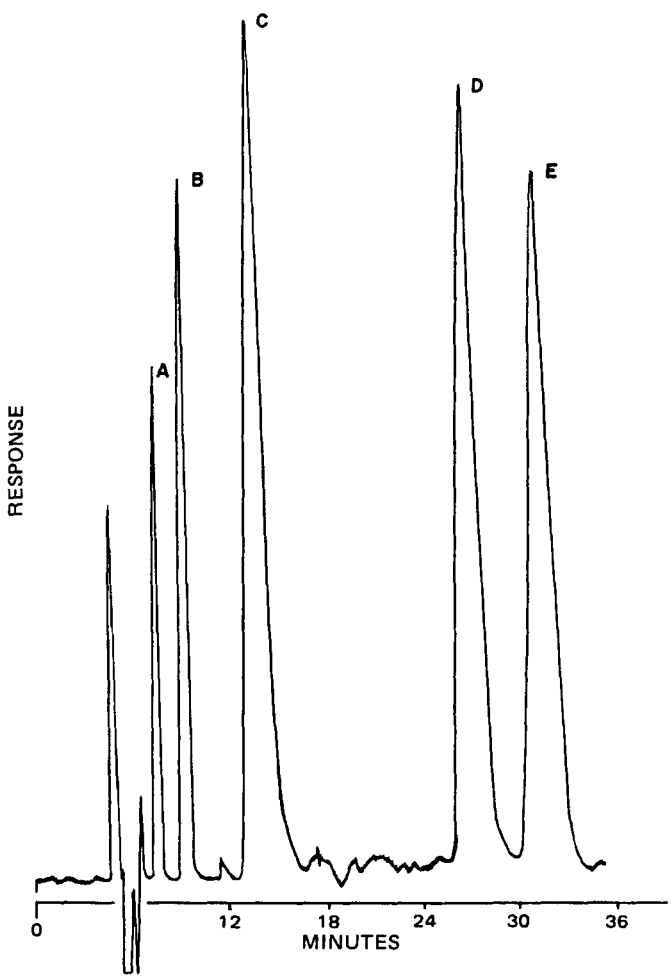

Figure 1—*Chromatographic trace of a standard mixture of niacin (A), niacinamide (B), pyridoxine (C), thiamine (D), and riboflavin (E). The conditions were: mobile phase, 25% methanol–75% 0.005 M sodium hexanesulfonate in 1% acetic acid; flow rate, 0.5 ml/min; detection, UV at 270 nm; and chart speed, 25.4 cm/hr.*

[1] Model 6000A, Waters Associates, Milford, Mass.
[2] Valco model CV-6-UHPa-C-20.
[3] Schoeffel model SF 770.
[4] μBondapak C_{18}, Waters Associates, Milford, Mass.
[5] Eastman-Kodak.
[6] Type LS, 47 mm, Millipore Corp.

0022-3549/78/1000-1444$01.00/0
© 1978, American Pharmaceutical Association

Table I—Precision of HPLC Method for the Determination of Niacin, Niacinamide, Pyridoxine, Thiamine, and/or Riboflavin in Five Multivitamin Blends

Multivitamin Blend	1 *RSD*, %				
	Niacin	Niacinamide	Pyridoxine	Thiamine	Riboflavin
1	—	1.0	—	1.3	1.0
2	—	1.0	0.9	2.6	1.2
3	2.8	—	—	3.0	2.8
4	1.0	—	—	0.5	—
5	—	2.4	0.9	—	1.0

Table II—Recovery of Niacin, Niacinamide, Pyridoxine, Thiamine, and/or Riboflavin from Five Multivitamin Blends

Multivitamin Blend	Recovery, %				
	Niacin	Niacinamide	Pyridoxine	Thiamine	Riboflavin
1	—	100	—	99	101
2	—	101	100	99	103
3	100	—	—	98	100
4	104	—	—	100	—
5	—	100	99	—	99

Sample Solution—No sample pretreatment was required for the multivitamin blends analyzed. Appropriate amounts of sample were dissolved directly in the aqueous portion of the mobile phase, placed in an ultrasonic bath for 10 min, diluted to volume, filtered if necessary, and chromatographed. Sample vitamin concentrations were determined *versus* single-point standards.

RESULTS AND DISCUSSION

Interest in the analysis of water-soluble vitamins in multivitamin preparations is immense. The complex matrixes of these preparations make chromatography an ideal choice for the determination, and the application of HPLC is particularly attractive due to its specificity, the lack of need for elaborate sample pretreatment schemes, and the physical properties of the vitamins themselves.

Recent literature reports indicated the successful application of reversed-phase ion-pair HPLC to the determination of niacin and niacinamide simultaneously (12, 13), riboflavin and thiamine simultaneously (13), and niacin, niacinamide, pyridoxine, and thiamine separately (13) in multivitamin preparations. A reversed-phase ion-pair HPLC technique for the simultaneous determination of niacinamide, pyridoxine, thiamine, and riboflavin analogous to the method described here was suggested previously (13); however, no reports of the application of this technique have appeared.

Liquid chromatographic methods involving ion exchange for the determination of niacinamide, niacin, pyridoxine, thiamine, and/or riboflavin were reported (14–17), but they are imprecise (18), result in limited column life (19), or are not amenable to the simultaneous determination of these vitamins. A normal phase chromatographic method for the determination of riboflavin in multivitamin preparations was reported (20), as was a reversed-phase system for folic acid, cyanocobalamin, and riboflavin (21). Relatively complicated sample pretreatment procedures are required for the application of many of these methods to the determination of water-soluble vitamins in multivitamin preparations.

In general, the complex matrixes of multivitamin preparations containing the water-soluble vitamins niacin, niacinamide, pyridoxine, thiamine, and riboflavin consist of polar diluents, fillers, oil-soluble vitamins, inorganic salts, dyes, preservatives, and other water-soluble vitamins such as folic acid and calcium pantothenate. Materials specifically tested for possible interference with the quantitation of niacin, niacinamide, pyridoxine, thiamine, or riboflavin and found to be either insoluble in the aqueous portion of the mobile phase or eluted at the solvent front include vitamins A, D, and E, butylated hydroxyanisole, butylated hydroxytoluene, calcium carbonate, elemental iron, yolk shade No. 2 dye, folic acid, and calcium pantothenate.

Cyanocobalamin was present in several multivitamin blend preparations but at levels not detectable (20 μg/g) by monitoring eluates at 270

Table III—Comparative Analyses between the HPLC Method, the Current Official Method, and the Amounts of Vitamin Added for Multivitamin Blend 1

Multivitamin Sample	Niacinamide, %			Thiamine, %			Riboflavin, %		
	HPLC	Official	Added	HPLC	Official	Added	HPLC	Official	Added
1-A	13.9 ± 0.3	14.5 ± 0.7	—[a]	2.8 ± 0.1	2.8 ± 0.1	—[a]	3.0 ± 0.1	2.8 ± 0.2	—[a]
1-B	13.9 ± 0.3	14.1 ± 0.7	—[a]	2.7 ± 0.1	2.7 ± 0.1	—[a]	3.0 ± 0.1	3.0 ± 0.2	—[a]
1-C	14.2 ± 0.3	14.5 ± 0.7	—[a]	2.7 ± 0.1	2.8 ± 0.1	—[a]	2.8 ± 0.1	2.8 ± 0.2	—[a]
1-D	13.9 ± 0.3	14.3 ± 0.7	14.5	1.9 ± 0.1	2.3 ± 0.1	2.1	2.6 ± 0.1	2.8 ± 0.2	2.8
1-E	14.2 ± 0.3	14.1 ± 0.7	14.5	2.0 ± 0.1	2.1 ± 0.1	2.1	2.5 ± 0.1	2.8 ± 0.2	2.8
1-F	13.4 ± 0.3	13.8 ± 0.7	14.5	2.0 ± 0.1	2.2 ± 0.1	2.1	2.8 ± 0.1	2.7 ± 0.2	2.8
1-G	13.3 ± 0.3	14.3 ± 0.7	14.5	2.2 ± 0.1	2.2 ± 0.1	2.1	2.9 ± 0.1	2.9 ± 0.2	2.8
1-H	14.0 ± 0.3	14.0 ± 0.7	14.5	2.2 ± 0.1	2.2 ± 0.1	2.1	2.9 ± 0.1	2.8 ± 0.2	2.8

[a] Values unavailable.

Table IV—Comparative Analyses between the HPLC Method, the Current Official Method, and the Amounts of Vitamin Added for Multivitamin Blend 2

Multivitamin Sample	Niacinamide, %			Pyridoxine, %			Thiamine, %			Riboflavin, %		
	HPLC	Official	Added	HPLC	Official	Added	HPLC	Official	Added	HPLC	Official	Added
2-A	3.7 ± 0.1	3.6 ± 0.2	3.8	0.46 ± 0.01	0.44 ± 0.03	0.45	0.58 ± 0.03	0.53 ± 0.03	0.52	0.34 ± 0.01	0.29 ± 0.02	0.30
2-B	3.7 ± 0.1	4.1 ± 0.2	3.9	0.44 ± 0.01	0.45 ± 0.03	0.46	0.54 ± 0.03	0.52 ± 0.03	0.53	0.33 ± 0.01	0.29 ± 0.02	0.31
2-C	3.6 ± 0.1	4.2 ± 0.2	3.8	0.43 ± 0.01	0.43 ± 0.03	0.45	0.53 ± 0.03	0.51 ± 0.03	0.52	0.42 ± 0.01	0.48 ± 0.03	—[a]
2-D	3.8 ± 0.1	4.1 ± 0.2	—[a]	0.42 ± 0.01	0.45 ± 0.03	—[a]	0.56 ± 0.03	0.53 ± 0.03	—[a]	0.34 ± 0.01	0.35 ± 0.02	—[a]
2-E	4.0 ± 0.1	4.1 ± 0.2	3.8	0.42 ± 0.01	0.45 ± 0.03	0.45	0.56 ± 0.03	0.53 ± 0.03	0.52	0.39 ± 0.01	0.35 ± 0.02	—[a]
2-F	3.7 ± 0.1	4.1 ± 0.2	—[a]	0.42 ± 0.01	0.45 ± 0.03	—[a]	0.55 ± 0.03	0.53 ± 0.03	—[a]	0.44 ± 0.01	0.35 ± 0.02	—[a]

[a] Values unavailable.

Table V—Comparative Analyses between the HPLC Method, the Current Official Method, and the Amounts of Vitamin Added for Multivitamin Blend 3

Multivitamin Sample	Niacin, %			Thiamine, %			Riboflavin, %		
	HPLC	Official	Added	HPLC	Official	Added	HPLC	Official	Added
3-A	13.6 ± 0.8	13.1 ± 0.7	—[a]	1.2 ± 0.1	0.9 ± 0.1	—[a]	1.1 ± 0.1	1.1 ± 0.1	—[a]
3-B	12.8 ± 0.7	12.9 ± 0.6	12.1	1.0 ± 0.1	0.9 ± 0.1	0.9	0.9 ± 0.1	1.0 ± 0.1	1.0
3-C	12.1 ± 0.7	13.1 ± 0.7	12.1	1.0 ± 0.1	0.9 ± 0.1	0.9	1.0 ± 0.1	1.0 ± 0.1	1.0
3-D	14.2 ± 0.8	12.8 ± 0.6	12.7	1.0 ± 0.1	1.0 ± 0.1	1.0	1.1 ± 0.1	1.0 ± 0.1	1.1
3-E	14.9 ± 0.8	13.5 ± 0.7	12.7	1.0 ± 0.1	1.0 ± 0.1	1.0	1.2 ± 0.1	1.1 ± 0.1	1.1

[a] Values unavailable.

Table VI—Comparative Analyses between the HPLC Method, the Current Official Method, and the Amounts of Vitamin Added for Multivitamin Blend 4

Multivitamin Sample	Niacin, %			Thiamine, %		
	HPLC	Official	Added	HPLC	Official	Added
4-A	9.8 ± 0.2	9.9 ± 0.5	10.0	0.95 ± 0.01	1.05 ± 0.05	1.00
4-B	10.6 ± 0.2	9.9 ± 0.5	—[a]	1.01 ± 0.01	1.06 ± 0.05	—[a]

[a] Values unavailable.

determining the vitamin content of the spiked samples *versus* single-point vitamin standards (Table II). Essentially quantitative recoveries were observed in all cases.

Comparative analytical data (between this HPLC procedure and the current official methods of analysis) are given in Tables III–VII for the five multivitamin blends. The average deviation of the HPLC method from the current official analytical procedures (percent relative to the current official analytical result) was 5.9% for niacin, 4.5% for niacinamide, 5.1% for pyridoxine, 6.4% for thiamine, and 4.5% for riboflavin. The HPLC assay (percent relative to the current official method analytical result) tended to give analytical values that were 3% high for niacin, 4% low for niacinamide, 2% low for pyridoxine, 0.5% low for thiamine, and

Table VII—Comparative Analyses between the HPLC Method, the Current Official Method, and the Amounts of Vitamin Added for Multivitamin Blend 5

Multivitamin Sample	Niacinamide, %			Pyridoxine, %			Riboflavin, %		
	HPLC	Official	Added	HPLC	Official	Added	HPLC	Official	Added
5-A	11.1 ± 0.5	11.4 ± 0.6	11.9	2.15 ± 0.04	2.3 ± 0.2	2.40	1.72 ± 0.03	1.7 ± 0.1	1.83
5-B	11.7 ± 0.6	11.8 ± 0.6	12.0	2.49 ± 0.04	2.3 ± 0.2	2.40	1.78 ± 0.04	1.7 ± 0.1	1.83

nm. Ascorbic acid, which elutes at the solvent front, tended to interfere with the quantitation of niacin when present in high concentrations; however, when the composition of the mobile phase was reduced from 25 to 22.5% methanol, the resolution of niacin from ascorbic acid was increased sufficiently to allow its accurate determination even in blends containing roughly 75% by weight of ascorbic acid. A small peak was noted just following the elution of pyridoxine due to the solubilization of small amounts of butylated hydroxytoluene, and a slight rise in the baseline of the chromatographic trace of multivitamin blends containing yolk shade No. 2 dye was noted; however, no interference with the quantitation of the water-soluble vitamins present was found.

All or portions of several multivitamin blend components are likely, if solubilized, to be retained on the column. A change in column performance was noted only after several days, however, during which time up to 20 samples containing varying amounts of the possible interferences were chromatographed. An overnight washing of the column with methanol regenerated it for further use.

The chromatographic trace of a standard mixture (50 μl injected) containing niacin (0.11 mg/ml, 0.1 aufs), niacinamide (0.11 mg/ml, 0.4 aufs), pyridoxine (0.026 mg/ml, 0.04 aufs), thiamine (0.011 mg/ml, 0.02 aufs), and riboflavin (0.019 mg/ml, 0.1 aufs) is presented in Fig. 1. The complete elution of all five water-soluble vitamins was accomplished within 35 min from injection. Recorder response *versus* vitamin concentration was linear for all five water-soluble vitamins over the concentration ranges described under *Experimental*. Correlation coefficients for standard curves were 0.9998, 0.9997, 0.9999, 0.9993, and 0.9998 for niacin, niacinamide, pyridoxine, thiamine, and riboflavin, respectively.

The mean y value and the y intercept were 2.52 and 0.12 for niacin, 3.47 and 0.22 for niacinamide, 3.85 and 0.17 for pyridoxine, 3.77 and 0.01 for thiamine, and 3.31 and 0.002 for riboflavin, respectively. The reproducibility of standard mixture injections as determined on 2 days with two separate standard mixtures was, at the worst, ±1.2% (2 *SD* relative to the average) for the five vitamins. Thus, single-point standards are amenable to the determination of these water-soluble vitamins by this procedure.

The precision of this method, as determined on four separate weighings of single samples of five different multivitamin blends, is presented in Table I. Although the water-soluble vitamin content of the five blends in solution varied widely (0.026–0.8 mg/ml for niacin, 0.032–0.076 mg/ml for niacinamide, 0.0036–0.016 mg/ml for pyridoxine, 0.002–0.008 mg/ml for thiamine, and 0.002–0.012 mg/ml for riboflavin), reproducibility was good in all cases. Decreases in precision noted for a particular water-soluble vitamin present in more than one sample matrix were directly proportional to the amount of vitamin present and the ease of dissolution of the sample matrix being assayed.

Recovery of the water-soluble vitamins present in each of the five multivitamin blend preparations was tested by adding the appropriate vitamins in amounts equal to those already present in the sample and

1% high for riboflavin. These deviations reflect the degree of imprecision and nonspecificity encountered using the current official methods of analysis.

The described HPLC method should be applicable to a variety of multivitamin preparations with little or no modification. Its flexibility with respect to sample concentration and composition and the lack of required elaborate sample pretreatment enhance accuracy and reduce analysis time greatly.

REFERENCES

(1) "Cereal Laboratory Methods," American Association of Cereal Chemists, St. Paul, Minn., 1967, p. 86.

(2) "The United States Pharmacopeia," 19th rev., Mack Publishing Co., Easton, Pa., 1975, p. 629.

(3) A. Y. Taura, *J. Assoc. Offic. Anal. Chem.*, **57**, 910 (1974).

(4) J. Lindquist and S. M. Farroha, *Analyst*, **100**, 377 (1975).

(5) J. Vessman and S. Stromberg, *J. Pharm. Sci.*, **64**, 311 (1975).

(6) Y. Itokava and J. R. Cooper, *Methods Enzymol.*, **18**, 91 (1970).

(7) H. Ahrens and W. Korytnyk, *Anal. Biochem.*, **30**, 413 (1969).

(8) S. A. Ismaiel and D. A. Yassa, *Analyst*, **98**, 816 (1973).

(9) V. D. Gupta and D. E. Cadwallader, *J. Pharm. Sci.*, **57**, 112 (1968).

(10) "The United States Pharmacopeia," 19th rev., Mack Publishing Co., Easton, Pa., 1975, p. 120.

(11) *Ibid.*, p. 627.

(12) S. P. Sood, D. P. Wittmer, S. A. Ismaiel, and W. G. Haney, *J. Pharm. Sci.*, **66**, 40 (1977).

(13) D. P. Wittmer and W. G. Haney, in "GLC and HPLC Analysis of Therapeutic Agents," K. Tsuji and W. Morozowitch, Eds., Dekker, New York, N.Y., 1976, chap. 29.

(14) "Chromatographic Application Bulletin DS019," Waters Associates, Milford, Mass., Feb. 1973.

(15) K. Callmer and L. Davies, *Chromatographia*, **7**, 644 (1974).

(16) R. C. Williams, D. R. Baker, and J. A. Schmidt, *J. Chromatogr. Sci.*, **11**, 618 (1973).

(17) K. Unger and D. Nyamah, *Chromatographia*, **7**, 63 (1974).

(18) M. Singh, *J. Assoc. Offic. Anal. Chem.*, **57**, 219 (1974).

(19) *Ibid.*, **57**, 358 (1974).

(20) D. P. Wittmer and W. G. Haney, Jr., *J. Pharm. Sci.*, **63**, 588 (1974).

(21) "Chromatographic Application Bulletin," Spectra-Physics, Santa Clara, Calif., 1974.

ACKNOWLEDGMENTS

The authors are indebted to R. Holmwood, J. Beyer, and R. May for assistance in the development and application of this analytical method.

Pharmacokinetics of Oral Cephalosporins: Cephradine and Cephalexin

E. FINKELSTEIN *, R. QUINTILIANI ‡, R. LEE §, A. BRACCI *, and C. H. NIGHTINGALE *x

Received November 18, 1977, from the *Department of Pharmacy, State University of New York at Buffalo, Amherst, NY 14260, the ‡Division of Infectious Diseases, Department of Medicine, Hartford Hospital, Hartford, CT 06100, and the §Department of Medicine, State University of New York at Buffalo, Buffalo, NY 14214. Accepted for publication February 8, 1978.

Abstract □ A crossover experiment was utilized to compare the pharmacokinetics of a 1-g dose of cephalexin tablets, cephalexin capsules, or cephradine capsules in nine normal human volunteers. These antibiotics were administered as three formulations: two 500-mg capsules of cephradine every 6 hr for five doses, two 500-mg capsules of cephalexin every 6 hr for five doses, and one 1000-mg tablet of cephalexin every 6 hr for five doses. Pharmacokinetic parameters in the experimental groups showed no statistical differences ($p > 0.1$), indicating that these drugs are equivalent pharmacokinetically.

Keyphrases □ Cephradine—pharmacokinetics compared to cephalexin, capsules and tablets, in humans □ Cephalexin—pharmacokinetics compared to cephradine, capsules and tablets, in humans □ Pharmacokinetics—cephradine and cephalexin compared, capsules and tablets in humans □ Antibacterials—cephradine and cephalexin, pharmacokinetics compared, capsules and tablets, in humans □ Cephalosporins—cephradine and cephalexin, pharmacokinetics compared, capsules and tablets, in humans

Cephalexin and cephradine are cephalosporin antibiotics available for oral administration. These agents have extremely similar spectra of microbiological activity and chemical structures. They are approved for the treatment of infections caused most commonly by sensitive strains of *Staphylococcus aureus, Streptococcus pyogenes, Streptococcus pneumoniae, Escherichia coli, Proteus mirabilis,* and *Klebsiella pneumoniae.* The usual therapeutic dose of these agents is 1–4 g/day, although doses of 6 g/day have been recommended (1–3).

Relatively few studies have appeared on the absorption and excretion characteristics of these drugs in 1-g doses in a single or multiple dosage regimen. This scarcity of information and the lack of any crossover studies, plus the fact that cephalexin is now available as a 1-g tablet, prompted a comparative study of these agents in doses of 4 g/day (4–12).

EXPERIMENTAL

Nine apparently normal, healthy volunteers, 23–38 years of age, underwent clinical-pathologic screening for liver, kidney, and hematologic function. This screen included serum electrolytes, creatinine, blood urea nitrogen, bilirubin, Coomb's test, complete blood count, serum glutamic-oxaloacetic transaminase, alkaline phosphatase, and creatinine clearance. All volunteers with a history of penicillin or cephalosporin allergy were excluded. No subject was receiving any other medications during this experiment.

A crossover design was utilized, with each subject undergoing a total of three experiments:

1. Two 500-mg capsules of cephradine[1] every 6 hr for five doses.
2. Two 500-mg capsules of cephalexin[2] every 6 hr for five doses.
3. One 1000-mg tablet of cephalexin[3] every 6 hr for five doses.

Cephalexin tablets, cephalexin capsules, or cephradine capsules were administered in a random fashion. At least 1 week separated all experiments. All subjects fasted overnight for 8 hr prior to each experiment and through the initial 2 hr of the testing. Water was provided in the following quantities: 200 ml initially, 200 ml at 1 hr, and *ad libitum* after 2 hr for the remainder of the sampling period.

Blood samples (1 ml) were collected through an indwelling butterfly catheter every 15 min for 1.5 hr and then every 30 min until the next dose was given. This schedule was followed for the first and final doses of each experiment. Urine was collected at hourly intervals between the first and second doses. Following the second dose, the total urine output during each dosing interval was collected. Once again, hourly urine output was collected following the final dose in the same manner as after the initial dose. The total urine output for the remainder of the 24 hr following the final dose also was collected.

Serum was separated from whole blood and frozen at −5°. Urine volume was measured, and an appropriate sample was frozen for analysis. Serum and urine concentrations were measured by a disk diffusion assay using *Bacillus subtilis* as the test organism (13). Serum and urine data were analyzed for appropriate pharmacokinetic parameters using a one-compartment open model with first-order absorption (14, 15). A nonlinear least-squares regression analysis computer program was used to fit the data (16).

RESULTS AND DISCUSSION

Nightingale *et al.* (14) suggested that cephalexin and cephradine be considered interchangeable. This suggestion was made after the pharmacokinetic evaluation of low maintenance dose (0.25–0.50 g) data. This study was undertaken to provide pharmacokinetic data for cephalexin tablet and capsule dosage forms and cephradine in large maintenance doses (1.0 g) in a well-controlled, crossover design.

The results (Fig. 1 and Tables I–III) illustrate that the serum con-

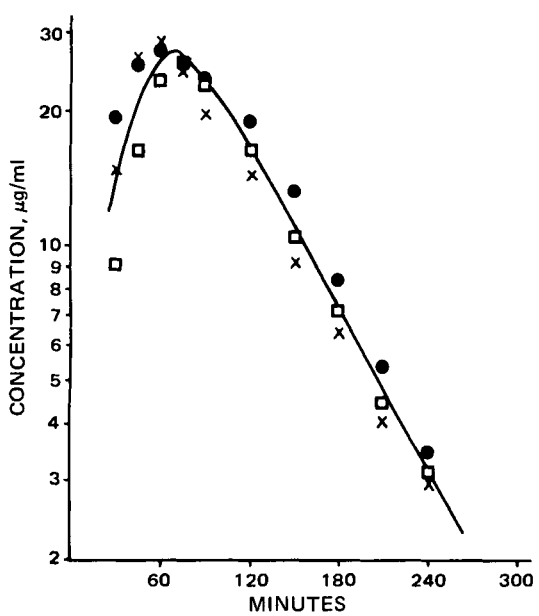

Figure 1—*Mean serum cephradine and cephalexin concentrations as a function of time. Key:* ●, *cephradine capsules;* ×, *cephalexin capsules; and* □, *cephalexin tablet.*

[1] Anspor capsules, 500 mg, lot 576A71, Smith Kline and French Laboratories, Philadelphia, Pa.
[2] Keflex Pulvules, 500 mg, lots 0DD32B and 0CN35B, Eli Lilly and Co., Indianapolis, Ind.
[3] Keflex tablets, 1 g, lot 9SH65A, Eli Lilly and Co., Indianapolis, Ind.

0022-3549/78/1000-1447$01.00/0
© 1978, American Pharmaceutical Association

Table I—Serum Cephradine Concentrations [a]

Subject	Minutes after Dose												
	15	30	45	60	75	90	120	150	180	210	240	270	300
BL	—	11.7	14.1	18.9	19.9	23.6	19.3	12.9	8.2	4.4	2.9	2.1	—
EM	—	3.5	12.3	21.6	22.6	25.0	20.1	16.1	7.6	5.5	3.9	2.5	1.7
CN	1.7	17.4	22.6	24.4	19.1	19.0	12.6	8.5	5.6	3.5	2.0	—	—
EF	6.6	30.6	35.6	31.6	26.6	23.2	17.8	10.8	6.4	3.4	1.9	—	—
TI	—	9.3	21.0	26.7	26.5	22.0	14.5	8.3	4.6	3.0	1.7	—	—
AM	12.4	44.5	44.2	40.1	32.0	26.7	17.9	10.9	7.7	4.7	3.1	—	—
AB	—	9.8	19.2	21.6	26.5	25.1	22.4	20.2	12.7	9.1	5.6	—	—
JO	—	36.3	43.9	41.5	34.8	30.5	21.6	9.9	8.6	4.9	3.1	—	—
GL	—	10.1	16.7	20.6	21.0	24.3	24.0	20.0	13.0	9.5	6.5	—	—
Mean	6.95	19.3	25.5	27.4	25.5	24.4	18.9	13.1	8.2	5.3	3.4		
SD	5.37	14.3	12.4	8.4	5.4	3.2	3.7	4.6	2.9	2.4	1.7		

[a] Data expressed as micrograms per milliliter.

Table II—Serum Cephalexin Capsule Concentrations [a]

Subject	Minutes after Dose												
	15	30	45	60	75	90	120	150	180	210	240	270	300
BL	—	23.3	33.7	30.4	24.1	20.9	16.4	9.6	7.2	4.2	2.8	1.7	—
EM	—	7.0	20.0	26.1	29.0	—	24.0	12.9	10.0	6.8	4.6	4.0	2.3
CN	—	21.1	27.9	22.2	19.3	16.0	9.0	6.5	3.3	3.0	—	—	—
EF	—	21.1	32.8	32.8	24.6	18.1	9.7	6.1	3.1	2.1	—	—	—
TI	—	14.3	29.5	33.9	26.3	22.2	16.3	10.2	7.5	4.8	2.2	1.8	—
AM	—	13.3	17.7	23.4	20.8	17.2	10.9	7.5	5.3	3.5	2.6	—	—
AB	—	12.2	—	29.0	25.9	24.8	18.9	15.0	10.4	6.5	3.9	—	—
JO	—	17.6	35.5	32.7	25.4	16.1	9.9	5.9	4.0	1.8	—	—	—
GL	—	2.5	13.3	23.9	—	20.6	14.2	7.4	5.3	3.4	1.7	—	—
Mean	—	14.7	26.3	28.3	24.4	19.5	14.4	9.0	6.3	4.0	3.0		
SD	—	6.9	8.3	4.5	3.1	3.2	5.0	3.2	2.7	1.7	1.1		

[a] Data expressed as micrograms per milliliter.

Table III—Serum Cephalexin Tablet Concentrations [a]

Subject	Minutes after Dose											
	15	30	45	60	75	90	120	150	180	210	240	270
BL	6.9	13.6	20.8	20.5	23.0	17.8	11.9	5.7	3.9	2.1	—	—
EM	—	7.1	14.6	22.4	24.3	20.8	16.0	12.1	8.3	5.6	3.1	2.2
CN	—	2.5	12.3	21.0	22.5	20.0	14.4	10.8	7.7	4.2	2.9	1.8
EF	—	19.7	28.5	28.6	25.2	23.6	14.1	9.0	6.2	4.7	2.7	—
TI	—	4.9	12.3	32.7	28.7	22.7	19.2	11.3	8.1	6.1	4.4	2.7
AM	—	21.8	30.1	27.4	23.6	22.2	14.5	9.5	6.2	3.9	2.7	—
AB	—	—	—	—	—	—	—	—	—	—	—	—
JO	—	1.2	7.8	19.8	36.3	32.5	19.6	10.8	7.6	3.6	2.2	—
GL	—	1.3	4.2	12.9	20.2	21.0	18.9	12.5	8.3	4.9	3.7	2.4
Mean	—	9.0	16.3	23.2	25.5	22.6	16.1	10.2	7.0	4.4	3.1	
SD	—	8.3	9.4	6.2	5.0	4.4	2.9	2.2	1.5	1.2	0.7	

[a] Data expressed in micrograms per milliliter.

Table IV—Peak Serum Concentration [a]

Subject	Cephradine Capsules		Cephalexin Capsules		Cephalexin Tablet	
	First Dose	Fifth Dose	First Dose	Fifth Dose	First Dose	Fifth Dose
CN	25.2[b]	23.7	27.9	27.9	17.6	27.6
EF	33.0	38.2	35.2	31.3	33.1	29.5
AM	47.2	48.2	24.3	27.9	25.0	36.4
JO	46.8	41.9	32.1	38.9	33.0	39.5
GL	28.8	28.8	24.5	31.1	23.8	22.3
TI	27.3	26.7	36.2	31.6	33.0	33.7
EM	29.0	26.7	30.6	27.7	30.9	21.6
BL	23.7	26.5	32.7	36.3	24.2	26.2
AB	33.5	27.8	23.9	35.5	—	—
Mean	32.7	32.0	29.7	30.9	27.6	29.6
SD	8.7	8.6	4.8	3.2	5.8	6.5

[a] Paired Student *t* tests were used to compare first- and fifth-dose peak serum concentrations in each of the three experimental groups. No statistical differences were found ($p > 0.1$). [b] Data expressed in micrograms per milliliter.

centration *versus* time profiles of these drugs at higher doses (1 g) are remarkably similar. No accumulation, as evidenced by lack of an increasing peak serum concentration, was observed after multiple dosing (Table IV). This result was not surprising since the half-lives of these drugs (approximately 45 min) are relatively short in relation to the dosing interval (6 hr).

It previously was established that the pharmacokinetics of cephalexin and cephradine (14, 15) are described most appropriately by two-compartment model analysis. Greene *et al.* (15) extensively studied the pharmacokinetics of cephalexin after one- and two-compartment model analysis and concluded that, for practical purposes, the pharmacokinetics could be described adequately by a one-compartment model. Comparison of the data reported in Table V shows that the pharmacokinetic parameters of cephalexin are not appreciably different from those reported by Greene *et al.* (15) after extensive two-compartment analysis. Accordingly, it was decided to analyze the data using a one-compartment model.

Table V—Pharmacokinetic Parameters [a]

Parameter	Cephradine Capsules[b]	Cephalexin Capsules	Cephalexin Tablet
AUC, μg-min/ml	3711.7 ± 671.8	3165.9 ± 561.5	3080.7 ± 417.9
Peak time, min	69.3 ± 22.0	60.4 ± 11.5	66.2 ± 14.5
Peak concentration, μg/ml	32.7 ± 8.1	30.6 ± 3.6	28.5 ± 14.5
Lag time, min	19.7 ± 5.7	22.3 ± 3.7	23.2 ± 8.2
$t_{1/2}$ elim., min	46.3 ± 4.5	46.2 ± 6.0	48.1 ± 7.1
$t_{1/2}$ abs., min	16.6 ± 6.3	12.4 ± 7.4	15.0 ± 4.0
Urinary recovery, %	85.5 ± 9.5	90.6 ± 8.7	89.6 ± 10.8
V_d, liters	18.4 ± 3.2	22.2 ± 4.4	22.7 ± 3.2[c]

[a] Paired Student *t* tests were used to compare all pharmacokinetic parameters between experimental groups. [b] Data expressed as mean ± *SD*. [c] $p < 0.01$ cephradine capsules *versus* cephalexin tablet.

Table VI—Cumulative Urinary Excretion [a]

Hours	Cephradine Capsules	Cephalexin Capsules	Cephalexin Tablet
First dose			
0–1	239.6 ± 90.2	284.0 ± 124.7	163.0 ± 96.8
1–2	599.1 ± 101.6	685.1 ± 140.6	535.0 ± 134.0
2–3	737.1 ± 128.8	795.9 ± 138.5	726.5 ± 113.3
3–4	801.3 ± 135.6	876.5 ± 153.6	804.6 ± 105.7
4–5	831.8 ± 148.0	915.5 ± 161.9	844.2 ± 111.5
5–6	845.1 ± 151.5	945.3 ± 161.5	863.7 ± 111.0
Fifth dose			
0–1	223.4 ± 108.7	266.6 ± 65.0	178.9 ± 96.0
1–2	586.2 ± 155.6	655.6 ± 101.3	602.2 ± 103.1
2–3	762.3 ± 139.0	839.2 ± 103.8	778.6 ± 125.0
3–4	858.4 ± 139.1	926.8 ± 111.1	889.4 ± 146.5
4–5	901.4 ± 143.2	972.2 ± 127.3	953.2 ± 184.7
5–6	921.4 ± 142.7	997.5 ± 137.4	988.7 ± 197.8
6–24	949.0 ± 148.5	1032.5 ± 139.8	1022.3 ± 200.2

[a] Data expressed as mean ± *SD* in milligrams.

Table VII—Urinary Recovery [a]

Dosing Interval	Cephradine Capsules	Cephalexin Capsules	Cephalexin Tablet
First	845.1 ± 151.5	945.3 ± 161.5	863.7 ± 111.0
Second	779.8 ± 104.5	797.6 ± 159.8	864.0 ± 178.1
Third	867.5 ± 91.1	798.1 ± 153.1	858.3 ± 158.4
Fourth	859.4 ± 162.6	951.9 ± 206.1	874.1 ± 161.7
Fifth	949.1 ± 148.5	1032.5 ± 139.8	1022.3 ± 200.2

[a] Data expressed as mean ± *SD* in milligrams.

Table VIII—Clearance Values [a]

	Cephradine Capsules		Cephalexin Capsules		Cephalexin Tablet	
Subject	Renal	TBC[b]	Renal	TBC	Renal	TBC
GL	217.8	234.3	518.3	416.0	415.0	359.7
JO	213.8	235.8	370.0	344.5	473.5	323.0
AB	155.5	241.8	264.3	268.3	—	—
AM	166.5	213.5	345.8	364.5	247.3	293.3
BL	231.2	315.0	255.7	268.8	370.5	412.0
EM	186.2	294.8	293.8	261.3	246.0	330.0
EF	235.5	264.5	188.7	350.0	182.2	288.8
CN	368.7	352.8	256.2	372.7	388.3	359.7
TI	379.0	346.7	283.7	284.8	247.7	270.1
Mean	239.3	277.7	308.5	325.7	321.3	329.7
SD	81.0	51.7	94.8	56.0	103.3	46.5

[a] Data expressed as milliliters per minute. [b] TBC = total body clearance.

However, the reported half-life for absorption, lag time, and volume of distribution should be considered as "apparent" parameters. A comparison of the model-independent parameters such as the peak concentration, time of peak concentration, clearance, area under the curve (*AUC*), elimination half-life, and urinary recovery allows one to determine if any differences exist in the pharmacokinetics of these drugs.

The data for the first and fifth doses of each patient were analyzed separately. Since no accumulation was noted after multiple dosing, the first and fifth dose parameters from each patient were averaged. The data from each experiment were compared and evaluated using paired Student *t* tests. Mean data for all subjects are shown in Table V.

No significant differences in the absorption or elimination half-life, *AUC*, peak serum concentration, time of peak, or lag time for absorption were observed. Analysis of the volume of distribution (V_d) data revealed a statistical difference between cephalexin tablets and cephradine capsules. No differences were found between either the cephalexin capsules and tablets or the cephalexin capsules and cephradine capsules. Since cephradine and cephalexin have similar protein binding (~10%) (14), one would expect similar V_d values as observed with the capsule data. No differences in the V_d values are expected due to dosage form effects. Although a statistical difference in V_d was found between cephalexin tablets and cephradine capsules, from a practical point of view the difference is not of sufficient magnitude to alter any pharmacokinetically derived dosage regimens and, therefore, is insignificant.

Cumulative urinary excretion data after the first and fifth doses (Table VI) illustrate that greater than 50% of both cephalexin and cephradine was excreted during the first 2 hr. Urinary recovery during each dosing interval is shown in Table VII. The amount recovered during any dosing interval was virtually identical for each experimental group. Since these drugs are eliminated unchanged in the urine (14), the percentage of the

total dose excreted can be used as indication of bioavailability. The data in Table V show that the percentage of the total dose recovered after 48 hr was similar for each drug and dosage form and that all were approximately 90–100% bioavailable. These findings are consistent with the results of other investigators (4–6, 12).

Renal clearances were calculated for each subject from the hourly urinary excretion rate data and the serum concentration at the midpoint of the collection period. Total body clearance was calculated from the volume of distribution and the elimination rate constant. Since no metabolites have been identified in humans for either cephalexin or cephradine (14), the renal and total body clearances would be expected to be identical. This expectation was found to be true (Table VIII). Renal and total body clearances of cephalexin and cephradine were also similar. Since both cephalexin and cephradine are eliminated by glomerular filtration and tubular secretion (14), clearances of greater than 125 ml/min were expected. This result is confirmed in Table VIII where it can be seen that the clearance values for these drugs are approximately 300 ml/min.

The present investigation, although not designed to investigate dose-dependent pharmacokinetics, firmly establishes in a carefully controlled manner that no difference exists in any measured parameter (Tables I–VIII) between cephradine and cephalexin in 1-g doses. This finding is consistent with previous pharmacokinetic analysis at low doses (0.25–0.50 g) (14). Rattie *et al.* (10) demonstrated that a linear relationship between dose (0.25–1.0 g) and both peak concentration and *AUC* exists for cephradine. Pfeffer *et al.* (9) reported that a linear relationship in peak concentration and *AUC* exists for cephalexin at doses of 0.25 and 0.5 g. The reported pharmacokinetic parameters from these studies are similar to the present findings; therefore, dose-dependent kinetics do not appear to exist with these drugs.

Since a 1-g tablet of cephalexin is available commercially, it was important to determine if the tablet and capsule dosage forms were equally bioavailable. Figure 1 and Tables II and III show that both the tablet and capsule yield similar serum concentration–time curves, indicating that no dosage form differences affecting the drug's pharmacokinetics exist. Statistical comparison of the *AUC*, percent of dose excreted, and all other pharmacokinetic parameters shown in Table V indicate that the bioavailability of the tablet and capsule dosage forms is similar. However, greater fluctuations in peak concentration and lag time were seen with the tablet dosage form. In addition, comparison of the cephalexin tablet to the cephradine capsules (Table V) reveals no statistically significant differences in any measured pharmacokinetic parameter.

The results of this study confirm that, from a pharmacokinetic view, these drugs in tablet or capsule form are essentially identical, both at low (0.25 g) and high (1.0 g) oral doses.

REFERENCES

(1) R. J. Fass, R. L. Perkins, and S. Saslaw, *Am. J. Med. Sci.*, **259,** 187 (1970).

(2) J. Klastersky, D. Daneau, and D. Weerts, *Chemotherapy*, **18,** 191 (1973).

(3) V. Macquet and P. L. Lafitte, *Postgrad. Med. J.*, **46S,** 128 (1970).

(4) P. E. Gower and C. H. Dash, *Br. J. Pharmacol.*, **37,** 737 (1969).

(5) R. S. Griffith and H. R. Black, *Clin. Med.*, **75,** 14 (1968).

(6) C. Harvengt, P. DeSchepper, F. Lamy, and J. Hansen, *J. Clin. Pharmacol.*, **13,** 36 (1973).

(7) C. H. O'Callaghan, J. P. R. Toothill, and W. D. Robinson, *J. Pharm. Pharmacol.*, **23,** 50 (1971).

(8) R. L. Perkins, H. N. Carlisle, and S. Saslaw, *Am. J. Med. Sci.*, **256,** 122 (1968).

(9) M. Pfeffer, A. Jackson, J. Ximenes, and J. P. DeMenezes, *Antimicrob. Agents Chemother.*, **11,** 331 (1977).

(10) E. S. Rattie, P. D. Bernardo, and L. J. Ravin, *ibid.*, **10,** 283 (1976).

(11) J. F. Scholand, G. R. Hodges, R. J. Fass, and S. Saslaw, *Am. J. Med. Sci.*, **267,** 111 (1974).

(12) A. Zaki and E. C. Schreiber, *J. Clin. Pharmacol.*, **14,** 118 (1974).

(13) H. P. Bassaris, R. Quintiliani, E. G. Maderazo, R. C. Tilton, and C. H. Nightingale, *Curr. Ther. Res.*, **19,** 110 (1976).

(14) C. H. Nightingale, D. S. Greene, and R. Quintiliani, *J. Pharm. Sci.*, **64,** 1899 (1975).

(15) D. S. Greene, D. R. Flanagan, R. Quintiliani, and C. H. Nightingale, *J. Clin. Pharmacol.*, **16,** 257 (1976).

(16) C. M. Metzler, G. L. Elfring, and A. J. McEwen, "A User's Manual for NONLIN and Associated Programs," Upjohn Co., Kalamazoo, Mich., 1974.

Versatile Kinetic Approach to Analysis of Dissolution Data

PETER VENG PEDERSEN *x and JAMES W. MYRICK ‡

Received December 5, 1977, from the **Department of Pharmacy, School of Pharmacy, University of California at San Francisco, San Francisco, CA 94143,* and the ‡*National Center for Drug Analysis, Food and Drug Administration, St. Louis, MO 63101.* Accepted for publication February 14, 1978.

Abstract □ A new kinetically based dissolution equation is presented that considers dissolution of polydisperse systems and disintegrating solid dosage forms. The equation is applicable under sink as well as nonsink conditions and enables the specific dissolution rate parameter, the dispersion parameter, the disintegration lag time, and a newly introduced parameter, the dissolution availability, to be evaluated simultaneously and directly from percent of label claim dissolved *versus* time data. The equation showed excellent fit to dissolution data for aminophylline tablets. The kinetic significance of the estimated parameters of the equation is discussed. The method of analysis is compared to an approach employing an empirical equation based on a modified Weibull distribution function.

Keyphrases □ Dissolution—kinetically based equation considers polydisperse systems and solid dosage forms, various conditions □ Models, mathematical—kinetically based equation considers dissolution of polydisperse systems and solid dosage forms, various conditions □ Kinetic approach—mathematical model considers dissolution of polydisperse systems and solid dosage forms, various conditions

The extensive literature on dissolution testing of drugs contains many theories and equations to describe observed behavior (1, 2). The equations often have limited application because they are derived for specific experimental conditions such as sink or nonsink conditions or they are based on unrealistic assumptions such as an ideal monodisperse system. Such equations often do not agree adequately with observed dissolution data.

Consequently, there has recently been interest in empirical equations for obtaining a better, more flexible

0022-3549/78/1000-1450$01.00/0

© 1978, American Pharmaceutical Association

total dose excreted can be used as indication of bioavailability. The data in Table V show that the percentage of the total dose recovered after 48 hr was similar for each drug and dosage form and that all were approximately 90–100% bioavailable. These findings are consistent with the results of other investigators (4–6, 12).

Renal clearances were calculated for each subject from the hourly urinary excretion rate data and the serum concentration at the midpoint of the collection period. Total body clearance was calculated from the volume of distribution and the elimination rate constant. Since no metabolites have been identified in humans for either cephalexin or cephradine (14), the renal and total body clearances would be expected to be identical. This expectation was found to be true (Table VIII). Renal and total body clearances of cephalexin and cephradine were also similar. Since both cephalexin and cephradine are eliminated by glomerular filtration and tubular secretion (14), clearances of greater than 125 ml/min were expected. This result is confirmed in Table VIII where it can be seen that the clearance values for these drugs are approximately 300 ml/min.

The present investigation, although not designed to investigate dose-dependent pharmacokinetics, firmly establishes in a carefully controlled manner that no difference exists in any measured parameter (Tables I–VIII) between cephradine and cephalexin in 1-g doses. This finding is consistent with previous pharmacokinetic analysis at low doses (0.25–0.50 g) (14). Rattie *et al.* (10) demonstrated that a linear relationship between dose (0.25–1.0 g) and both peak concentration and *AUC* exists for cephradine. Pfeffer *et al.* (9) reported that a linear relationship in peak concentration and *AUC* exists for cephalexin at doses of 0.25 and 0.5 g. The reported pharmacokinetic parameters from these studies are similar to the present findings; therefore, dose-dependent kinetics do not appear to exist with these drugs.

Since a 1-g tablet of cephalexin is available commercially, it was important to determine if the tablet and capsule dosage forms were equally bioavailable. Figure 1 and Tables II and III show that both the tablet and capsule yield similar serum concentration–time curves, indicating that no dosage form differences affecting the drug's pharmacokinetics exist. Statistical comparison of the *AUC*, percent of dose excreted, and all other pharmacokinetic parameters shown in Table V indicate that the bioavailability of the tablet and capsule dosage forms is similar. However, greater fluctuations in peak concentration and lag time were seen with the tablet dosage form. In addition, comparison of the cephalexin tablet to the cephradine capsules (Table V) reveals no statistically significant differences in any measured pharmacokinetic parameter.

The results of this study confirm that, from a pharmacokinetic view, these drugs in tablet or capsule form are essentially identical, both at low (0.25 g) and high (1.0 g) oral doses.

REFERENCES

(1) R. J. Fass, R. L. Perkins, and S. Saslaw, *Am. J. Med. Sci.*, **259,** 187 (1970).

(2) J. Klastersky, D. Daneau, and D. Weerts, *Chemotherapy*, **18,** 191 (1973).

(3) V. Macquet and P. L. Lafitte, *Postgrad. Med. J.*, **46S,** 128 (1970).

(4) P. E. Gower and C. H. Dash, *Br. J. Pharmacol.*, **37,** 737 (1969).

(5) R. S. Griffith and H. R. Black, *Clin. Med.*, **75,** 14 (1968).

(6) C. Harvengt, P. DeSchepper, F. Lamy, and J. Hansen, *J. Clin. Pharmacol.*, **13,** 36 (1973).

(7) C. H. O'Callaghan, J. P. R. Toothill, and W. D. Robinson, *J. Pharm. Pharmacol.*, **23,** 50 (1971).

(8) R. L. Perkins, H. N. Carlisle, and S. Saslaw, *Am. J. Med. Sci.*, **256,** 122 (1968).

(9) M. Pfeffer, A. Jackson, J. Ximenes, and J. P. DeMenezes, *Antimicrob. Agents Chemother.*, **11,** 331 (1977).

(10) E. S. Rattie, P. D. Bernardo, and L. J. Ravin, *ibid.*, **10,** 283 (1976).

(11) J. F. Scholand, G. R. Hodges, R. J. Fass, and S. Saslaw, *Am. J. Med. Sci.*, **267,** 111 (1974).

(12) A. Zaki and E. C. Schreiber, *J. Clin. Pharmacol.*, **14,** 118 (1974).

(13) H. P. Bassaris, R. Quintiliani, E. G. Maderazo, R. C. Tilton, and C. H. Nightingale, *Curr. Ther. Res.*, **19,** 110 (1976).

(14) C. H. Nightingale, D. S. Greene, and R. Quintiliani, *J. Pharm. Sci.*, **64,** 1899 (1975).

(15) D. S. Greene, D. R. Flanagan, R. Quintiliani, and C. H. Nightingale, *J. Clin. Pharmacol.*, **16,** 257 (1976).

(16) C. M. Metzler, G. L. Elfring, and A. J. McEwen, "A User's Manual for NONLIN and Associated Programs," Upjohn Co., Kalamazoo, Mich., 1974.

Versatile Kinetic Approach to Analysis of Dissolution Data

PETER VENG PEDERSEN *x and JAMES W. MYRICK ‡

Received December 5, 1977, from the **Department of Pharmacy, School of Pharmacy, University of California at San Francisco, San Francisco, CA 94143,* and the ‡*National Center for Drug Analysis, Food and Drug Administration, St. Louis, MO 63101.* Accepted for publication February 14, 1978.

Abstract □ A new kinetically based dissolution equation is presented that considers dissolution of polydisperse systems and disintegrating solid dosage forms. The equation is applicable under sink as well as nonsink conditions and enables the specific dissolution rate parameter, the dispersion parameter, the disintegration lag time, and a newly introduced parameter, the dissolution availability, to be evaluated simultaneously and directly from percent of label claim dissolved *versus* time data. The equation showed excellent fit to dissolution data for aminophylline tablets. The kinetic significance of the estimated parameters of the equation is discussed. The method of analysis is compared to an approach employing an empirical equation based on a modified Weibull distribution function.

Keyphrases □ Dissolution—kinetically based equation considers polydisperse systems and solid dosage forms, various conditions □ Models, mathematical—kinetically based equation considers dissolution of polydisperse systems and solid dosage forms, various conditions □ Kinetic approach—mathematical model considers dissolution of polydisperse systems and solid dosage forms, various conditions

The extensive literature on dissolution testing of drugs contains many theories and equations to describe observed behavior (1, 2). The equations often have limited application because they are derived for specific experimental conditions such as sink or nonsink conditions or they are based on unrealistic assumptions such as an ideal monodisperse system. Such equations often do not agree adequately with observed dissolution data.

Consequently, there has recently been interest in empirical equations for obtaining a better, more flexible

0022-3549/78/1000-1450$01.00/0

© 1978, American Pharmaceutical Association

representation of dissolution profiles (3–5). However, although empirical equations may fit some dissolution data better than equations derived from kinetic principles, they are usually of limited kinetic significance. Empirical equations may describe the general shape or nature of a dissolution curve (4) but are unable to resolve the dissolution data to describe adequately the intrinsic dissolution properties of a drug.

A new dissolution kinetic equation for characterizing dissolution properties of disintegrating solid dosage forms and multiparticulate systems is presented and tested. It is generally more applicable than other published equations and more completely describes a drug's dissolution properties. The intrinsic dissolution rate, the particle distribution effect, the disintegration effect, and the amount of drug available for dissolution can be evaluated directly from percent dissolved *versus* time data in simple and meaningful terms. This equation considers dissolution under sink as well as nonsink conditions and can be applied using most dissolution apparatus available.

THEORY

A previous paper (6) reported how the dissolution of multiparticulate systems under sink and nonsink conditions can be described rigorously according to a formula on the basis of the single-particle dissolution equation and the effective particle distribution (7). A mathematical model based on the well-established Noyes–Whitney kinetics (8) was derived for polydisperse systems with an effective particle distribution that is approximately log-normal (9). The mathematical model presented was:

$$\frac{W}{W_0} = \sum_{n=0}^{3} \binom{3}{n} (-G)^{(3-n)} \frac{F(T_2 - n\sigma) - F(T_1 - n\sigma)}{F(j - 3\sigma) - F(-i - 3\sigma)} \exp[(n^2 - 9)\sigma^2/2] \quad \text{(Eq. 1)}$$

where:

$$T_1 = \max(\ln G, -i\sigma)/\sigma \quad \text{(Eq. 2)}$$

$$T_2 = \max(\ln G, -j\sigma)/\sigma \quad \text{(Eq. 3)}$$

$$F(x) = \frac{1}{\sqrt{2\pi}} \int_{-\infty}^{x} \exp(-u^2/2)\, du \quad \text{(Eq. 4)}$$

$$G = \frac{\alpha^3 K^*}{1 + \alpha^3} t + \frac{K^*}{1 + \alpha^3} \int_0^t \frac{W}{W_0} dt \quad \text{(Eq. 5)}$$

$$\binom{3}{n} = \frac{3!}{(3-n)!n!} \quad \text{(Eq. 6)}$$

and where W/W_0 is the fraction undissolved at time t; K^* is the specific dissolution rate parameter (dimension = time^{-1}); σ is the dispersion parameter, a dimensionless measure of "how polydisperse" the effective particle distribution is; i and j (dimensionless) are the lower and upper truncation parameters of the effective particle distribution, respectively; and α (dimensionless) is the dissolution capacity coefficient, a measure of the dissolution capacity of the experimental system (6).

Equation 1 describes a general class of multiparticulate dissolution models considering both monodisperse ($\sigma = 0$) and polydisperse ($\sigma > 0$) systems and nonsink ($\alpha < \infty$) as well as sink ($\alpha = \infty$) conditions. The effective particle distribution can be considered truncated ($i, j < \infty$) or ideal ($i = j = \infty$), in which case Eq. 1 is simplified to (6):

$$\frac{W}{W_0} = \sum_{n=0}^{3} \binom{3}{n} (-G)^{(3-n)} \left[1 - F\left(\frac{1}{\sigma} \ln G - n\sigma\right)\right] \exp[(n^2 - 9)\sigma^2/2] \quad \text{(Eq. 7)}$$

In a study of the dissolution of micronized gliburide under sink conditions ($\alpha = \infty$), Eq. 7 was more appropriate than Eq. 1 because it contained fewer parameters, had the same kinetic significance, and gave essentially as good a fit as Eq. 1 (10). Simulation studies also showed that the effect of i and j is insignificant as long as the effective particle distribution is not extremely truncated (7). Therefore, it is appropriate to develop Eq. 7 to consider more complex systems such as the dissolution of disintegrating tablets, capsules, and compounded powders.

Two problems must be considered. The first arises from the fact that the dissolution of such systems cannot be followed in terms of W/W_0 *versus* time as in Eqs. 1 and 7 because W_0, the initial amount available for dissolution, and, therefore, also $W = W_0 - W_d$, where W_d is the amount dissolved, are not known. There are two reasons for this problem: (*a*) the drug content in a unit dose is usually not equal to the label claim because of the limited precision of the manufacturing process; and (*b*) the amount of drug available for dissolution, W_0, may be less than the actual drug content because of formulation problems such as incomplete disintegration and complexation.

However, the dissolution of solid dosage forms can always be expressed in terms of p, the percent of label claim dissolved *versus* time:

$$p = 100 W_d/(W_0)_1 \quad \text{(Eq. 8)}$$

where W_d and $(W_0)_1$ are the amount dissolved and the label claim, respectively. This problem can then be solved by introducing an additional parameter, F_d; it will be called the dissolution availability and be defined as the percent of label claim available for dissolution:

$$F_d = 100 W_0/(W_0)_1 \quad \text{(Eq. 9)}$$

Since $W/W_0 = 1 - W_d/W_0$, it follows from Eqs. 8 and 9 that:

$$W/W_0 = 1 - p/F_d \quad \text{(Eq. 10)}$$

This expression can then be inserted in Eq. 7 to replace the unknown variable W/W_0 with the variable p, which can be measured.

The second problem concerns the disintegration process. On the basis of some assumptions about disintegration, extensions to the model can be developed so that the kinetics of the disintegration process are considered. However, this consideration may complicate the dissolution kinetic model unnecessarily. A simpler approach is to consider that the dosage form has an ideal, instantaneous disintegration. This ideal is never the case, so a disagreement will exist between the dissolution data and the ideal model in the initial phase of the dissolution where the disintegration takes place. However, if the disintegration process is relatively short compared to the dissolution process, then the model is expected to agree with the data after this initial phase when the model is corrected for the dissolution lag time caused by disintegration, *i.e.*, when t in Eq. 7 is substituted with the expression $\max(t - \tau, 0)$ defined by[1]:

$$\max(t - \tau, 0) = 0 \qquad \text{for } t \le \tau \quad \text{(Eq. 11)}$$

$$\max(t - \tau, 0) = t - \tau \qquad \text{for } t > \tau \quad \text{(Eq. 12)}$$

where τ is the dissolution lag time. The value determined for τ gives a simple measure of the effect of the disintegration process on the dissolution.

When the expression for W/W_0 (Eq. 10) and the dissolution lag time τ is introduced in Eq. 7, it becomes:

$$p = F_d - F_d \sum_{n=0}^{3} \binom{3}{n} (-H)^{(3-n)} \left[1 - F\left(\frac{1}{\sigma} \ln H - n\sigma\right)\right] \exp[(n^2 - 9)\sigma^2/2] \quad \text{(Eq. 13)}$$

where:

$$H = K^* \max(t - \tau, 0) - \frac{K^*}{F_d(1 + \alpha^3)} \int_0^{\max(t-\tau,0)} p\, dt \quad \text{(Eq. 14)}$$

Equation 13 contains the normal probability integral F. This function is related to the error function, erf, and the complementary error function, erfc, by:

$$F(x) = \tfrac{1}{2}\left[\operatorname{erf}\left(\frac{x}{\sqrt{2}}\right) + 1\right] = 1 - \tfrac{1}{2} \operatorname{erfc}\left(\frac{x}{\sqrt{2}}\right) \quad \text{(Eq. 15)}$$

where:

$$\operatorname{erf}(x) = \frac{2}{\sqrt{\pi}} \int_0^x \exp(-u^2)\, du \quad \text{(Eq. 16)}$$

Therefore, Eq. 13 can also be expressed in terms of the complementary error function, which may be computationally more convenient[2]:

[1] The expression $\max(x - y, 0)$ is frequently denoted by $(x - y)_+$ in the mathematical literature. The former way of writing is used here because it is less ambiguous.

[2] The complementary error function is available as a built-in Fortran library function, ERFC, in IBM's Fortran; the probability integral Eq. 4 is not.

$$p = F_d - \frac{F_d}{2}\sum_{n=0}^{3}\binom{3}{n}(-H)^{(3-n)}\,\mathrm{erfc}\left[\left(\frac{1}{\sigma}\ln H - n\sigma\right)\Big/\sqrt{2}\right] \exp[(n^2-9)\sigma^2/2] \quad \text{(Eq. 17)}$$

where H is the expression defined by Eq. 14.

Equation 17, which describes the variation of p, the percent of label claim dissolved, with time, is applicable under a wide range of conditions. It considers polydisperse ($\sigma > 0$) as well as monodisperse ($\sigma = 0$) systems dissolving under nonsink ($\alpha < \infty$) or sink ($\alpha = \infty$) conditions.

Polydisperse Systems Dissolving under Sink Conditions—A sink condition is described by letting $\alpha \to \infty$ for which:

$$H = K^* \max(t = \tau, 0) - \frac{K^*}{F_d(1+\alpha^3)}\int_0^{\max(t-\tau,0)} p\,dt \to K^* \max(t-\tau, 0) \quad \text{(Eq. 18)}$$

so that Eq. 17 (and, similarly, Eq. 13) becomes:

$$p = F_d - \frac{F_d}{2}\sum_{n=0}^{3}\binom{3}{n}[-K^* \max(t-\tau,0)]^{(3-n)} \mathrm{erfc}\left\{\left[\frac{1}{\sigma}\ln[K^* \max(t-\tau,0)] - n\sigma\right]\Big/\sqrt{2}\right\} \exp[(n^2-9)\sigma^2/2] \quad \text{(Eq. 19)}$$

If H in Eq. 14 is written in the form:

$$H = K^*\left[\max(t-\tau,0) - \frac{1}{F_d(1+\alpha^3)}\int_0^{\max(t-\tau,0)} p\,dt\right] \quad \text{(Eq. 20)}$$

the only difference between the equation for nonsink conditions (Eq. 17) and sink conditions (Eq. 19) is the expression:

$$-\frac{1}{F_d(1+\alpha^3)}\int_0^{\max(t-\tau,0)} p\,dt$$

which, according to Eq. 20, can be considered as a "time-correcting term" accounting for the nonsink conditions. This term vanishes as the sink condition is approached ($\alpha \to \infty$).

The sink condition was previously (6) defined as "an interparticle independent dissolution," *i.e.*, a dissolution where the dissolution of any one particle does not affect the dissolution of the other particles[3]. This condition can be approximated closely in a noncumulating, open flow-through system (*e.g.*, Refs. 11 and 12). The drug dissolution in such systems is often followed by an automatic, continuously recording technique that provides data of differential form, *i.e.*, dW_d/dt *versus* t. To apply Eq. 19 would require the experimental data to be integrated, which may introduce numerical integration errors. To avoid this problem, it is more convenient to use the following differential form of Eq. 19, which can be derived readily (10):

$$\frac{dW_d}{dt} = \frac{3(W_0)_1 F_d K^*}{200}\sum_{n=0}^{2}\binom{2}{n}[-K^* \max(t-\tau,0)]^{(2-n)} \mathrm{erfc}\left\{\left[\frac{1}{\sigma}\ln[K^* \max(t-\tau,0)] - n\sigma\right]\Big/\sqrt{2}\right\} \exp[(n^2-9)\sigma^2/2] \quad \text{(Eq. 21)}$$

Monodisperse Systems Dissolving under Nonsink Conditions—A monodisperse system dissolving under nonsink conditions is described by $\sigma \to 0$ and $\alpha < \infty$, for which Eq. 13 (and, similarly, Eq. 17) reduces to (6):

$$p = F_d - F_d\sum_{n=0}^{3}\binom{3}{n}(-H)^{(3-n)} = F_d[1-(1-H)^3] \quad \text{(Eq. 22)}$$

Differentiation and rearrangement of Eq. 22 followed by integration give:

$$p = F_d[1 - x(K^*, \tau, \alpha)^3] \quad \text{(Eq. 23)}$$

where $x(K^*, \tau, \alpha)$ is the root of the equation:

$$\phi(x, \alpha) - \phi(1, \alpha) + K^* \max(t-\tau, 0) = 0 \quad \text{(Eq. 24)}$$

where the function ϕ is defined by:

$$\phi(x,\alpha) = \frac{\alpha^3+1}{\alpha^2}\frac{1}{6}\ln\frac{(x+\alpha)^2}{x-\alpha x+\alpha^2} + \frac{1}{\sqrt{3}}\tan^{-1}\frac{2x-\alpha}{\alpha\sqrt{3}} \quad \alpha \neq 0 \quad \text{(Eq. 25)}$$

[3] The nonsink condition was defined as the condition in a solute cumulating, closed system where the particles are exposed to the same bulk concentration of solute.

Equation 23 is preferable compared to Eq. 22 because it can be evaluated faster and more accurately on a digital computer.

For the special case $\alpha = 0$, Eq. 22 becomes:

$$p = F_d\{1 - [1 + 2K^* \max(t-\tau, 0)]^{-3/2}\} \quad \text{(Eq. 26)}$$

Monodisperse Systems Dissolving under Sink Conditions—For sink conditions ($\alpha \to 0$), Eq. 22 becomes:

$$p = F_d\{1 - \{\max[1 - K^* \max(t-\tau, 0), 0]\}^3\} \quad \text{(Eq. 27)}$$

where the max relationship ensures that $p \to F_d$ for $t \to \infty$ as expected[4].

The differential form of Eq. 27 is:

$$\frac{dW_d}{dt} = 3(W_0)_1 F_d K^*\{\max[1 - K^* \max(t-\tau, 0), 0]\}^2 \quad \text{(Eq. 28)}$$

which may be more appropriate than Eq. 27 when the dissolution data obtained are of differential form. For the special case $\tau = 0$, Eq. 27 can, according to Eq. 10, be written:

$$(W/W_0)^{1/3} = \max(1 - K^* t, 0) \quad \text{(Eq. 29)}$$

which is the well-known Hixson–Crowell cube root law (13). However, it would be incorrect to apply this equation directly to the dissolution of compounded drugs because W_0 and W are usually not accurately known for such systems.

EXPERIMENTAL

Commercially available aminophylline tablets with a label claim of 97.2 mg (1.5 gr) of aminophylline (theophylline ethylenediamine) were used for the dissolution tests. A Hanson dissolution apparatus[5] modified to accommodate a round-bottom resin kettle (14) was used at a stirring speed of 50 rpm witn 900 ml of water at 37°. Filtered aliquots were automatically withdrawn every 10 min from 3 to 113 min and analyzed spectrophotometrically at 273 nm.

The dissolution data, expressed as percent of label claim dissolved *versus* time, were analyzed[6] by a nonlinear least-squares regression technique according to the mathematical models discussed using FUNFIT, an interactive time-sharing program for general nonlinear regression and curve fitting (15).

RESULTS AND DISCUSSION

Although the dissolution kinetic equation, Eq. 17, mathematically may seem difficult to apply because the dependent variable, p, appears in both explicit and integral form, it can readily be fitted to p *versus* t dissolution data using a digital computer. To do so, p must be expressed numerically as an explicit function of t and the parameters K^*, F_d, σ, τ, and α. This is done as follows. Define:

$$y = \int_0^{\max(t-\tau,0)} p\,dt \quad \text{(Eq. 30)}$$

Then:

$$\frac{dy}{dt} = p \quad \text{(Eq. 31)}$$

and Eq. 17 can be written:

$$\frac{dy}{dt} = F_d - \frac{F_d}{2}\sum_{n=0}^{3}\binom{3}{n}(-A)^{(3-n)} \mathrm{erfc}\left[\left(\frac{1}{\sigma}\ln A - n\sigma\right)\Big/\sqrt{2}\right] \exp[(n^2-9)\sigma^2/2] \quad \text{(Eq. 32)}$$

where:

$$A = K^* \max(t-\tau, 0) - \frac{K^*}{F_d(1+\alpha^3)}y \quad \text{(Eq. 33)}$$

and:

$$y = 0 \qquad \text{for } t \leq \tau \quad \text{(Eq. 34)}$$

Equations 32–34 constitute an initial value problem that can be solved

[4] It is also readily verified using L' Hospital's rule that $W/W_0 \to 0$ for $t \to \infty$ in Eqs. 1 and 7, that $p \to F_d$ for $t \to \infty$ in Eqs. 13, 17, 19, 22, and 23, and that $dW_d/dt \to 0$ for $t \to \infty$ in Eq. 21.

[5] Hanson Research Corp., Northridge, CA 91324.

[6] The computations were done on an IBM 370/145 digital computer.

Table I—Dissolution Kinetic Parameters for Aminophylline Tablets Obtained by Nonlinear Least-Squares Regression Using Eq. 17

Tablet	Specific Dissolution Rate Parameter, $K^* \times 100$, min^{-1}	Dissolution Availability, F_d, %	Lag Time due to Disintegration, τ, min	Dispersion Parameter, σ	r
1	1.85	98.2	7.33	0.338	0.99882
2	1.96	99.9	6.19	0.302	0.99897
3	1.70	96.3	6.15	0.295	0.99854
4	2.25	96.5	6.71	0.431	0.99871
5	2.46	105	5.42	0.439	0.99848
6	1.82	98.3	6.20	0.374	0.99865
Mean	2.01	99.0	6.33	0.363	0.99870
CV, %	14.4	3.24	10.1	17.2	

numerically using a suitable integration algorithm such as a fourth-order Rhunge–Kutta method (16). The integration algorithm evaluates y as a function of time:

$$y(t) = \int_0^{\max(t-\tau,0)} p\,dt \qquad \text{(Eq. 35)}$$

which, when substituted into Eq. 32, gives p as a function of time, *i.e.*:

$$p = F_d - \frac{F_d}{2}\sum_{n=0}^{3}\binom{3}{n}(-A)^{(3-n)} \operatorname{erfc}\left[\left(\frac{1}{\sigma}\ln A - n\sigma\right)\Big/\sqrt{2}\right]\exp[(n^2-9)\sigma^2/2] \qquad \text{(Eq. 36)}$$

where:

$$A = K^*\max(t-\tau,0) - \frac{K^*}{F_d(1+\alpha^3)}y(t) \qquad \text{(Eq. 37)}$$

This procedure can be programmed and executed with a suitable nonlinear regression program to obtain the dissolution kinetic parameters K^*, F_d, τ, and σ directly from percent dissolved *versus* time dissolution data. The data treatment can readily be established as a simple routine procedure, either separately or directly in the form of a computer interface to a dissolution apparatus.

The practical value and power of Eq. 17 are substantiated by the significance and simplicity of its parameters. The specific dissolution rate parameter, K^*, is the most important parameter since it measures the dissolution rate. It has the remarkable property of not being dependent on the degree of sink or nonsink conditions in the dissolution or on the amount of drug used. It, therefore, allows a greater flexibility with respect to the design of the dissolution apparatus. This parameter can be interpreted as a dissolution rate parameter "extrapolated" to complete sink condition so it is automatically corrected for any degree of nonsink conditions (6). It gives a measure of the intrinsic dissolution rate properties of the drug.

A comparison of drug products on the basis of the K^* parameter is particularly simple and meaningful. For example, if $K_A^*/K_B^* = x$ in a comparison of Brand A and Brand B of tablets, capsules, or powders, then Brand A is x times faster dissolving than Brand B in the sense that it takes B x times as long to dissolve to the same extent (*e.g.*, 50, 95, or 100%) as Brand A. This is the case provided that the dissolution lag time, τ, and the dispersion parameter, σ, are not too different between the two products. This property is related to the concepts of intrinsic dissolution profiles and time scaling discussed previously (9).

In theory, the K^* ratio property extends over a wide range of experimental conditions. Therefore, the K^* parameter may be particularly valuable to consider in correlation analysis of *in vitro–in vivo* relationships.

The dissolution lag time, τ, is a more important and meaningful parameter to determine than the conventional disintegration time because it measures the effect of the disintegration on drug dissolution. This parameter is determined simultaneously with the other dissolution parameters and not in a separate "destructive" experiment as often is done in disintegration tests. This parameter is defined in a simple and meaningful way. It measures the time difference between the initial dissolution phase dominated by the disintegration reaction and the initial dissolution phase predicted under ideal conditions with instantaneous and complete disintegration.

Equation 17 appears to be the only kinetically based dissolution equation applicable under nonsink conditions that considers polydisperse systems. Other equations presented assume monodisperse systems that are never met in pharmaceutical preparations. For this reason, they are not able to describe or measure the distribution effect that shows up as a pronounced "tailing" in the later stage of dissolution if a fraction of the dispersed system is relatively slowly dissolving because it consists of particle aggregates, larger particles, or particles of a different crystal form (9). This inability is particularly unfortunate, because such dissolution behavior is important to detect and quantitate since it affects the systemic availability of drugs showing incomplete absorption due to dissolution rate-limited absorption.

Equation 17 does not have this deficiency. It is able to describe the distribution effect of polydisperse systems in terms of the dimensionless parameter σ, which is a measure of how "disperse" the effective particle distribution is. This parameter gives an intrinsic characterization of a particle system since it is essentially unaffected by experimental variables such as vehicle composition, pH, temperature, and agitation conditions (9).

The dissolution availability, F_d, measures a formulation's drug content in terms of the amount available for dissolution. In the biological context,

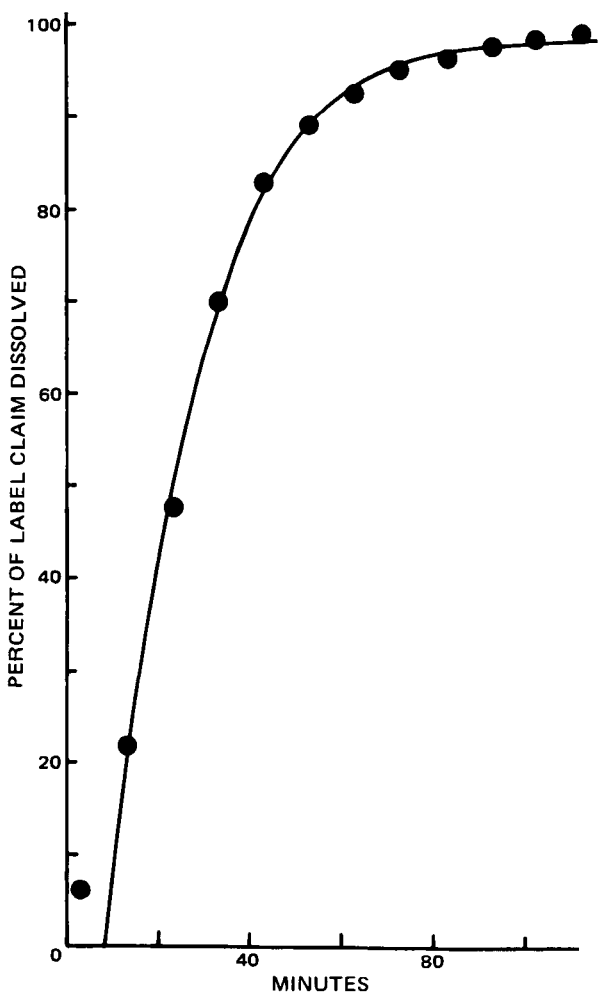

Figure 1—*Equation 17 fitted by nonlinear least-squares regression to dissolution data for an aminophylline tablet. The estimated dissolution kinetic parameters are given in the first row of Table I (Tablet 1).*

Table II—Dissolution Kinetic Parameters for Aminophylline Tablets Obtained by Nonlinear Regression Using Eq. 23 [a]

Tablet	Specific Dissolution Rate Parameter, $K^* \times 100$, min^{-1}	Dissolution Availability, F_d, %	Lag Time due to Disintegration, τ, min	r
1	2.04	110	9.43	0.99655
2	2.10	111	8.27	0.99790
3	2.17	107	8.90	0.99612
4	1.86	107	8.54	0.99787
5	1.84	116	7.17	0.99761
6	1.69	110	7.52	0.99832
Mean	1.95	110	8.305	0.997395
CV, %	9.37	3.01	10.19	

[a] Equation 23, which is identical to Eq. 17 with $\sigma = 0$, assumes that the dissolving particles are monodisperse.

this measure is more realistic than that obtained by conventional "drastic" analytical methods involving grinding followed by organic solvent extraction, which give an unrealistic measure of the amount available for dissolution *in vivo*.

The dissolution capacity coefficient, α, is a measure of the dissolution capacity of the experimental system. The parameter has a large value when the capacity is large, *i.e.*, when the solvent volume to drug weight ratio and the drug solubility are high. Its value decreases with the increasing degree of nonsink conditions (6). A flow-through system with complete sink conditions is described by letting $\alpha = \infty$. The dissolution capacity coefficient has the remarkable property that it provides an "automatic correction," so the other parameters, K^*, σ, τ, and F_d, can be determined unaffected by the degree of sink or nonsink conditions in the experimental design.

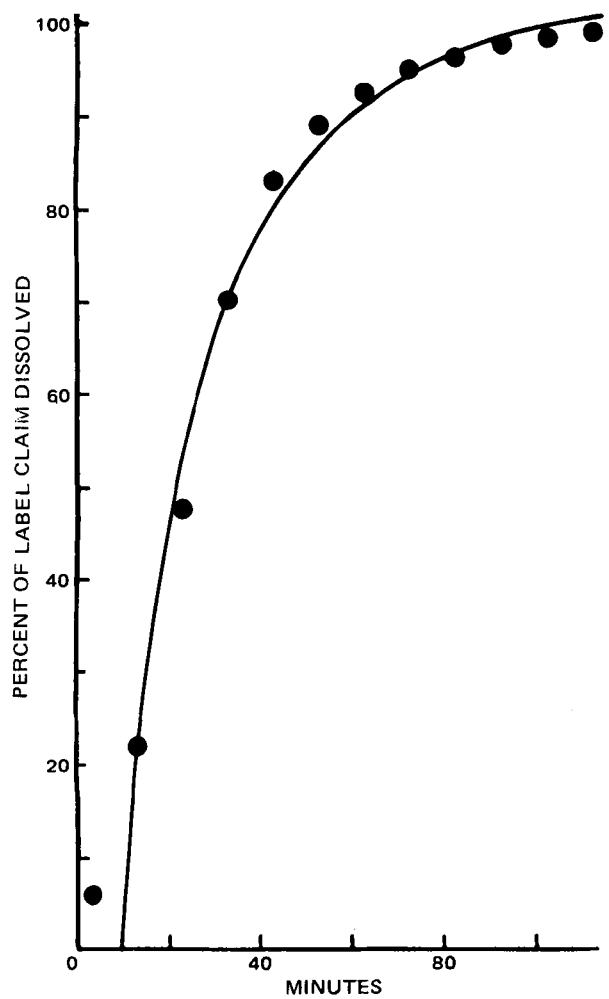

Figure 2—*Equation 23 fitted by nonlinear least-squares regression to dissolution data for an aminophylline tablet. Equation 23 is identical to Eq. 17 with $\sigma = 0$ and assumes a monodisperse particle system. The estimated dissolution kinetic parameters are given in the first row of Table II (Tablet 1).*

Characterization of Aminophylline Tablet Dissolution Properties—The dissolution data for six aminophylline tablets agreed well ($r = 0.99870$) with the kinetic model, Eq. 17 (Table I and Fig. 1). The agreement was consistent from tablet to tablet as reflected in the r values. The variability of each parameter appears to be of a magnitude that can be expected from the variation in physical properties and content uniformity caused by the limited reproducibility of the tablet manufacturing process. The variability is fairly small for F_d, as may be expected since the tablet size and the drug to excipient ratio facilitate a good drug uniformity in the manufacturing process.

The variability of the other parameters (K^*, τ, and σ) is considerably greater. These parameters are expected to be more dependent on the tablet's physical properties that mainly depend on the composition of the excipients and the compression dynamics. However, the variability does not seem to be greater than the mean values of the parameters, which can be considered to give a good representation of the overall dissolution properties of the batch from which the tablets are drawn.

There are ample opportunities for extensive statistical comparisons of brands and batches of tablets on the basis of the kinetic parameters given in Table I. With established statistical tests, it can be concluded whether tablets differ with respect to dissolution rate (K^*), disintegration (τ), drug uniformity (F_d), or dispersibility and particle aggregation (σ). The information may be used ultimately for more detailed analysis of *in vitro–in vivo* correlation than is possible using approaches based on "one-point" *in vitro* methods (*e.g.*, $t_{1/2}$), which give an incomplete characterization and ignore important aspects of the dissolution behavior.

It is of interest to investigate how well Eq. 17 fits the dissolution data if it is assumed that the dissolving particles are monodisperse, *i.e.*, $\sigma = 0$, which leads to Eq. 23 as a special case. Although the mean value for K^* obtained using Eq. 23 (Table II) does not differ significantly from that obtained using Eq. 17 (Table I), a pairwise comparison of the individual K^* values shows little agreement. This result seems to indicate that the assumption $\sigma = 0$ leads to a somewhat erratic determination of K^*. Judged from the r values, Eq. 17 also appears to fit the data significantly better than Eq. 23. Equation 23 tends to give significantly higher values for F_d and τ than Eq. 17 (Tables I and II). This bias is reflected in the definite consistent trend in the fitted curves as shown by Fig. 2, which clearly demonstrates the inadequacy of the model that assumes $\sigma = 0$. Thus, the size distribution effect must be considered to get a proper characterization of the drug's dissolution properties.

Comparison with an Empirical Equation—It is of interest to compare Eq. 17 with what appears to be the most flexible or versatile empirical dissolution equation presented:

$$p = p_\infty \{1 - \exp[-\max(t - T, 0)^b/a]\} \qquad \text{(Eq. 38)}$$

where p_∞ is the limit for p as $t \to \infty$, T is the location parameter, a is the scale parameter, and b is the shape parameter. This equation is a modification of the Weibull distribution function; it has been presented in various forms (3–5) and received much attention primarily because it has the ability to summarize dissolution profiles of pronounced sigmoid shape and of more regular shapes (3). However, because it is an empirical equation not derived from kinetic principles, it has several deficiencies:

1. The equation has no kinetic basis and can only summarize, but not adequately characterize, the dissolution kinetic properties of a drug.
2. It does not contain a single parameter that gives a simple measure

Table III—Dissolution Kinetic Parameters for Aminophylline Tablets Obtained by Nonlinear Least-Squares Regression Using Eq. 38

Tablet	p_∞, %	Location Parameter, T, min	Shape Parameter, b	Scale Parameter, a	r
1	97.9	4.89	1.28	58.8	0.99890
2	99.3	0[a]	1.36	92.3	0.99933
3	96.3	3.74	1.29	59.5	0.99863
4	95.6	4.09	1.16	43.2	0.99824
5	104	0[a]	1.20	56.9	0.99883
6	97.1	0[a]	1.26	74.8	0.99896
Mean	98.4	2.12	1.26	64.3	0.99882
CV, %	3.09	111	5.60	26.5	

[a] The fit is constrained by the lower limit (= 0) assigned to this parameter.

of the intrinsic drug dissolution rate. Instead, the rate is determined by a, b, and T in a way that seems extremely difficult to interpret.

3. The equation is of limited use for establishing *in vitro–in vivo* correlations.

4. Although the location parameter, T, gives an indication of when dissolution starts, the equation provides no measure of the effect of the disintegration reaction on the drug release. In fact, a negative value would have been obtained for T in two of the three cases if the lower limit was not set to zero for this parameter (Table III).

5. Equation 38 is not able to measure the distribution effect. It is not possible, from any of its parameters, to see whether some fraction of the particle system dissolves considerably slower than the rest.

The only advantages of Eq. 38 seem to be that it can summarize a great variety of dissolution curves and that it, because of its asymptotic property, can give an estimate of F_d by the parameter p_∞. Although Eq. 38, judged from the mean r value in Table III, appears to give a slightly better fit to the dissolution data than Eq. 17 (Table I and Fig. 3), this is not significant when compared by a t test (<0.05).

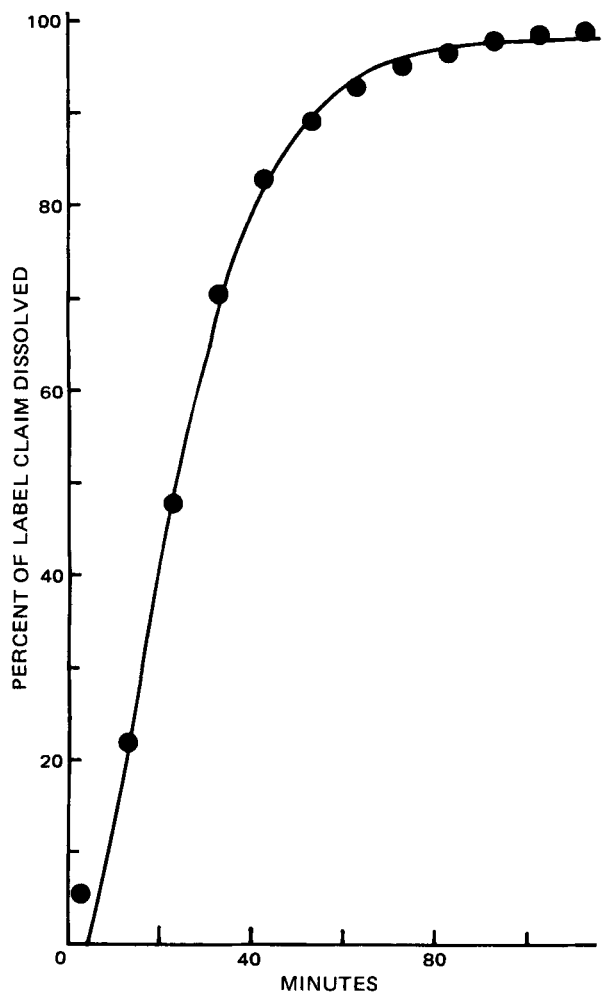

Figure 3—*Equation 38 fitted by nonlinear least-squares regression to dissolution data for an aminophylline tablet. The estimated parameters of the equation are given in the first row of Table III (Tablet 1).*

Among the many kinetically based dissolution equations published, there may well be some that fit the present dissolution data as well as Eq. 17. However, the adequacy of such equations for general usage can first be established when they are tested over a wide range of conditions and the kinetic significance of the parameters in the equation can be verified. Equation 17 in the form $\alpha = \infty$, $\beta = 100$, and $\tau = 0$ already has described accurately dissolution of the 60–85-mesh fraction of tolbutamide (12) and dissolution of micronized gliburide (10). Thus, with the present dissolution data included, the equation has accurately described the dissolution of a broad range of drug systems with widely different particle sizes, shapes, degrees of dispersity, and solubilities, dissolving under sink as well as nonsink conditions at various agitation conditions.

Although the approach presented provides a powerful tool for analysis of drug dissolution, the experimental requirements for its use can readily be met. For dissolution under nonsink conditions, the dissolving particles must be dispersed evenly in the dissolution liquid and be exposed to constant agitation, temperature, and pH. The sampling procedure must not significantly disturb the dissolution process and should be extensive enough to represent properly the complete dissolution process. For dissolution under sink conditions using a dissolution cell, the dissolving particles must be evenly dispersed over the cross section of the cell in a thin layer. Such conditions can be established readily for pure drug powders (10, 12). However, some engineering problems are expected for disintegrating dosage forms because of the possibility of uneven distribution and agitation conditions for the disintegrated particles. For such drug systems, it seems more appropriate to use a nonsink, constant volume-type dissolution apparatus.

Equation 17 shows great potential in characterizing the dissolution properties of disperse systems and disintegrating solid dosage forms with relevance to dosage form development and quality control. In future investigations, it would be valuable to investigate the biological significance of the dissolution kinetic parameters for drug systems showing dissolution rate-limited absorption. Hopefully, such investigations will lead to quality control standards of documented biological significance.

REFERENCES

(1) J. G. Wagner, "Biopharmaceutics and Relevant Pharmacokinetics," Drug Intelligence Publications, Hamilton, Ill., 1971, chap. 16.

(2) L. Z. Benet, in "Dissolution Technology," L. J. Leeson and J. T. Carstensen, Eds., Industrial Pharmaceutical Technology, APhA Academy of Pharmaceutical Sciences, Washington, D.C., 1974, chap. 2.

(3) F. Langenbucher, *J. Pharm. Pharmacol.*, **24**, 979 (1972).

(4) F. Langenbucher, *Pharm. Ind.*, **38**, 472 (1976).

(5) R. Gurny, C. Revillard, and E. Doelker, *ibid.*, **38**, 913 (1976).

(6) P. Veng Pedersen, *J. Pharm. Sci.*, **66**, 1435 (1977).

(7) *Ibid.*, **64**, 1192 (1975).

(8) A. Noyes and W. Whitney, *Z. Phys. Chem.*, **23**, 689 (1897).

(9) P. Veng Pedersen and K. F. Brown, *J. Pharm. Sci.*, **65**, 1981 (1976).

(10) P. Veng Pedersen, *ibid.*, **66**, 761 (1977).

(11) J. E. Tingstad and S. Riegelman, *ibid.*, **59**, 692 (1970).

(12) P. Veng Pedersen and K. F. Brown, *ibid.*, **65**, 1442 (1976).

(13) A. Hixson and J. Crowell, *Ind. Eng. Chem.*, **23**, 923 (1931).

(14) R. D. Kirchhoefer, *J. Assoc. Offic. Anal. Chem.*, **59**, 367 (1976).

(15) P. Veng Pedersen, *J. Pharmacokinet. Biopharm.*, **5**, 513 (1977).

(16) C. W. Gear, "Numerical Initial Value Problems in Ordinary Differential Equations," Prentice-Hall, Englewood Cliffs, N.J., 1971.

Bioavailability of Three Commercial Sustained-Release Tablets of Quinidine in Maintenance Therapy

THO HUYNH-NGOC *, MICHEL CHABOT ‡, and GERARD SIROIS ˣ

Received November 4, 1977, from the *Faculté de Pharmacie, Université de Montréal, Montréal, Québec, Canada, H3C 3J7.* Accepted for publication February 23, 1978. *Present address: A. H. Robins Canada Ltd., Montréal, Québec, Canada. ‡Present address: Institut de Cardiologie de Montréal, Montréal, Québec, Canada.

Abstract □ The bioavailability of three quinidine formulations was estimated during a dosing interval at steady state following their administration in 12 selected patients in accordance with a Latin-square 3 × 3. Each subject received the three dosage forms as two tablets every 12 hr for 6 days. Blood and urine samples were taken on the 7th day during the regular 12-hr dosing interval. Unchanged quinidine was determined by a reported spectrofluorometric procedure. The total fluorescence of plasma quinidine and metabolites also was monitored. The data obtained indicate that one dosage form gave a high peak level followed by a fall in the concentration. The two other forms presented a relatively lower peak followed by a plateau and then a decline. The differences between the dose-corrected values of $C_{p,max}$ were statistically significant. Secondary effects were observed particularly with one dosage form and could be related to the high $C_{p,max}$ value and/or the high percentage of quinidine liberated rapidly in the GI tract. Blood and urinary data indicated an equivalent degree of absorption. The dissolution behavior of the formulations and their absorption data suggest that there is a correlation between the quantity dissolved at 30 min and $C_{p,max}$.

Keyphrases □ Quinidine—pharmacokinetics and bioavailability of three dosage forms compared, humans □ Bioavailability—quinidine, three dosage forms compared, humans □ Pharmacokinetics—quinidine, three dosage forms compared, humans □ Antiarrhythmic agents—quinidine, pharmacokinetics and bioavailability of three dosage forms compared, humans

Quinidine is the most widely used oral antiarrhythmic in the prophylaxis and treatment of cardiac arrhythmias (1). There is a correlation between serum drug concentration and antiarrhythmic and toxic effects (2–4). The therapeutic drug level of unchanged quinidine and hydroquinidine is 0.8–2.5 mg/liter of plasma (5). To maintain a sufficiently steady therapeutic plasma level with quinidine sulfate tablets USP, this dosage form must be administered at relatively frequent intervals because of rapid drug absorption and elimination.

Sustained-release dosage forms offer the possibility of smoother blood level–time profiles with longer intervals between doses. The dissolution rate of some quinidine sustained-release tablets and its implication in bioavailability and therapeutic treatment were studied previously (6). The present study compared the bioavailability of three commercial dosage forms, considered as slow-release formulations, by measuring the plasma drug level and the degree of drug excretion during a regular dosing interval of a maintenance treatment.

EXPERIMENTAL

Subjects—Twelve patients[1], seven men and five women, who had received quinidine treatment for at least 6 months, were randomized into three groups of a Latin-square 3 × 3. These patients ranged in age from 28 to 65 years (mean of 45), in weight from 49.2 to 101.5 kg (mean of 75), and in height from 1.54 to 1.87 m (mean of 1.71). There was no evidence of hepatic, renal, or hematopoietic disease from urinalysis, complete blood count, and determination of serum levels of creatinine, bilirubin, alkaline phosphatase, glutamic-pyruvic transaminase, and glutamic-oxaloacetic transaminase. No patient exhibited evidence of congestive heart failure or GI disease from his or her history and physical examination. Before starting the study, the patients did not receive enzymatic drug inducers for 1 month and drugs likely to interfere with the analysis for 1 week.

Drug Administration—During three consecutive 7-day periods, the subjects received each of the three dosage forms: Tablet A[2] (250 mg of quinidine bisulfate, equivalent to 165.8 mg of quinidine base), Tablet B[3] (325 mg of quinidine gluconate, equivalent to 202.5 mg of quinidine base), and Tablet C[4] (325 mg of quinidine gluconate, equivalent to 202.5 mg of quinidine base). Two tablets of each dosage form were ingested every 12 hr for 6 days.

Each patient received a card to record the time at which each dose was taken. These cards indicated that the difference between the recorded and the prescribed times of ingestion was less than 20 min during the first 5 days and 10 min during the 6th day. On the 7th day, the morning dose of the dosage form that had been taken for 6 days was administered with 200 ml of water after an overnight fast of at least 10 hr. During the first 3 hr after drug administration, the subjects were not allowed to eat or to lie down but were asked to drink water at a rate approximately 70 ml/hr. Each subject received a standard meal after this period.

Specimen Collection and Assay—Blood sampling (6 ml) for quinidine determination was conducted with an indwelling catheter at 0.0, 0.5, 1.0, 1.5, 1.75, 2.0, 2.25, 2.5, 2.75, 3.0, 3.5, 4.0, 4.5, 5.0, 6.0, 8.0, 10.0, and 12.0 hr following the morning dose of the 7th day. Patency of the catheter was maintained with a slow infusion of 5% dextrose solution. Blood specimens were collected in heparinized tubes.

The tubes were subsequently centrifuged, and the plasma was removed and frozen until assayed by the specific spectrofluorometric procedure[5] of Armand and Badinand (5, 7). Although the specificity of this method is limited, it was sufficiently sensitive, accurate, and precise for the measurement of concentrations as low as 0.1 μg/ml (5). Total quinidine-derived fluorescence also was monitored by the protein precipitation method of Brodie and Udenfriend (8). For each urine void, the volume was determined and an aliquot was frozen until just prior to drug analysis by the method of Armand and Badinand (5, 7). Quinidine levels are reported in terms of quinidine base.

Hydroquinidine Determination—Since the two procedures used for quinidine also measure hydroquinidine (5), the percentage of hydroquinidine as a contaminant was determined in each product. The high-speed liquid chromatographic procedure[6] reported by Pound and Sears (9) was used.

Data Analysis—The bioavailability of the three dosage forms was determined by comparing the: (*a*) plasma concentrations at each sampling time, (*b*) dose-corrected[7] peak plasma concentration, (*c*) time to attain the peak plasma concentration, (*d*) area under the plasma concentration–time curve (*AUC*) during the dosing interval [corrected for the dose and normalized to (mg/liter)(hr/m^2)], and (*e*) percentage of the dose of quinidine excreted unchanged during the dosing interval. The efficacy of the three dosage forms was evaluated by comparing the duration of the different minimum effective plasma concentrations that could be required for different patients.

The *AUC* was estimated by means of the trapezoidal rule. Statistical significance was determined by analysis of variance (ANOVA) (10) after verifying the homogeneity of variances by the Bartlett test (11). Com-

[1] Written informed consent was obtained after discussing with each subject the inconveniences and hazards.

[2] Biquin, lot AM405, Astra Chemicals Ltd., Mississauga, Ontario, Canada.
[3] Quinate, lot 04TG, Rougier Inc., Chambly, Quebec, Canada.
[4] Quinaglute, lot R51002, Cooper Laboratories, Wayne, N.J.
[5] Aminco-Bowman spectrofluorometer, American Instrument Co., Silver Spring, Md.
[6] Model 8500 high-pressure liquid chromatograph, Varian Associates, Palo Alto, Calif.
[7] Parameters of Tablet A corrected for the dose are multiplied by 202.5/165.8.

0022-3549/78/1000-1456$01.00/0
© 1978, American Pharmaceutical Association

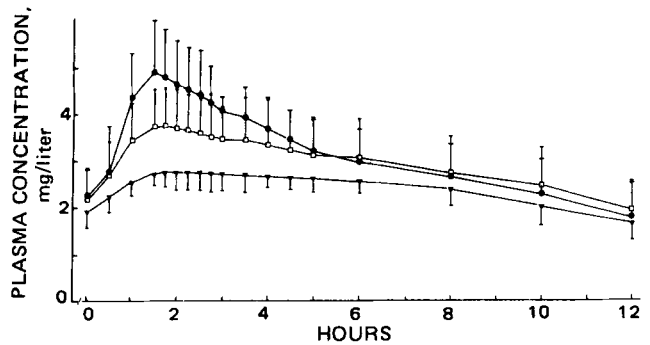

Figure 1—*Mean plasma concentration of intact drug for three different quinidine products during a 12-hr dosing interval of a maintenance treatment. Key: ●, Tablet B; □, Tablet C; and ▼, Tablet A. The vertical bar represents the standard deviation.*

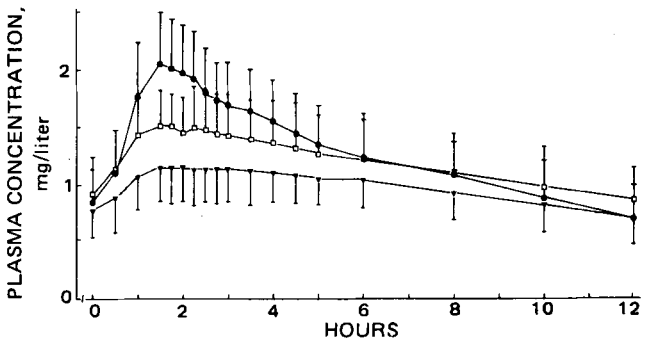

Figure 2—*Mean plasma concentration of total drug for three different quinidine products during a 12-hr dosing interval of a maintenance treatment. Key: ●, Tablet B; □, Tablet C; and ▼, Tablet A. The vertical bar represents the standard deviation.*

puter programs written in Fortran were used for the estimation of the *AUC* and the realization of the analysis of variance and the Bartlett test. Differences between individual treatments were determined by the Newman–Keuls multiple-range test (12).

Dissolution Test—Four dosage units of each product were subjected to a dissolution test using a USP dissolution assembly equipped with a continuous fluid exchange system to change the pH of the medium progressively. The method was described previously (13).

RESULTS

Figures 1 and 2 illustrate the mean plasma concentration–time profile of the corresponding unchanged and total drug during the 12-hr dosing interval for the three products tested. Although initial and final plasma concentrations for each product were similar, the values of the maximum plasma concentration varied considerably for a given method. The variation of plasma concentration at each sampling time was determined by the analysis of variance; Table I summarizes this analysis at time zero.

The statistical analysis at different blood sampling times indicated that a significant difference ($p < 0.05$) can be observed only with the intersubject and treatment factors. No significant difference ($p > 0.05$) was observed for the group, period, and period–treatment factors. For the intersubject factor of the plasma concentration of unchanged quinidine at different times after drug administration, a significant difference was observed at 0, 0.5, 4.0, 4.5, 5.0, 6.0, 8.0, 10.0, and 12.0 hr. The treatment factor of plasma concentration of intact quinidine was statistically significant from 0.5 to 5.0 hr following drug administration. For this latter period, the rank order of plasma concentration was Tablets A, C, and B. The Newman–Keuls *a posteriori* test indicated that there was a significant difference between each plasma concentration obtained with the three products between 1.0 and 4.5 hr. At 0.5 and 5.0 hr, the difference between plasma concentrations observed with Tablets B and C was not statistically significant. The statistical analysis of total quinidine plasma concentrations at different times yielded very similar results.

Some pharmacokinetic parameters estimated from plasma and urine data of unchanged quinidine are given in Table II. The analysis of variance on the parameters listed in this table showed that there was a significant difference for the intersubject factor with $C_{p,\min}$, Cl_p, *AUC*, $t_{0.8}$, $t_{1.0}$, and $t_{1.2}$ and for the treatment factor with some parameters. No significant difference was observed for the group, period, and period–treatment factors. The unifactorial analysis of variance (14) used for % D_u and Cl_r parameters, because of some missing urine samples, allows the variability evaluation of the treatment factor only.

The statistical analysis of the values of the dose-corrected *AUC* and the percentage of the dose excreted unchanged in the urine, % D_u, derived from each patient revealed that there was no significant difference in the degree of quinidine absorption from these dosage forms. A statistical difference was not observed for the time required to attain the peak concentration, t_{max}, of the individual plasma concentration–time curves exhibited with the three treatments. However, a statistical difference between the three products was evidenced for the dose-corrected maximum plasma concentration, $C_{p,max}$, obtained from the individual plasma concentration–time curves.

A statistical difference also was found for the three treatments in their difference between the dose-corrected maximum and minimum plasma concentrations measured at the end of the dosing interval, ΔC_p, in each patient. For the three products tested, the difference between the duration of a minimum effective plasma concentration of 1.0 or 1.2 mg/liter, but not of 0.8 mg/liter, was significant.

The dissolution behavior of the three formulations and their absorption data (Fig. 3) suggest that there is a correlation between the quantity dissolved at 30 min and the observed maximum plasma drug concentration.

DISCUSSION

With a consideration of the quinidine dose administered and the assumption of linear pharmacokinetics, the degree of drug absorption from the three products was similar. However, between 1 and 4.5 hr, a statistically significant difference was observed for plasma concentrations obtained with Tablets C and B, which were administered at the same dose. The highest level was obtained with Tablet B. The dose-corrected $C_{p,max}$ value of Tablet B was significantly different from that of A and C. Furthermore, the dose-corrected ΔC_p values demonstrated that Tablets A and C presented similar fluctuation in blood levels and that this fluctuation was less pronounced than for B. Consequently, the statistical analysis of the data and the plasma level–time profiles shown in Fig. 2 indicated that Tablet B did not present the sustained-release properties observed by Goldberg and Chakrabarti (15), who reported plasma levels based on the total fluorescence of quinidine and metabolites. Slow-release characteristics were not observed. Results of this in-

Table I—Analysis of Variance of the Plasma Concentrations of Unchanged Quinidine at Time Zero [a]

Source of Variation	Sum of Squares	Degrees of Freedom	Mean of Squares	*F*	*p*
Between subjects	2.050	11	0.186	6.41	<0.01
Groups	0.383	2	0.191	1.03	>0.25
Subjects within groups	1.667	9	0.185	—	—
Within subjects	0.698	24	0.029	0.16	>0.25
Periods	0.009	2	0.005	0.15	>0.25
Treatments	0.131	2	0.065	2.11	>0.10
Period–treatment	0.001	2	0.0004	0.01	>0.25
Error	0.557	18	0.031	—	—
Total	2.748	35	—	—	—

[a] The test of Bartlett (11) for the homogeneity of variances indicated that the value of the calculated χ-square is smaller than the critical χ-square value for $p = 0.05$.

Table II—Pharmacokinetic Parameters Estimated from Plasma Levels and Urinary Excretion of Intact Drug

Parameter[a]	$\bar{X}$[b] A	$\bar{X}$[b] B	$\bar{X}$[b] C	ANOVA F	ANOVA p	N.K.[c]
$C_{p,max}$, mg/liter	1.46 (0.36)	2.14 (0.41)	1.59 (0.34)	29.13	<0.01	A C B
$C_{p,min}$, mg/liter	0.84 (0.27)	0.69 (0.30)	0.84 (0.28)	3.12	>0.05	—
ΔC_p, mg/liter	0.62 (0.16)	1.46 (0.37)	0.75 (0.22)	51.66	<0.01	A C B
AUC, (mg/liter)(hr/m^2)	7.75 (2.38)	8.22 (2.31)	7.86 (2.86)	0.39	>0.05	—
% D_u	19.1 (4.0)	16.4[d] (6.5)	16.1[e] (2.9)	1.34[f]	>0.05	—
t_{max}, hr	1.81 (0.40)	1.65 (0.36)	1.62 (0.46)	0.75	>0.05	—
$t_{0.8}$, hr	8.35 (3.65)	9.72 2.73)	9.69 (3.12)	1.39	>0.05	—
$t_{1.0}$, hr	5.02 (4.59)	7.93 (3.41)	7.6 (4.3)[e]	4.75	<0.05	A C B
$t_{1.2}$, hr	2.29 (3.89)	6.05 (3.73)	5.38 (4.98)	5.97	<0.05	A C B
Cl_r, ml/min/m^2	50.75 (12.14)	44.96[d] (24.28)	46.47[e] (11.06)	0.36[f]	>0.05	—
Cl_p, ml/min/m^2	274.56 (82.83)	260.84 (93.28)	274.48 (72.33)	0.35	>0.05	—

[a] The abbreviations used for parameters are: $C_{p,max}$ = maximum drug plasma concentration corrected for the dose; $C_{p,min}$ = minimum drug plasma concentration corrected for the dose; $\Delta C_p = C_{p,max} - C_{p,min}$; AUC = area under the plasma concentration–time curve corrected for the dose; % D_u = percentage of dose excreted; t_{max} = time to attain peak plasma concentration; $t_{0.8}$, $t_{1.0}$, and $t_{1.2}$ = period of time where the plasma level of unchanged drug is greater than 0.8, 1.0, and 1.2 mg/liter, respectively; Cl_r = renal clearance estimated from the amount of unchanged quinidine base excreted in the urine during the dosing interval divided by the AUC; and Cl_p = plasma clearance estimated from the equation: Cl_p = (fraction of dose absorbed)(dose of quinidine base)/(AUC) in assuming that the absorption is complete. [b] Arithmetic mean value. The value in parenthesis is the standard deviation. [c] Newman–Keuls multiple-range test. Drug products underlined by the same line are not significantly different ($p > 0.05$). [d] Mean of 11 subjects. [e] Mean of 10 subjects. [f] Unifactorial analysis of variance.

vestigation and previous dissolution data (6) suggest that Tablet B must have been reformulated.

The effects of quinidine are related to high plasma levels and/or high local concentrations in the GI tract (2–4). In this study, Tablet B presented a high dissolution rate and a high maximum plasma concentration (Fig. 3). Therefore, a higher frequency of side effects after its administration would be expected. In this investigation, two patients complained of vertigo, visual disturbances, and cold sweat for 1–2 hr after ingestion of Tablet B during the 1-week treatment. Five subjects reported having some diarrhea: four with Tablet B (one patient for the whole duration of the treatment and three patients for several days during the 6-day loading portion) and one with Tablet C (for many days during the treatment). Patients demonstrating side effects after receiving Tablet B had a mean maximum plasma concentration of 2.0 mg/liter. This value did not differ significantly from the $C_{p,max}$ observed with patients receiving this product and not showing side effects. Therefore, this result was apparently due to the fact that toxic as well as therapeutic responses to quinidine are determined by individual patient sensitivity (16).

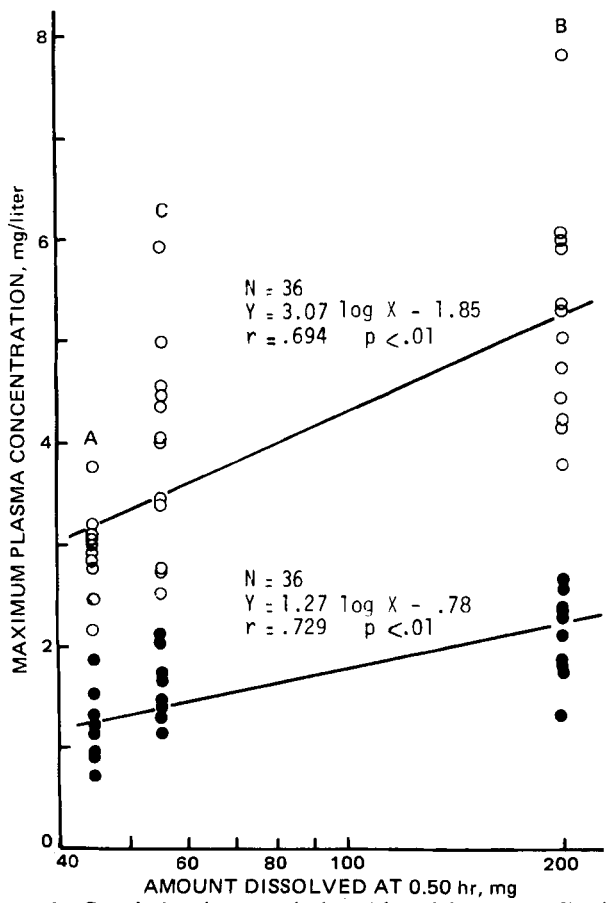

Figure 3—*Correlations between the logarithm of the amount dissolved at 0.5 hr and the maximum plasma concentration. Key:* ●, *intact quinidine; and* O, *total quinidine.*

In view of the sensitivity factor in a quinidine treatment (16), it is important to realize that the minimum effective concentration required for obtaining the desired pharmacological effect will vary from one patient to another. The efficacy of the three products can thus be evaluated by determining their ability to produce and to maintain a given minimum plasma concentration during the dosing intervals of a maintenance treatment. In patients requiring a plasma level of 0.8 mg of unchanged drug/liter, the statistical analysis of the data (Table II) indicated that the three products tested would give the same protection. Patients requiring a level of 1.0 or 1.2 mg/liter would get a relatively good prophylaxis with Tablets B and C. Consequently, the dose required to give these levels with Tablet A should be increased.

The biological half-life was estimated from the data of Tablet B by regression analysis on the linear terminal portion of the relation between ln C_p and time. The biological half-life was calculated using:

$$t_{1/2} = -0.693/\text{slope} \qquad \text{(Eq. 1)}$$

When using the plasma concentration of unchanged quinidine, the mean half-life for all subjects was 7.16 hr with a standard deviation of 2.29 and a range of 3.44–12.15 hr. This range corresponds closely to the results reported previously (17, 18). The mean half-life calculated from the plasma concentration of total quinidine gave nearly the same value (7.46 hr with a standard deviation of 2.36). The similarity between these two values demonstrates that the rate constants for overall elimination of metabolites must be greater than the overall elimination (metabolism and renal excretion of unchanged drug) rate constant of quinidine (19).

The mean renal clearance value given in Table II is very close to that reported previously (18, 20). The mean plasma clearance value is similar to the one reported by Mahon *et al.* (20) but higher than the one obtained by Ueda *et al.* (18) after infusion. This difference would result mainly

from first-pass hepatic drug removal when quinidine is administered orally (21).

The two procedures used in this work measure the total fluorescence of either the unchanged quinidine and hydroquinidine or the two unchanged alkaloids and their metabolites (5). As a result, the contamination by hydroquinidine would be expected to produce a certain error in the evaluation of quinidine pharmacokinetic parameters. However, the corresponding percentages of hydroquinidine in Tablets A, B, and C were only 8.23, 4.33, and 6.71, respectively. Furthermore, a study on the pharmacokinetics of quinidine and hydroquinidine by Ueda *et al.* (22) indicated that the differences in the distribution and elimination characteristics of the two alkaloids are not significant. In view of these facts, the bias introduced in the value of quinidine pharmacokinetic parameters estimated in this work (Table II) appears to be negligible.

Several parameters measured in this study demonstrated significant intersubject variability. This observation is in agreement with previously published works and demonstrates the need to individualize the dosage regimens of this drug (18). Drug monitoring with a given dosage form is usually based on the range of plasma concentrations known to produce the desired therapeutic response in most patients. However, better drug monitoring could be obtained if the adjustment of the dose is also based on therapeutic and toxic effects observed in individual patients.

REFERENCES

(1) *Pharm. Times*, **42**, 37 (1976).

(2) M. Sokolow and A. L. Edgar, *Circulation*, **1**, 576 (1950).

(3) R. H. Heissenbuttel and J. T. Bigger, Jr., *Am. Heart J.*, **80**, 453 (1970).

(4) I. R. Edwards and B. W. Hancock, *Br. J. Clin. Pharmacol.*, **1**, 455 (1974).

(5) T. Huynh-Ngoc and G. Sirois, *J. Pharm. Sci.*, **66**, 591 (1977).

(6) T. Huynh-Ngoc and G. Sirois, *J. Pharm. Belg.*, **32**, 67 (1977).

(7) J. Armand and A. Badinand, *Ann. Biol. Clin.*, **30**, 599 (1972).

(8) B. B. Brodie and S. Udenfriend, *J. Pharmacol. Exp. Ther.*, **78**, 154 (1943).

(9) N. J. Pound and R. W. Sears, *Can. J. Pharm. Sci.*, **10**, 122 (1975).

(10) B. J. Winer, "Statistical Principles in Experimental Design," McGraw-Hill, New York, N.Y., 1971, p. 713.

(11) *Ibid.*, p. 208.

(12) *Ibid.*, p. 191.

(13) T. Huynh-Ngoc and G. Sirois, *J. Pharm. Belg.*, **31**, 589 (1976).

(14) B. J. Winer, "Statistical Principles in Experimental Design," McGraw-Hill, New York, N.Y., 1971, p. 160.

(15) W. M. Goldberg and S. G. Chakrabarti, *Can. Med. Assoc. J.*, **91**, 991 (1964).

(16) J. P. Van Dueme and M. G. Bogaert, *Circulation*, **50**, 1284 (1974).

(17) J. D. Strum, J. L. Colaizzi, J. M. Jaffe, P. C. Martineau, and R. I. Poust, *J. Pharm. Sci.*, **66**, 539 (1977).

(18) C. T. Ueda, D. S. Hirschfeld, M. M. Scheinman, M. Rowland, B. J. Williamson, and B. S. Dzindzio, *Clin. Pharmacol. Ther.*, **19**, 30 (1976).

(19) M. Gibaldi and D. Perrier, "Pharmacokinetics," Dekker, New York, N.Y., 1975, p. 27.

(20) W. A. Mahon, M. Mayersohn, and T. Inaba, *Clin. Pharmacol. Ther.*, **19**, 566 (1976).

(21) C. T. Ueda, B. J. Williamson, and B. S. Dzindzio, *ibid.*, **20**, 260 (1976).

(22) C. T. Ueda, B. J. Williamson, and B. S. Dzindzio, *Res. Commun. Chem. Pathol. Pharmacol.*, **14**, 215 (1976).

ACKNOWLEDGMENTS

Supported by Medical Research Council of Canada Grant MA5337, Astra Chemicals Ltd., and Cooper Laboratories Inc.

Ditheophylline Succinate: Transfer of Theophylline across Everted Rat Intestinal Sacs

DILIP R. SANVORDEKER

Received June 27, 1977, from *Searle Laboratories, Chicago, IL 60680.*

Accepted for publication February 21, 1978.

Abstract □ The cumulative theophylline transfer rate across 10-cm everted rat intestinal sacs incubated at 37° in pH 7.4 Krebs phosphate buffer was determined. A suspension of ditheophylline succinate (a potential prodrug of theophylline) and a solution of theophylline at equimolar concentration were evaluated to determine the magnitude of the difference between the cumulative theophylline transfer rates from the two preparations. A linear concentration dependency for the rate across the intestinal wall was evidenced. The theophylline formation rate from ditheophylline succinate suspended in pH 7.4 Krebs buffer at 37° followed apparent zero-order kinetics. The observed difference (fourfold) between the cumulative transfer rates estimated for the theophylline solution and the ditheophylline succinate suspension was attributed to the prevailing theophylline concentration in the mucosal solutions. The biopharmaceutical implications of these observations are discussed.

Keyphrases □ Ditheophylline succinate—theophylline transfer rate across everted rat intestinal sacs □ Theophylline—transfer rate across everted rat intestinal sacs □ Transfer rate—theophylline from solution and ditheophylline succinate suspension across everted rat intestinal sacs □ Prodrugs—ditheophylline succinate, theophylline transfer rate across everted rat intestinal sacs □ Relaxants, smooth muscle—theophylline, transfer rate across everted rat intestinal sacs

7,7′-Ditheophylline succinate[1] (I) is a potential theophylline prodrug. In the presence of moisture or water, it hydrolyzes rapidly to yield two molecules of theophylline (II) and one molecule of succinic acid[2] (Scheme I).

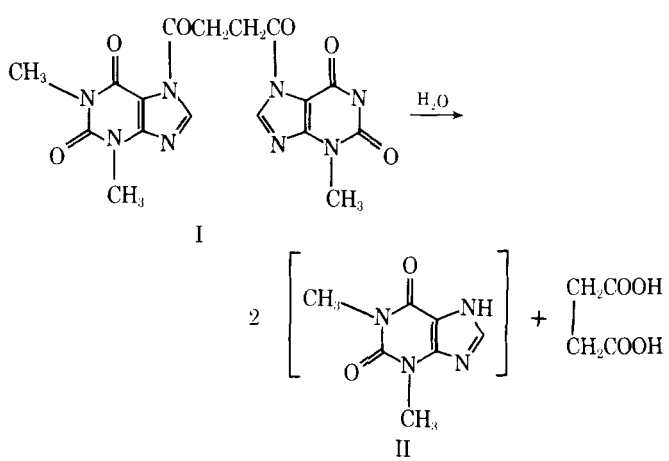

Scheme I

The aqueous solubility of I is less than 0.1 mg/ml; however, the dissolved material undergoes ultrafast hydrolysis

[1] SC-30163.

[2] H. K. Lee and H. Lambert, Internal Report DVR7611023, Searle Laboratories, Chicago, IL 60680.

0022-3549/78/1000-1459$01.00/0

© 1978, American Pharmaceutical Association

from first-pass hepatic drug removal when quinidine is administered orally (21).

The two procedures used in this work measure the total fluorescence of either the unchanged quinidine and hydroquinidine or the two unchanged alkaloids and their metabolites (5). As a result, the contamination by hydroquinidine would be expected to produce a certain error in the evaluation of quinidine pharmacokinetic parameters. However, the corresponding percentages of hydroquinidine in Tablets A, B, and C were only 8.23, 4.33, and 6.71, respectively. Furthermore, a study on the pharmacokinetics of quinidine and hydroquinidine by Ueda *et al.* (22) indicated that the differences in the distribution and elimination characteristics of the two alkaloids are not significant. In view of these facts, the bias introduced in the value of quinidine pharmacokinetic parameters estimated in this work (Table II) appears to be negligible.

Several parameters measured in this study demonstrated significant intersubject variability. This observation is in agreement with previously published works and demonstrates the need to individualize the dosage regimens of this drug (18). Drug monitoring with a given dosage form is usually based on the range of plasma concentrations known to produce the desired therapeutic response in most patients. However, better drug monitoring could be obtained if the adjustment of the dose is also based on therapeutic and toxic effects observed in individual patients.

REFERENCES

(1) *Pharm. Times*, **42**, 37 (1976).

(2) M. Sokolow and A. L. Edgar, *Circulation*, **1**, 576 (1950).

(3) R. H. Heissenbuttel and J. T. Bigger, Jr., *Am. Heart J.*, **80**, 453 (1970).

(4) I. R. Edwards and B. W. Hancock, *Br. J. Clin. Pharmacol.*, **1**, 455 (1974).

(5) T. Huynh-Ngoc and G. Sirois, *J. Pharm. Sci.*, **66**, 591 (1977).

(6) T. Huynh-Ngoc and G. Sirois, *J. Pharm. Belg.*, **32**, 67 (1977).

(7) J. Armand and A. Badinand, *Ann. Biol. Clin.*, **30**, 599 (1972).

(8) B. B. Brodie and S. Udenfriend, *J. Pharmacol. Exp. Ther.*, **78**, 154 (1943).

(9) N. J. Pound and R. W. Sears, *Can. J. Pharm. Sci.*, **10**, 122 (1975).

(10) B. J. Winer, "Statistical Principles in Experimental Design," McGraw-Hill, New York, N.Y., 1971, p. 713.

(11) *Ibid.*, p. 208.

(12) *Ibid.*, p. 191.

(13) T. Huynh-Ngoc and G. Sirois, *J. Pharm. Belg.*, **31**, 589 (1976).

(14) B. J. Winer, "Statistical Principles in Experimental Design," McGraw-Hill, New York, N.Y., 1971, p. 160.

(15) W. M. Goldberg and S. G. Chakrabarti, *Can. Med. Assoc. J.*, **91**, 991 (1964).

(16) J. P. Van Dueme and M. G. Bogaert, *Circulation*, **50**, 1284 (1974).

(17) J. D. Strum, J. L. Colaizzi, J. M. Jaffe, P. C. Martineau, and R. I. Poust, *J. Pharm. Sci.*, **66**, 539 (1977).

(18) C. T. Ueda, D. S. Hirschfeld, M. M. Scheinman, M. Rowland, B. J. Williamson, and B. S. Dzindzio, *Clin. Pharmacol. Ther.*, **19**, 30 (1976).

(19) M. Gibaldi and D. Perrier, "Pharmacokinetics," Dekker, New York, N.Y., 1975, p. 27.

(20) W. A. Mahon, M. Mayersohn, and T. Inaba, *Clin. Pharmacol. Ther.*, **19**, 566 (1976).

(21) C. T. Ueda, B. J. Williamson, and B. S. Dzindzio, *ibid.*, **20**, 260 (1976).

(22) C. T. Ueda, B. J. Williamson, and B. S. Dzindzio, *Res. Commun. Chem. Pathol. Pharmacol.*, **14**, 215 (1976).

ACKNOWLEDGMENTS

Supported by Medical Research Council of Canada Grant MA5337, Astra Chemicals Ltd., and Cooper Laboratories Inc.

Ditheophylline Succinate: Transfer of Theophylline across Everted Rat Intestinal Sacs

DILIP R. SANVORDEKER

Received June 27, 1977, from *Searle Laboratories, Chicago, IL 60680.*

Accepted for publication February 21, 1978.

Abstract □ The cumulative theophylline transfer rate across 10-cm everted rat intestinal sacs incubated at 37° in pH 7.4 Krebs phosphate buffer was determined. A suspension of ditheophylline succinate (a potential prodrug of theophylline) and a solution of theophylline at equimolar concentration were evaluated to determine the magnitude of the difference between the cumulative theophylline transfer rates from the two preparations. A linear concentration dependency for the rate across the intestinal wall was evidenced. The theophylline formation rate from ditheophylline succinate suspended in pH 7.4 Krebs buffer at 37° followed apparent zero-order kinetics. The observed difference (fourfold) between the cumulative transfer rates estimated for the theophylline solution and the ditheophylline succinate suspension was attributed to the prevailing theophylline concentration in the mucosal solutions. The biopharmaceutical implications of these observations are discussed.

Keyphrases □ Ditheophylline succinate—theophylline transfer rate across everted rat intestinal sacs □ Theophylline—transfer rate across everted rat intestinal sacs □ Transfer rate—theophylline from solution and ditheophylline succinate suspension across everted rat intestinal sacs □ Prodrugs—ditheophylline succinate, theophylline transfer rate across everted rat intestinal sacs □ Relaxants, smooth muscle—theophylline, transfer rate across everted rat intestinal sacs

7,7′-Ditheophylline succinate[1] (I) is a potential theophylline prodrug. In the presence of moisture or water, it hydrolyzes rapidly to yield two molecules of theophylline (II) and one molecule of succinic acid[2] (Scheme I).

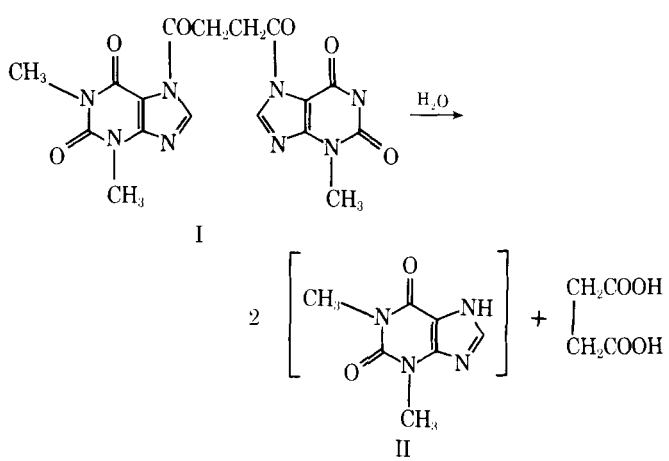

Scheme I

The aqueous solubility of I is less than 0.1 mg/ml; however, the dissolved material undergoes ultrafast hydrolysis

[1] SC-30163.

[2] H. K. Lee and H. Lambert, Internal Report DVR7611023, Searle Laboratories, Chicago, IL 60680.

0022-3549/78/1000-1459$01.00/0

© 1978, American Pharmaceutical Association

Table I—Cumulative Transfer of Theophylline (Milligrams ± *SD*) across 10-cm Everted Rat Intestinal Sacs ($n = 4$) Immersed in a Solution of Theophylline (10^{-3} *M*) or a Suspension (0.045% w/v) of Ditheophylline Succinate (I) in pH 7.4 Krebs Phosphate Buffer at 37°

Minutes	From Theophylline Solution	From I Suspension
15	0.079 ± 0.009	0.034 ± 0.007
30	0.166 ± 0.003	0.063 ± 0.032
45	0.252 ± 0.052	0.088 ± 0.032
60	0.348 ± 0.053	0.109 ± 0.035
75	0.455 ± 0.085	0.139 ± 0.042
90	0.548 ± 0.099	0.163 ± 0.051
Cumulative transfer rate	0.0063 mg/min	0.0017 mg/min

in an aqueous medium, thus providing a continuous and steady supply of theophylline in solution[2]. The advantage of this approach to theophylline therapy is that a dissolution-controlled theophylline formation is established and, consequently, its absorption through the GI wall can be controlled at a pseudo-zero-order rate.

The usefulness of everted rat intestinal sacs for evaluating the *in vitro* transfer of drugs and other organic compounds is well documented (1–5). This study was initiated to determine the theophylline transfer rate across everted rat intestinal sacs. Experiments were conducted with theophylline solutions and I suspensions to ascertain the difference between the cumulative theophylline transfer rates.

EXPERIMENTAL

Materials—All reagents used for the preparation of buffer solutions were analytical reagent grade. Theophylline[3] was used as supplied. 7,7′-Ditheophylline succinate[4] had a surface area of 1.4 m^2/g.

Methods—In Vitro *Transfer Rate Studies*—The general procedure adopted to determine the cumulative theophylline transfer rate across everted rat intestinal sacs was similar to that reported previously (4, 5). Briefly, everted intestinal segments of approximately 11-cm length were ligated at one end with surgical grade silk thread. The other (open) end was mounted and tied on a 3.5-cm long polytef tube, which protruded inward through a neoprene rubber stopper of suitable dimensions. The ligated end was then tied to the end of an L-shaped, blunt-edged, hypodermic needle[5].

The modified needle, which was fitted into the rubber stopper, was used to deliver gaseous 95% O_2–5% CO_2. A small hole drilled into the rubber stopper served as the outlet for escaping gas. The everted rat intestinal sac was restrained parallel to the needle, thus facilitating easy access to fill and empty it as desired. Four such intestinal preparations were immersed in 85 ml of a solution or a suspension (0.045% w/v) of the test compound in pH 7.4 Krebs phosphate buffer (6) without calcium and magnesium chlorides. A 12 × 3.3-cm glass test tube was used to hold each preparation. The rubber stoppers were fitted on the test tube mouths, and the gas was bubbled through the gas outlet port. The tube was agitated mechanically up and down by a disintegration test shaker[6] to maintain a coarse suspension of the compound in the test medium. Four assemblies of the intestinal preparation were immersed in a constant-temperature bath at 37 ± 0.5°.

At the start of the experiment, approximately 0.8 ml of Krebs buffer was placed in the intestinal sac, withdrawn, and discarded. This step was repeated a second time, and the withdrawn sample was collected to serve as a blank to quantify the theophylline by UV spectrophotometry. The intestinal sac was filled again with blank buffer, and the contents were withdrawn 15 min later, followed by a quick rinse of the sac with buffer. This procedure was repeated every 15 min for 90 min of incubation of the intestinal sacs in the corresponding mucosal medium. The sample and the rinse were mixed and diluted to 10 ml with blank buffer. For studies with the I suspension, a large excess of I was maintained in the dissolution (mucosal) medium during the entire incubation period.

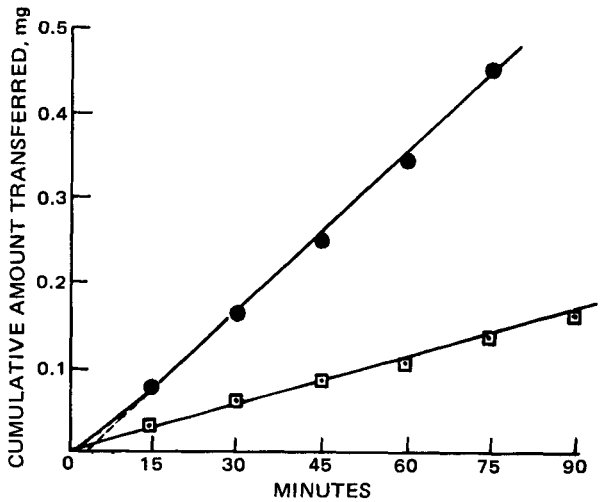

Figure 1—*Plot illustrating the cumulative transfer of theophylline across everted rat intestinal sacs immersed in pH 7.4 Krebs phosphate buffer at 37°. Key: ⊡, I suspension (10^{-3} M), slope = 0.0017 mg/min; and ●, theophylline solution (10^{-3} M), slope = 0.0063 mg/min.*

Theophylline Formation Rate in pH 7.4 Krebs Buffer at 37°—To determine the theophylline formation rate from I, the same assemblies without the rat intestinal sacs were used. A 38-mg portion of I was added to 85 ml of Krebs buffer. The suspension was shaken once vigorously, and then the loop-type stirrer was placed inside the test tube to provide the identical conditions of pH, temperature, and agitation adopted for the transfer rate studies.

Approximately 2 ml of sample from each tube was withdrawn in a syringe[5] using a hypodermic, 35.5-cm long needle[5]. It was filtered quickly through a membrane filter fitted in accompanying filtration units[7]. The samples thus collected every 15 min for 90 min after preparation of I suspensions were diluted appropriately and assayed for theophylline by the adopted procedure.

Quantitation of Theophylline—The samples from transfer rate studies with everted rat intestinal sacs were filtered through sintered-glass funnels and diluted with pH 7.4 Krebs buffer as required. UV absorption spectra were recorded on a dual-beam UV–visible recording spectrophotometer[8]. The absorbance of blank samples was subtracted from the absorbance of the samples at 270 nm (λ_{max} for theophylline) to quantitate the theophylline in the serosal solution. A calibration curve of absorbance (at 270 nm) *versus* theophylline concentration (in milligrams per milliliter) in Krebs phosphate buffer was prepared to assist in the quantitation of theophylline transfer as a function of time. The amount of theophylline transferred was calculated with:

$$\text{amount transferred per unit time} = \left(\text{corrected absorbance at 270 nm}\right)\left(\text{dilution factor}\right)\left(\frac{1}{m}\right) \quad \text{(Eq. 1)}$$

where m is the slope of the calibration curve for theophylline in Krebs buffer. All other samples were diluted appropriately with Krebs buffer and assayed by the adopted UV spectrophotometric procedure.

RESULTS AND DISCUSSION

Table I shows results of transfer rate studies conducted with four everted rat intestinal sac preparations. A plot of the cumulative amount of theophylline transferred from the mucosal to the serosal side is illustrated in Fig. 1. The slope of the line gives an estimated value for the cumulative theophylline transfer rate from the I suspension and theophylline solution at equimolar concentration. The cumulative transfer rate of theophylline from the I suspension was less than that observed for the theophylline solution.

With the I suspensions, one would expect that the theophylline transfer rate during the early incubation period (<15 min) would be concentration dependent. Since an adequate build-up of the concentration gradient

[3] Lot 13C-2810, Sigma Chemical Co., St. Louis, Mo.
[4] Lot A13177, synthesized by the Searle Chemical Development Department and released by Quality Control for investigational use.
[5] Becton-Dickinson Co., Rutherford, N.J.
[6] Model 39-133, Hansen Research Corp., New York, N.Y.
[7] Swinney type, Millipore Corp., Bedford, Mass.
[8] Coleman model 124 D, Perkin-Elmer Corp., Maywood, Ill.

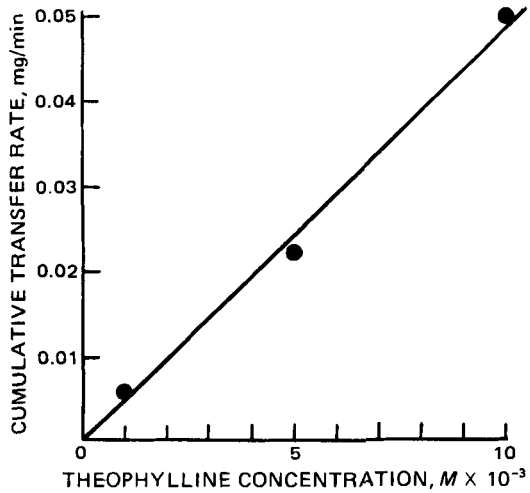

Figure 2—*Concentration dependency of theophylline transfer rate across everted 10-cm rat intestinal sacs immersed in theophylline solutions prepared with pH 7.4 Krebs buffer at 37°.*

was lacking during this period, a lag time for the appearance of theophylline in the serosal side is to be expected. Such a lag time of over 2 min (Fig. 1), as estimated from back-extrapolation (dotted line) of the amount transferred *versus* time plot, was evidenced for theophylline transfer from the I suspension. The cumulative transfer rate of theophylline formed from I in the mucosal side was retarded by as much as fourfold.

To assess whether a concentration dependency existed for the transfer rate process, theophylline solutions at three different concentrations in pH 7.4 Krebs buffer were prepared and tested by the described technique (Fig. 2). Consistent with Fick's law of diffusion (7), the concentration dependency of theophylline transfer rates across everted rat intestinal sacs was ascertained. To rationalize the observed differences between theophylline transfer rates from a I suspension and a theophylline solution at equimolar concentration, it became important to determine the theophylline formation rate from I suspension under identical conditions of pH, temperature, and stirring.

Figure 3 illustrates a concentration *versus* time profile for theophylline formation in pH 7.4 Krebs buffer containing a crude suspension (0.045% w/v) of I. After an initial induction period of 10 min, the theophylline formation rate followed zero-order kinetics; that is, the theophylline formation rate was constant in the presence of an excess of suspended I particles. The theophylline concentrations in solution ranged from an initial 2.07×10^{-4} *M* to a final 3.2×10^{-4} *M* during the incubation period. By assuming that a pseudo-steady-state concentration of 2.5×10^{-4} *M* (as estimated on the basis of a midpoint concentration at 45-min intervals) was prevalent during the course of intestinal incubation, a predicted value for the cumulative theophylline transfer rate from I suspensions could be obtained. This predicted value (calculated by multiplying the slope of the line in Fig. 2 by the estimated theophylline concentration at 2.5×10^{-4} *M*) was 0.00124 mg/min. The observed value of 0.0017 mg/min closely agreed with the predicted value. This evidence strongly suggested that only concentration-dependent theophylline transfer occurs from the mucosal to the serosal side of the everted rat intestinal sacs.

The utility of such an *in vitro* animal model for assessing *in vivo* availability of drugs and their metabolites was demonstrated previously (8, 9). The biopharmaceutical implications of these findings are obvious when the advantages of theophylline therapy with a solid oral dosage form

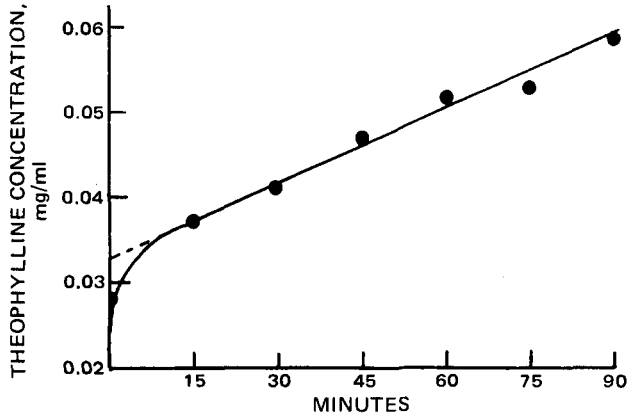

Figure 3—*Formation of theophylline from I suspension (0.045% w/v) in pH 7.4 Krebs phosphate buffer at 37°.*

of I are considered. Since the theophylline formation rate from I is constant at pH 7.4 and 37°, the availability of theophylline for absorption over a prolonged period apparently could be maintained *in vivo*. Consequently, a continuous appearance of theophylline into the vascular compartment would allow the maintenance of a constant plasma theophylline level over a prolonged period after dosing the patient with I. It is conceivable that the toxic manifestations associated with theophylline therapy might be controlled by such a prodrug approach.

In conclusion, this study demonstrated the usefulness of everted rat intestinal sacs for ascertaining the transfer rate of a drug, such as theophylline, from its prodrug entity, namely, ditheophylline succinate. These data provided meaningful biopharmaceutical support indicative of theophylline appearance on the serosal side of the intestinal sacs. The observed and predicted values for the cumulative theophylline transfer rate from a I suspension closely agreed. Evidence presented indicates that, under simulated conditions of physiological pH and temperature, the concentration-dependent transfer rate of theophylline across the intestinal barrier is controlled by the constant (steady) formation of theophylline in solution from a suspension of I in a given physiological medium.

REFERENCES

(1) R. K. Crane and T. H. Wilson, *J. Appl. Physiol.*, **12**, 145 (1958).
(2) G. Levy and W. J. Jusko, *J. Pharm. Sci.*, **54**, 219 (1965).
(3) S. Feldman and M. Gibaldi, *ibid.*, **58**, 425 (1969).
(4) W. H. Barr and S. Riegelman, *ibid.*, **59**, 155 (1970).
(5) M. Taraszka, *ibid.*, **60**, 946 (1971).
(6) H. A. Krebs, *Biochem. Biophys. Acta*, **4**, 249 (1950).
(7) R. M. Barrer, "Diffusion in and through Solids," Cambridge University Press, Cambridge, England, 1951.
(8) W. H. Barr and S. Riegelman, *J. Pharm. Sci.*, **59**, 164 (1970).
(9) W. H. Barr, in "Bioavailability of Drugs," B. B. Brodie and W. M. Heller, Eds., S. Karger, New York, N.Y., 1972, pp. 55–101.

ACKNOWLEDGMENTS

The author expresses appreciation to Ms. Slavena Pophristov for technical assistance and to Mr. S. Marshall for assistance in determining the surface area of ditheophylline succinate by the Brunauer, Emmett, and Teller nitrogen absorption method.

Rapid and Micro High-Pressure Liquid Chromatographic Determination of Plasma Phenytoin Levels

JOSEPH E. SLONEK, GEOFFREY W. PENG, and WIN L. CHIOU ˣ

Received November 14, 1977, from the *Clinical Pharmacokinetics Laboratory and Department of Pharmacy, University of Illinois, Chicago, IL 60612.* Accepted for publication February 28, 1978.

Abstract □ A rapid and simple high-pressure liquid chromatographic microanalytical method was developed for the determination of clinically encountered plasma phenytoin levels. This method is accurate down to about 1 μg of phenytoin/ml of plasma and requires as little as 10 μl of sample. Total analysis time is about 10 min. The method involves deproteinizing with acetonitrile followed by monitoring the deproteinized sample at 254 nm. Phenytoin's primary metabolite in humans, 5-(*p*-hydroxyphenyl)-5-phenylhydantoin, also can be quantitated when present in moderately high clinically encountered concentrations. Plasma profiles of phenytoin and its metabolite were followed with time after an intravenous bolus injection to a rabbit.

Keyphrases □ Phenytoin—high-pressure liquid chromatographic analysis in plasma □ High-pressure liquid chromatography—analysis, phenytoin in plasma □ Anticonvulsants—phenytoin, high-pressure liquid chromatographic analysis in plasma

Phenytoin is one of the most frequently prescribed anticonvulsants and also is used to treat various psychoses, trigeminal and related neuralgias, and various cardiac arrhythmias. It is considered the drug of choice in treating all forms of epilepsy except absence seizures (1).

BACKGROUND

Plasma concentrations of phenytoin may be related closely to its therapeutic as well as toxic effects (2). Phenytoin exerts a useful therapeutic effect at plasma concentrations of 10–20 μg/ml (1–3). Plasma levels higher than 20 μg/ml often are associated with adverse effects. The importance of plasma level monitoring also is increased by phenytoin's nonlinear elimination pharmacokinetics (4, 5).

No method of phenytoin measurement was available before 1956 (2). Since then, GLC (6–8), TLC (9, 10), mass fragmentographic (11), and high-pressure liquid chromatographic (HPLC) (12–15) methods have been used to determine phenytoin alone or in combination with other agents. Radioimmunoassay, enzyme immunoassay, spectrophotometric, and GLC determinations of phenytoin have been compared (16). All proposed methods suffer from one or more of the following requirements: (*a*) an excessive amount of time, (*b*) chemical derivatization, (*c*) extraction (either single or multiple steps) to "clean" the sample, (*d*) sample dilution, and (*e*) a fairly large plasma sample (1–2 ml).

The developed method has none of these drawbacks. Quantitation can be achieved within 10 min after obtaining the plasma sample. No derivatives are made nor extractions used. This method is ideally suited for assays of commonly encountered plasma phenytoin concentrations using as little as 10 μl of plasma. In addition, when present in moderately high plasma concentration, 5-(*p*-hydroxyphenyl)-5-phenylhydantoin (I), the major metabolite of phenytoin in humans, also may be quantitated.

EXPERIMENTAL

Reagents—Phenytoin[1], phenytoin sodium[2], 5-(*p*-hydroxyphenyl)-5-phenylhydantoin[3], and acetonitrile[4] were used.

Instruments—All determinations were made using an HPLC pump with an injector[5], an absorbance detector[6] with a 254-nm filter, a recorder[7], and a 30-cm × 3.9-mm (i.d.) reversed-phase column[8]. The system ran at ambient room temperature. The sensitivity was 0.005 absorbance unit full-scale deflection.

Standard Curve and Sample Preparation—A standard curve was prepared for phenytoin and I in the following manner. Aliquots of 200 μl of pooled human plasma were spiked with various quantities of concentrated acetonitrile–water stock solutions of phenytoin and I. The stock solutions were kept refrigerated and tightly sealed until use. A blank plasma and seven plasma samples with concentrations ranging from 1 to 40 μg of phenytoin/ml and from 0.1 to 4 μg of I/ml were vortex mixed[9] for about 5 sec. These samples were deproteinized by addition of 500 μl of acetonitrile, vortex mixed for about 5 sec, and centrifuged for 1 min at 2500 rpm.

Aliquots of 25 μl of the clear liquid fraction were chromatographed. Peak heights were used for quantitation. The flow rate was 2.0 ml/min with a mobile phase of acetonitrile–water (30:70 v/v), acidified with concentrated phosphoric acid to pH 2.65–2.69. Samples from *in vivo* experiments were analyzed similarly.

Drug Recovery Study—Three samples each of 100 μl of water and pooled human plasma were spiked with 4 μl of a stock solution of phenytoin and I to give a final concentration of 10 μg/ml. To each sample and plasma blank was added 250 μl of acetonitrile, and all were chromatographed as described.

Drug Interference Study—Many compounds were tested to determine if they would interfere: primidone[10], mephenytoin[11], salicylic acid[12], mephobarbital[13], trimethadione[14], ethotoin[14], phenacemide[14], methsuximide[15], ethosuximide[15], mephobarbital[16], phenobarbital sodium[17], hexobarbital[18], and heptabarbital[19]. Aliquots of 25 μl of 200-μg/ml acetonitrile–water stock solutions of each compound were injected and monitored at 254 nm.

***In Vivo* Study**—The solution for injection contained 20 mg of phenytoin sodium/ml in basified water. The right marginal ear vein of a 3.4-kg male albino rabbit was catheterized[20]. Phenytoin sodium, 40 mg, was injected *via* this route over 6–7 sec. Venous blood samples were collected in heparinized vials and were centrifuged within 30 min at 2500 rpm for 4 min to obtain plasma fractions. These fractions were stored frozen until analysis.

RESULTS AND DISCUSSION

Phenytoin and I standard curves were linear in the concentration ranges studied. For example, the phenytoin plot linear regression line was $y = 0.1431x - 0.0965$ ($\gamma = 0.9992$) and that for I was $y = 0.4407x - 0.0705$ ($\gamma = 0.9931$), where y is peak height in centimeters and x is concentration in micrograms per milliliter.

With the conditions of this analysis, the minimum concentrations that can be measured accurately by the procedure are about 1.0 μg of phenytoin and 1.0 μg of I/ml of plasma. This value for phenytoin is well below the therapeutic level. Lower concentrations give poor accuracy because of error in peak height measurement and, in the case of I, plasma interference. Retention times for I and phenytoin are 3.6 and 8.2 min, re-

[1] Prepared from phenytoin sodium.
[2] Sigma Chemical Co., St. Louis, Mo.
[3] Aldrich Chemical Co., Milwaukee, Wis.
[4] Burdick and Jackson Laboratories, Muskegon, Mich.
[5] Model M-6000A, U6K injector, Waters Associates, Milford, Mass.
[6] Model 440, Waters Associates, Milford, Mass.
[7] Ominscribe, Houston Instruments, Austin, Tex.
[8] μBondapak C_{18}, Waters Associates, Milford, Mass.
[9] Vortex-Genie, Scientific Industries, Springfield, Mass.
[10] Ayerst Laboratories, New York, N.Y.
[11] Sandoz Pharmaceuticals, Hanover, N.J.
[12] Merck Sharp & Dohme, West Point, Pa.
[13] Sterling-Winthrop Research Institute, Rensselaer, N.Y.
[14] Abbott, North Chicago, Ill.
[15] Parke-Davis and Co., Detroit, Mich.
[16] Eli Lilly Laboratories, Indianapolis, Ind.
[17] J. T. Baker Chemical Co., Phillipsburg, N.J.
[18] Gane's Chemical Works, Corlstadt, N.J.
[19] Geigy Pharmaceuticals, Ardsley, N.Y.
[20] Radiopaque/Teflon, 22-gauge, 1 in., Jelco Laboratories, Raritan, N.J.

0022-3549/78/1000-1462$01.00/0
© 1978, American Pharmaceutical Association

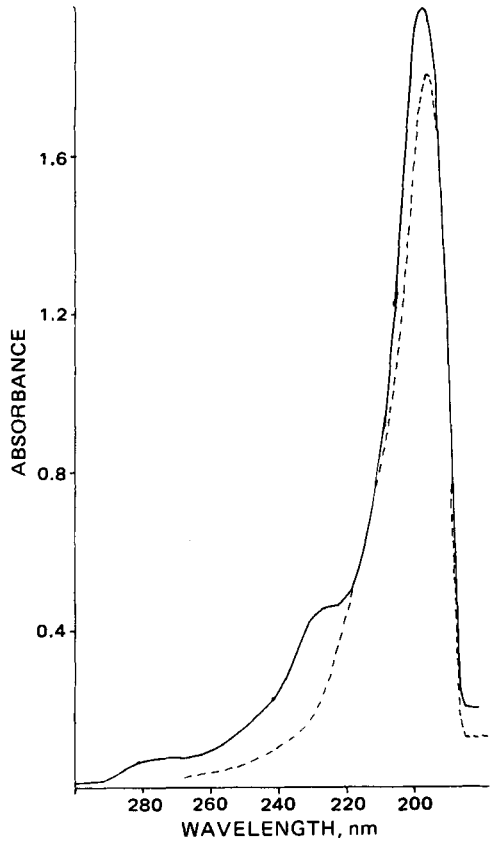

Figure 1—*UV spectra of phenytoin (- - -) and I (—), both at 1 mg % in acetonitrile–water (30:70 v/v) acidified to pH 2.65–2.69 with phosphoric acid. Spectra were obtained using 1-cm cells.*

spectively. The 2.0-ml/min flow rate and 25-μl injection volume were optimal.

At a concentration of 14.8 μg/ml, seven replicate analyses of phenytoin gave essentially identical peak heights. Similarly, at the same concentration and for the same number of assays, the coefficient of variation for I was only 1.9%. Under the same concentration conditions, four replicate analyses over 4 days gave interassay coefficients of variation of 2.2% for phenytoin and 1.2% for I. Placement of 50 ng each of phenytoin and I on-column resulted in signal-to-noise ratios of 12.5 and 76, respectively. The UV spectra of phenytoin and I are shown in Fig. 1. Although phenytoin and I showed maximal absorption at around 197 nm, detection at 254 nm using a mercury light souce had adequate sensitivity and an excellent signal-to-noise ratio.

The recovery study was done to show whether some of the drug was being lost during deproteinization. Recovery was essentially complete. Specifically, phenytoin was 100% recovered and I was 96% recovered, as calculated by relative average peak heights of plasma samples as compared to distilled water samples. There was some difficulty in I quantitation because of occasional minor blank interference, which had to be subtracted from peak height measurements. Had the small interfering peak height not been compensated for, I recovery would have been 107.4%, an overestimation of the plasma I concentration. No endogenous interference with the phenytoin signal was noted.

The drug interference study showed that phenobarbital sodium and ethotoin interfered with the I signal and that mephobarbital interfered with the phenytoin signal. The amounts injected were generally greatly in excess of plasma concentrations usually encountered clinically.

The rabbit data are graphically presented in Fig. 2. Plasma phenytoin levels declined biexponentially, with a terminal half-life of about 2 hr. At these levels, I can be monitored readily. Chromatograms of phenytoin and I in rabbit plasma are shown in Fig. 3. This preliminary rabbit study was done to show the ability of this procedure to follow plasma phenytoin and I concentrations.

The satisfactory amount of acetonitrile needed for deproteinization of the plasma was 2.5 times the plasma volume used. With this ratio, as little as 10 μl of plasma can be assayed to give good results. Acetonitrile proved excellent for plasma deproteinization, which obviates the need

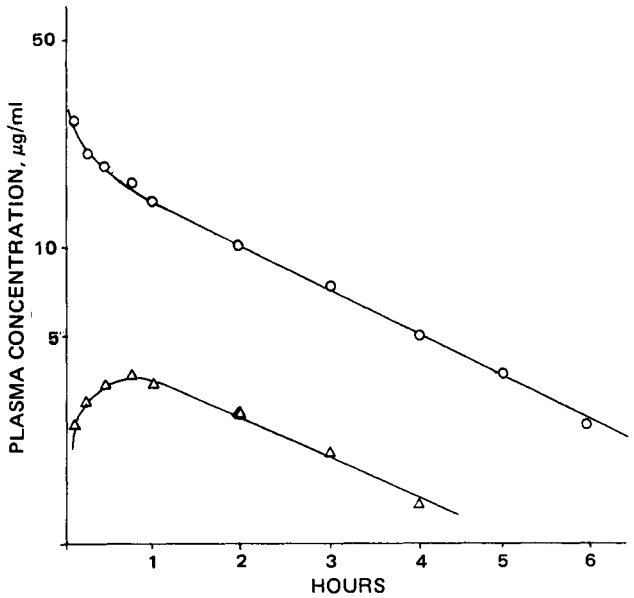

Figure 2—*Plasma concentration profiles of phenytoin (○) and I (△) in a rabbit after intravenous administration of phenytoin.*

for extraction. After centrifugation, the supernatant clear liquid may be poured into a screw-capped glass culture tube and refrigerated until the following morning if necessary; samples were stable overnight when stored in this manner. During storage or if a long break is taken between sample preparation and sample injection, the samples must be sealed from the air or volatile acetonitrile may evaporate and result in spuriously high drug concentration readings.

This assay was performed without column thermoregulation, and this omission contributed to the slight variations in retention times of the compounds from day to day. If used for routine clinical monitoring of plasma phenytoin levels, a standard solution of phenytoin (and I if analyzed) should be injected into the chromatographic system prior to sample analysis to obtain an exact retention time value for any given day; ther-

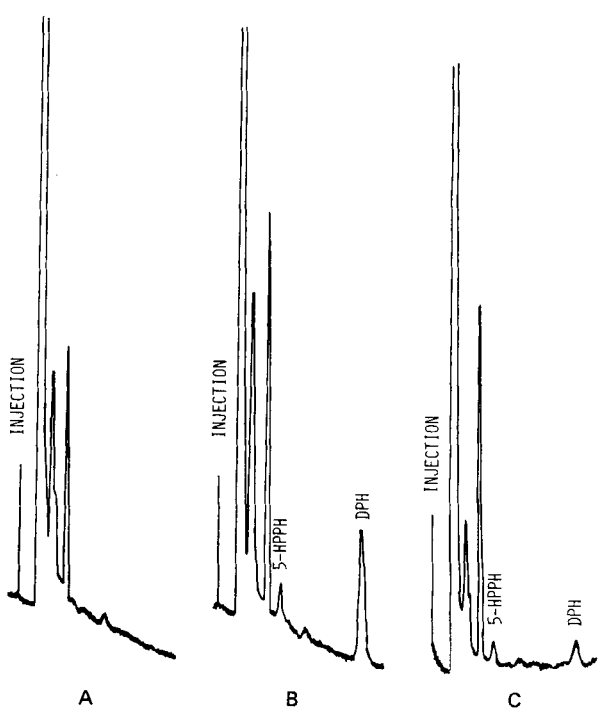

Figure 3—*Typical chromatograms of phenytoin (DPH) and I (5-HPPH) seen on analysis of rabbit plasma. Key: A, blank; B, 6 min after intravenous phenytoin administration; and C, 4 hr after intravenous phenytoin administration.*

moregulation of the column might also be desirable. The slight variations in retention times do not appreciably affect peak heights for quantitation.

Acidification of the mobile phase was shown to affect chromatography favorably. It shortened the retention times of plasma residues and lengthened retention times of phenytoin and I, thereby minimizing plasma interference with the assay.

The column gave good resolution of the compounds for at least 6 months of operation with systems of this sort, being used about 3 days/week.

In conclusion, this method should be useful for clinical monitoring of plasma phenytoin concentrations. Its metabolite, I, can be detected in moderately high concentrations, as shown by a preliminary *in vivo* rabbit investigation. The method is extremely rapid, economical of plasma and reagents, and simple.

REFERENCES

(1) D. M. Woodbury and E. Fingl, in "The Pharmacological Basis of Therapeutics," 5th ed., L. S. Goodman and A. Gilman, Eds., Macmillan, New York, N.Y., 1975, chap. 13.

(2) L. Lund, in "The Biological Effects of Drugs in Relation to Their Plasma Concentrations," D. S. Davies and B. N. C. Prichard, Eds., University Park Press, Baltimore, Md., 1973, chap. 18.

(3) "Physicians' Desk Reference," Medical Economics Co., Oradell, N.J., 1976, p. 1151.

(4) A. Richens and A. Dunlop, *Lancet*, **2**, 247 (1975).

(5) D. G. Lambie, R. H. Johnson, R. N. Nanda, and R. A. Shahir, *ibid.*, **2**, 386 (1976).

(6) K. K. Midha, I. J. McGilveray, and D. L. Wilson, *J. Pharm. Sci.*, **65**, 1240 (1976).

(7) R. J. Perchalski, K. N. Scott, B. J. Wilder, and R. H. Hammer, *ibid.*, **62**, 1735 (1973).

(8) J. MacGee, *Anal. Chem.*, **42**, 421 (1970).

(9) N. Wad, E. Hanifl, and H. Rosenmund, *J. Chromatogr.*, **143**, 89 (1977).

(10) G. E. Simon, P. I. Jatlow, H. T. Seligson, and D. Seligson, *Am. J. Clin. Pathol.*, **55**, 145 (1971).

(11) C. Hoppel, M. Garle, and M. Elander, *J. Chromatogr.*, **116**, 53 (1976).

(12) J. E. Evans, *Anal. Chem.*, **45**, 2428 (1973).

(13) R. F. Adams and F. L. Vandemark, *Clin. Chem.*, **22**, 25 (1976).

(14) K. S. Albert, M. R. Hallmark, M. E. Carroll, and J. G. Wagner, *Res. Commun. Chem. Pathol. Pharmacol.*, **6**, 845 (1973).

(15) P. M. Kabda, G. Gotelli, R. Stomfill, and L. J. Marton, *Clin. Chem.*, **22**, 824 (1976).

(16) V. Spiehler, L. Sun, D. S. Miyada, S. G. Sarandis, E. R. Walwick, M. W. Klein, D. B. Jordan, and B. Jessen, *ibid.*, **22**, 749 (1976).

Comparison of Adsorbed Films of a Polyvinylpyrrolidone Copolymer with Spread Monolayers

JOEL L. ZATZ

Received November 28, 1977, from the *College of Pharmacy, Rutgers—the State University, Piscataway, NJ 08854.* Accepted for publication February 23, 1978.

Abstract □ The adsorption of a polyvinylpyrrolidone–polyvinyl acetate graft copolymer from solution was studied by surface pressure measurement. Adsorption from the dilute solutions was slow, limited, in part, by diffusion of polymer molecules to the surface. When adsorbed monolayers were compressed on a surface balance, the resulting surface pressure values paralleled those of a spread monolayer, strongly suggesting that the structures of adsorbed and spread monolayers are the same.

Keyphrases □ Polyvinylpyrrolidone copolymer—adsorption from solution studied by surface pressure measurement, films compared to spread monolayers □ Adsorption—polyvinylpyrrolidone copolymer from solution, studied by surface pressure measurement, films compared to spread monolayers □ Surface pressure—measurement used to study polyvinylpyrrolidone copolymer adsorption from solution, films compared to spread monolayers □ Polymers—polyvinylpyrrolidone–vinyl acetate copolymer, adsorption from solution studied by surface pressure measurement, films compared to spread monolayers

The surface properties of polymers are studied conveniently by spreading them as monolayers on a water surface. In such studies, polymer molecules are spread onto an aqueous substrate in small quantity so as barely to disturb the surface tension. Once the spreading process is complete, the surface area is reduced to smaller values (thereby concentrating the two-dimensional polymer systems) and the surface properties are measured as a function of the area available to each unit of polymer.

However, in systems of practical interest such as pharmaceutical dispersions, a polymer in the formulation is in solution and polymer molecules migrate to the interface and are adsorbed. The first few polymer molecules adsorbed encounter an uncrowded interface and have space in which to adopt the energetically most favorable orientation. But the interfacial region gradually becomes crowded as adsorption proceeds, and polymer molecules arriving later may be unable to spread completely. The conformation of molecules in concentrated adsorbed monolayers may thus be different from that in spread monolayers, so the properties of the two types of systems may differ.

BACKGROUND

Most studies comparing the structures of spread and adsorbed monolayers have been carried out on proteins. Yamashita and Bull (1) found that adsorbed films of lysozyme were thicker than spread monolayers. They suggested that the adsorbed protein molecules largely retain their native configuration at the surface while spread lysozyme molecules unfold more completely. Surface films of trypsin formed by applying the enzyme to a clean surface showed a complete loss of enzymatic activity (2–4). However, when the films were formed by adding more trypsin to an interface that already had some trypsin present, some enzymatic activity was retained. In this situation, complete spreading did not occur and the film properties depended on the method of film formation.

Musselwhite and Palmer (5) prepared monolayers of bovine serum albumin using two different techniques. In one experiment, the monolayers were spread in the usual way, and the film was concentrated by compression to a smaller surface area. The second approach involved concentration of the monolayer by maintaining the same surface area and adding more protein to the surface. The newly added protein molecules encountered a surface already partially occupied. This mode of increasing the surface concentration of the protein is similar to the process that occurs during adsorption. The force–area diagrams for the two techniques were quite different. These reports indicated that adsorbed and spread films of proteins are not equivalent.

0022-3549/78/1000-1464$01.00/0

© 1978, American Pharmaceutical Association

moregulation of the column might also be desirable. The slight variations in retention times do not appreciably affect peak heights for quantitation.

Acidification of the mobile phase was shown to affect chromatography favorably. It shortened the retention times of plasma residues and lengthened retention times of phenytoin and I, thereby minimizing plasma interference with the assay.

The column gave good resolution of the compounds for at least 6 months of operation with systems of this sort, being used about 3 days/week.

In conclusion, this method should be useful for clinical monitoring of plasma phenytoin concentrations. Its metabolite, I, can be detected in moderately high concentrations, as shown by a preliminary *in vivo* rabbit investigation. The method is extremely rapid, economical of plasma and reagents, and simple.

REFERENCES

(1) D. M. Woodbury and E. Fingl, in "The Pharmacological Basis of Therapeutics," 5th ed., L. S. Goodman and A. Gilman, Eds., Macmillan, New York, N.Y., 1975, chap. 13.

(2) L. Lund, in "The Biological Effects of Drugs in Relation to Their Plasma Concentrations," D. S. Davies and B. N. C. Prichard, Eds., University Park Press, Baltimore, Md., 1973, chap. 18.

(3) "Physicians' Desk Reference," Medical Economics Co., Oradell, N.J., 1976, p. 1151.

(4) A. Richens and A. Dunlop, *Lancet*, **2**, 247 (1975).

(5) D. G. Lambie, R. H. Johnson, R. N. Nanda, and R. A. Shahir, *ibid.*, **2**, 386 (1976).

(6) K. K. Midha, I. J. McGilveray, and D. L. Wilson, *J. Pharm. Sci.*, **65**, 1240 (1976).

(7) R. J. Perchalski, K. N. Scott, B. J. Wilder, and R. H. Hammer, *ibid.*, **62**, 1735 (1973).

(8) J. MacGee, *Anal. Chem.*, **42**, 421 (1970).

(9) N. Wad, E. Hanifl, and H. Rosenmund, *J. Chromatogr.*, **143**, 89 (1977).

(10) G. E. Simon, P. I. Jatlow, H. T. Seligson, and D. Seligson, *Am. J. Clin. Pathol.*, **55**, 145 (1971).

(11) C. Hoppel, M. Garle, and M. Elander, *J. Chromatogr.*, **116**, 53 (1976).

(12) J. E. Evans, *Anal. Chem.*, **45**, 2428 (1973).

(13) R. F. Adams and F. L. Vandemark, *Clin. Chem.*, **22**, 25 (1976).

(14) K. S. Albert, M. R. Hallmark, M. E. Carroll, and J. G. Wagner, *Res. Commun. Chem. Pathol. Pharmacol.*, **6**, 845 (1973).

(15) P. M. Kabda, G. Gotelli, R. Stomfill, and L. J. Marton, *Clin. Chem.*, **22**, 824 (1976).

(16) V. Spiehler, L. Sun, D. S. Miyada, S. G. Sarandis, E. R. Walwick, M. W. Klein, D. B. Jordan, and B. Jessen, *ibid.*, **22**, 749 (1976).

Comparison of Adsorbed Films of a Polyvinylpyrrolidone Copolymer with Spread Monolayers

JOEL L. ZATZ

Received November 28, 1977, from the *College of Pharmacy, Rutgers—the State University, Piscataway, NJ 08854.* Accepted for publication February 23, 1978.

Abstract □ The adsorption of a polyvinylpyrrolidone–polyvinyl acetate graft copolymer from solution was studied by surface pressure measurement. Adsorption from the dilute solutions was slow, limited, in part, by diffusion of polymer molecules to the surface. When adsorbed monolayers were compressed on a surface balance, the resulting surface pressure values paralleled those of a spread monolayer, strongly suggesting that the structures of adsorbed and spread monolayers are the same.

Keyphrases □ Polyvinylpyrrolidone copolymer—adsorption from solution studied by surface pressure measurement, films compared to spread monolayers □ Adsorption—polyvinylpyrrolidone copolymer from solution, studied by surface pressure measurement, films compared to spread monolayers □ Surface pressure—measurement used to study polyvinylpyrrolidone copolymer adsorption from solution, films compared to spread monolayers □ Polymers—polyvinylpyrrolidone–vinyl acetate copolymer, adsorption from solution studied by surface pressure measurement, films compared to spread monolayers

The surface properties of polymers are studied conveniently by spreading them as monolayers on a water surface. In such studies, polymer molecules are spread onto an aqueous substrate in small quantity so as barely to disturb the surface tension. Once the spreading process is complete, the surface area is reduced to smaller values (thereby concentrating the two-dimensional polymer systems) and the surface properties are measured as a function of the area available to each unit of polymer.

However, in systems of practical interest such as pharmaceutical dispersions, a polymer in the formulation is in solution and polymer molecules migrate to the interface and are adsorbed. The first few polymer molecules adsorbed encounter an uncrowded interface and have space in which to adopt the energetically most favorable orientation. But the interfacial region gradually becomes crowded as adsorption proceeds, and polymer molecules arriving later may be unable to spread completely. The conformation of molecules in concentrated adsorbed monolayers may thus be different from that in spread monolayers, so the properties of the two types of systems may differ.

BACKGROUND

Most studies comparing the structures of spread and adsorbed monolayers have been carried out on proteins. Yamashita and Bull (1) found that adsorbed films of lysozyme were thicker than spread monolayers. They suggested that the adsorbed protein molecules largely retain their native configuration at the surface while spread lysozyme molecules unfold more completely. Surface films of trypsin formed by applying the enzyme to a clean surface showed a complete loss of enzymatic activity (2–4). However, when the films were formed by adding more trypsin to an interface that already had some trypsin present, some enzymatic activity was retained. In this situation, complete spreading did not occur and the film properties depended on the method of film formation.

Musselwhite and Palmer (5) prepared monolayers of bovine serum albumin using two different techniques. In one experiment, the monolayers were spread in the usual way, and the film was concentrated by compression to a smaller surface area. The second approach involved concentration of the monolayer by maintaining the same surface area and adding more protein to the surface. The newly added protein molecules encountered a surface already partially occupied. This mode of increasing the surface concentration of the protein is similar to the process that occurs during adsorption. The force–area diagrams for the two techniques were quite different. These reports indicated that adsorbed and spread films of proteins are not equivalent.

0022-3549/78/1000-1464$01.00/0

© 1978, American Pharmaceutical Association

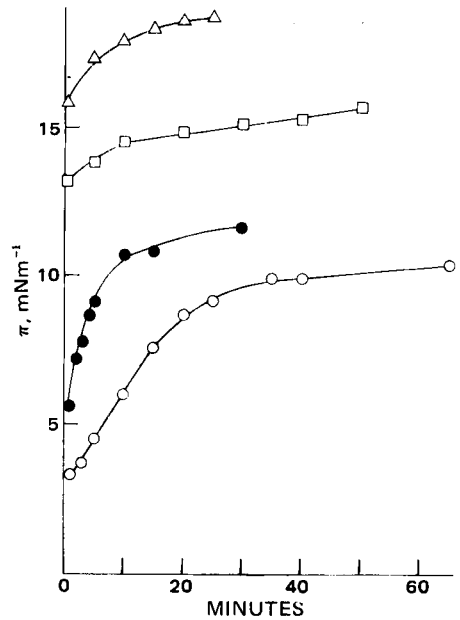

Figure 1—*Surface pressure of solutions of copolymer as a function of time. Key: △, 8.05 × 10⁻³%, unstirred; □, 2.75 × 10⁻³%, unstirred; ○, 0.20 × 10⁻³%, unstirred; and ●, 0.20 × 10⁻³%, stirred.*

Previously (6, 7), the properties of monolayers of some polyvinylpyrrolidone–polyvinyl acetate graft copolymers were presented. The copolymer with the smallest vinyl acetate content is sufficiently water soluble to permit study of its adsorption from aqueous solution. This report describes the adsorption of the copolymer at the air–water interface and compares adsorbed films with the monolayers studied earlier.

EXPERIMENTAL

The copolymer[1] [61.2% (w/w) vinylpyrrolidone and 38.8% vinyl acetate] was purified as described previously (3). Water was deionized and distilled from an all-glass still. Glassware was cleaned with chromic acid cleaning solution and then rinsed repeatedly with distilled water. Aspiration was used to remove impurities from the surfaces of the polymer solutions. Surface tension was measured by the Wilhelmy plate method. All experiments were performed at room temperature, 24.5 ± 1°.

RESULTS AND DISCUSSION

Surface tension of the polymer solutions was measured as a function of time. Results are expressed in terms of surface pressure, π, defined as the difference between the surface tension of pure water and that of the polymer solution. The solution surfaces were cleaned by aspiration, and surface pressure was monitored for 10 days. The values of surface pressure rose quickly at first and then leveled off. Attainment of a limiting value of surface pressure indicated that adsorption underwent no further change. The more concentrated solutions approached within 1 mNm^{-1} of the limiting value of surface pressure within 1 hr. Very dilute solutions required about 3 days to reach the same point.

Some data obtained during the first 60 min after aspiration of the solution surface are presented in Fig. 1. Previous work (8) showed that bulk diffusion is important in limiting the adsorption rate in very dilute solutions. The dependence of the rate of copolymer adsorption on bulk concentration suggests that diffusion is an important step in the adsorption process, at least during the early stages. Further evidence for this conclusion is provided by the fact that gentle stirring speeded adsorption from the very dilute solutions (Fig. 1).

At higher values of bulk concentration, the approach to apparent equilibrium is limited by the presence of previously adsorbed molecules. Molecules approaching the surface must find an opening to which to anchor and then bring other polymer segments into the interface. The attainment of a quasiequilibrium conformation at the interface requires expansion of the molecule against the force exerted by neighboring molecules. This condition has been referred to as a surface pressure barrier to adsorption (9).

[1] PVP/VA 735, GAF Corp., New York, N.Y.

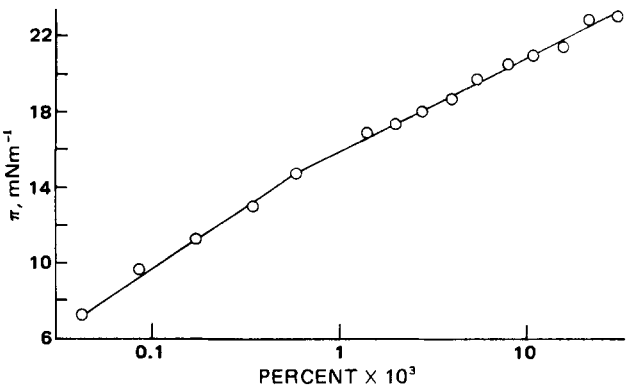

Figure 2—*Limiting values of surface pressure of solutions of the copolymer as a function of concentration.*

In Fig. 2, the limiting surface pressures are plotted against the logarithm of solution concentration. The experimental points may be resolved into two linear segments. The slope of the plot is steeper at low concentrations than at higher concentrations. This type of behavior is opposite to that found with compounds of low molecular weight but was observed in studies of other polymers (10, 11).

Unfortunately, the Gibbs isotherm cannot be employed to calculate values of surface excess. The Gibbs equation assumes a state of equilibrium, and there is no assurance that the reported surface pressures represent equilibrium values since surface films of polyvinylpyrrolidone copolymers are not readily desorbed (6). Furthermore, the copolymer molecules cannot be considered to be a single species since they differ in molecular weight and in relative composition of the monomeric building blocks. Therefore, the polymer solutions represent multicomponent systems, to which the Gibbs equation is inapplicable (12).

In several independent experiments, copolymer solutions were placed in a surface balance and permitted to stand for about 15 min after the surface was swept. The adsorbed monolayers were then compressed, and surface pressure readings were taken as a function of available surface area (Fig. 3). To determine whether compression of these adsorbed films yielded the same pattern as the spread monolayer, the specific surface area, in square meters per milligram, at full trough area was determined for each experiment from the π–A curve for spread monolayers of the copolymer (6). The surface area corresponding to the other surface pressures measured on the compressed adsorbed films then was calculated from the percent of the trough area. With these calculated areas and the experimentally measured surface pressures, it was possible to construct π–A curves representing compression of the adsorbed films.

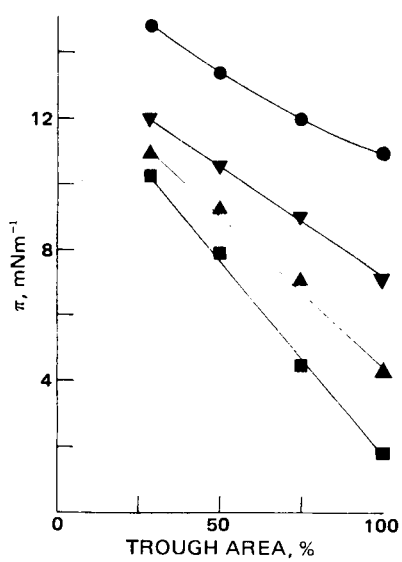

Figure 3—*Surface pressure of adsorbed monolayers compressed on a surface balance. Each symbol represents a different adsorbed monolayer.*

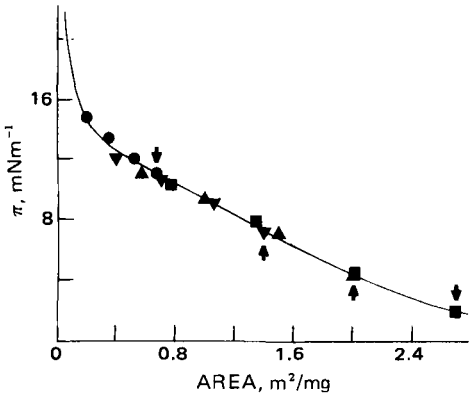

Figure 4—*Comparison of π–A results obtained from adsorbed films (see text for details) with those from a spread monolayer. This solid line is the π–A curve for the compressed monolayer (6). Symbols correspond to those in Fig. 3. Arrows indicate the data points that were fit to the π–A curve of the spread monolayer and from which surface area values of the other points were calculated.*

In Fig. 4, all of the data are combined and compared with the π–*A* curve for a spread monolayer. The correspondence obtained suggests that the structure of the adsorbed monolayers is identical or very similar to that of a spread monolayer, in contrast to what was observed with other polymers.

Concentration of a monolayer by addition of more of the copolymer (in solution) to the surface leads to surface pressure values equivalent to those obtained by compression of a monolayer (6). Therefore, the added copolymer molecules are incorporated to yield a system identical to that obtained by compression of an extremely dilute surface film. Spreading in the presence of a monolayer is similar to the process that occurs during adsorption in that the molecules arriving at the surface in both situations must take their place against the resistance of an existing surface pressure (5). Thus, the ability of the copolymer to spread in the presence of a monolayer to reach a quasiequilibrium state is consistent with the evidence obtained in the present study for the structural equivalence of spread and adsorbed monolayers of the copolymer.

Attainment of the final shape and orientation of an adsorbing polymer molecule is a two-step process. In the first step, the polymer molecule touches the interface and "sticks." At this point, the conformation of the molecule is the same, or nearly the same, as in the bulk phase. In the second step, if it occurs, the molecule rearranges itself to minimize contact of hydrophobic groups with the aqueous liquid while permitting immersion of polar groups. This rearrangement usually involves a change from a coiled conformation to one that is more extended.

Adsorption of the open conformation typical of completely spread molecules requires breaking intramolecular bonds, which represents an energy barrier to molecular rearrangement. In addition, the surface pressure of neighboring molecules in the interface must be overcome since the change to the extended conformation requires additional area at the interface. Another possible hindrance to spreading is intermolecular interaction between adsorbing molecules or between an adsorbing molecule and one that has achieved the open conformation. This interaction would tend to fix the adsorbing molecule in place, making it difficult to reorient in the interface. If these barriers are operative, molecular reorientation can be extremely slow, and the majority of adsorbed molecules will then retain a conformation similar to that in bulk.

Polyvinylpyrrolidone copolymer molecules are highly flexible, and the monolayers are fluid (6). These findings argue against significant intra- or intermolecular association and help to explain why adsorbed films are fully spread. Proteins, however, show significant interactions (13). This fact may account for the differences between spread and adsorbed monolayers of proteins.

REFERENCES

(1) T. Yamashita and H. B. Bull, *J. Colloid Interface Sci.*, **27**, 19 (1968).

(2) B. R. Ray and L. G. Augenstine, *J. Phys. Chem.*, **60**, 1193 (1956).

(3) L. G. Augenstine and B. R. Ray, *ibid.*, **61**, 1380 (1957).

(4) *Ibid.*, **61**, 1385 (1957).

(5) P. R. Musselwhite and J. Palmer, *J. Colloid Interface Sci.*, **28**, 168 (1968).

(6) J. L. Zatz and B. Knowles, *J. Pharm. Sci.*, **60**, 1731 (1971).

(7) J. L. Zatz and B. Knowles, *J. Colloid Interface Sci.*, **40**, 475 (1972).

(8) F. MacRitchie and A. E. Alexander, *J. Colloid Sci.*, **18**, 453 (1963).

(9) *Ibid.*, **18**, 458 (1963).

(10) J. E. Glass, *J. Phys. Chem.*, **72**, 4450 (1968).

(11) J. M. G. Lankveld and J. Lyklema, *J. Colloid Interface Sci.*, **41**, 454 (1972).

(12) G. L. Gaines, *J. Phys. Chem.*, **73**, 3143 (1969).

(13) F. MacRitchie, *J. Macromol. Sci. Chem.*, **A4**, 1169 (1970).

ACKNOWLEDGMENTS

Supported in part by a Merck Grant for Faculty Development.

The author thanks Beverly Knowles and Kam-Bor Ip for technical assistance.

NOTES

Polarographic Analysis of Cephalexin

J. A. SQUELLA, L. J. NUÑEZ-VERGARA ˣ, and E. M. GONZALEZ

Received November 14, 1977, from the *Department of Physical Chemistry and Chemical Pharmacology, Faculty of Chemical Sciences, University of Chile, Santiago 1, Chile.* Accepted for publication February 14, 1978.

Abstract □ Cephalexin was found to be polarographically reducible after hydrolysis in an acidic medium, producing two polarographic waves. Both waves were diffusion controlled. The concentration–diffusion plot method was used for the analysis of cephalexin in capsules.

Keyphrases □ Cephalexin—polarographic analysis in dosage forms □ Polarography—analysis of cephalexin in dosage forms □ Antibacterials—cephalexin, polarographic analysis in dosage forms

Cephalexin[1] is a semisynthetic analog of cephalosporin C in which the α-aminoadipic acid of cephalosporin C is replaced by phenylglycine and the ester-linked acetic acid is condensed to a simple methyl group.

Electrochemical analysis of cephalosporins, specifically, cephalosporin C and derivatives (1, 2) and cefamandole

[1] Recalcine Inc.

0022-3549/78/1000-1466$01.00/0
© 1978, American Pharmaceutical Association

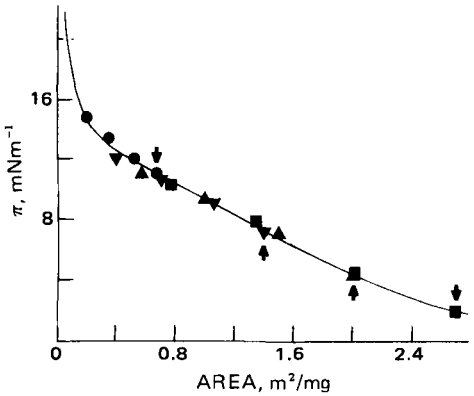

Figure 4—*Comparison of π–A results obtained from adsorbed films (see text for details) with those from a spread monolayer. This solid line is the π–A curve for the compressed monolayer (6). Symbols correspond to those in Fig. 3. Arrows indicate the data points that were fit to the π–A curve of the spread monolayer and from which surface area values of the other points were calculated.*

In Fig. 4, all of the data are combined and compared with the π–*A* curve for a spread monolayer. The correspondence obtained suggests that the structure of the adsorbed monolayers is identical or very similar to that of a spread monolayer, in contrast to what was observed with other polymers.

Concentration of a monolayer by addition of more of the copolymer (in solution) to the surface leads to surface pressure values equivalent to those obtained by compression of a monolayer (6). Therefore, the added copolymer molecules are incorporated to yield a system identical to that obtained by compression of an extremely dilute surface film. Spreading in the presence of a monolayer is similar to the process that occurs during adsorption in that the molecules arriving at the surface in both situations must take their place against the resistance of an existing surface pressure (5). Thus, the ability of the copolymer to spread in the presence of a monolayer to reach a quasiequilibrium state is consistent with the evidence obtained in the present study for the structural equivalence of spread and adsorbed monolayers of the copolymer.

Attainment of the final shape and orientation of an adsorbing polymer molecule is a two-step process. In the first step, the polymer molecule touches the interface and "sticks." At this point, the conformation of the molecule is the same, or nearly the same, as in the bulk phase. In the second step, if it occurs, the molecule rearranges itself to minimize contact of hydrophobic groups with the aqueous liquid while permitting immersion of polar groups. This rearrangement usually involves a change from a coiled conformation to one that is more extended.

Adsorption of the open conformation typical of completely spread molecules requires breaking intramolecular bonds, which represents an energy barrier to molecular rearrangement. In addition, the surface pressure of neighboring molecules in the interface must be overcome since the change to the extended conformation requires additional area at the interface. Another possible hindrance to spreading is intermolecular interaction between adsorbing molecules or between an adsorbing molecule and one that has achieved the open conformation. This interaction would tend to fix the adsorbing molecule in place, making it difficult to reorient in the interface. If these barriers are operative, molecular reorientation can be extremely slow, and the majority of adsorbed molecules will then retain a conformation similar to that in bulk.

Polyvinylpyrrolidone copolymer molecules are highly flexible, and the monolayers are fluid (6). These findings argue against significant intra- or intermolecular association and help to explain why adsorbed films are fully spread. Proteins, however, show significant interactions (13). This fact may account for the differences between spread and adsorbed monolayers of proteins.

REFERENCES

(1) T. Yamashita and H. B. Bull, *J. Colloid Interface Sci.*, **27**, 19 (1968).

(2) B. R. Ray and L. G. Augenstine, *J. Phys. Chem.*, **60**, 1193 (1956).

(3) L. G. Augenstine and B. R. Ray, *ibid.*, **61**, 1380 (1957).

(4) *Ibid.*, **61**, 1385 (1957).

(5) P. R. Musselwhite and J. Palmer, *J. Colloid Interface Sci.*, **28**, 168 (1968).

(6) J. L. Zatz and B. Knowles, *J. Pharm. Sci.*, **60**, 1731 (1971).

(7) J. L. Zatz and B. Knowles, *J. Colloid Interface Sci.*, **40**, 475 (1972).

(8) F. MacRitchie and A. E. Alexander, *J. Colloid Sci.*, **18**, 453 (1963).

(9) *Ibid.*, **18**, 458 (1963).

(10) J. E. Glass, *J. Phys. Chem.*, **72**, 4450 (1968).

(11) J. M. G. Lankveld and J. Lyklema, *J. Colloid Interface Sci.*, **41**, 454 (1972).

(12) G. L. Gaines, *J. Phys. Chem.*, **73**, 3143 (1969).

(13) F. MacRitchie, *J. Macromol. Sci. Chem.*, **A4**, 1169 (1970).

ACKNOWLEDGMENTS

Supported in part by a Merck Grant for Faculty Development.

The author thanks Beverly Knowles and Kam-Bor Ip for technical assistance.

NOTES

Polarographic Analysis of Cephalexin

J. A. SQUELLA, L. J. NUÑEZ-VERGARA ˣ, and E. M. GONZALEZ

Received November 14, 1977, from the *Department of Physical Chemistry and Chemical Pharmacology, Faculty of Chemical Sciences, University of Chile, Santiago 1, Chile.* Accepted for publication February 14, 1978.

Abstract □ Cephalexin was found to be polarographically reducible after hydrolysis in an acidic medium, producing two polarographic waves. Both waves were diffusion controlled. The concentration–diffusion plot method was used for the analysis of cephalexin in capsules.

Keyphrases □ Cephalexin—polarographic analysis in dosage forms □ Polarography—analysis of cephalexin in dosage forms □ Antibacterials—cephalexin, polarographic analysis in dosage forms

Cephalexin[1] is a semisynthetic analog of cephalosporin C in which the α-aminoadipic acid of cephalosporin C is replaced by phenylglycine and the ester-linked acetic acid is condensed to a simple methyl group.

Electrochemical analysis of cephalosporins, specifically, cephalosporin C and derivatives (1, 2) and cefamandole

[1] Recalcine Inc.

0022-3549/78/1000-1466$01.00/0
© 1978, American Pharmaceutical Association

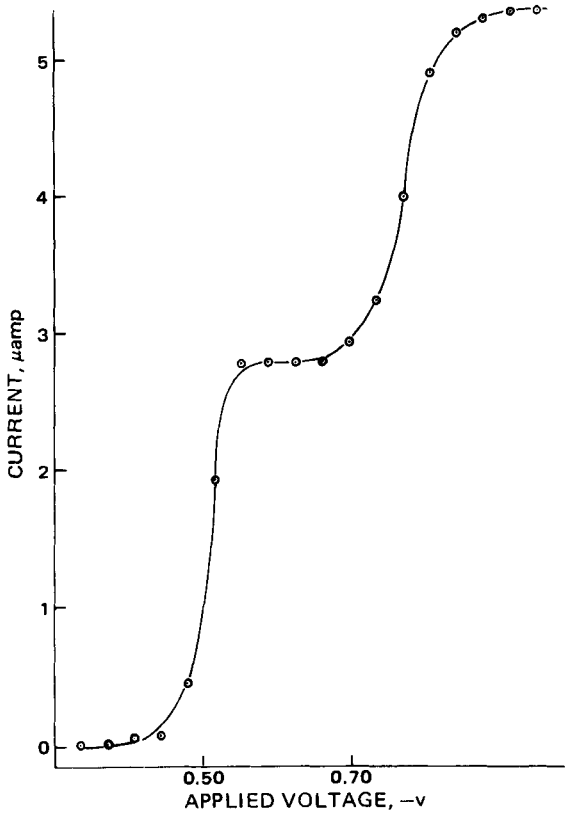

Figure 1—*Polarogram for 6.15 × 10⁻³ M cephalexin in 5.0 N HCl.*

nafate (3), was reported. This paper reports the polarographic behavior of cephalexin and its application to pharmaceutical analysis.

EXPERIMENTAL

Polarograms were recorded using a three-electrode polarograph[2] and a three-compartment polarographic cell. A saturated calomel reference electrode and a 0.5-cm² platinum foil counterelectrode were used. The dropping mercury electrode had an $m^{2/3}\,t^{1/6}$ value of 2.67 at −0.70 v *versus* the saturated calomel electrode in nitrogen-saturated 5.0 *N* HCl.

The current range was 5–7 μamp for the full scale of the recorder, and the potential scan rate was 2 mv/sec. The samples were scanned between −0.30 and −0.90 v *versus* the saturated calomel electrode.

Standards were prepared by accurately weighing 200–300 mg of standard cephalexin[3] and dissolving and diluting in 5.0 *N* HCl to 100 ml.

[2] Tacussel assembly, potentiostat type PRT 20-2, Pilote type Servovit, and recorder type EPL-2

[3] I.S.F. SpA. Rome and Recalcine Inc.

Table I—Results of Six Polarographic Analyses of Cephalexin in Capsules [a]

Analysis	i_d, μamp	Cephalexin per Capsule, mg
1	3.17	262.0
2	3.14	259.0
3	3.18	263.0
4	3.21	266.0
5	3.16	261.0
6	3.16	261.0
Average		262.0
SD		±2.4%

[a] Pentocetin capsules, Recalcine; analyzed by Recalcine Certificate of Analysis No. 10324. This sample contained 263 mg of cephalexin/capsule.

These solutions were heated to 80 ± 0.5° in a constant-temperature bath for 15 min. In a separate study, hydrolysis was complete after 12 min of treatment under the described conditions.

Each sample[1] (commercially available capsules) was dissolved completely in 5.0 *N* HCl, and the same procedure for the standard was followed.

Standard solution and samples were purged with oxygen-free nitrogen for 10 min and polarographed at 25 ± 1°.

The half-wave potentials, $E_{1/2}$, and the diffusion current, i_d, were determined graphically using the maximum of the recorder trace.

RESULTS AND DISCUSSION

Cephalexin does not exhibit polarographic waves without previous treatment. After hydrolysis in 5.0 *N* HCl at 80° for 15 min, two polarographic waves were obtained. The half-wave potentials of waves I and II were −0.50 and −0.78 v *versus* the saturated calomel electrode, respectively. A typical polarogram of cephalexin is shown in Fig. 1.

A plot of diffusion current against the square root of the mercury column height (corrected for back pressure) is a straight line. This result indicated that both reduction waves were diffusion controlled.

Wave I was selected for analytical purposes. Its polarographic current showed a linear relation for levels of cephalexin between 1×10^{-2} and 1×10^{-5} *M* in 5.0 *N* HCl (correlation coefficient for 10 values = 0.99).

The concentration–diffusion current plot method was used for the analysis of cephalexin capsules. The equation of this line is:

$$\text{concentration (mg/100 ml)} = -56.57 + 100.38\, i_d \text{ (μamp)} \qquad \text{(Eq. 1)}$$

Wave I was well developed, and the precision of the proposed method is indicated by Table I.

This method can be recommended for acidic degradation studies of cephalexin and analogous drugs.

REFERENCES

(1) I. F. Jones, J. E. Page, and C. T. Rhodes, *J. Pharm. Pharmacol., Suppl.*, **20**, 45S (1968).

(2) D. A. Hall, *J. Pharm. Sci.*, **62**, 980 (1973).

(3) E. C. Rickard and G. G. Cooke, *ibid.*, **66**, 379 (1977).

Analysis of Prazosin in Plasma by a Sensitive High-Performance Liquid Chromatographic–Fluorescence Method

THOMAS M. TWOMEY ˣ and DONALD C. HOBBS

Received December 2, 1977, from *Central Research, Pfizer, Inc., Groton, CT 06340.* Accepted for publication January 23, 1978.

Abstract □ A specific high-performance liquid chromatographic–fluorescence method for the quantitative analysis of prazosin in plasma at concentrations down to 0.2 ng/ml is described. The method involves the coextraction of drug and an internal standard from alkalinized plasma followed by a simple purification step prior to evaporation and high-performance liquid chromatographic–fluorescence analysis. The method is sufficiently sensitive to allow pharmacokinetic analyses of 1-mg doses through five half-lives, with a relative standard deviation of 12%.

Keyphrases □ Prazosin—high-performance liquid chromatographic–fluorescence analysis in plasma □ High-performance liquid chromatography–fluorometry—analysis, prazosin in plasma □ Antihypertensives—prazosin, high-performance liquid chromatographic–fluorescence analysis in plasma

Prazosin, an antihypertensive agent of the quinazoline family, lowers blood pressure in humans at doses as low as 0.5 mg (1). The determination of plasma drug concentrations after such low doses required an assay with a sensitivity capable of measuring levels below 1 ng/ml.

The quantitative determination of prazosin in human plasma has been accomplished by fluorometric–wet chemistry methods involving drug extraction from alkalinized plasma with ethyl acetate followed by back-extraction into dilute acid (2). Concentrations were calculated from the fluorescence measured at specific excitation and emission wavelengths as compared to externally standardized samples. The assay is rapid but limited in sensitivity to approximately 2 ng/ml and requires quantitative or carefully controlled aliquot transfer steps.

The method described here is specific and accurate. By use of an internal standard, the need for quantitative transfer steps has been eliminated.

EXPERIMENTAL

Reagents and Materials—Prazosin [1-(4-amino-6,7-dimethoxy-2-quinazolinyl)-4-(2-furoyl)piperazine] (I) and the internal standard 4-(4-amino-6,7,8-trimethoxy-2-quinazolinyl)-1-piperazine carboxylic acid, 2-methallyl ester (II) were prepared as methanolic stock solutions at 1.0 mg/ml and stored in the dark at 4°; no degradation was noted for at least 3 weeks. Appropriate dilutions of these solutions were made weekly with methanol to produce working standards containing 1, 0.1, and 0.01 μg of prazosin/ml and 1 μg of the internal standard/ml. Acetonitrile[1] and ethyl acetate[1] were glass distilled, as was the water used in preparing the reagents. Stock reagents were analytical reagent quality unless specified otherwise. Glassware was treated with a solution of sulfuric acid and sodium dichromate and rinsed well with water before use.

Sample Preparation—In a 15-ml centrifuge tube, 2.0 ml of plasma was fortified with 20 ng of internal standard, made alkaline with 0.5 ml of 1 *N* KOH, and extracted with 5 ml of ethyl acetate on a vortex mixer for 30 sec. Following centrifugation, the solvent was decanted into another 15-ml centrifuge tube, 1 ml of 0.1 *N* H_2SO_4 was added, and the contents of the tube were mixed on a vortex mixer for 10 sec. After centrifugation, the organic solvent layer was aspirated and discarded; the acidic aqueous fraction was made alkaline by the addition of 0.5 ml of 1 *N* KOH and extracted with 5 ml of ethyl acetate on a vortex mixer for 30 sec.

After centrifugation, the organic solvent was recovered, transferred to another 15-ml centrifuge tube with a disposable pipet (Pasteur), and evaporated to dryness at 50° in a water bath using a nitrogen stream. The residue was reconstituted with 50 μl of the chromatographic mobile phase (below), and aliquots (1–10 μl) were assayed by high-performance liquid chromatography (HPLC)–fluorescence. Samples at this stage could be held for at least 7 days when stored in the dark at 4°, as demonstrated by the same peak height ratio of prazosin to the internal standard measured on Days 1, 3, and 8. The peak height ratios were 0.99, 0.99, and 1.01, respectively, for a concentration of 2 ng/ml of drug and 10 ng/ml of the internal standard (n = 3).

Table I—Calibration Curve from Plasma

Fortification Level, ng/ml	Number of Samples	Average PHR[a], Drug/Internal Standard
0	3	0
0.2	2	0.083
0.5	2	0.20
1.0	2	0.47
2.0	4	0.85
5.0	2	1.81
10.0	2	3.75
20.0	2	7.24

[a] PHR = peak height ratio.

HPLC—An analytical liquid chromatograph[2], equipped with a 4 × 300-mm 10-μm column[3], was fitted with a fluorescence detector[4] using low dead-volume hardware. A mobile phase of acetonitrile–water–acetic acid (50:47:3) was filtered, degassed, and used at a flow rate of 2.4 ml/min (99.12 kg/cm²). The effluent stream was monitored at an excitation wavelength of 246 nm while employing the KV 389 emission filter. The range setting was varied from 0.2 to 1.0 μamp using a time constant of 2 sec. The signal was monitored with a 10-mv strip-chart recorder using a chart speed of 0.254 cm/min. Column effluent was recycled back into the mobile phase reservoir (700 ml) and prepared weekly.

Calibration curves were constructed by determining the response from known amounts of prazosin and the internal standard added to control plasma. Electronic integration offered no advantages and did not appear to yield results as reproducible as manual measurement of peak heights. Assay linearity was demonstrated over the 0.2–20-ng/ml range (Table I); the amount of the internal standard was held constant at 20 ng/sample.

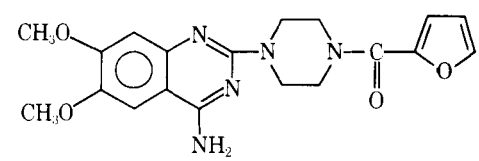

I

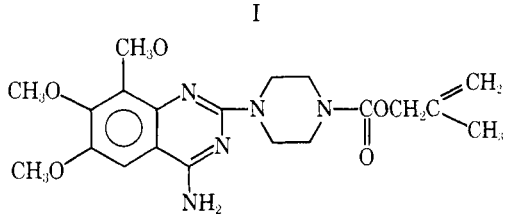

II

[1] Burdick & Jackson Laboratories, Muskegon, Mich.

[2] Spectra-Physics model 3500.

[3] The packing material was μBondapak CN; the column was Part 84042, Waters Associates.

[4] Model 970, Schoeffel Instrument Corp.

0022-3549/78/1000-1468$01.00/0
© 1978, American Pharmaceutical Association

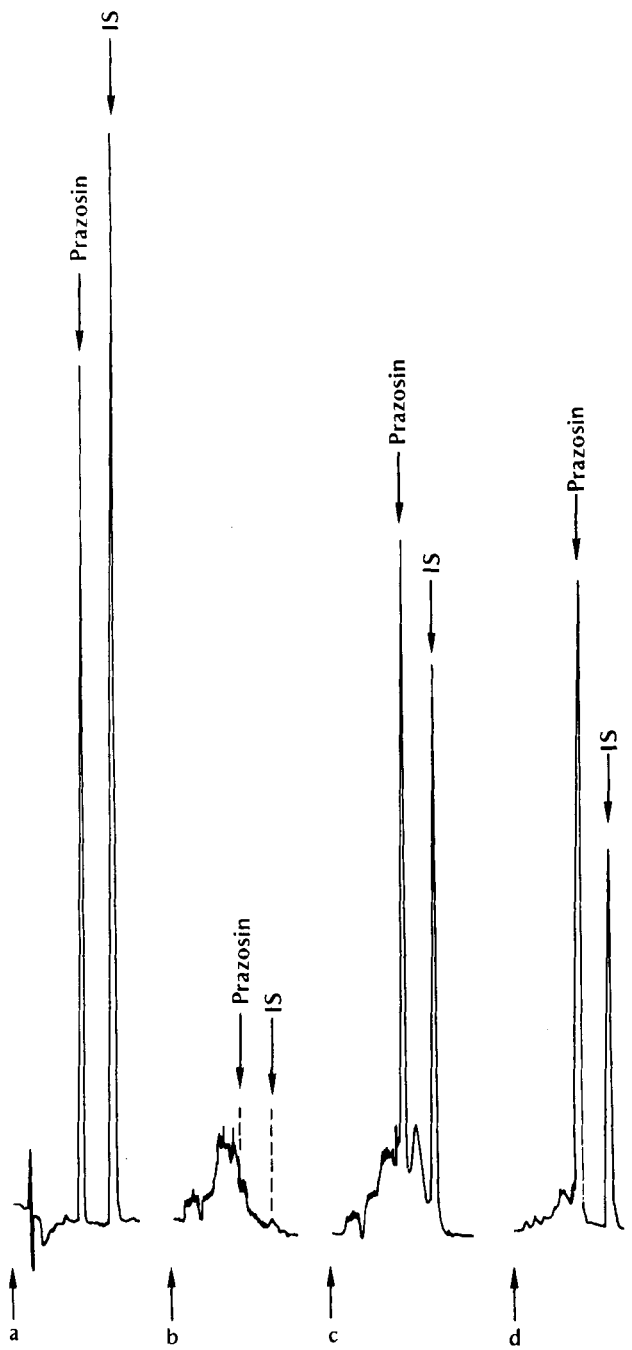

Figure 1—*Chromatograms showing the separation of drug and the internal standard (IS) (a), control plasma (b), control plasma fortified at 2 ng/ml with drug and at 10 ng/ml with the internal standard (c), and 8-hr plasma of Subject HS after a 1-mg dose with 10 ng/ml of the internal standard added (d). Retention times were prazosin, 4.2 min; and the internal standard, 6.2 min.*

For daily validation, five samples fortified at midrange (2.0 ng/ml) were processed with each group of test samples. The mean ratio of prazosin to the internal standard (IS) peak heights was determined, and the prazosin concentration in test samples was calculated from the formula:

$$\text{concentration (ng/ml)} = \frac{\text{peak height drug}}{\text{peak height IS}} \times \frac{C}{\text{mean ratio}} \quad \text{(Eq. 1)}$$

where C represents the concentration (nanograms per milliliter) of prazosin in the fortified standards.

To assess assay specificity, plasma samples from six volunteers receiving 5 mg of prazosin were pooled, made alkaline, and extracted with two volumes of ethyl acetate. The organic layer (180 ml) was recovered, extracted with 20 ml of 0.1 N H_2SO_4, and discarded. The acidic aqueous phase was then alkalinized and extracted with 40 ml of ethyl acetate. The organic layer was recovered and reduced in volume under vacuum to 0.2 ml, and 50-μl aliquots were applied to TLC plates[5].

Following development in equilibrated tanks containing ethyl acetate–diethylamine (95:5) (R_f 0.43) or chloroform–methanol–diethylamine (90:5:5) (R_f 0.63), the plates were visualized using 254-nm UV light. Only one fluorescent zone, migrating with the same R_f as prazosin, was visible on each plate. This evidence, together with the absence of additional peaks during HPLC (Fig. 1), indicated that only unchanged prazosin was being measured in the assay.

RESULTS AND DISCUSSION

Reproducibility was calculated by normalizing the observed ratios over the assay range (Table I) to 1.0 ng/ml. A relative standard deviation of 12.0% was found (n = 16). Assay recovery was determined by comparing the response from known amounts of drug and the internal standard with processed fortified plasma samples. Assay recoveries for prazosin and the internal standard were 58.6 and 50.2%, respectively.

Mean peak plasma levels of 14.9 ng/ml were reported following a 2-mg oral dose to hypertensive humans (1). In an extensive pharmacokinetic investigation with normal subjects, mean peak concentrations of 37.5 ng/ml following a 5-mg capsule were observed (3). Thus, peak concentrations of about 7.5 ng/ml after a 1-mg dose can be expected, assuming a continued linear relationship between dose and plasma levels. The 0.2-ng/ml sensitivity of the assay described here can be expected to permit the measurement of plasma prazosin levels through five half-lives following a 1-mg dose to humans.

REFERENCES

(1) R. M. Graham, I. R. Thornell, J. M. Gain, C. Bagnoli, H. F. Oates, and G. S. Stokes, *Br. Med. J.*, **2**, 1293 (1976).

(2) A. J. Wood, P. Bolli, and F. O. Simpson, *Br. J. Clin. Pharmacol.*, **3**, 199 (1976).

(3) D. C. Hobbs and T. M. Twomey, *J. Clin. Pharmacol.*, in press.

ACKNOWLEDGMENTS

The authors acknowledge the generous gifts of the internal standard and prazosin from Dr. L. J. Czuba and Dr. H.-J. Hess.

[5] Silica gel glass plates supplied by Brinkmann Instruments, Westbury, N.Y.

Distribution of Camazepam in Rats and Mice

F. MARCUCCI *x, E. MUSSINI *, L. COTELLESSA *, P. GHIRARDI ‡, M. PARENTI ‡, R. RIVA *, and P. SALVA §

Received December 1, 1977, from the **Istituto di Ricerche Farmacologiche "Mario Negri," Via Eritrea, 62, 20157 Milan, Italy,* and the ‡*Laboratorio di Ricerche Simes, Milan, Italy.* Accepted for publication February 1, 1978. §Present address: Universidad Autonoma, Barcelona, Spain.

Abstract □ Camazepam, 5 mg/kg iv, was injected in rats and mice to study its distribution in the blood and brain. Peak blood levels were about 0.9 μg/ml in rats and 0.6 μg/ml in mice. Peak brain levels were about 1.5 μg/g in rats and 0.8 μg/g in mice. The apparent blood half-life of camazepam was 9 min in mice and 20 min in rats.

Keyphrases □ Camazepam—blood and brain distribution in rats and mice □ Distribution, blood and brain—camazepam in mice and rats □ Psychoactive agents—camazepam, blood and brain distribution in rats and mice

Camazepam[1], 3-*N,N*-dimethylcarbamoyloxy-7-chloro-5-phenyl-1-methyl-1,3-dihydro-2*H*-1,4-benzodiazepin-2-one (I), is a new psychoactive benzodiazepine derivative with a carbamic group in position C-3. Pharmacologically, camazepam displays anxiolytic properties, very weak muscle relaxant activity, no cardiodepressant effect, and very low toxicity (1–3).

During the investigation of suitable analytical parameters for the analysis of camazepam, its response to electron-capture GLC was found to be sufficiently sensitive for quantitation in the nanogram range. The electron-capture GLC assay reported here was chosen for the determination of blood and brain levels of camazepam in rats and mice given doses of 5 mg/kg iv.

EXPERIMENTAL

Animals—Male CD-COBS Charles River rats, 220 ± 10 g, and male CD_1 mice, 25 ± 3 g, were used.

Drug Administration—Camazepam was injected at 5 mg/kg iv. It was dissolved in diethylacetamide–polysorbate 80[2] (1:10) and diluted with water to a suitable concentration so that the animals received less than 0.1 ml of polysorbate 80/kg.

At 5, 30, 60, and 180 min after drug injection, five animals were killed, blood samples were collected in heparinized test tubes, and the brain was rapidly removed and weighed.

Extraction from Blood—Aliquots of 1 ml of whole blood and 3 ml of benzene were pipetted into 10-ml test tubes with ground-glass stoppers. The tubes were stirred vigorously on a vortex mixer for 3 min and then centrifuged at 2000 rpm for 5 min. Then a 2-ml aliquot of the benzene extract was transferred to a 15-ml conical centrifuge tube, and the benzene was evaporated to dryness in the water bath of a rotary evaporator at 35–40°. The evaporation residue was dissolved in at least 100 μl of acetone in which 0.25 μg of penfluridol[3]/ml (internal standard) was dissolved. A suitable aliquot (1–2 μl) was injected into the gas chromatograph.

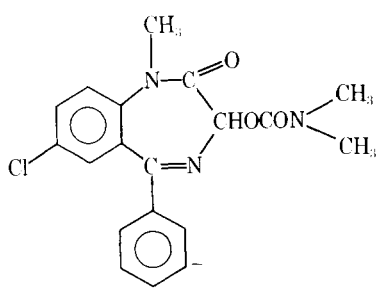

I

[1] SB 5833, obtained from Simes S.p.A., Milan, Italy.
[2] Tween 80.

Table I—Blood and Brain Levels of Camazepam after Administration of 5 mg/kg iv in Rats

Time after Injection, min	Blood Level, μg/ml ± *SE*[a]	Brain Level, μg/g ± *SE*[a]
5	0.910 ± 0.2	1.490 ± 0.1
30	0.300 ± 0.1	0.710 ± 0.1
60	0.120 ± 0.05	0.240 ± 0.08
180	0.005 ± 0.005	0.026 ± 0.001

[a] Each value represents the means ± *SE* of five animals.

Table II—Blood and Brain Levels of Camazepam after Administration of 5 mg/kg iv in Mice

Time after Injection, min	Blood Level, μg/ml ± *SE*[a]	Brain Level, μg/g ± *SE*[a]
5	0.640 ± 0.02	0.790 ± 0.03
30	0.060 ± 0.01	0.140 ± 0.02
60	0.010 ± 0.002	0.067 ± 0.003
180	<0.005	0.011 ± 0.001

[a] Each value represents the means ± *SE* of five determinations.

Extraction from Brain—The brains were homogenized (1:4 w/v) in 0.1 *M* glycine buffer, pH 10.2, with a polytef–glass homogenizer. Brain homogenate, 1 ml, was removed under stirring, and 3 ml of benzene was pipetted into a 10-ml test tube with a ground-glass stopper. Treatment was then identical with that for blood.

Conditions for GLC Analysis—*Column*—The column packing was a pretested preparation containing 3% OV-17 on 100–120-mesh Gas Chrom Q[4] packed into a 1-m glass column (3 mm i.d.).

Instrumental Conditions—A gas chromatograph[5] equipped with a ^{63}Ni-electron-capture detector was used. The flow rates of the carrier gas, nitrogen, and the detector purge gas were 60 and 30 ml/min, respectively. The temperature settings were: oven, 275°; injection port, 300°; and detector, 320°.

Quantitative Analysis—For quantitative camazepam analysis, the internal standard technique was used. Penfluridol [4-(4-chloro-α,α,α-trifluoro-*m*-tolyl)-1-[4,4-bis(*p*-fluorophenyl)butyl]-4-piperidinol] was chosen as an internal standard because of its suitable retention time.

Recovery studies of camazepam from the blood and brain of the two animal species were satisfactory, ranging from 80 ± 2 to 85 ± 3%. The sensitivity of the electron-capture GLC assay is 15 ng/ml of blood or g of brain. The identity of the GLC peak for camazepam was checked by mass spectrometry[6].

RESULTS AND DISCUSSION

The distribution of camazepam in rat blood and brain after administration of 5 mg/kg iv is shown in Table I. Camazepam entered the brain very rapidly from the bloodstream, giving constantly higher concentrations in the brain than in the blood from 5 min to 3 hr after administration. The highest blood and brain levels of camazepam were observed 5 min after injection; thereafter, concentration progressively decreased, reaching 5 ng/ml and 26 ng/g in the rat blood and brain, respectively, 3 hr after treatment.

Table II shows the levels of camazepam in the blood and brain of mice at different times after injection of 5 mg/kg iv. In mice, as in rats, brain

[3] Courtesy of Dr. P. Janssen, Janssen Pharmaceutica, Beerse, Belgium.
[4] Applied Science Laboratories, State College, Pa.
[5] Fractovap, model G I, Carlo Erba, Milan, Italy.
[6] LKB 9000 gas chromatograph–mass spectrometer.

0022-3549/78/1000-1470$01.00/0
© 1978, American Pharmaceutical Association

drug levels were higher than blood levels; but in both compartments, camazepam concentrations were considerably lower than those found in rats 5 min after injection. The drug declined faster in the blood of mice than in that of rats, the apparent half-lives in the two species being 9 and 20 min, respectively, as calculated according to Gibaldi (4).

REFERENCES

(1) R. Ferrini, G. Miragoli, and B. Taccardi, *Arzneim.-Forsch.*, **24**, 2029 (1974).

(2) L. Merlo, V. Noseda, R. Ferrini, G. Miragoli, and G. Marchetti, *ibid.*, **24**, 1759 (1974).

(3) M. Bianchi, P. Ghirardi, and F. Ravaccia, *ibid.*, **24**, 2032 (1974).

(4) M. Gibaldi, *Ann. N.Y. Acad. Sci.*, **179**, 19 (1971).

ACKNOWLEDGMENTS

The authors thank Mr. G. Meroni for technical assistance.

Synthesis of 1-Methyl-2-phenylcarbamoylpyrazolidines as Potential Anticonvulsant Agents

MILTON J. KORNET

Received November 28, 1977, from the *Division of Medicinal Chemistry, College of Pharmacy, University of Kentucky, Lexington, KY 40506.* Accepted for publication January 13, 1978.

Abstract □ Lithium aluminum hydride reduction of 1,4-dimethyl-3-pyrazolidinone yielded 1,4-dimethylpyrazolidine. The latter compound and 1-methylpyrazolidine reacted with aryl isocyanates to produce 1-methyl-2-phenylcarbamoylpyrazolidines. Several of these adducts displayed significant anticonvulsant activity in the maximal electroshock seizure and pentylenetetrazol seizure threshold tests.

Keyphrases □ Pyrazolidines, various substituted—synthesized, evaluated for anticonvulsant activity in mice □ Anticonvulsant activity—various substituted pyrazolidines evaluated in mice □ Structure–activity relationships—various substituted pyrazolidines evaluated for anticonvulsant activity in mice

Antiepileptic agents containing the semicarbazide functionality have been investigated only rarely (1–3). 1-Phenylsemicarbazide (I) is devoid of protective activity in the maximal electroshock test at 300 mg/kg (4). However, several tricyclic semicarbazides (II), which possess good potency and a favorable therapeutic ratio, have been described (5).

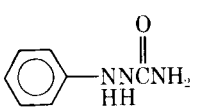

I

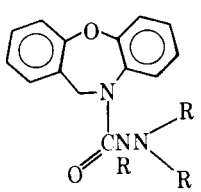

II

Interest in new anticonvulsant agents (6–8) as well as in pyrazolidine analogs of medicinals (9) prompted the synthesis and evaluation of a series of 1-methyl-2-phenylcarbamoylpyrazolidines (IV*a*–IV*w*).

DISCUSSION

Chemistry—The synthesis of the title compounds necessitated the preparation of the two pyrazolidine bases III*a* and III*b*. 1-Methylpyrazolidine (III*a*) was obtained by previously described methods (10). 1,4-Dimethylpyrazolidine (III*b*), a new base, resulted from the lithium aluminum hydride reduction of 1,4-dimethyl-3-pyrazolidinone. The latter precursor was prepared by condensing methylhydrazine with methacrylic acid (11) (Scheme I).

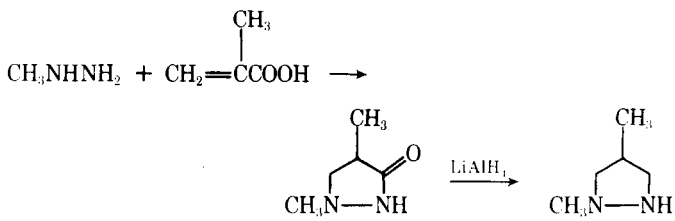

Scheme I

Addition of these pyrazolidines to aryl-substituted isocyanates occurred smoothly to give IV*a*–IV*w* (Scheme II). The physical properties of these adducts are given in Table I.

Biological Activity—All phenylcarbamoylpyrazolidines were tested for anticonvulsant activity and neurotoxicity by the methods described under *Experimental* (Table II). Of the 22 compounds tested, 19 exhibited some anticonvulsant activity. The *p*-bromo derivatives IV*b* and IV*p* were uniformly inactive.

Compounds IV*m*, IV*n*, and IV*v* showed the best activity against maximal electroshock. They all possess a 2,6-substitution pattern in the aromatic ring reminiscent of the local anesthetic–antiarrhythmic drug lidocaine, which can temporarily arrest *grand mal* as well as certain other epileptic seizures (12). However, the short time of peak effect (0.5 hr) for IV*m*, IV*n*, and IV*v* probably indicates a short duration of action and may limit their usefulness (5).

Compounds IV*e*, IV*i*, and IV*m* showed significant activity in the pentylenetetrazol test at 0.5 hr but were devoid of activity at 4 hr.

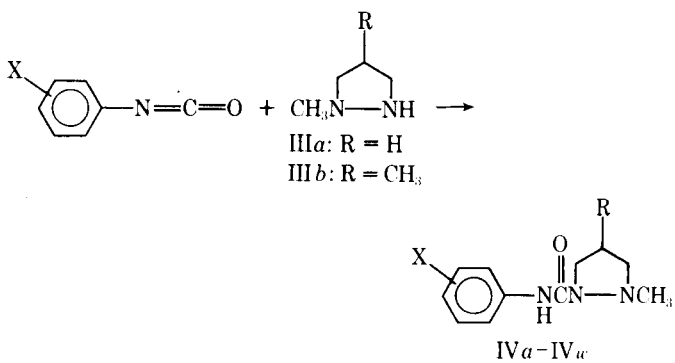

Scheme II

0022-3549/78/1000-1471$01.00/0

© 1978, American Pharmaceutical Association

drug levels were higher than blood levels; but in both compartments, camazepam concentrations were considerably lower than those found in rats 5 min after injection. The drug declined faster in the blood of mice than in that of rats, the apparent half-lives in the two species being 9 and 20 min, respectively, as calculated according to Gibaldi (4).

REFERENCES

(1) R. Ferrini, G. Miragoli, and B. Taccardi, *Arzneim.-Forsch.*, **24**, 2029 (1974).

(2) L. Merlo, V. Noseda, R. Ferrini, G. Miragoli, and G. Marchetti, *ibid.*, **24**, 1759 (1974).

(3) M. Bianchi, P. Ghirardi, and F. Ravaccia, *ibid.*, **24**, 2032 (1974).

(4) M. Gibaldi, *Ann. N.Y. Acad. Sci.*, **179**, 19 (1971).

ACKNOWLEDGMENTS

The authors thank Mr. G. Meroni for technical assistance.

Synthesis of 1-Methyl-2-phenylcarbamoylpyrazolidines as Potential Anticonvulsant Agents

MILTON J. KORNET

Received November 28, 1977, from the *Division of Medicinal Chemistry, College of Pharmacy, University of Kentucky, Lexington, KY 40506.* Accepted for publication January 13, 1978.

Abstract □ Lithium aluminum hydride reduction of 1,4-dimethyl-3-pyrazolidinone yielded 1,4-dimethylpyrazolidine. The latter compound and 1-methylpyrazolidine reacted with aryl isocyanates to produce 1-methyl-2-phenylcarbamoylpyrazolidines. Several of these adducts displayed significant anticonvulsant activity in the maximal electroshock seizure and pentylenetetrazol seizure threshold tests.

Keyphrases □ Pyrazolidines, various substituted—synthesized, evaluated for anticonvulsant activity in mice □ Anticonvulsant activity—various substituted pyrazolidines evaluated in mice □ Structure–activity relationships—various substituted pyrazolidines evaluated for anticonvulsant activity in mice

Antiepileptic agents containing the semicarbazide functionality have been investigated only rarely (1–3). 1-Phenylsemicarbazide (I) is devoid of protective activity in the maximal electroshock test at 300 mg/kg (4). However, several tricyclic semicarbazides (II), which possess good potency and a favorable therapeutic ratio, have been described (5).

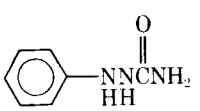

I

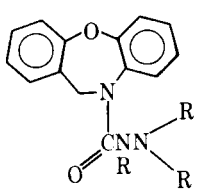

II

Interest in new anticonvulsant agents (6–8) as well as in pyrazolidine analogs of medicinals (9) prompted the synthesis and evaluation of a series of 1-methyl-2-phenylcarbamoylpyrazolidines (IV*a*–IV*w*).

DISCUSSION

Chemistry—The synthesis of the title compounds necessitated the preparation of the two pyrazolidine bases III*a* and III*b*. 1-Methylpyrazolidine (III*a*) was obtained by previously described methods (10). 1,4-Dimethylpyrazolidine (III*b*), a new base, resulted from the lithium aluminum hydride reduction of 1,4-dimethyl-3-pyrazolidinone. The latter precursor was prepared by condensing methylhydrazine with methacrylic acid (11) (Scheme I).

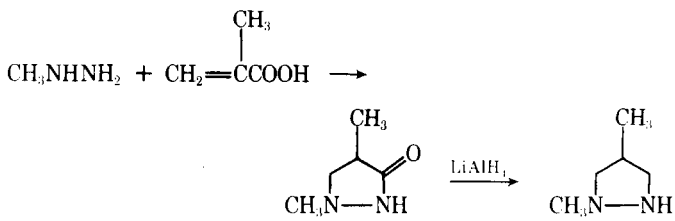

Scheme I

Addition of these pyrazolidines to aryl-substituted isocyanates occurred smoothly to give IV*a*–IV*w* (Scheme II). The physical properties of these adducts are given in Table I.

Biological Activity—All phenylcarbamoylpyrazolidines were tested for anticonvulsant activity and neurotoxicity by the methods described under *Experimental* (Table II). Of the 22 compounds tested, 19 exhibited some anticonvulsant activity. The *p*-bromo derivatives IV*b* and IV*p* were uniformly inactive.

Compounds IV*m*, IV*n*, and IV*v* showed the best activity against maximal electroshock. They all possess a 2,6-substitution pattern in the aromatic ring reminiscent of the local anesthetic–antiarrhythmic drug lidocaine, which can temporarily arrest *grand mal* as well as certain other epileptic seizures (12). However, the short time of peak effect (0.5 hr) for IV*m*, IV*n*, and IV*v* probably indicates a short duration of action and may limit their usefulness (5).

Compounds IV*e*, IV*i*, and IV*m* showed significant activity in the pentylenetetrazol test at 0.5 hr but were devoid of activity at 4 hr.

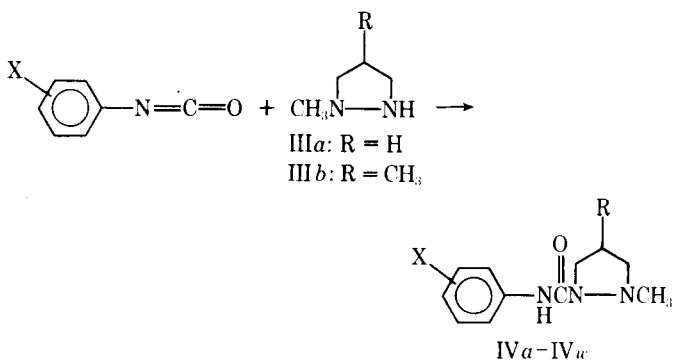

Scheme II

0022-3549/78/1000-1471$01.00/0

© 1978, American Pharmaceutical Association

Table I—Physical Properties of 1-Methyl-2-phenylcarbamoylpyrazolidines

Compound	R	X	Melting Point	Yield, %	Recrystallization Solvent[a]	Formula	Analysis, % Calc.	Found
IV*a*	H	H	71–73°	40	C	$C_{11}H_{15}N_3O$	C 64.38	64.32
							H 7.37	7.62
							N 20.47	20.67
IV*b*	H	*p*-Br	121–123°	56	A	$C_{11}H_{14}BrN_3O$	C 46.49	46.44
							H 4.97	5.14
							N 14.79	14.55
IV*c*	H	*m*-Cl	105–107°	65	A	$C_{11}H_{14}ClN_3O$	C 55.12	55.38
							H 5.89	6.06
							N 17.53	17.22
IV*d*	H	*p*-Cl	110–112°	62	A	$C_{11}H_{14}ClN_3O$	C 55.12	55.01
							H 5.89	5.94
							N 17.53	17.27
IV*e*	H	*p*-F	84–85°	82	A	$C_{11}H_{14}FN_3O$	C 59.18	59.33
							H 6.32	6.36
							N 18.82	18.85
IV*f*	H	*p*-CH_3O	72.5–73.5°	48	A	$C_{12}H_{17}N_3O_2$	C 61.26	60.89
							H 7.28	7.43
							N 17.86	17.73
IV*g*	H	*m*-CH_3	91–93°	71	A	$C_{12}H_{17}N_3O$	C 65.73	65.73
							H 7.81	7.74
							N 19.16	19.13
IV*h*	H	*p*-CH_3	87–89°	60	B	$C_{12}H_{17}N_3O$	C 65.73	65.81
							H 7.81	7.89
							N 19.16	18.87
IV*i*	H	*m*-NO_2	101.5–103.5°	60	E	$C_{11}H_{14}N_4O_3$	C 52.79	52.91
							H 5.64	5.85
							N 22.39	22.38
IV*j*	H	*p*-NO_2	112–113°	41	C	$C_{11}H_{14}N_4O_3$	C 52.79	53.16
							H 5.64	5.52
							N 22.39	22.65
IV*k*	H	*m*-CF_3	85.5–86.5°	57	A	$C_{12}H_{14}F_3N_3O$	C 52.75	52.92
							H 5.16	5.18
							N 15.38	15.32
IV*l*	H	3,4-Cl_2	94–95°	79	A	$C_{11}H_{13}Cl_2N_3O$	C 48.19	48.28
							H 4.78	4.88
							N 15.33	15.33
IV*m*	H	2-Cl, 6-CH_3	92–93°	71	A	$C_{12}H_{16}ClN_3O$	C 56.80	56.89
							H 6.36	6.59
							N 16.56	16.26
IV*n*	H	2,6-$(CH_3)_2$	110–112°	60	A	$C_{13}H_{19}N_3O$	C 66.92	67.01
							H 8.21	8.47
							N 18.01	17.87
IV*o*	CH_3	H	70–71°	58	A	$C_{12}H_{17}N_3O$	C 65.73	65.69
							H 7.81	7.72
							N 19.16	19.08
IV*p*	CH_3	*p*-Br	101–102°	66	A	$C_{12}H_{16}BrN_3O$	C 48.34	48.28
							H 5.41	5.54
							N 14.09	14.21
IV*q*	CH_3	*p*-Cl	99–101°	72	A	$C_{12}H_{16}ClN_3O$	C 56.80	56.94
							H 6.36	6.45
							N 16.56	16.71
IV*r*	CH_3	*p*-CH_3O	107–109°	60	A	$C_{13}H_{19}N_3O_2$	C 62.63	62.74
							H 7.68	7.84
							N 16.85	16.74
IV*s*	CH_3	*m*-CH_3	79–80°	94	A	$C_{13}H_{19}N_3O$	C 66.92	67.12
							H 8.21	8.31
							N 18.01	17.97
IV*t*	CH_3	*p*-CH_3	67–68°	46	A	$C_{13}H_{19}N_3O$	C 66.92	66.99
							H 8.21	8.25
							N 18.01	17.96
IV*u*	CH_3	*p*-NO_2	126–127°	64	D	$C_{12}H_{16}N_4O_3$	C 54.54	54.61
							H 6.10	6.23
							N 21.20	21.31
IV*v*	CH_3	2-Cl, 6-CH_3	72–73°	43	A	$C_{13}H_{18}ClN_3O$	C 58.31	58.34
							H 6.78	6.93
							N 15.69	15.88
IV*w*	CH_3	2,6-$(CH_3)_2$	113–115°	65	A	$C_{14}H_{21}N_3O$	C 67.98	68.14
							H 8.56	8.54
							N 16.99	17.16

[a] A = cyclohexane, B = hexane–cyclohexane, C = benzene–petroleum ether, D = benzene, and E = benzene–cyclohexane.

EXPERIMENTAL[1]

1,4-Dimethylpyrazolidine (III*b*)[2]—This compound was prepared by the lithium aluminum hydride reduction of 1,4-dimethyl-3-pyrazolidinone (11) in tetrahydrofuran by the same procedure utilized for the preparation of 1-methylpyrazolidine (10). The colorless liquid, bp 128–131°, was obtained in 39% yield; NMR ($CDCl_3$): δ 1.17 (d, 3, C-CH_3),

[1] Melting points were determined on a Thomas-Hoover apparatus and are uncorrected. IR spectra were taken on a Perkin-Elmer 700 spectrophotometer as either liquid films or potassium bromide pellets. NMR spectra were recorded on a Varian A-60A spectrometer, using tetramethylsilane as the internal reference. Elemental analyses were performed by PCR Inc., Gainesville, Fla., and Dr. Kurt Eder, Geneva, Switzerland.

[2] This experiment was carried out by W. J. Layton.

Table II—Anticonvulsant Effect

Compound	MES Activity[a] 0.5 hr	MES Activity[a] 4 hr	MES ED_{50}	sc Met Activity[a] 0.5 hr	sc Met Activity[a] 4 hr	sc Met ED_{50}	sc Met TD_{50}[b]
IV*a*	+	−	153 (144–163)	+	−	ND[c]	ND
IV*b*	−	−	ND	−	−	ND	ND
IV*c*	−	−	ND	+	−	ND	ND
IV*d*	−	−	ND	+	+	ND	ND
IV*e*	+	−	ND	++	−	ND	ND
IV*f*	+	−	ND	−	−	ND	ND
IV*g*	−	−	ND	+	−	ND	ND
IV*h*	−	−	ND	−	−	ND	ND
IV*i*	−	−	ND	++	−	181 (155–226)	ND
IV*j*	ND	ND	ND	ND	ND	ND	ND
IV*k*	−	−	ND	+	−	ND	ND
IV*l*	−	+	ND	−	−	ND	ND
IV*m*	++	+	55.7 (48.1–75.3)[d]	++	—[e]	ND	148 (134–166)[d]
IV*n*	++	−	48.8 (39.7–61.6)[d]	+	−	ND	150 (142–159)[d]
IV*o*	+	−	ND	+	−	ND	ND
IV*p*	−	−	ND	−	−	ND	ND
IV*q*	+	+	ND	−	+	ND	ND
IV*r*	+	−	ND	−	−	ND	ND
IV*s*	+	−	ND	+	+	ND	ND
IV*t*	+	−	ND	+	−	ND	ND
IV*u*	−	−	ND	+	−	ND	ND
IV*v*	++	−	62.2 (60.8–63.9)[d]	+	−	ND	174 (159–197)[d]
IV*w*	+	−	88.0 (75.5–99.3)[d]	−	−	ND	207 (177–245)[d]
Ethotoin			85.5 (72.0–92.2)			35.4 (19.0–56.1)	171 (144–250)

[a] +++, ++, and + signify activity at 30, 100, and 300 mg/kg, respectively; − denotes no activity observed at 300 mg/kg. [b] TD_{50} = median toxic dose in the rotorod test. [c] ND = not determined. [d] Determined at time of peak effect (0.5 hr). [e] No activity observed at 100 mg/kg.

2.80 (s, 3, NCH_3), and 1.60–3.47 (m, 6, NH and remaining ring H) ppm. Storage under a nitrogen atmosphere is necessary to avoid oxidation to 1,4-dimethyl-2-pyrazoline.

Anal.—Calc. for $C_5H_{12}N_2$: C, 59.96; H, 12.08; N, 27.97. Found: C, 59.74; H, 12.28; N, 27.83.

1-Methyl-2-phenylcarbamoylpyrazolidines (IV*a*–IV*w*)—A typical reaction is described, that for the preparation of 1-methyl-2-*p*-chlorophenylcarbamoylpyrazolidine (IV*d*). Table I lists the physical and analytical data.

To a solution of 2.58 g (0.030 mole) of 1-methylpyrazolidine (10) in 15 ml of dry benzene was added dropwise a solution of 4.12 g (0.0268 mole) of *p*-chlorophenyl isocyanate in 10 ml of dry benzene with magnetic stirring. The resulting mixture was refluxed for 3 hr, cooled, diluted with 25 ml of benzene, and extracted with 50 ml of 5% hydrochloric acid. The acidic extract was washed with 40 ml of ether and made basic by the addition of solid sodium carbonate (carbon dioxide evolution).

The aqueous solution was extracted twice with 40-ml portions of ether and dried (magnesium sulfate). Evaporation of the ether resulted in a crystalline residue. Recrystallization from cyclohexane afforded 3.95 g (62%) of colorless crystals, mp 110–112°; IR (KBr): 1662 (C=O) and 3325 (NH) cm^{-1}; NMR ($CDCl_3$): δ 2.57 (s, 3, NCH_3), 1.67–4.20 (m, 6, aliphatic ring H), 7.4 (m, 4, ArH), and 8.57 (broad s, 1, CONH) ppm.

Pharmacological Testing—All compounds were tested for anticonvulsant activity[3]. The compounds were evaluated using the Anticonvulsant Screening Project Test Systems (13, 14). Three tests were performed: MES (maximal electroshock seizure test), sc Met (subcutaneous pentylenetetrazol seizure threshold test), and the rotorod test to evaluate neurotoxicity. The ED_{50} and TD_{50} values and their confidence limits were determined by probit analysis. Additional details concerning the pharmacological testing were reported recently (7). All tests were performed on male Carworth Farms No. 1 mice.

[3] By the Antiepileptic Drug Development Program administered by the Section on Epilepsy, National Institutes of Health, Bethesda, MD 20014.

REFERENCES

(1) W. J. Close and M. A. Spielman, in "Medicinal Chemistry," vol. 5, W. H. Hartung, Ed., Wiley, New York, N.Y., 1961, p. 48.

(2) A. Spinks and W. S. Waring, in "Progress in Medicinal Chemistry," vol. 3, G. P. Ellis and G. B. West, Eds., Butterworths, Washington, D.C., 1963, p. 261.

(3) J. Mercier, in "Anticonvulsant Drugs," vol. 1, J. Mercier, Sect. Ed., Pergamon, Elmsford, N.Y., 1973, chap. 6.

(4) H. H. Merritt and T. J. Putnam, *Epilepsia*, **3**, 51 (1945).

(5) W. E. Coyne and J. W. Cusic, *J. Med. Chem.*, **11**, 1158 (1968).

(6) M. J. Kornet, J. H. Thorstenson, and W. C. Lubawy, *J. Pharm. Sci.*, **63**, 1090 (1974).

(7) M. J. Kornet, A. M. Crider, and E. O. Magarian, *J. Med. Chem.*, **20**, 405 (1977).

(8) *Ibid.*, **20**, 1210 (1977).

(9) M. J. Kornet and H. S. I. Tan, *J. Pharm. Sci.*, **61**, 235 (1972).

(10) M. J. Kornet, *ibid.*, **56**, 963 (1967).

(11) W. S. Wadsworth, Jr., *J. Org. Chem.*, **31**, 1704 (1966).

(12) J. Mercier, in "Anticonvulsant Drugs," vol. 1, J. Mercier, Sect. Ed., Pergamon, Elmsford, N.Y., 1973, p. 228.

(13) Anticonvulsant Screening Project, Antiepileptic Drug Development Program, National Institutes of Health, DHEW Publication No. (NIH) 76-1093, Bethesda, MD 20014.

(14) E. A. Swinyard, W. C. Brown, and L. S. Goodman, *J. Pharmacol. Exp. Ther.*, **106**, 319 (1952).

ACKNOWLEDGMENTS

The author is indebted to Mr. Gill D. Gladding, Antiepileptic Drug Development Program, National Institutes of Health, for providing the anticonvulsant activity data. He is also grateful to Mr. James Swencki for technical assistance.

Inhibition of Epinephrine Oxidation in Weak Alkaline Solutions

R. BONEVSKI, J. MOMIROVIĆ-ČULJAT ˣ, and L. BALINT

Received February 8, 1977, from the *Faculty of Pharmacy and Biochemistry, Department of Food Chemistry, University of Zagreb, Zagreb, Domagojeva 2, Yugoslavia.* Accepted for publication January 12, 1978.

Abstract □ The effect of sodium metabisulfite and cysteine on the oxidation of epinephrine in weak alkaline solutions was studied. The fluorescent intensity of the reacting mixture also was measured. Sodium metabisulfite in 2×10^{-3} *M* NaOH at concentrations lower than 3×10^{-5} *M* had no effect on epinephrine oxidation; however, in concentrations from 5×10^{-5} to 3×10^{-4} *M*, it greatly accelerated this process. Its inhibitory action appeared only in concentrations greater than 5×10^{-4} *M*. The mechanism of these reactions also was explained. Cysteine in 2×10^{-3} *M* NaOH inhibited the oxidation of epinephrine even in concentrations of 7×10^{-5} *M*.

Keyphrases □ Epinephrine—oxidation in alkaline solutions, effect of sodium metabisulfite and cysteine □ Oxidation—epinephrine in alkaline solutions, effect of sodium metabisulfite and cysteine □ Sodium metabisulfite—effect on oxidation of epinephrine in alkaline solutions □ Cysteine—effect on oxidation of epinephrine in alkaline solutions □ Adrenergics—epinephrine, oxidation in alkaline solutions, effect of sodium metabisulfite and cysteine

The stabilization of epinephrine (I) is a problem because present technological methods do not permit long storage of preparations including it (1, 2). The instability of epinephrine in solution is related to its spontaneous oxidation, caused by the oxygen from the air, which in alkaline solutions proceeds according to Scheme I (3–6). In addition to decreasing the pharmacological activity of the preparation, epinephrine oxidation yields epinephrine quinone (II), adrenochrome (III), and adrenolutine (IV), which are toxic (5).

The mechanism of the reaction between epinephrine and bisulfite leading to the formation of sulfonate was described previously (7, 8). Loss of epinephrine activity was determined by a modified triacetyl derivative procedure. The results of the investigations into accelerated loss in optical activity induced by bisulfite are in agreement with the triacetylation procedure (7, 8).

In this study, the oxidative changes of epinephrine under the influence of sodium metabisulfite were followed by the fluorescence method. Under certain conditions, bisulfite accelerated epinephrine degradation, creating fluorescent products. The objective of this work was to determine the activity of sodium metabisulfite and cysteine on epinephrine oxidation in weak alkaline solutions.

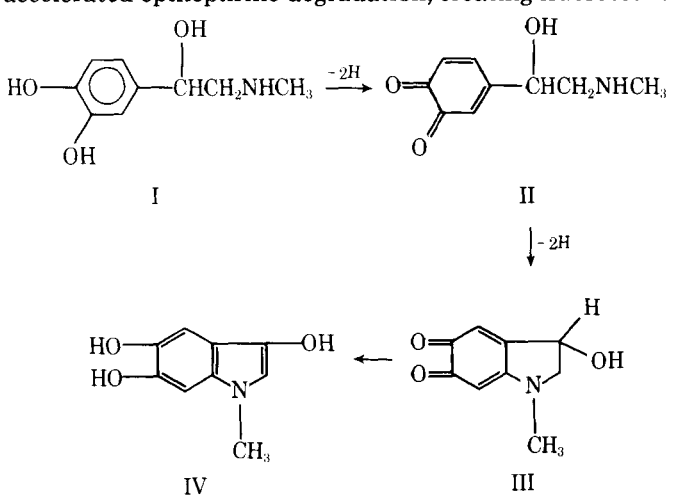

Scheme I

EXPERIMENTAL

Materials—All chemicals were either reagent or analytical grade. Epinephrine[1] (BP 1973 and USP XVIII), (−)-1-(3,4-dihydroxyphenyl)-2-methylaminoethanol, was dissolved in an equal amount of hydrochloric acid.

Cysteine chloride monohydrate[2], quinine sulfate (Ph. Jug. II), and sodium metabisulfite[2] were used as received.

Instrumentation—The intensity of the fluorescent reacting mixture was measured by the photoelectric fluorometer based on the principle of ray penetration (9).

Filter paper[3], 8 cm in diameter, was used as a fluorescence standard. It was soaked in 10 mg % quinine sulfate and 0.1 *M* H_2SO_4, air dried, and fixed to the bottom of a petri dish for easier handling while measuring. The photocurrent strength was regulated by a resistor so that the fluorescence standard showed a decline of 500 parts on the scale.

All measurements were performed in a 50-ml glass beaker (5.5 cm high and 3.5 cm in diameter). To maintain a constant thickness of the layer, the total volume of the reacting mixture was always a constant 10 ml. The oxidative changes of epinephrine were followed in free air and in nitrogen atmospheres at 22°.

RESULTS AND DISCUSSION

When following the spontaneous oxidation of epinephrine in relation to the concentration of sodium hydroxide, all measurements were performed with identical concentrations of epinephrine of 1.09×10^{-5} *M*. Figure 1 shows the changes in the intensity of fluorescence in relation to time in solutions of sodium hydroxide from 2×10^{-3} to 2×10^{-1} *M*. The acceleration of the oxidation of epinephrine and the intensity of the fluorescence of the reacting mixture increased correspondingly to the increase in the concentration of sodium hydroxide.

Under the same conditions in relation to the concentration of epi-

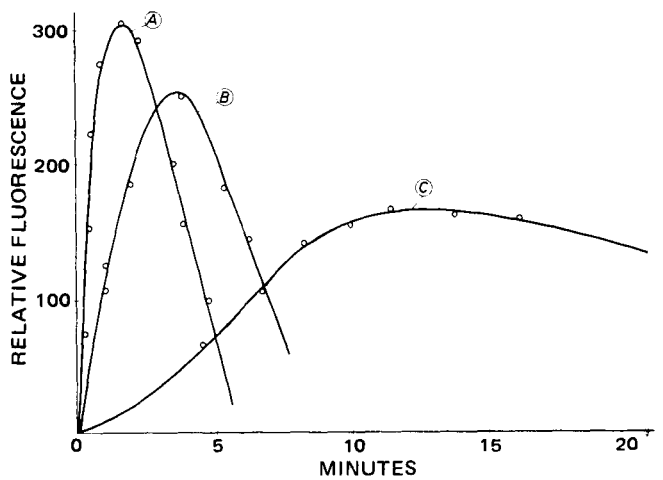

Figure 1—*Changes in fluorescent intensity of the* 1.09×10^{-5} M *epinephrine solution in relation to time and sodium hydroxide concentration. Key: A,* 2×10^{-1} M *NaOH, pH 13.2; B,* 2×10^{-2} M *NaOH, pH 12.2; and C,* 2×10^{-3} M *NaOH, pH 10.7.*

[1] Adrenalin.
[2] Merck.
[3] Whatman No. 1.

0022-3549/78/1000-1474$01.00/0
© 1978, American Pharmaceutical Association

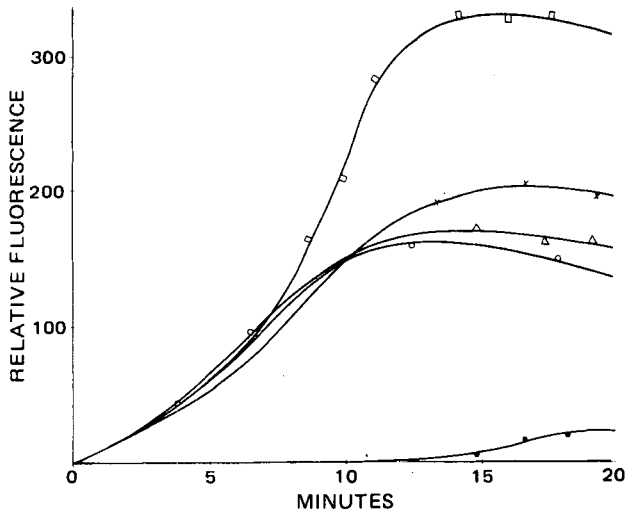

Figure 2—*Changes in fluorescent intensity in relation to time of the 1.09 × 10⁻⁵ M epinephrine solution in 2 × 10⁻³ M NaOH in the presence of different concentrations of sodium metabisulfate. Key:* ○, *control (2 × 10⁻³ M NaOH), pH 10.7;* △, *3 × 10⁻⁵ M $Na_2S_2O_5$, pH 10.5;* □, *5 × 10⁻⁵–3 × 10⁻⁴ M $Na_2S_2O_5$, pH 10.3–10.7;* ×, *4.5 × 10⁻⁴ M $Na_2S_2O_5$, pH 9.5; and* ●, *8 × 10⁻⁴ M $Na_2S_2O_5$, pH 8.4.*

nephrine and sodium hydroxide, the effects of different concentrations of sodium metabisulfite on the oxidation of epinephrine were followed (Figs. 2–4). Sodium metabisulfite in concentrations less than 3×10^{-5} *M* had no effect on the oxidation of epinephrine in 2×10^{-3} *M* NaOH. Increasing the concentration of sodium metabisulfite to 5.0×10^{-5} or 3×10^{-4} *M* doubled the effects of oxidation. However, these effects were decreased by an increase in the concentration of sodium metabisulfite of more than 5×10^{-4} *M*. At 8×10^{-4} *M*, the inhibition of the oxidation of epinephrine almost reached its maximum. Epinephrine oxidation was inhibited almost completely in higher concentrations of sodium metabisulfite.

If the sodium hydroxide concentration was increased 10 times (2×10^{-2} *M*), sodium metabisulfite had no stimulus on epinephrine oxidation, and the effects of inhibition were perceivable only when the sodium metabisulfite concentration in the reacting mixture was increased above 2.5×10^{-3} *M*. When the sodium hydroxide concentration was increased to 2×10^{-1} *M*, the effects of sodium metabisulfite were even less visible. To slow oxidation under such conditions, sodium metabisulfite concentrations greater than 1×10^{-2} *M* were needed.

From analysis of the results, it can be assumed that sodium metabisulfite, under the conditions in which it accelerates epinephrine oxidation, reacts according to Scheme II. Sodium metabisulfite dissolved in an alkaline solution in the presence of oxygen produces SO_4^{2-} ions. Increasing the bisulfite concentration increases the concentration of SO_3^{2-} ions, by which the oxidation of epinephrine is stopped.

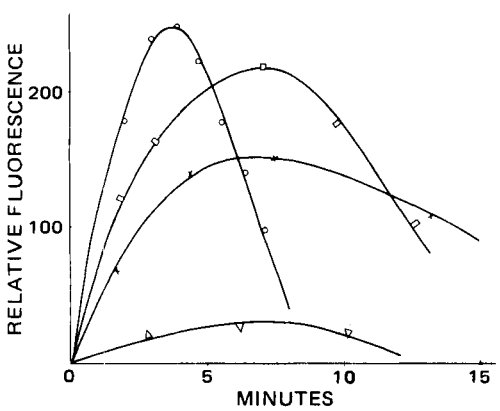

Figure 3—*Changes in fluorescent intensity in relation to time of the 1.09 × 10⁻⁵ M epinephrine solution in 2 × 10⁻² M NaOH in the presence of different concentrations of sodium metabisulfite. Key:* ○, *control (2 × 10⁻² M NaOH), pH 12.2;* □, *2.5 × 10⁻³ M $Na_2S_2O_5$, pH 12.1;* ×, *5 × 10⁻³ M $Na_2S_2O_5$, pH 12.0; and* △, *7 × 10⁻³ M $Na_2S_2O_5$, pH 11.9.*

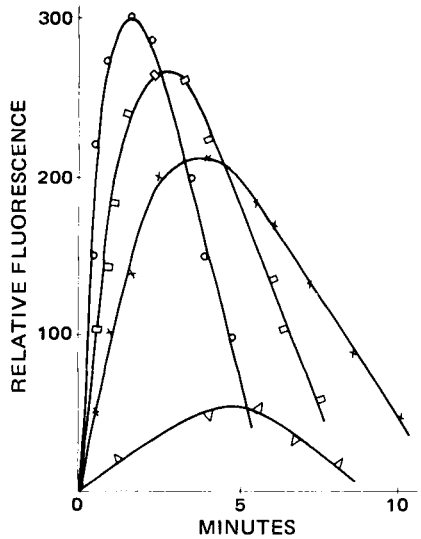

Figure 4—*Changes in fluorescent intensity in relation to time of the 1.09 × 10⁻⁵ M epinephrine solution in 2 × 10⁻¹ M NaOH in the presence of different concentrations of sodium metabisulfite. Key:* ○, *control (2 × 10⁻¹ M NaOH), pH 13.2;* □, *1 × 10⁻² M $Na_2S_2O_5$, pH 13.0;* ×, *1.5 × 10⁻² M $Na_2S_2O_5$, pH 12.8; and* △, *4 × 10⁻² M $Na_2S_2O_5$, pH 12.5.*

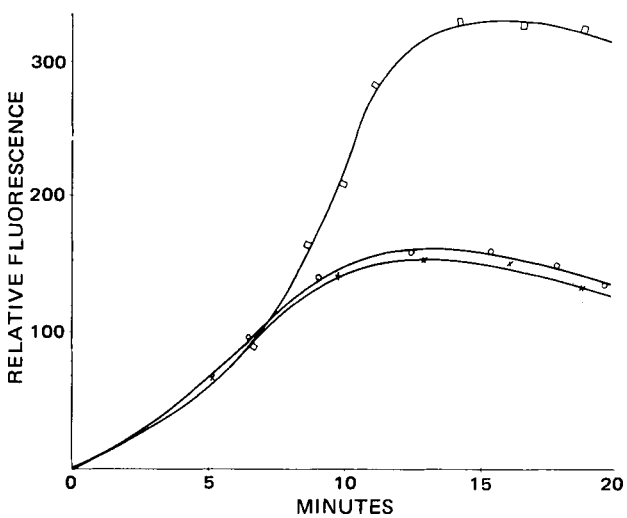

Figure 5—*Changes in fluorescent intensity in relation to time of the 1.09 × 10⁻⁵ M epinephrine solution in 2 × 10⁻³ M NaOH in the presence of the same concentration of sodium metabisulfite, in the presence of air, and in the nitrogen atmosphere. Key:* ○, *control (2 × 10⁻³ M NaOH, air), pH 10.7;* □, *1 × 10⁻⁴ M $Na_2S_2O_5$ (air), pH 9.8; and* ×, *1 × 10⁻⁴ M $Na_2S_2O_5$ (nitrogen), pH 9.8.*

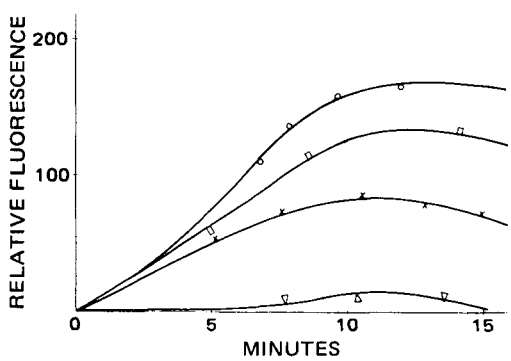

Figure 6—*Changes in fluorescent intensity in relation to time of the 1.09 × 10⁻⁵ M epinephrine solution in 2 × 10⁻³ M NaOH in the presence of different concentrations of cysteine. Key:* ○, *control (2 × 10⁻³ M NaOH), pH 10.7;* □, *2.5 × 10⁻⁵ M cysteine, pH 10.4–10.6;* ×, *5 × 10⁻⁵ M cysteine, pH 10.4–10.6; and* △, *7 × 10⁻⁵ M cysteine, pH 10.4–10.6.*

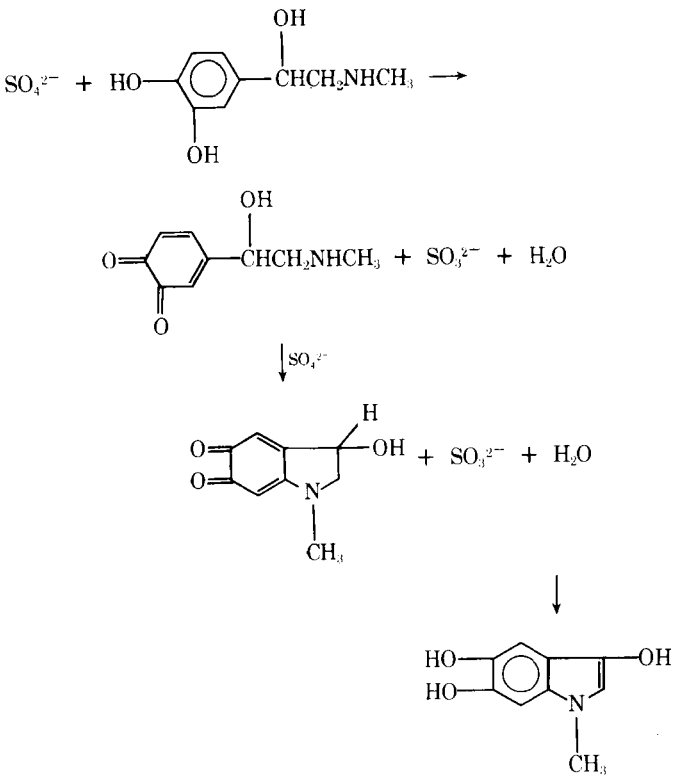

Scheme II

Previous success (10) in stabilizing different water solutions of epinephrine up to 5 years by preparing them in a nitrogen atmosphere confirms this hypothesis.

The results of the present experiments obtained in the nitrogen atmosphere show that oxygen in the reacting mixture is the most decisive factor for the stimulation of epinephrine oxidation in the presence of sodium metabisulfite in the given concentrations. Namely, the stimulating action of sodium metabisulfite on epinephrine oxidation is absent when dissolved oxygen from the air is eliminated from the solution of the reactant and when the reacting process goes on in the nitrogen atmosphere. In a highly alkaline medium, this process does not occur because of the strong influence of the hydroxide ions on epinephrine oxidation (Fig. 5).

Under the same experimental conditions, numerous experiments were performed using cysteine in different concentrations instead of sodium metabisulfite. Cysteine concentrations greater than 7×10^{-5} *M* efficiently inhibited epinephrine oxidation (Fig. 6). Since cysteine is an integral part of the human organism and since it maintains a kind of balance with the epinephrine concentration (11), it would be worthwhile to study its application in the stabilization of aqueous epinephrine solutions.

REFERENCES

(1) K. Backe-Hansen, G. Holst, A. M. Vennerod, and K. Briseid, *Acta Pharm. Suec.*, **3**, 269 (1966).

(2) W. Fuertig and I. Methke, *Pharm. Prax.*, **21**, 248 (1965).

(3) K. Breitschwerdt, T. Forster, and A. Weller, *Naturwissenschaften*, **43**, 443 (1965).

(4) K. Weber and D. Kodrnja, *Fotokem. Ind.*, **18**, 1 (1971).

(5) A. M. Kuzin, *Radiats. Biochem., Moskva, Atomizdat*, **1975**, 191–219.

(6) F. Martin, *J. Pharm. Belg.*, **41**, 151 (1969).

(7) L. C. Schroeter, T. Higuchi, and E. E. Schuler, *J. Am. Pharm. Assoc., Sci. Ed.*, **47**, 723 (1958).

(8) T. Higuchi and L. C. Schroeter, *J. Am. Chem. Soc.*, **82**, 1904 (1960).

(9) B. Uhlik and K. Wever, *Arh. Hig. Rada*, **17**, 329 (1965).

(10) P. Lundgren and S. Strom, *Acta Pharm. Suec.*, **3**, 273 (1966).

(11) D. Kovačević, G. Bjelobradič, and V. Stevanovič, *Yugosl. Physiol. Pharmacol. Acta*, **7**, 36 (1971).

Cardiovascular Effects of *Azadirachta indica* Extract

EMMANUEL B. THOMPSON ˣ and COMFORT C. ANDERSON *

Received October 25, 1977, from the *Department of Pharmacognosy and Pharmacology, College of Pharmacy, University of Illinois at the Medical Center, Chicago, IL 60612.* Accepted for publication February 10, 1978. *Present address: Department of Health Sciences, University of Ife, Ile-Ife, Nigeria.

Abstract □ A crude extract of the leaves of *Azadirachta indica* was studied for its effects on the cardiovascular system of anesthetized guinea pigs and rabbits. These effects include profound hypotension and a minimal negative chronotropic effect, which increased at higher doses. In one rabbit, 200 mg of extract/kg decreased the heart rate from 280 to 150 beats/min. The extract also exhibited a weak antiarrhythmic activity in rabbits against ouabain-induced dysrhythmia.

Keyphrases □ *Azadirachta indica*—extract of leaves, cardiovascular effects evaluated in guinea pigs and rabbits □ Cardiovascular effects—*Azadirachta indica* extract of leaves, evaluated in guinea pigs and rabbits

There is scanty literature information concerning the pharmacological properties of *Azadirachta indica*, an evergreen flowering plant belonging to the family Meliaceae. In Nigeria, this plant, called "dongoyaro," is used primarily to treat malaria, fever, abdominal disorders, and hemorrhoids and as an anthelmintic (1). Recent studies *in vivo* (2) failed to confirm the antimalarial effects attributed to this plant.

A preliminary pharmacological study (3) revealed that the extract acted as a spasmogen on isolated guinea pig ileum. It also increased the respiratory rate in the dog without a change in depth.

The present experiments were undertaken to elucidate further the pharmacological effects of an extract of the leaves of *A. indica* on the heart and circulatory system.

EXPERIMENTAL

Preparation of Crude Aqueous Extract—Air-dried powdered leaves[1] (1.8 kg) of *A. indica* were extracted with 3 liters of distilled water in a soxhlet apparatus for 1 week. The extract volume was then reduced to about 200 ml on low heat with constant stirring. The final 200 ml of

[1] The leaves were collected from plants on the University of Ife campus, Ile-Ife, Nigeria, during January. The plant material was identified as *A. indica* A. Juss. (Meliaceae) by Dr. E. A. Sofowora, Department of Pharmacognosy Incorporating Drug Research Unit, University of Ife, Ile-Ife, Nigeria, and authenticated by comparison with specimens in the Institute of Forest Research Herbarium, Ibadan, Nigeria. Voucher (preserved) specimens (No. UNIFE 426) are on deposit in the Museum and Herbarium of Nigerian Medicinal Plants of the University of Ife.

0022-3549/78/1000-1476$01.00/0

© 1978, American Pharmaceutical Association

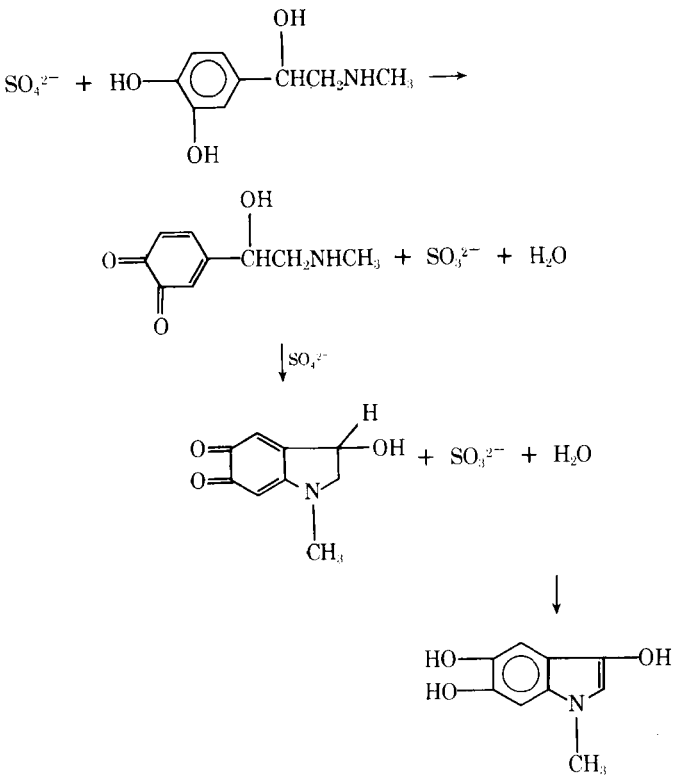

Scheme II

Previous success (10) in stabilizing different water solutions of epinephrine up to 5 years by preparing them in a nitrogen atmosphere confirms this hypothesis.

The results of the present experiments obtained in the nitrogen atmosphere show that oxygen in the reacting mixture is the most decisive factor for the stimulation of epinephrine oxidation in the presence of sodium metabisulfite in the given concentrations. Namely, the stimulating action of sodium metabisulfite on epinephrine oxidation is absent when dissolved oxygen from the air is eliminated from the solution of the reactant and when the reacting process goes on in the nitrogen atmosphere. In a highly alkaline medium, this process does not occur because of the strong influence of the hydroxide ions on epinephrine oxidation (Fig. 5).

Under the same experimental conditions, numerous experiments were performed using cysteine in different concentrations instead of sodium metabisulfite. Cysteine concentrations greater than 7×10^{-5} *M* efficiently inhibited epinephrine oxidation (Fig. 6). Since cysteine is an integral part of the human organism and since it maintains a kind of balance with the epinephrine concentration (11), it would be worthwhile to study its application in the stabilization of aqueous epinephrine solutions.

REFERENCES

(1) K. Backe-Hansen, G. Holst, A. M. Vennerod, and K. Briseid, *Acta Pharm. Suec.*, **3**, 269 (1966).

(2) W. Fuertig and I. Methke, *Pharm. Prax.*, **21**, 248 (1965).

(3) K. Breitschwerdt, T. Forster, and A. Weller, *Naturwissenschaften*, **43**, 443 (1965).

(4) K. Weber and D. Kodrnja, *Fotokem. Ind.*, **18**, 1 (1971).

(5) A. M. Kuzin, *Radiats. Biochem., Moskva, Atomizdat*, **1975**, 191–219.

(6) F. Martin, *J. Pharm. Belg.*, **41**, 151 (1969).

(7) L. C. Schroeter, T. Higuchi, and E. E. Schuler, *J. Am. Pharm. Assoc., Sci. Ed.*, **47**, 723 (1958).

(8) T. Higuchi and L. C. Schroeter, *J. Am. Chem. Soc.*, **82**, 1904 (1960).

(9) B. Uhlik and K. Wever, *Arh. Hig. Rada*, **17**, 329 (1965).

(10) P. Lundgren and S. Strom, *Acta Pharm. Suec.*, **3**, 273 (1966).

(11) D. Kovačević, G. Bjelobradič, and V. Stevanovič, *Yugosl. Physiol. Pharmacol. Acta*, **7**, 36 (1971).

Cardiovascular Effects of *Azadirachta indica* Extract

EMMANUEL B. THOMPSON ˣ and COMFORT C. ANDERSON *

Received October 25, 1977, from the *Department of Pharmacognosy and Pharmacology, College of Pharmacy, University of Illinois at the Medical Center, Chicago, IL 60612.* Accepted for publication February 10, 1978. *Present address: Department of Health Sciences, University of Ife, Ile-Ife, Nigeria.

Abstract □ A crude extract of the leaves of *Azadirachta indica* was studied for its effects on the cardiovascular system of anesthetized guinea pigs and rabbits. These effects include profound hypotension and a minimal negative chronotropic effect, which increased at higher doses. In one rabbit, 200 mg of extract/kg decreased the heart rate from 280 to 150 beats/min. The extract also exhibited a weak antiarrhythmic activity in rabbits against ouabain-induced dysrhythmia.

Keyphrases □ *Azadirachta indica*—extract of leaves, cardiovascular effects evaluated in guinea pigs and rabbits □ Cardiovascular effects—*Azadirachta indica* extract of leaves, evaluated in guinea pigs and rabbits

There is scanty literature information concerning the pharmacological properties of *Azadirachta indica*, an evergreen flowering plant belonging to the family Meliaceae. In Nigeria, this plant, called "dongoyaro," is used primarily to treat malaria, fever, abdominal disorders, and hemorrhoids and as an anthelmintic (1). Recent studies *in vivo* (2) failed to confirm the antimalarial effects attributed to this plant.

A preliminary pharmacological study (3) revealed that the extract acted as a spasmogen on isolated guinea pig ileum. It also increased the respiratory rate in the dog without a change in depth.

The present experiments were undertaken to elucidate further the pharmacological effects of an extract of the leaves of *A. indica* on the heart and circulatory system.

EXPERIMENTAL

Preparation of Crude Aqueous Extract—Air-dried powdered leaves[1] (1.8 kg) of *A. indica* were extracted with 3 liters of distilled water in a soxhlet apparatus for 1 week. The extract volume was then reduced to about 200 ml on low heat with constant stirring. The final 200 ml of

[1] The leaves were collected from plants on the University of Ife campus, Ile-Ife, Nigeria, during January. The plant material was identified as *A. indica* A. Juss. (Meliaceae) by Dr. E. A. Sofowora, Department of Pharmacognosy Incorporating Drug Research Unit, University of Ife, Ile-Ife, Nigeria, and authenticated by comparison with specimens in the Institute of Forest Research Herbarium, Ibadan, Nigeria. Voucher (preserved) specimens (No. UNIFE 426) are on deposit in the Museum and Herbarium of Nigerian Medicinal Plants of the University of Ife.

0022-3549/78/1000-1476$01.00/0

© 1978, American Pharmaceutical Association

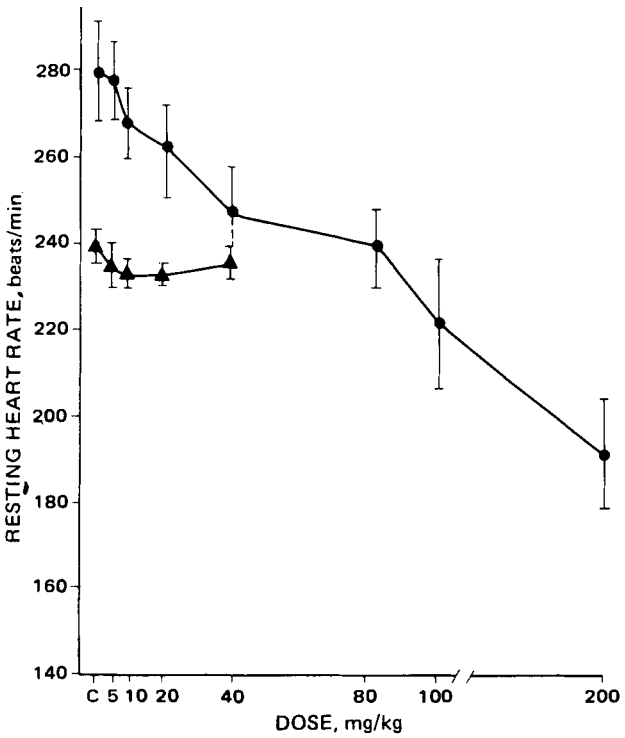

Figure 1—*Effect of* A. indica *extract on the spontaneous resting heart rate. Key:* ●, *rabbit response* (n = 3); *and* ▲, *guinea pig response* (n = 3).

brown extract was frozen and lyophilized to yield 250 g of a dark-brown powder, which was used for testing. Solutions (weight per volume) of this extract were freshly prepared in distilled water on the day of each experiment.

Preparation of Animals—Rabbits and guinea pigs of either sex, 1.0–2.2 kg and 200–250 g, respectively, were surgically prepared under urethan anesthesia (1000 mg/kg ip) for recording arterial blood pressure from a femoral artery and spontaneous heart rate and for intravenous drug administration by conventional methods (4). Only rabbits were tested for a 15-sec bilateral carotid occlusion response. This test involves the application of two bulldog clamps, one to each common carotid artery, to stop blood flow to the brain for 15 sec.

The cardiovascular effects of increasing doses of an aqueous extract of the leaves of *A. indica* were determined in three rabbits and three guinea pigs. Doses of 5, 10, 20, 40, 80, 100, and 200 mg/kg iv were tested. Each dose was administered at 30-min intervals while recordings of heart rate and arterial blood pressure were taken every 5 min. The antiarrhythmic potential of the extract also was determined in four other rabbits against ouabain-induced dysrhythmia according to a previously described method (5). The dose of the extract required to reverse sustained arrhythmia to normal sinus rhythm was determined.

RESULTS

Effect on Heart Rate—Figure 1 shows that increasing doses of the *A. indica* leaf extract progressively reduced the spontaneous heart rate of anesthetized rabbits. A dose of 200 mg of extract/kg greatly reduced the heart rate from both predrug and postdrug levels in these animals.

In anesthetized guinea pigs, the extract had no appreciable effect on the spontaneous heart rate, since the rate remained almost constant, varying only by two or three beats/min.

Effect on Blood Pressure—An extract of *A. indica* decreased arterial blood pressure (Fig. 2) but had no effect on the bilateral carotid occlusion response in anesthetized rabbits. The hypotensive effect of the extract was dose related and was much greater on diastolic than systolic pressure. Each dose level of the extract increased the arterial pulse width in these animals while it decreased the pulse rate.

In anesthetized guinea pigs, 5 and 10 mg of extract/kg transitorily increased arterial blood pressure; higher doses lowered the pressure. None of the three guinea pigs tested tolerated doses of the extract above 40 mg/kg without manifestations of toxicity and eventually death.

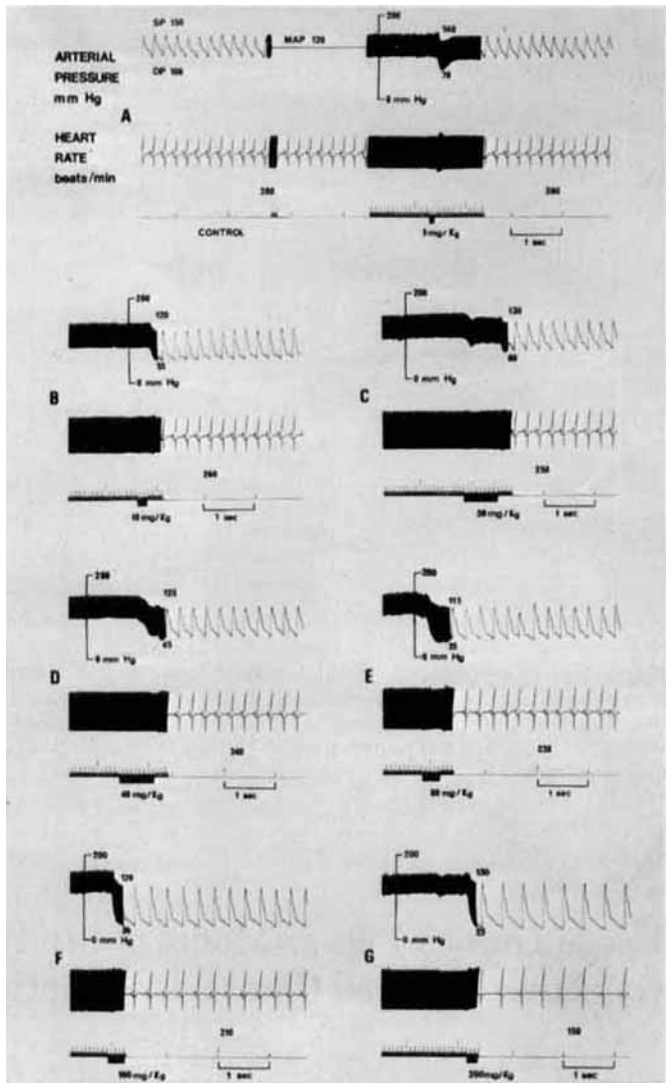

Figure 2—*Arterial blood pressure and heart rate response to* A. indica *extract. Key: A, control before drug administration; and B–G, responses to increasing doses of the drug.*

Effect on Ouabain[2]-Induced Cardiac Dysrhythmias—The sustained cardiac dysrhythmia induced by the serially administered doses of ouabain was reversed to normal sinus rhythm by 40 mg of extract/kg given in two equally divided doses. Normal rhythm returned within 8 min after the administration of the second dose (Fig. 3). It also decreased tachycardia from 380 beats/min, associated with the multifocal ventricular extrasystoles, to 220 beats/min.

DISCUSSION

In anesthetized guinea pigs and rabbits, an extract of the leaves of *A. indica* exerted some effects on the cardiovascular system. All doses tested had hypotensive effects. Reduction in arterial blood pressure was dose related. However, in anesthetized guinea pigs, small doses (5 and 10 mg/kg) induced a transient blood pressure rise. Since this effect was not observed in anesthetized rabbits, this difference seems to be species related.

The rise in arterial blood pressure observed in guinea pigs caused by low doses of the extract supports the suggestion (3) that the extract may have a biphasic effect on arterial blood pressure. In the anesthetized dog, intravenous administration of the extract produced an initial rise in arterial blood pressure, followed by a protracted fall below the normal level (3). In both species, the fall in arterial blood pressure was accompanied by an increase in the pulse width. This observation also confirms previous findings and suggests that the prolonged fall in blood pressure was due to the effect of the extract on vascular smooth muscle, probably giving

[2] Ouabain injection USP, Eli Lilly and Co.

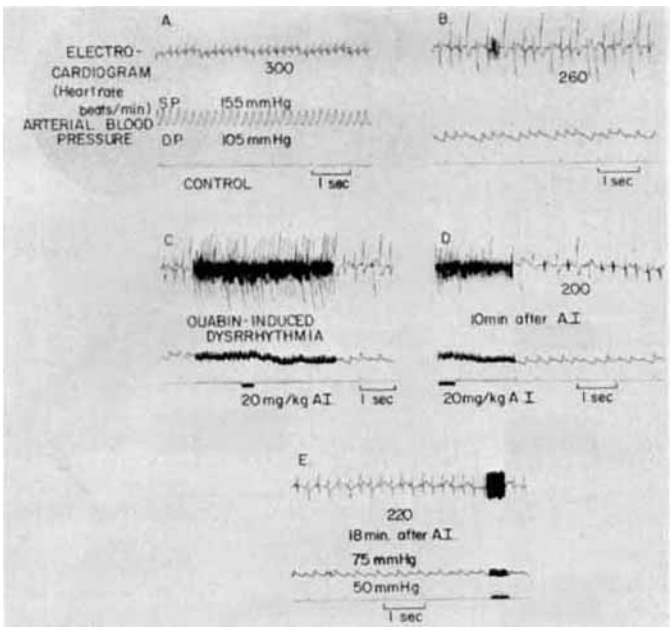

Figure 3—*Antiarrhythmic action of* A. indica *extract. Key: A, control before ouabain-induced dysrhythmia; B, 10 min after sustained dysrhythmia; C, after first dose (20 mg/kg) of extract; D, after second dose (20 mg/kg) of extract; and E, normal sinus rhythm 18 min after initial dose of extract.*

rise to a somewhat persistent vasodilation due to a reduction in arteriolar tone.

Heart rate remained nearly constant in the guinea pig, whereas there was a slight but progressive decrease in the rabbit. A direct depressant action of the compound is an untenable explanation of the mechanism of cardiac slowing in view of the observed increases in both pulse width and ECG amplitude, which may be evidence of a positive inotropic effect.

The extract of *A. indica* possessed weak antiarrhythmic activity against ouabain-induced cardiac dysrhythmias. The present experiments did not provide a satisfactory explanation of the mechanism involved, but the negative chronotropic effect of the drug appears to be beneficial in this respect.

REFERENCES

(1) B. Oliver, "Medicinal Plants in Nigeria," Nigerian College of Arts and Technology, Zaria, Nigeria, 1959, p. 48.

(2) A. Tella, *West Afr. J. Pharmacol. Drug Res.*, **3**, 80P (1976).

(3) S. O. Arigbabu and S. G. Don-Pedro, *Afr. J. Pharmacol. Pharm. Sci.*, **114**, 181 (1971).

(4) L. R. Klevans, J. L. Kovacs, and R. Kelly, *J. Pharmacol. Exp. Ther.*, **196**, 389 (1975).

(5) E. B. Thompson, *J. Pharm. Sci.*, **62**, 1638 (1973).

ACKNOWLEDGMENTS

The authors thank the Drug Research Unit of the University of Ife, Ile-Ife, Nigeria, for use of their facilities, Dr. O. O. Odebiyi who assisted in the phytochemical extraction of the plant material, and Mr. Toni Sanni for assistance.

This study was undertaken when E. B. Thompson was on a Sabbatical leave at the Drug Research Unit, University of Ife, Ile-Ife, Nigeria.

Use of Guinea Pigs as Model to Study Galactose-Induced Cataract Formation

DAVID C. KOSEGARTEN ˣ and TIMOTHY J. MAHER

Received December 5, 1977, from the *Department of Pharmacology, Massachusetts College of Pharmacy, Boston, MA 02115.* Accepted for publication February 10, 1978.

Abstract □ Because the dietary requirement for ascorbic acid is similar in humans and guinea pigs, galactose-induced cataract research with the guinea pig as an experimental model instead of the rat might be appropriate and may represent a closer analogy to galactosemic cataract formation in humans. In this study, dietary ascorbic acid was found in all guinea pigs to have a retarding or delaying effect on the development of galactose-induced cataracts.

Keyphrases □ Models, experimental—guinea pig for study of galactose-induced cataract formation, effect of ascorbic acid □ Galactose-induced cataract formation—studied in guinea pigs, effect of ascorbic acid □ Ascorbic acid—effect on galactose-induced cataract formation in guinea pigs

Galactose fed in high enough concentration causes cataracts in experimental animals (1–3). In humans, cataract formation is a prevalent complication of galactosemia, an inborn error of metabolism associated with impaired galactose biotransformation.

BACKGROUND

Classic galactosemia results from a deficiency of the enzyme galactose 1-phosphate uridyl transferase, which leads to tissue accumulation of galactose 1-phosphate and galactose. Once inside the lens, galactose is reduced by aldol reductase to galactitol, to which the lens is impermeable. A high concentration of galactitol within the lens of the galactosemic rat leads to an osmotic overhydration, which ultimately causes the formation of mature cataracts (4–6).

The early observation that scorbutic guinea pigs showed a decline in lens ascorbic acid content led to the production of cataracts in a small percentage of guinea pigs by feeding them a scorbutic diet (7). Galactose cataracts also developed in guinea pigs maintained on a scorbutic diet that included 30% casein (8).

There is a scarcity of literature on the use of the guinea pig as an animal model for the study of galactose cataracts, but a large number of studies used the rat. Of particular importance in this regard is the renewed interest in the use of flavonoids (9) or vitamin diets (10) to delay the formation of galactose-induced cataracts in the rat.

Unlike the rat, however, humans and guinea pigs cannot synthesize their own daily requirements of ascorbic acid, which is essential in the daily diet to prevent scurvy. Because of this similarity and because of the infrequent use of the guinea pig as an experimental model for the study of galactosemic cataracts, the present study was undertaken to determine if ascorbic acid could effectively delay the onset of galactosemic cataracts in the guinea pig.

EXPERIMENTAL

Fifteen Hartley strain guinea pigs, approximately 300 g, were housed in three gang cages, five per cage. The dietary protocol is shown in Table

0022-3549/78/1000-1478$01.00/0
© 1978, American Pharmaceutical Association

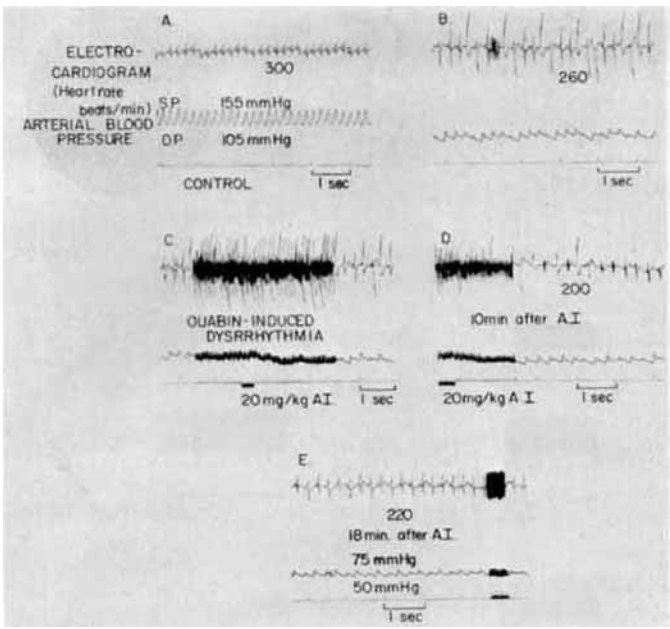

Figure 3—*Antiarrhythmic action of* A. indica *extract. Key: A, control before ouabain-induced dysrhythmia; B, 10 min after sustained dysrhythmia; C, after first dose (20 mg/kg) of extract; D, after second dose (20 mg/kg) of extract; and E, normal sinus rhythm 18 min after initial dose of extract.*

rise to a somewhat persistent vasodilation due to a reduction in arteriolar tone.

Heart rate remained nearly constant in the guinea pig, whereas there was a slight but progressive decrease in the rabbit. A direct depressant action of the compound is an untenable explanation of the mechanism of cardiac slowing in view of the observed increases in both pulse width and ECG amplitude, which may be evidence of a positive inotropic effect.

The extract of *A. indica* possessed weak antiarrhythmic activity against ouabain-induced cardiac dysrhythmias. The present experiments did not provide a satisfactory explanation of the mechanism involved, but the negative chronotropic effect of the drug appears to be beneficial in this respect.

REFERENCES

(1) B. Oliver, "Medicinal Plants in Nigeria," Nigerian College of Arts and Technology, Zaria, Nigeria, 1959, p. 48.

(2) A. Tella, *West Afr. J. Pharmacol. Drug Res.*, **3**, 80P (1976).

(3) S. O. Arigbabu and S. G. Don-Pedro, *Afr. J. Pharmacol. Pharm. Sci.*, **114**, 181 (1971).

(4) L. R. Klevans, J. L. Kovacs, and R. Kelly, *J. Pharmacol. Exp. Ther.*, **196**, 389 (1975).

(5) E. B. Thompson, *J. Pharm. Sci.*, **62**, 1638 (1973).

ACKNOWLEDGMENTS

The authors thank the Drug Research Unit of the University of Ife, Ile-Ife, Nigeria, for use of their facilities, Dr. O. O. Odebiyi who assisted in the phytochemical extraction of the plant material, and Mr. Toni Sanni for assistance.

This study was undertaken when E. B. Thompson was on a Sabbatical leave at the Drug Research Unit, University of Ife, Ile-Ife, Nigeria.

Use of Guinea Pigs as Model to Study Galactose-Induced Cataract Formation

DAVID C. KOSEGARTEN ˣ and TIMOTHY J. MAHER

Received December 5, 1977, from the *Department of Pharmacology, Massachusetts College of Pharmacy, Boston, MA 02115.* Accepted for publication February 10, 1978.

Abstract □ Because the dietary requirement for ascorbic acid is similar in humans and guinea pigs, galactose-induced cataract research with the guinea pig as an experimental model instead of the rat might be appropriate and may represent a closer analogy to galactosemic cataract formation in humans. In this study, dietary ascorbic acid was found in all guinea pigs to have a retarding or delaying effect on the development of galactose-induced cataracts.

Keyphrases □ Models, experimental—guinea pig for study of galactose-induced cataract formation, effect of ascorbic acid □ Galactose-induced cataract formation—studied in guinea pigs, effect of ascorbic acid □ Ascorbic acid—effect on galactose-induced cataract formation in guinea pigs

Galactose fed in high enough concentration causes cataracts in experimental animals (1–3). In humans, cataract formation is a prevalent complication of galactosemia, an inborn error of metabolism associated with impaired galactose biotransformation.

BACKGROUND

Classic galactosemia results from a deficiency of the enzyme galactose 1-phosphate uridyl transferase, which leads to tissue accumulation of galactose 1-phosphate and galactose. Once inside the lens, galactose is reduced by aldol reductase to galactitol, to which the lens is impermeable. A high concentration of galactitol within the lens of the galactosemic rat leads to an osmotic overhydration, which ultimately causes the formation of mature cataracts (4–6).

The early observation that scorbutic guinea pigs showed a decline in lens ascorbic acid content led to the production of cataracts in a small percentage of guinea pigs by feeding them a scorbutic diet (7). Galactose cataracts also developed in guinea pigs maintained on a scorbutic diet that included 30% casein (8).

There is a scarcity of literature on the use of the guinea pig as an animal model for the study of galactose cataracts, but a large number of studies used the rat. Of particular importance in this regard is the renewed interest in the use of flavonoids (9) or vitamin diets (10) to delay the formation of galactose-induced cataracts in the rat.

Unlike the rat, however, humans and guinea pigs cannot synthesize their own daily requirements of ascorbic acid, which is essential in the daily diet to prevent scurvy. Because of this similarity and because of the infrequent use of the guinea pig as an experimental model for the study of galactosemic cataracts, the present study was undertaken to determine if ascorbic acid could effectively delay the onset of galactosemic cataracts in the guinea pig.

EXPERIMENTAL

Fifteen Hartley strain guinea pigs, approximately 300 g, were housed in three gang cages, five per cage. The dietary protocol is shown in Table

0022-3549/78/1000-1478$01.00/0
© 1978, American Pharmaceutical Association

Table I—Protocol, Mean Animal Weight, and Food and Fluid Daily Intake

Group	Protocol	Animal Weight, g (*LSD* = ±86.9)	Food Intake, g/animal/day (*LSD* = ±4.72)	Fluid Intake, ml/animal/day (*LSD* = ±26.1)
I	Scorbutic, no galactose	363.1	53.44[a]	190.8[a]
II	Scorbutic with galactose	395.0	47.36	67.6[a]
III	Ascorbic acid with galactose	462.7[a]	48.16	111.8[a]

[a] Significant at $p = 0.05$.

I. All animals were fed a diet[1] lacking ascorbic acid. Group II animals received galactose as a 10% solution as their drinking supply, while the drinking supply of Group III animals contained both galactose (10%) and ascorbic acid (1%). Group I animals received tap water. Fresh solutions were prepared each day, and daily food and fluid consumption were recorded.

Throughout the 25 days, the animals were weighed and examined with an ophthalmoscope every other day. One drop of 0.25% atropine sulfate ophthalmic solution was applied to the ocular conjunctiva as a mydriatic. The presence or absence of cataract formation was recorded. When cataract formation was present, appropriate drawings were made to depict their extent and rate of change. Food and fluid consumption and animal weight data were subjected to least significant difference analysis of variance.

RESULTS AND DISCUSSION

By Day 7 of the study, two animals from Group II had faint rings on the periphery of both lenses. By Day 9, all animals in Group II had rings on the periphery of the lens, indicative of marginal cataracts (Fig. 1A). At the end of 25 days, these peripheral rings had progressed slightly to a more coarse and thicker opacity (Fig. 1B). At Day 25, none of the animals from Group I or III showed any signs of cataract formation (Fig. 1C). The daily food and fluid intake of Group II guinea pigs was less than that of the other two groups, yet their mean weight was not significantly different.

The appearance of cataracts in both eyes of all animals fed galactose and placed on a scorbutic diet and the absence of cataracts in any of the control groups indicate that ascorbic acid has a retarding or delaying effect on the development of galactose cataracts in the guinea pig.

[1] Charles River rabbit diet.

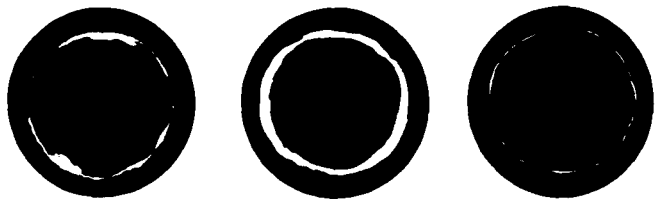

Figure 1—*Drawings of lenses illustrating the effect of ascorbic acid on the formation of galactose cataracts in the guinea pig.*

While it has been shown that rats have ample galactose 1-phosphate uridyl transferase (11), there have been no reports on the level of galactose 1-phosphate uridyl transferase in the guinea pig. Moreover, lens aldol reductase activity has been studied in rats (12, 13) but not guinea pigs.

Further investigations are being conducted in these laboratories on guinea pig galactose 1-phosphate uridyl transferase and lens aldol reductase activity in relation to galactosemic cataract formation. The present study demonstrates that the guinea pig is a suitable model for galactosemic cataract investigations, which is desirable considering the similarity between humans and the guinea pig with regard to the dietary requirement for ascorbic acid.

REFERENCES

(1) H. S. Mitchell and W. M. Dodge, *J. Nutr.*, **9**, 37 (1935).
(2) J. W. Patterson, *Am. J. Ophthalmol.*, **36** (6)II, 143 (1953).
(3) Z. Dische and E. Borenfreund, *ibid.*, **38**, 165 (1954).
(4) R. van Heyningen, *Nature (London)*, **184**, 194 (1959).
(5) J. H. Kinoshita, *Invest. Ophthalmol.*, **13**, 713 (1974).
(6) S. D. Varma and J. H. Kinoshita, *Exp. Eye Res.*, **19**, 577 (1974).
(7) N. K. Monjukowa and M. J. Fradkin, *Arch. Ophthalmol.*, **133**, 328 (1935).
(8) H. Tojo, *Acta Soc. Ophthalmol. Jpn.*, **58**, 556 (1954).
(9) S. D. Varma, E. Mikuni, and J. H. Kinoshita, *Science*, **188**, 1215 (1975).
(10) J. D. Heffley and R. J. Williams, *Proc. Natl. Acad. Sci. USA*, **71**, 4164 (1974).
(11) S. Kelly and L. DesJardins, *Proc. Soc. Exp. Biol. Med.*, **138**, 545 (1971).
(12) S. D. Varma and J. H. Kinoshita, *Biochem. Pharmacol.*, **25**, 2505 (1976).
(13) A. B. Segelman, F. P. Segelman, S. D. Varma, H. Wagner, and O. Seligman, *J. Pharm. Sci.*, **66**, 1358 (1977).

Quinazolinylformamidines and Quinazolinediylbisformamidines as Antihypertensive Agents

J. D. WARREN ˣ, S. A. LANG, Jr., P. S. CHAN, and J. W. MARSICO

Received October 12, 1977, from the *Chemical Research Department, Lederle Laboratories, American Cyanamid Co., Pearl River, NY 10965.* Accepted for publication February 9, 1978.

Abstract □ Eleven quinazolinylformamidines and quinazolinediylbisformamidines were synthesized and investigated for antihypertensive activity in spontaneous hypertensive rats. Several compounds showed moderate antihypertensive activity at 100 mg/kg po. The same compounds were not hypotensive in the normotensive dog.

Keyphrases □ Quinazolinylformamidines, substituted—synthesized, evaluated for antihypertensive activity in rats □ Antihypertensive activity—various substituted quinazolinylformamidines evaluated in rats □ Structure–activity relationships—various substituted quinazolinylformamidines evaluated for antihypertensive activity in rats

In an investigation of the potential antihypertensive activity of 2,4-diaminoquinazoline derivatives, the quinazolinediylbisformamidine (III) was observed to be a moderately active (25 mg/kg) antihypertensive agent when orally administered to spontaneously hypertensive rats (1). Further evaluation of III revealed it to be free of

0022-3549/78/1000-1479$01.00/0
© 1978, American Pharmaceutical Association

Table I—Protocol, Mean Animal Weight, and Food and Fluid Daily Intake

Group	Protocol	Animal Weight, g (*LSD* = ±86.9)	Food Intake, g/animal/day (*LSD* = ±4.72)	Fluid Intake, ml/animal/day (*LSD* = ±26.1)
I	Scorbutic, no galactose	363.1	53.44[a]	190.8[a]
II	Scorbutic with galactose	395.0	47.36	67.6[a]
III	Ascorbic acid with galactose	462.7[a]	48.16	111.8[a]

[a] Significant at $p = 0.05$.

I. All animals were fed a diet[1] lacking ascorbic acid. Group II animals received galactose as a 10% solution as their drinking supply, while the drinking supply of Group III animals contained both galactose (10%) and ascorbic acid (1%). Group I animals received tap water. Fresh solutions were prepared each day, and daily food and fluid consumption were recorded.

Throughout the 25 days, the animals were weighed and examined with an ophthalmoscope every other day. One drop of 0.25% atropine sulfate ophthalmic solution was applied to the ocular conjunctiva as a mydriatic. The presence or absence of cataract formation was recorded. When cataract formation was present, appropriate drawings were made to depict their extent and rate of change. Food and fluid consumption and animal weight data were subjected to least significant difference analysis of variance.

RESULTS AND DISCUSSION

By Day 7 of the study, two animals from Group II had faint rings on the periphery of both lenses. By Day 9, all animals in Group II had rings on the periphery of the lens, indicative of marginal cataracts (Fig. 1A). At the end of 25 days, these peripheral rings had progressed slightly to a more coarse and thicker opacity (Fig. 1B). At Day 25, none of the animals from Group I or III showed any signs of cataract formation (Fig. 1C). The daily food and fluid intake of Group II guinea pigs was less than that of the other two groups, yet their mean weight was not significantly different.

The appearance of cataracts in both eyes of all animals fed galactose and placed on a scorbutic diet and the absence of cataracts in any of the control groups indicate that ascorbic acid has a retarding or delaying effect on the development of galactose cataracts in the guinea pig.

[1] Charles River rabbit diet.

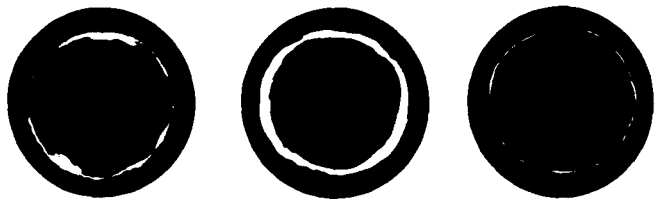

Figure 1—*Drawings of lenses illustrating the effect of ascorbic acid on the formation of galactose cataracts in the guinea pig.*

While it has been shown that rats have ample galactose 1-phosphate uridyl transferase (11), there have been no reports on the level of galactose 1-phosphate uridyl transferase in the guinea pig. Moreover, lens aldol reductase activity has been studied in rats (12, 13) but not guinea pigs.

Further investigations are being conducted in these laboratories on guinea pig galactose 1-phosphate uridyl transferase and lens aldol reductase activity in relation to galactosemic cataract formation. The present study demonstrates that the guinea pig is a suitable model for galactosemic cataract investigations, which is desirable considering the similarity between humans and the guinea pig with regard to the dietary requirement for ascorbic acid.

REFERENCES

(1) H. S. Mitchell and W. M. Dodge, *J. Nutr.*, **9**, 37 (1935).
(2) J. W. Patterson, *Am. J. Ophthalmol.*, **36** (6)II, 143 (1953).
(3) Z. Dische and E. Borenfreund, *ibid.*, **38**, 165 (1954).
(4) R. van Heyningen, *Nature (London)*, **184**, 194 (1959).
(5) J. H. Kinoshita, *Invest. Ophthalmol.*, **13**, 713 (1974).
(6) S. D. Varma and J. H. Kinoshita, *Exp. Eye Res.*, **19**, 577 (1974).
(7) N. K. Monjukowa and M. J. Fradkin, *Arch. Ophthalmol.*, **133**, 328 (1935).
(8) H. Tojo, *Acta Soc. Ophthalmol. Jpn.*, **58**, 556 (1954).
(9) S. D. Varma, E. Mikuni, and J. H. Kinoshita, *Science*, **188**, 1215 (1975).
(10) J. D. Heffley and R. J. Williams, *Proc. Natl. Acad. Sci. USA*, **71**, 4164 (1974).
(11) S. Kelly and L. DesJardins, *Proc. Soc. Exp. Biol. Med.*, **138**, 545 (1971).
(12) S. D. Varma and J. H. Kinoshita, *Biochem. Pharmacol.*, **25**, 2505 (1976).
(13) A. B. Segelman, F. P. Segelman, S. D. Varma, H. Wagner, and O. Seligman, *J. Pharm. Sci.*, **66**, 1358 (1977).

Quinazolinylformamidines and Quinazolinediylbisformamidines as Antihypertensive Agents

J. D. WARREN ˣ, S. A. LANG, Jr., P. S. CHAN, and J. W. MARSICO

Received October 12, 1977, from the *Chemical Research Department, Lederle Laboratories, American Cyanamid Co., Pearl River, NY 10965.* Accepted for publication February 9, 1978.

Abstract □ Eleven quinazolinylformamidines and quinazolinediylbisformamidines were synthesized and investigated for antihypertensive activity in spontaneous hypertensive rats. Several compounds showed moderate antihypertensive activity at 100 mg/kg po. The same compounds were not hypotensive in the normotensive dog.

Keyphrases □ Quinazolinylformamidines, substituted—synthesized, evaluated for antihypertensive activity in rats □ Antihypertensive activity—various substituted quinazolinylformamidines evaluated in rats □ Structure–activity relationships—various substituted quinazolinylformamidines evaluated for antihypertensive activity in rats

In an investigation of the potential antihypertensive activity of 2,4-diaminoquinazoline derivatives, the quinazolinediylbisformamidine (III) was observed to be a moderately active (25 mg/kg) antihypertensive agent when orally administered to spontaneously hypertensive rats (1). Further evaluation of III revealed it to be free of

0022-3549/78/1000-1479$01.00/0
© 1978, American Pharmaceutical Association

Table I—Substituted 2,4-Diaminoquinazolines

Compound	Substituents	Preparation Reference Number	Melting Point
Ia	$R_1 = R_2 = R_3 = H, R_4 = NH_2$	3	249–251°
Ib	$R_1 = NO_2, R_2 = R_3 = H, R_4 = NH_2$	3	>300°
Ic	$R_1 = Br, R_2 = R_3 = H, R_4 = NH_2$	4	188–190°
Id	$R_1 = R_4 = NH_2, R_2 = R_3 = H$	3	256–258°
Ie	$R_1 = R_2 = CH_3O, R_3 = H, R_4 = NH_2$	5	238–240°
If	$R_1 = Cl, R_2 = NO_2, R_3 = H, R_4 = NH_2$	4	—
Ig	$R_1 = H, R_2 = Cl, R_3 = CH_3, R_4 = NH_2$	4	227–227.5°
Ih	$R_1 = Cl, R_2 = R_3 = H, R_4 = NH_2$	4	265–267°
Ii	$R_1 = NC, R_2 = R_3 = H, R_4 = NH_2$	3	>300°
Ij	$R_1 = R_2 = R_3 = R_4 = H$	6	267–268°
Ik	$R_1 = NO_2, R_2 = R_3 = R_4 = H$	6	319–320°

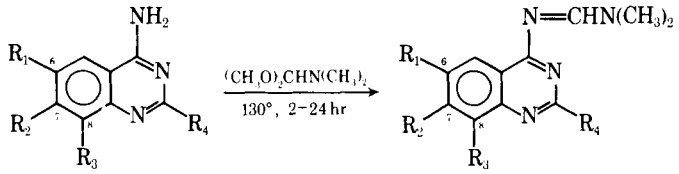

Ia–Ik IIa–IIk

Scheme I

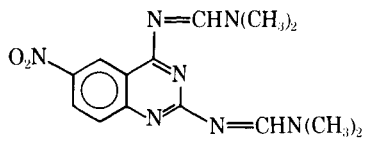

III

adverse side effects such as ataxia, sedation, agitation, or tachycardia at 25 mg/kg in the spontaneously hypertensive rat.

The only published biological activity for the quinazolinylformamidines or the quinazolinediylbisformamidines was the antiparasitic activity of a series of *N'*-(6-benzylamino-4-quinazolinyl) -*N,N*- dimethylformamidines (2).

These observations prompted the synthesis of 10 related formamidines and the investigation of their antihypertensive activity.

RESULTS AND DISCUSSION

Chemistry—The required starting materials, including the unsubstituted as well as the 10 substituted 2,4-diaminoquinazolines, were synthesized by routes analogous to published procedures. The substituents were either electron donating or withdrawing and attached to the benzene ring of the quinazoline nucleus at position 6, 7, or 8 (Table I).

The desired formamidines, IIa–IIk (Table II), were readily synthesized by the general procedure shown in Scheme I. Reaction of diaminoquinazolines Ia–Ik with excess dimethylformamide dimethyl acetal at 130°, either neat or in a dimethylformamide or dimethyl sulfoxide solution, yielded, after workup, IIa–IIk in 50–85% yield.

Biology—Formamidines IIa–IIk were administered orally in two doses of 100 mg/kg each to spontaneously hypertensive rats. The second dose was given 24 hr after the first. The mean arterial blood pressure was measured at 4 hr after the second dosing. All determinations were made in restrained, conscious animals by direct femoral puncture. The antihypertensive activity of the active formamidines in this series, together with the values for known reference agents, is listed in Table III.

Of the formamidines reported in Table II, IIa, IIb, IIe, and IIi decreased the mean arterial pressure of the spontaneously hypertensive rats at 100 mg/kg by 12–29%. The congeners IIa and IIb were the most

Table II—Quinazolinylformamidines and Quinazolinediylbisformamidines

Compound	Substituents	Melting Point	Yield, %	Formula	Analysis, %	Calc.	Found
IIa	$R_1 = R_2 = R_3 = H$, $R_4 = N{=}CHN(CH_3)_2$	142°	80	$C_{14}H_{18}N_6$	C	61.03	61.20
					H	6.70	6.71
					N	30.88	31.09
IIb	$R_1 = NO_2, R_2 = R_3 = H$, $R_4 = N{=}CHN(CH_3)_2$	228°	60	$C_{14}H_{17}N_7O_2$	C	52.94	53.32
					H	5.34	5.44
					N	31.00	31.09
IIc	$R_1 = Br, R_1 = H_3 = H$, $R_4 = N{=}CHN(CH_3)_2$	204°	50	$C_{14}H_{17}BrN_6$	C	48.15	47.95
					H	4.91	4.79
					Br	22.88	23.26
					N	24.06	24.25
IId	$R_1 = R_4 = N{=}CHN(CH_3)_2$, $R_2 = R_3 = H$	173°	70	$C_{17}H_{18}N_8$	C	61.06	60.95
					H	5.43	5.35
					N	33.51	33.21
IIe	$R_1 = R_2 = CH_3O, R_3 = H$, $R_4 = N{=}CHN(CH_3)_2$	216°	50	$C_{16}H_{22}N_6O_2$	C	56.62	56.72
					H	6.83	6.94
					N	24.76	24.52
IIf	$R_1 = Cl, R_2 = NO_2, R_3 = H$, $R_4 = N{=}CHN(CH_3)_2 \cdot \frac{1}{2}H_2O$	209°	56	$C_{14}H_{16}ClN_7O_2 \cdot \frac{1}{2}H_2O$	C	46.47	47.09
					H	4.78	4.47
					Cl	9.88	10.26
					N	27.33	27.17
IIg	$R_1 = H, R_2 = Cl, R_3 = CH_3$, $R_4 = N{=}CHN(CH_3)_2$	184°	69	$C_{15}H_{19}ClN_6$	C	56.51	56.51
					H	6.01	5.99
					Cl	11.12	11.10
					N	26.36	26.14
IIh	$R_1 = Cl, R_2 = R_3 = H$, $R_4 = N{=}CHN(CH_3)_2$	218°	61	$C_{14}H_{17}ClN_6$	C	55.17	55.09
					H	5.62	5.62
					Cl	11.60	11.55
					N	27.60	27.93
IIi	$R_1 = NC, R_2 = R_3 = H$, $R_4 = N{=}CHN(CH_3)_2$	270°	85	$C_{15}H_{17}N \cdot \frac{1}{2}H_2O$	C	59.20	59.54
					H	5.96	5.62
					N	32.22	32.20
IIj	$R_1 = R_2 = R_3 = R_4 = H$	69°	75	$C_{11}H_{12}N_4$	C	66.00	66.20
					H	6.04	6.17
					N	28.00	28.20
IIk	$R_1 = NO_2, R_2 = R_3 = R_4 = H$	153°	70	$C_{11}H_{11}N_5O_2$	C	53.90	53.80
					H	4.52	4.37
					N	28.60	28.90

Table III—Antihypertensive Quinazolinylformamides and Quinazolinediylbisformamidines

Compound	*n*	Mean Arterial Blood Pressure	Dose, mg/kg	Percent Decrease from Control
II*a*	2	131	100	21
II*b*	3	118	100	29
II*b*	3	129	25	22
II*e*	2	146	100	12
II*i*	2	139	100	16
II*i*	4	144	25	13
Guanabenz	20	123	25	26
Clonidine	6	96	0.5	43
Control	60	166	—	—

active of this series at the 100-mg/kg dose level. The most active congener was the 6-nitro derivative II*b*, while the least active congener was the 6,7-dimethoxy derivative II*e*. Of the active formamidines, only II*b* (6-nitro) and II*i* (6-cyano) were active at the 25-mg/kg dose level in the spontaneously hypertensive rat. Congener II*b* was approximately twice as active as II*i*, a 29 *versus* 13% decrease in mean arterial blood pressure. Thus, quinazolinediylbisformamidines bearing an electron-withdrawing group at C-6 of the quinazoline nucleus apparently are more active than the corresponding quinazolinediylbisformamidines bearing electron-donating substituents.

When II*a*–II*k* were administered in gelatin capsules to normotensive dogs, no effect on blood pressure was observed with a single dose of 25 mg/kg. Bradycardia was observed at doses greater than 25 mg/kg, which prevented further evaluation at higher doses.

The lack of hypotensive activity of II*a*–II*k* in the normotensive dog precludes further development of the quinazolinediylbisformamidines.

EXPERIMENTAL

All melting points are uncorrected. Samples for elemental analysis were dried at 55° under high vacuum for 5–24 hr. The general procedure employed in the synthesis of the quinazolinylformamidines is as follows for N^1,N^3-dimethyl -N^2,N^4- (7-chloro-8-methyl-2,4-quinazolinediyl)bisformamidine (II*g*).

A solution of 2.1 g (10.0 mmoles) of 7-chloro-8-methyl-2,4-diaminoquinazoline in 20 ml of dimethylformamide dimethyl acetal and 20 ml of dimethylformamide was refluxed for 16 hr and then cooled to room temperature. Excess solvent was removed under aspirator pressure, and the solid residue was recrystallized twice from ethyl acetate to yield 2.2 g (69%) of light-yellow crystals, mp 182–184°.

Anal.—Calc. for $C_{15}H_{19}ClN_6$: C, 56.51; H, 6.01; Cl, 11.12; N, 26.36. Found: C, 56.51; H, 5.99; Cl, 11.10; N, 26.14.

Compounds II*a*–II*k* (Table II) were prepared by a similar procedure by condensing dimethylformamide dimethyl acetal with the appropriate I*a*–I*k*.

These quinazolinediylbisformamidines were characterized by elemental analyses and the presence of characteristic resonances at 3.0–3.3 ppm (methyl group protons at the terminal nitrogen atom of the formamidine moiety) in their PMR spectra.

REFERENCES

(1) P. S. Chan, D. Poorvin, M. A. Ronsberg, G. Vice, F. Beyer, and P. Scully, *Pharmacologist*, **17**, 253 (1975).

(2) E. F. Eislager and D. F. Worth (Parke-Davis), U.S. pat. 3,668,205 (1972).

(3) J. Davoll and A. M. Johnson, *J. Chem. Soc. C*, **1970**, 997.

(4) K. Schofield, *ibid.*, **1952**, 1927.

(5) F. H. S. Curd, J. K. Landquist, and F. L. Rose, *ibid.*, **1948**, 1759.

(6) J. S. Morley and J. Simpson, *J. Chem. Soc.*, **1949**, 1354.

ACKNOWLEDGMENTS

The authors are grateful to Mr. W. Fulmor, Mr. L. Brancone, and their associates for technical assistance in obtaining spectral and microanalytical data.

Quantitative Determination of Cephalexin in Cephradine by NMR Spectroscopy

R. J. WARREN ˣ, J. E. ZAREMBO, D. B. STAIGER, and A. POST

Received July 20, 1977, from *Smith Kline & French Laboratories, Philadelphia, PA 19101.* Accepted for publication February 1, 1978.

Abstract □ An NMR method to determine quantitatively the presence of cephalexin in cephradine was developed. The method is applicable to the chemical itself as well as to capsules and oral suspension formulations. The determination is based on the NMR signal arising from the five aromatic protons of the cephalexin molecule. Integration of this signal relative to a signal from cephradine provides the data necessary to determine the percentage of cephalexin present. The precision at the 2% cephalexin level is ±0.18%. The time required to carry out a single analysis is about 10 min, and five analyses can be done in about 0.5 hr.

Keyphrases □ Cephalexin—NMR spectroscopic analysis in cephradine bulk drug and dosage forms □ NMR spectroscopy—analysis, cephalexin in cephradine bulk drug and dosage forms □ Antibacterials—cephalexin, NMR spectroscopic analysis in cephradine bulk drug and dosage forms

Cephalexin (I) may be present in a given lot of cephradine (II) as an impurity from the synthesis of cephradine or as a decomposition product of cephradine. A rapid, quantitative method was required to determine the cephalexin content of cephradine chemical as well as capsule and oral suspension formulations. Present methods (1, 2) were too slow for large numbers of samples.

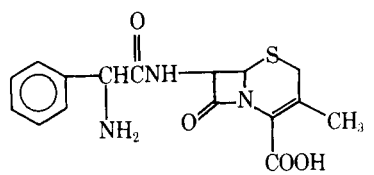

I

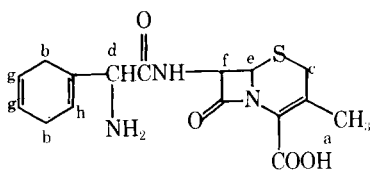

II

0022-3549/78/1000-1481$01.00/0

© 1978, American Pharmaceutical Association

Table III—Antihypertensive Quinazolinylformamides and Quinazolinediylbisformamidines

Compound	*n*	Mean Arterial Blood Pressure	Dose, mg/kg	Percent Decrease from Control
II*a*	2	131	100	21
II*b*	3	118	100	29
II*b*	3	129	25	22
II*e*	2	146	100	12
II*i*	2	139	100	16
II*i*	4	144	25	13
Guanabenz	20	123	25	26
Clonidine	6	96	0.5	43
Control	60	166	—	—

active of this series at the 100-mg/kg dose level. The most active congener was the 6-nitro derivative II*b*, while the least active congener was the 6,7-dimethoxy derivative II*e*. Of the active formamidines, only II*b* (6-nitro) and II*i* (6-cyano) were active at the 25-mg/kg dose level in the spontaneously hypertensive rat. Congener II*b* was approximately twice as active as II*i*, a 29 *versus* 13% decrease in mean arterial blood pressure. Thus, quinazolinediylbisformamidines bearing an electron-withdrawing group at C-6 of the quinazoline nucleus apparently are more active than the corresponding quinazolinediylbisformamidines bearing electron-donating substituents.

When II*a*–II*k* were administered in gelatin capsules to normotensive dogs, no effect on blood pressure was observed with a single dose of 25 mg/kg. Bradycardia was observed at doses greater than 25 mg/kg, which prevented further evaluation at higher doses.

The lack of hypotensive activity of II*a*–II*k* in the normotensive dog precludes further development of the quinazolinediylbisformamidines.

EXPERIMENTAL

All melting points are uncorrected. Samples for elemental analysis were dried at 55° under high vacuum for 5–24 hr. The general procedure employed in the synthesis of the quinazolinylformamidines is as follows for N^1,N^3-dimethyl -N^2,N^4- (7-chloro-8-methyl-2,4-quinazolinediyl)bisformamidine (II*g*).

A solution of 2.1 g (10.0 mmoles) of 7-chloro-8-methyl-2,4-diaminoquinazoline in 20 ml of dimethylformamide dimethyl acetal and 20 ml of dimethylformamide was refluxed for 16 hr and then cooled to room temperature. Excess solvent was removed under aspirator pressure, and the solid residue was recrystallized twice from ethyl acetate to yield 2.2 g (69%) of light-yellow crystals, mp 182–184°.

Anal.—Calc. for $C_{15}H_{19}ClN_6$: C, 56.51; H, 6.01; Cl, 11.12; N, 26.36. Found: C, 56.51; H, 5.99; Cl, 11.10; N, 26.14.

Compounds II*a*–II*k* (Table II) were prepared by a similar procedure by condensing dimethylformamide dimethyl acetal with the appropriate I*a*–I*k*.

These quinazolinediylbisformamidines were characterized by elemental analyses and the presence of characteristic resonances at 3.0–3.3 ppm (methyl group protons at the terminal nitrogen atom of the formamidine moiety) in their PMR spectra.

REFERENCES

(1) P. S. Chan, D. Poorvin, M. A. Ronsberg, G. Vice, F. Beyer, and P. Scully, *Pharmacologist*, **17**, 253 (1975).

(2) E. F. Eislager and D. F. Worth (Parke-Davis), U.S. pat. 3,668,205 (1972).

(3) J. Davoll and A. M. Johnson, *J. Chem. Soc. C*, **1970**, 997.

(4) K. Schofield, *ibid.*, **1952**, 1927.

(5) F. H. S. Curd, J. K. Landquist, and F. L. Rose, *ibid.*, **1948**, 1759.

(6) J. S. Morley and J. Simpson, *J. Chem. Soc.*, **1949**, 1354.

ACKNOWLEDGMENTS

The authors are grateful to Mr. W. Fulmor, Mr. L. Brancone, and their associates for technical assistance in obtaining spectral and microanalytical data.

Quantitative Determination of Cephalexin in Cephradine by NMR Spectroscopy

R. J. WARREN ˣ, J. E. ZAREMBO, D. B. STAIGER, and A. POST

Received July 20, 1977, from *Smith Kline & French Laboratories, Philadelphia, PA 19101.* Accepted for publication February 1, 1978.

Abstract □ An NMR method to determine quantitatively the presence of cephalexin in cephradine was developed. The method is applicable to the chemical itself as well as to capsules and oral suspension formulations. The determination is based on the NMR signal arising from the five aromatic protons of the cephalexin molecule. Integration of this signal relative to a signal from cephradine provides the data necessary to determine the percentage of cephalexin present. The precision at the 2% cephalexin level is ±0.18%. The time required to carry out a single analysis is about 10 min, and five analyses can be done in about 0.5 hr.

Keyphrases □ Cephalexin—NMR spectroscopic analysis in cephradine bulk drug and dosage forms □ NMR spectroscopy—analysis, cephalexin in cephradine bulk drug and dosage forms □ Antibacterials—cephalexin, NMR spectroscopic analysis in cephradine bulk drug and dosage forms

Cephalexin (I) may be present in a given lot of cephradine (II) as an impurity from the synthesis of cephradine or as a decomposition product of cephradine. A rapid, quantitative method was required to determine the cephalexin content of cephradine chemical as well as capsule and oral suspension formulations. Present methods (1, 2) were too slow for large numbers of samples.

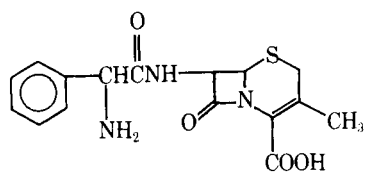

I

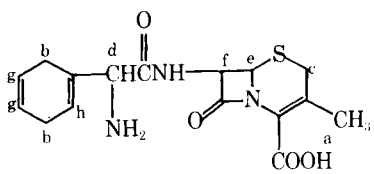

II

0022-3549/78/1000-1481$01.00/0

© 1978, American Pharmaceutical Association

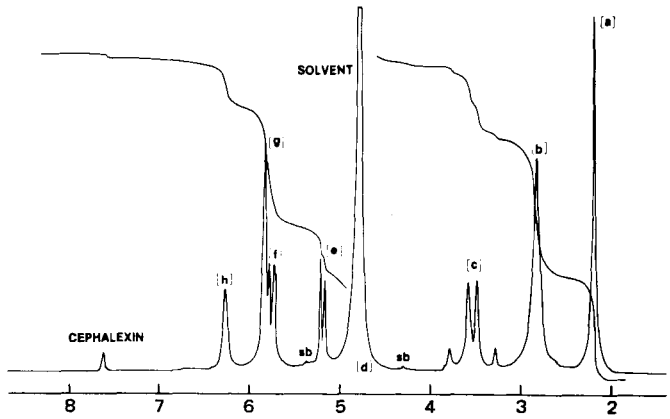

Figure 1—*NMR spectrum of cephradine containing 2.5% cephalexin.*

The purpose of this study was to establish the feasibility of using NMR to differentiate between the two compounds and for quantitative analysis of cephalexin when present. The described methods provide the data required for such analyses.

EXPERIMENTAL

All spectra were recorded on a 90-MHz spectrometer[1] using 3% deuterium chloride as the solvent. The spectra were recorded at 37° at a concentration of at least 200 mg/ml. Chemical shifts were measured relative to tetramethylsilane.

The quantitative NMR determination of cephalexin in cephradine is based on the integration of the five aromatic protons of the fully aromatic system in cephalexin (679 Hz) *versus* the integration of the olefinic proton of cephradine (558 Hz) (Figs. 1 and 2). A calibration curve was prepared by making known mixtures of the two components and plotting the ratio of their NMR integration *versus* the cephalexin concentration, usually expressed in percent. This calibration curve was then used for subsequent

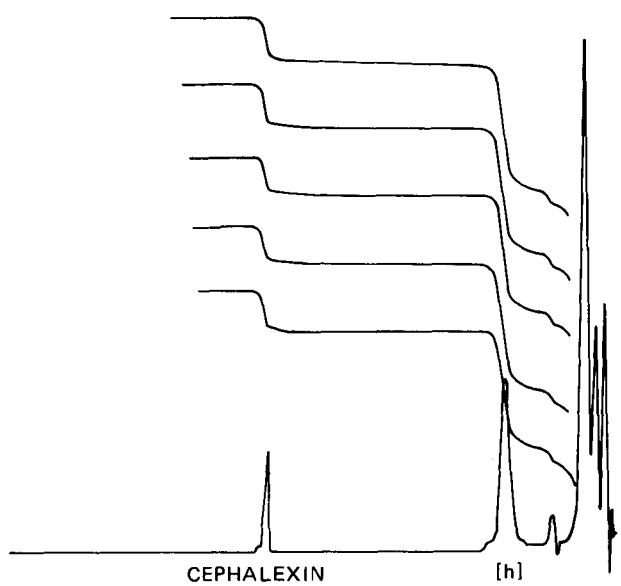

Figure 2—*The 300-MHz expansion of portion of Fig. 1.*

[1] Perkin-Elmer model R32.

Table I—Statistical Analysis of NMR Results

Group	Average, %	*SD*, %	*CV*, %
A	2.27	0.176	7.78
B	3.07	0.177	5.80
C	3.98	0.173	4.35

analyses of the chemical or dosage forms, *i.e.*, capsules or oral suspensions, according to the following procedures.

Chemical—Approximately 100 mg of sample was weighed and transferred to a small glass vial. Deuterium chloride (0.5 ml) was added, and the vial was shaken until the sample was dissolved. The solution was then transferred to an NMR tube. The NMR spectrum was run and integrated five times, and the average integral value was obtained. The ratio of the integral at 679 Hz representing the five aromatic protons of the cephalexin molecule and the integral at 558 Hz representing the olefinic proton of cephradine was recorded. The percentage of cephalexin then was calculated from a standard calibration plot.

Capsules—This determination can be carried out using a single capsule, but the contents of 10 capsules can be pooled to minimize capsule-to-capsule variation. The weight equivalent to a single capsule is then taken for assay.

A weight equivalent to a single capsule was transferred to a small glass vial, 0.5 ml of 3% deuterium chloride was added, and the vial was shaken. The cephalosporin materials dissolved in deuterium chloride, and the inorganic capsule filler (magnesium stearate) precipitated. The clear solution was removed by pipet or syringe and transferred to an NMR tube. From this point, the procedure followed was the same as that used for the chemical.

Oral Suspensions—Approximately 3 g of the oral suspension dry mix was weighed and transferred to a 250-ml erlenmeyer flask; 50 ml of methanolic 0.1 *N* HCl was added, and the flask was shaken. The slurry formed was filtered through filter paper. The residue was washed twice with 20-ml portions of methanolic 0.1 *N* HCl. The filtrate, which consisted of the cephalosporins, small amounts of sugar, and trace amounts of artificial coloring, was evaporated to dryness at room temperature under a nitrogen stream. The presence of the sugar and coloring in these amounts did not interfere with the determination. The dry sample was dissolved in 0.5 ml of 3% deuterium chloride, and the procedure followed from this point was the same as that for the chemical.

A statistical evaluation of the NMR method was carried out as follows: 18 samples of each of three levels of cephalexin (a total of 54 samples) were assayed. The samples were supplied as unknowns in sets of 18 and arbitrarily numbered within each set in such a way that if Samples 1–6 were analyzed on 1 day, 7–12 on a 2nd day, and 13–18 on a 3rd day, two samples of each cephalexin level would be analyzed on each day.

RESULTS AND DISCUSSION

A statistical analysis of the NMR results showed the variation among sets was not significant. There was no significant day-to-day variation. The standard deviation of the sample-to-sample variation is shown in Table I along with the average cephalexin content determined for each group and the coefficient of variation (standard deviation expressed as a percent of the average). The sample-to-sample standard deviations for the three groups were similar. With essentially a constant standard deviation (over this range of cephalexin content), the coefficient of variation steadily decreased as the cephalexin content increased.

REFERENCES

(1) E. H. Flynn, "Cephalosporins and Penicillins," Academic, New York, N.Y., 1972, p. 610.

(2) M. A. Carroll, E. R. White, Z. Jancsik, and J. E. Zarembo, *J. Antibiot.*, **30**, 397 (1977).

ACKNOWLEDGMENTS

The authors thank John F. Pauls of the Biostatistics Department for the statistical analysis of the data.

Mass Fragmentographic Determination of Methadyl Acetate in Urine Using Stable Isotope Labeled Analog as Internal Standard

SATYA P. JINDAL ˣ, PER VESTERGAARD, and THERESA LUTZ

Received December 19, 1977, from the *Rockland Research Institute, Orangeburg, NY 10962.* Accepted for publication February 16, 1978.

Abstract □ A quantitative GLC–mass spectrometric assay was developed for the determination of methadyl acetate in urine. The assay utilizes selective ion focusing to monitor, in a GLC effluent, the M − 15 ion generated by electron-impact ionization of methadyl acetate. Methadyl acetate-d_4 was used as an internal standard. The assay can measure 10 ng of drug/ml with about 6% precision. The curve relating the amounts of drug added to control urine *versus* the amounts experimentally found over a large concentration range is a straight line with a slope of 0.98 ± 0.02 and a nearly zero intercept. Assay specificity was confirmed by complete identity of the mass spectrum of methadyl acetate in the biological extract with that of the authentic material. The method was used for the urinary analysis of methadyl acetate in a rabbit given a single intravenous dose. The animal excreted less than 1% of the intact drug with a half-life of approximately 15 hr. Consequently, the long-acting characteristic of methadyl acetate must be attributed to its metabolism into active metabolites.

Keyphrases □ Methadyl acetate—GLC–mass spectrometric analysis in urine □ GLC–mass spectrometry—analysis, methadyl acetate in urine □ Narcotic analgesics—methadyl acetate, GLC–mass spectrometric analysis in urine

Methadyl acetate[1], 6-(dimethylamino)-4,4-diphenyl-3-heptanol acetate (I), a potent, long acting, synthetic narcotic analgesic (1, 2), is currently under clinical evaluation for the treatment of opiate addiction (3–5). Its usefulness as a substitute for methadone in opiate addiction therapy prompted the development of a sensitive and specific assay in biological fluids. Methadyl acetate is biotransformed to several metabolites (5, 6), some of which are structurally similar to the parent drug. Consequently, an assay must be specific and free from interference from these metabolites.

This report presents a GLC–mass spectrometric assay for I in urine. Selective ion monitoring, the technique built on combined GLC–mass spectrometry, with selective focusing on a suitable fragment of the molecular ion (mass fragmentography) is a well-established technique in biomedical research (7, 8). This technique was used to develop a very sensitive and specific assay of I in urine utilizing deuterium-labeled I as an internal standard.

EXPERIMENTAL

Materials—Analytical grade I hydrochloride[2], sodium borodeuteride[3], and acetic anhydride[4] were used without further purification. All solvents were analytical grade[4]. Silanized tubes[5] (10 ml) with screw caps[6] were used for urine extraction; final solvent evaporation was performed in 5-ml glass-stoppered centrifuge tubes[7]. Pasteur pipets with hand-drawn constricted tips were utilized for all solution transfers. Urine was collected by catheterization, an aliquot was taken, an appropriate amount of internal standard was added, and the mixture was stored frozen until analysis.

Methadone[8]-d_3 [6-(dimethylamino)-4,4-diphenyl-1,1,1-trideutero-3-heptanone], on treatment with sodium borodeuteride using an established procedure for reduction of carbonyl compounds (9), gave dimepheptanol-d_4. On subsequent reaction with acetic anhydride (10), dimepheptanol-d_4 afforded I-d_4 [6-(dimethylamino)-4,4-diphenyl-1,1,1,3-tetradeutero-3-heptanol acetate] in an overall yield of 80%. The labeled compound showed satisfactory mass spectral (electron-impact ionization) characteristics; a multiple-ion detection analysis showed the presence of an ion equivalent to 99 ± 0.4% (n = 4) I-d_4 and 0.61 ± 0.1% I-d_0.

Extraction of I from Urine—To 5 ml of urine was added an appropriate amount of I-d_4 (typically 97 ng/ml) as an internal standard. The solution was adjusted to pH 8.5 with 1 N NH_4OH and extracted twice with 10 ml of ether. The organic fractions were combined. To this solution was added 1 ml of 0.1 N HCl; the solution was shaken for 15 min and centrifuged. The organic phase was discarded, and the aqueous phase was adjusted to pH 8.5 with 0.4 N NH_4OH and extracted twice with 4 ml of cyclohexane.

The organic fractions were combined, dried with sodium sulfate, and filtered. Then the filtrate was evaporated to dryness at 40° under a gentle stream of nitrogen. The residue was taken up in 20 μl of benzene, and an aliquot was injected into the GLC–mass spectrometer for selective ion monitoring. Recovery of I, added to control urine, was studied at the 20-ng/ml level.

Instrumentation—A magnetic sector, single-focusing mass spectrometer[9] interfaced with a gas chromatograph and equipped with a multiple-ion detector/peak matcher accessory was used (7, 8). GLC was performed on a 1.8-m glass column (2 mm i.d.). The column was silanized with 5% dimethyldichlorosilane in toluene, packed with 1.5% OV-1 on 100–200-mesh Gas Chrom Q, and conditioned for 24 hr at 280° with a flow rate of 20 ml of helium/min.

During the mass fragmentography assay, the column temperature was maintained at 185°, the flash heater was at 230°, the separator was at 235°, and the ion source was at 250°. The accelerating voltage was 3.5 kv. The ionization potential was 70 ev in the scan mode and 30 ev in the multiple-ion detector mode, and the trap current was set at 60 μamp. The magnetic field was kept constant by focusing on the background ion (column bleed) at m/e 355; the additional voltages were 173 and 130 v for measuring ion intensities at m/e 338 and 342, respectively. The retention time for I was 6 min.

RESULTS AND DISCUSSION

The mass spectrum of I (Fig. 1A) shows a molecular ion, an ion at m/e 338 (M − 15), and a base peak at m/e 72 [$CH_3CH{=}N^+(CH_3)_2$]. The fragmentation pattern is consistent with the structure and is in agreement with the spectra of similar compounds (11, 12). The mass spectrum of I-d_4 is similar to the spectrum of unlabeled isomer. Most ions are shifted to higher mass by 4 amu except the ion at m/e 72, which is a common ion from both labeled and unlabeled I.

The ion at m/e 338 is specific for I (m/e 342 for I-d_4) and is not observed in the electron-impact ionization spectra of methadone, methadone metabolites, and known metabolites of α-l-acetylmethadone (6, 13–15). Consequently, I was quantitated by measuring the ion intensities at m/e 338 and 342.

Control urine samples subjected to the described procedure for I showed no significant background ions at m/e 338 and 342. Known amounts of I along with the internal standard I-d_4 in "fixed" amount were added to control urine and processed as already described. Analysis of the data (Fig. 2) gave a slope of 0.98 ± 0.02 and an intercept of 0.15 ± 0.2

[1] The International Nonproprietary Name is α-l-acetylmethadol.
[2] Gift from Dr. K. Verebey, N.Y. State Department Drug Addiction Control Commission, Brooklyn, N.Y.
[3] ICN Pharmaceuticals, Plainview, N.Y.
[4] Fisher Scientific Co., Pittsburgh, Pa.
[5] Kimble, Owens, Illinois.
[6] Pyrex 8084.
[7] Lined with Teflon (Dupont).
[8] Gift from Dr. J. C. Hsia, University of Toronto, Toronto, Canada.
[9] LKB 9000, LKB, Stockholm, Sweden.

0022-3549/78/1000-1483$01.00/0
© 1978, American Pharmaceutical Association

Table I—Urinary I Levels after Injection of 15 mg iv in a Rabbit [a]

Sample	Hours	I, ng/ml	Total I, μg
1	5.5	384.6 ± 4.5[b]	13.944
2	27.0	269.8 ± 5.3	20.774
3	51.5	332.7 ± 4.92	22.956
4	75.0	74.0 ± 3.10	3.700
5	101.5	6.0 ± 0.75	0.420
6	168.5	13.0 ± 0.55	0.975
7	216.5	12.2 ± 0.54	0.817

[a] At varying intervals during 9 days, seven urine specimens (1–7) were obtained following administration of 15 mg iv of I hydrochloride to a 6-kg rabbit. [b] Mean of duplicate determinations.

ng. These data affirm a linear relationship between the ion intensity ratios (*m/e* 338/342) and the concentration of I in the biological fluid and exclude any significant isotopic fractionation during extraction, GLC column adsorption, and the fragmentation process.

Five samples of control urine containing 20 ng of I/ml were analyzed by this method with 22 ng of I-d_4/ml as the internal standard. The result for these samples was 19.3 ± 0.7 ng. These samples were assayed in duplicate; exactly the same amounts were taken in this set as in the previous experiment, but the internal standards were added after the extraction. The recoveries for these samples, based on comparison of the ion intensity

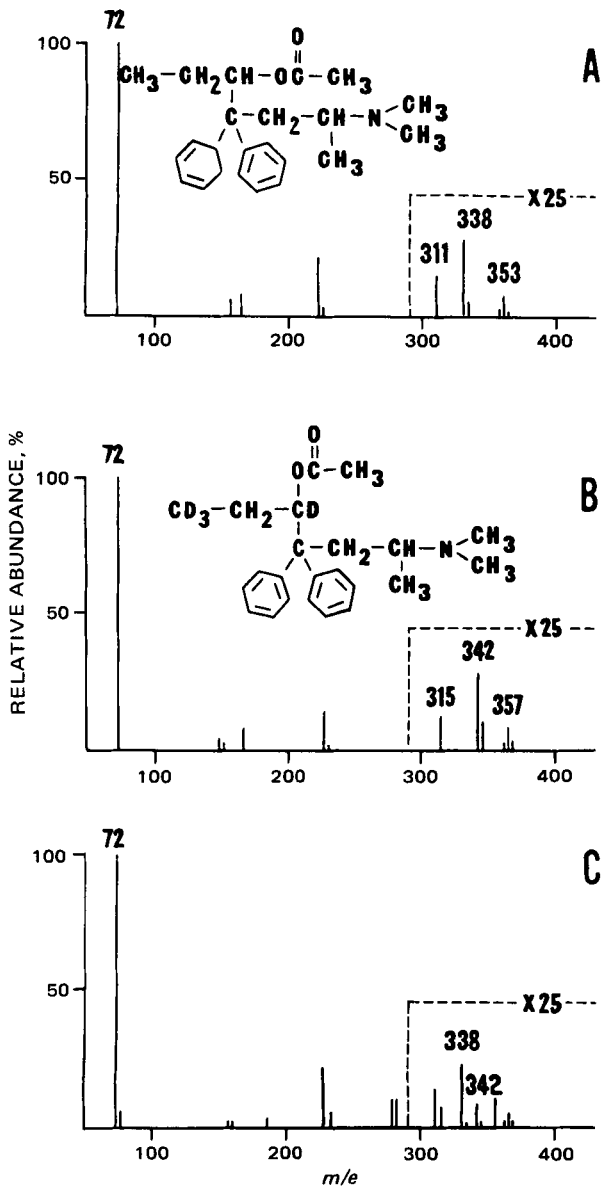

Figure 1—*Electron ionization (70 ev) mass spectrum of I (A), I-*d_4 *(B), and I in urine extract along with added I-*d_4 *(C).*

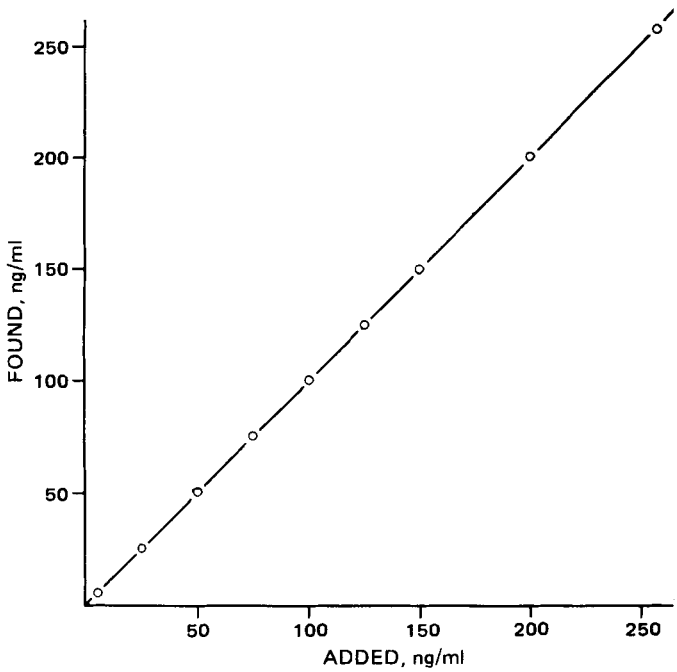

Figure 2—*Curve relating amount of I (0–250 ng) added to control urine versus the amounts found using the method described. For these samples, 97 ng of I-*d_4*/ml was used as the internal standard.*

ratios of the two sets, were 82 ± 8% (*m/e* 338/342). The variable recoveries observed are expected in the field of trace analysis and are attributed to variable glassware and GLC column adsorption. The use of I-d_4 as an internal standard in the assay presented here circumvents these problems.

A number of experiments were performed on rabbits[10] to determine urinary excretion after a single intravenous dose. In a typical experiment, a 6-kg rabbit was given 15 mg iv of I hydrochloride in water. Urine was collected by catherization periodically, starting at 5.5 hr. The last sample was collected 216 hr after the injection. Aliquots of urine samples were taken, appropriate amounts of the internal standard were added, and the samples were processed as described. The mass chromatograms (Fig. 3) at *m/e* 338/342 obtained from these samples show clean, symmetrical peaks and were used for analysis. The practical sensitivity of the assay in its current form is about 10 ng/ml of urine; furthermore, the assay is specific. Assay specificity was confirmed by a complete mass spectrum

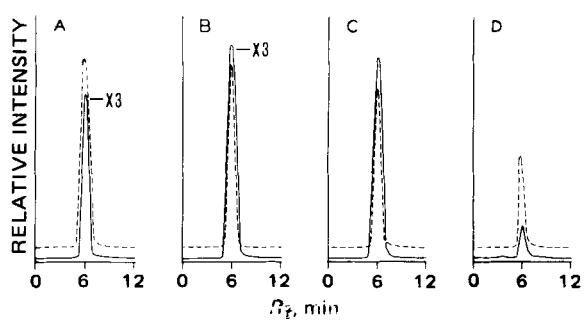

Figure 3—*Selective ion chromatograms for I (—,* m/e *338) along with I-*d_4 *(– –,* m/e *342). A: Urine was obtained 27 hr after the dose. The internal standard I-*d_4 *(*m/e *342) concentration was 97 ng/ml, and the I concentration was 269.8 ng/ml. B: Urine was obtained 51.5 hr after the dose. The internal standard I-*d_4 *(*m/e *342) concentration was 97 ng/ml, and I (*m/e *338) concentration was 332.7 ng/ml. C: Urine was obtained 75 hr after the dose. The internal standard I-*d_4 *(*m/e *342) concentration was 68 ng/ml, and the I (*m/e *338) concentration was 74 ng/ml. D: Urine was obtained 168.5 hr after the dose. The internal standard I-*d_4 *(*m/e *342) concentration was 39 ng/ml, and the I (*m/e *338) concentration was 13 ng/ml.*

[10] White New Zealand.

of the material (Fig. 1C) in the biological extract with added internal standard.

Table I shows the urinary analysis of I in the rabbit as a function of time. The cumulative urinary excretion indicates the half-life of excretion of the intact drug to be approximately 15 hr. Significantly, the animal excreted less than 1% of the drug in its native form. Evidently, its long acting characteristic must be attributed to its biotransformation into active metabolites.

REFERENCES

(1) R. E. Billing and R. E. McMahon, *Fed. Proc. Abstr.*, **32**, 764 (1973).

(2) R. N. Booher, *J. Med. Chem.*, **18**, 266 (1975).

(3) J. H. Jaffe and E. C. Senay, *J. Am. Med. Assoc.*, **216**, 1303 (1971).

(4) A. Zaks, M. Fink, and A. M. Freedman, *ibid.*, **220**, 811 (1972).

(5) G. L. Henderson, B. K. Wilson, and D. H. M. Lau, *Clin. Pharmacol. Ther.*, **21**, 16 (1977).

(6) M. M. Kochhar, P. P. Davidson, and R. S. Bhushan, *Res. Commun. Chem. Pathol. Pharmacol.*, **16**, 251 (1977).

(7) C. G. Hammar, B. Holmstedt, and R. Ryhage, *Anal. Biochem.*, **25**, 530 (1968).

(8) B. Holmstedt and L. Palmer, *Adv. Biochem. Psychopharmacol.*, **7**, 1 (1973).

(9) H. C. Brown and K. Ichikawa, *J. Am. Chem. Soc.*, **84**, 373 (1962).

(10) W. Steglich and G. Hofle, *Angew. Chem. Int. Ed.*, **8**, 981 (1969).

(11) H. R. Sullivan, S. E. Smits, S. L. Due, R. E. Booher, and R. B. McMahon, *Life Sci.*, **11**, 1093 (1972).

(12) H. R. Sullivan, S. L. Due, and R. E. McMahon, *Res. Commun. Chem. Pathol. Pharmacol.*, **6**, 1072(1973).

(13) H. R. Sullivan, F. J. Marshall, R. E. McMahon, E. Anggard, L. M. Gunne, and J. H. Holmstrand, *Biomed. Mass Spectrom.*, **2**, 197 (1975).

(14) H. R. Sullivan, S. L. Due, and R. E. McMahon, *J. Am. Chem. Soc.*, **94**, 4050 (1972).

(15) A. Pohland, H. E. Boaz, and H. R. Sullivan, *J. Med. Chem.*, **14**, 194 (1971).

ACKNOWLEDGMENTS

Supported by Grant DA 00327 and by the Department of Mental Hygiene, State of New York, Office of Research.

The authors thank Sidney Bernstein for the illustrations.

Color Analysis of Dextrose Solutions Using a Color Difference Meter

RAYMOND W. JURGENS, Jr.ˣ, JOSEPH P. LACZ, and ALAN D. WELCO

Received September 19, 1977, from *Pharmaceutical Product Development, McGaw Laboratories, Santa Ana, CA 92711.* Accepted for publication February 14, 1978.

Abstract□ A method for quantitating color measurements in dextrose solutions by using a color difference meter is described. This method was shown to correlate well with standard American Public Health Association (APHA) color measurements. A mathematical relationship was developed relating yellowness index values to APHA numbers as described in the USP for dextrose solutions. This relationship was tested by comparing the results from standard APHA color tests on laboratory samples of autoclaved dextrose solutions to APHA numbers calculated from yellowness index values for the same samples.

Keyphrases □ Dextrose solutions—color analysis, color difference meter compared to standard measurements □ Color—analysis, dextrose solutions, color difference meter compared to standard measurements

After sterilization, dextrose solutions may exhibit a brownish-yellow color as a result of dextrose degradation (1, 2). Currently, color measurement in many pharmaceutical solutions is performed by the American Public Health Association (APHA) method, which utilizes a concentration gradient of platinum–cobalt solutions in 100-ml Nessler tubes (3). The sample solution color can be measured by matching the color of the sample tube with one corresponding standard. Color is reported as parts per million of platinum–cobalt.

This study examined the correlation of yellowness index values, determined by a color difference meter[1], to the standard APHA colors. The practical use of the yellowness index for color evaluation of pharmaceutical dextrose solutions also was demonstrated. The advantage of this technique is that it allows an objective quantitation of color.

EXPERIMENTAL

A color difference meter, standardized using a calibrated white plate[2], was used for color measurement. Calibration values were derived by direct comparison to master standards traceable to measurements at the National Bureau of Standards.

A 6.4-cm optical cell[3] was the sample holder for each solution. The cell was filled with 80 ml of solution and placed over the 5.1-cm aperture of the detection head. A white reflective plate was placed over the cell; then a lightproof cover was placed over the detection head to exclude any ambient light. Light was transmitted through the bottom of the cell and reflected off the reflector plate into the detector head where an optical sensor transmitted a signal to the signal processor. The color meter then presented the color of solutions as four variables: L (brightness), a (green and red), b (blue and yellow), and YI (yellowness index) (4, 5). Color values were displayed by a digital readout to one decimal place.

Color values for a concentration gradient of platinum–cobalt solutions (0–80 ppm) were obtained using a color difference meter. Three readings were taken at each concentration level.

The practical application of the color difference meter was demonstrated through a comparison of observed APHA values for various autoclaved dextrose solutions to mathematically derived APHA values calculated from YI values. Solutions were made from various lots of dextrose[4] and were tested by USP methods (6). The particular solutions were chosen at random to represent various products with potential color variation.

The colors of five solutions of different dextrose concentrations were determined by six observers using the APHA method. The colors of these

[1] D25L-2, Hunter Associates Laboratory, Fairfax, Va.

[2] C2-6664, Hunter Associates Laboratory, Fairfax, Va.

[3] Agtron 13851210, Hunter Associates Laboratory, Fairfax, Va.

[4] Corn Products, Englewood Cliffs, NJ 07632.

0022-3549/78/1000-1485$01.00/0

© 1978, American Pharmaceutical Association

of the material (Fig. 1C) in the biological extract with added internal standard.

Table I shows the urinary analysis of I in the rabbit as a function of time. The cumulative urinary excretion indicates the half-life of excretion of the intact drug to be approximately 15 hr. Significantly, the animal excreted less than 1% of the drug in its native form. Evidently, its long acting characteristic must be attributed to its biotransformation into active metabolites.

REFERENCES

(1) R. E. Billing and R. E. McMahon, *Fed. Proc. Abstr.*, **32**, 764 (1973).

(2) R. N. Booher, *J. Med. Chem.*, **18**, 266 (1975).

(3) J. H. Jaffe and E. C. Senay, *J. Am. Med. Assoc.*, **216**, 1303 (1971).

(4) A. Zaks, M. Fink, and A. M. Freedman, *ibid.*, **220**, 811 (1972).

(5) G. L. Henderson, B. K. Wilson, and D. H. M. Lau, *Clin. Pharmacol. Ther.*, **21**, 16 (1977).

(6) M. M. Kochhar, P. P. Davidson, and R. S. Bhushan, *Res. Commun. Chem. Pathol. Pharmacol.*, **16**, 251 (1977).

(7) C. G. Hammar, B. Holmstedt, and R. Ryhage, *Anal. Biochem.*, **25**, 530 (1968).

(8) B. Holmstedt and L. Palmer, *Adv. Biochem. Psychopharmacol.*, **7**, 1 (1973).

(9) H. C. Brown and K. Ichikawa, *J. Am. Chem. Soc.*, **84**, 373 (1962).

(10) W. Steglich and G. Hofle, *Angew. Chem. Int. Ed.*, **8**, 981 (1969).

(11) H. R. Sullivan, S. E. Smits, S. L. Due, R. E. Booher, and R. B. McMahon, *Life Sci.*, **11**, 1093 (1972).

(12) H. R. Sullivan, S. L. Due, and R. E. McMahon, *Res. Commun. Chem. Pathol. Pharmacol.*, **6**, 1072(1973).

(13) H. R. Sullivan, F. J. Marshall, R. E. McMahon, E. Anggard, L. M. Gunne, and J. H. Holmstrand, *Biomed. Mass Spectrom.*, **2**, 197 (1975).

(14) H. R. Sullivan, S. L. Due, and R. E. McMahon, *J. Am. Chem. Soc.*, **94**, 4050 (1972).

(15) A. Pohland, H. E. Boaz, and H. R. Sullivan, *J. Med. Chem.*, **14**, 194 (1971).

ACKNOWLEDGMENTS

Supported by Grant DA 00327 and by the Department of Mental Hygiene, State of New York, Office of Research.

The authors thank Sidney Bernstein for the illustrations.

Color Analysis of Dextrose Solutions Using a Color Difference Meter

RAYMOND W. JURGENS, Jr.ˣ, JOSEPH P. LACZ, and ALAN D. WELCO

Received September 19, 1977, from *Pharmaceutical Product Development, McGaw Laboratories, Santa Ana, CA 92711.* Accepted for publication February 14, 1978.

Abstract□ A method for quantitating color measurements in dextrose solutions by using a color difference meter is described. This method was shown to correlate well with standard American Public Health Association (APHA) color measurements. A mathematical relationship was developed relating yellowness index values to APHA numbers as described in the USP for dextrose solutions. This relationship was tested by comparing the results from standard APHA color tests on laboratory samples of autoclaved dextrose solutions to APHA numbers calculated from yellowness index values for the same samples.

Keyphrases □ Dextrose solutions—color analysis, color difference meter compared to standard measurements □ Color—analysis, dextrose solutions, color difference meter compared to standard measurements

After sterilization, dextrose solutions may exhibit a brownish-yellow color as a result of dextrose degradation (1, 2). Currently, color measurement in many pharmaceutical solutions is performed by the American Public Health Association (APHA) method, which utilizes a concentration gradient of platinum–cobalt solutions in 100-ml Nessler tubes (3). The sample solution color can be measured by matching the color of the sample tube with one corresponding standard. Color is reported as parts per million of platinum–cobalt.

This study examined the correlation of yellowness index values, determined by a color difference meter[1], to the standard APHA colors. The practical use of the yellowness index for color evaluation of pharmaceutical dextrose solutions also was demonstrated. The advantage of this technique is that it allows an objective quantitation of color.

EXPERIMENTAL

A color difference meter, standardized using a calibrated white plate[2], was used for color measurement. Calibration values were derived by direct comparison to master standards traceable to measurements at the National Bureau of Standards.

A 6.4-cm optical cell[3] was the sample holder for each solution. The cell was filled with 80 ml of solution and placed over the 5.1-cm aperture of the detection head. A white reflective plate was placed over the cell; then a lightproof cover was placed over the detection head to exclude any ambient light. Light was transmitted through the bottom of the cell and reflected off the reflector plate into the detector head where an optical sensor transmitted a signal to the signal processor. The color meter then presented the color of solutions as four variables: L (brightness), a (green and red), b (blue and yellow), and YI (yellowness index) (4, 5). Color values were displayed by a digital readout to one decimal place.

Color values for a concentration gradient of platinum–cobalt solutions (0–80 ppm) were obtained using a color difference meter. Three readings were taken at each concentration level.

The practical application of the color difference meter was demonstrated through a comparison of observed APHA values for various autoclaved dextrose solutions to mathematically derived APHA values calculated from YI values. Solutions were made from various lots of dextrose[4] and were tested by USP methods (6). The particular solutions were chosen at random to represent various products with potential color variation.

The colors of five solutions of different dextrose concentrations were determined by six observers using the APHA method. The colors of these

[1] D25L-2, Hunter Associates Laboratory, Fairfax, Va.

[2] C2-6664, Hunter Associates Laboratory, Fairfax, Va.

[3] Agtron 13851210, Hunter Associates Laboratory, Fairfax, Va.

[4] Corn Products, Englewood Cliffs, NJ 07632.

0022-3549/78/1000-1485$01.00/0

© 1978, American Pharmaceutical Association

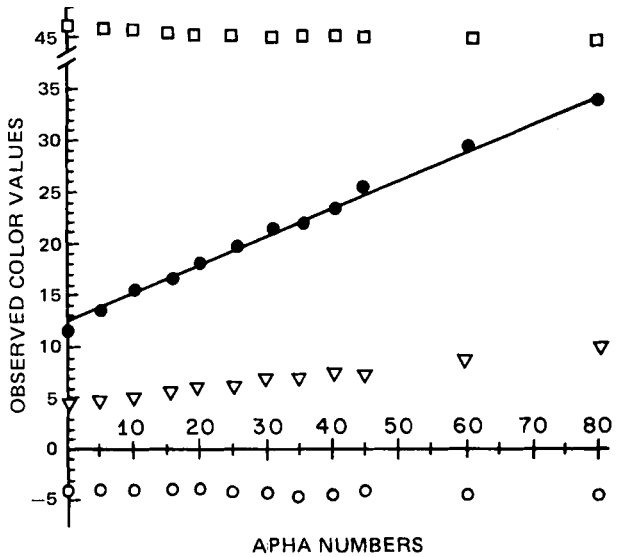

Figure 1—*Standard curve represents the relationship of L (□), a (○), b (▽), and YI (●) observed values to APHA numbers for platinum–cobalt solutions. The y intercept corresponds to the APHA number of the water standard (0 ppm platinum–cobalt). The slope of the YI line is 0.282, and the correlation coefficient is 0.9957.*

same five solutions were then determined using the color difference meter. The APHA values were calculated for these dextrose solutions and compared to the average observed APHA values.

RESULTS AND DISCUSSION

The L, a, b, and YI values were compared to the APHA numbers using regression analysis (Fig. 1). All color values had good correlation with the APHA colors (L, $r = 0.91$; a, $r = 0.77$; b, $r = 0.99$; and YI, $r = 0.99$). The variance of the points in L, a, and b values showed that these values were inappropriate for analytical use. The YI values, however, had a small individual point variance compared to differences between points. For this reason, the YI value, with the greatest correlation coefficient ($r = 0.99$), was selected for this study.

The relationship of YI to APHA color was linear over the entire range of the platinum–cobalt solutions studied. The following mathematical equation relating YI to APHA color was derived:

$$\text{APHA number} = \frac{[YI_s - YI_0]}{m} \qquad \text{(Eq. 1)}$$

Table I—Comparison of Calculated APHA Values to Observed APHA Numbers

Solution[a]	APHA Values Observed (Mean ± *SD*)[b]	Range of Individual Observations	APHA Values Determined by Yellowness Index	Range between Sample Readings[c]
5% Dextrose	3.0 ± 1.8	2–4	0.9	0.7–1.1
5% Dextrose in lactated Ringers	4.9 ± 1.5	2.5–7	4.0	3.9–4.1
30% Dextrose (diluted from 60%)	15.1 ± 2.3	12–18	12.9	Equal
25% Dextrose (diluted from 50%)	19.3 ± 2.3	17–23	20.7	Equal
60% Dextrose	32.1 ± 1.7	30–35	27.0	Equal
50% Dextrose	38.9 ± 2.1	37–42	40.0	38.4–41.7

[a] The solutions represent different lots of dextrose. [b] The average of six different observers. [c] Each solution was read twice at different times on the color difference meter.

where YI_s equals the YI value of the sample solution, YI_0 equals the YI value of a distilled water sample, and m corresponds to the slope of a line describing the relationship.

A comparison of APHA numbers calculated from the color difference meter and APHA numbers visually observed from various dextrose solutions is shown in Table I. The correlation of the observed APHA values with the calculated values indicated a 97% correlation ($r = 0.97$). The 50 and 60% dextrose solutions were diluted 1:1 to see if dilution of the solutions would result in a corresponding dilution of color and, as indicated in Table I, it did. Examination of the range of individual observations revealed that when six different observers graded the solutions using the APHA visual technique, the observed values differed considerably (approximately 5 ppm). Smaller differences were observed when the APHA values were determined from the yellowness index.

REFERENCES

(1) W. T. Wing, *J. Pharm. Pharmacol.*, **12**, 191T (1960).

(2) N. E. Webb, Jr., and G. J. Sperandio, *J. Am. Pharm. Assoc., Sci. Ed.*, **47**, 101 (1958).

(3) "Annual Book of ASTM Standards," parts 27 and 29, American Society for Testing Materials, Philadelphia, Pa., 1976, 01209-69.

(4) R. S. Hunter, "The Measurement of Appearance," Wiley, New York, N.Y., 1975, pp. 122, 123.

(5) "Annual Book of ASTM Standards," part 30, American Society for Testing Materials, Philadelphia, Pa., 1976, E450-75.

(6) "The United States Pharmacopeia," 19th rev., Mack Publishing Co., Easton, Pa., 1975, p. 765.

Evaluation of Commercial Ginseng Products

LAWRENCE E. LIBERTI and ARA DER MARDEROSIAN ˣ

Received December 5, 1977, from the *Department of Biological Sciences, Philadelphia College of Pharmacy and Science, Philadelphia, PA 19104.* Accepted for publication February 21, 1978.

Abstract □ The variation in panaxoside content of roots and commercial products of *Panax ginseng* and *P. quinquefolium* was evaluated by a new spectrodensitometric TLC method. The method is rapid and applicable to all commercial products, and it has a relative standard deviation of 6.4%. Panaxoside patterns of slurry-filled capsules and root extracts most closely resembled those of whole roots. Tablets did not contain detectable panaxosides while teas and granules for infusion yielded only low concentrations. The wide variation among these products indicates the need for more rigid control.

Keyphrases □ Ginseng—panaxoside content of various commercial products, TLC analysis □ Panaxoside content—ginseng, various commercial products, TLC analysis □ TLC—analysis, panaxoside content of various commercial ginseng products □ *Panax ginseng* and *P. quinquefolium*—panaxoside content of various commercial products, TLC analysis

A resurgence in the use of folkloric medicine has prompted a return to traditional herbal remedies. Ginseng, *Panax quinquefolium* L. and *P. ginseng* C. A. Meyer (Araliaceae), is receiving much attention. Ginseng, whose characteristic taste is disagreeable, is available as the dried root, which is chewed, taken as tea, or made into an elixir. It is also available as capsules, tablets, instant teas, extracts, and a line of cosmetics. The popularity of ginseng is attributed to the "adaptogenic" effect (stress protective) of the saponin (panaxoside) content (1), which appears to exert an antistress and rehabilitative action in test animals. Ginseng is also heavily promoted as an aphrodisiac.

Ginseng is not included in the Generally Recognized as Safe (GRAS) list, nor has the government set guidelines for the manufacture and quality control of commercial ginseng preparations. Seizures of ginseng tablets by the Food and Drug Administration as an unsafe food additive when no regulations describe conditions for safe ingestion (2) press the need for standardizing ginseng products.

The TLC assay in this report was developed as a rapid screen for the evaluation of the panaxoside content of the hundreds of commercially available ginseng products.

BACKGROUND

Although ginseng has been used for centuries, the problem of evaluating commercial ginseng products is recent. Ginseng has not been an official compendial drug in the United States since the U.S. Dispensatory dropped it after noting that the "extraordinary properties and medical virtues formerly ascribed to ginseng had no other existence than in the imagination of the Chinese" (3). In light of both traditional effectiveness and recent experiments supporting the adaptogenic effect of the panaxosides (1), ginseng is included in several modern compendia.

Official compendia (4–6) that include ginseng do not evaluate ginseng root in terms of chemical constituents but by physical and microscopic characteristics. The Russian pharmacopeia (7) lists a "reaction for quality" of ginseng roots, involving a subjective evaluation of color reaction and precipitate formation over 24 hr following the addition of silver nitrate.

Only recently have more sophisticated attempts been made to evaluate the saponin content of ginseng roots and products. Nine saponins (panaxosides Ro, Rb1, Rb2, Rc, Rd, Re, Rf, Rg1, and Rg2) are present in varying amounts in fresh ginseng roots, but their isolation with good recovery following recrystallization is difficult (8).

Table I—Determination of Recovery Rate (Theoretical Amount Present, 0.40 μg)

Sample	Amount Determined by TLC Method, μg	Recovery, %
Rb2	0.38	95
Rd	0.39	97
Rg1	0.38	95
	Average	96

Table II—Comparison of TLC and Spectrophotometric Methods

Sample	Total Milligrams of Panaxoside per 250-mg Sample: Spectrophotometric Method	TLC Method
1	3.0	3.3
7	2.2	1.9
10	None	None
13	1.6	1.7
15	None	None
16	0.5	None
21	1.0	1.0

A GLC method was reported for the evaluation of ginseng roots and extracts (9). The assay, based on the fact that the hydrolysis of the saponins yields panaxadiol, panaxatriol, and oleanolic acid genins, is incapable of quantitatively or qualitatively evaluating the individual panaxosides. A colorimetric reaction with vanillin–sulfuric acid was proposed for the spectrophotometric determination of total saponin content (10). Methods developed using rod-TLC (11) and countercurrent chromatography (12) for the quantitative and qualitative evaluation of individual panaxosides are reliable but not readily available for the large-scale screening of commercial products. Therefore, the following TLC method is proposed.

EXPERIMENTAL

Apparatus—A spectrodensitometer[1] was coupled to a density computer[2]. Plates[3] were scanned at 600 nm using a slit aperture of 2 cm and sensitivity of 0.4 absorbance unit.

Standard Solutions—Standard solutions of panaxosides Ro, Rb1, Rb2, Rc, Rd, Re, Rf, Rg1, and Rg2 were each prepared by dissolving the panaxoside in methanol to yield a final concentration of 1 mg/10 ml. All stock solutions were refrigerated.

Detection Reagent—A solution of 1 ml of *p*-anisaldehyde and 1 ml of concentrated sulfuric acid diluted to 100 ml with methanol was prepared fresh daily. Plates were heated for 15 min at 130° following spraying.

Sample Solution Preparation—After the contents of the dosage form were weighed, 250 mg was transfered to a 10-ml flask to which 5 ml of water had been added. The solution was shaken for 30 min. The flask was then filled to 10 ml, and shaking was continued for an additional 30 min. The solution was filtered through a 70-mm paper.

The first 3–4 ml of filtrate was discarded. The next 5-ml aliquot was transferred to a 10-ml flask to which a 5-ml aliquot of water-saturated 1-butanol was added. The flask was shaken gently for 30 min. Samples were drawn from the 1-butanol layer and applied as 8-μl spots.

Plate Structure and TLC Assay—Each scored plate was spotted on alternate lanes. The first 10 lanes were used for the Beer's law calibration. Samples of 2, 3, 4, 5, and 8 μl of standard Re were spotted. Samples for analysis were spotted alternately in quadruplicate in the last eight lanes.

[1] Schoeffel model SD-3000.
[2] SDC-300.
[3] Silica gel G 250 μm (Analtech) activated at 130° for 15 min.

0022-3549/78/1000-1487$01.00/0
© 1978, American Pharmaceutical Association

Table III—Comparison of Individual and Total Panaxoside Content of Roots and Commercial Products

Sample[a]	Individual Panaxoside Concentration, mg									Total Panaxoside Concentration per 250-mg Sample, mg
	Ro	Rb1	Rb2	Rc	Rd	Re	Rf	Rg1	Rg2	
SA-1	—	0.79	—	0.58	0.50	0.29	0.53	—	0.57	3.26
SA-2	—	1.2	3.7	—	—	1.5	—	1.2	—	7.6
SA-3	—	1.8	—	2.2	0.38	0.67	1.8	—	—	6.85
SA-4	No detectable panaxosides									
SA-5	0.49	0.26	—	0.29	0.42	0.13	0.19	—	—	1.78
SA-6	0.36	0.80	0.18	0.32	—	—	0.27	—	—	1.93
SA-7	—	0.86	—	0.69	—	—	—	—	0.31	1.86
SA-8	—	0.30	—	—	0.77	—	0.32	—	—	1.39
SA-9	No detectable panaxosides									
SA-10	No detectable panaxosides									
SA-11	No detectable panaxosides									
SA-12	0.42	0.45	0.10	0.26	—	0.17	0.40	—	—	1.8
SA-13	0.42	0.22	—	0.44	0.31	0.10	0.17	—	—	1.66
SA-14	No detectable panaxosides									
SA-15	No detectable panaxosides									
SA-15a	—	0.15	0.16	0.16	0.10	0.10	0.30	—	—	0.97
SA-16	No detectable panaxosides									
SA-17	—	0.36	—	—	—	—	0.26	—	0.29	0.91
SA-18	No detectable panaxosides									
SA-19	0.33	0.27	—	—	0.27	—	—	—	—	0.87
SA-20	—	0.26	—	—	—	—	—	—	—	0.26
SA-21	—	0.45	—	—	—	0.58	—	—	—	1.03
SA-22	—	—	—	—	—	0.26	—	—	—	0.26
SA-23	—	—	—	—	—	0.60	—	—	—	0.60

[a] Samples 1–6 were roots, Samples 7 and 8 were slurry-filled soft gelatin capsules, Samples 9–11 were tablets, Samples 12 and 13 were dry-filled capsules, Samples 14–15a were extracts, Samples 16–22 were granules and powders for water infusion, and Sample 23 was ginseng-containing soap.

Plates were single developed to 15 cm in methanol–chloroform–1-butanol (1:1:1), dried, sprayed, heated, and scanned.

A Beer's law plot was developed for each plate by evaluating the area under the curve (*AUC*) of the five reference spots. Plot linearity was evaluated with a linear least-squares weighted fit program. The average *AUC* values for the four sample runs were used for the calculation of individual panaxoside concentrations.

Recovery Rate—A mixture of 5 ml each of Rb2, Rd, and Rg1 stock solutions was used. A 10-ml aliquot of water-saturated 1-butanol was added to the mixture, which was then shaken for 30 min. Samples were drawn from the 1-butanol layer. Lanes were spotted with 8-μl samples (equivalent to 0.4 μg of each panaxoside/8 μl). The plates were developed and scanned, and the amount recovered was determined (Table I).

Limits of Detection—A standard solution of Re was spotted on TLC plates in the following concentrations: 0.05, 0.1, 0.2, 0.4, 0.8, 1.6, 2.0, 3.0, 4.0, and 6.4 μg. Plates were developed and scanned, and plot linearity was evaluated as described previously.

Microscopic Evaluation—Each sample was observed under low and high powers for the presence of characteristic plant parts. Tablets were triturated lightly. All slides were cleared with chloral hydrate solution; teas and powders for infusion were suspended with a drop of water and observed before and after dissolution.

Comparison to Spectrophotometric Method—The spectrophotometric method of Hiai *et al.* (10) is a rapid means of evaluating total panaxoside content. To 0.1 ml of aqueous solutions of each sample, 0.5 ml of 8% vanillin in ethanol and 5 ml of 72% H_2SO_4 were added and mixed well in an ice water bath. The tubes were warmed at 60° for 10 min and then cooled in an ice bath. The absorbance of the reaction mixture was read[4] at 544 nm against a blank solution, and the amount present was determined by molar ratios.

RESULTS AND DISCUSSION

Limits of Detection—The range of detection remained linear in accordance with Beer's law from 0.1 to 4.0 μg. A change in the spectrodensitometer sensitivity from 0.4 to 1.0 unit dropped the lower detectable value to 0.4 μg and included the 6.4-μg reading. Since most samples yielded panaxosides in the range of 0.1 to 1.0 μg, all readings were performed at the higher sensitivity.

A 1-butanol transfer step was incorporated to avoid the detection of free sugars in sample extracts. In this manner, glucose, glucuronic acid, sucrose, rhamnose, and arabinose [present in whole root samples (13, 14)] were not detectable upon development with *p*-anisaldehyde. Reagents with greater specificity for triterpene steroids, such as antimony(III) chloride and chlorosulfonic acid, yielded less intense spots, which conformed poorly to Beer's law upon quantitation. The lower limit of detection using these reagents was only 0.8 μg.

Microscopic Evaluation—Each sample was scanned under polarized light at 100 and 430×. Root samples of *P. ginseng*[5] and *P. quinquefolium*[6], ground lightly in a mortar and pestle, yielded pale-yellow powders with large quantities of fragmented parenchyma and an almost equal amount of fiber groups of varying sizes. Occasional calcium oxalate crystals (7) were found along with fragments of bordered pitted vessels.

The commercial products varied widely in characteristic root inclusions. Samples 7, 12, 13, and 17 yielded large quantities of parenchyma and fiber fragments. Sample 17 yielded starch granules identified by reaction with iodine. Tablets did not display characteristic root parts. Teas consisted primarily of lyophilized powders, which yielded no characteristic fragments either before or following dissolution. Calcium oxalate crystals were not found in any commercial product.

Comparison of TLC and Spectrophotometric Methods (10)—An agreement was observed between these two methods (Table II). The spectrophotometric method is a useful means of estimating total saponin content, and the TLC method quantitates both individual panaxoside content and total saponin content. The spectrophotometric assay has the disadvantage of being time dependent because of the reaction of vanillin with sugars in the test solution. The 1-butanol transfer step cleaned the sample of interfering sugars while affording a 96% recovery of panaxosides from water solution. Plate color development remained unchanged for 45 min following removal from the oven.

Product Assay—Results of the TLC assays of 24 roots and products are presented in Table III. Dried roots of *P. ginseng* and *P. quinquefolium* yielded the highest panaxoside contents, ranging from 0.5 to 3.0% of dry root weight. Dried ginseng roots generally contain 2.5% panaxoside[7], a figure that varies with root age, method of preservation, and season of harvest. Sample 4, a 60-year-old herbarium specimen ravaged by insects, yielded no panaxosides.

Soft gelatin capsules containing slurries of ground root and those containing powdered root showed total panaxoside levels comparable to dried root samples. That these samples exhibited characteristic root inclusions by microscopic evaluation supports the conclusion that their contents most closely resemble ground ginseng root. These products yielded TLC patterns similar to ground roots.

The lack of detectable panaxosides in tablet samples along with a lack of identifiable root parts in the granulation indicates that these products

[4] Hitachi-Perkin Elmer 139 UV-visible spectrophotometer.

[5] Tatra Herb Co., Morrisville, PA 19067.

[6] Authentic samples were obtained from the herbarium, Philadelphia College of Pharmacy and Science, Philadelphia, Pa.

[7] "Ginseng," Inverni Della Beffa Inc., Milan, Italy.

may be adulterated or diluted during manufacture. When the ginseng powder is reduced to 40 or 60 mesh in the granulation, microscopic evaluation becomes less confirmatory. However, panaxoside levels should still be detected. The absence of detectable amounts of panaxosides requires further investigation into the manufacturing of ginseng tablets.

Granules and powders for the preparation of ginseng water infusions yielded panaxoside levels in the low region (0.1–0.4% of product weight).

Extracts yielded surprisingly low panaxoside levels, probably because of the relatively short shelflife of the opened extracts. The cosmetic tested yielded 0.3% panaxoside, within the recommended level of 0.25–0.5% for creams and rinses (15).

The TLC pattern of the roots can be correlated with the patterns of the powder-filled capsules and extracts and, to a lesser extent, the slurry-filled soft gelatin capsules. Most roots present at least four detectable panaxosides. Six-year-old roots show more extensive patterns and may yield up to nine panaxosides. All root samples tested yielded Rb1, while four of five yielded Rc, Re, and Rf. A similar pattern was seen with the capsule and extract products.

It is difficult to explain the tremendous variation among ginseng products. The wide range of total panaxoside content may be a function of the amount of ginseng root incorporated into the product. The lack of a consistent pattern of individual panaxosides in these products requires further clarification. The possibility of panaxoside loss during the manufacture of ginseng tablets is under investigation.

In view of the high prices of these products, there is a need for regulations regarding the control of commercial ginseng products.

REFERENCES

(1) I. I. Brekman and I. V. Dardymov, *Lloydia*, **32**, 46 (1969).

(2) *Wkly. Pharm. Rep.*, **35**, 1 (1977).

(3) G. B. Wood and L. LaWall, "The Dispensatory of the United States," Lippincott, Philadelphia, Pa., 1937, p. 1393.

(4) "Pharmacopoeia Japonica," Ministry of Health and Welfare, Tokyo, Japan, 1951, p. 280.

(5) "Martindale, The Extra Pharmacopoeia," Pharmaceutical Press, London, England, 1941, p. 1371.

(6) "Pharmacopoeia of the American Institute of Homeopathy," Otis Clapp and Sons, Boston, Mass., 1941, p. 116.

(7) "The State Pharmacopoeia of the U.S.S.R., "Ministry of Health, Moscow, U.S.S.R., 1961, p. 377.

(8) S. Hiai, H. Oura, Y. Odaka, and T. Nakajima, *Planta Med.*, **28**, 363 (1975).

(9) I. Sakamoto, K. Morimoto, and O. Tanaka, *Yakugaku Zasshi*, **95**, 1456 (1975).

(10) S. Hiai, H. Oura, H. Hamanaka, and Y. Odaka, *Planta Med.*, **28**, 131 (1975).

(11) T. Namba, M. Yoshizaki, T. Tomimori, K. Kobashi, K. Mitsui, and J. Hase, *Yakugaku Zasshi*, **94**, 252 (1974).

(12) O. Yukio, O. Inoue, N. Hosokawa, and K. Hanawa, *Nagoya Nempo*, **23**, 54 (1975).

(13) T. Kaku, T. Miyata, T. Uruno, I. Sako, and A. Kinoshita, *Arzneim.-Forsch.*, **25**, 343 (1975).

(14) F. Gatriner and H. J. Vogt, *Arch. Pharm.*, **300**, 371 (1967).

(15) J. C. Chang, *Cosmet. Toiletries*, **92**, 50 (1977).

ACKNOWLEDGMENTS

The authors thank Dr. J. Shoji, Showa University, Tokyo, Japan, and Dr. S. Shibata, Meiji College of Pharmacy, Tokyo, Japan, for their help in obtaining authentic panaxoside reference samples.

Use of a Nitrogen Detector for GLC Determination of Fluorouracil in Plasma during Single- and Combined-Agent Chemotherapy

ROSEMARY E. FINCH *x, MICHAEL R. BENDING ‡, and ARIEL F. LANT *

Received January 3, 1978, from the **Department of Therapeutics and the* ‡*Medical Unit, Westminster Hospital, London, SW1P 2AP, England.* Accepted for publication February 24, 1978.

Abstract □ A GLC assay for fluorouracil was developed and used to monitor plasma drug levels in patients on both single- and combined-agent chemotherapy. Fluorouracil is extracted from plasma, derivatized by flash methylation, and estimated using a thermionic nitrogen–phosphorus detector. The GLC determination was accurate at concentrations as low as 0.1 μg/ml of human plasma. Other drugs commonly used in combination with fluorouracil did not interfere with the assay.

Keyphrases □ Fluorouracil—nitrogen-detector GLC analysis in plasma □ GLC, nitrogen detector—analysis, fluorouracil in plasma □ Antineoplastic agents—fluorouracil, nitrogen-detector GLC analysis in plasma

Since its synthesis in 1957, fluorouracil has been used extensively as an antimetabolite in the treatment of cancer, particularly of the breast and GI tract (1). More recently, it has been widely used in multiple-agent chemotherapy (2, 3). Despite this continued usage, the clinical response is often inconsistent, and a variety of empirical dosage schedules are still employed. Therefore, to optimize drug schedules for individual patients, it would be useful to relate the time course of fluorouracil in plasma, both alone and in combination with other cytotoxic drugs, to clinical response.

Most methods for measuring fluorouracil employ GLC techniques (4–6) or assay by analysis of microbial kinetics (7). The present study describes a GLC method with nitrogen detection capable of measuring fluorouracil in combination with other cytotoxic agents without interference.

EXPERIMENTAL

Materials—Fluorouracil[1] was used both in the solid form and as a solution for injection. Thymine[2], the internal standard, was obtained as the anhydrous solid. Trimethylanilinium hydroxide[3], 0.2 *M* in methanol, was the derivatizing agent. Buffer salts[4] and solvents[4] were analytical reagent grade.

GLC Conditions—A gas chromatograph[5] equipped with a thermionic

[1] Roche Products Ltd., Welwyn Garden City, Herts., England.
[2] Sigma Chemical Co. Ltd., Kingston-upon-Thames, Surrey, England.
[3] Pierce and Warriner (UK) Ltd., Chester, Cheshire, England.
[4] B.D.H. Chemicals Ltd., Poole, Dorset, England.
[5] Model F30, Series III, Perkin-Elmer Ltd., Beaconsfield, Bucks, England.

0022-3549/78/1000-1489$01.00/0

© 1978, American Pharmaceutical Association

may be adulterated or diluted during manufacture. When the ginseng powder is reduced to 40 or 60 mesh in the granulation, microscopic evaluation becomes less confirmatory. However, panaxoside levels should still be detected. The absence of detectable amounts of panaxosides requires further investigation into the manufacturing of ginseng tablets.

Granules and powders for the preparation of ginseng water infusions yielded panaxoside levels in the low region (0.1–0.4% of product weight).

Extracts yielded surprisingly low panaxoside levels, probably because of the relatively short shelflife of the opened extracts. The cosmetic tested yielded 0.3% panaxoside, within the recommended level of 0.25–0.5% for creams and rinses (15).

The TLC pattern of the roots can be correlated with the patterns of the powder-filled capsules and extracts and, to a lesser extent, the slurry-filled soft gelatin capsules. Most roots present at least four detectable panaxosides. Six-year-old roots show more extensive patterns and may yield up to nine panaxosides. All root samples tested yielded Rb1, while four of five yielded Rc, Re, and Rf. A similar pattern was seen with the capsule and extract products.

It is difficult to explain the tremendous variation among ginseng products. The wide range of total panaxoside content may be a function of the amount of ginseng root incorporated into the product. The lack of a consistent pattern of individual panaxosides in these products requires further clarification. The possibility of panaxoside loss during the manufacture of ginseng tablets is under investigation.

In view of the high prices of these products, there is a need for regulations regarding the control of commercial ginseng products.

REFERENCES

(1) I. I. Brekman and I. V. Dardymov, *Lloydia*, **32**, 46 (1969).

(2) *Wkly. Pharm. Rep.*, **35**, 1 (1977).

(3) G. B. Wood and L. LaWall, "The Dispensatory of the United States," Lippincott, Philadelphia, Pa., 1937, p. 1393.

(4) "Pharmacopoeia Japonica," Ministry of Health and Welfare, Tokyo, Japan, 1951, p. 280.

(5) "Martindale, The Extra Pharmacopoeia," Pharmaceutical Press, London, England, 1941, p. 1371.

(6) "Pharmacopoeia of the American Institute of Homeopathy," Otis Clapp and Sons, Boston, Mass., 1941, p. 116.

(7) "The State Pharmacopoeia of the U.S.S.R., "Ministry of Health, Moscow, U.S.S.R., 1961, p. 377.

(8) S. Hiai, H. Oura, Y. Odaka, and T. Nakajima, *Planta Med.*, **28**, 363 (1975).

(9) I. Sakamoto, K. Morimoto, and O. Tanaka, *Yakugaku Zasshi*, **95**, 1456 (1975).

(10) S. Hiai, H. Oura, H. Hamanaka, and Y. Odaka, *Planta Med.*, **28**, 131 (1975).

(11) T. Namba, M. Yoshizaki, T. Tomimori, K. Kobashi, K. Mitsui, and J. Hase, *Yakugaku Zasshi*, **94**, 252 (1974).

(12) O. Yukio, O. Inoue, N. Hosokawa, and K. Hanawa, *Nagoya Nempo*, **23**, 54 (1975).

(13) T. Kaku, T. Miyata, T. Uruno, I. Sako, and A. Kinoshita, *Arzneim.-Forsch.*, **25**, 343 (1975).

(14) F. Gatriner and H. J. Vogt, *Arch. Pharm.*, **300**, 371 (1967).

(15) J. C. Chang, *Cosmet. Toiletries*, **92**, 50 (1977).

ACKNOWLEDGMENTS

The authors thank Dr. J. Shoji, Showa University, Tokyo, Japan, and Dr. S. Shibata, Meiji College of Pharmacy, Tokyo, Japan, for their help in obtaining authentic panaxoside reference samples.

Use of a Nitrogen Detector for GLC Determination of Fluorouracil in Plasma during Single- and Combined-Agent Chemotherapy

ROSEMARY E. FINCH *x, MICHAEL R. BENDING ‡, and ARIEL F. LANT *

Received January 3, 1978, from the **Department of Therapeutics and the* ‡*Medical Unit, Westminster Hospital, London, SW1P 2AP, England.* Accepted for publication February 24, 1978.

Abstract □ A GLC assay for fluorouracil was developed and used to monitor plasma drug levels in patients on both single- and combined-agent chemotherapy. Fluorouracil is extracted from plasma, derivatized by flash methylation, and estimated using a thermionic nitrogen–phosphorus detector. The GLC determination was accurate at concentrations as low as 0.1 μg/ml of human plasma. Other drugs commonly used in combination with fluorouracil did not interfere with the assay.

Keyphrases □ Fluorouracil—nitrogen-detector GLC analysis in plasma □ GLC, nitrogen detector—analysis, fluorouracil in plasma □ Antineoplastic agents—fluorouracil, nitrogen-detector GLC analysis in plasma

Since its synthesis in 1957, fluorouracil has been used extensively as an antimetabolite in the treatment of cancer, particularly of the breast and GI tract (1). More recently, it has been widely used in multiple-agent chemotherapy (2, 3). Despite this continued usage, the clinical response is often inconsistent, and a variety of empirical dosage schedules are still employed. Therefore, to optimize drug schedules for individual patients, it would be useful to relate the time course of fluorouracil in plasma, both alone and in combination with other cytotoxic drugs, to clinical response.

Most methods for measuring fluorouracil employ GLC techniques (4–6) or assay by analysis of microbial kinetics (7). The present study describes a GLC method with nitrogen detection capable of measuring fluorouracil in combination with other cytotoxic agents without interference.

EXPERIMENTAL

Materials—Fluorouracil[1] was used both in the solid form and as a solution for injection. Thymine[2], the internal standard, was obtained as the anhydrous solid. Trimethylanilinium hydroxide[3], 0.2 *M* in methanol, was the derivatizing agent. Buffer salts[4] and solvents[4] were analytical reagent grade.

GLC Conditions—A gas chromatograph[5] equipped with a thermionic

[1] Roche Products Ltd., Welwyn Garden City, Herts., England.
[2] Sigma Chemical Co. Ltd., Kingston-upon-Thames, Surrey, England.
[3] Pierce and Warriner (UK) Ltd., Chester, Cheshire, England.
[4] B.D.H. Chemicals Ltd., Poole, Dorset, England.
[5] Model F30, Series III, Perkin-Elmer Ltd., Beaconsfield, Bucks, England.

0022-3549/78/1000-1489$01.00/0

© 1978, American Pharmaceutical Association

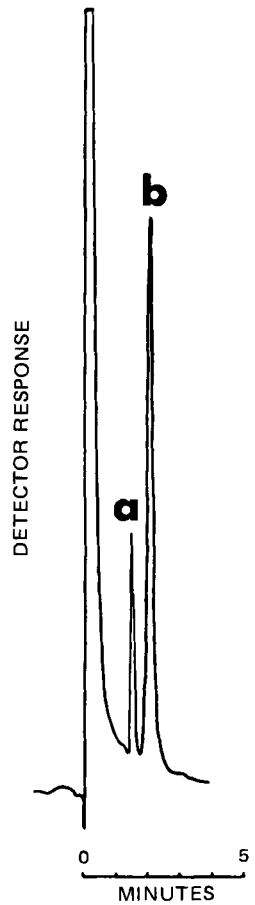

Figure 1—*Gas chromatogram showing fluorouracil (peak b, retention time = 2.00 min) and the internal standard, thymine (peak a, retention time = 1.45 min).*

nitrogen–phosphorus detector was used. A 2-m glass column packed with 0.75% Carbowax 20M–5% potassium hydroxide on 80–100-mesh Chromosorb G[6] was conditioned by temperature programming at 1°/min from 100 to 230° and maintained at 230° for 48 hr under low helium flow. The operating temperatures were: column, 210°; and injector and detector, 300°. Helium, the carrier gas, was maintained at a flow rate of 30 ml/min. The flow rates of air and hydrogen were optimized at 100 and 6 ml/min, respectively. Under these conditions, the retention times were 2.00 min for fluorouracil and 1.45 min for thymine (Fig. 1).

Procedure—Samples of 0.1–1 ml of plasma containing fluorouracil were diluted to 1 ml, where necessary, with blank plasma. This 1 ml of plasma was further diluted to 4 ml with 0.33 *M* phosphate buffer, pH 6.8, to give a final buffer concentration of 0.25 *M*. The mixture was heated in a water bath at 100° for 5 min, and the protein precipitate was removed by centrifugation at 3000×*g* for 5 min. A 2-ml aliquot of the supernate was removed and extracted by mixing with 25 ml of 16% propanol in ether for 1 min.

A 20-ml volume of the upper layer was removed and evaporated under nitrogen at 60° in a water bath. The dry residue was redissolved in 2 ml of methanol containing 0.5 or 1.0 μg of thymine as the internal standard. Then the mixture was transferred to a smaller tube and evaporated as previously described. The resultant residue was dissolved in 100 μl of 0.01 *M* trimethylanilinium hydroxide, and 1 μl was injected onto the column.

Standard curves over the ranges of 0.1–5.0 and 2–20 μg of fluorouracil/ml, containing 0.5 and 1.0 μg of thymine/ml, respectively, were prepared by extracting blank plasma and were linear.

Plasma samples not assayed immediately were stored at −20° for up to 4 weeks without any decrease in the measured fluorouracil levels.

RESULTS AND DISCUSSION

The described procedure can measure plasma fluorouracil levels accurately down to 0.1 μg/ml and is suitable for monitoring the time course of drug disappearance after oral and intravenous therapy. This method offers several advantages over previously published methods. It does not use contaminating silyl reagents for derivatization, thus obviating the need for frequent detector cleaning. It does not require the complex instrumentation of mass spectrometry, because use of the nitrogen detector increases the sensitivity of the assay 50–100 times in comparison with the responsiveness of the flame-ionization detector. Sensitivity was increased still further by adapting the extraction procedure of Hillcoat *et al.* (6) to omit the ether wash stage. Recovery of fluorouracil was 88 ± 5% (mean ± *SD*, n = 12), measured over the range of 0.2–10 μg of fluorouracil/ml of plasma. The coefficient of variation of the analyses was ±5.6%.

Unlike the mass spectrometric method, use of a nitrogen detector requires complete separation of the fluorouracil from the internal standard, thymine. Various stationary phases, over a wide range of polarity, were investigated to achieve this separation. The most suitable, 0.75% Carbowax 20M–5% potassium hydroxide, separated the two compounds with minimal retention times (Fig. 1).

The specificity of the assay in the presence of other cytotoxic drugs commonly used with fluorouracil was assessed in patients receiving 5-day cycles of quadruple chemotherapy. The cytotoxic regimen consisted of fluorouracil, cyclophosphamide, methotrexate, and vincristine, given in varying combinations intravenously over 3-min periods on different days[7]. Plasma samples were collected immediately after drug administration and were analyzed for fluorouracil. No interfering peaks attributable to cytotoxic agents other than fluorouracil were seen on the chromatograms.

The method is rapid, the compounds being eluted from the column in less than 3 min. It also does not require complex instrumentation, and it is specific for fluorouracil even in the presence of other antineoplastic drugs.

REFERENCES

(1) C. Heidelberger and F. J. Ansfield, *Cancer Res.*, **23,** 1226 (1963).

(2) V. T. DeVita, R. C. Young, and G. P. Canellos, *Cancer,* **35,** 98 (1975).

(3) J. J. Costanzi and C. A. Coltman, Jr., *ibid.,* **23,** 589 (1969).

(4) J. L. Cohen and P. B. Brennan, *J. Pharm. Sci.,* **62,** 572 (1973).

(5) K. V. Rao, K. Killon, and Y. Tanrikut, *ibid.,* **63,** 1328 (1974).

(6) B. L. Hillcoat, M. Kawai, P. B. McCulloch, J. Rosenfeld, and C. K. O. Williams, *Br. J. Clin. Pharmacol.,* **3,** 135 (1976).

(7) E. R. Garrett, G. H. Hurst, and J. R. Green, Jr., *J. Pharm. Sci.,* **66,** 1422 (1977).

[6] Phase Separations Ltd., Clwyd, Wales.

[7] Treatment courses followed the scheme used by Costanzi and Coltman (3).

Ascorbic Acid Elimination in Humans after Intravenous Administration

Keyphrases □ Ascorbic acid—elimination in humans after intravenous administration□ Elimination—ascorbic acid in humans after intravenous administration □ Vitamins—ascorbic acid, elimination in humans after intravenous administration

To the Editor:

Relatively few studies have examined the disposition kinetics of ascorbic acid in humans after administration of exogenous doses. The elimination half-life of the ascorbate pool in humans is approximately 16 days (1–3). In contrast to this relatively slow turnover time, exogenous ascorbic acid, in excess of the body store, appears to be eliminated rapidly. In human subjects whose body stores have been "saturated" with the vitamin, the elimination half-life was reported to be 2–3 hr (4–6). Recently, however, Zetler *et al.* (7) estimated the elimination half-life as 13–29 hr, values considerably greater than those previously reported.

As part of a study to determine factors influencing ascorbic acid absorption in humans[1], the elimination of ascorbic acid was evaluated after intravenous administration to five healthy normal volunteers (four males and one female; age of 25–32 years). All subjects had their body stores saturated with ascorbic acid by receiving 1 g of the vitamin daily for several weeks. After this dosing period, saturation was assumed when urinary recoveries of ascorbic acid (during 24 hr) on two occasions, separated by 3–7 days, were within ±10% of each other. One gram of ascorbic acid[2] was then administered intravenously into an arm vein over 3–4 min.

Subjects voided their bladders immediately prior to dosing, and frequent urine samples were collected thereafter at known time intervals for 24 hr. The total volume of each collection was recorded, and a 15-ml aliquot was taken and placed into a vial containing sufficient metaphosphoric acid to produce a 4% solution with this volume of urine. All samples were stored in a refrigerator and assayed within 4 days of collection.

Two days prior to and during the experimental period, the subjects avoided the ingestion of ascorbic acid either in vitamin preparations or in foods known to be high in ascorbic acid content. One day prior to the experiment, "blank" urine samples were obtained by collecting total urine for 1–2 hr during two collection periods (one in the morning and one in the afternoon). Urine was assayed to determine the concentrations of ascorbic acid, dehydroascorbic acid, and diketogulonic acid by the 2,4-dinitrophenylhydrazine method as outlined by Pelletier (8).

Urinary excretion data were corrected for blank ascorbic acid excretion. Semilogarithmic plots of excretion rate *versus* time were prepared to obtain initial estimates of the coefficients and exponents of the equation by the method of residuals. The data were fitted by nonlinear regression analysis to an equation appropriate for a two-compartment model, and the parameters of this equation were determined by conventional methods (9).

Table I—Pharmacokinetic Parameters Determined from Intravenous Ascorbic Acid Administration

Parameter[a]	Subject 1	2	3	4	5	Mean (±*SD*)
α, hr^{-1}	1.21	1.16	1.08	0.75	0.78	1.00 (0.22)
β, hr^{-1}	0.23	0.25	0.26	0.16	0.17	0.21 (0.05)
$t_{1/2\beta}$, hr	3.01	2.77	2.67	4.33	4.08	3.37 (0.78)
K_e, hr^{-1}	0.54	0.76	0.67	0.45	0.49	0.58 (0.13)
K_{10}, hr^{-1}	0.70	0.85	0.80	0.51	0.61	0.69 (0.14)
K_{12}, hr^{-1}	0.34	0.22	0.23	0.17	0.12	0.22 (0.08)
K_{21}, hr^{-1}	0.40	0.34	0.40	0.24	0.21	0.32 (0.09)
Percent dose recovered	74.0	86.7	87.3	84.6	81.3	82.6 (5.3)

[a] The α and β are hybrid first-order rate constants, $t_{1/2\beta}$, is the half-life associated with the terminal exponential process (*i.e.*, $t_{1/2\beta} = 0.693/\beta$), K_{10} is the first-order elimination rate constant from the central compartment, K_e is the first-order urinary excretion rate constant, and K_{12} and K_{21} are intercompartmental first-order transfer rate constants.

Figure 1 is a representative graph of the ascorbic acid excretion rate *versus* time for one subject. The data appear to be consistent with a two-compartment model. The solid line represents the best fit of the data. Table I summarizes the pharmacokinetic parameters generated from the analysis of the data. The urinary recovery values were corrected for the content of ascorbic acid determined from the assay of three vials of the parenteral solution (108.7% of the label claim). The values of urinary recovery represent total vitamin (*i.e.*, the sum of ascorbic, dehydroascorbic, and diketogulonic acids).

Ascorbic acid was eliminated relatively rapidly in these subjects, with an average half-life of 3.37 hr. This value is similar to some results reported previously (4, 6) but is considerably smaller than the values suggested by Zetler *et al.* (7). The degree of saturation of ascorbic acid body stores may partially explain this discrepancy. While the total urinary recoveries of the vitamin in these subjects were virtually identical, only about 83% of the dose ulti-

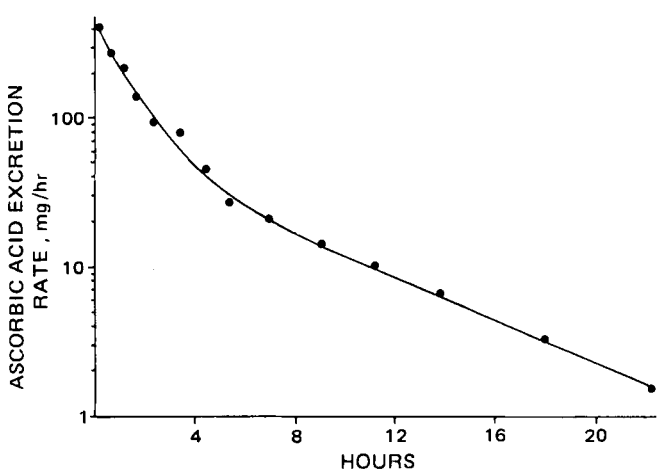

Figure 1—*Semilogarithmic plot of the ascorbic acid excretion rate as a function of time in one subject after the intravenous administration of 1 g of ascorbic acid. The solid line represents the best fit of the data obtained from nonlinear regression analysis.*

[1] Unpublished data.
[2] Lot 7509-1, Sterilab Corp. Ltd., Downsview, Ontario, Canada.

0022-3549/78/1000-1491$01.00/0
© 1978, American Pharmaceutical Association

mately was excreted. The remainder of the dose may be accounted for by other minor metabolites (*e.g.*, oxalic acid and ascorbate 2-sulfate) (10–12), or a portion of the dose may remain in the ascorbate body pool. Approximately 84% of the recovered vitamin was excreted in the form of ascorbic acid.

(1) L. Hellman and J. J. Burns, *J. Biol. Chem.*, **230**, 923 (1958).

(2) E. M. Baker, H. E. Sauberlich, S. J. Wolfskill, W. T. Wallace, and E. E. Dean, *Proc. Soc. Exp. Biol. Med.*, **109**, 737 (1962).

(3) G. L. Atkins, B. M. Dean, W. J. Griffin, and R. W. E. Watts, *J. Biol. Chem.*, **239**, 2975 (1964).

(4) J. S. Stewart and C. C. Booth, *Clin. Sci.*, **27**, 15 (1964).

(5) W. Kubler and J. Gehler, *Int. Z. Vit. Forsch.*, **40**, 442 (1970).

(6) J. Gehler and W. Kubler, *ibid.*, **40**, 454 (1970).

(7) G. Zetler, G. Siedel, C. P. Siegers, and H. Iven, *Eur. J. Clin. Pharmacol.*, **10**, 273 (1976).

(8) O. Pelletier, *J. Lab. Clin. Med.*, **72**, 674 (1968).

(9) M. Gibaldi and D. Perrier, "Pharmacokinetics," Dekker, New York, N.Y., 1975.

(10) M. Banay and E. Dimant, *Biochim. Biophys. Acta*, **59**, 313 (1962).

(11) B. M. Tolbert, M. Downing, R. W. Carlson, M. K. Knight, and E. M. Baker, *Ann. N.Y. Acad. Sci.*, **258**, 48 (1975).

(12) E. M. Baker, D. C. Hammer, S. C. March, B. M. Tolbert, and J. E. Canham, *Science*, **173**, 826 (1971).

Susanna Yung
Michael Mayersohn ˣ
J. Barry Robinson

Department of Pharmaceutical Sciences
College of Pharmacy
University of Arizona
Tucson, AZ 85721

Received June 16, 1978.

Accepted for publication July 28, 1978.

This study was conducted while the authors were at the Faculty of Pharmacy, University of Toronto, Toronto, Ontario, Canada.

The authors gratefully acknowledge the participation of the volunteers.

Comparative Pharmacokinetics of Coumarin Anticoagulants XXXVII: Simultaneous *In Vivo* Displacement of Dicumarol from Serum Protein and Tissue Binding Sites by Tolbutamide in Rats

Keyphrases □ Dicumarol—*in vivo* binding to serum proteins and tissues, effect of tolbutamide in rats □ Tolbutamide—effect on *in vivo* binding of dicumarol to serum proteins and tissues in rats □ Binding, serum protein and tissue—dicumarol *in vivo*, effect of tolbutamide in rats □ Anticoagulants, coumarin—dicumarol, *in vivo* binding to serum proteins and tissues, effect of tolbutamide in rats □ Antidiabetic agents—tolbutamide, effect on *in vivo* binding of dicumarol to serum proteins and tissues in rats

To the Editor:

The ability of some drugs and endogenous substances to displace other drugs or endogenous substances from serum or plasma protein binding sites has been studied extensively. However, there is only very limited information on such displacement effects in various organs and tissues, probably because of the technical difficulties of such investigations, which must be carried out *in vivo* (1). Recently developed pharmacokinetic theory indicates that a full appreciation of the pharmacokinetic implications of changes in drug binding can only be obtained by assessing the magnitude of such changes in serum as well as in tissues (2). During a study of pharmacokinetic and pharmacodynamic interactions between dicumarol and tolbutamide, we have found evidence that tolbutamide administration causes a displacement of dicumarol not only from serum proteins but also from binding sites in the liver.

Thirty adult male Sprague–Dawley rats, 250–350 g, received ^{14}C-dicumarol, 8 mg/kg iv, and the pharmacokinetics of this drug were determined by methods described previously (3) (Experiment I). Twenty of these animals were matched into pairs with nearly identical total clearance values. One month later, these rats again received a dicumarol injection (Experiment II), but one member of each pair also received tolbutamide, 125 mg/kg ip at the time of dicumarol administration and 62.5 mg/kg every 3–4 hr thereafter while the other member received saline injections at these times. The animals were killed when serum dicumarol concentrations were expected, by extrapolation of earlier concentrations (determined during the experiment), to have declined to about 7 μg/ml. The liver was removed and blood was expressed from it; it was homogenized, and the homogenate was assayed for dicumarol.

Another six pairs of rats (not from the original group of 30) with nearly identical dicumarol clearance received only tolbutamide (125 mg/kg for the first dose and then 62.5 mg/kg every 3–4 hr for 30 hr) or saline, but no dicumarol, one month after Experiment I. They were killed 3 hr after the last dose of tolbutamide; plasma was obtained from blood withdrawn from the abdominal aorta and diluted 1:10 with pH 7.4 isotonic sodium phosphate buffer. The liver was excised and homogenized with three volumes of ice-cold phosphate buffer. ^{14}C-Dicumarol, 10 μg/ml final concentration, was added to both plasma and liver homogenate, and the samples were dialyzed at 25° against an equal volume of phosphate buffer to equilibrium (4).

The effects of tolbutamide on the pharmacokinetics of dicumarol when both drugs were administered *in vivo* are summarized in Table I. Intentionally, animals with widely different total clearance values were selected for the study (range in Experiment I: 3.33–16.8 ml/hr/kg), so standard deviations are reported only for the mean of the individual ratios of various parameter values. The average total clearance, the volume of distribution, and the β value of the control and tolbutamide groups were almost identical in Experiment I; these values were also nearly identical in Experiments I and II of the control group. These results reflect the excellent matching of the two groups and the reproducibility of the pharmacokinetic parameter values in repeated experiments.

Concomitant administration of tolbutamide caused a pronounced increase in the total clearance and β and a smaller, but still statistically significant, increase in the volume of distribution (Experiment II, tolbutamide group). The free fraction of dicumarol in diluted plasma (mean ± *SD*, $n = 6$) was 0.000754 ± 0.000156 for control animals and 0.00213 ± 0.00095 for tolbutamide-treated animals ($p < 0.01$). A method to determine protein binding of dicumarol in undiluted plasma was not available when these studies were done.

Since tolbutamide administration was acute, it is unlikely to have caused enzyme induction. This conclusion

0022-3549/78/1000-1492$01.00/0

© 1978, American Pharmaceutical Association

mately was excreted. The remainder of the dose may be accounted for by other minor metabolites (*e.g.*, oxalic acid and ascorbate 2-sulfate) (10–12), or a portion of the dose may remain in the ascorbate body pool. Approximately 84% of the recovered vitamin was excreted in the form of ascorbic acid.

(1) L. Hellman and J. J. Burns, *J. Biol. Chem.*, **230**, 923 (1958).

(2) E. M. Baker, H. E. Sauberlich, S. J. Wolfskill, W. T. Wallace, and E. E. Dean, *Proc. Soc. Exp. Biol. Med.*, **109**, 737 (1962).

(3) G. L. Atkins, B. M. Dean, W. J. Griffin, and R. W. E. Watts, *J. Biol. Chem.*, **239**, 2975 (1964).

(4) J. S. Stewart and C. C. Booth, *Clin. Sci.*, **27**, 15 (1964).

(5) W. Kubler and J. Gehler, *Int. Z. Vit. Forsch.*, **40**, 442 (1970).

(6) J. Gehler and W. Kubler, *ibid.*, **40**, 454 (1970).

(7) G. Zetler, G. Siedel, C. P. Siegers, and H. Iven, *Eur. J. Clin. Pharmacol.*, **10**, 273 (1976).

(8) O. Pelletier, *J. Lab. Clin. Med.*, **72**, 674 (1968).

(9) M. Gibaldi and D. Perrier, "Pharmacokinetics," Dekker, New York, N.Y., 1975.

(10) M. Banay and E. Dimant, *Biochim. Biophys. Acta*, **59**, 313 (1962).

(11) B. M. Tolbert, M. Downing, R. W. Carlson, M. K. Knight, and E. M. Baker, *Ann. N.Y. Acad. Sci.*, **258**, 48 (1975).

(12) E. M. Baker, D. C. Hammer, S. C. March, B. M. Tolbert, and J. E. Canham, *Science*, **173**, 826 (1971).

Susanna Yung
Michael Mayersohn ˣ
J. Barry Robinson

Department of Pharmaceutical Sciences
College of Pharmacy
University of Arizona
Tucson, AZ 85721

Received June 16, 1978.

Accepted for publication July 28, 1978.

This study was conducted while the authors were at the Faculty of Pharmacy, University of Toronto, Toronto, Ontario, Canada.

The authors gratefully acknowledge the participation of the volunteers.

Comparative Pharmacokinetics of Coumarin Anticoagulants XXXVII: Simultaneous *In Vivo* Displacement of Dicumarol from Serum Protein and Tissue Binding Sites by Tolbutamide in Rats

Keyphrases □ Dicumarol—*in vivo* binding to serum proteins and tissues, effect of tolbutamide in rats □ Tolbutamide—effect on *in vivo* binding of dicumarol to serum proteins and tissues in rats □ Binding, serum protein and tissue—dicumarol *in vivo*, effect of tolbutamide in rats □ Anticoagulants, coumarin—dicumarol, *in vivo* binding to serum proteins and tissues, effect of tolbutamide in rats □ Antidiabetic agents—tolbutamide, effect on *in vivo* binding of dicumarol to serum proteins and tissues in rats

To the Editor:

The ability of some drugs and endogenous substances to displace other drugs or endogenous substances from serum or plasma protein binding sites has been studied extensively. However, there is only very limited information on such displacement effects in various organs and tissues, probably because of the technical difficulties of such investigations, which must be carried out *in vivo* (1). Recently developed pharmacokinetic theory indicates that a full appreciation of the pharmacokinetic implications of changes in drug binding can only be obtained by assessing the magnitude of such changes in serum as well as in tissues (2). During a study of pharmacokinetic and pharmacodynamic interactions between dicumarol and tolbutamide, we have found evidence that tolbutamide administration causes a displacement of dicumarol not only from serum proteins but also from binding sites in the liver.

Thirty adult male Sprague–Dawley rats, 250–350 g, received ^{14}C-dicumarol, 8 mg/kg iv, and the pharmacokinetics of this drug were determined by methods described previously (3) (Experiment I). Twenty of these animals were matched into pairs with nearly identical total clearance values. One month later, these rats again received a dicumarol injection (Experiment II), but one member of each pair also received tolbutamide, 125 mg/kg ip at the time of dicumarol administration and 62.5 mg/kg every 3–4 hr thereafter while the other member received saline injections at these times. The animals were killed when serum dicumarol concentrations were expected, by extrapolation of earlier concentrations (determined during the experiment), to have declined to about 7 μg/ml. The liver was removed and blood was expressed from it; it was homogenized, and the homogenate was assayed for dicumarol.

Another six pairs of rats (not from the original group of 30) with nearly identical dicumarol clearance received only tolbutamide (125 mg/kg for the first dose and then 62.5 mg/kg every 3–4 hr for 30 hr) or saline, but no dicumarol, one month after Experiment I. They were killed 3 hr after the last dose of tolbutamide; plasma was obtained from blood withdrawn from the abdominal aorta and diluted 1:10 with pH 7.4 isotonic sodium phosphate buffer. The liver was excised and homogenized with three volumes of ice-cold phosphate buffer. ^{14}C-Dicumarol, 10 μg/ml final concentration, was added to both plasma and liver homogenate, and the samples were dialyzed at 25° against an equal volume of phosphate buffer to equilibrium (4).

The effects of tolbutamide on the pharmacokinetics of dicumarol when both drugs were administered *in vivo* are summarized in Table I. Intentionally, animals with widely different total clearance values were selected for the study (range in Experiment I: 3.33–16.8 ml/hr/kg), so standard deviations are reported only for the mean of the individual ratios of various parameter values. The average total clearance, the volume of distribution, and the β value of the control and tolbutamide groups were almost identical in Experiment I; these values were also nearly identical in Experiments I and II of the control group. These results reflect the excellent matching of the two groups and the reproducibility of the pharmacokinetic parameter values in repeated experiments.

Concomitant administration of tolbutamide caused a pronounced increase in the total clearance and β and a smaller, but still statistically significant, increase in the volume of distribution (Experiment II, tolbutamide group). The free fraction of dicumarol in diluted plasma (mean ± *SD*, $n = 6$) was 0.000754 ± 0.000156 for control animals and 0.00213 ± 0.00095 for tolbutamide-treated animals ($p < 0.01$). A method to determine protein binding of dicumarol in undiluted plasma was not available when these studies were done.

Since tolbutamide administration was acute, it is unlikely to have caused enzyme induction. This conclusion

0022-3549/78/1000-1492$01.00/0

© 1978, American Pharmaceutical Association

Table I—Effect of Tolbutamide on the Pharmacokinetics of Dicumarol in Rats [a]

Pharmacokinetic Parameter	Control Group			Tolbutamide Group		
	Experiment I	Experiment II	Ratio, II/I	Experiment I	Experiment II	Ratio, II/I
Total clearance, ml/hr/kg	8.60	8.46	1.04 ± 0.18[b]	8.17	18.7[c]	2.40 ± 0.49[c]
Apparent volume of distribution, ml/kg	133	129	0.979 ± 0.081	126	156[c]	1.27 ± 0.26[c]
β, hr^{-1}	0.0651	0.0648	1.06 ± 0.184	0.0649	0.118[c]	1.90 ± 0.32[c]
Concentration in serum/concentration in liver[d]	—	2.15 ± 0.42	—	—	1.90 ± 0.40[c]	—
Amount in liver/amount in body[d]	—	0.113 ± 0.040	—	—	0.0887 ± 0.027[c]	—

[a] All animals received dicumarol, 8 mg/kg iv. Experiment II was carried out 4 weeks after Experiment I, at which time the tolbutamide group also received tolbutamide, 125 mg/kg ip at zero time and 62.5 mg/kg every 3–4 hr thereafter while the control group received saline injections at these times. There were 10 rats in each group. [b] All ± values are ± *SD*. [c] $p < 0.005$ compared to the corresponding value in the control group. [d] The serum concentrations at the time of determination were 7.13 ± 1.08 and 6.95 ± 0.70 μg/ml for control and tolbutamide groups, respectively.

is confirmed by the fact that the liver weights were not increased (mean ± *SD*: 10.7 ± 1.6 g and 10.4 ± 1.2 g for control and tolbutamide-treated animals, respectively). The pronounced increase in dicumarol clearance caused by tolbutamide is consistent with the strong displacing effect of the latter on the former in plasma and with the previously demonstrated direct proportionality between dicumarol clearance and the free fraction in serum (3). This direct proportionality suggests a 2.4-fold increase of the dicumarol free fraction in plasma (since clearance increased by that magnitude), similar to the change in the free fraction observed *in vitro*.

The *in vivo* serum to liver concentration ratio of dicumarol was only slightly affected by tolbutamide treatment; it decreased by about 12% on the average (Table I). This finding indicates that tolbutamide administration resulted in a displacement of dicumarol not only from plasma protein but also (and to an almost similar extent) from hepatic tissues. Had there been no appreciable displacement of dicumarol from binding sites in the liver, the plasma or serum to liver concentration ratio of dicumarol should have decreased by about 60%.

Confirmation of the displacing effect of tolbutamide (and, possibly, its metabolites) on dicumarol in the liver was obtained from a partly *in vitro* experiment. Homogenates were prepared from the livers of control rats and tolbutamide-treated rats, and the binding of dicumarol in these homogenates was determined following the *in vitro* addition of dicumarol. The free fraction of dicumarol in these homogenates (mean ± *SD*, $n = 6$) was 0.0121 ± 0.0050 for control rats and 0.0283 ± 0.0110 for tolbutamide-treated animals ($p < 0.01$). Thus, *in vivo* administration of tolbutamide caused a pronounced displacement of dicumarol from hepatic binding sites upon *in vitro* addition of the latter. While presently used methods for the *in vitro* determination of drug binding to tissues have pronounced limitations (1), the liver homogenate data can serve as supportive evidence, particularly since the displacing agent was administered *in vivo*.

The *in vivo* pharmacokinetic study revealed that tolbutamide treatment caused an increase in the apparent volume of distribution of dicumarol as well as a significant decrease in the ratio of the amount of drug in the liver to the amount of drug in the total body (estimated as concentration in plasma times apparent volume of distribution). This effect suggests a shift of the anticoagulant from the plasma and liver to other tissues. One may infer, therefore, that the displacing effect of tolbutamide on dicumarol in these other tissues considered together (*i.e.*, as a weighted average) is less pronounced than in the plasma and liver.

Recently developed pharmacokinetic theory suggests that changes in tissue binding can be more important than changes in plasma protein binding as a cause of alterations in the biological half-life of drugs (2). In view of these theoretical considerations and the indications of drug displacement from tissue binding sites reported here, it is important that future pharmacokinetic studies of drug interactions, particularly in animals, be designed to include assessment of possible displacement of drugs from tissues.

(1) G. Levy, C.-M. Lai, and A. Yacobi, *J. Pharm. Sci.*, **67**, 229 (1978).
(2) M. Gibaldi, G. Levy, and P. J. McNamara, *Clin. Pharmacol. Ther.*, **24**, 1 (1978).
(3) C.-M. Lai and G. Levy, *J. Pharm. Sci.*, **66**, 1739 (1977).
(4) A. Yacobi, C.-M. Lai, and G. Levy, *ibid.*, **64**, 1995 (1975).

Chii-Ming Lai
Gerhard Levy ˣ
Department of Pharmaceutics
State University of New York
at Buffalo
Amherst, NY 14260

Received March 10, 1978.
Accepted for publication July 13, 1978.
Supported in part by Grant GM 20852 from the National Institutes of Health.

Absorption of Saccharin from Rat Urinary Bladder

Keyphrases □ Saccharin—absorption from urinary bladder, rats □ Absorption, urinary bladder—saccharin in rats □ Sweeteners—saccharin, absorption from urinary bladder, rats

To the Editor:

The renal excretion of drugs and chemicals has generally been considered an elimination route. The absorption or reabsorption of compounds from the urinary bladder has not been studied widely. I have been studying saccharin pharmacokinetics in the rat and have discovered unusual plasma and urinary profiles for the compound. During renal clearance studies, it became apparent that saccharin was cleared from the plasma more quickly when the urine was removed from the urinary bladder at 5-min intervals than when it was left for 60 min. This communication discusses this observation and describes the absorption (reabsorption) of saccharin from the urinary bladder of the rat.

0022-3549/78/1000-1493$01.00/0
© 1978, American Pharmaceutical Association

Table I—Effect of Tolbutamide on the Pharmacokinetics of Dicumarol in Rats [a]

Pharmacokinetic Parameter	Control Group			Tolbutamide Group		
	Experiment I	Experiment II	Ratio, II/I	Experiment I	Experiment II	Ratio, II/I
Total clearance, ml/hr/kg	8.60	8.46	1.04 ± 0.18[b]	8.17	18.7[c]	2.40 ± 0.49[c]
Apparent volume of distribution, ml/kg	133	129	0.979 ± 0.081	126	156[c]	1.27 ± 0.26[c]
β, hr^{-1}	0.0651	0.0648	1.06 ± 0.184	0.0649	0.118[c]	1.90 ± 0.32[c]
Concentration in serum/concentration in liver[d]	—	2.15 ± 0.42	—	—	1.90 ± 0.40[c]	—
Amount in liver/amount in body[d]	—	0.113 ± 0.040	—	—	0.0887 ± 0.027[c]	—

[a] All animals received dicumarol, 8 mg/kg iv. Experiment II was carried out 4 weeks after Experiment I, at which time the tolbutamide group also received tolbutamide, 125 mg/kg ip at zero time and 62.5 mg/kg every 3–4 hr thereafter while the control group received saline injections at these times. There were 10 rats in each group. [b] All ± values are ± *SD*. [c] $p < 0.005$ compared to the corresponding value in the control group. [d] The serum concentrations at the time of determination were 7.13 ± 1.08 and 6.95 ± 0.70 μg/ml for control and tolbutamide groups, respectively.

is confirmed by the fact that the liver weights were not increased (mean ± *SD*: 10.7 ± 1.6 g and 10.4 ± 1.2 g for control and tolbutamide-treated animals, respectively). The pronounced increase in dicumarol clearance caused by tolbutamide is consistent with the strong displacing effect of the latter on the former in plasma and with the previously demonstrated direct proportionality between dicumarol clearance and the free fraction in serum (3). This direct proportionality suggests a 2.4-fold increase of the dicumarol free fraction in plasma (since clearance increased by that magnitude), similar to the change in the free fraction observed *in vitro*.

The *in vivo* serum to liver concentration ratio of dicumarol was only slightly affected by tolbutamide treatment; it decreased by about 12% on the average (Table I). This finding indicates that tolbutamide administration resulted in a displacement of dicumarol not only from plasma protein but also (and to an almost similar extent) from hepatic tissues. Had there been no appreciable displacement of dicumarol from binding sites in the liver, the plasma or serum to liver concentration ratio of dicumarol should have decreased by about 60%.

Confirmation of the displacing effect of tolbutamide (and, possibly, its metabolites) on dicumarol in the liver was obtained from a partly *in vitro* experiment. Homogenates were prepared from the livers of control rats and tolbutamide-treated rats, and the binding of dicumarol in these homogenates was determined following the *in vitro* addition of dicumarol. The free fraction of dicumarol in these homogenates (mean ± *SD*, $n = 6$) was 0.0121 ± 0.0050 for control rats and 0.0283 ± 0.0110 for tolbutamide-treated animals ($p < 0.01$). Thus, *in vivo* administration of tolbutamide caused a pronounced displacement of dicumarol from hepatic binding sites upon *in vitro* addition of the latter. While presently used methods for the *in vitro* determination of drug binding to tissues have pronounced limitations (1), the liver homogenate data can serve as supportive evidence, particularly since the displacing agent was administered *in vivo*.

The *in vivo* pharmacokinetic study revealed that tolbutamide treatment caused an increase in the apparent volume of distribution of dicumarol as well as a significant decrease in the ratio of the amount of drug in the liver to the amount of drug in the total body (estimated as concentration in plasma times apparent volume of distribution). This effect suggests a shift of the anticoagulant from the plasma and liver to other tissues. One may infer, therefore, that the displacing effect of tolbutamide on dicumarol in these other tissues considered together (*i.e.*, as a weighted average) is less pronounced than in the plasma and liver.

Recently developed pharmacokinetic theory suggests that changes in tissue binding can be more important than changes in plasma protein binding as a cause of alterations in the biological half-life of drugs (2). In view of these theoretical considerations and the indications of drug displacement from tissue binding sites reported here, it is important that future pharmacokinetic studies of drug interactions, particularly in animals, be designed to include assessment of possible displacement of drugs from tissues.

(1) G. Levy, C.-M. Lai, and A. Yacobi, *J. Pharm. Sci.*, **67**, 229 (1978).
(2) M. Gibaldi, G. Levy, and P. J. McNamara, *Clin. Pharmacol. Ther.*, **24**, 1 (1978).
(3) C.-M. Lai and G. Levy, *J. Pharm. Sci.*, **66**, 1739 (1977).
(4) A. Yacobi, C.-M. Lai, and G. Levy, *ibid.*, **64**, 1995 (1975).

Chii-Ming Lai
Gerhard Levy ˣ
Department of Pharmaceutics
State University of New York
at Buffalo
Amherst, NY 14260

Received March 10, 1978.
Accepted for publication July 13, 1978.
Supported in part by Grant GM 20852 from the National Institutes of Health.

Absorption of Saccharin from Rat Urinary Bladder

Keyphrases □ Saccharin—absorption from urinary bladder, rats □ Absorption, urinary bladder—saccharin in rats □ Sweeteners—saccharin, absorption from urinary bladder, rats

To the Editor:

The renal excretion of drugs and chemicals has generally been considered an elimination route. The absorption or reabsorption of compounds from the urinary bladder has not been studied widely. I have been studying saccharin pharmacokinetics in the rat and have discovered unusual plasma and urinary profiles for the compound. During renal clearance studies, it became apparent that saccharin was cleared from the plasma more quickly when the urine was removed from the urinary bladder at 5-min intervals than when it was left for 60 min. This communication discusses this observation and describes the absorption (reabsorption) of saccharin from the urinary bladder of the rat.

0022-3549/78/1000-1493$01.00/0
© 1978, American Pharmaceutical Association

Table I—Plasma Concentrations (Nanograms per Milliliter) following *In Vivo* Instillation of Various Doses of Saccharin into the Urinary Bladder of the Rat

Minutes after Dosing	10 μg/kg		1 mg/kg		100 mg/kg	
	Rat 1	Rat 2	Rat 3	Rat 4	Rat 5	Rat 6
5	4.62	2.94	81.6	130.0	25,200	13,500
15	3.95	3.30	105.0	173.0	39,500	18,300
30	3.88	2.66	100.0	137.0	48,200	18,100
45	3.85	3.52	82.7	114.0	53,000	17,500
60	3.28	3.23	73.8	113.0	53,000	13,800
90	4.62	3.37	73.6	92.3	51,400	14,200
120	4.32	2.87	63.2	88.8	39,100	11,900
Fraction of dose in urinary bladder at 120 min	0.43	0.48	0.57	0.69	0.58	0.80

^{35}S-Saccharin sodium was instilled in the urinary bladder of pentobarbital-anesthetized male Sprague–Dawley rats. Three groups of two rats, 200–240 g, were administered 10-μg/kg or 1- or 100-mg/kg doses in equimolar sodium solutions (pH 6.5) of 1 ml/kg *via* a bladder cannula. Blood samples were withdrawn through a jugular vein cannula at 5, 15, 30, 45, 60, 90, and 120 min after bladder instillation (1). At 120 min, the urine–dose solution was removed from the urinary bladder. Plasma samples and urine–dose solutions were counted for ^{35}S-activity by liquid scintillation counting.

The 1-mg/kg dose is comparable to a single-dose ingestion of diet soft drink or one cup of coffee with two saccharin tablets (~70 mg). The 10-μg/kg and 100-mg/kg doses were chosen to study the possible dose dependence in saccharin pharmacokinetics in the rat.

Since saccharin is not metabolized in the rat (2), ^{35}S-activity measurements can be assumed to reflect only saccharin. The results of the bladder instillation experiments are presented in Table I. Saccharin was absorbed extensively from the urinary bladder of the rat. These data, in conjunction with data from previously reported oral absorption studies (3) and data following intravenous administration from continuing studies in this laboratory, indicate that the absorption from the bladder is slower than from the GI tract and that approximately 50% to equal amounts of the bladder dose ultimately will reach the systemic circulation when compared to the oral route. Preliminary bladder absorption studies also indicate that the extent of initial absorption may be dose and pH dependent in the rat; *i.e.*, greater amounts reach the systemic circulation at higher doses and at higher pH.

In summary, significant absorption of saccharin occurs from the urinary bladder in the rat. The continued high plasma concentrations following bladder instillation are probably, at least in part, due to the closed system created by inhibiting urination during the present experiment. However, significant reabsorption of saccharin would also decrease the elimination rate for the compound in much the same way as would enterohepatic cycling and probably accounts for the retention of saccharin in urinary bladder tissue (3). The use of the rat as an acceptable model for carcinogenicity studies with saccharin will be highly dependent on interspecies differences with respect to the absorption phenomenon.

(1) J. R. Weeks and J. D. Davis, *J. Appl. Physiol.*, **19**, 540 (1964).

(2) L. M. Ball, A. G. Renwick, and R. T. Williams, *Xenobiotica*, **7**, 189 (1977).

(3) H. B. Matthews, M. Fields, and L. Fishbein, *Agr. Food Chem.*, **21**, 916 (1973).

Wayne A. Colburn

Laboratory of Pharmacokinetics
National Institute of Environmental Health Sciences
Research Triangle Park, NC 27709

Received May 17, 1978.
Accepted for publication August 2, 1978.
Present address: Department of Biochemistry and Drug Metabolism, Hoffmann–La Roche Inc., Nutley, NJ 07110.

Adsorption of Fluorouracil on Glass Surfaces

Keyphrases □ Fluorouracil—adsorption on glass surfaces □ Adsorption—fluorouracil on glass surfaces □ Antineoplastic agents—fluorouracil, adsorption on glass surfaces

To the Editor:

The determination of the cytostatic drug fluorouracil in plasma has been described (1–6). The experimental procedures leading to the isolation of fluorouracil from biological fluids and the subsequent sensitive determination are rather complicated (5) and sometimes require expensive equipment (3, 4). In attempts to design a GLC assay of underivatized fluorouracil, we encountered a phenomenon that could be responsible for problems during its analysis: when standard solutions of fluorouracil in methanol in a glass vial were evaporated under nitrogen and redissolved in methanol in the same vial, less fluorouracil was found than in a corresponding amount of the original standard solution. This finding prompted us to study the possible adsorption of fluorouracil on glass surfaces using GLC as well as radioactive measurements.

Standard solutions of fluorouracil[1] in methanol (0.05–0.6 μg/μl) were prepared in closed plastic containers. Aliquots of 10 μl of these standard solutions (0.5, 1, 2, 4, and 6 μg of fluorouracil) were evaporated under nitrogen in glass and plastic vials. The residue was redissolved carefully in 100 μl of methanol; 10 μl of this solution was analyzed by GLC.

The absolute peak heights of the fluorouracil samples were compared with those of the standard solutions in the plastic containers (Fig. 1). An almost quantitative recovery was obtained from the plastic vials, whereas a significant loss of fluorouracil was observed in glass vials.

The experiments were repeated with standard solutions

[1] Supplied by Hoffmann-La Roche B.V.

0022-3549/78/1000-1494$01.00/0
© 1978, American Pharmaceutical Association

Table I—Plasma Concentrations (Nanograms per Milliliter) following *In Vivo* Instillation of Various Doses of Saccharin into the Urinary Bladder of the Rat

Minutes after Dosing	10 μg/kg		1 mg/kg		100 mg/kg	
	Rat 1	Rat 2	Rat 3	Rat 4	Rat 5	Rat 6
5	4.62	2.94	81.6	130.0	25,200	13,500
15	3.95	3.30	105.0	173.0	39,500	18,300
30	3.88	2.66	100.0	137.0	48,200	18,100
45	3.85	3.52	82.7	114.0	53,000	17,500
60	3.28	3.23	73.8	113.0	53,000	13,800
90	4.62	3.37	73.6	92.3	51,400	14,200
120	4.32	2.87	63.2	88.8	39,100	11,900
Fraction of dose in urinary bladder at 120 min	0.43	0.48	0.57	0.69	0.58	0.80

^{35}S-Saccharin sodium was instilled in the urinary bladder of pentobarbital-anesthetized male Sprague–Dawley rats. Three groups of two rats, 200–240 g, were administered 10-μg/kg or 1- or 100-mg/kg doses in equimolar sodium solutions (pH 6.5) of 1 ml/kg *via* a bladder cannula. Blood samples were withdrawn through a jugular vein cannula at 5, 15, 30, 45, 60, 90, and 120 min after bladder instillation (1). At 120 min, the urine–dose solution was removed from the urinary bladder. Plasma samples and urine–dose solutions were counted for ^{35}S-activity by liquid scintillation counting.

The 1-mg/kg dose is comparable to a single-dose ingestion of diet soft drink or one cup of coffee with two saccharin tablets (~70 mg). The 10-μg/kg and 100-mg/kg doses were chosen to study the possible dose dependence in saccharin pharmacokinetics in the rat.

Since saccharin is not metabolized in the rat (2), ^{35}S-activity measurements can be assumed to reflect only saccharin. The results of the bladder instillation experiments are presented in Table I. Saccharin was absorbed extensively from the urinary bladder of the rat. These data, in conjunction with data from previously reported oral absorption studies (3) and data following intravenous administration from continuing studies in this laboratory, indicate that the absorption from the bladder is slower than from the GI tract and that approximately 50% to equal amounts of the bladder dose ultimately will reach the systemic circulation when compared to the oral route. Preliminary bladder absorption studies also indicate that the extent of initial absorption may be dose and pH dependent in the rat; *i.e.*, greater amounts reach the systemic circulation at higher doses and at higher pH.

In summary, significant absorption of saccharin occurs from the urinary bladder in the rat. The continued high plasma concentrations following bladder instillation are probably, at least in part, due to the closed system created by inhibiting urination during the present experiment. However, significant reabsorption of saccharin would also decrease the elimination rate for the compound in much the same way as would enterohepatic cycling and probably accounts for the retention of saccharin in urinary bladder tissue (3). The use of the rat as an acceptable model for carcinogenicity studies with saccharin will be highly dependent on interspecies differences with respect to the absorption phenomenon.

(1) J. R. Weeks and J. D. Davis, *J. Appl. Physiol.*, **19**, 540 (1964).

(2) L. M. Ball, A. G. Renwick, and R. T. Williams, *Xenobiotica*, **7**, 189 (1977).

(3) H. B. Matthews, M. Fields, and L. Fishbein, *Agr. Food Chem.*, **21**, 916 (1973).

Wayne A. Colburn

Laboratory of Pharmacokinetics
National Institute of Environmental Health Sciences
Research Triangle Park, NC 27709

Received May 17, 1978.
Accepted for publication August 2, 1978.
Present address: Department of Biochemistry and Drug Metabolism, Hoffmann–La Roche Inc., Nutley, NJ 07110.

Adsorption of Fluorouracil on Glass Surfaces

Keyphrases □ Fluorouracil—adsorption on glass surfaces □ Adsorption—fluorouracil on glass surfaces □ Antineoplastic agents—fluorouracil, adsorption on glass surfaces

To the Editor:

The determination of the cytostatic drug fluorouracil in plasma has been described (1–6). The experimental procedures leading to the isolation of fluorouracil from biological fluids and the subsequent sensitive determination are rather complicated (5) and sometimes require expensive equipment (3, 4). In attempts to design a GLC assay of underivatized fluorouracil, we encountered a phenomenon that could be responsible for problems during its analysis: when standard solutions of fluorouracil in methanol in a glass vial were evaporated under nitrogen and redissolved in methanol in the same vial, less fluorouracil was found than in a corresponding amount of the original standard solution. This finding prompted us to study the possible adsorption of fluorouracil on glass surfaces using GLC as well as radioactive measurements.

Standard solutions of fluorouracil[1] in methanol (0.05–0.6 μg/μl) were prepared in closed plastic containers. Aliquots of 10 μl of these standard solutions (0.5, 1, 2, 4, and 6 μg of fluorouracil) were evaporated under nitrogen in glass and plastic vials. The residue was redissolved carefully in 100 μl of methanol; 10 μl of this solution was analyzed by GLC.

The absolute peak heights of the fluorouracil samples were compared with those of the standard solutions in the plastic containers (Fig. 1). An almost quantitative recovery was obtained from the plastic vials, whereas a significant loss of fluorouracil was observed in glass vials.

The experiments were repeated with standard solutions

[1] Supplied by Hoffmann-La Roche B.V.

0022-3549/78/1000-1494$01.00/0
© 1978, American Pharmaceutical Association

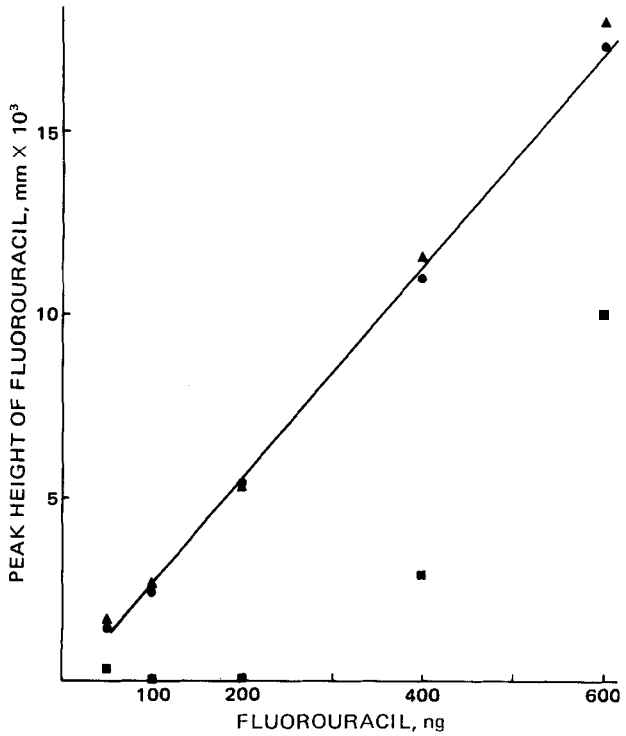

Figure 1—*Recovery of fluorouracil after evaporation of the test solution and reconstitution in plastic (▲) and glass (■) containers as compared to the initial solution (●).*

now enriched with 6-^{3}H-fluorouracil[2], thus permitting a radioactivity control of the GLC results. The recoveries of fluorouracil from glass and plastic vials obtained by the radiochemical determination were essentially the same as in Fig. 1.

The experiments were also extended to other materials. Silanized glass vials, several types of plastic (polyethylene and polypropylene) vials, and small Eppendorf tubes were investigated for their adhesive behavior. Adsorption was observed for glass, whereas fair to almost complete recoveries were found for silanized glass and plastic tubes.

Thus, a simple step in procedures used in the extraction of fluorouracil can produce a substantial loss of the compound in glass vials. We ascribe the observed loss to adsorption on the glass surface. So far, we have no indication that fluorouracil in solution also adheres to glass. However, we try to avoid any contact of fluorouracil with nondeactivated glass surfaces.

(1) J. L. Cohen and P. B. Brennan, *J. Pharm. Sci.*, **62**, 572 (1973).
(2) K. V. Rao, K. Killion, and Y. Tanrikut, *ibid.*, **63**, 1328 (1974).
(3) C. Finn and W. Sadée, *Cancer Chemother. Rep.*, **59**, 279 (1975).
(4) B. L. Hillcoat, M. Kawai, P. B. McCullough, J. Rosenfeld, and C. K. O. Williams, *Br. J. Clin. Pharm.*, **3**, 135 (1976).
(5) A. T. W. U. Schwandt, C. Finn, and W. Sadée, *Res. Commun. Chem. Pathol. Pharmacol.*, **14**, 89 (1976).
(6) D. S. Sitar, D. H. Shaw, M. P. Thirlwell, and J. R. Ruedy, *Cancer Res.*, **37**, 3981 (1977).

O. Driessen ˣ
D. de Vos
P. J. A. Timmermans
Department of Pharmacology
Leiden University Medical Center
Sylvius Laboratories
Wassenaarseweg 72
2333 AL Leiden, The Netherlands

Received March 30, 1978.
Accepted for publication July 24, 1978.
Supported by the Koningin Wilhelmina Foundation, The Netherlands Organization for Cancer Research.

[2] From the Radiochemical Center, Amersham, U.K.

Problems with Iodometric Assay of Penicillin V Benzathine

Keyphrases □ Penicillin V benzathine—iodometric analysis, interference by benzathine molecule □ Benzathine molecule—interference in iodometric analysis of penicillin V benzathine □ Iodometry—analysis, penicillin V benzathine, interference by benzathine molecule □ Antibacterials—penicillin V benzathine, iodometric analysis, interference by benzathine molecule

To the Editor:

Although antibiotics have traditionally been assayed by microbiological techniques, other chemical procedures are now used because of their advantages of speed, precision, and economy. The iodometric method for penicillins (1) is based on the observation that certain products of the inactivation of penicillin, but not the pure active substance, show a marked consumption of iodine.

Two identical samples are taken from a solution of penicillin. One is inactivated with alkali (or penicillinase) and then neutralized with acid. The same amount of iodine is added to both samples and, after a time, the excess iodine is back-titrated with thiosulfate. The difference in the consumption of iodine is a function of the amount of penicillin present.

In the original method, the pH of the iodine reaction solution was about 2. Ortenblad (2), however, found that the method did not always give reproducible values. At pH 4.5, the method was more accurate in the presence of iodine-absorbing impurities and more reproducible since the blank and the inactivated solutions are buffered at the same pH (2). However, with penicillin G procaine, the procaine interfered with the determination at a pH higher than 4.6. This modified procedure is the basis of the present European Pharmacopoeia (3) methods for penicillins G and V.

In 1959, Weiss (4) reviewed the factors affecting the reproducibility of the iodometric method, particularly interference from other antibiotics and excipients used in combination with penicillin. This interference is significant only in the blank determination part of the assay where it is evidenced by iodine absorption. In these cases, reducing the pH of the blank solution to below 2.0 almost completely eliminated the problem. Nevertheless, the present Code of Federal Regulations (CFR) procedure (5), which has recently become the conclusive assay for penicillins G and V and their salts (6), uses an iodine solution of about pH 4.

In the iodometric assay, a sample and reference standard of the same chemical species are normally analyzed under parallel conditions, and this method is probably one of the most rapid, accurate, and specific chemical tests available for a biologically active compound. With the benzathine

© 1978, American Pharmaceutical Association

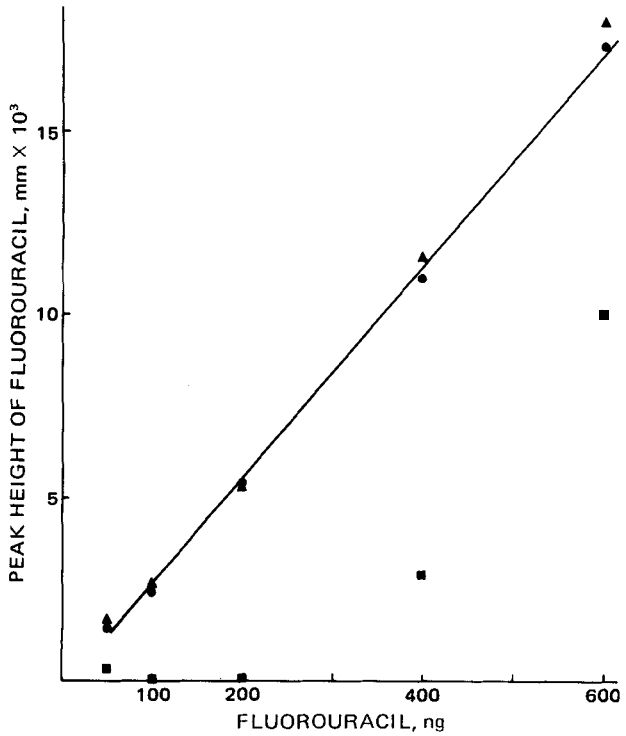

Figure 1—*Recovery of fluorouracil after evaporation of the test solution and reconstitution in plastic (▲) and glass (■) containers as compared to the initial solution (●).*

now enriched with 6-^{3}H-fluorouracil[2], thus permitting a radioactivity control of the GLC results. The recoveries of fluorouracil from glass and plastic vials obtained by the radiochemical determination were essentially the same as in Fig. 1.

The experiments were also extended to other materials. Silanized glass vials, several types of plastic (polyethylene and polypropylene) vials, and small Eppendorf tubes were investigated for their adhesive behavior. Adsorption was observed for glass, whereas fair to almost complete recoveries were found for silanized glass and plastic tubes.

Thus, a simple step in procedures used in the extraction of fluorouracil can produce a substantial loss of the compound in glass vials. We ascribe the observed loss to adsorption on the glass surface. So far, we have no indication that fluorouracil in solution also adheres to glass. However, we try to avoid any contact of fluorouracil with nondeactivated glass surfaces.

(1) J. L. Cohen and P. B. Brennan, *J. Pharm. Sci.*, **62**, 572 (1973).
(2) K. V. Rao, K. Killion, and Y. Tanrikut, *ibid.*, **63**, 1328 (1974).
(3) C. Finn and W. Sadée, *Cancer Chemother. Rep.*, **59**, 279 (1975).
(4) B. L. Hillcoat, M. Kawai, P. B. McCullough, J. Rosenfeld, and C. K. O. Williams, *Br. J. Clin. Pharm.*, **3**, 135 (1976).
(5) A. T. W. U. Schwandt, C. Finn, and W. Sadée, *Res. Commun. Chem. Pathol. Pharmacol.*, **14**, 89 (1976).
(6) D. S. Sitar, D. H. Shaw, M. P. Thirlwell, and J. R. Ruedy, *Cancer Res.*, **37**, 3981 (1977).

O. Driessen ˣ
D. de Vos
P. J. A. Timmermans
Department of Pharmacology
Leiden University Medical Center
Sylvius Laboratories
Wassenaarseweg 72
2333 AL Leiden, The Netherlands

Received March 30, 1978.
Accepted for publication July 24, 1978.
Supported by the Koningin Wilhelmina Foundation, The Netherlands Organization for Cancer Research.

[2] From the Radiochemical Center, Amersham, U.K.

Problems with Iodometric Assay of Penicillin V Benzathine

Keyphrases □ Penicillin V benzathine—iodometric analysis, interference by benzathine molecule □ Benzathine molecule—interference in iodometric analysis of penicillin V benzathine □ Iodometry—analysis, penicillin V benzathine, interference by benzathine molecule □ Antibacterials—penicillin V benzathine, iodometric analysis, interference by benzathine molecule

To the Editor:

Although antibiotics have traditionally been assayed by microbiological techniques, other chemical procedures are now used because of their advantages of speed, precision, and economy. The iodometric method for penicillins (1) is based on the observation that certain products of the inactivation of penicillin, but not the pure active substance, show a marked consumption of iodine.

Two identical samples are taken from a solution of penicillin. One is inactivated with alkali (or penicillinase) and then neutralized with acid. The same amount of iodine is added to both samples and, after a time, the excess iodine is back-titrated with thiosulfate. The difference in the consumption of iodine is a function of the amount of penicillin present.

In the original method, the pH of the iodine reaction solution was about 2. Ortenblad (2), however, found that the method did not always give reproducible values. At pH 4.5, the method was more accurate in the presence of iodine-absorbing impurities and more reproducible since the blank and the inactivated solutions are buffered at the same pH (2). However, with penicillin G procaine, the procaine interfered with the determination at a pH higher than 4.6. This modified procedure is the basis of the present European Pharmacopoeia (3) methods for penicillins G and V.

In 1959, Weiss (4) reviewed the factors affecting the reproducibility of the iodometric method, particularly interference from other antibiotics and excipients used in combination with penicillin. This interference is significant only in the blank determination part of the assay where it is evidenced by iodine absorption. In these cases, reducing the pH of the blank solution to below 2.0 almost completely eliminated the problem. Nevertheless, the present Code of Federal Regulations (CFR) procedure (5), which has recently become the conclusive assay for penicillins G and V and their salts (6), uses an iodine solution of about pH 4.

In the iodometric assay, a sample and reference standard of the same chemical species are normally analyzed under parallel conditions, and this method is probably one of the most rapid, accurate, and specific chemical tests available for a biologically active compound. With the benzathine

© 1978, American Pharmaceutical Association

Table I—Analysis of Oral Suspensions

Manufacturer	Reagent	
	Set A	Set B
1	50.95[a]	54.16
2	49.97	54.15

[a] Expressed as milligrams of penicillin V per gram of oral suspension to avoid the necessity of a specific gravity determination.

Table II—Analysis of Synthetic Mixtures of Penicillin V and Benzathine

Benzathine Added, mg	Penicillin V, mg		Recovery[a], %
	Added	Found	
	Set A		
Control	101.24	101.24	100
20.7	98.90	93.70	94.7
41.4	98.83	89.02	90.1
82.7	102.17	84.94	83.1
	Set B		
Control	102.92	102.92	100
20.7	99.86	99.88	100.0
41.4	104.49	102.05	97.7
82.7	100.22	92.10	91.9

[a] Relative to assigned value of 100% for penicillin V control.

salts of penicillins V and G, however, these products are assayed against penicillin V free acid and penicillin G sodium standards, respectively. In developing a high-performance liquid chromatographic (HPLC) assay for the penicillin V content of all penicillin V acid and salt formulations, we doubted the accuracy of the results obtained by the official CFR iodometric method for the penicillin V benzathine pure drug substance and formulations. That the erroneous results were caused by interference of the benzathine portion of the molecule was shown by the following experiments.

Two sets of reagents (iodine and thiosulfate) were used. Set A was prepared according to the CFR (5), and Set B differed only in that the pH of the iodine solution was adjusted to 2.8 [as originally suggested by Weiss (4)] and the thiosulfate solution was stabilized with chloroform (1 ml/liter) instead of sodium carbonate. Two samples of penicillin V benzathine powder for oral suspension from different manufacturers were reconstituted according to the label instructions and were assayed against the USP penicillin V reference standard on the same day by the same analyst with both sets of reagents.

The results in Table I are averages of two determinations and show that the CFR reagents gave lower potency values for both products. A similar discrepancy was obtained when a sample of penicillin V benzathine pure drug substance was assayed. No difference was encountered, however, when penicillin V free acid was assayed with both sets of reagents. The addition of common excipients, propylparaben, methylparaben, sorbitol, and sodium benzoate, to the penicillin V free acid had no effect on results.

The analysis of synthetic mixtures of benzathine and penicillin V provided evidence that the interference was caused by benzathine. For each set of reagents, approximately 100 mg of penicillin V was dissolved in 2 ml of methanol in four 100-ml volumetric flasks. Aliquots of 0, 10, 20, or 40 ml of a solution of benzathine (2.07 mg/ml) in 1% phosphate buffer (pH 6.0) were then added, the solutions were diluted to volume with buffer, and 2-ml aliquots were determined iodometrically. The results (Table II) conclusively indicate that iodine reacts with benzathine in the blank titration, leading to inaccurate values not only with the CFR method but, to a lesser extent, with the modified iodine reagent as well. Penicillin V benzathine contains approximately 25% benzathine, and Table II indicates that one would expect results from the CFR iodometric method to be from 5 to 10% low. With the more acidic iodine reagent, this error is reduced to about 2%.

The reaction of the iodine with benzathine no doubt involves one or both of the secondary amines in the benzathine molecule. This reaction explains the reduced interference with the iodine reagent at lower pH since the amine is probably present as the hydrochloride salt instead of as the free base. A reaction product has been isolated, and work is continuing to determine its structure and the mechanism of the reaction.

These results indicate that the iodometric assay as presently described (5) is unacceptably inaccurate when applied to the analysis of the benzathine salts of penicillins G and V and that its use as a regulatory procedure should be reevaluated. Alternatives include lowering the pH of the blank solution with accompanying reproducibility problems (2, 7), adoption of more specific methods such as HPLC, and use of the benzathine salts of the penicillins as the reference standards.

(1) J. F. Alicino, *Ind. Eng. Chem. Anal. Ed.*, **18**, 619 (1946).
(2) B. Ortenblad, *Acta Chem. Scand.*, **4**, 518 (1950).
(3) "European Pharmacopoeia," vol. II, Maisonneuve S.A., France, 1971, pp. 160, 339.
(4) P. J. Weiss, *Antibiot. Chemother.*, **9**, 660 (1959).
(5) "Code of Federal Regulations," Title 21, 436.204, U.S. Government Printing Office, Washington, D.C., 1977.
(6) *Fed. Regist.*, **42**, 59852 (1977).
(7) H. Vanderhaeghe, *J. Pharm. Belg.*, **30**, 497 (1975).

Michael J. LeBelle
William L. Wilson [x]
Drug Research Laboratories
Health Protection Branch
National Health and Welfare Canada
Ottawa, Ontario K1A 0L2, Canada

Received April 18, 1978.
Accepted for publication July 19, 1978.

REVIEWS

Textbook of Adverse Drug Reactions. Edited by D. M. DAVIES. Oxford University Press, 200 Madison Ave., New York, NY 10016. 1977. 503 pp. 19.5 × 25 cm. Price $33.95.

This comprehensive book fills the need for an authoritative reference on all major and minor adverse drug reactions. It is the collective work of 32 contributors authoring the 29 chapters and four appendixes.

The specific subject matter covered starts with the history, epidemiology, and pathogenesis of adverse drug reactions and then travels through all the body organs and systems that can possibly be affected by drugs in an unfavorable manner. Also included are the toxicity of opaque media used in X-ray diagnosis, as well as the medicolegal aspects and implications of adverse drug reactions and detection techniques.

The casual reader may be horrified by the great amount of information already available on undesirable effects of the approximately 650 drugs that are prescribed between one and 50,000 times per year and wonder, therefore, why these drugs are still being administered. However, one should be reminded that risk *versus* benefit must be considered when any drug is prescribed. Also, for any drug to be valuable and work, it will always be toxic at some dosage level. A completely safe drug does not exist. A reasonable amount of adverse drug reactions must, therefore, be tolerated in our unending quest for the amelioration of disease manifestations.

Throughout this book, the mechanisms of drug-induced reactions are noted where known and in all cases are explained clearly and concisely. The editor has done a magnificent job of making all the contributors not stray too far from the task at hand. The index is exhaustive, showing the extent of the available information. In addition, the reference material appended to each chapter is far more extensive then that usually seen in a book of this type.

This book is recommended for anyone requiring information on adverse drug reactions of most contemporary drugs. Among those in the health professions that would most likely benefit from it are physicians specializing in internal medicine, pharmacists performing patient counseling, and anyone on the health care team involved in the monitoring of adverse drug reactions including clinical pharmacologists.

Reviewed by Ronald F. Gautieri
Department of Pharmacology
School of Pharmacy
Temple University
Philadelphia, PA 19140

Industrial Bioavailability and Pharmacokinetics: Guidelines, Regulations, and Controls. Edited by ALFRED MARTIN and JAMES T. DOLUISIO. College of Pharmacy, Drug Dynamics Institute, University of Texas, Austin, TX 78712. 1977. 539 pp. 21 × 28 cm.

This book is a somewhat disorganized compilation of some of the presentations from the International Industrial Pharmacy Conference sponsored by the College of Pharmacy, University of Texas, over a 3-year period (1974–1976). The editors have done the best possible job of arranging the material; the fault lies primarily with the inclusion of too many subjects that have little or nothing to do with the title and expressed purpose of the book, "the publication of federal guidelines, regulations, and controls related to industrial problems in drug product bioavailability and pharmacokinetics." Considerable space is devoted to such diverse subjects as the future of compendia, standards for containers and closures, and chemical standards and quality control. The editors have tried valiantly to relate all this information, but it is a hopeless cause, considering the book's title and apparent purpose.

One can find little fault with the qualifications of the authors and editors; they represent some of the very best in the fields of academia, industry, compendia, and government. Furthermore, most presentations, taken individually, are very solid; there is a great deal of relevant information in this book. But its value is considerably lessened by three interrelated culprits: the aforementioned disorganization/diversity, acute redundancy, and mild pedestrianism.

One of the clearer examples of redundancy is the inclusion of three different and overlapping versions of the bioavailability guidelines: the 1974 and 1976 "unofficial" views and the official rules and regulations published in the January 7, 1977, "Federal Register." The repetitiousness of this approach—with its accompanying boredom—is not at all offset by the experience of "(watching) the edifice (i.e., the regulations) as it is being built." A far more efficient and economical way to obtain this information would be order the January 7, 1977 "Federal Register." Additional redundancy is heaped upon the reader when the identical subject (Contributions of Pharmacokinetics During Drug Development) is presented from two different points of view, industry and FDA. Obviously, there is some worthwhile additional information in each presentation, but this approach invites repetition and, while barely tolerable in oral presentations, is best avoided altogether in print.

The third offender, mild pedestrianism, is not the fault of the authors as individuals, nor can it really be attributed to the editors. The basic problem, that too much of the information in the book has appeared elsewhere, stems from our unfortunate tendency to hold too many symposia/conferences on the same subject at (essentially) the same time in different places with essentially the same people presenting and attending.

But in spite of these drawbacks and others (*e.g.*, one questions the added expense of a hard cover and double spacing), the basic value of the philosophies and technical information presented shines through—if one has the patience and mental discipline to put up with the redundancy. It is regrettable that the proceedings of such a worthwhile conference couldn't be published in a more meaningful and less expensive way.

Reviewed by James E. Tingstad
Riker Laboratories, Inc.
Saint Paul, MN 55101

NOTICES

Glucagon: Its Role in Physiology and Clinical Medicine. Edited by PIERO P. FOÀ, JASBIR S. BAJAJ, and NAOMI L. FOÀ. Springer-Verlag, 175 Fifth Ave., New York, NY 10010. 1977. 793 pp. 18 × 26 cm.

Inflammation: Mechanisms and Their Impact on Therapy. Proceedings of an Advanced Teaching Course Held in Rotterdam, November 1976. Edited by I. L. BONTA, J. THOMPSON, and K. BRUNE. Birkhäuser Verlag, P. O. Box 34, CH-4010 Basel, Switzerland. 1977. 197 pp. 16 × 24 cm. Price Sfr. 90.—.

Origins of Human Cancer. Book A, Incidence of Cancer in Humans, 602 pp; *Book B, Mechanisms of Carcinogenesis,* 1303 pp; *Book C, Human Risk Assessment,* 1889 pp. Edited by H. H. HIATT, J. D. WATSON, and J. A. WINSTEN. Cold Spring Harbor Laboratory, P. O. Box 100, Cold Spring Harbor, NY 11724. 1977. 18 × 26 cm. Price $45.00 (set of three).

Reviews of Physiology, Biochemistry and Pharmacology 79. Edited by R. H. ADRIAN *et al.* Springer-Verlag, 175 Fifth Ave., New York, NY 10010. 1977. 180 pp. 16 × 24 cm. Price $45.10.

This volume contains "The Binding of Saxitoxin and Tetrodotoxin to Excitable Tissue," by J. M. RITCHIE and R. B. ROGART; "The Physiology, Pharmacology, and Biochemistry of the Eccrine Sweat Gland," by K. SATO; and "H+ Transport by a Non-Electrogenic Gastric ATPase as a Model for Acid Secretion," by G. SACHS.

Hypertension. Mechanisms, Diagnosis & Management. Edited by JAMES O. DAVIS, JOHN H. LARAGH, and AMY SELWYN. HP Publishing, 575 Lexington Ave., New York, NY 10022. 1977. 274 pp. 21 × 24 cm.

Applications of Ion-Selective Membrane Electrodes in Organic Analysis. By GEORGE E. BAIULESCU and VASILE V. COSOFRET. Halsted,

REVIEWS

Textbook of Adverse Drug Reactions. Edited by D. M. DAVIES. Oxford University Press, 200 Madison Ave., New York, NY 10016. 1977. 503 pp. 19.5 × 25 cm. Price $33.95.

This comprehensive book fills the need for an authoritative reference on all major and minor adverse drug reactions. It is the collective work of 32 contributors authoring the 29 chapters and four appendixes.

The specific subject matter covered starts with the history, epidemiology, and pathogenesis of adverse drug reactions and then travels through all the body organs and systems that can possibly be affected by drugs in an unfavorable manner. Also included are the toxicity of opaque media used in X-ray diagnosis, as well as the medicolegal aspects and implications of adverse drug reactions and detection techniques.

The casual reader may be horrified by the great amount of information already available on undesirable effects of the approximately 650 drugs that are prescribed between one and 50,000 times per year and wonder, therefore, why these drugs are still being administered. However, one should be reminded that risk *versus* benefit must be considered when any drug is prescribed. Also, for any drug to be valuable and work, it will always be toxic at some dosage level. A completely safe drug does not exist. A reasonable amount of adverse drug reactions must, therefore, be tolerated in our unending quest for the amelioration of disease manifestations.

Throughout this book, the mechanisms of drug-induced reactions are noted where known and in all cases are explained clearly and concisely. The editor has done a magnificent job of making all the contributors not stray too far from the task at hand. The index is exhaustive, showing the extent of the available information. In addition, the reference material appended to each chapter is far more extensive then that usually seen in a book of this type.

This book is recommended for anyone requiring information on adverse drug reactions of most contemporary drugs. Among those in the health professions that would most likely benefit from it are physicians specializing in internal medicine, pharmacists performing patient counseling, and anyone on the health care team involved in the monitoring of adverse drug reactions including clinical pharmacologists.

Reviewed by Ronald F. Gautieri
Department of Pharmacology
School of Pharmacy
Temple University
Philadelphia, PA 19140

Industrial Bioavailability and Pharmacokinetics: Guidelines, Regulations, and Controls. Edited by ALFRED MARTIN and JAMES T. DOLUISIO. College of Pharmacy, Drug Dynamics Institute, University of Texas, Austin, TX 78712. 1977. 539 pp. 21 × 28 cm.

This book is a somewhat disorganized compilation of some of the presentations from the International Industrial Pharmacy Conference sponsored by the College of Pharmacy, University of Texas, over a 3-year period (1974–1976). The editors have done the best possible job of arranging the material; the fault lies primarily with the inclusion of too many subjects that have little or nothing to do with the title and expressed purpose of the book, "the publication of federal guidelines, regulations, and controls related to industrial problems in drug product bioavailability and pharmacokinetics." Considerable space is devoted to such diverse subjects as the future of compendia, standards for containers and closures, and chemical standards and quality control. The editors have tried valiantly to relate all this information, but it is a hopeless cause, considering the book's title and apparent purpose.

One can find little fault with the qualifications of the authors and editors; they represent some of the very best in the fields of academia, industry, compendia, and government. Furthermore, most presentations, taken individually, are very solid; there is a great deal of relevant information in this book. But its value is considerably lessened by three interrelated culprits: the aforementioned disorganization/diversity, acute redundancy, and mild pedestrianism.

One of the clearer examples of redundancy is the inclusion of three different and overlapping versions of the bioavailability guidelines: the 1974 and 1976 "unofficial" views and the official rules and regulations published in the January 7, 1977, "Federal Register." The repetitiousness of this approach—with its accompanying boredom—is not at all offset by the experience of "(watching) the edifice (i.e., the regulations) as it is being built." A far more efficient and economical way to obtain this information would be order the January 7, 1977 "Federal Register." Additional redundancy is heaped upon the reader when the identical subject (Contributions of Pharmacokinetics During Drug Development) is presented from two different points of view, industry and FDA. Obviously, there is some worthwhile additional information in each presentation, but this approach invites repetition and, while barely tolerable in oral presentations, is best avoided altogether in print.

The third offender, mild pedestrianism, is not the fault of the authors as individuals, nor can it really be attributed to the editors. The basic problem, that too much of the information in the book has appeared elsewhere, stems from our unfortunate tendency to hold too many symposia/conferences on the same subject at (essentially) the same time in different places with essentially the same people presenting and attending.

But in spite of these drawbacks and others (*e.g.*, one questions the added expense of a hard cover and double spacing), the basic value of the philosophies and technical information presented shines through—if one has the patience and mental discipline to put up with the redundancy. It is regrettable that the proceedings of such a worthwhile conference couldn't be published in a more meaningful and less expensive way.

Reviewed by James E. Tingstad
Riker Laboratories, Inc.
Saint Paul, MN 55101

NOTICES

Glucagon: Its Role in Physiology and Clinical Medicine. Edited by PIERO P. FOÀ, JASBIR S. BAJAJ, and NAOMI L. FOÀ. Springer-Verlag, 175 Fifth Ave., New York, NY 10010. 1977. 793 pp. 18 × 26 cm.

Inflammation: Mechanisms and Their Impact on Therapy. Proceedings of an Advanced Teaching Course Held in Rotterdam, November 1976. Edited by I. L. BONTA, J. THOMPSON, and K. BRUNE. Birkhäuser Verlag, P. O. Box 34, CH-4010 Basel, Switzerland. 1977. 197 pp. 16 × 24 cm. Price Sfr. 90.—.

Origins of Human Cancer. Book A, Incidence of Cancer in Humans, 602 pp; *Book B, Mechanisms of Carcinogenesis,* 1303 pp; *Book C, Human Risk Assessment,* 1889 pp. Edited by H. H. HIATT, J. D. WATSON, and J. A. WINSTEN. Cold Spring Harbor Laboratory, P. O. Box 100, Cold Spring Harbor, NY 11724. 1977. 18 × 26 cm. Price $45.00 (set of three).

Reviews of Physiology, Biochemistry and Pharmacology 79. Edited by R. H. ADRIAN *et al.* Springer-Verlag, 175 Fifth Ave., New York, NY 10010. 1977. 180 pp. 16 × 24 cm. Price $45.10.

This volume contains "The Binding of Saxitoxin and Tetrodotoxin to Excitable Tissue," by J. M. RITCHIE and R. B. ROGART; "The Physiology, Pharmacology, and Biochemistry of the Eccrine Sweat Gland," by K. SATO; and "H+ Transport by a Non-Electrogenic Gastric ATPase as a Model for Acid Secretion," by G. SACHS.

Hypertension. Mechanisms, Diagnosis & Management. Edited by JAMES O. DAVIS, JOHN H. LARAGH, and AMY SELWYN. HP Publishing, 575 Lexington Ave., New York, NY 10022. 1977. 274 pp. 21 × 24 cm.

Applications of Ion-Selective Membrane Electrodes in Organic Analysis. By GEORGE E. BAIULESCU and VASILE V. COSOFRET. Halsted,

REVIEWS

Textbook of Adverse Drug Reactions. Edited by D. M. DAVIES. Oxford University Press, 200 Madison Ave., New York, NY 10016. 1977. 503 pp. 19.5 × 25 cm. Price $33.95.

This comprehensive book fills the need for an authoritative reference on all major and minor adverse drug reactions. It is the collective work of 32 contributors authoring the 29 chapters and four appendixes.

The specific subject matter covered starts with the history, epidemiology, and pathogenesis of adverse drug reactions and then travels through all the body organs and systems that can possibly be affected by drugs in an unfavorable manner. Also included are the toxicity of opaque media used in X-ray diagnosis, as well as the medicolegal aspects and implications of adverse drug reactions and detection techniques.

The casual reader may be horrified by the great amount of information already available on undesirable effects of the approximately 650 drugs that are prescribed between one and 50,000 times per year and wonder, therefore, why these drugs are still being administered. However, one should be reminded that risk *versus* benefit must be considered when any drug is prescribed. Also, for any drug to be valuable and work, it will always be toxic at some dosage level. A completely safe drug does not exist. A reasonable amount of adverse drug reactions must, therefore, be tolerated in our unending quest for the amelioration of disease manifestations.

Throughout this book, the mechanisms of drug-induced reactions are noted where known and in all cases are explained clearly and concisely. The editor has done a magnificent job of making all the contributors not stray too far from the task at hand. The index is exhaustive, showing the extent of the available information. In addition, the reference material appended to each chapter is far more extensive then that usually seen in a book of this type.

This book is recommended for anyone requiring information on adverse drug reactions of most contemporary drugs. Among those in the health professions that would most likely benefit from it are physicians specializing in internal medicine, pharmacists performing patient counseling, and anyone on the health care team involved in the monitoring of adverse drug reactions including clinical pharmacologists.

Reviewed by Ronald F. Gautieri
Department of Pharmacology
School of Pharmacy
Temple University
Philadelphia, PA 19140

Industrial Bioavailability and Pharmacokinetics: Guidelines, Regulations, and Controls. Edited by ALFRED MARTIN and JAMES T. DOLUISIO. College of Pharmacy, Drug Dynamics Institute, University of Texas, Austin, TX 78712. 1977. 539 pp. 21 × 28 cm.

This book is a somewhat disorganized compilation of some of the presentations from the International Industrial Pharmacy Conference sponsored by the College of Pharmacy, University of Texas, over a 3-year period (1974–1976). The editors have done the best possible job of arranging the material; the fault lies primarily with the inclusion of too many subjects that have little or nothing to do with the title and expressed purpose of the book, "the publication of federal guidelines, regulations, and controls related to industrial problems in drug product bioavailability and pharmacokinetics." Considerable space is devoted to such diverse subjects as the future of compendia, standards for containers and closures, and chemical standards and quality control. The editors have tried valiantly to relate all this information, but it is a hopeless cause, considering the book's title and apparent purpose.

One can find little fault with the qualifications of the authors and editors; they represent some of the very best in the fields of academia, industry, compendia, and government. Furthermore, most presentations, taken individually, are very solid; there is a great deal of relevant information in this book. But its value is considerably lessened by three interrelated culprits: the aforementioned disorganization/diversity, acute redundancy, and mild pedestrianism.

One of the clearer examples of redundancy is the inclusion of three different and overlapping versions of the bioavailability guidelines: the 1974 and 1976 "unofficial" views and the official rules and regulations published in the January 7, 1977, "Federal Register." The repetitiousness of this approach—with its accompanying boredom—is not at all offset by the experience of "(watching) the edifice (i.e., the regulations) as it is being built." A far more efficient and economical way to obtain this information would be order the January 7, 1977 "Federal Register." Additional redundancy is heaped upon the reader when the identical subject (Contributions of Pharmacokinetics During Drug Development) is presented from two different points of view, industry and FDA. Obviously, there is some worthwhile additional information in each presentation, but this approach invites repetition and, while barely tolerable in oral presentations, is best avoided altogether in print.

The third offender, mild pedestrianism, is not the fault of the authors as individuals, nor can it really be attributed to the editors. The basic problem, that too much of the information in the book has appeared elsewhere, stems from our unfortunate tendency to hold too many symposia/conferences on the same subject at (essentially) the same time in different places with essentially the same people presenting and attending.

But in spite of these drawbacks and others (*e.g.*, one questions the added expense of a hard cover and double spacing), the basic value of the philosophies and technical information presented shines through—if one has the patience and mental discipline to put up with the redundancy. It is regrettable that the proceedings of such a worthwhile conference couldn't be published in a more meaningful and less expensive way.

Reviewed by James E. Tingstad
Riker Laboratories, Inc.
Saint Paul, MN 55101

NOTICES

Glucagon: Its Role in Physiology and Clinical Medicine. Edited by PIERO P. FOÀ, JASBIR S. BAJAJ, and NAOMI L. FOÀ. Springer-Verlag, 175 Fifth Ave., New York, NY 10010. 1977. 793 pp. 18 × 26 cm.

Inflammation: Mechanisms and Their Impact on Therapy. Proceedings of an Advanced Teaching Course Held in Rotterdam, November 1976. Edited by I. L. BONTA, J. THOMPSON, and K. BRUNE. Birkhäuser Verlag, P. O. Box 34, CH-4010 Basel, Switzerland. 1977. 197 pp. 16 × 24 cm. Price Sfr. 90.—.

Origins of Human Cancer. Book A, Incidence of Cancer in Humans, 602 pp; *Book B, Mechanisms of Carcinogenesis,* 1303 pp; *Book C, Human Risk Assessment,* 1889 pp. Edited by H. H. HIATT, J. D. WATSON, and J. A. WINSTEN. Cold Spring Harbor Laboratory, P. O. Box 100, Cold Spring Harbor, NY 11724. 1977. 18 × 26 cm. Price $45.00 (set of three).

Reviews of Physiology, Biochemistry and Pharmacology 79. Edited by R. H. ADRIAN *et al.* Springer-Verlag, 175 Fifth Ave., New York, NY 10010. 1977. 180 pp. 16 × 24 cm. Price $45.10.

This volume contains "The Binding of Saxitoxin and Tetrodotoxin to Excitable Tissue," by J. M. RITCHIE and R. B. ROGART; "The Physiology, Pharmacology, and Biochemistry of the Eccrine Sweat Gland," by K. SATO; and "H+ Transport by a Non-Electrogenic Gastric ATPase as a Model for Acid Secretion," by G. SACHS.

Hypertension. Mechanisms, Diagnosis & Management. Edited by JAMES O. DAVIS, JOHN H. LARAGH, and AMY SELWYN. HP Publishing, 575 Lexington Ave., New York, NY 10022. 1977. 274 pp. 21 × 24 cm.

Applications of Ion-Selective Membrane Electrodes in Organic Analysis. By GEORGE E. BAIULESCU and VASILE V. COSOFRET. Halsted,

605 Third Ave., New York, NY 10016. 1977. 235 pp. 15 × 23 cm.

Review of Inhalants: Euphoria to Dysfunction. NIDA Research Monograph 15. Edited by CHARLES W. SHARP and MARY LEE BREHM. National Institute on Drug Abuse, 5600 Fishers Lane, Rockville, MD 20857. 1977. 347 pp. 14 × 23 cm.

Entwicklung der Hypertoniemortalität und des Antihypertensiva-Verbrauchs in der Schweiz. By MARTIN ESCHER. Springer-Verlag, 175 Fifth Ave., New York, NY 10010. 1977. 106 pp. 16 × 24 cm. Price $11.10.

Research on Smoking Behavior. NIDA Research Monograph 17. Edited by MURRAY E. JARVIK, JOSEPH W. CULLEN, ELLEN R. GRITZ, THOMAS M. VOGT, and LOUIS JOLYON WEST. National Institute on Drug Abuse, 5600 Fishers Lane, Rockville, MD 20857. 1977. 381 pp. 14 × 24 cm.

The Epidemiology of Heroin and Other Narcotics. NIDA Research Monograph 16. Edited by JOAN DUNNE RITTENHOUSE. National Institute on Drug Abuse, 5600 Fishers Lane, Rockville, MD 20857. 1977. 249 pp. 14 × 23 cm.

Essays in Neurochemistry and Neuropharmacology. Vol. 2. Edited by M. B. H. YOUDIM, D. F. SHARMAN, W. LOVENBERG, and J. LAGNADO. Wiley, 605 Third Ave., New York, NY 10016. 1977. 174 pp. 15 × 23 cm. Price $19.95.

Progress in Drug Research. Vol. 21. Edited by ERNST JUCKER. Birkhäuser Verlag, P. O. Box 34, CH-4010 Basel, Switzerland, 1977. 499 pp. 16 × 24 cm. Price Sfr. 186.

The Freezing of Mammalian Embryos. Ciba Foundation Symposium 52 (new series). Elsevier/North-Holland, 52 Vanderbilt Ave., New York, NY 10017. 1977. 330 pp. 16 × 24 cm.

Iron Metabolism. Ciba Foundation Symposium 51 (new series). Elsevier/North-Holland, 52 Vanderbilt Ave., New York, NY 10017. 1977. 391 pp. 16 × 24 cm.

Health Needs of Society: A Challenge for Medical Education. 10th CIOMS Round Table Conference and Report of the Scientific Session of the 10th General Assembly of CIOMS, Geneva. Edited by A. GELLHORN, T. FÜLOP, and Z. BANKOWSKI. World Health Organization, 49 Sheridan Ave., Albany, NY 12210. 1977. 221 pp. 13 × 21 cm. Price $9.00.

The SI for the Health Professions. Prepared at the Request of the 30th World Health Assembly. World Health Organization, 49 Sheridan Ave., Albany, NY 12210. 1977. 75 pp. 11 × 19 cm. Price $2.25.

The Selection of Essential Drugs. Report of a WHO Expert Committee. World Health Organization, 49 Sheridan Ave., Albany, NY 12210. 1977. 36 pp. 14 × 20 cm. Price $2.25.

Iatrogenic Carcinogensis. By D. SCHMÄHL, C. THOMAS, and R. AUER. Springer-Verlag, 175 Fifth Ave., New York, NY 10010. 1977. 120 pp. 13 × 20 cm. Price $10.60.

Methods in Prenatal Toxicology. Evaluation of Embryotoxic Effects in Experimental Animals. Teratology Workshop, April 1977, Berlin. Edited by D. NEUBERT, H.-J. MERKER, and T. E. KWASIGROCH. Georg Tieme Verlag, Herdweg 63, P.O.B. 732, D-7000 Stuttgart 1, Germany. 1977. 474 pp. 15 × 23 cm.

Plasma Proteins: Analytical and Preparative Techniques. By PETER C. ALLEN, ELIZABETH A. HILL, and ALISTAIR M. STOKES. Lippincott, East Washington Square, Philadelphia, PA 19105. 1977. 254 pp. 16 × 24 cm. Price $32.00.

Reviews of Physiology, Biochemistry, and Pharmacology 80. Edited by R. H. ADRIAN, *et al.* Springer-Verlag, 175 Fifth Ave., New York, NY 10010. 1978. 197 pp. 16 × 24 cm. Price $39.60.

This volume contains "The Physiologic Determinants of Glomerular Ultrafiltration," by C. BAYLIS and B. M. BRENNER; "Models for the Ontogenetic Development of Higher Organisms," by H. MEINHARDT; and "Extraretinal Influences on the Lateral Geniculate Nucleus," by W. BURKE and A. M. COLE.

Serotonin in Health and Disease. Vol. II: Physiological Regulation and Pharmacological Action. Edited by WALTER B. ESSMAN. Spectrum, 175-20 Wexford Terrace, Jamaica, NY 11423. 1978. 443 pp. 15 × 23 cm. Price $37.50.

Guide des Plantes Dangereuses. By ANNE-MARIE DEBELMAS and PIERRE DELAVEAU. Maloine S. A. Editeur, 27 Rue de l'Ecole de Médecine, 75006 Paris, France. 1978. 190 pp. 15 × 22 cm. Price 68 Fr.

Gas Chromatography with Glass Capillary Columns. By WALTER JENNINGS. Academic, 111 Fifth Ave., New York, NY 10003. 1978. 184 pp. 14 × 23 cm. Price $16.50.

Noncatecholic Phenylethylamines. Part I, Phenylethylamine: Biological Mechanisms and Clinical Aspects. Edited by ARON D. MOSNAIM and MARION E. WOLF. Dekker, 270 Madison Ave., New York, NY 10016. 1978. 536 pp. 14 × 23 cm. Price $49.50.

Synthesis of Prostaglandins. Recent Developments in the Chemistry of Carbon Compounds, Vol. 8. By CS. SZÁNTAY and L. NOVAK. Akadémiai Kiadó, Publishing House of the Hungarian Academy of Sciences, V. Alkotmany U. 21, Budapest, Hungary. 1978. 267 pp. 16 × 24 cm. Price $16.00.

Paraquat Determination

The Open Forum item by Kaistha *et al.*[1] on Paraquat is very interesting and also appropriate due to the high risks involved in Paraquat-contaminated marijuana smoking. However, the described method is time consuming, particularly when one is looking for a quick answer.

I believe that a recent technique that utilizes sodium bicarbonate and sodium dithionate solutions in the marijuana washings for the development of a blue color is rather simple and convenient. Moreover, our laboratory has developed a single TLC and spot test technique[2] for the Paraquat-sprayed hallucinogen.

Nicolas H. Choulis
School of Pharmacy
Medical Center
West Virginia University
Morgantown, WV 26506

Received August 24, 1978.

[1] K. K. Kaistha, R. Tadrus, and D. Wojtulewicz, *J. Pharm. Sci.*, 67 (8), IV (1978).
[2] To be published.

PHARMACIST

We are a rapidly growing ethical pharmaceutical company presently building a research and product development team and seek a pharmacist with a B.S. degree to develop stability protocols for finished dosage, monitor stability and coordinate the necessary work. Will also conduct formulation studies to defend marketed products.

Send resume and salary requirement to

Adria
LABORATORIES INC.

582 Goodale St. Columbus, Ohio 43215

An equal opportunity employer, M/F.

manager product r & d

In 1977 we exceeded $1 billion...an increase of 15% from 1976 and *over double* our 1973 volume! We reinvested more than 5% of that volume in R & D. And we continued to market a wide range of health care products in over 150 countries worldwide.

All of the above indicates growth! A growth you can share in if you qualify for this challenging position. Responsibilities include managing a staff of approximately 30 professionals in research and development activities for pharmaceutical products.

To qualify, you should have a Ph.D. in Pharmacy, Pharmaceutics, Pharmaceutical Chemistry or Biopharmaceutics plus at least 5 years of solid experience involving:

- Managing pharmaceutical product scientists
- Scale-up activities
- Interfacing with manufacturing, Q.A., regulatory, clinical, and other areas
- Budget preparation and adherence
- Manpower planning and allocation
- General interpersonal management
- Exposure to solid dosage form pharmaceuticals (including filmcoating)

In addition to exceptional career potential, we offer an excellent salary and full benefits program. For consideration, send a resume with salary history, in complete confidence, to:

**Box 108, *J. Pharm. Sci.*, 2215 Constitution Avenue N.W.
Washington, DC 20037**

We are an Affirmative Action Employer

NOVEMBER 1978
VOLUME 67 NUMBER 11

JOURNAL OF PHARMACEUTICAL SCIENCES

MARY H. FERGUSON
Editor

SHELLY ELLIOTT
Production Editor

EDWARD G. FELDMANN
Contributing Editor

SAMUEL W. GOLDSTEIN
Contributing Editor

BELLE R. BECK
Editorial Secretary

DAVID BOHARDT
Director of Publications

L. LUAN CORRIGAN
Assistant Director of Publications

EDITORIAL ADVISORY BOARD

JOHN AUTIAN	HERBERT A. LIEBERMAN
NORMAN R. FARNSWORTH	DAVID E. MANN, JR.
WILLIAM O. FOYE	GERALD J. PAPARIELLO
WILLIAM J. JUSKO	EDWARD G. RIPPIE

The *Journal of Pharmaceutical Sciences* is published monthly by the American Pharmaceutical Association (APhA) at 2215 Constitution Ave., N.W., Washington, DC 20037. Second-class postage paid at Washington, D.C., and at additional mailing office.

All expressions of opinion and statements of supposed fact appearing in articles or editorials carried in this journal are published on the authority of the writer over whose name they appear and are not to be regarded as necessarily expressing the policies or views of APhA.

Offices—Editorial, Advertising, and Subscription: 2215 Constitution Ave., N.W., Washington, DC 20037. Printing: 20th & Northampton Streets, Easton, PA 18042.

Annual Subscriptions—United States and foreign, industrial and government institutions $50, educational institutions $50, individuals *for personal use only* $30; single copies $5. All foreign subscriptions add $5 for postage. Subscription rates are subject to change without notice. Members of APhA may elect to receive the *Journal of Pharmaceutical Sciences* as a part of their annual $70 (foreign $75) APhA membership dues.

Claims—Missing numbers will not be supplied if dues or subscriptions are in arrears for more than 60 days or if claims are received more than 60 days after the date of the issue, or if loss was due to failure to give notice of change of address. APhA cannot accept responsibility for foreign delivery when its records indicate shipment has been made.

Change of Address—Members and subscribers should notify at once both the Post Office and APhA of any change of address.

Photocopying—The code at the foot of the first page of an article indicates that APhA has granted permission for copying of the article beyond the limits permitted by Sections 107 and 108 of the U.S. Copyright Law provided that the copier sends the per copy fee stated in the code to the Copyright Clearance Center, Inc., P. O. Box 765, Schenectady, NY 12301. Copies may be made for personal or internal use only and not for general distribution.

Microfilm—Available from University Microfilms International, 300 N. Zeeb Road, Ann Arbor, MI 48106.

© Copyright 1978. American Pharmaceutical Association, 2215 Constitution Ave., N.W., Washington, DC 20037; all rights reserved.

RESEARCH FRONTIERS REMAIN RIPE

A hundred years ago, it is reported, some adventurous fellows complained that "there are no more new worlds to conquer!" In their view, the golden age of discovery and exploration which started with Columbus' epic voyage in 1492 had run its course; it had come to an end, they thought, because everything discoverable had been discovered, and everything explorable had been explored.

In the intervening years, however, we have learned that we really still don't know much about the polar regions, about the ocean depths, and about remote regions of mountains and jungle. For example, entire tribes and cultures, previously unknown, have only recently been found in the Philippine Islands and in South America. And all of this is aside from the dramatic space explorations of the last twenty years.

So, too, in the field of science, researchers are purported to have lamented at various times that all the great discoveries have taken place, and the well of innovation has literally run dry.

We were reminded of all this in September when we read the truly dramatic announcement that human insulin had been produced in a California research laboratory by bacteria through application and use of recombinant DNA research and methodology. The process involves the insertion of a synthetic gene into *E. coli* organisms, which are then grown *via* normal fermentation processes. Insulin is produced by the bacteria during the fermentation, and it is subsequently isolated and purified. The resulting product appears to be identical to human insulin.

Consequently, this discovery has several potential beneficial aspects:

- *First,* when the process is ultimately refined and made practical from a production standpoint, it should require far less time, equipment, and effort to produce insulin by this method compared to existing procedures; this translates into major cost savings.
- *Second,* availability of insulin will no longer be dependent upon the risky supply of vast quantities of animal organs—pancreas glands of cattle and swine—from which the hormone presently is obtained by extraction procedures. This means that any concern over future supplies of critical raw material would be eliminated.
- *Third,* the resulting form of insulin is structurally identical to that produced by the normal human pancreas, as well as being free from any animal protein or other animal by-products; this means a more effective product and virtually eliminates the possibility of allergic reactions.

Considering these remarkable advantages, we are tempted to offer the facetious comment that the people who think up slogans for automobile bumper stickers ought to design one reading: "Bacteria do it better!"

Seriously, however, the accomplishment is really magnificent, and all those who in any way contributed to the success of this feat have our sincere congratulations and compliments. It is recognized (*a*) that this test-tube scale laboratory success must yet be converted into practical production and manufacturing processes, (*b*) that considerable animal and clinical testing needs to be performed to demonstrate the safety and effectiveness of the product, and (*c*) that regulatory approvals also will be needed before the product can be marketed.

Nevertheless, the scientific breakthroughs reflected in this accomplishment constitute major achievements in hormone or protein synthesis (insulin) as well as genetic research (application of recombinant DNA). Either aspect by itself would be considered most noteworthy; coming together in a single stroke, the result is virtually mind-boggling.

This makes it the most convincing proof imaginable that there remain many scientific frontiers of research and discovery that simply await the attention of adventurous minds and imaginative approaches.

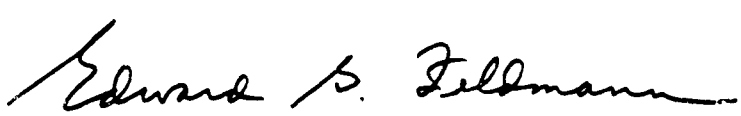

NOVEMBER 1978
VOLUME 67 NUMBER 11

JOURNAL OF PHARMACEUTICAL SCIENCES

MARY H. FERGUSON
Editor

SHELLY ELLIOTT
Production Editor

EDWARD G. FELDMANN
Contributing Editor

SAMUEL W. GOLDSTEIN
Contributing Editor

BELLE R. BECK
Editorial Secretary

DAVID BOHARDT
Director of Publications

L. LUAN CORRIGAN
Assistant Director of Publications

EDITORIAL ADVISORY BOARD

JOHN AUTIAN	HERBERT A. LIEBERMAN
NORMAN R. FARNSWORTH	DAVID E. MANN, JR.
WILLIAM O. FOYE	GERALD J. PAPARIELLO
WILLIAM J. JUSKO	EDWARD G. RIPPIE

The *Journal of Pharmaceutical Sciences* is published monthly by the American Pharmaceutical Association (APhA) at 2215 Constitution Ave., N.W., Washington, DC 20037. Second-class postage paid at Washington, D.C., and at additional mailing office.

All expressions of opinion and statements of supposed fact appearing in articles or editorials carried in this journal are published on the authority of the writer over whose name they appear and are not to be regarded as necessarily expressing the policies or views of APhA.

Offices—Editorial, Advertising, and Subscription: 2215 Constitution Ave., N.W., Washington, DC 20037. Printing: 20th & Northampton Streets, Easton, PA 18042.

Annual Subscriptions—United States and foreign, industrial and government institutions $50, educational institutions $50, individuals *for personal use only* $30; single copies $5. All foreign subscriptions add $5 for postage. Subscription rates are subject to change without notice. Members of APhA may elect to receive the *Journal of Pharmaceutical Sciences* as a part of their annual $70 (foreign $75) APhA membership dues.

Claims—Missing numbers will not be supplied if dues or subscriptions are in arrears for more than 60 days or if claims are received more than 60 days after the date of the issue, or if loss was due to failure to give notice of change of address. APhA cannot accept responsibility for foreign delivery when its records indicate shipment has been made.

Change of Address—Members and subscribers should notify at once both the Post Office and APhA of any change of address.

Photocopying—The code at the foot of the first page of an article indicates that APhA has granted permission for copying of the article beyond the limits permitted by Sections 107 and 108 of the U.S. Copyright Law provided that the copier sends the per copy fee stated in the code to the Copyright Clearance Center, Inc., P. O. Box 765, Schenectady, NY 12301. Copies may be made for personal or internal use only and not for general distribution.

Microfilm—Available from University Microfilms International, 300 N. Zeeb Road, Ann Arbor, MI 48106.

© Copyright 1978. American Pharmaceutical Association, 2215 Constitution Ave., N.W., Washington, DC 20037; all rights reserved.

RESEARCH FRONTIERS REMAIN RIPE

A hundred years ago, it is reported, some adventurous fellows complained that "there are no more new worlds to conquer!" In their view, the golden age of discovery and exploration which started with Columbus' epic voyage in 1492 had run its course; it had come to an end, they thought, because everything discoverable had been discovered, and everything explorable had been explored.

In the intervening years, however, we have learned that we really still don't know much about the polar regions, about the ocean depths, and about remote regions of mountains and jungle. For example, entire tribes and cultures, previously unknown, have only recently been found in the Philippine Islands and in South America. And all of this is aside from the dramatic space explorations of the last twenty years.

So, too, in the field of science, researchers are purported to have lamented at various times that all the great discoveries have taken place, and the well of innovation has literally run dry.

We were reminded of all this in September when we read the truly dramatic announcement that human insulin had been produced in a California research laboratory by bacteria through application and use of recombinant DNA research and methodology. The process involves the insertion of a synthetic gene into *E. coli* organisms, which are then grown *via* normal fermentation processes. Insulin is produced by the bacteria during the fermentation, and it is subsequently isolated and purified. The resulting product appears to be identical to human insulin.

Consequently, this discovery has several potential beneficial aspects:

- *First,* when the process is ultimately refined and made practical from a production standpoint, it should require far less time, equipment, and effort to produce insulin by this method compared to existing procedures; this translates into major cost savings.
- *Second,* availability of insulin will no longer be dependent upon the risky supply of vast quantities of animal organs—pancreas glands of cattle and swine—from which the hormone presently is obtained by extraction procedures. This means that any concern over future supplies of critical raw material would be eliminated.
- *Third,* the resulting form of insulin is structurally identical to that produced by the normal human pancreas, as well as being free from any animal protein or other animal by-products; this means a more effective product and virtually eliminates the possibility of allergic reactions.

Considering these remarkable advantages, we are tempted to offer the facetious comment that the people who think up slogans for automobile bumper stickers ought to design one reading: "Bacteria do it better!"

Seriously, however, the accomplishment is really magnificent, and all those who in any way contributed to the success of this feat have our sincere congratulations and compliments. It is recognized (*a*) that this test-tube scale laboratory success must yet be converted into practical production and manufacturing processes, (*b*) that considerable animal and clinical testing needs to be performed to demonstrate the safety and effectiveness of the product, and (*c*) that regulatory approvals also will be needed before the product can be marketed.

Nevertheless, the scientific breakthroughs reflected in this accomplishment constitute major achievements in hormone or protein synthesis (insulin) as well as genetic research (application of recombinant DNA). Either aspect by itself would be considered most noteworthy; coming together in a single stroke, the result is virtually mind-boggling.

This makes it the most convincing proof imaginable that there remain many scientific frontiers of research and discovery that simply await the attention of adventurous minds and imaginative approaches.

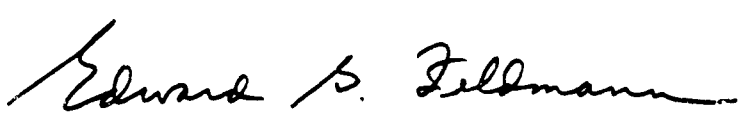

JOURNAL OF PHARMACEUTICAL SCIENCES

NOVEMBER 1978
VOLUME 67 NUMBER 11

RESEARCH ARTICLES

Rheology of Pharmaceutical Systems: Oscillatory and Steady Shear of Non-Newtonian Viscoelastic Liquids

GEORGE B. THURSTON ˣ and ALFRED MARTIN

Received December 8, 1977, from the *Departments of Mechanical and Biomedical Engineering and the Drug Dynamics Institute, College of Pharmacy, University of Texas at Austin, Austin, TX 78712.* Accepted for publication March 1, 1978.

Abstract □ A comparative analysis of oscillatory and steady shear rate measurements was made on carboxymethylcellulose solutions of two concentrations and two viscosity grades. In the oscillatory methods, the material is examined under nearly quiescent equilibrium conditions. Steady shear, conversely, produces large deformations and may yield false results, often interpreted as thixotropy, if the shear rate experiment is not conducted properly. Solutions of carboxymethylcellulose at concentrations ordinarily used in drug product formulations were examined by oscillatory and steady shear methods at low shear. Viscoelastic properties of pharmaceutical materials were measured using a newly developed oscillometric instrument. Mathematical expressions, formulated on the basis of a generalized Maxwell model for viscoelasticity and viscosity in steady shear, were correlated using these two rheological test methods. The results showed large increases in viscosity and relaxation time with increasing carboxymethylcellulose concentrations as well as with increasing molecular weights of the polymeric solute. The behavior of carboxymethylcellulose under both oscillatory and steady shear agreed with theory, linking the two methods of testing. Applications in pharmacy to this rheological analysis are presented. The present investigation attempted to bridge the gap between oscillatory and steady shear methods, demonstrating how both can find appropriate use in the analysis of non-Newtonian materials of pharmaceutical importance.

Keyphrases □ Carboxymethylcellulose—oscillatory and steady shear rate measurements compared, effect of concentration and viscosity grade □ Viscoelastic properties—carboxymethylcellulose, oscillatory and steady shear rate measurements compared, effect of concentration and viscosity grade □ Oscillatory measurements—compared to steady shear rate method, carboxymethylcellulose, effect of concentration and viscosity grade □ Steady shear rate measurements—compared to oscillatory method, carboxymethylcellulose, effect of concentration and viscosity grade

Polymer solutions such as carboxymethylcellulose dispersions and some pharmaceutical, food, and cosmetic products show shear thinning with increased shear rate. This phenomenon is characteristic of non-Newtonian liquids, which are referred to as pseudoplastic (1). When shear thinning is measured in a rotational viscometer of the concentric cylinder type or in the cone and plate configuration (2–4), the shear stress and shear rate often are varied in a cyclic sequence. Starting from rest, the stress is measured with shear rate increasing, either continuously or stepwise at some prescribed rate, and then decreasing to rest.

With a Newtonian fluid, this procedure gives a graph of shear stress *versus* rate that is linear, the up and down curves being superimposed. With non-Newtonian fluid, the graph is generally concave toward the shear rate axis since the shear stress increases less rapidly than the shear rate. If the cyclic time is too short, the down curve may not coincide with the up curve. With the broader classification of thixotropic materials, the up and down curves may not coincide in any event (5).

BACKGROUND

In a solution of long chain polymer molecules, non-Newtonian behavior results from chain elongation induced by high shear stress and, at high polymer concentrations, may also involve ordering and disentanglement of the chains (1, 6). In colloids and suspensions, non-Newtonian behavior results from particle orientation, deformation, aggregation, disaggregation, and other structural modifications.

Davis (7) pointed out disadvantages of continuous, steady shear rheometry, principally the unavoidable disruption of the solid structure of a material during measurement. It is often impossible to separate the true rheological properties of complex materials from the instrumental effects when using a rotational, steady shear instrument (7). Schnaare *et al.* (8) also confronted these inherent problems.

An alternative approach to the rheology of non-Newtonian materials, that of viscoelastic measurements performed using small deformations including creep analysis, does not ordinarily disrupt particle aggregates in suspension, destroy the network of gels, or force entanglement effects in polymers. Creep tests have been used in pharmacy and cosmetic science (9–18). The measurement flexes the structures of the dispersions without destroying rheological characteristics. Other workers (19–21) described oscillatory equipment for the measurement of suspensions, gels, and blood in the unperturbed state or in the "rheological ground state," as Barry (9) termed it. By a mathematical transformation from the theory on linear viscoelasticity, oscillatory and creep measurements can be related (22) to one another.

0022-3549/78/1100-1499$01.00/0
© 1978, American Pharmaceutical Association

Since the present work concerns a comparative analysis of oscillatory and steady shear rate measurements, it is necessary to make several distinctions in classifying these two conditions. First, oscillatory shear may be of either small or large amplitude. For small amplitude, the shear stress to shear rate relation is linear with a change in amplitude; therefore, a pure sinusoid of shear rate produces a pure sinusoid of shear stress at the same frequency. The material is thus examined under nearly quiescent, unperturbed, equilibrium conditions. For large amplitude, the state of the material may undergo some change because of finite deformations. The shear stress to shear rate relation may become nonlinear, and the sinusoidal waveforms take on some harmonic distortion.

Second, steady shear, unlike oscillatory shear, produces only large deformations, with the magnitude of deformation increasing at a constant rate with time. However, the growth rate of the deformation, *i.e.*, the shear rate, may be either low or high. Thus, continuous steady shear is incompatible with materials in the solid state since these materials can tolerate only limited deformations without destruction. Small oscillatory deformations can be employed for both solids and liquids, but steady shear is applicable only to liquids. Corresponding stress to strain rate relations probably are approached under conditions of very small shear rates using either steady shear measurements or oscillating measurements with the frequency of oscillation approaching zero. This limiting relationship is evaluated for the materials in the current investigation.

Within the framework of these concepts, the questions arise: Can thixotropy be meaningfully studied in steady shear? And, if conventional indications are found, is the material truly thixotropic? The fact that finite to infinite deformation of the material is involved in the test means that the material is a liquid, or it is a solid that has undergone disruption of the bulk material or slippage at the wall to permit deformation. Moreover, to achieve steady shear rate conditions, the shear rate must be maintained at a constant value for a time sufficiently long that equilibrium is attained and all recoverable effects from past deformational history are regained. The time needed for this effect is much longer than convenient for measurements on many materials. Measurements performed by instrumentation that continuously increases or decreases the shear rate may perpetuate the nonequilibrium condition and give a false indication of thixotropy. Careful attention is given to attainment of equilibrium in the work reported here.

In the present investigation, the behavior of the polymer, carboxymethylcellulose, in solutions of moderately high concentrations is examined using oscillatory shear measurements at low amplitudes and steady shear measurements. This comparison is done to examine limiting low shear rate–steady shear behavior with limiting low frequency oscillatory shear behavior. The extension to higher frequencies of oscillatory shear and higher rates of steady shear also is discussed. Mathematical expressions for viscoelasticity in oscillatory shear and for viscosity in steady shear are compared with the experimental results and provide a basis for the characterization of liquids under these two test methods.

THEORETICAL

Viscoelasticity in Oscillatory Shear—The conceptual definition for viscoelastic behavior in oscillatory shear is represented in Fig. 1*a*. An idealized thin layer of material is subjected to an oscillatory driving force, F, resulting in a surface motion of velocity, V. The shear stress induced in the material, τ, is directly proportional to F, while the shear rate, $\dot{\gamma}$, is proportional to V. If the frequency of this sinusoidal oscillation is $(\omega/2\pi)$ Hz, then the shear rate and shear stress have the time dependencies:

$$\dot{\gamma} = \dot{\gamma}_M \cos(\omega t) \qquad \text{(Eq. 1}a\text{)}$$

$$\tau = \tau_M \cos(\omega t - \phi) \qquad \text{(Eq. 1}b\text{)}$$

where ϕ is the phase difference between τ and $\dot{\gamma}$. These phased sinusoids are shown in Fig. 1*b*. For a purely viscous material, $\phi = 0$; for a purely elastic material, $\phi = (\pi/2)$ rad. In the general viscoelastic case, ϕ falls between these two limits. The shear rate and shear stress may be described using complex forms:

$$\dot{\gamma}^* = \dot{\gamma}_M \exp(i\omega t) \qquad \text{(Eq. 2}a\text{)}$$

$$\tau^* = \tau_M \exp(i\omega t - i\phi) \qquad \text{(Eq. 2}b\text{)}$$

the real parts of which are $\dot{\gamma}$ and τ. These are shown in a complex plane representation in Fig. 1*c*, where the phasors, $\dot{\gamma}^*$ and τ^*, rotate counterclockwise at an angular rotation rate, ω. By forming the ratio of τ^* to $\dot{\gamma}^*$, the complex coefficient of viscosity is defined. This ratio gives:

$$\eta^* = \tau^*/\dot{\gamma}^* \qquad \text{(Eq. 3}a\text{)}$$

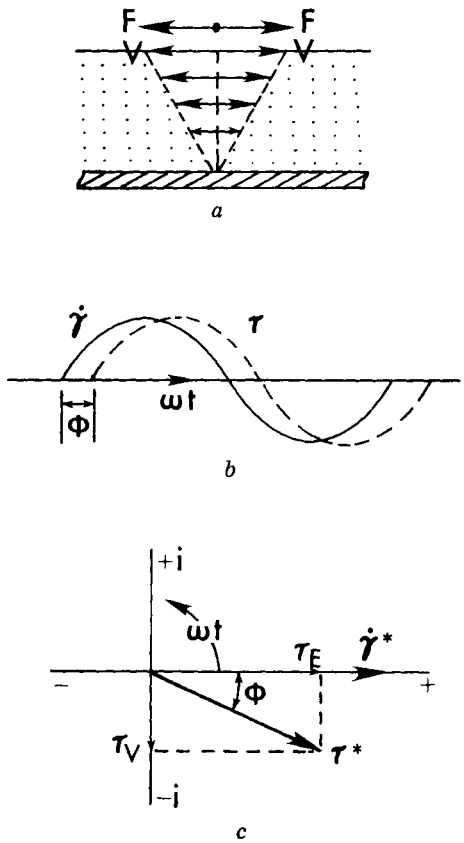

Figure 1—*Viscoelastic behavior in oscillatory shear. A sample is subjected to oscillatory force,* F, *and velocity,* V, *at a radian frequency,* ω. *The resulting shear stress,* τ, *and the time rate of shear strain,* $\dot{\gamma}$, *differ in phase by the angle,* ϕ. *These parameters are also shown in complex form by plotting in the complex plane.*

$$\eta^* = (\tau_M/\dot{\gamma}_M) \exp(-i\phi) \qquad \text{(Eq. 3}b\text{)}$$

$$\eta^* = \eta \exp(-i\phi) \qquad \text{(Eq. 3}c\text{)}$$

where η is the magnitude and ϕ is the phase of the viscoelastic modulus.

Equations 3*a*–3*c* may be resolved into real and imaginary terms, in which case the viscous and elastic parts are determined. In the diagram of the complex plane (Fig. 1), the complex shear stress, τ^*, is shown resolved into that part in phase, τ_V, with the shear rate, $\dot{\gamma}^*$, and that part in quadrature, τ_E. These shear stresses are the viscous and elastic parts of τ^*. Thus, the complex coefficient of viscosity is:

$$\eta^* = (\tau_V - i\tau_E)/\dot{\gamma}^* \qquad \text{(Eq. 4}a\text{)}$$

$$\eta^* = (\tau_M \cos\phi/\dot{\gamma}_M) - (\tau_M \sin\phi/\dot{\gamma}_M) \qquad \text{(Eq. 4}b\text{)}$$

$$\eta^* = \eta_V - i\eta_E \qquad \text{(Eq. 4}c\text{)}$$

where η_V and η_E are the viscous and elastic parts of η^*. To interpret these parameters further, the viscous parts are associated with energy loss during the cyclic shearing while the elastic parts give cyclic storage and recovery of energy. This relation is seen by calculating the work done per unit volume of material during a portion, $d(\omega t)$, of the cycle:

$$\text{(work/volume)} = (\dot{\gamma}_M{}^2/\omega)(\eta_V \cos^2\omega t + \eta_E \sin\omega t \cos\omega t)\, d(\omega t) \qquad \text{(Eq. 5)}$$

Averaging this work over one complete cycle gives the average power per unit value as:

$$\text{(power/volume)} = \eta_V(\dot{\gamma}_M{}^2/2) \qquad \text{(Eq. 6)}$$

which represents a nonrecoverable energy loss.

Characteristic Behavior of Viscoelastic Liquids in Oscillatory Shear—The viscoelastic behavior of liquids as seen by oscillatory shear measurements at small amplitudes of varying frequency can be analyzed using a generalized extension of the well-known Maxwell model (23)

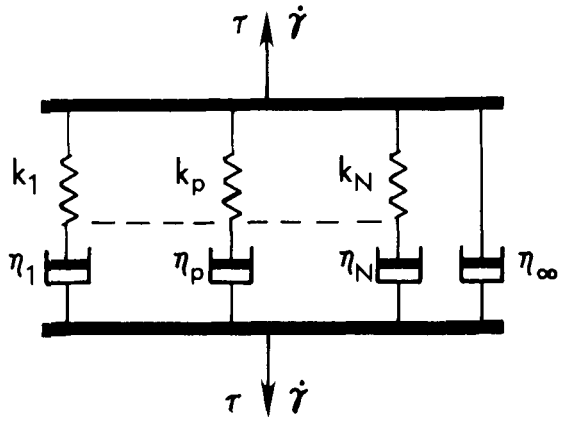

Figure 2—*Generalized extension of the Maxwell model for a unit cube of material in shear.*

shown in Fig. 2. The individual spring–dashpot combination in series is the element of Maxwell, N of these being shown in the model. The $(N + 1)$ element is a dashpot alone, represented by η_∞, this being the dissipative element controlling the viscoelasticity at infinite frequency.

At very low frequencies of excitation, the dashpot controls the mechanical behavior of the combination; at high frequencies, the strain becomes totally absorbed in the stretch and compression of the spring. The relaxation time, T_p, of the pth element serves as the "internal clock" that delineates the distinction between low and high frequencies according to whether (ωT_p) is very much less than 1 or very much greater than 1, respectively. The contribution of the single element to the viscoelasticity of the assemblage is:

$$\eta_p^* = \eta_p/(1 + i\omega T_p) = \tau_p/\dot{\gamma}_p \qquad \text{(Eq. 7)}$$

where T_p is related to the damping factor and the spring constant, K_p (Fig. 2), by:

$$T_p = \eta_p/K_p \qquad \text{(Eq. 8)}$$

In this model, each Maxwell element is subject to the same shear rate, $\dot{\gamma}$, while shear stress, τ_p, is additive for the stress, τ, of the total system. Thus, the viscoelastic modulus for the complete assemblage is:

$$\eta^* = \sum_{p=1}^{N} \eta_p^* + \eta_\infty \qquad \text{(Eq. 9)}$$

Equation 9 can be rewritten in the form:

$$\eta^* = \eta_\infty + (\eta_0 - \eta_\infty) \sum_{p=1}^{N} H_p/(1 + i\omega T_p) \qquad \text{(Eq. 10)}$$

where:

$$\eta_0 = \sum_{p=1}^{N} \eta_p + \eta_\infty \qquad \text{(Eq. 11)}$$

and:

$$H_p = \eta_p \Big/ \sum_{p=1}^{N} \eta_p \qquad \text{(Eq. 12)}$$

Therefore:

$$\sum_{p=1}^{N} H_p = 1 \qquad \text{(Eq. 13)}$$

By taking the limits in Eq. 10 as $\omega T_p \to 0$ and $\omega T_p \to \infty$, η_0 is the viscosity at zero frequency while η_∞ is the viscosity at infinite frequency, the elasticity vanishing at both limits.

The generalized Maxwell model can be considered an empirical model for a linear viscoelastic material. However, this model is produced exactly from two molecular theories for liquid solutions at low concentrations. One is for rigid, ellipsoidal macromolecules suspended in a viscous solvent (24, 25); the other is for flexible, linear polymer molecules (26). The more precise polymer chain theory including internal chain viscosity (27, 28) gives characteristics very similar to the Maxwell model (29–31). In going from dilute to concentrated polymer solutions, the theories are no longer strictly pertinent; however, the form of the model remains applicable (19). The Maxwell model can serve equally well as a basis for analysis of stress and strain rate relaxation experiments.

When a fluid containing N relaxation processes (*i. e.*, N Maxwell elements) is subjected to oscillatory shear at a radian frequency, ω, all processes contribute to the viscosity and elasticity but in differing amounts, depending on the individual values of ωT_p. Only by examining η^* over a wide range of frequencies can some assessment be made of the extent of the characteristic relaxation times for a material. While, in principle, it is necessary to vary ω from 0 to ∞ to establish the complete relaxation spectra, the significant contribution of a single Maxwell element seen as ωT_p ranges from 0.1 to 10. Thus, it is important to perform measurements in a particular frequency range to show the relaxation processes of interest.

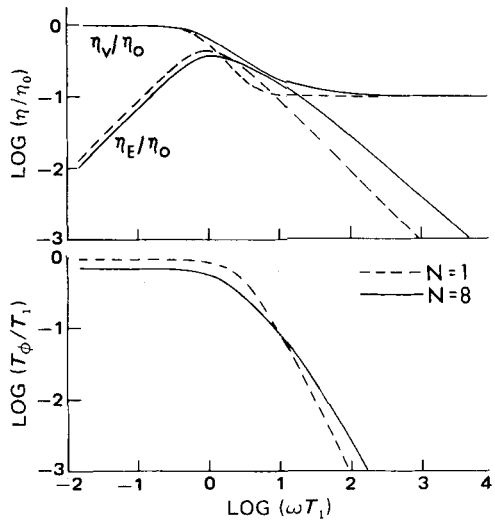

Figure 3—*Frequency dependence of the viscous component, η_V, and the elastic component, η_E, of the viscoelasticity and the effective relaxation time, T_ϕ; T_1 is the longest relaxation time of the system. Calculations are for the generalized Maxwell model of Fig. 2, the dashed line curves being for N = 1 and the solid line curves being for N = 8. Numerical parameters are given in the text.*

Precise matching of theory and experiment to establish the N values of a relaxation time, T_p, for the generalized Maxwell model is difficult when several Maxwell elements are involved. However, a useful parameter that gives good insight into the relaxation spectrum is the "effective relaxation time," calculated as though there were a single element only. If the high frequency limiting viscosity, η_∞, is known, this time is obtained from the phase of $(\eta^* - \eta_\infty)$. When η_∞ is not known, the phase of η^* alone can be used. The effective relaxation time is then:

$$T_\phi = (\tan \phi)/\omega \qquad \text{(Eq. 14)}$$

Applying this equation to the generalized model, using Eq. 9, gives:

$$T_\phi = \sum_{p=1}^{N} \frac{\eta_p T_p}{1 + (\omega T_p)^2} \Big/ \left[\sum_{p=1}^{N} \frac{\eta_p}{1 + (\omega T_p)^2} + \eta_\infty \right] \qquad \text{(Eq. 15)}$$

This function is frequency dependent and approaches an upper limit, as $\omega T_p \to 0$, of:

$$T_{\phi,0} = \sum_{p=1}^{N} \eta_p T_p \Big/ \left[\sum_{p=1}^{N} \eta_p + \eta_\infty \right] \qquad \text{(Eq. 16)}$$

The lower limit of this function is obtained for large values of ωT_p as:

$$T_{\phi,\infty} = \sum_{p=1}^{N} (\eta_p/T_p) \Big/ \left[\sum_{p=1}^{N} \eta_p/T_p{}^2 + \eta_\infty \omega^2 \right] \to 0 \text{ as } \omega T_p \to \infty \qquad \text{(Eq. 17)}$$

Thus, the function T_ϕ generally falls in the range of the relaxation times of the contributing Maxwell elements.

The character of the frequency dependence of the viscous and elastic components of the complex coefficient of viscosity is shown in Fig. 3. Here, the ratios η_V/η_0 and η_E/η_0 are plotted *versus* ωT_1, where T_1 is the longest relaxation time for the system of relaxing elements. This plot is shown for a single relaxing element, $N = 1$, and for a multiple system, $N = 8$. The curves are computed using Eq. 10 with the following values: $N = 1$ and $H_1 = 1$; and $N = 8$, $T_p/T_1 = 1, 0.3, 0.1, 0.03, 0.01, 0.003, 0.001$, and 0.0003, and H_p values are arbitrarily selected to be $H_p = T_p/\Sigma_{p=1}^{8} T_p$.

Characteristic Behavior of Liquids in Steady Shear—The shear stress and shear rate for a liquid in steady flow can be related by:

$$\tau_S = [\eta_S(\dot{\gamma}_S)]\dot{\gamma}_S \qquad \text{(Eq. 18)}$$

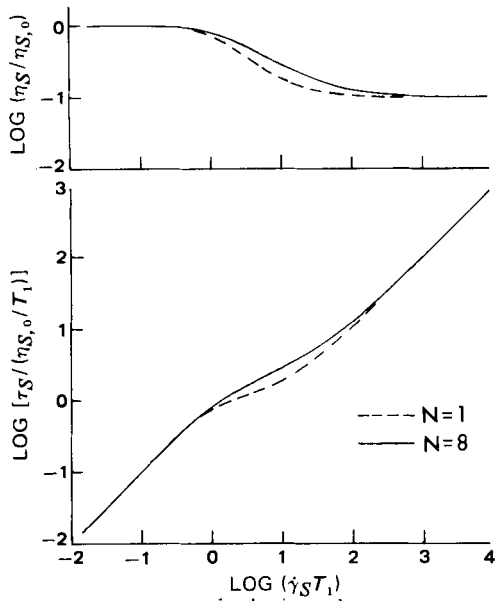

Figure 4—*Steady shear rate dependence of viscosity, η_S, and shear stress, τ_S, for the model of Fig. 2. The functions are calculated using Eqs. 24–26 and incorporating the same numerical factors used in Fig. 3 for the oscillatory flow case.*

where $\eta_S(\dot{\gamma}_S)$ is the shear rate dependent viscosity. For steady-state conditions and nonthixotropic materials, the η_S is independent of the past mechanical history of the sample and, thus, is the same when arrived at by either increasing or decreasing the shear rate. To make some determination of the time required to attain a steady-state flow condition, the stress is examined in the light of the generalized Maxwell model. The nonsteady-state solution for the contribution to the stress of a single Maxwell element is (32):

$$\tau_p = \int_{-\infty}^{t} [(\eta_p/T_p) \exp[-(t - t')/T_p]]\dot{\gamma}(t')\, dt' \qquad \text{(Eq. 19)}$$

When the shear rate, $\dot{\gamma}(t')$, is changed to a new value at time t_0, it can be shown by integration of Eq. 19 that the time factor $[(t - t_0)/T_p]$ must become very large compared to 1 so that the stress contribution, τ_p, becomes equal to $\eta_p\dot{\gamma}$ as is necessary for Eq. 18 to be valid. Thus, in performing steady shear measurements on systems where the longest relaxation time is the order of seconds, a waiting period on the order of minutes may be necessary to achieve an equilibrium steady shear measurement.

The shear rate dependent viscosity is generally a decreasing function of shear rate once the shear rate exceeds some initial value below which η_S is constant. For polymers, this critical shear rate is nearly equal in magnitude to the radian frequency at which the viscoelasticity begins its dispersion (33–35). This characteristic shear rate dependence is derivable from molecular theories for dilute solutions of rigid ellipsoidal molecules (25) and dumbbell shapes (36, 37) and for linear polymer chains with internal viscosity (27, 28). A number of constitutive equations also exhibiting this character were developed (32).

The similarities observed between $\eta^*(\omega)$ and $\eta_S(\dot{\gamma}_S)$ suggest that the same fluid structural mechanisms are responsible for both functions in liquids, particularly at low frequencies and low shear rates. The generalized Maxwell model may serve as a basis for describing this similarity. For small oscillatory shear in the limit as $\omega \to 0$:

$$\eta^*|_{\omega\to 0} = \eta_0 = \eta_\infty + \sum_{p=1}^{N} \eta_p \qquad \text{(Eq. 20)}$$

This limiting condition can be assumed to coincide with the steady shear result as $\dot{\gamma}_S \to 0$, in which case:

$$\eta_S|_{\dot{\gamma}_S\to 0} = \eta_{S,0} = \eta_\infty + \sum_{p=1}^{N} \eta_{S,p}(0) \qquad \text{(Eq. 21)}$$

where $\eta_{S,p}(0)$ is the limiting value of the damping factor for the Maxwell element as $\dot{\gamma}_S \to 0$ and, under this condition, is the same as η_p.

For polymer solutions, there is a cutoff of relaxation processes with increasing steady shear rate (38, 39). The processes having the longest relaxation times are the first to be suppressed. In terms of the generalized Maxwell model, this condition means that the η_p values are dependent upon the steady shear rate, $\dot{\gamma}_S$, and may be specified as $\eta_{S,p}(\dot{\gamma}_S)$. The character of this dependence may be written as:

$$\eta_{S,p}(\dot{\gamma}_S) = \eta_{S,p}(0)F(\dot{\gamma}_S T_p) \qquad \text{(Eq. 22)}$$

where the product $\dot{\gamma}_S T_p$ is dimensionless and T_p is the relaxation time of the pth Maxwell element.

Under these conditions, the model gives the steady flow viscosity as:

$$\eta_S(\dot{\gamma}_S) = \eta_\infty + \sum_{p=1}^{N} \eta_{S,p}(\dot{\gamma}_S) \qquad \text{(Eq. 23)}$$

Equation 23 may be put into a form similar to Eq. 10:

$$\eta_S(\dot{\gamma}_S) = \eta_\infty + (\eta_{S,0} - \eta_\infty) \sum_{p=1}^{N} B_p F(\dot{\gamma}_S T_p) \qquad \text{(Eq. 24)}$$

where:

$$B_p = \eta_{S,p}(0) \Big/ \sum_{p=1}^{N} \eta_{S,p}(0) \qquad \text{(Eq. 25)}$$

and $B_p = H_p$ under the assumption of the common model for oscillatory flow at low frequency and steady flow at low shear rates.

There are numerous possible functions $F(\dot{\gamma}_S T_p)$ with the generally desired properties that will truncate a relaxation process. Several such functions have appeared in the rheological literature in other contexts to describe the shear rate dependence of steady flow viscosity. The function $[1/(1 + X^2)]$ was used by Lamb (40) for lubricating oils, while the square root of this function appeared in the derivation of Williams (41) for polymer solutions using an elastic dumbbell model. Tanner and Simmons (38) obtained the function $[1 - (1 + 1/X) \exp(-1/X)]$ in an analysis of breakage of polymer entanglements.

The character of $\eta_S(\dot{\gamma}_S)$ from Eq. 24 is illustrated using:

$$F(\dot{\gamma}_S T_p) = 1/[1 + (\dot{\gamma}_S T_p)^2]^{1/2} \qquad \text{(Eq. 26)}$$

This relationship is shown in Fig. 4 where $(\eta_S/\eta_{S,0})$ is plotted *versus* $\dot{\gamma}_S T_1$. The curves are for the same series of Maxwell models as shown for the oscillatory flow in Fig. 3. Also in Fig. 4 are curves showing a factor proportional to shear stress plotted *versus* shear rate for the same two cases.

Measurement of Viscoelasticity—The basis for measurement of the complex coefficient of viscosity is from the analysis of the pressure to volume flow relation in a rigid straight tube of circular cross section. The theory for this oscillatory flow of viscoelastic liquids was developed by Thurston (42) and has been tested thoroughly in measurements (43). The pressure and volume flow are sinusoidal and follow a time variation in the complex plane that is proportional to $\exp(i\omega t)$. With a volume flow of U and a complex pressure drop per unit length of tube of P^*, this pressure can be resolved into component P' in phase with the flow and P'' in quadrature with the flow. Then:

$$P^* = P' + iP'' \qquad \text{(Eq. 27)}$$

The relation between P^*, U, the tube radius a, and the viscous and elastic components, η_V and η_E, is particularly simple in small tubes at low frequencies when the dimensionless parameter:

$$a[\rho\omega/|\eta^*|]^{1/2} < 1 \qquad \text{(Eq. 28)}$$

where ρ is the fluid density. Under this condition, the components of viscoelastic modulus are given by:

$$\eta_V = (\pi a^4/8)(P'/U) \qquad \text{(Eq. 29)}$$

$$\eta_E = (\pi a^4/8)[(4\rho\omega/3\pi a^2) - (P''/U)] \qquad \text{(Eq. 30)}$$

The complex shear stress at the tube wall is also determined from the pressure and flow:

$$\tau_\omega^* = (a/2)P^* - (i\omega\rho/2\pi a)U \qquad \text{(Eq. 31)}$$

With Eq. 31, the shear rate at the tube wall is given by:

$$\dot{\gamma}_\omega = \tau_\omega^*/\eta^* \qquad \text{(Eq. 32)}$$

EXPERIMENTAL

Measurements of the pressure and volume flow were obtained using an apparatus designed by Thurston (44) (Fig. 5). The oscillatory flow in this apparatus is developed by a piston-like driver, the motion of which is monitored by a velocity-sensitive transducer attached to the drive shaft. The product of this shaft velocity times the effective area of the driver gives the instantaneous representation of the flow, U. This flow is

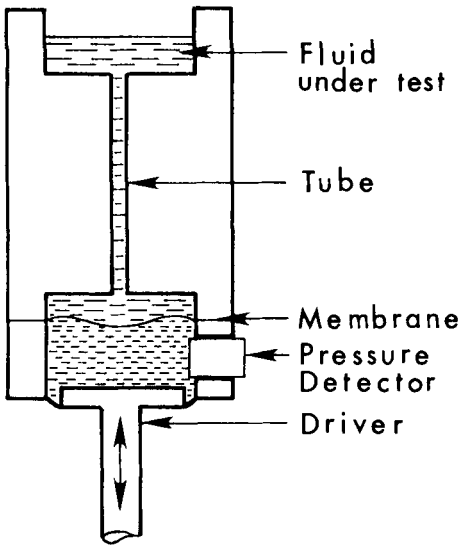

Figure 5—*Schematic drawing of apparatus for measuring oscillatory flow properties of a viscoelastic fluid in a small tube having a circular cross section (42).*

transmitted through a coupling fluid, water, through a flexible separating membrane, to the fluid under test that fills the tube. The pressure developed across the tube is monitored by the pressure detector, P.

Small corrections to the measured pressure and flow are made to compensate for residual chamber impedances. The electrical signals representing the pressure and volume flow are analyzed to obtain the desired in-phase and quadrative components of the pressure. The tube is always selected for the test fluid such that Eq. 28 is valid. Furthermore, the tube length is usually greater than the tube radius by a factor of 50 or more, thereby minimizing the effects of small tube length corrections. The complete system is calibrated using water as a viscosity standard.

The viscoelastic properties of the carboxymethylcellulose solutions were measured in the oscillatory flow frequency range of 0.05–100 Hz. In all cases, the amplitude of the oscillatory shear rate at the wall of the containing tube was held sufficiently low so that no nonlinear effects were evident. This condition was checked for each case by first increasing the amplitude to establish that the sample η^* remained unchanged. All measurements were made at 24°.

Measurement in Steady Flow—Steady flow of non-Newtonian liquids ordinarily is measured in a rotational viscometer, an instrument that continuously shears the material at various rates within the annular space between a stationary cup and a rotating inner cylinder or bob.

Measurements of steady shear were made by use of the steady shear rotational instrument[1], which was provided with both coaxial cylinder and plate and cone sensor systems. Only the coaxial cylinder attachment was used. The instrument allows measurement of Newtonian and non-Newtonian materials over a shear rate range of 10^{-3}–4×10^4 sec^{-1} and shear stress range of 2–10^7 dynes/cm^2. Viscosity from 0.02 to 10^8 poises can be measured. Temperature was controlled in the annular space of the concentric cylinders by means of a constant-temperature circulator adjusted to 25 ± 0.1°. Data were collected manually, point by point, with the rheometer or obtained automatically with a programmer attachment, and the up-and-down curves of shear stress *versus* shear rate were plotted continuously using an x-y recorder.

The instrument was programmed to provide speeds for rotation of the inner cylinder between 1 and 100 rpm. The speed was changed automatically at 10, 25, 50, 75, 100, 150, 200, 250, 300, and 400 rpm/min, depending on the dial setting chosen.

In preparation for measurement, a sample of the solution was poured into the outer cylinder using the proper rotating inner cylinder (rotor) found in preliminary tests to provide a suitable rheogram within the specified viscosity range. The sample was allowed to stand undisturbed in the cylinder (covered with plastic film to prevent evaporation) for approximately 30 min. The constant-temperature control maintained the sample at 25 ± 0.1° during the experiment.

For the concentric cylinder system, shear rate, $\dot{\gamma}_S$ sec^{-1}, is obtained

[1] Haake Rotovisco, RV2, Haake Instruments, Saddle Brook, NJ 07662.

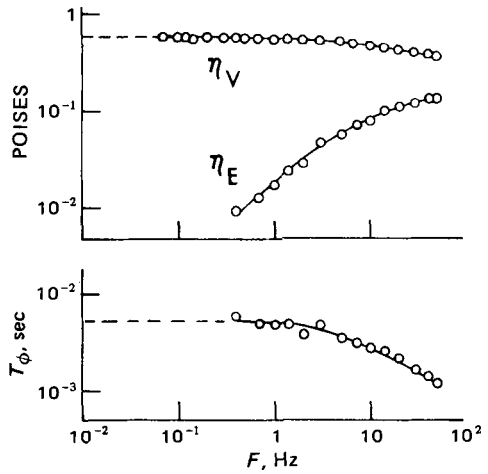

Figure 6—*Viscoelastic properties of 1% carboxymethylcellulose solution (medium viscosity grade) under oscillatory shear flow. The viscosity, η_V, and elasticity, η_E, are defined in Eq. 4; T_ϕ is the effective relaxation time defined in Eqs. 14–17.*

from the rotor speed and an appropriate shear rate factor, M. Shear stress, τ, depends on the scale value, S. It is obtained by multiplying S by an instrumental shear stress factor, A, to yield shear stress in dynes per square centimeter. The viscosity of a sample (in poises) at various shear rates is obtained from the scale reading, S, the revolutions per minute setting, n, and the instrumental constant, $G = 100A/M$, which varies depending on the measuring head and sensor used:

$$\eta = (G)(S/n) \qquad \text{(Eq. 33)}$$

The rotational instrument was supplied with calibration certificates giving the values of A and M for the various sensor systems, based upon the geometry of the measuring parts. These constants were checked using glycerin–water mixtures of established viscosities (45) and standard viscosity samples[2]. The results using both the instrument calibration values and the standard viscosity samples gave viscosity values that differed by less than 2% for the significant portions of the curve. Care must be taken not to make measurements below scale values of $S = 10$ or 15 where errors in results may become large.

To correlate oscillatory results with steady shear values, it is necessary to examine the steady shear data at low shear rates. The rotational instrument is not ordinarily capable of accurate results below shear rate values of 1–10 sec^{-1} and shear stress values below 10^2 dynes/cm^2.

A Couette instrument[3], giving accurate values at shear rates as low as 0.1 sec^{-1}, was used to extend the measurement range. By combining the data from the two instruments, the shear stress to shear rate characteristics were revealed over a range of four decades.

The same four samples used in the oscillatory analysis were measured in steady shear flow. The next section describes the materials used in this investigation. In each case, the shear stress *versus* shear rate was measured with the rotational viscometer using two modes of measurement: (*a*) by automatic stepping of the shear rate in which the sample was cycled from a low shear rate to a high one and then back to a low one, and (*b*) by a manual method in which the time between measurements was lengthened to try to assure equilibrium conditions (see discussion following Eq. 19). The rotational measurements were carried out at 25°. Similarly, manual equilibrium measurements were made with the Couette viscometer at low shear rates and at 24°.

Sample Preparation—Carboxymethylcellulose sodium[4], high viscosity food grade and medium viscosity grade powders, was obtained in sealed containers. The high viscosity food grade had a weight average molecular weight[5] of 700,000 and a degree of polymerization[5] of 3200. The medium food grade had a molecular weight[5] of 250,000 and a degree of polymerization[5] of 1100.

The polymer solutions were prepared by a standard procedure. Sam-

[2] Brookfield Engineering Laboratories, Houghton, MA 02072.
[3] Designed by G. B. Thurston.
[4] Cellulose Gum, Hercules Inc., Wilmington, Del.
[5] Values provided by the manufacturer.

Table I—Measurement Ranges and Rheological Limiting Values

Sample[a]	Frequency Range, Hz	Shear Rate Range, sec^{-1}	$\eta_{V,0}$, poises	$T_{\phi,0}$, sec
I	0.1–50	2.0–81	0.57	0.006
II	0.1–50	0.1–22	5.7	~0.17
III	0.05–50	0.02–23	12.3	>0.8
IV	0.07–100	0.007–4	≫162.0	≫1.5

[a] I = medium viscosity 1% solution, II = medium viscosity 2% solution, III = high viscosity 1% solution, and IV = high viscosity 2% solution.

Table II—Experimental Conditions and Results for the Four Samples of Carboxymethylcellulose Tested [a]

Sample[b]	Automated Total Average Time for Up and Down Plot, min	Manual Rate Average Time at Each Point, min	Manual Total Average Time for Up and Down Plot, min	$\eta_{S,0}$, poises
I	31	5	59	0.58
II	22	6	50	5.6
III	30	6	61	13.4
IV	41	4	50	≫80

[a] For all four samples, the automated increment rate (rate of change) was 10 rpm/min and the Couette manual rate was 30 sec/point. [b] The sample numbers are the same as in Table I.

ples were placed in a continuous air-flow oven at 55° and dried to constant weight. The loss in weight, assumed to be due to moisture, was thus accounted for; this procedure permitted calculation of the amount undried to be used in preparing the carboxymethylcellulose solutions. Solutions of high and medium grades were prepared in concentrations of 1.0 and 2.0% in water containing a preservative mixture consisting of 0.1 g of propylparaben and 0.1 g of methylparaben/100 g of solution.

The solutions were made in 300-g quantities using warm water and a propeller blade stirrer. The samples were stored at room temperature in wide-mouth glass containers with plastic screw caps and liners. Preliminary work without parabens present showed that preservation was required for product viscosity to remain constant over time. Later results showed that, at the concentration of preservatives used, viscosities began to decrease after 4 months.

Oscillatory Shear Results—The results of oscillatory shear measurements on the carboxymethylcellulose medium grade 1 and 2% and high viscosity grade 1 and 2% are shown in Figs. 6–9. In each figure, the viscoelasticity is given in terms of η_V and η_E (see Eqs. 3c and 4c). The effective relaxation time, T_ϕ, is also given.

The character of the theoretical frequency–response curves of Fig. 3 is clearly seen in the experimental curves (Figs. 6–9). However, the frequency range of the experimental data is not sufficient to reveal both the low and high frequency limits; with the high viscosity gums in 2% solution (Fig. 9), neither limit was seen. Table I summarizes the measurement conditions and low frequency limiting values. With increasing concentration, the breadth of the relaxation spectrum increased. Furthermore, $\eta_{V,0}$ and $T_{\phi,0}$ increased. These effects confirm that the polymer molecules in the solutions are highly interactive.

Steady Shear Results—The results of the steady shear measurements are shown in Figs. 10 and 11.

Table II summarizes the measurement conditions and the results obtained. The data in columns 2–5 were obtained using the commercial rotational viscometer. The values in column 6 are for the Couette instrument. The automated and manual results were identical for the medium viscosity samples but not for the high viscosity samples. Thus, because of the longer relaxation times of the higher molecular weight samples, the automated measurements were nonequilibrium values and could be misinterpreted as indicative of thixotropic behavior. But the longer manual waiting period between measurement results in equilibrium and removes this artifact.

Comparison of the experimental curves (Figs. 10 and 11) with the theoretical curves of Fig. 4 shows that the general behavior is in agreement with the theory. With the exception of the high viscosity 2% sample, the low shear rate-limiting condition ($\dot{\gamma}_S T_1 > 1$) was achieved, but the high shear rate limit was not.

Oscillatory and Steady Shear Correlations—Comparison of the low frequency limiting value of $\eta_{V,0}$ and the low shear rate value of $\eta_{S,0}$ (Tables I and II) shows that they do indeed approach the same limit. This result is in agreement with the postulate under *Theoretical*, in which the generalized Maxwell model is applied to both steady and oscillatory flow (Eqs. 20 and 21).

A second point for comparison is the relaxation times. Figures 10 and 11 show that the range of the relaxation spectrum becomes enlarged with both increasing concentration and increasing molecular weight. This result is consistent with that found in the oscillatory cases. A quantitative comparison can be made on the basis of estimates of the longest, dominant relaxation time for the sample. As shown by the sample theoretical curves of Fig. 3, when the shear stress has deviated approximately 15% from the linear extrapolated value, the product $\dot{\gamma}_S T_1 \simeq 1$. While the deviation is clearly a function of the polydispersity of the sample's relaxation spectrum, this value can be used as a basis for estimation.

Similarly, one can use a condition on the η_V for which η_V has decreased 30% from its limiting value, and this occurs when $\omega T_1 \simeq 1$. Table III summarizes this comparison. The data range for the high viscosity 2% Sample IV was not sufficient for this procedure. Table III lists the critical shear rate corresponding to the 15% deviation of τ_S, the critical frequency

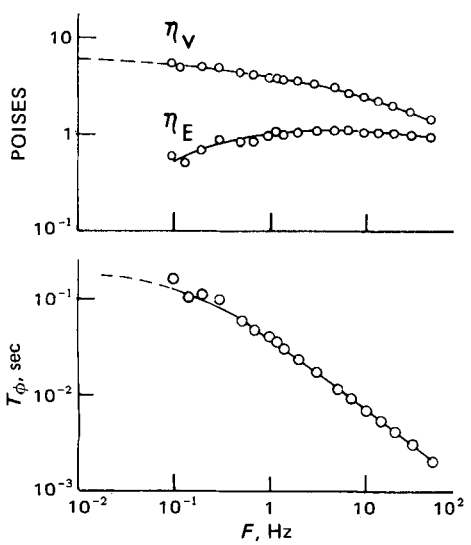

Figure 7—*Viscoelastic properties of 2% carboxymethylcellulose solution (medium viscosity grade). See Fig. 6 for explanation of symbols.*

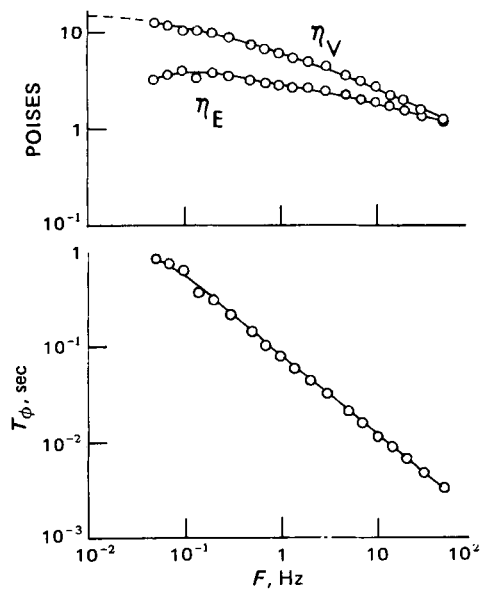

Figure 8—*Viscoelastic properties of 1% carboxymethylcellulose solution (high viscosity grade). See Fig. 6 for explanation of symbols.*

Table III—Comparison of Relaxation Times for Steady and Oscillatory Flow

Sample[a]	Critical Shear Rate, $\dot{\gamma}_S$, sec^{-1}	Critical Frequency, Hz	T_1, Steady, sec	T_1, Oscillatory, sec
I	80	30	0.012	0.0053
II	4.6	1.2	0.22	0.133
III	2.0	0.25	0.5	0.64

[a] The sample numbers are the same as in Table I.

corresponding to the 30% deviation of η_V, and the terminal relaxation time, T_1, calculated from these critical values.

The degree of agreement between the relaxation times is reasonable considering the method of estimation used. Complete characterization *via* the generalized Maxwell model requires specification of all the T_p and weighting factors, H_p (see Eqs. 10–13), as well as the zero frequency and high frequency limits, η_0 and η_∞. Before T_1 can be evaluated exactly, it is necessary to have all of the spectral information. Thus, the T_1 estimates will improve with increased information on the relaxation spectrum. Also, while the T_ϕ values have an exact definition, they cannot be related exactly to the T_1 values without additional information (Eqs. 14–16). These limitations on exact interpretations are common to all methods of rheological characterization when one seeks to describe multirelaxational molecular systems by means of only a few numerical factors.

Applications in Pharmacy—Added insights are gained through the analysis of the viscoelastic properties, η_V and η_E. For 1 and 2% medium viscosity carboxymethylcellulose, η_V remained relatively constant over a wide frequency range; η_E, on the other hand, passed through a maximum. The phase angle, ϕ, tended to rise, whereas the "effective relaxation time," T_ϕ, decreased in a linear manner. These phenomena are characteristic of solutions of long chain molecules and can be used to characterize samples of carboxymethylcellulose and similar polymeric materials found in pharmacy. The values of η_V, η_E, η, ϕ, and T_ϕ can serve as raw material specifications for commercial lots of suspending agents entering the manufacturing plant. They can also be used to adjust product characteristics in the research and design of new drug and cosmetic formulations. Studies on the rheology of disperse systems were reviewed by Barry (9). New approaches include the use of creep and oscillatory methods for the analysis of pharmaceutical and cosmetic products.

The present investigation attempts to bridge the gap between oscillatory and steady shear methods. The application of steady shear methods for anything more than estimations of flow properties of products in practical use was criticized (5, 7). It was thought that a product

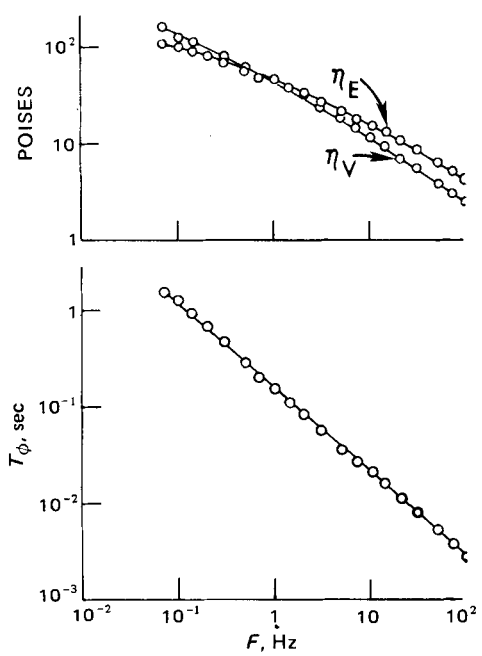

Figure 9—*Viscoelastic properties of 2% carboxymethylcellulose solution (high viscosity grade). See Fig. 6 for explanation of symbols.*

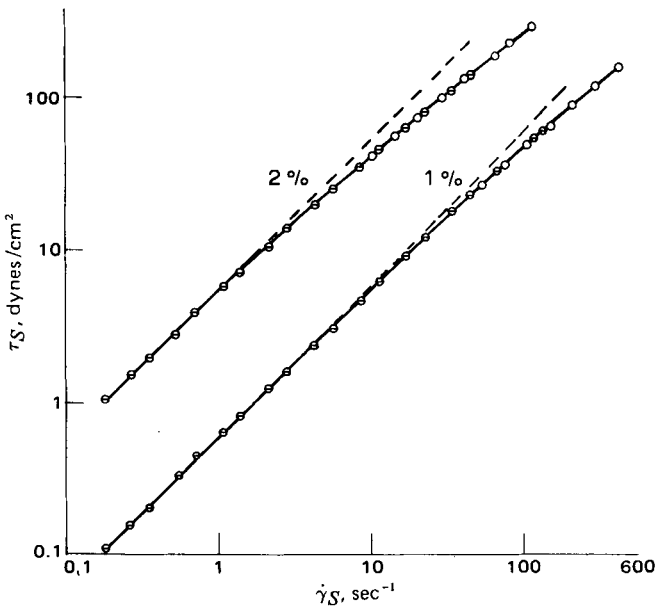

Figure 10—*Steady shear stress* versus *shear rate for 1 and 2% carboxymethylcellulose solutions (medium viscosity grade) in the rotational viscometer. Dashed lines show the deviation from linearity at high shear. Open circles are commercial viscometer values; cross-line circles are values obtained with the Couette instrument.*

under rotational shear is no longer in its "rheological ground state," its structure being so severely perturbed by the shearing action that fundamental characteristics of the material cannot be studied (5, 7). Although rotational viscometry, mainly of the cone and plate geometry (7), was used, the application of creep or oscillatory experiments was suggested to obtain basic understanding of rheological materials, for the testing of theories of molecular structure, and for studying effects of formulation changes, storage temperature, and use characteristics of ointments, creams, and lotions.

For the carboxymethylcellulose solutions, the present study has demonstrated how a joint study of oscillatory perturbation together with steady shear in a rotational instrument can provide insight into the nature of viscoelastic materials used in pharmacy. Similar investigations should be carried out for cosmetics, paints, plastics, and other industrial materials. Through such work, a better understanding of the materials and

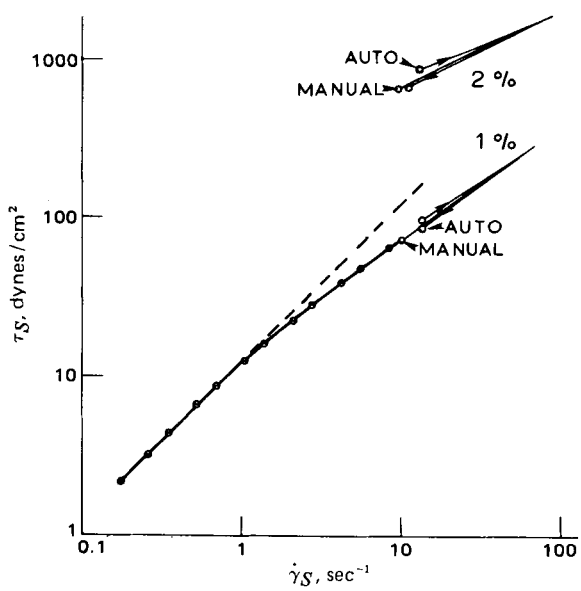

Figure 11—*Steady shear stress* versus *shear rate for 1 and 2% carboxymethylcellulose solutions (high viscosity grade). The results for both automatic and manual operations of the commercial rotational viscometer are shown. Open circles are commercial viscometer values; cross-line circles are values obtained using the Couette instrument.*

test methods of rheology can be obtained so that one may intelligently employ the equipment most appropriate to the preparation whose rheological properties are under investigation. Carboxymethylcellulose is a relatively well behaved material, a polymeric solution of practical use in pharmacy, and shows interesting rheological properties. It remains to be determined whether the analysis used here can be extended to gels, emulsions, and suspensions.

This analytic method offers a theoretical approach to steady shear measurements of non-Newtonian materials. It provides the possibility for a more fundamental understanding of results obtained with rotational and cone–plate steady shear viscometers. An evident suggestion uncovered by the work is that commercial rheometers should be designed to operate in the range of low shear rates of approximately 0.1 or 0.01 sec^{-1} where results correspond more nearly to oscillatory findings and thus provide a knowledge of rheological structures in the ground state. Then, proceeding from low to high shear rates, of which commercial instruments are quite capable, will provide useful data on how the unperturbed gel, emulsion droplet, or suspension structure is altered by processing, packaging, and actual use. In this manner, the gap between theoretical and practical knowledge of rheology can be bridged and advances in applied and structural rheology can be accelerated. It is hoped that this study will help join two important aspects of rheology, nondestructive oscillation of products vis à vis deformation at high shear in rotating instruments, and will provide theoretical and experimental approaches to this end.

The next study will extend the method to the characterization of thixotropic materials.

REFERENCES

(1) "Remington's Pharmaceutical Sciences," 15th ed., Mack Publishing Co., Easton, Pa., 1970, pp. 354, 356.

(2) J. C. Boylan, *Bull. Parenteral Drug Assoc.*, **19,** 98 (1965).

(3) J. C. Boylan, *J. Pharm. Sci.*, **55,** 710 (1966).

(4) *Ibid.*, **56,** 1164 (1967).

(5) G. W. S. Blair, "Elementary Rheology," Academic, New York, N.Y., 1969.

(6) W. W. Graessley, "Advances in Polymer Science," vol. 16, Springer-Verlag, New York, N.Y., 1974, pp. 1–179.

(7) S. S. Davis, *Pharm. Acta Helv.*, **40,** 161 (1974).

(8) R. L. Schnaare, R. M. Sheikh, P. J. Niebergall, and E. T. Sugita, *J. Pharm. Sci.*, **65,** 1385 (1976).

(9) B. W. Barry, in "Advances in Pharmaceutical Sciences," vol. 4, H. S. Bean, A. H. Beckett, and J. E. Carless, Eds., Academic, New York, N.Y., 1975, p. 1.

(10) W. H. Bauer and E. A. Collins, in "Rheology, Theory and Applications," vol. 4, F. R. Eirich, Ed., Academic, New York, N.Y., 1967, p. 425.

(11) S. S. Davis, *J. Pharm. Sci.*, **58,** 412 (1969).

(12) *Ibid.*, **60,** 1351 (1971).

(13) S. S. Davis, *J. Sci. Instrum.*, **1,** Series 2, 933 (1968).

(14) *Ibid.*, **2,** Series 2, 102 (1969).

(15) S. S. Davis, *J. Text. Stud.*, **4,** 15 (1973).

(16) T. Sherman, *J. Soc. Cosmet. Chem.*, **17,** 439 (1966).

(17) T. Sherman, *J. Colloid Interface Sci.*, **24,** 107 (1967).

(18) T. Sherman, "Emulsion Sciences," Academic, New York, N.Y., 1968.

(19) J. D. Ferry, "Viscoelastic Properties of Polymers," Wiley, New York, N.Y., 1970.

(20) J. R. Van Wazer, J. W. Lyons, K. Y. Kim, and R. E. Colwell, "Viscosity and Flow Measurements—A Laboratory Handbook of Rheology," Interscience, New York, N.Y., 1963.

(21) G. B. Thurston, *Biophys. J.*, **12,** 1205 (1972).

(22) D. R. Bland, "The Theory of Linear Viscoelasticity," Pergamon Press, Oxford, England, 1960.

(23) T. Alfred, Jr., and E. F. Gurnee, in "Rheology, Theory and Applications," E. R. Eirich, Ed., Academic, New York, N.Y., 1956, chap. 10.

(24) R. Cerf, *J. Phys. Radium*, **13,** 458 (1952).

(25) H. A. Scheraga, *J. Chem. Phys.*, **23,** 1526 (1955).

(26) B. H. Zimm, *ibid.*, **24,** 269 (1956).

(27) R. Cerf, *J. Phys. Radium*, **19,** 122 (1958).

(28) R. Cerf, *J. Polym. Sci.*, **23,** 125 (1957).

(29) A. Peterlin, *Kolloid-Z.*, **209,** 181 (1966).

(30) A. Peterlin, *J. Polym. Phys.*, **5,** 179 (1967).

(31) G. B. Thurston and A. Peterlin, *J. Chem. Phys.*, **46,** 4881 (1967).

(32) R. B. Bird, *Annu. Rev. Fluid Mech.*, **8,** 13 (1976).

(33) W. W. Graessley, *Adv. Polym. Sci.*, **16** (§8.2), 1 (1974).

(34) A. Dyson, *Trans. R. Soc. London*, **258,** 529 (1965).

(35) W. Philippoff, *J. Appl. Phys.*, **36,** 3033 (1965).

(36) W. E. Stewart and J. P. Sorensen, *Trans. Soc. Rheol.*, **16,** 1 (1972).

(37) R. B. Bird, H. R. Warner, and D. C. Evans, *Adv. Polym. Sci.*, **8,** 1 (1971).

(38) R. I. Tanner and J. M. Simmons, *Chem. Eng. Sci.*, **22,** 1803 (1967).

(39) R. I. Tanner, *AIChE J.*, **15,** 177 (1969).

(40) J. Lamb, "Viscoelastic Behavior and the Lubricating Properties of Liquids," Symposium on Rheology, ASME Applied Mechanics and Fluids Engineering Conference, Washington, D.C., June 1965.

(41) M. C. Williams, *AIChE J.*, **12,** 1064 (1966).

(42) G. B. Thurston, *J. Acoust. Soc. Am.*, **32,** 210 (1960).

(43) G. B. Thurston, *Biorheology*, **13,** 191 (1976).

(44) G. B. Thurston, *Microvasc. Res.*, **11,** 133 (1976).

(45) J. B. Segur and H. E. Oberstar, *Ind. Eng. Chem.*, **43,** 2117 (1951).

ACKNOWLEDGMENTS

The authors thank Ms. Gloria Querijero for assistance in preparing samples and for determinations of steady shear values.

Anticonvulsant and Antiproteolytic Properties of 3,5-Disubstituted Oxadiazole-2-thiones and Their Inhibition of Respiration in Rat Brain Homogenates

SUNIL K. CHAUDHARY *§, MAHIMA CHAUDHARY *, ANSHUMALI CHAUDHARI *, and SURENDRA S. PARMAR ‡x

Received December 5, 1977, from the **Jawahar Lal Nehru Laboratory of Molecular Biology, Department of Pharmacology and Therapeutics, King George's Medical College, Lucknow University, Lucknow 226003, India,* and the ‡*Department of Physiology, University of North Dakota School of Medicine, Grand Forks, ND 58202.* Accepted for publication March 1, 1978. §Present address: Environmental Biology and Chemistry Branch, National Institute of Environmental Health Sciences, Research Triangle Park, NC 27709.

Abstract □ Eight 5-(3,4-methylenedioxyphenyl)-3-arylaminomethyl-1,3,4-oxadiazole-2-thiones were synthesized, characterized by their sharp melting points, elemental analyses, and IR spectra, and evaluated for anticonvulsant activity. All substituted oxadiazole-2-thiones possessed anticonvulsant activity, which was reflected by their ability to provide 10–70% protection against pentylenetetrazol-induced convulsions in mice at 100 mg/kg ip. These compounds inhibited *in vitro* nicotinamide adenine dinucleotide (NAD)-dependent oxidation of pyruvate, α-ketoglutarate, and NADH by rat brain homogenates as well as NAD-independent oxidation of succinate by rat brain homogenates. Antiproteolytic activity of these substituted oxadiazole-2-thiones was reflected by their ability to inhibit trypsin hydrolysis of bovine serum albumin. These results indicated that the inhibition of cellular respiration and antiproteolytic activity of these substituted oxadiazole-2-thiones is not the biochemical basis for their anticonvulsant activity.

Keyphrases □ Oxadiazole-2-thiones, substituted—synthesized, evaluated for anticonvulsant activity in mice, effect on NAD-dependent and independent oxidations and antiproteolytic activity *in vitro* □ Anticonvulsant activity—various substituted oxadiazole-2-thiones evaluated in mice □ Oxidations, NAD dependent and independent—various substituted oxadiazole-2-thiones evaluated in rat brain homogenate □ Antiproteolytic activity—various substituted oxadiazole-2-thiones evaluated for effect on trypsin hydrolysis of bovine serum albumin □ Structure–activity relationships—various substituted oxadiazole-2-thiones synthesized, evaluated for anticonvulsant activity in mice, effect on NAD-dependent and independent oxidations and antiproteolytic activity *in vitro*

Earlier studies (1–4) suggested the anticonvulsant activity of substituted 1,3,4-oxadiazoles. Oxadiazoles also possess analgesic (5), muscle relaxant (6), tranquilizing (7), and anti-inflammatory (8) activities. The ability of oxadiazoles to inhibit trypsin hydrolysis of bovine serum albumin also was reported (2, 8).

These observations prompted the synthesis of 5-(3,4-methylenedioxyphenyl) -3- arylaminomethyl -1,3,4-oxadiazole-2-thiones by the methods outlined in Scheme I. These compounds also were evaluated for their anticonvulsant activity and their ability to inhibit cellular respiratory activity of rat brain homogenates and trypsin hydrolysis of bovine serum albumin with a view to studying their biochemical mechanism of action.

EXPERIMENTAL

Chemistry—3,4-Methylenedioxybenzoic acid (Ib) was prepared (9) by the oxidation of 3,4-methylenedioxybenzaldehyde (Ia) and was converted to its methyl ester (Ic) by refluxing with absolute methanol (10). The methyl ester, on refluxing with hydrazine hydrate (11), yielded 3,4-methylenedioxybenzohydrazide (Id), which was cyclized to the corresponding 5-(3,4-methylenedioxyphenyl)-1,3,4-oxadiazole-2-thione (Ie) in the presence of carbon disulfide and potassium hydroxide in ethanol (12). The various 5-(3,4-methylenedioxyphenyl)-3-arylaminomethyl-1,3,4-oxadiazole-2-thiones (II–IX, Table I) were synthesized through a Mannich reaction (13) from the thione (Ie).

Analyses for carbon, hydrogen, and nitrogen were performed; melting points were taken in open capillary tubes with a partial immersion thermometer and are corrected.

5-(3,4-Methylenedioxyphenyl)-1,3,4-oxadiazole-2-thione (Ie)—A mixture of 3,4-methylenedioxybenzohydrazide (0.2 mole), potassium hydroxide (0.2 mole), carbon disulfide (40 ml), and ethanol (200 ml) was refluxed on a steam bath until hydrogen sulfide evolution ceased. Excess ethanol was removed by distillation under reduced pressure. The residue was stirred with water, and the contents were filtered. The filtrate was acidified with dilute hydrochloric acid. The resulting compound was collected by filtration, washed with water, dried, and recrystallized with ethanol, yielding 80%, mp 238°.

Anal.—Calc. for $C_9H_6N_2O_3S$: C, 48.64; H, 2.70; N, 12.6. Found: C, 48.69; H, 2.62; N, 12.54.

5-(3,4-Methylenedioxyphenyl) -3- arylaminomethyl-1,3,4-oxadiazole-2-thiones (II–IX)—To an ethanolic solution of 5-(3,4-methylenedioxyphenyl)-1,3,4-oxadiazole-2-thione (0.01 mole) and formaldehyde (0.015 mole, 40%) was added slowly, with stirring, an ethanolic solution of the appropriate aromatic primary amine (0.01 mole). The reaction mixture was stirred for 1 hr at room temperature and left overnight in a refrigerator. The solid mass thus obtained was filtered, washed with cold ethanol, dried, and recrystallized with the appropriate solvent.

Compounds II–IX (Table I) were characterized by their sharp melting points and elemental analyses. The presence of the characteristic bands of C=S (~1090 cm^{-1}), C=N (~1600 cm^{-1}), and NH (~3300 cm^{-1}) in their IR spectra provided further support of their molecular structure.

Determination of Anticonvulsant Activity—Anticonvulsant activity was determined in albino mice, 25–30 g, of either sex. The mice were

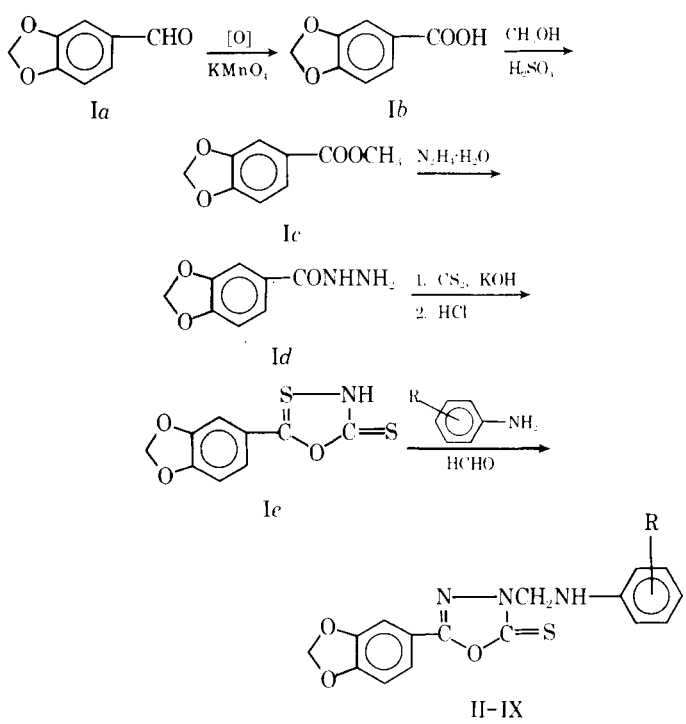

Scheme I

0022-3549/78/1100-1507$01.00/0
© 1978, American Pharmaceutical Association

Table I—Physical Constants of 5-(3,4-Methylenedioxyphenyl)-3-arylaminomethyl-1,3,4-oxadiazole-2-thiones

Compound[a]	R	Melting Point	Yield, %	Formula	Analysis, % Calc.	Found	Anticonvulsant Activity[b], % Protection	Pentylenetetrazol Mortality[c], % after 24 hr
II	H	142°	70	$C_{16}H_{13}N_3O_3S$	C 58.71	58.60	10	70
					H 3.97	4.00		
					N 12.84	12.92		
III	2-CH_3	164°	72	$C_{17}H_{15}N_3O_3S$	C 59.82	59.62	70	10
					H 4.39	4.40		
					N 12.31	12.20		
IV	3-CH_3	138°	68	$C_{17}H_{15}N_3O_3S$	C 59.82	59.94	50	30
					H 4.39	4.44		
					N 12.31	12.40		
V	4-CH_3	152°	65	$C_{17}H_{15}N_3O_3S$	C 59.82	59.65	30	30
					H 4.39	4.28		
					N 12.31	12.30		
VI	2-OCH_3	124°	53	$C_{17}H_{15}N_3O_4S$	C 57.14	57.00	70	Nil
					H 4.20	4.24		
					N 11.76	11.70		
VII	3-OCH_3	114°	62	$C_{17}H_{15}N_3O_4S$	C 57.14	57.26	30	50
					H 4.20	4.10		
					N 11.76	11.92		
VIII	4-OCH_3	106°	60	$C_{17}H_{15}N_3O_4S$	C 57.14	57.28	10	50
					H 4.20	4.20		
					N 11.76	11.70		
IX	4-Cl	198°	65	$C_{16}H_{12}ClN_3O_3S$	C 53.11	53.26	50	30
					H 3.31	3.34		
					N 11.61	11.58		

[a] These compounds were recrystallized with ethanol (II, IV, V, and IX), benzene–petroleum ether (VI and VIII), or ethanol–benzene (III). [b] The screening procedures are as indicated in the text. Administration of pentylenetetrazol (90 mg/kg sc) produced convulsions in all untreated mice and exhibited 100% mortality during 24 hr. [c] Mortality in pentylenetetrazol-treated mice was observed during the 24-hr period.

divided into groups of 10; group weights were kept as near the same as possible. Each oxadiazole-2-thione was suspended in 5% aqueous gum acacia at 1% (w/v). All test compounds were administered to a group of 10 mice at 100 mg/kg ip.

Four hours after the drug administration, the mice were injected with pentylenetetrazol (90 mg/kg sc). In the present experiments, this dose produced convulsions in all untreated mice and also exhibited 100% mortality during 24 hr (14). No mortality was observed during 24 hr in animals treated with the test compounds alone.

The mice were then observed for 60 min for seizures. An episode of clonic spasm that persisted for at least 5 sec was considered a threshold convulsion. Transient intermittent jerks and tremulousness were not counted. Animals devoid of the threshold convulsions during 60 min were considered protected. The number of animals protected in each group was recorded, and the anticonvulsant activity of these oxadiazole-2-thiones was represented by percent protection. No anticonvulsant activity was observed in animals treated with 5% aqueous gum acacia solution alone. The animals were then observed for 24 hr, and their mortality was recorded.

Assay of Cellular Respiratory Activity of Rat Brain Homogenates[1]—Albino rats, 100–150 g, were kept on an *ad libitum* diet. Rat brains isolated from decapitated animals were homogenized[2] immediately in ice-cold 0.25 *M* sucrose in a ratio of 1:9 (w/v). All incubations were conducted at 37°, and the oxygen uptake was measured by the conventional Warburg manometric technique with air as the gas phase (14).

Fresh brain homogenates equivalent to 100 mg wet weight were added to chilled Warburg vessels containing 6.7 mmoles of magnesium sulfate, 20 mmoles of dibasic sodium phosphate buffer (pH 7.4), 1 mmole of adenosine monophosphate (sodium salt), 33 mmoles of potassium chloride, and 500 μg of cytochrome c in a final volume of 3 ml, unless otherwise stated. The central well contained 0.2 ml of 20% KOH. Pyruvate, α-ketoglutarate, and succinate were used at a final concentration of 10 m*M*; the concentration of NADH was 0.5 m*M*. It was presumed that the endogenous NAD, present in the brain homogenates, was sufficient for these oxidative processes.

All oxadiazole-2-thiones were dissolved in propylene glycol (100%) and were incubated with rat brain homogenates at 37° for 10 min prior to the addition of different substrates. An equal volume of the solvent (0.2 ml) was added to the control vessels. The oxygen uptake was measured every 10 min for 60 min.

Assay of Proteolytic Activity of Trypsin—The antiproteolytic activity of substituted oxadiazole-2-thiones was determined by measuring their ability to inhibit trypsin hydrolysis of bovine serum albumin. The reaction mixture consisted of 0.05 *M* tromethamine buffer (pH 8.2), 0.075 mg of crystalline trypsin[3] (1 g of this crystalline trypsin preparation is capable, under certain conditions, of hydrolyzing 250 g of casein), and 0.03 m*M* bovine serum albumin[3] (substrate) in a total volume of 1 ml. The test compounds were dissolved in dimethylformamide and were used at final concentrations of 0.1, 0.5, and 1 m*M*. An equivalent amount of dimethylformamide, added to the control tubes, had no effect on the *in vitro* activity of trypsin with bovine serum albumin as the substrate.

The test compounds were incubated with trypsin for 10 min prior to the addition of bovine serum albumin (15). The reaction was stopped after 5 min by the addition of 0.5 ml of 15% (w/v) trichloroacetic acid. The acid-soluble products of protein breakdown, obtained after centrifugation in the supernatant fraction, were determined by the method of Lowry *et al.* (16). The decrease in the formation of protein breakdown products in the presence of the oxadiazole-2-thiones was used to determine their antiproteolytic activity.

RESULTS AND DISCUSSION

Table I illustrates the anticonvulsant activity of oxadiazole-2-thiones (100 mg/kg ip) against pentylenetetrazol-induced convulsions in mice. The anticonvulsant activity ranged from 10 to 70%; 5-(3,4-methylenedioxyphenyl) -3- (2-methylphenylaminomethyl)-1,3,4-oxadiazole-2-thione (III) and 5-(3,4-methylenedioxyphenyl)-3-(2-methoxyphenylaminomethyl)-1,3,4-oxadiazole-2-thione (VI) exhibited the greatest protection. 5-(3,4-Methylenedioxyphenyl)-3-phenylaminomethyl-1,3,4-oxadiazole-2-thione (II) and 5-(3,4-methylenedioxyphenyl)-3-(4-methoxyphenylaminomethyl)-1,3,4-oxadiazole-2-thione (VIII) possessed the least anticonvulsant activity. All compounds except II exhibited 50–100% protection against 24-hr pentylenetetrazol-induced mortality.

The effects of oxadiazole-2-thiones on the *in vitro* respiratory activity of rat brain homogenates are recorded in Table II. All compounds inhibited NAD-dependent oxidation of pyruvate, α-ketoglutarate, and NADH. These compounds also inhibited FAD-dependent oxidation of succinate by rat brain homogenates. The greatest inhibition of the oxidation of pyruvate and NADH was observed with III. The greatest inhibition of the oxidation of α-ketoglutarate and succinate was observed with II and VI, respectively.

The inhibitory effects of these compounds on the hydrolysis of bovine serum albumin by trypsin are recorded in Table III. All compounds

[1] Sodium pyruvate, sodium α-ketoglutarate, sodium succinate, NADH, adenosine monophosphate (sodium salt), and cytochrome c were obtained from Sigma Chemical Co., St. Louis, Mo.

[2] Potter-Elvehjem homogenizer.

[3] Sigma Chemical Co., St. Louis, Mo.

Table II—Inhibition of Respiratory Activity of Rat Brain Homogenates by 5-(3,4-Methylenedioxyphenyl)-3-arylaminomethyl-1,3,4-oxadiazole-2-thiones

Compound	Inhibition of Respiratory Activity[a], %			
	Pyruvate Oxidation	α-Ketoglutarate Oxidation	NADH Oxidation	Succinate Oxidation
II	67.3 ± 1.3	64.8 ± 1.3	51.9 ± 1.4	32.1 ± 1.0
III	78.6 ± 1.2	38.0 ± 1.2	84.0 ± 1.0	63.2 ± 1.1
IV	69.9 ± 1.4	26.4 ± 1.3	74.6 ± 1.3	17.6 ± 1.3
V	69.9 ± 1.4	33.5 ± 1.3	60.6 ± 1.4	49.1 ± 1.3
VI	76.6 ± 1.0	47.1 ± 1.3	68.1 ± 1.1	73.0 ± 1.5
VII	40.6 ± 1.1	21.4 ± 1.4	79.0 ± 1.0	55.4 ± 1.3
VIII	30.9 ± 1.3	13.1 ± 1.2	49.7 ± 1.2	16.2 ± 1.2
IX	55.9 ± 1.3	38.4 ± 1.4	66.7 ± 1.5	64.5 ± 1.4

[a] Assay procedures and the contents of the reaction mixture are as indicated in the text. Each experiment was done in duplicate. All values represent mean values of percent inhibition with ±*SEM* from three separate experiments. Inhibition was determined by the decrease in the oxygen uptake/100 mg of wet tissue weight/hr. All substituted oxadiazole-2-thiones were used at a final concentration of 2 m*M*. Different substrates and NADH were used at a final concentration of 10 and 0.5 m*M*, respectively.

possessed antiproteolytic activity, and the inhibition of trypsin activity was concentration dependent. The greatest inhibition in the activity of trypsin was observed with VI.

These results provided evidence for the changes in anticonvulsant activity of oxadiazole-2-thiones (Table I) on the introduction of a substituent in the phenyl nucleus of the arylamino moiety. In general, an increase in anticonvulsant activity was observed with the introduction of CH_3, OCH_3, or 4-Cl substituents; with VIII, however, no change in the anticonvulsant activity was observed as compared to the unsubstituted compound (II). The compounds possessing either a CH_3 (III) or OCH_3 (VI) group at position 2 of the phenyl nucleus provided the greatest protection against convulsions as compared to the unsubstituted compound.

The degree of protection against pentylenetetrazol-induced convulsions was decreased by the introduction of a CH_3 or OCH_3 substituent at position 2, 3, or 4 of the phenyl nucleus. Compounds with 4-CH_3 and 4-OCH_3 substituents showed low anticonvulsant activity. The order of the anticonvulsant activity of these compounds observed with respect to the substitution was 2-CH_3 or 2-OCH_3 > 3-CH_3 or 3-OCH_3 > 4-CH_3 or 4-OCH_3 > unsubstituted compound. The 4-Cl-substituted compound (IX) showed increased ability to provide protection as compared to the unsubstituted compound. The anticonvulsant activity of these substituted oxadiazole-2-thiones was related to their ability to provide protection against pentylenetetrazol-induced mortality during 24 hr.

Table III—Inhibition of Trypsin-Induced Hydrolysis of Bovine Serum Albumin by 5-(3,4-Methylenedioxyphenyl)-3-arylaminomethyl-1,3,4-oxadiazole-2-thiones

Compound	Inhibition[a], %		
	0.1 m*M*	0.5 m*M*	1 m*M*
II	23.2 ± 1.4	53.6 ± 1.2	62.6 ± 1.4
III	8.0 ± 0.2	15.9 ± 1.0	35.1 ± 0.6
IV	25.4 ± 1.3	50.7 ± 1.2	83.3 ± 1.7
V	32.0 ± 1.0	53.6 ± 1.2	65.2 ± 1.3
VI	40.4 ± 1.0	59.4 ± 1.7	90.5 ± 1.4
VII	8.0 ± 0.6	30.4 ± 1.3	40.5 ± 1.3
VIII	25.4 ± 1.3	33.3 ± 0.9	53.6 ± 1.4
IX	10.0 ± 1.4	13.0 ± 0.4	33.7 ± 0.7

[a] Assay procedures and the contents of the reaction mixture are as indicated in the text. Each experiment was done in triplicate. The figures indicate mean values of percent inhibition of trypsin activity during hydrolysis of bovine serum albumin with ±*SEM* calculated from three separate experiments. All substituted oxadiazole-2-thiones were used at final concentrations of 0.1, 0.5, and 1 m*M*.

Introduction of various substituents in the phenyl nucleus of the arylaminomethyl moiety of these substituted oxadiazole-2-thiones influenced their ability to inhibit respiratory activity of rat brain homogenates (Table II). The ability of these compounds to inhibit oxidation of pyruvate and NADH by rat brain homogenates corresponded well with the changes observed in their anticonvulsant activity due to substitution effects.

All substituted oxadiazole-2-thiones inhibited the activity of trypsin during hydrolysis of bovine serum albumin. These results (Table III) failed to show any definite role of substituents on antiproteolytic activity.

These results failed to provide a definite structure–activity relationship with respect to anticonvulsant activity, inhibition of cellular respiratory activity of rat brain homogenates, and antiproteolytic activity. However, determination of the activity of these substituted oxadiazole-2-thiones with other animal model systems could presumably prove useful in elucidating the relationship of molecular structure with anticonvulsant activity.

REFERENCES

(1) H. H. Singh, S. Nagar, A. Chaudhari, and S. S. Parmar, *Indian J. Pharm.*, **34,** 101 (1972).

(2) H. H. Singh, S. Nagar, A. Chaudhari, and S. S. Parmar, *J. Pharm. Sci.*, **62,** 504 (1973).

(3) S. S. Parmar, P. C. Joshi, B. Ali, and W. E. Cornatzer, *ibid.*, **63,** 872 (1974).

(4) S. S. Parmar, S. K. Chaudhary, S. Kumar, and M. Chaudhary, *Proc. Can. Fed. Biol. Soc.*, **19,** 81 (1976).

(5) H. Najer, R. Gindicelli, C. Morel, and J. Menin, *Bull. Soc. Chim. Fr.*, **1966,** 153.

(6) H. L. Yale and K. Losee, *J. Med. Chem.*, **9,** 478 (1966).

(7) J. J. Piala and H. L. Yale, U.S. pat. 3,142,022 (July 14, 1964); through *Chem. Abstr.*, **61,** 8317b (1964).

(8) V. Kishore, S. Kumar, S. S. Parmar, and V. I. Stenberg, *Res. Commun. Chem. Pathol. Pharmacol.*, **11,** 581 (1975).

(9) R. L. Shriner and E. C. Kleiderer, in "Organic Synthesis" coll. vol. III, A. H. Blatt, Ed., Wiley, New York, N.Y., 1955, p. 538.

(10) K. A. Bagdanov, *Maslob-Zhir. Prom.*, **30,** 29 (1964); through *Chem. Abstr.*, **61,** 14612f (1964).

(11) J. S. McFadyen and S. S. Thomas, *J. Chem. Soc.*, **1936,** 584.

(12) R. W. Young and K. H. Wood, *J. Am. Chem. Soc.*, **77,** 400 (1955).

(13) V. J. Ram and H. N. Pandey, *J. Indian Chem. Soc.*, **L.I.,** 634 (1974).

(14) S. S. Parmar, M. Chaudhary, S. K. Chaudhary, and H. R. Spiro, *Pharmacology,* **15,** 112 (1977).

(15) A. Chaudhari, S. S. Parmar, S. P. Singh, S. Kumar, and H. R. Spiro, *ibid.*, **15,** 24 (1977).

(16) O. H. Lowry, N. J. Rosenbrough, A. L. Farr, and R. J. Randall, *J. Biol. Chem.*, **193,** 265 (1951).

ACKNOWLEDGMENTS

Supported in part by the Council of Scientific and Industrial Research, Government of India, New Delhi, India, and U.S. Public Health Service NIDA Grant 7-R01-DA01893-01 and National Institutes of Health Grant 5-T01-HL05939-03.

The authors thank Professor K. P. Bhargava and Professor S. J. Brumleve for their advice and encouragement. Grateful acknowledgment is made to the Northwest Area Foundation, St. Paul, Minn., for providing a Hill Professorship to S. S. Parmar.

Simultaneous Quantitation of Morphine and Paraben Preservatives in Morphine Injectables

KEVIN L. AUSTIN and LAURENCE E. MATHER ˣ

Received June 2, 1977, from the *Department of Anaesthesia and Intensive Care, Flinders Medical Centre, Flinders University of South Australia, Bedford Park, S.A. 5042, Australia.* Accepted for publication February 28, 1978.

Abstract □ A high-performance liquid chromatographic method for the simultaneous determination of morphine sulfate, methylparaben, and propylparaben in morphine sulfate injection was developed. A reversed-phase system, based on an octadecylsilane stationary phase, was used with a binary solvent mobile phase consisting of methanol–phosphate buffer (pH 4.0) containing methanol (5%) delivered at a constant rate (0.6:0.4 ml/min) using a two-pump system. The detector response at 254 nm was linear with the amount injected over a wide range, allowing rapid and reproducible quantitation of each component.

Keyphrases □ Morphine sulfate—high-performance liquid chromatographic analysis simultaneously with parabens in dosage form □ Methylparaben—high-performance liquid chromatographic analysis simultaneously with morphine sulfate and propylparaben in dosage form □ Propylparaben—high-performance liquid chromatographic analysis simultaneously with morphine sulfate and methylparaben in dosage form □ High-performance liquid chromatography—simultaneous analyses, morphine sulfate and parabens in dosage form □ Narcotic analgesics—morphine sulfate, high-performance liquid chromatographic analysis simultaneously with parabens in dosage form

Although neither the USP (1) nor the BP (2) requires the determination of preservative agents in official preparations of morphine sulfate injection, a simple method for the simultaneous quantitation of morphine and preservative agents occasionally is required. Official methods for the determination of morphine in pharmaceutical preparations are tedious and time consuming (3). Although column chromatographic–UV spectrophotometric methods were reported for the determination of paraben preservatives (4) and morphine in the presence of paraben preservatives (5), they also are time consuming. During a project to assess the effects of sterilization procedures on drugs used in anesthetic practice, an extremely simple and fast method was developed to quantitate simultaneously morphine, methylparaben, and propylparaben in morphine injectables using high-performance liquid chromatography (HPLC).

EXPERIMENTAL

Reagents and Chemicals—Analytical reagent grade chemicals were used. Methanol and aqueous solutions were filtered through a 0.45-μm filter[1] and degassed using an ultrasonic bath immediately before use.

Morphine sulfate[2], methylparaben[2], and propylparaben[2], all BP grade, were prepared for calibration by dissolving in distilled water, both singly and in admixture, in concentrations similar to the final concentration in the injectable—*viz.*, morphine sulfate, 10.0 mg/ml; methylparaben sodium, 0.63 mg/ml; and propylparaben sodium, 0.33 mg/ml.

Apparatus—A high-performance liquid chromatograph[3] was equipped with an octadecylsilane column[4] for reversed-phase chromatography and a recording digital integrator[5]. The chromatograph detector was set at 254 nm. The absorbance scale was set at 1.0 unit full scale, and the recorder was set at 1 cm/min.

Mobile Phase—The mobile phase was delivered from two pumps. Pump A delivered pure methanol. Pump B delivered an aqueous solution of 0.1% monobasic sodium phosphate dihydrate containing 5% methanol at pH 4.0 (the pH was adjusted by dropwise addition of either 1% phosphoric acid or 1% dibasic sodium phosphate). A total flow rate of 1.0 ml/min consisted of 0.6 ml/min from Pump A and 0.4 ml/min from Pump B.

Determination of Calibration Curve—Triplicate volumes of each standard solution (1.0–10.0 μl), first individually and then in admixture, were injected into the chromatograph using a 10-μl microsyringe. Regression of the detector response for each component on volume injected was assessed in two ways: by manually measured peak heights and by electronically computed peak areas.

Determination of Components in Morphine Sulfate Injection—Exactly 3.0-μl aliquots of morphine sulfate injection (nominally containing 10.0 mg of morphine sulfate/ml, 0.63 mg of methylparaben so-

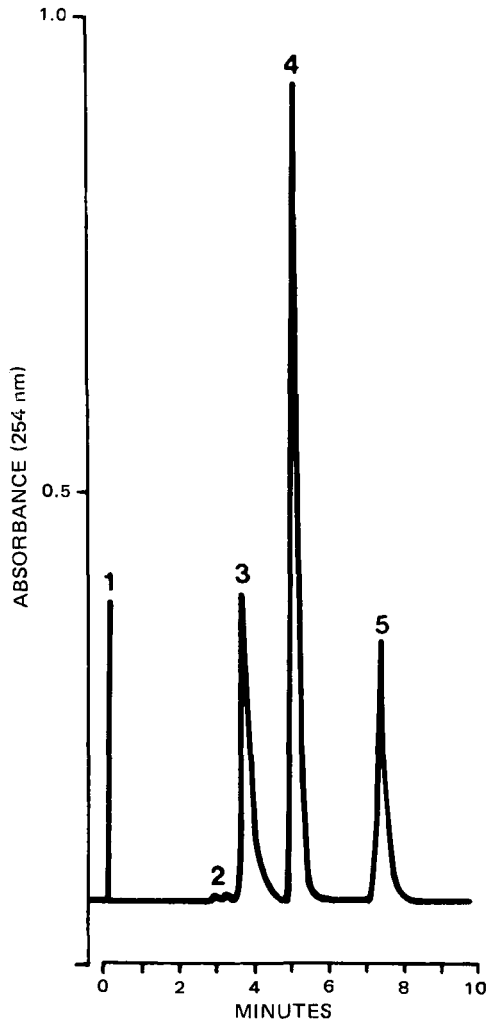

Figure 1—*High-pressure liquid chromatogram obtained with the described method. Key: peak 1, point of injection; peak 2, trace components found in morphine sulfate injections; peak 3, morphine; peak 4, methylparaben; and peak 5, propylparaben.*

[1] Gelman Metricel GA-6.
[2] Courtesy of David Bull Laboratories, Melbourne, Australia.
[3] Waters ALC/GPC 200 series with U6K universal injector, model 440 multiple wavelength absorbance detector, model M6000A pumps, and model 660 solvent programmer.
[4] μBondapack C_{18}, 10-μm particle size, 4 mm i.d. × 30 cm.
[5] Hewlett-Packard model 3380A.

0022-3549/78/1100-1510$01.00/0
© 1978, American Pharmaceutical Association

Table I—Regression Analysis of Detector Response (254 nm) Measured as Peak Height and Peak Area on Volume Injected

	Morphine	Methyl-paraben	Propyl-paraben
Peak height			
Intercept, mm	7.4	−2.5	−1.2
Slope, mm/μl	11.71	34.21	10.25
r^2	0.99406	0.99915	0.99731
Range, μl	1.0–10.0	1.0–7.0[a]	1.0–10.0
n	30	21	30
Peak area			
Intercept, (mv)(sec)	−1933	3840	−1386
Slope, (mv)(sec)/μl	20,769	31,285	15,214
r^2	0.99984	0.99581	0.99826
Range, μl	1.0–10.0	1.0–6.0[b]	1.0–10.0
n	30	18	30

[a] The response beyond 7.0 μl was off scale. [b] The response was nonlinear beyond 6.0 μl.

dium/ml, and 0.33 mg of propylparaben sodium/ml) were injected directly into the chromatograph. Peak area calibration curves were used to read off the equivalent volume injected (and, therefore, the drug amount injected). The results were calculated using:

$$\text{percent of strength claim} = \frac{V_0}{V_i} \times 100\% \qquad \text{(Eq. 1)}$$

where V_0 is the volume observed as equivalent from standard curve and V_i is the volume actually injected.

Effects of Sterilization on Active Ingredients—Ampuls from a test batch of morphine sulfate injection were obtained both before and after routine factory sterilization. Representative samples from each lot were divided into two groups and then subjected to three cycles of sterilization by autoclaving at 120–121° for 30 min. One group from each lot was cooled rapidly over 5–10 min while the other group was cooled slowly over 45–60 min.

Analysis of variance was used to detect any differences between the procedures.

RESULTS AND DISCUSSION

Mobile Phase—HPLC provides an excellent method of separation and quantitation of these compounds, which differ markedly in volatility and polarity. The analysis conditions finally chosen for routine use fulfilled the requirements of simplicity, speed, and separation. By varying the binary mixture, other drugs including lidocaine, mepivacaine, bupivacaine, and meperidine may readily be analyzed using the same combination of column and solvent systems. The separation of a wide range of chemical types using an octadecylsilane stationary phase with a methanol–water mobile phase has been reported (6).

Optimum operating conditions depend on the mobile phase pH. Operation at pH 4.0 produced symmetrical peaks for all components (Fig. 1). Preliminary studies using an unbuffered aqueous phase and aqueous phosphate buffer at pH 6.0 or 8.0 or an ammonium carbonate solution produced insufficiently symmetrical peaks for reproducible quantitation. Hays *et al.* (7) reported unsuccessful quantitation chromatography of morphine under a variety of mobile and stationary phase conditions because of peak asymmetry.

Liquid chromatography of weak bases such as morphine (pKa = 8.0) presents special problems because of the pH-dependent dissociation of the conjugate acid. This dissociation may be overcome using ion suppression techniques by operating at a pH where the free base is predominant. For morphine, operation in excess in pH 10 would be required, but it is not feasible because stationary phase decomposition occurs at pH 8 or greater. Recently, ion-pair techniques were developed to enable optimum separation of symmetrical peak shapes. The separation presently described separates the hydrophilic conjugate acid of morphine from the more hydrophobic neutral paraben esters. Under these conditions, morphine is retained on the column ($k' = 0.4$) long enough for highly reproducible separation and quantitation.

Table II—Reproducibility of 10 Replicate Simultaneous Determinations of Morphine, Methylparaben, and Propylparaben

Variable	Mean	CV, %	Range
Morphine			
Retention time, min	3.57	1.2	3.53–3.64
Peak height, mm	53.70	1.4	53.0–54.7
Peak area, (mv)(sec)	71,924	0.7	71,287–73,156
Methylparaben			
Retention time, min	5.27	0.4	5.22–5.29
Peak height, mm	120.70	0.7	119.5–121.7
Peak area, (mv)(sec)	118,352	0.6	117,687–119,521
Propylparaben			
Retention time, min	8.25	1.3	8.11–8.37
Peak height, mm	33.80	1.2	33.2–34.5
Peak area, (mv)(sec)	51,320	0.6	50,894–51,799

Table III—Concentrations of Morphine and Paraben Preservatives in Ampuls after Three Cycles of Pharmacy Autoclave Sterilization

	Not Factory Sterilized, Mean ± SD, mg/ml	Factory Sterilized, Mean ± SD, mg/ml
Control		
Morphine sulfate	11.31 ± 0.23	11.30 ± 0.45
Methylparaben sodium	0.76 ± 0.03	0.76 ± 0.04
Propylparaben sodium	0.38 ± 0.01	0.38 ± 0.00
Rapid cool		
Morphine sulfate	11.18 ± 0.50	10.92 ± 0.32
Methylparaben sodium	0.77 ± 0.05	0.76 ± 0.04
Propylparaben sodium	0.37 ± 0.01	0.39 ± 0.00
Slow cool		
Morphine sulfate	10.84 ± 0.35	11.35 ± 0.34
Methylparaben sodium	0.76 ± 0.05	0.77 ± 0.06
Propylparaben sodium	0.37 ± 0.01	0.38 ± 0.01

While determining optimum separation conditions, a problem of spurious detector response was encountered consistently at fractional flows of methanol between 20 and 80%. Both random fast and systematic slow noise signals were observed. This effect was attributed to the liberation of gas on mixing of the solvents. The liberated gas affected the constant flow rate solvent delivery system and occurred even with freshly degassed methanol and aqueous solutions. The problem was circumvented by the addition of 5% methanol to the aqueous phase prior to degassing.

Calibration Curve and Reproducibility—There is a longstanding dispute over the choice between peak height and peak area measurements in chromatographic determinations. For two of the three components, marginally higher correlation coefficients were obtained from analysis of the regression of peak area on volume injected when compared to the corresponding analysis using peak heights (Table I). A definite discontinuity appeared in the peak height calibration curve for morphine, which was not reflected in the peak area curve. Although injection of volumes greater than 7.0 μl of methylparaben resulted in peaks being off scale, they were still integrated. The peak area–volume injected relationship was linear to 6–7 μl injected; beyond this limit, distinct nonlinearity was observed. Both the peak height and peak area *versus* volume injected standard curves were linear for propylparaben over the 0–10-μl range tested.

Details of a reproducibility study for 10 replicate determinations are given in Table II. The method appears quite robust in that retention times of the compounds were very consistent with coefficients of variation in the order of 1% for all three components.

Excellent quantitative reproducibility was obtained using both peak height and peak area measurements. Coefficients of variation for peak height measurements were approximately double those for computed peak areas, confirming the preference for the latter method of calculation.

Effect of Sterilization Procedure—There were no significant differences between the two rates of cooling with respect to active ingredient concentration. No degradation of active ingredients was observed for any component measured (Table III).

REFERENCES

(1) The "United States Pharmacopeia," 19th rev., Mack Publishing Co., Easton, Pa., 1975, p. 332.

(2) "British Pharmacopoeia 1973," Her Majesty's Stationery Office, London, England, 1973, p. 331.

(3) V. D. Gupta, *J. Pharm. Sci.*, **65**, 1967 (1976).

(4) T. Higuchi, K. P. Patel, E. R. Bonow, and J. Ladsman, *J. Am. Pharm. Assoc., Sci. Ed.*, **41**, 293 (1952).

(5) I. J. Holcomb, R. B. Luers, and S. A. Fusari, *J. Pharm. Sci.*, **62**, 1504 (1973).

(6) P. J. Twitchett and A. C. Moffat, *J. Chromatogr.*, **111**, 149 (1975).

(7) S. E. Hays, L. T. Grady, and A. V. Kruegel, *J. Pharm. Sci.*, **62**, 1509 (1973).

Pharmacokinetics of Morphine and Its Surrogates I: Comparisons of Sensitive Assays of Morphine in Biological Fluids and Application to Morphine Pharmacokinetics in the Dog

EDWARD R. GARRETT ˣ **and TÜRKAN GÜRKAN** *

Received December 5, 1977, from *The Beehive, College of Pharmacy, J. Hillis Miller Health Center, University of Florida, Gainesville, FL 32610.* Accepted for publication March 2, 1978. *Present address: Department of Analytical Chemistry, Faculty of Pharmacy, University of Istanbul, Istanbul, Turkey.

Abstract □ A sensitive isotope derivatization assay was developed to quantify morphine in biological fluids in the nanogram per milliliter range. Morphine, derivatized with ^{3}H-dansyl chloride, was separated from the reaction products by TLC. The spots were scraped from the plate, and the eluted radioactivity was determined by liquid scintillation. The standard deviations of this morphine assay were ±18.6 ng/ml in 100 μl of plasma and ±1.86 ng/ml in 1 ml of plasma. The GLC analysis of pentafluoropropionated morphine in the range of 0–5 ng of morphine/ml of plasma had a standard deviation of ±0.46 ng/ml when 1 ml of plasma was taken. Liquid scintillation spectrometric analysis of ^{14}C-morphine had a sensitivity of 1.5 ng/ml of plasma at double the background. There were no significant differences among the liquid scintillation, electron-capture GLC, and radioisotope derivatization methods for morphine obtained from the plasma of a dog given 14.00 mg iv of morphine. Morphine conjugates were assayed as morphine after the acid hydrolysis of plasma and urine preextracted to remove unconjugated morphine, and the equivalence of various methods was demonstrated to monitor plasma and urine pharmacokinetics in a dog.

Keyphrases □ Morphine—radiochemical TLC analysis in biological fluids, compared to GLC and liquid scintillation spectrometric analyses, pharmacokinetics in dog □ Radiochemical TLC—analysis, morphine in biological fluids, compared to GLC and liquid scintillation spectrometric analyses □ Pharmacokinetics—morphine in dog, radiochemical TLC, GLC, and liquid scintillation spectrometric analyses compared □ Narcotic analgesics—morphine, radiochemical TLC analysis in biological fluids, compared to GLC and liquid scintillation spectrometric analyses, pharmacokinetics in dog

The disposition and pharmacokinetics of morphine have been studied in humans and animals (1–12). Assays with sufficient sensitivity to determine morphine at nanogram per milliliter levels in biological fluids used radioactive (13–16), spectrofluorometric (17–21), and GLC (22–29) techniques. Procedures utilizing radiolabeled morphine are highly sensitive but are relatively nonspecific unless accompanied by chromatographic separation. Fluorometric methods have high sensitivity but lack specificity and have high interfering backgrounds. Radioimmunoassay measures picogram amounts of morphine but also assays metabolites and analogs (30–32).

It is necessary to derivatize the polar morphine molecule for reliable GLC assay. Morphine has been converted to its trimethylsilyl and acetyl derivatives and quantified by flame-ionization detection (22–26, 29). Methods utilizing GLC–mass fragmentography with a practical lower limit of detection of 500 pg were reported (33–35). Electron-capture GLC assays of morphine derivatized with trifluoroacetic anhydride (27) and with pentafluoropropionic anhydride (28) were applied to biological samples.

In preparation for detailed studies on the pharmacokinetics of morphine and its surrogates, this paper reports the comparison of the modified electron-capture GLC assay of pentafluoropropionic anhydride derivatized morphine (28), a new radioisotopic derivatization technique using ^{3}H-dansyl chloride, and selected extraction techniques for liquid scintillation assay of *N*-methyl-labeled ^{14}C-morphine in biological fluids. The methods were applied to a pharmacokinetic study of morphine in the dog.

EXPERIMENTAL

Materials and Methods—Spectral grade benzene[1], 1-butanol[1], ethyl acetate[1], toluene[1], chloroform[1], isopropyl alcohol[1], acetone[1], and methanol[1] were used. A toluene-based scintillation cocktail[2] was used in the radioactive assays. Reagents were pentafluoropropionic anhydride[3], silylating fluid[4], ^{3}H-dansyl chloride in benzene solution[5] (8.3 Ci/mmole and 1 mCi/ml), and dansyl chloride[6]. High purity hydrochloric acid[7], sodium hydroxide[7], sodium carbonate[7], and sodium bicarbonate[7] were used to prepare buffer solutions.

N-Methyl-labeled ^{14}C-morphine[5] (60 mCi/mmole) and morphine sulfate crystalline[8] USP were used to prepare the dose (3.85 mCi/mmole) for the pharmacokinetic study. ^{14}C-Urea[9] (9.76 mCi/mmole) was the internal standard for the radioactive assay. Precoated silica gel plates[10] on aluminum supports were used for TLC separations. Nalorphine[8] was the internal standard for GLC assays.

Apparatus—The gas chromatograph[11] was equipped with a ^{63}Ni-electron-capture detector. The GLC separation was carried out with a silylated 3.05-m coiled glass column[12] at 215° with a detector temperature of 275°. The carrier (nitrogen) flow rate was 30 ml/min.

Radioactivity of the samples was determined with a liquid scintillation counter[13].

A chromatograph[14] equipped with a 6000-psi constant-flow pump and a 254-nm detector was used for high-pressure liquid chromatographic (HPLC) separation of morphine. The column[15] was designed for reversed-phase chromatography.

GLC Assay—An aliquot (0.5 ml) of plasma or urine was placed in a 15-ml centrifuge tube containing 1.5 ml of freshly prepared 1 *M* sodium bicarbonate adjusted to pH 8.9 with 1 *M* NaOH. An appropriate amount (2–10 μl) of the internal standard, nalorphine, in 0.1 *M* sulfuric acid was added and was usually between 3 and 350 ng. The amount of nalorphine was chosen to give a peak area ratio of the separated morphine pentafluoropropionate to nalorphine pentafluoropropionate between 0.5 and 2. Prior radioactivity measurements of radiolabeled morphine permitted the best estimates of the appropriate amounts of nalorphine to add.

The mixture was thoroughly mixed with 2 ml of benzene–1-butanol (85:15) on a vortex mixer for 30 sec. The phases were separated by centrifugation[16] for 10 min at 3000 rpm, and the organic phase was transferred with a silylated Pasteur pipet into another 15-ml centrifuge tube. The extraction was repeated with 2 ml of solvent. The aqueous phase was saved for subsequent assay of morphine conjugates.

[1] Burdick and Jackson Laboratories, Muskegon, Mich.
[2] Scinti Verse, Fisher Scientific Co., Fair Lawn, N.J.
[3] Reactivial, Pierce Chemical Co., Rockford, Ill.
[4] Silyl-8, Pierce Chemical Co., Rockford, Ill.
[5] Amersham/Searle Co., Arlington Heights, Ill.
[6] Aldrich Chemical Co., Milwaukee, Wis.
[7] J. T. Baker Chemical Co., Phillipsburg, N.J.
[8] Merck & Co., Rahway, N.J.
[9] Bionuclear Corp., Sun Valley, Calif.
[10] E. Merck Laboratories, Elmsford, N.Y.
[11] Model 3920-B, Perkin-Elmer, Norwalk, Conn.
[12] Supelco Inc., Bellefonte, Pa.
[13] Model LS 330, Beckman Instruments, Fullerton, Calif.
[14] Model ALC 202, Waters Associates, Milford, Mass.
[15] μBondapak C_{18} Porasil, Waters Associates, Milford, Mass.
[16] Model K, International Centrifuge, Needham Heights, Mass.

0022-3549/78/1100-1512$01.00/0
© 1978, American Pharmaceutical Association

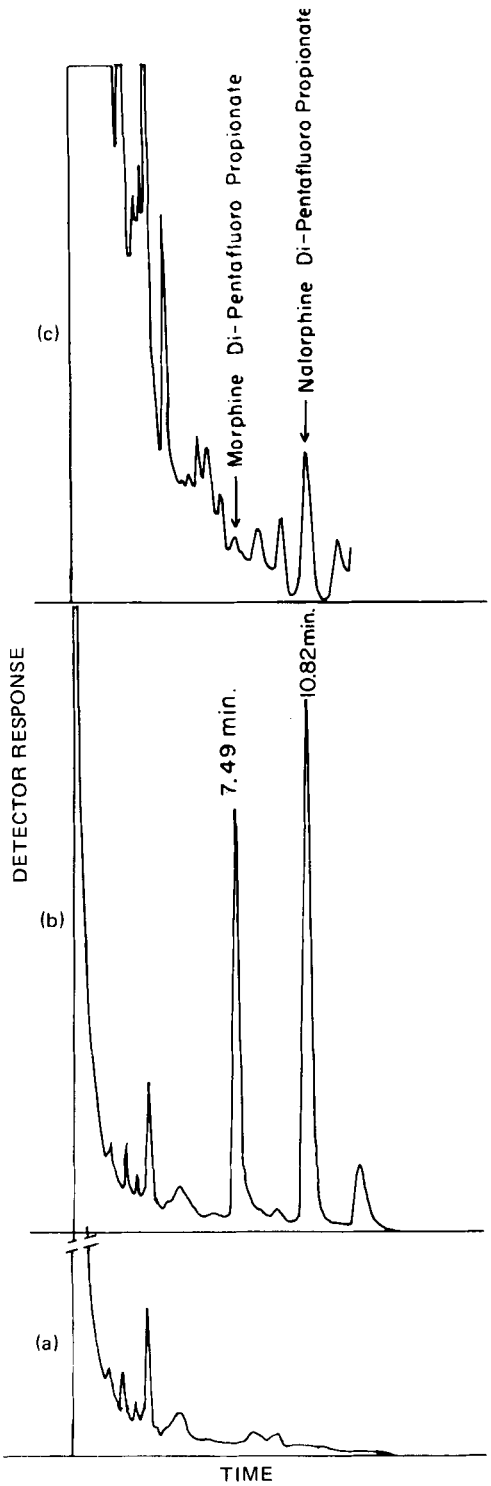

Figure 1—*Electron-capture GLC analysis of pentafluoropropionyl-derivatized morphine and nalorphine from dog plasma. The chromatograms represent the injection of 1 of 200 μl of the final solution from a derivatized extract of 1 ml of blank plasma (0 ng/ml) with an attenuation of 64 (a), the injection of 1 of 500 μl of the final solution of derivatized compound from 0.5 μl of plasma (525 ng/ml) taken 1.36 min after injection of 0.91 mg/kg iv as morphine base but with an attenuation of 128 (b), and the injection of 1 of 50 μl of the final solution of derivatized compound from 1 ml of plasma (1.32 mg/ml) taken 420 min after injection with an attenuation of 64 (c).*

The combined organic phases, containing morphine and internal standard, were back-extracted into 0.5 ml of 1 *M* HCl by mixing on a vortex mixer for 30 sec. The phases were separated by centrifugation for 10 min at 3000 rpm, and the organic phase was aspirated and discarded.

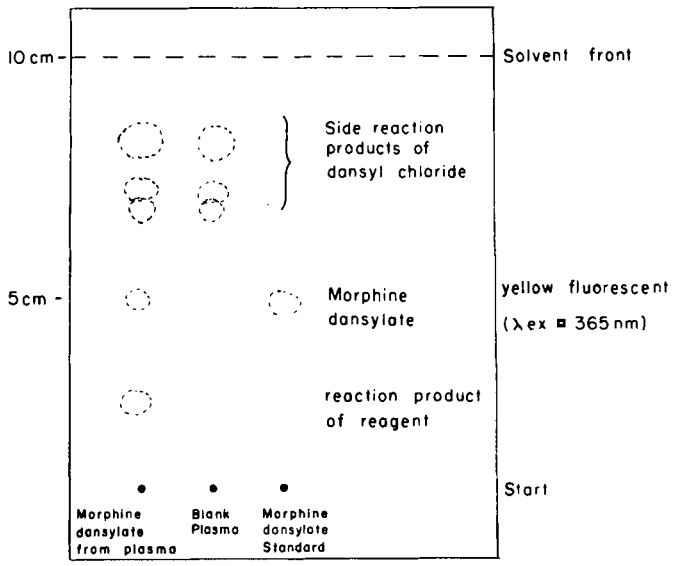

Figure 2—*Thin-layer chromatogram of morphine dansylate prepared from morphine extracted from plasma compared to a derivatized extract of blank plasma and pure morphine dansylate.*

The aqueous phase was washed with 2 ml of fresh organic solvent, and the solvent was aspirated and discarded. The acid phase was neutralized with 0.5 ml of 1 *M* NaOH, the pH was adjusted to 8.9 with the 1 *M* carbonate buffer, and the solution was twice reextracted as already described with 2 ml of benzene–1-butanol.

The organic phases were combined in a vial[3] (5 ml) and evaporated under a nitrogen stream at 55° on a heating block[17]. The thoroughly dried residue was derivatized with 100 μl of pentafluoropropionic anhydride in 50 μl of ethyl acetate for 30 min on a heating block at 55°. Excess reagent was evaporated under a nitrogen stream. The thoroughly dried residue was dissolved in 50 μl of toluene, and 1 μl of this solution was injected into the gas chromatograph. This solvent gave much less of a solvent peak than the previously used ethyl acetate (28).

Quantification was based on the peak area ratio of morphine pentafluoropropionate and nalorphine pentafluoropropionate. The peak areas were measured by an integrator[18]. Typical chromatograms of pentafluoropropionic esters of morphine and nalorphine extracted from plasma are given in Fig. 1. Linear calibration curves were established from morphine-spiked plasma samples for different concentration ranges. The 3.05-m column used gave the greater separation of morphine and nalorphine peaks with less interferences at low morphine concentrations than the 1.5-m column used previously (28).

Radioisotopic Derivatization Method with ^{3}H-Dansyl Chloride—Plasma (100 μl) was placed in a 5-ml centrifuge tube containing 400 μl of the previously described 1 *M* carbonate buffer (pH 8.9). The mixture was mixed with 1 ml of benzene–1-butanol (85:15) on a vortex mixer for 30 sec. The phases were separated by centrifugation for 15 min, and the organic phase was transferred to a 1-ml vial[3] with a Pasteur pipet. The extraction was repeated with 1 ml of solvent, and the combined solvent extracts were evaporated under a nitrogen stream at 55° on a heating block.

The vial walls were washed with 100 μl of solvent, and the contents of the vial were taken to dryness. A 100-μl benzene solution of ^{3}H-dansyl chloride, which was diluted to about 0.83-Ci/mmole specific activity with unlabeled dansyl chloride, was added to the dry residue, and the benzene was evaporated under a nitrogen stream at room temperature. The dry residue, containing the mixture of dansyl chloride and morphine, was dissolved in 20 μl of acetone, and 5 μl of 0.1 *M* sodium bicarbonate was added. The mixture was reacted in a dark place for 7 hr at room temperature. Excess reagent was destroyed with 50 μl of 0.1 *M* sodium carbonate, and the dansylated morphine was extracted with 200 μl of chloroform–isopropyl alcohol (3:1).

After the separation of the phases by centrifugation, the aqueous phase was removed carefully with a 50-μl syringe and discarded. The organic solvent was evaporated under a nitrogen stream at room temperature for

[17] Reacti-Term heating module, Pierce Chemical Co., Rockford, Ill.
[18] Model 3380A integrator, Hewlett-Packard, Avondale, Pa.

Table I—Regression Analyses ($R = mC + b$) of Calibration Curves for GLC Morphine Assay: Peak Area or Height Ratio (R) [a] against Morphine Concentration (C, mg/ml) in Plasma on Analysis of 0.5 ml

C, Range, ng/ml	Internal Standard, ng/ml	m ($\pm \sigma_m$)	b ($\pm \sigma_b$)	σ_R [b]	C_1 [c], ng/ml	σ_c	SD, % of C_1
926–3705	2122	$4.6\ (\pm 0.1) \times 10^{-4}$	$1.27\ (\pm 0.04) \times 10^{-2}$	0.012	2500	26	1.0
371–936	510	$1.70\ (\pm 0.10) \times 10^{-3}$	$1.27\ (\pm 0.78) \times 10^{-1}$	0.059	500	34	6.8
18.5–92.6	56.6	$1.06\ (\pm 0.04) \times 10^{-2}$	$1.9\ (\pm 2.6) \times 10^{-2}$	0.025	50	2.4	4.8
1.8–9.2 [d]	5.65	$1.24\ (\pm 0.11) \times 10^{-1}$	$3.0\ (\pm 6.1) \times 10^{-2}$	0.058	5	0.46	9.2

[a] Peak height ratios were used only in the 1.8–9.2 ng/ml (Fig. 2). [b] From variance about regression. [c] Value of C_1 to substitute in regression equation for calculation of $\pm\sigma_c$ from given $\pm\sigma_R$. [d] Plasma, 1.0 ml, was extracted in this case.

approximately 20 min. The dry residue was dissolved in 20 μl of chloroform–isopropyl alcohol (3:1), and 10 μl of this solution was spotted on a silica gel plate. The plate was developed with methanol (Fig. 2).

The spot assigned to morphine dansylate was identified under UV light (365 nm), marked, scraped, and transferred to a scintillation vial. Methanol (0.5 ml) was added and then shaken with the gel for 5 min, and liquid scintillation fluid (10 ml) was added. The capped samples were dark adapted for at least 6 hr before counting. A calibration curve (Fig. 3) was constructed from spiked plasma samples carried through the derivatization and TLC procedures at the same time as the samples to be analyzed.

Radioactive Assay of ^{14}C-Morphine—Plasma or urine (0.5 ml) was placed in a 15-ml centrifuge tube containing 1.5 ml of 1 *M* carbonate buffer (pH 8.9) prepared as described previously. The mixture was extracted with 4 ml of ethyl acetate–isopropyl alcohol (85:15) by mixing for 30 sec on a vortex mixer, and the tubes were centrifuged for 10 min at 3000 rpm. Then a portion (3 ml) of the organic phase was transferred into a liquid scintillation vial, and the residual organic phase was removed by aspiration. The aqueous phase was saved for subsequent assay of morphine conjugate.

The organic phase in the vial was evaporated under a nitrogen stream at 55° in a water bath. The dry residue was dissolved in 0.5 ml of methanol, 10 ml of liquid scintillation fluid was added, and the samples were dark adapted for at least 6 hr before counting. All samples also were counted after addition of a known amount of the internal standard, ^{14}C-urea (usually 50,000 dpm), to calculate the counting efficiency. The counts per minute values were converted to disintegrations per minute by dividing by the counting efficiency after subtracting background.

Total Radioactivity—The total radioactivity of a plasma or urine sample was determined from an aliquot (0.2 or 0.5 ml) of plasma or urine transferred to a liquid scintillation vial with 0.5 ml of water added. Liquid scintillation fluid (10 ml) was added to the vial, and the capped samples were dark adapted for at least 6 hr. The counting efficiency was calculated by the internal standard method already described. The total concentration of radiolabeled substances as morphine was calculated by dividing the disintegrations per minute values by the known specific activity of the morphine.

^{14}C-Morphine Glucuronide—Morphine glucuronide was hydrolyzed by the procedure of Yeh and Woods (15). The previously morphine-extracted and diluted plasma and urine samples (0.5 ml) were adjusted to about 3.2 *M* HCl with 4 ml of 6 *M* HCl. The capped tubes were maintained for 30 min at 4.54-kg pressure in an autoclave, and the hydrolyzed samples were carefully adjusted to pH 8.9 with solid sodium carbonate.

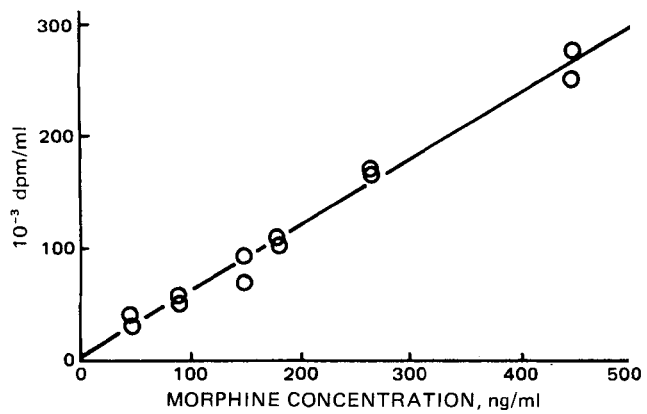

Figure 3—*Calibration curve for morphine derivatized with ^{3}H-dansyl chloride after extraction from 100 μl of plasma.*

The free morphine was extracted by the techniques previously described, and the content of the organic solvent was analyzed by liquid scintillation counting for morphine derived from its conjugates. For GLC, the organic extract was extracted by 3 ml of hydrochloric acid, and 1 ml of the hydrochloric acid was assayed by the procedures used in GLC monitoring.

Preparation of Morphine Dansylate—Crystalline morphine sulfate (0.125 m*M*) was dissolved in 2 ml of water, and 2 ml of the acetone solution of dansyl chloride (0.250 m*M*) and 1 g of sodium bicarbonate were added. The mixture was reacted for 2 hr at room temperature. The yellow precipitate was filtered, washed with water, and recrystallized from acetone–water. The filtrate was extracted with ethyl acetate. This procedure gave additional morphine dansylate, and the overall yield was 49%. The mass spectrum of the product was taken after TLC purification and showed the molecular peak at *m/e* 518 for monodansylated morphine (Fig. 4).

Determination of Extraction Efficiency of Morphine from Plasma—The extraction efficiency of a known amount of TLC-purified ^{14}C-morphine added to dog plasma (129 ng/ml) was determined using the method described under *Radioactive Assay of ^{14}C-Morphine* and was 97.3 ± 0.9% (*SD*).

Preparation of Pharmacokinetic Dose—*N*-Methyl-labeled ^{14}C-morphine hydrochloride[5], 60 mCi/mmole (1.197 mg as morphine base), was mixed with 20 mg of crystalline morphine sulfate (15.039 mg as morphine base) to give a theoretical specific activity of morphine of 4.39 μCi/mmole. The mixture was dissolved in 3.5 ml of sterile isotonic saline, and 3 ml was injected into the dog. The total dose was 13.91 mg as morphine base. The actual specific activity of the dose was determined by HPLC.

The *N*-methyl-labeled ^{14}C-morphine was spotted on a silica gel plate and developed with methanol–ammonia (99:1). Each centimeter of the plate was scraped, eluted with 0.5 ml of methanol, and counted after the addition of 10 ml of liquid scintillation fluid; 87% of the radioactivity was found at the morphine spot (R_f 0.43). This same method was used to prepare the purified ^{14}C-morphine used in studies of extraction efficiencies.

Aliquots of the prepared dose (5 μl) were analyzed for radiolabeled purity by HPLC with a reversed-phase column, using 45% methanol–0.0002 *M* dibasic sodium phosphate (adjusted to pH 7.8 with 0.1 *M* HCl) at a constant flow rate of 2 ml/min. The eluate was monitored for UV absorbance at 254 nm and collected in a scintillation vial over the range (6–7.5 min) where the retention volume of morphine was 6.7 min. The collected fraction was taken to dryness under nitrogen at 70° and dissolved in 0.5 ml of methanol.

Liquid scintillation fluid (10 ml) was added, and the pure radiolabeled morphine was counted after 6 hr of dark adaptation. The amount of

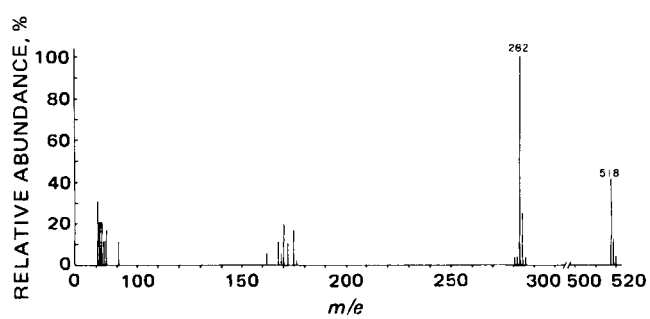

Figure 4—*Mass spectrum of morphine dansylate to demonstrate that the derivatization of morphine with cold dansyl chloride occurs at only one hydroxyl with a resultant product of mass* m/e *518.*

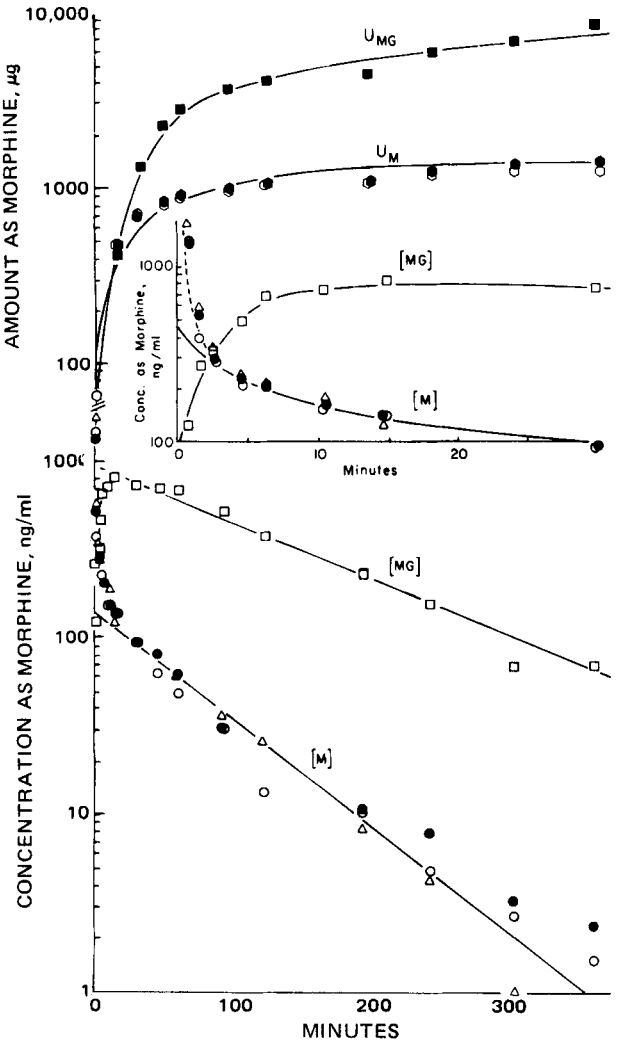

Figure 5—*Plots against time of morphine concentrations in plasma, [M], assayed by liquid scintillation spectrophotometry (○) and GLC (●) of the hexane extract of 0.5 ml of plasma and by dansyl chloride derivatization (△) of the hexane extract of 0.1 ml of plasma. The plot against time of morphine glucuronide, [MG], was based on the average of the values obtained from the total liquid scintillation counting of 0.2 ml of plasma and the counting of the hexane extract of 0.5 ml of solvolyzed plasma from which the morphine had been removed by extraction prior to solvolysis. The cumulative plots against time of morphine, U_M (○), and it glucuronide, U_{MG} (□), excreted in the urine were based on liquid scintillation counting of urine before and after hexane extraction. The values, U_M (●), based on the GLC assay of the hexane extract of urine are given also. The lines drawn through the [M] and [MG] data are those of best fit. The curve drawn through the U_{MG} data was generated from $U_M = Cl_M^{ren} \int_0^t [M]\,dt$, where Cl_M^{ren} was taken as 120 ml/min and $\int_0^t [M]\,dt$ is the area under the [M] versus time plot up to time t. The curve drawn through the U_{MG} data was generated from $U_{MG} = Cl_{MG}^{ren} \int_0^t [MG]\,dt$, where Cl_{MG}^{ren} was taken as 60 ml/min and $\int_0^t [MG]\,dt$ is the area under the [MG] versus time plot up to time t. The inset is for [M] and [MG] on an expanded time scale. The solid line through [M] is for calculated values based on a sum of two exponentials, which ignores the two points at the earliest times; the dashed line in the inset is based on a sum of three exponentials.*

morphine in the collection was determined with respect to a prior HPLC calibration of the UV peak heights on HPLC with pure cold morphine. Thus, the true specific activity was 29,993 dpm/μg or 3.85 μCi/mmole, and 4.216×10^8 dpm (14.0 mg) was administered to the 15.2-kg dog.

Treatment of the Animal—The dog was transferred to a metabolism cage 1 day before the experiment. It was weighed and anesthetized with pentobarbital (30 mg/kg iv). One external jugular vein of the neck was exposed and cannulated under sterile conditions with 30 cm of a catheter[19], and at least 20 cm was inserted into the vein. The incision was closed after the patency of the cannula was verified, and it was filled with heparinized saline. On the following day, the dog was placed on a table in a standing position and restrained by two straps around the fore- and hindlegs that were fixed to a horizontal bar above.

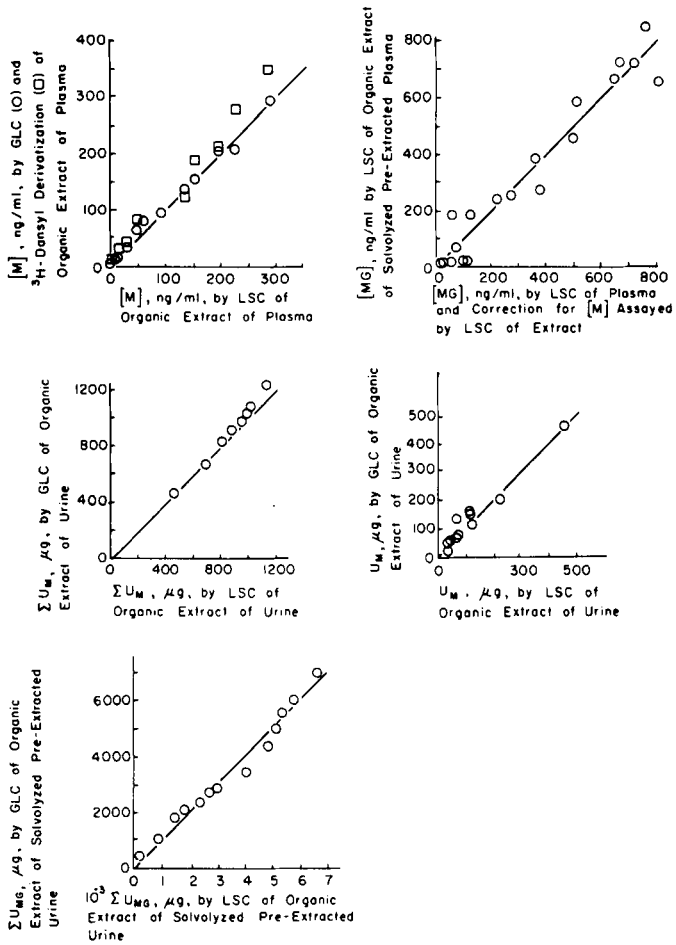

Figure 6—*Regression plots of one assay upon another for the various analytical methods used to determine concentrations of morphine, [M], and morphine conjugates, [MG], in plasma; amounts of morphine, U_M, in urine collections; and cumulative amounts of morphine, ΣU_M, and conjugate, ΣU_{MG}, in the urine of a dog administered a 14.00-mg iv dose of morphine. The theoretical lines drawn through the points have slopes of unity and intercepts of zero. LSC = liquid scintillation counting.*

^{14}C-Morphine solution was prepared in isotonic sterile saline and injected into the jugular catheter over 20 sec. The dosing syringe and catheter were flushed with 10 ml of normal saline. Blood was withdrawn from the jugular catheter, after the dead space of the catheter was filled with fresh undiluted blood, into a sterile, disposable syringe containing 0.01 ml of heparin (10,000 μl/min). The blood sample was transferred to a 5-ml centrifuge tube and centrifuged at 1500 rpm for 10 min. Plasma was transferred to another 5-ml centrifuge tube with a Pasteur pipet, and the tube was stoppered and refrigerated.

Blood (5 ml) was sampled at 0.5, 1, 2, 4, 6, 10, 15, 30, 45, 60, 90, 120, 190, 240, 300, 360, 420, 480, 540, 625, and 1435 min. Hematocrits were obtained on selected blood samples prior to centrifugation.

Urine was collected from the catheterized animal at approximately 15, 30, 50, 60, 90, 120, and 190 min and then every 60 min up to 420 min, every 120 min up to 640 min, and every 12 hr up to 2 days. The volumes of each collection were measured. Urine pH was determined, and an aliquot was removed to determine total carbon-14. The remaining urine was stored in a refrigerator.

The dog was returned to the metabolism cage 12 hr after drug administration.

[19] Medical grade tubing, Dow Corning Corp., Medical Products, Midland, MI 48640.

Table II—Comparisons of Various Assays of Biological Fluids with Time by Regression Analyses [$y \pm \sigma_y = m(\pm\sigma_m)x + b(\pm\sigma_b)$] of Concentrations of Morphine, *M*, and Morphine Conjugates, *MG*, in Plasma ([*M*] and [*MG*]), Amounts in a Urine Collection (U_M and U_{MG}), and Amounts Cumulatively Excreted in Urine (ΣU_M and ΣU_{MG}) after a Morphine Dose of 14.00 mg to a Dog

Assay	*y*	*x*	*n*	Range	$m \pm \sigma_m$	$b \pm \sigma_b$	σ_y	r^2
[*M*], ng/ml	GLC assay of organic extract of 0.5 ml of plasma	LSC[a] assay of organic extract of 0.5 ml of plasma	6	90–300	0.986 ± 0.070	1.4 ± 14	10.8	0.981
			10	10–300	0.956 ± 0.035	7.9 ± 5.4	9.8	0.989
			12	10–1400	0.970 ± 0.036	17 ± 16	45	0.987
			18	0.2–1400	0.979 ± 0.027	10 ± 9.7	36	0.988
	^{3}H-Dansyl derivatization of organic extract of 0.1 ml of plasma	LSC assay of organic extract of 0.5 ml of plasma	10	4–350	1.167 ± 0.057	−1.7 ± 8.5	18	0.981
			12	4–1811	1.31 ± 0.03	−10 ± 11	32	0.996
[*MG*], ng/ml	LSC of 4 or 5 of 12 ml of organic extract of solvolyzed preextracted 0.5 ml of plasma	Determination from LSC (total counts) of 0.1 ml of plasma and LSC of organic extract of 0.5 ml of plasma	11	200–900	0.992 ± 0.132	−1.3 ± 75	85	0.992
			20	14–900	0.992 ± 0.060	−1.9 ± 25	74	0.938
U_M, μg	GLC assay of organic extract of 0.5 ml of urine	LSC assay of organic extract of 0.5 ml of urine	5	60–500	0.960 ± 0.098	12 ± 24	33	0.970
			13	20–500	0.938 ± 0.065	22 ± 10	27	0.950
ΣU_M, μg	GLC assay of organic extract of 0.5 ml of urine	LSC assay of organic extract of 0.5 ml of urine	7	0–1100	1.11 ± 0.05	−72 ± 40	23	0.991
			13	0–1625	1.23 ± 0.05	−213 ± 47	41	0.988
ΣU_{MG}, μg	GLC assay of organic extract of 0.5 or 1.0 ml of 3 ml of aqueous solution from material in organic extract of solvolyzed preextracted 1.0 ml of urine	LSC of 5 of 12 ml of organic extract of solvolyzed preextracted 0.5 ml of urine	13	0–7000	0.963 ± 0.045	180 ± 177	320	0.977

[a] LSC = liquid scintillation counting.

RESULTS AND DISCUSSION

GLC Assay of Plasma Morphine—The regression analyses of linear calibration curves for plasma morphine obtained in four different concentration ranges are given in Table I. In three of the four cases, the intercepts were not significantly different from zero and the estimated standard deviations (in percent of concentration) of an assay from 0.5 ml of plasma ranged from 1% at 2500 ng/ml to 9.2% at 5 ng/ml.

Radioisotopic Derivatization Method for Morphine—Loh *et al.* (21) derivatized morphine extracted from biological samples with dansyl chloride and separated the dansylated morphine from reagent and other reaction products by TLC on polyamide plates. The detection of dansyl morphine was effected by fluorescent scanning or by radioactive counting when ^{14}C-morphine had been used. The sensitivity was claimed to be 5 ng.

The radioisotopic derivatization of morphine described herein was based on the reaction of ^{3}H-dansyl chloride with nonlabeled morphine after a single-step extraction from plasma. The facile TLC separation was applied with subsequent liquid scintillation counting of the ^{3}H-dansylated morphine. This procedure substituted for the extensive sequence of solvent extractions necessary for the cleanup prior to GLC assay of derivatized morphine. The radioisotopic derivatization assay of nonradiolabeled morphine in plasma demonstrated a linear calibration curve (Fig. 3) with a regression equation for the specific activity of ^{3}H-dansyl chloride used (0.83 Ci/mmole) of:

$$\text{dpm/ml } (\pm 11 \times 10^3) = 592\ (\pm 25)C + 3.0(\pm 5) \times 10^3 \quad \text{(Eq. 1)}$$

for a concentration, *C*, in nanograms of morphine per milliliter of plasma. The parenthetical values are the standard deviations. The first two parentheses are related to the variance about regression and the variance of the slope. The intercept is not significantly different from zero. The error about regression permitted an estimation of a concentration, *C*, from a given monitored disintegrations per minute of ±18 ng/ml when 0.1 ml of plasma was taken. The sensitivity could be increased to ±2 ng when 1 ml of plasma was taken. Calibration curves should be prepared on the day of assay since they demonstrated variation among days.

Comparisons of Assays—The plasma samples from a 15-kg dog injected with 14 mg of ^{14}C-morphine (30,000 dpm/μg) through a jugular catheter were analyzed for morphine concentrations, [*M*], as a function of time by the electron-capture GLC assay, the radioactive dansyl derivatization assay, and the direct radiochemical assay after selective extraction (Fig. 5). Linear relationships were found for both the GLC and radioactive dansyl derivatization assays with the direct radiochemical assay of the organic solvent extract for morphine (Fig. 6). The regression coefficients, *m*, were not significantly different than unity, nor were the intercepts significantly different than zero (Table II). There were no significant differences by the *t* test between the mean values of these methods.

The concentrations of morphine conjugates in plasma, [*MG*], were assayed with time (Fig. 5). There was a linear relation with a slope not significantly different than unity and with an intercept not significantly different than zero for the regression of morphine conjugate concentration by liquid scintillation counting of the organic extract of acid-hydrolyzed plasma, which had been preextracted to remove unconjugated morphine, and the conjugate assayed from the difference between total radioactive counts of plasma and the samples extracted as morphine in the organic solvent (Fig. 6 and Table II).

Similarly, the time courses of amounts of morphine excreted in the urine, U_M, by the GLC assay and radiolabeled counting of the organic extracts of urine were the same (Fig. 5). The regression coefficients of the values of the former on the latter (Fig. 6) were not significantly different than unity with an intercept of zero. Furthermore, the equivalence of methods for morphine conjugates in urine, U_{MG}, was demonstrated. GLC assay of the organic extract of solvolyzed preextracted urine plotted against the radiolabeled counting of the organic extract gave a slope of unity and an intercept of zero (Fig. 6 and Table II).

Initial Pharmacokinetic Study—The time course of morphine in the plasma of the 15.2-kg dog administered 14.0 mg iv of morphine (Fig. 5) demonstrated a dependency on the sum of three exponentials. If the initial two values taken at 0.75 and 1.6 min were ignored, a sum of two exponentials was adequate with respective apparent half-lives of 3.0 and 48.8 min. If the initial two points were accepted, an additional apparent half-life of 0.23 min was indicated. The calculated pharmacokinetic parameters for this study are listed in Table III for both models, and their methods of calculation are given in the footnotes.

On the premise of the two-compartment body model, the apparent volume of distribution of the central compartment for morphine was 31 liters; it was 1.3 liters for the three-compartment body model. The latter value is close to the plasma volume of a 15-kg dog (0.6–1.2 liters) whereas the former greatly exceeds the total body water (9–12 liters) (36). These facts strongly indicate that an α'-phase does exist. This finding is confirmed by achievement of three-fourths of the maximum in morphine conjugate concentration in the plasma within 5 min (Fig. 5) after administration when the renal clearance of this conjugate is a relatively slow process (58 ml/min).

The hepatic flow in the 15-kg dog is in the 900–1300-ml/min range (37), which corresponds well to the estimated metabolic clearance of morphine of 959–1234 ml/min. This result indicates complete metabolism of all morphine entering the liver, and an extremely high first-pass metabolism on oral administration would be anticipated. The 86–120-ml/min esti-

Table III—Pharmacokinetic Parameters on Intravenous Bolus Administration of 14.0 mg of Morphine to a 15.2-kg Dog

Body Model[a]	Two Compartment	Three Compartment
A', ng/ml	0	10,000
A	310	310
B	142	142
α', min^{-1}	∞	307
α	0.230	0.230
β	1.42×10^{-2}	1.42×10^{-2}
C_0, ng/ml[b]	452	10,452
V_C^M, ml[c]	30,973	1339
Cl_{ren}^M, ml/min[d]	120.0 ± 9.9 (*SD*)	86.2 ± 5.2
Cl_{ren}^{MG}, ml/min[e]	57.9 ± 5.5 (*SD*)	57.9 ± 5.5 (*SD*)
Cl_{tot}^M, ml/min[f]	1234	959
Cl_{met}^M, ml/min[g]	1176	901
Fraction of dose renally excreted as *MG*	0.643	0.643
Fraction of dose renally excreted as M[h]	0.102	0.102
$Cl^{M\text{-}MG}$, ml/min[i]	840	840
$k_{[MG],U_{MG}}$, min^{-1} [j]	7.09×10^{-3}	7.09×10^{-3}
V_{pss}^{MG}, ml[k]	8166	8166
V_{pss}^M, ml[l]	86,900	67,535

[a] The time course of concentration of morphine in plasma can be described by $[M] = A'e^{-\alpha' t} + Ae^{-\alpha t} + Be^{-\beta t}$. [b] $C_0 = A' + A + B$. [c] Volume of central compartment referenced to morphine concentration in plasma, $V_C^M = D/C_0$, where $D = 14 \times 10^6$ ng. [d] Renal clearance of morphine was calculated from the average of values, $Cl_{ren}^M = \Sigma U_M / \int_0^t [M]\,dt$, where ΣU_M is amount of morphine excreted in the urine up to time t obtained by interpolation of the ΣU_M *versus* t curve after 15 min and $\int_0^t [M]\,dt$ is the area under the $[M]$ *versus* t curve up to time t, $n = 13$. [e] Renal clearance of morphine conjugate calculated similarly where $Cl_{ren}^{MG} = \Sigma U_{MG} / \int_0^t [MG]\,dt$. [f] Total clearance of morphine $Cl_{tot}^M = D / \int_0^\infty [M]\,dt$, where $\int_0^\infty [M]\,dt$ is the total area under the $[M]$ *versus* time curve and can be calculated from $A'/\alpha' + A/\alpha + B/\beta$. [g] $Cl_{tot}^M - Cl_{ren}^M$. [h] Value by liquid scintillation counting where value by GLC was 0.116. [i] Clearance of morphine to analyzed conjugate estimated from fCl_{met}^M, where $f = \Sigma U_{MG}/(D - \Sigma U_M) = 0.71$. [j] Estimated from terminal slope of ln $[MG]$ *versus* time. [k] Pseudo-steady-state volume of distribution estimated from $Cl_{ren}^{MG}/k_{[MG],U_{MG}}$. [l] Pseudo-steady-state volume of distribution estimated from Cl_{tot}^M/β.

mates of renal clearance of morphine and the 58-ml/min clearance of the conjugates are well within the 40–130-ml/min range assigned to glomerular filtration by inulin clearance (36). The estimates of the renal clearances are consistent with the observed excretions of morphine and its conjugates in the urine (Fig. 5).

REFERENCES

(1) L. A. Woods, *J. Pharmacol. Exp. Ther.*, **112,** 158 (1954).

(2) E. L. Way and T. K. Adler, *Pharmacol. Rev.*, **12,** 383 (1960).

(3) E. L. Way and T. K. Adler, *Bull. WHO*, **25,** 227 (1961).

(4) K. Oguri, S. Ida, H. Yoshimura, and H. Tsukamoto, *Chem. Pharm. Bull.*, **18,** 2414 (1970).

(5) S. Spector, *Science*, **174,** 421 (1971).

(6) S. F. Brunk and M. Delle, *Clin. Pharmacol. Ther.*, **16,** 51 (1974).

(7) B. A. Berkowitz, K. V. Cerrata, and S. Spector, *J. Pharmacol. Exp. Ther.*, **191,** 527 (1974).

(8) S. Y. Yeh, *ibid.*, **192,** 201 (1975).

(9) B. A. Berkowitz, S. H. Ngai, J. C. Yang, J. Hempstead, and S. Spector, *Clin. Pharmacol. Ther.*, **17,** 629 (1975).

(10) B. E. Dahlstrom and L. K. Paalzow, *J. Pharmacokinet. Biopharm.*, **3,** 293 (1975).

(11) D. R. Stanski, D. J. Greenblatt, D. G. Lappas, J. K. Weser, and E. Lowenstein, *Clin. Pharmacol. Ther.*, **19,** 752 (1976).

(12) D. H. Catlin, *J. Pharmacol. Exp. Ther.*, **200,** 224 (1977).

(13) T. K. Adler, H. W. Elliott, and R. George, *ibid.*, **120,** 475 (1957).

(14) S. J. Mulé and L. A. Woods, *ibid.*, **136,** 232 (1962).

(15) S. Y. Yeh and L. A. Woods, *J. Pharm. Sci.*, **59,** 380 (1970).

(16) E. Brochmann-Hanssen, *ibid.*, **61,** 1118 (1972).

(17) H. Kupferberg, A. Burkhalter, and E. L. Way, *J. Pharmacol. Exp. Ther.*, **145,** 247 (1964).

(18) A. E. Takemori, *Biochem. Pharmacol.*, **17,** 1627 (1968).

(19) S. J. Mulé and P. L. Hushin, *Anal. Chem.*, **43,** 708 (1971).

(20) M. Sansur, A. Buccafuri, and S. Morgenstern, *J. Assoc. Offic. Anal. Chem.*, **55,** 880 (1972).

(21) H. H. Loh, I. K. Ho, T. M. Cho, and W. Lipscomb, *J. Chromatogr.*, **76,** 505 (1973).

(22) E. Brochmann-Hanssen and A. B. Svendsen, *J. Pharm. Sci.*, **52,** 1134 (1963).

(23) G. E. Martin and J. S. Swinehart, *Anal. Chem.*, **38,** 1789 (1966).

(24) G. R. Wilkinson and E. L. Way, *Biochem. Pharmacol.*, **18,** 1435 (1969).

(25) J. E. Wallace, J. D. Biggs, and K. Blum, *Clin. Chim. Acta*, **36,** 85 (1972).

(26) S. Y. Yeh, *J. Pharm. Sci.*, **62,** 1827 (1973).

(27) J. E. Wallace and H. E. Hamilton, *Anal. Chem.*, **46,** 2107 (1974).

(28) B. Dahlstrom and L. K. Paalzow, *J. Pharm. Pharmacol.*, **27,** 172 (1975).

(29) K. E. Rasmussen, *J. Chromatogr.*, **120,** 491 (1976).

(30) S. Spector and C. W. Parker, *Science*, **168,** 1347 (1970).

(31) S. Spector, *J. Pharmacol. Exp. Ther.*, **178,** 253 (1971).

(32) D. Catlin, R. Cleeland, and E. Grunberg, *Clin. Chem.*, **19,** 216 (1973).

(33) W. O. R. Ebbighausen, J. H. Mowat, P. Vestergaard, and N. S. Kline, *Adv. Biochem. Psychopharmacol.*, **7,** 135 (1973).

(34) P. A. Clarke and R. L. Foltz, *Clin. Chem.*, **20,** 465 (1974).

(35) P. P. Hipps, M. R. Eveland, E. R. Meyer, W. R. Sherman, and T. J. Cicero, *J. Pharmacol. Exp. Ther.*, **196,** 642 (1976).

(36) P. L. Altman and D. S. Dittmer, "Blood and Other Body Fluids," Biological Handbooks, American Societies for Experimental Biology, Washington, D.C., 1961, pp. 4, 52, 3907.

(37) P. L. Altman and D. S. Dittmer, "Respiration and Circulation," Biological Handbooks, American Societies for Experimental Biology, Bethesda, Md., 1971, p. 429.

ACKNOWLEDGMENTS

Supported in part by Grant 2-R01-DA-00743-04 from the National Institute on Drug Abuse, Rockville, MD 20852. A portion of T. Gürkan's stay was supported by a grant from the government of Turkey.

The technical assistance of Kathleen L. Eberst is gratefully acknowledged. The authors are grateful to Dr. Brian D. Andresen (Analytical Toxicology Laboratory) for the mass spectral studies.

Mechanism of Fluorometric Analysis of Tetracycline Involving Metal Complexation

STANLEY T. DAY, WILLIAM G. CROUTHAMEL *, LOUIS C. MARTINELLI, and JOSEPH K. H. MA ˣ

Received June 15, 1977, from the *School of Pharmacy, West Virginia University, Morgantown, WV 26506.* Accepted for publication March 3, 1978. *Present address: School of Pharmacy, University of Maryland, Baltimore, MD 21201.

Abstract □ Tetracycline complexation with calcium and organic ligands was studied using fluorescence, circular dichroism, and solvent extraction methods. The results were used to interpret the mechanism of the commonly used fluorometric methods for the analysis of tetracycline in biological fluids. Tetracycline formed ternary calcium complexes with barbital sodium and L-tryptophan in alkaline solutions. The circular dichroism studies indicate that the calcium ion in these complexes is bound to the C-4 dimethylamino and the C-12a hydroxyl groups of tetracycline. These ternary complexes are strongly fluorescent and can be extracted easily into 1-butanol or ethyl acetate. Based on the characteristics of the ternary complexes and of the tetracycline degradation products, it is concluded that only the active form of tetracycline can be complexed and extracted for fluorescence analysis.

Keyphrases □ Tetracycline—complexation with calcium and organic ligands, mechanism of fluorometric analysis □ Complexation—tetracycline with calcium and organic ligands, mechanism of fluorometric analysis □ Fluorometry—mechanism of analysis, tetracycline complexation with calcium and organic ligands □ Antibacterials—tetracycline, complexation with calcium and organic ligands, mechanism of fluorometric analysis

Tetracycline is amphoteric, forming salts with either acids or bases. The drug is commonly marketed as the hydrochloride salt (I), in which the tetracycline molecule is protonated at the C-4 dimethylamino group.

Tetracycline hydrochloride exhibits three pKa values (1): pK_1 at 3.3 is associated with the tricarbonyl methane system at the C-1, C-2, and C-3 positions; pK_2 at 7.8 is associated with the C-11–C-12 β-diketone system; and pK_3 at 9.5 indicates the deprotonation of the C-4 dimethylammonium ion.

BACKGROUND

The pH of the medium has a great effect on the stability of tetracycline and its interaction with other molecules. Most tetracyclines are unstable in basic solutions. Kelly *et al.* (2) reported that chlortetracycline converts rapidly into isochlortetracycline at pH 10, and similar reactions for other tetracyclines were observed (3). Tetracycline undergoes oxidation with atmospheric oxygen (4), which may be catalyzed by riboflavin under light (5). Epimerization occurs at the C-4 position and leads to the formation of anhydrotetracycline, a biologically inactive compound often found in aged tetracycline products (6, 7). Dehydration and aromatization of the C-ring lead to the formation of anhydro derivatives, a process occurring predominantly at low pH.

Several methods of tetracycline analysis were developed recently. Tetracycline in biological fluids has been assayed primarily by microbiological (8, 9) and fluorometric (10–14) techniques. The disadvantages inherent in the microbiological methods are that the results may be subjected to large errors (±15%) (15) and that the assay is of limited specificity since several tetracycline-like compounds have similar biological activity (16). The serum tetracycline concentrations determined by these methods are consistently lower than those determined by chemical analysis, presumably because of protein binding, which may inhibit the diffusion necessary in the microbiological procedures. Furthermore, the microbiological assay requires sample incubation at pH 4.5 for 3–4 hr, conditions conducive for epimerization to the biologically inactive epimer.

Fluorometric techniques have become popular because of their high sensitivity and reduced variability. The analysis is based on the fluorescence quantitation of tetracycline extracted from biological fluids. Since tetracycline is nearly nonfluorescent, the assays must provide complete extraction as well as large enhancement of the tetracycline fluorescence. Tetracycline forms complexes with many divalent and trivalent cations, and some of these complexes are strongly fluorescent when compared to nonchelated tetracycline. However, these complexes are fairly water soluble and difficult to extract with organic solvents at physiological concentrations. For these reasons, some early fluorometric procedures (10, 11) involved primarily the extraction of the lipid-soluble degradation products of tetracycline followed by treatment with alcoholic calcium or aluminum chloride to enhance the fluorescence.

A method combining both the extraction and fluorescence enhancement was first reported by Kohn (12); tetracycline was extracted with ethyl acetate from solutions containing 0.01 *M* calcium chloride and 0.3 *M* barbital sodium at pH 9. Similar success was reported (13, 14) using magnesium acetate buffer and different solvents. The function of barbital sodium in Kohn's method was to enhance both extraction and fluorescence by forming a neutral ternary complex with calcium and tetracycline. A structure of this complex (II) was proposed by Kohn based on his solvent distribution data. However, the structure and the role of barbital in fluorescence enhancement have been questioned (13, 14, 17).

Poiger and Schlatter (17) suggested that barbital sodium only enhances the fluorescence but does not facilitate tetracycline extraction, whereas others (13, 14) suggested that barbital sodium has no effect on tetracycline fluorescence. The contradictions may be partly due to the use of different analogs of tetracycline in different studies; nevertheless, the study of the ternary complex of calcium, tetracycline, and barbital is important for several reasons. While most fluorometric procedures are adequate for *in vivo* studies of tetracycline, information has not been presented to indicate whether the complex is extracted selectively from the active form of tetracycline. The drug is known to form nonactive degradation products under various conditions. The analytical results could be misleading if some of the results are due to the contribution of the nonactive products.

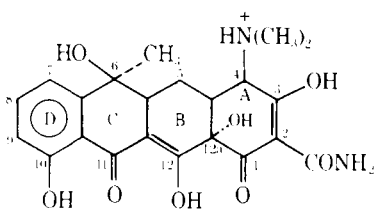

I

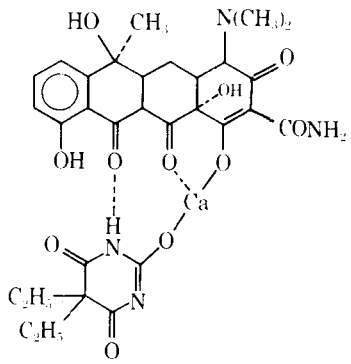

II

0022-3549/78/1100-1518$01.00/0
© 1978, American Pharmaceutical Association

Studies on the ternary complex will aid in understanding the extracted species. From the pharmacological point of view, metal binding of tetracycline has long been known to affect the drug's absorption in biological systems. Studies of the binary and ternary complexes of metal–tetracycline and other ligands should provide useful information on the action of the tetracycline antibiotics.

Under these guidelines, studies of the complexation involving calcium, tetracycline, and several other ligands were carried out using solvent extraction, fluorescence, and circular dichroism techniques. Emphasis was placed on the nature of these complexes and of their importance in the chemical analysis of tetracycline.

EXPERIMENTAL

Materials—Tetracycline hydrochloride[1], barbital sodium[2], and L-tryptophan[3] were obtained commercially. 1-Butanol and other solvents were spectroscopic grade. All other chemicals were analytical grade.

Instruments—Fluorescence measurements were made with a spectrophotofluorometer[4] equipped with a 150-w xenon lamp, a 1P21 photomultiplier tube, and an x–y spectral recorder[5]. Absorption studies were carried out with a spectrophotometer[6] using a matched set of UV cells. Circular dichroism measurements were made with a spectrophotometer[7] equipped with constant nitrogen flush.

Fluorescence Measurements—The fluorescence of tetracycline and its complexes was determined at the emission maximum of 512 nm with the excitation wavelength at 390 nm. A primary fluorescence standard (12) was prepared by mixing a 2-ml aliquot of 5×10^{-5} M tetracycline hydrochloride in water with 0.4 ml of 0.9 M barbital sodium in water. The mixture was then diluted to 50 ml with a solution of 3×10^{-4} M calcium chloride and 8×10^{-3} M barbital prepared in methanol.

After allowing the instrument to warm up for 1 hr, the standard was used to adjust the instrument to give a fluorescence reading of 90 on a fixed sensitivity setting. This adjustment was done periodically during the fluorescence measurements. All sample measurements were carried out at 25° using a matched set of fluorescence cells. Dilution of samples for fluorescence measurement, when necessary, was made with a microsyringe.

Fluorescence–pH Titrations—A 100-ml volume of aqueous solution containing 0.01 M calcium chloride and an appropriate ligand was adjusted to the desired pH with dilute sodium hydroxide or sulfuric acid. A 2-ml aliquot was pipetted into the cell, and to it was added 4 μl of 1×10^{-3} M tetracycline in methanol. The sample fluorescence was then measured. For titrations using only calcium and tetracycline, 20 μl of 1×10^{-2} M tetracycline in methanol was added to 100 ml of aqueous calcium chloride, and pH adjustments were made as described.

All solutions for the pH studies were prepared using double-distilled water. Argon gas was constantly used to prevent pH errors due to carbon dioxide interference in nonbuffered solutions prior to and during titrations.

Distribution Studies—Solvent extraction studies were carried out according to the following procedure. A 10-ml aliquot of tetracycline in a 0.01 M tris(hydroxymethyl)aminomethane–0.1 M hydrochloric acid buffer was equilibrated with 4 ml of the organic solvent (1-butanol or ethyl acetate) by hand shaking for 2 min, followed by centrifuging for 4 min at 2500 rpm; pH adjustments were made prior to extraction. The concentration of the extracted tetracycline was determined spectrophotometrically (Table I). The extracted tetracycline in the complexed forms showed an absorption at 385 nm in 1-butanol or ethyl acetate, whereas the uncomplexed tetracycline absorbed at 360 nm. The molar absorptivities of the complexed tetracycline in 1-butanol and ethyl acetate were determined to be 2.53×10^4 and 1.75×10^4 M^{-1} cm^{-1}, respectively.

Data Treatment—The solvent distribution data were used to determine the stability constants of the binary and ternary complexes involving calcium, tetracycline, and other ligands. In the calcium–tetracycline binary system, the stability constant, K, can be determined from:

$$K = [MT_n]/[M][T]^n \qquad \text{(Eq. 1)}$$

[1] Lot 1110/337, Mylan Laboratories, Morgantown, W.Va.
[2] Fisher Scientific, Pittsburgh, Pa.
[3] Nutritional Biochemical Corp.
[4] Aminco-Bowman, American Instruments, Silver Spring, Md.
[5] Omnigraphic model 2000, Houston Instruments, Houston, Tex.
[6] Cary 118, model C, Varian Instruments, Palo Alto, Calif.
[7] Jasco ORD/CD model 5.

Table I—Percent Extraction of Tetracycline Solutions with 1-Butanol

Solution[a]	pH	Extraction, %
—	7.5	2
—	9.0	43
0.3 M Barbital sodium	9.0	88
0.1 M Acetic acid	9.0	51
0.025 M L-Tryptophan	9.0	89

[a] All solutions contained 0.01 M calcium chloride and 1×10^{-6} M tetracycline (see *Experimental* for extraction procedure).

where $[MT_n]$ is the concentration of the tetracycline complex, $[M]$ is the free concentration of the calcium ion, $[T]$ is the unbound concentration of tetracycline, and n is the number of tetracycline molecules bound to one calcium ion.

In this study, $[MT_n]$ was determined in terms of the bound tetracycline concentration, $[T_b]$. The latter was taken to be the extracted concentration of tetracycline in the organic layer because: (*a*) no extraction can be made without the presence of calcium chloride; and (*b*) the measured absorption of the extracted species is at 385 nm, which is clearly different from that of the unbound tetracycline at 360 nm. Since the concentration of calcium chloride (0.01 M) used is much greater than that of tetracycline (in the range of 10^{-6} M), the initial concentration of calcium chloride, C_m, is essentially taken to be the free concentration, $[M]$. Substitution of C_m for $[M]$ and $[T_b]/n$ for $[MT_n]$ in Eq. 1 leads to:

$$K = [T_b]/n[T]^n C_m \qquad \text{(Eq. 2)}$$

and:

$$-\log[T] = (\log nKC_m)/n - \log[T_b]/n \qquad \text{(Eq. 3)}$$

The plot of $-\log[T]$ *versus* $-\log[T_b]$ should give a straight line with the intercept and slope equal to $(\log nKC_m)/n$ and $1/n$, respectively. From these results, K and n can be easily calculated.

In the ternary system, the overall stability constant for the reaction $M + T + A = MTA$ can be expressed as:

$$K = [MTA]/[M][T][A] \qquad \text{(Eq. 4)}$$

where $[MTA]$ is the concentration of the ternary complex, which is equal to $[T_b]$, and $[A]$ is the free concentration of the second ligand. Equation 4 is based on the assumption that only one molecule of T or A is involved in the complex. The validity of this assumption will be discussed under *Results*. In a condition such that the tetracycline concentration is much smaller than the concentrations of the calcium ion and the ligand A, $K[M][A]$ is essentially a constant. Thus, the plot of $-\log[T]$ *versus* $-\log[MTA]$ should yield a straight line. From the intercept of the plot, the stability constant can be calculated with known values of $[M]$ and $[A]$.

In the present study, the ligand A represents barbital, L-tryptophan, and acetate. These compounds show very weak binding with calcium; *i.e.*, the free concentrations of the ligand and the calcium ion, $[A]$ and $[M]$, may be approximated to be their initial concentrations. With this approximation, the stability constants for these complexes were then calculated. The constants calculated in this manner are slightly lower than the actual values; nevertheless, these results are adequate for comparison.

RESULTS

The pH profile of tetracycline fluorescence in solutions containing calcium chloride and barbital sodium is shown in Fig. 1. Tetracycline is only weakly fluorescent in a basic medium. Calcium chloride addition, however, results in a large enhancement of the tetracycline fluorescence, with a maximum at pH 7.5. Calcium chloride can cause a shift of the pK_2 of tetracycline to a more acidic pH (18), so that the deprotonation of the BCD-ring β-diketone system is nearly complete at pH 7.5. Therefore, the strong fluorescence of the calcium–tetracycline complex at pH 7.5 is due to the chelation of calcium at the β-diketone system of tetracycline. Model studies of the complex indeed show that the calcium ion forces the tetracycline molecule to maintain a planar, rigid conformation, which is optimal for fluorescence.

At pH 9 and above, the calcium–tetracycline solution shows a marked decrease in fluorescence. This result indicates that the calcium ion may have changed its binding site on the tetracycline molecule. At this pH, the C-4 dimethylammonium group of tetracycline undergoes proton dissociation and conformational change. Mitscher *et al.* (19, 20) found

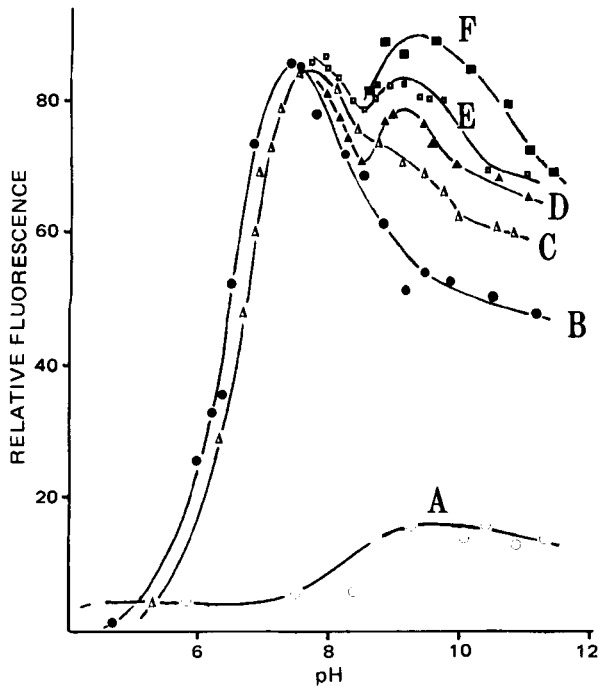

Figure 1—*The pH profile of tetracycline fluorescence (excitation, 390 nm; emission, 512 nm; and concentration of tetracycline, 2×10^{-6} M) in various solutions. Key: A, tetracycline alone; B, with 0.01 M calcium chloride; C, with 0.01 M calcium chloride and 0.025 M barbital sodium; D, with 0.01 M calcium chloride and 0.06 M barbital sodium; E, with 0.01 M calcium chloride and 0.08 M barbital sodium; and F, with 0.01 M calcium chloride and 0.1 M barbital sodium.*

that this conformational change may be enhanced by the presence of calcium and suggested that the calcium is bound to the A-ring system. The present study supports the A-ring binding theory, because the fluorescence of the solution should have been as strong as that in pH 7.5 if the calcium were bound predominantly at the β-diketone system.

In the presence of barbital sodium, the fluorescence of the solution at pH 7.5 remains unchanged; strong enhancement of the fluorescence, however, is observed at pH 9. As shown in Fig. 1, the peak becomes more prominent at higher barbital concentrations. The results indeed suggest the formation of a ternary calcium–tetracycline–barbiturate complex since, in the absence of calcium, barbital sodium has no effect on the tetracycline fluorescence. Furthermore, the mixture of calcium chloride and barbital sodium does not exhibit fluorescence at the wavelength measured.

The effect of barbital sodium on the fluorescence of the calcium–tetracycline solution at pH 9.5 can be used to determine the number of

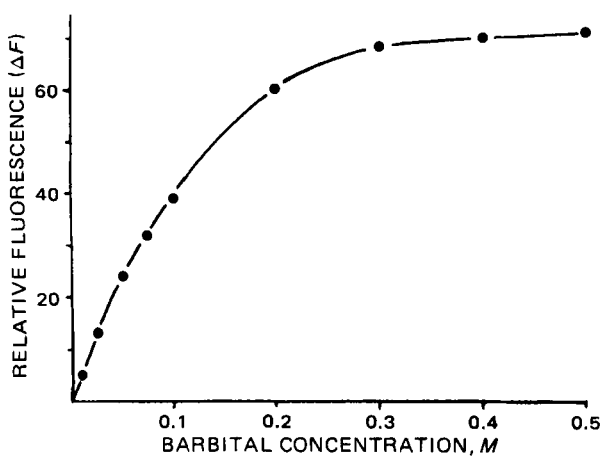

Figure 2—*Plot of the fluorescence enhancement, ΔF, as a function of barbital sodium concentration for solutions containing 0.01 M calcium chloride, 2×10^{-6} M tetracycline, and varying concentrations of barbital sodium at pH 9.5.*

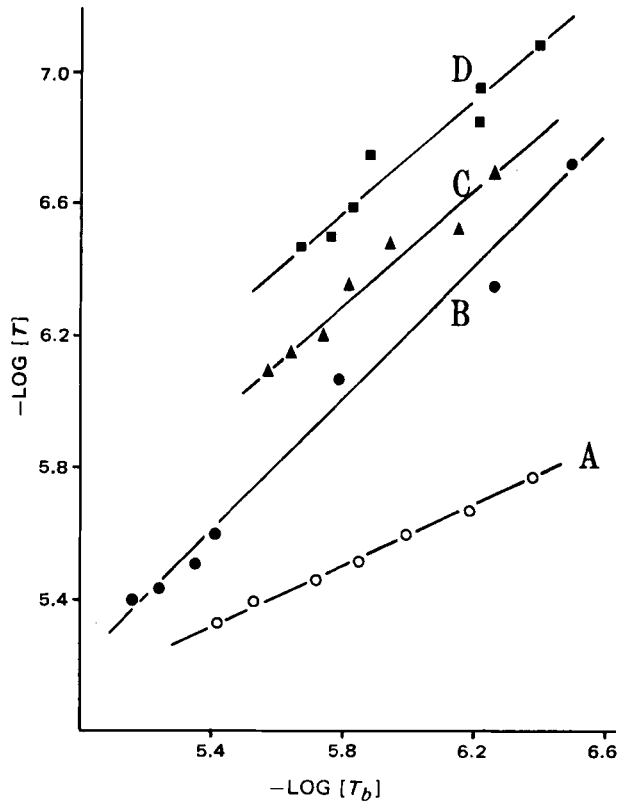

Figure 3—*Tetracycline distribution between pH 9 buffer and 1-butanol (expressed by the plot of $-log[T]$ versus $-log[T_b]$) for solutions containing 0.01 M calcium chloride (A), 0.01 M calcium chloride and 0.2 M acetic acid (B), 0.01 M calcium chloride and 0.025 M L-tryptophan (C), and 0.01 M calcium chloride and 0.1 M barbital sodium (D).*

barbiturate molecules involved in the ternary complex. Figure 2 shows the plot of the fluorescence enhancement, ΔF, induced by barbital sodium *versus* the barbital sodium concentrations, where ΔF is the difference in fluorescence between the ternary and binary systems. If it is assumed that the ternary complex is formed by the reaction $M + T + pA = MTA_p$, then $K = [MTA_p]/[M][T][A]^p$. Here K is the equilibrium constant, p is the number of barbiturate molecules, $[M]$ and $[A]$ are the respective concentrations of calcium and barbital sodium, and $[MTA_p]$ and $[T]$ are the concentrations of the bound and free tetracycline, respectively.

The plot of $\log[MTA_p]/[T]$ *versus* $\log[A]$ should yield a straight line with the slope equal to p. The values of $\log[MTA_p]/[T]$ may be taken to be the values of $\log \Delta F/(\Delta F_0 - \Delta F)$, where ΔF_0 is the maximum fluorescence enhancement, which may be seen in Fig. 2 as a plateau in the region of high barbiturate concentrations. From the data of Fig. 2, a slope of 1.1 was obtained from the plot. This result indicates that only one barbiturate molecule is involved in the ternary complex.

Table I shows the distribution data of the extraction of 1×10^{-6} *M* tetracycline with 1-butanol from solutions containing 0.01 *M* calcium chloride and various ligands. Acetic acid is used as a ligand because it was reported (13) to replace barbital sodium in a fluorometric assay of tetracycline. The results show that nearly complete extraction can be achieved by the presence of 0.3 *M* barbital sodium or 0.025 *M* L-tryptophan, whereas acetic acid shows only little or no effect on the extraction.

Figure 3 shows the log–log plots of the tetracycline distribution between water and 1-butanol in the absence (line A) and presence (lines B, C, and D) of acetic acid, L-tryptophan, and barbital sodium. In the absence of ligands, the plot gives a straight line with $n = 2$, indicating two tetracycline molecules in the extracted complex. In the presence of ligands, however, the plots give straight lines with a slope of 1. This result indicates that one tetracycline molecule in the binary complex is replaced by these ligands to form a ternary complex.

The equilibrium data of the binary and ternary complexes are shown in Table II. In the binary system, the log K values, determined from Eq. 3, were 5.90 at pH 7.5 and 7.04 at pH 9. These results are quite reliable, since similar studies (21) reported log $K = 3.0$ for a 1:1 calcium–oxytetracycline complex at pH 7.4. The equilibrium constant measured at pH

Table II—Equilibrium Data of Tetracycline Complexes

Complex[a]	pH	n	log K
A	7.5	2.1	5.90
B	9.0	2.0	7.04
C	9.0	1.2	5.07
D	9.0	1.2	4.92
E	9.0	1.0	2.90

[a] A = calcium–tetracycline; B = calcium–tetracycline, C = calcium–tetracycline–L-tryptophan, D = calcium–tetracycline–barbital, and E = calcium–tetracycline–acetate.

9 is about 14-fold greater than that at pH 7.5. The large difference between the two values also suggests that calcium forms two different complexes at these pH values. In the ternary system, the equilibrium constants for the barbiturate and the L-tryptophan complexes are about 100-fold greater than the constant of the acetate, indicating that the acetate is a poor agent for tetracycline extraction. Successful extraction of tetracycline in physiological concentrations using 1-butanol can be made with barbital sodium and L-tryptophan. The results show a linear relationship between fluorescence and the tetracycline concentration. L-Tryptophan appears to be more effective in inducing extraction but is less effective in enhancing fluorescence than barbital sodium. In contrast to some earlier reports (13, 14), this study shows that barbital sodium markedly affects the tetracycline fluorescence.

The circular dichroism spectra of tetracycline and of its calcium complexes at pH 7.5 and 9 are shown in Fig. 4. The BCD-ring chromophore is responsible for the bands at 360, 320, 285, and 225 nm; the A-ring chromophore contributes the 262-nm band (19). The circular dichroism spectrum is extremely sensitive to configuration change at the C-4 position of the tetracycline molecule (22). At pH 7.5, only the bands associated with the BCD-ring chromophore are affected by calcium ion (Fig. 4). At pH 9, however, binding of calcium to the A-ring is evident from the striking change of the 262-nm band.

Spectral differences between the two calcium complexes are also seen in the 350–400-nm region. At pH 7.5, the spectrum (C) shows a weak band at 370 nm and a trough at 400 nm; at pH 9, strong positive and negative bands (spectrum D) are observed at 360 and 400 nm, respectively. This result may indicate that the A-ring binding also produces a conformational change of the BCD-ring chromophore. Similar studies, reported by Newman and Frank (23), suggest that at pH 7.4 the calcium is bound to the BCD-ring and that the C-4 dimethylamino group of tetracycline is not involved. The A-ring binding occurs only in high pH solutions, with the deprotonation of the C-4 dimethylammonium group (pK_3 = 9.5) being critical.

To study the solvent effect on the complexation, the calcium–tetracycline complex formed in pH 9 buffer was extracted into 1-butanol and ethyl acetate. The circular dichroism spectra were then taken (Fig. 5, spectra B and C). For comparison, the spectrum obtained in pH 9 buffer (spectrum A) is also included in the figure. Besides the A-ring binding as indicated by the 262-nm band in all three spectra, a remarkable inversion of the peaks at 360 and 400 nm is observed as the complex is extracted into nonpolar solvents. This phenomenon resembles the reciprocal relationship found in the circular dichroism studies of adenosine 5-mononicotinate (24). Adenosine has an absorption at 259 nm, whereas nicotinate absorbs at 264 nm. In adenosine 5-mononicotinate, stacking of the two aromatic moieties results in a reciprocal relationship where the 259-nm band becomes more negative as the stacking becomes more prominent. In the calcium–tetracycline complex, the inversion of the 360- and 400-nm bands may indicate a certain interaction between the two tetracycline molecules in nonpolar solvents. In aqueous solution, this interaction becomes less likely because of the interaction of water with the complex.

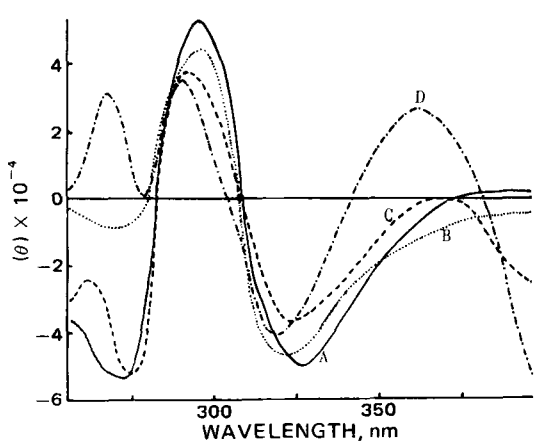

Figure 4—*Circular dichroism spectra of 1 × 10⁻⁴ M tetracycline in pH 7.5 buffer (A), 1 × 10⁻⁴ M tetracycline in pH 9 buffer (B), 1 × 10⁻⁴ M tetracycline and 0.01 M calcium chloride in pH 7.5 buffer (C), and 1 × 10⁻⁴ M tetracycline and 0.01 M calcium chloride in pH 9 buffer (D).*

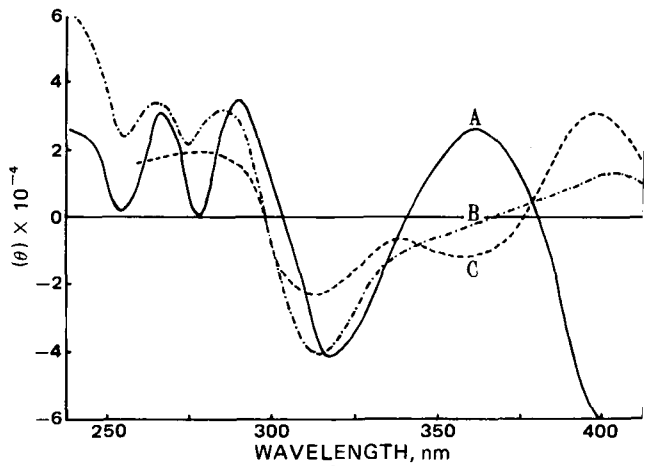

Figure 5—*Circular dichroism spectra of 0.01 M calcium chloride and 1 × 10⁻⁴ M tetracycline in pH 9 buffer (A), 1-butanol (B), and ethyl acetate (C).*

The effect of barbital sodium on the circular dichroism spectrum of the calcium–tetracycline complex in ethyl acetate is shown in Fig. 6. The positive band at 400 nm of the binary complex is diminished and becomes negative in the presence of barbital sodium. However, the 360-nm band increases with increasing barbiturate concentration. These results are consistent with the data shown in Fig. 5 since, in this case, the interaction between the tetracycline molecules is no longer possible as one tetracycline molecule is replaced by the barbiturate.

Figure 7 shows the circular dichroism spectrum of the ternary barbital complex in 1-butanol. The sharp peaks at 260 and 270 nm strongly indicate that, in the ternary complex, the calcium ion is bound to tetracycline at the A-ring binding site. A similar spectrum also was obtained for the ternary complex involving acetate as a ligand. However, the spectrum

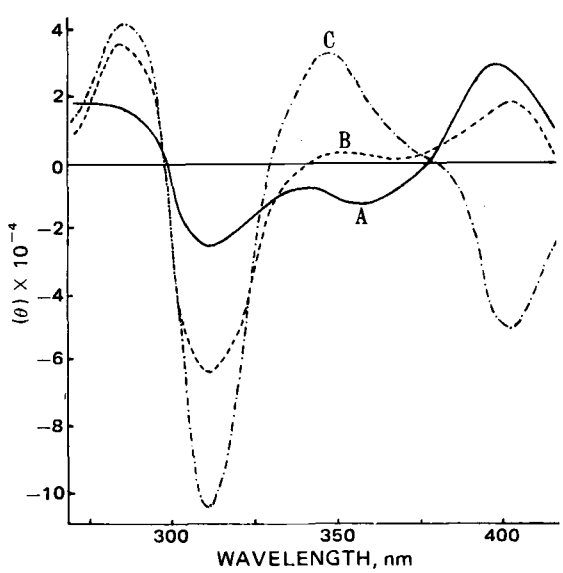

Figure 6—*Effect of barbital sodium on the circular dichroism spectrum of 0.01 M calcium chloride and 1 × 10⁻⁴ M tetracycline in ethyl acetate. Key (concentration of barbital sodium): A, 0; B, 0.01 M; and C, 0.05 M.*

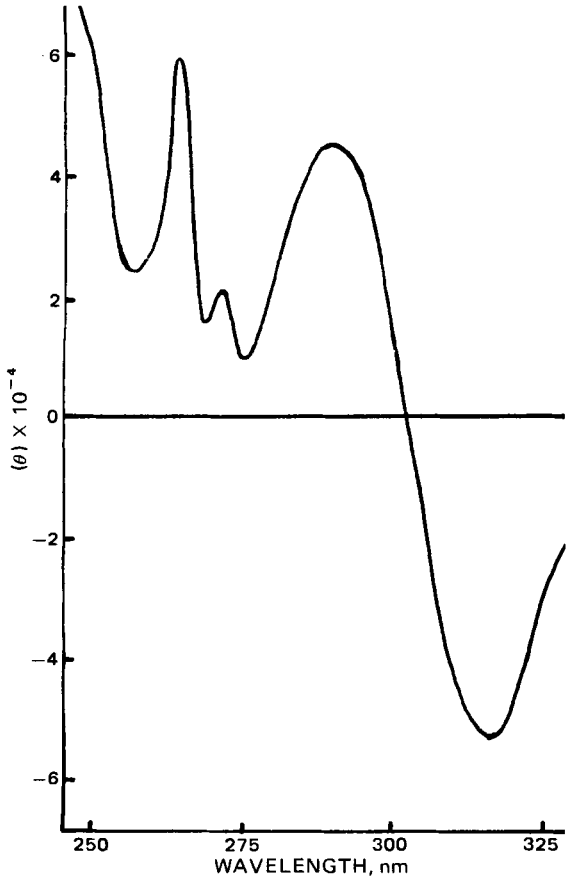

Figure 7—*Circular dichroism spectrum of the ternary calcium–tetracycline–barbiturate complex in 1-butanol (concentration of tetracycline was 1 × 10⁻⁴ M).*

for the ternary complex involving tryptophan cannot be obtained, because L-tryptophan exhibits strong absorptions in the low wavelength region.

DISCUSSION

Fluorometric analysis of tetracycline analogs, a method widely used in many laboratories, involves essentially the extraction of a highly fluorescent tetracycline complex. For tetracycline to be strongly fluorescent, the molecule has to maintain a planar structure in its BCD-ring-conjugated system. This structure may be achieved by rigid binding at the β-diketone system of the tetracycline molecule, as experimentally demonstrated by pH studies of calcium–tetracycline binding. As shown in Fig. 1, at pH 7.5, where the calcium ion is predominantly bound to the β-diketone groups, the complex exhibits the highest fluorescence. At pH 9 or above, the calcium–tetracycline complex is noticeably different from that of pH 7.5, as indicated by the fluorescence, solvent extraction, and circular dichroism studies. The circular dichroism studies, in particular, suggest that the binding occurs at the A-ring binding site. These results are in agreement with other studies (19, 20, 22, 25).

The calcium–tetracycline complex formed in basic solution produces lipid-soluble ternary complexes with barbital sodium and L-tryptophan. These compounds are very effective for tetracycline extraction. A structure of the ternary barbiturate complex was proposed by Kohn (12) (Structure II), but this arrangement is rather unfavorable considering the geometry of the tetracycline molecule. X-ray studies (26) on the structure of 4-hydroxytetracycloxide have shown that the A-ring is nonplanar with respect to the BCD-ring and that chelation at the C-1 and C-12 groups is quite impossible because of their different orientations. In tetracycline, under basic conditions, the C-4 dimethylamino and the C-12a hydroxyl groups rotate toward each other and force the A-ring away from the BCD-plane. This structural change not only results in a nonplanar relationship among the C-11, C-12, and C-1 groups but also creates an unfavorable situation at the C-1 and C-12 carbonyl groups.

In the present study, the calcium ion in the ternary complex is proposed to chelate to the C-4 dimethylamino and the C-12a hydroxyl functions because:

1. While barbital sodium induced the tetracycline extraction at pH 9, it showed no effect at pH 7.5 on either the fluorescence or extraction of the calcium–tetracycline complex, which indicates that barbital sodium does not affect the BCD-ring binding between calcium and tetracycline.
2. The circular dichroism spectrum for the ternary barbital complex strongly suggests the A-ring binding.
3. Circular dichroism studies (25) indicated that the calcium ion, even in large excess, does not exhibit A-ring binding with 4-dedimethylaminotetracycline at pH 9.
4. Kohn (12) reported that the use of barbital sodium is practically ineffective in the attempt to extract 12a-deoxytetracycline, 4-dedimethylaminotetracycline, and 4-epitetracycline.

The binding of calcium to the A-ring does not preclude the BCD-ring binding. Simultaneous binding of the calcium ion to the two binding sites can maintain the planar condition of the BCD-ring and, therefore, result in strong fluorescence. This reaction may explain the strong fluorescence of the barbiturate complex in basic solution. The tryptophan complex is equally effective in extraction but less fluorescent than the barbiturate complex, presumably because of the steric effect of the rather large tryptophan molecule, which may hinder the chance of the BCD-ring binding.

Tetracycline is known to have remarkable resistance toward metabolic changes (2). The chemical degradation, however, may present potential problems for the assay of tetracycline in biological fluids. The principal degradation products of tetracycline are anhydrotetracycline, 4-epitetracycline, and some oxidation and basic degradation products. Under basic conditions, chlortetracycline rapidly converts to isochlortetracycline, in which the C-6 hydroxyl group interacts with the β-diketone system to form a five-member ring including the C-6–O–C-11 linkage. The reaction is also known to result in a shift of the fluorescence maximum from 520 to 425 nm (27). A similar reaction, although less rapid, has been reported for other tetracyclines having C-5 or C-6 hydroxyl groups. For example, oxytetracycline is known to form the C-5–O–C-12 linkage under basic conditions (3).

In the present study, certain oxidation products were observed, although not yet identified, during the experiments. The degradation, which occurs rapidly under light, give a purple-colored water-soluble product. Based on the examination of the characteristics of these degradation products and of the calcium–tetracycline–barbiturate complex, it appears that Kohn's (12) method is quite specific for the assay of the active form of tetracycline. Serious structural changes in the tetracycline molecule, such as the chlortetracycline–isochlortetracycline reaction, affect the fluorescence spectrum greatly. Yet the fluorescence of the ternary complex is measured at about 510 nm, the fluorescence maximum common to all active tetracyclines. Structural change may also change the A-ring conformation, thus preventing the formation of the ternary complex. This reaction may explain why Kohn's method is not effective for the analysis of oxytetracycline, which undergoes similar degradation under basic conditions. In the case of epimerization, the ternary complex cannot be formed because of the unfavorable configuration of the C-4 dimethylamino group.

REFERENCES

(1) J. Colaizzi, *J. Pharm. Sci.*, **58**, 1185 (1969).

(2) R. G. Kelly, H. A. Floyd, and K. D. Hoyt, *Antimicrob. Agents Chemother.*, **1969**, 666.

(3) T. Perenyi, S. Szoke, and E. K. Novak, *Acta Pharm. Hung.*, **42**, 220 (1972).

(4) K. H. Ibsen, R. L. Saunders, and M. R. Urist, *Anal. Biochem.*, **5**, 505 (1963).

(5) L. J. Leeson and J. F. Weidenheimer, *J. Pharm. Sci.*, **58**, 355 (1969).

(6) E. G. Remmers, M. Sieger, and A. P. Doerschuk, *ibid.*, **52**, 752 (1963).

(7) K. R. Benitz and H. F. Diermeier, *Proc. Soc. Exp. Biol. Med.*, **115**, 930 (1964).

(8) C. H. Rammelkamp, *ibid.*, **51**, 95 (1942).

(9) A. E. Altmann, H. Beeuwkes, P. J. Brumbacher, H. J. Buytendijk, A. H. G. Gijzen, and F. P. V. Marsen, *Clin. Chim. Acta*, **20**, 185 (1968).

(10) J. Levine, E. A. Garlock, and H. Fishback, *J. Am. Pharm. Assoc., Sci. Ed.*, **38**, 473 (1949).

(11) R. G. Kelly, L. M. Peets, and K. D. Hoyt, *Anal. Biochem.*, **28**, 222 (1969).

(12) K. W. Kohn, *Anal. Chem.*, **33**, 862 (1961).
(13) D. M. Wilson, M. Lever, E. A. Brosnan, and A. Stillwell, *Clin. Chim. Acta*, **36**, 260 (1972).
(14) M. Lever, *Biochem. Med.*, **6**, 216 (1972).
(15) P. P. Ascione, J. B. Zager, and G. P. Chrekian, *J. Pharm. Sci.*, **56**, 1936 (1967).
(16) R. F. Miller, T. D. Sokoloski, L. A. Mitscher, A. C. Bonnaci, and B. J. Hoener, *ibid.*, **62**, 1143 (1973).
(17) H. Poiger and C. Schlatter, *Analyst*, **101**, 808 (1976).
(18) P. P. Regna, I. A. Solomons, K. Mural, A. E. Timreck, K. J. Brunings, and W. A. Lazier, *J. Am. Chem. Soc.*, **73**, 4211 (1951).
(19) L. A. Mitscher, A. C. Bonnaci, and T. D. Sokoloski, *Antimicrob. Agents Chemother.*, **1968**, 78.
(20) L. A. Mitscher, A. C. Bonnaci, and T. D. Sokoloski, *Tetrahedron Lett.*, **51**, 5361 (1968).
(21) K. Ibsen and M. Urist, *Proc. Soc. Exp. Biol. Med.*, **109**, 797 (1962).
(22) L. A. Mitscher, A. C. Bonnaci, B. Slater-Eng, A. K. Hacker, and T. D. Sokoloski, *Antimicrob. Agents Chemother.*, **1969**, 111.
(23) E. C. Newman and C. W. Frank, *J. Pharm. Sci.*, **65**, 1728 (1976).
(24) K. W. Urry, "Spectroscopic Applications to Biomolecular Conformation," American Medical Association, Chicago, Ill., 1970, p. 78.
(25) L. A. Mitscher, B. Slater-Eng, and T. D. Sokoloski, *Antimicrob. Agents Chemother.*, **1972**, 66.
(26) J. H. Van Den Hende, *J. Am. Chem. Soc.*, **87**, 925 (1965).
(27) S. Udenfriend, "Fluorescence Assay in Biology and Medicine," vol. II, Academic, New York, N.Y., 1962, p. 409.

ACKNOWLEDGMENTS

Presented at the Basic Pharmaceutics Section, APhA Academy of Pharmaceutical Sciences, New York meeting, May 1977.

Abstracted from a thesis submitted by S. T. Day to the Graduate School, West Virginia University, in partial fulfillment of the Master of Science degree requirements.

Degradative Behavior of a New Bronchodilator, Carbuterol, in Aqueous Solution

LOUIS J. RAVIN ˣ, ELISABETH S. RATTIE, ALICIA PETERSON, and DAVID E. GUTTMAN †

Received July 25, 1977, from the *Research and Development Division, Smith Kline and French Laboratories, Philadelphia, PA 19101.* Accepted for publication March 2, 1978. †Deceased.

Abstract □ The degradation kinetics of carbuterol in aqueous solution were investigated at 85° and constant ionic strength over the pH 0.25–13.3 range under anaerobic conditions. The results demonstrated a complex kinetic pattern involving specific acid and specific base catalyses at the pH extremes. Degradation resulted primarily from intramolecular catalysis and indicated that both the protonated and unprotonated phenolic groups participated in the reaction. High-pressure liquid chromatography was used to isolate carbuterol and its degradation product. Mass spectrometric examination showed that the degradation product was a cyclized derivative formed by intramolecular attack of the phenoxy group on the ureido carbonyl with ammonia expulsion. The apparent activation energy for carbuterol at pH 4.0 and 10.0 was 22.3 and 11.7 kcal/mole, respectively. The agreement between the calculated theoretical pH–rate profile and the experimental points supports the hypothesis presented concerning the reactions involved in carbuterol degradation.

Keyphrases □ Carbuterol—degradation kinetics in aqueous solution, pH effect □ Degradation kinetics—carbuterol in aqueous solution, pH effect □ Kinetics—carbuterol degradation in aqueous solution, pH effect □ Bronchodilators—carbuterol, degradation kinetics in aqueous solution, pH effect

Carbuterol, [5-[2-[(1,1-dimethylethyl)amino]-1-hydroxyethyl]-2-hydroxyphenyl]urea hydrochloride (I), is a new potent bronchodilator. It is stable in solid admixtures, capsules, and tablets. Like other bronchodilators of similar structure, carbuterol oxidizes readily in aqueous solution (1, 2). Unlike other similar bronchodilators, carbuterol exhibits significant solution degradation under anaerobic conditions in the presence of antioxidants. This study investigated the unusual degradative behavior of carbuterol in aqueous solution.

EXPERIMENTAL

Materials—All chemicals were analytical reagent grade.

Buffers—Hydrochloric acid–potassium chloride (pH 0.25–2.0), citrate buffer (pH 3.0–5.5), succinate buffer (pH 6.0), phosphate buffer (pH 6.5–8.0), borate buffer (pH 8.5–9.0), carbonate buffer (pH 9.35–11.0), trisodium phosphate buffer (pH 12.0), and sodium hydroxide–potassium chloride (pH 13.0–13.3) were used. The buffers were freshly prepared by dissolving hydrochloric acid, citric acid, succinic acid, monobasic sodium phosphate, boric acid, sodium bicarbonate, tribasic sodium phosphate, or sodium hydroxide together with potassium chloride in distilled water and adding concentrated sodium hydroxide to achieve the desired pH. The buffers were 0.1 *M* with respect to hydrochloride, citrate, succinate, phosphate, borate, carbonate, and hydroxide ions (except when buffer effects were investigated) and were adjusted to an ionic strength of 0.5 with potassium chloride (except when the primary salt effect was investigated).

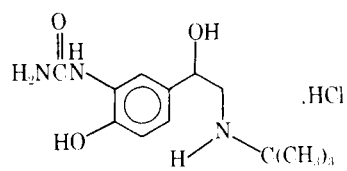

I

High-Pressure Liquid Chromatographic (HPLC) Isolation of Degradation Product—The liquid chromatograph[1] was fitted with a precision photometer at 254 nm. The column, 2 mm i.d. × 1 mm, was packed with strong cationic exchange[2] resin and was operated at ambient temperature, a pressure of 900 psig, and a flow rate of 1 ml/min.

The mobile phase was 0.01 *M* borate buffer containing 0.1 *M* anhydrous sodium sulfate adjusted to pH 10.0 with sodium hydroxide. The concentration was normal at about 2.5 mg/ml; the injection size was 5 μl in aqueous solution. The attenuation was 64×10^{-2}, and the chart speed was 2.54 cm/5 min.

Several injections of degraded solution were placed on the column, and the decomposition product was collected as it was eluted. The solution was evaporated to dryness, and the residue was washed several times with aliquots of methanol. The methanol subsequently was evaporated to dryness, and the residue was submitted for analysis by mass spectrometry.

[1] Dupont 820.
[2] Dupont 820960002.

0022-3549/78/1100-1523$01.00/0
© 1978, American Pharmaceutical Association.

(12) K. W. Kohn, *Anal. Chem.*, **33**, 862 (1961).
(13) D. M. Wilson, M. Lever, E. A. Brosnan, and A. Stillwell, *Clin. Chim. Acta*, **36**, 260 (1972).
(14) M. Lever, *Biochem. Med.*, **6**, 216 (1972).
(15) P. P. Ascione, J. B. Zager, and G. P. Chrekian, *J. Pharm. Sci.*, **56**, 1936 (1967).
(16) R. F. Miller, T. D. Sokoloski, L. A. Mitscher, A. C. Bonnaci, and B. J. Hoener, *ibid.*, **62**, 1143 (1973).
(17) H. Poiger and C. Schlatter, *Analyst*, **101**, 808 (1976).
(18) P. P. Regna, I. A. Solomons, K. Mural, A. E. Timreck, K. J. Brunings, and W. A. Lazier, *J. Am. Chem. Soc.*, **73**, 4211 (1951).
(19) L. A. Mitscher, A. C. Bonnaci, and T. D. Sokoloski, *Antimicrob. Agents Chemother.*, **1968**, 78.
(20) L. A. Mitscher, A. C. Bonnaci, and T. D. Sokoloski, *Tetrahedron Lett.*, **51**, 5361 (1968).
(21) K. Ibsen and M. Urist, *Proc. Soc. Exp. Biol. Med.*, **109**, 797 (1962).
(22) L. A. Mitscher, A. C. Bonnaci, B. Slater-Eng, A. K. Hacker, and T. D. Sokoloski, *Antimicrob. Agents Chemother.*, **1969**, 111.
(23) E. C. Newman and C. W. Frank, *J. Pharm. Sci.*, **65**, 1728 (1976).
(24) K. W. Urry, "Spectroscopic Applications to Biomolecular Conformation," American Medical Association, Chicago, Ill., 1970, p. 78.
(25) L. A. Mitscher, B. Slater-Eng, and T. D. Sokoloski, *Antimicrob. Agents Chemother.*, **1972**, 66.
(26) J. H. Van Den Hende, *J. Am. Chem. Soc.*, **87**, 925 (1965).
(27) S. Udenfriend, "Fluorescence Assay in Biology and Medicine," vol. II, Academic, New York, N.Y., 1962, p. 409.

ACKNOWLEDGMENTS

Presented at the Basic Pharmaceutics Section, APhA Academy of Pharmaceutical Sciences, New York meeting, May 1977.

Abstracted from a thesis submitted by S. T. Day to the Graduate School, West Virginia University, in partial fulfillment of the Master of Science degree requirements.

Degradative Behavior of a New Bronchodilator, Carbuterol, in Aqueous Solution

LOUIS J. RAVIN ˣ, ELISABETH S. RATTIE, ALICIA PETERSON, and DAVID E. GUTTMAN †

Received July 25, 1977, from the *Research and Development Division, Smith Kline and French Laboratories, Philadelphia, PA 19101.* Accepted for publication March 2, 1978. †Deceased.

Abstract □ The degradation kinetics of carbuterol in aqueous solution were investigated at 85° and constant ionic strength over the pH 0.25–13.3 range under anaerobic conditions. The results demonstrated a complex kinetic pattern involving specific acid and specific base catalyses at the pH extremes. Degradation resulted primarily from intramolecular catalysis and indicated that both the protonated and unprotonated phenolic groups participated in the reaction. High-pressure liquid chromatography was used to isolate carbuterol and its degradation product. Mass spectrometric examination showed that the degradation product was a cyclized derivative formed by intramolecular attack of the phenoxy group on the ureido carbonyl with ammonia expulsion. The apparent activation energy for carbuterol at pH 4.0 and 10.0 was 22.3 and 11.7 kcal/mole, respectively. The agreement between the calculated theoretical pH–rate profile and the experimental points supports the hypothesis presented concerning the reactions involved in carbuterol degradation.

Keyphrases □ Carbuterol—degradation kinetics in aqueous solution, pH effect □ Degradation kinetics—carbuterol in aqueous solution, pH effect □ Kinetics—carbuterol degradation in aqueous solution, pH effect □ Bronchodilators—carbuterol, degradation kinetics in aqueous solution, pH effect

Carbuterol, [5-[2-[(1,1-dimethylethyl)amino]-1-hydroxyethyl]-2-hydroxyphenyl]urea hydrochloride (I), is a new potent bronchodilator. It is stable in solid admixtures, capsules, and tablets. Like other bronchodilators of similar structure, carbuterol oxidizes readily in aqueous solution (1, 2). Unlike other similar bronchodilators, carbuterol exhibits significant solution degradation under anaerobic conditions in the presence of antioxidants. This study investigated the unusual degradative behavior of carbuterol in aqueous solution.

EXPERIMENTAL

Materials—All chemicals were analytical reagent grade.

Buffers—Hydrochloric acid–potassium chloride (pH 0.25–2.0), citrate buffer (pH 3.0–5.5), succinate buffer (pH 6.0), phosphate buffer (pH 6.5–8.0), borate buffer (pH 8.5–9.0), carbonate buffer (pH 9.35–11.0), trisodium phosphate buffer (pH 12.0), and sodium hydroxide–potassium chloride (pH 13.0–13.3) were used. The buffers were freshly prepared by dissolving hydrochloric acid, citric acid, succinic acid, monobasic sodium phosphate, boric acid, sodium bicarbonate, tribasic sodium phosphate, or sodium hydroxide together with potassium chloride in distilled water and adding concentrated sodium hydroxide to achieve the desired pH. The buffers were 0.1 *M* with respect to hydrochloride, citrate, succinate, phosphate, borate, carbonate, and hydroxide ions (except when buffer effects were investigated) and were adjusted to an ionic strength of 0.5 with potassium chloride (except when the primary salt effect was investigated).

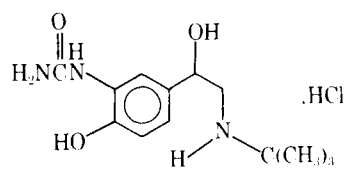

I

High-Pressure Liquid Chromatographic (HPLC) Isolation of Degradation Product—The liquid chromatograph[1] was fitted with a precision photometer at 254 nm. The column, 2 mm i.d. × 1 mm, was packed with strong cationic exchange[2] resin and was operated at ambient temperature, a pressure of 900 psig, and a flow rate of 1 ml/min.

The mobile phase was 0.01 *M* borate buffer containing 0.1 *M* anhydrous sodium sulfate adjusted to pH 10.0 with sodium hydroxide. The concentration was normal at about 2.5 mg/ml; the injection size was 5 μl in aqueous solution. The attenuation was 64×10^{-2}, and the chart speed was 2.54 cm/5 min.

Several injections of degraded solution were placed on the column, and the decomposition product was collected as it was eluted. The solution was evaporated to dryness, and the residue was washed several times with aliquots of methanol. The methanol subsequently was evaporated to dryness, and the residue was submitted for analysis by mass spectrometry.

[1] Dupont 820.
[2] Dupont 820960002.

0022-3549/78/1100-1523$01.00/0
© 1978, American Pharmaceutical Association.

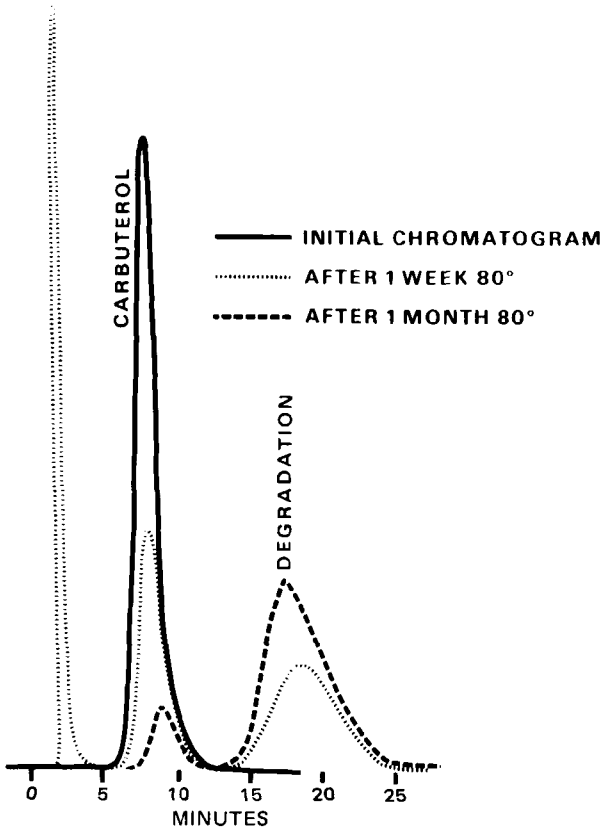

Figure 1—*HPLC separation of carbuterol from its degradation product at pH 4.0.*

Colorimetric Assay—A sensitive 4-aminoantipyrine method for phenolic compounds was used for the colorimetric determination of residual carbuterol (3).

The following reagents were added, in order, to a 100-ml volumetric flask: 50 ml of 0.4 *M* carbonate buffer (pH 10.0), 5 ml of carbuterol stock solution (0.5 mg/ml), 10 ml of 3% aqueous aminoantipyrine, and 15 ml of 4% aqueous potassium ferricyanide. The flask was brought to volume with the carbonate buffer. A reagent blank also was prepared. After

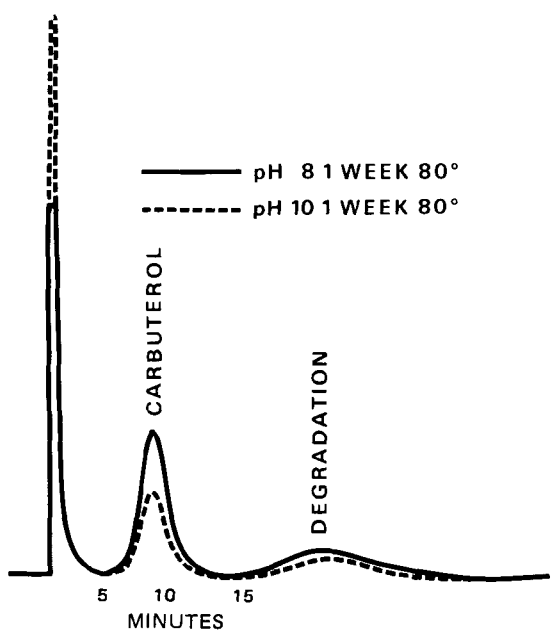

Figure 2—*Separation of carbuterol from its degradation product at pH 8.0 and 10.0.*

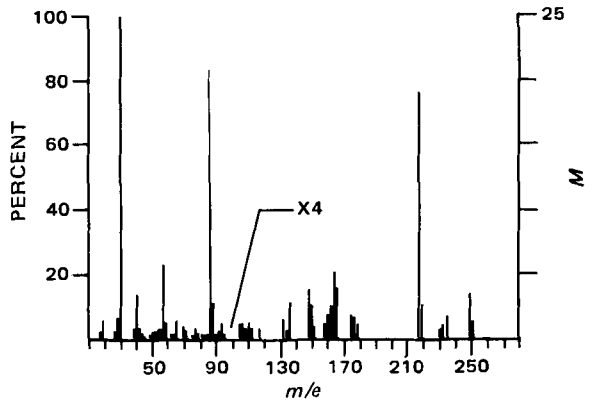

Figure 3—*Mass spectrum of carbuterol degradation product.*

standing for 10 min to allow color development, both solutions were analyzed spectrophotometrically at 520 nm in 1-cm cells.

Kinetic Procedure—Approximately 50 mg of carbuterol was weighed accurately and dissolved in 100 ml of the appropriate buffer. The resulting solution was flushed with nitrogen and subsequently filled into 15-ml glass ampuls. The ampuls were flushed with nitrogen, sealed, and placed in a constant-temperature oil bath set at 85°. Samples were taken at various intervals and assayed using the colorimetric procedure previously described.

RESULTS AND DISCUSSION

Characterization of Degradation Product—Figures 1 and 2, typical chromatograms, indicate that the degradation product can be separated from the parent compound. The compound isolated during the kinetic studies was subjected to spectral analysis (Fig. 3). This spectrum supports a structure with a molecular ion peak at *m/e* 250 and major fragmentation peaks at *m/e* 235, 232, 217, 164, 86, 57, 41, and 30.

This product was subsequently synthesized by an unambiguous route; it was also characterized by conventional analytical, spectral, and chromatographic methods[3]. The synthetic compound gave a mass spectrum identical with that observed for the degradation product (II).

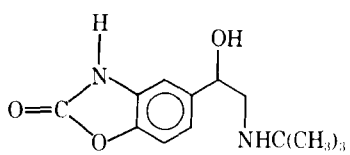

II

Reaction Order—The disappearance rate of carbuterol from aqueous solution was an overall pseudo-first-order reaction with respect to carbuterol at pH 0.25–13.0 and constant temperature and ionic strength. The relationship between time and the logarithm of the residual carbuterol concentration was linear (Fig. 4). The observed rate constants and the buffer systems are listed in Table I.

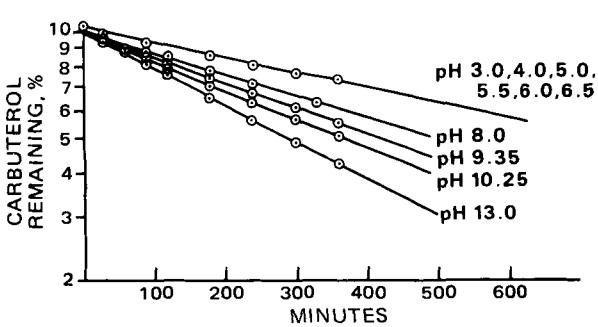

Figure 4—*Effect of pH on carbuterol degradation at 85° (μ = 0.5).*

[3] Information obtained through Dr. Carl Kaiser, Smith Kline and French Laboratories, Philadelphia, PA 19101.

Table I—Buffer Systems and Observed Rate Constants for Carbuterol Degradation at 85°

pH	Buffer System	k_{obs}, $min^{-1} \times 10^3$	k_0, $min^{-1} \times 10^3$
0.25	Hydrochloric acid	1.72	—
0.50	Hydrochloric acid–potassium chloride	1.359	—
1.0	Hydrochloric acid–potassium chloride	1.307	—
1.3	Hydrochloric acid–potassium chloride	1.195	—
2.0	Hydrochloric acid–potassium chloride	1.026	—
3.0	Citrate	0.969	—
4.0	Citrate	0.969	—
5.0	Citrate	0.976	—
5.5	Citrate	0.99	—
6.0	Succinate	0.962	—
6.5	Phosphate	1.04	—
7.0	Phosphate	1.127	1.05
7.5	Phosphate	1.233	0.972
8.0	Phosphate	1.428	1.045
8.5	Borate	1.215	—
9.0	Borate	1.52	—
9.35	Carbonate	1.66	—
10.0	Carbonate	1.925	—
10.25	Carbonate	2.05	—
10.5	Carbonate	2.09	—
10.61	Carbonate	2.10	—
11.0	Carbonate	2.068	—
12.0	Trisodium phosphate	2.27	—
13.0	Sodium hydroxide–potassium chloride	2.475	—
13.3	Sodium hydroxide	2.66	—

Catalytic Effects of Buffer Systems—The catalytic effect of the buffer systems used in the kinetic studies was determined at constant pH, temperature, ionic strength ($\mu = 0.5$), and carbuterol concentration; only the buffer concentration was varied. The citrate, borate, and carbonate buffer species did not appreciably affect carbuterol degradation. Figure 5 shows the phosphate buffer effect between pH 7.0 and 8.0. Within this pH range, only the mono- and dihydrogen phosphate ions are important. The observed rate constant is, therefore, a summation of the catalytic rate constants of the phosphate buffer species and the rate at zero buffer concentration. It may be expressed as:

$$k_{obs} = k_0 + k_{H_2PO_4^-}[H_2PO_4^-] + k_{HPO_4^{2-}}[HPO_4^{2-}] \quad \text{(Eq. 1)}$$

where k_0 is the rate constant at zero buffer concentration; the other rate constants are the catalytic rate constants due to the phosphate buffer species. By using the conservation equation and the acidity constant expression for the phosphate buffer system:

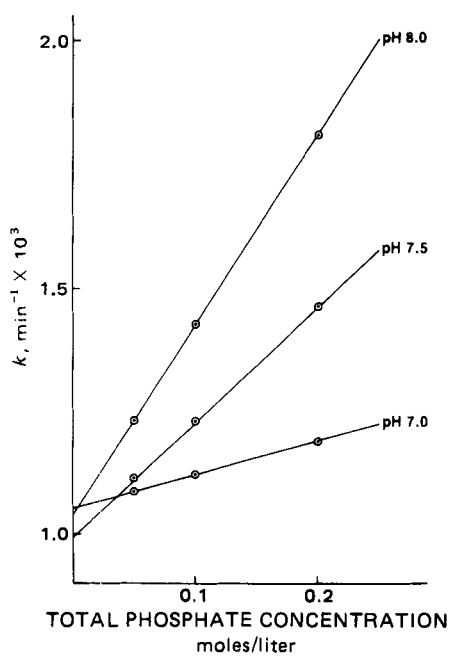

Figure 5—*Phosphate buffer catalytic effect on observed rate constants of carbuterol degradation at constant pH and 85° ($\mu = 0.5$).*

Table II—Slopes (S_{exp}) of the Lines in Fig. 5 and Slopes (S_{calc}) Calculated

pH	$S_{exp} \times 10^4$	$S_{calc} \times 10^4$
7.0	6.8	6.8
7.5	13	13
8.0	37	27

$$C_p = [H_2PO_4^-] + [HPO_4^{2-}] \quad \text{(Eq. 2)}$$

$$K_{a2} = \frac{[H^+][HPO_4^{2-}]}{[H_2PO_4^-]} \quad \text{(Eq. 3)}$$

the overall rate may be written as:

$$k_{obs} = k_0 + C_p \frac{k_{H_2PO_4^-}[H^+] + k_{HPO_4^{2-}} K_{a2}}{[H^+] + K_{a2}} \quad \text{(Eq. 4)}$$

A plot of k_{obs} *versus* the total phosphate concentration will yield a straight line with an intercept of k_0 and a slope of:

$$\text{slope} = \frac{k_{H_2PO_4^-}[H^+] + k_{HPO_4^{2-}} K_{a2}}{[H^+] + K_{a2}} \quad \text{(Eq. 5)}$$

As can be seen from Fig. 5, the phosphate buffer catalysis increased with an increase in pH. This result suggests that the monohydrogen phosphate ion is the catalyzing species for carbuterol. From Eq. 4, the phosphate buffer catalytic rate constants for carbuterol degradation at 85° were obtained and shown to be $k_{H_2PO_4^-} = 7.9 \times 10^{-4}\ min^{-1}$ and $k_{HPO_4^{2-}} = 4.87 \times 10^{-3}\ min^{-1}$. With these rate constants, theoretical slopes that agreed well with the experimental slopes were calculated for the phosphate buffer system (Table II).

Primary Salt Effect—The primary salt effect on carbuterol degradation was studied at constant pH and temperature; only the ionic strength was varied by the addition of potassium chloride. Studies were conducted at pH 4.0 and 9.0; no primary significant salt effect was observed.

pH Dependency—The pH–rate profile (Fig. 6) shows the relationship between pH and the observed reaction rate over the pH 0.25–13.0 range. The curve suggests that the overall degradation rate for carbuterol hydrolysis represents a summation of Reactions A–E shown in Scheme I.

$$\text{A:}\quad C^+ + [H^+] \xrightarrow{k_1} \text{products}$$

$$\text{B:}\quad C^+ \xrightarrow{k_2} \text{products}$$

$$\text{C:}\quad C^{\pm} \xrightarrow{k_3} \text{products}$$

$$\text{D:}\quad C^- \xrightarrow{k_4} \text{products}$$

$$\text{E:}\quad C^- + [OH^-] \xrightarrow{k_5} \text{products}$$

Scheme I

This scheme can be represented by the following equation:

$$-\frac{dC_T}{dt} = k_1[C^+][H^+] + k_2[C^+] + k_3[C^{\pm}] + k_4[C^-] + k_5[C^-][OH^-] \quad \text{(Eq. 6)}$$

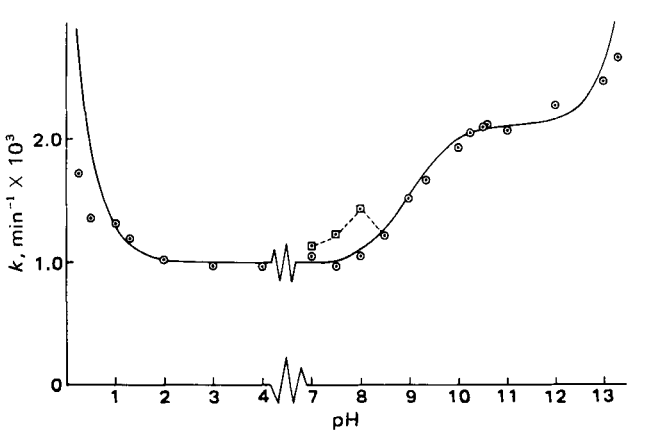

Figure 6—*The pH–rate profile of carbuterol degradation in aqueous solution at 85° ($\mu = 0.5$). Key: —, theoretical profile; ⊙, experimental profile; and ⊡, rates uncorrected for buffer effect.*

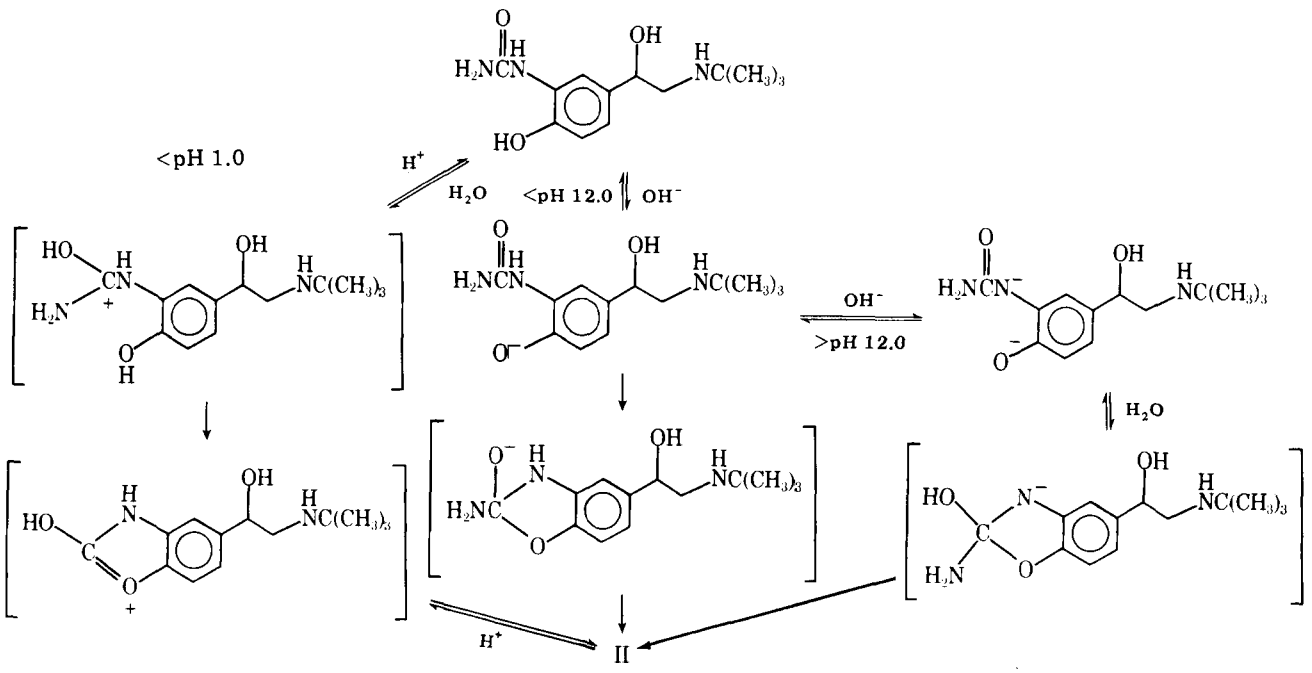

Scheme II

where:

$$C_T = [C^+] + [C^\pm] + [C^-] \quad \text{(Eq. 7)}$$

$$K_1 = \frac{[C^\pm][H^+]}{[C^+]} \quad \text{(Eq. 8)}$$

$$K_2 = \frac{[C^-][H^+]}{[C^\pm]} \quad \text{(Eq. 9)}$$

By combining these equations, the overall degradation rate can be represented by:

$$k_{obs} = \frac{k_1[H^+]^3 + k_2[H^+]^2 + k_3K_1[H^+] + k_4K_1K_2 + k_5K_1K_2K_W/[H^+]}{K_1K_2 + K_1[H^+] + [H^+]^2} \quad \text{(Eq. 10)}$$

The theoretical disappearance rate of carbuterol was calculated for the pH 0.25–13.0 range. The rate constants were approximated from the experimental data at pH intervals where the reactions in Scheme I were specifically involved. The following values provided the best fit: $k_1 = 3 \times 10^{-3}$ min^{-1}, $k_2 = 1 \times 10^{-3}$ min^{-1}, $k_3 = 2.1 \times 10^{-3}$ min^{-1}, $k_4 = 2.1 \times 10^{-3}$ min^{-1}, $k_5 = 5 \times 10^{-3}$ min^{-1}, $K_1 = 1.862 \times 10^{-8}$, $K_2 = 5 \times 10^{-12}$, and $K_W = 5.62 \times 10^{-13}$. The calculated rate (solid line in Fig. 6) is in good agreement with the experimentally determined rate.

The data indicate that below pH 1.0 the degradation rate is due to hydrogen-ion attack on the protonated species. The fact that the slope of the line below pH 1.0 is −1 suggests that Reaction A is solely responsible for the degradation. In the pH range from 1.0 to approximately 9.0, the degradation rate is essentially constant. Degradation proceeds spontaneously with water as the catalyzing species. Reaction B is responsible for this behavior.

In the pH 9.0–10.0 range, the reaction rate increases with a slope of nonintegral value. The reactions proceed spontaneously with water attack on both the protonated species and the zwitterion. These processes can be represented by Reactions B and C.

Between pH 10.0 and 12.0, the reaction rate remains constant. The reaction proceeds spontaneously with water attack on the zwitterionic species and can be represented by Reaction D.

Above pH 12.0, the reaction rate increases. The slope of the reaction rate plot is +1, suggesting that the principal reaction (E) in this range is hydroxide-ion attack on the ionized species.

Temperature Dependency—Rate constants for the overall disappearance of carbuterol were obtained from 60 to 85° at pH 4.0 and 10.0. Typical Arrhenius plots are shown in Fig. 7. From these data, the apparent activation energy at pH 4.0 and 10.0 was determined to be approximately 22.3 and 11.7 kcal/mole, respectively.

Possible Degradation Pathway—Scheme II illustrates the possible degradation pathway for carbuterol in aqueous buffered solutions. It involves the protonation or ionization of carbuterol and subsequent water attack, resulting in the appearance of II, which was isolated and characterized by mass spectral analysis. Compound II did not appear to be stable at elevated pH since the high-pressure liquid chromatograms in Fig. 2 indicated that there was no accumulation as the degradation increased.

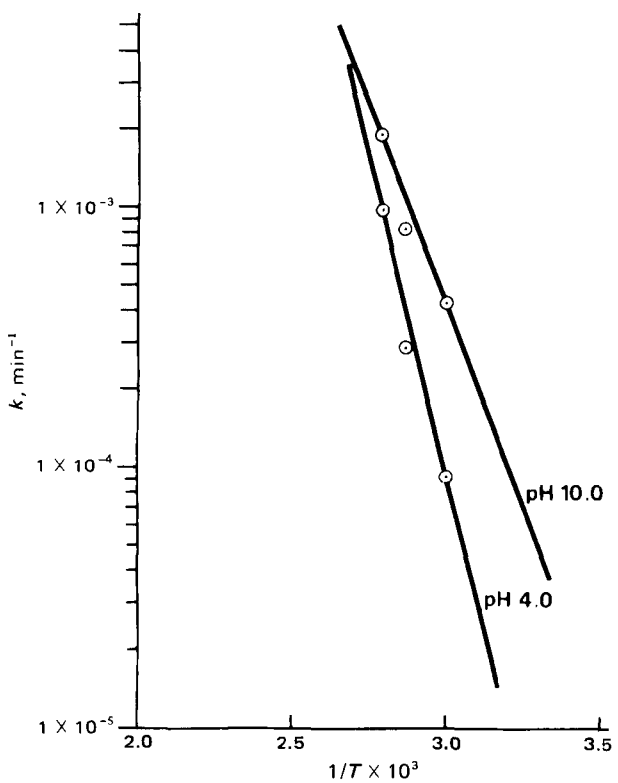

Figure 7—*Typical Arrhenius-type plot depicting the temperature dependency of carbuterol hydrolysis at pH 4.0 and 10.0.*

REFERENCES

(1) T. D. Sokoloski and T. Higuchi, *J. Pharm. Sci.*, **51**, 172 (1962).

(2) R. A. Heacock, *Chem. Rev.*, **59**, 181 (1959).

(3) M. B. Ettinger, C. C. Ruchhoft, and R. J. Lishka, *Anal. Chem.*, **23**, 1783 (1951).

Mechanism of Hydrolysis of Halogenated Nitrosoureas

DULAL C. CHATTERJI ˣ, RAYMOND F. GREENE, and JOSEPH F. GALLELLI

Received October 7, 1977, from the *Pharmaceutical Development Service, Pharmacy Department, The Clinical Center, National Institutes of Health, Bethesda, MD 20014.* Accepted for publication March 7, 1978.

Abstract □ The hydrolysis kinetics of halogenated nitrosoureas were investigated using chlorozotocin as a model. Evidence is presented to show that the hydrolytic reaction of halogenated nitrosoureas between pH 3 and 8 is a summation of spontaneous water and hydroxide-ion-catalyzed reactions; the later reaction is the sum of two parallel reactions. The relative contribution of each reaction changes with pH and results in different product distributions. Dianionic phosphate (HPO_4^{2-}) increased the amount of free chloride-ion production without significantly altering the hydrolysis rate. A mechanism is proposed to explain this behavior. The role of hydrolytic decomposition products produced at physiological pH on the biological activity of nitrosoureas is discussed.

Keyphrases □ Nitrosoureas, halogenated—kinetics and mechanism of hydrolysis, effect of pH □ Hydrolysis—kinetics and mechanism, halogenated nitrosoureas, effect of pH □ Kinetics—hydrolysis of halogenated nitrosoureas, effect of pH □ Mechanism—hydrolysis of halogenated nitrosoureas, effect of pH

Nitrosoureas are a mainstay of cancer chemotherapy, and several of them have undergone extensive clinical trials. Nevertheless, the mechanism of action of nitrosoureas (Table I) is not well understood. The difficulty in explaining their mechanism is related mainly to the instability of nitrosoureas in plasma, which gives rise to many possible reactive intermediates.

A useful approach to the understanding of these reactive intermediates has been chemical kinetic studies at or near physiological pH (1–8). A systematic kinetic study of nonhalogenated nitrosoureas (*i.e.*, where the N-1 substituent is a simple alkyl group, R) led Garrett and Goto (7) to propose a mechanism yielding a carbonium ion, R^+, at physiological pH. However, systematic kinetic studies on 1-(2-chloroethyl)nitrosoureas, which exhibit even greater antileukemic activity, have not been reported.

BACKGROUND

Previous kinetic studies on the hydrolysis of halogenated nitrosoureas II–IV (Table I) were contradictory (1–4). They primarily emphasized the analysis of hydrolytic products around physiological pH or pH 4. In the hydrolysis of nonhalogenated nitrosoureas, the major product arising from the N-1 alkyl substituent is the corresponding alcohol (1–6). However, with 1-(2-chloroethyl)nitrosoureas, the major products at pH 4 are acetaldehyde and the chloride ion instead of 2-chloroethanol. As the pH is increased, however, more 2-chloroethanol is produced at the expense of acetaldehyde.

These results indicate that additional hydrolytic mechanisms may exist for 1-(2-chloroethyl)nitrosoureas that are not available to nonhalogenated nitrosoureas (1, 3), and two mechanisms have been proposed (1–3) to account for the hydrolysis products. Neither mechanism, however, adequately explains the changes in product distribution observed at various pH values. Since the 1-(2-chloroethyl) substituent may partly determine the chemical and biological activity of these compounds, a systematic kinetic study of a 1-(2-chloroethyl)nitrosourea was warranted.

Since the rate and extent of chloride-ion production would be expected to yield valuable information on the role of the N-1 halogen substituent, chlorozotocin (I), a monochlorinated nitrosourea (*i.e.*, having a β-chloro substituent on N-1 only), was chosen as the major compound. By studying this monochlorinated compound, ambiguities about the source of the chloride ion produced could be eliminated. Furthermore, chlorozotocin has greater aqueous solubility than other monochlorinated nitrosoureas (III and IV), which allows quantitation in totally aqueous solvents. Also, a detailed kinetic study on streptozotocin (V) (a nonchlorinated analog of I) was available (5), and possible analysis of comparative kinetic values of I and V could be useful in understanding the role of the 1-(2-chloroethyl) substituent. Finally, it was necessary to conduct limited kinetic studies on II–IV and VI (Table I) to clarify some ambiguous results reported in the literature and to support the proposed hydrolytic pathways for other halogenated nitrosoureas.

EXPERIMENTAL

Materials—The nitrosoureas and their analogs[1], I[2], II[3], III[4], IV[5], V[6], VI[7], and 1-(2-chloroethyl)-3-(2-deoxy-D-glucopyranosyl)urea[8] (VII), were used as received. All other chemicals were reagent grade.

Buffers—Citrate and phosphate buffers (pH 2–8) were prepared from 0.25 *M* stock solutions of citric acid and monobasic sodium phosphate, respectively, by the addition of sodium hydroxide to the desired pH.

Tris(hydroxymethyl)aminomethane buffer (pH 6–8.5) was prepared by dissolving the appropriate amount of base in distilled water and adjusting the pH with hydrochloric acid. When chloride-ion determinations were to be made, nitric acid was used for pH adjustment.

No attempts were made to maintain a constant ionic strength because preliminary studies revealed that ionic strength did not appreciably affect the hydrolysis rate.

Equipment—Absorbance readings were determined using a recording spectrophotometer[9] equipped with a programmable thermostated cell holder[10]. Temperature in the cell compartment was regulated within ±0.1° using a circulating water bath. Chloride-ion determinations were made with an automatic chloride titrator[11]. Fluoride-ion determinations were made with a combination fluoride electrode[12] using the expanded scale of a pH meter[13]. All pH measurements were conducted at room temperature.

Kinetic Studies—*Spectrophotometric Determination*—The first-order rate constants for the hydrolysis of nitrosoureas were determined as reported (6, 7) by following the loss of UV absorption at 231 nm with time. The general procedure consisted of making a stock solution of nitrosourea (~1×10^{-2} *M*) in methanol, diluting the solution with thermally preequilibriated buffers in a 1-cm UV cell to an initial concentration of ~1×10^{-4} *M*, and recording the absorbance at 231 nm *versus* time. The solution pH remained constant (within 0.05 unit) throughout the kinetic runs.

Chloride-Ion Measurements—The decomposition rate of I also was determined by following the production of free chloride ion. A weighed amount of nitrosourea was dissolved in thermally equilibrated buffer (~1×10^{-3} *M*), and the chloride-ion concentration was determined by titrating an aliquot out of the reaction mixture at specified intervals. For this purpose, 2.0 ml of the reaction mixture was placed in a 6-ml beaker and 2.0 ml of titration reagent [consisting of 0.2 *M* HNO_3 and 20% (v/v) acetic acid] was added.

Titration was performed by an electrolysis of a silver wire to produce free silver ions at a constant rate, the end-point of titration being determined by an excess of free silver ions. The time of electrolysis (which is displayed by the titrator), after appropriate correction for the reagent blank, was proportional to the amount of free chloride ion. The titrator was calibrated with standard sodium chloride solution, and the medium range of the titrator was used. During the titration procedure, the mixture

[1] Obtained through the National Cancer Institute.
[2] Synthesized by Stark Associates, lot PH 37-43-1.
[3] Synthesized by Merck & Co., lot L-596025-0-7.
[4] Synthesized by Stark Associates, lot CC 52-21-1.
[5] Synthesized by Ash-Steven, lot JOS-01-282-1.
[6] Synthesized by Pfanstehl, lot 10337-B.
[7] Synthesized by Southern Research Institute, lot 4689-23-1.
[8] Synthesized by Stark Associates, lot PH 28-98-1.
[9] Cary-17, Varian Instruments, Palo Alto, Calif.
[10] Cary-1729 programmer, Varian Instruments, Palo Alto, Calif.
[11] Model 4-4433, American Instrument Co., Silver Spring, Md.
[12] Model 96-09, Orion Research, Cambridge, Mass.
[13] Model 76, Beckman Instruments, Fullerton, Calif.

0022-3549/78/1100-1527$01.00/0
© 1978, American Pharmaceutical Association

Table I—Structures of Various Nitrosoureas

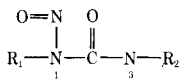

Drug	Chemical Name	R_1	R_2	Mol. Wt.
Chlorozotocin (I)	1-(2-Chloroethyl)-3-(2-deoxy-D-glucopyranosyl)-1-nitrosourea	CH_2CH_2Cl	*O*-Glucopyranosyl	313.7
II	1,3-Bis(2-chloroethyl)-1-nitrosourea	CH_2CH_2Cl	CH_2CH_2Cl	213.9
III	1-(2-Chloroethyl)-3-cyclohexyl-1-nitrosourea	CH_2CH_2Cl		233.5
IV	1-(2-Chloroethyl)-3-(*trans*-4-methylcyclohexyl)-1-nitrosourea	CH_2CH_2Cl	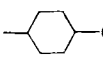	247.5
Streptozotocin (V)	1-Methyl-3-(2-deoxy-D-glucopyranosyl)-1-nitrosourea	CH_3	*O*-Glucopyranosyl	265.3
VI	1,3-Bis(2-fluoroethyl)-1-nitrosourea	CH_2CH_2F	CH_2CH_2F	181.0

pH was decreased to about 2. The short titration time (less than 1 min) along with the long half-life of I at pH 2 and room temperature (approximately 40 hr) assured that no significant nitrosourea degradation took place during the analytical procedure. The extent of chloride-ion liberation (or percentage chloride ion) was calculated as the percentage of the theoretical maximum (1 mole of drug liberating 1 mole of chloride ion). For this purpose, the drug powder was assumed to be pure; the weight of drug taken was converted to a molar basis directly to calculate the theoretical maximum of chloride liberation.

In the kinetic runs from chloride-ion measurements, particularly above pH 6.50, the end-points were slightly inaccurate, because other slow reactions probably were yielding some free chloride. Furthermore, a finite time period was needed to pipet accurately an aliquot out of the reaction mixture and then to add the titration reagent. Because of the gas bubbles (nitrogen, carbon dioxide, *etc.*) being generated during the reaction, there were some inaccuracies in pipetting. Therefore, the rate constants calculated by chloride-ion measurements have a higher uncertainty than those calculated from UV measurements.

Fluoride-Ion Measurements—A weighed amount of VI was dissolved in the buffer ($\sim 1 \times 10^{-3}$ *M*), and the fluoride-ion electrode was dipped into the reaction mixture. The millivolt reading on the pH meter was noted at different times, and the fluoride-ion concentration was determined from a standard calibration plot of millivolts *versus* sodium fluoride concentration prepared in the identical buffer. The limitation of the electrode allowed fluoride-ion measurements only between pH 5.0 and 7.0. These measurements were carried out at room temperature.

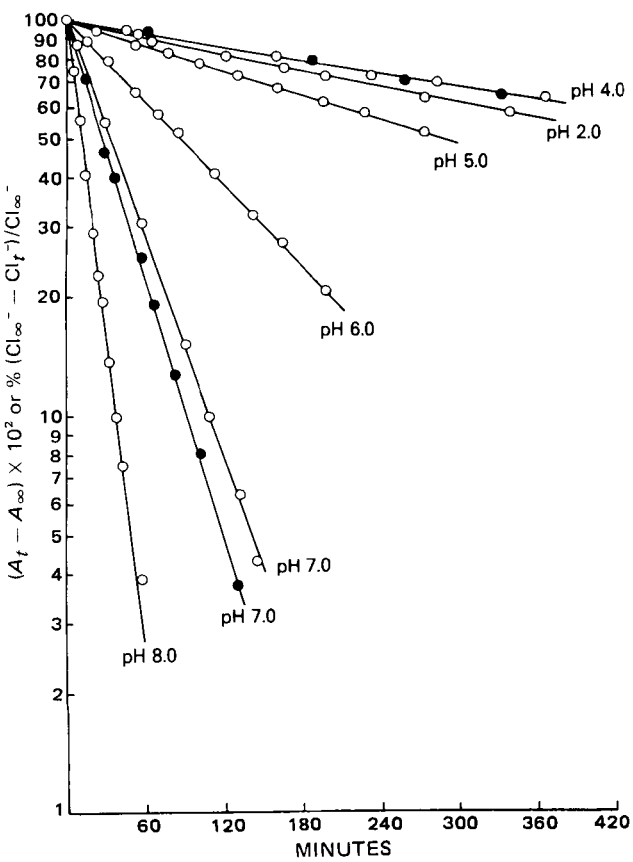

Figure 1—*Apparent first-order plots for the hydrolysis of I. Key:* ○, *from UV absorbance; and* ●, *from chloride-ion determination in 0.01* M *citrate buffer (pH 2.0, 4.0, and 5.0) and 0.01* M *phosphate buffer (pH 6.0, 7.0, and 8.0) at 37°. The* A_∞, A_t, *and* A_0 *are the absorbances at time infinity, time* t, *and time zero, respectively;* Cl_∞^- *and* Cl_t^- *are the amounts of the chloride ion produced at time infinity and time* t, *respectively. Infinity readings were taken after approximately seven half-lives.*

RESULTS AND DISCUSSION

Chlorozotocin (I) hydrolysis followed first-order kinetics between pH 1 and 9.5 as measured by either the rate of loss of UV absorbance at 231 nm or the rate of free chloride-ion production (Fig. 1). The observed rate constants for I hydrolysis as a function of pH are presented in Table II. The extent of free chloride-ion production changed with pH and buffer composition (Table III). These results suggest that three different mechanisms (Schemes I–III) exist for the hydrolysis of I and other 1-(2-haloethyl)nitrosoureas and that the relative contribution of each depends on the pH of the reaction mixture. The unstable intermediates formed during these first steps in Schemes II and III further decompose to yield the final products (Schemes IV and V).

Acid-Catalyzed Hydrolysis—In the acidic region (pH < 2) the hydrolytic rate of I increased sharply with decreasing pH, indicating hydrogen-ion catalysis. Scheme I presents the classical hydrogen-ion-catalyzed hydrolysis of the nitroso group to yield the nitrite ion but no chloride ion. In contrast, the water- and hydroxide-ion-catalyzed reac-

Table II—Observed First-Order Rate Constants, K_{obs}, for Chlorozotocin (I) Decomposition in Aqueous Solution at Various pH Values and Buffer Concentrations at 37°

Buffer Concentration, *M*	pH	Observed Rate Constants, min^{-1}: From Absorbance Measurements	From Chloride-Ion Determinations
Hydrochloric acid			
0.50	0.42	0.0289	—
0.01	2.00	0.00159	—
Citrate			
0.01	2.01	0.00145	—
0.01	2.81	0.00140	—
0.01	3.28	0.00138	—
0.01	4.00	0.00140	0.0017
0.01	5.00	0.00245	—
0.01	6.00	0.00785	0.0061
Phosphate			
0.01	6.00	0.0078	—
0.10	6.50	0.0139	—
0.01	7.00	0.024	0.021
0.10	7.00	0.025	0.022
0.20	7.00	0.025	0.024
0.01	8.00	0.062	—
0.10	8.00	0.068	—
Tris(hydroxymethyl)-aminomethane			
0.01	8.00	0.0552	—

Table III—Production of Chloride Ion from the Decomposition of Chlorozotocin (I) in Various Buffers at 37°

Buffer Concentration, *M*	pH	Total Percent Chloride Ion
Nitric acid		
0.5	0.40	18.7
0.10	1.10	57.1
0.03	1.50	72.0
Citrate		
0.10	2.00	81.4
0.10	2.63	84.8
0.10	3.00	87.8
0.10	3.13	90.5
0.10	3.50	91.6
0.10	4.00	90.5
0.10	5.02	67.9
0.10	5.55	47.0
0.10	6.00	41.6
0.10	6.50	35.1
0.10	7.00	30.0
0.02	7.00	29.6
Phosphate		
0.01	6.00	41.6
0.10	6.00	41.0
0.01	7.00	33.6
0.10	7.00	51.4
0.20	7.00	59.8
0.40	7.00	68.6
0.01	7.50	32.8
0.10	7.50	52.8
Tris(hydroxymethyl)aminomethane		
0.02	7.00	30.8
0.10	7.00	31.2
0.10	8.45	25.7
0.10	9.26	27.2

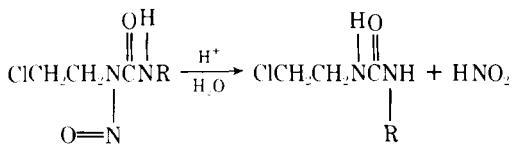

Scheme I

tions (Schemes II and III, respectively) yield chloride ion. Therefore, as the pH is lowered, the hydrogen-ion-catalyzed reaction becomes increasingly important, and there should be a decrease in chloride-ion production. As seen in Table III, the yield of chloride ion decreased as the pH was decreased below pH 3, thus supporting increasing hydrogen-ion catalysis at lower pH values.

Hydroxide-Ion-Catalyzed Reaction—Two separate mechanisms were proposed (2, 3) for hydroxide-ion-catalyzed hydrolysis of nitrosoureas, both involving prior ionization of the N-3 proton. These mechanisms were based on the product and kinetic analysis at various pH values. The major product arising from the hydrolysis of nonhalogenated nitrosoureas is the corresponding alcohol, and the rate of hydrolysis increases with increasing pH above about pH 4. This result led Garrett and Goto (7) to propose a mechanism yielding the corresponding carbonium ion (same as step K_2 in Scheme II, which yields the carbonium ion as shown in Scheme V) and Reed *et al.* (2) to propose the same mechanism for 1-(2-chloroethyl)nitrosoureas.

However, the major product arising from 1-(2-chloroethyl)nitrosoureas at pH 4 is not 2-chloroethanol but acetaldehyde (1, 3). Observation of this unusual product led Montgomery *et al.* (3) to propose a cyclic mechanism involving the attack of negatively charged carbonyl oxygen to form an unstable oxazolidine intermediate, which then decomposes to acetaldehyde (similar to step K_1 in Scheme II, except that the carbonyl oxygen instead of the nitroso oxygen displaces the chloride). Both mechanisms, however, do not explain fully the experimental findings. Thus, the cyclic mechanism, if it is valid over the pH 3–8 range, should yield similar amounts of the chloride ion irrespective of pH and should not yield any 2-chloroethanol. At pH 4, the chloride-ion yield was about 90% of the theoretical value, and no 2-chloroethanol formed. However, at pH 7, the chloride-ion yield was only about 30%, and a significant amount (40% of the theoretical) of 2-chloroethanol formed at the expense of acetaldehyde (1, 3). The cyclic mechanism of Montgomery *et al.* (3) alone fails to explain this change in product distribution.

Similarly, the 2-chloroethylcarbonium-ion intermediate proposed by Reed *et al.* (2) does not account for the acetaldehyde product. Reed's

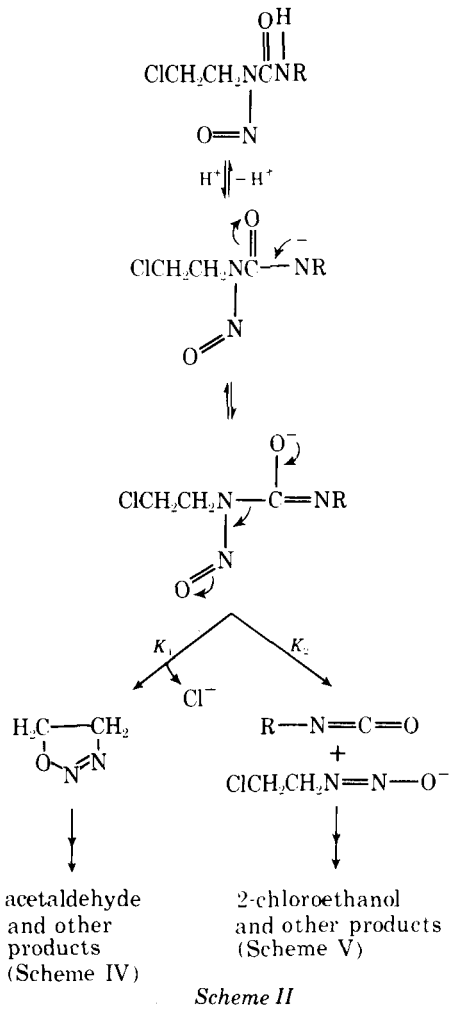

Scheme II

mechanism (2) postulates that dehydrohalogenation of the 2-chloroethylcarbonium ion yields vinyl cation, which subsequently forms vinyl alcohol and rearranges to acetaldehyde. It is difficult to explain why the

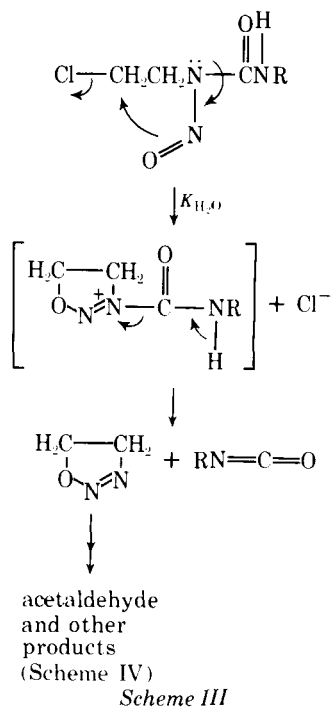

Scheme III

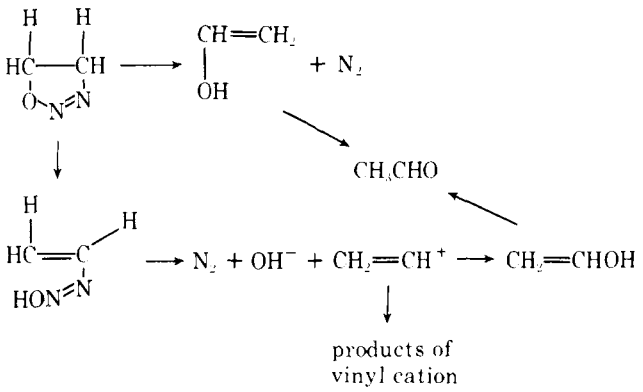

Scheme IV

yield of acetaldehyde should decrease with increasing pH. Moreover, 3-(2-chloroethyl)-1-triazinoimidazole-4-carboxamide, an excellent precursor of the 2-chloroethylcarbonium ion (9), was reported to yield mostly 2-chloroethanol in water (1). Therefore, the 2-chloroethylcarbonium ion does not appear to be the source of acetaldehyde; the cyclic structure, either the oxazolidine intermediate proposed by Montgomery or the oxadiazole intermediate proposed in Scheme II, is more likely the source. Furthermore, as will be discussed later, in unbuffered aqueous solution (pH ~4) where maximal acetaldehyde production is observed (1), ionization of the N-3 proton is not important and an alternative mechanism, other than the 2-chloroethylcarbonium ion, must yield the acetaldehyde.

Studies on I hydrolysis (Tables II and III) showed that, although the total amount of the chloride ion produced generally decreased with increasing pH, the hydrolytic rates determined by either the loss of UV absorbance or chloride-ion production were the same at each pH value. This result indicated that the reactions responsible for the loss of chloride ion and the loss of nitroso moiety (the chromophore at 231 nm) were not always the same. This observation provided the basis for proposing a parallel pathway for alkaline hydrolysis of I in which involvement of the chloroethyl moiety is the differentiating factor (Scheme II).

The scheme essentially integrates the two reported mechanisms (2, 3). Pathway K_1 involves a cyclic mechanism similar to that proposed by Montgomery *et al.* (3) for halogenated nitrosoureas, except that the nitroso oxygen rather than the carbonyl oxygen is considered the cyclizing nucleophile. The reasoning for a cyclic mechanism *via* the nitroso oxygen will be discussed later. Pathway K_2 is the same as that proposed by Reed *et al.* (2). The occurrence of both mechanisms around physiological pH was suggested, but no evidence was provided (10). The kinetic data reported in this paper support the parallel mechanism of Scheme II in which the change in product distribution with changing pH from 4 to 7 can be accounted for by assuming that increasing pH specifically favors pathway K_2 over K_1, thus yielding more 2-chloroethanol and smaller amounts of the chloride ion and acetaldehyde.

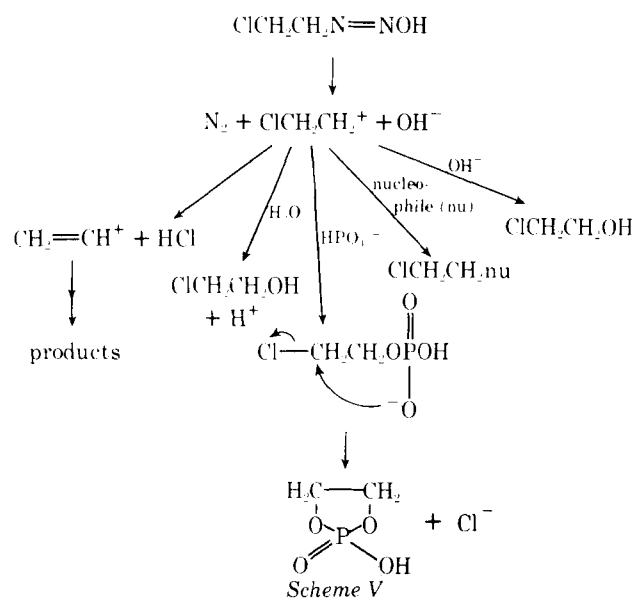

Scheme V

Table IV—Observed First-Order Rate Constants and Chloride-Ion Production from the Decomposition of the Urea Analogs of Chlorozotocin (VII) at pH 4.0–7.0 at Room Temperature

Buffer, 0.05 *M*	pH	Observed Rate Constant, min^{-1}	Total Percent Chloride Ion
Citrate	4.0	0.00085	36.8
Citrate	6.0	0.00064	39.4
Phosphate	6.0	0.00067	36.6
Phosphate	7.0	0.00073	36.9

Water Reaction—Careful analysis of the studies at pH 2–4 revealed that some results cannot be explained solely by the reactions presented in Schemes I and II. Thus, a plateau region was observed between pH 3.0 and 4.0, where observed rates of hydrolysis of I and extents of chloride-ion production were similar (Tables II and III). Based on Schemes I and II, similar yields of the chloride ion would be difficult to justify if this plateau region is due only to a competition between base- (Scheme II) and acid- (Scheme I) catalyzed reactions because acid-catalyzed hydrolysis does not yield any free chloride ion. Therefore, another reaction yielding free chloride ion must be considered.

This reasoning formed the basis for proposing a spontaneous water reaction in Scheme III. Evidence for the proposed water reaction on the unionized I was obtained by conducting kinetic studies on its urea analog, VII. Table IV shows the extent and the rate of chloride production from VII at pH 4–7. Between pH 4.0 and 7.0, the rate and extent of chloride-ion production were independent of pH and buffer species. Furthermore, the chloride-ion production rate was too fast (compared to hydrolysis of simple alkyl halides) to be explained by simple nucleophilic displacement by water and other buffer species. At pH 4–7, VII, a substituted urea, is not expected to ionize appreciably; therefore, the chloride ion must come from the cyclization involving the carbonyl oxygen of unionized VII.

The pKa of the N-3 proton of nitrosoureas is estimated to be 8–9 (5, 6); therefore, it is reasonable to conclude that no appreciable ionization of I would take place at pH 3–4. Thus, the major reaction at pH 3–4 is attributed to the water reaction involving the unionized drug (Scheme III) where hydroxide- and hydrogen-ion catalyses are least significant. On the acid side, the hydrogen-ion-catalyzed reaction becomes more important and, at pH > 4, hydroxide-ion catalysis is increasingly the dominant reaction. Scheme VI summarizes the pathways for the decomposition of nitrosoureas.

Further Evidence for Schemes II and III—The cyclic mechanisms K_{H_2O} (Scheme III) and K_1 (Scheme II), which are only available to 1-(2-haloethyl)nitrosoureas, are more evident from the kinetic studies of V (nonchlorinated analog of I). As presented in Table V, the hydrolysis rate of I at pH 4.0 was about seven times faster than that of V. As the pH became increasingly alkaline, the hydrolytic rates of I and V became closer (Table V), and the amount of chloride liberated from the hydrolysis of I decreased (Table III). This result indicates that, at higher pH (*i.e.*, ~pH 7–8), both I and V must be primarily hydrolyzing by a similar mechanism and that the increased reactivity of I at lower pH (~pH 3–4) may be related to a specific mechanism involving the 2-chloroethyl moiety available only to I.

The proposed mechanisms of Schemes II and III are supported also by kinetic studies conducted with VI, where the β-fluoro substituent, a poor leaving group, was shown to be resistant to decomposition by pathway K_{H_2O} (Scheme III). As seen in Table V, the decomposition rate of VI at pH 4.0 was about 10 times slower than that of its chlorinated analog, II, and was similar to that of the nonhalogenated nitrosourea, V. This result indicates that VI is relatively resistant to halogen-assisted hydrolysis as presented in Scheme III. However, at pH 7.0, the hydrolysis

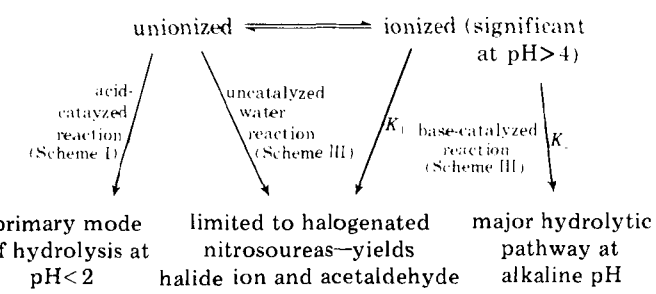

Scheme VI

Table V—Comparison of Observed Hydrolytic Rate Constants at pH 4.0 and 7.0 for Various Nitrosoureas at 37°

Nitrosourea	Buffer	pH	Observed Rate Constant, min^{-1} [a]	Total Percent Chloride Ion
Chloro-zotocin (I)	0.01 *M* Citrate	4.00	0.00136	90.5
	0.01 *M* Phosphate	7.00	0.0248	33.6
	—	9.25	0.693[b]	—
II	0.01 *M* Citrate	4.00	0.0013	94
	0.01 *M* Tris(hydroxy-methyl)aminomethane	7.00	0.0086	—
	0.01 *M* Phosphate	7.00	0.0109	41.3
	0.10 *M* Phosphate	7.00	0.0112	—
	0.20 *M* Phosphate	7.00	—	55.8
III	0.01 *M* Tris(hydroxy-methyl)aminomethane	7.00	0.00635	—
	0.10 *M* Phosphate	7.00	0.0089	—
IV	0.01 *M* Tris(hydroxy-methyl)aminomethane	7.00	0.0064	—
	0.10 *M* Phosphate	7.00	0.0091	—
Strepto-zotocin (V)	0.17 *M* Acetate	3.98	0.00020[c]	—
	0.125 *M* Phosphate	6.89	0.0054[c]	—
	—	9.25	0.594[b]	—
VI	0.10 *M* Citrate	4.00	0.00015	—
	0.01 *M* Tris(hydroxy-methyl)aminomethane	7.00	0.0072	—
	0.05 *M* Phosphate	7.00	0.011	—

[a] From absorbance measurements. [b] Room temperature. [c] Estimated by doubling the rate constant at 30.2° from Tables I and II, Ref. 5.

rates of II and VI were similar, indicating that the 2-chloroethyl-moiety-dependent water reaction is not important and that the reactions presented in Scheme II are dominant. Step K_2 is not expected to be affected by the fluoro group; in step K_1, the negatively charged nitroso group is expected to displace some fluoride (Table VI). These rate constants at pH 7.0 agreed well with those reported at pH 7.2 in phosphate buffer (1, 3).

Further evidence supporting the mixed water- and hydroxide-ion-catalyzed reaction from pH 3.0 to 8.0 comes from the calculation of values of the chloride ion produced at various pH values. At pH > 8, the major reaction is hydroxide-ion catalysis where the extent of the chloride ion produced plateaus at about 26% of the maximal theoretical value (Table III). Thus, at pH > 8, a ratio of K_1/K_2 of 26/74 is expected. If one assumes that this ratio does not change from pH 3 to 8, it can be concluded that, for each mole of ionized I degrading by Scheme II, 0.26 mole of chloride ion is produced. However, unionized chlorozotocin undergoing hydrolysis through Scheme III should yield ionic chloride on an equimolar basis. Thus, the theoretical amount of the chloride ion can be calculated from Eq. 1 if the fraction of chlorozotocin undergoing degradation by Schemes II and III is known:

Table VI—Effect of Various Nucleophiles on Observed Rate Constants and Fluoride-Ion Production from VI at pH 7.0 and Room Temperature

Buffer	Nucleophile	Observed Rate Constant[a], min^{-1}	Total Percent Fluoride Ion
0.10 *M* Tris(hydroxymethyl)-aminomethane	—	—	20.5
0.01 *M* Phosphate	—	0.00271	26.5
0.01 *M* Phosphate	0.05 *M* $Na_2S_2O_3$	0.00233	21.7
0.40 *M* Phosphate	—	0.00265	75.7
0.40 *M* Phosphate	0.05 *M* $Na_2S_2O_3$	0.00280	65.8
0.20 *M* Phosphate	—	0.00281	59.5
0.20 *M* Phosphate	0.20 *M* KNO_3	0.00299	59.0
0.20 *M* Phosphate	0.20 *M* KCl	0.00299	59.4
0.20 *M* Phosphate	0.20 *M* NaI	0.00305	50.0

[a] From fluoride-ion measurements.

Table VII—Comparison of Chloride-Ion Production Observed Experimentally and That Calculated from Eq. 1 for Chlorozotocin (I) Decomposition at 37°

pH	K_{obs}, min^{-1}	K_{H_2O}/K_{obs}	Total Percent Chloride Ion	
			Theoretical	Experimental
3.0	0.00140	0.8643	90.0	90.5
4.0	0.00140	0.8643	90.0	90.5
5.0	0.00245	0.4939	62.5	67.9
6.0	0.00785	0.1541	37.4	41.6
6.5	0.0139	0.0871	32.4	35.1
7.0	0.025	0.048	29.6	30.0
8.0	0.0610	0.0198	27.5	26.0

$$\text{total \% chloride} = 100\,(X) + 26\,(1 - X) \qquad \text{(Eq. 1)}$$

where X is the fraction of chlorozotocin undergoing hydrolysis by Scheme I and can be calculated from:

$$X = \frac{K_{H_2O}}{K_{obs}} \qquad \text{(Eq. 2)}$$

where K_{obs} is the observed first-order rate constant. Hydrogen-ion catalysis is assumed to be negligible above pH 3.0.

At pH 3.0–4.0, maximal chloride-ion formation is observed equivalent to 90% of the chlorozotocin decomposition. By substituting this value in Eq. 1, X at this pH is found to be 64/74 (0.865). By substituting this value of X and K_{obs} at pH 4.0 in Eq. 2:

$$0.865 = K_{H_2O}/(0.0014\ min^{-1}) \qquad \text{(Eq. 3)}$$

$$K_{H_2O} = (0.865)\,(0.0014) = 0.0012\ min^{-1} \qquad \text{(Eq. 4)}$$

The value of X at any pH can be calculated from Eq. 2 if K_{obs} at that pH is known. By substituting this value of X in Eq. 1, theoretical chloride values can be calculated. Table VII presents the theoretically calculated values of chloride ion along with the observed values at pH 3.0–8.0. The close agreement between theoretical and experimental values lends support to the proposed mechanisms and to the assumption that K_{H_2O} (Scheme III) and the ratio K_1/K_2 (Scheme II) are relatively unaffected by pH.

Cyclic Oxadiazole Intermediate—In Schemes II and III, formation of a cyclic oxadiazole intermediate involving the nitroso oxygen as the attacking nucleophile is proposed. Montgomery *et al.* (1, 3), however, proposed an oxazolidine intermediate involving the carbonyl oxygen as the attacking nucleophile. This proposal was not supported by any direct evidence but was based on the fact that acetaldehyde and products derived from vinyl cation were formed. However, the oxadiazole intermediate as proposed in Schemes II and III also could account for the production of acetaldehyde and products of vinyl cation as shown in Scheme IV. Therefore, based on product analysis alone, either of the two oxygens could act as the nucleophile in displacing the chloride ion.

Evidence supporting the cyclic oxazolidine intermediate comes from the fact that VII (urea analog of I), which does not contain the nitroso moiety, liberates the chloride ion at a rate comparable to I in aqueous buffers at pH 4.0 (Tables II and IV). The absence of the nitroso group in VII allows unequivocal assignment of the carbonyl oxygen as the attacking nucleophile. At this pH, the urea would be unionized and thus it must be the polarized carbonyl group that displaces the chloride group. However, the yield of the chloride ion from the urea compound was only 40%, whereas in I the yield was 90% at pH 4; the kinetic schemes presented in this paper dictate that the cyclic mechanism yield nearly 100% free chloride ion. Since the yield of chloride ion was only 40% in the absence of nitroso group, it is more reasonable to assume that nitroso oxygen is the primary cyclizing nucleophile in I.

Furthermore, although the carbonyl oxygen will be highly polarized in alkyl-substituted analogs (VII), this polarity will be less pronounced in nitrosoureas where the N-1 nitrogen lone pair of electrons will be strongly resonating with the nitroso group and thus be unavailable for amide resonance with the carbonyl group. This assumption is supported by the IR spectra[14] of I and VII where the carbonyl peak for VII appears as a doublet at 1575 and 1620 cm^{-1} (typical of ureas, showing considerable resonance), but that for I appears upfield at 1690 cm^{-1}, or roughly the same as that of an ordinary carbonyl group. This relative lack of polarity of the carbonyl in nitrosoureas (upfield shift of carbonyl peak indicating less single bond character) makes it an unlikely candidate to act as a

[14] In potassium bromide pellet.

nucleophile in displacing the β-chloro group of the N-1 substituent and favors the highly polarized *N*-nitroso group as the nucleophile giving a cyclic oxadiazole intermediate.

Also, if the carbonyl oxygen is the attacking species, then the cyclic oxazolidine intermediate formed will still have the nitroso group (the chromophore at 231 nm) and, therefore, must decompose instantly with the loss of the nitroso chromophore to account for the observed first-order hydrolysis kinetics as determined by the UV method. There is no reason to expect such instability of 2-oxazolidines. In contrast, the oxadiazole intermediate proposed in Schemes II and III has no nitroso group, so first-order kinetic behavior does not require its instant decomposition. Other evidence against the carbonyl oxygen acting as the cyclizing nucleophile (and thus favoring the nitroso oxygen as the primary nucleophile) is the similarity of rates observed for various nitrosoureas at pH 4.0 and 7.0 (Table V). Nucleophilic attack of the carbonyl oxygen on the β-chloro group should be influenced by steric and electronic effects of various N-3 substituents, whereas those effects would not be as significant for the attack by nitroso oxygen. Therefore, the cyclic structure presented in Schemes II and III is the more likely intermediate. However, because of the lack of strong direct evidence, this assignment in favor of the oxadiazole intermediate is tentative; the oxazolidine intermediate as proposed by Montgomery *et al.* (1, 3) cannot be ruled out.

Role of Phosphate in Hydrolysis—The role of the phosphate dianion (HPO_4^{2-}) in the catalysis of the overall hydrolysis rate of nitrosoureas has been controversial. Garrett (5) suggested a catalytic effect of HPO_4^{2-} on V hydrolysis. Loo *et al.* (4) demonstrated that phosphate buffer had no appreciable effect on the hydrolysis rate of II. Montgomery *et al.* (3) reported significant rate increases in phosphate buffer compared to tris(hydroxymethyl)aminomethane and acetate buffers at pH 7.2, specifically with III, where the rate in phosphate buffer was reported to be more than threefold faster than in acetate buffer. However, their reports (1, 3) did not mention the molarity of the acetate buffer used for comparison at pH 7.2 and its buffer capacity could not be ascertained. Therefore, it is difficult to compare data when the maintenance of pH is not demonstrated.

The present data (Table V) showed that the hydrolysis rates of nitrosoureas at pH 7.0 were about 25% faster in phosphate buffer than in tris(hydroxymethyl)aminomethane buffer. The present values at pH 7.0 in phosphate buffer agreed well with those reported (1, 3, 8).

Increased Chloride Production by Phosphate Dianion—The observation that the phosphate dianion increases the yield of chloride has not been reported. As can be observed from Table III, the yield of chloride increased substantially at pH 7.0 with an increase in the phosphate dianion concentration. However, at pH 6.0, where most of the phosphate would be monobasic, there was very little change in chloride production with increasing phosphate concentration. The yield of chloride was independent of buffer species and buffer concentration at pH 7.0 for other buffers tested [tris(hydroxymethyl)aminomethane and citrate (Table III)]. Although phosphate dianion appeared to have a specific effect in increasing the chloride-ion production, the overall decomposition rate (or the production rate of chloride) was unaffected by phosphate buffer concentration (Table II).

Indirect evidence for higher chloride production in phosphate buffer around pH 7 was presented when Montgomery *et al.* (1) reported a lower yield of 2-chloroethanol in phosphate buffer than in acetate buffer and Reed *et al.* (2) reported lower yields of 2-chloroethanol in phosphate buffer compared to the yield in tris(hydroxymethyl)aminomethane buffer. To determine if the reaction involved a simple nucleophilic displacement of chloride by phosphate dianion, studies were conducted with VII. As can be seen from Table IV, both the rate and extent of chloride-ion production were independent of pH and buffer species over pH 4–7. Therefore, simple nucleophilic substitution by phosphate dianion was ruled out. As the overall decomposition rate of I did not change with phosphate buffer strength (Table II), an almost twofold increase in the amount of chloride produced (by increasing the phosphate concentration from 0.01 to 0.2 *M*; Table III) must be explained by some other mechanism.

At pH 7.0, only the pathways presented in Scheme II are important. Therefore, higher production of chloride could come from either (*a*) phosphate dianion catalysis of the cyclic mechanism K_1, or (*b*) phosphate dianion reaction with 2-chloroethylcarbonium ion, which then cyclizes to yield free chloride (Scheme V). Route *a* could be ruled out on the basis that it would have to increase the overall rate. Pathway *b*, involving the intramolecular nucleophilic substitution, appears more likely because this reaction would not change the overall decomposition rate.

If pathway *b* is correct, then addition of strong nucleophiles, which would compete for 2-chloroethyldiazonium hydroxide (Scheme V), should decrease the yield of free chloride ion (*i.e.*, less 2-chloroethyl phosphate would form). Therefore, an attempt was made to determine the yield of chloride in phosphate buffer in the presence of strong nucleophiles such as sulfide, thiocyanate, thiosulfate, or iodide. However, the chloride ion could not be assayed in the presence of these nucleophiles by the method used in this study because the titration is based on precipitating chloride by silver cation, and the strong nucleophiles interfere with the assay of chloride.

An alternative compound, VI, was chosen because it liberates the fluoride ion, which could be assayed without being affected by the presence of strong nucleophiles. Also, if one assumes that both VI and other 2-(chloroethyl)nitrosoureas hydrolyze by similar mechanisms (Schemes I–V), the conclusion drawn in experiments with VI could be directly related to 1-(2-chloroethyl)nitrosoureas. As expected, increasing the phosphate concentration at pH 7.0 increased the yield of the fluoride ion (Table VI). However, addition of strong nucleophiles, thiosulfate or iodide ion, significantly decreased the yield of the fluoride ion (Table VI). In contrast, weaker nucleophiles (*i.e.*, chloride or nitrate ion) had no effect on the yield of the fluoride ion (Table VI). Therefore, it appears that strong nucleophiles, by competing with phosphate dianion, reduce the production of 2-fluoroethyl phosphate monoanion and thus reduce the yield of free fluoride ion by making smaller amounts of 2-fluoroethyl phosphate monoanion available for cyclic displacement (Scheme V). These results support the cyclic phosphate pathway presented in Scheme V. Simple nucleophilic displacement of fluorine is extremely difficult, and liberation of the fluoride ion almost certainly points to an intramolecular substitution by a negatively charged atom, both in Scheme II (K_1) and from 2-fluoroethyldiazonium hydroxide (Scheme V).

The problem of assigning the active alkylating intermediate under physiological conditions is still unanswered. Current reports favor 2-chloroethyl cation (or the corresponding diazonium hydroxide) as the active intermediate. The increased chloride-ion production by phosphate dianion led to a proposed mechanism whereby the 2-chloroethylcarbonium ion acts as a bifunctional alkylating agent of phosphate dianion (Scheme V). Other compounds having more than one nucleophilic center might react similarly with 2-chloroethylcarbonium ion. Low nucleophilic selectivity of the nitrosoureas led Veleminsky *et al.* (11) to suggest that the groups being alkylated are nitrogens or phosphates.

It is possible, therefore, that 2-chloroethylcarbonium ions derived from 1-(2-chloroethyl)nitrosoureas act as bifunctional alkylating agents to form interstrand or intrastrand nucleic acid cross-links. The inability of nonhalogenated nitrosoureas to form bifunctional reactive intermediates may be responsible for their lower activity. The higher activity of halogenated nitrosoureas also may be due to significant production of acetaldehyde and vinyl cation products at physiological pH (Scheme VI). Further experiments are needed to isolate and identify the complexes formed and to correlate the observed reactivity of phosphate dianion to the *in vivo* effects of chlorinated nitrosoureas.

REFERENCES

(1) J. A. Montgomery, R. James, G. S. McCaleb, M. C. Kirk, and T. P. Johnston, *J. Med. Chem.*, **18**, 568 (1975).

(2) D. J. Reed, H. E. May, R. B. Boose, K. M. Gregory, and M. A. Beilstein, *Cancer Res.*, **35**, 568 (1975).

(3) J. Montgomery, R. James, G. S. McCaleb, and T. P. Johnston, *J. Med. Chem.*, **10**, 668 (1967).

(4) T. L. Loo, R. L. Dion, R. L. Dixon, and D. P. Rall, *J. Pharm. Sci.*, **55**, 492 (1966).

(5) E. R. Garrett, *J. Am. Pharm. Assoc., Sci. Ed.*, **49**, 767 (1960).

(6) E. R. Garrett, S. Goto, and J. F. Stubbins, *J. Pharm. Sci.*, **54**, 119 (1965).

(7) E. R. Garrett and S. Goto, *Chem. Pharm. Bull.*, **21**, 1811 (1973).

(8) P. A. Laskar and J. W. Ayers, *J. Pharm. Sci.*, **66**, 1073 (1977).

(9) Y. F. Shealy, C. A. O'Dell, and C. A. Krauth, *ibid.*, **64**, 177 (1975).

(10) G. P. Wheeler, in "ACS Symposium Series 30, Cancer Chemotherapy," A. C. Sartorelli, Ed., American Chemical Society, Washington, D.C., 1976, p. 87.

(11) J. Veleminsky, S. Osterman-Golkar, and L. Ehrenberg, *Mutat. Res.*, **10**, 169 (1970).

Influence of Food and Fluid Ingestion on Aspirin Bioavailability

PATRICIA A. KOCH, CRAIG A. SCHULTZ, ROBERT J. WILLS, SHARON L. HALLQUIST, and PETER G. WELLING *x

Received December 5, 1977, from the *Center for Health Sciences, School of Pharmacy, University of Wisconsin, Madison, WI 53706.* Accepted for publication March 3, 1978. *Present address: Department of Clinical Pharmacology and Therapeutics, School of Medicine, University of Birmingham, Birmingham, B15 2TJ, England.

Abstract □ The influence of test meals and accompanying fluid volume on aspirin bioavailability from commercial tablets was determined following single oral doses to healthy male volunteers. Plasma aspirin and salicylate levels were determined simultaneously using a GLC end-point. Area analysis indicated that approximately 5–8% of absorbed drug entered the systemic circulation as unchanged aspirin in nonfasted subjects compared to 16–18% in fasted individuals. Food tended to reduce the appearance rate of aspirin into the circulation, resulting in lower and somewhat more sustained levels than with fasting. Plasma salicylate levels were not influenced markedly by the various treatments, although levels were higher in fasted than in nonfasted subjects during the 1st hr after dosing. After this time, fat pretreatment tended to produce higher levels than other treatments.

Keyphrases □ Aspirin—bioavailability in humans, effect of food and fluid volume □ Bioavailability—aspirin in humans, effect of food and fluid volume □ Absorption, GI—aspirin in humans, effect of food and fluid volume □ Analgesics—aspirin, bioavailability in humans, effect of food and fluid volume

Considerable attention has been paid to the absorption characteristics of aspirin from various dosage forms and dosage routes. Studies have concerned aspirin absorption from both oral (1) and rectal (2) routes; the influence of gastric pH, antacids, and buffering agents (3); particle size (4); and interactions with other medicinal agents (5). Other reports have discussed aspirin absorption from sustained-release (6) and conventional (7) tablets and from solutions (8). A bioavailability monograph for aspirin has been published (9).

The objective of this study was to examine the influence of food and fluid volume on the rate and extent of aspirin absorption following single doses to healthy male volunteers. Aspirin absorption is determined in terms of the circulating levels of both unchanged aspirin and salicylate.

EXPERIMENTAL

Protocols—The protocol was similar to that described previously (10). Six healthy males, 21–30 years old and weighing 66–87 kg, took no known enzyme-inducing agents for 1 month and no drugs for 1 week before the study. Subjects took no drugs other than the required doses of aspirin during the study.

Subjects fasted overnight before each dose of aspirin and ate no food, apart from test meals, until 4 hr after dosing. On the morning of a treatment, subjects drank 250 ml of water on arising, at least 1 hr before dosing. Aspirin was dosed at 8 am; blood samples (~5 ml) were drawn from a forearm vein into chilled vacuum tubes containing 50 μl of heparin solution (1000 units/ml) and 50 μl of 50% (w/v) aqueous potassium fluoride immediately before and at 10, 20, and 30 min and 1, 2, 3, 4, 6, 8, and 12 hr after dosing.

As soon as blood samples were drawn, the tubes were gently mixed in ice for 2 min and centrifuged for 3 min at 0°. The plasma was separated and stored at −20° until assayed, usually within 24 hr. This procedure effectively inhibits hydrolysis of aspirin to salicylate after sampling (11).

Treatments—Subjects received single 650-mg doses of aspirin[1] as two 325-mg tablets. Test meals were prepared as described previously (12). Aspirin was administered as follows:

Treatment 1—Two tablets with 250 ml of water immediately following a high carbohydrate meal.

Treatment 2—Two tablets with 250 of ml water immediately following a high fat meal.

Treatment 3—Two tablets with 250 ml of water immediately following a high protein meal.

Treatment 4—Two tablets with 25 ml of water on an empty stomach.

Treatment 5—Two tablets with 250 ml of water on an empty stomach.

All subjects received the same treatment at the same time. Treatments were administered 2 weeks apart, and all subjects received all treatments. Tablets were swallowed whole.

Assay—Plasma aspirin and salicylate were assayed by a GLC method (13) with *m*-toluic acid as internal standard. This method, in association with the described sampling procedure, minimizes hydrolysis of aspirin to salicylate. Any hydrolysis is accounted for by constructing standard curves based on known plasma concentrations of both aspirin and salicylate.

Linear regressions of peak height ratios of compound to internal standard *versus* compound concentration in plasma were $y = -0.007 + 0.159x$ ($r = +0.998$, $n = 14$) for aspirin over a concentration range of 0.5–10 μg/ml and $y = 0.315 + 0.151x$ ($r = +0.997$, $n = 14$) for salicylate over a concentration range of 0.5–100 μg/ml. Average values of peak height ratios divided by known compound concentrations were 0.15 ± 0.02 (*SD*) and 0.19 ± 0.02 for aspirin and salicylate, respectively. Assay reproducibility at the lower limits of the standard curves was ± 10%.

Analysis—The most simple model that may approximate absorption and elimination of salicylate is shown in Scheme I.

In this scheme, "aspirin in GI tract" represents unabsorbed aspirin, while C_{ASA} and C_{SA} represent concentrations of aspirin and salicylate in their respective body distribution volumes. All k's are first-order rate constants. The rate constant k_a represents drug loss from the GI tract due to absorption and hydrolysis. The rate constants k_1, k_2, k_3, and k_4 represent absorption of unchanged drug into the systemic circulation, formation of salicylate during absorption, hydrolysis of aspirin to salicylate once aspirin has entered the systemic circulation, and elimination of salicylate, respectively.

With this pharmacokinetic model, circulating levels of aspirin and salicylate are described by:

$$C_{ASA} = \frac{FDk_1}{V_{ASA}(k_3 - k_a)}[e^{-k_a t} - e^{-k_3 t}] \qquad \text{(Eq. 1)}$$

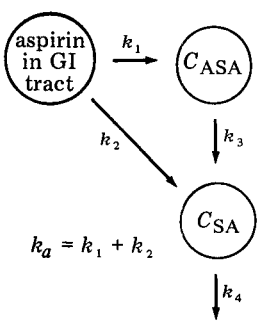

Scheme I

[1] Bayer Aspirin, lot A6009, Glenbrook Laboratories, New York, NY 10016.

0022-3549/78/1100-1533$01.00/0
© 1978, American Pharmaceutical Association

Table I—Mean Pharmacokinetic Values (±1 *SD*) for Aspirin

Value	Treatment 1	2	3	4	5	Paired *t* Test
k_a, hr^{-1}	1.4 ± 0.5	1.5 ± 0.5	2.9 ± 1.0	4.0 ± 1.4	4.3 ± 2.2	3–5 > 1,2
$t_{1/2(abs)}$, hr	0.55 ± 0.20	0.47 ± 0.10	0.28 ± 0.14	0.20 ± 0.11	0.20 ± 0.10	1,2 > 3–5
k_3, hr^{-1}	0.73 ± 0.23	0.76 ± 0.25	0.71 ± 0.30	1.61 ± 0.73	1.53 ± 0.57	4,5 > 1,2
$t_{1/2(elim)}$, hr	1.0 ± 0.3	0.98 ± 0.21	1.1 ± 0.4	0.55 ± 0.32	0.53 ± 0.29	5 > 2; 4 > 3
FDk_1/Vk_a[a], μg/ml	6.6 ± 3.0	7.2 ± 2.5	6.1 ± 2.1	15.8 ± 5.8	18.6 ± 4.2	4,5 > 1–3
area $^{0\to\infty}_{trap}$[b], μg/hr/ml	13.4 ± 5.5	10.9 ± 4.1	13.9 ± 8.9	9.1 ± 2.6	14.2 ± 6.0	NSD[c]
Peak height, μg/ml	5.0 ± 2.5	4.5 ± 1.3	5.4 ± 1.0	8.1 ± 2.9	11.0 ± 2.6	4 > 2,3; 5 > 1–3
Time of peak, hr	2.2 ± 1.2	1.3 ± 0.6	1.3 ± 1.5	0.44 ± 0.09	0.64 ± 0.67	1,2 > 4; 1 > 5

[a] Fraction of dose absorbed as unchanged aspirin, expressed as a concentration in its distribution volume. [b] Calculated by trapezoidal rule. [c] Not significantly different.

$$C_{SA} = \frac{FD}{V_{SA}}\left[\frac{k_1k_3}{(k_4-k_3)(k_a-k_3)}e^{-k_3t} + \frac{k_a(k_3-k_2)}{(k_4-k_a)(k_3-k_a)}e^{-k_at} + \frac{(k_ak_3-k_2k_4)}{(k_a-k_4)(k_3-k_4)}e^{-k_4t}\right] \quad \text{(Eq. 2)}$$

where F is the fraction of the aspirin dose absorbed as both aspirin and salicylate and V_{ASA} and V_{SA} are the respective distribution volumes.

Individual plasma aspirin levels were fitted graphically to Eq. 1. The small number of data points and the considerable variation in the absorptive phase of plasma aspirin levels made additional curve fitting by computer impractical. Although less variation was observed in plasma salicylate levels, it was not possible to analyze these data in terms of more than two exponents and, therefore, to distinguish further between k_3 and k_a. Salicylate data, therefore, were analyzed in terms of a biexponential expression with an elimination rate constant, k_4, and an appearance rate constant, k', representing the overall contribution of k_3 and k_a. In this case, improved computer estimates of rate constants were obtained (12).

The fraction of absorbed dose entering the systemic circulation as unchanged aspirin and the fraction appearing as salicylate were calculated by area analysis. Integration of Eqs. 1 and 2 yields, respectively:

$$\text{area}^{0\to\infty}_{ASA} = \frac{FDk_1}{V_{ASA}k_ak_3} \quad \text{(Eq. 3)}$$

$$\text{area}^{0\to\infty}_{SA} = \frac{FD}{V_{SA}k_4} \quad \text{(Eq. 4)}$$

The distribution volumes of aspirin and salicylate are similar (14), and FD is common to both equations. Areas under individual plasma level *versus* time curves were calculated by the trapezoidal rule. Residual areas following the last sampling time were obtained by dividing the drug concentration at that time by the appropriate elimination rate constant. Thus, with known values of the respective areas and of the rate constants k_3 from aspirin data and k_4 from salicylate data and with appropriate correction for molecular weights, the ratios k_1/k_a and k_2/k_a are obtained.

Statistical analysis included comparison of plasma aspirin levels, plasma salicylate levels, and all appropriate pharmacokinetic values between treatments by analysis of variance. Differences between individual treatments were examined for significance by a paired t test.

RESULTS

Mean plasma levels of aspirin and salicylate from all treatments are summarized in Figs. 1 and 2. Results of pharmacokinetic analysis are given in Tables I and II.

Plasma aspirin levels tended to be higher and to peak earlier in fasted individuals, while levels were lower and prolonged when aspirin was ingested with food. Prolonged absorption probably accounted for the apparent decrease in the elimination rate constant in nonfasted individuals. The elimination half-life from Treatments 4 and 5, although shorter than from the nonfasted treatments, was larger than values obtained when aspirin was dosed intravenously (14) and may also have been influenced by continued absorption but to a smaller extent than after Treatments 1–3. Although no differences were observed in areas under plasma level–time curves, these values were influenced by varied apparent elimination rates from the different treatments. A better indication of the absorption efficiency of aspirin as unchanged drug was given by FDk_1/Vk_a. This value was significantly higher following Treatments 4 and 5 than from nonfasted treatments.

The various treatments had less influence on plasma salicylate levels than those of aspirin. Fasting treatments tended to yield higher salicylate levels during the 1st hr after dosing. However, after that time, the only consistent trend among treatments was that of higher salicylate levels from the fat treatment compared to those obtained when aspirin was ingested with low fluid volume by fasted subjects.

The overall similarity of salicylate bioavailability characteristics from the five treatments is reflected in the pharmacokinetic values in Table II. No differences were obtained in the apparent appearance rate con-

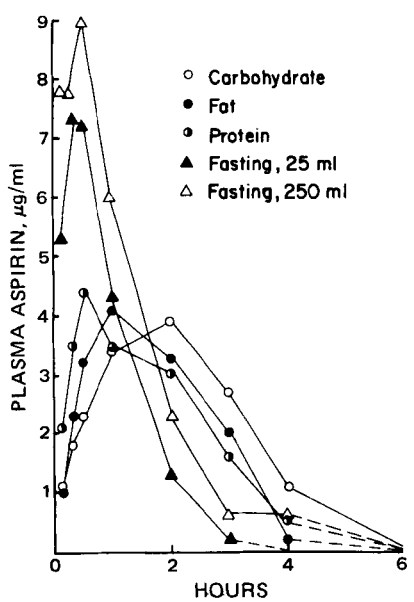

Figure 1—*Average plasma aspirin levels.*

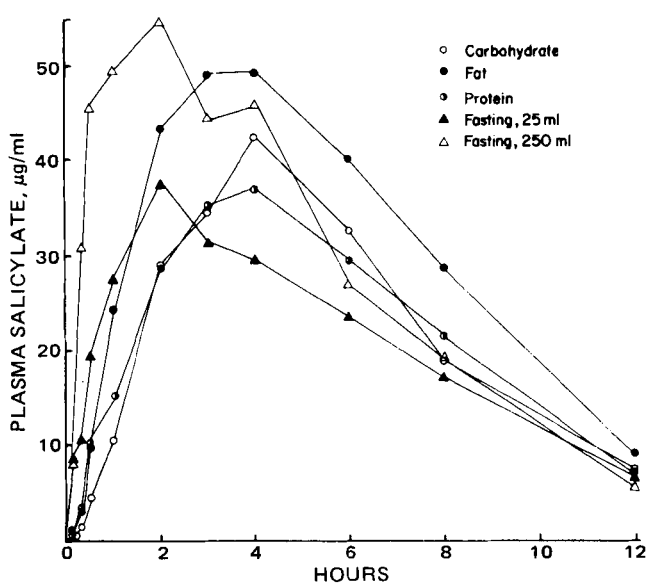

Figure 2—*Average plasma salicylate levels.*

Table II—Mean Pharmacokinetic Values (±1 *SD*) for Salicylate

Value	Treatment 1	2	3	4	5	Paired *t* Test
k', hr^{-1}	0.39 ± 0.14	0.45 ± 0.22	0.43 ± 0.05	0.56 ± 0.23	0.89 ± 0.55	NSD[c]
$t_{1/2}$[a], hr	2.0 ± 0.9	1.9 ± 0.9	1.6 ± 0.2	1.4 ± 0.5	1.1 ± 0.7	NSD
k_4, hr^{-1}	0.31 ± 0.14	0.28 ± 0.06	0.31 ± 0.07	0.25 ± 0.07	0.27 ± 0.10	NSD
$t_{1/2(elim)}$[b], hr	2.5 ± 0.7	2.6 ± 0.6	3.2 ± 0.4	3.0 ± 0.9	3.0 ± 1.3	NSD
FD/V, μg/ml	77 ± 16	109 ± 31	71 ± 11	65 ± 14	98 ± 31	2 > 1,4
area $_{trap}^{0\rightarrow\infty}$[d] μg/hr/ml	310 ± 113	409 ± 98	298 ± 59	289 ± 60	371 ± 68	2 > 1,3
Peak height, μg/ml	46.6 ± 15.2	53.2 ± 10.1	43.6 ± 16.4	46.8 ± 13.7	65.2 ± 16.4	5 > 1,4
Time of peak, hr	3.8 ± 1.3	3.7 ± 0.5	4.3 ± 2.3	1.8 ± 0.9	2.1 ± 1.3	1 > 4; 1, 3 > 5
r^{2e}	0.81 ± 0.19	0.92 ± 0.04	0.86 ± 0.07	0.92 ± 0.05	0.88 ± 0.17	

[a] $t_{1/2} = 0.693/k'$. [b] $t_{1/2(elim)} = 0.693/k_4$. [c] Not significantly different. [d] Area from 0 to 12 hr plus the terminal area, 12 → ∞ hr, calculated from C_{12hr}/k_4. [e] Coefficient of determination $(\Sigma^2_{obs} - \Sigma^2_{dev})/\Sigma^2_{obs}$.

stants or the elimination rate constants between treatments. Treatment 5 yielded the highest mean peak salicylate levels, and both fasting treatments resulted in earlier peak times. However, the overall bioavailability of salicylate from Treatments 2 and 5 tended to be higher than from other treatments. The elimination half-life of salicylate was similar to values previously reported at this dose level (15).

Calculation of the ratios k_1/k_a and k_2/k_a from area analysis and Eqs. 3 and 4 gave the values in Table III. Fasting treatments resulted in a greater percentage of absorbed drug entering the circulation in unchanged form.

DISCUSSION

The simple model utilized in this study is not intended to represent the complex events associated with aspirin pharmacokinetics (15). It is used in a relative sense to determine the influence of fasting and nonfasting treatments on circulating levels of aspirin and salicylate. Although the elimination kinetics of aspirin are saturable, they are essentially linear at the dose level used in this study, so the use of the linear Eqs. 1–4 is justified (15).

The results show that, after all oral treatments, aspirin is absorbed into the circulation predominantly as salicylate. Although circulating levels of aspirin were influenced more by the different treatments than salicylate levels, the latter values are of greater clinical significance.

Comparison of salicylate data among treatments indicates that dosing aspirin on an empty stomach produces higher circulating salicylate levels during the 1st hr after dosing. These levels are increased further if aspirin is taken with a large volume of water. However, the overall bioavailability of salicylate was influenced to only a small extent by food. Since salicylate has a relatively long biological half-life and is chemically stable compared to aspirin, it is not surprising that its overall absorption efficiency is not significantly changed by the delay in stomach emptying due to solid food.

Table III—Percentage (±1 *SD*) of Aspirin Absorbed into the Systemic Circulation as Unchanged Drug (k_1/k_a) and as Salicylate (k_2/k_a)

Treatment	$\frac{k_1}{k_a}$	$\frac{k_2}{k_a}$
1. Carbohydrate	8.6 ± 2.9	91.4 ± 2.9
2. Fat	5.8 ± 2.2	94.2 ± 2.2
3. Protein	5.9 ± 2.1	94.1 ± 2.1
4. Fasting, 25 ml of water	16.0 ± 7.1	84.0 ± 7.1
5. Fasting, 250 ml of water	17.8 ± 10.1	82.2 ± 10.1
Paired *t* test	4,5 > 1–3	2 > 4,5 3 > 5

It is concluded that ingestion of solid food prior to dosing aspirin tablets reduces circulating levels of both aspirin and salicylate during the 1st hr after dosing. This effect is not observed at later times. In fact, fatty meals may increase absorption, perhaps due to greater drug solubilization resulting from increased bile flow.

The absorption rate of aspirin, both as unchanged drug and as salicylate, was optimal when the drug was ingested with a relatively large volume of water on an empty stomach. These conclusions are consistent with observations made with other drugs examined under similar experimental conditions (10, 12).

REFERENCES

(1) G. Levy and A. Yacobi, *J. Clin. Pharmacol.*, **15**, 525 (1975).

(2) M. Gibaldi and B. Grundhofer, *J. Pharm. Sci.*, **64**, 1064 (1975).

(3) G. Levy, D. T. Lampman, B. L. Kamath, and L. K. Garrettson, *N. Engl. J. Med.*, **293**, 323 (1975).

(4) E. L. Parrott, *J. Pharm. Sci.*, **64**, 878 (1975).

(5) W. J. Decker, R. A. Shpall, D. G. Corby, H. F. Combs, and C. E. Payne, *Clin. Pharmacol. Ther.*, **10**, 710 (1969).

(6) S. Feldman and B. C. Carlstedt, *J. Am. Med. Assoc.*, **227**, 660 (1974).

(7) A. Perälä-Suominen, *Ann. Clin. Res., Suppl.*, **6**, 26 (1974).

(8) K. Frislid, E.-M. Haram, R. Norberg, and S. Oie, *Pharm. Acta Helv.*, **48**, 610 (1973).

(9) M. Mayersohn, *J. Am. Pharm. Assoc.*, **NS17**, 107 (1977).

(10) P. G. Welling, H. Huang, P. A. Koch, W. A. Craig, and P. O. Madsen, *J. Pharm. Sci.*, **66**, 549 (1977).

(11) M. Rowland and S. Riegelman, *ibid.*, **56**, 717 (1967).

(12) P. G. Welling, L. L. Lyons, W. A. Craig, and G. A. Trochta, *Clin. Pharmacol. Ther.*, **17**, 475 (1975).

(13) M. J. Rance, B. J. Jordan, and J. D. Nichols, *J. Pharm. Pharmacol.*, **27**, 425 (1975).

(14) M. Rowland and S. Riegelman, *J. Pharm. Sci.*, **57**, 1313 (1968).

(15) G. Levy, *ibid.*, **54**, 959 (1965).

ACKNOWLEDGMENTS

Supported by Public Health Service Grant GM 20327 from the National Institute of General Medical Sciences and by a grant from Glenbrook Laboratories.

Synthesis of Oximes, Aziridines, and Allyl Alcohols Derived from Substituted 1-Phenyl-1-nonen-3-ones as Potential Cytotoxic and Antitumor Agents

J. R. DIMMOCK *x, P. J. SMITH ‡, L. M. NOBLE ‡, and W. J. PANNEKOEK ‡

Received October 13, 1977, from the **College of Pharmacy and the* ‡*Department of Chemistry and Chemical Engineering, University of Saskatchewan, Saskatoon, Saskatchewan, S7N 0W0, Canada.* Accepted for publication March 7, 1978.

Abstract □ A number of nuclear-substituted 1-phenyl-1-nonen-3-one oximes were synthesized. Reduction of several of these compounds with lithium aluminum hydride yielded the corresponding 1-phenyl-2,3-epiminononanes, shown by 100-MHz NMR spectroscopy to be the *cis*-geometrical isomers. When several ring-substituted 4-dimethylaminomethyl-1-phenyl-1-nonen-3-ones were treated with hydroxylamine hydrochloride under forcing conditions, the product isolated was the corresponding oxime. Reaction under mild conditions led only to the isolation of the Michael addition product of the oxime in low yield. Reduction of some nuclear-substituted 4-dimethylaminomethyl-1-phenyl-1-nonen-3-ones with sodium borohydride led to the formation of the corresponding allyl alcohols, and the products were shown by ^{1}H- and ^{13}C-NMR spectroscopy to be the *threo*-isomers or, alternatively, a mixture of *erythro*- and *threo*-isomers. Reaction of phosphoric acid with one of the substituted allyl alcohols led to a diolefin, shown by NMR spectroscopy to be a mixture of (*E*, *E*)- and (*E*, *Z*)-isomers in a ratio of 65:35.

Keyphrases □ 1-Phenyl-1-nonen-3-one derivatives, various—synthesized □ Oximes—various 1-phenyl-1-nonen-3-one derivatives synthesized □ Aziridines—various 1-phenyl-1-nonen-3-one derivatives synthesized □ Allyl alcohols—various 1-phenyl-1-nonen-3-one derivatives synthesized

Drugs classified as alkylating agents are used extensively in cancer chemotherapy. While a number of these compounds are clinically available, additional alkylating agents are needed (1, 2). A group of novel alkylating agents that have received some attention are acyclic α,β-unsaturated ketones, some of which show antineoplastic activity (3–5). While the substituted styryl ketones I [$R_1 = R_2 = H$, Cl, or $N(CH_3)_2$] were virtually devoid of bioactivity (5), conversion to the corresponding Mannich bases led to compounds with promising antitumor and cytotoxic activities shown to be due, in part at least, to interference with mitochondrial function (6). It was decided, therefore, to prepare further analogs of I such as the oximes (II*a*–II*f*) and the Mannich bases of the oximes (V*a*–V*d*) (Scheme I).

A group of alkylating agents with marked antineoplastic activity are aziridines, including triethylenemelamine, which is used clinically (7). In addition, allyl alcohols have alkylating properties due to the stability of the carbonium ion. In the aryl-substituted allyl alcohols VI*a*–VI*d*, the carbonium ion would be expected to be further stabilized by delocalization of the positive charge on the ring. To this end, therefore, the preparation of the aziridines III*a*–III*d* and allyl alcohols was undertaken (Scheme I).

DISCUSSION

The ketones I were converted into the corresponding oximes (II*a*–II*f*) in yields ranging from 5 to 76%. 2-Benzylidenecyclohexanone oximes can be reduced with lithium aluminum hydride to give the corresponding 1-benzyl-1,2-epiminocyclohexanes in good yield (8). Reaction of the oximes with this reagent afforded the aziridines III*a*–III*d* in yields of approximately 20%.

Since steric factors in the reaction of aziridines with biological macromolecules are important (9), the configuration of the aziridines was determined using ^{1}H-NMR spectroscopy. The 100-MHz spectra of III*a*, III*c*, and III*d* were similar, with resonances at δ 2.6 (H_3 and H_4), 2.2 (H_2), and 2.0 (H_1) ppm (see Structure A). The resonance of H_1 was broadened because of coupling with the aliphatic side chain, so attention was focused on the coupling of protons 1 and 2 by examination of the H_2 resonance, which appeared as a quartet with J = 6.0 Hz. Decoupling of H_{3-4} changed the pattern to a doublet with $J_{1,2}$ = 6.0 Hz. The quartet at 2.2 ppm resulted from the combined effect of $H_{3,4}$ on H_2 with $J_{2-3,4}$ = 6.0 Hz and H_1 on H_2 with $J_{1,2}$ = 6.0 Hz, giving a doublet of triplets whose two inner lines coincided.

When an *ortho*-substituent was present on the phenyl ring (III*b*), a complex pattern for $H_{3,4}$ resulted since H_3 and H_4 were no longer magnetically equivalent. Decoupling H_3 and H_4 separately showed that $J_{2-3} = J_{2,4}$ = 6.0 Hz, with the coupling J_{1-2} being 6.0 Hz. Since the coupling between protons 1 and 2 was shown to be 6.0 Hz, the *cis*-configuration was attributed to the aziridines III*a*–III*d*. Several workers (10–12) reported the coupling of adjacent protons of *cis*-aziridines to be approximately 6 Hz while the coupling is approximately 3 Hz in the *trans*-isomers.

Oxime formation proceeded with difficulty in the attempted synthesis of V*a*–V*d*, and only V*b* and V*d* were obtained as crystalline solids in low yields. In an attempt to reduce by-product formation through lengthy heating conditions, IV*a* (as the free base) was reacted with hydroxylamine hydrochloride for a short time in methanol. From the reaction mixture, a low yield of colorless crystals was obtained and shown by ^{1}H-NMR spectroscopy, mass spectrometry, and elemental analysis to be the Michael addition product of the oxime of the Mannich base (VII).

The Mannich bases IV*b*, IV*d*, and IV*e* were reduced with sodium borohydride to give the allyl alcohols VI*a*–VI*c*, which allowed the possibility of a mixture of diastereoisomers. Examination of the ^{1}H-NMR spectrum of VI*b* gave an unresolved spectrum for which unequivocal assignments could not be made. The ^{13}C-NMR spectrum showed absorptions at 69.85, 59.05, and 39.64 ppm attributable to C-3 and C-4 as well as to the methylene carbon adjacent to the quadrivalent nitrogen atom. Off-resonance decoupling showed the peak at 59.05 ppm to be a triplet and was assigned to the methylene carbon atom. Since C-3 was situated at a position with increased deshielding relative to C-4, the peaks at 69.85 and 39.64 ppm were assigned to C-3 and C-4, respectively, with off-resonance decoupling indicating doublets centered at 69.85 and 39.64 ppm.

The ^{13}C-NMR spectra of VI*b* and the *threo*-isomer of VI*a* (13) were virtually superimposable. For VI*a*, the absorptions of C-3 and C-4 were at 70.04 and 39.76 ppm, respectively. ^{13}C-NMR spectroscopy of VI*c* showed absorptions at 69.48 and 39.83 ppm, which were assigned to C-3 and C-4, respectively, of the *threo*-isomer and at 76.41 and 40.32 ppm for the *erythro*-isomer. The ratio of the intensities of the *threo*- to the *erythro*-isomers was 40:60.

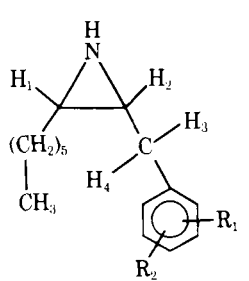

A

0022-3549/78/1100-1536$01.00/0
© 1978, American Pharmaceutical Association

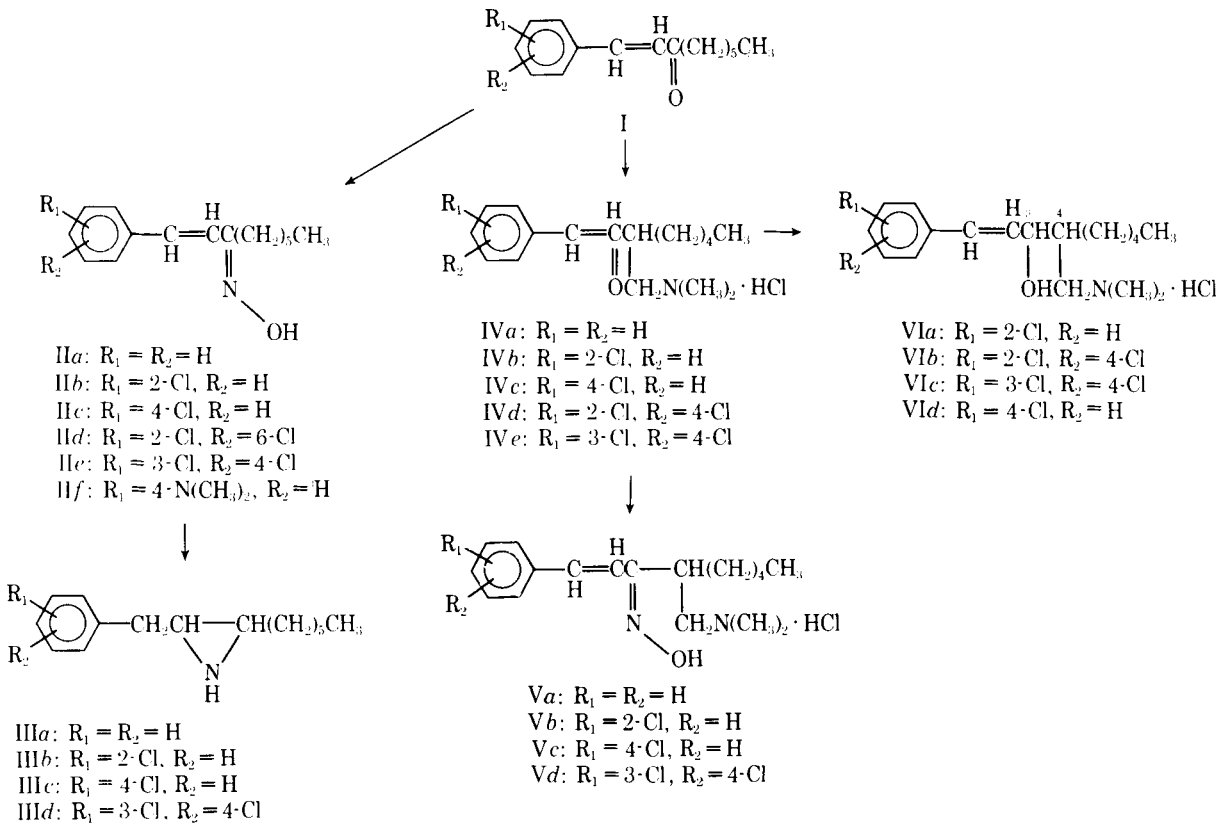

Scheme I

Reduction of IV*c* gave VI*d*, possessing the *threo*-configuration (13). This compound was treated with phosphoric acid in an attempt to prepare the phosphate ester as a candidate antineoplastic drug since certain cancerous tissue has a higher phosphatase content than other tissues (14). The product obtained was shown to be the corresponding diolefin. While the olefinic C-1 and C-2 atoms were seen from ^{1}H-NMR spectroscopy to have the (*E*)-configuration, the possibility exists of the product being a mixture of VIII*a* and VIII*b* because of variation in the spatial arrangements of the groups at C-3 and C-4.

In VIII*b*, the methylene group adjacent to the nitrogen is subject to steric impedance because the neighboring styryl group forces the electrons of the methylene protons toward the nitrogen atom, thereby causing a greater deshielding than in VIII*a*. ^{1}H-NMR spectroscopy indicated two *AB* quartets centered at 3.90 and 3.62 ppm, assigned to the methylene group adjacent to the nitrogen for VIII*b* and VIII*a*, respectively, in a ratio of 35:65.

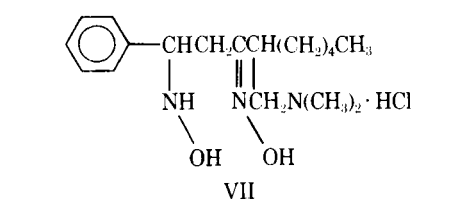

VII

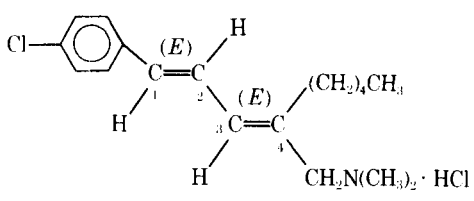

VIII*a*

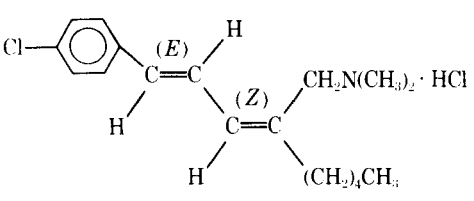

VIII*b*

EXPERIMENTAL[1]

Melting points are uncorrected. Organic extracts were washed with water and dried over anhydrous magnesium sulfate. After filtration, the solvent was removed *in vacuo*, using a water aspirator. NMR spectra[2] were carried out in deuterochloroform. GLC[3] was undertaken using a 3% methyl silicone gum rubber column[4] (1.524 m × 0.635 cm) unless otherwise stated.

1-Phenyl-1-nonen-3-one Oximes—1-Phenyl-1-nonen-3-one (15) (10.0 g, 0.046 mole) in ethanol (30 ml) was added to a stirring solution of hydroxylamine hydrochloride (3.6 g, 0.051 mole) and potassium acetate (5.0 g, 0.051 mole) in water (10 ml), and the mixture was heated to 60° for 1 hr. On cooling, the reaction mixture was extracted with ether to give a pale-yellow oil; its IR spectra showed the presence of unreacted ketone.

The oil was placed in sodium bisulfite solution (16) (200 ml), stirred for 1 hr, and extracted with ether, producing a colorless oil that solidified on cooling. Recrystallization from petroleum ether (bp 30–60°) gave 1-

[1] Elemental analyses were carried out by Mr. R. G. Teed of the Department of Chemistry and Chemical Engineering, University of Saskatchewan. Mass spectra (AE1 MS-12 mass spectrometer, Picker X-Ray Engineering Ltd., Montreal 304, Quebec, Canada) were determined at 70 ev by Mr. D. R. Bain, Department of Chemistry and Chemical Engineering, University of Saskatchewan. IR spectra (Beckman IR 8 spectrophotometer, Beckman Instruments Inc., Edmonton, Alberta, Canada) were determined as Nujol mulls with sodium chloride disks unless otherwise stated.

[2] For 60-MHz spectra: Bruker WP60 spectrophotometer, Brucker Spectrospin (Canada) Ltd., Mississauga, Ontario, L5L 1J9, Canada, and Varian T60 spectrophotometer, Varian Associates of Canada Ltd., Georgetown, Ontario, L7G 2J4, Canada. For 100-MHz spectra: Varian HA 100-12 spectrophotometer, Varian Associates of Canada Ltd., Georgetown, Ontario, L7G 2J4, Canada.

[3] Varian Aerograph model 90-P, Varian Associates of Canada Ltd., Georgetown, Ontario, L7G 2J4, Canada.

[4] All GLC columns were obtained from Varian Associates of Canada Ltd., Edmonton, Alberta, Canada.

Table I—Substituted 1-Phenyl-1-nonen-3-one Oximes

Compound	Yield, %	Melting Point	Molecular Formula	Analysis, % Calc.	Found
II*b*	39	74–75°	$C_{15}H_{20}ClNO$	C 67.80	67.84
				H 7.53	7.32
				N 5.27	5.30
II*c*	66	90–91°	$C_{15}H_{20}ClNO$	C 67.80	68.00
				H 7.53	7.67
				N 5.27	5.29
II*d*	5	56.5–57°	$C_{15}H_{19}Cl_2NO$	C 60.00	60.29
				H 6.33	6.38
				N 4.67	4.54
II*e*	76	101–102°	$C_{15}H_{19}Cl_2NO$	C 60.00	60.38
				H 6.33	6.40
				N 4.67	4.60
II*f*	30	88–89°	$C_{17}H_{26}NO$	C 74.45	74.37
				H 9.49	9.62
				N 10.22	10.25

Table II—Substituted 1-Phenyl-2,3-epiminononanes [a]

Compound	Yield, %	Boiling Point (°/mm)	Molecular Formula	Analysis, % Calc.	Found
III*a*	13	127°/0.05	$C_{15}H_{23}N$	C 82.95	83.15
				H 10.60	10.84
				N 6.45	6.37
III*b*	12	124°/0.07	$C_{15}H_{22}ClN$	C 71.57	71.45
				H 8.75	9.03
				N 5.57	5.50
III*c*	26	128°/0.05	$C_{15}H_{22}ClN$	C 71.57	71.63
				H 8.75	9.11
				N 5.57	5.44
III*d*	24	147°/0.06	$C_{15}H_{21}Cl_2N$	C 62.94	63.04
				H 7.34	7.53
				N 4.90	4.81

[a] The value of J_{2-3} was 6.0 Hz for each compound.

phenyl-1-nonen-3-one oxime (30% yield), mp 72–73°, as colorless needles; IR: 3220 (br) (OH), 1635 (w) (C=N), 1620 (w) (C=C), 965 (w) (HC=CH), and 950 (w) (NO) cm^{-1}; ^{1}H-NMR: δ 9.35 (broad, 1, NOH), 7.0–7.5 (m, 5, C_6H_5), 6.6 (s, 2, C_1H and C_2H), 2.2–2.85 (m, 2, C_4H_2), 1.1–2.0 [m, 8, $(CH_2)_4$], and 0.7–1.15 (m, 3, C_9H_3) ppm.

Anal.—Calc. for $C_{15}H_{21}NO$: C, 77.92; H, 9.09; N, 6.06. Found: C, 77.87; H, 9.24; N, 6.06.

Compounds II*b*, II*c*, II*e*, and II*f* were prepared similarly from the corresponding substituted 1-phenyl-1-nonen-3-ones (15), except that the use of sodium bisulfite solution was unnecessary and II*f* was recrystallized from petroleum ether (bp 100–120°). The oximes, except II*f*, appeared as colorless needles; II*f* appeared as yellow prisms.

In preparing II*d* from 1-(2,6-dichlorophenyl)-1-nonen-3-one (15), equimolar amounts of reactants were heated at 60° for 36 hr. The crude product was treated exhaustively with sodium bisulfite solution until no more unreacted ketone was present (IR evidence). The resultant oil was dissolved in petroleum ether (bp 30–60°), and flocculent colorless crystals of II*d* deposited after storage at −10° for 3 weeks. The structures of the oximes II*b*–II*f* were confirmed by IR and NMR spectroscopy, and some of the physical data are summarized in Table I.

1-Phenyl-2,3-epiminononanes (III)—A solution of 1-phenyl-1-nonen-3-one oxime (25.2 g, 0.109 mole) in dry ether (200 ml) was added dropwise to a stirring suspension of lithium aluminum hydride (6.6 g, 0.17 mole) in dry ether (120 ml), and the resultant mixture was heated under reflux for 24 hr. On cooling, the reaction complex was decomposed by the dropwise addition of methanol and subsequently water. After filtration, the ethereal extract was washed with water (3 × 100 ml) and dried.

Evaporation of the solvent gave a pale-yellow oil (7.5 g), showed by GLC to consist of two components in the ratio of 90:10. Fractional distillation gave 1-phenyl-2,3-epiminononane (5.4 g, 13% yield), bp 127°/0.05 mm, as a colorless oil, shown by GLC to be one component; IR (neat): 3225 (br) (NH) cm^{-1}; ^{1}H-NMR: δ 7.25 (s, 5, C_6H_5), 2.75 (d, 2, C_1H), 1.9–2.5 (br, 3, C_2H, C_3H, NH), 1.1–1.8 [m, 10, $(CH_2)_5$], and 0.65–1.1 (m, 3, C_9H_3) ppm.

Attempts to separate completely the two components of the crude reaction mixture by preparative GLC were unsuccessful. A 3% methyl silicone gum rubber column[5] (1.524 m × 0.635 cm) was best; columns (6.096 m × 0.953 cm) containing polyethylene glycol[6], methyl phenyl silicone[7], free fatty acid phase modified polyethylene glycol[8], octylphenoxyethanol[9], liquid methyl silicone[10], poly(*m*-phenyl) ether[11], and diethylene glycol succinate[12] gave only poor resolution. An oil containing the minor component of the crude reaction product as the principal product (60%) was obtained by preparative GLC, using a methyl silicone gum rubber column[5] (1.524 m × 0.635 cm), and examined by mass spectrometry. The parent ion, *m/e* 219, and a prominent peak at *m/e* 114, due probably to an α-cleavage fragment ion, suggested that the minor component in the crude reaction mixture was 3-amino-1-phenylnonane.

When the reaction between 1-phenyl-1-nonen-3-one oxime and lithium aluminum hydride was carried out in the presence of dry tetrahydrofuran in place of ether, the major product (85%) was 1-phenyl-2,3-epiminononane with the saturated amine as the minor product (15%).

Reaction of oximes II*b*, II*c*, and II*e* with lithium aluminum hydride in dry ether gave reaction products consisting of two components; these components could not be separated by preparative GLC. Purification of the crude mixtures by fractional distillation afforded 1-(2-chlorophenyl)-2,3-epiminononane (III*b*), 1-(4-chlorophenyl)-2,3-epiminononane (III*c*), and 1-(3,4-dichlorophenyl)-2,3-epiminononane (III*d*) (Table II).

Oximes V*a*–V*d* and VII—The free Mannich base (4.5 g, 0.015 mole), obtained from the hydrochloride salt IV*b* (17) by basifying with aqueous sodium hydroxide solution at 0° and extracting with ether, was heated with hydroxylamine hydrochloride (1.4 g, 0.02 mole) in methanol (10 ml) for 48 hr. Removal of the solvent gave a viscous yellow oil, which gave a semisolid on trituration with ether. The semisolid was boiled with acetone for 1 min, producing a finely divided powder (0.8 g). This powder was recrystallized from acetone–methanol to give V*b* as colorless prisms (0.53 g, 10% yield), mp 175°; IR: 3120 (br) (OH), 2650 (br) $[CN^+H(CH_3)_2]$, 1610 (w) (C=N), 1590 (w) (CH=CH), 960 (m) (CH=CH), and 930 (m) (NO) cm^{-1}; mass spectrum: *m/e* 322 (M^+ − HCl) (0.16%) and 58 (100).

Anal.—Calc. for $C_{18}H_{28}Cl_2N_2O$: C, 60.17; H, 7.80; N, 7.80. Found: C, 60.11; H, 7.27; N, 7.77.

The 3,4-dichloro derivative V*d* was prepared similarly as colorless prisms (13%), mp 192°; IR: 3120 (br) (OH), 2660 (br) $[CN^+H(CH_3)_2]$, 1620 (w) (C=N), 1590 (w) (CH=CH), 960 (m) (CH=CH), and 940 (m) (NO) cm^{-1}; mass spectrum: *m/e* 356 (M^+ − HCl) (0.01%) and 58 (100).

Anal.—Calc. for $C_{18}H_{27}Cl_3N_2O$: C, 54.89; H, 6.86; N, 7.12. Found: C, 54.65; H, 6.83; N, 7.04.

Attempts to form V*a* and V*c* gave only viscous oils from which no crystalline material could be obtained.

4-Dimethylaminomethyl-1-phenyl-1-nonen-3-one (50.0 g, 0.18 mole), obtained by neutralization of IV*a* (*vide supra*), was added to hydroxylamine hydrochloride (27.8 g, 0.4 mole) in methanol (100 ml) at 0°. The resultant mixture was heated under reflux for 2 hr. The solvent was removed partially, and ether was added. Upon refrigeration at −10°, colorless plates of 4-dimethylaminomethyl-1-hydroxyamino-1-phenylnonan-3-one oxime hydrochloride (VII) (3.2 g, 5% yield), mp 177–178°, were obtained; IR: 3220 and 3260 (br) (OH), 2680 (br) $[CN^+(CH_3)_2]$, 1640 (w) (C=N), and 935 (w) (NO) cm^{-1}; mass spectrum: *m/e* 321 (M^+ − HCl) (0.4%), 58 (100), and 44 (20.1).

Anal.—Calc. for $C_{18}H_{32}ClN_3O_2$: C, 60.42; H, 8.95; N, 11.75. Found: C, 59.21; H, 8.45; N, 11.28.

Allyl Alcohols VI—To a solution of 1-(3,4-dichlorophenyl)-4-dimethylaminomethyl-1-nonen-3-one (15.6 g, 0.045 mole), obtained by basification of IV*e* (*vide supra*) in methanol (90 ml) cooled at 0°, was added sodium borohydride (15.1 g, 0.04 mole) in water (150 ml, pH adjusted to 9 with aqueous sodium hydroxide). This solution was stirred at 5–8° for 1 hr and then heated under reflux for 3 hr. On cooling, aqueous hydrochloric acid was added to adjust the pH to 5. Evaporation of the solvent gave a white semisolid, which was dissolved in water and extracted with ether.

The aqueous extracts were basified with aqueous sodium hydroxide and extracted with ether. Evaporation of the ether gave a pale-yellow oil (10 g). On treatment with ethanolic hydrochloric acid (10% w/v), the oil deposited a colorless solid, which was recrystallized from dry acetone, yielding (*E*)-1-(3,4-dichlorophenyl)-4-dimethylaminomethyl-1-nonen-3-ol (VI*c*) (5.5 g, 32%), mp 139.5°, as colorless needles; IR: 3320 (br) (OH), 2670 (br) $[CN^+H(CH_3)_2]$, 1570 (w) (CH=CH), and 960 (m) (CH=CH)

[5] SE-30
[6] Carbowax 20M column (20%).
[7] OV-17 column (20%).
[8] FFAP column (20%).
[9] Triton X-100 column (20%).
[10] OV-101 column (3%).
[11] PMPE column (20%).
[12] DEGS column (30%).

cm^{-1}; mass spectrum: *m/e* 343 (M^+ − HCl) (1.8%), 345 (0.9), and 58 (100); ^{1}H-NMR: δ 7.67–6.07 (m, 5, C_6H_3, C_1H and C_2H), 4.9 (ragged t, 1, C_3H), 4.27–2.50 [m, 8, $CH_2N(CH_3)_2$], 2.50–1.77 (broad s, 1, C_4H), 1.28 [s, 8, $(CH_2)_4$], and 0.83 (t, 3, CH_3) ppm.

Anal.—Calc. for $C_{18}H_{28}Cl_3NO$: C, 56.76; H, 7.36; N, 3.68. Found: C, 56.82; H, 7.42; N, 3.67.

The 2,4-dichloro analog VI*b*, prepared in a similar manner in 38% yield, was recrystallized from dry acetone as colorless needles, mp 142.5°; IR: 3320 (br) (OH), 2680 (br) [$NH^+(CH_3)_2$], 1580 (w) (CH=CH), and 955 (m) (CH=CH); mass spectrum: *m/e* 343 (M^+ − HCl) (0.9%), 345 (0.6), and 58 (100); ^{1}H-NMR ($CDCl_3$): δ 7.56–6.70 (m, 4, C_6H_3 and C_1H), 6.50–5.96 (dd, 1, C_2H), 4.83 (ragged t, 1, C_3H), 4.08–2.53 [m, 8, $CH_2N(CH_3)_2$], 2.53–1.90 (broad s, 1, C_4H), 1.30 [s, 8, $(CH_2)_4$], and 0.87 (t, 3, CH_3) ppm.

Anal.—Calc. for $C_{18}H_{28}Cl_3NO$: C, 56.76; H, 7.36; N, 3.68. Found: C, 57.03; H, 7.14; N, 3.69.

1-(*p*-Chlorophenyl) - 4-dimethylaminomethyl - 1,3-nonadiene Hydrochloride—*threo*-(*E*)-1-(*p*-Chlorophenyl) - 4-dimethylaminomethyl-1-nonen-3-ol (10 g, 0.029 mole), mp 157° [lit. (13) mp 151–152°], prepared by the published procedure (13), was added to phosphoric acid (85% v/v). The solution was stirred at room temperature for 24 hr. The reaction mixture, on extraction with ether, gave a yellow oil (3.2 g). This oil was treated with ethanolic hydrochloric acid (10% w/v) to give a colorless solid.

Recrystallization of the precipitate from ether–ethanol gave 1-(*p*-chlorophenyl)-4-dimethylaminomethyl-1,3-nonadiene hydrochloride (1.4 g, 15%), mp 203°, as colorless plates; IR (free base, neat): 3020 (w) (CH=CH), 2760, 2800 (m) (NCH_3), 1625 (w) (CH=CH), and 945 (s) (CH=CH); mass spectrum: *m/e*: 291 (M^+ − HCl) (21%), 220 (35), and 58 (100); ^{1}H-NMR ($CDCl_3$): δ 7.30 (s, 4, C_6H_4), 7.27–6.17 (m, 3, C_1H, C_2H, C_3H), 4.10–2.30 [m, 8, $CH_2N(CH_3)_2$], 1.40 [s, 8, $(CH_2)_4$], and 0.83 (t, 3, CH_3) ppm.

Anal.—Calc. for $C_{18}H_{27}Cl_2N$: C, 74.10; H, 8.92; N, 4.80. Found: C, 74.73; H, 8.56; N, 4.80.

REFERENCES

(1) T. A. Connors, *Cancer Res.*, **29**, 2443 (1969).

(2) C. Heidelberger, *ibid.*, **29**, 2435 (1969).

(3) O. K. Kabiev and S. M. Vermenichev, *Izv. Akad. Nauk Kaz. SSR, Ser. Biol.*, **9**, 72 (1971); through *Chem. Abstr.*, **75**, 47091u (1971).

(4) A. Furst, W. C. Cutting, and R. H. Driesback, *Stanford Med. Bull.*, **12**, 190 (1954); through *Chem. Abstr.*, **49**, 515e (1955).

(5) J. R. Dimmock and W. G. Taylor, *J. Pharm. Sci.*, **64**, 241 (1975).

(6) J. R. Dimmock, N. W. Hamon, K. W. Hindmarsh, L. E. Negrave, D. G. Mills, G. H. Rank, and A. J. Robertson, *ibid.*, **65**, 482 (1976).

(7) J. A. Stock, in "Drug Design," vol. 2, E. J. Ariens, Ed., Academic, New York, N.Y., 1971, p. 531.

(8) J. R. Dimmock, W. A. Turner, P. J. Smith, and R. G. Sutherland, *Can. J. Chem.*, **51**, 427 (1973).

(9) Y. Hata, M. Watanabe, T. Matsubara, and A. Touchi, *J. Am. Chem. Soc.*, **98**, 6033 (1976).

(10) Y. Diab, A. Laurent, and P. Mison, *Tetrahedron Lett.*, **1974**, 1605.

(11) K. Kotera, Y. Matsukawa, H. Takahashi, T. Okada, and K. Kitahonoki, *Tetrahedron*, **24**, 6177 (1968).

(12) A. Hassner and C. C. Heathcock, *Tetrahedron Lett.*, **1964**, 1125.

(13) W. G. Taylor and J. R. Dimmock, *Can. J. Chem.*, **52**, 2522 (1974).

(14) H. Druckrey and S. Raabe, *Klin. Wochenschr.*, **30**, 882 (1952).

(15) P. J. Smith, J. R. Dimmock, and W. G. Taylor, *Can. J. Chem.*, **50**, 871 (1972).

(16) A. I. Vogel, "A Textbook of Practical Organic Chemistry," 3rd ed., Longmans, Green, London, England, 1956, p. 332.

(17) J. R. Dimmock and W. G. Taylor, *J. Pharm. Sci.*, **63**, 69 (1974).

ACKNOWLEDGMENTS

The authors thank the Medical Research Council of Canada for the award of an operating grant (MA 5538) to J. R. Dimmock and also the Prairie Regional Laboratory for access to their 100-MHz NMR spectrometer.

Effect of Antineoplastic and Cytotoxic Mannich Bases Derived from Conjugated Styryl Ketones on Mitochondrial Respiration in Rat Liver Cells

N. W. HAMON *x, D. L. BASSENDOWSKI *, D. E. WRIGHT *, J. R. DIMMOCK *, and L. M. NOBLE ‡

Received November 28, 1977, from the **College of Pharmacy and the* ‡*Department of Chemistry and Chemical Engineering, University of Saskatchewan, Saskatoon, Saskatchewan, S7N 0W0, Canada.* Accepted for publication March 7, 1978.

Abstract □ Five cytotoxic Mannich bases (5-dimethylamino-1-substituted phenyl-1-penten-3-ones), three having antineoplastic activity, were evaluated for respiratory-inhibiting properties in rat liver mitochondria in the presence of four substrates: succinate, glutamate, 3-hydroxybutyrate, and palmitylcarnitine. Four compounds (I*b*–I*e*) showed significant inhibiting properties which, on occasion, were reversed partially by coenzyme Q_{10}. Evaluation of the spectra of the mitochondrial cytochromes indicated that I*b*–I*e* blocked the electron transport chain prior to the sequence of cytochromes. Since inhibition occurred when different substrates were used, a common site of action for I*b*–I*e* is likely; competition of I*b*–I*e* with coenzyme Q_{10} probably occurs. Compounds I*a*–I*e* inhibited RNA polymerase from Swiss mouse kidney cells but were virtually bereft of activity *versus* RNA polymerase from L-1210 leukemia cells. Polarography of the Mannich bases and the related styryl ketones showed that antineoplastic activity was associated with higher half-wave potentials.

Keyphrases □ 1-Phenyl-1-penten-3-one derivatives—effect on enzyme activity in rat liver mitochondria, various substrates □ Enzyme activity—effect of 1-phenyl-1-penten-3-one derivatives in rat liver mitochondria □ Structure–activity relationships—1-phenyl-1-penten-3-one derivatives evaluated for effect on enzyme activity in rat liver mitochondria

Mannich bases have a wide range of biological activities including antimicrobial effects (1–3), analgesic activity (4), local anesthetic properties (5, 6), and psychotropic effects (7). Recently, a number of Mannich bases and related compounds including 5-dimethylamino-1-substituted phenyl-1-penten-3-ones I*a*–I*e* were shown to have cyto-

0022-3549/78/1100-1539$01.00/0

© 1978, American Pharmaceutical Association

cm^{-1}; mass spectrum: *m/e* 343 (M^+ − HCl) (1.8%), 345 (0.9), and 58 (100); ^{1}H-NMR: δ 7.67–6.07 (m, 5, C_6H_3, C_1H and C_2H), 4.9 (ragged t, 1, C_3H), 4.27–2.50 [m, 8, $CH_2N(CH_3)_2$], 2.50–1.77 (broad s, 1, C_4H), 1.28 [s, 8, $(CH_2)_4$], and 0.83 (t, 3, CH_3) ppm.

Anal.—Calc. for $C_{18}H_{28}Cl_3NO$: C, 56.76; H, 7.36; N, 3.68. Found: C, 56.82; H, 7.42; N, 3.67.

The 2,4-dichloro analog VI*b*, prepared in a similar manner in 38% yield, was recrystallized from dry acetone as colorless needles, mp 142.5°; IR: 3320 (br) (OH), 2680 (br) [$NH^+(CH_3)_2$], 1580 (w) (CH=CH), and 955 (m) (CH=CH); mass spectrum: *m/e* 343 (M^+ − HCl) (0.9%), 345 (0.6), and 58 (100); ^{1}H-NMR ($CDCl_3$): δ 7.56–6.70 (m, 4, C_6H_3 and C_1H), 6.50–5.96 (dd, 1, C_2H), 4.83 (ragged t, 1, C_3H), 4.08–2.53 [m, 8, $CH_2N(CH_3)_2$], 2.53–1.90 (broad s, 1, C_4H), 1.30 [s, 8, $(CH_2)_4$], and 0.87 (t, 3, CH_3) ppm.

Anal.—Calc. for $C_{18}H_{28}Cl_3NO$: C, 56.76; H, 7.36; N, 3.68. Found: C, 57.03; H, 7.14; N, 3.69.

1-(*p*-Chlorophenyl) - 4-dimethylaminomethyl - 1,3-nonadiene Hydrochloride—*threo*-(*E*)-1-(*p*-Chlorophenyl) - 4-dimethylaminomethyl-1-nonen-3-ol (10 g, 0.029 mole), mp 157° [lit. (13) mp 151–152°], prepared by the published procedure (13), was added to phosphoric acid (85% v/v). The solution was stirred at room temperature for 24 hr. The reaction mixture, on extraction with ether, gave a yellow oil (3.2 g). This oil was treated with ethanolic hydrochloric acid (10% w/v) to give a colorless solid.

Recrystallization of the precipitate from ether–ethanol gave 1-(*p*-chlorophenyl)-4-dimethylaminomethyl-1,3-nonadiene hydrochloride (1.4 g, 15%), mp 203°, as colorless plates; IR (free base, neat): 3020 (w) (CH=CH), 2760, 2800 (m) (NCH_3), 1625 (w) (CH=CH), and 945 (s) (CH=CH); mass spectrum: *m/e*: 291 (M^+ − HCl) (21%), 220 (35), and 58 (100); ^{1}H-NMR ($CDCl_3$): δ 7.30 (s, 4, C_6H_4), 7.27–6.17 (m, 3, C_1H, C_2H, C_3H), 4.10–2.30 [m, 8, $CH_2N(CH_3)_2$], 1.40 [s, 8, $(CH_2)_4$], and 0.83 (t, 3, CH_3) ppm.

Anal.—Calc. for $C_{18}H_{27}Cl_2N$: C, 74.10; H, 8.92; N, 4.80. Found: C, 74.73; H, 8.56; N, 4.80.

REFERENCES

(1) T. A. Connors, *Cancer Res.*, **29**, 2443 (1969).

(2) C. Heidelberger, *ibid.*, **29**, 2435 (1969).

(3) O. K. Kabiev and S. M. Vermenichev, *Izv. Akad. Nauk Kaz. SSR, Ser. Biol.*, **9**, 72 (1971); through *Chem. Abstr.*, **75**, 47091u (1971).

(4) A. Furst, W. C. Cutting, and R. H. Driesback, *Stanford Med. Bull.*, **12**, 190 (1954); through *Chem. Abstr.*, **49**, 515e (1955).

(5) J. R. Dimmock and W. G. Taylor, *J. Pharm. Sci.*, **64**, 241 (1975).

(6) J. R. Dimmock, N. W. Hamon, K. W. Hindmarsh, L. E. Negrave, D. G. Mills, G. H. Rank, and A. J. Robertson, *ibid.*, **65**, 482 (1976).

(7) J. A. Stock, in "Drug Design," vol. 2, E. J. Ariens, Ed., Academic, New York, N.Y., 1971, p. 531.

(8) J. R. Dimmock, W. A. Turner, P. J. Smith, and R. G. Sutherland, *Can. J. Chem.*, **51**, 427 (1973).

(9) Y. Hata, M. Watanabe, T. Matsubara, and A. Touchi, *J. Am. Chem. Soc.*, **98**, 6033 (1976).

(10) Y. Diab, A. Laurent, and P. Mison, *Tetrahedron Lett.*, **1974**, 1605.

(11) K. Kotera, Y. Matsukawa, H. Takahashi, T. Okada, and K. Kitahonoki, *Tetrahedron*, **24**, 6177 (1968).

(12) A. Hassner and C. C. Heathcock, *Tetrahedron Lett.*, **1964**, 1125.

(13) W. G. Taylor and J. R. Dimmock, *Can. J. Chem.*, **52**, 2522 (1974).

(14) H. Druckrey and S. Raabe, *Klin. Wochenschr.*, **30**, 882 (1952).

(15) P. J. Smith, J. R. Dimmock, and W. G. Taylor, *Can. J. Chem.*, **50**, 871 (1972).

(16) A. I. Vogel, "A Textbook of Practical Organic Chemistry," 3rd ed., Longmans, Green, London, England, 1956, p. 332.

(17) J. R. Dimmock and W. G. Taylor, *J. Pharm. Sci.*, **63**, 69 (1974).

ACKNOWLEDGMENTS

The authors thank the Medical Research Council of Canada for the award of an operating grant (MA 5538) to J. R. Dimmock and also the Prairie Regional Laboratory for access to their 100-MHz NMR spectrometer.

Effect of Antineoplastic and Cytotoxic Mannich Bases Derived from Conjugated Styryl Ketones on Mitochondrial Respiration in Rat Liver Cells

N. W. HAMON *x, D. L. BASSENDOWSKI *, D. E. WRIGHT *, J. R. DIMMOCK *, and L. M. NOBLE ‡

Received November 28, 1977, from the **College of Pharmacy and the* ‡*Department of Chemistry and Chemical Engineering, University of Saskatchewan, Saskatoon, Saskatchewan, S7N 0W0, Canada.* Accepted for publication March 7, 1978.

Abstract □ Five cytotoxic Mannich bases (5-dimethylamino-1-substituted phenyl-1-penten-3-ones), three having antineoplastic activity, were evaluated for respiratory-inhibiting properties in rat liver mitochondria in the presence of four substrates: succinate, glutamate, 3-hydroxybutyrate, and palmitylcarnitine. Four compounds (I*b*–I*e*) showed significant inhibiting properties which, on occasion, were reversed partially by coenzyme Q_{10}. Evaluation of the spectra of the mitochondrial cytochromes indicated that I*b*–I*e* blocked the electron transport chain prior to the sequence of cytochromes. Since inhibition occurred when different substrates were used, a common site of action for I*b*–I*e* is likely; competition of I*b*–I*e* with coenzyme Q_{10} probably occurs. Compounds I*a*–I*e* inhibited RNA polymerase from Swiss mouse kidney cells but were virtually bereft of activity *versus* RNA polymerase from L-1210 leukemia cells. Polarography of the Mannich bases and the related styryl ketones showed that antineoplastic activity was associated with higher half-wave potentials.

Keyphrases □ 1-Phenyl-1-penten-3-one derivatives—effect on enzyme activity in rat liver mitochondria, various substrates □ Enzyme activity—effect of 1-phenyl-1-penten-3-one derivatives in rat liver mitochondria □ Structure–activity relationships—1-phenyl-1-penten-3-one derivatives evaluated for effect on enzyme activity in rat liver mitochondria

Mannich bases have a wide range of biological activities including antimicrobial effects (1–3), analgesic activity (4), local anesthetic properties (5, 6), and psychotropic effects (7). Recently, a number of Mannich bases and related compounds including 5-dimethylamino-1-substituted phenyl-1-penten-3-ones I*a*–I*e* were shown to have cyto-

0022-3549/78/1100-1539$01.00/0

© 1978, American Pharmaceutical Association

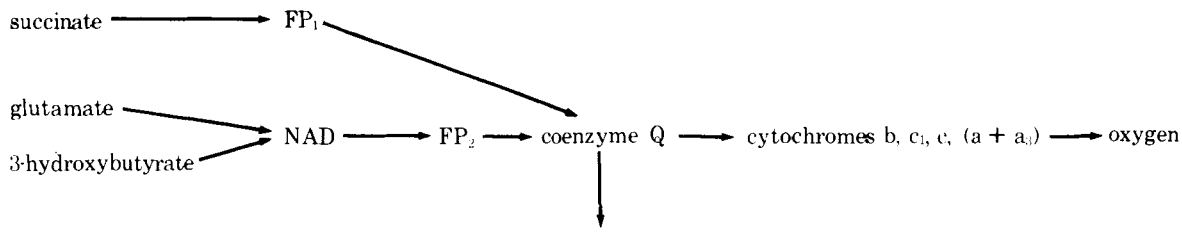

Scheme I

toxic activities in the KB *in vitro* screen (Table I) (8), which may be an indication of tumor-inhibiting properties (9). While I*a*–I*e* showed no activity in the L-1210 lymphoid leukemia screen in mice, three of the derivatives were assessed in the murine P-388 lymphocytic leukemia test system and showed antineoplastic activity at low dose levels (8).

Since certain compounds containing a benzylidene group attached to electron-withdrawing functions, such as cyano and nitro moieties, interfere with mitochondrial functions (10) and some anticancer agents interfere with mitochondria (11), solutions of I*a*–I*e* were added to disks on complex ethanol and complex glucose media inoculated with a strain of *Saccharomyces cerevisiae* (12). In the absence of mitochondrial function, the yeast will grow on complex glucose medium because energy is provided by glucose fermentation. However, the complex ethanol medium contains a nonfermentable energy source and interference with mitochondrial function prevents yeast growth. Thus, a comparison of the differential in growth on these two media in the presence of inhibitors gives a quantitative estimation of the efficacy in blocking mitochondrial function.

Table I shows that the biological activities of I*a*–I*e* may be attributed, in part at least, to interference with mitochondrial function in *S. cerevisiae*. The questions arise whether rat liver mitochondria are also inhibited by I*a*–I*e* and what processes occurring in the mitochondria are affected by these Mannich bases.

RESULTS AND DISCUSSION

A number of important biochemical events occur in the mitochondria, including oxidative phosphorylation, the fatty acid and citric acid cycles, and ion transport activities (13). In this study, the effect of I*a*–I*e* on respiration was investigated. In normal cells, respiration is coupled to phosphorylation in a process referred to as oxidative phosphorylation. This process occurs when a number of substrates such as succinate, pyruvate, and malate are reduced by dehydrogenases and the pairs of electrons formed are transferred to coenzyme Q *via* either flavoproteins or an NAD–flavoprotein route. The electrons are then transferred by a series of cytochromes from coenzyme Q_{10} to molecular oxygen, which is then reduced to water (14).

The various substrates added to isolated rat liver mitochondria were succinate, glutamate, 3-hydroxybutyrate, and palmitylcarnitine; electrons are transferred from these four substrates to coenzyme Q_{10} by three mechanisms involving separate flavoproteins designated FP_1, FP_2, and FP_3 (Scheme I). Table II shows the effects of various concentrations of the Mannich bases I*b*–I*e* on mitochondrial respiration in the presence of the four substrates. At the dose levels examined, all compounds except I*a* had inhibiting properties; I*a* showed the weakest effect on interference with mitochondrial function with *S. cerevisiae* and also had the lowest cytotoxicity in the KB screen.

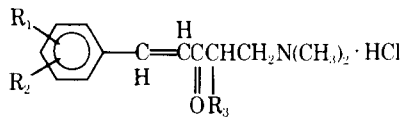

I*a*: $R_1 = R_2 = R_3 = H$

I*b*: $R_1 = R_2 = H$, $R_3 = (CH_2)_4CH_3$

I*c*: $R_1 = 2\text{-Cl}$, $R_2 = 4\text{-Cl}$, $R_3 = (CH_2)_4CH_3$

I*d*: $R_1 = 2\text{-Cl}$, $R_2 = 6\text{-Cl}$, $R_3 = (CH_2)_4CH_3$

I*e*: $R_1 = 3\text{-Cl}$, $R_2 = 4\text{-Cl}$, $R_3 = (CH_2)_4CH_3$

The inhibition of respiration that occurred on addition of the drug showed that only uncoupling of oxidative phosphorylation did not occur since well-known uncouplers such as 2,4-dinitrophenol added to the mitochondria gave a rapid increase in oxygen consumption. The question arises as to the site of action of I*a*–I*e* in the electron transport chain. An examination of the normal difference spectra of the mitochondria under both aerobic and anaerobic conditions revealed the presence of cytochromes c and a_3 in both the oxidized and reduced forms (15), respectively, after the addition of succinate to the anaerobic sample. However, in the presence of I*b*–I*e*, cytochromes c and a_3 remained in the oxidized state in the presence of succinate under anaerobic conditions. This result indicates that the point of blockage of these compounds likely occurs before cytochrome c.

When antimycin A was added to the mitochondria, cytochromes c and a were blocked, but, in addition, a difference spectrum also was obtained for cytochrome b. This finding confirms that antimycin A blocks the transfer of electrons to cytochrome b (16). The failure of the Mannich bases I*b*–I*e* to act in a similar manner to antimycin A suggests that they have a different point of inhibition than antimycin A or that blockade of the electron transport chain by these compounds occurred between cytochromes b and c. The possibility also exists that cytochrome b is not on the direct respiratory chain but may represent a side or shunt pathway.

The fact that I*b*–I*e* inhibited each substrate suggested a common site of action, namely, coenzyme Q_{10}. Table II shows that the inhibitory effect of I*b*–I*e* on respiration may be reversed by the addition of coenzyme Q_{10}. This finding strengthens the hypothesis that the Mannich bases, which

Table I—Effect of the Mannich Bases against the KB Tumor, P-388 Lymphocytic Leukemia, and Yeast Mitochondria [a]

Compound	KB [b]	P-388 Lymphocytic Leukemia [c]	Mean Area of Inhibition of *S. cerevisiae* [d] Growth in Presence of I [e]	
			Complex Ethanol Medium, mm^2	Complex Glucose Medium, mm^2
I*a*	11	N.A.	32.4	0.0
I*b*	1.5	N.A.	307.7	15.2
I*c*	1.0	130 (18)	123.2	41.5
I*d*	2.8	115 (28)	41.5	0.0
I*e*	1.2	142 (6.25)	128.7	27.9

[a] With the exception of the KB result for I*a*, the data are taken from Refs. 8 and 12 (reproduced with permission of the copyright owner). [b] The figures, in micrograms per milliliter, in the KB cell culture screen indicate the dose inhibiting 50% growth of human epidermoid carcinoma of the nasopharynx in Eagle's medium. [c] Compounds I*c* and I*e* were dissolved in saline, and I*d* was dissolved in hydroxypropylcellulose. The solutions of I*d* and I*e* were injected intraperitoneally into BDF_1 mice; with I*c*, the CDF_1 strain was used. Nine daily injections were made with I*c* and I*e*, and one injection every 4 days was made with I*d*. The figures quoted are the maximum activities obtained and are ratios of the survival time of treated animals to control animals expressed as a percentage. The figures in parentheses are the optimum doses in milligrams per kilogram. N.A. = result not available. [d] Strain GR 13 constructed in the Department of Biology, University of Saskatchewan, Saskatoon, Saskatchewan, Canada. [e] The concentration of solutions added to the medium was 5 mg/ml for I*a* and I*b* and 1 mg/ml for I*c*–I*e*.

Table II—Inhibition of Respiration in Rat Liver Mitochondria by Ib–Ie Using Different Substrates

Compound	Concentration, μmoles	Succinate				Glutamate				3-Hydroxybutyrate				Palmitylcarnitine			
		Inhibition, %	SE	Reversal with Ubiquinone, %	SE	Inhibition, %	SE	Reversal with Ubiquinone, %	SE	Inhibition, %	SE	Reversal with Ubiquinone, %	SE	Inhibition, %	SE	Reversal with Ubiquinone, %	SE
Ib	5	84.34	2.24	7.69	2.06	85.56	2.99	6.43	2.07	94.69	0.94	−0.07	0.10	79.81	1.69	0.24	3.50
	2.5	49.55	3.84	−3.51	10.61	80.98	2.69	7.91	4.52	91.83	1.85	0.31	2.94	69.29	4.29	−1.83	7.40
	0.5	0	—	—	—	2.88	7.66	−73.32	31.08	65.27	9.02	−41.34	36.81	2.48	9.12	11.38	184.46
Ic	5	97.58	0.56	0.67	0.25	86.36	2.86	11.61	4.56	95.50	1.83	3.04	1.14	88.59	3.57	5.10	6.35
	2.5	96.83	1.13	1.89	1.21	78.01	1.72	3.45	2.27	94.74	1.62	−0.43	3.68	84.32	3.70	14.14	5.77
	0.5	84.77	0.78	31.04	25.66	79.57	1.63	−0.37	2.54	95.00	1.21	1.88	0.95	66.53	7.69	−0.21	1.54
	0.1	10.88	16.17	18.17	9.90	80.12	2.61	0.17	5.30	89.66	1.64	−1.22	2.30	0	—	—	—
Id	5	95.13	0.95	2.32	1.74	83.67	2.97	8.40	2.88	93.34	1.76	2.89	0.83	78.92	2.49	−0.06	3.34
	2.5	95.52	0.79	−0.11	0.72	82.10	3.88	3.21	2.12	95.00	0.90	2.49	1.64	83.42	2.29	−4.70	3.50
	0.5	84.43	0.90	10.31	3.26	81.56	2.26	−0.01	5.73	93.82	1.18	4.67	0.56	41.38	4.66	0.66	7.71
	0.1	7.96	8.85	142.39	111.44	70.41	3.89	13.16	16.88	89.74	0.90	−2.69	1.72	0	—	—	—
Ie	5	96.76	1.21	−0.28	0.57	86.14	2.53	−1.34	3.65	102.30	4.52	3.56	1.63	80.12	4.18	7.80	8.05
	2.5	93.61	1.47	−1.23	0.93	89.99	1.68	5.44	1.44	98.32	0.92	1.71	1.08	87.92	3.24	−1.06	1.74
	0.5	79.46	2.72	15.55	5.45	82.63	4.08	0.73	2.13	90.92	1.89	−1.47	3.09	79.80	2.92	−1.03	3.50
	0.1	80.13	2.61	23.80	22.87	74.59	4.11	5.10	6.60	92.56	1.75	−123.53	120.64	0	—	—	—

contain an α,β-unsaturated keto group like coenzyme Q_{10}, may compete with coenzyme Q_{10} for the electrons produced from the various substrates.

With succinate as the substrate, increasing concentrations of coenzyme Q_{10} increased the degree of reversal of the inhibition produced by Ib–Ie (Table III). Coenzyme Q_{10} alone did not stimulate respiration when added to uninhibited mitochondrial preparations. The degree of reversal of inhibition by coenzyme Q_{10} caused by Ib–Ie varied between substrates, being highest with succinate. This variation may possibly be caused by Ib–Ie acting at a second site, prior to coenzyme Q_{10}, with glutamate, 3-hydroxybutyrate, and palmitylcarnitine. This possibility is under investigation.

Correlations between antitumor and antimicrobial activities with redox potentials were established previously (17–19). It was considered that if the Mannich bases act as receptors for electrons in place of ubiquinone, then a relationship between the half-wave potentials of I and respiratory-inhibiting properties may be found. Table IV indicates that the half-wave potentials ($E_{1/2}$) of Ia–Ie, although varying over a narrow range, parallel the effect on respiration; *i.e.*, the dichlorinated compounds have higher $E_{1/2}$ values than the unsubstituted nonenone Ib, which, in turn, has a half-wave potential higher than Ia, which was bereft of effect on respiration under the conditions employed. The α,β-unsaturated ketones IIa–IIe, which were inactive in the L-1210 lymphoid leukemia screen (8), had lower half-wave potentials than the corresponding Mannich bases, suggesting that higher $E_{1/2}$ values favor antineoplastic activity.

Efforts are underway to examine whether the antineoplastic and cytotoxic Mannich bases act at other sites in the mammalian cell than the mitochondria. Since a number of antitumor agents interfere with RNA polymerase (20), Ia–Ie were tested for inhibitory activity toward solubilized nuclear DNA-dependent RNA polymerases from L-1210 leukemia and Swiss mouse kidney cells. Table IV indicates that Ib was the most active compound in both tests.

EXPERIMENTAL

Syntheses—The compounds were prepared by the literature procedure (21).

Inhibition of Respiration in Rat Liver Mitochondria—Adult, male, Wistar rats, which had been starved for 18 hr, were sacrificed by decapitation. The livers were removed, and 10 g of the liver was placed in 10 ml of ice-cold 3.4 m*M* tromethamine[1] (III) hydrochloride buffer (pH 7.40 at room temperature). The 3.4 m*M* III hydrochloride buffer contained 0.25 *M* sucrose and 1 m*M* ethylene glycol bis(aminoethyl) tetraacetate. All following procedures were carried out at 0°.

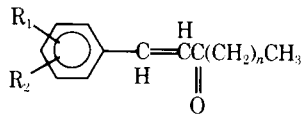

IIa: $R_1 = R_2 = H$, $n = 1$
IIb: $R_1 = R_2 = H$, $n = 5$
IIc: $R_1 = 2\text{-Cl}$, $R_2 = 4\text{-Cl}$, $n = 5$
IId: $R_1 = 2\text{-Cl}$, $R_2 = 6\text{-Cl}$, $n = 5$
IIe: $R_1 = 3\text{-Cl}$, $R_2 = 4\text{-Cl}$, $n = 5$

The liver was homogenized[2], and the homogenate was then diluted with buffer so that it contained 10% liver and 90% buffer. The homogenate was then centrifuged at 2000 rpm (500×*g*) for 10 min. The supernate was removed carefully and centrifuged at 9500 rpm (10,000×*g*) for 7 min. The supernate was discarded, and the mitochondrial pellet was resuspended in approximately 30 ml of buffer and recentrifuged at 9500 rpm (10,000×*g*) for 7 min. Resuspension of the pellet and recentrifugation was carried out once more. Finally, the pellet was resuspended in 10 ml of buffer. In the respiratory experiments (*vide infra*), 1 ml of this suspension was diluted with 5 ml of buffer to give a protein concentration of approximately 3.5 mg/ml.

The medium for the determination of Ia–Ie on mitochondrial respiration contained potassium chloride (0.1790 g), magnesium chloride (0.1708 g), III monophosphate (0.1315 g), and sucrose (9.24 g) dissolved in 100 ml of 10 m*M* III hydrochloride. The 10 m*M* III hydrochloride had a pH of 7.40 at 25°. The pH of the respiratory medium was adjusted to 7.40 at 37° using a 0.5 *M* III solution. The Mannich bases were dissolved in 10 m*M* III hydrochloride buffer in such concentrations that 10 μl of solution contained 5 μmoles of compound. Disodium succinate, monosodium glutamate, and β-hydroxybutyric acid (sodium salt) were dissolved in 10 m*M* III hydrochloride, and the palmitylcarnitine was dissolved in absolute ethanol.

The cells of an oxygen monitor[3] were surrounded by circulating water from a constant-temperature bath at 37°, and to a cell were added the medium (2.5 ml) and mitochondrial suspension (0.5 ml). After a baseline had been recorded, the substrate (15.0 μmoles of succinate, glutamate, or β-hydroxybutyrate or 1.0 μmole of palmitylcarnitine) was added, and the increase in respiration was recorded for approximately 2 min. With palmitylcarnitine, 0.5 ml of bovine serum albumin solution (60 mg/ml) also was added to protect the mitochondria from the detergent action of the substrate. The requisite volume of the solution of the drug was added, and the effect on mitochondrial respiration was noted.

In experiments attempting reversal of the effect of the Mannich bases on mitochondrial respiration with ubiquinone, 5 μl of a solution of ubiquinone in ethanol containing 2.25 nmoles/5 μl of ubiquinone was added to the cell approximately 2 min after the addition of the Mannich base, and the effect on respiration was noted. Preliminary experiments established that the ubiquinone and ethanol in these concentrations had no effect on respiration; in addition, solutions of the Mannich bases and ubiquinone were stable during the experiment (UV evidence). The literature method (15) was followed in examining the spectra of the cytochromes in rat liver mitochondria.

[1] Sigma Chemical Co., St. Louis, MO 63178.

[2] With a Potter-Elvehjem glass–Teflon (du Pont) homogenizer, Kontes Glass Co., Vineland, NJ 08360.

[3] YSI Model 53, Yellow Springs Instrument Co., Yellow Springs, OH 45387.

Table III—Effect of Increasing Concentrations of Coenzyme Q_{10} on Respiration Blocked by Ib–Ie

Compound	Concentration, μmoles	Reversal with 4.5 nmoles of Ubiquinone, %		Reversal with 9.0 nmoles of Ubiquinone, %	
		Trial 1	Trial 2	Trial 1	Trial 2
Ib	2.5	31.4	25.0	37.5	34.5
Ic	0.5	36.4	32.0	53.6	55.6
Id	0.5	16.7	17.0	28.6	32.4
Ie	0.5	32.5	30.4	46.1	35.0

Table IV—Measurement of Half-Wave Potentials of Ia–Ie and IIa–IIe and Assay of Ia–Ie against RNA Polymerases

Compound	$E_{1/2}$	Inhibition of RNA Polymerase, %	
		L-1210	Mouse Kidney
Ia	−1.25	0	20.3
Ib	−1.19	5.9	27.9
Ic	−1.06	0	12.5
Id	−1.09	0	7.6
Ie	−1.11	0	18.2
IIa	−1.40		
IIb	−1.38		
IIc	−1.25		
IId	−1.28		
IIe	−1.30		

The effect of increased concentration of ubiquinone on succinate-induced respiration after the addition of Mannich bases was shown using *Ib–Ie*. The concentrations of drugs used were: 2.5 μmoles of *Ib* and 0.5 μmole of *Ic–Ie*. The concentrations of ubiquinone were 4.5 and 9.0 nmoles. Each trial was repeated twice.

In every case that rat liver mitochondria were used, the protein content was determined by a modification (22) of the previously described procedure (23).

Effect of Ia–Ie on RNA Polymerases—The solubilized nuclear DNA-dependent RNA polymerases from L-1210 leukemia and Swiss mouse kidney cells were prepared according to the literature procedure (24), and each assay was carried out in duplicate using a concentration of 10 m*M*.

Measurement of Half-Wave Potentials—A polarograph[4] was calibrated in the following manner. A solution of 0.01 *N* cadmium chloride (5.0 ml) was diluted to 50.0 ml with 0.1 *N* potassium chloride. The mixture was purged with nitrogen, and five polarograms were obtained. The average half-wave potential ($E_{1/2}$) was compared to the literature value of −0.600 v (25). The half-wave potentials found in this experiment differed by 0.011 v from the value obtained when the solutions contained 40% (v/v) ethyl alcohol (*vide infra*).

Approximately 1 mg of *Ia–Ie* was dissolved in 1.0 ml of ethyl alcohol and placed in a 25-ml volumetric flask. The flask was filled to volume with a solution of 0.1 *N* potassium chloride containing 40% (v/v) ethyl alcohol. The solution was shaken and emptied into an electrolytic cell, and nitrogen was bubbled through the solution for 10 min. The temperature of the solutions varied from 21.7 to 22.5°; five determinations were undertaken (<2% variation), and the average result was obtained.

[4] Metrohm Polarecord E 261 model R, Fisher Scientific Co., Edmonton, Alberta, Canada.

REFERENCES

(1) J. R. Dimmock, W. A. Turner, and H. A. Baker, *J. Pharm. Sci.*, **64,** 995 (1975).

(2) J. R. Dimmock, A. M. Qureshi, L. M. Noble, P. J. Smith, and H. A. Baker, *ibid.*, **65,** 38 (1976).

(3) W. L. Noble and B. B. Thompson, *ibid.*, **53,** 1554 (1964).

(4) R. Viberbo, M. Mastursi, and G. Perri, German pat. 2,241,578; through *Chem. Abstr.*, **80,** 108064q (1974).

(5) F. F. Blicke and E. S. Blake, *J. Am. Chem. Soc.*, **52,** 235 (1930).

(6) W. Wilson and Z. Y. Kyi, *J. Chem. Soc.*, **1952,** 1321.

(7) R. N. Shut, F. E. Ward, and R. Rodriguez, *J. Med. Chem.*, **15,** 301 (1972).

(8) J. R. Dimmock and W. G. Taylor, *J. Pharm. Sci.*, **64,** 241 (1975).

(9) N. R. Farnsworth, *ibid.*, **62**(5), iv (1973).

(10) C. R. Bovell, L. Packer, and G. R. Schontaum, *Arch. Biochem. Biophys.*, **95,** 379 (1961).

(11) M. Gosalvez, M. Blanco, J. Hunter, M. Miko, and B. Chance, *Eur. J. Cancer*, **10,** 567 (1974).

(12) J. R. Dimmock, N. W. Hamon, K. W. Hindmarsh, D. G. Mills, L. E. Negrave, G. H. Rank, and A. J. Robertson, *J. Pharm. Sci.*, **65,** 482 (1976).

(13) C. S. Rossi and E. Carafoli, in "Fundamentals of Biochemical Pharmacology," Z. M. Bacq, Ed., Pergamon, Toronto, Canada, 1971, p. 153.

(14) A. L. Lehninger, "Biochemistry," Worth Publishers, New York, N.Y., 1970, p. 379.

(15) B. Chance and G. R. Williams, *J. Biol. Chem.*, **217,** 395 (1955).

(16) C. S. Rossi and E. Carafoli, in "Fundamentals of Biochemical Pharmacology," Z. M. Bacq, Ed., Pergamon, Toronto, Canada, 1971, p. 157.

(17) S. Kinoshita, K. Uzu, K. Nakano, M. Shimizu, T. Takahashi, and M. Matsui, *J. Med. Chem.*, **14,** 103 (1971).

(18) S. Kinoshita, K. Uzu, K. Nakano, and T. Takahashi, *ibid.*, **14,** 109 (1971).

(19) J. E. Page and F. A. Robinson, *Br. J. Exp. Pathol.*, **24,** 89 (1943).

(20) F. Zunino, R. Gambetta, and A. diMarco, *Biochem. Pharmacol.*, **24,** 309 (1975).

(21) J. R. Dimmock and W. G. Taylor, *J. Pharm. Sci.*, **63,** 69 (1974).

(22) G. L. Miller, *Anal. Chem.*, **31,** 964 (1959).

(23) O. H. Lowry, N. J. Rosebrough, L. Fair, and R. J. Randall, *J. Biol. Chem.*, **193,** 265 (1951).

(24) D. G. R. Blair, *J. Natl. Cancer Inst.*, **55,** 397 (1975).

(25) J. Heyrosky and P. Zuman, "Practical Polarography," Academic, New York, N.Y., 1968, p. 190.

ACKNOWLEDGMENTS

The authors thank the Medical Research Council of Canada for the award of an operating grant (MA 5538) to J. R. Dimmock. The assistance of Dr. D. G. R. Blair, Department of Biochemistry, University of Saskatchewan, is gratefully acknowledged.

Synthesis and Evaluation of 1-(Hydroxyphenyl)-1-nonen-3-ones and Related Compounds for Antineoplastic and Antimicrobial Activities

J. R. DIMMOCK *x, C. B. NYATHI ‡, and P. J. SMITH ‡

Received November 28, 1977, from the *College of Pharmacy and the ‡Department of Chemistry and Chemical Engineering, University of Saskatchewan, Saskatoon, Saskatchewan, S7N 0W0, Canada. Accepted for publication March 7, 1978.

Abstract □ Some 1-(hydroxyphenyl)-1-nonen-3-ones, the corresponding Mannich bases, and *O*-benzoyl esters were synthesized. Evaluation of these derivatives against murine P-388 lymphocytic leukemia indicated that, while the hydroxyphenyl styryl ketones and related esters were devoid of significant anticancer activities, etherification of the nuclear hydroxyl group gave compounds with a discernible increase in mean survival time. The hydroxyphenyl styryl ketones showed marked potencies against two pathogenic fungi and one yeast, while the corresponding ethers had diminished activities and the related esters were virtually devoid of antimicrobial activities. Two Mannich bases showed similar spectra of antimicrobial activities as the phenols and, in particular, were active against *Trichophyton mentagrophytes* and *Saccharomyces uvarum*.

Keyphrases □ 1-Phenyl-1-nonen-3-one derivatives—synthesized, evaluated for antineoplastic and antimicrobial activities □ Antineoplastic activity—various 1-phenyl-1-nonen-3-one derivatives evaluated in mice □ Antimicrobial activity—various 1-phenyl-1-nonen-3-one derivatives evaluated *in vitro* □ Structure–activity relationships—various 1-phenyl-1-nonen-3-one derivatives evaluated for antineoplastic activity in mice and antimicrobial activity *in vitro*

Recently (1, 2), some styryl ketones containing nuclear halogen and dimethylamino substituents and the related Mannich bases were examined for cytotoxic and antineoplastic activities. Metabolism of the cytotoxic (*E*)-2-benzylidenecyclohexanone was shown to proceed, in part at least, by nuclear hydroxylation (3). A convenient synthetic route to nuclear hydroxystyryl alkyl ketones would assist in identifying the structures of the metabolites; available methodology for the synthesis of these compounds indicates various problems such as dimer formation (4). Furthermore, certain nuclear hydroxy chalcones have tumor-inhibiting properties (5), and a number of cytotoxic sesquiterpenoid lactones have hydroxyl groups in close proximity to α,β-unsaturated keto functions (6).

A synthesis of hydroxystyryl alkyl ketones was initiated to evaluate them for antineoplastic activity. It was also considered that phenolic derivatives could be metabolized rapidly by conjugation (7) and that, by reacting the nuclear hydroxyl group with various benzoyl chlorides, esters could be produced which, on hydrolysis, would allow the gradual release of the parent phenol at a rate dependent on the Hammett value of the nuclear benzoyl substituent.

The interference of microsomal mixed function oxidase systems by methylenedioxyphenyl derivatives (8) suggested the synthesis of 1-(3,4-methylenedioxyphenyl)-1-nonen-3-one and the related Mannich base. Furthermore, as a continuing interest in the antimicrobial activities of Mannich bases and related compounds (9–11), it was proposed to examine the new derivatives for both antibacterial and antifungal activities.

DISCUSSION

An initial attempt to prepare 1-(hydroxyphenyl)-1-nonen-3-ones, utilizing the Claisen–Schmidt method (12), gave only a viscous oil and recovery of the starting material. This reaction depends on the formation of an intermediate aldol, produced by attack of the anion from the dialkyl ketone on the carbon atom of the aromatic aldehyde (13). In the presence of aqueous alkali, the phenoxide ion from the hydroxybenzaldehyde diminishes or abolishes the fractional positive charge on the carbonyl carbon atom of the benzaldehyde, thus inhibiting or preventing the synthesis of the intermediate aldol. Therefore, it was decided to protect the phenolic group by chemical modification prior to the condensation reaction. Since alkyloxymethyl ethers have been used previously for this purpose (14), the reaction sequence for the formation of I shown in Scheme I was followed successfully.

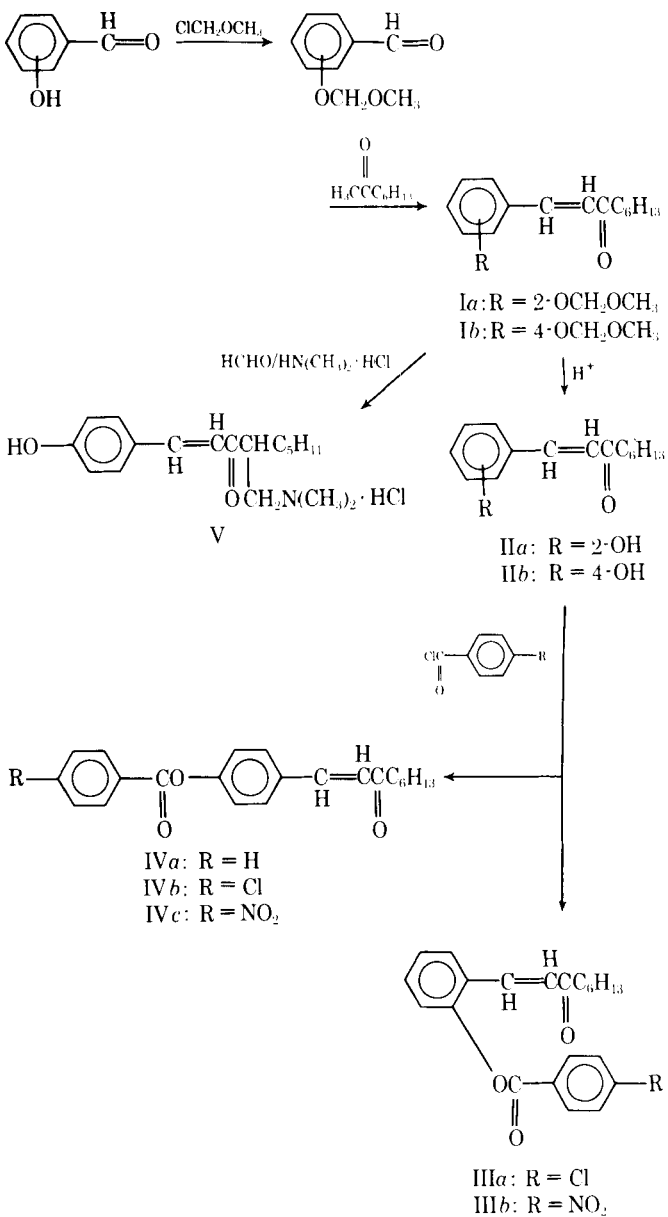

Scheme I

0022-3549/78/1100-1543$01.00/0
© 1978, American Pharmaceutical Association

Table I—Antineoplastic Evaluation of Substituted 1-(Hydroxyphenyl)-1-nonen-3-ones and Related Compounds against P-388 Lymphocytic Leukemia in Mice

Compound	Maximum Increase in Mean Survival Time (Dose in mg/kg)[a]
I*a*	116 (200)
I*b*	121 (100)[b]
II*a*	112 (200)
II*b*	105 (200)
III*a*	94 (200)
III*b*	99 (100)[c]
IV*a*	110 (200)
IV*b*	97 (6.25)
IV*c*	105 (12.5)
V	113 (100)[d]
VI*a*	102 (100)
VI*b*	123 (50)[e]

[a] The figures are the ratios of the survival time of treated animals to control animals expressed as a percentage. [b] On Day 5, there were 5/6 survivors at 200 and 100 mg/kg. [c] On Day 5, there were 5/6 survivors at 100 mg/kg and 6/6 survivors at 50 mg/kg. [d] On Day 5, there were 1/6 survivors at 200 mg/kg and 6/6 survivors at 100 mg/kg. [e] On Day 5, there were no survivors at 200 mg/kg and 6/6 survivors at 100 mg/kg.

Initial attempts to cleave the ethers I*a* and I*b* to the desired phenols II*a* and II*b* using hydrogen chloride, hydrogen bromide, acetic acid, sulfuric acid, and trifluoroacetic acid were unsuccessful. Aqueous formic acid led to the required compounds from which the corresponding *O*-benzoate esters III*a*, III*b*, and IV*a*–IV*c* were produced. It was decided that subjecting the phenols to the Mannich reaction might lead to ring aminomethylation (15) and that reaction of I*a* and I*b* under the Mannich conditions followed by cleavage of the protecting group would be feasible. However, reaction of I*b* with formaldehyde and dimethylamine hydrochloride led to the Mannich base V in 37% yield; *i.e.*, cleavage of the ether group occurred under the reaction conditions. Subsequently, it was shown that aminomethylation of II*b* gave V in 16% yield. The piperonylidene derivative VI*a* was prepared using the Claisen–Schmidt condensation and underwent the Mannich reaction to yield VI*b*.

The screening results of all compounds against P-388 lymphocytic leukemia in mice are summarized in Table I. Eight of the 12 compounds were nontoxic at the highest dose level examined (200 mg/kg); I*b* and III*b* had only marginal toxicity. With V and VI*b*, murine toxicity was noted at 200 mg/kg but was absent at 100 mg/kg. In compounds structurally related to these two Mannich bases, toxicity has been associated, in part at least, to impairment of mitochondrial function (16). The phenolic derivatives II*a* and II*b* gave small increases of approximately 9% in the mean survival time.

While the benzoate esters III*a*, III*b*, and IV*a*–IV*c* had lower antineoplastic activities than the precursor phenols, the corresponding ethers I*a* and I*b* increased the mean survival time by 19% on the average. This perceptible beneficial response could be due to preferential hydrolysis of the ether to the phenol in the tumorous cell since the claim has been made that the interstitial fluid surrounding certain cancers is more acidic than the plasma of blood afferent to the tumors (17). Alternatively, the diminished aqueous solubilities of the benzoate esters in comparison to the ethers may have retarded benzoate transport to the sites of action and, hence, diminished their anticancer potencies. Conversion of the styryl ketones II*b* and VI*a* to the corresponding Mannich bases V and VI*b* increased the antineoplastic activities in both cases.

Table II illustrates the evaluation of the 1-(hydroxyphenyl)-1-nonen-3-ones and related compounds for antimicrobial activities. The high potencies of the phenolic ketones II*a* and II*b* against the pathogenic fungi *Trichophyton mentagrophytes* and *Microsporum gypseum*, as well as the yeast *Saccharomyces uvarum*, are particularly noteworthy. The related ethers I*a* and I*b*, as well as the diether VI*a*, showed similar spectra of activities, but potencies were reduced and conversion of the phenols to the esters III*a*, III*b*, and IV*a*–IV*c* produced derivatives that were either bereft of activities at the higher concentrations tested (500 μg/ml) or showed very low levels of potencies. The Mannich bases V and VI*b* showed similar spectra of activities to the phenols and approached these derivatives in demonstrated bioactivities. With the exception of *Bacillus subtilis*, the compounds appeared to be virtually devoid of antibacterial activities.

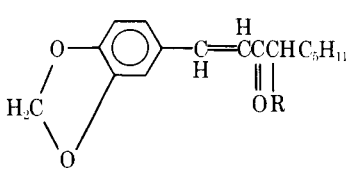

VI*a*: R = H
VI*b*: R = $CH_2N(CH_3)_2 \cdot HCl$

EXPERIMENTAL[1]

Melting points and boiling points are uncorrected. Organic extracts were washed several times with water and dried over anhydrous magnesium sulfate. After filtration, the solvent was removed *in vacuo*, using a water aspirator.

(*E*)-1-(Methoxymethoxyphenyl)-1-nonen-3-ones (I*a* and I*b*)—The methoxymethoxybenzaldehydes were prepared by the literature method (14), except that the sodium hydride dispersion was added in one operation rather than intermittently and the reaction mixture was stirred for 1 hr after sodium hydride addition. *o*-Methoxymethoxybenzaldehyde, bp 102°/0.55 mm [lit. (18) bp 100–102°/2.5 mm], was prepared as a colorless oil in 68% yield. The corresponding *para*-derivative, bp 113°/0.2 mm [lit. (19) bp 122°/2 mm], was prepared as a colorless oil in 74% yield. NMR spectroscopy and mass spectrometry were in accord with the proposed structures.

A mixture of *o*-methoxymethoxybenzaldehyde (83.1 g, 0.5 mole), 2-octanone (76.9 g, 0.6 mole), and sodium hydroxide (10 g, 0.25 mole) in water (300 ml) was heated under reflux for 18 hr. On cooling, the two phases were separated. The aqueous layer was extracted with benzene, and the organic extracts were combined with the original organic layer. Removal of both the benzene and excess 2-octanone gave a viscous brown oil, which was distilled to give (*E*)-1-(*o*-methoxymethoxyphenyl)-1-nonen-3-one (I*a*) in 59% yield, bp 178°/0.5 mm, as a yellow viscous oil; mass spectrum: *m/e* 276 ($M^{\cdot+}$, 2%) and 45 (100).

Anal.—Calc. for $C_{17}H_{24}O_3$: C, 73.88; H, 8.75. Found: C, 72.80; H, 8.78.

The corresponding *para*-isomer, I*b*, was prepared in a similar manner as a yellow viscous oil, bp 191°/0.7 mm, in 42% yield. On standing, the oil solidified to a very pale-yellow waxy solid; mass spectrum: *m/e* 276 ($M^{\cdot+}$, 11%) and 45 (100).

Anal.—Calc. for $C_{17}H_{24}O_3$: C, 73.88; H, 8.75. Found: C, 73.51; H, 8.43.

(*E*)-1-(Hydroxyphenyl)-1-nonen-3-ones (II*a* and II*b*)—A solution of (*E*)-1-(*o*-methoxymethoxyphenyl)-1-nonen-3-one (10 g, 0.036 mole) and aqueous formic acid (85% v/v, 15 ml, 0.338 mole) in petroleum ether (bp 100–120°, 250 ml) was heated under reflux for 20 min. On cooling, the layers were separated. The petroleum ether layer was concentrated to 50 ml and placed in a refrigerator (5°) to yield the desired ketone, II*a* (5.8 g), mp 98–100°. The aqueous phase, on refrigeration, deposited a further quantity of the required compound (0.41 g), mp 92–94°. Repeated recrystallization of the crude product from petroleum ether (bp 100–120°) afforded (*E*)-1-(*o*-hydroxyphenyl)-1-nonen-3-one (II*a*) (67% yield) as pale-yellow granular crystals, mp 101–102°; NMR ($CDCl_3$): δ 8.48 (s, 1, OH), 8.02 (d, 1, C_1H, $J_{1,2}$ = 16.2), 7.67–6.58 (m, 4, aromatic H), 6.97 (d, 1, C_2H, $J_{1,2}$ = 16.2), 2.70 (t, 2, C_4H), and 2.00–0.58 [m, 11, $(CH_2)_4CH_3$] ppm; mass spectrum: *m/e* 232 ($M^{\cdot+}$, 5%) and 147 (100).

Anal.—Calc. for $C_{15}H_{20}O_2$: C, 77.54; H, 8.68. Found: C, 78.03; H, 8.62.

The corresponding *para*-compound, II*b*, was prepared in an analogous manner, except that petroleum ether was not added to the reaction mixture. It crystallized from petroleum ether (bp 100–120°) as pale-yellow granular crystals (71% yield), mp 76–77°; mass spectrum: *m/e* 232 ($M^{\cdot+}$, 12%) and 147 (100).

Anal.—Calc. for $C_{15}H_{20}O_2$: C, 77.54; H, 8.68. Found: C, 77.89; H, 8.42.

Other attempts at cleaving I*b* to the desired hydroxy ketones II*a* and II*b* gave either viscous oils or a mixture of products. When hydrogen chloride or hydrogen bromide was bubbled through an ethereal solution of I*b* at room temperature for 1.5 hr, only brown viscous oils were formed. A solution of I*b* in ether and a twice molar ratio of acetic acid were stirred

[1] Elemental analyses were carried out by Mr. R. G. Teed of the Department of Chemistry and Chemical Engineering, University of Saskatchewan. Mass spectra (AEI MS-12 mass spectrometer, Picker X-Ray Engineering Ltd., Montreal 304, Quebec, Canada) were determined at 70 ev by Mr. D. R. Bain, Department of Chemistry and Chemical Engineering, University of Saskatchewan. The 60-MHz NMR spectra (Varian T60 spectrophotometer, Varian Associates of Canada Ltd., Georgetown, Ontario, L7G 2J4, Canada) were carried out in deuterochloroform.

Table II—Antimicrobial Evaluation of Substituted 1-(Hydroxyphenyl)-1-nonen-3-ones and Related Compounds [a]

Microorganism	Ia	Ib	IIa	IIb	IIIa	IIIb	IVa	IVb	IVc	V	VIa	VIb
Escherichia coli (ATCC 8739)	>500	>500	>500	>500	>500	>500	>500	>500	>500	>500	>500	>500
Pseudomonas aeruginosa (ATCC 10145)	>500	>500	>500	>500	>500	>500	>500	>500	>500	>500	>500	>500
Klebsiella pneumoniae (ATCC 4352)	>500	>500	>500	>500	>500	>500	>500	>500	>500	>500	>500	>100
Salmonella typhimurium (G 46)	>500	>500	>100	>500	>500	>500	>500	>500	>500	>500	>500	>500
Bordetella bronchiseptica (ATCC 4617)	>500	>500	>500	>500	>500	>500	>500	>500	>500	>100	>500	>500
Staphylococcus aureus (ATCC 6538)	>500	>500	<100	<100	>500	>500	>500	>500	>500	>100	>500	>100
Streptococcus faecalis (ATCC 8030)	>500	>500	>500	>500	>500	>500	>500	>500	>500	>100	>500	>100
Bacillus subtilis (ATCC 6633)	<100	<100	<100	<100	>500	<100	>500	>500	<100	<100	<100	<100
Trichophyton mentagrophytes (ATCC 9533)	>250	<100	<10	<10	>500	>500	>100	>500	>250	<10	<100	<10
Microsporum gypseum (ATCC 14683)	<100	>100	<10	<10	>500	>500	>100	>500	>250	<100	>100	<100
Aspergillus niger (ATCC 10535)	>500	>500	>500	>500	>500	>500	>500	>500	>500	>500	>500	>100
Candida albicans (ATCC 10231)	>250	>500	<100	>500	>500	>500	>500	>500	>500	>100	>500	>100
Saccharomyces uvarum (ATCC 9080)	>500	>100	<10	<10	>500	>500	>500	>500	>500	<10	>500	<10
Average antimicrobial activity [b]	92	115	712	654	0	39	39	0	54	539	96	558

[a] The figures are the minimum inhibitory concentrations of the compounds in micrograms per milliliter. [b] Figures were calculated from the following expression: (combined antimicrobial activity × 100)/number of microorganisms in the screen. The combined antimicrobial activity was determined by giving the following scores at the highest potency of the compound against the microorganism: >250, 1; >100, 2.5; <100, 5; and <10, 25.

at room temperature for 2 hr, but only a quantitative recovery of I*b* was obtained. A solution of I*b* in benzene and acetic acid (5:1 v/v) was brought to reflux, 5 drops of sulfuric acid were added, and the resultant mixture was heated under reflux for 5 min. The product obtained was a mixture of I*b* and II*b* (PMR and mass spectral evidence). When a solution of I*b* in a mixture of equal parts of benzene and trifluoroacetic acid was heated under reflux for 48 hr, a mixture of I*b* and II*b* was obtained (PMR and mass spectral evidence).

An initial attempt to prepare II*a* and II*b* by the conventional Claisen–Schmidt reaction (12) from the appropriate hydroxybenzaldehyde, 2-octanone, and aqueous sodium hydroxide (3% w/v) produced only brown tars and unreacted hydroxybenzaldehyde (33%).

(*E*)-1-(Benzoyloxyphenyl)-1-nonen-3-ones (III*a*, III*b*, and IV*a*–IV*c*)—The esters III*a*, III*b*, and IV*a*–IV*c* were prepared by the following general method. The appropriate benzoyl chloride (0.025 mole) was added to a solution of either II*a* or II*b* (0.022 mole) in dry pyridine (20 ml), and the mixture was heated on a steam bath for 10 min and then stirred at room temperature for 24 hr. The solution was then poured onto crushed ice (20 g). After the ice melted, the crude reaction product was extracted with ether and purified by recrystallization.

(*E*)-1-[*o*-(*p*-Chlorobenzoyloxy)phenyl]-1-nonen-3-one (III*a*) crystallized from methanol as colorless needles in a 68% yield, mp 47–48.5°.

Anal.—Calc. for $C_{22}H_{23}ClO_3$: C, 71.23; H, 6.26. Found: C, 71.43; H, 6.23.

The corresponding *p*-nitro ester, III*b*, crystallized from methanol as pale-yellow needles in a 59% yield, mp 62–63.5°.

Anal.—Calc. for $C_{22}H_{23}NO_5$: C, 69.26; H, 6.08; N, 3.67. Found: C, 69.81; H, 6.18; N, 3.62.

(*E*)-1-[*p*-(Benzoyloxy)phenyl]-1-nonen-3-one (IV*a*) crystallized from ether as colorless flakes in an 83% yield, mp 85–86°.

Anal.—Calc. for $C_{22}H_{24}O_3$: C, 78.57; H, 7.20. Found: C, 79.11; H, 7.03.

The corresponding *p*-chloro ester, IV*b*, crystallized from ether as colorless flakes in an 85% yield, mp 115–116°.

Anal.—Calc. for $C_{22}H_{23}ClO_3$: C, 71.23; H, 6.26. Found: C, 71.62; H, 6.13.

The corresponding *p*-nitro ester, IV*c*, crystallized from ether as cream flakes in a 65% yield, mp 99–101°.

Anal.—Calc. for $C_{22}H_{23}NO_5$: C, 69.26; H, 6.08; N, 3.68. Found: C, 67.45; H, 5.94; N, 3.52.

PMR and mass spectral studies also confirmed the structures.

The crude reaction product from II*a* and benzoyl chloride was distilled to give an orange oil, bp 198–206°/0.2 mm. TLC of the distillate, using silica gel and a solvent mixture of chloroform–ethyl acetate–diethylamine (92:5:3), indicated the presence of unreacted ketone II*a*, which was not separated from the desired ester by a chromatography column packed with silica gel and eluted with the solvent mixture used for TLC. Attempted redistillation of the oil led only to the formation of a yellowish-brown viscous mass.

(*E*)-4-Dimethylaminomethyl-1-(*p*-hydroxyphenyl)-1-nonen-3-one Hydrochloride (V)—A mixture of (*E*)-I*b* (15 g, 0.054 mole), dimethylamine hydrochloride (4.4 g, 0.054 mole), and paraformaldehyde (4.9 g, 0.054 mole) in ethanol (100 ml) containing hydrochloric acid (0.5–2.0%) was heated under reflux for 24 hr. On cooling, the alcohol was removed *in vacuo;* the residue was suspended in water and extracted with ether. Separation of the organic phase, followed by removal of ether, afforded (*E*)-II*b* (2.1 g, 17% yield). The aqueous layer was cooled with ice water and basified to pH 9 with aqueous sodium hydroxide (0.1 *M*).

The liberated oil was extracted with ether, and the organic extract was washed with water, dried, and then acidified with ethanolic hydrochloric acid (20% w/v). The solution was concentrated and placed in a refrigerator, and the colorless solid that deposited was recrystallized from acetone to give V (6.5 g, 37% yield) as a colorless powder, mp 174–176°; NMR: δ 10.56 (s, 1, N^+H), 10.22 (s, 1, OH), 7.72 (d, l, C_1H, $J_{1,2}$ = 16.0), 7.64 (d, 2, aromatic H, $J_{2',3'}$ = 8.7), 6.90 (d, 2, aromatic H, $J_{5',6'}$ = 8.7), 6.90 (d, l, C_2H, $J_{1,2}$ = 16.0), 3.80–3.00 (m, 3, C_4H, CH_2), 2.72 [s, 6, $N(CH_3)_2$], and 1.90–0.57 [m, 11, $(CH_2)_4CH_3$] ppm; mass spectrum: *m/e* 289 (M^+ − HCl, 2%) and 58 (100).

Anal.—Calc. for $C_{18}H_{28}ClNO_2$: C, 66.34; H, 8.66; N, 4.30. Found: C, 62.03; H, 8.71; N, 4.08.

(*E*)-1-(3,4-Methylenedioxyphenyl)-1-nonen-3-one (VI*a*) and the Related Mannich Base (VI*b*)—A mixture of 3,4-methylenedioxybenzaldehyde (24.0 g, 0.16 mole), 2-octanone (23.1 g, 0.18 mole), and sodium hydroxide (4 g, 0.1 mole) in water (100 ml) was heated under reflux for 23 hr. On cooling, the reaction mixture was extracted with benzene. Evaporation of the solvent produced a yellow solid, which was recrystallized from petroleum ether (bp 100–120°) to give VI*a* (16.4 g, 39% yield) as colorless needles, mp 56.5–58° [lit. (20) mp 61°]; mass spectrum: *m/e* 260 ($M^{\cdot+}$, 22%) and 175 (100).

Anal.—Calc. for $C_{16}H_{20}O_3$: C, 73.81; H, 7.75. Found: C, 73.92; H, 7.95.

A solution of hydrochloric acid (10 ml) in ethanol (250 ml) was added to a mixture of VI*a* (41.2 g, 0.16 mole), dimethylamine hydrochloride (12.9

g, 0.16 mole), and paraformaldehyde (4.8 g, 0.16 mole) in methanol (12.5 ml), and the resultant mixture was heated under reflux for 1 hr. On cooling, a colorless solid deposited, which was recrystallized from acetone to give (*E*)-4-dimethylamino-1-(3,4-methylenedioxyphenyl)-1-nonen-3-one hydrochloride (VI*b*) (18.3 g, 32% yield) as colorless needles, mp 149–150°; mass spectrum: *m/e* 317 (M^+ − HCl, 2%) and 58 (100).

Anal.—Calc. for $C_{19}H_{28}ClNO_3$: C, 64.47; H, 7.98; N, 3.96. Found: C, 64.78; H, 8.07; N, 3.81.

Screening—For anticancer screening[2], the compounds were administered in saline (II*a*, IV*a*–IV*c*, and V), saline with polysorbate 80 (II*b*, III*a*, III*b*, VI*a*, and VI*b*), saline with alcohol (I*b*), and hydroxypropylcellulose (I*a*) intraperitoneally to CD_2F_1 mice. Injections were made daily for 9 consecutive days.

For the antimicrobial screen[3], the compounds were dissolved in water or dimethyl sulfoxide and diluted serially to various concentrations. The concentrations of stock solutions were prepared in such a way that when 0.5 ml was added to 15 ml of agar medium, the desired final concentrations were obtained. Trypticase soy agar medium was employed for the bacteria, and modified Sabouraud agar was used for the fungi and yeasts. The test organisms were grown previously for 2 days at 35° for bacteria and yeasts and 1 week for fungi at 24° on slants of the same medium.

The agar plates were streaked with a loopful of cell suspension that had been washed off from the slants and diluted to approximately 10^5 organisms/ml. The plates were incubated for 2–14 days at 24° for fungi and at 35° for bacteria. The bacteria were assessed at 500 and 100 μg/ml; therefore, >100 indicates a compound showing inhibition of growth at 100, but not 500, μg/ml. The fungal growth was measured at concentrations of 500, 250, 100, and 10 μg/ml; >100 indicates, for example, that growth was inhibited at 100, but not 250, μg/ml.

REFERENCES

(1) J. R. Dimmock and W. G. Taylor, *J. Pharm. Sci.*, **64,** 241 (1975).

(2) J. R. Dimmock, G. B. Baker, and R. G. Sutherland, *Can. J. Pharm. Sci.*, **10,** 53 (1975).

(3) J. R. Dimmock, N. W. Hamon, K. W. Hindmarsh, A. P. Sellar, W. A. Turner, G. H. Rank, and A. J. Robertson, *J. Pharm. Sci.*, **65,** 538 (1976).

(4) I. M. Heilbron and F. Irving, *J. Chem. Soc.*, **1929,** 934.

(5) O. K. Kabiev and S. M. Vermenichev, *Izv. Akad. Nauk Kaz. SSR, Ser. Biol.*, **9,** 72 (1971); through *Chem. Abstr.*, **75,** 47091u (1971).

(6) S. M. Kupchan, M. A. Eakin, and A. M. Thomas, *J. Med. Chem.*, **14,** 1147 (1971).

(7) A. Goldstein, L. Aronow, and S. M. Kalman, "Principles of Drug Action: The Basis of Pharmacology," 2nd ed., Wiley, Toronto, Canada, 1974, p. 258.

(8) E. Hodgson and J. E. Casida, *Biochem. Pharmacol.*, **8,** 179 (1961).

(9) J. R. Dimmock, A. M. Qureshi, L. M. Noble, P. J. Smith, and H. A. Baker, *J. Pharm. Sci.*, **65,** 38 (1976).

(10) J. R. Dimmock, W. A. Turner, and H. A. Baker, *ibid.*, **64,** 995 (1975).

(11) J. R. Dimmock, D. K. Kowal, W. A. Turner, P. J. Smith, L. M. Noble, and W. J. Pannekoek, *ibid.*, **67,** 401 (1978).

(12) P. J. Smith, J. R. Dimmock, and W. G. Taylor, *Can. J. Chem.*, **50,** 871 (1972).

(13) J. Packer and J. Vaughan, "A Modern Approach to Organic Chemistry," Oxford University Press, London, England, 1958, p. 760.

(14) P. J. Nelson and A. F. A. Wallis, *Tappi*, **56,** 132 (1973).

(15) F. F. Blicke, in "Organic Reactions," vol. I, R. Adams, Ed., Wiley, New York, N.Y., 1942, p. 311.

(16) J. R. Dimmock, N. W. Hamon, K. W. Hindmarsh, D. G. Mills, L. E. Negrave, G. H. Rank, and A. J. Robertson, *J. Pharm. Sci.*, **65,** 482 (1976).

(17) P. M. Gullino, F. H. Crantham, S. H. Smith, and A. C. Haggerty, *J. Natl. Cancer Inst.*, **34,** 857 (1965).

(18) H. Bohnsack and W. Seibert, *Riechstoffe, Aromen, Koerperpflegemittel*, **15,** 407 (1965); through *Chem. Abstr.*, **64,** 17458f (1966).

(19) *Ibid.*, **15,** 321 (1965); through *Chem. Abstr.*, **64,** 17349g (1966).

(20) O. F. Hedenburg and H. Wachs, *J. Am. Chem. Soc.*, **70,** 2216 (1948).

(21) R. I. Geran, N. H. Greenberg, M. M. MacDonald, A. M. Schumacher, and B. J. Abbott, *Cancer Chemother. Rep., Part 3,* **3** (Sept. 1972).

[2] Carried out by the Drug Research and Development Division, National Cancer Institute, Bethesda, Md., using their protocols (21).

[3] Bio-Research Laboratories Ltd., Montreal, Quebec, Canada.

ACKNOWLEDGMENTS

The authors thank the Medical Research Council of Canada for the award of an operating grant (MA 5538) to J. R. Dimmock. They also thank Connlab Holdings Ltd. for financial assistance. The United Nations provided a stipend to C. B. Nyathi, which is gratefully acknowledged.

Effect of Diphenhydramine on Methaqualone Metabolism: An *In Vitro* Study

K. W. HINDMARSH ˣ, N. W. HAMON, D. F. LeGATT, and S. M. WALLACE

Received November 21, 1977, from the *College of Pharmacy, University of Saskatchewan, Saskatoon, Saskatchewan, Canada, S7N 0W0.* Accepted for publication March 7, 1978.

Abstract □ A GLC assay to quantitate the methaqualone metabolite 2-methyl-3-(2-hydroxymethylphenyl)-4(3*H*)-quinazolinone was developed. Standard curves were linear, and recovery of the metabolite from tissue homogenates averaged 89%. *In vitro* metabolism of methaqualone by the 10,000×*g* supernatant fraction of rat liver homogenate was measured by monitoring metabolite formation with the GLC assay. Diphenhydramine inhibited the *in vitro* metabolism of methaqualone. The percentage inhibition increased with increasing diphenhydramine concentration. The significance of this inhibition in relation to use and abuse of methaqualone–diphenhydramine combinations is discussed.

Keyphrases □ Diphenhydramine—effect on methaqualone metabolism in rat liver homogenate □ Methaqualone—metabolism, effect of diphenhydramine in rat liver homogenate □ Metabolism—methaqualone, effect of diphenhydramine in rat liver homogenate □ GLC—analysis, methaqualone metabolite in rat liver homogenate □ Antihistaminics—diphenhydramine, effect on methaqualone metabolism in rat liver homogenate □ Hypnotic–sedatives—methaqualone, metabolism, effect of diphenhydramine in rat liver homogenate

The abuse of methaqualone [2-methyl-3-*O*-tolyl-4(3*H*)-quinazolinone], a nonbarbiturate hypnotic, has been recognized as a serious problem among drug addicts (1). Methaqualone also was reported to be a street drug (2–6). The abuse of methaqualone and diphenhydramine in combination (7–9) and poisoning cases arising from such abuse have been reported (10–13). A combination pharmaceutical product containing both drugs emerged as an abuse drug among soldiers stationed in West Germany (14, 15). There has been no clearcut rationale for the combination of diphenhydramine and methaqualone in commercial drug preparations or for supplementation of methaqualone with diphenhydramine by abusers.

In vitro, the 10,000×*g* supernatant fraction of rat liver homogenate metabolizes methaqualone to 2-methyl-3-(2-hydroxymethylphenyl)-4(3*H*)-quinazolinone (16). This metabolite is also one major metabolite identified in human and rat urine (17). The monohydroxy metabolites do not show any marked biological activity (18, 19). Inhibition of metabolism may result in increased pharmacological activity of methaqualone.

The objective of this present study was to determine the effect of diphenhydramine on the metabolism of methaqualone *in vitro* by the rat hepatic 10,000×*g* supernatant fraction. Metabolism of methaqualone to 2-methyl-3-(2-hydroxymethylphenyl)-4(3*H*)-quinazolinone was monitored by GLC.

EXPERIMENTAL

Materials—Methaqualone hydrochloride[1], diphenhydramine hydrochloride[2], 1-chlorobutane[3], glucose 6-phosphate monosodium salt[4], nicotinamide adenine dinucleotide phosphate[4], sucrose[5], semicarbazide hydrochloride[5], concentrated hydrochloric acid[5] (reagent grade), and magnesium chloride[6] were obtained commercially, and appropriate aqueous solutions were prepared. Tris(hydroxymethyl)aminomethane hydrochloride (pH 7.4) buffer containing sucrose was prepared using 25 ml of 3.4 m*M* tris(hydroxymethyl)aminomethane, 20.7 ml of 3.4 m*M* HCl, and 5.58 g of sucrose. This mixture was diluted to 100 ml with distilled water.

Tris(hydroxymethyl)aminomethane hydrochloride (pH 5.5) buffer containing semicarbazide hydrochloride was prepared from 25 ml of 0.5 *M* tris(hydroxymethyl)aminomethane, 15 ml of 0.5 *M* HCl, and 0.17 g of semicarbazide hydrochloride. This solution was diluted to 100 ml with distilled water and heated for 1 hr at 40° prior to use. 2-Methyl-3-(2-hydroxymethylphenyl)-4(3*H*)-quinazolinone was synthesized according to previously described methods (16, 20).

Preparation of 10,000×*g* Supernatant Fraction—Adult male albino rats of the Wistar strain, 250 g, were fasted for 18 hr and then sacrificed by decapitation. The livers were removed and immediately placed in 15 ml of an ice-cold solution of tris(hydroxymethyl)aminomethane hydrochloride buffer and sucrose. The tissue was minced, weighed, and homogenized[7] in a volume of the same buffer equal to two times the liver weight. The homogenate was centrifuged[8] at 600×*g* for 10 min, and the resulting supernate was centrifuged twice at 10,000×*g* for 20 min.

The protein concentration of the 10,000×*g* supernate was determined using the colorimetric method described by Lowry *et al.* (21) and modified by Miller (22). Protein standards were prepared using bovine serum albumin.

***In Vitro* Metabolism of Methaqualone**—*Control Studies*—The following reagents were added in the order given to a series of 25-ml erlenmeyer flasks: 1 ml of tris(hydroxymethyl)aminomethane hydrochloride buffer containing semicarbazide hydrochloride, 2 ml of 0.07 *M* magnesium chloride, 1 ml of 21.3 m*M* glucose 6-phosphate, 1 ml of 4.4

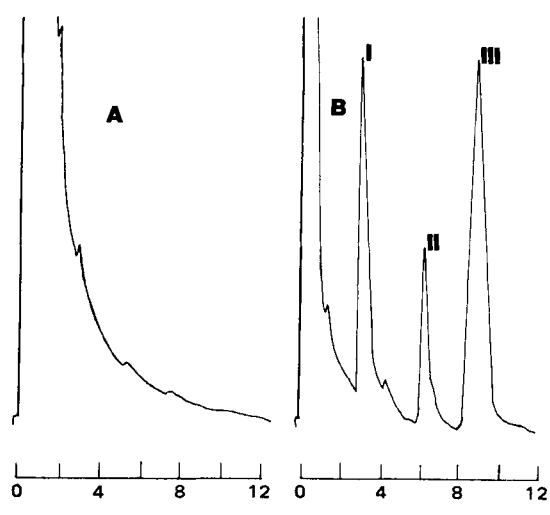

Figure 1—*Gas chromatograms of: A, control homogenate; and B, methaqualone (peak I), trimethylsilyl derivative of 2-methyl-3-(2-hydroxymethylphenyl)-4-(3H)-quinazolinone (peak II), and trimethylsilyl derivative of codeine (peak III).*

[1] William H. Rorer (Canada) Ltd., Bramalea, Ontario, Canada.
[2] Parke-Davis and Co., Brockville, Ontario, Canada.
[3] J. T. Baker Chemical Co., Phillipsburg, N.J.
[4] Sigma Chemical Co., St. Louis, Mo.
[5] Fisher Scientific Co., Fair Lawn, N.J.
[6] British Drug Houses (Canada) Ltd., Toronto, Ontario, Canada.
[7] Virtis "45," Virtis Co., Gardiner, N.Y.
[8] Model B-20, International Equipment Co., Needham Heights, Mass.

0022-3549/78/1100-1547$01.00/0
© 1978, American Pharmaceutical Association

Table I—GLC Estimation of 2-Methyl-3-(2-hydroxymethylphenyl)-4(3*H*)-quinazolinone (n = 3)

Concentration of Metabolite, μg/μl	Peak Height Ratio	*SD*
5	0.89	0.008
10	2.22	0.006
15	2.69	0.02
20	3.97	0.02
30	6.39	0.006
40	8.37	0.02

m*M* nicotinamide adenine dinucleotide phosphate, and the 10,000×*g* supernatant fraction. Varying amounts of methaqualone hydrochloride (2.6–26.4 μmoles) were added to each flask, and the flasks were then incubated at 37° for 20 min in a metabolic shaker bath[9]. Three separate flasks were prepared for incubation at each methaqualone concentration.

Inhibition Studies—A 1-ml aliquot of 1, 3, or 5 m*M* diphenhydramine hydrochloride was added to an incubation mixture similar to that already described. To maintain the same total volume of incubation mixture as in the control studies, the volume of the magnesium chloride solution added was decreased to 1 ml.

Extraction Procedure—At the completion of the 20-min incubation period, 1 *N* NaOH (1 ml) was added to each flask. The flask contents were extracted separately with 4 × 6-ml portions of 1-chlorobutane using a shaker[10]. The shaker was maintained at a constant speed (15 oscillations/5 sec) for 10 min. The organic extracts from each flask were pooled and centrifuged[11] at 2500 rpm for 10 min. The upper organic layer was evaporated to dryness at room temperature under a gentle flow of air.

The residues were transferred quantitatively to 1-ml vials[12] using a small quantity of 1-chlorobutane. A 55-μl aliquot of aqueous codeine stock solution (1 μg/ml) was added to each vial, and the solvent was removed using a gentle flow of air. Silyl ethers were prepared by adding 15 μl of *pyridine*[12] (*silylation* grade), 30 μl of bis(trimethylsilyl)acetamide[12], and 10 μl of trimethylchlorosilane[12] to the resulting residue in each vial. Then the vials were stoppered and incubated at 100° for 1 hr. Aliquots (2–3 μl) of the silylated solution were injected into the gas chromatograph.

GLC Analysis—A gas chromatograph[13] equipped with a flame-ionization detector was employed. The chromatographic column was 1.2-m × 3.1-mm o.d., coiled, stainless steel tubing packed with 3% OV-101 on 80–100-mesh, high performance Chromosorb W[14]. The column was conditioned by maintaining the oven at 290° for 18 hr with low nitrogen flow. Operating temperatures were: injection port, 255°; column, 180°; and detector, 255°. The nitrogen flow rate was 80 ml/min. Hydrogen and compressed air flow rates were adjusted to give maximum response.

The metabolite concentration in the incubation medium was calculated from a standard curve plotted as the peak height ratio of the metabolite to the internal standard against known metabolite concentrations. Standard curves consisted of five concentrations of the metabolite ranging from 5 to 40 μg/μl.

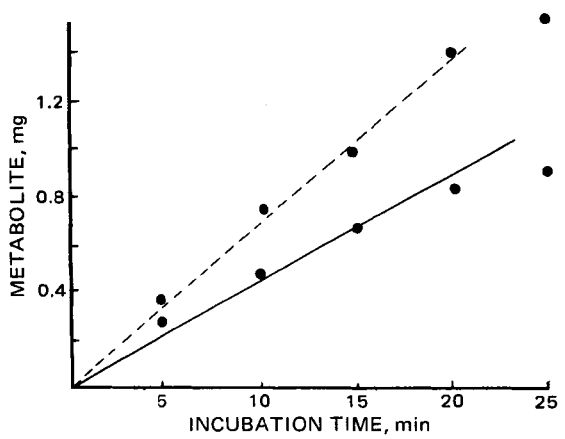

Figure 2—*2-Methyl-3-(2-hydroxymethylphenyl)-4(3H)-quinazolinone formation as a function of incubation time at methaqualone concentrations of 2.18 (●- -●) and 0.43 (●—●) m*M.

[9] Dubnoff incubator, GCA Precision Scientific, Chicago, Ill.
[10] Eberbach, Ann Arbor, Mich.
[11] International clinical centrifuge, International Equipment Co., Needham Heights, Mass.
[12] Reacti vials, Pierce Chemical Co., Rockford, Ill.
[13] Model 5750B, Hewlett-Packard, Avondale, Pa.
[14] Chromatographic Specialties, Brockville, Ontario, Canada.

Table II—Recovery of 2-Methyl-3-(2-hydroxymethylphenyl)-4(3*H*)-quinazolinone from Incubation Media Determined by GLC Assay

Concentration Added, μg/μl	Concentration Recovered, μg/μl	Percentage Recovery, mean
5	4.2, 4.4, 4.6	88.0
10	8.6, 8.6, 8.6	86.0
15	13.6, 13.6, 14.0	91.5
20	17.8, 18.0, 18.2	90.0
30	25.0, 25.0, 25.0	83.3
40	37.0, 37.5, 40.0	95.4
Mean ± *SD*		89.0 ± 4.5

RESULTS AND DISCUSSION

A method suitable for quantitation of the major *in vitro* metabolite was developed. Under the GLC conditions described, the retention times were 3.2 min for methaqualone (peak I), 6.5 min for the silyl derivative of 2-methyl-3-(2-hydroxymethylphenyl)-4(3*H*)-quinazolinone (peak II), and 9.2 min for silylated codeine (peak III) (Fig. 1B). No interfering peaks were observed on chromatographic analysis of an extract of control liver homogenate (Fig. 1A). The standard curves for the methaqualone metabolite were linear (r^2, coefficient of determination, 0.994) over the range of 5–40 μg/μl of the standard (Table I). Recovery of the metabolite from the homogenate was 89.0 ± 4.5% when compared to samples chromatographed directly without extraction (Table II).

A preliminary study indicated that diphenhydramine inhibited methaqualone metabolism when added to the incubation mixture. Three different diphenhydramine concentrations (1, 3, and 5 m*M*) were added to incubation mixtures containing the same amount of methaqualone (2.6 μmoles), and the peak heights for metabolite formation were compared to control samples to which no diphenhydramine was added. The percentage inhibition increased (45.9, 75.4, and 96.1%, respectively) as the diphenhydramine concentration increased. Neither diphenhydramine nor methaqualone affected the generation of reduced cofactor from the nicotinamide adenine dinucleotide phosphate added to the incubation mixture (as monitored spectrophotometrically at 340 nm).

Further experiments to investigate the kinetics of the enzymatic degradation of methaqualone and the effect of diphenhydramine on the reaction were initiated. A standard incubation time of 20 min was chosen after verifying that the conversion rate of the substrate, methaqualone, to the metabolite was constant for that time period under the study conditions. At methaqualone concentrations of 0.43 and 2.18 m*M*, the conversion of substrate to metabolite was linear for the 20 min (Fig. 2).

The velocity of the metabolite formation increased with increasing substrate concentration over a range of 0.43–4.4 μmoles of methaqualone/ml of incubation mixture. At substrate concentrations greater than 2.15 μmoles/ml, velocity increased only minimally (Fig. 3), suggesting

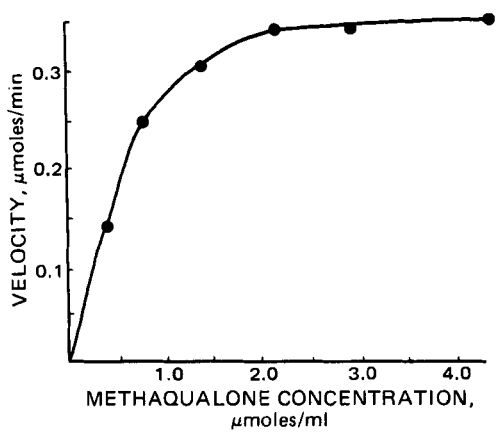

Figure 3—*Effect of increasing concentrations of methaqualone on the velocity of metabolite formation at a 20-min incubation time.*

Table III—Effect of Diphenhydramine on the Conversion of Methaqualone to 2-Methyl-3-(2-hydroxymethylphenyl)-4-(3*H*)-quinazolinone by Rat Liver Homogenate

Methaqualone Concentration, μmoles/ml	Inhibition of Metabolism, %	
	0.5 m*M* Diphenhydramine	0.83 m*M* Diphenhydramine
0.43	40.63	59.38
0.72	32.35	47.06
1.01	35.90	46.15
1.43	26.20	38.10
2.15	26.00	40.00

that the enzyme is saturated at concentrations greater than 2.15 μmoles/ml.

In the presence of diphenhydramine at concentrations of 0.5 and 0.83 m*M*, the velocity of metabolite production decreased (Fig. 4). Inhibition of conversion of methaqualone to 2-methyl-3-(2-hydroxymethylphenyl)-4(3*H*)-quinazolinone increased with increasing diphenhydramine concentration (Table III).

To evaluate maximal velocity, V_m, the Michaelis constant, K_m, and the inhibitory constant, standard methods for linearizing enzyme kinetic data were applied. Data for the velocity of metabolite formation at various substrate concentrations were plotted as $1/V$ against $1/S$ (Fig. 5) and as V against V/S. Although the correlation coefficients, r, for all data sets were significant ($p < 0.05$), systematic deviations from linearity were apparent. Curvature was more obvious without inhibitor than with 0.83 m*M* diphenhydramine and in plots of V against V/S than in plots of $1/V$ against $1/S$.

While recognizing the difficulties in interpreting nonlinear plots, K_m and V_m were estimated from the slope and intercept of the double-reciprocal plots (as calculated by least-squares linear regression) for five substrate and two inhibitor concentrations. The maximal velocity altered only slightly from 0.26 mmoles/min without diphenhydramine to 0.23 and 0.22 mmole/min with 0.5 and 0.83 m*M* diphenhydramine, respectively. The K_m as estimated from data obtained without inhibitor added was 0.30 m*M*. The apparent K_m with diphenhydramine concentrations of 0.5 and 0.83 m*M* increased to 0.62 and 1.06, respectively. The similarity in V_m values and the significant difference in apparent K_m values determined in the presence and absence of inhibitor suggest that diphenhydramine inhibition of methaqualone metabolism is competitive rather than noncompetitive.

One may speculate that such nonlinearity is due to independent binding sites with different binding affinities for the substrate (*e.g.*, isoenzymes) or to cooperative binding of more than one substrate molecule. Isoenzymes have been demonstrated for a number of enzyme systems (23). Methaqualone metabolism is catalyzed by liver microsomal oxidoreductases (24). Functionally independent isoenzymes of microsomal oxidoreductases with different binding affinities for the substrate may exist. Naturally occurring enzymes appear to consist of a small number of similar subunits (22). Binding of a single substrate molecule may enhance or inhibit binding of subsequent substrate molecules. Therefore, affinity of binding appears to change as the substrate concentration is increased.

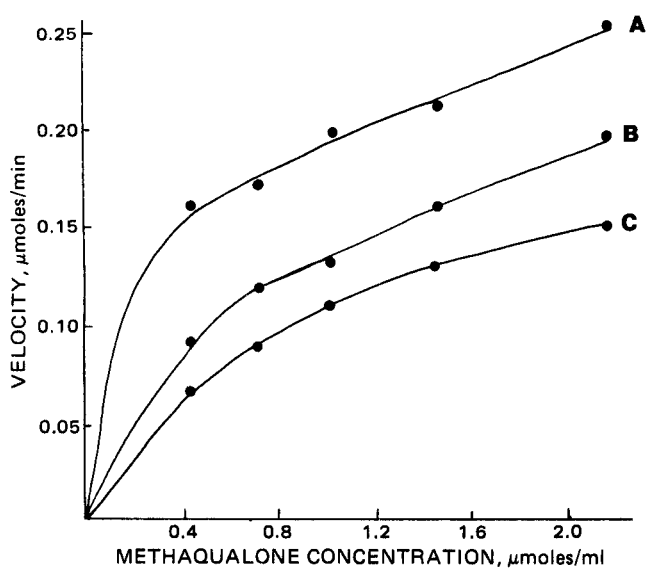

Figure 4—*Effect of diphenhydramine on the velocity of metabolite formation at varying methaqualone (substrate) concentrations. Key: A, 0.00 m*M *diphenhydramine; B, 0.50 m*M *diphenhydramine; and C, 0.83 m*M *diphenhydramine.*

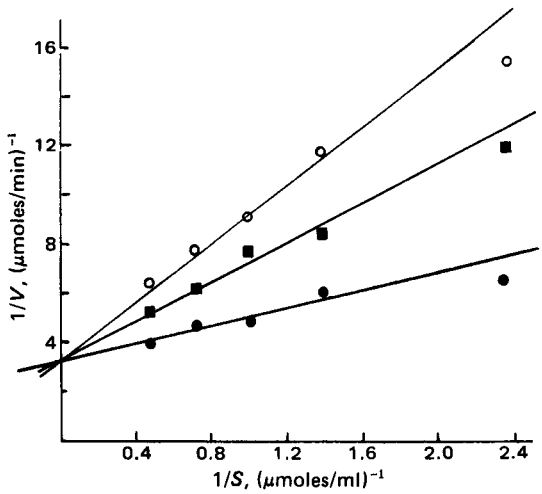

Figure 5—*Double-reciprocal plot of the effect of methaqualone (substrate) concentration on the initial velocity of metabolite formation in the presence of diphenhydramine at concentrations of 0 (●), 0.5 (■), and 0.83 (○) m*M.

In conclusion, it has been demonstrated *in vitro* that diphenhydramine inhibits the metabolism of methaqualone by rat liver homogenate. The inhibition of the conversion of the pharmacologically active methaqualone to an inactive metabolite (18, 19) may explain the enhanced effect claimed by drug abusers for a methaqualone–diphenhydramine combination.

The significance of inhibition of methaqualone metabolism by diphenhydramine detected *in vitro* is presently being investigated *in vivo*.

REFERENCES

(1) G. E. Kochansky, T. S. Hemenway, C. Saltzman, and R. I. Shader, *Dis. Nerv. Syst.*, **36**, 348 (1975).

(2) J. A. Ostrenga, *Clin. Toxicol.*, **6**, 607 (1973).

(3) A. T. Shulgin, *ibid.*, **8**, 405 (1975).

(4) J. R. Gamage and E. L. Zerkin, *Nat. Clear. House Drug Abuse Info.*, **18** (1), (Oct. 1973).

(5) P. Marriott, *Commun. Psychol.*, **17**, 779 (1976).

(6) T. P. Bridge and E. H. Ellinwood, *Am. J. Psychol.*, **130**, 217 (1973).

(7) M. Mitcheson, J. Davidson, D. Hawks, L. Hitchins, and S. Malone, *J. Psychol. Drugs*, **4**, 123 (1971).

(8) R. De Alarcon, *Br. Med. J.*, **1**, 122 (1969).

(9) P. A. L. Chappell, *Med. News*, **Feb. 21, 1969**, 4.

(10) H. Matthew, A. T. Proudfoot, S. S. Brown, and A. C. A. Smith, *Br. Med. J.*, **2**, 101 (1968).

(11) K. Constantinidis, *ibid.*, **2**, 370 (1975).

(12) N. L. Rock and R. J. Moore, *Int. J. Addict.*, **11**, 237 (1976).

(13) A. A. H. Lawson and S. S. Brown, *Br. Med. J.*, **2**, 1455 (1966).

(14) F. S. Tennant, *Br. J. Addict.*, **68**, 327 (1973).

(15) F. S. Tennant, *J. Am. Med. Assoc.*, **221**, 1146 (1972).

(16) K. W. Hindmarsh, D. F. LeGatt, and N. W. Hamon, *Can. J. Pharm. Sci.*, **12**, 103 (1977).

(17) W. G. Stillwell, P. A. Gregory, and M. G. Horning, *Drug Metab. Dispos.*, **3**, 287 (1975).

(18) S. S. Brown and S. Goenechea, *Clin. Pharmacol. Ther.*, **14**, 314 (1973).

(19) H. Nowak, G. Schorre, and R. Struller, *Arzneim.-Forsch.*, **16**, 407 (1966).

(20) J. A. Cella, *J. Pharm. Sci.*, **63**, 1627 (1974).

(21) O. H. Lowry, N. J. Rosebrough, L. Fair, and R. J. Randall, *J. Biol. Chem.*, **193**, 265 (1951).

(22) G. L. Miller, *Anal. Chem.*, **31**, 964 (1954).

(23) M. Dixon and E. C. Webb, "Enzymes," Academic, New York,

N.Y., 1964, pp. 656–659.
(24) R. K. Nyak, R. D. Smyth, J. H. Chamberlain, A. Polk, A. F. DeLong, T. Herczeg, P. B. Chemburkar, R. S. Joslin, and N. H. Reavey-Cantwell, *J. Pharmacokin. Biopharm.*, **2**, 107 (1974).

ACKNOWLEDGMENTS

The award of a Medical Research Council Studentship (to D. F. LeGatt) is gratefully acknowledged.

Potential Antitumor Agents *via* Inhibitors of L-Asparagine Synthetase: Substituted Sulfonamides and Sulfonyl Hydrazides Related to Glutamine

STEVEN BRYNES *§x, VICTOR J. FIORINA *, DAVID A. COONEY ‡, and HARRY A. MILMAN ‡

Received November 21, 1977, from the **Organic Chemistry Division, Microbiological Associates, Bethesda, MD 20016*, and the ‡*Laboratory of Toxicology, National Cancer Institute, National Institutes of Health, Bethesda, MD 20014.* Accepted for publication March 7, 1978. §Present address: Food and Drug Administration, HFF-144, DCH/RAMIB, Washington, DC 20204.

Abstract □ A series of 4-(substituted aminosulfonyl)- and 4-(substituted hydrazinosulfonyl)-2-aminobutanoic acids, compounds structurally related to glutamine, was synthesized as potential inhibitors of L-asparagine synthetase and subjected to screening as antitumor agents. Target amino acids were obtained by condensation of a blocked reactive sulfonyl chloride with the appropriate amine or hydrazide, followed by deblocking with hydrogen–palladium or liquid hydrogen fluoride–anisole. Neither the target compounds nor their protected precursors inhibited the enzyme from L5178Y/AR or prolonged the life of mice with P-388 lymphocytic leukemia. However, DL-4,4′-dithiobis[2-(benzyloxycarbonylamino)butanoic acid], an intermediate in the synthesis of the target amino acids, exhibited 90% inhibition of L-asparagine synthetase at 10 m*M*.

Keyphrases □ Sulfonamides, various—synthesized, evaluated for antineoplastic activity in mice and effect on L-asparagine synthetase activity *in vitro* □ Sulfonyl hydrazides, various—synthesized, evaluated for antineoplastic activity in mice and effect on L-asparagine synthetase activity *in vitro* □ Antineoplastic activity—various sulfonamides and sulfonyl hydrazides evaluated in mice □ L-Asparagine synthetase activity—effect of various sulfonamides and sulfonyl hydrazides evaluated *in vitro* □ Enzyme activity—effect of various sulfonamides and sulfonyl hydrazides on L-asparagine synthetase evaluated *in vitro* □ Structure–activity relationships—various sulfonamides and sulfonyl hydrazides evaluated for antineoplastic activity in mice and effect on L-asparagine synthetase activity *in vitro*

Asparaginase, the enzyme responsible for hydrolyzing L-asparagine to L-aspartic acid, is therapeutically useful in the treatment of certain tumors (1). However, its effectiveness is diminished by several factors, including an induced resistance by formerly susceptible tumor cells. Various reports (2–4) indicated that such resistance is attributable to the appearance of high levels of the biosynthetic enzyme L-asparagine synthetase (I), which catalyzes the transfer of the amide nitrogen of L-glutamine to L-aspartic acid to form L-asparagine (5). The relation between resistance to asparaginase and high levels of I and sensitivity to asparaginase and absence of I provides a distinct biochemical difference between certain tumors (high levels of I) and normal tissue (low levels of I), which should be capable of being exploited chemotherapeutically.

In studies aimed at developing inhibitors of I and potential antitumor agents, Brynes *et al.* (6) recently described the synthesis and biological activity of asparagine analogs characterized by replacement of the amide carbonyl with a sulfonyl group. The compounds generally produced moderate (30–40% at 2 m*M*) inhibition of I isolated from Novikoff hepatoma, although 3-(hydroxysulfamoyl)-L-alanine displayed quantitative inhibition at 2 m*M* (6). Noting the importance of glutamine as a substrate for I (as well as for other significant biochemical events such as the biosynthesis of purines), this report describes the preparation and biochemical testing of several similar sulfonamides and sulfonyl hydrazides (VI*a*–VI*g*, Scheme I).

EXPERIMENTAL[1]

Chemistry—The route employed in obtaining target compounds VI*a*–VI*g* was analogous to that established previously (6) for a series of L-asparagine analogs. Generally, homocystine was fully protected by treatment first with benzyloxycarbonyl chloride and then with benzyl bromide in the presence of dicyclohexylamine. Subsequent cleavage of the blocked homocystine (III) with chlorine in aqueous acetic acid provided the reactive sulfonyl chloride IV, which was, in turn, allowed to react with the appropriate amine or hydrazide, yielding the blocked intermediates V*a*–V*g*. Hydrogenolysis or treatment with hydrogen fluoride gave the desired free amino acids (Scheme I). All compounds were characterized by their melting points, elemental analyses, IR spectra, and homogeneity on TLC (visualization with ninhydrin).

DL-4,4′-Dithiobis[2-(benzyloxycarbonylamino)butanoic Acid] (II)—This protected amino acid was prepared from DL-homocystine and benzyloxycarbonyl chloride in exactly the same manner as described for *N,N′*-di(benzyloxycarbonyl)-L-cystine (7). The use of 5.3 g (0.02 mole) of homocystine afforded 9.2 g (86%) of crystalline product from chloroform, mp 119–127°. Recrystallization from ethanol–water yielded an analytical sample, mp 138–139.5°.

Anal.—Calc. for $C_{24}H_{28}N_2O_8S_2$: C, 53.72; H, 5.26; N, 5.22. Found: C, 53.90; H, 5.44; N, 5.36.

Dibenzyl DL-4,4′-Dithiobis[2-(benzyloxycarbonylamino)butanoate] (III)—Diacid II (26.8 g, 0.05 mole), benzyl bromide (13.6 ml, 0.10 mole), and dicyclohexylamine (21.6 ml, 0.11 mole) were combined in 500 ml of dimethylformamide and allowed to stir overnight at room temperature. Following removal of the solvent *in vacuo*, the white solid was thoroughly

[1] Melting points were determined on a Mel-Temp apparatus and are uncorrected. Microanalyses were performed by Galbraith Laboratories, Knoxville, Tenn. The petroleum ether used had a boiling-point range of 30–60°. Commercially unavailable monoethyl fumarylhydrazide, needed for the synthesis of V*g*, was prepared as previously described (6).

0022-3549/78/1100-1550$01.00/0
© 1978, American Pharmaceutical Association

N.Y., 1964, pp. 656–659.
(24) R. K. Nyak, R. D. Smyth, J. H. Chamberlain, A. Polk, A. F. DeLong, T. Herczeg, P. B. Chemburkar, R. S. Joslin, and N. H. Reavey-Cantwell, *J. Pharmacokin. Biopharm.*, **2**, 107 (1974).

ACKNOWLEDGMENTS

The award of a Medical Research Council Studentship (to D. F. LeGatt) is gratefully acknowledged.

Potential Antitumor Agents *via* Inhibitors of L-Asparagine Synthetase: Substituted Sulfonamides and Sulfonyl Hydrazides Related to Glutamine

STEVEN BRYNES *§x, VICTOR J. FIORINA *, DAVID A. COONEY ‡, and HARRY A. MILMAN ‡

Received November 21, 1977, from the **Organic Chemistry Division, Microbiological Associates, Bethesda, MD 20016*, and the ‡*Laboratory of Toxicology, National Cancer Institute, National Institutes of Health, Bethesda, MD 20014.* Accepted for publication March 7, 1978. §Present address: Food and Drug Administration, HFF-144, DCH/RAMIB, Washington, DC 20204.

Abstract □ A series of 4-(substituted aminosulfonyl)- and 4-(substituted hydrazinosulfonyl)-2-aminobutanoic acids, compounds structurally related to glutamine, was synthesized as potential inhibitors of L-asparagine synthetase and subjected to screening as antitumor agents. Target amino acids were obtained by condensation of a blocked reactive sulfonyl chloride with the appropriate amine or hydrazide, followed by deblocking with hydrogen–palladium or liquid hydrogen fluoride–anisole. Neither the target compounds nor their protected precursors inhibited the enzyme from L5178Y/AR or prolonged the life of mice with P-388 lymphocytic leukemia. However, DL-4,4′-dithiobis[2-(benzyloxycarbonylamino)butanoic acid], an intermediate in the synthesis of the target amino acids, exhibited 90% inhibition of L-asparagine synthetase at 10 m*M*.

Keyphrases □ Sulfonamides, various—synthesized, evaluated for antineoplastic activity in mice and effect on L-asparagine synthetase activity *in vitro* □ Sulfonyl hydrazides, various—synthesized, evaluated for antineoplastic activity in mice and effect on L-asparagine synthetase activity *in vitro* □ Antineoplastic activity—various sulfonamides and sulfonyl hydrazides evaluated in mice □ L-Asparagine synthetase activity—effect of various sulfonamides and sulfonyl hydrazides evaluated *in vitro* □ Enzyme activity—effect of various sulfonamides and sulfonyl hydrazides on L-asparagine synthetase evaluated *in vitro* □ Structure–activity relationships—various sulfonamides and sulfonyl hydrazides evaluated for antineoplastic activity in mice and effect on L-asparagine synthetase activity *in vitro*

Asparaginase, the enzyme responsible for hydrolyzing L-asparagine to L-aspartic acid, is therapeutically useful in the treatment of certain tumors (1). However, its effectiveness is diminished by several factors, including an induced resistance by formerly susceptible tumor cells. Various reports (2–4) indicated that such resistance is attributable to the appearance of high levels of the biosynthetic enzyme L-asparagine synthetase (I), which catalyzes the transfer of the amide nitrogen of L-glutamine to L-aspartic acid to form L-asparagine (5). The relation between resistance to asparaginase and high levels of I and sensitivity to asparaginase and absence of I provides a distinct biochemical difference between certain tumors (high levels of I) and normal tissue (low levels of I), which should be capable of being exploited chemotherapeutically.

In studies aimed at developing inhibitors of I and potential antitumor agents, Brynes *et al.* (6) recently described the synthesis and biological activity of asparagine analogs characterized by replacement of the amide carbonyl with a sulfonyl group. The compounds generally produced moderate (30–40% at 2 m*M*) inhibition of I isolated from Novikoff hepatoma, although 3-(hydroxysulfamoyl)-L-alanine displayed quantitative inhibition at 2 m*M* (6). Noting the importance of glutamine as a substrate for I (as well as for other significant biochemical events such as the biosynthesis of purines), this report describes the preparation and biochemical testing of several similar sulfonamides and sulfonyl hydrazides (VI*a*–VI*g*, Scheme I).

EXPERIMENTAL[1]

Chemistry—The route employed in obtaining target compounds VI*a*–VI*g* was analogous to that established previously (6) for a series of L-asparagine analogs. Generally, homocystine was fully protected by treatment first with benzyloxycarbonyl chloride and then with benzyl bromide in the presence of dicyclohexylamine. Subsequent cleavage of the blocked homocystine (III) with chlorine in aqueous acetic acid provided the reactive sulfonyl chloride IV, which was, in turn, allowed to react with the appropriate amine or hydrazide, yielding the blocked intermediates V*a*–V*g*. Hydrogenolysis or treatment with hydrogen fluoride gave the desired free amino acids (Scheme I). All compounds were characterized by their melting points, elemental analyses, IR spectra, and homogeneity on TLC (visualization with ninhydrin).

DL-4,4′-Dithiobis[2-(benzyloxycarbonylamino)butanoic Acid] (II)—This protected amino acid was prepared from DL-homocystine and benzyloxycarbonyl chloride in exactly the same manner as described for *N,N′*-di(benzyloxycarbonyl)-L-cystine (7). The use of 5.3 g (0.02 mole) of homocystine afforded 9.2 g (86%) of crystalline product from chloroform, mp 119–127°. Recrystallization from ethanol–water yielded an analytical sample, mp 138–139.5°.

Anal.—Calc. for $C_{24}H_{28}N_2O_8S_2$: C, 53.72; H, 5.26; N, 5.22. Found: C, 53.90; H, 5.44; N, 5.36.

Dibenzyl DL-4,4′-Dithiobis[2-(benzyloxycarbonylamino)butanoate] (III)—Diacid II (26.8 g, 0.05 mole), benzyl bromide (13.6 ml, 0.10 mole), and dicyclohexylamine (21.6 ml, 0.11 mole) were combined in 500 ml of dimethylformamide and allowed to stir overnight at room temperature. Following removal of the solvent *in vacuo*, the white solid was thoroughly

[1] Melting points were determined on a Mel-Temp apparatus and are uncorrected. Microanalyses were performed by Galbraith Laboratories, Knoxville, Tenn. The petroleum ether used had a boiling-point range of 30–60°. Commercially unavailable monoethyl fumarylhydrazide, needed for the synthesis of V*g*, was prepared as previously described (6).

0022-3549/78/1100-1550$01.00/0
© 1978, American Pharmaceutical Association

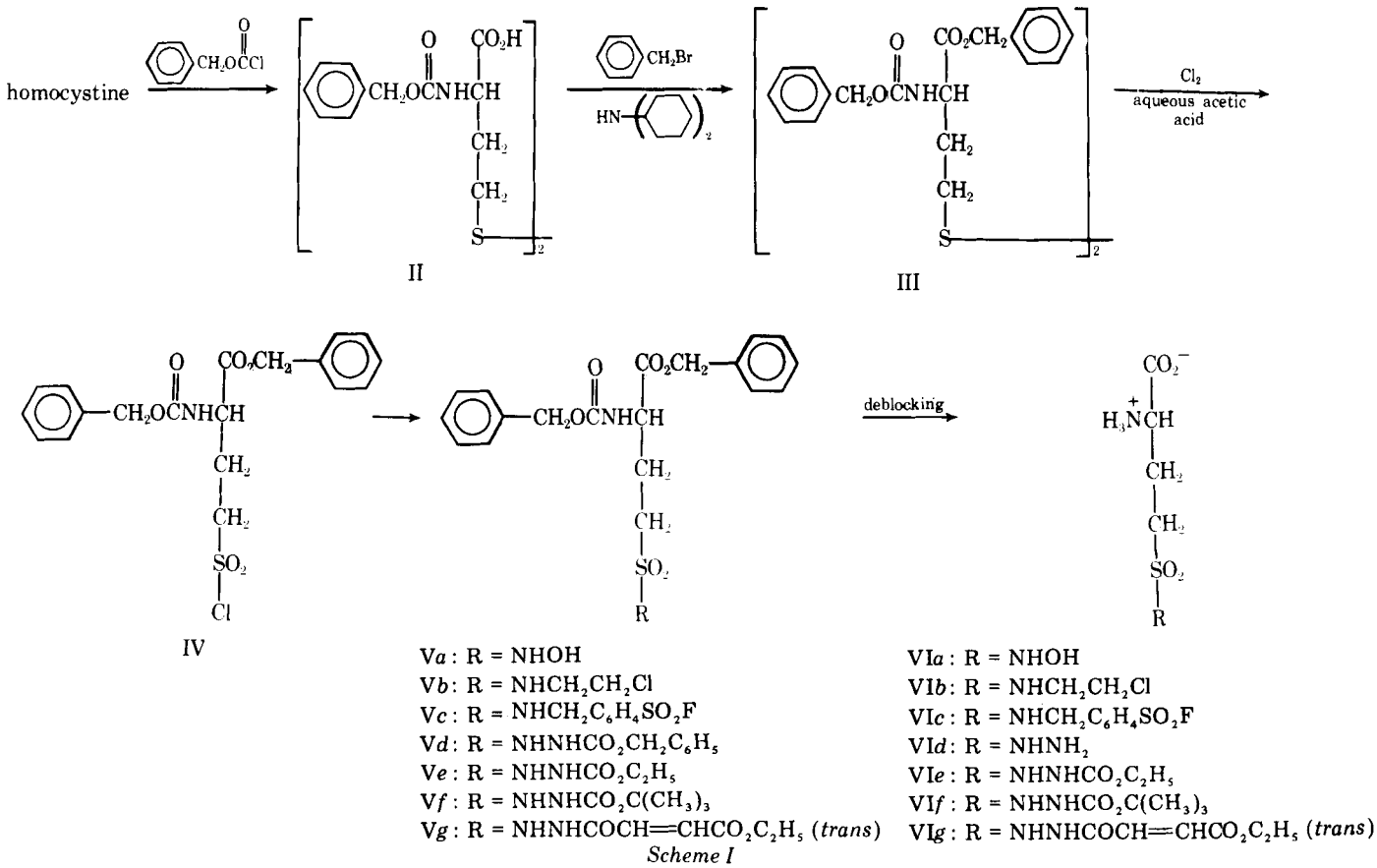

Scheme I

triturated with ethyl acetate. The insoluble material was removed by filtration, and the filtrate was washed twice with 1 *N* HCl, twice with 6.9% $NaHCO_3$, and once with 35% NaCl. The organic solvent was dried and evaporated. The oil remaining was crystallized from ether–petroleum ether, affording 28.9 g (81%) of desired product III, mp 84–101°. Repeated recrystallization from the same solvent system yielded an analytical sample, mp 92–96°.

Anal.—Calc. for $C_{38}H_{40}N_2O_8S_2$: C, 63.67; H, 5.62; N, 3.91. Found: C, 63.66; H, 5.72; N, 3.99.

Benzyl DL-4-(Chlorosulfonyl)-2-(benzyloxycarbonylamino)butanoate (IV)—Diester III (21.5 g, 0.03 mole) was dissolved in 700 ml of acetic acid containing 2 ml of water. Chlorine (14 ml, 0.30 mole) was condensed in a test tube surrounded by dry ice–acetone. When the tube was removed from the ice bath, the chlorine slowly distilled and was introduced just above the surface of the reaction solution, which was stirred at 0°. Following complete distillation of the chlorine, the reaction mixture was allowed to warm to room temperature, and solvent was removed by co-distillation with carbon tetrachloride. The remaining oil was crystallized from ether–petroleum ether, yielding 18.8 g (70%) of sulfonyl chloride IV, mp 51–57° (softens) and 57–61° (melts). Preparative TLC (silica, chloroform) afforded an analytical sample, mp 39–42°.

Anal.—Calc. for $C_{19}H_{20}ClNO_6S$: C, 53.58; H, 4.73; N, 3.29. Found: C, 53.66; H, 4.76; N, 3.45.

Protected 4-(Substituted aminosulfonyl)- and 4-(Substituted hy-

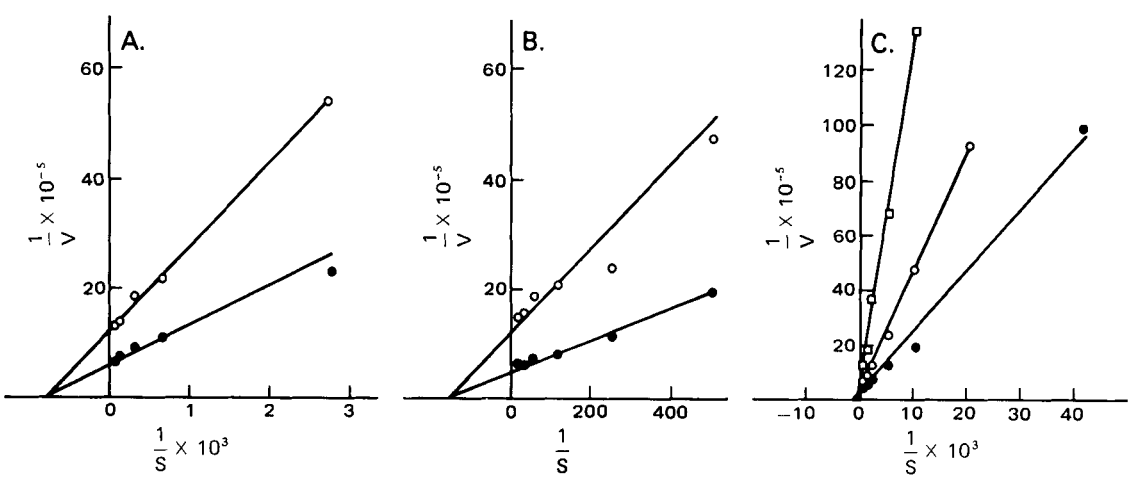

Figure 1—*Double-reciprocal plots of II* versus *L-glutamine, ammonium chloride, and L-aspartic acid for asparagine synthetase of L5178Y/AR. In a final volume of 15 μl were admixed 4 (○) or 8 (□) mM II or water (●), ATP (10 mM), magnesium chloride (25 mM), and the following: A, L-glutamine (13, 6, 3, 1.5, or 0.35 mM) and L-4-^{14}C-aspartic acid (0.05 mM); B, ammonium chloride (66, 33, 17, 8, 4, or 2 mM) and L-4-^{14}C-aspartic acid (0.056 mM); and C, L-4-^{14}C-aspartic acid (specific radioactivity of 12.9 μCi/μmole; 1.46, 0.74, 0.37, 0.18, 0.09, 0.045, and 0.02 mM) and L-glutamine (13 mM). A 5-μl aliquot of the 27,000×g (20 min) supernate of L5178Y/AR homogenate (1:4, w/v) was used to initiate the reaction. All vessels were incubated at 37° for 30 min, after which the reaction was terminated by heating the closed vessels at 95° for 5 min. Subsequent steps for the recovery of synthesized L-4-^{14}C-asparagine were conducted as previously described (9). V = cpm; S = molarity.*

Table I—4-(Substituted aminosulfonyl)- and 4-(Substituted hydrazinosulfonyl)-2-aminobutanoic Acids and Antitumor Activity [a]

Compound	Reaction Solvent (Method) [b]	Yield, %	Melting Point	Recrystallization Solvent	Formula		Analysis, % Calc.	Analysis, % Found	Antitumor Activity Dose [c]	Antitumor Activity T/C [d]
II	*Experimental* section	86	138–139.5°	Ethanol–water	$C_{24}H_{28}N_2O_8S_2$	C	53.72	53.90	400 [e]	103
						H	5.26	5.44		
						N	5.22	5.36		
III	*Experimental* section	81	92–96°	Ether–petroleum ether	$C_{38}H_{40}N_2O_8S_2$	C	63.67	63.66	400 [e]	94
						H	5.62	5.72		
						N	3.91	3.99		
V*a*	1% Water–acetonitrile	30	112–114°	Ether–petroleum ether	$C_{19}H_{22}N_2O_7S$	C	54.02	53.86	400 [e]	109
						H	5.25	5.37		
						N	6.63	6.43		
V*b*	Chloroform–water [f]	34	91–93°	Carbon tetrachloride	$C_{21}H_{25}ClN_2O_6S$	C	53.79	53.57	400 [e]	92
						H	5.37	5.15		
						N	5.97	5.80		
V*c*	Acetonitrile	55	114–115°	Ethyl acetate–petroleum ether	$C_{26}H_{27}FN_2O_8S_2$	C	53.97	54.06	200 [e]	98
						H	4.70	4.80		
						N	4.84	4.76		
V*d*	Chloroform	54	123°	Carbon tetrachloride	$C_{27}H_{29}N_3O_8S$	C	58.37	58.13	400 [e]	111
						H	5.26	5.10		
						N	7.56	7.44		
V*e*	Chloroform	59	114–118°	Ethanol–water	$C_{22}H_{27}N_3O_8S$	C	53.54	53.53	400 [e]	91
						H	5.51	5.65		
						N	8.51	8.54		
V*f*	Chloroform	76	68°	Carbon tetrachloride	$C_{24}H_{31}N_3O_8S$	C	55.27	55.12	400 [e]	93
						H	5.99	6.11		
						N	8.06	7.97		
V*g*	Pyridine	25	143–145°	Ethyl acetate–petroleum ether	$C_{25}H_{29}N_3O_9S$	C	54.84	54.74	200 [e]	86
						H	5.34	5.40		
						N	7.67	7.66		
VI*a*	A	86	186–187° dec.	Water–ethanol	$C_4H_{10}N_2O_5S$	C	24.24	24.33	400 [g]	101
						H	5.09	5.16		
						N	14.13	14.15		
VI*b*	A	82	230° dec.	Water	$C_6H_{13}ClN_2O_4S$	C	29.45	29.59	400 [g]	99
						H	5.36	5.36		
						N	11.45	11.29		
VI*c*	B	58	226–230°	Water	$C_{11}H_{15}FN_2O_6S_2$	C	37.28	37.51	200 [g]	88
						H	4.27	4.42		
						N	7.90	7.96		
VI*d*	A	79	187–193° dec.	Water–ethanol	$C_4H_{11}N_3O_4S$	C	24.36	24.45	100 [g]	98
						H	5.62	5.75		
						N	21.31	21.26		
VI*e*	A	83	234–237°	Water	$C_7H_{15}N_3O_6S$	C	31.22	31.03	400 [g]	111
						H	5.61	5.70		
						N	15.60	15.51		
VI*f*	A	72	189° dec.	Water–acetone	$C_9H_{19}N_3O_6S$	C	36.36	36.18	400 [e]	93
						H	6.44	6.44		
						N	14.13	13.98		
VI*g*	B	58	203–204° dec.	Water–acetone	$C_{10}H_{17}N_3O_7S \cdot H_2O$	C	35.18	35.34	100 [g]	116
						H	5.61	5.73		
						N	12.31	12.45		

[a] Antitumor activity determined *versus* P-388 lymphocytic leukemia; QD 1–9 treatments, drug given ip. Protocols and tumor systems were described in Ref. 10. [b] The letter refers to general procedure given in *Experimental* section. [c] In milligrams per kilogram. [d] T/C (treated survival/control survival) × 100. [e] Water + Tween 80 as vehicle. [f] A two-phase solvent system was used in this synthesis: blocked sulfonyl chloride IV in chloroform and 2-chloroethylamine hydrochloride and sodium carbonate in an equal volume of water were combined with vigorous stirring. [g] Water as vehicle.

drazinosulfonyl)-2-aminobutanoic Acids (V*a*–V*g*)—For benzyl DL-4-(hydroxyaminosulfonyl)-2-(benzyloxycarbonylamino)butanoate (V*a*), sulfonyl chloride IV (20.0 g, 0.047 mole) in 1% aqueous acetonitrile was allowed to stir with hydroxylamine hydrochloride (13.0 g, 0.19 mole) and sodium bicarbonate (19.7 g, 0.24 mole) for 3 hr at room temperature. The solvent was removed *in vacuo*, and the remaining salts were washed with ethyl acetate. Following removal of the salts by filtration, the ethyl acetate was washed twice with 1 *N* HCl, 6.9% $NaHCO_3$, and 35% NaCl and dried. Removal of the ethyl acetate yielded an oil. This oil was purified with column chromatography (silica, 4% methanol–chloroform) and subsequently crystallized from ether–petroleum ether, affording 5.9 g (30%) of V*a*, mp 112–114°.

Anal.—Calc. for $C_{19}H_{22}N_2O_7S$: C, 54.02; H, 5.25; N, 6.63. Found: C, 53.86; H, 5.37; N, 6.43.

Compounds V*b*–V*g* were prepared similarly in the solvents indicated in Table I with reaction times varying between 3 and 6 hr. Triethylamine served as the acid acceptor for *p*-(fluorosulfonyl)benzylamine hydrochloride (8) in the synthesis of V*c*.

Preparation of Free Amino Acids VI*a*–VI*g*—*Method A*—Blocked amino acid (0.003 mole) was dissolved in 50 ml of 20% aqueous ethanol and hydrogenated at atmospheric pressure in the presence of 350 mg of palladium black. Following removal of the catalyst by filtration and evaporation of the filtrate, the residue was crystallized from the appropriate solvent (Table I). Yields were in the 70–90% range.

Method B—Blocked amino acid (0.01 mole) and anisole (0.02 mole) were allowed to stir with 20 ml of liquid hydrogen fluoride at 0° for 1 hr. Following complete removal of hydrogen fluoride by aspiration, the residue was dissolved in 100 ml of 6% aqueous acetic acid and washed several times with ethyl acetate. The aqueous solution was lyophilized, and the residue was crystallized from the appropriate solvent (Table I).

Preparation of I, Assay for I, and Inhibition—Generally, I was extracted from subcutaneous nodules of leukemia 5178Y resistant to L-asparaginase (L5178Y/AR) grown in BDF_1 mice. The 105,000×*g* supernate (specific activity of 0.001 IU/mg of protein) was used as the enzyme source. L-4-^{14}C-Aspartic acid was incubated with ATP, magnesium chloride, L-glutamine, and I; any L-4-^{14}C-asparagine synthesized was determined as previously described (9). Further details can be found in Ref. 9.

Antitumor Activity—Antitumor activity *versus* lymphocytic leukemia P-388 was determined by standard protocols[2] (10). Compounds were considered active if they gave T/C activity (10) values in the P-388 system equal to or greater than 125%, where T/C represents the ratio of

[2] Division of Cancer Treatment, National Cancer Institute, National Institutes of Health.

the median survival times of the treated animals over those of the control animals expressed as a percentage.

RESULTS AND DISCUSSION

All synthesized compounds except IV were subjected both to an *in vitro* inhibition assay with I and to screening for antitumor activity. At 10 m*M*, II and VI*a* with glutamine as the nitrogen donor inhibited I by 90 and 32%, respectively; at 1 m*M*, both compounds were devoid of activity. The remainder of the compounds possessed negligible or no activity when tested at 1 and 10 m*M*. The results for the antitumor screen are given in Table I; none of the analogs displayed significant (T/C ≥ 125%) activity.

Only diacid II exhibited significant inhibition of I *in vitro*. In double-reciprocal plots (Fig. 1), II was competitive with L-aspartic acid for crude I, but noncompetitive with L-glutamine. From the results for II, one might expect that either homocystine or diester III would also show some inhibition with I; however, neither compound showed activity in the assay. Dithiothreitol (10 m*M*) did not prevent the inhibition of I by II, indicating that the agent was not acting by virtue of sulfhydryl groups. Since enzymes utilizing amino acids are usually highly substrate specific (11), it appears improbable that structurally bulky (as compared to aspartic acid) II is acting directly at the aspartic acid site of I. The observed inhibition probably results from an allosteric effect by II upon the aspartic acid site of the synthetase.

It is somewhat surprising that none of the target free amino acids of this study exhibited significant inhibitory action with I. In particular, results from an earlier study indicated 3-(hydroxysulfamoyl)-L-alanine (normethylene analog of VI*a*) to be a moderately good inhibitor of I from L5178Y/AR (81 and 23% at 10 and 1 m*M*, respectively) (6). Compound VI*a*, on the other hand, exhibited reduced activity (32 and 0% at 10 and 1 m*M*, respectively). Kinetic studies with 3-(hydroxysulfamoyl)-L-alanine and I revealed that the amino acid was acting as an analog of aspartic acid rather than of asparagine (6). By extrapolation, VI*a* becomes an analog not of glutamine but of glutamic acid. Because I does not utilize glutamic acid, the lowered activity of VI*a* is understandable.

REFERENCES

(1) J. M. Hill, J. Roberts, E. Loev, A. Kahn, A. MacLellan, and R. W. Hill, *J. Am. Med. Assoc.*, **202**, 116 (1967).

(2) M. K. Patterson, Jr., and G. Orr, *Biochem. Biophys. Res. Commun.*, **26**, 228 (1967).

(3) M. D. Prager and N. Bachynsky, *ibid.*, **31**, 43 (1968). M. D. Prager and N. Bachynsky, *Arch. Biochem. Biophys.*, **127**, 645 (1968).

(4) C. M. Haskell and G. P. Canellos, *Biochem. Pharmacol.*, **18**, 2578 (1969).

(5) A. Meister, in "The Enzymes," 3rd ed., vol. 10, P. D. Boyer, Ed., Academic, New York, N.Y., 1974, p. 561.

(6) S. Brynes, G. J. Burckart, and M. Mokotoff, *J. Med. Chem.*, **21**, 45 (1978).

(7) V. duVigneaud and G. L. Miller, in "Biochemical Preparations," vol. 2, E. G. Ball, Ed., Wiley, New York, N.Y., 1952, p. 74.

(8) M. Mokotoff, S. Brynes, and J. F. Bagaglio, *J. Med. Chem.*, **18**, 888 (1975).

(9) H. A. Milman and D. A. Cooney, *Biochem. J.*, **142**, 27 (1974).

(10) R. I. Geran, N. H. Greenberg, M. M. Macdonald, A. M. Schumacher, and B. J. Abbott, *Cancer Chemother. Rep., Part 3*, **3**, 1 (1972).

(11) W. Shive and C. G. Skinner, in "Metabolic Inhibitors," R. M. Hochster and J. H. Quastel, Eds., Academic, New York, N.Y., 1963, p. 1.

ACKNOWLEDGMENTS

Supported by Contract N01-CM-43761 from the Division of Cancer Treatment, National Cancer Institute, National Institutes of Health, Department of Health, Education, and Welfare.

Radioimmunoassay of Oxfendazole in Bovine, Equine, or Canine Plasma or Serum

C. NERENBERG, R. A. RUNKEL, and S. B. MATIN ˣ

Received October 31, 1977, from the *Department of Drug Metabolism, Syntex Research, Palo Alto, CA 94304.* Accepted for publication March 8, 1978.

Abstract □ A simple radioimmunoassay was developed for the determination of oxfendazole in plasma. Oxfendazole *N*-1(3)-valerate was coupled to polylysine *via* a carbodiimide reaction, and antiserum was developed in rabbits after inoculation with oxfendazole–polylysine conjugate. The assay was developed so that oxfendazole could be measured directly in a 0.1-ml aliquot of diluted or undiluted plasma. With the developed procedure, 200 pg of oxfendazole/ml of plasma can be determined quantitatively. Cross-reactivity was determined for closely related compounds and metabolites. The method was used to determine plasma concentration–time profiles in dogs and calves.

Keyphrases □ Oxfendazole—radioimmunoassay in plasma or serum □ Radioimmunoassay—oxfendazole in plasma or serum □ Anthelmintics—oxfendazole, radioimmunoassay in plasma or serum

Oxfendazole (I) is active against a broad spectrum of GI nematodes, lungworms, and tapeworms found in cattle, sheep, and pigs (1).

This paper describes an assay for I that was developed to provide data for the determination of certain pharmacokinetic parameters, *e.g.*, plasma clearance, half-lives, and absorption. The sensitivity requirement for these determinations was the low nanogram range.

EXPERIMENTAL

Materials—Freund's complete and incomplete adjuvants were purchased in sealed glass ampuls[1]. Activated powdered charcoal[2] was used.

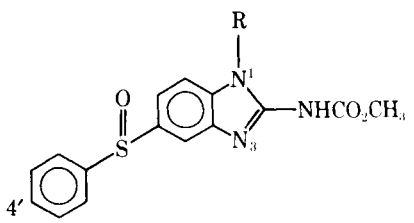

I: R = H

II: R = $(CH_2)_4COOH$

[1] Difco Laboratories, Detroit, Mich.

[2] Norit A, Matheson, Coleman and Bell, Norwood, Ohio.

0022-3549/78/1100-1553$01.00/0

© 1978, American Pharmaceutical Association

the median survival times of the treated animals over those of the control animals expressed as a percentage.

RESULTS AND DISCUSSION

All synthesized compounds except IV were subjected both to an *in vitro* inhibition assay with I and to screening for antitumor activity. At 10 m*M*, II and VI*a* with glutamine as the nitrogen donor inhibited I by 90 and 32%, respectively; at 1 m*M*, both compounds were devoid of activity. The remainder of the compounds possessed negligible or no activity when tested at 1 and 10 m*M*. The results for the antitumor screen are given in Table I; none of the analogs displayed significant (T/C ≥ 125%) activity.

Only diacid II exhibited significant inhibition of I *in vitro*. In double-reciprocal plots (Fig. 1), II was competitive with L-aspartic acid for crude I, but noncompetitive with L-glutamine. From the results for II, one might expect that either homocystine or diester III would also show some inhibition with I; however, neither compound showed activity in the assay. Dithiothreitol (10 m*M*) did not prevent the inhibition of I by II, indicating that the agent was not acting by virtue of sulfhydryl groups. Since enzymes utilizing amino acids are usually highly substrate specific (11), it appears improbable that structurally bulky (as compared to aspartic acid) II is acting directly at the aspartic acid site of I. The observed inhibition probably results from an allosteric effect by II upon the aspartic acid site of the synthetase.

It is somewhat surprising that none of the target free amino acids of this study exhibited significant inhibitory action with I. In particular, results from an earlier study indicated 3-(hydroxysulfamoyl)-L-alanine (normethylene analog of VI*a*) to be a moderately good inhibitor of I from L5178Y/AR (81 and 23% at 10 and 1 m*M*, respectively) (6). Compound VI*a*, on the other hand, exhibited reduced activity (32 and 0% at 10 and 1 m*M*, respectively). Kinetic studies with 3-(hydroxysulfamoyl)-L-alanine and I revealed that the amino acid was acting as an analog of aspartic acid rather than of asparagine (6). By extrapolation, VI*a* becomes an analog not of glutamine but of glutamic acid. Because I does not utilize glutamic acid, the lowered activity of VI*a* is understandable.

REFERENCES

(1) J. M. Hill, J. Roberts, E. Loev, A. Kahn, A. MacLellan, and R. W. Hill, *J. Am. Med. Assoc.*, **202**, 116 (1967).

(2) M. K. Patterson, Jr., and G. Orr, *Biochem. Biophys. Res. Commun.*, **26**, 228 (1967).

(3) M. D. Prager and N. Bachynsky, *ibid.*, **31**, 43 (1968). M. D. Prager and N. Bachynsky, *Arch. Biochem. Biophys.*, **127**, 645 (1968).

(4) C. M. Haskell and G. P. Canellos, *Biochem. Pharmacol.*, **18**, 2578 (1969).

(5) A. Meister, in "The Enzymes," 3rd ed., vol. 10, P. D. Boyer, Ed., Academic, New York, N.Y., 1974, p. 561.

(6) S. Brynes, G. J. Burckart, and M. Mokotoff, *J. Med. Chem.*, **21**, 45 (1978).

(7) V. duVigneaud and G. L. Miller, in "Biochemical Preparations," vol. 2, E. G. Ball, Ed., Wiley, New York, N.Y., 1952, p. 74.

(8) M. Mokotoff, S. Brynes, and J. F. Bagaglio, *J. Med. Chem.*, **18**, 888 (1975).

(9) H. A. Milman and D. A. Cooney, *Biochem. J.*, **142**, 27 (1974).

(10) R. I. Geran, N. H. Greenberg, M. M. Macdonald, A. M. Schumacher, and B. J. Abbott, *Cancer Chemother. Rep., Part 3*, **3**, 1 (1972).

(11) W. Shive and C. G. Skinner, in "Metabolic Inhibitors," R. M. Hochster and J. H. Quastel, Eds., Academic, New York, N.Y., 1963, p. 1.

ACKNOWLEDGMENTS

Supported by Contract N01-CM-43761 from the Division of Cancer Treatment, National Cancer Institute, National Institutes of Health, Department of Health, Education, and Welfare.

Radioimmunoassay of Oxfendazole in Bovine, Equine, or Canine Plasma or Serum

C. NERENBERG, R. A. RUNKEL, and S. B. MATIN ˣ

Received October 31, 1977, from the *Department of Drug Metabolism, Syntex Research, Palo Alto, CA 94304.* Accepted for publication March 8, 1978.

Abstract □ A simple radioimmunoassay was developed for the determination of oxfendazole in plasma. Oxfendazole *N*-1(3)-valerate was coupled to polylysine *via* a carbodiimide reaction, and antiserum was developed in rabbits after inoculation with oxfendazole–polylysine conjugate. The assay was developed so that oxfendazole could be measured directly in a 0.1-ml aliquot of diluted or undiluted plasma. With the developed procedure, 200 pg of oxfendazole/ml of plasma can be determined quantitatively. Cross-reactivity was determined for closely related compounds and metabolites. The method was used to determine plasma concentration–time profiles in dogs and calves.

Keyphrases □ Oxfendazole—radioimmunoassay in plasma or serum □ Radioimmunoassay—oxfendazole in plasma or serum □ Anthelmintics—oxfendazole, radioimmunoassay in plasma or serum

Oxfendazole (I) is active against a broad spectrum of GI nematodes, lungworms, and tapeworms found in cattle, sheep, and pigs (1).

This paper describes an assay for I that was developed to provide data for the determination of certain pharmacokinetic parameters, *e.g.*, plasma clearance, half-lives, and absorption. The sensitivity requirement for these determinations was the low nanogram range.

EXPERIMENTAL

Materials—Freund's complete and incomplete adjuvants were purchased in sealed glass ampuls[1]. Activated powdered charcoal[2] was used.

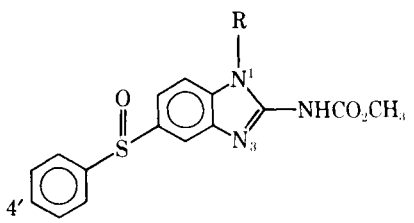

I: R = H

II: R = $(CH_2)_4COOH$

[1] Difco Laboratories, Detroit, Mich.

[2] Norit A, Matheson, Coleman and Bell, Norwood, Ohio.

0022-3549/78/1100-1553$01.00/0

© 1978, American Pharmaceutical Association

Table I—Radioimmunoassay Protocol

Tube Number	Description	Number of Replicates	Buffer, ml	Tritiated Oxfendazole, ml	Cold Oxfendazole, ml	Unknowns, ml	Antiserum, ml	Total Volume, ml
0	Zero standard	6	0.4	0.1	—	—	0.1	0.6
1	20-pg standard	3	0.3	0.1	0.1	—	0.1	0.6
2	50-pg standard	3	0.3	0.1	0.1	—	0.1	0.6
3	100-pg standard	3	0.3	0.1	0.1	—	0.1	0.6
4	200-pg standard	3	0.3	0.1	0.1	—	0.1	0.6
5	500-pg standard	3	0.3	0.1	0.1	—	0.1	0.6
6	1000-pg standard	3	0.3	0.1	0.1	—	0.1	0.6
7	1500-pg standard	3	0.3	0.1	0.1	—	0.1	0.6
N1[a], N2, *etc.*	Nonspecific traps (plasma)	6	0.4	0.1	—	0.1	—	0.6
NB[b]	Nonspecific trap (buffer)	3	0.5	0.1	—	—	—	0.6
TC	Total counts	3	0.5	0.1	—	—	—	0.6
U1, U2, *etc.*	Unknowns	3	0.3	0.1	—	0.1	0.1	0.6

[a] N1, N2, *etc.*, are nonspecific traps containing an aliquot of plasma equivalent to the dilutions used for the unknowns. [b] NB is the nonspecific trap for buffer only and it applies to the standard curve.

The buffer used throughout was 0.05 or 0.1 *M* phosphate-buffered saline, pH 8.0, with or without 0.1% gelatin.

Labeled oxfendazole was synthesized in-house[3] and was tritiated at the 4′-phenyl position with a specific activity of 24–27 Ci/mmole. The *N*-1(3)-valerate derivative (II) of oxfendazole and the oxfendazole–polylysine conjugate were synthesized in-house[3]. The oxfendazole derivatives used in the cross-reactivity experiments also were synthesized in-house[3].

Antiserum Production—The oxfendazole–polylysine conjugate used for immunization was prepared by coupling II to polylysine with a water-soluble carbodiimide coupling reagent (2). The reaction mixture was dialyzed exhaustively against normal saline. The extent of conjugation was determined by measuring the polylysine concentration by the method of Lowry *et al.* (3) and the oxfendazole residues by UV absorption. The molar ratio of oxfendazole to polylysine varied between 60 and 120 moles of oxfendazole/mole of polylysine.

An emulsion of the conjugate in saline was prepared by mixing with an equal volume of Freund's complete adjuvant. The polylysine concentration was 100 μg/ml, and 0.25 ml was injected subcutaneously into four sites in New Zealand White rabbits. Six weeks after the initial injection, all animals were placed on a regimen of weekly booster shots in which the conjugate was prepared in incomplete Freund's adjuvant. After 4–5 months, antiserum dilutions of 1:1000 and 1:2000 yielded 50% binding or more. At this stage, development of the assay was begun.

Radioimmunoassay—Oxfendazole standards for the standard curve were obtained by dilution of a stock solution of 1.0 mg of oxfendazole in 10.0 ml of propylene glycol–0.2 *N* HCl (1:1). The series of standard solutions, 20, 50, 100, 200, 500, 1000, and 1500 pg/0.1 ml, was prepared in 0.05 *M* phosphate-buffered saline, pH 8.0, without gelatin in 10.0-ml volumes and stored in the refrigerator. Gelatin was withheld from the buffer in the standards to give them a longer shelflife.

The labeled oxfendazole was prepared in 0.05 *M* phosphate-buffered saline, pH 8.0, with 0.1% gelatin such that a 0.1-ml aliquot contained approximately 10,000–12,000 cpm. This solution was normally prepared in a volume sufficient for one or two assays only and was not kept longer than 3–4 days. Radioisotope purity was checked periodically by TLC using chloroform–methanol (95:5).

The antiserum was diluted in 0.05 *M* phosphate-buffered saline, pH 8.0, with 0.1% gelatin to yield a total binding of between 35 and 50%. Depending on the quality of the antiserum, this binding was achieved by diluting 1:500, 1:1000, or 1:2000; a 0.1-ml aliquot was added to each tube.

The charcoal stock suspension (1% in water) was diluted as required with 0.05 *M* phosphate-buffered saline, pH 8.0, with 0.1% gelatin immediately before use. A 0.2-ml aliquot of the diluted charcoal suspension was added to blocks of 12–15 tubes at a time. The tubes were vortexed, and the 30-min time cycle was started. Midway through this cycle, additions were made to a second block of tubes and they were started on their 30-min cycle. This staggered array procedure was repeated until all tubes were processed. At the end of the 30-min cycle, each block of tubes was centrifuged immediately and sampled for counting.

A typical radioimmunoassay protocol is given in Table I, and a stepwise procedure for setting up the assay is as follows:

1. Add buffer, label, standards, unknown, antiserums, *etc.*, to the appropriate tubes. Use 12 × 75 disposable culture tubes.
2. After all additions have been made, vortex all tubes for 1–3 sec.
3. Cover the tubes with sheets of waxed film[4] cut to fit test tube racks.
4. Incubate the tubes overnight at 40° in a covered temperature-controlled water bath.
5. After overnight incubation, place the tubes in an ice bath and start the charcoal addition regimen. Add 0.2 ml of charcoal to blocks of 12–15 tubes. Vortex the tubes for 6 sec and then start the 30-min time cycle.
6. After 30 min, centrifuge the tubes at 2000 rpm for 4 min and immediately transfer 0.3 ml of the supernate into scintillation vials. Add 10.0 ml of scintillation fluid.
7. Count for 10 min.
8. Process the data with the Rodbard and Lewald Model I program (4) or manually plot percent bound *versus* oxfendazole concentration and determine unknowns by interpolation.

The centrifuge[5] used was a bench top model with swing out head. Liquid scintillation counting was done in a scintillation spectrometer[6], using commercially available scintillation fluid[7].

^{14}C-Radiochemical Assay—Three calves were given an oral dose of ^{14}C-oxfendazole (3 mg/kg) having the following specific activities: 8.8×10^6 dpm/mg for Calf 1 and 50.2×10^6 dpm/mg for Calves 2 and 3. Blood samples were taken at 2, 4, 8, 24, and 48 hr after dosing.

To 1.0 ml of plasma were added 0.5 ml of phosphate buffer, pH 8.0, and 2.0 ml of chloroform. The tubes were shaken and centrifuged, and the chloroform layer was removed. The extraction was carried out three times, and the chloroform extracts were combined. Then the chloroform extracts were taken to dryness under nitrogen, and the residue was resuspended in a minimum volume of solvent. The residue was spotted on TLC plates, and the peak corresponding to oxfendazole was scraped into a scintillation vial and counted in liquid scintillation fluid.

Specificity—Cross-reactivities were determined from displacement curves generated for oxfendazole free amine (III), oxfendazole thio ether (IV), oxfendazole free amine thio ether (V), and oxfendazole sulfone (VI). This family of curves was compared to the oxfendazole displacement curve. The concentration of each compound that corresponded to the 50% inhibition point on the oxfendazole curve was then used to calculate the percent of cross-reactivity.

Data Processing, Sensitivity, and Precision—Data processing was done with the aid of the Rodbard and Lewald Model I computer program (4), a logit–log transformation that linearizes the sigmoid curve normally obtained in a displacement reaction. The advantages of this system are that it eliminates operator variation both in plotting the standard curve and estimating the unknowns and it increases the speed with which the computations can be made, especially if a teletype punched tape system is coupled to the program. Since the program does not have the capability to subtract different nonspecific traps, this step was either done manually

[3] Syntex Research, Palo Alto, Calif.

[4] Parafilm.
[5] IEC centrifuge model HN-S.
[6] Packard Tri-Carb model 3330.
[7] Aquasol or Oxifluor-H_2O, New England Nuclear.

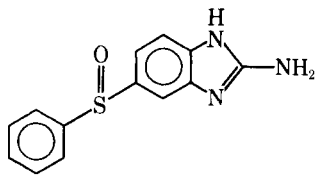

III

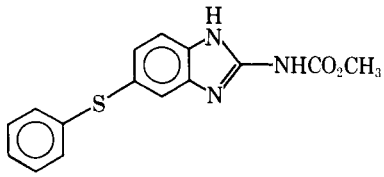

IV

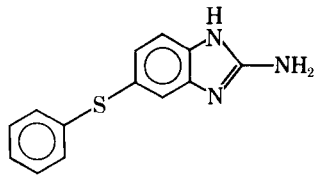

V

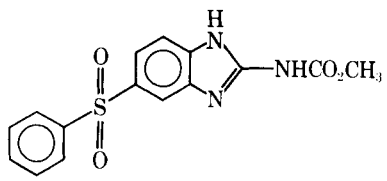

VI

beforehand or by the use of a small preprogram that then fed the corrected data into the Rodbard and Lewald program.

The accuracy and precision of the assay were determined by adding known amounts of oxfendazole to equine, bovine, and canine plasma or serum and then assaying six replicates of each concentration for each plasma.

RESULTS AND DISCUSSION

Assay Conditions—The parameters optimized in this assay were the charcoal contact time and its influence on the separation of bound from free oxfendazole, the effect of pH on total binding, the effect of temperature on the antigen–antibody equilibrium process, and the optimum amount of charcoal required for the separation of bound from free oxfendazole.

The amount of charcoal used to separate bound from free oxfendazole (5) was such that the buffer nonspecific bound would run from 2 to 4% of the total radioactivity added and the nonspecific bound containing an aliquot of undiluted plasma would range from 3 to 8%.

The charcoal contact time is defined as that interval from the instant of addition to when an aliquot is removed for counting. Figure 1 illustrates the time dependence of this process. The procedure outlined, *i.e.*, processing small blocks of tubes at a time, had as its primary purpose to maintain the contact time as nearly alike for all tubes as possible. It would be difficult to maintain a constant time for a large block of 200–300 tubes. However, by processing a staggered array of smaller blocks of tubes, this factor could be controlled.

The effect of buffer pH on the total binding obtained showed that slightly higher binding was achieved at pH 8.0 than at lower pH values. Therefore, pH 8.0 buffers were routinely employed.

The effect of incubation temperature on the antigen–antibody reaction was investigated, and the results failed to show any clearcut advantage. Assays were carried out at 40° in a constant-temperature water bath or at room temperature.

The final assay conditions chosen were as follows. The amount of charcoal required to maintain the nonspecific bound in the specified range was around 0.4%, the charcoal contact time was 30 min plus the time required for centrifugation and aliquoting, the buffer pH was 8.0, and the radioimmunoassay incubation was carried out overnight at 40° or room temperature.

Table II—Validity of Using Nonspecific Traps to Correct Serum or Plasma Unknowns

Experiment	Oxfendazole Added, ng/0.1 ml of Serum	Oxfendazole Measured, ng/0.1 ml of Serum	Ratio of Measured to Added
A[a]	0.50	0.52 ± 0.013[b]	1.04
	1.00	1.08 ± 0.014	1.08
	1.50	1.49 ± 0.037	0.99
	2.00	1.96 ± 0.054	0.98
B[c]	0.50	0.43 ± 0.015	0.86
	1.00	1.04 ± 0.017	1.04
	1.50	1.50 ± 0.038	1.00

[a] In Experiment A, the standard curve was run in buffer only. Samples were prepared by fortifying with known amounts of oxfendazole in the presence of a 0.1-ml aliquot of serum diluted 1:10. The nonspecific trap contained an equivalent amount of diluted serum. The samples were corrected by subtracting the nonspecific bound and then reading these values from the buffer standard curve. [b] Standard errors calculated from six replicates. [c] In Experiment B, the standard curve was run in buffer only. The fortified samples and nonspecific traps were prepared in undiluted plasma but otherwise were treated as in Experiment A.

In this assay, the appropriate nonspecific bound values were subtracted from the unknowns and these values were then interpolated from a

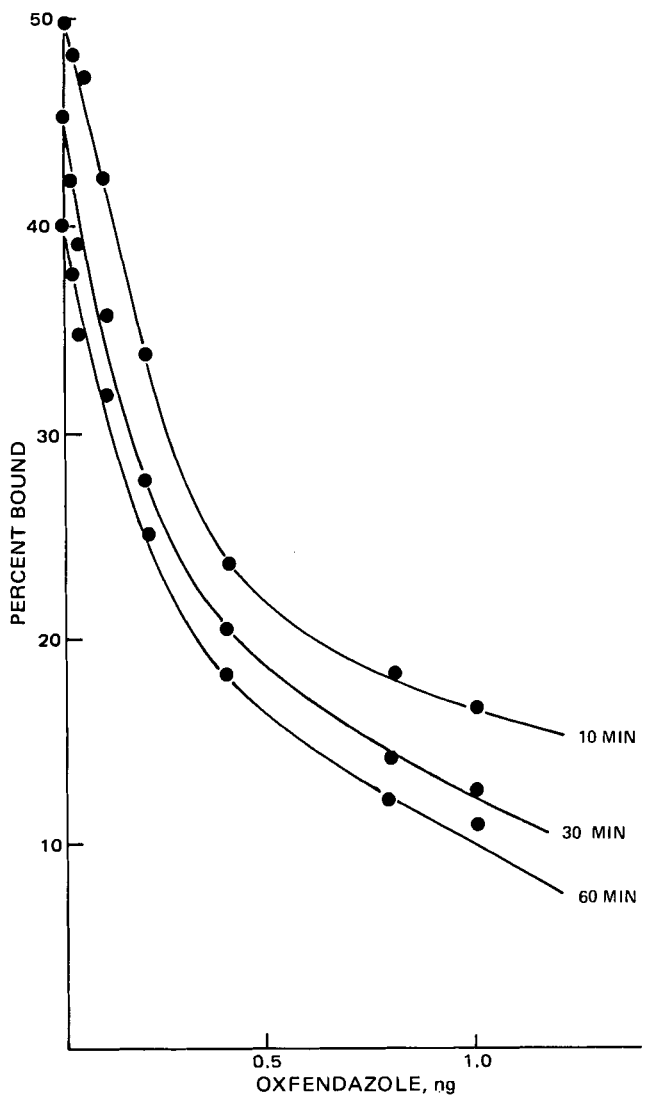

Figure 1—*Effect of charcoal contact time on the separation of bound from free radioactivity. Three displacement curves were run simultaneously under identical conditions while the charcoal contact time was varied.*

Table III—Estimation of Oxfendazole in Bovine Plasma

Oxfendazole Added, ng	Oxfendazole Measured, ng	Mean ± *SE*	Ratio of Assayed to Added
0.20	0.14	0.16 ± 0.006	0.80
	0.16		
	0.17		
	0.15		
	0.18		
	0.17		
0.50	0.53	0.52 ± 0.013	1.04
	0.49		
	0.51		
	0.53		
	0.58		
	0.50		
1.00	1.12	1.08 ± 0.014	1.08
	1.08		
	1.11		
	1.08		
	1.02		
	1.08		
1.50	1.40	1.49 ± 0.037	0.99
	1.52		
	1.44		
	1.45		
	1.66		
	1.49		
2.00	2.08	1.96 ± 0.054	0.98
	1.95		
	2.10		
	1.82		
	1.78		
	2.00		
2.50	2.39	2.52 ± 0.069	1.01
	2.33		
	2.80		
	2.56		
	2.44		
	2.60		

standard curve run in buffer only. The data in Table II are given in support of this procedure. The appropriate nonspecific bound simply means that if the plasma samples are run undiluted, then the nonspecific bound tubes also consist of an aliquot of undiluted plasma; if the unknowns are diluted, then there must be correspondingly diluted nonspecific bound tubes. The alternative would be to add an aliquot of untreated plasma to all points of the standard curve, thereby creating a chemical environment equivalent to the unknowns.

Specificity—To investigate cross-reactivities, a number of known oxfendazole metabolites (III–VI) were selected. The sulfide (IV) and

Table IV—Estimation of Oxfendazole in Equine Serum

Oxfendazole Added, ng	Oxfendazole Measured, ng	Mean ± *SE*	Ratio of Assayed to Added
0.200	0.198	0.210 ± 0.009	1.05
	0.206		
	0.184		
	0.228		
	0.238		
0.500	0.479	0.429 ± 0.021	0.86
	0.407		
	0.504		
	0.419		
	0.405		
	0.359		
1.00	1.02	1.02 ± 0.064	1.02
	0.91		
	0.78		
	1.09		
	1.19		
	1.17		
2.00	2.58	2.19 ± 0.085	1.09
	2.25		
	1.99		
	2.18		
	2.06		
	2.11		

Table V—Estimation of Oxfendazole in Canine Plasma

Oxfendazole Added, ng	Oxfendazole Measured, ng	Mean ± *SE*	Ratio of Assayed to Added
0.05	0.040	0.041 ± 0.0027	0.82
	0.045		
	0.030		
	0.043		
	0.038		
	0.050		
0.10	0.100	0.082 ± 0.0045	0.82
	0.070		
	0.075		
	0.090		
	0.080		
	0.077		
0.50	0.520	0.466 ± 0.014	0.94
	0.485		
	0.475		
	0.450		
	0.435		
	0.435		
1.0	1.20	1.05 ± 0.12	1.05
	0.84		
	1.60		
	0.88		
	0.85		
	0.97		

sulfone (VI) metabolites known to circulate in bovine and sheep plasma after oral oxfendazole cross reacted to the extent of 2.00 and 0.25%, respectively. Compound V cross reacted at 0.33%. The oxfendazole free amine (III) showed higher cross-reactivity, 11.3%. Although this metabolite was present in the urine of sheep and cattle, its presence was not established in plasma. Thus, the major cross-reacting metabolite very likely does not interfere in the plasma radioimmunoassay.

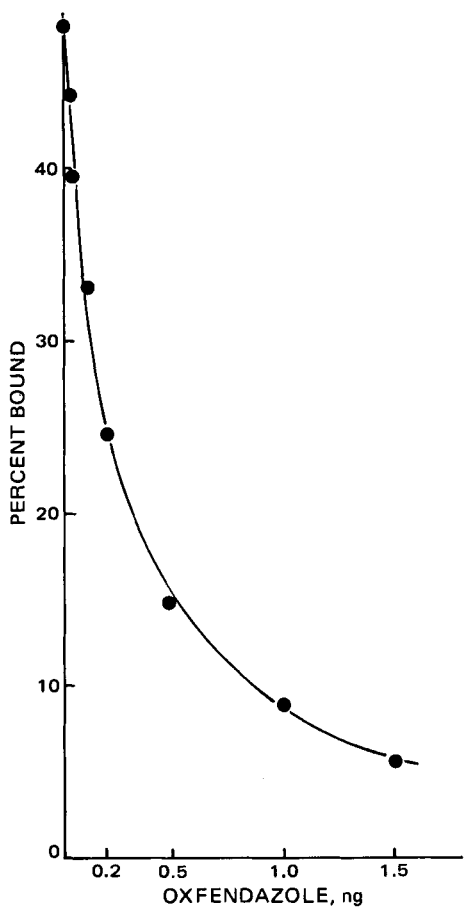

Figure 2—*Plot of the displacement curve (or standard curve). The antiserum dilution was 1:1000. The reaction was carried out overnight at room temperature.*

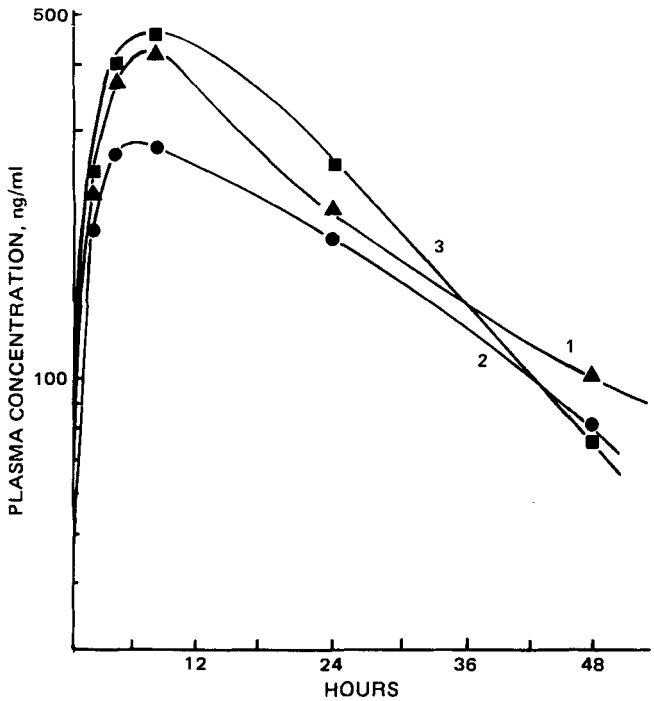

Figure 3—*Plot of the plasma concentration–time profile in calves after an oxfendazole dose of 3 mg/kg.*

Sensitivity, Accuracy, and Precision—A typical displacement (or standard) curve is shown in Fig. 2. The displacement curve is linear in logit–log coordinates in the range of 20–1500 pg. The displacement curve shows the 20-pg point to be uniquely different from zero, and it was taken as the lower limit of sensitivity. In this assay, this limit corresponds to a value of 200 pg/ml of plasma or serum.

Accuracy and precision of the assay were determined by adding known amounts of oxfendazole to plasma or serum and then assaying these samples (Tables III–V). The ratios of assayed to added indicated by their proximity to unity that the accuracy of the assay was at an acceptable level. The precision was also acceptable in that the standard errors of the replicates were 5% or less of the mean value for each concentration measured.

The validity of the assay was further established by comparing the values obtained by radioimmunoassay to values obtained from a ^{14}C-oxfendazole radiochemical assay. The results (Table VI) indicated a relatively good agreement. Most of the values obtained by the two assays were within 20% of one another. The difference in the results was probably due to variability in the TLC procedure.

Table VI—Comparison of Oxfendazole Levels as Measured by Radioimmunoassay and ^{14}C-Radiochemical Assay

Calf	Postdose Time, hr	Plasma Oxfendazole Levels, ng/ml	
		Radioimmunoassay	^{14}C-Radiochemical
1	2	226	203
	4	376	310
	8	447	337
	24	209	258
	48	102	171
2	2	195	185
	4	266	246
	8	269	286
	24	188	224
	48	80	150
3	2	250	271
	4	400	354
	8	443	365
	24	257	291
	48	74	143

Plasma Concentration in Experimental Animals—Plasma concentration–time profiles were determined in the calf after administering an oral dose of oxfendazole (Fig. 3). The profile indicated that the method has sufficient sensitivity to be useful in a variety of oral or intravenous experiments. Similarly, the profiles obtained in dogs showed that the sensitivity was adequate. The peak plasma levels achieved after 11- and 33-mg/kg doses varied between 1100 and 1400 ng/ml, respectively.

In summary, the method is sensitive, specific, and relatively simple. Analytical measurements can be performed directly on an aliquot of plasma without prior extraction or purification.

REFERENCES

(1) N. E. Downey, *Vet. Rec.*, **90**, 267 (1976).

(2) J. C. Sheehan and J. J. Hlavka, *J. Org. Chem.*, **21**, 439 (1956).

(3) O. H. Lowry, N. J. Rosebrough, A. L. Farr, and R. Randall, *J. Biol. Chem.*, **193**, 265 (1951).

(4) D. Rodbard and J. E. Lewald, *Acta Endocrinol. (Kobenhavn) (Suppl.)*, **147**, 79 (1970).

(5) M. A. Binoux and W. D. Odell, *J. Clin. Endocrinol. Metab.*, **36**, 303 (1973).

ACKNOWLEDGMENTS

The authors acknowledge Dr. Colin Beard for synthesis of the oxfendazole valerate derivative, Dr. Howard Parnes for synthesis of the tritiated oxfendazole, Dr. Pamela Burton for synthesis of the oxfendazole–polylysine conjugate, and Mr. William Leitch for production of the antiserum. Recognition is also given to the competent assistance of Ms. Anna Bury in applying the method to experimentally treated animals.

Temperature and Surfactant Dependence of Accumulation of 4-Aminoantipyrine and Ethanol in Fish

JUZAR S. KAKA and WILLIAM L. HAYTON ˣ

Received September 19, 1977, from the *College of Pharmacy, Washington State University, Pullman, WA 99164.* Accepted for publication March 24, 1978.

Abstract □ The accumulation of 4-aminoantipyrine and ethanol by goldfish placed in solutions of the drugs was determined from 10 to 35° in the presence and absence of 0.01% polysorbate 80. The volume of distribution of ethanol, 0.68 ml/g of fish, was not affected by surfactant or temperature. The volume of distribution of 4-aminoantipyrine also was not affected by surfactant, but it increased linearly from 0.43 to 0.76 ml/g over 10–35°. The clearance constants for the absorption of both drugs were temperature sensitive. The clearance constant for 4-aminoantipyrine, 11.6 μl/min/g of fish at 20°, conformed to the Arrhenius equation; the activation energy was 12.9 kcal/mole, indicating that 4-aminoantipyrine absorption was probably membrane controlled. Polysorbate 80 increased the clearance constant of 4-aminoantipyrine, and the increase occurred at a measurable rate rather than instantaneously. The clearance constant for ethanol, 46.5 μl/min/g at 20°, was not described by the Arrhenius equation. The activation energy appeared to decrease with increasing temperature, perhaps reflecting a change in the rate-limiting barrier to absorption from the membrane to the aqueous stagnant layer. Alternatively, the ethanol absorption rate may have been limited by blood flow to the absorbing surface. The ethanol absorption rate was not affected by polysorbate 80.

Keyphrases □ 4-Aminoantipyrine—accumulation by goldfish, effect of temperature and surfactant □ Ethanol—accumulation by goldfish, effect of temperature and surfactant □ Absorption—4-aminoantipyrine and ethanol by goldfish, effect of temperature and surfactant □ Distribution, tissue—4-aminoantipyrine and ethanol by goldfish, effect of temperature and surfactant □ Antipyretic–analgesics—4-aminoantipyrine, accumulation by goldfish, effect of temperature and surfactant

Recent reports (1, 2) discussed the effects of temperature on the toxicity of chemical pollutants to fish and showed the complex interrelationships between chemical toxicity and temperature in fish. While the uptake rate of pollutants may increase with temperature, metabolism and excretion rates also may be affected. In addition, the dissolved oxygen concentration, which may affect metabolism, is decreased as temperature increases. Thus, it is not surprising that the toxicity to fish of some pollutants, *e.g.*, endrin and toxaphene, increases with a temperature increase while the toxicity of others, *e.g.*, chlorophenothane (DDT) and methoxychlor, decreases with a temperature increase (1).

The toxicity of a chemical present in the environment of fish is generally a function of the amount of chemical accumulated by the fish. To understand the effects of temperature on the toxicity of pollutants to fish, it is necessary to know the temperature dependence of the processes that determine the extent of accumulation: absorption, distribution, and elimination. Toward this end, the accumulation of 4-aminoantipyrine and ethanol was studied in goldfish at various temperatures. The absorption and distribution of these drugs are rapid compared to their elimination by metabolism or excretion. Thus, their accumulation is related primarily to absorption and distribution, and it was possible to focus on the temperature dependence of these processes. The temperature dependence of the absorption-enhancing effect of a premicellar concentration of polysorbate 80 also was studied.

THEORETICAL

The accumulation rate of substances toxic to fish has been characterized by measuring the time required for fish to turn over or to die (*e.g.*, 3–7). This approach requires no chemical analysis, and it is useful for detection of the relative absorption rates of compounds that elicit the end-point. The time required to produce the end-point depends on both the absorption rate and the dose that causes overturn or death (3). Since the dose required to produce the end-point as well as the absorption rate may be sensitive to temperature, the following alternative approach was used in this study.

The accumulation process was followed by measuring the amount of xenobiotic present in the fish as a function of time. This approach is commonly used; the data are generally modeled as an equilibrium with two first-order rate constants, with units of time^{-1}, for absorption and exsorption of the xenobiotic. For example, an equilibrium model was used recently as the basis for an accelerated test to predict the extent of accumulation of xenobiotics (8). The equilibrium has also been used to model time-for-overturn and time-for-death data (6, 7, 9). For many compounds studied, the accumulation process appears to be represented adequately as a simple equilibrium.

A problem associated with the use of absorption and exsorption rate constants for characterizing accumulation is that the rate constants reflect not only the permeability of barriers to absorption but also the volumes of the fish and bathing solution (7). To overcome this problem, the equilibrium model was modified so that the accumulation process is characterized by two pharmacokinetic constants: a clearance constant, k, that reflects only the permeability of barriers to absorption and exsorption, and a volume of distribution, V, that reflects the capacity for accumulation.

The fish was treated as a single compartment with the xenobiotic equilibrating between it and the external solution. The accumulation rate of the xenobiotic (dX/dt) is:

$$\frac{dX}{dt} = k(C_o - C_i) \qquad \text{(Eq. 1)}$$

where X is the amount of the xenobiotic absorbed in units of milligrams per gram of fish; k is in units of milliliters per minute per gram of fish; and C_o and C_i are the concentrations of the xenobiotic in the external solution and the body water of the fish, respectively, in units of milligrams per milliliter. Experiments with 4-aminoantipyrine showed that the uptake rate was directly related to the size of the fish (Fig. 1). When expressed on a per gram basis, however, uptake was independent of fish size over a range of 1–3 g (Fig. 1); therefore, k and X were normalized to body weight.

The following assumptions were made:

1. Under fixed conditions, uptake obeys the principle of superposition. This assumption appears valid since the uptake of ethanol (Fig. 2) and 4-aminoantipyrine (data not shown) was directly proportional to C_o.
2. There is no absorption from the gut of the fish. This assumption seems to be reasonable since freshwater fish generally do not swallow water (10).
3. Except for exsorption, the elimination of ethanol and 4-aminoantipyrine is negligible during the experiment. While one report suggests that goldfish may metabolize ethanol (11), the metabolism rate apparently is small compared to the absorption rate of ethanol in this study and the effect of metabolism on the shape of the accumulation curves would be negligible. 4-Aminoantipyrine is apparently not metabolized in goldfish (12).

The volume of the solution bathing the fish was sufficiently large that C_o could be considered constant; it decreased less than 0.5% during any

0022-3549/78/1100-1558$01.00/0
© 1978, American Pharmaceutical Association

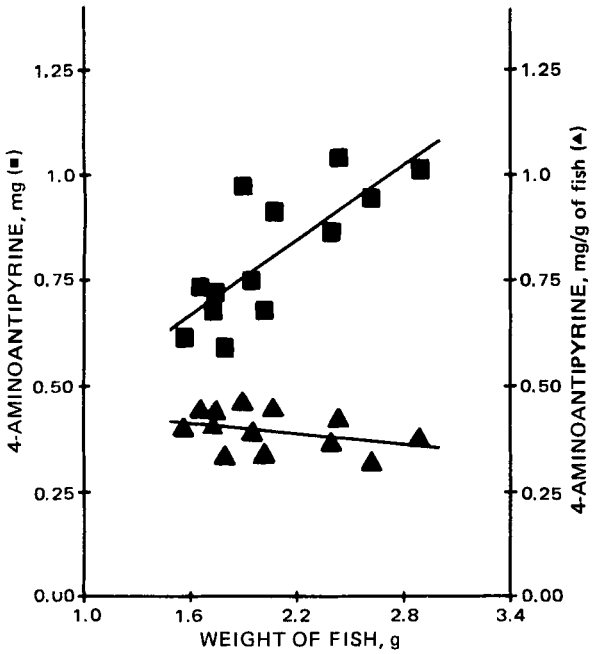

Figure 1—*4-Aminoantipyrine (■) and 4-aminoantipyrine per gram of fish (▲) as a function of the weight of the fish. Fish were in the solution for 30 min at 35°. Each point represents one fish; the lines were fit by the least-squares method.*

absorption experiment. A volume of distribution, V, was defined such that $C_i = X/V$, where V has units of milliliters per gram of fish. Equation 1 may be integrated to:

$$X = VC_o[1 - e^{-(kt/V)}] \qquad \text{(Eq. 2)}$$

Equation 2 predicts that X approaches an equilibrium value of VC_o, and the half-life for equilibration is 0.693 V/k. The volume of distribution is somewhat different from that used in standard compartmental pharmacokinetic models (13) in that the "reference tissue" is the external solution rather than blood or plasma.

The interpretation of k depends on the rate-limiting step or steps operative for a particular xenobiotic. When the uptake rate is controlled by an aqueous stagnant layer, the clearance constant is:

$$k = (D_a)(A/h) \qquad \text{(Eq. 3)}$$

where D_a is the diffusion coefficient of the xenobiotic in the aqueous layer in units of square centimeters per minute, A is the effective area of the absorbing surface in square centimeters per gram of fish, and h is the effective thickness of the aqueous stagnant layer in centimeters. When the uptake rate is limited by diffusion across a membrane, the clearance constant is:

$$k = (D_m)(A)(K_m/\delta) \qquad \text{(Eq. 4)}$$

where D_m is the diffusion coefficient of the xenobiotic in the membrane, K_m is the membrane–water partition coefficient of the xenobiotic, and δ is the thickness of the membrane in centimeters. For compounds with high membrane permeability, the uptake rate may be limited by blood flow and:

$$k = (Q)(K_b) \qquad \text{(Eq. 5)}$$

where Q is the blood flow rate to the absorbing surface in milliliters per minute per gram of fish and K_b is the effective blood–external solution partition coefficient of the xenobiotic. In the general case, the absorption rate may be limited by all three barriers and the clearance constant for absorption would be:

$$k = \left[\frac{h}{D_a A} + \frac{\delta}{D_m A K_m} + \frac{1}{QK_b}\right]^{-1} \qquad \text{(Eq. 6)}$$

Any one of the three terms on the right can be omitted to give an expression relevant to an absorption barrier composed of two rate-limiting steps.

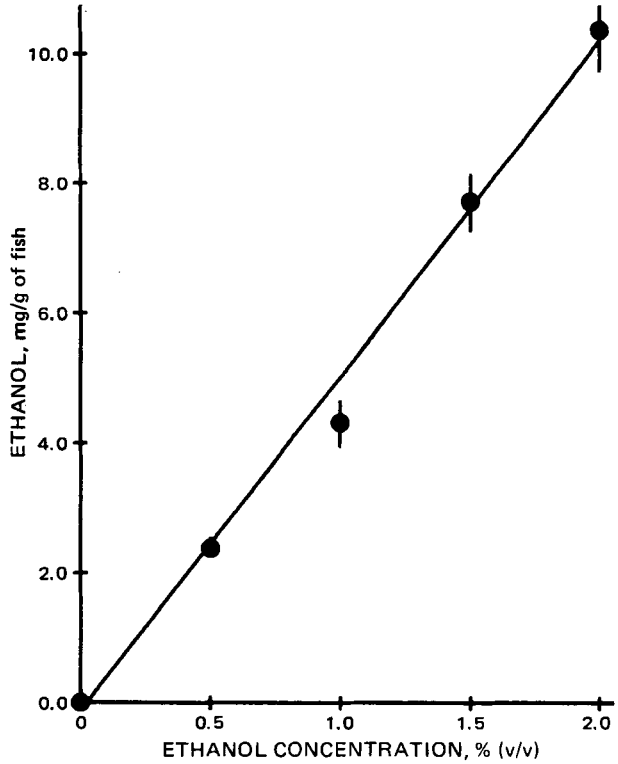

Figure 2—*Ethanol absorbed by fish as a function of ethanol concentration. Fish were in each ethanol solution for 30 min at 25°. Each point represents the mean of five fish; bars represent ±1 SD. The line was fit by the least-squares method.*

EXPERIMENTAL

Materials—4-Aminoantipyrine[1], ethanol[2], tromethamine[3], and polysorbate 80[4] were used as received. ^{14}C-Ethanol[5] was dissolved in distilled water and stored at 4°; all other reagents and solvents were reagent grade.

Absorption—Goldfish (*Crassius auratus*), 1–3 g, were housed in a rectangular glass tank containing 56 liters of 0.075% NaCl solution that was aerated and filtered continuously. The tank was suspended in a water bath that could be maintained at constant temperature[6] over 10–35°. Five lots of fish were used. All fish used in each experiment were from the same lot to overcome the problem of lot-to-lot variability.

Preliminary experiments showed that the absorption rate rapidly stabilized after a change in temperature (Fig. 3). Fish were acclimated to the temperature being studied for a minimum of 24 hr. They were placed individually in 100 ml of 4-aminoantipyrine (1.5 mg/ml) or 75 ml of ethanol (1.0%) solution buffered at pH 7.0 with 0.05 M tromethamine. When present, polysorbate 80 was at a concentration of 0.01%. Ethanol solutions contained 7 nCi of ^{14}C-ethanol/ml; all solutions were prepared on the day of use. After immersion in drug solution for varying periods, the fish were rinsed with distilled water, blotted with tissue paper, and weighed. Fish were immediately either assayed for drug or frozen for assay later.

Analytical Methods—Fish exposed to 4-aminoantipyrine were homogenized with 15 ml each of chloroform and 0.05 M, pH 7.0 tromethamine solution. The homogenate was centrifuged, and 5.0 ml of the chloroform layer was removed and shaken with 10 ml of 0.01 N HCl solution for 20 min. To 2 ml of the aqueous phase were added 7.0 ml of water and 2 ml of p-dimethylaminobenzaldehyde reagent (14). The absorbance was measured[7] at 430 nm and converted to the amount of 4-aminoantipyrine per gram of fish.

[1] Sigma Chemical Co., St. Louis, Mo.
[2] U.S. Industrial Chemical Co., New York, N.Y.
[3] J. T. Baker Chemical Co., Phillipsburg, N.J.
[4] Atlas Chemical Industries, Wilmington, Del.
[5] New England Nuclear, Boston, Mass.
[6] Model TE9 Tamson circulating bath and model PBC-4 bath cooler, Neslab Instruments, Portsmouth, N.H.
[7] Beckman DU, Beckman Instruments, Fullerton, Calif.; with Gilford model 2000 multiple sample recorder, Gilford Instrument Laboratories, Oberlin, Ohio.

Table I—Volume of Distribution of 4-Aminoantipyrine and Ethanol with and without 0.01% Polysorbate 80 at Various Temperatures

Temperature	Volume of Distribution[a], ml/g of Fish			
	4-Aminoantipyrine		Ethanol	
	With	Without	With	Without
10°	0.448	0.427	0.655	0.680
20°	0.581	0.554	0.675	0.681
30°	0.709	0.724	0.673	0.688
35°	—[b]	0.765	0.705	0.722

[a] Estimated from nonlinear least-squares fit of Eq. 2 to data shown in Figs. 4–7. [b] Not determined.

To measure the extent of adsorption of 4-aminoantipyrine to the fish surface, fish were immersed in the drug solution for 30 sec and analyzed for 4-aminoantipyrine; the amount detected was negligible. There was no detectable difference between the absorbances of blanks prepared without fish and with fish that had not been exposed to 4-aminoantipyrine. Blanks prepared without fish were used routinely as a reference.

To determine the amount of ethanol absorbed, each fish was homogenized with 5 ml of distilled water and the homogenate was centrifuged. One-half milliliter of the supernate was transferred to a scintillation vial, mixed with 10 ml of scintillation fluid[8], and counted[9] until a minimum of 10,000 counts was collected. ^{14}C-Toluene was used as an internal standard to correct for quenching; the efficiency of the counting system was approximately 75%. The recovery of ethanol added to fish homogenate was 100%.

RESULTS AND DISCUSSION

Equation 2 adequately described the accumulation of both drugs at various temperatures and in the presence and absence of 0.01% polysorbate 80 (Figs. 4–7). Equation 2 was fit to the data by a nonlinear least-squares method to obtain estimates of V and k.

The volume of distribution characterizes the capacity of the fish to accumulate drug. The volume of distribution of 4-aminoantipyrine increased with temperature while that of ethanol was relatively temperature independent (Fig. 8). This result suggests that the distribution of 4-aminoantipyrine involves temperature-sensitive equilibria, possibly tissue or plasma protein binding, or partitioning into a nonaqueous phase. The lack of temperature dependence of V for ethanol indicates that its distribution is limited primarily to body water. Polysorbate 80 did not affect the V values of either drug (Table I).

For both drugs, the clearance constants for absorption were quite sensitive to temperature (Table II). Two of the potential barriers to absorption involve diffusion (Eqs. 3 and 4); therefore, the clearance constants were plotted according to the Arrhenius equation. The plots were linear for 4-aminoantipyrine but convex for ethanol (Fig. 9). The activation energy for the absorption of 4-aminoantipyrine in the absence of surfactant was determined from the slope of the Arrhenius plot to be 12.9 kcal/mole. Since this activation energy is considerably greater than the activation energy for diffusion of a substance in water, approximately

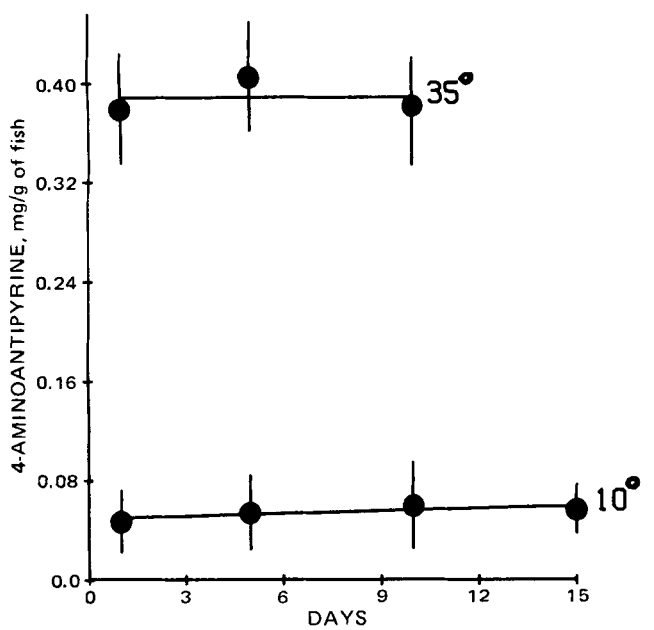

Figure 3—*4-Aminoantipyrine absorbed by fish at various times after adjusting the temperature of the fish tank from room temperature to either 10 or 35°. Fish were exposed to the drug solution for 30 min. Each point represents the mean of five fish; bars represent ±1 SD. The lines were fit by least squares.*

[8] PCS solubilizer, Amersham/Searle, Arlington Heights, Ill.
[9] Packard Tri-Carb 3320, Packard Instrument Co., Downers Grove, Ill.

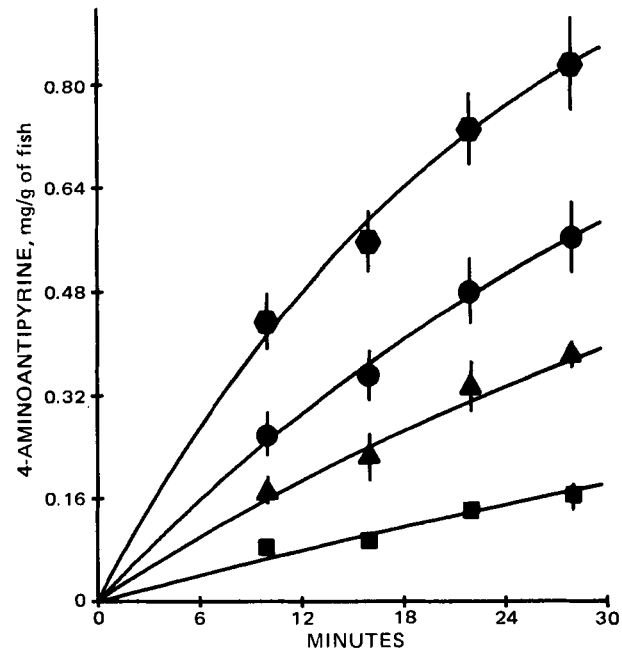

Figure 4—*4-Aminoantipyrine absorbed by fish as a function of time at 10° (■), 20° (▲), 30° (●), and 35° (●). Each point represents the mean of five fish; bars represent ±1 SD. Lines were fit by nonlinear least squares according to Eq. 2. The experiments were performed in the sequence: 10, 20, 30, and 35°.*

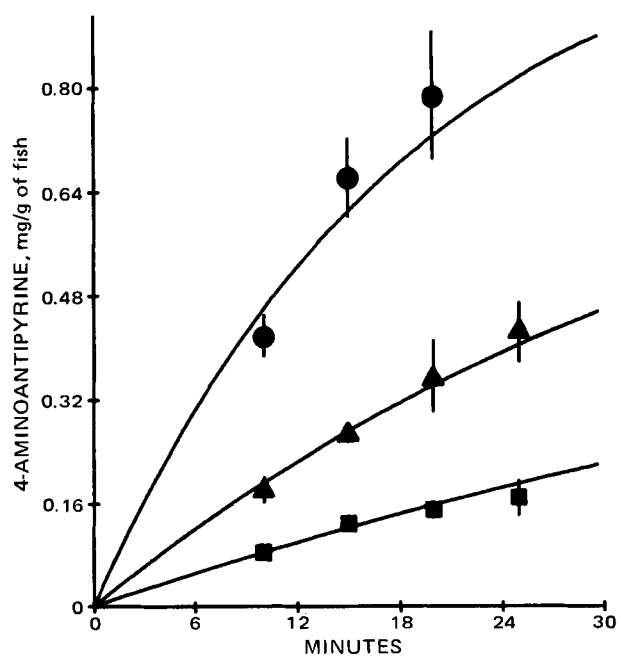

Figure 5—*Same as Fig. 4 except that 0.01% polysorbate 80 was present in the 4-aminoantipyrine solution. The experiments were performed in the sequence: 30, 20, and 10°.*

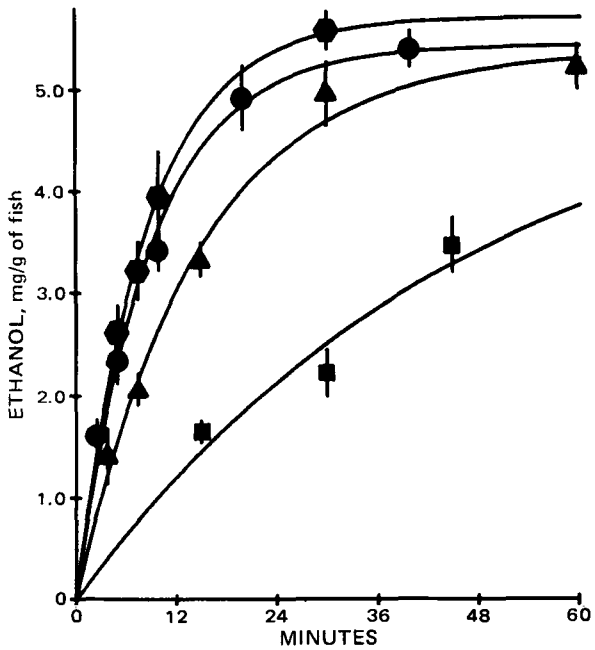

Figure 6—*Ethanol absorbed by fish as a function of time at 10° (■), 20° (▲), 30° (●), and 35° (●). Each point represents the mean of five fish; bars represent ±1 SD. Lines were fit by nonlinear least squares according to Eq. 2. The experiments were performed in the sequence: 30, 35, 10, and 20°.*

5 kcal/mole, the rate-limiting step in 4-aminoantipyrine absorption appears to be diffusion across a biological membrane rather than an aqueous stagnant layer. Similar activation energies were reported for the passive transport of small molecules across lipoid membranes. For example, the activation energies for transport of malonamide and urea across egg–lecithin liposomes were 13.0 and 9.3 kcal/mole, respectively (15), and activation energies for urea and antipyrine transport through rabbit gallbladder epithelium were 10.1 and 10.5 kcal/mole, respectively (16).

The rate constant (k/V) for equilibration of 4-aminoantipyrine was also plotted according to the Arrhenius equation. This rate constant is equivalent to the absorption rate constant when the equilibrium is characterized by absorption and exsorption rate constants (see *Theoretical*). The activation energy was 9.3 kcal/mole, considerably less than the value obtained when the clearance constant alone was used. The discrepancy occurs because the absorption rate constant is a function of both membrane permeability and the volume of distribution. Both parameters are temperature sensitive for 4-aminoantipyrine, and the activation energy determined from the absorption rate constant reflects this fact. The clearance constant is a better characterization of the permeability of barriers to absorption than the absorption rate constant because changes in the latter may be due to a change in either absorption or distribution of drug. The clearance constant is less ambiguous because it reflects only the permeability of barriers to absorption.

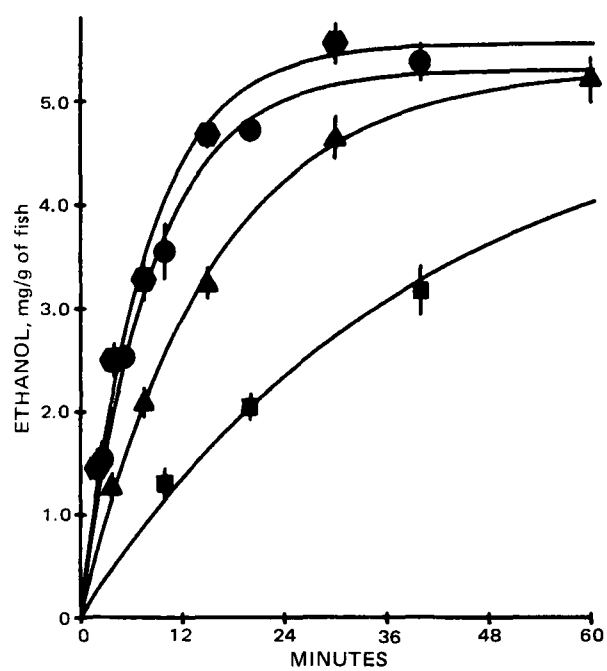

Figure 7—*Same as Fig. 6 except that 0.01% polysorbate 80 was present in the ethanol solution. The experiments were performed in the sequence: 10, 20, 30, and 35°.*

Table II—Clearance Constants of 4-Aminoantipyrine and Ethanol with and without 0.01% Polysorbate 80 at Various Temperatures

Temperature	Clearance Constant[a], μl/min/g of Fish			
	4-Aminoantipyrine		Ethanol	
	With	Without	With	Without
10°	6.0	4.8	16.4	14.3
20°	14.5	11.6	44.3	46.5
30°	39.7	20.0	80.6	76.9
35°	—[b]	33.5	92.5	85.4

[a] Estimated from nonlinear least-squares fit of Eq. 2 to data shown in Figs. 4–7. [b] Not determined.

In the presence of 0.01% polysorbate 80, the clearance constant of 4-aminoantipyrine increased significantly over the 10–35° range (Fig. 9). The absorption-enhancing effect of premicellar concentrations of surfactants is well known (17). It is due to an increase in the permeability of the absorbing membrane rather than to a nonmicellar surfactant–drug complex. The mechanism of the surfactant effect is not well understood. It has been postulated that the surfactant molecules enter the lipid portion of membranes and either increase the fluidity of the hydrocarbon lipid chains (18) or cause dissociation of structural lipoproteins (19, 20).

While the presence of polysorbate 80 appeared to increase the energy of activation for the absorption of 4-aminoantipyrine (Fig. 9), this result may be an artifact. The increased slope of the Arrhenius plot may reflect a temperature dependence of the effect of the surfactant on the membrane. Thus, at higher temperatures, the membrane would be more susceptible to the effects of the surfactant than at lower temperatures and the slope of the Arrhenius plot would appear to be increased.

Alternatively, if the structure of the membrane in the presence of polysorbate 80 is unchanged over the 10–35° range, the increased slope of the Arrhenius plot and Eq. 4 suggest that the surfactant reduces the diffusion coefficient of 4-aminoantipyrine in the membrane and that the reduced diffusion coefficient is more than compensated for by: (*a*) an increase in the area available for absorption, (*b*) an increase in the

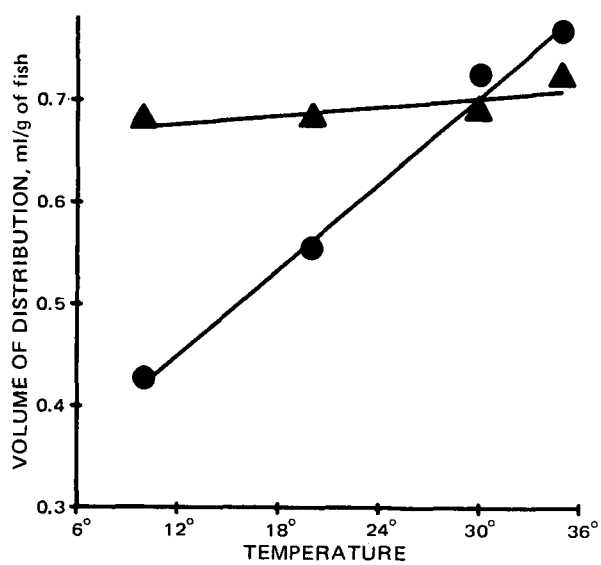

Figure 8—*Volume of distribution as a function of temperature for 4-aminoantipyrine (●) and ethanol (▲). The volumes of distribution were obtained from fits of Eq. 2 to the plots shown in Figs. 4 and 6.*

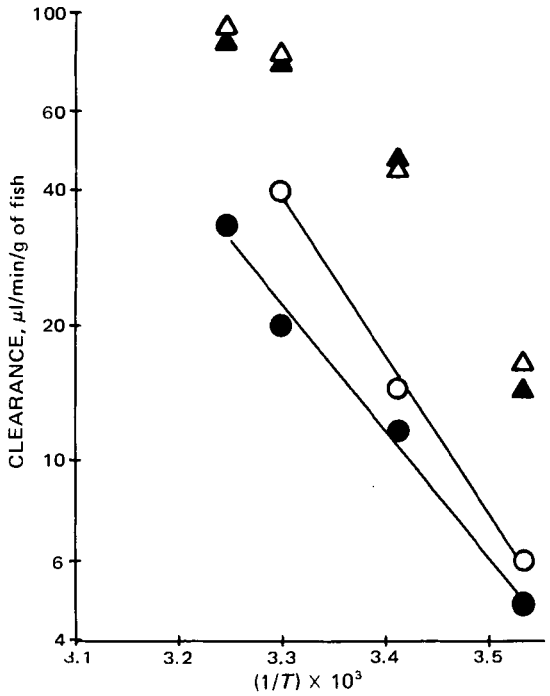

Figure 9—*Arrhenius plots for the absorption clearance constants of 4-aminoantipyrine (circles) and ethanol (triangles) in the absence (closed) and presence (open) of 0.01% polysorbate 80.*

membrane-water partition coefficient of the drug, and/or (c) a decrease in the thickness of the membrane.

The initial absorption rate of 4-aminoantipyrine was lower than would be predicted if polysorbate 80 produced an instantaneous increase in membrane permeability. For example, the amount of 4-aminoantipyrine absorbed at 10 min at 30° was appreciably below the least-squares fitted line (Fig. 5). To determine whether the absorption-enhancing effect of the surfactant was instantaneous, the amount of 4-aminoantipyrine absorbed was measured after a 5-min exposure of the fish to 1.5 mg of 4-aminoantipyrine/ml under the following conditions: A, control fish were exposed for 5 min to 1.5 mg of 4-aminoantipyrine/ml; B, fish were exposed for 5 min to 1.5 mg of 4-aminoantipyrine/ml containing 0.01% polysorbate 80; C, fish were immersed in 0.01% polysorbate 80 solution for 10 min, removed, rinsed, and placed for 5 min in 1.5 mg of 4-aminoantipyrine/ml of solution containing 0.01% polysorbate 80; and D, fish were pretreated with surfactant as in Condition C and then placed in 1.5 mg of 4-aminoantipyrine/ml of solution without surfactant.

As shown in Table III, the absorption rate of 4-aminoantipyrine under Condition B tended to be greater than the control as observed previously (Figs. 4 and 5). However, pretreatment of the fish with 0.01% polysorbate 80 for 10 min (Condition C) further increased the absorption rate of 4-aminoantipyrine. Thus, the action of the surfactant apparently is not instantaneous. When fish are placed in drug solutions containing surfactant, membrane permeability apparently is at or near the control value, and it increases with time until it reaches a maximum value. This observation agrees with the results of *in vitro* studies of the kinetics of the surface pressure of an air–aqueous solution interface after injection of cetrimonium bromide beneath the interface into the stirred subphase (21). The surface pressure exponentially approached an equilibrium value with a half-life of approximately 5 min, consistent with the concept of a potential energy barrier to surfactant adsorption at the interface.

The absorption rate of 4-aminoantipyrine under Condition D was also significantly greater ($p < 0.05$) than the control absorption rate. The permeability-enhancing effect of the surfactant persists after the surfactant has been removed from the drug solution. The surfactant-mediated alteration in the permeability of the absorbing membrane apparently is relatively slow. A similar observation was made with regard to the effect of 1% poloxalene on pentobarbital absorption (22).

The relatively small surfactant-induced increase in the k of 4-aminoantipyrine at low temperature (Fig. 9) may be explained in part by the kinetics of the surfactant effect. At low temperatures, a longer time may be required for the surfactant to increase permeability than is required

Table III—4-Aminoantipyrine Absorption in Fish Pretreated with Polysorbate 80

Condition[a]	4-Aminoantipyrine[b], mg/g of Fish
A	0.138 ± 0.013[c,d]
B	0.162 ± 0.020[e]
C	0.251 ± 0.030[c,e]
D	0.209 ± 0.025[d]

[a] A = control, B = 0.01% polysorbate 80 present in the drug solution, C = 10-min pretreatment in 0.01% polysorbate 80 and 0.01% polysorbate 80 present in the drug solution, and D = 10-min pretreatment in 0.01% polysorbate 80 and no surfactant in drug solution. [b] Mean of five fish ±1 *SD*. [c,d,e] Values having same superscript are significantly different ($p < 0.05$).

for equilibration of 4-aminoantipyrine between the fish and the external solution.

The convex curvature of the Arrhenius plot for ethanol clearance constants (Fig. 9) indicates that the activation energy for ethanol absorption decreases with a temperature increase. Such curvature has been attributed to a phase change in the lipids of absorbing membranes. For example, the kinetics of absorption of chlortetracycline by *Staphylococcus aureus* are temperature dependent, and there is a pronounced change in the slope of the Arrhenius plot at 27° (23). This transition temperature is sensitive to the fatty acid composition of the *S. aureus* cells and to the temperature at which the cells are cultured. Since no break in the Arrhenius plot of the 4-aminoantipyrine clearance constants was evident, the curvature of the Arrhenius plot for the ethanol clearance constants apparently was not due to a phase change in the membrane.

An alternative explanation for the curved Arrhenius plot is that the absorption rate of ethanol is controlled both by diffusion to the membrane across a stagnant aqueous layer and by diffusion across the membrane. Since the activation energy for diffusion to the membrane would be lower than for diffusion across the membrane, the former process would be less sensitive to a change in temperature than the latter. Thus, at high temperature the rate-limiting barrier could be an aqueous stagnant layer, with the permeability of the underlying membrane being sufficiently large that the membrane would not act as a barrier. A decrease in temperature would cause a greater decrease in the permeability of the membrane than the aqueous stagnant layer. At low temperature, the rate-limiting barrier would be the membrane, with the permeability of the aqueous layer being large enough not to control the absorption rate. A similar mechanism was proposed to explain a convex Arrhenius plot observed for the permeation of 1-butanol across the toad urinary bladder (24). The plot was linear if the permeability coefficients were corrected for unstirred layer effects.

If the membrane controlled the absorption rate of ethanol at low temperature, the absorption rate should have been increased by polysorbate 80 at low temperature; it was not (Fig. 9). This lack of effect may have resulted from a relatively slow onset of surfactant-induced permeability. Alternatively, it may reflect the existence of two separate routes, membrane lipid and pores, for 4-aminoantipyrine and ethanol, the permeability of the latter being insensitive to surfactant (25). However, the existence of a pore route is open to question (24, 26).

The convex curvature noted in the Arrhenius plot for ethanol also may be explained by postulating that the absorption rate of ethanol is controlled by the blood flow rate to the absorbing membranes. There is no theoretical basis for the blood flow rate to follow the Arrhenius equation. The relationship between k for ethanol and temperature would mirror the relationship between blood flow and temperature. In addition, postulation of blood flow as the rate-limiting step is consistent with the lack of effect of polysorbate 80 on the ethanol absorption rate. While the surfactant may increase the permeability of the absorbing membranes to ethanol, the permeability in the absence of surfactant is sufficiently large so that it would not control the absorption rate. A further increase in permeability when surfactant was present would not alter the capacity of the blood to remove absorbed ethanol.

REFERENCES

(1) J. Cairns, Jr., A. G. Heath, and B. C. Parker, *J. Water Poll. Control Fed.*, **47**, 267 (1975).

(2) J. Cairns, Jr., A. G. Heath, and B. C. Parker, *Hydrobiologia*, **47**, 135 (1975).

(3) G. Levy and S. P. Gucinski, *J. Pharmacol. Exp. Ther.*, **146**, 80 (1964).

(4) N. A. Hall and W. L. Hayton, *J. Pharm. Sci.*, **56**, 304 (1967).
(5) M. Gibaldi and C. H. Nightingale, *ibid.*, **57**, 226 (1968).
(6) A. R. DiSanto and J. G. Wagner, *ibid.*, **58**, 1077 (1969).
(7) S. H. Yalkowsky, O. S. Carpenter, G. L. Flynn, and T. G. Slunick, *ibid.*, **62**, 1949 (1973).
(8) D. R. Branson, G. E. Blau, H. C. Alexander, and W. B. Neely, *Trans. Am. Fish. Soc.*, **104**, 785 (1975).
(9) C. H. Nightingale and M. Gibaldi, *J. Pharm. Sci.*, **60**, 1360 (1971).
(10) H. W. Smith, *Am. J. Physiol.*, **93**, 480 (1930).
(11) R. R. Ryback, B. Percarpio, and J. Vitale, *Nature*, **222**, 1068 (1969).
(12) B. B. Brodie and R. P. Maickel, *Proc. Int. Pharmacol. Mtg.*, **6**, 299 (1962).
(13) M. Gibaldi and D. Perrier, "Pharmacokinetics," Dekker, New York, N.Y., 1975, pp. 175–187.
(14) C. Brun, *J. Lab. Clin. Med.*, **37**, 955 (1951).
(15) B. E. Cohen, *J. Membr. Biol.*, **20**, 205 (1975).
(16) C. H. van Os, M. D. de Jong, and J. F. G. Slegers, *ibid.*, **15**, 363 (1974).
(17) M. Gibaldi and S. Feldman, *J. Pharm. Sci.*, **59**, 579 (1970).
(18) A. T. Florence and J. M. N. Gillan, *J. Pharm. Pharmacol.*, **27**, 152 (1975).
(19) F. Alhaique, D. Giacchetti, M. Marchetti, and F. M. Riccieri, *ibid.*, **27**, 811 (1975).
(20) F. Alhaique, M. Marchetti, F. M. Riccieri, and E. Santucci, *Experientia*, **31**, 215 (1975).
(21) E. R. Garrett and F. A. Vilallonga, *J. Pharm. Sci.*, **64**, 1782 (1975).
(22) M. W. Gouda, *Can. J. Pharm. Sci.*, **9**, 37 (1974).
(23) M. E. Dokter and J. A. Magnuson, *Arch. Biochem. Biophys.*, **168**, 81 (1975).
(24) N. Bindslev and E. M. Wright, *J. Membr. Biol.*, **29**, 265 (1976).
(25) G. Levy, K. E. Miller, and R. H. Reuning, *J. Pharm. Sci.*, **55**, 394 (1966).
(26) E. M. Wright and N. Bindslev, *J. Membr. Biol.*, **29**, 289 (1976).

ACKNOWLEDGMENTS

Presented at the Basic Pharmaceutics Section, APhA Academy of Pharmaceutical Sciences, New Orleans meeting, April 1976.

Abstracted from a dissertation submitted by J. S. Kaka to Washington State University in partial fulfillment of the Master of Science degree requirements.

Supported in part by funds provided for biological and medical research by Washington State Initiative Measure No. 171.

Radioimmunoassay for Psychotropic Drugs I: Synthesis and Properties of Haptens for Chlorpromazine

J. W. HUBBARD *, K. K. MIDHA ‡x, I. J. McGILVERAY ‡, and J. K. COOPER ‡

Received August 22, 1977, from the **Faculty of Pharmacy, University of Manitoba, Winnipeg, Manitoba, Canada,* and the ‡*Drug Research Laboratories, Health Protection Branch, Health and Welfare Canada, Ottawa, Ontario, Canada.* Accepted for publication April 6, 1978.

Abstract □ For the development of radioimmunoassay procedures for chlorpromazine and its active metabolites, three chlorpromazine haptens, 7-(or 8-)(3-carboxypropionyl)chlorpromazine, *N*-(3-carboxypropionyl)desmethylchlorpromazine, and *N*-(2-carboxyethyl)desmethylchlorpromazine, were synthesized and characterized by GLC–mass spectrometry, PMR spectrometry, and IR spectrophotometry. Each hapten was coupled to bovine serum albumin, and the number of hapten residues per mole of bovine serum albumin was calculated by UV spectrophotometric methods. Antibodies to each hapten–protein conjugate were obtained in rabbits, and titers of the antiserums were checked by evaluating their binding characteristics to tritiated chlorpromazine.

Keyphrases □ Chlorpromazine—three haptens synthesized and characterized, antibodies developed in rabbits, antiserum titers determined □ Haptens, chlorpromazine—three synthesized and characterized, antibodies developed in rabbits, antiserum titers determined □ Antibodies—to three chlorpromazine haptens developed in rabbits □ Tranquilizers—chlorpromazine, three haptens synthesized and characterized, antibodies developed in rabbits, antiserum titers determined

Chlorpromazine is widely used in the treatment of certain psychiatric disorders. It is extensively metabolized in humans, and several of its metabolites are pharmacologically active. For thorough study of the metabolism, pharmacokinetics, and clinical monitoring of this drug, sensitive specific procedures are required for the determination of chlorpromazine levels in biological fluids.

BACKGROUND

Various current techniques with adequate sensitivity to determine plasma chlorpromazine concentrations are GLC with electron-capture detection (1), labeled derivative formation (2), fluorescent labeling with dansyl chloride (3), TLC of a quaternary ammonium derivative (with 9-bromomethylacridine) followed by UV photolysis and subsequent spectrofluorometric determination (4), and GLC with mass spectrometric detection (5). But these methods are tedious, require extraction of the drug from biological fluids and/or its derivatization, and are not easily amenable for routine clinical monitoring.

Radioimmunoassay also may be applicable for determining plasma chlorpromazine concentrations. This technique is simple, requires no extraction, and is readily applied to routine analysis. A reported radioimmunoassay procedure for chlorpromazine (6), in which the protein (bovine serum albumin) was presumably coupled through the side chain of the drug, is not sufficiently sensitive (*cf.*, 7) and does not differentiate between chlorpromazine and its didemethylated metabolite at any level or among chlorpromazine, 7-hydroxychlorpromazine, and chlorpromazine sulfoxide at the 20-ng level.

Another published procedure (7), in which the bovine serum albumin was coupled to the ring system of chlorpromazine through a carboxyphenylazo bridge, was claimed to distinguish to some extent between chlorpromazine and several of its ring-modified and side-chain-modified metabolites, but it has not been widely evaluated or applied.

The present approach toward a sensitive, specific radioimmunoassay for chlorpromazine and other tricyclic antidepressants was to synthesize three chlorpromazine–protein conjugates in which the drug was coupled through a modified side chain as well as through a ring-modified chlorpromazine hapten. These conjugates will subsequently be evaluated to determine which had the specificity and sensitivity to measure the concentration of unchanged chlorpromazine and the total concentration of chlorpromazine and its active metabolites such as monodesmethyl- and didesmethylchlorpromazine.

This paper describes the synthesis and characterization of three new drug–protein conjugates, the production of antibodies to these conjugates in rabbits, and the titers of the antiserums.

0022-3549/78/1100-1563$01.00/0
© 1978, American Pharmaceutical Association

(4) N. A. Hall and W. L. Hayton, *J. Pharm. Sci.*, **56**, 304 (1967).
(5) M. Gibaldi and C. H. Nightingale, *ibid.*, **57**, 226 (1968).
(6) A. R. DiSanto and J. G. Wagner, *ibid.*, **58**, 1077 (1969).
(7) S. H. Yalkowsky, O. S. Carpenter, G. L. Flynn, and T. G. Slunick, *ibid.*, **62**, 1949 (1973).
(8) D. R. Branson, G. E. Blau, H. C. Alexander, and W. B. Neely, *Trans. Am. Fish. Soc.*, **104**, 785 (1975).
(9) C. H. Nightingale and M. Gibaldi, *J. Pharm. Sci.*, **60**, 1360 (1971).
(10) H. W. Smith, *Am. J. Physiol.*, **93**, 480 (1930).
(11) R. R. Ryback, B. Percarpio, and J. Vitale, *Nature*, **222**, 1068 (1969).
(12) B. B. Brodie and R. P. Maickel, *Proc. Int. Pharmacol. Mtg.*, **6**, 299 (1962).
(13) M. Gibaldi and D. Perrier, "Pharmacokinetics," Dekker, New York, N.Y., 1975, pp. 175–187.
(14) C. Brun, *J. Lab. Clin. Med.*, **37**, 955 (1951).
(15) B. E. Cohen, *J. Membr. Biol.*, **20**, 205 (1975).
(16) C. H. van Os, M. D. de Jong, and J. F. G. Slegers, *ibid.*, **15**, 363 (1974).
(17) M. Gibaldi and S. Feldman, *J. Pharm. Sci.*, **59**, 579 (1970).
(18) A. T. Florence and J. M. N. Gillan, *J. Pharm. Pharmacol.*, **27**, 152 (1975).
(19) F. Alhaique, D. Giacchetti, M. Marchetti, and F. M. Riccieri, *ibid.*, **27**, 811 (1975).
(20) F. Alhaique, M. Marchetti, F. M. Riccieri, and E. Santucci, *Experientia*, **31**, 215 (1975).
(21) E. R. Garrett and F. A. Vilallonga, *J. Pharm. Sci.*, **64**, 1782 (1975).
(22) M. W. Gouda, *Can. J. Pharm. Sci.*, **9**, 37 (1974).
(23) M. E. Dokter and J. A. Magnuson, *Arch. Biochem. Biophys.*, **168**, 81 (1975).
(24) N. Bindslev and E. M. Wright, *J. Membr. Biol.*, **29**, 265 (1976).
(25) G. Levy, K. E. Miller, and R. H. Reuning, *J. Pharm. Sci.*, **55**, 394 (1966).
(26) E. M. Wright and N. Bindslev, *J. Membr. Biol.*, **29**, 289 (1976).

ACKNOWLEDGMENTS

Presented at the Basic Pharmaceutics Section, APhA Academy of Pharmaceutical Sciences, New Orleans meeting, April 1976.

Abstracted from a dissertation submitted by J. S. Kaka to Washington State University in partial fulfillment of the Master of Science degree requirements.

Supported in part by funds provided for biological and medical research by Washington State Initiative Measure No. 171.

Radioimmunoassay for Psychotropic Drugs I: Synthesis and Properties of Haptens for Chlorpromazine

J. W. HUBBARD *, K. K. MIDHA ‡x, I. J. McGILVERAY ‡, and J. K. COOPER ‡

Received August 22, 1977, from the **Faculty of Pharmacy, University of Manitoba, Winnipeg, Manitoba, Canada,* and the ‡*Drug Research Laboratories, Health Protection Branch, Health and Welfare Canada, Ottawa, Ontario, Canada.* Accepted for publication April 6, 1978.

Abstract □ For the development of radioimmunoassay procedures for chlorpromazine and its active metabolites, three chlorpromazine haptens, 7-(or 8-)(3-carboxypropionyl)chlorpromazine, *N*-(3-carboxypropionyl)desmethylchlorpromazine, and *N*-(2-carboxyethyl)desmethylchlorpromazine, were synthesized and characterized by GLC–mass spectrometry, PMR spectrometry, and IR spectrophotometry. Each hapten was coupled to bovine serum albumin, and the number of hapten residues per mole of bovine serum albumin was calculated by UV spectrophotometric methods. Antibodies to each hapten–protein conjugate were obtained in rabbits, and titers of the antiserums were checked by evaluating their binding characteristics to tritiated chlorpromazine.

Keyphrases □ Chlorpromazine—three haptens synthesized and characterized, antibodies developed in rabbits, antiserum titers determined □ Haptens, chlorpromazine—three synthesized and characterized, antibodies developed in rabbits, antiserum titers determined □ Antibodies—to three chlorpromazine haptens developed in rabbits □ Tranquilizers—chlorpromazine, three haptens synthesized and characterized, antibodies developed in rabbits, antiserum titers determined

Chlorpromazine is widely used in the treatment of certain psychiatric disorders. It is extensively metabolized in humans, and several of its metabolites are pharmacologically active. For thorough study of the metabolism, pharmacokinetics, and clinical monitoring of this drug, sensitive specific procedures are required for the determination of chlorpromazine levels in biological fluids.

BACKGROUND

Various current techniques with adequate sensitivity to determine plasma chlorpromazine concentrations are GLC with electron-capture detection (1), labeled derivative formation (2), fluorescent labeling with dansyl chloride (3), TLC of a quaternary ammonium derivative (with 9-bromomethylacridine) followed by UV photolysis and subsequent spectrofluorometric determination (4), and GLC with mass spectrometric detection (5). But these methods are tedious, require extraction of the drug from biological fluids and/or its derivatization, and are not easily amenable for routine clinical monitoring.

Radioimmunoassay also may be applicable for determining plasma chlorpromazine concentrations. This technique is simple, requires no extraction, and is readily applied to routine analysis. A reported radioimmunoassay procedure for chlorpromazine (6), in which the protein (bovine serum albumin) was presumably coupled through the side chain of the drug, is not sufficiently sensitive (*cf.*, 7) and does not differentiate between chlorpromazine and its didemethylated metabolite at any level or among chlorpromazine, 7-hydroxychlorpromazine, and chlorpromazine sulfoxide at the 20-ng level.

Another published procedure (7), in which the bovine serum albumin was coupled to the ring system of chlorpromazine through a carboxyphenylazo bridge, was claimed to distinguish to some extent between chlorpromazine and several of its ring-modified and side-chain-modified metabolites, but it has not been widely evaluated or applied.

The present approach toward a sensitive, specific radioimmunoassay for chlorpromazine and other tricyclic antidepressants was to synthesize three chlorpromazine–protein conjugates in which the drug was coupled through a modified side chain as well as through a ring-modified chlorpromazine hapten. These conjugates will subsequently be evaluated to determine which had the specificity and sensitivity to measure the concentration of unchanged chlorpromazine and the total concentration of chlorpromazine and its active metabolites such as monodesmethyl- and didesmethylchlorpromazine.

This paper describes the synthesis and characterization of three new drug–protein conjugates, the production of antibodies to these conjugates in rabbits, and the titers of the antiserums.

0022-3549/78/1100-1563$01.00/0
© 1978, American Pharmaceutical Association

EXPERIMENTAL

GLC—The gas chromatograph[1] was equipped with a flame-ionization detector. The columns[2] were of coiled glass tubing, 1.83 m (6 ft) long × 2 mm i.d., packed with 5% OV-7[2] (Column 1) or 2% OV-25[2] (Column 2) on acid-washed dimethylchlorosilane-treated high performance 100–120-mesh Chromosorb W. The columns were conditioned by maintaining the oven at 310° for 18 hr with a low nitrogen flow.

Operating temperatures were: injection port, 325°; detector, 325°; and ovens, 300° (Column 1) and 270° (Column 2). The nitrogen flow rates for Columns 1 and 2 were 60 and 65 ml/min, respectively. Hydrogen and compressed air flow rates were adjusted to give maximum response.

GLC–Mass Spectrometry—GLC–mass spectrometry was carried out on a mass spectrometer[3] coupled to a gas chromatograph[4] through a two-stage jet separator. The ionization potential was 70 ev. The GLC column and conditions were the same as for direct GLC. For accurate mass measurement[5], the sample of reacted product was collected from the detector at its appropriate retention time after the flame was extinguished.

PMR—All PMR spectra were recorded on a spectrometer[6] operating at 60 mHz at ambient temperature with deuterated chloroform as the solvent and tetramethylsilane as the internal standard.

IR—All IR spectra were recorded on a spectrophotometer[7] at ambient temperature.

Synthesis of 7-(or 8-)(3-Methoxycarbonylpropionyl)chlorpromazine (III)—A solution of 3-methoxycarbonylpropionyl chloride[8] (2.03 g, 13.5 mmoles) in methylene dichloride[9] (30 ml) was added to a solution of anhydrous aluminum chloride[10] (3.60 g, 27 mmoles) dissolved in methylene dichloride (100 ml). The mixture was stirred at room temperature for 30 min, after which a solution of 3.19 g (10 mmoles) of chlorpromazine[11] free base (I) in methylene dichloride (30 ml) was added all at once. The dark-red reaction mixture was stirred at room temperature in the dark for 72 hr, and then the stirring was stopped to allow the solids to settle. The solvent was decanted and discarded since it was shown by GLC to contain unreacted I (1.25 g, 3.98 mmoles after evaporation).

Ice water (50 ml) was cautiously added to the solid residue, followed by 100 ml of 1.0 *N* NaOH. The greenish-yellow aqueous suspension was then extracted by ether[12] (6 × 100 ml). The combined ethereal extracts were washed with water (100 ml) and saturated brine (2 × 100 ml) and dried over anhydrous magnesium sulfate[8]. Evaporation[13] under reduced pressure afforded III as a yellow oil (2.6 g, 60%).

GLC showed one major peak (90% by area) with a retention time (T_R) of 5.2 min (Column 1); IR (chloroform): ν 1738 (ester C=O) and 1680 (aromatic keto C=O) cm^{-1}; PMR [after purification by preparative high-performance liquid chromatography (HPLC)[14]] (deuterated chloroform): δ 1.96 (m, 2H), 2.28 (s, 6H), 2.57 (m, 4H), 3.17 (m, 2H), 3.70 (s, 3H), 3.97 (m, 2H), 6.93 (m, 4H), and 7.80 (m, 2H) ppm (Fig. 1B). GLC–mass spectrometry gave a molecular ion at *m/e* 432/434 and other diagnostic ions (Fig. 2).

Synthesis of 7-(or 8-)(3-Carboxypropionyl)chlorpromazine (IV)—Sodium hydroxide (5 ml, 1.0 *N*) was added to a rapidly stirred solution of III (1.0 g, 2.3 mmoles) in 100 ml of water containing 2.3 ml of 1.0 *N* HCl. A fine oily precipitate appeared and was kept in suspension by continual rapid stirring as the mixture was heated to a gentle reflux. After 3 hr, the precipitate had all dissolved, and the solution was allowed to cool to room temperature. It was washed (at pH 11.5) with ether (5 × 100 ml) to remove any unreacted I or III. The pH was then adjusted to 6.2 with 1.0 *N* HCl.

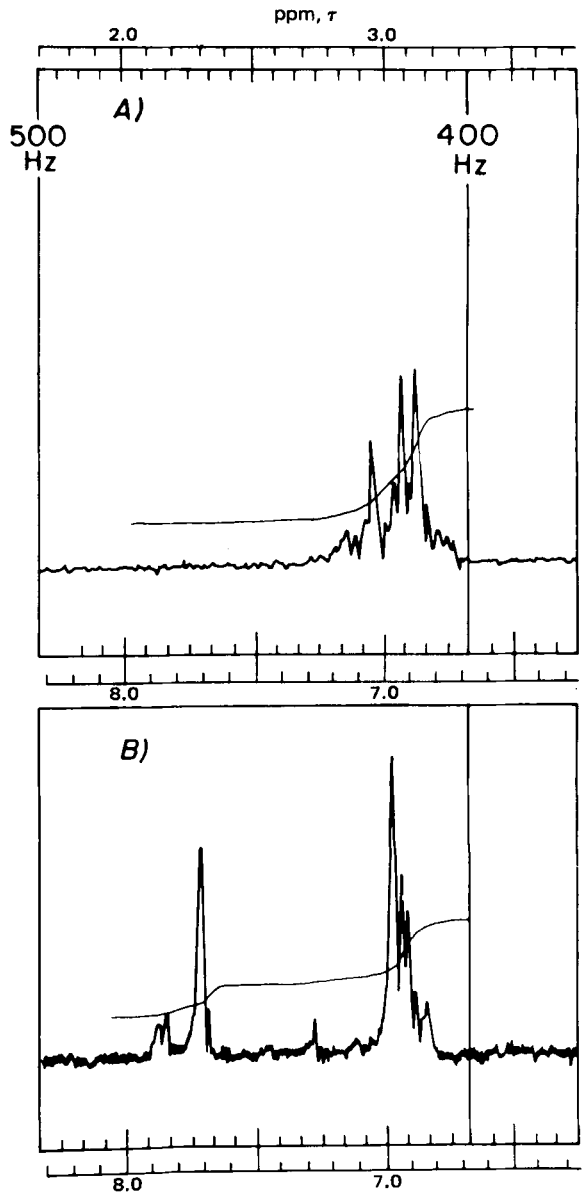

Figure 1—*PMR spectra of aromatic protons of I (A) and III (B) in deuterated chloroform*

The product was recovered by continuous extraction[15] (56 hr) with ether (500 ml) to yield IV as a yellow oily solid (0.9 g); IR (chloroform): ν 1710–1720 (carboxylic acid C=O) and 1680 (keto C=O) cm^{-1}. GLC analysis of this material showed no peak corresponding to III. However, on treatment with diazomethane[16] and subsequent GLC (Column 1), a single peak corresponding to III (T_R 5.2 min) was obtained. GLC–mass spectrometry of the diazomethane-treated material was identical to that of III (Fig. 2), as were the IR and PMR spectra. Accurate mass determi-

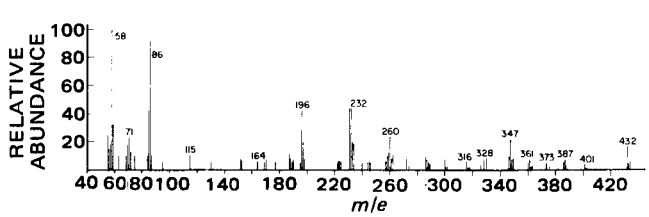

Figure 2—*GLC–mass spectrum (normalized) of III.*

[1] Model 3920, Perkin-Elmer, Montreal, Quebec, Canada.
[2] Chromatographic Specialties, Brockville, Ontario, Canada.
[3] Hitachi Perkin-Elmer, model RMU 6L.
[4] Model 990, Perkin-Elmer, Montreal, Quebec, Canada.
[5] Varian MAT 311, Varian of Canada, Georgetown, Ontario, Canada.
[6] Varian A-60A, Varian of Canada, Georgetown, Ontario, Canada.
[7] Unicam SP-1000, Canlab, Montreal, Quebec, Canada.
[8] Aldrich Chemical Co., Milwaukee, Wis.
[9] Caledon Laboratories, Georgetown, Ontario, Canada.
[10] Baker Analyzed Reagent, J. T. Baker Chemical Co., Phillipsburg, N.J.
[11] Poulenc Laboratories, Montreal, Quebec, Canada.
[12] Mallinckrodt Chemical Works Ltd., Montreal, Quebec, Canada.
[13] Flash-Evaporator, Buchler Instruments, Fort Lee, N.J.
[14] Carried out on a Lichrosorb Si 60 column (230 × 4.6 mm i.d.) with a mobile phase of 15% 2-propanol–15% methylene dichloride–15% methanol–0.1% triethylamine in *n*-hexane. Under these conditions, κ' values for chlorpromazine and the desired product were 2.7 and 8.7, respectively. A. G. Butterfield, Drug Research Laboratories, Health Protection Branch, Health and Welfare Canada, Ottawa, Ontario, Canada, personal communication.
[15] Kontes Glass Co., Vineland, N.J.
[16] Prepared from Diazald, Aldrich Chemical Co., Milwaukee, Wis.

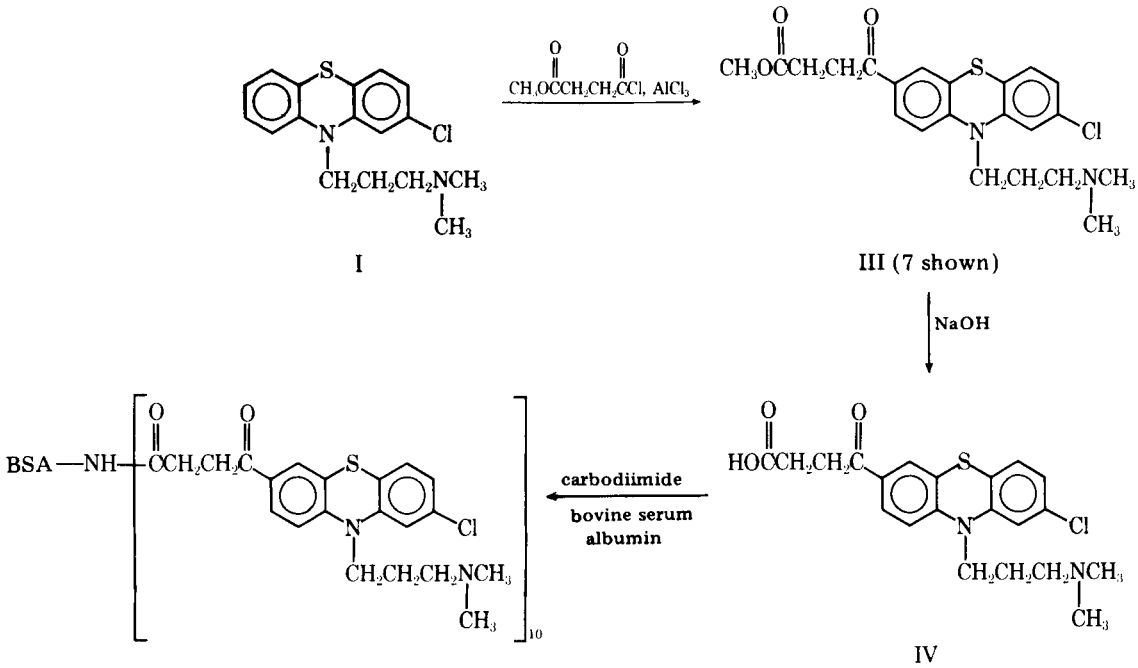

Scheme I

nation for $C_{22}H_{25}ClN_2O_3S$: calculated for $C_{22}H_{25}{}^{35}ClN_2O_3S$, 432.1274; found, 432.1270; calculated for $C_{22}H_{25}{}^{37}ClN_2O_3S$, 434.1245; found, 434.1259.

Coupling of IV to Bovine Serum Albumin—Compound IV was coupled to bovine serum albumin[17] by the carbodiimide method (8–12). A solution of bovine serum albumin (0.07 g, 0.001 mmole) in 5 ml of distilled water was added to a solution of IV (0.042 g, 0.1 mmole) in 10 ml of water. A solution of 1-ethyl-3-(3-dimethylaminopropyl)carbodiimide hydrochloride[17] (0.057 g, 0.3 mmole) in 1.0 ml of water was added, and the solution was adjusted to pH 4.5 by the dropwise addition of 0.01 *N* HCl.

The mixture was then allowed to stand in the dark at room temperature for 24 hr before dialysis[18] against running distilled water (pH 5.5) for 24 hr. After lyophilization, the conjugate was obtained as a yellow crystalline solid (0.06 g). A blank was prepared in the same manner but without IV. The number of hapten residues per mole of conjugate was calculated by the UV method (13, 14) to be 10.

Synthesis of *N*-(3-Carboxypropionyl)desmethylchlorpromazine (V)—Desmethylchlorpromazine[19] free base (II) (0.342 g, 1.12 mmoles) and succinic anhydride[20] (0.112 g, 1.12 mmoles) were dissolved in ethanol (50 ml) and stirred at room temperature in the dark for 48 hr. The ethanol was evaporated[13], and the oily residue was dissolved in 20 ml of 1.0 *N* NaOH. Then the solution was washed with ether (3 × 20 ml). On acidification with 1.0 *N* HCl, an oily precipitate separated at pH 7.5.

This precipitate was extracted with ether (2 × 20 ml). The combined ether extracts were dried over molecular sieves[21] and evaporated[13] to give V as a colorless oil (0.43 g); IR (chloroform): ν 1715–1730 (carboxylic acid C=O) and 1640 (amide C=O) cm^{-1}; PMR (deuterated chloroform): δ 2.02 (bm, 2H), 2.40 (m, 2H), 2.58 (m, 2H), 2.88 (m, 3H), 3.47 (bm, 2H), 3.88 (bm, 2H), 7.03 (bm, 7H), and 7.67 (bs, 1H) ppm. The single proton signal at δ 7.67 ppm exchanged with deuterium oxide.

Compound V was converted into its methyl ester with diazomethane. The ester gave only one peak (T_R 8.4 min) on GLC analysis (Column 1). GLC–mass spectrometry gave a molecular ion at 418/420 and other diagnostic ions (Fig. 3). Accurate mass determination for $C_{21}H_{23}ClN_2O_3S$: calculated for $C_{21}H_{23}{}^{35}ClN_2O_3S$, 418.1118; found 418.1101; calculated for $C_{21}H_{23}{}^{37}ClN_2O_3S$, 420.1088; found 420.1078. In the PMR spectrum of the methyl ester, the broad singlet at δ 7.67 ppm in the spectrum of V was replaced by a 3H singlet at δ 3.68 ppm; IR (chloroform): ν 1735 (ester C=O) and 1640 (amide C=O) cm^{-1}.

Coupling of V to Bovine Serum Albumin—A solution of V (0.04 g, 0.1 mmole) in 10 ml of 0.1 *N* NaOH was adjusted to pH 8.0 with 0.1 *N* HCl. The bovine serum albumin (0.07 g, 0.001 mmole) in 5 ml of water was added, followed by a solution of 1-ethyl-3-(3-dimethylaminopropyl)carbodiimide hydrochloride in 1.0 ml of water. The solution (final pH 7.0) was mixed by swirling and allowed to stand at room temperature in the dark for 24 hr. It was then dialyzed against bicarbonate buffer containing 0.2% sodium azide[22] (0.042 *M*, pH 8, 6 × 500 ml) and then against running distilled water (pH 6.2) for 12 hr. After lyophilization, the conjugate was obtained as a white crystalline solid (0.063 g).

A blank was prepared in the same manner but without V. The number of hapten residues per mole of bovine serum albumin was calculated by the UV method (13, 14) to be 50.

Synthesis of *N*-(2-Methoxycarbonylethyl)desmethylchlorpromazine (VI)—Methyl acrylate[22] (0.353 g, 4.1 mmoles) was added all at once to a solution of II (1.19 g, 3.9 mmoles) in 50 ml of methanol. The mixture was maintained at a gentle reflux for 48 hr, and the solvent was then evaporated[13] to yield a pale-yellow oil (1.35 g). GLC analysis of this material (Column 2) showed two peaks. The major peak (69% by area) had a retention time of 5.2 min. GLC–mass spectrometry gave a molecular ion at *m/e* 390/392 and other diagnostic ions (Fig. 4).

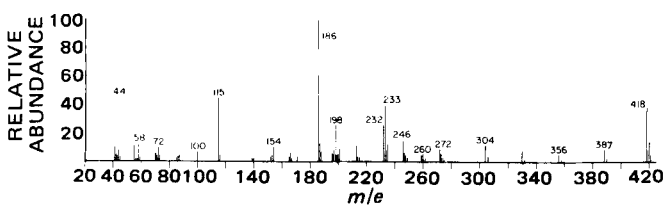

Figure 3—*GLC–mass spectrum (normalized) of methyl ester of V.*

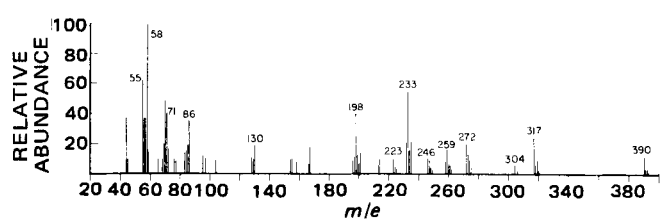

Figure 4—*GLC–mass spectrum (normalized) of VI.*

[17] Sigma Chemical Co., St. Louis, Mo.
[18] Fisher dialyzer tubing (Size C), Fisher Scientific Co., Pittsburg, Pa.
[19] Rhône-Poulenc, Centre Nicolas Grillet, France (supplied as the maleate salt).
[20] Eastman Kodak Co., Rochester, N.Y.
[21] Davison Chemical Co., Baltimore, Md.
[22] British Drug Houses, Poole, England.

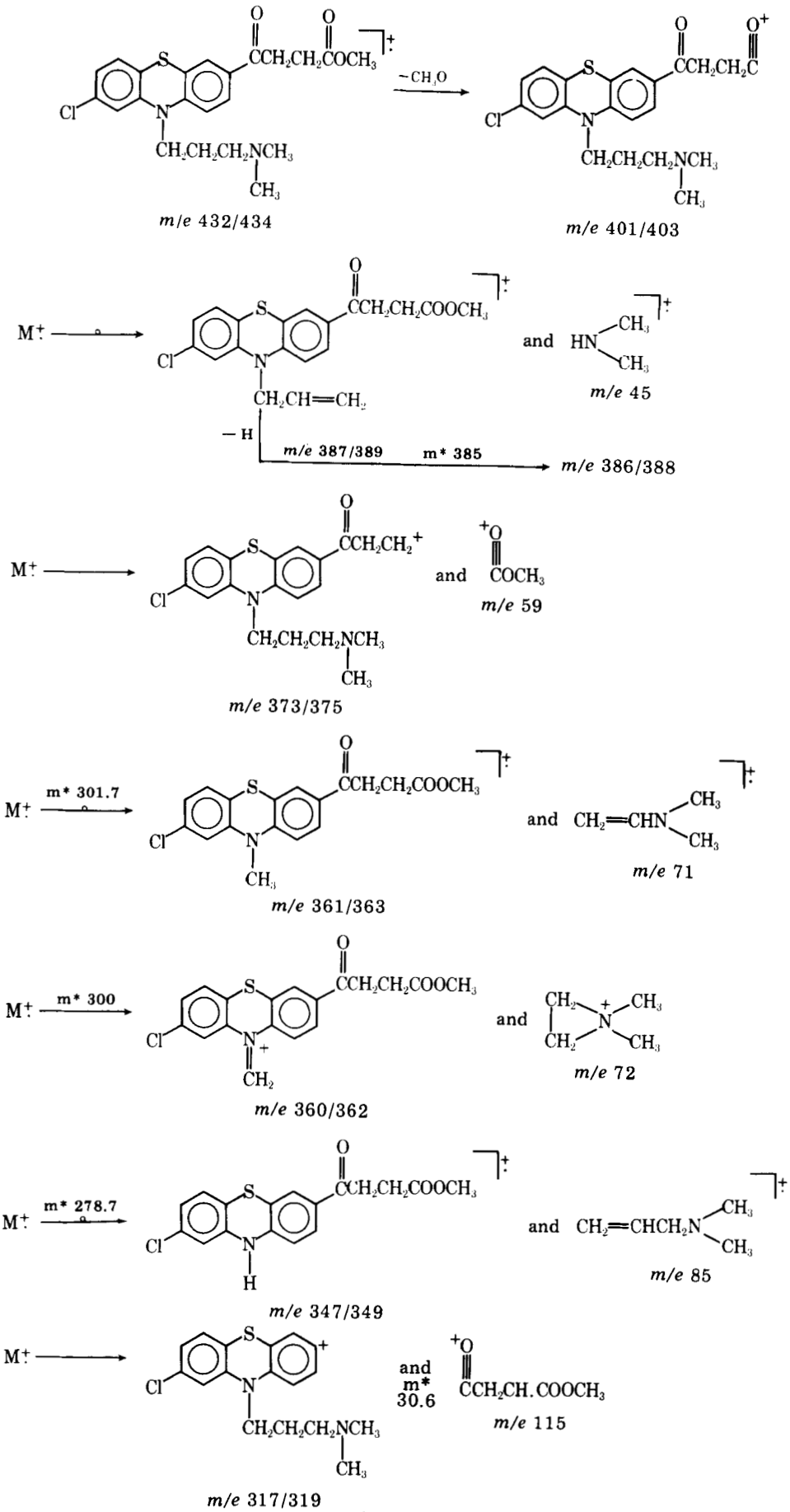
m/e 432/434
−CH2O
m/e 401/403
M+
and
m/e 45
m/e 387/389
m* 385
m/e 386/388
M+
and
m/e 59
m/e 373/375
M+
m* 301.7
and
m/e 71
m/e 361/363
M+
m* 300
and
m/e 72
m/e 360/362
M+
m* 278.7
and
m/e 85
m/e 347/349
M+
and
m* 30.6
m/e 115
m/e 317/319

Scheme II

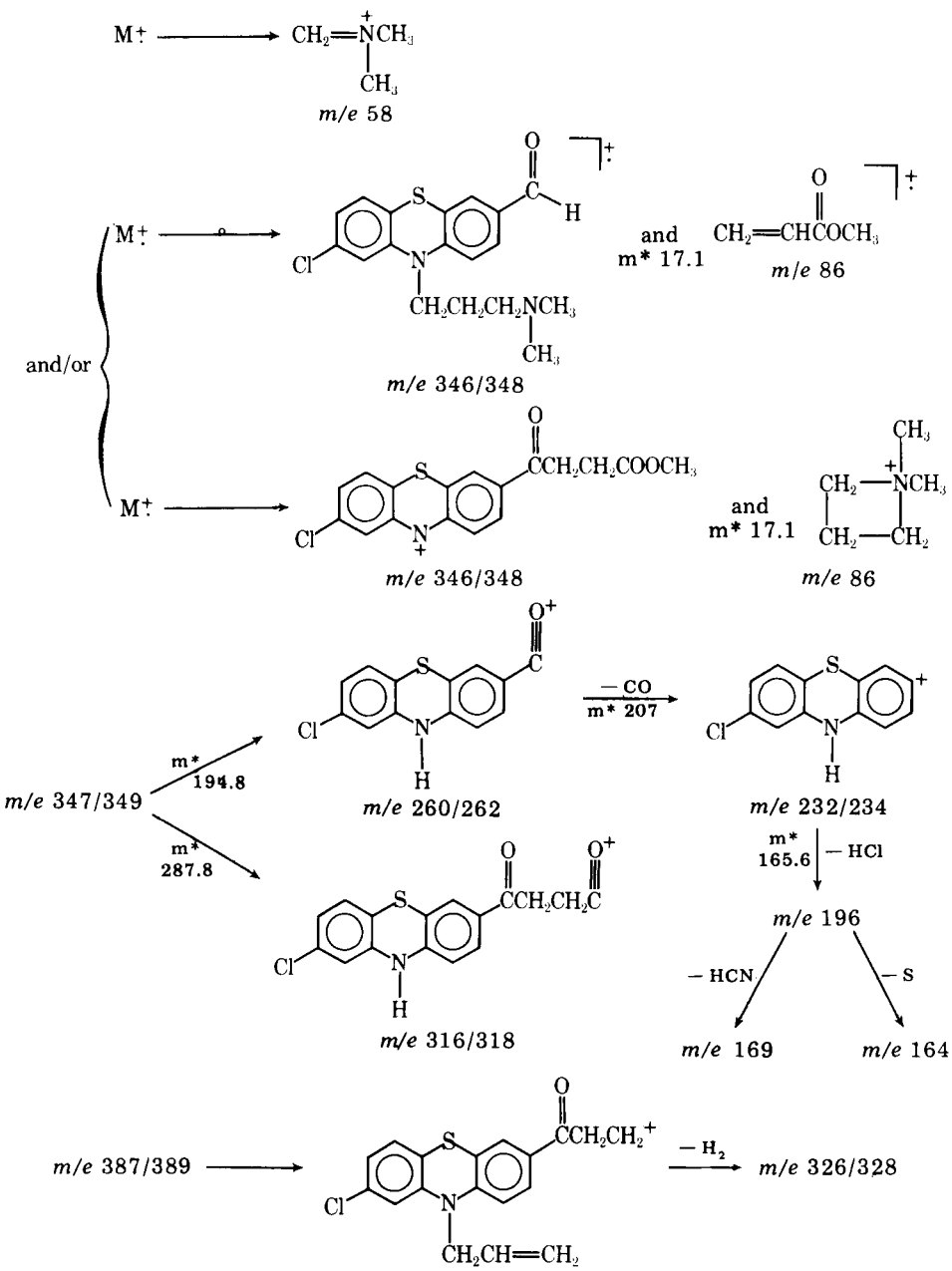

Scheme III

The second peak (31% by area) had the same retention time (1.8 min) as II. There was no change in the ratio of these peaks if the reaction was allowed to continue beyond 48 hr or if additional methyl acrylate was added. No attempt was made to remove the unreacted II until after the hydrolysis step.

Synthesis of *N*-(2-Carboxyethyl)desmethylchlorpromazine (VII)—The hydrolysis of VI was carried out in a manner similar to that for IV. After the wash step at pH 11.5, the reaction mixture pH was adjusted to 7.5 with 1.0 *N* HCl, and the product separated as a colorless oil. The mixture was allowed to stand at 4° overnight, and the aqueous layer was then decanted and discarded. The oil was taken up in benzene (50 ml) and washed with distilled water (50 ml).

Evaporation of the benzene gave VII in quantitative yield; IR (chloroform): ν 1720 (carboxylic acid C=O) cm^{-1}; PMR (deuterated chloroform): δ 2.00 (m, 2H), 2.33 (m, 5H), 2.75 (m, 4H), 3.92 (m, 2H), 7.00 (m, 7H), and 7.83 (bs, 1H) ppm. The broad singlet at δ 7.83 ppm exchanged with deuterium oxide.

GLC analysis of this material showed no peak corresponding to VI or to unreacted II. However, after treatment with diazomethane[16] and subsequent GLC (Column 2) analysis, a single peak corresponding to VI was obtained (T_R 5.2 min). The GLC–mass spectrum and IR spectrum of this product were identical to those of VI. In the PMR spectrum (deuterated chloroform), the broad singlet at δ 7.83 ppm in the spectrum of VII was replaced by a 3H singlet at δ 3.65 ppm. Accurate mass determination for $C_{20}H_{23}ClN_2O_2S$: calculated for $C_{20}H_{23}{}^{35}ClN_2O_2S$, 390.1169; found 390.1173; calculated for $C_{20}H_{23}{}^{37}ClN_2O_2S$, 392.1139; found 392.1146.

Coupling of VII to Bovine Serum Albumin—Compound VII was coupled to bovine serum albumin by a modified mixed anhydride method (13, 14). Compound VII (0.049 g, 0.13 mmole) and isobutyl chloroformate[10] (0.017 g, 0.13 mmole) were dissolved in freshly distilled dioxane[22] (2.6 ml), and the solution was cooled to 15° and allowed to react for 20 min. The mixture was then added in 0.5-ml aliquots to a stirred, well-cooled (4°) solution of bovine serum albumin (0.182 g, 0.0026 mmole) in 50% dioxane–water (25 ml), which had been adjusted to pH 9.3 with 1.0 *N* NaOH. Throughout the addition, the pH was maintained at 9.0–9.8 with 1.0 *N* NaOH. After the addition was complete, the solution was clear and was allowed to react at 4° for 12 hr with continuous stirring.

The solution was dialyzed[18] against bicarbonate buffer (0.042 *M*, pH 8.0, 6 × 500 ml) and then against acetate buffer (0.012 *M*, pH 4.0, 6 × 500

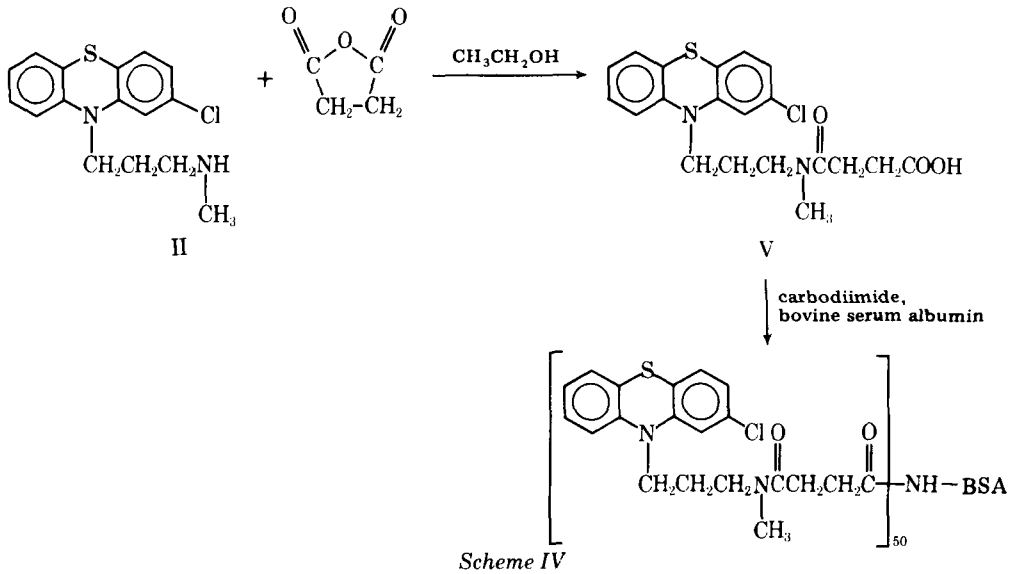

II V

Scheme IV

ml); both buffer systems contained 0.2% sodium azide[22]. A fine colloidal precipitate appeared during the dialysis procedure and was removed by centrifugation[23] and discarded. After lyophilization, the conjugate was obtained as a white crystalline solid (0.171 g). A blank was prepared in the same manner but without VII. The number of hapten residues per mole of bovine serum albumin was calculated by the UV method (13, 14) to be 17.

Compound VII also was coupled to bovine serum albumin by the carbodiimide procedure as described for V. The number of hapten residues per mole of bovine serum albumin was calculated to be 5.

Immunization—Each hapten–protein conjugate (4 mg) was dissolved in normal saline (2.0 ml) and emulsified with complete Freund's adjuvant[24] (2.0 ml). Each conjugate was administered to four New Zealand White female rabbits[25] by injection of 0.5 ml of the emulsion into each flank. At 2-week intervals thereafter, the injections were repeated with an emulsion prepared as already described, except that complete Freund's adjuvant was replaced by incomplete. The antiserum titer of each rabbit was checked 1 week after the third injection.

Serum was obtained from the marginal ear vein at weekly intervals after the third injection. The antiserum titer of each rabbit was checked by evaluating the binding characteristic of tritiated chlorpromazine[26] to each antiserum. After optimal titer values were achieved, blood was obtained from each rabbit by cardiac puncture. The harvested serum was immediately lyophilized in 1.0-ml samples and stored at −70°.

RESULTS AND DISCUSSION

To couple the ring system of chlorpromazine to bovine serum albumin (BSA), a ring-modified hapten was prepared by the Friedel–Crafts acylation of chlorpromazine with 3-methoxycarbonylpropionyl chloride (Scheme I). GLC analysis of the hapten showed that it contained 90% III (by peak area, T_R 5.2 min). The GLC–mass spectrum of III gave a molecular ion at m/e 432/434 and other diagnostic ions (Fig. 2). Formation of these ions is rationalized in Schemes II and III. In most cases, the fragmentations are supported by the observation of appropriate metastables. Fragments associated with the basic chlorpromazine nucleus are consistent with literature spectra (15).

The minor product (10% by peak area) (T_R 4.2 min) gave essentially the same GLC–mass spectrum as III and was assumed to be a positional isomer of III. Various attempts to hasten the Friedel–Crafts reaction by raising the temperature, changing the molar proportions of the reactants, or changing the order of mixing led to a reduced yield of III and the production of disubstituted chlorpromazine derivatives. Thus, a mixture of III, its positional isomer, and two disubstituted products was obtained when the reaction mixture was heated to reflux under conditions similar to those described by Schmitt *et al.* (16), who prepared some 3-acetylphenothiazine derivatives by a Friedel–Crafts technique.

Attempts to prepare the carboxylic acid IV (Scheme I) directly, by treating I with succinic anhydride in the presence of aluminum chloride, were unsuccessful. Experimental conditions similar to those described for III, or similar to published procedures for the reaction of aromatic compounds with succinic anhydride (17–19), gave either unreacted I or an unidentified compound, the mass spectrum of which bore no resemblance to that of IV. The alkaline hydrolysis of the methyl ester III, however, gave IV in excellent yield.

In the PMR spectrum of III, the aromatic protons gave two distinct signals. The first of these was a 4H multiplet, centered at δ 6.93 (6.80–7.07) ppm (Fig. 1B), comparable to the chemical shift (δ 6.98 ppm) of the aromatic protons of chlorpromazine (deuterated chloroform), δ 6.73–7.23 ppm (m, 7H) (Fig. 1A). The remaining two aromatic protons of III appeared as a 2H multiplet centered at δ 7.8 (7.67–7.92) ppm (Fig. 1B), consistent with a deshielding effect produced by an adjacent keto substituent. These two aromatic protons must be located *ortho* to the keto group of III, which precludes the possibility of the side chain being attached to the 1-, 3-, 4-, 6-, or 9-position of chlorpromazine. The only positions in which the side chain can be situated with two *ortho* protons are, therefore, the 7- and 8-positions.

Kawashima *et al.* (7) suggested that the 3- and 7-positions would be optimum for electrophilic substitution of I because of the participation of the lone pair on the nitrogen. The present PMR evidence, together with the fact that chlorine generally deactivates an aromatic ring to electrophilic attack, suggests that the principal site for electrophilic attack on chlorpromazine is at the 7-position. Full details on the further elucidation of the structure of III will be published elsewhere.

To couple the side chain of chlorpromazine with bovine serum albumin, desmethylchlorpromazine was treated with succinic anhydride to give the amido acid V (Scheme IV) in excellent yield without the addition of

Table I—Rabbit Antiserum Titers of Chlorpromazine Hapten–Protein Conjugates

Immunizing Antigen	Number of Positives/ Number Tested	Number of Boosters	Titers
IV–bovine serum albumin	4/4	0	1:500
		0	1:1200
		0	1:1500
		0	1:200
V–bovine serum albumin	2/12[a]	—	1:80
		—	1:100
VII–bovine serum albumin	4/4	0	1:500
		1	1:200
		2	1:500
		2	1:1000

[a] Compound V–bovine serum albumin only produced titers after two intravenous boosters.

[23] Sorvall Inc. RC2-B, Ingram and Bell Ltd., Don Mills, Ontario, Canada.
[24] Grand Island Biological Co., Grand Island, N.Y.
[25] Double Rabbit Ranch, Smith Falls, Ontario, Canada.
[26] Radioactive chlorpromazine generally labeled with tritium having a specific activity of 5.5 Ci/mmole; Nuclear Research Center, Negev, Israel. Radiochemical purity was checked by analytical TLC and HPLC.

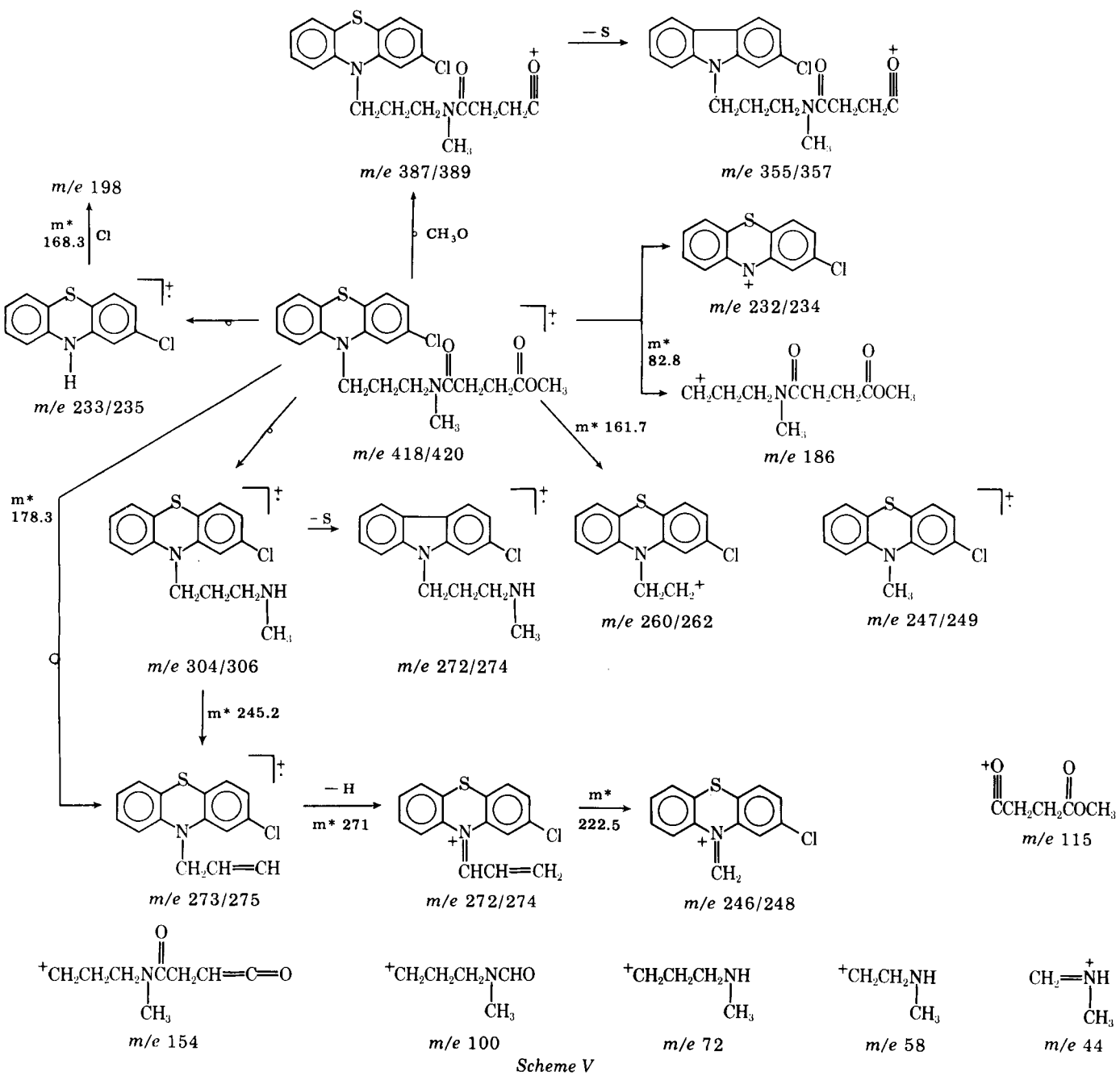

Scheme V

a catalyst. The IR and PMR spectra of V were entirely consistent with the given structure. To facilitate GLC–mass spectrometry, V was converted to its methyl ester by treatment with diazomethane.

The GLC–mass spectrum of the methyl ester of V gave a molecular ion at *m/e* 418/420 and other diagnostic ions (Fig. 3). A rationale for formation of these ions is given in Scheme V. (Fragmentation pathways were not assigned where unsupported by metastables or corresponding fragments.)

The ion at *m/e* 272/274 could be formed by loss of sulfur (*cf.*, 15) from *m/e* 304/306 and/or by loss of a hydrogen radical from *m/e* 273/275; the latter is supported by the observation of a metastable ion (Scheme V).

With the formation of the amido acid derivative of II, the side-chain nitrogen function is changed from a secondary amine to a carboxamide, which has different physical and chemical properties. To determine if this change has any effect on the sensitivity or specificity of the antibody, II was converted into its *N*-methoxycarbonylethyl derivative VI (Scheme VI). The addition of II to the α,β-unsaturated ester methyl acrylate proceeded smoothly without a catalyst to yield the desired product.

The GLC–mass spectrum of VI (Fig. 4) gave a molecular ion at *m/e* 390/392 and other diagnostic ions as rationalized in Scheme VII. Ions at *m/e* 272/274 and 273/275 are considered to have the same structures as those in Scheme V.

The ions at *m/e* 130 and 260/262 arise from the molecular ion by cleavage of the same carbon–carbon bond. The formation of the ion at *m/e* 130 from the molecular ion is supported by observation of an appropriate metastable ion at *m/e* 43.3.

Similar twin fragment ions at *m/e* 304/306 and 86 from the molecular ion were observed, and the formation of the ion at *m/e* 304/306 is again supported by a metastable ion at *m/e* 237.0. Alternative structures are suggested for the ion or ions giving rise to the base peak at *m/e* 58, both of which appear to arise from daughter ions at *m/e* 317/319 and/or 304/306.

The methyl ester VI was hydrolyzed with alkali to the corresponding carboxylic acid VII. The IR and PMR spectra of VII were entirely consistent with this structure.

The conjugation of IV, V, and VII to bovine serum albumin by the carbodiimide method was carried out according to established procedures with minor adaptations. In the coupling of VII by the mixed anhydride method, however, the addition of tributylamine (13, 14) was unnecessary since VII contains a tertiary amino residue in it structure. If one equiv-

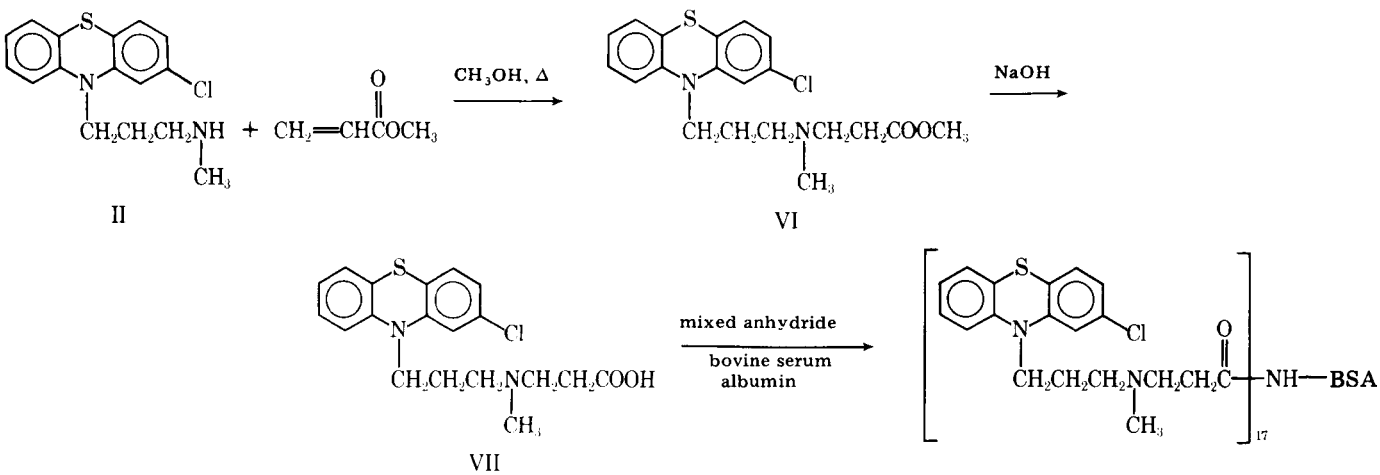

Scheme VI

alent of tributylamine was added to the solution of VII in dioxane, a precipitate was formed on addition of the isobutyl chloroformate. In the absence of tributylamine, the solution remained clear.

If the addition of the mixed anhydride of VII to the bovine serum albumin solution was rapid (13, 14), a precipitate was immediately formed. It did not redissolve when the pH was readjusted to 9.5, even after prolonged stirring. The addition was successfully completed if the mixed anhydride solution was added in small aliquots (0.5 ml) and the pH was maintained at ~9.5 throughout the procedure by dropwise addition of 1.0 *N* NaOH; the initial precipitate redissolved and the final solution was clear.

The preliminary assessment of the antiserums is presented in Table I. All four rabbits immunized with IV–bovine serum albumin (Scheme I) produced operational titers after the fourth injection. Of the four rabbits immunized with VII–bovine serum albumin, one produced an operational titer after the fourth injection, one required a booster shot

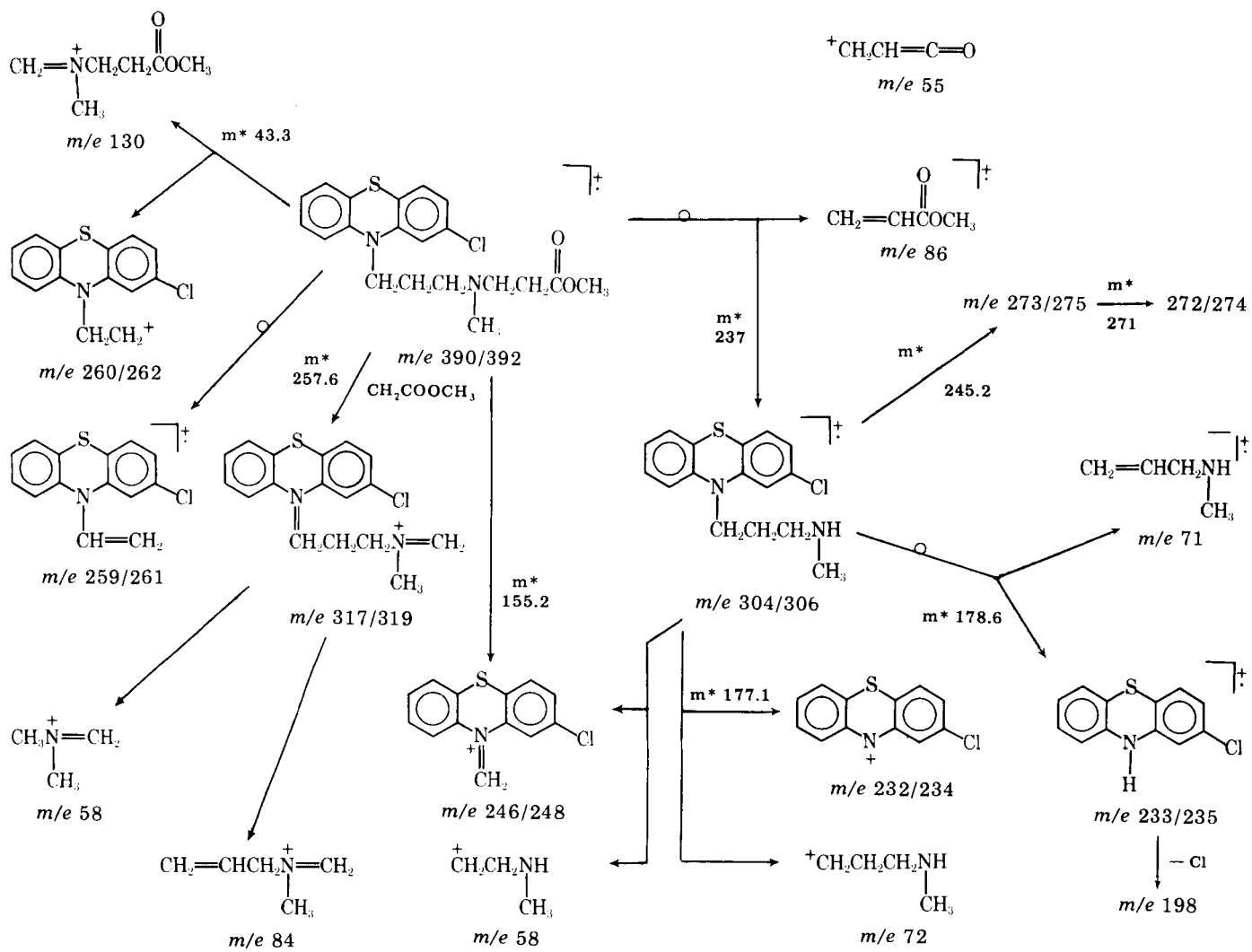

Scheme VII

at double the previous dose, and the remaining two each required two booster shots before satisfactory titers were obtained.

Radioimmunoassay sensitive down to the nanogram range was developed using antibodies to IV-bovine serum albumin and VII-bovine serum albumin. The assays were not influenced by plasma and endogenous substances. Details of these procedures will be described in depth in a subsequent publication.

REFERENCES

(1) S. H. Curry, *Psychopharmacol. Commun.*, **2**, 1 (1976).

(2) D. H. Efron, S. R. Harris, A. A. Manian, and L. E. Gaudette, *Psychopharmacologia*, **19**, 207 (1971).

(3) I. S. Forrest, S. D. Rose, L. G. Brookes, B. Halpern, V. A. Bacon, and L. A. Silberg, *Agressologie*, **12**, 127 (1970).

(4) P. N. Kaul, L. R. Whitfield, and M. L. Clark, *J. Pharm. Sci.*, **65**, 689 (1976).

(5) C. G. Hammar, B. Holmstedt, and R. Ryhage, *Anal. Biochem.*, **25**, 532 (1968).

(6) M. Shostak, in "The Phenothiazines and Structurally Related Drugs," I. S. Forrest, C. J. Carr, and E. Usdin, Eds., Raven, New York, N.Y., 1974.

(7) K. Kawashima, R. Dixon, and S. Spector, *Eur. J. Pharmacol.*, **32**, 195 (1975).

(8) J. C. Sheeham and J. S. Hlavka, *J. Org. Chem.*, **21**, 439 (1956).

(9) B. F. Erlanger, *Pharmacol. Rev.*, **25**, 271 (1973).

(10) P. T. Tsui, K. A. Kelly, M. M. Pompipom, M. Strahilevitz, and A. H. Sehan, *Can. J. Biochem.*, **52**, 252 (1974).

(11) T. A. Williams and K. A. Pittman, *Res. Commun. Chem. Pathol. Pharmacol.*, **7**, 119 (1974).

(12) B. Africa and E. Haker, *Immunochemistry*, **8**, 479 (1971).

(13) B. F. Erlanger, F. Borèk, S. M. Beiser, and S. Lieberman, *J. Biol. Chem.*, **228**, 713 (1957).

(14) *Ibid.*, **234**, 1090 (1959).

(15) J. N. T. Gilbert and B. J. Millard, *Org. Mass Spectrom.*, **2**, 17 (1969).

(16) J. Schmitt, J. Boitard, P. Comoy, A. Hallot, and M. Suquet, *Bull. Soc. Chim. Fr.*, **1957**, 938.

(17) L. F. Fieser and E. B. Hershberg, *J. Am. Chem. Soc.*, **58**, 2314 (1936).

(18) D. G. Thomas and H. L. Nathan, *ibid.*, **70**, 331 (1948).

(19) F. Koelsch, *ibid.*, **55**, 3385 (1933).

ACKNOWLEDGMENTS

Presented at the Pharmaceutical Analysis and Control Section, APhA Academy of Pharmaceutical Sciences, New York meeting, May 1977.

The authors acknowledge the technical assistance of Mr. T. Young, Mr. C. Charette, Mrs. N. Jordan, and Mrs. M. Rowe and the helpful discussions with Dr. J. C. K. Loo and Dr. K. Bailey. They also thank Mr. J.-C. Ethier for mass spectra, Mr. H. Avdovich for PMR spectra, and Mr. A. Trottier for drafting.

Appreciation is extended to the University of Manitoba (Winnepeg) for the study leave to J. W. Hubbard.

Radioimmunoassay for Psychotropic Drugs II: Synthesis and Properties of Haptens for Tricyclic Antidepressants

J. W. HUBBARD *, K. K. MIDHA ‡x, J. K. COOPER ‡, and C. CHARETTE ‡

Received September 26, 1977, from the **Faculty of Pharmacy, University of Manitoba, Winnipeg, Manitoba, Canada,* and the ‡*Drug Research Laboratories, Health Protection Branch, Health and Welfare Canada, Ottawa, Ontario, Canada.* Accepted for publication March 21, 1978.

Abstract □ For the development of radioimmunoassay procedures for tricyclic antidepressants, two drug haptens were synthesized for each of the two amitriptyline–nortriptyline and imipramine–desipramine groups. In one case, nortriptyline or desipramine was treated with succinic anhydride to yield *N*-(3-carboxypropionyl) derivatives; in the other case, the haptens were novel *N*-(2-carboxyethyl) derivatives. The hapten and its corresponding ester were characterized by GLC–mass spectrometry, PMR spectrometry, and IR spectrophotometry. Each hapten was coupled to bovine serum albumin, and the number of hapten residues per mole of bovine serum albumin was determined by UV spectrophotometric methods. Antibodies to each hapten–protein conjugate were developed in rabbits, and titers of the antiserums were checked by evaluating their binding characteristics to tritiated drug.

Keyphrases □ Antidepressants, various tricyclic—haptens synthesized, coupled to bovine serum albumin, antibodies developed in rabbits □ Haptens—of various tricyclic antidepressants, synthesized, coupled to bovine serum albumin, antibodies developed in rabbits □ Antibodies—to hapten–bovine serum albumin conjugates of various tricyclic antidepressants, developed in rabbits

Tricyclic antidepressants are widely used in the treatment of mental disorders, and recent evidence suggests that routine monitoring of plasma levels should provide useful clinical information (1). Some frequently prescribed tricyclic compounds used for the treatment of endogenous depression are imipramine, amitriptyline, and their desmethyl metabolites, desipramine and nortriptyline, respectively.

The determination of the levels of these antidepressant drugs in biological fluids is desirable to study the pharmacokinetics, metabolism, and correlation between blood levels and therapeutic response.

BACKGROUND

Analytical techniques for determining the concentration of the tricyclic antidepressants in biological fluids include spectrophotometry (2, 3), quantitative TLC (4–7), GLC with flame-ionization detection (8–11), GLC with alkali flame (nitrogen specific) detection (12–19), GLC with electron-capture detection (20–23), GLC with mass fragmentographic detection (24–31), GLC with chemical-ionization mass spectrometric detection (32), radioisotope labeling (33–37), and high-pressure liquid chromatography (38). These procedures suffer from a lack of sensitivity or specificity, tedious extraction procedures and/or derivatization techniques, and/or the use of expensive and sophisticated instrumentation. Since they are not easily amenable to routine clinical monitoring, a procedure that may be employed routinely in a standard hospital laboratory is needed.

Radioimmunoassay techniques are simple, usually requiring no extraction, and are readily applied to routine analysis. Of the two published radioimmunoassay procedures, the method for desipramine–imipramine

0022-3549/78/1100-1571$01.00/0

© 1978, American Pharmaceutical Association

at double the previous dose, and the remaining two each required two booster shots before satisfactory titers were obtained.

Radioimmunoassay sensitive down to the nanogram range was developed using antibodies to IV-bovine serum albumin and VII-bovine serum albumin. The assays were not influenced by plasma and endogenous substances. Details of these procedures will be described in depth in a subsequent publication.

REFERENCES

(1) S. H. Curry, *Psychopharmacol. Commun.*, **2**, 1 (1976).

(2) D. H. Efron, S. R. Harris, A. A. Manian, and L. E. Gaudette, *Psychopharmacologia*, **19**, 207 (1971).

(3) I. S. Forrest, S. D. Rose, L. G. Brookes, B. Halpern, V. A. Bacon, and L. A. Silberg, *Agressologie*, **12**, 127 (1970).

(4) P. N. Kaul, L. R. Whitfield, and M. L. Clark, *J. Pharm. Sci.*, **65**, 689 (1976).

(5) C. G. Hammar, B. Holmstedt, and R. Ryhage, *Anal. Biochem.*, **25**, 532 (1968).

(6) M. Shostak, in "The Phenothiazines and Structurally Related Drugs," I. S. Forrest, C. J. Carr, and E. Usdin, Eds., Raven, New York, N.Y., 1974.

(7) K. Kawashima, R. Dixon, and S. Spector, *Eur. J. Pharmacol.*, **32**, 195 (1975).

(8) J. C. Sheeham and J. S. Hlavka, *J. Org. Chem.*, **21**, 439 (1956).

(9) B. F. Erlanger, *Pharmacol. Rev.*, **25**, 271 (1973).

(10) P. T. Tsui, K. A. Kelly, M. M. Pompipom, M. Strahilevitz, and A. H. Sehan, *Can. J. Biochem.*, **52**, 252 (1974).

(11) T. A. Williams and K. A. Pittman, *Res. Commun. Chem. Pathol. Pharmacol.*, **7**, 119 (1974).

(12) B. Africa and E. Haker, *Immunochemistry*, **8**, 479 (1971).

(13) B. F. Erlanger, F. Borèk, S. M. Beiser, and S. Lieberman, *J. Biol. Chem.*, **228**, 713 (1957).

(14) *Ibid.*, **234**, 1090 (1959).

(15) J. N. T. Gilbert and B. J. Millard, *Org. Mass Spectrom.*, **2**, 17 (1969).

(16) J. Schmitt, J. Boitard, P. Comoy, A. Hallot, and M. Suquet, *Bull. Soc. Chim. Fr.*, **1957**, 938.

(17) L. F. Fieser and E. B. Hershberg, *J. Am. Chem. Soc.*, **58**, 2314 (1936).

(18) D. G. Thomas and H. L. Nathan, *ibid.*, **70**, 331 (1948).

(19) F. Koelsch, *ibid.*, **55**, 3385 (1933).

ACKNOWLEDGMENTS

Presented at the Pharmaceutical Analysis and Control Section, APhA Academy of Pharmaceutical Sciences, New York meeting, May 1977.

The authors acknowledge the technical assistance of Mr. T. Young, Mr. C. Charette, Mrs. N. Jordan, and Mrs. M. Rowe and the helpful discussions with Dr. J. C. K. Loo and Dr. K. Bailey. They also thank Mr. J.-C. Ethier for mass spectra, Mr. H. Avdovich for PMR spectra, and Mr. A. Trottier for drafting.

Appreciation is extended to the University of Manitoba (Winnepeg) for the study leave to J. W. Hubbard.

Radioimmunoassay for Psychotropic Drugs II: Synthesis and Properties of Haptens for Tricyclic Antidepressants

J. W. HUBBARD *, K. K. MIDHA ‡x, J. K. COOPER ‡, and C. CHARETTE ‡

Received September 26, 1977, from the **Faculty of Pharmacy, University of Manitoba, Winnipeg, Manitoba, Canada,* and the ‡*Drug Research Laboratories, Health Protection Branch, Health and Welfare Canada, Ottawa, Ontario, Canada.* Accepted for publication March 21, 1978.

Abstract □ For the development of radioimmunoassay procedures for tricyclic antidepressants, two drug haptens were synthesized for each of the two amitriptyline–nortriptyline and imipramine–desipramine groups. In one case, nortriptyline or desipramine was treated with succinic anhydride to yield *N*-(3-carboxypropionyl) derivatives; in the other case, the haptens were novel *N*-(2-carboxyethyl) derivatives. The hapten and its corresponding ester were characterized by GLC–mass spectrometry, PMR spectrometry, and IR spectrophotometry. Each hapten was coupled to bovine serum albumin, and the number of hapten residues per mole of bovine serum albumin was determined by UV spectrophotometric methods. Antibodies to each hapten–protein conjugate were developed in rabbits, and titers of the antiserums were checked by evaluating their binding characteristics to tritiated drug.

Keyphrases □ Antidepressants, various tricyclic—haptens synthesized, coupled to bovine serum albumin, antibodies developed in rabbits □ Haptens—of various tricyclic antidepressants, synthesized, coupled to bovine serum albumin, antibodies developed in rabbits □ Antibodies—to hapten–bovine serum albumin conjugates of various tricyclic antidepressants, developed in rabbits

Tricyclic antidepressants are widely used in the treatment of mental disorders, and recent evidence suggests that routine monitoring of plasma levels should provide useful clinical information (1). Some frequently prescribed tricyclic compounds used for the treatment of endogenous depression are imipramine, amitriptyline, and their desmethyl metabolites, desipramine and nortriptyline, respectively.

The determination of the levels of these antidepressant drugs in biological fluids is desirable to study the pharmacokinetics, metabolism, and correlation between blood levels and therapeutic response.

BACKGROUND

Analytical techniques for determining the concentration of the tricyclic antidepressants in biological fluids include spectrophotometry (2, 3), quantitative TLC (4–7), GLC with flame-ionization detection (8–11), GLC with alkali flame (nitrogen specific) detection (12–19), GLC with electron-capture detection (20–23), GLC with mass fragmentographic detection (24–31), GLC with chemical-ionization mass spectrometric detection (32), radioisotope labeling (33–37), and high-pressure liquid chromatography (38). These procedures suffer from a lack of sensitivity or specificity, tedious extraction procedures and/or derivatization techniques, and/or the use of expensive and sophisticated instrumentation. Since they are not easily amenable to routine clinical monitoring, a procedure that may be employed routinely in a standard hospital laboratory is needed.

Radioimmunoassay techniques are simple, usually requiring no extraction, and are readily applied to routine analysis. Of the two published radioimmunoassay procedures, the method for desipramine–imipramine

0022-3549/78/1100-1571$01.00/0

© 1978, American Pharmaceutical Association

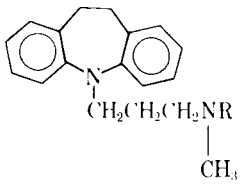

I: R = H
IIa: R = $COCH_2CH_2COOH$
IIb: R = $COCH_2CH_2COOCH_3$
IIIa: R = CH_2CH_2COOH
IIIb: R = $CH_2CH_2COOCH_3$

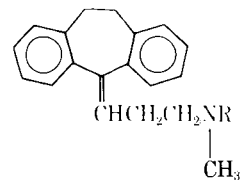

IV: R = H
Va: R = $COCH_2CH_2COOH$
Vb: R = $COCH_2CH_2COOCH_3$
VIa: R = CH_2CH_2COOH
VIb: R = $CH_2CH_2COOCH_3$

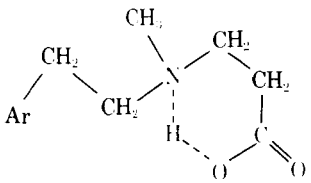

VII

(39), in which the protein (bovine serum albumin) is coupled to the ring system through a carboxyphenylazo bridge, lacks specificity and does not distinguish between a drug and its metabolites. The other radioimmunoassay (40) procedure for amitriptyline–nortriptyline, in which a linkage occurs through the alkylamine side chain to the bovine serum albumin, is not sensitive enough to monitor plasma levels following single or therapeutic dosage.

In the present study, two drug–protein conjugates were prepared for each of the two amitriptyline–nortriptyline and imipramine–desipramine groups. Prior to coupling to bovine serum albumin, the structural integrity of the four haptens was established by GLC–mass spectrometry, PMR spectrometry, and IR spectroscopy to establish a basis for an understanding of the antigenic determinants. The production of antibodies to these conjugates in rabbits and the titers of the antiserums are reported.

EXPERIMENTAL

GLC—The gas chromatograph[1] was equipped with a flame-ionization detector. The column[2] was coiled glass tubing, 1.83 m (6 ft) long × 2 mm i.d., packed with 5% OV-25[2] on acid-washed dimethylchlorosilane-treated high-performance Chromosorb W[2] support (100–120 mesh). The column was conditioned by maintaining the oven at 310° for 18 hr with a low nitrogen flow. Operating conditions were: injection port temperature, 325°; detector temperature, 325°; oven temperature, 300°; and nitrogen flow rate, 60 ml/min. Hydrogen and compressed air flow rates were adjusted to give maximum response.

GLC–Mass Spectrometry—The mass spectrometer[3] was coupled to a gas chromatograph[4] through a two-stage jet separator. The ionization potential was 70 ev. The GLC column and conditions were the same as for direct GLC.

PMR—All PMR spectra were recorded on a spectrometer[5] operating at 60 MHz at ambient temperature with deuterated chloroform as the solvent and tetramethylsilane as the internal standard.

[1] Model 3920, Perkin-Elmer, Montreal, Quebec, Canada.
[2] Chromatographic Specialties, Brockville, Ontario, Canada.
[3] Hitachi Perkin-Elmer, model RMU 6L.
[4] Model 990, Perkin-Elmer, Montreal, Quebec, Canada.
[5] Varian A-60A, Varian of Canada, Georgetown, Ontario, Canada.

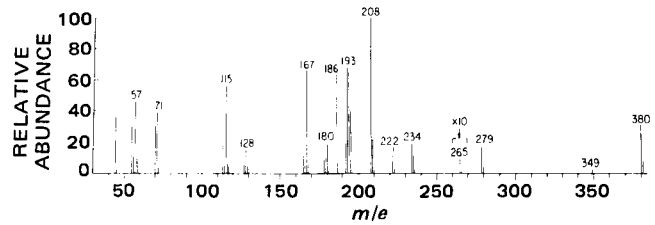

Figure 1—*GLC–mass spectrum (normalized) of IIb.*

IR—All IR spectra were recorded on a spectrophotometer[6] at ambient temperature.

Synthesis of *N*-(3-Carboxypropionyl) Derivative of Desipramine (IIa)—Succinic anhydride[7] (0.45 g, 4.5 mmoles) was added to a solution of desipramine[8] free base (I) (1.16 g, 4.34 mmoles) in ethanol[9] (50 ml). The mixture was stirred at room temperature for 48 hr, and the ethanol was then evaporated[10].

The pale-yellow oil thus obtained was dissolved in aqueous sodium hydroxide (50 ml, 1.0 *N*) and washed with ether[11] (3 × 50 ml) to remove any unreacted I. The aqueous solution pH was then adjusted to 7.5 with aqueous hydrochloric acid (1.0 *N*), whereupon IIa separated as fine white crystals. These crystals were filtered by suction, washed with distilled water (20 ml), and dried in a vacuum desiccator (1.52 g yield, 94%); IR (chloroform): 1715–1740 (carboxylic acid ν C=O) and 1635 (amide ν C=O) cm^{-1}; PMR (deuterated chloroform): δ 1.5–2.0(b, 2H), 2.38(m, 2H), 2.61 (m, 2H), 2.82 (s, 3H), 3.19 (s, 4H), 3.29 (m, 2H), 3.74 (m, 2H), 7.08 (m, 8H), and 9.36 (bs, 1H) ppm. The proton giving rise to the signal at 9.36 ppm exchanged with deuterium oxide.

Compound IIa was converted to its methyl ester IIb by reaction with an ethereal solution of diazomethane[12]. The ester gave only one peak (T_r 11.26 min) on GLC analysis. GLC–mass spectrometry gave a molecular ion at *m/e* 380 and other diagnostic ions (Fig. 1); IR (chloroform): 1730 (ester ν C=O) and 1635 (amide ν C=O) cm^{-1}. In the PMR spectrum of IIb, the singlet at δ 9.36 (1H) ppm was absent and a singlet appeared at δ 3.69 (3H) ppm.

Coupling of IIa to Bovine Serum Albumin—A solution of IIa (0.037 g, 0.1 mmole) in sodium hydroxide (10 ml, 0.1 *N*) was adjusted to pH 8.0 with aqueous hydrochloric acid (0.1 *N*). The bovine serum albumin[13] (0.07 g, 0.001 mmole) in 5 ml of water was added, followed by a solution of 1-ethyl-3-(3-dimethylaminopropyl)carbodiimide hydrochloride (0.057 g, 0.3 mmole) in 1.0 ml of water. The solution was mixed by swirling (pH 6.8) and allowed to stand at room temperature for 24 hr.

The mixture was then dialyzed[14] against bicarbonate buffer containing 0.2% sodium azide[15] (0.042 *M*, pH 8.0, 6 × 500 ml) and then against acetate buffer (0.012 *M*, pH 4.0, 6 × 500 ml, with 0.2% sodium azide[15]). After lyophilization[16], the conjugate was obtained as a white crystalline solid (0.064 g). A blank was prepared in the same manner without IIa. The number of hapten residues per mole of conjugate was calculated by the UV method (41, 42) to be 23.

Synthesis of *N*-(2-Carboxyethyl) Derivative of Desipramine (IIIa)—Methyl acrylate[15] (0.39 g, 4.5 mmoles) was added all at once to a solution of I (1.56 g, 4.34 mmoles) in 50 ml of methanol[9]. The mixture was maintained at a gentle reflux for 48 hr, after which the solvent was evaporated[10] to yield a pale-yellow oil (1.33 g). This material was dissolved in hydrochloric acid (4.0 ml, 1.0 *N*) and diluted to 100 ml with distilled water. Aqueous sodium hydroxide (10 ml, 1.0 *N*) was then added, giving a fine oily precipitate.

This precipitate was kept in suspension by continuous rapid stirring as the mixture was heated to a gentle reflux. After 1 hr, the precipitate had all dissolved, and the solution was allowed to cool to room temperature. It was then washed with ether[11] (3 × 100 ml) to remove any unreacted I. The pH was then adjusted to 7.5 with aqueous hydrochloric acid (1.0 *N*), and the mixture was allowed to stand overnight at 4°.

Fine white crystals were collected, washed with distilled water (30 ml), and dried in a vacuum desiccator (1.46 g, 89.4%); IR (chloroform):

[6] Unicam SP-1000, Canlab, Montreal, Quebec, Canada.
[7] Eastman Kodak Co., Rochester, N.Y.
[8] Ciba-Geigy Ltd., Basel, Switzerland (supplied as the hydrochloride).
[9] Burdick & Jackson Laboratories, Muskegon, Mich.
[10] Flash-Evaporator, Buchler Instruments, Fort Lee, N.J.
[11] Mallinckrodt Chemical Works Ltd., Montreal, Quebec, Canada.
[12] Prepared from Diazald, Aldrich Chemical Co., Milwaukee, Wis.
[13] Sigma Chemical Co., St. Louis, Mo.
[14] Fisher dialyzer tubing (size C), Fisher Scientific Co., Pittsburgh, Pa.
[15] British Drug Houses, Poole, England.
[16] Virtis, Fisher Scientific Co., Montreal, Quebec, Canada.

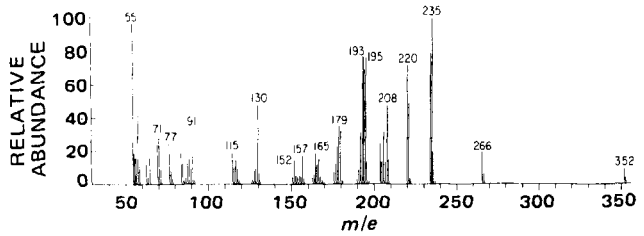

Figure 2—*GLC–mass spectrum (normalized) of IIIb.*

1710–1725 (carboxylic acid ν C=O) cm^{-1}; PMR (deuterated chloroform): δ 1.83 (b, 2H), 2.29 (s) and 2.36 (m) overlapping (5H), 2.67 (m, 4H), 3.16 (s, 4H), 3.78 (m, 2H), 7.08 (m, 8H), and 11.27 (bs, 1H) ppm. The proton giving rise to the broad singlet at δ 11.27 ppm exchanged with deuterium oxide.

Compound IIIa was converted into its methyl ester IIIb by reaction with an ethereal solution of diazomethane[12]. GLC analysis of this material showed only one peak (T_r 2.5 min). GLC–mass spectrometry gave a molecular ion at *m/e* 352 and other diagnostic ions (Fig. 2). In the PMR spectrum (deuterated chloroform) of IIIb, the broad singlet (1H) at δ 11.27 ppm in the spectrum of IIIa was absent and a singlet (3H) appeared at δ 3.63 ppm; IR (chloroform): 1735 (ester ν C=O) cm^{-1}.

Coupling of IIIa to Bovine Serum Albumin—*Carbodiimide Method (IIIa–Bovine Serum Albumin A)*—A solution of IIIa (0.034 g, 0.1 mmole) in sodium hydroxide (1.0 ml, 0.1 *N*) was added dropwise to the stirred mixture of bovine serum albumin[13] (0.070 g, 0.001 mmole) and 1-ethyl-3-(3-dimethylaminopropyl)carbodiimide hydrochloride[13] (0.057 g, 0.3 mmole) in 1 ml of distilled water. The solution pH was 9.0 and was then adjusted to 7.2 with aqueous hydrochloric acid (0.1 *N*); then the mixture was allowed to stand at room temperature overnight.

The solution was then dialyzed against bicarbonate and acetate buffers as described for IIa–bovine serum albumin. After lyophilization[16], the conjugate was obtained as a white crystalline solid (0.065 g). A blank was prepared in the same manner without IIIa. The number of hapten molecules per mole of conjugate was calculated by the UV method (41, 42) to be 1.0.

Mixed Anhydride Method (IIIa–Bovine Serum Albumin B)—Isobutyl chloroformate[17] (0.017 g, 0.13 mmole) and IIIa (0.044 g, 0.13 mmole) were dissolved in freshly distilled dioxane[15] (2.5 ml). The solution was cooled to 13° and allowed to react for 20 min. The mixture was then added in 0.5-ml aliquots to a stirred, cooled (4°) solution of bovine serum albumin (0.182 g, 0.0026 mmole) in 50% dioxane–water (25 ml), previously adjusted to pH 9.3 with aqueous sodium hydroxide (1.0 *N*). Throughout the addition, the pH was maintained between 9.0 and 9.5 with aqueous sodium hydroxide (1.0 *N*). After the addition was complete, the clear solution was allowed to react for 12 hr at 4° with continuous stirring.

The solution was dialyzed as described for IIa–bovine serum albumin. During the dialysis procedure with the acetate buffer, the protein slowly precipitated. This material was separated by centrifugation[18] (0.5 hr at 2500 rpm) and redissolved in bicarbonate buffer (0.05 *M*, pH 9.3) before lyophilization. The conjugate, a white crystalline solid (0.167 g), was found to contain eight hapten residues per mole by the UV method (41, 42).

Synthesis of *N*-(3-Carboxypropionyl) Derivative of Nortriptyline (Va)—Succinic anhydride[7] (0.10 g, 1.0 mmole) and nortriptyline[19] (IV) (0.24 g, 0.91 mmole) were reacted as described for IIa. The residue was dissolved with aqueous sodium hydroxide, washed with ether, and adjusted to pH 7.5 with aqueous hydrochloric acid (1.0 *N*). The product separated as a colorless oil and was extracted with ether[11] (3 × 50 ml).

The combined ether extract was washed with distilled water (2 × 75 ml) and saturated brine (2 × 75 ml), dried over molecular sieves[20] (3Å), and evaporated[10] to give Va as a colorless oil (0.30 g, 82%); IR (chloroform): 1715–1740 (carboxylic acid ν C=O) and 1635 (amide ν C=O) cm^{-1}; PMR (deuterated chloroform): δ 2.20–3.68 (overlapping multiplets, 15H), 5.81 (t, J = 7 Hz, 1H), 7.17 (m, 8H), and 8.87 (bs, 1H) ppm. The proton giving rise to the singlet at δ 8.87 ppm exchanged with deuterium oxide.

Compound Va was converted to its methyl ester Vb by treatment with diazomethane[12]. The ester gave only one peak on GLC analysis (T_r 5.9 min); when scanned by GLC–mass spectrometry, it gave a molecular ion at *m/e* 377 and other diagnostic ions (Fig. 3). The PMR spectrum of Vb showed that the signal (1H) at 8.87 in the spectrum of Va was absent and a singlet (3H) appeared at δ 3.67 ppm; IR (chloroform): 1730 (ester ν C=O) and 1635 (amide ν C=O) cm^{-1}.

Coupling of Va to Bovine Serum Albumin (Va–Bovine Serum Albumin)—Compound Va was coupled to bovine serum albumin[13] using the carbodiimide method and dialysis procedure described for IIa–bovine serum albumin. The conjugate was obtained as a white crystalline solid (0.67 g), which was shown by the UV method (41, 42) to contain 18 moles of hapten/mole of protein.

Synthesis of *N*-(3-Carboxyethyl) Derivative of Nortriptyline (VIa)—Nortriptyline[19] (0.27 g, 1.02 mmoles) was reacted with methyl acrylate[15] (0.088 g, 1.02 mmoles) under the conditions described for IIIa. After the aqueous medium pH was adjusted to 7.5, the product separated as a colorless oil and was extracted with ether[11] (3 × 50 ml).

The combined ether extract was washed with water (2 × 75 ml) and saturated brine (2 × 75 ml), dried over molecular sieves[20] (3Å), and evaporated[10] to yield VIa as a colorless oil (0.275 g, 82%); IR (chloroform): 1715–1720 (carboxylic acid ν C=O) cm^{-1}; PMR (deuterated chloroform): δ 2.10–3.35 (overlapping multiplets, 15H), 5.78 (t, J = 7 Hz, 1H), 7.18 (m, 8H), and 10.45 (s, 1H) ppm. The proton giving rise to the signal at δ 10.45 ppm exchanged with deuterium oxide.

Compound VIa was converted to its methyl ester VIb by reaction with diazomethane[12]. GLC analysis of the ester showed only one peak (T_r 2.1 min); when scanned by GLC–mass spectrometry, it gave a molecular ion at *m/e* 349 and other diagnostic ions (Fig. 4). The PMR spectrum of the methyl ester showed that the signal (1H) at δ 10.45 ppm in the spectrum of VIa was absent and a singlet (3H) appeared at δ 3.62 ppm; IR (chloroform): 1735 (ester ν C=O) cm^{-1}.

Coupling of VIa to Bovine Serum Albumin—*Carbodiimide Method (VIa–Bovine Serum Albumin A)*—Compound VIa was coupled to bovine serum albumin[13] using the carbodiimide method escribed for IIIa–bovine serum albumin A and the dialysis procedure described for IIa–bovine serum albumin. The conjugate was obtained as a white crystalline solid (0.066 mg) and was shown by the UV method (41, 42) to contain 0.5 hapten residues/mole.

Mixed Anhydride Method (VIa–Bovine Serum Albumin B)—Compound VIa was coupled to bovine serum albumin[13] by the mixed anhydride technique described for IIIa–bovine serum albumin B and the dialysis procedure described for IIa–bovine serum albumin. The conjugate, a white crystalline solid (0.176 g), was shown by the UV method (41, 42) to contain 10 hapten molecules/mole.

Immunization—Each hapten–protein conjugate (4 mg) was dissolved in normal saline (2.0 ml) and emulsified with complete Freund's adjuvant[21] (2.0 ml). Each conjugate was administered to four New Zealand White female rabbits[22] by injection of 0.5 ml of the emulsion into each flank. At 2-week intervals thereafter, the injections were repeated with the emulsion prepared as described except that complete Freund's adjuvant was replaced by incomplete. The antiserum titer of each rabbit was checked 1 week after the third injection.

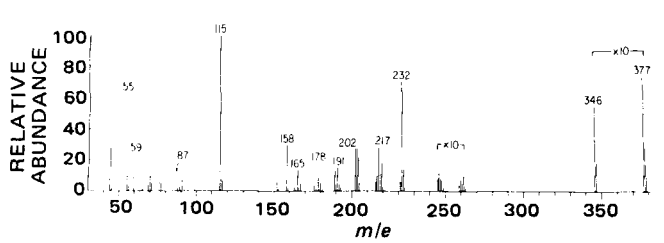

Figure 3—*GLC–mass spectrum (normalized) of Vb.*

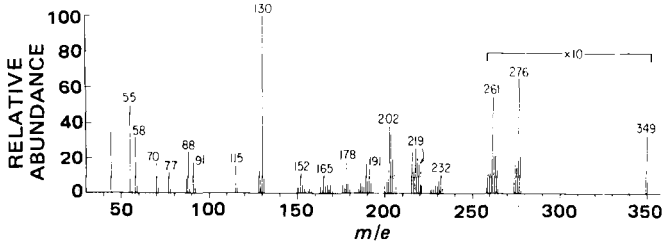

Figure 4—*GLC–mass spectrum (normalized) of VIb.*

[17] Aldrich Chemical Co., Milwaukee, Wis.
[18] Sorval Inc. RC2-B, Ingram and Bell Ltd., Don Mills, Ontario, Canada.
[19] Eli Lilly Co. Ltd., Toronto, Ontario, Canada.

[20] Davison Chemical Co., Baltimore, Md.
[21] Grand Island Biological Co., Grand Island, N.Y.
[22] Double Rabbit Ranch, Smith Falls, Ontario, Canada.

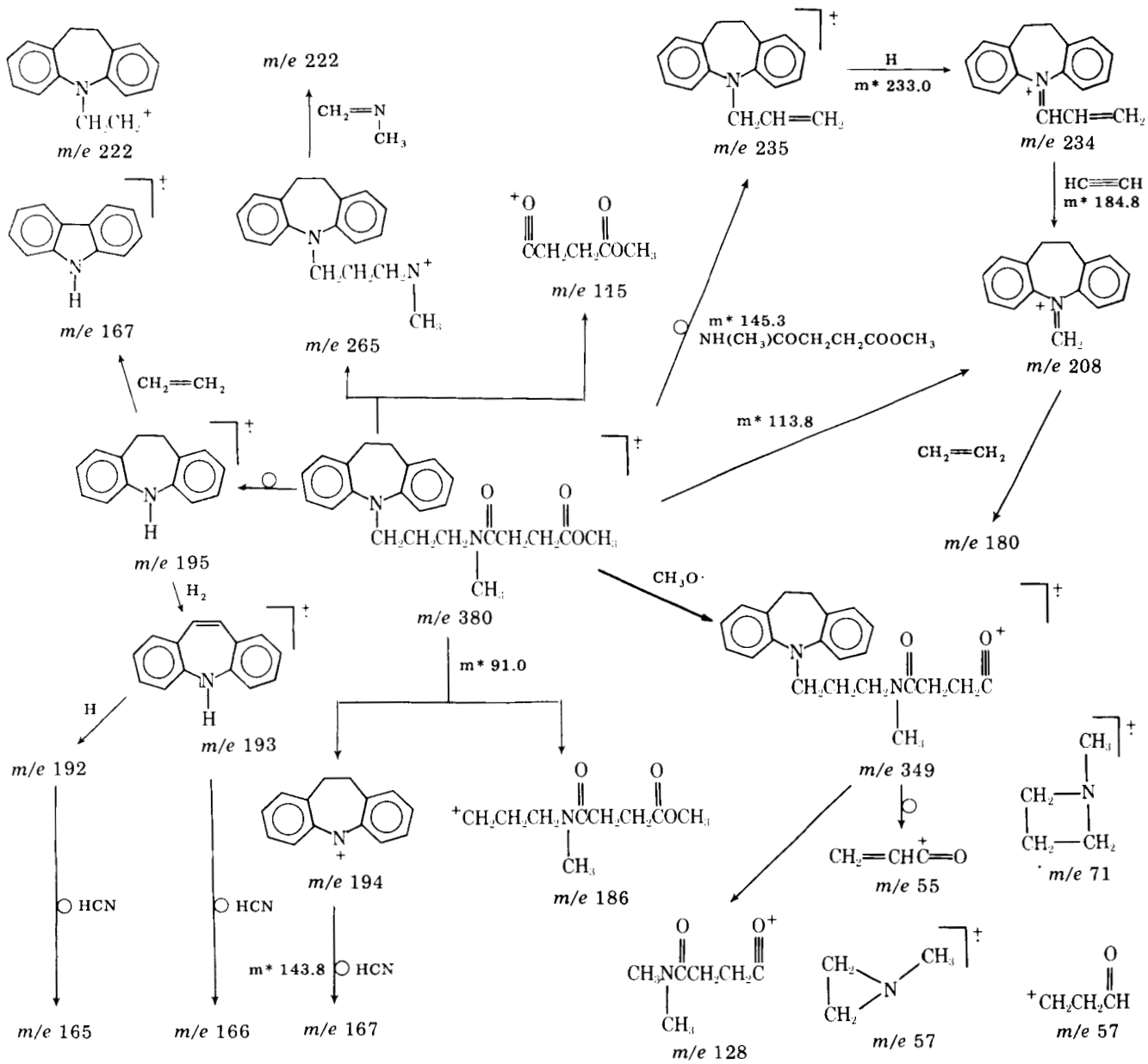

Scheme I

Serum was obtained from the marginal ear vein at weekly intervals after the third injection. The antiserum titer of each rabbit was checked by evaluating the binding characteristic of tritiated I[23] or tritiated IV[24] to each antiserum. After optimal titers were achieved, blood was obtained from each rabbit by cardiac puncture. The harvested serum in each case was immediately lyophilized in 1-ml samples and stored at −70°.

RESULTS AND DISCUSSION

The four haptens were obtained in good yields as described under *Experimental*. They were characterized by IR and PMR spectral data and by GLC–mass spectrometry of their respective methyl esters, prepared by reacting the carboxylic acids with diazomethane prior to coupling to bovine serum albumin. All IR and PMR spectra of the carboxylic acids and their respective methyl esters were entirely consistent with their proposed structures.

The GLC–mass spectrum of the methyl ester II*b* gave a molecular ion at *m/e* 380 and other diagnostic ions shown in Fig. 1 and rationalized in Scheme I. The base peak at *m/e* 208 apparently arises directly from the molecular ion at *m/e* 380 by cleavage of the bond between C-1 and C-2 of the side chain and also indirectly from the molecular ion through ions at *m/e* 235 and 234 (Scheme I). The observation of appropriate metastable ions (Scheme I) gives support to both pathways.

The formation of an ion at *m/e* 186 from the molecular ion, as supported by the appropriate metastable ion at *m/e* 91.0, suggests the loss of the ring system. The presence of an ion at *m/e* 194 (65%) indicates that, on cleavage of the intact side chain, the charge is accommodated to a similar extent by the ring system.

By contrast, in the fragmentation pattern of the methyl ester III*b* (Scheme II), the ion at *m/e* 194 (Fig. 2) seems to arise by a different pathway since no ion corresponds to the intact side chain. In this case, the ion at *m/e* 157 and the corresponding ion at *m/e* 195 (supported by an appropriate metastable ion at *m/e* 108.0) indicate that the molecular ion undergoes cleavage by a rearrangement involving the transfer of a proton from the side chain. The ion at *m/e* 194 seems to arise by loss of a hydrogen radical from the ion at *m/e* 195.

In the mass spectrum of III*b*, the base peak is observed at *m/e* 235 with a corresponding ion at *m/e* 117, with both fragments supported by appropriate metastable ions (Scheme II). This result indicates that the base peak at *m/e* 235 is formed by a rearrangement involving a 1–4 shift. The ion at *m/e* 234 (79%) is formed by loss of a hydrogen radical from the ion

[23] Radioactive imipramine generally labeled with tritium having a specific activity of 20 Ci/mmole; Nuclear Research Center, Negev, Israel. Radiochemical purity was checked by TLC.

[24] Radioactive nortriptyline generally labeled with tritium having a specific activity of 3.2 Ci/mmole; Nuclear Research Center, Negev, Israel. Radiochemical purity was checked by TLC.

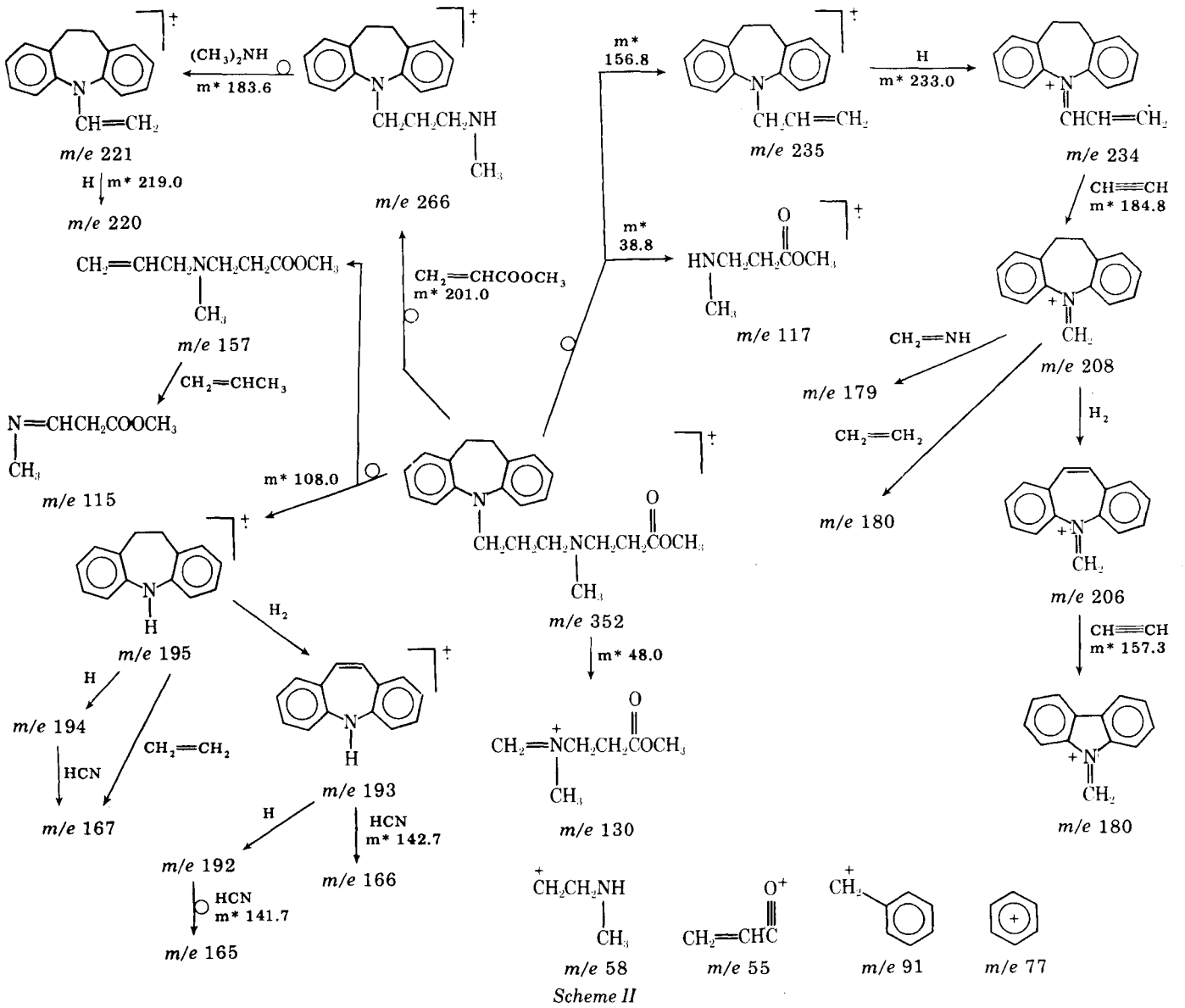

Scheme II

at *m/e* 235, as supported by the observation of a metastable ion at *m/e* 233.0. This sequence was observed in the mass spectrum of imipramine (43). Structures for the ions at *m/e* 179, 165, and 152 (Fig. 2) were proposed (44).

In the mass spectrum of the methyl ester V*b* (Fig. 3), the ion at *m/e* 115, which is the base peak (Scheme III), has the same structure as the equivalent ion (56%) in the mass spectrum of the amido ester II*b* of desipramine (Scheme I). The ion at *m/e* 232 (70%) (Scheme III), which arises from the molecular ion at *m/e* 377 with an appropriate metastable ion at *m/e* 142.8, has the same structure as was previously reported in the mass spectrum of *N*-trifluoroacetylnortriptyline (45).

Similarly, in the mass spectrum of the methyl ester VI*b* (Fig. 4 and Scheme IV), the ion at *m/e* 130 is the base peak, in contrast to the mass spectrum of the amino ester III*b* of desipramine (Fig. 2) in which the same ion occurs to a lesser extent (50%). Thus, the relative abundances of the ions at *m/e* 130 and 115 in the amino esters III*b* and VI*b* and in the amido esters II*b* and V*b*, respectively, reflect the influence of the two ring systems on the cleavage of the side chain under electron impact.

The amino acids II*a* and V*a* were coupled to bovine serum albumin by the carbodiimide method, with only minor modifications of established procedures (46–51). The number of moles of hapten coupled per mole of bovine serum albumin was calculated by the UV method (41, 42) to be 23 and 18, respectively. By contrast, the amino acids III*a* and VI*a* proved resistant to coupling by the carbodiimide method, even when the procedure was adapted for the poor solubility of these haptens between pH 3.5 and 9.5. The poor solubility of III*a* and VI*a* may be related to the formation of a stable, intramolecular, hydrogen-bonded, six-membered ring system VII. Aherne *et al.* (40) similarly found that an aminoalkyl derivative of nortriptyline coupled poorly with bovine serum albumin by the carbodiimide procedure.

The amino acids III*a* and VI*a* were successfully coupled to bovine serum albumin by a modified mixed anhydride procedure (41, 42, 51),

Table I—Rabbit Antiserum Titers of Antidepressant Hapten–Protein Conjugates

Immunizing Antigen	Number of Positives/ Number Tested	Number of Boosters	Titers
II*a*–bovine serum albumin	3/4	0	1:200
		0	1:400
		0	1:400
		—	—
III*a*–bovine serum albumin	4/4	0	1:1500
		0	1:1600
		0	1:1000
		0	1:1500
V*a*–bovine serum albumin	2/4	1	1:500
		2	1:200
		—	—
VI*a*–bovine serum albumin	4/4	0	1:500
		0	1:500
		0	1:200
		0	1:1000

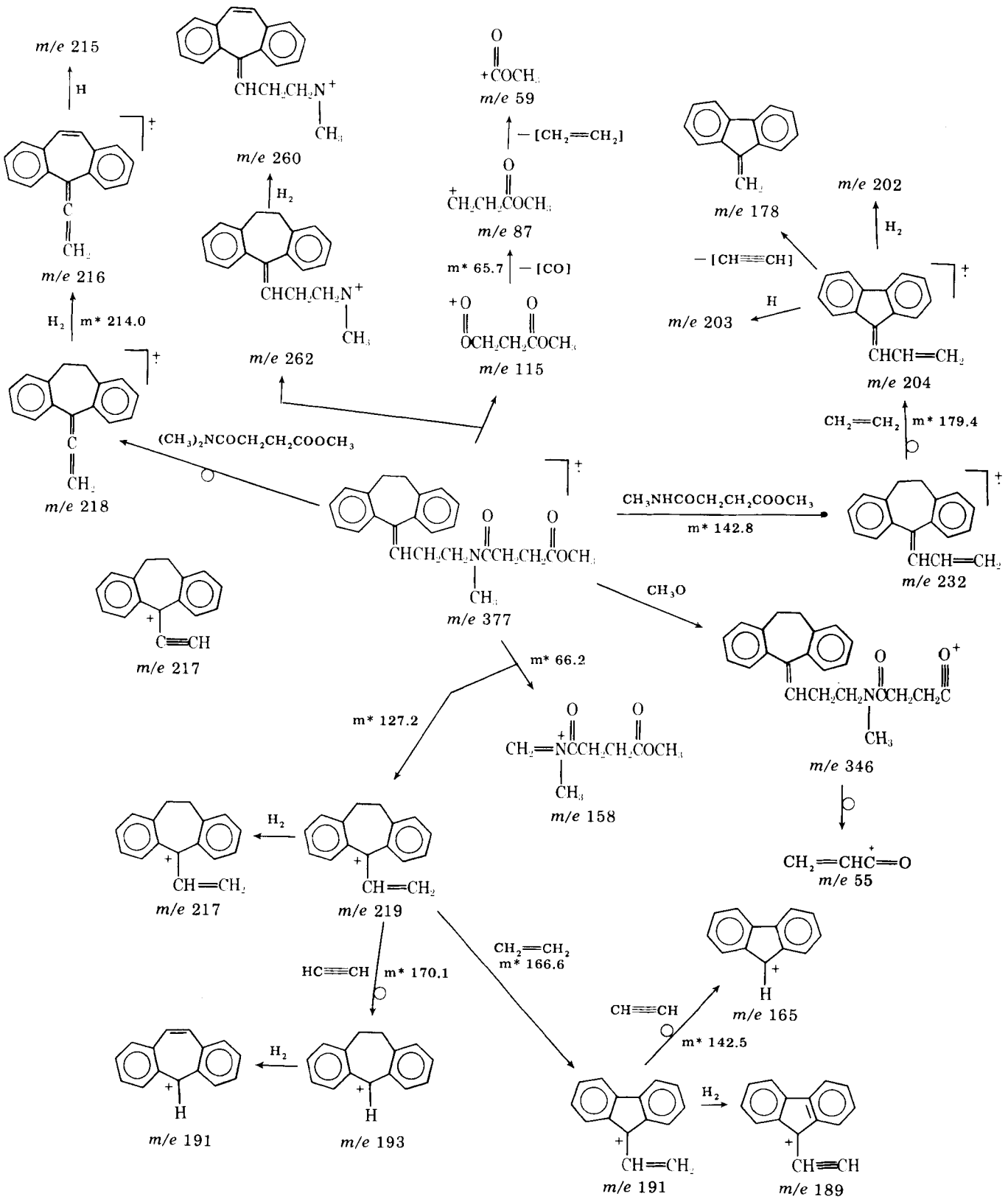

Scheme III

which gave 8 and 10 moles of hapten/mole of bovine serum albumin, respectively.

The preliminary assessment of the antiserums is presented in Table I. Three out of four rabbits immunized with II*a*–bovine serum albumin produced operational titers after the fourth injection. The fourth rabbit died because of a bacterial lung infection after the first injection. All rabbits immunized with III*a*–bovine serum albumin and VI*a*–bovine serum albumin produced operational titers after the fourth injection. Of the four rabbits immunized with V*a*–bovine serum albumin, two did not produce any titer, one rabbit required one booster shot intravenously at double the previous dose, and the remaining rabbit required two intravenous boosters before satisfactory titers were produced.

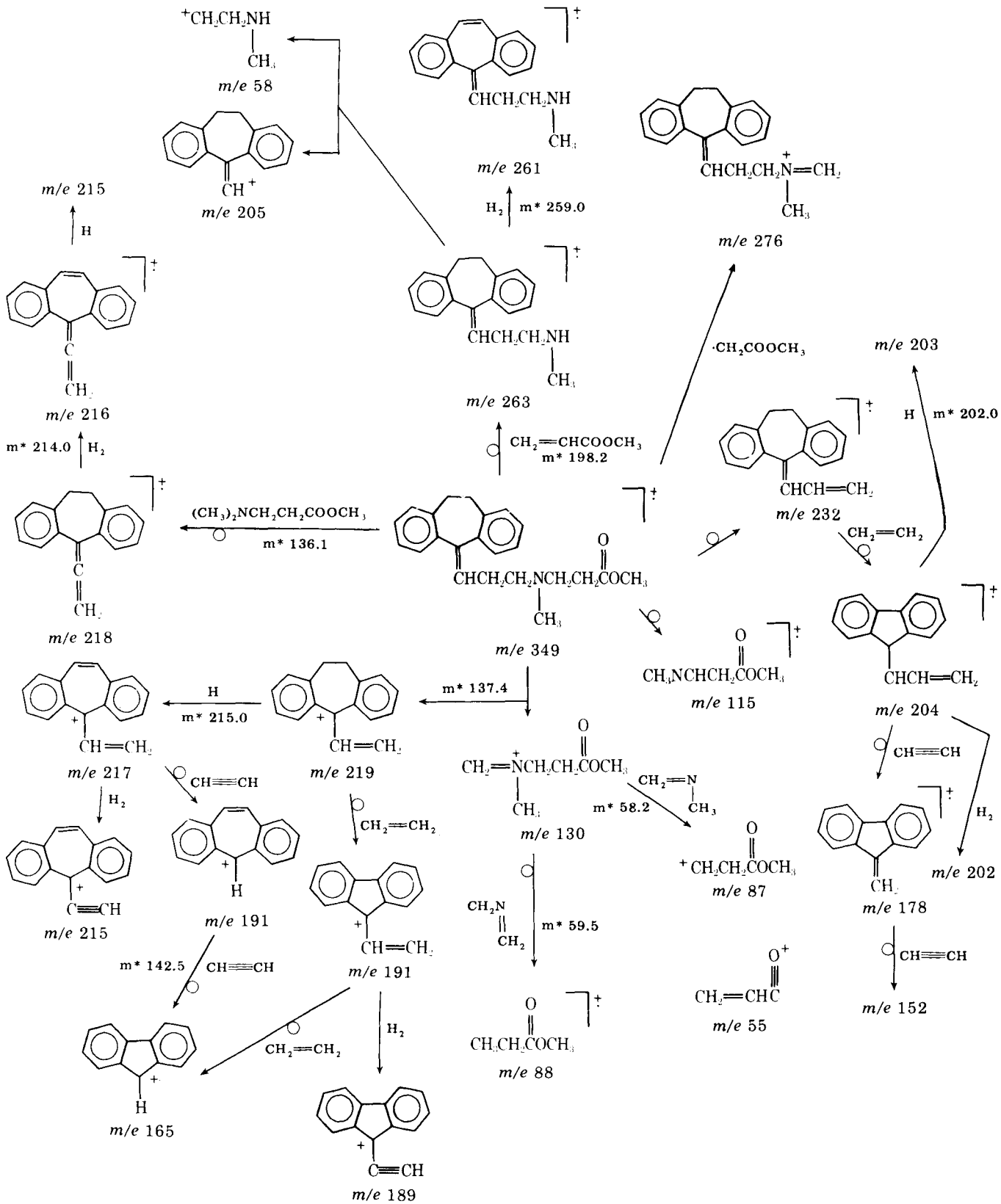

Scheme IV

Radioimmunoassays sensitive down to the nanogram range were developed for imipramine and desipramine using antibodies to IIα-bovine serum albumin and IIIα-bovine serum albumin; for amitriptyline and nortriptyline, antibodies to Vα-bovine serum albumin and VIα-bovine serum albumin were used. The assays were not influenced by plasma and endogenous substances. The procedures will be described in depth in a subsequent publication.

REFERENCES

(1) M. Lader, *Br. J. Clin. Pharmacol.*, **1**, 281 (1974).

(2) H. E. Hamilton, J. E. Wallace, and K. Blum, *Anal. Chem.*, **47**, 1139 (1975).

(3) J. S. Oliver and H. Smith, *Forensic Sci.*, **3**, 181 (1974).

(4) A. Nagy, *J. Pharm. Pharmacol.*, **29**, 104 (1977).

(5) D. B. Faber, C. Mulder, and W. A. Man In T Veld, *J. Chromatogr.*, **100,** 55 (1974).
(6) J. Christiansen and L. F. Gram, *J. Pharm. Pharmacol.*, **25,** 604 (1973).
(7) A. Nagy and L. Treiber, *ibid.*, **25,** 599 (1973).
(8) P. C. N. Eichholtz, *J. Chromatogr.*, **111,** 456 (1975).
(9) G. L. Coroner and B. Bonferoni, *ibid.*, **124,** 401 (1976).
(10) H. B. Hucker and S. S. Stauffer, *J. Pharm. Sci.*, **63,** 296 (1974).
(11) R. A. Braithwaite and B. Widdop, *Clin. Chim. Acta,* **35,** 461 (1971).
(12) R. N. Gupta, G. Molnar, R. E. Hill, and M. L. Gupta, *Clin. Biochem.*, **9,** 247 (1976).
(13) D. N. Bailey and P. I. Jatlow, *Clin. Chem.*, **22,** 1697 (1976).
(14) *Ibid.*, **22,** 777 (1976).
(15) J. Vasiliades and K. C. Bush, *Anal. Chem.*, **48,** 1708 (1976).
(16) T. B. Cooper, D. Allen, and G. M. Simpson, *Psychopharmacol. Commun.*, **1,** 445 (1975).
(17) L. A. Gifford, P. Turner, and C. M. B. Pare, *J. Chromatogr.*, **105,** 107 (1975).
(18) A. Jorgensen, *Acta Pharmacol. Toxicol.*, **36,** 79 (1975).
(19) S. Reite, B. Salvesen, and O. Skaug, *Medd. Nor. Farm. Selsk.*, **37,** 55 (1975).
(20) P. Hartvig, S. Strandberg, and B. Näslund, *J. Chromatogr.*, **118,** 65 (1976).
(21) J. E. Wallace, H. E. Hamilton, L. K. Gogin, and K. Blum, *Anal. Chem.*, **47,** 1516 (1975).
(22) T. Walle and H. Ehrsson, *Acta Pharm. Suec.*, **8,** 27 (1971).
(23) O. Borgå and M. Garle, *J. Chromatogr.*, **68,** 77 (1972).
(24) J. T. Biggs, W. H. Holland, S. Chang, P. P. Hipps, and W. R. Sherman, *J. Pharm. Sci.*, **65,** 261 (1976).
(25) V. E. Ziegler, T. A. Fuller, and J. T. Biggs, *J. Pharm. Pharmacol.*, **28,** 849 (1976).
(26) J.-P. Dubois, W. Kung, W. Theobald, and B. Wirz, *Clin. Chem.*, **22,** 892 (1976).
(27) A. Frigerio, G. Belvedere, F. D. Nadai, R. Fanelli, C. Pantarotto, E. Riva, and P. L. Morselli, *J. Chromatogr.*, **74,** 201 (1972).
(28) O. Borgå, L. Palmér, A. Linnarsson, and B. Holmstedt, *Anal. Lett.*, **4,** 837 (1971).
(29) C.-G. Hammar, B. Alexanderson, B. Holmstedt, and F. Sjöquist, *Clin. Pharmacol. Ther.*, **12,** 496 (1971).
(30) C.-G. Hammar, B. Holmstedt, and R. Ryhage, *Anal. Biochem.*, **25,** 532 (1968).
(31) W. Hammer and F. Sjoquist, *Life Sci.*, **6,** 1895 (1967).
(32) W. A. Garland, *J. Pharm. Sci.*, **66,** 77 (1977).
(33) F. R. Zuleski, A. Loh, and F. J. DiCarlo, *J. Chromatogr.*, **132,** 45 (1977).
(34) G. Carnis, J. Godbillon, and J. P. Metayer, *Clin. Chem.*, **22,** 817 (1976).
(35) K. P. Maguire, G. D. Burrows, J. P. Coghlan, and B. A. Scoggins, *ibid.*, **22,** 761 (1976).
(36) S. R. Harrys, L. E. Gaudette, E. H. Daniel, and A. A. Mannian, *Life Sci. (I),* **9,** 781 (1970).
(37) W. Hammer and B. B. Brodie, *J. Pharmacol. Exp. Ther.*, **157,** 503 (1967).
(38) I. D. Watson and M. J. Stewart, *J. Chromatogr.*, **132,** 155 (1977).
(39) S. Spector, N. L. Spector, and M. P. Almeida, Jr., *Psychopharmacol. Commun.*, **1,** 421 (1975).
(40) G. W. Aherne, E. M. Piall, and V. Marks, *Br. J. Clin. Pharmacol.*, **3,** 561 (1976).
(41) B. F. Erlanger, F. Borèk, S. M. Beiser, and S. Lieberman, *J. Biol. Chem.*, **228,** 713 (1957).
(42) *Ibid.*, **234,** 1090 (1959).
(43) A. Frigerio and P. L. Morselli, *Boll. Chim. Farm.*, **112,** 429 (1973).
(44) L. J. Kricka and A. Ledwith, *Chem. Rev.*, **74,** 102 (1974).
(45) D. R. Knapp, T. E. Gaffney, R. E. McMahon, and G. Kiplinger, *J. Pharmacol. Exp. Ther.*, **180,** 784 (1971).
(46) J. C. Sheehan and J. S. Hlavka, *J. Org. Chem.*, **21,** 439 (1956).
(47) B. F. Erlanger, *Pharmacol. Rev.*, **25,** 271 (1973).
(48) P. T. Tsui, K. A. Kelly, M. M. Pompipom, M. Strahilevitz, and A. H. Sehan, *Can. J. Biochem.*, **52,** 252 (1974).
(49) T. W. Williams and K. A. Pittman, *Res. Commun. Chem. Pathol. Pharmacol.*, **7,** 119 (1974).
(50) B. Africa and E. Haker, *Immunochemistry,* **8,** 479 (1971).
(51) J. W. Hubbard, K. K. Midha, I. J. McGilveray, and J. K. Cooper, *J. Pharm. Sci.*, **67,** 1563 (1978).

ACKNOWLEDGMENTS

The authors acknowledge the technical assistance of Mrs. M. Rowe and the helpful discussions with Dr. J. C. K. Loo and Dr. I. J. McGilveray. They also thank Mr. J.-C. Ethier for mass and IR spectra, Mr. H. Avdovich for PMR spectra, and Mr. A. Trottier for drafting. Appreciation is extended to the University of Manitoba (Winnipeg) for the study leave to J. W. Hubbard.

Pharmacokinetic Evaluation of a Drug Interaction between Kaolin–Pectin and Clindamycin

K. S. ALBERT ˣ, K. A. DeSANTE, R. D. WELCH, and A. R. DiSANTO

Received December 12, 1977, from *The Upjohn Company, Kalamazoo, MI 49001.* Accepted for publication March 20, 1978.

Abstract □ The effect of a kaolin–pectin antidiarrheal suspension on the bioavailability of orally administered clindamycin was evaluated by model-dependent pharmacokinetic techniques. Each subject's serum clindamycin concentration–time data in the absence of the kaolin–pectin suspension were fitted to a one-compartment open model with first-order absorption and lag time. The resulting disposition parameters were used to construct individual Wagner–Nelson absorption profiles, expressed as the cumulative relative fraction of clindamycin absorbed *versus* time following combined antidiarrheal–antibiotic therapy. For each subject, absorption persisted to varying degrees through 14 hr. On the average, the half-time for absorption was prolonged 20-fold (from about 16 min to more than 300 min). In contrast, extrapolation of the individual time courses of relative absorption to infinity revealed that the antidiarrheal had no effect on the extent of clindamycin absorption.

Keyphrases □ Kaolin–pectin suspension—effect on bioavailability of orally administered clindamycin in humans □ Clindamycin—orally administered, effect of kaolin–pectin suspension on bioavailability in humans □ Bioavailability—orally administered clindamycin, effect of kaolin–pectin suspension in humans □ Antidiarrheals—kaolin–pectin suspension, effect of bioavailability of orally administered clindamycin in humans □ Antibacterials—clindamycin, orally administered, effect of kaolin–pectin suspension on bioavailability in humans

That an antidiarrheal suspension containing kaolin and pectin[1] can irreversibly adsorb coadministered drugs *in vivo*, resulting in decreased bioavailability, was first documented by Wagner (1, 2). When a single oral dose of lincomycin was administered together with a dose of a kaolin–pectin suspension, the resulting serum antibiotic levels were reduced to one-tenth those obtained when the antibiotic was given alone (1, 2). Subsequent studies showed that concomitant kaolin–pectin and drug administration decreased the bioavailability of tetracycline (3, 4) and digoxin (5–7) but not of ampicillin (3) and warfarin[2], indicating that the drug interaction potential of the antidiarrheal was not absolute.

This report describes the effects of a kaolin–pectin suspension on the bioavailability of orally administered clindamycin when both products were given concomitantly. Although the antidiarrheal dramatically reduced the clindamycin absorption rate, it had no effect on the extent of drug absorption.

EXPERIMENTAL

Sixteen normal, nonobese adult volunteers, whose average age was 29 years (range of 23–51 years) and whose average weight was 69 kg (range of 57–94 kg), exhibited normal vital signs and selected laboratory parameters and were without any evidence of cardiac, renal, or GI abnormalities. The subjects did not receive any medication for 7 days, any antibacterial agents for 15 days, and any long-acting antibacterial medication (such as penicillin G benzathine) for 30 days prior to the study. During the study, volunteers received only the medication prescribed, with 7 days separating each administered treatment.

Subjects were fasted (food and beverage) from 10:00 pm the night before their allocated treatment to 4 hr after their medication. Smoking was permitted only if it was the subject's usual custom. Volunteers did not engage in strenuous and athletic activities during the days of drug administration.

Each subject received a 150-mg dose of clindamycin capsules[3] with and without the kaolin–pectin suspension[4] (Treatments A and B, respectively) in crossover fashion (Table I). Serum samples were harvested at 0, 0.33, 0.67, 1.0, 1.5, 2.0, 2.5, 3.0, 4.0, 5.0, 6.0, 8.0, 10.0, 12.0, and 14.0 hr after the drug was given and frozen until assayed microbiologically for clindamycin-like activity (8).

RESULTS

Model-Independent Approach—The effect of the kaolin–pectin suspension on average serum clindamycin levels when both products were given concomitantly is summarized in Table II. At all sampling times except the 6-hr time point, there was a highly significant difference between treatment means. Furthermore, the average of individual peak serum antibiotic concentrations was reduced by 61%, with a concomitant delay in time to peak from 1.01 to 2.34 hr. Since the terminal slope of the serum concentration–time curve following the kaolin–pectin treatment appeared to be less steep for all subjects than when antibiotic was given alone, these results suggested that either the disposition of clindamycin was perturbed or the absorption of clindamycin was prolonged after coadministration of the antidiarrheal. Based on other drug interaction studies (1–7), however, the latter possibility seemed more plausible.

Table II also shows that the average area under the clindamycin serum–time curve through 14 hr (AUC) was reduced by 23% in the presence of the kaolin–pectin suspension. Attempts to estimate relative bioavailability by extrapolating individual AUC values to infinity were unsuccessful because of the erratic temporal change in clindamycin-like activity for Treatment A beyond the peak. Therefore, model-dependent pharmacokinetic techniques were utilized to assess the effect of the antidiarrheal on serum clindamycin concentrations.

Model-Dependent Approach—*Estimation of Pharmacokinetic Parameters for Treatment B*—The kinetics of absorption and disposition of clindamycin can be represented by a one-compartment open model with first-order absorption and lag time (possibly associated with stomach emptying) as shown in Scheme I:

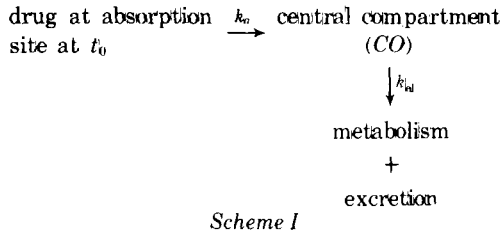

Scheme I

where t_0 is lag time; k_a and k_{el} are the first-order rate constants for the designated processes; and CO is equivalent to FD/V, where F is the fraction of the dose, D, absorbed and V is the apparent volume of distribution for the central compartment including blood serum.

Model parameters estimated from individual serum concentration curves following Treatment B (clindamycin alone) by the technique described in the *Appendix* are shown in Table III. Good fits of the data to the model were obtained in all cases, as judged by low coefficients of

[1] Kaopectate (18% kaolin and 0.4% pectin), The Upjohn Co., Kalamazoo, MI 49001.

[2] The Upjohn Co., Kalamazoo, MI 49001, unpublished data.

[3] Cleocin Hydrochloride capsules, 150 mg, The Upjohn Co., Kalamazoo, MI 49001.

[4] Kaopectate Concentrate (27% kaolin and 0.6% pectin), The Upjohn Co., Kalamazoo, MI 49001.

0022-3549/78/1100-1579$01.00/0
© 1978, American Pharmaceutical Association

Table I—Dosage Schedule and Treatments [a]

Group	Subjects in Group	Treatment for Phase I	Treatment for Phase II
1	1–8	A	B
2	9–16	B	A

[a] Treatment A, 90 ml of Kaopectate Concentrate (Upjohn, lot 902CX) followed immediately by one Cleocin Hydrochloride 150-mg capsule (Upjohn, lot 033PA) administered orally with 90 ml of water; and Treatment B, one Cleocin Hydrochloride 150-mg capsule (Upjohn, lot 033PA) administered orally with 180 ml of water.

variation of the estimates and high correlation coefficients (r_1 and r_2^2) of observed *versus* model-predicted serum concentrations (see *Appendix* for further discussion). The mean parameter estimates reported here were in excellent agreement with previously reported average values (9, 10).

Estimation of Cumulative Relative Fraction Absorbed—On the presumption that the kaolin–pectin suspension had no effect on the disposition of clindamycin, the cumulative fraction of the dose absorbed of Treatment A relative to Treatment B, $[A^A(t)/V]/F^BD$, is given by (11):

$$\frac{A^A(t)}{V}\Big/F^BD = \frac{C^A(t) + k_{el}\int_0^t C^A(t)\,dt}{CO} \qquad \text{(Eq. 1)}$$

where $C^A(t)$ is the observed serum concentration following Treatment A, the integral is estimated by the trapezoidal rule, and k_{el} and CO are the parameter estimates from Treatment B (Table III).

Individual time courses of relative oral absorption constructed with the aid of Eq. 1 are shown in Table IV; the average data are depicted graphically in Fig. 1. Among individuals, relative absorption persisted to varying degrees through the 14th hr. On the average, at least 86% of the dose relative to Treatment B was absorbed within 14 hr following kaolin–pectin and clindamycin administration, the fractional value of which tested statistically significantly different from unity.

An attempt was made to estimate the relative fraction absorbed at infinite time by constructing a plot of the reciprocal of the cumulative relative fraction absorbed *versus* the reciprocal of time, fitting the points to an exponential curve, and determining the ordinate value at 1/time

Table II—Effect of the Kaolin–Pectin Suspension on Serum Clindamycin Levels

Parameter	Treatment Mean[a] A	Treatment Mean[a] B	Significance Level of Treatment Differences
Serum clindamycin level, μg/ml, at:			
0.00 hr	0.00	0.00	N.S.[b]
0.33 hr	0.41	1.13	$p < 0.025$
0.67 hr	0.74	2.34	$p < 0.0001$
1.0 hr	0.73	2.48	$p < 0.0001$
1.5 hr	0.71	2.13	$p < 0.0001$
2.0 hr	0.67	1.81	$p < 0.0001$
2.5 hr	0.66	1.53	$p < 0.0001$
3.0 hr	0.66	1.38	$p < 0.0001$
4.0 hr	0.64	1.12	$p < 0.0001$
5.0 hr	0.71	0.88	$p < 0.025$
6.0 hr	0.74	0.70	N.S.
8.0 hr	0.64	0.45	$p < 0.010$
10.0 hr	0.50	0.23	$p < 0.001$
12.0 hr	0.39	0.11	$p < 0.0005$
14.0 hr	0.30	0.06	$p < 0.0005$
Average of individual peak serum levels, μg/ml	1.06	2.77	$p < 0.0001$
Average time of individual peaks, hr	2.37	1.01	$p < 0.05$
Area under clindamycin serum–time curve through 14 hr, μg/ml × hr	8.05	10.5	$p < 0.0005$

[a] Treatment A, clindamycin and kaolin–pectin; and Treatment B, clindamycin alone. [b] Not significant.

Table III—Final Parameter Estimates for Treatment B (Clindamycin Alone) following NONLIN Fit to One-Compartment Model [a]

Subject	k_a, hr^{-1}	k_{el}, hr^{-1}	CO, μg/ml	Lag Time, hr
1	28.2	0.409	4.08	0
2	60[b]	0.333	3.54	0
3	9.94	0.263	1.91	0
4	3.82	0.270	4.39	0
5	1.67	0.315	1.93	0
6	1.14	0.270	2.90	0.0600
7	4.88	0.324	1.96	0
8	1.73	0.196	2.56	0.186
9	2.32	0.250	3.47	0
10	3.81	0.225	3.13	0.276
11	1.49	0.348	5.23	0
12	1.99	0.279	2.21	0
13	4.36	0.244	3.12	0.0696
14	6.11	0.303	3.30	0.285
15	2.82	0.256	3.49	0
16	2.46	0.370	2.69	0
Mean	5.12	0.291	3.12	0.0548
SD	6.78	0.0562	0.932	0.100

[a] Points weighted equally. [b] Excluded from mean estimate.

= 0[5]. Individual subject values are given in Table V. The average ratio, $F^A/F^B = 1.08$, which was not statistically significantly different from unity, indicates that the kaolin–pectin suspension had no effect on the extent of clindamycin absorption.

Estimation of Time for Half-Absorption—The time for half-absorption of clindamycin ($t_{1/2}^{abs}$) for Treatment B (clindamycin alone) can be calculated using:

$$(t_{1/2}^{abs})^B = 0.693/k_a \qquad \text{(Eq. 2)}$$

where k_a is the absorption rate constant listed in Table III for each subject. As shown in the *Appendix*, this value corresponds to the time when $A(t) = \frac{1}{2}A_\infty$, where $A(t)$ is the amount of drug absorbed at any given time, t, and A_∞ is the total amount of drug absorbed, FD. For Treatment A where relative bioavailability was estimated, $(t_{1/2}^{abs})^A$ may

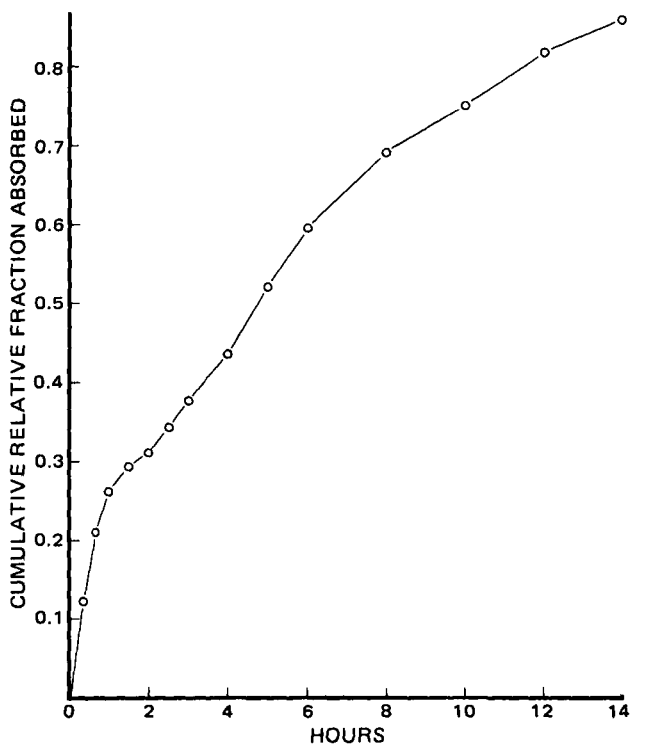

Figure 1—*Profile of the average time course of relative oral absorption for clindamycin.*

[5] As 1/time → 0, $1/[A^A(t)/V]/F^BD \to 0$, corresponding to $[A^A(t)/V]/F^BD \to \infty$. The range in r^2 was between 0.97 and 1.00.

Table IV—Relative Absorption Profiles of Clindamycin following Coadministration of the Kaolin–Pectin Suspension and Clindamycin

Subject	Cumulative Relative Fraction Absorbed[a]													
	0.33	0.67	1.0	1.5	2.0	2.5	3.0	4.0	5.0	6.0	8.0	10.0	12.0	14.0
1	0	0.254	0.279	0.359	0.321	0.358	0.390	0.433	0.506	0.589	0.730	0.810	0.867	0.929
2	0.459	0.493	0.447	0.490	0.452	0.467	0.463	0.470	0.484	0.507	0.567	0.505	0.505	0.505
3	0	0.408	0.455	0.535	0.552	0.559	0.594	0.636	0.732	0.814	0.969	1.07	1.13	1.20
4	0.133	0.482	0.419	0.417	0.446	0.435	0.472	0.519	0.623	0.771	0.916	1.01	1.09	1.14
5	0	0	0	0	0	0.129	0.209	0.306	0.517	0.713	0.770	0.811	0.833	—
6	0.183	0.238	0.241	0.246	0.243	0.242	0.282	0.315	0.413	0.485	0.609	0.698	0.760	0.804
7	0	0	0.209	0.252	0.253	0.265	0.297	0.387	0.452	0.504	0.606	0.665	0.737	0.803
8	0	0	0.278	0.316	0.327	0.341	0.350	0.383	0.419	0.432	0.465	0.489	0.515	—
9	0.460	0.459	0.462	0.500	0.558	0.556	0.564	0.623	0.753	0.837	0.894	0.917	0.939	0.941
10	0	0	0	0	0	0.152	0.212	0.364	0.595	0.757	0.900	0.975	1.01	1.08
11	0	0.299	0.306	0.280	0.299	0.324	0.346	0.372	0.432	0.489	0.564	0.613	0.667	0.708
12	0	0	0	0	0.102	0.144	0.180	0.287	0.399	0.458	0.598	0.699	0.774	0.806
13	0	0.108	0.142	0.202	0.263	0.319	0.406	0.437	0.489	0.539	0.599	0.696	0.760	0.767
14	0.317	0.392	0.429	0.472	0.484	0.493	0.514	0.555	0.614	0.647	0.743	0.832	0.913	0.983
15	0.423	0.443	0.416	0.450	0.512	0.517	0.529	0.562	0.583	0.627	0.675	0.727	0.771	0.808
16	0	0.184	0.144	0.165	0.186	0.224	0.244	0.313	0.375	0.405	0.446	0.506	—	0.570
Mean[b]	0.123	0.235	0.264	0.293	0.312	0.345	0.378	0.435	0.524	0.598	0.690	0.751	0.818	0.860
SD	0.184	0.196	0.169	0.183	0.181	0.147	0.134	0.114	0.116	0.143	0.162	0.180	0.182	0.201

[a] Estimated by Eq. 1. [b] All mean values were statistically significantly different from unity as judged by the t-statistic, $t_{n-1} = (\bar{x} - 1)/(x_i - \bar{x})^2/[n(n-1)]$.

be interpolated from individual graphs of the cumulative relative fraction absorbed *versus* time data (Table IV) where $[A^A(t)/V]/F^BD = \frac{1}{2}F^A/F^B$. Individual values for $t_{1/2}^{abs}$ for both treatments are given in Table V. In every case, $t_{1/2}^{abs}$ was dramatically prolonged in the presence of the kaolin–pectin suspension. On the average, the time for half-absorption increased 20-fold, from about 16 min to more than 300 min.

DISCUSSION

The influence of the kaolin–pectin suspension on the bioavailability of orally administered clindamycin when both products were given concomitantly was evaluated by model-dependent pharmacokinetic techniques. On the assumption that the disposition of the antibiotic was unaltered by the kaolin–pectin suspension, it was found that the antidiarrheal had no effect on the extent of clindamycin absorption, but it markedly reduced its absorption rate. Hence, continuing absorption through 14 hr most likely accounted for the prolonged serum levels exhibited by clindamycin when coadministered with the antidiarrheal.

Structurally, clindamycin differs from lincomycin only at the 7-position because of the (*S*)-chloro substitution of the (*R*)-hydroxyl group of lincomycin. In terms of a drug interaction with the kaolin–pectin suspension, however, lincomycin appeared to be adsorbed irreversibly to components of the antidiarrheal, as judged by its 90% reduction in relative bioavailability (1, 2). In marked contrast, the continuing absorption of clindamycin beyond the last sampling time suggests that this antibiotic was desorbed from components of the antidiarrheal mixture such that its relative bioavailability was unaltered. Thus, 7-chloro substitution of the hydroxyl group of lincomycin dramatically influenced the *in vivo* behavior of the parent compound. This aspect of the study, as well as mechanistic considerations in general, is currently under investigation and will be reported subsequently.

Table V—Effect of the Kaolin–Pectin Suspension on the Rate and Extent of Clindamycin Absorption

Subject	Half-Time for Absorption, min		Relative Extent of Absorption, F^A/F^B
	Treatment A	Treatment B	
1	414	1.47	1.30
2	—	—	0.505
3	336	4.18	1.56
4	375	10.9	1.59
5	291	24.9	0.976
6	462	34.5	1.18
7	390	8.52	1.06
8	104	24.1	0.581
9	92.4	17.9	1.01
10	328	10.9	1.34
11	322	27.9	0.909
12	510	20.9	1.24
13	288	9.54	0.959
14	432	6.78	1.41
15	101	14.7	0.943
16	260	16.9	0.671
Mean	314[a]	15.6[a]	1.08[b]
% *SD*	41.5	60.4	30.0

[a] Statistically significantly different from one another by ANOVA. [b] Not statistically significantly different from unity by t test.

APPENDIX

Fit of Data to Model—Individual sets of serum concentration data following Treatment B (clindamycin alone) were fitted to the integrated equation describing the one-compartment open model with first-order absorption and lag time, *i.e.*:

$$C(t) = (CO)\left[\frac{k_a}{k_a - k_{el}}\right] e^{-k_{el}(t-t_0)} - e^{-k_a(t-t_0)} \qquad \text{(Eq. A1)}$$

where CO is equivalent to FD/V, F being the fraction of dose, D, that is absorbed and V being the volume of distribution of the central compartment which includes blood serum; k_a and k_{el} are the first-order absorption and elimination rate constants, respectively; t is clock time; and t_0 is lag time.

The nonlinear least-squares computer program NONLIN (12) was employed to estimate the parameters CO, k_a, k_{el}, and t_0; initial estimates were obtained with the program CSTRIP (13). The least-squares estimates of the parameters were obtained by minimizing the weighted sum of deviation squared, *i.e.*:

$$\sum_{i=1}^{n} w_i(\hat{C}_i - C_i)^2 \qquad \text{(Eq. A2)}$$

where w_i is the weighting factor taken to be equal to 1.0 in this case, $\hat{C}_i$ is the estimated concentration, and C_i is the observed concentration at time t_i.

Criteria used to assess the adequacy of the fit of the data to the model were: (*a*) r_1, the correlation coefficient for the linear regression of the model predicted *versus* the observed plasma concentration; (*b*) r_2^2, the coefficient of determination equivalent to the difference between the sum of observed concentrations squared and the sum of the deviations squared, divided by the sum of observed concentrations squared, *i.e.*, $[(\Sigma^2_{obs} - \Sigma^2_{dev})/\Sigma^2_{obs}]$; (*c*) the magnitudes of the coefficients of variation (CV%) of the estimated parameters; and (*d*) the lack of trends or regions of poor fit. Individual values for r_1, r_2^2, and CV% indicated that excellent fits were obtained in all cases[6].

Estimation of $t_{1/2}^{abs}$—As shown by Wagner and Nelson (11), the amount of drug absorbed having entered the volume of distribution V up to time t is given by:

$$\frac{A(t)}{V} = C(t) + k_{el}\int_0^t C(t)\,dt \qquad \text{(Eq. A3)}$$

The maximum value of the function is:

$$\frac{A_\infty}{V} = k_{el}\int_0^\infty C(t)\,dt \qquad \text{(Eq. A4)}$$

[6] Data available from the authors on request.

Since $A_\infty/V = FD/V$, the fraction absorbed is given by (11):

$$\frac{A(t)}{V}\Big/\frac{FD}{V} = \frac{C(t) + k_{el}\int_0^t C(t)\,dt}{k_{el}\int_0^\infty C(t)\,dt} \qquad \text{(Eq. A5)}$$

If two or more treatments are being compared at equal doses and if the assumption is made that disposition is invariant among treatments, the cumulative fraction absorbed of Treatment X relative to Treatment S can be expressed as:

$$\frac{A^x(t)}{F^sD} = \frac{C^x(t) + k_{el}\int_0^t C^x(t)\,dt}{CO^s} \qquad \text{(Eq. A6)}$$

where k_{el} is the elimination rate constant obtained from Treatment S; $CO^s = F^sD/V$, which is equivalent to $k_{el}\int_0^\infty C^s(t)\,dt$; and the superscripts refer to the designated treatments. At $t = \infty$, the asymptotic value of Eq. A6 is F^x/F^s. Therefore, the time for half-absorption relative to Treatment S, $(t_{1/2}^{abs})^x$, is the time when $A^x(t)/F^sD = \frac{1}{2}F^x/F^s$.

For Treatment S, if the assumption of first-order absorption is made:

$$\frac{A^s(t)}{V} = \frac{A_\infty{}^s}{V}(1 - e^{-k_a t}) \qquad \text{(Eq. A7)}$$

When $t = (t_{1/2}^{abs})^s$:

$$\frac{A^s(t)}{V} = \frac{1}{2}\frac{A_\infty{}^s}{V} \qquad \text{(Eq. A8)}$$

and:

$$e^{-k_a(t_{1/2}^{abs})^s} = 0.5 \qquad \text{(Eq. A9)}$$

where:

$$(t_{1/2}^{abs})^s = 0.693/k_a \qquad \text{(Eq. A10)}$$

REFERENCES

(1) J. G. Wagner, *Can. J. Pharm. Sci.*, **1**, 55 (1966).

(2) J. G. Wagner, *Drug. Intel.*, **2**, 38 (1968).

(3) W. M. Gouda, "Academy of Pharmaceutical Sciences Abstracts," **6**, 117 (1976).

(4) K. A. DeSante, A. R. DiSanto, R. G. Stoll, R. D. Welch, T. J. Vecchio, and K. S. Albert, *ibid.*, **7(2)**, 116 (1977).

(5) P. F. Binnion, in "Symposium on Digitalis," O. Storstein, Ed., Gyldendal Norsk Forlag, Oslo, Norway, 1973, p. 216.

(6) D. D. Brown and R. P. Juhl, *N. Engl. J. Med.*, **295**, 1034 (1976).

(7) K. S. Albert, J. W. Ayres, D. J. Weidler, E. Sakmar, M. R. Hallmark, R. G. Stoll, K. A. DeSante, A. R. DiSanto, and J. G. Wagner, "Academy of Pharmaceutical Sciences Abstracts," **7(2)**, 116 (1977).

(8) W. L. Lummis, G. M. R. Davison, and J. W. Wilson, "Clindamycin," accepted in "Laboratory Methods for Antimicrobial Chemotherapy," I. P. Phillips, J. D. Williams, R. Wise, and D. S. Reeves, Eds., Churchill and Livingston, Edinburg, Scotland, 1978.

(9) R. M. DeHaan, C. M. Metzler, D. Schellenberg, W. D. VandenBosch, and E. L. Mason, *Int. J. Clin. Pharmacol.*, **6**, 105 (1972).

(10) C. M. Metzler, R. M. DeHaan, D. Schellenberg, and W. D. VandenBosch, *J. Pharm. Sci.*, **62**, 591 (1973).

(11) J. G. Wagner and E. Nelson, *ibid.*, **52**, 610 (1963).

(12) C. M. Metzler, "A User's Manual for NONLIN," The Upjohn Co., Kalamazoo, Mich., 1969.

(13) A. J. Sedman and J. G. Wagner, *J. Pharm. Sci.*, **65**, 1006 (1976).

ACKNOWLEDGMENTS

Presented at the APhA Academy of Pharmaceutical Sciences, Phoenix meeting, November 1977.

Influence of Kaolin–Pectin Suspension on Digoxin Bioavailability

K. S. ALBERT *x, J. W. AYRES ‡, A. R. DiSANTO *, D. J. WEIDLER ‡, E. SAKMAR ‡, M. R. HALLMARK ‡, R. G. STOLL *§, K. A. DeSANTE *, and J. G. WAGNER ‡

Received December 20, 1977, from **The Upjohn Company, Kalamazoo, MI 49001*, and ‡*The Upjohn Center for Clinical Pharmacology, University of Michigan, Ann Arbor, MI 48109.* Accepted for publication March 20, 1978. §Present address: Arnar-Stone Laboratories, Mt. Prospect, Ill.

Abstract □ The effect of a kaolin–pectin suspension on the bioavailability of orally administered digoxin was evaluated when both drugs were given concomitantly and when their time of administration was separated by 2 hr. Coadministration of the antidiarrheal with the cardiac glycoside delayed absorption of the latter and, at the same time, decreased by 62% the amount of drug absorbed. Intersubject variation in digoxin bioavailability also was increased more than twofold. When the kaolin–pectin suspension was given 2 hr before the cardiac glycoside, the digoxin absorption rate was not affected, although its relative extent of absorption was reduced by about 20%. In contrast, when the antidiarrheal was given 2 hr after digoxin, neither the rate nor the extent of absorption of the cardiac glycoside was perturbed. No change in the intersubject variability in digoxin bioavailability was noted whether the antidiarrheal was given 2 hr before or 2 hr after the cardiac glycoside.

Keyphrases □ Digoxin—GI absorption and bioavailability, effect of kaolin–pectin suspension in humans □ Kaolin–pectin suspension—effect on GI absorption and bioavailability of digoxin in humans □ Absorption, GI—digoxin, effect of kaolin–pectin suspension in humans □ Bioavailability—digoxin, effect of kaolin–pectin suspension in humans □ Cardiotonic agents—digoxin, GI absorption and bioavailability, effect of kaolin–pectin suspension in humans □ Antidiarrheals—kaolin–pectin suspension, effect on GI absorption and bioavailability of digoxin in humans

The decreased bioavailability of digoxin due to coadministration of an antidiarrheal suspension containing 18% kaolin and 0.4% pectin[1] was first reported by Binnion (1) after observing ineffective blood levels of cardiac glycoside in a patient who had taken the antidiarrheal at the same time as digoxin. Brown and Juhl (2) subsequently verified Binnion's findings in a crossover study employing 10 normal volunteers. When 60 ml of kaolin–pectin was given with 0.75 mg of digoxin, the area under the serum digoxin concentration–time curve through 8 hr was decreased by 41% while 6-day urinary recovery of digoxin was reduced by 42% relative to digoxin alone (2). Furthermore, terminal half-lives based on urinary excretion following the two

[1] Kaopectate, The Upjohn Co., Kalamazoo, MI 49001.

0022-3549/78/1100-1582$01.00/0

© 1978, American Pharmaceutical Association

Since $A_\infty/V = FD/V$, the fraction absorbed is given by (11):

$$\frac{A(t)}{V}\Big/\frac{FD}{V} = \frac{C(t) + k_{el}\int_0^t C(t)\,dt}{k_{el}\int_0^\infty C(t)\,dt} \qquad \text{(Eq. A5)}$$

If two or more treatments are being compared at equal doses and if the assumption is made that disposition is invariant among treatments, the cumulative fraction absorbed of Treatment X relative to Treatment S can be expressed as:

$$\frac{A^x(t)}{F^sD} = \frac{C^x(t) + k_{el}\int_0^t C^x(t)\,dt}{CO^s} \qquad \text{(Eq. A6)}$$

where k_{el} is the elimination rate constant obtained from Treatment S; $CO^s = F^sD/V$, which is equivalent to $k_{el}\int_0^\infty C^s(t)\,dt$; and the superscripts refer to the designated treatments. At $t = \infty$, the asymptotic value of Eq. A6 is F^x/F^s. Therefore, the time for half-absorption relative to Treatment S, $(t_{1/2}^{abs})^x$, is the time when $A^x(t)/F^sD = \frac{1}{2}F^x/F^s$.

For Treatment S, if the assumption of first-order absorption is made:

$$\frac{A^s(t)}{V} = \frac{A_\infty{}^s}{V}(1 - e^{-k_a t}) \qquad \text{(Eq. A7)}$$

When $t = (t_{1/2}^{abs})^s$:

$$\frac{A^s(t)}{V} = \frac{1}{2}\frac{A_\infty{}^s}{V} \qquad \text{(Eq. A8)}$$

and:

$$e^{-k_a(t_{1/2}^{abs})^s} = 0.5 \qquad \text{(Eq. A9)}$$

where:

$$(t_{1/2}^{abs})^s = 0.693/k_a \qquad \text{(Eq. A10)}$$

REFERENCES

(1) J. G. Wagner, *Can. J. Pharm. Sci.*, **1**, 55 (1966).

(2) J. G. Wagner, *Drug. Intel.*, **2**, 38 (1968).

(3) W. M. Gouda, "Academy of Pharmaceutical Sciences Abstracts," **6**, 117 (1976).

(4) K. A. DeSante, A. R. DiSanto, R. G. Stoll, R. D. Welch, T. J. Vecchio, and K. S. Albert, *ibid.*, **7(2)**, 116 (1977).

(5) P. F. Binnion, in "Symposium on Digitalis," O. Storstein, Ed., Gyldendal Norsk Forlag, Oslo, Norway, 1973, p. 216.

(6) D. D. Brown and R. P. Juhl, *N. Engl. J. Med.*, **295**, 1034 (1976).

(7) K. S. Albert, J. W. Ayres, D. J. Weidler, E. Sakmar, M. R. Hallmark, R. G. Stoll, K. A. DeSante, A. R. DiSanto, and J. G. Wagner, "Academy of Pharmaceutical Sciences Abstracts," **7(2)**, 116 (1977).

(8) W. L. Lummis, G. M. R. Davison, and J. W. Wilson, "Clindamycin," accepted in "Laboratory Methods for Antimicrobial Chemotherapy," I. P. Phillips, J. D. Williams, R. Wise, and D. S. Reeves, Eds., Churchill and Livingston, Edinburg, Scotland, 1978.

(9) R. M. DeHaan, C. M. Metzler, D. Schellenberg, W. D. VandenBosch, and E. L. Mason, *Int. J. Clin. Pharmacol.*, **6**, 105 (1972).

(10) C. M. Metzler, R. M. DeHaan, D. Schellenberg, and W. D. VandenBosch, *J. Pharm. Sci.*, **62**, 591 (1973).

(11) J. G. Wagner and E. Nelson, *ibid.*, **52**, 610 (1963).

(12) C. M. Metzler, "A User's Manual for NONLIN," The Upjohn Co., Kalamazoo, Mich., 1969.

(13) A. J. Sedman and J. G. Wagner, *J. Pharm. Sci.*, **65**, 1006 (1976).

ACKNOWLEDGMENTS

Presented at the APhA Academy of Pharmaceutical Sciences, Phoenix meeting, November 1977.

Influence of Kaolin–Pectin Suspension on Digoxin Bioavailability

K. S. ALBERT *x, J. W. AYRES ‡, A. R. DiSANTO *, D. J. WEIDLER ‡, E. SAKMAR ‡, M. R. HALLMARK ‡, R. G. STOLL *§, K. A. DeSANTE *, and J. G. WAGNER ‡

Received December 20, 1977, from **The Upjohn Company, Kalamazoo, MI 49001*, and ‡*The Upjohn Center for Clinical Pharmacology, University of Michigan, Ann Arbor, MI 48109.* Accepted for publication March 20, 1978. §Present address: Arnar-Stone Laboratories, Mt. Prospect, Ill.

Abstract □ The effect of a kaolin–pectin suspension on the bioavailability of orally administered digoxin was evaluated when both drugs were given concomitantly and when their time of administration was separated by 2 hr. Coadministration of the antidiarrheal with the cardiac glycoside delayed absorption of the latter and, at the same time, decreased by 62% the amount of drug absorbed. Intersubject variation in digoxin bioavailability also was increased more than twofold. When the kaolin–pectin suspension was given 2 hr before the cardiac glycoside, the digoxin absorption rate was not affected, although its relative extent of absorption was reduced by about 20%. In contrast, when the antidiarrheal was given 2 hr after digoxin, neither the rate nor the extent of absorption of the cardiac glycoside was perturbed. No change in the intersubject variability in digoxin bioavailability was noted whether the antidiarrheal was given 2 hr before or 2 hr after the cardiac glycoside.

Keyphrases □ Digoxin—GI absorption and bioavailability, effect of kaolin–pectin suspension in humans □ Kaolin–pectin suspension—effect on GI absorption and bioavailability of digoxin in humans □ Absorption, GI—digoxin, effect of kaolin–pectin suspension in humans □ Bioavailability—digoxin, effect of kaolin–pectin suspension in humans □ Cardiotonic agents—digoxin, GI absorption and bioavailability, effect of kaolin–pectin suspension in humans □ Antidiarrheals—kaolin–pectin suspension, effect on GI absorption and bioavailability of digoxin in humans

The decreased bioavailability of digoxin due to coadministration of an antidiarrheal suspension containing 18% kaolin and 0.4% pectin[1] was first reported by Binnion (1) after observing ineffective blood levels of cardiac glycoside in a patient who had taken the antidiarrheal at the same time as digoxin. Brown and Juhl (2) subsequently verified Binnion's findings in a crossover study employing 10 normal volunteers. When 60 ml of kaolin–pectin was given with 0.75 mg of digoxin, the area under the serum digoxin concentration–time curve through 8 hr was decreased by 41% while 6-day urinary recovery of digoxin was reduced by 42% relative to digoxin alone (2). Furthermore, terminal half-lives based on urinary excretion following the two

[1] Kaopectate, The Upjohn Co., Kalamazoo, MI 49001.

0022-3549/78/1100-1582$01.00/0

© 1978, American Pharmaceutical Association

Table I—Effect of the Kaolin–Pectin Suspension on Serum Digoxin Levels following Concomitant Administration of Both Drugs

Parameter	Treatment Mean[a] A	Treatment Mean[a] B	Significance Level of Treatment Differences[b]
Serum digoxin level, ng/ml, at:			
0.25 hr	0.00	0.34	N.S.[c]
0.50 hr	0.02	0.90	$p < 0.001$
0.75 hr	0.10	1.25	$p < 0.0001$
1.0 hr	0.19	1.20	$p < 0.0001$
1.5 hr	0.25	0.98	$p < 0.0001$
3.0 hr	0.15	0.64	$p < 0.0001$
5.0 hr	0.17	0.51	$p < 0.010$
7.0 hr	0.13	0.31	$p < 0.001$
9.0 hr	0.13	0.25	$p = 0.001$
12.0 hr	0.12	0.23	$p < 0.001$
16.0 hr	0.11	0.21	$p < 0.001$
24.0 hr	0.12	0.23	$p < 0.010$
36.0 hr	0.07	0.15	$p < 0.025$
48.0 hr	0.07	0.14	$p < 0.05$
AUC through 48 hr, ng/ml × hr	4.98	12.48	$p = 0.0001$
Average of individual peak serum levels, ng/ml	0.33	1.45	$p < 0.0001$
Time of individual peak serum levels, hr	3.16	0.86	$p < 0.010$

[a] Treatment A, digoxin and kaolin–pectin; and Treatment B, digoxin alone. [b] Based on results of analysis of variance. [c] Not significant.

Table II—Individual Estimates of Relative Absorption of Digoxin following Coadministration with the Kaolin–Pectin Suspension

Subject[a]	*AUC* through 48 hr, ng/ml × hr[b] A	*AUC* through 48 hr, ng/ml × hr[b] B	F^A/F^B [c]
1	13.2	13.2	1.00
2	3.74	17.1	0.219
3	1.88	9.33	0.202
4	3.35	12.1	0.277
5	1.16	12.3	0.094
6	10.5	19.2	0.547
7	4.73	12.5	0.378
8	2.50	10.8	0.231
10	1.30	6.64	0.196
11	4.72	12.0	0.393
12	7.76	12.2	0.636
Average	4.98	12.5	0.379
SD[d], %	78.8	27.1	69.0

[a] Subject 9 did not complete the study. [b] Treatment A, digoxin and kaolin–pectin; and Treatment B, digoxin alone. [c] Relative bioavailability calculated as the ratio of the *AUC* through 48 hr (see text for discussion). [d] $(SD/\bar{X}) \times 100$.

Table III—Effect of Concomitant Administration of Kaolin–Pectin Suspension on the Treatment Variability of Digoxin

Parameter	Intersubject Treatment Variability[a] A Low	A High	B Low	B High	*SD*, %[b] A	*SD*, %[b] B
Peak concentration, ng/ml	0.10	0.82	0.82	1.98	69.7	23.3
Time to peak, hr	0.75	7.0	0.50	0.50	75.8	31.6
AUC through 48 hr, ng/ml × hr	1.30	13.2	6.64	17.1	78.5	27.0

[a] Treatment A, digoxin and kaolin–pectin; and Treatment B, digoxin alone. [b] $(SD/\bar{X}) \times 100$.

treatments were similar, suggesting that the interaction probably affected only absorption and not disposition. Brown and Juhl (2) speculated that the decreased digoxin bioavailability could not be related entirely to physical adsorption to kaolin–pectin or to an alteration in gut transit time by the antidiarrheal.

This report describes the effect of a more concentrated antidiarrheal, containing 27% kaolin and 0.6% pectin[2], on the bioavailability of orally administered digoxin when both drugs were given concomitantly (Study 1) and when the antidiarrheal was given 2 hr before and 2 hr after the cardiac glycoside (Study 2). Although coadministration of both drugs markedly decreased the rate and extent of digoxin absorption, the interaction could be essentially circumvented by giving the medication at separated time intervals.

EXPERIMENTAL

Normal, nonobese adult volunteers exhibited normal vital signs and selected laboratory parameters and had no evidence of cardiac, renal, and GI abnormalities. Each subject underwent a complete physical examination before acceptance. Subjects did not receive any medication for 7 days or any enzyme-inducing drugs for 30 days before the study. During each study, subjects received only the medication prescribed, with 14 days separating each administered treatment.

Subjects were required to fast (food and beverage) from 10:00 pm the night before their allocated treatment until 4 hr after the medication. Except in Study 2, where meals were standardized, food and beverages were permitted *ad libitum* after the fasting period. Smoking was only permitted if it was the subject's usual custom. Volunteers did not engage in strenuous and athletic activities during the days of drug administration.

Blood was drawn at selected time intervals after each specified treatment. Serum was harvested from all blood during Study 1; plasma[3] was collected during Study 2. Twenty-four-hour urine specimens also were collected for Study 2. All samples were frozen immediately and kept frozen until assayed for digoxin by radioimmunoassay (3).

Study 1—Treatments A and B were randomly administered to 11 subjects whose average age was 29.7 years (range of 24–39 years) and whose average weight was 80.7 kg (range of 63.5–98.8 kg[4]).

Treatment A—Two 0.25-mg digoxin compressed tablets[5] and 90 ml of the kaolin–pectin suspension[6] were administered at zero time. The antidiarrheal mixture was administered first, with 90 ml of water being used to rinse the dispensing container and aid in swallowing the digoxin tablets.

Treatment B—Two 0.25-mg digoxin compressed tablets[5] were administered with 180 ml of water at zero time.

Serum samples were collected at 0, 0.25, 0.50, 0.75, 1.0, 1.5, 2.0, 3.0, 5.0, 7.0, 9.0, 12.0, 16.0, 24.0, 36.0, and 48.0 hr after dosing.

Study 2—Treatments A–C were randomly administered to 15 subjects whose average age was 27.3 years (range of 21–34 years) and whose average weight was 73.5 kg (range of 64.0–86.2 kg).

Treatment A—Two 0.25-mg digoxin compressed tablets[5] were administered at zero time with 180 ml of water.

Treatment B—Ninety milliliters of the kaolin–pectin suspension[7] administered 2 hr before zero time, followed immediately by 90 ml of water to rinse the dispensing container. Then two 0.25-mg digoxin compressed tablets[5] were administered at zero time with 180 ml of water.

Treatment C—Two 0.25-mg digoxin compressed tablets[5] were administered at zero time. Then 90 ml of the kaolin–pectin suspension[7] was administered 2 hr after zero time, followed immediately by 90 ml of water to rinse the dispensing container.

[2] Kaopectate Concentrate, The Upjohn Co., Kalamazoo, MI 49001.
[3] Vacutainers, Becton-Dickinson No. 477, containing dry-filled edetate disodium as an anticoagulant.
[4] Twelve subjects began the study, but one subject dropped out after Phase I.
[5] Lanoxin, lot 776-0, supplied by Burroughs Wellcome, Research Triangle Park, N.C.
[6] Kaopectate Concentrate, lot 402CX, The Upjohn Co., Kalamazoo, MI 49001.
[7] Kaopectate Concentrate, lot 333A3L, The Upjohn Co., Kalamazoo, MI 49001.

Table IV—Effect of the Kaolin–Pectin Suspension on Plasma Digoxin Levels following a Dosing Interval of 2 hr between Drugs

Parameter	Treatment Average[a] A	B	C	Level of Significance	Significance Level of Treatment Differences[b] B *versus* A	C *versus* A	B *versus* C
Plasma digoxin level, ng/ml, at:							
0.25 hr	0.31	0.18	0.33	N.S.[c]	–	–	–
0.5 hr	1.05	0.81	1.08	N.S.	–	–	–
0.75 hr	1.50	1.23	1.57	N.S.	–	–	–
1.0 hr	1.53	1.40	1.70	N.S.	–	–	–
1.5 hr	1.31	1.06	1.23	N.S.	–	–	–
3.0 hr	0.73	0.58	0.64	$p < 0.025$	+	–	–
5.0 hr	0.48	0.42	0.39	$p < 0.025$	–	+	–
7.0 hr	0.39	0.33	0.31	$p < 0.005$	+	+	–
9.0 hr	0.34	0.32	0.32	N.S.	–	–	–
12.0 hr	0.29	0.24	0.23	$p < 0.01$	+	+	–
24.0 hr	0.26	0.23	0.22	$p < 0.05$	–	+	–
48.0 hr	0.18	0.15	0.16	N.S.	–	–	–
72.0 hr	0.13	0.11	0.11	$p < 0.025$	+	–	–
96.0 hr	0.08	0.07	0.07	N.S.	–	–	–
Average of individual peak plasma levels, ng/ml	1.71	1.53	1.81	N.S.	–	–	–
Time of individual peak plasma levels, hr	1.02	0.93	0.88	N.S.	–	–	–
AUC through 96 hr, ng/ml × hr	21.8	18.4	18.8	$p < 0.01$	+	+	–
Amount excreted in urine through 24 hr, μg	85.6	70.4	87.1	N.S.	–	–	–
Elimination rate constant, hr^{-1}	0.018	0.020	0.020	N.S.	–	–	–
Half-life, hr	43.8	40.5	43.5	N.S.	–	–	–
Renal clearance, ml/min	144	136	165	N.S.	–	–	–

[a] Treatment A, digoxin alone; Treatment B, kaolin–pectin 2 hr before digoxin; and Treatment C, kaolin–pectin 2 hr after digoxin. [b] Tested only at the 0.05 level using Tukey's allowable difference, where (+) = $p \leq 0.05$ and (–) = $p > 0.05$. [c] Not significant.

To ensure adequate urine output, subjects were required to drink 360 ml of water upon arising in the morning.

Plasma samples were harvested at 0, 0.25, 0.50, 0.75, 1.0, 1.5, 3.0, 5.0, 7.0, 9.0, 12.0, 24.0, 48.0, 72.0, and 96.0 hr after drug administration. Urine specimens were collected for 24 hr before each treatment to serve as a control (−24–0 hr) and for the next 24 hr postdosing (0–24 hr).

RESULTS

Study 1—Administration of the kaolin–pectin suspension concomitantly with digoxin markedly reduced average serum levels of the cardiac glycoside at all sampling times (Table I and Fig. 1). The average of individual peak serum digoxin concentrations was depressed by 77% with a corresponding delay in the average time to peak (Table I).

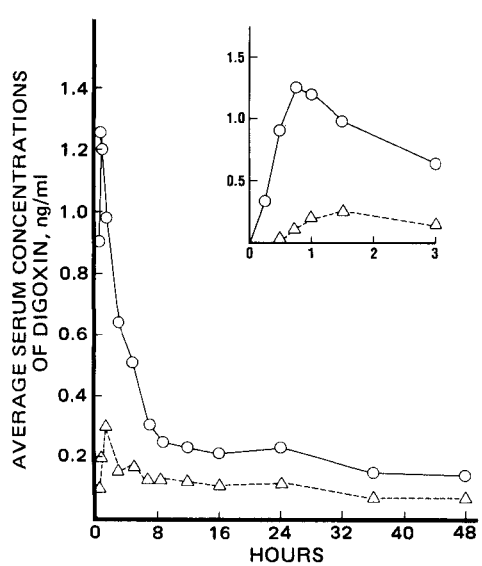

Figure 1—*Effect of the kaolin–pectin suspension on serum digoxin levels following concomitant administration of both drugs. Insert shows expanded 0–3-hr data. Key: ○, digoxin alone; and △, digoxin plus kaolin–pectin.*

These results suggested that the antidiarrheal mixture decreased the absorption rate of digoxin. In addition, average areas under the serum digoxin concentration–time curve through 48 hr were reduced from 12.5 to 4.98 ng/ml × hr, indicative of a 62% decrease in the relative amount of drug absorbed (Table II)[8]. Table III illustrates that more than a twofold increase in the intersubject treatment variability in digoxin bioavailability also resulted when the cardiac glycoside was given with the antidiarrheal.

Study 2—The effect of the kaolin–pectin suspension on plasma digoxin concentrations when the dosing of both products was separated by 2 hr is summarized in Table IV and Fig. 2. Through the first 1.5 hr, no significant differences among treatment average plasma levels were found. Since the average of individual peak plasma digoxin levels of 1.71, 1.53, and 1.81 ng/ml following Treatments A, B, and C, respectively, or their corresponding times to peak of 1.02, 0.93, and 0.88 hr, respectively, did not test significantly differently, these results suggested that the ad-

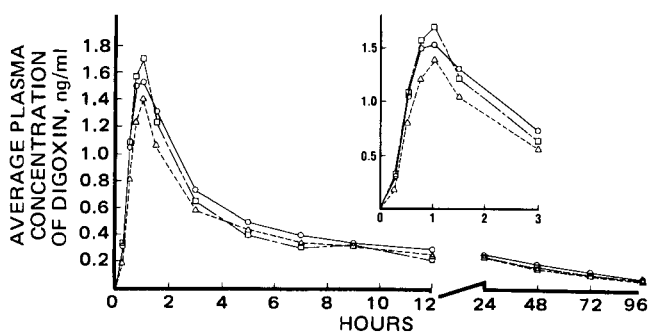

Figure 2—*Effect of the kaolin–pectin suspension on plasma digoxin levels following a dosing interval of 2 hr between drugs. Insert shows expanded 0–3-hr data. Key: ○, digoxin alone; △, kaolin–pectin 2 hr before digoxin; and □, kaolin–pectin 2 hr after digoxin.*

[8] It was impossible to estimate the terminal slope for all subjects since blood was not collected for a long enough time. Hence, the *AUC* through 48 hr was used to estimate relative bioavailability.

Table V—Individual Estimates of Relative Absorption of Digoxin when Given before or after the Kaolin–Pectin Suspension [a]

Subject	$\dot{V}_{cl,r}$, ml/min [b]			AUC_∞, ng/ml × hr [c]			Bioavailability Ratios [d] F^B/F^A			F^C/F^A		
	A	B	C	A	B	C	I	II	III	I	II	III
1	208	127	145	27.1	26.1	24.2	0.709	0.588	0.963	0.710	0.623	0.893
2	156	143	188	26.7	28.9	20.8	1.04	0.992	1.08	0.859	0.939	0.779
3	178	134	174	18.2	15.0	19.0	0.750	0.620	0.824	1.04	1.02	1.04
4	98.1	186	172	31.2	27.6	19.7	1.18	1.68	0.885	0.806	1.11	0.631
5	153	106	146	24.8	24.8	22.1	0.860	0.613	1.00	0.873	0.850	0.891
6	140	120	143	25.0	20.0	23.1	0.752	0.686	0.800	0.932	0.944	0.924
7	92.4	178	157	31.5	25.6	30.2	1.08	1.57	0.813	1.19	1.63	0.959
8	155	150	279	22.8	24.5	26.0	1.06	1.04	1.08	1.53	2.05	1.14
9	146	63.7	195	39.1	21.4	18.5	0.336	0.239	0.547	0.582	0.632	0.473
10	181	158	192	22.4	29.0	19.4	1.22	1.13	1.30	0.892	0.919	0.866
11	113	120	95.5	32.4	26.2	36.5	0.831	0.859	0.809	1.05	0.952	1.13
12	125	130	197	27.3	9.05	18.4	0.337	0.345	0.332	0.833	1.06	0.674
13	117	134	143	26.3	28.5	25.5	0.845	0.902	0.787	0.784	0.861	0.704
14	95.1	141	86.9	22.6	15.7	25.2	0.781	1.03	0.695	1.09	1.02	1.12
15	211	146	167	21.7	15.0	25.3	0.574	0.478	0.691	1.03	0.923	1.17
Mean,	144	136	165	27.2	22.5	23.6	0.824	0.857	0.840	0.947	1.04	0.892
SD, % [e]							32.7	47.5	27.7	23.8	34.8	23.4
t-Value							2.54	1.37	2.65	1.37	0.380	1.98
Significance level							$p < 0.05$	$p > 0.10$	$p < 0.02$	$p > 0.10$	$p > 0.25$	$p > 0.10$

[a] Treatment A, digoxin alone; Treatment B, kaolin–pectin 2 hr before digoxin; and Treatment C, kaolin–pectin 2 hr after digoxin. [b] Renal clearance calculated as the ratio of the amount of digoxin excreted in the urine in 24 hr to the AUC through 24 hr. [c] Area through infinity estimated by trapezoidal rule through 96 hr and classical extrapolation techniques beyond 96 hr. [d] Assumption I, nonrenal clearance is constant; Assumption II, renal and nonrenal clearances change proportionally; and Assumption III, plasma clearance is constant. [e] $(SD/\bar{X}) \times 100$.

ministration of the kaolin–pectin suspension either 2 hr before or 2 hr after digoxin had no effect on the absorption rate of the cardiac glycoside. In contrast, mean areas under the plasma digoxin concentration–time curve through 96 hr were significantly depressed relative to Treatment A by 16% for Treatment B and 14% for Treatment C (Table IV). These results parallel the significant differences among treatment average plasma levels beyond 1.5 hr that were observed.

Table IV also gives treatment average elimination half-lives, renal clearances, and 24-hr urinary recoveries of digoxin. The kaolin–pectin suspension did not perturb these parameters, suggesting that the antidiarrheal had no effect on the mean renal elimination of digoxin.

Observed plasma levels and urinary recovery of digoxin are functions not only of the drug absorption and renal elimination rates, as already delineated, but also of the extent of drug absorption and the effects of the kaolin–pectin suspension on absorption. An estimate of this influence can be made utilizing the model-independent method of Kwan and Till (4). This technique, which uses plasma level and urinary recovery data together, is based on the determination of renal clearance and assumptions regarding the constancy of nonrenal clearance among treatments.

Individual assessments of relative absorption, with the assumptions that nonrenal clearance for a given subject was constant and that individual values for nonrenal clearance varied in proportion to observed changes in renal clearance (4), are given in Table V. Included for comparison are individual relative bioavailability estimates based on the assumption of constant plasma clearance. This assumption ignores observed differences in renal clearance on the premise that the nonrenal components of plasma clearance are compensating. Equations appropriate to the methods, as applied here, are given in the *Appendix*.

When the kaolin–pectin suspension was given 2 hr before digoxin, the average ratio F^B/F^A of about 0.8 was significantly less than unity with the assumption that nonrenal clearance was either constant (Assumption I) or compensating (Assumption III) (Table V). When renal and nonrenal clearances change in proportion to one another (Assumption II), 10 out of 15 subjects had ratios less than 1.0. These results suggested that when the antidiarrheal dose preceded the cardiac glycoside dose, absorption was reduced by about 20% (Table V). In contrast, when the kaolin–pectin suspension was administered 2 hr after digoxin, absorption was not appreciably perturbed, as evidenced by the average ratio F^C/F^A not being different from 1.0 regardless of which assumption was utilized.

The effect of the antidiarrheal mixture on the intersubject treatment variability in the bioavailability of digoxin is summarized in Table VI. The ranges of coefficients of variation of the tested parameters were similar among the three treatments, suggesting no change in the treatment variability of digoxin whether the kaolin–pectin suspension was given 2 hr before or 2 hr after the cardiac glycoside.

DISCUSSION

When both drugs were given concomitantly, the digoxin absorption rate was delayed and, based on 48-hr areas under the concentration–time curve, the relative extent of digoxin absorption was reduced by 62%. In contrast, the interaction was virtually eliminated by giving the antidiarrheal 2 hr after the cardiac glycoside; administration of the kaolin–pectin suspension 2 hr before the cardiac glycoside did not perturb the rate of digoxin absorption, although the relative extent of its absorption was reduced by about 20%.

Apparently, a 2-hr dosing interval, within the parameters of rational therapy, exists for the kaolin–pectin suspension and oral digoxin administration, particularly since digoxin is given chronically once a day.

Table VI—Effect of Kaolin–Pectin Suspension on the Treatment Variability of Digoxin following a Dosing Interval of 2 hr between Drugs

Parameter	Intersubject Treatment Variability [a] A Low	A High	B Low	B High	C Low	C High	SD, % [b] A	B	C
Peak concentration, ng/ml	1.04	2.57	0.83	2.86	0.89	2.29	28.6	34.0	24.1
Time to peak, hr	0.50	1.50	0.50	1.50	0.50	1.00	32.8	31.2	18.1
AUC through 96 hr, ng/ml × hr	16.4	29.2	8.57	2.50	12.9	22.7	19.6	25.3	14.1
24-hr urinary recovery, μg	65.5	119	50.5	109	62.5	145	19.2	17.8	13.1
Half-life, hr	14.9	69.7	12.8	77.4	11.1	81.9	31.4	41.3	42.5
Renal clearance, ml/min	92.4	211	63.7	186	95.5	279	26.5	21.5	27.5

[a] Treatment A, digoxin alone; Treatment B, kaolin–pectin 2 hr before digoxin; and Treatment C, kaolin–pectin 2 hr after digoxin. [b] $(SD/\bar{X}) \times 100$.

Since the half-life of the cardiac glycoside is about 40 hr, accumulation occurs. Therefore, the effect of the antidiarrheal mixture on a given dose of digoxin with respect to steady state would be considerably less than that reported herein after a single dose. The influence of the kaolin–pectin suspension on steady-state plasma digoxin levels is under investigation.

The decreased digoxin bioavailability after coadministration with the kaolin–pectin suspension appears to be related to a mechanism involving physical adsorption. This conclusion is supported by *in vitro* experiments that show that the antidiarrheal mixture removes digoxin from solution[9]. The mechanism probably also involves differences in gut transit time between digoxin and the kaolin–pectin suspension, with the latter persisting for a longer time in the GI tract. This hypothesis is consistent with the observation that when the antidiarrheal was administered before the cardiac glycoside, an interaction occurred; no such interaction was noted, however, when the antidiarrheal was given after the cardiac glycoside. Hence, mechanisms involving physical absorption and alterations in gut transit time appear to explain the interaction of the kaolin–pectin suspension with digoxin, a conclusion not totally supported by others (2).

APPENDIX

In accordance with the model-independent method of Kwan and Till (4), the following equation was derived to estimate relative bioavailability under the assumption of constant nonrenal clearance:

$$\frac{F^x}{F^s} = \frac{AUC_\infty{}^x}{AUC_\infty{}^s} - \frac{AUC_\infty{}^x}{D^x}(\dot{V}^s_{cl,r} - \dot{V}^x_{cl,r}) \qquad \text{(Eq. A1)}$$

where F is the fraction of the dose, D, that reaches the general circulation unchanged; $\dot{V}_{cl,r}$ is renal clearance; AUC_∞ is the area under the plasma concentration–time curve through infinity; and the superscripts x and s refer to test treatment and standard treatment, respectively.

For the case of nonrenal clearance changing in proportion to observed changes in renal clearance:

$$\frac{F^x}{F^s} = \frac{AUC_\infty{}^x}{AUC_\infty{}^s}\left(\frac{\dot{V}^x_{cl,r}}{\dot{V}^s_{cl,r}}\right) \qquad \text{(Eq. A2)}$$

With the assumption of constant plasma clearance:

$$\frac{F^x}{F^s} = \frac{AUC_\infty{}^x}{AUC_\infty{}^s} \qquad \text{(Eq. A3)}$$

This equation ignores observed changes in renal clearance by assuming that nonrenal clearance compensates.

[9] The Upjohn Co., Kalamazoo, MI 49001, unpublished data.

REFERENCES

(1) P. F. Binnion, in "Symposium on Digitalis," O. Storstein, Ed., Gyldendal Norsk Forlag, Oslo, Norway, 1973, p. 216.

(2) D. D. Brown and R. P. Juhl, *N. Engl. J. Med.*, **295**, 1034 (1976).

(3) R. G. Stoll, M. S. Christensen, E. Sakmar, and J. G. Wagner, *Res. Commun. Chem. Pathol. Pharmacol.*, **4**, 503 (1972).

(4) K. C. Kwan and A. E. Till, *J. Pharm. Sci.*, **62**, 1494 (1973).

ACKNOWLEDGMENTS

Presented at the APhA Academy of Pharmaceutical Sciences, Phoenix meeting, November 1977.

Pentobarbital Absorption from Capsules and Suppositories in Humans

JAMES T. DOLUISIO *x, RANDALL B. SMITH ‡, A. H. C. CHUN §, and LEWIS W. DITTERT ‡

Received May 16, 1977, from the **College of Pharmacy, University of Texas at Austin, Austin, TX 78712*, the ‡*College of Pharmacy, University of Kentucky, Lexington, KY 40506*, and §*Abbott Laboratories, North Chicago, IL 60064*. Accepted for publication March 20, 1978.

Abstract □ Serum pentobarbital levels following administration of the sodium salt as a 100-mg capsule orally and as two 120-mg suppository formulations (A and B) rectally were measured. From these data and previously determined kinetic constants after intravenous administration, the absorption rates and bioavailability of pentobarbital from each dosage form were determined. All three dosage forms were 100% absorbed. Peak serum pentobarbital levels occurred at 1, 4, and 10 hr for the capsule, Suppository A, and Suppository B, respectively. *In vitro* studies agreed with the serum data in that Suppository A released drug in an *in vitro* aqueous pH 7.4 system at a much greater rate than Suppository B. The capsule and Suppository A both appeared to be absorbed by simple first-order processes; however, Suppository B had a complex absorption pattern, which was modeled using sequential zero-order and first-order absorption.

Keyphrases □ Pentobarbital—absorption rates and bioavailability from capsules and suppositories in humans □ Absorption rates—pentobarbital from capsules and suppositories in humans □ Bioavailability—pentobarbital from capsules and suppositories in humans □ Hypnotic-sedatives—pentobarbital, absorption rates and bioavailability from capsules and suppositories in humans

Studies in rats on the oral absorption of phenobarbital demonstrated that food decreases the rate but not the extent of absorption (1). This delayed but complete absorption markedly influenced the pharmacological responses observed. In humans, the absorption rate of orally administered pentobarbital was decreased in the presence of food (2). It can be expected that the alteration of absorption of barbiturates into the blood by any factor (*e.g.*, food, dosage formulation, or route of administration) will influence desired pharmacological responses.

This investigation compares the rectal and oral absorption of pentobarbital in human subjects and evaluates two different suppository vehicles to determine the influence of formulation on the rectal absorption of pentobarbital.

EXPERIMENTAL

Chemicals—The following drug products were used: pentobarbital sodium capsules[1] containing 100 mg of pentobarbital sodium; pentobarbital suppositories, A and B[2], prepared with two different vehicles, containing 120 mg of pentobarbital sodium[2]; and mephobarbital NF. All chemicals were reagent grade. Suppository A contained a synthetic base, and Suppository B contained a cocoa butter–spermaceti base.

[1] Nembutal Sodium, lot 09-091, Abbott Laboratories.

[2] Supplied by Abbott Laboratories.

0022-3549/78/1100-1586$01.00/0

© 1978, American Pharmaceutical Association

Since the half-life of the cardiac glycoside is about 40 hr, accumulation occurs. Therefore, the effect of the antidiarrheal mixture on a given dose of digoxin with respect to steady state would be considerably less than that reported herein after a single dose. The influence of the kaolin–pectin suspension on steady-state plasma digoxin levels is under investigation.

The decreased digoxin bioavailability after coadministration with the kaolin–pectin suspension appears to be related to a mechanism involving physical adsorption. This conclusion is supported by *in vitro* experiments that show that the antidiarrheal mixture removes digoxin from solution[9]. The mechanism probably also involves differences in gut transit time between digoxin and the kaolin–pectin suspension, with the latter persisting for a longer time in the GI tract. This hypothesis is consistent with the observation that when the antidiarrheal was administered before the cardiac glycoside, an interaction occurred; no such interaction was noted, however, when the antidiarrheal was given after the cardiac glycoside. Hence, mechanisms involving physical absorption and alterations in gut transit time appear to explain the interaction of the kaolin–pectin suspension with digoxin, a conclusion not totally supported by others (2).

APPENDIX

In accordance with the model-independent method of Kwan and Till (4), the following equation was derived to estimate relative bioavailability under the assumption of constant nonrenal clearance:

$$\frac{F^x}{F^s} = \frac{AUC_\infty{}^x}{AUC_\infty{}^s} - \frac{AUC_\infty{}^x}{D^x}(\dot{V}^s_{cl,r} - \dot{V}^x_{cl,r}) \qquad \text{(Eq. A1)}$$

where F is the fraction of the dose, D, that reaches the general circulation unchanged; $\dot{V}_{cl,r}$ is renal clearance; AUC_∞ is the area under the plasma concentration–time curve through infinity; and the superscripts x and s refer to test treatment and standard treatment, respectively.

For the case of nonrenal clearance changing in proportion to observed changes in renal clearance:

$$\frac{F^x}{F^s} = \frac{AUC_\infty{}^x}{AUC_\infty{}^s}\left(\frac{\dot{V}^x_{cl,r}}{\dot{V}^s_{cl,r}}\right) \qquad \text{(Eq. A2)}$$

With the assumption of constant plasma clearance:

$$\frac{F^x}{F^s} = \frac{AUC_\infty{}^x}{AUC_\infty{}^s} \qquad \text{(Eq. A3)}$$

This equation ignores observed changes in renal clearance by assuming that nonrenal clearance compensates.

[9] The Upjohn Co., Kalamazoo, MI 49001, unpublished data.

REFERENCES

(1) P. F. Binnion, in "Symposium on Digitalis," O. Storstein, Ed., Gyldendal Norsk Forlag, Oslo, Norway, 1973, p. 216.

(2) D. D. Brown and R. P. Juhl, *N. Engl. J. Med.*, **295**, 1034 (1976).

(3) R. G. Stoll, M. S. Christensen, E. Sakmar, and J. G. Wagner, *Res. Commun. Chem. Pathol. Pharmacol.*, **4**, 503 (1972).

(4) K. C. Kwan and A. E. Till, *J. Pharm. Sci.*, **62**, 1494 (1973).

ACKNOWLEDGMENTS

Presented at the APhA Academy of Pharmaceutical Sciences, Phoenix meeting, November 1977.

Pentobarbital Absorption from Capsules and Suppositories in Humans

JAMES T. DOLUISIO *x, RANDALL B. SMITH ‡, A. H. C. CHUN §, and LEWIS W. DITTERT ‡

Received May 16, 1977, from the **College of Pharmacy, University of Texas at Austin, Austin, TX 78712*, the ‡*College of Pharmacy, University of Kentucky, Lexington, KY 40506*, and §*Abbott Laboratories, North Chicago, IL 60064*. Accepted for publication March 20, 1978.

Abstract □ Serum pentobarbital levels following administration of the sodium salt as a 100-mg capsule orally and as two 120-mg suppository formulations (A and B) rectally were measured. From these data and previously determined kinetic constants after intravenous administration, the absorption rates and bioavailability of pentobarbital from each dosage form were determined. All three dosage forms were 100% absorbed. Peak serum pentobarbital levels occurred at 1, 4, and 10 hr for the capsule, Suppository A, and Suppository B, respectively. *In vitro* studies agreed with the serum data in that Suppository A released drug in an *in vitro* aqueous pH 7.4 system at a much greater rate than Suppository B. The capsule and Suppository A both appeared to be absorbed by simple first-order processes; however, Suppository B had a complex absorption pattern, which was modeled using sequential zero-order and first-order absorption.

Keyphrases □ Pentobarbital—absorption rates and bioavailability from capsules and suppositories in humans □ Absorption rates—pentobarbital from capsules and suppositories in humans □ Bioavailability—pentobarbital from capsules and suppositories in humans □ Hypnotic-sedatives—pentobarbital, absorption rates and bioavailability from capsules and suppositories in humans

Studies in rats on the oral absorption of phenobarbital demonstrated that food decreases the rate but not the extent of absorption (1). This delayed but complete absorption markedly influenced the pharmacological responses observed. In humans, the absorption rate of orally administered pentobarbital was decreased in the presence of food (2). It can be expected that the alteration of absorption of barbiturates into the blood by any factor (*e.g.*, food, dosage formulation, or route of administration) will influence desired pharmacological responses.

This investigation compares the rectal and oral absorption of pentobarbital in human subjects and evaluates two different suppository vehicles to determine the influence of formulation on the rectal absorption of pentobarbital.

EXPERIMENTAL

Chemicals—The following drug products were used: pentobarbital sodium capsules[1] containing 100 mg of pentobarbital sodium; pentobarbital suppositories, A and B[2], prepared with two different vehicles, containing 120 mg of pentobarbital sodium[2]; and mephobarbital NF. All chemicals were reagent grade. Suppository A contained a synthetic base, and Suppository B contained a cocoa butter–spermaceti base.

[1] Nembutal Sodium, lot 09-091, Abbott Laboratories.

[2] Supplied by Abbott Laboratories.

0022-3549/78/1100-1586$01.00/0

© 1978, American Pharmaceutical Association

Table I—Serum Pentobarbital Levels (Micrograms per Milliliter) following Oral Administration of Pentobarbital Sodium 100-mg Capsules

Hour	Subject										
	PIM	BG	RB	GB	TB	LM	HS	KD	SD	RM	Mean + *SD*
0.5	1.57	0.76	1.28	1.63	1.13	0.54	1.57	0.96	0.67	1.07	1.12 ± 0.39
1.0	(1.60)[a]	0.87	1.18	1.69	1.50	0.42	2.71	1.19	1.39	1.17	1.37 ± 0.60
1.5	1.66	0.57	1.12	0.50	1.46	1.46	1.49	0.99	1.45	1.13	1.18 ± 0.40
2.5	1.36	0.52	0.59	0.64	1.08	0.94	1.23	1.00	1.09	0.84	0.93 ± 0.28
4.0	1.13	0.70	0.52	0.75	0.77	(0.90)	0.94	0.74	1.08	0.73	0.83 ± 0.19
6.0	0.75	0.71	0.50	(0.74)	0.66	0.89	0.88	0.57	0.33	0.68	0.67 ± 0.17
8.0	(0.70)	0.22	0.44	0.74	0.63	0.56	1.24	0.72	0.51	1.08	0.68 ± 0.30
24.0	0.67	0.43	0.33	(0.70)	0.49	0.36	0.79	0.70	0.73	0.70	0.59 ± 0.17

[a] Parentheses equal approximate value.

Table II—Serum Pentobarbital Levels (Micrograms per Milliliter) following Rectal Administration of Pentobarbital Sodium 120-mg Suppositories

Hour	Subject						
	LN	GB	BG	RB	RM	LM	Mean + *SD*
				Suppository A			
0.5	0.221	0.109	0.295	0.346	0.310	0.300	0.263 ± 0.086
1.0	0.354	0.319	0.612	0.714	0.620	0.614	0.537 ± 0.162
1.5	0.566	0.596	0.714	0.968	0.661	0.679	0.696 ± 0.143
2.5	0.643	1.097	0.932	1.062	0.838	0.903	0.897 ± 0.164
4.0	0.820	1.280	1.015	0.956	0.897	0.932	0.982 ± 0.159
6.0	0.968	1.050	0.991	0.938	0.785	0.950	0.947 ± 0.089
8.0	1.121	0.932	0.944	0.885	0.720	0.897	0.915 ± 0.129
10.0	1.027		0.773			0.767	0.861 ± 0.148
12.0			0.743			0.749	(0.746)[a]
				Suppository B			
0.5	N.M.[b]	N.M.	N.M.	N.M.	N.M.	N.M.	N.M.
1.0	N.M.	0.171	N.M.	0.087	N.M.	N.M.	(0.043)
1.5	0.048	0.230	0.039	0.133	0.083	0.056	0.099 ± 0.072
2.5	0.071	0.566	0.139	0.173	0.230	0.182	0.227 ± 0.174
4.0	0.483	0.661	0.291	0.225	0.679	0.444	0.464 ± 0.185
6.0	0.814	1.056	0.749	0.560	0.791	0.649	0.770 ± 0.169
8.0	0.897	1.156	1.103	0.944	0.784	0.826	0.952 ± 0.149
10.0		1.133		1.056	0.867		1.019 ± 0.232
12.0		0.944		0.9991	0.761		0.899 ± 0.121

[a] Parentheses equal approximate value. [b] Not measurable.

Selection of Subjects—*Oral Study*—The 10 healthy male volunteers were 21 years or older and ranged in weight from 69.0 to 89.5 kg. Five of these volunteers participated in the suppository study.

Suppository Studies—The six healthy male volunteers were 21 years or older and ranged in weight from 69.0 to 89.5 kg. These volunteers had not consumed any drug substances for at least 1 week prior to the study. These subjects had participated in a previous study of intravenous pentobarbital pharmacokinetics. The intravenous, oral capsule, and rectal suppository studies all were conducted within 10 months.

Study Design—*Oral Study*—The 10 subjects fasted overnight and were given a single oral capsule containing 100 mg of pentobarbital sodium. No food or water, other than that taken with the capsule, was allowed until the 3rd experimental hr. Venous blood specimens (15 ml) were collected before dosing and at 0.5, 1.0, 1.5, 2.5, 4.0, 6.0, and 8.0 hr following capsule administration.

Suppository Studies—The six subjects were randomly divided into two groups of three subjects.In the first part of the crossover study, Group I volunteers were given Suppository A and Group II volunteers were given Suppository B. One week later, in the second part of the crossover study, the test was repeated and medications were reversed.

The studies began in the early morning following an overnight fast. Each subject was given a breakfast consisting of orange juice, two eggs, two slices of bacon, two slices of toast, and coffee with cream and sugar. After breakfast, each subject was given an enema. One suppository was administered 1 hr postenema. The subjects were not confined to bed, but strenuous activity was prohibited. The suppositories were retained by all subjects. Experimental timing began with suppository administration. Venous blood specimens (15 ml) were collected before dosing and at 0.5,

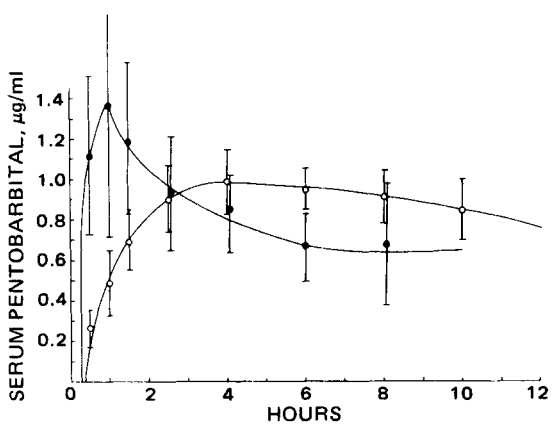

Figure 1—*Serum pentobarbital levels with standard deviations following oral administration to 10 subjects of 100 mg of pentobarbital sodium by capsule (○) and following rectal administration to six subjects of 120 mg by Suppository A (●).*

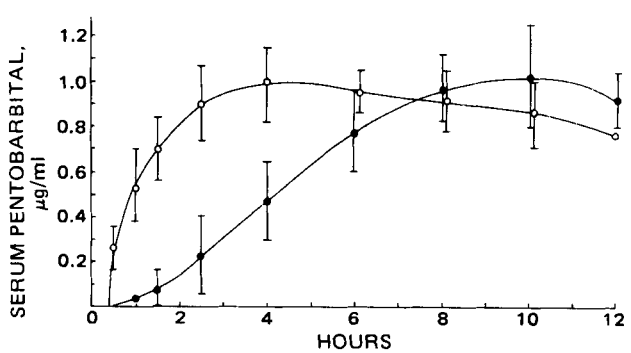

Figure 2—*Serum pentobarbital levels with standard deviations following rectal administration to six subjects of 100 mg by Suppository A (○) and Suppository B (●).*

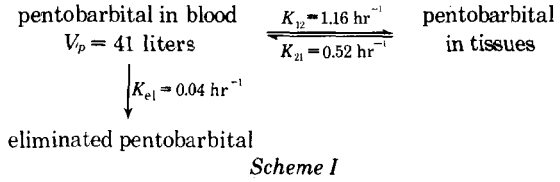

Scheme I

1.0, 1.5, 4.0, 6.0, and 8.0 hr following suppository administration in the first part of the crossover. Analysis of the samples collected indicated that further samples should be taken. In the second part of the crossover, samples also were taken at 10.0 and 12.0 hr.

Assay of Serum Pentobarbital—The concentration of unmetabolized pentobarbital in serum was determined by GLC as previously described (2).

***In Vitro* Release Studies**—The apparatus used in the *in vitro* studies consisted of a 38-mm o.d. × 10-cm glass tube centered in a 600-ml beaker and immersed 5.08 cm (2 in.) below the fluid surface. A 500-ml volume of pH 7.5 buffer at 50° was used. Sealed to the bottom of the tube was a 12-mesh stainless steel screen to allow for more uniform agitation. After the fluid reached the desired temperature, a suppository was placed in the tube, and the fluid was stirred with a 2.54-cm magnetic bar at 100 rpm.

Samples were taken every 5 min for the first 30 min and at 45, 60, and 90 min. These samples were diluted 1:6 with 1.5% ammonium hydroxide and assayed by UV spectroscopy at 240 nm.

RESULTS AND DISCUSSION

Serum pentobarbital levels following oral administration of 100 mg of pentobarbital sodium by capsule and rectal administration of 120 mg by Suppositories A and B are shown in Tables I and II and Figs. 1 and 2.

In a previous study (2) of five subjects, the average serum pentobarbital levels were determined following a 50-mg iv dose. From these data, the constants for pentobarbital distribution and elimination were calculated (2). The model employed and the appropriate constants are shown in Scheme I. The mean total clearance rate of pentobarbital was 1.64 liters/hr or 27.33 ml/min in these subjects.

Serum levels following oral administration of a 50-mg pentobarbital sodium capsule also were obtained after an overnight fast in the previous study (2). It was estimated that 100% of the 50-mg oral dose was absorbed. A time lag of 0.30 hr occurred prior to the onset of absorption, the absorption half-life was 0.35 hr (k_a = 2.00 hr^{-1}), and peak serum levels occurred 1.0 hr after dosing.

The absorption rate constant, k_a, for the 100-mg pentobarbital sodium capsule in the present investigation was calculated according to Loo and Riegelman (3) using the mean serum level data from the present investigation and the mean rate constants after intravenous administration from the previous study as already described. Mean data were employed since kinetic constants following intravenous administration were not available for all subjects. [Also, results from the previous study (2) indicated the same outcome when average data were used as compared to average parameters from individual data.] The k_a calculated by this method was 2.0 hr^{-1} with a lag time of 0.30 hr.

A comparison of the area under the curve (*AUC*) with the *AUC* from previously reported intravenous data in the same subjects (2) indicated 100% absorption from the 100-mg capsule. The theoretical line for these data shown in Fig. 1 was calculated using the mean rate constants from the previous study and the absorption rate constant of 2.0 hr^{-1}. From the good approximation of the data using these rate constants, it appears that

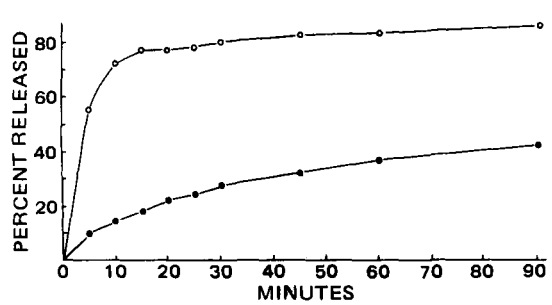

Figure 3—In vitro *dissolution of Suppository A* (○) *and Suppository B* (●) *in an aqueous pH 7.4 system.*

Table III—Absorption Characteristics of Pentobarbital Sodium from Oral and Rectal Dosage Forms

Formulation	Time of Peak Concentration, hr	Lag Time, hr	$t_{1/2}$, hr	*AUC*/Dose[a], hr/liter	F^b
50.0-mg Capsule[c]	1.0	0.3	0.35	0.630	1.11
100-mg Capsule	1.0	0.3	0.35	0.25	1.05
Suppository A	4.0	0.4	1.70	0.669	1.15
Suppository B	9–10	0.5	—[d]	0.767	1.33

[a] Values represent the mean of subjects who received all dosage forms and an intravenous injection (data from Ref. 2). [b] $(AUC_{form} \cdot dose_{iv}/AUC_{iv} \cdot dose_{form})$; intravenous data from Ref. 2. [c] Taken from Ref. 2. [d] Complex absorption pattern; see text.

no significant changes in parameters had occurred since the previous study.

Serum levels in six subjects following rectal administration of Suppositories A and B are shown in Table II and Figs. 1 and 2. The *AUC* for both suppositories was calculated from the mean data with the trapezoidal rule up to the last data point. The *AUC* from the last data point to infinity was estimated by dividing the plasma concentration at the last time point by the mean value of the slope of the elimination phase of the intravenous data (2). A comparison of these calculated *AUC* values with the *AUC* after intravenous administration, when corrected for difference in the doses, indicated that both suppositories were approximately 100% absorbed.

The data also were analyzed according to the method of Loo and Riegelman (3). However, the absorption of pentobarbital following administration of Suppository A was appreciably faster than that of Suppository B. Suppository A showed a peak serum level 4 hr after administration, and the absorption half-life was calculated to be 1.7 hr (k_a = 0.40 hr^{-1}). Suppository B showed a peak serum level approximately 9 or 10 hr after administration, and the serum curve could be fitted only when a complex absorption pattern [involving zero-order (k_0 = 0.07 μg/ml/hr) and first-order (k_1 = 0.35 hr^{-1}) processes] was assumed. The complex absorption pattern is most likely a result of the release characteristics of Suppository B.

Other models involving mixed zero- and first-order, pure first-order, and pure zero-order absorption processes were tested. However, none resulted in a better fit of the data. Without further data, no conclusions about the release and absorption rates from Suppository B can be made other than that the overall process was not simple first order.

The absorption characteristics for the oral and rectal dosage forms are shown in Table III. Table III and Fig. 1 illustrate that, although pentobarbital was efficiently absorbed after rectal administration, even the better formulation was absorbed more slowly than when the drug was administered by oral capsule.

The results of pharmacokinetic calculations from serum levels following administration of pentobarbital sodium indicate that:

1. The rate and extent of oral absorption following administration of 50- and 100-mg capsules are similar. The absorption half-life in each case was 0.35 hr, and each dose was totally absorbed.

2. Pentobarbital absorption after administration of rectal suppositories was influenced dramatically by product formulation. Both suppository products studied allowed total absorption of pentobarbital, but Suppository A give a peak serum level 4 hr after administration whereas Suppository B gave a peak serum level 9–10 hr after administration.

3. Oral absorption of pentobarbital sodium was faster than rectal absorption from the suppositories studied. As shown in Fig. 3, *in vitro* studies agreed with absorption estimates following suppository administration in that Suppository A released pentobarbital at a much faster rate than Suppository B in an *in vitro* aqueous pH 7.4 system.

Thus, the route of pentobarbital sodium administration as well as product formulation may markedly influence the rate of absorption and, consequently, the serum level–time profile. *In vitro* release characteristics may be helpful as a guide in formulation of pentobarbital suppositories with optimal absorption properties. Based on previous studies, these effects may influence pharmacological responses seen in patients.

REFERENCES

(1) S. Kojima, R. B. Smith, and J. T. Doluisio, *J. Pharm. Sci.*, **60**, 1639 (1971).

(2) R. B. Smith, L. W. Dittert, W. O. Griffen, Jr., and J. T. Doluisio, *J. Pharmacokinet. Biopharm.*, **1**, 5 (1973).

(3) J. C. K. Loo and S. Riegelman, *J. Pharm. Sci.*, **57**, 919 (1968).

Hemolytic Properties of Synthetic Glycosides

RUTH SEGAL ˣ, FRIEDA SHUD, and ILANA MILO-GOLDZWEIG

Received December 22, 1977, from the *Department of Pharmacognosy, School of Pharmacy, Hebrew University of Jerusalem, Jerusalem, Israel.* Accepted for publication March 21, 1978.

Abstract □ Cholesteryl α-L-rhamnopyranoside, tigogenyl α-L-rhamnopyranoside, tigogenyl β-D-fucopyranoside, smilagenyl β-D-fucopyranoside, cholesteryl β-maltoside, tigogenyl β-maltoside, and smilagenyl β-maltoside were synthesized and characterized. The rhamnosides and fucosides, as well as some other steroid monoglycosides, proved to be extremely insoluble in water. The concentration giving 50% hemolysis, H_{50}, was of the same order of magnitude for all synthetic glycosides. Ghost cells collected from blood hemolyzed by smilagenyl maltoside and tigogenyl maltoside had appreciable amounts of absorbed aglycones. All results are in accordance with previous investigations on the mechanism of saponin and sapogenin hemolysis.

Keyphrases □ Glycosides, various—synthesized, hemolytic activity evaluated □ Hemolytic activity—various glycosides evaluated

Saponins have a wide range of biological activity, some of which might be of medical value. Most saponins possess antibiotic properties (1), especially against fungi (2–4). Escin (5), the active principle of *Aesculus hippocastanum*, has antiexudative and anti-inflammatory activities. Various saponins are antiviral agents (6, 7), and tumor inhibitory saponins were isolated from *Acer negundo* (8, 9) and *Entada phaseolides* (10). However, therapeutic application of saponins is very limited. When taken orally, they are poorly absorbed from the intestine; when administered by injection, especially intravenously, they are very toxic and induce marked hemolysis.

BACKGROUND

Saponins in their original form are generally nonhemolytic (11, 12) and nonfungicidic (13), but these properties are attained after the glycosidic bonds are hydrolyzed by appropriate membrane glycosidase enzymes to liberate the active aglycone[1]. The presence of several glycosidases in extracts of human erythrocytes was described (14). The mechanism by which saponins induce hemolysis is the basis for the biological activity of various glycosides, *i.e.*, anthraglycosides (15) and phloridzin (16, 17). It can be assumed that biological activities other than hemolysis are also based on the same mechanism.

Since the nature of the glycosidases varies from one type of cell to another, it should be possible to synthesize nonhemolytic saponins whose glycosidic bonds will be hydrolyzed only by some target cell and thereby set free the active aglycones. The synthesis of such glycosides should obviously be guided by the glycosidases active in whole erythrocytes. However, slight hemolysis was obtained when erythrocytes were incubated with nitrophenyl glycosides, so the nature of whole erythrocyte glycosidases could not be determined.

The purposes of the present investigation were to synthesize various new glycosides of hemolytically active aglycones and to test their hemolytic activity.

RESULTS AND DISCUSSION

The glycosides were synthesized according to the Koenigs–Knorr method (18–20) by condensing the acetyl bromoglycosides with the sapogenins in the presence of silver oxide as described by Wulff *et al.* (21). Optimal yields were obtained when the final hydrolytic step, usually performed according to Zemplen and Pacsu (22), was modified. Instead of methanolysis with catalytic amounts of sodium methoxide under reflux, hydrolysis was performed with 0.25 *M* sodium methoxide at room temperature.

The following new glycosides were synthesized: cholesteryl α-L-rhamnopyranoside (I), tigogenyl α-L-rhamnopyranoside (II), tigogenyl β-D-fucopyranoside (III), smilagenyl β-D-fucopyranoside (IV), cholesteryl β-maltoside (V), tigogenyl β-maltoside (VI), and smilagenyl β-maltoside (VII). The constitution of the glycosides was assured by elemental analysis and TLC of the products obtained after acid hydrolysis. The stereochemical assignments of the glycosidic bonds were deduced from the synthetic methods applied (23).

Generally, β-glycosides are obtained from sugars belonging to the D-series, while L-sugars give rise to α-glycosides. The configuration was further confirmed from molecular rotation differences according to Klyne (24) who showed that the rotation contribution of the carbohydrate component, ΔC, in steroid glycosides is almost independent of the steroid component and is approximately equal to the molecular rotation, $[M]_D$, of the corresponding α- or β-methyl glycosides:

$$[M]_D = [\alpha]_D \times \text{mol. wt.}/100 \qquad \text{(Eq. 1)}$$

The value of ΔC is determined from:

$$\Delta C = [M]_D \text{ of steroid glycoside} - [M]_D \text{ of free steroid} \qquad \text{(Eq. 2)}$$

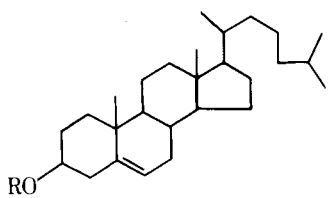

I: R = α-L-rhamnopyranose
V: R = β-maltose
XII: R = β-D-glucopyranose

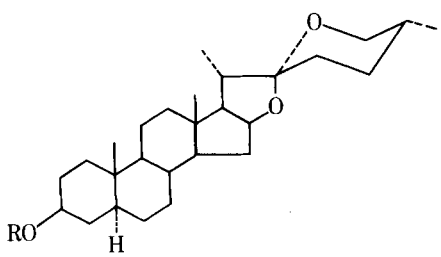

II: R = α-L-rhamnopyranose
III: R = β-D-fucopyranose
VI: R = β-maltose
VIII: R = H
IX: R = β-D-glucopyranose

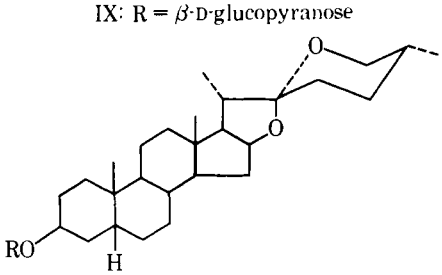

IV: R = β-D-fucopyranose
VII: R = β-maltose
X: R = H
XI: R = β-D-glucopyranose

[1] Saponins possessing very high surface activities (*e.g.*, digitonin) may induce hemolysis by a parallel mechanism, probably similar to that of other surfactants.

0022-3549/78/1100-1589$01.00/0
© 1978, American Pharmaceutical Association

Table I—$[M]_D$ Values of the Synthesized Glycosides and the Corresponding Aglycones and Calculated ΔC Values and Literature $[M]$ Values for the α- and β-Methyl Glycosides

Compound	Proposed Configuration	$[M]_D$ Glycoside	$[M]_D$ Aglycone	ΔC	$[M]_D$ Methyl Glycopyranosides[a] α	β
I	α	−300	−153	−147	−111 (24)	+170 (24)
II	α	−568	−258	−310	−111 (24)	+170 (24)
III	β	−340	−258	−82	+332 (25)	—
IV	β	−310	−287	−23	+332 (25)	—
V	β	+120	−153	+273	—	+273 (26)
VI	β	−100	−258	+158	—	+273 (26)
VII	β	−40	−287	+247	—	+273 (26)

[a] Literature reference in parentheses.

Table I summarizes the ΔC values obtained for the new synthetic glycosides and the available $[M]_D$ values for the methyl glycosides. Considerable differences between some observed and literature data exist. This discrepancy may be attributed to the difference in the solvents used (24); the methyl glycosides were measured in water whereas the steroid glycosides were measured in chloroform or methanol. However, the ΔC values are all of the same sign and order of magnitude as the corresponding methyl glycosides.

The configurations of the glycosidic bonds could not be confirmed by either one of the two most reliable methods, NMR spectroscopy or degradation with specific glycosidases, because of the extremely low solubility of the glycosides in all organic solvents and in water.

The hemolytic activities of the synthetic glycosides, tested on bovine erythrocytes, are expressed by the H_{50} values, the concentrations inducing 50% hemolysis. These values were determined by plotting percentage hemolysis *versus* hemolysin concentration (27). Some sapogenin monoglycosides also were tested. All data are summarized in Table II.

Most tested monoglycosides proved to be extremely water insoluble. In previous investigations (27) on the hemolytic activity of various sapogenins and steroids, dimethyl sulfoxide–water was an excellent system for dissolving these compounds and for performing the hemolysis tests. However, contrary to expectation, this system was completely inadequate for dissolving monoglycosides. Higher solubility was attained with isopropyl alcohol, which was nonhemolytic[2] at a final concentration of 10%. This solvent system was adequate for dissolving smilagenyl glucoside and, to some extent, tigogenyl glucoside for which the activity was tested on the saturated solution without determining its concentration. However, neither dimethyl sulfoxide nor isopropyl alcohol could be used for dissolving the glycosides of the desoxy sugars, *i.e.*, the rhamnosides and the fucosides. Although these compounds are by themselves soluble in both solvents, they precipitate from the solution on the addition of water.

Awareness of the fact that the monoglycosides are extremely insoluble, often even less soluble than the corresponding aglycones, is important in preparing water-soluble derivatives of lipophilic compounds.

In contrast to the monoglycosides, the maltosides (which are diglucosides) proved to be fairly soluble in dimethyl sulfoxide and isopropyl alcohol and could be diluted with water without precipitation. All three maltosides tested were highly hemolytic (Table II). All maltosides gave 50% hemolysis at the same concentration. The same concentration also gave 50% hemolysis in the only soluble glucoside, smilagenyl glucoside, and was determined previously (28) for the aglycone itself.

Ghost cells were collected from blood hemolyzed with either tigogenyl or smilagenyl maltoside and were extracted with dichloromethane. The extracts, when tested by TLC, were found to contain significant quantities of absorbed free aglycones, although the original maltoside solutions were devoid of any aglycone. These findings agree with previous conclusions that hydrolysis of the glycosidic bonds by membrane glycosidases, which free the active aglycones, precedes the hemolytic phase (11). Such a mechanism also rationalizes the identical H_{50} values of smilagenin, smilagenyl glucoside, and smilagenyl maltoside, as well as the identical H_{50} values of the three maltosides, since all monohydroxy steroids and sapogenins possess identical hemolytic activity (28).

Saponin hemolysis generally is ascribed to the fact that saponins form stable insoluble complexes with cholesterol (29). Since cholesterol is an erythrocyte membrane constituent, it is assumed that hemolysis is induced by the formation of an insoluble complex between the saponin (or sapogenin) and this constituent (30). The finding that cholesteryl maltoside is exactly as active as smilagenyl and tigogenyl maltosides is of special relevance to this theory. In tigogenyl and smilagenyl maltosides, the aglycones were detected in extracts of the ghost cells.

Because of the presence of cholesterol in every erythrocyte membrane extract, the aglycone could not be demonstrated in cholesteryl maltoside but may be assumed. (The use of isotopically labeled cholesteryl maltoside was not feasible because of the very low yields in which the maltosides were obtained.) Consequently, the generally accepted conception that a stable insoluble complex between the hemolysin and the membrane cholesterol is the factor inducing hemolysis must be reconsidered. The possibility that the sapogenins, including cholesterol, combine with

[2] The identity of the H_{50} values of tigogenin maltoside in dimethyl sulfoxide and isopropyl alcohol (Table III) indicates that the latter has no enhancing or inhibiting effect on hemolysis.

Table II—H_{50} Values of Glycosides and Aglycones

	Compound	H_{50}, M[a]	Solvent
VIII	Tigogenin	2.5×10^{-5} (25)	Dimethyl sulfoxide
II	Tigogenyl α-L-rhamnopyranoside	Insoluble	Dimethyl sulfoxide and isopropyl alcohol
III	Tigogenyl β-D-fucopyranoside	Insoluble	Dimethyl sulfoxide and isopropyl alcohol
VI	Tigogenyl β-maltoside	1×10^{-5}	Dimethyl sulfoxide and isopropyl alcohol
IX	Tigogenyl β-D-glucopyranoside[b]	5[c]	Isopropyl alcohol
X	Smilagenin	3.9×10^{-5} (25)	Dimethyl sulfoxide
IV	Smilagenyl β-D-fucopyranoside	Insoluble	Dimethyl sulfoxide and isopropyl alcohol
XI	Smilagenyl β-D-glucopyranoside[b]	1.2×10^{-5}	Isopropyl alcohol
VII	Smilagenyl β-maltoside	1.1×10^{-5}	Dimethyl sulfoxide
I	Cholesteryl α-L-rhamnopyranoside	Insoluble	Dimethyl sulfoxide and isopropyl alcohol
XII	Cholesteryl β-D-glucopyranoside	Insoluble	Dimethyl sulfoxide and isopropyl alcohol
V	Cholesteryl β-maltoside	1.5×10^{-5}	Dimethyl sulfoxide

[a] Literature reference in parentheses. [b] Obtained from Professor G. Wulff, University of Bonn, Federal Republic of Germany. [c] Percent hemolysis of saturated solution.

Table III—TLC Data for Acetylated Steroid Glycosides and Their Corresponding Aglycones

Acetylated Glycoside	R_f	Aglycone	R_f	Solvent System
Cholesteryltriacetyl α-L-rhamnoside	0.85	Cholesterol	0.78	Acetone–petroleum ether (bp 60–80°) (2:3)
Tigogenyltriacetyl α-L-rhamnoside	0.83	Tigogenin	0.77	Acetone–petroleum ether (bp 60–80°) (2:3)
Tigogenyltriacetyl β-D-fucoside	0.89	Tigogenin	0.83	Acetone–petroleum ether (bp 60–80°) (1:1)
Smilagenyltriacetyl β-D-fucoside	0.80	Smilagenin	0.78	Acetone–petroleum ether (bp 60–80°) (2:3)
Cholesterylheptaacetyl β-maltoside	0.73	Cholesterol	0.78	Acetone–petroleum ether (bp 60–80°) (2:3)
Tigogenylheptaacetyl β-maltoside	0.73	Tigogenin	0.78	Acetone–petroleum ether (bp 60–80°) (2:3)
Smilagenylheptaacetyl β-maltoside	0.73	Smilagenin	0.78	Acetone–petroleum ether (bp 60–80°) (2:3)

Table IV—Solvent Systems and R_f Values for TLC of Glycosides

Compound	Solvent System	R_f
I	Chloroform–methanol (9:1)	0.36
II	Chloroform–methanol (9:1)	0.46
III	Acetone–petroleum ether (bp 60–80°) (2:1)	0.42
IV	Chloroform–methanol (9:1)	0.43
V	Chloroform–methanol (9:1)	0.72
VI	Chloroform–methanol (9:1)	0.70
VII	Chloroform–methanol (9:1)	0.73

Table V—Analytical Data of Synthetic Glycosides

Compound	Solvent Used for Column Chromatography[a]	Solvent for Crystallization	Melting Point	Yield, %	$[\alpha]_D$[b] (Solvent Concentration)	Formula	Analysis, %	Calc.	Found
I	A	Methanol	213–214°	42	−58° (0.38 chloroform)	$C_{33}H_{56}O_5$	C	74.40	74.71
							H	10.52	10.67
II	A	Methanol	229–231°	50	−101° (0.20 chloroform)	$C_{33}H_{54}O_7 \cdot CH_3OH$	C	67.0	67.38
							H	9.76	9.18
III	B	Methanol	216–217°	45	−60.4 (0.3 chloroform)	$C_{33}H_{54}O_7 \cdot H_2O$	C	68.02	67.96
							H	9.6	9.5
IV	A	Methanol	196–198°	54	−55.4° (0.20 chloroform)	$C_{33}H_{54}O_7 \cdot \frac{1}{2}CH_3OH$	C	69.4	69.76
							H	9.63	9.86
V	B	Chloroform–methanol (4:1)	213°	21	+16.9° (0.28 methanol)	$C_{39}H_{66}O_{11} \cdot 2H_2O$	C	62.6	62.97
							H	9.38	9.12
VI	C	Chloroform–methanol (4:1)	157°	28	−14.7° (0.3 methanol)	$C_{39}H_{64}O_{13} \cdot H_2O$	C	61.74	61.57
							H	8.71	8.85
VII	C	Chloroform–methanol (4:1)	298–300°	25	−5.4°	$C_{39}H_{64}O_{17} \cdot H_2O$	C	61.74	61.27
							H	8.71	8.75

[a] Solvent system A, chloroform–methanol (36:1); B, petroleum ether (bp 60–80°)–acetone (6:1); and C, chloroform–methanol (6:1). [b] Optical rotations were determined on a Perkin-Elmer polarimeter-241.

membrane cholesterol in some micellar structure resulting in hemolysis is, of course, not precluded.

The role of membrane cholesterol in the hemolyzing mechanism is now being investigated.

EXPERIMENTAL

The following materials were obtained commercially: L-rhamnose[3], D-fucose[3], maltose[4], tigogenin[4], smilagenin[4], cholesterol[4], crystalline silver nitrate[5], and hydrogen bromide solution in acetic acid[6].

TLC was performed on silica gel G coated plates.

Synthesis of Peracetylated Sugars (31–33)—To a solution of the sugar (30 m*M*) in pyridine (20–40 ml) at 4°, an equal volume of acetic anhydride was added. The reaction solution was stirred for several hours at 4° and monitored by TLC [acetone–petroleum ether (bp 60–80°) (2:3)]. The R_f of the sugar component was 0; the R_f of peracetylated sugars was 0.4–0.7. When the components with low R_f values had disappeared, ether and ice water were added.

The organic phase was collected, washed with cold aqueous sulfuric acid (5%), sodium bicarbonate (5%), and ice water, and dried (magnesium sulfate). Then the solvent was evaporated. The monosugars yielded yellow viscous products, and maltose yielded a white solid. The acetates were stored over phosphorus pentoxide and used without further purification.

Synthesis of Acetyl Sugar 1-Bromides (34–36)—To a solution of the peracetylated sugar in acetic acid (3 ml for monosaccharides and 30 ml for maltose), excess hydrogen bromide–acetic acid was added (7 ml for monosaccharides and 23 ml for maltose). The reaction was monitored by TLC [acetone–petroleum ether (bp 60–80°) (2:3)]. The bromoacetates generally had slightly higher R_f values than the peracetylated sugars.

After 2–3 hr, the reaction was complete (*i.e.*, all peracetylated sugars disappeared). Chloroform and then ice water were added. The organic phase was collected, washed with cold sodium bicarbonate (5%) and ice water, and dried (magnesium sulfate); then the solvent was evaporated. The bromoacetates were used for glycoside synthesis without purification immediately after their preparation.

Glycoside Syntheses—The general method was a modification of the Koenigs–Knorr reaction (18–20). A solution of the aglycone (1.5 moles, about 600 mg) in freshly prepared (37) dry ether (30–50 ml), finely powdered silver oxide (11 mmoles, 2.6 g), and several grains of calcium sulfate[7] were stirred in the dark in a two-necked bottle equipped with a calcium chloride tube and a separator. A solution of the bromoacetyl glycoside in dry ether (10 ml) containing a few grains of calcium sulfate was added slowly (~30 min).

The reaction mixture was stirred vigorously until no more aglycone could be detected by TLC. The chromatographic data are summarized in Table III. When the reaction was completed after 2–4 hr, the mixture was filtered, and the solvent was evaporated. The residue, a white powder, was stored over phosphorus pentoxide until alcoholysis was performed.

Basic Alcoholysis of Acetyl Glycoside—The general method was a modification of the Zemplen and Pacsu method (22). Sodium methoxide was added to a solution of the acetyl glycoside in absolute methanol (dried over molecular sieve 3) to give a final concentration of 0.25 *M* with a total volume of ~50 ml. The reaction mixture was stirred at room temperature and monitored by TLC (solvent systems and R_f values are summarized in Table IV).

When alcoholysis was complete, the solvent was evaporated. Then the residue was washed several times with cold water and chromatographed on a column of silica gel. Crystallization yielded the pure glycosides. All analytical data concerning the individual glycosides are summarized in Table V.

Acid Hydrolysis of Synthetic Glycosides—A solution of the glycoside (3 mg) dissolved in methanol (10–20 ml), with concentrated hydrochloric acid added to give a final concentration of 1 *N*, was heated under reflux for 3 hr. It was then neutralized with concentrated ammonia, and most of the solvent was evaporated. The aglycones were extracted from the aqueous methanolic residue; both fractions were tested on TLC, authentic aglycones and sugars being used as references. The TLC data for the aglycones are given in Table III. For TLC of sugars, chloroform–methanol (7:6) was used as the developing solvent; the R_f values were: glucose, 0.47; rhamnose, 0.57; and fucose, 0.52.

Hemolysis Test—*Hemolysin Solutions*—The glycosides were dissolved in dimethyl sulfoxide or isopropyl alcohol. The dimethyl sulfoxide solutions were diluted with water to give a final concentration of 30%, and the isopropyl alcohol solutions were diluted to give a final concentration of 10%. All solutions were checked carefully to determine whether the solute had precipitated on addition of water.

Blood—Citrated bovine blood was used in all experiments.

Determination of Hemolytic Activity—The method employed was described previously (28). Ghost cells were collected, extracted, and tested by TLC by the method described recently (38).

[3] Sigma.
[4] Merck, A. G. Darmstadt.
[5] J.T. Baker Chemical Co., New York, N.Y.
[6] B.D.H.
[7] Drierite.

REFERENCES

(1) R. Tschesche and G. Wulff, *Naturforschung*, **20b**, 543 (1965).
(2) B. Wolters, *Planta*, **79**, 77 (1968).
(3) E. Schlosser, *Acta Phytopathol.*, **6**, 85 (1971).
(4) E. Schlosser, *Z. Pflanzenkr. Pflanzenschutz*, **80**, 704 (1974).
(5) R. Tschesche and G. Wulff, in "Progress in the Chemistry of Organic Natural Products," vol. 30, W. Herz, H. Griesbach, and G. W. Kirby, Eds., Springer, Vienna, Austria, 1973, p. 461, and references cited therein.
(6) J. E. Sinsheimer, *Experientia*, **24**, 302 (1968).
(7) G. S. Rao and J. E. Sinsheimer, *J. Pharm. Sci.*, **63**, 471 (1974).
(8) S. M. Kupchan, R. J. Hemingway, J. R. Knox, S. J. Barboutis, D. Werner, and M. A. Barboutis, *ibid.*, **56**, 603 (1967).
(9) S. M. Kupchan, M. Takasugi, R. M. Smith, and P. S. Steyn, *J. Org. Chem.*, **36**, 1972 (1971).
(10) W. C. Liu, M. Kugelman, R. A. Wilson, and K. V. Rao, *Phytochemistry*, **11**, 171 (1972).

(11) R. Segal, P. Shatkovsky, and I. Milo-Goldzweig, *Biochem. Pharmacol.*, **23**, 973 (1974).
(12) R. Segal and I. Milo-Goldzweig, *ibid.*, **24**, 77 (1975).
(13) R. Segal and E. Schlosser, *Arch. Microbiol.*, **104**, 147 (1975).
(14) R. B. Bosmann, *J. Membr. Biol.*, **4**, 113 (1971).
(15) W. Schmid, in "Modern Methods of Plant Analysis," vol. 3, K. Peach and M. V. Tracey, Eds., Springer, Berlin, Germany, 1955, p. 549.
(16) W. Wildebrandt, *Arch. Exp. Pathol. Pharmacol.*, **212**, 9 (1950).
(17) P. G. Lefevere, *Symp. Soc. Exp. Biol. Med.*, **8**, 118 (1954).
(18) W. Koenigs and E. Knorr, *Sitzungber. Bayr. Akad. Wiss.*, **30**, 103 (1900).
(19) W. Koenigs and E. Knorr, *Chem. Ber.*, **34**, 957 (1901).
(20) P. L. Durrete and D. Horton, *Adv. Carbohydr. Chem. Biochem.*, **26**, 49 (1971).
(21) G. Wulff, G. Rhole, and W. Kruger, *Chem. Ber.*, **105**, 1097 (1972).
(22) G. Zemplen and E. Pacsu, *ibid.*, **62**, 1613 (1929).
(23) G. Wulff and G. Rhole, *Angew. Chem. (Int. Ed.)*, **13**, 157 (1974).
(24) W. Klyne, *Biochem. J.*, **47**, XLI (1950).
(25) B. Iselin and T. Reichstein, *Helv. Chim. Acta*, **29**, 508 (1946).
(26) R. E. Reeves, *J. Am. Chem. Soc.*, **76**, 4595 (1954).
(27) R. Segal, M. Mansour, and D. V. Zaitschek, *Biochem. Pharmacol.*, **15**, 1411 (1966).
(28) R. Segal and I. Milo-Goldzweig, *ibid.*, **20**, 2163 (1971).
(29) R. Tschesche and G. Wulff, *Planta Med.*, **12**, 272 (1964).
(30) S. Shany, A. W. Bernheimer, P. S. Grushoff, and K. S. Kim, *Mol. Cell. Biochem.*, **3**, 179 (1974).
(31) G. P. Ellis and J. Honeyman, in "Carbohydrate Chemistry," vol. 10, E. L. Hirst and A. G. Ross, Eds., Academic, New York, N.Y., 1955, p. 95.
(32) M. N. Wolform and A. Thompson, in "Methods in Carbohydrate Chemistry," vol. 1, R. H. Whistler and M. L. Wolform, Eds., Academic, New York, N.Y., 1955, p. 334.
(33) D. Horton and J. H. Lauterbach, *Carbohydr. Res.*, **43**, 9 (1975).
(34) R. E. Deriaz, W. B. Overend, M. Stacey, E. G. Teece, and L. F. Wiggins, *J. Chem. Soc.*, **1949**, 1879.
(35) A. M. Gakhokize, *J. Gen. Chem. (USSR)*, **18**, 60 (1948); through *Chem. Abstr.*, **42**, 4948i (1948).
(36) E. Fischer, *Chem. Ber.*, **44**, 1903 (1911).
(37) B. Helferich and W. Klein, *Justus Liebigs Ann. Chem.*, **450**, 219 (1928).
(38) R. Segal, I. Milo-Goldzweig, D. V. Zaitschek, and M. Noam, *Anal. Biochem.*, **84**, 78 (1978).

ACKNOWLEDGMENTS

Supported in part by a grant from the Joint Research Fund of the Hebrew University and Hadassah.

The authors thank Professor G. Wulff (University of Bonn, Federal Republic of Germany) for samples of monoglycosides and for valuable discussions.

Nonisothermal Aqueous Calorimetry: Computation of Process-Dependent Temperature Change and Aspects of Calorimeter Design

R. GARY HOLLENBECK *, GARNET E. PECK, and DANE O. KILDSIG ˣ

Received July 29, 1977, from the *Department of Industrial and Physical Pharmacy, School of Pharmacy and Pharmacal Sciences, Purdue University, West Lafayette, IN 47907.* Accepted for publication March 23, 1978. *Present address: School of Pharmacy, University of Maryland, Baltimore, MD 21201.

Abstract □ A general method for determining the process-dependent (intrinsic) temperature change in a nonisothermal calorimeter is presented. The nonisothermal approach to calorimetric investigations requires an estimate of the magnitude of the process independent (extrinsic) temperature change during the reaction period. The proposed method can be applied to any calorimeter whose output is a discrete or continuous temperature–time profile. It is based on a first-derivative transformation of the temperature–time profile and the partitioning of the observed temperature variation into two components: pure extrinsic variation, which occurs outside the reaction period, and the combined extrinsic and intrinsic effects during the reaction period. Close examination of the pure extrinsic variation was considered essential, since it provided the basis for identifying the form of a descriptive mathematical function consistent with the observed extrinsic behavior. Once a suitable function was selected, parameters for the equation were determined through a linear regression procedure. The resulting equation was used to predict the extrinsic variation within the reaction period. Subtraction of predicted extrinsic variation from the observed total variation and integration over the time course of the experiment provide an estimate of the process-dependent temperature change. The differential approach was examined for processes performed in a calorimeter of simple design. Aspects of calorimeter design and advantages of the proposed method of data analysis are discussed.

Keyphrases □ Calorimetry, nonisothermal—general method for determining process-dependent temperature change, aspects of calorimeter design □ Instrument design—nonisothermal calorimeter, general method for determining process-dependent temperature change

Immersional calorimetry is a remarkably versatile technique for investigation of the wetting of hydrophilic and hydrophobic solids (1). Some applications of this analytical method were reported (2–7); yet, in view of its utility, these applications are few and limited.

The information available from calorimetric investigations could be of value in the formulation and evaluation of pharmaceutical products. Implementation of this general experimental technique has proceeded slowly, primarily because of the apparent sophistication necessary in the equipment.

Aspects of calorimeter design and data analysis were included in a general review of calorimetry (8). This paper presents a general method of data analysis and demonstrates its rational development for a calorimeter of simple design.

0022-3549/78/1100-1592$01.00/0
© 1978, American Pharmaceutical Association

(11) R. Segal, P. Shatkovsky, and I. Milo-Goldzweig, *Biochem. Pharmacol.*, **23**, 973 (1974).
(12) R. Segal and I. Milo-Goldzweig, *ibid.*, **24**, 77 (1975).
(13) R. Segal and E. Schlosser, *Arch. Microbiol.*, **104**, 147 (1975).
(14) R. B. Bosmann, *J. Membr. Biol.*, **4**, 113 (1971).
(15) W. Schmid, in "Modern Methods of Plant Analysis," vol. 3, K. Peach and M. V. Tracey, Eds., Springer, Berlin, Germany, 1955, p. 549.
(16) W. Wildebrandt, *Arch. Exp. Pathol. Pharmacol.*, **212**, 9 (1950).
(17) P. G. Lefevere, *Symp. Soc. Exp. Biol. Med.*, **8**, 118 (1954).
(18) W. Koenigs and E. Knorr, *Sitzungber. Bayr. Akad. Wiss.*, **30**, 103 (1900).
(19) W. Koenigs and E. Knorr, *Chem. Ber.*, **34**, 957 (1901).
(20) P. L. Durrete and D. Horton, *Adv. Carbohydr. Chem. Biochem.*, **26**, 49 (1971).
(21) G. Wulff, G. Rhole, and W. Kruger, *Chem. Ber.*, **105**, 1097 (1972).
(22) G. Zemplen and E. Pacsu, *ibid.*, **62**, 1613 (1929).
(23) G. Wulff and G. Rhole, *Angew. Chem. (Int. Ed.)*, **13**, 157 (1974).
(24) W. Klyne, *Biochem. J.*, **47**, XLI (1950).
(25) B. Iselin and T. Reichstein, *Helv. Chim. Acta*, **29**, 508 (1946).
(26) R. E. Reeves, *J. Am. Chem. Soc.*, **76**, 4595 (1954).
(27) R. Segal, M. Mansour, and D. V. Zaitschek, *Biochem. Pharmacol.*, **15**, 1411 (1966).
(28) R. Segal and I. Milo-Goldzweig, *ibid.*, **20**, 2163 (1971).
(29) R. Tschesche and G. Wulff, *Planta Med.*, **12**, 272 (1964).
(30) S. Shany, A. W. Bernheimer, P. S. Grushoff, and K. S. Kim, *Mol. Cell. Biochem.*, **3**, 179 (1974).
(31) G. P. Ellis and J. Honeyman, in "Carbohydrate Chemistry," vol. 10, E. L. Hirst and A. G. Ross, Eds., Academic, New York, N.Y., 1955, p. 95.
(32) M. N. Wolform and A. Thompson, in "Methods in Carbohydrate Chemistry," vol. 1, R. H. Whistler and M. L. Wolform, Eds., Academic, New York, N.Y., 1955, p. 334.
(33) D. Horton and J. H. Lauterbach, *Carbohydr. Res.*, **43**, 9 (1975).
(34) R. E. Deriaz, W. B. Overend, M. Stacey, E. G. Teece, and L. F. Wiggins, *J. Chem. Soc.*, **1949**, 1879.
(35) A. M. Gakhokize, *J. Gen. Chem. (USSR)*, **18**, 60 (1948); through *Chem. Abstr.*, **42**, 4948i (1948).
(36) E. Fischer, *Chem. Ber.*, **44**, 1903 (1911).
(37) B. Helferich and W. Klein, *Justus Liebigs Ann. Chem.*, **450**, 219 (1928).
(38) R. Segal, I. Milo-Goldzweig, D. V. Zaitschek, and M. Noam, *Anal. Biochem.*, **84**, 78 (1978).

ACKNOWLEDGMENTS

Supported in part by a grant from the Joint Research Fund of the Hebrew University and Hadassah.

The authors thank Professor G. Wulff (University of Bonn, Federal Republic of Germany) for samples of monoglycosides and for valuable discussions.

Nonisothermal Aqueous Calorimetry: Computation of Process-Dependent Temperature Change and Aspects of Calorimeter Design

R. GARY HOLLENBECK *, GARNET E. PECK, and DANE O. KILDSIG ˣ

Received July 29, 1977, from the *Department of Industrial and Physical Pharmacy, School of Pharmacy and Pharmacal Sciences, Purdue University, West Lafayette, IN 47907.* Accepted for publication March 23, 1978. *Present address: School of Pharmacy, University of Maryland, Baltimore, MD 21201.

Abstract □ A general method for determining the process-dependent (intrinsic) temperature change in a nonisothermal calorimeter is presented. The nonisothermal approach to calorimetric investigations requires an estimate of the magnitude of the process independent (extrinsic) temperature change during the reaction period. The proposed method can be applied to any calorimeter whose output is a discrete or continuous temperature–time profile. It is based on a first-derivative transformation of the temperature–time profile and the partitioning of the observed temperature variation into two components: pure extrinsic variation, which occurs outside the reaction period, and the combined extrinsic and intrinsic effects during the reaction period. Close examination of the pure extrinsic variation was considered essential, since it provided the basis for identifying the form of a descriptive mathematical function consistent with the observed extrinsic behavior. Once a suitable function was selected, parameters for the equation were determined through a linear regression procedure. The resulting equation was used to predict the extrinsic variation within the reaction period. Subtraction of predicted extrinsic variation from the observed total variation and integration over the time course of the experiment provide an estimate of the process-dependent temperature change. The differential approach was examined for processes performed in a calorimeter of simple design. Aspects of calorimeter design and advantages of the proposed method of data analysis are discussed.

Keyphrases □ Calorimetry, nonisothermal—general method for determining process-dependent temperature change, aspects of calorimeter design □ Instrument design—nonisothermal calorimeter, general method for determining process-dependent temperature change

Immersional calorimetry is a remarkably versatile technique for investigation of the wetting of hydrophilic and hydrophobic solids (1). Some applications of this analytical method were reported (2–7); yet, in view of its utility, these applications are few and limited.

The information available from calorimetric investigations could be of value in the formulation and evaluation of pharmaceutical products. Implementation of this general experimental technique has proceeded slowly, primarily because of the apparent sophistication necessary in the equipment.

Aspects of calorimeter design and data analysis were included in a general review of calorimetry (8). This paper presents a general method of data analysis and demonstrates its rational development for a calorimeter of simple design.

0022-3549/78/1100-1592$01.00/0
© 1978, American Pharmaceutical Association

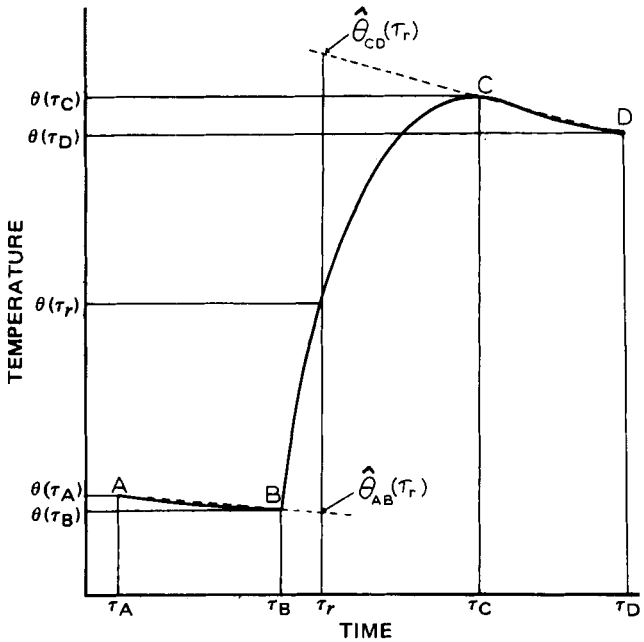

Figure 1—*Typical temperature–time profile for an exothermic process.*

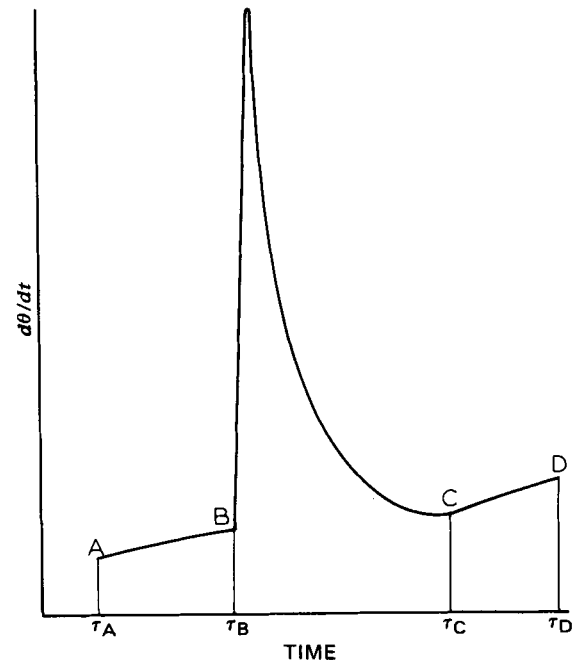

Figure 2—*First-derivative transformation of Fig. 1.*

THEORETICAL

Background—Equation 1 describes the basic relationship between the heat released by a process and the subsequent temperature change in a nonisothermal calorimeter:

$$-q = C\,\Delta\theta_i \qquad \text{(Eq. 1)}$$

where $-q$ is the heat released (calories), C is the heat capacity of the system (calories per degree celsius), and $\Delta\theta_i$ is the intrinsic temperature change (degrees celsius) in the calorimeter contents.

The term "intrinsic temperature change" refers to that portion of the total temperature change in the contents of the calorimeter that can be attributed to the process performed. Such a distinction is necessary, because it is not possible to insulate the reaction perfectly from its surroundings. In this manner, the total temperature change in the calorimeter contents, $\Delta\theta$, can be partitioned into two quantities:

$$\Delta\theta = \Delta\theta_i + \Delta\theta_e \qquad \text{(Eq. 2)}$$

where $\Delta\theta_e$ is the "extrinsic" or process-independent temperature change. The extrinsic change is primarily a consequence of heat lost or gained from the environment and of heat contributed by stirring.

Figure 1 depicts a typical temperature–time profile for a calorimetric investigation of an exothermic process, where point B represents the initiation of the process and point C is its completion. Periods A–B and C–D are often termed the initial and final rating periods, respectively, and correspond to extrinsic variation. In the ideal case of perfect insulation, the slope of these lines would be zero.

These periods are generally approximated by straight lines and the intrinsic temperature change determined by extrapolation of these lines through the reaction period BC:

$$\Delta\theta_i = \hat{\theta}_{CD}(\tau_r) - \hat{\theta}_{AB}(\tau_r) \qquad \text{(Eq. 3)}$$

where $\hat{\theta}_{CD}(\tau_r)$ and $\hat{\theta}_{AB}(\tau_r)$ refer to the temperature values at reference time τ_r obtained by linear extrapolation of the final and initial rating periods, respectively. This procedure is demonstrated graphically by the dashed lines in Fig. 1.

A frequently chosen reference point is the time when the actual system temperature, $\theta(\tau_r)$, is equal to the arithmetic mean of the temperature at points C and B:

$$\theta(\tau_r) = \frac{\theta(\tau_B) + \theta(\tau_C)}{2} \qquad \text{(Eq. 4)}$$

The method of rating period extrapolations, which is essentially empirical, can be used with acceptable accuracy for examination of a process with three characteristics: short duration, large intrinsic temperature change, and rating periods that can be expressed as linear functions of time.

A more sophisticated method of data analysis was developed in which the extrinsic temperature variation is characterized on theoretical grounds (8). This method is based on a modified form of Newton's law of cooling:

$$\frac{d\theta_e}{dt} = K[\theta_S - \theta(t)] + w \qquad \text{(Eq. 5)}$$

where $d\theta_e/dt$ is the extrinsic temperature variation, θ_S is the environmental temperature, $\theta(t)$ is the temperature of the calorimeter contents at time t, K is a proportionality constant termed the thermal leakage modulus, and w is another constant included to account for the effect of stirring.

If it is assumed that θ_S is known and constant, the parameters K and w can be obtained from the initial and final rating periods by employing a linear approximation in each period. The value of $\theta(t)$ is taken at the rating period midpoint, and $d\theta_e/dt$ is estimated by the slope of the line. A set of two simultaneous equations results from the substitution of corresponding values for $d\theta_e/dt$ and $\theta(t)$ into Eq. 5. These equations can be solved for K and w, so the extrinsic temperature change during the reaction period can be determined by integration of Eq. 5:

$$\Delta\theta_e = \int_{\tau_B}^{\tau_C} [K[\theta_S - \theta(t)] + w]\,dt \qquad \text{(Eq. 6)}$$

In explicit form, the expression for the intrinsic temperature change is obtained by expansion of Eq. 6 and substitution into Eq. 2:

$$\Delta\theta_i = \Delta\theta - \Delta\theta_e = \theta(\tau_C) - \theta(\tau_B) - (K\theta_S + w)(\tau_C - \tau_B) + K\int_{\tau_B}^{\tau_C} \theta(t)\,dt \qquad \text{(Eq. 7)}$$

Equation 7 represents an exact procedure for determining $\Delta\theta_i$ when Eq. 5 describes the extrinsic temperature variation of the system.

Because of the assumptions on which Eqs. 3 and 7 are based, neither is generally applicable to all data; nonlinearity with respect to time prohibits the use of Eq. 3, and nonlinearity with respect to temperature prohibits the use of Eq. 7.

The proposed method for the determination of the intrinsic temperature change is general and based solely on the observed extrinsic variation of the calorimeter.

Proposed Method for Computation of Intrinsic Temperature Changes—A series of steps can be taken to characterize explicitly the extrinsic temperature variation of a calorimeter and, thus, to determine the intrinsic temperature change on a rational basis.

Figure 2 represents the first-derivative transformation of the temperature–time profile presented in Fig. 1. As a result of this procedure, segments A–B and C–D comprise part of a "baseline," which represents the extrinsic variation. Substantial deviations from this baseline occur

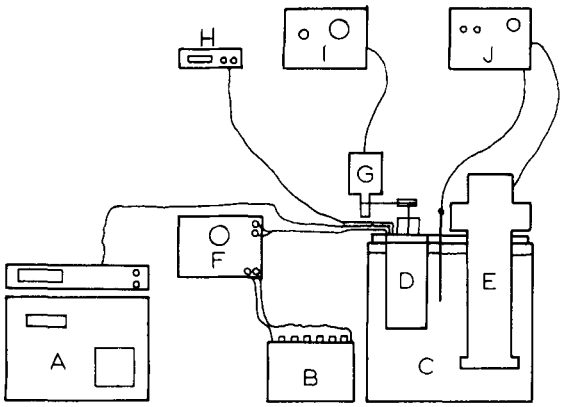

Figure 3—*Organizational schematic for components of the nonisothermal calorimeter. Key: A, digital quartz thermometer and digitial recorder; B, 12-v lead storage battery as dc power supply; C, environmental thermostat (insulated water reservoir covered with 1.9-cm acrylic); D, calorimeter cell; E, heating and water circulation unit; F, cell calibration control unit; G, stirring unit; H, digital voltmeter; I, control unit for stirrer; and J, control unit for constant-temperature water bath.*

in the reaction period B–C, and the observed $d\theta/dt$ values during this period represent the combination of intrinsic and extrinsic variations:

$$\frac{d\theta}{dt} = \frac{d\theta_i}{dt} + \frac{d\theta_e}{dt} \qquad \text{(Eq. 8)}$$

where $d\theta_i/dt$ is the intrinsic variation.

When the extrinsic temperature variation can be represented by a function capable of predicting its values *during* the reaction period, Eq. 8 may be rearranged and solved for $\Delta\theta_i$:

$$\Delta\theta_i = \int_{\tau_B}^{\tau_C} \left(\frac{d\theta}{dt} - g_e\right) dt \qquad \text{(Eq. 9)}$$

where g_e represents the function used to generate values of $d\theta_e/dt$.

The form of the function g_e should be elucidated from actual experimental data. Equation 5 is one form that may be suitable. This equation essentially states that the extrinsic variation is a first-order function of temperature:

$$\frac{d\theta_e}{dt} = g_e[\theta(t)] = B_0 + B_1\theta(t) \qquad \text{(Eq. 10)}$$

where $B_0 = K\theta_S + w$ and $B_1 = -K$. Substitution of Eq. 10 into Eq. 9, followed by integration between the limits of the reaction period, results in Eq. 7.

This linear form for g_e should only be used when the extrinsic variation is a linear function of temperature. Equation 11 represents a first-order function of time and temperature that was found to be more satisfactory than Eq. 5 for the calorimeter employed in this study:

$$\frac{d\theta_e}{dt} = B_0 + B_1 t + B_2\theta(t) \qquad \text{(Eq. 11)}$$

Parameters for either Eq. 10 or 11 can be obtained through a least-squares linear regression analysis based on the transformed data in periods A–B and C–D. Once these parameters are established, the solution of Eq. 9 is straightforward.

EXPERIMENTAL

Calorimeter—A nonisothermal calorimeter was designed and constructed to investigate immersional processes in water. Figure 3 represents the organization of the various components. The temperature recording device, A, and the calorimeter cell, D, are the primary components. Remaining components contribute partially or totally to one of three auxiliary functions: maintenance of constant environmental temperature, steady and efficient stirring of the calorimeter cell contents, and calibration of the cell (heat capacity determination).

A detailed drawing of the calorimeter cell is presented in Fig. 4. This cell was designed to fit into the acrylic[1] cover of an insulated water bath (C in Fig. 3) maintained at 25.00 ± 0.05°.

[1] Plexiglas.

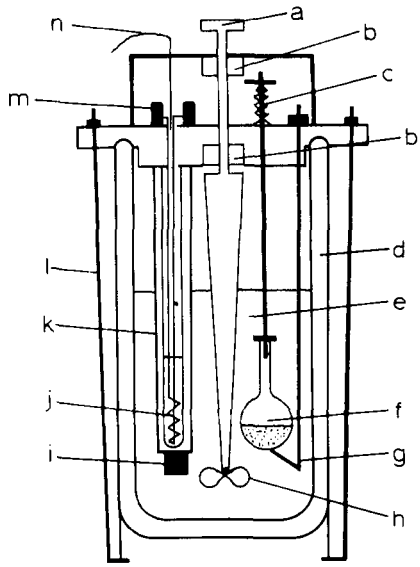

Figure 4—*Calorimeter cell. Key: a, belt guide for propeller drive shaft; b, ball bearing; c, spring-loaded sample bulb fracturing rod; d, insulated vessel; e, liquid (distilled water); f, thin-walled glass bulb containing sample; g, sample bulb support; h, propeller; i, quartz crystal thermometer probe; j, resistance heater; k, acrylic support; l, assembly rod; m, resistance heater leads; and n, thermometer lead.*

The temperature of the contents of the calorimeter cell was measured and recorded using a digital quartz thermometer[2] and output recorder[3]. With maximum resolution of 0.0001°, the output consisted of a concomitant temperature and time recording, which was updated at approximately 10-sec intervals. The quartz thermometer probe was affixed to a 16.0 × 1.5 × 0.32-cm acrylic[1] support (k in Fig. 4) within the calorimeter cell, which also served as a baffle and, thus, promoted mixing. Any thermal effect associated with the temperature measurement itself was assumed to be constant, contributing to and being characterized by the extrinsic variation.

Mounted on the opposite side of the acrylic support was a resistance heater for liquid temperature adjustment and determination of the cell heat capacity. This heater consisted of a section of wound nickel alloy[4] wire placed in a 10-mm diameter glass tube sealed at one end. Distilled water was added to cover the wire completely and to provide a medium for heat transfer. The leads from the heater were indirectly attached to a 12-v lead storage battery[5] (B in Fig. 3) through a calibration control unit (F in Fig. 3).

Within the cell, stirring was provided by an axially mounted propeller (h in Fig. 4) attached by a heavy gauge rubber band to the high revolutions per minute shaft of a commercially available stirring unit[6] (G in Fig. 3). A digital tachometer[7], based upon a photoelectric counter, was used to calibrate the stirrer. With a setting of 1500 rpm on the control unit, measurements throughout several experiments showed a tendency for the stirring rate to increase as time passed, starting at 1550 ± 25 rpm and eventually stabilizing at 1620 ± 5 rpm. The setting of 1500 rpm was used in all experiments.

The remaining components within the calorimeter cell comprise an assembly designed to contain the sample under investigation and to release it into the liquid at the appropriate time. A thin-walled glass bulb (f in Fig. 4), blown from 10-mm o.d. glass tubing, was used to contain the sample and isolated it from the immersion liquid. The bulb containing the sample was attached to an actuation rod (c in Fig. 4). Depression of the rod forced the sample bulb against a stationary support, resulting in fracture of the glass. After fracture, a spring mechanism returned the assembly to its original position so that the heat capacity of the cell was only slightly altered.

All components of the cell and all processes therein were isolated from

[2] Model 2801A, Hewlett-Packard, Palo Alto, CA 94303.
[3] Model 5050B, Hewlett-Packard, Palo Alto, CA 94303.
[4] Nichrome.
[5] Delco energizer E5000-R59, Delco Remy Division, General Motors Corp.
[6] Stedi-Speed stirrer, Fisher Scientific Co., Chicago, Ill.
[7] Designed by Professor G. Peck and Mr. T. McDaniels, Purdue University, West Lafayette, Ind.

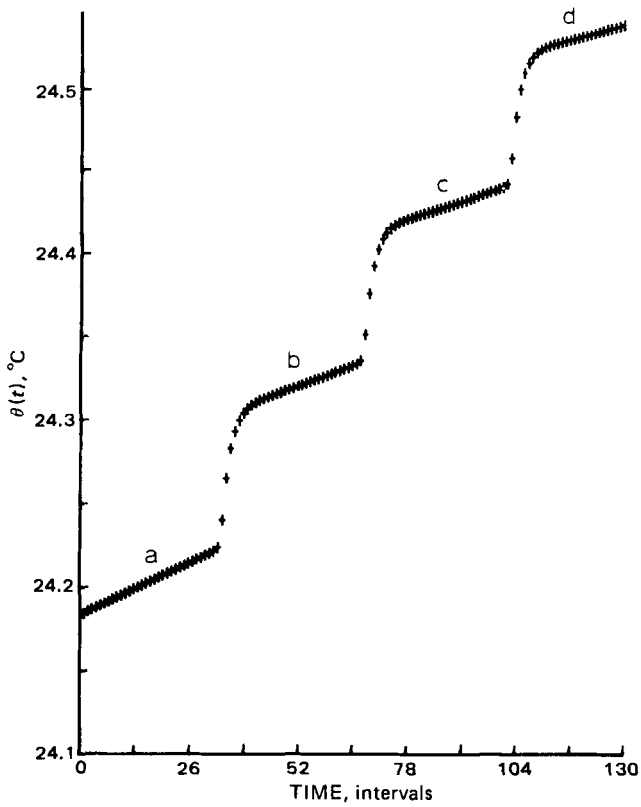

Figure 5—*Temperature–time profile for calibrations 1–3 in Table I. The periods a–d are the rating periods corresponding to the extrinsic temperature variation when the system temperature is below the environmental temperature.*

the environment by virtue of the Dewar flask (d in Fig. 4) in which they were contained. Unless otherwise specified, 250 ml of distilled water was placed in this flask and served as the immersional liquid.

Calibration—Calibration of the calorimeter consisted of a procedure used to determine the heat capacity of the cell. This procedure involved introducing a known amount of thermal energy into the cell and measuring the associated intrinsic temperature change. Completion of the circuit containing the resistance heater for a period of time, D, resulted in the release of a quantity of heat calculated from the following equation:

$$-q = V^2D/4.184R \qquad \text{(Eq. 12)}$$

where $-q$ is the heat released (calories), V is the voltage drop across the heater, and R is the resistance of the heater (ohms).

The calibration control unit (F in Fig. 3), which was directly attached to the power supply, was designed and manufactured to serve two purposes: voltage stabilization and heater activation. A center-off double-throw toggle switch was employed; when the switch was in the LOAD position, a circuit containing three 1-ohm resistors was completed. This circuit served as an external load to stabilize the power supply. When the switch was in the RUN position, the circuit containing the resistance heater was completed and, simultaneously, an elapsed time indicator[8] was actuated.

During actuation, the voltage across the terminals of the cell was measured using a digital voltmeter[9] with a resolution of 0.001 v. Movement of the control switch to the center-off position simultaneously opened the heater circuit and stopped the timer. The elapsed time was recorded with an accuracy of ±0.05 sec.

Also contained within the control unit was a 5-ohm variable resistor in series with the heater. Before a calibration was performed, the total resistance of this circuit was adjusted so that it equaled the resistance of the external load circuit. In this manner, movement of the control switch from the LOAD to RUN position did not result in a change in the potential drop across the power supply.

[8] Model 635K, Cramer/Cleveland, Cleveland, Ohio.
[9] Model 1450, Data Precision Corp., Wakefield, Me.

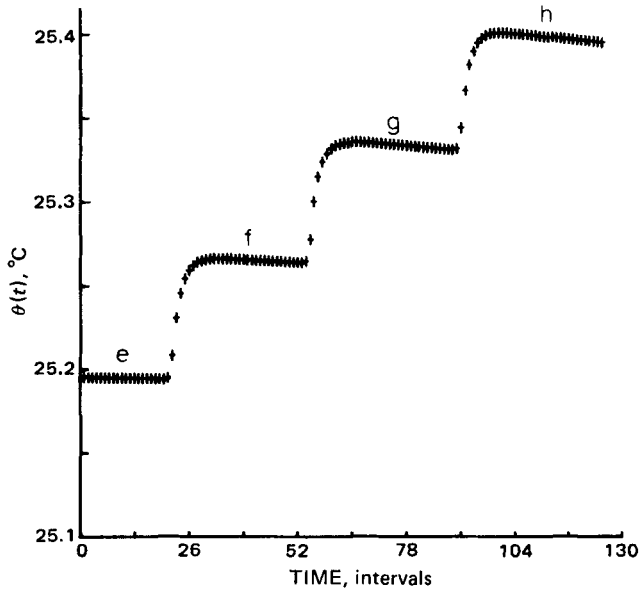

Figure 6—*Temperature–time profile for calibrations 4–6 in Table I. The periods e–h are the rating periods corresponding to the extrinsic temperature variation when the system temperature is above the environmental temperature.*

Solution of Eq. 12 for q requires a value for R, the resistance of the nickel alloy wire heater. This value is difficult to obtain by direct measurement, because the resistance is low and its value changes as the wire is heated. A retrogressive technique was employed to obtain an "effective" resistance for the heater. This technique consisted of performing a process of known magnitude in the calorimeter and comparing the temperature change induced in this manner with the intrinsic change associated with a calibration. The dissolution of coarse sodium chloride was examined, and Eqs. 1 and 12 were combined to give:

$$R' = \frac{V^2D\ \Delta\theta_{i(\text{soln})}}{q_{\text{soln}}\ \Delta\theta_{i(\text{calib})}} \qquad \text{(Eq. 13)}$$

where R' is the effective resistance, $\Delta\theta_{i(\text{soln})}$ is the intrinsic temperature change associated with dissolution, $q_{(\text{soln})}$ is the heat of solution of sodium chloride, and $\Delta\theta_{i(\text{calib})}$ is the intrinsic temperature change resulting from calibration.

A value of 0.475 ohm was obtained in this manner.

Examination of Temperature Effect on Extrinsic Variation—The applicability of Eq. 10 was tested by examining the extrinsic variation at several temperatures above and below the environmental temperature.

The calorimeter cell was filled with 250 ml of distilled water, cooled slightly to approximately 24°. After assembly of the calorimeter cell and placement in the constant-temperature water bath, stirring was initiated and 30 min was allowed for thermal stabilization. The thermometer was then turned on, and the temperature of the calorimeter contents was recorded with a resolution of 0.0001° at approximately 10-sec intervals.

The external load resistance was applied across the power supply for at least 5 min (30 intervals). After this voltage stabilization, the heater was actuated for approximately 10 sec, during which the voltage across the resistance was measured and recorded. When the heater was turned off, the duration of the heating process was recorded; sufficient time was allowed for stabilization of the extrinsic behavior. This heating procedure was repeated two more times.

After the third calibration was completed, the heater was actuated until the system temperature reached approximately 25°. The system also was altered by securing the sample bulb breaker rod in the depressed position. This action was taken to produce a significant change in the heat capacity of the calorimeter and, thus, to test the sensitivity of calibration.

When the system had stabilized, another three calibrations were subsequently performed at these higher temperatures. Thus, the calorimeter response and extrinsic temperature change were observed at temperatures both above and below the environmental temperature. Figures 5 and 6 show the temperature–time plots for the six processes. The extrinsic temperature change has a positive slope when the temperature is below that of the environment (Fig. 5) and a negative slope when the temperature is above that of the environment (Fig. 6).

Table I—Temperature–Time Output Data for the Investigation of the Wetting of Microcrystalline Cellulose

t[a]	$\theta(t)$	t[a]	$\theta(t)$
1	25.0094	50	25.0344
2	25.0093	51	25.0345
3	25.0093	52	25.0347
4	25.0092	53	25.0348
5	25.0092	54	25.0349
6	25.0092	55	25.0352
7	25.0091	56	25.0353
8	25.0092	57	25.0355
9	25.0091	58	25.0355
10	25.0092	59	25.0358
11	25.0091	60	25.0359
12	25.0091	61	25.0361
13	25.0091	62	25.0362
14	25.0092	63	25.0364
15	25.0093	64	25.0366
16	25.0092	65[b]	25.0373
17	25.0093	66[b]	25.0483
18	25.0094	67[b]	25.0676
19	25.0095	68[b]	25.0809
20	25.0095	69[b]	25.0894
21	25.0096	70[b]	25.0943
22	25.0096	71[b]	25.0976
23	25.0097	72[b]	25.0096
24	25.0099	73[b]	25.1008
25	25.0099	74[b]	25.1017
26	25.0100	75[b]	25.1024
27	25.0101	76[b]	24.1025
28	25.0102	77[b]	25.1028
29	25.0103	78[b]	25.1031
30	25.0104	79[b]	25.1032
31[c]	25.0251	80	25.1034
32[c]	25.0325	81	25.1035
33[c]	25.0326	82	25.1036
34	25.0326	83	25.1037
35	25.0327	84	25.1039
36	25.0327	85	25.1039
37	25.0329	86	25.1040
38	25.0329	87	25.1041
39	25.0330	88	25.1043
40	25.0331	89	25.1044
41	25.0333	90	25.1045
42	25.0334	91	25.1046
43	25.0335	92	25.1048
44	25.0336	93	25.1049
45	25.0338	94	25.1050
46	25.0339	95	25.1051
47	25.0340	96	25.1052
48	25.0342	97	25.1053
49	25.0342	98	25.1055

[a] Time expressed in intervals, where each interval is approximately 10 sec. [b] Time point included in calibration period where $V = 2.035$ v and $D = 10.10$ sec. [c] Time point included in reaction period.

Sample Process Investigation—The wetting of a sample of dried microcrystalline cellulose was examined to demonstrate the application of the differential method of process analysis and the validity of Eq. 11. An accurately weighed quantity of powder was placed in a glass sample bulb and attached to the breaker rod in the calorimeter cell. The cell was filled with 250 ml of distilled water and assembled. After stirring was initiated, 15 min of stabilization was allowed.

When the system appeared to be at thermal equilibrium, the temperature recording was started. After 5 min (30 intervals), the sample bulb was broken. Following another 5 min, during which the external load was applied across the storage battery, a calibration was performed.

Table I contains the thermometer output and calibration data from this experiment.

Data Transformation—The first derivative of the experimental data was approximated by finding the difference between successive temperature recordings. This approximation corresponds to the slope of the temperature–time profile, $\Delta\theta/\Delta t$, at the midpoint of each interval.

The actual data from the first calibration in Fig. 5 are given in Table II, where the transformation was explicitly performed. The entire data associated with Figs. 5 and 6 were transformed in this manner, and the resulting differential values are presented in Fig. 7. Transformed data from the sample wetting process are presented in Fig. 8.

These figures include only $\Delta\theta/\Delta t$ values less than 0.0020°.

Estimation of Parameters—The differential transformation (Figs. 7 and 8) provided a method for determining parameters of the function g_e. The points that should be identified with the reaction periods were clearly distinguished from those belonging to the rating periods. For example, in the first calibration (Table II), the $\Delta\theta/\Delta t$ values at times 1.5–31.5 and 44.5–64.5 were identified as belonging to rating periods a and b (Fig. 7), respectively. The $\Delta\theta/\Delta t$ values at times 32.5–43.5 were considered to be associated with the reaction period.

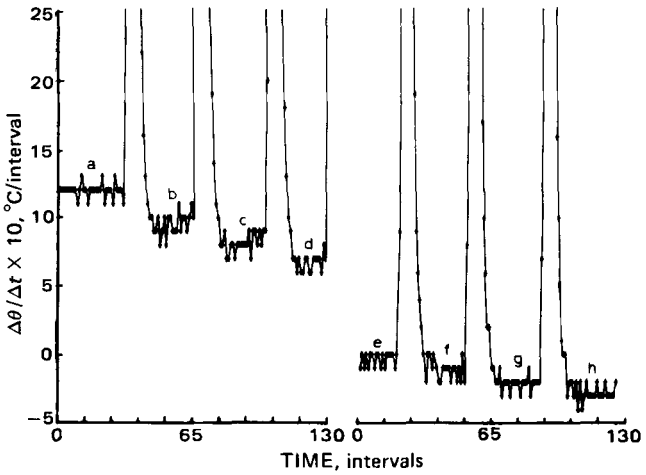

Figure 7—*Differential transformation of temperature–time profiles for calibrations 1–6 of Table I. The rating periods a–h with essentially constant $\Delta\theta/\Delta t$ values are easily distinguished from the reaction periods where these values are considerably greater in magnitude.*

Once identified as such, the entire rating period information from an experiment was used to estimate the parameters of the function g_e. For an investigation where Eq. 10 was employed as the descriptive equation for extrinsic variation, $[\Delta\theta/\Delta t, \theta(t)]$ coordinates from the rating periods were entered into a linear regression analysis to predict B_0 and B_1. When the form of Eq. 11 was employed for g_g, $[\Delta\theta/\Delta t, t, \theta(t)]$ values were entered into a multiple linear regression analysis to predict B_0, B_1, and B_2. In both cases, $\theta(t)$ was taken as the arithmetic mean interval temperature.

Computation of $\Delta\theta_i$—For computational purposes, Eq. 9 can be rewritten as:

$$\Delta\theta_i = \sum_{\substack{\text{reaction}\\ \text{period}}} \left(\frac{\Delta\theta}{\Delta t} - \frac{\Delta\hat{\theta}_e}{\Delta t}\right) \Delta t \qquad \text{(Eq. 14)}$$

where $\Delta\hat{\theta}_e/\Delta t$ is the predicted value of the extrinsic variation during the reaction at each successive time interval midpoint. These predicted values were obtained from the function g_e whose parameters were identified in the previous section. Equation 14 represents the sum of the residuals in the reaction period.

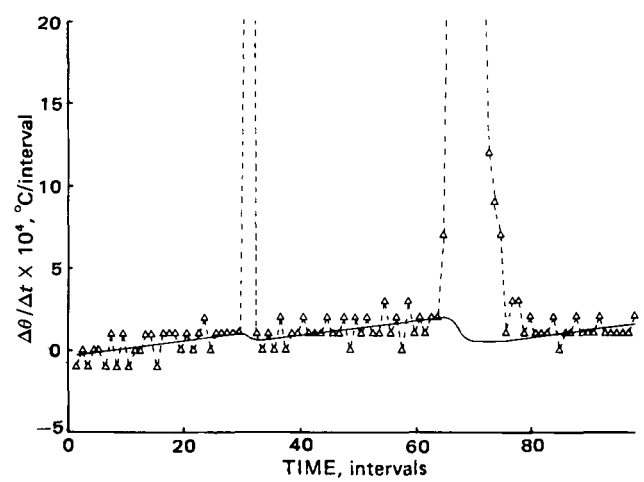

Figure 8—*Differential transformation of temperature–time data in Table II. Key: Δ, actual $\Delta\theta/\Delta t$ values; —, continuous prediction function, $\hat{g}_e$.*

Table II—Transformation of Thermometer Output for Calibration 1 of Fig. 5 and Predicted Extrinsic Variation

t, intervals	$\theta(t)$, °C	t, intervals	$\Delta\theta/\Delta t$, °C/interval	$\Delta\hat{\theta}_e/\Delta t$, °C/interval	t^b, intervals	$\theta(t)$, °C	t, intervals	$\Delta\theta/\Delta t$, °C/interval	$\Delta\hat{\theta}_e/\Delta t^a$, °C/interval
1	24.184	1.5	0.0012	0.00121	34	24.2403	34.5	0.0253	0.00111
2	24.1859	2.5	0.0012	0.00120	35	24.2656	35.5	0.0176	0.00107
3	24.1871	3.5	0.0012	0.00120	36	24.2832	36.5	0.0101	0.00105
4	24.1883	4.5	0.0012	0.00120	37	24.2933	37.5	0.0066	0.00104
5	24.1895	5.5	0.001	0.00120	38	24.2999	38.5	0.0042	0.00103
6	24.1907	6.5	0.0012	0.00120	39	24.3041	39.5	0.0027	0.00102
7	24.1919	7.5	0.0012	0.00120	40	24.3068	40.5	0.0022	0.00102
8	24.1931	8.5	0.0012	0.00119	41	24.3090	41.5	0.0016	0.00102
9	24.1943	9.5	0.0011	0.00119	42	24.3106	42.5	0.0013	0.00101
10	24.1954	10.5	0.0012	0.00119	43	24.3119	43.5	0.0011	0.00101
11	24.1966	11.5	0.0013	0.00119	44	24.3130	44.5	0.0010	0.00101
12	24.1979	12.5	0.0012	0.00119	45	24.3140	45.5	0.0010	0.00101
13	24.1991	13.5	0.0012	0.00119	46	24.3150	46.5	0.0009	0.00101
14	24.2003	14.5	0.0011	0.00118	47	24.3159	47.5	0.0009	0.00101
15	24.2014	15.5	0.0012	0.00118	48	24.3168	48.5	0.0010	0.00101
16	24.2026	16.5	0.0012	0.00118	49	24.3178	49.5	0.0008	0.00101
17	24.2038	17.5	0.0012	0.00118	50	24.3186	50.5	0.0009	0.00100
18	24.2040	18.5	0.0012	0.00118	51	24.3195	51.5	0.0010	0.00100
19	24.2062	19.5	0.0012	0.00118	52	24.3205	52.5	0.0008	0.00100
20	24.2074	20.5	0.0012	0.00117	53	24.3213	53.5	0.0010	0.00100
21	24.2086	21.5	0.0013	0.00117	54	24.3223	54.5	0.0010	0.00100
22	24.2099	22.5	0.0011	0.00117	55	24.3233	55.5	0.0009	0.00100
23	24.2110	23.5	0.0012	0.00117	56	24.3242	56.5	0.0009	0.00100
24	24.2122	24.5	0.0012	0.00117	57	24.3251	57.5	0.0009	0.00099
25	24.2134	25.5	0.0012	0.00116	58	24.3260	58.5	0.0011	0.00099
26	24.2146	26.5	0.0011	0.00116	59	24.3271	59.5	0.0009	0.00099
27	24.2157	27.5	0.0013	0.00116	60	24.3280	60.5	0.0010	0.00099
28	24.2170	28.5	0.0012	0.00116	61	24.3290	61.5	0.0010	0.00099
29	24.2182	29.5	0.0012	0.00116	62	24.3300	62.5	0.0009	0.00099
30	24.2194	30.5	0.0012	0.00116	63	24.3309	63.5	0.0010	0.00099
31	24.2206	31.5	0.0011	0.00115	64	24.3319	64.5	0.0011	0.00099
32	24.2217	32.5	0.0023	0.00115	65	24.330	65.5		
33	24.2240	33.5	0.0163	0.00114		24.3340			

[a] Predicted extrinsic temperature variation at interval midpoint. [b] One interval ≃ 10 sec.

RESULTS AND DISCUSSION

Examination of Extrinsic Variation—Examination of the differential curve in Fig. 7 indicated that temperature was an important independent variable for purposes of characterizing the extrinsic temperature variation. Figure 9 depicts this relationship over the combined temperature range of both calibration experiments. The $\Delta\theta_e/\Delta t$ values used in the construction of this figure were obtained by averaging the last 10 values in each rating period of Fig. 7. These estimates of $d\theta_e/dt$ were plotted at the final temperature in the period.

Over a relatively large temperature range (0.2°), Eq. 10 appeared to describe the data reasonably well. However, there was evidence that this form of g_e was not satisfactory during the rating period.

Solution of Eq. 10 in the time domain results in an expression containing an exponentially decreasing term. The absolute values of $d\theta_e/dt$ within any period should always decrease with time. This behavior clearly did not occur in Fig. 7 where $\Delta\theta_e/\Delta t$ values are quite constant. In periods b, c, and d, there actually appears to be an increasing trend.

The increasing trend in the rating periods is not obvious because of the short duration of these periods. It is somewhat more discernible in the extrinsic periods of Fig. 8. In fact, having established that temperature is an important independent variable, the extrinsic behavior in a typical experiment such as the one represented in Fig. 8 should be scrutinized. It is in this scrutiny that several fallacies of the generally employed methods of analysis can be recognized.

The method of rating period extrapolations is based upon the assumption that $d\theta_e/dt$ is a constant throughout the rating period. In Fig. 8, the values of $\Delta\theta_e/\Delta t$ tend to increase slightly in each period throughout the experiment, indicating that the temperature is not a first-order function of time alone.

A somewhat philosophical consequence of the actual nonlinearity of the extrinsic variation becomes important when the method of rating period extrapolations is employed. Assuming that the rating periods provide information about the nature of the system, it seems wise to collect as much information as possible, *i.e.*, to use a relatively long rating period. However, the more information obtained, the less acceptable is the linear hypothesis. The two extreme alternatives that arise from this contradiction are both unacceptable: extrapolation of a "poor" line based on a lot of information and extrapolation of a "good" line based on very little information. The acceptable linear fit obtained by using a short rating period should not be construed as a valid basis for extrapolation of the line over a relatively long reaction period.

A good general rule to follow when using this empirical method is to consider rating periods of a duration equal to or greater than the process itself. If the linear approximation is still reasonable, the method can be employed with negligible error.

The alternative method presented in the theoretical background sec-

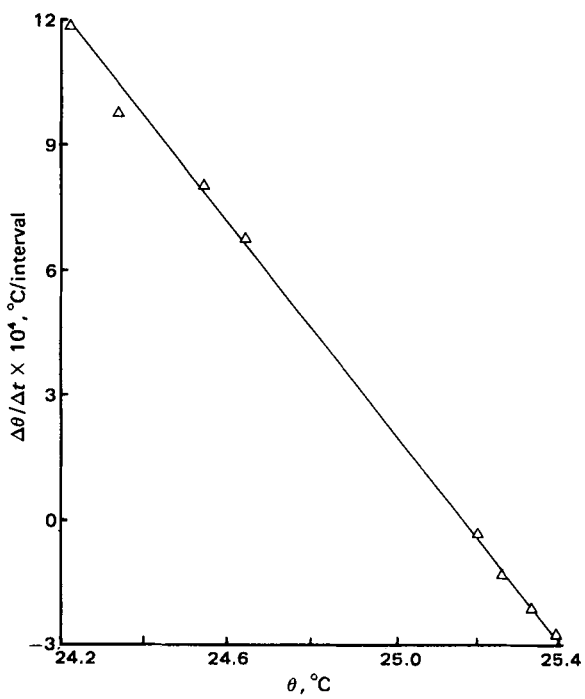

Figure 9—*Relationship between system temperature, θ, and extrinsic temperature variation, Δθ/Δt.*

Table III—Heat Capacity Values Determined from the Calibration Processes of Fig. 7 and Table II

Calibration	$-q$, cal	$\Delta\theta_i$, °C	C, cal/deg
1	21.732	0.07825	277.7
2	20.984	0.07563	277.4
3	21.046	0.07642	275.4
4	20.984	0.07145	293.7
5	20.860	0.07175	290.7
6	20.942	0.07143	293.2

tion represents an exact procedure when Eq. 10 describes the extrinsic variation; however, this method should not be used perfunctorily. The positive values for $d\theta_e/dt$ in Fig. 8 indicate a system whose temperature is below environmental temperatures. Therefore, any exothermic process should result in a postprocess rating period whose $d\theta/dt$ values are lower than the preprocess period. Both the wetting and calibration processes in Fig. 8 are exothermic, but neither reaction is followed by a decrease in $d\theta_e/dt$.

On the basis of these observations, the form used for g_e was that presented in Eq. 10: a function of time and temperature. The solid line in Fig. 8 was constructed from values generated through the following equation:

$$\frac{\Delta\hat{\theta}_e}{\Delta t} = 0.07509 - (4.9776 \times 10^{-6})t - (3.0042 \times 10^{-3})\theta(t) \quad \text{(Eq. 15)}$$

This equation was predicted using multiple least-squares regression based on $[\Delta\theta/\Delta t, t, \theta(t)]$ coordinates at time intervals 1.5–29.5, 33.5–63.5, and 80.5–97.5. The line appears to describe the experimental data, including the increasing trends within each period.

Table II also includes $\Delta\hat{\theta}_e/\Delta t$ values predicted from an equation of the form of Eq. 11 for the first calibration process of Figs. 5 and 7. These values compare well with the observed $\Delta\theta/\Delta t$ values in rating periods a and b.

There is no reason why an equation of the form of Eq. 11 cannot be used routinely. If either time or temperature proves to be negligible, the coefficients will reflect that fact.

Computation of $\Delta\theta_i$—Equation 14 was used to compute the intrinsic temperature changes associated with all processes investigated.

Table III contains the results of the six successive calibrations. The closeness of the heat capacity measurement in each set of determinations is reasonable considering the error associated with calculation of $-q$ from Eq. 12. Fixing the breaker rod in the depressed position resulted in a heat capacity increase of approximately 16 cal/°C.

For the wetting of the solid represented in Table I, intrinsic temperature changes of 0.02200 and 0.06546° were obtained for the wetting and calibration processes, respectively. A heat capacity of 321.15 cal/°C and a heat of wetting of −7.07 cal were obtained from these data.

SUMMARY AND CONCLUSIONS

Determination of the process-dependent temperature change in any nonisothermal calorimeter is predicated on a mathematical characterization of the process-independent or extrinsic temperature variation. With respect to the most frequently employed methods of data analysis, the following points should be emphasized:

1. The method of linear extrapolations is based, implicitly, on the assumption that the rating periods can be described by a function of time alone. When employing this method, the assumption should be critically tested by an examination of rating periods equal to or, preferably, greater in duration than the process itself.

2. More sophisticated methods are generally based on a form of Newton's law of cooling. When employing these methods, the actual extrinsic experimental behavior must be described adequately by a function of temperature alone.

The experiment presented can be used to assess the influence of temperature on the extrinsic variation of any calorimeter. Through an experiment of this type and a close investigation of a typical process, a rational decision can be made regarding the method used to compute the intrinsic change. In many cases, a conventional method is satisfactory; however, no method should be employed indiscriminately. For example, the described calorimeter required a first-order function of time and temperature to describe the extrinsic variation.

In lieu of an examination of each calorimetric experiment, it is recommended that a first-order function of time and temperature be used routinely to characterize a system's extrinsic variation. If either variable in this expression is insignificant, the function automatically reduces to one of those previously described.

The digital transformation (first-derivative approximation) method outlined in this paper has some benefits that support its use in conjunction with the chosen function for the extrinsic variation: (*a*) easy identification of the extrinsic periods, (*b*) compatibility with extrinsic variation functions because the data are in the form necessary to employ linear regression analysis of the actual data, and (*c*) computational procedures that are easily programmable.

Of course, greater confidence is associated with the results when a rigorous approach is used to describe the system. In this case, the proposed method actually permits the investigation of many processes with small thermal effects that may require a relatively long time to reach completion.

REFERENCES

(1) J. J. Chessick and A. C. Zettlemoyer, *Adv. Cat.*, **XI**, 263 (1959).

(2) H. Matsumaru, *Pharm. Soc. Jpn.*, **79**, 63 (1959).

(3) *Ibid.*, **79**, 64 (1959).

(4) H. Nogami, J. Hasegawa, and Y. Nakai, *Chem. Pharm. Bull.*, **7**, 331 (1959).

(5) *Ibid.*, **7**, 337 (1959).

(6) Y. Nakai and Y. Kubo, *Chem. Pharm. Bull.*, **8**, 634 (1960).

(7) Y. Nakai, *ibid.*, **8**, 641 (1960).

(8) J. M. Sturtevant, in "Physical Methods of Organic Chemistry," vol. 1, A. Weissberger, Ed., Interscience, New York, N.Y., 1945, pp. 335–344.

ACKNOWLEDGMENTS

Supported in part by a Biomedical Research Grant, National Institutes of Health.

The authors acknowledge the technical assistance of Mr. T. McDaniels throughout the design, construction, and modification of the calorimeter.

R. G. Hollenbeck is an American Foundation for Pharmaceutical Education Fellow.

Application of Immersional Calorimetry to Investigation of Solid–Liquid Interactions: Microcrystalline Cellulose–Water System

R. GARY HOLLENBECK *, GARNET E. PECK, and DANE O. KILDSIG ˣ

Received July 29, 1977, from the *Department of Industrial and Physical Pharmacy, School of Pharmacy and Pharmacal Sciences, Purdue University, West Lafayette, IN 47907.* Accepted for publication March 23, 1978. *Present address: School of Pharmacy, University of Maryland, Baltimore, MD 21201.

Abstract □ A comprehensive characterization of the specific solid–liquid interaction for microcrystalline cellulose and water is presented. The procedure consisted of a conjoint vapor adsorption and immersional wetting experiment. The following information was obtained with respect to the solid. Estimates of the total surface area (138 m^2/g) and the external surface (9.2 m^2/g) were calculated from the adsorption and immersion data, respectively. Existence of an energetically homogeneous surface was verified by a linear decrease in the heat of immersion of samples containing adsorbed moisture approximately up to monolayer capacity. Integral and differential free energy, enthalpy, and entropy changes accompanying the adsorption process were calculated, and a lack of swelling was substantiated by comparison with a similar study of cellulose fibers. Immersional hysteresis was observed, and its magnitude suggested that sorption hysteresis was of enthalpic as well as entropic origin. The experimental method is potentially valuable for routine characterization of hydrophilic powders.

Keyphrases □ Solid–liquid interactions—microcrystalline cellulose–water system characterized, immersional calorimetry–vapor adsorption procedure □ Cellulose, microcrystalline–water system—solid–liquid interactions characterized by immersional calorimetry–vapor adsorption procedure □ Calorimetry, immersional—combined with vapor adsorption procedure to characterize solid–liquid interactions of microcrystalline cellulose–water system □ Adsorption, vapor—combined with immersional calorimetry procedure to characterize solid–liquid interactions of microcrystalline cellulose–water system

Most problems encountered in the production and performance of solid and liquid dosage forms can be resolved in terms of solid–liquid interactions. The basis for an experimental characterization of these interactions (1) involved the confluence of immersional calorimetry and vapor adsorption. The combination of these two powerful techniques has been used to describe the wetting of hydrophilic and hydrophobic solids (1–12).

This study represents a comprehensive investigation of the specific solid–liquid interaction for microcrystalline cellulose and water.

THEORETICAL

The thermodynamics of wetting deal with the entire spectrum of solid–liquid interactions, ranging from the adsorption of a small amount of vapor by a relatively large amount of solid to the immersion of a small quantity of solid into a large amount of liquid. Both the adsorption and immersion processes involve the same fundamental interactions; they differ only in the relative amounts of each component. An experimental investigation involving both of these processes can provide a complete characterization of the mutual affinity of the solid and liquid.

Free Energy Changes—At constant temperature, the net integral free energy change, ΔF, associated with the adsorption of a volatile liquid (Component 1) on a nonvolatile solid (Component 2) is given as:

$$\Delta F = \overline{\Delta F_1} n_1 + \overline{\Delta F_2} n_2 \qquad \text{(Eq. 1)}$$

where $\overline{\Delta F_1}$ and $\overline{\Delta F_2}$ are the partial molal free energy changes of the volatile and nonvolatile components, respectively; and n_1 and n_2 are the numbers of moles of each, respectively.

Since the adsorption process is most often regarded with respect to the thermodynamic characteristics of the volatile component, $\overline{\Delta F_1}$ is referred to simply as the differential free energy change of adsorption. The equilibrium adsorption isotherm provides the information necessary to determine both the differential and integral free energy changes.

The differential free energy change is given as the difference between the chemical potential of liquid in the adsorbed state and pure liquid:

$$\overline{\Delta F_1} = u_1 - u_1^0 = RT \ln P/P_0 \qquad \text{(Eq. 2)}$$

where u_1 and u_1^0 are the chemical potentials of the adsorbate and pure liquid, respectively; P is the actual vapor pressure; P_0 is the vapor pressure of pure liquid at experimental temperature T; and R is the gas constant.

With a form of the Gibbs–Duhem relation:

$$\overline{\Delta F_2} = \int -(n_1/n_2)\, d\, \overline{\Delta F_1} \qquad \text{(Eq. 3)}$$

an expression for the integral free energy change can be obtained. By substitution of the partial molal equalities of Eqs. 2 and 3 into Eq. 1, the integral free energy change is obtained as:

$$\Delta F = n_1 RT \ln P/P_0 - RT \int n_1\, d \ln P/P_0 \qquad \text{(Eq. 4)}$$

Equations 2 and 4 were presented explicitly by Dole and McLaren (13).

Evaluation of the integral on the right-hand side of Eq. 4 can be performed graphically from a plot of n_1P_0/P *versus* P/P_0, recognizing the identity:

$$-RT \int_0^{P/P_0} n_1\, d \ln \left(\frac{P}{P_0}\right) \equiv -RT \int_0^{P/P_0} \frac{n_1 P_0}{P}\, d\left(\frac{P}{P_0}\right) \qquad \text{(Eq. 5)}$$

Errors associated with low pressure extrapolation to $P = 0$ are smaller with this technique than with a plot of n_1 *versus* $\ln P/P_0$.

The differential free energy change has units of energy per mole of adsorbate, because it refers to the volatile component. The integral free energy change simply has units of energy, because the entire process is specified for a certain number of moles of each component.

Enthalpy Changes—Figure 1 is a pictorial representation of the interrelationship between the various enthalpy changes associated with the wetting of a solid by a liquid. Step 1 represents the immersion of a dry solid into a large quantity of liquid. The enthalpy change associated with this process is referred to as the "heat of immersion of the dry solid" and is designated $\Delta H_i(S/L)$, the parenthetical S/L indicating the process of going from a clean solid to a solid–liquid interface (3).

Step 4 also represents an immersional process, only now the solid contains adsorbed moisture. The heat of immersion of this wet solid is designated $\Delta H_i(S_f/L)$, where the f indicates that the solid possesses a "film" of adsorbed liquid (3). The value of $\Delta H_i(S_f/L)$ depends on the number of moles of water adsorbed, n_1.

The final states of Steps 1 and 4 are identical, and the enthalpy change associated with Step 1 is clearly equivalent to the sum of Steps 2–4:

$$\Delta H_i(S/L) = n_1\lambda + \Delta H(\text{ads}) + \Delta H_i(S_f/L) \qquad \text{(Eq. 6)}$$

where λ is the molar heat of vaporization of the liquid and $\Delta H(\text{ads})$ is the heat of adsorption.

The net integral enthalpy change associated with the adsorption process, ΔH, is the heat change in excess of the normal condensation of the liquid:

$$\Delta H = \Delta H(\text{ads}) - (-n_1\lambda) \qquad \text{(Eq. 7)}$$

Therefore, from Eq. 6:

$$\Delta H = \Delta H_i(S/L) - \Delta H_i(S_f/L) \qquad \text{(Eq. 8)}$$

0022-3549/78/1100-1599$01.00/0
© 1978, American Pharmaceutical Association

Table I—Initial Conditions of Relative Humidity Chambers at 25°

Chamber	H_2SO_4, % (w/w)	Relative Humidity, %
1	68.79	5.75
2	63.87	10.75
3	59.16	18.00
4	55.30	24.75
5	52.20	30.50
6	43.48	48.75
7	33.16	70.00
8	25.44	81.50
9	17.61	90.25
10	—	100.00

The integral enthalpy change once again has units of energy; by measuring the heats of immersion of solids with varying moisture contents, the entire range of ΔH values can be obtained.

The partial molal enthalpy change with respect to the volatile component, $\overline{\Delta H_1}$, can easily be obtained by estimating the slope of the ΔH *versus* n_1 curve, where the data have been normalized for a constant amount of solid. This thermodynamic quantity is often referred to as the differential heat of adsorption and has units of energy per mole of adsorbate.

Where swelling of the solid occurs, the integral and differential enthalpies of adsorption calculated through an immersional procedure are influenced by the endothermic swelling term. The effect is a decrease in both thermodynamic quantities.

Entropy Changes—Both the integral and differential entropy changes can be obtained from the defining equations once the other thermodynamic variables are determined:

$$\Delta S = (\Delta H - \Delta F)/T \qquad \text{(Eq. 9)}$$

$$\overline{\Delta S_1} = (\overline{\Delta H_1} - \overline{\Delta F_1})/T \qquad \text{(Eq. 10)}$$

Surface Area Analysis—Both adsorption and immersion data can be used to estimate a surface area relative to the solid. In adsorption studies, the surface area calculated is the area accessible to adsorption by the adsorbate. In an immersion study, the area represents the area of a film of liquid on the solid particle.

The constant-temperature adsorption data are generally analyzed using the linear form of the Brunauer, Emmett, and Teller (BET) equation (14, 15):

$$\frac{P/P_0}{v(1 - P/P_0)} = \frac{1}{cv_m} + \frac{(c-1)}{cv_m}(P/P_0) \qquad \text{(Eq. 11)}$$

where P/P_0 is the relative vapor pressure, v is the amount of gas adsorbed at P/P_0, and v_m and c are parameters of the equation.

The value of v_m is used as an estimate of the monolayer capacity, so the solid surface area can be calculated from the known area of one adsorbate molecule. In these experiments, values of 16.2 and 12.5 A^2 were used as the molecular areas of nitrogen and water, respectively.

The parameter c is related by theory to the average energy of adsorption:

$$c = e^{-(\Delta E/RT)} = e^{-(E_1 - E_L)} \qquad \text{(Eq. 12)}$$

where E is the net energy of adsorption, E_1 is the energy of adsorption of the first layer of adsorbate, and E_L is the energy of liquefaction of the adsorbate.

A second estimate of the surface area can be obtained through application of the "absolute" method of Harkins and Jura (16). This method is based on the immersion of samples equilibrated at $P/P_0 = 1$. These samples are assumed to be covered with liquid to the extent that the film-covered surface has an enthalpy not unlike that of pure liquid. Therefore, the immersion of the film-covered sample results in the release of a quantity of heat directly proportional to the surface area of the film destroyed.

From surface tension measurements, the heat content of pure liquid water was determined to be 118 ergs/cm^2. By using the heat of immersion of the solid equilibrated at 100% relative humidity (RH), the surface area, A, is given by:

$$A = \frac{\Delta H_i(S_f/L)^*}{118 \text{ ergs/cm}^2} \qquad \text{(Eq. 13)}$$

where $\Delta H_i(S_f/L)^*$ is the heat of immersion of the sample equilibrated at 100% RH expressed in ergs per amount of solid. The surface area obtained in this manner is an estimate of the "external" surface area of the solid material since the capillaries and some intra-aggregate spaces are filled with water.

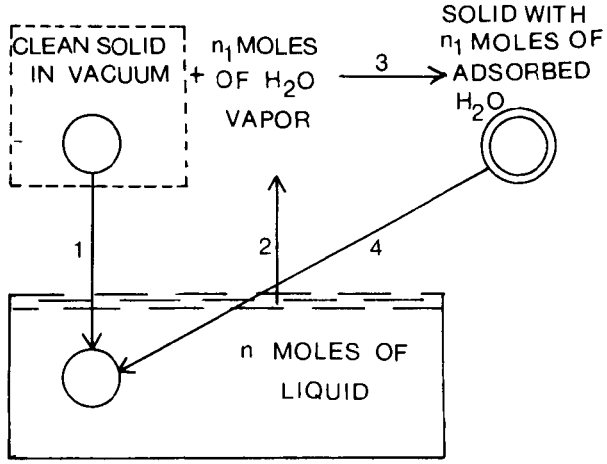

Figure 1—*Relationship between adsorption and immersion (adapted from Ref. 3).*

EXPERIMENTAL

Microcrystalline cellulose[1], dried at approximately 70° in a vacuum oven (= 0.1 mm Hg) for 24 hr, was used as the starting material in all experiments. The average moisture content of the dried material was measured gravimetrically by further drying at 100° and determined to be about 0.2% on a dry weight basis. This value was based on two independent determinations; the solid turned brown at elevated temperature (100°).

A water vapor sorption study was performed to obtain a complete adsorption–desorption isotherm as well as to generate samples with varying moisture contents. Equilibrated samples were subsequently used in an immersional study.

For comparative purposes, a low pressure nitrogen adsorption isotherm was also obtained and analyzed as an independent estimate of the surface area.

Water Vapor Sorption—Relative humidity chambers, varying from 5 to 100% RH, were prepared. Glass[2] containers, normally used as desiccators, were employed as chambers; the relative humidity was controlled by using sulfuric acid solutions of varying concentration, based upon the relationship established by Stokes and Robinson (17). Actual concentrations of sulfuric acid were determined by titrating aliquots of the final solutions with standardized sodium hydroxide. Table I contains the initial conditions obtained for each chamber.

Water adsorption was followed by a simple gravimetric method. Two previously weighed containers were filled with dry powder, weighed, and placed in each chamber. For these experiments, 60 × 15-mm petri dish[3] tops were used as containers.

All weighings were performed on an analytical balance[4] with a resolution of ±0.1 mg. Initial sample weights, from approximately 4.5 to 7.0 g, were determined by difference. Subsequent weighings were made at 3, 4, and 7 days. Humidity chambers were stored in a constant-temperature room maintained at 25 ± 0.5°.

Desorption studies were performed in essentially the same manner with samples equilibrated at 100% RH for 1 week. Weight determinations were made at 5, 7, and 8 days.

Nitrogen Adsorption—A commercially available apparatus[5] was employed to obtain a nitrogen adsorption isotherm at low relative pressures. The microcrystalline cellulose sample was degassed until the rate of pressure increase in the closed system (not exposed to vacuum) was less than 0.0001 mm Hg/min at room temperature. Adsorption data were generated at 77 °K by sequential addition in such a manner that six data points were obtained in the relative pressure range of 0.05–0.35.

Aqueous Immersional Calorimetry—Heats of immersion of mi-

[1] Avicel pH 101, FMC Corp., Marcus Hook, Pa.
[2] Pyrex.
[3] Kimax, Owens-Illinois, Toledo, Ohio.
[4] Mettler H18 analytical balance, Mettler Instrument Corp., Princeton, N.J.
[5] Orr surface area–pore volume analyzer, model 2100, Micromeretics Instrument Co., Norcross, Ga.

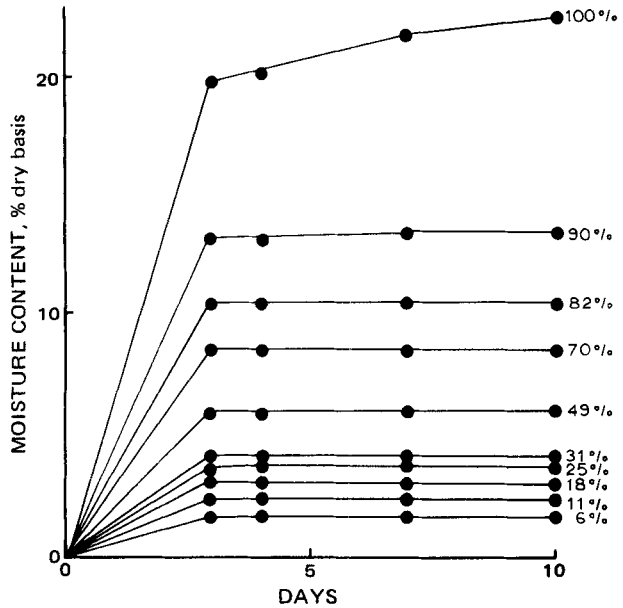

Figure 2—*Adsorption of water by microcrystalline cellulose at various relative humidities.*

crocrystalline cellulose containing various amounts of adsorbed water and water remaining after the desorption process were determined in a nonisothermal calorimeter (18). The design of this calorimeter and aspects of its operation were presented previously (19).

A thin-walled glass sample bulb was tared and partially filled with powder equilibrated under one of the previously described conditions. The weight of the sample was obtained by the difference between the filled and empty sample bulbs.

The calorimeter cell was filled with an accurately measured quantity of distilled water (either 200 or 250 ml), and the entire unit was assembled. Stirring was initiated, and the temperature of the calorimeter contents, θ, was adjusted to approximately 25° by actuation of the calibration heater.

Thermal equilibration of the system was assumed complete when the observed $\Delta\theta/\Delta t$ values were not greater than ±0.0002°/interval. (The digital thermometer reports the temperature at 10-sec intervals when operated at a resolution of 0.0001°.) After stabilization, the recorder was turned on and a preprocess rating period of at least 5 min (30 intervals) was allowed. The sample bulb was then fractured by a rapid depression and release of the beaker rod.

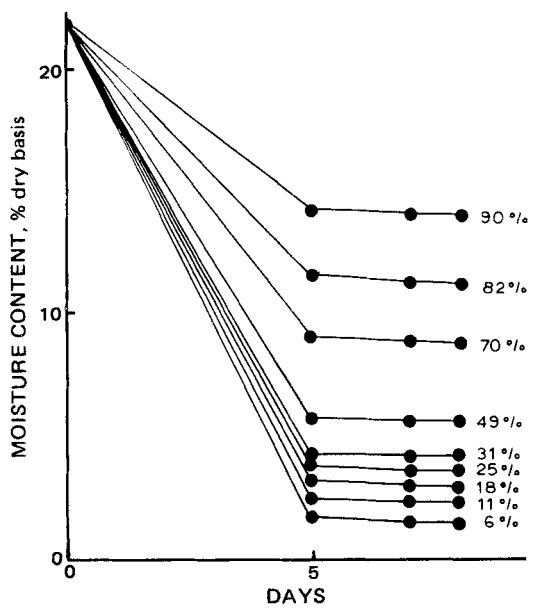

Figure 3—*Desorption of saturated microcrystalline cellulose at various relative humidities.*

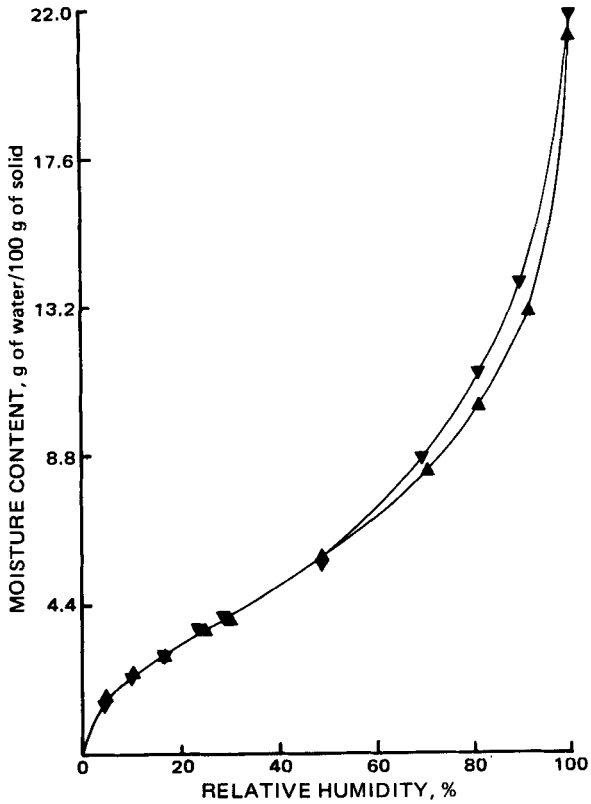

Figure 4—*Water vapor sorption isotherm for microcrystalline cellulose at 25°. Key: ▲, adsorption; and ▼, desorption.*

During the 5 min allowed after process initiation, the calibration heater power supply was stabilized by discharge through a 3-ohm external resistance circuit. A calibration was then accomplished by an actuation of the resistance heater in the calorimeter cell for approximately 10 sec, during which the voltage across the heater was measured. After termination of the heating process, the duration of the actuation was recorded.

A 5-min period was allowed before termination of the experiment. This procedure was employed for all samples.

Intrinsic temperature changes for the wetting and calibration processes were computed using the differential transformation method described previously (19). The heat capacity used to compute the heats of wetting was obtained by averaging the results of all calibrations within the same set of experiments. The accuracy of all heats of wetting is related to the accuracy of the heat capacity determination for the system (see Table III, Ref. 19). The accuracy of the heat capacity determinations is approximately ±0.6%.

Immersional experiments were performed in three sets; samples containing adsorbed water taken after 3 and 7 days of equilibration and samples containing water remaining after the 8-day desorption process.

RESULTS AND DISCUSSION

Water Vapor Sorption—Figures 2 and 3 represent the adsorption and desorption of water by dry microcrystalline cellulose and saturated microcrystalline cellulose, respectively. These processes occurred relatively fast, reaching virtual completion in 5 days or less for all samples, except the adsorption of water at 100% RH.

The equilibration adsorption–desorption isotherm is presented in Fig. 4. This isotherm is clearly a Type II, with a slight degree of hysteresis in the upper pressure region. The sorption hysteresis is shown for microcrystalline cellulose is classical for cellulosics, although its magnitude is considerably less than that for standard cellulose (11).

The etiology of sorption hysteresis in these systems was discussed previously (9, 11, 20–22). Gregg (22) stated that, in many cases, the phenomenon is due to a very slow rate of equilibrium attainment and, hence, is actually an artifact. His view considers that the desorption branch represents a kind of supersaturation effect and, if a long enough time is allowed, the hysteresis will disappear. There is some evidence in

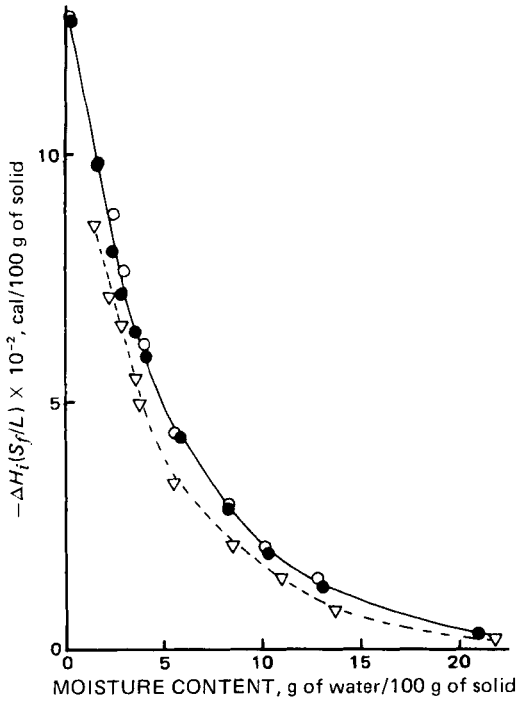

Figure 5—*Heats of wetting of microcrystalline cellulose containing various amounts of adsorbed and desorbed water. Key:* ○, *samples equilibrated for 3 days at varying humidity (adsorption);* ●, *samples equilibrated for 7 days at varying humidity (adsorption); and* ▽, *samples equilibrated for 8 days at varying humidity (desorption).*

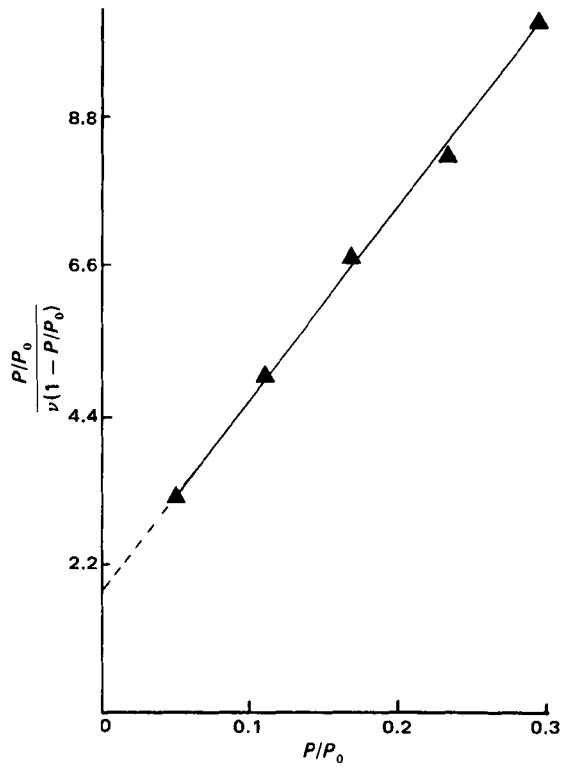

Figure 6—*BET plot for water vapor adsorption on microcrystalline cellulose where* ν = *grams of water per gram of solid.*

this work with microcrystalline cellulose that the system may not be at equilibrium. At high relative humidities, the adsorption and desorption moisture contents may indeed be approaching each other at a very slow rate.

However, other thermodynamic evidence indicates that the hysteresis may be real. When the system is thermodynamically stable, the sorption hysteresis reflects a difference in the free energy of the two systems at the same relative pressure. It follows that the hysteresis may be due to a difference in specific surface area (irreversible swelling), solid–liquid bonding strengths (enthalpy effect), molecular ordering (entropy), or a combination of these effects. Therefore, a complete thermodynamic analysis can help identify the origin of the hysteresis. Such an analysis is presented in the following sections.

Heats of Immersion—Figure 5 represents the immersional isotherm for microcrystalline cellulose containing various amounts of adsorbed water and water remaining after the desorption process.

The initial region of the curve for solid containing adsorbed water demonstrates a nearly linear decrease in the heat of wetting as the moisture content increases. Zettlemoyer *et al.* (8) considered this type of relationship to be indicative of an energetically homogeneous surface. The heat evolved on wetting appears to depend simply on the amount of bare surface present. If there were a distribution of energy sites on the surface of the solid, the high energy sites would preferentially adsorb vapor molecules and the heat of immersion would not be proportional to the amount of surface but, instead, would depend on which sites were occupied.

The desorbed samples had heats of wetting consistently lower than the samples containing an equivalent amount of adsorbed water. Thus, a hysteresis of the immersional isotherm also exists.

Argue and Maass (20) also found an immersional hysteresis in the wetting of cellulose samples, but it was the opposite of that in Fig. 5; their desorbed samples exhibited the greater heats of wetting. Argue and Maass (20) concluded that this behavior was characteristic of a solid that swells irreversibly when immersed in water.

Swelling is an endothermic process involving the rupture of some solid–solid bonds. Their solid samples containing adsorbed water exhibited a lower heat of immersion than expected, because some of the energy released in wetting was consumed in the swelling process. Alternatively, the heat of immersion of solid with water remaining after desorption did not involve this endothermic term since the solid already had the opportunity to swell during its long exposure to 100% RH.

After desorption, the standard cellulose employed by Argue and Maass (20) had a higher specific surface area than the solid containing adsorbed water. This information is important in identifying the origin of sorption hysteresis.

Microcrystalline cellulose clearly does not show irreversible swelling. The sorption hysteresis for this solid cannot be explained on the basis of specific surface area changes.

Morrison and Dzieciuch (11) found no differences between the heats of wetting of adsorbed and partially desorbed cellulose samples containing equivalent amounts of water. The coincidental wetting curves indicate either no swelling or completely reversible swelling. In either event, since the enthalpies are the same for equivalent moisture contents, the sorption hysteresis is of entropic origin.

The observed hysteresis in the present study represents the final possibility: lower heats of wetting for the partially desorbed samples. Dunford and Morrison (9) found a similar, though smaller, hysteresis in their study involving silk fibroin. These authors remarked: "At equal moisture contents, water is more tightly held on the desorption branch. Therefore, we would expect the heat of wetting to be less for the desorption side if there are no phenomena occurring other than pure adsorption." Actually, this statement involves some circular reasoning; it may be better to emphasize that this type of immersional hysteresis stands as evidence that the water is "held" more tightly on the desorption branch of the isotherm than it is on the adsorption branch. For the microcrystalline cellulose–water system, the strength of the solid–liquid interaction plays a role in the production of sorption hysteresis. In a later section, the extent to which this role accounts for the entire phenomenon will be assessed by observing the relative changes in the enthalpy and entropy values.

Surface Area Analysis—Based on the information collected in this study, three independent estimates of the surface area of microcrystalline cellulose were obtained.

An analysis of the water vapor adsorption data indicated that the BET theory (14, 15) could be applied in the range of 5–30% RH. Figure 6 depicts the low pressure adsorption data when plotted using the linear form of the BET equation (Eq. 11). The monolayer capacity of 0.0330 g of water/g of solid obtained in this manner corresponds to a surface area of 138 m^2/g. A value of 149 m^2/g was obtained by Nakai *et al.* (23) in a similar study.

Figure 7 represents the results of the nitrogen adsorption study. With the BET theory for these data, a surface area of 1.5 m^2/g was estimated. Surface area measurements of 11.2 and 1.0 m^2/g were reported for mi-

Table II—Calculated Thermodynamic Properties for the Adsorption of Water on Microcrystalline Cellulose

n_1[a], moles of Water	P/P_0	$-\Delta H^*$, cal	$-\Delta F^*$, cal	$-\Delta S^*$, eu	$-\Delta\overline{H}$, cal/mole of Water	$-\Delta\overline{F}_1$, cal/mole of Water	$-\Delta\overline{S}$, eu/mole of Water
0.01	—	40	—	—	3750	—	—
0.02	—	75	—	—	3500	—	—
0.03	—	110	—	—	3500	—	—
0.04	—	145	—	—	3500	—	—
0.05	0.0216	180	147.2	0.11	3500	2271	4.12
0.06	0.0276	215	169.2	0.15	3500	2126	4.61
0.07	0.0343	250	190.0	0.20	3500	1997	5.04
0.08	0.0419	285	209.1	0.26	3500	1879	5.44
0.09	0.505	320	227.4	0.31	3500	1768	5.81
0.10	0.0602	355	244.6	0.37	3500	1664	6.16
0.11	0.075	390	260.6	0.43	3500	1534	6.60
0.12	0.088	425	275.4	0.50	3500	1439	6.92
0.13	0.105	460	289.3	0.57	3500	1335	7.27
0.14	0.120	495	302.3	0.65	3500	1255	7.53
0.15	0.135	530	314.5	0.72	3250	1186	8.32
0.16	0.152	560	326.0	0.79	3000	1115	6.33
0.17	0.170	590	336.8	0.85	3000	1049	6.55
0.18	0.195	620	347.0	0.92	2750	968	5.98
0.19	0.212	645	356.4	0.97	2400	918	4.97
0.20	0.235	668	365.2	1.02	2325	857	4.93
0.22	0.282	713	381.4	1.11	1925	750	3.94
0.24	0.330	745	395.5	1.17	1600	656	3.17
0.26	0.370	777	407.9	1.24	1575	589	3.31
0.28	0.410	808	419.1	1.31	1525	528	3.35
0.30	0.445	838	429.1	1.37	1450	479	3.26
0.32	0.480	866	438.3	1.44	1375	435	3.15
0.34	0.512	893	446.6	1.50	1275	396	2.95
0.36	0.542	917	454.2	1.55	1175	363	2.72
0.38	0.575	940	461.1	1.61	1150	328	2.76
0.40	0.605	963	467.3	1.66	1075	298	2.61
0.42	0.635	983	472.9	1.71	975	269	2.37
0.44	0.665	1002	478.1	1.76	925	242	2.29
0.46	0.690	1020	482.7	1.80	900	220	2.28
0.48	0.715	1038	486.9	1.85	900	199	2.35
0.50	0.738	1056	490.6	1.90	805	180	2.10
0.60	0.835	1124	504.9	2.08	560	107	1.52
0.70	0.897	1168	5i3.4	2.20	370	64	1.03
0.80	0.935	1198	518.6	2.28	260	40	0.74
0.90	0.967	1220	521.5	2.34	145	20	0.42
1.00	0.987	1237	523.0	2.40	—	—	—

[a] With respect to 100 g of solid.

crocrystalline cellulose based on similar nitrogen adsorption studies (23, 24).

The difference between the size of the nitrogen and water molecules is not sufficient to account for the monumental difference observed in the results of these two methods. Young and Healey (6) observed a similar phenomenon in adsorption studies on asbestos. They showed that the source of the difference between nitrogen and water vapor adsorption studies is associated with the difficulty in removing water from a solid where it is held by strong capillary and adsorption forces. Residual water, which is likely a solid at the 77 °K used in the nitrogen adsorption study, occludes a significant amount of surface in the nitrogen study. In this sense, the surface area values determined should be quite sensitive to the sample pretreatment, so the variation in reported values is understandable.

It may be considered from this observation that nitrogen adsorption provides an estimate of the "external" area of the solid.

As indicated under *Theoretical*, the immersional data provide another estimate of the external area of the film-covered solid. A value for $\Delta H_i(S_fL)^*$ of 26 cal/100 g of solid was obtained from Fig. 5. With Eq. 13, a value of 9.2 m^2/g was obtained for the area of microcrystalline cellulose.

Microcrystalline cellulose aggregates into clusters during spray drying (25). The low pressure analysis represented by the BET analysis provides an estimate of the total surface area of the microcrystals. Conversely, at the high relative moisture pressures used in the method of Harkins and Jura (16), the "internal" space of these aggregates is filled with water.

Following the analysis of Zettlemoyer *et al.* (8), the total surface of the aggregates is then 140–280 m^2/g. The upper limit of this range comes from the consideration that if one layer of adsorbed water molecules occupies the space between two close layers of solid, the calculated surface area (approximately 140 m^2/g) is actually only one-half of the total surface area. Also, considering an estimate of 10 m^2/g for the external area, it appears that the internal surface area is 130–270 m^2/g.

Thermodynamics of Adsorption—The smooth adsorption isotherm in Fig. 4 was used to calculate the differential, $\Delta\overline{F}_1$, and integral, ΔF, free energy changes associated with the adsorption of water by microcrystalline cellulose using Eqs. 2 and 4. The first two columns of Table II represent the coordinate moisture content and partial pressure values chosen at regular intervals from the adsorption branch of the isotherm in Fig. 4. The calculated integral and differential free energies are found in columns 4 and 7 of Table II, respectively.

The integral and differential enthalpy changes associated with adsorption were determined from the data in Fig. 5. An estimate of 1300 cal/100 g of solid was obtained for $\Delta H_i(SL)$ by extrapolation of the linear portion of the immersional isotherm to zero moisture content. The integral enthalpy change (column 3 of Table II) was calculated from Eq. 8 by choosing $\Delta H_i(S_fL)$ values from the smooth curve of Fig. 5 at each value for n_1.

As mentioned previously, the differential enthalpy of adsorption was determined by approximating the slope of a plot of ΔH *versus* n_1 at each n_1 given in Table II. This approximation was performed by determining the slope of a straight-line segment through adjacent experimental values. These values are also included in Table II.

Computation of integral, ΔS, the differential, $\Delta\overline{S}_1$, entropies was performed from the defining equations, Eqs. 9 and 10. Table II includes these values in columns 5 and 8. Figures 8 and 9 are graphical representations of the variation in integral and differential thermodynamic variables throughout adsorption.

Enthalpy Analysis—The integral enthalpy of immersion was characterized by a linear decrease in the heat of wetting throughout the period of low moisture contents. This relationship is consistent with the nearly constant differential enthalpy of adsorption shown in Fig. 9.

The constant differential enthalpy observed in the range of 0–0.15 mole of adsorbate/100 g of solid for microcrystalline cellulose is quite a contrast to the behavior observed in the wetting of standard cellulose (Fig. 10) presented by Morrison and Dzieciuch (11). These authors concluded that

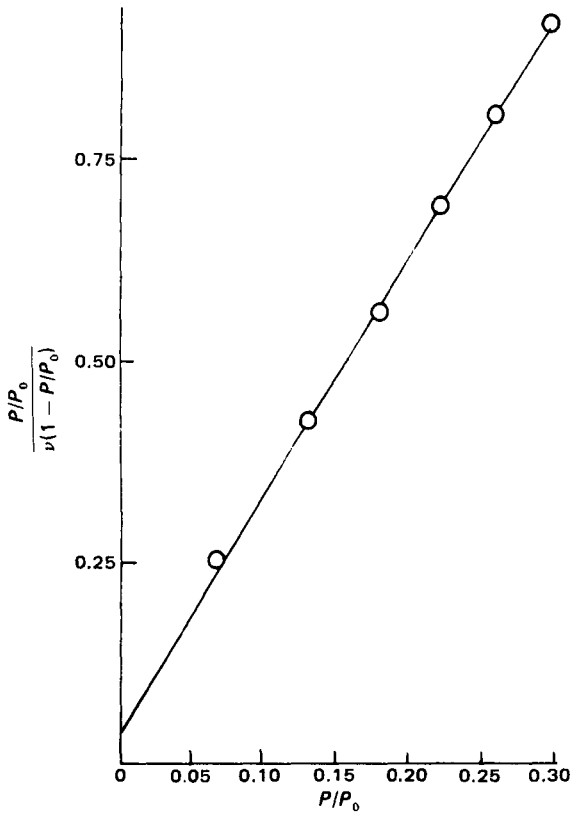

Figure 7—*BET plot for the adsorption of nitrogen by microcrystalline cellulose.*

the initial decrease in the value of $-\overline{\Delta H_1}$ was due to a peptization (swelling) of the solid. The energy consumed in the disruption of solid–solid bonds produced a heat of immersion lower than expected and was not a constant effect. This effect, which is carried implicitly throughout the determination of $\overline{\Delta H_1}$ from immersional data, is not present in the study of microcrystalline cellulose. Therefore, the constant $-\overline{\Delta H_1}$ period seems to be an indication of no swelling as well as an indication of an energetically homogeneous surface.

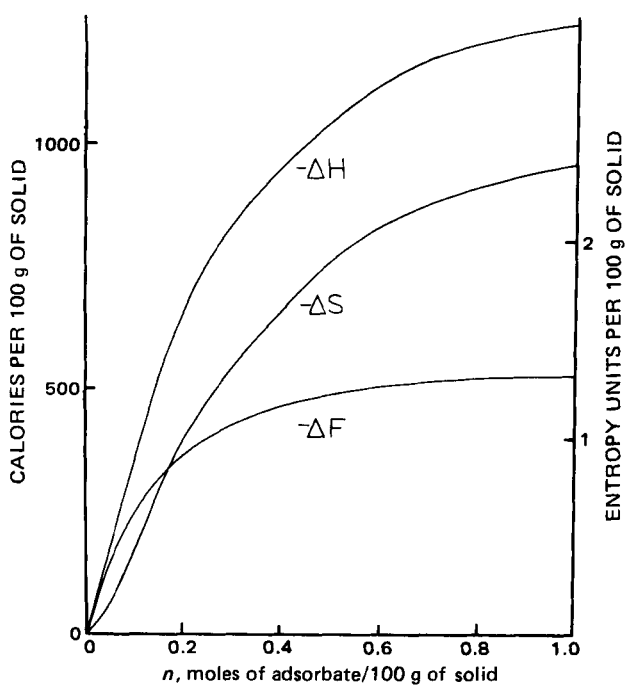

Figure 8—*Integral thermodynamic properties of adsorption for the microcrystalline cellulose–water system.*

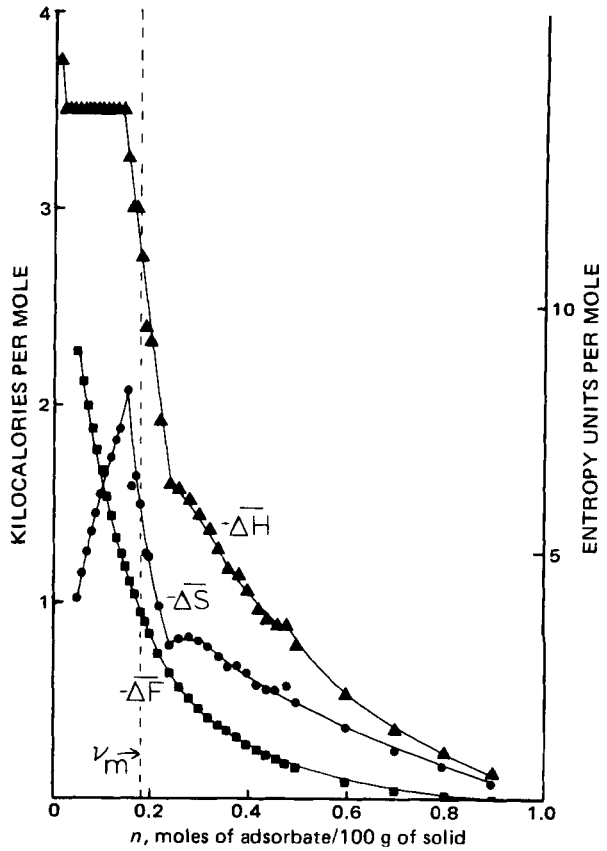

Figure 9—*Differential thermodynamic properties of the microcrystalline cellulose–water system. Key:* ▲, *differential enthalpy;* ●, *differential entropy;* ■, *differential free energy; and* ν_m, *BET monolayer capacity.*

The dashed line in Fig. 9 represents the monolayer capacity as estimated from the BET treatment of the sorption data. Slightly before completion of the monolayer, $-\overline{\Delta H_1}$ begins to decrease rapidly. The end of the constant period indicates the point where lateral adsorbate interactions begin to influence the heat of adsorption. The sharply decreasing values of $-\overline{\Delta H_1}$ seem to indicate the transition from a situation where the majority of water molecules interact by forming two bonds with cellulose to a completed monolayer involving one solid–liquid bond per water molecule.

Values of $\overline{\Delta H_1}$ in Fig. 7 are net values above the heat of condensation to liquid water. A value of $\overline{\Delta H_1} = 0$ indicates that the bonds formed during vapor adsorption have an energy equivalent to the bond strength in liquid water. The heat of condensation of water is approximately −9 kcal/mole; thus, each mole of hydrogen bonds in water has an energy of approximately −4.5 kcal.

At low moisture contents (<0.15 mole of water/100 g of solid), an adsorbed water molecule is likely to form two bonds with the cellulose substrate. In this range, the $\overline{\Delta H_1}$ values of −3.5 kcal/mole represents the bond energy in excess of the normal hydrogen bonds in water: −1.75 kcal/mole of hydrogen bonds. A total hydrogen bond energy between water and cellulose of −6.25 kcal/mole can be calculated by adding the energy for 1 mole of hydrogen bonds in water (−4.5 kcal/mole) to the experimentally measured excess (−1.75 kcal/mole). The inflection point that occurs slightly after ν_m in Fig. 7 has a value of −1.6 kcal/mole. If this entire excess is assigned to the formation of one bond between cellulose and water, a hydrogen bond energy of −6.1 kcal/mole is calculated.

Since the hydrogen bond energy between cellulose and water should be relatively constant despite the orientation of the adsorbed molecule, the closeness of the −6.25- and −6.1-kcal/mole values supports the hypothesis that a partial transition from solid–liquid to liquid–liquid bonding is responsible for the observed decrease in $-\overline{\Delta H_1}$.

The values of −1.75 and −1.6 kcal/mole obtained calorimetrically compare reasonably well to the net interaction energy estimated from the BET theory. The parameter c had a value of 16.48 and, with Eq. 12, this value leads to a net interaction of −1.66 kcal/mole.

Entropy Analysis—Entropy represents disorder. Therefore, a neg-

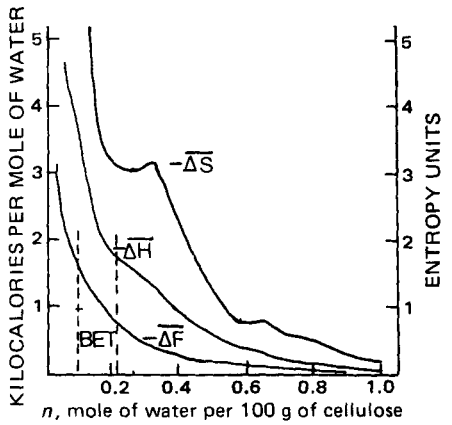

Figure 10—*Net differential enthalpy, free energy, and entropy of adsorption of water by cotton cellulose (adapted from Ref. 11).*

ative change of entropy corresponds to an ordering process. The increase in $-\Delta S$ (Fig. 8) throughout the adsorption process corresponds to an overall increase in the ordering of the system.

The differential entropy curve determined from immersional data reflects the influence of four factors: (*a*) a decrease in entropy associated with the change of three-dimensional molecular motion to two-dimensional motion (transition effect), (*b*) an increase in entropy due to the separation of liquid molecules in surface spreading (separation effect), (*c*) an increase in entropy associated with the disordering or peptization of the solid, and (*d*) a decrease in entropy associated with ordering in the surface film.

As Wahba (4) indicated, the very early stages of adsorption must always be characterized by a positive differential entropy. This conclusion is a direct result of the fact that while the differential heat of adsorption has a finite value at $P/P_0 = 0$, the differential free energy is infinite (see Eq. 2).

From a conceptual point of view, the positive value of $\overline{\Delta S_1}$ is due to the predominance of the separation effect of liquid molecules. The decrease in this thermodynamic quantity corresponds with the decrease in the separation effect as more molecules are adsorbed. A value of zero for $\overline{\Delta S}$ at low moisture contents does not indicate that the adsorbate is the same as bulk water; it merely represents the point where the separation effect is balanced by the transition from three-dimensional motion to the two-dimensional surface phase.

Generally, experimental free energy values are not available at low relative pressures, so few studies include the $+\overline{\Delta S}$ values of this region. The initial region of the differential entropy curve for the adsorption of water on microcrystalline cellulose (Fig. 9) corresponds to an increase in $-\overline{\Delta S_1}$. This region of the curve is primarily a result of a decrease in the separation effect. In other words, this region corresponds to a period of ordering, due primarily to the approach of monolayer completion. If there were any perturbation of the solid during this period such as swelling, that effect would oppose the experimental results in the sense that the perturbation would represent an increase in entropy.

Ideally, the maximum in $-\overline{\Delta S_1}$ observed around $n = 0.15$ would represent the point where the separation effect reached a minimum and the ordering due to surface packing reached a maximum, *i.e.*, completion of the monolayer. Wahba (4) commented that actually the maximum will occur slightly before monolayer completion because there is undoubtedly some premature multilayer formation. Indeed, in this study, the maximum appears slightly before the monolayer capacity as estimated from adsorption data.

A comparison of the results for standard cellulose, obtained by Morrison and Dzieciuch (11) (Fig. 10), with the results of the microcrystalline cellulose study reveals major differences between these two materials in the low pressure region where the standard cellulose curve does not exhibit a maximum. Morrison and Dzieciuch (11) indicate that the rapid decrease of $-\overline{\Delta S_1}$ is due in part to the disordering of the dried gel and in part to the replacement of two or more hydrogen bonds per water molecule by one per molecule. Peptization of the standard cellulose represents swelling of the fibers and, hence, an increase in entropy. This swelling only occurs in regions where moisture can penetrate, and the entropy change associated with the microcrystalline product was not influenced by such perturbation.

Thus, with microcrystalline cellulose, the decreasing region of $-\overline{\Delta S_1}$ near the BET monolayer capacity is exclusively due to the change from a surface cellulose interaction involving two hydrogen bonds per water molecule to an interaction consisting of one such bond and not to swelling of the solid.

Table III—Calculated Differential Thermodynamic Properties for the Desorption of Water from Saturated Microcrystalline Cellulose Samples

n, moles of Water/ 100 g of Solid	P/P_0	$-\Delta\overline{H}$, cal/mole	$-\Delta\overline{F}$, cal/mole	$-\Delta\overline{S}$, eu/mole
1.00	0.987	—	—	—
0.90	0.960	145	24	0.41
0.80	0.911	210	55	0.52
0.70	0.858	270	91	0.60
0.60	0.781	460	146	1.05
0.50	0.711	680	202	1.60
0.48	0.685	650	224	1.43
0.46	0.661	650	245	1.36
0.44	0.638	800	266	1.79
0.42	0.615	850	288	1.89
0.40	0.590	825	312	1.72
0.38	0.562	900	341	1.88
0.36	0.535	950	370	1.95
0.34	0.512	1025	396	2.11
0.32	0.480	1225	435	2.65
0.30	0.445	—	—	—

Both standard cellulose (11) and microcrystalline cellulose exhibit a minimum in $-\overline{\Delta S_1}$ around $n = 0.25$, followed by another maximum. This region represents the moisture content where the surface is covered and further adsorption occurs with much less ordering. Since the value of $-\overline{\Delta S_1}$ drops off faster for cellulose than it does for microcrystalline cellulose, the nature of the microcrystalline solid apparently is still influential at higher relative pressures.

Such behavior seems characteristic of the difference between adsorption with a fibrous solid and adsorption involving discrete particles of essentially the same material. Fibers tend to confine the adsorption so that interactions between adjacent layers of adsorbate are inevitable. The immersional data of the cellulose–water system (11) confirm this hypothesis by showing a negligible heat of wetting for saturated solid. In contrast, the heat of wetting of saturated microcrystalline cellulose has been used as a method for estimating the external solid surface area.

Origin of Hysteresis—The strength of the solid–liquid bond plays a role in the origin of hysteresis in the microcrystalline cellulose–water system. Possibly, an increase in enthalpy at a given partial pressure could entirely account for an increase in free energy (see Eq. 10). If so, the entropy of water molecules on the surface of microcrystalline cellulose would be the same regardless of whether the water is adsorbed or remains after partial desorption. Table III contains the calculated differential quantities based upon desorption data. A comparison of these differential entropies with those for adsorbed water (Table II) at the same partial pressures shows that the hysteresis is real and does indeed involve both enthalpic and entropic factors since the $\overline{\Delta S_1}$ values are not identical.

SUMMARY AND CONCLUSIONS

Surface characteristics of powders, especially hydrophilic powders, are not easily characterized through experimental methods such as contact angle measurement or tensile strength determinations. The calorimetric approach represents an almost exclusive and particularly appropriate procedure. Immersion in an aqueous environment is, after all, the ultimate fate of most pharmaceutical dosage forms.

With the calorimetric technique, the following surface characteristics have been quantified for microcrystalline cellulose powder:

1. The solid has a strong affinity for water, demonstrated by a heat of wetting of −13.00 cal/g and monolayer coverage occurring at approximately 20% RH.
2. The surface is energetically uniform, showing a linear decrease in the heat of wetting of samples with adsorbed moisture up to monolayer coverage.
3. The powder is relatively porous with an internal surface area of 130–270 m^2/g. This surface area represents at least 95% of the surface that interacts with water. Nitrogen adsorption does not give a reasonable estimate of the total surface area.
4. The powder does not swell during the adsorption or wetting process.

5. Hysteresis of the immersional isotherm indicates that, once wetted, the solid holds water tighter at the same moisture content than when the water is adsorbed by dry solid.

6. Sorption hysteresis is of enthalpic and entropic origin.

The widespread use of microcrystalline cellulose powder in the pharmaceutical industry as a tablet excipient makes this specific information of particular relevance. However, the general experimental procedure represents a technique that has as its greatest potential application the determination of changes in surface characteristics as a result of formulation and/or processing.

REFERENCES

(1) G. E. Boyd and W. D. Harkins, *J. Am. Chem. Soc.*, **64**, 1190 (1942).

(2) W. D. Harkins and G. E. Boyd, *ibid.*, **64**, 1195 (1942).

(3) W. D. Harkins and G. Jura, *ibid.*, **66**, 919 (1944).

(4) M. Wahba, *J. Phys. Colloid Chem.*, **54**, 1148 (1950).

(5) G. J. Young, J. J. Chessick, F. H. Healey, and A. C. Zettlemoyer, *J. Phys. Chem.*, **58**, 313 (1954).

(6) G. J. Young and F. H. Healey, *ibid.*, **58**, 881 (1954).

(7) F. H. Healey and G. J. Young, *ibid.*, **58**, 885 (1954).

(8) A. C. Zettlemoyer, G. J. Young, and J. J. Chessick, *ibid.*, **59**, 962 (1955).

(9) H. B. Dunford and J. L. Morrison, *Can. J. Chem.*, **33**, 904 (1955).

(10) J. L. Morrison and J. F. Hanlan, *Nature*, **179**, 528 (1957).

(11) J. L. Morrison and M. A. Dzieciuch, *Can. J. Chem.*, **37**, 1379 (1959).

(12) Y. C. Wu and L. E. Copeland, *Adv. Chem. Ser.*, No. 33, 357 (1961).

(13) M. Dole and A. D. McLaren, *J. Am. Chem. Soc.*, **69**, 651 (1947).

(14) S. Brunauer, P. H. Emmett, and E. Teller, *J. Am. Chem. Soc.*, **60**, 309 (1938).

(15) S. Brunauer, L. S. Deming, W. E. Deming, and E. Teller, *ibid.*, **62**, 1723 (1940).

(16) W. D. Harkins and G. Jura, *ibid.*, **66**, 1362 (1944).

(17) R. H. Stokes and R. A. Robinson, *Ind. Eng. Chem.*, **41**, 2013 (1949).

(18) J. M. Sturtevant, in "Physical Methods of Organic Chemistry," vol. 1, A. Weissburger, Ed., Interscience, New York, N.Y., 1945, pp. 335–344.

(19) R. G. Hollenbeck, G. E. Peck, and D. O. Kildsig, *J. Pharm. Sci.*, **67**, 1592 (1978).

(20) G. H. Argue and O. Maass, *Can. J. Res.*, **12**, 564 (1935).

(21) J. D. Babbitt, *ibid.*, **20**, 143 (1942).

(22) S. J. Gregg, "The Surface Chemistry of Solids," Reinhold, New York, N.Y., 1951, pp. 24–26.

(23) Y. Nakai, E. Fukuska, S. Nakajima, and J. Hasegawa, *Chem. Pharm. Bull.*, **25**, 96 (1977).

(24) K. Marshall and D. Sixsmith, *Drug Dev. Commun.*, **1**, 51 (1974–75).

(25) F. W. Billmeyer, "Textbook of Polymer Science," 2nd ed., Wiley-Interscience, New York, N.Y., 1971.

ACKNOWLEDGMENTS

Supported in part by a Biomedical Research Grant, National Institutes of Health.

The authors acknowledge the technical assistance of Mr. T. McDaniels throughout the design, construction, and modification of the calorimeter.

R. G. Hollenbeck is an American Foundation for Pharmaceutical Education Fellow.

Glass Formation in Barbiturates and Solid Dispersion Systems of Barbiturates with Citric Acid

M. P. SUMMERS

Received September 19, 1977, from the *Department of Pharmaceutics, School of Pharmacy, University of London, London WC1N 1AX, England.* Accepted for publication March 13, 1978.

Abstract □ Glasses were prepared from a number of barbiturates. The viscosities and glass transition temperatures of the glasses were dependent on the structure of the groups present on the C-5 and N-1 atoms. Solid dispersions were prepared from three selected barbiturates formulated with citric acid. The glass transition temperatures of these systems indicated that a 1:1 molar ratio complex was formed between the two components and that intermolecular bonding was stronger in the complex than in the individual components.

Keyphrases □ Barbiturates, various—glass formation and solid dispersion systems evaluated □ Glass formation—various barbiturates evaluated □ Solid dispersion systems—various barbiturates evaluated □ Central depressants—various barbiturates, glass formation and solid dispersion systems evaluated

The use of citric acid as a glass-forming carrier in solid dispersions was studied previously (1–3). Although the dissolution rate of primidone formulated in such a system was faster than that of the pure drug, the glassy phase of this system was unstable and studies had to be performed on the devitrified solid (2).

To study the full potential of a glass system for improved drug dissolution, it is necessary to find a system with a glass transition temperature well above room temperatures so that a hard, usable glass can be formed. It would probably be advantageous if the drug could exist as a glass, which may stabilize the glass formed by the carrier.

The purpose of the present work was to study glass formation in a series of barbiturates and the formation of binary glass systems with citric acid to find a system that complied with the suggested criteria.

EXPERIMENTAL

Preparation of Barbiturate Glasses and Solid Dispersion Systems—Glass formation was studied in the following barbiturates: barbital[1], mephobarbital[2], phenylmethylbarbituric acid[3], pentobarbital[2], hexobarbital[4], phenobarbital[5], heptabarbital[6], butethal[3], amobarbital[3], ethylpropylbarbituric acid, cyclobarbital, and 5-ethyl-5-cycloheptenyl-1-methylbarbituric acid[6].

[1] BDH Chemicals Ltd., Poole, England.
[2] Siegfried, Zofingen, Switzerland.
[3] May and Baker Ltd., Dagenham, England.
[4] Sigma Chemical Co., St. Louis, Mo.
[5] Macarthys, Romford, England.
[6] Geigy Pharmaceuticals, Macclesfield, England.

0022-3549/78/1100-1606$01.00/0

© 1978, American Pharmaceutical Association

5. Hysteresis of the immersional isotherm indicates that, once wetted, the solid holds water tighter at the same moisture content than when the water is adsorbed by dry solid.

6. Sorption hysteresis is of enthalpic and entropic origin.

The widespread use of microcrystalline cellulose powder in the pharmaceutical industry as a tablet excipient makes this specific information of particular relevance. However, the general experimental procedure represents a technique that has as its greatest potential application the determination of changes in surface characteristics as a result of formulation and/or processing.

REFERENCES

(1) G. E. Boyd and W. D. Harkins, *J. Am. Chem. Soc.*, **64**, 1190 (1942).

(2) W. D. Harkins and G. E. Boyd, *ibid.*, **64**, 1195 (1942).

(3) W. D. Harkins and G. Jura, *ibid.*, **66**, 919 (1944).

(4) M. Wahba, *J. Phys. Colloid Chem.*, **54**, 1148 (1950).

(5) G. J. Young, J. J. Chessick, F. H. Healey, and A. C. Zettlemoyer, *J. Phys. Chem.*, **58**, 313 (1954).

(6) G. J. Young and F. H. Healey, *ibid.*, **58**, 881 (1954).

(7) F. H. Healey and G. J. Young, *ibid.*, **58**, 885 (1954).

(8) A. C. Zettlemoyer, G. J. Young, and J. J. Chessick, *ibid.*, **59**, 962 (1955).

(9) H. B. Dunford and J. L. Morrison, *Can. J. Chem.*, **33**, 904 (1955).

(10) J. L. Morrison and J. F. Hanlan, *Nature*, **179**, 528 (1957).

(11) J. L. Morrison and M. A. Dzieciuch, *Can. J. Chem.*, **37**, 1379 (1959).

(12) Y. C. Wu and L. E. Copeland, *Adv. Chem. Ser.*, No. 33, 357 (1961).

(13) M. Dole and A. D. McLaren, *J. Am. Chem. Soc.*, **69**, 651 (1947).

(14) S. Brunauer, P. H. Emmett, and E. Teller, *J. Am. Chem. Soc.*, **60**, 309 (1938).

(15) S. Brunauer, L. S. Deming, W. E. Deming, and E. Teller, *ibid.*, **62**, 1723 (1940).

(16) W. D. Harkins and G. Jura, *ibid.*, **66**, 1362 (1944).

(17) R. H. Stokes and R. A. Robinson, *Ind. Eng. Chem.*, **41**, 2013 (1949).

(18) J. M. Sturtevant, in "Physical Methods of Organic Chemistry," vol. 1, A. Weissburger, Ed., Interscience, New York, N.Y., 1945, pp. 335–344.

(19) R. G. Hollenbeck, G. E. Peck, and D. O. Kildsig, *J. Pharm. Sci.*, **67**, 1592 (1978).

(20) G. H. Argue and O. Maass, *Can. J. Res.*, **12**, 564 (1935).

(21) J. D. Babbitt, *ibid.*, **20**, 143 (1942).

(22) S. J. Gregg, "The Surface Chemistry of Solids," Reinhold, New York, N.Y., 1951, pp. 24–26.

(23) Y. Nakai, E. Fukuska, S. Nakajima, and J. Hasegawa, *Chem. Pharm. Bull.*, **25**, 96 (1977).

(24) K. Marshall and D. Sixsmith, *Drug Dev. Commun.*, **1**, 51 (1974–75).

(25) F. W. Billmeyer, "Textbook of Polymer Science," 2nd ed., Wiley-Interscience, New York, N.Y., 1971.

ACKNOWLEDGMENTS

Supported in part by a Biomedical Research Grant, National Institutes of Health.

The authors acknowledge the technical assistance of Mr. T. McDaniels throughout the design, construction, and modification of the calorimeter.

R. G. Hollenbeck is an American Foundation for Pharmaceutical Education Fellow.

Glass Formation in Barbiturates and Solid Dispersion Systems of Barbiturates with Citric Acid

M. P. SUMMERS

Received September 19, 1977, from the *Department of Pharmaceutics, School of Pharmacy, University of London, London WC1N 1AX, England.* Accepted for publication March 13, 1978.

Abstract □ Glasses were prepared from a number of barbiturates. The viscosities and glass transition temperatures of the glasses were dependent on the structure of the groups present on the C-5 and N-1 atoms. Solid dispersions were prepared from three selected barbiturates formulated with citric acid. The glass transition temperatures of these systems indicated that a 1:1 molar ratio complex was formed between the two components and that intermolecular bonding was stronger in the complex than in the individual components.

Keyphrases □ Barbiturates, various—glass formation and solid dispersion systems evaluated □ Glass formation—various barbiturates evaluated □ Solid dispersion systems—various barbiturates evaluated □ Central depressants—various barbiturates, glass formation and solid dispersion systems evaluated

The use of citric acid as a glass-forming carrier in solid dispersions was studied previously (1–3). Although the dissolution rate of primidone formulated in such a system was faster than that of the pure drug, the glassy phase of this system was unstable and studies had to be performed on the devitrified solid (2).

To study the full potential of a glass system for improved drug dissolution, it is necessary to find a system with a glass transition temperature well above room temperatures so that a hard, usable glass can be formed. It would probably be advantageous if the drug could exist as a glass, which may stabilize the glass formed by the carrier.

The purpose of the present work was to study glass formation in a series of barbiturates and the formation of binary glass systems with citric acid to find a system that complied with the suggested criteria.

EXPERIMENTAL

Preparation of Barbiturate Glasses and Solid Dispersion Systems—Glass formation was studied in the following barbiturates: barbital[1], mephobarbital[2], phenylmethylbarbituric acid[3], pentobarbital[2], hexobarbital[4], phenobarbital[5], heptabarbital[6], butethal[3], amobarbital[3], ethylpropylbarbituric acid, cyclobarbital, and 5-ethyl-5-cycloheptenyl-1-methylbarbituric acid[6].

[1] BDH Chemicals Ltd., Poole, England.
[2] Siegfried, Zofingen, Switzerland.
[3] May and Baker Ltd., Dagenham, England.
[4] Sigma Chemical Co., St. Louis, Mo.
[5] Macarthys, Romford, England.
[6] Geigy Pharmaceuticals, Macclesfield, England.

0022-3549/78/1100-1606$01.00/0

© 1978, American Pharmaceutical Association

Table I—Properties of the Barbiturate Series

Barbiturate	C-5 Groups	N-1 Group	Melting Point	Glass Transition Temperature (°C)	Glass Transition Temperature (°K) / Melting Point (°K)	Heat of Fusion, ΔH_f, cal/mole	Entropy of Fusion, ΔS_f, cal/mole/K	Solubility, g/liter	−Log Ideal Solubility
Cyclobarbital	Ethyl, cyclohexenyl	Hydrogen	163.0°	41.5	0.721	2025	4.64	430	0.4953
Phenobarbital	Ethyl, phenyl	Hydrogen	177.0°	40.5	0.697	6058	13.46	228.5	1.5762
Heptabarbital	Ethyl, cycloheptenyl	Hydrogen	176.5°	32.0	0.678	7288	16.23	50	1.8924
Phenylmethylbarbituric acid	Methyl, phenyl	Hydrogen	226.0°	—[a]	—	6594	13.21	48.0	—
Hexobarbital	Methyl, cyclohexenyl	Methyl	145.5°	9	0.674	5309	12.70	29.5	1.1874
5-Ethyl-5-cycloheptenyl-1-methylbarbituric acid	Ethyl, cycloheptenyl	Methyl	100.0°	7	0.751	5549	14.88	125	0.3655
Mephobarbital	Ethyl, phenyl	Methyl	181.3°	−3	0.594	9034	19.90	7.7	2.3921
Butethal	Ethyl, butyl	Hydrogen	126.0°	5	0.697	3630	9.1	612.5	0.7202
Pentobarbital	Ethyl, 1-methylbutyl	Hydrogen	132.0°	4	0.683	4919	12.15	300	1.1939
Amobarbital	Ethyl, isopentyl	Hydrogen	160.0°	−4	0.621	5297	12.23	275	1.2774
Ethylpropylbarbituric acid	Ethyl, propyl	Hydrogen	150.5°	—[a]	—	4340	10.25	300	—
Barbital	Diethyl	Hydrogen	188.5°	—[a]	—	5710[b]	12.37	180	—

[a] Crystallization of melt occurred. [b] Includes ΔH of polymorphic transition that occurred on heating.

Cyclobarbital was prepared from the calcium salt[3] by boiling with acidified water followed by extraction of the free barbiturate from the aqueous phase with ether[7]. After evaporation of the ether phase, the crystals were purified by recrystallization from 70% alcohol–water.

Glass formation was investigated by gently melting barbiturate samples in small Pyrex tubes and pouring the melt into glass petri dishes. A barbiturate was considered to be a glass former if the melt did not crystallize at room temperature or when quenched in liquid nitrogen.

Solid dispersion systems of citric acid monohydrate[7] and the selected barbiturates were prepared as described previously (2) using concentrations of citric acid from 10 to 90% (w/w).

Melting Points, Glass Transition Temperatures, and Heats of Fusion—The melting points of the original samples were determined[8] as outlined previously (2), but the samples were not sieved before the determination. The glass transition temperatures of the barbiturate glasses and solid dispersion systems were determined[8] as described previously (3).

Heats of fusion were measured by determining[8] the area under the fusion peak of a known weight of each barbiturate and comparing it to the area under the fusion peak of a known weight of metal standard. Indium[9] (heat of fusion, ΔH_f, 781 cal/g mole) was used as the standard metal, and the same operating conditions of the differential scanning calorimeter were used for both barbiturate samples and reference metal. The areas under the peaks were determined by weighing the peaks after cutting them from chart paper equilibrated for 24 hr at room temperature. The heat of fusion of the barbiturate could then be found using the formula:

$$\Delta H_f(\text{barbiturate}) = \frac{\Delta H_f(\text{standard}) \times \text{weight of standard} \times \text{peak weight of barbiturate} \times \text{molecular weight of barbiturate}}{\text{weight of barbiturate} \times \text{peak weight of standard} \times \text{molecular weight of standard}} \text{ cal/mole} \quad \text{(Eq. 1)}$$

Three determinations were performed for each sample, and the mean value was calculated.

Solubility Determination—Solubilities were determined by equilibrating suspensions of the barbiturates in methanol[7] at 20° on a shaking water bath for 24 hr. Then 1-ml samples were withdrawn using a pipet fitted with a grade 3 sintered-glass filter stick, and the samples were diluted to suitable concentrations before assay. Replicate determinations were performed for each barbiturate.

The solutions were assayed using a UV spectrophotometer[10], and the concentrations of the solutions were calculated from a previously constructed calibration curve.

X-Ray Diffraction—X-ray diffraction[11] was used to assess the amorphous nature of those dispersions and barbiturate glasses that could be tested before they devitrified.

[7] Analar grade, BDH Chemicals Ltd., Poole, England.
[8] Using a differential scanning calorimeter 1B, Perkin-Elmer, Beaconsfield, Bucks, England.
[9] Koch Light Laboratories, Colnebrook, Bucks, England.
[10] SP 1800, Pye Unicam, Cambridge, England.
[11] Nonius Mk 2 self-focusing Guinier diffractometer.

RESULTS AND DISCUSSION

Table I shows the melting points (T_m) and glass transition temperatures (T_g) of the barbiturates studied.

Many barbiturates are capable of glass formation, and glass transition temperatures varied throughout the series. Low molecular weight compounds have the same viscosity at the glass transition temperature (4); above this temperature, their viscosity decreases as the temperature increases. Barbiturates with a glass transition temperature below ambient temperature are viscous liquids at this temperature, so only barbiturates having a glass transition temperature well above ambient temperature can be considered to be rigid glasses. Thus, phenobarbital, cyclobarbital, and heptabarbital are the only compounds in this category. However, the heptabarbital glass was relatively unstable when prepared in a large batch and showed evidence of devitrification (as shown by X-ray diffraction) after a few hours at room temperature. Phenobarbital and cyclobarbital glasses were more stable and remained amorphous for longer than 24 hr.

Although a full understanding of the reasons for glass formation has not been achieved (5), an attempt was made to elucidate the reasons for the difference in the glass transition temperature of the barbiturates. Two general types of glass-forming systems have been studied extensively: the inorganic glasses such as silicon dioxide glass and organic polymer glasses such as polystyrene. Different criteria for glass formation have been developed for both types; although some similarities exist, the two systems are generally different. The barbiturates probably more closely resemble the polymer glasses, although their low molecular weight may result in some differences.

The main factors affecting the glass transition temperature of the high molecular weight polymers are molecular chain stiffness, intermolecular forces, and molecular geometry (4). The glass transition temperature increases as the first two factors increase. Many attempts have been made to correlate the glass transition temperature with the melting point since the same factors affect both transitions. Lee and Knight (6), however, showed that no simple relationship exists between glass transition and melting point because of the fundamental differences between the crystal–liquid (T_m) and glass–liquid (T_g) transitions. Nevertheless, a plot of glass transition temperature against melting point has been useful to divide polymers into two groups, "sterically restricted" and "sterically nonrestricted" polymers (4), with the former having higher ratios of glass transition temperature to melting point.

The values of the ratio of glass transition temperature to melting point given in Table I appear to have little correlation, as does the relationship between glass transition temperature and melting point shown in Fig. 1. Amobarbital and mephobarbital were the only melts that required

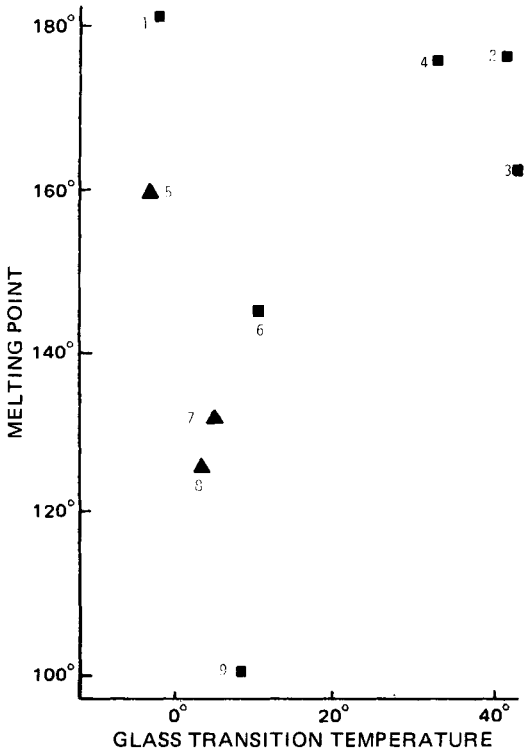

Figure 1—*Relationship between melting point and glass transition temperature. Key: 1, mephobarbital; 2, phenobarbital; 3, cyclobarbital; 4, heptabarbital; 5, amobarbital; 6, hexobarbital; 7, pentobarbital; 8, butethal; and 9, 5-ethyl-5-cycloheptenyl-1-methylbarbituric acid.*

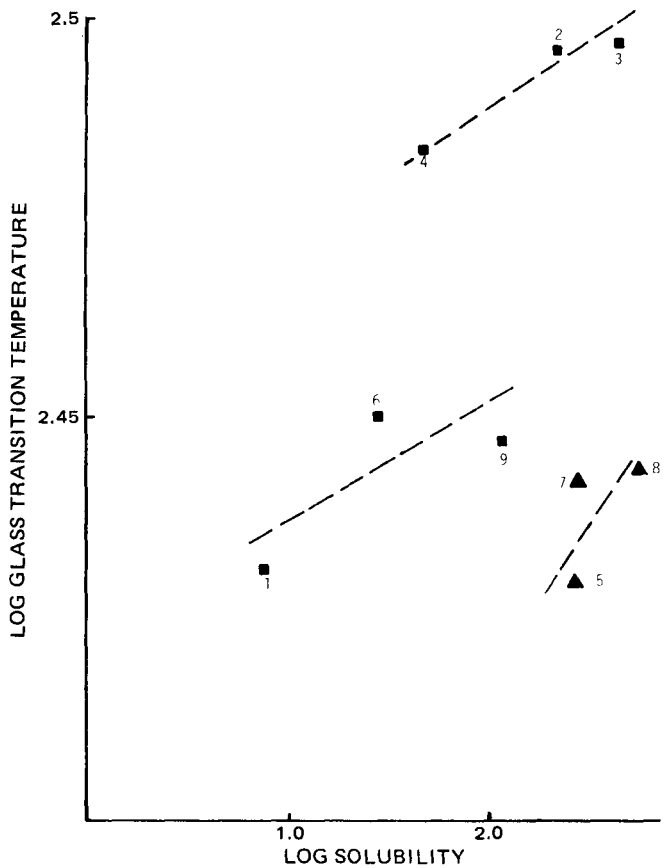

Figure 2—*Relationship between log solubility and log glass transition temperature. Key: same as Fig. 1.*

cooling in liquid nitrogen to form glasses, and they showed the lowest ratios of glass transition temperature to melting point. Therefore, Fig. 1 may separate the barbiturates into a main group of compounds that formed glasses with relative ease and the two that had to be quenched in liquid nitrogen. There do not appear to be any structural features, however, to separate these compounds from the others.

The substitution of different groups in the 5-position affects the polarity of the molecule. Since this factor may affect intermolecular bonding and, thus, affect the glass transition temperature, a correlation was attempted between glass transition temperature and solubility in an alcohol of short alkyl chain length.

The solubilities of barbiturates in methanol are given in Table I, and Fig. 2 shows log glass transition temperature plotted against log solubility. Plotted in this manner, the barbiturate series is divided into two or three groups. For reasons that will be evident later, it is convenient to divide the data into three groups: (*a*) barbiturates with a ring substituent on C-5, (*b*) barbiturates with a ring substituent on C-5 and a group other than hydrogen on N-1, and (*c*) barbiturates with alkyl substituents on C-5.

A similar relationship exists between log ideal solubility (as shown in Table I) and log glass transition temperature. The use of the ideal solubility removes any effect on the measured solubility of the crystal lattice energy that will oppose the solution process.

The ideal mole fraction solubility can be calculated from:

$$\log \text{ideal solubility} = \frac{-\Delta H_f}{2.303R}\left(\frac{T_m - T}{T_m T}\right) \qquad \text{(Eq. 2)}$$

where R is the gas constant and T (°K) is the temperature of solubility measurement.

Within each group, both sets of data are the converse of the partition coefficients (octanol–water) determined and calculated by Hansch and Anderson (7). Since these partition coefficients are considered to increase as the barbiturate polarity decreases, the methanol solubilities increase as the polarity increases.

The solubilities of barbiturates in Groups *a* and *c* are very similar, although the glass transition temperatures of compounds in Group *a* are much greater than those in Group *c*. This result is probably due to the ring substituent on C-5, which hinders molecular flow so that the glass–liquid transition occurs at a higher temperature. Differences within a group may be due to differences in intermolecular bonding, with those of higher glass transition temperature being more polar (having greater methanol solubility) and having greater molecular bonding. Molecular bond strength is important for the same reasons as the size of group substituents. If the size of the ring substituent is the only determining factor, one would expect that heptabarbital would have a greater glass transition temperature than cyclobarbital; therefore, both C-5 substituents and intermolecular bonding are important, the glass transition temperature being determined by a balance of these two effects.

The third group (*b*) contains the barbiturates with a C-5 ring and an N-1 methyl group. The N-1 substituent replaces a hydrogen and thus reduces hydrogen bonding, which, in turn, reduces intermolecular attraction and glass transition temperature. 5-Ethyl-5-cycloheptenyl-1-methylbarbituric acid deviates from the general trend in Fig. 2, having a relatively low glass transition temperature. The reason for this deviation is unknown. These results are consistent with the self-association constants of barbiturates calculated by Kyogoku *et al.* (8). Phenobarbital and pentobarbital had similar self-association constants (8.1 and 7.0 M^{-1}, respectively) but those for the N-1-substituted barbiturates were very much lower.

For three barbiturates in Table I, glass transition temperatures could not be obtained. Probably with barbital and ethylpropylbarbituric acid, the groups on the 5-position were not bulky enough to hinder free molecular movement when the melt was cooled, so crystallization took place. The intermolecular attraction of phenylmethylbarbituric acid molecules was probably insufficient to cause glass formation, despite the large group on the 5-position. High bonding in the melt prevents crystallization because these bonds have to be broken to reorganize the molecules into the lattice.

The thermodynamics of glass formation were discussed by Pye (5), and these aspects can be applied to the barbiturate systems. The heat of fusion (ΔH_f) and entropy of fusion (ΔS_f) are given in Table I; ΔS_f was calculated from:

$$\Delta S_f = \frac{\Delta H_f}{T_m \text{ (°K)}} \qquad \text{(Eq. 3)}$$

When the barbiturate series is divided into the three groups previously discussed, a general trend is evident; as the glass transition temperature

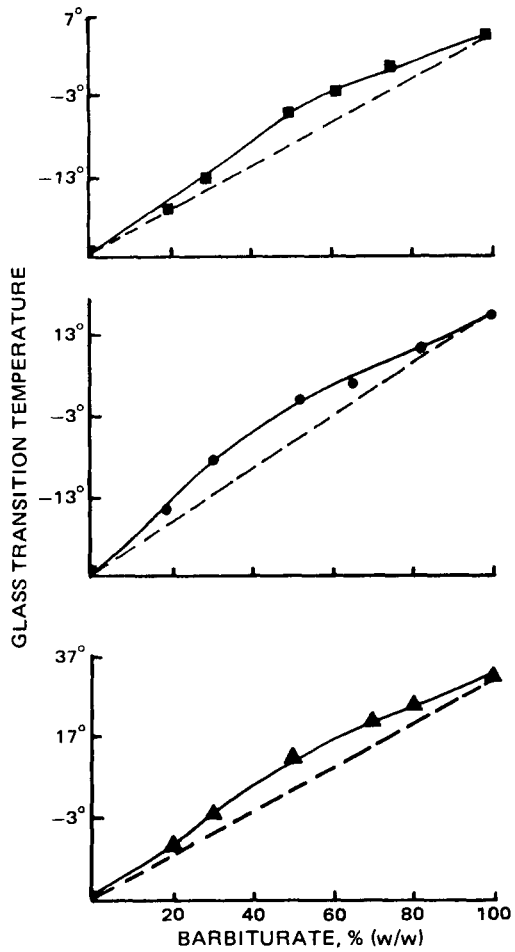

Figure 3—*Variation in glass transition temperature with barbiturate concentration. Key: ---, theoretical relationship; —, observed relationship; ■, pentobarbital; ●, hexobarbital; and ▲, heptabarbital.*

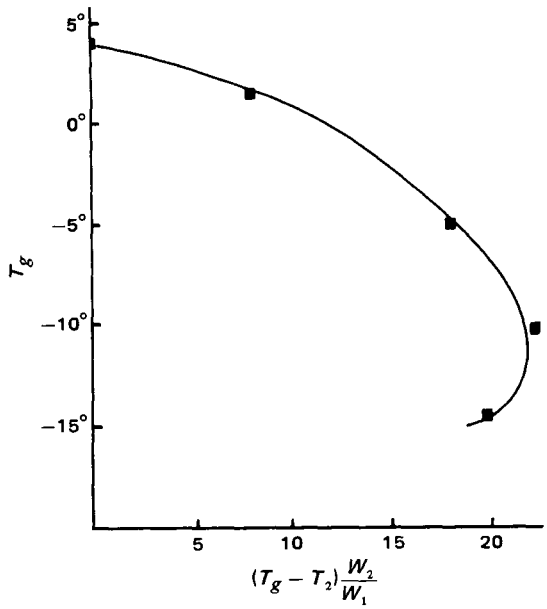

Figure 4—*Deviation of pentobarbital solid dispersion systems from the Gordon and Taylor equation.*

within the group decreases, ΔH_f, ΔS_f, and the melting point increase. It might be expected that ΔS_f would decrease as the glass-forming tendency decreases, since large structural differences between the melt and the crystal would be expected to hinder crystallization. This behavior apparently does not occur. In this respect, the system resembles silicon dioxide, which shows little structural difference between the melt and the crystal (ΔS_f 0.7 cal/K/mole).

The increase in ΔH_f as the glass-forming tendency decreases is consistent with the hypothesis that large energy differences between the crystal and the melt cause unstable supercooling. Thus, the crystalline phase is thermodynamically more favored as ΔH_f increases and the melt is more prone to crystallization. Amobarbital and mephobarbital required rapid quenching to prevent crystallization; within their respective groups, they had the largest ΔH_f values.

Within the barbiturate series as a whole, however, there was little correlation among ΔH_f, ΔS_f, and the glass transition temperature. This result is in general agreement with the observation of Pye (5), who suggested that there is no correlation between thermodynamic parameters and the glass-forming tendency when a large number of glass-forming materials is studied. Furthermore, the similarity of the thermodynamic parameters of materials with different glass transition temperatures and glass-forming tendencies suggests that the structural features previously outlined are more important in determining the ease of glass formation.

Attempts to investigate the structure of the glasses were unsuccessful because of their instability. Even the hard and relatively stable systems devitrified on grinding.

Solid Dispersions of Citric Acid and Barbiturates—An initial study was conducted, using citric acid solid dispersions, to investigate the possibility of producing stable glassy dispersions containing barbiturates of a low glass transition temperature. Summers and Enever (3) showed that the glass transition temperature of solid dispersions may be greater than the expected glass transition temperature of the system based on the additivity principle inherent in the Gordon and Taylor (9) treatment of the glass transition temperature of copolymers. Illers (10) showed that the glass transition temperature of a copolymer system of vinylidene chloride and methyl acrylate can rise well above the glass transition temperature of either pure component. Therefore, it may be possible to produce solid dispersions having glass transition temperatures above ambient temperature but containing barbiturates of a low glass transition temperature.

Hexobarbital, heptabarbital, and pentobarbital were studied. Figure 3 shows the variation in the glass transition temperature with composition for these solid dispersion systems. All three compounds showed similar behavior when fused with citric acid, the glass transition temperature of the mixed glass rising and falling from the glass transition temperature of citric acid to that of the barbiturate. There was little effect at low concentrations of either component, and the effect was most marked at concentrations around 50% (w/w) of the barbiturate. None of these systems complied with the Gordon and Taylor (9) equation and thus resembled the citric acid–primidone system previously described (3). This equation:

$$T_g = -k(T_g - T_2)\frac{W_2}{W_1} + T_1 \qquad \text{(Eq. 4)}$$

predicts a linear relationship between the glass transition temperature of the mixture (T_g) and $(T_g - T_2)(W_2/W_1)$, where T_2 is the glass transition temperature of the second component, W_2 is its weight fraction in the mixture, and T_1 and W_1 are the glass transition temperature and weight fraction of the first component, respectively. Figure 4 shows the pentobarbital–citric acid system plotted in this manner to illustrate the deviation.

The increase in the glass transition temperature shown in Fig. 3 and the deviation from the Gordon and Taylor equation indicate that the strength of the interaction between the two components is stronger than the arithmetic mean of the bond strengths of the individual components (3). This situation could arise because of the formation of very strong bonds between the components, the formation of a greater number of bonds in the mixture than between the individual components, and some steric factors such as the restriction of movement of part of one molecule because of the presence of the second molecule.

Kyogoku *et al.* (8) showed that the interaction between barbiturates and 9-ethyladenine was stronger than that between the individual components, the association constants of the complexes being approximately 10 times greater than the self-association constants of the barbiturates. The different proton-donating properties of the individual components were responsible for the formation of stronger bonds, and a greater number of hydrogen bonds formed in the complex. The solid dispersion systems of this work show similar properties.

With 9-ethyladenine, the barbiturates formed dimers in solution (8).

A 1:1 mole ratio complex also was formed between 9-ethyladenine and barbital in the solid state (11), but a continuous chain of molecules was formed in this case. The formation of strongly bonded dimers or chains of molecules would increase the glass transition temperature of the barbiturate–citric acid glass, and evidence of a 1:1 molecular reaction is found in the presence of the glass transition temperature maximum, which occurs at approximately 50 mole % [51.8% (w/w) pentobarbital, 52.9% (w/w) hexobarbital, and 54.4% (w/w) heptabarbital, respectively]. At this concentration, each barbiturate molecule is complexed with one citric acid molecule. Therefore, the interaction and the deviation of the glass transition temperature are greater.

X-ray diffraction could not be used to investigate complex formation because the glass phase was amorphous. The devitrified glasses were simple eutectic mixtures, which suggested that crystallization involved the breakage of citric acid–barbiturate bonds to produce crystals of the pure components. Therefore, the X-ray diffraction patterns of the devitrified systems could not help to elucidate the structures of the complexes.

The increase in the glass transition temperature in these three dispersions was not great and did not exceed the glass transition temperature of the pure barbiturate. It may be possible to increase the glass transition temperature further by selecting other glass-forming compounds as carriers or formulating three-component glass systems. By selection of suitable barbiturates, glassy dispersions can be prepared for further studies to test the feasibility of the glass phase as a solid dispersion system. Work is continuing on this aspect.

Conclusions—Many barbiturates will form glasses when fused; the viscosity and glass transition temperature of the glass vary with the molecular configuration of the barbiturate molecule. The position of the glass transition temperature within the barbiturate series can be rationalized in terms of the intermolecular bonding in the glass and the restriction of molecular movement imposed by substituents in the C-5 position. Substituting a methyl group for hydrogen on the N-1 position reduces intermolecular hydrogen bonding and results in a relatively low glass transition temperature.

When fused with citric acid, heptabarbital, hexobarbital, and pentobarbital form binary glasses. The glass transition temperatures of these systems do not show a linear increase with composition but attain a maximum at approximately 50% (w/w) of the barbiturate. This deviation is consistent with the formation of a 1:1 mole ratio complex between the two components; it is postulated that there is a greater number of hydrogen bonds in the complex, probably of greater strength, than in glasses of the individual components.

REFERENCES

(1) W. L. Chiou and S. Riegelman, *J. Pharm. Sci.*, **58**, 1505 (1969).
(2) M. P. Summers and R. P. Enever, *ibid.*, **65**, 1613 (1976).
(3) *Ibid.*, **66**, 825 (1977).
(4) R. F. Boyer, *Rubber Chem. Technol.*, **36**, 1303 (1963).
(5) L. D. Pye, in "Introduction to Glass Science," L. D. Pye, H. J. Stevens, and W. C. La Course, Eds., Plenum, New York, N.Y., 1972.
(6) W. A. Lee and G. J. Knight, *Br. Polym. J.*, **2**, 73 (1970).
(7) C. Hansch and S. M. Anderson, *J. Med. Chem.*, **10**, 745 (1967).
(8) Y. Kyogoku, R. C. Lord, and A. Rich, *Nature*, **218**, 69 (1968).
(9) M. Gordon and J. S. Taylor, *J. Appl. Chem.*, **2**, 493 (1952).
(10) K. H. Illers, *Kolloid-Z.*, **190**, 16 (1963).
(11) D. Voet, *J. Am. Chem. Soc.*, **94**, 8213 (1972).

ACKNOWLEDGMENTS

The author thanks Dr. R. J. Gilbert (School of Pharmacy) and the following companies for barbiturate samples: Siegfried (Switzerland), May and Baker Ltd. (England), and Geigy Pharmaceuticals (England). Thanks are also due to W. Dissanayake for technical assistance.

Improved Spectrophotometric Determination of Antazoline

NABIL M. OMAR

Received January 12, 1978, from the *Department of Pharmaceutical Chemistry, University of Assiut, Assiut, Egypt.* Accepted for publication March 21, 1978.

Abstract □ A simple, precise, and accurate spectrophotometric determination of antazoline salts was developed by improving the ceric sulfate procedure. Replacement of water with acetic acid for the preparation of all assay solutions permitted reproducible measurements of the chromogen that absorbed at 505 nm. An appreciable increase in color stability was attained by the controlled addition of perchloric acid to the ceric reagent prior to interaction with antazoline at room temperature. Evidence is provided to account for the oxidation of antazoline at the expense of a complex ceric species. Other 2-imidazolines or phenylephrine did not interfere with the investigated color reaction. In addition to the high value of the chromogen molar absorptivity, ideal adherence of color absorption to Beer's law permitted accurate and reproducible estimation of antazoline over the 1–10-μg range. The procedure was applied to the analysis of different antazoline dosage forms.

Keyphrases □ Antazoline—spectrophotometric analysis in prepared solutions and dosage forms □ Spectrophotometry—analysis, antazoline in prepared solutions and dosage forms □ Antihistaminics—antazoline, spectrophotometric analysis in prepared solutions and dosage forms

The frequent formulation of antazoline[1], 2-[(*N*-phenyl)benzylaminomethyl]-2-imidazoline, with other pharmaceutical amines and 2-imidazoline congeners motivated the development of a selective determination of this antihistamine.

BACKGROUND

Previous antazoline analyses primarily were based on spectrophotometry (1–8). Of the diverse chromogenic reagents adopted, only the sodium nitrite (5–7) and ceric sulfate procedures showed pronounced selectivity. The well-documented and popular ammonium reineckate (1, 2), sodium nitroprusside (3), and dipicrylamine (4) methods are not specific; other pharmaceutical amines and 2-imidazoline derivatives, likely to be present along with antazoline, interfere (9). Moreover, the nitroprusside method, while apparently specific for the intact imidazoline ring, is affected by the experimental buffer concentration and species, the age of reagents, and the intrinsic color of the sample (10).

The utility of the nitrite method is handicapped by interference of phenylephrine with color production (6), and the accuracy of the ceric sulfate procedure is questionable. Discrepancies in recovery studies attained by this latter method reveal considerable nonreproducibility, especially when compared to the nitrite procedure (11). In addition, no quantitative data could be supplied when the ceric reagent was not properly cooled prior to interaction with antazoline or when much water was present. These findings attest to the thermolabile nature of the antazoline–ceric chromogen as well as to its marked sensitivity to pH variations.

Such shortcomings in the available methods for the estimation of an-

[1] Antistine.

0022-3549/78/1100-1610$01.00/0

© 1978, American Pharmaceutical Association

A 1:1 mole ratio complex also was formed between 9-ethyladenine and barbital in the solid state (11), but a continuous chain of molecules was formed in this case. The formation of strongly bonded dimers or chains of molecules would increase the glass transition temperature of the barbiturate–citric acid glass, and evidence of a 1:1 molecular reaction is found in the presence of the glass transition temperature maximum, which occurs at approximately 50 mole % [51.8% (w/w) pentobarbital, 52.9% (w/w) hexobarbital, and 54.4% (w/w) heptabarbital, respectively]. At this concentration, each barbiturate molecule is complexed with one citric acid molecule. Therefore, the interaction and the deviation of the glass transition temperature are greater.

X-ray diffraction could not be used to investigate complex formation because the glass phase was amorphous. The devitrified glasses were simple eutectic mixtures, which suggested that crystallization involved the breakage of citric acid–barbiturate bonds to produce crystals of the pure components. Therefore, the X-ray diffraction patterns of the devitrified systems could not help to elucidate the structures of the complexes.

The increase in the glass transition temperature in these three dispersions was not great and did not exceed the glass transition temperature of the pure barbiturate. It may be possible to increase the glass transition temperature further by selecting other glass-forming compounds as carriers or formulating three-component glass systems. By selection of suitable barbiturates, glassy dispersions can be prepared for further studies to test the feasibility of the glass phase as a solid dispersion system. Work is continuing on this aspect.

Conclusions—Many barbiturates will form glasses when fused; the viscosity and glass transition temperature of the glass vary with the molecular configuration of the barbiturate molecule. The position of the glass transition temperature within the barbiturate series can be rationalized in terms of the intermolecular bonding in the glass and the restriction of molecular movement imposed by substituents in the C-5 position. Substituting a methyl group for hydrogen on the N-1 position reduces intermolecular hydrogen bonding and results in a relatively low glass transition temperature.

When fused with citric acid, heptabarbital, hexobarbital, and pentobarbital form binary glasses. The glass transition temperatures of these systems do not show a linear increase with composition but attain a maximum at approximately 50% (w/w) of the barbiturate. This deviation is consistent with the formation of a 1:1 mole ratio complex between the two components; it is postulated that there is a greater number of hydrogen bonds in the complex, probably of greater strength, than in glasses of the individual components.

REFERENCES

(1) W. L. Chiou and S. Riegelman, *J. Pharm. Sci.*, **58**, 1505 (1969).
(2) M. P. Summers and R. P. Enever, *ibid.*, **65**, 1613 (1976).
(3) *Ibid.*, **66**, 825 (1977).
(4) R. F. Boyer, *Rubber Chem. Technol.*, **36**, 1303 (1963).
(5) L. D. Pye, in "Introduction to Glass Science," L. D. Pye, H. J. Stevens, and W. C. La Course, Eds., Plenum, New York, N.Y., 1972.
(6) W. A. Lee and G. J. Knight, *Br. Polym. J.*, **2**, 73 (1970).
(7) C. Hansch and S. M. Anderson, *J. Med. Chem.*, **10**, 745 (1967).
(8) Y. Kyogoku, R. C. Lord, and A. Rich, *Nature*, **218**, 69 (1968).
(9) M. Gordon and J. S. Taylor, *J. Appl. Chem.*, **2**, 493 (1952).
(10) K. H. Illers, *Kolloid-Z.*, **190**, 16 (1963).
(11) D. Voet, *J. Am. Chem. Soc.*, **94**, 8213 (1972).

ACKNOWLEDGMENTS

The author thanks Dr. R. J. Gilbert (School of Pharmacy) and the following companies for barbiturate samples: Siegfried (Switzerland), May and Baker Ltd. (England), and Geigy Pharmaceuticals (England). Thanks are also due to W. Dissanayake for technical assistance.

Improved Spectrophotometric Determination of Antazoline

NABIL M. OMAR

Received January 12, 1978, from the *Department of Pharmaceutical Chemistry, University of Assiut, Assiut, Egypt.* Accepted for publication March 21, 1978.

Abstract □ A simple, precise, and accurate spectrophotometric determination of antazoline salts was developed by improving the ceric sulfate procedure. Replacement of water with acetic acid for the preparation of all assay solutions permitted reproducible measurements of the chromogen that absorbed at 505 nm. An appreciable increase in color stability was attained by the controlled addition of perchloric acid to the ceric reagent prior to interaction with antazoline at room temperature. Evidence is provided to account for the oxidation of antazoline at the expense of a complex ceric species. Other 2-imidazolines or phenylephrine did not interfere with the investigated color reaction. In addition to the high value of the chromogen molar absorptivity, ideal adherence of color absorption to Beer's law permitted accurate and reproducible estimation of antazoline over the 1–10-μg range. The procedure was applied to the analysis of different antazoline dosage forms.

Keyphrases □ Antazoline—spectrophotometric analysis in prepared solutions and dosage forms □ Spectrophotometry—analysis, antazoline in prepared solutions and dosage forms □ Antihistaminics—antazoline, spectrophotometric analysis in prepared solutions and dosage forms

The frequent formulation of antazoline[1], 2-[(*N*-phenyl)benzylaminomethyl]-2-imidazoline, with other pharmaceutical amines and 2-imidazoline congeners motivated the development of a selective determination of this antihistamine.

BACKGROUND

Previous antazoline analyses primarily were based on spectrophotometry (1–8). Of the diverse chromogenic reagents adopted, only the sodium nitrite (5–7) and ceric sulfate procedures showed pronounced selectivity. The well-documented and popular ammonium reineckate (1, 2), sodium nitroprusside (3), and dipicrylamine (4) methods are not specific; other pharmaceutical amines and 2-imidazoline derivatives, likely to be present along with antazoline, interfere (9). Moreover, the nitroprusside method, while apparently specific for the intact imidazoline ring, is affected by the experimental buffer concentration and species, the age of reagents, and the intrinsic color of the sample (10).

The utility of the nitrite method is handicapped by interference of phenylephrine with color production (6), and the accuracy of the ceric sulfate procedure is questionable. Discrepancies in recovery studies attained by this latter method reveal considerable nonreproducibility, especially when compared to the nitrite procedure (11). In addition, no quantitative data could be supplied when the ceric reagent was not properly cooled prior to interaction with antazoline or when much water was present. These findings attest to the thermolabile nature of the antazoline–ceric chromogen as well as to its marked sensitivity to pH variations.

Such shortcomings in the available methods for the estimation of an-

[1] Antistine.

0022-3549/78/1100-1610$01.00/0

© 1978, American Pharmaceutical Association

Table I—Effect of Perchloric Acid Addition to Antazoline Reaction Medium on Color Development (c 5 μg/ml)

Milliliters Added per 10 ml of Assay Solution			
0.05% Ceric Reagent	Perchloric Acid	Absorbance	Stability, min
0.5	1.0	0.400	60
0.5	2.0	0.360	70
0.5	3.0	0.310	80
1.0	1.0	0.395	70
1.0	2.0	0.410	90
1.0	3.0	0.405	90
2.0	1.0	0.385	70
2.0	2.0	0.390	80
2.0	3.0	0.378	80

tazoline prompted development of a more accurate and precise method. The antazoline–ceric color reaction and its application to the analysis of pure antazoline salts and some of their pharmaceutical formulations were investigated.

EXPERIMENTAL

Instrumentation—A double-beam UV–visible spectrophotometer[2] with 1-cm glass cells and an analytical balance[3] were used.

Materials—Pharmaceutical grade hydrochloride and methanesulfonate salts of antazoline were utilized as the working standards. The following commercially available formulations were analyzed: antazoline tablets[4], antazoline injection[5], and antazoline–naphazoline solution[6]. Other chemicals were analytically pure.

Reagents—*Ceric Sulfate Solution*—By gentle warming, 50 mg of the dried salt was dissolved in 50 ml of 98% (w/w) sulfuric acid. This solution was then cooled and diluted stepwise and quantitatively to 100 ml with formate-free acetic acid. The clear and bright-yellow solution obtained was quite stable at room temperature.

Standard Antazoline Solution—An accurately weighed amount of the appropriate, well-dried antazoline salt was dissolved in acetic acid, and the solution was diluted quantitatively and stepwise with the same solvent to obtain a final concentration of 50 μg of the working standard/ml of the solution.

Assay Samples—*Tablets*—A single powdered tablet, or its equivalent (150 mg) from a composite of 20 tablets, was placed in a 100-ml volumetric flask. Then ~25 ml of acetic acid was added, and the flask was allowed to stand for 30 min with occasional shaking. The solution was diluted to volume with acetic acid, mixed well, and filtered through a dry filter into a dry flask, the first portions of the filtrate being rejected. An aliquot of this sample was properly diluted with acetic acid to obtain ~50 μg of the claimed antazoline salt content/ml of the assay solution.

Injections and Solutions—For these dosage forms, 1.0 ml of the injection, or the measured content of a single-dose container, was pipetted into a suitable volumetric flask and diluted with acetic acid to obtain ~50 μg of the claimed antazoline salt content/ml of the assay solution.

Procedure—Ceric sulfate reagent (1.0 ml) was transferred into a 10-ml volumetric flask, 2.0 ml of 70% (w/w) perchloric acid was added, and the solution was mixed well. Then 1.0 ml of the standard or assay solution of antazoline was added, and the solution was diluted to volume with acetic acid and mixed well. The solution was transferred directly into a 1-cm glass cell, and the absorbance of the color was determined at 505 nm *versus* a blank prepared from 1.0 ml of acetic acid and treated similarly.

RESULTS AND DISCUSSION

Antazoline–Cerium(IV) Interaction—The original application of ceric sulfate as a color reagent for the identification of medicinal imidazoline derivatives revealed its high sensitivity for the detection of antazoline (12). However, this test could not be quantified because of the instability of the red color formed in 15% aqueous sulfuric acid at room temperature. Enhancing chromogen stability for not more than 30 min by raising the acid concentration to 50%, added with essential cooling before interaction, could not bring about a fully accurate estimation of antazoline; the recovery was ~94–99% (11).

Table II—Effect of Temperature Rise on Antazoline–Ceric Interaction (c 5 μg/ml)

Temperature[a]	Absorbance[b]
25°	0.408
40°	0.383
75°	0.255
95°	0.125

[a] Of a thermostated water bath, as the reaction temperature. [b] At 505 nm after 10-min interaction time.

Water was utilized for the preparation of antazoline and ceric sulfate solutions (11). The chromogen formed is much less stable on addition of water to the reaction mixture (11, 12); therefore, the antazoline–ceric sulfate reaction was performed in 50% sulfuric acid, and the chromogen formed was extracted by organic solvents. However, this procedure was handicapped by the insolubility of the color in chloroform, ether, or benzene.

Further investigation of the behavior of the chromogen in different nonaqueous solvents revealed its complete instability in absolute ethanol, methanol, dimethylformamide, dimethyl sulfoxide, dioxane, acetonitrile, and formic acid. However, marked stability was noticed with acetic acid as the reaction solvent, an observation that recommended its use for the preparation of all solutions. The utility of acetic acid for the ceric sulfate oxidation of organic compounds is well documented (13).

Preliminary interaction at room temperature of antazoline hydrochloride with a 0.05% (w/v) ceric sulfate solution in a 50% (v/v) sulfuric–acetic acid mixture resulted in the instantaneous production of a purple-red color with a maximum absorption at 505 nm. Maximum color intensity was manifested directly after mixing and measurement, with a steady rate of light absorption over 45 min. Repetition of this interaction using lower concentrations of sulfuric acid brought about a measurable decrease in the stability of the chromogen, with a negligible drop of its maximum absorption (Fig. 1).

These data reflect the significance of protonation for the stabilization of the chromogen formed. Further investigation of the effect of higher sulfuric acid concentrations was hindered by the syrupy consistency of the solutions during preparation of the corresponding mixtures in acetic acid. However, this problem was overcome by addition of a measured volume of 70% (w/w) perchloric acid to the ceric reagent, prepared in a 50% (v/v) sulfuric–acetic acid mixture, prior to interaction with the antazoline solution. In contrast to sulfuric acid, perchloric acid offered no

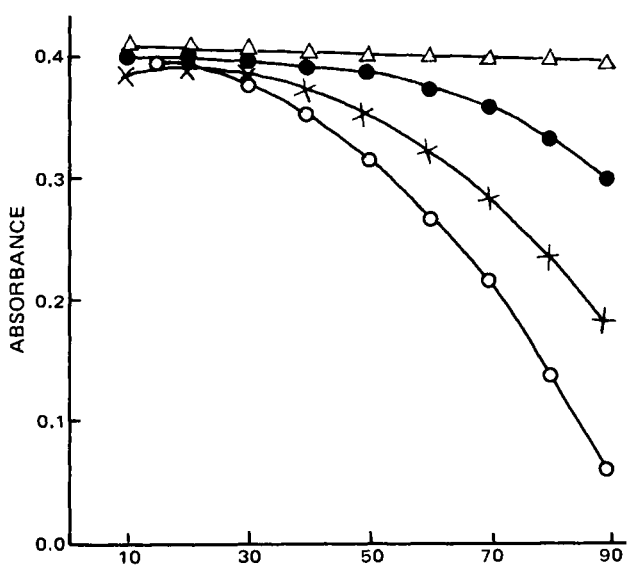

Figure 1—*Absorbance–stability behavior of antazoline chromogen at different sulfuric acid concentrations. Key:* ●, *50% sulfuric acid in glacial acetic acid;* ×, *30% sulfuric acid in glacial acetic acid;* ○, *15% sulfuric acid in glacial acetic acid; and* △, *same as* ● *after addition of 2 ml of perchloric acid.*

[2] MOM, Budapest, Hungary.
[3] WA-33, Warsaw, Poland.
[4] Antistine (Ciba-Geigy, West Germany) contains 100 mg of antazoline hydrochloride/tablet.
[5] Histazine (CID, Egypt) contains 100 mg of antazoline methanesulfonate/2-ml ampul.
[6] Antistine-Privine (Ciba-Geigy) contains 5 mg of antazoline sulfate and 0.25 mg of naphazoline nitrate/1 ml of solution.

Table III—Replicate Analysis of Antazoline Hydrochloride Working Solutions (c 5 μg/ml)

Replication	Absorbance at 505 nm
1	0.410
2	0.408
3	0.408
4	0.409
5	0.410
6	0.412
7	0.407
Average	0.409
SD	$\pm 1.676 \times 10^{-3}$

difficulties with respect to consistency or exothermic interactions. As revealed from the data given in Table I, 90 min of maximum stability was demonstrated by the color developed when 1.0 ml of the ceric reagent was mixed with 2.0 ml of 70% (w/w) perchloric acid and the mixture formed was further interacted with 1.0 ml of the working antazoline hydrochloride solution.

Under optimum conditions for color production, interaction of antazoline with ceric sulfate was seriously affected by a temperature rise (Table II), thus confirming the thermolability of the chromogen as initially postulated. Discrepancies in antazoline estimation, as achieved by the "aqueous" ceric sulfate method, can be attributed to some inaccuracies in controlling the local exothermic effect brought about by water–acid mixing.

Investigation of the effect of the mode of addition on the sensitivity of color production indicated that the antazoline solution should be added to the ceric reagent. Slightly lowered light absorption values were observed with the reverse order.

Reaction Interpretation—Substitution of phenylephrine or other 2-imidazoline derivatives for antazoline in the given interaction failed to induce color formation. These derivatives included 2-methyl-2-imidazoline, naphazoline[7], oxymetazoline[8], tolazoline[9], xylometazoline[10], and tetrahydrozoline[11] hydrochloride salts. With phentolamine[12], a transient blue color appeared for a few moments and faded into pale yellow However, with different aniline derivatives, including *N*-ethylaniline, *N,N*-dimethylaniline, and *o*-toluidine, an instantaneous red-brown color was observed.

These data and the fact that different aniline derivatives are frequently utilized as redox indicators in cerimetric titrations (14) suggested that the antazoline–cerium(IV) color interaction could be explained in terms of the oxidation of the antazoline aniline moiety. That the imidazoline ring is not vulnerable to such an effect is in accord with the stability of this heterocycle toward oxidation (15). This stability is further enhanced in the antazoline salts by their resonance-stabilized guanidinium function. The appreciable stabilization of the antazoline chromogen in the presence of strong acids is also in agreement with the properties of other *N*-disubstituted aniline chromogens (16). Establishment of the exact nature of the investigated color product was not attempted because of its insolubility in different organic solvents, sensitivity to pH variations, thermolability, and instability in aqueous solutions.

Addition of excess perchloric acid to the ceric sulfate reagent prior to the interaction with antazoline lowered reaction sensitivity (Table I). Such lowering was not observed when this excess was added after the interaction of antazoline with the reagent alone. This paradox in the effect of perchloric acid attests to the role of an anionic complex cerium species (17), mostly as $Ce(SO_4)_3^{2-}$, for an effective oxidation of antazoline. The formation of this complex in the presence of higher perchloric acid concentrations is doubtful (18). In support of this view, no color response could be evidenced up to a sensitivity limit of ~100 μg of antazoline/ml when a 0.05% solution of ceric perchlorate in a 50% (v/v) perchloric–acetic acid mixture was reacted under the optimum conditions mentioned.

Quantitative Analysis—For the investigated antazoline–cerium(IV) interaction, the intensity of color absorption was a function of the amount of antazoline interacted. A linear regression analysis of the Beer's plot of antazoline hydrochloride revealed an excellent correlation ($r = 0.9996$) over a concentration range of 1.0–10 μg/ml, with a slope value of 0.082 and an apparent molar absorptivity of 2.47×10^4. For antazoline methanesulfonate, these values were r, 0.9995; concentration range, 2.0–12 μg/ml; slope, 0.066; and apparent molar absorptivity, 2.05×10^4. These results permitted the development of the investigated color reaction into a sensitive spectrophotometric analysis of antazoline salts.

[7] Privine.
[8] Nasivin.
[9] Priscol.
[10] Otrivine.
[11] Tyzine.
[12] Regitine.

Table IV—Recovery Analysis of Antazoline Hydrochloride Working Solutions

	Antazoline Hydrochloride			
Sample	Weight, mg	Level of Analysis, μg/ml	Found[a], mg	Recovery, %
1	25	4	24.9	99.6
2	25	8	25.1	100.4
3	50	3	49.9	99.8
4	50	6	50.8	101.6
5	100	2	99.5	99.5
6	100	10	99.3	99.3
Mean recovery, %				100.03
Relative *SD*				$\pm 8.545 \times 10^{-3}$

[a] Average of four determinations.

Table V—Analysis of Antazoline Commercial Formulations

	Antazoline Salt Content, mg/unit			
Preparation[a]	Label Claim	Found[b]	Added	Recovered[b]
Tablets	100	101.4	50	151.2
Injections[c]	50	49.3	10	59.4
Solution[d]	5.0	5.1	100	105.5

[a] See *Experimental* for details. [b] Average of three determinations. [c] Antazoline methanesulfonate per milliliter. [d] Calculated as antazoline hydrochloride and multiplied by 1.0415.

Replicate analysis of these salts by the improved method (Table III) proved to be very precise, with a relative standard deviation of 4.098×10^{-3}. Recovery studies of working solutions of antazoline hydrochloride, analyzed at different concentrations (Table IV), afforded a mean percent recovery of 100.03 ± 0.85, in comparison to 102.6 ± 0.4 attained by the sodium nitrite method (5–7). No discrepancies in the recovery data of antazoline assayed by the presented method were observed, in contrast to the former ceric sulfate procedure (8, 11). Application of the presented color reaction to the analysis of different, commercially available antazoline dosage forms (Table V) proved satisfactory.

The presented improved ceric sulfate colorimetric determination of antazoline salts offers several advantages over the previously reported method in terms of accuracy, precision, and convenience and surpasses the sodium nitrite procedure on account of its high selectivity and stability of the ceric reagent. These considerations recommend the method for the automated analysis of antazoline formulations.

REFERENCES

(1) F. J. Bandelin, E. D. Slifer, and R. E. Pankratz, *J. Am. Pharm. Assoc., Sci. Ed.*, **39**, 277 (1950).

(2) K. I. Lee, *J. Pharm. Pharmacol.*, **12**, 666 (1960).

(3) S. C. Slack and W. J. Mader, *J. Am. Pharm. Assoc., Sci. Ed.*, **46**, 742 (1957).

(4) E. Selles and A. M. Rodriguez, *Galenica Acta*, **9**, 33 (1956).

(5) S. A. Ibrahim and A. F. Youssef, *Indian J. Pharm. Sci.*, **36**, 73 (1974).

(6) N. M. Sanghavi and H. S. Chardramohan, *ibid.*, **36**, 137 (1974).

(7) M. M. Amer, M. S. Tawakkol, and S. A. Ismaiel, *Analyst*, **99**, 487 (1974).

(8) M. M. Amer, M. S. Tawakkol, and S. A. Ismaiel, *Aust. J. Pharm. Sci.*, **3**, 58 (1974).

(9) P. F. G. Boon and W. Sudds, *J. Pharm. Pharmacol.*, **19**, 88S (1967).

(10) J. A. Mollica, G. R. Padmanabhan, and R. Strusz, *Anal. Chem.*, **45**, 1859 (1973).

(11) S. A. Ismaiel, Master dissertation, Cairo University, Cairo, Egypt, 1974, p. 119.

(12) A. Pitrowska, *Farm. Pol.*, **24**, 71B (1968).

(13) S. V. Gorbachev and Y. I. Vabel, *Zh. Fiz. Khim.*, **28**, 1782 (1954).

(14) L. Chatten, "Pharmaceutical Analysis," vol. I, Dekker, New York, N.Y., 1966, p. 163.

(15) K. Hoffmann, in "The Chemistry of Heterocyclic Compounds,"

vol. 6, A. Weissberger, Ed., Wiley–Interscience, New York, N.Y., 1953, pp. 1–420.
(16) H. S. Tan, G. A. Bruemmer, and D. Shelton, *J. Pharm. Sci.*, **66**, 1037 (1977).
(17) T. J. Hardwick and E. Robertson, *Can. J. Chem.*, **29**, 828 (1951).
(18) E. L. King and M. L. Pandow, *J. Am. Chem. Soc.*, **74**, 1966 (1952).

Effect of Formulation and Process Variables on Bioequivalency of Nitrofurantoin I: Preliminary Studies

ROBERT W. MENDES ˣ, SHABIR Z. MASIH, and R. RANGA KANUMURI

Received December 1, 1977, from the *Department of Industrial Pharmacy, Massachusetts College of Pharmacy, Boston, MA 02115.* Accepted for publication March 22, 1978.

Abstract □ Fifty-two combinations of nitrofurantoin were developed to assess the effect of dosage form type, particle size, diluent, and process on *in vitro* availability. With the official procedure and conditions, dissolution rates fell in a 66-fold range. Statistical analysis of the dissolution rates indicated no significant differences as a result of particle size, processing method, or compression force. The diluent choice and dosage form type significantly influenced the dissolution rate. Based on *in vitro* screening, six formulations presenting a broad range of dissolution rates were selected for further study relating to human bioavailability and bioequivalence.

Keyphrases □ Nitrofurantoin—*in vitro* dissolution rate, effect of formulation and process variables □ Dissolution rate, *in vitro*—nitrofurantoin, effect of formulation and process variables □ Antibacterials, urinary—nitrofurantoin, *in vitro* dissolution rate, effect of formulation and process variables

Nitrofurantoin, an antibacterial agent used in urinary tract infections, was included by the Food and Drug Administration on its list of drugs requiring bioavailability/bioequivalence testing (1). Because of its physicochemical properties, dissolution testing might be used as a means for eliciting inferences concerning its bioavailability. Formulation and manufacturing processes may affect its dissolution and ultimate bioavailability (2), and dissolution is particle size dependent (3–5).

No useful correlation was observed between the extent of urinary excretion and either the disintegration or dissolution characteristics of nitrofurantoin tablets (6, 7). However, the third supplement of USP XIX (8) requires that not less than 25% of the labeled amount of nitrofurantoin must dissolve in 60 min. Since the bioavailability characteristics of commercially produced nitrofurantoin tablets were examined in previous investigations without regard to specific formulation and process variability information, a study was undertaken utilizing predetermined variables to assess their effect on bioequivalence.

EXPERIMENTAL

Particle-Size Reduction and Analysis—To determine the effect of particle size, crystalline nitrofurantoin USP[1] was used both in its commercially available form and in micronized form prepared by processing the commercial material through a fluid energy jet mill[2]. A differential pressure of 30% was used between the inlet and opposing jets.

The original and micronized crystals were then suspended in peanut oil, and the particle size was determined by microscopy (9).

Formulations and Processing—Fifty-two formulations were prepared, incorporating the following variables:

1. Three types of dosage forms (chewable tablets, swallow tablets, and hard gelatin capsules).
2. Two particle sizes of nitrofurantoin crystals.
3. Two processes of incorporation (wet granulation and direct blending–compression).
4. Two diluents [compressible sugar[3] and mannitol[4]–lactose[5] (2:1)].
5. Three levels of hardness or compression force for the tablet formulations.

The formulations are summarized in Tables I–III.

For wet granulation, all ingredients except the lubricant were blended in a cuboidal blender[6] for 10 min at 35 rpm. Granulation then was accomplished in a planetary mixer[7] at 120 rpm for 10 min, using sufficient distilled water to produce the proper consistency. This mixture was granulated through a 12-mesh screen, dried overnight at 48°, and sized through a 16-mesh screen. The granulation was blended with the lubricant in the cuboidal blender for 10 min at 35 rpm. Compression was accomplished on an instrumented rotary tablet press[8] at three levels of force.

For direct compression, all ingredients were blended in the cuboidal blender for 10 min at 35 rpm and compressed as described.

For the hard gelatin capsules, the blends were prepared as for direct compression. The blend was filled into hard gelatin capsules[9] (size 0) using a hand-operated capsule-filling machine[10].

The tablets were physically evaluated on the basis of weight variation, hardness variation, friability, and disintegration. The capsules were physically evaluated on the basis of weight variation only. All dosage forms were evaluated chemically on the basis of composite average assay and content uniformity using a slight modification of the method originally proposed by Conklin and Hollifield (10). An accurate sample equivalent to approximately 100 mg of nitrofurantoin was mixed with approximately 10 ml of dimethylformamide, filtered, quantitatively transferred with adequate rinsing, and diluted to 50 ml with dimethylformamide. A 1.0-ml aliquot of this solution was diluted to 50.0 ml with 10% dimethylformamide. A 1.0-ml aliquot of this dilution was acidified with 2.0 ml of 0.2 *M* HCl and extracted with 5.0 ml of nitromethane. Then 3.0 ml of the nitromethane layer was combined with 0.5 ml of 0.04 *M*

[1] Lot 12060, Berry and Withington Co., Cambridge, Mass.

[2] Gem-T research model, Trost Air Mill Department, Newton, Pa.
[3] Nu-Tab, lot DB917M, Specialty Products by SuCrest, Pennsauken, N.J.
[4] Granular, lot 1219, ICI America, Wilmington, Del.
[5] Anhydrous, lot 4NM10, Sheffield Chemical Co., Union, N.J.
[6] Model KB-15, Erweka-G.m.b.H., Frankfurt, West Germany.
[7] Model N-50, Hobart Manufacturing Co., Troy, Ohio.
[8] Model B-2, Stokes Division, Pennwalt Corp., Warminster, Pa.
[9] Elanco Products Co., Indianapolis, Ind.
[10] Model SGR-O Capsulator, Spielman and Co., Clifton, N.J.

0022-3549/78/1100-1613$01.00/0
© 1978, American Pharmaceutical Association

vol. 6, A. Weissberger, Ed., Wiley–Interscience, New York, N.Y., 1953, pp. 1–420.
(16) H. S. Tan, G. A. Bruemmer, and D. Shelton, *J. Pharm. Sci.*, **66**, 1037 (1977).
(17) T. J. Hardwick and E. Robertson, *Can. J. Chem.*, **29**, 828 (1951).
(18) E. L. King and M. L. Pandow, *J. Am. Chem. Soc.*, **74**, 1966 (1952).

Effect of Formulation and Process Variables on Bioequivalency of Nitrofurantoin I: Preliminary Studies

ROBERT W. MENDES ˣ, SHABIR Z. MASIH, and R. RANGA KANUMURI

Received December 1, 1977, from the *Department of Industrial Pharmacy, Massachusetts College of Pharmacy, Boston, MA 02115.* Accepted for publication March 22, 1978.

Abstract □ Fifty-two combinations of nitrofurantoin were developed to assess the effect of dosage form type, particle size, diluent, and process on *in vitro* availability. With the official procedure and conditions, dissolution rates fell in a 66-fold range. Statistical analysis of the dissolution rates indicated no significant differences as a result of particle size, processing method, or compression force. The diluent choice and dosage form type significantly influenced the dissolution rate. Based on *in vitro* screening, six formulations presenting a broad range of dissolution rates were selected for further study relating to human bioavailability and bioequivalence.

Keyphrases □ Nitrofurantoin—*in vitro* dissolution rate, effect of formulation and process variables □ Dissolution rate, *in vitro*—nitrofurantoin, effect of formulation and process variables □ Antibacterials, urinary—nitrofurantoin, *in vitro* dissolution rate, effect of formulation and process variables

Nitrofurantoin, an antibacterial agent used in urinary tract infections, was included by the Food and Drug Administration on its list of drugs requiring bioavailability/bioequivalence testing (1). Because of its physicochemical properties, dissolution testing might be used as a means for eliciting inferences concerning its bioavailability. Formulation and manufacturing processes may affect its dissolution and ultimate bioavailability (2), and dissolution is particle size dependent (3–5).

No useful correlation was observed between the extent of urinary excretion and either the disintegration or dissolution characteristics of nitrofurantoin tablets (6, 7). However, the third supplement of USP XIX (8) requires that not less than 25% of the labeled amount of nitrofurantoin must dissolve in 60 min. Since the bioavailability characteristics of commercially produced nitrofurantoin tablets were examined in previous investigations without regard to specific formulation and process variability information, a study was undertaken utilizing predetermined variables to assess their effect on bioequivalence.

EXPERIMENTAL

Particle-Size Reduction and Analysis—To determine the effect of particle size, crystalline nitrofurantoin USP[1] was used both in its commercially available form and in micronized form prepared by processing the commercial material through a fluid energy jet mill[2]. A differential pressure of 30% was used between the inlet and opposing jets.

The original and micronized crystals were then suspended in peanut oil, and the particle size was determined by microscopy (9).

Formulations and Processing—Fifty-two formulations were prepared, incorporating the following variables:

1. Three types of dosage forms (chewable tablets, swallow tablets, and hard gelatin capsules).
2. Two particle sizes of nitrofurantoin crystals.
3. Two processes of incorporation (wet granulation and direct blending–compression).
4. Two diluents [compressible sugar[3] and mannitol[4]–lactose[5] (2:1)].
5. Three levels of hardness or compression force for the tablet formulations.

The formulations are summarized in Tables I–III.

For wet granulation, all ingredients except the lubricant were blended in a cuboidal blender[6] for 10 min at 35 rpm. Granulation then was accomplished in a planetary mixer[7] at 120 rpm for 10 min, using sufficient distilled water to produce the proper consistency. This mixture was granulated through a 12-mesh screen, dried overnight at 48°, and sized through a 16-mesh screen. The granulation was blended with the lubricant in the cuboidal blender for 10 min at 35 rpm. Compression was accomplished on an instrumented rotary tablet press[8] at three levels of force.

For direct compression, all ingredients were blended in the cuboidal blender for 10 min at 35 rpm and compressed as described.

For the hard gelatin capsules, the blends were prepared as for direct compression. The blend was filled into hard gelatin capsules[9] (size 0) using a hand-operated capsule-filling machine[10].

The tablets were physically evaluated on the basis of weight variation, hardness variation, friability, and disintegration. The capsules were physically evaluated on the basis of weight variation only. All dosage forms were evaluated chemically on the basis of composite average assay and content uniformity using a slight modification of the method originally proposed by Conklin and Hollifield (10). An accurate sample equivalent to approximately 100 mg of nitrofurantoin was mixed with approximately 10 ml of dimethylformamide, filtered, quantitatively transferred with adequate rinsing, and diluted to 50 ml with dimethylformamide. A 1.0-ml aliquot of this solution was diluted to 50.0 ml with 10% dimethylformamide. A 1.0-ml aliquot of this dilution was acidified with 2.0 ml of 0.2 *M* HCl and extracted with 5.0 ml of nitromethane. Then 3.0 ml of the nitromethane layer was combined with 0.5 ml of 0.04 *M*

[1] Lot 12060, Berry and Withington Co., Cambridge, Mass.

[2] Gem-T research model, Trost Air Mill Department, Newton, Pa.
[3] Nu-Tab, lot DB917M, Specialty Products by SuCrest, Pennsauken, N.J.
[4] Granular, lot 1219, ICI America, Wilmington, Del.
[5] Anhydrous, lot 4NM10, Sheffield Chemical Co., Union, N.J.
[6] Model KB-15, Erweka-G.m.b.H., Frankfurt, West Germany.
[7] Model N-50, Hobart Manufacturing Co., Troy, Ohio.
[8] Model B-2, Stokes Division, Pennwalt Corp., Warminster, Pa.
[9] Elanco Products Co., Indianapolis, Ind.
[10] Model SGR-O Capsulator, Spielman and Co., Clifton, N.J.

0022-3549/78/1100-1613$01.00/0
© 1978, American Pharmaceutical Association

Table I—Preliminary Formulation of Nitrofurantoin Chewable Tablets

Formulation	Ingredients[a], %							
	X_1	X_2	Li	Ca	Sa	Mg	D_1	D_2
IA, IB, IC	6.67	—	0.67	1.67	1.00	0.50	89.50	—
ID, IE, IF	—	6.67	0.67	1.67	1.00	0.50	89.50	—
IG, IH, I-I	6.67	—	0.67	1.67	1.00	0.50	—	89.50
IJ, IK, IL	—	6.67	0.67	1.67	1.00	0.50	—	89.50
IM, IN, IO	6.67	—	0.67	1.67	1.00	0.50	89.50	—
IP, IQ, IR	—	6.67	0.67	1.67	1.00	0.50	89.50	—
IS, IT, IU	6.67	—	0.67	1.67	1.00	0.50	—	89.50
IV, IW, IX	—	6.67	0.67	1.67	1.00	0.50	—	89.50

[a] X_1 = nitrofurantoin crystal USP, X_2 = nitrofurantoin micronized crystals, Li = lime flavor, Ca = citric acid, Sa = saccharin sodium powder, Mg = magnesium stearate USP, D_1 = compressible sugar, and D_2 = mannitol–lactose (2:1).

quaternary ammonium hydroxide[11] in absolute methanol. The absorbance was determined spectrophotometrically[12] at 400 nm against a blank sample prepared by carrying 1.0 ml of 10% dimethylformamide through the extraction procedure. The resulting absorbance then was compared to a previously constructed standard curve to determine concentration.

All dosage forms were evaluated for dissolution rate using the USP XIX procedure (11). The dissolution medium consisted of 900 ml of pH 7.2 phosphate buffer maintained at 37° in a constant-temperature bath, and the basket was rotated at 100 rpm. Samples of 2.5 ml were collected at 5, 10, 15, 20, 30, 40, 50, 60, 75, and 90 min. Each sample withdrawal was replaced by an equivalent amount of dissolution medium.

The samples were assayed by diluting 1.0 ml of each sample to 10.0 ml with buffer and determining the absorbance at 380 nm against a blank consisting of the buffer. The dissolution rate was then calculated for each formulation. All resulting evaluation data were subjected to a factorial design analysis of variance to determine which variables affected the dissolution rate. Ultimately, six formulations were selected for Phase II of the study.

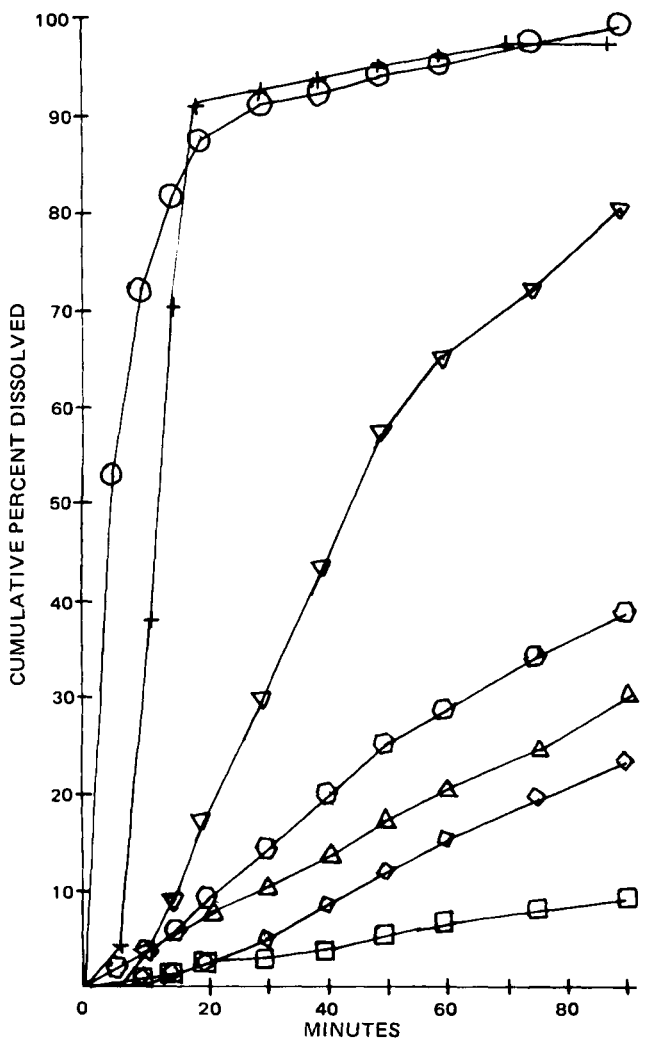

Figure 1—*Mean cumulative percent of nitrofurantoin dissolved in phosphate buffer. Each data point is the mean of three determinations. Key: ○, Formulation IIIC; +, Formulation IG; ○, Formulation CTL; □, Formulation IIA; ◇, Formulation IIM; △, Formulation IA; and ▽, Formulation IIIA.*

[11] Hyamine.
[12] Model DB-GT, Beckman Instrument Co., Fullerton, Calif.

RESULTS AND DISCUSSION

The microscopic particle-size analysis, based on the examination of 100 particles, revealed a geometric mean diameter for the commercial material of 3.0 μm with a standard deviation of 1.66. The micronized product had a geometric mean diameter of 0.75 μm with a standard deviation of 2.0. There was, therefore, a fourfold difference in the average particle sizes of the two forms of nitrofurantoin.

All tablet formulations were produced without difficulty to contain 100 mg of active ingredient. Because of bulk density and a desire for reasonable size, the capsules were produced to contain 50 mg each; two capsules were then used as one unit dose.

The dosage form evaluation data are summarized categorically by dosage form type and processing method in Tables IV–VIII.

The weight variation for all formulations was well within compendial limits, *i.e.*, ±5% for tablets and ±10% for capsules. In general, the weight variation for formulations produced with compressible sugar was better than for those produced with the mannitol–lactose combination. Presumably, this result is due to the better flowability of the former excipient.

Table II—Preliminary Formulation of Nitrofurantoin Swallow Tablets

Formulation	Ingredients[a], %					
	X_1	X_2	Mg	Vg	D_1	D_2
IIA, IIB, IIC	16.67	—	0.50	—	82.83	—
IID, IIE, IIF	—	16.67	0.50	—	82.83	—
IIG, IIH, II-I	16.67	—	0.50	5.00	77.83	—
IIJ, IIK, IIL	—	16.67	0.50	5.00	77.83	—
IIM, IIN, IIO	16.67	—	0.50	—	—	82.83
IIP, IIQ, IIR	—	16.67	0.50	—	—	82.83
IIS, IIT, IIU	16.67	—	0.50	5.00	—	77.83
IIV, IIW, IIX	—	16.67	0.50	5.00	—	77.83

[a] X_1 = nitrofurantoin crystal USP, X_2 = nitrofurantoin micronized, Mg = magnesium stearate, Vg = aluminum magnesium silicate (Veegum) medium fine, D_1 = compressible sugar, and D_2 = mannitol–lactose (2:1).

Table III—Preliminary Formulation of Nitrofurantoin Capsules

Formulation	Ingredients[a], %				
	X_1	X_2	Mg	D_1	D_2
IIIA	9.52	—	1.00	89.48	—
IIIB	—	9.52	1.00	89.48	—
IIIC	11.36	—	1.00	—	87.89
IIID	—	11.36	1.00	—	87.89

[a] X_1 = nitrofurantoin crystal USP, X_2 = nitrofurantoin micronized, Mg = magnesium stearate, D_1 = compressible sugar, and D_2 = mannitol–lactose (2:1).

Table IV—Evaluation Summary for 12 Nitrofurantoin Chewable Tablet Formulations Produced by Direct Compression

Diluent	Particle Size of Nitrofurantoin, μm	Compression Force, kg	Hardness, SCU	Disintegration, min	Dissolution Rate, mg/min
Compressible sugar	USP, 3.0	1571–2200	8–11	8–12	0.0021–0.0026
	Micronized, 0.75	1571–2200	9–12	8–12	0.0021–0.0036
Mannitol–lactose	USP, 3.0	1257–1885	9–14	6–10	0.0300–0.0418
	Micronized, 0.75	1257–1885	12–17	8–10	0.0141–0.0529

Table V—Evaluation Summary for 12 Nitrofurantoin Chewable Tablet Formulations Produced by Wet Granulation

Diluent	Particle Size of Nitrofurantoin, μm	Compression Force, kg	Hardness, SCU	Disintegration, min	Dissolution Rate, mg/min
Compressible sugar	USP, 3.0	1571–2200	12–15	8–12	0.0022–0.0024
	Micronized, 0.75	1571–2200	12–17	8–12	0.0014–0.0019
Mannitol–lactose	USP, 3.0	1257–1414	15–18	8–10	0.0140–0.0209
	Micronized, 0.75	1257–1414	15–18	7–10	0.0166–0.0213

Table VI—Evaluation Summary for 12 Nitrofurantoin Swallow Tablet Formulations Produced by Direct Compression

Diluent	Particle Size of Nitrofurantoin, μm	Compression Force, kg	Hardness, SCU	Disintegration, min	Dissolution Rate, mg/min
Compressible sugar	USP, 3.0	943–1257	8–10	14–16	0.0012
	Micronized, 0.75	1100–1414	9–11	14–16	0.0013
Mannitol–lactose	USP, 3.0	629–943	9–14	8–15	0.0022–0.0029
	Micronized, 0.75	471–943	8–14	6–12	0.0023–0.0041

Table VII—Evaluation Summary for 12 Nitrofurantoin Swallow Tablet Formulations Produced by Wet Granulation

Diluent	Particle Size of Nitrofurantoin, μm	Compression Force, kg	Hardness, SCU	Disintegration, min	Dissolution Rate, mg/min
Compressible sugar	USP, 3.0	707–1021	9–13	14–16	0.0090–0.0091
	Micronized, 0.75	707–1021	10–14	14–16	0.0080–0.0090
Mannitol–lactose	USP, 3.0	550–943	9–13	2–4	0.0018–0.0048
	Micronized, 0.75	550–943	9–13	2–5	0.0020–0.0043

Tablet hardness fell generally in a range of 8–18 Strong–Cobb units (SCU) with a standard deviation of approximately ±1.0.

Friability for the tablet formulations fell within a range of 0.12–2.03%. In general, the friability of formulations produced with mannitol–lactose was higher than for formulations produced with compressible sugar. The friability of the chewable tablets was generally greater than that of the swallow tablets, no doubt because of their greater size, weight, and surface area. The disintegration times for the tablets fell within a range of 2–16 min. In general, disintegration was more rapid for formulations made with mannitol–lactose than for those made with compressible sugar. The composite assays for all formulations fell within the compendial limits of 95–105% of the labeled amount. Content uniformity testing also fell within the compendial limits of 85–115%.

The dissolution rates for the formulations ranged from 0.0008 to 0.0529 mg/min (Fig. 1). Statistical analysis indicated that the difference in the two particle sizes of nitrofurantoin did not significantly affect dissolution. Apparently, the particle size of commercially available nitrofurantoin is sufficiently small to elicit the maximum dissolution rate for this material. Surprisingly, neither process method (wet granulation *versus* dry blending–compression) nor compression force–hardness significantly affected the dissolution rate of the tablets. This result indicates that the intrinsic solubility of the drug is sufficient to overcome the binding of individual particles through both wet granulation and void space reduction as a result of applied compression force.

The diluent choice produced significantly ($p < 0.05$) different dissolution rates. Dissolution of the formulations made with mannitol–lactose was significantly faster than that of formulations made with compressible sugar. A viable explanation for this difference is not apparent. It appears that the presence of compressible sugar definitely depressed the nitrofurantoin dissolution rate. This effect could be due to competitive solubility, gelatinization–encapsulation, or chemical complexation.

Dosage form type also produced a significant ($p < 0.05$) difference in dissolution rate. The hard gelatin capsules produced the most rapid dissolution, followed by the chewable tablets and, finally, by the swallow tablets. The rapid dissolution of the capsules was, of course, anticipated since the disintegration of a capsule shell is generally faster than the disintegration of tablets and since no binding force is applied during encapsulation. The percentage concentration of active ingredient in the chewable tablets was considerably lower (6.67%) than in the swallow tablets (16.67%). This concentration difference could have led to more rapid dissolution as disintegration took place since greater surface area would be provided to the dissolution medium by the physically larger chewable tablets.

Based on the foregoing results, six formulations were selected for Phase II (bioequivalence) of the study. Two capsules (IIIA and IIIC), two chewable tablets (IA and IG), and two swallow tablets (IIA and IIM) were chosen to provide a broad range of dissolution rates, the objective being to conduct the bioequivalence study with a group of formulations that could be expected to produce diverse bioavailability.

Table VIII—Evaluation Summary for 12 Nitrofurantoin Capsule Formulations

Diluent	Particle Size of Nitrofurantoin, μm	Dissolution Rate, mg/min
Compressible sugar	USP, 3.0	0.0176
	Micronized, 0.75	0.0143
Mannitol–lactose	USP, 3.0	0.0460
	Micronized, 0.75	0.0518

REFERENCES

(1) *Fed. Regist.*, **40**, 26164 (1975).

(2) G. Levy, in "Physico-Chemical Aspects of Drug Action," E. J. Ariens, Ed., Pergamon, New York, N.Y., 1968, p. 48.

(3) F. J. Hailey and H. W. Glassocle, *Curr. Ther. Res.*, **1**, 600 (1967).

(4) H. E. Paul, J. H. Keyon, M. F. Paul, and A. R. Borgman, *J. Pharm. Sci.*, **56**, 882 (1967).

(5) R. G. Stoll, R. B. Bates, and J. Swarbrick, *ibid.*, **62**, 65 (1973).

(6) G. L. Mattok, R. D. Hossie, and I. J. McGilveray, *Can J. Pharm. Sci.*, **7**, 3 (1972).

(7) M. C. Meyer, G. W. A. Slywka, R. E. Dann, and P. L. Whyatt, *J. Pharm. Sci.*, **63**, 1693 (1974).

(8) "Third Supplement to The United States Pharmacopeia XIX and The National Formulary XIV," Mack Publishing Co., Easton, Pa., 1977, p. 103.

(9) I. C. Edmundson, in "Advances in Pharmaceutical Sciences," vol. 2, H. S. Bean, S. E. Carless, and A. H. Beckett, Eds., Academic, London, England, 1967, p. 95.

(10) J. D. Conklin and R. D. Hollifield, *Clin. Chem.*, **11**, 925 (1965).

(11) "The United States Pharmacopeia," 19th rev., Mack Publishing Co., Easton, Pa., 1975, p. 343.

ACKNOWLEDGMENTS

Presented at the Industrial Pharmaceutical Technology Section, APhA Academy of Pharmaceutical Sciences, Phoenix meeting, November 1977.

Abstracted from a thesis submitted by R. R. Kanumuri to the Massachusetts College of Pharmacy in partial fulfillment of the Doctor of Philosophy degree requirements.

Effect of Formulation and Process Variables on Bioequivalency of Nitrofurantoin II: *In Vivo–In Vitro* Correlation

ROBERT W. MENDES ˣ, SHABIR Z. MASIH, and R. RANGA KANUMURI

Received December 1, 1977, from the *Department of Industrial Pharmacy, Massachusetts College of Pharmacy, Boston, MA 02115.* Accepted for publication March 22, 1978.

Abstract □ Based on preliminary *in vitro* evaluation, six formulations presenting a broad range of dissolution rates were selected for bioequivalency determination in a randomized complete block crossover. *In vitro–in vivo* correlations were developed relating cumulative percent dissolved to cumulative percent excreted. These correlations appear to be useful for comparing different formulations as well as different batches of the same formulation.

Keyphrases □ Nitrofurantoin—various formulations, bioavailability in humans correlated to dissolution rate *in vitro* □ Bioavailability—various formulations of nitrofurantoin in humans, correlated to dissolution rate *in vitro* □ Dissolution rate, *in vitro*—various formulations of nitrofurantoin correlated with bioavailability in humans □ Antibacterials, urinary—nitrofurantoin, various formulations, bioavailability in humans correlated to dissolution rate *in vitro*

Numerous reports (1–5) provided support for the contention that not all commercially available products meeting compendial requirements necessarily exhibit equivalent bioavailability. Nitrofurantoin exhibits this problem (3–5). The Food and Drug Administration included nitrofurantoin on its list (6) of drugs requiring bioavailability testing for market preclearance, and the American Pharmaceutical Association included it in their bioavailability monograph project (7).

Previous studies on the bioinequivalence of nitrofurantoin utilized commercially available products for testing without regard to formulation and process variables that might affect bioequivalency. A preliminary study (8) concerned the development and screening of 52 nitrofurantoin products having controlled variables in formulation and processing. This screening on the basis of *in vitro* test procedures led to the selection of six final formulations for bioequivalency testing and attempts at correlation with *in vitro* test results.

Table I—Final Formulations of Nitrofurantoin Tablets and Capsules

Formulation[a]	IA	IG	IIA	IIM	IIIA	IIIC
Nitrofurantoin crystals USP, %	6.67	6.67	16.67	16.67	9.52	11.36
Lime flavor, %	0.67	0.67	—	—	—	—
Citric acid monohydrate, powdered USP, %	1.67	1.67	—	—	—	—
Saccharin sodium USP, %	1.00	1.00	—	—	—	—
Magnesium stearate USP, %	0.50	0.50	0.50	0.50	1.00	1.00
Compressible sugar, %	89.5	—	82.83	—	89.48	—
Lactose, anhydrous USP, %	—	30.0	—	27.67	—	29.30
Mannitol, granular USP, %	—	59.5	—	55.16	—	58.59

[a] IA = nitrofurantoin chewable tablets, IG = nitrofurantoin chewable tablets, IIA = nitrofurantoin swallow tablets, IIM = nitrofurantoin swallow tablets, IIIA = nitrofurantoin swallow capsules, and IIIC = nitrofurantoin swallow capsules.

Table II—Experimental Design for Nitrofurantoin Bioavailability Evaluation [a]

Subject	Day 1	4	7	10	13	16	19
1	IG	CTL	IIA	IIM	IIIA	IIIC	IA
2	CTL	IIA	IIM	IIIA	IIIC	IA	IG
3	IIA	IIM	IIIA	IIIC	IA	IG	CTL
4	IIM	IIIA	IIIC	IA	IG	CTL	IIA
5	IIIC	IA	IG	CTL	IIA	IIM	IIIA

[a] Each item within the matrix corresponds to a specific formulation as described in Table I; CTL = control.

EXPERIMENTAL

Formulations—Based on preliminary dissolution data (8), six formulations (Table I) were selected to provide a broad range of dissolution rates with the expectation that this range would lead to a wide variation in bioavailability. The six formulations consisted of three dosage forms

0022-3549/78/1100-1616$01.00/0

© 1978, American Pharmaceutical Association

REFERENCES

(1) *Fed. Regist.*, **40**, 26164 (1975).

(2) G. Levy, in "Physico-Chemical Aspects of Drug Action," E. J. Ariens, Ed., Pergamon, New York, N.Y., 1968, p. 48.

(3) F. J. Hailey and H. W. Glassocle, *Curr. Ther. Res.*, **1**, 600 (1967).

(4) H. E. Paul, J. H. Keyon, M. F. Paul, and A. R. Borgman, *J. Pharm. Sci.*, **56**, 882 (1967).

(5) R. G. Stoll, R. B. Bates, and J. Swarbrick, *ibid.*, **62**, 65 (1973).

(6) G. L. Mattok, R. D. Hossie, and I. J. McGilveray, *Can J. Pharm. Sci.*, **7**, 3 (1972).

(7) M. C. Meyer, G. W. A. Slywka, R. E. Dann, and P. L. Whyatt, *J. Pharm. Sci.*, **63**, 1693 (1974).

(8) "Third Supplement to The United States Pharmacopeia XIX and The National Formulary XIV," Mack Publishing Co., Easton, Pa., 1977, p. 103.

(9) I. C. Edmundson, in "Advances in Pharmaceutical Sciences," vol. 2, H. S. Bean, S. E. Carless, and A. H. Beckett, Eds., Academic, London, England, 1967, p. 95.

(10) J. D. Conklin and R. D. Hollifield, *Clin. Chem.*, **11**, 925 (1965).

(11) "The United States Pharmacopeia," 19th rev., Mack Publishing Co., Easton, Pa., 1975, p. 343.

ACKNOWLEDGMENTS

Presented at the Industrial Pharmaceutical Technology Section, APhA Academy of Pharmaceutical Sciences, Phoenix meeting, November 1977.

Abstracted from a thesis submitted by R. R. Kanumuri to the Massachusetts College of Pharmacy in partial fulfillment of the Doctor of Philosophy degree requirements.

Effect of Formulation and Process Variables on Bioequivalency of Nitrofurantoin II: *In Vivo–In Vitro* Correlation

ROBERT W. MENDES ˣ, SHABIR Z. MASIH, and R. RANGA KANUMURI

Received December 1, 1977, from the *Department of Industrial Pharmacy, Massachusetts College of Pharmacy, Boston, MA 02115.* Accepted for publication March 22, 1978.

Abstract □ Based on preliminary *in vitro* evaluation, six formulations presenting a broad range of dissolution rates were selected for bioequivalency determination in a randomized complete block crossover. *In vitro–in vivo* correlations were developed relating cumulative percent dissolved to cumulative percent excreted. These correlations appear to be useful for comparing different formulations as well as different batches of the same formulation.

Keyphrases □ Nitrofurantoin—various formulations, bioavailability in humans correlated to dissolution rate *in vitro* □ Bioavailability—various formulations of nitrofurantoin in humans, correlated to dissolution rate *in vitro* □ Dissolution rate, *in vitro*—various formulations of nitrofurantoin correlated with bioavailability in humans □ Antibacterials, urinary—nitrofurantoin, various formulations, bioavailability in humans correlated to dissolution rate *in vitro*

Numerous reports (1–5) provided support for the contention that not all commercially available products meeting compendial requirements necessarily exhibit equivalent bioavailability. Nitrofurantoin exhibits this problem (3–5). The Food and Drug Administration included nitrofurantoin on its list (6) of drugs requiring bioavailability testing for market preclearance, and the American Pharmaceutical Association included it in their bioavailability monograph project (7).

Previous studies on the bioinequivalence of nitrofurantoin utilized commercially available products for testing without regard to formulation and process variables that might affect bioequivalency. A preliminary study (8) concerned the development and screening of 52 nitrofurantoin products having controlled variables in formulation and processing. This screening on the basis of *in vitro* test procedures led to the selection of six final formulations for bioequivalency testing and attempts at correlation with *in vitro* test results.

Table I—Final Formulations of Nitrofurantoin Tablets and Capsules

Formulation[a]	IA	IG	IIA	IIM	IIIA	IIIC
Nitrofurantoin crystals USP, %	6.67	6.67	16.67	16.67	9.52	11.36
Lime flavor, %	0.67	0.67	—	—	—	—
Citric acid monohydrate, powdered USP, %	1.67	1.67	—	—	—	—
Saccharin sodium USP, %	1.00	1.00	—	—	—	—
Magnesium stearate USP, %	0.50	0.50	0.50	0.50	1.00	1.00
Compressible sugar, %	89.5	—	82.83	—	89.48	—
Lactose, anhydrous USP, %	—	30.0	—	27.67	—	29.30
Mannitol, granular USP, %	—	59.5	—	55.16	—	58.59

[a] IA = nitrofurantoin chewable tablets, IG = nitrofurantoin chewable tablets, IIA = nitrofurantoin swallow tablets, IIM = nitrofurantoin swallow tablets, IIIA = nitrofurantoin swallow capsules, and IIIC = nitrofurantoin swallow capsules.

Table II—Experimental Design for Nitrofurantoin Bioavailability Evaluation [a]

Subject	Day 1	4	7	10	13	16	19
1	IG	CTL	IIA	IIM	IIIA	IIIC	IA
2	CTL	IIA	IIM	IIIA	IIIC	IA	IG
3	IIA	IIM	IIIA	IIIC	IA	IG	CTL
4	IIM	IIIA	IIIC	IA	IG	CTL	IIA
5	IIIC	IA	IG	CTL	IIA	IIM	IIIA

[a] Each item within the matrix corresponds to a specific formulation as described in Table I; CTL = control.

EXPERIMENTAL

Formulations—Based on preliminary dissolution data (8), six formulations (Table I) were selected to provide a broad range of dissolution rates with the expectation that this range would lead to a wide variation in bioavailability. The six formulations consisted of three dosage forms

0022-3549/78/1100-1616$01.00/0

© 1978, American Pharmaceutical Association

Table III—*In Vitro* Data Summary for Nitrofurantoin Solid Dosage Forms

Test	Formulation[a]						
	CTL[b]	IA	IG	IIA	IIM	IIIA	IIIC
Disintegration, min	9	10	5	13	7	—	—
Hardness[c], SCU	18.0	8.8	8.9	8.8	9.1	—	—
Dissolution, mg/min							
Phosphate buffer	0.0057	0.0040	0.0423	0.0011	0.0032	0.0196	0.0381
Acid buffer	—	—	—	—	—	0.0030	0.0090

[a] For description of formulations, see Table I. [b] Control. [c] Mean of 20 determinations.

(chewable tablet, swallow tablet, and hard gelatin capsule) produced with two diluent excipients [compressible sugar[1] and mannitol[2]–lactose[3] (2:1)]. All dosage forms were prepared using commercially available nitrofurantoin crystals[4] by direct blending–granulation and, for tablets, at the lowest compression force necessary to make physically satisfactory tablets. A commercially available nitrofurantoin tablet[5] was used as the control.

Bioavailability Protocol—Five male volunteers[6] between the ages of 20 and 40 years and with a weight range of 43–75 kg were given a blood chemistry analysis[7] to ensure inclusion of only those subjects in good health. All subjects were instructed to refrain from taking any other medication during the study. Each subject was given a 100-mg dose (one tablet or two capsules) of a nitrofurantoin product once every 72 hr until all dosage forms were administered in accordance with the experimental design (Table II).

Since bioavailability has been shown to be greater if nitrofurantoin is taken with food (9), the dose was taken in the morning after a light breakfast of 240 ml of milk and 30 g of cold cereal[8]. Since urinary excretion studies are the method of choice (approximately 40% of the drug is excreted in the urine as unchanged drug following oral administration) and since clearance is independent of urinary pH (10), urine samples were collected at 0, 0.5, 1.0, 1.5, 2.0, 3.0, 6.0, 8.0, 12.0, and 24.0 hr. A volume of 150 ml of water was provided at 0, 0.5, 1.0, 2.0, 3.0, and 4.0 hr to ensure adequate urine volume.

The volume of each urine sample was recorded along with the time of collection, and an aliquot was taken. Preliminary experimentation indicated that nitrofurantoin frozen in urine exhibited excellent stability for several days. Therefore, the samples were frozen to provide convenience in analysis and were allowed to thaw immediately before use.

Urinalysis—An aliquot (0.5 ml) of each urine sample was acidified with 2.0 ml of 0.2 *N* HCl. Nitromethane (5.0 ml) was added, mixed, and centrifuged. From the nitromethane layer, 3.0 ml was removed and transferred to a test tube. A quaternary ammonium hydroxide[9] solution (0.5 ml of 0.04 *M*) was added, and the solution was mixed and allowed to stand for at least 2, but not more than 30, min. Absorbance was determined spectrophotometrically[10] at 400 nm against a blank, and concentration was determined from a previously constructed standard curve.

Correlation Methodology—The urinary excretion data obtained from the randomized complete block experimental design were analyzed according to a one-compartment open model using the following relationship (11):

$$X_t = 100\left[\left(1 - \frac{1}{K_a - K}\right)(K_a e^{-Kt} - K e^{-K_a t})\right] \quad \text{(Eq. 1)}$$

where X_t is the percent of drug excreted to time t, K_a is the absorption rate constant, and K is the elimination rate constant.

Initial estimates of the absorption and elimination rate constants were obtained graphically by a semilog plot of the excretion rate *versus* time. With the initial estimates of K and K_a, the data were subjected to digital computer least-squares iterations using the program NONLIN (12) to obtain the best estimates.

A two-way analysis of variance was performed on the cumulative amount excreted, the absorption rate, the peak excretion rate, the peak excretion time, and the elimination rate. Where significant f ratios were

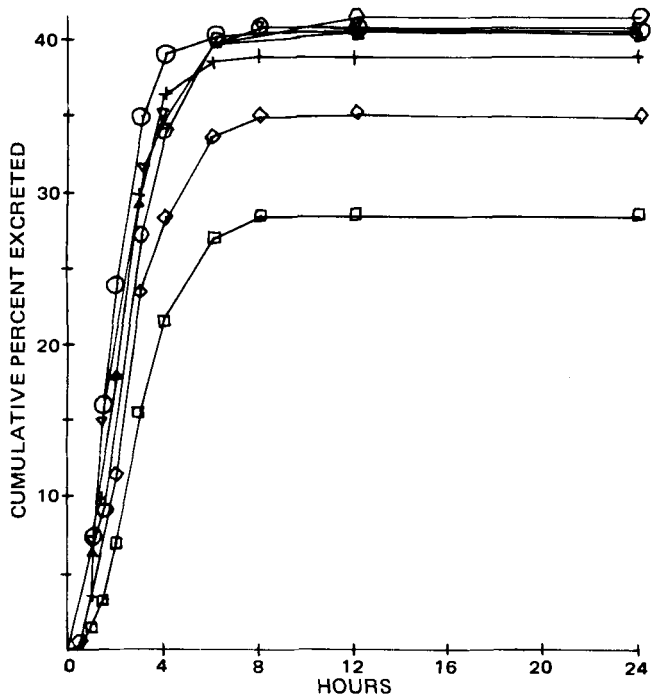

Figure 1—*Mean cumulative percent of nitrofurantoin excreted following the oral administration of nitrofurantoin products. Each data point is the mean cumulative percent excreted for all five subjects. Key: ○, Formulation CTL; ▽, Formulation IG; △, Formulation IA; ○, Formulation IIIC; □, Formulation IIA; ◇, Formulation IIM; and +, Formulation IIIA.*

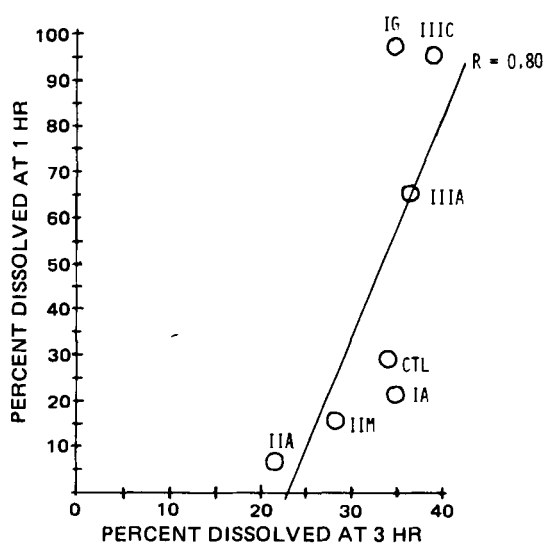

Figure 2—*Linear correlation of excretion in urine after 3 hr* versus *dissolution in phosphate buffer after 1 hr for seven nitrofurantoin formulations.*

[1] Nu-Tab, lot BD917M, Specialty Products by SuCrest, Pennsauken, N.J.
[2] Granular, lot 1219, ICI America, Wilmington, Del.
[3] Anhydrous, lot 4NM10, Sheffield Chemical Co., Union, N.J.
[4] Lot 12060, Berry and Withington Co., Cambridge, Mass.
[5] Furadantin, lot 810315, Eaton Laboratories, Norwich, N.Y.
[6] Each subject gave written informed consent.
[7] SMA 18/60.
[8] Product 19, Kellogg Co., Battle Creek, MI 49016.
[9] Hyamine.
[10] Model DB-GT, Beckman Instrument Co., Fullerton, Calif.

Table IV—Bioavailability Parameters for Nitrofurantoin Tablets and Capsules

Formulation[a]	Cumulative Amount[b], mg	Absorption Rate Constant[b], hr^{-1}	Peak Excretion Rate[b], mg/hr	Peak Excretion Time[b], hr	Duration min	
					30 μg/ml Maintained[b]	75 μg/ml Maintained
CTL	41.48	0.6900	13.37	2.40	272	127
	(2.01)	(0.1729)	(4.02)	(1.23)	(112)	(73)
IA	40.74	0.8270	12.99	1.73	256	101
	(2.44)	(0.1630)	(3.34)	(0.50)	(49)	(79)
IG	40.63	1.0559	14.20	1.55	235	107
	(2.99)	(0.2746)	(3.69)	(0.45)	(113)	(88)
IIA	28.30	0.6313	8.49	2.85	257	64
	(1.24)	(0.2385)	(2.31)	(1.11)	(77)	(76)
IIM	35.74	0.8299	11.60	2.42	265	171
	(1.02)	(0.2583)	(2.76)	(0.65)	(109)	(159)
IIIA	38.81	0.9667	14.40	2.25	228	85
	(3.22)	(0.2005)	(2.81)	(0.53)	(60)	(93)
IIIC	40.10	0.9826	17.44	1.70	226	135
	(3.54)	(0.1735)	(3.80)	(0.54)	(63)	(73)

[a] For description of formulations, see Table I. [b] Mean values of five subjects with standard deviation in parentheses.

detected, linear contrasts were utilized to elicit the specific factors related to their cause.

To derive *in vitro–in vivo* correlations, two approaches were taken. The cumulative percent excreted at various times was compared to the cumulative percent dissolved at various times using the Spearman rank correlation method. The times giving best correlation by this method were then plotted using simple linear regression analysis.

Next, to determine the correlation for each formulation, the percent excreted at various times was compared to the cumulative percent dissolved at various times. When dissolution was very rapid, it was necessary to change the conditions to produce the best correlation.

RESULTS AND DISCUSSION

Bioequivalency—Pertinent *in vitro* evaluative data for the six formulations and the control are presented in Table III. The mean hardnesses of the four tablet formulations were essentially identical, ranging from 8.8 to 9.1 Strong-Cobb units (SCU), while that of the control was significantly higher at 18. Disintegration time ranged from a low of 5 to a high of 13 min, with the control at 9 min. This result obviously precluded any correlation between hardness and disintegration time. The dissolution rate in phosphate buffer ranged from a low of 0.0011 to a high of 0.0423 mg/min. The significant differences among the tablet formulations precluded any correlation with tablet hardness. The dissolution profiles for the six formulations and the control in phosphate buffer were presented previously (8).

Nonlinear regression indicated that the urinary excretion data analyzed according to a one-compartment open model gave a correlation coefficient of at least 0.98. Table IV lists the means of the computer estimates of each bioavailability parameter for each formulation. Two-way analysis of variance, followed by linear contrast, revealed significant differences among the formulations with respect to all parameters. However, for all except cumulative amount excreted, the intersubject variability exceeded the interformulation variability.

Figure 1 shows the profiles for cumulative amount excreted as a function of time. Linear contrasts indicated that the chewable tablets and hard gelatin capsules were not significantly different ($p < 0.05$) from the control. The swallow tablets prepared with mannitol–lactose had a slightly lower (84.5%) bioavailability than the control, while the swallow tablets made with compressible sugar had a significantly lower bioavailability (68%).

The urine concentration of nitrofurantoin was also examined. A previous study (5) indicated that a urine concentration of 30 μg/ml should be effective against 90% of the strains of *Escherichia coli*, although levels of 75 μg/ml may be required against some strains. The urinary concentration of nitrofurantoin at each sampling time for each product in each subject was examined. Formulation differences were insignificant, but subject variability was significant. This result was due to extreme differences in the urine volume for each subject. It was concluded that a determination of this type would require a large number of subjects, preferably actual patients with urinary tract infections.

***In Vitro–In Vivo* Correlation**—The Spearman rank correlation test for the 3-hr cumulative excretion and 1-hr cumulative dissolution (Table V) produced a correlation coefficient of 0.93 and a t value of 5.59. Both values indicate good rank-order correlation between the parameters. When the data relative to these ranks were subjected to linear regression analysis, a correlation coefficient of 0.80 resulted (Fig. 2). This value was judged to be relatively acceptable for overall correlation of *in vitro–in vivo* data for seven different formulations.

For the individual tablet formulations, when the cumulative percent excreted at each available sample time was plotted against the cumulative percent dissolved at each sample time (0, 0.5, 1, 1.5, 2, 3, and 4 hr *versus* 0.5, 10, 15, 20, 30, and 40 min, respectively), excellent correlation was achieved ($R > 0.94$) (Fig. 3). Data for the six possible excretion sampling

Table V—Spearman's Rank Correlation for All Formulations

Formulation[a]	1-hr Dissolution Rank	3-hr Excretion Rank
IIA	1	1
IIM	2	2
IA	3	4
CTL	4	3
IIIA	5	5
IIIC	6	7
IG	7	6
	$R_s = 0.93$	
	$t = 5.59$	
	Critical $t_{0.975}$ (5 df) = 2.57	

[a] For description of formulations, see Table I.

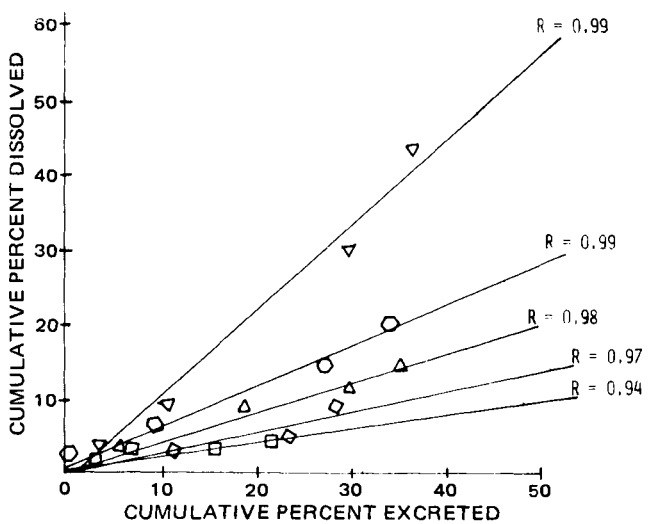

Figure 3—*Correlation of mean cumulative percent of nitrofurantoin excreted in 0, 0.5, 1.0, 1.5, 2.0, 3.0, and 4.0 hr following the oral administration of nitrofurantoin products with mean cumulative percent dissolved in 0, 5, 10, 15, 20, 30, and 40 min in phosphate buffer. Key: △, Formulation IA; ▽, Formulation IIIA; ○, Formulation CTL; □, Formulation IIA; and ◇, Formulation IIM.*

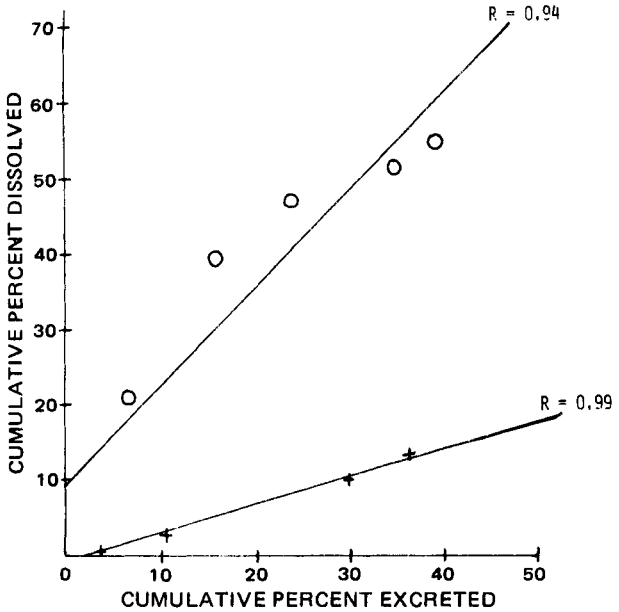

Figure 4—*Correlation of mean cumulative percent of nitrofurantoin excreted in 0, 0.5, 1.0, 1.5, 2.0, 3.0, and 4.0 hr following the oral administration of nitrofurantoin products with mean cumulative percent dissolved in 0, 5, 10, 15, 20, 30, and 40 min in hydrochloric acid buffer. Key: O, Formulation IIIC; and +, Formulation IIIA.*

times were not always available for all subjects because of individual variability in urination time. For any sampling time where data for all subjects were not available for a given formulation, the period was omitted from consideration to minimize error due to intersubject variability.

For the capsule formulations, correlation was not as good because of their very rapid dissolution. Therefore, the dissolution test conditions were modified to bring about rates more closely aligned with those for the tablets. The dissolution medium was changed to pH 1.2 hydrochloric acid buffer, and the stirring rate was reduced from 100 to 50 rpm. These changes produced dissolution rates for the capsules that were of a similar magnitude as the tablet dissolution rates while at the same time strongly differentiating between the two capsule formulations. Based on the dissolution rates in acid buffer, good correlation ($R > 0.94$) was found (Fig. 4). This correlation method appears useful for batch-to-batch testing on a given formulation or product.

All formulations in which at least 25% dissolved in 60 min were bioequivalent. Formulations that produced less than 25% dissolution exhibited significantly inferior bioavailability. Therefore, the existing USP specifications (13) appear to be adequately capable of eliminating formulations with a potential for poor bioavailability.

REFERENCES

(1) J. G. Wagner, M. Christensen, E. Sakmar, D. Blair, J. D. Yate, P. W. Willis, A. J. Sedman, and R. G. Stoll, *J. Am. Med. Assoc.*, **224**, 199 (1973).

(2) K. Arnold and N. Gerber, *Clin. Pharmacol. Ther.*, **11**, 121 (1970).

(3) I. J. McGilveray, G. L. Mattok, and R. D. Hossie, *J. Pharm. Pharmacol.*, **23**, 246S (1971).

(4) I. J. McGilveray, G. L. Mattok, and R. D. Hossie, *Rev. Can. Biol.*, **32**, 99 (1973).

(5) M. C. Meyer, G. W. A. Slywka, R. E. Dann, and P. L. Wyatt, *J. Pharm. Sci.*, **63**, 1693 (1974).

(6) *Fed. Regist.*, **40**, 26164 (1975).

(7) D. E. Cadwallader, T. R. Bates, and J. Swarbrick, *J. Am. Pharm. Assoc.*, **NS15**, 409 (1975).

(8) R. W. Mendes, S. Z. Masih, and R. R. Kanumuri, *J. Pharm. Sci.*, **67**, 1613 (1978).

(9) T. W. Bates, H. A. Rosenbury, and A. V. Tembo, *Clin. Pharmacol Ther.*, **16**, 63 (1974).

(10) I. J. McGilveray and G. L. Mattok, presented at the APhA Academy of Pharmaceutical Sciences, Chicago meeting, 1972.

(11) W. A. Ritschel, "Handbook of Basic Pharmacokinetics," Drug Intelligence Publications, Hamilton, Ill., 1976.

(12) C. M. Metzler, " 'NONLIN'–A Computer Program for Parameter Estimation in Nonlinear Situations," The Upjohn Co., Kalamazoo, Mich., 1969.

(13) "Third Supplement to The United States Pharmacopeia XIX and The National Formulary XIV," Mack Publishing Co., Easton, Pa., 1977, p. 103.

ACKNOWLEDGMENTS

Presented at the Industrial Pharmaceutical Technology Section, APhA Academy of Pharmaceutical Sciences, Phoenix meeting, November 1977.

Abstracted from a thesis submitted by R. R. Kanumuri to the Massachusetts College of Pharmacy in partial fulfillment of the Doctor of Philosophy degree requirements.

Evaluation of an Oral Prolonged-Release Antibiotic Formulation

H. SCHNEIDER [§], C. H. NIGHTINGALE [*¶], R. QUINTILIANI [‡], and D. R. FLANAGAN [*‖x]

Received May 19, 1977, from the *School of Pharmacy, University of Connecticut, Storrs, CT 06268, and the ‡Infectious Disease Division, Department of Medicine, Hartford Hospital, Hartford, CT 06100. Accepted for publication March 21, 1978. §School of Medicine, University of Connecticut, Farmington, CT 06032. ¶Present address: Department of Pharmacy, Hartford Hospital, Hartford, CT 06100. ‖Present address: College of Pharmacy, University of Iowa, Iowa City, IA 52242.

Abstract □ The antibiotic cephalexin was formulated as an oral prolonged-release tablet and evaluated by *in vitro* dissolution testing as well as *in vivo* in 10 human subjects. Comparisons were made of the time course of the blood levels among the prolonged-release formulation, the commercially available capsule, and intravenous administration. Even though lower peak blood levels were attained in the prolonged-release tablet, absorption continued for at least 6 hr. Comparison with *in vitro* dissolution data showed that absorption was dissolution rate limited. Bioavailability comparisons showed that the prolonged-release formulation was completely available, as was the commercial oral capsule.

Keyphrases □ Cephalexin—prolonged-release tablet compared to capsule and intravenous administration, dissolution *in vitro* and bioavailability in humans □ Dissolution, *in vitro*—prolonged-release cephalexin tablet □ Bioavailability—prolonged-release cephalexin tablet compared to capsule and intravenous administration in humans □ Antibacterials—cephalexin, prolonged-release tablet compared to capsule and intravenous administration, dissolution *in vitro* and bioavailability in humans

A prolonged-release oral antibiotic dosage form has several potential advantages compared to nonprolonged release formulations: better patient compliance, more constant blood levels resulting in shorter treatment periods, and reduced cost. The usual parenteral or oral antibiotic regimen results in high peak blood levels that fall well below therapeutic concentrations before administration of the next dose. Although it is generally believed that antibiotic efficiency is enhanced by wide excursions of the blood levels, which periodically fall below the minimum inhibitory concentration (MIC), this hypothesis has not been demonstrated clinically.

One study (1) indicated that the antibiotic levels must be above the MIC for a specified period to eradicate an infection and that this action is relatively independent of whether the level is achieved by constant infusion or intermittent bolus dosing. Since antibiotic levels may be below the MIC for significant periods after parenteral or oral bolus dosing, there may be unnecessary prolongation of treatment and excess drug consumption. In certain circumstances, a prolonged-release antibiotic regimen may allow outpatient treatment of diseases like bacterial endocarditis, where continuous therapy is indicated after disappearance of clinical manifestations to ensure against relapse.

This paper reports studies conducted with cephalexin to show that prolonged-release oral dosage forms can give reasonable blood levels for extended periods. Studies also were conducted with human volunteers after intravenous and oral administration of commercially available capsules. A comparison was made between the commercial oral capsule and the prolonged-release formulation.

EXPERIMENTAL

In vitro release studies were conducted by placing the test dosage form in a USP dissolution basket and rotating the basket at 120 rpm in the release medium. The release medium was maintained at 150 ml and was thermostated to 37° in a jacketed beaker. Samples were removed at regular intervals and assayed for cephalexin by UV spectrophotometry at 260 nm.

To approximate the pH change encountered as the dosage form travels along the GI tract, the release medium was changed at definite times. Dissolution studies were begun in 0.1 *N* HCl for 1 hr and continued for 1 additional hr in 0.01 *N* HCl; finally, the medium was changed to pH 7 phosphate buffer or distilled water for 3–4 hr. Distilled water was preferred because less degradation of cephalexin occurred in water than in phosphate buffer and little difference in release rate was observed between the two media.

The *in vivo* studies were performed using 10 healthy volunteers (seven males and three females, average age of 25 years). Cephalexin was given on 4 experimental days, with a 1-week interval between each administration. Various blood samples were drawn at 0.5-hr intervals for 3 hr and then hourly for a total of 8 hr after drug administration.

Initially, each subject received 500 mg of cephalexin orally after an overnight fast. The dosage form was two commercial 250-mg capsules[1]. One week later, each subject received a rapid intravenous injection of 500 mg of cephalexin[1] dissolved in 9.6 ml of sodium bicarbonate (8.4%). The solution was administered within 2 min of preparation to minimize degradation. In the 3rd and 4th weeks of the study, each subject received two 250-mg prolonged-release tablets; cephalexin was mixed with the other components as powders and compressed into tablets (12.7 mm in diameter and 6 mm thick) with a hydraulic press[2] at 2500 kg of total pressure for 5 min.

Serum was removed from blood samples after centrifugation and stored at −20° until assayed. Assays were performed by an agar–diffusion method with *Sarcina lutea* (ATCC 9341). Seeded agar plates were prepared as follows. One liter of molten medium[3] was inoculated with 1.0 ml of an overnight growth of *S. lutea*. Aliquots of 9 ml were then dispensed into sterile plastic petri dishes (100 × 15 mm) and allowed to solidify. The samples (15 μl) were spotted on paper disks and incubated at 37° for 24 hr, the inhibition zone was measured, and the samples were compared to standards. All assays were performed in triplicate.

A few urinary excretion studies were used as a screen to establish *in vivo* drug release from the products. Commercial cephalexin capsules and the prolonged-release tablets were administered after an overnight fast with 200 ml of water to two subjects, and drug excretion was monitored as a function of time. Urine samples were obtained initially, every 30 min after dosing for 2 hr, and then every hour thereafter for 3 hr; cumulative urine was collected for a total of 24 hr. The urine samples were centrifuged at 5000 rpm for 5 min and assayed microbiologically.

The serum levels obtained after intravenous and oral (commercial capsule) administration were fit to a two-compartment open model with the aid of a nonlinear least-squares regression program, NONLIN (2). The results were reported previously (3), with NONLIN fits giving $R^2 \geq 0.92$ for all subject data (intravenous and oral). The serum levels obtained after administration of the prolonged-release tablet were not modeled but were graphically compared to the oral capsule data.

Absorption rate constants for the capsule data were calculated from the slopes of semilogarithmic plots of the percentage unabsorbed *versus* time (4) as well as from nonlinear least-squares fits (3). The absorption rate constants obtained by these two methods did not differ significantly (*i.e.*, 1.93 ± 0.91 hr^{-1} from percentage unabsorbed plots and 1.90 ± 0.68 hr^{-1} from NONLIN fits). Bioavailability was determined as the ratio of

[1] Eli Lilly & Co., Indianapolis, Ind.
[2] Model C laboratory press, F. S. Carver, Summit, N.J.
[3] Antibiotic Medium No. 1, Difco Laboratories, Detroit, Mich.

0022-3549/78/1100-1620$01.00/0
© 1978, American Pharmaceutical Association

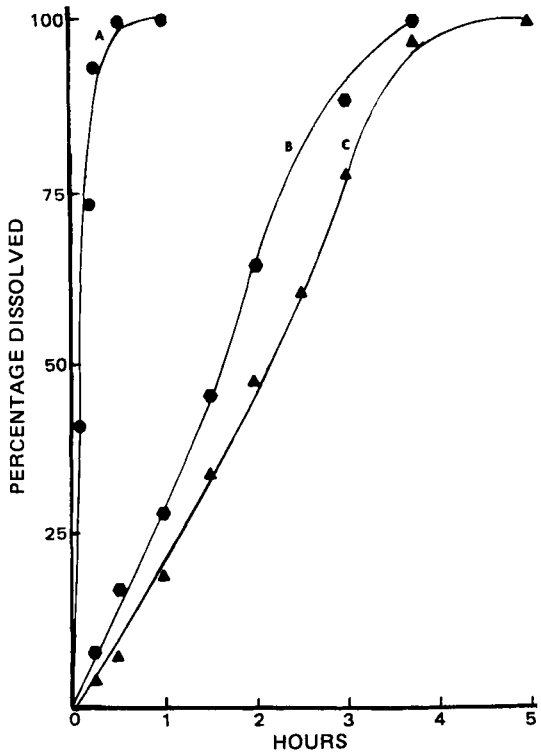

Figure 1—*Dissolution results for cephalexin dosage forms. Key: ●, commercial capsule; ●, prolonged-release tablet containing 50% carboxymethylcellulose and 50% cephalexin; and ▲, prolonged-release tablet containing 40% carboxymethylcellulose, 10% dicalcium phosphate, and 50% cephalexin.*

the total area under the serum concentration–time curve (obtained graphically) for the oral preparations compared to the intravenous administration.

RESULTS AND DISCUSSION

The results from the *in vitro* dissolution studies are shown in Fig. 1. The carboxymethylcellulose formulations (curves B and C) released cephalexin much more slowly than the commercial capsule formulation (curve A), which dissolved completely in 20 min. The retarding effect of the dicalcium phosphate (dibasic calcium phosphate) is seen when curve C is compared to curve B.

The dissolution rate differences between the commercial capsule and the prolonged-release formulation also were reflected in the urinary excretion of cephalexin after oral administration (Fig. 2). These studies (*in vitro* dissolution and urinary excretion) served as a screen to test formulations for the best candidate for further study. Such a formulation contained cephalexin, carboxymethylcellulose, and dicalcium phosphate dihydrate in the ratio of 5:4:1, respectively.

The average blood level–time curves are shown in Fig. 3[4]. The curve for the prolonged-release formulation was constructed without excluding the results from any individual subject. Thus, this curve includes the results from two subjects that showed little prolongation of blood levels and one subject that exhibited significantly delayed absorption. By comparing the average blood level–time curves obtained for the three formulations, three observations can be made:

1. With the commercial oral capsule, absorption was rapid, being essentially complete in 2 hr as signified by the parallel β-phases for the blood levels after intravenous and oral administration.
2. The prolonged-release formulation produced significantly lower blood levels than the commercial capsule.
3. Absorption continued for at least 6 hr for the prolonged-release formulation.

The lower peak blood level with the prolonged-release formulation is not surprising with a well-absorbed antibiotic like cephalexin, because it would be impossible to prolong blood levels and also to achieve the same peak levels as the commercial capsule without increasing the amount of drug in the prolonged-release formulation. Upon multiple dosing at 6-hr intervals, the peak levels for the prolonged-release formulation would rise 1–2 μg/ml, but no significant accumulation would occur upon multiple dosing with the commercial capsule.

[4] Individual subject data are available from the authors upon request.

Table I—Average Percentage Unabsorbed for Oral Cephalexin Dosage Forms

Hours	Commercial Capsule[a]	Prolonged Release
0.50	87.5 (4.0)[b]	92.1 (5.0)[b]
0.75	54.4 (10.6)	78.7 (8.6)
1.00	33.9 (10.9)	85.5 (6.5)
1.50	13.1 (6.9)	63.7 (13.7)
2.00	5.1 (3.4)	49.8 (18.0)
2.50	2.0 (1.5)	38.8 (18.7)
3.00	0.3 (0.2)	28.9 (18.0)
4.00	—	15.6 (14.2)
5.00	—	5.1 (4.0)

[a] Calculated using k_a = 1.9 hr^{-1} with an absorption lag time (t_0) of 0.43 hr (3). [b] Values within parentheses are standard deviations.

Besides prolonging the blood levels, another important consideration with prolonged-release formulations is the extent of absorption or bioavailability. When formulated as prolonged-release products, many well-absorbed drugs exhibit significant reductions in bioavailability. For cephalexin, this formulation was essentially completely bioavailable when compared to the intravenous administration (96 ± 20% with the intravenous taken as 100%). The commercial capsule exhibited 120 ± 16% availability when compared to the intravenous administration. This high value may be accounted for by overfill on the part of the manufacturer and/or loss of potency in the cephalexin powder used to prepare the intravenous and prolonged-release formulations as well as microbiological assay standards. Nevertheless, the prolonged-release formulation is completely available, although with more variability, suggesting that all drug is released from the formulation and available for absorption. Therefore, either the formulation does not travel far down the GI tract in 6 hr or cephalexin can be well absorbed for a long distance along the

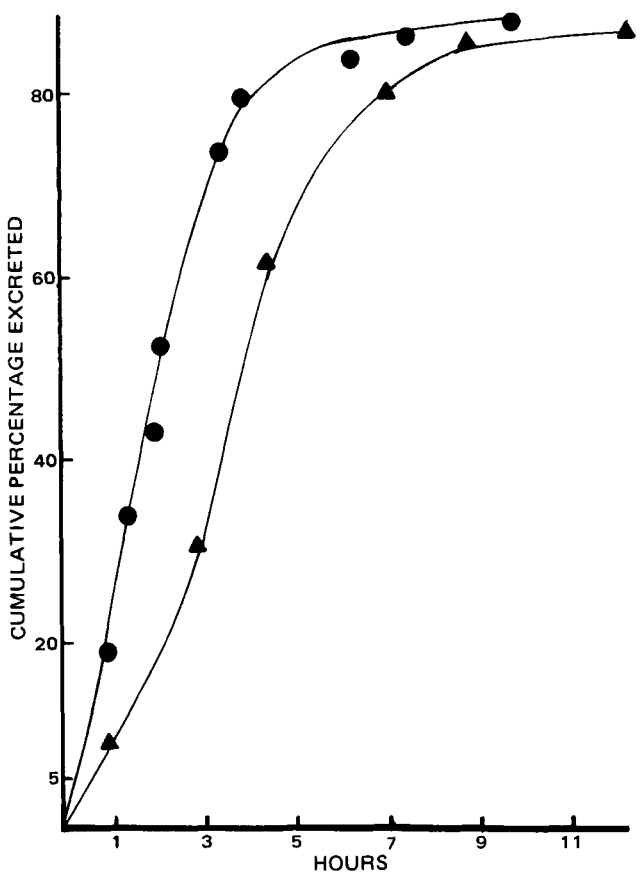

Figure 2—*Urinary excretion data for cephalexin dosage forms. Key: ●, commercial capsule; and ▲, prolonged-release tablet containing 40% carboxymethylcellulose, 10% dicalcium phosphate, and 50% cephalexin.*

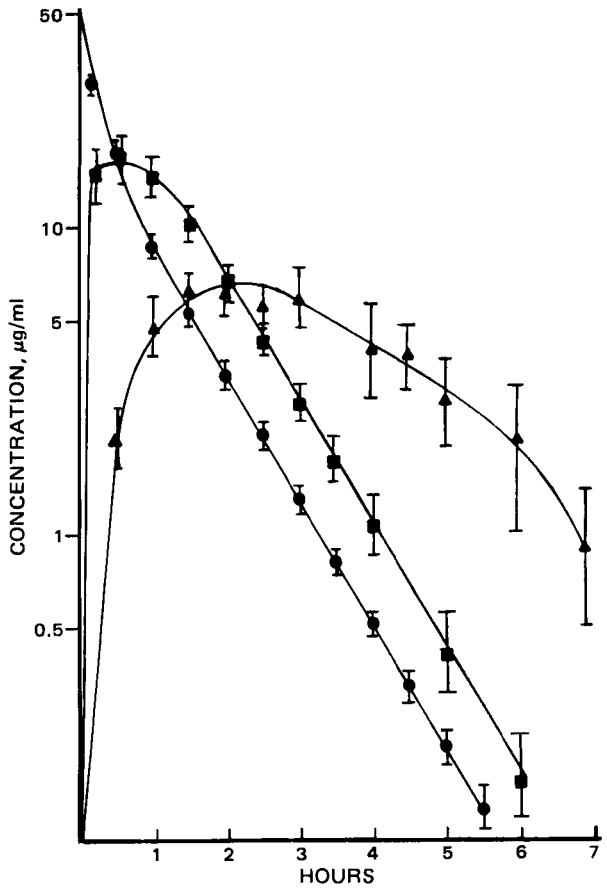

Figure 3—*Average blood level* versus *time data for cephalexin dosage forms. Key:* ●, *intravenous administration;* ■, *commercial capsule; and* ▲, *prolonged-release tablet containing 40% carboxymethylcellulose, 10% dicalcium phosphate, and 50% cephalexin.*

GI tract. Further studies will be required to differentiate between these two possibilities.

Table I shows the average percentage unabsorbed as a function of time for both oral dosage forms. Semilogarithmic plots of these data show that while the absorption of cephalexin from the capsule followed first-order kinetics, the absorption from the prolonged-release formulation followed no single kinetic order. Initially, the log percentage unabsorbed–time plot curves downward with apparent linearity at later times. This nonlinear behavior is most likely the result of the complex release pattern from the dosage form.

Figure 4 depicts the proposed model for drug released from this formulation. Initially, in the acidic conditions of gastric fluids, the dicalcium phosphate dissolves, releasing calcium, which binds to the carboxymethylcellulose. This binding, in turn, decreases the tablet's dissolution rate by decreasing its hydration rate. The cephalexin is released by dissolving in the gelatin matrix and diffusing out. As the carboxymethylcellulose matrix hydrates, the outer layers dissolve or erode from the periphery of the matrix. Thus, the initial matrix hydration, diffusion of cephalexin, and later the erosion of the matrix probably control the release rate, resulting in a system that would not be expected to exhibit a simple first-order release pattern.

To demonstrate that absorption is dosage form limited, Fig. 5 shows a plot of percentage unabsorbed *versus* percentage undissolved. While no correlation was seen between the absorption and dissolution rates of the commercial capsule, there was a high correlation between these rates for the prolonged-release formulation. Thus, for this type of formulation, *in vitro* dissolution rates are a reasonable reflection of the availability rate *in vivo*.

This study showed that cephalexin can be reasonably formulated to give prolonged blood levels after oral administration. Absorption of cephalexin apparently takes place for at least 6 hr, resulting in complete availability. Blood levels probably could be prolonged for more than 6 hr and higher levels attained if more cephalexin is incorporated into the formulation. Since the objective of this study was to determine whether 6-hr prolonged release and complete absorption could be attained, these

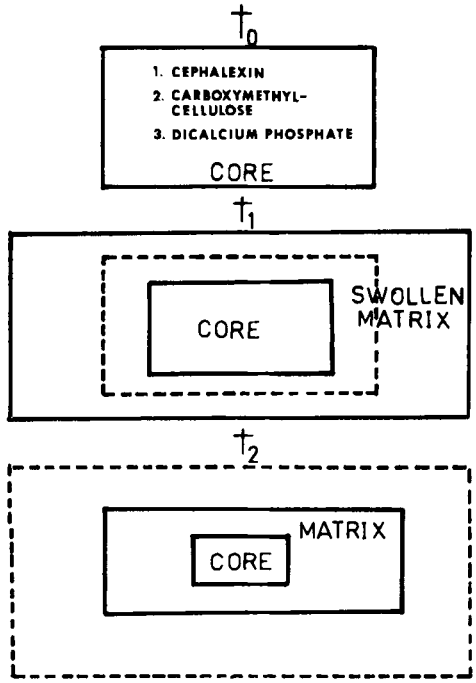

Figure 4—*Physical changes in the prolonged-release tablet at various times. Key:* t_0, *initial dosage form;* t_1, *dosage form shortly after introduction into GI fluids (dashed line represents original tablet size); and* t_2, *dosage form after matrix erosion has begun (dashed line represents swollen matrix size at largest extent).*

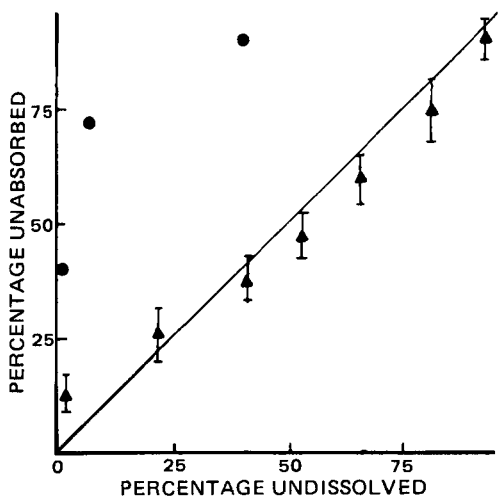

Figure 5—*Comparison of percentage undissolved with percentage unabsorbed. Key:* ●, *commercial capsule; and* ▲, *prolonged-release tablet. The line is a reference line with a slope of 1.*

possibilities were not explored. Moreover, the developed formulation controls the absorption rate of cephalexin, with a good correlation between *in vitro* dissolution and *in vivo* absorption results.

REFERENCES

(1) L. Weinstein, G. K. Darkos, and T. S. Perrin, *J. Lab. Clin. Med.*, **38**, 712 (1951).

(2) C. M. Metzler, G. L. Elfring, and A. J. McErven, "A User's Manual for NONLIN and Associated Programs," The Upjohn Co., Kalamazoo, Mich., 1974.

(3) D. S. Greene, D. R. Flanagan, R. Quintiliani, and C. H. Nightingale, *J. Clin. Pharmacol.*, **16**, 257 (1976).

(4) J. C. K. Loo and S. Reigelman, *J. Pharm. Sci.*, **57**, 918 (1968).

ACKNOWLEDGMENTS

Supported in part by Eli Lilly & Co., Indianapolis, Ind.

High-Pressure Liquid Chromatographic Determination of 8-Hydroxycarteolol in Plasma and Urine Using Electrochemical Detection

SOU-YIE CHU

Received November 16, 1977, from the *Drug Analysis Section, Drug Metabolism Department, Abbott Laboratories, North Chicago, IL 60064.* Accepted for publication March 23, 1978.

Abstract □ Assay of 8-hydroxycarteolol (a metabolite of carteolol) was achieved using high-pressure liquid chromatography with electrochemical detection. Plasma or urine samples alkalinized by addition of a sodium carbonate solution were extracted with ethyl acetate or chloroform. The residues from evaporation of the organic extracts were redissolved in pH 2.1 phosphate buffer, and the solutions were chromatographed on a Partisil 10 SCX chromatographic column. The detection of 8-hydroxycarteolol was accomplished using an electrochemical detector. The procedure is rapid, specific, and highly sensitive. Reproducible results can be obtained, with relative standard deviations from analysis of replicate samples within ±8%. With 1-ml samples, the lower quantifiable concentrations of 8-hydroxycarteolol in plasma and urine are approximately 5 and 25 ng/ml, respectively.

Keyphrases □ 8-Hydroxycarteolol—high-pressure liquid chromatographic analysis in plasma and urine □ High-pressure liquid chromatography—analysis, 8-hydroxycarteolol in plasma and urine □ Antiadrenergics—8-hydroxycarteolol, high-pressure liquid chromatographic analysis in plasma and urine □ Metabolites—8-hydroxycarteolol, high-pressure liquid chromatographic analysis in plasma and urine

Carteolol hydrochloride [5-(3-*tert*-butylamino-2-hydroxypropoxy)-3,4-dihydrocarbostyril hydrochloride] is a potent β-adrenergic blocking agent (1). One of its major metabolites in animals and humans was identified as 8-hydroxy-5-(3-*tert*-butylamino-2-hydroxypropoxy)-3,4-dihydrocarbostyril, 8-hydroxycarteolol (I) (2). This metabolite also possesses β-adrenergic blocking activity (3).

BACKGROUND

To assess the correlation between plasma drug levels and responses of β-adrenergic blockade following administration of carteolol, the plasma concentrations of the active metabolite, I, must be considered together with the levels of the parent compound. Furthermore, in conjunction with pharmacokinetic and bioavailability studies, information on the time course and extent of formation of such an active metabolite should be highly pertinent. Therefore, the development of a sensitive method for the determination of I in biological fluids was undertaken.

Data from high-pressure liquid chromatographic (HPLC) analysis of I solutions showed that the compound could be readily eluted from both reversed-phase and strong cation-exchange columns. Detection using a UV (254 nm) photometer had a lower sensitivity limit of about 5 ng of I injected on-column. This method was inadequate for the measurement of clinically achievable plasma levels of I.

Recently, a simple design for an electrochemical detector for liquid chromatography was described (4, 5). The usefulness of this detector was demonstrated in the HPLC analysis of catecholamines (6–8), uric acid (5), ascorbic acid (5, 9), acetaminophen (10), and β-cetotetrine (11) in tissues, body fluids, and pharmaceutical preparations. In all reported cases, the electrochemical detections were characteristically highly sensitive, with lower detection limits at picomole quantities. Additionally, because only electrochemically active compounds can evoke responses from the detector, the electrochemical HPLC technique frequently offers an opportunity to mask interfering peaks appearing in HPLC–UV chromatograms.

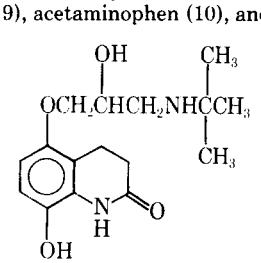

I

Based on these published observations, it was conceived that the electrochemical HPLC technique should be of great potential in the analysis of phenolic drug metabolites in biological fluids, especially when highly efficient microparticulate columns were utilized in combination with this sensitive detector. In the present study, this approach was examined for the analysis of I. The detection of I in HPLC effluent by the electrochemical technique was considerably more sensitive than that by a UV photometer, with a minimum detectable quantity of about 0.22 ng. A simple and specific method was developed for the determination of I in plasma and urine using the electrochemical HPLC technique.

EXPERIMENTAL

Reagents—8-Hydroxycarteolol maleate[1] was at least 98% pure, based on HPLC–UV analysis on μBondapak-C_{18} and Partisil 10 SCX columns. Its electron-impact and chemical-ionization mass spectral data were consistent with the proposed 8-hydroxycarteolol structure. A stock solution of I maleate was prepared at 1 mg/ml in freshly prepared 0.01 *M* sodium bisulfite. Standard solutions of I maleate at 10 and 1 μg/ml were prepared by serial dilutions of the stock solution with the sodium bisulfite solution. All standard solutions were refrigerated until used.

All chemicals were analytical reagent grade[2]. A 1 *M* sodium bisulfite solution in distilled water was prepared fresh weekly and stored under refrigeration. This solution was used in the preparation of the eluent and the 0.01 *M* sodium bisulfite. A 3 *M* sodium carbonate solution was prepared in distilled water to which was added sodium metabisulfite to a concentration of 2% (w/v). The reconstituting buffer was prepared fresh by adding 100 μl of 1 *M* sodium bisulfite to 10 ml of an acidic phosphate buffer (0.1 *M* monobasic ammonium phosphate–0.1 *M* phosphoric acid, pH ~2.1).

Chromatographic System—The HPLC system consisted of a solvent delivery pump[3], a Partisil 10 SCX chromatographic column[4] (4.6 mm i.d. × 25 cm), and an electrochemical detector[5]. Injection was accomplished with a sample injection valve[6] modified with a homemade sample loading port to allow syringe loading of variable sample sizes at atmospheric pressure. The electrochemical potential of the working electrode was set at +0.65 ± 0.02 v *versus* a silver–silver chloride reference electrode.

The aqueous mobile phase was composed of sodium sulfate (0.2 *M*), 2-propanol (5% v/v), sodium dihydrogen phosphate (0.02 *M*), phosphoric acid (0.01 *M*), and sodium bisulfite (1 m*M*). The mobile phase was degassed under reduced pressure before use. The chromatographic system was operated at ambient temperature, with an eluent flow rate of 1.0 ml/min.

Procedures—To minimize the loss of 8-hydroxycarteolol because of oxidation, the centrifuge tubes (which had been washed with chromic acid) were rinsed with 5% (w/v) sodium bisulfite and dried before use.

Assay of Plasma Samples—A 1.0-ml aliquot of plasma, with sodium bisulfite preservative added to a concentration of about 100 mg/ml, was transferred to a screw-capped centrifuge tube. To the sample were added

[1] Otsuka Pharmaceutical Co., Osaka, Japan.
[2] Mallinckrodt, St. Louis, Mo.
[3] Model M-6000, Waters Associates, Milford, Mass.
[4] Whatman Co., Clifton, N.J.
[5] Model LC-2, Bioanalytical Systems, West Lafayette, Ind.
[6] Model 70-10, Rheodyne, Berkeley, Calif.

0022-3549/78/1100-1623$01.00/0
© 1978, American Pharmaceutical Association

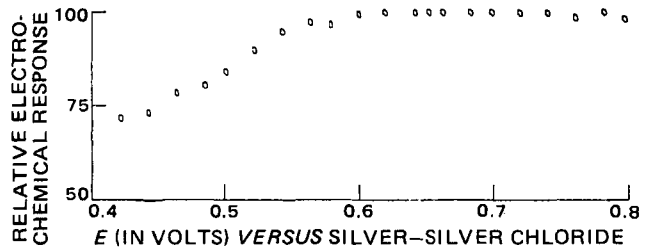

Figure 1—*Relative electrochemical response of I at various potentials.*

1 ml of 3 *M* sodium carbonate and 4.0 ml of ethyl acetate. The mixture was shaken for 5 min at low speed on a reciprocating shaker and centrifuged for 10 min at ~1000×*g*. A 3.0-ml aliquot of the organic layer was transferred to a clean conical centrifuge tube, and the solution was evaporated to dryness at 45° under a nitrogen stream. The residue was mixed with 100 μl of the reconstituting buffer; then a 20-μl aliquot of this mixture was injected into the HPLC system and analyzed.

A set of standard samples prepared from blank plasma spiked with known amounts of I was analyzed along with the unknown samples. Typically, 20-, 40-, 60-, 100-, and 200-μl aliquots of a standard solution of I maleate at 1 μg/ml were transferred to centrifuge tubes. To each tube plus a blank were added 1.0 ml of blank control plasma and 100 mg of sodium bisulfite. After the volumes were equalized by addition of distilled water, these standard samples were carried through the analytical procedure. A calibration curve was constructed from resulting data, and the concentrations of the unknown samples were derived.

Assay of Urine Samples—A procedure identical to the plasma assay was followed, except that chloroform (4 ml) was used instead of ethyl acetate. A set of standard urine samples prepared from blank urine spiked with known quantities of I was analyzed along with the unknown samples. The levels of I added to the blank urine may be varied to suit the concentration ranges of the anticipated analyses. Typically, 5-, 10-, 50-, 100-, and 200-μl aliquots of the standard I maleate solution at 10 μg/ml were transferred to centrifuge tubes. To each of the tubes plus a blank were added 1.0 ml of blank control urine and 100 mg of sodium bisulfite powder. These samples were carried through the analytical procedure, and their results were used to construct a calibration curve of peak height *versus* the corresponding urinary concentration of I.

RESULTS AND DISCUSSION

When I was subjected to electrochemical HPLC analysis, the compound evoked a large electrochemical response. To study the effect that varying the potential had on the response, an aqueous solution of I maleate was analyzed at various working electrode potentials. The peak heights observed were compared to those obtained at 0.66 v, which was arbitrarily set at 100%. The results (Fig. 1) indicated that electrochemical responses of I increased as the potential on the carbon paste electrode was raised from +0.4 to +0.6 v, with no significant changes at potentials between +0.6 and +0.8 v. Based on these observations and on the rationale that the potential should be at the lower end of the optimum potential ranges to increase the electrochemical specificity, a potential of +0.65 ± 0.02 v was chosen.

The relative sensitivities of the two modes of detection were examined by subjecting the column effluent to both UV and electrochemical de-

Table I—Data for the Determination of Linearity of the Electrochemical HPLC Assay of I in Plasma

Theoretical Plasma I Concentration, ng/ml	I Peak Height, Arbitrary Units	Recalculated Plasma I Concentration, ng/ml	Percent of Theory
15.5	24.4[a]	14.0	90.2
31.1	55.0[a]	30.9	99.5
93.3	155	86.3	92.5
155	316	176	113.3
311	585	325	104.4
933	1820	1009	108.1
1860	3330	1846	99.2
3110	5450	3020	97.1
6219	11250	6234	100.2

[a] These are mean values obtained from replicate plasma samples, five each spiked with I at 15.5 and 31.1 ng/ml.

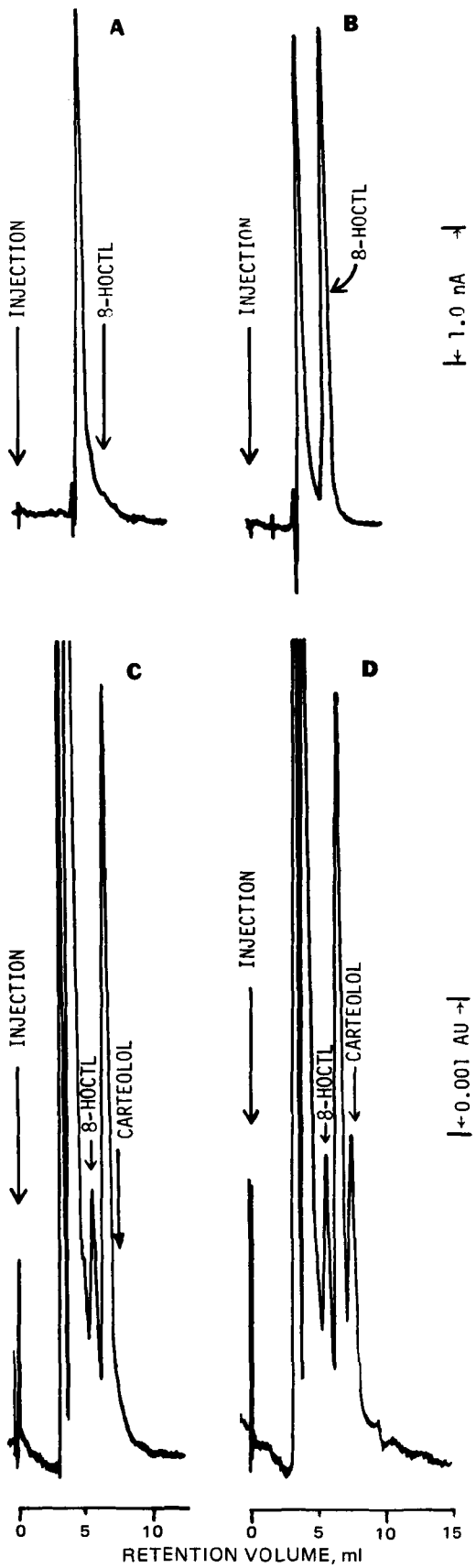

Figure 2—*HPLC chromatograms of samples prepared from blank plasma (A and C) and blank plasma spiked with I (8-HOCTL) at 155 ng/ml and carteolol hydrochloride at 492 ng/ml (B and D), analyzed according to the HPLC conditions specified under* Experimental. *Chromatograms A and B are tracings of the electrochemical detection, and chromatograms C and D are recordings of UV absorption.*

Table II—Data for the Determination of Linearity of the Electrochemical HPLC Assay of I in Urine

Spiked Urine I Concentration, ng/ml	I Peak Height, Arbitrary Units	Recalculated I Concentration in Urine, ng/ml	Percent of Theory
36.3	15	33.0	90.9
72.7	40	73.4	100.4
109	64[a]	113	103.8
182	100	170	93.4
363	211[a]	350	96.4
727	450	736	101.2

[a] These are mean values from analysis of replicate urine samples, five each spiked with I at 109 and 363 ng/ml.

tections. The column outlet was connected to the UV detector, from which the effluent was led to the inlet of the electrochemical detector, using a zero dead volume union and a short piece of 0.23-mm i.d. stainless steel tubing. HPLC analyses of both aqueous solutions of I and samples from plasma spiked with I were performed using the dual-detection system. The results indicated that the electrochemical detection was about 15-fold more sensitive than UV detection and that approximately 0.22 ng (0.7 picomole) of I on-column would be detected.

Figure 2 shows typical chromatograms of samples prepared from plasma using this dual-detection system. When UV detection was used, the I peak was lost in the background peaks as shown in chromatograms C and D. In contrast, the electrochemical detector provided more selectivity, yielding a well-resolved I peak, with cleaner backgrounds (chromatograms A and B). Thus, the use of the electrochemical HPLC technique eliminates the need for extensive sample cleanup procedures which would be required for UV detection.

As mentioned previously, I could be eluted readily under reversed-phase conditions; however, the increased concentrations of organic solvents required for the elution caused a considerable reduction in the electrochemical detector sensitivity. Furthermore, the resolution of the desired peak of I from the background peaks was inferior to that attainable using the proposed procedure with a strong cation-exchange column.

Because of the susceptibility of I to oxidative degradation, addition of preservative to plasma and urine samples was required to obtain reproducible results and good linear standard curves. Among the antioxidants tested, sodium bisulfite at 100 mg/ml of plasma or urine was most satisfactory. Based on these observations, some precautions are recommended in handling plasma or urine specimens when assaying for their I contents. Sodium bisulfite should be added at 100 mg/ml, and the samples should be stored immediately at about −10°.

To assess the precision and range of linearity of the proposed assay, 17 plasma samples spiked with known amounts of I were prepared from blank plasma and carried through the proposed analytical procedure (Table I). The method was reproducible with relative standard deviations of ±7.8 and ±3.6% from analysis of replicate plasma samples at levels of 15.5 and 31.1 ng/ml, respectively. Linear regression was performed on the data of Table I. The equation y (peak height) = $1.805x$ (concentration) − 0.821 was obtained, with the y-intercept of −0.821 being not significantly different from zero. The correlation coefficient was 0.9995, clearly demonstrating the linearity of the data. The observed peak heights were then inserted back into the equation to calculate the determined concentrations. The recalculated concentrations were all within 90–113% of theoretical values.

For the assay of I in urine, chloroform was used for the extraction of I instead of ethyl acetate. This modification was necessary since ethyl acetate extracts of urine samples gave broad background peaks that interfered with the analyses. After several unsuccessful attempts to clean up the sample by back-extraction steps, chloroform was chosen as the extraction solvent. Typical chromatograms are shown in Fig. 3. Assay of replicate urine samples to which I had been added to levels of 109 and 363 ng/ml were performed using the proposed procedure. The results showed relative standard deviations of ±2.7 and ±3.2%, respectively. Data for the determination of the linearity of the assay are listed in Table II. From these results, a linear equation was derived by least-squares analysis: y (peak height) = $0.619x$ (concentration) − 5.432, with the y-intercept of −5.432 being not significantly different from zero. The correlation coefficient was 0.9992, indicating linearity of the data.

The method was used for the analysis of plasma and urine samples collected from dogs or humans that had been orally dosed with carteolol.

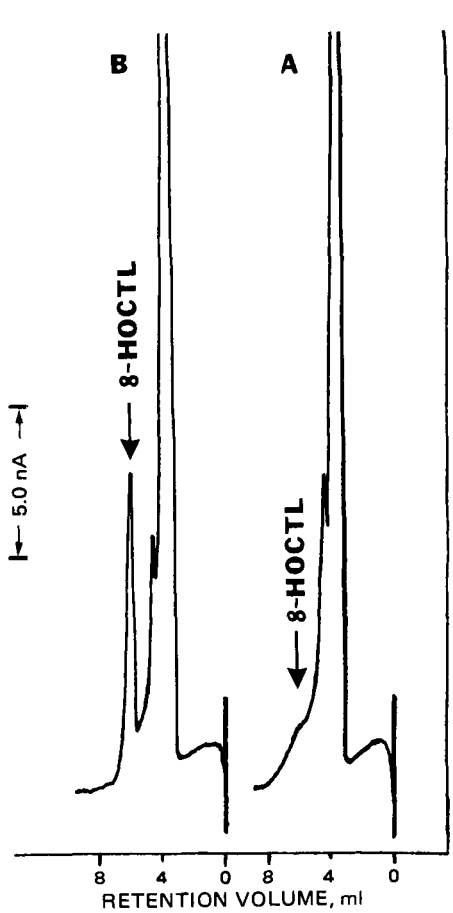

Figure 3—*Electrochemical HPLC chromatograms of samples prepared from blank urine (A) and blank urine spiked with I (8-HOCTL) at 182 ng/ml (B).*

Chromatograms were identical to those shown in this report, and no interfering peaks were observed. Minor metabolites such as 5-hydroxy-3,4-dihydrocarbostyril and 5,8-dihydroxy-3,4-dihydrocarbostyril have been found in dog urine (2); however, these compounds do not interfere with the assay of I because they are well resolved from I.

REFERENCES

(1) K. Nakagawa, N. Murakami, S. Yoshizaki, M. Tominaga, H. Mori, Y. Yabuuchi, and S. Shintani, *J. Med. Chem.*, **17**, 529 (1974).

(2) H. Mori, M. Kido, N. Murakami, S. Morita, H. Kohri, K. Nakagawa, T. Uno, and T. Ishihara, *Yakugaku Zasshi*, **97**, 350 (1977).

(3) M. Uchida, M. Tominaga, K. Oka, H. Tone, T. Ishihara, and K. Nakagawa, *ibid.*, **96**, 571 (1976).

(4) P. T. Kissinger, C. Refshauge, R. Dreiling, and R. N. Adams, *Anal. Lett.*, **6**, 465 (1973).

(5) P. T. Kissinger, L. J. Felice, R. M. Riggin, L. A. Pachla, and D. C. Wenke, *Clin. Chem.*, **20**, 992 (1972).

(6) C. Refshauge, P. T. Kissinger, R. Dreiling, L. Blank, R. Freeman, and R. N. Adams, *Life Sci.*, **14**, 311 (1974).

(7) R. M. Riggin, L.-D. Rau, R. L. Alcorn, and P. T. Kissinger, *Anal. Lett.*, **7**, 791 (1974).

(8) P. T. Kissinger, R. M. Riggin, R. L. Alcorn, and L.-D. Rau, *Biochem. Med.*, **13**, 299 (1975).

(9) L. A. Pachla and P. T. Kissinger, *Anal. Chem.*, **48**, 364 (1976).

(10) R. M. Riggin, A. L. Schmidt, and P. T. Kissinger, *J. Pharm. Sci.*, **64**, 680 (1975).

(11) S. E. Magic, *J. Chromatogr.*, **129**, 73 (1976).

ACKNOWLEDGMENTS

The author acknowledges the assistance of Mr. Raymond Gudgeon and Mr. Kap Ahn and the helpful discussions of Dr. Lawrence T. Sennello.

Intrinsic Factor-Mediated Binding of Cyanocobalamin to Cholestyramine

KNUT-JAN ANDERSEN ˣ **and HENNING SCHJØNSBY**

Received December 12, 1977, from the *Section for Clinical Research and Molecular Medicine, Medical Department A, University of Bergen, 5016 Haukeland Sykehus, Bergen, Norway.* Accepted for publication February 28, 1978.

Abstract □ The intrinsic factor-mediated binding of cyanocobalamin to cholestyramine was studied *in vitro* under varying conditions of pH, added electrolyte, and bile salt. The intrinsic factor–cyanocobalamin complex was adsorbed strongly by the resin at pH 3 in the presence of neutral salt and low concentrations of glycocholic acid. An increase in glycocholic acid concentration as well as neutral pH decreased the observed binding, although significant amounts of cyanocobalamin–intrinsic factor complex remained bound after incubation at pH 6.8. Cyanocobalamin alone was not adsorbed by the resin.

Keyphrases □ Cyanocobalamin—intrinsic factor-mediated binding to cholestyramine *in vitro*, effect of pH, added electrolyte, and bile salt □ Binding, intrinsic factor mediated—cyanocobalamin to cholestyramine *in vitro*, effect of pH, added electrolyte, and bile salt □ Cholestyramine—intrinsic factor-mediated binding of cyanocobalamin, effect of pH, added electrolyte, and bile salt □ Vitamins—cyanocobalamin, intrinsic factor-mediated binding to cholestyramine *in vitro*, effect of pH, added electrolyte, and bile salt □ Ion-exchange resins—cholestyramine, intrinsic factor-mediated binding of cyanocobalamin, effect of pH, added electrolyte, and bile salt

Cholestyramine resin is effective in removing bile salts from the intestinal lumen (1, 2) and in decreasing the intragastric bile salt content (3–5). Cholestyramine also binds other compounds in the intestine, including chlorothiazide, phenylbutazone, anticoagulants, and various digitalis preparations (6). Since cholestyramine impairs the intestinal absorption of cyanocobalamin in normal patients and patients with pernicious anemia (7), it is feasible that cholestyramine decreases cyanocobalamin absorption either by binding to the sites on the intrinsic factor molecules that normally bind cyanocobalamin (7) or by binding the whole cyanocobalamin–intrinsic factor complex.

The purpose of this study was to investigate *in vitro* the molecular events in the interaction of cholestyramine with cyanocobalamin (I) and intrinsic factor as well as the effect of the bile salt, glycocholic acid, on this interaction.

EXPERIMENTAL

Materials—Commercially available ^{57}Co-labeled I[1] (10–20 μCi/μg), glycocholic acid (sodium salt)[2], and and cholestyramine[3] were used.

Normal human gastric juice was collected after stimulation with pentagastrin, depepsinized (8), diluted 1:1 with isotonic saline, and stored in aliquots at −20°. All other reagents were the highest purity commercially available.

Incubation—Cholestyramine particles (22.2 mg of cholestyramine) were weighed into the incubation tubes. Buffer to give a final volume of 5.25 ml was then added, followed by 300 μl of human gastric juice (12 intrinsic factor units) and 50 μl of ^{57}Co-I (5 ng). Glycocholic acid was added, and incubation was performed at 25° by end-over-end incubation for 2 hr.

The cholestyramine particles were then collected by centrifugation, and the particles were washed in the incubation buffer and resedimented twice. The radioactivity in the final sediment was determined in an automatic β–γ-spectrometer to a precision of ±2%.

In some experiments, a buffer of a different pH was added to the sediment. The sediment was washed once and incubated in this buffer without glycocholic acid for 30 min at 25° as described. Finally, the sediment was washed twice in the buffer, and the radioactivity was determined.

Buffers of different ionic strength (0.05 and 0.1 *M* NaCl) and different pH (3.0, 6.8, and 7.4) were used in the incubations. The results were corrected by performing blank incubations, *i.e.*, incubations without cholestyramine.

RESULTS AND DISCUSSION

The effect of pH and ionic strength on the intrinsic factor-mediated binding of ^{57}Co-I to cholestyramine is shown in Fig. 1. A high proportion of the I–intrinsic factor complex adsorbed to the resin at pH 3 and low ionic strength. An increase in ionic strength as well as pH decreased binding. There was no significant binding of I by the resin when human gastric juice was omitted from the incubation mixture.

These results indicate that cholestyramine binds the whole I–intrinsic factor complex, which apparently contrasts with the suggestion that cholestyramine binds to the sites on the intrinsic factor molecules that normally bind I (7). However, the present incubations were done at an acid pH to simulate the pH of the stomach while the previous incubations were performed at a neutral pH (7). The observed binding of the I–intrinsic factor complex to cholestyramine at pH 3 is probably of a hydrophobic nature (9) since cholestyramine is an anion-exchange resin and the isoelectric point of the intrinsic factor has been reported to vary between 4.84 and 5.73, depending on the sialic acid content (10). Furthermore, the binding must be weak since there is competition for the exchange sites by chloride ions at low as well as neutral pH (Fig. 1).

The effect of glycocholic acid on the intrinsic factor-mediated binding

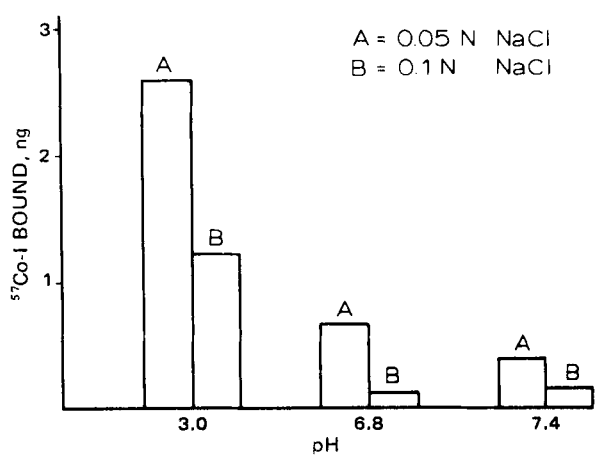

Figure 1—*Effect of pH and ionic strength on the intrinsic factor-mediated binding of ^{57}Co-I to cholestyramine.*

[1] Radiochemical Center, Amersham, Bucks., England.
[2] Sigma Chemical Co., St. Louis, Mo.
[3] Questran, containing 4 g of cholestyramine chloride/9 g.

0022-3549/78/1100-1626$01.00/0
© 1978, American Pharmaceutical Association

Table I—Effect of Glycocholic Acid, pH, and Ionic Strength on the Intrinsic Factor-Mediated Binding of I to Cholestyramine [a]

Glycocholic Acid Added, μmoles	Cyanocobalamin Bound, pg			
	Incubated in Buffer A		Incubated in Buffer B	
	Washed in Buffer A	Incubated and Washed in Buffer C	Washed in Buffer B	Incubated and Washed in Buffer C
0	2560	1370	1230	280
1.25	2589	1386	1247	262
2.5	3393	1696	1519	487
3.75	3465	2113	1480	674
5.0	3364	2444	605	257
7.5	3210	1806	76	60
10.0	1638	686	54	46

[a] The values given are the arithmetic means of two determinations, each run in triplicate. Incubations were performed as described in the text. The following buffers were used: 0.05 *M* NaCl, pH 3.0 (Buffer A); 0.1 *M* NaCl, pH 3.0 (Buffer B); and 0.05 *M* NaCl, pH 6.8 (Buffer C).

of I to cholestyramine at two different ionic strengths is shown in Table I. At very low concentrations of glycocholic acid, binding of the I–intrinsic factor complex to the resin increased, but when the glycocholic acid concentration was increased, complex binding gradually decreased, which suggests that glycocholic acid blocked the possible binding sites of the I–intrinsic factor complex. A further decrease in the amount of the I–intrinsic factor complex bound was observed when the ionic strength was increased by increasing the sodium chloride concentration from 0.05 to 0.1 *M* (Table I), which is compatible with the hypothesis that binding at this pH must be due to hydrophobic interactions. However, significant amounts of the complex remained bound to the resin after incubation at pH 6.8 (Table I), which suggests that the forces taking part in the binding also are coulombic.

The results show that binding of the I–intrinsic factor complex was partly reversible at neutral pH as well as at a glycocholic acid concentration similar to that found in the lumen of the small intestine. Hence, it is uncertain whether cholestyramine binds sufficient quantities of the complex in the lumen of the small intestine to impair intestinal vitamin absorption. Furthermore, results of absorption tests are conflicting; *i.e.*, cholestyramine increased as well as decreased intestinal vitamin absorption (11).

REFERENCES

(1) T. B. Van Itallie, S. A. Hashim, R. S. Crampton, and D. M. Tennent, *N. Engl. J. Med.*, **265**, 469 (1961).

(2) S. A. Hashim and T. B. Van Itallie, *J. Am. Med. Assoc.*, **192**, 289 (1965).

(3) R. S. Fisher and S. Cohen, *N. Engl. J. Med.*, **288**, 273 (1973).

(4) H. H. Scudamore, E. E. Eckstam, W. J. Fencil, and C. A. Jaramillo, *Am. J. Gastroenterol.*, **60**, 9 (1973).

(5) R. B. Black, J. Rhodes, G. T. Davies, H. Gravelle, and P. Sweetnam, *Gastroenterology*, **61**, 821 (1971).

(6) "The Pharmacological Basis of Therapeutics," 5th ed., L. S. Goodman and A. Gilman, Eds., Macmillan, New York, N.Y., 1975, p. 749.

(7) A. Coronato and G. B. J. Glass, *Proc. Soc. Exp. Biol. Med.*, **142**, 1341 (1973).

(8) R. Gräsbeck, *Acta Med. Scand., Suppl. 314*, **154**, 1 (1956).

(9) S. Lindenbaum and T. Higuchi, *J. Pharm. Sci.*, **64**, 1887 (1975).

(10) R. Gräsbeck, *Acta Chem. Scand.*, **22**, 1041 (1968).

(11) J. G. Spenney and B. J. Hirschowitz, *Gastroenterology*, **58**, 996 (1970).

Simultaneous Programmed Temperature GLC Assay of Phenol, Chloroxylenol, and Lidocaine Hydrochloride in Topical Antiseptic Cream

PHILIP J. PALERMO ˣ and J. BRIAN LUNDBERG

Received October 25, 1977, from *Norwich-Eaton Pharmaceuticals, Norwich, NY 13815.* Accepted for publication February 28, 1978.

Abstract □ A simultaneous programmed temperature GLC assay for the active ingredients in a topical antiseptic cream is described. The sample is extracted directly using a dimethyl sulfoxide solution of *p*-cresol, 4-chlorophenol, and 2-amino-4-phenylthiazole as internal standards for phenol, chloroxylenol, and lidocaine hydrochloride, respectively. The resulting solution is chromatographed by temperature programming on an OV-225 column from 90 to 225°. The internal standard calculation is accomplished using peak heights or peak areas. The relative standard deviation of all assays is less than 2%.

Keyphrases □ Phenol—GLC analysis simultaneously with other active ingredients in commercial preparations □ Chloroxylenol—GLC analysis simultaneously with other active ingredients in commercial preparations □ Lidocaine hydrochloride—GLC analysis simultaneously with other active ingredients in commercial preparations □ GLC—simultaneous analyses, phenol, chloroxylenol, and lidocaine hydrochloride in commercial preparations

Existing assay methods for products with multiple active ingredients can often be tedious and time consuming. Current procedures for phenol, chloroxylenol (*p*-chloro-*m*-xylenol), and lidocaine hydrochloride in a topical cream formulation required 2 days of laboratory time and three separate assays for the active ingredients. A simultaneous procedure for the three active ingredients was desirable. In addition, a specific method was necessary for stability-indicating purposes.

GLC has been used successfully to determine lidocaine (1–3), phenol (4–6), and chloroxylenol (7–9). These techniques have inherent specificity qualities. The range of boiling points and polarities of these three components required a programmed temperature method.

EXPERIMENTAL

Materials and Reagents—Phenol and lidocaine hydrochloride meeting USP specifications were used as standards. Chloroxylenol standard material was assayed by a GLC procedure. *p*-Cresol, 4-chlorophenol, and 2-amino-4-phenylthiazole at 99+ % purity were used as received[1]. All other chemicals were ACS reagent grade or equivalent.

The column was 1.8-m × 3-mm silanized stainless steel filled with 3% OV-225 on 80–100-mesh Supelcoport adapted for on-column injection.

[1] Aldrich Chemical Co. and Fairfield Chemical Co.

0022-3549/78/1100-1627$01.00/0

© 1978, American Pharmaceutical Association

Table I—Effect of Glycocholic Acid, pH, and Ionic Strength on the Intrinsic Factor-Mediated Binding of I to Cholestyramine [a]

Glycocholic Acid Added, μmoles	Cyanocobalamin Bound, pg			
	Incubated in Buffer A		Incubated in Buffer B	
	Washed in Buffer A	Incubated and Washed in Buffer C	Washed in Buffer B	Incubated and Washed in Buffer C
0	2560	1370	1230	280
1.25	2589	1386	1247	262
2.5	3393	1696	1519	487
3.75	3465	2113	1480	674
5.0	3364	2444	605	257
7.5	3210	1806	76	60
10.0	1638	686	54	46

[a] The values given are the arithmetic means of two determinations, each run in triplicate. Incubations were performed as described in the text. The following buffers were used: 0.05 *M* NaCl, pH 3.0 (Buffer A); 0.1 *M* NaCl, pH 3.0 (Buffer B); and 0.05 *M* NaCl, pH 6.8 (Buffer C).

of I to cholestyramine at two different ionic strengths is shown in Table I. At very low concentrations of glycocholic acid, binding of the I–intrinsic factor complex to the resin increased, but when the glycocholic acid concentration was increased, complex binding gradually decreased, which suggests that glycocholic acid blocked the possible binding sites of the I–intrinsic factor complex. A further decrease in the amount of the I–intrinsic factor complex bound was observed when the ionic strength was increased by increasing the sodium chloride concentration from 0.05 to 0.1 *M* (Table I), which is compatible with the hypothesis that binding at this pH must be due to hydrophobic interactions. However, significant amounts of the complex remained bound to the resin after incubation at pH 6.8 (Table I), which suggests that the forces taking part in the binding also are coulombic.

The results show that binding of the I–intrinsic factor complex was partly reversible at neutral pH as well as at a glycocholic acid concentration similar to that found in the lumen of the small intestine. Hence, it is uncertain whether cholestyramine binds sufficient quantities of the complex in the lumen of the small intestine to impair intestinal vitamin absorption. Furthermore, results of absorption tests are conflicting; *i.e.*, cholestyramine increased as well as decreased intestinal vitamin absorption (11).

REFERENCES

(1) T. B. Van Itallie, S. A. Hashim, R. S. Crampton, and D. M. Tennent, *N. Engl. J. Med.*, **265**, 469 (1961).

(2) S. A. Hashim and T. B. Van Itallie, *J. Am. Med. Assoc.*, **192**, 289 (1965).

(3) R. S. Fisher and S. Cohen, *N. Engl. J. Med.*, **288**, 273 (1973).

(4) H. H. Scudamore, E. E. Eckstam, W. J. Fencil, and C. A. Jaramillo, *Am. J. Gastroenterol.*, **60**, 9 (1973).

(5) R. B. Black, J. Rhodes, G. T. Davies, H. Gravelle, and P. Sweetnam, *Gastroenterology*, **61**, 821 (1971).

(6) "The Pharmacological Basis of Therapeutics," 5th ed., L. S. Goodman and A. Gilman, Eds., Macmillan, New York, N.Y., 1975, p. 749.

(7) A. Coronato and G. B. J. Glass, *Proc. Soc. Exp. Biol. Med.*, **142**, 1341 (1973).

(8) R. Gräsbeck, *Acta Med. Scand., Suppl. 314*, **154**, 1 (1956).

(9) S. Lindenbaum and T. Higuchi, *J. Pharm. Sci.*, **64**, 1887 (1975).

(10) R. Gräsbeck, *Acta Chem. Scand.*, **22**, 1041 (1968).

(11) J. G. Spenney and B. J. Hirschowitz, *Gastroenterology*, **58**, 996 (1970).

Simultaneous Programmed Temperature GLC Assay of Phenol, Chloroxylenol, and Lidocaine Hydrochloride in Topical Antiseptic Cream

PHILIP J. PALERMO ˣ and J. BRIAN LUNDBERG

Received October 25, 1977, from *Norwich-Eaton Pharmaceuticals, Norwich, NY 13815.* Accepted for publication February 28, 1978.

Abstract □ A simultaneous programmed temperature GLC assay for the active ingredients in a topical antiseptic cream is described. The sample is extracted directly using a dimethyl sulfoxide solution of *p*-cresol, 4-chlorophenol, and 2-amino-4-phenylthiazole as internal standards for phenol, chloroxylenol, and lidocaine hydrochloride, respectively. The resulting solution is chromatographed by temperature programming on an OV-225 column from 90 to 225°. The internal standard calculation is accomplished using peak heights or peak areas. The relative standard deviation of all assays is less than 2%.

Keyphrases □ Phenol—GLC analysis simultaneously with other active ingredients in commercial preparations □ Chloroxylenol—GLC analysis simultaneously with other active ingredients in commercial preparations □ Lidocaine hydrochloride—GLC analysis simultaneously with other active ingredients in commercial preparations □ GLC—simultaneous analyses, phenol, chloroxylenol, and lidocaine hydrochloride in commercial preparations

Existing assay methods for products with multiple active ingredients can often be tedious and time consuming. Current procedures for phenol, chloroxylenol (*p*-chloro-*m*-xylenol), and lidocaine hydrochloride in a topical cream formulation required 2 days of laboratory time and three separate assays for the active ingredients. A simultaneous procedure for the three active ingredients was desirable. In addition, a specific method was necessary for stability-indicating purposes.

GLC has been used successfully to determine lidocaine (1–3), phenol (4–6), and chloroxylenol (7–9). These techniques have inherent specificity qualities. The range of boiling points and polarities of these three components required a programmed temperature method.

EXPERIMENTAL

Materials and Reagents—Phenol and lidocaine hydrochloride meeting USP specifications were used as standards. Chloroxylenol standard material was assayed by a GLC procedure. *p*-Cresol, 4-chlorophenol, and 2-amino-4-phenylthiazole at 99+ % purity were used as received[1]. All other chemicals were ACS reagent grade or equivalent.

The column was 1.8-m × 3-mm silanized stainless steel filled with 3% OV-225 on 80–100-mesh Supelcoport adapted for on-column injection.

[1] Aldrich Chemical Co. and Fairfield Chemical Co.

0022-3549/78/1100-1627$01.00/0

© 1978, American Pharmaceutical Association

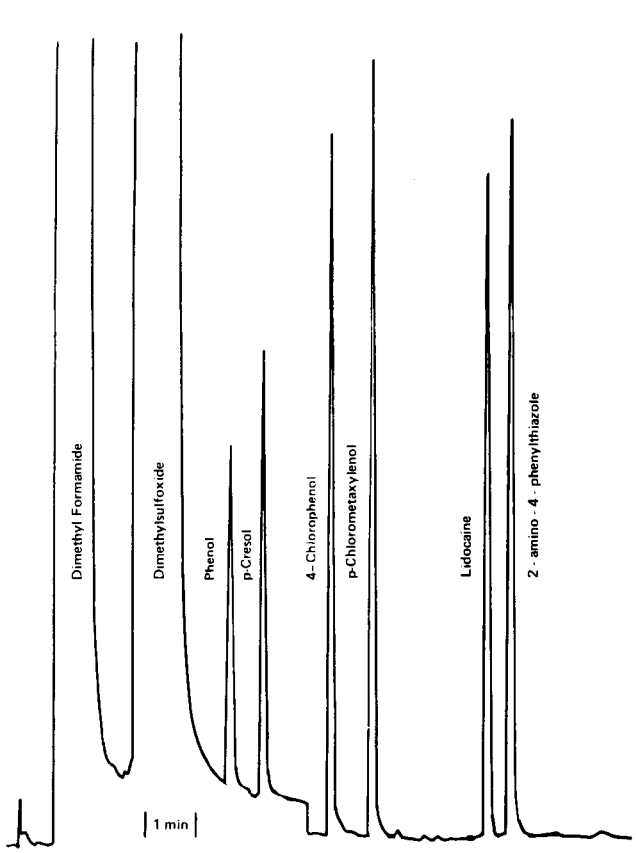

Figure 1—*Chromatogram of standard solution.*

The liquid phase was dissolved in chloroform and coated on the stationary phase by evaporation of the solvent. The column required overnight conditioning at 250° with helium flow.

Apparatus—The method was validated on two commercial gas chromatographs[2] using a flame-ionization detector. The instrument parameters were: column temperature, 90–225°; program rate, 20°/min; postinjection time, 2 min; upper limit time, 4 min; injector temperature, 250°; detector temperature, 300°; carrier gas flow rate (helium), 30 ml/min; hydrogen gas flow rate, 25 ml/min; air flow rate, 500 ml/min; attenuation, 4 for phenol and *p*-cresol and 8 for subsequent peaks; range, 1000; and recorder[3] chart speed, 1.25 cm/min.

Standard Solutions—The internal standard was prepared to contain about 0.35 g of *p*-cresol, 1.5 g of 4-chlorophenol, and 1.8 g of 2-amino-4-phenylthiazole/100 ml of dimethyl sulfoxide. (Exact weights are not necessary but should be within 20% of the recommended amounts.) A standard solution of the analytes was prepared by accurately weighing (±0.1 mg) and diluting 0.12 g of phenol, 0.48 g of chloroxylenol, and 0.43 g of lidocaine to 100 ml with dimethylformamide. The standard for injection was made by pipetting exactly 10.00 ml of internal standard and 25.00 ml of the standard analyte solution and diluting to 50 ml with dimethylformamide.

Sample Solution—Six grams of the sample was introduced into a 40-ml glass-stoppered centrifuge tube, and 10.0 ml of internal standard solution was added. This tube was then swirled in a vortex-type mixer and shaken vigorously until the sample was completely homogenized. Dimethylformamide, 10 ml, was added, and the sample was shaken briefly again. The resulting suspension was centrifuged, and the solution was decanted and diluted to 50 ml with dimethylformamide. A portion of this mixture was centrifuged.

The sample and standard solutions were injected into the gas chromatograph (Figs. 1 and 2). The injection volume was about 1 μl. This volume corresponds to about 0.7 μg of phenol, 0.8 μg of *p*-cresol, 2.7 μg of chloroxylenol, 3.0 μg of 4-chlorophenol, 2.3 μg of lidocaine, and 4.0 μg of 2-amino-4-phenylthiazole injected.

The response curve characteristics are shown in Table I for peak heights.

As an additional test of the method's viability, a solution containing

[2] Hewlett-Packard model 5750B and Perkin-Elmer model 3920.
[3] Hewlett-Packard model 7128 A.

Table I—Linear Regression Analysis

	Phenol	Chloro-xylenol	Lidocaine
Amount injected, μg	0–1	0–4	0–4
Slope, cm/μg	14.8	8.4	7.4
Correlation coefficient	0.9992	0.9996	0.9999
y-Intercept, cm	−0.92	−0.90	0.05
Standard error of estimate (Sy/x)	0.11	0.17	0.05
Percent variation $[(Sy/x)/\bar{y}] \times 100$	1.24	0.79	0.32

all internal standards and active drugs was prepared. This solution was used for adding known amounts (spiking) of analytes and internal standards to an appropriate amount of placebo material. The resulting chromatogram showed no significant difference in the peak height ratios from a portion of the solution not treated with placebo within the precision of the method.

RESULTS AND DISCUSSION

Because the phenolic compounds are acids and lidocaine is a base, quantitative partition of all compounds from a diphasic system was not investigated. Rather, a leaching procedure that leaves the excipient residue behind was employed. The excipient base consisted mainly of a saturated polyethylene glycol ether and white petrolatum. Dimethylformamide and dimethyl sulfoxide were the best solvents for breaking up the cream and getting the analytes into solution. Dimethyl sulfoxide extracted fewer excipients but eluted closer to phenol than did dimethylformamide. To keep the dimethyl sulfoxide to a minimum, a compromise procedure was to extract the sample with dimethyl sulfoxide and to dilute it to a workable volume with dimethylformamide. Quantitative recovery of the leach liquor was not necessary since the internal standards were incorporated into the dimethyl sulfoxide solution so that the ratios of each analyte to its internal standard were fixed at this point.

The sample dosage levels were: phenol, 0.5%; chloroxylenol, 2.0%; and lidocaine hydrochloride, 2.0%. A 6-g sample extracted and diluted to 50 ml gave a good response. The sample was extracted with 10 ml of dimethyl

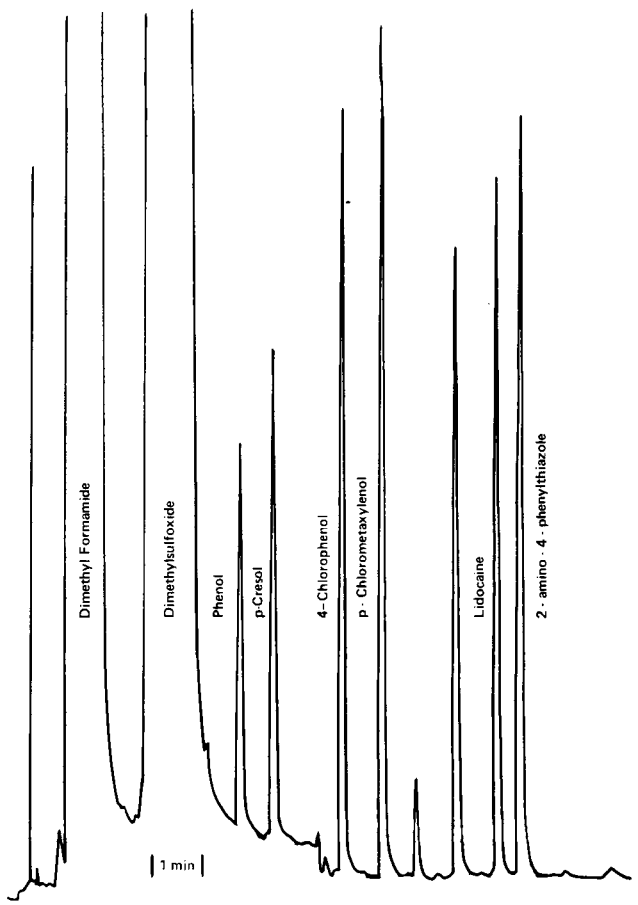

Figure 2—*Chromatogram of sample solution.*

Table II—Interlaboratory Collaborative Evaluation

Run	First Laboratory	Second Laboratory
Phenol, %	0.499	0.509
	0.490	0.519
	0.505	0.503
$\bar{X}$	0.498	0.510
RSD, %	1.5	1.6
Chloroxylenol, %	1.95	1.98
	2.01	1.97
	2.02	2.01
$\bar{X}$	2.00	1.99
RSD, %	1.9	0.9
Lidocaine hydrochloride, %	2.04	2.02
	2.04	2.03
	2.06	2.01
$\bar{X}$	2.04	2.02
RSD, %	0.33	0.68

sulfoxide internal standard solution and then diluted with dimethylformamide.

An internal standard for each analyte was preferable because of the temperature programming. Comparisons of all three drugs to any one of the internal standards did not yield acceptable precision for all of them. Phenol and *p*-cresol eluted during the initial constant-temperature period, chloroxylenol and 4-chlorophenol eluted at about 180° during the program, and lidocaine and 2-amino-4-phenylthiazole eluted during the final upper level temperature (225°). The attenuation was lowered for the first part of the chromatogram because of the lower dosage of phenol.

Two synthetic samples were prepared at the label values and assayed 10 times by two analysts on 4 different days. The sample size was varied from 80 to 120% of the recommended amount. Since the response curves are linear over the range of interest and have acceptably low *y*-intercepts, the calculations may be performed using a single-point ratio of peak response. There was no statistical difference in results between calculations using peak heights or areas. The ratios (R) are calculated as the peak response (heights or areas) of the analyte divided by the peak response of its internal standard.

The final calculation for each component is:

$$\text{percent drug} = \frac{R_{\text{sample}}}{R_{\text{std}}} \times \frac{g_{\text{std}}}{g_{\text{sample}}} \times K \qquad \text{(Eq. 1)}$$

where K is a constant incorporating dilution factors and, for lidocaine, the molecular weight ratio of lidocaine hydrochloride to lidocaine.

The average percent recovery and relative standard deviations (%) were: phenol, 100.6 ± 1.4; chloroxylenol, 100.3 ± 1.1; and lidocaine hydrochloride, 99.1 ± 1.4.

Eighteen analyses were performed on a 2-year-old actual sample by one analyst on 4 different days. The relative standard deviations of the assays were: phenol, ±0.9%; chloroxylenol, ±0.8%; and lidocaine hydrochloride, ±1.2%.

This method was further evaluated by simultaneous interlaboratory collaborative analyses on identical samples (Table II).

This simultaneous three-assay procedure represents a significant saving in time. Approximately eight samples (24 assays) can be performed per worker day.

REFERENCES

(1) A. Cometti, G. Bagnasco, and N. Maggi, *J. Pharm. Sci.*, **60**, 1074 (1971).

(2) N. D. Greenwood and I. W. Guppy, *Analyst*, **99**, 313 (1974).

(3) N. Benowitz and M. Rowland, *Anesthesiology*, **39**, 639 (1973).

(4) C. C. Douglas, *J. Assoc. Offic. Anal. Chem.*, **55**, 610 (1972).

(5) J. Hrivnak and J. Macak, *Anal. Chem.*, **43**, 1039 (1971).

(6) J. B. Johnson and V. S. Venturello, *Bull. Parenter. Drug Assoc.*, **25**, 239 (1971).

(7) S. Husain, *Indian J. Technol.*, **6**, 94 (1968).

(8) H. Koenig, *Fresenius Z. Anal. Chem.*, **266**, 119 (1973).

(9) I. Takemura, *Bunseki Kagaka*, **20**, 61 (1971).

Drug Resistance Studies with Topical Antiseptics

HERBERT N. PRINCE ˣ, WALTER S. NONEMAKER, RICHARD C. NORGARD, and DANIEL L. PRINCE

Received January 23, 1978, from the *Research Department, Gibraltar Biological Laboratories, Inc., Fairfield, NJ 07006.* Accepted for publication March 6, 1978.

Abstract □ Species of *Proteus, Serratia,* and *Pseudomonas* became resistant to chlorhexidine after five to eight transfers *in vitro*. Cross-resistance to benzalkonium chloride also was detected. Resistance to povidone-iodine was not encountered. Chlorhexidine resistance was stable after drug-free transfers of *Serratia* and *Pseudomonas* but was transitory for *Proteus*.

Keyphrases □ Chlorhexidine gluconate—resistance by various microorganisms *in vitro* □ Povidone-iodine—resistance by various microorganisms *in vitro* □ Resistance—various microorganisms to chlorhexidine gluconate and povidone-iodine *in vitro* □ Antiseptics, topical—chlorhexidine gluconate and povidone-iodine, resistance by various microorganisms *in vitro*

Chlorhexidine, *N,N″*-bis(4-chlorophenyl)-3,12-diimino-2,4,11,13-tetraazatetradecanediimidamide, first described in 1954 by Davies *et al.* (1), has been used extensively in England and Europe as a preservative, disinfectant, and topical antiseptic. It recently was introduced in the United States for use in hospitals as a topical antimicrobial cleanser.

Resistant strains of *Proteus mirabilis* were isolated from postoperative urinary infections and in paraplegics undergoing catheterization of the bladder following repeated use of chlorhexidine for cleansing the external genitalia (2–4). More recently, Stickler (5) examined 104 clinical isolates of *P. mirabilis* for sensitivity to chlorhexidine and found minimum inhibitory concentrations

Table I—Baseline *In Vitro* Activity of Three Topical Antiseptics against Parent Gram-Negative Rods

Organism	MIC, μg/ml (in Dubos Broth, 48 hr at 35°)		
	Chlorhexidine Gluconate	Benzalkonium Chloride	Available Iodine from Povidone-Iodine
P. mirabilis	8	16	8
Ps. aeruginosa	8	128	8
Ps. cepacia	1	1000	16
Ser. marcescens	8	16	8
Ser. rubidae	32	512	32
Sal. enteritidis	8	32	16

0022-3549/78/1100-1629$01.00/0

© 1978, American Pharmaceutical Association

Table II—Interlaboratory Collaborative Evaluation

Run	First Laboratory	Second Laboratory
Phenol, %	0.499	0.509
	0.490	0.519
	0.505	0.503
$\bar{X}$	0.498	0.510
RSD, %	1.5	1.6
Chloroxylenol, %	1.95	1.98
	2.01	1.97
	2.02	2.01
$\bar{X}$	2.00	1.99
RSD, %	1.9	0.9
Lidocaine hydrochloride, %	2.04	2.02
	2.04	2.03
	2.06	2.01
$\bar{X}$	2.04	2.02
RSD, %	0.33	0.68

sulfoxide internal standard solution and then diluted with dimethylformamide.

An internal standard for each analyte was preferable because of the temperature programming. Comparisons of all three drugs to any one of the internal standards did not yield acceptable precision for all of them. Phenol and *p*-cresol eluted during the initial constant-temperature period, chloroxylenol and 4-chlorophenol eluted at about 180° during the program, and lidocaine and 2-amino-4-phenylthiazole eluted during the final upper level temperature (225°). The attenuation was lowered for the first part of the chromatogram because of the lower dosage of phenol.

Two synthetic samples were prepared at the label values and assayed 10 times by two analysts on 4 different days. The sample size was varied from 80 to 120% of the recommended amount. Since the response curves are linear over the range of interest and have acceptably low *y*-intercepts, the calculations may be performed using a single-point ratio of peak response. There was no statistical difference in results between calculations using peak heights or areas. The ratios (R) are calculated as the peak response (heights or areas) of the analyte divided by the peak response of its internal standard.

The final calculation for each component is:

$$\text{percent drug} = \frac{R_{\text{sample}}}{R_{\text{std}}} \times \frac{g_{\text{std}}}{g_{\text{sample}}} \times K \qquad \text{(Eq. 1)}$$

where K is a constant incorporating dilution factors and, for lidocaine, the molecular weight ratio of lidocaine hydrochloride to lidocaine.

The average percent recovery and relative standard deviations (%) were: phenol, 100.6 ± 1.4; chloroxylenol, 100.3 ± 1.1; and lidocaine hydrochloride, 99.1 ± 1.4.

Eighteen analyses were performed on a 2-year-old actual sample by one analyst on 4 different days. The relative standard deviations of the assays were: phenol, ±0.9%; chloroxylenol, ±0.8%; and lidocaine hydrochloride, ±1.2%.

This method was further evaluated by simultaneous interlaboratory collaborative analyses on identical samples (Table II).

This simultaneous three-assay procedure represents a significant saving in time. Approximately eight samples (24 assays) can be performed per worker day.

REFERENCES

(1) A. Cometti, G. Bagnasco, and N. Maggi, *J. Pharm. Sci.*, **60**, 1074 (1971).

(2) N. D. Greenwood and I. W. Guppy, *Analyst*, **99**, 313 (1974).

(3) N. Benowitz and M. Rowland, *Anesthesiology*, **39**, 639 (1973).

(4) C. C. Douglas, *J. Assoc. Offic. Anal. Chem.*, **55**, 610 (1972).

(5) J. Hrivnak and J. Macak, *Anal. Chem.*, **43**, 1039 (1971).

(6) J. B. Johnson and V. S. Venturello, *Bull. Parenter. Drug Assoc.*, **25**, 239 (1971).

(7) S. Husain, *Indian J. Technol.*, **6**, 94 (1968).

(8) H. Koenig, *Fresenius Z. Anal. Chem.*, **266**, 119 (1973).

(9) I. Takemura, *Bunseki Kagaka*, **20**, 61 (1971).

Drug Resistance Studies with Topical Antiseptics

HERBERT N. PRINCE ˣ, WALTER S. NONEMAKER, RICHARD C. NORGARD, and DANIEL L. PRINCE

Received January 23, 1978, from the *Research Department, Gibraltar Biological Laboratories, Inc., Fairfield, NJ 07006.* Accepted for publication March 6, 1978.

Abstract □ Species of *Proteus, Serratia,* and *Pseudomonas* became resistant to chlorhexidine after five to eight transfers *in vitro*. Cross-resistance to benzalkonium chloride also was detected. Resistance to povidone-iodine was not encountered. Chlorhexidine resistance was stable after drug-free transfers of *Serratia* and *Pseudomonas* but was transitory for *Proteus*.

Keyphrases □ Chlorhexidine gluconate—resistance by various microorganisms *in vitro* □ Povidone-iodine—resistance by various microorganisms *in vitro* □ Resistance—various microorganisms to chlorhexidine gluconate and povidone-iodine *in vitro* □ Antiseptics, topical—chlorhexidine gluconate and povidone-iodine, resistance by various microorganisms *in vitro*

Chlorhexidine, *N,N″*-bis(4-chlorophenyl)-3,12-diimino-2,4,11,13-tetraazatetradecanediimidamide, first described in 1954 by Davies *et al.* (1), has been used extensively in England and Europe as a preservative, disinfectant, and topical antiseptic. It recently was introduced in the United States for use in hospitals as a topical antimicrobial cleanser.

Resistant strains of *Proteus mirabilis* were isolated from postoperative urinary infections and in paraplegics undergoing catheterization of the bladder following repeated use of chlorhexidine for cleansing the external genitalia (2–4). More recently, Stickler (5) examined 104 clinical isolates of *P. mirabilis* for sensitivity to chlorhexidine and found minimum inhibitory concentrations

Table I—Baseline *In Vitro* Activity of Three Topical Antiseptics against Parent Gram-Negative Rods

Organism	MIC, μg/ml (in Dubos Broth, 48 hr at 35°)		
	Chlorhexidine Gluconate	Benzalkonium Chloride	Available Iodine from Povidone-Iodine
P. mirabilis	8	16	8
Ps. aeruginosa	8	128	8
Ps. cepacia	1	1000	16
Ser. marcescens	8	16	8
Ser. rubidae	32	512	32
Sal. enteritidis	8	32	16

0022-3549/78/1100-1629$01.00/0

© 1978, American Pharmaceutical Association

Table II—Development of Resistance to Chlorhexidine Gluconate [a] by the Serial Passage Technique

Organism	MIC, μg/ml (in Dubos Broth, 48 hr at 35°)																			Geometric Increase at[c]
	1[b]	2	3	4	5	6	7	8	9	10	11	12	13	14	15	16	17	18	20	
P. mirabilis	8	8	16	32	32	32	64	*128*	*128*	*128*	*128*	*128*	*128*	*256*	*255*	*256*	*256*	*512*	*1024*	128×
Ser. marcescens	8	4	16	64	*128*	*128*	*128*	*256*	*256*	*512*	*1024*	*1024*	*1024*	*2048*	*2048*	*1024*	*2048*	*2048*	*2048*	256×
Ser. rubidae	32	120	256	256	256	256	256	*512*	*1024*	*1024*	*1024*	*1024*	*1024*	*1024*	*1024*	*1024*	*1024*	*1024*	*2048*	128×
Ps. cepacia	1	2	2	4	4	4	8	*16*	*32*	*32*	*64*	*64*	*16*	*16*	*32*	*32*	*32*	*128*	*128*	128×
Ps. aeruginosa	8	4	4	8	8	8	16	32	16	16	16	8	8	16	16	16	8	32	16	2×
Sal. enteritidis	8	8	16	16	16	16	16	8	16	16	32	16	32	16	16	8	16	16	16	2×

[a] Hibiclens. [b] Transfer number. [c] Resistance was considered to have occurred when the MIC value was 10-fold greater than the parent strain (Transfer 1); italicized figure equals resistance.

ranging from 10 to 800 μg/ml with cross-resistance to benzalkonium chloride.

The present study was undertaken to determine the: (*a*) rate and extent to which resistance to chlorhexidine gluconate could be induced in Gram-negative rods as compared to povidone-iodine, (*b*) presence or absence of cross-resistance to topical antiseptics widely used in this country, and (*c*) possible coinduction of other phenotypic changes in strains selected for resistance.

EXPERIMENTAL

Drugs—Chlorhexidine gluconate cleanser[1] as the 4% (w/v) solution, 7.5% povidone-iodine[2], and benzalkonium chloride[3] antiseptic, 1:750 aqueous, were studied.

Procedure—All formulations were diluted in unsupplemented Dubos broth base without glycerin or albumin since this minimally organic medium allowed detection of reproducible values with povidone-iodine. Twofold serial dilutions were prepared in this broth, ranging from 4000 to 0.125 μg of active ingredients/ml. Aliquots of 2 ml of drug were added to 2 ml of broth to achieve the twofold dilution; a fresh pipet was used for each dilution step.

Baseline minimum inhibitory concentrations (MIC values) were obtained by inoculating tubes with 0.1 ml of a 1:1000 dilution of 24-hr trypticase soy broth cultures (~10^4 cells/tube of broth–drug mixture). The inhibitory end-point in micrograms per milliliter was taken as the lowest concentration free of gross turbidity after 48 hr at 35°. The development of drug resistance was then determined by the serial passage technique of Grunberg and Prince (6).

Studies with chlorhexidine gluconate and povidone-iodine were performed concurrently. After 48 hr, the tubes containing growth in the presence of the highest tolerated concentration of drug were diluted 1:1000 and used as the inoculum for the following transfer. A total of 20 passages was performed with each of the following organisms, all initially purified from an isolated colony on MacConkey's agar: *Proteus mirabilis* (ATCC 7002, GBL 15), *Pseudomonas aeruginosa* (ATCC 15442, GBL 67), *Pseudomonas cepacia* (wild strain GBL 110), *Serratia marcescens* (clinical isolate GBL 104), *Serratia rubidae* (wild strain GBL 181), and *Salmonella enteritidis* (clinical isolate GBL 78). The baseline MIC values for the seven organisms are shown in Table I.

Drug resistance was considered to have occurred if the MIC value increased at least 10-fold above the baseline. When resistance was detected, biochemical tests employing freeze-dried miniaturized cupules[4] and intraperitoneal virulence assays in mice (septicemia and death) were performed (7), and the results were compared with the parent strains. These tests included the fermentation of glucose, arabinose, mannitol, sorbitol, rhamnose, sucrose, lactose, and amygdalin; dissimilation of arginine, lysine, ornithine, tryptophan, urea, and citrate; and production of hydrogen sulfide, nitratase, and cytochrome oxidase. When resistant strains emerged, cross-resistance to benzalkonium chloride and povidone-iodine was determined employing the same broth dilution technique in Dubos broth.

[1] Hibitane, Ayerst Laboratories, Montreal, Canada; Hibiclens, Stuart Pharmaceuticals, Wilmington, Del.
[2] Betadine Surgical Scrub, Purdue-Frederick Co., Norwalk, Conn.
[3] Zephiran, Winthrop Laboratories, New York, N.Y.
[4] API System, Analytical Products, South Plainfield, N.J.

RESULTS AND DISCUSSION

The data in Table I show that chlorhexidine gluconate and povidone-iodine were of similar activity in the broth dilution assay and that both were superior to benzalkonium chloride.

The effect of serial transfer on the development of resistance to chlorhexidine gluconate is summarized in Table II. Four of the six organisms studied became resistant to chlorhexidine.

P. mirabilis displayed a 128-fold increase in resistance to chlorhexidine gluconate, with initial resistance seen to emerge by the eighth transfer. Transfer 20 showed MIC values of 512 μg/ml against benzalkonium chloride and 8 μg/ml against povidone-iodine. Thus, resistance to chlorhexidine developed rapidly and extensively with cross-resistance to benzalkonium chloride but not to povidone-iodine. Resistance to chlorhexidine was not permanent since three drug-free transfers produced a strain for which the MIC decreased to 32 μg/ml, a value similar to the value obtained in Transfer 1 with the parent strain. The resistant strains were not altered with respect to biochemical properties or virulence for mice.

Ser. marcescens developed a 256-fold increase in resistance to chlorhexidine gluconate, with initial resistance seen as early as the fifth transfer. Transfer 20 was cross-resistant to benzalkonium chloride (MIC = 512 μg/ml) but not to povidone-iodine (MIC = 8 μg/ml). A similar pattern of resistance and cross-resistance was detected for *Ser. rubidae*. Resistance of these two species of *Serratia* to chlorhexidine was stable, since three drug-free transfers produced strains with MIC values remaining at 512–1024 μg/ml. The resistant strains were not altered with respect to biochemical properties or mouse virulence.

Ps. cepacia developed a 128-fold increased resistance to chlorhexidine. This organism, initially insensitive to benzalkonium chloride (MIC = 1000 μg/ml), did not display baseline cross-resistance to chlorhexidine (Table I). Such resistance had to be induced in a stepwise manner, indicating, perhaps, that chlorhexidine and benzalkonium chloride differ in their mechanism of action against this organism. Resistance of *Ps. cepacia* to chlorhexidine was stable, since three drug-free transfers produced strains with an MIC value remaining at 128 μg/ml. This chlorhexidine-resistant strain also failed to ferment lactose, the only coinduced phenotypic change encountered in this study. Deletion of β-galactosidase was as stable as the acquisition of resistance, since the lac^- condition was maintained after three drug-free transfers.

Neither strain of *Ps. aeruginosa* nor *Sal. enteritidis* became resistant to chlorhexidine gluconate, and additional strains are under test. Similarly, *Staphylococcus aureus* (FDA 209, ATCC 6538) failed to develop resistance to this drug.

In contrast to chlorhexidine, resistance to povidone-iodine was not induced after 20 transfers in any of the six Gram-negative rods studied. The MIC ranges for *P. mirabilis*, *Ser. marcescens*, *Ser. rubidae*, *Ps. cepacia*, *Ps. aeruginosa*, and *Sal. enteritidis* were 8–16, 8–16, 16–64, 8–16,

8–16, and 16–64 μg/ml, respectively, variations normal to the twofold serial dilution technique. These results confirm the work of Houang *et al.* (8), who were unable to detect resistance to this drug.

These studies show that the development of drug resistance can be an important factor in the choice of a skin antiseptic. Pharmaceutical scientists should share equal awareness of this limitation with microbiologists and physicians. There is no evidence from either the literature (8) or the present work that resistance to povidone-iodine is a potential problem in medical practice. However, previous observations of resistance to chlorhexidine and benzalkonium chloride (5) were confirmed and extended. Development of resistance to chlorhexidine in the genus *Serratia* is newly reported here (MIC = 2000 μg/ml). This concentration can be obtained easily in the hospital with only a 20-fold dilution of full-strength surgical scrub.

The practical significance of these findings with respect to nosocomial infections should not be underestimated, especially with increased use of chlorhexidine as a preservative, antiseptic, and oral drug.

REFERENCES

(1) G. E. Davies, J. Francis, A. R. Martin, F. L. Rose, and G. Swain, *Br. J. Pharmacol.*, **9**, 192 (1954).

(2) W. A. Gillespie, G. G. Lennon, K. B. Linton, and G. A. Phippen, *Br. Med. J.*, **3**, 90 (1967).

(3) J. D. O'Flynn and D. J. Stickler, *Lancet*, **1**, 489 (1972).

(4) D. J. Sticker, C. B. Wilmont, and J. D. O'Flynn, *Paraplegia*, **8**, 243 (1971).

(5) D. J. Stickler, *J. Clin. Pathol.*, **27**, 284 (1974).

(6) E. Grunberg and H. N. Prince, "IIId International Congress of Chemotherapy," Georg Thieme Verlag, Stuttgart, West Germany, 1964, pp. 51–58.

(7) E. Grunberg, J. Berger, G. Beskid, R. Cleeland, H. N. Prince, and E. Titsworth, *Chemotherapia*, **12**, 272 (1967).

(8) E. T. Houang, O. J. A. Gilmore, C. Reid, and E. J. Shaw, *J. Clin. Pathol.*, **29**, 752 (1976).

Aspirin Stability in Solid Dispersion Binary Systems

H. M. EL-BANNA ˣ, N. A. DAABIS, and S. ABD EL-FATTAH

Received December 7, 1977, from the *Department of Pharmaceutics, Faculty of Pharmacy, University of Alexandria, Alexandria, Egypt.* Accepted for publication February 27, 1978.

Abstract □ The stability of aspirin in its solid dispersion with urea or povidone was investigated at two accelerated storage conditions. The observed aspirin degradation in both systems followed the first-order rate equation. The water sorption ability of the two carriers as well as the alkalinity imparted by urea could possibly be the most important factors responsible for the observed acceleration of aspirin decomposition. The results also showed that the temperature effect was more pronounced than the humidity effect. Generally, coprecipitated samples exhibited slightly higher degradation rates than physically mixed ones.

Keyphrases □ Aspirin—stability in solid dispersion binary systems with urea or povidone, effect of temperature and humidity □ Solid dispersions—aspirin in binary systems with urea or povidone, effect of temperature and humidity □ Stability—aspirin in solid dispersion binary systems with urea or povidone, effect of temperature and humidity □ Dosage forms—solid dispersion binary systems, aspirin with urea or povidone, effect of temperature and humidity on stability □ Analgesics—aspirin, stability in solid dispersion binary systems with urea or povidone, effect of temperature and humidity

Aspirin decomposition in the solid form is considered to be due to a hydrolytic reaction in the presence of water. The first reported humidity- and temperature-controlled experiments with aspirin tablets was conducted by Canback (1). Stability studies on aspirin incorporated with antacids or lubricants in solid dosage forms were reviewed (2), and aspirin stability in various liquid and semisolid bases was investigated (3, 4). Blocking free hydroxyl groups on polyethylene glycols retarded aspirin decomposition resulting from transesterification (5, 6).

BACKGROUND

In 1961, a unique approach was demonstrated (7) to reduce the particle size and increase the dissolution rates and absorption of poorly soluble drugs *via* the formation of solid dispersions with inert, highly soluble carriers. Since then, this concept has been applied successfully to the formulation of fast-release dosage forms containing sparingly water-soluble drugs (8–12). An investigation of possible enhancement of the dissolution rate of aspirin *via* coprecipitation with polyethylene glycol 6000 was reported (8). Urea and povidone were used commonly as inert carriers in solid dispersion binary systems (9–12).

A literature review revealed that the effect of aging or storage under various conditions on the fast-release characteristics and chemical stability of drugs in solid dispersion systems had not been reported extensively. Aging effects were manifested only as coarsening of eutectic mixtures (13), precipitation from solid solutions (14) or glass solutions (15), and polymorphic transformations or changes in dissolution rates (16).

The present study was undertaken to evaluate the chemical stability of aspirin in its solid dispersion with a water-soluble carrier such as urea or povidone and to determine the influence of solid dispersion systems on drug stability.

EXPERIMENTAL

Materials—Aspirin[1], urea[2], povidone[3], and calcium chloride hexahydrate[4] were used as obtained. Absolute ethanol[5] and chloroform[5] were analytical grade.

Sample Preparation—Solid dispersion samples of aspirin with urea or povidone were prepared by the solvent method to avoid any possible aspirin decomposition if samples were prepared by the melt method (17). Coprecipitates of aspirin with both carriers in a ratio of 3:1 were obtained by dissolving the components in the minimum volume of absolute ethanol and subsequently evaporating the solvent *in vacuo* at room temperature using a rotary evaporator. The residue was finely ground, sieved to a particle-size range of 80–125 μm, and stored in a desiccator over anhydrous calcium sulfate.

Physical mixtures of the same compositions as the coprecipitates were prepared by simple mixing of ingredients possessing the same particle-size range. Pure crystalline aspirin (80–125 μm) served as a control sample.

Accelerated Storage Conditions—Samples, equivalent to 50 mg of aspirin, were placed in separate small beakers and kept in a desiccator under controlled relative humidity (R.H.) and temperature conditions of 100% R.H.–40° and 42% R.H.–65°. The latter condition was attained by using a saturated solution of calcium chloride hexahydrate. No ap-

[1] Bayer, Leverkusen, West Germany.
[2] E. Merck, Darmstadt, West Germany.
[3] BASF, Ludwigshafen/Rhein, West Germany.
[4] Riedel-De Haen AG, Seelze-Hannover, West Germany.
[5] BDH Chemicals Ltd., Poole, England.

0022-3549/78/1100-1631$01.00/0

© 1978, American Pharmaceutical Association

8–16, and 16–64 μg/ml, respectively, variations normal to the twofold serial dilution technique. These results confirm the work of Houang *et al.* (8), who were unable to detect resistance to this drug.

These studies show that the development of drug resistance can be an important factor in the choice of a skin antiseptic. Pharmaceutical scientists should share equal awareness of this limitation with microbiologists and physicians. There is no evidence from either the literature (8) or the present work that resistance to povidone-iodine is a potential problem in medical practice. However, previous observations of resistance to chlorhexidine and benzalkonium chloride (5) were confirmed and extended. Development of resistance to chlorhexidine in the genus *Serratia* is newly reported here (MIC = 2000 μg/ml). This concentration can be obtained easily in the hospital with only a 20-fold dilution of full-strength surgical scrub.

The practical significance of these findings with respect to nosocomial infections should not be underestimated, especially with increased use of chlorhexidine as a preservative, antiseptic, and oral drug.

REFERENCES

(1) G. E. Davies, J. Francis, A. R. Martin, F. L. Rose, and G. Swain, *Br. J. Pharmacol.*, **9**, 192 (1954).

(2) W. A. Gillespie, G. G. Lennon, K. B. Linton, and G. A. Phippen, *Br. Med. J.*, **3**, 90 (1967).

(3) J. D. O'Flynn and D. J. Stickler, *Lancet*, **1**, 489 (1972).

(4) D. J. Sticker, C. B. Wilmont, and J. D. O'Flynn, *Paraplegia*, **8**, 243 (1971).

(5) D. J. Stickler, *J. Clin. Pathol.*, **27**, 284 (1974).

(6) E. Grunberg and H. N. Prince, "IIId International Congress of Chemotherapy," Georg Thieme Verlag, Stuttgart, West Germany, 1964, pp. 51–58.

(7) E. Grunberg, J. Berger, G. Beskid, R. Cleeland, H. N. Prince, and E. Titsworth, *Chemotherapia*, **12**, 272 (1967).

(8) E. T. Houang, O. J. A. Gilmore, C. Reid, and E. J. Shaw, *J. Clin. Pathol.*, **29**, 752 (1976).

Aspirin Stability in Solid Dispersion Binary Systems

H. M. EL-BANNA ˣ, N. A. DAABIS, and S. ABD EL-FATTAH

Received December 7, 1977, from the *Department of Pharmaceutics, Faculty of Pharmacy, University of Alexandria, Alexandria, Egypt.* Accepted for publication February 27, 1978.

Abstract □ The stability of aspirin in its solid dispersion with urea or povidone was investigated at two accelerated storage conditions. The observed aspirin degradation in both systems followed the first-order rate equation. The water sorption ability of the two carriers as well as the alkalinity imparted by urea could possibly be the most important factors responsible for the observed acceleration of aspirin decomposition. The results also showed that the temperature effect was more pronounced than the humidity effect. Generally, coprecipitated samples exhibited slightly higher degradation rates than physically mixed ones.

Keyphrases □ Aspirin—stability in solid dispersion binary systems with urea or povidone, effect of temperature and humidity □ Solid dispersions—aspirin in binary systems with urea or povidone, effect of temperature and humidity □ Stability—aspirin in solid dispersion binary systems with urea or povidone, effect of temperature and humidity □ Dosage forms—solid dispersion binary systems, aspirin with urea or povidone, effect of temperature and humidity on stability □ Analgesics—aspirin, stability in solid dispersion binary systems with urea or povidone, effect of temperature and humidity

Aspirin decomposition in the solid form is considered to be due to a hydrolytic reaction in the presence of water. The first reported humidity- and temperature-controlled experiments with aspirin tablets was conducted by Canback (1). Stability studies on aspirin incorporated with antacids or lubricants in solid dosage forms were reviewed (2), and aspirin stability in various liquid and semisolid bases was investigated (3, 4). Blocking free hydroxyl groups on polyethylene glycols retarded aspirin decomposition resulting from transesterification (5, 6).

BACKGROUND

In 1961, a unique approach was demonstrated (7) to reduce the particle size and increase the dissolution rates and absorption of poorly soluble drugs *via* the formation of solid dispersions with inert, highly soluble carriers. Since then, this concept has been applied successfully to the formulation of fast-release dosage forms containing sparingly water-soluble drugs (8–12). An investigation of possible enhancement of the dissolution rate of aspirin *via* coprecipitation with polyethylene glycol 6000 was reported (8). Urea and povidone were used commonly as inert carriers in solid dispersion binary systems (9–12).

A literature review revealed that the effect of aging or storage under various conditions on the fast-release characteristics and chemical stability of drugs in solid dispersion systems had not been reported extensively. Aging effects were manifested only as coarsening of eutectic mixtures (13), precipitation from solid solutions (14) or glass solutions (15), and polymorphic transformations or changes in dissolution rates (16).

The present study was undertaken to evaluate the chemical stability of aspirin in its solid dispersion with a water-soluble carrier such as urea or povidone and to determine the influence of solid dispersion systems on drug stability.

EXPERIMENTAL

Materials—Aspirin[1], urea[2], povidone[3], and calcium chloride hexahydrate[4] were used as obtained. Absolute ethanol[5] and chloroform[5] were analytical grade.

Sample Preparation—Solid dispersion samples of aspirin with urea or povidone were prepared by the solvent method to avoid any possible aspirin decomposition if samples were prepared by the melt method (17). Coprecipitates of aspirin with both carriers in a ratio of 3:1 were obtained by dissolving the components in the minimum volume of absolute ethanol and subsequently evaporating the solvent *in vacuo* at room temperature using a rotary evaporator. The residue was finely ground, sieved to a particle-size range of 80–125 μm, and stored in a desiccator over anhydrous calcium sulfate.

Physical mixtures of the same compositions as the coprecipitates were prepared by simple mixing of ingredients possessing the same particle-size range. Pure crystalline aspirin (80–125 μm) served as a control sample.

Accelerated Storage Conditions—Samples, equivalent to 50 mg of aspirin, were placed in separate small beakers and kept in a desiccator under controlled relative humidity (R.H.) and temperature conditions of 100% R.H.–40° and 42% R.H.–65°. The latter condition was attained by using a saturated solution of calcium chloride hexahydrate. No ap-

[1] Bayer, Leverkusen, West Germany.
[2] E. Merck, Darmstadt, West Germany.
[3] BASF, Ludwigshafen/Rhein, West Germany.
[4] Riedel-De Haen AG, Seelze-Hannover, West Germany.
[5] BDH Chemicals Ltd., Poole, England.

0022-3549/78/1100-1631$01.00/0

© 1978, American Pharmaceutical Association

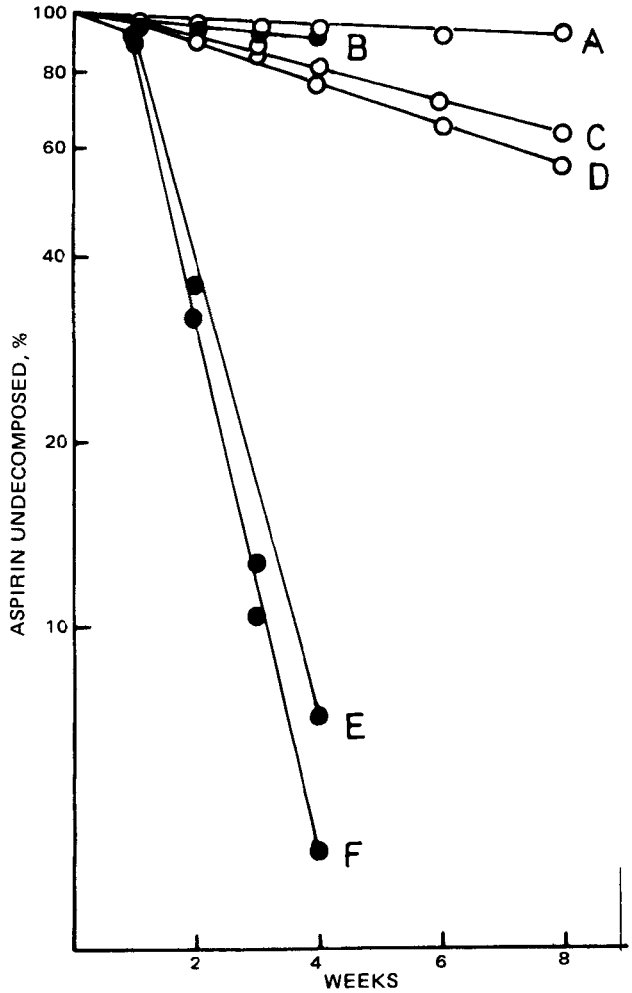

Figure 1 —*Semilogarithmic plots of percentage of aspirin undecomposed in aspirin–urea system (3:1 ratio) against time at 100% R.H.–40° (○) and at 42% R.H.–65° (●). Key: A and B, crystalline aspirin; C and E, physical mixture; and D and F, coprecipitate.*

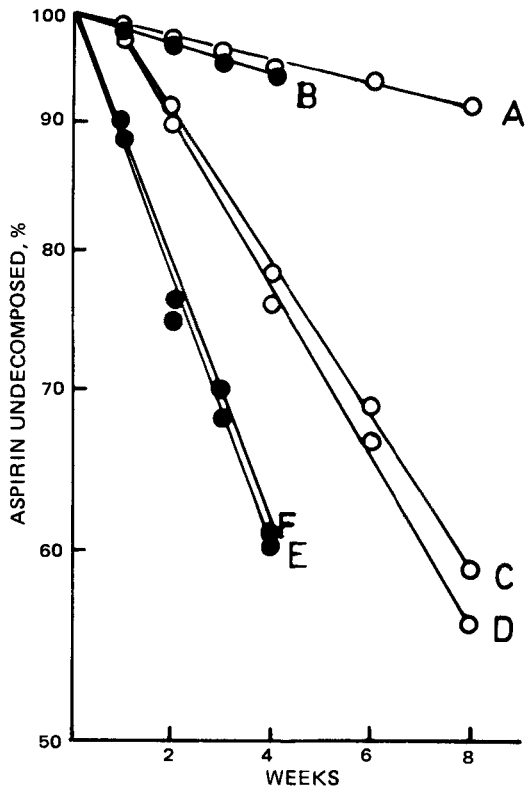

Figure 2—*Semilogarithmic plots of percentage of aspirin undecomposed in aspirin–povidone system (3:1 ratio) against time at 100% R.H. –40° (○) and at 42% R.H.–65° (●). Key: A and B, crystalline aspirin; C and E, physical mixture; and D and F, coprecipitate.*

preciable change in humidity was observed during the experiment. At frequent intervals, samples were withdrawn and assayed.

Assay—UV spectrophotometric analysis, as reported by Tinker and McBay (18), was employed to measure aspirin and salicylic acid. The content of each beaker, equivalent to 50 mg of aspirin, was dissolved in 20 ml of chloroform containing 1% acetic acid. After filtration and further appropriate dilution, the absorbance was read[6] at 282 nm for aspirin and 310 nm for salicylic acid. The calculation of the quantities of aspirin and salicylic acid was based on the standard method of simultaneous spectrophotometric determinations.

RESULTS AND DISCUSSION

Accelerated storage conditions were applied to evaluate aspirin stability in solid dispersion systems. Only samples having the same mesh size were investigated to avoid any discrepancies due to particle-size effect (19). Figures 1 and 2 show the semilogarithmic plots of the percentage of aspirin undecomposed in the control sample and physically mixed and coprecipitated samples with urea and povidone, respectively, against time after storage at 100% R.H.–40° and 42% R.H.–65°.

Under the accelerated storage conditions, an initial induction period, which could be attributed to water absorption, was generally observed (Figs. 1 and 2). After this lag period, aspirin degradation appeared to follow the first-order rate equation.

Crystalline Aspirin System—As may be seen from Figs. 1 and 2, crystalline aspirin (curve A) was the most stable. In this sample, no decomposition was noted during the 1st week of storage at either studied condition. Less than 10% degradation was detected after either 8 weeks of storage at 100% R.H.–40° (curve A) or 4 weeks at 42% R.H.–65° (curve B); the degradation rate constants were 0.008 and 0.015 week^{-1}, respectively. This relatively slight amount of aspirin decomposition could have been caused by small moisture sorption by the hydrophobic aspirin (20).

Aspirin–Urea System—Contrary to the reported stability of aspirin mixed with urea as a powder or tablet after 1 year of storage (21), urea showed an adversely affected aspirin degradation in the present study. The physically mixed aspirin–urea sample exhibited a high degradation rate constant of 0.061 week^{-1} after 8 weeks of storage at 100% R.H.–40° (Fig. 1, curve C). Furthermore, a comparison of curves C and E of Fig. 1 shows a drastic difference in the aspirin decomposition rate in the physically mixed sample stored at 100% R.H.–40° compared to that stored at 42% R.H.–65°. At the former condition, the decomposition reached approximately 35% after 8 weeks; at the latter storage condition, the decomposition was greater than 90% after only 4 weeks, the samples being melted and changed in color.

The acceleration of aspirin hydrolysis in the presence of urea could possibly be due to the hydrophilicity of this carrier and its ability to absorb water. One could describe this system as a suspension of aspirin in a minimum quantity of water in which urea is dissolved or as particles with each surrounded by a thin film of solubilized aspirin in a saturated urea solution. Moreover, urea itself imparts a slight alkalinity to this humid microatmospheric film, which further increases the degradation rate. This film is likely to be present at the two humidities studied.

Therefore, it was not surprising that, at the low humidity and high temperature condition (42% R.H.–65°), aspirin in this system exhibited a much higher degradation rate of 0.891 week^{-1} compared to that at the other storage condition. The marked instability of aspirin at this high temperature could be due to the effect of increased pH on the medium by ammonia caused by the partial decomposition of urea during heating (17). In addition, an increase in temperature could enhance the passage of aspirin to the surrounding film of urea solution, resulting in further degradation.

As may be seen from Fig. 1, the degradation rate constants of aspirin from the coprecipitated samples were 0.077 and 1.05 week^{-1} (curves D and F, respectively), which were higher than those from the physically mixed samples of identical composition (curves C and E). Aspirin par-

[6] Unicam SP 1800 UV spectrophotometer.

ticles in the coprecipitated samples are in a fine state of subdivision and in intimate contact with urea. In such a solid dispersion system, the reduced particle size of aspirin, the concomitant increase in its surface area exposed to the suggested film layer of urea solution, and the resultant increase in its solubility appear to be the major factors responsible for the observed acceleration of aspirin degradation. Traces of alcohol in the coprecipitated sample also may play a part (22).

Aspirin–Povidone System—In the aspirin–povidone system, the effects of humidity, temperature, and aspirin solubilization by this water-soluble carrier seem to be operating in the microenvironment surrounding aspirin particles at the two storage conditions studied. The physically mixed and coprecipitated aspirin–povidone samples (curves C and D) exhibited decomposition rate constants of 0.069 and 0.077 $week^{-1}$, respectively (Fig. 2), which were comparable to those found with the aspirin–urea system. Possibly, the degradation-enhancing effect due to the high moisture sorption inherent to povidone (23), compared to that with urea, would be outweighed by the slight alkalinity imparted by urea.

However, for comparable times, the percent decomposition of both physically mixed and coprecipitated aspirin–povidone samples stored at 42% R.H.–65° was approximately one-seventh that observed with the same samples in the aspirin–urea system. This difference in aspirin stability could be attributed to the partial decomposition of urea at this high temperature. The apparent similarity between the stability of both physically mixed and coprecipitated aspirin–povidone samples stored at 42% R.H.–65° may be due to a complex reaction (24) that seems to be temperature dependent. This complex formation was reported for aspirin with other similar, structurally related compounds (25).

From these results, it can be concluded that the polar and perhaps the hygroscopic nature of urea and povidone tend to allow aspirin to degrade when incorporated into this type of carrier as physical mixtures or coprecipitates. Although the aspirin–povidone system exhibited lower degradation rates than those for the aspirin–urea system, the percent of decomposition in the former system was still prohibitively high. Consequently, the application of solid dispersion should be handled with care for drugs showing stability problems.

REFERENCES

(1) T. Canback, *Sv. Farm. Tidskr.*, **47**, 621 (1943); through *Chem. Abstr.*, **38**, 5644[6] (1944).

(2) C. A. Kelly, *J. Pharm. Sci.*, **59**, 1053 (1970).

(3) C. W. Whitworth, L. A. Luzzi, B. B. Thompson, and H. W. Jun, *ibid.*, **62**, 1372 (1973).

(4) C. W. Whitworth and A. Asker, *ibid.*, **64**, 2018 (1975).

(5) C. W. Whitworth, H. W. Jun, and L. A. Luzzi, *ibid.*, **62**, 1184 (1973).

(6) H. W. Jun, C. W. Whitworth, and L. A. Luzzi, *ibid.*, **61**, 1160 (1972).

(7) K. Sekiguchi and N. Obi, *Chem. Pharm. Bull.*, **9**, 866 (1961).

(8) A. F. Asker and C. W. Whitworth, *Pharmazie*, **30**, 530 (1975).

(9) H. M. El-Banna, S. Abd El-Fattah, and N. A. Daabis, *ibid.*, **29**, 396 (1974).

(10) N. A. Daabis, S. Abd El-Fattah, and H. M. El-Banna, *ibid.*, **29**, 400 (1974).

(11) A. P. Simonelli, S. C. Mehta, and W. I. Higuchi, *J. Pharm. Sci.*, **58**, 538 (1969).

(12) T. R. Bates, *J. Pharm. Pharmacol.*, **21**, 710 (1969).

(13) R. P. Rastogi and P. S. Bassi, *J. Phys. Chem.*, **98**, 2398 (1964).

(14) R. Smoluchoweski, "Phase Transformation in Solids," Wiley, New York, N.Y., 1951.

(15) W. L. Chiou and S. Riegelman, *J. Pharm. Sci.*, **60**, 1281 (1971).

(16) W. L. Chiou and S. Niazi, *ibid.*, **60**, 1333 (1971).

(17) C. C. Edison and M. G. Ines, *Ann. R. Acad. Farm.*, **40**, 487 (1974).

(18) R. B. Tinker and A. J. McBay, *J. Am. Pharm. Assoc., Sci. Ed.*, **43**, 315 (1954).

(19) R. Yamamoto and T. Takahashi, *Ann. Rep. Shionogi Res. Lab.*, **3**, 112 (1953).

(20) L. J. Leeson and A. M. Mattocks, *J. Am. Pharm. Assoc., Sci. Ed.*, **47**, 329 (1958).

(21) I. Grabowska, *Gdansk. Tow. Nauk., Rozpr. Wydz.*, **3**, 193 (1964); through *Chem. Abstr.*, **64**, 14029a (1966).

(22) E. R. Garrett, *J. Am. Chem. Soc.*, **79**, 3401 (1957).

(23) "Martindale, The Extra Pharmacopoeia," N. W. Blacow, Ed., 26th ed., Pharmaceutical Press, London, England, 1972, p. 1085.

(24) S. M. Blaug and J. W. Weslowski, *J. Am. Pharm. Assoc., Sci. Ed.*, **48**, 691 (1959).

(25) A. N. Martin, J. Swarbrick, and A. Cammarata, "Physical Pharmacy," 2nd ed., Lea & Febiger, Philadelphia, Pa., 1973, p. 334.

Odoratin and Paucin: Cytotoxic Sesquiterpene Lactones from *Baileya pauciradiata* (Compositae)

JOSEPH J. HOFFMANN, SHIVANAND D. JOLAD, STERLING J. TORRANCE, DORI J. LUZBETAK, RICHARD M. WIEDHOPF, and JACK R. COLE ˣ

Received December 23, 1977, from the *Division of Pharmaceutical Chemistry, College of Pharmacy, University of Arizona, Tucson, AZ 85721.* Accepted for publication March 2, 1978.

Abstract □ An ethanol extract of *Baileya pauciradiata* exhibited cytotoxic activity against the human epidermoid carcinoma of the nasopharynx and the lymphocytic leukemia test systems. Two constituents responsible for this activity were isolated and identified as odoratin and paucin. Their identities were proven by IR, PMR, and mass spectral data; elemental analysis; preparation of their acetates; and melting-point determinations. Odoratin was confirmed by comparison with an authentic sample.

Keyphrases □ *Baileya pauciradiata*—whole plant ethanol extract, odoratin and paucin isolated and identified □ Paucin—isolated and identified from whole plant ethanol extract of *Baileya pauciradiata* □ Odoratin—isolated and identified from whole plant ethanol extract of *Baileya pauciradiata* □ Cytotoxic sesquiterpene lactones—odoratin and paucin, isolated from whole plant ethanol extract of *Baileya pauciradiata*

In the continuing search for plants having antitumor properties, an ethanol extract of the whole plant of *Baileya pauciradiata* Harv. and Gray (Compositae)[1] exhibited cytotoxic activity against the human epidermoid carcinoma of the nasopharynx (KB) and lymphocytic leukemia (P-388) test systems[2].

[1] The plant was collected in California in March 1972. Identification was confirmed by Dr. Robert E. Perdue, Medicinal Plant Resources Laboratory, U.S. Department of Agriculture, Beltsville, Md., where a reference specimen (PR25375) is maintained.

[2] Data on the cytotoxic and *in vivo* activity were provided through the courtesy of the Division of Cancer Treatment, National Cancer Institute, National Institutes of Health, Bethesda, Md.

0022-3549/78/1100-1633$01.00/0

© 1978, American Pharmaceutical Association

ticles in the coprecipitated samples are in a fine state of subdivision and in intimate contact with urea. In such a solid dispersion system, the reduced particle size of aspirin, the concomitant increase in its surface area exposed to the suggested film layer of urea solution, and the resultant increase in its solubility appear to be the major factors responsible for the observed acceleration of aspirin degradation. Traces of alcohol in the coprecipitated sample also may play a part (22).

Aspirin–Povidone System—In the aspirin–povidone system, the effects of humidity, temperature, and aspirin solubilization by this water-soluble carrier seem to be operating in the microenvironment surrounding aspirin particles at the two storage conditions studied. The physically mixed and coprecipitated aspirin–povidone samples (curves C and D) exhibited decomposition rate constants of 0.069 and 0.077 $week^{-1}$, respectively (Fig. 2), which were comparable to those found with the aspirin–urea system. Possibly, the degradation-enhancing effect due to the high moisture sorption inherent to povidone (23), compared to that with urea, would be outweighed by the slight alkalinity imparted by urea.

However, for comparable times, the percent decomposition of both physically mixed and coprecipitated aspirin–povidone samples stored at 42% R.H.–65° was approximately one-seventh that observed with the same samples in the aspirin–urea system. This difference in aspirin stability could be attributed to the partial decomposition of urea at this high temperature. The apparent similarity between the stability of both physically mixed and coprecipitated aspirin–povidone samples stored at 42% R.H.–65° may be due to a complex reaction (24) that seems to be temperature dependent. This complex formation was reported for aspirin with other similar, structurally related compounds (25).

From these results, it can be concluded that the polar and perhaps the hygroscopic nature of urea and povidone tend to allow aspirin to degrade when incorporated into this type of carrier as physical mixtures or coprecipitates. Although the aspirin–povidone system exhibited lower degradation rates than those for the aspirin–urea system, the percent of decomposition in the former system was still prohibitively high. Consequently, the application of solid dispersion should be handled with care for drugs showing stability problems.

REFERENCES

(1) T. Canback, *Sv. Farm. Tidskr.*, **47**, 621 (1943); through *Chem. Abstr.*, **38**, 5644[6] (1944).

(2) C. A. Kelly, *J. Pharm. Sci.*, **59**, 1053 (1970).

(3) C. W. Whitworth, L. A. Luzzi, B. B. Thompson, and H. W. Jun, *ibid.*, **62**, 1372 (1973).

(4) C. W. Whitworth and A. Asker, *ibid.*, **64**, 2018 (1975).

(5) C. W. Whitworth, H. W. Jun, and L. A. Luzzi, *ibid.*, **62**, 1184 (1973).

(6) H. W. Jun, C. W. Whitworth, and L. A. Luzzi, *ibid.*, **61**, 1160 (1972).

(7) K. Sekiguchi and N. Obi, *Chem. Pharm. Bull.*, **9**, 866 (1961).

(8) A. F. Asker and C. W. Whitworth, *Pharmazie*, **30**, 530 (1975).

(9) H. M. El-Banna, S. Abd El-Fattah, and N. A. Daabis, *ibid.*, **29**, 396 (1974).

(10) N. A. Daabis, S. Abd El-Fattah, and H. M. El-Banna, *ibid.*, **29**, 400 (1974).

(11) A. P. Simonelli, S. C. Mehta, and W. I. Higuchi, *J. Pharm. Sci.*, **58**, 538 (1969).

(12) T. R. Bates, *J. Pharm. Pharmacol.*, **21**, 710 (1969).

(13) R. P. Rastogi and P. S. Bassi, *J. Phys. Chem.*, **98**, 2398 (1964).

(14) R. Smoluchoweski, "Phase Transformation in Solids," Wiley, New York, N.Y., 1951.

(15) W. L. Chiou and S. Riegelman, *J. Pharm. Sci.*, **60**, 1281 (1971).

(16) W. L. Chiou and S. Niazi, *ibid.*, **60**, 1333 (1971).

(17) C. C. Edison and M. G. Ines, *Ann. R. Acad. Farm.*, **40**, 487 (1974).

(18) R. B. Tinker and A. J. McBay, *J. Am. Pharm. Assoc., Sci. Ed.*, **43**, 315 (1954).

(19) R. Yamamoto and T. Takahashi, *Ann. Rep. Shionogi Res. Lab.*, **3**, 112 (1953).

(20) L. J. Leeson and A. M. Mattocks, *J. Am. Pharm. Assoc., Sci. Ed.*, **47**, 329 (1958).

(21) I. Grabowska, *Gdansk. Tow. Nauk., Rozpr. Wydz.*, **3**, 193 (1964); through *Chem. Abstr.*, **64**, 14029a (1966).

(22) E. R. Garrett, *J. Am. Chem. Soc.*, **79**, 3401 (1957).

(23) "Martindale, The Extra Pharmacopoeia," N. W. Blacow, Ed., 26th ed., Pharmaceutical Press, London, England, 1972, p. 1085.

(24) S. M. Blaug and J. W. Weslowski, *J. Am. Pharm. Assoc., Sci. Ed.*, **48**, 691 (1959).

(25) A. N. Martin, J. Swarbrick, and A. Cammarata, "Physical Pharmacy," 2nd ed., Lea & Febiger, Philadelphia, Pa., 1973, p. 334.

Odoratin and Paucin: Cytotoxic Sesquiterpene Lactones from *Baileya pauciradiata* (Compositae)

JOSEPH J. HOFFMANN, SHIVANAND D. JOLAD, STERLING J. TORRANCE, DORI J. LUZBETAK, RICHARD M. WIEDHOPF, and JACK R. COLE ˣ

Received December 23, 1977, from the *Division of Pharmaceutical Chemistry, College of Pharmacy, University of Arizona, Tucson, AZ 85721.* Accepted for publication March 2, 1978.

Abstract □ An ethanol extract of *Baileya pauciradiata* exhibited cytotoxic activity against the human epidermoid carcinoma of the nasopharynx and the lymphocytic leukemia test systems. Two constituents responsible for this activity were isolated and identified as odoratin and paucin. Their identities were proven by IR, PMR, and mass spectral data; elemental analysis; preparation of their acetates; and melting-point determinations. Odoratin was confirmed by comparison with an authentic sample.

Keyphrases □ *Baileya pauciradiata*—whole plant ethanol extract, odoratin and paucin isolated and identified □ Paucin—isolated and identified from whole plant ethanol extract of *Baileya pauciradiata* □ Odoratin—isolated and identified from whole plant ethanol extract of *Baileya pauciradiata* □ Cytotoxic sesquiterpene lactones—odoratin and paucin, isolated from whole plant ethanol extract of *Baileya pauciradiata*

In the continuing search for plants having antitumor properties, an ethanol extract of the whole plant of *Baileya pauciradiata* Harv. and Gray (Compositae)[1] exhibited cytotoxic activity against the human epidermoid carcinoma of the nasopharynx (KB) and lymphocytic leukemia (P-388) test systems[2].

[1] The plant was collected in California in March 1972. Identification was confirmed by Dr. Robert E. Perdue, Medicinal Plant Resources Laboratory, U.S. Department of Agriculture, Beltsville, Md., where a reference specimen (PR25375) is maintained.

[2] Data on the cytotoxic and *in vivo* activity were provided through the courtesy of the Division of Cancer Treatment, National Cancer Institute, National Institutes of Health, Bethesda, Md.

0022-3549/78/1100-1633$01.00/0

© 1978, American Pharmaceutical Association

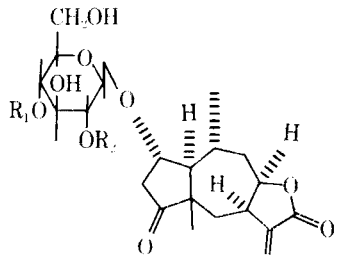

I: R_1 or R_2 = CH_3CO

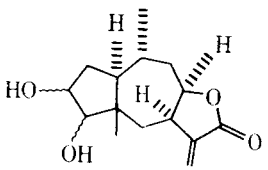

II

DISCUSSION

A literature search revealed that several sesquiterpene lactones have been isolated from various *Baileya* species. The germacranolide, baileyin, the closely related guaianolide, pleniradin, and the pseudoguaianolides, fastigilin C, radiatin, and baileyolin, were isolated from *B. multiradiata* and *B. pleniradiata* (1, 2). Plenolin was isolated from *B. pleniradiata* as was paucin, which also was isolated from *B. pauciradiata* (1, 3).

This paper reports the isolation of odoratin from *B. pauciradiata* and the fact that paucin is responsible for the high cytotoxic activity. Plenolin, paucin (I), and odoratin (II) are also pseudoguaianolides.

Paucin was isolated by a modification of the previously reported procedure (4). Its identity was confirmed by comparisons of the PMR, IR, and mass spectra and melting points of the parent compound and its triacetate with reported data and spectra (3, 4). Odoratin (5) was isolated from the mother liquor by column and preparative thick-layer chromatography. Its identity was verified by the mass spectrum, comparison of the PMR spectrum with the reported spectrum (6), preparation of its diacetate, and comparison with an authentic sample (mixed melting point and superimposable IR spectra).

Paucin exhibited cytotoxic activity at 0.016 and 0.4 μg/ml in the P-388 and KB test systems, respectively. Odoratin demonstrated an activity of 3.1 μg/ml in the KB test system. Activity in these test systems is defined[3] as an $ED_{50} \leq 4$ μg/ml. Paucin demonstrated *in vivo* activities of 135, 137, and 137% test/control (T/C) at dose levels of 35, 22, and 9.6 mg/kg, respectively, in the PS (lymphocytic leukemia) test system. Activity in the PS test system is defined[3] as an increase in the survival of treated animals over that of controls resulting in a T/C ≥ 130%.

EXPERIMENTAL[4]

Isolation Procedure—The whole plant (7 kg) of *B. pauciradiata* was ground to a powder and extracted exhaustively with 95% ethanol in a Lloyd-type extractor. The air-dried ethanol extract was partitioned between chloroform and water (1:1). The air-dried chloroform phase was taken up in hot ethanol, and two parts of hot water was added. After cooling, the resultant precipitate was removed by filtration and the filtrate was extracted with chloroform.

Isolation of Paucin—The air-dried chloroform phase (26 g) was taken up in 6% methanolic dichloromethane. The resultant residue was recrystallized from methanol and dichloromethane to yield a crystalline paucin, mp 172–173° [lit. (3) mp 171–173°].

Triacetylpaucin—Acetylation of paucin in pyridine with acetic anhydride yielded the triacetate, mp 240–242° [lit. (3) mp 241–243°].

Isolation of Odoratin—The mother liquor from the isolation was chromatographed on a silica gel 60[5] (600 g) column (7 × 40 cm) and was eluted with 6% methanolic dichloromethane. Fractions (30 ml each) 93–139 were combined and further fractionated on preparative TLC plates developed in chloroform–acetone (7:3). The major spot was further purified on preparative TLC plates developed in benzene–ether–methanol (5:10:1) and crystallized from acetone, methanol, and isopropyl ether to yield odoratin, mp 155°. Recrystallization from acetone yielded fine needles, mp 166° [lit. (5) mp 165–167°]. The mixed melting point with an authentic sample[6] showed no depression.

Anal.—Calc. for $C_{15}H_{22}O_4$: C, 67.64; H, 8.33; mol. wt. 266. Found: C, 67.29; H, 8.33; *m/e* 266 (M^+).

Diacetylodoratin—Acetylation of odoratin in pyridine with acetic anhydride yielded the diacetate, mp 132–133° [lit. (5) mp 132–133°].

REFERENCES

(1) T. G. Waddell and T. A. Geissman, *Phytochemistry*, **8**, 2371 (1969).

(2) A. Yoshitake and T. A. Geissman, *ibid.*, **8**, 1753 (1969).

(3) T. G. Waddell and T. A. Geissman, *Tetrahedron Lett. No. 7*, **1969**, 515.

(4) T. G. Waddell, Ph.D. dissertation, University of California, Los Angeles, Calif., 1969.

(5) A. Ortega, A. Romo de Vivar, and J. Romo, *Can. J. Chem.*, **46**, 1539 (1968).

(6) H. Yoshioka, T. J. Mabry, and B. N. Timmermann, "Sesquiterpene Lactones," University of Tokyo Press, Tokyo, Japan, 1973, p. 290.

ACKNOWLEDGMENTS

Supported by Contract N01-CM-33750 from the Division of Cancer Treatment, National Cancer Institute, National Institutes of Health, Department of Health, Education, and Welfare, Bethesda, MD 20014, and the Elsa U. Pardee Foundation, Midland, MI 48640.

[3] J. Douros, National Cancer Institute, Bethesda, Md., Oct. 1977, personal communication.

[4] Carbon and hydrogen analyses were performed by Chemalytics, Inc., Tempe, Ariz. PMR, IR, and mass spectral data were determined using a Varian T-60 spectrophotometer, a Beckman IR-33, and a Hewlett-Packard model 5930 spectrometer, respectively. Melting points were determined on a Kofler hot-stage apparatus and are uncorrected.

[5] Merck.

[6] Courtesy of J. Romo, Instituto de Quimica, Universidad Nacional Autónoma de México, Mexico 20, D.F., México.

Determination of Phenylpropanolamine Salts in Dosage Forms through Fluorescent Derivative Formation

L. L. SHANKLE

Received January 30, 1978, from the *Applied Pharmaceutics Laboratory, Consumer Products Division, Miles Laboratories, Inc., Elkhart, IN 46514.* Accepted for publication March 22, 1978.

Abstract □ Phenylpropanolamine was determined by measuring its fluorescent fluorescamine derivative. The method is rapid, sensitive, and easily automated. Statistics are presented for an effervescent cold product, and recovery data are presented for other commercially available products.

Keyphrases □ Phenylpropanolamine—fluorometric analysis in dosage forms □ Fluorometry—analysis, phenylpropanolamine in dosage forms □ Adrenergics—phenylpropanolamine, fluorometric analysis in dosage forms

Phenylpropanolamine can be determined by several different methods (1–7). Although they provide acceptable results, these methods are time consuming because of their complexity or the manipulations required. The need arose in this laboratory for a simple, rapid, and sensitive method for the determination of phenylpropanolamine bitartrate in a combination effervescent tablet containing aspirin and chlorpheniramine maleate. None of the existing methods was considered fast enough.

The fluorescent derivative of fluorescamine[1], 4-phenylspiro[furan-2(3*H*),1′-phthalan]-3,3′-dione (I), has been used (8, 9) to determine quantitatively primary amines in various media. This paper reports the application of this technique to the analysis of phenylpropanolamine in dosage forms. This approach is a valuable alternative to existing procedures, especially where simplicity and rapidity are important.

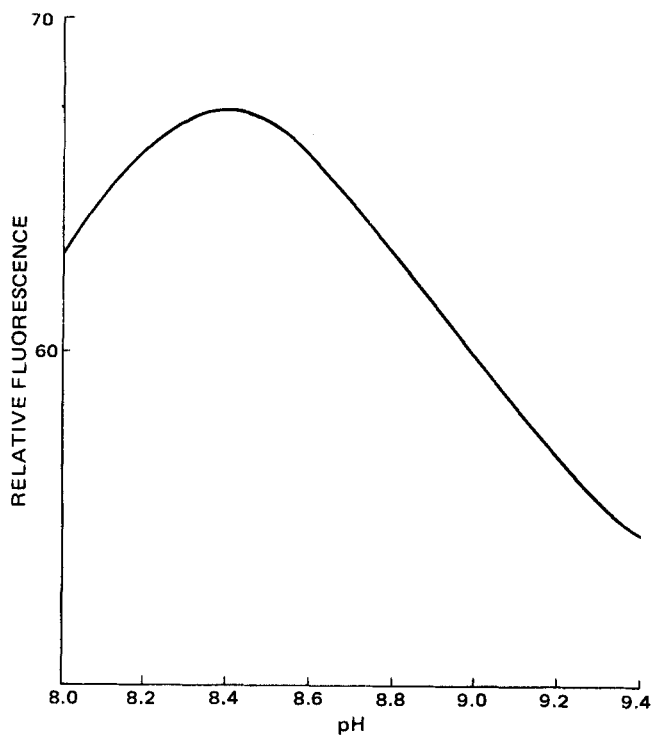

Figure 1—*Effect of pH on the intensity of fluorescence.*

[1] Fluram, Roche Diagnostic, Nutley, N.J.

Table I—Statistical Evaluation of Proposed Method

Level	Recovery, %	*CV*, %
1 (−20%)	97.3	4.52
2	96.2	1.78
3 (+20%)	97.9	1.66
Overall	97.3	2.81

EXPERIMENTAL

Reagents—To prepare borate buffer, 6.2 g of reagent grade boric acid was dissolved in 500 ml of water and the pH was adjusted to 8.4 with 10% NaOH.

A 0.3% solution of I was prepared in reagent grade acetone. The standard solution was an aqueous solution containing an accurately known concentration of phenylpropanolamine salt equivalent to approximately 2 μg of free base/ml.

Procedure—A representative sample was dissolved and diluted to obtain a final concentration of approximately 2 μg/ml as the free base. Exactly 2 ml of standard, sample, and water (blank) was transferred to separate cells or 19 × 150-mm test tubes. To each tube, 2.0 ml of borate buffer was added. Then, while mixing on a vortex mixer, 1.0 ml of I was added rapidly. Within 35 min, the fluorescence was determined at 480 nm while exciting at 398 nm.

RESULTS AND DISCUSSION

The relation of the subsequent fluorescence intensity *versus* the test medium pH is shown in Fig. 1. Although the pH effect was not pronounced, the greatest sensitivity and reproducibility were obtained at pH 8.4. The fluorescence of the reagent blank was pH independent.

The suggested concentration range for I is 0.015–0.030%[2]. In this case, the highest concentration was used since greater precision resulted, as evidenced by a 3.3% decrease in the coefficient of variation.

The fluorescence was stable under normal benchtop conditions for at least 35 min, while limited data suggested constancy over several hours. Extended intervals were not investigated since 35 min was considered ample to obtain readings on normal batch runs.

The intended use of the proposed assay required that it be stability indicating. Stressed samples of a typical formulation were assayed by periodate (5) and ninhydrin (7) methods as well as by the proposed method. Highly precise first-order data were obtained by the fluorometric method over three half-lives. Although the data of the other two methods were more variable, the results confirmed the fluorometric data. Claims have been made for the stability-indicating capabilities of the periodate method (5), and these data support the conclusion that the fluorometric method is stability indicating.

The range of 0–3 μg/ml as the free base was selected since the fluorescence obtained at this level could be read using the midrange sensitivity of the spectrofluorometer. A linear calibration curve was obtained over this range. Some indications suggest that this linearity extends over a much broader range. However, evidence of quenching was noticed in samples that were an order of magnitude higher in concentration.

It is desirable to operate at peak excitation and emission wavelengths, but good results were obtained with much simpler filter instruments[3].

A statistical analysis was accomplished by assaying three sets of five

[2] Roche Diagnostics package insert issued May 1973.

[3] Coleman 12 c photofluorometer with filters 12-221 and 14-221.

0022-3549/78/1100-1635$01.00/0
© 1978, American Pharmaceutical Association

Table II—Assay Results of Commercial Products

Product	Phenylpropanolamine Hydrochloride		Additional Active Ingredients[a]
	Labeled	Found	
Uncoated tablet	12.5 mg/tablet	13.1	2, 4
Syrup	37.5 mg/5 ml	34.6	4, 5
Film-coated tablet	18.75 mg/tablet	19.9	2, 4
Capsule	25 mg/capsule	25.5	3, 4
Spray	0.2%	0.224	6, 7, 9
Capsule	18 mg/capsule	19.0	1
Uncoated tablet	25 mg/tablet	24.1	2
Sugar-coated tablet	18.75 mg/tablet	17.7	2, 4
Uncoated tablet	25 mg/tablet	24.2	1, 8
Press-coated tablet	25 mg/tablet	25.2	2, 3, 4

[a] 1 = acetaminophen, 2 = aspirin, 3 = caffeine, 4 = chlorpheniramine maleate, 5 = dextromethorphan hydrobromide, 6 = naphazoline, 7 = phenylephrine hydrochloride, 8 = phenyltoloxamine citrate, and 9 = pyrilamine maleate.

synthetic samples (Table I). One set contained phenylpropanolamine at the level of interest while the other two sets contained levels 20% above and below that level.

To demonstrate the utility of the proposed method, several commercially available products were assayed (Table II). An attempt was made to select products representing a wide variety of dosage form types as well as accompanying active ingredients. Duplicate analyses were carried out on two individual unit dose samples or, with liquids, on two aliquots containing between 12 and 25 mg of phenylpropanolamine hydrochloride. The object was merely to illustrate the applicability of the assay and not to establish accurate phenylpropanolamine hydrochloride levels for the various products.

For dosage forms where phenylpropanolamine is the only primary amine present, this method provides a convenient, specific, sensitive, and easily automated alternative to existing methods. It has been employed routinely and successfully in this laboratory for more than 2 years.

REFERENCES

(1) B. R. Rader and E. A. Aranda, *J. Pharm. Sci.*, **57**, 847 (1968).

(2) L. L. Chafetz, L. A. Gosser, H. Schriftman, and R. E. Daly, *Anal. Chim. Acta*, **52**, 374 (1970).

(3) D. J. Smith, *J. Assoc. Offic. Anal. Chem.*, **53**, 116 (1970).

(4) E. Smith, L. F. Worrel, and J. E. Sinsheimer, *Anal. Chem.*, **35**, 58 (1963).

(5) N. H. Brown and G. A. Portmann, *J. Pharm. Sci.*, **60**, 1229 (1971).

(6) D. J. Smith, *J. Assoc. Offic. Anal. Chem.*, **49**, 536 (1966).

(7) D. Burke, V. S. Ventruella, and B. Z. Senkowski, *J. Pharm. Sci.*, **63**, 269 (1974).

(8) S. Udenfriend, S. Stein, P. Bohlen, W. Dairman, W. Leimgruber, and M. Weigele, *Science*, **178**, 871 (1972).

(9) J. A. F. deSilva and N. Strojny, *Anal. Chem.*, **47**, 714 (1975).

ACKNOWLEDGMENTS

The author gratefully acknowledges the counsel received from Dr. R. N. Duvall and Mr. A. E. Troup and also thanks Mrs. Jane Graybosch for her assistance.

Thimerosal Determination by High-Pressure Liquid Chromatography

ROGER C. MEYER ˣ and LAWRENCE B. COHN

Received December 30, 1977, from *Allergan Pharmaceuticals, Inc., Irvine, CA 92713.* Accepted for publication March 24, 1978.

Abstract □ A sensitive and useful high-pressure liquid chromatographic method for the determination of intact thimerosal was developed. This method is extremely fast and reliable, and its inherent specificity makes it a breakthrough over other common wet chemical methods.

Keyphrases □ Thimerosal—high-pressure liquid chromatographic analysis in aqueous pharmaceutical preparations □ High-pressure liquid chromatography—analysis, thimerosal in aqueous pharmaceutical preparations □ Anti-infectives, topical—thimerosal, high-pressure liquid chromatographic analysis in aqueous pharmaceutical preparations

Thimerosal, ethyl (sodium *o*-mercaptobenzoato)mercury (I), is a relatively stable organomercurial that has long been used as both a topical antiseptic and a preservative. It is the preservative of choice for soft contact lens care solutions. Its stability, compatibility, and low toxicity account for its wide use.

BACKGROUND

The low concentrations of thimerosal typically used (10–50 ppm) have led to difficulties in development of suitable assays. Early analysis methods for organic mercurials involved the decomposition of the metallo-organic compounds (1) and detection with a complexing agent such as diphenylthiocarbazone (dithizone) or diphenylcarbazone (2, 3). More specificity was obtained by the use of better extraction procedures (4) or column chromatography (5). More sophisticated analytical methods such as atomic absorption (6), neutron activation (7), and GLC (8) detect degradation products as well as intact thimerosal.

Thimerosal degrades in aqueous solution to form ethylmercury salts and thiosalicylic acid (9, 10). Therefore, techniques based on either total mercury or total organic mercury do not reflect accurately the amount of intact thimerosal present in solution. Since some degradation products may have a higher toxicity potential than the original thimerosal (11, 12), accurate analytical techniques are essential.

Quantitative high-pressure liquid chromatography (HPLC) has been suggested as a simple, specific method that meets these objectives (13).

The HPLC method described here is a rapid, specific determination of intact thimerosal at 5–25 ppm (μg/g) in aqueous samples. In many cases, no sample cleanup is needed before determination. However, interferences are sometimes encountered because of components of the formulation. In such cases, a simple extraction procedure can be used.

To facilitate the handling of large numbers of samples, the assay is designed for the smallest retention time consistent with good chromatography. Thimerosal content of several commercial soft contact lens formulations was determined using this method to verify the usefulness of the procedure.

EXPERIMENTAL

Apparatus—The HPLC system consisted of a pump[1], a UV detector[2], and an automatic sampler[3].

Reagents—All reagents were analytical reagent grade unless noted otherwise. The mobile phase was 0.1 *M* ammonium carbonate with the pH adjusted to 7.9 with acetic acid. To prepare pH 4 acetate buffer, 410

[1] Waters Associates model 6000 pump.
[2] Chromatonix model 260 UV detector (254 nm).
[3] DuPont Instruments model 834 autoinjector with a 50-μl loop.

0022-3549/78/1100-1636$01.00/0

© 1978, American Pharmaceutical Association

Table II—Assay Results of Commercial Products

Product	Phenylpropanolamine Hydrochloride		Additional Active Ingredients[a]
	Labeled	Found	
Uncoated tablet	12.5 mg/tablet	13.1	2, 4
Syrup	37.5 mg/5 ml	34.6	4, 5
Film-coated tablet	18.75 mg/tablet	19.9	2, 4
Capsule	25 mg/capsule	25.5	3, 4
Spray	0.2%	0.224	6, 7, 9
Capsule	18 mg/capsule	19.0	1
Uncoated tablet	25 mg/tablet	24.1	2
Sugar-coated tablet	18.75 mg/tablet	17.7	2, 4
Uncoated tablet	25 mg/tablet	24.2	1, 8
Press-coated tablet	25 mg/tablet	25.2	2, 3, 4

[a] 1 = acetaminophen, 2 = aspirin, 3 = caffeine, 4 = chlorpheniramine maleate, 5 = dextromethorphan hydrobromide, 6 = naphazoline, 7 = phenylephrine hydrochloride, 8 = phenyltoloxamine citrate, and 9 = pyrilamine maleate.

synthetic samples (Table I). One set contained phenylpropanolamine at the level of interest while the other two sets contained levels 20% above and below that level.

To demonstrate the utility of the proposed method, several commercially available products were assayed (Table II). An attempt was made to select products representing a wide variety of dosage form types as well as accompanying active ingredients. Duplicate analyses were carried out on two individual unit dose samples or, with liquids, on two aliquots containing between 12 and 25 mg of phenylpropanolamine hydrochloride. The object was merely to illustrate the applicability of the assay and not to establish accurate phenylpropanolamine hydrochloride levels for the various products.

For dosage forms where phenylpropanolamine is the only primary amine present, this method provides a convenient, specific, sensitive, and easily automated alternative to existing methods. It has been employed routinely and successfully in this laboratory for more than 2 years.

REFERENCES

(1) B. R. Rader and E. A. Aranda, *J. Pharm. Sci.*, **57**, 847 (1968).

(2) L. L. Chafetz, L. A. Gosser, H. Schriftman, and R. E. Daly, *Anal. Chim. Acta*, **52**, 374 (1970).

(3) D. J. Smith, *J. Assoc. Offic. Anal. Chem.*, **53**, 116 (1970).

(4) E. Smith, L. F. Worrel, and J. E. Sinsheimer, *Anal. Chem.*, **35**, 58 (1963).

(5) N. H. Brown and G. A. Portmann, *J. Pharm. Sci.*, **60**, 1229 (1971).

(6) D. J. Smith, *J. Assoc. Offic. Anal. Chem.*, **49**, 536 (1966).

(7) D. Burke, V. S. Ventruella, and B. Z. Senkowski, *J. Pharm. Sci.*, **63**, 269 (1974).

(8) S. Udenfriend, S. Stein, P. Bohlen, W. Dairman, W. Leimgruber, and M. Weigele, *Science*, **178**, 871 (1972).

(9) J. A. F. deSilva and N. Strojny, *Anal. Chem.*, **47**, 714 (1975).

ACKNOWLEDGMENTS

The author gratefully acknowledges the counsel received from Dr. R. N. Duvall and Mr. A. E. Troup and also thanks Mrs. Jane Graybosch for her assistance.

Thimerosal Determination by High-Pressure Liquid Chromatography

ROGER C. MEYER ˣ and LAWRENCE B. COHN

Received December 30, 1977, from *Allergan Pharmaceuticals, Inc., Irvine, CA 92713.* Accepted for publication March 24, 1978.

Abstract □ A sensitive and useful high-pressure liquid chromatographic method for the determination of intact thimerosal was developed. This method is extremely fast and reliable, and its inherent specificity makes it a breakthrough over other common wet chemical methods.

Keyphrases □ Thimerosal—high-pressure liquid chromatographic analysis in aqueous pharmaceutical preparations □ High-pressure liquid chromatography—analysis, thimerosal in aqueous pharmaceutical preparations □ Anti-infectives, topical—thimerosal, high-pressure liquid chromatographic analysis in aqueous pharmaceutical preparations

Thimerosal, ethyl (sodium *o*-mercaptobenzoato)mercury (I), is a relatively stable organomercurial that has long been used as both a topical antiseptic and a preservative. It is the preservative of choice for soft contact lens care solutions. Its stability, compatibility, and low toxicity account for its wide use.

BACKGROUND

The low concentrations of thimerosal typically used (10–50 ppm) have led to difficulties in development of suitable assays. Early analysis methods for organic mercurials involved the decomposition of the metallo-organic compounds (1) and detection with a complexing agent such as diphenylthiocarbazone (dithizone) or diphenylcarbazone (2, 3). More specificity was obtained by the use of better extraction procedures (4) or column chromatography (5). More sophisticated analytical methods such as atomic absorption (6), neutron activation (7), and GLC (8) detect degradation products as well as intact thimerosal.

Thimerosal degrades in aqueous solution to form ethylmercury salts and thiosalicylic acid (9, 10). Therefore, techniques based on either total mercury or total organic mercury do not reflect accurately the amount of intact thimerosal present in solution. Since some degradation products may have a higher toxicity potential than the original thimerosal (11, 12), accurate analytical techniques are essential.

Quantitative high-pressure liquid chromatography (HPLC) has been suggested as a simple, specific method that meets these objectives (13).

The HPLC method described here is a rapid, specific determination of intact thimerosal at 5–25 ppm (μg/g) in aqueous samples. In many cases, no sample cleanup is needed before determination. However, interferences are sometimes encountered because of components of the formulation. In such cases, a simple extraction procedure can be used.

To facilitate the handling of large numbers of samples, the assay is designed for the smallest retention time consistent with good chromatography. Thimerosal content of several commercial soft contact lens formulations was determined using this method to verify the usefulness of the procedure.

EXPERIMENTAL

Apparatus—The HPLC system consisted of a pump[1], a UV detector[2], and an automatic sampler[3].

Reagents—All reagents were analytical reagent grade unless noted otherwise. The mobile phase was 0.1 *M* ammonium carbonate with the pH adjusted to 7.9 with acetic acid. To prepare pH 4 acetate buffer, 410

[1] Waters Associates model 6000 pump.
[2] Chromatonix model 260 UV detector (254 nm).
[3] DuPont Instruments model 834 autoinjector with a 50-μl loop.

0022-3549/78/1100-1636$01.00/0

© 1978, American Pharmaceutical Association

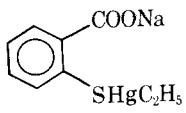

I

ml of Solution A (11.55 ml of concentrated acetic acid/liter of water) and 90 ml of Solution B (2.72 g of sodium acetate trihydrate/100 ml of water) were mixed with 500 ml of water. To prepare pH 10 carbonate buffer, 27.5 ml of Solution C (2.12 g of sodium carbonate/100 ml of water) and 22.5 ml of Solution D (1.68 g of sodium bicarbonate/100 ml of water) were mixed and diluted to 200 ml with water.

Standards—A stock solution was prepared by dissolving 200 mg of thimerosal in 100 ml of distilled deionized water. The working standard (20 ppm or 0.0020%) was a 1:100 dilution of the stock solution.

Chromatography—A 3.9 × 500-mm, Vydac C-18 reversed-phase 30–44-μm column was equilibrated with acetonitrile by overnight conditioning at a low flow rate. The next morning, the mobile phase was pumped through the system followed by five to 10 injections of the stock standard to saturate the column. Reproducibility usually was obtained with a few injections of a 20-ppm standard solution.

Polymers such as polysorbate 80 possess no UV absorption that can interfere. However, these and other compounds do build up slowly on the column; slowly decreasing retention times with increasing peak heights are observed as the compound coats the column packing. This problem can be alleviated by flushing the column with acetonitrile.

The chromatographic conditions were as follows: flow rate, 2 ml/min; pressure, ~2000 psi; temperature, ambient; detector wavelength, 254 nm; detector sensitivity, 0.08 aufs; and chart speed, 20 cm/hr.

Sample Preparation—Many formulations can be injected on the column, and thimerosal can be determined directly. Samples containing certain surfactants, polymers, and other excipients that interfere with the assay can be cleaned up with a simple extraction procedure. A 5-ml sample (20 ppm of thimerosal) is added to 50 ml of pH 4 acetate buffer and extracted with 50 ml of chloroform. The chloroform is then extracted with 5 ml of pH 10 carbonate buffer. The carbonate buffer is then chromatographed as any other sample. The initial sample volume can be altered appropriately so that the final thimerosal concentration is within the range of the standard.

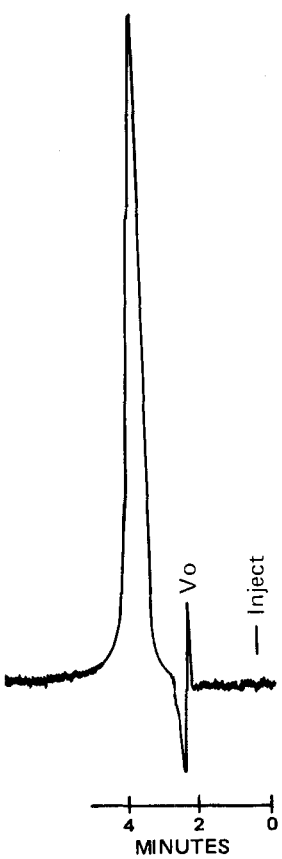

Figure 1—*Chromatogram of thimerosal.*

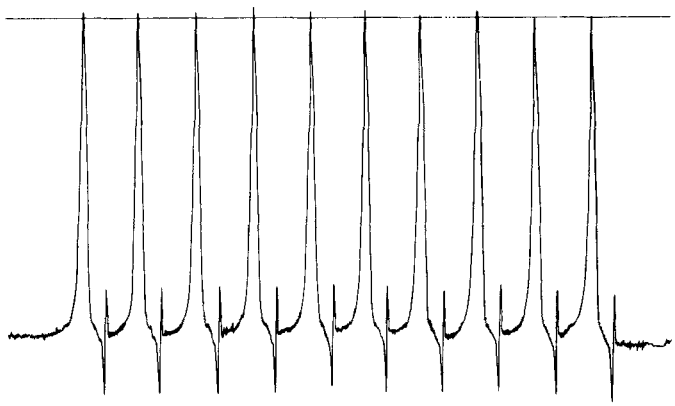

Figure 2—*Typical reproducibility of thimerosal.*

Calculation—The results are calculated using:

$$\text{concentration of thimerosal (sample)} = \frac{\text{peak height (sample)}}{\text{peak height (standard)}} \times \text{concentration of thimerosal (standard)} \quad \text{(Eq. 1)}$$

Test Solutions—Several soft lens products containing thimerosal formulated in this laboratory were determined using the method. In addition, several solutions labeled as containing thimerosal were bought from commercial sources both outside and within the United States. All laboratory samples were within their shelflife expiration date, and one commercial sample was past it. Exact age could not always be determined. When extraction cleanup was necessary, a sample of the product was spiked with thimerosal and tested immediately.

RESULTS

As seen in Fig. 1, thimerosal eluted as a sharp peak soon after the baseline had been reestablished following the initial injection spike (V_0). This behavior allows for an analysis time of approximately 4 min/sample.

The calibration curve of thimerosal concentration *versus* peak height was linear over the 0–25-ppm range and passed through the origin (r = 0.99994). Replicate injections of a standard solution had a relative

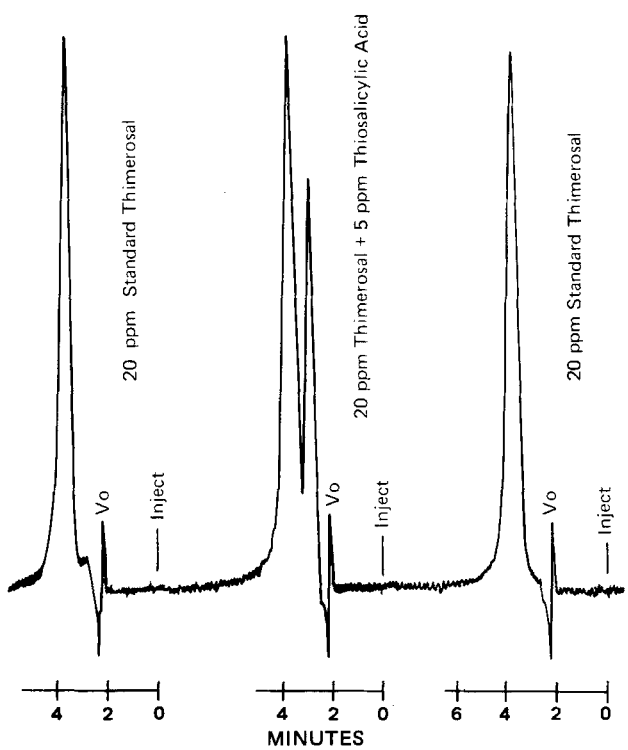

Figure 3—*Separation of thimerosal and thiosalicylic acid.*

Table I—Thimerosal Assay of Soft Contact Lens Products

Product/ Major Ingredients	Sample	Expiration Date	Date of Assay	Age at Assay, months	Method	Percent of Label Found	Spike Recovery, %
Product A: 0.001% thimerosal, 0.01%	1	6/77	12/76	18	Direct injection	122	—
ethylenediaminetetraacetic acid (II) and 0.85% sodium	2	10/78	6/77	6	Direct injection	122	—
chloride (III) boric acid	3	12/78	4/77	6	Direct injection	110	—
Product B: 0.002% thimerosal and 0.03%	1	4/77	3/77	20	Direct injection	97	—
alkyltriethanolammonium chloride	2	1/78	3/77	12	Direct injection	101	—
	3	9/78	3/77	4	Direct injection	106	—
Product C: 0.001% thimerosal, 0.005% chlorhexidine, 0.1%	1	5/77	10/76	9	Extraction	<5	102
II, 0.9% III, and povidone (IV)	2	12/77	2/77	6	Extraction	16	—
	3	1/78	3/77	2	Extraction	41	—
	4	9/77	10/76	5	Extraction	<5	—
Product D: 0.001% thimerosal, 0.1% II, and 0.005%	1	10/78	2/77	4	Extraction	101	103
chlorhexidine	2	12/78	3/77	3	Extraction	114	—
Product E: 0.001% thimerosal, 0.1% II, and 0.7% III	1	1/78	2/77	13	Extraction	65	94
Product F: 0.001% thimerosal, 0.1% II, and 0.7% III	1	5/78	2/77	9	Extraction	113	103
Product G: 0.001% thimerosal, 0.1% II, and 0.7% III	1	11/76	2/77	26	Extraction	52	102
	2	11/78	2/77	3	Extraction	112	—
	3	1/79	2/77	2	Extraction	113	—
	4	11/78	2/77	3	Extraction	100	—

standard deviation of ±0.91% (Fig. 2). Replicate injections of samples yielded slightly higher relative standard deviations of ±1–2%. The minimum detectable concentration of thimerosal is less than 0.5 ppm with a 50-μl sample loop.

One degradation product of thimerosal is thiosalicylic acid. Its peak appears before that of thimerosal, however, so it does not interfere with the assay (Fig. 3). Ethylenediaminetetraacetic acid interferes at concentrations greater than approximately 0.02% but can be eliminated by the extraction cleanup procedure.

DISCUSSION

The data in Table I indicate the utility of the method. All samples tested, except G_1, were within their expiration dates. However, one-third of the 18 products tested contained significantly less than the labeled amount of thimerosal, with two showing virtually none present at all. When these products were spiked with thimerosal, the assay did detect appropriate amounts, showing that there was no interference with the assay.

The fact that all four samples of Product C showed inadequate amounts of thimerosal suggests that the expiration data for the product may be based on an inadequate assay and that the thimerosal may not be stable in the formulation. Sample C_3 was only 2 months old but contained only 41% of its labeled thimerosal in the intact form. Samples C_1 and C_4, at 9 and 5 months, respectively, had virtually no intact thimerosal present.

REFERENCES

(1) J. L. A. Webb, I. S. Bhatia, A. H. Corwin, and A. G. Sharp, *J. Am. Chem. Soc.*, **72**, 91 (1950).

(2) V. L. Miller, D. Polley, and C. J. Gould, *Anal. Chem.*, **23**, 1286 (1951).

(3) D. Pollye and V. L. Miller, *ibid.*, **24**, 1622 (1952).

(4) E. Hoffman, *Fresenius Z. Anal. Chem.*, **174**, 48 (1960).

(5) S. Ishikura and K. Yokota, *Chem. Pharm. Bull.*, **11**, 939 (1963).

(6) W. H. Harper, *Proc. Soc. Anal. Chem.*, **7**, 104 (1970).

(7) M. Margosis and J. T. Tanner, *J. Pharm. Sci.*, **61**, 936 (1972).

(8) J. E. Longbottom, R. C. Dressman, and J. J. Lichtenberg, *J. Assoc. Offic. Anal. Chem.*, **56**, 1297 (1973).

(9) F. Tanaka and M. Mitsuna, *Takedo Kenkyusho Nempo*, **10**, 65 (1951).

(10) E. O. Davisson, H. M. Powell, J. O. MacFarlane, R. Hodgson, R. L. Stone, and C. G. Culbertson, *J. Lab. Clin. Med.*, **47**, 8 (1956).

(11) T. W. Clarkson, *Annu. Rev. Pharmacol.*, **12**, 375 (1972).

(12) A. M. J. N. Blair, B. Clark, A. J. Clarke, and P. Wood, *Toxicology*, **3**, 171 (1975).

(13) C. Fu and M. J. Sibley, *J. Pharm. Sci.*, **66**, 738 (1977).

Hypotensive Effect Induced by a Cyclic Dopamine Analog, *trans*-4-Methyl-7,8-dihydroxy-1,2,3,4,4a,5,6,10b-octahydrobenzo[*f*]quinoline

FOUAD M. SHARABI [§], **JOHN P. LONG** [*x], **and JOSEPH G. CANNON** [‡]

Received December 30, 1976, from the [*]*Department of Pharmacology, College of Medicine, and the* [‡]*Division of Medicinal Chemistry and Natural Products, College of Pharmacy, University of Iowa, Iowa City, IA 52242.* Accepted for publication March 3, 1978. [§]Present address: Department of Pharmacology, Faculty of Pharmacy, University of Alexandria, Alexandria, Egypt.

Abstract □ The antihypertensive effects of *trans*-4-methyl-7,8-dihydroxy-1,2,3,4,4a,5,6,10b-octahydrobenzo[*f*]quinoline, a dopamine agonist, were investigated in dogs and spontaneous hypertensive rats. Intravenous administration of low doses of this cyclic analog of dopamine (0.25–1.00 μg/kg) consistently reduced blood pressure and heart rate, concurrently recorded in the dog. This effect was antagonized by haloperidol, a specific dopamine antagonist. The dopamine analog also reduced systolic blood pressure of spontaneous hypertensive rats. This study confirmed the possibility that the decrease in blood pressure and heart rate elicited by the dopamine analog is attributable to an effect on specific dopaminergic receptors.

Keyphrases □ *trans*-4-Methyl-7,8-dihydroxy-1,2,3,4,4a,5,6,10b-octahydrobenzo[*f*]quinoline—hypotensive activity evaluated in dogs and spontaneous hypertensive rats □ Benzo[*f*]quinoline, substituted—hypotensive activity evaluated in dogs and spontaneous hypertensive rats □ Hypotensive activity—substituted benzo[*f*]quinoline evaluated in dogs and spontaneous hypertensive rats □ Dopamine analogs, cyclic—hypotensive activity evaluated in dogs and spontaneous hypertensive rats

Dopamine acts on α- or β-adrenergic and dopaminergic receptors (1–9). It has received considerable attention as a potential therapeutic agent because of its ability to dilate renal and sphanchnic vasculature in experimental animals (2, 3, 6, 7, 10–13). Previously, depressor responses were elicited with small doses of dopamine, biphasic responses with intermediate doses, and pressor responses with large doses in dogs and cats. Dopamine in rabbits induced only a fall in blood pressure at all doses (1, 9, 14–19).

The depressor effect of dopamine and other dopaminergic agonists is assumed to be achieved through an action on specific dopaminergic receptors (12, 20–23). *trans*-4-Methyl-7,8-dihydroxy-1,2,3,4,4a,5,6,10b-octahydrobenzo[*f*]quinoline (I) is a potent inhibitor of adrenergic nerve terminals in cats (24, 25). The present investigation was undertaken to determine if I would affect blood pressure of dogs and rats in the same manner as dopamine by acting on dopaminergic receptors.

EXPERIMENTAL

Dog Arterial Blood Pressure and Heart Rate—Mongrel dogs (14–18 kg) were anesthetized with pentobarbital sodium (30 mg/kg iv). The animals were intubated and artificially ventilated with a respiration pump. Blood pressure was measured using a recorder and pressure transducer connected to a catheter inserted in the right femoral artery. Heart rate was monitored using a cardiotachometer. Drugs were injected through a catheter inserted in the left femoral vein.

Systolic Blood Pressure of Spontaneous Hypertensive Rats—The systolic blood pressures of conscious spontaneous hypertensive rats were determined by tail-cuff plethysmography. The rats were prewarmed by placing them in a glass-doored incubator at 30° for 20 min. The tail cuff was then applied while the rat was loosely restrained, and five consecutive readings of systolic blood pressure were obtained. The procedure was similar to that described by Friedman and Freed (26) in which occlusion cuff pressure was monitored visually while systolic pulses, detected by a pulse transducer, were monitored with an audiosignal.

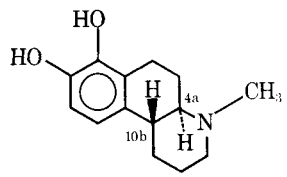

I

Consistent readings were obtained by following a fixed routine and ensuring that the same person performed the measurements at the same time on each occasion. It was important that the tail cuff was placed on the same part of the tail and that extraneous noise was kept to a minimum. The rats were trained for 2 weeks before injection of the compound.

The hydrobromide salt of I was synthesized[1]. The data were analyzed statistically by the paired *t* test (27). A *p* value <0.05 was regarded as significant. Relative potencies of I before and after haloperidol were obtained from a split plot design six-point bioassay (28).

RESULTS

Effect of I on Arterial Blood Pressure and Heart Rate—The resting mean arterial blood pressure and heart rate of the anesthetized dogs were 120 ± 4 mm Hg and 182 ± 6 beats/min, respectively. Intravenous injections of I were given in dosage increments from 0.25 to 1.00 μg/kg. These doses elicited a depressor effect associated with a decrease in heart rate; both the depressor effect and decrease in heart rate were dose dependent. The effects persisted 15–30 min, depending on the doses used, showing that I possessed a short duration of action.

After initial resting blood pressure returned to normal, haloperidol, 100 μg/kg, was slowly infused over 15 min. It did not significantly alter blood pressure or heart rate. Compound I, in doses that previously produced inhibition of blood pressure and heart rate, was then administered after haloperidol infusion, and the degree of inhibition was determined. Compound I (0.25–2.00 μg/kg) hardly affected blood pressure and heart rate after haloperidol. The need for increasing the doses of I to 16.0 μg/kg to obtain maximal depressor response showed that haloperidol antagonized its inhibitory effect on blood pressure and heart rate (Fig. 1).

Effect of Intraperitoneal Injection of I on Systolic Blood Pressure—Measurements of systolic blood pressure were made before the injection of I and were considered as controls. Systolic blood pressure was measured 20 min after the injection of I. Low intraperitoneal doses of I reduced arterial systolic blood pressure of spontaneous hypertensive rats from 238 ± 8 to 218 ± 7 mm Hg. The 3.1-μg/kg dose elicited an 8.4% reduction of the initial resting blood pressure. A high dose of 25.0 μg/kg reduced arterial systolic blood pressure from 236 ± 7 to 206 ± 5 mm Hg, amounting to a 12.7% reduction of initial resting blood pressure.

All doses elicited a significant pressure decrease ($p < 0.01$) (Fig. 2). Higher doses of I tended to excite the rats, and measurements of systolic blood pressure became difficult. Saline injected intraperitoneally to spontaneous hypertensive rats in volumes similar to those used when injecting I produced no significant effect on blood pressure.

The blood pressure of seven spontaneous hypertensive rats (group mean systolic pressure of 240 ± 7 mm Hg) was reduced by a single dose of I (25.0 μg/kg ip). The nadir of the depressor effect occurred 20 min after I injection ($p < 0.01$), and the mean systolic blood pressure was reduced to 204 ± 2 mm Hg. Second measurements after 80 min showed a still-

[1] Division of Medicinal Chemistry and Natural Products, University of Iowa.

0022-3549/78/1100-1639$01.00/0
© 1978, American Pharmaceutical Association

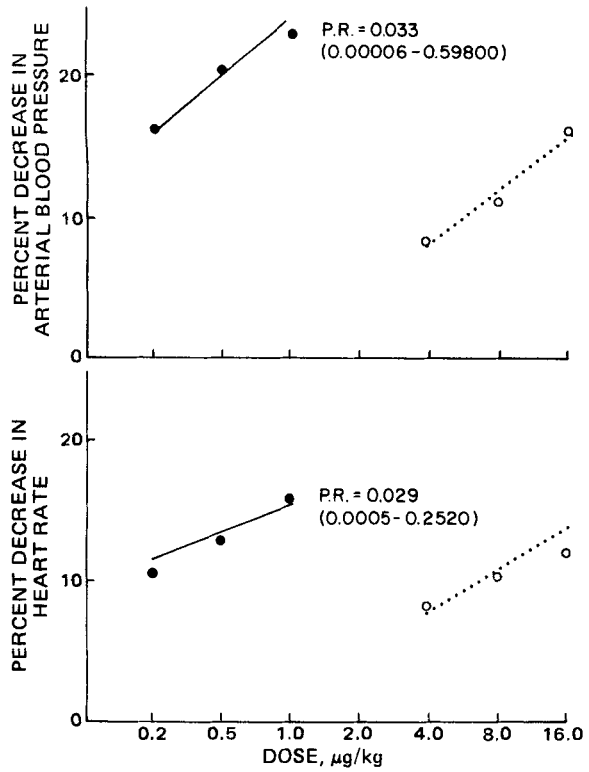

Figure 1—*Dose-response curves illustrating the effect of I on blood pressure and heart rate and the antagonism by haloperidol in anesthetized dogs. Each point represents the mean of seven experiments before (●) and after (○) haloperidol infusion (100 μg/kg over 15 min). The initial resting blood pressure and heart rate before intravenous administration of I were 120 ± 4 mm Hg and 182 ± 6 beats/min, respectively. The blood pressure and heart rate after the infusion of haloperidol (100 μg/kg) were 106 ± 7 mm Hg and 197 ± 13 beats/min, respectively. P.R. equals the relative potency as defined by Finney (28).*

significant decrease in systolic blood pressure ($p < 0.01$). The blood pressure returned to pretreatment level after 140 min (Fig. 3).

DISCUSSION

Intravenous administration of I resulted in a depressor effect similar to that reported for low doses of dopamine in the dog (1, 2, 9, 19, 21). Haloperidol caused a shift to the right in the dose–response curves of I.

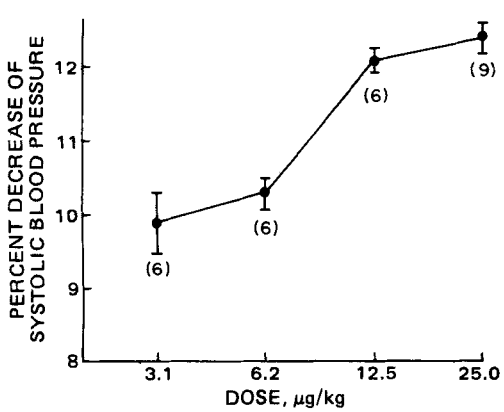

Figure 2—*Dose–response curve illustrating the effect of intraperitoneal I on systolic blood pressure of spontaneous hypertensive rats. Values within parentheses indicate the number of rats used at each dose. Each point is the mean ± SE. For the doses of 3.12, 6.25, 12.50, and 25.00 μg/kg, the control initial systolic blood pressure was 238 ± 8, 235 ± 10, 255 ± 8, and 236 ± 7 mm Hg, respectively.*

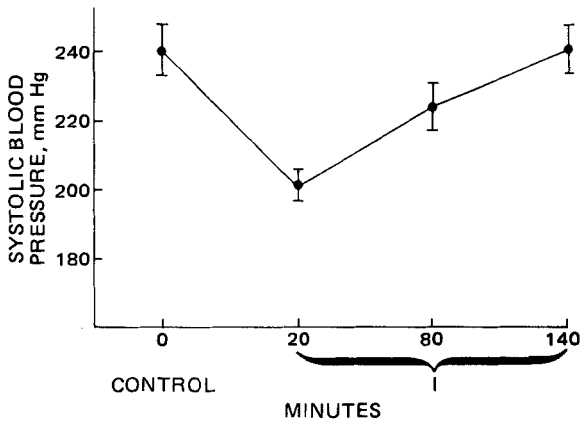

Figure 3—*Effect of I on systolic blood pressure of spontaneous hypertensive rats at different time intervals. Compound I was injected at a dose of 25 μg/kg ip, and systolic blood pressure was measured 20, 80, and 140 min after injection. Each value is the mean ± SE of seven rats.*

The fact that the before and after haloperidol curves do not deviate significantly from parallel suggests that haloperidol is a competitive antagonist. The results support the concept of specific dopaminergic receptors mediating a vasodilation, which is thus antagonized by haloperidol. Haloperidol is a known dopamine receptor blocker (6, 18, 29, 30). The vasodilation induced by dopamine in the different vascular beds is said to contribute to its depressor effect (6, 21, 31, 32).

Compound I has been postulated to be a potent dopaminergic agonist, impairing sympathetic transmission, an effect blocked by haloperidol (25). This inhibitory effect might involve dopaminergic receptors located on the nerve endings as well as on the autonomic ganglia. The resultant vascular dilatation would probably participate in the depressor effect of I. The decrease in heart rate could be attributed to the decrease of sympathetic discharges to the heart. The effect of dopamine on blood pressure was reported to differ from one species to another. Compound I lowered systolic blood pressure of spontaneous hypertensive rats in doses from 3.1 to 25.0 μg/kg. It was not possible to study the effect of higher doses of I in the rats since these doses produced excitement, probably because compulsive gnawing doses for these animals were approached.

Haloperidol affected the systolic blood pressure of spontaneous hypertensive rats; therefore, the antagonism of the depressor effect seen in the dog could not be demonstrated in the rat. The depressor effect of dopamine in anesthetized rats was antagonized by metoclopramide, another dopamine antagonist (22). The significance of the effect of I on blood pressure lies in the fact that I can be used to study some of the physiological properties of dopamine that are likely involved in regional circulatory beds where there are large numbers of dopaminergic receptors. With alterations of the chemical structure of dopamine, the intensity of its pharmacological actions can be changed. Compound I in the doses used in this study seems to be more potent as a hypotensive agent than dopamine since the reported doses of dopamine required to exert a similar hypotensive effect are greater. Since the duration of action of I on blood pressure is very short, it does not seem to be a promising hypotensive agent for clinical use.

REFERENCES

(1) R. H. McDonald and L. I. Goldberg, *J. Pharmacol. Exp. Ther.*, **140**, 60 (1963).

(2) J. N. Eble, *ibid.*, **145**, 64 (1964).

(3) J. L. McNay and L. I. Goldberg, *ibid.*, **151**, 23 (1966).

(4) J. L. McNay, R. H. McDonald, Jr., and L. I. Goldberg, *Circ. Res.*, **16**, 510 (1965).

(5) K. M. Dhasmana, K. S. Dixit, K. N. Dhawan, and G. P. Gupta, *Jpn. J. Pharmacol.*, **19**, 168 (1969).

(6) B. K. Yeh, J. L. McNay, and L. I. Goldberg, *J. Pharmacol. Exp. Ther.*, **168**, 303 (1969).

(7) L. I. Goldberg and B. K. Yeh, *Eur. J. Pharmacol.*, **15**, 36 (1971).

(8) M. Endoh, *Br. J. Pharmacol.*, **55**, 475 (1975).

(9) P. E. Setler, R. G. Pendleton, and E. Finlay, *J. Pharmacol. Exp. Ther.*, **192**, 702 (1975).

(10) M. B. Meyer, J. L. McNay, and L. I. Goldberg, *ibid.*, **156,** 192 (1967).
(11) G. Ross and W. Brown, *Am. J. Physiol.*, **212,** 823 (1967).
(12) L. I. Goldberg, *Pharm. Rev.*, **24,** 1 (1972).
(13) H. Morishita and T. Furukawa, *Arch. Int. Pharmacodyn. Ther.*, **212,** 317 (1974).
(14) P. Holtz, K. Credner, and W. Koepp, *Arch. Exp. Pathol. Pharmakol.*, **200,** 356 (1942).
(15) J. H. Burn and M. J. Rand, *Br. J. Pharmacol.*, **13,** 471 (1958).
(16) L. I. Goldberg and A. Sjoerdsma, *J. Pharmacol. Exp. Ther.*, **127,** 212 (1959).
(17) G. M. Maxwell, G. G. Rowe, C. A. Castillo, J. E. Clifford, S. Afonson, and C. W. Crumpton, *Arch. Int. Pharmacodyn. Ther.*, **129,** 62 (1960).
(18) J. M. van Rossum, *ibid.*, **160,** 492 (1966).
(19) T. Furukawa, K. Kushiku, and T. Kawagoe, *Jpn. J. Pharmacol.*, **24,** 635 (1974).
(20) A. Barnett and J. W. Fiore, *Eur. J. Pharmacol.*, **14,** 206 (1971).
(21) R. G. Sampson, G. C. Scroop, and W. J. Louis, *Clin. Exp. Pharmacol. Physiol.*, **1,** 3 (1974).
(22) M. D. Day and P. R. Blower, *J. Pharm. Pharmacol.*, **27,** 276 (1975).
(23) R. G. Pendleton, E. Finlay, and S. Sherman, *Naunyn-Schmiedeberg's Arch. Pharmacol.*, **289,** 171 (1975).
(24) J. G. Cannon, G. J. Hatheway, J. P. Long, and F. M. Sharabi, *J. Med. Chem.*, **19,** 987 (1976).
(25) F. M. Sharabi, J. P. Long, J. G. Cannon, and G. J. Hatheway, *J. Pharmacol. Exp. Ther.*, **199,** 630 (1976).
(26) M. Friedman and S. C. Freed, *Proc. Soc. Exp. Biol. Med.*, **70,** 670 (1949).
(27) R. G. D. Steel and J. H. Torrie, "Principles and Procedures of Statistics," McGraw-Hill, New York, N.Y., 1960, p. 67.
(28) D. J. Finney, "Statistical Method in Biological Assays," Griffin, London, England, 1952, p. 139.
(29) N. E. Andén, A. Rubenson, K. Fuxe, and R. Hökfelt, *J. Pharm. Pharmacol.*, **19,** 627 (1967).
(30) D. M. Schuelke, A. L. Mark, P. G. Schmid, and J. W. Eckstein, *J. Pharmacol. Exp. Ther.*, **176,** 320 (1971).
(31) M. G. Bogaert and A. F. DeSchaepdryver, *Arch. Int. Pharmacodyn. Ther.*, **166,** 203 (1967).
(32) T. C. Hamilton, *Br. J. Pharmacol.*, **44,** 442 (1972).

ACKNOWLEDGMENTS

Supported in part by National Institutes of Health Grant GM-22365.

Determination of Flucytosine in Tablets by Differential Pulse Polarography

F. W. TEARE *x, R. N. YADAV *, and M. SPINO ‡

Received November 9, 1976, from the **Faculty of Pharmacy, University of Toronto, Toronto, Ontario, Canada M5S 1A1,* the ‡*Division of Clinical Pharmacology, Toronto Western Hospital, Toronto, Ontario, Canada,* and the ‡*Clinical Institute, Addiction Research Foundation, Toronto, Ontario, Canada.* Accepted for publication March 31, 1978.

Abstract □ A differential pulse polarographic assay was developed for determining flucytosine in tablets. The drug is extracted from the sample with water and hydrochloric acid and, after the pH is adjusted, an aliquot is added to the cell and the solution is polarographed at the dropping mercury electrode *versus* the saturated calomel electrode with 0.066 *M* Sørensen phosphate buffer (pH 5.6) as the supporting electrolyte. The polarographic peak height enables precise quantitative determination. The E_p value for flucytosine is −1.54 v *versus* the saturated calomel electrode. The mean recovery of the drug is 101.5% ± 1.9 (*SD*). The method is simple, rapid, and precise.

Keyphrases □ Flucytosine—differential pulse polarographic analysis in dosage forms □ Polarography, differential pulse—analysis, flucytosine in dosage forms □ Antifungal agents—flucytosine, differential pulse polarographic analysis in dosage forms

Flucytosine, 5-fluorocytosine (I), is a fluorinated pyrimidine that has shown *in vitro* and *in vivo* antifungal activity. Microbiological (1), fluorometric (2, 3), and high-pressure liquid chromatographic (4) procedures were reported for the estimation of I in biological fluids. The USP (5) employs a spectrophotometric method for the estimation of I in capsules. The mechanism of polarographic reduction of pyrimidine derivatives was reported previously (6–8). This paper reports a simple, convenient, and rapid differential pulse polarographic analysis of I in tablets.

EXPERIMENTAL

Apparatus and Conditions—Polarograms were obtained using a polarographic analyzer[1] equipped with a drop timer[2]; the differential pulse mode was used. A three-electrode cell (5–50 ml) was comprised of a dropping mercury electrode, a saturated calomel electrode (SCE), and a platinum wire auxiliary electrode. The drop time t, was 2 sec, the drop mass was 1.4 mg/sec, and the capillary characteristic was $m^{2/3}t^{1/6} = 1.3$, measured in 0.066 *M* Sørensen phosphate buffer (pH 5.6) with an open circuit and at a mercury column height of 95 cm. The current range was either 5 or 10 μamp for a peak response of full-scale deflection, the scan range was from −1.2 to −1.95 v, the peak potential was −1.54 v, the modulation amplitude was 25 mv, and the scan rate was 2 mv/sec. The polarogram was recorded on an x–y recorder[3].

A pH meter[4], fitted with a combination glass–saturated calomel electrode electrode pair, was used to monitor the pH of all solutions.

Reagents and Chemicals—All chemicals were analytical reagent grade. The Sørensen buffer was prepared by mixing stock solutions A (9.073 g of monobasic potassium phosphate/liter) and B (11.87 g of dibasic sodium phosphate dihydrate/liter) in varying proportions to produce the desired pH (9). Flucytosine[5] was used as a standard.

Calibration Curve—An aqueous stock solution of I was prepared at 1×10^{-2} *M*. A range of 1×10^{-3}–1×10^{-4} *M* was employed for the preparation of the diffusion current *versus* concentration calibration curve. All standard solutions were prepared by pipetting an aliquot of the aqueous stock solution and adding 13.0 ml of Sørensen phosphate buffer (pH 5.6) and sufficient distilled water to a final volume of 20 ml.

These solutions were transferred to the cell and deoxygenated with pure nitrogen for 10 min prior to obtaining the polarograms in quiescent solution. A layer of nitrogen was maintained over the solution surface during the electroreduction. Polarograms were obtained using the differential pulse polarographic mode.

[1] Princeton Applied Research (PAR) model 174A.
[2] Princeton Applied Research (PAR) model 172A.
[3] Houston Omnigraphic model 2000.
[4] Fisher, Accumet model 230 pH/ion meter.
[5] Hoffmann–La Roche lot I-898.

0022-3549/78/1100-1641$01.00/0
© 1978, American Pharmaceutical Association

(10) M. B. Meyer, J. L. McNay, and L. I. Goldberg, *ibid.*, **156,** 192 (1967).
(11) G. Ross and W. Brown, *Am. J. Physiol.*, **212,** 823 (1967).
(12) L. I. Goldberg, *Pharm. Rev.*, **24,** 1 (1972).
(13) H. Morishita and T. Furukawa, *Arch. Int. Pharmacodyn. Ther.*, **212,** 317 (1974).
(14) P. Holtz, K. Credner, and W. Koepp, *Arch. Exp. Pathol. Pharmakol.*, **200,** 356 (1942).
(15) J. H. Burn and M. J. Rand, *Br. J. Pharmacol.*, **13,** 471 (1958).
(16) L. I. Goldberg and A. Sjoerdsma, *J. Pharmacol. Exp. Ther.*, **127,** 212 (1959).
(17) G. M. Maxwell, G. G. Rowe, C. A. Castillo, J. E. Clifford, S. Afonson, and C. W. Crumpton, *Arch. Int. Pharmacodyn. Ther.*, **129,** 62 (1960).
(18) J. M. van Rossum, *ibid.*, **160,** 492 (1966).
(19) T. Furukawa, K. Kushiku, and T. Kawagoe, *Jpn. J. Pharmacol.*, **24,** 635 (1974).
(20) A. Barnett and J. W. Fiore, *Eur. J. Pharmacol.*, **14,** 206 (1971).
(21) R. G. Sampson, G. C. Scroop, and W. J. Louis, *Clin. Exp. Pharmacol. Physiol.*, **1,** 3 (1974).
(22) M. D. Day and P. R. Blower, *J. Pharm. Pharmacol.*, **27,** 276 (1975).
(23) R. G. Pendleton, E. Finlay, and S. Sherman, *Naunyn-Schmiedeberg's Arch. Pharmacol.*, **289,** 171 (1975).
(24) J. G. Cannon, G. J. Hatheway, J. P. Long, and F. M. Sharabi, *J. Med. Chem.*, **19,** 987 (1976).
(25) F. M. Sharabi, J. P. Long, J. G. Cannon, and G. J. Hatheway, *J. Pharmacol. Exp. Ther.*, **199,** 630 (1976).
(26) M. Friedman and S. C. Freed, *Proc. Soc. Exp. Biol. Med.*, **70,** 670 (1949).
(27) R. G. D. Steel and J. H. Torrie, "Principles and Procedures of Statistics," McGraw-Hill, New York, N.Y., 1960, p. 67.
(28) D. J. Finney, "Statistical Method in Biological Assays," Griffin, London, England, 1952, p. 139.
(29) N. E. Andén, A. Rubenson, K. Fuxe, and R. Hökfelt, *J. Pharm. Pharmacol.*, **19,** 627 (1967).
(30) D. M. Schuelke, A. L. Mark, P. G. Schmid, and J. W. Eckstein, *J. Pharmacol. Exp. Ther.*, **176,** 320 (1971).
(31) M. G. Bogaert and A. F. DeSchaepdryver, *Arch. Int. Pharmacodyn. Ther.*, **166,** 203 (1967).
(32) T. C. Hamilton, *Br. J. Pharmacol.*, **44,** 442 (1972).

ACKNOWLEDGMENTS

Supported in part by National Institutes of Health Grant GM-22365.

Determination of Flucytosine in Tablets by Differential Pulse Polarography

F. W. TEARE *x, R. N. YADAV *, and M. SPINO ‡

Received November 9, 1976, from the **Faculty of Pharmacy, University of Toronto, Toronto, Ontario, Canada M5S 1A1,* the ‡*Division of Clinical Pharmacology, Toronto Western Hospital, Toronto, Ontario, Canada,* and the ‡*Clinical Institute, Addiction Research Foundation, Toronto, Ontario, Canada.* Accepted for publication March 31, 1978.

Abstract □ A differential pulse polarographic assay was developed for determining flucytosine in tablets. The drug is extracted from the sample with water and hydrochloric acid and, after the pH is adjusted, an aliquot is added to the cell and the solution is polarographed at the dropping mercury electrode *versus* the saturated calomel electrode with 0.066 *M* Sørensen phosphate buffer (pH 5.6) as the supporting electrolyte. The polarographic peak height enables precise quantitative determination. The E_p value for flucytosine is −1.54 v *versus* the saturated calomel electrode. The mean recovery of the drug is 101.5% ± 1.9 (*SD*). The method is simple, rapid, and precise.

Keyphrases □ Flucytosine—differential pulse polarographic analysis in dosage forms □ Polarography, differential pulse—analysis, flucytosine in dosage forms □ Antifungal agents—flucytosine, differential pulse polarographic analysis in dosage forms

Flucytosine, 5-fluorocytosine (I), is a fluorinated pyrimidine that has shown *in vitro* and *in vivo* antifungal activity. Microbiological (1), fluorometric (2, 3), and high-pressure liquid chromatographic (4) procedures were reported for the estimation of I in biological fluids. The USP (5) employs a spectrophotometric method for the estimation of I in capsules. The mechanism of polarographic reduction of pyrimidine derivatives was reported previously (6–8). This paper reports a simple, convenient, and rapid differential pulse polarographic analysis of I in tablets.

EXPERIMENTAL

Apparatus and Conditions—Polarograms were obtained using a polarographic analyzer[1] equipped with a drop timer[2]; the differential pulse mode was used. A three-electrode cell (5–50 ml) was comprised of a dropping mercury electrode, a saturated calomel electrode (SCE), and a platinum wire auxiliary electrode. The drop time t, was 2 sec, the drop mass was 1.4 mg/sec, and the capillary characteristic was $m^{2/3}t^{1/6} = 1.3$, measured in 0.066 *M* Sørensen phosphate buffer (pH 5.6) with an open circuit and at a mercury column height of 95 cm. The current range was either 5 or 10 μamp for a peak response of full-scale deflection, the scan range was from −1.2 to −1.95 v, the peak potential was −1.54 v, the modulation amplitude was 25 mv, and the scan rate was 2 mv/sec. The polarogram was recorded on an x–y recorder[3].

A pH meter[4], fitted with a combination glass–saturated calomel electrode electrode pair, was used to monitor the pH of all solutions.

Reagents and Chemicals—All chemicals were analytical reagent grade. The Sørensen buffer was prepared by mixing stock solutions A (9.073 g of monobasic potassium phosphate/liter) and B (11.87 g of dibasic sodium phosphate dihydrate/liter) in varying proportions to produce the desired pH (9). Flucytosine[5] was used as a standard.

Calibration Curve—An aqueous stock solution of I was prepared at 1×10^{-2} *M*. A range of 1×10^{-3}–1×10^{-4} *M* was employed for the preparation of the diffusion current *versus* concentration calibration curve. All standard solutions were prepared by pipetting an aliquot of the aqueous stock solution and adding 13.0 ml of Sørensen phosphate buffer (pH 5.6) and sufficient distilled water to a final volume of 20 ml.

These solutions were transferred to the cell and deoxygenated with pure nitrogen for 10 min prior to obtaining the polarograms in quiescent solution. A layer of nitrogen was maintained over the solution surface during the electroreduction. Polarograms were obtained using the differential pulse polarographic mode.

[1] Princeton Applied Research (PAR) model 174A.
[2] Princeton Applied Research (PAR) model 172A.
[3] Houston Omnigraphic model 2000.
[4] Fisher, Accumet model 230 pH/ion meter.
[5] Hoffmann–La Roche lot I-898.

0022-3549/78/1100-1641$01.00/0
© 1978, American Pharmaceutical Association

Table I—Effect of Supporting Electrolyte Concentration on the Peak Height of Flucytosine

Molarity of Buffer	Current, μamp
0.200	4.52
0.100	4.46
0.066	4.15
0.050	3.97
0.040	3.78

Tablet Analysis—Twenty tablets were weighed and finely crushed. A portion of the powder equivalent to 200 mg of I was weighed accurately and transferred to a 250-ml volumetric flask. About 50 ml of dilute hydrochloric acid (1:100) was added, and the flask was shaken for 30 min on a mechanical shaker and diluted to volume with the dilute hydrochloric acid. The contents were mixed, and the excipients were allowed to settle.

A 10-ml aliquot was adjusted to pH 5.6 using dilute sodium hydroxide, quantitatively transferred to a 25-ml volumetric flask, and diluted to volume with water. An aliquot of the solution sufficient to give a peak height in the middle of the calibration curve was pipetted into the polarographic cell. The remainder of the procedure was identical to that described for the preparation of the calibration curve.

RESULTS AND DISCUSSION

Preliminary experiments revealed that I exhibits a single sharp differential pulse polarographic peak in Sørensen phosphate buffer over pH 5–8. In the dc mode, a single well-defined reduction wave was obtained (10) having a half-wave potential of −1.49 v *versus* the saturated calomel reference electrode (Fig. 1). That this electrode process was diffusion controlled was evident from a linear plot of the diffusion current *versus* the square root of the mercury column height corrected for back pressure (10). The fact that this plot did not quite pass through the origin on extrapolation may indicate that some small additional process such as adsorption or a rate-limiting reaction may occur at the surface of the dropping mercury electrode (11).

To select optimal conditions for the quantitative determination of I, the effects of both the concentration and pH of the buffer on the peak potential, E_p, and the corresponding peak current were investigated (Table I and Fig. 2). The E_p value shifted to more negative values with

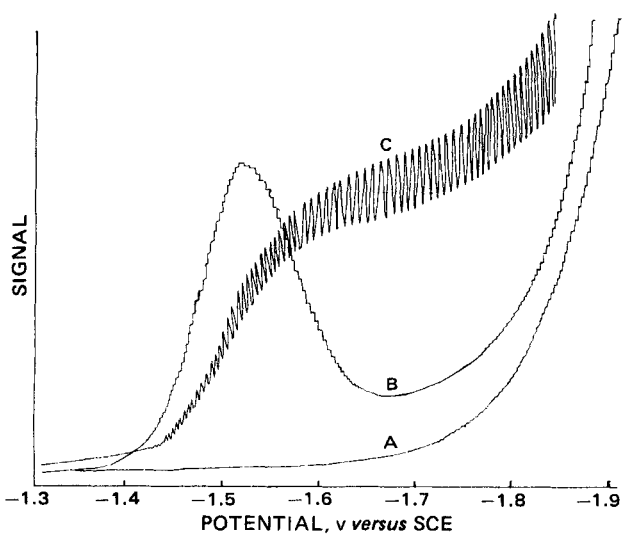

Figure 1—*Polarograms of 6 × 10⁻⁴ M I in 0.066 M Sørensen phosphate buffer (pH 5.6); $m^{2/3}t^{1/6}$ = 1.29; mercury column height = 95 cm; potential scan rate = 2 mv/sec; and drop time = 2 sec. Curves A and B represent the supporting electrolyte and I, respectively, in the differential pulse mode with a modulation amplitude of 25 mv. Curve C represents the drug run in the dc mode. The current sensitivity (full-scale deflection) for A and B was 10 μamp; for C, it was 5 μamp.*

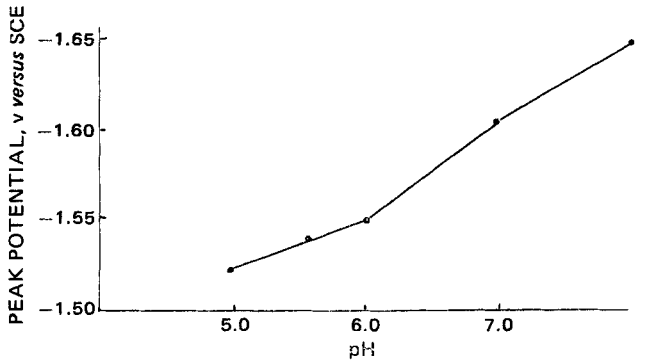

Figure 2—*Effect of pH on peak potential for the electroreduction of I at a concentration of 6 × 10⁻⁴ M in Sørensen phosphate buffer (0.066 M).*

increasing pH. The I concentration did not affect the E_p value in this buffer at pH 5.6. Increasing molarity of the buffer caused a slight increase in the current measured at the E_p (Table I). The final supporting electrolyte used in the assay of I was 0.066 *M* Sørensen phosphate buffer (pH 5.6).

A linear relationship existed between the current measured at an E_p of −1.54 v (*versus* the saturated calomel electrode) and the concentration of I in the range of 1×10^{-3}–1×10^{-4} *M*. This plot had a correlation coefficient of 0.9976, a *y*-intercept of 0.0604, and a slope of 0.6605 (10). The failure of this calibration curve to pass through the origin is not important since the size of the aliquot of the sample was selected to give a current peak height reading falling in the middle portion of this plot.

The mean assay result of 10 replicate determinations of I in commercial tablets[6] was 101.5% ± 1.9 (*SD*) of the labeled amount. Tablets from the same bottle were assayed by the USP XIX method for I capsules, involving UV spectrophotometry at 285 nm. The plot of absorbance *versus* concentration of the same reference material (I) used for the polarographic method resulted in a straight line with a slope of 0.0699, a *y*-intercept of −0.007, and a correlation coefficient of 0.9997. The mean result of three replicate determinations of I in the same lot of tablets was 102.2%. This excellent agreement of results obtained by two unrelated methods indicates that the tablet excipients in this formulation do not interfere with either assay.

Filtration of the tablet sample suspension was not required. This differential pulse polarographic method is simple, rapid, and convenient for analysis of flucytosine in commercial tablets.

The quantitative determination of I in biological fluids by differential pulse polarography (10) will be reported elsewhere.

REFERENCES

(1) R. G. Blaker and B. J. Doutt, *Antimicrob. Agents Chemother.*, **2**, 502 (1972).

(2) D. Wade and G. Sudlow, *J. Pharm. Sci.*, **62**, 828 (1973).

(3) R. A. Richardson, *Clin. Chim. Acta*, **63**, 109 (1975).

(4) A. D. Blair, A. W. Forrey, B. T. Meijsen, and R. E. Cutler, *J. Pharm. Sci.*, **64**, 1334 (1975).

(5) "The United States Pharmacopeia," 19th rev., Mack Publishing Co., Easton, Pa., 1975, p. 199.

(6) D. L. Smith and P. J. Slving, *J. Am. Chem. Soc.*, **84**, 2741 (1962).

(7) L. F. Cavalieri and B. A. Lowy, *Arch. Biochem. Biophys.*, **35**, 83 (1952).

(8) E. Palecek and B. Janik, *ibid.*, **98**, 527 (1962).

(9) "Scientific Tables," 7th ed., J. R. Geigy S.A., Basel, Switzerland, 1970, p. 281.

(10) R. N. Yadav, M.S. thesis, University of Toronto, Toronto, Ontario, Canada, 1977.

(11) P. Zuman, "The Elucidation of Organic Electrode Processes," Academic, New York, N.Y., 1969.

[6] Ancotil tablets (500 mg), lot I-891, Hoffmann-La Roche Inc., Nutley, N.J.

Effects of Pharmacological Intervention on Infarct Size following Induced Myocardial Infarction in Rats

MICHAEL A. BARLETTA ˣ, ROBERT STAAB, CESAR LAU CAM, and VINCENT dePAUL LYNCH

Received December 15, 1977, from the *Department of Pharmaceutical Sciences, College of Pharmacy and Allied Health Professions, St. John's University, Jamaica, NY 11439.* Accepted for publication March 17, 1978.

Abstract □ Several therapeutic agents that alter infarct size were administered to rats with myocardial infarcts induced by electrocauterization. The myocardial tissue damage and infarct size correlated well with the creatine phosphokinase myocardial band activity, and these markers were utilized to assess the action of the therapeutic agents on myocardial tissue damage. Hyaluronidase, insulin, potassium chloride, and isoproterenol increased myocardial tissue damage whereas heparin and prednisolone administration resulted in decreased myocardial tissue damage after induced myocardial infarction in rats.

Keyphrases □ Infarct size—effect of various therapeutic agents, rats with induced myocardial infarctions □ Myocardial tissue damage—effect of various therapeutic agents, rats with induced myocardial infarctions □ Creatine phosphokinase myocardial band—correlated with infarct size and myocardial tissue damage, rats with induced myocardial infarctions

Currently available methods for assessing myocardial ischemia include measurements for coronary blood flow, serum lactate levels, angiography, radioactive scanning, and ECG mapping (1–3). However, these methods study the qualitative aspects of myocardial ischemia without quantitatively ascertaining the infarct size.

BACKGROUND

Correlations between infarct size and myocardial enzyme levels have been recognized for many years. Myocardial infarct size, measured by excision and weighing of the damaged tissue, correlated well with the extent of the release of myocardial creatine phosphokinase (4, 5). This enzyme offered many advantages over the other myocardial enzymes since it rose first following an infarction and returned to normal levels in approximately 3 days (6). Sequential serum changes in creatine phosphokinase monitored myocardial infarction in experimentally infarcted dogs (7).

The presence of the cardiac specific creatine phosphokinase fraction, creatine phosphokinase myocardial band, in elevated amounts is a much better index of necrotic damage since this enzyme is exclusively of myocardial origin (8). Evidence supports the contention that enzyme release from the ischemic myocardium occurs once necrosis is either inevitable or complete (9). One could prevent cellular mortality by preventing necrosis in endangered, but not yet necrotic or irreversibly damaged, myocardium.

Serial determinations of creatine phosphokinase have been performed to predict the infarct size by utilizing data from only the first 7 hr postinfarction in patients and after 5 hr postinfarction in animals (10). With clinical experimentation, the variation between observed infarction and the enzymatically predicted infarction was only 5%. It appeared that the jeopardized zone was a reflection of the creatine phosphokinase predicted infarct size and that this zone would ultimately become necrotic without a beneficial intervention (10).

Experimental models show that brief coronary occlusions do not alter creatine phosphokinase activity and do not produce histological necrosis. An occlusion of sufficient duration, however, results in creatine phosphokinase release (9, 11). The myocardial depletion of creatine phosphokinase reflects the infarct size in experimental animals (12, 13) and is indicative of necrosis as determined with radioactive microspheres.

In this study, the activity of the creatine phosphokinase cardiac specific myocardial band fraction was correlated to the grams of damaged necrotic myocardium produced after induced infarction. These biochemical and histological markers are used to illustrate the degree of myocardial tissue necrosis following pharmacological interventions in rats with induced myocardial infarction. This study demonstrates a model for evaluating various therapeutic agents capable of altering infarct size. The pharmacological agents studied were prednisolone, heparin, hyaluronidase, insulin, potassium chloride, and isoproterenol.

EXPERIMENTAL

Animals—One hundred and five Sprague–Dawley[1] male rats, 300–400 g, were divided into seven groups. Group I (45 rats) was used as a control to establish a correlation between infarct size and creatine phosphokinase myocardial band activity. The remaining rats were divided into six groups of 10 rats each.

Group II was treated with 100 units of heparin/kg iv by the penile vein at 15 min postinfarction. Group III was treated with 1.5 units of insulin sc 15 min following infarction. Group IV animals were treated with 0.025 mEq of potassium chloride subcutaneously at 15 min postinfarction. Group V was treated at the same time interval following infarction with prednisolone butylacetate at 11.4 mg/kg im. Group VI received 100 U iv of hyaluronidase.

Group VII was used as a positive control since many reports on isoproterenol suggest that the increased chronotropic and inotropic activity of this drug would increase the expected infarct size. This final group received a dosage of isoproterenol of 0.02 mg/kg.

All animals were given food[2] and water *ad libitum*.

Procedure for Inducing Infarction—The animals were anesthetized with pentobarbital sodium[3] (35 mg/kg ip), and the ECG was monitored throughout the surgical procedure. Following depilatation and sterilization with povidone-iodine[4], a 2.54-cm long incision was made through the skin in the left thoracic area to the skeletal muscle. The muscle layers were separated with minimal damage, using blunt dissection, and a purse string suture was prepared around the incision site.

After the ribs had been spread, the thorax opened, and the heart exposed, a branch of the left anterior descending artery was cauterized[5] carefully. Artificial respiration was not employed since the procedure involved an open thorax for only 15 sec. The chest was slightly compressed to create a negative intrathoracic pressure, and the purse string suture was closed.

For the measurement of the creatine phosphokinase levels, blood was taken from the tail at 0, 6, 18, 30, 42, and 54 hr since creatine phosphokinase activity previously returned to baseline by this time. After each experiment, the surviving animals were sacrificed, their hearts were removed, and the infarcted tissues were excised carefully. The necrotic tissue was weighed for future correlation with enzyme release data.

Assay of Creatine Phosphokinase Myocardial Band—A 0.1-ml volume of serum was used for the assay of creatine phosphokinase levels in a commercial spectrophotometric kit[6].

RESULTS

Group II (heparin) was treated with a dose expected to increase clotting time and result in a diminished clot surrounding the occluded vasculature. Clotting at the infarction site has been implicated with the extension of ischemia in the immediate area of the occlusion as well as in the distal vasculature. The current finding of a diminished necrosis and released enzyme is in total agreement with previous work (14–19) demonstrating

[1] Taconic Farms, Germantown, N.Y.
[2] Purina Rat Chow, Ralston-Purina, St. Louis, Mo.
[3] Sedasol, EVSCO Pharmaceutical Corp., Oceanside, N.Y.
[4] Betadine, Purdue-Frederick, Yonkers, N.Y.
[5] Lawton Co., New York, N.Y.
[6] Creatine phosphokinase 45-UV, Sigma Chemical Co., St. Louis, Mo.

0022-3549/78/1100-1643$01.00/0
© 1978, American Pharmaceutical Association

Table I—Mean Necrosis *versus* Mean Enzyme Released

Group	Necrotic Mass[a]	Enzymes[b]	Treatment[c]	Correlation Coefficient[d]
I	0.175	47.52	Control	0.930
II	0.173	32.65	Heparin	0.924
III	0.193	65.50	Insulin	0.836
IV	0.197	74.80	Potassium chloride	0.984
V	0.151	24.10	Prednisolone	0.672
VI	0.184	52.40	Hyaluronidase	0.963
VII	0.277	153.90	Isoproterenol	0.819

[a] Necrotic mass = necrosis in grams. [b] Enzymes = mean creatine phosphokinase myocardial band released in 54 hr. [c] Treatment = agent administered to the group. [d] Correlation coefficient between creatine phosphokinase myocardial band and necrotic mass.

that decreased infarct size is associated with an inhibition of platelet aggregation. Although not statistically less than the experimental group, there was a mean decrease in infarct size. A similar minimal decrease in the enzymes demonstrated a definite trend.

Insulin treatment was carried out as a positive control because Smith and Bird (20) showed that hypoglycemia increases infarct size by eliminating anaerobic metabolism of glucose as an energy source. The inhibition of glucose from access to the cell enhances the damage to the ischemic myocardium. This agent is often given with glucose to overcome hypoglycemia and with potassium to replenish the ion lost to the interstitial space during infarction. In this study, a nonsignificant increase in infarct size was shown by the mean increase in the necrotic mass at postmortem and also by the mean increase in the released enzyme.

Potassium was administered to the myocardially infarcted rats to determine if an increase in intracellular potassium in the deficient myocardial cell would affect myocardial salvage. The dosage was administered subcutaneously in an attempt to release the ion slowly into the circulation. A small dosage was chosen to eliminate the chance of toxicity associated with larger doses. The cells of the body store this ion, once administered, if it is administered at a rate exceeding the body's ability to utilize it or to excrete it *via* the kidney (21). An increase in necrosis was associated with this drug, which can probably be attributed to the toxic effect of the ion on the myocardium.

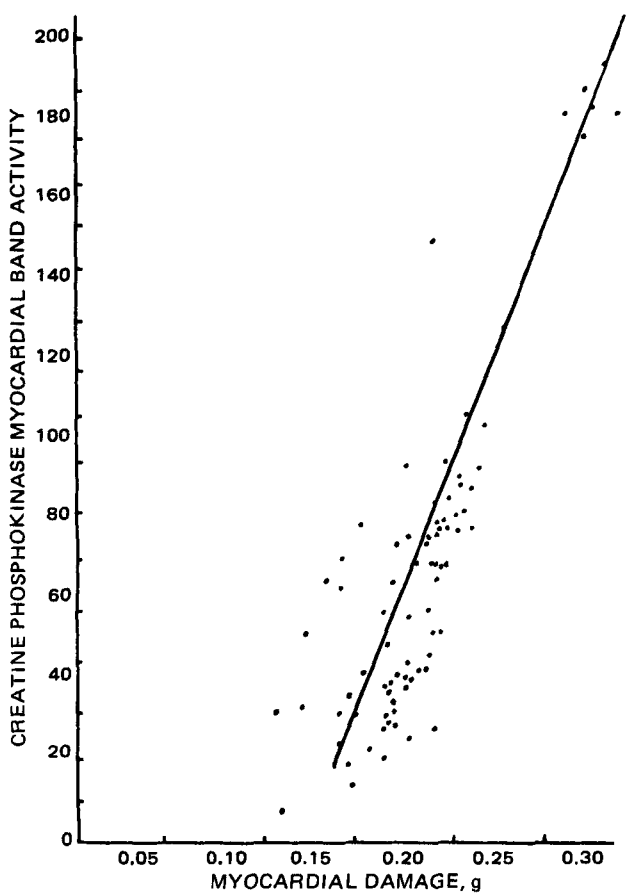

Figure 1—*Linear regression of all animals.*

Although the use of steroids to protect the ischemic myocardium has been studied extensively, controversy still surrounds this application. In the present study, there was a definite reduction in necrotic tissue as well as a reduction in the observed serum creatine phosphokinase attributed to this drug.

Steroids are thought to stabilize the lysosomal membrane and the cellular membrane itself. These effects limit the spread of lysosomal hydrolases capable of further damaging the myocardium (22). The efficacy of the glucocorticoids in decreasing infarct size was undoubtedly demonstrated in this study. This work supports the clinical finding of Morrison *et al.* (23) when a single dose of methylprednisolone decreased infarct size.

The effect of hyaluronidase on the extent of myocardial necrosis following infarction was studied to determine if the spreading factor associated with this agent would efficiently allow the transport of nutrients and oxygen to the ischemic portion of the myocardium and thus salvage the tissue. Hyaluronidase increased the level of necrosis and also the enzyme release but not significantly.

Isoproterenol was administered to assess the effect of the positive inotropic and chronotropic activities of this drug and its oxygen-wasting activity on the ischemic myocardium. Studies (24) utilizing such an intervention on the surgically occluded left ventricle of the dog demonstrated an increase in infarct size. The present study agrees with this work since the increased workload and oxygen requirements associated with the drug significantly increased infarct size in this group. The serial determination of the creatine phosphokinase myocardial band also correlated with the increased necrotic mass observed at postmortem.

The proof of the sensitivity of this model is depicted in Table I where it is demonstrated that each group correspondingly increases, *i.e.*, potassium chloride is the sixth in both total enzymes and necrotic mass. The two groups in which statistically significant alterations were observed were at the extreme ends of the experimental animal groups.

Although several drugs significantly reduced infarct size and enzyme release, Table I displays an important insight into the sensitivity of the model; in each case, the group with the lowest mean released enzyme had the lowest mean necrotic mass and the group with the highest release of enzymes had the highest necrotic mass as well. The middle groups responded sequentially.

Figure 1, a scatter diagram, shows the linear regression of all animals in which the analysis with creatine phosphokinase myocardial band was carried out.

The procedure offers a simple, easily performed method for the induction of myocardial infarction in the rat. The model offers enzyme sensitivity, reliability, and speed with a minimum of mortality following the intervention. Therefore, this procedure can be part of a routine screening for the pharmacological efficacy of agents that limit the extent of infarction in the rat.

REFERENCES

(1) R. B. Jennings, J. H. Baum, and P. B. Herdson, *Arch. Pathol.*, **79**, 135 (1965).

(2) "The Pathological Diagnosis of Acute Ischemic Heart Disease," WHO Technical Report Series 441, Geneva, Switzerland, 1970.

(3) F. T. Zugibe, P. Bell, and T. Conley, *Arch. Pathol.*, **81**, 409 (1966).

(4) J. G. McVie, *J. Clin. Pathol.*, **23**, 203 (1970).

(5) R. Staab, V. Lynch, C. Lau Cam, and M. Barletta, *J. Pharm. Sci.*, **66**, 1483 (1977).

(6) J. T. Lie, *Am. J. Clin. Pathol.*, **50**, 317 (1968).

(7) B. Bouchardy and G. Manjo, *Am. J. Pathol.*, **74**, 301 (1974).

(8) R. Roberts, H. D. Ambros, E. M. Carlson, and B. E. Sobel, *Am. J. Cardiol.*, **35**, 166 (1975).

(9) W. E. Shell and B. E. Sobel, in "Progress in Cardiology," vol. 4, P. Yu and J. F. Goodwin, Eds., Lea & Febiger, Philadelphia, Pa., 1975.

(10) W. E. Shell, J. F. Lavelle, J. W. Covell, and B. E. Sobel, *J. Clin. Invest.*, **52**, 2579 (1973).

(11) S. A. Ahmed, J. Williamson, R. Roberts, and B. E. Sobel, *Circulation*, **45**, 186 (1975).

(12) J. K. Kjeckshush and B. E. Sobel, *Circ. Res.*, **27**, 403 (1970).

(13) W. E. Shell and B. E. Sobel, *Am. J. Cardiol.*, **31**, 474 (1972).

(14) P. R. Maroko, J. K. Kjeckshush, B. E. Sobel, T. Watanabe, J. W. Corell, J. Ross, and E. Braunwald, *Circulation*, **43**, 67 (1971).

(15) P. R. Maroko and E. Braunwald, *Ann. Intern. Med.*, **79**, 720

(1973).
(16) K. A. Reimer, M. M. Rasmussen, and R. B. Jennings, *Circ. Res.*, **33**, 353 (1973).
(17) P. A. Serrano, B. Chavez-Lara, A. Bisteni, and D. Sodi-Pollares, *J. Mol. Cell. Cardiol.*, **2**, 91 (1971).
(18) P. P. Steele, H. S. Weilly, H. Davies, and E. Genton, *Circulation*, **48**, 1194 (1973).
(19) E. A. Murphy and J. F. Mustard, *ibid.*, **25**, 114 (1962).
(20) A. L. Smith and J. W. C. Bird, *J. Mol. Cell. Cardiol.*, **7**, 39 (1975).
(21) "Drill's Pharmacology in Medicine," 4th ed., J. R. DiPalma, Ed., McGraw-Hill, New York, N.Y., 1971.
(22) J. A. Spath, D. L. Lane, and A. M. Lefer, *Circ. Res.*, **35**, 44 (1974).
(23) J. Morrison, L. Reduto, R. Pizzarello, K. Geller, T. Maley, and S. Gulotta, *Circulation*, **53**, 1 (1976).
(24) P. R. Maroko, E. Braunwald, J. W. Covell, and J. Ross, *ibid.*, **40**, 111 (1969).

Effect of Surfactants on Percutaneous Absorption of Naproxen II: *In Vivo* and *In Vitro* Correlations in Rats

Z. T. CHOWHAN ˣ, R. PRITCHARD, W. H. ROOKS, II, and A. TOMOLONIS

Received May 9, 1977, from the *Institute of Pharmaceutical Sciences, Syntex Research, Palo Alto, CA 94304.* Accepted for publication March 20, 1978.

Abstract □ The effect of surfactants on percutaneous absorption of naproxen was studied using rat *in vivo* models. The *in vivo* normalized relative absorption rates were in good agreement with the *in vitro* relative flux. An antipyretic model in the rat could not show relatively small increases in percutaneous absorption caused by the surfactants. Based on these results, it is apparent that reliance on the rat, using either *in vitro* or *in vivo* models, may lead to erroneous conclusions when considering the effect of surfactants on human percutaneous absorption of drugs such as naproxen.

Keyphrases □ Surfactants, various—effect on percutaneous absorption of naproxen, *in vivo* and *in vitro* correlations in rats □ Naproxen—percutaneous absorption, effect of various surfactants, *in vivo* and *in vitro* correlations in rats □ Absorption, percutaneous—naproxen, effect of various surfactants, *in vivo* and *in vitro* correlations in rats □ Anti-inflammatory agents—naproxen, percutaneous absorption, effect of various surfactants, *in vivo* and *in vitro* correlations in rats

Percutaneous absorption generally is studied by two types of model systems: those employing excised skin in some type of a diffusion cell and those using living animals or humans *in situ*. Many studies suggested that these two model systems may differ in their mode of percutaneous absorption, namely, the *in vitro* measurement of steady-state flux *versus* the pharmacological activity mainly induced by the small amount of drug penetrating through the appendageal route in the early stages of diffusion.

BACKGROUND

Penetration through sweat ducts under a potential gradient occurred within 1–5 min, with no comparable transport through the stratum corneum within this period (1). Histological studies (2) also demonstrated follicular diffusion occurring within 5 min. Similarly, perifollicular wheals were observed 5 min after the application of 10% histamine free base (3). Some studies also related the *in vitro* steady-state flux to the *in vivo* steady-state flux. For example, the *in vitro* and *in vivo* transport of alkylmethyl sulfoxide across rabbit skin was studied, and the steady-state urinary elimination rate was about one-half of the *in vitro* steady-state flux (4).

Because of the question of the absorption mechanism, *i.e.*, intra-appendageal or transepidermal, in *in vivo versus* model systems and further complications due to variations in skin permeability from site to site, human to human, and species to species, comparable quantitative data between *in vivo* and *in vitro* model systems are sparse. A notable exception may be data (5) showing a similarity between the *in vitro* skin penetration and *in vivo* vasoconstriction response of fluocinonide and fluocinolone acetonide.

Previously (6), an *in vitro* model using excised skin from laboratory animals and humans was used to study the effect of surfactants on percutaneous naproxen absorption. The results suggested that excised skin of laboratory animals may lead to erroneous conclusions about the effect of surfactants on excised human skin.

This paper reports the effect of surfactants on percutaneous naproxen absorption in the rat *in vivo*. Comparisons between the *in vivo* normalized relative absorption rates and the *in vitro* relative flux in the rat indicate good correlation between the two model systems. Since surfactants showed only a small increase in percutaneous absorption in the rat, an antipyretic bioassay model in the rat could not show a similar correlation.

EXPERIMENTAL

Materials—The surfactants sodium lauryl sulfate[1], sodium laurate[2], and methyldecyl sulfoxide[3] were used as received.

Nonlabeled naproxen[4] was at least 99% pure. The tritiated naproxen was purified by radiochromatography and was at least 98% pure. The two solvent systems used were hexane–ethyl acetate (85:15) and benzene–tetrahydrofuran–acetic acid (90:9:3). All other chemicals were analytical reagent grade unless otherwise indicated.

Preparation of Creams—The method for the preparation of creams was as described previously (6).

***In Vivo* Percutaneous Absorption in Rats**—Male Sprague–Dawley rats[5], 250–300 g, were employed. Hair was removed[6] from the skin of the dorsal area between the forelegs and hindlegs on both sides of the spine, 18 hr prior to the application of cream. Throughout the shaving and dosing operations, the animals were kept under light anesthesia with anesthetic grade ether[7].

A cardboard template with an outside measurement of 4 × 5 cm and an inside measurement of 2 × 3 cm was devised to restrict and control the contact area between the cream and skin of the rat. The cardboard was covered on both sides with waterproof plastic tape[8] and was held in position by medical adhesive tape[9]. An accurately measured dose (0.5 ml) was delivered with a 1-ml tuberculin syringe to a 2 × 3-cm area. A

[1] E. I. du Pont de Nemours & Co., Menlo Park, Calif.
[2] Eastman Kodak Co., Rochester, N.Y.
[3] Institute of Organic Chemistry, Syntex Research, Palo Alto, CA 94304.
[4] *d*-2-(6′-Methoxy-2′-naphthyl)propionic acid, Syntex Research, Palo Alto, CA 94304.
[5] Simonsen Laboratories, Gilroy, Calif.
[6] Model-A2 animal electric clipper with size 40 blade, John Oster Manufacturing Co., Milwaukee, WI 53200.
[7] Mallinckrodt Chemical Works, St. Louis, MO 63100.
[8] Scotch No. 471, 3M Co., St. Paul, Minn.
[9] Zonar Porous Tape, Johnson & Johnson.

0022-3549/78/1100-1645$01.00/0
© 1978, American Pharmaceutical Association

(1973).
(16) K. A. Reimer, M. M. Rasmussen, and R. B. Jennings, *Circ. Res.*, **33**, 353 (1973).
(17) P. A. Serrano, B. Chavez-Lara, A. Bisteni, and D. Sodi-Pollares, *J. Mol. Cell. Cardiol.*, **2**, 91 (1971).
(18) P. P. Steele, H. S. Weilly, H. Davies, and E. Genton, *Circulation*, **48**, 1194 (1973).
(19) E. A. Murphy and J. F. Mustard, *ibid.*, **25**, 114 (1962).
(20) A. L. Smith and J. W. C. Bird, *J. Mol. Cell. Cardiol.*, **7**, 39 (1975).
(21) "Drill's Pharmacology in Medicine," 4th ed., J. R. DiPalma, Ed., McGraw-Hill, New York, N.Y., 1971.
(22) J. A. Spath, D. L. Lane, and A. M. Lefer, *Circ. Res.*, **35**, 44 (1974).
(23) J. Morrison, L. Reduto, R. Pizzarello, K. Geller, T. Maley, and S. Gulotta, *Circulation*, **53**, 1 (1976).
(24) P. R. Maroko, E. Braunwald, J. W. Covell, and J. Ross, *ibid.*, **40**, 111 (1969).

Effect of Surfactants on Percutaneous Absorption of Naproxen II: *In Vivo* and *In Vitro* Correlations in Rats

Z. T. CHOWHAN ˣ, R. PRITCHARD, W. H. ROOKS, II, and A. TOMOLONIS

Received May 9, 1977, from the *Institute of Pharmaceutical Sciences, Syntex Research, Palo Alto, CA 94304.* Accepted for publication March 20, 1978.

Abstract □ The effect of surfactants on percutaneous absorption of naproxen was studied using rat *in vivo* models. The *in vivo* normalized relative absorption rates were in good agreement with the *in vitro* relative flux. An antipyretic model in the rat could not show relatively small increases in percutaneous absorption caused by the surfactants. Based on these results, it is apparent that reliance on the rat, using either *in vitro* or *in vivo* models, may lead to erroneous conclusions when considering the effect of surfactants on human percutaneous absorption of drugs such as naproxen.

Keyphrases □ Surfactants, various—effect on percutaneous absorption of naproxen, *in vivo* and *in vitro* correlations in rats □ Naproxen—percutaneous absorption, effect of various surfactants, *in vivo* and *in vitro* correlations in rats □ Absorption, percutaneous—naproxen, effect of various surfactants, *in vivo* and *in vitro* correlations in rats □ Anti-inflammatory agents—naproxen, percutaneous absorption, effect of various surfactants, *in vivo* and *in vitro* correlations in rats

Percutaneous absorption generally is studied by two types of model systems: those employing excised skin in some type of a diffusion cell and those using living animals or humans *in situ*. Many studies suggested that these two model systems may differ in their mode of percutaneous absorption, namely, the *in vitro* measurement of steady-state flux *versus* the pharmacological activity mainly induced by the small amount of drug penetrating through the appendageal route in the early stages of diffusion.

BACKGROUND

Penetration through sweat ducts under a potential gradient occurred within 1–5 min, with no comparable transport through the stratum corneum within this period (1). Histological studies (2) also demonstrated follicular diffusion occurring within 5 min. Similarly, perifollicular wheals were observed 5 min after the application of 10% histamine free base (3). Some studies also related the *in vitro* steady-state flux to the *in vivo* steady-state flux. For example, the *in vitro* and *in vivo* transport of alkylmethyl sulfoxide across rabbit skin was studied, and the steady-state urinary elimination rate was about one-half of the *in vitro* steady-state flux (4).

Because of the question of the absorption mechanism, *i.e.*, intra-appendageal or transepidermal, in *in vivo versus* model systems and further complications due to variations in skin permeability from site to site, human to human, and species to species, comparable quantitative data between *in vivo* and *in vitro* model systems are sparse. A notable exception may be data (5) showing a similarity between the *in vitro* skin penetration and *in vivo* vasoconstriction response of fluocinonide and fluocinolone acetonide.

Previously (6), an *in vitro* model using excised skin from laboratory animals and humans was used to study the effect of surfactants on percutaneous naproxen absorption. The results suggested that excised skin of laboratory animals may lead to erroneous conclusions about the effect of surfactants on excised human skin.

This paper reports the effect of surfactants on percutaneous naproxen absorption in the rat *in vivo*. Comparisons between the *in vivo* normalized relative absorption rates and the *in vitro* relative flux in the rat indicate good correlation between the two model systems. Since surfactants showed only a small increase in percutaneous absorption in the rat, an antipyretic bioassay model in the rat could not show a similar correlation.

EXPERIMENTAL

Materials—The surfactants sodium lauryl sulfate[1], sodium laurate[2], and methyldecyl sulfoxide[3] were used as received.

Nonlabeled naproxen[4] was at least 99% pure. The tritiated naproxen was purified by radiochromatography and was at least 98% pure. The two solvent systems used were hexane–ethyl acetate (85:15) and benzene–tetrahydrofuran–acetic acid (90:9:3). All other chemicals were analytical reagent grade unless otherwise indicated.

Preparation of Creams—The method for the preparation of creams was as described previously (6).

***In Vivo* Percutaneous Absorption in Rats**—Male Sprague–Dawley rats[5], 250–300 g, were employed. Hair was removed[6] from the skin of the dorsal area between the forelegs and hindlegs on both sides of the spine, 18 hr prior to the application of cream. Throughout the shaving and dosing operations, the animals were kept under light anesthesia with anesthetic grade ether[7].

A cardboard template with an outside measurement of 4 × 5 cm and an inside measurement of 2 × 3 cm was devised to restrict and control the contact area between the cream and skin of the rat. The cardboard was covered on both sides with waterproof plastic tape[8] and was held in position by medical adhesive tape[9]. An accurately measured dose (0.5 ml) was delivered with a 1-ml tuberculin syringe to a 2 × 3-cm area. A

[1] E. I. du Pont de Nemours & Co., Menlo Park, Calif.
[2] Eastman Kodak Co., Rochester, N.Y.
[3] Institute of Organic Chemistry, Syntex Research, Palo Alto, CA 94304.
[4] *d*-2-(6′-Methoxy-2′-naphthyl)propionic acid, Syntex Research, Palo Alto, CA 94304.
[5] Simonsen Laboratories, Gilroy, Calif.
[6] Model-A2 animal electric clipper with size 40 blade, John Oster Manufacturing Co., Milwaukee, WI 53200.
[7] Mallinckrodt Chemical Works, St. Louis, MO 63100.
[8] Scotch No. 471, 3M Co., St. Paul, Minn.
[9] Zonar Porous Tape, Johnson & Johnson.

0022-3549/78/1100-1645$01.00/0
© 1978, American Pharmaceutical Association

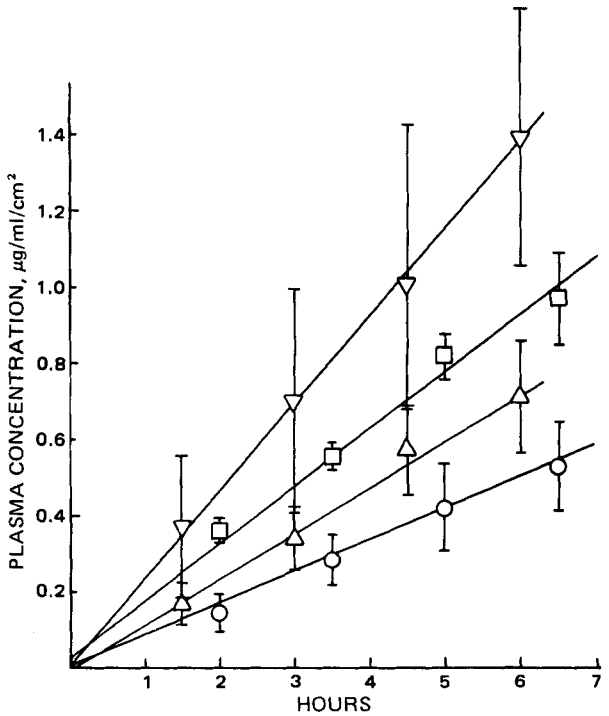

Figure 1—*Effect of surfactants on the* in vivo *percutaneous absorption of naproxen in the rat. Experimental points are averages of three rats, and vertical bars represents standard errors. Lines are the regression lines. Key:* ○, *control,* $y = -0.008 + 0.083x$, $r = 0.999$; △, *2% sodium lauryl sulfate,* $y = -0.007 + 0.121x$, $r = 0.998$; ▽, *2% sodium laurate,* $y = 0.029 + 0.150x$, $r = 0.996$; *and* □, *1% methyldecyl sulfoxide,* $y = 0.01 + 0.231x$, $r = 1.00$.

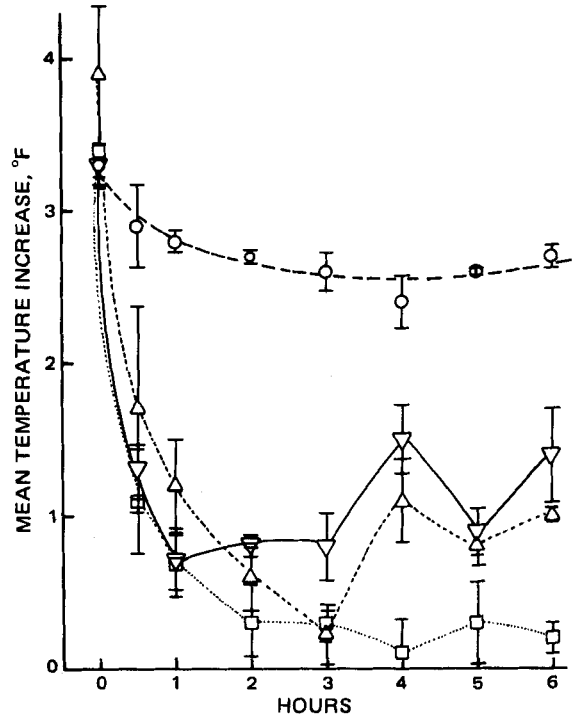

Figure 2—*Antipyretic activity of naproxen following topical application of cream formulations with and without surfactants. The curves indicate onset, intensity, and duration of antipyretic activity. Key:* ○, *placebo control;* △, *naproxen cream without surfactant;* ▽, *naproxen cream containing 1% methyldecyl sulfoxide; and* □, *naproxen cream containing 2% sodium lauryl sulfate. Points are averages of five rats, and vertical lines represent standard error.*

plastic film[10], 4 × 5 cm, was placed over the dose and the template and taped in place.

The cream was uniformly spread in the restricted area with a stainless steel spatula, and the rats were then transferred to individual cages. At appropriate intervals, blood was withdrawn by making an incision in the tail vein. Heparinized microhematocrit capillary tubes[11] were used to collect blood samples. These tubes were centrifuged immediately, and 50 μl of plasma was added to 15 ml of scintillation cocktail contained in a scintillation vial. Then the radioactive counts were determined[12].

The counts per minute of plasma samples were corrected for the quench effect, and the total radioactivity was converted to micrograms of naproxen per milliliter of plasma using an internal standard. Three animals were used for each evaluation.

***In Vivo* Studies Using a Rat Antipyretic Model**—The procedure described by Roszkowski *et al.* (7) was used. The dorsal fur of female rats[5], 90–100 g, was clipped 1 day prior to taking the "normal" rectal temperature at 0 hr, after which pyresis was induced by subcutaneous administration, dorsally and ventrally, of 2 ml of a 44% suspension of yeast (one 0.6-oz cake of bakers yeast[13] in 22 ml of 0.9% NaCl). The injection sites were then massaged to spread the suspension beneath the skin.

At 17 hr, the rats were massaged again to stimulate a further increase in body temperature. At 18 hr, the rectal temperature was recorded for the second time, which served as the baseline from which antipyresis was determined. An accurately measured dose (0.1 ml) of naproxen cream was delivered to a specific skin area and spread uniformly over an area 2 cm². Subsequent rectal temperatures were recorded at appropriate intervals.

RESULTS

The initial plasma naproxen concentration *versus* time profiles obtained following topical application of the four cream formulations are given in Fig. 1. The relative rates were obtained from the linear regression lines. These rates were normalized for making comparisons to the *in vitro* relative flux data. Table I shows that excellent correlation exists between the *in vitro* flux and the *in vivo* normalized rates, with the possible exception of the formulation containing 1% methyldecyl sulfoxide. These results suggest that the *in vitro* skin penetration model provides a good index of the *in vivo* percutaneous naproxen absorption in the rat.

A bioassay model using rats was developed (7) for determining antipyretic effects of naproxen. This model has been utilized to investigate the differences, if any, in the antipyretic activity of naproxen due to the presence of surfactants in the formulation applied topically. The mean temperature increase *versus* time plots following injection of a yeast suspension and the application of the placebo control and creams under study are given in Fig. 2. A definite antipyretic effect occurred from topical application of creams containing naproxen. However, the effect of the surfactants in enhancing percutaneous absorption of naproxen could not be demonstrated. The creams with and without surfactants showed similar onset, intensity, and duration of antipyretic activity. This result is probably because of the lack of sensitivity of the bioassay model to show small enhancement in percutaneous absorption in the rat from creams containing surfactants.

DISCUSSION

Percutaneous absorption studies using an *in vitro* skin penetration model assume that the living processes and the skin surface conditions do not affect medicament penetration. The main barrier to skin penetration is the stratum corneum; *i.e.*, the model also assumes that the steady-state flux obtained after a long lag time may serve as a good index of the *in vivo* situations, where percutaneous absorption is frequently measured during the lag time. In view of these assumptions of the *in vitro* model, it is important to establish a correlation between *in vitro* and *in vivo* models. The results of this study show some correlation between the results of *in vitro* and *in vivo* models in the rat. Additional studies directed specifically at the correlation of *in vitro* and *in vivo* topical absorption are clearly required to clarify this point.

[10] Saran Wrap, Dow Chemical Co., Midland, Mich.
[11] Sherwood Medical Industries, St. Louis, Mo.
[12] Unilux II, Nuclear-Chicago, Chicago, Ill.
[13] Fleischmann's

Table I—Comparison of the *In Vitro* Relative Flux of Naproxen Using Excised Rat Skin and the Normalized Relative Rates of Percutaneous Absorption in the *In Vivo* Rat

Formulation	*In Vitro* Relative Flux[a]	*In Vivo* Normalized Relative Rates[b]
No added surfactant (control)	1	1
Sodium lauryl sulfate (2%)	1.3	1.5
Sodium laurate (2%)	1.7	1.8
Methyldecyl sulfoxide (1%)	1.5	2.8

[a] Data from Table II, Ref. 6. [b] Slopes of the linear regression lines in Fig. 2 were normalized.

It is also apparent that reliance on the rat using either *in vitro* or *in vivo* models may lead to erroneous conclusions regarding the effect of surfactants on human percutaneous absorption of drugs similar to naproxen. A great degree of caution should be exercised in using animal bioassay models in evaluating the effect of formulation changes on topical absorption.

REFERENCES

(1) H. A. Abramson and M. H. Gorin, *J. Phys. Chem.*, **44**, 1094 (1940).

(2) G. M. McKee, M. B. Sulzberger, F. Herrmann, and R. L. Baer, *J. Invest. Dermatol.*, **6**, 43 (1945).

(3) W. B. Shelley and F. M. Melton, *ibid.*, **13**, 61 (1949).

(4) D. L. Sekura and J. Scala, in "Pharmacology and the Skin," W. Montagna, R. B. Stoughton, and E. J. Van Scott, Eds., Appleton-Century-Crofts, New York, N.Y., 1972.

(5) J. Ostrenga, C. Steinmetz, and B. Poulsen, *J. Pharm. Sci.*, **60**, 1175 (1971).

(6) Z. T. Chowhan and R. Pritchard, *ibid.*, **67**, 1272 (1978).

(7) A. P. Roszkowski, W. H. Rooks, II, A. J. Tomolonis, and L. M. Miller, *J. Pharmacol. Exp. Ther.*, **179**, 141 (1971).

ACKNOWLEDGMENTS

The authors are grateful to Dr. Boyd J. Poulsen for helpful discussions.

Rapid GLC Determination of Chlordiazepoxide and Metabolite in Serum Using On-Column Methylation

SY-RONG SUN ˣ and D. J. HOFFMAN

Received December 12, 1977, from the *Pharmaceutical Products Division, Abbott Laboratories, North Chicago, IL 60064.* Accepted for publication March 13, 1978.

Abstract □ A rapid GLC method was developed for the assay of chlordiazepoxide in serum. After chlordiazepoxide was extracted with ether, it was methylated with trimethylanilinium hydroxide in the injection port and detected by electron capture. The assay is simple and sensitive and can be automated for large-scale clinical analysis.

Keyphrases □ Chlordiazepoxide—electron-capture GLC analysis in serum □ GLC, electron capture—analysis, chlordiazepoxide in serum □ Tranquilizers—chlordiazepoxide, electron-capture GLC analysis in serum

Electron-capture GLC determination of chlordiazepoxide in biological fluids was accomplished by assaying for either its hydrolysis product (1, 2) or the intact moiety (3, 4). These procedures were somewhat tedious and required large amounts of sample. The following method is rapid and has a sensitivity of about 45 ng/ml using 0.4 ml of serum.

EXPERIMENTAL

Reagents—Chlordiazepoxide hydrochloride[1] (I), trimethylanilinium hydroxide[2] in methanol (0.1 *M*), and 1,3-dimethyl-6-methoxy-4-(*p*-chlorophenyl)-1*H*-pyrazolo[3,4-*b*]pyridine[3] (II) as the internal standard were used as supplied. Ether[4] was anesthetic grade, and other chemicals were analytical reagent grade.

Instrumentation—A gas chromatograph[5], equipped with a ^{63}Ni-electron-capture detector containing a 2-mCu ^{63}Ni-β-ionization source, and an electronic integrator were used. The glass column was 1.21 m (4 ft) × 4 mm (i.d.), packed with 5% OV-225[6] on 80–100-mesh Gas Chrom Q[6]. The column was conditioned at 265° for at least 18 hr with a carrier gas [argon–methane[7] (95:5)] flow rate of 50 ml/min. The cylinder of the carrier gas was fitted with an oxygen trap filter[8].

The operating conditions were: column oven temperature, 265°; electron-capture detector temperature, 300°; injection port temperature, 270°; detector pulse interval, 150 μsec; electrometer range, 10^3; recorder presentation, 2 mv; and slope sensitivity, 0.3 mv/min. Under these conditions, the internal standard and chlordiazepoxide had retention times of 1.8 and 3.0 min, respectively (Fig. 1).

Table I—Assay Reproducibility

Serum Chlordiazepoxide Concentration, μg/ml	Calculated Serum Concentration[a], μg/ml	*RSD*, %
0	0	—
0.10	0.099 ± 0.0098	9.9
0.25	0.229 ± 0.062	27.2
0.75	0.758 ± 0.013	1.7
1.00	1.04 ± 0.14	13.7
1.50	1.48 ± 0.068	4.6

[a] Mean ± *SD* of triplicate determinations at each concentration.

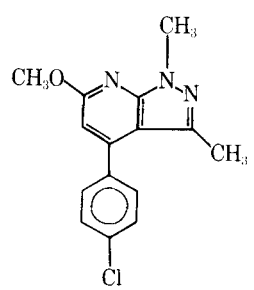

II

[1] Lot 351074, Hoffmann–La Roche, Nutley, N.J.
[2] Eastman Kodak Chemicals, Rochester, N.Y.
[3] Lot 3827-LRS-25, synthesized from methylation of Compound 22 in *J. Heterocycl. Chem.*, **12**, 1137 (1975).
[4] Mallinckrodt Chemicals, St. Louis, Mo.
[5] Hewlett-Packard model 7620A.
[6] Applied Science Laboratories, State College, Pa.
[7] Matheson Gas Products, Elk Grove Village, Ill.
[8] Altech Associates, Arlington Heights, Ill.

0022-3549/78/1100-1647$01.00/0

© 1978, American Pharmaceutical Association

Table I—Comparison of the *In Vitro* Relative Flux of Naproxen Using Excised Rat Skin and the Normalized Relative Rates of Percutaneous Absorption in the *In Vivo* Rat

Formulation	*In Vitro* Relative Flux[a]	*In Vivo* Normalized Relative Rates[b]
No added surfactant (control)	1	1
Sodium lauryl sulfate (2%)	1.3	1.5
Sodium laurate (2%)	1.7	1.8
Methyldecyl sulfoxide (1%)	1.5	2.8

[a] Data from Table II, Ref. 6. [b] Slopes of the linear regression lines in Fig. 2 were normalized.

It is also apparent that reliance on the rat using either *in vitro* or *in vivo* models may lead to erroneous conclusions regarding the effect of surfactants on human percutaneous absorption of drugs similar to naproxen. A great degree of caution should be exercised in using animal bioassay models in evaluating the effect of formulation changes on topical absorption.

REFERENCES

(1) H. A. Abramson and M. H. Gorin, *J. Phys. Chem.*, **44**, 1094 (1940).

(2) G. M. McKee, M. B. Sulzberger, F. Herrmann, and R. L. Baer, *J. Invest. Dermatol.*, **6**, 43 (1945).

(3) W. B. Shelley and F. M. Melton, *ibid.*, **13**, 61 (1949).

(4) D. L. Sekura and J. Scala, in "Pharmacology and the Skin," W. Montagna, R. B. Stoughton, and E. J. Van Scott, Eds., Appleton-Century-Crofts, New York, N.Y., 1972.

(5) J. Ostrenga, C. Steinmetz, and B. Poulsen, *J. Pharm. Sci.*, **60**, 1175 (1971).

(6) Z. T. Chowhan and R. Pritchard, *ibid.*, **67**, 1272 (1978).

(7) A. P. Roszkowski, W. H. Rooks, II, A. J. Tomolonis, and L. M. Miller, *J. Pharmacol. Exp. Ther.*, **179**, 141 (1971).

ACKNOWLEDGMENTS

The authors are grateful to Dr. Boyd J. Poulsen for helpful discussions.

Rapid GLC Determination of Chlordiazepoxide and Metabolite in Serum Using On-Column Methylation

SY-RONG SUN ˣ and D. J. HOFFMAN

Received December 12, 1977, from the *Pharmaceutical Products Division, Abbott Laboratories, North Chicago, IL 60064.* Accepted for publication March 13, 1978.

Abstract □ A rapid GLC method was developed for the assay of chlordiazepoxide in serum. After chlordiazepoxide was extracted with ether, it was methylated with trimethylanilinium hydroxide in the injection port and detected by electron capture. The assay is simple and sensitive and can be automated for large-scale clinical analysis.

Keyphrases □ Chlordiazepoxide—electron-capture GLC analysis in serum □ GLC, electron capture—analysis, chlordiazepoxide in serum □ Tranquilizers—chlordiazepoxide, electron-capture GLC analysis in serum

Electron-capture GLC determination of chlordiazepoxide in biological fluids was accomplished by assaying for either its hydrolysis product (1, 2) or the intact moiety (3, 4). These procedures were somewhat tedious and required large amounts of sample. The following method is rapid and has a sensitivity of about 45 ng/ml using 0.4 ml of serum.

EXPERIMENTAL

Reagents—Chlordiazepoxide hydrochloride[1] (I), trimethylanilinium hydroxide[2] in methanol (0.1 *M*), and 1,3-dimethyl-6-methoxy-4-(*p*-chlorophenyl)-1*H*-pyrazolo[3,4-*b*]pyridine[3] (II) as the internal standard were used as supplied. Ether[4] was anesthetic grade, and other chemicals were analytical reagent grade.

Instrumentation—A gas chromatograph[5], equipped with a ^{63}Ni-electron-capture detector containing a 2-mCu ^{63}Ni-β-ionization source, and an electronic integrator were used. The glass column was 1.21 m (4 ft) × 4 mm (i.d.), packed with 5% OV-225[6] on 80–100-mesh Gas Chrom Q[6]. The column was conditioned at 265° for at least 18 hr with a carrier gas [argon–methane[7] (95:5)] flow rate of 50 ml/min. The cylinder of the carrier gas was fitted with an oxygen trap filter[8].

The operating conditions were: column oven temperature, 265°; electron-capture detector temperature, 300°; injection port temperature, 270°; detector pulse interval, 150 μsec; electrometer range, 10^3; recorder presentation, 2 mv; and slope sensitivity, 0.3 mv/min. Under these conditions, the internal standard and chlordiazepoxide had retention times of 1.8 and 3.0 min, respectively (Fig. 1).

Table I—Assay Reproducibility

Serum Chlordiazepoxide Concentration, μg/ml	Calculated Serum Concentration[a], μg/ml	*RSD*, %
0	0	—
0.10	0.099 ± 0.0098	9.9
0.25	0.229 ± 0.062	27.2
0.75	0.758 ± 0.013	1.7
1.00	1.04 ± 0.14	13.7
1.50	1.48 ± 0.068	4.6

[a] Mean ± *SD* of triplicate determinations at each concentration.

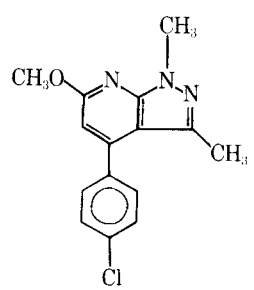

II

[1] Lot 351074, Hoffmann–La Roche, Nutley, N.J.
[2] Eastman Kodak Chemicals, Rochester, N.Y.
[3] Lot 3827-LRS-25, synthesized from methylation of Compound 22 in *J. Heterocycl. Chem.*, **12**, 1137 (1975).
[4] Mallinckrodt Chemicals, St. Louis, Mo.
[5] Hewlett-Packard model 7620A.
[6] Applied Science Laboratories, State College, Pa.
[7] Matheson Gas Products, Elk Grove Village, Ill.
[8] Altech Associates, Arlington Heights, Ill.

0022-3549/78/1100-1647$01.00/0

© 1978, American Pharmaceutical Association

Table II—Assay Sensitivity

Serum Chlordiazepoxide Concentration, μg/ml	Peak Area Ratio, Chlordiazepoxide to Internal Standard
0	0
0	0
0	0
0.10	0.09
0.10	0.11
0.10	0.11
0.25	0.23
0.25	0.34
0.25	0.20
0.50	0.55
0.50	0.56
0.75	0.88
0.75	0.87
0.75	0.90
1.00	1.29
1.00	1.35
1.00	1.03
1.50	1.72
1.50	1.82
1.50	1.66
Least-Squares Linear Regression Calculation (7)	
Slope	1.1841
y-Intercept ± 95% confidence limit	−0.0141 ± 0.0533
Correlation coefficient	0.993
Calculated sensitivity, μg/ml[a]	0.0450

[a] The calculated sensitivity was the x value (in concentration) corresponding to the upper part of the 95% confidence interval of the y-intercept (in peak area ratio).

Preparation of Standards—A serum standard at 1.5 μg/ml for chlordiazepoxide was prepared from a freshly prepared primary standard solution at 100 μg/ml in water. Other serum standards were prepared from serial dilutions (with serum) of the 1.5-μg/ml serum standard.

An internal standard solution at 3 μg/ml in 0.1 M K_2HPO_4 was prepared from an initial standard at 100 μg/ml in methanol.

Extraction Procedure—To a 15-ml conical glass centrifuge tube were added 1.0 ml of the internal standard solution, 0.4 ml of serum, and 3 ml of ether. After mixing[9] for 15 sec and centrifuging at 2500 rpm for 5 min at 10°, 2 ml of the organic layer (top) was transferred into a conical tube and evaporated to dryness at 40° with filtered air. The residue was reconstituted with 1 ml of 0.01 M trimethylanilinium hydroxide in methanol; after mixing, the solution was transferred into disposable GLC vials[10]. After the vial was capped, a 2-μl aliquot was injected into the gas chromatograph using an automatic sampler[11].

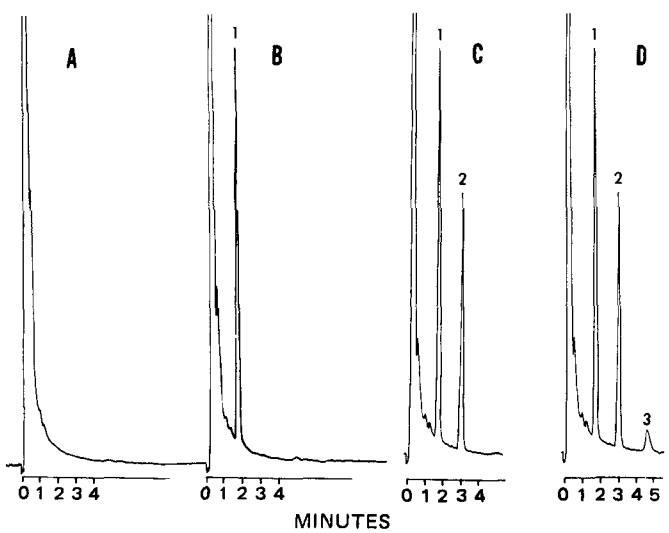

Figure 1—*GLC tracings of extracted serum samples. Key: A, serum blank; B, serum standard containing the internal standard; C, serum standard containing the internal standard and chlordiazepoxide at 0.6 μg/ml of serum; D, serum standard containing the internal standard, chlordiazepoxide, and demoxepam at 4 μg/ml of serum; peak 1, internal standard; peak 2, chlordiazepoxide; and peak 3, demoxepam.*

Table III—Assay Accuracy

Chlordiazepoxide Concentration, μg/ml		Percent Difference
Actual[a]	Calculated	
0.10	0.12	+20.0
0.25	0.21	−16.0
0.75	0.80	+6.7
1.00	1.04	+4.0
1.50	1.54	+2.7
0.62	0.60	−3.2
1.25	1.10	−12.0
0	0	0

[a] Serum spiked with chlordiazepoxide at the indicated concentrations.

Calculations—A calibration curve was constructed by plotting the peak area ratio (chlordiazepoxide to internal standard) against the serum chlordiazepoxide concentration. The unknowns were calculated using least-squares linear regression analysis.

RESULTS AND DISCUSSION

Figure 1 shows a chromatogram of an extract from 0.4 ml of serum spiked with chlordiazepoxide. Peak shapes were sharp and symmetrical. Injection of methanolic trimethylanilinium hydroxide solutions of chlordiazepoxide produced a thermal reaction in the injection port to give the methyl derivative. The flash-heater methylation technique was used previously for the barbiturates assay (5, 6).

The serum blank sample (Fig. 1) gave a very clean background on the chromatogram. The short retention time of chlordiazepoxide (R_t = 3.0 min) allows assay of many samples per day.

The precision of the assay is shown in Table I. Relative standard deviations ranged from 1.7 to 27.2%. The calculated sensitivity (Table II) was 0.045 μg/ml. The accuracy of this assay was estimated by analyzing eight spiked serum unknowns under "blind" conditions. The results (Table III) show good accuracy.

Demoxepam, a metabolite of chlordiazepoxide, also can be analyzed by this procedure. Under the same assay condition, its retention time was 4.4 min (Fig. 1) and the amount of demoxepam detectable was about 0.8 ng/injection.

REFERENCES

(1) J. A. F. de Silva, M. A. Schwartz, V. Stefanovic, J. Kaplan, and L. D'Arconte, *Anal. Chem.*, **36**, 2099 (1964).

(2) J. A. F. de Silva, B. A. Koechlin, and G. Bader, *J. Pharm. Sci.*, **55**, 692 (1966).

(3) I. A. Zingales, *J. Chromatogr.*, **61**, 237 (1971).

(4) J. A. F. de Silva, I. Bekersky, C. V. Puglisi, M. A. Brooks, and R. E. Weinfeld, *Anal. Chem.*, **48**, 10 (1976).

(5) G. W. Stevenson, *ibid.*, **38**, 1948 (1966).

(6) E. Brochmann-Hanssen and T. O. Oke, *J. Pharm. Sci.*, **58**, 370 (1969).

(7) A. Goldstein, "Biostatistics: An Introductory Text," Macmillan, New York, N.Y., 1967.

ACKNOWLEDGMENTS

Technical assistance from S. Kulkarni and helpful discussions with Dr. S. Borodkin are gratefully acknowledged.

[9] Maxi-Mix model M-16715, Thermodyne, Sybron Corp.
[10] Hewlett-Packard, Avondale, Pa.
[11] Hewlett-Packard model 7670A.

REVIEWS

Major Medicinal Plants: Botany, Culture and Uses. By JULIA F. MORTON. Charles C Thomas, 301-327 E. Lawrence Ave., Springfield, IL 62717. 1977. 429 pp. 17 × 25 cm. Price $49.50.

The forward by Norman R. Farnsworth and Maynard W. Quimby justifies the need for an authoritative current book on the subject of medicinal plants for pharmacy students, botanists, natural products chemists, and consumers. As stated in the introduction, the book is intended as a supplement to a pharmacology textbook, and its purpose is to delineate briefly but concisely the physical and chemical aspects of the major medicinal plants currently utilized in the United States.

To survey the literature on major medicinal plants in a single volume of about 400 pages is an enormous undertaking. Dr. Julia F. Morton has presented in this book a concise review on this subject. The book covers 28 plant families with 92 figures and 16 color illustrations. With the exception of several poor photoreproductions, *i.e.*, figures 28, 79, and 86 and color illustration 4, the printing is of exceptional quality in an otherwise error-free book.

The bibliography of 635 entries, although limited for such a large field, is relatively up to date and should be sufficient as a starting point for the student.

Principal subdivisions of the text are by plant family with minor subdivisions being botanical name, other names, family, descriptions, origin and distribution, constituents, propagation, cultivation, harvesting, medicinal uses, toxicity, other uses, and related species. In addition, there are two appendixes that list about 70 medicinal plants no longer official in the United States and about 60 plants that serve as pharmaceutical aids or adjuncts. The text makes a useful integration of the disciplines of pharmacognosy, botany, and chemistry.

Each section of the chapters is well balanced and contains a wealth of information. I highly recommend this book for students and professionals.

Reviewed by Phillip G. Vincent
Agricultural Environmental Quality Institute
Beltsville Agricultural Research Center
Beltsville, MD 20705

Progress in Drug Metabolism, Vol. 2. Edited by J. W. BRIDGES and L. F. CHASSEAUD. Wiley, 605 Third Ave., New York, NY 10016. 1977. ix + 348 pp. 15.5 × 23.5 cm. Price $29.50.

This volume is the second of a new series devoted to reviewing selected topics in the field of drug metabolism research. Thus far, as intended, these topics have been of a general nature, emphasizing principles, methods, and techniques applicable to a wide variety of drugs. The current volume, consisting of six chapters, offers a well-balanced selection of such material.

The first chapter, Newer Aspects of Glucuronidation, by G. J. Dutton and B. Burchell, deals primarily with the properties of UDP-glucuronyltransferase and factors affecting glucuronidation. Although this subject is reviewed often, the authors have presented an informative and particularly comprehensive account of recent work. Because of the vast amount of material reviewed (nearly 600 references, of which only 15% appeared before 1970) and the detailed presentation, this review may be more suitable for those experienced in drug metabolism research than for those just entering the field.

The next chapter, The Metabolism of Xenobiotics in Cell Suspensions and Cell Cultures, by J. R. Fry and J. W. Bridges, addresses a subject likely to be unfamiliar to many of those engaged in drug metabolism research. In a brief introduction, the authors compare the use of cell suspensions and cultures with *in vivo* and other *in vitro* methods for studying drug metabolism. They then discuss the preparation, characteristics, and application of isolated and cultured cells. This timely review should be particularly valuable to anyone engaged in drug metabolism research.

The third chapter, Transplacental Transfer of Foreign Compounds and their Metabolism by the Foetus, by O. Pelkonen, deals primarily with drug metabolism in the fetus and neonate. Throughout the review, species differences are emphasized, particularly the ability of the human fetus, in contrast to fetuses of common laboratory animals, to metabolize drugs.

The next two chapters deal with two important analytical techniques useful in drug metabolism research. The Role of Stable Isotopes in Drug Metabolism by D. R. Hawkins reviews the use of such isotopes for detecting and identifying metabolites, measuring drug and metabolite concentrations in biological fluids, and investigating metabolic pathways. Some general principles are presented, but much of the review is devoted to examples drawn from these three areas of application.

The second analytical technique reviewed, Ion-Pair Extraction Methods, by G. Schill *et al.* describes the use of ion-pair methods for batch extraction and partition chromatography of drugs and their metabolites. Both the principles and applications of the methods are discussed in detail. Substantially the same material has been presented by these authors in another review series also published during 1977.

The final chapter, Bioavailability and Drug Dissolution, by G. L. Mattock *et al.*, briefly describes concepts and methods for measuring drug dissolution and absorption and factors affecting these parameters. The major part of the chapter, however, is devoted to reviewing the application of these concepts and methods to studies with 23 drugs. Particular attention is given to possible correlations between a drug's bioavailability in humans and its *in vitro* dissolution rate.

The chapters comprising this second volume of "Progress in Drug Metabolism" were well selected by the editors and uniformly well written by the authors. Those with broad involvement in drug metabolism research should find the entire volume both interesting and valuable. Others, with a more specific involvement, will likely find most of the chapters interesting and, perhaps, certain ones valuable. Libraries should add this volume and, indeed, the entire series to their collection.

Reviewed by Richard C. Thomas
Drug Metabolism Research
The Upjohn Company
Kalamazoo, MI 49001

Inflammation and Antiinflammatories. By EDOARDO ARRIGONI-MARTELLI. Spectrum, 175-20 Wexford Terrace, Jamaica, NY 11432. 1977. 343 pp. 15 × 23 cm. Price $30.00.

"Inflammation and Antiinflammatories" is a comprehensive review covering the current theories on the etiology, pathology, and treatment of inflammation. It is a well-referenced book and is illustrated with appropriate tables and figures (the last figure in the book, No. 48, is for some reason poorly reproduced). The review will be most useful to pharmacologists, biochemists, and immunologists who have a sound background in the areas of inflammation and anti-inflammatories; it is too advanced for the novice in the area who is not familiar with the vernacular.

The review is well organized with an introductory chapter on the "Release of Mediators from Inflammatory Cells" followed by chapters on specific mediators of inflammation including histamine, serotonin, bradykinin, and prostaglandins. Each chapter discusses the chemistry, synthesis, and degradation of the mediator; the role of the mediator in the inflammatory response; and the present methods available for its assay.

Succeeding chapters discuss complement and properdin, slow reacting substances, lysosomal inflammatory materials, and nonantibody lymphocyte activation products (lymphokines). A chapter is also included on the cyclic nucleotides as modulators of inflammation.

Three chapters in the middle of the review are concerned with the experimental evaluation of anti-inflammatory agents and their clinical efficacy.

The third main part of the book deals with the anti-inflammatory agents currently in use or under investigation. Chapters cover the toxicity and proposed mechanisms of actions of nonsteroidal anti-inflammatory agents and immunosuppressive agents. Chapter 16, on nonsteroidal anti-inflammatory agents, is organized according to chemical class and is well illustrated with chemical structures.

While the review is comprehensive, the reader is often confronted with a large number of experimental, well-referenced observations without an attempt by the author to tie them together, although this is done at times.

REVIEWS

Major Medicinal Plants: Botany, Culture and Uses. By JULIA F. MORTON. Charles C Thomas, 301-327 E. Lawrence Ave., Springfield, IL 62717. 1977. 429 pp. 17 × 25 cm. Price $49.50.

The forward by Norman R. Farnsworth and Maynard W. Quimby justifies the need for an authoritative current book on the subject of medicinal plants for pharmacy students, botanists, natural products chemists, and consumers. As stated in the introduction, the book is intended as a supplement to a pharmacology textbook, and its purpose is to delineate briefly but concisely the physical and chemical aspects of the major medicinal plants currently utilized in the United States.

To survey the literature on major medicinal plants in a single volume of about 400 pages is an enormous undertaking. Dr. Julia F. Morton has presented in this book a concise review on this subject. The book covers 28 plant families with 92 figures and 16 color illustrations. With the exception of several poor photoreproductions, *i.e.*, figures 28, 79, and 86 and color illustration 4, the printing is of exceptional quality in an otherwise error-free book.

The bibliography of 635 entries, although limited for such a large field, is relatively up to date and should be sufficient as a starting point for the student.

Principal subdivisions of the text are by plant family with minor subdivisions being botanical name, other names, family, descriptions, origin and distribution, constituents, propagation, cultivation, harvesting, medicinal uses, toxicity, other uses, and related species. In addition, there are two appendixes that list about 70 medicinal plants no longer official in the United States and about 60 plants that serve as pharmaceutical aids or adjuncts. The text makes a useful integration of the disciplines of pharmacognosy, botany, and chemistry.

Each section of the chapters is well balanced and contains a wealth of information. I highly recommend this book for students and professionals.

Reviewed by Phillip G. Vincent
Agricultural Environmental Quality Institute
Beltsville Agricultural Research Center
Beltsville, MD 20705

Progress in Drug Metabolism, Vol. 2. Edited by J. W. BRIDGES and L. F. CHASSEAUD. Wiley, 605 Third Ave., New York, NY 10016. 1977. ix + 348 pp. 15.5 × 23.5 cm. Price $29.50.

This volume is the second of a new series devoted to reviewing selected topics in the field of drug metabolism research. Thus far, as intended, these topics have been of a general nature, emphasizing principles, methods, and techniques applicable to a wide variety of drugs. The current volume, consisting of six chapters, offers a well-balanced selection of such material.

The first chapter, Newer Aspects of Glucuronidation, by G. J. Dutton and B. Burchell, deals primarily with the properties of UDP-glucuronyltransferase and factors affecting glucuronidation. Although this subject is reviewed often, the authors have presented an informative and particularly comprehensive account of recent work. Because of the vast amount of material reviewed (nearly 600 references, of which only 15% appeared before 1970) and the detailed presentation, this review may be more suitable for those experienced in drug metabolism research than for those just entering the field.

The next chapter, The Metabolism of Xenobiotics in Cell Suspensions and Cell Cultures, by J. R. Fry and J. W. Bridges, addresses a subject likely to be unfamiliar to many of those engaged in drug metabolism research. In a brief introduction, the authors compare the use of cell suspensions and cultures with *in vivo* and other *in vitro* methods for studying drug metabolism. They then discuss the preparation, characteristics, and application of isolated and cultured cells. This timely review should be particularly valuable to anyone engaged in drug metabolism research.

The third chapter, Transplacental Transfer of Foreign Compounds and their Metabolism by the Foetus, by O. Pelkonen, deals primarily with drug metabolism in the fetus and neonate. Throughout the review, species differences are emphasized, particularly the ability of the human fetus, in contrast to fetuses of common laboratory animals, to metabolize drugs.

The next two chapters deal with two important analytical techniques useful in drug metabolism research. The Role of Stable Isotopes in Drug Metabolism by D. R. Hawkins reviews the use of such isotopes for detecting and identifying metabolites, measuring drug and metabolite concentrations in biological fluids, and investigating metabolic pathways. Some general principles are presented, but much of the review is devoted to examples drawn from these three areas of application.

The second analytical technique reviewed, Ion-Pair Extraction Methods, by G. Schill *et al.* describes the use of ion-pair methods for batch extraction and partition chromatography of drugs and their metabolites. Both the principles and applications of the methods are discussed in detail. Substantially the same material has been presented by these authors in another review series also published during 1977.

The final chapter, Bioavailability and Drug Dissolution, by G. L. Mattock *et al.*, briefly describes concepts and methods for measuring drug dissolution and absorption and factors affecting these parameters. The major part of the chapter, however, is devoted to reviewing the application of these concepts and methods to studies with 23 drugs. Particular attention is given to possible correlations between a drug's bioavailability in humans and its *in vitro* dissolution rate.

The chapters comprising this second volume of "Progress in Drug Metabolism" were well selected by the editors and uniformly well written by the authors. Those with broad involvement in drug metabolism research should find the entire volume both interesting and valuable. Others, with a more specific involvement, will likely find most of the chapters interesting and, perhaps, certain ones valuable. Libraries should add this volume and, indeed, the entire series to their collection.

Reviewed by Richard C. Thomas
Drug Metabolism Research
The Upjohn Company
Kalamazoo, MI 49001

Inflammation and Antiinflammatories. By EDOARDO ARRIGONI-MARTELLI. Spectrum, 175-20 Wexford Terrace, Jamaica, NY 11432. 1977. 343 pp. 15 × 23 cm. Price $30.00.

"Inflammation and Antiinflammatories" is a comprehensive review covering the current theories on the etiology, pathology, and treatment of inflammation. It is a well-referenced book and is illustrated with appropriate tables and figures (the last figure in the book, No. 48, is for some reason poorly reproduced). The review will be most useful to pharmacologists, biochemists, and immunologists who have a sound background in the areas of inflammation and anti-inflammatories; it is too advanced for the novice in the area who is not familiar with the vernacular.

The review is well organized with an introductory chapter on the "Release of Mediators from Inflammatory Cells" followed by chapters on specific mediators of inflammation including histamine, serotonin, bradykinin, and prostaglandins. Each chapter discusses the chemistry, synthesis, and degradation of the mediator; the role of the mediator in the inflammatory response; and the present methods available for its assay.

Succeeding chapters discuss complement and properdin, slow reacting substances, lysosomal inflammatory materials, and nonantibody lymphocyte activation products (lymphokines). A chapter is also included on the cyclic nucleotides as modulators of inflammation.

Three chapters in the middle of the review are concerned with the experimental evaluation of anti-inflammatory agents and their clinical efficacy.

The third main part of the book deals with the anti-inflammatory agents currently in use or under investigation. Chapters cover the toxicity and proposed mechanisms of actions of nonsteroidal anti-inflammatory agents and immunosuppressive agents. Chapter 16, on nonsteroidal anti-inflammatory agents, is organized according to chemical class and is well illustrated with chemical structures.

While the review is comprehensive, the reader is often confronted with a large number of experimental, well-referenced observations without an attempt by the author to tie them together, although this is done at times.

REVIEWS

Major Medicinal Plants: Botany, Culture and Uses. By JULIA F. MORTON. Charles C Thomas, 301-327 E. Lawrence Ave., Springfield, IL 62717. 1977. 429 pp. 17 × 25 cm. Price $49.50.

The forward by Norman R. Farnsworth and Maynard W. Quimby justifies the need for an authoritative current book on the subject of medicinal plants for pharmacy students, botanists, natural products chemists, and consumers. As stated in the introduction, the book is intended as a supplement to a pharmacology textbook, and its purpose is to delineate briefly but concisely the physical and chemical aspects of the major medicinal plants currently utilized in the United States.

To survey the literature on major medicinal plants in a single volume of about 400 pages is an enormous undertaking. Dr. Julia F. Morton has presented in this book a concise review on this subject. The book covers 28 plant families with 92 figures and 16 color illustrations. With the exception of several poor photoreproductions, *i.e.*, figures 28, 79, and 86 and color illustration 4, the printing is of exceptional quality in an otherwise error-free book.

The bibliography of 635 entries, although limited for such a large field, is relatively up to date and should be sufficient as a starting point for the student.

Principal subdivisions of the text are by plant family with minor subdivisions being botanical name, other names, family, descriptions, origin and distribution, constituents, propagation, cultivation, harvesting, medicinal uses, toxicity, other uses, and related species. In addition, there are two appendixes that list about 70 medicinal plants no longer official in the United States and about 60 plants that serve as pharmaceutical aids or adjuncts. The text makes a useful integration of the disciplines of pharmacognosy, botany, and chemistry.

Each section of the chapters is well balanced and contains a wealth of information. I highly recommend this book for students and professionals.

Reviewed by Phillip G. Vincent
Agricultural Environmental Quality Institute
Beltsville Agricultural Research Center
Beltsville, MD 20705

Progress in Drug Metabolism, Vol. 2. Edited by J. W. BRIDGES and L. F. CHASSEAUD. Wiley, 605 Third Ave., New York, NY 10016. 1977. ix + 348 pp. 15.5 × 23.5 cm. Price $29.50.

This volume is the second of a new series devoted to reviewing selected topics in the field of drug metabolism research. Thus far, as intended, these topics have been of a general nature, emphasizing principles, methods, and techniques applicable to a wide variety of drugs. The current volume, consisting of six chapters, offers a well-balanced selection of such material.

The first chapter, Newer Aspects of Glucuronidation, by G. J. Dutton and B. Burchell, deals primarily with the properties of UDP-glucuronyltransferase and factors affecting glucuronidation. Although this subject is reviewed often, the authors have presented an informative and particularly comprehensive account of recent work. Because of the vast amount of material reviewed (nearly 600 references, of which only 15% appeared before 1970) and the detailed presentation, this review may be more suitable for those experienced in drug metabolism research than for those just entering the field.

The next chapter, The Metabolism of Xenobiotics in Cell Suspensions and Cell Cultures, by J. R. Fry and J. W. Bridges, addresses a subject likely to be unfamiliar to many of those engaged in drug metabolism research. In a brief introduction, the authors compare the use of cell suspensions and cultures with *in vivo* and other *in vitro* methods for studying drug metabolism. They then discuss the preparation, characteristics, and application of isolated and cultured cells. This timely review should be particularly valuable to anyone engaged in drug metabolism research.

The third chapter, Transplacental Transfer of Foreign Compounds and their Metabolism by the Foetus, by O. Pelkonen, deals primarily with drug metabolism in the fetus and neonate. Throughout the review, species differences are emphasized, particularly the ability of the human fetus, in contrast to fetuses of common laboratory animals, to metabolize drugs.

The next two chapters deal with two important analytical techniques useful in drug metabolism research. The Role of Stable Isotopes in Drug Metabolism by D. R. Hawkins reviews the use of such isotopes for detecting and identifying metabolites, measuring drug and metabolite concentrations in biological fluids, and investigating metabolic pathways. Some general principles are presented, but much of the review is devoted to examples drawn from these three areas of application.

The second analytical technique reviewed, Ion-Pair Extraction Methods, by G. Schill *et al.* describes the use of ion-pair methods for batch extraction and partition chromatography of drugs and their metabolites. Both the principles and applications of the methods are discussed in detail. Substantially the same material has been presented by these authors in another review series also published during 1977.

The final chapter, Bioavailability and Drug Dissolution, by G. L. Mattock *et al.*, briefly describes concepts and methods for measuring drug dissolution and absorption and factors affecting these parameters. The major part of the chapter, however, is devoted to reviewing the application of these concepts and methods to studies with 23 drugs. Particular attention is given to possible correlations between a drug's bioavailability in humans and its *in vitro* dissolution rate.

The chapters comprising this second volume of "Progress in Drug Metabolism" were well selected by the editors and uniformly well written by the authors. Those with broad involvement in drug metabolism research should find the entire volume both interesting and valuable. Others, with a more specific involvement, will likely find most of the chapters interesting and, perhaps, certain ones valuable. Libraries should add this volume and, indeed, the entire series to their collection.

Reviewed by Richard C. Thomas
Drug Metabolism Research
The Upjohn Company
Kalamazoo, MI 49001

Inflammation and Antiinflammatories. By EDOARDO ARRIGONI-MARTELLI. Spectrum, 175-20 Wexford Terrace, Jamaica, NY 11432. 1977. 343 pp. 15 × 23 cm. Price $30.00.

"Inflammation and Antiinflammatories" is a comprehensive review covering the current theories on the etiology, pathology, and treatment of inflammation. It is a well-referenced book and is illustrated with appropriate tables and figures (the last figure in the book, No. 48, is for some reason poorly reproduced). The review will be most useful to pharmacologists, biochemists, and immunologists who have a sound background in the areas of inflammation and anti-inflammatories; it is too advanced for the novice in the area who is not familiar with the vernacular.

The review is well organized with an introductory chapter on the "Release of Mediators from Inflammatory Cells" followed by chapters on specific mediators of inflammation including histamine, serotonin, bradykinin, and prostaglandins. Each chapter discusses the chemistry, synthesis, and degradation of the mediator; the role of the mediator in the inflammatory response; and the present methods available for its assay.

Succeeding chapters discuss complement and properdin, slow reacting substances, lysosomal inflammatory materials, and nonantibody lymphocyte activation products (lymphokines). A chapter is also included on the cyclic nucleotides as modulators of inflammation.

Three chapters in the middle of the review are concerned with the experimental evaluation of anti-inflammatory agents and their clinical efficacy.

The third main part of the book deals with the anti-inflammatory agents currently in use or under investigation. Chapters cover the toxicity and proposed mechanisms of actions of nonsteroidal anti-inflammatory agents and immunosuppressive agents. Chapter 16, on nonsteroidal anti-inflammatory agents, is organized according to chemical class and is well illustrated with chemical structures.

While the review is comprehensive, the reader is often confronted with a large number of experimental, well-referenced observations without an attempt by the author to tie them together, although this is done at times.

Other criticisms include the placement of Chapter 16, "Non-Steroidal Antiinflammatory Agents." This chapter should logically precede and not succeed the other two chapters on nonsteroidal anti-inflammatories (Chapters 14 and 15).

In summary, "Inflammation and Antiinflammatories" is a well organized and well-written review on the current concepts of the field. It will prove a valuable resource to the laboratory investigator as well as to the clinician.

Reviewed by Russell Buchman
Diamond Shamrock Corporation
T. R. Evans Research Center
Painesville, OH 44077

Recent Advances in the Chemistry of β-Lactam Antibiotics. Edited by J. ELKS. The Chemical Society, Burlington House, London W1V OBN, England. 1977. 313 pp. 14 × 21 cm. Price $29.00.

This volume consists of 32 papers presented at a Chemical Society Symposium held in June 1976 in Cambridge, England. Included are two papers on the biosynthesis of β-lactams, nine papers dealing primarily with modification or incorporation of unique side chains on the penam or cephem nucleus, and 15 papers on the synthesis of the β-lactam ring systems or incorporation of substituents into the cephem or penam ring systems. While most papers in the last group deal with the synthesis of penicillins or cephalosporins, Ajay Bose discusses his general β-lactam synthesis. Also of special note are the papers outlining synthetic approaches to the biologically interesting 3-chloro and 3-hydroxy cephems.

The remaining six chapters include a paper on extraction of cephalosporins from fermentation broth, a chiroptical study of penicillinates, a study of the nonenzymatic hydrolysis of β-lactams, and a review by R. B. Woodward of the work at the Woodward Research Institute. Also included are one paper on the norcardicins, monocyclic β-lactams with antibacterial activity, and one paper covering clavulanic acid, a bicyclic β-lactam, which is a potent irreversible inhibitor of β-lactamase enzymes.

Although the prime emphasis of this volume is the chemistry of β-lactam antibiotics, nine chapters contain tables of antibacterial activity of various analogs. As with most symposium volumes, no subject or author indexes are included. With the exception of Woodward's article, which contains no references, the papers are for the most part adequately referenced (references into the early 1976 literature are included). As is expected in a symposium paper, some authors make liberal use of references to unpublished results.

This volume is a valuable updating of the voluminous literature on β-lactam antibiotic chemistry. It should prove to be a useful information source not only to individuals involved in antibiotic research but also to individuals with teaching responsibilities in this field.

Reviewed by Larry J. Powers
Diamond Shamrock Corporation
T. R. Evans Research Center
Painesville, OH 44077

NOTICES

Phenomenology and Treatment of Schizophrenia. Edited by WILLIAM E. FANN, ISMET KARACAN, ALEX D. POKORNY, and ROBERT L. WILLIAMS. Spectrum, 175-20 Wexford Terrace, Jamaica, NY 11432. 1978. 549 pp. 15 × 23 cm. Price $30.00.

Predicting the Properties of Mixtures: Mixture Rules in Science and Engineering. By LAWRENCE E. NIELSEN. Dekker, 270 Madison Ave., New York, NY 10016. 1978. 96 pp. 15 × 23 cm. Price $12.50.

Receptors in Pharmacology. (Modern Pharmacology-Toxicology Series, Vol. 11). Edited by JOHN R. SYMTHIES and RONALD J. BRADLEY, Jr. Dekker, 270 Madison Ave., New York, NY 10016. 1978. 506 pp. 15 × 23 cm. Price $45.00.

Current Chemotherapy. Vols. I and II. Proceedings of the 10th International Congress of Chemotherapy. Edited by WALTER SIEGENTHALER and RUEDI LUTHY. American Society for Microbiology, 1913 I St., N.W., Washington, DC 20006. 1978. Vol. I, 736 pp; Vol. II, 1361 pp. 17 × 26 cm. Price $75.00 (two-volume set).

Zinc and Copper in Clinical Medicine. Edited by K. MICHAEL HAMBIDGE and BUFORD L. NICHOLS, Jr. Spectrum, 175-20 Wexford Terrace, Jamaica, NY 11432. 1978. 132 pp. 15 × 23 cm. Price $15.00.

The Molecular Biology of Animal Viruses, Vol. 2. Edited by DEBI PROSAD NAYAK. Dekker, 270 Madison Ave., New York, NY 10016. 1978. 1006 pp. 15 × 23 cm. Price SFr. 140.—

pH Measurements. By C. CLARK WESTCOTT. Academic, 111 Fifth Ave., New York, NY 10003. 1978. 172 pp. 15 × 23 cm. Price $16.00.

Behavioral Neurology. 2nd Ed. By JONATHAN H. PINCUS and GARY J. TUCKER. Oxford University Press, 200 Madison Ave., New York, NY 10016. 1978. 284 pp. 12 × 21 cm. Price $5.95 (paper), $11.95 (cloth).

Behavioral Tolerance: Research and Treatment Implications. NIDA Research Monograph 18. Edited by NORMAN A. KRASNEGOR. National Institute on Drug Abuse, 5600 Fishers Lane, Rockville, MD 20852. 1978. 151 pp. 14 × 24 cm.

Neisseria gonorrhoeae and Gonococcal Infections. World Health Organization, 49 Sheridan Ave., Albany, NY 12210. 1978. 142 pp. 13 × 20 cm. Price $5.40.

Handbook of Clinical Pharmacology. By FELIX BOCHNER, GEORGE CARRUTHERS, JENS KAMPMANN, and JANICE STEINER. Little, Brown, 34 Beacon St., Boston, MA 02106. 1978. 313 pp. 11 × 20 cm. Price $9.95.

Handbook of Clinical Drug Data. 4th Ed. By JAMES E. KNOBEN, PHILIP O. ANDERSON, and ARTHUR S. WATANABE. Drug Intelligence Publications, Hamilton, IL 62341. 1978. 467 pp. 11 × 18 cm.

Nursing Pharmacology: A Systems Approach to Drug Therapy and Nursing Practice. By ALVIN K. SWONGER. Little, Brown, 34 Beacon St., Boston, MA 02106. 1978. 329 pp. 19 × 24 cm. Price $9.95.

Respiratory Tract Mucus. Ciba Foundation Symposium 54 (new series). Elsevier Scientific, 52 Vanderbilt Ave., New York, NY 10017. 1978. 334 pp. 16 × 24 cm.

The Economics of Medical Malpractice. Edited by SIMON ROTTENBERG. American Enterprise Institute for Public Policy Research, 1150 Seventeenth St., N. W., Washington DC 20036. 1978. 293 pp. 15 × 23 cm. Price $5.75.

Polymeric Drugs. Edited by L. GUY DONARUMA and OTTO VOGL. Academic, 111 Fifth Ave., New York, NY 10003. 1978. 397 pp. 15 × 23 cm. Price $19.50.

Mycotoxic Fungi, Mycotoxins, and Mycotoxicoses. An Encyclopedic Handbook, Vol. 2. Edited by THOMAS D. WYLLIE and LAWRENCE G. MOREHOUSE. Dekker, 270 Madison Ave., New York, NY 10016. 1978. 570 pp. 17 × 26 cm. Price $75.00.

Actualités Pharmacologiques. Edited by RENE HAZARD. Masson, 120 Boulevard Saint-Germain, 75280 Paris Cedex 06, France. 1978. 222 pp. 16 × 24 cm. Price 180 Fr.

The Biochemical Basis of Neuropharmacology, 3rd Ed. By JACK R. COOPER, FLOYD E. BLOOM, and ROBERT H. ROTH. Oxford University Press, 200 Madison Ave., New York, NY 10016. 1978. 327 pp. 13 × 21 cm. Price $6.95 (paper), $13.95 (cloth).

Advances in Chromatography, Vol. 16. Edited by J. CALVIN GIDDINGS, ELI GRUSHKA, JACK CAZES, and PHYLLIS R. BROWN. Dekker, 270 Madison Ave., New York, NY 10016. 1978. 290 pp. 14 × 23 cm. Price $28.75.

Further Perspectives in Organic Chemistry. Ciba Foundation Symposium 53 (new series). Elsevier North-Holland, 52 Vanderbilt Ave., New York, NY 10017. 1978. 212 pp. 16 × 24 cm.

Gaddum's Pharmacology. 8th Ed. By A. S. V. BURGEN and J. F. MITCHELL. Oxford University Press, 200 Madison Ave., New York, NY 10016. 1978. 269 pp. 15 × 24 cm. Price $11.95.

Ophthalmica. Band II. Pharmazeutische Grundlagen ihrer Zubereitung. By R. DOLDER and F. S. SKINNER. Wissenschaftliche Verlagsgesellschaft mbH 40, 7000 Stuttgart 1, Germany. 1978. 638 pp. 14 × 21 cm. Price $94.00.

Effectors of Thermogenesis. Proceedings of a Symposium Held at Geneva (Switzerland) 14–16 July 1977. Edited by G. GIRARDIER and J. SEYDOUX. Birkhauser Verlag, P. O. Box 34, CH-4010 Basel, Switzerland. 1978. 345 pp. 17 × 24 cm. Price Sfr. 68.

Other criticisms include the placement of Chapter 16, "Non-Steroidal Antiinflammatory Agents." This chapter should logically precede and not succeed the other two chapters on nonsteroidal anti-inflammatories (Chapters 14 and 15).

In summary, "Inflammation and Antiinflammatories" is a well organized and well-written review on the current concepts of the field. It will prove a valuable resource to the laboratory investigator as well as to the clinician.

Reviewed by Russell Buchman
Diamond Shamrock Corporation
T. R. Evans Research Center
Painesville, OH 44077

Recent Advances in the Chemistry of β-Lactam Antibiotics. Edited by J. ELKS. The Chemical Society, Burlington House, London W1V OBN, England. 1977. 313 pp. 14 × 21 cm. Price $29.00.

This volume consists of 32 papers presented at a Chemical Society Symposium held in June 1976 in Cambridge, England. Included are two papers on the biosynthesis of β-lactams, nine papers dealing primarily with modification or incorporation of unique side chains on the penam or cephem nucleus, and 15 papers on the synthesis of the β-lactam ring systems or incorporation of substituents into the cephem or penam ring systems. While most papers in the last group deal with the synthesis of penicillins or cephalosporins, Ajay Bose discusses his general β-lactam synthesis. Also of special note are the papers outlining synthetic approaches to the biologically interesting 3-chloro and 3-hydroxy cephems.

The remaining six chapters include a paper on extraction of cephalosporins from fermentation broth, a chiroptical study of penicillinates, a study of the nonenzymatic hydrolysis of β-lactams, and a review by R. B. Woodward of the work at the Woodward Research Institute. Also included are one paper on the norcardicins, monocyclic β-lactams with antibacterial activity, and one paper covering clavulanic acid, a bicyclic β-lactam, which is a potent irreversible inhibitor of β-lactamase enzymes.

Although the prime emphasis of this volume is the chemistry of β-lactam antibiotics, nine chapters contain tables of antibacterial activity of various analogs. As with most symposium volumes, no subject or author indexes are included. With the exception of Woodward's article, which contains no references, the papers are for the most part adequately referenced (references into the early 1976 literature are included). As is expected in a symposium paper, some authors make liberal use of references to unpublished results.

This volume is a valuable updating of the voluminous literature on β-lactam antibiotic chemistry. It should prove to be a useful information source not only to individuals involved in antibiotic research but also to individuals with teaching responsibilities in this field.

Reviewed by Larry J. Powers
Diamond Shamrock Corporation
T. R. Evans Research Center
Painesville, OH 44077

NOTICES

Phenomenology and Treatment of Schizophrenia. Edited by WILLIAM E. FANN, ISMET KARACAN, ALEX D. POKORNY, and ROBERT L. WILLIAMS. Spectrum, 175-20 Wexford Terrace, Jamaica, NY 11432. 1978. 549 pp. 15 × 23 cm. Price $30.00.

Predicting the Properties of Mixtures: Mixture Rules in Science and Engineering. By LAWRENCE E. NIELSEN. Dekker, 270 Madison Ave., New York, NY 10016. 1978. 96 pp. 15 × 23 cm. Price $12.50.

Receptors in Pharmacology. (Modern Pharmacology-Toxicology Series, Vol. 11). Edited by JOHN R. SYMTHIES and RONALD J. BRADLEY, Jr. Dekker, 270 Madison Ave., New York, NY 10016. 1978. 506 pp. 15 × 23 cm. Price $45.00.

Current Chemotherapy. Vols. I and II. Proceedings of the 10th International Congress of Chemotherapy. Edited by WALTER SIEGENTHALER and RUEDI LUTHY. American Society for Microbiology, 1913 I St., N.W., Washington, DC 20006. 1978. Vol. I, 736 pp; Vol. II, 1361 pp. 17 × 26 cm. Price $75.00 (two-volume set).

Zinc and Copper in Clinical Medicine. Edited by K. MICHAEL HAMBIDGE and BUFORD L. NICHOLS, Jr. Spectrum, 175-20 Wexford Terrace, Jamaica, NY 11432. 1978. 132 pp. 15 × 23 cm. Price $15.00.

The Molecular Biology of Animal Viruses, Vol. 2. Edited by DEBI PROSAD NAYAK. Dekker, 270 Madison Ave., New York, NY 10016. 1978. 1006 pp. 15 × 23 cm. Price SFr. 140.—

pH Measurements. By C. CLARK WESTCOTT. Academic, 111 Fifth Ave., New York, NY 10003. 1978. 172 pp. 15 × 23 cm. Price $16.00.

Behavioral Neurology. 2nd Ed. By JONATHAN H. PINCUS and GARY J. TUCKER. Oxford University Press, 200 Madison Ave., New York, NY 10016. 1978. 284 pp. 12 × 21 cm. Price $5.95 (paper), $11.95 (cloth).

Behavioral Tolerance: Research and Treatment Implications. NIDA Research Monograph 18. Edited by NORMAN A. KRASNEGOR. National Institute on Drug Abuse, 5600 Fishers Lane, Rockville, MD 20852. 1978. 151 pp. 14 × 24 cm.

Neisseria gonorrhoeae and Gonococcal Infections. World Health Organization, 49 Sheridan Ave., Albany, NY 12210. 1978. 142 pp. 13 × 20 cm. Price $5.40.

Handbook of Clinical Pharmacology. By FELIX BOCHNER, GEORGE CARRUTHERS, JENS KAMPMANN, and JANICE STEINER. Little, Brown, 34 Beacon St., Boston, MA 02106. 1978. 313 pp. 11 × 20 cm. Price $9.95.

Handbook of Clinical Drug Data. 4th Ed. By JAMES E. KNOBEN, PHILIP O. ANDERSON, and ARTHUR S. WATANABE. Drug Intelligence Publications, Hamilton, IL 62341. 1978. 467 pp. 11 × 18 cm.

Nursing Pharmacology: A Systems Approach to Drug Therapy and Nursing Practice. By ALVIN K. SWONGER. Little, Brown, 34 Beacon St., Boston, MA 02106. 1978. 329 pp. 19 × 24 cm. Price $9.95.

Respiratory Tract Mucus. Ciba Foundation Symposium 54 (new series). Elsevier Scientific, 52 Vanderbilt Ave., New York, NY 10017. 1978. 334 pp. 16 × 24 cm.

The Economics of Medical Malpractice. Edited by SIMON ROTTENBERG. American Enterprise Institute for Public Policy Research, 1150 Seventeenth St., N. W., Washington DC 20036. 1978. 293 pp. 15 × 23 cm. Price $5.75.

Polymeric Drugs. Edited by L. GUY DONARUMA and OTTO VOGL. Academic, 111 Fifth Ave., New York, NY 10003. 1978. 397 pp. 15 × 23 cm. Price $19.50.

Mycotoxic Fungi, Mycotoxins, and Mycotoxicoses. An Encyclopedic Handbook, Vol. 2. Edited by THOMAS D. WYLLIE and LAWRENCE G. MOREHOUSE. Dekker, 270 Madison Ave., New York, NY 10016. 1978. 570 pp. 17 × 26 cm. Price $75.00.

Actualités Pharmacologiques. Edited by RENE HAZARD. Masson, 120 Boulevard Saint-Germain, 75280 Paris Cedex 06, France. 1978. 222 pp. 16 × 24 cm. Price 180 Fr.

The Biochemical Basis of Neuropharmacology, 3rd Ed. By JACK R. COOPER, FLOYD E. BLOOM, and ROBERT H. ROTH. Oxford University Press, 200 Madison Ave., New York, NY 10016. 1978. 327 pp. 13 × 21 cm. Price $6.95 (paper), $13.95 (cloth).

Advances in Chromatography, Vol. 16. Edited by J. CALVIN GIDDINGS, ELI GRUSHKA, JACK CAZES, and PHYLLIS R. BROWN. Dekker, 270 Madison Ave., New York, NY 10016. 1978. 290 pp. 14 × 23 cm. Price $28.75.

Further Perspectives in Organic Chemistry. Ciba Foundation Symposium 53 (new series). Elsevier North-Holland, 52 Vanderbilt Ave., New York, NY 10017. 1978. 212 pp. 16 × 24 cm.

Gaddum's Pharmacology. 8th Ed. By A. S. V. BURGEN and J. F. MITCHELL. Oxford University Press, 200 Madison Ave., New York, NY 10016. 1978. 269 pp. 15 × 24 cm. Price $11.95.

Ophthalmica. Band II. Pharmazeutische Grundlagen ihrer Zubereitung. By R. DOLDER and F. S. SKINNER. Wissenschaftliche Verlagsgesellschaft mbH 40, 7000 Stuttgart 1, Germany. 1978. 638 pp. 14 × 21 cm. Price $94.00.

Effectors of Thermogenesis. Proceedings of a Symposium Held at Geneva (Switzerland) 14–16 July 1977. Edited by G. GIRARDIER and J. SEYDOUX. Birkhauser Verlag, P. O. Box 34, CH-4010 Basel, Switzerland. 1978. 345 pp. 17 × 24 cm. Price Sfr. 68.

Other criticisms include the placement of Chapter 16, "Non-Steroidal Antiinflammatory Agents." This chapter should logically precede and not succeed the other two chapters on nonsteroidal anti-inflammatories (Chapters 14 and 15).

In summary, "Inflammation and Antiinflammatories" is a well organized and well-written review on the current concepts of the field. It will prove a valuable resource to the laboratory investigator as well as to the clinician.

Reviewed by Russell Buchman
Diamond Shamrock Corporation
T. R. Evans Research Center
Painesville, OH 44077

Recent Advances in the Chemistry of β-Lactam Antibiotics. Edited by J. ELKS. The Chemical Society, Burlington House, London W1V OBN, England. 1977. 313 pp. 14 × 21 cm. Price $29.00.

This volume consists of 32 papers presented at a Chemical Society Symposium held in June 1976 in Cambridge, England. Included are two papers on the biosynthesis of β-lactams, nine papers dealing primarily with modification or incorporation of unique side chains on the penam or cephem nucleus, and 15 papers on the synthesis of the β-lactam ring systems or incorporation of substituents into the cephem or penam ring systems. While most papers in the last group deal with the synthesis of penicillins or cephalosporins, Ajay Bose discusses his general β-lactam synthesis. Also of special note are the papers outlining synthetic approaches to the biologically interesting 3-chloro and 3-hydroxy cephems.

The remaining six chapters include a paper on extraction of cephalosporins from fermentation broth, a chiroptical study of penicillinates, a study of the nonenzymatic hydrolysis of β-lactams, and a review by R. B. Woodward of the work at the Woodward Research Institute. Also included are one paper on the norcardicins, monocyclic β-lactams with antibacterial activity, and one paper covering clavulanic acid, a bicyclic β-lactam, which is a potent irreversible inhibitor of β-lactamase enzymes.

Although the prime emphasis of this volume is the chemistry of β-lactam antibiotics, nine chapters contain tables of antibacterial activity of various analogs. As with most symposium volumes, no subject or author indexes are included. With the exception of Woodward's article, which contains no references, the papers are for the most part adequately referenced (references into the early 1976 literature are included). As is expected in a symposium paper, some authors make liberal use of references to unpublished results.

This volume is a valuable updating of the voluminous literature on β-lactam antibiotic chemistry. It should prove to be a useful information source not only to individuals involved in antibiotic research but also to individuals with teaching responsibilities in this field.

Reviewed by Larry J. Powers
Diamond Shamrock Corporation
T. R. Evans Research Center
Painesville, OH 44077

NOTICES

Phenomenology and Treatment of Schizophrenia. Edited by WILLIAM E. FANN, ISMET KARACAN, ALEX D. POKORNY, and ROBERT L. WILLIAMS. Spectrum, 175-20 Wexford Terrace, Jamaica, NY 11432. 1978. 549 pp. 15 × 23 cm. Price $30.00.

Predicting the Properties of Mixtures: Mixture Rules in Science and Engineering. By LAWRENCE E. NIELSEN. Dekker, 270 Madison Ave., New York, NY 10016. 1978. 96 pp. 15 × 23 cm. Price $12.50.

Receptors in Pharmacology. (Modern Pharmacology-Toxicology Series, Vol. 11). Edited by JOHN R. SYMTHIES and RONALD J. BRADLEY, Jr. Dekker, 270 Madison Ave., New York, NY 10016. 1978. 506 pp. 15 × 23 cm. Price $45.00.

Current Chemotherapy. Vols. I and II. Proceedings of the 10th International Congress of Chemotherapy. Edited by WALTER SIEGENTHALER and RUEDI LUTHY. American Society for Microbiology, 1913 I St., N.W., Washington, DC 20006. 1978. Vol. I, 736 pp; Vol. II, 1361 pp. 17 × 26 cm. Price $75.00 (two-volume set).

Zinc and Copper in Clinical Medicine. Edited by K. MICHAEL HAMBIDGE and BUFORD L. NICHOLS, Jr. Spectrum, 175-20 Wexford Terrace, Jamaica, NY 11432. 1978. 132 pp. 15 × 23 cm. Price $15.00.

The Molecular Biology of Animal Viruses, Vol. 2. Edited by DEBI PROSAD NAYAK. Dekker, 270 Madison Ave., New York, NY 10016. 1978. 1006 pp. 15 × 23 cm. Price SFr. 140.—

pH Measurements. By C. CLARK WESTCOTT. Academic, 111 Fifth Ave., New York, NY 10003. 1978. 172 pp. 15 × 23 cm. Price $16.00.

Behavioral Neurology. 2nd Ed. By JONATHAN H. PINCUS and GARY J. TUCKER. Oxford University Press, 200 Madison Ave., New York, NY 10016. 1978. 284 pp. 12 × 21 cm. Price $5.95 (paper), $11.95 (cloth).

Behavioral Tolerance: Research and Treatment Implications. NIDA Research Monograph 18. Edited by NORMAN A. KRASNEGOR. National Institute on Drug Abuse, 5600 Fishers Lane, Rockville, MD 20852. 1978. 151 pp. 14 × 24 cm.

Neisseria gonorrhoeae and Gonococcal Infections. World Health Organization, 49 Sheridan Ave., Albany, NY 12210. 1978. 142 pp. 13 × 20 cm. Price $5.40.

Handbook of Clinical Pharmacology. By FELIX BOCHNER, GEORGE CARRUTHERS, JENS KAMPMANN, and JANICE STEINER. Little, Brown, 34 Beacon St., Boston, MA 02106. 1978. 313 pp. 11 × 20 cm. Price $9.95.

Handbook of Clinical Drug Data. 4th Ed. By JAMES E. KNOBEN, PHILIP O. ANDERSON, and ARTHUR S. WATANABE. Drug Intelligence Publications, Hamilton, IL 62341. 1978. 467 pp. 11 × 18 cm.

Nursing Pharmacology: A Systems Approach to Drug Therapy and Nursing Practice. By ALVIN K. SWONGER. Little, Brown, 34 Beacon St., Boston, MA 02106. 1978. 329 pp. 19 × 24 cm. Price $9.95.

Respiratory Tract Mucus. Ciba Foundation Symposium 54 (new series). Elsevier Scientific, 52 Vanderbilt Ave., New York, NY 10017. 1978. 334 pp. 16 × 24 cm.

The Economics of Medical Malpractice. Edited by SIMON ROTTENBERG. American Enterprise Institute for Public Policy Research, 1150 Seventeenth St., N. W., Washington DC 20036. 1978. 293 pp. 15 × 23 cm. Price $5.75.

Polymeric Drugs. Edited by L. GUY DONARUMA and OTTO VOGL. Academic, 111 Fifth Ave., New York, NY 10003. 1978. 397 pp. 15 × 23 cm. Price $19.50.

Mycotoxic Fungi, Mycotoxins, and Mycotoxicoses. An Encyclopedic Handbook, Vol. 2. Edited by THOMAS D. WYLLIE and LAWRENCE G. MOREHOUSE. Dekker, 270 Madison Ave., New York, NY 10016. 1978. 570 pp. 17 × 26 cm. Price $75.00.

Actualités Pharmacologiques. Edited by RENE HAZARD. Masson, 120 Boulevard Saint-Germain, 75280 Paris Cedex 06, France. 1978. 222 pp. 16 × 24 cm. Price 180 Fr.

The Biochemical Basis of Neuropharmacology, 3rd Ed. By JACK R. COOPER, FLOYD E. BLOOM, and ROBERT H. ROTH. Oxford University Press, 200 Madison Ave., New York, NY 10016. 1978. 327 pp. 13 × 21 cm. Price $6.95 (paper), $13.95 (cloth).

Advances in Chromatography, Vol. 16. Edited by J. CALVIN GIDDINGS, ELI GRUSHKA, JACK CAZES, and PHYLLIS R. BROWN. Dekker, 270 Madison Ave., New York, NY 10016. 1978. 290 pp. 14 × 23 cm. Price $28.75.

Further Perspectives in Organic Chemistry. Ciba Foundation Symposium 53 (new series). Elsevier North-Holland, 52 Vanderbilt Ave., New York, NY 10017. 1978. 212 pp. 16 × 24 cm.

Gaddum's Pharmacology. 8th Ed. By A. S. V. BURGEN and J. F. MITCHELL. Oxford University Press, 200 Madison Ave., New York, NY 10016. 1978. 269 pp. 15 × 24 cm. Price $11.95.

Ophthalmica. Band II. Pharmazeutische Grundlagen ihrer Zubereitung. By R. DOLDER and F. S. SKINNER. Wissenschaftliche Verlagsgesellschaft mbH 40, 7000 Stuttgart 1, Germany. 1978. 638 pp. 14 × 21 cm. Price $94.00.

Effectors of Thermogenesis. Proceedings of a Symposium Held at Geneva (Switzerland) 14–16 July 1977. Edited by G. GIRARDIER and J. SEYDOUX. Birkhauser Verlag, P. O. Box 34, CH-4010 Basel, Switzerland. 1978. 345 pp. 17 × 24 cm. Price Sfr. 68.

DECEMBER 1978
VOLUME 67 NUMBER 12

JOURNAL OF PHARMACEUTICAL SCIENCES

MARY H. FERGUSON
Editor

SHELLY ELLIOTT
Production Editor

JANIS KELLY
Copy Editor

EDWARD G. FELDMANN
Contributing Editor

SAMUEL W. GOLDSTEIN
Contributing Editor

BELLE R. BECK
Editorial Secretary

DAVID BOHARDT
Director of Publications

L. LUAN CORRIGAN
Assistant Director of Publications

EDITORIAL ADVISORY BOARD

JOHN AUTIAN
NORMAN R. FARNSWORTH
WILLIAM O. FOYE
WILLIAM J. JUSKO
HERBERT A. LIEBERMAN
DAVID E. MANN, JR.
GERALD J. PAPARIELLO
EDWARD G. RIPPIE

The *Journal of Pharmaceutical Sciences* is published monthly by the American Pharmaceutical Association (APhA) at 2215 Constitution Ave., N.W., Washington, DC 20037. Second-class postage paid at Washington, D.C., and at additional mailing office.

All expressions of opinion and statements of supposed fact appearing in articles or editorials carried in this journal are published on the authority of the writer over whose name they appear and are not to be regarded as necessarily expressing the policies or views of APhA.

Offices—Editorial, Advertising, and Subscription: 2215 Constitution Ave., N.W., Washington, DC 20037. Printing: 20th & Northampton Streets, Easton, PA 18042.

Annual Subscriptions—United States and foreign, industrial and government institutions $50, educational institutions $50, individuals *for personal use only* $30; single copies $5. All foreign subscriptions add $5 for postage. Subscription rates are subject to change without notice. Members of APhA may elect to receive the *Journal of Pharmaceutical Sciences* as a part of their annual $70 (foreign $75) APhA membership dues.

Claims—Missing numbers will not be supplied if dues or subscriptions are in arrears for more than 60 days or if claims are received more than 60 days after the date of the issue, or if loss was due to failure to give notice of change of address. APhA cannot accept responsibility for foreign delivery when its records indicate shipment has been made.

Change of Address—Members and subscribers should notify at once both the Post Office and APhA of any change of address.

Photocopying—The code at the foot of the first page of an article indicates that APhA has granted permission for copying of the article beyond the limits permitted by Sections 107 and 108 of the U.S. Copyright Law provided that the copier sends the per copy fee stated in the code to the Copyright Clearance Center, Inc., P. O. Box 765, Schenectady, NY 12301. Copies may be made for personal or internal use only and not for general distribution.

Microfilm—Available from University Microfilms International, 300 N. Zeeb Road, Ann Arbor, MI 48106.

© Copyright 1978. American Pharmaceutical Association, 2215 Constitution Ave., N.W., Washington, DC 20037; all rights reserved.

TOWARD A UNIFORM LEVEL OF PERFORMANCE

No one likes to be told how to perform. On the other hand, almost everyone feels that it is perfectly proper to tell others how they should conduct themselves.

For example, we subscribe to the idea of having speed limits posted on our roads and highways. But we feel these restrictions are needed "for the other guy," who often doesn't have sense to drive with care. For ourselves, such restrictions are not necessary even though we may exceed the speed limit and mentally justify doing so by reminding ourselves that our own superior driving skill makes it all right. It is simply human nature to rationalize things in this manner.

The September 29 issue of the *Federal Register* carried a 75-page edict telling an entire industry how to perform in the day-to-day business of manufacturing its products. The product involved is drugs; the industry is the pharmaceutical manufacturers; and the government agency spelling out the rules is the federal Food and Drug Administration.

The rules themselves are formally titled Current Good Manufacturing Practice (CGMP) regulations; they are more commonly known and referred to as "GMPs." Most of our readers are at least casually familiar with the term but have only a vague idea of their impact and bearing on the drug manufacturing operation.

The GMPs first came into being in 1963 as a result of a new provision which was added to the Federal Food, Drug, and Cosmetic Act as part of the 1962 Kefauver–Harris Drug Amendments. Those original 1963 regulations were pretty skimpy by today's standards, and over the years they have undergone the normal process of refinement and expansion to flesh out and to fine tune the original set of rules. In making such changes, the FDA also has tried to consider new technology both in drug product manufacturing and in assessing quality of drug products.

Until this year, the last such revision was completed in 1971, so a thorough overhaul of the GMPs had become timely. However, the result did not come about overnight. The preamble statement in the September 29 document includes a brief historical account of the stepwise adoption of these finalized regulations, beginning with the initial draft version proposed in February 1976. Moreover, some related actions on specific aspects of manufacturing practice—such as how to deal with returned and salvaged drug products—dated back to January 1975.

The general purpose of the GMPs is to establish requirements for such matters as the adequacy of drug processing facilities, the training of personnel working in drug plants, quality assurance procedures, and company procedures for handling consumer complaints.

The big focus of the revised regulations seems to stress the need for companies to adhere strictly to modern quality control practices in drug product manufacture. They mandate the inclusion of a quality assurance unit in each manufacturing plant, with full authority to accept or reject all raw materials as well as finished products. They require special batch-by-batch evaluations at specified time intervals for the purpose of identifying the need for new manufacturing specifications or for changes in manufacturing or quality controls. They require the inclusion of expiration dates on practically all drug products.

So much for the content of the GMPs. What will be their impact or effect?

For the drug industry, they will mean more tests to perform, more records to keep, more analysts to hire, more borderline batches of products to reject. For some companies, the impact will be relatively minor—they have been doing much of this already. For some others, the impact will be much greater. All will be affected to some degree, and all will be forced up to a new standard of performance and acceptability.

Many in the industry probably will feel that—as in the example of the speed laws mentioned above—the requirements are needed for their competitors but not for them. Perhaps so. But whether needed or not, they do need to apply to all manufacturers.

For too long, pharmacists and others have been asked to judge and select drug products on the basis of the ethereal concept of "reputable manufacturers." It is time to separate the sheep and the goats. There is room in the American drug marketplace for only reputable manufacturers, and the new GMPs should go a long way toward creating and assuring that single standard of performance.

—EGF

DECEMBER 1978
VOLUME 67 NUMBER 12

JOURNAL OF PHARMACEUTICAL SCIENCES

MARY H. FERGUSON
Editor

SHELLY ELLIOTT
Production Editor

JANIS KELLY
Copy Editor

EDWARD G. FELDMANN
Contributing Editor

SAMUEL W. GOLDSTEIN
Contributing Editor

BELLE R. BECK
Editorial Secretary

DAVID BOHARDT
Director of Publications

L. LUAN CORRIGAN
Assistant Director of Publications

EDITORIAL ADVISORY BOARD

JOHN AUTIAN
NORMAN R. FARNSWORTH
WILLIAM O. FOYE
WILLIAM J. JUSKO
HERBERT A. LIEBERMAN
DAVID E. MANN, JR.
GERALD J. PAPARIELLO
EDWARD G. RIPPIE

The *Journal of Pharmaceutical Sciences* is published monthly by the American Pharmaceutical Association (APhA) at 2215 Constitution Ave., N.W., Washington, DC 20037. Second-class postage paid at Washington, D.C., and at additional mailing office.

All expressions of opinion and statements of supposed fact appearing in articles or editorials carried in this journal are published on the authority of the writer over whose name they appear and are not to be regarded as necessarily expressing the policies or views of APhA.

Offices—Editorial, Advertising, and Subscription: 2215 Constitution Ave., N.W., Washington, DC 20037. Printing: 20th & Northampton Streets, Easton, PA 18042.

Annual Subscriptions—United States and foreign, industrial and government institutions $50, educational institutions $50, individuals *for personal use only* $30; single copies $5. All foreign subscriptions add $5 for postage. Subscription rates are subject to change without notice. Members of APhA may elect to receive the *Journal of Pharmaceutical Sciences* as a part of their annual $70 (foreign $75) APhA membership dues.

Claims—Missing numbers will not be supplied if dues or subscriptions are in arrears for more than 60 days or if claims are received more than 60 days after the date of the issue, or if loss was due to failure to give notice of change of address. APhA cannot accept responsibility for foreign delivery when its records indicate shipment has been made.

Change of Address—Members and subscribers should notify at once both the Post Office and APhA of any change of address.

Photocopying—The code at the foot of the first page of an article indicates that APhA has granted permission for copying of the article beyond the limits permitted by Sections 107 and 108 of the U.S. Copyright Law provided that the copier sends the per copy fee stated in the code to the Copyright Clearance Center, Inc., P. O. Box 765, Schenectady, NY 12301. Copies may be made for personal or internal use only and not for general distribution.

Microfilm—Available from University Microfilms International, 300 N. Zeeb Road, Ann Arbor, MI 48106.

© Copyright 1978. American Pharmaceutical Association, 2215 Constitution Ave., N.W., Washington, DC 20037; all rights reserved.

TOWARD A UNIFORM LEVEL OF PERFORMANCE

No one likes to be told how to perform. On the other hand, almost everyone feels that it is perfectly proper to tell others how they should conduct themselves.

For example, we subscribe to the idea of having speed limits posted on our roads and highways. But we feel these restrictions are needed "for the other guy," who often doesn't have sense to drive with care. For ourselves, such restrictions are not necessary even though we may exceed the speed limit and mentally justify doing so by reminding ourselves that our own superior driving skill makes it all right. It is simply human nature to rationalize things in this manner.

The September 29 issue of the *Federal Register* carried a 75-page edict telling an entire industry how to perform in the day-to-day business of manufacturing its products. The product involved is drugs; the industry is the pharmaceutical manufacturers; and the government agency spelling out the rules is the federal Food and Drug Administration.

The rules themselves are formally titled Current Good Manufacturing Practice (CGMP) regulations; they are more commonly known and referred to as "GMPs." Most of our readers are at least casually familiar with the term but have only a vague idea of their impact and bearing on the drug manufacturing operation.

The GMPs first came into being in 1963 as a result of a new provision which was added to the Federal Food, Drug, and Cosmetic Act as part of the 1962 Kefauver–Harris Drug Amendments. Those original 1963 regulations were pretty skimpy by today's standards, and over the years they have undergone the normal process of refinement and expansion to flesh out and to fine tune the original set of rules. In making such changes, the FDA also has tried to consider new technology both in drug product manufacturing and in assessing quality of drug products.

Until this year, the last such revision was completed in 1971, so a thorough overhaul of the GMPs had become timely. However, the result did not come about overnight. The preamble statement in the September 29 document includes a brief historical account of the stepwise adoption of these finalized regulations, beginning with the initial draft version proposed in February 1976. Moreover, some related actions on specific aspects of manufacturing practice—such as how to deal with returned and salvaged drug products—dated back to January 1975.

The general purpose of the GMPs is to establish requirements for such matters as the adequacy of drug processing facilities, the training of personnel working in drug plants, quality assurance procedures, and company procedures for handling consumer complaints.

The big focus of the revised regulations seems to stress the need for companies to adhere strictly to modern quality control practices in drug product manufacture. They mandate the inclusion of a quality assurance unit in each manufacturing plant, with full authority to accept or reject all raw materials as well as finished products. They require special batch-by-batch evaluations at specified time intervals for the purpose of identifying the need for new manufacturing specifications or for changes in manufacturing or quality controls. They require the inclusion of expiration dates on practically all drug products.

So much for the content of the GMPs. What will be their impact or effect?

For the drug industry, they will mean more tests to perform, more records to keep, more analysts to hire, more borderline batches of products to reject. For some companies, the impact will be relatively minor—they have been doing much of this already. For some others, the impact will be much greater. All will be affected to some degree, and all will be forced up to a new standard of performance and acceptability.

Many in the industry probably will feel that—as in the example of the speed laws mentioned above—the requirements are needed for their competitors but not for them. Perhaps so. But whether needed or not, they do need to apply to all manufacturers.

For too long, pharmacists and others have been asked to judge and select drug products on the basis of the ethereal concept of "reputable manufacturers." It is time to separate the sheep and the goats. There is room in the American drug marketplace for only reputable manufacturers, and the new GMPs should go a long way toward creating and assuring that single standard of performance.

—EGF

JOURNAL OF PHARMACEUTICAL SCIENCES

DECEMBER 1978
VOLUME 67 NUMBER 12

RESEARCH ARTICLES

Rapid Attainment of Successively Higher Steady-State Plasma Levels Using the Wagner Two-Step Infusion Method

JAMES J. ZIMMERMAN

Received August 15, 1977, from the *Department of Pharmaceutics, School of Pharmacy, Temple University, Philadelphia, PA 19140.* Accepted for publication March 24, 1978.

Abstract □ The Wagner equation describing the plasma concentration–time relationship for the two-step infusion method is presented in general form for application to both the fast and slow infusion phases of single- and multiple-cycle infusions. The generalized parameters C (steady-state concentration), Q (infusion rate), A (amount of drug), and t' (time) are defined for each case. Plasma concentrations are simulated for a hypothetical two-compartment drug, X, to illustrate the uses of the equation and to examine error effects in the Q^F/Q^S ratio, T, and k_{e1}. For the single-cycle case, it is shown that positive or negative (±) errors in Q^F/Q^S and T delay the approach to the steady-state plasma value, C_1^{ss}, but such errors would not be of clinical importance when they are $\leq \pm 2.5\%$. Errors in k_{e1} prevent attainment of C_1^{ss} and more greatly affect the plasma concentration at the end of the dose cycle, $C_1^{\prime}$, than do the same errors in Q^F/Q^S or T. Therefore, the use of an average population value for k_{e1} instead of the actual patient value is more likely to produce large deviations from C_1^{ss} than experimental errors in flow rate and T. The utility of the two-step infusion method in reaching successively higher steady-state values, $C_{1,(n)}^{ss}$, for drugs with a high therapeutic index is also demonstrated for drug X over a range of multiple cycles. The examination of error effects for the multiple-cycle case revealed that errors in Q^F/Q^S and T yield $C_{1,(n)}^{\prime}$ values that tend to converge toward the desired value of $C_{1,(n)}^{ss}$ as the dose cycle increases, while such errors in k_{e1} yield $C_{1,(n)}^{\prime}$ values that increasingly diverge from $C_{1,(n)}^{ss}$ as dosing increases. Thus, individual patient differences as reflected in k_{e1} become increasingly more important as a source of error in $C_{1,(n)}^{\prime}$ with successively higher dosing, while experimental errors in Q^F/Q^S become less important.

Keyphrases □ Plasma levels—successively higher at steady state, obtained using two-step infusion method, simulated data for hypothetical drug □ Infusion methods, two step—used to obtain successively higher plasma levels at steady state, simulated data for hypothetical drug □ Pharmacokinetics—successively higher plasma levels at steady state obtained using two-step infusion method, simulated data for hypothetical drug

Methods for reducing the characteristic slow approach to steady state for drugs administered by infusion include: A, an initial intravenous (1, 2) or intramuscular (3) loading dose followed by a constant rate infusion; B, a two-step infusion process using two consecutive constant rate infusions (4, 5); and C, an initial intravenous loading dose followed by a real or simulated exponential infusion (6).

The loading dose methods (A) have the disadvantage of exhibiting a large early overshoot component in reaching the steady state (2) or mimicking the usual infusion process by eventually exhibiting a slow approach to the steady state (1, 3). These disadvantages are potentially minimized by Methods B and C. Method C (6), however, is difficult to employ since it requires either a special pump capable of exponential delivery or a series of consecutive constant rate infusions to simulate an exponential input.

The two-step infusion method of Wagner (4) appears to be the most ideal, because of its relative ease of employment and potential for producing a rapid steady state. While an overshoot component is associated with the two-step infusion method, the degree of overshoot can be predetermined and, therefore, controlled.

The purpose of this report is to expand upon the Wagner method to demonstrate its utility in attaining successively higher steady-state plasma levels for cases where a drug must be given at successively higher doses to achieve continued therapeutic response. The effect of error in key pharmacokinetic parameters on the simulated plasma concentrations is also examined.

THEORETICAL

Use of the two-step infusion method requires that an initial fast infusion rate, Q^F, be employed for a time interval, T, after which the infusion rate is immediately reduced to a slower infusion rate, Q^S, to attain and maintain the desired steady-state plasma level. At T, the plasma concentration, C_1^{max}, will be greater than the steady-state plasma level, C_1^{ss}, producing the overshoot component mentioned. The relative overshoot, C_1^{max}/C_1^{ss}, defined by Eq. 1 (4) is dependent on T and the kinetic constants α, β, and k_{e1} for a two-compartment drug (7):

$$\frac{C_1^{max}}{C_1^{ss}} = \frac{1}{1-e^{-\beta T}}\left[1 - \left\{\frac{k_{e1}-\beta}{\alpha-\beta}\right\}e^{-\alpha T} - \left\{\frac{\alpha-k_{e1}}{\alpha-\beta}\right\}e^{-\beta T}\right] \quad \text{(Eq. 1)}$$

Any degree of overshoot can be selected, depending on the choice of T.

0022-3549/78/1200-1651$01.00/0
© 1978, American Pharmaceutical Association

In general, the larger T is, the smaller is the overshoot. The required value of T can be obtained by inserting the values of α, β, and k_{e1} into Eq. 1 and subsequently varying T to obtain the desired relative overshoot.

The plasma concentration, C_1, of a two-compartment drug administered by the two-step infusion method is expressed in general form by:

$$C_1 = C + \left\{\frac{(k_{21}-\alpha)(Q-\alpha A_1)-\alpha k_{21}A_2}{\alpha(\alpha-\beta)V_1}\right\} e^{-\alpha t'} - \left\{\frac{(k_{21}-\beta)(Q-\beta A_1)-\beta k_{21}A_2}{\beta(\alpha-\beta)V_1}\right\} e^{-\beta t'} \quad \text{(Eq. 2)}$$

where subscripts 1 and 2 refer to the central and peripheral compartments, respectively; A represents the amount of drug in the respective compartments; and Q represents either Q^F or Q^S, depending on whether the concentration being calculated is that of the fast or slow infusion phase. The values of C, Q, A, and t' are defined differently within the fast and slow phases of single- and multiple-cycle cases.

Single Cycle—*Fast Phase*—Within the fast phase of a single cycle, the value of C in Eq. 2 becomes $C_1^{ss'}$ (Eq. 3), the hypothetical plasma concentration that results if the fast infusion rate, Q^F, is allowed to proceed to steady state:

$$C_1^{ss'} = Q^F/V_1k_{e1} \quad \text{(Eq. 3)}$$

where Q^F is given by (4):

$$Q^F = Q^S/(1-e^{-\beta T}) \quad \text{(Eq. 4)}$$

and Q^S is defined by:

$$Q^S = C_1^{ss}V_1k_{e1} \quad \text{(Eq. 5)}$$

where C_1^{ss} is the desired steady-state plasma concentration. Furthermore, t' assumes values from $0 \rightarrow T$, and the constants A_1 and $A_2 = 0$.

Slow Phase—Within the slow phase of a single cycle, the value of C in Eq. 2 becomes C_1^{ss}, Q is substituted by Q^S (Eq. 5), and t' is given by:

$$t' = t - T \quad \text{(Eq. 6)}$$

where t is the continuous time period within the fast–slow infusion cycle and T is the required value calculated from Eq. 1. The values of A_1 and A_2 are equal to A_1^T (Eq. 7) and A_2^T (Eq. 8), respectively (4):

$$A_1^T = \frac{Q^F}{k_{e1}} + \left\{\frac{Q^F(k_{21}-\alpha)}{\alpha(\alpha-\beta)}\right\} e^{-\alpha T} - \left\{\frac{Q^F(k_{21}-\beta)}{\beta(\alpha-\beta)}\right\} e^{-\beta T} \quad \text{(Eq. 7)}$$

$$A_2^T = \frac{k_{12}Q^F}{k_{21}k_{e1}} + \left\{\frac{k_{12}Q^F}{\alpha(\alpha-\beta)}\right\} e^{-\alpha T} - \left\{\frac{k_{12}Q^F}{\beta(\alpha-\beta)}\right\} e^{-\beta T} \quad \text{(Eq. 8)}$$

where the superscript T indicates that the quantities calculated are for amounts of drug in the respective compartments at the end of the fast infusion phase.

Multiple Cycles—The expressions given apply to cycles initiated after a steady-state plasma level is established for any given cycle.

Fast Phase—Within the fast phase of the nth infusion cycle, the value of C in Eq. 2 is equal to $C_{1,(n)}^{ss'}$ as given by:

$$C_{1,(n)}^{ss'} = Q_{(n)}^F/V_1k_{e1} \quad \text{(Eq. 9)}$$

where the subscript (n) refers to the cycle number and $Q_{(n)}^F$ is the fast infusion rate for cycle n defined by:

$$Q_{(n)}^F = Q_{(1)}^F + Q_{(n-1)}^S \quad \text{(Eq. 10)}$$

where $Q_{(1)}^F$ is the fast infusion rate for cycle 1 and $Q_{(n-1)}^S$ is the slow infusion rate for cycle $(n-1)$ defined by:

$$Q_{(n-1)}^S = C_{1,(n-1)}^{ss}V_1k_{e1} \quad \text{(Eq. 11}a\text{)}$$

Equation 11a reduces to Eq. 11b when the steady-state concentration is increased by constant increments:

$$Q_{(n-1)}^S = (n-1)Q_{(1)}^S \quad \text{(Eq. 11}b\text{)}$$

where $Q_{(1)}^S$ is the slow infusion rate for cycle 1.

Within cycles, t' assumes values from $0 \rightarrow T$; but when cycles are initiated at constant time intervals, t' is generalized by:

$$t' = t - (n-1)\tau \quad \text{(Eq. 12)}$$

where t is the continuous time period from time zero, t' is the time within any given cycle, and τ is the length of each cycle.

Corresponding values of A_1 and A_2 at the beginning of the fast phase are equal to $A_{1,(n-1)}^{ss}$ (Eq. 13) and $A_{2,(n-1)}^{ss}$ (Eq. 14), respectively:

$$A_{1,(n-1)}^{ss} = Q_{(n-1)}^S/k_{e1} \quad \text{(Eq. 13)}$$

$$A_{2,(n-1)}^{ss} = k_{12}Q_{(n-1)}^S/k_{21}k_{e1} \quad \text{(Eq. 14)}$$

By definition, the value of $Q_{(n-1)}^S$ for cycle 1 equals zero, producing values of A_1 and A_2 in agreement with those set for the fast phase of the single-cycle case.

Slow Phase—In the slow phase of the nth infusion cycle, C in Eq. 2 is substituted by $C_{1,(n)}^{ss}$, which represents the desired steady-state plasma level for cycle n. The parameter Q is defined by:

$$Q_{(n)}^S = C_{1,(n)}^{ss}V_1k_{e1} \quad \text{(Eq. 15}a\text{)}$$

Equation 15a reduces to Eq. 15b when the steady-state plasma concentration is increased by constant increments:

$$Q_{(n)}^S = (n)Q_{(1)}^S \quad \text{(Eq. 15}b\text{)}$$

The parameter t' assumes values from $0 \rightarrow (\tau - T)$ within any given cycle; but when cycles are initiated at constant time intervals, t' is generalized by:

$$t' = t - (n-1)\tau - T \quad \text{(Eq. 16)}$$

Corresponding values of A_1 and A_2 at the beginning of the slow phase of the nth infusion cycle are equal to $A_{1,(n)}^{tot}$ (Eq. 17) and $A_{2,(n)}^{tot}$ (Eq. 18), respectively:

$$A_{1,(n)}^{tot} = A_{1,(n-1)}^{ss} + A_1^T \quad \text{(Eq. 17)}$$

$$A_{2,(n)}^{tot} = A_{2,(n-1)}^{ss} + A_2^T \quad \text{(Eq. 18)}$$

where A_1^T and A_2^T are calculated from Eqs. 7 and 8, respectively, using a Q value of $Q_{(1)}^F$.

RESULTS AND DISCUSSION

The applications of Eqs. 1–18 are demonstrated by use of the following pharmacokinetic constants for hypothetical drug X: $V_1 = 1.50$ liters/kg, $\alpha = 3.6\ hr^{-1}$, $\beta = 0.2\ hr^{-1}$, $k_{e1} = 0.6\ hr^{-1}$, $k_{12} = 2.0\ hr^{-1}$, and $k_{21} = 1.2\ hr^{-1}$. It is assumed that the drug has a usual therapeutic concentration of 0.60 μg/ml and a toxic level of 5.0 μg/ml in normal adults, thereby lending itself to use in multiple-cycle infusions.

Single-Cycle Case—Figure 1 illustrates the use of Eqs. 1–8 for the single-cycle case (error free) with variations in T where $C_1^{ss} = 0.60$ μg/ml. The corresponding value of $Q^S = 0.54$ mg/kg/hr; Q^F values were calculated from Eq. 4 using appropriate values of T. The T values of 0.5, 1, and 1.5 hr were selected for the simulations for which the corresponding relative overshoot values, C_1^{max}/C_1^{ss}, are 1.914, 1.514, and 1.334, respectively. The larger overshoot associated with the smaller T values is clearly visible in the figure.

A steady value of 0.60 μg/ml is easily reached for all three values of T within 3 hr. By contrast, the single-infusion method (lower curve, Q^S = 0.54 mg/kg/hr) after a dosing cycle of 4 hr produces a plasma level of only 0.604 C_1^{ss}, with 22.4 hr being required to reach 99% of the steady-state value.

Errors in Q^F *and* T—Rapid attainment of the steady state as shown in Fig. 1 is highly dependent on the correctness of the Q^F/Q^S ratio and the T value. Figures 2 and 3 demonstrate the effect of error in these two quantities relative to the time required to reach the steady state.

Figure 2 represents simulations for an extreme error of ±50% in the Q^F/Q^S ratio, achieved by varying Q^F while maintaining Q^S constant at 0.54 mg/kg/hr for $C_1^{ss} = 0.60$ μg/ml and $T = 1$ hr. The corresponding error-free value for $Q^F = 2.979$ mg/kg/hr, as calculated from Eq. 4. These simulations depict the effect of a ±50% error in Q^F used in Eqs. 2, 7, and 8 on the time required to reach a steady-state value of 0.60 μg/ml. When Q^F is reduced by 50% of its original value (lower curve), overshoot of the steady state does not occur, but approach to the steady state is very slow. Alternatively, when Q^F is increased by 50% of its original value (upper curve), there is a larger than normal overshoot of the steady state; the plasma level remains elevated above normal (middle curve) for an extended time, again producing a very slow approach to the steady state. At 4 hr, the plasma concentrations for +50 and −50% errors in Q^F are 1.242 C_1^{ss} and 0.758 C_1^{ss}, respectively.

Figure 3 represents simulations for an extreme error of ±50% in T based on an error-free value of $T = 1$ hr. The Q^F/Q^S is maintained constant using the error-free values for Q^F and Q^S at $C_1^{ss} = 0.60$ μg/ml.

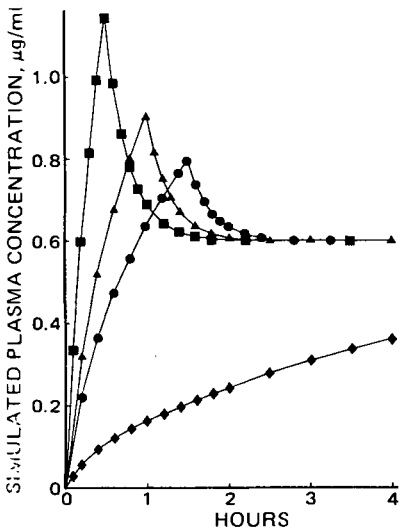

Figure 1—*Simulated plasma concentration–time curves for drug* X *comparing the two-step infusion method at* T *values of 0.5 (■), 1.0 (▲), and 1.5 (●) hr with the single-infusion rate method (♦). For all curves,* C_1^{ss} *= 0.60 μg/ml and* Q^S *= 0.54 mg/kg/hr.*

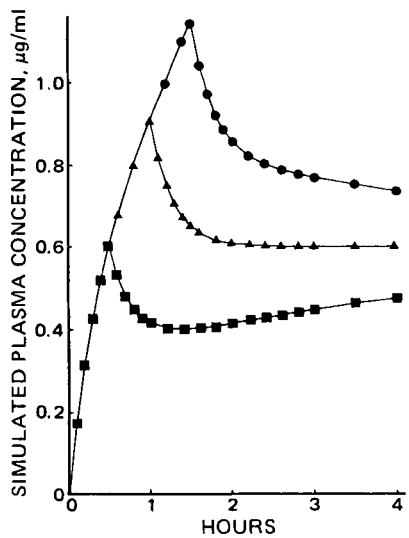

Figure 3—*Plasma concentration–time curves for drug* X *simulated by the two-step infusion method comparing the effects of −50% (■) and +50% (●) error in* T *with the error-free curve (▲). For all curves,* C_1^{ss} *= 0.60 μg/ml,* Q^S *= 0.54 mg/kg/hr, and* Q^F *= 2.979 mg/kg/hr.*

Qualitatively, the results of these simulations are completely analogous to those for Fig. 2; *i.e.*, a 50% reduction in T (lower curve) eliminates overshoot of the steady state while a 50% increase in T (upper curve) yields a larger than normal overshoot of the steady state followed by plasma levels that are elevated above normal (middle curve) for an extended period. The end result of both errors is a very slow approach to the steady state. The corresponding plasma concentrations at the end of the 4-hr dosing cycle for +50 and −50% errors in T are 1.230 $C_1^{ss}$and 0.792 C_1^{ss}, respectively.

In general, Figs. 2 and 3 show that the presence of error in the Q^F/Q^S ratio or the T value increases the time required to reach the steady state. This condition is further illustrated in Table I where the percent error in Q^F for drug X is compared with the time, t, required to reach 99% of the steady-state value. An error as small as 2.5% in Q^F increases the time required to reach 99% of steady state by a factor of approximately 2.5 times (*i.e.*, 4.96 hr *versus* 2.09 hr). Larger errors even more greatly extend the time required to reach 99% of the steady-state value. An analogous table based on the percent error in T yields very similar values of t.

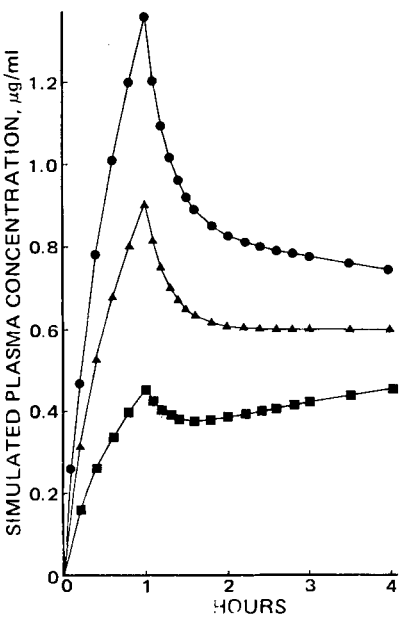

Figure 2—*Plasma concentration–time curves for drug* X *simulated by the two-step infusion method comparing the effects of −50% (■) and +50% (●) error in* Q^F *with the error-free curve (▲). For all curves,* C_1^{ss} = 0.60 μg/ml, Q^S *= 0.54 mg/kg/hr, and* T = *1 hr.*

Table II summarizes the error effects in Q^F and T at intermediate values within the ±50% error range. Errors in plasma concentrations are tabulated as $\%C_1^{max}$ (*i.e.*, percent of error-free concentration at the end of the fast infusion phase) and $\%C_1^{\tau}$ (*i.e.*, percent of error-free concentration at the end of the 4-hr dosing cycle). In contrast to the large displacements of the concentration–time profiles in Figs. 2 and 3 for ±50% errors, it is apparent from Table II that relatively small errors in Q^F and T of approximately ±2.5% will have only minor effects on C_1^{max} and C_1^{τ} after a single cycle. Therefore, errors in Q^F and T would not be expected to affect greatly the peak and steady-state plasma levels in well-controlled clinical studies.

Errors in k_{el} *and* β—Rapid attainment of the steady state using the two-step infusion method largely depends on an accurate assessment of the pharmacokinetic constants V_1, α, β, and k_{e1} used in Eqs. 1–5. Often, however, infusion therapy may be initiated using average population values for these constants instead of actual patient values. In this case, the patient may never exhibit plasma levels corresponding to C_1^{ss} even when Q^F, Q^S, and T are error free.

While intersubject variation is expected to exist for any of the pharmacokinetic parameters of a two-compartment drug, the greatest variability is often seen in the elimination rate constant, k_{e1}. Figure 4 was constructed to demonstrate the effect of error in k_{e1} in preventing attainment of C_1^{ss}. The simulations in Fig. 4 represent ±50% errors in k_{e1}, with concomitant changes in α and β calculated according to Eqs. 19 and 20 (7), respectively:

$$\alpha = \tfrac{1}{2}\left[(k_{12} + k_{21} + k_{e1}) + \sqrt{(k_{12} + k_{21} + k_{e1})^2 - 4k_{21}k_{e1}}\right] \quad \text{(Eq. 19)}$$

$$\beta = \tfrac{1}{2}\left[(k_{12} + k_{21} + k_{e1}) - \sqrt{(k_{12} + k_{21} + k_{e1})^2 - 4k_{21}k_{e1}}\right] \quad \text{(Eq. 20)}$$

Table I—Effect of Error in Q^F on the Time Required to Reach 99% of Steady State [a]

Error in Q^F, ±%	t, hr [b]
0	2.09
1.0	2.40
2.5	4.96
5.0	8.43
10.0	11.89
25.0	16.47
50.0	19.94

[a] Calculated by varying Q^F while maintaining Q^S constant at 0.54 mg/kg/hr for C_1^{ss} = 0.60 μg/ml and T = 1 hr. The error-free value of Q^F = 2.979 mg/kg/hr. [b] t = time required to reach 99% of the steady-state value.

Table II—Values [a] of $\%C_1^{max}$ and $\%C_1^{\tau}$ as a Function of Error in Q^F and T for the Single-Cycle Case [b]

Error, %	Q^F		T	
	$\%C_1^{max}$	$\%C_1^{\tau}$	$\%C_1^{max}$	$\%C_1^{\tau}$
+50.0	150.0	124.2	126.0	123.0
+25.0	125.0	112.1	113.5	111.2
+10.0	110.0	104.9	105.6	104.4
+5.0	105.0	102.4	102.8	102.2
+2.5	102.5	101.2	101.4	101.1
0	100.0	100.0	100.0	100.0
−2.5	97.5	98.8	98.6	98.9
−5.0	95.0	97.6	97.1	97.8
−10.0	90.0	95.2	94.2	95.7
−25.0	75.0	87.9	84.8	89.3
−50.0	50.0	75.8	66.4	79.2

[a] $\%C_1^{max}$ = percent of error-free concentration at the end of the fast infusion cycle; $\%C_1^{\tau}$ = percent of error-free concentration at the end of the 4-hr dosing cycle. [b] The C_1^{max} and C_1^{τ} values as a function of error in Q^F and T were calculated for the respective conditions given in Figs. 2 and 3. The 100% values for $\%C_1^{max}$ and $\%C_1^{\tau}$ correspond to C_1^{max} = 0.9082 μg/ml and C_1^{τ} = 0.60 μg/ml, respectively.

Table III—Values [a] of $\%C_1^{max}$ and $\%C_1^{\tau}$ as a Function of Error in k_{e1} and β for the Single-Cycle Case [b]

Error in k_{e1}, %	Error[c] in β, %	$\%C_1^{max}$	$\%C_1^{\tau}$
+90	+71.1	84.6	61.5
+70	+56.7	87.6	67.8
+50	+41.5	90.9	75.1
+30	+25.5	94.4	83.8
+10	+8.7	98.1	94.1
0	0	100.0	100.0
−10	−8.9	102.0	106.4
−30	−27.5	106.2	121.2
−50	−47.0	110.6	139.1
−70	−67.4	115.3	160.9
−90	−88.9	120.3	187.7

[a] See footnote *a* of Table II. [b] The C_1^{max} and C_1^{τ} values as a function of error in k_{e1} were calculated for the conditions given in Fig. 4. The 100% values of $\%C_1^{max}$ and $\%C_1^{\tau}$ correspond to C_1^{max} = 0.9082 μg/ml and C_1^{τ} = 0.60 μg/ml, respectively. [c] The β values as a function of error in k_{e1} were calculated from Eq. 20.

The constants k_{12}, k_{21}, and V_1 were assumed to be error free; Q^S and Q^F were assumed to be error free for the conditions of C_1^{ss} = 0.60 μg/ml and T = 1 hr. The ±50% errors in k_{e1} correspond to +41.5 and −47% errors in β and +5.7 and −6% errors in α. The calculated values (after rounding off) of α, β, and k_{e1} used in the simulations for a +50% error in k_{e1} were 3.187, 0.2829, and 0.9 hr^{-1}, respectively. For a −50% error in k_{e1}, the values of these constants were 3.394, 0.1061, and 0.3 hr^{-1}, respectively.

Because of the imposed errors in k_{e1}, the simulated upper and lower curves in Fig. 4 converge upon new steady-state values in accordance with Eq. 5. Thus, when k_{e1} is increased by 50% of its original value (lower curve), there is slight reduction in the normal overshoot value followed by a rapid drop in the plasma concentration below the desired value of C_1^{ss} = 0.60 μg/ml and then a gradual approach to a new steady-state value of 0.40 μg/ml. This simulation represents a hypothetical patient eliminating the drug more rapidly than the average patient.

When k_{e1} is decreased by 50% of its original value (upper curve), there is a slight increase in the normal overshoot value followed by a continued elevation above 0.60 μg/ml and then a gradual approach to a new steady-state value of 1.20 μg/ml. This simulation represents a slower-than-average eliminator of the drug. At 4 hr, the plasma concentrations for +50 and −50% errors in k_{e1} are 0.751 C_1^{ss} and 1.391 C_1^{ss}, respectively.

Table III summarizes the error effects in k_{e1} over a ± 90% error range. In addition to providing a tabulation of $\%C_1^{max}$ and $\%C_1^{\tau}$ values, Table III also gives corresponding percent errors in β for any given percent error in k_{e1}. A comparison of the error effects on C_1^{max} between Tables II and III shows that errors in k_{e1} have less influence on the peak concentration at the end of the fast infusion phase than do errors in Q^F and T. For example, a +50% error in k_{e1} and corresponding −50% errors in Q^F and T yield $\%C_1^{max}$ values of 90.9, 50, and 66.4%, respectively, while a −50% error in k_{e1} and corresponding +50% errors in Q^F and T yield $\%C_1^{max}$ values of 110.6, 150, and 126%, respectively. Relatively small errors in k_{e1} of ±10% yield errors in C_1^{max} of only 2%.

In contrast, however, negative errors in k_{e1} have a more pronounced effect on C_1^{τ}, the plasma concentration at the end of the dosing cycle, than corresponding errors in Q^F and T. For example, a −50% error in k_{e1} and corresponding +50% errors in Q^F and T yield $\%C_1^{\tau}$ values of 139.1, 124.2, and 123%, respectively. For a +50% error in k_{e1}, the resulting $\%C_1^{\tau}$ values are very similar to the −50% errors in Q^F and T (*i.e.*, 75.1, 75.8, and 79.2%, respectively).

For the extreme range of + and −90% errors in k_{e1}, the resulting $\%C_1^{\tau}$ values are 61.5 and 187.7%, respectively (Table III). Since it is not unlikely to find such a range of actual patient values that deviate from the average literature value in any clinical study, actual patient values may need to be determined, *a priori*, to avoid potential subtherapeutic or toxic plasma concentrations.

Multiple-Cycle Case—The applications of Eqs. 2 and 7–18 for the multiple-cycle case (error-free) are illustrated in Fig. 5 for the conditions $C_{1,(1)}^{ss}$ = 0.60 μg/ml and T = 1 hr. Accordingly, $Q_{(1)}^S$ = 0.54 mg/kg/hr and $Q_{(1)}^F$ = 2.979 mg/kg/hr. The values of Q required in Eq. 2 for the various cycles were calculated using Eqs. 10, 11*b*, and 15*b*, assuming equal doses and dosing intervals. Thus, for the third cycle: $Q_{(3)}^F = Q_{(1)}^F + (n-1)Q_{(1)}^S$ = [2.979 + 2(0.54)] mg/kg/hr = 4.059 mg/kg/hr and $Q_{(3)}^S = nQ_{(1)}^S$ = 3 (0.54) mg/kg/hr = 1.62 mg/kg/hr.

Drug X is depicted as having a usual therapeutic level of 0.60 μg/ml and a toxic level of 5 μg/ml, thereby possessing the property of a drug with a high therapeutic index. This property safely permits the use of successively higher plasma concentrations to achieve and maintain a continued therapeutic response. Seven cycles are simulated in Fig. 5 at a regular dosing interval of τ = 4 hr. All $C_{1,(n)}^{max}$ values fall safely within the therapeutic region, including the value for cycle 7 for which $C_{1,(7)}^{max}$ = 4.508 μg/ml.

The value of τ = 4 hr in Fig. 5 was selected for convenience in display purposes only since the dosing cycles could actually be initiated at any time following attainment of the steady state. Thus, for drug X, successive cycles may be as short as 2.5 hr, at which time C_1 is within 0.2% of

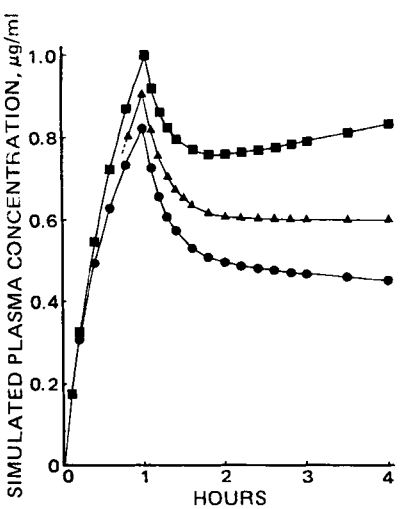

Figure 4—*Plasma concentration–time curves for drug* X *simulated by the two-step infusion method comparing the effects of −50% (■) and +50% (●) error in* k_{el} *with the error-free curve (▲). For all curves,* Q^S *= 0.54 mg/kg/hr,* T *= 1 hr, and* Q^F *= 2.979 mg/kg/hr.*

Table IV—Values [a] of $\%C_{1,(n)}^{\tau}$ as a Function of Various Error Conditions for the Multiple-Cycle Case [b]

Error Condition	Dose Cycle (n)		
	1	3	6
+50% k_{e1}	75.1	70.7	68.7
−50% Q^F	75.8	86.7	92.7
−50% T	79.2	88.5	93.8
0	100.0	100.0	100.0
+50% T	123.0	112.7	106.9
+50% Q^F	124.2	113.3	107.3
−50% k_{e1}	139.1	157.7	173.0

[a] $\%C_{1,(n)}^{\tau}$ = percent of error-free concentration at the end of the 4-hr dose cycle for the specified cycle, (n). [b] The $C_{1,(1)}^{\tau}$ values as a function of error in Q^F, T, and k_{e1} were calculated for the respective conditions given in Figs. 2–4. The 100% values of $\%C_{1,(n)}^{\tau}$ for cycles 1, 3, and 6 correspond to 0.6, 1.8, and 3.6 μg/ml, respectively.

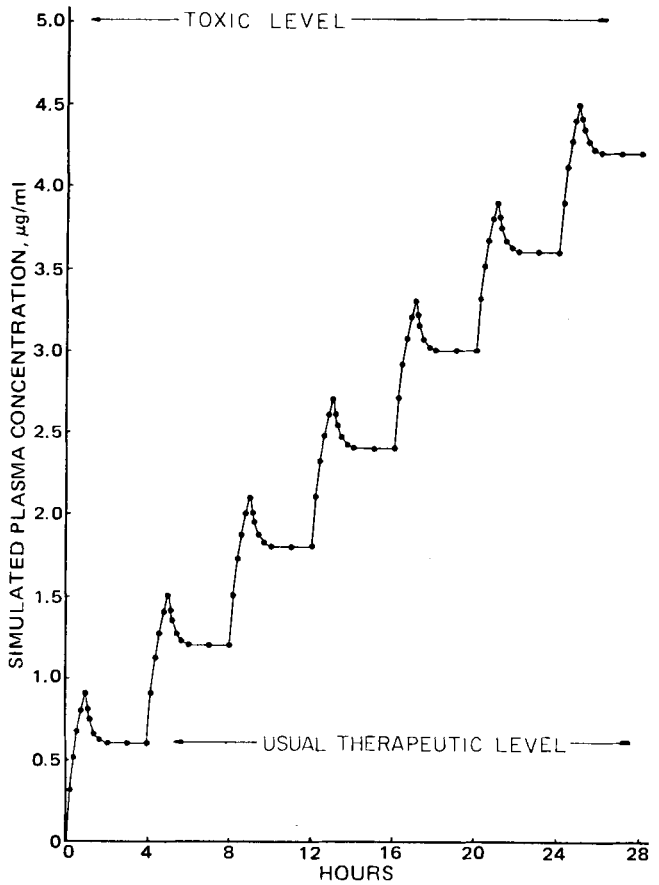

Figure 5—*Plasma concentration–time curves for drug* X *simulated by the two-step infusion method for the multiple-cycle case with* $C^{ss}_{1,(1)}$ = *0.60 μg/ml,* $Q^S_{(1)}$ = *0.54 mg/kg/hr,* T = *1 hr,* $Q^F_{(1)}$ = *2.979 mg/kg/hr, and* τ = *4 hr.*

$C^{ss}_{1,(n)}$, or longer than 4 hr, depending on the therapeutic need. Furthermore, the dosing cycles need not be spaced at regular intervals but may be sporadic, again depending on the therapeutic need.

Errors in Q^F, T, *and* k_{el}—Tables IV–VI summarize the errors in $C^{\tau}_{1,(n)}$, $C^{max}_{1,(n)}$, and $AUC|^{\tau}_{0,(n)}$ for six successively higher doses during 24 hr (*i.e.*, one dosing cycle every 4 hr) under various conditions. The conditions of ±50% error in Q^F, T, and k_{el} were used in these tables.

Since Eqs. 9–19 require that the steady state be attained prior to beginning the next dose, these equations could not be used for calculating the plasma concentrations required in compiling Tables IV–VI. Instead, the superposition principle was utilized (7). For each condition specified in these tables, the plasma concentrations for cycle 1 were computed with Eqs. 2–7 for specifically selected time intervals over 24 hr. The plasma concentrations of successive cycles were computed by simply stacking the cycle 1 data stepwise every 4 hr and summing the resulting concentration values at each point in time. The number of selected time intervals

Table V—Values[a] of $\%C^{max}_{1,(n)}$ as a Function of Various Error Conditions for the Multiple-Cycle Case[b]

Error Condition	Dose Cycle (*n*) 1	3	6
+50% k_{el}	90.9	79.5	73.7
−50% Q^F	50.0	70.3	83.0
−50% T	66.4	77.8	87.0
0	100.0	100.0	100.0
+50% T	126.0	118.2	110.7
+50% Q^F	150.0	129.7	117.0
−50% k_{el}	110.6	135.7	157.8

[a] $\%C^{max}_{1,(n)}$ = percent of error-free concentration at the end of the fast infusion phase for the specified cycle, (n). [b] The $C^{max}_{1,(n)}$ values as a function of error in Q^F, T, and k_{el} were calculated for the respective conditions given in Figs. 2–4. The 100% values of $\%C^{max}_{1,(n)}$ for cycles 1, 3, and 6 correspond to 0.9082, 2.1082, and 3.9082 μg/ml, respectively.

Table VI—Values[a] of $\%AUC|^{\tau}_{0,(n)}$ as a Function of Various Error Conditions for the Multiple-Cycle Case[b]

Error Condition	Dose Cycle (*n*) 1	3	6
+50% k_{el}	83.8	74.7	70.8
−50% Q^F	62.0	79.2	88.6
−50% T	70.4	83.1	90.7
0	100.0	100.0	100.0
+50% T	127.6	116.9	109.4
+50% Q^F	138.4	121.0	111.4
−50% k_{el}	122.9	146.8	166.0

[a] $\%AUC|^{\tau}_{0,(n)}$ = percent of error-free area under the curve from 0 → τ at the end of the 4-hr dose cycle for the specified cycle, (n). [b] The $AUC|^{\tau}_{0,(1)}$ values as a function of error in Q^F, T, and k_{el} were calculated for the respective conditions given in Figs. 2–4. The 100% values of $\%AUC|^{\tau}_{0,(n)}$ for cycles 1, 3, and 6 correspond to 2.4436, 7.2436, and 14.4436 μg hr/ml, respectively.

during each 4-hr cycle ranged between 8 and 12, depending on the specified condition. The same number of time intervals was used to calculate values of $AUC|^{\tau}_{0,(n)}$ by the trapezoidal rule for specified conditions.

Table IV gives $\%C^{\tau}_{1,(n)}$ values at the end of the slow infusion cycles during multiple dosing. Within any cycle, it is apparent that $\%C^{\tau}_{1,(n)}$ follows the order: +50% k_{el} < −50% Q^F < −50% T < EF < +50% T < +50% Q^F < −50% k_{el}, with extreme effects being imposed by ±50% errors in k_{el}. This order is not observed, however, for cycle 1 in Table V ($\%C^{max}_{1,(n)}$) or in Table VI ($\%AUC|^{\tau}_{0,(n)}$) where the extreme effects are imposed by ±50% errors in Q^F. Nevertheless, errors in k_{el} become increasingly important as the number of dosing cycles increases, and the order followed by $\%C^{\tau}_{1,(n)}$ is duplicated by $\%C^{max}_{1,(n)}$ and $\%AUC|^{\tau}_{0,(n)}$ beginning in dose cycles 5 and 3, respectively.

For ±50% errors in k_{el}, the calculated percentages, $\%C^{\tau}_{1,(n)}$, $\%C^{max}_{1,(n)}$, and $\%AUC|^{\tau}_{0,(n)}$, all increasingly diverge from 100% as the dosing cycle increases (Tables IV–VI). In contrast, for the conditions of ±50% errors

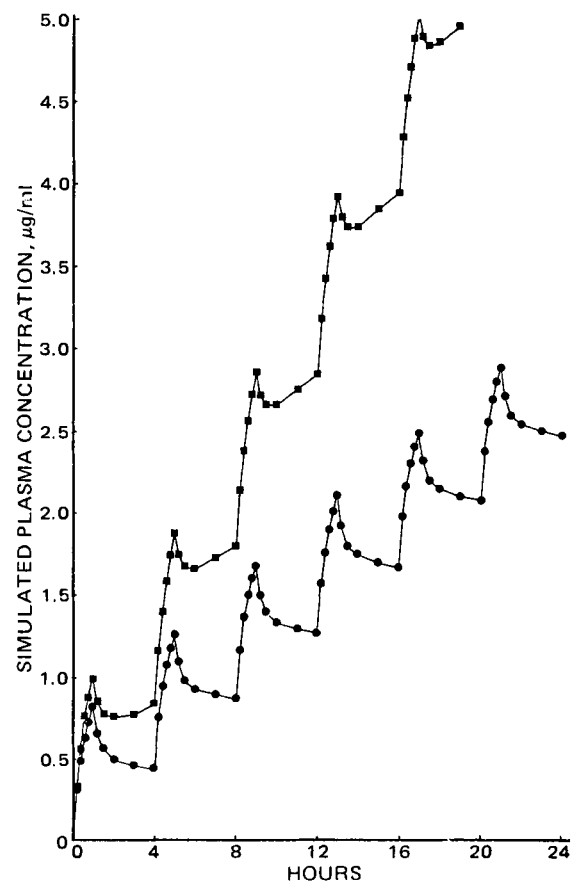

Figure 6—*Plasma concentration–time curves for drug* X *simulating the two-step infusion approach for the multiple-cycle case and comparing the effects of −50% (■) with +50% (●) error in* k_{el}. *For both curves,* $Q^S_{(1)}$ = *0.54 mg/kg/hr,* T = *1 hr, and* $Q^F_{(1)}$ = *2.979 mg/kg/hr.*

in Q^F and T, the calculated percentages all tend to converge toward 100% as dosing increases. For example, in the sixth dosing cycle of Table IV + and −50% errors in k_{el} yield $\%C^{\tau}_{1,(n)}$ values of 68.7 and 173%, respectively, while ±50% errors in Q^F and T produce $\%C^{\tau}_{1,(n)}$ values of 92.7–107.3%. Similar results are found in Tables V and VI for $\%C^{max}_{1,(n)}$ and $\%AUC|^{\tau}_{0,(n)}$, respectively.

The effect of ±50% errors in k_{el} during multiple-dose cycles is further illustrated in Fig. 6 for six successively higher doses over 24 hr. The shapes of the plasma profiles are obviously distorted when compared with the error-free profile in Fig. 5. The pronounced effect of a −50% error in k_{el} is evidenced by values of $C^{max}_{1,(n)}$ and $C^{\tau}_{1,(n)}$ that begin to exceed the hypothetical toxic level of 5 μg/ml after only five dose cycles. Values of $C^{max}_{1,(n)}$ and $C^{\tau}_{1,(n)}$ for a +50% error in k_{el} all safely fall within the therapeutic region over the total 24 hr as expected. The increasingly larger differences between the areas under the curve for ±50% errors in k_{el} as the dose cycle increases are immediately apparent.

It may be concluded that individual patient differences in elimination, as reflected in k_{el}, become increasingly more important as a source of error in $C^{max}_{1,(n)}$, $C^{\tau}_{1,(n)}$, and $AUC|^{\tau}_{0,(n)}$ with successively higher doses while experimental error in Q^F and T become less and less important.

Finally, it is cautioned that the attainment clinically of profiles as ideal as that in Fig. 5 depends on an accurate estimation of the pharmacokinetic parameters for the individual patient, a constancy in the values of the pharmacokinetic parameters during therapy, and careful administration of the drug with respect to both flow rate and T.

REFERENCES

(1) R. N. Boyes, D. B. Scott, R. J. Jebson, M. J. Godman, and D. G. Julian, *Clin. Pharmacol. Ther.*, **12**, 105 (1971).

(2) P. A. Mitenko and R. I. Ogilvie, *ibid.*, **14**, 509 (1973).

(3) D. Shen and M. Gibaldi, *J. Clin. Pharmacol.*, **14**, 339 (1974).

(4) J. G. Wagner, *Clin. Pharmacol. Ther.*, **16**, 691 (1974).

(5) D. P. Vaughan and G. T. Tucker, *Eur. J. Clin. Pharmacol.*, **9**, 235 (1975).

(6) *Ibid.*, **10**, 433 (1976).

(7) J. G. Wagner, "Fundamentals of Clinical Pharmacokinetics," 1st ed., Drug Intelligence Publications, Hamilton, Ill., 1975, chaps. 2 and 3.

Synthesis and Biological Activity of Cocaine Analogs I: *N*-Alkylated Norcocaine Derivatives

EDWARD S. LAZER *, NARANJAN D. AGGARWAL *, GILBERT J. HITE *, KARL A. NIEFORTH *x, ROGER T. KELLEHER ‡, ROGER D. SPEALMAN ‡, CHARLES R. SCHUSTER §, and WILLIAM WOLVERTON §

Received January 30, 1978, from the **Section of Medicinal Chemistry and Pharmacognosy, School of Pharmacy, University of Connecticut, Storrs, CT 06268,* the ‡*Harvard Medical School New England Regional Primate Research Center, Southborough, MA 01772,* and the §*Department of Psychiatry, University of Chicago, Chicago, IL 60637.* Accepted for publication March 22, 1978.

Abstract □ *N*-Allylnorcocaine, *N*-dimethylallylnorcocaine, and *N*-cyclopropylmethylnorcocaine were prepared and examined for cocaine-like activity. The compounds were prepared by alkylation of norcocaine, which was obtained by demethylation of cocaine with 2,2,2-trichloroethyl chloroformate followed by zinc–acetic acid reduction. The compounds were evaluated by comparison with cocaine in causing disruption of milk intake in rats, behavioral modification in squirrel monkeys, and inhibition of ^{3}H-serotonin uptake by rat synaptosomes. The compounds showed cocaine-like activity less potent than cocaine in the latter two tests and were inactive in the milk intake test.

Keyphrases □ Cocaine analogs, various—synthesized, evaluated for effect on milk intake in rats, behavioral modifications in monkeys, and effect on ^{3}H-serotonin uptake by rat synaptosomes □ Structure–activity relationships—various cocaine analogs evaluated for effect on milk intake in rats, behavioral modifications in monkeys, and effect on ^{3}H-serotonin uptake by rat synaptosomes

Structural modifications of cocaine have been undertaken to derive compounds with the ability to interact at the cocaine receptor but with a lower intrinsic activity. Such an approach ultimately may lead to compounds with the ability to antagonize the euphoric effects of cocaine (I) as an adjunct to the treatment of cocaine abuse. Another desirable effect would be to attenuate the potent central nervous system (CNS) stimulant properties (1) of cocaine to obtain mood elevation without the prolonged latency period of tricyclic antidepressants and monoamine oxidase inhibitors. Although not defensible on any theoretical basis, previous reports on narcotic analgesics (2–6), CNS stimulants (7), and hallucinogens (8) strongly suggested the synthesis of *N*-allylnorcocaine[1] (IV), *N*-dimethylallylnorcocaine (V), and *N*-cyclopropylmethylnorcocaine (VI). This paper reports the syntheses and evaluations of IV–VI.

EXPERIMENTAL[2]

Norcocaine (III) was prepared by treatment of carbamate II with zinc and 95% acetic acid. The carbamate (II) was obtained by treating cocaine with 2,2,2-trichloroethyl chloroformate (10) and potassium carbonate in refluxing benzene. The procedure varied slightly from that described by Borne *et al.* (11) and provided similar yields. Alkylated norcocaine derivatives IV–VII were prepared by treating III with the appropriate alkyl bromide and triethylamine in refluxing benzene. Cyclopropylmethyl bromide, the only alkyl bromide not available commercially, was prepared by treating cyclopropylcarbinol with triphenylphosphine and bromine in dimethylformamide.

N-Cyclopropylmethylnorcocaine (VI) was purified by column chro-

[1] While the biological studies on these compounds were being carried out, the synthesis of *N*-allylnorcocaine and its effects on temperature, respiration, and heart rate in monkeys were reported (9).

[2] Melting points were determined on a Thomas-Hoover Uni-Melt apparatus and are uncorrected. Elemental analyses were performed by Baron Consultants, Orange, Conn. NMR spectra were obtained on a Hitachi Perkin-Elmer R-24 high-resolution NMR spectrometer using deuterated chloroform as the solvent. TLC was run on silica gel GF-254 (type 60) (EM Reagents). Column chromatography was run on silica gel 60 with a particle size of 0.063–0.200 mm (70–230 mesh ASTM) (EM Reagents). Benzene–ethanol–ammonium hydroxide (10:1:1), top phase, served as the solvent system for all chromatography.

0022-3549/78/1200-1656$01.00/0

© 1978, American Pharmaceutical Association

in Q^F and T, the calculated percentages all tend to converge toward 100% as dosing increases. For example, in the sixth dosing cycle of Table IV + and −50% errors in k_{el} yield $\%C^{\tau}_{1,(n)}$ values of 68.7 and 173%, respectively, while ±50% errors in Q^F and T produce $\%C^{\tau}_{1,(n)}$ values of 92.7–107.3%. Similar results are found in Tables V and VI for $\%C^{max}_{1,(n)}$ and $\%AUC|^{\tau}_{0,(n)}$, respectively.

The effect of ±50% errors in k_{el} during multiple-dose cycles is further illustrated in Fig. 6 for six successively higher doses over 24 hr. The shapes of the plasma profiles are obviously distorted when compared with the error-free profile in Fig. 5. The pronounced effect of a −50% error in k_{el} is evidenced by values of $C^{max}_{1,(n)}$ and $C^{\tau}_{1,(n)}$ that begin to exceed the hypothetical toxic level of 5 μg/ml after only five dose cycles. Values of $C^{max}_{1,(n)}$ and $C^{\tau}_{1,(n)}$ for a +50% error in k_{el} all safely fall within the therapeutic region over the total 24 hr as expected. The increasingly larger differences between the areas under the curve for ±50% errors in k_{el} as the dose cycle increases are immediately apparent.

It may be concluded that individual patient differences in elimination, as reflected in k_{el}, become increasingly more important as a source of error in $C^{max}_{1,(n)}$, $C^{\tau}_{1,(n)}$, and $AUC|^{\tau}_{0,(n)}$ with successively higher doses while experimental error in Q^F and T become less and less important.

Finally, it is cautioned that the attainment clinically of profiles as ideal as that in Fig. 5 depends on an accurate estimation of the pharmacokinetic parameters for the individual patient, a constancy in the values of the pharmacokinetic parameters during therapy, and careful administration of the drug with respect to both flow rate and T.

REFERENCES

(1) R. N. Boyes, D. B. Scott, R. J. Jebson, M. J. Godman, and D. G. Julian, *Clin. Pharmacol. Ther.*, **12**, 105 (1971).

(2) P. A. Mitenko and R. I. Ogilvie, *ibid.*, **14**, 509 (1973).

(3) D. Shen and M. Gibaldi, *J. Clin. Pharmacol.*, **14**, 339 (1974).

(4) J. G. Wagner, *Clin. Pharmacol. Ther.*, **16**, 691 (1974).

(5) D. P. Vaughan and G. T. Tucker, *Eur. J. Clin. Pharmacol.*, **9**, 235 (1975).

(6) *Ibid.*, **10**, 433 (1976).

(7) J. G. Wagner, "Fundamentals of Clinical Pharmacokinetics," 1st ed., Drug Intelligence Publications, Hamilton, Ill., 1975, chaps. 2 and 3.

Synthesis and Biological Activity of Cocaine Analogs I: *N*-Alkylated Norcocaine Derivatives

EDWARD S. LAZER *, NARANJAN D. AGGARWAL *, GILBERT J. HITE *, KARL A. NIEFORTH *x, ROGER T. KELLEHER ‡, ROGER D. SPEALMAN ‡, CHARLES R. SCHUSTER §, and WILLIAM WOLVERTON §

Received January 30, 1978, from the **Section of Medicinal Chemistry and Pharmacognosy, School of Pharmacy, University of Connecticut, Storrs, CT 06268,* the ‡*Harvard Medical School New England Regional Primate Research Center, Southborough, MA 01772,* and the §*Department of Psychiatry, University of Chicago, Chicago, IL 60637.* Accepted for publication March 22, 1978.

Abstract □ *N*-Allylnorcocaine, *N*-dimethylallylnorcocaine, and *N*-cyclopropylmethylnorcocaine were prepared and examined for cocaine-like activity. The compounds were prepared by alkylation of norcocaine, which was obtained by demethylation of cocaine with 2,2,2-trichloroethyl chloroformate followed by zinc–acetic acid reduction. The compounds were evaluated by comparison with cocaine in causing disruption of milk intake in rats, behavioral modification in squirrel monkeys, and inhibition of ^{3}H-serotonin uptake by rat synaptosomes. The compounds showed cocaine-like activity less potent than cocaine in the latter two tests and were inactive in the milk intake test.

Keyphrases □ Cocaine analogs, various—synthesized, evaluated for effect on milk intake in rats, behavioral modifications in monkeys, and effect on ^{3}H-serotonin uptake by rat synaptosomes □ Structure–activity relationships—various cocaine analogs evaluated for effect on milk intake in rats, behavioral modifications in monkeys, and effect on ^{3}H-serotonin uptake by rat synaptosomes

Structural modifications of cocaine have been undertaken to derive compounds with the ability to interact at the cocaine receptor but with a lower intrinsic activity. Such an approach ultimately may lead to compounds with the ability to antagonize the euphoric effects of cocaine (I) as an adjunct to the treatment of cocaine abuse. Another desirable effect would be to attenuate the potent central nervous system (CNS) stimulant properties (1) of cocaine to obtain mood elevation without the prolonged latency period of tricyclic antidepressants and monoamine oxidase inhibitors. Although not defensible on any theoretical basis, previous reports on narcotic analgesics (2–6), CNS stimulants (7), and hallucinogens (8) strongly suggested the synthesis of *N*-allylnorcocaine[1] (IV), *N*-dimethylallylnorcocaine (V), and *N*-cyclopropylmethylnorcocaine (VI). This paper reports the syntheses and evaluations of IV–VI.

EXPERIMENTAL[2]

Norcocaine (III) was prepared by treatment of carbamate II with zinc and 95% acetic acid. The carbamate (II) was obtained by treating cocaine with 2,2,2-trichloroethyl chloroformate (10) and potassium carbonate in refluxing benzene. The procedure varied slightly from that described by Borne *et al.* (11) and provided similar yields. Alkylated norcocaine derivatives IV–VII were prepared by treating III with the appropriate alkyl bromide and triethylamine in refluxing benzene. Cyclopropylmethyl bromide, the only alkyl bromide not available commercially, was prepared by treating cyclopropylcarbinol with triphenylphosphine and bromine in dimethylformamide.

N-Cyclopropylmethylnorcocaine (VI) was purified by column chro-

[1] While the biological studies on these compounds were being carried out, the synthesis of *N*-allylnorcocaine and its effects on temperature, respiration, and heart rate in monkeys were reported (9).

[2] Melting points were determined on a Thomas-Hoover Uni-Melt apparatus and are uncorrected. Elemental analyses were performed by Baron Consultants, Orange, Conn. NMR spectra were obtained on a Hitachi Perkin-Elmer R-24 high-resolution NMR spectrometer using deuterated chloroform as the solvent. TLC was run on silica gel GF-254 (type 60) (EM Reagents). Column chromatography was run on silica gel 60 with a particle size of 0.063–0.200 mm (70–230 mesh ASTM) (EM Reagents). Benzene–ethanol–ammonium hydroxide (10:1:1), top phase, served as the solvent system for all chromatography.

0022-3549/78/1200-1656$01.00/0

© 1978, American Pharmaceutical Association

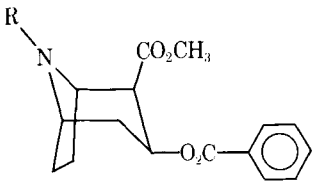

I: R = CH_3
II: R = $CO_2CH_2C(Cl)_3$
III: R = H
IV: R = $CH_2CH{=}CH_2$
V: R = $CH_2CH{=}C(CH_3)_2$
VI: R = CH_2—⟨△⟩
VII: R = $CH_2CH_2CH{=}CH_2$

matography because of formation of a small amount (5–10%) of side product. The identity of the side product, *N*-(3-butenyl)norcocaine (VII), was determined by isolation of a small amount from the column and comparison (TLC and NMR) with a separately prepared sample. The homoallylic by-product probably forms by S_N2' attack of III on cyclopropylmethyl bromide. No homoallyl bromide was detectable (NMR) in the cyclopropylmethyl bromide.

The norcocaine derivatives were tested in three biological systems: milk intake in rats, ^{3}H-serotonin uptake in rat brain synaptosomal preparations, and behavioral effects on squirrel monkeys.

Norcocaine (III)—To a stirred refluxing mixture of cocaine (8 g, 0.026 mole), potassium carbonate (0.8 g, 0.0058 mole), and 140 ml of dry benzene, 2,2,2-trichloroethyl chloroformate (16 g, 0.0757 mole) was added over 30 min. The reaction mixture was refluxed for 40 hr. It was then cooled and poured into 150 ml of ice water. The benzene layer was separated, and the aqueous layer was extracted thoroughly with chloroform. The combined organic layers were washed with saturated sodium chloride solution, dried over anhydrous sodium sulfate, and evaporated to yield II as an oil.

Without further purification, II was dissolved in 130 ml of 95% acetic acid. Zinc dust (20 g, 0.306 mole) was added slowly. The mixture was stirred for 23 hr and then filtered. The zinc salts were rinsed with a small amount of 95% acetic acid. The filtrate was diluted with 450 ml of water and extracted thoroughly with chloroform. The combined chloroform extracts were then washed with 5% sodium hydroxide solution until the aqueous phase remained basic. The organic phase was washed with water, dried over anhydrous sodium sulfate, and evaporated to give norcocaine as an oil.

A small amount of the oil was triturated in cold petroleum ether. The petroleum ether was decanted, and the process was repeated until the norcocaine solidified. Two recrystallizations from petroleum ether gave norcocaine (III), mp 82.5–83.5° [lit. (12) mp 82°]. The remaining oil, without further purification, was converted to its hydrochloride salt, mp 115–117° (from acetone) [lit. (11) mp 111–113°]. Norcocaine hydrobromide, mp 164–165° (from acetone–ethanol), also was prepared. In several parallel runs, the overall yield (based on the yield of crude hydrochloride salt) ranged from 54 to 65%.

Cyclopropylmethyl Bromide—Cyclopropylmethyl bromide was prepared from cyclopropylcarbinol in 30% yield by the method used by Wiley *et al.* (13) to prepare *n*-butyl bromide from *n*-butyl alcohol. However, instead of an aqueous workup, the product was distilled, bp 95–115°/760 mm [lit. (14) bp 102–110°/760 mm]. Its NMR spectrum indicated that it still contained about 30% reaction solvent [dimethylformamide, δ 2.75 (s, CH_3) and 2.9 (s, CH_3) ppm]. The crude cyclopropylmethyl bromide was used in the alkylation reaction with norcocaine without further purification.

General Procedure for Alkylation of Norcocaine—N-*Dimethylallylnorcocaine Hydrochloride* (*V Hydrochloride*)—A solution of norcocaine (1.15 g, 0.004 mole), 1-bromo-3-methyl-2-butene (0.59 g, 0.004 mole), triethylamine (0.6 g, 0.006 mole), and 10 ml of anhydrous benzene was refluxed. The progress of the reaction was monitored by TLC at 1- or 2-hr intervals. At each interval, a few drops of the alkyl bromide was added. After 7 hr, TLC indicated that all of the norcocaine had reacted. The reaction mixture was then diluted with 10 ml of ether, and the mixture was filtered and evaporated under reduced pressure to afford an oil.

The oil was dissolved in ether and extracted into 1.5 *N* HCl. The aqueous solution was made basic with 6 *N* NaOH, and the product was extracted back into ether. The ether layer was dried over anhydrous sodium sulfate and evaporated under reduced pressure to give V as an oil. The hydrochloride salt was prepared by dissolving the oil in anhydrous ether and adding an ethereal solution of hydrochloric acid. In several parallel runs, the yields ranged from 67 to 72% of hydrochloride, mp 161.5–162° (from acetone); NMR: δ 1.85 (6H, s, CH_3), 3.76 (3H, s, OCH_3), and 7.4–8.1 (5H, m, aromatic) ppm.

Anal.—Calc. for $C_{21}H_{18}ClNO_4$: C, 64.03; H, 7.17; N, 3.56. Found: C, 63.75; H, 7.06; N, 3.69.

N-*Allylnorcocaine Hydrochloride* (*IV Hydrochloride*)—This compound was obtained in 60–67% yield, mp 154–155°; NMR: δ 5.35–5.9 (4H, m, vinyl and CHOCO-phenyl), 3.75 (3H, s, OCH_3), and 7.4–8.1 (5H, m, aromatic) ppm.

Anal.—Calc. for $C_{19}H_{24}ClNO_4$: C, 62.38; H, 6.61; N, 3.83. Found: C, 62.18; H, 6.66; N, 3.80.

N-*Cyclopropylmethylnorcocaine Hydrochloride* (*VI Hydrochloride*)—The hygroscopic salt, mp 98–103°, was obtained in 54–80% yield after purification of the free base by column chromatography to remove VII, which was identified by comparison (NMR and TLC) with an authentic sample; NMR: δ 0.46–0.82 (5H, m, cyclopropyl), 3.78 (3H, s, OCH_3), and 7.4–8.1 (5H, m, aromatic) ppm.

Anal.—Calc. for $C_{20}H_{26}ClNO_4$: C, 63.24; H, 6.90; N, 3.69. Found: C, 62.95; H, 6.80; N, 3.81.

N-(*3-Butenyl*)*norcocaine Hydrochloride* (*VII Hydrochloride*)—This compound was obtained in 50% yield, mp 125–127°; NMR: δ 4.9–6.0 (4H, m, vinyl and CHOCO-phenyl), 3.75 (3H, s, OCH_3), and 7.4–8.2 (5H, m, aromatic) ppm.

Anal.—Calc. for $C_{20}H_{26}ClNO_4$: C, 63.24; H, 6.90; N, 3.69. Found: C, 62.86; H, 6.76; N, 4.00.

Biological Methods—In the milk intake studies, eight experimentally naive female Sprague–Dawley-derived rats weighed between 210 and 290 g at the beginning of the experiments. They were housed individually in stainless steel cages; water was available at all times except during experimental sessions. Experimental sessions consisted of 15 min/day access to a sweetened condensed milk solution (two parts of tap water to one part of commercial sweetened condensed milk[3]), which was placed on the front of the cage in a graduated drinking tube with a drinking spout. The volume of milk intake was measured at the end of the session. Each rat received 4–6 g of food after the session.

The effects of the experimental compounds on milk intake were determined in the following manner. After milk intake was stable for the group of rats (±10% for 3 days), each rat was injected 15 min before the session with saline or a dose of the test compound in a volume of 1 ml/kg ip. After dose–effect relations of all compounds had been determined, the effects of several doses of each compound plus cocaine were determined to test for possible antagonism of the effects of cocaine on intake. Interaction studies were carried out by injecting the test drug intraperitoneally 5 min before the intraperitoneal injection of cocaine, which preceded access to milk by 15 min.

For the inhibition of serotonin uptake study, subcellular fractions of rat brain (striatum hypothalamus, hippocampus, and midbrain) were prepared by the method of Gray and Whittaker (15). A crude nucleus fraction was obtained by centrifugation of 10% brain homogenate in 0.32 *M* sucrose at 1000×*g* for 10 min. The supernate was sedimented further at 12,000×*g* for 20 min to obtain the P2 pellet (crude mitochondria fraction). Synaptosomes and mitochondria were fractioned from resuspended P2 by a discontinuous sucrose gradient procedure (15). The P2B layer (containing the nerve ending particles) was aspirated, and the sucrose concentration was adjusted to 0.32 *M*. It then was resedimented at 12,000×*g* for 20 min to obtain the synaptosomal fraction.

The uptake of serotonin by isolated synaptosomes was measured by a modification of the procedure of Neckers and Sze (16). A 600-μl aliquot of the incubation mixture contained 0.5 nmole of unlabeled 5-hydroxytryptamine, 30 nmoles of test drug, 1 μCi of labeled biogenic amine, and synaptosomal preparation equivalent to 1.2–1.7 mg of protein resuspended in a modified Krebs–Ringer phosphate buffer, pH 7.4, containing 12 m*M* glucose and 0.08 m*M* pargyline hydrochloride. The mixture was allowed to incubate for 5 min at 30°. After incubation, the synaptosomal suspension was immediately cooled in ice for 2 min after the addition of ice-cold Ringer solution (3 ml) and centrifuged at 12,000×*g* for 15 min. The supernate was poured out, and the tubes were cleaned cautiously with cotton swabs without touching the pellet. The pellet was vortexed in 250 μl of 50% ethanol, and 100 μl was pipetted into the scintillation vial containing 10 ml of Bray's solution. Radioactivity in the samples was then measured[4].

[3] Borden.
[4] Packard Tri-Carb liquid scintillation spectrometer.

Table I—Inhibition of Milk Intake by Cocaine and Analogs in Rats

Compound (Hydrochloride Salt)	Dose, mg/kg	n	Mean Intake, ml	*SEM*, ml
Saline		8	29.5	0.4
I	4	4	25.5	2.3
	8	4	19.0	2.1
	16	4	22.0	1.2
	32	4	15.7	2.7
IV	4	7	20.1	0.87
	8	8	30.6	2.3
	16	8	27.2	2.2
	32	8	26.0	1.8
	64	4	20.5	2.2
V	4	4	31.6	3.3
	8	4	33.2	2.8
	16	4	26.1	3.8
	32	4	30.7	1.9
	64	2	26.0	0
VI	16	2	25	20–30
	32	2	24	22–26

Table II—Interaction of Cocaine and Analogs in Inhibition of Milk Intake in Rats

Compound (Hydrochloride Salt)	Dose, mg/kg	n	Mean Intake, ml	*SEM*, ml
Saline		8	29.5	0.4
I	16	4	22.0	1.2
IV + I	32 + 16	4	13.2	2.2
V + I	8 + 16	4	10.5	6.1
V + I	16 + 16	4	20.7	2.0
V + I	64 + 16	4	22.5[a]	3.0
V + I	64 + 32	4	0[b]	0
VI + I	32 + 16	1	6.0	—

[a] Convulsions in one rat; prostration in one rat. [b] Stereotypy, frothing, and intermittent convulsions in one rat.

To study the behavioral effects of the compounds on squirrel monkeys, IV and VI (0.3, 1.0, 10.0, and 30.0 mg/kg im) and V (0.3, 1.0, 3.0, and 10.0 mg/kg im) were administered to each of two mature male squirrel monkeys. Each monkey received a single administration of each dose, and successive administrations were separated by at least 48 hr. Two observers recorded the effects of each dose at various times after administration (1–60 min). Four other mature male squirrel monkeys responded under a multiple 5-min fixed-interval (FI), 30-response fixed-ratio (FR) schedule of termination of a stimulus associated with electric shock. A description of this test is given in detail elsewhere (17). Cocaine (0.1, 0.3, 1.0, and 3.0 mg/kg im) and IV–VI (0.3, 1.0, 3.0, and 10.0 mg/kg im) were administered 5 min before the beginning of a 75-min experimental session. Each monkey received duplicate administrations of each dose, and at least 48 hr separated successive administrations.

RESULTS AND DISCUSSION

Compounds IV–VI were compared to cocaine (I) for their ability to disrupt milk intake in rats (18, 19). They were also coadministered with cocaine to test for possible inhibition of cocaine-induced disruption of milk intake. Dose–effect results for each compound are presented in Table I. There was a dose-related decrease in milk intake following injections of cocaine. Compound IV showed weak activity at the lowest and highest doses tested but not in a dose-related manner. Compounds V and VI did not disrupt milk intake at a significant level at any dose tested.

The data for the interaction studies are shown in Table II. None of the compounds showed evidence of antagonism of the effects of cocaine. Differences between the combination of drugs and cocaine alone were in the direction of a greater disruption of intake, although these effects were not statistically significant because of high variability. With high doses (64 mg of V/kg with 32 mg of I/kg), milk intake was precluded completely due to convulsions and frothing.

Compounds IV–VI also were compared with cocaine in their ability to inhibit ^{3}H-serotonin uptake by synaptosomes isolated from the rat midbrain. The results (Table III) indicate that these compounds inhibited ^{3}H-serotonin uptake, as cocaine does. However, approximately 10 times the concentration of IV–VI was required to bring about the range of inhibition exhibited by cocaine.

Table III—Cocaine Derivatives as Inhibitors of ^{3}H-Serotonin Uptake in Rat Synaptosomal Preparations

Compound (5×10^{-5} *M*)[a] (Hydrochloride Salt)	Inhibition[b,c], %
Cocaine (5.3×10^{-6} *M*)	26
IV	25
V	15
VI	32.4

[a] Concentration unless otherwise stated. [b] The value for cocaine was an average value obtained over six experiments ($\bar{X}$ = 26.033, *SD* = 1.426). [c] The values for IV–VI were averages of two determinations.

In behavioral tests with squirrel monkeys, at the highest doses tested, V and VI produced convulsions almost immediately after injection (3 min or less) and continued to do so for up to 10 (V) or 30 (VI) min. The highest dose of IV produced marked incoordination and rapid and shallow respirations but not convulsions. Doses of 10.0 (IV and VI) or 3.0 (V) mg/kg or less produced no gross behavioral effects in either monkey.

Some doses of cocaine (0.3 and 1.0 mg/kg) or of IV–VI (1.0 and 3.0 mg/kg) increased responding under the FI schedule to 130–180% of control (control mean, 0.68 response/sec); the largest dose of cocaine (3.0 mg/kg) or of VI (10.0 mg/kg) decreased FI responding. Cocaine and IV–VI only decreased responding under the FR schedule (control mean, 2.14 responses/sec). The 3.0-mg/kg dose of cocaine and the 10.0-mg/kg dose of IV and VI decreased FR responding to about the same extent, 30–60% of control. The behavioral effects of IV–VI were qualitatively similar to those of cocaine, but each compound was less potent than cocaine.

In conclusion, these *N*-alkylated norcocaine derivatives exhibited cocaine-like activity in two of the three biological test systems. This result suggests that these or similar compounds can interact at the cocaine receptor. The fact that these compounds were less potent than cocaine is encouraging considering the possible implications mentioned earlier.

REFERENCES

(1) S. Cohen, *J. Am. Med. Assoc.*, **231**, 74 (1975).

(2) E. R. Hart and E. L. McCawley, *J. Pharmacol. Exp. Ther.*, **82**, 339 (1944).

(3) C. A. Winter and L. Flataker, *ibid.*, **112**, 99 (1954).

(4) J. Telford, C. N. Papadopoulos, and A. S. Keats, *ibid.*, **133**, 106 (1961).

(5) M. Gates and T. A. Montzka, *J. Med. Chem.*, **7**, 127 (1964).

(6) S. Archer, N. F. Albertson, L. S. Harris, A. K. Pierson, and J. G. Bird, *ibid.*, **7**, 123 (1964).

(7) F. Leuschner, *Arch. Exp. Pathol. Pharmakol.*, **225**, 95 (1955).

(8) F. DeSantis, Jr., and K. A. Nieforth, *J. Pharm. Sci.*, **65**, 1479 (1976).

(9) A. H. Kibbe, J. A. Bedford, R. F. Borne, and M. C. Wilson, *Pharmacol. Res. Commun.*, **9**, 367 (1977).

(10) T. A. Montzka, J. D. Matiskella, and R. A. Partyka, *Tetrahedron Lett.*, **1974**, 1325.

(11) R. F. Borne, J. A. Bedford, J. L. Buelke, C. B. Craig, T. C. Hardin, A. H. Kibbe, and M. C. Wilson, *J. Pharm. Sci.*, **66**, 119 (1977).

(12) H. L. Schmidt and G. Werner, *Justus Liebigs Ann. Chem.*, **653**, 184 (1962).

(13) G. A. Wiley, R. L. Hershkowitz, B. M. Rein, and B. C. Chung, *J. Am. Chem. Soc.*, **86**, 964 (1964).

(14) A. E. Drukker, Neth. Appl. 6,613, 986; through *Chem. Abstr.*, **68**, 59608m (1968).

(15) E. Gray and V. P. Whittaker, *J. Anat. (London)*, **96**, 79 (1962).

(16) L. Neckers and P. Y. Sze, *Brain Res.*, **93**, 123 (1975).

(17) W. H. Morse and R. T. Kelleher, *J. Exp. Anal. Behav.*, **9**, 267 (1966).

(18) D. Kandel, D. Doyle, and M. W. Fischman, *Pharmacol. Biochem. Behav.*, **3**, 705 (1975).

(19) P. L. Carlton and D. L. Wolgin, *Physiol. Behav.*, **7**, 221 (1971).

ACKNOWLEDGMENTS

The authors thank the Connecticut Drug Dependency Trust for supporting this research. They also thank Dr. P. Y. Sze, Biobehavioral Sciences Department, University of Connecticut, for help in the serotonin uptake studies.

Bioavailability of Sulfadiazine Solutions, Suspensions, and Tablets in Humans

MARVIN C. MEYER *x, ARTHUR B. STRAUGHN *, GOLLAMUDI RAMACHANDER *, JERRY C. CAVAGNOL *, and A. F. BIOLA MABADEJE ‡

Received January 3, 1978, from the *Department of Medicinal Chemistry, College of Pharmacy, University of Tennessee Center for the Health Sciences, Memphis, TN 38163, and the ‡Department of Pharmacology, College of Medicine, University of Lagos, Lagos, Nigeria. Accepted for publication March 23, 1978.

Abstract □ A four-way crossover sulfadiazine bioavailability study was conducted in 16 normal healthy male volunteers. The subjects were divided into groups of eight. Each group received four different oral dosage forms of sulfadiazine at 1-week intervals: a solution as a reference, a suspension, and two different tablets. All dosage forms were equivalent to 500 mg of sulfadiazine. Blood samples were obtained at 0, 0.5, 1.0, 2.0, 3.0, 4.0, 6.0, 8.0, 10.0, 25.0, 33.0, and 49.0 hr. Analysis of variance indicated no statistically significant difference ($p > 0.05$) between the dosage forms in terms of area under the plasma level–time curve, peak plasma concentration, and time of peak plasma concentration. In both groups, there were differences between products at isolated sampling times. It was concluded that the four tablet formulations of sulfadiazine exhibited bioavailability characteristics equivalent to those of the solution and the suspension.

Keyphrases □ Sulfadiazine—bioavailability of various dosage forms compared in humans □ Bioavailability—sulfadiazine, various dosage forms compared in humans □ Antibacterials—sulfadiazine, bioavailability of various dosage forms compared in humans

Sulfadiazine, an anti-infective sulfonamide, is used mainly in the treatment of chancroid, trachoma, nocardiosis, and acute urinary tract infections. The drug has an aqueous solubility of less than 0.2 mg/ml (1). Bioavailability differences among sulfadiazine products have been noted (1–5). Sulfadiazine also has appeared on several lists of drugs with potential or actual bioavailability differences (6, 7). In addition, the Food and Drug Administration (FDA) recently implemented a bioequivalence requirement for sulfadiazine tablets (8). In view of the potential for sulfadiazine dosage forms to exhibit bioinequivalence, this study was undertaken to assess the relative bioavailability of currently marketed products.

EXPERIMENTAL

Selection of Products—Four lots of 500-mg sulfadiazine tablets manufactured by different companies met the USP XIX specifications for sulfadiazine tablets[1]. A commercially available suspension containing 500 mg of sulfadiazine/5 ml was employed as a reference product. The suspension was administered with an oral syringe.

A solution of sulfadiazine also was utilized as a reference dosage form. The oral solution was prepared from 10 ml of sulfadiazine sodium (0.25 g/ml) ampuls[2]. A 2.8-ml aliquot was removed from the ampul, equivalent to 500 mg of sulfadiazine, and combined with 20 ml of a chocolate syrup in a 100-ml beaker. The mixture was further diluted with 50 ml of water prior to administration. Care was taken that the entire contents of the beaker were ingested by the subjects.

The individual products are identified in Table I.

Clinical Protocol—Sixteen male volunteers[3] underwent urine analysis and hematological and blood chemistry[4] determinations to ensure that they were in good health. The 16 individuals were divided into groups of eight (Groups I and II). The subjects ranged in age from 20 to 30 years, in weight from 66.8 to 93.2 kg, and in height from 168 to 193 cm. The weight of each subject was within ±10% of the ideal weight for his age, sex, height, and build.

Each subject received a single tablet, suspension dose, or oral solution equivalent to 500 mg of sulfadiazine once a week for 4 weeks. The administration sequence was based on a crossover matrix designed to minimize the influence of any residual or cumulative effects of the preceding doses (9). Each group received two tablet products, the suspension, and the solution. The administration sequence of the drug formulations is presented in Table I.

The subject initially designated as Subject 6 in Group I exhibited signs of an allergic reaction to the first dose of sulfadiazine and was replaced by a new subject. All data reported relative to Subject 6 of Group I concern the subject who replaced the individual experiencing the reaction.

The subjects were given the sulfadiazine products along with 200 ml of water in the morning following an overnight fast. No food or liquid, other than water, was permitted until 4 hr after ingestion. The subjects avoided the use of any other medication during the study.

Blood samples, 10 ml, were collected in heparinized containers at 0, 0.5, 1.0, 2.0, 3.0, 4.0, 6.0, 8.0, 10.0, 25.0, 33.0, and 49.0 hr. The blood samples were centrifuged immediately, and the plasma fraction was removed and frozen until assayed. Aliquots of 2 ml of plasma were assayed in duplicate, using an adaptation of the Bratton–Marshall (10) procedure as previously described (11).

RESULTS AND DISCUSSION

Analysis of variance was used to evaluate statistically significant differences in plasma sulfadiazine levels ($p < 0.05$) at each sampling time. In addition, the time of peak plasma level, peak plasma level, and area under the plasma level–time curve (*AUC*) were subjected to statistical analysis. Where statistically significant differences occurred, the Newman–Keuls *a posteriori* test was used to determine which subjects, treatment sequence, or dosage forms were different ($p < 0.05$).

Plasma Levels at Each Sampling Time—The mean values for plasma sulfadiazine levels at each sampling time for both groups are summarized in Table II and graphically presented in Figs. 1 and 2. In both groups, the plasma levels exhibited considerable variability at each sampling time, with a relative standard deviation generally greater than 20%.

The variability of Product 3 in Group I was greater than that of the

Table I—Experimental Design for Bioavailability Study

Study Group	Subject	Sulfadiazine Products[a] Week 1	Week 2	Week 3	Week 4
I	1, 2	1	2	4	3
I	3, 4	2	3	1	4
I	5, 6	3	4	2	1
I	7, 8	4	1	3	2
II	1, 2	1	2	4	3
II	3, 4	2	3	1	4
II	5, 6	3	4	2	1
II	7, 8	4	1	3	2

[a] Numbers represent product code numbers. Product 1, the oral solution prepared as described in the text, and Product 2, the suspension (Coco-Diazine, 0.5 g/5 ml, lot 0BT91A, Eli Lilly), were common to both groups. The tablet code numbers are as follows: Group I, Product 3, 0.5-g tablets, lot 9SW20A, Eli Lilly; Group I, Product 4, 0.5-g tablets, lot 474206, Lederle Laboratories; Group II, Product 3, 0.5-g tablets, lot 116510, Stanlabs; and Group II, Product 4, 0.5-g tablets, lot 30565, Richlyn Laboratories.

[1] Tablets and data were provided by FDA.
[2] Injection, Lederle Labs, lot 458-151.
[3] Staff and students of the University of Tennessee Center for the Health Sciences. Written informed consent was obtained.
[4] SMA 18/90.

0022-3549/78/1200-1659$01.00/0
© 1978, American Pharmaceutical Association

Table II—Plasma Sulfadiazine Levels at Each Sampling Time [a]

Product [b]	0.5 hr	1 hr	2 hr	3 hr	4 hr	6 hr	8 hr	10 hr	25 hr	33 hr	49 hr
					Group I						
1	15.8	16.9	18.0	17.7	17.3	15.1	12.6	10.8	4.3	2.6	1.0
	(46.6)	(36.2)	(30.6)	(26.5)	(19.0)	(21.1)	(19.1)	(19.3)	(33.5)	(53.0)	(67.9)
2	6.5	9.4	15.3	17.5	17.3	15.1	13.0	11.5	5.0	3.1	1.3
	(59.7)	(44.1)	(21.2)	(13.9)	(17.3)	(15.6)	(15.4)	(17.6)	(32.1)	(50.8)	(81.0)
3	2.5	7.0	11.9	14.5	16.7	16.0	i3.6	11.8	5.3	3.3	1.4
	(138.8)	(104.0)	(58.0)	(37.9)	(30.0)	(25.1)	(23.4)	(24.4)	(34.1)	(50.4)	(70.5)
4	3.0	8.8	13.4	14.8	16.0	15.0	13.1	11.5	4.8	3.0	1.3
	(88.5)	(50.9)	(33.7)	(27.9)	(13.6)	(18.1)	(16.3)	(20.2)	(30.9)	(49.5)	(68.4)
					Group II						
1	14.1	15.4	17.5	18.4	18.3	15.9	13.3	11.3	4.5	2.6	0.9
	(27.3)	(23.2)	(18.1)	(12.4)	(12.3)	(10.2)	(12.3)	(i6.3)	(31.2)	(38.0)	(71.9)
2	7.2	11.3	15.4	17.3	17.2	15.1	13.2	11.3	4.7	2.4	0.9
	(53.0)	(41.7)	(27.1)	(15.8)	(16.8)	(18.4)	(12.5)	(16.7)	(23.7)	(35.8)	(63.8)
3	6.1	11.8	15.6	17.5	17.6	16.7	14.5	12.9	5.7	3.4	1.3
	(67.4)	(48.4)	(35.4)	(22.4)	(20.7)	(19.9)	(25.4)	(27.3)	(43.0)	(50.6)	(66.1)
4	2.5	5.7	11.7	17.0	18.1	17.6	15.0	12.9	5.6	3.2	1.3
	(104.7)	(83.1)	(49.0)	(26.3)	(20.8)	(14.5)	(18.9)	(21.0)	(39.4)	(52.0)	(68.2)

[a] Average data for eight subjects; concentration in micrograms per milliliter; relative standard deviation in percent given in parentheses. [b] See Table I for product code numbers.

Table III—Sulfadiazine Bioavailability Parameters [a]

Product	Peak Plasma Level, μg/ml	Time of Peak Level, hr	$AUC_{(0-49\ hr)}$, μg/ml × hr	$AUC_{(0-\infty)}$, μg/ml × hr	*AUC* Normalized, (μg/ml)(kg/mg)
			Group I		
1	19.3	3.3	317.9	336.6	3.15
	(21.3)	(27.3)	(25.5)	(28.4)	(11.8)
2	17.8	3.9	327.8	354.1	3.11
	(14.7)	(29.1)	(21.1)	(26.7)	(15.4)
3	17.7	3.5	328.5	355.9	3.18
	(28.3)	(68.3)	(24.6)	(28.5)	(21.3)
4	17.4	2.9	314.8	340.4	3.13
	(13.2)	(57.9)	(21.7)	(25.7)	(17.8)
			Group II		
1	19.0	3.0	326.4	342.2	3.31
	(14.4)	(30.9)	(18.6)	(21.6)	(9.3)
2	18.2	3.6	313.2	328.8	3.24
	(17.7)	(53.0)	(17.3)	(19.4)	(10.8)
3	19.0	3.9	358.3	382.0	3.56
	(20.9)	(48.6)	(26.9)	(29.6)	(15:4)
4	18.9	4.5	349.8	373.7	3.49
	(16.0)	(29.1)	(27.7)	(31.1)	(12.0)

[a] Each value is the mean of eight subjects with relative standard deviation given in parentheses.

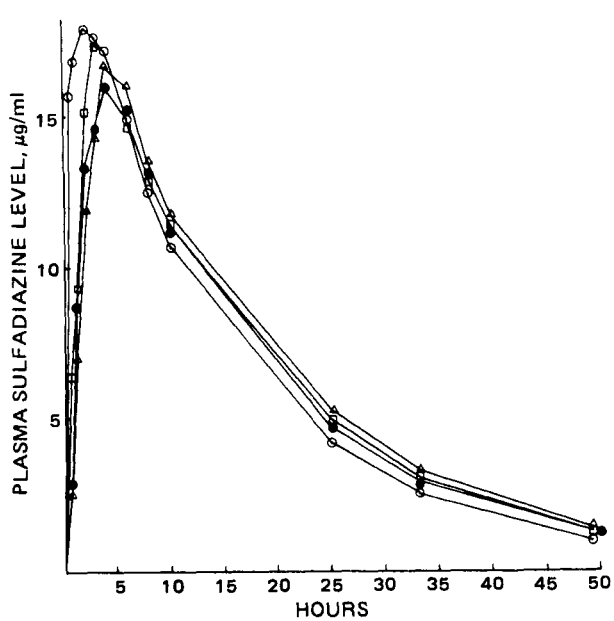

Figure 1—*Mean plasma sulfadiazine levels for Group I. Each data point represents the mean of eight subjects. Key:* ○, *Product 1;* □, *Product 2;* △, *Product 3; and* ●, *Product 4.*

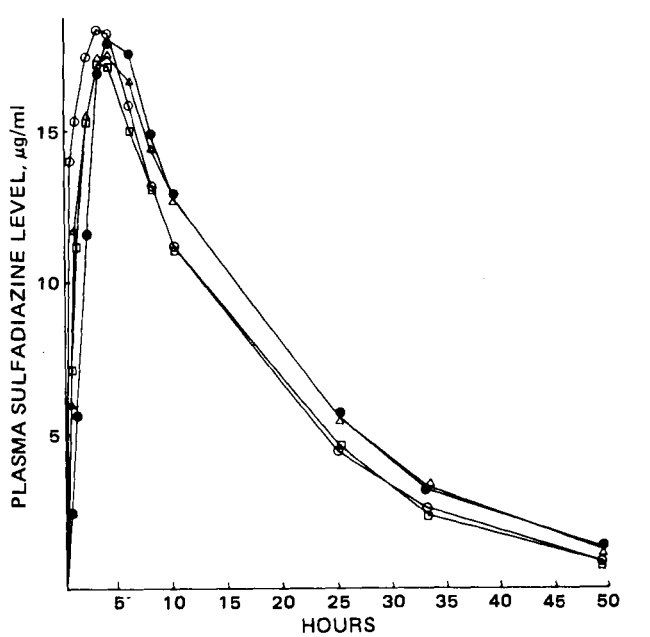

Figure 2—*Mean plasma sulfadiazine levels for Group II. Each data point represents the mean of eight subjects. Key:* ○, *Product 1;* □, *Product 2;* △, *Product 3; and* ●, *Product 4.*

Table IV—Power Analysis Table [a]

Parameter	Minimum Number of Subjects for 20% Difference		Minimum Detectable Difference, %	
	Group I	Group II	Group I	Group II
0.5 hr	≥30	20	54.8	33.3
1.0 hr	≥30	≥30	61.9	45.9
2.0 hr	≥30	20	56.8	34.0
3.0 hr	≥30	10	43.5	24.5
4.0 hr	10	10	23.7	23.4
6.0 hr	8	6	21.4	17.8
8.0 hr	4	4	14.1	16.5
10.0 hr	8	6	20.3	19.2
25.0 hr	4	16	15.0	32.7
33.0 hr	16	16	29.5	32.9
49.0 hr	≥30	≥30	46.8	46.2
Peak plasma concentration, μg/ml	6	8	19.2	20.5
Time of peak plasma concentration, hr	≥30	≥30	63.8	55.4
$AUC_{(0\text{-}49\ hr)}$, μg/ml × hr	4	6	13.6	18.2
$AUC_{(0\text{-}\infty)}$, μg/ml × hr	4	6	12.3	19.7
AUC (normalized), (μg/ml)(kg/mg)	10	6	24.6	19.6

[a] $\alpha = 0.05$, and $\beta = 0.2$.

other tablet (Product 4) in Group I, and both tablet products exhibited greater variability in plasma levels than did the solution (Product 1) or the suspension (Product 2). In the Group II study, one tablet (Product 4) showed greater variability than did the other tablet product (Product 3); both tablet formulations were more variable than either the solution (Product 1) or the suspension (Product 2).

The Newman–Keuls *a posteriori* test indicated significance differences ($p < 0.05$) between products at 0.5 and 1.0 hr for Group I and at 0.5, 1.0, and 2.0 hr for Group II. In the Group I study, the solution (Product 1) exhibited plasma levels greater than those of the other three dosage forms at 0.5 and 1.0 hr. In the Group II study, Product 4 resulted in significantly lower levels at 0.5, 1.0, and 2.0 hr. At 0.5 hr, Product 1 yielded significantly higher drug levels than those of the other dosage forms. At 25 hr, Product 1 exhibited significantly lower plasma levels than those of the other three dosage forms. No other significant differences ($p > 0.05$) between dosage forms were observed at any other sampling time in either the Group I or the Group II study.

Except for the 25-hr sample in the Group I study, there were no significant differences with respect to the sequence of dosage form administration. The Newman–Keuls *a posteriori* test did, however, indicate numerous significant differences at the various sampling times between individual subjects.

Peak Plasma Level, Time of Peak Level, and *AUC*—Table III summarizes the mean peak plasma concentrations, time of peak concentration, and *AUC*.

In both groups, the highest peak concentration was achieved with the solution (Product 1), although there were no statistically significant differences ($p > 0.05$) between the products in either group with respect to this parameter. The time of peak plasma concentration was also not significantly different among the solution, the suspension, and the tablet in either group. The relatively long mean peak level time of 3.0–3.3 hr for the solution may reflect an inherently slow absorption of sulfadiazine, or it may be related to drug precipitation from solution in the acid environment of the stomach. The actual time of peak plasma level may have been overestimated and the magnitude of the peak plasma level may have been underestimated, because the plasma samples were only obtained hourly from 1 to 4 hr after dose administration.

The $AUC_{(0\text{-}49\ hr)}$, computed using the trapezoidal rule, ranged from 314.8 (Product 4) to 328.5 (Product 3) μg/ml × hr in Group I and from 313.2 (Product 2) to 358.3 (Product 3) μg/ml × hr in Group II. In both groups, the $AUC_{(0\text{-}49\ hr)}$ did not differ by more than 13% between any two products. The *AUC* also was computed to time infinity, as previously described (11), and this value was normalized for half-life and a milligram per kilogram dose as suggested by Wagner (12). Neither of these parameters indicated any significant differences between the dosage forms included in either study group.

Biological Half-Life—The apparent half-life, estimated from the terminal slope of a semilog plot of plasma concentration *versus* time, was computed for each dose administered to each subject. In Group I, the mean half-life ranged from 11.1 (*SD* = 2.4) hr for Product 1 to 12.1 (*SD* = 3.3) hr for Product 2. Individual mean subject half-lives, computed for the four formulations, ranged from 9.0 (*SD* = 1.2) to 16.2 (*SD* = 0.9) hr.

In Group II, the mean half-life ranged from 10.0 (*SD* = 3.2) hr for Product 4 to 11.3 (*SD* = 2.9) hr for Product 3. Individual subject half-lives ranged from 9.4 (*SD* = 0.4) to 11.5 (*SD* = 0.9) hr. The observed range of half-lives was similar to previously reported values of 8–17 hr for sulfadiazine (13).

Significant differences were noted between subjects in terms of *AUC*. These differences could be related to the apparent half-life estimated for each subject. The subjects in each group with the lowest $AUC_{(0\text{-}49\ hr)}$ and $AUC_{(0\text{-}\infty)}$ values also exhibited the shortest half-life. Similarly, the subjects with the largest *AUC* values were those with the longest half-life.

Power Analysis—Table IV summarizes the results of the power analysis of the experimental design. The use of eight subjects in each study group was adequate to detect a 20% difference ($p < 0.05$) between formulations in terms of peak plasma concentration, $AUC_{(0\text{-}49\ hr)}$, and $AUC_{(0\text{-}\infty)}$. Because of the variability of the plasma levels at the early sampling times and at the terminal portion of the study, greater than 30 subjects would have been required for differences of this magnitude to be statistically significant at these times.

REFERENCES

(1) W. A. Ritschel, G. Ritschel, C. R. Buncher, and J. Rotmensch, *Drug Intel. Clin. Pharm.*, **10**, 402 (1976).

(2) J. G. Reinhold, F. J. Phillips, and H. F. Flippin, *Am. J. Med. Sci.*, **210**, 141 (1945).

(3) E. M. Boyd and R. W. Dingwall, *ibid.*, **213**, 549 (1947)

(4) G. R. Van Petten, G. C. Becking, R. J. Withey, and H. F. Lettau, *J. Clin. Pharmacol.*, **11**, 27 (1971).

(5) A. Maleque and K. Ahmad, *Bangladesh Pharm. J.*, **3**, 13 (1974).

(6) *J. Am. Pharm. Assoc.*, **NS 13**, 278 (1973).

(7) *F-D-C Reports*, July 15, 1974.

(8) *Fed. Regist.*, **42** (5), 1624 (Jan. 7, 1977).

(9) E. G. Williams, *Aust. J. Sci. Res. A*, **2**, 149 (1949).

(10) A. C. Bratton and E. K. Marshall, *J. Biol. Chem.*, **128**, 537 (1939).

(11) G. W. A. Slywka, A. P. Melikian, A. B. Straughn, P. L. Whyatt, and M. C. Meyer, *J. Pharm. Sci.*, **65**, 1494 (1976).

(12) J. G. Wagner, "Fundamentals of Clinical Pharmacokinetics," Drug Intelligence Publications, Hamilton, Ill., 1975, pp. 347, 348.

(13) W. A. Ritschel, in "Perspectives in Clinical Pharmacy," 1st ed., D. E. Francke and H. A. K. Whitney, Jr., Drug Intelligence Publications, Hamilton, Ill., 1972, pp. 286–324.

ACKNOWLEDGMENTS

Supported in part by a contract from the Tennessee Department of Public Health and by FDA Contract 223-74-3097.

The authors gratefully acknowledge the support of Mr. Herbert Bates, Jr., Pharmacist Consultant, Tennessee Department of Public Health; the technical assistance of Mrs. Cathy Wibking, Mrs. Vicki Proefrock, and Mrs. Peg Westmoreland; the assistance of Mrs. Ann McEachran in the statistical and computer analysis of the data; and the medical supervision provided by Dr. Philip Liberman.

Quantitation of the Anti-Inflammatory Agent Fenbufen and Its Metabolites in Human Serum and Urine Using High-Pressure Liquid Chromatography

G. E. VAN LEAR ˣ, F. S. CHICCARELLI, P. A. BONENFANT, and A. BARR

Received December 27, 1977, from *Lederle Laboratories, A Division of American Cyanamid Company, Pearl River, NY 10965.* Accepted for publication March 30, 1978.

Abstract □ Specific procedures are described for the determination of fenbufen and its metabolites in serum and urine using high-pressure liquid chromatography. Serum or urine extracts were chromatographed on a bonded reversed-phase partitioning column. The sensitivity of the assay for fenbufen was 0.5 μg/ml in serum with 2-ml samples and 1.0 μg/ml in urine with 1-ml samples. The procedures are suitable for bioavailability and pharmacokinetic studies.

Keyphrases □ Fenbufen—high-pressure liquid chromatographic analysis in serum and urine □ High-pressure liquid chromatography—analysis, fenbufen in serum and urine □ Anti-inflammatory agents—fenbufen, high-pressure liquid chromatographic analysis in serum and urine

Fenbufen[1], 3-(4-biphenylylcarbonyl)propionic acid (I), is an orally effective, nonsteroidal, anti-inflammatory analgesic and antipyretic agent (1) and has been shown to be an effective and safe treatment for rheumatoid arthritis in humans (2–4). In a program to determine the structure–activity relationships of a series of analogs (5), two major human serum metabolites of fenbufen, 3-(4-biphenylylhydroxymethyl)propionic acid (II) and 4-biphenylacetic acid (III), were found to possess the same spectrum of activity as fenbufen itself. A TLC assay[2] for fenbufen and these metabolites, based on chromatographic separation followed by quantitation, was reported (6).

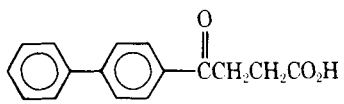

I

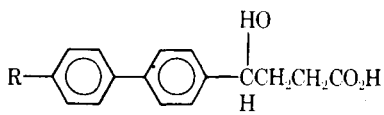

II: R = H
V: R = OH

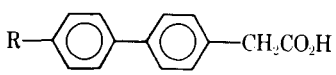

III: R = H
IV: R = OH

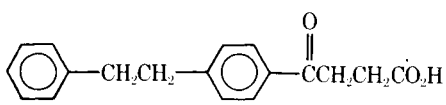

VI

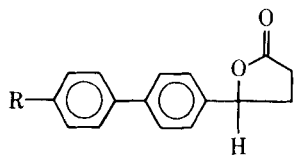

VII: R = H
VIII: R = OH

For bioavailability studies where large numbers of samples must be analyzed, a simpler analytical procedure was required. This paper describes a quantitative assay for I–III as well as two additional fenbufen serum and urinary metabolites, 4′-hydroxy-4-biphenylacetic acid (IV) and 3-(4′-hydroxy-4-biphenylylhydroxymethyl)propionic acid (V), based on high-pressure liquid chromatography (HPLC).

Table I—Retention Volumes, V_R, for I–V on Reversed-Phase HPLC [a]

Compound	V_R, ml
I	40.52
II (VII)[b]	54.00
III	31.38
IV	14.60
V (VIII)[b]	21.72
VI	82.94

[a] Chromatographic conditions are described under *Experimental.* [b] Compounds II and V form lactones VII and VIII, respectively, during the assay.

Table II—Absolute Recovery (Percent ± *SD*) of I–V from Spiked Serum Specimens [a]

Compound[b]	Amount Added, μg/ml[c]			
	2.5	0.625	50.0	12.5
I	93.03 ± 4.38	—	92.11 ± 4.23	—
II	93.60 ± 4.43	—	87.09 ± 4.68	—
III	98.75 ± 5.55	—	93.73 ± 4.08	—
IV	—	69.15 ± 5.87	—	61.42 ± 2.72
V	—	94.59 ± 7.91	—	85.35 ± 3.09

[a] The procedure to determine these values is described under *Experimental.* [b] Absolute recovery of VI was 93.72 ± 2.45%. [c] Five samples at each concentration level.

Table III—Absolute Recovery (Percent ± *SD*) of I–V from Spiked Urine Samples [a]

Compound[b]	Amount Added, μg/ml[c]		
	5	25	200
I	102.36 ± 5.65	107.80 ± 4.12	91.44 ± 1.44
II	76.88 ± 1.92	86.59 ± 5.00	92.45 ± 1.76
III	101.21 ± 9.85	106.10 ± 2.39	94.48 ± 1.22
IV	76.80 ± 0.68	87.62 ± 7.02	99.59 ± 1.47
V	63.09 ± 2.48	69.46 ± 3.60	71.31 ± 1.16

[a] The procedure to determine these values is described under *Experimental.* [b] Absolute recovery of VI was 95.68 ± 2.31% from spiked urine samples. [c] With the exception of I at 5 μg/ml where there were only four determinations, all other values are for five determinations.

[1] Cinopal.

[2] F. S. Chiccarelli, unpublished data.

0022-3549/78/1200-1662$01.00/0
© 1978, American Pharmaceutical Association

Table IV—Precision Data for the Determination of I–V in Spiked Serum

Amount Added, I–III, μg/ml	Amount Added, IV and V, μg/ml	Assay Concentration, μg/ml of Serum[a] I	II	III	IV	V
100	25	96.54 ± 2.16	96.17 ± 2.36	93.90 ± 3.01	24.47 ± 1.08	25.53 ± 1.05
50	12.5	47.87 ± 1.96	47.85 ± 2.29	46.88 ± 2.60	12.17 ± 0.39	12.49 ± 0.48
25	6.25	24.42 ± 0.61	25.36 ± 2.58	24.67 ± 1.96	6.37 ± 0.52	6.41 ± 0.41
10	2.5	9.99 ± 0.28	9.97 ± 0.40	9.83 ± 0.26	2.52 ± 0.19	2.49 ± 0.12
5	1.25	5.00 ± 0.11	4.99 ± 0.19	4.93 ± 0.14	1.24 ± 0.08	1.23 ± 0.04
2.5	0.625	2.57 ± 0.07	2.57 ± 0.06	2.42 ± 0.42	0.63 ± 0.06	0.63 ± 0.09
1.25	0.312	1.37 ± 0.08	1.31 ± 0.06	1.42 ± 0.10	0.33 ± 0.06	0.32 ± 0.05
Mean percent recovery ± *RSD*		100.32 ± 4.72	100.06 ± 3.32	99.03 ± 6.85	100.83 ± 2.82	100.85 ± 1.62

[a] Mean ± *SD* for six determinations at each level.

Table V—Precision Data for the Determination of I–V in Spiked Urine

Amount Added, μg/ml	Assay Concentration, μg/ml of Urine[a] I	II	III	IV	V
200	205.95 ± 12.23	200.45 ± 14.12	201.30 ± 8.29	197.25 ± 9.53	200.37 ± 2.69
100	103.12 ± 3.09	99.02 ± 4.75	101.95 ± 1.12	102.10 ± 3.41	101.33 ± 3.43
50	52.60 ± 1.60	50.50 ± 2.26	51.34 ± 1.53	52.40 ± 2.96	51.10 ± 1.99
25	26.32 ± 1.30	25.30 ± 1.37	25.75 ± 0.90	26.45 ± 1.60	25.90 ± 0.98
10	9.68 ± 0.43	10.52 ± 0.84	10.01 ± 0.28	10.02 ± 0.29	10.15 ± 0.31
5	4.98 ± 0.48	5.13 ± 0.56	4.98 ± 0.47	4.78 ± 0.33	4.90 ± 0.42
Mean percent recovery ± *RSD*	102.25 ± 3.36	102.60 ± 2.10	101.33 ± 1.39	101.19 ± 3.79	101.14 ± 1.94

[a] Mean ± *SD* for five determinations at each level.

EXPERIMENTAL

Reagents—Fenbufen, its metabolites, and the internal standard[3] (VI) were used as received[4]. Spectroquality solvents were used in the chromatography. All other solvents were analytical grade.

Standard Solutions—A solution of the internal standard was prepared in methanol (100 μg/ml). For the serum assay, a solution containing I–III, each at a concentration of 100 μg/ml, and IV and V, each at a concentration of 25 μg/ml, was prepared in methanol. A stock solution containing I–V, each at a concentration of 50 μg/ml, was prepared in methanol for the urine assay.

Chromatographic Conditions—The high-pressure liquid chromatograph[5] was equipped with a variable wavelength UV absorbance detector set at 265 nm with a sensitivity of 0.05 aufs. The column used for chromatography of serum and urine extracts was 10-μm porous silica bonded with octadecylsilane for reversed-phase chromatography[6]. The mobile phase was chloroform–methanol–water–acetic acid (0.33:33:66:0.67 v/v) at a flow rate of 2.50 ml/min. The chromatograph oven was maintained at 45°. Retention volumes for fenbufen and its metabolites are shown in Table I.

Assay—*Serum*—The internal standard (2 ml) containing 200 μg of VI was added to a 20-ml screw-capped test tube. After removal of the methanol with a nitrogen stream, the standard was redissolved in 0.25 ml of 0.1 *N* NaOH. To this alkaline solution was added 2 ml of human serum, and the contents of the tube were thoroughly mixed for 45 sec. Then a 2.0-ml aliquot of concentrated hydrochloric acid was carefully added, and the tube was shaken for 30 sec. After standing for 5 min, the acid solution was extracted with 15 ml of cyclohexane–ether (7:3 v/v).

Following centrifugation, as much as possible of the organic phase was transferred to a new tube, and the solvent was evaporated to dryness under a stream of clean dry nitrogen. The residue was redissolved in 1.5 ml of chloroform–methanol–acetic acid–water (0.95:94.05:0.05:4.95 v/v), and the solution was filtered through a 0.5-μm filter[7] into a clean, dry tube. A 36-μl aliquot of the final extract was injected into the chromatograph.

The concentrations of fenbufen and its metabolites were determined from standard curves, employing peak area ratios of drug-related material to internal standard *versus* concentrations in normal serum. A laboratory computer system[8] was used for these calculations.

Urine—The procedure for extraction of urine (1 ml) aliquots was exactly as for serum, except that only 100 μg of the internal standard and 1 ml of concentrated hydrochloric acid were used and the extraction solvent was chloroform–ether (8:3 v/v) in two portions, 15 and 10 ml.

Absolute Recovery of Fenbufen and Metabolites—Aliquots of serum (2 ml) and urine (1 ml) were spiked with known quantities of fenbufen and its metabolites to give drug concentrations as detailed in Tables II and III, respectively. After the samples were treated as described under *Assay*, the peak areas for the respective components were compared to peak areas from the same amount of material[9] that did not go through the extraction procedure to give absolute recoveries.

Precision Determinations—Aliquots of normal human serum and urine were spiked with known amounts of fenbufen and its metabolites to give several concentrations of drug-related material (Tables IV and V, respectively). The samples were assayed using the analytical conditions

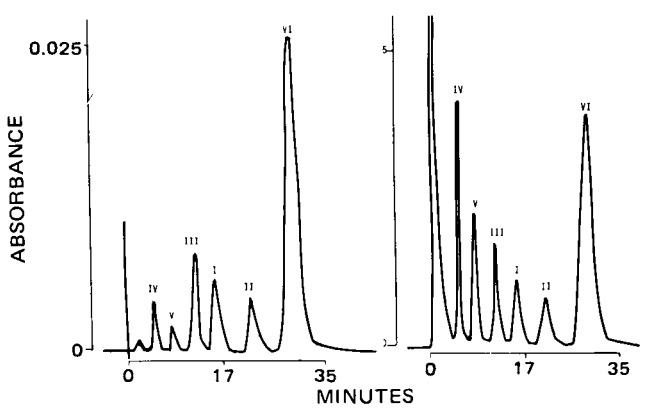

Figure 1—*Representative chromatograms of serum (left) and urine (right) extracts containing I–V plus an internal standard (VI).*

[3] 3-[4-(2-Phenylethyl)benzoyl]propanoic acid.
[4] Supplied by Lederle Laboratories.
[5] Model 7114-24 chromatograph, model 785 UV absorbance detector, and model 725 autoinjector, Micromeritics Instrument Corp., Norcross, Ga.
[6] Partisil-10 ODS column (4.6 mm i.d. × 25 cm), Whatman, Inc., Clifton, N.J.
[7] Fluoropore, FHLP 01300, Millipore Corp., Bedford, Mass.
[8] Model 3352 data system, Hewlett-Packard, Cupertino, Calif.
[9] Instead of II and V, respectively, the respective lactones VII and VIII were substituted. As described later, the lactones are actually the species chromatographed in the assay.

Table VI—Serum Concentrations of I–V following a Single Oral Dose of 600 mg of I [a]

Hours after Dose	Concentration in Serum, μg/ml				
	I	II	III	IV	V
0	0	0	0	0	0
0.16	<0.50	<0.50	<0.50	<0.50	<0.50
0.33	<0.50	<0.50	<0.50	<0.50	<0.50
0.50	3.48	5.98	<0.50	<0.50	<0.50
0.75	8.69	27.97	0.65	<0.50	<0.50
1	6.21	39.25	0.91	<0.50	<0.50
2	6.97	71.47	2.45	<0.50	1.00
4	2.97	61.86	4.91	<0.50	1.27
6	1.98	49.73	5.60	0.59	0.85
12	1.58	33.64	6.29	0.50	0.50
24	1.02	19.43	5.31	0.56	<0.50
36	0.76	13.36	4.34	<0.50	<0.50
48	<0.50	6.27	2.13	<0.50	<0.50

[a] Chromatographic conditions are described under *Experimental.*

Table VII—Total I–V (Milligrams) Excreted over 2 Days in Urine of an Adult Male after a Single Oral Dose of 600 mg of I [a]

Day[b]	I	II	III	IV	V	Total Percent of Dose[c]
1	19.3	7.5	28.6	68.0	103.4	38.87
2	3.0	—	8.1	30.3	26.0	11.79
Total	22.3	7.5	36.7	98.3	129.4	50.66

[a] Chromatographic conditions are described under *Experimental.* [b] Values noted are sum of individual results for fractional urines collected during Days 1 and 2. [c] Values were collected for stoichiometric differences.

detailed under *Assay.*

Clinical Study—One adult male volunteer was given two 300-mg capsules of I. Serum samples were obtained at 0, 10, 20, 30, and 45 min and 1, 2, 4, 6, 12, 24, 36, and 48 hr after the dose. Urine samples were collected for 48 hr after the dose. The urine volume of each collection was measured, and an aliquot was frozen at −10° until analyzed.

RESULTS AND DISCUSSION

Fenbufen and its metabolites, II–V, have similar chemical properties, and all are strongly bound to serum proteins. In this procedure, treatment of serum specimens with concentrated hydrochloric acid breaks the protein binding and converts II and V essentially quantitatively to their corresponding lactones, 5-(4-biphenylyl)-2(3*H*)-dihydrofuranone (VII) and 5-(4′-hydroxy-4-biphenylyl)-2(3*H*)-dihydrofuranone (VIII). Metabolite III and lactone VII exhibit strong maxima in the UV at 254 nm while the absorption maximum for fenbufen occurs at 280 nm. Since the isosbestic point for I, III, and VII is at 265 nm, which is the maximum for UV absorption of IV and VIII, the lactone of V, this wavelength was chosen to monitor the chromatographic effluent. Typical chromatograms are shown in Fig. 1.

The HPLC conditions and the selection of the internal standard were established through several experiments. Initial efforts to develop an HPLC method led to a procedure based on absorption chromatography. Although this method was adequate for the determination of fenbufen and the major serum metabolites, II and III, it was not suitable for the determination of IV and V, which are the major urine metabolites. In addition, salicylic acid interfered. Neither deficiency is present in the procedure based on reversed-phase HPLC. Comparative retention volumes for I–VI[10] are presented in Table I. Representative chromatograms are shown in Fig. 1. No interfering peaks from normal serum or urine extracts were observed.

Absolute recoveries of I–V from spiked serum and urine are presented in Tables II and III, respectively. The recoveries from serum ranged from 69.15 to 98.75% with standard deviations less than 10%. Absolute recoveries from urine ranged from 63.09 to 107.80% with standard deviations less than 10%.

Precision data for the determination of fenbufen and its metabolites in serum are presented in Table IV. The mean relative accuracies were ±1% of the amount of I–III added over the 1.25–100-μg/ml range with relative standard deviations less than 7%. For IV and V, the relative accuracies observed were ±1% of the compound added for concentrations in the 0.312–25-μg/ml range; relative standard deviations were less than 3%. The lower limit of sensitivity for all components in the assay was 0.5 μg/ml with a 2-ml serum sample.

Precision data for the assay of normal urine specimens spiked with known concentrations of I–V are presented in Table V. The mean relative accuracies were ±3% of the amount added with relative standard deviations less than 5% over the 5–200-μg/ml range. The lower limits of sensitivity for the assay were 1.0 μg/ml for I–IV and 2.0 μg/ml for V with 1.0 ml of urine.

To demonstrate the utility of this method, serum and urine concentrations of fenbufen and its metabolites were measured in a normal male volunteer after oral administration of a 600-mg dose of fenbufen (Tables VI and VII). Serum and urine concentrations of I–V were readily measured during the 2-day period after drug ingestion.

The described reversed-phase HPLC method for fenbufen and its metabolites is both rapid and sensitive and can serve as a useful means for studying the pharmacokinetics and bioavailability of fenbufen.

REFERENCES

(1) A. E. Sloboda and A. C. Osterberg, *Inflammation*, **1**, 415 (1970).

(2) C. H. Nunes, *J. Rheum.*, **1**, 68 (1974).

(3) I. DeSalcedo, L. F. Arias, and B. P. Greenberg, *Curr. Ther. Res.*, **18**, 295 (1975).

(4) J. M. Vergara-Castro, L. F. Arias, and B. P. Greenberg, *J. Int. Med. Res.*, **4**, 418 (1976).

(5) R. G. Child, A. C. Osterberg, A. E. Sloboda, and A. S. Tomcufcik, *J. Pharm. Sci.*, **66**, 406 (1977).

(6) H. Yoshizawa, Y. Tada, T. Naruke, and M. Mizumura, *Basic Pharm. Ther.*, **2**, 31 (1974).

ACKNOWLEDGMENTS

The authors thank Dr. R. G. Kelly, Lederle Laboratories, for advice and support.

[10] Retention volumes quoted for II and V are actually those of their lactones VII and VIII, respectively.

Phase Solubility Analysis and PMR Study of Complexing Behavior of Dinoprostone with β-Cyclodextrin in Water

SYLVAN G. FRANK * **and MOO J. CHO** ‡x

Received May 11, 1977, from the *Division of Pharmaceutics and Pharmaceutical Chemistry, College of Pharmacy, Ohio State University, Columbus, OH 43210, and the ‡Pharmacy Research Unit, The Upjohn Company, Kalamazoo, MI 49001. Accepted for publication March 30, 1978.

Abstract □ The mechanism of inclusion compound formation by dinoprostone (prostaglandin E_2) with β-cyclodextrin was studied by phase solubility analysis and PMR spectroscopy. As indicated by the linear increase of aqueous solubility of dinoprostone with β-cyclodextrin concentration, some types of molecular interactions definitely exist between dinoprostone and the complexing ligands. The temperature dependence of a 1:1 complex formation constant yielded the following thermodynamic data at 20°: $\Delta G°$ = −4.11 kcal/mole, $\Delta H°$ = 7.20 kcal/mole, and $\Delta S°$ = 10.5 e.u. Since water was the solvent system, these parameters appear to be largely determined by solvent reorganization through hydrogen bonding rather than solely by the binding of desolvated free dinoprostone and β-cyclodextrin entities. PMR data indicate that dinoprostone is included within the cavity and also interacts with protons on the exterior of the β-cyclodextrin molecule. A model consisting of a 1:1 complex, in which a dinoprostone molecule is partially included within the cavity and the remainder of the molecule extends around the edge of the opening of the cavity to the exterior of the β-cyclodextrin molecule, is proposed as the most probable structure of this inclusion compound.

Keyphrases □ Dinoprostone—complexation with β-cyclodextrin, phase solubility and PMR analyses □ β-Cyclodextrin—complexation with dinoprostone, phase solubility and PMR analyses □ Complexation—dinoprostone with β-cyclodextrin, phase solubility and PMR analyses □ Phase solubility—analysis of complexation of dinoprostone with β-cyclodextrin □ PMR—analysis of complexation of dinoprostone with β-cyclodextrin□ Prostaglandins—dinoprostone, complexation with β-cyclodextrin, phase solubility and PMR analyses

Various molecules of pharmaceutical interest form inclusion compounds with cyclodextrins (1–4). The cyclodextrins, which are also known as Schardinger dextrins or cycloamyloses, are water-soluble, macrocyclic polymers that contain glucose units joined by α-1,4-linkages (5). The most common is β-cyclodextrin, which is formed by glucose units oriented in a ring, enclosing an internal cavity of about 8 Å diameter.

BACKGROUND

The cyclodextrins readily form relatively insoluble inclusion compounds with many substances of sizes able to be held wholly or partially within the cavity (1, 2, 5–11). The degree of reactivity of the host and guest is dependent on the presence of a suitable group or ring capable of entering the cyclodextrin cavity.

The chemical stability of dinoprostone (prostaglandin E_2) can be improved in the form of solid molecular complexes with polyvinylpyrrolidone (12), β-cyclodextrin (13), polyalkyl ethers (14), and other similar complexing ligands (15). In a given solvent system, if the molecular interaction between dinoprostone and these ligands is strong enough to produce a molecular complex with a definite stoichiometric ratio, then the apparent physicochemical properties of dinoprostone will differ from its intrinsic properties. The magnitude of the property change that occurs in the presence of a complexing ligand will depend not only on the difference of the property between pure dinoprostone and the complex but also on the concentration of the ligand in the system, because it will determine the equilibrium position of the reaction.

Changes in various physical properties of a compound can be followed as a quantitative measure of its molecular interactions with other ligands. The apparent solubility is perhaps the most commonly measured property, mainly because of its high sensitivity toward the formation of a complex and the simplicity involved in the determination. In this study, the apparent aqueous solubility of dinoprostone was measured as a function of the concentration of β-cyclodextrin at 10, 20, and 30°. From the thermodynamic parameters associated with the molecular interactions, the nature of the intermolecular forces involved was evaluated.

Experimental evidence indicates that dinoprostone undergoes hydrogen bonding with various functional groups, particularly hydroxyl groups; that it has a relatively long retention time on a silica gel column; and that it has extremely high and low solubilities in alcohols and simple aliphatic hydrocarbons, respectively. Consequently, the hydrogen bonding ability of dinoprostone with a compound known to complex with it was examined specifically. Even though water can participate competitively in hydrogen bonding, it was chosen as the solvent system, because β-cyclodextrin is sufficiently soluble in water [up to 1.85% at room temperature (5)] to cover a wide range of ligand concentrations.

NMR and X-ray investigations established that the cyclodextrin glucose units were in the C-1 chair configuration (4, 16). This arrangement had primary and secondary hydroxyl groups around the opening of the cavity on both sides of the molecule, with H-3, H-5, and, possibly, H-6 located within the cavity and H-1, H-2, and H-4 on the exterior. Atoms H-3 and H-5 were shielded by guest molecule protons on formation of an inclusion compound with cyclodextrins (17, 18).

The technique in these studies (17, 18) was based on the shielding of the interior protons of the cyclodextrin ring as a result of the anisotropy of the guest aromatic moiety; increasing chemical shifts could be detected with increasing concentrations of the guest species up to the saturation concentration. In the present work, this NMR technique was used to investigate the mechanism of formation of the β-cyclodextrin–dinoprostone inclusion compound.

EXPERIMENTAL

Into a series of 7-ml vials containing different amounts of β-cyclodextrin[1] in 5.0 ml of glass-distilled water, a large excess of dinoprostone was added. The vials were then shaken for 12 hr in a temperature-controlled water bath. At solubility equilibrium, each vial was left standing for 1 hr; then an aliquot of supernate was withdrawn and directly diluted with 1.0 *N* KOH. The absorbance was read[2] at 282 nm.

In calculating the dinoprostone concentration, an apparent absorptivity value of 52.0 A_{282} ml/mg cm was used. β-Cyclodextrin solutions were transparent at 282 nm. The concentrations of β-cyclodextrin stock solutions were calculated on the basis of the weight of the solutes.

Samples for NMR spectroscopy were prepared by saturating a 2% (w/v) solution of β-cyclodextrin in deuterium oxide[3] with dinoprostone. The excess β-cyclodextrin inclusion compound was allowed to precipitate, and the supernate was decanted. PMR spectra[4] at 100 MHz were determined on the supernate of the inclusion compound at 34 ± 1° in standard 5-mm tubes.

RESULTS AND DISCUSSION

Phase Solubility Analysis—As shown in Fig. 1, the apparent solubility of dinoprostone increased linearly with the concentration of β-cyclodextrin at all temperatures studied. For such a phase diagram, it is generally adopted that the complex formed is first order in ligand; the equilibrium constant for the formation of a 1:1 complex is given by:

$$K = \frac{\text{slope}}{S_0\,(1 - \text{slope})} \qquad \text{(Eq. 1)}$$

where S_0 is the solubility of the substrate in the absence of ligand, β-

[1] Nutritional Biochemicals, Inc. (used without further purification).
[2] Beckman model DB-G spectrophotometer.
[3] Bio-Rad Laboratories (99.85 mole % D_2O).
[4] Varian XL-100 NMR spectrometer.

0022-3549/78/1200-1665$01.00/0
© 1978, American Pharmaceutical Association

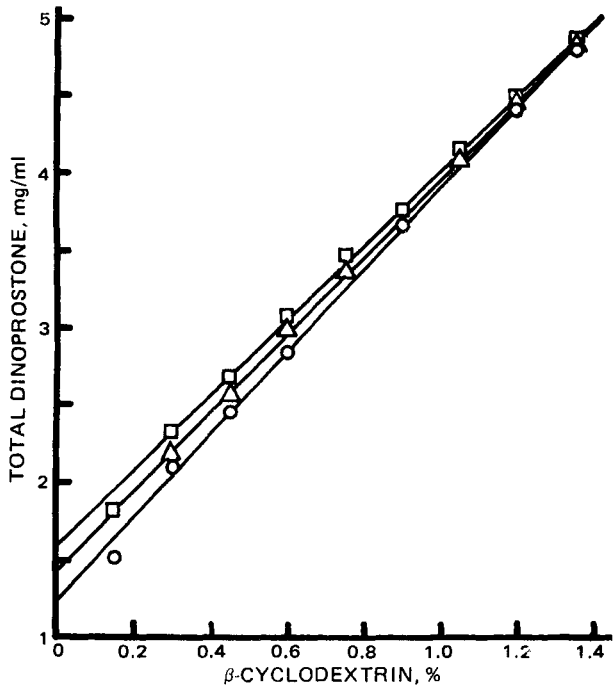

Figure 1—*Apparent aqueous solubility of dinoprostone as a function of the concentration of β-cyclodextrin at 10 (○), 20 (△), and 30° (□).*

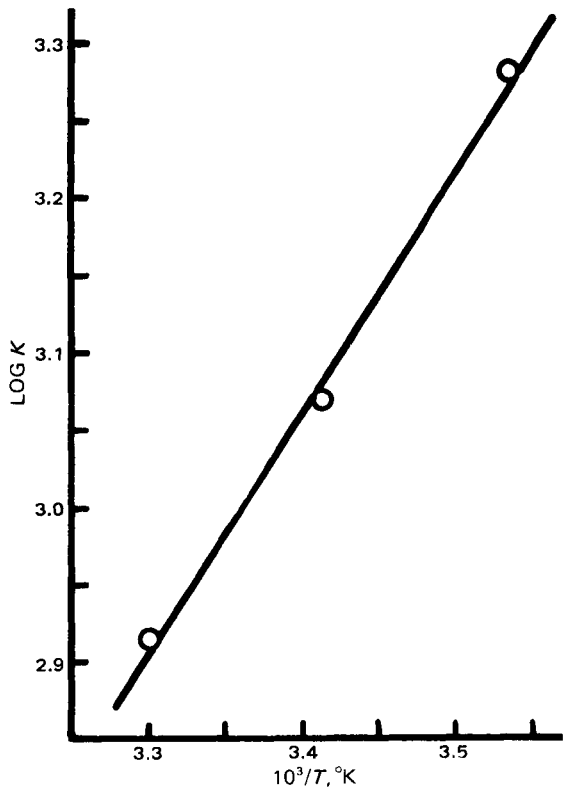

Figure 2—*Van't Hoff plot for the formation of a 1:1 complex of dinoprostone and β-cyclodextrin.*

cyclodextrin (19). The equilibrium constants calculated by Eq. 1 are listed in Table I. The key assumption was that the 1:1 complex was the only significant species present in the system besides free dinoprostone and β-cyclodextrin. All thermodynamic parameters (20) associated with the 1:1 complex formation are listed in Table I. As shown in Fig. 2, within experimental error, $\Delta H°$ appears to be independent over the temperature range of 10–30°.

Cyclodextrins bind a vast array of guest molecules equally well with little substrate specificity. The intermolecular forces involved can be hydrogen bonding (21), nonspecific van der Waals forces (21), hydrophobic interactions (22), or their combinations. As shown in Table I, the favorable enthalpy changes overcompensate for the unfavorable entropy changes, resulting in negative free energy changes at all temperatures. The magnitudes are very similar to those associated with the interaction of hydrocinnamic acid ($C_6C_5CH_2CH_2COOH$) with α-cyclodextrin [$(C_6H_{10}O_5)_6$], where, at 25°, $\Delta G° = -4.2$ kcal/mole, $\Delta H° = -7.5$ kcal/mole, and $\Delta S° = 11$ e.u. (23).

Since the size of the cavity provided by cyclodextrins plays the most important role in forming inclusion compounds, hydrocinnamic acid, being smaller than dinoprostone in size, conceivably fits better to α-cyclodextrin, whereas dinoprostone binds to β-cyclodextrin to the same extent. Hydrocinnamic acid does not form a complex with the β-form (23, 24), and the interaction of dinoprostone with the α-form is much less than its interaction with the β-form (13).

Since water, which may solvate dinoprostone and β-cyclodextrin in free entities through hydrogen bonding, was the solvent system employed, it is a very complicated task to interpret the thermodynamic data presented in Table I. However, if the mechanism involved in the interaction between hydrocinnamic acid and α-cyclodextrin is followed, then the heat gained on formation of a complex by the increased hydrogen bonding of water molecules released from the cyclodextrin cavity and the dinoprostone surroundings appears to be the major driving force of the interactions.

Even though dinoprostone is assumed to undergo hydrogen bonding actively with β-cyclodextrin, its contribution to the overall $\Delta H°$ reported in Table I may not be significant, simply because the number of hydrogen bonds involved must be smaller than that accompanied with the solvent reorganization. An unfavorable entropy change can result from the ordering effect of solvent reorganization as well as the reduced degrees of freedom of dinoprostone when it is confined in and around the cyclodextrin cavity.

PMR Studies—The PMR spectra of β-cyclodextrin and the β-cyclodextrin–dinoprostone inclusion compound in deuterium oxide are shown in Fig. 3. The β-cyclodextrin spectrum (Fig. 3B) is broken for ease in comparison of the two spectra; the large peak at approximately 4.6 ppm

Table I—Thermodynamic Parameters Associated with the Reaction Dinoprostone + β-Cyclodextrin ⇌ 1:1 Complex

Temperature	$10^{-3}K$, liter/mole	$\Delta G°$, kcal/mole	$\Delta H°$, kcal/mole	$\Delta S°$, e.u.
10°	1.917	−4.25	−7.20	−10.4
20°	1.170	−4.11	−7.20	−10.5
30°	0.819	−4.04	−7.20	−10.4

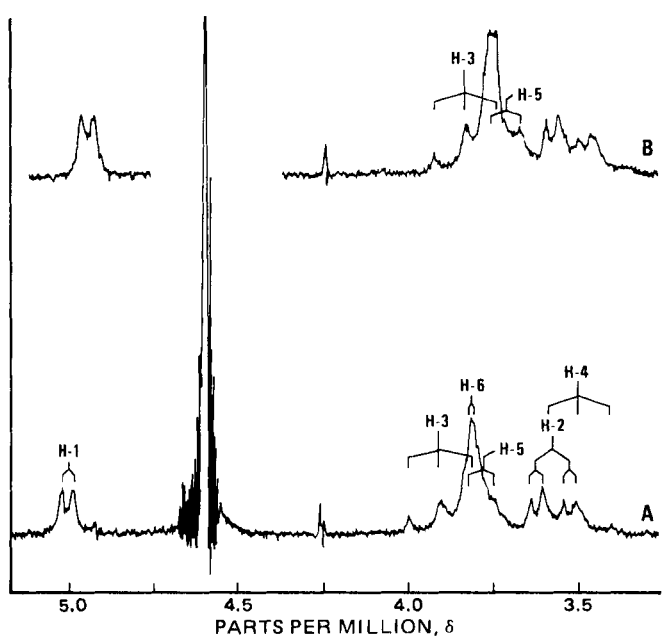

Figure 3—*PMR spectra of β-cyclodextrin (A) and the β-cyclodextrin–dinoprostone inclusion compound (B) in deuterium oxide.*

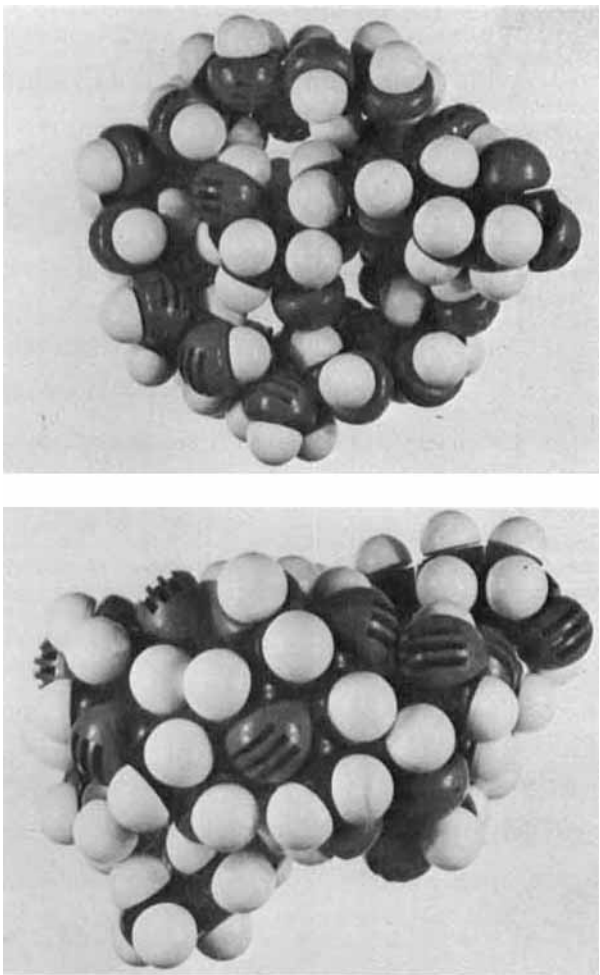

Figure 4—*CPK space-filling molecular model of the proposed dinoprostone–β-cyclodextrin (1:1) inclusion complex. Top: View from above with β-cyclodextrin in the plane of the page (the dinoprostone molecule extends from the right side of the β-cyclodextrin torus into the cavity). Bottom: View from the side with dinoprostone in the plane of the page, extending from upper right to lower left through the β-cyclodextrin cavity.*

due to small amounts of deuterium hydroxide and water as impurities is common to both spectra. No other peaks appear on the full 100-MHz spectrum; except for the deuterium hydroxide–water peak, all of the peaks observed in Fig. 3 are those of β-cyclodextrin.

In the presence of dinoprostone, the β-cyclodextrin spectrum is shifted upfield. The anomeric hydrogens, H-1, appear as a doublet at the farthest downfield position and are gauche, whereas the rest of the β-cyclodextrin protons are axial. Farther upfield is the large deuterium hydroxide–water peak. Due to its fixed position, this peak was used as an internal standard in the measurement of the chemical shifts of the portions of the β-cyclodextrin moiety in the presence of dinoprostone relative to their positions in the absence of dinoprostone. Still farther upfield is a side band, 4.25 and 4.80 ppm (Fig. 3A), followed by a group of peaks corresponding to the remainder of the β-cyclodextrin protons. The sideband appears only on the β-cyclodextrin spectrum.

From the chemical shift data in Table II, it appears that all of the protons are experiencing a shielding effect, suggesting that a portion of the dinoprostone molecule in the inclusion compound is proximate to each proton. Corey–Pauling–Koltan (CPK) space-filling molecular models indicate that the entire dinoprostone molecule cannot enter the β-cyclodextrin cavity from either side of the β-cyclodextrin torus, regardless of whether the approach is made by the ring portion or the combined, parallel-oriented chain portions of the molecule. However, if the dinoprostone chains are not parallel but oriented at angles to each other, tending toward a linear arrangement, one chain can enter the β-cyclodextrin cavity. The rather loose fit of the dinoprostone chain and the expected corresponding weaker anisotropic shielding effect on the

Table II—Dinoprostone-Induced Chemical Shifts of β-Cyclodextrin Protons

Proton	Δδ, ppm
H-1	0.06
H-2	0.05
H-3	0.08
H-4	0.03
H-5	0.08
H-6	0.07

interior protons of the β-cyclodextrin ring are reflected in the lower chemical shift values for these protons.

A possible molecular arrangement for the inclusion compound is that the molecule of dinoprostone wraps itself around the open end of the β-cyclodextrin ring in a configuration in which one chain is buried in the cavity, the five-membered ring is adjacent to the edge of the torus, and the other chain extends over the exterior of the β-cyclodextrin molecule. CPK space-filling molecular models indicate that the dinoprostone molecule is capable of such a configuration (Fig. 4). The virtually identical values of the chemical shift for H-3, H-5, and H-6 indicate that a single dinoprostone chain could enter from either direction on the PMR time scale. Since H-1 and H-4 are both located close to the equator of the exterior of the torus, the lower value of the chemical shift of H-4 as compared to that of H-1 may also indicate that the dinoprostone chain preferentially orients proximate to H-1 on the PMR time scale.

While clustering of dinoprostone molecules in and around the β-cyclodextrin torus could also possibly explain the PMR observations, such an arrangement can be expected to be thermodynamically unstable since molecular models indicate that only a portion of one dinoprostone molecule can occupy the cavity. Thus, the most probable arrangement of the complex is that in which the chain of the dinoprostone molecule bearing the carboxyl group extends over the exterior of the β-cyclodextrin molecule. This orientation, while admittedly speculative, would be consistent with the 1:1 complex suggested by phase solubility analysis.

Information on the solution process of dinoprostone in water was obtained. The solubility of dinoprostone in water is shown in Fig. 5 as a function of temperature. The apparent heat of solution calculated from the slope when a mole fraction unit was used for the solubility was 2.16 kcal/mole. In the mole fraction calculation, 55.5 moles/liter was used as the concentration of water. If the solution process is considered as the sum of two steps, fusion of solid dinoprostone to liquid and a subsequent mixing of liquid dinoprostone with water, then the second process should be exothermic in nature with $\Delta H°$ of about −6 kcal/mole since the heat of dinoprostone fusion is about 8 kcal/mole.

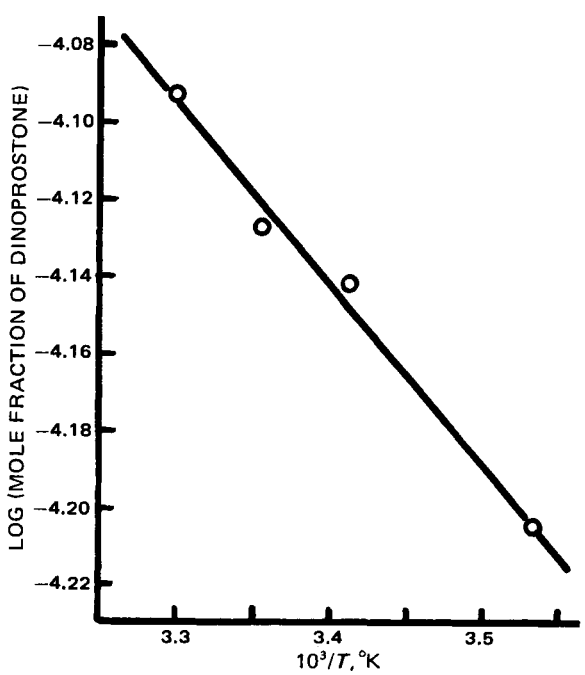

Figure 5—*Estimation of the apparent heat of solution of dinoprostone in water.*

REFERENCES[5]

(1) J. L. Lach and T. F. Chin, *J. Pharm. Sci.*, **53**, 69 (1964).
(2) W. A. Pauli and J. L. Lach, *ibid.*, **54**, 1745 (1965).
(3) H. Schlenk, D. M. Sand, and J. A. Tillotson, *J. Am. Chem. Soc.*, **77**, 3587 (1955).
(4) C. A. Glass, *Can. J. Chem.*, **43**, 2652 (1965).
(5) D. French, *Adv. Carbohydr. Chem.*, **12**, 189 (1957).
(6) J. A. Thoma and L. Stewart, in "Starch Chemistry and Technology," vol. 1, R. L. Whistler and E. F. Paschall, Eds., Academic, New York, N.Y., 1965.
(7) F. Cramer and H. Hettler, *Naturwissenschaften*, **54**, 625 (1967), and references cited therein.
(8) R. Breslow and P. Campbell, *J. Am. Chem. Soc.*, **91**, 3085 (1969).
(9) J. Cohen and J. L. Lach, *J. Pharm. Sci.*, **52**, 132 (1963).
(10) J. L. Lach and J. Cohen, *ibid.*, **52**, 137 (1963).
(11) J. L. Lach and W. A. Pauli, *ibid.*, **55**, 32 (1966).
(12) A. C. O'Rourke and J. S. Kent (Syntex, Inc.), U.S. pat. 3,826,823 (1974).
(13) Ono Pharm. Co., West German pat. 2353-797 (1974).
(14) G. F. Thompson (Syntex Inc.), U.S. pat. 3,833,725 (1974).
(15) Ono Pharm. Co., Japanese pat. 8033-013 (1973).
(16) A. Hybl, R. E. Rundle, and D. E. Williams, *J. Am. Chem. Soc.*, **87**, 2779 (1965).
(17) P. V. Demarco and A. L. Thakkar, *Chem. Commun.*, **1970**, 2.
(18) A. L. Thakkar and P. V. Demarco, *J. Pharm. Sci.*, **60**, 652 (1971).
(19) T. Higuchi and K. A. Connors, in "Advances in Analytical Chemistry and Instrumentation," vol. 4, C. N. Reilley, Ed., Interscience, New York, N.Y., 1965, pp. 117–212.
(20) G. M. Barrow, "Physical Chemistry," McGraw-Hill, New York, N.Y., 1961, chap. 7.
(21) F. Cramer, *Angew. Chem.*, **73**, 49 (1967).
(22) G. Nemethy and H. A. Scheraga, *J. Chem. Phys.*, **36**, 3401 (1962).
(23) E. A. Lewis and L. D. Hansen, *J. Chem. Soc. Perkin Trans.*, **2**, 2081 (1973).
(24) W. A. Pauli and J. L. Lach, *J. Pharm. Sci.*, **54**, 1745 (1965).

[5] After the present study was completed, the authors became aware of the work of K. Uekama *et al.* on a very similar subject [*J. Pharm. Sci.*, **66**, 706 (1977)]. The present results are in general agreement in that the equilibrium constants for the molecular interaction are in the order of 10^3 mole^{-1} at 25°.

ACKNOWLEDGMENTS

Grateful appreciation is extended by S. G. Frank to The Upjohn Co. for a Summer Visiting Professorship in Pharmacy Research (1972), during which a portion of this project was completed.

Simultaneous Determination of Pseudoephedrine and Chlorpheniramine in Pharmaceutical Dosage Forms

AVRAHAM YACOBI ˣ, ZEE M. LOOK, and CHII-MING LAI

Received October 17, 1977, from the *Department of Biopharmaceutical Sciences, Research and Medical Affairs, Arnar-Stone Laboratories, Inc., McGaw Park, IL 60085.* Accepted for publication March 23, 1978.

Abstract □ A simple and sensitive high-pressure liquid chromatographic (HPLC) determination of pseudoephedrine and chlorpheniramine in a pharmaceutical dosage form is described. Quantities of 1.5 μg of pseudoephedrine and 0.1 μg of chlorpheniramine are sufficient to determine concentrations in an aqueous solution. Small volume samples, without any extraction procedures, can be treated for direct drug concentration measurement with a high-pressure liquid chromatograph. The stability-indicating property and the accuracy of this method are comparable to those of an established GLC method. The HPLC method can be applied directly and successfully for dissolution studies. The latter application eliminates the need for volume replacement or subsequent mathematical corrections.

Keyphrases □ Pseudoephedrine—high-pressure liquid chromatographic analysis, simultaneously with chlorpheniramine, in dosage forms □ Chlorpheniramine—high-pressure liquid chromatographic analysis, simultaneously with pseudoephedrine, in dosage forms □ High-pressure liquid chromatography—simultaneous analyses, pseudoephedrine and chlorpheniramine in dosage forms □ Adrenergics—pseudoephedrine, high-pressure liquid chromatographic analysis, simultaneously with chlorpheniramine, in dosage forms □ Antihistaminics—chlorpheniramine, high-pressure liquid chromatographic analysis, simultaneously with pseudoephedrine, in dosage forms

Some cough–cold–allergy dosage forms contain both pseudoephedrine hydrochloride, a nasal decongestant, and chlorpheniramine maleate, an antihistamine. These compounds are usually determined individually by GLC and/or UV spectrophotometry following TLC for drug separation. These methods require tedious extraction and lengthy reaction procedures. High-pressure liquid chromatographic (HPLC) systems also have been utilized for the determination of pseudoephedrine in cough–cold mixtures (1) and of chlorpheniramine in combination with other antihistamines (2) and antitussive preparations (3) and for quantitation of other antihistamines including chlorpheniramine in cough syrups (4).

This paper describes a suitable HPLC method for the simultaneous determination of pseudoephedrine and chlorpheniramine in pharmaceutical dosage forms.

EXPERIMENTAL

Instrumentation—A liquid chromatograph[1] was equipped with a UV detector operated at 254 nm and a nonpolar column[2] (30 cm long × 4 mm i.d.). The column was eluted with a mobile phase consisting of acetonitrile–methanol–sodium nitrate (35:40:25) and 1-heptanesulfonic acid[3] (0.001 *M* each), pH 5, at a flow rate of 2 ml/min. The output of the detector was recorded[4] at 10 mv.

A gas–liquid chromatograph[5] was equipped with a flame-ionization detector. A glass column (1.8 m long × 4 mm i.d.) was packed with 3% OV-17 on 100–120-mesh Chromosorb W-HP; helium was used as the carrier gas at a rate of 40 ml/min. The temperatures of the injection port, column, and detector were 225, 165, and 300°, respectively, for pseudoephedrine and 225, 235, and 300°, respectively, for chlorpheniramine.

[1] Model ALC/GPC 204, Waters Associates, Milford, Mass.
[2] μBondapak C_{18}, Waters Associates, Milford, Mass.
[3] Pic B-7 Waters Associates, Milford, Mass.
[4] Omniscribe recorder, Houston Instruments, Austin, Tex.
[5] Model 65, Beckman Instruments, Irvine, Calif.

0022-3549/78/1200-1668$01.00/0

© 1978, American Pharmaceutical Association

REFERENCES[5]

(1) J. L. Lach and T. F. Chin, *J. Pharm. Sci.*, **53**, 69 (1964).
(2) W. A. Pauli and J. L. Lach, *ibid.*, **54**, 1745 (1965).
(3) H. Schlenk, D. M. Sand, and J. A. Tillotson, *J. Am. Chem. Soc.*, **77**, 3587 (1955).
(4) C. A. Glass, *Can. J. Chem.*, **43**, 2652 (1965).
(5) D. French, *Adv. Carbohydr. Chem.*, **12**, 189 (1957).
(6) J. A. Thoma and L. Stewart, in "Starch Chemistry and Technology," vol. 1, R. L. Whistler and E. F. Paschall, Eds., Academic, New York, N.Y., 1965.
(7) F. Cramer and H. Hettler, *Naturwissenschaften*, **54**, 625 (1967), and references cited therein.
(8) R. Breslow and P. Campbell, *J. Am. Chem. Soc.*, **91**, 3085 (1969).
(9) J. Cohen and J. L. Lach, *J. Pharm. Sci.*, **52**, 132 (1963).
(10) J. L. Lach and J. Cohen, *ibid.*, **52**, 137 (1963).
(11) J. L. Lach and W. A. Pauli, *ibid.*, **55**, 32 (1966).
(12) A. C. O'Rourke and J. S. Kent (Syntex, Inc.), U.S. pat. 3,826,823 (1974).
(13) Ono Pharm. Co., West German pat. 2353-797 (1974).
(14) G. F. Thompson (Syntex Inc.), U.S. pat. 3,833,725 (1974).
(15) Ono Pharm. Co., Japanese pat. 8033-013 (1973).
(16) A. Hybl, R. E. Rundle, and D. E. Williams, *J. Am. Chem. Soc.*, **87**, 2779 (1965).
(17) P. V. Demarco and A. L. Thakkar, *Chem. Commun.*, **1970**, 2.
(18) A. L. Thakkar and P. V. Demarco, *J. Pharm. Sci.*, **60**, 652 (1971).
(19) T. Higuchi and K. A. Connors, in "Advances in Analytical Chemistry and Instrumentation," vol. 4, C. N. Reilley, Ed., Interscience, New York, N.Y., 1965, pp. 117–212.
(20) G. M. Barrow, "Physical Chemistry," McGraw-Hill, New York, N.Y., 1961, chap. 7.
(21) F. Cramer, *Angew. Chem.*, **73**, 49 (1967).
(22) G. Nemethy and H. A. Scheraga, *J. Chem. Phys.*, **36**, 3401 (1962).
(23) E. A. Lewis and L. D. Hansen, *J. Chem. Soc. Perkin Trans.*, **2**, 2081 (1973).
(24) W. A. Pauli and J. L. Lach, *J. Pharm. Sci.*, **54**, 1745 (1965).

[5] After the present study was completed, the authors became aware of the work of K. Uekama *et al.* on a very similar subject [*J. Pharm. Sci.*, **66**, 706 (1977)]. The present results are in general agreement in that the equilibrium constants for the molecular interaction are in the order of 10^3 mole^{-1} at 25°.

ACKNOWLEDGMENTS

Grateful appreciation is extended by S. G. Frank to The Upjohn Co. for a Summer Visiting Professorship in Pharmacy Research (1972), during which a portion of this project was completed.

Simultaneous Determination of Pseudoephedrine and Chlorpheniramine in Pharmaceutical Dosage Forms

AVRAHAM YACOBI ˣ, ZEE M. LOOK, and CHII-MING LAI

Received October 17, 1977, from the *Department of Biopharmaceutical Sciences, Research and Medical Affairs, Arnar-Stone Laboratories, Inc., McGaw Park, IL 60085.* Accepted for publication March 23, 1978.

Abstract □ A simple and sensitive high-pressure liquid chromatographic (HPLC) determination of pseudoephedrine and chlorpheniramine in a pharmaceutical dosage form is described. Quantities of 1.5 μg of pseudoephedrine and 0.1 μg of chlorpheniramine are sufficient to determine concentrations in an aqueous solution. Small volume samples, without any extraction procedures, can be treated for direct drug concentration measurement with a high-pressure liquid chromatograph. The stability-indicating property and the accuracy of this method are comparable to those of an established GLC method. The HPLC method can be applied directly and successfully for dissolution studies. The latter application eliminates the need for volume replacement or subsequent mathematical corrections.

Keyphrases □ Pseudoephedrine—high-pressure liquid chromatographic analysis, simultaneously with chlorpheniramine, in dosage forms □ Chlorpheniramine—high-pressure liquid chromatographic analysis, simultaneously with pseudoephedrine, in dosage forms □ High-pressure liquid chromatography—simultaneous analyses, pseudoephedrine and chlorpheniramine in dosage forms □ Adrenergics—pseudoephedrine, high-pressure liquid chromatographic analysis, simultaneously with chlorpheniramine, in dosage forms □ Antihistaminics—chlorpheniramine, high-pressure liquid chromatographic analysis, simultaneously with pseudoephedrine, in dosage forms

Some cough–cold–allergy dosage forms contain both pseudoephedrine hydrochloride, a nasal decongestant, and chlorpheniramine maleate, an antihistamine. These compounds are usually determined individually by GLC and/or UV spectrophotometry following TLC for drug separation. These methods require tedious extraction and lengthy reaction procedures. High-pressure liquid chromatographic (HPLC) systems also have been utilized for the determination of pseudoephedrine in cough–cold mixtures (1) and of chlorpheniramine in combination with other antihistamines (2) and antitussive preparations (3) and for quantitation of other antihistamines including chlorpheniramine in cough syrups (4).

This paper describes a suitable HPLC method for the simultaneous determination of pseudoephedrine and chlorpheniramine in pharmaceutical dosage forms.

EXPERIMENTAL

Instrumentation—A liquid chromatograph[1] was equipped with a UV detector operated at 254 nm and a nonpolar column[2] (30 cm long × 4 mm i.d.). The column was eluted with a mobile phase consisting of acetonitrile–methanol–sodium nitrate (35:40:25) and 1-heptanesulfonic acid[3] (0.001 *M* each), pH 5, at a flow rate of 2 ml/min. The output of the detector was recorded[4] at 10 mv.

A gas–liquid chromatograph[5] was equipped with a flame-ionization detector. A glass column (1.8 m long × 4 mm i.d.) was packed with 3% OV-17 on 100–120-mesh Chromosorb W-HP; helium was used as the carrier gas at a rate of 40 ml/min. The temperatures of the injection port, column, and detector were 225, 165, and 300°, respectively, for pseudoephedrine and 225, 235, and 300°, respectively, for chlorpheniramine.

[1] Model ALC/GPC 204, Waters Associates, Milford, Mass.
[2] μBondapak C_{18}, Waters Associates, Milford, Mass.
[3] Pic B-7 Waters Associates, Milford, Mass.
[4] Omniscribe recorder, Houston Instruments, Austin, Tex.
[5] Model 65, Beckman Instruments, Irvine, Calif.

0022-3549/78/1200-1668$01.00/0

© 1978, American Pharmaceutical Association

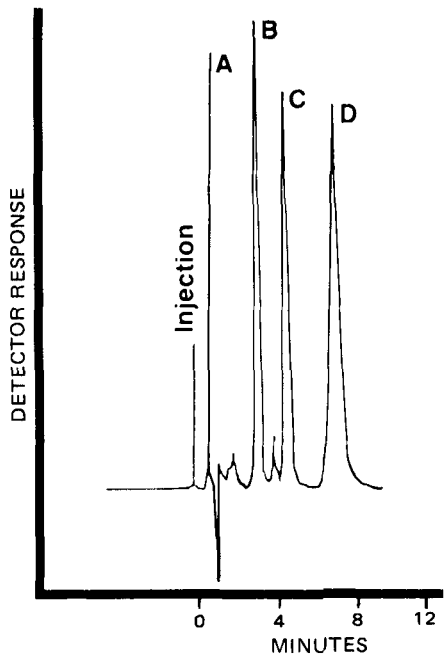

Figure 1—*Typical chromatogram obtained by HPLC analysis of the contents of sustained-release capsules. Key: A, maleic acid; B, pseudoephedrine; C, chlorpheniramine; and D, internal standard (chlorpromazine). The reaction times for A–D were 0.95, 3.1, 4.6, and 7.3, respectively.*

Pseudoephedrine also was determined spectrophotometrically with a UV spectrophotometer[6] at 256 nm.

Preparation—A stock solution containing pseudoephedrine hydrochloride[7] and chlorpheniramine maleate[8] (3.0 and 0.2 g, respectively, in 200 ml of purified water) was diluted to prepare a series of standard solutions for the determination of calibration curves for each drug. As the internal standard for the HPLC method, 5 mg of chlorpromazine hydrochloride[9] was dissolved in 100 ml of purified water. As internal standards for the GLC determination, 75 mg of mephentermine sulfate[10] (for pseudoephedrine) and 25 mg of pyrilamine maleate[9] (for chlorpheniramine) in 100 ml of purified water were used.

Sustained-release capsules[11] containing 120 mg of pseudoephedrine hydrochloride and 8 mg of chlorpheniramine maleate were sampled randomly, and their contents were ground to produce a fine powder. An accurate amount corresponding to one capsule weight was dissolved in purified water, and the solution was filtered through a filter paper[12]. The filtered solution then was diluted to prepare a series of working solutions with different concentrations. The final concentration of pseudoephedrine ranged from 0.3 to 3.6 mg/ml, and that of chlorpheniramine ranged from 20 to 240 μg/ml.

Capsules[13] containing 120 mg of pseudoephedrine hydrochloride also were processed in a similar manner to prepare a series of solutions, which were then determined by UV spectrophotometry.

For stability testing, solutions containing 600 μg of pseudoephedrine hydrochloride/ml and 40 μg of chlorpheniramine maleate/ml in water, 3 *N* NaOH, and buffers of various pH values (2.5, 4.5, 6.5, and 8) were prepared. The buffer solutions were heated at 90° for 1 hr. The water and alkaline solutions containing the drugs were heated for 24 hr at 100°. Then all solutions were allowed to cool overnight, adjusted for loss of volume, and subsequently assayed for pseudoephedrine and chlorpheniramine by the HLPC and GLC methods. The water solution, which was not exposed to heat, was used as the control.

Assay—For the HPLC method, 1 ml of each solution and 0.1 ml of the internal standard solution were mixed together and 5 μl was injected into the instrument. For the GLC methods[14], 2 ml of each solution and 2 ml of the internal standard solution were mixed together. Then about 2 g of sodium chloride, 2 drops of 10 *N* NaOH, and 2 ml of extraction solution (cyclohexane–benzene, 55:45) were added. The mixture was shaken and then centrifuged. Aliquots of 1–2 μl of the organic layer were injected into the instrument for determination of either pseudoephedrine or chlorpheniramine.

In both HPLC and GLC methods, the concentration of each drug was determined by means of peak height ratios of individual compounds and the respective internal standard. For UV spectrophotometry, solutions containing pseudoephedrine hydrochloride were determined directly. All samples were determined in duplicate.

Dissolution Study—For the dissolution test, an NF rotating basket assembly was used. The dissolution medium consisted of 900 ml of 0.01 *M* sodium phosphate buffer, pH 4.5. The contents of two capsules were put into the basket and immersed in the medium. The study was done in triplicate at 100 rpm and 37°. Serial 0.1-ml samples of the dissolution medium were taken immediately before and after immersion of the baskets and at appropriate sampling times. To each 0.1-ml sample, 0.05 ml of the internal standard (5 μg of chlorpromazine hydrochloride/ml) was added. The mixture was vortexed, and a 25-μl aliquot was injected for HPLC analysis.

Table I—Percent Error in Determination of Pseudoephedrine and Chlorpheniramine by the GLC and HPLC Methods

Drug	Method	Concentration Range[a], mg/ml	Percent Error[b] Range	Mean	*SD*
Pseudoephedrine hydrochloride	GLC	0.30–3.60	0.65–16.1	4.63	5.43
	HPLC		1.01–8.50	3.03	2.52
Chlorpheniramine maleate	GLC	0.02–0.24	0.48–4.73	1.73	1.45
	HPLC		0.92–3.84	1.92	1.20

[a] Total of seven concentrations. The assay for each concentration was done in duplicate. [b] These are absolute values and were determined by (absolute values of the difference between two determinations/concentration) × 100.

Table II—Precision and Reproducibility of the GLC and HPLC Methods for Determination of Pseudoephedrine and Chlorpheniramine in Sustained-Release Capsules

Sample	Relative Amount in Capsules, % Pseudoephedrine Hydrochloride GLC	HPLC	Chlorpheniramine Maleate GLC	HPLC
1	103.0	97.0	102.0	97.3
2	101.0	97.4	89.4	98.8
3	97.2	101.0	107.0	100.0
4	97.4	97.4	98.1	96.6
5	101.0	104.0	106.0	102.0
6	98.0	101.0	98.2	100.0
7	100.0	98.6	92.6	99.7
8	103.0	104.0	107.0	105.0
Mean	100.1	100.0	100.0	99.9
SD	2.35	2.88	6.68	2.65

RESULTS AND DISCUSSION

Figure 1 depicts a typical chromatogram obtained by the HPLC analysis of the contents of the sustained-release capsules. Chlorpheniramine maleate underwent hydrolysis in the system to chlorpheniramine and maleic acid, resulting in the earlier appearance of the latter on the chromatogram, which appears to be characteristic of maleic acid in this system. There was a clear separation of each component with no indication of any interference due to the hydrolysis of chlorpheniramine maleate or the presence of other molecules resulting from degradation of one of the compounds. The retention times of each species are listed in Fig. 1. These values show that the entire procedure for simultaneous analyses of pseudoephedrine and chlorpheniramine in the same sample can be completed within 10 min.

For comparison purposes, established stability-indicating GLC methods for the determination of pseudoephedrine and chlorpheniramine

[6] Model 25, Beckman Instruments, Irvine, Calif.
[7] Knoll, A. G., Whippany, N.J.
[8] E. M. Labs, Elmsford, N.Y.
[9] H. Reisman Corp., Orange, N.J.
[10] Arapahoe Chemicals, Inc., Boulder, Colo.
[11] Isoclor Timesule Capsules, Arnar-Stone Laboratories, Inc., McGaw Park, Ill.
[12] Whatman No. 1, W & R Balston, Ltd., London, England.
[13] Novafed Capsules, Dow Pharmaceuticals, Dow Chemical Co., Indianapolis, Ind.
[14] An unpublished in-house analytical procedure, Arnar-Stone Laboratories, McGaw Park, IL 60085.

Table III—Results of Stability Testing of Pseudoephedrine and Chlorpheniramine by the GLC and HPLC Methods

	Percent of Control[a]			
	Pseudoephedrine Hydrochloride		Chlorpheniramine Maleate	
Sample	GLC[b]	HPLC	GLC[b]	HPLC
pH 2.5	93.3 ± 4.32[c]	97.8 ± 2.35	99.3 ± 0.65	96.9 ± 1.17
pH 4.5	98.1 ± 1.26	97.4 ± 1.34	99.7 ± 3.39	100.3 ± 0.66
pH 6.5	97.5 ± 2.23	94.7 ± 1.63	97.3 ± 0.64	102.3 ± 1.26
pH 8.0	99.0 ± 1.29	95.6 ± 2.40	97.9 ± 0.40	100.4 ± 0.57
Water[d]	88.9 ± 1.54	78.2 ± 4.20	46.8 ± 1.68	47.4 ± 2.76
3 *N* NaOH[d]	80.8 ± 3.88	87.2 ± 2.34	29.2 ± 0.46	30.8 ± 0.55

[a] The control solution was prepared in water and reserved for assay together with the buffer solutions. The buffer solutions were heated for 1 hr at 90°. All solutions contained 600 μg of pseudoephedrine hydrochloride/ml and 40 μg of chlorpheniramine maleate/ml. [b] Pseudoephedrine and chlorpheniramine were determined individually by the GLC methods and simultaneously by the HPLC procedure. [c] Mean ± *SD*, $n = 4$. [d] These solutions were heated at 100° for 24 hr, $n = 6$.

were used. There were excellent correlations between: (*a*) the theoretical concentrations and those obtained by GLC and HPLC for pseudoephedrine and chlorpheniramine, respectively; (*b*) concentrations of pseudoephedrine determined by GLC and HPLC ($r = 0.976$, $p < 0.001$); and (*c*) concentrations of chlorpheniramine determined by GLC and HPLC ($r = 0.999$, $p < 0.001$). The lowest corresponding quantities injected into the HPLC system are 1.5 μg of pseudoephedrine hydrochloride and 0.1 μg of chlorpheniramine maleate.

Table I shows the values of the percent error involved with each procedure. For pseudoephedrine and chlorpheniramine, the mean values were 3.03 and 1.92% by HPLC and 4.63 and 1.73% by GLC, respectively. The variations in the measurement by HPLC were very low and comparable to those of the GLC procedures. Similar results were obtained when the HPLC method was tested against a UV spectrophotometric determination with respect to pseudoephedrine ($r = 0.989$, $p < 0.001$).

The precision and reproducibility of the HPLC method for the determination of potency of pseudoephedrine and chlorpheniramine in the sustained-release capsule, using a standard sample preparation and dilution procedure, were examined (Table II). The HPLC as well as the GLC method showed a high degree of accuracy, precision, and reproducibility. Table III compares the results of the stability testing of pseudoephedrine and chlorpheniramine. There was no statistically significant difference between the results obtained by the HPLC and the GLC methods, indicating that both methods are equally stability indicating.

Both compounds appeared to be stable at various pH values and moderate temperature conditions. However, when the aqueous and the alkaline samples were heated for about 24 hr, there was significant degradation of both molecules, particularly chlorpheniramine (Table III). The HPLC and GLC methods showed good separation of the parent compounds from their degradation products. The results were almost identical for both methods.

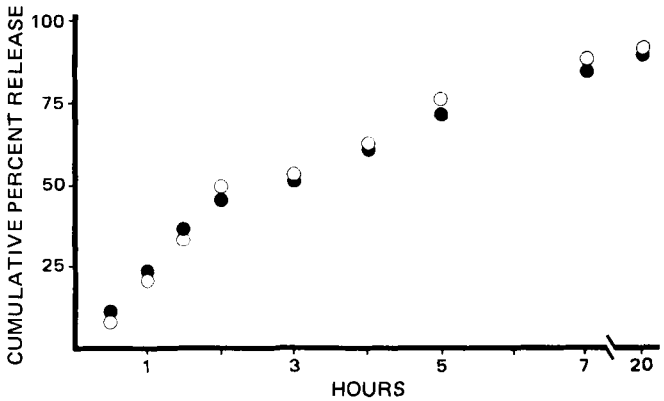

Figure 2—*Cumulative percentage released* versus *time profile of pseudoephedrine (○) and chlorpheniramine (●), observed from the dissolution test of a sustained-release capsule. Each data point represents the average of three values.*

Figure 2 shows the results for the dissolution test of the capsule content. About 85 and 92% of pseudoephedrine and chlorpheniramine, respectively, were released in 20 hr, comparable to results obtained in in-house dissolution studies utilizing the GLC method. The simplicity of this HPLC method for the determination of the two ingredients permits a rapid characterization of the dissolution profile of the drug with maximum accuracy. In addition, the size of samples (0.1 ml) taken from the dissolution medium is extremely small and eliminates the need for volume replacement or subsequent mathematical corrections.

The results indicate that the HPLC method can be considered for the determination of pseudoephedrine and chlorpheniramine in the evaluation of pharmaceutical dosage forms. This procedure does not involve any extraction or reaction steps. A sample can be easily mixed with an internal standard solution and analyzed *via* HPLC. The method is simple, rapid, accurate, stability indicating, and reproducible. Additionally, the sensitivity and reliability of the HPLC method over a wide range of concentrations will extend the use of this method to measurement of the urinary excretion of the active ingredients following ingestion of oral dosage forms containing one or both compounds. Such a study is presently in progress.

REFERENCES

(1) I. L. Honigberg, J. T. Stewart, and A. P. Smith, *J. Pharm. Sci.*, **63**, 766 (1974).

(2) A. G. Ghanekar and V. D. Gupta, *Am. J. Hosp. Pharm.*, **34**, 651 (1977).

(3) A. Menyharth, F. P. Mahn, and J. E. Heveran, *J. Pharm. Sci.*, **63**, 430 (1974).

(4) V. D. Gupta and A. G. Ghanekar, *ibid.*, **66**, 895 (1977).

Polyamine Metabolism III: Urinary Acetyl Polyamines in Human Cancer

MAHMOUD M. ABDEL-MONEM [x] **and KOSEI OHNO** *

Received February 6, 1978, from the *College of Pharmacy, University of Minnesota, Minneapolis, MN 55455.* Accepted for publication March 23, 1978. *Present address: Faculty of Pharmaceutical Sciences, Higashi Nippon Gakuen University, Ishikari-Tobetsu, Hokkaido, 061-02 Japan.

Abstract □ Polyamine levels were determined by high-pressure liquid chromatography in the unhydrolyzed 24-hr urine obtained from 15 cancer patients and nine normal subjects. N^1-Acetylspermine, N^4-acetylspermine, N^4-acetylspermidine, and N-(3-aminopropyl)acetamide were not detected in any samples. N^1-Acetylspermidine, N^8-acetylspermidine, acetylputrescine, and acetylcadaverine were present in all samples. Furthermore, acetylspermidine and acetylputrescine were excreted in much greater quantities than the respective amines in the urine of both cancer patients and normal subjects. The levels of N^1-acetylspermidine were considerably higher than the levels of N^8-acetylspermidine in the 24-hr urine of cancer patients, resulting in a ratio of N^1- to N^8-acetylspermidine in the urine of cancer patients significantly higher than that in normal subjects. The urinary levels of acetylputrescine were also significantly higher in cancer patients. The urinary polyamines in 13 of the 15 cancer patients were outside the 95% confidence limits of the normal mean for the ratio of N^1- to N^8-acetylspermidine and acetylputrescine. All cancer patients showed values outside the 95% confidence limits of the mean for either of these two parameters. Diurnal variation was observed in the urinary excretion of the acetyl polyamines but not for the free amines in two normal subjects.

Keyphrases □ Polyamines, various acetyl—high-pressure liquid chromatographic analyses in urine of normal humans and cancer patients □ High-pressure liquid chromatography—analyses, various acetyl polyamines in urine of normal humans and cancer patients

Since the initial report (1) describing elevated levels of polyamines in urine of cancer patients, interest in the possible use of urinary polyamine levels as biochemical markers of tumor presence and growth has increased. Independent studies involving large numbers of patients showed that the levels of these amines were elevated in the urine of a majority of the cancer patients (2–12). One comprehensive study indicated that the potential usefulness of the urinary polyamines as biological markers was less promising than originally anticipated (13). However, a recent study demonstrated the usefulness of urinary and serum polyamines as markers of response and disease activity in cancer chemotherapy (14, 15). Elevated polyamine concentration in the cerebrospinal fluid of patients with untreated malignant central nervous system tumors also was demonstrated (16).

Polyamines are present predominantly in human urine as conjugates that produce the free amines after hydrolysis. In most previous studies, the biological samples (urine, serum, and cerebrospinal fluid) were hydrolyzed prior to analysis. The data presented (1–15) pertain to the quantities of total polyamines excreted in urine and not to the nature of these amines.

In preliminary studies (17–19), the polyamines were examined in the unhydrolyzed urine of a limited number of cancer patients and normal subjects. The polyamines were present primarily in the form of the monoacetyl conjugates in all samples. This paper reports a more complete examination of the unhydrolyzed urine of additional subjects.

EXPERIMENTAL

Materials—All chemicals were the highest purity available or were purified before use. Chloroform (ACS grade) was stored over anhydrous calcium chloride overnight and distilled. 2-Propanol (ACS grade) was distilled from magnesium and a catalytic amount of iodine. Triethylamine[1] was distilled over potassium hydroxide and then over *p*-toluenesulfonyl chloride. Other high-pressure liquid chromatographic (HPLC) solvents were obtained from commercial sources[2]. All solvents were degassed before use by HPLC.

Urine Collection—Twenty-four-hour urine samples were obtained from nine healthy adults (six males and three females) as normal controls and from 15 patients with diagnosed cancer[3]. Urine was obtained from patients who had not received therapy except for one patient (DE) who had received intravenous fluorouracil weekly for 10 months. Samples for the study of diurnal variation were obtained from two normal males at 6-hr intervals.

Urine was collected in polyethylene bottles under toluene and kept refrigerated. The volume of urine was determined, and aliquots (2 ml each) were stored at −20° until analysis.

Analysis of Urine Samples—Each urine sample was analyzed in duplicate. Each urine aliquot (2 ml) was adjusted to pH 10–12 with 2 *N* NaOH (0.1 ml) and mixed with isoamyl alcohol (5 ml) on a vortex mixer for 2 min. The organic solvent extract was transferred into a centrifuge tube, and nitrogen gas was bubbled through the solvent for 30 min to remove ammonia. Concentrated hydrochloric acid (0.1 ml) was added, and the solvents were mixed on a vortex mixer for 30 sec.

The solvents were then evaporated[4] at 45° and 0.2 mm Hg. A 1-ml aliquot of sodium carbonate (50 mg/ml) and 2 ml of dansyl chloride (10.1 mg/ml in acetone) were added to the residue and mixed. Then the tubes were shaken at room temperature in the dark for 12 hr. Acetone was evaporated at 35° in a nitrogen stream, and the residue was mixed with water (1 ml) to dissolve the inorganic salts and then with benzene (5 ml). The solution was mixed on a vortex mixer for 30 sec. The benzene extract (4.8 ml) was transferred into a centrifuge tube, and the solvent was evaporated at 35° in a nitrogen stream. The residue was dissolved in chloroform (25–50 μl).

An aliquot of the chloroform solution (10 μl) was applied on a TLC silica gel GF plate[5] (20 × 20 cm, 250 μm), and the plate was developed as described previously (19). The spots on the plate corresponding to the position of N^1-acetylspermidine (VI), N^8-acetylspermidine (VII), acetylputrescine (III), acetylcadaverine (IV), putrescine (II), spermidine (V), and spermine (IX) were scraped separately. The adsorbent obtained from each spot was extracted immediately with a mixture of equal volumes of triethylamine and 2-propanol (10 ml). The extract was evaporated to dryness in a nitrogen stream at 40°, and the residue was stored at 2–4° until HPLC analysis.

The HPLC analysis was performed as described previously using two silica gel columns[6] (120 cm × 2.2 mm i.d.). One column was for the analysis of the dansyl derivatives of the monoacetyl polyamines with a solvent of chloroform–2-propanol (50:3). The flow rates were 0.3 ml/min for the analysis of VI and VII and 0.6 ml/min for the analysis of III and IV. The second column was for the analysis of the dansyl derivatives of the polyamines with a solvent of chloroform–triethylamine (50:1) at a flow rate of 0.4 ml/min.

Standard solutions of II, V, IX, and III, containing 1, 2, 3, or 4 nmoles

[1] Aldrich, Milwaukee, Wis.
[2] Burdick and Jackson Laboratories, Muskegon, Mich.
[3] Medical Oncology Service, University of Minnesota Hospitals, Minneapolis, Minn.
[4] Evapomix, Buchler Instruments, Fort Lee, N.J.
[5] Analtech, Newark, Del.
[6] Corasil II, Waters Associates, Milford, Mass.

0022-3549/78/1200-1671$01.00/0
© 1978, American Pharmaceutical Association

Table I—Pretreatment Levels of Polyamines in the 24-hr Urine of Cancer Patients and Normal Subjects

Patient	Micromoles per 24 hr							
	VI	VII	Ratio of VI to VII	III	IV	II	V	IX
FL	4.3	3.0	1.43	25.9	8.4	0.5	—[a]	—[a]
GB	2.2	1.6	1.34	17.1	—[b]	0.9	—[a]	—[a]
MH	26.5	3.9	6.76	41.0	2.5	1.3	—[c]	—[a]
CM	0.4	0.7	0.54	18.1	0.8	0.6	—[a]	—[a]
WM	27.2	8.0	3.41	65.5	—[b]	3.8	—[c]	—[c]
EN	4.9	1.5	3.16	17.4	—[b]	1.0	0.2	—[a]
WT	12.8	4.3	3.02	17.0	4.7	0.7	0.9	22.0
FL	2.2	1.0	2.21	5.5	—[b]	1.0	—[c]	—[c]
MV	5.3	4.4	1.20	34.3	—[b]	2.4	0.7	—[a]
FM	3.3	6.0	0.55	20.5	0.6	0.6	—[a]	—[a]
MB	3.4	3.4	1.02	17.5	3.1	1.1	—[c]	—[c]
LB	2.5	3.0	0.82	30.6	—[b]	—[c]	—[c]	—[c]
DE	3.7	5.2	0.70	18.3	0.4	2.0	—[a]	1.1
NL	3.0	2.1	1.47	14.6	—[b]	2.3	—[c]	—[c]
ET	4.8	4.2	1.17	14.8	0.6	0.83	0.5	3.3
Mean (*SE*)	7.1 (±2.2)	3.5 (±0.9)	1.92[d] (±0.41)	23.9[d] (±3.7)	2.6 (±1.0)	1.4	0.6	8.8
Normal mean (*SE*)	2.91 (±0.6)	2.84 (±0.5)	0.94[d] (±0.09)	11.7[d] (±1.5)	1.9 (±0.9)	1.6 (±0.4)	0.2 (±0.04)	2.1 (±1.0)

[a] The amine was detected by TLC and HPLC, but the levels were too low for quantitative measurement. [b] Acetylcadaverine was detected by TLC but was not determined by HPLC. [c] The sample was not analyzed for the amine. [d] Differences are significant at $p < 0.05$.

of each in water (2 ml), were analyzed concurrently with the urine samples. The percent recovery for each compound was calculated and used for correcting for losses during the analytical procedure. Since authentic samples of IV, VI, and VII were not available, the recovery of III was used for correcting the results.

$RHN(CH_2)_nNH_2$
I: R = $COCH_3$, $n = 3$
II: R = H, $n = 4$
III: R = $COCH_3$, $n = 4$
IV: R = $COCH_3$, $n = 5$

$R_1HN(CH_2)_3N(CH_2)_4NHR_3$
$|$
R_2
V: $R_1 = R_2 = R_3 = H$
VI: $R_1 = COCH_3$, $R_2 = R_3 = H$
VII: $R_1 = R_2 = H$, $R_3 = COCH_3$
VIII: $R_1 = R_3 = H$, $R_2 = COCH_3$

$R_1HN(CH_2)_3N(CH_2)_4NH(CH_2)_3NH_2$
$|$
R_2
IX: $R_1 = R_2 = H$
X: $R_1 = COCH_3$, $R_2 = H$
XI: $R_1 = H$, $R_2 = COCH_3$

RESULTS

Examination of the crude mixture of the dansyl derivatives of the polyamines obtained from unhydrolyzed human urine by TLC or HPLC alone indicated the complexity of the mixture. The combination of TLC and HPLC allowed the simultaneous determination of the free polyamines and the monoacetyl polyamines in the unhydrolyzed urine samples. Representative TLC and HPLC separations of the dansyl derivatives from the urine of normal subjects and cancer patients were described previously[7] (19).

The concentrations of each polyamine and monoacetyl polyamine in the urine samples were calculated by comparison of the HPLC peak height of its dansyl derivative with those obtained from known concentrations of the authentic sample of the derivative. The calculated values were corrected for losses during the analytical procedure, using the percent recovery determined concurrently for standard solutions. Fractions of HPLC column eluates corresponding to each polyamine and monoacetyl polyamine were collected and examined by two-dimensional TLC. All examined fractions contained only one fluorescent component with chromatographic mobility similar to the authentic compound.

Table I indicates the concentrations of the free polyamines and monoacetyl polyamines found in the 24-hr urine from 15 cancer patients as well as the mean values obtained for nine normal subjects. The free polyamines were not determined in all samples from cancer patients because these compounds were present in relatively low concentrations, which complicated the analytical procedure. The values reported in Table I have been corrected for losses during the analytical procedures and are accurate estimates of the actual urine concentrations.

N^1-Acetylspermine (X), N^4-acetylspermine (XI), N^4-acetylspermidine (VIII), and *N*-(3-aminopropyl)acetamide (I) were not detected in any urine sample obtained from the 24 subjects. On the other hand, N^1-acetylspermidine (VI), N^8-acetylspermidine (VII), acetylputrescine (III), and acetylcadaverine (IV) were present in all samples. Only a few samples were analyzed for the free amines, and some did not contain detectable levels of one or more of the free amines. The normal range for spermine (IX) was 0.7–5.1 μmoles/24 hr (mean = 2.1). The range for IX in the urine of three cancer patients was 1.1–22.0 μmoles/24 hr.

The levels of free spermidine (V) in the 24-hr urine of normal subjects were considerably lower than those of acetylspermidines VI and VII. The normal range for V was 0.1–0.3 μmole/24 hr (mean = 0.2). The normal range for the ratio of VI and VII to V was 14–89 (mean = 44). The range for V in the urine of the cancer patients was 0.2–0.9 μmole/24 hr (mean = 0.6), and the range for the ratio of VI and VII to V was 14–32 (mean = 21).

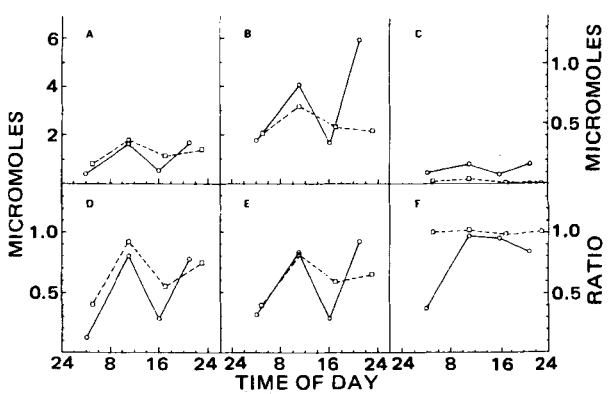

Figure 1—*Diurnal variation of urinary polyamines in two normal subjects, MA (—) and CC (- - -). Key: A, total acetylspermidines; B, acetylputrescine; C, acetylcadaverine; D,* N^1*-acetylspermidine; E,* N^8*-acetylspermidine; and F, ratio of* N^1*-acetylspermidine to* N^8*-acetylspermidine. On the abscissa, micromoles indicates the micromoles of polyamine/24 hr and ratio indicates the ratio of* N^1*-acetylspermidine to* N^8*-acetylspermidine.*

[7] Complete chemical names for compounds described in this article can be found in Ref. 19.

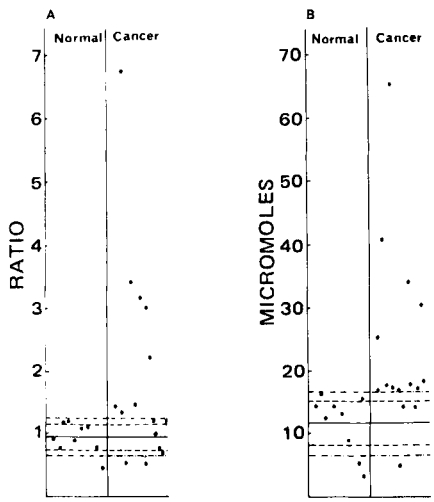

Figure 2—*Ratio of* N^1*-acetylspermidine to* N^8*-acetylspermidine (A) and urinary levels of acetylputrescine (B) in cancer patients and normal subjects. On the abscissa, ratio indicates the ratio of* N^1*- to* N^8*-acetylspermidine and micromoles indicates micromoles of acetylputrescine/24 hr.*

The concentration of II in the 24-hr unhydrolyzed urine of normal subjects was considerably higher than that for V. The normal range was 0.7–3.0 μmoles (mean = 1.6). The concentration of free II in the urine from the cancer patients was not significantly higher than that in the normal subjects. The range for free II in the urine of these patients was 0.5–3.8 μmoles/24 hr (mean = 1.4). The ratio of III to II in the urine of normal subjects was lower than that for VI and VII to V. The normal range for this ratio was 5–20 (mean = 11) in normal subjects and 5–50 (mean = 21) in cancer patients. These data indicate the much greater amounts of the acetylated II and V excreted in the urine of both normal and cancer patients relative to the amounts of the respective amines. This result is to be contrasted with the undetectable levels of X and XI in urine.

Compound IV appears to be a normal constituent of urine of both normal subjects and cancer patients. The normal range was 0.4–5.8 μmoles/24 hr (mean = 1.9), and the range in the urine of cancer patients was 0.4–8.4 μmoles/24 hr (mean = 2.6).

Both VI and VII were present in the unhydrolyzed 24-hr urine collected from the 24 subjects examined. The normal range for VI was 0.2–5.3 (mean = 2.9); for VII, it was 0.5–4.5 (mean = 2.8) μmoles/24 hr. The normal range for the ratio of VI to VII was 0.4–1.3 (mean = 0.9). The range for VI in the cancer patients was 0.4–27.0 μmoles/24 hr (mean = 7.1); for VII, it was 0.7–8.0 μmoles/24 hr (mean = 3.5). The ratio of VI to VII ranged from 0.5 to 6.8 (mean = 1.9) and was significantly higher than that in the normal subjects ($p < 0.05$).

The diurnal variation in the excretion of polyamines in the urine of two normal subjects is shown in Fig. 1. Periodicity was observed for the urinary excretion of VI, VII, and III for both subjects. One subject showed diurnal variation for urinary levels of IV. The second subject had considerably lower levels of acetylcadaverine in urine, and variation was not observed for this substance. One subject (MA) showed a relatively constant ratio of VI to VII. The second subject had a much lower ratio of VI to VII in the morning urine collection. The urinary excretion of the free polyamines did not show diurnal variation for either subject.

DISCUSSION

The results indicate that the differences in the urinary excretion of polyamines between normal subjects and cancer patients are not only in their levels but also in the nature of the polyamine conjugates. Cancer patients excreted considerably higher levels of VI than VII. The ratio of VI to VII in the urine of cancer patients was significantly higher than that in normal subjects (Fig. 2). The results obtained are in agreement with those observed earlier with only three cancer patients and three normal subjects (17, 19).

Compounds II and V were present primarily as acetyl conjugates in the urine of normal subjects and cancer patients. Compounds X and XI were not detected in any sample examined. In preliminary studies, III, VI, and VII were not detected in the serum of one normal subject, indicating that the acetyl compounds are not present in serum or that the serum concentration of the acetyl conjugates is much lower than that for the free polyamines. These preliminary findings suggest that either the acetylation of the polyamines takes place primarily in the kidneys or the renal clearance of the acetyl compounds is much greater than that for the free amines. The mechanisms of urinary excretion of the polyamines are not clear and are currently under investigation.

Diurnal variation was observed in the urinary excretion of the acetyl polyamines but not for the free amines in two normal subjects. Diurnal variation in polyamine excretion in normal and tumor-bearing rats was reported (20). However, diurnal variation of the urinary polyamines in humans has not been described.

Rosenblum *et al.* (21, 22) reported the formation of conjugates of radiolabeled V and II in rats and humans, but preliminary studies indicated that the conjugates in rat urine were not the acetyl compounds (22).

Comparison of the urinary profiles of polyamines in normal subjects and cancer patients indicates that the mean urinary levels for III and the ratio of VI to VII were significantly higher in cancer patients ($p < 0.05$). The levels of III and the ratio of VI to VII in the urine of cancer patients were outside the 95% confidence limits of the normal mean in 13 of 15 patients (Fig. 2). All cancer patients showed values outside the 95% confidence limits for either the ratio of VI to VII or levels of III.

REFERENCES

(1) D. H. Russell, *Nature New Biol.*, **233**, 144 (1971).

(2) D. H. Russell, C. C. Levy, S. C. Schimpff, and I. A. Hawk, *Cancer Res.*, **31**, 1555 (1971).

(3) F. Dreyfuss, R. Chayen, G. Dreyfuss, R. Dvir, and J. Ratan, *Isr. J. Med. Sci.*, **11**, 785 (1975).

(4) A. Lipton, L. M. Sheehan, and G. F. Kessler, Jr., *Cancer*, **35**, 464 (1975).

(5) D. C. Tormey, T. P. Waalkes, D. Ahmann, C. W. Gehrke, R. W. Zumwalt, J. Snyder, and H. Hansen, *ibid.*, **35**, 1095 (1975).

(6) M. Tsuji, T. Nakajima, and I. Sano, *Clin. Chim. Acta*, **59**, 161 (1975).

(7) Y. Takeda, T. Tominaga, M. Kitamura, T. Taguchi, T. Takeda, and T. Miwatani, *Gann*, **66**, 445 (1975).

(8) W. R. Fair, N. Wehner, and U. Brorsson, *J. Urol.*, **114**, 88 (1975).

(9) A. Lipton, L. Sheehan, and H. A. Harvey, *Cancer*, **36**, 2351 (1975).

(10) D. Bartos, R. A. Campbell, F. Bartos, and D. P. Grettie, *Cancer Res.*, **35**, 2056 (1975).

(11) A. Lipton, L. Sheehan, R. Mortel, and H. A. Harvey, *Cancer*, **38**, 1344 (1976).

(12) K. Fujita, T. Nagatsu, K. Maruta, M. Ito, H. Senba, and K. Miki, *Cancer Res.*, **36**, 1320 (1976).

(13) T. P. Waalkes, C. W. Gehrke, D. C. Tormey, R. W. Zumwalt, J. N. Hueser, K. C. Kuo, D. B. Lakingo, D. L. Ahmann, and C. G. Moertel, *Cancer Chemother. Rep.*, **59**, 1103 (1975).

(14) D. H. Russell, B. G. M. Durie, and S. E. Salmon, *Lancet*, **2**, 797 (1975).

(15) B. G. M. Durie, S. E. Salmon, and D. H. Russell, *Cancer Res.*, **37**, 214 (1977).

(16) L. J. Marton, O. Heby, V. A. Levin, W. P. Lubich, D. C. Crafts, and C. B. Wilson, *ibid.*, **36**, 973 (1976).

(17) M. M. Abdel-Monem, K. Ohno, I. E. Fortuny, and A. Theologides, *Lancet*, **2**, 1210 (1975).

(18) M. M. Abdel-Monem and K. Ohno, *J. Pharm. Sci.*, **66**, 1089 (1977).

(19) *Ibid.*, **66**, 1195 (1977).

(20) F. Halberg, C. W. Gehrke, H. H. Zinneman, K. Kuo, W. L. Nelson, D. P. Dubey, L. M. Cadotte, E. Haus, L. E. Scheving, R. A. Good, A. Rosenberg, L. Soong, H. Bazin, and M. M. Abdel-Monem, *Chronobiologia*, **3**, 309 (1976).

(21) M. G. Rosenblum, B. G. M. Durie, S. E. Salmon, S. Chang, and D. H. Russell, *Proc. Am. Assoc. Cancer Res.*, **17** (1976).

(22) M. G. Rosenblum and D. H. Russell, *Cancer Res.*, **37**, 47 (1977).

ACKNOWLEDGMENTS

The authors thank Dr. I. Fortuny for assistance in providing the urine samples from the cancer patients.

Supported by U.S. Public Health Service Grant CA14239.

Dissolution of Nonspherical Powders

NOBUYUKI KITAMORI [x] **and KATSUMI IGA**

Received December 8, 1977, from the *Pharmaceutical Research Laboratories, Central Research Division, Takeda Chemical Industries, Ltd., Yodogawa-ku, Osaka 532, Japan.* Accepted for publication March 29, 1978.

Abstract □ To elucidate the effect of particle shape on the dissolution profile of a powder, an equation was derived for the dissolution of powders whose particles are rectangular parallelepipeds and log-normally distributed by introducing three-dimensional parameters instead of diameter in the Brooke equation for the spherical powder dissolution. By using some hypothetical values for constants in the equation, it is shown that the smallest side length, a_0, does greatly affect the dissolution profile but that the other two side lengths, αa_0 and βa_0, do not, even with rather large values of α and β. Nonisotropic dissolution also is discussed.

Keyphrases □ Dissolution profiles—nonspherical powders, effect of particle shape, equations derived □ Powders, nonspherical—dissolution profiles, effect of particle shape, equations derived

Theoretical considerations of drug dissolution in relation to particle-size distribution were first presented by Higuchi and Hiestand (1, 2). Recently, Brooke (3, 4) and Pedersen and Brown (5) developed more exact equations that permit the calculation of the dissolution rate of spherical particles obeying the log-normal distribution law. Most dissolution theories describing the particle-size distribution effect considered spherical particles.

Little attention has been given to the influence of shape factors on dissolution, except that Carstensen and Patel (6) reported the dissolution of nonspherical particles of a log-normal distribution. The dissolution of nonspherical single particles was approximated by the dissolution equation for a hypothetical spherical particle of a specified diameter by Pedersen and Brown (7).

The purpose of this paper is to elucidate the effect of particle shape on dissolution profiles. An equation was derived for the dissolution of powders whose particles are rectangular parallelepipeds and log-normally distributed by introducing three-dimensional parameters instead of diameter into the Brooke equation for the spherical powder dissolution. The shape effect in cubes, needles, and plates was examined on the basis of this theory. Nonisotropic dissolution is also discussed.

THEORETICAL

For a powder whose particles are rectangular parallelepipeds and log-normally distributed, it is assumed that the side lengths of a particle initially are a_0, αa_0, and βa_0 on the edges, where α and β are constants larger than unity. Its initial volume is then $\alpha\beta a_0^3$ ($= V_0$). If it dissolves isotropically under sink conditions, then its volume after t can be written:

$$V_t = [a_0 - (2k_i/p)t][\alpha a_0 - (2k_i/p)t][\beta a_0 - (2k_i/p)t] \quad \text{(Eq. 1)}$$

where k_i is the intrinsic dissolution rate constant and p is the density. After $t = a_0 p/2k_i$, the particle volume is zero ($V_t = 0$). A log-normal particle-size distribution is given by:

$$f = \frac{1}{\sigma\sqrt{2\pi}} \exp[-(\ln M - \ln a_0)^2/2\sigma^2] \quad \text{(Eq. 2)}$$

where $\ln M$ is the logarithmic mean of a_0 and σ is the standard deviation. The weight undissolved after t is given by:

$$W_t = \int_{\ln[(2k_i/p)t]}^{\infty} pV_t N_0 f \, d(\ln a_0) \quad \text{(Eq. 3)}$$

After inserting Eq. 1 into Eq. 3 by expanding the cubic term and letting $\alpha\beta p N_0 = r$ and $(2k_i/p)t = \tau$, Eq. 3 becomes:

$$W_\tau = r\int_{\ln\tau}^{\infty} a_0^3 f \, d(\ln a_0) - \left(1 + \frac{1}{\alpha} + \frac{1}{\beta}\right) r\tau \int_{\ln\tau}^{\infty} a_0^2 f \, d(\ln a_0) + \left(\frac{1}{\alpha} + \frac{1}{\beta} + \frac{1}{\alpha\beta}\right) r\tau^2 \int_{\ln\tau}^{\infty} a_0 f \, d(\ln a_0) - \frac{1}{\alpha\beta} r\tau^3 \int_{\ln\tau}^{\infty} f \, d(\ln a_0) \quad \text{(Eq. 4)}$$

By employing a standard normal distribution function $F(x)$, as was done by Brooke (3, 4) for spherical particles, Eq. 4 becomes:

$$W_\tau = r\exp[3(\ln M + 3\sigma^2/2)]\left(1 - F\left[\frac{\ln(\tau/M) - 3\sigma^2}{\sigma}\right]\right) - \left(1 + \frac{1}{\alpha} + \frac{1}{\beta}\right) r\tau \exp[2(\ln M + \sigma^2)]\left(1 - F\left[\frac{\ln(\tau/M) - 2\sigma^2}{\sigma}\right]\right) + \left(\frac{1}{\alpha} + \frac{1}{\beta} + \frac{1}{\alpha\beta}\right) r\tau^2 \exp(\ln M + \sigma^2/2)\left(1 - F\left[\frac{\ln(\tau/M) - \sigma^2}{\sigma}\right]\right) - \frac{1}{\alpha\beta} r\tau^3 \left(1 - F\left[\frac{\ln(\tau/M)}{\sigma}\right]\right) \quad \text{(Eq. 5)}$$

The initial weight of the particles, W_0, is:

$$W_0 = r\exp[3(\ln M + 3\sigma^2/2)] \quad \text{(Eq. 6)}$$

Then the weight fraction dissolved, $S_\tau (= 1 - W_\tau/W_0)$, can be written:

$$S_\tau = F\left[\frac{\ln(\tau/M) - 3\sigma^2}{\sigma}\right] + \left(1 + \frac{1}{\alpha} + \frac{1}{\beta}\right)(\tau/M)\exp(-5\sigma^2/2)\left(1 - F\left[\frac{\ln(\tau/M) - 2\sigma^2}{\sigma}\right]\right) - \left(\frac{1}{\alpha} + \frac{1}{\beta} + \frac{1}{\alpha\beta}\right)(\tau/M)^2\exp(-4\sigma^2)\left(1 - F\left[\frac{\ln(\tau/M) - \sigma^2}{\sigma}\right]\right) + \frac{1}{\alpha\beta}(\tau/M)^3\exp(-9\sigma^2/2)\left(1 - F\left[\frac{\ln(\tau/M)}{\sigma}\right]\right) \quad \text{(Eq. 7)}$$

RESULTS AND DISCUSSION

In the dissolution equation for a powder consisting of rectangular parallelepipeds, three-dimensional parameters (a_0, α, and β) were introduced instead of diameter. Brooke (3, 4), in his equation for spherical powders, showed that the expression of the weight fraction undissolved, W_τ/W_0, is a function of only τ/M when σ is constant. Similarly, for rectangular parallelepipeds, W_τ/W_0 is dependent only on the ratio of time length to mean side length when α, β, and σ are constant.

In this paper, S_τ in Eq. 6 was calculated with a computer, using hypothetical values of these parameters, where the standard normal function $F(x)$ was approximated (8) by:

$$F(x) = 1 - \frac{1}{\sqrt{2\pi}}\exp(-x^2/2)(ay + by^2 + cy^3 + dy^4 + ey^5) \quad \text{(Eq. 8)}$$

where $y = 1/(1 + 0.2316419x)$, $a = 0.319381530$, $b = -0.356563782$, $c = 1.781477937$, $d = -1.821255978$, and $e = 1.330274429$.

Exactly calculated dissolution profiles for the hypothetical powders consisting of cubes, needles, and plates with isotropic behavior are presented in Table I as weight percent dissolved *versus* t. The parameters are based on $k_i = 0.1$, $M = 1.0$, $p = 1.5$, and $\sigma = 0$–0.7. Figure 1 shows the dissolution profiles when $\sigma = 0.5$ in Table I. In this figure, curve a is for cubes ($1 \times 1 \times 1$ on the edges; *i.e.*, $\alpha = 1.0$ and $\beta = 1.0$), curve b is for needles ($1 \times 1 \times 10$ on the edges; *i.e.*, $\alpha = 1.0$ and $\beta = 10.0$), curve c is for plates ($1 \times 10 \times 10$ on the edges; *i.e.*, $\alpha = 10.0$ and $\beta = 10.0$), and curve d is for cubes 10 times larger in size than the cubes in curve a. The ratio of the time necessary for 50% dissolution is 1:1.36:2.11:10 for the profiles.

0022-3549/78/1200-1674$01.00/0
© 1978, American Pharmaceutical Association

Table I—Exactly Calculated Isotropic Dissolution Profiles for the Powders Consisting of Cubes, Needles, and Plates [a] (M = 1.0, p = 1.5, and k_i = 0.1)

Time	Cube (α = 1.0, β = 1.0)					Needle (α = 1.0, β = 10.0)					Plate (α = 10.0, β = 10.0)				
	$\sigma = 0$ [b]	0.1	0.3	0.5	0.7	0 [b]	0.1	0.3	0.5	0.7	0 [b]	0.1	0.3	0.5	0.7
1.0	34.90	34.11	28.38	19.53	11.03	25.89	25.28	20.89	14.21	7.93	15.63	15.53	12.52	8.43	4.65
2.0	60.56	59.34	50.26	35.59	20.70	47.66	46.60	38.89	26.90	15.27	30.53	30.34	24.52	16.58	9.19
3.0	78.40	77.04	66.60	48.65	29.19	65.44	64.09	54.11	38.11	22.04	44.70	44.44	36.03	24.47	13.63
4.0	89.84	88.56	78.35	59.16	36.64	79.38	77.89	66.63	47.90	28.27	58.18	57.84	47.03	32.07	17.95
5.0	96.30	95.28	86.43	67.56	43.17	89.63	88.13	76.59	56.35	33.99	70.96	70.55	57.46	39.33	22.15
10.0	99.99	99.99	99.09	89.55	6.590	99.99	99.99	97.52	82.63	55.99	99.99	99.99	91.95	68.43	40.84
15.0			99.99	96.40	78.50			99.82	93.08	70.00			99.19	84.80	55.39
20.0				98.66	85.87			99.99	97.13	79.05			99.93	92.78	66.28
30.0				99.77	93.30				99.43	89.12			99.99	98.28	80.26
60.0				99.99	98.85				99.99	97.80				99.99	95.09

[a] The values in the table are percent dissolved. [b] Since Eq. 7 does not hold for σ = 0, the dissolution profiles for monosized powders were calculated at σ = 0.0001.

Figure 1 reveals that the increase in the smallest side length, a_0, greatly affects the dissolution profiles, whereas the influence of the other two side lengths, αa_0 and βa_0, on dissolution is not severe, even with rather large values of α and β. Thus, rough evaluation of the dissolution for the powders consisting of rectangular parallelepipeds using Eq. 7 is possible, even though the particles in the powder are not exactly similar in shape.

Several investigators (1–5) approximated particles as spheres in their theories. On the other hand, by letting α and β be unity (the condition for cubes), Eq. 6 reduces to the one equation for spherical powders. This finding shows that the weight fraction dissolved for spherical powders having mean diameter M is equal to that for cubic powders having mean side length M.

The comparison of the dissolution profile for powder of acicular particles (1 × 1 × 10 on the edges) with the dissolution profiles of hypothetical spherical particles having the same volume or surface area with

Table II—Exactly Calculated Isotopic Dissolution Profiles for the Powders Consisting of Rectangular Parallelepipeds (1 × 1 × 10 on the Edges) and the Spheres Having the Same Volume or Surface Area [a] (σ = 0.5, p = 1.5, and k_i = 0.1)

Time	Rectangular Parallelepipeds (M = 1.0)	Hypothetical Spheres Having Same Volume (M = 2.673)	Hypothetical Spheres Having Same Surface Area (M = 3.656)
1.0	14.21	7.74	5.71
2.0	26.90	14.95	11.14
3.0	38.11	21.67	16.29
4.0	47.90	27.90	21.18
5.0	56.35	33.69	25.81
10.0	82.63	56.66	45.45
15.0	93.08	71.82	60.11
20.0	97.13	81.63	70.88
30.0	99.99	92.01	84.40
60.0		99.15	97.30

[a] The values in the table are percent dissolved.

Table III—Exactly Calculated Dissolution Profiles for the Powders Consisting of Rectangular Parallelepipeds (1 × 1 × 10 on the Edges) with Three Dissolution Rate Constants Proportional to the Corresponding Side Lengths and with the Average Dissolution Rate Constant k_{ia} [a] (M = 1.0, σ = 0.5, p = 1.5, α = 1.0, and β = 10.0)

Time	Nonisotropic Dissolution (k_i = 0.1, 0.1, 10.0)	Isotropic Dissolution (k_{ia} = 0.14286)
1.0	19.53	19.83
2.0	35.59	36.59
3.0	48.65	50.45
4.0	59.16	61.63
5.0	67.56	70.46
10.0	89.55	92.12
15.0	96.40	97.75
20.0	98.66	99.29
30.0	99.77	99.91
60.0	99.99	99.99

[a] The values in the table are percent dissolved.

isotropic behavior is given in Table II. The ratio of the time necessary for 50% dissolution is 1:1.97:2.69 for the profiles. For nonspherical single-particle dissolution, Pedersen and Brown (7) showed that spherical approximations give somewhat slower dissolution than the best approximations for fitting to the exact dissolution curves. The situation is also true in the dissolution of nonspherical powders.

Actually, acicular or flaky crystals do not grow isotropically, so they probably dissolve nonisotropically. The dissolution rate constant may be smaller for a larger side; *i.e.*, particles may dissolve faster from the smaller surface at the end of an acicular crystal (6). If it is assumed that three dissolution rate constants for rectangular parallelepipeds are proportional to the corresponding side lengths, as illustrated in Fig. 2, the particles are similar in shape throughout the dissolution. Then V_t in Eq. 1 can be written:

$$V_t = [a_0 - (2k_i/p)t][\alpha a_0 - (2k_i/p)t][\beta a_0 - (2k_i/p)t] \quad \text{(Eq. 9a)}$$

$$V_t = \alpha\beta[a_0 - (2k_i/p)t]^3 \quad \text{(Eq. 9b)}$$

In this case, $[1 + (1/\alpha) + (1/\beta)]$, $[(1/\alpha) + (1/\beta) + (1/\alpha\beta)]$, and $(1/\alpha\beta)$ in Eq. 5 are replaced by 3, 3, and 1, respectively. Hence, the final equation for S_T remains the same as the dissolution equation for the powder consisting of cubes or spheres.

In general, however, it is difficult to obtain the value of k_i; some average value is usually obtained, for example, by means of the disk method. The mean dissolution rate, k_{ia}, of three rates on the surface-area basis can be expressed by:

$$k_{ia} = \frac{(\alpha \times \beta)k_i + (1 \times \alpha)\beta k_i + (1 \times \beta)\alpha k_i}{(\alpha \times \beta) + (1 \times \alpha) + (1 \times \beta)} = \frac{3\alpha\beta}{\alpha\beta + \alpha + \beta} k_i \quad \text{(Eq. 10)}$$

The dissolution profile for needle-shaped particles (1 × 1 × 10 on the edges) with dissolution rate constants k_i, k_i, and $10k_i$ (M = 1.0, σ = 0.5, and p = 1.5) and the dissolution profile for these same particles with the

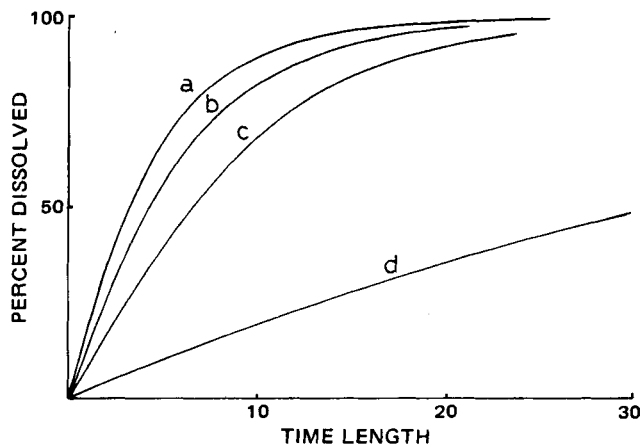

Figure 1—*Typical dissolution profiles for powders of cubic, acicular, and flaky particles with isotropic behavior. The constants used are* k_i *= 0.1,* M *= 1.0,* σ *= 0.5, and* p *= 1.5. Key: curve a, powder of cubic particles (1 × 1 × 1 on the edges); curve b, powder of acicular particles (1 × 1 × 10 on the edges); curve c, powder of flaky particles (1 × 10 × 10 on the edges); and curve d, powder of cubic particles (10 × 10 × 10 on the edges).*

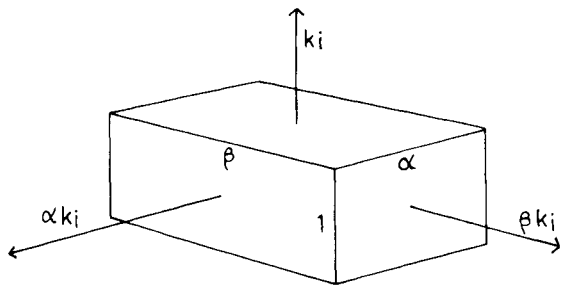

Figure 2—*Rectangular parallelepiped having the dissolution rate constants* k_i, αk_i, *and* βk_i.

average dissolution rate constant, k_{ia} ($M = 1.0$, $\sigma = 0.5$, $p = 1.5$, $\alpha = 1.0$, and $\beta = 10.0$), and with isotropic behavior are presented in Table III. Both profiles are almost the same. The ratio of the time necessary for 50% dissolution is 1:0.95. This result implies that the evaluation of the dissolution for the acicular or flaky particles with nonisotropic behavior is roughly possible by means of Eq. 6 using the mean dissolution rate constant, k_{ia}, which may be obtained experimentally as described.

The basic assumptions behind the theory are that the constituent particles are rectangular parallelepipeds that are similar in shape and dissolve isotropically under sink conditions. In actual situations, more factors may affect the overall dissolution profiles such as deviation from the log-normal law, irregularity in shape, and differences in the diffusion barrier for each particle, none of which is easily available. But these factors do not prevent an understanding of particle-shape effects on drug dissolution profiles, since they normally act independently of the effects.

In practical terms, the sizes of acicular or flaky particles measured microscopically or by an automated counter tend to be larger than those available for the evaluation of their dissolution profiles since the microscopic method does not always give the smallest side length but gives a larger one and the automated counter method gives volume diameter.

REFERENCES

(1) W. I. Higuchi and E. N. Hiestand, *J. Pharm. Sci.*, **52**, 67 (1963).

(2) W. I. Higuchi, E. L. Rowe, and E. N. Hiestand, *ibid.*, **52**, 162 (1963).

(3) D. Brooke, *ibid.*, **62**, 795 (1973).

(4) *Ibid.*, **63**, 344 (1974).

(5) P. V. Pedersen and K. F. Brown, *J. Pharm. Sci.*, **64**, 1192 (1975).

(6) J. T. Carstensen and M. Patel, *ibid.*, **64**, 1770 (1975).

(7) P. V. Pedersen and K. F. Brown, *ibid.*, **65**, 1437 (1976).

(8) "Handbook of Mathematical Functions with Formulas, Graphs, and Mathematical Tables," M. Abramowitz and I. A. Stegun, Eds., National Bureau of Standards, Washington, D.C., 1965.

Autoxidation of Polysorbates

M. DONBROW ˣ, E. AZAZ, and A. PILLERSDORF

Received September 6, 1977, from the *Pharmacy Department, School of Pharmacy, Hebrew University, Jerusalem, Israel.* Accepted for publication March 31, 1978.

Abstract □ Aqueous solutions of polysorbate 20 undergo autoxidation on storage, with the peroxide number increasing and subsequently decreasing again, the acidity increasing continuously, the pH and surface tension falling and tending to level off, and the cloud point dropping sharply until turbidity begins at room temperature. The changes are accelerated by light, elevation of temperature, and a copper sulfate catalyst. At the same time, hydrolysis occurs, liberating lauric acid. Analysis of the alterations in these properties leads to the conclusion that hydrolysis has the major influence near room temperature and that oxyethylene undergoes chain shortening at temperatures above 40°. However, evidence of degradation is detectable even in previously unopened commercial samples of polysorbates 20, 40, and 60, warranting attention to the stability of and standards for these surfactants as compared with the solid alkyl ether type of nonionic surfactant.

Keyphrases □ Polysorbates, various—autoxidation on storage, effect of light, temperature, and copper sulfate □ Oxidation—various polysorbates on storage, effect of light, temperature, and copper sulfate □ Stability—various polysorbates, autoxidation on storage, effect of light, temperature, and copper sulfate □ Degradation—various polysorbates, autoxidation on storage, effect of light, temperature, and copper sulfate □ Surfactants—various polysorbates, autoxidation on storage, effect of light, temperature, and copper sulfate

In view of accumulating evidence of the ease of autoxidation of polyethylene glycols and polyoxyethylene fatty alcohol ethers (1–4), it was suspected that other nonionic surfactants might undergo a similar process. Information about such reactions could increase the understanding of drug instability in aqueous solutions containing nonionic surfactants (1, 3).

The only systematic investigation of autoxidation in nonionic surfactants was carried out on cetomacrogol (1, 2). Peroxides were formed and decomposed spontaneously at rates increasing with temperature and decreasing with surfactant concentration. Furthermore, the induction period for peroxide chain propagation was shortened by an increase of temperature, a reduction of pH, a copper sulfate catalyst. The period was also reduced by the addition of chemical initiators, such as hydrogen peroxide or partially oxidized surfactant, and by free radical-initiating processes, such as exposure to light or thermal treatment as in sterilization by autoclaving.

During storage, the pH and cloud point fell and the acid content rose while the surface tension characteristics changed drastically. Polyglycols exhibited parallel changes in peroxide and acid content and in pH after autoclaving. These changes were interpreted as showing that degradation occurred in the hydrophilic chain with progressive reduction of the oxyethylene content until the hydrophilic–lipophilic balance fell below the critical value for solubility in water, when phase separation of the surfactant occurred at room temperature.

Since sorbitan derivatives are used widely, knowledge of their stability is important. Their behavior relative to the fatty alcohol ether type of surfactant may govern the choice between these two agents in a formulation. In the present work, the decomposition of polysorbate 20 (polyoxyethylene 20 sorbitan monolaurate) was studied systematically at controlled temperatures. The results are also

0022-3549/78/1200-1676$01.00/0
© 1978, American Pharmaceutical Association

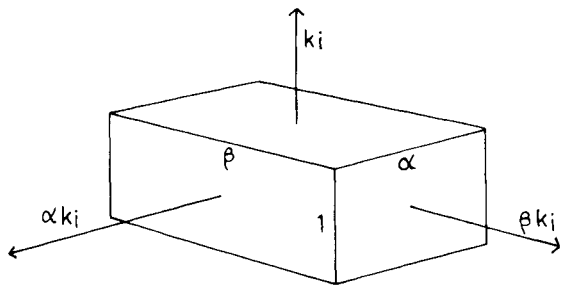

Figure 2—*Rectangular parallelepiped having the dissolution rate constants* k_i, αk_i, *and* βk_i.

average dissolution rate constant, k_{ia} ($M = 1.0$, $\sigma = 0.5$, $p = 1.5$, $\alpha = 1.0$, and $\beta = 10.0$), and with isotropic behavior are presented in Table III. Both profiles are almost the same. The ratio of the time necessary for 50% dissolution is 1:0.95. This result implies that the evaluation of the dissolution for the acicular or flaky particles with nonisotropic behavior is roughly possible by means of Eq. 6 using the mean dissolution rate constant, k_{ia}, which may be obtained experimentally as described.

The basic assumptions behind the theory are that the constituent particles are rectangular parallelepipeds that are similar in shape and dissolve isotropically under sink conditions. In actual situations, more factors may affect the overall dissolution profiles such as deviation from the log-normal law, irregularity in shape, and differences in the diffusion barrier for each particle, none of which is easily available. But these factors do not prevent an understanding of particle-shape effects on drug dissolution profiles, since they normally act independently of the effects.

In practical terms, the sizes of acicular or flaky particles measured microscopically or by an automated counter tend to be larger than those available for the evaluation of their dissolution profiles since the microscopic method does not always give the smallest side length but gives a larger one and the automated counter method gives volume diameter.

REFERENCES

(1) W. I. Higuchi and E. N. Hiestand, *J. Pharm. Sci.*, **52**, 67 (1963).

(2) W. I. Higuchi, E. L. Rowe, and E. N. Hiestand, *ibid.*, **52**, 162 (1963).

(3) D. Brooke, *ibid.*, **62**, 795 (1973).

(4) *Ibid.*, **63**, 344 (1974).

(5) P. V. Pedersen and K. F. Brown, *J. Pharm. Sci.*, **64**, 1192 (1975).

(6) J. T. Carstensen and M. Patel, *ibid.*, **64**, 1770 (1975).

(7) P. V. Pedersen and K. F. Brown, *ibid.*, **65**, 1437 (1976).

(8) "Handbook of Mathematical Functions with Formulas, Graphs, and Mathematical Tables," M. Abramowitz and I. A. Stegun, Eds., National Bureau of Standards, Washington, D.C., 1965.

Autoxidation of Polysorbates

M. DONBROW ˣ, E. AZAZ, and A. PILLERSDORF

Received September 6, 1977, from the *Pharmacy Department, School of Pharmacy, Hebrew University, Jerusalem, Israel.* Accepted for publication March 31, 1978.

Abstract □ Aqueous solutions of polysorbate 20 undergo autoxidation on storage, with the peroxide number increasing and subsequently decreasing again, the acidity increasing continuously, the pH and surface tension falling and tending to level off, and the cloud point dropping sharply until turbidity begins at room temperature. The changes are accelerated by light, elevation of temperature, and a copper sulfate catalyst. At the same time, hydrolysis occurs, liberating lauric acid. Analysis of the alterations in these properties leads to the conclusion that hydrolysis has the major influence near room temperature and that oxyethylene undergoes chain shortening at temperatures above 40°. However, evidence of degradation is detectable even in previously unopened commercial samples of polysorbates 20, 40, and 60, warranting attention to the stability of and standards for these surfactants as compared with the solid alkyl ether type of nonionic surfactant.

Keyphrases □ Polysorbates, various—autoxidation on storage, effect of light, temperature, and copper sulfate □ Oxidation—various polysorbates on storage, effect of light, temperature, and copper sulfate □ Stability—various polysorbates, autoxidation on storage, effect of light, temperature, and copper sulfate □ Degradation—various polysorbates, autoxidation on storage, effect of light, temperature, and copper sulfate □ Surfactants—various polysorbates, autoxidation on storage, effect of light, temperature, and copper sulfate

In view of accumulating evidence of the ease of autoxidation of polyethylene glycols and polyoxyethylene fatty alcohol ethers (1–4), it was suspected that other nonionic surfactants might undergo a similar process. Information about such reactions could increase the understanding of drug instability in aqueous solutions containing nonionic surfactants (1, 3).

The only systematic investigation of autoxidation in nonionic surfactants was carried out on cetomacrogol (1, 2). Peroxides were formed and decomposed spontaneously at rates increasing with temperature and decreasing with surfactant concentration. Furthermore, the induction period for peroxide chain propagation was shortened by an increase of temperature, a reduction of pH, a copper sulfate catalyst. The period was also reduced by the addition of chemical initiators, such as hydrogen peroxide or partially oxidized surfactant, and by free radical-initiating processes, such as exposure to light or thermal treatment as in sterilization by autoclaving.

During storage, the pH and cloud point fell and the acid content rose while the surface tension characteristics changed drastically. Polyglycols exhibited parallel changes in peroxide and acid content and in pH after autoclaving. These changes were interpreted as showing that degradation occurred in the hydrophilic chain with progressive reduction of the oxyethylene content until the hydrophilic–lipophilic balance fell below the critical value for solubility in water, when phase separation of the surfactant occurred at room temperature.

Since sorbitan derivatives are used widely, knowledge of their stability is important. Their behavior relative to the fatty alcohol ether type of surfactant may govern the choice between these two agents in a formulation. In the present work, the decomposition of polysorbate 20 (polyoxyethylene 20 sorbitan monolaurate) was studied systematically at controlled temperatures. The results are also

0022-3549/78/1200-1676$01.00/0
© 1978, American Pharmaceutical Association

relevant to the stability of other polysorbates. Some data on the purity of polysorbates 40, 60, and 80 indicative of the state of commercial samples also are reported.

For comparison with cetomacrogol, the peroxide content, pH, and total acidity were measured as parameters of chemical decomposition; cloud point and surface tension were used as criteria of physical changes bearing on both the decomposition process and the possible failure of the surfactant as a solubilizer or emulsifier in a formulation.

THEORETICAL

Apart from peroxide formation, which might be expected to occur in all oxyethylene-containing materials under suitable conditions, the possibility of hydrolysis also must be considered in the polysorbate ester surfactants. The first process is a chain reaction analogous to the peroxidation of oils and ethers (5) and occurs by autoxidation reactions as shown in Schemes I and II:

$$RH + \text{light or catalyst} \rightarrow R^{\cdot} + H^{\cdot}$$

Scheme I—Initiation

$$R^{\cdot} + O_2 \rightarrow ROO^{\cdot}$$

$$ROO^{\cdot} + RH \rightarrow ROOH + R^{\cdot}$$

Scheme II—Propagation

Free radicals also may be formed by the processes in Scheme III and removed by those in Scheme IV:

$$ROOH \rightarrow ROO^{\cdot} + H^{\cdot}$$

$$ROOH \rightarrow RO^{\cdot} + {}^{\cdot}OH$$

$$2ROOH \rightarrow ROO^{\cdot} + RO^{\cdot} + H_2O$$

Scheme III

$$2RO_2^{\cdot} \xrightarrow{(a)} \text{inactive products}$$

$$RO_2^{\cdot} + R^{\cdot} \xrightarrow{(b)} \text{inactive products}$$

$$2R^{\cdot} \xrightarrow{(c)} \text{inactive products}$$

Scheme IV—Termination

On the basis that the peroxidation occurs in the hydrophilic chain in polyoxyethylene surfactants (1, 2), the initiation and propagation steps (Schemes I and II) yield hydroperoxides of the oxyethylene units according to Scheme V:

$$-(OCH_2CH_2)O- + O_2 \rightarrow -(OCH_2\underset{\displaystyle OOH}{\underset{|}{CH}})O-$$

Scheme V

The hydroperoxide concentration is measured iodometrically in oils and polyglycol solutions, and results are expressed as the hydroperoxide equivalent to the iodine liberated in milliequivalents or millimoles per liter (5, 6). Recalculation with respect to the weight of material undergoing autoxidation gives the peroxide number (P.N.), expressed in milliequivalents per kilogram of surfactant (1, 5).

Peroxide Decomposition—Degradation of both hydroperoxides and peroxide free radicals may occur by a number of routes (7–10), as summarized elsewhere (11, 12). The peroxide formation rate during the initial stage of propagation is normally faster than that of its decomposition. The rates subsequently become equal, giving rise to a short plateau representing a temporary steady state, following which decomposition is the faster reaction. The analytical data give the residual peroxide content, which is determined by the rates of the various simultaneous reactions involved (8, 9); these reactions are temperature, concentration, and catalyst dependent in aqueous surfactant systems (1).

The typical kinetic pattern, showing the rise to the maximum P.N. value and then the fall, is a clear indication of autoxidation with degradation. The presence of more than minimal quantities of peroxide (P.N. > 5) signifies that autoxidation is underway and has probably passed the lag phase, but a low P.N. value may also be obtained if the decomposition rate is or has been high. Therefore, a low P.N. value is not in itself a criterion of nondegradation of the surfactant.

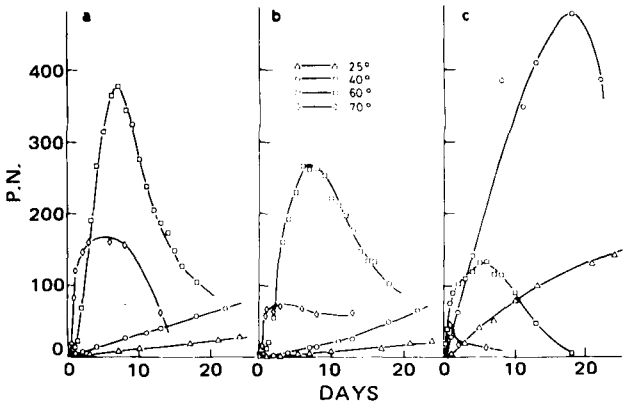

Figure 1—*Rate of peroxide formation in 3% aqueous polysorbate 20 at 70, 60, 40, and 25° in daylight* (a), *darkness* (b), *or daylight with 1* × 10^{-4} M *copper sulfate catalyst* (c). *P.N. = peroxide number in milliequivalents per kilogram.*

Surfactant Chain Degradation—Various chemical degradation products have been detected, including carbonyl compounds and acidic products (12), but no stoichiometric relationship with the degree of decomposition of the surfactant has been established. Acid formation is readily measured by the change in pH and the total acid content, and it is an important indicator of the extent of degradation and the quality of the surfactant (1, 12). Increased degradation leads to larger amounts of low molecular weight acids and, thus, a lower pH. The terminal hydroxyl groups are relatively stable compared with hydroperoxide and free radicals, requiring highly acidic conditions with strong oxidizing agents for their oxidation to terminal aldehydic and carboxylic groups.

However, substitution of a hydroperoxide radical in the α- or β-position to the terminal hydroxyl leads to instability, which generally causes migration and/or C–C or C–O fission (9, 11, 12) with consequent formation of a two-carbon acid or formic acid, respectively. The latter has been identified as a degradation product (12).

In view of the complexity of the degradation reactions and the difficulty of performing separations quantitatively in dilute aqueous surfactant solutions, physical-chemical methods have particular importance. Surface tension–concentration curves enable measurement of changes in the critical micelle concentrations (CMC); furthermore, the sub-CMC slope is determined by the surfactant area per molecule at the air–liquid interface if the molecules are close packed. In the oxyethylene type of nonionic surfactant, the area per molecule at close packing is determined by the number of oxyethylene groups present in the molecule and is relatively independent of the hydrophobic group due to coiling of the polyglycol groups (13). The surface tension value above the CMC is relatively constant and is also a characteristic property, becoming progressively lower in a series based on the same hydrophobic group as the hydrophilic chain is shortened (2).

The cloud point of nonionic surfactants is the temperature at which turbidity appears on heating their aqueous solutions. It is related to the hydrophilic–lipophilic balance; in a series based on the same hydrophobic group, phase separation occurs at progressively lower temperature as the oxyethylene chain length is reduced (2), but the cloud point is also sensitive to the presence of additives (14).

Changes in surface tension and cloud point properties were used to establish that degradation occurred in the hydrophilic chain in cetomacrogol and to estimate the rate of loss of oxyethylene groups at 50° (2).

For polysorbate 20, chain breakdown may be represented as shown in Scheme VI:

$$C_{11}H_{23}CO(OR)\,(OCH_2CH_2)_{n-x}\,(OCH_2CH_2)_xOH \rightarrow C_{11}H_{23}CO(OR)\,(OCH_2CH_2)_{n-x}\,OH + \text{short chain degradation products}$$

Scheme VI

where R is the sorbitan ring, n is the number of oxyethylene groups originally present, and x is the number of oxyethylene groups peroxidized and subsequently degraded.

Hydrolysis of Polysorbate—Hydrolysis, which may be acid, base,

Table I—Peroxide Formation in Polysorbate 20 at Different Temperatures

Temperature	Conditions[a]	Induction Period[b], hr	Maximum[c] P.N., mEq/kg	Time of[c] Maximum P.N., days
70°	C + L	<2	50	1
	L	5.5	168	5
	D	—	75	2.5
60°	C + L	<2	130	5.5
	L	10	368	7
	D	—	268	7
40°	C + L	<5	440	17
	L	~50	(>70)	(>20)
	D	—	(>70)	(>20)
25°	C + L	<24	(>140)	(>25)
	L	144	(>70)	(>50)
	D	—	(>50)	(>50)

[a] C = catalyst (1×10^{-4} *M* $CuSO_4$), L = light, and D = dark. [b] Based on P.N. of 5 (1). [c] Numbers in parentheses indicate values at end of experiment before termination was reached.

or solvent catalyzed (15), would be expected to proceed at an increasing rate as the pH falls on formation of acidic degradation products, following the reaction in Scheme VII:

$$C_{11}H_{23}CO(OR)\,(OCH_2CH_2)_nOH \rightarrow C_{11}H_{23}COOH + H(OR)\,(OCH_2CH_2)_nOH$$

Scheme VII

Of the products, lauric acid is stable and micelle soluble. The micelle saturation point would be determined by the increasing quantity of lauric acid and decreasing quantity of micelles, both functions of the hydrolysis rate, and also by changes in the micelle-solubilizing capacity as a result of chain shortening. The sorbitan polyglycol would pass out of the micellar phase, raising the aqueous concentration of hydrophilic solute progressively and possibly reducing the cloud point of the surfactant. It would be expected to undergo peroxidation and degradation by the reactions outlined for the parent surfactant; but since the process would occur outside the micellar phase, the rate constants and mechanism might not be identical with those of the polysorbate.

Turbidity in the solution could be the result of either lauric acid separation or reduction of the cloud point.

EXPERIMENTAL

Polysorbate 20 was neutralized before use to pH 6.00 with sodium hydroxide.

Autoxidation was effected under the same conditions as used previously in studies on cetomacrogol (1, 2). The method was designed to ensure adequate agitation and free access of air during storage, without loss of solvent by evaporation. Therefore, the oxygen concentration remained constant and was not rate limiting.

The acid content, pH, cloud point (1), and surface tension (2) were determined as described previously.

The peroxide number was determined using the spectrophotometric method developed for determining hydroperoxide in micellar solutions (6). Final readings were made at a concentration level of 1% polysorbate containing pH 6.00 buffer and potassium iodide at the same concentrations as described for cetomacrogol. Readings were taken at 360 nm (ϵ = 11,400) and were time independent in this system. Dilutions, when necessary, were made with solutions of 1% polysorbate 20; readings were corrected by deducting the amount of iodine liberated by the polysorbate content of the diluent. The polysorbate used as the diluent was stored under nitrogen and refrigerated.

RESULTS AND DISCUSSION

Development of Peroxides—The three stages of autoxidation—*viz.*, induction, propagation, and termination, were observed (Fig. 1). The peroxide number (P.N.) values at each stage varied with conditions but were comparable with those of cetomacrogol under parallel conditions (1).

Elevation of temperature from 25 to 70° reduced the induction period and raised the peroxide formation rate under all conditions. Copper sulfate and light had the expected catalytic effects, shortening induction and raising the peroxide formation rate relative to the dark uncatalyzed reaction. Pronounced catalysis of peroxide breakdown by the metal ions at 60 and 70° occurred (1, 3, 11), with a shorter time required to reach the maximum P.N. value and a lower value of P.N. obtained (Table I). Elevation of temperature also catalyzed the decomposition of peroxide.

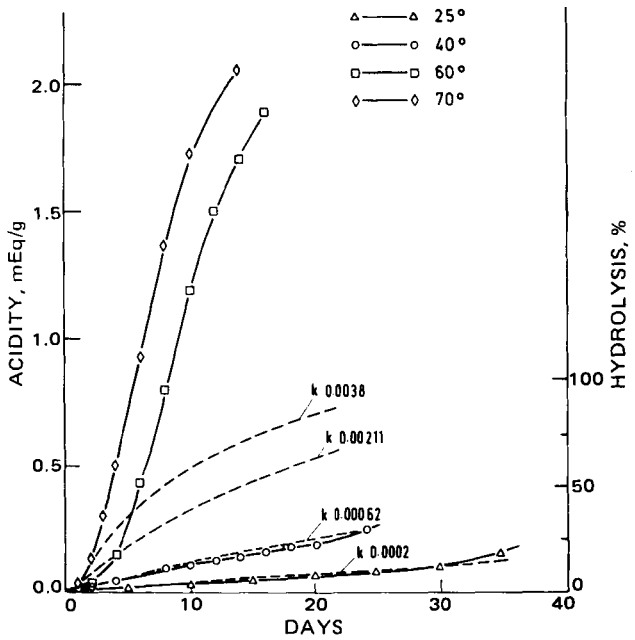

Figure 2—*Rate of acid formation in 3% aqueous polysorbate 20 at 70, 60, 40, and 25° in daylight with no catalyst. Broken lines represent lauric acid produced by hydrolysis and were calculated using the indicated values of* k ($hour^{-1}$), *the first-order hydrolysis constant, on both acidity and percent hydrolysis scales.*

Generally speaking, the greater the peroxide decomposition rate, the lower was the P.N. value at the termination stage, in which the degradation rate of the peroxides equaled or exceeded their formation rate. The enhancement of formation and decomposition rates by the temperature–catalyst combinations was such that termination was reached even at 40°; yet at this temperature, the rate balance brought about the highest P.N. value. Even at 25° with the catalyst, the P.N. rose to 150 within 25 days, and there was virtually no induction period (Fig. 1*c*).

pH and Acidity—As observed with cetomacrogol (1), the increase in acidity (Fig. 2) continued after the P.N. fell and was, therefore, the most reliable factor for following the degree of deterioration. The phenomenon of incessant increase in acidity in short chain polyglycols also was described by McKenzie (11). The rate of development of acidity had an inverse relation to the time of onset of propagation (Fig. 1*a*) and also to the initial rate of formation of peroxides.

The pH value approached 4.0 at 25 and 40°, whereas at 60 and 70° it fell rapidly and continuously to 2.5 (Fig. 3*a*). The relation between pH and acid concentration, *c* (Fig. 3*b*), indicated that the acids developed at the lower temperatures contained weaker functions. Log acid concentration–pH plots were linear at 40, 60, and 70° and tended to converge at high acidity. By use of the equation $pH = \frac{1}{2}(pKa + \log c)$, the intercepts at $\log c = 0$ enabled estimation of apparent pKa values[1], which were 3.6 ± 0.5 at 60 and 70° and 4.9 ± 0.8 at 40°.

These results suggest the presence of a larger fraction of stronger acids at the higher temperatures, which is consistent with greater rupture of the oxyethylene chains (Scheme VI). Indeed, in cetomacrogol, an ether for which hydrolysis is not to be expected, formic acid (pKa 3.75) constituted 50% or more of the acid formed during the initial stages of autoxidation under drastic conditions (12). The weaker acids present at 25° could be constituted of micelle-solubilized lauric acid (Scheme VII), carboxylated surfactant, or acetic acid (12).

The hydrolysis rate of polysorbate 80 was reported to be relatively constant and lowest between pH 3 and 7.6, increasing rapidly as a function of pH below 3 and above 7.6 (15). There was little difference between the hydrolysis rates of different polysorbate esters. To estimate the degree

[1] These pKa values represent mixed acid systems. The linearity over one order of concentration could indicate that the acid mixture has a relatively constant composition over this region in the aqueous phase. Lyophobic acids solubilized in the micelles would have a lesser influence on the experimental pH (16), and the pKa estimate would relate to their apparent pKa values in the micellar solutions and not to their aqueous pKa values.

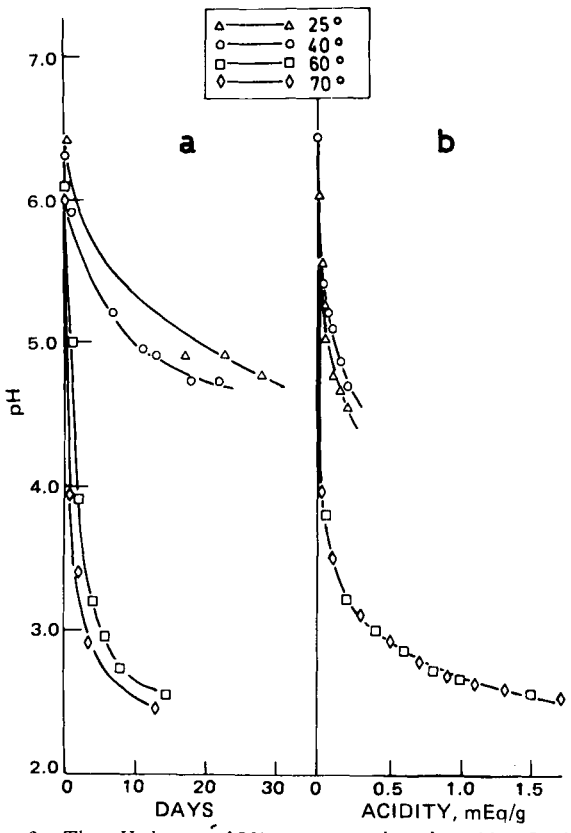

Figure 3—*The pH change of 3% aqueous polysorbate 20 at 70, 60, 40, and 25° in daylight with no catalyst, with time* (a), *and as a function of total acidity at the corresponding time* (b).

of hydrolysis expected at the temperatures used in the present work, approximate rate constants, k, were calculated based on the rate constant reported for 0.02% polysorbate 80 at pH 3.95 and 80°, utilizing the reported energy of activation (15). This calculation gave k values of 3.80, 2.65, 1.21, and 0.62×10^{-3} hr^{-1} at 70, 60, 40, and 25°, respectively, and these values were used to calculate the respective quantities of lauric acid that would be yielded at various times.

Some of these results have been included in Fig. 2 for comparison. The values are of the same order as the observed acidities at 25 and 40°, although somewhat overestimated[2]; the curves are also similar in form. However, at 70 and 60°, the quantity of acid formed on storage after 3 and 6 days, respectively, greatly exceeded that expected theoretically from hydrolysis. Again, the upward curvature indicates a rate rising with time, as in cetomacrogol (1), characteristic of degradation processes of the chain-reaction type[3].

Surface Tension (γ) Changes—The surface tension above the CMC decreased on storage and ultimately reached a constant value (Fig. 4). The rate of fall of γ increased systematically with a temperature rise; the minimum values for $\gamma_{3\%}$ developed at 60 and 70° were lower than at 40 and 25° (about 28 and 30 dynes/cm, respectively). The rate was much greater than observed under parallel conditions in cetomacrogol (1); a typical result is included in Fig. 4. There was a rank correlation among the rates of fall of γ, increase of acidity, and fall in pH suggestive of an acidic reaction product increasing in quantity with temperature and influencing surface tension.

For the consideration of the hydrolysis of the fatty acid ester, temperature acceleration has already been discussed. The increasing quantity

[2] Hydrolysis rates are concentration dependent in acid solution, with the rate constant falling by some 60% at high surfactant concentration (15). This fact is the probable reason for the discrepancy; the 40 and 25° experimental acidities accord better when the estimated k values are reduced by some 60%, as do the acidities at 60 and 70° during the first 2 days (Fig. 2). A similar reduction of the rate constant at a high surfactant concentration also was observed for peroxide formation in cetomacrogol (1).

[3] The general picture and conclusions drawn would not be altered by the errors inherent in this treatment due to the approximated k values or to the possibility that the hydrolysis data on which they are based (15) are uncorrected for acids formed by autoxidation, which could be a serious source of error at 80°, particularly at low pH values.

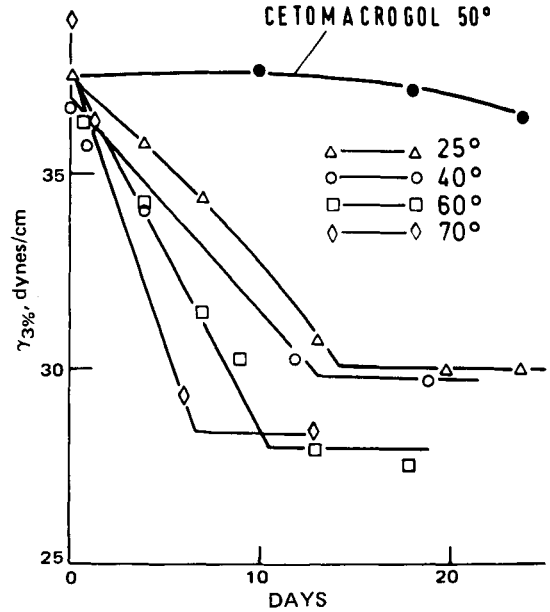

Figure 4—*Rate of change of surface tension, γ, of 3% aqueous polysorbate 20 at 70, 60, 40, and 25° in daylight with no catalyst. (Cetomacrogol, 3% aqueous solution at 50°, is shown for comparison.)*

of hydrophobic lauric acid formed would be largely solubilized in the micelles. However, being in equilibrium with the surface, some acid would tend to be adsorbed there, forming a mixed surface film with the more hydrophilic surface-active monomers of the polysorbate. Mixed films are closer packed and are expected to give lower surface tension values than the separate amphiphiles (13). Confirmation that this was the probable explanation was obtained by measurement of the surface tensions of mixtures of lauric acid and polysorbate 20 (Fig. 5).

The $\gamma_{1\%}$ value of the polysorbate fell steeply and almost linearly as the lauric acid concentration was raised to about 2.2% (w/w) in polysorbate [$\Delta\gamma/\Delta c$: ~ -3.1 dynes/cm/1% (w/w) lauric acid in polysorbate or -61 dynes/cm/mEq of lauric acid/g of polysorbate]. Above 2.2% lauric acid (equivalent to about 10% hydrolysis of the polysorbate), the rate of fall decreased greatly to 0.32 dyne/cm/1% but remained approximately linear up to saturation concentration [9% (w/w) lauric acid, 0.45 mEq/g,

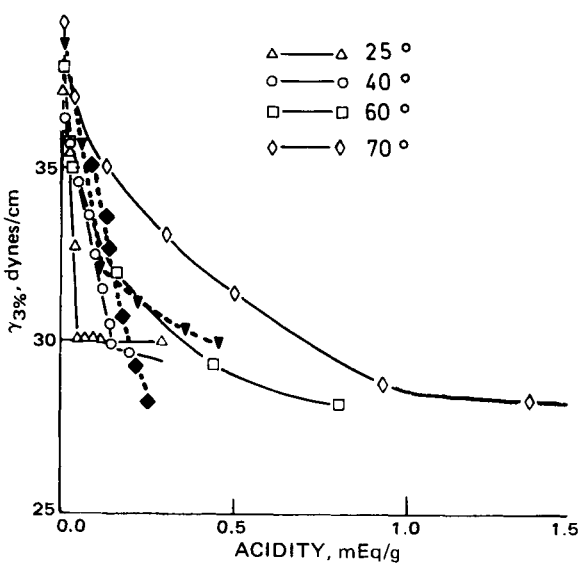

Figure 5—*Surface tension of 3% aqueous polysorbate 20 at 70, 60, 40, and 25° as a function of total acidity at the corresponding time. Broken lines represent surface tension of lauric acid solutions in polysorbate 20 (1% w/v), expressed as milliequivalents of lauric acid per gram of polysorbate (▼); and experimental surface tensions at 70° "corrected" for acidity due to autoxidation by plotting against hydrolyzed polysorbate at the corresponding time using k = 0.00211 hr^{-1} (♦).*

Table II—Phase Separation Time as Measured by Surface Tension, γ, and Cloud Point

Temperature	Phase Separation Time, days	
	γ Constant	Cloud Point 59°
25°	14.5	12.5
40°	12–13	15.5
60°	10.5	11
70°	6.5	6

equivalent to about 50% hydrolysis; $\Delta\gamma$(total) = −9 dynes/cm approximately to saturation][4].

The γ-time curves of Fig. 4 are closely predictable by using selected values of the hydrolysis constants and estimating surface tensions from the data for the prepared mixtures corresponding to the amount of lauric acid formed at the time intervals, but they are highly sensitive to the k values selected. There was reasonable agreement on a γ-acidity scale (Fig. 5) between the lauric acid solubilizate curve and the experimental curves at the three lower temperatures initially, but the 70° curve deviated almost from the start and the 60° curve deviated at a later stage toward increased acidity at corresponding γ values; both fell ultimately to lower γ values than were accounted for by the lauric acid–polysorbate mixtures.

Degradation of the oxyethylene chains (Scheme VI) also would be expected to be temperature accelerated and, as noted, to give rise to short chain acids. The residual surfactant would have a lower hydrophilic–lipophilic balance and, hence, be preferentially adsorbed on the surface or from a mixed surface film, as described for lauric acid. Consequently, lowering of surface tension should also occur during degradation and was, in fact, demonstrated in cetomacrogol where a series of hexadecyl polyoxyethylene ethers was used to determine the degree of degradation (2, 13). One must assume that the γ values at 70 and 60° in particular reflect the added effects of hydrolysis and chain shortening in view of the pattern of acid formation noted earlier.

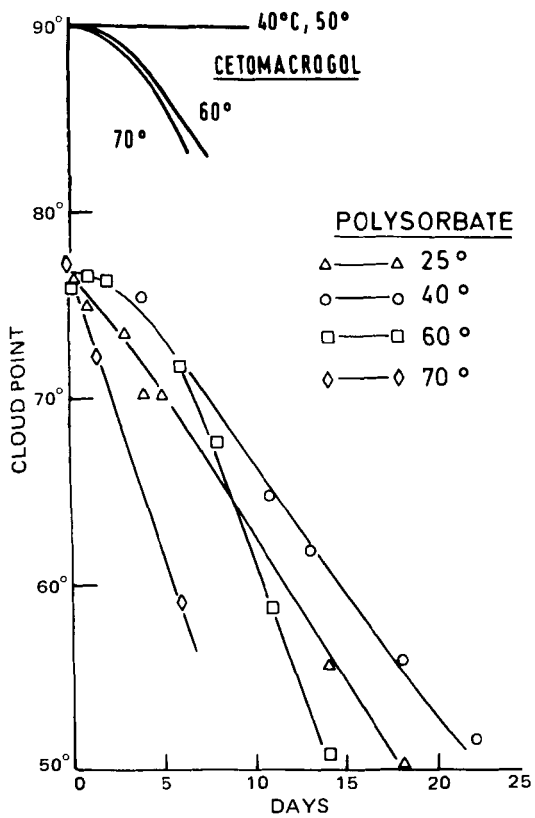

Figure 6—*Rate of change of cloud point of 3% aqueous polysorbate 20 at 70, 60, 40, and 25° in daylight with no catalyst, measured after addition of 1 M NaCl. (Cetomacrogol is shown for comparison.)*

This hypothesis was borne out by the γ–total acid plot (Fig. 5). At the higher temperatures, the acid content was greatly in excess of the amount of lauric acid that could be solubilized in the micelles, this excess acid being constituted of short chain autoxidation products that were probably not very surface active. To test this proposition, the total acid formed at 70° was "corrected," with γ being replotted against the amount of lauric acid formed hypothetically by hydrolysis on the basis that k was about 0.0021 hr^{-1}. This approach brought the curve more closely into line with the data for the lower temperatures and with the curve for the lauric acid–polysorbate mixtures. Thus, at low acid concentration, most of the acid formed at 25, 40, and 60° was accounted for by lauric acid; at 70° and at the higher acidities at 60°, the acids formed by autoxidation became predominant. At the same time, the sharper fall than expected of γ at the lowest temperatures may indicate that oxyethylene chain degradation occurs here as well.

The region of time independence of γ (Fig. 4) is explained by phase separation at room temperature, as evidenced by the appearance of cloudiness, with the nature and concentration of water-soluble surface-active species at the surface remaining virtually constant. Phase separations occurred earlier as the temperature was raised because of the accumulation of larger quantities of the hydrophobic products. At the same time, the higher terminal γ values at 40 and 25°, close to the lauric acid saturation γ value, imply that the main reaction was that of lauric acid formation. The greater surface activity at 60 and 70° was compatible with the summated effect of the two reactions.

Cloud Point—As in cetomacrogol (1, 2), the cloud point of polysorbate 20 solutions (3% containing 1 *M* NaCl) decreased during autoxidation (Fig. 6); but unlike in cetomacrogol, the rates of fall were not in rank order of temperature change. Results could not be determined accurately below 60° because of cloudiness appearing at room temperature (the cloudy phase partially dissolved on heating but interfered with observations). The turbidity stage corresponded fairly well to the time at which $\gamma_{3\%}$ reached a constant value at 70 and 60° but less closely at 40 and 25° (Table II).

The cloud point dropped unexpectedly rapidly at 25 and 40°, and room temperature turbidity appeared well within 15–20 days. Under comparable conditions, cetomacrogol exhibited little change in the cloud point at 50°, phase separation being evident only after 60 days of storage; even catalyzed solutions remained optically clear for some 30 days or more (2). At 60 and 70°, cetomacrogol ultimately exhibited a similar rate of fall of the cloud point to that of polysorbate, but there was a longer induction period (Fig. 6). These differences again point to the hydrolysis reaction as a probable explanation. Lauric acid will be taken almost entirely into the micelles up to saturation concentration, above which turbidity will appear at room temperature; warming will clarify the solution due to a solubility increase.

The phenomenon was studied in some depth for benzoic acid and a series of substituted phenols (14). Except for certain aliphatic hydrocarbons, most solubilizates lower the cloud point. The effect is not straightforward, however, being dependent on factors such as concentration, type of polar group present, and site of solubilization in the micelle (see references in 14). In the present work, saturation with lauric acid (90 mg/g of polysorbate) lowered the cloud point of 3% polysorbate to 59° and that of 3% cetomacrogol to 64° (150 mg of lauric acid/g of cetomacrogol).

The form of the 60° curve was deviant, showing a lag during the first 6 days and then falling more steeply; *i.e.*, the initial stage resembled 40°, and the later stage resembled 70°. To the extent that the cloud point fall in polysorbate is a function of polyglycol chain shortening, as demonstrated in cetomacrogol (2), the chain breakdown is presumed to occur *via* reactions of the hydroperoxides formed in the initial stages (Scheme V) and modified by acid catalysis (Figs. 7 and 8 in Ref. 1). The P.N. data (Fig. 1 and Table I) show that the peroxide stability was enhanced at 60° relative to 70°, which could explain the initial lag in chain breakdown at 60°. However, the absolute peroxide concentration increased greatly by the 7th day (P.N. 368), which would enhance the rate of reactions involving the peroxide species, and, indeed, the slope of the cloud point–time relation increased at the time corresponding to the peak P.N. value[5].

This time was also close to the time at which the pH drops below the critical value of 3 (15). Therefore, autocatalytic effects would also operate[5] here, as well as at 70°.

[4] Cetomacrogol 1000 gave a similar picture [$\Delta\gamma/\Delta c$: ~ −1.9 dynes/cm/1% lauric acid up to 6% (w/w) lauric acid, after which the rate fell to −0.44 dyne/cm]. The total fall was about 12 dynes/cm because of higher lauric acid solubility [15% (w/w)].

[5] For example, with the assumption of a first-order dependence on the hydroperoxide concentration in decomposition reactions, the rate will follow equations of the type $dx/dt = k_t[H^+][P.N.]$, where k_t is the temperature-dependent rate constant and $k_{70} > k_{60} \gg k_{40} > k_{25}$.

Table III—Physicochemical Data for Surfactants from Different Sources

Surfactant	Sample[a]	Solubility[b] at 20% (w/v)	pH	Acidity, mEq/g	P.N., mEq/kg	Cloud[c] Point	$\gamma_{1\%}$, dynes/cm
Polysorbate 20	A	+	4.6	0.040	14.6	76°	—
	B	+	3.8	0.050	4.5	—	—
	C	+	4.2	0.016	0.13	77°	40.9
	D	+	4.5	0.027	0.07	—	41.2
	E	+	5.2	0.033	0.05	76°	40.0
Polysorbate 40	A	−	—	—	—	—	—
(polyoxyethylene	B	−	6.6	0.016	—	—	—
20 sorbitan	Ca	+	4.9	0.023	0.21	72.8°	42.8
monopalmitate)	Cb	−	—	0.022 d[d]	—	—	—
	Da	−	—	0.033 d	—	—	—
	Db	−	3.6	0.065 f[d]	0.04 f	74.3° f	42.3 f
Polysorbate 60	A	−	4.2 d, 4.1 f	0.02 d, 0.014 f	0.36 f	80.3° f	—
(polyoxyethylene	B	−	—	0.013 d, 0.0095 f	0.1 f	69.5° f	—
20 sorbitan	C	−	5.1 f	0.012 d, 0.006 f	0.5 f	76.8° f	45.9 d, 46.0 f
monostearate)	D	−	4.3 d, 4.0 f	0.33 d, 0.017 f	0.06 f	80.7° f	—
Polysorbate 80	A	+	6.1	0.021	3.7	65°	—
(polyoxyethylene	B	+	6.5	0.022	0.17	—	—
20 sorbitan	D	+	5.5	0.034	—	—	—
monooleate)							
Cetomacrogol	F	+	7.2	0.025	0	90.2°	38.0
1000 BPC	G	+	7.4	0.0	0	89.2°	38.5

[a] A, B, and C, I.C.I.-Atlas, Wilmington, Del.; D, Sigma, St. Louis, Mo.; E, NBC, Cleveland, Ohio; and F and G, Glovers, Liverpool, England. Sample b is about 1 month older than Sample a. [b] All surfactants stated by the manufacturers to be soluble at this concentration (+, soluble; and −, turbid). [c] In 3% solution containing 1 *N* NaCl. [d] d = dispersed, and f = filtered.

One may assume that the rapid fall in the cloud point at 70° results from the two decomposition processes (Schemes VI and VII). However, since the curves are more ambiguous with respect to temperature effects than those of the other properties studied and different from those of ether-type surfactants, further investigation is warranted[6]. Nevertheless, the falls in cloud points in the polysorbate 20 systems were much greater than those occurring over a similar period in the cetomacrogol systems (1).

General and Pharmaceutical Aspects—There are some important differences between the stability behavior of the polysorbate ester and alkyl ether types of nonionic surfactant exemplified by polysorbate 20 and cetomacrogol. Although both types undergo degradation of the polyglycol chains rapidly at elevated temperatures and in the presence of light, air, and catalysts but more slowly at room temperature and in the absence of these factors, polysorbate 20 shows some surprising differences in cloud point behavior, and the early phase separation is a limitation to its use as a solubilizer. The main disadvantages arise from its potential for hydrolysis to lauric acid[7] and its more rapid autoxidation than cetomacrogol, which may be a function of its liquid state, conducive to rapid diffusion of oxygen and free radicals into the bulk. Evidence of the difficulty of preventing autoxidation is presented in Table III, which gives analytical data on commercial samples intended for the present study and determined as received without purification.

Many of the samples contained a measurable amount of peroxide; several were approaching the propagation stage (P.N. 3–4). The acid content and low pH values indicated that even if the P.N. was low, decomposition had progressed and decreased the induction period. Some samples contained insoluble components and showed inconsistencies in the cloud point. Cetomacrogol samples were generally free from these impurities and had a longer induction period. One must assume that these variations are reflected in the instability of many products containing oxidizable or pH-sensitive drugs (17), formulated with polysorbate surfactants containing peroxides, or having undergone partial autoxidation. Additional and tighter standards are needed for the quality control and storage of these materials.

[6] Free polyglycols, when formed in significant quantities by hydrolysis, might influence the cloud point. Short chain acids, aldehydes, and ketones (11, 12) in the trace amounts expected should have little effect on bulk phase properties while the concentration of polysorbate remains high. The latter argument is supported by the agreement between γ and cloud point estimations of oxyethylene chain degradation based on reference data from a series of surfactants (2).

[7] The acid content of 3% polysorbate 20 solutions stored at 25° was equivalent to about 5% hydrolysis after 10 days and 10% after 20 days; at 40°, the 5% level was reached in about 4 days and the 10% level was reached in about 8 days.

REFERENCES

(1) R. Hamburger, E. Azaz, and M. Donbrow, *Pharm. Acta Helv.*, **50,** 10 (1975).

(2) M. Donbrow, R. Hamburger, and E. Azaz, *J. Pharm. Pharmacol.*, **27,** 160 (1975).

(3) J. W. McGinity, J. A. Mill, and A. L. Lavia, *J. Pharm. Sci.*, **64,** 356 (1975).

(4) J. W. McGinity, T. R. Patel, A. H. Naqvi, and J. A. Hill, *Drug. Dev. Commun.*, **2,** 505 (1976).

(5) G. Scott, "Atmospheric Oxidation and Antioxidants," Elsevier, Amsterdam, The Netherlands, 1965.

(6) E. Azaz, M. Donbrow, and R. Hamburger, *Analyst*, **98,** 663 (1973).

(7) J. L. Bolland, *Q. Rev. Chem. Soc.*, **25,** 265 (1949).

(8) P. Grosborne, *Rev. Inst. Fr. Petrole Ann. Combust. Liquides*, **23,** 508 (1968).

(9) L. Dulog and G. Storck, *Macromol. Chem.* **91,** 50 (1966).

(10) H. R. Rawls and P. J. Van Senten, *J. Am. Oil Chem. Soc.*, **47,** 121 (1969).

(11) D. A. McKenzie, "Technical Service Report," Union Carbide Corp., Tarrytown, N.Y., 1970, Part I.

(12) M. Donbrow, R. Hamburger, E. Azaz, and A. Pillersdorf, *Analyst*, **103,** 400 (1978).

(13) M. Donbrow, *J. Colloid Interface Sci.*, **53,** 145 (1975).

(14) M. Donbrow and E. Azaz, *ibid.*, **57,** 20 (1976).

(15) T. R. Bates, C. H. Nightingale, and E. Dixon, *J. Pharm. Pharmacol.*, **25,** 470 (1973).

(16) M. Donbrow and C. T. Rhodes, *ibid.*, **15,** 233 (1963).

(17) M. J. Amin and J. T. Bryan, *J. Pharm. Sci.*, **62,** 1769 (1973).

ACKNOWLEDGMENTS

Supported in part by a grant to Dr. E. Azaz from the Joint Fund of the Hebrew University and the Hadassah Medical Organization.

The authors thank Mrs. Ester Dror for technical assistance.

Anticonvulsant Activity and Inhibition of Respiration in Rat Brain Homogenates by Substituted Trimethoxybenzamides

SHIVA P. SINGH *, BHAGWAN R. PANDEY ‡, SUSHIL KUMAR ‡§, and SURENDRA S. PARMAR *x

Received November 28, 1977, from the *Department of Physiology, University of North Dakota School of Medicine, Grand Forks, ND 58202, and the ‡Jawahar Lal Nehru Laboratory of Molecular Biology, Department of Pharmacology and Therapeutics, King George's Medical College, Lucknow University, Lucknow, India. Accepted for publication April 18, 1978. §Present address: Department of Biochemistry and Psychiatry, Medical School of Ohio at Toledo, Toledo, OH 43606.

Abstract □ Ten *N*-[4-[4-(arylthiosemicarbazido)carbonyl]phenyl]-3,4,5-trimethoxybenzamides were synthesized and characterized by their sharp melting points, elemental analyses, and IR and NMR spectra. All substituted benzamides were evaluated for their anticonvulsant activity. The degree of protection afforded by these compounds (100 mg/kg ip) against pentylenetetrazol (90 mg/kg sc)-induced convulsions in mice ranged from 10 to 80%. The ability of substituted benzamides to inhibit respiratory activity was observed by inhibition of oxidation of pyruvate, α-ketoglutarate, NADH, and succinate by rat brain homogenates. Inhibition of pyruvic acid oxidation was concentration dependent. The anticonvulsant activity of substituted benzamides was not related to their ability to inhibit cellular respiratory activity.

Keyphrases □ Trimethoxybenzamides, various substituted—synthesized, evaluated for anticonvulsant activity in mice and effect on enzyme activity in rat brain homogenates □ Anticonvulsant activity—various substituted trimethoxybenzamides evaluated in mice □ Enzyme activity—NAD dependent and independent oxidations in rat brain homogenates, effect of various substituted trimethoxybenzamides □ Oxidations, NAD dependent and independent—effect of various substituted trimethoxybenzamides in rat brain homogenates □ Structure–activity relationships—various substituted trimethoxybenzamides evaluated for anticonvulsant activity in mice and effect on enzyme activity in rat brain homogenates

Central nervous system (CNS) depressant and hypotensive properties associated with reserpine are due to the presence of a 3,4,5-trimethoxybenzene moiety (1–6). Many drugs affecting CNS activity have amide or thioamide linkage as the common molecular structural units (7, 8). CNS-affecting properties of trimethoxybenzamides were reported (9, 10). Amides also possess greater CNS depressant activity as compared to their corresponding esters (11). The anticonvulsant activity of nitrobenzamides and their ability to inhibit nicotinamide adenine dinucleotide (NAD)-dependent oxidations by rat brain homogenates were reported recently (12, 13).

These observations and the functional role of the 3,4,5-trimethoxyphenyl moiety for CNS activity (14) prompted the synthesis of some *N*-[4-[4-(arylthiosemicarbazido)carbonyl]phenyl]-3,4,5-trimethoxybenzamides. These substituted trimethoxybenzamides were evaluated for their anticonvulsant activity. The ability of these compounds to inhibit cellular respiratory activity of rat brain homogenates also was investigated to elucidate their biochemical mechanism of action. The various trimethoxybenzamides were synthesized by following the methods outlined in Scheme I.

EXPERIMENTAL

Chemistry—The condensation of 3,4,5-trimethoxybenzoyl chloride (Ia, Scheme I) with ethyl *p*-aminobenzoate (Ib) gave ethyl 4-(3,4,5-trimethoxybenzamido)benzoate (Ic) which, on reaction with hydrazine hydrate, yielded 4-(3,4,5-trimethoxybenzamido)benzohydrazide (Id). This trimethoxybenzamide, on treatment with suitable aryl isothiocyanates, gave *N*-[4-[4-(arylthiosemicarbazido)carbonyl]phenyl]-3,4,5-trimethoxybenzamides (II–XI).

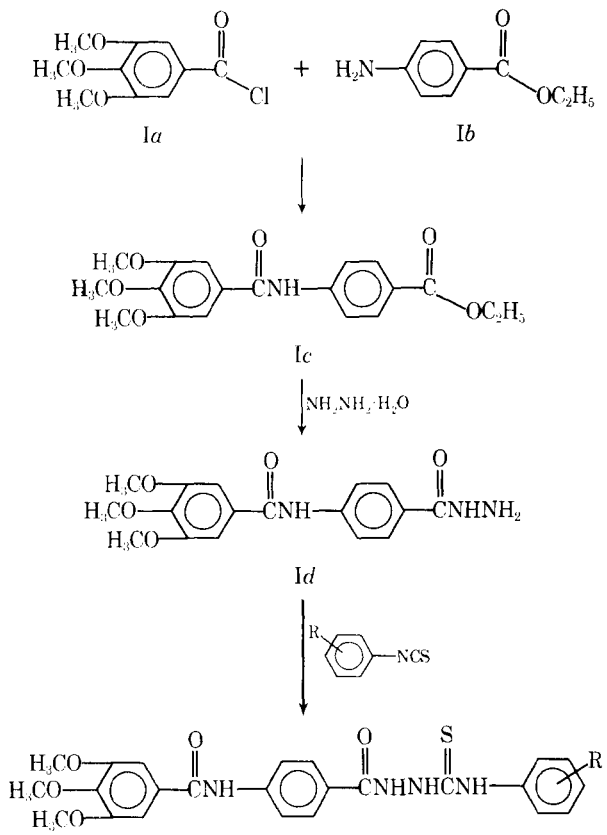

Scheme I

Analyses for carbon, hydrogen, and nitrogen were performed; melting points were taken in open capillary tubes and are corrected. IR spectra were taken[1] in mineral oil mulls in the range of 1000 to 4000 cm^{-1}. The NMR spectra were obtained[2] using dimethyl sulfoxide-d_6 as solvent and tetramethylsilane as a reference.

Ethyl 4-(3,4,5-Trimethoxybenzamido)benzoate (*Ic*)—A solution of Ia (0.2 mole) in dry tetrahydrofuran was added slowly, with stirring, to a cooled (below 10°) solution of Ib (0.4 mole) in the same solvent. The mixture was stirred for 1 hr and allowed to stand overnight in a refrigerator. The solvent was removed by distillation under reduced pressure. The solid residue was collected by filtration and washed first with 5% HCl, then with 5% sodium carbonate, and then with water repeatedly.

The compound was recrystallized from ethanol, mp 120° [lit. (14) mp 117°]. The IR spectrum showed peaks at 1690 ($COOC_2H_5$), 1675 (CONH), and 3350 (CO*NH*) cm^{-1}. The NMR spectrum gave signals at δ 1.27 (t, 3H, $COOCH_2CH_3$, J = 7 Hz), 3.75 (s, 3H, 4-OCH_3), 3.87 (s, 6H, 3- and 5-OCH_3), 4.33 (q, 2H, $COOCH_2CH_3$), 7.33 (s, 2H, C_6H_2), 8.00 (s, 4H, C_6H_4), and 10.35 (b, 1H, CONH) ppm.

4-(3,4,5-Trimethoxybenzamido)benzohydrazide (*Id*)—A mixture of

[1] Beckman IR-12 spectrophotometer.
[2] Varian Associates model A-60.

0022-3549/78/1200-1682$01.00/0
© 1978, American Pharmaceutical Association

Table I—Physical Constants and Anticonvulsant Activity of *N*-[4-[4-(Arylthiosemicarbazido)carbonyl]phenyl]-3,4,5-trimethoxybenzamides

Compound	R	Melting Point	Yield, %	Molecular Formula		Analysis, % Calc.	Analysis, % Found	Anticonvulsant Activity, % Protection[a]	Anticonvulsant Activity, % Mortality[b]
II	H	144°	70	$C_{24}H_{24}N_4O_5S$	C	60.00	60.32	20	80
					H	5.00	4.81		
					N	11.66	11.42		
III	2-CH_3	128°	75	$C_{25}H_{26}N_4O_5S$	C	61.13	60.84	60	40
					H	5.26	5.38		
					N	11.33	11.67		
IV	3-CH_3	172°	80	$C_{25}H_{26}N_4O_5S$	C	61.13	61.44	10	90
					H	5.26	5.34		
					N	11.33	11.12		
V	4-CH_3	121°	72	$C_{25}H_{26}N_4O_5S$	C	61.13	61.43	80	20
					H	5.26	5.32		
					N	11.33	11.61		
VI	2-OCH_3	214°	78	$C_{25}H_{26}N_4O_6S$	C	58.82	58.64	10	90
					H	5.09	5.00		
					N	10.90	11.15		
VII	4-OCH_3	113°	70	$C_{25}H_{26}N_4O_6S$	C	58.82	59.11	20	60
					H	5.09	5.27		
					N	10.90	10.65		
VIII	2-OC_2H_5	168°	68	$C_{26}H_{28}N_4O_6S$	C	59.54	59.76	40	60
					H	5.34	5.41		
					N	10.68	10.47		
IX	4-OC_2H_5	128°	65	$C_{26}H_{28}N_4O_6S$	C	59.54	59.29	50	40
					H	5.34	5.23		
					N	10.68	10.48		
X	4-Cl	116°	80	$C_{24}H_{23}ClN_4O_5S$	C	55.97	56.18	10	80
					H	4.47	4.53		
					N	10.88	10.59		
XI	4-Br	125°	82	$C_{24}H_{23}BrN_4O_5S$	C	51.52	51.79	20	40
					H	4.11	4.37		
					N	10.01	10.25		

[a] Anticonvulsant activity is represented as percent protection against pentylenetetrazol-induced seizures. [b] Toxicity is represented as percent deaths of animals treated with pentylenetetrazol during 24 hr.

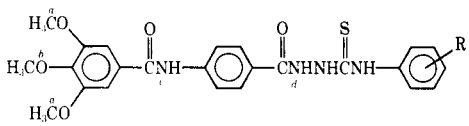

Table II—Chemical Shifts of Some Protons of *N*-[4-[4-(Arylthiosemicarbazido)carbonyl]phenyl]-3,4,5-trimethoxybenzamides

Compound	Chemical Shift[a] OCH_3 (*a*)	OCH_3 (*b*)	CONH (*c*)	CONH (*d*)	R
II	3.90 (s, 6H)	3.78 (s, 3H)	10.50 (b, 1H)	9.80 (b, 1H)	—
III	3.90 (s, 6H)	3.77 (s, 3H)	10.43 (b, 1H)	9.50 (b, 1H)	2.23 (s, 3H)
IV	3.91 (s, 6H)	3.76 (s, 3H)	10.37 (b, 1H)	9.50 (b, 1H)	2.25 (s, 3H)
V	3.88 (s, 6H)	3.77 (s, 3H)	10.28 (b, 1H)	9.60 (b, 1H)	2.28 (s, 3H)
VI	3.90 (s, 6H)	3.78 (s, 3H)	10.38 (b, 1H)	9.30 (b, 1H)	3.78 (s, 3H)
VII	3.88 (s, 6H)	3.75 (s, 3H)	10.30 (b, 1H)	9.60 (b, 1H)	3.75 (s, 3H)
VIII	3.88 (s, 6H)	3.75 (s, 3H)	10.40 (b, 1H)	9.13 (b, 1H)	1.10 (t, 3H, J = 7 Hz) and 4.00 (q, 2H)
IX	3.90 (s, 6H)	3.78 (s, 3H)	10.36 (b, 1H)	9.75 (b, 1H)	1.3 (t, 3H, J = 7 Hz) and 4.03 (q, 2H)
X	3.91 (s, 6H)	3.80 (s, 3H)	10.23 (b, 1H)	9.76 (b, 1H)	—
XI	3.90 (s, 6H)	3.75 (s, 3H)	10.35 (b, 1H)	9.93 (b, 1H)	—

[a] Chemical shifts are expressed in parts per million downfield relative to tetramethylsilane as the internal standard. All spectra were taken in dimethyl sulfoxide-d_6. Multiplicities of the peaks are expressed as singlet (s), triplet (t), and quartet (q). All amidic protons were exchangeable with deuterium oxide.

Ic (0.01 mole) and hydrazine hydrate (0.02 mole, 99–100%) was refluxed on a steam bath in absolute ethanol (200 ml) for 8–10 hr. Excess solvent was distilled under reduced pressure, and the hydrazide that separated out was collected by filtration and recrystallized from ethanol in a 70% yield, mp 202°.

The IR spectrum showed peaks at 1670 (CONH) and 3370 (CONHNH_2) cm^{-1}. The NMR spectrum gave the signals at δ 3.75 (s, 3H, 4-OCH_3), 3.88 (s, 6H, 3- and 5-OCH_3), 4.45 (b, 2H, CONHNH_2), 7.33 (s, 2H, C_6H_2), 7.90 (s, 4H, C_6H_4), 9.91 (b, 1H, CON*H*NH_2), and 10.53 (b, 1H, CON*H*) ppm.

Anal.—Calc. for $C_{17}H_{19}N_3O_5$: C, 59.13; H, 5.50; N, 12.17. Found: C, 59.38; H, 5.41; N, 11.86.

N-[4-[4-(*Arylthiosemicarbazido)carbonyl*]*phenyl*] *-3,4,5- trimethoxybenzamides (II–XI)*—Suitable aryl isothiocyanates (0.01 mole) were added to Id (0.01 mole) in 25 ml of absolute ethanol, and the mixture was refluxed on a steam bath for 6 hr. Then the reaction mixture was concentrated under reduced pressure. On cooling, the solid mass that separated out was filtered and washed with ether. The product thus obtained was dried and recrystallized from ethanol.

The various substituted trimethoxybenzamides (Table I) were characterized by their sharp melting points, elemental analyses, and IR and NMR spectra. The IR spectra showed peaks between 1660 and 1675 cm^{-1} and 3320 and 3360 cm^{-1}, characteristic of *CO*NH and CO*NH* groups, respectively. The chemical shifts in NMR spectra of these compounds are recorded in Table II.

Determination of Anticonvulsant Activity—Anticonvulsant activity against pentylenetetrazol-induced seizures was determined in albino mice of either sex weighing 25–30 g. The mice were divided into groups of 10, and the group weights were kept as near the same as possible. Each test compound was suspended in a 5% aqueous suspension of gum acacia to give a concentration of 1% (w/v). The test compounds (100 mg/kg) were injected intraperitoneally in a group of 10 animals. Pentylenetetrazol (90 mg/kg) was injected subcutaneously 4 hr after drug administration.

This dose of pentylenetetrazol produces not only convulsions in almost all untreated mice but also exhibits 100% mortality over 24 hr. No mortality was observed over 24 hr in animals pretreated with 100-mg/kg doses of test compound. The mice were then observed for seizures for 60 min.

Table III—Effect of *N*-[4-[4-(Arylthiosemicarbazido)carbonyl]phenyl]-3,4,5-trimethoxybenzamides on Rat Brain Respiratory Activity

Compound	Inhibition[a], %					
	Pyruvate			α-Ketoglutarate,	NADH,	Succinate,
	1.0×10^{-3} M[b]	5.0×10^{-4} M[b]	1.0×10^{-4} M[b]	1.0×10^{-3} M[b]	1.0×10^{-3} M[b]	1.0×10^{-3} M[b]
II	65.40 ± 0.52	24.88 ± 0.37	Nil	93.72 ± 0.82	18.92 ± 0.71	Nil
III	95.21 ± 0.81	60.38 ± 0.58	19.74 ± 0.55	38.31 ± 0.50	23.15 ± 0.42	31.78 ± 0.51
IV	88.49 ± 0.77	51.77 ± 0.61	19.30 ± 0.63	98.12 ± 0.78	26.18 ± 0.56	Nil
V	70.38 ± 0.54	52.85 ± 0.91	11.36 ± 0.85	98.41 ± 0.61	Nil	Nil
VI	38.01 ± 0.32	31.08 ± 0.79	Nil	64.01 ± 0.53	Nil	7.35 ± 0.82
VII	36.24 ± 0.79	20.44 ± 0.54	14.39 ± 0.61	60.38 ± 0.49	11.01 ± 0.82	Nil
VIII	54.03 ± 0.82	46.48 ± 0.39	30.26 ± 0.73	46.43 ± 0.37	5.87 ± 0.94	33.17 ± 0.69
IX	66.82 ± 0.92	56.84 ± 0.65	48.89 ± 0.65	88.24 ± 0.12	25.17 ± 0.66	Nil
X	42.86 ± 0.79	27.43 ± 0.87	5.89 ± 0.97	88.81 ± 0.75	53.89 ± 0.71	16.86 ± 0.59
XI	39.02 ± 0.59	15.04 ± 0.73	Nil	56.28 ± 0.34	37.61 ± 0.67	Nil

[a] Each experiment was done in duplicate. All values represent mean values of percent inhibition with the standard error calculated from three separate experiments. Inhibition was determined by the decrease in oxygen uptake per 100 mg wet weight of tissue per hour. [b] Molar concentrations given are the final concentrations of II–XI in the assay system. Assay conditions are as indicated in the text.

An episode of clonic spasm that persisted for a minimum of 5 sec was considered a threshold convulsion. Transient intermittent jerks and tremulousness were not counted.

Animals devoid of threshold convulsions during 60 min were considered protected. The number of animals protected in each group was recorded, and the anticonvulsant activity of these substituted trimethoxybenzamides was represented as percent protection. The mortality was recorded after 24 hr to obtain an idea of the toxicity of these compounds in pentylenetetrazol-treated experimental animals.

Determination of Respiratory Activity of Rat Brain Homogenate[3]—Male albino rats were kept on an *ad libitum* diet. Rat brains, isolated from decapitated animals, were immediately homogenized in ice-cold 0.25 *M* sucrose in a homogenizer[4] in a ratio of 1:9 (w/v). All incubations were carried out at 37°, and the oxygen uptake was measured using air as the gas phase (13). Fresh rat brain homogenate (1 ml), equivalent to 100 mg wet weight, was added to chilled Warburg vessels containing 6.7 m*M* magnesium sulfate, 20 m*M* sodium hydrogen phosphate buffer solution (pH 7.4), 1 m*M* adenosine monophosphate (sodium salt), 33 m*M* potassium chloride, and 500 μg of cytochrome c in a final volume of 3 ml, unless otherwise stated. The central well contained 0.2 ml of 20% KOH.

The final concentration of pyruvate, α-ketoglutarate, and succinate was 1 m*M* while that of NADH was 0.5 m*M*. It was presumed that endogenous NAD, present in rat brain homogenates, was sufficient for these oxidative processes. All substituted trimethoxybenzamides were dissolved in propylene glycol and were used at final concentrations of 1 m*M* during oxidation of α-ketoglutarate, NADH, and succinate and of 0.1, 0.5, and 1 m*M* during oxidation of pyruvate by rat brain homogenates. An equal volume of propylene glycol was added to the control vessels.

RESULTS AND DISCUSSION

The anticonvulsant activity of II–XI is recorded in Table I. All compounds provided protection against pentylenetetrazol-induced seizures at a dose of 100 mg/kg. The degree of protection ranged from 10 to 80%. Most compounds exhibited significantly low anticonvulsant activity. The maximum degree of protection was observed with the compound having a methyl group at position 4 of the phenyl nucleus (V), and minimum protection was observed with IV, VI, and X.

The replacement of the methyl group by a methoxy, ethoxy, or halogen group caused a marked decrease in the anticonvulsant activity. Compounds possessing an ethoxy group on the phenyl moiety possessed higher anticonvulsant activity as compared to compounds having a methoxy group. As is evident from Table I, compounds having low anticonvulsant activity produced less protection against 24-hr mortality in pentylenetetrazol-treated animals. These results failed to provide evidence for any definite structural requirements in the molecular makeup of these substituted trimethoxybenzamides that could be responsible for their anticonvulsant activity.

The inhibition of cellular respiratory activity of rat brain homogenates by II–XI is recorded in Table III. Almost all compounds inhibited oxidation of pyruvate, α-ketoglutarate, NADH, and succinate. The inhibition of pyruvate oxidation was concentration dependent; an increase in the concentration of test compound increased the inhibition of pyruvic acid oxidation by rat brain homogenates. The degree of inhibition by substituted trimethoxybenzamides was of low order during oxidation of NADH and succinate while maximum inhibition by most compounds was observed during oxidation of α-ketoglutarate by rat brain homogenates. However, it can be assumed that the use of higher concentrations of compounds devoid of the inhibitory property could possibly inhibit the respiratory activity of rat brain homogenates.

These results indicated the unspecific inhibition of both the NAD-dependent oxidation of pyruvate and α-ketoglutarate and the NAD-independent oxidation of succinate by rat brain homogenates. The *in vitro* inhibition of the oxidation of NADH was observed, as reported earlier for nitrobenzamides (XII). In general, the nature of different substituents on the phenyl moiety of these compounds did not contribute significantly in their ability to inhibit respiratory activity of rat brain homogenates. These results provided evidence regarding the possible sensitivity of substituted trimethoxybenzamides toward both NADH-COQ (oxido) reductase (Complex I) and succinate-COQ (oxido) reductase (Complex II) of the electron transport chain. Hydro COQ-cytochrome c (oxido) reductase (Complex III) and/or cytochrome c-O_2 (oxido) reductase (Complex IV) also may be susceptible to these substituted trimethoxybenzamides, which might account for their ability to inhibit flavine adenine dinucleotide-dependent oxidation of succinate (NAD-independent) and NAD-dependent oxidation of pyruvate and α-ketoglutarate.

These results did not provide a correlation between the anticonvulsant activity of substituted trimethoxybenzamides and their ability to inhibit the respiratory activity of rat brain homogenates as a biochemical basis of their anticonvulsant activity. Further studies dealing with the synthesis of related structures carrying different substituents on the phenyl moiety and the determination of effectiveness to inhibit purified enzyme preparation may possibly reflect the biochemical basis for the anticonvulsant activity of these compounds.

[3] Sodium pyruvate, sodium α-ketoglutarate, NADH, sodium succinate, adenosine monophosphate (AMP), and cytochrome c were obtained from Sigma Chemical Co., St. Louis, Mo.

[4] Potter-Elvehjem homogenizer.

REFERENCES

(1) H. J. Bein, *Pharmacol. Rev.*, **8**, 435 (1956).

(2) H. J. Bein, *Experientia*, **9**, 107 (1953).

(3) J. Tripod, H. J. Bein, and R. Meier, *Arch. Int. Pharmacodyn. Ther.*, **36**, 406 (1954).

(4) H. J. Bein, F. Gross, J. Tripod, and R. Meier, *Schweiz. Med. Wochenschr.*, **83**, 1007 (1953).

(5) J. C. Gupta, B. S. Kahali, and A. Dutta, *Indian J. Med. Res.*, **32**, 183 (1944).

(6) A. J. Plummer, W. E. Barrett, G. Wagle, and F. F. Yonkman, *Fed. Proc.*, **12**, 357 (1953).

(7) A. Burger, "Medicinal Chemistry," 2nd ed., Interscience, New York, N.Y. 1960.

(8) C. O. Wilson, O. Gisvold, and R. F. Doerge, "Textbook of Organic Medicinal and Pharmaceutical Chemistry," 5th ed., Lippincott, Philadelphia, Pa., 1966.

(9) K. Brosy, B. Dumbovich, L. Vargha, and L. Farkas, Hungarian pat. 147, 687 (1960).

(10) P. C. Dandiya, P. K. Sharma, and M. K. Menon, *Indian J. Med. Res.*, **50**, 750 (1962).

(11) R. B. Moffett, *J. Med. Chem.*, **7**, 319 (1964).

(12) S. S. Parmar, C. Dwivedi, B. Ali, and R. S. Misra, *ibid.*, **15**, 846

(1972).
(13) S. P. Singh, A. Chaudhari, S. S. Parmar, and W. E. Cornatzer, *Can. J. Pharm. Sci.*, **9**, 110 (1974).
(14) S. K. Sogani and P. C. Dandiya, *J. Med. Chem.*, **8**, 139 (1965).

ACKNOWLEDGMENTS

Supported in part by U.S. Public Health Service NIDA Grant 7-R01-DA01893-01, National Institutes of Health Grant 5-T01-HL05939-03, and the National Science Foundation Institutional Grant for Science Program administered through the University of North Dakota (Faculty Research Grant), Grand Forks.

The authors thank Professor S. J. Brumleve and Professor K. P. Bhargava for their advice and encouragment. Grateful acknowledgment is made to the State Council of Scientific and Industrial Research of Uttar Pradesh, Lucknow, India, for providing a Research Fellowship to S. Kumar and to the Northwest Area Foundation, St. Paul, Minn., for providing a Hill Professorship to S. S. Parmar.

Effect of Repeated Skin Application on Percutaneous Absorption of Salicylic Acid

M. S. ROBERTS *x and ELIZABETH HORLOCK ‡

Received October 11, 1977, from the *Department of Pharmacy, Tasmanian College of Advanced Education, Hobart, Tasmania, Australia 7001.* Accepted for publication April 27, 1978. *Present address: School of Pharmacy, University of Tasmania, Hobart, Tasmania, Australia 7001. ‡Present address: Department of Pharmacy, Queen Victoria Medical Centre, Melbourne, Australia 3000.

Abstract □ Various concentrations of salicylic acid in hydrophilic ointment were applied repeatedly at daily or weekly intervals to rats *in vivo*. Salicylic acid absorption through treated skin was monitored by determining the penetration fluxes of salicylic acid through skin excised at various times. A gradual decrease in the salicylic acid penetration flux was observed following weekly applications of either 5 or 10% salicylic acid in hydrophilic ointment. The penetration flux of 1% salicylic acid remained constant. In the daily applications of 5 and 10% salicylic acid, the penetration flux increased after approximately 2 days of treatment and declined thereafter. The penetration flux of salicylic acid from the 1% salicylic acid increased slightly after 3–4 days of treatment.

Keyphrases □ Salicylic acid—percutaneous absorption, effect of repeated application, rats □ Absorption, percutaneous—salicylic acid, effect of repeated application, rats □ Keratolytic agents—salicylic acid, percutaneous absorption, effect of repeated application, rats

The percutaneous absorption of salicylates has been reported extensively (1–5). Barry *et al.* (6) examined blood salicylate levels in rabbits treated with 10% salicylic acid in hydrophilic ointment at weekly intervals. They reported that a progressive and statistically significant decrease in percutaneous absorption of salicylic acid occurred over the treatment period. Skin dehydration and decreased emotional arousal of the animals were suggested as possible explanations for this result.

BACKGROUND

Since salicylic acid is usually applied to the skin in topical therapy with repeated applications, it was decided to evaluate the effect of repeated applications of salicylic acid on its percutaneous absorption. Blood salicylate levels resulting from salicylic acid absorption following repeated topical applications (6) may reflect not only changes in absorption rates due to the dermatological effects of salicylic acid but also other pharmacokinetic alterations in metabolism and excretion due to the prolonged therapy.

Müller *et al.* (7) reported decreased steady-state plasma salicylic acid levels associated with chronic aspirin ingestion. Percutaneous absorption of substances was examined using excised skin (8, 9). Excised skin allows intracutaneous penetration to be measured simply, directly, reproducibly, and precisely, the fundamental assumption being that the stratum corneum is a dead tissue whose impermeability is unaffected by excision. The use of skin excised following repeated applications of salicylic acid to the skin *in vivo* was employed in the present study to examine directly the consequences of the dermatological effects of salicylic acid on its absorption.

The wide range of dermatotherapeutic effects of salicylic acid is also concentration dependent (10). In concentrations of 5% or more, salicylic acid exerts a keratolytic effect on the skin; in concentrations of less than 5%, a keratoplastic effect is apparent (10). Consequently, the objective of this study was to assess: (*a*) the effect of daily or weekly repeated topical applications of salicylic acid on its absorption, and (*b*) the effect of the concentration of salicylic acid in the hydrophilic ointment on its absorption.

EXPERIMENTAL

Animals—Female Wistar rats[1], 250–300 g, were housed in a constant-temperature room and given food[2] and water *ad libitum*.

Ointment Base—Salicylic acid BP was passed through an 80-mesh sieve, and appropriate amounts were incorporated into hydrophilic ointment USP. Accordingly, hydrophilic ointments containing 10, 5, and 1% salicylic acid were prepared.

Test Procedures—Under light ether anesthesia (anesthetic ether BP), the rats were weighed and hair was removed from the flanks with an animal clipper[3]. A sample of ointment was rubbed into the area of shaved skin; this area (3 cm^2) was approximately twice the cross-sectional area for diffusion in the diffusion cells. Additional ointment (total ~2 g) was spread uniformly over the area on the dull side of a sheet of aluminum foil. The foil was held in place by adhesive tape and an elastic bandage.

The animals were kept in restraining cages for the duration of the treatment. After the 7.5-hr test period, the bandages were removed from the animals and the animals were returned to the animal house. Repeated treatments at daily or weekly intervals were then employed. At various stages during the treatment, the animals were asphyxiated by an overdose of ether, the skin immediately was excised, and the appropriate ointment was applied to the epidermis. The treated excised skin was placed in a diffusion cell (9); the receptor compartment contained 0.1% chlorhexidine solution to prevent microbial growth at 37°.

To measure the amount of salicylic acid penetrating the skin, 3-ml aliquots of receptor solution were removed and treated with 1 ml of 13.2% ferric chloride in 0.4 *N* HCl. The resultant color was measured[4] at 540 nm, and the salicylate concentration was computed from a Beer's law plot. The 3-ml aliquot of solution removed from the diffusion cell was replaced with 3 ml of the chlorhexidine solution. A minimum of three animals was used in the estimation of each reported penetration flux. The possible interaction between salicylic acid and the skin on the initial application was examined by comparing the fluxes of various concentrations of salicylic acid in hydrophilic ointment to its flux across an inert membrane

[1] Southern Biological Services, Parkdale, Victoria.
[2] M & V Mouse Cubes, W. M. Charlick, Adelaide, South Australia.
[3] Breville model 900.
[4] Beckman spectrophotometer.

0022-3549/78/1200-1685$01.00/0
© 1978, American Pharmaceutical Association

(1972).
(13) S. P. Singh, A. Chaudhari, S. S. Parmar, and W. E. Cornatzer, *Can. J. Pharm. Sci.*, **9**, 110 (1974).
(14) S. K. Sogani and P. C. Dandiya, *J. Med. Chem.*, **8**, 139 (1965).

ACKNOWLEDGMENTS

Supported in part by U.S. Public Health Service NIDA Grant 7-R01-DA01893-01, National Institutes of Health Grant 5-T01-HL05939-03, and the National Science Foundation Institutional Grant for Science Program administered through the University of North Dakota (Faculty Research Grant), Grand Forks.

The authors thank Professor S. J. Brumleve and Professor K. P. Bhargava for their advice and encouragment. Grateful acknowledgment is made to the State Council of Scientific and Industrial Research of Uttar Pradesh, Lucknow, India, for providing a Research Fellowship to S. Kumar and to the Northwest Area Foundation, St. Paul, Minn., for providing a Hill Professorship to S. S. Parmar.

Effect of Repeated Skin Application on Percutaneous Absorption of Salicylic Acid

M. S. ROBERTS *x and ELIZABETH HORLOCK ‡

Received October 11, 1977, from the *Department of Pharmacy, Tasmanian College of Advanced Education, Hobart, Tasmania, Australia 7001.* Accepted for publication April 27, 1978. *Present address: School of Pharmacy, University of Tasmania, Hobart, Tasmania, Australia 7001. ‡Present address: Department of Pharmacy, Queen Victoria Medical Centre, Melbourne, Australia 3000.

Abstract □ Various concentrations of salicylic acid in hydrophilic ointment were applied repeatedly at daily or weekly intervals to rats *in vivo*. Salicylic acid absorption through treated skin was monitored by determining the penetration fluxes of salicylic acid through skin excised at various times. A gradual decrease in the salicylic acid penetration flux was observed following weekly applications of either 5 or 10% salicylic acid in hydrophilic ointment. The penetration flux of 1% salicylic acid remained constant. In the daily applications of 5 and 10% salicylic acid, the penetration flux increased after approximately 2 days of treatment and declined thereafter. The penetration flux of salicylic acid from the 1% salicylic acid increased slightly after 3–4 days of treatment.

Keyphrases □ Salicylic acid—percutaneous absorption, effect of repeated application, rats □ Absorption, percutaneous—salicylic acid, effect of repeated application, rats □ Keratolytic agents—salicylic acid, percutaneous absorption, effect of repeated application, rats

The percutaneous absorption of salicylates has been reported extensively (1–5). Barry *et al.* (6) examined blood salicylate levels in rabbits treated with 10% salicylic acid in hydrophilic ointment at weekly intervals. They reported that a progressive and statistically significant decrease in percutaneous absorption of salicylic acid occurred over the treatment period. Skin dehydration and decreased emotional arousal of the animals were suggested as possible explanations for this result.

BACKGROUND

Since salicylic acid is usually applied to the skin in topical therapy with repeated applications, it was decided to evaluate the effect of repeated applications of salicylic acid on its percutaneous absorption. Blood salicylate levels resulting from salicylic acid absorption following repeated topical applications (6) may reflect not only changes in absorption rates due to the dermatological effects of salicylic acid but also other pharmacokinetic alterations in metabolism and excretion due to the prolonged therapy.

Müller *et al.* (7) reported decreased steady-state plasma salicylic acid levels associated with chronic aspirin ingestion. Percutaneous absorption of substances was examined using excised skin (8, 9). Excised skin allows intracutaneous penetration to be measured simply, directly, reproducibly, and precisely, the fundamental assumption being that the stratum corneum is a dead tissue whose impermeability is unaffected by excision. The use of skin excised following repeated applications of salicylic acid to the skin *in vivo* was employed in the present study to examine directly the consequences of the dermatological effects of salicylic acid on its absorption.

The wide range of dermatotherapeutic effects of salicylic acid is also concentration dependent (10). In concentrations of 5% or more, salicylic acid exerts a keratolytic effect on the skin; in concentrations of less than 5%, a keratoplastic effect is apparent (10). Consequently, the objective of this study was to assess: (*a*) the effect of daily or weekly repeated topical applications of salicylic acid on its absorption, and (*b*) the effect of the concentration of salicylic acid in the hydrophilic ointment on its absorption.

EXPERIMENTAL

Animals—Female Wistar rats[1], 250–300 g, were housed in a constant-temperature room and given food[2] and water *ad libitum*.

Ointment Base—Salicylic acid BP was passed through an 80-mesh sieve, and appropriate amounts were incorporated into hydrophilic ointment USP. Accordingly, hydrophilic ointments containing 10, 5, and 1% salicylic acid were prepared.

Test Procedures—Under light ether anesthesia (anesthetic ether BP), the rats were weighed and hair was removed from the flanks with an animal clipper[3]. A sample of ointment was rubbed into the area of shaved skin; this area (3 cm^2) was approximately twice the cross-sectional area for diffusion in the diffusion cells. Additional ointment (total ~2 g) was spread uniformly over the area on the dull side of a sheet of aluminum foil. The foil was held in place by adhesive tape and an elastic bandage.

The animals were kept in restraining cages for the duration of the treatment. After the 7.5-hr test period, the bandages were removed from the animals and the animals were returned to the animal house. Repeated treatments at daily or weekly intervals were then employed. At various stages during the treatment, the animals were asphyxiated by an overdose of ether, the skin immediately was excised, and the appropriate ointment was applied to the epidermis. The treated excised skin was placed in a diffusion cell (9); the receptor compartment contained 0.1% chlorhexidine solution to prevent microbial growth at 37°.

To measure the amount of salicylic acid penetrating the skin, 3-ml aliquots of receptor solution were removed and treated with 1 ml of 13.2% ferric chloride in 0.4 *N* HCl. The resultant color was measured[4] at 540 nm, and the salicylate concentration was computed from a Beer's law plot. The 3-ml aliquot of solution removed from the diffusion cell was replaced with 3 ml of the chlorhexidine solution. A minimum of three animals was used in the estimation of each reported penetration flux. The possible interaction between salicylic acid and the skin on the initial application was examined by comparing the fluxes of various concentrations of salicylic acid in hydrophilic ointment to its flux across an inert membrane

[1] Southern Biological Services, Parkdale, Victoria.
[2] M & V Mouse Cubes, W. M. Charlick, Adelaide, South Australia.
[3] Breville model 900.
[4] Beckman spectrophotometer.

0022-3549/78/1200-1685$01.00/0
© 1978, American Pharmaceutical Association

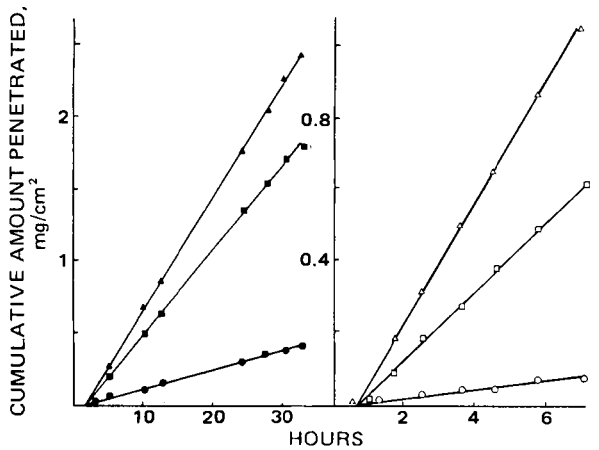

Figure 1—*Typical plots of cumulative amount of salicylic acid penetrating through excised rat skin (left) and dimethyl polysiloxane membranes (right) with time. Key: ●○, 1% salicylic acid in hydrophilic ointment; ■□, 5% salicylic acid in hydrophilic ointment; and ▲△, 10% salicylic acid in hydrophilic ointment.*

(dimethyl polysiloxane[5]) according to the method of Roberts and Anderson (9).

Thick sections for light microscopic observations were prepared by the method of Roberts *et al.* (8), except that Spurs resin[6] was used as the embedding medium.

RESULTS AND DISCUSSION

The relation between the cumulative amount of salicylic acid penetrating through single samples of excised skin and dimethyl polysiloxane with time following a single application is shown in Fig. 1. Similar plots were observed for repeated applications. After a lag time, the plot of the cumulative amount of solute penetrating against time was linear, the slope of this line being the steady-state penetration flux.

Table I shows the mean penetration fluxes observed through dimethyl polysiloxane and excised skin with the ratio of the fluxes. The ratio of fluxes decreased with increasing concentrations of salicylic acid. This result may be ascribed to the suspended salicylic acid particles reducing the occlusive properties of the hydrophilic ointment or to a dehydrating effect of the salicylic acid. However, Loveday (2) showed that the rate of penetration of salicylic acid from aqueous solutions (pH 2.2) through excised pig skin was directly proportional to the concentration of salicylic acid used. The decreased ratio suggests that a single application of salicylic acid does not damage the skin significantly. Marked increases in the ratio of fluxes (skin to inert membrane) were observed when high damaging concentrations of phenol were applied to the skin (8, 9).

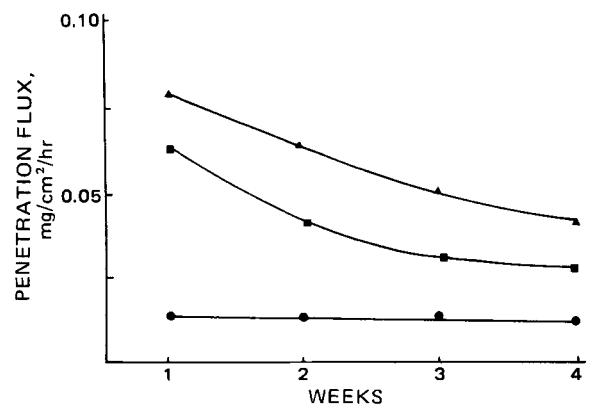

Figure 2—*Mean penetration fluxes of salicylic acid through excised rat skin following weekly treatments with salicylic acid* in vivo. *Key: ●, 1% salicylic acid in hydrophilic ointment; ■, 5% salicylic acid in hydrophilic ointment; and ▲, 10% salicylic acid in hydrophilic ointment.*

[5] Dow Corning Silastic sheeting 501-1.
[6] Ladd Chemicals, New York, N.Y.

Table I—Mean Penetration Fluxes (±*SE*) of Salicylic Acid in Hydrophilic Ointment Base through Dimethyl Polysiloxane Membranes and Excised Rat Skin following a Single Treatment

Salicylic Acid Concentration (w/w)	Penetration Flux of Salicylic Acid (± *SE*), mg/cm²/hr		Ratio of Fluxes: Skin–Dimethyl Polysiloxane
	Excised Skin	Dimethyl Polysiloxane	
1	0.014 ± 0.002	0.016 ± 0.001	0.88
5	0.061 ± 0.003	0.099 ± 0.001	0.62
10	0.078 ± 0.003	0.159 ± 0.001	0.49

The mean penetration fluxes of salicylic acid through rat skin following repeated weekly applications of 5 and 10% salicylic acid in hydrophilic ointment over 4 weeks of treatment are shown in Fig. 2. An analysis of variance of the penetration fluxes observed for each week of treatment revealed a significant difference between the treatments with both the 5% ($F = 58.6, df = 3/12, p < 0.001$) and 10% ($F = 9.97, df = 3/12, p < 0.01$) concentrations. The decline in fluxes paralleled the reduction in blood levels observed when rabbits were treated with 10% salicylic acid in hydrophilic ointment at weekly intervals (6). These results suggest that the reduction in fluxes or blood levels may be attributed directly to the local effects of the salicylic acid. The treatment with 1% salicylic acid in hydrophilic ointment did not alter the salicylic acid penetration flux. The relative changes in fluxes produced by the 5 and 10% salicylic acid ointments were similar.

Figure 3 shows the mean penetration fluxes of salicylic acid following repeated daily applications. An analysis of variance of the penetration fluxes observed for each day of treatment revealed a statistically significant difference between the treatments of all concentrations (1%, $F = 8.87, df = 4/10, p < 0.01$; 5%, $F = 20.2, df = 4/10, p < 0.001$; and 10%, $F = 4.14, df = 4/10, p < 0.05$).

For the higher concentrations of salicylic acid, an increase in penetration flux was observed after 2 days. Following further treatment, this flux gradually decreased. The increase in flux was quite substantial and supports reports that treatment of the skin with salicylic acid may facilitate the absorption of other medicaments (10). Daily treatment with 1% salicylic acid in hydrophilic ointment also increased flux, but this flux was not readily apparent before 3–4 days.

The histological changes resulting from the topical application of ointments containing salicylic acid were reported previously (11, 12). The histological changes to the rat skin following treatment with salicylic acid preparations in this study were consistent with the observations of Strakosch (11), who observed that the keratolytic changes began after 2–3 days of treatment with 5 or 10% salicylic acid in an oxycholesterol–petrolatum base and after 7 days of treatment with 1% salicylic acid in this base.

The initial increases in the penetration flux observed for daily treatment with 1, 5, and 10% salicylic acid in hydrophilic ointment (Fig. 3) corresponded to the histological observations of swelling and exfoliation. The times for keratolysis implicit from the penetration fluxes and his-

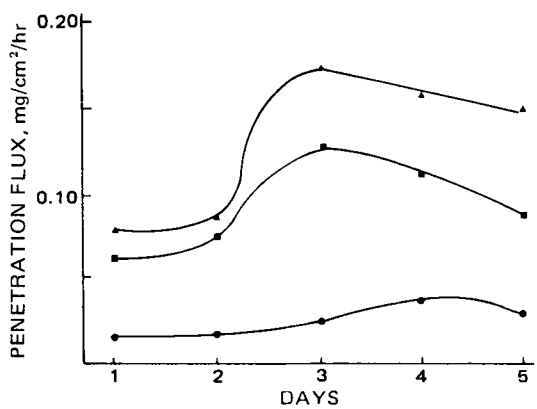

Figure 3—*Mean penetration fluxes of salicylic acid through excised rat skin following daily treatments with salicylic acid* in vivo. *Key: ●, 1% salicylic acid in hydrophilic ointment; ■, 5% salicylic acid in hydrophilic ointment; and ▲, 10% salicylic acid in hydrophilic ointment.*

tological changes in this study were shorter than those reported by Strakosch (11). These differences may be ascribed to the use of rat rather than human skin or different base formulations. Strakosch also found that the onset of keratolysis was markedly dependent on the base used, the onset being two to three times more rapid for salicylic acid in the oxycholesterol–petrolatum base than in the petrolatum base. Since higher blood salicylic acid levels were observed from the topical application of salicylic acid in a hydrophilic ointment base compared to a petrolatum base (1), keratolysis apparently depends on the absorption rate of the salicylic acid from the particular formulation.

Following the initial keratolytic process in which morphological changes were observed in the stratum spinosum, stratum granulosum, and stratum corneum, further repeated applications of salicylic acid gave rise to the formation of a broad stratum corneum. The process by which this broad stratum corneum formed was not clearly evident but may have resulted from diminished fluxes after prolonged daily (Fig. 3) or weekly (Fig. 2) treatments.

Since the salicylic acid being applied still exerts its surface keratolytic effect, reduced absorption *in vivo* may be due not only to the thicker horny layer but also to the process of desquamation. The results of this study, using an *in vitro* diffusion apparatus, suggest that the thicker horny layer does offer greater resistance to the penetration of salicylic acid.

Recent work by Davies and Marks (12) did not substantiate the increased epidermopoiesis resulting from the application of salicylic acid to human skin as described by Strakosch (11). Davies and Marks did observe differences in the horny layer structure and thickness in treated and untreated samples of skin. As stated by Davies and Marks (12), it is possible that their experimental conditions were not sufficiently severe or of a sufficient duration for increased epidermopoiesis to be observed.

Although the present histological and physiochemical results are consistent with a dynamic equilibrium between keratolysis and regeneration of the epidermis, the precise cytological changes in the epidermis following salicylic acid therapy have yet to be fully documented. The changes resulting from the present experimental conditions are being examined using transmission electron microscopy.

REFERENCES

(1) M. E. Stolar, G. V. Rossi, and M. Barr, *J. Am. Pharm. Assoc., Sci. Ed.*, **49**, 144 (1960).

(2) D. E. Loveday, *J. Soc. Cosmet. Chem.*, **12**, 224 (1961).

(3) F. Gstirner and R. Elsner, *Arzneim.-Forsch.*, **14**, 281 (1964).

(4) J. N. Hlynka, A. J. Anderson, and B. E. Riedel, *Can. J. Pharm. Sci.*, **4**, 92 (1969).

(5) M. Washitake, T. Anmo, I. Tanaka, T. Arita, and M. Nakano, *J. Pharm. Sci.*, **64**, 397 (1975).

(6) H. Barry, III, F. Marcus, and J. L. Colaizzi, *ibid.*, **61**, 172 (1972).

(7) F. O. Müller, H. K. L. Hundt, and A. C. deKock, *Curr. Med. Res. Opin.*, **3**, 417 (1975).

(8) M. S. Roberts, C. D. Shorey, R. Arnold, and R. A. Anderson, *Aust. J. Pharm. Sci.*, **NS3**, 81 (1974).

(9) M. S. Roberts and R. A. Anderson, *J. Pharm. Pharmacol.*, **27**, 599 (1975).

(10) E. G. Weirich, *Dermatologica*, **151**, 268 (1975).

(11) E. A. Strakosch, *Arch. Dermatol. Syphilol.*, **47**, 16 (1943).

(12) M. Davies and R. Marks, *Br. J. Dermatol.*, **95**, 187 (1976).

ACKNOWLEDGMENTS

Supported by a grant from the National Health and Medical Research Council of Australia.

The authors gratefully acknowledge the technical assistance of Mrs. L. Trout, Department of Pathology, University of Tasmania, in the preparation of thick sections of epidermis for light microscopic examination.

ESTRIP, a BASIC Computer Program for Obtaining Initial Polyexponential Parameter Estimates

R. DON BROWN ˣ and JOSEPH E. MANNO

Received January 30, 1978, from the *Department of Pharmacology and Therapeutics, Louisiana State University School of Medicine in Shreveport, Shreveport, LA 71130.* Accepted for publication April 6, 1978.

Abstract □ A new BASIC exponential stripping program, ESTRIP, allows the relatively rapid calculation of initial polyexponential parameter estimates, as does the previously published FORTRAN IV program, CSTRIP. The potential advantages of the new program are that it can be run on microcomputers and minicomputers with BASIC capability and a relatively small core and that it can be easily modified by the user.

Keyphrases □ Computer programs—ESTRIP for calculation of initial polyexponential parameter estimates □ Pharmacokinetic models—ESTRIP computer program for calculation of initial polyexponential parameter estimates □ Models, pharmacokinetic—ESTRIP computer program for calculation of initial polyexponential parameter estimates

The mathematical solutions of classical linear pharmacokinetic models are given by the sums of exponential terms. The generalized equation for these models can be written as:

$$C = \sum_{i=1}^{u} a_i e^{-b_i t} \qquad \text{(Eq. 1)}$$

where C is the concentration of drug at time t, u is the number of exponential terms, and a_i and b_i are the parameters to be determined.

Computer programs for the estimation of these polyexponential parameters (1, 2) generally require sophisticated computers utilizing BMD, BMDP, SAS, or other expensive software packages and are usually available on a time-sharing, batch-job basis. One exception is the CSTRIP program (3), which can be used to obtain preliminary polyexponential parameter estimates *via* an automated stripping (feathering, peeling-off, or back-projection) technique; this program requires the use of FORTRAN IV.

The purposes of this paper are to describe a new exponential stripping computer program[1] and to illustrate its use. The potential advantages of the new program are that

[1] A complete photocopy of the program listing will be supplied upon request. The program is also available, for a fee, on paper tape or a Scotch DC300A Data Cartridge.

0022-3549/78/1200-1687$01.00/0

© 1978, American Pharmaceutical Association

tological changes in this study were shorter than those reported by Strakosch (11). These differences may be ascribed to the use of rat rather than human skin or different base formulations. Strakosch also found that the onset of keratolysis was markedly dependent on the base used, the onset being two to three times more rapid for salicylic acid in the oxycholesterol–petrolatum base than in the petrolatum base. Since higher blood salicylic acid levels were observed from the topical application of salicylic acid in a hydrophilic ointment base compared to a petrolatum base (1), keratolysis apparently depends on the absorption rate of the salicylic acid from the particular formulation.

Following the initial keratolytic process in which morphological changes were observed in the stratum spinosum, stratum granulosum, and stratum corneum, further repeated applications of salicylic acid gave rise to the formation of a broad stratum corneum. The process by which this broad stratum corneum formed was not clearly evident but may have resulted from diminished fluxes after prolonged daily (Fig. 3) or weekly (Fig. 2) treatments.

Since the salicylic acid being applied still exerts its surface keratolytic effect, reduced absorption *in vivo* may be due not only to the thicker horny layer but also to the process of desquamation. The results of this study, using an *in vitro* diffusion apparatus, suggest that the thicker horny layer does offer greater resistance to the penetration of salicylic acid.

Recent work by Davies and Marks (12) did not substantiate the increased epidermopoiesis resulting from the application of salicylic acid to human skin as described by Strakosch (11). Davies and Marks did observe differences in the horny layer structure and thickness in treated and untreated samples of skin. As stated by Davies and Marks (12), it is possible that their experimental conditions were not sufficiently severe or of a sufficient duration for increased epidermopoiesis to be observed.

Although the present histological and physiochemical results are consistent with a dynamic equilibrium between keratolysis and regeneration of the epidermis, the precise cytological changes in the epidermis following salicylic acid therapy have yet to be fully documented. The changes resulting from the present experimental conditions are being examined using transmission electron microscopy.

REFERENCES

(1) M. E. Stolar, G. V. Rossi, and M. Barr, *J. Am. Pharm. Assoc., Sci. Ed.*, **49**, 144 (1960).

(2) D. E. Loveday, *J. Soc. Cosmet. Chem.*, **12**, 224 (1961).

(3) F. Gstirner and R. Elsner, *Arzneim.-Forsch.*, **14**, 281 (1964).

(4) J. N. Hlynka, A. J. Anderson, and B. E. Riedel, *Can. J. Pharm. Sci.*, **4**, 92 (1969).

(5) M. Washitake, T. Anmo, I. Tanaka, T. Arita, and M. Nakano, *J. Pharm. Sci.*, **64**, 397 (1975).

(6) H. Barry, III, F. Marcus, and J. L. Colaizzi, *ibid.*, **61**, 172 (1972).

(7) F. O. Müller, H. K. L. Hundt, and A. C. deKock, *Curr. Med. Res. Opin.*, **3**, 417 (1975).

(8) M. S. Roberts, C. D. Shorey, R. Arnold, and R. A. Anderson, *Aust. J. Pharm. Sci.*, **NS3**, 81 (1974).

(9) M. S. Roberts and R. A. Anderson, *J. Pharm. Pharmacol.*, **27**, 599 (1975).

(10) E. G. Weirich, *Dermatologica*, **151**, 268 (1975).

(11) E. A. Strakosch, *Arch. Dermatol. Syphilol.*, **47**, 16 (1943).

(12) M. Davies and R. Marks, *Br. J. Dermatol.*, **95**, 187 (1976).

ACKNOWLEDGMENTS

Supported by a grant from the National Health and Medical Research Council of Australia.

The authors gratefully acknowledge the technical assistance of Mrs. L. Trout, Department of Pathology, University of Tasmania, in the preparation of thick sections of epidermis for light microscopic examination.

ESTRIP, a BASIC Computer Program for Obtaining Initial Polyexponential Parameter Estimates

R. DON BROWN ˣ and JOSEPH E. MANNO

Received January 30, 1978, from the *Department of Pharmacology and Therapeutics, Louisiana State University School of Medicine in Shreveport, Shreveport, LA 71130.* Accepted for publication April 6, 1978.

Abstract □ A new BASIC exponential stripping program, ESTRIP, allows the relatively rapid calculation of initial polyexponential parameter estimates, as does the previously published FORTRAN IV program, CSTRIP. The potential advantages of the new program are that it can be run on microcomputers and minicomputers with BASIC capability and a relatively small core and that it can be easily modified by the user.

Keyphrases □ Computer programs—ESTRIP for calculation of initial polyexponential parameter estimates □ Pharmacokinetic models—ESTRIP computer program for calculation of initial polyexponential parameter estimates □ Models, pharmacokinetic—ESTRIP computer program for calculation of initial polyexponential parameter estimates

The mathematical solutions of classical linear pharmacokinetic models are given by the sums of exponential terms. The generalized equation for these models can be written as:

$$C = \sum_{i=1}^{u} a_i e^{-b_i t} \qquad \text{(Eq. 1)}$$

where C is the concentration of drug at time t, u is the number of exponential terms, and a_i and b_i are the parameters to be determined.

Computer programs for the estimation of these polyexponential parameters (1, 2) generally require sophisticated computers utilizing BMD, BMDP, SAS, or other expensive software packages and are usually available on a time-sharing, batch-job basis. One exception is the CSTRIP program (3), which can be used to obtain preliminary polyexponential parameter estimates *via* an automated stripping (feathering, peeling-off, or back-projection) technique; this program requires the use of FORTRAN IV.

The purposes of this paper are to describe a new exponential stripping computer program[1] and to illustrate its use. The potential advantages of the new program are that

[1] A complete photocopy of the program listing will be supplied upon request. The program is also available, for a fee, on paper tape or a Scotch DC300A Data Cartridge.

0022-3549/78/1200-1687$01.00/0

© 1978, American Pharmaceutical Association

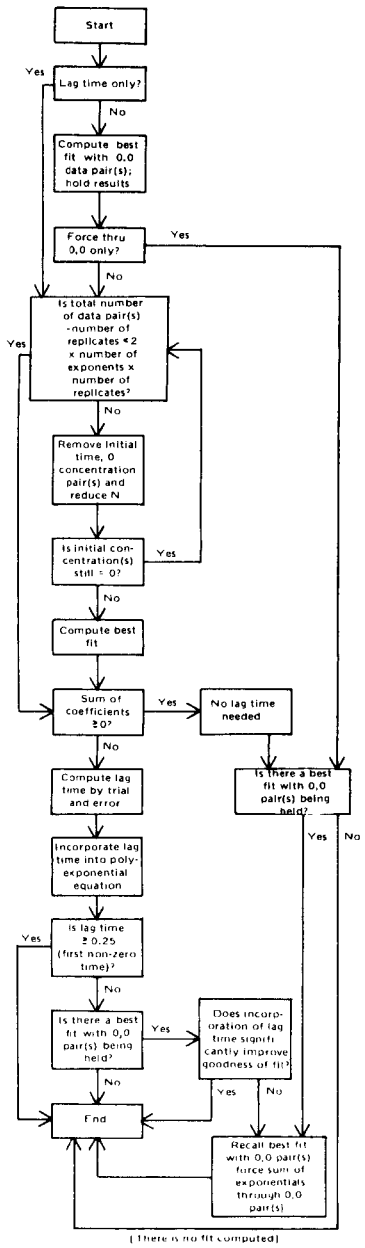

Figure 1—*Flowsheet for LGTME subroutine.*

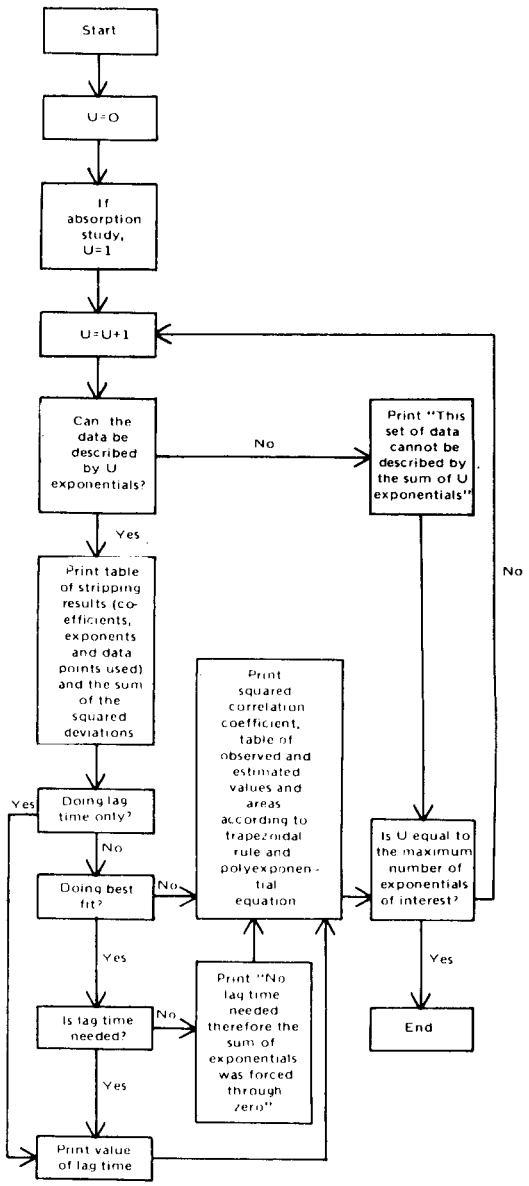

Figure 2—*Schematic diagram of ESTRIP output.*

it can be run on minicomputers and microcomputers with BASIC capability and a relatively small core (16 K or less) and that it can be easily modified by the user[2].

DISCUSSION

Computer Program—ESTRIP, a BASIC computer program for obtaining initial polyexponential parameter estimates, is based on a computer adaptation of the residual, back-projection technique. ESTRIP is composed of eight major subroutines; the most important will be discussed briefly and compared to those with similar functions in CSTRIP (3).

EXP STRIP[3]—This subroutine strips curves described by from one to five exponentials. It differs from the subroutines in CSTRIP with a similar function (3) on two observable points. To conserve core, this subroutine was written to strip one, two, three, four, *or* five exponentials rather than utilizing a separate stripping subroutine to estimate the parameters of each of the five possible exponential equations. In addition, the minimum number of points for a computer calculation of a_i and b_i is fixed at two rather than being dependent on the number of distinct time values and the number of exponential terms, with a minimum value of two.

As in CSTRIP, the value F (the sum of squares of the deviations) is used to evaluate the goodness of fit of the estimates:

$$F = \sum_{i=1}^{n} (C_i - \hat{C}_i)^2 \qquad \text{(Eq. 2)}$$

where $\hat{C}_i$ is the estimated drug concentration and n is the total number of data points.

The set of parameters obtained with EXP STRIP that has the minimum F value is chosen as the best estimate. As with CSTRIP, exponential terms describing intravenous or postabsorption (or postinfusion) data cannot have negative coefficients and, with all data, the value of b_{i-1} is required to be $\geq 1.33\ b_i$ and exponents b_i cannot assume values ≤ 0. An additional constraint in ESTRIP is that a_1 is required to be <0 in the absorption studies.

LEAST SQR—This subroutine, nested within EXP STRIP, calculates the appropriate residual regression lines using standard least-squares linear regression techniques.

[2] Finnigan BASIC was used in writing this program. The specific data system used was the Finnigan 6110, which is intended primarily for the operation of the Finnigan 3300 gas chromatograph–mass spectrometer but can be used in a non-gas chromatograph–mass spectrometer BASIC mode. The 6110 includes a Computer Automations, Inc. naked minicomputer with 16 kilobytes of random access memory.

[3] Names of subroutines are not used in BASIC; they are given in this paper for clarification purposes.

Table I—ESTRIP Output Parameters

Parameter	Comment
Subscript 1, 2, *etc.*	Subscripts of terms in polyexponential equation
A_1, A_2, *etc.*	Coefficients of exponential terms of polyexponential equation
B_1, B_2, *etc.*	Exponents of polyexponential equation
Data points used	Number of data pairs used in calculation of particular subscripted coefficient and exponent (counting backward beginning with last data)
F	Sum of squared deviations between observed data and data predicted by use of polyexponential equation
r^2	Squared correlation coefficient
Number	Data point number
Time	Abscissa values
C(obs)	Observed ordinate values
C(est)	Ordinate values predicted by use of polyexponential equation
Percent deviation	Percent deviation of observed from predicted ordinate values
Area using trapezoidal rule	$AUC_{0-t} = \sum_{i=0}^{n-1} \frac{t_{i+1} - t_i}{2} (C_i + C_{i+1})$
Area using polyexponential equation	$AUC_{0-\infty} = \sum_{i=1}^{U} A_i/B_i$

Table II—Tetracycline Data

Hours	Serum Concentration of Tetracycline Hydrochloride, μg/ml
0	0
1	0.7
2	1.2
3	1.4
4	1.4
6	1.1
8	0.8
10	0.6
12	0.5
16	0.3

SSQR DEV—This subroutine, also nested within EXP STRIP, is used to select the best fit of the sets of calculated estimates. If the constraints placed on the polyexponential parameter estimates are met in a particular set of estimates and if the F of this set is less than that of a previous set being held, the previous set is replaced. A modification of this subroutine is also used, as another nested subroutine within EXP STRIP, to determine the value of the sign placed on the coefficient a_i.

RSQR—This subroutine calculates r^2:

$$r^2 = \left[\sum_{i=1}^{n} C_i^2 - \frac{\left(\sum_{i=1}^{n} C_i\right)^2}{n} - \sum_{i=1}^{n} (C_i - \hat{C}_i)^2 \right] \Bigg/ \left[\sum_{i=1}^{n} C_i^2 - \frac{\left(\sum_{i=1}^{n} C_i\right)^2}{n} \right] \quad \text{(Eq. 3)}$$

which, with F, is used to evaluate the goodness of fit of the estimates.

LGTME—This subroutine determines whether a lag time is needed to describe the data from absorption studies. A flowsheet for the LGTME algorithm is given in Fig. 1. The lag time, t_1, is determined by a trial-and-error solution of:

$$\sum_{i=1}^{u} a_i e^{-b_i t_1} = 0 \quad \text{(Eq. 4)}$$

Use of ESTRIP Program—*Input of Time–Drug Concentration Data*—Data statements are inserted between lines 2985 and 9999 in the program before the Run command is initiated. The first Data statement contains the total number of data points and is followed by the time–drug concentration data. The following restrictions apply to the input of data to both ESTRIP and CSTRIP:

1. Abscissa (time) values must be ascendingly ordered.

```
MAXIMUM NUMBER OF EXPONENTS INTERESTED IN = ?5

IV OF POST-ABSOPPTION STUDIES = 1;
ABSORPTION STUDIES; AS DATA IS = 2; FORCE THRU 0,0 = 3;
                    BEST FIT = 4; LAG TIME = 5;?4

NO. OF REPLICATIONS = ?1

              THE NO. OF EXPONENTIALS =  2
  SUMMARY OF EXP. STRIPPING; REPORTED FROM LAST TO FIRST;

SUBSCRIPT      COEFF. (A)        EXP. (B)      DATA PTS. USED
    1          2.13352          0.128894            6
    2         -2.13351          1.03423             3

                    F =  2.6531E-02

              THE LAG TIME =  0.618479

              R SQUARE ( 2  ) =  0.979416

NO.          TIME          C(OBS)          C(EST)          % DEV
 1             1             0.7          0.682992        -13.8584
 2             2             1.2          1.27671          6.39227
 3             3             1.4          1.38774         -0.875694
 4             4             1.4          1.31428         -6.12309
 5             6             1.1          1.05763         -3.90616
 6             8             0.8          0.822865         2.75809
 7            10             0.6          0.635919         5.98652
 8            12             0.5          0.491496        -1.70088
 9            16             0.3          0.293589        -2.16364

AREA USING TRAPEZOIDAL RULE =  12.15
AREA USING POLYEXPONENTIAL EQUATION =  14.4896


              THE NO. OF EXPONENTIALS =  3
  SUMMARY OF EXP. STRIPPING; REPORTED FROM LAST TO FIRST;

SUBSCRIPT      COEFF. (A)        EXP. (B)      DATA PTS. USED
    1          1.84719          0.117265            3
    2          0.969024         0.462893            3
    3         -2.81621          0.896823            3

                    F =  2.69583E-02

              THE LAG TIME =  0.588749

              R SQUARE ( 3  ) =  0.979084

NO.          TIME          C(OBS)          C(EST)          % DEV
 1             1             0.7          0.613722        -12.3254
 2             2             1.2          1.27535          6.27897
 3             3             1.4          1.38565         -1.02517
 4             4             1.4          1.30583         -6.72642
 5             6             1.1          1.03651         -5.7718
 6             8             0.8          0.802304         0.288017
 7            10             0.6          0.62448          4.08607
 8            12             0.5          0.489403        -2.11942
 9            16             0.3          0.303919         1.30634

AREA USING TRAPEZOIDAL RULE =  12.15
AREA USING POLYEXPONENTIAL EQUATION =  14.7855


THIS SET CAN'T BE DESCRIBED BY THE SUM OF 4  EXPONENTIALS!


THIS SET CAN'T BE DESCRIBED BY THE SUM OF 5  EXPONENTIALS!
```

Figure 3—*ESTRIP analysis of tetracycline concentration and time data.*

Table III—Haloperidol Data

Hours	Plasma Concentration of Haloperidol, ng/ml
0	0
0.167	2.99
0.333	4.82
0.667	2.86
1	2.23
1.5	1.65
2	1.33
3	1.05
4	0.945
6	0.679
8	0.619
12	0.462
24	0.336
48	0.178
72	0.084

MAXIMUM NUMBER OF EXPONENTS INTERESTED IN = ? 5

IV OR POST-ABSORPTION STUDIES = 1;
ABSORPTION STUDIES: AS DATA IS = 2 FORCE THRU 0,0 = 3;
BEST FIT = 4; LAG TIME = 5; ? 4

NO. OF REPLICATIONS = ? 1

THE NO. OF EXPONENTIALS = 2
SUMMARY OF EXP. STRIPPING; REPORTED FROM LAST TO FIRST:

SUBSCRIPT	COEFF. (A)	EXP. (B)	DATA PTS. USED
1	1.52907	4.52019E-02	13
2	- 1.52907	0.226037	2

F = 45.3066

NO LAG TIME WAS NEEDED SO DATA WAS FORCED THRU 0,0 !

R SQUARE (2) = -0.760874

NO.	TIME	C(OBS)	C(EST)	% DEV
1	0	0	0	. . . . .
2	0.167	2.99	4.51448E-02	-98.4901
3	0.333	4.82	8.80252E-02	-98.1738
4	0.667	2.86	0.168583	-94.1055
5	1	2.23	0.241771	-89.1583
6	1.5	1.65	0.339457	-79.4269
7	2	1.33	0.423943	-68.1246
8	3	1.05	0.559047	-46.7574
9	4	0.945	0.657056	-30.4702
10	6	0.679	0.77191	13.6834
11	8	0.619	0.81441	31.5686
12	12	0.462	0.787416	70.4364
13	24	0.336	0.510019	51.7914
14	48	0.178	0.17461	-1.90455
15	72	8.4E-02	5.902E-02	-29.7381

AREA USING TRAPEZOIDAL RULE = 26.1144
AREA USING POLYEXPONENTIAL EQUATION = 27.0629

THE NO. OF EXPONENTIALS = 3
SUMMARY OF EXP. STRIPPING; REPORTED FROM LAST TO FIRST:

SUBSCRIPT	COEFF. (A)	EXP. (B)	DATA PTS. USED
1	0.965666	3.55743E-02	9
2	3.68443	1.14207	2
3	-4.65009	8.9605	3

F = 3.40128

THE LAG TIME = 8.465E-02

R SQUARE (3) = 0.85697

NO.	TIME	C(OBS)	C(EST)	% DEV
1	0.167	2.99	2.09326	-29.9914
2	0.333	4.82	3.22935	-33.0009
3	0.667	2.86	2.81532	-1.56224
4	1	2.23	2.22873	-5.71456E-02
5	1.5	1.65	1.64998	-9.10325E-04
6	2	1.33	1.31545	-1.09362
7	3	1.05	1.00247	-4.52651
8	4	0.945	0.882218	-6.64358
9	6	0.679	0.786703	15.862
10	8	0.619	0.729117	17.7895
11	12	0.462	0.632035	36.8041
12	24	0.336	0.412422	22.7446
13	48	0.178	0.17561	-1.34293
14	72	8.4E-02	7.47748E-02	-10.9824

AREA USING TRAPEZOIDAL RULE = 25.8648
AREA USING POLYEXPONENTIAL EQUATION = 29.8522

THE NO. OF EXPONENTIALS = 4
SUMMARY OF EXP. STRIPPING; REPORTED FROM LAST TO FIRST:

SUBSCRIPT	COEFF. (A)	EXP. (B)	DATA PTS. USED.
1	0.711191	2.96516E-02	5
2	1.8277	0.515867	4
3	4.3739	3.13509	3
4	-6.91242	29.9048	2

F = 2.44106E-02

THE LAG TIME = 0.14532

R SQUARE (4) = 0.998973

NO.	TIME	C(OBS)	C(EST)	% DEV
1	0.167	2.99	2.99	-7.97387E-06
2	0.333	4.82	4.76951	-1.04742
3	0.667	2.86	2.949	3.11186
4	1	2.23	2.16948	-2.71401
5	1.5	1.65	1.65443	0.268582
6	2	1.33	1.38826	4.38075
7	3	1.05	1.07317	2.2062
8	4	0.945	0.884614	-6.39003
9	6	0.679	0.687023	1.18159
10	8	0.619	0.595207	-3.84384
11	12	0.462	0.504448	9.18782
12	24	0.336	0.350596	4.34399
13	48	0.178	0.172082	-3.32473
14	72	8.4E-02	8.44645E-02	0.553011

AREA USING TRAPEZOIDAL RULE = 25.8648
AREA USING POLYEXPONENTIAL EQUATION = 28.6918

THE NO. OF EXPONENTIALS = 5
SUMMARY OF EXP. STRIPPING; REPORTED FROM LAST TO FIRST:

SUBSCRIPT	COEFF (A)	EXP. (B)	DATA PTS. USED
1	0.795918	3.12903E-02	2
2	-0.182529	6.23796E-02	2
3	1.15287	0.315505	3
4	4.96586	2.18112	5
5	-6.73225	21.3679	2

F = 8.38743E-02

THE LAG TIME = 0.13496

R SQUARE (5) = 0.996473

NO.	TIME	C(OBS)	C(EST)	% DEV
1	0.167	2.99	2.99	-5.58171E-05
2	0.333	4.82	4.82	0
3	0.667	2.86	3.13689	9.6814
4	1	2.23	2.23187	8.38955E-02
5	1.5	1.65	1.59736	-3.19011
6	2	1.33	1.31338	-1.24995
7	3	1.05	1.05149	0.142279
8	4	0.945	0.903468	-4.39496
9	6	0.679	0.717077	5.60776
10	8	0.619	0.606936	-1.9489
11	12	0.462	0.489291	5.90704
12	24	0.336	0.336619	0.184242
13	48	0.178	0.168783	-5.1782
14	72	8.4E-02	8.19373E-02	-2.45562

AREA USING TRAPEZOIDAL RULE = 25.8648
AREA USING POLYEXPONENTIAL EQUATION = 28.1262

Figure 4—*ESTRIP analysis of haloperidol concentration and time data (composer reproduction of teletype output).*

2. Data collected during an intravenous infusion cannot be analyzed, although postinfusion values may be analyzed.
3. Outliers should not be included in data sets.
4. Replicate abscissa and/or ordinate values are permitted.

Additionally, when replicate abscissa values are used in ESTRIP, the numerical value is entered only once in the Data statement, and it is followed by the corresponding ordinate values. All of these abscissa values must be associated with the same number of ordinate values. Any other data are entered as the abscissa–ordinate pairs.

Input of Data during Operation of ESTRIP—When Run is initiated, three questions are asked of the user. The first question is "Maximum Number of Exponents Interested In = ?" The answer can be from one through five. The second question gives the user the option of running the data with the constraints related to intravenous (postinjection or postinfusion) or postabsorption studies (answer = 1) or with the constraints related to absorption studies (answer = 2–5).

When doing absorption studies, the user can select to answer the second question with the number two (2, As Data Is). This option is useful in estimating the elimination half-life, *etc.*, of a drug in a patient who has been on the medication prior to determination of the blood drug levels since neither estimating a lag time nor forcing the sum of the exponentials through 0,0 is feasible in this type of patient with ESTRIP. If the user selects to answer this question with the number three, four, or five (3, Force Thru 0,0 only; 4, Best Fit; or 5, Lag Time only), the LGTME algorithm (Fig. 1) is used to arrive at the solution.

An additional restriction placed on the input of time–drug concentration data is related to the numerical answer given to this second question. If the answer is three or four, the initial time–drug concentration value(s) of 0 must be included in the Data statements or the program will give an error message after Run is initiated. To conserve core space, a subroutine to add the 0,0 data pair(s) is not included in ESTRIP. A subroutine to remove the initial time–0 concentration(s) data is included in the LGTME algorithm, because it is essential to the function of the algorithm.

The third and final question asked the user is "No. of Replications = ?" After this question is answered, the program runs to completion.

Data Output—The ESTRIP output format (Fig. 2) is dependent on the type of data being analyzed and the answer of the user to the second question of the program. The output parameters are defined in Table I.

Examples—Forty sets of data, some simulated and the rest from the literature, were used to evaluate the capabilities of ESTRIP. Two rep-

Table IV—Comparison of Automated and Graphical Curve Stripping of Haloperidol Concentration and Time Data[a]

Parameter	Value of Parameter Estimate			
		ESTRIP[c]		
	Graphical[b]	As Data Is and Force Thru 0,0[e]	Best Fit	AUTOAN[d]
A_1	0.661	0.661	0.711	0.671
B_1	0.0283	0.0283	0.0297	0.0284
A_2	1.341	1.20	1.83	1.347
B_2	0.355	0.338	0.516	0.369
A_3	5.525	6.60	4.37	20.57
B_3	2.147	2.21	3.14	2.97
A_4	−7.527	−8.47	−6.91	−22.80
B_4	5.94	5.52	29.9	4.22
Lag time (t_1)	0	0	0.145	0
Sum of squared deviations	1.73[f]	1.64	0.0244	0.977[f]
Squared correlation coefficient	0.932[f]	0.936	0.999	0.962[f]

[a] Data fitted to a quadriexponential equation of the form: $C = \sum_{i=1}^{4} A_i e^{-Bi(t-t1)}$. [b] From Wagner (5); data pairs grouped differently than with CSTRIP. [c] All ESTRIP estimates were rounded to three significant digits after calculation. [d] From Wagner (5): AUTOAN has incorporated in it nonlinear least-square analysis. No estimate of a lag time was made, and the data were not forced through 0,0. [e] Both options produced the same fit, because only two data pairs are used in the calculation of A_4 and B_4, one of which is the 0,0 pair. [f] Other parameters in these columns are as reported by Wagner (5). These estimates were calculated from the other estimates and the concentration data.

resentative data sets reported in the literature were used to illustrate the performance of ESTRIP. Table II gives oral tetracycline data (4), and Table III gives data collected after intramuscular haloperidol (5). The input of data during the operation of ESTRIP is illustrated in Figs. 3 and 4. The input format for the time–drug concentration values of the tetracycline data is:

9900 Data 10,0,0,1,.7,2,1.2,3,1.4,4,1.4,6,1.1,8,.8,10,.6,12,.5,16,.3

To conserve core, the figures are typed in with no spaces between data pairs and with a minimum number of individual data statements.

RESULTS

Tetracycline Data—These data were used to illustrate the operation of ESTRIP (Fig. 3) since they also were used to illustrate the operation of CSTRIP (3). The output resulting from both analyses was virtually identical. (ESTRIP analysis of the spectinomycin data used to illustrate CSTRIP performance also yielded a virtually identical output.)

Haloperidol Data—The output resulting from ESTRIP analysis of data collected after the intramuscular administration of haloperidol is given in Fig. 4. These data were described well by both the sum of four exponentials and the sum of five exponentials. Wagner (5) fitted them to the sum of four exponentials. A comparison between his estimates (graphical and with AUTOAN, a program that incorporates nonlinear least-squares analysis) and those produced by ESTRIP is given in Table IV.

The estimates given by ESTRIP for the As Data Is and the Force Thru 0,0 options were the same since only two data pairs were used in calculating A_4 and B_4, one of which was the 0,0 pair. These fits were comparable to those obtained by Wagner using a graphical method. However, the fit produced by the Best Fit option of ESTRIP included a lag time and was different from and slightly better than the AUTOAN fit of Wagner (5). An estimate of lag time was not included in the AUTOAN fit. The lag time obtained by ESTRIP was 0.145 hr (8.72 min).

ESTRIP usually gives results comparable to or better than graphical techniques and provides accurate parameter estimates. In addition, since this program is written in BASIC, it may provide a more readily available means of analysis than does CSTRIP, which is in FORTRAN IV. The primary disadvantage of ESTRIP compared to CSTRIP is the longer computing time required, because of the different computer languages being used.

REFERENCES

(1) J. G. Wagner, "Fundamentals of Clinical Pharmacokinetics," Drug Intelligence Publications, Hamilton, Ill., 1975, pp. 397–437.

(2) M. Gibaldi and D. Perrier, "Drugs and the Pharmaceutical Sciences," vol. 1, Dekker, New York, N.Y., 1975, pp. 307, 308.

(3) A. J. Sedman and J. G. Wagner, *J. Pharm. Sci.*, **65**, 1006 (1976).

(4) J. G. Wagner, *Clin. Pharmacol. Ther.*, **8**, 20 (1967).

(5) J. G. Wagner, "Fundamentals of Clinical Pharmacokinetics," Drug Intelligence Publications, Hamilton, Ill., 1975, pp. 60–63.

Assay of Tocainide in Blood by High-Pressure Liquid Chromatography

E. M. WOLSHIN *x, M. H. CAVANAUGH, C. V. MANION, M. B. MEYER, E. MILANO, C. R. REARDON, and S. M. WOLSHIN

Received December 12, 1977, from the *Astra Pharmaceutical Laboratory of Clinical Pharmacology, St. Vincent Hospital, Worcester, MA 01604.* Accepted for publication April 5, 1978. *Present address: Astra Pharmaceutical Products, Inc., Framingham, MA 01702.

Abstract □ A sensitive, specific, high-pressure liquid chromatographic assay for the determination of tocainide in whole blood is described. The residue from a methylene chloride extract of alkalinized blood was resolvated in a mobile phase of methanol–water (47:53) containing 1% acetic acid and 6.16 m*M* 1-octanesulfonic acid, adjusted to pH 4.0. Chromatography was performed on a reversed-phase column with detection at 254 or 225 nm. The limits of accurate measurement were 2 μg/ml for a 1-ml blood sample monitored at 254 nm and 0.2 μg/ml for a 2-ml sample monitored at 225 nm. The assay was tested on samples from emergency protocol patients and was also found suitable for single-dose pharmacokinetic studies.

Keyphrases □ Tocainide—high-pressure liquid chromatographic analysis in blood □ High-pressure liquid chromatography—analysis, tocainide in blood □ Cardiac depressants—tocainide, high-pressure liquid chromatographic analysis in blood

Tocainide, 2-amino-*N*-(2,6-dimethylphenyl)propanamide (I), is an oral antiarrhythmic agent currently under investigation. Its effectiveness, oral route of administration, long half-life (12 hr), and low order of toxicity indicate that this agent may have advantages over other existing antiarrhythmic agents (1–3).

GLC assays for tocainide have used heptafluorobutyrate (4) and trifluoroacetamide (1) derivatives. Tocainide also has been assayed by high-pressure liquid chromatography (HPLC), but the drug required derivatization with dansyl chloride to be detectable with precision (5).

This report describes a new HPLC assay that requires no derivatization and that has a high degree of precision, linearity, and reproducibility in the range of therapeutic and subtherapeutic concentrations.

EXPERIMENTAL

Reagents and Materials—Tocainide and the internal standards, *N*-(2,6-dimethylphenyl)-2-aminobutanamide (II) and glycinexylidide (III), were obtained in purified form as the hydrochloride salts[1]. ^{3}H-Tocainide, of 97.5% radiochemical purity, was obtained with the label in the 4-position on the aromatic ring[2]. 1-Octanesulfonic acid was supplied as the sodium salt and used without further purification[3].

Methanol and methylene chloride were supplied and used as triple-distilled solvents[4]. Water was distilled and deionized by ion-exchange resins, filtered through charcoal, and passed through a 0.45-μm filter prior to use. All other reagents were analytical grade or better.

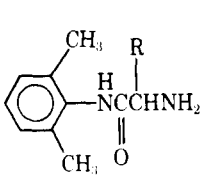

I: R = CH_3
II: R = CH_2CH_3
III: R = H

Instrumentation—The liquid chromatograph consisted of a high-pressure pump[5], a valve and loop injector[6], a 10-liter water bath with a circulating heater, a fixed wavelength UV detector[7], and a variable wavelength detector[8]. The solvent from the mobile phase reservoir was filtered through a 30-μm inlet filter[9]. A 2-μm filter[10] and 0.5-μm filter[11] in series were placed between the pump outlet and the injection valve inlet to remove any remaining particulate matter from the solvent.

Separations were done on a 30 × 4-mm i.d. column containing 10-μm silica with bonded octadecylsilane[12]. Chromatograms were produced on a strip-chart recorder[13] with 2-, 5-, and 10-mv inputs.

Chromatographic Conditions—The mobile phase was pumped through the column at 2.0 ml/min. The back-pressure of the system was 3500 psig. The column effluent was monitored at either 254 nm with the fixed wavelength detector or at 225 nm with the variable wavelength detector. Columns were flushed each morning with mobile phase for 1 hr at 1.0 ml/min prior to sample analysis. For clinical specimens run at 254 nm, the 0.02 absorbance scale was expanded to 0.01 and 0.004 by recording the 10-mv detector output on the 5- and 2-mv scales of the recorder, respectively. The column water bath was maintained at 25 ± 0.2°.

The mobile phase was prepared by combining 47 parts of a methanolic solution with 53 parts of an aqueous solution. Each solution contained 6.16 m*M* 1-octanesulfonic acid and 1% (v/v) acetic acid. The methanolic solution was adjusted to pH 4.0 with 1.0 *N* KOH in methanol, and the aqueous solution was adjusted to the same pH with 5.0 *N* NaOH in water. Acetonitrile (1%) was added to the aqueous component as a preservative.

Extraction—The extraction was done in 15-ml conical bottom centrifuge tubes capped with polyethylene stoppers.

The extraction mixture consisted of 1.0 or 2.0 ml of sample, 1.0 ml of internal standard, 1.0 ml of 1.0 *N* NaOH, enough water to bring the volume of the aqueous phase to 5.0 ml, and 5.0 ml of methylene chloride. The two phases were rotary mixed[14] for 15 min and separated by centrifugation[15] at 500 rpm for 10 min. The aqueous (upper) phase and coagulated proteins at the interface were removed by vacuum aspiration. The methylene chloride was poured into a 16 × 100-mm glass culture tube and evaporated at approximately 55° in a water bath.

The extracts were stored at room temperature (not more than 6 hr) until reconstituted with 50 μl of HPLC mobile phase. The extracted drug was solvated by vortexing[16] for 30 sec and sonicating[17] for 1 min. Aliquots of 20 μl were chromatographed.

Assay Reproducibility and Linearity—The linearity and precision of the assay in the 5–15-μg/ml range were determined by adding known amounts of tocainide hydrochloride to pooled human plasma, extracting 1.0-ml aliquots, and monitoring the chromatographic eluant at 254 nm. To test the subtherapeutic range (0.5–5.0 μg/ml), microliter volumes of a tocainide stock solution were added to 2-ml aliquots of pooled blood. The samples were extracted and chromatographed with detection at 225 nm. The slope, intercept, and correlation coefficient were determined

[1] Astra Pharmaceutical Products, Framingham, Mass.
[2] New England Nuclear, Boston, Mass.
[3] Eastman Organic Chemical, Rochester, N.Y.
[4] Burdick & Jackson Laboratories, Muskegon, Mich.
[5] Model M6000, Waters Associates, Milford, Mass.
[6] Model CV-6-UHPa-N60, Valco Valve, Houston, Tex.
[7] Model 202, Waters Associates, Milford, Mass.
[8] Model SF 770, Schoeffel Instruments, Westwood, N.J.
[9] Inlet solvent assembly filter 25551, Waters Associates, Milford, Mass.
[10] SS-2-F-2 Swagelok, Crawford Fitting Co., Cleveland, Ohio.
[11] SS-200-6-1-SR12 Swagelok, Crawford Fitting Co., Cleveland, Ohio.
[12] μBondapak C_{18}, Waters Associates, Milford, Mass.
[13] Model DSRG, Sargent Welch Scientific Co., Skokie, Ill.
[14] Rotary mixer, Drummond Scientific, Broomall, Pa.
[15] Model H-NS centrifuge, International Equipment Co., Needham Heights, Mass.
[16] Model K-550-G Vortex Genie, Scientific Instruments, Springfield, Mass.
[17] Model 220, Branson Cleaning Equipment Co., Shelton, Conn.

0022-3549/78/1200-1692$01.00/0
© 1978, American Pharmaceutical Association

Table I—UV Spectrum of Tocainide Hydrochloride in Distilled Water [a]

Wavelength, nm	19.9-μg/ml Absorbance	125-μg/ml Absorbance
200	—	—
205	1.25	—
210	0.960	—
215	0.720	—
220	0.450	—
225	0.280	—
230	0.190	1.37
235	0.120	0.850
240	0.070	0.480
245	0.040	0.370
250	0.035	0.200
255	0.025	0.190
260	0.025	0.215
265	0.025	0.230
270	0.025	0.190
275	0.010	0.050
280	0.000	0.020

[a] Spectrum was taken on a Perkin-Elmer model 202 UV-visible spectrophotometer with the slit at 25 and a 1-cm light path.

by a least-squares regression analysis.

Daily Calibration Curves and Analysis—A four-point calibration curve was run with each day's set of samples. The levels of internal standard were 10 μg/ml for clinical samples and 1.0 μg/ml for pharmacokinetic studies. The slope, intercept, and correlation coefficient were determined by a least-squares regression as already described.

Interferences—Stock solutions of the following pure drug substances were prepared in the mobile phase, and their retention times relative to tocainide were determined: procainamide, *N*-acetylprocainamide, quinidine, dihydroquinidine, lidocaine, theophylline, caffeine, diazepam, and chlordiazepoxide.

Also chromatographed were intravenous solutions of other common drugs containing no preservatives, including isoproterenol, epinephrine, levarterenol, propranolol, phenytoin, penicillin G, and furosemide. Compounds that were isographic with either tocainide or the internal standard were tested for their extractability from alkalinized blood with methylene chloride.

Blood Level Study—Tocainide was administered to patients with life-threatening arrhythmias. To monitor blood levels and to adjust the dose, samples of venous blood were periodically drawn in heparinized containers[18]. Tocainide, 400 mg, also was given to a normal volunteer fasted 12 hr prior to administration. Samples were drawn at appropriate intervals for 48 hr after dosing. Blood and plasma samples were stored at 4° until assayed.

Partition and Recovery—^{3}H-Tocainide was used to determine the partition coefficient and absolute recovery of the extraction procedure. A solution of 5.0 μg of tocainide/ml containing 0.5 μg of labeled species/ml was extracted by the described method. The radioactivity of the organic phase, aqueous phase, precipitated proteins, and reconstituted extract was determined by scintillation counting.

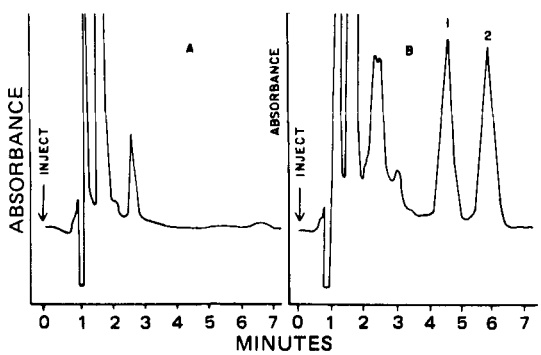

Figure 1—*A: extract of drug-free blood. B: patient sample containing 5 μg of tocainide/ml. Key: peak 1, tocainide; and peak 2, 2-amino-N-(2,6-dimethylphenyl)butanamide. HPLC conditions were: flow, 2.0 ml/min; detection, 254 nm; and 0.01 aufs.*

[18] Vacutainers, Becton-Dickinson, Rutherford, N.J.

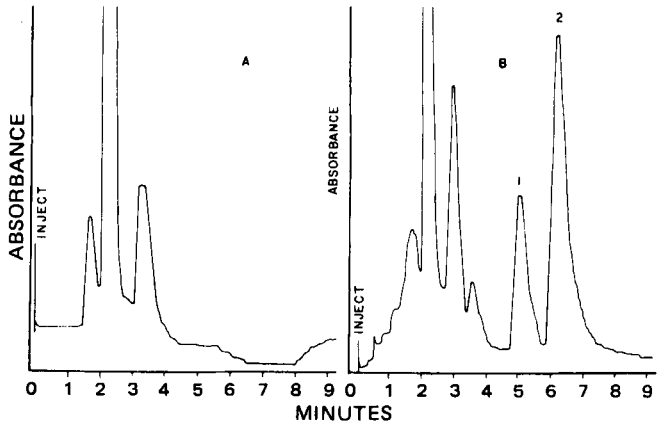

Figure 2—*A: extract of drug-free blood. B: sample from normal volunteer containing 1 μg of tocainide/ml. Key: peak 1, tocainide; and peak 2, 2-amino-N-(2,6-dimethylphenyl)butanamide. HPLC conditions were: flow, 2.4 ml/min; detection, 225 nm; and 0.02 aufs.*

The walls of both the extraction and evaporation tubes were etched with a solution containing 0.5 *M* HNO_3 and 0.5 *M* KF, and the etchant was checked for radioactivity. A quench correction (6) was calculated by adding a known amount of ^{3}H-tocainide to each scintillation vial and recounting the samples.

RESULTS AND DISCUSSION

Tocainide may be detected by UV absorbance at wavelengths below 275 nm (Table I). Figures 1 and 2 show chromatograms of samples monitored at 254 and 225 nm, respectively. Detection at 225 nm yielded a ninefold increase in sensitivity over detection at 254 nm (Fig. 3). Detection at 254 nm had a limit of useful measurement of 2.0 μg/ml for a 1.0-ml sample and was adequate for the monitoring of blood levels in the therapeutic range (4–10 μg/ml) (3). In pharmacokinetic studies, a subtherapeutic dose was administered and blood levels did not exceed 2.0 μg/ml. These levels were measured at 225 nm.

Most clinical data were obtained by monitoring at 254 nm. Use of 225 nm was a compromise between increased sensitivity and ability to null out the background absorbance of the mobile phase. This wavelength is presently recommended for the measurement of both therapeutic and subtherapeutic levels. The 225-nm setting also offered increased specificity. In several patient samples, a large peak at 254 nm interfered with quantitation of the internal standard but did not interfere at 225 nm.

The data from two standard curves are summarized in Table II. The

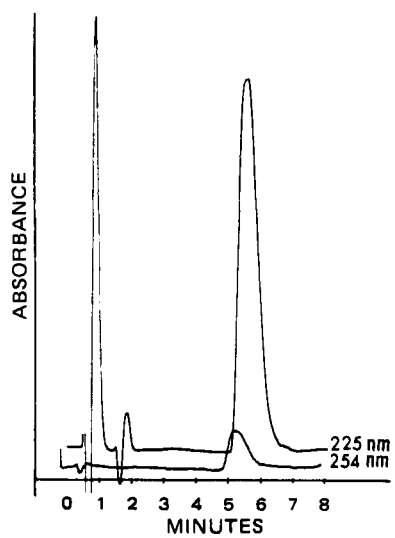

Figure 3—*Comparison of detection response at 254 and 225 nm. Both detectors were operated at 0.04 aufs; 4.0 μg of tocainide was injected. The flow was 2.0 ml/min.*

Table II—Standard Curves: Tocainide to Internal Standard Peak Height Ratios *versus* Micrograms per Milliliter Extracted

Blood Tocainide Concentration, μg/ml	Peak Height Ratio[a], Mean ± *SD* (n = 5)	*CV*, %
15[b]	2.366 ± 0.0928	3.9
10[b]	1.570 ± 0.0507	3.2
7.5[b]	1.101 ± 0.0500	4.5
5.0[b]	0.695 ± 0.025	3.6
5.0[c]	3.22 ± 0.111	3.4
1.5[c]	0.936 ± 0.0361	3.9
1.0[c]	0.642 ± 0.0248	3.9
0.5[c]	0.3470 ± 0.0214	6.2

[a] Internal standard was 2-amino-*N*-(2,6-dimethylphenyl)butanamide. [b] Column effluent was monitored at 254 nm; internal standard = 10 μg/ml. [c] Column effluent was monitored at 225 nm; internal standard = 2 μg/ml.

Table III—Mean Coefficient of Variation Calculated from Duplicate Analysis of Samples Monitored at 254 nm

Number of Samples, N	Concentration Range of Means, μg/ml	Mean *CV*[a], %
3	0.0–1.0	34
11	1.0–2.0	23
4	2.0–3.0	10
18	3.0–4.0	5.7
14	4.0–5.0	5.2
8	5.0–6.0	6.6
11	6.0–7.0	3.9
8	7.0–8.0	5.6
3	8.0–9.0	2.9
11	9.0–13.0	3.3

[a] Calculated from the formula:

$$\overline{CV} = \frac{(100)}{(N)}\sqrt{2}\sum_{i=1}^{N}\frac{|(A_i - B_i)|}{|(A_i + B_i)|}$$

where A_i and B_i are duplicate extractions of the same sample.

coefficients of variation were less than 4.5% in the 1.0–15-μg/ml range and only 6.2% at 0.5 μg/ml. Both curves were linear, with correlation coefficients of 0.99.

Daily four-point calibration curves showed a similar degree of linearity and reproducibility at 254 nm. The average slope for 20 calibration curves in the 5.0–15.0-μg/ml range was 0.1365 ± 0.0148 (mean ± *SD*), and the correlation coefficient ranged from 0.981 to 0.999. At 225 nm, the average slope over the 0.5–5.0-μg/ml range was 0.668 ± 0.078 (mean ± *SD*, n = 11), and the minimum correlation coefficient was 0.978. In Tables III and IV, the mean coefficients of variation as calculated from replicate patient samples provide a measure of the reproducibility that may be expected from actual samples rather than from spiked blood.

The partition coefficient for the organic to alkaline aqueous phases was determined from the extraction of ^{3}H-tocainide. No statistical difference was found between the extraction of blood or plasma. The mean partition coefficient was 0.64 ± 0.01 (mean ± *SD*, n = 4). Negligible (2%) quantities of tocainide adhered to the precipitated proteins and the walls of the extraction tubes. Sixty-three percent of the extracted drug was recovered upon reconstitution by the mobile phase. The balance was adsorbed to the evaporation tube.

Table IV—Mean Coefficient of Variation Calculated from Duplicate Analysis of Samples Monitored at 225 nm

Number of Samples, N	Concentration Range of Mean, μg/ml	Mean *CV*[a], %
8	0.2–0.4	5.9
10	0.4–0.6	6.0
18	0.6–0.8	6.0
43	0.8–1.0	3.0
43	1.0–1.2	8.1
27	1.2–1.4	8.2
34	1.4–1.6	6.8
62	1.6–1.8	9.9
20	1.8–2.0	13.7

[a] Same as footnote *a* in Table III.

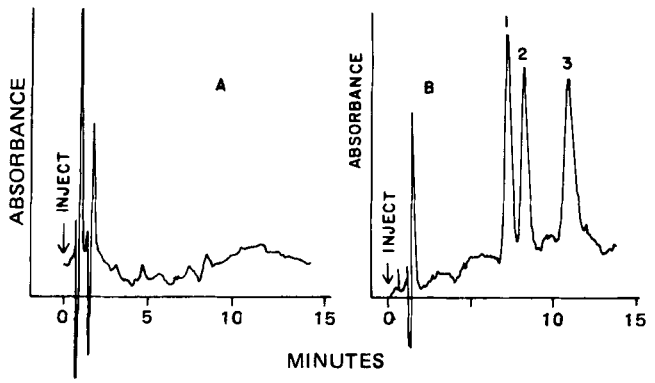

Figure 4—*Use of glycinexylidide as an alternative internal standard for analysis of samples from patients receiving both tocainide and lidocaine. A: extract of drug-free blood. B: extract of samples containing 5 μg/ml each of tocainide (peak 2), lidocaine (peak 3), and glycinexylidide (peak 1). HPLC conditions were: flow, 2.0 ml/min; detector, 225 nm; and 0.04 aufs.*

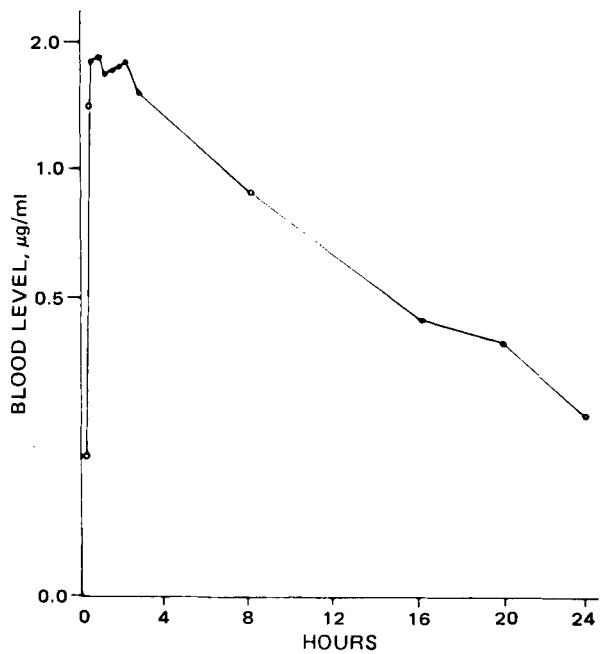

Figure 5—*Blood levels curve for a normal volunteer given 400 mg po of tocainide hydrochloride* ($t_{1/2}$ = ~8 *hr*).

None of the drugs evaluated for interference coeluted with tocainide. Lidocaine and phenytoin, however, were isographic with the internal standard.

Lidocaine, but not phenytoin, was extracted with the described method. For samples containing both lidocaine and tocainide, another internal standard, glycinexylidide (Fig. 4), was used. This compound was resolved from tocainide and other substances in a solvent system of methanol–water (40:60) with the same concentrations of 1-octanesulfonic acid and acetic acid and the same pH.

For samples without lidocaine, 2-amino-*N*-(2,6-dimethylphenyl)-butanamide was the internal standard of choice. Elution times were shorter, and the larger peak height to peak width ratio for a fixed amount injected produced increased assay sensitivity.

A typical blood level curve is shown in Fig. 5. The drug appears to have a rapid phase of distribution and a terminal half-life of approximately 8 hr.

REFERENCES

(1) D. G. McDevitt, A. S. Nies, G. R. Wilkinson, R. F. Smith, and R. L. Woosely, *Clin. Pharmacol. Ther.*, **19**, 396 (1976).

(2) D. Lalka, M. B. Meyer, B. Duce, and A. T. Elvin, *ibid.*, **19**, 757

(1976).
(3) R. A. Winkle, P. J. Meffin, J. W. Fitzgerald, and D. C. Harrison, *Circulation*, **54**, 884 (1976).
(4) D. J. Coltart, T. B. Berndt, R. Kernuff, and D. C. Harrison, *Am. J. Cardiol.*, **34**, 35 (1974).
(5) P. J. Meffin, S. R. Harapat, and D. C. Harrison, *J. Pharm. Sci.*, **66**, 588 (1977).
(6) D. L. Horrochs "Applications of Liquid Scintillation Counting," Academic, New York, N.Y., 1974, p. 210.

ACKNOWLEDGMENTS

The authors thank Dr. Robert Ronfeld for his comments and Ms. Deborah Higgins and Ms. Trudy DiBello for assistance.

New Microporous Cholestyramine Analog for Treatment of Hypercholesterolemia

RENATO DE SIMONE *, FRANCO CONTI ‡, M. ROSA LOVATI ‡, MARINA SIRTORI ‡, ENZO COCUZZA *, and CESARE R. SIRTORI ‡x

Received October 12, 1977, from the **Spemsa, Florence, Italy, and the* ‡*Center E. Grossi Paoletti, University of Milano, Via A. del Sarto 21, 20129 Milano, Italy.* Accepted for publication May 5, 1978.

Abstract □ A new, microporous, uniformly reticulated preparation of cholestyramine is described. The preparation, cholpor, has a higher exchange capacity for chloride than does cholestyramine and swells very little in water. It is 15–20% more potent than cholestyramine in the *in vitro* binding of sodium cholate; moreover, the binding velocity is considerably higher than that of cholestyramine. Colestipol hydrochloride, also used as a reference anion-exchange resin, is about half as potent as the other two resins; its binding velocity is similar to that of cholpor. Cholpor may be prepared in a suspension form of good palatability. Preliminary clinical findings in short-term trials showed a cholesterol-lowering effect similar to that of cholestyramine with lower doses and fewer side effects.

Keyphrases □ Cholestyramine analog—cholpor synthesized, *in vitro* binding of sodium cholate and cholesterol lowering effect in humans evaluated □ Cholpor—cholestyramine analog synthesized, *in vitro* binding of sodium cholate and cholesterol lowering effect in humans evaluated □ Antihypercholesterolemic activity—cholestyramine analog synthesized, *in vitro* binding of sodium cholate and cholesterol lowering effect in humans evaluated

Lowering of plasma cholesterol appears to be a major goal in the prevention of atherosclerosis (1). Anion-exchange resins are the most effective pharmaceutical agents in the clinical management of hypercholesterolemia (2); cholestyramine[1], a styrene-divinylbenzene copolymer with a free quaternary ammonium group, is currently the most widely used agent. Although the clinical efficacy of cholestyramine is not disputed, its unpleasant taste as well as the difficulty encountered by patients in mixing it with water upon each administration makes continued treatments rather difficult (3). The newer anion-exchange resin, colestipol hydrochloride[2] (4), is better tolerated but also requires several daily extemporary preparations.

This report describes a new microporous analog of cholestyramine, cholpor, which may be prepared in suspension form, is of good palatability, and is easily accessible to the patient.

EXPERIMENTAL

Analytical Methods—Swelling of the resins in water was determined by adding 1 g of cholestyramine[1], colestipol hydrochloride[2], or cholpor to enough water (10–30 ml) to provide a suspension. After 24 hr, the suspension was shaken and the volume of resin under water was determined.

Exchange Capacity—Chloride-ion absorption from a 5% NaCl solution, after regeneration of the resin with a 4% NaOH[3] solution, was measured by titrating with 0.1 *N* HCl[3] the sodium hydroxide resulting from the resin and sodium chloride reaction.

Pharmacology—Binding of sodium cholate[4] *in vitro* was estimated essentially according to Whiteside *et al.* (5). Preparations of cholestyramine (100–200 mesh), colestipol hydrochloride (60–150 mesh), and cholpor (60–80 mesh) were added to scintillation vials[5] containing 10 ml of 0.02 *M* phosphate buffer with 2 mg of sodium cholate/ml.

The significance of the differences in the various experiments was determined by the Student *t* test.

RESULTS AND DISCUSSION

Chemistry—Cholpor (6) is obtained by starting with a porous matrix. Porosity is first achieved during preparation of the copolymer. During chloromethylation, porosity is protected by maintaining reaction conditions that do not alter the physical structure of the matrix (low reaction temperature, low acidity of the catalysts, and marked swelling of the polymer chains with appropriate solvents).

Before polymerization, a mixture of compatible organic substances, chemically inert, is added to the monomers. During polymerization, this "porogenic" mixture regulates the molecular weights of the growing monomeric chains by causing precipitation when the chain length exceeds solubility. The copolymer precipitates in the form of microspheres, which, in the presence of the last nonreacted monomers, stably bind to each other. This copolymer is thus composed of numerous microspheres, and the empty space between one microsphere and another constitutes porosity.

Another function of the porogenic mixture is to avoid cross-linking of the macromolecules, allowing a uniform reticulation. Cross-linking inside the porous cavities would alter them, so that the specific properties of the resin, *i.e.*, velocity of diffusion, particularly important in the macroanion exchange, would be lost.

To achieve porosity in cholpor, several methods were tried (6). One method used squalane[3]–1-octanol[3]–paraffin[3] (mp 42–45°) (70:20:10), with the ratio of monomers to porogens being 1.2:1.1. The porogenic mixture, following copolymerization, was removed by prolonged extraction in a soxhlet extractor with a swelling solvent mixture (ether[3]–methylene chloride[3]). Proof of the completed extraction was provided by the final measurement of the extracted porogenic mixture. The general charac-

[1] Cuemid, courtesy of Merck Sharp & Dohme, Rahway, N.J.
[2] Colestid, courtesy of The Upjohn Co., Kalamazoo, Mich.
[3] Carlo Erba, Milan, Italy.
[4] Merck, Darmstadt, West Germany.
[5] Packard Instruments, Downers Grove, Ill.

0022-3549/78/1200-1695$01.00/0
© 1978, American Pharmaceutical Association

(1976).
(3) R. A. Winkle, P. J. Meffin, J. W. Fitzgerald, and D. C. Harrison, *Circulation*, **54**, 884 (1976).
(4) D. J. Coltart, T. B. Berndt, R. Kernuff, and D. C. Harrison, *Am. J. Cardiol.*, **34**, 35 (1974).
(5) P. J. Meffin, S. R. Harapat, and D. C. Harrison, *J. Pharm. Sci.*, **66**, 588 (1977).
(6) D. L. Horrochs "Applications of Liquid Scintillation Counting," Academic, New York, N.Y., 1974, p. 210.

ACKNOWLEDGMENTS

The authors thank Dr. Robert Ronfeld for his comments and Ms. Deborah Higgins and Ms. Trudy DiBello for assistance.

New Microporous Cholestyramine Analog for Treatment of Hypercholesterolemia

RENATO DE SIMONE *, FRANCO CONTI ‡, M. ROSA LOVATI ‡, MARINA SIRTORI ‡, ENZO COCUZZA *, and CESARE R. SIRTORI ‡x

Received October 12, 1977, from the **Spemsa, Florence, Italy, and the* ‡*Center E. Grossi Paoletti, University of Milano, Via A. del Sarto 21, 20129 Milano, Italy.* Accepted for publication May 5, 1978.

Abstract □ A new, microporous, uniformly reticulated preparation of cholestyramine is described. The preparation, cholpor, has a higher exchange capacity for chloride than does cholestyramine and swells very little in water. It is 15–20% more potent than cholestyramine in the *in vitro* binding of sodium cholate; moreover, the binding velocity is considerably higher than that of cholestyramine. Colestipol hydrochloride, also used as a reference anion-exchange resin, is about half as potent as the other two resins; its binding velocity is similar to that of cholpor. Cholpor may be prepared in a suspension form of good palatability. Preliminary clinical findings in short-term trials showed a cholesterol-lowering effect similar to that of cholestyramine with lower doses and fewer side effects.

Keyphrases □ Cholestyramine analog—cholpor synthesized, *in vitro* binding of sodium cholate and cholesterol lowering effect in humans evaluated □ Cholpor—cholestyramine analog synthesized, *in vitro* binding of sodium cholate and cholesterol lowering effect in humans evaluated □ Antihypercholesterolemic activity—cholestyramine analog synthesized, *in vitro* binding of sodium cholate and cholesterol lowering effect in humans evaluated

Lowering of plasma cholesterol appears to be a major goal in the prevention of atherosclerosis (1). Anion-exchange resins are the most effective pharmaceutical agents in the clinical management of hypercholesterolemia (2); cholestyramine[1], a styrene-divinylbenzene copolymer with a free quaternary ammonium group, is currently the most widely used agent. Although the clinical efficacy of cholestyramine is not disputed, its unpleasant taste as well as the difficulty encountered by patients in mixing it with water upon each administration makes continued treatments rather difficult (3). The newer anion-exchange resin, colestipol hydrochloride[2] (4), is better tolerated but also requires several daily extemporary preparations.

This report describes a new microporous analog of cholestyramine, cholpor, which may be prepared in suspension form, is of good palatability, and is easily accessible to the patient.

EXPERIMENTAL

Analytical Methods—Swelling of the resins in water was determined by adding 1 g of cholestyramine[1], colestipol hydrochloride[2], or cholpor to enough water (10–30 ml) to provide a suspension. After 24 hr, the suspension was shaken and the volume of resin under water was determined.

Exchange Capacity—Chloride-ion absorption from a 5% NaCl solution, after regeneration of the resin with a 4% NaOH[3] solution, was measured by titrating with 0.1 *N* HCl[3] the sodium hydroxide resulting from the resin and sodium chloride reaction.

Pharmacology—Binding of sodium cholate[4] *in vitro* was estimated essentially according to Whiteside *et al.* (5). Preparations of cholestyramine (100–200 mesh), colestipol hydrochloride (60–150 mesh), and cholpor (60–80 mesh) were added to scintillation vials[5] containing 10 ml of 0.02 *M* phosphate buffer with 2 mg of sodium cholate/ml.

The significance of the differences in the various experiments was determined by the Student *t* test.

RESULTS AND DISCUSSION

Chemistry—Cholpor (6) is obtained by starting with a porous matrix. Porosity is first achieved during preparation of the copolymer. During chloromethylation, porosity is protected by maintaining reaction conditions that do not alter the physical structure of the matrix (low reaction temperature, low acidity of the catalysts, and marked swelling of the polymer chains with appropriate solvents).

Before polymerization, a mixture of compatible organic substances, chemically inert, is added to the monomers. During polymerization, this "porogenic" mixture regulates the molecular weights of the growing monomeric chains by causing precipitation when the chain length exceeds solubility. The copolymer precipitates in the form of microspheres, which, in the presence of the last nonreacted monomers, stably bind to each other. This copolymer is thus composed of numerous microspheres, and the empty space between one microsphere and another constitutes porosity.

Another function of the porogenic mixture is to avoid cross-linking of the macromolecules, allowing a uniform reticulation. Cross-linking inside the porous cavities would alter them, so that the specific properties of the resin, *i.e.*, velocity of diffusion, particularly important in the macroanion exchange, would be lost.

To achieve porosity in cholpor, several methods were tried (6). One method used squalane[3]–1-octanol[3]–paraffin[3] (mp 42–45°) (70:20:10), with the ratio of monomers to porogens being 1.2:1.1. The porogenic mixture, following copolymerization, was removed by prolonged extraction in a soxhlet extractor with a swelling solvent mixture (ether[3]–methylene chloride[3]). Proof of the completed extraction was provided by the final measurement of the extracted porogenic mixture. The general charac-

[1] Cuemid, courtesy of Merck Sharp & Dohme, Rahway, N.J.
[2] Colestid, courtesy of The Upjohn Co., Kalamazoo, Mich.
[3] Carlo Erba, Milan, Italy.
[4] Merck, Darmstadt, West Germany.
[5] Packard Instruments, Downers Grove, Ill.

0022-3549/78/1200-1695$01.00/0
© 1978, American Pharmaceutical Association

Table I—Characteristics of One Preparation of Cholpor Compared with Cholestyramine and Colestipol Hydrochloride

	Cholpor	Cholestyramine	Colestipol Hydrochloride
Copolymer type	Styrene	Styrene	Epoxide
Monomer	Styrene-divinylbenzene	Styrene-divinylbenzene	Diethylenetriamine-epichlorohydrin
Reticulation[a], % wt.	11.3	2	Not significant
Exchange capacity for chloride, mEq/g	4.5	2.9–3.1	4.5
Mean diameter of pores[b], Å	~190	0	0
Specific surface[c], m^2/g	82	<1	<1
Real density[d], g/cm^3	1.11	1.09	1.07
Apparent density[e], g/cm^3	0.50	0.44	0.60
Porosity[f], cm^3/g	0.6	0	0
Granulometry, μ	250–177	150–80	250–100

[a] Percentage in weight of the divinylbenzene monomer in the total mixture of monomers. [b] Reference 7. [c] Reference 8. [d] Determined with a helium–air comparison pycnometer, model 930, Beckman Instruments, Palo Alto, Calif. [e] Determined with an SM3 dilatometer (3-mm capillary). [f] Difference between the reciprocals of apparent density and real density.

teristics of this preparation, as well as those of cholestyramine and colestipol hydrochloride, are reported in Table I.

The exchange capacity for chloride of different preparations of cholpor ranged between 3.9 and 5.7 mEq/g; this capacity exceeded that found with several preparations of cholestyramine, *i.e.*, 2.9–3.1 mEq/g. The exchange capacity of colestipol hydrochloride was similar to that of cholpor, *i.e.*, 4.5 mEq/g. Swelling of cholpor in water was about one-fifth that found with cholestyramine and about one-half that of colestipol hydrochloride (Fig. 1).

Pharmacology—In the first experiment (Fig. 2), a fixed amount of sodium cholate (2 mg/ml) and a fixed amount of each resin (30 mg) were incubated; the pH of the buffer solution was varied from 5 to 8. In the second experiment (Fig. 3), increasing amounts of each resin were added to the sodium cholate solution (pH 6). In the third experiment (Fig. 4), the percentage of binding was measured at successive time intervals after addition of 30 mg of each resin to the sodium cholate solution (pH 6).

Incubations always were carried out at 25° in a Dubnoff-type bath[6]. Unbound cholate was determined by filtering the content of each vial on paper[7] and measuring cholate spectrophotometrically[8] according to Kier (9).

Binding of sodium cholate *in vitro* was significantly higher for cholpor, as compared to cholestyramine and colestipol hydrochloride, in all experiments (Figs. 2–4). Colestipol had a binding capacity of about one-half that of the other two resins, thus confirming previous data (10), whereas cholpor was about 15–20% more potent than cholestyramine. The binding capacity of all three resins was scarcely modified by the pH of the buffer solution (Fig. 2).

Cholestyramine and cholpor differed in the velocity of binding *in vitro*. Whereas cholpor reached 80% of its maximal binding capacity after just 2 min and 100% after 10 min, the maximal binding for cholestyramine was found after 20 min of incubation (Fig. 4). Colestipol hydrochloride had a binding velocity similar to that of cholpor.

Pilot Clinical Study—After the chronic toxicity tests in animals, a 3-week clinical trial in patients was designed to evaluate both the hypocholesterolemic activity and the general acceptance of cholpor. Twenty patients with type IIA hyperlipoproteinemia (11) were selected (five females and 15 males, ages 37–72 years). All had been following a therapeutic diet, low in cholesterol and saturated fats (12), for at least 3 months and had stable weights. Eight out of the 20 patients had been treated previously with cholestyramine but had discontinued because of side effects.

Cholpor was made available in plastic ampuls containing 3 g of resin suspended in a solution of sorbitol[3] (3.4 g), yellow orange[9] (E 102 and E 124) (2.0 mg), and *p*-hydroxybenzoic acid esters[10] (14 mg) in demineralized water to a final volume of 17 ml. The drug was given immediately before meals. All patients were started with 1 ampul/day. As suggested by Farah *et al.* (13), plasma cholesterol (14) and triglycerides (15) were estimated twice weekly and eventual dose increases were decided at the end of each week; the dose was not increased if plasma cholesterol levels had dropped more than 20%. One patient, with severe familial hypercholesterolemia, was treated in a metabolic ward; the dose was initially 9 g/day and gradually was increased to 15 g/day.

This short-term clinical trial indicated an excellent palatability of the resin. Only two patients dropped out of the study, one (5%) because of

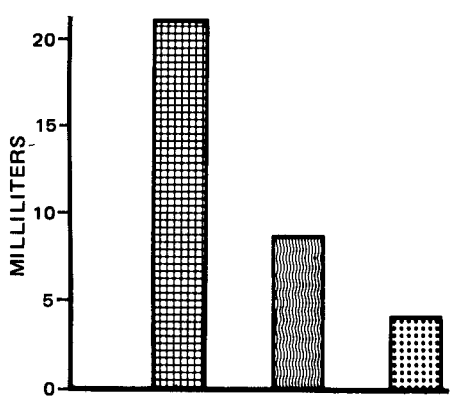

Figure 1—*Swelling of cholestyramine (left), colestipol hydrochloride (middle), and cholpor (right) after 24 hr in water. One gram of each resin was placed in an appropriate amount of water, and the volume was determined after 24 hr. Each column gives the mean volume (milliliters of water) of three different lots of each resin.*

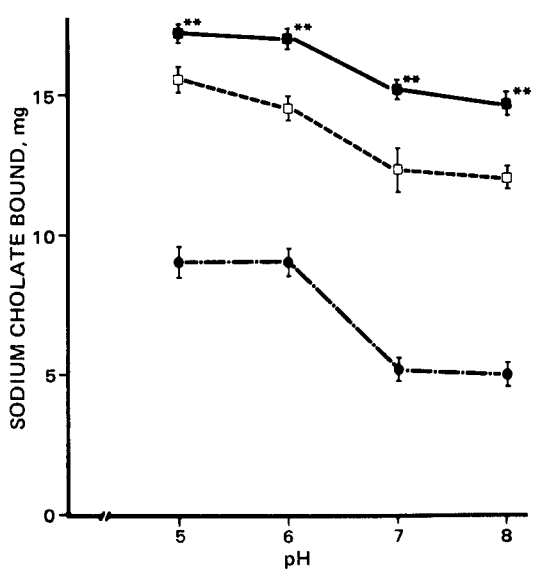

Figure 2—*Milligrams of sodium cholate bound by each resin after 30 min (2 mg of cholate/ml in 10 ml of 0.02 M phosphate buffer with 30 mg of each resin). The pH of the solution was appropriately changed before incubation. Each point gives the mean ± SD from six determinations. Key: ■, cholpor; □, cholestyramine; ●, colestipol hydrochloride; ★, $p < 0.05$; and ★★, $p < 0.01$ as compared to cholestyramine.*

[6] Bagno Valentini, Milan, Italy.
[7] Whatman type 42 ashless filter papers.
[8] Gilford model 2400 spectrophotometer, Gilford Instrument Laboratories, Oberlin, Ohio.

[9] Curt Georgi, Milan, Italy.
[10] Paracombin, Formenti Boots, Milan, Italy.

Table II—Results of a 3-Week Study with Cholpor in Hypercholesterolemic Patients

Final Daily Dose, g	Number of Patients	Age Range, years	Pretreatment Lipid Levels[a], mg/dl		Posttreatment[a], mg/dl	
			Plasma Cholesterol[b]	Triglycerides[b]	Cholesterol	Triglycerides
6	4	37–68	265.7 (7.1)	129.2 (27.2)	196.5 (16.3)[c]	135.0 (20.3)
9	13	37–72	317.4 (17.3)	145.7 (14.0)	240.6 (17.7)[d]	148.0 (14.0)
15	1	49	480	130	242	190

[a] Mean (*SEM*). [b] The mean of three pretreatment determinations was used for each patient. [c] $p < 0.01$ *versus* pretreatment. [d] $p < 0.001$ *versus* pretreatment.

constipation (she had the same symptom with cholestyramine previously) and the other for family reasons. A transient, very mild constipation was noted in three more patients. The final results (Table II) show that 6 g of resin/day was sufficient in four cases to achieve a cholesterol reduction of more than 20%. A dose of 9 g/day (given in two or three daily administrations, according to the patient's convenience) was adequate in 13 cases. The case treated in the hospital had a normalization of serum cholesterol levels with 15 g/day. Many of the patients have continued treatment for longer periods, generally maintaining the results achieved in this short trial.

Cholpor was prepared with the objective of eliminating some major problems of the available cholestyramine preparations, *i.e.*, bad taste and smell, relatively low activity, and constipating effect. Bad taste, mostly due to the release of trimethylamine groups, is reduced upon hydration, when the concentration of active groups is lower than in the dry state, and may be eliminated by the addition of a binding agent (16). The activity of cholestyramine, on the other hand, may be improved if all functional groups are readily accessible. A microporous, very uniformly reticulated resin, by making functional groups wholly available, may increase the velocity of the reaction.

Constipation is also probably a consequence of the relatively low activity of cholestyramine; the high doses employed in therapy require, in fact, large volumes of liquid (4 g corresponds to a final volume of approximately 85 ml). Probably the bulky masses of hydrated resin in the intestine, following the normal draining of liquid, leave a solid residue that the intestinal contractions do not easily eliminate.

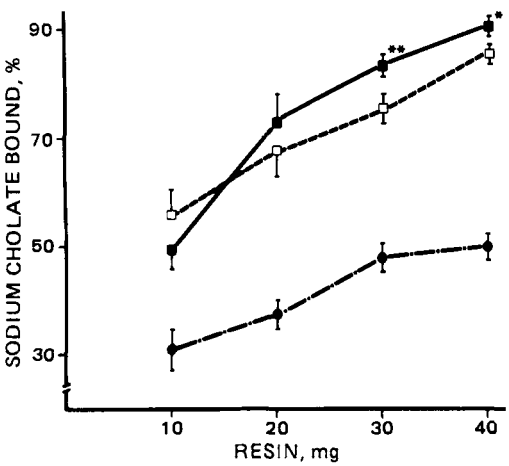

Figure 3—*Percentage of binding of sodium cholate (2 mg/ml in 10 ml of 0.02 M phosphate buffer, pH 6) after 30 min of incubation in the presence of increasing amounts of each resin (means ± SD of six determinations). Key: same as Fig. 2.*

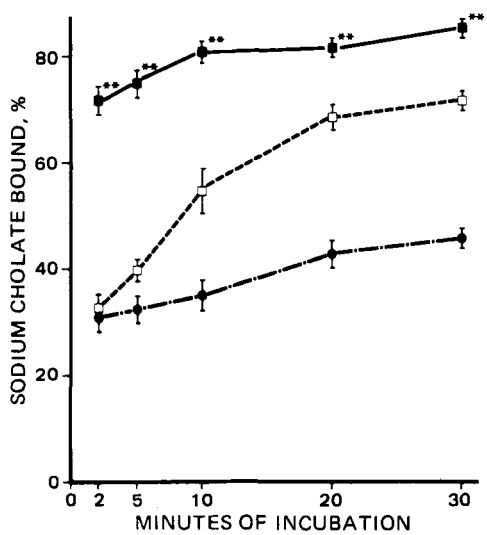

Figure 4—*Percentage of binding of sodium cholate (conditions similar to Fig. 3) in the presence of 30 mg of each resin after increasing intervals of incubation (means ± SD of six determinations). Key: same as Fig. 2.*

CONCLUSIONS

Results obtained with cholpor confirm that a porous, uniformly reticulated preparation of cholestyramine may be better suited for clinical use in hypercholesterolemia than the parent preparation. Cholpor has a higher exchange capacity for chloride than cholestyramine and a remarkably higher *in vitro* capacity for bile acids; it also binds bile acids *in vitro* significantly more rapidly than does cholestyramine. Moreover, possibly because of its uniform reticulation, cholpor swells very little in water, allowing the preparation of suspensions for clinical use.

The reported short-term clinical trial showed that relatively low doses of cholpor may be sufficient for the treatment of the most frequent forms of hypercholesterolemia. With these dosages, constipation is seldom encountered. Doses in the general range of cholestyramine may be necessary for the more severe forms. Longer studies will be needed to confirm both the efficacy and safety of cholpor.

Cholpor may provide a solution to some of the biggest obstacles in a wide-scale administration of anion-exchange resins for hypercholesterolemia. Its satisfactory palatability, ready availability in suspension form, and low constipating effect, in addition to the rapid *in vitro* activity which may allow administration immediately before meals, are possibly relevant for its use even for relatively mild forms of hypercholesterolemia where physicians may find cholestyramine powder too demanding for the patient.

REFERENCES

(1) D. S. Fredrickson, *Br. Med. J.*, **2**, 187 (1971).

(2) R. I. Levy, *Ann. Intern. Med.*, **77**, 267 (1972).

(3) H. R. Casdorph, *Vasc. Dis.*, **4**, 305 (1967).

(4) C. J. Glueck, S. Ford, Jr., D. Scheel, and P. Steiner, *J. Am. Med. Assoc.*, **222**, 676 (1972).

(5) C. H. Whiteside, H. B. Fluckinger, and H. P. Sarett, *Proc. Soc. Exp. Biol. Med.*, **121**, 153 (1966).

(6) Viridis, Spemsa, Belgium pat. 855,044 (Sept. 16, 1977).

(7) L. C. Drake and M. L. Ritter, *Ind. Eng. Chem. Anal. Ed.*, **17**, 786 (1945).

(8) S. Brunauer, "Physical Adsorptions," vol. 1, Princeton University Press, Princeton, N.J., 1943.

(9) C. L. Kier, *J. Lab. Clin. Med.*, **40**, 755 (1952).

(10) T. M. Parkinson, K. Gundersen, and N. A. Nelson, *Atherosclerosis*, **11**, 531 (1970).

(11) J. L. Beaumont, L. A. Carlson, G. Cooper, Z. Fejfar, D. S. Fredrickson, and T. Strasser, *Bull. W.H.O.*, **43**, 891 (1970).

(12) R. I. Levy, M. Bonnell, and N. D. Ernst, *J. Am. Diet. Assoc.*, **58**, 406 (1977).

(13) J. R. Farah, P. O. Kwiterovich, and C. A. Neill, *Lancet*, **1**, 59 (1977).

(14) W. D. Block, J. Jarrett, and J. B. Levine, in "Technicon Symposia

on Automation in Analytical Chemistry," Mediad Inc., New York, N.Y., 1965, p. 345.
(15) R. P. Noble and F. M. Campbell, *Clin. Chem.*, **16**, 166 (1970).
(16) R. Kunin, "Ion Exchange Resins," 2nd ed., Wiley, New York, N.Y., 1958.

ACKNOWLEDGMENTS

Prof. Rodolfo Paoletti is gratefully acknowledged for helpful advice and discussion. Miss Aurora Maccalli and Miss Mariella Parlavecchia were responsible for carefully editing the text.

Crystal and Molecular Structure of Quinidine

RUTH DOHERTY *, WALTER R. BENSON ‡x, MILLARD MAIENTHAL ‡, and JAMES McD. STEWART *

Received January 25, 1978, from the **Chemistry Department and Computer Science Center, University of Maryland, College Park, MD 20742,* and the ‡*Division of Drug Chemistry, Food and Drug Administration, Washington, DC 20204.* Accepted for publication April 27, 1978.

Abstract □ The structure of the free base quinidine was determined by single crystal X-ray diffraction. Quinidine crystallizes from absolute ethanol as the ethanolate, with the molecular formula $C_{20}H_{24}N_2O_2 \cdot C_2H_6O$ and molar mass 370.491 units. It crystallizes in the orthorhombic space group $P2_12_12_1$ with unit cell dimensions a = 1321.1(3), b = 989.3(2), and c = 1651.5(3) pm. The measured density was 1.15 g/cm^3; the density calculated for $Z = 4$ was 1.164 g/cm^3. The diffraction data were collected by using MoKα radiation. A final R value of 0.055 was obtained. Evidence for intermolecular hydrogen bonding was found. The crystal analysis is in agreement with the structure proposed by other methods. The absolute configuration is based on the published structure of 10-bromo-10,11-dihydroepiquinidine.

Keyphrases □ Quinidine—crystal and molecular structure, X-ray diffraction determination □ X-ray diffraction—determination, crystal and molecular structure of quinidine □ Cardiac depressants—quinidine, crystal and molecular structure determined by X-ray diffraction

The drug substance quinidine (I) contains several naturally occurring impurities (1). Commercial samples of I contain 3–22.1% of 10,11-dihydroquinidine (II). Compounds I and II are both potent antiarrhythmic agents, II being significantly more effective than I (2). Although structures for I and II have been determined by other techniques (3–7), no absolute configuration studies by single crystal X-ray diffraction have been reported. Because of the therapeutic significance of I and II, X-ray diffraction studies were undertaken.

One crystal study (8) was reported for 10-bromo-10,11-dihydroepiquinidine (III), a derivative of 10,11-dihydroepiquinidine (IV). Compounds II and IV differ only in the configuration about the carbon bearing the hydroxyl group. In the study of III, evidence was found for intramolecular hydrogen bonding between the hydroxyl group and the nitrogen in the quinuclidine ring. From models of II and IV, it was concluded that intramolecular hydrogen bonding in II and I is less favorable than in III and IV because of steric interactions of the quinoline and

Table I—Crystal Structure Analysis of Quinidine Ethanolate ($C_{20}H_{24}N_2O_2 \cdot C_2H_6O$)

Property	Analysis
Unit cell dimensions	a = 1321.1(3), b = 989.3(2), c = 1651.5(3) pm
Space group	$P2_12_12_1$
Density, g/cm^3	1.15 (measured), 1.164 ($Z = 4$) (calculated)
Radiation	MoKα
Number of observations	Total number of reflections = 1404, number of reflections less than 3σ above background = 586
Scattering factors	C,N,O (Ref. 11); H (Ref. 12)
Method of solution	Direct methods for partial structure, translation function, Fourier transform to complete
Method of refinement	Full-matrix least-squares
Weights	Unit
Programs used	XRAY76
Final R value ($\Sigma \Delta F/\Sigma\|F_0\|$)	0.055
Final difference synthesis	No significant peaks
Atomic coordinates	See Table II
Bond lengths	See Fig. 1
Bond angles	See Fig. 2
Hydrogen bonds between	O-12–H-12- - -N-1 O-9–H-91- - -N-1′

Distance from	Distance, pm
O-12–N-1	281(1)
H-12–N-1	160(8)
O-9–N-1′	279(1)
H-91–N-1′	243(8)

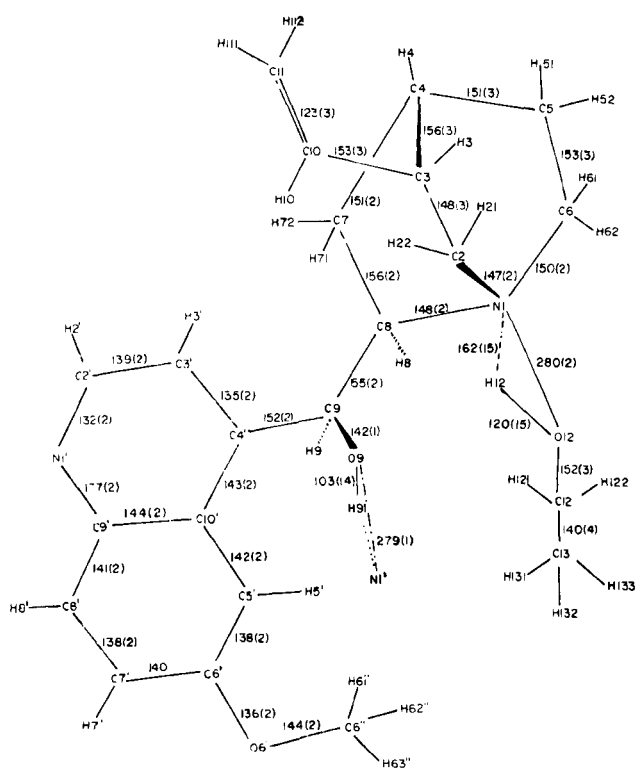

Figure 1—*Bond lengths (pm) for quinidine ethanolate.*

0022-3549/78/1200-1698$01.00/0
© 1978, American Pharmaceutical Association

on Automation in Analytical Chemistry," Mediad Inc., New York, N.Y., 1965, p. 345.
(15) R. P. Noble and F. M. Campbell, *Clin. Chem.*, **16**, 166 (1970).
(16) R. Kunin, "Ion Exchange Resins," 2nd ed., Wiley, New York, N.Y., 1958.

ACKNOWLEDGMENTS

Prof. Rodolfo Paoletti is gratefully acknowledged for helpful advice and discussion. Miss Aurora Maccalli and Miss Mariella Parlavecchia were responsible for carefully editing the text.

Crystal and Molecular Structure of Quinidine

RUTH DOHERTY *, WALTER R. BENSON ‡x, MILLARD MAIENTHAL ‡, and JAMES McD. STEWART *

Received January 25, 1978, from the **Chemistry Department and Computer Science Center, University of Maryland, College Park, MD 20742,* and the ‡*Division of Drug Chemistry, Food and Drug Administration, Washington, DC 20204.* Accepted for publication April 27, 1978.

Abstract □ The structure of the free base quinidine was determined by single crystal X-ray diffraction. Quinidine crystallizes from absolute ethanol as the ethanolate, with the molecular formula $C_{20}H_{24}N_2O_2 \cdot C_2H_6O$ and molar mass 370.491 units. It crystallizes in the orthorhombic space group $P2_12_12_1$ with unit cell dimensions a = 1321.1(3), b = 989.3(2), and c = 1651.5(3) pm. The measured density was 1.15 g/cm^3; the density calculated for $Z = 4$ was 1.164 g/cm^3. The diffraction data were collected by using MoKα radiation. A final R value of 0.055 was obtained. Evidence for intermolecular hydrogen bonding was found. The crystal analysis is in agreement with the structure proposed by other methods. The absolute configuration is based on the published structure of 10-bromo-10,11-dihydroepiquinidine.

Keyphrases □ Quinidine—crystal and molecular structure, X-ray diffraction determination □ X-ray diffraction—determination, crystal and molecular structure of quinidine □ Cardiac depressants—quinidine, crystal and molecular structure determined by X-ray diffraction

The drug substance quinidine (I) contains several naturally occurring impurities (1). Commercial samples of I contain 3–22.1% of 10,11-dihydroquinidine (II). Compounds I and II are both potent antiarrhythmic agents, II being significantly more effective than I (2). Although structures for I and II have been determined by other techniques (3–7), no absolute configuration studies by single crystal X-ray diffraction have been reported. Because of the therapeutic significance of I and II, X-ray diffraction studies were undertaken.

One crystal study (8) was reported for 10-bromo-10,11-dihydroepiquinidine (III), a derivative of 10,11-dihydroepiquinidine (IV). Compounds II and IV differ only in the configuration about the carbon bearing the hydroxyl group. In the study of III, evidence was found for intramolecular hydrogen bonding between the hydroxyl group and the nitrogen in the quinuclidine ring. From models of II and IV, it was concluded that intramolecular hydrogen bonding in II and I is less favorable than in III and IV because of steric interactions of the quinoline and

Table I—Crystal Structure Analysis of Quinidine Ethanolate ($C_{20}H_{24}N_2O_2 \cdot C_2H_6O$)

Property	Analysis
Unit cell dimensions	a = 1321.1(3), b = 989.3(2), c = 1651.5(3) pm
Space group	$P2_12_12_1$
Density, g/cm^3	1.15 (measured), 1.164 ($Z = 4$) (calculated)
Radiation	MoKα
Number of observations	Total number of reflections = 1404, number of reflections less than 3σ above background = 586
Scattering factors	C,N,O (Ref. 11); H (Ref. 12)
Method of solution	Direct methods for partial structure, translation function, Fourier transform to complete
Method of refinement	Full-matrix least-squares
Weights	Unit
Programs used	XRAY76
Final R value ($\Sigma \Delta F/\Sigma\|F_0\|$)	0.055
Final difference synthesis	No significant peaks
Atomic coordinates	See Table II
Bond lengths	See Fig. 1
Bond angles	See Fig. 2
Hydrogen bonds between	O-12–H-12- - -N-1 O-9–H-91- - -N-1′

Distance from	Distance, pm
O-12–N-1	281(1)
H-12–N-1	160(8)
O-9–N-1′	279(1)
H-91–N-1′	243(8)

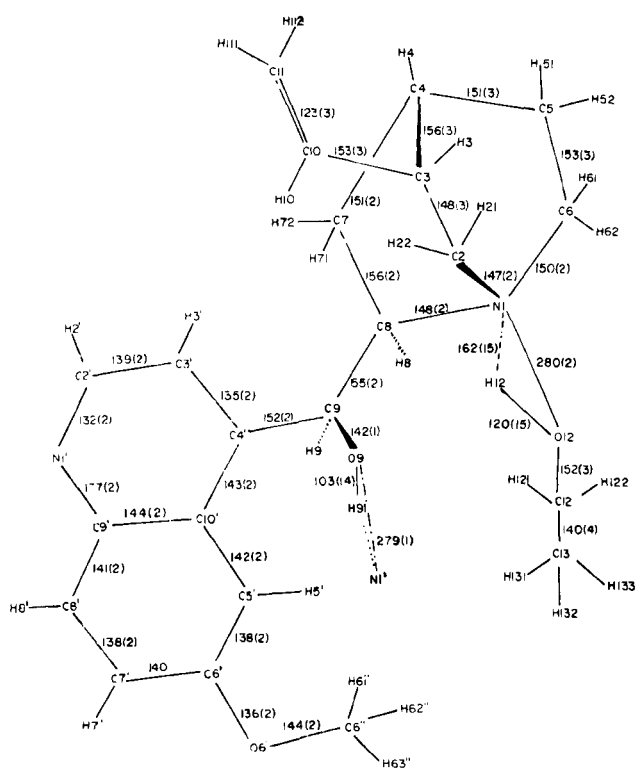

Figure 1—*Bond lengths (pm) for quinidine ethanolate.*

0022-3549/78/1200-1698$01.00/0
© 1978, American Pharmaceutical Association

Table II—Fractional Coordinates, Temperature Factors ($pm^2 \times 10^{-2}$), and Estimated Standard Deviations (in Parentheses)[a]

Atom	x	y	z	U_{11} or U	U_{22}	U_{33}	U_{12}	U_{13}	U_{23}
C-6″	0.6924(12)	0.8118(15)	0.5846(11)	7.7(1.0)	5.7(0.9)	13.8(1.4)	−1.5(0.9)	−1.3(1.1)	1.6(1.0)
O-6′	0.6142(7)	0.8031(8)	0.5242(6)	7.5(0.7)	4.0(0.5)	10.2(0.7)	−1.5(0.5)	−0.3(0.6)	0.6(0.5)
N-1′	0.4388(8)	0.3084(12)	0.4433(7)	5.9(0.7)	5.6(0.7)	8.6(0.8)	−0.6(0.7)	−1.8(0.6)	−0.4(0.7)
C-2′	0.4765(11)	0.1882(14)	0.4714(9)	6.3(1.0)	4.9(0.9)	9.1(1.1)	−1.5(0.8)	−1.4(0.9)	−0.6(0.9)
C-3′	0.5597(11)	0.1811(14)	0.5231(9)	5.6(0.9)	4.9(0.8)	8.5(1.0)	−0.2(0.8)	−1.0(0.8)	0.1(0.8)
C-4′	0.6078(9)	0.2966(12)	0.5479(7)	5.0(0.7)	4.4(0.8)	5.4(0.8)	0.3(0.7)	0.7(0.7)	−0.1(0.7)
C-5′	0.6194(8)	0.5536(12)	0.5375(7)	3.5(0.8)	4.5(0.7)	6.6(0.9)	−0.2(0.7)	0.3(0.7)	−0.2(0.7)
C-6′	0.5791(10)	0.6741(14)	0.5071(8)	4.4(0.9)	6.2(1.0)	7.4(0.9)	−1.0(0.7)	0.0(0.7)	0.5(0.8)
C-7′	0.4964(11)	0.6735(14)	0.4544(9)	6.1(0.9)	5.4(0.9)	8.4(1.1)	0.8(0.8)	0.7(0.9)	1.4(0.8)
C-3′	0.4505(10)	0.5513(15)	0.4328(9)	5.2(0.8)	6.9(0.9)	6.3(0.9)	−0.1(0.8)	−0.9(0.7)	1.4(0.8)
C-9′	0.4862(10)	0.4254(13)	0.4645(8)	5.4(0.9)	5.5(0.8)	6.4(0.9)	0.3(0.7)	−0.2(0.7)	0.9(0.8)
C-10′	0.5735(10)	0.4225(12)	0.5169(8)	5.2(0.9)	4.7(0.8)	5.6(0.8)	−0.4(0.7)	0.0(0.7)	0.5(0.7)
C-9	0.6939(9)	0.2917(11)	0.6086(7)	4.5(0.7)	4.0(0.7)	6.3(0.8)	0.5(0.6)	−0.2(0.7)	−0.3(0.7)
O-9	0.7394(6)	0.1593(7)	0.6095(5)	5.2(0.5)	4.6(0.5)	7.9(0.6)	0.2(0.4)	−0.2(0.5)	0.4(0.5)
N-1	0.7290(9)	0.3725(11)	0.7506(6)	6.4(0.7)	6.9(0.7)	6.7(0.8)	0.0(0.6)	−0.5(0.7)	−0.4(0.6)
C-2	0.7806(13)	0.2542(18)	0.7875(10)	9.3(1.2)	10.9(1.3)	7.8(1.1)	2.8(1.1)	−1.7(1.0)	−0.5(1.0)
C-3	0.7126(18)	0.1678(19)	0.8374(10)	15.2(1.9)	9.0(1.3)	7.3(1.2)	2.6(1.4)	−0.3(1.2)	1.7(1.0)
C-4	0.6024(16)	0.2182(19)	0.8220(10)	15.0(1.8)	8.9(1.3)	9.0(1.3)	−1.9(1.4)	6.2(1.3)	−0.9(1.1)
C-5	0.5907(16)	0.3645(19)	0.8525(10)	13.3(1.6)	11.1(1.4)	7.9(1.1)	−0.5(1.3)	2.7(1.2)	−1.0(1.0)
C-6	0.6772(15)	0.4503(16)	0.8172(10)	12.0(1.4)	7.3(1.0)	8.7(1.2)	−0.2(1.1)	0.5(1.1)	−2.4(1.0)
C-7	0.5828(11)	0.2172(15)	0.7316(8)	8.0(1.1)	7.2(1.0)	7.1(0.9)	−1.6(0.9)	2.0(0.9)	0.2(0.9)
C-8	0.6500(9)	0.3317(13)	0.6921(8)	4.6(0.8)	5.1(0.7)	7.2(0.8)	0.5(0.7)	−0.5(0.7)	0.4(0.7)
C-10	0.7273(31)	0.0125(20)	0.8252(13)	40.0(4.8)[b]	8.4(1.4)	9.6(1.5)	3.3(2.2)	1.2(2.5)	2.6(1.2)
C-11	0.7034(32)	−0.0733(23)	0.8766(13)	50.1(5.6)[b]	9.7(1.5)	10.8(1.8)	−0.7(2.7)	8.6(2.8)	1.3(1.4)
C-12	0.9439(18)	0.5832(23)	0.7222(16)	11.9(1.7)	9.7(1.5)	18.5(2.2)	−1.2(1.4)	0.7(1.7)	3.1(1.7)
C-13	0.9077(25)	0.7034(31)	0.7587(17)	22.1(2.9)	16.0(2.2)	18.4(2.6)	−4.3(2.5)	−2.3(2.4)	6.4(2.3)
O-12	0.8572(9)	0.5497(13)	0.6646(7)	11.8(1.0)	12.2(1.0)	10.5(0.8)	−4.7(0.9)	−2.2(0.8)	0.5(0.8)
H-2′	0.44[c]	0.11	0.46	9.5[d]					
H-3′	0.59	0.09	0.54						
H-5′	0.68	0.55	0.57						
H-7′	0.47	0.76	0.44						
H-8′	0.38	0.55	0.40						
H-62″	0.67	0.77	0.64						
H-63″	0.71	0.91	0.60						
H-61″	0.75	0.76	0.56						
H-9	0.74	0.36	0.59						
H-91	0.81	0.17	0.59						
H-21	0.84	0.28	0.83						
H-22	0.80	0.20	0.74						
H-3	0.72	0.18	0.89						
H-4	0.55	0.16	0.84						
H-51	0.59	0.37	0.92						
H-52	0.53	0.40	0.83						
H-61	0.73	0.47	0.85						
H-62	0.65	0.54	0.80						
H-71	0.59	0.13	0.70						
H-72	0.51	0.24	0.71						
H-8	0.60	0.41	0.68						
H-10	0.74	0.00	0.79						
H-111	0.70	−0.17	0.86						
H-112	0.70	−0.05	0.92						
H-12	0.81	0.46	0.70						
H-121	1.00	0.60	0.68						
H-122	0.96	0.50	0.76						
H-131	0.85	0.67	0.79						
H-132	0.86	0.78	0.72						
H-133	0.96	0.73	0.79						

[a] The form of the anisotropic thermal parameters is $\exp[-2\pi^2(U_{11}h^2a^{*2} + \ldots + 2U_{23}klb^*c^*)]$. [b] There is evidence for disorder in the C-10–C-11 side chain. [c] All hydrogen values are ±1 in the last figure. [d] No attempt was made to refine the hydrogen thermal parameters. All were set to 9.5.

quinuclidine rings in II. These same interactions occur in I.

The crystal structure analysis for I is in agreement with the structure proposed by other methods. The structure of II was not determined since it would be a duplication of the work for I.

EXPERIMENTAL

Because of impurities (1), the commercial samples of I could not be used as received. Compound I was prepared free of natural II by the method of Smith *et al.* (1). Mercuric acetate was added to I; II was separated from this addition product, and I was regenerated by removal of the mercuric acetate. Compound I was recrystallized from absolute ethanol, mp 174°, as determined by differential thermal analysis[1] [lit. (1) mp 174–175°].

The crystal used for X-ray analysis was grown in 95% ethanol. Crystals similarly grown were heated in a thermal balance[2], and the weight loss of the crystal at 110° corresponded to a loss of one molecule of ethanol for each molecule of quinidine. The IR spectrum[3] bands at 910 and 990 cm^{-1} for the CH=CH (9) are in agreement with the proposed structure. For other tests performed, see Refs. 1 and 10.

Compounds I and II undergo photodecomposition under laboratory light (1). However, they were stable when kept refrigerated and in the dark. After standing for several days, the crystals of both I and II crumbled to powder, probably because of the loss of the ethanol of crystallization.

The X-ray crystallographic analysis[4,5] of I is summarized in Tables I and II. The bond lengths and angles are shown in Figs. 1 and 2. A view of the molecule and of a hydrogen-bonded fragment of a symmetrically

[1] DuPont thermal analyzer model 990.

[2] DuPont thermal gravimetric analyzer model 951.
[3] Perkin-Elmer model 621 recording IR spectrophotometer.
[4] Picker automated FACS I diffractometer.
[5] XRAY76 is part of the XRAY system of crystallographic programs, Technical Report TR-446 Computer Science Center, University of Maryland, Mar. 1976.

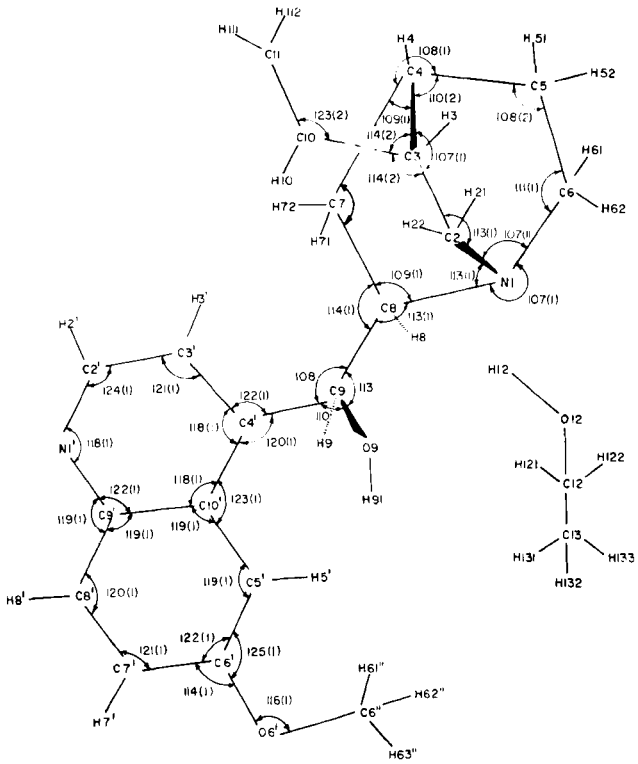

Figure 2—*Bond angles for quinidine ethanolate.*

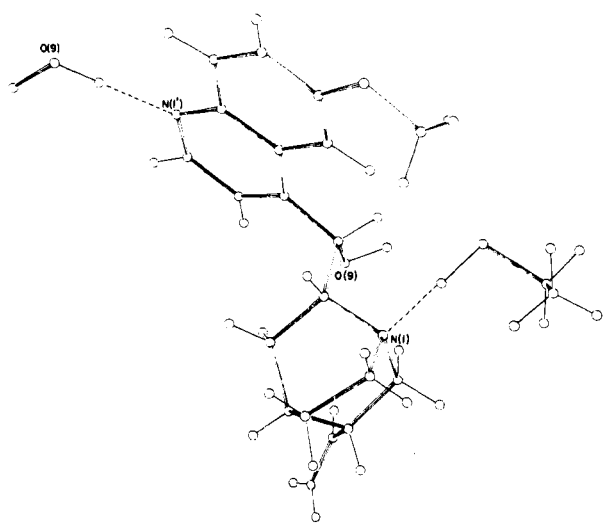

Figure 3—*Three-dimensional view of quinidine and ethanol molecules and a hydrogen-bonded fragment of a symmetrically related molecule.*

related molecule at $x - \frac{1}{2}, \frac{1}{2} - y$, and $-z$ is shown in Fig. 3. This plot was produced by ORTEP[6].

All other calculations were carried out by using the XRAY76 system[5]. The methods of solution and refinement were routine (Table I). The methods used in the calculations were found in a standard text on crystallographic analysis (13). The structure factor lists from which the values in Table II were obtained are available[7].

RESULTS AND DISCUSSION

Griffiths (14) previously reported the space group and cell dimensions

[6] See C. K. Johnson, "ORTEP," Report ORNL 5138 (3rd Rev. of ORNL 3794), UC-4-Chemistry, Oak Ridge National Laboratory (ORNL), Oak Ridge, Tenn.

[7] The structure factor lists are deposited with the Division of Drug Chemistry, Food and Drug Administration, Washington, DC 20204, and are available on request to the authors.

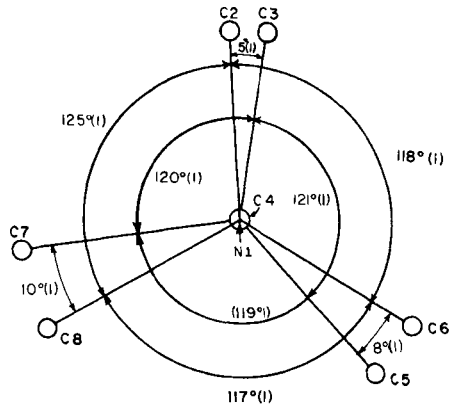

Figure 4—*Projection showing dihedral angles of the quinuclidine ring with special reference to the two bridgehead atoms, N-6 and C-4.*

of quinidine ethanolate to be $P2_12_12_1$ with a = 1310, b = 1660, and c = 960 pm. He reported a density of 1.18 g/cm^3 for $Z = 4$ under the conditions used. No structure was reported. The present study confirmed the assigned space group and approximate cell dimensions. The absolute configuration of I reported here (Fig. 3) is based on the published configuration of III (8). The relative configurations of I and epiquinidine (V) were established by chemical means (4), and the preparation of III from V does not affect the configurations about any of the asymmetric atoms in V. The difference between I and V is the configuration around C-9, so that I should have the same configurations as III around N-1, C-3, C-4, and C-8 and the opposite configuration around C-9. The absolute configuration reported for III (8) is 1*S*,3*S*,4*S*,8*S*,9*S*,10*S*. Therefore, the configuration for I is 1*S*,3*S*,4*S*,8*S*,9*R*.

The crystal structure of III (8) revealed strong intramolecular hydrogen bonding between the hydroxyl group and N-1. In the hydrogen-bonded conformation of III, the quinoline and quinuclidine rings are directed away from each other so there is no steric interaction between the rings. If I were to assume an analogous conformation, there would be a very strong steric interaction between the two rings. Thus, I does not exhibit intramolecular hydrogen bonding but crystallizes as the ethanolate in which N-1 is hydrogen bonded to the hydroxyl group of the molecule of ethanol.

A projection showing the dihedral angles of the quinuclidine ring with special reference to the two bridgehead atoms (N-1 and C-4) is given in Fig. 4.

REFERENCES

(1) E. Smith, S. Barkan, B. Ross, M. Maienthal, and J. Levine, *J. Pharm. Sci.*, **62,** 1151 (1973).

(2) T. Balazs, E. Herman, and J. Atkinson, *ibid.*, **67,** 1355 (1978).

(3) G. Grethe, H. L. Lee, T. Mitt, and M. R. Uskokovic, *Helv. Chim. Acta*, **56,** 1485 (1973).

(4) R. H. F. Manske and H. L. Holmes, "The Alkaloids," vol. III, Academic, New York, N.Y., 1953.

(5) J. Gutzwiller and M. R. Uskokovic, *Helv. Chim. Acta*, **56,** 1494 (1973).

(6) V. Prelog and E. Zalan, *ibid.*, **27,** 535 (1944).

(7) W. E. Doering, G. Cortes, and L. H. Knox, *J. Am. Chem. Soc.*, **69,** 1700 (1947).

(8) A. N. Chekhlov, Z. Kaluski, Y. T. Struchkov, G. Maluszynska, and A. I. Kitaigorodskii, *Zh. Strukt. Khim.*, **15,** 886 (1974).

(9) K. Nakanishi, "Infra-red Absorption Spectroscopy," Holden-Day, San Francisco, Calif., 1962, p. 24.

(10) W. A. Garland, W. F. Trager, and S. D. Nelson, *J. Biomed. Mass Spectrom.*, **1,** 124 (1974).

(11) D. Cromer and J. Mann, *Acta Crystallogr.*, **A24,** 321 (1968).

(12) R. F. Stewart, E. Davidson, and W. Simpson, *J. Chem. Phys.*, **42,** 3175 (1965).

(13) G. Stout and L. H. Jensen, "X-Ray Structure Determination—A Practical Guide," Macmillan, New York, N.Y., 1968.

(14) P. J. F. Griffiths, *Acta Crystallogr.*, **5,** 290 (1952).

ACKNOWLEDGMENTS

Presented in part at the 91st annual meeting of the Association of

Official Analytical Chemists, Washington, D.C., October 1977.

Abstracted from a dissertation to be submitted by R. M. Doherty to the Chemistry Department, University of Maryland, in partial fulfillment of the Doctor of Philosophy degree requirements.

The authors thank W. L. Brannon and Myron M. Smith, Jr., both from the Food and Drug Administration, for obtaining the IR spectra of some compounds involved in this study and for preparing Figs. 1, 2, and 4. They also thank John Statler, Computer Science Center, University of Maryland, for assistance in gathering the intensity data. The Computer Science Center provided support for computer time.

GI Absorption of β-Lactam Antibiotics I: Kinetic Assessment of Competing Absorption and Degradation in GI Tract

AKIRA TSUJI, ETSUKO MIYAMOTO, IZUMI KAGAMI, HIROMITSU SAKAGUCHI, and TSUKINAKA YAMANA ˣ

Received September 22, 1977, from the *Faculty of Pharmaceutical Sciences, Kanazawa University, Takara-machi, Kanazawa 920, Japan.* Accepted for publication April 4, 1978.

Abstract □ An equation was derived for the simultaneous assessment of rate constants for absorption and nonenzymatic degradation of unstable drugs in *in situ* absorption experiments. The equation was substantiated by using a variety of β-lactam antibiotics in the recirculation technique through the rat small intestine. Plots of the apparent first-order rate constant for the disappearance of the drug from the gut lumen *versus* the reciprocal of the volume of recirculating solution yielded a straight line with a slope equal to the intrinsic absorption rate constant and with an intercept equal to the nonenzymatic degradation rate constant in the GI lumen. The kinetic method for evaluation of the absorption rate constant also was developed for a more complex situation in the GI lumen involving absorption, nonenzymatic degradation, and enzymatic metabolism. The proposed method was confirmed with carbenicillin indanyl, which was metabolized rapidly to carbenicillin by the action of nonspecific esterase in the intestine. In the absence of information on Michaelis–Menten kinetic parameters, the present method is advantageous for evaluation of the intrinsic absorption rate of all unstable drugs.

Keyphrases □ β-Lactam antibiotics—kinetics of GI absorption and nonenzymatic degradation in rats □ Absorption, GI—β-lactam antibiotics, kinetics in rats □ Degradation, nonenzymatic GI—β-lactam antibiotics, kinetics in rats □ Antibiotics, β-lactam—kinetics of GI absorption and nonenzymatic degradation in rats

Penicillins are susceptible, depending on the nature of the side chain, to acid degradation and attack by β-lactamase in the GI tract (1). Since such degradations and absorption processes compete at the absorption site, the GI absorption of penicillins is difficult to study. A great deal of information is now available concerning the serum levels after oral administration of a variety of penicillins to experimental animals and humans (1, 2). It is, however, not always easy to discuss the absorption rate and mechanism from serum level data only because of the complex kinetic processes for the degradation in the GI tract and distribution in and elimination from the body (3).

In situ animal techniques are suitable for the quantitative determination of absorption rates and the clarification of the transport mechanism of a drug from the GI walls. A single perfusion method (4), a recirculation method (4, 5), and the method of Doluisio *et al.* (6) were used to study drug absorption. The present investigation was undertaken to establish a kinetic method for the evaluation of chemically and enzymatically unstable drugs such as β-lactam antibiotics by use of the recirculation technique. This technique has advantages of accurate pH control and suitable change in the perfusion volume. In the accompanying paper (7), the techniques developed were applied to study the *in situ* absorption of penicillins.

EXPERIMENTAL

Materials—The following β-lactam antibiotics were used as supplied: carbenicillin indanyl sodium[1] (704 μg/mg as carbenicillin free acid), propicillin potassium[2] (993 μg/mg), penicillin V potassium[3] (1490 units/mg), penicillin G potassium[3] (1600 units/mg), carbenicillin disodium[1] (799 μg/mg), and cephalothin sodium[4] (930 μg/mg).

All other chemicals were analytical reagent grade. Imidazole was recrystallized from benzene, followed by a thorough washing with ether (8).

Test Animals—Male albino Wistar rats, 180 ± 45 g, were fasted 20 hr prior to the experiment. Water was given freely..

Rat *In Situ* Intestinal Absorption, Degradation, and Metabolism—The recirculation method was based on those of Schanker *et al.* (4) and Koizumi *et al.* (5). The rats were anesthetized with urethan, 1.3 g/kg ip, approximately 1 hr prior to surgery. A midline abdominal incision was made, and the small intestine was exposed. The glass tubings connected to silicone tubing were cannulated into both ends of the small intestine. The double ligations were made with a 000 silk thread, with care being taken not to interfere with blood flow. The bile duct was ligated to avoid any flow of fluid into the intestinal lumen during the absorption experiments. The intestine was replaced in the abdomen, the incision was closed with metal clips, and the cannula was connected to a microtube pump[5].

The small intestine was washed with 100 (at pH 4.0) or 50 (at pH 7.0) ml of a perfusion solution (6) maintained at 37°. Then the desired volume of the perfusion solution containing the antibiotic was recirculated from the duodenum to the ileum (~100 cm in length) at pH 4.0 or to the jejunum (~30 cm in length) at pH 7.0. The perfusion solution consisted of 1–2 mg/ml, unless otherwise stated, of a β-lactam antibiotic together with the following compounds per liter at pH 4.0: hydrochloric acid, 3.8 ml; citric acid, 12.6 g; sodium hydroxide, 1.8 g; and sodium chloride, 2.1 g (5). At pH 7.0, the compounds used were: dibasic sodium phosphate, 14.3 g; monobasic potassium phosphate, 3.6 g; and sodium chloride, 4.3 g (5).

The solution was maintained at 37° and perfused with a pump at 10 ml/min at pH 4.0 or at 2 ml/min at pH 7.0. The perfusion solution pH was kept constant at the desired value during the absorption experiments by a pH-stat[6]. The samples (0.1–0.2 ml, unless otherwise stated) were taken at suitable time intervals and analyzed.

At pH 4.0, the volume changes were almost negligible. For carbenicillin indanyl sodium, a 0.025-mg/ml drug solution was used because of its low

[1] Taito Pfizer Co., Tokyo, Japan.
[2] Takeda Chemical Industries, Osaka, Japan.
[3] Meiji Seika Kaisha, Tokyo, Japan.
[4] Shionogi and Co., Osaka, Japan.
[5] Tokyo Rika Kikai Co. or Mitsumi Scientific Industries, Tokyo, Japan.
[6] pH-Stat titrator assembly consisting of TTT2 titrator and ABU12b autoburet, Radiometer, Copenhagen, Denmark.

0022-3549/78/1200-1701$01.00/0
© 1978, American Pharmaceutical Association

Official Analytical Chemists, Washington, D.C., October 1977.

Abstracted from a dissertation to be submitted by R. M. Doherty to the Chemistry Department, University of Maryland, in partial fulfillment of the Doctor of Philosophy degree requirements.

The authors thank W. L. Brannon and Myron M. Smith, Jr., both from the Food and Drug Administration, for obtaining the IR spectra of some compounds involved in this study and for preparing Figs. 1, 2, and 4. They also thank John Statler, Computer Science Center, University of Maryland, for assistance in gathering the intensity data. The Computer Science Center provided support for computer time.

GI Absorption of β-Lactam Antibiotics I: Kinetic Assessment of Competing Absorption and Degradation in GI Tract

AKIRA TSUJI, ETSUKO MIYAMOTO, IZUMI KAGAMI, HIROMITSU SAKAGUCHI, and TSUKINAKA YAMANA ˣ

Received September 22, 1977, from the *Faculty of Pharmaceutical Sciences, Kanazawa University, Takara-machi, Kanazawa 920, Japan.* Accepted for publication April 4, 1978.

Abstract □ An equation was derived for the simultaneous assessment of rate constants for absorption and nonenzymatic degradation of unstable drugs in *in situ* absorption experiments. The equation was substantiated by using a variety of β-lactam antibiotics in the recirculation technique through the rat small intestine. Plots of the apparent first-order rate constant for the disappearance of the drug from the gut lumen *versus* the reciprocal of the volume of recirculating solution yielded a straight line with a slope equal to the intrinsic absorption rate constant and with an intercept equal to the nonenzymatic degradation rate constant in the GI lumen. The kinetic method for evaluation of the absorption rate constant also was developed for a more complex situation in the GI lumen involving absorption, nonenzymatic degradation, and enzymatic metabolism. The proposed method was confirmed with carbenicillin indanyl, which was metabolized rapidly to carbenicillin by the action of nonspecific esterase in the intestine. In the absence of information on Michaelis–Menten kinetic parameters, the present method is advantageous for evaluation of the intrinsic absorption rate of all unstable drugs.

Keyphrases □ β-Lactam antibiotics—kinetics of GI absorption and nonenzymatic degradation in rats □ Absorption, GI—β-lactam antibiotics, kinetics in rats □ Degradation, nonenzymatic GI—β-lactam antibiotics, kinetics in rats □ Antibiotics, β-lactam—kinetics of GI absorption and nonenzymatic degradation in rats

Penicillins are susceptible, depending on the nature of the side chain, to acid degradation and attack by β-lactamase in the GI tract (1). Since such degradations and absorption processes compete at the absorption site, the GI absorption of penicillins is difficult to study. A great deal of information is now available concerning the serum levels after oral administration of a variety of penicillins to experimental animals and humans (1, 2). It is, however, not always easy to discuss the absorption rate and mechanism from serum level data only because of the complex kinetic processes for the degradation in the GI tract and distribution in and elimination from the body (3).

In situ animal techniques are suitable for the quantitative determination of absorption rates and the clarification of the transport mechanism of a drug from the GI walls. A single perfusion method (4), a recirculation method (4, 5), and the method of Doluisio *et al.* (6) were used to study drug absorption. The present investigation was undertaken to establish a kinetic method for the evaluation of chemically and enzymatically unstable drugs such as β-lactam antibiotics by use of the recirculation technique. This technique has advantages of accurate pH control and suitable change in the perfusion volume. In the accompanying paper (7), the techniques developed were applied to study the *in situ* absorption of penicillins.

EXPERIMENTAL

Materials—The following β-lactam antibiotics were used as supplied: carbenicillin indanyl sodium[1] (704 μg/mg as carbenicillin free acid), propicillin potassium[2] (993 μg/mg), penicillin V potassium[3] (1490 units/mg), penicillin G potassium[3] (1600 units/mg), carbenicillin disodium[1] (799 μg/mg), and cephalothin sodium[4] (930 μg/mg).

All other chemicals were analytical reagent grade. Imidazole was recrystallized from benzene, followed by a thorough washing with ether (8).

Test Animals—Male albino Wistar rats, 180 ± 45 g, were fasted 20 hr prior to the experiment. Water was given freely..

Rat *In Situ* Intestinal Absorption, Degradation, and Metabolism—The recirculation method was based on those of Schanker *et al.* (4) and Koizumi *et al.* (5). The rats were anesthetized with urethan, 1.3 g/kg ip, approximately 1 hr prior to surgery. A midline abdominal incision was made, and the small intestine was exposed. The glass tubings connected to silicone tubing were cannulated into both ends of the small intestine. The double ligations were made with a 000 silk thread, with care being taken not to interfere with blood flow. The bile duct was ligated to avoid any flow of fluid into the intestinal lumen during the absorption experiments. The intestine was replaced in the abdomen, the incision was closed with metal clips, and the cannula was connected to a microtube pump[5].

The small intestine was washed with 100 (at pH 4.0) or 50 (at pH 7.0) ml of a perfusion solution (6) maintained at 37°. Then the desired volume of the perfusion solution containing the antibiotic was recirculated from the duodenum to the ileum (~100 cm in length) at pH 4.0 or to the jejunum (~30 cm in length) at pH 7.0. The perfusion solution consisted of 1–2 mg/ml, unless otherwise stated, of a β-lactam antibiotic together with the following compounds per liter at pH 4.0: hydrochloric acid, 3.8 ml; citric acid, 12.6 g; sodium hydroxide, 1.8 g; and sodium chloride, 2.1 g (5). At pH 7.0, the compounds used were: dibasic sodium phosphate, 14.3 g; monobasic potassium phosphate, 3.6 g; and sodium chloride, 4.3 g (5).

The solution was maintained at 37° and perfused with a pump at 10 ml/min at pH 4.0 or at 2 ml/min at pH 7.0. The perfusion solution pH was kept constant at the desired value during the absorption experiments by a pH-stat[6]. The samples (0.1–0.2 ml, unless otherwise stated) were taken at suitable time intervals and analyzed.

At pH 4.0, the volume changes were almost negligible. For carbenicillin indanyl sodium, a 0.025-mg/ml drug solution was used because of its low

[1] Taito Pfizer Co., Tokyo, Japan.
[2] Takeda Chemical Industries, Osaka, Japan.
[3] Meiji Seika Kaisha, Tokyo, Japan.
[4] Shionogi and Co., Osaka, Japan.
[5] Tokyo Rika Kikai Co. or Mitsumi Scientific Industries, Tokyo, Japan.
[6] pH-Stat titrator assembly consisting of TTT2 titrator and ABU12b autoburet, Radiometer, Copenhagen, Denmark.

0022-3549/78/1200-1701$01.00/0
© 1978, American Pharmaceutical Association

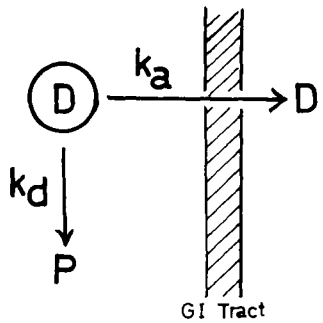

Scheme I—Simultaneous absorption and nonenzymatic degradation. Key: D, intact drug; P, product; k_a, absorption rate constant; and k_d, degradation rate constant.

solubility. Aliquots (5 ml) were taken, 5 ml of drug-free perfusion solution was added to maintain a constant solution volume, and the arithmetical correction of concentration resulting from the dilution was made. At pH 7.0, a sample was taken at each time period, the intestine was emptied, and the perfusion solution corresponding to the reduction in volume, except for sampling, was added to the recirculating drug solution. The volume added was only 1.5 ml.

Analysis—The samples were diluted appropriately, filtered with a 0.45-μm filter[7], and then analyzed.

Propicillin, penicillin V, and penicillin G were determined by the method of Bundgaard and Ilver (8). Carbenicillin indanyl was determined according to a spectrophotometric method developed for the simultaneous determination of carbenicillin indanyl and carbenicillin[8], based on the method reported by Bundgaard and Ilver (8). Cephalothin was determined by high-pressure liquid chromatography (HPLC)[9]. The eluant was 0.25 *M* acetate buffer (9), and the pressure was 100 kg/cm^2. The sample was injected in a 10-μl portion and detected at 254 nm[10].

RESULTS AND DISCUSSION

Case I: Simultaneous Absorption and Nonenzymatic Degradation in GI Tract—*Theoretical*—Scheme I represents the simultaneous absorption of a drug from the GI tract and nonenzymatic degradation of the drug in the perfusion solution. If the absorption kinetics obey Fick's law, if the overall transfer of a drug from the gut lumen to blood is irreversible, if drug accumulation in the gut membrane is negligible, and if first-order degradation proceeds, then the total disappearance of the amount of a drug in the perfusion solution can be expressed as:

$$-\frac{dA}{dt} = k_a(C - C_b) + k_dA \qquad \text{(Eq. 1)}$$

where A represents the amount of drug; C and C_b represent the drug concentrations in the perfusion solution and blood, respectively; k_a is the intrinsic absorption rate constant having a unit of volume × time^{-1}; and k_d is the competitive first-order rate constant having a unit of time^{-1}. For nonenzymatic and parallel degradation to produce n kinds of products, k_d can be expressed as:

$$k_d = \sum_i^n (k_d)_i \qquad \text{(Eq. 2)}$$

The parameter A can be expressed by the drug concentration, C, and the volume of the drug solution, V, as follows:

$$-\frac{d(VC)}{dt} = k_a(C - C_b) + k_d(VC) \qquad \text{(Eq. 3)}$$

Under the experimental conditions of the constant volume of the drug solution and $C \gg C_b$, Eq. 3 becomes:

$$-\frac{dC}{dt} = \left(\frac{k_a}{V} + k_d\right)C \qquad \text{(Eq. 4)}$$

[7] Sartorius-Membranfilter GmbH, 34 Göttingen, Germany.

[8] Details of the analytical method and the stability kinetics of the carbenicillin prodrug will be published; A. Tsuji, E. Miyamoto, T. Terasaki, and T. Yamana.

[9] Model 830, Shimadzu-DuPont, Kyoto, Japan. SAX on Zipax, 2.1 mm i.d. × 0.5 m, DuPont.

[10] UV 202 recording double-beam spectrophotometer, Shimadzu, Kyoto, Japan.

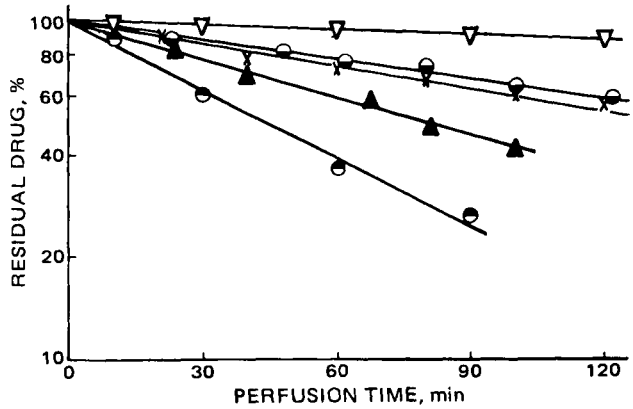

Figure 1—*First-order plots of percent β-lactam antibiotics remaining in the* in situ *rat intestinal recirculating experiments at pH 4.0 and at a perfusion flow rate of 10 ml/min. The pH of the drug solution was maintained constant by a pH-stat. Key (volume of the perfusion solution): ●, carbenicillin indanyl, 80 ml; ▲, propicillin, 70 ml; ×, penicillin G, 50 ml; ◒, penicillin V, 60 ml; and ▽, cephalothin, 50 ml.*

By integration:

$$\log\left(\frac{C}{C_0}\right) = -\frac{k_{app}}{2.303}t \qquad \text{(Eq. 5)}$$

where C_0 is the concentration at $t = 0$ and k_{app} is:

$$k_{app} = k_a\frac{1}{V} + k_d \qquad \text{(Eq. 6)}$$

Equation 5 predicts that the semilogarithmic plots of C/C_0 *versus* time show a straight line to give the apparent first-order rate constant, k_{app}.

Method 1—When the quantitative determination of all degradation products at time t after the start of the recirculating experiments yields the values of $\Sigma(C_d)_i$, the apparent first-order rate constant for the absorption, $(k_a)_{app}$, can be calculated easily according to:

$$(k_a)_{app} = k_a\frac{1}{V} \qquad \text{(Eq. 7}a\text{)}$$

Table I—Apparent Rate Constants, k_{app}, of β-Lactam Antibiotics for Various Volumes of Perfusion Solution from the *In Situ* Rat Small Intestine at pH 4.0 [a], 37°, and a Flow Rate of 10 ml/min

Compound	Perfusion Volume, ml	$k_{app} \times 10^3$, min^{-1}
Carbenicillin indanyl	80	15.27
	200	6.05
	400	3.80
Propicillin	47	11.55
	50	11.11
	70	8.44
	80	6.55
	100	5.42
	200	3.00
	400	1.52
	1000	0.85
Penicillin V	37	7.22
	50	5.40
	60	4.22
	70	4.22
	100	2.80
	200	1.67
Penicillin G	50	4.98
	60	5.30
	80	4.57
	100	4.53
	145	3.97
	200	4.07
Cephalothin	50	0.90
	70	0.72

[a] The pH of the perfusion solution was maintained constant with a pH-stat. No significant volume changes were observed during the absorption experiments.

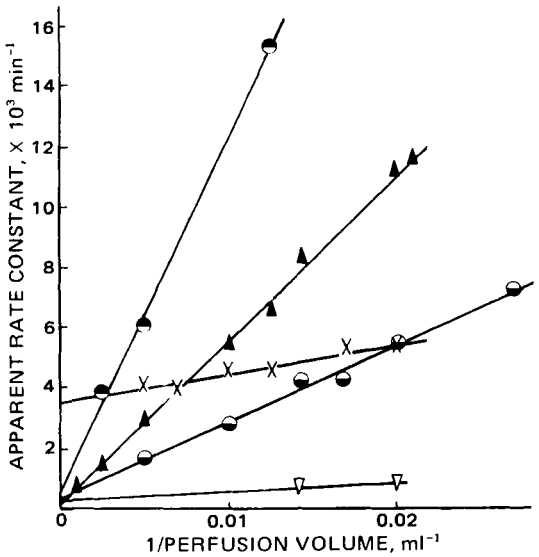

Figure 2—*Effect of the volume of the perfusion solution on the absorption of β-lactam antibiotics from the* in situ *rat small intestine at pH 4.0 and 37°. Key: ●, carbenicillin indanyl; ▲, propicillin; ×, penicillin G; ◒, penicillin V; and ▽, cephalothin.*

$$(k_a)_{app} = k_{app}\left[1 - \frac{\sum(C_d)_i}{C_0\,[1 - \exp(-k_{app}t)]}\right] \qquad \text{(Eq. 7b)}$$

Method 2—When the quantitative analysis of the degradation products is difficult and/or impossible for the test drug, the following kinetic technique should be suitable for the simultaneous assessment of k_a and k_d.

Equation 6 predicts that plots of k_{app} *versus* the reciprocal of the volume of the drug solution, $1/V$, give a straight line under constant experimental conditions, except for the change of the perfusion volume. The absorption rate constant, k_a, can be obtained from the slope; the total degradation rate constant, k_d, can be obtained from the intercept value.

Application of Theory to β-Lactam Antibiotics—In an acidic environment, penicillins are easily degraded by intramolecular attack of the side-chain amide on the β-lactam moiety, depending on the nature of the side chain, to produce the corresponding penicillenic, penillic, and penicilloic acids (1, 10). Although the β-lactam moiety of cephalosporins is relatively acid stable, the initial degradation product corresponding to penicilloic acid is not stable and is readily fragmented in aqueous solution (1, 10). Additionally, the ester bond of acetylcephalosporins is easily hydrolyzed in acidic solutions to produce deacetylcephalosporin and its lactone (1, 11, 12). Because of these circumstances, quantitative determination of the acid degradation products resulting from β-lactam antibiotics seems to be experimentally difficult or impossible. Therefore, the absorption rates of β-lactam antibiotics may be suitably evaluated with the kinetic technique of Method 2.

Figure 1 illustrates the disappearance of β-lactam antibiotics from the *in situ* rat intestinal lumen when the pH of the lumen solution was continuously controlled to pH 4.0 by a pH-stat. Disappearance followed first-order kinetics as predicted from Eq. 5. The rate constants, k_{app}, determined from the slopes by the least-squares treatment are listed in Table I; plots of k_{app} *versus* $1/V$ are illustrated in Fig. 2. For all β-lactam antibiotics, good straight lines with various slopes and intercepts were obtained, in agreement with Eq. 6.

Table II—Absorption and Degradation Rate Constants Determined from the *In Situ* and *In Vitro* Experiments at pH 4.0 and 37°

Compound	k_a[a], ml min^{-1}	k_d, × 10^3 [b] min^{-1}	k'_d, × 10^3 [c] min^{-1}
Carbenicillin indanyl	1.17	0.60	0.25
Propicillin	0.54	0.23	0.28
Penicillin V	0.25	0.36	0.28
Penicillin G	0.08	3.62	4.00
Cephalothin	0.02	0.28	0.43

[a] Evaluated from the slope in Fig. 2. [b] Evaluated from the intercepts in Fig. 2. [c] Pseudo-first-order rate constant for the *in vitro* degradation in isotonic buffer solution of pH 4.0 at 37°.

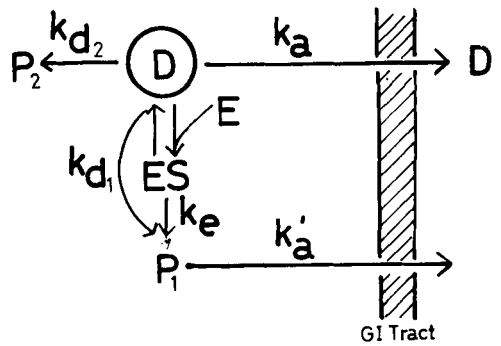

Scheme II—Simultaneous absorption and enzymatic degradation. Key: D, intact drug; E, specific or nonspecific enzyme; ES, substrate–enzyme complex; P, product; k_a *and* k'_a*, absorption rate constants of intact drug and products, respectively;* $(k_d)_1$ *and* $(k_d)_2$*, degradation rate constants of nonenzymatic reaction; and* k_e*, degradation rate constant of* ES *complex.*

The values of k_a and k_d estimated according to Eq. 6 are given in Table II. The k_d values were in relatively good agreement with those determined *in vitro* under the same conditions (Table II), suggesting that drug degradation in recirculating solution through the rat small intestine depends only on the bulk pH of the perfusion solution. The more lipophilic β-lactam antibiotics exhibited larger absorption rate constants. The absorption mechanism and the relationship between the absorption rate and the structure of β-lactam antibiotics are discussed in detail elsewhere (7).

Case II: Simultaneous Absorption and Both Enzymatic and Nonenzymatic Degradations in GI Tract—*Theoretical*—Drug-metabolizing enzymes existing in intestinal secretions and microflora (13) may influence the kinetics of disappearance of a drug during *in situ* absorption experiments. Scheme II shows the processes involving the competing first-order absorption with rate constant k_a, first-order nonenzymatic degradation with rate constants $(k_d)_1$ and $(k_d)_2$ to yield the corresponding products P_1 and P_2, and enzymatic degradation obeying Michaelis–Menten kinetics to produce the metabolite P_1, which is also absorbed with the rate constant k'_a.

The differential equations of a drug, D, and a metabolite, P_1, can be expressed as Eqs. 8 and 9, respectively, according to Scheme II:

$$\frac{dC}{dt} = -\left[k_a\frac{1}{V} + (k_d)_1 + (k_d)_2\right]C - \frac{k_e(A_e/V)C}{K_m + C} \qquad \text{(Eq. 8)}$$

$$\frac{d(C_p)_1}{dt} = (k_d)_1 C - k'_a\frac{1}{V}(C_p)_1 + \frac{k_e(A_e/V)C}{K_m + C} \qquad \text{(Eq. 9)}$$

where K_m is the Michaelis–Menten constant, A_e is the amount of enzyme, k_e is the degradation rate constant for the drug–enzyme complex, and $(C_p)_1$ is the concentration of the metabolite P_1.

Method 3—When a nonspecific enzyme, such as esterase, participates in the drug metabolism, the K_m value is unknown, and/or the amount of enzyme cannot be assumed to be constant during the experiments, the following kinetic approach is the most covenient for determining the absorption rate constant of a drug.

Summation of Eqs. 8 and 9 leads to:

$$\frac{dC}{dt} + \frac{d(C_p)_1}{dt} = -[(k_a)_{app} + (k_d)_2]C - (k'_a)_{app}(C_p)_1 \qquad \text{(Eq. 10)}$$

where $(k_a)_{app}$ and $(k'_a)_{app}$ represent the apparent absorption rate constants of the drug and its metabolite P_1, respectively, depending on the perfusion volume as shown in Eq. 7b. Integration of Eq. 10 from $t = 0$ to $t = t$ yields:

$$\int_0^t \frac{dC}{dt}\,dt + \int_0^t \frac{d(C_p)_1}{dt}\,dt = -[(k_a)_{app} + (k_d)_2]\int_0^t C\,dt - (k'_a)_{app}\int_0^t (C_p)_1\,dt \qquad \text{(Eq. 11)}$$

Since $C = C_0$ and $(C_p)_1 = 0$ at $t = 0$, Eq. 11 gives:

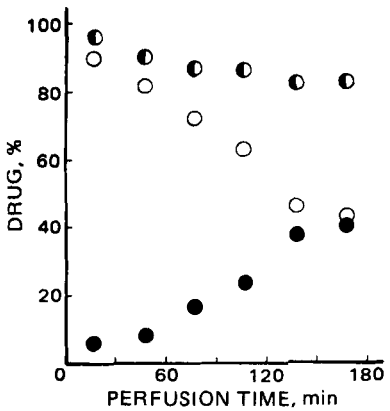

Figure 3—*Time course of absorption and metabolism of carbenicillin indanyl during the* in situ *recirculating experiment in a rat at pH 7.0. The following conditions were used: perfusion volume, 25 ml; initial drug concentration, 2 mg/ml; and flow rate, 2 ml/min. The pH of the drug solution was maintained constant with a pH-stat. Key:* ◐, *total antibiotics;* ○, *carbenicillin indanyl; and* ●, *carbenicillin.*

$$(k_a)_{app} + (k_d)_2 = k_{app}$$

$$= \frac{C_0 - C - (C_p)_1 - (k'_a)_{app} \int_0^t (C_p)_1 \, dt}{\int_0^t C \, dt} \quad \text{(Eq. 12)}$$

If the quantitative determination of the concentrations of both the drug and its metabolite at time t is possible, the apparent first-order rate constant, k_{app}, can be calculated from Eq. 12, where $\int_0^t C \, dt$ and $\int_0^t (C_p)_1 \, dt$ are the areas under the respective concentration of the drug and the metabolite *versus* time curves from time zero to t. The values of $(k'_a)_{app}$ can be obtained from another absorption experiment of the metabolite under the same conditions with the same volume of recirculating perfusion solution, V. Therefore, by plotting the k_{app} values determined according to Eq. 12 *versus* $1/V$, the absorption rate constant, k_a, and the nonenzymatic degradation rate constant, $(k_d)_2$, of the test drug can be obtained from the slope and the intercept, respectively.

Application of Method 3 to β-Lactam Antibiotics and Prodrug—Carbenicillin indanyl, which is the carbenicillin α-ester of 5-indanol, is a carbenicillin prodrug. It has been used orally with a sufficient therapeutic effect (14–17). Figure 3 illustrates the time course of the prodrug and the parent drug (carbenicillin, P_1) during recirculation of carbenicillin indanyl through the rat small intestine at pH 7.0. This graph indicates the slow absorption of the prodrug and rapid cleavage of the α-ester bond to yield carbenicillin. Since the ester was relatively stable with a half-life of ~17 hr at pH 7.0 and 37° *in vitro*[8], the rapid formation of carbenicillin is virtually the result of the action of a nonspecific intestinal esterase. Therefore, the behavior of carbenicillin indanyl in the perfusion solution essentially follows Scheme II. Under this condition, the absorption of carbenicillin itself was negligible [*i.e.*, $(k'_a)_{app} \simeq 0$)]. The apparent rate constant, k_{app}, could be calculated from the data of Fig. 3 according to Eq. 12.

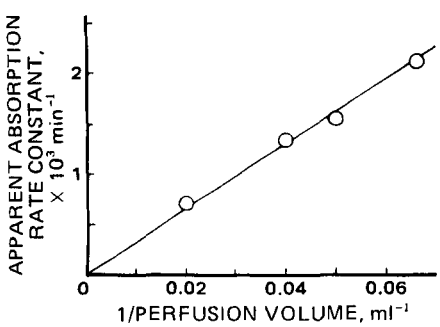

Figure 4—*Effect of the volume of the perfusion solution on the absorption rate of carbenicillin indanyl from the* in situ *rat small intestine at pH 7.0. The pH of the drug solution was maintained constant with a pH-stat.*

Figure 4 shows the plot of k_{app} *versus* $1/V$, yielding a good straight line with a slope equal to the absorption rate constant, k_a, of carbenicillin indanyl and almost through the origin. This result suggests that a nonenzymatic degradation process of carbenicillin indanyl other than that producing carbenicillin is essentially negligible. At pH 7.0 at 35°, the nonenzymatic β-lactam degradation of both carbenicillin indanyl and carbenicillin was only 1% during 2 hr[8].

Method 3 can also be utilized for the metabolism of penicillins by β-lactamase to produce the corresponding penicilloic acid, if the metabolite can be determined by a suitable analytical method.

SUMMARY AND CONCLUSIONS

A kinetic method was developed, allowing the simultaneous determination of rate constants for both absorption and nonenzymatic degradation of unstable drugs only by changing the volume of the drug solution from *in situ* absorption experiments. The method was experimentally confirmed for several β-lactam antibiotics by utilizing an *in situ* recirculation technique on the rat small intestine. The present kinetic approach provides vital information for the intrinsic GI absorption process of some drugs whose absorption experiments have been difficult because of their lability in the GI lumen.

For the more complex situation *in situ*, involving enzymatic metabolism of drugs, a method was developed for the accurate assessment of the absorption rate constant and was substantiated by a carbenicillin prodrug, which was metabolized rapidly to carbenicillin by the action of nonspecific intestinal esterase.

The present methods, although based on simple kinetic considerations, may be widely applicable to evaluate the intrinsic absorption rate from *in situ* absorption experiments for all drugs enzymatically or nonenzymatically unstable.

REFERENCES

(1) J. P. Hou and J. W. Poole, *J. Pharm. Sci.*, **60**, 503 (1971).

(2) G. N. Rolinson and R. Sutherland, in "Advances in Pharmacology and Chemotherapy," vol. 11, G. Garrattini, A. Goldin, F. Hawking, and I. J. Kopin, Eds., Academic, New York, N.Y., 1973, p. 151.

(3) R. E. Notari, J. L. Deyound, and R. H. Reuning, *J. Pharm. Sci.*, **61**, 135 (1972).

(4) L. S. Schanker, D. J. Tocco, B. B. Brodie, and C. A. M. Hogben, *J. Pharmacol. Exp. Ther.*, **123**, 81 (1958).

(5) T. Koizumi, T. Arita, and K. Kakemi, *Chem. Pharm. Bull.*, **12**, 412 (1964).

(6) J. T. Doluisio, N. F. Billups, L. W. Dittert, E. T. Sugita, and J. V. Swintosky, *J. Pharm. Sci.*, **58**, 1196 (1969).

(7) A. Tsuji, E. Miyamoto, N. Hashimoto, and T. Yamana, *ibid.*, **67**, 1705 (1978).

(8) H. Bundgaard and K. Ilver, *J. Pharm. Pharmacol.*, **24**, 790 (1972).

(9) R. P. Buhs, T. E. Maxim, N. Allen, T. A. Jacob, and F. J. Wolf, *J. Chromatogr.*, **99**, 609 (1974).

(10) M. A. Schwartz, *J. Pharm. Sci.*, **58**, 643 (1969).

(11) T. Yamana and A. Tsuji, *ibid.*, **65**, 1563 (1976).

(12) J. Konecny, E. Felber, and J. Gruner, *J. Antibiot.*, **26**, 135 (1973).

(13) R. R. Schline, *Pharmacol. Rev.*, **25**, 451 (1973).

(14) J. F. Wallace, E. Atlas, D. M. Bear, N. K. Brown, H. Clark, and M. Turck, *Antimicrob. Agents Chemother., 1970*, **1971**, 223.

(15) K. Butler, A. R. English, A. K. Knirsch, and J. J. Korst, *Del. Med. J.*, **43**, 366 (1971).

(16) A. R. English, J. A. Retsema, V. A. Ray, and J. E. Lynch, *Antimicrob. Agents Chemother.*, **1**, 185 (1972).

(17) D. C. Hobbs, *ibid.*, **2**, 272 (1972).

ACKNOWLEDGMENTS

Presented in part at the 97th Annual Meeting of the Pharmaceutical Society of Japan, Tokyo, Japan, April 1977.

The authors acknowledge the gifts of β-lactam antibiotics from Meiji Seika Kaisha, Shionogi & Co., Taito Pfizer Co., and Takeda Chemical Industries. They also thank Mr. T. Terasaki for assistance.

GI Absorption of β-Lactam Antibiotics II: Deviation from pH-Partition Hypothesis in Penicillin Absorption through *In Situ* and *In Vitro* Lipoidal Barriers

AKIRA TSUJI, ETSUKO MIYAMOTO, NAOHUMI HASHIMOTO, and TSUKINAKA YAMANA ˣ

Received September 22, 1977, from the *Faculty of Pharmaceutical Sciences, Kanazawa University, Takara-machi, Kanazawa 920, Japan.* Accepted for publication April 4, 1978.

Abstract □ The absorption of propicillin from the rat stomach and small intestine *in situ* was examined as a function of recirculating solution pH. The *in vitro* interphase transport from an aqueous buffer of various pH values to the octanol phase was also studied for several penicillins by the use of a two-phase rolling cell. The rate–pH profiles obtained from both *in situ* and *in vitro* experiments deviated significantly from the dissociation curves. The degrees of the shifts were approximately 2 pH units for the *in situ* intestinal absorption of propicillin and *in vitro* transport of propicillin and cloxacillin, approximately 1.5 pH units for the *in vitro* transport of penicillin V, and 0.8 pH unit for the *in situ* stomach absorption of propicillin. These discrepancies from the classical pH-partition hypothesis can be interpreted by the permeation through the lipoidal barrier of the undissociated species of penicillins transported through the aqueous diffusion layer adjacent to the lipoidal surface. All *in situ* and *in vitro* experiments tend to support this theory.

Keyphrases □ β-Lactam antibiotics—propicillin, GI absorption, deviation from pH-partition hypothesis, rats □ Propicillin—GI absorption, deviation from pH-partition hypothesis, rats □ Absorption, GI—propicillin, deviation from pH-partition hypothesis, rats □ pH-partition hypothesis—propicillin, GI absorption, rats □ Antibiotics, β-lactam—propicillin, GI absorption, deviation from pH-partition hypothesis, rats

The mucosal surface of the GI tract acts as a lipoidal barrier to drug absorption. To characterize absorption of foreign compounds through such a barrier, Schanker *et al.* (1) proposed the pH-partition hypothesis that the degree of absorption of weakly acidic and basic drugs depends on their lipid solubility and degree of ionization.

Penicillins are weakly acidic antibiotics with pKa values close to 2.7–2.8 (2, 3) and exhibit a wide range of lipid solubility, depending on the nature of the side chain (3–5). Much attention has been focused on the relative serum concentrations after oral administration, and GI absorption was evaluated from comparative serum level and urinary recovery data (6–10). Although some basic studies on the absorption mechanism for β-lactam antibiotics recently appeared (11–14), it is not clearly understood yet whether the absorption of penicillins obeys the pH-partition hypothesis or another specialized mechanism.

Previously, a novel kinetic method to determine simultaneously the rate constants of both absorption and degradation in the GI tract was reported (15). Based on this kinetic approach, the present investigation was performed to elucidate the pH dependency of the absorption rate and its mechanism for the undissociated penicillin from the rat GI tract. To evaluate the fundamental importance of diffusion transport of penicillins through a lipoidal barrier of the GI tract, the *in vitro* two-phase transport kinetics of penicillins also were studied.

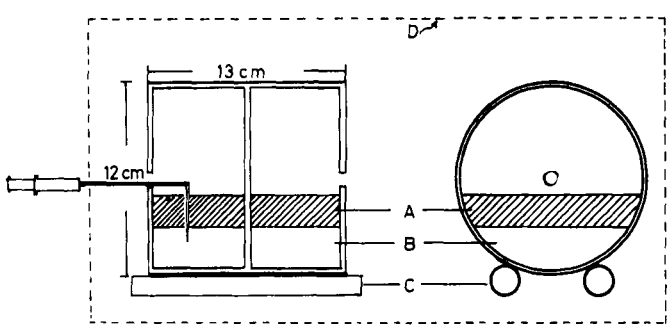

Figure 1—*Apparatus for rolling cell used for the* in vitro *two-phase transport study. Key: A, lipoidal phase; B, aqueous phase; C, rollers; and D, oven.*

EXPERIMENTAL

Materials—Dicloxacillin sodium[1] (900 μg/mg), cloxacillin sodium[1] (907 μg/mg), and oxacillin sodium[2] (840 μg/mg) were used as supplied. Other penicillins were the same as those used previously (15).

All other chemicals were reagent grade and were used without further purification, except octanol, cyclohexane, and imidazole. Octanol was purified according to a literature method (16), and cyclohexane was used after a single distillation. Imidazole was purified by double recrystallization from benzene, followed by a thorough washing with ether (17).

***In Situ* Recirculation Procedure**—Male albino Wistar rats, 165 ± 17 g, were fasted for 20 hr prior to the experiments. Water was allowed freely. The rats were anesthetized with urethan, 1.3 g/kg ip, approximately 1 hr prior to surgery.

Intestinal Absorption Procedure—The procedure for studying drug disappearance from the intestine (duodenum to ileum; ~100 cm in length) was described previously (15). A solution of propicillin (1 mg/ml) dissolved in an isotonic buffer of the desired pH (18) was perfused at the rate of 10 ml/min, unless otherwise stated. The recirculating solution was maintained at 37°, and its pH was kept constant at the desired value during the absorption experiments with a pH-stat[3]. Aliquots, 0.2 ml, of the sample solution were taken at suitable time intervals and analyzed. The apparent first-order rate constants, k_{app}, were determined by least-squares analysis.

Stomach Absorption Procedure—In a similar manner to that for the intestinal absorption experiments, the stomach was exposed, cannulated at the cardiac and duodenal ends, and washed from the cardiac end with approximately 100 ml of the perfusion solution (19). The perfusion solution was expelled with air, and the penicillin solution of various volumes (4.5–50 ml) was recirculated with a pump at 10 ml/min.

Propicillin sodium was dissolved in an isotonic buffer (18) for a final concentration of 0.5–1 mg/ml, depending on the solubility. The solution was maintained at 37°, and the solution pH was kept constant at the desired value for 3 hr with a pH-stat. After 3 hr, the remaining penicillin solution was collected, the stomach was washed thoroughly with the isotonic buffer, and the solutions were combined to make the desired volume. No significant volume change was observed, and the apparent disappearance first-order rate constant of propicillin from the perfusion solution was calculated from:

[1] Meiji Seika Kaisha, Tokyo, Japan.
[2] Banyu Pharmaceutical Co., Tokyo, Japan.
[3] pH-Stat titrator, assembly consisting of TTT2 titrator ABU12b autoburet, Radiometer, Copenhagen, Denmark.

0022-3549/78/1200-1705$01.00/0
© 1978, American Pharmaceutical Association

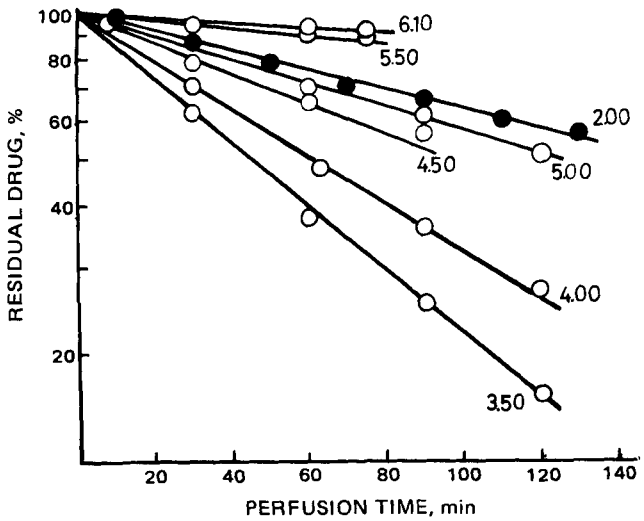

Figure 2—*Typical first-order plots of the percentage of propicillin remaining in the* in situ *rat GI recirculating perfusion experiments at various pH values and 37°. The 50-ml drug solution was perfused at the flow rate of 10 ml/min, and the pH of the solution was maintained constant with a pH-stat. Key: ●, experimental points from the stomach; and ○, experimental points from the intestine.*

$$k_{app} = -\frac{1}{3}\ln\frac{C^f}{C^0} \qquad \text{(Eq. 1)}$$

where C^0 and C^f are the concentrations of propicillin at initial and final stages, respectively.

Analytical Method—The samples were diluted with distilled water to produce a final concentration of 1×10^{-5}–1×10^{-4} *M*. They were then passed through a 0.45-μm filter[4] to remove any solid materials and assayed spectrophotometrically[5] at 325 nm by the method of Bundgaard and Ilver (17). No materials in the samples from the *in situ* experiments below pH 6 interfered significantly. This condition was confirmed by the use of recirculating solutions without the antibiotics.

Two-Phase Transport Procedure by Rolling Cell—A rolling cell (Fig. 1), similar to that described by Robertson and Madsen (20), was used for the *in vitro* transport study of penicillin. The apparatus consisted of a glass cell slowly rotated on rollers in an oven thermostated at a constant temperature of 32 ± 1°, unless otherwise stated. The cell was divided into two parts of an identical volume by a central partition.

All aqueous buffer solutions and lipid solutions were mutually saturated before the diffusion experiments. The buffers were citrate, acetate, and phosphate systems, depending on the pH range; their ionic strength was adjusted to 0.15 with potassium chloride. The pH of the aqueous phase was measured[6] before use and at the end of the experiments, and no significant change was observed. All experimental conditions, pH of the aqueous phase, temperature, and diffusion period, were chosen so that the degradation of the β-lactam moiety of penicillins may occur within 2% during the experiments.

The cell was rotated at a constant speed, followed by the addition of 25 ml of penicillin stock solution. This solution was prepared with the buffer used for the transport study to make a final concentration of 5×10^{-5}–2×10^{-4} *M*, according to the penicillin solubilities. At various time intervals, 3-ml samples were removed from the aqueous phase and 3 ml of aqueous buffer, preheated to the temperature studied, was added successively to maintain the constant surface area to volume ratio. All additions and withdrawals were made through a stainless steel tube inserted into the aqueous phase, which was connected with a 5-ml injector to the exterior of the oven (Fig. 1).

To measure the infinite concentration, C^∞, the same two-phase experiment was conducted in the other part of the cell without sampling for 20–120 min, depending on the rate of both the transfer and the degradation. The final sample aliquot then was taken from the aqueous phase.

All samples from the aqueous phase were centrifuged at 3000 rpm; after appropriate dilution with distilled water, if necessary, they were analyzed by UV spectrophotometry at 260 nm and/or by the method of Bundgaard and Ilver (17). The concentration of penicillins in the aqueous solution was determined from the previously prepared Beer's law plot for the respective antibiotics and was corrected for the dilution arising from each sampling.

[4] Sartorius-Membranfilter GmbH, 34 Göttingen, Germany.
[5] UV-200S double-beam spectrophotometer, Shimadzu, Kyoto, Japan.
[6] PHM 26 meter, Radiometer, Copenhagen, Denmark.

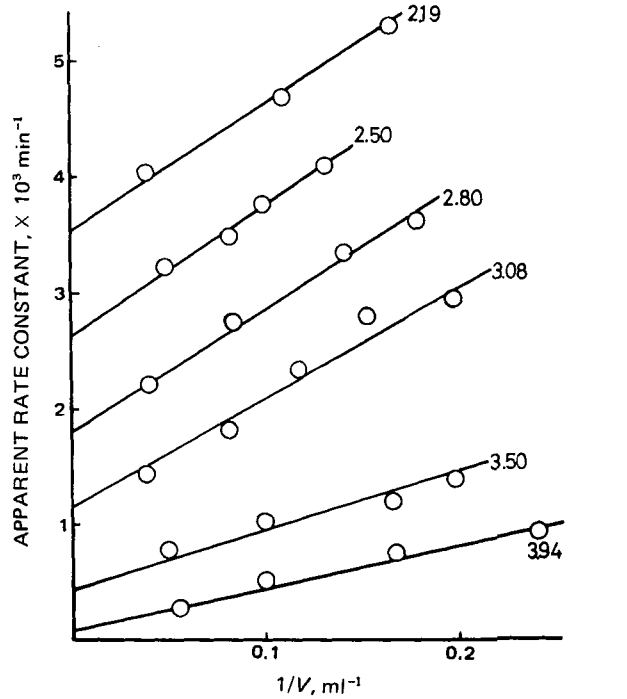

Figure 3—*Effect of the volume of the perfusion solution on absorption rate constants of propicillin from the* in situ *rat stomach at various pH values and 37°. The drug solution was perfused at the flow rate of 10 ml/min, and the pH of the solution was maintained constant with a pH-stat.*

RESULTS

Absorption of Propicillin from Rat Stomach and Intestine *In Situ*—*Rates of Nonenzymatic Degradation and Absorption*—Semilogarithmic plots, showing the disappearance of propicillin from the perfusion solution through the rat stomach and intestine, are shown in Fig. 2. The total disappearance followed first-order kinetics, as observed previously for other semisynthetic β-lactam antibiotics (15).

The apparent first-order rate constants, k_{app}, can be expressed as (15):

$$k_{app} = k_a\frac{1}{V} + k_d \qquad \text{(Eq. 2)}$$

where k_a is the first-order absorption rate constant with units of milliliters time^{-1}, k_d is the first-order nonenzymatic degradation rate constant with units of time^{-1}, and V is the volume of the recirculating drug solution. According to Eq. 2, a plot of k_{app} *versus* $1/V$ provides a straight line with

Table I—Absorption Rate Constant of Propicillin from the *In Situ* Rat GI Tract at Various pH Values and 37°

Stomach		Intestine	
pH[a]	$k_a \times 10^3$, ml min^{-1} [b]	pH[a]	$k_a \times 10^2$, ml min^{-1} [c]
2.19	11.0	3.30	68.2
2.50	11.2	3.50	63.2
2.80	10.5	3.50	75.8
3.08	9.33	4.00	53.8[d]
3.50	5.17	4.50	35.8
3.94	3.42	5.00	28.0
		5.50	8.32
		6.10	4.82

[a] The pH of the perfusion solution was maintained constant with a pH-stat. [b] Obtained from the slope in Fig. 3 according to Eq. 2. [c] Calculated according to Eq. 2. [d] Values determined previously (15).

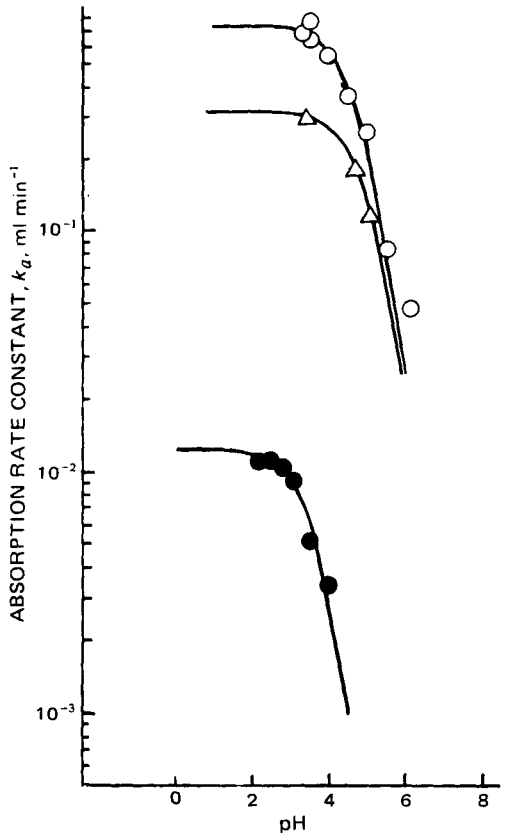

Figure 4—*Plots of the* in situ *rat GI absorption rate constants,* k_a, *of propicillin* versus *the pH of the perfusion solution at 37°. Key:* ●, *experimental points from the stomach at the flow rate of 10 ml/min;* ○, *experimental points from the intestine at the flow rate of 10 ml/min; and* △, *experimental points from the intestine at the flow rate of 10 ml/min for 2.5 min and with perfusion stopped for 10 min. The solid lines were generated from Eq. 17 and the parameters listed in Table VII.*

an intercept equal to k_d and a slope equal to k_a if the absorption process obeys Fick's law. This equation was substantiated previously in the *in situ* rat intestinal absorption experiments of various β-lactam antibiotics at pH 4.0 (15).

For the stomach recirculation experiments with propicillin at various pH values, plots according to Eq. 2 are shown in Fig. 3. Good straight lines were obtained with different slopes and intercepts at every pH of the propicillin solution. The k_d values determined from the intercepts were almost equal to those determined *in vitro* at the same pH, suggesting that the nonenzymatic degradation of penicillin in perfusion solution through the rat stomach depends only on the bulk pH values, as observed previously in the experiment on rat small intestinal absorption (15). Table I summarizes the absorption rate constants, k_a, determined according to Eq. 2 for the gastric and intestinal absorption of propicillin.

Table II—Degree of the pH Shift of the *In Situ* Absorption Rate- and *In Vitro* Transfer Rate-pH Profiles for Propicillin, Cloxacillin, and Penicillin V under Various Hydrodynamic Conditions

Penicillin	Rotating Speed, rpm, or GI Tract	pKa[a]	pKa^{app} [b]	Degree of pH Shift[c]
		In Vitro		
Propicillin	10	2.76	5.08 ± 0.07	2.32
Propicillin	20	2.76	5.02 ± 0.11	2.26
Propicillin	38	2.76	4.89 ± 0.05	2.13
Cloxacillin	20	2.78	4.72 ± 0.04	1.94
Penicillin V	10	2.79	4.35 ± 0.12	1.56
Penicillin V	38	2.79	4.00 ± 0.18	1.21
		In Situ		
Propicillin	Stomach[d]	2.76	3.49 ± 0.08	0.73
Propicillin	Intestine[d]	2.76	4.61 ± 0.10	1.85
Propicillin	Intestine[e]	2.76	4.87 ± 0.03	2.11

[a] Reference 3. [b] pKa^{app} ± *SD*, computed from the data in Fig. 4 and Figs. 8–10 according to Eq. 17 by nonlinear regression analysis[7]. [c] pKa^{app} − pKa. [d] Perfused at 10 ml/min. [e] Perfused at 10 ml/min for 2.5 min and statically for 10 min (see text).

pH–Absorption Rate Profile of Propicillin—In Fig. 4, the absorption rate constants, k_a, from the rat stomach and small intestine are plotted against the bulk pH of the perfusion solution. Intestinal absorption rates of propicillin were about 100 times faster than the gastric absorption rates at every pH, undoubtedly because of the relative surface areas and physiological organization of the two sites (19, 21).

From these pH–rate profiles, it is apparent that the major absorbable species of propicillin is its undissociated form rather than the ionized one at both absorption sites. If the pH–partition hypothesis is valid for propicillin absorption, the theory described by Eq. 3 gives, for the apparent pKa^{app} values (Table II) to be best fit[7] with the data for the perfusion flow rate of 10 ml/min (Fig. 4), 4.61 and 3.49 for the intestinal and gastric absorption, respectively:

$$k_a = k_u \left(\frac{a_H}{a_H + K_a^{app}}\right) \qquad \text{(Eq. 3)}$$

where a_H is the bulk hydrogen-ion activity of the drug solution, K_a^{app} is the apparent dissociation constant of the drug, and k_u is the absorption rate constant for the undissociated drug. The pKa^{app} values thus computed, however, significantly differ from the true pKa = 2.76 (3) of propicillin itself. This discrepancy is not well interpreted by the classical pH–partition theory.

***In Vitro* Transport of Penicillins in Water–Oil Two-Phase Model**—*Kinetics of Interphase Transfer*—When the transfer of a drug from the aqueous phase to the lipid phase obeys Fick's law of diffusion, Eq. 4 can be derived by assuming that a rapid partition equilibrium is always present at the interphase:

$$-\frac{dC_I}{dt} = k_{app}\left(C_I - \frac{C_{II}}{P_{app}}\right) \qquad \text{(Eq. 4)}$$

where C_I and C_{II} represent the concentrations of the drug in the aqueous phase (Compartment I) and in the oil phase (Compartment II), respectively; P_{app} is the apparent partition coefficient; and k_{app} is the apparent first-order transfer rate constant. The total quantity of the drug in two phases is given as:

$$Q_0 = Q_I + Q_{II} \qquad \text{(Eq. 5)}$$

Therefore:

$$V_I C_0 = V_I C_I + V_{II} C_{II} \qquad \text{(Eq. 6)}$$

where Q_I and Q_{II} represent the quantities of the drug in the aqueous and oil phases, respectively; Q_0 and C_0 are the quantity and concentration in the aqueous phase at time zero, respectively; and V_I and V_{II} are the volumes of the respective phases.

Combination of Eqs. 4–6 leads to:

$$-\frac{dC_I}{dt} = k_{app}[(F+1)C_I - FC_0] \qquad \text{(Eq. 7)}$$

where:

$$F = \frac{V_I}{P_{app} V_{II}} \qquad \text{(Eq. 8)}$$

Integration of Eq. 7 yields:

$$\log(C_I - C_I^\infty) = \log(C_0 - C_I^\infty) - \frac{k_{obs}}{2.303} t \qquad \text{(Eq. 9)}$$

where:

$$C_I^\infty = \frac{F}{1+F} C_0 \qquad \text{(Eq. 10)}$$

$$k_{obs} = k_{app} \frac{C_0}{C_0 - C_I^\infty} \qquad \text{(Eq. 11)}$$

where C_I^∞ represents the concentration of the drug in the aqueous phase at infinite time.

According to Eq. 9, it is predicted that a plot of the logarithm of $C_I - C_I^\infty$ *versus* time provides a straight line with a slope of $-k_{obs}/2.303$. Typical plots for propicillin, cloxacillin, and penicillin V are shown in Fig.

[7] A nonlinear regression analysis by the Fortran IV computer program written by the authors. The digital computer, FACOM 230-35, was used at the Data Processing Center, Kanazawa University.

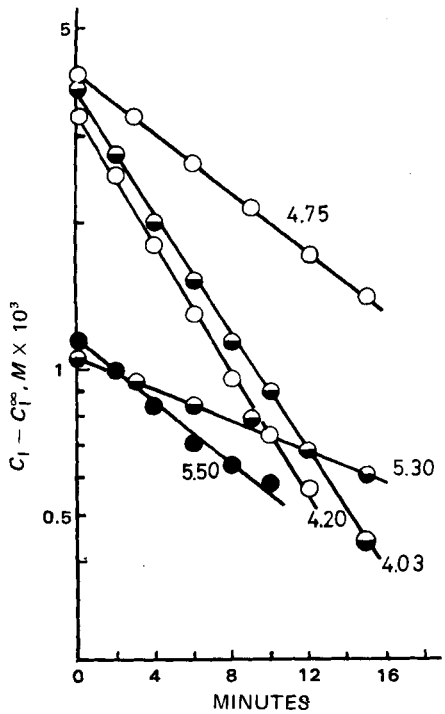

Figure 5—*Typical plots of* ($C_l - C_l^\infty$) versus *time for the two-phase transport of penicillins at various pH values and 32 ± 1°. Key:* ●, *cloxacillin, pH 5.50 (20 rpm);* ○, *propicillin, pH 4.20 (20 rpm) and pH 4.75 (10 rpm); and* ◒, *penicillin V, pH 5.30 (10 rpm) and pH 4.03 (38 rpm). The aqueous phase was acetate and citrate buffers of 0.15 ionic strength, and the oil phase was octanol.*

5, giving good straight lines in accordance with the prediction. The observed first-order rate constants, k_{obs}, can be converted to the apparent first-order transfer rate constant, k_{app}, with Eq. 11.

Factors Affecting Apparent Intestinal Transfer Rates—The diffusion rate constant, k_{app}, can generally be represented as:

$$k_{app} = \Phi \frac{DS}{V_I L_I} \qquad \text{(Eq. 12)}$$

where D is the diffusion coefficient of the drug, L_I is the aqueous diffusion layer thickness, S is the geometrical surface area of the interphase, and Φ represents a factor affected by the degree of ionization of diffusion molecule, solvent composition, and hydrodynamic situations. If Eq. 12 is valid for the interphase transfer of penicillins, k_{app} should be affected by the change in L_I, V_I, and S.

Table III demonstrates the effect of rotating speed on the cloxacillin transport rate from the aqueous phase, pH 4.0 acetate buffer, to the lipoidal phase, octanol–cyclohexane (1:1 v/v). The enhanced transport rates with an increasing rotating rate may exclusively be the result of a decrease in the diffusion layer thickness, L_I, since D, V_I, and S remain constant.

Equation 12 predicts that k_{app} depends on the change in the surface of the aqueous phase to volume ratio. As shown in Fig. 6 for the transfer of cloxacillin at 30 rpm from the aqueous pH 4.0 acetate buffer into octanol–cyclohexane (1:1 v/v), a plot of k_{app} *versus* S/V_I yields a straight line through the origin in accordance with the theory (Eq. 12).

The temperature effect on the transfer rate of penicillins from the

Table III—Effect of Rotating Rate on the Transfer Rate Constant of Cloxacillin at 33° from the Aqueous Phase [a] to the Lipoidal Phase [b]

Rotating Rate, rpm	Transfer Rate Constant, k_{app}, min^{-1}
9	0.05
20	0.10
30	0.12
38	0.17

[a] Acetate buffer (0.02 *M*) of 0.15 ionic strength and pH 4.0. [b] Octanol–cyclohexane (1:1 v/v).

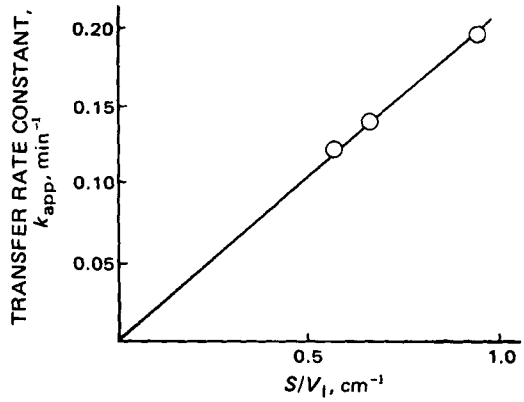

Figure 6—*Effect of the surface area to volume ratio on the transfer rate constant,* k_{app}, *for the* in vitro *two-phase transport of cloxacillin at 30 rpm at pH 4.0 and 33°. The aqueous phase was 0.02* M *acetate buffer of 0.15 ionic strength, and the oil phase was octanol–cyclohexane (1:1 v/v).*

aqueous phase into the octanol phase was examined for various penicillins. The Arrhenius equation predicts:

$$k_{app} = k_0 e^{-\Delta E_a/RT} \qquad \text{(Eq. 13)}$$

where k_0 represents the transfer rate constant independent of temperature and ΔE_a is the activation energy for the interphase transfer. Arrhenius plots (Fig. 7) yielded good straight lines for all penicillins studied. The activation enthalpies, $\Delta H^{\neq}$ ($= \Delta E_a - RT$), at 37° (Table IV) ranged from 1 to 4 kcal/mole and were similar to those obtained for the interphase transport of sulfonamides (22). Such small activation enthalpies may reflect those of diffusion coefficients (23).

All results obtained suggest strongly that *in vitro* interphase transport of penicillins in the two-phase rolling cell follows the rate-limiting diffusion in accordance with Eq. 12.

pH Dependency of Apparent Interphase Transfer Rates—Since quasi-steady-state and perfect sink conditions can be achieved in a system where the drug concentration transferred into the oil phase may be sufficiently diluted, experiments in such a transport system are expected to be sufficient for theoretical consideration of the diffusion kinetics. Rate constants, k_{app}, determined under sink conditions, which could be obtained by the dilution of the oil phase with fresh octanol through a recirculating pump, were considered to be approximately equal to those determined in the system with an equal volume phase of 100 ml (Table V).

For experimental convenience, therefore, k_{app} values were all determined as a function of pH over the 3.0–6.0 range in the two-phase system of 100 ml each of aqueous buffer and octanol under various hydrodynamic conditions, being regarded approximately as quasi-steady-state rate constants.

For comparison between *in situ* and *in vitro* absorption and transport,

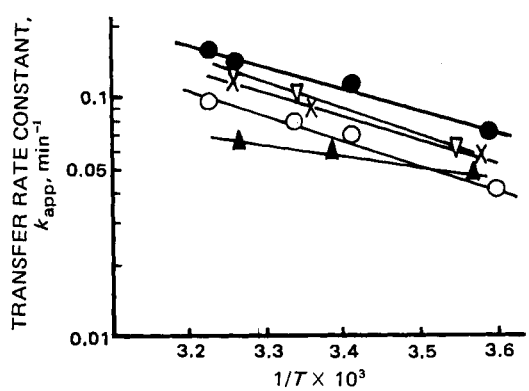

Figure 7—*Arrhenius plots for the* in vitro *two-phase transport rate constants of penicillins at 20 rpm. The aqueous phase was 0.15* M *acetate buffer of pH 4.20, except for dicloxacillin at pH 4.70, and of 0.15 ionic strength. The oil phase was octanol. Key:* ▲, *dicloxacillin;* ▽, *cloxacillin;* ×, *oxacillin;* ●, *propicillin; and* ○, *penicillin V.*

Table IV—Activation Enthalpy at 37° for the Transfer Rate at 20 rpm of Penicillins from the Aqueous Phase [a] to the Lipoidal Phase [b]

Penicillin	$\Delta H^{\neq}$ [c], kcal/mole
Dicloxacillin	1.4
Cloxacillin	4.4
Oxacillin	3.7
Propicillin	3.5
Penicillin V	4.0

[a] Acetate buffer (0.15 *M*) of 0.15 ionic strength. [b] Octanol. [c] $\Delta H^{\neq} = \Delta Ea - RT$ at pH 4.20, except dicloxacillin at pH 4.70.

Table V—Effect of Dilution of the Lipoidal Phase to Examine Sink Conditions for the Transfer Rate Constant of Propicillin at 10 rpm at 31°

pH	Aqueous Phase[a], ml	Lipoidal Phase[b], ml	Transfer Rate Constant, $k_{app} \times 10^2$ min^{-1}
5.27	100	600[c]	2.60
5.25	100	350[d]	2.59
5.23	100	100	3.38

[a] Citrate buffer (0.03 *M*) of 0.15 ionic strength. [b] Octanol. [c] The oil phase of 100 ml was exchanged continuously with 500 ml of fresh octanol through a circulation pump. [d] The oil phase of 100 ml was exchanged continuously with 250 ml of fresh octanol through a circulation pump.

Table VI—Effect of the Initial Concentration for the Transfer Rate Constant of Propicillin from the Aqueous Phase [a] to the Lipoidal Phase [b] at 20 rpm and 31°

pH	Initial Concentration, *M*	Transfer Rate Constant, k_{app}, min^{-1}
4.20	1×10^{-2}	0.154
4.20	5×10^{-3}	0.140
4.10	1×10^{-3}	0.150
4.10	5×10^{-4}	0.152
4.10	1×10^{-4}	0.153

[a] Acetate buffer (0.15 *M*) of 0.15 ionic strength. [b] Octanol.

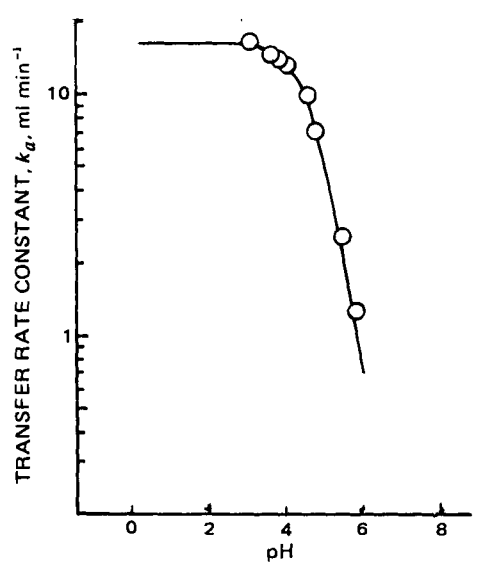

Figure 8—*Plots of the transfer rate constant,* k_a, *of cloxacillin* versus *the pH of the aqueous phase in* in vitro *two-phase transfer experiments at 20 rpm and 33°. The points are experimental values, and the solid line was generated from Eq. 17 and the parameters listed in Table VII.*

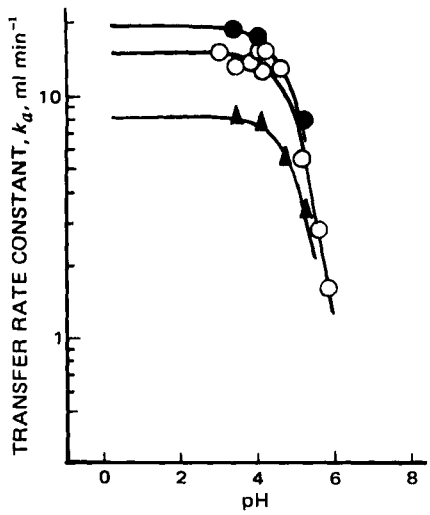

Figure 9—*Plots of the transfer rate constant,* k_a, *of propicillin at various rotating rates* versus *the pH of the aqueous phase in* in vitro *two-phase transfer experiments at 31°. Key:* ▲, *10 rpm;* ○, *20 rpm; and* ●, *38 rpm. The points are experimental values, and the solid lines were generated from Eq. 17 and the parameters listed in Table VII.*

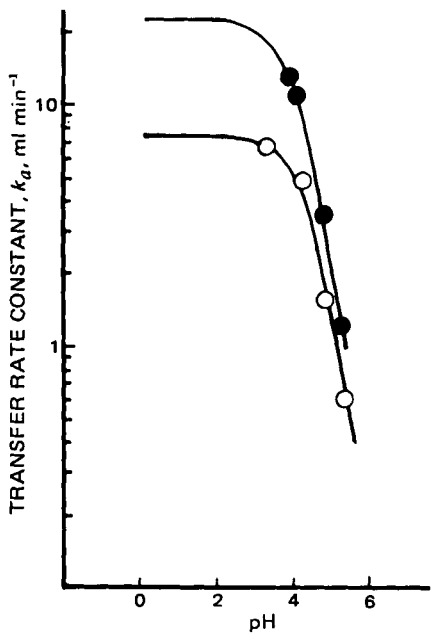

Figure 10—*Plots of the transfer rate constant,* k_a, *of penicillin V at various rotating rates* versus *the pH of the aqueous phase in* in vitro *two-phase transfer experiments at 31°. Key:* ○, *10 rpm; and* ●, *38 rpm. The points are experimental values, and the solid lines were generated from Eq. 17 and the parameters listed in Table VII.*

the first-order interphase transfer rate constants, k_a, can be defined as:

$$k_{app} = k_a \frac{1}{V} \qquad \text{(Eq. 14)}$$

These results are illustrated in Figs. 8–10 as plots of log k_a for cloxacillin, propicillin, and penicillin V *versus* the bulk pH of the aqueous phase. The k_a–pH profiles showed apparently rightward shifts relative to the corresponding dissociation curves. The best fitting pKa^{app} values were computed according to Eq. 3 in a manner similar to that already described (Table II). These values differed by 1–2 pKa units from the respective true pKa values (3).

In the present *in vitro* two-phase experiments, the extent of the penicillin degradation in the aqueous phase was within 2% during transport kinetics. No significant change in the rates was observed by the change in the initial concentration of penicillins (Table VI). Below pH 5, trans-

port of ionized species of penicillin can be regarded as almost negligible, considering that the partition ratios of undissociated to ionized species between water and octanol are approximately 10^3 for the respective penicillins (3).

From these findings, the deviation of Eq. 3 from the pH–partition theory can be concluded to be virtually due to the diffusion kinetics of undissociated penicillin species.

DISCUSSION

Discrepancies from the pH–partition hypothesis occur in the GI absorption of some drugs (19, 24–35). The contribution of physiological factors such as the requirement of a higher acid pH, *i.e.*, virtual pH at the membrane surface (24, 27, 28), or drug binding to the intestinal mucosal surface (25, 26, 29) was proposed as being responsible for deviation from this hypothesis. The two possibilities cannot explain the shifts of pH–rate curves of penicillins observed for *in vitro* interphase transport, where the presence of complicated physiological factors can be completely excluded. Therefore, there is no reason to apply both the virtual pH and binding hypotheses for the harmonious interpretation of both *in situ* and *in vitro* data observed for penicillins.

In situ kinetic evaluation of the absorption of ionic species of the drug was successful in the interpretation of deviation from the pH–partition equation for intestinal absorption of sulfaethidole and barbital (31), salicylic acid (30), and carbenoxolone (26). Ionized penicillin can be absorbed by the rat intestine to a considerable extent in neutral and alkaline pH regions[8], but this contribution to the total intestinal absorption rates had no significant effect on the pH–intestinal absorption curve. For a similar deviation from the pH–partition hypothesis in the *in vitro* experiments for propicillin, cloxacillin, and penicillin V, contribution of the transport rate of the ionic species was also negligible in the water–octanol system, as already discussed.

Therefore, attribution of both *in situ* and *in vitro* deviations observed for penicillins to the hydrodynamic diffusion theory involving the aqueous diffusion layer seems to be the most reasonable explanation.

A two-compartment diffusion model related to drug transport and absorption was developed (33–35). The first compartment (mucosal side; aqueous phase) consists of a bulk aqueous drug solution phase and a diffusion layer of thickness L_I, and it is in series with the second compartment consisting of a lipid phase (membrane) of thickness L_{II}. If there is a perfect sink on the second side after the lipid barrier and only the nonionized drug species permeates through the lipid membrane, the diffusion model yields the apparent quasi-steady-state first-order absorption rate constant, k_{app}, for acidic drugs (33):

$$k_{app} = \frac{SD_{aq}}{V_I L_I}\left[\frac{1}{\left[1 + \frac{K_a}{(a_H)s}\right]T + 1}\right] \qquad \text{(Eq. 15)}$$

where:

$$T = \frac{L_{II} D_{aq}}{L_I D_{lip} P_u R} \qquad \text{(Eq. 16)}$$

where D_{aq} and D_{lip} are the diffusion coefficients of the drug in water and lipid, respectively; P_u is the partition coefficient of the undissociated drug between the lipid and aqueous solution; $(a_H)s$ is the hydrogen-ion activity at the surface of the lipoid phase (membrane); and R is the ratio of the true interfacial area to the geometrical area. In a well-buffered solution, as in the present *in situ* and *in vitro* experiments, the pH at the lipoidal surface would not differ substantially from that in the bulk of the solution (36). Hence, $(a_H)s = a_H$.

Rearrangement of Eq. 15 yields:

$$k_a = k_u' \frac{a_H}{\left(1 + \frac{1}{T}\right)a_H + K_a} \qquad \text{(Eq. 17)}$$

where:

$$k_u' = \frac{SD_{lip} P_u R}{L_{II}} \qquad \text{(Eq. 18)}$$

where k_a is equal to $k_{app} V_I$ and the first-order rate constant is independent of the volume of the bulk drug solution. If T is large, the T^{-1} term in Eq. 17 becomes negligible compared to 1 and Eq. 17 can be reduced to an equation similar to Eq. 3, predicted by the pH–partition hypothesis.

[8] To be published.

Table VII—Computed Parameters in Accordance with Aqueous Diffusion Layer Theory for pH–k_a Profiles of *In Situ* Rat Intestinal and Gastric Absorption of Propicillin and *In Vitro* Interphase Transport of Propicillin, Cloxacillin, and Penicillin V under Various Hydrodynamic Conditions

Penicillin	Rotating Speed, rpm, or GI Tract	k_u'[a], ml min^{-1}	$T \times 10^3$
		In Vitro	
Propicillin	10	1697 ± 250	4.79 ± 0.81
Propicillin	20	2748 ± 706	5.53 ± 1.57
Propicillin	38	2593 ± 288	7.52 ± 0.93
Cloxacillin	20	1397 ± 116	11.73 ± 1.14
Penicillin V	10	266 ± 67	28.66 ± 9.06
Penicillin V	38	367 ± 87	65.42 ± 3.15
		In Situ	
Propicillin	Stomach[b]	0.07 ± 0.01	229.70 ± 54.08
Propicillin	Intestine[b]	51.14 ± 12.31	128.70 ± 9.16
Propicillin	Intestine[c]	40.77 ± 2.39	69.80 ± 19.63

[a] Computed from the data in Figs. 4 and 8–10 according to Eq. 17 by nonlinear regression analysis. [b] Perfused at 10 ml/min. [c] Perfused at 10 ml/min and statically for 10 min (see text).

If T is not large or if it cannot be ignored, Eq. 17 predicts the rightward deviation from the pH–partition curve depending on the magnitude of T. This physical model was applied to various *in situ* absorption rates involving buccal, gastric, intestinal, and rectal absorption with satisfactory results (34, 35, 37).

If both *in situ* and *in vitro* deviations from the pH–partition hypothesis presently observed for penicillins were to be substantially attributed to the aqueous diffusion layer theory described by Eq. 17, rather than to the extraction theory (32) derived from the distribution model of the permeating substance between the barrier and bulk phase solution, a change in the T value should produce a change in the shift of pH–absorption profiles. The increasing thickness of the aqueous diffusion layer, L_I, should lower the T value and thereby not only decrease the absorption rate but also yield a rightward shift of the pH–rate curve from the dissociation curve.

Such a prediction was examined for both *in vitro* interphase transport and *in situ* absorption experiments. Figures 9 and 10 show that the effect of the rotating speed decreased the transfer rates and also produced a significant rightward shift of the profile. Figure 4 shows the *in situ* absorption rate–pH profiles of propicillin under two different hydrodynamic conditions; one was carried out at the flow rate of 10 ml/min for 2.5 min with a static situation for 10 min. When the drug solution was less agitated, the intestinal absorption rates were significantly decreased and the profile shifted rightward, in accordance with the prediction from Eq. 17. The best fit parameters[7] according to Eq. 17 for various pH–k_a data are summarized in Table VII.

All experimental evidence obtained in this study strongly suggested the importance of the aqueous diffusion layer adjacent to the lipid, both for the *in vitro* transport and the *in situ* absorption of penicillin molecules. The deviation of the *in situ* gastric and intestinal absorption rate–pH profiles by approximately 0.8 and 2 pH units, respectively, from the dissociation curve can be regarded as the result of the membrane transport of undissociated species of penicillin permeating through the barrier of the aqueous diffusion layer rather than other possibilities such as the virtual pH hypothesis and drug–mucosal binding theory, which can be easily ruled out in the *in vitro* simple diffusion experiment. The difference in the extent of the shifts observed between the gastric and intestinal absorption rate–pH profiles is probably due to the ratio of the aqueous diffusion layer permeability, D_{aq}/L_I, to the lipoidal membrane permeability, $D_{lip}P_u/L_{II}$, and/or the different ratio of the true interfacial area to geometrical area, R, at the respective absorption sites.

The results of the intestinal absorption behavior of various penicillins in the region of pH 4–9 will be presented in a subsequent paper, and the quantitative relationship between the rates and the structural properties will be discussed according to the aqueous diffusion layer theory.

REFERENCES

(1) L. S. Schanker, D. J. Tocco, B. B. Brodie, and C. A. M. Hogben, *J. Pharmacol. Exp. Ther.*, **123**, 81 (1958).

(2) H. D. C. Rapson and A. E. Bird, *J. Pharm. Pharmacol.*, **15**, 222 T (1963).

(3) A. Tsuji, O. Kubo, E. Miyamoto, and T. Yamana, *J. Pharm. Sci.*, **66**, 1675 (1977).
(4) A. E. Bird and A. C. Marshall, *J. Chromatogr.*, **63**, 313 (1971).
(5) G. L. Biagi, A. M. Barbaro, M. C. Guerra, and M. F. Gamba, *ibid.*, **44**, 195 (1969).
(6) H. Juncher and F. Raaschou, *Antibiot. Med. Clin. Ther.*, **4**, 497 (1957).
(7) C. G. McCarthy and M. Finland, *N. Engl. J. Med.*, **263**, 315 (1960).
(8) I. M. Rollo and D. M. Burley, *Br. Med. J.*, **13**, 76 (1962).
(9) C. M. Kunin, *Antimicrob. Agents Chemother.*, **1966**, 1025.
(10) G. N. Rolinson and R. Sutherland, in "Advances in Pharmacology and Chemotherapy," vol. 11, G. Garrattini, A. Goldin, F. Hawking, and I. P. Kopin, Eds., Academic, New York, N.Y., 1973, p. 151.
(11) I. M. Rollo, *Can. J. Physiol. Pharmacol.*, **50**, 986 (1972).
(12) D. Perrier and M. Gibaldi, *J. Pharm. Sci.*, **62**, 1486 (1973).
(13) S. C. Penzotti, Jr., and J. W. Poole, *ibid.*, **63**, 1803 (1974).
(14) M. Yasuhara, Y. Miyoshi, T. Kimura, S. Muranishi, and H. Sezaki, *Chem. Pharm. Bull.*, **25**, 675 (1977).
(15) A. Tsuji, E. Miyamoto, I. Kagami, H. Sakaguchi, and T. Yamana, *J. Pharm. Sci.*, **67**, 1701 (1978).
(16) T. Fujita, J. Iwasa, and C. Hansch, *J. Am. Chem. Soc.*, **86**, 5175 (1964).
(17) H. Bundgaard and K. Ilver, *J. Pharm. Pharmacol.*, **24**, 790 (1972).
(18) T. Koizumi, T. Arita, and K. Kakemi, *Chem. Pharm. Bull.*, **12**, 413 (1964).
(19) J. T. Doluisio, N. F. Billups, L. W. Dittert, E. T. Sugita, and J. V. Swintosky, *J. Pharm. Sci.*, **58**, 1196 (1969).
(20) J. S. Robertson and B. W. Madsen, *ibid.*, **63**, 234 (1974).
(21) J. B. Houston, D. G. Upshall, and J. W. Bridges, *J. Pharmacol. Exp. Ther.*, **195**, 67 (1975).
(22) G. E. Schumacher and J. B. Nagwekar, *J. Pharm. Sci.*, **63**, 240 (1974).
(23) S. Glasstone, K. J. Laidler, and H. Eyring, "The Theory of Rate Processes," McGraw-Hill, New York, N.Y., 1941.
(24) T. Koizumi, T. Arita, and K. Kakemi, *Chem. Pharm. Bull.*, **12**, 421 (1964).
(25) K. Kakemi, T. Arita, R. Hori, R. Konishi, K. Nishimura, H. Matsui, and T. Nishimura, *ibid.*, **17**, 255 (1969).
(26) J. W. Bridges, J. B. Houston, M. J. Humphrey, W. E. Lindup, D. V. Parke, J. S. Shillingford, and D. G. Upshall, *J. Pharm. Pharmacol.*, **28**, 117 (1976).
(27) C. A. M. Hogben, D. J. Tocco, B. B. Brodie, and L. S. Schanker, *J. Pharmacol. Exp. Ther.*, **125**, 275 (1959).
(28) D. Winne, *J. Pharmacokinet. Biopharm.*, **5**, 53 (1977).
(29) S. Furusawa, K. Okumura, and H. Sezaki, *J. Pharm. Pharmacol.*, **24**, 272 (1971).
(30) H. Nogami and T. Matsuzawa, *Chem. Pharm. Bull.*, **9**, 532 (1961).
(31) W. G. Crouthamel, G. H. Tan, L. W. Dittert, and J. T. Doluisio, *J. Pharm. Sci.*, **60**, 1160 (1971).
(32) J. G. Wagner and A. J. Sedman, *J. Pharmacokinet. Biopharm.*, **1**, 23 (1973).
(33) A. Suzuki, W. I. Higuchi, and N. F. H. Ho, *J. Pharm. Sci.*, **59**, 644 (1970).
(34) *Ibid.*, **59**, 651 (1970).
(35) N. H. F. Ho and W. I. Higuchi, *J. Pharm. Sci.*, **63**, 686 (1974).
(36) V. F. Smolen, *ibid.*, **62**, 77 (1973).
(37) K. R. M. Vora, W. I. Higuchi, and N. F. H. Ho, *ibid.*, **61**, 1785 (1972).

ACKNOWLEDGMENTS

Presented in part at the 97th Annual Meeting of the Pharmaceutical Society of Japan, Tokyo, Japan, April 1977.

The authors acknowledge the gifts of penicillins from Banyu Pharmaceutical Co., Meiji Seika Kaisha, and Takeda Chemical Industries. They thank Dr. A. Suzuki for helpful discussions and Miss E. Kosugi for assistance.

Dissolution Kinetics of Cholesterol in Simulated Bile II: Influence of Simulated Bile Composition

K. H. KWAN *, W. I. HIGUCHI *x, and A. F. HOFMANN ‡

Received November 18, 1977, from the **College of Pharmacy, University of Michigan, Ann Arbor, MI 48109*, and the ‡*University Hospital, Department of Medicine, Division of Gastroenterology, University of California at San Diego, San Diego, CA 92103.* Accepted for publication April 26, 1978.

Abstract □ Normal human gallbladder bile and gallbladder bile of patients undergoing chenodeoxycholic acid therapy were simulated by using appropriate combinations of taurine and glycine conjugates of cholic, chenodeoxycholic, and deoxycholic acids. Also, the total bile acid concentration and the total bile acid to lecithin ratio were varied over physiological ranges. Dissolution rates of cholesterol monohydrate pellets (model gallstone) in these solutions were 90–99% interfacially controlled. Even under conditions favorable for dissolution, *i.e.*, high bile acid concentration and high bile acid to lecithin ratio, the interfacial resistances were extremely large. These results are of the same order of magnitude as those found in the limited studies with actual gallbladder bile and suggest that the bile acids, lecithin, and the electrolytes are the primary determinants of the interfacial resistance for cholesterol dissolution. Furthermore, the kinetics of dissolution were always much faster with the chenodeoxycholic acid-rich compositions than with the corresponding normal compositions. This finding suggests, therefore, that in addition to desaturating bile with respect to cholesterol, the feeding of chenodeoxycholic acid further facilitates cholesterol gallstone dissolution by reducing the interfacial resistance of the process.

Keyphrases □ Cholesterol—dissolution kinetics in simulated bile, effect of bile composition □ Dissolution kinetics—cholesterol in simulated bile, effect of bile composition □ Bile composition—effect on dissolution kinetics of cholesterol in simulated bile

Recent studies (1–7) on the dissolution of human cholesterol gallstones and cholesterol monohydrate pellets in bile acid–lecithin solutions and in human gallbladder bile indicated that:

1. The dissolution of both cholesterol gallstones and cholesterol monohydrate pellets (model gallstones) was interfacially controlled rather than diffusion–solubility controlled, providing a possible explanation for the rather slow rate of stone dissolution *in vivo* (8).

2. The interfacial resistance to dissolution was a function of the composition of the simulated bile solution—*viz.*, the bile acid type and concentration, the bile acid to lecithin ratio, and the electrolyte type and concentration.

3. The magnitudes of the interfacial resistances in both the simulated bile solutions and the human gallbladder biles were indeed comparable.

0022-3549/78/1200-1711$01.00/0
© 1978, American Pharmaceutical Association

(3) A. Tsuji, O. Kubo, E. Miyamoto, and T. Yamana, *J. Pharm. Sci.*, **66**, 1675 (1977).
(4) A. E. Bird and A. C. Marshall, *J. Chromatogr.*, **63**, 313 (1971).
(5) G. L. Biagi, A. M. Barbaro, M. C. Guerra, and M. F. Gamba, *ibid.*, **44**, 195 (1969).
(6) H. Juncher and F. Raaschou, *Antibiot. Med. Clin. Ther.*, **4**, 497 (1957).
(7) C. G. McCarthy and M. Finland, *N. Engl. J. Med.*, **263**, 315 (1960).
(8) I. M. Rollo and D. M. Burley, *Br. Med. J.*, **13**, 76 (1962).
(9) C. M. Kunin, *Antimicrob. Agents Chemother.*, **1966**, 1025.
(10) G. N. Rolinson and R. Sutherland, in "Advances in Pharmacology and Chemotherapy," vol. 11, G. Garrattini, A. Goldin, F. Hawking, and I. P. Kopin, Eds., Academic, New York, N.Y., 1973, p. 151.
(11) I. M. Rollo, *Can. J. Physiol. Pharmacol.*, **50**, 986 (1972).
(12) D. Perrier and M. Gibaldi, *J. Pharm. Sci.*, **62**, 1486 (1973).
(13) S. C. Penzotti, Jr., and J. W. Poole, *ibid.*, **63**, 1803 (1974).
(14) M. Yasuhara, Y. Miyoshi, T. Kimura, S. Muranishi, and H. Sezaki, *Chem. Pharm. Bull.*, **25**, 675 (1977).
(15) A. Tsuji, E. Miyamoto, I. Kagami, H. Sakaguchi, and T. Yamana, *J. Pharm. Sci.*, **67**, 1701 (1978).
(16) T. Fujita, J. Iwasa, and C. Hansch, *J. Am. Chem. Soc.*, **86**, 5175 (1964).
(17) H. Bundgaard and K. Ilver, *J. Pharm. Pharmacol.*, **24**, 790 (1972).
(18) T. Koizumi, T. Arita, and K. Kakemi, *Chem. Pharm. Bull.*, **12**, 413 (1964).
(19) J. T. Doluisio, N. F. Billups, L. W. Dittert, E. T. Sugita, and J. V. Swintosky, *J. Pharm. Sci.*, **58**, 1196 (1969).
(20) J. S. Robertson and B. W. Madsen, *ibid.*, **63**, 234 (1974).
(21) J. B. Houston, D. G. Upshall, and J. W. Bridges, *J. Pharmacol. Exp. Ther.*, **195**, 67 (1975).
(22) G. E. Schumacher and J. B. Nagwekar, *J. Pharm. Sci.*, **63**, 240 (1974).
(23) S. Glasstone, K. J. Laidler, and H. Eyring, "The Theory of Rate Processes," McGraw-Hill, New York, N.Y., 1941.
(24) T. Koizumi, T. Arita, and K. Kakemi, *Chem. Pharm. Bull.*, **12**, 421 (1964).
(25) K. Kakemi, T. Arita, R. Hori, R. Konishi, K. Nishimura, H. Matsui, and T. Nishimura, *ibid.*, **17**, 255 (1969).
(26) J. W. Bridges, J. B. Houston, M. J. Humphrey, W. E. Lindup, D. V. Parke, J. S. Shillingford, and D. G. Upshall, *J. Pharm. Pharmacol.*, **28**, 117 (1976).
(27) C. A. M. Hogben, D. J. Tocco, B. B. Brodie, and L. S. Schanker, *J. Pharmacol. Exp. Ther.*, **125**, 275 (1959).
(28) D. Winne, *J. Pharmacokinet. Biopharm.*, **5**, 53 (1977).
(29) S. Furusawa, K. Okumura, and H. Sezaki, *J. Pharm. Pharmacol.*, **24**, 272 (1971).
(30) H. Nogami and T. Matsuzawa, *Chem. Pharm. Bull.*, **9**, 532 (1961).
(31) W. G. Crouthamel, G. H. Tan, L. W. Dittert, and J. T. Doluisio, *J. Pharm. Sci.*, **60**, 1160 (1971).
(32) J. G. Wagner and A. J. Sedman, *J. Pharmacokinet. Biopharm.*, **1**, 23 (1973).
(33) A. Suzuki, W. I. Higuchi, and N. F. H. Ho, *J. Pharm. Sci.*, **59**, 644 (1970).
(34) *Ibid.*, **59**, 651 (1970).
(35) N. H. F. Ho and W. I. Higuchi, *J. Pharm. Sci.*, **63**, 686 (1974).
(36) V. F. Smolen, *ibid.*, **62**, 77 (1973).
(37) K. R. M. Vora, W. I. Higuchi, and N. F. H. Ho, *ibid.*, **61**, 1785 (1972).

ACKNOWLEDGMENTS

Presented in part at the 97th Annual Meeting of the Pharmaceutical Society of Japan, Tokyo, Japan, April 1977.

The authors acknowledge the gifts of penicillins from Banyu Pharmaceutical Co., Meiji Seika Kaisha, and Takeda Chemical Industries. They thank Dr. A. Suzuki for helpful discussions and Miss E. Kosugi for assistance.

Dissolution Kinetics of Cholesterol in Simulated Bile II: Influence of Simulated Bile Composition

K. H. KWAN *, W. I. HIGUCHI *x, and A. F. HOFMANN ‡

Received November 18, 1977, from the **College of Pharmacy, University of Michigan, Ann Arbor, MI 48109*, and the ‡*University Hospital, Department of Medicine, Division of Gastroenterology, University of California at San Diego, San Diego, CA 92103.* Accepted for publication April 26, 1978.

Abstract □ Normal human gallbladder bile and gallbladder bile of patients undergoing chenodeoxycholic acid therapy were simulated by using appropriate combinations of taurine and glycine conjugates of cholic, chenodeoxycholic, and deoxycholic acids. Also, the total bile acid concentration and the total bile acid to lecithin ratio were varied over physiological ranges. Dissolution rates of cholesterol monohydrate pellets (model gallstone) in these solutions were 90–99% interfacially controlled. Even under conditions favorable for dissolution, *i.e.*, high bile acid concentration and high bile acid to lecithin ratio, the interfacial resistances were extremely large. These results are of the same order of magnitude as those found in the limited studies with actual gallbladder bile and suggest that the bile acids, lecithin, and the electrolytes are the primary determinants of the interfacial resistance for cholesterol dissolution. Furthermore, the kinetics of dissolution were always much faster with the chenodeoxycholic acid-rich compositions than with the corresponding normal compositions. This finding suggests, therefore, that in addition to desaturating bile with respect to cholesterol, the feeding of chenodeoxycholic acid further facilitates cholesterol gallstone dissolution by reducing the interfacial resistance of the process.

Keyphrases □ Cholesterol—dissolution kinetics in simulated bile, effect of bile composition □ Dissolution kinetics—cholesterol in simulated bile, effect of bile composition □ Bile composition—effect on dissolution kinetics of cholesterol in simulated bile

Recent studies (1–7) on the dissolution of human cholesterol gallstones and cholesterol monohydrate pellets in bile acid–lecithin solutions and in human gallbladder bile indicated that:

1. The dissolution of both cholesterol gallstones and cholesterol monohydrate pellets (model gallstones) was interfacially controlled rather than diffusion–solubility controlled, providing a possible explanation for the rather slow rate of stone dissolution *in vivo* (8).

2. The interfacial resistance to dissolution was a function of the composition of the simulated bile solution—*viz.*, the bile acid type and concentration, the bile acid to lecithin ratio, and the electrolyte type and concentration.

3. The magnitudes of the interfacial resistances in both the simulated bile solutions and the human gallbladder biles were indeed comparable.

0022-3549/78/1200-1711$01.00/0
© 1978, American Pharmaceutical Association

Table I—Bile Acid Compositions of Normal Human Gallbladder Bile (N) and Gallbladder Bile of Patients Undergoing Chenodeoxycholic Acid Therapy (C)

Type of Bile	Mole Percent					
	I	II	III	IV	V	VI
N	10	30	5	15	10	30
C	15	75	1	4	1	4

4. The kinetics of cholesterol gallstone dissolution in bile may be explainable on the basis of the principal bile acids, lecithin, and the electrolytes in the particular bile.

In the present study, an attempt was made to simulate normal human gallbladder bile, which has been shown to dissolve cholesterol stones very slowly (2, 7), as well as the gallbladder bile of patients undergoing chenodeoxycholic acid therapy for the dissolution of cholesterol gallstones (8–12). The following parameters were varied: the composition of the six principal bile acids, the total concentration of these bile acids, the lecithin concentration, and, hence, the total bile acid to lecithin ratio. A wide range of conditions was simulated with regard to these parameters to cover the likely situations in both populations. All simulated solutions contained 0.10 *M* sodium chloride since the concentration of this predominant bile electrolyte seems to remain rather constant in human bile. In addition, the solutions were maintained at pH 7.40 at 37° with 0.01 *M* phosphate buffer.

The rate of dissolution per unit area, J/A, and the equilibrium solubility, C_s, of cholesterol monohydrate in these simulated solutions were determined experimentally, and the total resistance to dissolution, R, was calculated using (6, 7):

$$J/A = \frac{C_s}{R} \qquad \text{(Eq. 1)}$$

for sink conditions. In Eq. 1, R represents the sum of the diffusional resistance, h/D, and the interfacial resistance, $1/P$, where h is the Nernst effective diffusion layer thickness, D is the diffusion coefficient of micelle-solubilized cholesterol in solution, and P is the effective permeability coefficient of the solid–solution interface (1–7). In the present consideration, however, since $1/P$ is much greater than h/D in all situations, $R \cong 1/P$ = interfacial resistance.

EXPERIMENTAL

Materials—Commercial cholesterol[1] was recrystallized three times from 95% ethanol. Radioactive cholesterol monohydrate was prepared by mixing 5 g of the recrystallized cholesterol with 100 μCi of a benzene solution of 4-^{14}C-cholesterol[2] in 400 ml of 95% ethanol at 60°. This solution was filtered while hot, and the filtrate was allowed to stand for 48 hr at room temperature. Then the cholesterol monohydrate crystals were filtered and dried *in vacuo* for 24 hr. The crystals obtained were stored in the dark in a desiccator saturated with water vapor at room temperature.

NMR studies quantitatively confirmed the monohydrate nature of the crystals. TLC indicated the absence of any impurities (13). X-ray crystallography[3] indicated that they were cholesterol monohydrate crystals and that they had a lattice system similar to that of cholesterol found in human biliary calculi (14). These monohydrate crystals lose their water content readily on exposure to low humidity and light.

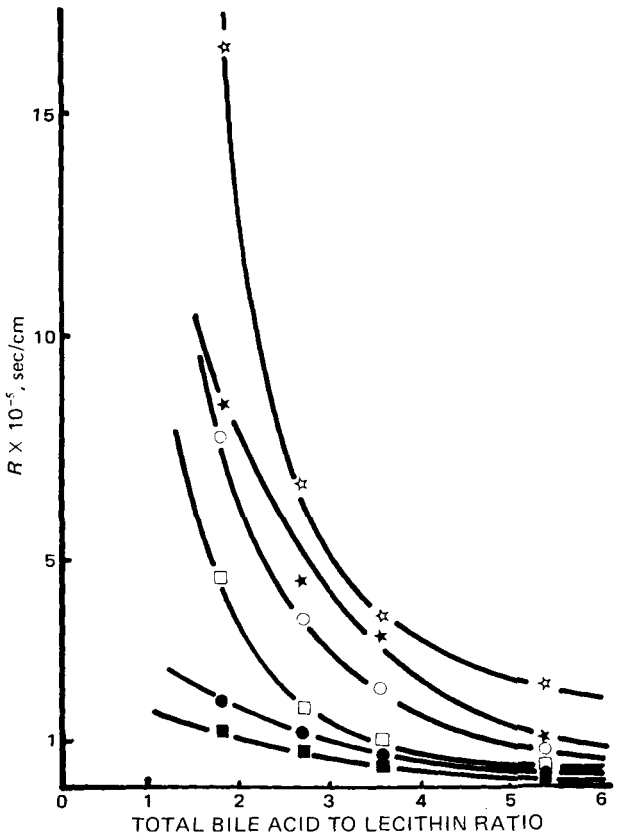

Figure 1—*Profile of* R *dependence on [total bile acid] to [lecithin] ratio at various total bile acid concentrations for simulated normal gallbladder bile (open symbols) and simulated gallbladder bile of patients undergoing chenodeoxycholic acid therapy (closed symbols). Key (concentration of bile acid):* ☆, ★, *46.4 m*M; ○,●, *116.0 m*M; *and* □,■, *174.0 m*M.

The sodium salts of chenodeoxycholyltaurine (I) and chenodeoxycholylglycine (II) were prepared by the method of Norman (15) with certain modifications (16). The sodium salts of deoxycholyltaurine[4] (III) and deoxycholylglycine[4] (IV) were used as received. The sodium salts of cholyltaurine (V) and cholylglycine (VI) were prepared using the method of Norman (15) with certain modifications by Pope (17) and Hofmann[5]. The purity of these compounds was checked and confirmed by TLC using a destructive detection method (18).

Egg lecithin was prepared from fresh egg yolks and subsequently stored according to the method of Singleton *et al.* (19). Chromatographically homogeneous lecithin (mol. wt. ≅ 771) was obtained. Monobasic sodium phosphate, dibasic sodium phosphate, and sodium chloride[6] were analytical grade and were used as received.

Dissolution Rate Determination—Pellets of ^{14}C-cholesterol monohydrate were prepared by directly compressing 100 mg of the material in a die, 1.27 cm i.d., under a force of 1360.8 kg with a laboratory press[7]. The exposed surface area of the resulting pellets was 1.267 cm^2. The pellet was held firmly in a die by covering the bottom with melted paraffin. This die was then placed on the bottom of a water-jacketed cylinder, with the pellet facing a stirring paddle inserted at the top of the cylinder (6). The stirring speed was maintained at 150 rpm during dissolution by a constant-speed motor[8].

Exactly 10 ml of the dissolution medium, preequilibrated at 37°, was added into the cylinder. Immediately, the first 0.50-ml sample was withdrawn using a pipet. Four other samples were taken at suitable time intervals. The ^{14}C-labeled samples were subsequently counted with a

[1] Eastman Kodak Co., Rochester, N.Y.
[2] New England Nuclear Corp., Boston, Mass.
[3] Performed by Dr. C. Nordman, Department of Chemistry, University of Michigan, Ann Arbor, Mich.
[4] Calbiochem, Los Angeles, Calif.
[5] A. F. Hofmann, unpublished data.
[6] Matheson, Coleman and Bell, Norwood, Ohio.
[7] Model B, Fred Carver Inc., Summit, N.J.
[8] Model CA, Hurst, Princeton, Ind.

Table II—Influence of Total Bile Acid Concentration and [Bile Acid] to [Lecithin] Ratio on Solubility, C_s, Dissolution Rate, J/A, and Resistance, R, for Simulated Normal Gallbladder Bile

Total [Bile Acid], mM	Total [Lecithin], mM	[Bile Acid] to [Lecithin] Ratio	$J/A \times 10^4$, mg/cm^2/sec	C_s, mg/ml	$R \times 10^{-3}$, sec/cm
174	96	1.81	0.219	10.27	469
174	64	2.72	0.470	7.65	163
174	48	3.63	0.548	5.86	107
174	32	5.44	0.914	4.55	50
116	64	1.81	0.0914	7.16	783
116	42.6	2.72	0.128	4.80	375
116	32	3.63	0.164	3.60	220
116	21.3	5.44	0.296	2.50	85
46.4	25.6	1.81	0.0146	2.43	1664
46.4	17.0	2.72	0.0301	2.04	678
46.4	12.8	3.63	0.0438	1.70	388
46.4	8.53	5.44	0.0532	1.24	233

Table III—Influence of Total Bile Acid Concentration and [Bile Acid] to [Lecithin] Ratio on Solubility, C_s, Dissolution Rate, J/A, and Resistance, R, for Simulated Gallbladder Bile of Patients Undergoing Chenodeoxycholic Acid Treatment

Total [Bile Acid], mM	Total [Lecithin], mM	[Bile Acid] to [Lecithin] Ratio	$J/A \times 10^4$, mg/cm^2/sec	C_s, mg/ml	$R \times 10^{-3}$, sec/cm
174	96	1.81	0.726	9.07	125
174	64	2.72	0.824	6.59	80
174	48	3.63	1.37	5.71	41.7
174	32	5.44	1.64	4.40	26.8
116	64	1.81	0.367	6.98	190
116	42.6	2.72	0.411	4.56	111
116	32	3.63	0.548	3.67	67.0
116	21.3	5.44	0.685	2.82	41.2
46.4	25.6	1.81	0.0274	2.30	839
46.4	17.0	2.72	0.0392	1.81	462
46.4	12.8	3.63	0.0477	1.63	342
46.4	8.53	5.44	0.107	1.06	99.1

Table IV—Comparison of Experimental and Estimated R Values for Human Gallbladder Bile Samples (7)

Bile Sample	Total [Bile Acid], mM	Total [Lecithin], mM	[Bile Acid] to [Lecithin] Ratio	$R \times 10^{-3a}$, sec/cm	$R \times 10^{-3b}$, sec/cm
1	194.1	41.3	4.70	26.6	55
2	133.7	24.9	5.38	30.6	75
3	237.2	64.9	3.65	40.1	35
4	206.5	46.3	4.46	24.5	55

[a] Determined from $R = AC_s/J$. [b] Estimated from Fig. 1.

liquid scintillation counter[9], and the amount of cholesterol dissolved in the solvent was plotted against time.

Solubility Determination—The solubilities of cholesterol monohydrate in various solvent media were determined by introducing an excess amount of ^{14}C-cholesterol monohydrate of about 20 mg into 2 ml of a solvent in a test tube. The tube was then flushed with nitrogen, capped, and shaken by a wrist-action shaker[10] in a water bath at 37°. After 4 days, a sample was taken and quickly filtered through a glass wool-wrapped, long tipped pipet preequilibrated at 37°. Exactly 0.2 ml of the filtrate was then assayed for cholesterol with a liquid scintillation counter. More samples were taken every 2 days and assayed for cholesterol. The solubility of cholesterol monohydrate in the medium was obtained when the concentration reached a constant level.

RESULTS AND DISCUSSION

The average bile acid compositions in normal human gallbladder bile (20) and in gallbladder bile of patients undergoing chenodeoxycholic acid therapy (10) are presented in Table I. The selected ranges of the total bile acid concentration, the lecithin concentration, and, hence, the bile acid to lecithin ratio were representative of over 100 human bile samples analyzed in several published reports (21–24).

Tables II and III and Fig. 1 summarize the dissolution kinetic data obtained with the simulated bile solutions. The R values were about 20–700 times the diffusion–convection resistance previously reported for similar systems[11] (Tables II and III); *i.e.*, the dissolution rates in these solutions were essentially 90–99% interfacially controlled. The magnitudes of these R values seemed to be comparable to those found in the situations where only one bile acid was present in solution (6). In addition, as shown previously with the individual bile acids (6), R decreased with an increasing bile acid concentration and an increasing bile acid to lecithin ratio. While this result occurred for both compositions of bile acids, the corresponding R values for the chenodeoxycholic acid-rich solutions were consistently lower than those with normal compositions (Fig. 1).

Even under the most favorable conditions with regard to the composition of the bile, *i.e.*, high bile acid concentration, high bile acid to lecithin ratio, and high chenodeoxycholate concentration, the R values were much larger than the diffusion–convection resistance. This result confirms the hypothesis (2, 5–7) that the interfacial resistance may indeed be an important rate-determining factor in cholesterol stone dissolution *in vivo*. Moreover, in the region where the bile acid concentration and the bile acid to lecithin ratio are low, the observation that three- to fourfold smaller R values were found with the chenodeoxycholic acid-rich compositions may have the following clinical implications:

1. Even if the oral administration of cholic acid had been as effective as chenodeoxycholic acid in desaturating bile with respect to cholesterol, from the kinetic viewpoint it would not have been as effective as cheno-

[9] Model LS 200, Beckman Instruments, Southfield, Mich.
[10] Burrell Corp., Pittsburgh, Pa.

[11] The h/D value for these systems $\cong 2.3 \times 10^3$ sec/cm (6).

deoxycholic acid.

2. In addition to its primary effect on cholesterol desaturation, the feeding of chenodeoxycholic acid also appears to promote stone dissolution by lowering the interfacial resistance in bile, thereby facilitating the kinetics of dissolution as well.

Recent clinical efforts (25) indicated that the oral administration of ursodeoxycholic acid may also be effective in promoting cholesterol gallstone dissolution but without some of the side effects attributed to chenodeoxycholic acid. Therefore, the dissolution kinetics in simulated bile acid mixtures should be studied using the ursodeoxycholic conjugates (glycine and taurine) and the results from these studies should be used to assess the relative effectiveness of ursodeoxycholic acid and chenodeoxycholic acid in speeding up the kinetics of stone dissolution.

At low bile acid concentrations and/or low bile acid to lecithin ratios, the R values are extremely large (Table III). These large R values are believed to be clinically significant since, in many instances, necessary treatment periods for significant stone dissolution have been very long, often extending beyond 12 months. In some cases, little or no dissolution was found (8–12) even after such long times. In view of this fact, it was suggested previously (26, 27) that dissolution rate accelerators might have therapeutic value in effecting more rapid stone dissolution when administered simultaneously with chenodeoxycholic acid.

Table IV shows some preliminary dissolution data on human gallbladder bile reported earlier (7). Based on the total bile acid concentration and the bile acid to lecithin ratio, a rough estimate of R was obtained for each bile sample by extrapolation and interpolation of the curves in Fig. 1. The magnitudes of these R values are reasonably comparable to the experimental values found in the present studies. Since the bile acid composition and the electrolyte content of these samples are not known, a better estimation of R based on the simulated solution data is not possible at this time. Nonetheless, the results suggest that the bile acids, lecithin, and the electrolytes are the primary determinants of interfacial resistance in cholesterol dissolution.

REFERENCES

(1) W. I. Higuchi, F. Sjuib, D. Mufson, A. P. Simonelli, and A. F. Hofmann, *J. Pharm. Sci.*, **62,** 942 (1973).

(2) W. I. Higuchi, S. Prakongpan, and F. Young, *ibid.*, **62,** 945 (1973).

(3) W. I. Higuchi, S. Prakongpan, V. Surpuriya, and F. Young, *Science*, **178,** 633 (1972).

(4) W. I. Higuchi, M. Surpuriya, S. Prakongpan, and F. Young, *J. Pharm. Sci.*, **62,** 695 (1973).

(5) S. Prakongpan, W. I. Higuchi, K. H. Kwan, and A. M. Molokhia, *ibid.*, **65,** 685 (1976).

(6) K. H. Kwan, W. I. Higuchi, A. M. Molokhia, and A. F. Hofmann, *ibid.*, **66,** 1094 (1977).

(7) A. M. Molokhia, A. F. Hofmann, W. I. Higuchi, M. Tuchinda, K. Feld, S. Prakongpan, and R. G. Danzinger, *ibid.*, **66,** 1101 (1977).

(8) R. G. Danzinger, A. F. Hofmann, L. J. Schoenfield, and J. L. Thistle, *N. Engl. J. Med.*, **286,** 1 (1972).

(9) J. L. Thistle and A. F. Hofmann, *ibid.*, **289,** 655 (1973).

(10) A. F. Hofmann and G. Paumgartner, "Chenodeoxycholic Acid Therapy of Gallstones," Progress Report 1975, Schattauer Verlag, Stuttgart, West Germany, 1975.

(11) R. G. Danzinger, A. F. Hofmann, J. L. Thistle, and L. J. Schoenfield, *J. Clin. Invest.*, **52,** 2809 (1973).

(12) G. D. Bell, B. Whitney, and R. H. Dowling, *Lancet*, **2,** 1213 (1972).

(13) A. T. James and L. J. Morris, "New Biochemical Separations," Van Nostrand, London, England, 1964, chap. 10.

(14) H. Bogren and K. Larsson, *Biochim. Biophys. Acta*, **75,** 65 (1963).

(15) A. Norman, *Ark. Kemi*, **8,** 331 (1955).

(16) A. F. Hofmann, *Acta Chem. Scand.*, **17,** 173 (1963).

(17) J. L. Pope, *J. Lipid Res.*, **8,** 146 (1967).

(18) A. F. Hofmann, *ibid.*, **3,** 127 (1962).

(19) W. S. Singleton, M. S. Gray, M. L. Brown, and J. L. White, *J. Am. Oil Chem. Soc.*, **42,** 53 (1965).

(20) A. F. Hofmann and D. M. Small, *Ann. Rev. Med.*, **18,** 333 (1967).

(21) H. Dam, I. Kruse, H. E. Kallehauge, O. E. Hartkopp, and M. K. Jensen, *Scand. J. Clin. Lab. Invest.*, **18,** 385 (1966).

(22) Z. R. Vlahcevic, C. C. Bell, and L. Swell, *Gastroenterology*, **59,** 62 (1970).

(23) D. M. Small and S. Rapo, *N. Engl. J. Med.*, **283,** 53 (1970).

(24) H. Dam, I. Kruse, I. Prange, H. E. Kallehauge, H. J. Fenger, and M. K. Jensen, *Z. Ernaehrungswiss.*, **10,** 160 (1971).

(25) I. Makino, K. Shinozaki, and K. Yoshino, *Jpn. J. Gastroenterol.*, **72,** 690 (1975).

(26) W. I. Higuchi, S. Prakongpan, and F. Young, *J. Pharm. Sci.*, **62,** 1207 (1973).

(27) K. H. Kwan, W. I. Higuchi, A. M. Molokhia, and A. F. Hofmann, *ibid.*, **66,** 1105 (1977).

ACKNOWLEDGMENTS

Supported by Grants AM 16694 and AM 16770 from the National Institutes of Health.

Kinetic and Thermodynamic Aspects of *In Vitro* Interphase Transfer of Tetracyclines I: Influence of Hydroxyl Group Substitution

G. E. SCHUMACHER ˣ and DONNA MAN LEI

Received December 23, 1977, from the *College of Pharmacy and Allied Health Professions, Wayne State University, Detroit, MI 48202.* Accepted for publication April 20, 1978.

Abstract □ The influence of hydroxyl group substitution on the kinetic and thermodynamic aspects of the interphase transfer of three tetracycline derivatives was studied in a two-phase *in vitro* system composed of an aqueous pH 5.5 buffer and 1-octanol. Data are reported on the kinetic and thermodynamic parameters of activation, the net thermodynamic parameters for interphase transfer, and the contribution of hydroxyl group substituents to the energy changes associated with partitioning. For each derivative, ΔH, ΔS, $T\,\Delta S$, and ΔF were positive with enthalpy dominating the entropic energy contribution. Introduction of a hydroxyl group at C-5 on the tetracycline nucleus promoted partitioning through an entropy-dominated decrease in the "apparent" free energy of partitioning, whereas shifting the hydroxyl group to C-6β retarded partitioning due to an enthalpy-dominated gain in the apparent free energy.

Keyphrases □ Tetracyclines—partitioning in aqueous–octanol system, kinetics and thermodynamics, effect of hydroxyl group □ Partitioning—tetracyclines in aqueous–octanol system, kinetics and thermodynamics, effect of hydroxyl group □ Kinetics—partitioning of tetracyclines in aqueous–octanol system □ Thermodynamics—partitioning of tetracyclines in aqueous–octanol system □ Antibacterials—tetracyclines, partitioning in aqueous–octanol system, kinetics and thermodynamics, effect of hydroxyl group

Previous papers (1, 2) concerned the influence of hydrophobic methyl group substitution and interface composition on the kinetic and thermodynamic aspects of the interphase transfer of sulfonamides in a liquid two-phase *in vitro* system. This report concerns the influence of hydrophilic hydroxyl group substitution on the kinetic and thermodynamic parameters for the interphase transfer of tetracyclines. Tetracycline, oxytetracycline, and doxycycline were studied because they differ from each other only in the number and placement of hydroxyl groups on the tetracycline nucleus.

EXPERIMENTAL

The apparatus, the method of performing the diffusion experiments, and the procedure for determining the partition coefficients were discussed previously (1).

Materials—The following reagents were the highest quality obtainable: tetracycline hydrochloride[1] (98% potency), oxytetracycline hydrochloride[1] (91% potency), doxycycline hyclate[1] (86% potency), 1-octanol, monobasic and dibasic sodium phosphates, sodium chloride, sodium hydroxide, and hydrochloric acid.

Diffusion Experiments—To study tetracycline diffusion, 5.2×10^{-4} M solutions[2] of each tetracycline derivative were prepared in aqueous phosphate buffer adjusted to pH 5.5 and ionic strength 0.15. The studies were performed at 23, 30, and 37° using water baths maintained at ±0.5°. Absorbance was measured with a UV spectrophotometer at 365 nm for tetracycline, 360 nm for oxytetracycline, and 355 nm for doxycycline.

[1] Pfizer and Co., Brooklyn, N.Y.; potency supplied by company.

[2] Although tetracycline and oxytetracycline were used as hydrochloride salts, doxycycline was used as the hyclate, which is the hydrochloride hemiethanolate hemihydrate. Therefore, doxycycline contributes a small quantity of ethyl alcohol ($\sim 10^{-4}$ M) to the aqueous buffer phase whereas tetracycline and oxytetracycline do not. This variable may have a small influence on the thermodynamic parameters observed for doxycycline.

RESULTS AND DISCUSSION

General Considerations—The structures of the three tetracyclines, their reported macrodissociation constants (3, 4), and their apparent partition coefficients in pH 5.5 phosphate buffer–1-octanol are summarized in Table I.

The complete ionization scheme for the tetracyclines is complex as a consequence of the three acidic moieties present, resulting in a dissociation sequence including 15 microionization steps (4, 5). A pH value of 5.5 was selected for the aqueous buffer solution to ensure that the zwitterionic form of the tetracyclines would be the predominant species, although other species are present for each derivative at this pH (4–6). Partitioning has been attributed to the zwitterionic form because maximum partitioning was observed in the general pH range of maximum zwitterionic concentration (5, 6). However, other reports (7) indicated that the unionized species of tetracycline is the dominant form for partitioning.

Because their pK values are the same, the concentration of various species at pH 5.5 should be the same for tetracycline and doxycycline. For oxytetracycline, the concentration of species will be slightly varied. Selection of pH 5.5 also minimized the epimerization of the various tetracyclines at the C-4 dimethylamino group commonly observed at lower pH values (8).

Tetracycline, oxytetracycline, and doxycycline were selected to examine the influence of hydroxyl group substitution and its position in these molecules on the interphase transfer characteristics. As shown in Table I, tetracycline differs from doxycycline only in a shift of the hydroxyl group from C-6β in the former to C-5 in the latter; this shift results in a ninefold increase in the apparent partition coefficient at pH 5.5. Oxytetracycline differs from tetracycline and doxycycline by the addition of a hydroxyl group; with respect of oxytetracycline, tetracycline and doxycycline are dehydroxylated at C-5 and C-6β, respectively.

Kinetic and Thermodynamic Data—Methods for obtaining the kinetic and thermodynamic data for the interphase transfer of tetracyclines in the two-phase system were discussed previously (1, 2). General mechanisms postulated for the interphase transfer of sulfonamides were used to interpret the data for the tetracyclines.

The activated complex for interphase transfer consists of an association of a tetracycline molecule with 1-octanol and water molecules. The octanol molecules interact primarily through hydrogen bonding and secondarily through hydrophobic interaction between the nonpolar moieties of the tetracycline and octanol molecules. The water molecules associate through hydrogen bonding and the formation of "icebergs" (9) of water molecules around the nonpolar groups of the tetracycline. Differences in the magnitude of the thermodynamic parameters for the interphase transfer of the three derivatives are attributed to variations in solute–solvate interactions arising from the extent of hydrogen bond and hydrophobic interactions among the tetracycline, octanol, and water molecules. As mentioned previously, it is unresolved whether the zwitterionic species, the unionized species, or both forms of the tetracyclines are capable of forming the activated complex and partitioning across the interface.

The kinetic and thermodynamic parameters of activation for the interphase transfer of the tetracyclines at 37° are summarized in Table II. Slight variations in structure lead to profound changes in the kinetic and thermodynamic parameters of activation. For example, since tetracycline and doxycycline differ only in the site of a hydroxyl substituent C-6β or C-5, respectively, and their pK values are the same, variation in the kinetic and thermodynamic parameters for these compounds may be attributed to the influence of the site of the hydroxyl group.

Doxycycline shows a greater k_f/k_b ratio and more positive $\Delta H_f^{\ddagger}$, $\Delta S_f^{\ddagger}$, $\Delta H_b^{\ddagger}$, and $\Delta S_b^{\ddagger}$ values than does tetracycline. This behavior is probably the effect of: (*a*) the larger continuous, uninterrupted hydrophobic surface on doxycycline, resulting from shifting the hydroxyl group from C-6β

0022-3549/78/1200-1715$01.00/0
© 1978, American Pharmaceutical Association

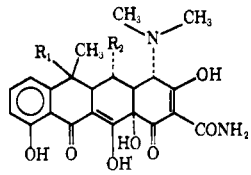

Table I—Structures and Physical Data for the Tetracyclines

Tetracycline	R_1 (C-6β)	R_2 (C-5)	Apparent Dissociation Constants at 25° (3) pK_1	pK_2	pK_3	Apparent Partition Coefficient at pH 5.5[a] 23°	30°	37°
Tetracycline hydrochloride	OH	H	3.3	7.7	9.7	0.075	0.083	0.092
Oxytetracycline hydrochloride	OH	OH	3.3	7.3	9.1	0.101	0.116	0.136
Doxycycline hyclate	H	OH	3.4	7.7	9.7	0.789	0.810	0.837

[a] Expressed in terms of the ratio of solute concentrations in octanol–aqueous pH 5.5 phosphate buffer phases as obtained from interphase transfer experiments.

Table II—Kinetic and Thermodynamic Parameters of Activation for the Interphase Transfer of Tetracyclines in a Two-Phase System at 37°

Tetracycline	k[a], hr^{-1} k_f	k_b	ΔH^*, cal/mole ΔH_f^*	ΔH_b^*	ΔS^*, cal/mole degree ΔS_f^*	ΔS_b^*	ΔF^*, cal/mole ΔF_f^*	ΔF_b^*	E_a, cal/mole E_{a_f}	E_{a_b}
Tetracycline hydrochloride	0.038	0.413	8,435	5683	−54.2	−58.3	25,237	23,767	9,051	6,299
Oxytetracycline hydrochloride	0.016	0.118	8,415	4622	−56.0	−64.2	25,770	24,539	9,031	5,238
Doxycycline hyclate	0.211	0.252	10,551	9783	−44.0	−46.1	24,181	24,071	11,167	10,399

[a] With the t test for independent means, there are significant differences between the k_f values for tetracycline *versus* oxytetracycline and oxytetracycline *versus* doxycycline ($p < 0.01$); there are also significant differences between the k_b values for tetracycline *versus* oxytetracycline and oxytetracycline *versus* doxycycline ($p < 0.01$). The data are based on nine determinations for each tetracycline.

in tetracycline to C-5 in doxycycline, which promotes greater hydrophobic interaction between solute and 1-octanol molecules in doxycycline; and (*b*) the greater potential for intramolecular hydrogen bonding of the C-5 hydroxyl group as compared to the C-6β hydroxyl substituent, which decreases hydrogen bonding between solute and solvate molecules in doxycycline. These factors alter the thermodynamic parameters of activation resulting from desolvation and resolvation of the tetracycline derivatives in forming the activated complex for interphase transfer.

Of course, the specific kinetic and thermodynamic parameters (Table II) depend on the cell design and stirring rate used in the interphase transfer experiments. The interphase transfer rates are influenced by the thickness of the aqueous diffusion layer, which, in turn, depends on the agitation rate (10).

By using the concept of the partition coefficient energy (1, 11), the differences in thermodynamic parameters of activation for forward minus backward transfer (*e.g.*, ΔF_f^* minus ΔF_b^*), termed net thermodynamic parameters (*e.g.*, ΔF), was calculated (Table III). The net thermodynamic parameters can be obtained directly, without consideration of the thermodynamic parameters of activation, by determining the partition coefficients at various temperatures and applying an Arrhenius treatment of the data. The relationships among the partition coefficient, rate constants, and net thermodynamic parameters of interphase transfer are given in Eqs. 1 and 2:

$$K_w^0 = \frac{k_f}{k_b} = \frac{e^{-\Delta F_f^*/RT}}{e^{-\Delta F_b^*/RT}} = e^{-\Delta F/RT} \qquad \text{(Eq. 1)}$$

$$K_w^0 = \frac{k_f}{k_b} = e^{(-\Delta H/RT + \Delta S/R)} \qquad \text{(Eq. 2)}$$

For all three tetracycline derivatives, the net free energy, ΔF, of interphase transfer is positive for partitioning between aqueous pH 5.5 and 1-octanol phases. Therefore, the net transfer of these tetracyclines from aqueous to 1-octanol phases is not favored ($K_w^0 < 1$). The net enthalpy, ΔH, and net entropy, ΔS, are also positive for each tetracycline derivative. In all cases, however, ΔH dominates the entropic energy, $T\,\Delta S$, and makes the major contribution to the positive ΔF. These results contrast with the previous observation for the more hydrophobic sulfonamide derivatives that the addition of methyl groups resulted in an entropy-dominated decrease in ΔF (1).

Table III—Net Thermodynamic Parameters and Apparent Partition Coefficients for the Interphase Transfer of Tetracyclines in a Two-Phase System at 37°

Tetracycline	$K_w^{0\,a,b}$	$\Delta H^{b,c}$, cal/mole	$\Delta S^{b,c}$, cal/mole degree	$T\,\Delta S^{b,c}$, cal/mole	$\Delta F^{b,c}$, cal/mole
Tetracycline hydrochloride	0.092	2752	4.1	1271	1470
Oxytetracycline hydrochloride	0.136	3793	8.2	2542	1231
Doxycycline hyclate	0.837	768	2.1	651	110

[a] As defined by Eqs. 1 and 2. [b] With the t test for independent means, there are significant differences between the values for tetracycline *versus* oxytetracycline and oxytetracycline *versus* doxycycline ($p < 0.01$). The data are based on nine determinations for each tetracycline. [c] Net values representing the difference between activation parameters for forward transfer minus back transfer. Values are calculated from the data in Table II.

The number and placement of hydroxyl groups appear to affect partitioning and net thermodynamic parameters significantly for the tetracycline derivatives. When doxycycline is modified to tetracycline by shifting the hydroxyl group from C-5 to C-6β, the ΔH, ΔS, and ΔF values increase markedly. This effect appears to be the consequence of the increased hydrophilic contribution of the hydroxyl group when substituted at C-6β rather than C-5, as discussed previously. When tetracycline is then modified to oxytetracycline by adding another hydroxyl group, ΔH and ΔS values increase again.

The positive ΔH and ΔS values observed for the three tetracycline derivatives suggest a net liberation of solvate molecules in forming the activated complex for interphase transfer.

"Apparent" Contribution of Hydroxyl Group Substitution to Energy Changes for Partitioning of Tetracyclines—To estimate the contribution of the C-5 and C-6β hydroxyl groups to the energy changes for partitioning of tetracyclines at pH 5.5, the method of Hansch (12, 13) was used. The contribution of individual substituents is measured by comparing the partitioning of the "parent" compound to that of a derivative differing by only a single substituent group. Equations 3 and 4 were used to calculate the data summarized in Table IV:

$$\pi = \log (K_w^{0''}/K_w^{0'}) = \Delta F_{G\ \Delta F}/-2.303RT \qquad \text{(Eq. 3)}$$

$$\Delta F_{G\ \Delta F} = \Delta F'' - \Delta F' \qquad \text{(Eq. 4)}$$

where π represents the log of the substituent group contribution factor (the log of $K_w^{0''}/K_w^{0'}$); $K_w^{0''}$ and $K_w^{0'}$ denote the partition coefficients for the derivative and parent compounds, respectively; and $\Delta F_{G\ \Delta F}$ represents the substituent group free energy contribution. The thermodynamic data in Table IV were obtained using the form of Eq. 4 and the data of Table III in which the appropriate net thermodynamic parameter for the parent drug was subtracted from the corresponding parameters for the derivative. When comparing the three derivatives, only a qualitative interpretation of the data is possible since the slight variation in pK values for oxytetracycline compared to tetracycline and doxycycline results in a small variation in the ratio of ionized to unionized species at pH 5.5. This change in species composition may in itself alter the apparent partition coefficient and, thus, the thermodynamic parameters observed. Because of this limitation, the data in Table IV are denoted as "apparent" values.

Table IV—Apparent [a] Contribution of Hydroxyl Groups to Net Thermodynamic Parameters for the Interphase Transfer of Tetracyclines in a Two-Phase System at 37°

Functional Group	π [b]	$\Delta F_{G\ \Delta F}$ [c], cal/mole	$\Delta H_{G\ \Delta H}$ [c], cal/mole	$\Delta S_{G\ \Delta S}$ [c], cal/mole degree	$T\Delta S_{GT\ \Delta S}$ [c], cal/mole
C-5 hydroxyl [d]	0.170	−239	1041	4.1	1271
C-6β hydroxyl [e]	−0.789	1121	3025	6.1	1891

[a] Apparent values because the composition of species is not constant for each tetracycline at pH 5.5. [b] The log of substituent constant calculated using Eq. 3. [c] The functional group free energy, enthalpy, entropy, and entropic energy of partitioning calculated using Eq. 4 and the net thermodynamic parameters of Table III; the net value of one derivative is subtracted from a second derivative to obtain the functional group thermodynamic contribution. [d] Obtained by subtracting tetracycline data from oxytetracycline data. [e] Obtained by subtracting doxycycline data from oxytetracycline data.

Substitution of a hydroxyl group at C-5 promotes partitioning by decreasing the apparent free energy of partitioning through an entropy-dominated effect. Shifting the hydroxyl group to C-6β, however, inhibits partitioning due to an enthalpy-dominated gain in the apparent free energy of partitioning. This small variation in position of the hydroxyl group from C-5 to C-6β results in substantial changes in the energy contributions of the hydroxyl group, as estimated by subtracting the C-5 hydroxyl data in Table IV from the C-6β data. For this shift in hydroxyl group, ΔF = 1360 cal/mole, ΔH = 1984 cal/mole, ΔS = 2.0 cal/mole degree, and $T\ \Delta S$ = 620 cal/mole. These observations suggest the fundamental importance of desolvation and resolvation processes in forming the activated complex for interphase transfer. In moving the hydroxyl group from C-5 to C-6β, a shift that probably accentuates the hydrophilic contribution of the hydroxyl group and diminishes the hydrophobic interaction of the tetracycline derivative with 1-octanol molecules in forming the activated complex, a ninefold decrease in the apparent partition coefficient is observed.

As shown in Tables III and IV, the addition of a hydrophilic substituent such as a hydroxyl group to a tetracycline derivative does not necessarily decrease the apparent partition coefficient. When tetracycline is converted to oxytetracycline by adding another hydroxyl group at C-5, the apparent partition coefficient increases because of a negative apparent $\Delta F_{G\ \Delta F}$ contribution. However, in converting doxycycline to oxytetracycline by adding an additional hydroxyl group at C-6β, the apparent partition coefficient decreases because of a positive apparent $\Delta F_{G\ \Delta F}$ contribution. For both examples, an additional hydroxyl group is substituted on the tetracycline derivative, but the effect on the apparent partition coefficient varies due to the fundamental influence on solute–solvate interactions in forming the activated complex for interphase transfer.

The data provide additional support for the mechanisms of solute transfer previously proposed (1, 2). While the simple model system used does not simulate the complexity of biological membranes, the similarity in intermolecular forces governing the transfer of solute across liquid–liquid and liquid–membrane interfaces suggests that studies such as these may furnish insight into *in vitro* and *in vivo* interphase transfer processes.

REFERENCES

(1) G. E. Schumacher and J. B. Nagwekar, *J. Pharm. Sci.*, **63**, 240 (1974).

(2) *Ibid.*, **63**, 245 (1974).

(3) W. C. Barringer, W. Shultz, G. M. Sieger, and R. A. Nash, *Am. J. Pharm.*, **146**, 179 (1974).

(4) L. J. Leeson, J. E. Krueger, and R. Nach, *Tetrahedron Lett.*, **18**, 1155 (1963).

(5) J. L. Colaizzi and P. R. Klink, *J. Pharm. Sci.*, **58**, 1184 (1969).

(6) T. F. Chin and J. L. Lach, *Am. J. Hosp. Pharm.*, **32**, 625 (1975).

(7) H. Terada and T. Inagi, *Chem. Pharm. Bull.*, **23**, 1960 (1975).

(8) E. G. Remmers, G. M. Sieger, and A. P. Doerschuk, *J. Pharm. Sci.*, **52**, 752 (1963).

(9) H. S. Frank and M. W. Evans, *J. Chem. Phys.*, **13**, 507 (1945).

(10) S. A. Howard, M. A. Farvar, A. Suzuki, and W. I. Higuchi, *J. Pharm. Sci.*, **58**, 1325 (1969).

(11) J. T. Davies, *J. Phys. Colloid Chem.*, **54**, 185 (1950).

(12) C. Hansch and A. Steward, *J. Med. Chem.*, **7**, 691 (1964).

(13) G. L. Flynn, *J. Pharm. Sci.*, **60**, 345 (1971).

ACKNOWLEDGMENTS

Abstracted in part from a thesis submitted by D. M. Lei to Wayne State University in partial fulfillment of the Master of Science degree requirements.

Kinetic and Thermodynamic Aspects of *In Vitro* Interphase Transfer of Tetracyclines II: Influence of Divalent Metal Salts

G. E. SCHUMACHER ˣ and EDWARDS E. LINN

Received December 23, 1977, from the *College of Pharmacy and Allied Health Professions, Wayne State University, Detroit, MI 48202.* Accepted for publication April 20, 1978.

Abstract □ With a two-phase *in vitro* model composed of an aqueous pH 5.5 buffer and 1-octanol, the kinetics of the interphase transfer of tetracycline derivatives were examined in the presence and absence of calcium and magnesium salts, and the contribution of some functional group substituents to the "apparent" free energy changes for partitioning of tetracyclines was evaluated. Only small changes were observed in k_f, k_b, K_w^0, and apparent functional group free energy changes, $\Delta F_{G\ \Delta F}$, in the presence of divalent metals as compared to values observed in the absence of these metals. Introduction of the C-6β hydroxyl group on the tetracycline nucleus decreased the apparent K_w^0 because of a positive apparent $\Delta F_{G\ \Delta F}$ contribution, whereas introduction of C-5 hydroxyl, C-6α methyl, or C-7 chloro groups increased the apparent K_w^0 through negative apparent $\Delta F_{G\ \Delta F}$ contributions.

Keyphrases □ Tetracyclines—partitioning in aqueous-octanol system, kinetics and thermodynamics, effect of divalent metal salts □ Partitioning—tetracyclines in aqueous-octanol system, kinetics and thermodynamics, effect of divalent metal salts □ Kinetics—partitioning of tetracyclines in aqueous-octanol system □ Thermodynamics—partitioning of tetracyclines in aqueous-octanol system □ Metal salts, divalent—effect on partitioning of tetracyclines in aqueous-octanol system □ Antibacterials—tetracyclines, partitioning in aqueous-octanol system, kinetics and thermodynamics, effect of divalent metal salts

The absorption of a tetracyclines is depressed in the presence of antacids and dairy products (1). Yet no evidence has been reported that calcium and magnesium ions, commonly present in antacid preparations, are capable of

0022-3549/78/1200-1717$01.00/0

© 1978, American Pharmaceutical Association

Table IV—Apparent [a] Contribution of Hydroxyl Groups to Net Thermodynamic Parameters for the Interphase Transfer of Tetracyclines in a Two-Phase System at 37°

Functional Group	π [b]	$\Delta F_{G\ \Delta F}$ [c], cal/mole	$\Delta H_{G\ \Delta H}$ [c], cal/mole	$\Delta S_{G\ \Delta S}$ [c], cal/mole degree	$T\Delta S_{GT\ \Delta S}$ [c], cal/mole
C-5 hydroxyl [d]	0.170	−239	1041	4.1	1271
C-6β hydroxyl [e]	−0.789	1121	3025	6.1	1891

[a] Apparent values because the composition of species is not constant for each tetracycline at pH 5.5. [b] The log of substituent constant calculated using Eq. 3. [c] The functional group free energy, enthalpy, entropy, and entropic energy of partitioning calculated using Eq. 4 and the net thermodynamic parameters of Table III; the net value of one derivative is subtracted from a second derivative to obtain the functional group thermodynamic contribution. [d] Obtained by subtracting tetracycline data from oxytetracycline data. [e] Obtained by subtracting doxycycline data from oxytetracycline data.

Substitution of a hydroxyl group at C-5 promotes partitioning by decreasing the apparent free energy of partitioning through an entropy-dominated effect. Shifting the hydroxyl group to C-6β, however, inhibits partitioning due to an enthalpy-dominated gain in the apparent free energy of partitioning. This small variation in position of the hydroxyl group from C-5 to C-6β results in substantial changes in the energy contributions of the hydroxyl group, as estimated by subtracting the C-5 hydroxyl data in Table IV from the C-6β data. For this shift in hydroxyl group, ΔF = 1360 cal/mole, ΔH = 1984 cal/mole, ΔS = 2.0 cal/mole degree, and $T\ \Delta S$ = 620 cal/mole. These observations suggest the fundamental importance of desolvation and resolvation processes in forming the activated complex for interphase transfer. In moving the hydroxyl group from C-5 to C-6β, a shift that probably accentuates the hydrophilic contribution of the hydroxyl group and diminishes the hydrophobic interaction of the tetracycline derivative with 1-octanol molecules in forming the activated complex, a ninefold decrease in the apparent partition coefficient is observed.

As shown in Tables III and IV, the addition of a hydrophilic substituent such as a hydroxyl group to a tetracycline derivative does not necessarily decrease the apparent partition coefficient. When tetracycline is converted to oxytetracycline by adding another hydroxyl group at C-5, the apparent partition coefficient increases because of a negative apparent $\Delta F_{G\ \Delta F}$ contribution. However, in converting doxycycline to oxytetracycline by adding an additional hydroxyl group at C-6β, the apparent partition coefficient decreases because of a positive apparent $\Delta F_{G\ \Delta F}$ contribution. For both examples, an additional hydroxyl group is substituted on the tetracycline derivative, but the effect on the apparent partition coefficient varies due to the fundamental influence on solute–solvate interactions in forming the activated complex for interphase transfer.

The data provide additional support for the mechanisms of solute transfer previously proposed (1, 2). While the simple model system used does not simulate the complexity of biological membranes, the similarity in intermolecular forces governing the transfer of solute across liquid–liquid and liquid–membrane interfaces suggests that studies such as these may furnish insight into *in vitro* and *in vivo* interphase transfer processes.

REFERENCES

(1) G. E. Schumacher and J. B. Nagwekar, *J. Pharm. Sci.*, **63**, 240 (1974).

(2) *Ibid.*, **63**, 245 (1974).

(3) W. C. Barringer, W. Shultz, G. M. Sieger, and R. A. Nash, *Am. J. Pharm.*, **146**, 179 (1974).

(4) L. J. Leeson, J. E. Krueger, and R. Nach, *Tetrahedron Lett.*, **18**, 1155 (1963).

(5) J. L. Colaizzi and P. R. Klink, *J. Pharm. Sci.*, **58**, 1184 (1969).

(6) T. F. Chin and J. L. Lach, *Am. J. Hosp. Pharm.*, **32**, 625 (1975).

(7) H. Terada and T. Inagi, *Chem. Pharm. Bull.*, **23**, 1960 (1975).

(8) E. G. Remmers, G. M. Sieger, and A. P. Doerschuk, *J. Pharm. Sci.*, **52**, 752 (1963).

(9) H. S. Frank and M. W. Evans, *J. Chem. Phys.*, **13**, 507 (1945).

(10) S. A. Howard, M. A. Farvar, A. Suzuki, and W. I. Higuchi, *J. Pharm. Sci.*, **58**, 1325 (1969).

(11) J. T. Davies, *J. Phys. Colloid Chem.*, **54**, 185 (1950).

(12) C. Hansch and A. Steward, *J. Med. Chem.*, **7**, 691 (1964).

(13) G. L. Flynn, *J. Pharm. Sci.*, **60**, 345 (1971).

ACKNOWLEDGMENTS

Abstracted in part from a thesis submitted by D. M. Lei to Wayne State University in partial fulfillment of the Master of Science degree requirements.

Kinetic and Thermodynamic Aspects of *In Vitro* Interphase Transfer of Tetracyclines II: Influence of Divalent Metal Salts

G. E. SCHUMACHER ˣ and EDWARDS E. LINN

Received December 23, 1977, from the *College of Pharmacy and Allied Health Professions, Wayne State University, Detroit, MI 48202.* Accepted for publication April 20, 1978.

Abstract □ With a two-phase *in vitro* model composed of an aqueous pH 5.5 buffer and 1-octanol, the kinetics of the interphase transfer of tetracycline derivatives were examined in the presence and absence of calcium and magnesium salts, and the contribution of some functional group substituents to the "apparent" free energy changes for partitioning of tetracyclines was evaluated. Only small changes were observed in k_f, k_b, K_w^0, and apparent functional group free energy changes, $\Delta F_{G\ \Delta F}$, in the presence of divalent metals as compared to values observed in the absence of these metals. Introduction of the C-6β hydroxyl group on the tetracycline nucleus decreased the apparent K_w^0 because of a positive apparent $\Delta F_{G\ \Delta F}$ contribution, whereas introduction of C-5 hydroxyl, C-6α methyl, or C-7 chloro groups increased the apparent K_w^0 through negative apparent $\Delta F_{G\ \Delta F}$ contributions.

Keyphrases □ Tetracyclines—partitioning in aqueous-octanol system, kinetics and thermodynamics, effect of divalent metal salts □ Partitioning—tetracyclines in aqueous-octanol system, kinetics and thermodynamics, effect of divalent metal salts □ Kinetics—partitioning of tetracyclines in aqueous-octanol system □ Thermodynamics—partitioning of tetracyclines in aqueous-octanol system □ Metal salts, divalent—effect on partitioning of tetracyclines in aqueous-octanol system □ Antibacterials—tetracyclines, partitioning in aqueous-octanol system, kinetics and thermodynamics, effect of divalent metal salts

The absorption of a tetracyclines is depressed in the presence of antacids and dairy products (1). Yet no evidence has been reported that calcium and magnesium ions, commonly present in antacid preparations, are capable of

0022-3549/78/1200-1717$01.00/0

© 1978, American Pharmaceutical Association

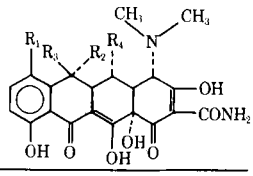

Table I—Structures and Physical Data for the Tetracyclines

Tetracycline	R_1 (C-7)	R_2 (C-6α)	R_3 (C-6β)	R_4 (C-5)	Apparent Dissociation Constants at 25° pK_1	pK_2	pK_3	Apparent Partition Coefficient at 37° and pH 5.5[a]
Tetracycline hydrochloride (8)[b]	H	CH_3	OH	H	3.3	7.7	9.7	0.074
Oxytetracycline hydrochloride (8)	H	CH_3	OH	OH	3.3	7.3	9.1	0.129
Chlortetracycline hydrochloride (8)	Cl	CH_3	OH	H	3.3	7.4	9.3	0.439
Demeclocycline hydrochloride (17)	Cl	H	OH	H	3.3	7.2	9.4	0.317
Doxycycline hyclate (17)	H	CH_3	H	OH	3.4	7.7	9.7	0.947

[a] Expressed in terms of the ratio of solute concentrations in 1-octanol–aqueous pH 5.5 phosphate buffer phases as obtained from interphase transfer experiments. [b] Denotes reference number.

Table II—Kinetic Parameters for the Interphase Transfer of Tetracyclines in the Presence[a] and Absence of Divalent Metal Salts at pH 5.5 and 37°

Tetracycline	k_f, hr^{-1} Absence of Metal	Presence of Calcium	Presence of Magnesium	k_b, hr^{-1} Absence of Metal	Presence of Calcium	Presence of Magnesium
Tetracycline hydrochloride	0.017	0.024	0.020	0.229	0.349	0.312
Oxytetracycline hydrochloride	0.017	0.015	0.014	0.133	0.125	0.130
Chlortetracycline hydrochloride	0.116	0.039	—	0.264	0.113	—
Demeclocycline hydrochloride	0.111	0.079	—	0.350	0.271	—
Doxycycline hyclate	0.288	0.271	0.215	0.304	0.319	0.276

[a] The molar ratio of tetracycline to divalent metal salt was 1:10.

chelating tetracycline derivatives at pH values achieved after administering antacids (2, 3). Therefore, some other mechanism may be responsible for the impaired absorption of tetracyclines (4).

Previously (5–7), a liquid two-phase *in vitro* system to study the kinetic and thermodynamic aspects of the interphase transfer of sulfonamides and tetracyclines was described. The system is applied here to investigate the influence of divalent metal salts on the kinetic and thermodynamic parameters for the partitioning of various tetracycline derivatives.

EXPERIMENTAL

The apparatus, the method of performing the diffusion experiments, and the procedure for determining the partition coefficients were discussed previously (5).

Materials—The following reagents were the highest quality obtainable: tetracycline hydrochloride[1] (98% potency), oxytetracycline hydrochloride[1] (91% potency), doxycycline hyclate[1] (86% potency), chlortetracycline hydrochloride[2] (92% potency), demeclocycline hydrochloride[2] (92% potency), 1-octanol, monobasic and dibasic sodium phosphates, sodium chloride, calcium chloride, magnesium chloride, and hydrochloric acid.

Diffusion Experiments—To study tetracycline diffusion from aqueous to 1-octanol phases, 5.2×10^{-4} *M* solutions[3] of each tetracycline derivative were prepared in aqueous phosphate buffer adjusted to pH 5.5. The same conditions were observed for tetracycline solutions also containing 5.2×10^{-3} *M* calcium chloride or magnesium chloride. All solutions were adjusted to an ionic strength of 0.15.

The studies were performed at 23, 30, and 37° using water baths maintained at ±0.5°. Absorbance was measured with a UV spectrophotometer at 375 nm for chlortetracycline and demeclocycline, 360 nm for tetracycline and oxytetracycline, and 355 nm for doxycycline.

[1] Pfizer and Co., Brooklyn, N.Y.; potency supplied by company.
[2] Lederle Laboratories, Pearl River, N.Y.; potency supplied by company.
[3] All tetracycline derivatives were used as the hydrochloride salts except for doxycycline hyclate, which is the hydrochloride hemiethanolate hemihydrate. Therefore, doxycycline contributes a small quantity of ethyl alcohol ($\sim 10^{-4}$ *M*) to the aqueous buffer phase whereas the other derivatives do not. This variable may have a small influence on the thermodynamic parameters observed for doxycycline.

RESULTS AND DISCUSSION

General Considerations—The structures of the three tetracyclines, their reported macrodissociation constants, and their apparent partition coefficients in pH 5.5 phosphate buffer–1-octanol are summarized in Table I.

The tetracyclines exhibit a complex dissociation scheme of 15 microionization steps resulting from the three acidic moieties present (8, 9). A pH value of 5.5 was selected for the aqueous phase to: (*a*) ensure maximum partitioning of the tetracycline derivatives as observed previously (9, 10) within a range including pH 5.5, (*b*) minimize the epimerization of the various tetracyclines at the C-4 dimethylamino group commonly observed at lower pH values (11), and (*c*) achieve a pH within the range observed after administration of antacid preparations. It is unresolved whether the zwitterionic species (3, 9), the unionized species (10), or both forms of the tetracyclines are capable of partitioning across the interface. Maximum partitioning has been observed in the general pH range of maximum zwitterionic concentration (9).

The concentration of tetracyclines used for the interphase transfer experiments, 5.2×10^{-4} *M*, is within the concentration range achieved in the stomach when the common dose of 250 mg is administered. The concentration of divalent metal salts used, 5.2×10^{-3} *M*, simulates a

Table III—Apparent Partition Coefficients for the Interphase Transfer of Tetracyclines in the Presence[a] and Absence of Divalent Metal Salts at pH 5.5 and 37°

Tetracycline	Apparent K_w^{0}[b] Absence of Metal	Presence of Calcium	Presence of Magnesium
Tetracycline hydrochloride	0.074	0.069	0.064
Oxytetracycline hydrochloride	0.129	0.120	0.108
Chlortetracycline hydrochloride	0.439	0.345	—
Demeclocycline hydrochloride	0.317	0.292	—
Doxycycline hyclate	0.947	0.850	0.779

[a] The molar ratio of tetracycline to divalent metal salt was 1:10. [b] As defined by Eq. 1.

Table IV—Apparent [a] Functional Group Free Energy Contributions for Partitioning of Tetracyclines in the Presence [b] and Absence of Divalent Metal Salts at pH 5.5 and 37°

Functional Group	π [c]			$\Delta F_{G\ \Delta F}$ [d], cal/mole		
	Absence of Metal	Presence of Calcium	Presence of Magnesium	Absence of Metal	Presence of Calcium	Presence of Magnesium
C-6α methyl [e]	0.141	0.074	—	−201	−105	—
C-5 hydroxyl [f]	0.238	0.247	0.223	−338	−350	−315
C-7 chloro [g]	0.773	0.705	—	−1097	−1000	—
C-6β hydroxyl [h]	−0.870	−0.850	−0.862	1233	1250	1222

[a] Apparent values because the composition of species is not constant for each tetracycline at pH 5.5 [b] The molar ratio of tetracycline to divalent metal salt was 1:10. [c] The log of the functional group constant calculated using Eq. 2. [d] The functional group free energy of partitioning calculated using Eq. 2. [e] Obtained by subtracting demeclocycline data from chlortetracycline data. [f] Obtained by subtracting tetracycline data from oxytetracycline data. [g] Obtained by subtracting tetracycline data from chlortetracycline data. [h] Obtained by subtracting doxycycline data from oxytetracycline data.

gastric concentration achieved with the commonly administered dosage of antacids. Under these study conditions, the tetracycline to divalent metal salt molar ratio is 1:10.

The five tetracycline derivatives (Table I) were chosen because they are commonly used in practice; they demonstrate small structural changes, facilitating the study of the contribution of discrete functional groups; and they exhibit greater than a 10-fold range in the apparent partition coefficient.

Kinetic and Partitioning Data—The kinetic scheme for the reversible interphase transfer of the tetracyclines in the two-phase system, as well as the methods for obtaining the kinetic and thermodynamic data, were discussed previously (5).

The kinetic parameters for the interphase transfer of the tetracycline derivatives in the presence and absence of calcium and magnesium salts are summarized in Table II. For all derivatives except tetracycline, the forward rate constants, k_f, for transfer from aqueous to 1-octanol phases were decreased in the presence of the divalent metals. These changes were generally small, although they were statistically significant ($p < 0.05$; t test for independent means, nine determinations for each experiment). The backward rate constants, k_b, for transfer from 1-octanol to aqueous phases were also, again with the exception of tetracycline, subject to small but statistically significant decreases in the presence of the metals. Of course, the specific kinetic parameters (Table II) depend on the cell design and stirring rate used in the interphase transfer experiments. The interphase transfer rates are influenced by the thickness of the aqueous diffusion layer, which, in turn, depends on the agitation rate (12).

The apparent partition coefficients for the interphase transfer of the tetracyclines in the presence and absence of the divalent metal salts at pH 5.5 are summarized in Table III. Changes in the presence of metals generally represented small to negligible decreases; only the variations observed for chlortetracycline and doxycycline were statistically significant ($p < 0.01$). Apparent partition coefficients were calculated using:

$$K_w^0 = \frac{k_f}{k_b} = e^{-\Delta F/RT} \qquad \text{(Eq. 1)}$$

Perhaps the changes observed in the k_f, k_b, and K_w^0 values in the environment of metals result from the presence of the divalent cations at the interface. The cations may alter the structural order of water and octanol molecules in the boundary region, decreasing the escaping tendencies of these molecules into the interface and resulting in changes in desolvation and resolvation of solvent molecules associated with the solute during formation of the activated complexes for interphase transfer (6). In studying the partitioning of phenothiazines across a water–octanol interface, large changes in the apparent partition coefficient were observed when various salts were added to the system (13). These changes were attributed to the influence of the salts on water-structuring effects in hydrophobic interactions and ion-pair formation.

"Apparent" Contribution of Functional Group Substitution to Energy Changes for Partitioning—The method of Hansch (14, 15) was used to estimate the contribution of functional groups to the free energy of partitioning of tetracycline derivatives. With this approach, the contribution of individual substituents is calculated by comparing the partitioning of the "parent" compound to that of a derivative differing by only a single substituent group:

$$\pi = \log (K_w^{0\prime\prime}/K_w^{0\prime}) = \Delta F_{G\ \Delta F}/-2.303RT \qquad \text{(Eq. 2)}$$

where π represents the log of the functional group contribution factor (the log of $K_w^{0\prime\prime}/K_w^{0\prime}$); $K_w^{0\prime\prime}$ and $K_w^{0\prime}$ denote the partition coefficients for the derivative and parent compounds, respectively; and $\Delta F_{G\ \Delta F}$ represents the functional group free energy contribution. When comparing the tetracycline derivatives, only a qualitative interpretation of the data is possible since the slight variation in pK values results in a small change in the ratio of ionized to unionized species at pH 5.5. This change in species composition may in itself alter the apparent partition coefficient and, thus, the free energy data observed. Because of this limitation, the data in Table IV are denoted as "apparent" values.

Introduction of the C-6β hydroxyl group on the tetracycline nucleus decreased the apparent partition coefficient due to a positive apparent $\Delta F_{G\ \Delta F}$ contribution leading to an increase in the free energy of partitioning. Introduction of C-5 hydroxyl, C-6α methyl, or C-7 chloro substituents, however, increased partitioning due to negative apparent $\Delta F_{G\ \Delta F}$ contributions leading to decreases in the free energy of partitioning. Contributions of each of these functional groups were essentially unchanged in the presence and absence of the divalent metal salts.

Tetracycline demonstrated a smaller apparent partition coefficient than its analogs oxytetracycline and chlortetracycline, three derivatives containing the C-6β hydroxyl group, because tetracycline lacks the additional substituent providing a negative apparent $\Delta F_{G\ \Delta F}$ contribution possessed by oxytetracycline and chlortetracycline. Chlortetracycline exhibited a larger apparent partition coefficient than demeclocycline because the addition of a methyl group at C-6α for chlortetracycline promotes partitioning through a negative apparent $\Delta F_{G\ \Delta F}$ contribution. The hydrophobic effect of methyl group substitution was demonstrated previously (5, 15, 16). Converting tetracycline to chlortetracycline by adding a C-7 chloro group resulted in a greater negative apparent $\Delta F_{G\ \Delta F}$ contribution than did the conversion of tetracycline to oxytetracycline by addition of a C-5 hydroxyl group. This result demonstrates the inductive effect of the chloro substituent as well as the more hydrophilic character of the hydroxyl group (16).

A small variation in the placement of the hydroxyl group, shifting from C-6β in tetracycline to C-5 in doxycycline, yielded a large increase in the apparent partition coefficient through a substantial decrease in the apparent $\Delta F_{G\ \Delta F}$. This small change in substituent site demonstrates the fundamental importance of desolvation and resolvation processes in forming the activated complexes for interphase transfer; the potential for hydrophobic interaction between 1-octanol and tetracycline molecules is expected to be greater for deoxycycline than tetracycline because of the larger hydrophobic surface on the tetracycline nucleus when the hydroxyl group is substituted at C-5 rather than C-6β (7).

The relatively small changes in kinetic, thermodynamic, and spectral[4] properties observed at pH 5.5 for the tetracycline derivatives in the presence and absence of divalent metal salts provide indirect evidence *in vitro* that the decreased absorption *in vivo* of some tetracyclines in the presence of magnesium and calcium ions is not the result of chelation between these solutes.

REFERENCES

(1) P. J. Neuvonen, *Drugs*, **11**, 45 (1976).

(2) L. A. Mitscher, A. C. Bonacci, A. K. Hacker, and T. D. Sokoloski, *Antimicrob. Agents Chemother. 1969*, **1970**, 111.

(3) T. F. Chin and J. L. Lach, *Am. J. Hosp. Pharm.*, **32**, 625 (1975).

(4) K. Kakemi, H. Sezaki, H. Ogata, and T. Nadai, *Chem. Pharm. Bull.*, **16**, 2200 (1968).

(5) G. E. Schumacher and J. B. Nagwekar, *J. Pharm. Sci.*, **63**, 240 (1974).

(6) *Ibid.*, **63**, 245 (1974).

[4] No changes in the wavelength of maximum absorbance were observed for any of the tetracycline derivatives over the 350–425-nm range in the presence and absence of calcium and magnesium salts.

(7) G. E. Schumacher and D. M. Lei, *J. Pharm. Sci.*, **67**, 1715 (1978).
(8) L. J. Leeson, J. E. Krueger, and R. Nach, *Tetrahedron Lett.*, **18**, 1115 (1963).
(9) J. L. Colaizzi and P. R. Klink, *J. Pharm. Sci.*, **58**, 1184 (1969).
(10) H. Terada and T. Inagi, *Chem. Pharm. Bull.*, **23**, 1960 (1975).
(11) E. G. Remmers, G. M. Sieger, and A. P. Doerschuk, *J. Pharm. Sci.*, **52**, 752 (1963).
(12) S. A. Howard, M. A. Farvar, A. Suzuki, and W. I. Higuchi, *ibid.*, **58**, 1325 (1969).
(13) K. S. Murthy and G. Zografi, *ibid.*, **59**, 1281 (1970).
(14) C. Hansch and A. Steward, *J. Med. Chem.*, **7**, 691 (1964).
(15) G. L. Flynn, *J. Pharm. Sci.*, **60**, 345 (1971).
(16) J. M. Diamond and E. M. Wright, *Proc. R. Soc. B*, **172**, 273 (1969).
(17) W. Barringer, W. Schultz, G. Sieger, and R. Nash, *Am. J. Pharm.*, **146**, 179 (1974).

ACKNOWLEDGMENTS

Abstracted in part from a thesis submitted by E. E. Linn to Wayne State University in partial fulfillment of the Master of Science degree requirements.

GLC Determination of Nanogram Quantities of a New Analgesic, Nefopam, in Human Plasma

D. SCHUPPAN *, C. S. HANSEN, and R. E. OBER ˣ

Received June 6, 1977, from the *Drug Metabolism Group, Riker Laboratories, Inc., a Subsidiary of 3M Company, St. Paul, MN 55101.* Accepted for publication April 27, 1978. *Present address: Klinikum der Johann Wolfgang Goethe Universität, 6000 Frankfurt Main 70, West Germany.

Abstract □ A sensitive and specific method was developed for the quantitative GLC determination of plasma nefopam levels. The method includes a multiple-step solvent extraction of the analgesic drug and the internal mass standard, orphenadrine. The accuracy, expressed as the relative error, was −4, 6, 6, and 4% at 20, 40, 70, and 130 ng/ml, respectively. The precision, expressed as relative standard deviation, was 17, 7, 3, and 5% at these same concentrations, respectively. Quantitation of nefopam in human plasma is possible down to 20 ng/ml with a 2-ml plasma sample; the sensitivity can be increased by using larger plasma samples. The method was applied successfully to the determination of plasma nefopam levels in humans in pharmacokinetic studies at therapeutic doses.

Keyphrases □ Nefopam—GLC analysis in plasma □ GLC—analysis, nefopam in plasma □ Analgesics—nefopam, GLC analysis in plasma

Nefopam[1], 3,4,5,6-tetrahydro-5-methyl-1-phenyl-1*H*-2,5-benzoxazocine hydrochloride (I), is a member of a new class of analgesics with a unique heterocyclic structure. It was originally synthesized by Klohs *et al.* (1) and was introduced as an analgesic drug in 1975 in Mexico and in 1976 in the Federal Republic of Germany. It is currently in the late stages of clinical testing in the United States, and a number of studies concerning the analgesic properties of I were reported[2] (2–5). *In vitro* metabolic data were published (6).

A prerequisite for *in vivo* metabolic and pharmacokinetic studies is a sensitive and specific assay. Since the recommended therapeutic dose of this basic drug for humans is relatively low, the plasma I concentrations are in the low nanogram per milliliter range. This report describes a sensitive and specific GLC method for the accurate determination of small amounts of I in human plasma. The method has been used to follow plasma pharmacokinetics of I. Another similar GLC method recently was published by a group collaborating with this laboratory (7).

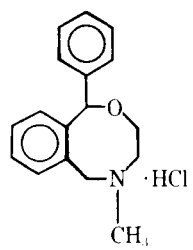

I

EXPERIMENTAL

Reagents—Ether was freshly distilled each day; all other reagents were analytical reagent grade. A *d,l*-mixture of I was used, and the ^{14}C-I (^{14}C-label in the 1- and 6-positions of the oxazocine ring; radiochemical purity >99%) employed for recovery studies was also the racemate. The internal standard (orphenadrine, II) and I were dissolved in methanol. Aqueous solutions of 0.1 *N* HCl and 0.1 *N* NaOH were prepared in distilled water. Carbon disulfide was diluted with methanol to give a final concentration of 2% methanol.

Blank Plasma—Human plasma was obtained from volunteers who had fasted overnight and had not been on any medication for the previous week.

Apparatus—GLC was carried out on a chromatograph[3] with a hydrogen flame-ionization detector. Glass columns (182 cm × 2 mm i.d.) were rinsed with methanol and acetone and dried. They were packed with 3% 100–120-mesh cyclohexanedimethyl succinate on Gas Chrom Q[4]. The column oven was operated at 221° while the injection port and detector were operated at 225 and 260°, respectively. The accuracy and sensitivity of the assay were enhanced markedly by use of a digital electronic integrator[5] for calculating the relative detector response.

For the maximal detector response of I, the flow rates were set as follows: helium carrier gas, 40 ml/min; hydrogen, 40 ml/min; and air, 250 ml/min. The recorder chart speed was 1.25 cm/min. The integrator was operated under the following conditions: noise suppression, 2; recorder presentation, 20; slope sensitivity, 0.03 (up slope and down slope); baseline reset, 0; area threshold, 100; front shoulder, off; and rear shoulder, 1000 mv.

Standard Solutions—The internal standard solution contained 10

[1] Riker Laboratories, St. Paul, Minn.
[2] In Ref. 2, blood level data should read nanogram instead of microgram.
[3] Fisher Victoreen model 4400, equipped with a Varactor electrometer.
[4] Applied Science Laboratories, State College, Pa.
[5] Hewlett-Packard model 3370 B.

0022-3549/78/1200-1720$01.00/0
© 1978, American Pharmaceutical Association

(7) G. E. Schumacher and D. M. Lei, *J. Pharm. Sci.*, **67**, 1715 (1978).
(8) L. J. Leeson, J. E. Krueger, and R. Nach, *Tetrahedron Lett.*, **18**, 1115 (1963).
(9) J. L. Colaizzi and P. R. Klink, *J. Pharm. Sci.*, **58**, 1184 (1969).
(10) H. Terada and T. Inagi, *Chem. Pharm. Bull.*, **23**, 1960 (1975).
(11) E. G. Remmers, G. M. Sieger, and A. P. Doerschuk, *J. Pharm. Sci.*, **52**, 752 (1963).
(12) S. A. Howard, M. A. Farvar, A. Suzuki, and W. I. Higuchi, *ibid.*, **58**, 1325 (1969).
(13) K. S. Murthy and G. Zografi, *ibid.*, **59**, 1281 (1970).
(14) C. Hansch and A. Steward, *J. Med. Chem.*, **7**, 691 (1964).
(15) G. L. Flynn, *J. Pharm. Sci.*, **60**, 345 (1971).
(16) J. M. Diamond and E. M. Wright, *Proc. R. Soc. B*, **172**, 273 (1969).
(17) W. Barringer, W. Schultz, G. Sieger, and R. Nash, *Am. J. Pharm.*, **146**, 179 (1974).

ACKNOWLEDGMENTS

Abstracted in part from a thesis submitted by E. E. Linn to Wayne State University in partial fulfillment of the Master of Science degree requirements.

GLC Determination of Nanogram Quantities of a New Analgesic, Nefopam, in Human Plasma

D. SCHUPPAN *, C. S. HANSEN, and R. E. OBER ˣ

Received June 6, 1977, from the *Drug Metabolism Group, Riker Laboratories, Inc., a Subsidiary of 3M Company, St. Paul, MN 55101.* Accepted for publication April 27, 1978. *Present address: Klinikum der Johann Wolfgang Goethe Universität, 6000 Frankfurt Main 70, West Germany.

Abstract □ A sensitive and specific method was developed for the quantitative GLC determination of plasma nefopam levels. The method includes a multiple-step solvent extraction of the analgesic drug and the internal mass standard, orphenadrine. The accuracy, expressed as the relative error, was −4, 6, 6, and 4% at 20, 40, 70, and 130 ng/ml, respectively. The precision, expressed as relative standard deviation, was 17, 7, 3, and 5% at these same concentrations, respectively. Quantitation of nefopam in human plasma is possible down to 20 ng/ml with a 2-ml plasma sample; the sensitivity can be increased by using larger plasma samples. The method was applied successfully to the determination of plasma nefopam levels in humans in pharmacokinetic studies at therapeutic doses.

Keyphrases □ Nefopam—GLC analysis in plasma □ GLC—analysis, nefopam in plasma □ Analgesics—nefopam, GLC analysis in plasma

Nefopam[1], 3,4,5,6-tetrahydro-5-methyl-1-phenyl-1*H*-2,5-benzoxazocine hydrochloride (I), is a member of a new class of analgesics with a unique heterocyclic structure. It was originally synthesized by Klohs *et al.* (1) and was introduced as an analgesic drug in 1975 in Mexico and in 1976 in the Federal Republic of Germany. It is currently in the late stages of clinical testing in the United States, and a number of studies concerning the analgesic properties of I were reported[2] (2–5). *In vitro* metabolic data were published (6).

A prerequisite for *in vivo* metabolic and pharmacokinetic studies is a sensitive and specific assay. Since the recommended therapeutic dose of this basic drug for humans is relatively low, the plasma I concentrations are in the low nanogram per milliliter range. This report describes a sensitive and specific GLC method for the accurate determination of small amounts of I in human plasma. The method has been used to follow plasma pharmacokinetics of I. Another similar GLC method recently was published by a group collaborating with this laboratory (7).

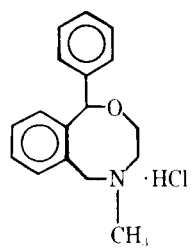

I

EXPERIMENTAL

Reagents—Ether was freshly distilled each day; all other reagents were analytical reagent grade. A *d,l*-mixture of I was used, and the ^{14}C-I (^{14}C-label in the 1- and 6-positions of the oxazocine ring; radiochemical purity >99%) employed for recovery studies was also the racemate. The internal standard (orphenadrine, II) and I were dissolved in methanol. Aqueous solutions of 0.1 *N* HCl and 0.1 *N* NaOH were prepared in distilled water. Carbon disulfide was diluted with methanol to give a final concentration of 2% methanol.

Blank Plasma—Human plasma was obtained from volunteers who had fasted overnight and had not been on any medication for the previous week.

Apparatus—GLC was carried out on a chromatograph[3] with a hydrogen flame-ionization detector. Glass columns (182 cm × 2 mm i.d.) were rinsed with methanol and acetone and dried. They were packed with 3% 100–120-mesh cyclohexanedimethyl succinate on Gas Chrom Q[4]. The column oven was operated at 221° while the injection port and detector were operated at 225 and 260°, respectively. The accuracy and sensitivity of the assay were enhanced markedly by use of a digital electronic integrator[5] for calculating the relative detector response.

For the maximal detector response of I, the flow rates were set as follows: helium carrier gas, 40 ml/min; hydrogen, 40 ml/min; and air, 250 ml/min. The recorder chart speed was 1.25 cm/min. The integrator was operated under the following conditions: noise suppression, 2; recorder presentation, 20; slope sensitivity, 0.03 (up slope and down slope); baseline reset, 0; area threshold, 100; front shoulder, off; and rear shoulder, 1000 mv.

Standard Solutions—The internal standard solution contained 10

[1] Riker Laboratories, St. Paul, Minn.
[2] In Ref. 2, blood level data should read nanogram instead of microgram.
[3] Fisher Victoreen model 4400, equipped with a Varactor electrometer.
[4] Applied Science Laboratories, State College, Pa.
[5] Hewlett-Packard model 3370 B.

0022-3549/78/1200-1720$01.00/0
© 1978, American Pharmaceutical Association

Table I—Extraction Recovery of ^{14}C-Nefopam from Human Plasma

Nefopam Added, ng/ml	Nefopam Recovered[a], ng/ml	Recovery, %
10	10.40	104.0
10	10.60	106.0
10	10.33	103.3
30	30.70	102.5
30	30.78	102.6
30	30.99	103.3
100	99.5	99.5
100	101.2	101.2
100	108.9	108.9
300	279.6	93.2
300	272.1	90.7
300	274.2	91.4
		Mean ± *SD* 100.6 ± 5.8

[a] After correcting for aliquot factor (× 0.64).

Table II—Accuracy and Precision of Nefopam Analysis in Human Plasma by GLC

Nefopam Added to Human Plasma, ng/ml	Nefopam Detected, ng/ml		Difference
20.0	19.9		−0.1
	21.6		1.6
	13.5		−6.5
	21.2		1.2
	19.8		−0.2
	Mean ± *SD*	19.2 ± 3.3	Mean error −0.8
	RSD	17%	Relative error −4%
40.0	41.3		1.3
	39.2		−0.8
	42.1		2.1
	42.8		2.8
	47.1		7.1
	Mean ± *SD*	42.5 ± 2.9	Mean error 2.5
	RSD	7%	Relative error 6%
70.0	77.8		7.8
	77.2		7.2
	71.7		1.7
	73.9		3.9
	73.4		3.4
	Mean ± *SD*	74.8 ± 2.6	Mean error 4.8
	RSD	3%	Relative error 6%
130.0	126.1		−3.9
	131.1		1.1
	143.7		13.7
	133.5		3.5
	141.2		11.2
	Mean ± *SD*	135.1 ± 7.3	Mean error 5.1
	RSD	5%	Relative error 4%

μg of orphenadrine (II)/ml of methanol. The standard solution of I contained 1 μg/ml.

Extraction of I from Plasma—To a 16 × 125-mm culture tube were added 2 ml of experimental plasma and 0.20 ml of methanol containing 2 μg of internal standard. Along with the experimental samples, 40, 80, 140, and 260 ng of I in methanol were added to 2 ml of blank plasma. Then 3.0 ml of 0.1 *N* NaOH and 5.0 ml of freshly distilled ether were added. The tubes were shaken for 10 min on a mechanical shaker[6] and centrifuged[7] for 5 min at about 1000×*g*. Then 4.0 ml of the top (ether) layer was transferred to a clean culture tube, 3.0 ml of 0.1 *N* HCl was added, and the tubes were shaken for 5 min and centrifuged for 2 min.

The ether was aspirated and discarded, and the aqueous phase was washed with another 5.0 ml of ether. To the washed aqueous phase were added 3.5 ml of 0.1 *N* NaOH and 5.0 ml of ether. The tube was shaken for 10 min and centrifuged for 5 min. Then 4.5 ml of the ether layer was transferred to a 12-ml conical extraction tube and concentrated down under nitrogen at 50° to a volume of about 100 μl. The final evaporation of ether down to dryness was controlled carefully, and immediately thereafter the residue was dissolved in 10 μl of methanolic carbon disulfide. Then 4.0-μl aliquots of the methanolic carbon disulfide solution were injected into the gas chromatograph.

All values are in terms of nefopam hydrochloride equivalents.

Recovery Tracer Study—Radiolabeled ^{14}C-nefopam was employed to investigate the extraction efficiency of the method. The labeled drug was added to samples, and the described method was carried out. Samples taken at various steps during extraction were analyzed for ^{14}C-content by liquid scintillation counting[8]. Corrections for quenching were made by an external standard method.

***In Vivo* Study**—An *in vivo* evaluation provided information about the applicability and limitations of the method for analysis of human plasma samples. Subjects received single oral doses of 60 mg of I in two different tablet formulations. Subjects fasted overnight and for 4 hr after drug administration. Blood samples were drawn into heparinized containers[9] at 0.5, 1, 1.5, 2, 3, 4, 6, 8, and 12 hr after drug administration. Red blood cells were separated immediately by centrifugation, and the plasma was removed and stored at −20° until assayed.

RESULTS

Recovery—Chemically, I is a tertiary amine, and attempts were directed toward optimal recovery of the free base from plasma. An extraction recovery study with ether and ^{14}C-labeled I was conducted at four concentrations: 10, 30, 100, and 300 ng of I/ml. Excellent recovery

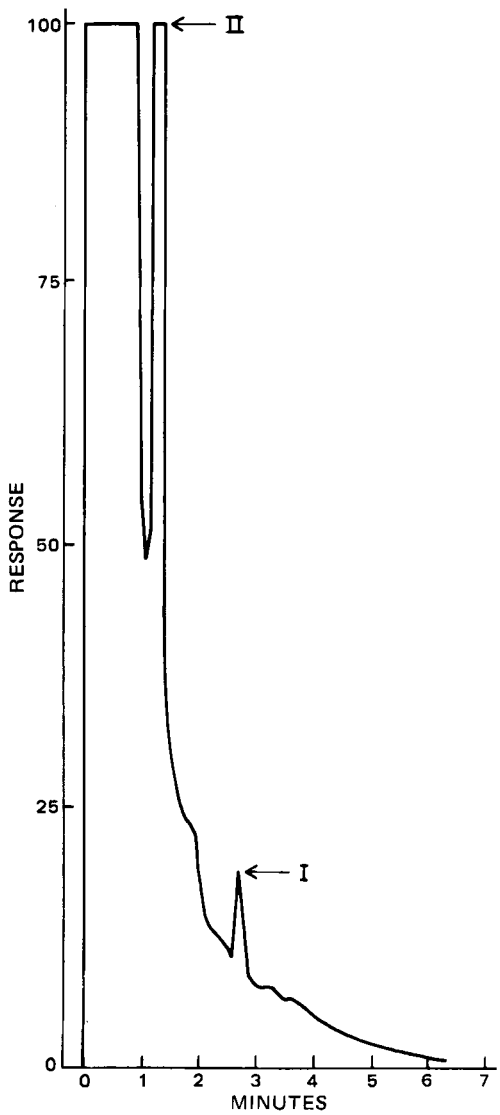

Figure 1—*Chromatogram tracing from human plasma extract.*

[6] Precision Scientific Co. model 65855.
[7] International Equipment Co. model XED, explosion proof.
[8] Model 3380 liquid scintillation spectrometer, Packard Instrument Co.
[9] Vacutainers.

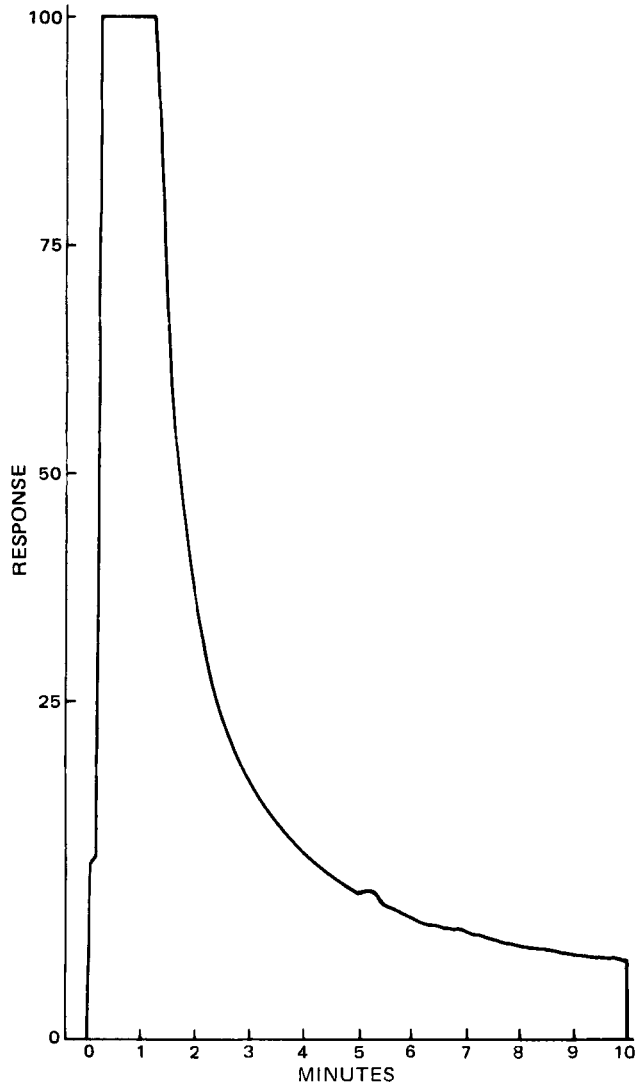

Figure 2—*Typical chromatogram tracing of a blank human plasma extract.*

was obtained (Table I) over this concentration range; the mean extraction recovery from plasma was 100.6% with a standard deviation of 5.8% (Table I). These results indicate that quantitative extraction from human plasma was achieved over a concentration range of 10–300 ng/ml, which covers the concentrations found in most biological samples analyzed so far from pharmacokinetic studies of I.

At lower nanogram per milliliter concentrations, problems were encountered initially in obtaining acceptable recovery of I. The drug was sometimes adsorbed to the surface of the glass tubes, from which it could be recovered by addition of an excess of other amines in solution. To keep the loss of I to a minimum during extraction, the amount of the internal standard added was in large excess compared to I in plasma samples. Orphenadrine was chosen as the mass internal standard. Methanolic solutions of I and the internal standard, when kept refrigerated, were stable for several months. The ether must be freshly distilled on each analysis day to avoid interfering peaks.

Accuracy and Precision—The accuracy of the method was checked by carrying samples at 20, 40, 70, and 130 ng/ml in replicates of five through the entire method; concentrations were calculated from a pooled standard curve constructed by linear regression (Table II). The mean detected concentrations were 19.2, 42.5, 74.8, and 135.1 ng/ml, respectively. The standard deviations were 3.3, 2.9, 2.6, and 7.3 and the relative standard deviations were 17, 7, 3, and 5%, respectively.

The accuracy of this method is indicated by the small mean error between the detected and theoretical values. The mean errors were −0.8, 2.5, 4.8, and 5.1 for 20, 40, 70, and 130 ng/ml, respectively. The corresponding relative errors were −4, 6, 6, and 4%.

Chromatographic Separation—Some packings (OV-17 and OV-1) did not give the desired separation or result in enough detector response at low nanogram per milliliter concentrations of I. The cyclohexanedimethyl succinate packing gave good chromatographic separation plus considerably improved detector response (Fig. 1). Pure I in methanol gave discernible peaks in absolute amounts as low as 100 pg under the conditions described.

When plasma extracts in chloroform, ether, or methyl acetate were injected into the chromatograph, interference from the solvent peak tracing decreased the sensitivity considerably. The use of methanolic carbon disulfide as the final solvent largely eliminated this problem, because it gave only minimal detector response. The 2% methanol content was necessary to dissolve the residue of I completely.

Specificity—*Interference from Endogenous Materials in Plasma*—There was no significant interference with I or the internal standard by any endogenous materials in normal human plasma. None of the predose samples from a human study demonstrated any significant GLC peaks corresponding to I or the internal standard. There was an extremely small peak close to the internal standard, but it contributed no more than 1% in area to the internal standard. Correction for this insignificant interference was not included in the routine calculation of the unknown. A typical GLC tracing of blank human plasma extract is shown in Fig. 2.

Interference from Metabolites of I—One metabolite of I found in urine, desmethylnefopam (III), did not interfere. The GLC tracing following injection of ≈ 400 ng of III did not give any discernible peak. The lack of interference by III was further supported by the report that carbon disulfide decomposes primary and secondary amines (8). There exist no GLC data on other likely metabolites. Since metabolites of I are likely to be more polar if also present in the plasma, they would, theoretically, be less readily extractable and require longer elution times than I under the present GLC operating conditions.

Human Plasma Standard Curves—Several standard curves covering the 10–130-ng/ml range were generated over 1 year. Linearity extended, however, up to 1500 ng/ml. Standard curves constructed by linear regression fitting indicated an excellent linear relationship between response and drug concentration present in the 10–130-ng/ml range. The sensitivity of the assay was 20 ng/ml with a 2-ml sample. Coefficients of correlation of individual curves were always better than 0.99. A pooled standard curve (n = 12) yielded a correlation coefficient of 0.9998, and the good linear fit was indicated by the coefficient of determination, r^2 = 0.9996.

Human Plasma Analysis for I—Typical plasma I levels in a healthy subject (selected from determinations in 24 individual subjects after a 60-mg po dose) are given in Fig. 3. The curve shown was created by a single determination per time point. A peak plasma level of 99 ng/ml was

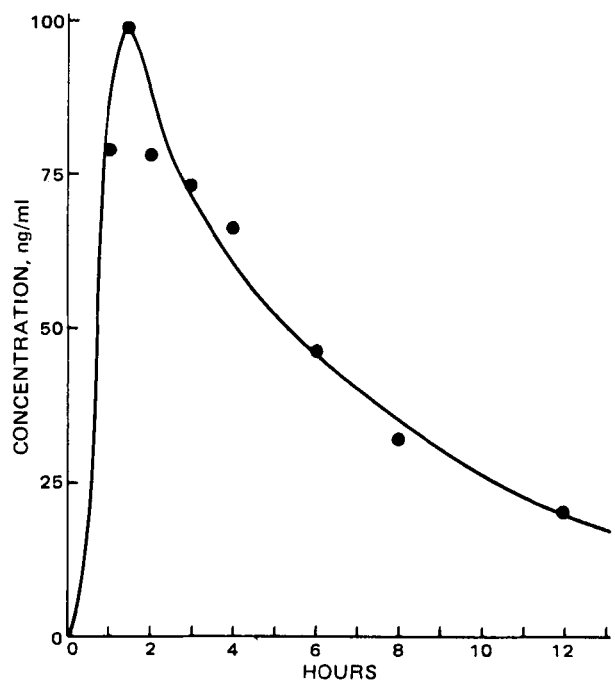

Figure 3—*Plasma levels of nefopam in one human subject following a single oral dose of 60 mg of nefopam hydrochloride.*

reached 60 min postdosing, and the decrease in plasma level between 3 and 12 hr was not a simple monoexponential decline. These results indicate that the method is applicable for determination of plasma concentrations of I in humans at this therapeutic dose.

DISCUSSION

The results demonstrate that GLC with a flame-ionization detector is very effective for the determination of the lipophilic drug, I, in biological fluids in the low nanogram per milliliter concentration range. Most of the endogenous material and one metabolite of I did not interfere. A minor interference peak from a blank human plasma extract was sometimes observed, but its amount was insignificant (<1% of the internal standard peak).

The lower limit of sensitivity is 20 ng/ml with a 2-ml plasma sample; however, the sensitivity can be improved to 10 ng/ml by employing larger plasma samples.

Both the accuracy and the precision of the method are good. The 20-ng/ml value shown in Table II has a larger relative standard deviation than the other three. One of the five values is approximately 60% lower than the mean of the other four values. If the 13.5-ng/ml value had been excluded, the relative standard error would have been 6%. This value is well within the range of the other relative standard errors. The 13.5-ng/ml value was probably due to random error. Since this analytical method is intended for samples from biological experiments, the levels of precision and accuracy are more than adequate. For 32 samples, including six standards, the total extraction and analysis time is 8 hr. Close to 500 human plasma samples have been analyzed successfully by this method over 1 year.

REFERENCES

(1) M. W. Klohs, M. D. Draper, F. J. Petracek, K. H. Ginzel, and O. N. Re', *Arzneim-Forsch.*, **22,** 132 (1972).

(2) A. Cohen, *Curr. Ther. Res. Clin. Exp.*, **16,** 184 (1974).

(3) F. C. Workmon and L. Winter, Jr., *ibid.*, **16,** 609 (1974).

(4) A. Sunshine and E. Laska, *Clin. Pharmacol. Ther.*, **18,** 530 (1975).

(5) M. M. Gassel, E. Diamantopoulos, V. Petropoulos, A. C. R. Hughes, M. L. Fernandez Ballesteros, and O. N. Re', *J. Clin. Pharmacol.*, **16,** 34 (1976).

(6) A. G. Bolt, G. Graham, and P. Wilson, *Xenobiotica*, **4,** 355 (1974).

(7) H. Ehrsson and S. Eksborg, *J. Chromatogr.*, **136,** 154 (1977).

(8) P. J. Kothari and M. M. Sharma, *Chem. Eng.*, **21,** 391 (1966).

ACKNOWLEDGMENTS

The authors thank W. J. Hammar and J. E. Bunker for the synthesis of ^{14}C-nefopam and S. F. Chang for valuable discussions. They also acknowledge the early GLC work by A. R. Hansen and G. Graham and participation in the clinical blood level study by Dr. D. T. Calderwood and Dr. B. J. Baltes.

Differential Pulse Polarographic Determination of Clorazepate Monopotassium and Dipotassium

S. HANNA ˣ, F. DIANA, J. SLEVINSKI, K. VERONICH, and L. LACHMAN

Received March 3, 1978, from the *Analytical Research and Development Department, Endo Laboratories, Inc., Subsidiary of E. I. du Pont de Nemours & Co., Inc., Garden City, NY 11530.* Accepted for publication May 1, 1978.

Abstract □ Polarographic investigation of clorazepate monopotassium and dipotassium showed two cathodic waves at about −1.28 and −1.66 v. The cathodic wave associated with clorazepate monopotassium or dipotassium at about −1.66 v was a pH-independent, diffusion-controlled wave. This wave was used to develop a specific stability-indicating procedure for clorazepate monopotassium and dipotassium in the presence of their degradation products, namely, nordiazepam, 2-amino-5-chlorobenzophenone, and glycine. The method involves a 10^{-2} *M* LiOH–10^{-1} *M* LiCl extraction of the active ingredient from the formulation, filtration, dilution with the same supporting electrolyte, and then use of the standard addition technique for drug quantitation in capsules. Typical formulation excipients did not interfere with the analysis. Accuracy and precision of the procedure were 99.55 ± 0.68%.

Keyphrases □ Clorazepate monopotassium and dipotassium—differential pulse polarographic analyses in pharmaceutical preparations □ Polarography, differential pulse—analyses, clorazepate monopotassium and dipotassium in pharmaceutical preparations □ Tranquilizers—clorazepate monopotassium and dipotassium, differential pulse polarographic analyses in pharmaceutical preparations

Several methods have been reported for the quantitative analysis of clorazepate monopotassium (I) and dipotassium (II) and their capsule formulations, including UV spectrophotometry (1), fluorometry (2), colorimetry (3), potentiometry (4), GLC (2, 5), TLC (1), and high-pressure liquid chromatography (6). One method utilized ac and differential pulse polarography for the assay of clorazepate dipotassium in its capsules (7). In this polarographic procedure, the clorazepate dipotassium was dissolved in an acetate buffer containing 10% dimethylformamide to give *N*-desmethyldiazepam after 10 min. Then quantitation was achieved through measurement of the reducible double bond C=N moiety.

The reported procedures lack specificity and, consequently, cannot be used for stability studies. In this study, differential pulse polarography was applied to achieve a specific stability-indicating procedure for the analysis of clorazepate monopotassium or dipotassium in capsule formulations.

EXPERIMENTAL

Apparatus—A polarograph[1] was equipped with a 4.0 *N* saturated calomel fiber junction reference electrode, a dropping mercury electrode at 40 cm (62 cm corrected), a platinum wire auxiliary electrode, and a drop timer[2]. An *x–y* recorder[3] was attached to the polarograph.

Reagents and Solutions—All chemicals were reagent grade[4]. The potency and purity of clorazepate monopotassium and dipotassium reference standards[5] were 94.27 and 99.77%, respectively, as ascertained by the manufacturers' physicochemical and analytical procedures.

Working standards contained 40.0 and 51.0 mg of I and II/100 ml, respectively.

The supporting electrolyte was 10^{-2} *M* LiOH–10^{-1} *M* LiCl.

[1] Model 174, Princeton Applied Research, Princeton, N.J.
[2] Model 170, Princeton Applied Research, Princeton, N.J.
[3] Model 2000, Houston Co., Houston, Tex.
[4] Fisher Scientific Co., Fair Lawn, N.J.
[5] Abbott Laboratories, North Chicago, Ill.

0022-3549/78/1200-1723$01.00/0

© 1978, American Pharmaceutical Association

reached 60 min postdosing, and the decrease in plasma level between 3 and 12 hr was not a simple monoexponential decline. These results indicate that the method is applicable for determination of plasma concentrations of I in humans at this therapeutic dose.

DISCUSSION

The results demonstrate that GLC with a flame-ionization detector is very effective for the determination of the lipophilic drug, I, in biological fluids in the low nanogram per milliliter concentration range. Most of the endogenous material and one metabolite of I did not interfere. A minor interference peak from a blank human plasma extract was sometimes observed, but its amount was insignificant (<1% of the internal standard peak).

The lower limit of sensitivity is 20 ng/ml with a 2-ml plasma sample; however, the sensitivity can be improved to 10 ng/ml by employing larger plasma samples.

Both the accuracy and the precision of the method are good. The 20-ng/ml value shown in Table II has a larger relative standard deviation than the other three. One of the five values is approximately 60% lower than the mean of the other four values. If the 13.5-ng/ml value had been excluded, the relative standard error would have been 6%. This value is well within the range of the other relative standard errors. The 13.5-ng/ml value was probably due to random error. Since this analytical method is intended for samples from biological experiments, the levels of precision and accuracy are more than adequate. For 32 samples, including six standards, the total extraction and analysis time is 8 hr. Close to 500 human plasma samples have been analyzed successfully by this method over 1 year.

REFERENCES

(1) M. W. Klohs, M. D. Draper, F. J. Petracek, K. H. Ginzel, and O. N. Re', *Arzneim-Forsch.*, **22,** 132 (1972).

(2) A. Cohen, *Curr. Ther. Res. Clin. Exp.*, **16,** 184 (1974).

(3) F. C. Workmon and L. Winter, Jr., *ibid.*, **16,** 609 (1974).

(4) A. Sunshine and E. Laska, *Clin. Pharmacol. Ther.*, **18,** 530 (1975).

(5) M. M. Gassel, E. Diamantopoulos, V. Petropoulos, A. C. R. Hughes, M. L. Fernandez Ballesteros, and O. N. Re', *J. Clin. Pharmacol.*, **16,** 34 (1976).

(6) A. G. Bolt, G. Graham, and P. Wilson, *Xenobiotica*, **4,** 355 (1974).

(7) H. Ehrsson and S. Eksborg, *J. Chromatogr.*, **136,** 154 (1977).

(8) P. J. Kothari and M. M. Sharma, *Chem. Eng.*, **21,** 391 (1966).

ACKNOWLEDGMENTS

The authors thank W. J. Hammar and J. E. Bunker for the synthesis of ^{14}C-nefopam and S. F. Chang for valuable discussions. They also acknowledge the early GLC work by A. R. Hansen and G. Graham and participation in the clinical blood level study by Dr. D. T. Calderwood and Dr. B. J. Baltes.

Differential Pulse Polarographic Determination of Clorazepate Monopotassium and Dipotassium

S. HANNA ˣ, F. DIANA, J. SLEVINSKI, K. VERONICH, and L. LACHMAN

Received March 3, 1978, from the *Analytical Research and Development Department, Endo Laboratories, Inc., Subsidiary of E. I. du Pont de Nemours & Co., Inc., Garden City, NY 11530.* Accepted for publication May 1, 1978.

Abstract □ Polarographic investigation of clorazepate monopotassium and dipotassium showed two cathodic waves at about −1.28 and −1.66 v. The cathodic wave associated with clorazepate monopotassium or dipotassium at about −1.66 v was a pH-independent, diffusion-controlled wave. This wave was used to develop a specific stability-indicating procedure for clorazepate monopotassium and dipotassium in the presence of their degradation products, namely, nordiazepam, 2-amino-5-chlorobenzophenone, and glycine. The method involves a 10^{-2} *M* LiOH–10^{-1} *M* LiCl extraction of the active ingredient from the formulation, filtration, dilution with the same supporting electrolyte, and then use of the standard addition technique for drug quantitation in capsules. Typical formulation excipients did not interfere with the analysis. Accuracy and precision of the procedure were 99.55 ± 0.68%.

Keyphrases □ Clorazepate monopotassium and dipotassium—differential pulse polarographic analyses in pharmaceutical preparations □ Polarography, differential pulse—analyses, clorazepate monopotassium and dipotassium in pharmaceutical preparations □ Tranquilizers—clorazepate monopotassium and dipotassium, differential pulse polarographic analyses in pharmaceutical preparations

Several methods have been reported for the quantitative analysis of clorazepate monopotassium (I) and dipotassium (II) and their capsule formulations, including UV spectrophotometry (1), fluorometry (2), colorimetry (3), potentiometry (4), GLC (2, 5), TLC (1), and high-pressure liquid chromatography (6). One method utilized ac and differential pulse polarography for the assay of clorazepate dipotassium in its capsules (7). In this polarographic procedure, the clorazepate dipotassium was dissolved in an acetate buffer containing 10% dimethylformamide to give *N*-desmethyldiazepam after 10 min. Then quantitation was achieved through measurement of the reducible double bond C=N moiety.

The reported procedures lack specificity and, consequently, cannot be used for stability studies. In this study, differential pulse polarography was applied to achieve a specific stability-indicating procedure for the analysis of clorazepate monopotassium or dipotassium in capsule formulations.

EXPERIMENTAL

Apparatus—A polarograph[1] was equipped with a 4.0 *N* saturated calomel fiber junction reference electrode, a dropping mercury electrode at 40 cm (62 cm corrected), a platinum wire auxiliary electrode, and a drop timer[2]. An *x–y* recorder[3] was attached to the polarograph.

Reagents and Solutions—All chemicals were reagent grade[4]. The potency and purity of clorazepate monopotassium and dipotassium reference standards[5] were 94.27 and 99.77%, respectively, as ascertained by the manufacturers' physicochemical and analytical procedures.

Working standards contained 40.0 and 51.0 mg of I and II/100 ml, respectively.

The supporting electrolyte was 10^{-2} *M* LiOH–10^{-1} *M* LiCl.

[1] Model 174, Princeton Applied Research, Princeton, N.J.
[2] Model 170, Princeton Applied Research, Princeton, N.J.
[3] Model 2000, Houston Co., Houston, Tex.
[4] Fisher Scientific Co., Fair Lawn, N.J.
[5] Abbott Laboratories, North Chicago, Ill.

0022-3549/78/1200-1723$01.00/0

© 1978, American Pharmaceutical Association

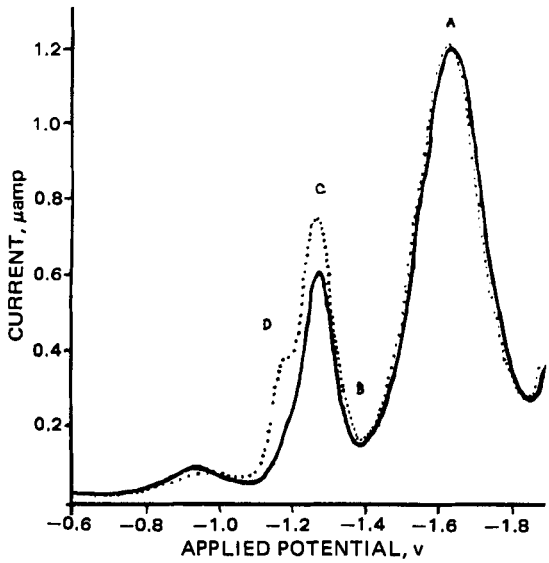

Figure 1—*Differential pulse polarogram for I, excipients, and its degradation products at a 10% level. Key: —, I reference standard and excipients; . . . ., I reference standard, excipients, and degradation products; A, I; B, 2-amino-5-chlorobenzophenone; C, increase in current due to glycine; and D, nordiazepam.*

Polarographic Conditions—The conditions were: drop time, 1 sec; scan rate, 2–5 mv/sec; display direction, positive; scan direction, negative; initial potential, −0.6 v; range, 3.0 v; sensitivity, 2–5 μafs; modulation amplitude, 25–50 mv; temperature, ambient; low pass filter, off; and output offset, off.

Polarographic Analysis of Samples—Prior to sample analysis, 50.0 ml of blank solution (10^{-2} *M* LiOH–10^{-1} *M* LiCl) was transferred into the polarographic cell, deaerated for 10 min with high purity nitrogen, and scanned from −0.6 to −2.0 v. The circuit was opened, and the cell was emptied. Then the cell was rinsed with distilled water and dried. With the previously described operating conditions, the blank polarogram should be an essentially straight, horizontal line over the whole range from −0.6 to −1.8 v.

The contents of five capsules were transferred into a 100-ml volumetric flask, about 75 ml of the supporting electrolyte solution was added, and the stoppered flask was mechanically shaken for 15 min. Then the solution was brought to volume with the same supporting electrolyte solution and filtered; the first 20 ml of filtrate was discarded. An aliquot, equivalent to 5.406 mg of I or 5.752 mg of II, of the filtered sample solution was transferred to the polarographic cell and adjusted to 45 ml with the supporting electrolyte solution. The solution was then deaerated with nitrogen for 10 min and allowed to stand for 1 min under a blanket of nitrogen. The differential pulse polarogram was recorded between −0.6 and −2.0 v. The resulting peak height at about −1.66 v was the sample peak height, *S*.

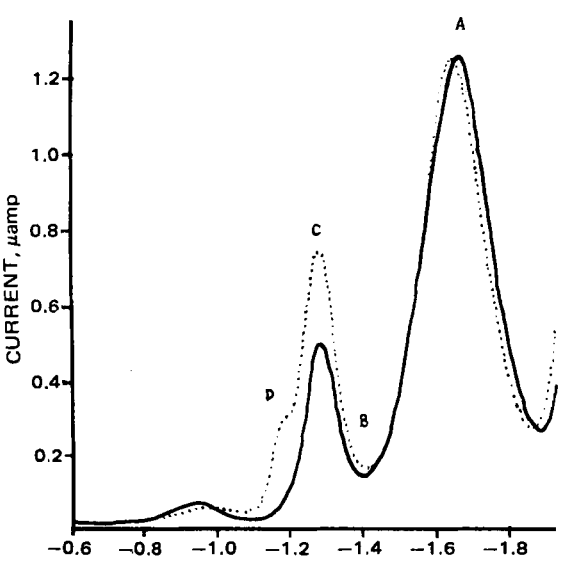

Figure 2—*Differential pulse polarogram of II, excipients, and its degradation products as a 10% level. Key: —, II reference standard and excipients; . . . ., II reference standard, excipients, and degradation products; A, II; B, 2-amino-5-chlorobenzophenone; C, increase in current due to glycine; and D, nordiazepam.*

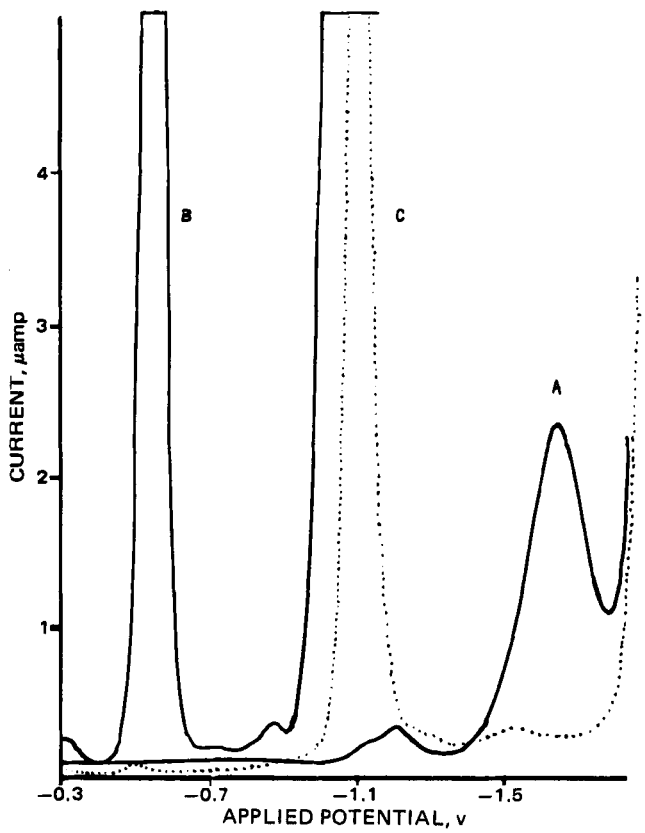

Figure 3—*Composite polarogram for the carboxylate functionality polarographic behavior of I. Polarograms of I reference standard and placebo were in 0.01* M *LiOH (A), 1.0* M *HCl (to pH 1) (B), and 1.0* M *LiOH (to pH 12) (C).*

A standard addition technique was used for quantitation. Without removing the cell, a 5.0-ml aliquot of standard solution was added. The cell was then again deaerated for 5 min with nitrogen and allowed to stand for 1 min under nitrogen, and a polarogram was recorded. The resulting peak height was the total peak height, *T*. Triplicate runs were carried out on each sample solution.

Calculations—Peak heights, *S* and *T*, were measured by drawing a horizontal line through the low point in the polarogram. The baseline was extrapolated so that it passed under the actual peak, and the peak height was then measured in millimeters:

$$\text{mg of I or II/capsule} = \frac{\text{peak height } S \times \text{clorazepate standard weight (mg)} \times \text{purity factor} \times \text{sample dilution factor}}{\left(\text{peak height } T \times \frac{50}{45} - \text{peak height } S\right) \times 100} \quad \text{(Eq. 1)}$$

RESULTS AND DISCUSSION

Determination of the polarographic behavior of I and II with typical excipients and degradation products was conducted using a 10^{-2} *M* LiOH–10^{-1} *M* LiCl solution as the supporting electrolyte. The polarograms for both I (Fig. 1) and II (Fig. 2) showed two major cathodic waves at about −1.28 and −1.66 v. The peak current for the second cathodic wave at about −1.66 v was unaffected by the presence of 10% levels of nordiazepam, 2-amino-5-chlorobenzophenone, and glycine. Nordiazepam produced a prewave on the first cathodic wave at about −1.16 v, 2-

Table I—Effect of Variation of pH on the Cathodic Waves at about −1.28 and −1.66 v ([LiCl] = 10^{-1} *M*)

	First Peak Potential at −1.28 v		Second Peak Potential at −1.66 v	
[LiOH], *M*	Peak Potential, v	Peak Height, mm	Peak Potential, v	Peak Height, mm
10^{-4}	−1.15	51.0	−1.62	43.0
10^{-3}	−1.18	28.5	−1.61	48.5
10^{-2}	−1.24	16.5	−1.62	48.5
10^{-1}	−1.28	7.9	−1.67	49.0

Table II—Effect of Variation of Ionic Strength on the Cathodic Waves at about −1.28 and −1.66 v

		First Peak Potential at −1.28 v		Second Peak Potential at −1.66 v	
[LiOH], *M*	[LiCl], *M*	Peak Potential, v	Peak Height, mm	Peak Potential, v	Peak Height, mm
10^{-2}	0	−1.24	5.5	−1.74	57.0
	10^{-2}	−1.29	6.0	−1.71	52.5
	10^{-1}	−1.24	16.5	−1.62	48.5
10^{-1}	0	−1.28	5.5	−1.71	52.0
	10^{-2}	−1.29	6.5	−1.70	51.0
	10^{-1}	−1.28	7.9	−1.67	48.0

amino-5-chlorobenzophenone produced a slight wave between the two major waves at about −1.42 v, and glycine increased the observed current at the first peak potential at about −1.28 v.

The peak potential observed at about −1.28 v is believed to be associated with the azomethine functionality (8). To establish that the cathodic wave at about −1.66 v is related to the carboxylate functionality on the intact drug molecule, the pH of the solution in the cell was adjusted to approximately pH 1 by the addition of 1.0 *N* HCl, and the polarogram for this solution was recorded. A single peak at −0.55 v was observed. Ten minutes after the addition of acid, the pH of the solution was returned to its initial pH 12 using 1.0 *M* LiOH and rescanned. The peak at about −1.66 v was no longer present, and the peak current at about −1.16 v corresponding to the nordiazepam increased significantly, indicating that complete degradation of the drug had occurred (Fig. 3). Addition of a 10-fold excess of the two possible carboxylate degradation materials, namely, carbonate and formate, produced a slight shift in peak potential, but peak current remained constant in both cases.

The behavior of the cathodic wave at about −1.66 v with variation of pH and ionic strength was studied with 8.10×10^{-5} *M* I. Basicity and supporting electrolyte concentrations were varied while polarograms were recorded in both dc and differential pulse modes in a range of 1.5 v. The range of pH studies was from pH 10 to 13 because of the relative instability of I and II in neutral or acidic media. There was no correlation between either differential pulse peak height or peak potential with the pH or ionic strength of the cathodic wave at about −1.66 v (Tables I and II).

Solutions of I in 10^{-2} *M* LiOH–10^{-1} *M* LiCl ranging from 5.04×10^{-5} to 1.90×10^{-3} *M* were used to study the effect of concentration on the cathodic wave at about −1.66 v. Polarograms were recorded in both dc and differential pulse modes. The peak current and differential pulse peak heights observed depicted the linearity of the polarographic response over the concentration range studied.

A 2.016×10^{-4} *M* solution of monopotassium clorazepate in 10^{-2} *M* LiOH–10^{-1} *M* LiCl was used to study the effect of the height of the mercury column on the cathodic wave at about −1.66 v. The height of the mercury column, corrected to include the distance to the capillary tip of the dropping mercury electrode, was varied from 28.2 to 101.9 cm. Polarograms were recorded in the dc mode with scan rate and sensitivity adjusted to give approximately the same millivolts per drop under all mercury heights (Table III). Graphical representation of current *versus* the square root of height showed a linear dependency.

Use of II instead of I in the polarographic investigation resulted only in a difference in peak current for the carboxylate functionality at about −1.66 v due to the higher molecular weight of the dipotassium salt.

Accuracy and precision of fortified sample studies are presented in Table IV.

The results obtained using the differential pulse polarographic procedure for the analysis of 3.25, 6.5, and 13.0 mg of I[6]/capsule and 3.75, 7.5, and 15.0 mg of II[7]/capsule are summarized in Table V.

Table III—Effect of Variation of Height of Mercury Column on the Cathodic Wave at about −1.66 v

Clorazepate Wave Current, μamp ($E_{1/2}$ = −1.66 v)	Corrected Height, cm	√Corrected Height, cm
0.429	28.2	5.31
0.543	43.0	6.56
0.634	57.9	7.61
0.728	73.9	8.60
0.776	88.1	9.39
0.843	101.9	10.09

Table IV—Accuracy and Precision of I and II Fortified Capsules

Added, mg/capsule		Percent[a]	
I	II	Recovery	±*SD*
3.25	—	99.7	1.4
6.5	—	100.4	1.8
13.0	—	99.8	1.0
—	3.75	99.2	1.3
—	7.50	99.8	0.8
—	15.0	98.4	2.8

[a] Mean of 10 results.

Table V—Analysis of I and II Capsules

Labeled, mg/capsule		Found, mg/capsule		
I	II	I[a]	II[b]	±*SD*
3.25	—	3.21	—	0.05
6.5	—	6.41	—	0.07
13.0	—	12.8	—	0.3
—	3.75	—	3.65	0.03
—	7.5	—	7.4	0.00
—	15.0	—	14.67	0.04

[a] Mean of six results. [b] Mean of three results.

REFERENCES

(1) J. Laguleau, R. Crockett, and P. Mesnard, *Bull. Soc. Pharm., Bordeaux*, **110**, 10 (1971).

(2) P. LaFargue, J. Meunier, and Y. Lemontey, *J. Chromatogr.*, **62**, 423 (1971).

(3) P. Gros and R. Raveux, *Chim. Ther.*, **4**, 312 (1969).

(4) J. A. Raihle and V. E. Papendick, "Analytical Profiles," vol. IV, Academic, New York, N.Y., 1975, p. 111.

(5) A. Valia, J. P. Cano, and A. Angeletti-Philippe, *J. Eur. Toxicol.*, **3**, 109 (1971).

(6) C. G. Scott and P. Brommer, *J. Chromatogr. Sci.*, **8**, 446 (1970).

(7) H. Oelschlager and F. I. Segun, *Arch. Pharm. (Weinheim, Ger.)*, **307**, 401 (1974).

(8) B. Z. Senkowski, M. S. Levin, J. R. Urbigkit, and E. G. Wollish, *Anal. Chem.*, **36**, 1991 (1964).

[6] Azene Capsules, Endo Laboratories, Garden City, N.Y.

[7] Tranxene Capsules, Abbott Laboratories, North Chicago, Ill.

Antineoplastic Agents III: Effects of Dibromoethyl and Vinyl Esters of *N*-Benzyloxycarbonyl-L-phenylalanine on Ehrlich Ascites Tumor Cell Metabolism

IRIS H. HALL ˣ, ZIAODIN SAJADI, and LARRY J. LOEFFLER

Received January 3, 1978, from the *Division of Medicinal Chemistry, School of Pharmacy, University of North Carolina at Chapel Hill, Chapel Hill, NC 27514.* Accepted for publication May 1, 1978.

Abstract □ Evidence is presented that *N*-benzyloxycarbonyl-L-phenylalanine vinyl ester and 1,2-dibromoethyl ester are inhibitors of Walker 256 carcinosarcoma and Ehrlich ascites carcinoma tumor growth. The major effects of these two agents on Ehrlich ascites cell metabolism were the inhibition of deoxyribonucleic acid and protein synthesis and the alteration of cellular regulatory processes controlling cytokinetics. Deoxynucleotide (purine) kinase enzymes appeared to be the focal site for inhibition of deoxyribonucleic acid synthesis with marginal inhibition of thymidylate synthetase activity. Cyclic adenosine monophosphate levels were elevated by drug treatment whereas chromatin protein phosphorylation, cell respiration, and lysosomal activities were inhibited. *N*-Benzyloxycarbonyl-L-phenylalanine 1,2-dibromoethyl ester was a latent *in vitro* chymotrypsin inhibitor. Some preliminary evidence suggests that these activated esters may inhibit cellular enzymatic activity by alkylating imidazole and lysine residues of proteins.

Keyphrases □ *N*-Benzyloxycarbonyl-L-phenylalanine esters—effect on tumor cell metabolism in mice □ Phenylalanine esters, substituted—effect on tumor cell metabolism in mice □ Antineoplastic activity—substituted phenylalanine esters, effect on tumor cell metabolism in mice □ Metabolism, tumor cell—effect of substituted phenylalanine esters in mice □ Structure–activity relationships—effect of substituted phenylalanine esters on tumor cell metabolism in mice

The antitumor activity of *N*-protected vinyl, 1,2-dibromoethyl, and cyanomethyl esters of amino acids was reported previously (1, 2). Of this series of 50 compounds, the *N*-benzyloxycarbonyl-L-phenylalanine analogs were the most active in the Walker 256 carcinosarcoma and Ehrlich ascites screens. These compounds are structurally related to tosylphenylalanyl chloromethyl ketone (I), which effectively inhibited carcinogenesis initiated by 7,12-dimethylbenz[*a*]anthracene and growth of Swiss SV-3T3 transformed tissue culture cells (3–6).

At that time, it was postulated that I may inhibit the acquired proteolytic activity associated with cell transformation and increased malignant invasiveness of neoplastic tissue. However, I then was shown to inhibit protein synthesis of tumor cells (7). *N*-Benzyloxycarbonyl-L-phenylalanine vinyl ester (II) and *N*-benzyloxycarbonyl-L-phenylalanine 1,2-dibromoethyl ester (III) were investigated for their effects on tumor cell metabolism, and the preliminary results are now reported.

EXPERIMENTAL

Chemical Synthesis—*N-Benzyloxycarbonyl-L-phenylalanine Vinyl Ester (II)*—The starting material, *N*-benzyloxycarbonyl-L-phenylalanine (IV), was prepared according to the procedure of Bergman and Zervas (8). A mixture of 1.5 g (4 mmoles) of IV, 20 ml of vinyl acetate, and 20 mg of palladium chloride–sodium chloride was refluxed (70–75°) for 5 hr. After cooling, 34 mg of activated charcoal was added in one portion and the mixture was stirred for 5 min. The reaction mixture was filtered, and solvents were removed *in vacuo*. The residue was dissolved in 10 ml of vinyl acetate, then 20 mg of palladium chloride–sodium chloride was added, and the mixture was refluxed for 5 hr.

After the mixture was cooled to room temperature, the procedure was repeated. When the reaction was complete, as demonstrated by TLC, purification of the product was carried out by column chromatography on silica gel [benzene–chloroform (1:1)]. A colorless oily product was obtained in a 75–80% yield; $[\alpha]_D^{24}$ −11.0° (c in $CHCl_3$).

Anal.—Calc. for $C_6H_{16}N_2O_3$: C, 70.13; H, 5.19; N, 9.02. Found: C, 70.07; H, 5.27; N, 9.01.

N-Benzyloxycarbonyl-L-phenylalanine 1,2-Dibromoethyl Ester (III)—To a solution of 0.97 g (3 mmoles) of II in 45 ml of benzene, a solution of 0.47 g (3 mmoles) of bromine in 40 ml of benzene was added dropwise over 30 min with vigorous stirring. The reaction mixture was stirred for an additional 3 hr at room temperature, and then the solvent was removed under high vacuum. The product was impure, as shown by TLC with chloroform–ethyl acetate (2:1), and was purified by column chromatography on silica gel eluted with chloroform–ethyl acetate (2:1).

Further purification was carried out by recrystallization from chloroform and low boiling ligroin to yield 1.05 g of product (70–75%), mp 78–80°; $[\alpha]_D^{24}$ −33.5° (c in CH_3OH); IR: 1775 (ester carbonyl) cm^{-1}; NMR: δ 4.05 (2H, d, CH_2Br) and 6.8 (1H, t, OCHBr) ppm.

Anal.—Calc. for $C_{19}H_{19}NO_4$: C, 47.20; H, 3.93; Br, 32.71; N, 2.89. Found: C, 47.00; H, 3.95; Br, 32.88; N, 2.88.

L-Phenylalanine Vinyl Ester Hydrochloride (V)—This compound was prepared by a modification of a reported procedure (9). Trifluoroacetic acid (10 ml) was added gradually at −15° to a mixture of 1.89 g (5 mmoles) of II and 2 ml of anisole. Upon completion of the reaction, the mixture was kept at room temperature for 20 min and then refluxed in an oil bath (70–75°) for 20 min. Most of the trifluoroacetic acid was then distilled off *in vacuo*, and the remaining oil was dissolved in absolute ether. The ester hydrochloride was precipitated from this solution by introduction of gaseous hydrogen chloride at −10°. The yield was 0.95 g (70–75%), mp 155–157° [lit. (9) mp 159–160°].

Tosylphenylalanyl chloromethyl ketone (I), benzaldehyde (VI), acetaldehyde (VII), phenylalanine mustard (VIII), mercaptopurine (IX), fluorouracil, and iodoacetate were purchased.

***In Vivo* Tumor Screens**—In the Ehrlich ascites screen, 10^6 cells were implanted on Day 0. Test compounds were suspended in 0.05% polysorbate 80–water and homogenized to obtain a fine suspension. Each compound was injected intraperitoneally (1 mg/day; *i.e.*, 33.3 mg/kg) into CF_1 male mice (~30 g). On the 7th day, the mice were sacrificed; the total volumes of ascites fluid and packed cells (ascites-crit) were determined, and the percentage inhibition was calculated (1). Phenylalanine mustard and mercaptopurine were used as positive controls.

In the Walker 256 carcinosarcoma screen, 10^6 tumor cells were implanted intraperitoneally into Sprague–Dawley male rats (75 ± 10 g). Test compounds were injected intraperitoneally at 2.5 mg/kg/day, and the day of death was recorded. Treated/control (T/C) values were calculated for the average survival time of each group according to the National Institutes of Health protocol (10). The LD_{50} values were determined in CF_1 male mice by the Litchfield and Wilcoxon method (11).

Macromolecular Synthesis—Unless otherwise stated, all biochemical studies were carried out on 8-day Ehrlich ascites tumor-bearing CF_1 male mice treated with I–III at a subacute dose of 16 mg/kg/day on Days 5–7. ^{14}C-Thymidine incorporation into deoxyribonucleic acid was determined by the method of Chae *et al.* (12). One hour prior to sacrifice of the animal on Day 8, 10 μCi of [*methyl*-^{14}C]thymidine (54 mCi/mmole) in 0.1 ml of isotonic sodium chloride was injected intraperitoneally. The deoxyribonucleic acid was isolated, and the ^{14}C-content was determined by placing an aliquot in 10 ml of scintillation fluid (two parts toluene, one part octoxynol, 0.4% 2,5-diphenyloxazole, and 0.01% 1,4-bis[2-(5-phenyloxazolyl)]benzene).

0022-3549/78/1200-1726$01.00/0
© 1978, American Pharmaceutical Association

Table I—Effects of *N*-Benzyloxycarbonyl-L-phenylalanine Esters on Tumor Cell Growth

Compound	n^a	Ehrlich Ascites Tumor, CF_1 Male Mice, 33.3 mg/kg/day				Walker 256 Carcinosarcoma, Sprague–Dawley Rats, 2.5 mg/kg/day		LD_{50}, CF_1 Mice, mmoles/kg
		Survival at Day 7	Ascites-Crit	Volume	Inhibition, %	Average Days Survived	T/C	
I[b]	6	5/6	0.05	0.01	100.0	—	—	0.21
II	6	6/6	0.40	0.10	99.9	18.1	226	6.15
III	6	6/6	1.40	0.01	100.0	23.0	305	0.15
IV	6	6/6	4.70	0.60	75.0	—	—	0.84
V	6	4/6	27.0	2.20	41.0	—	—	—
VI[c]	6	6/6	49.0	0.80	69.0	—	—	—
VII[d]	6	5/6	27.3	2.04	43.0	—	—	—
VIII[e]	6	6/6	3.00	0.10	99.0	23.0	305	—
IX[f]	6	6/6	0.30	0.70	99.6	—	—	—
X[g]	6	6/6	32.75	41.0	—	7.5	—	—

[a] Number of animals in group. [b] Cyclo chemical. [c] Matheson, Coleman and Bell. [d] Aldrich. [e] 4-[Bis(2-chloroethyl)amino]phenylalanine, Burroughs Wellcome Co. [f] Calbiochem. [g] Water–0.05% Tween 80.

The deoxyribonucleic acid concentration per aliquot was determined by UV spectrophotometry at 260 nm. Uridine incorporation into ribonucleic acid was determined in an analogous manner with 10 μCi of 5-^{3}H-uridine (26.2 Ci/mmole). Ribonucleic acid was extracted by the method of Shibko *et al.* (13). Leucine incorporation into protein was determined by the method of Sartorelli (14) with 1 μCi of 1-^{14}C-leucine (56.9 mCi/mmole). *In vitro* incorporation of 1-^{14}C-acetic acid (57 mCi/mmole) into cholesterol of 8-day Ehrlich ascites cells was determined by the assay of Haven *et al.* (15), and cholesterol was extracted by the method of Wada *et al.* (16) with 6 μmoles of I–III.

Enzymatic Studies—Nuclear deoxyribonucleic acid polymerase activity was determined on washed (three times) isolated nuclei from 8-day Ehrlich ascites cells, prepared by the method of Hymer and Kuff (17). The incubation medium was that described by Sawada *et al.* (18), except that 2-^{14}C-deoxyribothymidine triphosphate (45 mCi/mmole) was used and the insoluble nucleic acids were collected on glass fiber paper GF/F by vacuum suction. Thymidylate synthetase activity was determined by the method of Kampf *et al.* (19) with a postmitochondrial supernate (9000×*g*) from 8-day Ehrlich ascites cells, 1.5 μmoles of test compound, and 5 μCi of 5′-^{3}H-deoxyuridine monophosphate (11 Ci/mmole).

Deoxythymidylate kinase, deoxyguanylate kinase, deoxyadenylate kinase, and deoxythymidylate diphosphate kinase activities were determined by the method of Maley and Ochoa (20) with 1.5 μmoles of test compound. Nucleotide kinase activity was based on the disappearance of 0.1 μmole of reduced nicotinamide adenosine dinucleotide at 340 nm for 20 min. Deoxyribonuclease activity was determined by the method of Hall *et al.* (21) with 1.5 μmoles of test compound.

Nonhistone chromatin (3′,5′-cyclic monophosphate dependent) protein kinase activity was determined on isolated nuclei (17) by the method of Kish and Kleinsmith (22) with 1.5 μmoles of test compounds. Chromatin protein was collected on nitrocellulose membrane filters. 3′,5′-Cyclic adenosine monophosphate levels were determined[1] on 10^6 8-day tumor cells (23). Phosphorus incorporation into histones was determined by the method of Rainer *et al.* (24). One hour prior to sacrifice, 10 μCi of γ-^{32}P-adenosine 5′-triphosphate (8.23 Ci/mmole) was injected intraperitoneally. The nuclear fraction was isolated, and the histones were extracted and counted.

Cathepsin protease activity (pH 5) was determined on 8-day Ehrlich ascites cells by the method of Cho-Chung and Guillino (25). Since I is a chymotrypsin inhibitor, the possibility also existed that *N*-benzyloxycarbonyl-L-phenylalanine esters inhibited chymotrypsin activity. The inhibition of protease activity by II and III was followed with a pH-stat with *N*-acetyl-L-tyrosine ethyl ester ($K_m = 0.83 \times 10^{-3}$ *M*) as the substrate (26). The preincubation medium at 25° contained 0.1 *M* $CaCl_2$, 0.1 *M* tris(hydroxymethyl)aminomethane (pH 7.8), and 50 μmoles of II or III in an ethanolic solution. The reaction was started by adding α-chymotrypsin (in 0.001 *N* HCl) to a final concentration of 3.2 μmoles. At various times (0–390 min), a 4.5-ml aliquot was removed to determine the hydrolysis rate of the substrate by titrating to pH 7.8 with 0.01 *N* NaOH. A Lineweaver–Burke plot was employed to determine chymotrypsin inhibition by II or III.

The *in vitro* aerobic respiration of Ehrlich ascites tumor cell homogenates with succinate, dependent on a flavin adenine dinucleotide-linked dehydrogenase, as the substrate in the presence and absence of adenosine diphosphate was measured in the presence of 0.6 μmole of test compound (27).

[1] Schwarz/Mann radioimmunoassay kit.

UV Spectrophotometric and NMR Studies—UV spectrophotometric binding studies were performed with 75 μg of deoxyribonucleic acid or deoxyguanosine monophosphate, 0.15 μmole of imidazole, or 2 μmoles of lysine after incubation with II, III, VI, or VII in concentrations of 1–5 μmoles in 0.1 *M* phosphate buffer (pH 7.2) over 190–360 nm for 24 hr (23).

Clear solutions for NMR studies were obtained by homogenizing benzaldehyde (0.094 mmole) with imidazole (0.94 mmole) in deuterated chloroform containing 1% tetramethylsilane and adjusting the pH to 6. Benzaldehyde (0.188 mmole) and L-cysteine (0.188 mmole) were dissolved in deuterated water with 1% 3-(trimethylsilyl)-1-propanesulfonic acid, and the pH was adjusted to 9. Benzaldehyde (0.188 mmole) and imidazole (0.188 mmole) were homogenized in deuterated chloroform containing 1% tetramethylsilane. Compound II (0.061 mmole) and imidazole (0.147 mmole) were incubated in deuterated methanol containing 1% tetramethylsilane (pH 6.0).

Compound II (0.061 mmole) and lysine (0.061 mmole) were homogenized in deuterated methanol and deuterated water (pH 11.0) with 1% 2,2-dimethyl-2-silapentane-5-sulfonate as the standard. Compound II (0.061 mmole) and L-cysteine (0.061 mmole) were homogenized in deuterated chloroform with 1% tetramethylsilane (pH 8.0). Compound III (0.092 mmole) was incubated with imidazole (0.147 mmole) (pH 6.0) in deuterated chloroform with 1% tetramethylsilane (pH 6.0). Compound III (0.092 mmole) and lysine (0.092 mmole) were homogenized in deuterated chloroform containing 1% tetramethylsilane and deuterated water (pH 10). Compound III (0.092 mmole) and L-cysteine (0.092 mmole) were reacted in deuterated chloroform containing 1% tetramethylsilane (pH 8.0).

RESULTS

Compounds I–III significantly inhibited Ehrlich ascites tumor cell growth. Compounds II and III increased the survival of Walker 256 carcinosarcoma-bearing rats two and three times, respectively (Table I).

Subacute doses of II and III on Days 5–7 inhibited deoxyribonucleic acid synthesis 57 and 49%, respectively. Ribonucleic acid synthesis and content were unaffected by the drug treatment. Protein synthesis was reduced 53% by II and 50% by III. Cholesterol synthesis was inhibited 25% by II and III. Interference with macromolecular synthesis also was reflected in the deoxyribonucleic acid content per milliliter of ascites fluid in that II reduced this content by 85% and III reduced it by 83%. The protein content per milliliter of ascites fluid was lowered by II to 53% and by III to 45% (Table II). The number of ascites cells per milliliter for the control was 233×10^6; treatment with II resulted in 70.4×10^6 cells/ml, and treatment with III resulted in 83.2×10^6 cells/ml.

Initial studies on nuclear deoxyribonucleic acid polymerases demonstrated that treatment with II and III did not reduce significantly the activity of these enzymes. *In vitro* studies of thymidylate synthetase activity showed that II and III inhibited this enzyme 21 and 27%, respectively. Other sites required for deoxyribonucleic acid synthesis also were examined. Deoxythymidylate kinase activity was inhibited 31 and 37%, respectively. Deoxythymidylate diphosphate kinase activity was reduced 20 and 42% by II and III, respectively. Deoxyguanylate kinase activity was suppressed 51 and 53% by II and III, respectively, and deoxyadenylate kinase activity was reduced 46 and 66%, respectively (Table III). The proteolytic inhibitor I significantly reduced these deoxyribonucleotide kinase enzymes also.

Hydrolytic enzymatic activity measured as cathepsin (pH 5) was significantly reduced by I–III. Deoxyribonuclease activity was marginally

Table II—Effects of *N*-Benzyloxycarbonyl-L-phenylalanine Esters on Macromolecular Synthesis of 8-Day Ehrlich Ascites Tumor Cells

Compound[a]	n[b]	Percent Control, Mean ± *SD*: ^{14}C-Thymidine Incorporation into Deoxyribonucleic Acid	Deoxyribonucleic Acid, mg/ml	^{3}H-Uridine Incorporation into Ribonucleic Acid	^{14}C-Leucine Incorporation into Protein	Protein, mg/ml	^{14}C-Acetic Acid Incorporation into Cholesterol
Control	8	100 ± 26[c]	100 ± 25[d]	100 ± 3[e]	100 ± 5[f]	100 ± 5[g]	100 ± 4[h]
II	6	43 ± 21[i]	15 ± 4[i]	81 ± 25	47 ± 25[i]	46 ± 8[i]	75 ± 8[j]
III	6	51 ± 18[i]	17 ± 5[i]	108 ± 12	50 ± 19[i]	55 ± 9[i]	75 ± 12[j]

[a] One milliliter of control ascites fluid contained 158 × 10^6 cells/ml. Compound II contained 70.4 × 10^6 cells/ml, and III contained 83.2 × 10^6 cells/ml. [b] Number of animals in group. [c] Control value of 263.948 dpm/mg of deoxyribonucleic acid. [d] Control value of 1.3 mg/ml of ascites fluid. [e] Control value of 21,975 dpm/mg of ribonucleic acid. [f] Control value of 814 dpm/mg of protein. [g] Control value of 6.32 mg/ml of ascites fluid. [h] Control value of 132,809 dpm/mg of protein. [i] $p = 0.001$ determined by Student t test (62). [j] $p = 0.010$.

Table III—Effects of *N*-Benzyloxycarbonyl-L-phenylalanine Esters on Enzymes Required in Deoxyribonucleic Acid Synthesis of 8-Day Ehrlich Ascites Tumor Cells

Compound	n[a]	Percent Control Activity, Mean ± *SD*: Thymidylate Synthetase, dUMP → dTMP	Deoxythymidylate Kinase, dTMP → dTDP	Deoxythymidylate Diphosphate, dTDP → dTTP	Deoxyguanylate Kinase, dGMP → dGDP	Deoxyadenosylate Kinase, dAMP → dADP	Nuclear Deoxyribonucleic Polymerase
Control	8	100 ± 3[b]	100 ± 10[c]	100 ± 11[d]	100 ± 16[e]	100 ± 13[f]	100 ± 18[g]
I	5	81 ± 5	58 ± 12[h]	40 ± 8[h]	45 ± 9[h]	80 ± 8[i]	123 ± 32
II	6	79 ± 7[h]	69 ± 14[h]	80 ± 9[j]	49 ± 8[h]	54 ± 5[h]	95 ± 17
III	6	73 ± 5[h]	67 ± 8[h]	58 ± 14	47 ± 11[h]	34 ± 10[h]	—
VI	4	—	52 ± 9[h]	83 ± 11	43 ± 12[h]	34 ± 12[h]	—
Fluorouracil	5	39 ± 7[h]	—	—	—	—	—
Iodoacetate	5	—	—	—	—	—	41 ± 4[h]

[a] Number of animals in group. [b] Control value of 103,328 dpm/mg of protein. [c] ΔO.D. unit = 0.413/mg of protein. [d] ΔO.D. unit = 0.557/mg of protein. [e] ΔO.D. unit = 0.314/mg of protein. [f] ΔO.D. unit = 0.456/mg of protein. [g] Control value of 47,424 dpm/mg of DNA. [h] $p = 0.001$. [i] $p = 0.025$. [j] $p = 0.010$.

Table IV—Effects (Mean ± *SD*) of *N*-Benzyloxycarbonyl-L-phenylalanine Esters on 8-Day Ehrlich Ascites Tumor Cell Metabolism

Compound	n[a]	Hydrolytic Enzyme Activity: Cathepsin	Hydrolytic Enzyme Activity: Deoxyribonuclease	3′,5′-Cyclic Adenosine Monophosphate Level	Nonhistone Chromatin Protein Kinase Activity	^{32}P-Incorporation into Nuclear Histones	Milligrams of Chromatin Protein per Milliliter
Control	6	100 ± 32[b]	100 ± 8[c]	100 ± 14[d]	100 ± 3[e]	100 ± 18[f]	100 ± 13[g]
I	6	6 ± 6[h]	88 ± 8[i]	—	39 ± 2[h]	—	—
II	6	10 ± 7[h]	73 ± 4[h]	164 ± 11[h]	42 ± 7[h]	48 ± 9[h]	74 ± 13[j]
III	6	20 ± 20	83 ± 13[i]	133 ± 7[h]	49 ± 6[h]	43 ± 12[h]	71 ± 16[j]

[a] Number of animals in group. [b] Control value of 435 μg of protein hydrolyzed per 30 min/mg of protein. [c] Control value of 35 μg of deoxyribonucleic acid hydrolyzed per 30 min/mg of protein. [d] Control value of 3.48 pmoles/10^6 cells. [e] Control value of 97,238 dpm/mg of protein. [f] Control value of 7989 dpm/mg of crude histone protein. [g] Control value of 1.20 mg/ml of ascites fluid. [h] $p = 0.001$. [i] $p = 0.050$. [j] $p = 0.010$.

suppressed by I–III (Table IV). 3′,5′-Cyclic adenosine monophosphate levels were elevated in tumor cells 64% by II and 33% by III. Nonhistone chromatin protein kinase activity, which requires 3′,5′-cyclic adenosine monophosphate for regulation, was suppressed 61% by I, 58% by II, and 51% by III. ^{32}P-Incorporation into crude histones was reduced 52% by II and 57% by III. Chromatin protein also was reduced 26% by II and 29% by III, reflecting the inhibition of protein synthesis observed earlier (Table IV).

Compounds I and III significantly reduced oxidative phosphorylation processes (state 3) of Ehrlich ascites cells. Basal respiration, electron transport system (state 4), was reduced significantly by I and III and uncoupled in the case of II (Table V). These results indicate that I and III interfered with aerobic glycolysis of tumor cells.

Compound II demonstrated no inhibitor activity for the enzyme chymotrypsin. Rather, II appeared to be a reasonably good substrate for chymotrypsin enzymatic activity, resulting in a K_m value of 2.05 × 10^{-3} as compared to 0.8 × 10^{-3} for *N*-acetyl-L-tyrosine ethyl ester. On the other hand, chymotrypsin showed no ability to hydrolyze III. Preincubation periods of longer than 30 min resulted in significant inhibition by III of chymotrypsin activity with the substrate *N*-acetyl-L-tyrosine ethyl ester (Table VI).

UV spectrophotometric studies indicated that there was no interaction between deoxyribonucleic acid or the purine nucleophile guanosine and II, III, VI, and VII. However, when benzaldehyde (VI) was incubated with imidazole, the UV absorption magnitude of benzaldehyde was reduced 50% at 248 nm. Imidazole's maximum peak was at 206 nm, and benzaldehyde had a second peak at 202 nm. This second peak of benzaldehyde also was suppressed in magnitude from the anticipated absorption of two species in solution. Compounds II and III had maximum absorption peaks at 207 and 206 nm, respectively. Interaction with imidazole again resulted in reduction of the expected magnitude of these two independent molecules in solution. When benzaldehyde was incubated with lysine, there

Table V—Effects (Mean ± *SD*) of *N*-Benzyloxycarbonyl-L-phenylalanine Esters of 8-Day Ehrlich Ascites Homogenate Respiration with Succinate as Substrate

Compound	n[a]	State 4 Basal Respiration	State 3 Adenosine Monophosphate Stimulated Respiration
Control	6	100 ± 10[b]	100 ± 8[c]
I	6	69 ± 12[d]	62 ± 12[d]
II	6	129 ± 16[e]	40 ± 16[d]
III	6	74 ± 14[e]	70 ± 5[d]
VI	6	72 ± 11[e]	63 ± 6[d]

[a] Number of animals per group. [b] Control value of 5.506 μl of O_2/hr/mg of protein. [c] Control value of 6.487 μl of O_2/hr/mg of protein. [d] $p = 0.001$. [e] $p = 0.005$.

Table VI—Effects of III on Hydrolysis of *N*-Acetyl-L-tyrosine Ethyl Ester by Chymotrypsin

Preincubation Time, hr	Percent of Original Activity[a] ($V/V_0 \times 100$)
0	100
1	90
2	48
3	25
4	17
6	5

[a] The initial velocity of the enzyme at zero time and in the absence of the inhibitor for substrate was expressed as V_0 (100% activity), where V represents values of enzymatic activity after specific incubation time. The velocity of the control was not altered over the 6-hr period.

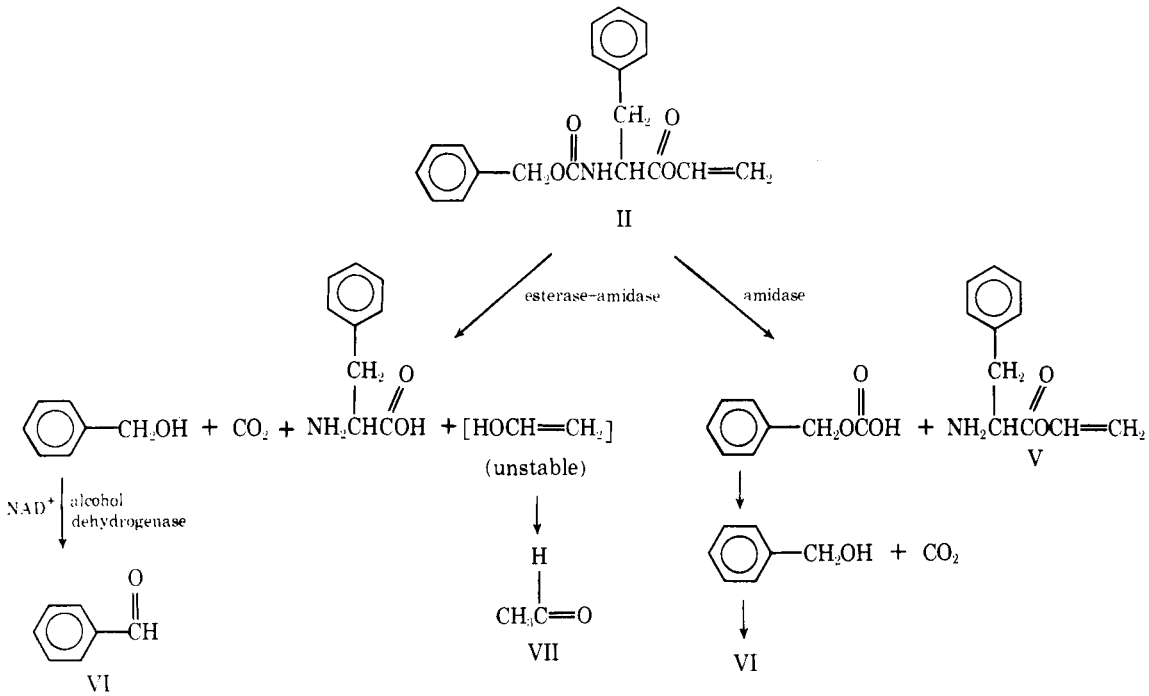

Scheme I

was a reduction of 25% of the benzaldehyde peaks at 240 and 202 nm. Compound II, when incubated with lysine, resulted in a shift of the absorption peak from 207 to 198 nm with a drastic increase in magnitude.

Under the conditions used, NMR studies afforded no evidence that II, III, or VI interacted in any way with the nucleophilic sulfhydryl groups of L-cysteine. Compound VI interacted with lysine, showing clear evidence of a Schiff base formation between the lysine ϵ-amino group and the aldehyde function; *i.e.*, a methinyl (CH=N) proton appeared at δ 8.5 ppm along with a reduction in the intensity of the aldehyde absorption at δ 9.9 ppm. The NMR spectrum of III also was altered in the presence of lysine; however, distinction between amine alkylation and simple dehydrobromination and/or decomposition of III was not possible.

There was no evidence for the interaction of II and lysine under the conditions of incubation. Some spectral changes were observed during the interaction of benzaldehyde and imidazole; however, no assignments were possible. The vinyl ester showed no alteration when incubated with imidazole. However, III appeared to alkylate imidazole through the involvement of the terminal (primary) bromine atom. Changes in the spectrum involved a shift of the absorption assigned to the CH_2Br grouping from δ 3.9 to 3.1 ppm while the absorption of the OCH(Br) was only slightly altered in its splitting pattern but not its chemical shift.

Probable (p) significant difference was determined by the Student t test. Data are expressed in Tables II–V as percent of control and standard deviation; n equals the number of animals per group.

DISCUSSION

Establishment of a molecular mechanism of action for II and III would be premature based on these data. These analogs probably are acted on by tissue kinases, esterases, and proteases once they are introduced into the body. Previous studies indicated that an *N*-benzyloxycarbonyl-L-phenylalanine ether analog is not active (1). Biotransformation according to Schemes I and II would result in the generation of a number of aldehyde derivatives. Benzaldehyde (VI) has been shown to inhibit Ehrlich tumor growth 69%. *N*-Benzyloxycarbonyl-L-phenylalanine (IV) was slightly higher in inhibitory activity, *i.e.*, 75%. Since L-phenylalanine is actively transported across membranes, this moiety may facilitate the movement of the benzaldehyde into the tumor cells. L-Phenylalanine vinyl ester (V) also inhibited tumor growth by 41%, which was of the same magnitude as acetaldehyde (VII), 43%. Compounds V and VII are extremely unstable in solution. The low antitumor activity may be due to drug decomposition.

Compounds VI and VII would be converted quickly to the acid analogs when administered *in vivo*, possibly resulting in less activity than anticipated. However, if these metabolites were released in the tumor cells or in close proximity of the tumor cells, they might be more active.

The major effects of II and III on Ehrlich ascites tumor cells were on deoxyribonucleic acid and protein metabolism. Since neither proteolytic nor deoxyribonuclease activity was accelerated by II and III treatment, increased catabolism of protein or deoxyribonucleic acid could not account for the reduced incorporation of labeled precursors into these macromolecules. A number of enzymes required for deoxyribonucleic acid synthesis were examined, and the kinases required to phosphorylate deoxynucleotides to the di- and triphosphate forms were inhibited by the same magnitude as thymidine incorporation into deoxyribonucleic acid. Thymidylate synthetase was inhibited marginally, and nuclear deoxyribonucleic acid polymerase was unaffected by II and III. Both of these enzymes are sulfhydryl bearing.

Furthermore, II and III did not significantly inhibit ribonucleic acid synthesis. Since both polymerase activity and ribonucleic acid synthesis require an intact template of exposed deoxyribonucleic acid to function, the nucleic acids themselves appear unharmed by treatment with II and III. This result was confirmed by the spectrophotometric studies on nucleic acid. Thus, the major effect of II and III on tumor cell metabolism involves inhibition of specific enzymes required for deoxyribonucleic acid synthesis, *e.g.*, nucleotide kinases, and cellular regulatory processes that affect cytokinetics. For a cell to enter into the cell cycle and accelerate nucleic acid synthesis (Go → S), a number of preliminary events occur, *e.g.*, increased proteolytic activity on the cell membrane surface (28), decreased cyclic adenosine monophosphate, increased cyclic guanosine monophosphate (29), phosphorylation of the lysine-rich F-1 fraction of histones, and synthesis of enzymes required for nucleic acid synthesis such as deoxyribonucleic acid polymerases (29).

Treatment with II and III reduced protein synthesis and chromatin protein content. Other protein inhibitors, *e.g.*, hydroxyurea and cycloheximide, inhibited the phosphorylation of histones, regulatory proteins of gene activity (30). Phosphorylation of the F-1 (H-1) fraction of histones during G_1 by a protein kinase dependent on high cyclic guanosine monophosphate and low cyclic adenosine monophosphate concentrations was dependent on the γ-phosphorus of adenosine 5′-triphosphate derived from oxidative phosphorylation in the mitochondria (31–34). Various structurally nonrelated antitumor agents including methotrexate inhibited respiration and energy production by Ehrlich ascites cells (35–38). Protein inhibitors also inhibited respiration (39). Compounds I–III inhibited phosphorylation of histones and oxidative phosphorylation (state 3), processes of Ehrlich ascites cells, and thus reduced the energy available for synthesis.

Inhibition of histone phosphorylation could also be due to the elevation of cyclic adenosine monophosphate concentration after treatment with II and III. Increased levels of cyclic adenosine monophosphate in cancer cells, according to the Ying-Yang theory of Goldberg *et al.* (40), compete with the elevated levels of cyclic guanosine monophosphate observed in

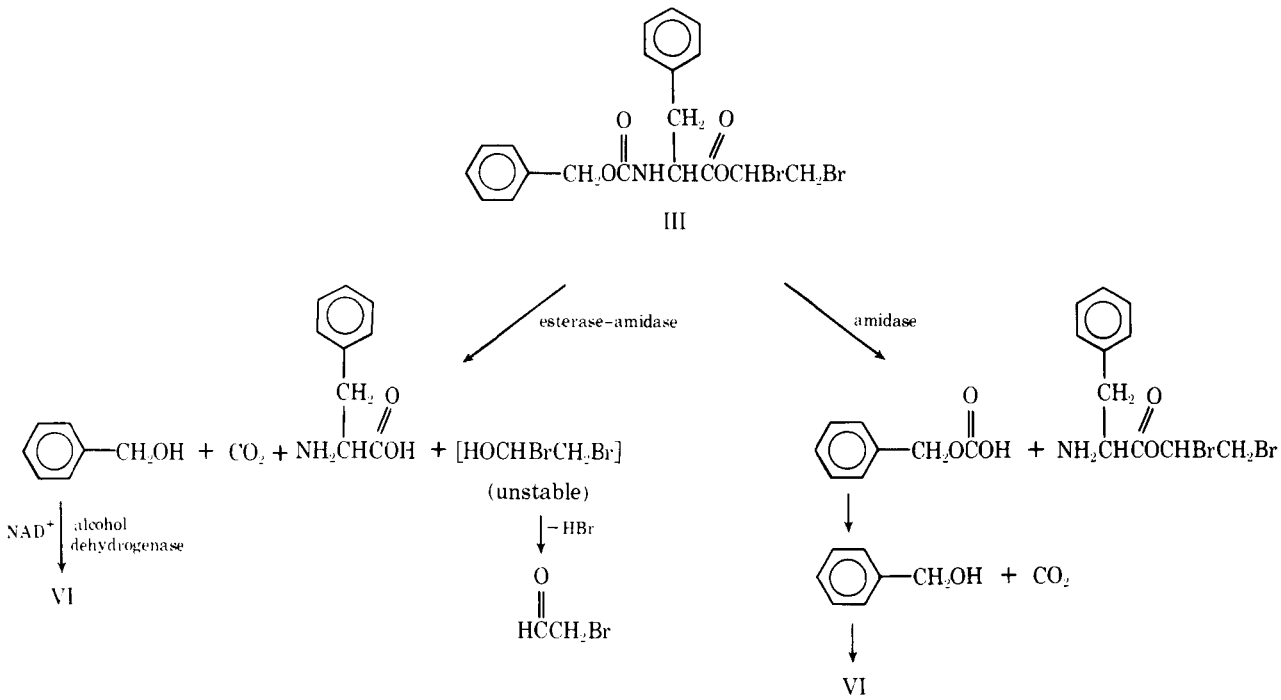

Scheme II

rapidly dividing cells for the binding sites on nuclear portein kinases that regulate histone phosphorylation. Other protein kinases modulated by cyclic nucleotides phosphorylate nonhistone chromatin protein and also regulate transcription and differentiation. Johnson and Hadden (41) observed that a particular fraction, mol. wt. 52,000, is not phosphorylated in the presence of high cyclic adenosine monophosphate, and this result correlates with a cessation of lymphocyte proliferation. Apparently, this protein kinase is also under the control of the Ying-Yang modulation of cyclic nucleotides. Compounds I–III significantly reduced the activity of nonhistone cyclic adenosine monophosphate-dependent protein kinase.

Compounds I–III were potent inhibitors of cathepsin activity in tumor cells. Proteolytic agents such as trypsin and the protease components of serum mimic virus transformation of cells and result in a decreased cyclic adenosine monophosphate level (42). Proteolytic inhibitors, *e.g.*, I, block the transformation process (43–45), and dibutyryl cyclic adenosine monophosphate inhibits the growth-stimulating action of trypsin and serum (46, 47). Arrest of cancer growth can be achieved by elevating cyclic adenosine monophosphate levels in the cells by administering dibutyryl cyclic adenosine monophosphate (48) or by blocking the enzyme responsible for hydrolysis of the cyclic nucleotide, *i.e.*, phosphodiesterase, with theophylline (49).

Cholesterol synthesis required for newly synthesized membranes, *etc.*, was also impaired by treatment with II and III. Both cholesterol and triglyceride synthesis in the liver was inhibited when the cyclic adenosine monophosphate level was elevated (50, 51). A similar phenomenon also was observed in tumor cells treated with α-methylene-γ-lactone containing antineoplastic agents (27). Cancer patients are hyperlipidemic (52) because of the failure of a cyclic adenosine monophosphate-dependent regulatory feedback mechanism, resulting in the tumor releasing cholesterol into the serum (50, 53).

Based on the premise that II and III are metabolized as outlined in Scheme I, several species are generated that can attack functional groups of specific enzymes like the kinases. Benzaldehyde, bromoacetaldehyde, and acetaldehyde are good candidates. Warburg (54) postulated that glyceraldehyde reacts with the sulfhydryl groups of glycolytic enzymes to form thiohemiacetals, resulting in cancer cell death. Glutaraldehyde forms Schiff bases with lysine residues (55, 56). α,β-Unsaturated glutaraldehydes can form stable Michael-type adducts with the amino groups of lysine (56). Formaldehyde reacts with proteins, enzymes, and nucleic acids (57). Short-term exposure to formaldehyde results in substantial covalent bonding between histones and deoxyribonucleic acids, thus inhibiting gene activity (58).

Compound I is known to alkylate the active site histidine residue of chymotrypsin, thus inhibiting the enzymatic activity. Evidence indicates that active vinyl and dihaloethyl esters of L-phenylalanine containing *N*-protecting groups are latent alkylating agents dependent on catalytic release of a reactive metabolite within the active site of the proteases or esterase enzyme (59), *e.g.*, suicide substrates. As a latent alkylating agent, II would produce acetaldehyde, which reacts with histidine and lysine (60). Compound III would produce bromoacetaldehyde with the potential of reacting with cysteine, lysine, histidine, and guanine (61). Alternatively, these active esters might conceivably function through direct alkylation of a bionucleophilic moiety within the active or allosteric site of enzymes.

In vitro, UV and NMR special data support the thesis that benzaldehyde, possibly arising by catabolism of the *N*-benzyloxycarbonyl group, is capable of interacting with functional groups, *e.g.*, imidazole groups of histidine residues of enzymes, and of forming Schiff bases with lysine residues of enzymes. There is no NMR evidence that sulfhydryl groups are being alkylated by II, III, or VI. UV spectral studies support the idea that II forms Schiff bases with lysine residues, but this hypothesis is not confirmed by NMR spectral data. Compound III interacts with lysine residues according to NMR data, but it is difficult to interpret what chemical species evolve. According to UV data, both II and III can interact with imidazole groups (*e.g.*, histidine); however, NMR evidence indicates a reaction only with III. These spectral studies with II, III, and VI are inconclusive. However, they suggest that a lysine and imidazole nucleophilic attack of activated esters of phenylalanine may be a possible mode of action *in vivo*.

REFERENCES

(1) L. J. Loeffler, Z. Sajadi, and I. H. Hall, *J. Med. Chem.*, **20**, 1578 (1977).

(2) *Ibid.*, **20**, 1584 (1977).

(3) W. Troll, A. Klassen, and A. Janoff, *Science*, **169**, 1211 (1970).

(4) E. Shaw, M. Mares-Guia, and W. Cohen, *Biochemistry*, **2**, 252 (1965).

(5) G. Schoellman and E. Shaw, *ibid.*, **2**, 252 (1963).

(6) H. P. Schnebli and N. N. Burger, *Proc. Natl. Acad. Sci. USA*, **69**, 3825 (1972).

(7) I. Chou, P. H. Black, and R. O. Roblin, *ibid.*, **71**, 1748 (1974).

(8) M. Bergman and L. Zervas, *Chem. Ber.*, **65**, 1119 (1932).

(9) A. Weygand and M. W. Beyerman, *Recueil*, **84**, 213 (1965).

(10) R. I. Geran, N. H. Greenberg, M. M. MacDonald, A. Schymacher, and B. Abbott, *Cancer Chemother. Rep., Part 3*, **3**, 1 (1972).

(11) J. T. Litchfield and F. Wilcoxon, *J. Pharmacol. Exp. Ther.*, **96**, 99 (1949).

(12) C. B. Chae, J. L. Irvin, and C. Piantadosi, *J. Med. Chem.*, **11**, 506 (1968).

(13) I. Shibko, P. Koivistainen, C. A. Tratnyek, and A. R. Newhall,

Anal. Biochem., **19**, 514 (1967).
(14) A. C. Sartorelli, *Biochem. Biophys. Res. Commun.*, **27**, 26 (1967).
(15) G. T. Haven, J. R. Krzemien, and T. T. Nquyea, *Res. Commun. Chem. Pathol. Pharmacol.*, **6**, 253 (1973).
(16) F. Wada, K. Hirata, and Y. Sakamoto, *J. Biochem.*, **65**, 171 (1969).
(17) W. C. Hymer and E. L. Kuff, *J. Histochem. Cytochem.*, **12**, 359, (1964).
(18) H. Sawada, K. Tatsumi, M. Sasada, K. Shirakawa, T. Nakumura, and G. Wakisaka, *Cancer Res.*, **34**, 3341 (1974).
(19) A. Kampf, R. L. Barfknecht, P. J. Shaffer, S. Osaki, and M. P. Mertes, *J. Med. Chem.*, **19**, 903 (1976).
(20) F. Maley and S. Ochoa, *J. Biol. Chem.*, **233**, 1538 (1958).
(21) I. H. Hall, K. S. Ishaq, and C. Piantadosi, *J. Pharm. Sci.*, **63**, 625 (1974).
(22) Y. M. Kish and L. J. Kleinsmith, *Methods Enzymol.*, **40**, 201 (1975).
(23) A. L. Steiner, D. M. Kipnis, R. Utiger, and C. Parker, *Proc. Natl. Acad. Sci. USA*, **64**, 367 (1969).
(24) A. Rainer, R. C. Simsiman, and R. K. Boutwell, *Cancer Res.*, **33**, 134 (1973).
(25) Y. S. Cho-Chung and P. M. Guillino, *J. Biol. Chem.*, **248**, 4743 (1973).
(26) G. W. Schwert and Y. Takemata, *Biochim. Biophys. Acta*, **16**, 570 (1955).
(27) I. H. Hall, K. H. Lee, E. C. Mar, C. O. Starnes, and T. G. Waddell, *J. Med. Chem.*, **20**, 333 (1977).
(28) H. P. Schnebli, in "Proteinase Inhibitors, Proceedings," H. Fritz, H. Tschnesche, L. J. Green, and E. Truscheit, Eds., Springer-Verlag, New York, N.Y., 1974, p. 615.
(29) R. R. Burk, *Nature*, **219**, 1272 (1968).
(30) R. Balhorn, T. Nongnuj, R. Chalkley, and D. R. Garner, *Biochemistry*, **12**, 5146 (1973).
(31) R. C. Huang and J. Bonner, *Proc. Natl. Acad. Sci. USA*, **48**, 1716 (1962).
(32) R. Balhorn, W. O. Reik, and R. Chalkley, *Biochemistry*, **11**, 1094 (1971).
(33) D. Sherod, G. Johnson, and R. Chalkley, *ibid.*, **9**, 4611 (1970).
(34) C. S. Rubin and O. M. Roseu, *Ann. Rev. Biochem.*, **44**, 831 (1975).
(35) M. Gosalvez, R. Garcia-Canero, M. Blanco, and Gurmcharri-Llyd, *Cancer Chemother. Rep.*, **60**, 1 (1976).
(36) C. Piantadosi, C. S. Kim, and J. L. Irvin, *J. Pharm. Sci.*, **58**, 821 (1969).
(37) J. J. Figueras and M. Gosalvez, *Eur. J. Cancer*, **9**, 527 (1973).
(38) R. A. Tobey, D. F. Peterson, and E. C. Anderson, in "Biochemistry of Cell Division," R. Baserga, Ed., Charles C Thomas, Springfield, Ill., 1969, p. 34.
(39) S. B. Wilson and A. L. Moore, *Biochim. Biophys. Acta*, **292**, 603 (1973).
(40) N. D. Goldberg, M. K. Haddox, R. Estensen, J. G. White, C. Lopez, and J. W. Hadden, in "Cyclic AMP, Cell Growth and the Immune Responses," W. Braum, C. M. Lichtenstein, and C. W. Parker, Eds., Springer-Verlag, New York, N.Y., 1974, p. 247.
(41) E. M. Johnson and J. W. Hadden, *Science*, **107**, 1198 (1975).
(42) J. R. Sheppard, *Nature, New Biol.*, **236**, 14 (1972).
(43) G. S. Johnson, R. M. Friedman, and I. Pastau, *Proc. Natl. Acad. Sci. USA*, **68**, 425 (1971).
(44) A. W. Hsie, C. Jones, and T. T. Puck, *ibid.*, **68**, 1648 (1971).
(45) C. V. Perry, G. S. Johnson, and I. Pastau, *J. Biol. Chem.*, **246**, 5785 (1971).
(46) W. Troll, A. Klassen, and A. Janoff, *Science*, **169**, 1211 (1970).
(47) A. L. Latner, E. Longstaff, and K. Pardham, *Br. J. Cancer*, **27**, 460 (1973).
(48) M. M. Burger, B. M. Bombik, B. M. Breckenridge, and J. R. Sheppard, *Nature*, **239**, 161 (1972).
(49) P. M. Guillino and Y. S. Cho-Chung, *Science*, **183**, 87 (1974).
(50) L. A. Bricker and G. S. Levy, *J. Biol. Chem.*, **247**, 4914 (1972).
(51) D. O. Allen, J. Munshower, H. P. Morris, and G. Weber, *Cancer Res.*, **31**, 557 (1971).
(52) W. C. Mattick and K. W. Buckwald, *J. Cancer Res.*, **13**, 157 (1929).
(53) M. D. Siperstein and V. M. Fagan, *Cancer Res.*, **24**, 1108 (1963).
(54) O. Warburg, *Ann. Rev. Biochem.*, **33**, 1 (1964).
(55) B. R. Brook, *Eur. J. Biochem.*, **5**, 178 (1968).
(56) T. M. Richard, *J. Mol. Biol.*, **37**, 231 (1968).
(57) C. J. Martin and D. P. Lam, *Bioorg. Chem.*, **4**, 22 (1975).
(58) D. Burtlag, C. Schellenhuber, and J. Bonner, *Biochemistry*, **8**, 3214 (1969).
(59) R. R. Rando, *Science*, **185**, 320 (1974).
(60) W. C. J. Ross, "Biological Alkylating Agents," Butterworth, London, England, 1962, p. 176.
(61) E. Shaw, *Physiol. Rev.*, **50**, 244 (1970).
(62) G. W. Snedecor, "Statistical Methods," Iowa State College Press, Ames, Iowa, 1956, sect. 2.

ACKNOWLEDGMENTS

Supported by a University of North Carolina Research Council Grant and by American Cancer Society Institutional Grant MC157.

The authors thank Ron K. Levy for assistance with the NMR studies.

Comparison of Operational Characteristics of Different Dissolution Testing Systems

E. A. HARDWIDGE ˣ, A. C. SARAPU, and W. C. LAUGHLIN

Received September 16, 1977, from the *Control Division, The Upjohn Company, Kalamazoo, MI 49001.* Accepted for publication April 25, 1978.

Abstract □ Three dissolution apparatus, the rotating basket, the rotating paddle, and the rotating filter–stationary basket, were evaluated for their suitability as production control tools and their relation to blood level studies in dogs. The rotating basket and rotating paddle assemblies were easier to use and less variable than the rotating filter–stationary basket. When relative levels of agitation and the pH of the dissolution medium were held constant, all three apparatus correlated with each other and equally well with the serum drug levels from experimental formulations of an oral hypoglycemic drug after administration to dogs. Such an observed relationship cannot, of course, be used to predict blood levels in other species; however, it does suggest that the choice of one apparatus over another cannot be made *a priori*.

Keyphrases □ Dissolution testing systems—three apparatus compared, suitability for use as production control tools and relation to blood level studies in dogs evaluated □ Apparatus, dissolution testing—three systems compared, suitability for use as production control tools and relation to blood level studies in dogs evaluated

When relative merits of dissolution apparatus design are discussed, there often are no data available to compare results directly with other apparatus in the same laboratory. Thus, differences in parameters such as the dissolution medium or relative levels of agitation, recognized as having profound influence on dissolution results (1), often make direct comparison impossible. Therefore, different dissolution apparatus were evaluated to provide data on comparative operational characteristics under controlled experimental conditions and in a quality control environment.

The rotating basket and rotating paddle are Apparatus 1 and 2, respectively, in the official compendia (2, 3). The rotating filter–stationary basket system was described previously (4, 5).

EXPERIMENTAL

All equipment was obtained commercially. All dissolution tests were conducted on a six-station dissolution apparatus[1]. The rotation speed of the dissolution apparatus was measured with a hand-held digital tachometer[2] in direct friction contact with the rotating basket or rotating paddle shift.

The speed of the rotating filters on the rotating filter–stationary basket apparatus was determined with a digital phototachometer[3] so that measurements could be made on the rotational speed of the filter assembly itself while submerged and in operation. During a test, the dissolution fluid was continuously circulated through flowcells and absorbance was read on a UV spectrophotometer[4]. A peristaltic pump[5] was used to maintain a flow rate of about 40 ml/min. A 60-mesh wire screen was used to filter the solution on the rotating basket and rotating paddle apparatus; the 1-μm stainless steel filter was used on the rotating filter–stationary basket.

Prednisone Tablets (50 mg)—All tests were conducted in 900 ml of deionized water at 37°. Absorbance was read at 244 nm with 1.0-cm flowcells. The apparatus was operated at 25–200 rpm for the rotating basket, at 25–150 rpm for the rotating paddle, and at 150–600 rpm for the rotating filter–stationary basket.

Tetracycline Hydrochloride Capsules (250 mg)—Tests were conducted in 900 ml of deionized water at 37°. Absorbance was read at 268 nm with 0.5-mm flowcells. Since the capsules float in water, a loop of copper wire was used as a weight with the rotating paddle apparatus. This approach was described previously (6). For these capsules, the rotating filter–stationary basket was operated at 600 rpm, the rotating basket was operated at 150 rpm, and the rotating paddle was operated at 100 rpm.

Experimental Hypoglycemic Tablets (500 mg)—All tests were conducted in 900 ml of the dissolution medium at 37°. A tris(hydroxymethyl)aminomethane solution (1:40), adjusted to pH 7.6 with hydrochloric acid, or 0.05 *M* phosphate buffer, pH 7.2, was used. Absorbance was read at 226 nm with 0.5-mm flowcells. Tests were conducted at 600 rpm with the rotating filter–stationary basket apparatus, at 100 rpm with the rotating paddle, and at 150 rpm with the rotating basket.

All dissolution tests were run using a single tablet or capsule in each of the six flasks. On occasion, one spinning filter would stop spontaneously during a rotating filter–stationary basket test. In the 18 tests reported, this problem occurred five times. In this case, the tablet or capsule was dropped from the treatment and the values of the remaining five were used to calculate the average results. In all other cases, reported data are the averages of six tablets.

Serum Level Studies—Sixteen male beagle dogs were employed in a 4 × 4 crossover design. The dogs were fasted overnight and orally administered one 0.5-g oral hypoglycemic tablet. Blood samples were withdrawn just prior to dosing and at 2, 4, 6, 8, 12, 24, and 48 hr after

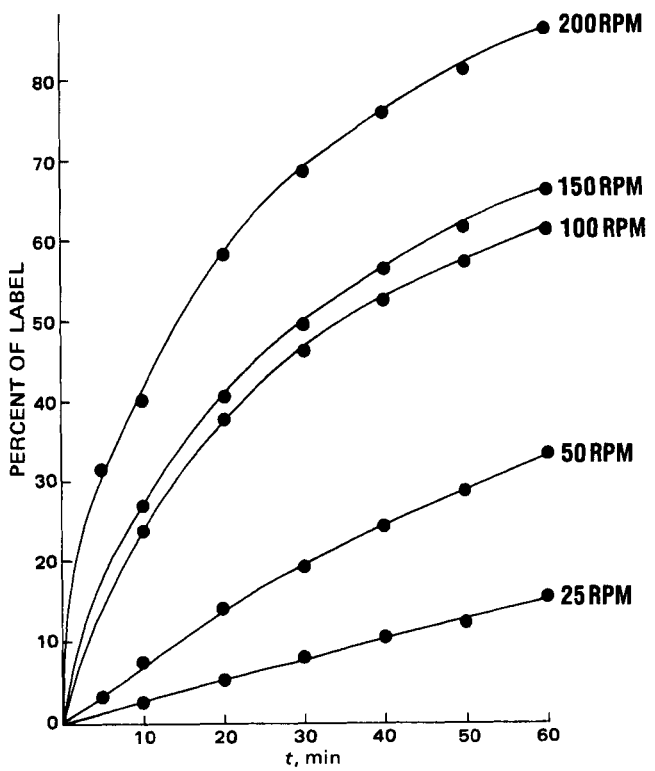

Figure 1—*Dissolution profile for 50-mg prednisone tablets with varying rotation speed in the rotating basket apparatus.*

[1] Hansen model 72B-115 or Coffman Industries model 7401 rotating filter–stationary basket apparatus.
[2] Biddle model 9970.
[3] Pioneer model DT-9600.
[4] Beckman Kintrac VII or Beckman 25-7.
[5] Harvard model 1210.

0022-3549/78/1200-1732$01.00/0
© *1978, American Pharmaceutical Association*

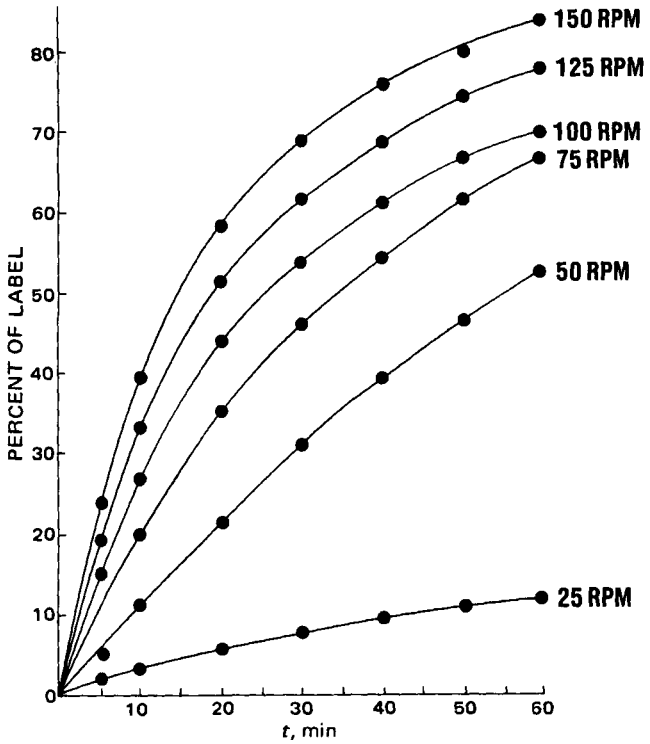

Figure 2—*Dissolution profile for 50-mg prednisone tablets with varying rotation speed in the rotating paddle apparatus.*

dosing. Average individual serum peak levels were observed at 7 hr, and the half-life of elimination for this drug was approximately 16 hr.

RESULTS AND DISCUSSION

Criteria for evaluation of these apparatus were based on their suitability as production control tools and their potential ability to produce correlations with blood level data. Effects of changes in agitation speed on dissolution, ease of operation in a quality control environment, sensitivity to production and formulation changes, and variability were all considered.

The prednisone tablets and tetracycline capsules were used primarily to examine relative agitation and variability. The oral hypoglycemic tablets provided data for comparison of dog blood levels with dissolution test results.

Effect of Rotation Speed—The three dissolution apparatus all agitate the solution with a rotating device, *i.e.*, a basket, paddle, or filter. To compare the effect of changes in rotation speed for each device, the dissolution of 50-mg prednisone tablets, known to have a relatively long dissolution time, was studied. Use of these tablets thus made it possible to run the dissolution test for a long enough period to assure that differences observed would be valid.

Each apparatus generated a family of curves that appear similar in shape (Figs. 1–3). With the basket and paddle apparatus, the dissolution rate increased with increasing rotational speed. However, while similar behavior with the rotating filter device was observed from 150 to 300 rpm, little change in the dissolution rate occurred from 350 to 600 rpm. The plateauing of the apparent level of agitation for the rotating filter in that range is surprising and unexplained at this time.

Direct comparison of agitation levels for the three apparatus is possible when the percent of label claim dissolved at a given time, 30 min, is plotted as a function of the revolutions per minute (Fig. 4). Thus, values of 75–125 rpm for the rotating paddle, 100–150 rpm for the rotating basket, and 350–600 rpm for the rotating filter–stationary basket gave approximately equivalent agitation since they gave about 50% of label claim in solution at 30 min. This comparison is based on the results obtained for the 50-mg prednisone tablet results only; however, it provides good initial values for comparison with other dosage forms, and large differences would not be anticipated.

Variability—During the comparisons, it was important to observe the variability obtained with the three apparatus. Variability is defined as the relative standard deviation of observed dissolution rates for the

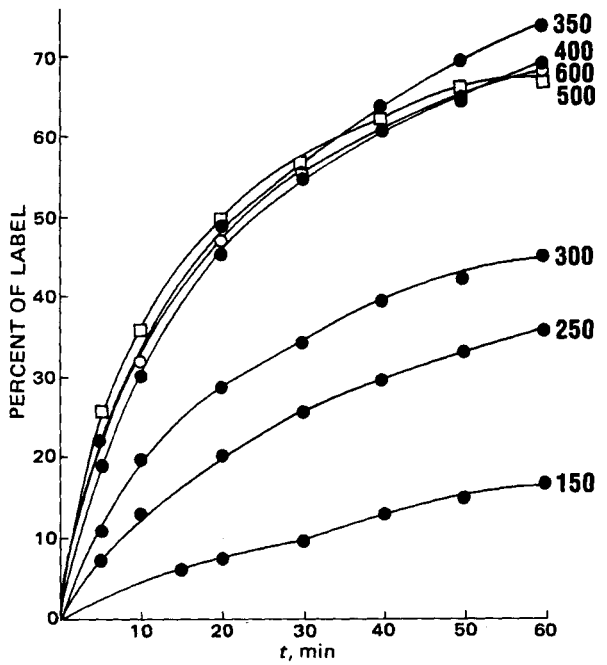

Figure 3—*Dissolution profile for 50-mg prednisone tablets with varying rotation speed in the rotating filter–stationary basket apparatus.*

dosage forms studied simultaneously in a single dissolution test. This parameter is a measure of within-run reproducibility. With the percent dissolved at 30 min for the 50-mg prednisone tablets (Figs. 1–3) as a test point, the observed relative standard deviation was calculated and plotted as a function of rotation speed for each apparatus. These data (Fig. 5) show that the rotating filter–stationary basket generated significantly greater variability than either the rotating basket or the rotating paddle. This variability was very pronounced at intermediate speeds (*i.e.*, 300–350 rpm) with the rotating filter–stationary basket apparatus.

A major contributor to the high variability of the rotating filter–stationary basket probably is the tendency of the spinning filter to wobble occasionally. Where a spinning filter had developed a noticeable wobble,

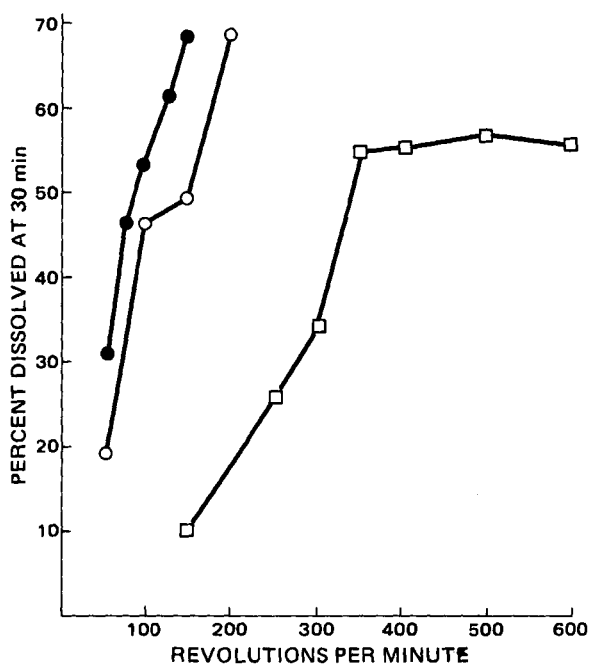

Figure 4—*Comparison of dissolution rate* versus *rotation speed for three dissolution apparatus using 50-mg prednisone tablets. Key:* ●, *rotating paddle;* ○, *rotating basket; and* □, *rotating filter–stationary basket.*

Table I—Summary of 250-mg Tetracycline Hydrochloride Capsule $T_{50\%}$ Values

Manufacturer	Rotating Filter–Stationary Basket (600 rpm)	Rotating Basket (150 rpm)	Rotating Paddle (100 rpm)
A	5.8 (33)[a]	7.1 (22)	5.0 (12)
B	4.1 (17)	5.6 (21)	5.6 (36)
C	5.5 (25)	6.5 (16)	5.6 (26)

[a] Values in parentheses are percent relative standard deviations.

the dissolution rate in that particular flask increased qualitatively. No attempt was made to quantitate these effects, but wobble occurred more often at the intermediate speeds and the apparatus operated more smoothly at higher speeds.

The only other study in which the variability of the rotating filter–stationary basket was compared directly to another apparatus using the same formulation, dissolution medium, and relative level of agitation was reported by Shah *et al.* (4). They compared dissolution results for the rotating filter–stationary basket and the rotating basket. A single six-place dissolution run of an unidentified tablet sample was reported for each apparatus. The observed relative standard deviations were 3.28 and 41.7% for the rotating filter–stationary basket and rotating basket, respectively. For the tablets examined, the rotating basket test gave considerably greater variability than the rotating filter–stationary basket.

The formulation dependence of such a result may be important since the rotating basket test was operated at an unusually high level of agitation (300 rpm), well outside the operational limits of the USP test. The high relative standard deviation reported (4) for the rotating basket in this case is not typical of results obtained when drug products are tested by compendial dissolution methods. On the other hand, the variability reported (4) for the rotating filter–stationary basket is much less than that reported for the capsules and tablets in the present work. The differences may be attributable to the choice of test samples or differences in apparatus performance.

Capsule Dissolution Testing—To test the relative behavior of the three dissolution apparatus with capsules, 250-mg tetracycline hydrochloride capsules produced by three different manufacturers were obtained. Results are presented in Table I as $T_{50\%}$ in each case. The three methods gave comparable dissolution rates and did not demonstrate significant differences in dissolution behavior between the capsules. Furthermore, the relative standard deviations for all three methods were nearly the same, unlike the results with the prednisone tablets. Based on the observed variability for tablets plotted in Fig. 5, it appears that the rotating basket and rotating paddle gave relatively higher variability with the capsules than with the tablets. The rotating filter–stationary basket apparatus gave uniformly high variability for both capsules and tablets.

Ease of Use—The rotating basket and rotating paddle apparatus were comparable in the ease of use in a quality control environment. Of the three apparatus, the rotating filter–stationary basket was the most difficult to operate and clean. It was necessary to dismantle the entire filter assembly for cleaning, which involves manipulation of the seals and several other parts. Some of these parts are relatively fragile, particularly the pilot tube, a glass capillary on which the filter assembly rotates. Breakage of two pilot tubes occurred during this study.

Moreover, dynamic seals on the top of the filter assembly at the point where the pilot tube enters the rotating filter assembly were defective at the start of the study and had to be replaced. They were leaking and admitting solid particles into the continuous flow stream as the dissolution medium was pumped without passing through the filter. After replacement, the problem did not recur. The time required for setup and breakdown on a per run basis was considerably greater for the rotating filter–stationary basket system compared to the rotating paddle and rotating basket apparatus.

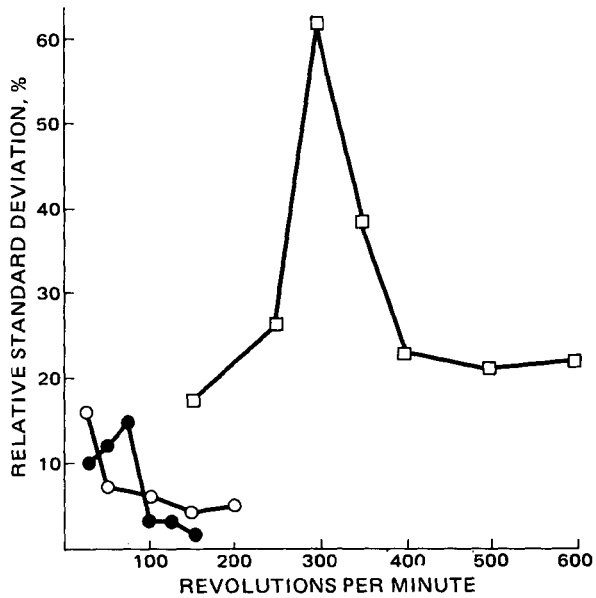

Figure 5—*Observed apparatus variability as a function of rotation speed (50-mg prednisone tablets). Key: ●, rotating paddle; ○, rotating basket; and □, rotating filter–stationary basket.*

Dissolution Rates and Serum Level Data—Relative serum level data in dogs were obtained previously in these laboratories for four experimental lots of an oral hypoglycemic drug intentionally formulated to give a range of dissolution results (Table II). Each apparatus gave $T_{50\%}$ values of approximately 30 min for Lot C at pH 7.6 and significantly longer times for Lot D. The trend to lower serum drug levels with increased dissolution rate became highly significant ($p < 0.05$) for Lot D, which had a dissolution $T_{50\%}$ of greater than 80 min at pH 7.6 for all three apparatus.

The observations that there was a range of dissolution rates over which drug absorption was not significantly affected and that there was some critical value beyond which absorption was affected were noted previously (7). The correlation coefficients tabulated provide only a rough guide for comparison in such a case but do, nevertheless, indicate that all three apparatus give essentially equivalent results. When all lots were retested in pH 7.2 buffer and the correlation coefficients were recalculated, differences were noted. For example, the rank-order exchange of Lots B and C observed for the rotating filter–stationary basket apparatus results in an improved apparent correlation. Such results emphasize the importance of the dissolution medium on observed dissolution rates. To be valid, direct comparisons of one apparatus with another must be made using the same dissolution medium and approximately equivalent agitation.

SUMMARY AND CONCLUSIONS

Production Control—Of the three apparatus studied, the rotating

Table II—Canine Serum Levels and Dissolution $T_{50\%}$ Values for Oral Hypoglycemic Experimental Lots (500 mg)

Lot	Rotating Filter–Stationary Basket (600 rpm)		Rotating Paddle (100 rpm)		Rotating Basket (150 rpm)		$AUC_{0\text{-}48hr}$[a], μg-hr/ml	*AUC* Differences[b] ($p \leq 0.05$)
	pH 7.6[c]	pH 7.2[d]	pH 7.6	pH 7.2	pH 7.6	pH 7.2		
A	2.0 (17)[e]	2.0 (17)	1.6 (10)	2.4 (3)	2.5 (7)	4.1 (11)	4250	A > D
B	40.8 (33)	21.1 (43)	29.3 (26)	14.4 (52)	26.4 (24)	13.6 (21)	4120	B > D
C	33.5 (28)	32.1 (62)	30.9 (16)	16.3 (38)	30.3 (15)	20.8 (36)	3706	None
D	94.5 (17)	61.5 (53)	85.2 (25)	38.6 (9)	83.8 (15)	33.6 (31)	3017	D < A,B
Correlation coefficient, $T_{50\%}$ *versus AUC*	−0.92	−0.98	−0.95	−0.96	−0.96	−0.97		

[a] Area under the serum concentration–time curve. [b] Tukey's multiple comparison test. [c] With 0.21 *M* tris(hydroxymethyl)aminomethane buffer. [d] With 0.05 *M* phosphate buffer. [e] Values in parentheses are percent relative standard deviations for each run.

basket and rotating paddle were relatively easy to use, reliable, and amenable for routine use in a quality control environment. The rotating filter–stationary basket apparatus was more difficult to operate, required more time per test, and generally gave greater variability.

Serum Level Data—Dissolution times measured with all three apparatus correlated equally well with serum drug levels in dogs for the four experimental hypoglycemic lots. None of these three apparatus gave substantially better correlations when other test conditions, such as the dissolution medium and relative agitation levels, were kept constant. These data cannot be used, of course, to prove or disprove ability to predict a relation between dissolution and blood levels in other species. On the contrary, since there is a high degree of correlation of dissolution results between apparatus when experimental conditions are kept as similar as possible, claims that one apparatus or another is *a priori* superior for prediction of *in vivo* behavior should be critically assessed.

REFERENCES

(1) M. Pernarowski, in "Dissolution Technology," L. J. Leeson and J. T. Carstensen, Eds., APhA Academy of Pharmaceutical Sciences, Washington, D.C., 1974, pp. 58–92.

(2) "The United States Pharmacopeia," 19th rev., Mack Publishing Co., Easton, Pa., 1975, p. 651.

(3) "Fourth Supplement to USP XIX and NF XIV," The United States Pharmacopeial Convention, Rockville, Md., 1978, pp. 194, 195.

(4) A. C. Shah, C. B. Peot, and J. F. Ochs, *J. Pharm. Sci.*, **62**, 671 (1973).

(5) A. C. Shah and J. F. Ochs, *ibid.*, **63**, 2968 (1974).

(6) J. W. Poole, *Drug Inf. Bull.*, **3**, 8 (1969).

(7) T. J. Sullivan, E. Sakmar, and J. G. Wagner, *J. Pharmacokinet. Biopharm.*, **4**, 173 (1976).

ACKNOWLEDGMENTS

Presented at the APhA Academy of Pharmaceutical Sciences, Orlando meeting, November 1976.

The authors thank Dr. R. H. Buller and Mr. W. M. Kooyers of The Upjohn Co. for making available previously unpublished canine blood level data on several oral hypoglycemic experimental lots.

High-Pressure Liquid Chromatographic Analysis of Estrogens in Pharmaceuticals by Measurement of Their Dansyl Derivatives

ROBERT W. ROOS

Received February 17, 1978, from the *Food and Drug Administration, Department of Health, Education, and Welfare, Brooklyn, NY 11232.* Accepted for publication April 27, 1978.

Abstract □ A high-pressure liquid chromatographic method is described for the analysis of estrogens in pharmaceutical tablet and injectable dosage forms. In general, the estrogens are isolated, an internal standard is added, the dansyl derivatives are formed, and the dansyl estrogen solution is injected into a liquid chromatograph. Linear response is experienced between the mass of estrogen and the ratio of the estrogen peak height to the internal standard peak height, using a microparticle silica column and chloroform–*n*-heptane mobile phases. With fluorometric measurement, limits of detectability for ethinyl estradiol and estradiol were 0.04 and 0.05 ng, respectively. Methyltestosterone, an androgen in combination with ethinyl estradiol, was analyzed simultaneously. Commercial pharmaceutical preparations containing estrone, ethinyl estradiol, and estradiol were analyzed by the proposed method. The results indicate the method to be sensitive, reasonably precise (<2%), and accurate in the analysis of estrogen in dosage forms.

Keyphrases □ Estrogens, various—high-pressure liquid chromatographic analyses of dansyl derivatives, pharmaceutical preparations □ High-pressure liquid chromatography—analyses, dansyl derivatives of various estrogens, pharmaceutical preparations □ Dansyl derivatives—various estrogens, high-pressure liquid chromatographic analyses, pharmaceutical preparations

Dansyl chloride, 5-(dimethylamino)-1-naphthalenesulfonyl chloride (I), is a useful reagent for the production of fluorescent derivatives (fluorogenic labeling) with several functional groups, including primary and secondary amines, imidazoles, and phenols. However, since I can decompose to yield dansyl hydroxide (actually a sulfonic acid), dansyl dimethylamide, and other compounds (1) under the conditions used for derivatization, analyses involving I usually include a procedure to separate the dansyl derivative from any other fluorescent compounds present in the solution.

The ability of various classes of compounds to form dansyl derivatives that can be detected at low levels is advantageous. Some analytical applications were reviewed by Seiler and Wiechmann (1). Recently, high-pressure liquid chromatographic (HPLC) methods for the analysis of carbamate insecticides (2), hydroxybiphenyls (3), and barbiturates (4) used dansyl derivatives and demonstrated the value of this approach.

Better methods of analysis for the determination of estrogens in pharmaceutical dosage forms are needed (5, 6). Penzes and Oertel (7, 8) described the TLC separation of the dansyl derivatives of estrone, estradiol, and estriol, and Fishman (5) introduced a conventional fluorescence method for some estrogens using dansyl estrogen derivatives.

This study was conducted to determine the utility of the formation of dansyl derivatives of estrogens in an HPLC analytical procedure. The procedure was adapted satisfactorily to the analysis of estradiol, ethinyl estradiol, and estrone in pharmaceutical dosage forms. Ethinyl estradiol, the estrogen receiving the most attention owing to its small dose, is frequently found in combination with a progestin (oral contraceptive) and an androgen such as methyltestosterone. Fortunately, some nonestrogen steroids are separated from the dansyl estrogens, so they can be analyzed with the same column. A simultaneous method for

0022-3549/78/1200-1735$01.00/0

© 1978, American Pharmaceutical Association

basket and rotating paddle were relatively easy to use, reliable, and amenable for routine use in a quality control environment. The rotating filter–stationary basket apparatus was more difficult to operate, required more time per test, and generally gave greater variability.

Serum Level Data—Dissolution times measured with all three apparatus correlated equally well with serum drug levels in dogs for the four experimental hypoglycemic lots. None of these three apparatus gave substantially better correlations when other test conditions, such as the dissolution medium and relative agitation levels, were kept constant. These data cannot be used, of course, to prove or disprove ability to predict a relation between dissolution and blood levels in other species. On the contrary, since there is a high degree of correlation of dissolution results between apparatus when experimental conditions are kept as similar as possible, claims that one apparatus or another is *a priori* superior for prediction of *in vivo* behavior should be critically assessed.

REFERENCES

(1) M. Pernarowski, in "Dissolution Technology," L. J. Leeson and J. T. Carstensen, Eds., APhA Academy of Pharmaceutical Sciences, Washington, D.C., 1974, pp. 58–92.

(2) "The United States Pharmacopeia," 19th rev., Mack Publishing Co., Easton, Pa., 1975, p. 651.

(3) "Fourth Supplement to USP XIX and NF XIV," The United States Pharmacopeial Convention, Rockville, Md., 1978, pp. 194, 195.

(4) A. C. Shah, C. B. Peot, and J. F. Ochs, *J. Pharm. Sci.*, **62**, 671 (1973).

(5) A. C. Shah and J. F. Ochs, *ibid.*, **63**, 2968 (1974).

(6) J. W. Poole, *Drug Inf. Bull.*, **3**, 8 (1969).

(7) T. J. Sullivan, E. Sakmar, and J. G. Wagner, *J. Pharmacokinet. Biopharm.*, **4**, 173 (1976).

ACKNOWLEDGMENTS

Presented at the APhA Academy of Pharmaceutical Sciences, Orlando meeting, November 1976.

The authors thank Dr. R. H. Buller and Mr. W. M. Kooyers of The Upjohn Co. for making available previously unpublished canine blood level data on several oral hypoglycemic experimental lots.

High-Pressure Liquid Chromatographic Analysis of Estrogens in Pharmaceuticals by Measurement of Their Dansyl Derivatives

ROBERT W. ROOS

Received February 17, 1978, from the *Food and Drug Administration, Department of Health, Education, and Welfare, Brooklyn, NY 11232.* Accepted for publication April 27, 1978.

Abstract □ A high-pressure liquid chromatographic method is described for the analysis of estrogens in pharmaceutical tablet and injectable dosage forms. In general, the estrogens are isolated, an internal standard is added, the dansyl derivatives are formed, and the dansyl estrogen solution is injected into a liquid chromatograph. Linear response is experienced between the mass of estrogen and the ratio of the estrogen peak height to the internal standard peak height, using a microparticle silica column and chloroform–*n*-heptane mobile phases. With fluorometric measurement, limits of detectability for ethinyl estradiol and estradiol were 0.04 and 0.05 ng, respectively. Methyltestosterone, an androgen in combination with ethinyl estradiol, was analyzed simultaneously. Commercial pharmaceutical preparations containing estrone, ethinyl estradiol, and estradiol were analyzed by the proposed method. The results indicate the method to be sensitive, reasonably precise (<2%), and accurate in the analysis of estrogen in dosage forms.

Keyphrases □ Estrogens, various—high-pressure liquid chromatographic analyses of dansyl derivatives, pharmaceutical preparations □ High-pressure liquid chromatography—analyses, dansyl derivatives of various estrogens, pharmaceutical preparations □ Dansyl derivatives—various estrogens, high-pressure liquid chromatographic analyses, pharmaceutical preparations

Dansyl chloride, 5-(dimethylamino)-1-naphthalenesulfonyl chloride (I), is a useful reagent for the production of fluorescent derivatives (fluorogenic labeling) with several functional groups, including primary and secondary amines, imidazoles, and phenols. However, since I can decompose to yield dansyl hydroxide (actually a sulfonic acid), dansyl dimethylamide, and other compounds (1) under the conditions used for derivatization, analyses involving I usually include a procedure to separate the dansyl derivative from any other fluorescent compounds present in the solution.

The ability of various classes of compounds to form dansyl derivatives that can be detected at low levels is advantageous. Some analytical applications were reviewed by Seiler and Wiechmann (1). Recently, high-pressure liquid chromatographic (HPLC) methods for the analysis of carbamate insecticides (2), hydroxybiphenyls (3), and barbiturates (4) used dansyl derivatives and demonstrated the value of this approach.

Better methods of analysis for the determination of estrogens in pharmaceutical dosage forms are needed (5, 6). Penzes and Oertel (7, 8) described the TLC separation of the dansyl derivatives of estrone, estradiol, and estriol, and Fishman (5) introduced a conventional fluorescence method for some estrogens using dansyl estrogen derivatives.

This study was conducted to determine the utility of the formation of dansyl derivatives of estrogens in an HPLC analytical procedure. The procedure was adapted satisfactorily to the analysis of estradiol, ethinyl estradiol, and estrone in pharmaceutical dosage forms. Ethinyl estradiol, the estrogen receiving the most attention owing to its small dose, is frequently found in combination with a progestin (oral contraceptive) and an androgen such as methyltestosterone. Fortunately, some nonestrogen steroids are separated from the dansyl estrogens, so they can be analyzed with the same column. A simultaneous method for

0022-3549/78/1200-1735$01.00/0

© 1978, American Pharmaceutical Association

ethinyl estradiol and methyltestosterone also was developed.

EXPERIMENTAL

Apparatus—The liquid chromatograph[1] was equipped with a UV (254 nm) absorption photometer and, in series, a fluorescence detector[2] containing a broad band (240–420 nm) excitation filter and a 440-nm cutoff emission filter. Injections were made with a 10-μl injection valve.

Column and Mobile Phases—The column was a 25-cm × 3.2-mm i.d. × 0.63-cm o.d. stainless steel tube, slurry-packed with LiChrosorb Si 60[3] (5 μm). Mobile phases were simple combinations of *n*-heptane[4] and chloroform[5]. Prior to use, the mobile phases were degassed by ultrasonics for 10 min.

Chemicals, Solvents, and Standards—Unless otherwise specified, all chemicals were reagent grade. Certified ACS grade solvents were used, except where mobile phase requirements dictated otherwise. Standard estrogens were laboratory working grade materials with conventional assay values established above 99.0%. Prior to use in quantitative analysis, estradiol and estrone were dried at 105° for 4 hr; ethinyl estradiol was dried over silica gel for 4 hr at room temperature.

Assay of Estradiol and Ethinyl Estradiol in Commercial Preparations—*Estradiol Standard Solution A*—Accurately weigh and quantitatively transfer approximately 50 mg of estradiol to a 250-ml volumetric flask and bring to volume with acetone.

Estradiol Standard Solution B—Dilute 10.0 ml of estradiol standard solution A to 100.0 ml with acetone.

Ethinyl Estradiol Standard Solution A—Accurately weigh and quantitatively transfer approximately 40 mg of ethinyl estradiol to a 250-ml volumetric flask and bring to volume with acetone.

Ethinyl Estradiol Standard Solution B—Dilute 10.0 ml of ethinyl estradiol standard solution A to 100.0 ml with acetone.

Preparation of Standard Mixture Solution—Transfer 10.0 ml of estradiol standard solution A and 10.0 ml of ethinyl estradiol standard solution A to a 100-ml volumetric flask and bring to volume with acetone. Transfer 1.25 ml to a 125-ml glass-stoppered flask and evaporate just to dryness on a steam bath with an air current to obtain the standard estradiol–ethinyl estradiol residue. Continue with the procedure entitled *Dansylation and Extraction of Dansyl Estrogens.*

Estradiol in Sesame Oil (1.0 mg/ml)—Accurately measure and quantitatively transfer 5.0 ml of the estradiol in sesame oil sample to a 100-ml volumetric flask, add 25.0 ml of ethinyl estradiol standard solution A, and bring to volume with acetone. Transfer 20.0 ml of the latter solution to a 100-ml volumetric flask and bring to volume with methanol.

Centrifuge a portion of this solution at 2000 rpm for 10 min to separate most of the sesame oil. Then transfer 2.50 ml of the acetone–methanol solution (upper layer after centrifugation) to a 125-ml glass-stoppered flask and evaporate just to dryness on a steam bath with an air current to obtain the estradiol residue. Continue with the procedure entitled *Dansylation and Extraction of Dansyl Estrogens.*

Estradiol in Aqueous Suspension (1.0 mg/ml)—Accurately measure and quantitatively transfer 5.0 ml of estradiol in an aqueous suspension to a 250-ml volumetric flask, add 25.0 ml of ethinyl estradiol standard solution A, mix, bring to volume with acetone, and filter. Transfer 1.25 ml to a 125-ml glass-stoppered flask and evaporate just to dryness on a steam bath with an air current to obtain the estradiol residue. Continue with the procedure entitled *Dansylation and Extraction of Dansyl Estrogens.*

Estradiol in Tablets (0.5 mg/Tablet)—Accurately weigh and finely powder a representative number (usually 20) of tablets to pass through a 60-mesh sieve. Accurately weigh a portion of the powder, estimated to contain 1.0 mg of estradiol, and quantitatively transfer it to a 100-ml volumetric flask using methanol. Add 5.0 ml of ethinyl estradiol standard solution A and bring to approximately 50 ml with methanol.

Mix on a laboratory shaker for 30 min, bring to volume with acetone, and filter. Then transfer 2.50 ml of the filtrate to a 125-ml glass-stoppered flask and evaporate just to dryness on a steam bath with an air current to obtain the estradiol residue. Continue with the procedure entitled *Dansylation and Extraction of Dansyl Estrogens.*

Ethinyl Estradiol in Tablets (0.5 mg/Tablet)—Proceed as directed for estradiol in tablets (0.5 mg/tablet) but use the sample and internal standard as given here. Accurately weigh a portion of ethinyl estradiol in tablets sample powder, estimated to contain 0.8 mg of ethinyl estradiol, and add 5.0 ml of estradiol standard solution A. Label the final residue as ethinyl estradiol residue.

Ethinyl Estradiol in Tablets (0.01–0.05 mg/Tablet)—Just prior to use, prepare a conventional partition column in the following manner. To a 250 × 25-mm glass column containing a glass wool plug, add 8 g of anhydrous sodium sulfate, 2 g of diatomaceous earth impregnated with 1.0 ml of water (pack tightly), and 3 g of diatomaceous earth impregnated with 2.0 ml of 10% aqueous anhydrous sodium carbonate (pack tightly).

Accurately weigh and finely powder a representative number (usually 20) of tablets to pass through a 60-mesh sieve. Accurately weigh a portion of the powder, estimated to contain 80 μg of ethinyl estradiol, and quantitatively transfer it to a 100-ml beaker containing 4 g of diatomaceous earth. Dry mix thoroughly, add 3.0 ml of water, and mix until uniform. Quantitatively transfer the mixture to the prepared column, packing tightly after each one-third addition.

Dry wash the beaker with 1 g of diatomaceous earth, transfer to the column, and wipe the spatula, tamping rod, and beaker with glass wool. Then transfer the glass wool to the column. Elute the ethinyl estradiol with 175 ml of benzene, collecting the eluate in a 200-ml volumetric flask. Add 5.0 ml of estradiol standard solution B to the volumetric flask, mix, and bring to volume with acetone.

Transfer 50 ml of this solution to a 125-ml glass-stoppered flask and add 30 ml of acetone. Mix, evaporate on a steam bath using an air current to approximately 10 ml, add 10 ml of acetone, and continue evaporation just to dryness to obtain the ethinyl estradiol residue. Continue with the procedure entitled *Dansylation and Extraction of Dansyl Estrogens.*

Assay of Estrone in Aqueous Suspensions (5 mg/ml)—*Preparation of Standard Mixture Residue*—Accurately weigh and quantitatively transfer approximately 25 mg of estrone and 50 mg of ethinyl estradiol to a 250-ml volumetric flask and dilute to volume with acetone. Transfer 10.0 ml of this solution to a 100-ml volumetric flask and dilute to volume with acetone. Transfer 8.0 ml of the latter solution to a 125-ml glass-stoppered flask and evaporate just to dryness on a steam bath with an air current to obtain the standard mixture residue. Continue with the procedure entitled *Dansylation and Extraction of Dansyl Estrogens.*

Sample Preparation—Accurately weigh about 50 mg of ethinyl estradiol, quantitatively transfer to a 250-ml volumetric flask containing 25 ml of acetone, and mix until the solute dissolves. Transfer 5.0 ml of the estrone aqueous suspension, using an appropriate sampling technique, to the 250-ml volumetric flask; then swirl, dilute to volume with acetone, and filter.

Dilute 10.0 ml of the filtrate to volume with acetone in a 100.0-ml volumetric flask. Transfer 8.0 ml of this solution to a 125-ml glass-stoppered flask and evaporate just to dryness on a steam bath with an air current to obtain the estrone residue. Continue with the procedure entitled *Dansylation and Extraction of Dansyl Estrogens.*

Dansylation and Extraction of Dansyl Estrogens—*Preparation of Reagents*—Prepare a 0.10-mg/ml acetone solution of I and filter. To prepare the base solution, add 0.3667 g of anhydrous sodium carbonate to 300 ml of water, mix to dissolve, add 150 ml of acetone, and mix well.

Dansylation Reaction—To the 125-ml glass-stoppered flask containing the appropriate estrogen residue, add 5.0 ml of I solution and swirl to dissolve. Add 7.5 ml of base solution, mix, stopper, and allow to stand in the dark for 30 min.

Extraction of Dansyl Estrogen Derivatives—Transfer the dansylation reaction solution to a 60-ml separator with 25 ml of ether. Shake for several minutes, transfer the lower aqueous layer to a second 60-ml separator containing 25 ml of ether, shake, and discard the aqueous phase. Wash both ether extracts consecutively with 15- and 10-ml portions of water and discard the washings.

Transfer the ether extracts in both separators to a 50-g anhydrous sodium sulfate column, collecting the eluate in a 125-ml glass-stoppered flask. Wash both separators with 10 ml of ether, transfer the washings to the column, and wash the column with 25 ml of ether. Evaporate the total ether eluate on a steam bath with an air current just to dryness and then continue the evaporation for an additional 2 min[6]. Cool, add 2.0 ml of chloroform, swirl to dissolve the residue, and transfer to a 15-ml glass-stoppered centrifuge tube (label dansyl estrogen solution).

HPLC Measurement of Estradiol and Ethinyl Estradiol—Inject

[1] DuPont model 841.
[2] DuPont model 836.
[3] Altex Scientific, Berkeley, CA 94710.
[4] Spectranalyzed grade, Fisher Scientific Co., Fair Lawn, NJ 07410.
[5] ACS reagent, Eastman Kodak Co., Rochester, NY 14650.

[6] Additional evaporation causes I decomposition products to vaporize.

Table I—Chromatographic Behavior of Some Estrogens, Dansyl Estrogen Derivatives, Progestins, and Androgens [a]

Compound	Relative Retention Time [b]
Dansyl estradiol cypionate	—[c]
Dansyl estradiol valerate	—[c] (1.16)[d]
Dansyl estrone	1.60 (1.92)[d]
Testosterone enanthate	1.78
Dansyl ethinyl estradiol	2.26 (3.56)[d]
Norethindrone acetate	2.28
Estradiol cypionate	2.35
Estradiol valerate	2.70
Dansyl α-estradiol	3.00 (4.92)[d]
Estradiol benzoate	3.07
Dansyl estradiol	3.92 (6.72)[d]
Estrone	4.24
Norethindrone	6.08
Ethinyl estradiol	6.71
Methyltestosterone	7.12
α-Estradiol	8.71
Testosterone	9.48
Estradiol	11.25
Dansyl estriol	—[e]
Chloroform	1.00 (1.00)[d]

[a] Chromatography conditions were: column, LiChrosorb Si 60 (5 μm), 25 cm × 3.2 mm; mobile phase, 20% (v/v) *n*-heptane in chloroform; column temperature, ambient; inlet pressure, 1500 psig; flow rate, 0.75 ml/min; and detection, UV (254 nm) and fluorescence. [b] Retention times are expressed relative to chloroform (UV detection) with an absolute retention of 1.97 min in both mobile phases. [c] Less than 1.05. [d] Mobile phase of 30% (v/v) *n*-heptane in chloroform. [e] Requires a 6–10% absolute ethanol in chloroform mobile phase for elution.

the standard dansyl estrogen mixture solution onto a LiChrosorb Si 60 column, using a 20% (v/v) *n*-heptane in chloroform mobile phase (0.75-ml/min flow rate). Adjust the fluorescence settings to provide a 50–80% full-scale response.

Once reproducible behavior is observed, inject the sample dansyl estrogen solution. Calculate the quantity of estrogen present in the dosage

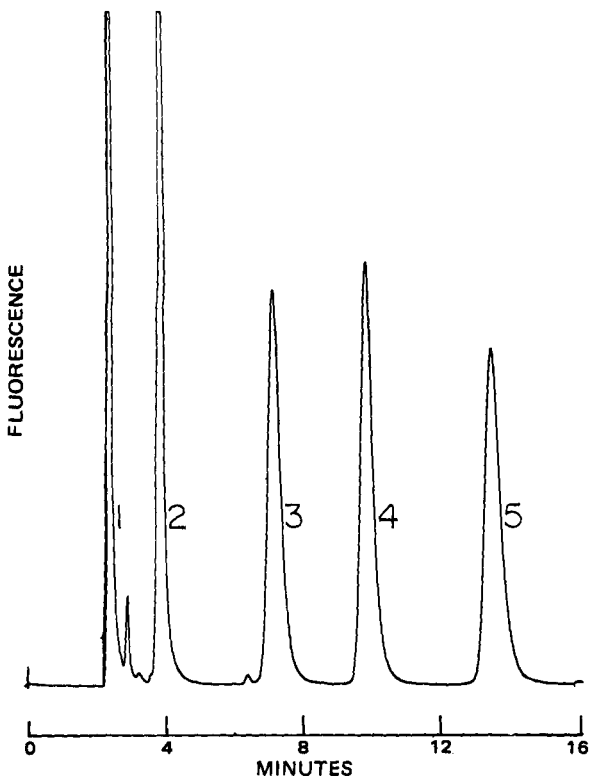

Figure 1—*Separation of five dansyl estrogen derivatives on a LiChrosorb Si 60 (5-μm microparticle silica) column with a 30% (v/v) n-heptane in chloroform mobile phase. Chromatography conditions were: temperature, ambient; pressure at inlet, 1500 psig; flow rate, 0.75 ml/min; and fluorescence sensitivity, 128 setting with a 7-54 excitation filter (broad band) and a 3-72 emission filter. Key (dansyl derivatives): 1, estradiol valerate; 2, estrone; 3, ethinyl estradiol; 4, α-estradiol; and 5, estradiol.*

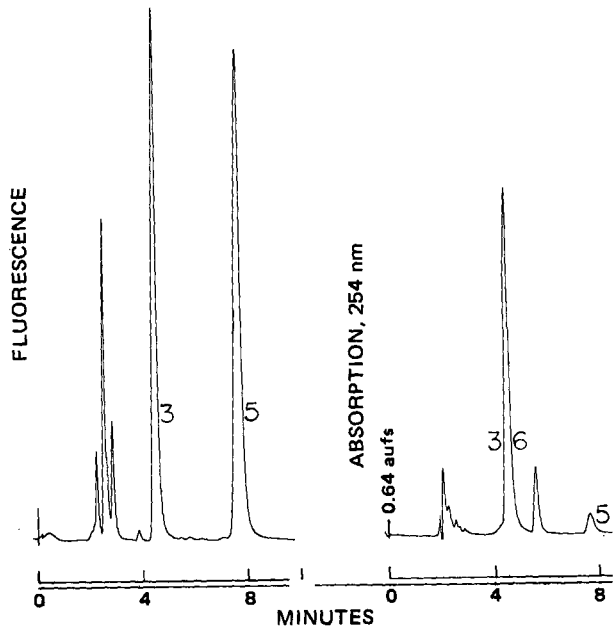

Figure 2—*Chromatograms recorded in the assay for ethinyl estradiol in norethindrone acetate and ethinyl estradiol tablets using fluorescence and UV (254 nm) detection. Chromatography conditions were: column, LiChrosorb Si 60 (5 μm); mobile phase, 20% (v/v) n-heptane in chloroform; temperature, ambient; pressure at inlet, 1500 psig; flow rate, 0.75 ml/min; and fluorescence sensitivity, 128 setting with a 7-54 excitation filter and a 3-72 emission filter. Key: same as Fig. 1; and 6, norethindrone acetate.*

form with standard peak height equations.

HPLC Measurement of Estrone—Proceed as directed for the measurement of estradiol and ethinyl estradiol; however, use a 30% (v/v) *n*-heptane in chloroform mobile phase.

RESULTS AND DISCUSSION

The conditions used for the formation of the dansyl estrogen derivatives are based on the work of Fishman (5). The solvent composition, as well as the base and its concentration, were described by Fishman; however, the I reagent concentration at the time of reaction was twice that used by Fishman, and the reaction time of 30 min was one-half that described (5). These conditions were satisfactory and ensured completed dansyl estrogen reaction as indicated by the following criteria.

1. Fishman found that 30 min would be adequate even with a smaller I reagent concentration than that used in this work.
2. The yellow color of I in the reaction medium was decreased to a constant intensity in about 15 min, indicating that the reaction was at a constant level.
3. Analysis of estrogens using the dansylation procedure to produce the dansyl estrogen and including the selected internal standard showed results that demonstrated a linear relationship (going through the origin) between the ratio of the estrogen analyte and the estrogen internal standard concentration.

The dansyl estrogen derivatives exhibited both strong UV absorption at 254 nm and useful fluorescent properties, as observed by Fishman. The fluorescence detector was sensitive to about 0.05 ng of estrogen (0.04 ng of ethinyl estradiol and 0.05 ng of estradiol), measured as the appropriate dansyl derivative; this sensitivity makes fluorescence detection the preferred method.

The elution behavior of seven estrogens, seven dansyl estrogens, two progestins, and three androgens on a microparticle silica adsorption column with 20% (v/v) *n*-heptane in chloroform as the mobile phase is summarized in Table I. The inclusion of progestins and androgens was based on their presence in pharmaceutical dosage forms in combination with ethinyl estradiol or as potential internal standards. The free estrogens, detectable owing to their UV absorption, were included to demonstrate their separability from their respective dansyl derivatives and to provide data useful for identifying the parent estrogen.

With dansyl estrone, the use of the 20% *n*-heptane in chloroform mobile phase did not yield satisfactory separation from the solvent; 30% (v/v)

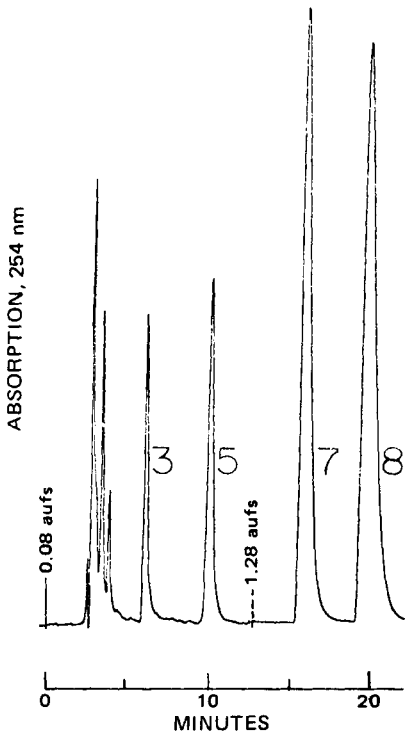

Figure 3—*Chromatogram recorded in the simultaneous assay for ethinyl estradiol and methyltestosterone in a commercial capsule dosage form. Chromatography conditions were: column, LiChrosorb Si 60 (5 μm); mobile phase, 20% (v/v) n-heptane in chloroform; temperature, ambient; pressure at inlet, 1500 psig; and flow rate, 0.75 ml/min. Key: same as Fig. 1; 7, norethindrone; and 8, methyltestosterone.*

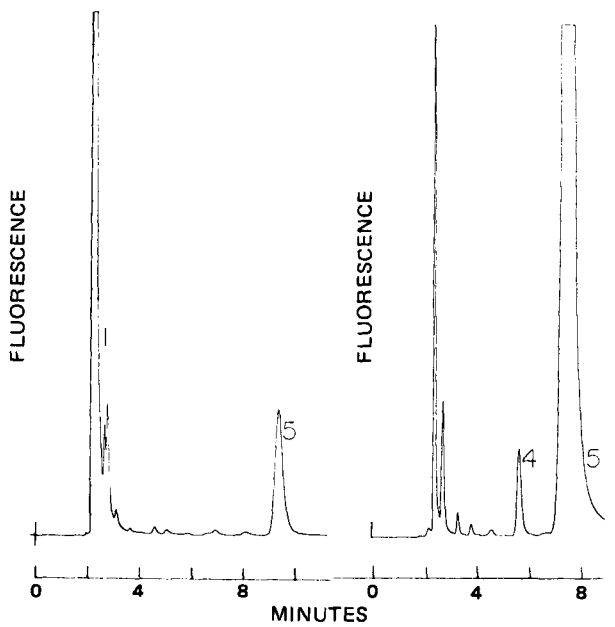

Figure 4—*Chromatograms recorded in the detection of estradiol and α-estradiol as impurities at the 1% level in estradiol valerate and estradiol, respectively. Chromatography conditions were: column, LiChrosorb Si 60 (5 μm); mobile phase, 20% (v/v) n-heptane in chloroform; temperature, ambient; inlet pressure, 1500 psig; flow rate, 0.75 ml/min (approximately ±20%); and fluorescence sensitivity, 128 setting with a 7-54 excitation filter and a 3-72 emission filter. Key: same as Fig. 1.*

n-heptane in chloroform as the mobile phase resulted in an improved mobility. The value of this mobile phase is demonstrated in Fig. 1. This chromatogram indicates that a useful separation of five different dansyl estrogens takes place with the 30% (v/v) *n*-heptane in chloroform mobile solvent.

The general approach to the analysis of estrogens in dosage forms is relatively simple. HPLC analysis of the estrogen is undertaken after the estrogen is separated from the dosage form matrix by dissolution in acetone and methanol followed by filtration or centrifugation. With the lower dosage ethinyl estradiol tablets (0.01 and 0.05 mg), the isolation step was a partition chromatographic procedure. This variation was useful since a large quantity of powdered tablet sample was necessary, making the simpler "dissolve and filter" approach unreliable. In each case, a steroid was chosen as the internal standard; not only did such a choice respect the usual guideline for structural similarity between analyte and internal standard, but it also made the dansyl estrogen formation possible for the internal standard, allowing for a straightforward quantitative measurement.

The chromatograms demonstrate the reasons for some of the experimental choices made in planning the procedures. Figure 2 is a pair of chromatograms recorded during the assay of ethinyl estradiol in norethindrone acetate and ethinyl estradiol tablets. Fluorescence is the detection method of choice owing to its greater sensitivity. The ability of fluorescence to detect selectively and to measure fluorescent compounds is important because, although dansyl ethinyl estradiol and norethindrone acetate have the same chromatographic mobility, only the dansyl estrogen is measured using the fluorescence detector; the UV detector would measure both steroids. Furthermore, if fluorescence detection is to be used, then the chosen internal standards must be estrogens to ensure formation of the dansyl estrogen for analytical comparison.

The UV absorption properties do have value when no fluorescence is present. Figure 3 is a chromatogram observed during the simultaneous analysis of ethinyl estradiol and methyltestosterone in a capsule. The analysis of the ethinyl estradiol would be carried out first with the fluo-

Table II—Analysis of Estrogens in Commercial Dosage Forms

Sample	Estrogen Declared	Percent Found: Dansyl Estrogen HPLC[a,b]	Percent Found: Alternative Method
Estradiol in sesame oil	1.0 mg/ml	95.8, 96.1	—[c]
Estradiol in aqueous suspension[d]	1.0 mg/ml	92.3, 90.6	—[e]
Estradiol tablets	0.5 mg/tablet	103.6, 103.3	102.4, 103.2[f]
Ethinyl estradiol tablets	0.5 mg/tablet	102.6, 101.2	100.2, 100.3[g]
Ethinyl estradiol tablets (coated) (Manufacturer 1)	0.05 mg/tablet	108.0, 110.7	104.1, 105.5[h] 107.9, 107.2[i]
Ethinyl estradiol tablets (coated) (Manufacturer 2)	0.05 mg/tablet	97.8, 97.5	91.5, 88.2[h] 90.9, 92.5[i]
Norethindrone acetate and ethinyl estradiol tablets NF[j]	0.05 mg/tablet	96.6, 95.8	94.5, 96.7[h]
Ethinyl estradiol and methyltestosterone slow-release capsules[k]	0.03 mg/capsule	103.9, 102.6	98.1, 96.0[h]
Ethinyl estradiol tablets	0.02 mg/tablet	101.5, 102.4	97.3, 95.8[h]
Ethinyl estradiol tablets	0.01 mg/tablet	94.3, 95.9	90.7, 87.5[h]
Estrone in aqueous suspension	5.0 mg/ml	97.9, 96.0	97.3, 96.7[l]

[a] Chromatography conditions were: column, LiChrosorb Si 60 (5 μm), 25 cm × 3.2 mm; mobile phase for estradiol and ethinyl estradiol, 20% (v/v) *n*-heptane in chloroform; mobile phase for estrone, 30% (v/v) *n*-heptane in chloroform; column temperature, ambient; pressure at inlet, 1500 psig; flow rate, 0.75 ml/min; and detection, fluoresence. [b] Internal standards were estradiol for ethinyl estradiol and ethinyl estradiol for estradiol and estrone. [c] Study showed 99.3% recovery of a synthetic preparation. [d] Contained declared 5.0 mg/ml of phenol. [e] No alternative assay performed. [f] Extraction and UV. [g] USP XIX, pp. 186, 187. [h] AOAC 12th ed., 39.031–39.034. [i] Modified AOAC 12th ed., 39.031–39.034. [j] Contained 1.0 mg of norethindrone acetate/tablet. [k] Contained 3.5 mg of methyltestosterone/capsule. [l] HPLC analysis without derivatization.

rescence detector. Then norethindrone would be added as an internal standard for methyltestosterone, followed by HPLC, which permits detection of all components and quantitative measurement of methyltestosterone. This procedure was carried out using a commercial capsule dosage form and yielded results of 100.4 and 100.1% of methyltestosterone.

The two chromatograms in Fig. 4 demonstrate another use of the analytical system described in this work. The high sensitivity of the fluorescence detector in measuring dansyl estrogens allows the monitoring of impurities of one estrogen in another. The chromatograms in Fig. 4 are measurements of estradiol (at the 1% level) in estradiol valerate and α-estradiol (1% added as an impurity) in estradiol. The USP (9) has a limit of 1% estradiol in estradiol valerate, whereas the NF (10) has a specification of 3% foreign steroids and other impurities in estradiol.

The results of the analysis of 11 different pharmaceutical dosage forms by the proposed procedure are presented in Table II. The values obtained are within 2% of each other, except for the ethinyl estradiol coated tablets. As a test of the accuracy of the method, a sesame oil solution of estradiol was prepared and assayed. Results of 99.0 and 99.6% estradiol indicated that the procedure was accurate to within 1% for this dosage form.

For comparison, analyses of all but two of the dosage forms were carried out by alternative procedures (given in the footnotes to Table II). The agreement between members in pairs of results was within an average of less than 2%, but three pairs of values differed by more than 2%. In each case, the alternative method average values were lower than the HPLC method. The greatest difference was observed for the lower dosage ethinyl estradiol (0.01 and 0.05 mg) dosage forms.

The AOAC method (footnote *h* of Table II) was collaboratively studied for antifertility tablets and gave results comparable to the HPLC method with norethindrone acetate and ethinyl estradiol tablets. With the lower dosage ethinyl estradiol dosage forms, the variation was wider. In two instances (footnote *i* in Table II), the AOAC method was modified in that chloroform was replaced by benzene and the chromogenic reaction was carried out in benzene. In both cases, somewhat higher results, closer to the HPLC results, were achieved. The alternative method (footnote *l* in Table II) consisted of extracting the estrone aqueous suspension with a chloroform solution of estradiol valerate (internal standard), followed by filtration and direct injection for HPLC (UV detection) analysis. Good agreement was observed with the HPLC procedure.

REFERENCES

(1) N. Seiler and M. Wiechmann, in "Progress in Thin Layer Chromatography and Related Methods," A. Niederwieser and G. Pataki, Eds., vol. 1, Ann Arbor-Humphrey Science Publishers, Ann Arbor, Mich., 1970, p. 94.

(2) R. W. Frei, J. F. Lawrence, J. Hope, and R. M. Cassidy, *J. Chromatogr. Sci.*, **12**, 40 (1974).

(3) R. M. Cassidy and D. S. LeGay, *ibid.*, **12**, 85 (1974).

(4) W. Dunges, *ibid.*, **12**, 655 (1974).

(5) S. Fishman, *J. Pharm. Sci.*, **64**, 674 (1975).

(6) J. Y. P. Wu, *J. Assoc. Off. Anal. Chem.*, **57**, 747 (1974).

(7) L. P. Penzes and G. W. Oertel, *J. Chromatogr.*, **51**, 325 (1970).

(8) *Ibid.*, **74**, 359 (1972).

(9) "The United States Pharmacopeia," 19th rev., Mack Publishing Co., Easton, Pa., 1975, p. 180.

(10) "The National Formulary," 14th ed., Mack Publishing Co., Easton, Pa., 1975, p. 264.

ACKNOWLEDGMENTS

Presented in part at the 91st annual meeting of the Association of Official Analytical Chemists (Abstract 90), October 1977.

The author thanks Dr. Thomas Medwick, Science Advisor, Food and Drug Administration, New York District, and Professor of Pharmaceutical Chemistry, Rutgers—The State University, New Brunswick, N.J., for assistance in the preparation of this paper. He also thanks Matthew Go, Altex Scientific, Inc., for support and advice.

Synthesis and Evaluation of Sulfur-Containing Steroids against Methylmercuric Chloride Toxicity

LARRY K. STEINRAUF *‡, **BRIAN COX** ‡, **EMERSON FOSTER** §, **AMIRA SATTAR** *¶, and **ROBERT T. BLICKENSTAFF** *§x

Received March 9, 1978, from the *Departments of *Biochemistry and ‡Biophysics, Indiana University School of Medicine,* and the §*Veterans Administration Hospital, Indianapolis, IN 46202.* Accepted for publication May 10, 1978. ¶Present address: Department of Physiological Chemistry, College of Medicine, University of Baghdad, Baghdad, Iraq.

Abstract □ Sulfur-containing steroids, analogs, and derivatives were synthesized for evaluation in mice suffering acute toxicity from methylmercuric chloride. Steroids were administered by intraperitoneal injection, by stomach tube feeding, or by absorption through the tail skin. Thiocholesterol and the thiocholanoic acids were effective if given prior to poisoning. The thiosteroids were significantly more effective than penicillamine or dimercaprol under these conditions.

Keyphrases □ Sulfur-containing steroids—synthesized, evaluated in treatment of methylmercuric chloride toxicity in mice □ Steroids, sulfur containing—synthesized, evaluated in treatment of methylmercuric chloride toxicity in mice □ Methylmercuric chloride toxicity—treatment by various sulfur-containing steroids evaluated in mice □ Chelating agents—various sulfur-containing steroids synthesized, evaluated in treatment of methylmercuric chloride toxicity in mice □ Structure–activity relationships—various sulfur-containing steroids evaluated in treatment of methylmercuric chloride toxicity in mice

Heavy metal poisoning traditionally is treated with chelating agents such as penicillamine, dimercaprol, and ethylenediamine tetraacetic acid, which are thought to combine with the metal and facilitate rapid elimination through the kidneys. Because the effectiveness of these agents frequently is limited by toxicity, novel chemotherapeutic agents of low toxicity are needed.

To minimize the burden placed on the kidney by heavy metal poisoning, such agents could include sulfhydryl-type chelators with lipophilic character that might form more nearly irreversible complexes with the heavy metal and be eliminated by other than the urinary route. Sulfhydryl analogs of bile components, specifically mercapto analogs of cholesterol and the bile acids, are such candidates.

The protective action of thiocholesterol (I*a*) and 3β-mercapto-5β-cholanic acid (VII*a*) against lethal doses of methylmercuric chloride was reported recently (1). Spironolactone (III) protects against mercuric chloride toxicity in rats (2) and mice (3). The present report describes continuing efforts to test other sulfur-containing steroids and their esters and analogs as therapy for methylmercuric chloride intoxication.

EXPERIMENTAL

Steroids—Thiocholesterol was converted to its acetate (I*b*) (4) and

0022-3549/78/1200-1739$01.00/0

© 1978, American Pharmaceutical Association

rescence detector. Then norethindrone would be added as an internal standard for methyltestosterone, followed by HPLC, which permits detection of all components and quantitative measurement of methyltestosterone. This procedure was carried out using a commercial capsule dosage form and yielded results of 100.4 and 100.1% of methyltestosterone.

The two chromatograms in Fig. 4 demonstrate another use of the analytical system described in this work. The high sensitivity of the fluorescence detector in measuring dansyl estrogens allows the monitoring of impurities of one estrogen in another. The chromatograms in Fig. 4 are measurements of estradiol (at the 1% level) in estradiol valerate and α-estradiol (1% added as an impurity) in estradiol. The USP (9) has a limit of 1% estradiol in estradiol valerate, whereas the NF (10) has a specification of 3% foreign steroids and other impurities in estradiol.

The results of the analysis of 11 different pharmaceutical dosage forms by the proposed procedure are presented in Table II. The values obtained are within 2% of each other, except for the ethinyl estradiol coated tablets. As a test of the accuracy of the method, a sesame oil solution of estradiol was prepared and assayed. Results of 99.0 and 99.6% estradiol indicated that the procedure was accurate to within 1% for this dosage form.

For comparison, analyses of all but two of the dosage forms were carried out by alternative procedures (given in the footnotes to Table II). The agreement between members in pairs of results was within an average of less than 2%, but three pairs of values differed by more than 2%. In each case, the alternative method average values were lower than the HPLC method. The greatest difference was observed for the lower dosage ethinyl estradiol (0.01 and 0.05 mg) dosage forms.

The AOAC method (footnote *h* of Table II) was collaboratively studied for antifertility tablets and gave results comparable to the HPLC method with norethindrone acetate and ethinyl estradiol tablets. With the lower dosage ethinyl estradiol dosage forms, the variation was wider. In two instances (footnote *i* in Table II), the AOAC method was modified in that chloroform was replaced by benzene and the chromogenic reaction was carried out in benzene. In both cases, somewhat higher results, closer to the HPLC results, were achieved. The alternative method (footnote *l* in Table II) consisted of extracting the estrone aqueous suspension with a chloroform solution of estradiol valerate (internal standard), followed by filtration and direct injection for HPLC (UV detection) analysis. Good agreement was observed with the HPLC procedure.

REFERENCES

(1) N. Seiler and M. Wiechmann, in "Progress in Thin Layer Chromatography and Related Methods," A. Niederwieser and G. Pataki, Eds., vol. 1, Ann Arbor-Humphrey Science Publishers, Ann Arbor, Mich., 1970, p. 94.

(2) R. W. Frei, J. F. Lawrence, J. Hope, and R. M. Cassidy, *J. Chromatogr. Sci.*, **12**, 40 (1974).

(3) R. M. Cassidy and D. S. LeGay, *ibid.*, **12**, 85 (1974).

(4) W. Dunges, *ibid.*, **12**, 655 (1974).

(5) S. Fishman, *J. Pharm. Sci.*, **64**, 674 (1975).

(6) J. Y. P. Wu, *J. Assoc. Off. Anal. Chem.*, **57**, 747 (1974).

(7) L. P. Penzes and G. W. Oertel, *J. Chromatogr.*, **51**, 325 (1970).

(8) *Ibid.*, **74**, 359 (1972).

(9) "The United States Pharmacopeia," 19th rev., Mack Publishing Co., Easton, Pa., 1975, p. 180.

(10) "The National Formulary," 14th ed., Mack Publishing Co., Easton, Pa., 1975, p. 264.

ACKNOWLEDGMENTS

Presented in part at the 91st annual meeting of the Association of Official Analytical Chemists (Abstract 90), October 1977.

The author thanks Dr. Thomas Medwick, Science Advisor, Food and Drug Administration, New York District, and Professor of Pharmaceutical Chemistry, Rutgers—The State University, New Brunswick, N.J., for assistance in the preparation of this paper. He also thanks Matthew Go, Altex Scientific, Inc., for support and advice.

Synthesis and Evaluation of Sulfur-Containing Steroids against Methylmercuric Chloride Toxicity

LARRY K. STEINRAUF *‡, **BRIAN COX** ‡, **EMERSON FOSTER** §, **AMIRA SATTAR** *¶, and **ROBERT T. BLICKENSTAFF** *§x

Received March 9, 1978, from the *Departments of *Biochemistry and ‡Biophysics, Indiana University School of Medicine,* and the §*Veterans Administration Hospital, Indianapolis, IN 46202.* Accepted for publication May 10, 1978. ¶Present address: Department of Physiological Chemistry, College of Medicine, University of Baghdad, Baghdad, Iraq.

Abstract □ Sulfur-containing steroids, analogs, and derivatives were synthesized for evaluation in mice suffering acute toxicity from methylmercuric chloride. Steroids were administered by intraperitoneal injection, by stomach tube feeding, or by absorption through the tail skin. Thiocholesterol and the thiocholanoic acids were effective if given prior to poisoning. The thiosteroids were significantly more effective than penicillamine or dimercaprol under these conditions.

Keyphrases □ Sulfur-containing steroids—synthesized, evaluated in treatment of methylmercuric chloride toxicity in mice □ Steroids, sulfur containing—synthesized, evaluated in treatment of methylmercuric chloride toxicity in mice □ Methylmercuric chloride toxicity—treatment by various sulfur-containing steroids evaluated in mice □ Chelating agents—various sulfur-containing steroids synthesized, evaluated in treatment of methylmercuric chloride toxicity in mice □ Structure–activity relationships—various sulfur-containing steroids evaluated in treatment of methylmercuric chloride toxicity in mice

Heavy metal poisoning traditionally is treated with chelating agents such as penicillamine, dimercaprol, and ethylenediamine tetraacetic acid, which are thought to combine with the metal and facilitate rapid elimination through the kidneys. Because the effectiveness of these agents frequently is limited by toxicity, novel chemotherapeutic agents of low toxicity are needed.

To minimize the burden placed on the kidney by heavy metal poisoning, such agents could include sulfhydryl-type chelators with lipophilic character that might form more nearly irreversible complexes with the heavy metal and be eliminated by other than the urinary route. Sulfhydryl analogs of bile components, specifically mercapto analogs of cholesterol and the bile acids, are such candidates.

The protective action of thiocholesterol (I*a*) and 3β-mercapto-5β-cholanic acid (VII*a*) against lethal doses of methylmercuric chloride was reported recently (1). Spironolactone (III) protects against mercuric chloride toxicity in rats (2) and mice (3). The present report describes continuing efforts to test other sulfur-containing steroids and their esters and analogs as therapy for methylmercuric chloride intoxication.

EXPERIMENTAL

Steroids—Thiocholesterol was converted to its acetate (I*b*) (4) and

0022-3549/78/1200-1739$01.00/0

© 1978, American Pharmaceutical Association

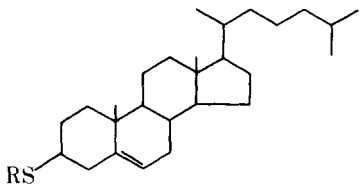

Ia: R = H
Ib: R = CH_3CO

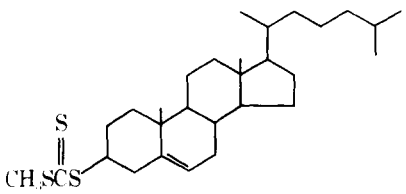

II

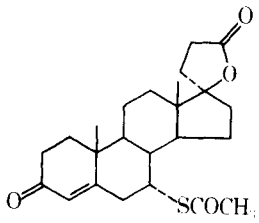

III

to the trithiocarbonate (II), the latter by treatment of the sodium salt of Ia with carbon disulfide and then methyl iodide, following the procedure for converting cholesterol to its xanthate (5). 3β-Mercapto-5β-cholan-24-oic acid (VIa) and 12α-hydroxy-3β-mercapto-5β-cholan-24-oic acid (VIb) were prepared (Scheme I) from the 3-tosylates (IVa and IVb) (6) *via* the intermediate isothiouronium salts (Va and Vb), as in the synthesis of thiocholesterol (7). Ethyl 17β-acetoxy-3-oxo-5α-androstan-2α-ylxanthate (VII, Table I) was prepared from 17β-acetoxy-2α-bromo-5α-androstan-3-one[1] (8), following the conditions for the synthesis of 2α-mercapto-5α-cholestan-3-one (9). Two additional xanthates were synthesized similarly, ethyl 11β,17α-dihydroxy-3,20-dioxo-4-pregnen-21-ylxanthate (VIII) from cortisol mesylate (10) and ethyl 17-oxo-5α-androstan-3α-ylxanthate (IX) from epiandrosterone tosylate (11).

Cholesteryl thiocyanate (X) was prepared from cholesteryl tosylate

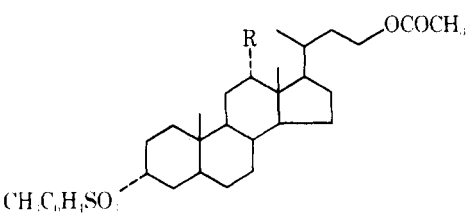

IVa: R = H
IVb: R = OH

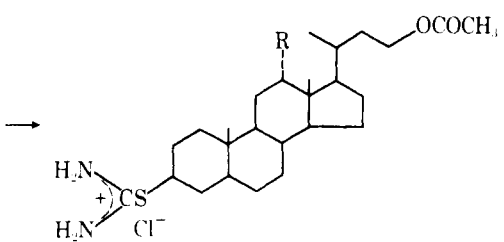

Va: R = H
Vb: R = OH

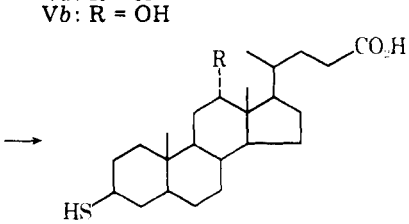

VIa: R = H
VIb: R = OH

Scheme I

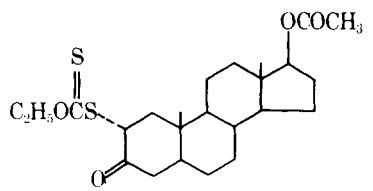

VII

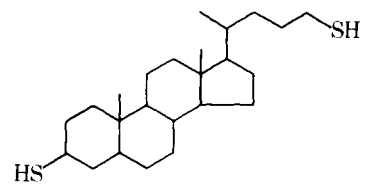

XII

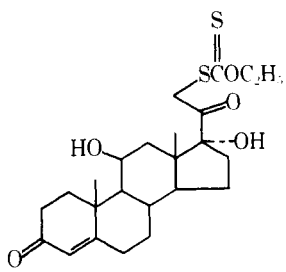

XIII

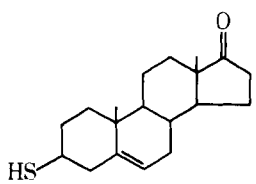

XVI

and potassium thiocyanate (5). 3-Cholestanone was converted to its thiosemicarbazone (XI) by standard means. Methyl lithocholate was reduced to 5α-cholane-3β,24-diol (12), the ditosylate of which was treated with thiourea; alkaline hydrolysis of the bisisothiouronium salt gave 5α-cholane-3β,24-dithiol (XII) in a sequence analogous to the preparation of VIa and VIb. Deoxycorticosterone tosylate (13) and potassium thioacetate (14) reacted to give 21-acetylthio-4-pregnene-3,20-dione (XIII), and 2α-bromo-5α-cholestan-3-one was similarly converted into 2α-acetylthio-5α-cholestan-3-one (XIV). Physical constants of all new compounds are reported in Table I. 3α-Mercapto-5α-androstan-17-one (XV) (11, 15, 16) and 3β-mercapto-5-androsten-17-one (XVI) (17–19) were prepared *via* the corresponding isothiouronium intermediates.

Toxic effects of the steroids themselves were investigated beyond 14-day survival only for thiocholesterol. Mice were fed or injected twice weekly with 400 mg of thiocholesterol/kg for 2 months without showing any obvious ill effects.

Liposomes—In a typical preparation, 500 mg of lecithin (L-α-phosphatidyl choline[2]) and 200 mg of the steroid were dissolved in 10 ml of acetone and 4 ml of chloroform, with warming if necessary. The solution was diluted with 10 ml of warm water, producing a milky suspension, which was concentrated[3] slowly to 2 ml. Occasionally, a second phase separated; it could be homogenized, however, by trituration. The resulting syrup was diluted to 4 ml with water and kept in the refrigerator. A 25-g mouse received 0.2 ml of the liposomal preparation containing 10 mg of steroid (400 mg/kg), unless otherwise indicated (Tables II–IV).

Suspensions—For the suspensions used in Experiment 2, a mixture of 200 mg of steroid, 20 mg of cholic acid, 4 drops of polysorbate 80, and 1 ml of corn oil was diluted to 4 ml with water and mixed in a tissue grinder. The suspensions used in Experiment 5 were similar, but they lacked corn oil and cholic acid.

For Experiment 8, 250 mg of steroid was dissolved in 1 ml of 1% methylcellulose solution, except with thiocholesteryl acetate because its limited solubility allowed a suspension of only 125 mg/ml. For Experiment 9, the spironolactone suspension was diluted 1:5 and the thiocholesteryl acetate suspension was diluted 2:5.

Methylmercuric Chloride—Crystalline methylmercuric chloride[4] was dissolved in warm water at a concentration of 1 mg/ml.

Mice—Male Swiss-Webster mice, 25 ± 4 g, were weighed daily. The amounts of methylmercuric chloride or steroid to be administered were calculated for each mouse from the initial weight, except for the results in Table IV, where the amount of methylmercuric chloride injected on

[1] This sample, prepared by bromination of 17β-acetoxy-5α-androstan-3-one in glacial acetic acid, had the same properties as the product prepared by bromination with *N*-bromosuccinimide and hydrofluoric acid (8).

[2] Sigma.
[3] Rotovap.
[4] R.E.L. Laboratories, Plainfield, N.J.

Table I—Sulfur-Containing Steroids and Their Analogs

Compound	Yield, %	Melting Point	IR[a], cm^{-1}	Formula	Analysis[b], %	Calc.	Found
II	63	129–131°[c]	1062, 958, 816	$C_{29}H_{48}S_3$	C	70.66	70.54
					H	9.81	9.70
					S	19.51	19.72
Va	86	260–261°[d]	3315 and 3100 (NH), 1739 (C=O), 1655 (C=N), 1220, 1170 (SO_3), 1120, 1038, 1012, 820, 678	$C_{33}H_{52}N_2O_5S_2$	C	63.84	63.54
					H	8.44	8.25
					N	4.51	4.42
					S	10.33	10.27
Vb	75	250–251°[d]	3580, 3555, and 3450 (OH), 3300 and 3190 (NH), 1720, 1170 (SO_3), 1120, 1036, 1012, 820, 680	$C_{33}H_{52}N_2O_6S_2$	C	62.23	62.11
					H	8.23	8.43
					N	4.40	4.19
					S	10.07	9.72
VIa	71	143–149°[e]	3400–3200 (OH), 1712 (C=O), 1275, 1100, 720	$C_{24}H_{40}O_2S \cdot 1\frac{1}{2} CH_3OH$	C	69.50	69.75
					H	10.52	9.72
					S	7.27	7.07
VIb	67	99–107°[d]	3570–3240 (OH), 1690 (C=O), 1280, 1030	$C_{24}H_{40}O_3S \cdot H_2O$	C	67.88	68.01
					H	9.97	9.83
					S	7.55	7.59
VII	68	143–144°[f]	1738 and 1718 (C=O), 1260, 1220 (C=S), 1060, 908	$C_{24}H_{36}O_4S_2$	C	63.68	63.82
					H	8.02	7.94
					S	14.17	13.97
VIII	90	196–197°[c]	3480 and 3440 (OH), 1700 (C=O), 1638, 1220 (C=S), 1110, 1054, 870	$C_{24}H_{23}O_5S_2$	C	61.77	62.05
					H	7.34	7.47
					S	13.74	14.09
IX	37	145–147°[d]	1728 (C=O), 1210, 1043, 924	$C_{22}H_{34}O_2S_2$	C	66.96	66.67
					H	8.68	8.47
					S	16.25	16.20
XI		204–206°[g]	3210 and 3140 (NH), 1584, 1500, 1302, 1092, 878	$C_{28}H_{47}N_3S$	C	73.46	73.61
					H	9.18	9.03
					N	10.35	10.17
					S	7.00	6.93
XII	10	88–92°[h]	2600 (SH), 720	$C_{24}H_{42}S_2$	C	73.02	73.12
					H	10.72	10.65
					S	16.25	16.19
XIII	80	170–172°[c]	1708 (20 C=O), 1662 (3 C=O and acetyl C=O), 1610 (C=C), 1278, 1230, 1078, 962, 722	$C_{23}H_{32}O_3S$	C	71.09	71.27
					H	8.30	8.15
					S	8.25	8.47
XIV	58	117–118°[c]	1730 and 1698 (C=O), 1148, 1120, 964	$C_{29}H_{48}O_2S$	C	75.64	75.37
					H	10.50	10.50
					S	6.96	6.93

[a] IR spectra were taken as mineral oil mulls on a Perkin-Elmer spectrophotometer, model 247. [b] Analyses by Galbraith Laboratories, Knoxville, Tenn. [c] Recrystallized from acetone. Melting points were taken on a Hoover-Thomas apparatus and are corrected. [d] Recrystallized from methanol–water. [e] Dissolved in methanolic sodium hydroxide and precipitated with hydrochloric acid. [f] Recrystallized from acetone–water. [g] Recrystallized from dimethylformamide, methanol, and water. [h] Recrystallized from methanol–acetone. The yield of dithiol was 10% from the 3,24-diol; a 6% yield of a monothiol also was obtained, tentatively identified as 5β-chol-3-ene-24-thiol, mp 64–65° (from acetone). *Anal.*—Calc. for $C_{24}H_{40}S$: C, 79.93; H, 11.18; S, 8.89. Found: C, 79.83; H, 11.15; S, 8.69.

Day 3 was calculated from the mouse weight on that day. Mice receiving the steroid by stomach tube were first deprived of food and water for 1 hr; otherwise, they received standard mouse feed and water *ad libitum*.

Male Swiss-Webster albino mice[5] were not constant in their response to methylmercuric chloride poisoning during this investigation (24 months). Therefore, controls were included with each animal study. Dose–response studies for methylmercuric chloride were carried out during June 1976, May 1977, and October 1977 with approximately 100 animals each time. Determinations of the LD_{50} for the three dates were 11.3 ± 0.7, 15.1 ± 1.3, and 17.5 ± 1.8 mg/kg, respectively; the LD_{95} values were 16.3 ± 2.0, 33.1 ± 3.5, and 29.4 ± 2.5, respectively. All observations in any experiment were collected within a 30-day interval. Comparisons from one experiment to another are not necessarily valid since the response of the control group may have changed.

Experiment 1—This experiment compared sulfur-containing steroids with dimercaprol and penicillamine (Table II).

Experiment 2—Six sulfur-containing steroids were assayed by oral administration *via* a stomach tube. All mice received 16 mg of methylmercuric chloride/kg ip. Steroids were administered as suspensions in corn oil, water, and polysorbate 80. In addition, thiocholesterol and its control contained diethylaminoethylcellulose. Animals were fed 400 mg of steroid/kg on each of 2 days before and 1 day following the methylmercuric chloride injection.

The compounds, survivors, number of test animals, and p values (where calculated) were: Ia, 11, 20, <0.059; control, 6, 20; Ib, 18, 24, <0.089; II, 9, 20; X, 11, 24; XI, 11, 24; VIb, 5, 24; and control, 10, 20.

Experiment 3—In the first attempt to devise a screening assay that would utilize only a few mice, sulfur-containing steroids (400 mg/kg) were incorporated into lipsomes and administered by stomach tube on each of 2 days before and 1 day following 16 mg of methylmercuric chloride/kg ip. Neither XII nor XV performed (six mice each) significantly differently from the control group (one survivor out of nine).

Experiment 4—This experiment tested the feasibility of administering the steroids by absorption through skin (Table III).

Experiment 5—Mice were fed aqueous suspensions of steroids (400 mg/kg) every 12 hr following 16 mg of methylmercuric chloride/kg ip. The control group was fed cholesterol to balance any possible nutrient effect of the steroids. The compounds, survivors, and numbers of test animals were: XIII, 2, 11; XIV, 4, 11; and cholesterol, 3, 11.

Experiment 6—In a second attempt to devise a screening assay, ste-

Table II—Effects of Chemotherapy on Methylmercuric Chloride Toxicity[a]

Chemotherapy[b]	Method[c]	Time[d]	Survivors	Percent	p[e]
None			7/53	13	
Dimercaprol	A	C	15/63	24	0.1336
Dimercaprol	B	C	23/61	38	0.0027
Dimercaprol	B	D	5/20	25	0.2301
Penicillamine	A	C	4/12	33	0.1000
Penicillamine	B	D	13/46	28	0.0719
Ia	A	C	16/20	80	0.0001
VIa	A	C	12/15	80	0.0001
Ia–VIa (10:1)	A	C	55/73	75	0.0001
Ia–VIa (2:1)	A	C	30/32	94	0.0001

[a] Survivors were gaining weight 14 days after a 16-mg/kg ip dose of methylmercuric chloride in water, pH 7. [b] Total chemotherapeutic dose: steroid, 3 × 400 mg/kg; dimercaprol, 3 × 120 mg/kg; and penicillamine, 3 × 160 mg/kg. [c] A, intraperitoneal injection of liposomes; and B, intraperitoneal injection of the thiol dissolved in acetate buffer, pH 6. [d] C, administered 48 hr before, 24 hr before, and 24 hr after methylmercuric chloride injection; and D, administered 3 hr before, 3 hr after, and 24 hr after methylmercuric chloride injection. [e] Normal difference test (20) as compared to the control group.

[5] Cox, Indianapolis, Ind.

Table III—Administration of Thiosteroids by Absorption through Tail Skin after Methylmercuric Chloride Injection [a]

Steroid [b]	Daily Dosage for 4 Days, mg/kg	Survivors [c]	Percent
Control (no thiosteroid)		6/20	30
XVI	400	3/12	25
XII	400	3/12	25
VII	400	1/11	9
XIII	400	6/11	55 [d]

[a] All mice received 16 mg of methylmercuric chloride/kg ip. [b] Steroids administered at the level of 400 mg/kg, except XII, which was less soluble (see text). [c] Animals alive and gaining weight at 14 days after methylmercuric chloride injection. [d] $p < 0.0587$; normal difference test (20).

roids (400 mg/kg) were incorporated into liposomes and administered to six mice by stomach tube at 0, 12, 24, and 36 hr after 18 mg of methylmercuric chloride/kg ip. The compounds and numbers of survivors were: I*a*, 2; I*b*, 1; XII, 1; IX, 1; III, 2; VIII, 0; and cholesterol, 3.

Experiment 7—In a similar experiment employing 12 mice/group, steroids (400 mg/kg) were incorporated into liposomes and administered by stomach tube at 0, 12, 24, and 36 hr after 18 mg of methylmercuric chloride/kg ip. The compounds and numbers of survivors were: I*a*, 3; III, 5; cholesterol, 4; and no drug, 3.

Experiment 8—To determine the effect of massive doses, steroids suspended in 1% methylcellulose were administered by stomach tube at 0, 8, 24, 32, and 48 hr after 35 mg of methylmercuric chloride/kg ip. The dose of I*b* was 1250 mg/kg at each feeding; for all other steroids, the dose was 2500 mg/kg. Compounds I*b*, VIII, and III had no survivors out of 12 for each steroid, while cholesterol had three out of 16 survivors.

Experiment 9—Compounds I*b* and III were compared with I*a* (Table IV).

Experiment 10—The toxicity of 1:1 complexes formed between methylmercuric chloride and penicillamine, dimercaprol, or thiocholesterol was evaluated (Table V).

RESULTS AND DISCUSSION

Both penicillamine and dimercaprol provided, as expected, some protection against methylmercuric chloride poisoning (Table II). All results were obtained with the therapeutic agent given a few hours to 1 day before and after the methylmercuric chloride. Penicillamine and dimercaprol were equally effective at either time period. Compounds I*a* and VI*a*, alone or in combination, were considerably more effective in protecting against acute methylmercuric chloride poisoning than were penicillamine or dimercaprol.

In the search for orally active compounds, the steroids in Experiment 2 and some analogs were administered as aqueous suspensions *via* stomach tube. It was assumed that esters like the thioacetate (I*b*), the trithiocarbonate (II), and (less likely) the thiocyanate (X) might hydrolyze to thiocholesterol. The thiosemicarbazone (XII) was tested because of its structural resemblance to diphenylthiocarbazone [$C_6H_5NHNHC(=S)N=NC_6H_5$], which binds mercuric and methylmercuric ions. Although both I*a* and I*b* had more survivors than their respective controls, the results were not significant at the 95% confidence level. Compound X gave poorer results than controls (not tabulated).

Compounds XII and XV were compared in a screening procedure designed to detect promising compounds with few mice (six for each compound) (see Experiment 3). Neither compound was active.

It was of interest to find new ways of administering the test steroid.

Table IV—Comparison of Spironolactone and Cholesteryl Thioacetate with Thiocholesterol [a]

Steroid [b]	Route [c]	Survivors [d]	Percent
Control (no thiosteroid)		4/14	29
I*a*	A	9/12	75 [e]
I*a*	B	3/12	25
I*b*	C	2/13	15
III	C	2/12	17

[a] All mice received 22 mg of methylmercuric chloride/kg ip. [b] Steroids were administered at the level of 400 mg/kg. [c] A, liposomes injected intraperitoneally each of 2 days before and 1 day after methylmercuric chloride; B, liposomes administered orally at 0, 8, 24, and 32 hr after methylmercuric chloride; and C, suspension in 1% methylcellulose administered each of 2 days before and 1 day after methylmercuric chloride. [d] Animals alive and gaining weight 14 days after methylmercuric chloride. [e] $p < 0.0278$; normal difference test (20).

Table V—Toxicity of Complexes of Methylmercuric Chloride with Penicillamine, Dimercaprol, or Thiocholesterol [a]

Complex of Methylmercuric Ion	Dose: Complex, μM	Dose: Methylmercuric Chloride [b], mg/kg	Survivors
Penicillamine	32	320	4/6
Penicillamine	40	400	1/7
Dimercaprol	32	320	4/6
Dimercaprol	40	400	2/7
Thiocholesterol	32	320	5/5
Thiocholesterol	40	400	6/6
Thiocholesterol	80	800	6/6

[a] Complexes were incorporated into liposomes and injected intraperitoneally. [b] In the other experiments, survivals of 11–50% in control groups were observed with dosages of 16–35 mg of methylmercuric chloride.

Compounds VII*b*, XII, XIII, and XVI (Table III) were dissolved in dimethyl sulfoxide, and the tail of each mouse was soaked in the solution until it was absorbed (15 min). Each animal was treated at 0, 24, 48, and 72 hr after the methylmercuric chloride injection. The soluble compounds were administered at 400 mg/kg; XII, however, slowly crystallized out, and the amount actually absorbed is unknown. Only the xanthate (IX) had more survivors than the control group; the difference was barely significant.

Because of the possible activity in I*b* (Experiment 2) and XIII, other thioesters were examined (Experiment 5). In this case, the control group was fed cholesterol to balance the possible nutritional value of the thioesters, XIII and XIV. No significant activity was observed. The same result was obtained from screening the compounds listed in Experiment 6, made up as liposomes and administered by stomach tube following the methylmercuric chloride injection.

In previous studies (3), massive doses (2500 mg/kg) of spironolactone (III), given orally, protected rats and mice following a lethal dose of mercuric chloride. In the present study, spironolactone had no protective effects against methylmercuric chloride (Experiment 8). However, the protective effects against mercuric chloride observed by Eyble *et al.* (3) could be due to the strong diuretic action of spironolactone and are, therefore, not as appropriate against methylmercuric chloride. It was recommended (21) that spironolactone be used with other diuretics such as organic mercurials to obtain the additive effects of more than one diuretic. Such therapeutic doses are at the 1-mg/kg level, however.

Spironolactone was assayed and compared with thiocholesterol and its acetate (Table IV). Only the mice receiving thiocholesterol before and after methylmercuric chloride injection exhibited increased survival.

Since the dissociation of a molecule into ionized parts should be favored by a polar solvent and restricted by a nonpolar solvent, it might be expected that the methylmercuric–thiocholesterol complex, being more lipid soluble than the corresponding complex of penicillamine or dimercaprol, would dissociate less to release free methylmercury. To test this idea, each complex was synthesized by mixing equimolar amounts of methylmercuric chloride with thiocholesterol, penicillamine, or dimercaprol in absolute ethanol. Each complex was incorporated into liposomes and injected in mice intraperitoneally. Results (Table V) strongly imply that the methylmercuric–thiocholesterol complex is indeed of very low toxicity, indicating a very stable complex. To depress the toxic effects of methylmercury, it may be almost as good to form an irreversible complex as to promote the rapid excretion.

Almost no information about the metabolism of thiocholesterol and the thio bile acids is available. Thus far, only the first of the possible metabolic products of thiocholesterol, the disulfide, has been tested, and it was devoid of any possible effects.

No ill effects from thiocholesterol, administered orally or intraperitoneally for several weeks, were observed. On the other hand, 6 days of penicillamine or dimercaprol produced fatalities. The combination of thiocholesterol with either penicillamine or dimercaprol produced even more fatalities. This result is under further investigation.

In conclusion, thiocholesterol and mercaptocholanic acid are more effective orally or intraperitoneally than either penicillamine or dimercaprol in protecting against acute doses of methylmercuric chloride. The assumption is that the thiosteroids form irreversible complexes with methylmercuric ion that enhance excretion through the bile, thereby protecting the kidneys.

REFERENCES

(1) L. K. Steinrauf, B. Cox, A. Sattar, E. L. Foster, and R. T. Blick-

enstaff, in "Abstracts of the 173rd ACS National Meeting," New Orleans, La., Mar. 1977, ORGN 13.
(2) H. Seyle, I. Meces, and S. Szabo, *Int. Urol. Nephrol.*, **2**, 287 (1970). H. Seyle, *Science*, **169**, 775 (1970).
(3) V. Eyble, J. Sýkora, M. Koutenská, J. Koutenský, and F. Mertl, *Arzneim.-Forsch.*, **23**, 867 (1973).
(4) J. Strating and H. J. Backer, *Rec. Trav. Chim.*, **69**, 909 (1950).
(5) G. L. O'Connor and H. R. Nace, *J. Am. Chem. Soc.*, **75**, 2118 (1953).
(6) F. C. Chang, R. T. Blickenstaff, A. Feldstein, J. R. Gray, G. S. McCaleb, and D. H. Sprunt, *ibid.*, **79**, 2164 (1957).
(7) L. C. King, R. M. Dodson, and L. A. Subluskey, *ibid.*, **70**, 1176 (1948).
(8) A. Bowers, L. C. Ibáñez, E. Denot, and R. Becerra, *ibid.*, **82**, 4001 (1960).
(9) D. A. Lightner and C. Djerassi, *Steroids*, **2**, 583 (1963).
(10) J. E. Herz and J. Fried, U.S. pat. 2,842,568 (July 9, 1958); through *Chem. Abstr.*, **53**, 456i (1959).
(11) D. A. Swann and J. H. Turnbull, *Tetrahedron*, **20**, 1265 (1964).
(12) R. T. Blickenstaff and F. C. Chang, *J. Am. Chem. Soc.*, **80**, 2726 (1958).
(13) C. R. Engel and G. Just, *ibid.*, **76**, 4909 (1954).
(14) B. Bannister and F. Kagan, *ibid.*, **82**, 3363 (1960).
(15) J. H. Turnbull, *Chem. Ind.*, **1959**, 515.
(16) J. Kawanami, Japanese pat. 8348 (1966); through *Chem. Abstr.*, **65**, 10641f (1966).
(17) F. A. Kincl, *Chem. Ber.*, **93**, 1043 (1960).
(18) A. Segaloff and R. B. Gabbard, *Steroids*, **5**, 219 (1965).
(19) D. A. Swann and J. H. Turnbull, *Tetrahedron*, **22**, 231 (1966).
(20) A. K. Bahn, "Basic Medical Statistics," Grune & Stratton, New York, N.Y., 1972, pp. 52–55.
(21) "Physicians' Desk Reference," 22nd ed., Medical Economics Inc., Oradell, N.J., 1968, p. 1063.

ACKNOWLEDGMENTS

Supported by PHS-R01-ES-942-03 and by Veterans Administration Research Project 8-583.
The spironolactone was a gift of G. D. Searle and Co.

Molecular Connectivity and Substructure Analysis

LOWELL H. HALL *x and LEMONT B. KIER ‡

Received February 21, 1978, from the **Department of Chemistry, Eastern Nazarene College, Quincy, MA 02170*, and the ‡*Department of Pharmaceutical Chemistry, Medical College of Virginia, Richmond, VA 23298.* Accepted for publication May 19, 1978.

Abstract □ Antimicrobial and antiviral data sets were analyzed by molecular connectivity. Standard structure–activity relationship equations of high quality were produced in both cases. For phenyl propyl ether activity against *Staphylococcus aureus*, the three variables ${}^{1}\chi$, ${}^{3}\chi_P$, and ${}^{4}\chi^{u}_{PC}$ yielded an r of 0.957, significantly better than a π,σ analysis. Analysis of benzimidazole antiviral data (Lee strain, B flu virus) revealed that the one variable, ${}^{6}\chi_P$, yielded an r of 0.950, also better than a reported Hansch analysis. Both data sets were further analyzed by partitioning the important regression variables into terms representing various structural features of the molecules. For the phenyl propyl ethers, the *para*-region of the phenyl ring is important for improved activity and the negative coefficient on ${}^{3}\chi_P$ corresponds to decreased activity for *vic*-dihydroxy compounds. For the alkylbenzimidazoles, substitution on the five-membered ring is highly important. No discrimination of six-membered ring positions was revealed. These structure–activity relationship observations can form the basis for synthetic decisions to improve activity.

Keyphrases □ Molecular connectivity—antimicrobial and antiviral data sets analyzed, structure–activity relationships produced □ Structure–activity relationships—antimicrobial and antiviral data sets analyzed by molecular connectivity method □ Antimicrobial data sets—analyzed by molecular connectivity method, structure–activity relationships produced □ Antiviral data sets—analyzed by molecular connectivity method, structure–activity relationships produced □ Topological indexes—molecular connectivity, antimicrobial and antiviral data sets analyzed, structure–activity relationships produced

Before there was any serious effort to quantify structure–activity relationships, it was popular to draw structural conclusions in terms of molecular fragments. Thus, combinations of atoms and groups were judged essential, based on studies of series of molecules with similar biological actions (1–3). This approach attempted to convey direct structural information to permit the familiar iterative process: synthesis → test → synthesis → test.

BACKGROUND

These fragment proposals are certainly in an understandable and convenient form. However, the results of structure–activity relationship analyses frequently are stated in terms of values of physical properties, information far less valuable to the synthetic chemist. This approach has led to a greater quantification of structure–activity relationship results but also a loss of more useful information, *i.e.*, information directly related to structures.

The basic problem has been the lack of a numerical structural description that can be applied universally to all fragments and that can be translated from numbers back to structural fragments. Such a method, molecular connectivity (4–11), is now available for the numerical representation of molecular structure in a form suitable for multiple regression analysis. The molecular connectivity indexes give quantitative expression to structural variations described traditionally in such qualitative terms as branching, cyclization, and bond type, as well as number and kind of atoms. Structural information is encoded in the set of connectivity indexes, which may be calculated for any molecular structure.

The molecular connectivity indexes, referred to as χ indexes, are based on the hydrogen-suppressed graph; this graph is simply the molecular skeleton, including all atoms (except hydrogen) and the bonds between them. Information describing the molecular structure is extracted in numerical form from the connectivity relationships in the hydrogen-suppressed graph (4).

This paper discusses methods of identifying molecular fragments that the structure–activity relationship regression equation suggests are important. In a systematic fashion, the important molecular fragments or atomic arrangements may be identified. In this further development of the connectivity method, a high quality regression equation first is established with one or more χ indexes. Each χ index is a summation of subgraphs of a specific type. Then the subgraphs may be divided into chemically sensible sets. By regression analysis, the most important sets are picked out. Based on the topology of the important subgraphs, structure–activity relationship conclusions may be drawn as an aid to drug design.

Formalism of Method—Each ${}^{m}\chi_t$ is a sum of terms called subgraph terms:

$$ {}^{m}\chi_t = \sum {}^{m}S_j \qquad \text{(Eq. 1)} $$

Each term ${}^{m}S_j$ is defined for a subgraph—a skeletal fragment of m bonds arranged in a particular fashion (type t)—and the summation is over all such subgraphs in the hydrogen-suppressed graph. The symbol m is called the order or the index of the subgraph. The zero-order subgraph is simply a skeletal atom (graph vertex), and ${}^{0}\chi$ is a sum of the numerical

0022-3549/78/1200-1743$01.00/0
© 1978, American Pharmaceutical Association

enstaff, in "Abstracts of the 173rd ACS National Meeting," New Orleans, La., Mar. 1977, ORGN 13.
(2) H. Seyle, I. Meces, and S. Szabo, *Int. Urol. Nephrol.*, **2**, 287 (1970). H. Seyle, *Science*, **169**, 775 (1970).
(3) V. Eyble, J. Sýkora, M. Koutenská, J. Koutenský, and F. Mertl, *Arzneim.-Forsch.*, **23**, 867 (1973).
(4) J. Strating and H. J. Backer, *Rec. Trav. Chim.*, **69**, 909 (1950).
(5) G. L. O'Connor and H. R. Nace, *J. Am. Chem. Soc.*, **75**, 2118 (1953).
(6) F. C. Chang, R. T. Blickenstaff, A. Feldstein, J. R. Gray, G. S. McCaleb, and D. H. Sprunt, *ibid.*, **79**, 2164 (1957).
(7) L. C. King, R. M. Dodson, and L. A. Subluskey, *ibid.*, **70**, 1176 (1948).
(8) A. Bowers, L. C. Ibáñez, E. Denot, and R. Becerra, *ibid.*, **82**, 4001 (1960).
(9) D. A. Lightner and C. Djerassi, *Steroids*, **2**, 583 (1963).
(10) J. E. Herz and J. Fried, U.S. pat. 2,842,568 (July 9, 1958); through *Chem. Abstr.*, **53**, 456i (1959).
(11) D. A. Swann and J. H. Turnbull, *Tetrahedron*, **20**, 1265 (1964).
(12) R. T. Blickenstaff and F. C. Chang, *J. Am. Chem. Soc.*, **80**, 2726 (1958).
(13) C. R. Engel and G. Just, *ibid.*, **76**, 4909 (1954).
(14) B. Bannister and F. Kagan, *ibid.*, **82**, 3363 (1960).
(15) J. H. Turnbull, *Chem. Ind.*, **1959**, 515.
(16) J. Kawanami, Japanese pat. 8348 (1966); through *Chem. Abstr.*, **65**, 10641f (1966).
(17) F. A. Kincl, *Chem. Ber.*, **93**, 1043 (1960).
(18) A. Segaloff and R. B. Gabbard, *Steroids*, **5**, 219 (1965).
(19) D. A. Swann and J. H. Turnbull, *Tetrahedron*, **22**, 231 (1966).
(20) A. K. Bahn, "Basic Medical Statistics," Grune & Stratton, New York, N.Y., 1972, pp. 52–55.
(21) "Physicians' Desk Reference," 22nd ed., Medical Economics Inc., Oradell, N.J., 1968, p. 1063.

ACKNOWLEDGMENTS

Supported by PHS-R01-ES-942-03 and by Veterans Administration Research Project 8-583.
The spironolactone was a gift of G. D. Searle and Co.

Molecular Connectivity and Substructure Analysis

LOWELL H. HALL *x and LEMONT B. KIER ‡

Received February 21, 1978, from the **Department of Chemistry, Eastern Nazarene College, Quincy, MA 02170*, and the ‡*Department of Pharmaceutical Chemistry, Medical College of Virginia, Richmond, VA 23298.* Accepted for publication May 19, 1978.

Abstract □ Antimicrobial and antiviral data sets were analyzed by molecular connectivity. Standard structure–activity relationship equations of high quality were produced in both cases. For phenyl propyl ether activity against *Staphylococcus aureus*, the three variables ${}^{1}\chi$, ${}^{3}\chi_P$, and ${}^{4}\chi^{u}_{PC}$ yielded an r of 0.957, significantly better than a π,σ analysis. Analysis of benzimidazole antiviral data (Lee strain, B flu virus) revealed that the one variable, ${}^{6}\chi_P$, yielded an r of 0.950, also better than a reported Hansch analysis. Both data sets were further analyzed by partitioning the important regression variables into terms representing various structural features of the molecules. For the phenyl propyl ethers, the *para*-region of the phenyl ring is important for improved activity and the negative coefficient on ${}^{3}\chi_P$ corresponds to decreased activity for *vic*-dihydroxy compounds. For the alkylbenzimidazoles, substitution on the five-membered ring is highly important. No discrimination of six-membered ring positions was revealed. These structure–activity relationship observations can form the basis for synthetic decisions to improve activity.

Keyphrases □ Molecular connectivity—antimicrobial and antiviral data sets analyzed, structure–activity relationships produced □ Structure–activity relationships—antimicrobial and antiviral data sets analyzed by molecular connectivity method □ Antimicrobial data sets—analyzed by molecular connectivity method, structure–activity relationships produced □ Antiviral data sets—analyzed by molecular connectivity method, structure–activity relationships produced □ Topological indexes—molecular connectivity, antimicrobial and antiviral data sets analyzed, structure–activity relationships produced

Before there was any serious effort to quantify structure–activity relationships, it was popular to draw structural conclusions in terms of molecular fragments. Thus, combinations of atoms and groups were judged essential, based on studies of series of molecules with similar biological actions (1–3). This approach attempted to convey direct structural information to permit the familiar iterative process: synthesis → test → synthesis → test.

BACKGROUND

These fragment proposals are certainly in an understandable and convenient form. However, the results of structure–activity relationship analyses frequently are stated in terms of values of physical properties, information far less valuable to the synthetic chemist. This approach has led to a greater quantification of structure–activity relationship results but also a loss of more useful information, *i.e.*, information directly related to structures.

The basic problem has been the lack of a numerical structural description that can be applied universally to all fragments and that can be translated from numbers back to structural fragments. Such a method, molecular connectivity (4–11), is now available for the numerical representation of molecular structure in a form suitable for multiple regression analysis. The molecular connectivity indexes give quantitative expression to structural variations described traditionally in such qualitative terms as branching, cyclization, and bond type, as well as number and kind of atoms. Structural information is encoded in the set of connectivity indexes, which may be calculated for any molecular structure.

The molecular connectivity indexes, referred to as χ indexes, are based on the hydrogen-suppressed graph; this graph is simply the molecular skeleton, including all atoms (except hydrogen) and the bonds between them. Information describing the molecular structure is extracted in numerical form from the connectivity relationships in the hydrogen-suppressed graph (4).

This paper discusses methods of identifying molecular fragments that the structure–activity relationship regression equation suggests are important. In a systematic fashion, the important molecular fragments or atomic arrangements may be identified. In this further development of the connectivity method, a high quality regression equation first is established with one or more χ indexes. Each χ index is a summation of subgraphs of a specific type. Then the subgraphs may be divided into chemically sensible sets. By regression analysis, the most important sets are picked out. Based on the topology of the important subgraphs, structure–activity relationship conclusions may be drawn as an aid to drug design.

Formalism of Method—Each ${}^{m}\chi_t$ is a sum of terms called subgraph terms:

$$ {}^{m}\chi_t = \sum {}^{m}S_j \qquad \text{(Eq. 1)} $$

Each term ${}^{m}S_j$ is defined for a subgraph—a skeletal fragment of m bonds arranged in a particular fashion (type t)—and the summation is over all such subgraphs in the hydrogen-suppressed graph. The symbol m is called the order or the index of the subgraph. The zero-order subgraph is simply a skeletal atom (graph vertex), and ${}^{0}\chi$ is a sum of the numerical

0022-3549/78/1200-1743$01.00/0
© 1978, American Pharmaceutical Association

values computed for each atom. First-order subgraphs are the skeletal bonds, and $^1\chi$ is a sum of values computed for each bond.

Second-order subgraphs consist of pairs of adjacent bonds, and $^2\chi$ is a summation of the values for all distinct sets of adjacent pairs of bonds in the skeleton. The number of second-order subgraphs (paths of length two) in a graph depends heavily on the complexity of skeletal branching. For example, in normal alkanes, the number of second-order subgraphs is $n - 2$. The count of second-order paths increases steadily with branching complexity, so that in 2,2,3-trimethylbutane there are nine compared to five in *n*-heptane.

There are three types of third-order subgraphs: path ($t = P$), cluster ($t = C$), and chain ($t = CH$) (see Ref. 4, chap. 3). Third-order path subgraphs consist of three consecutive skeletal bonds (*n*-butane skeleton). Third-order cluster subgraphs consist of three skeletal bonds sharing a common skeletal atom as in the isobutane skeleton. And third-order chain subgraphs consist of three bonds joined as a triangle (cyclopropane skeleton).

For fourth order, a new type of subgraph is encountered in addition to path (*n*-pentane skeleton), cluster (neopentane skeleton), and chain (cyclobutane skeleton). The new type is path-cluster ($t = PC$) and corresponds to the isopentane skeleton. The number of such types depends heavily on the number of three-way and four-way branch points, as well as the adjacency of such branch points. Higher order χ indexes, $^m\chi_t$, may be defined analogously.

As this brief discussion emphasizes, the concept of molecular connectivity is based on a point of view that begins with the molecular skeletal structure and develops the structural information in systematic numerical manner. A central aspect is the recognition and identification of fragments as subgraphs.

The numerical value computed for each subgraph depends on the vertex delta value, δ, the number of bonded neighbor atoms, for each skeletal atom:

$$^mS_j = \prod_{i=1}^{m+1} \delta_i^{-1/2} \qquad \text{(Eq. 2)}$$

The subgraph term is the reciprocal square root of the product of the vertex delta values, δ_i, for all atoms in the subgraph. For example, for the zero- and first-order indexes:

$$^0\chi = \sum_{i=1}^{N_a} \delta_i^{-1/2} \qquad \text{(Eq. 3)}$$

and:

$$^1\chi = \sum_{k=1}^{N_e} (\delta_i \delta_j)^{-1/2} \qquad \text{(Eq. 4)}$$

where N_a is the number of atoms and N_e is the number of edges in the whole graph and k refers to the kth bond.

Identification and recognition of subgraphs depend only on the connections (bonds) in the molecular skeleton, not the identity of the individual atoms. For example, the isobutane skeleton, as well as those of trimethylamine and isopropyl alcohol, correspond to a cluster-3 subgraph. The simple connectivity index, $^3\chi_c$, is independent of the atom types and has a value of 0.577 for the three molecules. However, there is also a χ cluster index defined as above but depending on the specific identity of the atoms in the skeleton. The atom type is entered into the calculation through a modification of the vertex delta value. Atoms such as nitrogen, oxygen, and fluorine influence properties through the number of valence electrons and attached hydrogens. Thus, the valence delta is defined as:

$$\delta^v = Z^v - h \qquad \text{(Eq. 5)}$$

being the difference between the number of valence electrons and the number of hydrogen atoms bonded to the atom[1]. Thus, δ^v is a count of valence electrons involved in lone pairs and skeletal bonding. Chi indexes based on valence delta values are symbolized with the superscript v as in $^0\chi^v$, $^1\chi^v$, $^4\chi^v_{PC}$, *etc.* For atoms beyond the first row, the inner shell electrons are included as follows:

$$\delta^v = (Z^v - h/Z - Z^v) \qquad \text{(Eq. 6)}$$

Each χ index is a weighted count of the specific type of subgraph (skeletal fragment). The summation includes a contribution from each distinct subgraph in the molecule. This method then replaces a separate listing of all fragments with a single numerical value by assigning a weight, ^mS_j, to each fragment. For example, the following path four fragments may appear in a given molecule in a biological study: $HOCH_2CH_2CH_2$, $CH_3OCH_2CH_2$, $CH_3CH_2CH_2CH_2$, $ClCH_2CH_2CH_2$, $CH_3NHCH_2CH_2$, *etc.* Each fragment may be assigned a value, ^4S_P, and summed to give the $^4\chi^v_P$ value.

In published molecular connectivity studies, the various $^m\chi_t$ indexes have been used in many high quality correlations, singly and in sets of two, three, or more. This present study shows how the $^m\chi_t$ indexes in a high quality correlation may be dissected to determine which of the contributing subgraphs are most important in the molecules under investigation. This isolation of a portion of the molecule or a particular arrangement of substituents is a systematic identification of a fragment of significance. A quantification of the fragment influence is also determined on the basis of a regression equation.

Two sets of biological data were examined, one of antimicrobial activity and the other of antiviral activity.

Antimicrobial Activity of Phenyl Propyl Ethers—A number of ethers of glycerol and trimethyleneglycol were prepared and tested against skin fungi (12). Chlorphenesin, 3-*p*-chlorophenoxy-1,2-propanediol, has been marketed as an antifungal agent[2], but other agents in this chemical class have considerably greater antifungal potency (12). In this study, 28 alkyl- and chloro-substituted phenyl propyl ethers were examined for their action against *Trichophyton mentagrophytes*.

The phenyl propyl ethers in this data set present an interesting problem from the standpoint of structure–activity relationships. Five positions on the phenyl ring and two on the ether side chain were modified to develop the series shown in Table I. Hansch and Lien (13) used partition coefficients and Hammett σ terms to evaluate a property–activity relationship. Their analysis led to a modest correlation but only after the deletion of two molecules from the data set.

In the present study, the antifungal activity of these molecules was examined using molecular connectivity (4). In addition, the different skeletal patterns in the list are described by evaluating the significant contributions of specific molecular structure features as reflected in molecular connectivity indexes for salient subgraphs.

Antiviral Activity of Alkyl-Substituted Benzimidazoles—Sixteen alkyl-substituted derivatives of benzimidazole were examined for their effectiveness against the Lee strain of influenza B virus (Table II). Only one compound in the series studied by Tamm *et al.* (14) was an *N*-alkyl derivative. Since this compound, *N*-methylbenzimidazole, has significantly different acid–base properties and may act *via* a different mechanism, it was not considered in the present study (although its inclusion does not adversely affect the correlation statistics). Alkyl groups were substituted on all five available carbon atoms in the benzimidazole nucleus. Substituents included methyl, ethyl, propyl, isopropyl, and butyl in various combinations. The inhibitory concentrations covered over a 40-fold range.

RESULTS

The general procedure for application of molecular connectivity was the same for both sets of biological data. Chi indexes through the sixth order were computed both for simple and valence connectivity indexes. After checking the molecular structure input data—the connectivity matrix and numbers of valence electrons—for accuracy, the following indexes were stored on computer file for further analysis: $^0\chi$, $^1\chi$, and path terms $^2\chi$ through $^6\chi_P$, $^3\chi_C$, $^4\chi_{PC}$, and $^6\chi_{CH}$, as well as the corresponding valence indexes for a total of 20 variables.

With standard multiple linear regression computer programs, all possible one- and two-variable equations were computed for both data sets. In addition, three-variable equations were examined for the phenyl propyl ether set.

Phenyl Propyl Ether Antifungal Data Set—Examination of the three-variable multiple regressions reveals that two equations are of very high quality and give good account of the experimental data. The two equations differ in one variable:

$$\log(1/c) = 2.44\ (\pm 0.09)^1\chi - 3.29\ (\pm 0.09)^3\chi_P + 2.71\ (\pm 0.03)^4\chi^v_{PC} - 1.31\ (\pm 2.4) \qquad \text{(Eq. 7)}$$

$$r = 0.957 \quad s = 0.149 \quad F = 87.4 \quad n = 28$$

$$\log(1/c) = 1.30\ (\pm 0.10)^1\chi - 2.70\ (\pm 0.08)^3\chi_P + 2.74\ (\pm 0.04)^3\chi^v_P + 0.01\ (\pm 2.5) \qquad \text{(Eq. 8)}$$

$$r = 0.955 \quad s = 0.152 \quad F = 83.8 \quad n = 28$$

[1] For fluorine, the negative sign is taken for the square root in ^mS_j so that the sign of ^mS_j is negative for any subgraph containing fluorine.

[2] Mycil.

Table I—Antimicrobial Activity for Substituted Phenyl Propyl Ethers

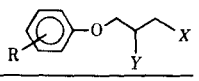

R	X	Y	$^1\chi$	$^3\chi_P$	$^4\chi^v_{PC}$	Observed	Calculated[a]	Difference
2-Methyl	OH	OH	6.236	4.016	0.505	2.26	2.07	0.19
2-Methyl	OH	H	5.698	3.404	0.469	2.46	2.68	−0.22
2-Methyl	H	OH	5.842	3.468	0.394	2.79	2.62	0.17
2-Chloro	OH	OH	6.236	4.016	0.560	2.31	2.22	0.09
2-Chloro	OH	H	5.698	3.404	0.524	2.84	2.83	0.01
4-Chloro	OH	OH	6.219	3.900	0.467	2.31	2.31	−0.00
4-Chloro	OH	H	5.681	3.288	0.431	2.81	2.92	−0.11
4-Chloro	H	OH	5.826	3.351	0.357	3.07	2.86	0.21
2,6-Dichloro	OH	OH	6.647	4.470	0.840	2.37	2.49	−0.12
2,6-Dichloro	OH	H	6.109	3.858	0.804	3.04	3.09	−0.05
2,4-Dichloro	OH	H	6.092	3.724	0.726	3.35	3.28	0.07
2,4-Dichloro	OH	OH	6.630	4.336	0.761	2.61	2.68	−0.07
2-Methyl-4-chloro	OH	H	6.092	3.724	0.672	3.30	3.14	0.16
2-Methyl-4-chloro	OH	OH	6.630	4.336	0.708	2.33	2.53	−0.20
3-Methyl-4-chloro	OH	OH	6.630	4.471	0.932	2.90	2.69	0.21
3-Methyl-4-chloro	OH	H	6.092	3.859	0.896	3.30	3.30	0.00
2-Methyl-6-chloro	OH	OH	6.647	4.470	0.788	2.33	2.35	−0.02
2-Methyl-6-chloro	OH	H	6.109	3.858	0.752	2.70	2.95	−0.25
2-Methyl-6-chloro	H	OH	6.253	3.922	0.678	2.78	2.89	−0.11
2,6-Dimethyl-4-chloro	OH	OH	7.041	4.700	0.913	2.76	2.89	−0.13
2,6-Dimethyl-4-chloro	OH	H	6.503	4.087	0.877	3.51	3.50	0.01
2,6-Dimethyl-4-chloro	H	OH	6.647	4.151	0.803	3.51	3.44	0.07
3,5-Dimethyl-4-chloro	OH	OH	7.041	4.970	1.332	3.24	3.14	0.10
2,4,6-Trimethyl	OH	OH	7.041	4.700	0.980	3.10	3.08	0.02
3,5-Dimethyl-4-chloro	OH	H	6.503	4.358	1.296	3.68	3.74	−0.06
2,4,6-Trimethyl	OH	H	6.503	4.087	0.944	3.47	3.68	−0.21
3,5-Dimethyl-4-chloro	H	OH	6.647	4.421	1.221	3.93	3.68	0.25
2,6-Dichloro-4-methyl	H	OH	6.647	4.151	0.870	3.67	3.62	0.05

[a] Based on Eq. 7.

where r is the correlation coefficient, s is the standard error, F is the F statistic, and n is the number of observations.

Both Eqs. 7 and 8 are highly significant in the statistical sense. The F test value exceeds the table value at the 99.5% level: $F(3, 25, 0.005) = 5.51$. The Student t values for each coefficient also are very large: 26.9, 37.3, and 80.8 for Eq. 7 and 13.8, 32.3, and 76.7 for Eq. 8. Furthermore, the addition of each variable is highly significant on statistical grounds. The F for the addition of $^3\chi_P$ as a second variable in Eq. 10 is significant at the 99.9% level: $F = 29.2 > F(1, 25, 0.001) = 13.9$. The F for the addition of $^1\chi$ as the third variable in Eq. 7 is equally significant: $F = 67.3 > F(1, 24, 0.001) = 14.0$. The χ indexes for Eq. 7 along with the observed, calculated, and residual values are shown in Table I based on Eq. 7. There are no residuals greater than 1.7 s, where s is the standard error of the regression. A plot of observed *versus* calculated values shows no systematic trends in the residuals such as curvature or general increase/decrease as a function of log $1/c$.

To test the integrity of the regression equation, about 15% (four) of the observations were randomly deleted and the three-variable regression was rerun for the remaining 24 observations. The procedure was repeated 10 times, and all of the regression statistics were averaged. None of the regression parameters for the diminished data sets is significantly different from those for the full data set (Table III). This procedure has the effect of testing the predictive power of the equation. When the regression coefficients do not change significantly on deletion of randomly selected sets of observations, one can conclude that the activity of similar compounds will be well predicted also. Furthermore, the average absolute value of the residuals for the deleted observations is 0.15, about the same (0.11) as for the residuals for all 28 observations based on Eq. 7. The range of residuals is also only slightly larger, from −0.34 to +0.30, compared to from −0.25 to +0.25.

Table II—Antiviral Activity for Substituted Benzimidazoles

Compound	$^6\chi_P$	Observed	Calculated[a]	Difference
1 Benzimidazole	0.937	2.14	2.20	−0.06
2 2-Methyl	1.111	2.51	2.44	0.07
3 5-Methyl	1.236	2.72	2.62	0.10
4 5,6-Dimethyl	1.452	2.72	2.92	−0.20
5 4,6-Dimethyl	1.468	2.82	2.94	−0.12
6 2,5-Dimethyl	1.438	2.89	2.90	−0.01
7 4,5-Dimethyl	1.394	2.96	2.84	0.12
8 2,5,6-Trimethyl	1.715	3.05	3.29	−0.24
9 2,4,5-Trimethyl	1.627	3.20	3.16	0.04
10 5,6-Diethyl	1.912	3.39	3.56	−0.17
11 2-Propyl-5-methyl	1.936	3.60	3.60	0.00
12 2,4,5,6,7-Pentamethyl	2.051	3.66	3.76	−0.10
13 2-Ethyl-5-methyl	1.757	3.74	3.35	0.39
14 2-Butyl-5-methyl	2.014	3.77	3.71	0.06
15 2-Isopropyl-5-methyl	1.979	3.77	3.66	0.11

[a] Based on Eq. 9.

Benzimidazole Antiviral Data Set—The one-variable correlation with the antiviral data, expressed as the logarithm of concentration to give 75% inhibition of multiplication log $(1/c)$, revealed that the $^6\chi_P$ index gives a very good correlation:

$$\log(1/c) = 1.40\ (\pm 0.016)^6\chi_P + 1.11\ (\pm 0.29) \qquad \text{(Eq. 9)}$$

$$r = 0.950 \quad s = 0.166 \quad F = 120.3 \quad n = 15$$

The statistical significance of the equation is indicated by the fact that the calculated F value exceeds the tabulated value at the 99.5% level: $F = 120.3 > F(1, 13, 0.005) = 11.8$.

The addition of $^4\chi^v_P$ as a second variable improves the correlation:

$$\log(1/c) = 1.89\ (\pm 0.058)^6\chi_P - 0.677\ (\pm 0.087)^4\chi^v_P + 1.04\ (\pm 0.59) \qquad \text{(Eq. 10)}$$

$$r = 0.966 \quad s = 0.144 \quad F = 86.6 \quad n = 15$$

As shown by the appropriate F test, the addition of $^4\chi^v_P$ as a second variable is significant above the 95% level: $F = 5.7 > 4.61 = F(1, 13, 0.05)$. Observed, calculated, and residual PC values are shown in Table II along with values for $^6\chi_P$. Table II is based on Eq. 9.

DISCUSSION

For both sets of data, the connectivity correlations are of excellent quality with a reasonable number of variables. For the phenyl propyl ethers, the ratio of observations to variables is 28/3 = 9.3; for the benzimidazoles, it is 15/1.

Phenyl Propyl Ether Antifungal Activity—For this data set, three variables are required to give a good account of the variation in the biological data. Such a result suggests that more than one structural feature is important in determining the biological activity. If the activity is the result of a generalized dispersion interaction or a simple size effect, the data probably should be described with a single variable, such as $^1\chi$ or $^1\chi^v$, which has been shown to be important for such effects (4–6).

Equations 1 and 2 account equally well for the experimental data as indicated by their regression statistics. Since the two equations differ only in one variable, $^4\chi^v_{PC}$ or $^3\chi^v_P$, these two variables probably encode the same information for this data set. Moreover, these two variables should be

Table III—Comparison of Regression Parameters for Diminished and Full Antimicrobial Data Sets for Phenyl Propyl Ethers

Data Set	Coefficients			Regression Parameters	
	$^1\chi$	$^3\chi_P$	$^4\chi^v_{PC}$	r	s
Diminished[a]	2.45 (±0.07)	−3.39 (±0.09)	2.71 (±0.10)	0.957 (±0.007)	0.147 (±0.007)
Full[b]	2.44 (±0.09)	−3.29 (±0.09)	2.71 (±0.03)	0.957	0.149

[a] See text for definition. Values are averages of 10 separate runs and in parentheses are given the standard error of the average. [b] From Eq. 7.

highly intercorrelated, an expectation borne out by an examination of the correlation matrix; $^4\chi^v_{PC}$ correlates with $^3\chi^v_P$ with $r = 0.97$. Hence, either equation represents the structure–activity relationship of the data set and may be used for prediction. Subsequent discussion and analysis are limited to Eq. 7 somewhat arbitrarily but also because the $^4\chi^v_{PC}$ index is important for other phenyl ring systems (4, 15).

The two statistically most significant variables in Eq. 7 are $^4\chi^v_{PC}$ and $^3\chi_P$. Whereas $^1\chi$ contains contributions uniformly from the overall molecule, both $^4\chi^v_{PC}$ and $^3\chi_P$ depend heavily upon specific branching characteristics and substitution patterns in the molecular skeleton (4). Thus, the spatial arrangement determined by molecular connections is important in determining an optimum interaction; the optimum interaction is reflected by the nature of the $^4\chi^v_{PC}$ and $^3\chi_P$ indexes. Chemical intuition may suggest a possible hydrogen bonding involving the hydroxyl groups at *X* and/or *Y*. In addition, as subsequent analysis suggests, an interaction involving the substituted phenyl ring, centered at the *para*-position, may be hypothesized.

The two most active compounds (Compounds 25 and 27) are characterized by the largest $^4\chi^v_{PC}$ values, 1.302 and 1.227, respectively. Hence, a search for more active compounds should center on this fact. The negative coefficient on $^3\chi_P$ suggests an unfavorable condition arising from the presence of substituent groupings that lead to large $^3\chi_P$ values. The 1,3,4,5-pattern on the phenyl ring leads to large values for both $^3\chi_P$ and $^4\chi^v_{PC}$. However, the $^4\chi^v_{PC}$ index is increased by the presence of chlorine (and, of course, bromine) whereas the nonvalence (simple connectivity) index $^3\chi_P$ reflects only the atomic arrangement and not the identity of the atoms. The presence of the 1,2-dihydroxy pattern (*X*/*Y* occupancy) on the side chain also increases $^3\chi_P$ and decreases the calculated activity.

It would be meaningful if specific structural interpretation could be extracted from the regression equation. This analysis was accomplished by a partitioning on the $^4\chi^v_{PC}$ and $^3\chi_P$ indexes.

As already discussed, each χ index, $^m\chi_t$, is a summation of subgraph terms, ^mS_j; the index represents the whole molecule summation of topological features. However, it is possible to factor out of the summation those terms that isolate specific structural features or substructures and to identify those most significantly related to the biological activity. In this manner, the structure–activity relationship study may be focused on selected features of the molecular structure so that significant fragments or substructures may be identified. In this present case, for example, it seems meaningful to explore the substitution pattern in the aromatic ring to determine the arrangement that elicits maximum response.

In this second stage of connectivity analysis, subgraph terms are factored out to explore the specific attributes of structure in the *X*/*Y* region of the side chain and the *para*-region of the phenyl ring. The symbol $^m\overline{S}_t$ (the subgraph term symbol with a bar) is used to denote the restricted sum of subgraph terms that encompass only specified portions of the molecular skeleton. For the *X*/*Y* region, the symbol $^3\overline{S}_P$ stands for the sum of path-three subgraphs that include the OH at position *X* or position *Y* or both. Such subgraphs may be the following molecular fragments: $CH_2CH_2CH_2OH$, $CH_2\underset{Y}{C}HCH_2OH$, $CHOHCH_2OH$, and $OCH_2\underset{Y}{C}HOH$.

The symbol $^4\overline{S}^v_{PC}$ is defined to contain only path/cluster-four subgraphs containing a *para*-substituent. Some of the possible subgraphs are CHCClCHCH, $CHCClC(CH_3)$, and $>CCClC(CH_3)$. To determine the possible significance of these partial χ indexes, a regression was run in which the $^m\overline{S}_t$ terms were put in place of the complete $^m\chi_t$ indexes. For the equation with $^3\overline{S}_P$, $^4\overline{S}^v_{PC}$, and $^1\chi$, the correlation coefficient is $r = 0.924$. When compared to $r = 0.957$ for Eq. 7, it appears that the partial subgraph terms $^3\overline{S}_P$ and $^4\overline{S}^v_{PC}$ must be capturing the major part of the important structural information in the total indexes $^3\chi_P$ and $^4\chi^v_{PC}$. Furthermore, the correlation strongly suggests that the *X*/*Y* region and the ring *para*-region play very important roles in the biological action. That is, the action arises from major interactions centered in these two portions of the molecules rather than from generalized whole molecule effects.

Benzimidazole Antiviral Activity—Examination of the regression equations shows that only one variable is required for a very good correlation with the antiviral data. The addition of a second variable does improve the results, $r = 0.962$ compared to $r = 0.950$ (93% variation explained compared to 88%). Either equation can be used for prediction.

In a property–activity relationship study, Hansch found only a modest correlation with the partition coefficient, $r = 0.903$ (16). The alkyl π values used in the study are proportional to the number of substituent carbon atoms. Such analysis suggests that only the number of substituent atoms is important and that the substituent size, branching, and pattern of substitution are less important. However, the appearance of high order connectivity path terms, sixth and fourth order, and one valence term in Eqs. 9 and 10 strongly indicates the importance of the alkyl chain length and the pattern of substitution.

To investigate further the question of substitution pattern, the constituent subgraphs were analyzed in a manner somewhat like that described for the phenyl propyl ether data set. In this case, major attention was focused on the efficacy of substitution on the five-membered ring in comparison to the six-membered ring.

All of the subgraphs contributing to the $^6\chi_P$ index are subdivided in various ways. For example, some sixth-order path subgraphs are contained wholly in the benzimidazole nucleus. These subgraphs, given the symbol R_{56}, do not include any substituent atoms. Examples are shown in Fig. 1. The symbol S_6R_6 stands for the sum of subgraph terms including a substituent on the six-membered ring (S_6) and extending only over the six-membered ring (R_6). Other subgraphs include a substituent on the six-membered ring but also extend over both the six- and five-membered rings; these substituents contribute to S_6R_{56}. In similar fashion, terms may be defined for the five-membered ring as S_5R_5 and S_5R_{56}. Finally, some sixth-order path subgraphs include substituents on both rings and also extend over parts of both rings; these substituents contribute to $S_6S_5R_{56}$. Thus, for sixth-order paths, there are six subclassifications: $^6S_6R_6$, $^6S_6R_{56}$, $^6S_5R_5$, $^6S_5R_{56}$, $^6S_5S_6R_{56}$, and $^6R_{56}$. The superscript 6 refers to sixth order. An analogous set of subgraph classifications may be obtained for the $^4\chi^v_P$ index as follows: $^4S_6R_6$, $^4S_6R_{56}$, $^4S_5R_5$, $^4S_5R_{56}$, and $^4R_{56}$. Fourth-order paths are not long enough to span the distance involving substituents on both rings. All of these subclassifications may be obtained routinely from the XFUNC computing system that produces the file of χ indexes.

The first observation to be made is that sixth-order subgraphs contained wholly in the benzimidazole nucleus, $^6R_{56}$, do not contribute much to the correlation: $r^2 = 0.25$. This result is expected since such terms do not vary greatly with substituent changes. Hence, it is expected that subtracting $^6R_{56}$ terms from the total $^6\chi_P$ index would not greatly affect its correlation. The r for $^6\chi_P - {}^6R_{56}$ is 0.92, not a great deal less than the 0.95 found for $^6\chi_P$ alone.

The two best single subgraph terms for correlation with the activity involve five-membered ring substitution: $r = 0.69$ for $^6S_5R_{56}$ and $r = 0.72$

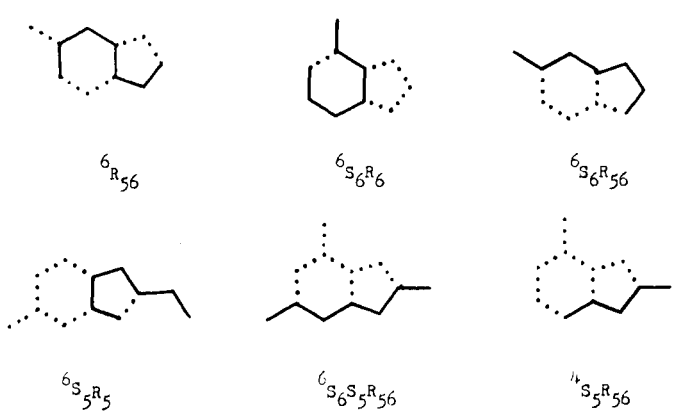

Figure 1—*Some constituent subgraphs of* $^6\chi_P$ *and* $^4\chi^v_P$ *in alkylbenzimidazoles. Subgraphs are shown in full dark lines; the rest of the graph is in dotted lines.*

for $^4S_5R_5$. These partial χ indexes, each containing contributions from only a few of the total number of subgraphs, account for about 50% of the variation. This result suggests the importance of substitution on the five-membered ring.

Only six pairs of these subgraph variables yield a correlation equal in quality to Eq. 9, which utilizes all of the subgraphs in $^6\chi_P$; $r \geq 0.93$. Three of the six equations contain $^6S_5R_{56}$; the other three contain $^4S_5R_5$. Thus, a partial subgraph term involving five-membered ring substitution is required for quality correlation. No combination of terms that excludes five-membered ring substitution yields a high quality correlation. The best of these two variables is based on $^6S_6R_{56}$ in addition to $^6S_5R_{56}$, for which $r = 0.941$.

These observations indicate the importance of: (*a*) alkyl substitution on the 2-position (five-membered ring) and (*b*) the combination of substitution on both five- and six-membered rings. The compound with the largest value of $^6S_5R_{56}$, 0.6193, is Compound 15, the compound of highest activity.

The subgraph analysis may be continued by examination of three-variable equations involving the $^m\overline{S}_t$ terms. There are 19 sets of three-variable equations with $r \geq 0.94$. Sixteen sets include $^6S_5R_{56}$, again underscoring the importance of substitution on the five-membered ring. The other equations contain either $^6S_5R_5$ or $^4S_5R_{56}$. Furthermore, of the seven equations with $r \geq 0.95$, all contain $^6S_5R_{56}$. Also prominent in these high quality correlations are $^6S_6R_6$ and $^6S_6R_{56}$. It is significant that the $^6S_6S_5R_{56}$ term does not play an important role in any of the regression equations. Its appearance would suggest that substitution on the 4- and 7-positions is more efficacious than on the 5- and 6-positions. However, there seems to be no discrimination among the six-membered ring positions.

The key term, $^6S_5R_{56}$, is enhanced by large alkyl groups on the 2-position; branched groups produce greater activity. Compare Compound 15 (2-isopropyl) with Compound 11 (2-propyl). Also, Compound 15 (2-isopropyl) is as active as Compound 14 (2-butyl), four carbon atom-substituent unbranched compared to three branched. Apparently, cyclopropyl, *sec*-butyl, and *tert*-butyl groups may enhance activity as substituents on the 2-position.

CONCLUSIONS

Two general conclusions can be drawn from these studies. First, for both data sets, molecular connectivity provides excellent structure–activity relationship equations; in both cases, these results are superior to previously published Hansch π, σ analyses. Moreover, by systematic elimination of randomly selected phenyl propyl ethers, the significance and reliability of the regression equation were further substantiated. For both data sets, the significant regression variables were partitioned into subgraph terms related to various structural features of the molecules. These partial subgraph terms, $^m\overline{S}_t$, were then entered into regression studies.

For the phenyl propyl ether data set, the results suggest the following conclusions. The principal interactions are related to the *para*-position of the phenyl ring and the X/Y portion (Table I) of the ether side chain. Substitution leading to increased $^4\chi^v_{PC}$ values augments the activity. Bromine in the *para*-position and methyl in the *meta*-position may increase activity. *vic*-Dihydroxy substitution decreases activity. In addition to these specific structural effects, there is a general whole molecule interaction, perhaps related to dispersion effects.

For the alkylbenzimidazole data set, subgraph analysis shows that substitution of branched (or cyclic) alkyl groups on the 2-position (five-membered ring) is important for high activity. There is no discrimination between the four positions on the six-membered ring.

By use of the partial subgraph terms, $^m\overline{S}_t$, structurally significant portions of the biologically active molecule may be identified in cases where the activity may be highly related to a specific structural feature. The significance of the molecular fragment or substructure may even be put into quantitative terms by using the regression equation for the partial subgraph terms. The method of substructure identification by partial subgraph analysis can now be applied to more complex chemical systems.

REFERENCES

(1) W. C. Holland, R. L. Klein, and A. H. Briggs, "Introduction to Molecular Pharmacology," Macmillan, New York, N.Y., 1964.

(2) A. Korolkovas, "Essentials of Molecular Pharmacology," Wiley-Interscience, New York, N.Y., 1970.

(3) R. B. Barlow, "Introduction to Chemical Pharmacology," Wiley, New York, N.Y., 1964.

(4) L. B. Kier and L. H. Hall, "Molecular Connectivity in Chemistry and Drug Research," Academic, New York, N.Y., 1976.

(5) L. B. Kier, L. H. Hall, W. J. Murray, and M. Randić, *J. Pharm. Sci.*, **64**, 1971 (1975).

(6) L. B. Kier, W. J. Murray, and L.H. Hall, *J. Med. Chem.*, **18**, 1272 (1975).

(7) L. B. Kier and L. H. Hall, *J. Pharm. Sci.*, **65**, 1806 (1976).

(8) L. H. Hall and L. B. Kier, *ibid.*, **66**, 642 (1977).

(9) T. DiPaolo, L. B. Kier, and L. H. Hall, *Mol. Pharmacol.*, **13**, 31 (1977).

(10) L. B. Kier, T. DiPaolo, and L. H. Hall, *J. Theor. Biol.*, **67**, 585 (1977).

(11) L. B. Kier and L. H. Hall, *Eur. J. Med. Chem.*, **12**, 307 (1977).

(12) F. M. Berger, C. V. Hubbard, and B. J. Ludwig, *Appl. Microbiol.*, **1**, 146 (1953).

(13) C. Hansch and E. J. Lien, *J. Med. Chem.*, **14**, 653 (1971).

(14) I. Tamm, K. Folkers, C. H. Shunk, D. Heyl, and F. L. Horofall, *J. Exp. Med.*, **98**, 245 (1953).

(15) L. B. Kier and L. H. Hall, *J. Med. Chem.*, **12**, 1631 (1977).

(16) "Biological Correlations, The Hansch Approach," W. van Valkenburg, Ed., ACS Advances in Chemistry Series 114, American Chemical Society, Washington, D.C., 1972.

ACKNOWLEDGMENTS

The authors thank Mr. James D. Fisk and Mr. Philip A. Coy for assistance with the computer calculations. They also appreciate use of the computer centers at Eastern Nazarene College and the Massachusetts College of Pharmacy.

GLC–Mass Spectrometry of Several Important Anticancer Drugs II: Doxorubicin and Daunorubicin Aglycone Analogs

KENNETH K. CHAN ˣ **and ERIC WATSON**

Received November 28, 1977, from the *School of Pharmacy, University of Southern California, Los Angeles, CA 90033.* Accepted for publication March 31, 1978.

Abstract □ By using previously developed pertrimethylsilylation and methoxime formation procedures, the GLC–mass spectra of pertrimethylsilyl and pertrimethylsilyl methoxime derivatives of 12 doxorubicin and daunorubicin glycone analogs, mostly synthesized in this laboratory, were studied. The fragmentation pathways were readily interpretable, and the patterns were highly specific for corresponding structural changes, thus supporting the previous contention that this method has potential for the identification of doxorubicin and daunorubicin metabolites. Four aglycone metabolites were identified, on the basis of their GLC–mass spectra, in the hydrolysate of the 1-butanol extract of bile obtained from a doxorubicin-treated rabbit.

Keyphrases □ Doxorubicin glycone analogs, various—GLC–mass spectral analyses, prepared samples □ Daunorubicin glycone analogs, various—GLC–mass spectral analyses, prepared samples □ GLC–mass spectrometry—analyses, various doxorubicin and daunorubicin glycone analogs, prepared samples □ Antineoplastic agents—doxorubicin and daunorubicin, various glycone analogs, GLC–mass spectral analyses, prepared samples □ Metabolites, aglycone—GLC–mass spectral identification in bile of doxorubicin-treated rabbit

The anthracycline antitumor agents doxorubicin[1,2] (I*a*) and daunorubicin[2,3] (II*a*) undergo extensive metabolism (1–11). Isolation of their metabolites involved usual extraction of the material from biological fluids followed by extensive chromatographic separations. Identification methods were based on spectroscopic and mass spectral data obtained from these isolated components. In all cases, these components had to be pure.

GLC–mass spectrometry often offers advantages in the separation of properly derivatized substances. This method simplifies purification procedures and yields good mass spectral data. Previously (12), stable volatile pertrimethylsilyl and pertrimethylsilyl methoxime derivatives were obtained for doxorubicinone (I*b*), daunorubicinone (II*b*), carminomycinone (III*b*), and mithramycinone/chromomycinone, and these derivatives exhibited excellent GLC properties and readily interpretable mass fragments. This paper reports the application of this method to study the fragmentation patterns of the derivatives of I*a* and II*a*. Several of these derivatives have been reported as metabolites of these agents.

EXPERIMENTAL

Instrumental Conditions—A magnetic sector mass spectrometer interfaced with a gas chromatograph[4] was used to obtain the mass spectra under the previously described conditions (12).

Chemicals and Reagents—Compounds I*a*, II*a*, carminomycin[5,6] (III*a*), daunomycinol[5] (IX*a*), 7-deoxydaunomycinone[3] (VI), and doxorubicin carboxylic acid[7] (XIV*a*) were found to be greater than 95% pure by TLC[8]. The aglycones of these compounds were obtained as described previously (12). Silylating mixtures composed of trimethylsilylimidazole–bis(trimethylsilyl)trifluoroacetamide–trimethylchlorosilane[9] (3:3:2) and methoxyamine hydrochloride[10] were obtained commercially. Pyridine was silylation grade. Aluminum chloride, sodium dithionite, sodium bicarbonate, disodium ethylenediaminetetraacetate, benzene, ethyl acetate, and methylene dichloride were all analytical grade and were used without further purification.

Compound III*b* was obtained by hydrolysis of III*a* or was synthesized by the procedure of Kende *et al.* (13), starting from II*b*. 4-Demethyldoxorubicinone (IV) was synthesized by a procedure identical to that used for III*b* (13). Red crystals, obtained after crystallization in ethyl acetate, gave a melting point of 237–240°. The electron-impact mass spectrum did not yield a substantial parent ion; the GLC–mass spectrum of the pertrimethylsilyl derivative (Table I) was consistent with the assigned structure.

Compound VI was synthesized by the procedure of Smith *et al.* (14). The product obtained was identical in all respects (UV and mass spectra and melting point) with an authentic sample[5]. 7-Deoxydoxorubicinone (V) was synthesized by an identical procedure. After crystallization from dichloromethane, the red crystals gave a melting point of 246–249°. The high-resolution electron-impact mass spectrum[11] gave a prominent peak at *m/e* 338.076, corresponding to M − 60 [HC(=O)CH_2OH] ($C_{19}H_{14}O_6$). The GLC–mass spectrum (Table I) was consistent with the expected structure.

Similarly, 7-deoxycarminomycinone (4-demethyl-7-deoxydaunorubicinone, VIII), was synthesized according to the same procedure. After crystallization from dichloromethane, the red crystals gave a parent ion at *m/e* 368.090, corresponding to $C_{20}H_{16}O_7$, under high-resolution electron-impact mass spectrometry.

Doxorubicinol (X*a*) was isolated from I*a*-treated rabbit bile according to the modified procedure of Takanashi and Bachur (11). The bile was extracted extensively with 1-butanol. The residue obtained after evaporation of the solvent was chromatographed on an XAD resin[10] and eluted first with water and then with methanol. The red band corresponding to X*a* eluted off the column by methanol was collected. The red residue obtained after removal of the solvent *in vacuo* was purified on semipreparative TLC plates[12] with chloroform–methanol–water (80:40:4) as the eluting solvent. The isolated band was chromatographically identical with reported X*a* (11). The fluorescence spectrum was identical with that of I*a*.

The aglycones of IX*a* and X*a*, *i.e.*, IX*b* and X*b*, respectively, were obtained by acid hydrolysis as reported previously (12).

Alternatively, X*a* was synthesized by reduction of I*a* *via* sodium cyanoborohydride in an aqueous solution; the pH was controlled at 3.5[13] The isolated product was identical in all respects (TLC and UV and GLC–mass spectra of its aglycone) with the product of metabolic origin[14].

4-Demethyl-7-deoxydoxorubicinone (VII) was synthesized by demethylation of previously synthesized V by the procedure described for the synthesis of IV. After crystallization from dichloromethane, the red

[1] Adriamycin, NSC-123127.
[2] Supplied by the Drug Synthesis and Chemistry Branch, Developmental Therapeutic Program, Division of Cancer Treatment, National Cancer Institute, Bethesda, Md.
[3] Daunomycin, rubidomycin, NSC-82151.
[4] Varian model CH-7, Springfield, N.J.
[5] Gift of Dr. F. Arcamone, Farmatalia, Milan, Italy.
[6] NSC-180024.
[7] Gift of Dr. David Henry, Stanford Research Institute, Palo Alto, Calif.
[8] Silica gel GH with chloroform–methanol–acetic acid (80:20:4).
[9] Powersil, Pierce Chemical Co., Rockford, Ill.
[10] Applied Science Laboratories, State College, Pa.
[11] DuPont mass spectrometer model 21-492B, at the California Institute of Technology, Pasadena, Calif.
[12] Gelman ITLC, SA type, Ann Arbor, Mich.
[13] Dr. David Henry, Stanford Research Institute, provided the reduction procedure.
[14] No identical stereochemistry is implied.

0022-3549/78/1200-1748$01.00/0
© 1978, American Pharmaceutical Association

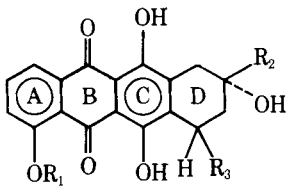

Ia: $R_1 = CH_3$, $R_2 = C(=O)CH_2OH$, R_3 =

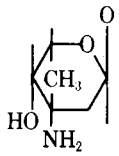

Ib: $R_1 = CH_3$, $R_2 = C(=O)CH_2OH$, $R_3 = OH$

IIa: $R_1 = CH_3$, $R_2 = C(=O)CH_3$, R_3 =

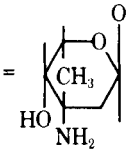

IIb: $R_1 = CH_3$, $R_2 = C(=O)CH_3$, $R_3 = OH$

IIIa: $R_1 = H$, $R_2 = C(=O)CH_3$, R_3 =

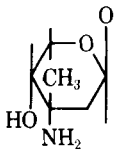

IIIb: $R_1 = H$, $R_2 = C(=O)CH_3$, $R_3 = OH$

IV: $R_1 = H$, $R_2 = C(=O)CH_2OH$, $R_3 = OH$

V: $R_1 = CH_3$ $R_2 = C(=O)CH_2OH$, $R_3 = H$

VI: $R_1 = CH_3$, $R_2 = C(=O)CH_3$, $R_3 = H$

VII: $R_1 = R_3 = H$, $R_2 = C(=O)CH_2OH$

VIII: $R_1 = R_3 = H$, $R_2 = C(=O)CH_3$

IXa: $R_1 = CH_3$, $R_2 = CH(OH)CH_3$, R_3 =

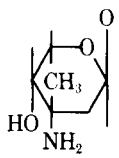

IXb: $R_1 = CH_3$, $R_2 = CH(OH)CH_3$, $R_3 = OH$

Xa: $R_1 = CH_3$, $R_2 = CH(OH)CH_2OH$, R_3 =

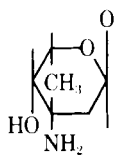

Xb: $R_1 = CH_3$, $R_2 = CH(OH)CH_2OH$, $R_3 = OH$

XI: $R_1 = CH_3$, $R_2 = CH(OH)CH_2OH$, $R_3 = H$

XII: $R_1 = H$, $R_2 = CH(OH)CH_2OH$, $R_3 = OH$

XIII: $R_1 = R_3 = H$, $R_2 = CH(OH)CH_2OH$

XIVa: $R_1 = CH_3$, $R_2 = COOH$, R_3 =

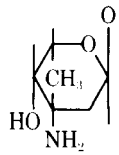

XIVb: $R_1 = CH_3$, $R_2 = COOH$, $R_3 = OH$

XV: $R_1 = H$, $R_2 = COOH$, $R_3 = OH$

crystals gave a melting point of 167°. The high-resolution electron-impact mass spectrum gave a major fragment at *m/e* 324.063, corresponding to M − 60 [HC(=O)CH_2OH] ($C_{18}H_{12}O_6$), which is consistent with the expected structure.

Similarly, 4-demethyldoxorubicinol aglycone (XII) and 4-demethyldoxorubicinone carboxylic acid (XV) were prepared. The mass spectra of the respective pertrimethylsilylated derivatives gave fragments (Table II) consistent with their expected structures.

7-Deoxydoxorubicinol aglycone (XI) was synthesized in a manner similar to that used for V. 4-Demethyl-7-deoxydoxorubicinol aglycone (XIII) was synthesized by a procedure similar to that used for VII. The GLC–mass spectral data (Table II) of their respective pertrimethylsilyl derivatives were consistent with their expected structures.

Pertrimethylsilyl derivatives of these aglycones were prepared using the previously published procedure (12). *O*-Methoxime derivatives and *O*-methoxime silyl derivatives also were obtained (12).

Table I—Mass Spectral Analysis [a] of Pertrimethylsilyl Derivatives of Ia and IIa Analogs

Presumed Fragmentation	*m/e* (Percent Relative Intensity) Trimethylsilyl IIIb	Trimethylsilyl IV	Trimethylsilyl VI	Trimethylsilyl V
M	744 (0)	832 (0)	598 (0)	686 (0)
M − 15	729 (40)	817 (10)	583 (15)	671 (8)
M − 30	714 (90)	802 (20)	568 (100)	656 (25)
M − 15 − side chain	686 (20)	686 (10)	540 (10)	540 (16)
M − 90 − side chain	611 (100)	611 (100)	—	—
M − 15 − 90 − side chain	596 (25)	596 (20)	—	—
M − 30 − 90 − side chain	581 (50)	581 (30)	—	—

[a] Only common major fragments are presented.

Table II—Mass Spectral Analysis [a] of Pertrimethylsilyl Derivatives of I*a* Analogs

Presumed Fragmentation	*m/e* (Percent Relative Intensity) Trimethylsilyl XIV*b*	Trimethylsilyl XV	Trimethylsilyl XII	Trimethylsilyl XI	Trimethylsilyl XIII
M	760 (0)	818 (0)	906 (0)	760 (0)	818 (0)
M − 15	745 (55)	803 (45)	891 (2)	745 (12)	803 (16)
M − 30	730 (100)	788 (85)	876 (1.5)	730 (45)	768 (31)
M − 15 − 90	655 (11)	713 (5)	—	655 (10)	713 (4)
M − 30 − 90	640 (20)	698 (9)	786 (2)	640 (8)	698 (5)
M − side chain	—	—	—	555 (8)	613 (8)
M − 15 − side chain	—	—	686 (3)	540 (20)	598 (17)
M − 30 − side chain	—	670 (4)	—	525 (15)	—
M − 90 − side chain	553 (17)	611 (16)	611 (17)	—	—
M − 15 − 90 − side chain	—	596 (16)	—	—	—
M − 30 − 90 − side chain	523 (26)	581 (20)	581 (7)	—	—
M − 30 − 320 (retro-Diels-Alder)	—	—	—	—	468 (5)

[a] Only common major fragments are presented.

RESULTS AND DISCUSSION

The mass spectra of pertrimethylsilyl derivatives of I*b* and II*b* were reported previously (12). The major common fragments are shown in Table III. As indicated, these two compounds underwent quantitatively and qualitatively similar fragmentations.

Common major mass fragments of the pertrimethylsilyl derivatives[15] of II*b* analogs (III*b*, VI, VIII, and IX*b*) are listed in pairs with the pertrimethylsilyl derivatives of the corresponding analogs of I*b* in Tables I and IV. Similar data for their corresponding pertrimethylsilyl methoxime derivatives[15] are shown in Tables V and VI. In all cases, mass fragmentations were consistent with the proposed structures.

As previously indicated (12), one major mass fragment of trimethyl silyl I*b* and trimethylsilyl II*b*, *m/e* 553, resulting from silanol and side-chain cleavages (Table III), appears to possess diagnostic value capable of reflecting changes on the anthracycline rings. This notion was tested for trimethylsilyl III*b*, where the fragment at *m/e* 611 was the base peak (12) consistent with silanol and side-chain cleavages. A mass unit gain of 58 was observed, representing the addition of a trimethylsilyl group on the demethylated ring A relative to the parent compound, as expected.

Similar fragmentation would be expected for trimethylsilyl IV. Major mass fragmentation of trimethylsilyl IV included cleavages of methyl radicals, the side chain, silanol, and their combinations (Table I). The base peak was at *m/e* 611 (M − silanol − side chain), identical to trimethylsilyl III*b*, as expected. Other fragments exhibited quantitative and qualitative similarity to trimethylsilyl III*b*.

One prominent metabolic pathway of II*a* is a reductive cleavage product at the glycosidic linkage of the D ring (11). By using this approach, the structural change at the D ring could be similarly revealed. The mass spectral data of VI (Table I) showed the usual fragmentations expected for silylated derivatives and the base peak was, indeed, at *m/e* 568 (M − 30). However, unlike other pertrimethylsilyl aglycones, elimination of silanol did not appear to be a favorable process, because of the lack of a hydroxy group at the 7-position. Instead, methyl and side-chain cleavages gave a substantial fragment at *m/e* 540.

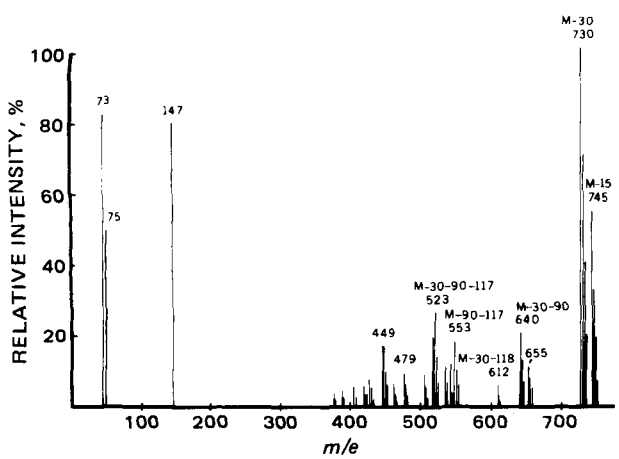

Figure 1—*GLC–mass spectrum of pertrimethylsilyl derivative of XIV*a.

Similar fragmentations were expected for trimethylsilyl V. Its fragmentation data (Table I) exhibited a substantial mass fragment at *m/e* 540 and an overall qualitative resemblance to fragments of trimethylsilyl VI.

The keto side chains of I*b* and II*b* form stable *O*-methoximes with methoxyamine. When this procedure was coupled with persilylation, a volatile derivative with good GLC characteristics was obtained (12). The methoxime appeared to stabilize that side chain with respect to cleavage. Little or no cleavage occurred between the carbonyl side chain and ring D. Thus, a comparison of the mass fragments of the pertrimethylsilyl derivative to those of pertrimethylsilyl methoxime could possibly reveal structural changes of the side chain. The methoxime derivatives of trimethylsilyl III*b* and trimethylsilyl IV (Table V) gave typical fragmentations of silylated compounds without significant side-chain cleavage. However, the lack of an $OSi(CH_3)_3$ group at the 7-position, as in the pertrimethylsilyl methoxime derivatives of V and VI, appeared to decrease the stabilizing effect on the side chain. Consequently, a substantial fragment at *m/e* 524 (M − 30 − side chain) was still observed for these derivatives (Table V).

Minor structural change such as side-chain carbonyl reduction would not be expected to result in a significant alteration in the fragmentation. Thus, trimethylsilyl IX*b* and X*b* gave quantitatively and qualitatively similar fragmentations to each other as well as to their respective parent compounds (Table IV). The mass fragment at *m/e* 553, representing side-chain and silanol elimination, was still one prominent peak of these derivatives. Identical spectra were obtained on their pertrimethylsilyl derivatives after pretreatment with methoxyamine, consistent with a lack of the carbonyl side chain.

A more drastic alteration of the side chain was examined for the corresponding change in fragmentation. Compound XIV*a*, which could conceivably be generated metabolically by oxidation from either I*a* or X*a*, was selected. The mass spectrum of the pertrimethylsilyl derivative of its aglycone, XIV*b*, gave a base peak at *m/e* 730 (M − 30) and two significantly abundant fragments at *m/e* 553 and 523 (Table II and Fig. 1), representing the M − 90 − side chain and M − 30 − side chain, re-

Table III—Mass Spectral Analysis [a] of Pertrimethylsilyl I*b* and II*b*

Presumed Fragmentation	*m/e* (Percent Relative Intensity) Trimethylsilyl I*b*	Trimethylsilyl II*b*
M	774 (1)	686 (1)
M − 15	759 (20)	671 (37)
M − 30	744 (15)	656 (45)
M − side chain	643 (5)	643 (2)
M − 15 − side chain	628 (5)	628 (3)
M − 90 − side chain	553 (100)	553 (80)
M − 15 − 90 − side chain	538 (10)	538 (20)
M − 30 − 90 − side chain	523 (10)	523 (20)
$(CH_3)_2Si\overset{+}{O}Si(CH_3)_3$	147 (20)	147 (10)

[a] Only major fragments are presented.

[15] Mass spectra are available from the authors upon request.

Table IV—Mass Spectral Analysis [a] of Pertrimethylsilyl Derivatives of Ia and IIa Analogs

Presumed Fragmentation	*m/e* (Percent Relative Intensity) Trimethylsilyl VIII	Trimethylsilyl VII	Trimethylsilyl IX*b*	Trimethylsilyl X*b*
M	656 (0)	744 (0)	760 (0)	840 (0)
M − 15	641 (37)	729 (5)	745 (25)	833 (8)
M − 30	626 (100)	714 (9)	730 (12)	818 (8)
M − 15 − side chain	598 (10)	598 (5)	628 (3)	628 (6)
M − 30 − neutral side chain	582 (13)	582 (5)	—	—
M − 30 − 72 − side chain	510 (15)	510 (7)	—	—
M − 90 − side chain	—	—	553 (100)	553 (50)
M − 30 − 90 − side chain	—	—	523 (10)	523 (12)

[a] Only common major fragments are presented.

Table V—Mass Spectral Analysis [a] of Pertrimethylsilyl Methoxime Derivatives of Ia and IIa Analogs

Presumed Fragmentation	*m/e* (Percent Relative Intensity) Pertrimethylsilyl III*b* Methoxime	Pertrimethylsilyl IV Methoxime	Pertrimethylsilyl VI Methoxime	Pertrimethylsilyl V Methoxime
M	773 (10)	861 (0)	627 (0)	715 (0)
M − 15	758 (45)	846 (8)	612 (7)	700 (10)
M − 30	743 (21)	831 (3)	597 (8)	685 (30)
M − 15 − 90	668 (75)	756 (6)	522 (10)	610 (20)
M − 30 − 90	653 (70)	741 (14)	507 (20)	595 (60)
M − 30 − side chain	—	—	524 (10)	524 (75)

[a] Only common major fragments are presented.

spectively. The abundance of the mass fragment at *m/e* 553 is again consistent with the fragmentation trend for I*b* and trimethylsilyl II*b*. As expected from its structure, no derivative was formed with methoxyamine.

A single change of the structure of I*b* and II*b* capable of being derived from metabolic origin reflected definitive and interpretable mass spectral changes as discussed when subjected to the GLC–mass spectral conditions. A combination of these single structural changes should still be reflected by the combined changes in the corresponding mass spectral fragmentation patterns. To test this hypothesis, GLC–mass spectra[15] of the pertrimethylsilyl and pertrimethylsilyl methoxime derivatives of VII, VIII, XI–XIII, and XV were examined (Tables II and IV).

The mass spectrum of VII gave major fragments at *m/e* 729 (M − 15), 714 (M − 30), 598 (M − 15 − side chain), and 582 (M − 30 − neutral side chain), consistent with its structure (Table IV). Its pertrimethylsilyl methoxime derivative (Table VI) also yielded a fragmentation pattern similar to the pertrimethylsilyl methoxime derivative of V. In this case, the mass fragments are interpretable as a combination of methyl and silanol cleavages.

The mass spectral data of the pertrimethylsilyl derivative of XII (Table II) followed closely the combined fragmentation patterns of trimethylsilyl IV and trimethylsilyl X*b*. As expected, a prominent peak at *m/e* 611, representing side-chain and silanol cleavages, was present. Similarly, trimethylsilyl XI gave fragments consistent with its structure (Table II). Side-chain and methyl cleavages giving rise to a fragment at *m/e* 540 appeared to be favorable processes, although the M − 30 peak was also prominent.

Plausible combined metabolic changes on the A and D rings and the side chain resulted in XIII. The pertrimethylsilyl derivative of this synthetic compound exhibited major mass fragments (Table II) at *m/e* 768, 698, 613, 598, and 468, corresponding to M − 30, M − 30 − 90, M − 205 (side chain), M − 15 − 205, and M − 30 − 320, respectively. The last fragment is accountable by a retro-Diels–Alder fragmentation reaction involving the D ring. These fragmentation patterns are essentially the appropriate combinations of those of pertrimethylsilyl derivatives of XI and XII. In addition, no mass spectral changes were observed for this compound after double treatment with methoxime and pertrimethylsilyl formation, indicating a reduction of the carbonyl group.

Combination of side-chain oxidation and demethylation on ring A generated XV (Table II). Major fragments of its pertrimethylsilyl derivatives included the usual methyl and combination of methyl and silanol cleavages. Similar to the acid, the fragment at *m/e* 788 (M − 30) represented one prominent pathway. Nevertheless, a substantial fragment at *m/e* 611 (M − 90 − side chain) marked the demethylation characteristic of the A ring. Consistent with its structure, no methoxime formation was observed.

Table VI—Mass Spectral Analysis [a] of Pertrimethylsilyl Methoxime Derivatives of Ia and IIa Analogs

Presumed Fragmentation	*m/e* (Percent Relative Intensity) Pertrimethylsilyl VIII Methoxime	Pertrimethylsilyl[b] VII Methoxime
M	685 (0)	773 (0)
M − 15	670 (24)	758 (6)
M − 30	655 (28)	743 (60)
M − 73	—	700 (3)
M − 15 − 90	580 (52)	668 (8)
M − 30 − 90	565 (100)	653 (30)
M − 30 − side chain	582 (52)	582 (60)

[a] Only common major fragments are presented. [b] All of the intensities here have been multiplied by 10.

METABOLISM

Both I*a* and II*a* undergo rather extensive hepatic metabolism, giving rise to several fluorescent metabolites (7, 8, 11). Metabolic changes involving *O*-demethylation on the A ring, reduction of the carbonyl group on the side chain, and reductive glycosidic cleavage were proposed on the basis of solid probe mass spectral analysis of the aglycone and other spectroscopic data. With the described GLC–mass spectral techniques, VII, X*b*, XI, and XIII were identified in the hydrolysate of a partially purified rabbit bile 1-butanol extract. The GLC properties of these pertrimethylsilyl and pertrimethylsilyl methoxime derivatives gave excellent chromatographic peaks, and the GLC–mass spectra of these metabolites were identical in all respects with those of the synthetic samples. Details of the isolation and identification of these metabolites, including the evidence of a lack of a metabolic change of the amino sugar moiety on the I*a* metabolites, will be published separately.

REFERENCES

(1) N. R. Bachur and J. C. Craddock, *J. Pharmacol. Exp. Ther.*, **175**, 331 (1970).

(2) N. R. Bachur, *ibid.*, **177**, 153 (1971).

(3) D. H. Huffman, R. S. Benjamin, and N. R. Bachur, *Clin. Pharmacol. Ther.*, **13**, 895 (1972).

(4) D. H. Huffman and N. R. Bachur, *Cancer Res.*, **32**, 600 (1972).

(5) F. H. Bullock, R. J. Bruni, and M. A. Asbell, *J. Pharmacol. Exp. Ther.*, **182**, 70 (1972).

(6) M. A. Asbell, E. Schwartzbach, F. J. Bullock, and D. W. Yesair, *ibid.*, **182**, 63 (1972).

(7) N. R. Bachur, M. J. Egorin, and R. C. Hildebrand, *Biochem. Med.*,

8, 352 (1973).
(8) N. R. Bachur, R. C. Hildebrand, and R. S. Jaenke, *J. Pharmacol. Exp. Ther.*, **191**, 331 (1974).
(9) R. S. Benjamin, C. E. Riggs, Jr., and N. R. Bachur, *Clin. Pharmacol. Ther.*, **14**, 592 (1973).
(10) R. L. Felsted, M. Gee, and N. R. Bachur, *J. Biol. Chem.*, **249**, 3672 (1974).
(11) S. Takanashi and N. R. Bachur, *Drug Metab. Disp.*, **4**, 79 (1976).
(12) E. Watson and K. K. Chan, *J. Pharm. Sci.*, **67**, 1243 (1978).
(13) A. S. Kende, Y. G. Tsay, and J. E. Mills, *J. Am. Chem. Soc.*, **98**, 1967 (1976).
(14) T. H. Smith, A. N. Fujiwara, D. W. Henry, and W. W. Lee, *ibid.*, **98**, 1978 (1976).

ACKNOWLEDGMENTS

Supported by Contracts N01-CM-23241 and N01-CM-67065 of the Division of Cancer Treatment, National Cancer Institute.

The assistance of Dr. Sue Rotschaeffer, Analytical Facilities, California Institute of Technology, Pasadena, Calif., for the high-resolution mass spectra is appreciated.

NOTES

Limit Test for Determination of Free Ferricyanide and Ferrocyanide in Sodium Nitroferricyanide

CHARLESWORTH E. PHILIP, FELISA S. MANALILI, HERMINIA J. UMAGAT, ROBERT B. HAGEL, and RALPH GOMEZ ˣ

Received January 12, 1978, from the *Research Products and Diagnostics Section, Quality Control Department, Hoffmann-La Roche Inc., Nutley, NJ 07110.* Accepted for publication April 25, 1978.

Abstract □ A simple and rapid procedure for the isolation and determination of free ferricyanide and ferrocyanide in sodium nitroferricyanide (nitroprusside) was developed. The method, employing aluminum oxide column chromatography, was sensitive enough to detect ferricyanide and ferrocyanide at the 0.05% level.

Keyphrases □ Sodium nitroferricyanide (nitroprusside)—prepared solutions, chromatographic separation and spectrophotometric analyses of free ferricyanide and ferrocyanide □ Ferricyanide and ferrocyanide, free—chromatographic separation and spectrophotometric analyses in prepared solutions of sodium nitroferricyanide (nitroprusside) □ Antihypertensives—sodium nitroferricyanide (nitroprusside), prepared solutions, chromatographic separation and spectrophotometric analyses of free ferricyanide and ferrocyanide

Sodium nitroferricyanide (nitroprusside) (I) has been used extensively as an analytical reagent, primarily for the detection of organic compounds such as ketones and aldehydes, and recently it has gained stature as a potent antihypertensive in acute hypertensive crises (1–6). Since the mode of administration is intravenous infusion, a high quality substance is required. As a result, analytical methodology for the determination of purity and potency of I in pharmaceutical preparations is needed. Methodology and specifications are available for reagent grade material (7–9), but these methods are not suitable for a parenteral grade pharmaceutical product.

Two potential contaminants in I are free ferricyanide and ferrocyanide. Existing methods for the analysis of these two impurities are limit tests in which a faint color or turbidity is detected in the solution if the contaminants are present (7, 9). However, at levels near and below 0.05% ferricyanide and ferrocyanide, it is extremely difficult to detect these subtle changes in the sample solution. This paper reports a simple and rapid procedure for the isolation and determination of ferricyanide and ferrocyanide in I at the 0.05% level. The method involves the chromatographic separation of ferricyanide and ferrocyanide from I on an alumina column by a series of elutions of increasing acid strengths. Ferricyanide and ferrocyanide are determined spectrophotometrically at 415 nm.

The limit of 0.05% is realistic because of the relatively lower toxicity of ferricyanide and ferrocyanide *versus* I. The oral LD_{50} in rats for ferricyanide and ferrocyanide is 1600 mg/kg; for I, it is 20 mg/kg (10, 11).

EXPERIMENTAL

Reagents—Neutral aluminum oxide[1], activity grade I, was used as received. All other chemicals were ACS reagent grade or equivalent and were used without further purification.

Column Preparation—Amber glass columns, 1.45 cm i.d., fitted with polytef stopcocks, were each dry filled with 7 g of aluminum oxide.

Standard Solution—A solution containing 15.5 mg of potassium ferricyanide and 19.9 mg of potassium ferrocyanide trihydrate in 100 ml of 1 *N* HNO_3 was prepared.

Sample Solutions—Solutions of sodium nitroferricyanide at a concentration of 200 mg/ml were prepared in 1 *N* HNO_3.

Procedure—Aliquots of 2.0 ml of sample solutions and 2.0 ml of standard solution were placed on individual columns. The columns were eluted with 35 ml of 0.5 *N* HNO_3, which was discarded. Ferricyanide was then eluted with 25 ml of 2 *N* HNO_3, and ferrocyanide was eluted with 25 ml of 6 *N* HNO_3. The absorbances of the solutions were measured in 1-cm cells at 415 nm. If the sample absorbances were lower than the standard absorbances, the sample contained less than 0.05% each of ferricyanide and ferrocyanide.

RESULTS AND DISCUSSION

Complete separation of ferricyanide $[Fe(CN)_6^{3-}]$ and ferrocyanide $[Fe(CN)_6^{4-}]$ from I $[Na_2Fe(CN)_5NO]$ was achieved by column chromatography with aluminum oxide as the adsorbent. Determination at the 0.05% level was achieved by comparing the sample absorbances at 415 nm to those of the standards.

The dependence of ferricyanide and ferrocyanide recovery on the acid strength of the final elution was investigated. To each of several columns, 0.2 mg of ferricyanide was applied and the columns were eluted as pre-

[1] Woelm, ICN Pharmaceuticals.

0022-3549/78/1200-1752$01.00/0
© 1978, American Pharmaceutical Association

8, 352 (1973).
(8) N. R. Bachur, R. C. Hildebrand, and R. S. Jaenke, *J. Pharmacol. Exp. Ther.*, **191**, 331 (1974).
(9) R. S. Benjamin, C. E. Riggs, Jr., and N. R. Bachur, *Clin. Pharmacol. Ther.*, **14**, 592 (1973).
(10) R. L. Felsted, M. Gee, and N. R. Bachur, *J. Biol. Chem.*, **249**, 3672 (1974).
(11) S. Takanashi and N. R. Bachur, *Drug Metab. Disp.*, **4**, 79 (1976).
(12) E. Watson and K. K. Chan, *J. Pharm. Sci.*, **67**, 1243 (1978).
(13) A. S. Kende, Y. G. Tsay, and J. E. Mills, *J. Am. Chem. Soc.*, **98**, 1967 (1976).
(14) T. H. Smith, A. N. Fujiwara, D. W. Henry, and W. W. Lee, *ibid.*, **98**, 1978 (1976).

ACKNOWLEDGMENTS

Supported by Contracts N01-CM-23241 and N01-CM-67065 of the Division of Cancer Treatment, National Cancer Institute.

The assistance of Dr. Sue Rotschaeffer, Analytical Facilities, California Institute of Technology, Pasadena, Calif., for the high-resolution mass spectra is appreciated.

NOTES

Limit Test for Determination of Free Ferricyanide and Ferrocyanide in Sodium Nitroferricyanide

CHARLESWORTH E. PHILIP, FELISA S. MANALILI, HERMINIA J. UMAGAT, ROBERT B. HAGEL, and RALPH GOMEZ ˣ

Received January 12, 1978, from the *Research Products and Diagnostics Section, Quality Control Department, Hoffmann-La Roche Inc., Nutley, NJ 07110.* Accepted for publication April 25, 1978.

Abstract □ A simple and rapid procedure for the isolation and determination of free ferricyanide and ferrocyanide in sodium nitroferricyanide (nitroprusside) was developed. The method, employing aluminum oxide column chromatography, was sensitive enough to detect ferricyanide and ferrocyanide at the 0.05% level.

Keyphrases □ Sodium nitroferricyanide (nitroprusside)—prepared solutions, chromatographic separation and spectrophotometric analyses of free ferricyanide and ferrocyanide □ Ferricyanide and ferrocyanide, free—chromatographic separation and spectrophotometric analyses in prepared solutions of sodium nitroferricyanide (nitroprusside) □ Antihypertensives—sodium nitroferricyanide (nitroprusside), prepared solutions, chromatographic separation and spectrophotometric analyses of free ferricyanide and ferrocyanide

Sodium nitroferricyanide (nitroprusside) (I) has been used extensively as an analytical reagent, primarily for the detection of organic compounds such as ketones and aldehydes, and recently it has gained stature as a potent antihypertensive in acute hypertensive crises (1–6). Since the mode of administration is intravenous infusion, a high quality substance is required. As a result, analytical methodology for the determination of purity and potency of I in pharmaceutical preparations is needed. Methodology and specifications are available for reagent grade material (7–9), but these methods are not suitable for a parenteral grade pharmaceutical product.

Two potential contaminants in I are free ferricyanide and ferrocyanide. Existing methods for the analysis of these two impurities are limit tests in which a faint color or turbidity is detected in the solution if the contaminants are present (7, 9). However, at levels near and below 0.05% ferricyanide and ferrocyanide, it is extremely difficult to detect these subtle changes in the sample solution. This paper reports a simple and rapid procedure for the isolation and determination of ferricyanide and ferrocyanide in I at the 0.05% level. The method involves the chromatographic separation of ferricyanide and ferrocyanide from I on an alumina column by a series of elutions of increasing acid strengths. Ferricyanide and ferrocyanide are determined spectrophotometrically at 415 nm.

The limit of 0.05% is realistic because of the relatively lower toxicity of ferricyanide and ferrocyanide *versus* I. The oral LD_{50} in rats for ferricyanide and ferrocyanide is 1600 mg/kg; for I, it is 20 mg/kg (10, 11).

EXPERIMENTAL

Reagents—Neutral aluminum oxide[1], activity grade I, was used as received. All other chemicals were ACS reagent grade or equivalent and were used without further purification.

Column Preparation—Amber glass columns, 1.45 cm i.d., fitted with polytef stopcocks, were each dry filled with 7 g of aluminum oxide.

Standard Solution—A solution containing 15.5 mg of potassium ferricyanide and 19.9 mg of potassium ferrocyanide trihydrate in 100 ml of 1 *N* HNO_3 was prepared.

Sample Solutions—Solutions of sodium nitroferricyanide at a concentration of 200 mg/ml were prepared in 1 *N* HNO_3.

Procedure—Aliquots of 2.0 ml of sample solutions and 2.0 ml of standard solution were placed on individual columns. The columns were eluted with 35 ml of 0.5 *N* HNO_3, which was discarded. Ferricyanide was then eluted with 25 ml of 2 *N* HNO_3, and ferrocyanide was eluted with 25 ml of 6 *N* HNO_3. The absorbances of the solutions were measured in 1-cm cells at 415 nm. If the sample absorbances were lower than the standard absorbances, the sample contained less than 0.05% each of ferricyanide and ferrocyanide.

RESULTS AND DISCUSSION

Complete separation of ferricyanide $[Fe(CN)_6^{3-}]$ and ferrocyanide $[Fe(CN)_6^{4-}]$ from I $[Na_2Fe(CN)_5NO]$ was achieved by column chromatography with aluminum oxide as the adsorbent. Determination at the 0.05% level was achieved by comparing the sample absorbances at 415 nm to those of the standards.

The dependence of ferricyanide and ferrocyanide recovery on the acid strength of the final elution was investigated. To each of several columns, 0.2 mg of ferricyanide was applied and the columns were eluted as pre-

[1] Woelm, ICN Pharmaceuticals.

0022-3549/78/1200-1752$01.00/0
© 1978, American Pharmaceutical Association

Table I—Addition of Ferricyanide and Ferrocyanide to I

Amount Added, %			Number of
Ferricyanide	Ferrocyanide	Recovery, %	Runs
0.05	—	0.047 ± 0.004	7
—	0.05	0.047 ± 0.005	7
0.04	—	0.037 ± 0.008	5
—	0.04	0.041 ± 0.014	5
0.03	—	0.031 ± 0.005	6
—	0.03	0.024 ± 0.004	6

viously described with the exception of the final wash. Here the nitric acid concentration was varied on individual columns from 1.0 to 2.5 *N*, and 25.0 ml of eluate was collected. A similar experiment using ferrocyanide was carried out using nitric acid strengths up to 6 *N*.

At nitric acid concentrations of 1.0 *N* and below, no ferricyanide was eluted; full recovery was obtained at an acid strength of 1.8 *N* and above. Ferrocyanide started eluting when the nitric acid concentration reached 2.5 *N*. At nitric acid strengths of 4.0 *N*, there was evidence that elution was still incomplete. An acid strength of 6.0 *N* eluted ferrocyanide completely. As a result of these data, nitric acid concentrations of 2.0 and 6.0 *N* were chosen for the ferricyanide and ferrocyanide elutions, respectively.

To verify the column results, a TLC separation of I, ferricyanide, and ferrocyanide was performed on aluminum oxide plates with 2.0 *N* HNO_3 as the developer. As with the column separation, I and ferricyanide traveled to the solvent front while ferrocyanide remained at the origin.

The linearity of the spectrophotometric response to changes in ferricyanide and ferrocyanide concentrations was evaluated. Known amounts of potassium ferricyanide and potassium ferrocyanide trihydrate were subjected to chromatography, and the absorbances of the solutions were determined spectrophotometrically. A plot of absorbance *versus* concentration was linear from 2 to 30 μg of ferricyanide and ferrocyanide/ml. Since a sample size of 400 mg was chosen to assure nonoverloading of the column, 8 μg each of ferricyanide and ferrocyanide/ml represented 0.05% of the I content. This concentration is well within the region of linear response.

To determine whether ferricyanide and ferrocyanide could be determined accurately at levels below 0.05%, known concentrations of each were added to I and the solutions were analyzed according to the procedure (Table I). The data indicate that the precision and accuracy of the method are lower than those normally acceptable for a quantitative determination. However, its use as a limit test is justified since the recoveries of both ferricyanide and ferrocyanide are at least semiquantitative when added to I.

Compared to the limit tests currently available for the determination of ferricyanide and ferrocyanide in I, this procedure offers the following advantages:

1. Semiquantitation of the contaminants, if more than a limit test is required, is possible.
2. The results are reproducible.
3. The preparation of reagents, samples, and standards is simple.
4. The procedure can be carried out rapidly.

Since I is now accepted and used as a pharmaceutical preparation, this improved procedure for controlling two possible contaminants will help in maintaining and ensuring the purity and integrity of the product.

REFERENCES

(1) N. H. Guiha, J. H. Cohn, E. Mikulic, J. Franciosa, and C. J. Limas, *N. Engl. J. Med.*, **291**, 587 (1974).

(2) G. O. Jones and P. Cole, *Br. J. Anaesth.*, **40**, 804 (1968).

(3) N. P. Keaney, O. G. McDowell, J. M. Turner, J. R. Lane, and Y. Okuda, *ibid.*, **45**, 639 (1973).

(4) J. Koch-Weser, *Arch. Intern. Med.*, **133**, 1017 (1974).

(5) I. H. Page, A. C. Corcoran, H. P. Dustan, and T. Koppanyi, *Circulation*, **11**, 188 (1955).

(6) I. H. Tuzel, *J. Clin. Pharmacol.*, **14**, 494 (1974).

(7) J. Rosin, "Reagent Chemicals and Standards," 5th ed., Van Nostrand, Princeton, N.J., 1967, p. 472.

(8) "Reagent Chemicals, American Chemical Society Specifications," 4th ed., American Chemical Society, Washington, D.C., 1968, p. 551.

(9) "British Pharmacopoeia 1973," Her Majesty's Stationery Office, London, England, 1973, p. A47.

(10) "Registry of Toxic Effects of Chemical Substances," U.S. Department of Health, Education, and Welfare, Rockville, Md., 1976, pp. 537, 538.

(11) "Industrial Hygiene and Toxicology," vol. II, F. A. Patty, Ed., Interscience, New York, N.Y., 1963, p. 2036.

ACKNOWLEDGMENTS

The authors acknowledge the assistance of the Scientific Literature Department of Hoffmann-La Roche Inc.

Determination of Carbocysteine from Human Plasma

WILLIAM R. MAYNARD ˣ, R. B. BRUCE, and GENEVIEVE G. FOX

Received August 3, 1977, from the *A. H. Robins Company, Inc., Richmond, VA 23220.* Accepted for publication March 30, 1978.

Abstract □ A fast and accurate GLC procedure for determining carbocysteine, using a sulfur photometric detector, is described. Interferences from nonsulfur constituents are eliminated. The method is linear from 2 to 15 μg. Results from the application of this method to a bioavailability study in humans are given.

Keyphrases □ Carbocysteine—GLC analysis in plasma □ GLC—analysis, carbocysteine in plasma □ Mucolytic agents—carbocysteine, GLC analysis in plasma

Carbocysteine, *S*-(carboxymethyl)cysteine, has been undergoing clinical evaluation as a mucolytic agent. Therefore, it was of interest to determine the pharmacokinetic parameters of this drug, and an analytical method was needed.

Carbocysteine has properties typical of amino acids and has been determined in biological materials by ion-exchange chromatography (1). That method is time consuming and did not appear practical. GLC procedures are more rapid and have varying degrees of success using trifluoroacetic anhydride derivatization with flame-ionization detection (2–8). In general, these methods require temperature programming, which is undesirable.

Since carbocysteine contains a sulfur atom, the use of a flame photometric detector in the sulfur mode appeared logical. Concentration of the drug through extraction into an organic solvent would also help in derivatization. Such a method was found to be of value by adopting Maynard's (9) procedure for extracting piperazine from an aqueous solution. That this method may be applicable to the analysis of other amino acids was demonstrated by

0022-3549/78/1200-1753$01.00/0

© 1978, American Pharmaceutical Association

Table I—Addition of Ferricyanide and Ferrocyanide to I

Amount Added, %			Number of
Ferricyanide	Ferrocyanide	Recovery, %	Runs
0.05	—	0.047 ± 0.004	7
—	0.05	0.047 ± 0.005	7
0.04	—	0.037 ± 0.008	5
—	0.04	0.041 ± 0.014	5
0.03	—	0.031 ± 0.005	6
—	0.03	0.024 ± 0.004	6

viously described with the exception of the final wash. Here the nitric acid concentration was varied on individual columns from 1.0 to 2.5 *N*, and 25.0 ml of eluate was collected. A similar experiment using ferrocyanide was carried out using nitric acid strengths up to 6 *N*.

At nitric acid concentrations of 1.0 *N* and below, no ferricyanide was eluted; full recovery was obtained at an acid strength of 1.8 *N* and above. Ferrocyanide started eluting when the nitric acid concentration reached 2.5 *N*. At nitric acid strengths of 4.0 *N*, there was evidence that elution was still incomplete. An acid strength of 6.0 *N* eluted ferrocyanide completely. As a result of these data, nitric acid concentrations of 2.0 and 6.0 *N* were chosen for the ferricyanide and ferrocyanide elutions, respectively.

To verify the column results, a TLC separation of I, ferricyanide, and ferrocyanide was performed on aluminum oxide plates with 2.0 *N* HNO_3 as the developer. As with the column separation, I and ferricyanide traveled to the solvent front while ferrocyanide remained at the origin.

The linearity of the spectrophotometric response to changes in ferricyanide and ferrocyanide concentrations was evaluated. Known amounts of potassium ferricyanide and potassium ferrocyanide trihydrate were subjected to chromatography, and the absorbances of the solutions were determined spectrophotometrically. A plot of absorbance *versus* concentration was linear from 2 to 30 μg of ferricyanide and ferrocyanide/ml. Since a sample size of 400 mg was chosen to assure nonoverloading of the column, 8 μg each of ferricyanide and ferrocyanide/ml represented 0.05% of the I content. This concentration is well within the region of linear response.

To determine whether ferricyanide and ferrocyanide could be determined accurately at levels below 0.05%, known concentrations of each were added to I and the solutions were analyzed according to the procedure (Table I). The data indicate that the precision and accuracy of the method are lower than those normally acceptable for a quantitative determination. However, its use as a limit test is justified since the recoveries of both ferricyanide and ferrocyanide are at least semiquantitative when added to I.

Compared to the limit tests currently available for the determination of ferricyanide and ferrocyanide in I, this procedure offers the following advantages:

1. Semiquantitation of the contaminants, if more than a limit test is required, is possible.
2. The results are reproducible.
3. The preparation of reagents, samples, and standards is simple.
4. The procedure can be carried out rapidly.

Since I is now accepted and used as a pharmaceutical preparation, this improved procedure for controlling two possible contaminants will help in maintaining and ensuring the purity and integrity of the product.

REFERENCES

(1) N. H. Guiha, J. H. Cohn, E. Mikulic, J. Franciosa, and C. J. Limas, *N. Engl. J. Med.*, **291**, 587 (1974).

(2) G. O. Jones and P. Cole, *Br. J. Anaesth.*, **40**, 804 (1968).

(3) N. P. Keaney, O. G. McDowell, J. M. Turner, J. R. Lane, and Y. Okuda, *ibid.*, **45**, 639 (1973).

(4) J. Koch-Weser, *Arch. Intern. Med.*, **133**, 1017 (1974).

(5) I. H. Page, A. C. Corcoran, H. P. Dustan, and T. Koppanyi, *Circulation*, **11**, 188 (1955).

(6) I. H. Tuzel, *J. Clin. Pharmacol.*, **14**, 494 (1974).

(7) J. Rosin, "Reagent Chemicals and Standards," 5th ed., Van Nostrand, Princeton, N.J., 1967, p. 472.

(8) "Reagent Chemicals, American Chemical Society Specifications," 4th ed., American Chemical Society, Washington, D.C., 1968, p. 551.

(9) "British Pharmacopoeia 1973," Her Majesty's Stationery Office, London, England, 1973, p. A47.

(10) "Registry of Toxic Effects of Chemical Substances," U.S. Department of Health, Education, and Welfare, Rockville, Md., 1976, pp. 537, 538.

(11) "Industrial Hygiene and Toxicology," vol. II, F. A. Patty, Ed., Interscience, New York, N.Y., 1963, p. 2036.

ACKNOWLEDGMENTS

The authors acknowledge the assistance of the Scientific Literature Department of Hoffmann-La Roche Inc.

Determination of Carbocysteine from Human Plasma

WILLIAM R. MAYNARD ˣ, R. B. BRUCE, and GENEVIEVE G. FOX

Received August 3, 1977, from the *A. H. Robins Company, Inc., Richmond, VA 23220.* Accepted for publication March 30, 1978.

Abstract □ A fast and accurate GLC procedure for determining carbocysteine, using a sulfur photometric detector, is described. Interferences from nonsulfur constituents are eliminated. The method is linear from 2 to 15 μg. Results from the application of this method to a bioavailability study in humans are given.

Keyphrases □ Carbocysteine—GLC analysis in plasma □ GLC—analysis, carbocysteine in plasma □ Mucolytic agents—carbocysteine, GLC analysis in plasma

Carbocysteine, *S*-(carboxymethyl)cysteine, has been undergoing clinical evaluation as a mucolytic agent. Therefore, it was of interest to determine the pharmacokinetic parameters of this drug, and an analytical method was needed.

Carbocysteine has properties typical of amino acids and has been determined in biological materials by ion-exchange chromatography (1). That method is time consuming and did not appear practical. GLC procedures are more rapid and have varying degrees of success using trifluoroacetic anhydride derivatization with flame-ionization detection (2–8). In general, these methods require temperature programming, which is undesirable.

Since carbocysteine contains a sulfur atom, the use of a flame photometric detector in the sulfur mode appeared logical. Concentration of the drug through extraction into an organic solvent would also help in derivatization. Such a method was found to be of value by adopting Maynard's (9) procedure for extracting piperazine from an aqueous solution. That this method may be applicable to the analysis of other amino acids was demonstrated by

0022-3549/78/1200-1753$01.00/0

© 1978, American Pharmaceutical Association

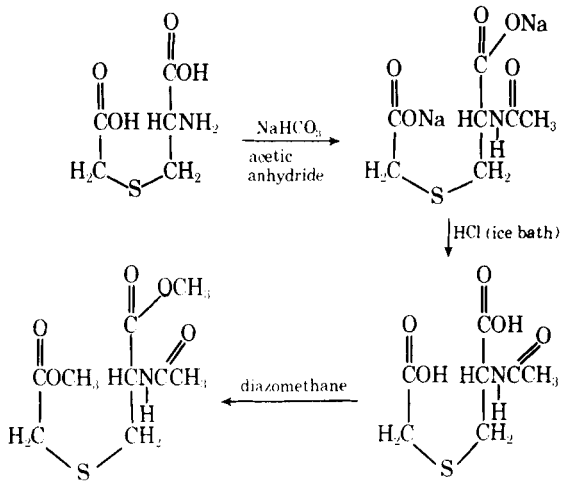

Scheme I

applying it to methionine, cystine, and cysteine.

EXPERIMENTAL

Reagents—Ethyl acetate and chloroform were ultrapure[1]; sodium bicarbonate, hydrochloric acid, and anhydrous sodium sulfate were reagent grade. Diazomethane was generated from nitrosomethylurea with 40% potassium hydroxide in chloroform and redistilled (10).

S-(2-Carboxyethyl)cysteine, the internal standard, was synthesized by refluxing a sodium hydroxide solution of L-cysteine hydrochloride with chloropropionic acid under nitrogen. The resulting compound was precipitated by adjusting to pH 2–3 with 6 *N* HCl. It was further purified by reprecipitation from water with 6 *N* HCl, mp 230° dec.

Anal.—Calc. for $C_6H_{11}NO_4S$: C, 32.29; H, 5.74; N, 7.25. Found: C, 36.88; H, 5.74; N, 7.20.

Equipment—The gas chromatograph[2] was equipped with a sulfur–phosphorus emission detector[2]. The column was glass, 1.2 m × 2 mm i.d., packed with 15% Apiezon-L on 100–120-mesh Gas Chrom P and silanized[3]. The column temperature was 185°; the injector and detector were at 295°. The carrier was nitrogen at a flow rate of 25 ml/min.

Structures of all compounds and their derivatives (Scheme I) were confirmed with a mass spectrometer[4] by a direct probe method.

Drug Administration—Eleven healthy, normal male subjects[5] received 1.0-g doses of carbocysteine orally. On 1 day, they received the drug as a capsule; 3 days later, they received it as a suspension. Blood samples were taken at intervals, and the plasma was separated and analyzed for carbocysteine.

Analytical Method—The plasma sample (1.0 ml) was pipetted into a 50-ml glass-stoppered centrifuge tube, and 10 μg of the internal standard in water was added. Then the solution was diluted to 4.0 ml with water and saturated with sodium bicarbonate (Scheme I). An excess of approximately 25 mg of sodium bicarbonate was added. Then 1.0 ml of acetic anhydride was added cautiously; the mixture was shaken gently and then mixed for 1 min on a vortex mixer or until there was no further evolution of carbon dioxide. The sample was then cooled in an ice bath and made acidic with concentrated hydrochloric acid (~2 ml).

The aqueous mixture was extracted with two 20-ml portions of ethyl acetate, and each extract was filtered through a layer of anhydrous sodium sulfate into a large test tube (~25 × 200 mm). The sodium sulfate was washed with 3 ml of ethyl acetate. The solution was evaporated in a hot water bath (about 80°) under a nitrogen stream to 5 ml, and the ethyl acetate solution was transferred to a 15-ml centrifuge tube. This solution was evaporated to dryness using the same conditions. The tube was cooled in an ice bath, and diazomethane in chloroform was added with mixing until the solution remained yellow for 1 min. Then this solution was evaporated to approximately 200 μl and mixed, and 10 μl was injected into the gas chromatograph.

The retention times of the derivatives of carbocysteine and the internal standard were 4.9 and 6.7 min, respectively.

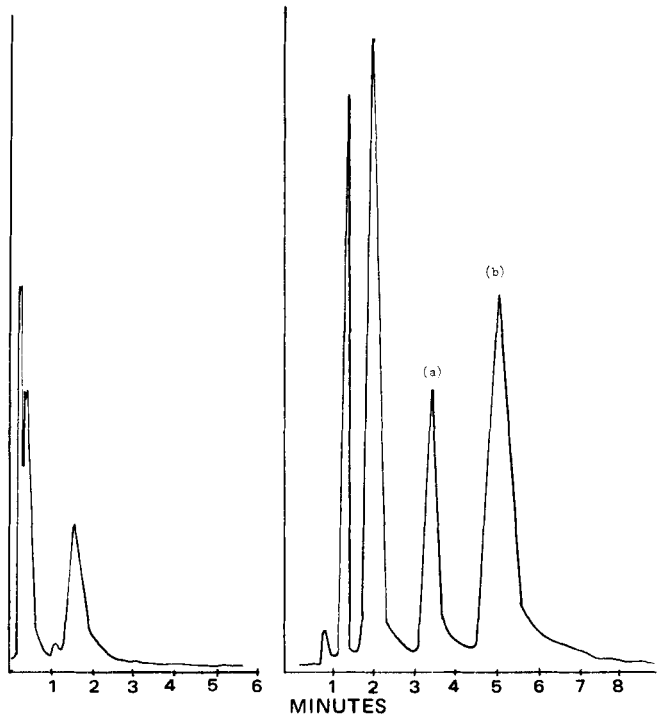

Figure 1—*Chromatograms of control plasma (left) and plasma containing carbocysteine (a) and S-(2-carboxyethyl)cysteine (b).*

Standard Curve and Calculations—A standard curve was prepared using 1.0 ml of plasma for each determination. Known concentrations of carbocysteine from 2.0 to 15.0 μg were added to each tube, followed by 10.0 μg of the internal standard.

The response of the flame photometric detector, as pointed out by Brody and Chaney (11), is exponentially proportional to the number of sulfur atoms in the molecule. To obtain a straight-line relationship between the response and concentration of carbocysteine, the square root of the peak height must be used rather than the simple peak height. The ratio obtained by dividing the square root of the peak height of the known concentration of the sample by the square root of the peak height of the internal standard was plotted against the amount added to obtain the calibration curve. The concentration of the sample in the aliquot taken for analysis was calculated from this calibration curve.

RESULTS AND DISCUSSION

Typical chromatograms obtained following the analysis of control plasma and of plasma containing both the internal standard and carbocysteine are shown in Fig. 1. These chromatograms do not show solvent peaks usually associated with GLC because early eluting gases, including solvents, were vented away from the detector to prevent undue contamination. However, the retention times were specific and easily repeated. No interferences were found from control samples carried through the procedure. It was necessary to silanize the column and to clean the detector following the injection of 150–200 samples.

The possibility existed of interference of other sulfur-containing amino acids whose derivatives might be extracted from blood. Aqueous solutions of methionine, L-cystine, and L-cysteine were carried through the described procedure. The structures of their derivatives were confirmed by mass spectra and then chromatographed. The cysteine derivative had a retention time of 3 min at a column temperature of 160°, the methionine derivative had a retention time of 3 min at 170°, and cystine had a retention time of 4 min at 250°. These compounds would not interfere under the method conditions. Similar GLC procedures for these amino acids probably could be easily developed.

Another source of possible interference is metabolites of the administered drug. Biotransformation of carbocysteine was studied[6] (12, 13). The major metabolites in humans, monkeys, dogs, and rats are inorganic

[1] Nanograde, Mallinckrodt Chemical Co.
[2] Bendix 2500 Series, Bendix Corp., Lewisburg, W. Va.
[3] Rejuv-8, Supelco, Inc.
[4] Hitachi RMU-6.
[5] Informed written consent was obtained.
[6] To be published.

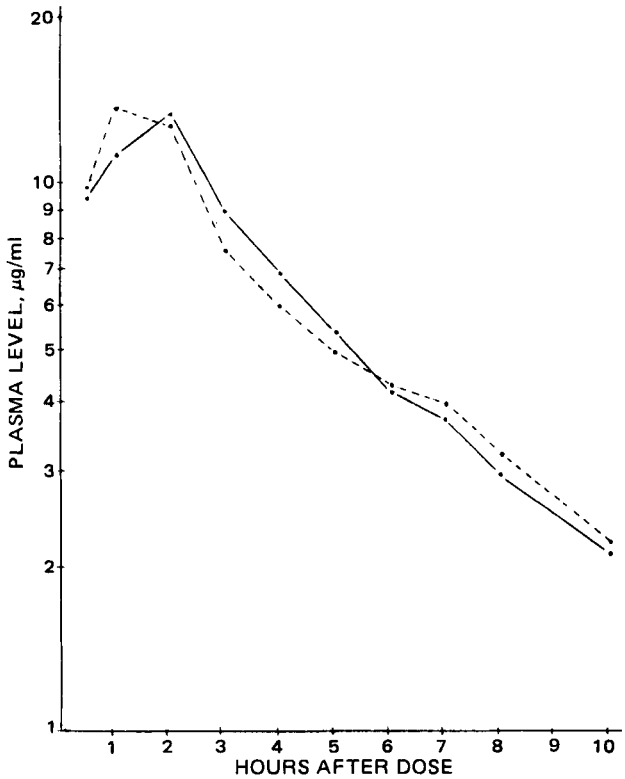

Figure 2—*Mean plasma carbocysteine levels in humans. Key: - - -, suspension; and —, tablet.*

sulfate and thiodiglycolic acid. A sample of this acid was carried through the described procedure and did not interfere. The dimethyl ester formed had a retention time of approximately 4 min at 170°. Like the cysteine and methionine derivatives, this compound would be discarded in the vented gas.

Recoveries of known amounts of carbocysteine added to control plasma are shown in Table I, together with standard deviations at low, medium, and high levels. These results indicate that the described procedure should be satisfactory for the determination of this compound in plasma.

The extraction procedure used for the amino acid was of primary interest and warranted further investigation. A consistent amount is extracted in this procedure, but the absolute amount is not indicated. This value was determined with ^{34}S-carbocysteine. A solution of 15 μg/ml of control plasma was prepared, and the radioactivity was determined before extraction and in the extract. The experiment was done with four samples of plasma; 72.8 ± 5.4% was extracted as the *N*-acetyl derivative.

Table I—Recovery of Known Amounts of Carbocysteine Added to Control Human Plasma

Amount Added, μg/ml	Amount Found (±*SD*[a]), μg/ml
2.0	2.08
2.5	2.58 (±0.050)
3.0	3.27
4.0	3.91
6.0	6.01
7.5	7.58 (±0.136)
9.0	9.23
10.0	10.1
12.0	12.1
15.0	15.3 (±0.39)

[a] From six determinations.

To illustrate the usefulness of this method, the results obtained from a bioavailability study are plotted in Fig. 2. This figure gives the mean values of the plasma levels for the 11 subjects (see *Experimental*). Maximum levels were obtained within 2 hr and were approximately 13 μg/ml; after 10 hr, they had declined to about 2 μg/ml. Standard errors at the two intervals were 1.38 and 0.46, respectively.

REFERENCES

(1) F. W. Wagner and S. L. Shepherd, *Anal. Biochem.*, **41**, 314 (1971).

(2) C. Zomzely, G. Marco, and E. Emergy, *Anal. Chem.*, **34**, 1414 (1962).

(3) P. A. Cruickshank and J. C. Sheehan, *ibid.*, **36**, 1191 (1965).

(4) S. Makisumi and H. A. Saroff, *J. Gas Chromatogr.*, **3**, 21 (1965).

(5) C. W. Gehrke, W. M. Lamkin, D. L. Stalling, and F. Shahrokhi, *Biophys. Res. Commun.*, **19**, 328 (1965).

(6) W. M. Lamkin and C. W. Gehrke, *Anal. Chem.*, **37**, 383 (1965).

(7) N. Ikekawa, O. Hoshino, and R. Watanuki, *Anal. Biochem.*, **17**, 16 (1966).

(8) C. W. Gehrke, K. Kuo, and R. W. Zumwalt, *J. Chromatogr.*, **57**, 209 (1971).

(9) W. R. Maynard, *J. Assoc. Offic. Anal. Chem.*, **42**, 610 (1959).

(10) F. Arndt, "Organic Syntheses," coll. vol. 2, 2nd ed., Wiley, New York, N.Y., 1943, p. 165.

(11) S. S. Brody and J. E. Chaney, *J. Gas Chromatogr.*, **4**, 42 (1966).

(12) F. R. Blood and H. B. Lewis, *J. Biol. Chem.*, **139**, 407 (1941).

(13) A. Fiori, M. Costa, and E. Banoni, *Physiol. Chem. Phys.*, **4**, 457 (1972).

ACKNOWLEDGMENTS

The authors thank Dr. Lina Teng for the preparation and purification of the *S*-(2-carboxyethyl)cysteine used as the internal standard.

High-Pressure Liquid Chromatographic Determination of Plasma Dobutamine Concentrations

D. W. McKENNON and R. E. KATES *x

Received February 17, 1978, from the *College of Pharmacy, Ohio State University, Columbus, OH 43210.* Accepted for publication March 31, 1978. *Present address: Cardiology Division, Stanford University Medical Center, Stanford, CA 94305.

Abstract □ A sensitive and specific high-pressure liquid chromatographic method was developed for measuring dobutamine in human plasma samples. Nylidrin is employed as an internal standard. Following extraction and separation on a C_{18} reversed-phase column, the drug is detected by a fluorescence detector with an excitation wavelength of 195 nm and a 330-nm emission cutoff filter. The retention times of dobutamine and nylidrin are 5.2 and 19.2 min, respectively. The minimum level of sensitivity is 10 ng/ml. Reproducibility was ±5% over a 25–300-ng/ml range. Several drugs were screened for possible interference, but none interfered with the dobutamine analysis.

Keyphrases □ Dobutamine—high-pressure liquid chromatographic analysis in plasma □ High-pressure liquid chromatography—analysis, dobutamine in plasma □ Cardiotonic agents—dobutamine, high-pressure liquid chromatographic analysis in plasma

Dobutamine (I), a synthetic catecholamine, was developed in an effort to find an ideal inotropic drug (1). Studies in patients with severe heart failure showed that dobutamine increases ventricular contractility and cardiac output without substantially increasing heart rate or systemic blood pressure (2). Dobutamine is structurally similar to dopamine (II) but does not appear to share the positive chronotropic or pressor effects seen with dopamine or other inotropic agents.

To investigate the pharmacokinetics and plasma level–effect relationships for this drug, it was necessary first to develop a rapid, specific, and sensitive analytical method for measuring dobutamine in human plasma samples. Since dobutamine is a naturally fluorescing compound, a high-pressure liquid chromatographic (HPLC) procedure utilizing a fluorescence detector was developed.

EXPERIMENTAL

Chemicals and Reagents—Dobutamine[1] and nylidrin[2] were obtained as the hydrochloride salts, and methoxydobutamine[1] was obtained as the free base. Glass-distilled[3] ethyl acetate, methanol, and acetonitrile were used as obtained without further purification. A solution of 5 *M* K_2HPO_4 and 0.1 *M* phosphate buffer (pH 2) were prepared using double-distilled deionized water.

HPLC—A 4.6-mm × 25-cm, 5-μm particle-size, C_{18} reversed-phase column[4] was used. The eluting solvent was 22% acetonitrile–78% 0.1 *M* phosphate buffer (pH 2.0). The solvent was routinely degassed prior to use by applying a vacuum. A dual-piston reciprocating pump[5] was used to pump the solvent isocratically through the column at 2.0 ml/min, which developed a precolumn pressure of about 2500 psi (175.75 kg/cm^2).

A valve loop injector[6] was used with a 50-μl loop. On the variable wavelength fluorescence detector[7], the range was set at 0.5 and the time constant was set at 3. The excitation wavelength was 195 nm, and an emission cutoff filter of 330 nm was employed.

Procedure—To 1 ml of plasma were added 1000 ng of nylidrin, 0.1 ml of 5 *M* K_2HPO_4, and 4 ml of ethyl acetate. The mixture was then shaken for 5 min and centrifuged to separate the organic and aqueous layers. The organic layer then was transferred to a clean tube. A second 4-ml aliquot of ethyl acetate was added to the plasma, which was then shaken and centrifuged. The second ethyl acetate extract was added to the first and evaporated to dryness on a nitrogen evaporator[8] at 70°.

To the residue was added 0.5 ml of methanol. Following adequate mixing, the methanol was transferred to a clean tube, leaving behind an oily residue, which was discarded. The methanol then was evaporated under nitrogen, and the residue was dissolved in 200 μl of the eluting solvent. After adequate mixing, a 50-μl sample was injected onto the column.

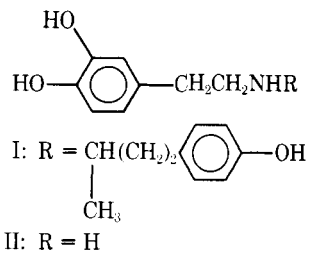

RESULTS AND DISCUSSION

The only previously published assay for dobutamine is an enzymatic procedure utilizing ^{3}H-methyl-*S*-adenosylmethionine (3). In this procedure, dobutamine is converted to the labeled methyl derivative by reaction in the presence of catechol *O*-methyltransferase. General procedures for measuring catecholamines in biological fluids include HPLC separations of dansyl derivatives (4), GLC separation after derivatization with trimethylsilane–imidazole (5), and extensive extraction procedures involving adsorption and selective desorption from aluminum oxide (6). The method reported here is relatively simple and rapid and does not require derivatization.

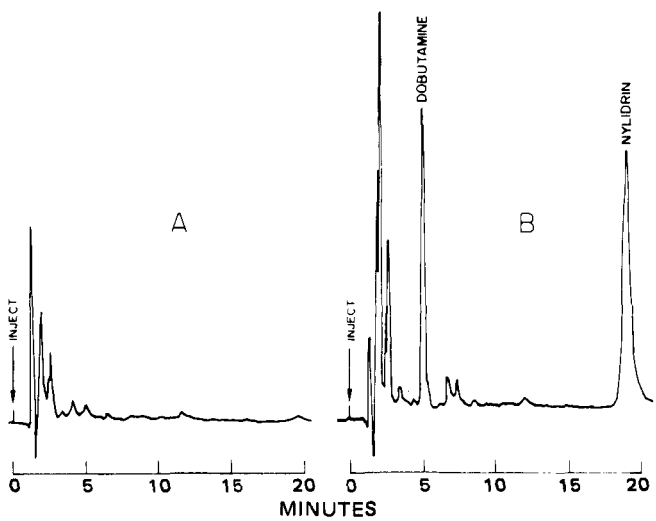

Figure 1—*Chromatograms of a blank plasma sample (A) and a plasma sample to which had been added 150 ng of dobutamine/ml and 1000 ng of nylidrin/ml (B).*

[1] Eli Lilly & Co., Indianapolis, Ind.
[2] Zenith Laboratories, Northvale, N.J.
[3] Burdick and Jackson Laboratories, Muskegon, Mich.
[4] Laboratory Data Control, Riviera Beach, Fla.
[5] Constametric II G, Laboratory Data Control, Riviera Beach, Fla.
[6] Model 7120, Rheodyne, Berkeley, Calif.
[7] Schoeffel Instrument Corp., Westwood, N.J.
[8] N-Evap, Organomation Associates, Shrewsbury, Mass.

0022-3549/78/1200-1756$01.00/0
© 1978, American Pharmaceutical Association

Dobutamine extraction from plasma was evaluated with several buffers at various pH levels. The optimal condition was found with 0.1 ml of 5 *M* K_2HPO_4. The resulting pH of the plasma was 8.9–9.1. The use of a pH 9 borate buffer or 1.0 *M* $NaHCO_3$ did not yield as adequate an extraction. The extraction efficiency, as determined by adding known amounts of dobutamine to plasma and comparing the peak heights with nonextracted samples, was 76.7 ± 4.3%. Since an internal standard was employed when analyzing plasma samples, variability in the extraction efficiency did not create any difficulties.

A fairly polar solvent was needed for extraction. Nonpolar solvents such as benzene were not effective in extracting dobutamine from plasma. Following extraction of the plasma with ethyl acetate and subsequent evaporation of the organic layer, the residue was partially dissolved in methanol. While dobutamine and nylidrin are readily soluble in methanol, an oily component did not dissolve in the alcohol. It is important to separate out this oily component prior to injecting the sample, because it collects on the precolumn filter and necessitates frequent filter replacement.

The nonpolar C_{18} column was selected for use after comparison studies with a moderately polar μ-CN column. The more polar column resulted in longer retention times for dobutamine, its metabolite, and the internal standard. For both columns, the use of an organic–aqueous mixture was necessary to elute the desired catechols. Higher concentrations of the organic phase, acetonitrile, lowered the retention times of the catechols while higher pH values in the aqueous media increased the retention times. Both columns gave the same elution order: dobutamine, 3-methoxydobutamine, and nylidrin.

Chromatograms of an extracted blank plasma sample (A) and an extract of a plasma sample to which was added 150 ng of dobutamine/ml (B) are shown in Fig. 1. The retention times of dobutamine and nylidrin were 5.2 and 19.2 min, respectively. As can be seen in the chromatogram of the blank plasma, no endogenous catecholamines present in plasma eluted with retention times that would interfere with the analysis of dobutamine.

Pure samples of epinephrine and L-norepinephrine were injected directly onto the column. They eluted together very rapidly with a retention time of about 2 min. When injected onto the column, dopamine also eluted with a retention time of about 2 min. The primary nonconjugated metabolite of dobutamine is the 3-methoxy derivative (3). This metabolite had a retention time of 7.9 min. It is apparently very rapidly conjugated to the glucuronide since only very low concentrations have been detected in plasma.

Several drugs commonly administered to cardiology patients were tested for possible interference with the assay. Included were allopurinol, colchicine, warfarin, chlorothiazide, digoxin, lidocaine, procainamide, furosemide, spironolactone, and quinidine. With the exception of quinidine, none of these drugs or their metabolites present in patient plasma interfered with the assay. Quinidine eluted with a retention time similar to that of dobutamine, and the fluorescence was extremely intense. It was necessary to extract quinidine from the plasma prior to extracting dobutamine. Since quinidine can be selectively extracted into benzene without removing dobutamine, an initial extraction with benzene can be performed before the ethyl acetate extraction.

Standard curves are routinely prepared from spiked plasma samples containing 25, 100, and 300 ng of dobutamine/ml. Each concentration is evaluated in triplicate. Peak height ratios (dobutamine to nylidrin) are plotted as a function of concentration of dobutamine added. The mean slope obtained from averaging six standard curves was 0.0061 ± 0.0002. Intercepts were not significantly different from the origin. Standard curves were linear up to 500 ng of dobutamine/ml.

The lower limit of sensitivity of the assay is around 10 ng/ml. However, this limit can be extended downward by using a larger injection loop and a smaller final dilution volume. To date, however, no patient samples with a dobutamine concentration of less than 10 ng/ml have been analyzed.

The assay reproducibility and precision were evaluated over a range of 25–300 ng of dobutamine/ml. Seven replicates of each concentration (25, 50, 150, and 300 ng/ml) were analyzed; the concentrations of dobutamine measured were 24.7 ± 0.87, 52.2 ± 3.01, 148.9 ± 4.05, and 303.1 ± 7.10 ng/ml ± *SD*, respectively. The average standard deviation was only 3.6% of the mean, and the measured mean concentrations only differed from the added concentrations by an average of 1.8%.

Metabolism of dobutamine in the plasma must be prevented once the sample has been drawn from a patient. Catechol *O*-methyltransferase, the enzyme primarily responsible for the metabolism of dobutamine, is present in plasma. By immediately placing samples in ice, this metabolic process can be arrested.

Whole blood, as well as plasma, may be analyzed by the described procedure. It was found that, following addition of dobutamine to whole blood, whole blood and plasma concentrations are equal. This result indicates that dobutamine readily partitions into red blood cells and reaches a rapid equilibrium.

This procedure has been used routinely to analyze patient samples containing dobutamine. Patients are generally administered the drug by constant infusion at rates of 2.5–15.0 μg/kg/min. Plasma dobutamine levels of 50–350 ng/ml have been observed in patient samples.

REFERENCES

(1) R. R. Tuttle and J. Mills, *Circ. Res.*, **36,** 185 (1975).

(2) C. V. Leier, J. Webel, and C. A. Bush, *Circulation,* **56,** 468 (1977).

(3) P. J. Murphy, T. L. Williams, and D. L. Kau, *J. Pharmacol. Exp. Ther.*, **199,** 423 (1976).

(4) G. Schwedt and H. H. Bussemas, *Chromatographia,* **9,** 17 (1976).

(5) Y. Maruyama and A. E. Takemori, *Anal. Biochem.*, **49,** 240 (1972).

(6) A. H. Anton and D. F. Sayre, *J. Pharmacol. Exp. Ther.*, **138,** 360 (1962).

ACKNOWLEDGMENTS

Supported in part by Health Professions Special Projects Grant 05D000714-010 of the Department of Health, Education, and Welfare.

The authors thank Ms. Suzanne Hessler for assistance in preparation of the manuscript.

Drug Contamination of Mortars and Pestles

EWART A. SWINYARD ˣ **and JOSE H. WOODHEAD**

Received March 13, 1978, from the *Department of Biochemical Pharmacology and Toxicology, College of Pharmacy, University of Utah, Salt Lake City, UT 84112.* Accepted for publication April 5, 1978.

Abstract □ Evidence is presented suggesting that potent water-insoluble antipentylenetetrazol agents triturated in porcelain mortars and pestles are not removed from this mixing device by the usual laboratory washing procedure. Moreover, amounts sufficient to contaminate the next substance triturated in this vessel can be demonstrated by the subcutaneous pentylenetetrazol seizure threshold test. The data show that a rigorous washing routine must be followed to achieve a "clean" mortar and pestle. Attention is also directed to the importance of using disposable hypodermic syringes, test tubes, *etc.*, whenever possible and of designing an internal control test to determine when implements that must be reused are "clean."

Keyphrases □ Contamination—mortars and pestles washed by usual procedures, demonstrated by pentylenetetrazol seizure threshold test □ Equipment, laboratory—contamination of mortars and pestles washed by usual procedures demonstrated by pentylenetetrazol seizure threshold test

Previously (1), lipophilic solvents were shown to increase hexobarbital sleep time in mice. This observation suggested that other factors might compromise the results obtained in pharmacological experiments. Consequently, when marked variations appeared in the evaluation of standard and candidate antiepileptic agents subjected to the subcutaneous pentylenetetrazol test, a search for the cause of such aberrant results was begun. Careful study disclosed that highly potent, insoluble, antipentylenetetrazol agents, such as clonazepan (ED_{50} *versus* pentylenetetrazol seizures in mice, 0.009 mg/kg), can be carried over on the mortar and pestle despite careful washing.

This article discusses the possibility of cross-contamination when testing highly potent water-insoluble substances and the precautions necessary to avoid such pitfalls.

EXPERIMENTAL

Male albino mice[1] (CF No. 1 strain, 18–25 g) were allowed free access to food[2] and water, except when they were removed from their cages for the experimental procedure. Pentylenetetrazol seizures were induced by the technique of Swinyard *et al.* (2). Briefly, pentylenetetrazol[3] is administered subcutaneously as a 0.85% solution in 0.9% NaCl, in a dose of 85 mg/kg, in a loose fold of skin on the back of the neck. Seizures are induced in 97+% of normal mice. The mice are observed for 30 min after administration. Absence of a 5-sec episode of clonic spasm (a threshold seizure) is defined as protection in this test.

Clonazepam (50 mg) was triturated for 30–60 sec in a 6.5-cm (o.d.) glazed porcelain mortar and pestle with 2.5 ml of 30% polyethylene glycol, and the resulting suspension was discarded. The mortar and pestle were washed with various combinations of hot water, 0.1 *N* HCl, absolute ethanol, detergent[4], and water rinse and then dried with a paper towel. An inactive control substance (10 or 25 mg of 3,3,5,5-tetramethylcyclohexanespirohydantoin) was placed in the same mortar and triturated for 30–60 sec with 2.5 ml of 30% polyethylene glycol. Then 0.01 ml/g was injected intraperitoneally into eight animals.

At the previously determined time of peak effect for clonazepam (0.5 hr), the mice were subjected to the subcutaneous pentylenetetrazol test, and the presence or absence of a seizure in each animal was recorded. This procedure was repeated with various washing routines until the mortar and pestle were "clean," as indicated by the inability of the inactive substance to protect against pentylenetetrazol-induced seizures.

[1] Charles Rivers, Wilmington, Mass.
[2] S/L Custom Lab Diet-G4.5.
[3] Metrazol, courtesy of Knoll Pharmaceutical Co.
[4] Liqui-Mox, Alconox Inc., New York, NY 10003.

Table I—Cross-Contamination of an Inactive Substance with Clonazepam as Determined by the Subcutaneous Pentylenetetrazol Test in Mice

Prewash Procedure[a]	Washing Procedure[b]	Postwash[c] Procedure	Dose	Subcutaneous Pentylenetetrazol Test Result[d]
Disposable test tube	—	Control	30% polyethylene glycol, 0.01 ml/g	0/8
Uncontaminated mortar and pestle	—	25 mg inactive substance triturated mortar and pestle	100 mg/kg ip	0/6
Clonazepam, 50 mg, triturated mortar and pestle	1, 7, 8	10 mg inactive substance triturated mortar and pestle	40 mg/kg ip in polyethylene glycol, 0.01 ml/g	8/8
	1, 2, 7, 8	10 mg inactive substance triturated mortar and pestle	40 mg/kg ip in polyethylene glycol, 0.01 ml/g	8/8
	1, 4, 7, 8	10 mg inactive substance triturated mortar and pestle	40 mg/kg ip in polyethylene glycol, 0.01 ml/g	2/8
	1, 3, 6–8	10 mg inactive substance triturated mortar and pestle	40 mg/kg ip in polyethylene glycol, 0.1 ml/g	2/8
	1–8	10 mg inactive substance triturated mortar and pestle	40 mg/kg ip in polyethylene glycol, 0.01 ml/g	0/8

[a] Clonazepam, 50 mg, triturated with 2.5 ml of 30% polyethylene glycol in 6.5-cm o.d. porcelain mortar and pestle.
[b] 1 = wash mortar and pestle thoroughly with hot tap water, using fingers to remove any residue of suspension.
2 = rinse mortar and pestle with 0.1 *N* HCl, using trituration motion.
3 = rinse mortar and pestle with water.
4 = rinse mortar and pestle with absolute ethyl alcohol, using trituration motion.
5 = rinse mortar and pestle with water.
6 = wash mortar and pestle with detergent, using scrubbing brush.
7 = rinse mortar and pestle with water.
8 = wipe dry with paper towel.
[c] Either 10 or 25 mg inactive substance triturated with 2.5 ml of 30% polyethylene glycol in washed mortar and pestle. [d] Number of mice protected/number of mice tested.

RESULTS AND DISCUSSION

The vehicle employed (30% polyethylene glycol) and the inactive control substance are devoid of antipentylenetetrazol activity in mice (Table I). Preliminary tests indicated that the control substance was inactive in intraperitoneal doses of 1000 mg/kg when tested from 0.5 to 6 hr after administration. Table I also shows that a mortar and pestle previously used to prepare a polyethylene glycol suspension of clona-

0022-3549/78/1200-1758$01.00/0
© 1978, American Pharmaceutical Association

zepam could not be thoroughly cleaned by washing with hot tap water and rinsing with water and/or rinsing with 0.1 *N* HCl followed by a water rinse since all animals tested were protected from pentylenetetrazol seizures when these procedures were employed. Although rinsing the mortar and pestle with absolute ethanol or washing with detergent reduced the amount of clonazepam remaining (two animals protected out of eight tested), neither procedure alone was adequate. Indeed, a clean mortar and pestle were obtained only when all of these procedures were employed in sequence (none protected out of eight tested).

The benzodiazepines in general (3) and clonazepam in particular are the most potent antipentylenetetrazol agents tested in this laboratory. The ED_{50} (and its 95% confidence interval) by the subcutaneous pentylenetetrazol test is 0.009 (0.0046–0.0165) mg/kg. Thus, a dose of only 180 ng is sufficient to protect 50% of the mice (20 g). Since the ED_{99} for clonazepam is approximately 0.013 mg/kg, at least 3.25 μg apparently was carried over on the mortar and pestle and subsequently incorporated in the polyethylene glycol suspension of the inactive substance. Chemical analysis[5] of 2.5 ml of 30% polyethylene glycol triturated in a contaminated mortar and pestle revealed that 66.25 μg (26.5 μg/ml) was, in fact, carried over in the solvent. This quantity is approximately 20 times the ED_{99} for clonazepam.

[5] Performed by Mr. Tom Jennison, Center for Human Toxicology, University of Utah.

The results presented reveal only a small fraction of the total problem. Many laboratories are working with highly potent, water-insoluble substances. Various methods such as a mortar and pestle, a sonicator, a homogenizer, a tissue grinder, and a micromixer are used to achieve a suitable solution or suspension. Subsequent use of this equipment to solubilize or suspend other chemicals could result in significant contamination unless appropriate precautions are taken. These precautions include the use of disposable laboratory utensils such as syringes, needles, test tubes, and spatulas and internal controls to determine when reused utensils are clean. One cannot help but wonder to what extent this problem has been unrecognized, ignored, or explained away on the basis of "biological variability."

REFERENCES

(1) E. A. Swinyard, J. H. Woodhead, and R. V. Petersen, *J. Pharm. Sci.*, **65**, 733 (1976).

(2) E. A. Swinyard, W. C. Brown, and L. S. Goodman, *J. Pharmacol. Exp. Ther.*, **106**, 319 (1952).

(3) E. A. Swinyard and A. W. Castellion, *ibid.*, **151**, 369 (1966).

ACKNOWLEDGMENTS

Supported by Contract NIH-N01-NS-5-2302.

Quaternary Acetate and Propionate Esters of 3-Hydroxyquinolizidine

RICHARD JUNEAU *x and CURTIS TABER ‡

Received February 16, 1977, from the **Department of Medicinal Chemistry and the* ‡*Department of Pharmacology, School of Pharmacy, Southwestern Oklahoma State University, Weatherford, OK 73096.* Accepted for publication April 18, 1978.

Abstract □ The preparation of the quaternary acetate and propionate esters of 3-hydroxyquinolizidine is described. Tentative structures are assigned on the basis of NMR data. Results of preliminary pharmacological screening of the methiodide and hydrochloride salts are given.

Keyphrases □ 3-Hydroxyquinolizidine esters, various—synthesized, structures assigned, cholinergic activity evaluated *in vitro* □ Cholinergic activity—various 3-hydroxyquinolizidine esters evaluated *in vitro* □ Structure–activity relationships—various 3-hydroxyquinolizidine esters evaluated for cholinergic activity *in vitro*

The quinolizidine ring system has been used to prepare semirigid analogs of several classes of biologically active compounds (1–4). The reported reversal of configuration of the *trans*-fused rings of quinolizidine to the *cis*-configuration upon quaternization of the acetate and propionate esters of axial and equatorial 1-hydroxyquinolizidine (1) led to the present investigation of the analogous esters at the 3-position.

This report describes the preparation of the acetate and propionate esters of axial and equatorial 3-hydroxyquinolizidine and their behavior upon quaternization with methyl iodide. These isomers were screened for cholinergic activity since they are structurally related to acetylcholine.

DISCUSSION

The synthesis of the desired compounds began with the preparation of 3-oxoquinolizidine (I) by the method of Counsell and Soine (5). Then, I was reduced according to the method of Aaron *et al.* (6). The structures of II and III (Scheme I) were assigned (6, 7) primarily on the basis of IR spectral data. The intermediate esters, IV and V (Scheme I), were obtained by reaction of the appropriate alcohol with either acetic or propionic anhydride and pyridine as a catalyst. The esters so prepared were assigned the same configuration as the respective parent alcohols since the conditions used for ester formation would not be expected to result in epimerization. The assignments appear valid since all esters exhibited Bohlmann bands (Table I) in their IR spectra, which is usually taken as empirical evidence for *trans*-ring fusion (6–8).

The desired quaternary salts were obtained by treating the purified esters with excess methyl iodide in refluxing acetone. The NMR spectra of each quaternized ester exhibited only one *N*-methyl signal, which appeared as a three-proton singlet (Table I). The appearance of only one *N*-methyl signal, along with the small differences in the chemical shifts of the signals, suggested that the quaternized esters were configurationally pure and probably all of the same configuration. These conclusions seem reasonable in view of the work of Williamson *et al.* (9), who showed a 12-Hz difference between the *N*-methyl groups of *trans*- (171 Hz) and *cis*- (183 Hz) fused *N*-methylquinolizidinium iodide. Also, since the *N*-methyl signals of the quaternary salts prepared have chemical shifts very close to the *N*-methyl signals of the analogous *cis*-fused quaternary salts substituted at the 1-position (see introduction and Ref. 1), the *cis*-configuration was tentatively assigned to the quaternary salts prepared.

Examination of Drieding models of the *cis*-fused products revealed that difficultly interconvertible conformers were probably in equilibrium as depicted in Scheme II. It was reasonable to assign a conformational preference to the products, and this assignment was made on the basis that less steric interaction would occur if the ester function was in the equatorial position in the *cis*-fused system. Therefore, XII and XVI (Table I) were tentatively assigned Structure VI, where R is methyl and ethyl, respectively. Likewise, XIII and XVII (Table I) were assigned Structure IX. Support for this conclusion was obtained by the observation

0022-3549/78/1200-1759$01.00/0

© 1978, American Pharmaceutical Association

zepam could not be thoroughly cleaned by washing with hot tap water and rinsing with water and/or rinsing with 0.1 *N* HCl followed by a water rinse since all animals tested were protected from pentylenetetrazol seizures when these procedures were employed. Although rinsing the mortar and pestle with absolute ethanol or washing with detergent reduced the amount of clonazepam remaining (two animals protected out of eight tested), neither procedure alone was adequate. Indeed, a clean mortar and pestle were obtained only when all of these procedures were employed in sequence (none protected out of eight tested).

The benzodiazepines in general (3) and clonazepam in particular are the most potent antipentylenetetrazol agents tested in this laboratory. The ED_{50} (and its 95% confidence interval) by the subcutaneous pentylenetetrazol test is 0.009 (0.0046–0.0165) mg/kg. Thus, a dose of only 180 ng is sufficient to protect 50% of the mice (20 g). Since the ED_{99} for clonazepam is approximately 0.013 mg/kg, at least 3.25 μg apparently was carried over on the mortar and pestle and subsequently incorporated in the polyethylene glycol suspension of the inactive substance. Chemical analysis[5] of 2.5 ml of 30% polyethylene glycol triturated in a contaminated mortar and pestle revealed that 66.25 μg (26.5 μg/ml) was, in fact, carried over in the solvent. This quantity is approximately 20 times the ED_{99} for clonazepam.

[5] Performed by Mr. Tom Jennison, Center for Human Toxicology, University of Utah.

The results presented reveal only a small fraction of the total problem. Many laboratories are working with highly potent, water-insoluble substances. Various methods such as a mortar and pestle, a sonicator, a homogenizer, a tissue grinder, and a micromixer are used to achieve a suitable solution or suspension. Subsequent use of this equipment to solubilize or suspend other chemicals could result in significant contamination unless appropriate precautions are taken. These precautions include the use of disposable laboratory utensils such as syringes, needles, test tubes, and spatulas and internal controls to determine when reused utensils are clean. One cannot help but wonder to what extent this problem has been unrecognized, ignored, or explained away on the basis of "biological variability."

REFERENCES

(1) E. A. Swinyard, J. H. Woodhead, and R. V. Petersen, *J. Pharm. Sci.*, **65**, 733 (1976).

(2) E. A. Swinyard, W. C. Brown, and L. S. Goodman, *J. Pharmacol. Exp. Ther.*, **106**, 319 (1952).

(3) E. A. Swinyard and A. W. Castellion, *ibid.*, **151**, 369 (1966).

ACKNOWLEDGMENTS

Supported by Contract NIH-N01-NS-5-2302.

Quaternary Acetate and Propionate Esters of 3-Hydroxyquinolizidine

RICHARD JUNEAU *x and CURTIS TABER ‡

Received February 16, 1977, from the **Department of Medicinal Chemistry and the* ‡*Department of Pharmacology, School of Pharmacy, Southwestern Oklahoma State University, Weatherford, OK 73096.* Accepted for publication April 18, 1978.

Abstract □ The preparation of the quaternary acetate and propionate esters of 3-hydroxyquinolizidine is described. Tentative structures are assigned on the basis of NMR data. Results of preliminary pharmacological screening of the methiodide and hydrochloride salts are given.

Keyphrases □ 3-Hydroxyquinolizidine esters, various—synthesized, structures assigned, cholinergic activity evaluated *in vitro* □ Cholinergic activity—various 3-hydroxyquinolizidine esters evaluated *in vitro* □ Structure–activity relationships—various 3-hydroxyquinolizidine esters evaluated for cholinergic activity *in vitro*

The quinolizidine ring system has been used to prepare semirigid analogs of several classes of biologically active compounds (1–4). The reported reversal of configuration of the *trans*-fused rings of quinolizidine to the *cis*-configuration upon quaternization of the acetate and propionate esters of axial and equatorial 1-hydroxyquinolizidine (1) led to the present investigation of the analogous esters at the 3-position.

This report describes the preparation of the acetate and propionate esters of axial and equatorial 3-hydroxyquinolizidine and their behavior upon quaternization with methyl iodide. These isomers were screened for cholinergic activity since they are structurally related to acetylcholine.

DISCUSSION

The synthesis of the desired compounds began with the preparation of 3-oxoquinolizidine (I) by the method of Counsell and Soine (5). Then, I was reduced according to the method of Aaron *et al.* (6). The structures of II and III (Scheme I) were assigned (6, 7) primarily on the basis of IR spectral data. The intermediate esters, IV and V (Scheme I), were obtained by reaction of the appropriate alcohol with either acetic or propionic anhydride and pyridine as a catalyst. The esters so prepared were assigned the same configuration as the respective parent alcohols since the conditions used for ester formation would not be expected to result in epimerization. The assignments appear valid since all esters exhibited Bohlmann bands (Table I) in their IR spectra, which is usually taken as empirical evidence for *trans*-ring fusion (6–8).

The desired quaternary salts were obtained by treating the purified esters with excess methyl iodide in refluxing acetone. The NMR spectra of each quaternized ester exhibited only one *N*-methyl signal, which appeared as a three-proton singlet (Table I). The appearance of only one *N*-methyl signal, along with the small differences in the chemical shifts of the signals, suggested that the quaternized esters were configurationally pure and probably all of the same configuration. These conclusions seem reasonable in view of the work of Williamson *et al.* (9), who showed a 12-Hz difference between the *N*-methyl groups of *trans*- (171 Hz) and *cis*- (183 Hz) fused *N*-methylquinolizidinium iodide. Also, since the *N*-methyl signals of the quaternary salts prepared have chemical shifts very close to the *N*-methyl signals of the analogous *cis*-fused quaternary salts substituted at the 1-position (see introduction and Ref. 1), the *cis*-configuration was tentatively assigned to the quaternary salts prepared.

Examination of Drieding models of the *cis*-fused products revealed that difficultly interconvertible conformers were probably in equilibrium as depicted in Scheme II. It was reasonable to assign a conformational preference to the products, and this assignment was made on the basis that less steric interaction would occur if the ester function was in the equatorial position in the *cis*-fused system. Therefore, XII and XVI (Table I) were tentatively assigned Structure VI, where R is methyl and ethyl, respectively. Likewise, XIII and XVII (Table I) were assigned Structure IX. Support for this conclusion was obtained by the observation

0022-3549/78/1200-1759$01.00/0

© 1978, American Pharmaceutical Association

Table I—Quinolizidine Hydrochlorides and Methiodides

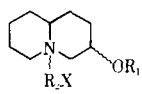

Compound	R_1	R_2	X	Melting Point	Analysis, %	Calc.	Found	Bohlmann Bands[a], cm^{-1}	NMR *N*-Methyl Signal[b], Hz
X	$OCOCH_3$ (ax)[c]	H	Cl	240–245°	C	56.53	56.70	2760, 2800	—
					H	8.63	8.64		
					N	5.99	6.15		
XI	$OCOCH_3$ (eq)[c]	H	Cl	195–197°	C	56.53	56.37	2760, 2805	—
					H	8.63	8.79		
					N	5.99	6.19		
XII	$OCOCH_3$ (eq)[d]	CH_3	I	175–178°	C	42.49	42.50	—	200
					H	6.54	6.61		
					N	4.13	4.08		
XIII	$OCOCH_3$ (eq)[d]	CH_3	I	200–205°	C	42.49	42.60	—	196
					H	6.54	6.48		
					N	4.13	4.21		
XIV	$OCOCH_2CH_3$ (ax)[c]	H	Cl	—[e]	C	58.18	—	2770, 2800	—
					H	8.95	—		
					N	5.65	—[e]		
XV	$OCOCH_2CH_3$ (eq)[c]	H	Cl	194–195°	C	58.18	58.28	2780, 2805	—
					H	8.95	8.98		
					N	5.65	5.76		
XVI	$OCOCH_2CH_3$ (eq)[d]	CH_3	I	148–150°	C	44.20	44.37	—	201
					H	6.85	6.74		
					N	3.97	3.92		
XVII	$OCOCH_2CH_3$ (eq)[d]	CH_3	I	190–192°	C	44.20	44.37	—	198
					H	6.85	6.76		
					N	3.97	3.91		

[a] Bohlmann bands in the IR were determined on the free bases, all of which were oils. [b] All signals were singlets integrating to three protons. [c] Axial or equatorial designation refers to the free base. [d] Equatorial designation refers to the *cis*-fused products as depicted in Scheme II. [e] The hydrochloride decomposed upon recrystallization.

that the NMR signals for the methine protons on the oxygen-bearing carbons of the quinolizidine ring all showed bandwidths at half-height (W_h) indicative of axial orientation (Table II). Only *cis*-fused products were obtained, probably as the result of small but steady-state concentrations of *cis*-fused esters that react preferentially due to much greater accessibility of the nitrogen electron pair[1].

Of the seven compounds tested, two exerted powerful, consistent, and reproducible effects on the rat jejunum. Compound XVII (Table I) inhibited contractile activity of the muscle. This effect was essentially instantaneous following injection and was reproducible at bath concentrations as low as 1 μg/ml. The IC_{50} of XVII was calculated to be 8 μg/ml (2.3×10^{-5} *M*), determined from seven experiments (*SD* ±4 μg/ml). Both spontaneous contractions and acetylcholine-induced contractions were inhibited.

Conversely, X (Table I) exerted a spasmogenic effect at concentrations as low as 25 μg/ml. This effect was not immediate but took 5–15 min to become maximal and was readily reversed by atropine sulfate. An average concentration of 62 μg/ml (2.7×10^{-4} *M*) determined from six experiments was required to produce contractions equal to approximately 0.03 μg/ml (1.3×10^{-7} *M*) of acetylcholine. Thus, X was approximately 0.0005 as potent as acetylcholine in this preparation.

The remaining compounds elicited weak, inconsistent, and nonreproducible effects at all concentrations tested up to the maximum of 100 μg/ml and were thus deemed inactive.

The lack of agonist activity displayed by the prepared quaternary salts was unexpected since all active decalin acetylcholine analogs have the antiplanar nitrogen–ester oxygen orientation (10). Drieding models of the quaternary salts prepared show that, regardless of the product formed (Structure VI or IX of Scheme II), there will be an antiplanar nitrogen–ester oxygen relationship. Even more enigmatic is the agonist activity of X (Table I), a hydrochloride salt. If it is assumed that the quinolizidine ring in the compound remains in the *trans*-fused configuration (since it is not quaternized), then Drieding models demonstrate that the nitrogen–ester oxygen relationship is synclinal. The synclinal arrangement is also thought to be present in acetylcholine (10) and thus may account for the agonist activity of the hydrochloride salt. However, acetylcholine-like agonists are normally quaternized. This finding is rather unusual, especially since the other amine salts prepared did not show activity of any sort. The nature of the agonist activity displayed by this hydrochloride salt will be explored in the future.

It is also reasonable to anticipate antagonistic activity from the prepared quaternary salts because of the greater number of hydrophobic interactions of the quinolizidine ring relative to acetylcholine. However, only one member of the series is antagonistic. Intuitively, since structural differences between these compounds are so minimal, any biological activity should be shared by all members. Further study will be required to clarify this anomaly.

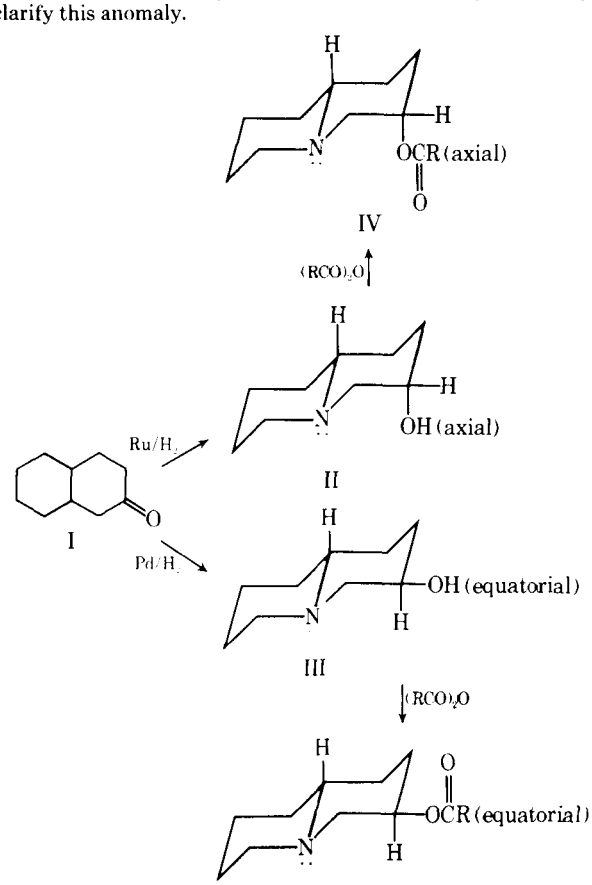

Scheme I

[1] This explanation was suggested by a reviewer.

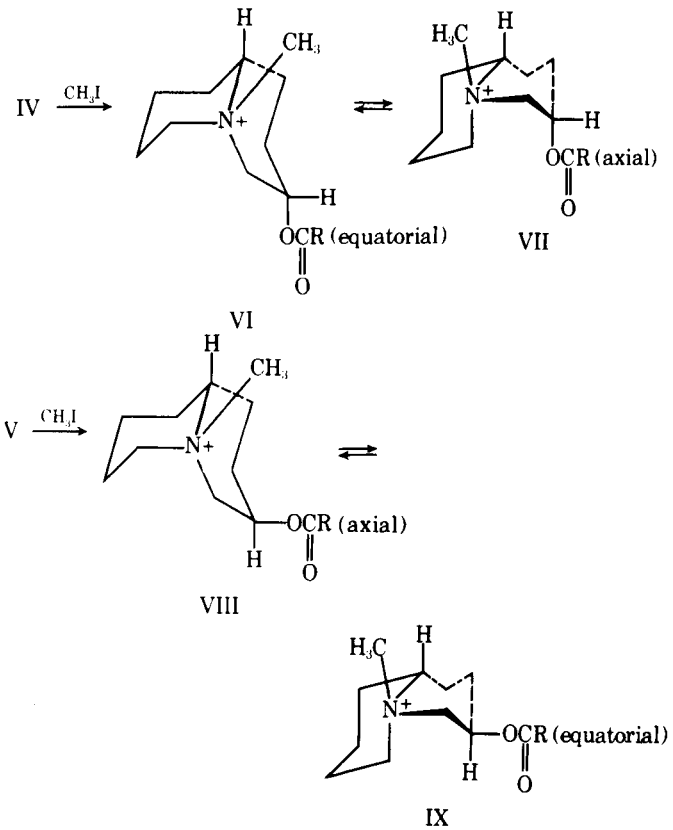

Scheme II

EXPERIMENTAL[2]

3-Hydroxyquinolizidine—3-Oxoquinolizidine was prepared according to the method of Counsell and Soine (5) and reduced catalytically by the procedure of Aaron *et al.* (6). A 5% ruthenium-on-carbon reduction gave a 72:28 axial to equatorial alcohol ratio, and a 10% palladium-on-carbon reduction yielded a 3:97 axial to equatorial alcohol ratio (6, 7). The epimeric mixtures were separated by fractional distillation. Homogeneity of the separated epimers was easily established by TLC.

Esters (Table I)—Approximately 4 g (0.04 mole) of the respective 3-hydroxyquinolizidine was mixed with 10 ml (0.1 mole) of fresh acetic anhydride and 1 ml of pyridine. The mixture was stirred for 24 hr at room temperature. The dark brown-black solution was then poured over crushed ice, and the mixture was saturated with potassium carbonate while ice bath temperatures were maintained. The resulting mixture, pH 8, was extracted with four 50-ml portions of chloroform.

The combined chloroform extracts were dried over anhydrous sodium sulfate, and the solvent was removed under water aspirator vacuum. The resulting oil was then taken up in a mixture of petroleum ether (bp 60–90°)–ethyl acetate (9:1) and passed through a silica gel column. Hydrochloride salts were prepared by dissolving the ester in a minimum of ether and adding, dropwise, a saturated solution of hydrogen chloride gas in anhydrous ether until precipitation ceased. The precipitate was then crystallized from ethanol–ether.

Methiodides (Table I)—Approximately 0.02 mole of the ester and 5 ml (0.08 mole) of methyl iodide were dissolved in 25 ml of acetone. This mixture was refluxed overnight, and the solvent was removed and yielded yellow-white crystals. These crystals were readily recrystallized from ethanol or ethanol–ether.

Biological—The compounds were tested on strips of rat jejunum suspended in oxygenated Tyrode solution in a 100-ml bath maintained at 37°. The muscles were attached to a myograph transducer, and contractions were recorded on a physiograph. Responses to test compounds were observed in comparison to responses to standard solutions of acetylcholine chloride. Typical contractions in response to acetylcholine occurred at concentrations ranging from 0.01 to 0.1 μg/ml of bath solution.

In appropriate experiments, atropine sulfate (0.01-μg/ml final concentration) was utilized to block muscarinic receptors. Test compounds were injected into the bath in volumes of 1.0 ml or less to yield final bath concentrations of 100 μg/ml or less. All doses are expressed in micrograms per milliliter of bathing solution.

Dose–response curves were constructed for the pharmacologically active compounds. Average concentrations of antagonists required to inhibit acetylcholine-induced contractions 50% (IC_{50}) were calculated. Average concentrations of cholinomimetics required to equal acetylcholine-induced contractions also were calculated. Standard deviations were computed for such averages.

[2] Melting points were taken with a Thomas-Hoover Uni-Melt apparatus and are uncorrected. IR spectra were determined with a Beckman Accu Lab Spectrophotometer. NMR spectra were obtained with a Varian model A-60-A spectrometer relative to an internal standard of tetramethylsilane with deuterochloroform as solvent. Column chromatography was performed with 28–200-mesh silica gel. Elemental analyses were performed by Galbraith Laboratories, Knoxville, Tenn.

Table II—NMR Bandwidth Data of Methine Protons on Oxygen-Bearing Carbon

Compound	W_h, Hz	Chemical Shift, Hz
XII[a]	12	320
XIII[a]	15	320
XVI[a]	12	322
XVII[a]	18	320
Axial 3-hydroxyquinolizidine (II)[b]	6.5	225
Equatorial 3-hydroxyquinolizidine (III)[b]	19	217

[a] All measurements were obtained for 10% $CDCl_3$ solutions. [b] Data were taken from Ref. 6. Measurements were obtained for 10% carbon tetrachloride solutions.

REFERENCES

(1) J. D. England, D. Temple, and J. Sam, *J. Med. Chem.*, **11**, 353 (1968).

(2) J. D. England and J. Sam, *J. Heterocycl. Chem.*, **3**, 482 (1966).

(3) A. H. Beckett, R. G. Lingard, and A. E. Theobald, *J. Med. Chem.*, **12**, 563 (1969).

(4) M. E. Rogers, J. Sam, and N. P. Plotnikoff, *ibid.*, **17**, 726 (1974).

(5) R. E. Counsell and T. O. Soine, *J. Am. Pharm. Assoc., Sci. Ed.*, **49**, 289 (1960).

(6) H. S. Aaron, G. E. Wicks, and C. P. Rader, *J. Org. Chem.*, **29**, 2248 (1964).

(7) C. P. Rader, G. E. Wicks, R. L. Young, and H. S. Aaron, *ibid.*, **29**, 2252 (1964).

(8) F. Bohlmann, *Chem. Ber.*, **91**, 2157 (1958).

(9) K. L. Williamson, T. Howell, and T. A. Spencer, *J. Am. Chem. Soc.*, **88**, 325 (1966).

(10) "Progress in Medicinal Chemistry," vol. 11, G. P. Ellis and G. P. West, Eds., Elsevier, New York, N.Y., 1975, pp. 5–20.

Mesoionic Xanthine Analogs as Inhibitors of Cyclic AMP Phosphodiesterase

R. A. GLENNON ˣ, M. E. ROGERS, R. G. BASS, and S. B. RYAN

Received August 25, 1977, from the *Departments of Pharmaceutical Chemistry and Chemistry, Medical College of Virginia, Virginia Commonwealth University, Richmond, VA 23298.* Accepted for publication April 26, 1978.

Abstract □ Several derivatives of two mesoionic xanthine analogs, mesoionic thiazolo[3,2-*a*]pyrimidine-5,7-diones and mesoionic 1,3,4-thiadiazolo[3,2-*a*]pyrimidine-5,7-diones, were synthesized and evaluated as inhibitors of cyclic AMP phosphodiesterase. A significant number of these compounds demonstrated theophylline-like activity.

Keyphrases □ Xanthine analogs, mesoionic—synthesized, evaluated for effect on cyclic AMP phosphodiesterase activity *in vitro* □ Thiazolo[3,2-*a*]pyrimidines, various—synthesized, evaluated for effect on cyclic AMP phosphodiesterase activity *in vitro* □ Thiadiazolo[3,2-*a*]-pyrimidines, various—synthesized, evaluated for effect on cyclic AMP phosphodiesterase activity *in vitro* □ Cyclic AMP phosphodiesterase—effect of various thiazolo- and thiadiazolo[3,2-*a*]pyrimidines *in vitro* □ Enzyme activity—cyclic AMP phosphodiesterase, effect of various thiazolo- and thiadiazolo[3,2-*a*]pyrimidines *in vitro* □ Structure–activity relationships—various thiazolo- and thiadiazolo[3,2-*a*]pyrimidines evaluated for effect on cyclic AMP phosphodiesterase activity *in vitro*

Methylated xanthines, such as theophylline, inhibit cyclic nucleotide phosphodiesterases, an effect believed to be responsible for their clinical utility (1). Structural modification of the xanthines has led to more potent and more selective inhibitors (2, 3). Although molecular modification of purines and pyrimidines continues to be extensively studied, mesoionic purinone analogs represent a virtually unknown class of heterocyclic compounds.

Mesoionic purinones are divided into several subclasses, *i.e.*, xanthine, hypoxanthine, and purin-2-one analogs, based on either five-membered ring (Class I) or six-membered ring (Class II) mesoionic systems (4). Mesoionic thiazolo[3,2-*a*]pyrimidine-5,7-diones (8-substituted anhydro-5-hydroxy-7-oxothiazolo[3,2-*a*]pyrimidinium hydroxides, I*a*–I*i*, Table I) and mesoionic 1,3,4-thiadiazolo[3,2-*a*]pyrimidine-5,7-diones (8-substituted anhydro-5-hydroxy-7-oxo-1,3,4-thiadiazolo[3,2-*a*]pyrimidinium hydroxides, II*a*–II*g*) are examples of Class II mesoionic xanthine analogs (5, 6).

Because of their close structural similarity with methylated xanthines, it was suggested previously (7) that such derivatives be evaluated as inhibitors of adenosine 3′,5′-monophosphate (cyclic AMP) phosphodiesterase. Coburn[1] found that several derivatives similar to II*a*–II*g* possess such activity.

The synthesis of 8-alkyl derivatives I*a*–I*i* is reported here, along with preliminary findings on their ability to inhibit cyclic AMP phosphodiesterase. For comparative purposes, the activities of II*a*–II*g* also were examined.

DISCUSSION

Compounds I*a*–I*i* (Table I) were prepared conveniently according to Scheme I. 2-Aminothiazole (III) was acylated using either an acid anhydride or an acyl chloride to give the 2-acylaminothiazoles IV*a*–IV*g*

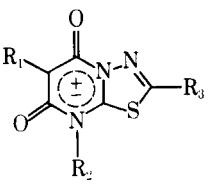

II*a*: $R_1 = R_2 = R_3 = CH_3$
II*b*: $R_1 = CH_3$, $R_2 = C_2H_5$, $R_3 = H$
II*c*: $R_1 = R_2 = C_2H_5$, $R_3 = H$
II*d*: $R_1 = CH_3$, $R_2 = C_3H_7$, $R_3 = H$
II*e*: $R_1 = CH_3$, $R_2 = CH(CH_3)_2$, $R_3 = H$
II*f*: $R_1 = CH_3$, $R_2 = CH(CH_3)CH_2CH_3$, $R_3 = H$
II*g*: $R_1 = CH_3$, $R_2 = C_5H_{11}$, $R_3 = H$

(Table II). Lithium aluminum hydride reduction of IV*a*–IV*g* afforded the 2-alkylaminothiazoles V*a*–V*g* (Table III), which were condensed with bis(2,4,6-trichlorophenyl) malonate ester VI*a* or VI*b* to yield the desired mesoionic thiazolopyrimidines (Table I).

Most phosphodiesterase preparations, including bovine heart phosphodiesterase, contain both high and low affinity enzymes or enzyme forms (2, 3). The preparations can be assayed at a low cyclic AMP concentration to observe effects on the high affinity enzyme and at a high concentration to observe inhibition of the low affinity enzyme (actually this high concentration reflects total enzyme activity). Initial results of inhibitor studies for I*a*–I*i*, II*a*–II*g*, and theophylline are given in Table IV.

Compounds I*c*, I*i*, II*c*, and II*e*–II*g* are theophylline like in inhibitor potency against both forms of the enzyme. Generally, I_{50} values obtained at the higher substrate concentration were two to three times greater than those obtained at the lower substrate concentration. Ethanol (2.5% final assay mixture concentration) was required to solubilize some inhibitors. The I_{50} values for theophylline in the absence and presence of ethanol were essentially the same, although the amount of ethanol utilized diminished enzyme activity by 15–25%.

For I*a*–I*i*, an alkyl substituent on the 6-position appears beneficial. The low order of activity of I*g* indicates that increasing the chain length of the 8-substituent does not necessarily increase activity; however, branching of the chain may be important (I*i*). Compound II*a*, the only compound with a 2-substituent other than hydrogen, was inactive. Increasing the chain length of the 8-substituent appears beneficial (II*g* > II*d* ≥ II*b*) as does branching (II*e* > II*d*). Interestingly, increasing the chain length of the 6-substituent from methyl (II*b*) to ethyl (II*c*) improved activity fourfold. These results parallel, somewhat, the results with the alkylated xanthines where increased chain length and branching at N-1 and N-3 were favorable, although alkyl chains at C-8 also increased activity; none of the mesoionic compounds thus far examined is as potent as the alkylated xanthines (2).

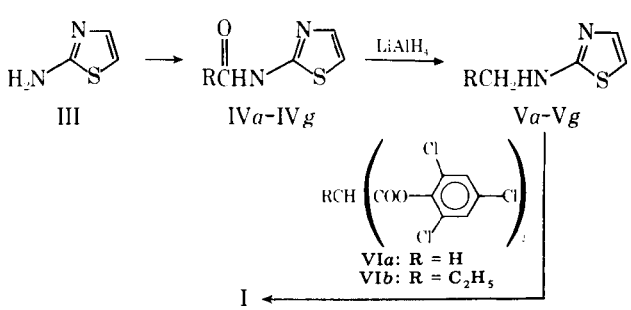

Scheme I

[1] R. A. Coburn, State University of New York at Buffalo, Amherst, N.Y., personal communication.

0022-3549/78/1200-1762$01.00/0
© 1978, American Pharmaceutical Association

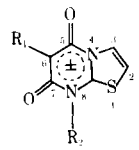

Table I—Properties of Mesoionic Thiazolo[3,2-*a*]pyrimidine-5,7-diones

Compound	R_1	R_2	Formula	Melting Point[a]	Yield, %	Analysis, % Calc.	Found
I*a*	H	$CH_2CH_2CH_2CH_3$	$C_{10}H_{12}N_2O_2S$	127–128°	63	C 53.56 H 5.40 N 12.49	53.50 5.41 12.48
I*b*	H	$CH_2CH(CH_3)_2$	$C_{10}H_{12}N_2O_2S$	155–157°	74	C 53.56 H 5.40 N 12.49	53.78 5.39 12.29
I*c*	C_2H_5	$CH_2CH(CH_3)_2$	$C_{12}H_{16}N_2O_2S$	136–137°	45	C 57.13 H 6.39 N 11.11	57.26 6.16 11.14
I*d*	H	$(CH_2)_4CH_3$	$C_{11}H_{14}N_2O_2S$	141–142°	51	C 55.45 H 5.92 N 11.76	55.27 5.83 11.66
I*e*	H	$CH_2CH_2CH(CH_3)_2$	$C_{11}H_{14}N_2O_2S$	159–161°	51	C 55.45 H 5.92 N 11.76	55.07 5.86 11.51
I*f*	H	$CH_2C(CH_3)_3$	$C_{11}H_{14}N_2O_2S$	183–184°	76	C 55.45 H 5.92 N 11.76	55.23 5.90 11.52
I*g*	H	$(CH_2)_5CH_3$	$C_{12}C_{16}N_2O_2S$	132–133°	50	C 57.13 H 6.39 N 11.11	56.97 6.32 10.84
I*h*	C_2H_5	$(CH_2)_5CH_3$	$C_{14}H_{20}N_2O_2S$	129–130°	47	C 59.98 H 7.19 N 10.00	59.97 7.22 9.98
I*i*	H	CH_2–C$_6$H$_5$	$C_{13}H_{16}N_2OS$	207–208°	40	C 59.30 H 5.74 N 10.64	59.26 6.10 10.53

[a] Ethyl acetate was the recrystallization solvent.

Table II—Properties of 2-Acylaminothiazoles

Compound	R	Formula	Melting Point	Recrystallization Solvent[a]	Yield, %	Analysis, % Calc.	Found
IV*a*	$CH_2CH_2CH_3$	$C_7H_{10}N_2OS$	133–134°[b]	E	71	—	—
IV*b*	$CH(CH_3)_2$	$C_7H_{10}N_2OS$	136–137°	M	73	C 49.39 H 5.92 N 16.46	49.37 5.93 16.55
IV*c*	$CH_2CH_2CH_2CH_3$	$C_8H_{12}N_2OS$	103–104°	M	86	C 52.15 H 6.56 N 15.20	51.92 6.44 15.10
IV*d*	$CH_2CH(CH_3)_2$	$C_8H_{12}N_2OS$	79–80°	E	89	C 52.15 H 6.56 N 15.20	51.95 6.23 15.20
IV*e*	$C(CH_3)_3$	$C_8H_{12}N_2OS$	139–140°	M	80	C 52.15 H 6.56 N 15.20	51.82 6.60 15.05
IV*f*	$(CH_2)_4CH_3$	$C_9H_{14}N_2OS$	99–100°[c]	M	91	—	—
IV*g*	C$_6$H$_{11}$	$C_{10}H_{14}N_2OS$	160–161°	M	30	C 57.11 H 6.71 N 13.32	56.71 6.68 13.19

[a] The recrystallization solvent was either 95% ethanol (E) or aqueous methanol (M). [b] Lit. (8) mp 128–130°. [c] Lit. (8) mp 102–103°.

These results must be tempered by the realization that the stabilities of these ring systems under the conditions of the enzyme assay and the measures taken to solubilize the inhibitors have not been fully investigated. These studies, as well as pharmacological studies, are in progress.

In conclusion, these limited data indicate that it may be possible to prepare new mesoionic xanthine analogs that will be significantly more potent than theophylline as cyclic AMP phosphodiesterase inhibitors.

EXPERIMENTAL[2]

***N*-(2-Thiazolyl)isobutyramide (IV*b*)**—Isobutyryl chloride (5.35 g, 50 mmoles) was added dropwise, with stirring, to a solution of 2-aminothiazole (5.0 g, 50 mmoles) and triethylamine (5.0 g, 50 mmoles) in 40 ml of tetrahydrofuran at 0°. After the addition, the reaction mixture was stirred at room temperature for 2 hr and was then filtered. The filtrate was dried with anhydrous sodium sulfate and evaporated *in vacuo* to yield an oil, which crystallized upon standing.

Recrystallizaion from aqueous methanol gave 6.2 g (72%) of IV*b* as white crystals, mp 136–137°; IR (KBr): 1690 cm^{-1}; NMR ($CDCl_3$): δ 1.35 (d, 6H, methyl protons), 2.75 (m, 1H, methine proton), 7.00 (d, 1H, thiazole proton), and 7.45 (d, 1H, thiazole proton) ppm. Table II lists the analytical data.

The 2-acylaminothiazoles IV*c*–IV*g* (Table II) were prepared in the same manner as IV*b*. Compound IV*a* was prepared using *n*-butyric anhydride in place of acyl chloride.

2-(Isobutylamino)thiazole (V*b*)—A solution of IV*b* (5.1 g, 30 mmoles) in 30 ml of tetrahydrofuran was added dropwise to a stirred suspension of lithium aluminum hydride (1.2 g, 32 mmoles) in 40 ml of tetrahydrofuran at 0°. After refluxing for 3 hr, water was added dropwise at 0° until hydrogen evolution ceased. The mixture was filtered, and the

[2] PMR spectra were obtained on a Perkin-Elmer R-24 spectrometer, and chemical shifts are reported relative to tetramethylsilane. IR spectra were obtained on a Perkin-Elmer 257 spectrophotometer. Microanalyses were performed at A. H. Robins, Richmond, Va. Melting points were determined on a Thomas-Hoover apparatus and are uncorrected. Compounds II*a*–II*g* were prepared following literature procedures (7).

Table III—Properties of 2-Alkylaminothiazoles

Compound	R	Formula	Melting Point	Recrystallization Solvent[a]	Yield, %	Analysis, %	Calc.	Found
V*a*	$CH_2CH_2CH_3$	$C_7H_{12}N_2S$	68–69°[b]	E	50	C	43.88	43.59
						H	5.73	5.61
						N	11.36	11.06
V*b*	$CH(CH_3)_2$	$C_7H_{12}N_2S$	94–95°[b]	A	73	C	43.88	43.82
						H	5.73	5.77
						N	11.36	11.23
V*c*	$CH_2CH_2CH_2CH_3$	$C_8H_{14}N_2S$	44–46°	M	72	C	56.43	56.30
						H	8.29	8.01
						N	16.45	16.24
V*d*	$CH_2CH(CH_3)_2$	$C_8H_{14}N_2S$	79–80°[b]	A	66	C	46.14	45.91
						H	6.20	6.15
						N	10.76	10.62
V*e*	$C(CH_3)_3$	$C_8H_{14}N_2S$	63–64°	M	58	C	56.43	56.34
						H	8.29	8.24
						N	16.45	16.30
V*f*	$(CH_2)_4CH_3$	$C_9H_{16}N_2S$	59–60°	M	23	C	58.64	58.61
						H	8.77	8.81
						N	15.20	15.09
V*g*		$C_{10}H_{16}N_2S$	82–85°	M	49	C	61.19	60.83
						H	8.22	8.04
						N	14.27	13.91

[a] The recrystallization solvent was 95% ethanol (E), aqueous methanol (M), or absolute ethanol (A). [b] Melting points and analytical data for V*a*, V*b*, and V*d* are for the hydrogen oxalate salt.

Table IV—Inhibition of Phosphodiesterase[a]

Compound	I_{50}, μM 1 μM cAMP[b]	I_{50}, μM 100 μM cAMP[b]
I*a*	(30)[c]	(25)[c]
I*b*	792	1888
I*c*	498	928
I*d*	(36)[c]	(20)[c]
I*e*	—	(34)[c]
I*f*	—	(14)[c]
I*g*	1139[d]	1802[d]
I*h*	—	(29)[e]
I*i*	307[d]	882[d]
II*a*	—	(1)[c]
II*b*	828	1463
II*c*	208	444
II*d*	711	1709
II*e*	245	840
II*f*	338	1131[d]
II*g*	300	571
Theophylline	306 (349[d])	917

[a] Bovine heart phosphodiesterase was used. [b] Substrate concentration. [c] Values in parentheses are the percent inhibition obtained at an inhibitor concentration of 500 μM; insufficient sample was available to determine the I_{50}. [d] Determined in the presence of 2.5% ethanol needed to solubilize inhibitors. [e] Same as *c* with inhibitor concentration at 250 μM.

filtrate was dried with anhydrous sodium sulfate. Removal of solvent *in vacuo* gave 3.4 g of an oil, which failed to crystallize. Dropwise addition of an ethereal solution of the oil to a solution of oxalic acid (1.96 g) in 50 ml of anhydrous ether at 0° resulted in a quantitative yield of the oxalate salt. Recrystallization from absolute ethanol gave the oxalate salt of V*b* as small white crystals, mp 94–95°.

The 2-alkylaminothiazoles V*a*–V*g* (Table III) were prepared in the same manner as V*b*.

Anhydro-5-hydroxy-7-oxo-8-isobutylthiazolo[3,2-*a*]pyrimidinium Hydroxide (I*b*)—Compound V*b* (0.55 g, 3.6 mmoles) and bis(2,4,6-trichlorophenyl) malonate (VI*a*) (9) (1.66 g, 3.6 mmoles) were heated neat at 160°, under a slow stream of nitrogen, until a clear melt resulted (~3 min). When cool, the resultant oil was triturated with 20 ml of anhydrous ether; the crude product crystallized and was collected.

Recrystallization from ethyl acetate gave 0.6 g (74%) of I*b* as off-white crystals, mp 155–157°; IR (KBr): 1630 cm^{-1}; NMR ($CDCl_3$): δ 0.80–1.28 (m, 7H), 3.84 (d, 2H, CH_2), 5.11 (s, 1H, C-6 H), 7.05 (d, 1H, thiazole proton), and 8.13 (d, 1H, thiazole proton) ppm. Table I lists the analytical data. Compounds I*a*–I*i* (Table I) were prepared in the same manner as I*b* with either VI*a* or VI*b* (9).

Enzyme Assays—The assay of Klee (10) was used, employing bovine heart phosphodiesterase[3], cyclic 8-^{3}H-adenosine monophosphate[4] (specific activity of 30 Ci/mmole), and ^{14}C-adenosine 5′-monophosphate[5] (specific activity of 570 Ci/mmole).

Ion-exchange resin[6], 200–400 mesh, H^+ form, was suspended in water; enough slurry was poured into disposable polypropylene columns[7] (0.7 × 4 cm) to provide a column volume of 1 ml. Prior to use, the columns were washed with 4 ml of 1 *N* NaOH, 4 ml of 1 *N* HCl, and 8 ml of water. The reaction mixtures (0.2 ml) contained routinely 3.8 μg of protein (8×10^{-4} enzyme unit) at the high substrate concentration or 1.3 μg of protein (2.7×10^{-4} enzyme unit) at the low substrate concentration along with 0.05 *M* tris(hydroxymethyl)aminomethane hydrochloride buffer (pH 8.0), 1 m*M* disodium ethylenediaminetetraacetate, 3 m*M* $MgCl_2$, and 1×10^{-6}–10^{-4} *M* (150,000–200,000 cpm) ^{3}H-cyclic AMP. Incubation at 37° was started by addition of enzyme, and the reaction was stopped after 20 min by addition of 1 ml of 5% trichloroacetic acid containing 1 m*M* cyclic AMP [1 m*M* ^{14}C-5′-AMP (2000–3000 cpm)]. ^{14}C-5′-AMP was added to permit estimation of the recovery of AMP after chromatography and correction of assay values for losses.

The sample was applied to the tops of the columns, which were then washed twice with 1 ml of water and three times with 3 ml of water. The eluate from these washes was discarded. Then 5′-AMP was eluted with 4 ml of 0.4 *M* sodium citrate (adjusted to pH 7.5 with citric acid), and the 4 ml was collected directly into a scintillation vial. The fraction containing 5′-AMP was counted after addition of 12 ml of scintillation fluor[8]. The enzyme was shown to contain both high and low K_m activities comparable to those reported (11). Initial rate measurements were linear with enzyme concentration and time (to 40 min).

The I_{50} values were determined by plotting uninhibited velocity/inhibited velocity (V_0/V) *versus* the inhibitor concentration. The I_{50} is the inhibitor concentration when $V_0/V = 2$. Five different inhibitor concentrations, giving 25–75% inhibition, were used for each inhibitor.

[3] Sigma Chemical Co., St. Louis, Mo.
[4] Amersham/Searle Corp, Chicago, Ill.
[5] New England Nuclear, Boston, Mass.
[6] AG-50W × 8.
[7] Biorad Laboratories, Richmond, Calif.
[8] Aquasol, New England Nuclear Co.

REFERENCES

(1) "The Pharmacological Basis of Therapeutics," 5th ed., L. S. Goodman and A. Gilman, Eds., Macmillan, New York, 1975, chap. 19.

(2) M. S. Amer and W. E. Kreighbaum, *J. Pharm. Sci.*, **64**, 1 (1975).

(3) M. Chasin and D. Harris, *Adv. Cycl. Nucl. Res.*, **7**, 225 (1976).

(4) R. A. Coburn, R. A. Carapellotti, and R. A. Glennon, *J. Heterocycl. Chem.*, **10**, 479 (1973).

(5) R. A. Coburn and R. A. Glennon, *ibid.*, **10**, 487 (1973).

(6) R. A. Coburn and R. A. Glennon, *J. Pharm. Sci.*, **62**, 1785 (1973).

(7) R. A. Coburn, R. A. Glennon, and Z. Chmielewicz, *J. Med. Chem.*, **17**, 1025 (1974).

(8) F. Ueda, T. Ueda, and S. Toyoshima, *Yakugaku Zasshi*, **79**, 920 (1959); through *Chem. Abstr.*, **53**, 21888 (1959).
(9) T. Kappe, *Monatsh. Chem.*, **98**, 874 (1967).
(10) C. B. Klee, *Biochemistry*, **16**, 1017 (1977).
(11) S. M. Hecht, R. D. Faulkner, and S. D. Hawrelak, *Proc. Natl. Acad. Sci., USA*, **71**, 4670 (1974).

ACKNOWLEDGMENTS

Presented in part at the Southeast Regional American Chemical Society meeting, Tampa, Fla., November 1977.

Supported in part by an A. D. Williams Fluid Fund Grant, Medical College of Virginia, Virginia Commonwealth University.

GLC Determination of Tilidine, Nortilidine, and Bisnortilidine in Biological Fluids with a Nitrogen-Sensitive Detector

H. HENGY ˣ, K.-O. VOLLMER, and V. GLADIGAU

Received January 30, 1978, from the *Department of Biochemistry, Gödecke Research Institute, D-7800 Freiburg, West Germany.* Accepted for publication April 25, 1978.

Abstract □ A sensitive and specific GLC method is described to determine therapeutic levels of tilidine and its two main metabolites, nortilidine and bisnortilidine, in plasma and urine. The method involves the extraction of the compounds and an internal standard with cyclohexane from alkalinized samples, followed by back-extraction into 1 *N* HCl. The hydrochloric acid solution is evaporated to dryness. After liberation of the free bases with ammonia, the residue is subjected to GLC analysis with a nitrogen–phosphorus detector and a 1.8-m (6-ft) glass column packed with 1% CRS 101 and 1.5% LAC-4-R-886 on Gas Chrom Q. Sensitivity in plasma and urine is ~1 ng/ml for a 5-ml sample.

Keyphrases □ Tilidine and metabolites—GLC analyses in biological fluids □ GLC—analyses, tilidine and metabolites in biological fluids □ Analgesics—tilidine and metabolites, GLC analyses in biological fluids

Tilidine hydrochloride[1] [ethyl DL-*trans*-2-(dimethylamino)-1-phenyl-3-cyclohexene-1-carboxylate hydrochloride] is a potent analgesic (1). Tilidine is metabolized rapidly to form the corresponding *N*-desmethyl- and *N*-bis(desmethyl) derivatives (2). A specific and sensitive analytical method was needed for the quantitative determination of tilidine and its two main metabolites, nortilidine and bisnortilidine, in biological fluids to study their kinetics in the body.

A GLC method (3) was used in previous pharmacokinetic studies, but the GLC column exhibited adsorption of bisnortilidine after a short time. A modified GLC column, well suited for the analytical control of the substances, was described recently (4).

This paper reports a new, sensitive, and selective GLC assay for tilidine, nortilidine, and bisnortilidine in plasma and urine. A thermoionic detector and a column packed with 1% CRS and 1.5% LAC-4-R-886 on Gas Chrom Q are used. The advantages of this method in comparison to the previous method are improved column stability, increased

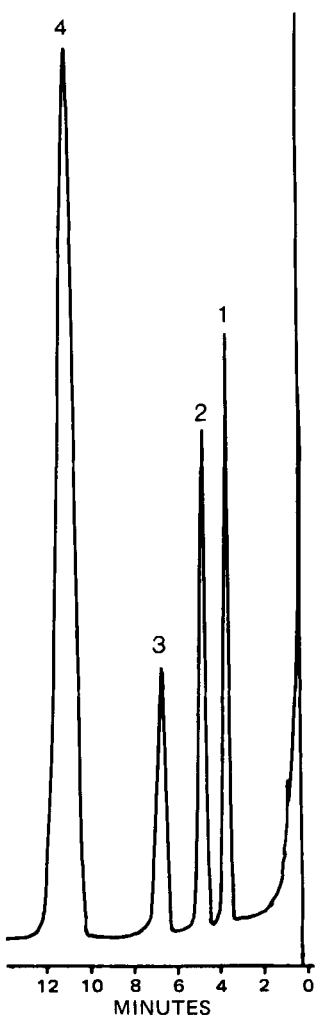

Figure 1—*Chromatogram of standards directly injected onto the columns. Key: 1, 20 ng of tilidine; 2, 20 ng of nortilidine; 3, 20 ng of bisnortilidine; and 4, 150 ng of internal standard. Attenuation was 16 × 1.*

[1] Valoron, Gödecke AG, Freiberg, West Germany (IND approved in the United States).

0022-3549/78/1200-1765$01.00/0
© 1978, American Pharmaceutical Association

(8) F. Ueda, T. Ueda, and S. Toyoshima, *Yakugaku Zasshi*, **79**, 920 (1959); through *Chem. Abstr.*, **53**, 21888 (1959).
(9) T. Kappe, *Monatsh. Chem.*, **98**, 874 (1967).
(10) C. B. Klee, *Biochemistry*, **16**, 1017 (1977).
(11) S. M. Hecht, R. D. Faulkner, and S. D. Hawrelak, *Proc. Natl. Acad. Sci., USA*, **71**, 4670 (1974).

ACKNOWLEDGMENTS

Presented in part at the Southeast Regional American Chemical Society meeting, Tampa, Fla., November 1977.

Supported in part by an A. D. Williams Fluid Fund Grant, Medical College of Virginia, Virginia Commonwealth University.

GLC Determination of Tilidine, Nortilidine, and Bisnortilidine in Biological Fluids with a Nitrogen-Sensitive Detector

H. HENGY ˣ, K.-O. VOLLMER, and V. GLADIGAU

Received January 30, 1978, from the *Department of Biochemistry, Gödecke Research Institute, D-7800 Freiburg, West Germany.* Accepted for publication April 25, 1978.

Abstract □ A sensitive and specific GLC method is described to determine therapeutic levels of tilidine and its two main metabolites, nortilidine and bisnortilidine, in plasma and urine. The method involves the extraction of the compounds and an internal standard with cyclohexane from alkalinized samples, followed by back-extraction into 1 *N* HCl. The hydrochloric acid solution is evaporated to dryness. After liberation of the free bases with ammonia, the residue is subjected to GLC analysis with a nitrogen–phosphorus detector and a 1.8-m (6-ft) glass column packed with 1% CRS 101 and 1.5% LAC-4-R-886 on Gas Chrom Q. Sensitivity in plasma and urine is ~1 ng/ml for a 5-ml sample.

Keyphrases □ Tilidine and metabolites—GLC analyses in biological fluids □ GLC—analyses, tilidine and metabolites in biological fluids □ Analgesics—tilidine and metabolites, GLC analyses in biological fluids

Tilidine hydrochloride[1] [ethyl DL-*trans*-2-(dimethylamino)-1-phenyl-3-cyclohexene-1-carboxylate hydrochloride] is a potent analgesic (1). Tilidine is metabolized rapidly to form the corresponding *N*-desmethyl- and *N*-bis(desmethyl) derivatives (2). A specific and sensitive analytical method was needed for the quantitative determination of tilidine and its two main metabolites, nortilidine and bisnortilidine, in biological fluids to study their kinetics in the body.

A GLC method (3) was used in previous pharmacokinetic studies, but the GLC column exhibited adsorption of bisnortilidine after a short time. A modified GLC column, well suited for the analytical control of the substances, was described recently (4).

This paper reports a new, sensitive, and selective GLC assay for tilidine, nortilidine, and bisnortilidine in plasma and urine. A thermoionic detector and a column packed with 1% CRS and 1.5% LAC-4-R-886 on Gas Chrom Q are used. The advantages of this method in comparison to the previous method are improved column stability, increased

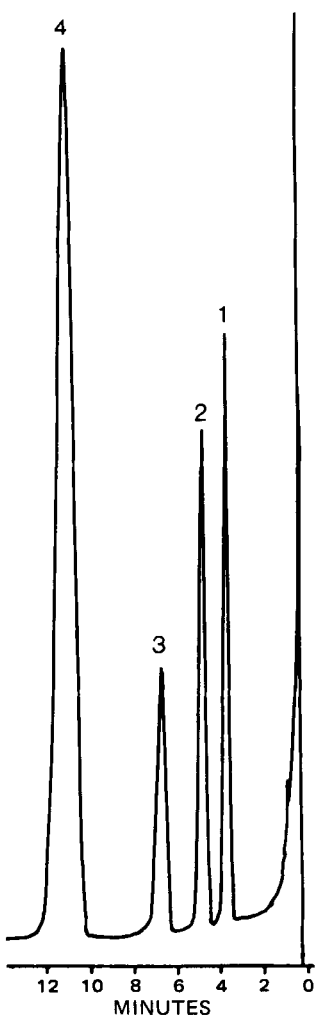

Figure 1—*Chromatogram of standards directly injected onto the columns. Key: 1, 20 ng of tilidine; 2, 20 ng of nortilidine; 3, 20 ng of bisnortilidine; and 4, 150 ng of internal standard. Attenuation was 16 × 1.*

[1] Valoron, Gödecke AG, Freiberg, West Germany (IND approved in the United States).

0022-3549/78/1200-1765$01.00/0
© 1978, American Pharmaceutical Association

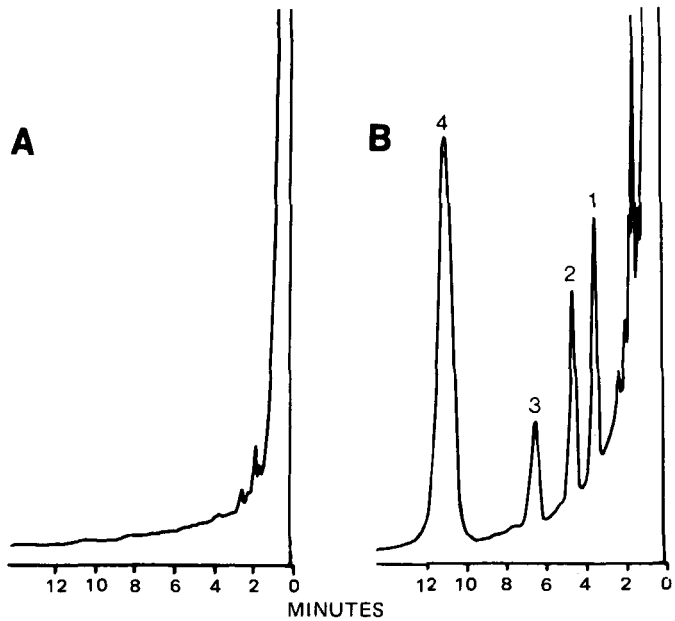

Figure 2—*Chromatograms of a blank plasma extract (A) and an extract from 10 ml of plasma spiked with 50 ng of tilidine, nortilidine, and bisnortilidine and 500 ng of internal standard (B). Key: 1, tilidine; 2, nortilidine; 3, bisnortilidine; and 4, internal standard. Attenuation was 16 × 1.*

sensitivity, and simplified cleanup. The utility of the method is shown after administration of 50 mg iv of tilidine hydrochloride to humans.

Table I—Peak Area Ratios (Tilidine, Nortilidine, and Bisnortilidine *versus* Internal Standard) after Three Calibration Runs with Spiked Human Plasma

Amount, ng	Peak Area Ratio						
	Calibration						
	1	2	3	Mean	*SD*	*CV*, %	*SEM*
			Tilidine				
25	0.0850	0.0930	0.0880	0.0887	0.0040	4.56	0.0023
50	0.1800	0.1900	0.1700	0.1800	0.0100	5.56	0.0058
100	0.4100	0.4400	0.3600	0.4033	0.0404	10.02	0.0233
250	1.1000	1.2050	1.0500	1.1183	0.0791	7.07	0.0457
500	2.0500	2.1800	2.0500	2.0933	0.0750	3.59	0.0433
1000	3.7500	4.0800	3.9700	3.9333	0.1680	4.27	0.0970
			Nortilidine				
25	0.0920	0.1000	0.0890	0.0937	0.0057	6.07	0.0033
50	0.1950	0.2100	0.1800	0.1950	0.0150	7.69	0.0087
100	0.4100	0.4300	0.4000	0.4133	0.0153	3.70	0.0088
250	1.1500	1.0800	1.0500	1.0933	0.0513	4.69	0.0296
500	2.2100	2.3000	2.1600	2.2233	0.0709	3.19	0.0410
1000	4.0700	4.2800	4.1200	4.1567	0.1097	2.64	0.0633
			Bisnortilidine				
25	0.0680	0.0820	0.0650	0.0717	0.0091	12.66	0.0052
50	0.1400	0.1600	0.1400	0.1467	0.0115	7.87	0.0067
100	0.3000	0.2800	0.3200	0.3000	0.0200	6.67	0.1155
250	0.7200	0.7100	0.7700	0.7333	0.0321	4.38	0.0186
500	1.4100	1.4800	1.5200	1.4700	0.0557	3.79	0.0321
1000	2.7800	2.9500	2.9800	2.9033	0.1079	3.71	0.0623

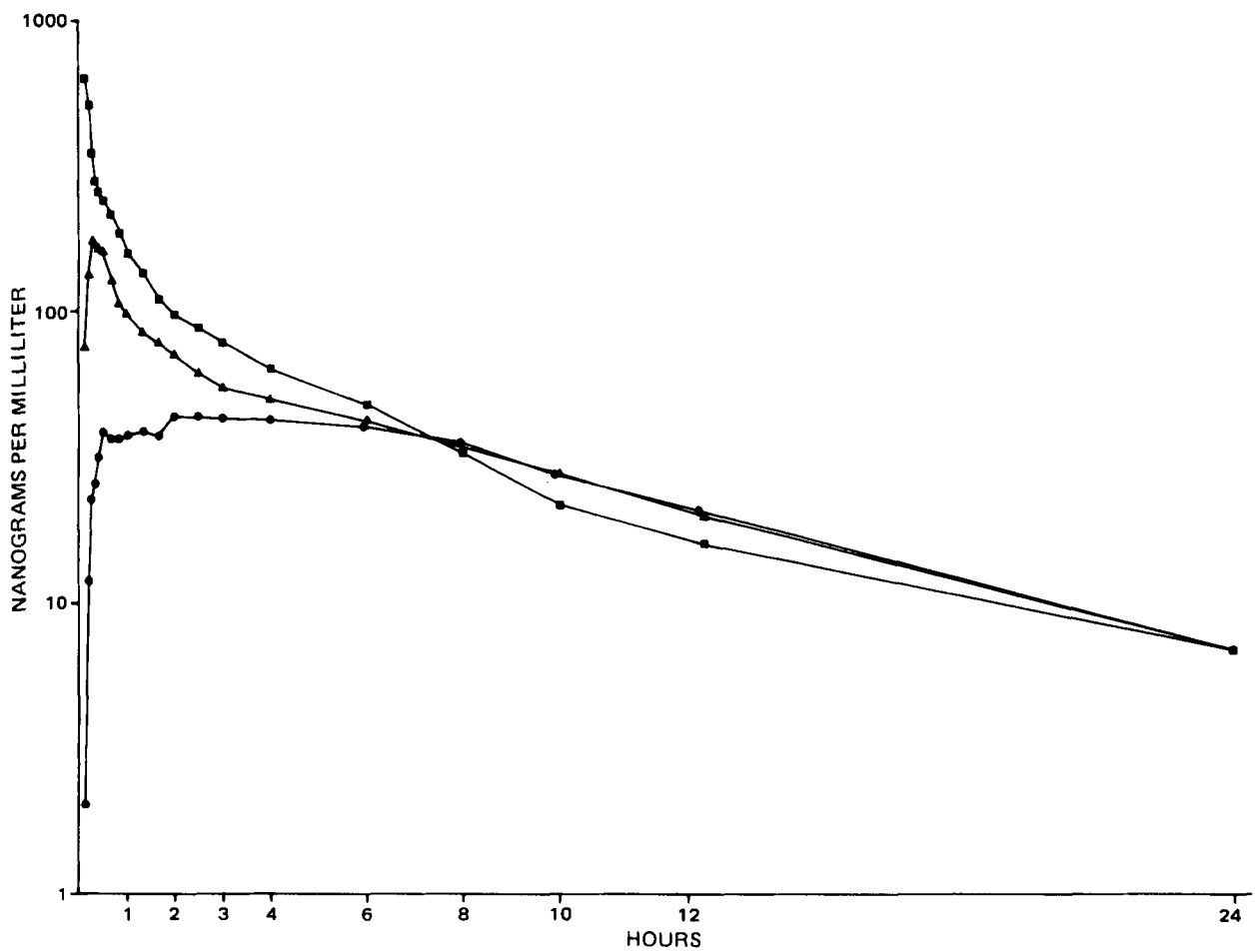

Figure 3—*Tilidine, nortilidine, and bisnortilidine concentrations in human plasma following single intravenous dose of 50 mg of tilidine hydrochloride.*

EXPERIMENTAL

Reagents and Standards—All reagents[2] were analytical grade. Aqueous solutions were prepared in double-distilled water. The following reagents and standards were used: 1 *N* NaOH, aqueous; 0.01 *N* NaOH, aqueous; 0.1 *N* HCl, aqueous; cyclohexane, distilled; sodium sulfate, anhydrous; chloroform; ethyl acetate; tilidine hydrochloride[1]; nortilidine hydrochloride[3]; bisnortilidine hydrochloride[4]; and 1[(*R*)-*N*-(dipropyl)-amino]-4-phenyl-4-ethoxycarbonylcyclohexene as the internal standard[5].

Apparatus—Measurements were carried out with a gas chromatograph equipped with a nitrogen–phosphorus detector and a 0.001–10-v recorder[6]. Retention times and peak areas were determined with a computing integrator[7]. For the sample preparations, an automatic shaker[8] and rotary evaporators[9] were used. All glassware was washed in detergent, thoroughly rinsed with water, soaked in chromic acid overnight, rinsed with water again, and dried in an oven at 70°.

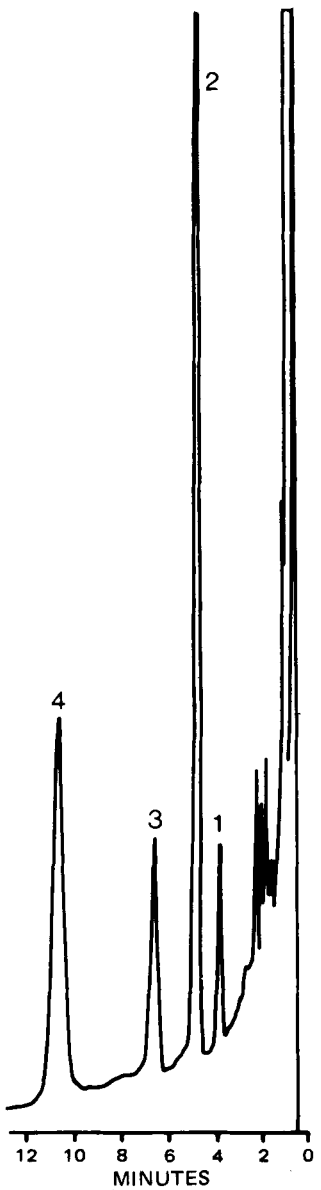

Figure 4—*Chromatogram of a plasma extract 80 min after oral administration of 50 mg of tilidine hydrochloride to a male subject. Key: 1, tilidine; 2, nortilidine; 3, bisnortilidine; and 4, internal standard. Attenuation was 8 × 1.*

GLC Conditions—The 1.8-m × 2-mm silanized glass column was packed with 1% CRS 101[10] and 1.5% LAC-4-R-886[11] on 80–100-mesh Gas Chrom Q[12]. To prepare the column packing, the stationary phases were dissolved in chloroform, poured over Gas Chrom Q, mixed well, and left to stand for ~15 min. Most of the solvent was then evaporated at 70° (without vacuum), followed by final evaporation on a rotary evaporator under vacuum at 50°. During the filling of the column, it was held in an ultrasonic bath[13] from time to time to ensure optimal packing. The column was conditioned for 24 hr at 180° prior to use.

The temperature settings were: injection port, 190°; outlet manifold, 200°; and column oven, 165°. The duo-dial knob of the temperature unit of the nitrogen detector was set at 600. The detector gases were hydrogen at 2 ml/min and synthetic air at 100 ml/min. The carrier gas was nitrogen at 20 ml/min. The recorder was set at 2-mv full-scale deflection, and the chart speed was 5 mm/min.

Procedure—Plasma or urine 1–5 ml (amount depended on the concentration), was placed in a separator. Internal standard, 500 ng, dissolved in 100 μl of double-distilled water, and 0.5 ml of 1 *N* NaOH were added. The sample was extracted three times for 2 min with 20-ml portions of cyclohexane on an automatic shaker. The combined cyclohexane solutions were washed once with 5 ml of 0.01 *N* NaOH and 5 ml of double-distilled water. Then the cyclohexane was reextracted with 10 and 5 ml of 0.1 *N* HCl.

The cyclohexane solution was discarded, and the combined hydrochloric acid solutions were evaporated to dryness on a rotary evaporator in a 25-ml round-bottom flask at 40°. The residue was transferred into a 5-ml tapered flask with 0.1 *N* HCl (3 × 1 ml) and again evaporated to dryness. The content of the flask was redissolved in 200 μl of chloroform, followed by evaporation with a gentle stream of nitrogen to concentrate the compounds in the tip of the flask.

Dry ammonia vapors were blown into the flask, and ~10–20 μl of ethyl acetate was added. The flask was stored in ice; 1–4 μl of this solution was injected into the gas chromatograph. The peak areas were calculated with a computing integrator. The computing integrator also calculated the amounts directly with previously determined stored calibration factors.

Standard Calibration Curves—Blank plasma (5 ml) was spiked with known concentrations (25–1000 ng) of aqueous solutions of tilidine, nortilidine, and bisnortilidine and with 500 ng of internal standard in 100 μl of water. The analyses were carried out as described. Standard curves were prepared by plotting the peak area ratios (substances to internal standard) *versus* nanograms of the determined substances (Table I).

RESULTS AND DISCUSSION

GLC analysis of secondary and primary amines is often hampered by the adsorption of these compounds on the GLC columns. In earlier studies, the support material (80–100-mesh Chromosorb G H.P.) was coated with 0.5% PEI and 0.75% LAC-4-R-886 to suppress column support activity. The alkaline properties of polyethyleneimine resulted in a GLC column on which nortilidine and bisnortilidine could be chromatographed over a long period without any noticeable adsorption. A number of biological samples were analyzed with this type of column.

During these experiments, a flame-ionization detector was used for GLC analysis. When a nitrogen-selective detector became available, polyethyleneimine was replaced by CRS 101 (amine-substituted silicone phase), which also possesses alkaline properties and deactivating adsorption sites. CRS 101 appeared to be a thermally stable stationary phase because of its low volatility; polyethyleneimine, in combination with the nitrogen-selective detector, showed a permanent baseline drift and extensive noise, limiting the advantages of a nitrogen-selective detector.

On the ethylene glycol succinate–CRS 101 column, the retention times of the substances to be determined were: tilidine, 3.7 min; nortilidine, 4.8 min; bisnortilidine, 6.7 min; and internal standard, 11.0 min. A typical chromatogram of standards directly injected onto the column is shown

[2] Merck, Darmstadt, West Germany.

[3] Ethyl DL-*trans*-2-(methylamino)-1-phenyl-3-cyclohexene-1-carboxylate hydrochloride. Prepared by the Chemical Department, Gödecke Research Institute, Freiburg, West Germany.

[4] Ethyl DL-*trans*-2-amino-1-phenyl-3-cyclohexene-1-carboxylate hydrochloride [isolated from rabbit urine (2)].

[5] Prepared by the Chemical Department, Gödecke Research Institute, Freiburg, West Germany.

[6] Model 900, Perkin-Elmer Corp., Überlingen, West Germany.

[7] Autolab System I, Spectraphysics GmbH, Darmstadt, West Germany.

[8] Bühler, Tübingen, West Germany.

[9] Büchi, Buchs, Switzerland.

[10] Chemical Research Services, Addison, Ill.

[11] Varian GmbH, Darmstadt, West Germany.

[12] WGA, Düsseldorf, West Germany.

[13] Bransonic 32, Branson Europe B.V., Soest, The Netherlands.

in Fig. 1. Chromatograms of a blank plasma sample (A) and a 10-ml plasma sample spiked with 50 ng of tilidine, nortilidine, and bisnortilidine and 500 ng of internal standard (B) are shown in Fig. 2.

The internal standard showed similar extraction properties to tilidine and the metabolites and was consequently well suited for quantitative analysis. The recovery of all substances from plasma ranged from 88 to 92%.

The accuracy and precision of this method are reflected by the data obtained from triplicate analyses of spiked plasma samples at different concentrations (Table I). The sensitivity limit was ~1 ng/ml for all three substances with a 5-ml sample.

The usefulness of an integrator system was checked by a special case regression analysis with the assumption that the line passes through the origin. For tilidine, nortilidine, and bisnortilidine, correlation indexes of 99.74, 99.38, and 99.90%, respectively, were found. In all three cases, the correlation coefficient was above 0.996. The slopes of the regression lines pressed through the origin did not differ from those obtained by a regression analysis with both degrees of freedom. With both methods, slopes of 0.0040, 0.0042, and 0.0029 for tilidine, nortilidine, and bisnortilidine, respectively, were calculated.

Some drugs or their metabolites were responsible for peaks appearing later in the chromatographic run and delayed the analysis. These substances must be eluted by increasing the column temperature prior to the next analysis. Therefore, volunteers who have taken no medication should be used for pharmacokinetic studies.

The described method is well suited for the determination of tilidine, nortilidine, and bisnortilidine in plasma and urine following therapeutic doses of the analgesic tilidine hydrochloride to humans. The results of a plasma level study after a single administration of 50 mg iv of tilidine hydrochloride to a fasting male volunteer (age 32, 70 kg) are given in Fig. 3. Figure 4 shows a typical chromatogram of a plasma sample after oral administration of tilidine hydrochloride to a male volunteer. This method is currently employed for routine analyses of biological samples.

REFERENCES

(1) K.-O. Vollmer and A. Poisson, *Arzneim.-Forsch.*, **26,** 1827 (1976).

(2) K.-O. Vollmer and H. Achenbach, *ibid.*, **24,** 1237 (1974).

(3) K.-O. Vollmer and F. Zimmermann, *ibid.*, **20,** 995 (1970).

(4) G. Satzinger, W. Herrmann, and F. Zimmermann, *Pharm. Ind.*, **40,** 657 (1978).

Toxic Substances Produced by *Fusarium* V: Occurrence of Zearalenone, Diacetoxyscirpenol, and T-2 Toxin in Moldy Corn Infected with *Fusarium moniliforme* Sheld.

S. GHOSAL ˣ, K. BISWAS, R. S. SRIVASTAVA, D. K. CHAKRABARTI *, and K. C. BASU CHAUDHARY *

Received July 14, 1977, from the *Pharmaceutical Chemistry Research Laboratory, Department of Pharmaceutics, Banaras Hindu University, Varanasi-5, India.* Accepted for publication April 27, 1978. *Department of Plant Pathology, Banaras Hindu University, Varanasi-5, India.

Abstract □ Sweet corn infected with *Fusarium moniliforme* Sheld. (CMI-IMI 204057) while growing in the fields was shown to contain zearalenone, diacetoxyscirpenol, and T-2 toxin. Assays by spectral, chemical, and biological methods established the presence of these substances, with zearalenone being the most abundant. *In vitro* cultures of the fungus also produced the three toxins.

Keyphrases □ *Fusarium moniliforme* mold—infected sweet corn and *in vitro* cultures, toxins isolated and identified □ Toxins—isolated and identified in extracts of sweet corn infected with *Fusarium moniliforme* mold and *in vitro* cultures

Toxicity of natural products from *Fusarium* has received wide attention because of its greater incidence and, perhaps, greater importance than aflatoxins (1, 2). As part of a continuing study on *Fusarium*-induced toxicity of foodstuffs (3–6), this paper reports the isolation, characterization, and quantitation of three mycotoxins, zearalenone, diacetoxyscirpenol, and T-2 toxin, from moldy sweet corn (*Zea mays* Linn., local variety) infected with *Fusarium moniliforme*[1] Sheld. while growing in the fields. The samples were collected from the valley of the Ganges in the Varanasi District of Uttar Pradesh, India, during July 1976, when they were ready for table use.

EXPERIMENTAL

Extraction of Mycotoxins—The ground moldy corn (about 500 g) was macerated in a blender[2] with chloroform (2 liters), and the mixture was kept at 35 ± 5° for 1 week. It then was filtered, and the solvent was removed from the chloroform extract when a thick brown oily liquid was obtained. This substance was dissolved in methanol–water (80:20, 100 ml) and extracted with *n*-hexane (3 × 30-ml portions) to remove the lipid materials.

The aqueous methanol layer was further diluted with water (50 ml) and then extracted with chloroform–ethyl acetate (1:1, 2 × 30-ml portions). Evaporation of the chloroform–ethyl acetate extract gave a light-brown oily substance (1.08 g), which was found to be biologically active when tested according to literature methods (7, 8). It showed several fluorescent and Ehrlich-positive spots on TLC on silica gel G[3]. Benzene–methanol–acetic acid (24:2:1) was used as the developer.

A portion of the oily liquid (0.52 g) was dissolved in chloroform (10 ml) and chromatographed over a column of silica gel[4] (60–120 mesh, 1.8 × 40 cm). Elution was carried out with benzene–ethyl acetate (80:20, 200 ml). Fractions (10 ml) were collected.

Zearalenone—The residue from fractions 4–7, an amorphous solid (8 mg), showed a faint blue fluorescent spot, R_f 0.48, under UV light and an olive-green fluorescent spot when sprayed with concentrated sulfuric acid with subsequent heat treatment (100–110° for 10 min) on thin-layer plates.

Attempts to crystallize the solid from common organic solvents were unsuccessful. The compound fragmented before giving any molecular

[1] The identity of the fungus, Strain CMI-IMI 204057, was confirmed by the Commonwealth Mycological Institute, Kew, England.

[2] Waring.

[3] E. Merck, Darmstadt, West Germany.

[4] British Drug Houses, Poole, England.

0022-3549/78/1200-1768$01.00/0

© 1978, American Pharmaceutical Association

in Fig. 1. Chromatograms of a blank plasma sample (A) and a 10-ml plasma sample spiked with 50 ng of tilidine, nortilidine, and bisnortilidine and 500 ng of internal standard (B) are shown in Fig. 2.

The internal standard showed similar extraction properties to tilidine and the metabolites and was consequently well suited for quantitative analysis. The recovery of all substances from plasma ranged from 88 to 92%.

The accuracy and precision of this method are reflected by the data obtained from triplicate analyses of spiked plasma samples at different concentrations (Table I). The sensitivity limit was ~1 ng/ml for all three substances with a 5-ml sample.

The usefulness of an integrator system was checked by a special case regression analysis with the assumption that the line passes through the origin. For tilidine, nortilidine, and bisnortilidine, correlation indexes of 99.74, 99.38, and 99.90%, respectively, were found. In all three cases, the correlation coefficient was above 0.996. The slopes of the regression lines pressed through the origin did not differ from those obtained by a regression analysis with both degrees of freedom. With both methods, slopes of 0.0040, 0.0042, and 0.0029 for tilidine, nortilidine, and bisnortilidine, respectively, were calculated.

Some drugs or their metabolites were responsible for peaks appearing later in the chromatographic run and delayed the analysis. These substances must be eluted by increasing the column temperature prior to the next analysis. Therefore, volunteers who have taken no medication should be used for pharmacokinetic studies.

The described method is well suited for the determination of tilidine, nortilidine, and bisnortilidine in plasma and urine following therapeutic doses of the analgesic tilidine hydrochloride to humans. The results of a plasma level study after a single administration of 50 mg iv of tilidine hydrochloride to a fasting male volunteer (age 32, 70 kg) are given in Fig. 3. Figure 4 shows a typical chromatogram of a plasma sample after oral administration of tilidine hydrochloride to a male volunteer. This method is currently employed for routine analyses of biological samples.

REFERENCES

(1) K.-O. Vollmer and A. Poisson, *Arzneim.-Forsch.*, **26,** 1827 (1976).

(2) K.-O. Vollmer and H. Achenbach, *ibid.*, **24,** 1237 (1974).

(3) K.-O. Vollmer and F. Zimmermann, *ibid.*, **20,** 995 (1970).

(4) G. Satzinger, W. Herrmann, and F. Zimmermann, *Pharm. Ind.*, **40,** 657 (1978).

Toxic Substances Produced by *Fusarium* V: Occurrence of Zearalenone, Diacetoxyscirpenol, and T-2 Toxin in Moldy Corn Infected with *Fusarium moniliforme* Sheld.

S. GHOSAL ˣ, K. BISWAS, R. S. SRIVASTAVA, D. K. CHAKRABARTI *, and K. C. BASU CHAUDHARY *

Received July 14, 1977, from the *Pharmaceutical Chemistry Research Laboratory, Department of Pharmaceutics, Banaras Hindu University, Varanasi-5, India.* Accepted for publication April 27, 1978. *Department of Plant Pathology, Banaras Hindu University, Varanasi-5, India.

Abstract □ Sweet corn infected with *Fusarium moniliforme* Sheld. (CMI-IMI 204057) while growing in the fields was shown to contain zearalenone, diacetoxyscirpenol, and T-2 toxin. Assays by spectral, chemical, and biological methods established the presence of these substances, with zearalenone being the most abundant. *In vitro* cultures of the fungus also produced the three toxins.

Keyphrases □ *Fusarium moniliforme* mold—infected sweet corn and *in vitro* cultures, toxins isolated and identified □ Toxins—isolated and identified in extracts of sweet corn infected with *Fusarium moniliforme* mold and *in vitro* cultures

Toxicity of natural products from *Fusarium* has received wide attention because of its greater incidence and, perhaps, greater importance than aflatoxins (1, 2). As part of a continuing study on *Fusarium*-induced toxicity of foodstuffs (3–6), this paper reports the isolation, characterization, and quantitation of three mycotoxins, zearalenone, diacetoxyscirpenol, and T-2 toxin, from moldy sweet corn (*Zea mays* Linn., local variety) infected with *Fusarium moniliforme*[1] Sheld. while growing in the fields. The samples were collected from the valley of the Ganges in the Varanasi District of Uttar Pradesh, India, during July 1976, when they were ready for table use.

EXPERIMENTAL

Extraction of Mycotoxins—The ground moldy corn (about 500 g) was macerated in a blender[2] with chloroform (2 liters), and the mixture was kept at 35 ± 5° for 1 week. It then was filtered, and the solvent was removed from the chloroform extract when a thick brown oily liquid was obtained. This substance was dissolved in methanol–water (80:20, 100 ml) and extracted with *n*-hexane (3 × 30-ml portions) to remove the lipid materials.

The aqueous methanol layer was further diluted with water (50 ml) and then extracted with chloroform–ethyl acetate (1:1, 2 × 30-ml portions). Evaporation of the chloroform–ethyl acetate extract gave a light-brown oily substance (1.08 g), which was found to be biologically active when tested according to literature methods (7, 8). It showed several fluorescent and Ehrlich-positive spots on TLC on silica gel G[3]. Benzene–methanol–acetic acid (24:2:1) was used as the developer.

A portion of the oily liquid (0.52 g) was dissolved in chloroform (10 ml) and chromatographed over a column of silica gel[4] (60–120 mesh, 1.8 × 40 cm). Elution was carried out with benzene–ethyl acetate (80:20, 200 ml). Fractions (10 ml) were collected.

Zearalenone—The residue from fractions 4–7, an amorphous solid (8 mg), showed a faint blue fluorescent spot, R_f 0.48, under UV light and an olive-green fluorescent spot when sprayed with concentrated sulfuric acid with subsequent heat treatment (100–110° for 10 min) on thin-layer plates.

Attempts to crystallize the solid from common organic solvents were unsuccessful. The compound fragmented before giving any molecular

[1] The identity of the fungus, Strain CMI-IMI 204057, was confirmed by the Commonwealth Mycological Institute, Kew, England.

[2] Waring.

[3] E. Merck, Darmstadt, West Germany.

[4] British Drug Houses, Poole, England.

0022-3549/78/1200-1768$01.00/0

© 1978, American Pharmaceutical Association

ion peak in its mass spectrum. However, co-TLC behavior with an authentic sample of zearalenone[5] and the UV molar extinction values [λ_{max} (ethyl alcohol) (log ϵ) of the compound from the moldy corn: 235 (4.46), 275 (4.04), and 315 (3.77) nm; λ_{max} (ethyl alcohol) (log ϵ) of zearalenone reported in the literature (9): 236 (4.47), 274 (4.14), and 316 (3.77) nm] suggested that the compound was almost pure zearalenone.

The isolated compound was tested for estrogenic activity (10) in the mice uterus bioassay. An alcoholic solution of the compound, in doses of 40 μg/mouse, was mixed with a ground corn supplement ration and fed to five ovariectomized mice for 3 days. The animals were sacrificed on the 4th day, and their uteri were weighed; a 38–45% increase in uterine weight was recorded. On the basis of the bioassay, the amount of zearalenone present in the moldy corn was estimated as 30 μg/g.

Diacetoxyscirpenol—Fractions 12–15, on evaporation, gave a brown oily liquid (16 mg). It showed an Ehrlich-positive spot on TLC, R_f 0.27. Co-TLC with an authentic sample of diacetoxyscirpenol[6] using ethyl alcohol–ethyl acetate–acetone (1:4:4), ethyl alcohol–chloroform–acetone (1:4:4), and ethyl alcohol–benzene–acetone (1:3:3) suggested that the major component in the brown oily liquid was diacetoxyscirpenol.

The major component was separated by preparative TLC as a colorless amorphous solid (7 mg). It showed $[\alpha]_D^{24}$ +17.8° (c 0.78, ethyl alcohol); mass spectrum: *m/e* 306 (relative abundance 58%), 278 (25), 263 (18), 233 (12), 124 (78), 123 (70), 122 (68), and 105 (100). These values are indistinguishable from those reported in the literature (3).

In the rat skin dermal toxicity test (8), the compound from the moldy corn produced reddish wheals in doses of 200 μg/rat.

T-2 Toxin—The residue from fractions 18–20, another brown oily liquid (11 mg), showed a blue fluorescent spot, R_f 0.08, in addition to three minor gray spots of higher R_f values when the plate was sprayed with concentrated sulfuric acid, treated with heat, and viewed under UV light. The fluorescent component was separated by preparative TLC as a homogeneous gummy material (2 mg). Attempts to crystallize the compound were unsuccessful, presumably because of the scarcity of material.

Co-TLC of the homogeneous gummy material with authentic T-2 toxin[5] in the three different solvent systems suggested that they were identical. The major fragment ion peaks of the compound isolated from the moldy corn were: *m/e* 382 (relative intensity, 11%), 365 (16), 364 (28), 277 (22), 205 (45), 180 (72), 126 (55), 122 (68), and 121 (100). These values were similar to those exhibited by the authentic T-2 toxin[5] and indistinguishable from those reported for T-2 toxin (11).

A chloroform solution of the brown oily liquid, in 400-μg doses, caused necrosis and hemorrhaging in all animals when applied on the shaved skin of four albino rats. Pure T-2 toxin and the homogeneous gummy material from the moldy corn produced similar necrosis and hemorrhaging in albino rats in doses of 100 μg/rat.

Extraction of Intra- and Extracellular Toxins of *F. moniliforme*—The fungus was grown in Richard's solution (200 ml) in a still culture flask (1 liter) at 21° for 21 days. Workup of the intra- and extracellular extractives in the usual fashion (3) afforded a brown oily substance (0.47 g) which, when tested according to published methods, demonstrated emetic activity and dermal toxicity as reported for T-2 toxin (7, 8) and was positive in the hyperestrogenism test as reported for zearalenone (10). It was partitioned in solvents of graded polarity, as already described, and a light-brown semisolid (0.05 g) was obtained.

Identification by TLC indicated that the three toxins, isolated from the moldy corn, were also present in the semisolid substance. From this mixture, the toxins were separated into individual entities by TLC and column chromatography. UV absorption spectra, optical rotation data, and biological assay indicated that the amounts of zearalenone, diacetoxyscirpenol, and T-2 toxin were 5, 3, and 0.8 mg, respectively, from the extra- and intracellular extracts of a 1-liter flask.

RESULTS AND DISCUSSION

Extraction of moldy corn infected with *F. moniliforme* Sheld. with chloroform, followed by partitioning in solvents of graded polarity, column chromatography, and preparative TLC, afforded three recognized mycotoxins—*viz.*, zearalenone, diacetoxyscirpenol, and T-2 toxin, in quantities sufficient for their characterization.

Table I—Toxins Isolated from Infected Sweet Corn

Source	Zearalenone	Diacetoxyscirpenol	T-2
Naturally infected sweet corn	16 μg/g	14 μg/g	4 μg/g
Artificially infected sweet corn[a]	48 μg/g	17 μg/g	5 μg/g
Flask culture	5 mg/flask	3 mg/flask	0.8 mg/flask

[a] In closed polythene bags.

On the basis of chemical, spectral, and biological analyses, the amounts of zearalenone, diacetoxyscirpenol, and T-2 toxin present in the naturally infected moldy corn were estimated as 16, 14, and 4 μg/g, respectively. Zearalenone is known to cause severe genital disorders in dairy cattle (9, 10), diacetoxyscirpenol causes dermal toxicity in albino mice and rats in small doses and death in high doses (8), and T-2 toxin causes necrosis and hemorrhaging in albino rats and demonstrated emetic activity when tested according to published methods (7, 8, 12).

The intra- and extracellular extracts of the fungus, grown in Richard's medium, produced emetic activity in pigeons, dermal toxicity in albino rats, and hyperestrogenism in albino mice when tested according to published methods (7, 8, 10, 12). These observations indicate that the CMI-IMI 204057 strain of the fungus is a producer of diacetoxyscirpenol, T-2 toxin, and zearalenone. The individual toxins from the culture extracts subsequently were isolated and quantitated.

The three toxins were isolated from three sources of fungi, and their relative amounts are shown in Table I. The three toxins were isolated from moldy sweet corn, infected while growing in the valley of the Ganges during July 1976 (a rainy season; temperature 35 ± 5°; relative humidity 41–79%) in India. This is the first report of the toxins being produced in relatively high temperature (35 ± 5°); previously, their occurrence was reported in overwintered corn (9, 12). People in India consume sizable amounts of sweet corn as a vegetable in semibaked form so that toxins would probably not be destroyed in cooking. Prolonged ingestion of the moldy corn presents a high risk of poisoning in humans.

REFERENCES

(1) C. J. Mirocha and C. M. Christensen, *Ann. Rev. Phytopathol.*, **12**, 303 (1974).

(2) G. N. Wogan, *Ann. Rev. Pharmacol.*, **15**, 437 (1975).

(3) S. Ghosal, D. K. Chakrabarti, and K. C. Basu Chaudhary, *J. Pharm. Sci.*, **65**, 160 (1976).

(4) D. K. Charkrabarti, K. C. Basu Chaudhary, and S. Ghosal, *Experientia*, **32**, 608 (1976).

(5) S. Ghosal, K. Biswas, D. K. Chakrabarti, and K. C. Basu Chaudhary, *Phytopathology*, **67**, 548 (1977).

(6) S. Ghosal, D. K. Chakrabarti, and K. C. Basu Chaudhary, *Experientia*, **33**, 574 (1977).

(7) R. A. Ellison and F. N. Kotsonis, *Appl. Microbiol.*, **26**, 540 (1973).

(8) R.-D. Wei, E. B. Smalley, and F. M. Strong, *ibid.*, **23**, 1029 (1972).

(9) C. J. Mirocha, C. M. Christensen, and G. H. Nelson, in "Microbial Toxins," vol. 7, S. Kadis, A. Ciegler, and S. J. Ajl, Eds., Academic, New York, N.Y., 1971, p. 107.

(10) R. W. Caldwell and J. Tuite, *Appl. Microbiol.*, **20**, 31 (1970).

(11) J. R. Bamburg, N. V. Riggs, and F. M. Strong, *Tetrahedron*, **24**, 3329 (1968).

(12) K. Ishii, Y. Ando, and Y. Ueno, *Chem. Pharm. Bull.*, **23**, 2162 (1975).

ACKNOWLEDGMENTS

The authors acknowledge Dr. N. Viswanathan, Ciba-Geigy Research Centre, Bombay, India, and Dr. S. C. Pakrashi, Indian Institute of Experimental Medicine, Calcutta, India, for providing mass spectral and optical rotational data, respectively. K. Biswas, R. S. Srivastava, and D. K. Chakrabarti are indebted to the Council of Scientific and Industrial Research and the University Grants Commission, New Delhi, India, for providing research fellowships.

[5] Provided by Dr. S. Nesheim, U.S. Department of Health, Education, and Welfare, Washington, D.C.

[6] Provided by Dr. D. Hauser and Dr. A. Closse, Sandoz, Basel, Switzerland.

Tautomerism of Singly Protonated Chloroquine and Quinacrine

LEONARD S. ROSENBERG and STEPHEN G. SCHULMAN ×

Received February 17, 1978, from the *College of Pharmacy, University of Florida, Gainesville, FL 32610.* Accepted for publication April 26, 1978.

Abstract □ Differential absorptiometric pH titrations of the antimalarials chloroquine and quinacrine, employing the respective uncharged species at pH 12.5 in the reference cell, show that protolytic dissociation from the heterocyclic ring nitrogen atoms occurs over pH 6–12. This finding indicates that the singly charged cations of the drugs exist measurably in two tautomeric forms. The tautomeric equilibrium constants were calculated from the titration data. The existence of these tautomeric equilibria may have significance in the pharmacodynamics of chloroquine and quinacrine.

Keyphrases □ Chloroquine—protolytic dissociation, spectrophotometric evaluation □ Quinacrine—protolytic dissociation, spectrophotometric evaluation □ Spectrophotometry—evaluation, protolytic dissociation of chloroquine and quinacrine □ Dissociation, protolytic—chloroquine and quinacrine, spectrophotometric evaluation □ Antimalarials—chloroquine and quinacrine, protolytic dissociation, spectrophotometric evaluation

The well-known antimalarials chloroquine (1) and quinacrine (2, 3) exist as singly and doubly charged cations at physiological pH. The doubly charged cations form strong complexes with native DNA (4, 5). It was implied (6–8) that their biological activities are derived from this interaction. Although no direct evidence has been presented to demonstrate the binding of the singly charged cations to the nucleic acids, the possible biological significance of the singly charged cations cannot be dismissed. Richard and Garrett (9), for example, showed that the efficacy of quinacrine against *Escherichia coli* increases with increasing pH and is minimal at low pH where the dication is predominant. This result could indicate either a transport problem involving the dication or the activity of the monocation. In either case, the importance of the monocation for biological effect is apparent.

The dissociation constants related to the dication $\rightleftharpoons$ monocation equilibria (pK_1) and the monocation $\rightleftharpoons$ neutral molecule equilibria (pK_2) of chloroquine (1) and quinacrine (3) were reported, on the basis of spectroscopic evidence, to correspond to dissociation from the heterocyclic nitrogen atom and the aliphatic ammonium group of the side chain, respectively, as shown for chloroquine in Scheme I. However, the proximities of pK_1 and pK_2 for both drugs (for chloroquine, $pK_1 - pK_2 = 2.0$; for quinacrine, $pK_1 - pK_2 = 2.5$) suggested that some dissociation from the alkylamino groups probably would occur in the doubly charged cations. This dissociation would give rise to tautomeric monocations. To examine this possibility more closely, the present spectrophotometric reinvestigation of the protolytic dissociations of chloroquine and quinacrine was undertaken.

EXPERIMENTAL

Chloroquine phosphate[1] and quinacrine hydrochloride[1] were used without further purification. Buffer solutions were prepared by titrating 0.005 *M* dibasic sodium phosphate or boric acid with 0.1 *M* NaOH. Solutions of pH ≥ 11 were prepared by dilution of 1 *M* NaOH with distilled deionized water.

Absorption spectra were taken in 1-cm matched silica cells, thermostated at 30°, on a spectrophotometer[2]. A series of 10-ml volumetric flasks, each containing a buffer solution of a different pH, was injected, each with 100 μl of a stock solution of chloroquine or quinacrine. The final concentrations of chloroquine and quinacrine in each flask were 1.61×10^{-5} and 1.93×10^{-5} *M*, respectively.

The spectrum of each solution was scanned against the appropriate buffer blank for the direct titrations and against a blank containing chloroquine or quinacrine at pH 12.5 for the difference titrations. The difference titrations were carried out, with the scale expansion capability of the spectrophotometer's recorder, at 0–0.25 absorbance unit full-scale deflection. The direct titrations were carried out at 0–1.0 absorbance unit full-scale deflection.

RESULTS AND DISCUSSION

The absorption spectrum of chloroquine [$pK_1 = 8.1$ and $pK_2 = 10.1$ (1)] shifted to shorter wavelengths and demonstrated hypochromism with increasing pH in the pH 6–9.5 region. At pH > 9.5, any further changes in the spectrum of chloroquine were essentially imperceptible, in agreement with previous observations (1, 4). The absorption spectrum of quinacrine [$pK_1 = 7.7$ and $pK_2 = 10.2$ (3)] demonstrated hypsochromism and hypochromism with increasing pH from pH 6 to 12. However, changes in the spectrum of quinacrine were quite pronounced from pH 6 to 9 and considerably less so from pH 9 to 12. The pH dependence of the difference spectra, employing chloroquine and quinacrine at pH 12.5 (the neutral species) in the reference cell (Figs. 1 and 2), clearly shows that the absorption spectra moved to shorter wavelengths and lower intensities with increasing pH over pH 6–12.

Since the alkylamino nitrogen atoms are well removed from the aromatic portions of the drugs, the spectroscopic changes observed must be due to ionization of the heterocyclic nitrogen atoms over the pH 6–12 range. This hypothesis indicates that in the region from pH 9 or 10 to 12, where the monocation is virtually the only acidic species present, some dissociation must occur from the heterocyclic nitrogen atoms. Hence, tautomers of the monocations protonated at the ring nitrogen atoms must exist, to a measurable extent, in equilibrium with the tautomers of the

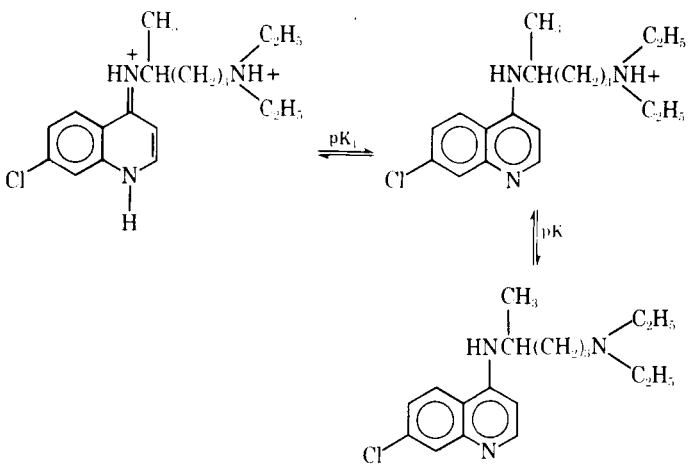

Scheme I

[1] Gift of Dr. S. Archer, Winthrop Research Institute, Rensselaer, N.Y.

[2] Model 25, Beckman Instruments, Fullerton, Calif.

0022-3549/78/1200-1770$01.00/0
© 1978, American Pharmaceutical Association

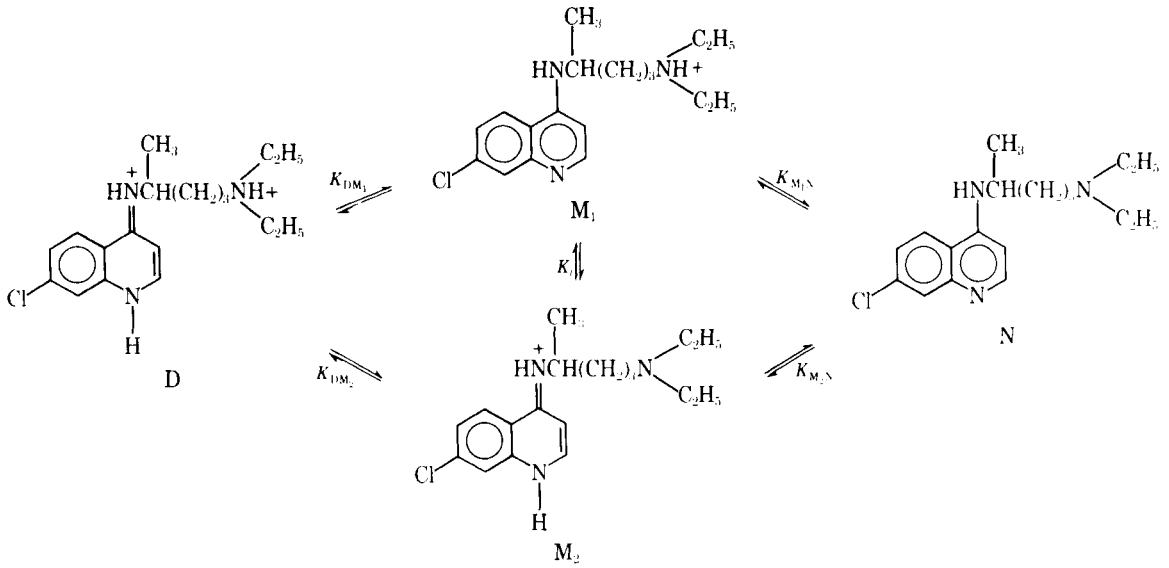

Scheme II

monocations protonated at the alkylamino nitrogen atoms, as shown for chloroquine in Scheme II where D is dication, M_1 and M_2 are monocations, and N is the neutral species.

The tautomeric ratio K_t of the equilibrium concentration ($[M_1]$) of cation M_1 to that ($[M_2]$) of M_2 may be evaluated as follows. According to Robinson and Biggs (10), for a doubly charged diprotic acid with overlapping protolytic equilibria:

$$(a - \epsilon_D C_B l)[H^+]^2 + (a - \epsilon_M C_B l)K_1[H^+] + (a - \epsilon_N C_B l)K_1K_2 = 0 \quad \text{(Eq. 1)}$$

where a is the absorbance at the analytical wavelength, C_B is the formal concentration of drug, l is the optical depth of the sample, K_1 and K_2 are the prototropic equilibrium constants of the drug, and ϵ_D, ϵ_M, and ϵ_N are the molar absorptivities of the dication, monocation, and neutral species, respectively.

From absorbance measurements at $[H^+] \gg K_1$ and $[H^+] \ll K_2$, ϵ_D and ϵ_N can easily be evaluated. However, since the successive equilibria overlap, the monocation cannot be isolated, and ϵ_M may be evaluated along with K_1 and K_2 from the simultaneous solution of Eq. 1 for at least three different values of $[H^+]$ and a. If the dissociating groups of the dication D are dissimilar, ϵ_M is not a true molar absorptivity, because [M] is not the concentration of a single species but rather a sum of the concentrations ($[M_1] + [M_2]$) of two tautomeric monocations. Since the absorbance of all monocationic species is equal to the sum of the absorbances of the tautomers, *i.e.*:

$$\epsilon_M[M]l = \epsilon_M[M_1]l + \epsilon_M[M_2]l = \epsilon_{M_1}[M_1]l + \epsilon_{M_2}[M_2]l \quad \text{(Eq. 2)}$$

the tautomeric ratio K_t is given by:

$$K_t = \frac{[M_1]}{[M_2]} = \frac{\epsilon_{M_2} - \epsilon_M}{\epsilon_M - \epsilon_{M_1}} \quad \text{(Eq. 3)}$$

Because the monocation M_2 differs from the dication D only in the absence of a proton on the aliphatic amino group, M_2 and D are essentially identical electronically in their aromatic (chromophoric) systems. Hence, it is reasonable to write $\epsilon_D = \epsilon_{M_2}$. Similarly, the monocation M_1 and the neutral molecule N have virtually identical chromophores and $\epsilon_N = \epsilon_{M_1}$. Substituting ϵ_D for ϵ_{M_2} and ϵ_N for ϵ_{M_1} in Eq. 3 yields:

$$K_t = \frac{\epsilon_D - \epsilon_M}{\epsilon_M - \epsilon_N} \quad \text{(Eq. 4)}$$

The preceding approach may be applied directly to differential titrations, such as those carried out here, without evaluation of the molar absorptivities at the analytical wavelength. In Eq. 1, let $\epsilon_D C_B l = a_D$, $\epsilon_M C_B l = a_M$, and $\epsilon_N C_B l = a_N$ so that:

$$(a - a_D)[H^+]^2 + (a - a_M)K_1[H^+] + (a - a_N)K_1K_2 = 0 \quad \text{(Eq. 5)}$$

If the reference cell in the spectrophotometer contains the analyte of concentration C_B at a pH high enough that it is all in the N form, each absorbance measurement will give the difference between the total absorbance of the solution in the sample cell and a_N:

$$([a - a_N] - [a_D - a_N])[H^+]^2 + ([a - a_N] - [a_M - a_N])K_1[H^+] + ([a - a_N] - [a_N - a_N])K_1K_2 = 0 \quad \text{(Eq. 6)}$$

If $a - a_N = \Delta a$, $a_D - a_N = \Delta a_D$, and $a_M - a_N = \Delta a_M$:

$$(\Delta a - \Delta a_D)[H^+]^2 + (\Delta a - \Delta a_M)K_1[H^+] + \Delta a K_1K_2 = 0 \quad \text{(Eq. 7)}$$

Equation 7 can be solved simultaneously in the titration of the analyte for K_1, K_2, and a_M. Multiplying the numerator and denominator of Eq.

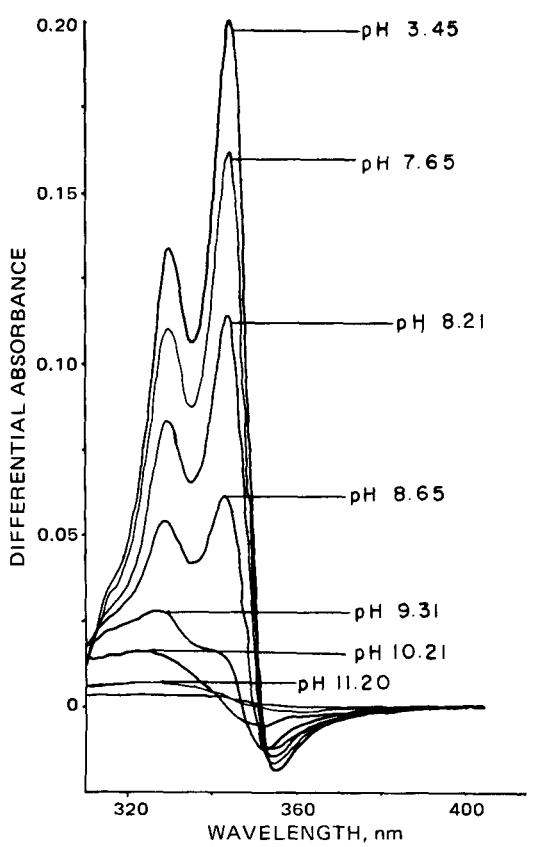

Figure 1—*The pH dependence of the differential absorption spectrum of 1.61 × 10⁻⁵ M chloroquine at 30°. The reference cell of the spectrophotometer contained 1.61 × 10⁻⁵ M chloroquine at a fixed pH of 12.5. Recorder scale expansion was 0–0.25 absorbance unit full-scale deflection.*

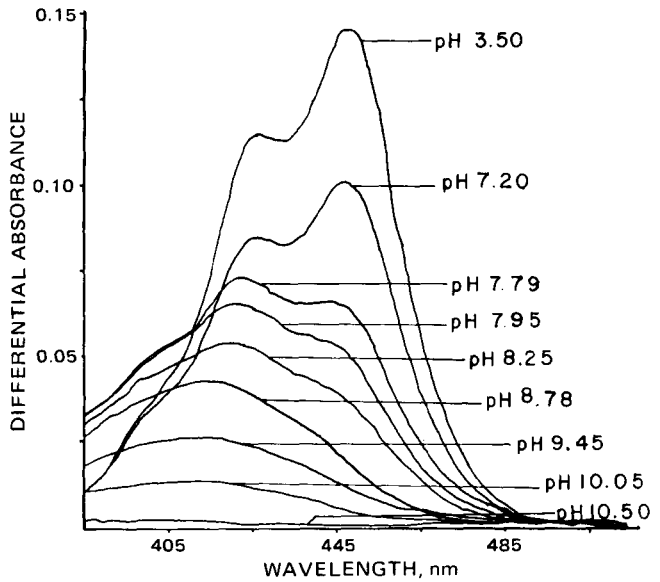

Figure 2—*The pH dependence of the differential absorption spectrum of 1.93 × 10^{-5} M quinacrine at 30°. The reference cell of the spectrophotometer contained 1.93 × 10^{-5} M quinacrine at a fixed pH of 12.5. Recorder scale expansion was 0–0.25 absorbance unit full-scale deflection.*

4 by $C_B l$ yields:

$$K_t = \frac{a_D - a_M}{a_M - a_N} \qquad \text{(Eq. 8)}$$

Moreover:

$$K_t = \frac{(a_D - a_N) - (a_M - a_N)}{(a_M - a_N) - (a_N - a_N)} \qquad \text{(Eq. 9)}$$

or:

$$K_t = \frac{\Delta a_D - \Delta a_M}{\Delta a_M} \qquad \text{(Eq. 10)}$$

Consequently, the value of Δa_M determined by the solution of Eq. 7 and that of Δa_D taken from the low pH limit of the differential titration can be used to calculate K_t directly.

Values of pK_1, pK_2, and Δa_M for chloroquine and quinacrine, calculated from the differential titrations, are presented in Table I. The analytical wavelengths of 330 nm for chloroquine and 445 nm for quinacrine were chosen for these calculations. The values of K_t resulting from these calculations are listed in Table II.

Table I—Spectroscopic and Thermodynamic Parameters of the Absorptiometric pH Titrations at 30° of Chloroquine and Quinacrine Calculated from Eq. 7 and the Data Represented in Figs. 1 and 2

	Δa_D	Δa_M	pK_1	pK_2
Chloroquine (λ = 330 nm)	0.128	0.013	8.35 ± 0.05 (8.08)[a]	10.40 ± 0.05 (10.1)[a]
Quinacrine (λ = 445 nm)	0.146	0.0158	7.72 ± 0.03 (7.69)[b]	10.39 ± 0.03 (10.18)[b]

[a] Reference 1. [b] Reference 3.

Table II—Tautomerization Constant K_t and Microequilibrium Constants for the Prototropic Equilibria of Chloroquine and Quinacrine (Scheme II) Calculated from the Data of Table I

	K_t	pK_{DM_1}	pK_{DM_2}	pK_{M_1N}	pK_{M_2N}
Chloroquine	8.9 ± 1.0	8.40	9.32	10.35	9.43
Quinacrine	8.2 ± 0.5	7.77	8.69	10.34	9.42

The tautomeric ratio K_t and the macroequilibrium constants K_1 and K_2 can be used to calculate the microequilibrium constants for the prototropic equilibria of chloroquine and quinacrine represented in Scheme II (11). The microequilibrium constants are presented in Table II.

The fact that two tautomers of chloroquine and quinacrine occur, each as substantial fractions of the population of singly charged molecules, may be of great significance in the pharmacodynamics of these drugs. For example, it is possible that one tautomer could be responsible for biological response and the other for the transport or metabolic disposition of either drug. This area is worthy of further consideration.

REFERENCES

(1) J. L. Irvin and E. M. Irvin, *J. Am. Chem. Soc.*, **69**, 1091 (1947).
(2) S. R. Christophers, *Ann. Trop. Med. Parasitol.*, **31**, 43 (1937).
(3) J. L. Irvin and E. M. Irvin, *J. Am. Chem. Soc.*, **72**, 2745 (1950).
(4) S. N. Cohen and K. L. Yielding, *J. Biol. Chem.*, **240**, 3123 (1965).
(5) D. S. Drummond, V. F. W. Simpson-Gildmeister, and A. R. Peacocke, *Biopolymers*, **3**, 135 (1965).
(6) S. N. Cohen and K. L. Yielding, *Proc. Natl. Acad. Sci. USA*, **54**, 521 (1965).
(7) J. Ciak and F. E. Hahn, *Science*, **156**, 655 (1967).
(8) M. L. Seligman and H. G. Mandel, *J. Gen. Microbiol.*, **68**, 135 (1971).
(9) A. J. Richard and E. R. Garrett, *J. Pharm. Sci.*, **63**, 894 (1974).
(10) R. A. Robinson and A. I. Biggs, *Aust. J. Chem.*, **10**, 128 (1957).
(11) R. J. Sturgeon and S. G. Schulman, *J. Pharm. Sci.*, **66**, 958 (1977).

Synthesis and Evaluation of 3-Substituted 1-[4-(2-Indol-3-ylethyl)piperazinyl]ureas as Potential Antihypertensive Agents

EDWARD J. GLAMKOWSKI *x, PHILIP A. REITANO *, and DAVID L. WOODWARD ‡

Received February 6, 1978, from the *Chemical Research Department and the ‡Department of Pharmacology, Hoechst-Roussel Pharmaceuticals, Inc., Somerville, NJ 08876. Accepted for publication May 2, 1978.

Abstract □ A series of 3-substituted 1-[4-(2-indol-3-ylethyl)piperazinyl]ureas was synthesized and screened for antihypertensive activity in spontaneously hypertensive rats. Two compounds with aryl urea substituents were very potent and lowered blood pressure 55 mm or more at oral doses of 100 mg/kg. However, both compounds failed to produce a cardiovascular response in the normotensive dog.

Keyphrases □ (Indolylethyl)piperazinylureas, substituted—synthesized, evaluated for antihypertensive activity in rats and dogs □ Antihypertensive activity—substituted (indolylethyl)piperazinylureas evaluated in rats and dogs □ Structure–activity relationships—substituted (indolylethyl)piperazinylureas evaluated for antihypertensive activity in rats and dogs

Previously (1), the synthesis and antihypertensive activity of 3-(4-acylaminopiperazinylalkyl)indoles of type I were described. These compounds are structurally related to indoramin (II), a drug clinically useful in lowering blood pressure (2, 3). The substituted indoles were derived by replacing the central portion of the indoramin molecule with the pharmacologically interesting *N*-aminopiperazine moiety.

It was of interest to modify the indoramin structure further by changing the connection between the phenyl and the piperazine rings from the amide to a urea linkage. Such a modification provided 3-substituted 1-[4-(2-indol-3-ylethyl)piperazinyl]ureas III*a*–III*h* (Table I), whose synthesis and antihypertensive effects are the subject of this report.

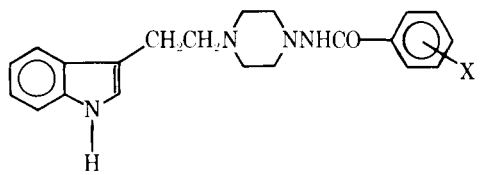

I

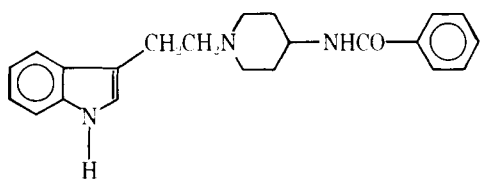

II

EXPERIMENTAL

Chemistry[1]—This class of compounds was synthesized by reacting the amino group of IV*a* and IV*b* (Scheme I) with a variety of aryl and alkyl isocyanates in dichloromethane as the solvent. The physical properties and analytical data for the resulting ureas (III*a*–III*h*) are recorded in Table I. The preparation of the precursors (IV*a* and IV*b*) was reported previously (1).

General Procedure for III*a*–III*h*.—The common method used to prepare the ureas of Table I is illustrated for 1-[4-(2-indol-3-ylethyl)-piperazinyl]-3-phenylurea (III*a*). To a stirred solution of 6.13 g (0.025 mole) of 3-[2-(4-aminopiperazinyl)ethyl]indole (IV*a*) in 100 ml of dry dichloromethane was added dropwise 3.53 g (0.035 mole) of phenyl isocyanate[2] while the reaction temperature was kept below 35°. After 3 hr at room temperature, 100 ml of ether was added to promote precipitation. The solid was filtered, washed well with ether, and dried. After two recrystallizations from ethanol–water (1:1), 5.5 g (61% yield) of pure urea, mp 168–171°, was obtained.

Pharmacology—Compounds III*a*–III*h* were tested for antihypertensive activity using genetically spontaneous hypertensive rats by an indirect tail cuff method (1, 4). In a standard 3-day test, systolic blood pressure readings were made at 0 hr (control) on Days 1 and 3 and at 2 hr after administration of the compound on Days 1 and 3. The dose administered was 100 mg/kg po at 0 hr on Days 1, 2, and 3 to groups of six rats per test.

An equal number of nondosed rats were used in each test as a control. Blood pressure for the latter group generally varied from −2 to −10 mm during the test, with readings mostly near the lower value. Activity was determined by comparison of the treatment blood pressure values with the zero-time (control) blood pressure readings. Comparisons were made using the paired *t* test method for evaluation of statistical significance (5). A value of −15 mm or more is considered significant.

RESULTS AND DISCUSSION

The pharmacological data in Table II show that compounds with either aryl or alkyl groups at R_3 were active in lowering blood pressure. Various substituents at the *para*-position in the phenyl ring (III*b*–III*e*) reduced potency relative to the parent molecule (III*a*), a nitro group being particularly deleterious. Cyclohexyl (III*g*) was better than a small alkyl group (III*f*). An analog with 2-methyl and 5,6-dimethoxy substituents (III*h*) in the indole portion of the molecule was less active than III*a* where these groups are absent.

Compound III*a*, which more closely resembles indoramin in structure than the others, was the most potent member of this series. At 100 mg/kg po, III*a* was about as active by Day 3 in lowering blood pressure as 50 mg of indoramin/kg. Compounds III*a* and III*e* were selected for further evaluation in the unanesthetized normotensive dog. Over a 3-day test period, dosing orally each day with 50 mg/kg, no significant decrease in blood pressure was observed for either compound.

The latter result is in sharp contrast to the related and previously described (1) series of formula I, which was very active in both rats and dogs,

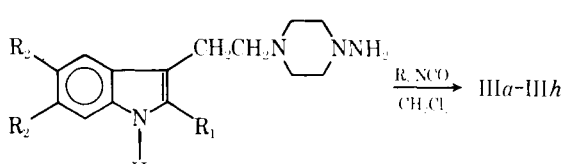

IV*a*: $R_1 = R_2 = H$
IV*b*: $R_1 = CH_3$, $R_2 = CH_3O$

Scheme I

[1] Melting points were taken on a Thomas-Hoover capillary melting-point apparatus and are uncorrected. Elemental analyses were performed by MicroTech Laboratories, Skokie, Ill. The structures of all novel compounds were confirmed by their IR (Perkin-Elmer 457) and NMR (Jeolco $C_{60}HL$) spectra.

[2] The various isocyanates required to prepare the target ureas were obtained from Aldrich Chemical Co., Milwaukee, Wis.

0022-3549/78/1200-1773$01.00/0
© 1978, American Pharmaceutical Association

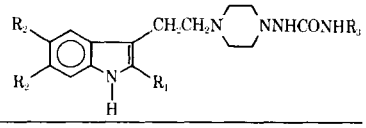

Table I—3-Substituted 1-[4-(2-Indol-3-ylethyl)piperazinyl]ureas

Compound	R_1	R_2	R_3	Yield[a], %	Melting Point	Recrystallization Solvent[b]	Formula	Analysis, %	Calc.	Found
III*a*	H	H		61	168–171°	A	$C_{21}H_{25}N_5O$	C	69.40	69.00
								H	6.92	6.97
								N	19.27	19.45
III*b*	H	H		64	203–205°	B	$C_{21}H_{24}FN_5O$	C	66.13	65.96
								H	6.34	6.30
								N	18.36	18.22
III*c*	H	H		55	212–214°	C	$C_{21}H_{24}ClN_5O$	C	63.38	63.25
								H	6.07	5.98
								N	17.60	17.50
III*d*	H	H	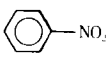	60	206–208°	B	$C_{21}H_{24}N_6O_3$	C	61.75	61.75
								H	5.92	5.88
								N	20.57	20.23
III*e*	H	H	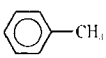	58	201–203°	B	$C_{22}H_{27}N_5O$	C	70.00	69.64
								H	7.21	7.31
								N	18.55	18.58
III*f*	H	H	CH_2CH_3	63	196–199°	C	$C_{17}H_{25}N_5O$	C	64.74	64.60
								H	7.99	7.93
								N	22.20	21.88
III*g*	H	H		63	178–180°	B	$C_{21}H_{31}N_5O$	C	68.26	68.55
								H	8.46	8.55
								N	18.95	18.72
III*h*	CH_3	CH_3O		45	170–173°	C	$C_{24}H_{31}N_5O_3$	C	66.79	66.60
								H	6.95	7.11
								N	15.57	15.92

[a] Yield of analytically pure product; no effort was made to optimize yields. [b] A = dimethylformamide–water, B = ethanol–water, and C = ethyl acetate.

Table II—Hypotensive Response in Spontaneously Hypertensive Rats

Compound[a]	Change in Blood Pressure, mm Hg Day 1	Day 3
III*a*	−47	−77
III*b*	−13	−35
III*c*	−12	−54
III*d*	±[b]	±
III*e*	±	−55
III*f*	−14	−20
III*g*	−46	−44
III*h*	−36	−38
Indoramin hydrochloride	−63	−79[c]

[a] At an oral dose of 100 mg/kg. [b] The ± indicates marginal or transient activity. [c] At an oral dose of 50 mg/kg.

in the latter by a mechanism primarily of α-blockade. Evidently, a subtle change in the linkage between the phenyl and the piperazine rings from amide to urea in structures of this type leads to marked differences in hypotensive activity in the dog.

REFERENCES

(1) E. J. Glamkowski, P. A. Reitano, and D. L. Woodward, *J. Med. Chem.*, **20,** 1485 (1977).

(2) J. L. Archibald, B. J. Alps, J. F. Cavalla, and J. L. Jackson, *ibid.*, **14,** 1054 (1971).

(3) R. B. Royds, D. J. Coltart, and J. D. F. Lockhart, *Clin. Pharmacol. Ther.*, **13,** 380 (1972).

(4) "Methods in Pharmacology," vol. I, A. Schwartz, Ed., Appleton-Century-Crofts, New York, N.Y., 1971, p. 135.

(5) H. C. Batson, "An Introduction to Statistics in the Medical Sciences," Burgess, Minneapolis, Minn., 1956, p. 16.

ACKNOWLEDGMENTS

The authors thank Lee O'Donnell and Romana Fedasiuk for the IR and NMR spectra, Jeffrey Wilker and his group for performing the pharmacological assays, and Irene Field for assistance in the preparation of this manuscript.

Direct Determination of Acetaminophen in Plasma by Differential Pulse Voltammetry

JAMES W. MUNSON ˣ **and HASSAN ABDINE**

Received December 27, 1977, from the *College of Pharmacy, University of Kentucky, Lexington, KY 40506.* Accepted for publication April 27, 1978.

Abstract □ A rapid, simple method for the direct determination of acetaminophen in plasma at toxic levels was developed. The method is based on the oxidation of the phenolic moiety of acetaminophen at a carbon paste electrode in a differential pulse voltammetric mode. Linear calibration curves are obtained from 20 to 400 μg/ml. No sample cleanup is required.

Keyphrases □ Acetaminophen—differential pulse voltammetric analysis in plasma □ Differential pulse voltammetry—analysis, acetaminophen in plasma □ Analgesics—acetaminophen, differential pulse voltammetric analysis in plasma

The increasing use of acetaminophen as a nonprescription analgesic has led to an increase in the occurrence of accidental and intentional ingestion of toxic amounts of this material. In the United Kingdom, deaths from acetaminophen ingestion have increased steadily since 1966 (1). Death from acetaminophen toxicity is usually attributable to liver failure. In all cases of acetaminophen overdose, some degree of liver damage is present.

BACKGROUND

Since plasma acetaminophen levels are indicative of the severity of probable liver damage, the determination of plasma levels is necessary for the selection of the appropriate treatment procedures.

An assay for plasma acetaminophen levels should be rapid and simple. Since overdose patients may be admitted at any time, the assay must be of sufficient simplicity to be performed in the emergency room. A method of estimation frequently employed is the differential absorbance procedure of Routh *et al.* (2), but this method has been criticized because of interferences by other drugs (3). Several methods are based on the nitration procedure of Chafetz *et al.* (4). This reaction was used to determine acetaminophen in plasma following the precipitation of plasma proteins by trichloroacetic acid (5, 6).

The described method is based on oxidation of acetaminophen at a carbon paste electrode (graphite–mineral oil) using differential pulse voltammetry. This method is similar to differential pulse polarography, with the principal difference being in the construction of the working electrode. The current measured in the oxidation of acetaminophen is proportional to the amplitude of the applied potential pulse, the surface area of the working electrode, and the concentration of the electroactive species.

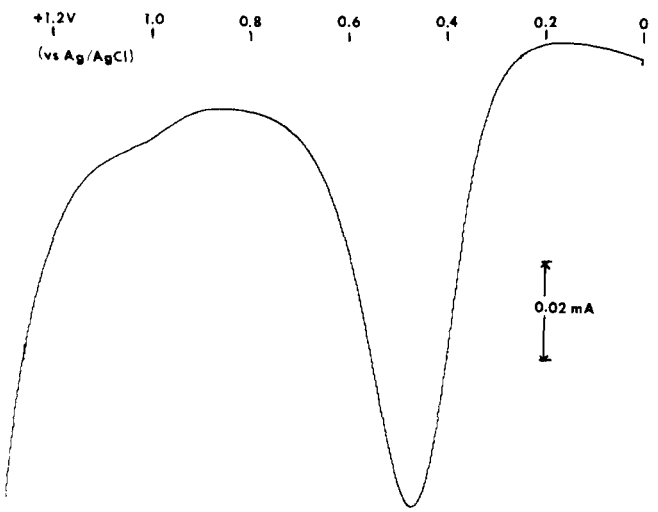

Figure 1—*Differential pulse voltammogram for acetaminophen in plasma. The concentration was 200 μg/ml. The plasma sample was diluted with an equal volume of pH 8 phosphate buffer.*

Differential pulse polarography was utilized in assays for various drugs including chlordiazepoxide (7), diazepam (8), and nitrazepam (9). The differential pulse mode also was applied to the *in vivo* detection of catecholamines with a surface-modified platinum electrode (10). Recently, differential pulse voltammetry at the carbon paste electrode was used to measure trace levels of phenols and aromatic amines (11). This configuration also was used for the determination of theophylline in plasma (12).

Acetaminophen was analyzed in a variety of dosage forms by a method based on linear dc voltammetry at the glassy carbon electrode (13).

This paper describes a method for determining acetaminophen directly in plasma at concentrations of toxicological interest.

EXPERIMENTAL

Reagents—All water was double distilled. Inorganic chemicals were analytical reagent grade and were used without further purification. Acetaminophen[1] was used as received. Individual plasma was obtained from the local blood bank. Phenobarbital, salicylic acid, theophylline, and aspirin were USP grade and were used directly. Theobromine[2] also was used without purification.

Apparatus—A polarographic analyzer system[3] was used for all measurements. A three-electrode configuration with a carbon paste electrode (14) as the working electrode, a silver–silver chloride reference electrode, and a platinum wire auxiliary electrode was used. The surface area (circular) of the carbon paste was 33 cm^2. All scans were taken at a rate of 10 mv/sec with a modulation amplitude of 50 mv and a drop time of 0.5 sec. All measurements were made in the differential pulse mode at ambient temperatures (21–24°).

The working electrode was prepared from a polytef plug (20 mm long × 15-mm diameter). A well (6-mm diameter, 4-mm depth) was drilled in one end of the polytef plug, and a 1-mm hole was drilled through the bottom of the well. A platinum wire (20 gauge) was glued (epoxy resin) into this hole so that 2 mm of the wire protruded into the well. The other end of the wire was soldered to a copper wire, and the polytef plug was glued (epoxy resin) into an open glass tube.

The carbon paste was prepared by levigating 3 g of powdered graphite[4] with 2 g of mineral oil. The paste was packed into the well to exclude any air bubbles, and the surface of the paste was smoothed with a stiff paper card (14).

Procedure—A spiked plasma sample (5.0 ml) was diluted with 5.0 ml of pH 8 phosphate buffer (0.5 *M*). The electrodes were inserted into this mixture, and 5 min was allowed to ensure a quiet solution. Then a differential pulse voltammogram was obtained from +0.2 to 0.8 v. The diffusion current was determined from the peak height and the appropriate scaling factor (current range) of the instrument.

RESULTS AND DISCUSSION

Figure 1 shows a typical differential pulse voltammogram for acetaminophen in plasma with the peak potential of +0.51 v *versus* the silver–silver chloride reference electrode. A typical calibration curve for

[1] McNeil Laboratories, Ft. Washington, Pa.
[2] Pfaltz and Bauer.
[3] Princeton Applied Research Co., model 174.
[4] Ultra Carbon, UCP-1-325, Ultra Carbon Corp., Bay City, MI 48706.

0022-3549/78/1200-1775$01.00/0
© 1978, American Pharmaceutical Association

Table I—Precision Study on Spiked Plasma Samples [a]

Acetaminophen, μg/ml	Current, μamp	CV, %
41	22.7, 21.5, 19.3, 19.5, 17.9 16.9, 18.3, 19.3, 19.3[b]	9.23
101	50.3, 49.1, 51.5, 47.6, 49.9 53.1, 51.1, 53.8, 55.0, 55.4	4.99
202	118.1, 118.1, 114.1, 106.3, 107.0 105.1, 103.1, 101.5, 99.9, 96.8	6.84
403	191.1, 195.0, 191.1, 193.1, 200.9 199.0, 199.0, 195.0[c]	1.97

[a] The data in Table I can be fitted by the equation: current (microamperes) = [acetaminophen (μg/ml)] + 2.88, with $r = 0.9960$ and $S_{y \cdot x} = 5.93$. [b] One determination was rejected because of an irregular peak shape. [c] Two determinations were rejected on a statistical basis according to the method of Dean and Dixon (16).

the range of 20–400 μg/ml can be described by the equation: current (μamp) = 0.438 concentration (μg/ml) + 12.9, with a correlation coefficient of 0.991 and a standard error of the estimate ($S_{y \cdot x}$) of 7.76. Determination of multiple spiked samples gave the results presented in Table I.

Daily minor variations in the slopes of standard curves were attributed to aging of the electrode surface. Consequently, it was necessary to prepare standard curves daily. Plasma samples containing phenobarbital, salicylic acid, theobromine, theophylline, or aspirin at levels of 100 μg/ml gave voltammograms (+0.2–0.8 v) identical to those of blank plasma at a sensitivity setting that produced a half-scale response for acetaminophen at 100 μg/ml.

This method is sufficiently simple and sensitive for the rapid determination of acetaminophen in plasma at levels likely to be encountered in cases of toxic overdosage. Since no sample preparation is required and the instrumentation requires virtually no startup time, this method represents an extremely rapid method for acetaminophen. Since the measurements are made at potentials positive with respect to the reference electrode, dissolved oxygen does not interefere. Hence, sample degassing is not required.

Since the major biotransformation of acetaminophen in humans is direct conjugation with sulfate and glucuronic acid to form the sulfate and glucuronate metabolites (15), these metabolites should not interfere in this assay. In both of these metabolites, the phenolic group, which is oxidized at the carbon paste electrode, is conjugated and unavailable for electrochemical oxidation. Although the instrumentation required for this method is probably not available in many clinical laboratories, the recent introduction of a low-priced unit[5] will undoubtedly make differential pulse voltammetry a more common tool.

REFERENCES

(1) B. G. Gazzard, M. Davis, J. B. Spooner, and R. S. Williams, *J. Int. Med. Res., Suppl. 4*, **4**, 25 (1976).

(2) J. I. Routh, N. A. Shane, E. G. Arrendondo, and W. D. Paul, *Clin. Chem.*, **14**, 882 (1968).

(3) K. Wiener, M. G. Longlands, and B. H. A. Tan, *Ann. Clin. Biochem.*, **13**, 452 (1976).

(4) L. Chafetz, R. E. Daly, H. Schriftman, and J. J. Lomner, *J. Pharm. Sci.*, **60**, 463 (1971).

(5) J. P. Glynn and S. E. Kendal, *Lancet*, **1**, 1147 (1975).

(6) K. Wiener, *Ann. Clin. Biochem.*, **14**, 55 (1977).

(7) M. R. Hackman, M. A. Brooks, J. A. F. de Silva, and T. S. Mas, *Anal. Chem.*, **46**, 1075 (1974).

(8) M. A. Brooks, J. A. F. de Silva, and M. R. Hackman, *Am. Lab.*, **5**, 23 (1973).

(9) S. Halvorsen and E. Jacobsen, *Anal. Chim. Acta*, **59**, 127 (1972).

(10) R. F. Lane, A. T. Hubbard, K. Funkunaga, and R. J. Blanchard, *Brain Res.*, **114**, 346 (1976).

(11) W. M. Chey and R. N. Adams, *J. Electroanal. Chem.*, **75**, 731 (1977).

(12) J. W. Munson and H. Abdine, *Talanta*, **25**, 221 (1978).

(13) C. M. Shearer, K. Christenson, A. Mukheji, and G. J. Papariello, *J. Pharm. Sci.*, **61**, 1627 (1972).

(14) P. T. Kissinger, C. Refshauge, R. Dreiling, and R. N. Adams, *Anal. Lett.*, **6**, 465 (1973).

(15) R. S. Andrews, C. C. Bond, J. Bernett, A. Saunders, and K. Watson, *J. Int. Med. Res., Suppl. 4*, **4**, 34 (1976).

(16) R. B. Dean and W. J. Dixon, *Anal. Chem.*, **23**, 636 (1951).

ACKNOWLEDGMENTS

The authors thank Mr. John Fowler for assistance.

[5] Model 364, Princeton Applied Research, Princeton, N.J.

COMMUNICATIONS

Simplified Derivation of Chiou–Hsu Equation for Rapid Estimation of Total Body Drug Clearance during Constant-Rate Intravenous Infusion

Keyphrases □ Total body drug clearance—rapid estimation during constant-rate intravenous infusion, equation derived □ Clearance, total body drug—rapid estimation during constant-rate intravenous infusion, equation derived □ Pharmacokinetics—rapid estimation of total body drug clearance during constant-rate intravenous infusion, equation derived

To the Editor:

An equation using two sets of plasma level data to estimate the total body clearance (*TBC*) of a substance during a zero-order input to the body was reported previously by Chiou and Hsu (1). The equation is:

$$TBC = \frac{2K_0}{C_{p_1} + C_{p_2}} + \frac{2V_d(C_{p_1} - C_{p_2})}{(C_{p_1} + C_{p_2})(t_2 - t_1)} \qquad \text{(Eq. 1)}$$

where K_0 is the zero-order input rate constant, V_d is the literature estimated apparent volume of distribution based on the linear one-compartment open model, and C_{p_1} and C_{p_2} are plasma levels of the substance at times t_1 and t_2 during the zero-order input, respectively.

This equation was originally proposed to estimate the total body clearance of endogenous creatinine and renal creatinine clearance in patients after a slight modification (1). It also was proposed recently to estimate rapidly the total body clearance of a drug in patients during a constant-rate intravenous infusion (2). Some precautions in using the equation for dosing individualization were discussed (2).

The derivation of Eq. 1 involved the Laplace transform

0022-3549/78/1200-1776$01.00/0

© 1978, American Pharmaceutical Association

Table I—Precision Study on Spiked Plasma Samples [a]

Acetaminophen, μg/ml	Current, μamp	CV, %
41	22.7, 21.5, 19.3, 19.5, 17.9 16.9, 18.3, 19.3, 19.3[b]	9.23
101	50.3, 49.1, 51.5, 47.6, 49.9 53.1, 51.1, 53.8, 55.0, 55.4	4.99
202	118.1, 118.1, 114.1, 106.3, 107.0 105.1, 103.1, 101.5, 99.9, 96.8	6.84
403	191.1, 195.0, 191.1, 193.1, 200.9 199.0, 199.0, 195.0[c]	1.97

[a] The data in Table I can be fitted by the equation: current (microamperes) = [acetaminophen (μg/ml)] + 2.88, with $r = 0.9960$ and $S_{y \cdot x} = 5.93$. [b] One determination was rejected because of an irregular peak shape. [c] Two determinations were rejected on a statistical basis according to the method of Dean and Dixon (16).

the range of 20–400 μg/ml can be described by the equation: current (μamp) = 0.438 concentration (μg/ml) + 12.9, with a correlation coefficient of 0.991 and a standard error of the estimate ($S_{y \cdot x}$) of 7.76. Determination of multiple spiked samples gave the results presented in Table I.

Daily minor variations in the slopes of standard curves were attributed to aging of the electrode surface. Consequently, it was necessary to prepare standard curves daily. Plasma samples containing phenobarbital, salicylic acid, theobromine, theophylline, or aspirin at levels of 100 μg/ml gave voltammograms (+0.2–0.8 v) identical to those of blank plasma at a sensitivity setting that produced a half-scale response for acetaminophen at 100 μg/ml.

This method is sufficiently simple and sensitive for the rapid determination of acetaminophen in plasma at levels likely to be encountered in cases of toxic overdosage. Since no sample preparation is required and the instrumentation requires virtually no startup time, this method represents an extremely rapid method for acetaminophen. Since the measurements are made at potentials positive with respect to the reference electrode, dissolved oxygen does not interefere. Hence, sample degassing is not required.

Since the major biotransformation of acetaminophen in humans is direct conjugation with sulfate and glucuronic acid to form the sulfate and glucuronate metabolites (15), these metabolites should not interfere in this assay. In both of these metabolites, the phenolic group, which is oxidized at the carbon paste electrode, is conjugated and unavailable for electrochemical oxidation. Although the instrumentation required for this method is probably not available in many clinical laboratories, the recent introduction of a low-priced unit[5] will undoubtedly make differential pulse voltammetry a more common tool.

REFERENCES

(1) B. G. Gazzard, M. Davis, J. B. Spooner, and R. S. Williams, *J. Int. Med. Res., Suppl. 4*, **4**, 25 (1976).

(2) J. I. Routh, N. A. Shane, E. G. Arrendondo, and W. D. Paul, *Clin. Chem.*, **14**, 882 (1968).

(3) K. Wiener, M. G. Longlands, and B. H. A. Tan, *Ann. Clin. Biochem.*, **13**, 452 (1976).

(4) L. Chafetz, R. E. Daly, H. Schriftman, and J. J. Lomner, *J. Pharm. Sci.*, **60**, 463 (1971).

(5) J. P. Glynn and S. E. Kendal, *Lancet*, **1**, 1147 (1975).

(6) K. Wiener, *Ann. Clin. Biochem.*, **14**, 55 (1977).

(7) M. R. Hackman, M. A. Brooks, J. A. F. de Silva, and T. S. Mas, *Anal. Chem.*, **46**, 1075 (1974).

(8) M. A. Brooks, J. A. F. de Silva, and M. R. Hackman, *Am. Lab.*, **5**, 23 (1973).

(9) S. Halvorsen and E. Jacobsen, *Anal. Chim. Acta*, **59**, 127 (1972).

(10) R. F. Lane, A. T. Hubbard, K. Funkunaga, and R. J. Blanchard, *Brain Res.*, **114**, 346 (1976).

(11) W. M. Chey and R. N. Adams, *J. Electroanal. Chem.*, **75**, 731 (1977).

(12) J. W. Munson and H. Abdine, *Talanta*, **25**, 221 (1978).

(13) C. M. Shearer, K. Christenson, A. Mukheji, and G. J. Papariello, *J. Pharm. Sci.*, **61**, 1627 (1972).

(14) P. T. Kissinger, C. Refshauge, R. Dreiling, and R. N. Adams, *Anal. Lett.*, **6**, 465 (1973).

(15) R. S. Andrews, C. C. Bond, J. Bernett, A. Saunders, and K. Watson, *J. Int. Med. Res., Suppl. 4*, **4**, 34 (1976).

(16) R. B. Dean and W. J. Dixon, *Anal. Chem.*, **23**, 636 (1951).

ACKNOWLEDGMENTS

The authors thank Mr. John Fowler for assistance.

[5] Model 364, Princeton Applied Research, Princeton, N.J.

COMMUNICATIONS

Simplified Derivation of Chiou–Hsu Equation for Rapid Estimation of Total Body Drug Clearance during Constant-Rate Intravenous Infusion

Keyphrases □ Total body drug clearance—rapid estimation during constant-rate intravenous infusion, equation derived □ Clearance, total body drug—rapid estimation during constant-rate intravenous infusion, equation derived □ Pharmacokinetics—rapid estimation of total body drug clearance during constant-rate intravenous infusion, equation derived

To the Editor:

An equation using two sets of plasma level data to estimate the total body clearance (*TBC*) of a substance during a zero-order input to the body was reported previously by Chiou and Hsu (1). The equation is:

$$TBC = \frac{2K_0}{C_{p_1} + C_{p_2}} + \frac{2V_d(C_{p_1} - C_{p_2})}{(C_{p_1} + C_{p_2})(t_2 - t_1)} \qquad \text{(Eq. 1)}$$

where K_0 is the zero-order input rate constant, V_d is the literature estimated apparent volume of distribution based on the linear one-compartment open model, and C_{p_1} and C_{p_2} are plasma levels of the substance at times t_1 and t_2 during the zero-order input, respectively.

This equation was originally proposed to estimate the total body clearance of endogenous creatinine and renal creatinine clearance in patients after a slight modification (1). It also was proposed recently to estimate rapidly the total body clearance of a drug in patients during a constant-rate intravenous infusion (2). Some precautions in using the equation for dosing individualization were discussed (2).

The derivation of Eq. 1 involved the Laplace transform

0022-3549/78/1200-1776$01.00/0

© 1978, American Pharmaceutical Association

method. However, the same equation can be derived in a much simpler manner, which will be the subject of this communication.

The differential equation for describing the change of concentration of the substance with time during the zero-order input process is:

$$\frac{dC_p}{dt} = \frac{K_0}{V_d} - KC_p \qquad \text{(Eq. 2)}$$

where K is the apparent first-order elimination rate constant for the substance in the body. Equation 2 can be approximated to:

$$\frac{\Delta C_p}{\Delta t} = \frac{C_{p2} - C_{p1}}{t_2 - t_1} = \frac{K_0}{V_d} - KC_{p\,\text{mid}} \qquad \text{(Eq. 3)}$$

Since $C_{p\,\text{mid}}$ can be approximated to be equal to:

$$C_{p\,\text{mid}} = \frac{C_{p1} + C_{p2}}{2} \qquad \text{(Eq. 4)}$$

substitution of Eq. 4 into Eq. 3 results in the following relationship:

$$KV_d = \frac{2K_0}{C_{p1} + C_{p2}} + \frac{2V_d(C_{p1} - C_{p2})}{(C_{p1} + C_{p2})(t_2 - t_1)} \qquad \text{(Eq. 5)}$$

Since $TBC = KV_d$, Eq. 5 is the same as Eq. 1.

(1) W. L. Chiou and F. H. Hsu, *Res. Commun. Chem. Pathol. Pharmacol.*, **10**, 315 (1975).

(2) W. L. Chiou, M. A. F. Gadalla, and G. W. Peng, *J. Pharmacokinet. Biopharm.*, **6**, 135 (1978).

Win L. Chiou

Clinical Pharmacokinetics Laboratory
and Department of Pharmacy
University of Illinois at the Medical Center
Chicago, IL 60612

Received July 21, 1978.
Accepted for publication September 27, 1978.

Dose-Dependent Pharmacokinetics of 7-Chloro-1,3-dihydro-5-(2′-chlorophenyl)-2*H*-1,4-benzodiazepin-2-one in Dogs

Keyphrases ☐ 1,4-Benzodiazepine, substituted—chlorodesmethyldiazepam, pharmacokinetics in dogs ☐ Metabolites—chlorodesmethyldiazepam, pharmacokinetics in dogs ☐ Chlorodesmethyldiazepam—pharmacokinetics in dogs ☐ Pharmacokinetics—chlorodesmethyldiazepam in dogs

To the Editor:

7-Chloro-1,3-dihydro-5-(2′-chlorophenyl)-2*H*-1,4-benzodiazepin-2-one (chlorodesmethyldiazepam, I) is a major metabolite of 2-*o*-chlorobenzoyl-4-chloro-*N*-methyl-*N*′-glycylglycinanilide, a recently developed[1] minor tranquilizer. Compound I undergoes hydroxylation at the C-3 position and is converted to lorazepam (II) by liver microsomal enzymes of rats and mice (1).

When I was administered to dogs intravenously, its plasma level–time curves were dose dependent. No report has appeared concerning the dose-dependent metabolism and nonlinear pharmacokinetics of 1,4-benzodiazepines, in spite of many investigations on their metabolism and pharmacokinetics.

This communication describes a nonlinear pharmacokinetic model to explain the dose-dependent plasma concentration–time curve of I. Simulation values of parameters were derived from this model.

Two male dogs were injected with 0.5, 2.0, and 3.0 mg of I/kg iv. Plasma samples were collected from 10 min to 30 hr after injection. Compound I and free lorazepam were determined by GLC with an electron-capture detector[2]. Lorazepam glucuronide (III) in urine was determined after hydrolysis with glucuronidase–sulfatase. The plasma concentration–time curve following administration of 0.5 mg/kg declined linearly in two phases (distribution and elimination) on a semilogarithmic plot; the 2.0- and 3.0-mg/kg doses gave curves of convex shape after distribution had been completed, with a more pronounced curvature for the higher dose. However, the apparent plasma half-lives of I estimated from the terminal straight region of the curves were nearly equal for the three doses. The plasma concentration–time curves of I, as already mentioned, would exclude enterohepatic circulation as a main elimination pathway of I and/or a conjugate of I. In urine, the major metabolite was lorazepam glucuronide (35%), and only 0.05% of the unchanged drug (total of free and conjugated forms) was excreted over 54 hr. Other metabolites were not detected.

Ethyl alcohol (2) and phenytoin (3) show dose-dependent pharmacokinetics that fit a one-compartment model including the Michaelis–Menten equation.

The most simplified model for the plasma concentration–time curves of I is elaborated on the following assumptions: enterohepatic circulation of I and/or its glucuronide is negligible, and enzymes concerned with the metabolism of I have the same enzyme constants (V_m and K_m). Model equations employed for the plasma level–time curves of I are shown as Eqs. 1 and 2 but cannot be solved with the data of plasma levels only:

$$V_1\frac{dC_1}{dt} = V_2k_{21}C_2 - V_1\left(k_{12}C_1 + \frac{V_mC_1}{K_m + C_1}\right) \qquad \text{(Eq. 1)}$$

$$V_2\frac{dC_2}{dt} = V_1k_{12}C_1 - V_2k_{21}C_2 \qquad \text{(Eq. 2)}$$

Therefore, digital computer simulation was performed by the Runge–Kutta method using the kinetic parameters k_{12}, k_{21}, V_1, and V_2 estimated from the linear two-compartment open model at 0.5 mg/kg. The simulation curves produced a satisfactory fit for the 2.0- and 3.0-mg/kg data. The simulation values obtained were 0.58 and 1.30 μM/hr for V_m and 0.50 and 1.00 μM for K_m in Dogs 1 and 2, respectively. Ten- and one-tenthfold multiple transformations of the simulated V_m and K_m values gave curves significantly different from the experimental data.

These results support the kinetics in which the plasma decline of I obeys the two-compartment model, including

[1] Unpublished results.

[2] To be published.

0022-3549/78/1200-1777$01.00/0
© 1978, American Pharmaceutical Association

method. However, the same equation can be derived in a much simpler manner, which will be the subject of this communication.

The differential equation for describing the change of concentration of the substance with time during the zero-order input process is:

$$\frac{dC_p}{dt} = \frac{K_0}{V_d} - KC_p \qquad \text{(Eq. 2)}$$

where K is the apparent first-order elimination rate constant for the substance in the body. Equation 2 can be approximated to:

$$\frac{\Delta C_p}{\Delta t} = \frac{C_{p2} - C_{p1}}{t_2 - t_1} = \frac{K_0}{V_d} - KC_{p\,\text{mid}} \qquad \text{(Eq. 3)}$$

Since $C_{p\,\text{mid}}$ can be approximated to be equal to:

$$C_{p\,\text{mid}} = \frac{C_{p1} + C_{p2}}{2} \qquad \text{(Eq. 4)}$$

substitution of Eq. 4 into Eq. 3 results in the following relationship:

$$KV_d = \frac{2K_0}{C_{p1} + C_{p2}} + \frac{2V_d(C_{p1} - C_{p2})}{(C_{p1} + C_{p2})(t_2 - t_1)} \qquad \text{(Eq. 5)}$$

Since $TBC = KV_d$, Eq. 5 is the same as Eq. 1.

(1) W. L. Chiou and F. H. Hsu, *Res. Commun. Chem. Pathol. Pharmacol.*, **10**, 315 (1975).

(2) W. L. Chiou, M. A. F. Gadalla, and G. W. Peng, *J. Pharmacokinet. Biopharm.*, **6**, 135 (1978).

Win L. Chiou

Clinical Pharmacokinetics Laboratory
and Department of Pharmacy
University of Illinois at the Medical Center
Chicago, IL 60612

Received July 21, 1978.
Accepted for publication September 27, 1978.

Dose-Dependent Pharmacokinetics of 7-Chloro-1,3-dihydro-5-(2′-chlorophenyl)-2*H*-1,4-benzodiazepin-2-one in Dogs

Keyphrases ☐ 1,4-Benzodiazepine, substituted—chlorodesmethyldiazepam, pharmacokinetics in dogs ☐ Metabolites—chlorodesmethyldiazepam, pharmacokinetics in dogs ☐ Chlorodesmethyldiazepam—pharmacokinetics in dogs ☐ Pharmacokinetics—chlorodesmethyldiazepam in dogs

To the Editor:

7-Chloro-1,3-dihydro-5-(2′-chlorophenyl)-2*H*-1,4-benzodiazepin-2-one (chlorodesmethyldiazepam, I) is a major metabolite of 2-*o*-chlorobenzoyl-4-chloro-*N*-methyl-*N*′-glycylglycinanilide, a recently developed[1] minor tranquilizer. Compound I undergoes hydroxylation at the C-3 position and is converted to lorazepam (II) by liver microsomal enzymes of rats and mice (1).

When I was administered to dogs intravenously, its plasma level–time curves were dose dependent. No report has appeared concerning the dose-dependent metabolism and nonlinear pharmacokinetics of 1,4-benzodiazepines, in spite of many investigations on their metabolism and pharmacokinetics.

This communication describes a nonlinear pharmacokinetic model to explain the dose-dependent plasma concentration–time curve of I. Simulation values of parameters were derived from this model.

Two male dogs were injected with 0.5, 2.0, and 3.0 mg of I/kg iv. Plasma samples were collected from 10 min to 30 hr after injection. Compound I and free lorazepam were determined by GLC with an electron-capture detector[2]. Lorazepam glucuronide (III) in urine was determined after hydrolysis with glucuronidase–sulfatase. The plasma concentration–time curve following administration of 0.5 mg/kg declined linearly in two phases (distribution and elimination) on a semilogarithmic plot; the 2.0- and 3.0-mg/kg doses gave curves of convex shape after distribution had been completed, with a more pronounced curvature for the higher dose. However, the apparent plasma half-lives of I estimated from the terminal straight region of the curves were nearly equal for the three doses. The plasma concentration–time curves of I, as already mentioned, would exclude enterohepatic circulation as a main elimination pathway of I and/or a conjugate of I. In urine, the major metabolite was lorazepam glucuronide (35%), and only 0.05% of the unchanged drug (total of free and conjugated forms) was excreted over 54 hr. Other metabolites were not detected.

Ethyl alcohol (2) and phenytoin (3) show dose-dependent pharmacokinetics that fit a one-compartment model including the Michaelis–Menten equation.

The most simplified model for the plasma concentration–time curves of I is elaborated on the following assumptions: enterohepatic circulation of I and/or its glucuronide is negligible, and enzymes concerned with the metabolism of I have the same enzyme constants (V_m and K_m). Model equations employed for the plasma level–time curves of I are shown as Eqs. 1 and 2 but cannot be solved with the data of plasma levels only:

$$V_1\frac{dC_1}{dt} = V_2k_{21}C_2 - V_1\left(k_{12}C_1 + \frac{V_mC_1}{K_m + C_1}\right) \qquad \text{(Eq. 1)}$$

$$V_2\frac{dC_2}{dt} = V_1k_{12}C_1 - V_2k_{21}C_2 \qquad \text{(Eq. 2)}$$

Therefore, digital computer simulation was performed by the Runge–Kutta method using the kinetic parameters k_{12}, k_{21}, V_1, and V_2 estimated from the linear two-compartment open model at 0.5 mg/kg. The simulation curves produced a satisfactory fit for the 2.0- and 3.0-mg/kg data. The simulation values obtained were 0.58 and 1.30 μM/hr for V_m and 0.50 and 1.00 μM for K_m in Dogs 1 and 2, respectively. Ten- and one-tenthfold multiple transformations of the simulated V_m and K_m values gave curves significantly different from the experimental data.

These results support the kinetics in which the plasma decline of I obeys the two-compartment model, including

[1] Unpublished results.

[2] To be published.

0022-3549/78/1200-1777$01.00/0
© 1978, American Pharmaceutical Association

the Michaelis–Menten equation. Further investigations on the metabolism and extrarenal excretion of I should confirm the described model.

(1) E. Mussini, F. Marcucci, L. Airoldi, T. Facchinetti, and S. Garattini, *J. Pharm. Sci.*, **66**, 1482 (1977).
(2) J. G. Wagner and J. A. Patel, *Res. Commun. Chem. Pathol. Pharmacol.*, **4**, 61 (1972).
(3) N. Gerber and J. G. Wagner, *ibid.*, **3**, 455 (1972).

Masaharu Konishi
Shionogi Research Laboratory
Shionogi & Co., Ltd.
Fukushima-ku, Osaka, 553
Japan

Received June 20, 1978.
Accepted for publication September 26, 1978.
The author thanks Mr. N. Yoshitani of the Shionogi Research Laboratory for allowing the use of his computer program and his assistance in programming the specific model.

BOOKS

REVIEWS

Drug Disposition During Development. Edited by PAOLO LUCIO MORSELLI. Spectrum, 170-20 Wexford Terrace, Jamaica, NY 11423. 1977. 490 pp. 15 × 25 cm. Price $40.00.

The editor of this multiauthored book is outstanding in the field of developmental pharmacology and has gained an international reputation of excellence.

The book is intended to provide investigators, clinical pharmacologists, pediatricians, general practitioners, and medical students with an understanding of the information available on the influence of age on drug disposition and effects from birth to adulthood.

It should be especially valuable to clinical pharmacists and certainly to those relating to children's therapy. There are a number of basic chapters, *e.g.*, pharmacokinetics, DME, and development of enzymes and organs as related to children.

The remaining chapters deal with various drug classes, all as related to the several age groups of childhood. The book accomplishes its purpose clearly and concisely and provides for further excursions into the literature by well-chosen references.

Those who are concerned with children's drug treatment need this book. It is clinically oriented and will be frequently consulted.

Reviewed by Harry C. Shirkey
Department of Pediatrics
University of Cincinnati
Cincinnati, OH 45229

New Drugs: Discovery and Development. (Drugs and the Pharmaceutical Sciences Series, Vol. 5). Edited by ALAN A. RUBIN. Dekker, 270 Madison Ave., New York, NY 10016. 1978. 328 pp. 15 × 23 cm. Price $35.00.

This fifth volume of the Drugs and the Pharmaceutical Sciences Series reviews pertinent background, methodology, present status, and future expectations of nine selected topics in modern drug research. It is unique in that it offers this information from the vantage point of the industrial researcher. All contributors to this volume conduct their research in pharmaceutical company settings where high screening capacity, cost effectiveness, and judicious manpower allocations play a critical role in the search for new drugs. This book discusses the fine balance between these scientific and economic considerations which is vital for successful industrial research.

The nine subjects covered in this volume were selected on the basis of their broad research appeal; they include four chapters on the central nervous system (major and minor tranquilizers, antidepressants, and analgesics), three chapters on the cardiovascular system (antianginals, antiarrhythmics, and antihypertensives), and one each on allergy and arthritis. The authors discuss their personal views concerning the strengths and weaknesses of current drug evaluation methodology, the profile of an ideal drug, and anticipated future developments in their respective areas of expertise.

With 896 references and comprehensive author and subject indexes, this book serves as a timely laboratory guide and desk reference for biologists and chemists involved in pharmaceutical research, whether it be in private industry or academia. It is of particular interest to pharmacologists responsible for evaluation and development of drugs affecting arthritis, allergies, the central nervous system, and the cardiovascular system.

Reviewed by William P. Heilman
Diamond Shamrock Corporation
T. R. Evans Research Center
Painesville, OH 44077

NOTICES

Affinity Chromatography. Journal of Chromatography Library, Vol. 12. By JAROSLAVA TURKOVA. Elsevier Scientific, 52 Vanderbilt Ave., New York, NY 10017. 1978. 405 pp. 18 × 24 cm. Price $69.75.

Fiches de Dosages des Medicaments dans les Millieux Biologiques. Edited by B. FLOUVAT. Expansion Scientifique, 15 Rue Saint-Benoit, 75278 Paris Cedex 06, France. 1978. 21 × 27 cm. Price 75 F.

IARC Monographs on the Evaluation of Carcinogenic Risk of Chemicals to Man. World Health Organization, 49 Sheridan Ave., Albany, NY 12210. 18 × 24 cm.

Vol. 1: Background, Purpose and Scope. 1972. 184 pp.
Vol. 2: Some Inorganic and Organometallic Compounds. 1973. 181 pp.
Vol. 3: Certain Polycyclic Aromatic Hydrocarbons and Heterocyclic Compounds. 1973. 271 pp.
Vol. 4: Some Aromatic Amines, Hydrazine and Related Substances, *N*-Nitroso Compounds, and Miscellaneous Alkylating Agents. 1974. 286 pp.
Vol. 5: Some Organochlorine Pesticides. 1974. 239 pp.
Vol. 6: Sex Hormones. 1974. 243 pp.
Vol. 7: Some Anti-Thyroid and Related Substances, Nitrofurans, and Industrial Chemicals. 1974. 326 pp.
Vol. 8: Some Aromatic Azo Compounds. 1975. 357 pp.
Vol. 9: Some Aziridines, *N*-, *S*-, and *O*-Mustards, and Selenium. 1975. 268 pp.
Vol. 10: Some Naturally Occurring Substances. 1976. 353 pp.
Vol. 11: Cadmium, Nickel, Some Epoxides, Miscellaneous Industrial Chemicals, and General Considerations on Volatile Anaesthetics. 1976. 306 pp.
Vol. 12: Some Carbamates, Thiocarbamates, and Carbazides. 1976. 282 pp.
Vol. 13: Some Miscellaneous Pharmaceutical Substances. 1977. 255 pp.
Vol. 14: Asbestos. 1977. 106 pp.
Vol. 15: Some Fumigants, the Herbicides, 2,4-D and 2,4,5-T, chlorinated Dibenzodioxins, and Miscellaneous Industrial Chemicals. 1977. 354 pp.

the Michaelis–Menten equation. Further investigations on the metabolism and extrarenal excretion of I should confirm the described model.

(1) E. Mussini, F. Marcucci, L. Airoldi, T. Facchinetti, and S. Garattini, *J. Pharm. Sci.*, **66**, 1482 (1977).
(2) J. G. Wagner and J. A. Patel, *Res. Commun. Chem. Pathol. Pharmacol.*, **4**, 61 (1972).
(3) N. Gerber and J. G. Wagner, *ibid.*, **3**, 455 (1972).

Masaharu Konishi
Shionogi Research Laboratory
Shionogi & Co., Ltd.
Fukushima-ku, Osaka, 553
Japan

Received June 20, 1978.
Accepted for publication September 26, 1978.
The author thanks Mr. N. Yoshitani of the Shionogi Research Laboratory for allowing the use of his computer program and his assistance in programming the specific model.

BOOKS

REVIEWS

Drug Disposition During Development. Edited by PAOLO LUCIO MORSELLI. Spectrum, 170-20 Wexford Terrace, Jamaica, NY 11423. 1977. 490 pp. 15 × 25 cm. Price $40.00.

The editor of this multiauthored book is outstanding in the field of developmental pharmacology and has gained an international reputation of excellence.

The book is intended to provide investigators, clinical pharmacologists, pediatricians, general practitioners, and medical students with an understanding of the information available on the influence of age on drug disposition and effects from birth to adulthood.

It should be especially valuable to clinical pharmacists and certainly to those relating to children's therapy. There are a number of basic chapters, *e.g.*, pharmacokinetics, DME, and development of enzymes and organs as related to children.

The remaining chapters deal with various drug classes, all as related to the several age groups of childhood. The book accomplishes its purpose clearly and concisely and provides for further excursions into the literature by well-chosen references.

Those who are concerned with children's drug treatment need this book. It is clinically oriented and will be frequently consulted.

Reviewed by Harry C. Shirkey
Department of Pediatrics
University of Cincinnati
Cincinnati, OH 45229

New Drugs: Discovery and Development. (Drugs and the Pharmaceutical Sciences Series, Vol. 5). Edited by ALAN A. RUBIN. Dekker, 270 Madison Ave., New York, NY 10016. 1978. 328 pp. 15 × 23 cm. Price $35.00.

This fifth volume of the Drugs and the Pharmaceutical Sciences Series reviews pertinent background, methodology, present status, and future expectations of nine selected topics in modern drug research. It is unique in that it offers this information from the vantage point of the industrial researcher. All contributors to this volume conduct their research in pharmaceutical company settings where high screening capacity, cost effectiveness, and judicious manpower allocations play a critical role in the search for new drugs. This book discusses the fine balance between these scientific and economic considerations which is vital for successful industrial research.

The nine subjects covered in this volume were selected on the basis of their broad research appeal; they include four chapters on the central nervous system (major and minor tranquilizers, antidepressants, and analgesics), three chapters on the cardiovascular system (antianginals, antiarrhythmics, and antihypertensives), and one each on allergy and arthritis. The authors discuss their personal views concerning the strengths and weaknesses of current drug evaluation methodology, the profile of an ideal drug, and anticipated future developments in their respective areas of expertise.

With 896 references and comprehensive author and subject indexes, this book serves as a timely laboratory guide and desk reference for biologists and chemists involved in pharmaceutical research, whether it be in private industry or academia. It is of particular interest to pharmacologists responsible for evaluation and development of drugs affecting arthritis, allergies, the central nervous system, and the cardiovascular system.

Reviewed by William P. Heilman
Diamond Shamrock Corporation
T. R. Evans Research Center
Painesville, OH 44077

NOTICES

Affinity Chromatography. Journal of Chromatography Library, Vol. 12. By JAROSLAVA TURKOVA. Elsevier Scientific, 52 Vanderbilt Ave., New York, NY 10017. 1978. 405 pp. 18 × 24 cm. Price $69.75.

Fiches de Dosages des Medicaments dans les Millieux Biologiques. Edited by B. FLOUVAT. Expansion Scientifique, 15 Rue Saint-Benoit, 75278 Paris Cedex 06, France. 1978. 21 × 27 cm. Price 75 F.

IARC Monographs on the Evaluation of Carcinogenic Risk of Chemicals to Man. World Health Organization, 49 Sheridan Ave., Albany, NY 12210. 18 × 24 cm.

Vol. 1: Background, Purpose and Scope. 1972. 184 pp.
Vol. 2: Some Inorganic and Organometallic Compounds. 1973. 181 pp.
Vol. 3: Certain Polycyclic Aromatic Hydrocarbons and Heterocyclic Compounds. 1973. 271 pp.
Vol. 4: Some Aromatic Amines, Hydrazine and Related Substances, *N*-Nitroso Compounds, and Miscellaneous Alkylating Agents. 1974. 286 pp.
Vol. 5: Some Organochlorine Pesticides. 1974. 239 pp.
Vol. 6: Sex Hormones. 1974. 243 pp.
Vol. 7: Some Anti-Thyroid and Related Substances, Nitrofurans, and Industrial Chemicals. 1974. 326 pp.
Vol. 8: Some Aromatic Azo Compounds. 1975. 357 pp.
Vol. 9: Some Aziridines, *N*-, *S*-, and *O*-Mustards, and Selenium. 1975. 268 pp.
Vol. 10: Some Naturally Occurring Substances. 1976. 353 pp.
Vol. 11: Cadmium, Nickel, Some Epoxides, Miscellaneous Industrial Chemicals, and General Considerations on Volatile Anaesthetics. 1976. 306 pp.
Vol. 12: Some Carbamates, Thiocarbamates, and Carbazides. 1976. 282 pp.
Vol. 13: Some Miscellaneous Pharmaceutical Substances. 1977. 255 pp.
Vol. 14: Asbestos. 1977. 106 pp.
Vol. 15: Some Fumigants, the Herbicides, 2,4-D and 2,4,5-T, chlorinated Dibenzodioxins, and Miscellaneous Industrial Chemicals. 1977. 354 pp.

the Michaelis–Menten equation. Further investigations on the metabolism and extrarenal excretion of I should confirm the described model.

(1) E. Mussini, F. Marcucci, L. Airoldi, T. Facchinetti, and S. Garattini, *J. Pharm. Sci.*, **66**, 1482 (1977).
(2) J. G. Wagner and J. A. Patel, *Res. Commun. Chem. Pathol. Pharmacol.*, **4**, 61 (1972).
(3) N. Gerber and J. G. Wagner, *ibid.*, **3**, 455 (1972).

Masaharu Konishi
Shionogi Research Laboratory
Shionogi & Co., Ltd.
Fukushima-ku, Osaka, 553
Japan

Received June 20, 1978.
Accepted for publication September 26, 1978.
The author thanks Mr. N. Yoshitani of the Shionogi Research Laboratory for allowing the use of his computer program and his assistance in programming the specific model.

BOOKS

REVIEWS

Drug Disposition During Development. Edited by PAOLO LUCIO MORSELLI. Spectrum, 170-20 Wexford Terrace, Jamaica, NY 11423. 1977. 490 pp. 15 × 25 cm. Price $40.00.

The editor of this multiauthored book is outstanding in the field of developmental pharmacology and has gained an international reputation of excellence.

The book is intended to provide investigators, clinical pharmacologists, pediatricians, general practitioners, and medical students with an understanding of the information available on the influence of age on drug disposition and effects from birth to adulthood.

It should be especially valuable to clinical pharmacists and certainly to those relating to children's therapy. There are a number of basic chapters, *e.g.*, pharmacokinetics, DME, and development of enzymes and organs as related to children.

The remaining chapters deal with various drug classes, all as related to the several age groups of childhood. The book accomplishes its purpose clearly and concisely and provides for further excursions into the literature by well-chosen references.

Those who are concerned with children's drug treatment need this book. It is clinically oriented and will be frequently consulted.

Reviewed by Harry C. Shirkey
Department of Pediatrics
University of Cincinnati
Cincinnati, OH 45229

New Drugs: Discovery and Development. (Drugs and the Pharmaceutical Sciences Series, Vol. 5). Edited by ALAN A. RUBIN. Dekker, 270 Madison Ave., New York, NY 10016. 1978. 328 pp. 15 × 23 cm. Price $35.00.

This fifth volume of the Drugs and the Pharmaceutical Sciences Series reviews pertinent background, methodology, present status, and future expectations of nine selected topics in modern drug research. It is unique in that it offers this information from the vantage point of the industrial researcher. All contributors to this volume conduct their research in pharmaceutical company settings where high screening capacity, cost effectiveness, and judicious manpower allocations play a critical role in the search for new drugs. This book discusses the fine balance between these scientific and economic considerations which is vital for successful industrial research.

The nine subjects covered in this volume were selected on the basis of their broad research appeal; they include four chapters on the central nervous system (major and minor tranquilizers, antidepressants, and analgesics), three chapters on the cardiovascular system (antianginals, antiarrhythmics, and antihypertensives), and one each on allergy and arthritis. The authors discuss their personal views concerning the strengths and weaknesses of current drug evaluation methodology, the profile of an ideal drug, and anticipated future developments in their respective areas of expertise.

With 896 references and comprehensive author and subject indexes, this book serves as a timely laboratory guide and desk reference for biologists and chemists involved in pharmaceutical research, whether it be in private industry or academia. It is of particular interest to pharmacologists responsible for evaluation and development of drugs affecting arthritis, allergies, the central nervous system, and the cardiovascular system.

Reviewed by William P. Heilman
Diamond Shamrock Corporation
T. R. Evans Research Center
Painesville, OH 44077

NOTICES

Affinity Chromatography. Journal of Chromatography Library, Vol. 12. By JAROSLAVA TURKOVA. Elsevier Scientific, 52 Vanderbilt Ave., New York, NY 10017. 1978. 405 pp. 18 × 24 cm. Price $69.75.

Fiches de Dosages des Medicaments dans les Millieux Biologiques. Edited by B. FLOUVAT. Expansion Scientifique, 15 Rue Saint-Benoit, 75278 Paris Cedex 06, France. 1978. 21 × 27 cm. Price 75 F.

IARC Monographs on the Evaluation of Carcinogenic Risk of Chemicals to Man. World Health Organization, 49 Sheridan Ave., Albany, NY 12210. 18 × 24 cm.

Vol. 1: Background, Purpose and Scope. 1972. 184 pp.
Vol. 2: Some Inorganic and Organometallic Compounds. 1973. 181 pp.
Vol. 3: Certain Polycyclic Aromatic Hydrocarbons and Heterocyclic Compounds. 1973. 271 pp.
Vol. 4: Some Aromatic Amines, Hydrazine and Related Substances, *N*-Nitroso Compounds, and Miscellaneous Alkylating Agents. 1974. 286 pp.
Vol. 5: Some Organochlorine Pesticides. 1974. 239 pp.
Vol. 6: Sex Hormones. 1974. 243 pp.
Vol. 7: Some Anti-Thyroid and Related Substances, Nitrofurans, and Industrial Chemicals. 1974. 326 pp.
Vol. 8: Some Aromatic Azo Compounds. 1975. 357 pp.
Vol. 9: Some Aziridines, *N*-, *S*-, and *O*-Mustards, and Selenium. 1975. 268 pp.
Vol. 10: Some Naturally Occurring Substances. 1976. 353 pp.
Vol. 11: Cadmium, Nickel, Some Epoxides, Miscellaneous Industrial Chemicals, and General Considerations on Volatile Anaesthetics. 1976. 306 pp.
Vol. 12: Some Carbamates, Thiocarbamates, and Carbazides. 1976. 282 pp.
Vol. 13: Some Miscellaneous Pharmaceutical Substances. 1977. 255 pp.
Vol. 14: Asbestos. 1977. 106 pp.
Vol. 15: Some Fumigants, the Herbicides, 2,4-D and 2,4,5-T, chlorinated Dibenzodioxins, and Miscellaneous Industrial Chemicals. 1977. 354 pp.

ERRATA

In the article titled "GLC Determination of Phenylbutazone in Human Plasma" (1), the following corrections should be made:

On page 243, column 2, the fourth line of the second paragraph should read "4-butyl-1,2-di(*p*-tolyl)-3,5-pyrazolidinedione (II)."

On page 243, column 2, Structure II should be:

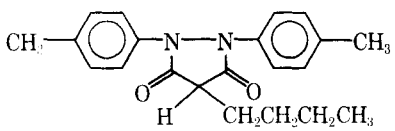

(1) A. Sioufi, F. Caudal, and F. Marfil, *J. Pharm. Sci.*, **67**, 243 (1978).

In the article titled "Rapid High-Pressure Liquid Chromatographic Determination of Quinidine and Dihydroquinidine in Plasma Samples" (1), the following correction should be made:

On page 269, column 2, under *Mobile Phase Preparation*, the third line should read "(0.01 mole)" instead of "(0.001 mole)."

(1) R. E. Kates, D. W. McKennon, and T. J. Comstock, *J. Pharm. Sci.*, **67**, 269 (1978).

In the article titled "Recommendations to Eliminate Subjective Olfactory Methods from Compendial Identification Tests" (1), the following correction should be made:

On page 542, column 1, under *Phenylmercuric Acetate*, the first line of the second paragraph should read "1000-ml erlenmeyer flask" instead of "10-ml erlenmeyer flask."

(1) G. Schwartzman, *J. Pharm. Sci.*, **67**, 539 (1978).

In the article titled "Electronic Structure–Activity Relationships of Antibacterial Acridines" (1), the following corrections should be made:

On page 707, column 2, the *F* values in Eqs. 7, 8, and 9 should be 25.87, 6.63, and 5.03, respectively.

(1) P. Singh and S. P. Gupta, *J. Pharm. Sci.*, **67**, 706 (1978).

Hydrocortisone Stability in Ethanol

In reference to my paper[1] "Effect of Vehicle and Other Active Ingredients on Stability of Hydrocortisone" and the recent comments by Chen[2], I would like to report that hydrocortisone is very stable in alcohol. In my experience of about 8 years, heating the sample in alcohol on a hot plate just to boiling has never caused any stability problem.

V. Das Gupta
College of Pharmacy
University of Houston
Houston, TX 77004

Received October 2, 1978.

[1] V. D. Gupta, *J. Pharm. Sci.*, **67**, 299 (1978).
[2] J. R. Chen, *ibid.*, 67(9), IV (1978).

U.S. Postal Service
Statement of Ownership, Management and Circulation
(Required by 39 U.S.C. 3685)

1. Title of publication: Journal of Pharmaceutical Sciences
2. Date of filing: Oct. 10, 1978
3. Frequency of issue: Monthly
4. Location of known office of publication: 2215 Constitution Ave. NW, Washington, DC 20037
5. Location of headquarters or general business offices of the publishers: 2215 Constitution Ave. NW, Washington, DC 20037
6. Names and complete addresses of publisher, editor and managing editor: American Pharmaceutical Association, publisher; Mary H. Ferguson, editor; William S. Apple, Managing Editor; 2215 Constitution Ave. NW, Washington, DC 20037
7. Owner: American Pharmaceutical Association, 2215 Constitution Ave. NW, Washington, DC 20037
8. Known bondholders, mortgagees and other security holders owning or holding one percent or more of total amount of bonds, mortgages or other securities: None
9. *For completion by nonprofit organizations authorized to mail at special rates* (section 132. 122, PSM). The purpose, function, and nonprofit status of this organization and the exempt status for federal income tax purposes have not changed during preceding 12 months
10. Extent and nature of circulation:

	Average no. copies each issue preceding 12 months	Actual no. copies of single issue published nearest to filing date
A. Total number of copies printed (net press run)	9,681	9,604
B. Paid circulation		
1. Sales through dealers and carriers, street vendors and counter sales:	0	0
2. Mail subscriptions	9,157	8,895
C. Total paid circulation (sum of 10B1 and 10B2)	9,157	8,895
D. Free distribution by mail carrier or other means, samples, complimentary and other free copies	133	133
E. Total distribution (sum of C and D):	9,290	9,028
F. Copies not distributed		
1. Office use, left over, unaccounted, spoiled after printing	391	576
2. Returns from news agents	0	0
G. Total (sum of E, F1, and F2—should equal net press run shown in A)	9,681	9,604

I certify that the statements made by me above are correct and complete, Mary H. Ferguson, editor

College of Pharmacy and Allied Health Professions
Wayne State University
Faculty Position in Pharmaceutics

Applications are invited for a faculty position in pharmaceutics at the assistant professor or associate professor level. The candidates must have a Ph.D. degree in physical pharmacy. An undergraduate degree in pharmacy is required.

The successful candidate is expected to contribute to the undergraduate and graduate teaching programs in pharmaceutics and initiate a vigorous research program.

This position is a 12-month appointment and salary is negotiable based on qualifications. This position is to be filled by July 1, 1979.

Interested individuals should send letters of application, curriculum vitae and names of three references to: **Dr. J. B. Nagwekar, Chairman, Search Committee, Wayne State University, College of Pharmacy and Allied Health Professions, 511 Health Sciences Building, Detroit, Michigan 48202.**

Wayne State University is an Equal Opportunity/Affirmative Action Employer.

PHARMACEUTICS/PHYSICAL PHARMACY

Applications are invited for a tenurable faculty position. The rank of assistant or associate professor and the salary on a 9-month basis are negotiable. The successful candidate must have the Ph.D. in pharmaceutics. A B.S. degree in pharmacy is desired.

Teaching responsibilities include presentations in principles of dosage form design and physical pharmacy. The development of an active research program in pharmaceutics is necessary. Other responsibilities include individual or committee activities that may be assumed or assigned in relation to the effective functioning of a health sciences professional school.

Starting date is September 1, 1979. Send curriculum vitae, graduate school transcript, and three letters of reference to: **Dr. Richard E. Lindstrom, Chairman, Pharmaceutics Section, School of Pharmacy, The University of Connecticut, Storrs, CT 06268.**

An Equal Opportunity Employer

PHYSICAL ORGANIC CHEMIST

San Francisco Peninsula

SYNTEX RESEARCH, a leader in the Health Care field, has an opportunity for a Scientist interested in physical-organic chemistry. This entry-level position in the Preformulation Department requires a PhD in Chemistry or Pharmacy, with major research emphasis in Physical-Organic Chemistry.

Responsibilities of this position include:

- **Chemical kinetic investigation for the purpose of elucidating reaction mechanisms & predicting the chemical reactivity of potential new drugs;**
- **Isolation, identification & synthesis of decomposition products of potential new drugs;**
- **Development of analytical methodology for new drug substances with major emphasis on high pressure liquid chromatography.**

SYNTEX offers a stimulating environment in which to advance your professionalism. Our compensation & complete benefits are most attractive. Please send resume to **A. Hall,** (Refer to Job # 7750), **SYNTEX, 3401 Hillview Ave., Palo Alto, CA 94304.** We are an equal opportunity employer.

SYNTEX